Intramolecular Interaction between Hydroxyl Group and π-Electrons. XVIII[1]. *Proton Magnetic Resonance Spectra of Aryldimethylcarbinols and Related Compounds*

By Michinori Ōki and Hiizu Iwamura

(Received June 26, 1962)

It has been recognized that aryldimethylcarbinols are the examples which have the intramolecular interaction between the hydroxyl group and the π-electrons (II). In a previous paper[2] the effect of the substituents on the equilibrium between I and II was investigated

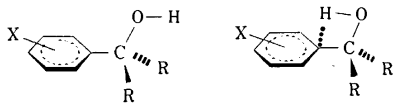

I II

by infrared spectroscopy. In short, the ratios of the two absorption intensities, A_{II}/A_{I}, which may be regarded to express the equilibrium constant, K, are in linear relation with the Hammett's sigma constants with the negative inclination of $\rho = -0.358$ and the phenomenon has been attributed to the varied π-electron density on the benzene ring as a proton acceptor.

Recent exploitation of NMR spectroscopy as a tool of studying the hydrogen bonding[3] and of detecting the weaker interaction involving hydrogen atom prompted the present authors to study the above system by this newer method.

The chemical shifts of OH proton should differ greatly in I and II. Since the population of the molecular species depends remarkably on the ring substituents, the apparent chemical shifts of OH proton, which will appear singly at the average position between the signals characteristic of I and II, is expected to vary with the substituents.

Owing to the associative nature of the aryldimethylcarbinols, the data obtainable at the most dilute solution (ca. 10^{-2} mol./l.) with use of a nowadays available spectrometer have the contribution of the associated species and cannot reflect directly the status of the aforementioned equilibrium of monomeric nature. In these connections, measurement must be carried out over a range of finite concentration to describe the nature of the association and the data obtained was extrapolated to those at infinite dilution with which the discussion of the equilibrium, I ⇌ II, was attempted.

Experimental

Spectral Measurements.—NMR spectra were obtained by a Varian DP-60 high resolution NMR spectrometer at 60 Mc./sec. The samples were dissolved to a given concentration in carbon tetrachloride and sealed in glass tubes with outside diameter of 5 mm., the chemical shifts in p. p. m. being referred to cyclohexane as an internal standard. The side-band technique was employed to measure the precise chemical shifts[4].

Materials.—Preparation and purity of the compounds have been described in the previous paper[2].

Results and Discussion

The assignments of the NMR signals of the aryldimethylcarbinols which consist of a methyl signal with the intensity of six protons, an OH signal, multiplet signals due to the ring protons, and signals due to the ring substituents, if any, are straightforward. Out of these only the OH proton signal moves significantly with the varying concentration. In Figs. 1 and 2 are illustrated the displacement, due to the change in concentration, of the chemical shift of the OH proton of dimethylphenylcarbinol. It is well known that in a solution of associable solute, there is a definite composition at a given concentration between the several species possible, e.g., monomer, dimer, trimer, and the higher polymers. Although they have different kinds of the hydroxyl group and thus show different ν_{O-H}'s at the same time in the infrared absorption, NMR spectrum of the system shows usually a single OH proton signal, owing to the rapid exchange between, and consequent averaging of, the protons of various kinds. That is, the apparent chemical shift (δ^{a}) of the OH proton at a given concentration can be expressed as follows, where

1) Part XVII: M. Ōki and H. Iwamura, This Bulletin, 35, 1744 (1962).
2) Part XVI: M. Ōki and H. Iwamura, ibid., 35, 1552 (1962).
3) J. A. Pople, W. G. Schneider and H. J. Bernstein, "High-Resolution Nuclear Magnetic Resonance", McGraw-Hill Book Co., Inc., New York, N. Y. (1959), p. 400.
4) J. T. Arnold and M. E. Packard, *J. Chem. Phys.*, **19**, 1608 (1951).

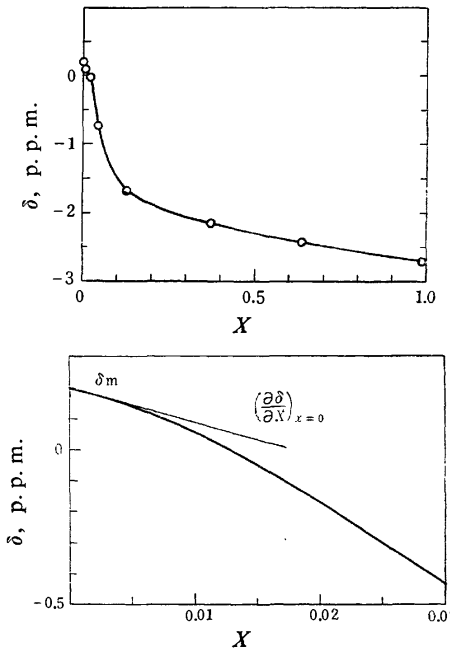

Figs. 1 and 2. Dilution shifts of OH proton signal, δ (in p. p. m. from cyclohexane) versus mole fraction (X) of dimethylphenylcarbinol.

δ_i and x_i represent the chemical shift characteristic of, and the mole fraction of, the i'th

$$\delta^a=\sum_i \delta_i x_i \qquad \sum_i x_i=1 \tag{1}$$

species, respectively, and the summation is made over the whole species present. x_i's are related each other by the respective equilibrium constant, K_{ij}. Since the change in the total concentration (X) accompanies the redistribution between x_i's, δ^a becomes dependent on the concentration.

$$K_{ij}=\frac{(x_j)^n}{(x_i)^m} \tag{2}$$

Although it is almost impossible to analyze the formula 1 over a whole range of concentration, it may be possible to derive Eq. 3 as an approximation in the lower concentration region ($X\leq 0.02$) where the contribution of only the first two terms, that is, monomer and dimer, may be regarded to be major. Here δ_m and δ_d represent the chemical shifts of the OH protons characteristic of monomer and dimer,

$$\delta^a=\delta_m x_m+\delta_d x_d \tag{3}$$ [5]

respectively. K stands for the equilibrium constant of dimerization (Eq. 4). Equation 5 is obtained by differentiating Eq. 3 and taking the limit. Since the left side of Eq. 5 is obtainable from the limiting slope of the δ

$$K=\frac{x_d}{x_m{}^2} \tag{4}$$

$$\left(\frac{\partial\delta^a}{\partial X}\right)_{x=0}=2K(\delta_d-\delta_m) \tag{5}$$

versus X curve in each carbinol (Fig. 2), it is now possible to derive either K or $\delta_d-\delta_m$, if the data of the other are available. It was the authors' choice to determine $\delta_m-\delta_d$ with use the value of K which is available independently from the infrared spectroscopy. To this purpose, the variation of ε at the absorption maximum of the monomeric ν_{O-H}, 3606 cm^{-1}, with concentration, was measured. Supposing that this ε_m represents the apparent absorption coefficient of the band due only to monomer, and that dimer is cyclic, the limiting slope of the ε_m versus concentration curve is found to be related to the equilibrium constant for dimer formation by Eq. 6;

$$\left(\frac{\partial\varepsilon_m}{\partial C}\right)_{c=0}=-2K_c\,\varepsilon_m{}^0 \tag{6}$$ [6]

where $\varepsilon_m{}^0$ stands for ε_m at infinite dilution. The equilibrium constant expressed in terms of mole fraction (K_x) can be related to K_c by $K_x=K_c\times 10$ for the carbon tetrachloride solution.

In Table I are listed the OH proton chemical shift at infinite dilution, δ_m, the limiting slope of the δ versus X curve, $-\left(\frac{\partial\delta^a}{\partial X}\right)_{x=0}$, the equilibrium constant for dimer formation, K, and the difference in the chemical shift between monomer and dimer, $\delta_m-\delta_d$.

As shown in Fig. 3, K and $\delta_m-\delta_d$ are roughly in linear relation with the Hammett's sigma constants. They are also proportional to each other. Strictly speaking, the linearity with a positive slope which reign over the substituents of positive sigma value does not hold true for those of negative sigma constant. It is naturally expected that any ring substitution produces counteracting effect on dimerization. Those substituents which strengthen the proton donor ability of the hydroxyl group are weakening its proton accepting power at the same time. The above finding indicates that, while the electron-withdrawing substituents strengthen the dimerization in effect, the action is just balanced in the case of the electron-donating substituents. Since $\delta_m-\delta_d$ may be regarded to correspond to the strength ($-\Delta E$) of the association[7], the linearity between $\delta_m-\delta_d$ and

5) E. D. Becker, U. Liddel and J. N. Shoolery, *J. Mol. Spectroscopy*, 2, 1 (1958).

6) U. Liddel and E. D. Becker, *Spectrochim. Acta*, 10, 70 (1957).

7) L. W. Reeves, E. A. Allan and K. O. Strømme, *Can. J. Chem.*, 38, 1249 (1960).

K is satisfying the relation, $-RT \ln K = \Delta E - T\Delta S$, where no anomaly in ΔS term is involved. This implies that the dimers of the aryldimethylcarbinols must have a similar structure.

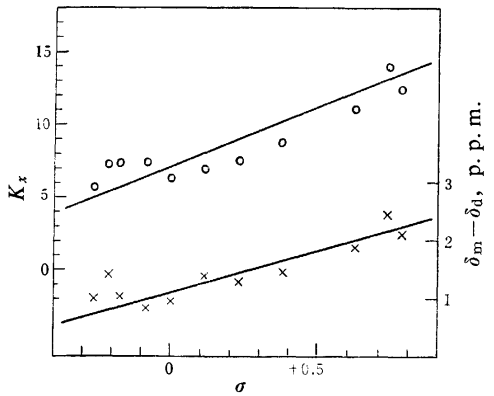

Fig. 3. The effect of the nuclear substitution on the dimer formation of aryldimethylcarbinols; the circle and the cross representing the equilibrium constant K_x and dimerization shift, $\delta_m-\delta_d$, respectively.

TABLE I. THE CHEMICAL SHIFTS OF OH PROTON AT INFINITE DILUTION IN CARBON TETRACHLORIDE AND THE DATA FOR THE DIMER FORMATION OF ARYLDIMETHYLCARBINOLS AND RELATED COMPOUNDS

$X\text{-}C_6H_4C(CH_3)_2OH$

X	δ_m p.p.m.	$-\left(\frac{\partial\delta^a}{\partial X}\right)_{x=0}$	K	$\delta_m-\delta_d$ p.p.m.
p-NO_2	0.26	54	12.5	2.17
m-NO_2	0.25	68	14.0	2.43
p-CO_2CH_3	0.24	45	11.2	2.01
m-Cl	0.28	25	8.7	1.44
p-Cl	0.23	20	7.4	1.35
m-MeO	0.26	19	6.9	1.38
H	0.20	12.7	6.5	0.98
m-CH_3	0.28	13	7.2	0.90
p-CH_3	0.29	14	7.2	0.98
m-Me_2N	0.23	20	7.3	1.38
p-MeO	0.33	12	5.6	1.09
p-$PhCH_2O$	0.29	15	6.2	1.21
Diethylphenylcarbinol	0.25	7	3.6	0.97
1-Methyl-1, 2, 3, 4-tetrahydro-1-naphthol	0.30	19	9.3	1.02
1-Phenylcyclohexanol	0.33	10	5.9	0.85

δ_m obtained by extrapolating δ versus X curve to the infinite dilution is only concerned with the monomeric hydroxyl proton. Since aryldimethylcarbinols have the equilibrium I $\rightleftharpoons$ II at this state, δ_m may be put as follows.

$$\delta_m = \delta_I x_I + \delta_{II} x_{II} \qquad (7)$$

The previous finding by infrared spectroscopy[2] that x_{II}/x_I ranges from 0.85 (for *p*-nitrophenyldimethylcarbinol) to 4.0 (for 1-phenylcyclohexanol) may make one to expect that δ_m would vary considerably with different substituents according to Eq. 7. However, as shown in Fig. 4, it is not the case and δ_m's are almost independent of the substituents.

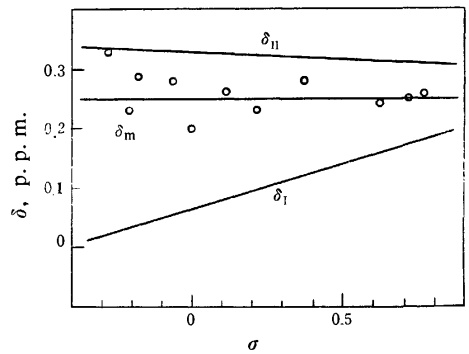

Fig. 4. The effect of the ring substituents on the monomeric OH proton shifts in aryldimethylcarbinols.

As regards the conformation of isomers, I and II, now assume that the plane made by C_α-O-H group will be situated perpendicularly to that of the benzene ring[8] and that the bonds, Ar-C_α and O-H, will be disposed around the C_α-O bond to be "trans" and "cis", for I and II, respectively. Then through the diamagnetic anisotropy of the benzene ring with the π-current of $J=\frac{3e^2H_o}{2\pi mc}$ [9], the hydroxyl proton in I will be deshielded by 0.234 p. p. m., while that of II will suffer from diamagnetic shift of 0.035 p. p. m., with respect to the hydroxyl proton indifferent to the ring current. A measure of $\delta_{II}-\delta_I=0.27$ p. p. m. has now been obtained.

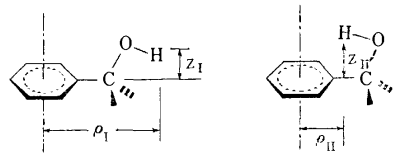

I' II'

In order to see whether the above postulate on the conformations I and II be valid, δ_I and δ_{II} were actually determined, by solving Eq. 7 and $\delta_{II}-\delta_I=0.27$ simultaneously, for the selected examples listed in Table II in which the π-electron density on the benzene ring may be considered to be equivalent. Fairly

8) J. C. Evans, *Spectrochim. Acta*, 17, 129 (1961).
9) E. C. Johnson, Jr. and F. A. Bovey, *J. Chem. Phys.*, 29, 1012 (1958).

good constancy of the calculated values of δ_I and δ_{II} obtained suggests the adequacy of the above conformations, I and II.

If δ_I and δ_{II} were constant over a whole range of the aryldimethylcarbinols, δ_m should have decreased with the increasing sigma value, because x_{II}/x_I has been shown to decrease in this order. The observed apparent indifference irrespective of the substituents must be ascribed to the change in the π-ring current. The reduced π-current density caused by the substitution with electron-withdrawing substituent will bring about the diminution of the ring current effect for both hydroxyl groups in I and II. However, the degree of this suffering may be seven times (derived from 0.234/0.035) greater in I than in II. That is, the absolute value of the positive slope of δ_I must be seven times greater than that of the negative inclination in δ_{II}, when they are plotted to the sigma constants, as illustrated in Fig. 4. Therefore, δ_m does not necessarily decrease proportionally to the decrease in x_{II}/x_I when the electron-withdrawing substituent is present.

TABLE II. THE COMPUTED OH PROTON SHIFTS IN THE CONFORMATION II

Carbinol	δ_m p. p. m.	x_I*	δ_{II}** p. p. m.
Dimethylphenylcarbinol	0.20	0.35	0.30
Dimethyl-*p*-methylphenylcarbinol	0.29	0.31	0.37
Dimethyl-*m*-methylphenylcarbinol	0.28	0.36	0.38
Diethylphenylcarbinol	0.25	0.56	0.40
1-Methyl-1, 2, 3, 4-tetrahydro-1-naphthol	0.30	0.41	0.41
1-Phenylcyclohexanol	0.33	0.21	0.39

* $x_I=\frac{A_I}{A_I+A_{II}}$, where A stands for the integrated intensity[2].

** $\delta_{II}=\delta_m+0.27\,x_I$

The authors are indebted to Professor Yoshiyuki Urushibara and Professor Shizuo Fujiwara for their encouragement and valuable discussion, and to Dr. Yo-ichiro Mashiko and Dr. Kenkichi Nukada for permitting the use of the spectrometer.

Department of Chemistry
Faculty of Science
The University of Tokyo
Hongo, Tokyo

Etude sur l'Équilibre de l'Échange d'Ion des Terres Rares avec la Solution Complexe des Métaux Lourds et des Acides Aminopolycarboxyliques

Par Haruo NATSUME*

(Reçu le 16 Février, 1962)

L'acide éthylènediaminetétraacétique a été, ainsi que d'autres acides complexants, un des premiers éluants essayés pour la séparation de terres rares en microquantité sur résine échangeuse d'ion. Son efficacité s'était révélée bien supérieure à celle d'autres acides, cependant on avait renoncé à l'employer à cause de son insuffisante solubilité dans le domaine utile de pH[1]. Plus tard, Ichikawa a séparé le Ce et le Pm à l'aide de cet acide[2] et Suzuki a constaté une anomalie[3], c'est que lorsque l'on baisse progressivement le pH de la solution éluante pour les mieux séparer, l'élution devient tout d'un coup impossible vers pH 3.2. Nous en concluons que cet acide se trouverait sous forme cationique par les atomes d'azote au dessous d'une certaine valeur de pH, et pourrait être fixé lui-même sur la colonne de résine[4]. Dans ces expériences on n'est jamais arrivé à l'efficacité de séparation que faisaient espérer les constantes de formation des complexes que forment cet acide avec les terres rares.

Pendant ce temps l'utilisation de cet acide, et des acides aminopolycarboxyliques en

* Adresse présente, Institut de Recherche de l'Energie Atomique du Japon, Tokai, Ibaraki.

1) S. W. Mayer et F. C. Freiling, *J. Am. Chem. Soc.*, 75, 5647 (1953).

2) K. Noguchi et F. Ishikawa, "Traité des Expériences Chimiques", Vol. 12 Radiochimie (en Japonais), Maruzén, Tokyo (1956), p. 385.

3) Y. Suzuki, non publié.

4) Ce phénomène a été constaté dans le cas de l'acide hydroxyéthyléthylènediaminetriacétique; communication privée par Z. Hagiwara.

générale, a donné lieu à de remarquables succès dans le cas de séparations et de purifications de terres rares en grande quantité. De ces nombreuses communications nous citons ici la découverte de l'élution du Cd dans les fractions de terres rares pour le cas de l'acide iminodiacétique[5], les interpolations de métaux lourds[6] et l'utilisation de résine cuivrique pour éviter la précipitation de l'acide libre dans le cas de l'acide éthylènediaminetétraacétique[7]. Fuger a publié recemment les résultats de recherches sur les réactions d'équilibre entre l'acide éthylènediaminetétraacétique et les éléments transuraniens en présence de résine échangeuse[8], puis plus tard il a proposé comme solution éluante le complexe entre cet acide et le Zn, la résine étant aussi sous forme zincique pour la séparation de terres rares[9]. Loriers a montré la possibilité d'employer comme la solution complexe de l'acide éthylènediaminetétraacétique et du Cu[10].

L'auteur aussi était déjà arrivé à cette méthode d'employer les solution de complexes de l'acide éthylènediaminetétraacétique avec les métaux lourds[11]. Il a montré une étude sur les réactions d'équilibres qui ont lieu sur le Ce et l'Y sans entraîneur entre la résine sous forme ammonium et les solutions de complexes du Mn^{2+}, du Co^{2+} et du Cu^{2+} avec l'acide éthylènediaminetétraacétique. Il a essayé la séparation de ces deux éléments sur colonne en employant comme la solution éluante le complexe du Co^{2+} avec l'acide éthylènediaminetétraacétique, on a trouvé alors une longue trainée de l'Y après son élution due probablement à l'effet des ions libres du Co^{2+}, le Ce radioactif était cependant resté fixé près du sommet de la colonne après l'élution complète de l'Y. Il semblait que l'on eût obtenu l'efficacité à peu près raisonnable, quoique l'on n'eût pas précisé le facteur de séparation à cause de l'élution impossible à la même condition.

Nous allons maintenant considérer les différentes caractéristiques de l'acide éthylènediaminetétraacétique. Il fait partie des acides aminopolycarboxyliques, parmi lesquels se trouvent les acides nitriletriacétique, cyclohexanediaminetétraacétique etc., à la différence des acides hydroxycarboxyliques tels que les acides lactique, α-hydroxyisobutylique généralement employés pour les séparations de terres rares et d'éléments alcalinoterreux.

L'acide éthylènediaminetétraacétique :

1. Il a la solubilité minimum au pH correspondant au point isoélectrique, vers pH 2.5～3.0, au dessous duquel il pourrait être à l'état cationique.

2. Il n'a pas beaucoup d'action de temponnement.

3. Il est capable de complexer presque complètement les terres rares, et la plupart des métaux lourds. Ce fait n'est pas toujours favorable, en provoquant les changements brusques de conditions à la solution tels que l'abaissement relativement grand de pH, la diminution à la concentration de l'anion.

En remplaçant cet acide par ses complexes avec les métaux lourds, il est possible d'améliorer ces caractéristiques mais par contre un problème se pose, celui de la présence d'ions libres des métaux lourds. Il est plutôt curieux qu'aucune étude poussée n'ait été faite sur ce sujet jusqu'à présent, où l'on a des succès assez remarquables, mais seulement partiels de divers points de vue. Ces expériences sont justement destinées à éclaircir les caractéristiques de ces solutions complexes plus systématiquement. Nous avons cherché à connaître le comportement des coéfficients de répartition et des facteurs de séparation en fonction des diverses variables.

A partir de considérations sur les constantes de formation des complexes et sur les différences d'affinité pour la résine entre les terres rares et les métaux lourds, on aurait trois ions convenables, Co^{2+}, Cd^{2+} et Zn^{2+}. L'auteur a préféré utiliser l'ion Co^{2+} parce qu'il est facile d'en observer le comportement de l'ion libre sur la résine grâce à sa couleur, quoique les deux autres ions, Cd^{2+} et Zn^{2+}, soient très faciles à éliminer par la fixation sur résine anionique en milieu chlorhydrique, s'il est nécessaire. Cependant nous avons expecté qu'il n'y aurait pas très grande différence sur les réactions d'équilibles entre le complexe du Co^{2+} et les deux autres.

Procédéd Experimental

Procédé Général d'Expérience. — Toutes les mesures des coéfficients de répartition ont été effectuées par la méthode qui consiste à mesurer la répartition des activités des deux terres rares, le Sm et l'Eu, entre la résine et la solution éluante, équilibrées en tube à essai.

Une certaine quantité de résine séchée à l'air, équilibrée pour l'humidité atmosphérique, dont le poids correspondra à environ 0.5 g. de résine sous forme de sel d'ammonium séchée en étuve, autrement dit la même capacité d'échange pour les

5) F. T. Fitch et S. Russel, *Can. J. Chem.*, **29**, 363 (1951).
6) R. C. Vickery, *J. Chem. Soc.*, **1952**, 4357.
7) F. H. Spedding, J. E. Powell et E. J. Wheelwright, *J. Am. Chem. Soc.*, **76**, 2557 (1954).
8) J. Fuger, *J. Inorg. Nucl. Chem.*, **5**, 332 (1958).
9) J. Fourage et J. Fuger, "Radioisotopes in Scientific Research", Vol. II, Proceeding of the First (UNESCO) International Conference, Pergamon Press, London (1957), p. 211.
10) J. Loriers et C. Lenoir, *Compt. rend.*, **247**, 468 (1958).
11) H. Natsume, Conférences de la Société de la Chimie Analytique du Japon (1954); Conférences de la Société Chimique du Japon (1956).

diverses formes, est introduite dans un tube à essai en lustéroïde général ou en verre si c'est nécessaire. On y ajoute le mélange de deux solutions en proportion variable suivant la composition à obtenir, de façon à avoir la composition prévue dans le volume total de 10 ml. avec la dilution par addition de 2 ml. de la solution de l'activité mélangée de l'Eu et du Sm. Outre un certain nombre de tubes préparés ainsi, on en prépare quelques autres de l'activité mélangée tout à fait de même que les précédants contenant une solution de composition moyenne ou bien des compositions représentatives, en général des deux solution à mélanger, sans résine qui serviront de témoins, et enfin quelques autres contenant un seul radioélément afin de déterminer l'efficacité de comptage et de déceler la présence d'impuretés.

Ces tubes sont agités pendant une vingtaine d'heures de manière discontinue, puis on laisse sédimenter les particules de résine, on prend une partie aliquote de la solution surnageante que l'on verse dans une coupelle en aluminium et on la sèche sous une lampe infrarouge. On en mesure d'abord l'activité qui est au début celle du mélange Sm-Eu, d'une part au moyen d'un spectromètre γ à un canal et/ou d'autre part au compteur G. M, puis plus tard après décroissances suffisamment complète du Sm, on mesure l'activité de l'Eu seule au compteur à scintillateur et/ou au compteur G. M. Ayant comparé l'activité de ces sources à celles du témoin, on peut calculer le coéfficient de répartition. On mesure aussi le pH de la solution restée dans le tube après la décroissance de la plupart du Sm.

La Résine Échangeuse d'Ion.—La résine échangeuse d'ion utilisées pour toutes ces expériences est la Diaïon SK-1 de la classe analytique, spécialement fabriquée par la Section de Réactif Analytique, Institut de Recherche, Société Industrielle de Produits Chimiques Mitsubishi. Elle est essentiellement identique à la Dowex 50W, X-8, c'est-à-dire une résine brune claire copolymérisées de styrène contenant 8% de divinylebenzène, ayant l'acide sulfonique comme groupement fonctionnel mais préparés très soigneusement, particulièrement au point de vue de la polymérisation uniforme et de l'élimination des impuretés. La taille des grains était de 60~80 mesh autant que possible triées par sédimentation dans l'eau.

Dans la plupart des expériences la résine employée est sous forme de sel d'ammonium. La nouvelle résine, on l'a traitée dans un bécher successivement par les solutions suivantes ; NH_4OH 3 N, eau distillée, HCl 3 N et eau distillée, ce traitement est répété 2 fois, puis, on l'a transformée sous forme ammonium sur colonne par la solution NH_4Cl 2 N, finalement la résine est bien lavée, filtrée sur un filtre en verre fritté et séchée à l'air dans un cristallisoir à l'abri des poussières. La résine après avoir fixé les radioéléments peut être décontaminée au moyen d'une solution à peu près neutre d'éthylènediaminetétraacétate d'ammonium, c'est très efficace surtout avec un léger chauffage sur bain-marie pendant plusieurs heures ; on peut ainsi décontaminer parfaitement la résine jusqu'à avoir une activité inférieure à 0.5 coups par minute par gramme de résine au compteur γ, pour une contamination par l'Eu de quelques centaines de milliers de coups.

La résine sous forme de sel cobalteux a été préparée par passage sur colonne d'une solution de chlorure de cobalt 1 N jusqu'à saturation complète. Pour la préparation des résines sous forme de sel de terre rare, on expliquera à l'expérience concernante.

Un certain nombre de parties de résine, dont le poids correspondra à 0.5 g. de résine séchée à l'étuve, sont pesées à l'aide d'une balance Metler B5. La teneur en eau de la résine sous forme ammonium variait de 8.5% à 17% suivant la durée de séchage et l'humidité atmosphérique ; sous forme cobalteuse elle variait entre 18 et 27% ; c'est pourquoi il faut la mesurer chaque fois sur une autre fraction de résine de 0.5 à 2 g. Cette dernière fraction de résine est utilisée aussi pour mesurer la capacité spécifique d'échange et pour contrôler la différence de poids due à la perte en eau de la résine au cours de pesée ; cette perte en effet, mesurée avant et après une vingtaiue de prises au moins pendant une heure, était inférieure à 0.1%, donc négligeable.

La mesure de la capacité spécifique d'échange est nécessaire pour savoir le poids équivalent de résine sous forme cabalteuse et sous forme ammonium. Elle est faite ainsi : après avoir mesuré la teneur en eau de la résine par séchage à poids constant à 110°C, en général pendant 1.5 à 2 heures, on en remplite une petite colonne, sur laquelle on passe environ 30 ml. de HCl 3 N, on lave parfaitement à l'eau distillée jusqu'à ce que la solution éluée ait le même pH, on passe ensuite environ 30 ml. de la solution de NaCl 2 N, on détermine enfin la capacité totale d'échange par titrage de l'acide dans cette dernière solution éluée à l'aide d'une solution de NaOH N/4. On peut de ces données calculer la capacité spécifique connaissant la teneur en eau. La capacité spécifique était de 4.81_5 méq. pour la résine sous forme ammonium, 4.50_3 méq. pour la résine sous forme cobalteuse.

Préparation de Terres Rares Radioactives.—Les terres rarres ont été employées à partir d'oxydes de qualité "Specpure" de la Société Johnson Mathey sans plus de purification. En cas de nécessité de connaître le poids précis, ces échantillons sont calcinés pour éliminer le gaz carbonique contenu.

Eu—10.0 mg. de Eu_2O_3 calciné est irradié pendant 4 semaines sous un flux de neutrons de 1.5×10^{12} n/cm^2/sec. dans le réacteur EL-2, puis laissé plusieurs mois pour faire décroître les activités possibles de période courte provenant des impuretés, dissous dans un petit bécher par 1 ml. de HCl concentré en chauffant légèrement au bain-marie, puis dilué à 10 ml. A partir de cette solution on prépare une deuxiéme solution 25 fois diluée.

Sm—499.2 mg. de Sm_2O_3 calciné est dissous par HCl concentré, l'excès d'acide est chassé doucement, puis la solution est étendue à 25 ml.; en la diluant de 12.5 fois on obtient une solution du Sm à 1.60 mg./ml. On irradie soit 1 ml. de cette solution dans un petit tube en polyéthylène pendant 1 week-end, c'est-à-dire 36 hr. au flux de neutrons

de 1.4×10^{11} n/cm²/sec. dans EL-1, soit 0.35 ml. dans un petit tube en silice pendant 1 semaine par 1.5×10^{2} n/cm²/sec. dans EL-2. Pour ouvrir le tube en polyéthylène, il est convenable d'en couper par une lame de rasoir la partie supérieure sans toucher la solution, pour le tube en silice, on peut le casser de même à l'aide d'un couteau à verre. On transmet la solution dans un petit bécher à l'aide d'une pipette à bout effilé en prenant soin de laver l'intérieur du tube.

On met 2 à 5 ml. de la solution d'Eu radioactif dans un petit bécher, ajoute quelques gouttes de HCl concentré pour assurer l'absence de radiocolloïde, amène presqu'à sec. deux ou trois fois sur bain-marie en reprenant chaque fois par 5 ml. d'eau distillée, puis ajoute 0.1 ml. de HCl 0.1 N et 2 à 3 ml. d'eau, en mouillant soigneusement la paloi intérieure du bécher on laisse refroidir, enfin on dilue à 25 ou 50 ml. dans une fiole jaugée. On en prend une partie aliquote dans un tube à essai pour le controle de l'activité. Parallèlement on traite tout le volume de la solution du Sm irradié. Sauf pour les contrôles, on prend 2 ml. de la solution de l'activité par une seule pipette, après avoir bien mélangé ces deux solutions ci-dessus, afin de rendre plus petite l'erreur de pipetage pour les calcules de facteur de séparation. La solution radioactive a été ajoutée en général après l'addition de solution de complexe.

Les Solutions de Complexe de l'Acide Éthylènediaminetétraacétique avec les Métaux Lourds.—Après une quinzaine d'expériences sur colonne, on est arrivé au choix entre trois sels suivants: le sel acide de l'EDTA*) et du métal, le sel double d'ammonium et du métal avec l'EDTA et le sel contenant plus de métal lourd. La présence des ions étrangers ne sera pas favorable à cause de la diminution du coéfficient de répartition en général sans aucun intérêt, c'est pour cette raison que nous avons préféré les préparer sur colonne. Nous allons examiner d'abord le cas des complexes de l'EDTA et du Co.

A) La Solution Acide. — On dissout 25.000 g. de $Na_2H_2Y\cdot2H_2O$ c'est-à-dire 0.067186 mol. dans environ 800 ml. d'eau distillée, on fait passer la solution successivement sur deux colonnes, l'une de NH_4R (15 mm$\phi\times$32.5 cm. ca. 58 ml. 78 méq. de capacité) l'autre de CoR_2 (15 mm$\times$65 cm. ca. 115 ml. 155 méq.), la première, servant à remplaçer le Na^+ par l'NH_4^+, n'est peut être pas nécessaire. La solution éluée est étendue à 1 l. dans une fiole jaugée que l'on remplit jusqu'à la ligne marquée par la solution de lavage après avoir passé la solution de l'EDTA.

Plus tard le sel disodique a été remplacé par la quantité équivalente d'acide, c'est-à-dire 19.6254 g. de H_4Y plus convenable, car on peut le passer sur la colonne de CoR_2 tout de suite après l'avoir neutralisé par l'ammoniaque concentré jusqu'à pH 5 à 7. Cette neutralisation qualitative est représentée dans Fig. 1.

La solution acide du complexe de l'EDTA avec le Co, obtenue par cette méthode, a un pH de 1.9~2.0, elle ne contient pas d'ion ammonium

* Nous appellerons l'acide éthylènediaminetétraacétique H_4Y ou EDTA, l'acid nitriletriacétique H_3X ou NTA.

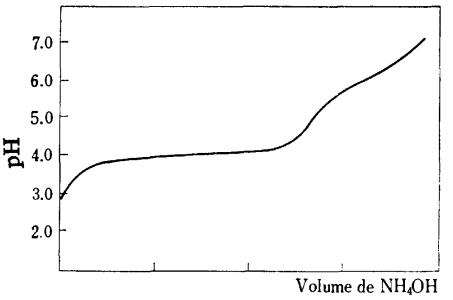

Fig. 1. Courbe de titrage de H_4Y par NH_4OH.

dosable d'après la méthode Kjeldahl, même si elle a été préparés à partir de la solution à pH 7; mais elle contient peut-être un peu d'ions libres Co^{2+}, dont l'élimination a été essayée sans succès.

Elle était stable au moins pendant plusieurs mois sans aucun précipité. Les solutions plus concentrées comme celle à 80 g./l. de Na_2H_2Y 2 aq. ne peuvent pas être préparées par cette méthode à cause de la faible solubilité du complexe. Quoiqu'elle ne corresponde pas exactement à la formule H_2CoY, on la désignera ainsi par la suite.

B) La Solution Neutre Libre du Co^{2+}.—La solution neutre n'est pas convenable à préparer par la méthode sur colonne, car en faisant passer sur colonne une solution non seulement calculée comme $(NH_4)_4Y$ mais encore contenant un excès d'ammoniaque, la solution éluée a au commencement un pH vers 3.5 à 4.5 à cause de l'absorption de l'ammoniaque par le CoR_2. Les composés, $[Co(NH_3)_6]R_2$ et surtout l'état oxydé $[Co(NH_3)_6]R_3$, étant ennuyeux à éliminer à cause de leur forte absorption, on a modifié la méthode de la manière suivante:

On prend la même quantité de H_4Y dans un bécher de 400 ml., on ajoute 200 à 250 ml. d'eau distillée, et la quantité suffisante de résine CoR_2, puis on neutralise jusqu'à pH 7.0 par l'ammoniaque concentré. Pour le cas d'une addition excessive d'ammoniaque, la résine HR peut être employée pour abaisser à 7.0 le pH de la solution. On filtre cette solution sur un filtre en verre fritté, lave complètement à l'eau distillée et dilue jusqu'à 750 à 800 ml. dans une éprouvette graduée, on passe ensuite sur une colonne de NH_4R tout à fait de même manière que précédemment, mais finalement on règle à 7.0 de nouveau le pH.

Cette solution manque un peu de Co^{2+} en comparaison de concentrations équivalentes pour l'H_4Y; nous l'appellerons quand même $(NH_4)_2CoY$.

C) La Solution Neutre Saturée du Co^{2+}.—Au lieu de NH_4R, on emploie CoR_2, à peu près la moitié des ions NH_4^+ sera alors remplacé par des ions Co^{2+}, d'après les observations de la longueur des bandes de NH_4R et de CoR_2, donc notons comme $[(NH_4)_2, Co]CoY$.

D) Les Solutions Complexes de l'EDTA et du Cu^{2+}.—On peut les préparer de la même manière que dans le cas du Co^{2+} sauf quelques légères différences. La première est que par neutralisation en présence de résine CuR_2, on ne peut pas élever le pH à plus de 6.55 à cause de la faible basicité de l'ions Cu^{2+}, on a en effet remarqué un peu de précipité

bleu pâle de $Cu(OH)_2$ après une nuit, ensuite pendant le lavage, tous les deux cas, après l'enlèvement et la saturation du Cu^{2+} la solution passée est colorée longtemps en bleu, peut-être à cause de la faible combinaison de la résine cuivrique et du complexe. Pour la solution acide du complexe il n'y a aucune différence particulière et la solution H_2CuY a pour pH à peu près 1.6.

E) Acide Nitriletriacétique.—Les solutions complexes de l'H_3X et du Co^{2+} sont préparées tout à fait de la même manière que dans le cas de l'EDTA, mais plus facilement encore car cet acide et ses dérivés ont toujours une solubilité plus grande que les composés correspondants de l'EDTA. La solution contient 25.000 gr. de cet acide c'est-à-dire 0.1308 mol./l.

Procédés à Equilibrer.—Dans les tubes à essai, on introduit la résine, on ajoute 8 ml. de solution de complexe mélengée comme expliqué ci-dessous, puis 2 ml. de la solution radioactive, la solution est diluée finalement 1.25 fois, donc 0.05373 mol./l. en EDTA et 0.10463 mol./l. en NTA. Pour une série d'expériences, on prépare d'abord deux des solutions ci-dessus ou des solutions plus ou moins modifiées sans changer la concentration en acide, les mélange progressivement aux taux différents, ainsi on peut réaliser des mélanges de compositions bien définies, ce qui est très important pour cette sorte d'études. En cas de nécessité, on a adapté l'addition sous la forme solide comme NH_4ClO_4 ou bien sous la forme absorbée par la résine comme SmR_3.

Après avoir ainsi préparé les tubes, on les bouche et les agite de temps en temps, une dizaine de fois au cours de la journée, puis encore quelques fois le lendemain. D'après quelques expériences, cette maniére était suffisante pour atteindre à l'équilibre, on les débouche soigneusement à l'aide d'un papier pour ne pas contaminer, laisse sédimenter les particules de résine et prélève une partie aliquote de la solution dans une coupelle en aluminium pour en mesurer l'activité. Cependant du point de vue des vitesses d'échange et de diffusion des ions à l'intérieur de particule, il sera réalisé vraisemblablement en 3 ou 4 hr. par l'agitation continuelle de la machine.

Mesures de l'Activité.—A) Préparation des Sources de Comptage.—Il est très important surtout pour les comptages de préparer des sources dont l'épaisseur de dépôt soit le plus uniforme possible. Une feuille de papier filtre collée au fond de la coupelle peut améliorer ce dépôt. La solution prise a été séchée sous une lampe infrarouge, il est efficace d'éloigner la source de la lampe pendant quelques temps vers la fin du séchage pour avoir un dépôt uniforme. Au cas où la solution contient beaucoup d'électrolyte, on vernit légèrement d'huile Silicone la paroi intérieure de la coupelle pour éviter un dépôt sur le haut de la paroi. Quelques fois 2 ml. solution prise était trop pour avoir une bonne source à cause de la faible solubilité de complexe. Les volumes des pipettes pour le témoin et les échantillons doivent être identiques et il vaut mieux choisir les pipettes les plus semblables possibles.

Les measures de l'activité en solution sont en général plus précises mais dans ces expériences. cette méthode n'était pas adaptée, car les corrections de la décroissance du Sm et de l'évaporation de l'eau seront très compliquées.

B) Comptages.—Toutes les sources sont mesurées au moins 2 fois aux compteurs avant et après la décroissance complète du Sm, c'est-à-dire à peu près 3 à 4 semaines après. L'activité du Sm est prise 10 à 30 fois plus forte au moment de l'addition que l'Eu pour éviter l'erreur de calculer l'activité du Sm. Les efficacités de comptage sont mesurées par l'étalon de l'Eu et aussi du Sm quelque fois, de la solution à la composition moyenne, et toujours surveillées contre la variation légère même pour la condition identique. La correction pour la décroissance du Sm pendant une série de mesures durant 2 à 3 hr. est calculée par la période considérée comme 47.1 hr.

Les caractéristiques des rayonnements de radioéléments employés sont montrées au Tableau I.

B. 1) Comptage β. — Le tube ordinaire G. M. cloche à fenêtre en mica mince est employé. L'activité relativement forte du mélange a été comptée en petite géométrie, au 5^e ou 4^e étage, l'activité de l'Eu seule en grande géométrie comme au 1er ou 2^e étage. Dans certains cas où les coefficients de répartition sont assez grands, l'activité du mélange est aussi mesurée au 1er étage, pour rendre plus petite l'erreur statistique, quoique ce ne soit pas favorable du point de vue de la reproductibilité.

Le plus important, c'est de choisir l'activité du témoin, assez forte, sans cependant donner lieu à de trop fortes pertes de comptage. Il ne faut pas mesurer une activité pour laquelle les pertes de comptage obligent à une correction de plus de 10%. La perte de comptage a été calculée en employant la méthode bien connue qui consiste à mesurer deux sources actives séparément de ^{143}Pr, puis ensemble, et d'en déduire par calcul le temps mort de l'installation de comptage. Les activités dues aux impuretés doivent être prises les précautions puisqu'il n'y a pas moyen de les séparer.

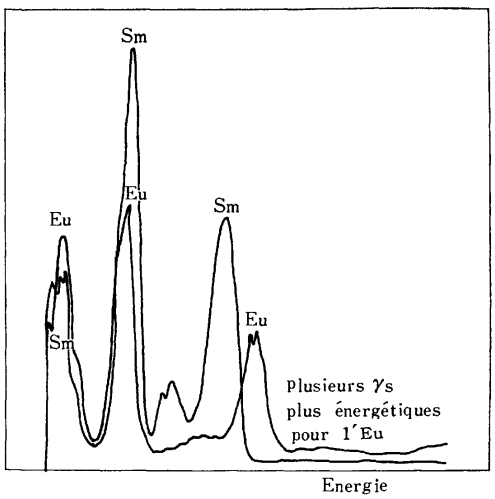

Fig. 2. Spectrographe γ du Sm et de l'Eu irradiés.

TABLEAU I. CARACTÉRISTIQUES DES RADIOÉLÉMENTS UTILISÉS*

Nucldie de cible (abondance)	Radio-élément produit	Période	Désintégration	Rayonnements β	Rayonnements γ
^{144}Sm (3.16%)	^{145}Sm	340 j	CE		0.0613 (+106) 0.485 (+0.02)
^{147}Sm (15.07%)		1.3×10^{11} an	α		2.18(α)
	^{148}Sm	stable			
^{150}Sm (7.47%)	^{151}Sm	93 an	β^-	0.076	0.021
^{152}Sm (26.63%)	^{153}Sm	47.1 hr.	β^-	0.80 (21%) 0.69 (70%) 0.26 (9%)	0.10318(+100) 0.06966(+ 7)
^{154}Sm (22.53%)	^{155}Sm	24.5 min.	β^-	1.8	0.105 (+100) 0.246 (+100)
	^{155}Eu	1.7 an	β^-	0.154(80%) 0.243(20%)	0.0189 0.0265 0.04529 0.06000 0.08654(+100) 0.10532(+ 63)
^{151}Eu (47.77%)	^{152}Eu	9.2 hr.	CE(K) (25%) β^- (75%) β^+ (faible)	1.88, 0.55(?) 0.82 (β^+)	0.122 0.837 (+140) 0.961 (+100) 1.41
		12.7 an	CE(K) (73%) β^- (27%)	1.46 (+21) 1.05 (+ 6) 0.68 (+51) 0.36 (+13) 0.22 (+ 9)	0.12179 0.24484(+ 40) 0.860 (+ 15) 0.965 (+ 60) 1.05 (+ 50) 1.20 (+ 20) 1.42 (+ 90) 0.3443 (+100) 0.420 (+ 4) 0.755 (+ 40)
^{153}Eu (52.23%)	^{154}Eu	16 an	β^-	1.84 (7%) 1.60 (3%) 0.83 (20%) 0.55 (30%) 0.25 (28%) 0.15 (12%)	0.123 (35%) 0.248 0.593 (4%) 0.694 0.706 0.725 (21%) 0.759 0.875 (13%) 0.998 (14%) 1.007 (17%) 1.277 (42%)

* D. Steominger, J. M. Hollander et G. T. Seaborg, UCRL-1928, "Table of Isotopes" (1958).

Cette contribution était également toujours surveillée par la comparaison du reste du Sm seul et des activités des échantillons.

B. 2) Comptage γ.—Deux appareils sont employés pour les comptages γ, l'un le spectromètre γ SGE-2 de l'Intertechnique sous la licence du CEA dans le cas du mélange, l'autre le compteur automatique N-530-P avec le scintillateur du NaI de l'EKCO pour l'Eu seul.

Puisque l'on peut négliger la différence de l'absorption par le dépôt et la perte de comptage, les mesures de γ sont en général plus précises et plus faciles que de β. Cependant les changements possibles de l'efficacité de comptage avec le temps et les mouvements propres doivent être souvent surveillés. En particulier si l'on mesure une faible activité, les mesures successives de mouvements propres sont indispensables, car une légère différence

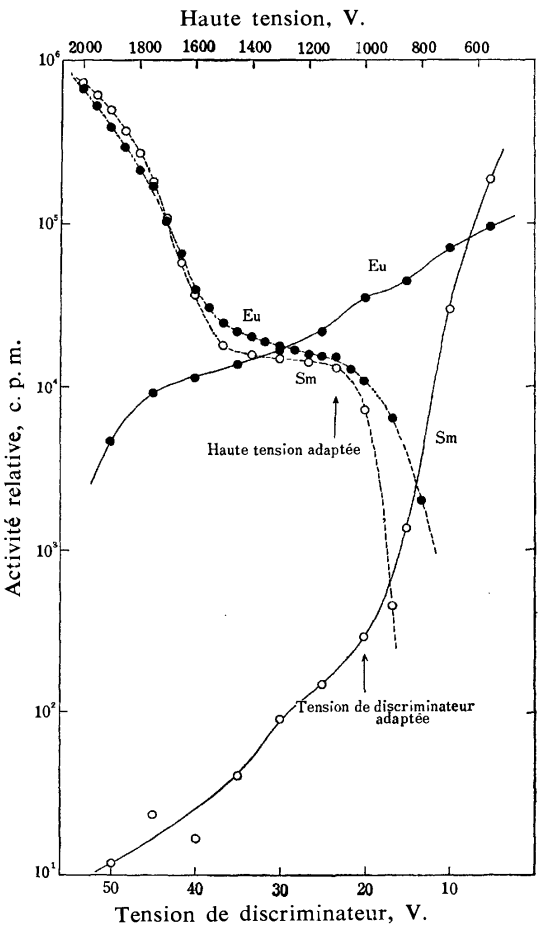

Fig. 3. Détermination des tensions pour le compteur γ.
----- Courbe d'intégration
—— Courbe de discrimination

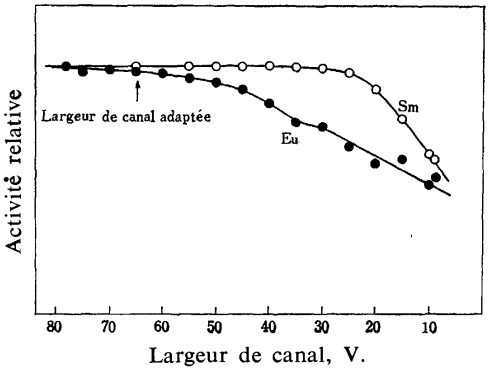

Fig. 4. Détermination de la largeur de canal pour le spectromètre γ.

de tension par température, ou bien le transport ou le déplacement d'une forte source dans les laboratoires voisins peuvent le faire varier.

Pour mesurer l'activité du Sm en présence de l'Eu, il n'y avait pas de condition particulièrement favorable. Les spectrographes γ de ces radioéléments sont montrés dans Fig. 3. Nous avons préféré le 1er pic de Sm 0.103 MeV. avec la largeur du canal qui pourra comprendre le pic 0.122 MeV. tout entier de l'Eu. Ces courbes intégrales sont montrées dans Fig. 4.

Au contraire, l'Eu peut être mesuré au compteur γ, avec une plus grande efficacité que le Sm, et les γs qu'il émet ont des énergies assez différentes de celles du Sm et des impuretés possibles; 90% de l'activité due à aux impuretés se trouve ainsi éliminée. Nous avons mesuré cette activité à la condition H. T. 1100 V., tension de discrimination 20 V.

Mesures de pH.—Comme on le montrera plus tard, le pH ne joue pas un rôle important dans ce système; donc les mesures de pH servent simplement à savoir les comportements de complexe du métal lourd. Après décroissance de la plus grande partie de l'activité due au Sm, on mesure le pH de la solution au moyen d'un pH-mètre Metrohm à électrode en verre dont l'erreur est indiquée comme étant de ± 0.04 unité, cependant on trouve souvent une erreur plus grande surtout au cours d'une série assez longue de mesures.

Causes d'Erreurs sur la Mesure du Coefficient de Répartition et du Facteur de Séparation.—Autant que possible on a essayé de rendre les erreurs inférieures à 0.3%. Les causes importantes d'erreurs sont les pipetages et les mesures des activités. Les premières pourront être diminuées par contrôle du poids de la prise; les deuxièmes comportent plusieurs facteurs: préparation des sources, mesures du témoin, différence des poids de dépôt entre le témoin et les échantillons pour les comptage β, variation des efficacités de comptages, variation du mouvement propre en cas de faibles activités pour le comptage γ.

Des expériences suivantes, on pourrait déduire que la répartition des activités elle-même réalisée par cette méthode expliquée ci-dessus, sera bien établie et cette variation ne dépasse jamais les erreurs expérimentales, et que l'erreur peut être considérée comme inférieure à 2 à 3% pour les coefficients de répartition moyens, c'est-à-dire 0.5 à 100, un peu plus grande pour les coefficients relativement grands c'est-à-dire plus de 100 et très grande pour les coefficients inférieurs à 0.5.

Pour comparer l'efficacité de séparation c'est-à-dire les facteurs de séparation, il faudra faire plus attention, en considérant les conditions de mesures, le degré des erreurs, quelques fois demander les aides de considérations théoriques. Il est presque impossible de comparer les facteurs de séparation d'une série à une autre des expériences sauf les séries effectuées par la même condition.

Resultats des Experiences

Etant donné que l'on peut prévoir d'assez grandes différances entre les caractéristiques de ce système et celles des acides hydroxycarboxyliques, on doit étudier les influences de divers facteurs sur le coéfficient de répartition. Puisque le coéfficent de répartition dans ces expériences dépend du rapport entre le volume de solution et le poids de résine, nous désignons le coéfficient de répartition dans ce système Cr comme

TABLEAU II

EXP. 1. SYSTÈME NH_4R-[H_2CoY, $(NH_4)_2CoY$]

N° d'exp.	NH_4R g.	H_2CoY ml.	$(NH_4)_2CoY$ ml.	pH	Cr_{Sm}	Cr_{Eu}	α
101	0.4921	8.0	0.0	2.65	36.0_9	23.2_7	1.55_1
102	0.4987	7.2	0.8	2.65	26.9_5	17.0_2	1.58_4
103	0.4929	6.4	1.6	2.64	18.8_5	11.7_1	1.58_4
104	0.4910	5.6	2.4	2.76	12.8_2	7.91_6	1.61_9
105	0.4932	4.8	3.2	2.90	8.01_7	4.93_5	1.62_4
106	0.4930	4.0	4.0	3.05	5.52_5	3.23_4	1.70_8
107	0.4924	3.2	4.8	3.22	3.41_1	2.03_4	1.67_7
108	0.4939	2.4	5.6	3.43	1.93_5	1.15_7	1.67_2
109	0.4928	1.6	6.4	3.69	1.07_6	0.62_6	1.72_0
110	0.4931	0.8	7.2	4.05	0.44_5	0.25_8	1.72_7
111	0.4934	0.0	8.0	5.25	0.04_2	0.03_7	(1.13_8)

Résine: Diaïon SK-1 sous forme de NH_4R, 60~80 mesh, poids montré calculé comme séché en étuve

Solution: Volume totale 10 ml., 0.05373 mol. en CoY^{2-} aux compositions montrées

Terres rares: Eu 2.2 μg., Sm 57 μg. comme en oxyde

Mesures: Eu par β et γ, Sm par γ

$$Cr = \frac{Act_{témoin} - Act_{échan}}{Act_{échan}}$$

et le facteur de séparation comme

$$\alpha = (Cr)_{Sm}/(Cr)_{Eu}$$

Les poids de résine sont exprimés en résine séchée, ils sont calculés connaissant la teneur en eau de la résine, celle-ci ayant été mesurée une fois sur une autre partie de résine.

1) Le Système NH_4R-[H_2CoY, $(NH_4)_2CoY$].—Une combination possible c'est le cas où l'on emploie NH_4R comme résine et le mélange des solutions de $(NH_4)_2CoY$ et de H_2CoY comme solution, dont, comme il a été dit précédement, la prmière est équiliblée avec NH_4R, mais cette dernière ayant été équiliblée avec CoR_2, donc on ne peut éviter la différence de concentration en ion libre Co^{2+} dans le mélange de ces deux solutions.

Les résultats sont donnés dans Tableau II et dans Fig. 5. La courbe est en convexe en haut, cette diminution du coéfficient de répartition pour les fortes teneurs de la solution en complexe acide est peut-être due à la différence de stabilité des complexes du Co et des terres rares, et pour les fortes teneurs en complexe neutre, elle a nettement pour cause une diminution de la concentration en ion libre Co^{2+}.

Comme facteur de séparation, on obtient la valeur à peu près raisonnable que l'on espére que pouvaient laisser prévoir les valeurs des constantes de formation des complexes, soit $\log Kc_{Eu}/\log Kc_{Sm} = 0.21 \pm 0.09$[12].

2) Le Système CoR_2-[H_2CoY, {$(NH_4)_2$, Co}CoY].— L'autre combinaison possible, c'est le cas où l'on emploie CoR_2 comme résine et la solution mélangée de H_2CoY et de [$(NH_4)_2$, Co]CoY qui sont toutes les deux équiliblées avec la résine CoR_2. Les résultats sont données dans Tableau III et dans Fig. 6.

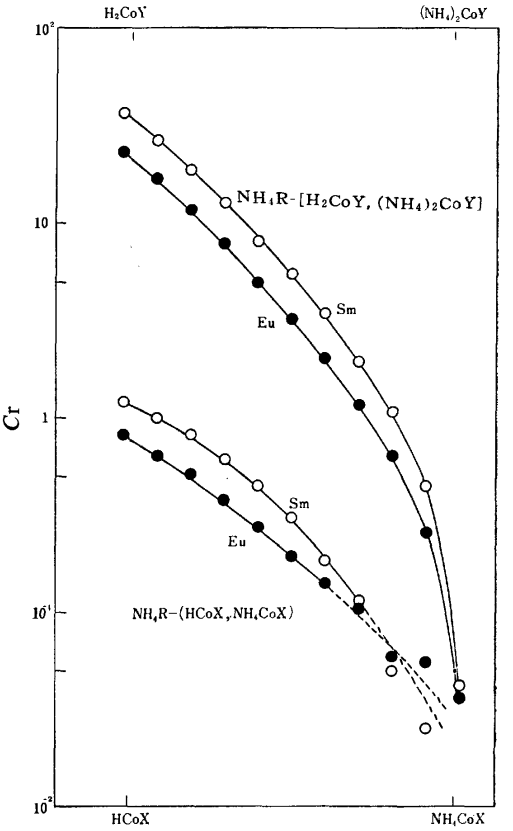

Fig. 5. Exp. 1. NH_4R-[H_2CoY, $(NH_4)_2CoY$] et Exp. 5. NH_4R-[HCoX, NH_4CoX].

Ces résultats indiquent la présence d'ion Co^{2+} en grande quantité n'est pas favorable à la séparation, au moins du Sm et de l'Eu. Il peut y avoir deux raisons possibles à cela, l'une serait l'augmentation de la force ionique, l'autre la formation

12) G. Schwarzenbach, R. Gut et G. Anderegg, *Helv. Chim. Acta*, 37, 937 (1954).

TABLEAU III

EXP. 2. SYSTÈME CoR_2-[H_2CoY, {$(NH_4)_2$,Co}CoY]

N° d'exp.	CoR_2 g.	NH_4R équiv. g.	H_2CoY ml.	$[(NH_4)_2,Co]CoY$ ml.	pH	Cr_{Sm}	Cr_{Eu}	α
201	0.7342	0.5107_7	8.0	0.0	2.09	89.8_9	74.8_9	1.20_0
202	0.7347	0.5111_3	7.2	0.8	2.21	72.4_0	56.1_7	1.28_9
203	0.7343	0.5108_5	6.4	1.6	2.36	55.0_5	32.5_2	1.26_8
204	0.7338_5	0.5105_3	5.6	2.4	2.60	42.7_0	32.5_2	1.31_3
205	0.7341	0.5107_1	4.8	3.2	2.77	33.1_0	25.3_1	1.30_8
206	0.7343	0.5108_5	4.0	4.0	2.96	26.1_2	19.9_5	1.30_9
207	0.7340_5	0.5106_7	3.2	4.8	3.14	20.8_9	15.6_5	1.33_5
208	0.7346	0.5110_5	2.4	5.6	3.35	16.9_8	13.2_3	1.28_5
209	0.7342	0.5107_7	1.6	6.4	3.65	14.6_9	10.9_8	1.33_8
210	0.7342	0.5107_7	0.8	7.2	4.07	12.3_3	9.44_0	1.30_6
211	0.7343	0.5108_5	0.0	8.0	6.66	11.2_1	9.01_2	1.24_4

Résine: Diaïon SK-1 sous forme de CoR_2, 60~80 mesh, poids comme montré
Solution: Volume total 10 ml., 0.05373 mol. en CoY^{2-} aux compositions montrées
Terres rares: Eu 2.25 μg., Sm 14.0 μg. comme en oxyde
Mesures: Eu, Sm tous les deux par γ

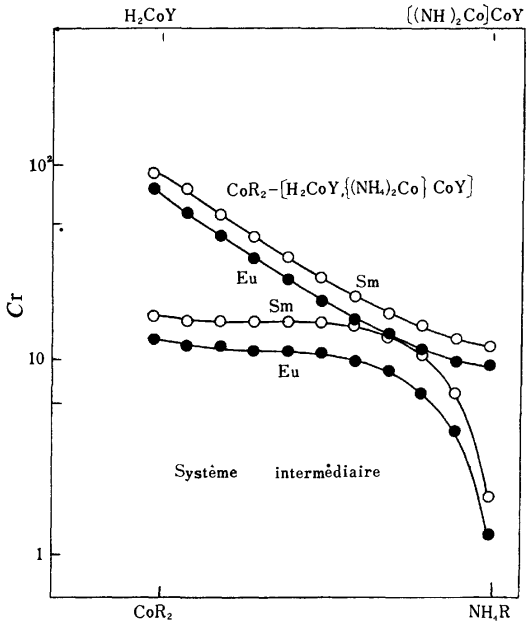

Fig. 6. Exp. 2. CoR_2-[H_2CoY, {$(NH_4)_2$, Co}·CoY] et Exp. 4. système intermédiaire.

d'un complexe polynucléaire où les terres rares sont complexées en état tri- ou tétradentatées au lieu de hexadentatées[13]. Dans la phase de résine occupée par le Co^{2+}, qui est bien hydraté, la séléctivité d'absorption des terres rares sera probablement aussi affaiblie.

3) Solution des Complexes entre l'EDTA et le Cu^{2+}.—Dans le cas de l'expérience 1, la solution $(NH_4)_2CoY$ ne contient que la quantité la moindre du Co^{2+}, c'est-à-dire la quantité qui peut être libérée du complexe en présence d'un grand excès de NH_4R. Les *C*rs dans ce cas sont relativement petits, il est donc difficile d'en constater les variations. Pour les constater, il vaut mieux employer une solution complexe plus stable, on en pourra réaliser une rempaçant le Co^{2+} par le Cu^{2+}.

Les *C*rs des terres rares en présence de NH_4R et des mélanges de solutions H_2CuY et $(NH_4)_2CuY$, sont étudiés, ces résultats figurent dans Tableau IV. Les valeurs de *C*r obtenues étaient très grandes, sauf pour les mélanges constitués presque totalement de $(NH_4)_2CuY$, cependant l'activité due aux impuretés nous a géné et nous n'avons pas pu l'éliminer complètement même en faisant les mesures au compteur γ après supprimé par discrimination la pluspart de l'activité due aux impuretés; on a donc essayé de l'éliminer grâce aux différences dans les efficacité de comtage β, γ, et aussi nous avons assuré par le spectromètre γ ce que l'activité des échantillons était prédominée par le Sm au moins au commencement. Tout de même nous n'avons pas pu obtenir une grade précision satisfaisante, sauf les deux dernières expériences.

De cette série d'expériences, on comprend que la solution $(NH_4)_2CuY$ est très susceptible pour la quantité de l'ion libre de Cu^{2+} à cause de sa teneur moindre, et par la différence dans les constantes de formation de complexe entre le Co et le Cu, on peut déduire que les *C*rs de l'Eu et du Sm pour la solution $(NH_4)_2CoY$ dans l'expérience 1 seraient sûrement presque zéro.

On remarque aussi les facteurs de séparation toujours inférieurs avec la solution complexe du Cu à avec celle du Co, même dans la dernière expérience, où le *C*r est aussi petit que les cas du Co.

4) Les Compositions Intermédiaires des Phases de Résine et de Solution.—Entre les duex systèmes, expériences 1 et 2, on a essayé d'étudier les variations en chageant progressivement la composition des deux phases, c'est-à-dire de la résine et de la solution. Comme les mélanges représentatifs, nous avons choisi 30% de la solution complexe acide toujours, pour le reste de 70%, la solution neutre libre de

13) A. E. Martell and M. Calvin, "Chemistry of the Metal Chelate Compounds", New York Prentice-Hall, Inc., New York (1952), p. 205.

TABLEAU IV

EXP. 3. SYSTÈME NH_4R-[H_2CuY, $(NH_4)_2CuY$]

N° d'exp.	NH_4R g.	H_2CuY ml.	$(NH_4)_2CuY$ ml.	pH	Cr_{Sm}	Cr_{Eu}	α
301	0.5021	8.0	0.0	2.94	1540.	1379.	(1.11_6)
302	0.5021	7.2	0.8	3.01	1532.	1280.	(1.19_7)
303	0.5018	6.4	1.6	3.09	1487.	1458.	(1.02_1)
304	0.5021	5.6	2.4	3.21	1439.	1356.	(1.06_1)
305	0.5020	4.8	3.2	3.30	1177.	1197.	(0.98_3)
306	0.5017	4.0	4.0	3.45	$901._1$	$810._4$	1.11_3
307	0.5018	3.2	4.8	3.62	$748._9$	$665._9$	1.12_6
308	0.5018	2.4	5.6	3.80	$551._3$	$486._0$	1.13_4
309	0.5018	1.6	6.4	3.95	$503._0$	$431._5$	1.16_3
310	0.5019	0.8	7.2	4.24	$314._1$	$234._3$	1.33_4
311	0.5020	0.0	8.0	5.66	4.98_4	3.31_5	1.54_3

Résine : Diaïon SK-1 sous forme de NH_4R, 60~80 mesh, poids comme montré
Solution : Volume total 10 ml., 0.05373 mol. en CuY^{2-} aux compositions montrées
Terres rares : Eu 2.25 μg., Sm 14.0 μg. comme en oxyde
Mesures : Eu par β et γ, Sm par γ

TABLEAU V

EXP. 4. LES COMPOSITIONS INTERMÉDIAIRES

N° d'exp.	NH_4R g.	CoR_2 g.	NH_4R équiv. de CoR_2 g.	$\frac{CoR_2}{CoR_2+NH_4R}$ %	Soln. A ml.	Soln. B ml.	pH	Cr_{Sm}	Cr_{Eu}	α
401	0.5024_5	0.0	0.0	0.0	8.0	0.0	3.55	1.85_8	1.17_3	1.58_4
402	0.4523_0	0.0545_8	0.0510_4	10.14	7.2	0.8	3.55	6.50_0	4.17_5	1.55_7
403	0.4019_8	0.1091_2	0.1020_5	20.25	6.4	1.6	3.54	10.1_0	6.58_2	1.53_5
404	0.3527_8	0.1637	0.1531_3	30.27	5.6	2.4	3.53	12.9_2	8.60_4	1.53_7
405	0.3014_2	0.2186_5	0.2044_8	40.42	4.8	3.2	3.51	14.3_6	9.56_1	1.50_2
406	0.2511_4	0.2730_4	0.2553_5	50.42	4.0	4.0	3.52	15.3_1	10.3_5	1.47_8
407	0.2009_9	0.3276_2	0.3063_6	60.39	3.2	4.8	3.51	15.2_9	10.5_8	1.44_5
408	0.1507_5	0.3825_3	0.3577_5	70.35	2.4	5.6	3.47	15.4_0	10.9_0	1.41_3
409	0.1007_3	0.4368_5	0.4085_5	80.22	1.6	6.4	3.43	15.8_4	11.4_7	1.38_1
410	0.0502_4	0.4913_9	0.4595_5	90.15	0.8	7.2	3.40	15.7_4	11.5_2	1.36_6
411	0.0	0.5462_3	0.5108_4	100.0	0.0	8.0	3.36	16.3_8	12.6_6	1.29_3

Résine : Diaïon SK-1, 60~80 mesh, sous forme mélangée de NH_4R et de CoR_2.
Solution : Volume total 10 ml., 0.05373 mol. en CoY^{2-}
Composition de soln. A: 30% de H_2CoY et 70% de $(NH_4)_2CoY$
Composition de soln. B: 30% de H_2CoY et 70% de $[(NH_4)_2,Co]CoY$
Terres rares : Eu 2.25 μg., Sm 14.0 μg. comme en oxyde
Mesures : Eu, Sm tous les deux par γ

Co^{2+} avec la résine NH_4R, saturée de Co^{2+} avec CoR_2. Les compositions intermédiaires ont été faites par ces deux solutions mélangées et les prises espérées de NH_4R et de CoR_2.

La variation de Cr est représentée dans Tableau V et dans Fig. 6.

5) Le Système du Complexe entre le NTA et le Co.—Si l'on compare les constantes de formation des complexes que forment les acides aminopolycarboxyliques avec les métaux lourds, d'une part, et les terres rares d'autre part, on constate que les métaux lourds ont une plus forte tendance à se complexer que les terres rares pour l'acide plus complexant—de plus les différences entre leurs constantes de formation sont plus grandes, sauf cependant dans quelques cas, tels que les terres rares du groupe gadolinium* avec les acides H_3V et DTPA**.

Dans les cas de séparation de terres rares sans entraîneur, le facteur de séparation doit être proportionnel au rapport entre ces constantes de formation, pourvu que l'on se serve toujours de résine identique ; de ce point de vue l'acide H_4Z** sera plus interressant et l'acide H_3X moins que l'acide H_4Y.

Dans cette série d'expériences nous voulons constater si l'acide H_3X nous donne le facteur de séparation moins grand que l'acide H_4Y comme

* Nous désignons les terres rares à partir du Gd jusqu' au Lu comme groupe gadolinium au lieu d'yttrium, car on peut remarquer certaines différences entre les terres rares et l'Y.

** Nous appellerons l'acide hydroxyéthyléthylènediaminetriacétique H_3V, l'acide diéthylènetriaminepentaacétique DTPA et l'acide cyclohexanediaminetétraacétique H_4Z.

TABLEAU VI

EXP. 5. SYSTÈME NH_4R-($HCoX$,NH_4CoX)

N° d'exp.	NH_4R g.	$HCoX$ ml.	NH_4CoX ml.	pH	Cr_{Sm}	Cr_{Eu}	α
501	0.5019	8.0	0.0	2.86	1.20_5	0.806_6	1.49_4
502	0.5015	7.2	0.8	2.97	0.991_5	0.634_0	1.56_4
503	0.5016	6.4	1.6	3.08	0.817_2	0.504_3	1.62_0
504	0.5016	5.6	2.4	3.20	0.602_1	0.379_7	1.58_6
505	0.5018	4.8	3.2	3.33	0.445_6	0.275_2	1.61_9
506	0.5012	4.0	4.0	3.50	0.308_5	0.193_8	1.59_2
507	0.5018	3.2	4.8	3.69	0.184_4	0.141_4	1.30_5
508	0.5013	2.4	5.6	3.95	0.114_3	0.106_0	(1.07_8)
509	0.5016	1.6	6.4	4.35	(0.049_4)	(0.056_7)	(0.82_8)
510	0.5016	0.8	7.2	5.00	(0.025_7)	(0.056_0)	(0.47_5)
511	0.5021	0.0	8.0	6.15	<0.02	<0.02	—

Résine: Diaïon SK-1 sous forme de NH_4R, 60~80 mesh, poids comme montré
Solution: Volume total 10 ml., 0.1046 mol. en CoX^- aux compositions montrées
Terres rares: Eu 2.25 μg., Sm 57.0 μg en oxyde
Mesures: Eu par β et γ, Sm par β

TABLEAU VII

EXP. 6. EFFET DE LA DILUTION

N° d'exp.	NH_4R g.	Solution de complexe ml.	H_2O ml.	Concen. en CoY^{2-} mol.	pH	Cr_{Sm}	Cr_{Eu}	α
601	0.4674	8.00	0.0	0.05373	3.50	1.88_6	1.15_9	1.63_3
602	0.4675	6.40	1.60	0.04298	3.55	2.17_1	1.30_3	1.66_6
603	0.4672	5.00	3.00	0.03358	3.80	2.44_5	1.56_4	1.56_3
604	0.4671	4.00	4.00	0.02687	3.61	2.65_1	1.75_0	1.51_5
605	0.4682	3.20	4.80	0.02149	3.58	2.76_6	1.92_4	1.43_8
606	0.4750	2.56	5.44	0.01719	3.78	2.81_5	2.04_0	1.38_0
607	0.4764	2.04	5.96	0.01370	3.85	2.80_8	2.11_1	1.33_0
608	0.4759	1.64	6.36	0.01101	3.94	2.74_4	2.13_3	1.28_7
609	0.4759	5.12*	2.88	0.008596	4.04	2.60_1	2.07_0	1.25_6
610	0.4762	4.00	4.00	0.006716	4.12	2.29_8	1.89_4	1.18_7
611	0.4753	3.20	4.80	0.005373	4.25	1.99_4	1.68_3	1.18_5
612	0.4761	2.56	5.44	0.004298	4.37	1.72_3	1.50_2	1.14_8
613	0.4769	2.04	5.96	0.003425	4.33	1.51_2	1.29_5	1.16_8
614	0.4770	1.64	6.36	0.002754	4.61	1.10_0	0.961	1.14_5
615	0.4774	1.28	6.72	0.002149	4.58	0.951	0.852	1.11_6
616	0.4760	1.00	7.00	0.001679	4.90	0.734	0.653	1.12_5

Résine: Diaïon SK-1 60~80 mesh, poids comme montré
Solution: Volume total 10 ml., 30%H_2CoY+70%$(NH_4)_2CoY$
Terres rares: Eu 2.92 μg., Sm 13.6 μg. en oxyde.
Mesures: Eu, Sm tous les deux par γ
* à partir N° 609 la solution préalablement 4 fois diluée

prévu par les considérations ci-dessus, et aussi les Crs plus petits prévu par les rapports des constantes de formation des complexes des terres rares pour des métaux lourds.

Les résultats figurés dans Tableau VI et Fig. 5, montrent exactement comme il était prévu, une efficacité de séparation moins grande et les valeurs de Cr plus petites, quoique ces résultats soient un peu moins précis à cause des valeurs de Cr trop petites à mesurer surtout vers les compositions auprès de NH_4CoX.

6) Effet de la Dilution.—A la suite de ces variations en fonction de la composition, nous voulons connaître les influences de divers facteurs sur les coéfficients de répartition. D'abord nous avons étudié l'effet de la dilution progressive de la solution complexe, car on dit qu'une concentration plus faible donne une séparation moins efficace[14].

Les variations du coéfficient de répartition sont représentées dans Tableau VII et Fig. 7, lorsqu'on a dilué la solution, en maintenant la même composition, c'est-à-dire dilué la solution de complexe mélangée 30% de H_2CoY et 70% de $(NH_4)_2CoY$.

14) R. C. Vickery, *J. Chem. Soc.*, **1952**, 4357.

TABLEAU VIII

EXP. 7. EFFET DE DILUTION POUR UNE CONCENTRATION CONSTANTE EN ION AMMONIUM

N° d'exp.	NH_4R	Solution de complexe	NH_4ClO_4	pH	Concen. finale en CoY^{2-}	Cr_{Sm}	Cr_{Eu}	α
	g.	ml.	ml.		mol.			
701	0.4790	8.00	0.0	3.67	0.05373	1.67_4	1.08_4	1.54_5
702	0.4789	5.60	2.40	3.59	0.03761	1.67_4	1.11_2	1.50_6
703	0.4786	4.00	4.00	3.55	0.02686	1.75_6	1.15_1	1.52_5
704	0.4791	2.88	5.12	3.53	0.01934	1.77_4	1.19_0	1.49_1
705	0.4790	2.04	5.96	3.45	0.01370	1.82_8	1.28_6	1.42_1
706	0.4787	1.44	6.56	3.45	0.00967_1	1.89_3	1.27_3	1.48_7
707	0.4786	1.04	6.96	3.47	0.00698_5	2.02_9	1.32_0	1.53_7
708	0.4790	0.74	7.26	3.46	0.00497_0	1.97_9	1.38_5	1.42_9
709	0.4793	0.52	7.48	3.66	0.00349_2	1.98_3	1.33_5	1.48_6
710	0.4789	0.26	7.74	3.46	0.00174_6	2.14_1	1.41_4	1.51_5
711	0.4791	0.14	7.86	3.50	0.00094_0	2.45_2	1.64_8	1.48_8
712	0.4791	0.08	7.92	3.50	0.00053_7	2.56_7	1.73_6	1.47_9

Résine: Diaïon SK-1, sous forme de NH_4R, 60~80 mesh poids comme montré
Solution: Volume total 10 ml., concentration en CoY^{2-} comme montrée
Solution de complexe: 30%H_2CoY+70%$(NH_4)_2CoY$
Solution de NH_4ClO_4: 0.09402 mol.
Terres rares: Eu 2.25 μg, Sm 57.0 μg., comme en oxyde
Mesures: Eu par β et γ, Sm par γ

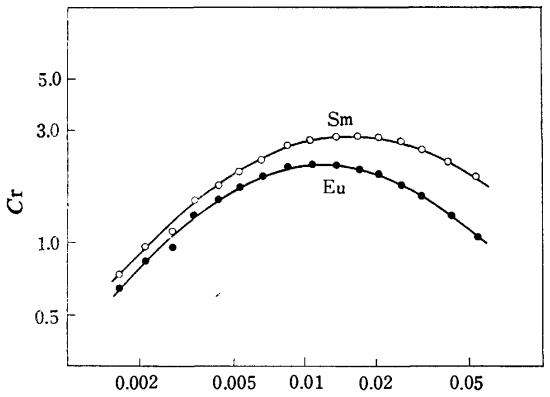

Fig. 7. Effet de la dilution.

On voit d'une part que le coéfficient de répartition augmente d'abord avec la dilution, devient ensuite à peu près constant, puis commence à diminuer, et d'autre part que le facteur de séparation décroît nettement de plus en plus. Il semble que ces variations soient assez difficile à analyser, peut-être on pourra considérer comme suivant. Aux fortes concentrations, l'effet de la diminution en NH_4^+ sera prédominant, tandis que pour les fortes dilution, la résine NH_4R pourra commencer à décomposer le complexe, après avoir fini l'élimiation complète de l'ion libre Co^{2+}, ainsi les terres rares commencent à passer en solution; aux concentration moyennes ces deux effets sont à peu près du même ordre, donc la répartition varie peu.

Cependant la diminution remarquable du facteur de séparation reste plus difficile à expliquer surtout à la comparaison de l'expérience suivante. Il sera possible d'y avoir une certaine quantité du NH_4^+ nécessaire pour tenir l'équilibre du Co^{2+} entre deux phases afin de réaliser l'éfficacité de séparation.

7) Effet de la Dilution pour une Concentration Constante en Ion Ammonium.—Ensuite nous avons étudié l'influence de la dilution en maintenant la concentration en ion NH^{4+} constante. Dans cette série, on a dilué la solution de complexe en remplaçant l'eau distillée, qui était employée dans l'expérience précédante, par une solution de perchlorate d'ammonium 0.09402 mol., soit 1.1048 g. dans 100 ml., qui correspond à la concentration calculée de la composition mélangée 30% H_2CoY et 70% $(NH_4)_2CoY$ 0.05373 mol., c'est pourquoi il est possible qu'elle soit de concentration un peu inférieure à celle de la solution complexe, dans laquelle une légère partie de Co^{2+} a été remplacé par le NH_4^+ au moment de l'élimination de l'excès de l'ion libre Co^{2+} dans la colonne NH_4R.

La légère augmentation de Crs pour les fortes dilutions du complexe viendrait probablement d'une concentration plus faible en ions Co^{2+} dans la phase de résine, et aussi de la dissociation du complexe du Co en ses composants. Cependant cette différence est vraiment légère surtout lorsqu'on compare aux cas des acides hydroxycarboxyliques pour lesquels les coéfficients de répartition varient proportionnellement presqu'au cube de la concentration. Il semble que la dilution provoque une légère diminution de l'efficacité de séparation.

8) Effet de la Concentration en Ion Ammonium.—L'effet de l'augmentation de la concentration en ion NH_4^+ peut être prévus à peu près par les considérations théoriques sur les réactions d'équilibre entre la phase résine et la phase solution. Pour savoir la validité de ces considérations, nous avons fait cette série d'expériences.

Comme solution de départ, on prend le mélenge, 80% de H_2CoY et 20% de $(NH_4)_2CoY$, à cause de sa faible teneur en ion NH_4^+ et des grands coéfficients de répartition qu'il peut obtenir. 50 ml. de cette solution divisée, on en ajoute 9.4367 g. de

TABLEAU IX

EXP. 8. EFFET DE LA CONCENTRATION EN ION AMMONIUM

N° d'exp.	NH_4R g.	Soln. de complexe ml.	Complexe $+NH_4ClO_4$ ml.	NH_4^+ ajouté mol.	Concen. fin.* en NH_4^+ mol.	pH	Cr_{Sm}	Cr_{Eu}	α
801	0.4781	8.00	0.00	0.0-	0.0215	2.86	15.7_2	10.3_9	1.51_3
802	0.4780	7.75	0.25	0.0040	0.0255	2.68	12.6_8	8.26_1	1.53_6
803	0.4781	7.44	0.56	0.0090	0.0305	2.47	9.93_4	6.60_6	1.50_4
804	0.4775	7.10	0.90	0.0145	0.036	2.40	7.94_3	5.34_2	1.48_7
805	0.4780	6.66	1.34	0.0215	0.043	2.28	6.39_6	4.54_4	1.43_6
806	0.4774	6.16	1.84	0.0295	0.051	2.16	5.34_7	3.80_5	1.40_5
807	0.4773	5.54	2.46	0.0395	0.061	2.14	4.29_0	3.19_6	1.34_2
808	0.4776	4.79	3.21	0.0515	0.073	2.22	3.52_2	2.58_4	1.36_3
809	0.4777	3.92	4.08	0.0665	0.087	2.14	2.88_7	2.15_6	1.33_9
810	0.4779	2.99	5.01	0.0805	0.102	2.12	2.51_8	1.81_5	1.38_7
811	0.4774	1.68	6.32	0.1015	0.123	2.07	1.95_1	1.47_2	1.32_5
812	0.4779	0.00	8.00	0.1285	0.150	2.04	1.65_3	1.25_2	1.32_0

Résine : Diaïon SK-1, sous forme NH_4R, 60～80 mesh, poids comme montré
Solution : Volume total 10 ml., concentration en NH_4^+ comme montrée
Concentration en CoY^{2-} 0.05373 mol.
Solution de complexe : $70\%H_2CoY+30\%(NH_4)_2CoY$
Solution de complexe$+NH_4ClO_4$: la même solution$+9.4367$ g. de NH_4ClO_4
Terres rares : Eu 2.25 μg., Sm 57.0 μg. comme en oxyde
Mesures : Eu, Sm tous les deux par β et γ
* Concentration finale, après l'addition de la solution des terres rares

TABLEAU X

EXP. 9. EFFET DE pH

N° d'exp.	NH_4R g.	$H_2CoY+NH_4ClO_4$ ml.	$(NH_4)_2CoY$ ml.	pH	Cr_{Sm}	Cr_{Eu}	α
901	0.4756	8.00*	0.00	7.11	0.13_4	0.13_8	(0.97_3)
902	0.4768	8.00**	0.00	6.76	0.09_9	0.11_8	(0.98_1)
903	0.4756	8.00***	0.00	6.74	0.11_6	0.10_1	(1.14_8)
904	0.4683	8.00	0.00	6.44	0.11_4	0.09_9	1.14_7
905	0.4655	7.97	0.03	6.35	0.14_0	0.11_8	1.18_6
906	0.4762	7.94	0.06	6.25	0.17_4	0.14_0	1.24_3
907	0.4775	7.90	0.10	5.87	0.18_5	0.15_3	1.21_1
908	0.4663	7.85	0.15	5.40	0.18_7	0.14_4	1.30_0
909	0.4759	7.80	0.20	5.15	0.19_0	0.14_4	1.32_4
910	0.4759	7.70	0.30	4.84	0.24_1	0.19_4	1.24_1
911	0.4759	7.60	0.40	4.60	0.27_0	0.20_1	1.34_6
912	0.4758	7.45	0.55	4.41	0.31_8	0.21_6	1.47_0
913	0.4757	7.25	0.75	4.20	0.43_3	0.29_2	1.48_3
914	0.4760	7.00	1.00	4.04	0.55_8	0.38_4	1.45_4
915	0.4757	6.40	1.60	3.75	0.92_5	0.61_4	1.50_7
916	0.4748	5.80	2.20	3.53	1.16_3	0.88_3	1.31_7
917	0.4761	5.20	2.80	3.34	1.85_6	1.22_7	1.51_3
918	0.4748	4.10	3.90	3.06	3.21_5	2.11_4	1.52_1
919	0.4758	3.20	4.80	2.85	4.90_6	3.28_3	1.49_5
920	0.4668	2.46	5.64	2.67	7.41_7	4.91_5	1.50_9
921	0.4764	1.50	6.50	2.48	10.92_4	7.56_2	1.44_5
922	0.4753	0.00	8.00	2.33	18.48_8	13.80_5	1.33_9

Résine : Diaïon SK-1, sous forme NH_4R, 60～80 mesh, poids comme montré
Solution : Volume total 10 ml., 0.05373 mol. en CoY^{2-}, 0.1075 mol. en NH_4^+
Terres rares : Eu 2.92 μg., Sm 13.6 μg. en oxyde
Mesures : Eu, Sm tous les deux par γ
* 1 Goutte de NH_4OH 1 N
** 1 Goutte de NH_4OH N/4
*** 1 Goutte de NH_4OH N/10

NH_4ClO_4 dans une partie, alors on obtient une solution à 0.05373 mol. en CoY^{2-} et à 0.150 mol. en NH_4^+, tandis que l'autre partie reste à 0.0215 mol. en NH_4^+, après addition de la solution de terres rares radioactives. A partir de ces deux solutions on obtient les concentrations différentes en ion NH_4^+, comme dans le tableau suivant.

On voit que le coéfficient de répartition décroît à peu près proportionellement à la concentration en ion NH_4^+ et que l'éfficacité de séparation diminue, comme on prévoyait. Les valeurs obtenues des facteurs de séparation ne sont pas très précises à cause de la difficulté à préparer de bonnes sources, étant donné la quantité relativement grande de perchlorate d'ammonium, qui se dépose d'abord en laissant la solution de complexe, pour cette raison on ne pouvait faire les mesures qu'aux compteurs γ pour quelques sources préparées de solutions concentrées en ion NH_4^+.

9) Effet du pH.—Il est possible de prévoir que le pH aura moins d'influence sur les coéfficients de répartition des terres rares dans le cas où l'on emploie l'EDTA que dans celui où l'on emploie les acides hydroxycarboxyliques, étant donné que la formation du complexe acide non dissocié n'est pas remarquable, et de plus, elle est de même ordre presque tous les métaux, contrairement aux acides hydroxycarboxyliques qui sont sensibles à se dissocier par la différence du pH, donc la concentration d'anion, à qui le coéfficient de répartition sera proportionnel presqu'au cube, varie beaucoup avec le pH.

Pour ces expériences, nous avons préparé les solutions aux pH différents, en partant des solutions du H_2CoY et du $(NH_4)_2CoY$, qui contiennent la quantité équivalente d'ammonium. Les résultats sont dans Tableau X.

La prévision était à peu près constatée, c'est-à-dire. il n'y a pas de différence remarquable dans le domaine des pHs entre 3.5 et 7.0. Notons que dans les cas des acides hydroxycarboxyliques, il est suffisant de changer la valeur de pH d'ordre de 1.0 pour augmenter le coéfficient de répartition 1000 fois plus grand. Cependant dans cette série d'expériences, nous n'avions pas prêté assez d'attention à l'effet de différence par les teneurs en ion libre de Co^{2+} dans les deux solutions de départ. L'augmentation de coéfficients de répartition pour les solutions aux pHs inférieurs à 3.5, sera certainement plutôt à cause de l'augmentation de la concentration de l'ion libre de Co^{2+}. Les coéfficients de répartition pour les pHs supérieurs à 5.0 sont trop petits pour nous permettre de les déterminer avec une grande précision. Il vaudrait mieux préparer les solutions à essayer par mélanger des deux solutions préparées d'une solution de H_2CoY, mais à la manière comme suivante; l'une neutralisée par l'ammoniaque jusqu'à pH 7.0, l'autre ajustée à la concentration en ion ammonium équivalente par l'addition de perchlorate d'ammonium, ainsi on pourrait éviter la différence à la teneur en ion libre du Co^{2+}, et obtenir les coéfficients de répartition convenable, dans ce cas il sera possible de savoir les comportements différents entre les complexes acides non dissociés de terres rares et de Co.

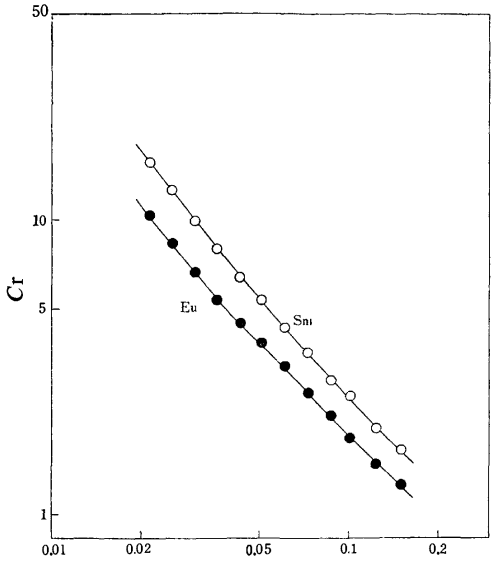

Fig. 8. Effet de concentration en NH_4^+.

10) Effet des Entraineurs Isotopique et non Isotopiques. En ce qui concerne les variations de l'efficacité deséparation en fonction de la différence de la quantité d'une terre rare par rapport à l'autre, il n'y a presque pas d'expérience, bien qu'il soit extrêmement important. Sur ce sujet, l'analyse des résultats de quelques expériences de séparation sur colonne n'a pas permis de préciser le comportement d'une terre rare en présence d'autres en grand quantité; la difficulté était de doser précisément la première. A l'aide de radioélément, on pourrait la determiner facilement. C'est essentiellement nécessaire à savoir surtout pour les préparations de terres rares extrêmement pures ou bien la séparation d'une terre rare sans entraîneur produite partir d'une voisine.

Dans ce but, nous avons choisi parmi les terres rares, le Sm comme entraîneur isotopique, le La, le Nd et l'Y comme non isotopiques mais les deux premières qui doivent être éluées plus tard, le troisième plus avant que l'Eu et le Sm, afin de savoir s'il y a les différences par leurs positions pour l'influence des coéfficients de répartition et de l'efficacité de séparation du Sm et de l'Eu. Plutôt que de partir d'une solution de terres rares nous avons préféré les fixer d'abord sur une petite quantité de résine dans une colonne, pour réaliser des conditions semblables à la séparation sur colonne, et aussi pour ne pas ajouter d'ion inutile.

Une quantité suffisante de résine sous forme d'ammonium séchée dans l'air a été prise par la balance chimique, versée dans une petite colonne avec de l'eau, puis transformée sous forme du sel d'une terre rare, en faisant passer la solution de cette terre rare. La saturation de la résine par terre rare a été verifiée par précipitation des terres rares par l'acide oxalique dans la solution passée. La résine lavée à l'eau distillée est versée sur un petit filtre en verre fritté, lavée une fois par un peu d'alcool puis laissée sécher à l'air. La quantité

de terres rares à ajouter selon la composition espérée peut être calculée par le poids de la résine prise sous forme ammonium et le poids de résine ainsi préparée. La composition de la solution choisie, c'est aussi le mélange de 30% de H_2CoY et de 70% de $(NH_4)_2CoY$, mais dans cette série d'expériences, le poids de résine et le volume total sont tous les deux juste moitié que dans les autres séries.

A la suite de l'agitation après avoir ajouté la solution complexe, on a remarqué le changement de couleur de la solution en rose plus claire assez net dans le dernier tube de chaque série LaR_3, NdR_3 et SmR_3 dans les deux derniers de la série YR_3, ce qui montre la diminution en ion de Co dans la solution et probablement aussi l'abaissement du pH ; à ces trois premiers tubes, on a remarqué les précipités, cependant la durée de ses commencements de l'apparition était différente ; dans le cas de LaR_3, bientôt après l'agitation, un peu plus tard dans le cas de NdR_3, et la quantité de précipité du premier était plus grande que du deuxième ; dans le cas de SmR_3, on n'a pas trouvé de précipité dans la première journée, mais le

TABLEAU XI

EXP. 10. EFFET DES ENTRAÎNEURS NON ISOTOPIQUES ET ISOTOPIQUE

N° d'exp.	LnR_3 g.	NH_4R éq. de LnR_3 g.	NH_4R g.	Capacité de LnR_3 %	pH	Cr_{Sm}		Cr_{Eu}		α	
						β	γ	β	γ	β	γ
1001	0.0–	0.0–	0.2524	0.0–	3.55	1.83_0	1.85_6	1.17_6	1.17_8	1.55_7	1.57_6
LaR_3											
1002	0.0001_5	0.0001_0	0.2530	0.04_1	3.52	1.84_6	1.86_3	1.17_3	1.15_6	1.57_4	1.61_2
1003	0.0004_5	0.0003_1	0.2522	0.12_3	3.53	1.82_5	1.85_0	1.15_8	1.16_8	1.57_6	1.58_4
1004	0.0015	0.0010_4	0.2518	0.41_1	3.53	1.85_2	1.82_4	1.12_9	1.16_9	1.64_0	1.56_0
1005	0.0048	0.0033_2	0.2499	1.31_1	3.53	1.77_8	1.78_3	1.13_9	1.14_6	1.56_1	1.55_3
1006	0.0148	0.0102_3	0.2424	4.05_2	3.53	1.79_0	1.78_3	1.14_7	1.14_3	1.56_1	1.56_0
1007	0.0434	0.0300_9	0.2227	11.90_3	3.52	1.67_8	1.64_0	1.05_4	1.04_0	1.59_2	1.57_7
1008	0.1450	0.1002_6	0.1515	39.82_3	3.52	1.21_4	1.23_4	0.76_4	0.79_0	1.58_8	1.56_2
1009	0.3618_5	0.2502	0.0–	100.0–	3.14	1.88_6	1.88_6	(1.04_8)	1.20_2	(1.80_0)	1.56_9
NdR_3											
1010	0.0002	0.0001_4	0.2527	0.05_4	3.53	1.86_9	1.85_4	1.16_6	1.17_5	1.60_3	1.57_8
1011	0.0006	0.0004_1	0.2523	0.16_3	3.53	1.83_0	1.83_5	1.14_6	1.16_3	1.59_6	1.57_9
1012	0.0015_5	0.0010_6	0.2519	0.41_9	3.53	1.83_1	1.86_5	1.15_3	1.18_5	1.58_6	1.57_4
1013	0.0046	0.0031_5	0.2496	1.24_5	3.53	1.85_4	1.86_3	1.18_7	1.17_3	1.56_2	1.58_9
1014	0.0149_5	0.0102_3	0.2424	4.05_0	3.53	1.95_5	1.93_5	1.22_1	1.23_4	1.60_1	1.56_7
1015	0.0439_5	0.0300_8	0.2223	11.91_6	3.52	2.00_5	2.00_2	1.27_4	1.21_8	1.64_2	1.57_3
1016	0.1466_5	0.1003_5	0.1519	39.78_4	3.50	2.22_4	2.24_1	1.42_8	1.27_3	(1.74_6)	1.54_9
1017	0.3661	0.2505_2	0.0–	100.0–	3.02	5.09_2	5.07_1	(2.90_5)	1.44_7	(1.72_7)	1.59_0
SmR_3											
1018	0.0002	0.0001_4	0.2522	0.05_4	3.53	1.88_6	1.86_0	1.17_9	1.18_4	1.59_9	1.57_3
1019	0.0004_5	0.0003_1	0.2522	0.12_3	3.53	1.88_9	1.87_2	1.16_5	1.16_7	1.62_2	1.60_4
1020	0.0015_5	0.0010_6	0.2521	0.41_7	3.52	1.88_8	1.87_3	1.17_9	1.18_6	1.60_2	1.58_0
1021	0.0045_5	0.0031_0	0.2497	1.22_7	3.52	1.95_2	1.96_3	1.26_1	1.24_9	1.68_2	1.57_2
1022	0.0155_5	0.0106_0	0.2424	4.18_8	3.47	2.17_5	2.19_7	1.36_6	1.41_8	1.59_3	1.54_9
1023	0.0442_5	0.0301_6	0.2226	11.93_1	3.47	2.65_2	2.68_4	1.69_2	1.69_9	1.56_7	1.58_0
1024	0.1501_5	0.1023_3	0.1514	40.33_5	3.43	2.96_6	3.11_2	(1.77_7)	1.95_9	(1.66_9)	1.58_8
1025	0.3677	0.2506_0	0.0–	100.0–	3.01	6.17_1	6.25_2	(3.49_5)	3.95_0	(1.76_6)	1.58_3
YR_3											
1026	0.0001_5	0.0001_1	0.2527	0.04_3	3.51	1.88_1	1.87_3	1.17_8	1.19_7	1.59_6	1.56_6
1027	0.0002_9	0.0002_9	0.2526	0.11_4	3.50	1.89_5	1.89_3	1.17_1	1.18_2	1.61_8	1.60_1
1028	0.0014	0.0010_1	0.2515	0.40_0	3.50	1.93_9	1.93_1	1.23_9	1.22_1	1.56_5	1.58_1
1029	0.0042	0.0030_3	0.2501	1.19_6	3.48	2.15_1	2.17_1	1.39_7	1.37_6	1.53_9	1.57_8
1030	0.0134	0.0096_6	0.2426	3.82_9	3.43	2.95_1	2.95_0	1.87_7	1.90_3	1.57_5	1.55_0
1031	0.0420	0.0302_8	0.2221	11.99_5	3.38	4.82_1	4.82_9	2.94_1	3.04_7	1.63_9	1.58_5
1032	0.1396	0.1006_4	0.1517	39.88_6	3.28	10.71_8	10.58_6	(6.24_6)	6.60_5	1.71_6	1.60_3
1033	0.3483_5	0.2511_3	0.0–	100.0–	2.83	15.11_1	15.06_5	(8.92_6)	10.05_7	1.69_3	1.49_8

Résine : Diaïon SK-1, sous forme NH_4R+LnR_3 aux compositions montrées, 60～80 mesh
Solution : Volum total 5 ml, $30\%H_2CoY+70\%(NH_4)_2CoY$
Terres rares : Eu 0.96 μg., Sm 4.48 μg. en oxyde
Mesures : Sm, Eu tous les deux par β et γ

lendemain une quantité plus petite de précipité crystallin au lieu de pulvérulent dans les deux cas précédants. Dans les tubes de YR_3, aucun précipité n'était pas remarqué même quelques jours après. Probablement ces précipités seront l'acide libre d'EDTA, mais on n'a pas examiné s'ils ne contenaient aucun métal, soit sous forme de complexe acide d'un ou de deux métaux, soit comme coprécipitation.

Les résultats sont donnés dans Tableau XI et Fig. 9, où nous pouvons citer ces points intéressants.

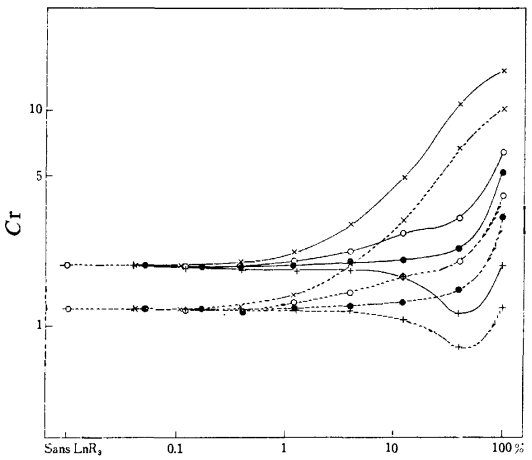

Fig. 9. Effet des entraîneurs isotopique et non isotopiques.

—— Sm × YR_3 ○ SmR_3
---- Eu ● NdR_3 + LaR_3

D'abord selon la quantité de terre rare, dont le complexe est plus fort ou plus faible que celui du Co, les coéfficients de répartition de l'Eu et du Sm sont diminués ou augmentés. Avec l'augmentation d'entraîneur, ces influences sont renforcées, enfin les coefficients de répartition montent plus vite dans tous les quatre cas, lorsque la quantité de terre rare dépasse la quantité équivalente de l'EDTA.

Ensuite il est vraiment remarquable que, dans tous les cas, les comportements de l'Eu et du Sm sont tout à fait identiques, c'est-à-dire le facteur de séparation reste toujours constant, quelle que soit la quantité de l'entaîneur, non seulement non isotopique mais aussi isotopique, soit 0.000895 à 1.20 méq., de plus même s'il y a la décomposition dans la solution à cause de l'excès d'une des terres rares. On doit faire attention ce qu'il y a une grande différence entre les comportements d'une terre rare et d'un métal lourd. Cependant on ne peut pas assurer pour moment si ce fait reste toujours vrai pour une autre couple de terres rares quelconques, car il est possible que ce fait vienne de la différence très petite du facteur de séparation à cause d'une paire des ions la plus semblable, le Sm et l'Eu, même parmis les terres rares.

De la comparaison des comportements du Sm et de l'Eu par les présences du Sm d'un côté et des autres terres rares d'autre, il semble qu'il n'y ait aucune différence entre les entraîneurs isotopiques et non isotopiques, au moins pour ces ions assez samblables.

De la comparaison des comportements de l'Eu à la présence du Sm minimum et maximum, on pourra sûrement appliquer ce facteur de séparation à un cas où il n'y a plus petite quantité de l'Eu que dans ces expérience, même jusqu'à l'état sans entraîneur, car c'est une grande qualité bien constatée géneralement à la séparation par la résine échangeuse d'ion, que le comportement d'un ion au dessous d'une certaine quantité, soit à peu près de l'ordre de quelques milligrammes, est tout à fait identique à celui qu'il est sans entraîneur, pourvu que cet ion reste vraiment à l'état d'ion. Quant à la séparation des terres rares à l'aide de la résine sous forme Zn[15], on a déjà montré jusqu'à la quantité la moindre dosable par la méthode d'absorption; ici c'est étendu jusqu'au cas limite.

Discussion

Etant donné que la solution complexe de l'acide aminopolycarboxylique et du métal lourd peut libérer une quantité plus ou moins grande d'ion libre du métal lourd, qui jouent un rôle important dans l'action de la solution et aussi dans la composition de la phase de résine, le coéfficient de répartition n'est plus indépendant du rapport du volume de solution au poids de résine, tout à fait différent de l'acide hydroxycarboxylique. Le contrôle de cet ion libre sera probablement le grand problème pour la séparation sur colonne, à ce point de vue, le système saturé en métal lourd est moins sensible pour la quantité de l'ion libre, cependant l'excès du métal lourd diminue l'éfficacité de séparation, certainement à cause de la formation des complexes polynucléaires.

Pour cette même raison l'effet de la concentration en ion ammonium aussi a une influence plus faible que dans le cas de l'acide hydroxycarboxylique, ainsi d'ailleur que le pH étant donné la différence entre la tendance à former les complexes acides et à former l'acide hydroxycarboxylique relativement peu dissocié avec l'augmentation de l'ion d'hydrogène. Des effets semblables sont remarqués aussi dans les dilutions de la solution complexe, or la dilution simple nous montre la complexité de cet acide, on doit remarquer aussi qu'il y a de grandes différences dans les facteur de séparation selon qu'on dilue la solution simplement par l'eau ou bien en conservant une concentration constante en ion ammonium;

15) P. Krumholz, K. Bril et al., "Proceedings of the Second United Nations International Conference on the Peaceful Uses of Atomic Energy", p/2491, **28**, 184, Geneva (1958).

dans le premier cas, le facteur de séparation décroît énormément avec la dilution, tandis qu'il décroît légèrement dans le deuxième cas. Nous ne pouvons dire à présent si c'est à cause de l'effet direct des ions ammonium à la concentration nécessaire minimum ou bien des qualités particulières de complexes mais sûrement ces points seront un des motifs pour lesquels on n'a pas pu obtenir une bonne séparation au moyen de l'acide éthylènediaminetétraacétique seule.

Les diminutions du facteur de séparation avec l'augmentation des ions ammonium et aux bas pHs, peuvent être considérés comme probablement dues dans le premier cas à l'augmentation de la force ionique et dans l'autre cas sûrement aux différences moins grandes dans les constantes de formation des complexes acides de ces deux terres rares.

Ces connaissances nous donne la suggestion qu'il vaudra mieux employer la solution de sel presque tétraammoniaque d'acide éthylènediaminetétracétique pour les séparations de terres rares en grande quantité sur colonne pour avoir une concentration plus forte en terres rares dans les solutions éluées et pour éviter la formation des complexes acides dont la solubilité est plus petite. La possibilité de précipitation des hydroxydes de terres rares dans la zone au commencement de la bande absorbée de terres rares où il y a un changement très grand du pH, pourra éviter à l'aide du magnésium par exemple, comme montré par Brunisholtz[16].

D'autre part il est tout à fait remarquable que le facteur de séparation reste toujours constant avec l'augmentation de la quantité d'entaîneurs non seulement non isotopiques mais aussi isotopique, ainsi qu'en présence d'une précipitation provoquée probablement de l'acide libre. Cette constance du facteur de séparation sera réalisée même en l'absence de métal lourd, c'est-à-dire si les terres rares en grande quantité sont séparées sur colonne par élution au moyen de l'éthylènediaminetétraacétate d'ammonium.

De ces connaissance, en bref la solution de complexe a une action remarquable presque tous les variants des études de l'échange d'ion, qui sera favorable à étudier la chimie de complexe surtout de la quantité impondérable de terres rares par la méthode d'équilibre, cependant pour effectuer la séparation sur colonne, il faudra encore beaucoup plus d'attentions pour maintenir la concentration de l'ion libre, de ce point de vue l'acide hydroxycarboxylique sera plus facile à employer.

16) G. Brunisholtz, Communication privée et aussi voir *Helv. Chim. Acta.* 40, 2004 (1957).

Résumé

Pour avoir l'efficacité de séparation que peuvent faire espérer les données sur les réactions d'équilibre de l'acide aminopolycarboxylique avec les terres rares, la solution du complexe de ces acides avec les métaux lourds est considérée comme meilleure que l'acide simple, à cause surtout de sa plus grande stabilité et de son comportement à faible concentration et à faible pH.

Les méthodes de préparation de ces solutions de complexes, leurs caractéristiques essentielles vis-à-vis des résines sous forme ammonium et sous forme métal lourd, les comportements des coéfficients de répartition en fonction de la dilution simple et pour une concentration en ion ammonium, en fonction de la concentration en ion ammonium et en fonction du pH sont étudiés. Les motifs qui peuvent diminuer le facteur de séparation sont aussi essayés de discuter, mais il est remarquable qu'ils restent constants en présence d'une grande quantité d'entreîneurs isotopiqus ou non. Les discussions ont été faites sur ces résultats.

L'auteur veut exprimer ses remercients les plus profonds à Monsieur Ch. Fisher, chef de Service de Radioéléments Artificiels, à Monsieur R. Henry, chef de Section de Préparation des Radioéléments du même Service, Département de Chimie, Commissariat à l'Energie Atomique de la France, qui lui permettaient d'étudier ces expériences, à Mademoiselle J. Beydon qui se donnait la peine de discuter les analyses des résultats, et aussi à d'autres ingénieurs de ce Service, au Centre d'Etudes Nucléaires de Saclay qui s'occupaient d'irradier les échantillons, de lui permettre de se servir des diverses appareils de mesure.

Il lui faut remercier profondément à l'Agence Internationale de l'Energie Atomique à Vienne, dont la bourse d'études lui permettait de devenir possible ses séjours à ce Centre au cours de ces expériences.

Département de Chimie
Centre d'Etudes Nucléaires de Saclay
France

Asymmetric Hydrogenation with Modified Raney Nickel. I. Studies on Modified Hydrogenation Catalyst. II[1]

By Yoshiharu IZUMI, Masami IMAIDA, Hideaki FUKAWA and Shiro AKABORI

(Received July 25, 1962)

Although a number of methods for asymmetric hydrogenation have been attempted, few reports are available on the asymmetric hydrogenation based on the assymmetric function of catalysts, except enzymatic hydrogenation. Akabori et al.[2-3] reported on asymmetric hydrogenation observed in the experiments using silk-palladium catalyst. However, the efficiency of their asymmetric hydrogenetion was very low and the results were not reproducible. Isoda et al.[4] also reported that asymmetric hydrogenation occurred by the use of silk-palladium catalyst and with R-Ni*, on which optically active amino acid has been adsorbed.

In the previous paper of this series[1] it was reported that the treatment of R-Ni with amino acid solution e. g. Glu* diminished the hydrogenation activity for the carbonyl group without any appreciable effect on the activity toward the C=C double bond.

The present paper deals with the asymmetric hydrogenation of carbonyl compounds carried out with R-Ni modified with optically active amino acid. It has been confirmed that R-Ni treated with L- or D-Glu solution has a definite ability to catalyze the hydrogenation of carbonyl compounds asymmetrically. Ethyl acetoacetate, methyl acetoacetate and acetophenone were asymmetrically hydrogenated with the use of this modified catalyst yielding the corresponding, optically active alcohols. An excellent result was obtained in the hydrogenation of methyl acetoacetate to methyl 2-hydroxybutyrate by the use of R-Ni treated with L- or D-Glu.

$$CH_3\text{-}CO\text{-}CH_2\text{-}CO_2Me \xrightarrow{+H_2} CH_3\text{-}\underset{\displaystyle OH}{\underset{|}{CH}}\text{-}CH_2CO_2Me$$

The treatment of R-Ni with other amino acids showed the same effect to a lesser extent. R-Ni treated with D-tartaric acid also had the capacity to catalyze asymmetric hydrogenation.

The results of experiments described above were reproducible and products of high optical activity were obtained. R-Ni treated with L- and D-Glu respectively gave levo- and dextrorotatory 2-hydroxybutyrate. When R-Ni treated with DL-Glu the product was fully inactive as could naturally be expected. Hydrogenation of benzalazlactone with R-Ni treated with L-Glu gave, however, optically inactive phenylalanine.

The catalyst modified with Glu had no asymmetric activity for the hydrogenation of benzalazlactone. As reported in the previous paper modification of R-Ni with amino acids had no effect on the hydrogenation activity toward the C=C double bond, while it showed a strong inhibition of the activity toward the carbonyl group. On the other hand, the modified catalysts had asymmetric hydrogenation activity toward the carbonyl group above 60°C.

The results described above and that reported in the previous paper suggest that the hydrogenation of the carbonyl group and C=C double bond may take place at different active centers.

Results and Discussion

Effect of the pH of Modifying Solution.— Asymmetric yields of catalytic hydrogenation by R-Ni treated with 2% L-Glu solution of various pH at 0°C were investigated. The pH of the Glu solution was adjusted with 1 N (f=0.833) sodium hydroxide solution according to the titration curve shown in Fig. 1.

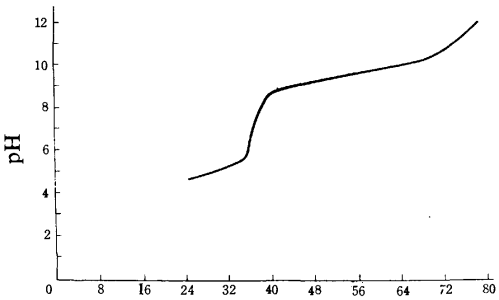

Fig. 1. Titrating curve of 2% L-Glu solution with 1 N NaOH.

* Abbreviation: R-Ni, Raney nickel; Glu, Glutamic acid.

1) H. Fukawa, Y. Izumi, S. Komatsu and S. Akabori, This Bulletin, 35. 1703 (1962).
2) S. Akabori, Y. Izumi, Y. Fujii and S. Sakurai, *J. Chem. Soc. Japan, Pure Chem. Sec.* (*Nippon Kagaku Zassi*), 77, 1374 (1956); S. Akabori, Y. Izumi and Y. Fujii, ibid., 78, 886 (1957).
3) Y. Izumi, This Bulletin, 32, 932 (1959).
4) T. Isoda, A. Ichikawa and T. Shimamoto, *J. Sci. Res. Inst.* (*Rikenhokoku*), 34, 134 (1958); 34, 143 (1958).

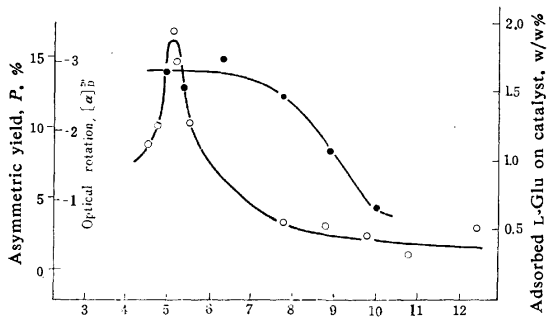

Fig. 2. Effect of pH of modifying solution.
○ Optical rotatory power of reduction product
● Adsorbed L-Glu on R-Ni

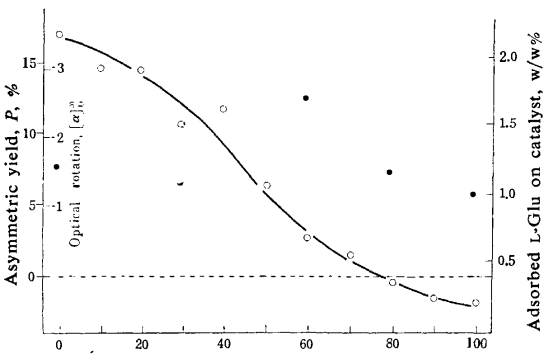

Fig. 3. Effect of modifying temperature.
○ Optical rotatory power of reduction product
● Adsorbed L-Glu on R-Ni

As shown in Fig. 2, the pH of the Glu solution greatly influenced the capacity of the catalyst for asymmetric hydrogenation and adsorbed L-Glu. There was a distinct optimum capacity at pH 5.1 with considerable diminution observed both at higher and lower pH values. It is interesting that the modifying solution turned green on treating R-Ni below pH 5 and blue above pH 5.

Effect of Modifying Temperature.—The relationship between the asymmetric capacity and the temperature of modifying solution was studied using R-Ni immersed in 2% L-Glu at pH 5.0~5.2. The highest asymmetric yield was obtained with R-Ni modified at 0~20°C, and the asymmetric yield was decreased at higher temperatures as shown in Fig. 3. If R-Ni was treated with the same modifying solution at temperatures higher than 80°C the product showed reverse optical rotation. Reaction velocity of hydrogenation decreased as the modifying temperature was increased. However, no relationship between the quantity of adsorbed amino acid and catalytic activity could be established, because exact determination of adsorbed Glu was impossible. The facts mentioned above might sugget that the mode of modification of the catalyst at higher temperature is different from that at lower temperature.

Effect of Concentration of Modifying Solution.—The asymmetric capacity of the modified R-Ni was independent of the concentration of L-Glu within the range of 6 to 0.0625% as can be seen in Fig. 4. This result shows that adsorption of Glu on R-Ni reaches saturation at the lower concentration.

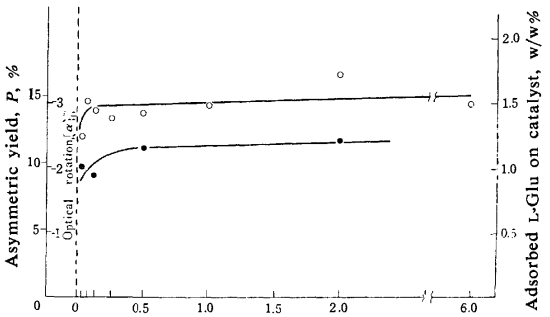

Fig. 4. Effect of concentration of modifying solution.
○ Optical rotatory power
● Adsorbed L-Glu on R-Ni

Effect of Immersion Time for Modification.—The effect of immersion time of R-Ni in Glu solution upon the asymmetric hydrogenation is shown in Table I. The adsorption equilibrium appears to be attained within 15 min.

TABLE I. EFFECT OF IMMERSION TIME FOR MODIFICATION

Immertion time	Optical rotation $[\alpha]_D^{20}$	Asymmetric yield P, %
2 min.	−2.56	12.2
10 min.	−3.51	16.8
1.5 hr.	−3.46	16.5
19 hr.	−3.30	15.8
47 hr.	−2.98	14.3

TABLE II. EFFECT OF MIXTURE D- AND L-GLU IN DIFFERENT RATIO UPON THE ASYMMETRIC YIELD

Mixing ratio		Optical rotation $[\alpha]_D^{20}$	Asymmetric yield P, %
L-Glu	D-Glu		
10	0	−2.86	13.7
9	1	−1.90	9.1
6	4	−0.45	2.2
0	10	+2.95	14.1

Effect of Mixing L- and D-Glutamic Acid.— The effect of mixtures D- and L-Glu in different ratios upon the asymmetric yield has been measured and has been compared with the effects of pure D- and L-Glu. A nearly linear relationship between the activity of the reaction products and the mixing ratio was observed as shown in Table II.

TABLE III. EFFECT OF DOUBLE MODIFICATION

Exp. No.	Modifying agent 1st	Modifying agent 2nd	Optical rotation $[\alpha]_D^{20}$
1	L-Glu	L-Glu	−3.14
2	L-Glu	D-Glu	+4.84
3	D-Glu	L-Glu	−3.58
4	D-Glu	D-Glu	+4.89

Effect of Double Modification.—When R-Ni was first treated with L- or D-Glu, and then D- or L-Glu, the capacity of asymmetric hydrogenation was determined by the configuration of the second modifying agents as shown in Table III.

Effect of Relative Amount of Catalyst.—The effect of varying the proportion of catalyst to substrate was investigated. Seventeen grams of methyl acetoacetate were reduced completely to methyl 2-hydroxybutyrate in the presence of modified catalyst which prepared from 1～7 g. of R-Ni alloy and modified with 225 ml. of 2% Glu solution.

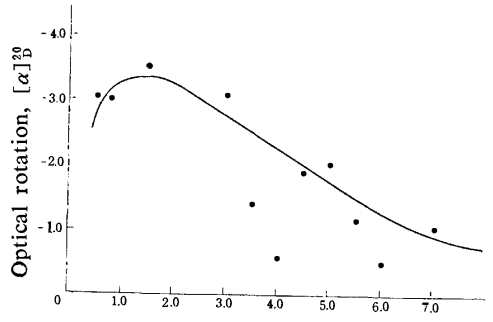

Fig. 5. Effect of the amount of catalyst prepared at 0°C.

When the catalyst was prepared at 0°C, increasing of the amount of catalyst decreased the asymmetric yield (Fig. 5). Catalyst prepared from 1.5 g. of alloy yielded a product with optical rotation $[\alpha]_D^{20}$, of −3.5. A product with the small rotation value, α −0.5, was obtained when a catalyst prepared from 6 g. of alloy was used; however, when the latter catalyst was recovered and one-fourth of it was used, the product showed an optical rotation of α −3.5.

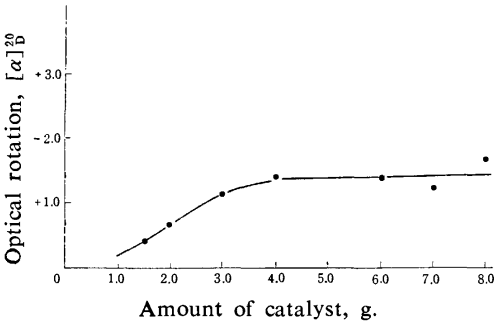

Fig. 6. Effect of the amount of catalyst prepared at 100°C.

The use of increased amounts of catalyst prepared at 100°C increased the asymmetric yield, as shown in Fig. 6. For example a catalyst prepared from 1.5 g. R-Ni alloy yielded a product with an optical rotation, α +0.4, while a catalyst prepared from 6 g. of alloy yielded a product with optical rotation, α +1.65. Recovery of the latter catalyst and the use of about a half and a third of the recovered material for reduction, yield products with rotation, α +0.60 and +0.41, respectively.

These results show that catalyst prepared in small or large amounts have the same activity when used under the same conditions. Therefore the effects shown in Figs. 5 and 6 resulted from the ratio of catalyst to substrate and not from the quantity in which the catalyst was prepared.

Desorption of Glutamic Acid from Asymmetric Catalyst. — The asymmetric catalyst prepared by contact with L-Glu solution of pH 5.2 at 0°C or 100°C was used for study. When this preparation was treated with N sodium hydroxide solution in boiling water for 1 hr., adsorbed Glu on R-Ni was removed from it, and the catalyst lost the adsorbed Glu and the asymmetric activity.

These results show that the presence of glutamic acid absorbed on the R-Ni was necessary for its asymmetric activity.

The results described above suggest that the asymmetric hydrogenation by the modified R-Ni was affected by many factors, particularly by pH and temperature of the modifying solution.

TABLE IV. ASYMMETRIC ACTIVITY OF DIFFERENT LOT OF R-Ni ALLOY

Lot	Optical rotation $[\alpha]_D^{20}$	Asymmetric yield *P*, %
A	−3.02	14.4
B	−3.30	15.8
C	−3.51	16.8

Catalysts were modified with 2% L-Glu solution at 0°C in pH 5.0.

However, so far as the authors experienced with the hydrogenation of methyl acetoacetate by the modified R-Ni prepared from different lots of R-Ni alloy of the same metal composition (Ni : Al = 4 : 6) gave 2-hydroxybutyrate of almost the same optical activity as shown in Table IV.

Further experiments on the asymmetric modification of hydrogenation catalysts are going on in the authors' laboratory.

Experimenal

Preparation of Catalyst.—R-Ni Catalyst used in the present work was prepared by a method similar to that described in the previous paper[4]. One and a half grams of powdered R-Ni alloy (Ni : Al = 40 : 60) was added to 20 ml. of 20% sodium hydroxide solution in small portions during 5 min. and was allowed to stand for 45 min. at 80°C. The nickel catalyst was washed several times with water. All of the hydrogenation experiments were carried out with this quantity of R-Ni catalyst.

Modification of Catalyst. — Two hundred and twenty-five milliliters of 2% L-Glu solution, the pH of which had been adjusted to a specified value, was added to newly prepared R-Ni and was allowed to stand with occasional shaking at 0°C for 1.5 hr. After the modifying solution was removed by decantation the catalyst was washed once with distilled water and twice with methanol, and was then separated by centrifugation.

Hydrogenation of Methyl Acetoacetate.—Commercial methyl acetoacetate was purified by washing with saturated sodium bicarbonate solution and then distilling under reduced pressure. Redistilled methyl acetoacetate (17.0 g.) was hydrogenated in the presence of modified R-Ni which was prepared from 1.5 g. of alloy. The reaction was run at 60°C under initial hydrogen pressure of 90 kg./cm^2 in a shaking autoclave. Hydrogen uptake was almost complete in about 12 hr. Reaction velocity was calculated as per cent hydrogen uptake during the first 3 hr. The reduction product was filtered off from R-Ni and distilled under reduced pressure. The main fraction boiling at 61~62°C/12 mmHg was identified as methyl 2-hydroxybutyrate by an elemental analysis of its hydrazide. The purity of methyl 2-hydroxybutyrate was tested by gas chromatography.

Asymmetric Yield. — Optical rotatory power of the distilled product was measured by a conventional polarimeter at 20°C without dilution in 1 dm. tube and the value was taken as the specific rotation because the density of methyl acetoacetate is nearly 1.0. According to Levene and Haller[5] the optical rotatory power of methyl-L-2-hydroxybutyrate is $[\alpha]_D^{20}$ −20.9, and therefore the percentage asymmetric yield, P, was calculated by the equation $P = ([\alpha]_D^{20}/20.9) \times 100$.

Identification of Methyl 2-Hydroxybutyrate.—Forty five grams of the reduction product ($[\alpha]_D^{20}$ −0.8) was boiled with 40 ml. 6 N hydrochloric acid for about 5 hr. and brought to dryness under reduced pressure. The residue was esterified by reacting it with ethanol (30 ml.) in the presence of benzene (20 ml.) and *p*-toluenesulfonic acid (0.5 g.). After the product was cooled, it was extracted with benzene and washed with water. Removal of the solvent followed by distillation gave ethyl 2-hydroxybutyrate (15.6 g.), b. p. 62°C/12 mmHg, $[\alpha]_D^{20}$ −0.7.

To 3.3 g. of ethyl 2-hydroxybutyrate 4.2 ml. of 80% hydrazine hydrate was added, the mixture was refluxed for 1 hr. and allowed to stand overnight. The crystalline product was stirred with 2 ml. ethanol, filtered and washed with a small quantity of ethanol. The yield was 2.6 g. ; m. p. 124~126°C, $[\alpha]_D^{20} < -0.04$.

Found : C, 40.71 ; H, 8.58 ; N, 23.49. Calcd. for $C_4H_{10}O_2N_2$: C, 40.66 ; H, 8.35 ; N, 23.71%.

This first crop is apparently DL-2-hydroxybutyric hydrazide. A second crop was obtained by adding ethanol to the mother liquor and recrystallizing from a mixture of ethyl acetate and ethanol. Yield 0.5 g. m. p. 123~124°C, $[\alpha]_D^{20}$ −5.67 in water.

Found : C, 40.93 ; H, 8.62 ; N, 23.26. Calcd. for $C_4H_{10}O_2N_2$: C, 40.66 ; H, 8.53 ; N, 23.71%.

Determination of Glutamic Acid Adsorbed on R-Ni Catalyst.—The modified catalysts were washed with water two times and were allowed to stand overnight. Then, the catalyst was filtered after the addition of a few drops of 1% methanol solution of lauric acid and dried in a desiccator. Glutamic acid was eluted with 1 N sodium hydroxide solution by heating for 1 hr. in a boiling water bath. The eluted glutamic acid was determined by the ninhydrin-photometric method of Stein and Moore[6].

Effect of Double Modification of L- and D-Glutamic Acid (Treatment of the R-Ni with D- after L- or L- after D-Glu).—R-Ni catalyst used in this cases was treated with 225 ml. of 2% L- or D-Glu solution adjusted to pH 5.0~5.2 at 0°C and washed once with distilled water. Then the catalyst was treated with 100 ml. of D- or L-Glu solution by the usual method as described above.

Hydrogenation of Ethyl Acetoacetate. — The catalyst was prepared by treating 1.5 g. of R-Ni alloy first with alkali and then with 225 ml. of L-Glu solution adjusted to pH 5.0 at 0°C, as described above. This catalyst was used in the hydrogenation of 16 g. of ethylacetoacetate. The reducing product, ethyl 2-hydroxybutyrate was purified by distillation and its optical rotation was measured, as above mentioned, $[\alpha]_D^{20}$ −2.00.

Hydrogenation of Acetophenone.—Sixteen grams of acetophenone was reduced and its optical rotation was measured by a similar method to the above, $[\alpha]_D^{20}$ +0.90.

Summary

1. Raney nickel catalyst treated with optically active glutamic acid has the property

5) P. A. Levene and H. L. Haller, *J. Biol. Chem.*, **65**, 51 (1925).

6) S. Moore and W. H. Stein *J. Biol. Chem.*, **176**, 367 (1948).

of catalyzing the hydrogenation of carbonyl compounds asymmetrically with high reproducibility and efficiency.

2. Excellent results were obtained in the hydrogenation of methyl acetoacetate to optically active methyl 2-hydroxybutyrate in the presence of Raney nickel catalyst treated with L- or D-glutamic acid.

3. The capacity for asymmetric hydrogenation was strongly dependent upon the pH of the modifying solution. The highest capacity was obtained when modifying solutions were adjusted to pH 4.8~5.5.

4. With elevation of the temperature of the modifying process, the asymmetric capacity of the catalyst decreased markedly, nearly disappearing at 60°C, and yielding products with reverse optical rotation above 80°C.

5. The asymmetric capacity was independent of the concentration of the modifying solution within the range of 6 to 0.0625%.

6. Hydrogenation in the presence of catalyst modified with D-glutamic acid yielded a product with reverse optical rotation to that obtained when L-glutamic acid was used.

7. Asymmetric yield of the reducing product of methyl acetoacetate by the catalyst treated with Glu was varied with the relative amount of the substrate and the catalyst.

The authors with to express their sincere thanks to Dr. Harvey A. Itano of the National Institutes of Health, U. S. A., for his advice on preparing this manuscript and to the Miss Kiku Koike and Miss Masako Kawakita of this Institute for the elemental analysis. This research was made possible through a support of Raney nickel alloy by the Kawakami Institute Ltd. Co., Tokyo. The authors are indebted to the Company for this fellowship.

Division of Organic Chemistry
Institute for Protein Research
Osaka University
Kita-ku, Osaka

A Synthesis of L-Proline from L-Glutamine

By Tamio Itoh

(Received July 28, 1962)

Since the resolution of racemic proline is difficult, it would be advantageous to develope a practical method for the synthesis of optically active proline. Two successful syntheses of L-proline in which L-glutamic acid was the starting material have been described to date. The method described by Pravda and Rudinger[1], which makes use of the selective reduction of the lactam group of tosyl-L-pyrrolidonecarboxylic acid derivatives by lithium aluminum hydride, resulted in an overall yield of 12% from L-glutamic acid in seven steps. Tanaka et al.[2] obtained L-proline in a 34% yield from methyl L-pyrroglutamate by means of sodium borohydride reduction.

In the course of an investigation of the dehydration products of L-glutamine derivatives, the author developed a novel method for the synthesis of optically active proline. It was found that catalytic hydrogenation of γ-cyano-α-L-carbobenzoxyaminobutyric acid esters in aqueous solvents produced L-proline in high yield under suitable conditions. Thus a single hydrogenation treatment in the presence of water effects pyrrolidine ring formation between the γ-carbon atom and the α-amino nitrogen atom without racemization by successive hydrogenation, hydrolysis and ring closure. The schematic representation of the synthesis of proline from carbobenzoxyglutamine is as follows:

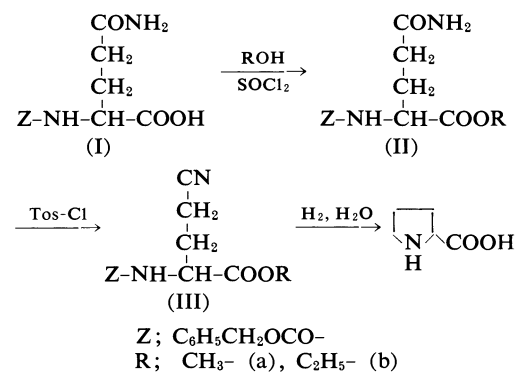

Z; $C_6H_5CH_2OCO-$
R; CH_3- (a), C_2H_5- (b)

The author feels that the method will be of

1) Z. Pravda and J. Rudinger, *Colletion Czech. Chem. Commun.*, **20**, 1 (1955).
2) M. Tanaka, T. Kishi and S. Kinoshita, *J. Agr. Chem. Soc. Japan* (*Nippon Nōgei-Kagaku Kaishi*), **34**, 782 (1960).

practical value for the synthesis of optically active proline because the starting material, L- or D-glutamine, is readily prepared from L- or D-glutamic acid, respectively, by a method previously reported by Akabori and Narita[3].

Results and Discussion

Preparation of Carbobenzoxy-L-glutamine Esters. — The methyl ester IIa was prepared from carbobenzoxy-L-glutamine[4-7] by the action of diazomethane[8], or by esterification with methanol in the presence of thionyl chloride at room temperature. In the latter case, increasing the reaction time or amount of thionyl chloride, or elevating the temperature resulted in increase of alcoholysis of the amide group to produce dimethyl carbobenzoxy-L-glutamate. The ethyl ester IIb was obtained by esterification with ethanol in the presence of thionyl chloride.

Taschner and Wasielewski[9] proposed the use of sulfuryl chloride as catalysts for the esterification of acylated amino acids. In the present work it was found that thionyl chloride is also a useful reagent under suitable conditions.

Dehydration of Carbobenzoxy-L-glutamine Esters.—Procedures for converting carboxamide residues of glutamine or asparagine derivatives to nitrile residue with suitable dehydrating reagents, *p*-toluenesulfonyl chloride, phosphorous oxychloride or *N*,*N'*-dicyclohexylcarbodiimide, were reported recently[10-12].

The author observed that carbobenzoxy-L-glutamine esters in pyridine solution were dehydrated to the corresponding cyano compounds in excellent yield by the action of *p*-toluenesulfonyl chloride, phosphorous oxychloride or thionyl chloride at 50°C for 30 to 50 min. *p*-Toluenesulfonyl chloride was the most suitable dehydrating reagent in these cases. Methyl γ-cyano-α-L-carbobenzoxyaminobutyrate (IIIa) was obtained as long crystalline needles, m. p. 52°C, from ethyl acetate-petroleum benzine mixture. The corresponding ethyl ester IIIb was obtained as crystalline leaflets, m. p. 60°C, from the same solvent system.

The infrared spectra of these cyano compounds showed characteristic nitrile absorption in the 2250 cm^{-1} region.

Hydrogenation of Methyl γ-Cyano-α-L-carbobenzoxyaminobutyrate. — Methyl γ-cyano-α-L-carbobenzoxyaminobutyrate was hydrogenated in a pressure bottle under various conditions as listed in the table.

After the catalyst was removed by filtration, the reaction mixture was hydrolyzed with hydrochloric acid, and the hydrolyzate was analyzed qualitatively by paper chromatography and quantitatively by colorimetry.

The main product was either proline or

TABLE I. HYDROGENATION OF METHYL γ-CYANO-α-L-CARBOBENZOXYAMINOBUTYRATE

Exp. no.	Catalyst	Solvent, ml.			Temp. °C	Time hr.	Yield of proline, %
		H_2O	MeOH	AcOH			
1	Silk-palladium 50 mg.	12	—	—	80	4	65
2	Silk-palladium 50 mg.	6	6	—	80	2	68
3	Silk-palladium 50 mg.	6	6	0.2	80	2	70
4	Silk-palladium 50 mg.	8	—	4	80	2	76
5	Silk-palladium 50 mg.	8	—	4	110	2	76
6	Silk-palladium 50 mg.	8	—	4	150	2	82
7	Silk-palladium 50 mg.	8	—	4	50	16	33
8	Silk-palladium 50 mg.	—	—	12	80	2	0*
9	Silk-platinum 10 mg.	8	—	4	80	2	0**
10	Silk-rhodium 10 mg.	8	—	4	80	2	0**
11	Raney nickel 100 mg.	8	—	4	80	2	0**
12	Raney nickel 100 mg.	—	—	12	80	2	0**

Each experiment was carried out in a 100 ml. stainless steel autoclave, with 0.5 g. substrate and initial pressure of hydrogen 70 kg./cm^2.

* Almost unreacted ** Main product was ornithine.

3) S. Akabori and K. Narita, *J. Chem. Soc. Japan, Pure Chem. Sec.* (*Nippon Kagaku Zassi*), **74**, 829 (1953).
4) D. Coleman, *J. Chem. Soc.*, **1951**, 2294.
5) R. A. Boissonnas, St. Guttmann, p.-A. Jaquenoud and J.-p. Waller, *Helv. Chim. Acta*, **38**, 1491 (1955).
6) H. K. Miller and H. Waelsch, *Arch. Biochim. Biophys.*, **35**, 176 (1952).
7) P. G. Katsoyannis, D. T. Gish, G. P. Hess and V. du Vigneaud, *J. Am. Chem. Soc.*, **80**, 2558 (1958).
8) E. Sondheimer and R. W. Holley, ibid., **76**, 2467 (1954).
9) E. Taschner and C. Wasielewski, *Ann.*, **640**, 137 (1961).
10) Z. Zaoral and J. Rudinger, *Collection Czech. Chem. Commun.*, **24**, 1993 (1959).
11) B. Liberek, *Chem. & Ind.*, **1961**, 987.
12) C. Ressler and H. Ratzkin, *J. Org. Chem.*, **26**, 3356 (1961).

ornithine, and the major side product was glutamic acid in all cases. One more ninhydrin positive spot which was believed to be δ-hydroxy-*n*-valine was present in some cases (Exp. no. 1-6, 11).

In order to determine the yield of proline by the ninhydrin method, ammonia formed in the hydrogenation was removed from the hydrolyzates by the addition of aqueous sodium hydroxide and evaporation under diminished pressure. The residue was dissolved in water and evaporated to dryness twice more, and the final residue was dissolved in water and adjusted pH to 7 with hydrochloric acid. The composition of this solution was determined colorimetrically by the ninhydrin method as usual[13]. The yield of proline was calculated from the optical densities at 440 and 570 mμ.

As catalyst for hydrogenation, silk-palladium[14], silk-platinum[15], silk-rhodium[16] and Raney nickel were used.

In aqueous solvent, silk-palladium catalyst produced proline as the main product with some ornithine, glutamic acid and δ-hydroxy-*n*-valine as by-products (Exp. no. 1-7). In acetic acid no hydrogenation occurred and glutamic acid was the only reaction product observed on paper chromatogram (Exp. no. 8). Rather low yield of proline and relatively high yield of ornithine was observed in water or water-methanol system (Exp. no. 1, 2). The pH of the reaction mixture was 9 and the high pH of the reaction media was believed responsible for the increased yield of ornithine. Water-acetic acid system increased the yield of proline (Exp. no. 3—6).

The three other catalysts, silk-platinum, silk-rhodium and Raney nickel, produced ornithine as almost the sole product in water-acetic acid mixture (Exp. no. 9—11). In these cases, only traces of proline were detected on paper chromatogram, and yield of ornithine was estimated to be over 80%.

The schematic representation of the hydrogenation yielding proline, ornithine, glutamic acid and δ-hydroxy-*n*-valine from γ-cyano-α-carbobenzoxyaminobutyric ester is shown in Scheme 1.

Hydrogenation of aldimine (C) to yield ornithine ester (D) is competitive with hydrolysis to yield aldehyde intermediate (E) which forms a pyrroline ring (F) by spontaneous ring closure. The pyrroline ring is hydrogenated to yield a pyrrolidine ring (G). The

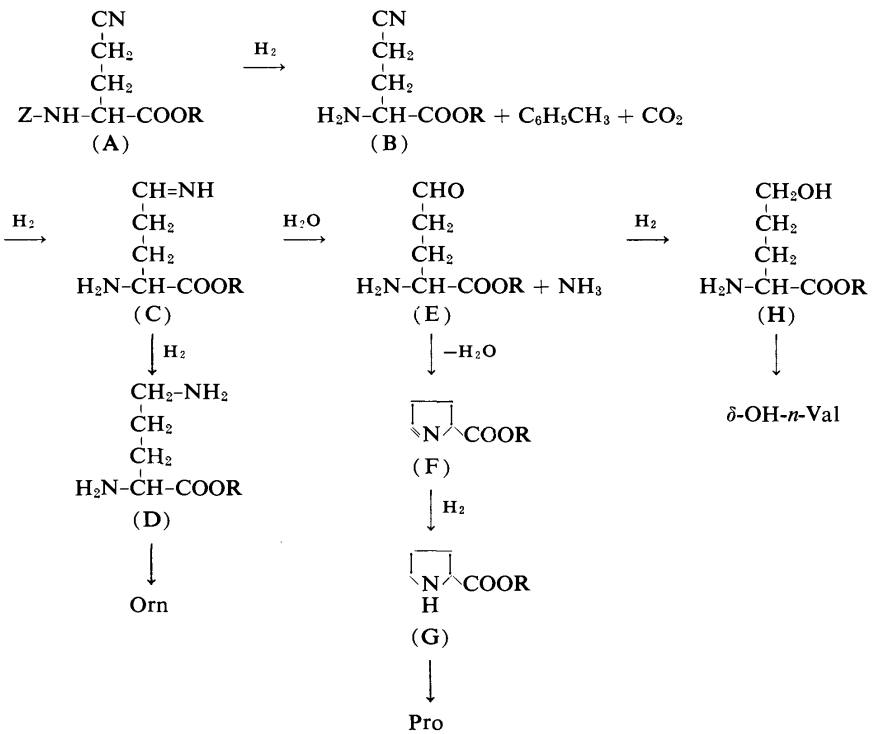

Scheme 1. Reaction scheme of hydrogenation

13) S. Moore and W. H. Stein, *J. Biol. Chem.*, 211. 907 (1954).
14) Y. Izumi, This Bulletin, 32. 932, 936, 942 (1959).
15) A. Akamatsu, Y. Izumi and S. Akabori, ibid., 34. 1067, 1302 (1961).
16) A. Akamatsu, Y. Izumi and S. Akabori, ibid., 35. 1706 (1962).

aldehyde intermediate (E) is also hydrogenated to form δ-hydroxy-*n*-valine ester (H).

According to this scheme, Raney nickel, silk-platinum and silk-rhodium are highly active catalysts for the reduction of aldimine (C), but silk-palladium has low activity; consequently the hydrolytic reaction of aldimine to produce aldehyde (E) occurs predominantly.

Experimental*

Carbobenzoxy-L-glutamine Methyl Ester (IIa).—Carbobenzoxy-L-glutamine (I), 28 g. (100 mmol.), was dissolved in 200 ml. of methanol containing thionyl chloride, 0.6 g. (5 mmol.), and the mixture was allowed to stand at 15°C for 48 hr. The methanol was distilled off under reduced pressure, and the residual crystalline product was washed thoroughly with cold water and dried. The crude product was recrystallized from methanol-ether. Aggregated colorless needles. Yield 25 g. (85%), m. p. 141~142°C (lit. 140~141°C[8]). $[\alpha]_D^{18}$ −23.6° (*c* 3, MeOH) (lit. $[\alpha]_D^{23}$ −19.4° (*c* 1, MeOH[8])).

Found: N, 9.26. Calcd. for $C_{14}H_{18}O_5N_2$: N, 9.52%.

From the mother liquor of recrystallization a colorless syrup was obtained which became a solid of very low melting point after several days. Elementary analysis and infrared spectra showed that this compound was the alcoholytic product of IIa, dimethyl carbobenzoxy-L-glutamate.

Found: C, 58.27; H, 6.26; N, 4.51. Calcd. for $C_{15}H_{19}O_6N$: C, 58.24; H, 6.19; N, 4.53%.

Carbobenzoxy-L-glutamine Ethyl Ester (IIb).—This compound was prepared from carbobenzoxy-L-glutamine, 14 g. (50 mmol.), and thionyl chloride 0.6 g. (5 mmol.), in 100 ml. of ethanol according to the procedure described for the preparation of the methyl ester IIa. Aggregated needles. Yield 80%, m. p. 125~126°C, $[\alpha]_D^{18}$ −20.6° (*c* 3, MeOH).

Found: C, 58.55; H, 6.53; N, 8.98. Calcd. for $C_{15}H_{20}O_5N_2$: C, 58.43; H, 6.54; N, 9.09%.

Methyl γ-Cyano-α-L-carbobenzoxyaminobutyrate (IIIa).—To a solution of carbobenzoxy-L-glutamine methyl ester (IIa), 18.4 g. (626 mmol.) in pyridine (120 g.), *p*-toluenesulfonyl chloride, 15 g. (788 mmol.) was added, and the mixture kept at 50°C for 30 min. The resulting dark red solution was concentrated under reduced pressure to obtain an oily residue, which was treated with 30 ml. of water and extracted three-times with ethyl acetate. The combined ethyl acetate extracts were washed successively with diluted hydrochloric acid, water, aqueous sodium bicarbonate and water, then decolorized with active charcoal and dried over magnesium sulfate. The concentrated ethyl acetate solution, to which petroleum benzine had been added just to the cloudy point, was stored in a refrigerator overnight. Long featherlike needles were collected and recrystallized from an ethyl acetate-petroleum benzine mixture to yield 14.2 g. (82%) of the ester (IIIa). M. p. 51~52°C, $[\alpha]_D^{21}$ −34.5° (*c* 3, MeOH).

Found: C, 60.82; H, 5.80; N, 10.04. Calcd. for $C_{14}H_{16}O_4N_2$: C, 60.86; H, 5.84; N, 10.14%.

* All melting points are not corrected.

Ethyl γ-Cyano-α-L-carbobenzoxyaminobutyrate (IIIb).—This compound was prepared as described for the methyl ester IIIa from carbobenzoxy-L-glutamine ethyl ester (IIb). Crystalline leaflets. Yield 70%, m. p. 59~60°C, $[\alpha]_D^{18}$ −30.7° (*c* 3, MeOH).

Found: C, 61.85; H, 6.15; N, 9.51. Calcd. for $C_{15}H_{18}O_4N_2$: C, 62.05; H, 6.25; N, 9.65%.

L-Proline.—In a 100 ml. autoclave were placed methyl γ-cyano-α-L-carbobenzoxyaminobutyrate (IIIa), 2.76 g. (10 mmol.), water, 15 ml., acetic acid, 10 ml. and silk-palladium catalyst, 138 mg. An initial pressure of 80 kg./cm² of hydrogen was applied. After 2 hr. of shaking at 120°C, the reaction was stopped, and the catalyst was removed by filtration. The reaction mixture was concentrated under reduced pressure, then hydrolyzed with 60 ml. of 3 N hydrochloric acid for 3 hr. After the hydrolyzate was evaporated in vacuo to remove excess hydrochloric acid, the residue was dissolved in 300 ml. of deionized water and passed through a column (16×400 mm.) of Amberlite CG-45 (OH cycle) then CG-50 (H cycle). The combined effluents and washings were evaporated to dryness. The residue was taken up in absolute ethanol and the proline precipitated by addition of ether. Repeated recrystallization gave 0.75 g. (65%) of non-hygroscopic white crystals of optically and chromatographically pure L-proline. The identity of thus obtained L-proline with authentic L-proline was also confirmed by infrared spectra. M. p. (decomp.) 216~218°C (lit. 226~228°C[1]), $[\alpha]_D^{23}$ −83.0° (*c* 1, H_2O) (lit. $[\alpha]_D^{24}$ −84.6°[1]).

Found: N, 12.02. Calcd. for $C_5H_9O_2N$: N, 12.17%.

D-Ornithine Hydrochloride.—In a 100 ml. autoclave were placed methyl γ-cyano-α-D-carbobenzoxyaminobutyrate (prepared starting from D-glutamic acid) (IIIa), 5.00 g. (18.1 mmol.), acetic acid, 30 ml. and Raney nickel catalyst prepared from 2 g. of the alloy*. High pressure hydrogenation at 90 kg./cm² of initial pressure at 100°C was continued for 2 hr. After removal of the catalyst by filtration and the acetic acid by vacuum evaporation, the residue was hydrolyzed with concentrated hydrochloric acid for 3 hr. under reflux. After excess of hydrochloric acid was removed by vacuum evaporation, the residue was diluted to 100 ml. and adjusted pH to 3 by addition of sodium bicarbonate. Hydrogen sulfide gas was bubbled to precipitate traces of nickel ion, the filtrate was evaporated to dryness. The residue was extracted three times with 95% ethanol. The combined ethanol extract was treated with pyridine to obtain crude crystals of D-ornithine hydrochloride which was recrystallized three times from water-ethanol. Yield 2 g. (63%), m. p. (decomp.) 227~228°C (lit. 236~237°C[10]), $[\alpha]_D^{20}$ −21.7° (*c* 3, 6 N HCl) (lit. −22.5°[10]).

Found: N, 16.48. Calcd. for $C_5H_{13}N_2O_2Cl$: N, 16.61%.

* The alloy was added to 20 ml. of 20% aqueous sodium hydroxide solution, and the mixture was warmed at 80°C for 20 min. The sodium hydroxide solution was decanted, and the catalyst was washed three times with water and twice with acetic acid by decantation.

Summary

1. Novel syntheses of optically active proline and ornithine from optically active glutamine are described.

2. Carbobenzoxy-L-glutamine esters were dehydrated to γ-cyano-α-L-carbobenzoxyaminobutyric acid esters with *p*-toluenesulfonyl chloride, phosphorous oxychloride or thionyl chloride.

3. Hydrogenation of γ-cyano-α-L-carbobenzoxyaminobutyric acid esters in aqueous solvent systems were effected by silk-palladium catalyst to yield mainly L-proline.

4. By hydrogenation in the presence of Raney nickel in non-aqueous solvent, L-ornithine was obtained.

The author wishes to express his hearty thanks to Professor Shiro Akabori and Dr. Yoshiharu Izumi for their cordial guidance and encouragement throughout this work. He is also grateful to Miss Kiku Koike and Miss Masako Kawakita for microanalysis.

Division of Organic Chemistry
Institute for Protein Research
Osaka University
Kita-ku, Osaka

Electrochemical Fluorination of 2, 2, 3, 3-Tetrafluoro-1-propanol

By Shunji NAGASE, Hajime BABA and Rimpei KOJIMA

(Received August 27, 1962)

Earlier work[1] of the present authors has shown that the electrochemical fluorination of alcohols gives perfluorocarboxylic acids in a significant yield. The present paper describes work extended further to the fluorination of C3 fluoroalcohol, 2, 2, 3, 3-tetrafluoro-1-propanol. The fluorocarboxylic acid with the corresponding number of carbon atoms, 3*H*-tetrafluoropropionic acid, which is easily obtained by oxidation from the C3 fluoroalcohol, was also fluorinated for the sake of comparison.

It is well known that the effect of enhancing the oil repellency of cotton fabrics treated by derivatives of perfluorocarboxylic acids or fluoroalcohols is markedly lessened if one hydrogen atom is present, instead of fluorine, at the ω-position of these fluorochemicals[2]. The ω-hydrogen of fluoroalcohols is relatively stable to chlorination[3]. From these facts, along with the results obtained from a series of electrochemical fluorinations of esters[4], ketones[5], aldehydes[6] and ethers[7], undertaken in order to prepare perfluorocarboxylic acids, the electrochemical fluorination of fluoroalcohols seemed of interest 2, 2, 3, 3-tetrafluoro-1-propanol was taken up.

No report has been made on the fluorination of fluoroalcohols. As expected, the ω-hydrogen was substituted for by fluorine, and perfluoropropionic acid containing a small amount of trifluoroacetic acid was obtained in quite a good yield from 2, 2, 3, 3-tetrafluoro-1-propanol. The yield was much higher than that obtained from propanol[1]. On the other hand, the amount of perfluorocarboxylic acid obtained from 3*H*-tetrafluoropropionic acid was extremely small.

The mechanism of the formation of perfluorocarboxylic acid fluorides from the fluoroalcohols should be similar to that for common alcohols[1].

Experimental

Materials.—2, 2, 3, 3-Tetrafluoro-1-propanol, given for research purposes by the Osaka Metal Industries Co., was purified by fractional distillation. 3*H*-Tetrafluoropropionic acid was prepared in this laboratory from 2, 2, 3, 3-tetrafluoro-1-propanol by oxidation with potassium permanganate according to Berry's method[8]. Hydrogen fluoride of about 99.4% purity was furnished by the Osaka Metal Industries Co.

1) S. Nagase and R. Kojima, *J. Chem. Soc. Japan, Ind. Chem. Sec.* (*Kogyo Kagaku Zasshi*), **64**, 1397 (1961).
2) F. J. Philips, L. Segal and L. Loeb, *Textile Research J.*, **27**, 369 (1957); S. Komori and T. Nishikagi, *J. Chem. Soc. Japan, Ind. Chem. Sec.* (*Kogyo Kagaku Zasshi*), **65**, 368 (1962).
3) N. O. Brace, *J. Org. Chem.*, **26**, 4005 (1961).
4) S. Nagase and R. Kojima, This Bulletin, **34**, 1468 (1961).
5) S. Nagase, H. Baba and R. Kojima, *J. Chem. Soc. Japan, Ind. Chem. Sec.* (*Kogyo Kagaku Zasshi*), **64**, 2126 (1961).
6) S. Nagase, H. Baba and R. Kojima, This Bulletin, **35**, 1907 (1962).
7) S. Nagase, H. Baba and R. Kojima, *J. Chem. Soc. Japan, Ind. Chem. Sec* (*Kogyo Kagaku Zasshi*), **65**, 1183 (1962).
8) K. L. Berry, U. S. Pat. 2559629 (1951).

Apparatus.—The apparatus used for this work consisted essentially of a nickel electrolytic cell of a 1 l. capacity, provided with a reflux codenser at the top and a drain at the bottom, a sodium fluoride pellet tube, and a pair of polyethylene bottles in which perfluorocarboxylic acid fluorides generated from the cell reacted with water and were converted into perfluorocarboxylic acids. In this system, gaseous products which are inert to water are allowed to escape as gases. Nickel electrodes with an effective surface area of 9.2 dm^2 were used as usual. The details of the apparatus have been fully described previously[1,4].

Standard Procedure.—Hydrogen fluoride (1 l.) was introduced into the cell, and, in order to remove a trace of water, electrolysis was carried out in a nitrogen atmosphere, prior to the addition of the sample, with the anodic current density of 2.7 A./dm^2 and at 5~6°C, until the cell voltage rose to 5.7 V. Then 35 g. (0.265 mol.) of 2, 2, 3, 3-tetrafluoro-1-propanol was introduced into the cell, and electrolysis was carried out with the anodic current density of 2.7 A./dm^2 at about 5.2~5.6 V. and at 5~6°C until the cell voltage rose to 6.0 V. The amount of electricity required for this fluorination reaction was 55.4 A. hr.; the same amout of electricity was supplied for the reaction under other current densities and temperatures.

In the case of 3*H*-tetrafluoropropionic acid, 38.7 g. (0.265 mol.) of the sample was used. The amount of electricity required to raise the cell voltage to 6.0 V. was 44.4 A. hr. at 5~6°C, with the anodic current density of 2.7 A./dm^2.

By the same method as has been reported before, perfluorocarboxylic acids were obtained as their sodium salts; these were analyzed quantitatively by the base-line technique of the infrared absorption spectrum.

Results and Discussion

Electrolysis was carried out under a variety of operating conditions, achieved by changing the current density and the cell temperature, in order to find the conditions which would make the fluorination reaction mild and which would give the products in a good yield. The results are shown in Table I. The calculation of the current efficiencies shown was based on the amount of electricity assumed to be required to form fluorine by discharging the fluoride ion which would substitute for hydrogen in the sample. This means that the amount of electricity corresponding to that needed for the formation of 3 mol. of fluorine would be required to convert 1 mol. of 2, 2, 3, 3-tetrafluoro-1-propanol into 1 mol. of sodium perfluoropropionate.

In general, the yield of perfluoropropionic acid increased with an increase in the anodic current density and in the temperature of fluorination, but the amount of degraded acid, trifluoroacetic acid, formed also increased. Under the reaction conditions used, perfluorocarboxylic acids were obtained in the highest yield with an anodic current density of 1.6 A./dm^2 and at 16°C. Though the ratio of trifluoroacetic acid to perfluoropropionic acid decreased when the reaction was carried out at a lower temperature (which shows the reaction to be milder), the yield of perfluorocarboxylic acids decreased considerably. The least degraded products were obtained by the reaction at −10°C, with an anodic current density of 2.7 or 1.6 A./dm^2. The product obtained at −10°C with an anodic current density of 1.1 A./dm^2 contained rather a higher percentage of trifluoroacetic acid. This might be attributed to the smaller degree of agitation brought about by the evolved gases and to the fact that the reaction was less mild, because the rate of gas evolution should be smaller under this condition.

It is interesting to note that the composition of the perfluorocarboxylic acids obtained

TABLE I. FLUORINATION OF 2, 2, 3, 3-TETRAFLUORO-1-PROPANOL

D_A* A./dm^2	Temp. °C	Product obtained g.	Composition wt. %		Yield mol. %			Current efficiency %
			CF_3COONa	C_2F_5COONa	CF_3COONa	C_2F_5COONa	Total	
2.7	16	22.1**	11	89	6.8	39.9	46.7	34.5
2.7	5~6	22.5	8.0	92	4.9	42.1	47.0	35.2
2.7	−10	13.7	5.8	94	2.2	26.2	28.4	21.5
1.6	16	29.0	11	89	8.9	52.3	61.2	45.5
1.6	5~6	18.2	8.1	92	4.1	33.9	38.0	28.7
1.6	−10	11.0	5.7	94	1.7	21.1	22.8	17.2
1.1	16	26.9	14	86	10.2	47.0	57.2	42.2
1.1	5~6	14.7	8.2	92	3.4	27.3	30.7	23.0
1.1	−10	9.4	7.9	92	2.0	17.5	19.5	14.7

* Anodic current density

** The amout of electricity supplied for this reaction is 41 A. hr., because the cell voltage rose to 6.2 V. at this point.

by the fluorination of 2, 2, 3, 3-tetrafluoro-1-propanol is almost identical with those obtained from propanol[1], propyl propionate[4], diethyl ketone[5], or dipropyl ether[7]. As expected, the composition of the products formed was not affected by the change in the anodic current density.

The mechanism for the formation of perfluorocarboxylic acid fluorides from fluoroalcohols is possibly similar to that for common alcohols[1]. This involves the first attack by fluorine on the α-carbon atom of the fluoroalcohols, and dehydrofluorination followed by exhaustive fluorination of the fluorocarboxylic acid fluorides thus formed into perfluorocarboxylic acid fluorides.

For the sake of comparison, electrochemical fluorination of 3*H*-tetrafluoropropionic acid was carried out with an anodic current density of 2.7 A./dm^2 at 5~6°C, and of 1.6 A./dm^2 at 16°C and at 5~6°C. By these reactions, the sample was degraded and fragmented seriously; only a trace of perfluorocarboxylic acids (0.2, 0.2 and 0.1 g. respectively) was obtained as their sodium salts. The product consisted of trifluoroacetic acid and perfluoropropionic acid in the ratio of 68 : 32, 61 : 39, and 60 : 40 under the respective reaction conditions given above. One reason for this result might be that given by Simons et al.[9] for the electrochemical fluorination of carboxylic acids. 3*H*-Tetrafluorocarboxylic acid is a highly fluorinated acid, strong enough to form the $HC_2F_4CO_2^-$ ion in hydrogen fluoride; the Kolbe-type electrochemical process would then decompose this ion into fluorocarbons and carbon dioxide.

With both samples, a trace of polymeric material (0.2~0.3 g.) was found in the residue in the electrolytic cell.

9) J. H. Simons et al., *J. Electrochem. Soc.*, **95**, 53 (1949).

Summary

Perfluoropropionic acid, accompanied by a small amount of trifluoroacetic acid, was obtained in a good yield by the electrochemical fluorination of 2, 2, 3, 3-tetrafluoro-1-propanol. The yield or current efficiency increased with an increase in the anodic current density and cell temperature. Although the yield decreased at lower temperatures, the reaction became milder, giving a smaller amout of trifluoroacetic acid in the product. The composition of the perfluorocarboxylic acids obtained by this fluorination reaction is very similar to that of those obtained by the fluorination of propanol, propyl propionate, diethyl ketone, and dipropyl ether. Only a trace of perfluorocarboxylic acid was formed by the electrochemical fluorination of 3*H*-tetrafluoropropionic acid.

The authors are much indebted to Professor Ikumi Kagawa of Nagoya University for his invaluable advice and encouragement throughout this work. They wish also to express their thanks to Osaka Metal Industries Co. for supplying the chemicals used in this work.

Government Industrial Research Institute, Nagoya
Kita-ku, Nagoya

Sterically-hindered Organosilicon Compounds Containing Cyclohexyl Groups. I. Reactions of Organolithium Compounds with Tricyclohexylfluorosilane

By Michio TAKAKUSA

(Received August 29, 1962)

Since organolithium compounds were reported to be very effective in obtaining highly-substituted organosilicon compounds[1], most studies on steric hindrance have been done with the reactions between silicon tetrachloride and alkyl- or aryl-lithiums. By these reactions tetra(*o*-phenoxyphenyl)silane[2], tetra-*o*-anisylsilane[3] and tetra-*o*-tolylsilane[3,4] were successfully obtained, while, with 1-naphthyl[5],

1) For example, H. Gilman and R. N. Clark, *J. Am. Chem. Soc.*, **68**, 1675 (1946).
2) K. Oita and H. Gilman, *J. Org. Chem.*, **21**, 1009 (1956).
3) H. Gilman and G. N. R. Smart, ibid., **15**, 720 (1950).
4) G. N. R. Smart, H. Gilman and H. W. Otto, *J. Am. Chem. Soc.*, **77**, 5193 (1955).
5) H. Gilman and C. G. Brannen, ibid., **73**, 4640 (1951).

2-biphenylyl[6], cyclohexyl[7] and isopropyl[8] groups, only a trisubstituted silane was obtained even when an excess of the lithium compound was used.

$$R_3SiCl + RLi \not\longrightarrow R_4Si$$

R ; 1-$C_{10}H_7$, *o*-Ph-C_6H_4, C_6H_{11} or *iso*-Pr

An attempt to introduce a third *t*-butyl group was unsuccessful in the reaction of di-*t*-butyldichlorosilane with the lithium compound[9].

These results provide some rough idea about the steric nature of those groups, but more detailed knowledge on the steric hindrance can be obtained by comparing difficulties with which various types of groups are introduced into a fixed radical (for example, R_3Si-).

Advantage of using fluorosilanes in preparation of sterically-hindered organosilicon compounds was shown by Eaborn[10] who paid attention to the smaller atomic size of fluorine. Thus, Grignard reactions with fluorosilanes gave many compounds that had not been obtained through interaction of Grignard reagents and chlorosilanes.

$$(C_6H_{11})_2SiF_2 + C_6H_{11}MgX \rightarrow (C_6H_{11})_3SiF$$

It was proved by Petrov and Chernysheva[11] that the feature was the case also in reactions of organolithium compounds. They reported that the combination of fluorosilanes and the alkyl- or aryl-lithium gave three tetraorgano-substituted silanes, tetra-1-naphthylsilane, tetraisopropylsilane and tetracyclohexylsilane, which had not been obtained by the reactions with chlorosilanes.

At the present stage, an interaction of alkyllithium with alkylfluorosilanes under drastic conditions is thought to be the most effective way of obtaining a highly-substituted organosilicon compound with some bulky groups, and hence, reactions of some organolithium compounds with tricyclohexylfluorosilane were studied in the present work.

$$(C_6H_{11})_3SiF + RLi \rightarrow$$

R ; *n*-Bu, *iso*-Pr, C_6H_{11} or Ph

Prolonged treatment of tricyclohexylfluorosilane with an excess of butyllithium in boiling petroleum ether (90~110°C)[12] yielded 41% of tricyclohexylbutylsilane which melts at 160°C. This compound was identical with tricyclohexylbutylsilane[13] obtained from hydrogenation of triphenylbutylsilane, but not the same as the tricyclohexylbutylsilane[11] that Petrov and Chernysheva obtained from a similar butyllithium reaction[14]. Tricyclohexylphenylsilane was obtained in a pretty high yield from the reaction after 12 hrs' refluxing in petroleum ether. Tricyclohexylfluorosilane did not react with an excess of isopropyllithium nor an excess of cyclohexyllithium even at an elevated temperature. The results obtained here show that the presence of three cyclohexyl groups on a silicon atom allows introduction of only a less bulky group such as *n*-alkyl or phenyl but not that of the *sec*-alkyl group, though[14] tetracyclohexylsilane has been reported by Petrov and Chernysheva[11] to be obtained through a similar route. No evidence was obtained that would indicate any difference in the reactivity between isopropyl and cyclohexyl groups.

Experimental*

Tricyclohexylfluorosilane. — A typical example was shown here. A mixture of 5.2 g. of tricyclohexylsilanol, 350 ml. of ethanol and 50 ml. of 58% hydrofluoric acid solution was kept at about 70~75°C for 2.5 hr., and then poured onto 1 l. of cold water. The product was extracted with petroleum ether (50~70°C), and the extract dried over Drierite. On concentration of the extract, 2.3 g. of tricyclohexylfluorosilane melting at 44.5~46°C was obtained. Recrystallization from ethanol gave 2.1 g. of the fluorosilane, m. p. 45.8~46.5°C (reported[15], 45~46°C).

Isopropyl Bromide. — Reagent grade isopropyl bromide was dried over Drierite and distilled. B. p. 59.2~59.4°C.

Cyclohexyl Bromide.—The bromide was prepared by introducing hydrogen bromide to cyclohexanol. A fraction boiling at 74~76°C/33 mmHg was collected. n_D^{20} 1.4866. A commercial material was also used after distillation.

Petroleum Ether.—High boiling petroleum ether was shaken with concentrated sulfuric acid until it did not give a yellow color, washed with alkali and water repeatedly, dried over calcium chloride and then over sodium, and distilled again. A fraction boiling at about 90~110°C was collected and dried over sodium.

Tricyclohexylbutylsilane.—Butyllithium was prepared from 1.2 g. of lithium and 10.2 g. of butyl

6) H. Gilman and K. Oita, *J. Org. Chem.*, 20, 862 (1955).
7) W. H. Nebergall and O. H. Johnson, *J. Am. Chem. Soc.*, 71, 4022 (1949).
8) H. Gilman and R. N. Clark, ibid., 69. 1499 (1947).
9) L. J. Tyler, L. H. Sommer and F. C. Whitmore, ibid., 70, 2876 (1948).
10) C. Eaborn, *J. Chem. Soc.*, 1952, 2840.
11) A. D. Petrov and T. I. Chernysheva, *Zhur. Obshchei Khim.*, 24, 1189 (1954).
12) Throughout this study, petroleum ether boiling at 90~110°C was used as a reaction solvent.
13) M. Takakusa, This Bulletin, in press. The preparation and physical properties of this compound were reported orally by T. Yoshimoto and M. Takakusa at Autumn Meeting of the Chemical Societies of Japan, Tokyo, Sept., 1956.
14) Discussions on this discrepance will be done in a subsequent paper. M. Takakusa, This Bulletin, in press.
* All melting points reported here are uncorrected.
15) C. Eaborn, *J. Chem. Soc.*, 1952, 2846.

bromide in the usual method[16]. To the butyllithium solution in ethyl ether, 4.1 g. of tricyclohexylfluorosilane in 30 ml. of ethyl ether was added with stirring, the mixture warmed to reflux for 8 hr., ether distilled off, 40 ml. of petroleum ether added, and the content of the flask heated to reflux (oil bath, 120~130°C) for 7 hr. After cooling, some petroleum ether was added, and the mixture was shaken with about 150 ml. of water. The organic layer was washed with water, and dried over anhydrous sodium sulfate. Concentration of the liquid gave 1.5 g. of tricyclohexylbutylsilane melting at 156~159°C. From the mother liquor, on chromatography, was obtained 0.4 g. of crude material with a combined yield of 41%. Duplicated recrystallization from benzene-ethanol gave pure material melting at 159.2~160.0°C. Further recrystallization did not raise the melting point. (Found: C, 78.90; H, 12.08. Calcd. for $C_{22}H_{42}Si$: C, 78.95; H, 12.65%.) The infrared spectrum of this compound was completely identical to that of tricyclohexylbutylsilane obtained by hydrogenation of triphenylbutylsilane, the mixed melting point with the authentic sample did not show any depression.

Tricyclohexylisopropylsilane (Attempted).—Isopropyllithium was prepared in ethyl ether from 0.9 g. of lithium shots and about 10 g. of isopropyl bromide. Preparation in petroleum ether was not successful. To the isopropyllithium solution was added 1.8 g. of tricyclohexylfluorosilane dissolved in 20 ml. of ethyl ether, the mixture was refluxed for 4 hr., the ether was substituted by petroleum ether, and refluxed for 10 hr. The reaction mixture was worked up in the same way as above, but only crude tricyclohexylfluorosilane, m. p. 43~46°C, was recovered.

Tetracyclohexylsilane (Attempted).—Cyclohexyllithium solution was prepared from 17 g. of lithium and 162.3 g. of cyclohexyl bromide in petroleum ether, and 2.5 g. of tricyclohexylfluorosilane dissolved in 20 ml. of petroleum ether was added to it. The mixture was refluxed (oil bath, 150~160°C) for 12 hr., and worked up in the usual way. Tricyclohexylfluorosilane was recovered.

Tricyclohexylphenylsilane. — Phenyllithium was prepared in the usual way[16] from 1.8 g. of lithium and 16.8 g. of phenyl bromide in 140 ml. of ethyl ether. To the stirred phenyllithium solution 3.7 g. of tricyclohexylfluorosilane dissolved in 20 ml. of ethyl ether was added, the mixture refluxed for 3 hr., the solvent substituted by petroleum ether, and then refluxed (oil bath, 100°C) for 12 hr. The reaction mixture was worked up in the usual way, and 4.1 g. of crude material melting at 202~207°C was obtained. Recrystallization from petroleum ether-ethanol gave 3.2 g. (72%) of tricyclohexylphenylsilane melting at 206.8~208.2°C. Further recrystallizations from petroleum ether-ethanol did not change the melting point. Infrared spectrum offered a structural support.

Found: C, 81.21; H, 10.80. Calcd. for $C_{24}H_{38}Si$: C, 81.28; H, 10.80%.

16) R. G. Jones and H. Gilman, "Organic Reactions", Vol. VI, R. Adams ed., John Wiley and Sons, Inc., New York (1951), p. 339.

Summary

The reactions of tricyclohexylflurosilane with *n*-butyl-, phenyl-, isopropyl- and cyclohexyllithiums in boiling petroleum ether (90~110°C) were studied, and tricyclohexylbutylsilane and tricyclohexylphenylsilane were prepared (41 and 72%, respectively) for the first time. A secondary alkyl group can not be bonded to the silicon of tricyclohexylsilyl group even under these drastic conditions.

The author expresses his hearty thanks to Dr. Motonori Kanazashi for his kind advice during this work.

Electrotechnical Laboratory
Agency of Industrial Science and Technology
Tanashi-machi, Tokyo

Reactions of Alicyclic Aminonitrile

By Rokuro SUDO and Shigehiro ICHIHARA

(Received September 1, 1962)

α-Aminonitriles are generally unstable and directly hydrolyzed to the corresponding amino acids commonly without their isolation in Strecker's synthesis.

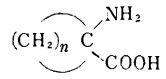

I: $n=5$
I': $n=4$

In an attempted synthesis of alicyclic amino acids I, I', some of which have been known as physiologically interesting substances[1,2], the authors found some characteristic reactions of alicyclic aminonitriles.

1-Aminocyclohexylonitrile (II) could be isolated only as an oily product by ether extraction from the reaction mixture of cyclohexanone, potassium cyanide and ammonium chloride, and this aminonitrile was characterized by the quantitative conversion into its benzoyl-derivative III and by hydrolysis to 1-aminocyclohexanecarboxylic acid (I).

This oily 1-aminocyclohexylonitrile (II) was, however, solidified after being kept at room temperature for a few weeks or heating under reduced pressure for a few hours giving a crystalline substance (m. p. 138°C). This substance was confirmed by elemental analysis and infrared spectrum to be 1, 1'-imino-dicyclohexylonitrile (V) and seemed to be identical with the compound, which Bucherer[3] isolated as a by-products in a rather low yield from the reaction mixture of aminonitrile and carbon dioxide. V was also hydrolyzed with concentrated hydrochloric acid giving I.

While, II was softly hydrolyzed in the presence of sodium hydroxide in the ethanol solution to give the compound of formula $C_{13}H_{22}ON_2$, which melted at 213°C. This compound was confirmed to be 2, 4-dicyclohexyl-iminazolidone-(5) (VI) by elemental analysis and infrared spectrum, which showed strong absorption bands at 3280 cm^{-1} (–NH–) and at 1710 cm^{-1} (ring forming amide), and then no band at 1500~1600 cm^{-1} region (free amide). Analogous to 2, 4-dicyclohexyl-5-thiaiminazolidone which was prepared by Gatewood[4] from α-aminonitrile and hydrogen sulfide, formation of VI was thought to proceed through the intermediate of V by the fact that V was similarly treated giving the same product VI. In addition, the structure VI may be explained by the following equation, because VI gave equimolecular I and ammonium chloride on heating with concentrated hydrochloric acid.

Moreover, V was allowed to stand with concentrated sulfuric acid at room temperature giving 1, 1'-iminodicyclohexanecarboximide sulfate (VII), which was neutralized yielding 1, 1'-iminodicyclohexanecarboximide (VIII). VIII was heated in 10% sodium hydroxide solution to give mono-amide IX, which was cyclized again to imide salt with

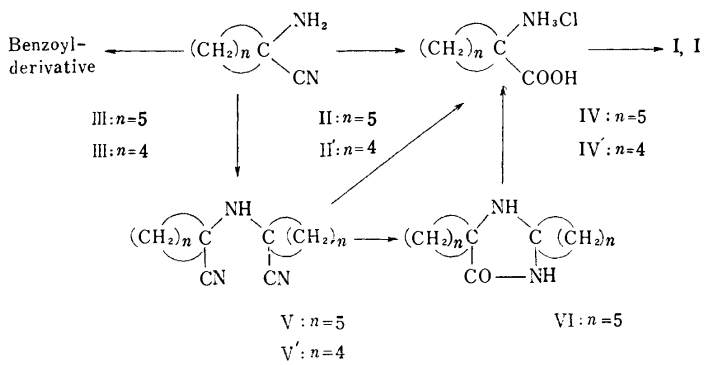

1) R. B. Ross, *J. Chem. Edu.*, **36**, 368 (1959).
2) T. A. Connors and W. C. J. Ross, *J. Chem. Soc.*, **1960**, 2119.
3) H. T. Bucherer and K. Dahlem, *J. prakt. Chem.*, **140**, 278 (1934).
4) E. S. Gatewood and T. B. Johnson, *J. Am. Chem. Soc.*, **50**, 1424 (1928).

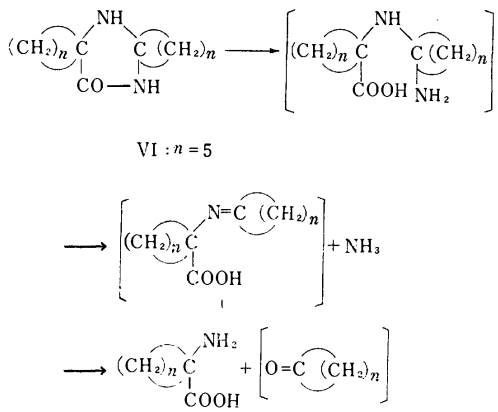

mineral acid, but was heated for a long time (16 hr.), giving 1, 1'-iminodicyclohexanecarboxylic acid (X).

This synthetic schema was also repeated beginning with cyclopentane derivatives, which involved physiologically interesting compounds[2], 1-aminocyclopentanecarboxylic acid (I') and 1, 1'-iminodicyclopentanecarboxylic acid (X'). 1, 1'-Iminodicyclopentylonitrile (V') was similarly prepared from 1-aminocyclopentylonitrile (II') but in a rather low yield.

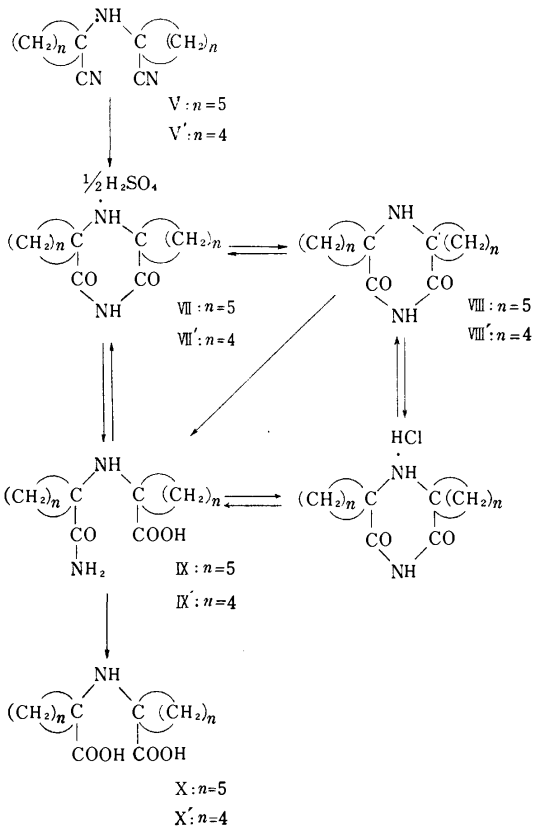

In view of above results, it is very interesting that imino-dinitrile was synthesized easily from aminonitrile and was hydrolyzed to amino acid as following equations a and b. In addition, aminonitrile can be prepared from hydroxynitrile (Eq. c)[5] and imino-dinitrile from hydroxynitrile and aminonitrile (Eq. d)[6].

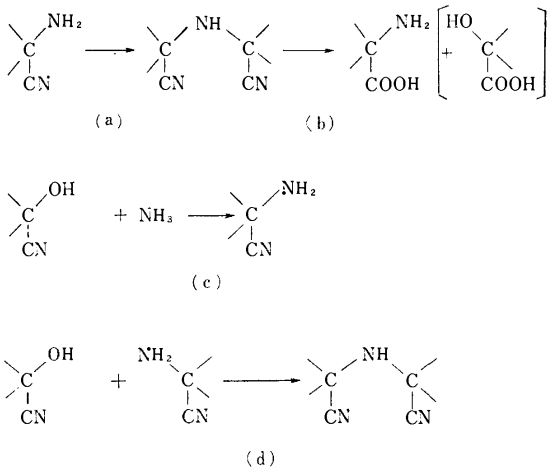

In this consideration, it was desirable to investigate the behavior of ammonolysis of iminodinitrile. In fact, it was discovered that 1, 1'-iminodicyclohexylonitrile (V) was heated with aqueous ammonia in a sealed tube giving 2 mol. of 1-aminocyclohexylonitrile (II), which was confirmed by conversion into its benzoyl-derivative.

Further experiments were tried in order to acertain that aliphatic iminodinitrile could be converted into α-aminonitrile. α, α'-Iminodipropionitrile (XII) was similarly treated

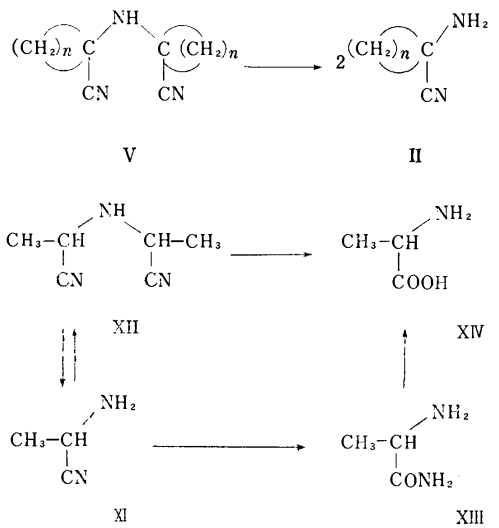

5) H. T. Bucherer and H. Barsch, *J. prakt. Chem.*, **140**, 79 (1934).
6) J. V. Dubsky, *Ber.*, **49**, 1045 (1916).

TABLE I

Substance	Amino-nitrile yield	Hydro-chloride m. p.	Benzoyl-deriv.		Amino-acid hydrochloride		Amino acid	
			M. p.	Yield	M. p.	Yield	M. p.	Yield
	%	°C	°C	%	°C	%	°C	%
Cyclohexane	80~90	190[a]	139[b]	95	298[c] decomp.	75	320[d] decomp.	65
Cyclopentane	70	174	129[e]	90	274[f] decomp.	72	330[g] subli.	60

a) Found: N, 17.34. Calcd. for $C_7H_{13}N_2Cl$: N, 17.40.
b) Found: N, 12.55. Calcd. for $C_{14}H_{16}ON_2$: N, 12.27.
c) Found: N, 7.78. Calcd. for $C_7H_{14}O_2NCl$: N, 7.82.
d) Found: N, 9.66. Calcd. for $C_7H_{13}O_2N$: N, 9.78.
e) Found: N, 13.13. Calcd. for $C_{13}H_{14}ON_2$: N, 13.08.
f) Found: N, 8.34. Calcd. for $C_6H_{12}O_2NCl$: N, 8.47.
g) Found: C, 49.24; H, 8.77; N, 9.79. Calcd. for $C_6H_{11}O_2N \cdot H_2O$: C, 48.96; H, 8.90; N, 9.59.

TABLE II

Substance	Iminodinitrile		Analysis of iminodinitrile					
			C		H		N	
	M. p. °C	Yield %	Found	Calcd.	Found	Calcd.	Found	Calcd.
Cyclohexane	138	80	72.60	72.68	9.28	9.15	18.12	18.17
Cyclopentane	52~53	25	71.05	70.90	8.52	8.43	20.66	20.67

with aqueous ammonia giving 2 mol. of α-aminopropionitrile (XI), which was confirmed conversion into benzoyl derivative. In this case, the benzoyl derivative isolated was α-benzaminopropionic amide (XIII) which was hydrolyzed to DL-alanine (XIV) in good yield. XIII was also hydrolyzed with hydrochloric acid giving 1 mol. of XIV (90%) and was treated after ammonolysis giving 2 mol. of XIV (60%).

Experimental

Alicyclic Aminonitrile II, II''. — Aminonitriles were prepared by Strecker's method[7] and extracted with ether. The ether solutions were dried with anhydrous sodium sulfate and gave a syrupy residue after removal of the solvent. These syrups were confirmed to be aminonitrile by conversion into benzoyl derivatives and α-amino acids. Benzoyl derivatives III, III' were prepared by Schotten-Baumann's method. Aminonitriles were suspended in sodium bicarbonate solution and benzoyl chloride added under stirring. Precipitates were filtered off and recrystallized from ethanol-water giving prisms.

Alicyclic Amino Acid I, I'.—Aminonitriles were heated in ten times the volume of concentrated hydrochloric acid for 4 hr. The reaction mixtures were concentrated to half the volume and allowed to stand overnight. The precipitates of their hydrochloride IV, IV' were collected and gave prisms by recrystallization (from water). These hydrochlorides were dissolved in a little water and neutralized with sodium bicarbonate. The precipitates were collected and recrystallized from ethanol-water. Colorless crystals were obtained. These data are summarized in Table I.

Alicyclic 1, 1'-Iminodinitriles (V), (V').—Syrup of II or II' was warmed for 5~6 hr. under reduced pressure and allowed to stand overnight at room temperature. Solidified compounds were collected and recrystallized from ethanol giving prisms. The infrared spectrum of V showed -C≡N band at 2260 cm^{-1} and -NH- band at 3380 cm^{-1}. These data were summarized in Table II.

Hydrolysis of V.—A solution of V (5 g.) in 50 ml. of concentrated hydrochloric acid was heated for 4 hr. The reaction mixture was concentrated to 10 ml. volume and allowed to stand at room temperature. Two grams of precipitates was collected. This product was identical to IV.

2, 4-Dicyclohexyliminazolidon-(5) (VI). — To a solution of II (2 g.) in 10 ml. of ethanol was added 2 ml. of 10% sodium hydroxide solution. The mixture was refluxed on a water-bath for 6 hr. and allowed to stand overnight at room temperature. The precipitates were collected and recrystallized from ethanol giving 1 g. of colorless prisms, melted at 213°C.

Found: C, 70.27; H, 10.11; N, 12.51. Calcd. for $C_{13}H_{22}ON_2$: C, 70.23; H, 9.97; N, 12.60%.

Infrared spectrum of VI showed strong bands at 1710 cm^{-1} (-CONH-) and at 3280 cm^{-1} (-NH-). V was similarly treated to give the same product VI.

1, 1' - Imino - dicyclohexanecarboximide Sulfate (VII).—V (5 g.) was dissolved in 30 ml. of concentrated sulfuric acid under cooling and allowed to stand overnight at room temperature. The mixture was added in ice-water and then gave precipitates. This product was collected and recrystallized from water giving 4 g. of crystals, melted at 273~274°C (decomp.).

7) V. Zelinsky and G. Stadnikoff, ibid., 39, 1728 (1906).

Found: N, 9.40. Calcd. for $C_{14}H_{22}O_2N_2 \cdot 1/2 \cdot H_2SO_4$: N, 9.36%.

1, 1'-Iminodicyclohexanecarboximide (VIII).—VII (2 g.) was dissolved in small water and neutralized with a solution of sodium bicarbonate. The precipitated product was collected and recrystallized from ethanol giving 1 g. of colorless crystals, melted at 164°C.

Found: C, 67.52; H, 8.71; N, 11.30. Calcd. for $C_{14}H_{22}O_2N_2$: C, 67.17; H, 8.86; N, 11.19%.

Hydrochloride of VIII.—A solution of VIII in hydrochloric acid was concentrated to give precipitates. The product was collected and recrystallized from ethanol-water giving colorless crystals, melted at 268°C (decomp.).

Found: N, 9.63. Calcd. for $C_{14}H_{22}O_2N_2 \cdot HCl$: N, 9.67%.

In a similar manner, a solution of VIII in sulfuric acid gave VII.

Mono-amide of 1, 1'-Iminodicyclohexanecarboxylic Acid (IX).—Two grams of VIII was heated for 30 min. in 20 ml. of 10% sodium hydroxide solution. The mixture acidified with acetic acid to give precipitates. The product was collected and recrystallized from ethanol, giving 1.8 g. of colorless crystals, melted at 204°C (decomp.).

Found: C, 62.48; H, 8.84; N, 10.42. Calcd. for $C_{14}H_{24}O_3N_2$: C, 62.66; H, 9.02; N, 10.44%.

1, 1'-Iminodicyclohexanecarboxylic Acid (X).—One gram of IX was heated with 10ml. of 10% sodium hydroxide solution for 10 hr. After cooling, the mixture was acidified with acetic acid to give precipitates. This product was collected and recrystallized from ethanol-water giving 0.4 g. of crystals, melted at 134°C. (decomp.).

Found: C, 62.31; H, 8.63; N, 5.50. Calcd. for $C_{14}H_{23}O_4N$: C, 62.43; H, 8.61; N, 5.20%.

1, 1'-Iminodicyclopentanecarboximide Sulfate (VII').—Four grams of this sulfate from 5 g. of V' was obtained in a manner similar to VII and melted at 274~275°C (decomp.)

Found: N, 10.78. Calcd. for $C_{12}H_{18}O_{12}N_2 \cdot 1/2H_2 \cdot SO_4$: N, 10.33%.

1, 1'-Iminodicyclopentanecarboximide (VIII').—In a manner similar to VIII, 1.3 g. of this imide was obtained from 2 g. of VII' and melted at 146°C.

Found: C, 64.57; H, 8.05; N, 12.49. Calcd. for $C_{12}H_{18}O_2N_2$: C, 64.84; H, 8.39; N, 12.66%.

Mono-amide of 1, 1'-Iminodicyclopentanecarboxylic Acid (IX).—In a manner similar to IX, 1.5 g. of IX' was obtained from 2 g. of VIII' and melted at 188~181°C (decomp.).

Found: N, 11.25. Calcd. for $C_{12}H_{20}O_3N_2$: N, 11.66%.

1, 1'-Iminodicyclopentanecarboxylic Acid (X).—IX' (1 g.) was heated in 10 ml. of 10% sodium hydroxide solution for 16 hr. The mixture was treated in a manner similar to X giving crystals (0.4 g.), which did not show clear melting point and sublimed at high temperature (above 200°C).

Found: C, 60.41; H, 8.36; N, 5.73. Calcd. for $C_{12}H_{19}O_4N$: C, 59.73; H, 7.94; N, 5.81%.

Ammonolysis of 1,1'-Iminodicyclophexylonitrile.—V (1 g.) was heated with 30 ml. of 28% aqueous ammonia in a sealed tube for 6 hr. The reaction mixture was extracted with ether. The ether solution was dried with anhydrous sodium sulfate and afforded syrupy residue after removal of the solvent and the syrup was confirmed by conversion into benzoyl derivative in a manner similar to III. 1.8 g. of crystals was obtained, (m. p. 138°C) and was identical to III. The melting point did not depress by mixing III.

α, α'-Iminodipropionitrile (XII).—This iminodinitrile was prepared from acetaldehyde by Dubsky's method[6], m. p. 66.5°C (reported m. p. 68°C).

Ammonolysis of α, α-Imino-dipropionitrile.—XII (6 g.) was treated with 28% aqeous ammonia in a manner described above. Oily syrup (crude 7 g.) was obtained. This syrup (1 g.) was converted into benzoylderivative (2 g.), which melted at 230~231°C and was confirmed to be α-benzaminopropionic amide (XIII) by elemental analysis.

Found: C, 62.36; H, 6.36; N, 14.42. Calcd. for $C_{10}H_{12}O_2N_2$: C, 62.48; H, 6.29; N, 14.58%.

This amide (4 g.) was heated in 40 ml. of hydrochloric acid. The reaction mixture was concentrated to dryness. After removal of ammonium chloride, the ethanol solution was neutralized with aniline giving crystalline (3 g., m. p. 260°C (decomp.)), which was identical to DL-alanine (XIV).

Hydrolysis of XII with Hydrochloric Acid.—a) XII (5 g.) was heated in 50 ml. hydrochloric acid and treated in a manner described above giving crystals of XIV (3 g., 90% to 1 mol.).

b) XII (5 g.) was treated similarly after ammonolysis giving 4.2 g. of XIV (60% to 2 mol.).

The authors wish to express deep gratitude to Professor Masaki Ohta for his kind and constant guidance throughout this study and to Dr. Tadashi Sato for the measurement of the infrared spectrum.

Laboratory of Organic Chemistry
Tokyo Institute of Technology
Meguro-ku, Tokyo

Synthesis of 1-Oxaazulan-2-imine Derivatives from Tropone[1]

By Tetsuo NOZOE, Toshio MUKAI and Tsunao SUZUKI*

(Received September 3, 1962)

The authors have investigated the reaction of tropones with an active methylene compound as a part of their continuing study of the chemistry of the troponoid system. A few years ago[2], it was found that the reaction of tropone (I) with malononitrile, in the presence of piperidine as a catalyst, afforded pale yellow crystals (II), m. p. 149°C, with a formula $C_{10}H_8ON_2$, in about 75% of yield. Since this reaction was considered to proceed by 1,8-addition mechanism[3,4], the authors proposed the structure of IIa or IIb for II[2]. A few months later, Kitahara and Doi[5] suggested that IIc would be more reasonable than IIa or IIb on the basis of its ultraviolet and infrared spectra.

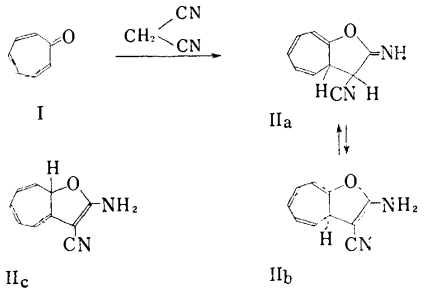

In the present paper, the authors wish to report the results of the reexamination of the structure of II and dehydrogenation of II, which resulted in the formation of derivatives of 1-oxaazulan-2-imine (2*H*-cyclohepta[b]furan-2-imine) in a fairly good yield.

As shown in Fig. 1, the ultraviolet spectrum of II exhibits a maximum around 320 mμ, which can not be explained by IIa or IIb as pointed out by Kitahara and Doi[5]. In infrared spectrum of II (see experimental part), there is a sharp band at 2210 cm^{-1} for the cyano group conjugated with unsaturated bond, besides three bands at 3230~3460 cm^{-1} for amino

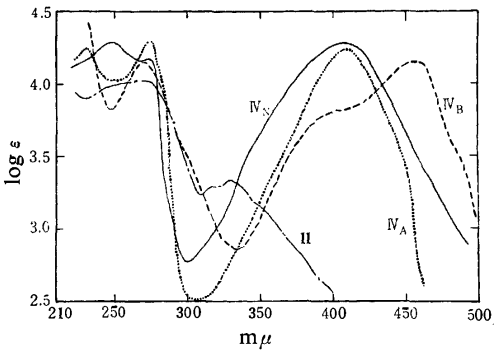

Fig. 1. UV spectra of II in methanol and of 3-cyano-1-oxaazulan-2-imine in methanol (IV_N), in 1 N HCl (IV_A) and in 1 N NaOH (IV_B).

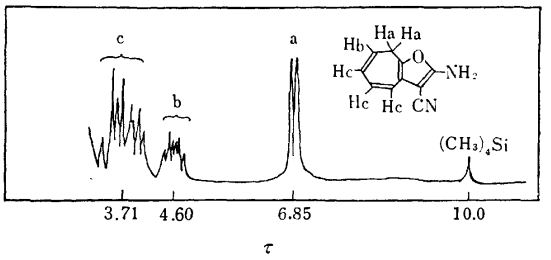

Fig. 2. NMR spectrum of II in pyridine (60 Mc.), with tetramethylsilane as an internal reference.

group. To elucidate the structure more clearly, the nuclear magnetic resonance spectrum of II was measured in a pyridine solution (Fig. 2). The signals appear as three groups, a, b and c with an area appropriate to 2, 1 and 3 protons respectively. The doublet signal a which appears at 6.85 τ with J=6.6 c. p. s. is ascribed to Ha and the multiplet signals b (centred at 4.60 τ) and c (centred at 3.71 τ) are attributed to Hb and Hc, respectively. This result is accommodated much better by the structure of 2-amino-3cyano-8*H*-cyclohepta-[b] furan (IId) than by IIa, II_b or IIc. The observed shift of the Ha peak to the lower field, compared with the NMR spectrum of cycloheptatriene[6], is ascribed to the paramagnetic shielding of the adjacent oxygen atom. 2-Amino-3-cyano-8*H*-cyclohepta [b] furan (IId) is

1) Presented at the 56th Tohoku Local Meeting of the Chemical Society of Japan, Yamagata, June, 1962.

* Present Address: Nihon Zeon Co., Takaoka, Toyama.

2) Presented at the 49th Tohoku Local Meeting of the Chemical Society of Japan, Yamagata, June, 1959.

3) T. Nozoe, T. Mukai and T. Tezuka, This Bulletin, 34, 619 (1961).

4) O. L. Chapman, D. J. Pasto and A. A. Griswold, *J. Am. Chem. Soc.*, 84, 1213 (1962).

5) Presented at the General Meeting of Tohoku District of the Chemical Society of Japan, Akita, October, 1959.

6) G. Frankel, R. E. Carter, A. McLachlan and J. H. Richards, *J. Am. Chem. Soc.*, 82, 5846 (1960).

assumed to be formed through the intermediate[7] as depicted below.

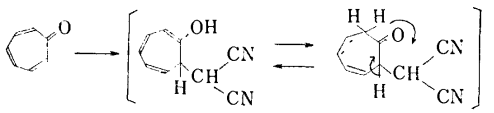

I

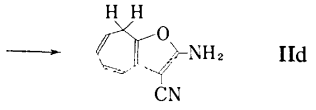

IId

The dehydrogenation of II with tetrachloro-1, 2-benzoquinone in benzene or chloroform afforded dark red complex (III). The treatment of III with dilute hydrochloric acid gave tetrachlorocatechol and 3-cyano-1-oxaazulan-2-imine (IV) in a good yield. When II was treated with selenium dioxide, the dehydrogenation was accompanied by simultaneous hydrolysis of the cyano group at 3-position and 3-carbamoyl-1-oxaazulan-2-imine (V), m. p. 192°C (decomp.), was obtained[8].

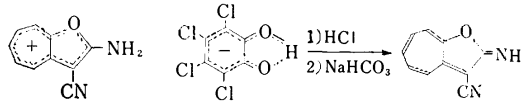

III IV

As shown in Figs. 1 and 3, the ultraviolet spectra of IV and V are very similar to that of 1-oxaazulan-2-one (2*H*-cyclohepta[b]furan-2-one)[9]. The infrared spectrum of IV shows an absorption band at 3300 cm^{-1} for the imino group and at 2207 cm^{-1} for the conjugated cyano group. In the infrared spectrum of V, there are bands at 3310 and 3155 cm^{-1} for the imino and amino groups and at 1650 cm^{-1} for the conjugated carbonyl group. IV and V are amphoteric substances, and soluble in both dilute acid and alkali. Passage of hydrogen chloride gas through a solution of IV in chloroform precipitated out the hydrochloride (VI) as pale yellow crystals, from which IV was regenerated by neutralization with sodium hydrogen carbonate. VI is much more stable than IV and it is possible to purify VI by sublimation under reduced pressure. Addition of sodium ethoxide to a solution of IV in chloroform gave the sodium salt VII as yellow crystals. From the fact that infrared spectrum

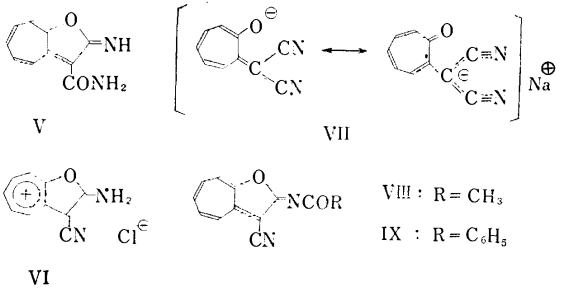

V VII

VI

VIII : R = CH_3
IX : R = C_6H_5

of VII showed two bands at 2210 and 2170 cm^{-1} for the cyano group, it is clear that the ring is opened as depicted above. The infrared spectrum of VII was similar to that of sodium troponate[10] (experimental part). There are no absorption bands from 2000 to 1600 cm^{-1}, but a band at 1595 cm^{-1}. It is not clear, however, whether this band should be due to the polarized carbonyl group or carbon-carbon double bond vibration as in the case of sodium troponate[10].

The ultraviolet spectra of IV in 1 N hydrochloric acid and 1 N sodium hydroxide solution are shown in Fig. 1. In an alkaline solution, the bathochromic shift ascribed to the formation of VII was observed, whereas in an acidic solution there is no remarkable shift in spite of the formation of VI.

Attempts to obtain 1-hydroxy-8, 8-dicyanoheptafulvene or its derivatives such as 1-methoxy-[11] or 1-acetoxy-8, 8-dicyanoheptafulvene did not succeed. For example, neutralization of VII with dilute acetic acid resulted in the ring closure to give IV. Acylation of

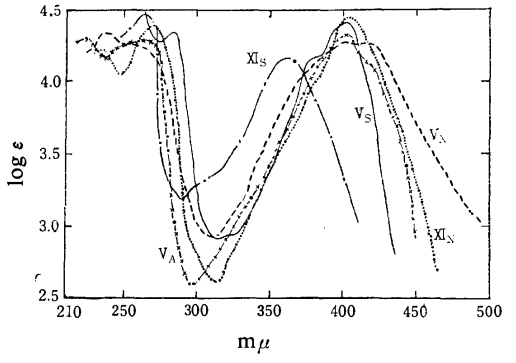

Fig. 3. UV spectra of 3-carbamoyl-1-oxaazulan-2-imine in methanol (V_N) in 1 N HCl (V_A) in conc. H_2SO_4 (V_S) and of 3-carbamoyl-1-oxaazulan-2-one in methanol (XI_N) and in conc. H_2SO_4 (XI_S).

7) In the addition reaction of tropones, the adducts same type as the intermediate have been obtained by. K. Takase and M. Yasunami (unpublished data), cf. Ref. 4.

8) Kitahara and Doi reported that dehydrogenation of II with selenium dioxide afforded 3-cyano-1-oxaazulan-2-imine, m. p. 161°C. Cf. Ref. 5.

9) S. Seto, *Sci. Repts. Tohoku Univ,, Ser. I*, 37, 367 (1954).

10) Y. Ikegami, *Kagaku-no-Ryoiki*, (*Extra* Vol.) 38, 70, Nankodo, Tokyo (1959).

11) Kitahara and Doi reported that, on using acetic anhydride as condensation reagent, reaction of tropolone methyl ether with malononitrile afforded 1-methoxy-8, 8-dicyanoheptafulvene, m. p. 206°C. Presented at the 15th Annual Meeting of the Chemical Society of Japan, Kyoto, April, 1962.

VII with acetyl or benzoyl chloride resulted also in the ring closure giving VIII or IX, which were obtained by acylation of IV. The infrared spectrum of VIII shows a band at 2164 cm^{-1} for the cyano group and at 1666 cm^{-1} for the carbonyl group. The latter supported the presence of the *N*-acetyl group rather than the *O*-acetyl group. The ultraviolet spectrum of VIII is shifted to a longer wavelength region than that of IV, because of the extension of the conjugate system (Fig. 4).

Previously, Nozoe and his coworkers reported that the reaction of tropolone methyl ether with ethyl cyanoacetate in the presence of sodium ethoxide afforded the azulene derivatives in a good yield[12]. However, Matsumura found that, under the same condition as above, the reaction of tropolone methyl ether and malononitrile resulted in the formation of the unknown compound, m. p. > 300°C, instead of the expected azulene derivative[13]. By comparison of the infrared spectra, it was found to be identical with VII. Furthermore, it was confirmed that, in the presence of sodium ethoxide, the reaction of VII with malononitrile did not yield the azulene derivatives, but resulted almost in the recovery of VII.

The heating of 3-cyano-1-oxaazulan-2-imine (IV) with 1 N hydrochloric acid gave 3-cyano-1-oxaazulan-2-one[14] (X) and 3-carbamoyl-1-oxaazulan-2-imine (V). On the other hand, X was not affected by heating with 1 N hydrochloric acid. This fact shows that the presence of imino group in IV assists the hydrolysis of the cyano group.

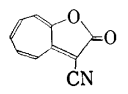

X

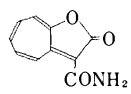

XI

The formation of V instead of IV, on dehydrogenation of II with selenium dioxide as mentioned before, may be explained as the result of hydrolysis of the cyano group with selenic acid. Upon treatment of IV with acid, an increase in acid concentration suppressed the hydrolysis of the imino group of 2-position. The same tendency was also observed in the acid-hydrolysis of V. The heating of V with 1 N hydrochloric acid afforded 3-carbamoyl-1-oxaazulan-2-one (XI) in a good yield, whereas heating of V in concentrated sulfuric acid resulted in the recovery of V accompanied with a small amount of XI. These facts indicated that, in an acid solution, IV and V were stabilized by the formation of the corresponding conjugate acid making the hydrolysis of the 2-imino group difficult. It is well known that the carbamoyl group of 1- or 3-position of azulenes is difficult to be hydrolyzed by acid treatment[15]. The heating of 3-carbamoyl-1-oxaazulan-2-one (XI) with concentrated or 50% sulfuric acid or the treatment of XI with sodium nitrite in sulfuric acid resulted almost in recovery of the starting material. The ultraviolet absorption spectra of V and XI are measured in methanol and concentrated sulfuric acid (Fig. 3). There is no distinguishable shift between V and its conjugate acid (in concentrated sulfuric acid), whereas the spectrum of the conjugate acid of XI is shifted to the shorter wavelength region as compared with that of XI in methanol.

The behavior of 3-carbamoyl-1-oxaazulan-2-imine (V) against alkali was studied by Nozoe and his coworkers[16] who discovered that V gave 3-cyano-1-azaazulan-2-one (3-cyano-cyclohepta[b]pyrole-2(1*H*)-one) (XII) in a quantitative yield. To obtain X exclusively, hydrolysis of the acylated compounds VIII or IX was attempted by using acid or alkali. The heating of VIII with dilute acid resulted in the formation of V and XI via IV. The treatment of VIII with dilute alkali, even ice-cooling, afforded unexpected XII in a good yield the formation of which is explained as follows.

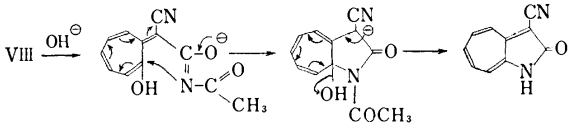

XII

By application of the method mentioned above, it is possible to synthesize not only 1-oxaazulan-2-ones but 1-azaazulan-2-ones from the tropone derivatives.

The reaction with malononitrile was extended to other tropone derivatives. Almost in the same way as the case of II, 2-phenyltropone afforded the condensation product XIII as pale yellow crystals, m. p. 150°C, in about 80% of yield. On the basis of its ultraviolet spectrum (Fig. 4), infrared spectrum (experimental part) and analytical value, $C_{16}H_{12}ON_2$, XIII was proved to be the phenyl derivative

12) T. Nozoe, S. Seto, S. Matsumura and T. Asano, *Proc. Japan Acad.*, 32, 339 (1956); T. Nozoe, S. Seto, S. Matsumura and Y. Murase, This Bulletin, 35, 1179 (1962).
13) S. Matumura, Private communication.
14) A. Sato succeeded in the synthesis of X by dehydration of the oxime of 3-formyl-1-oxaazulan-2-one. (Unpublished work.)
15) W. Schroth and W. Treibs, *Ann.*, 643, 108 (1961); T. Asano, presented at the 12th Annual Meeting of the Chemical Society of Japan, Kyoto, April, 1959; J. Tsunetsugu, Unpublished works.
16) T. Nozoe, K. Takase and T. Nakazawa, To be published.

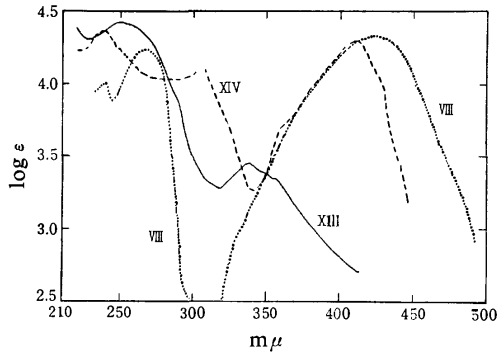

Fig. 4. UV spectra of VIII, XIII and 3-cyano-8-phenyl-1-oxaazulan-2-imine (XIV) in methanol.

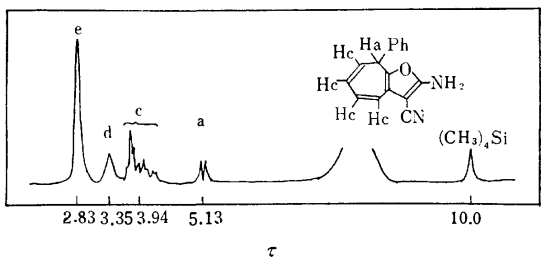

Fig. 5. NMR spectrum of XIII in acetone (60 Mc.). Tetramethylsilane as an internal reference.

of II, 2-amino-3-cyano-8-phenyl-8*H*-cyclohepta-[b]furan. Especially, the NMR spectrum of XIII, shown in Fig. 5, furnished the additional evidence concerning the protons of XIII. There are four groups of the absorption signal, a, c, d and e with an area appropriate about 1 : 4 : 2 : 5 protons respectively. The signals a (doublet at 5.13τ, J=7.4 c. p. s.) and c (multiplet centred at 3.94τ) are ascribed to Ha and Hc of XIII and correspond to the signals a, and b and c of II (Fig. 2). The peak corresponding to b of II may be shifted to the lower field by the paramagnetic effect of the adjacent phenyl group and included to the signal c. The observed shift of Ha to the low field, compared with that of II, seemed due to the same effect of the phenyl group. The hydrogens of the phenyl group appear at 2.83τ and the signal d at 3.35τ seemed due to the amino group at 2-position of XIII.

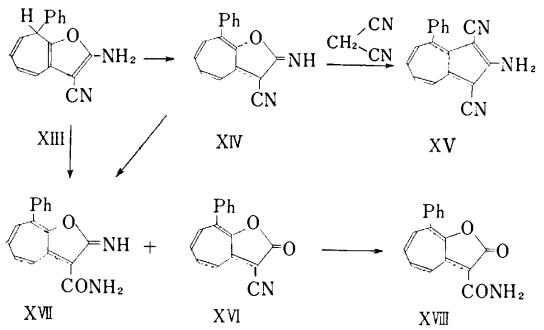

The dehydrogenation of XIII with tetrachloro-1, 2-benzoquinone was carried out in two steps and 3-cyano-8-phenyl-1-oxaazulan-2-imine (XIV) was obtained. Application of malononitrile to XIV in the presence of *tert*-butylamine yielded 2-amino-1, 3-dicyano-4-phenylazulene (XV)[17]. The yield of XIV was about 50% and that of XV was about 45% from 2-phenyltropone. The structure of XV was confirmed by the independent synthesis of XV from 2-chloro-7-phenyltropone and malononitrile[18].

The heating of XIV with 4 N hydrochloric acid afforded 3-cyano-8-phenyl-1-oxaazulan-2-one (XVI) and 3-carbamoyl-8-phenyl-1-oxaazulan-2-imine (XVII) with the recovery of considerable amount of XIV. XVII was also obtained by the dehydrogenation of XIII with selenium dioxide. The heating of XVI in concentrated sulfuric acid gave 3-carbamoyl-8-phenyl-1-oxaazulan-2-one (XVIII).

These approaches to the synthesis of the compounds from XIV to XVIII are of considerable significance from the view point of the synthetic tool for derivatives of 1-oxaazulan-2-one and azulene, not only because of the advantage of yield but the simplicity of the method.

Experimental[19,20]

Condensation of Tropone (I) and Malononitrile (Formation of II).—To a solution of 5 g. (0.047 mol.) of I and 3.6 g. (0.052 mol.) of malononitrile in 20 ml. of ethanol was added 0.2 ml. of piperidine. The solution turned to dark red with the heat formation and gave pale yellow prisms immediately. After standing overnight, the filtration gave 6.4 g. (75% of yield) of II as pale yellow prisms, m. p. 141~143°C, which on recrystallization from ethanol showed m. p. 149°C. IR (Nujol): 3460, 3340, 3230, 2210, 1640, 1592, 1422, 1346, 1235, 1160, 1110, 1042, 993, 850, 763, 706 and 687 cm^{-1}.

Found: C, 69.80; H, 4.36; N, 16.18. Calcd. for $C_{10}H_8ON_2$: C, 69.75; H, 4.68; N, 16.27%.

Dehydrogenation of II with Tetrachloro-1, 2-benzoquinone (Formation of IV).—Addition of a solution of 1.5 g. (6.1 mmol.) of tetrachloro-1, 2-benzoquinone dissolved in benzene into a solution of 1 g. (5.8 mmol.) of II in 150 ml. of benzene resulted in immediate precipitation of dark red crystals. After let to stand for 30 min. at room

17) The method for synthesizing azulene derivatives from 1-oxaazulan-2-ones or 1-oxaazulan-2-imines was established by T. Nozoe, K. Takase and N. Shimazaki. Presented at the 15th Annual Meeting of the Chemical Society of Japan, Kyoto, April, 1962.

18) H. Tsuruta, Unpublished data.

19) All melting points are uncorrected.

20) The microanalyses were carried out by Miss A. Iwanaga and M. Suzuki of this laboratory to whom the authors are indebted.

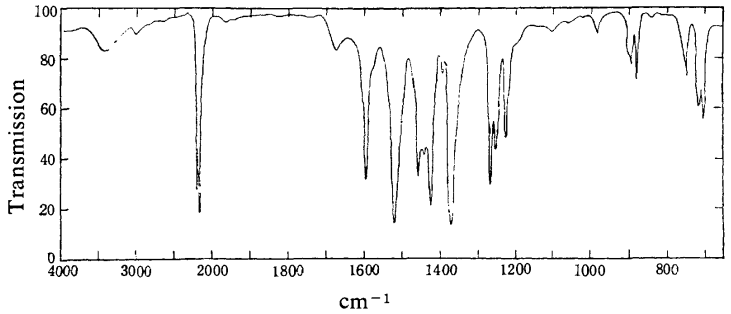

Fig. 6. IR spectrum of VII in KBr.

temperature, 2.2 g. (90% of yield) of complex (III), m. p. 130°C (decomp.) was filtered off. Three hundred milligrams of III ware also obtained by addition of 0.3 g. of tetrachloro-1,2-benzoquinone to a solution of 0.2 g. of II in 11 ml. of chloroform. IR (Nujol): 3340, 2220, 1672, 1587, 1345, 1270, 958, 805 and 751 cm^{-1}.

Found: C, 45.60; H, 1.83; N, 6.58. Calcd. for $C_{16}H_8O_3N_2Cl_4$: C, 45.96; H, 1.93; N, 6.70%.

To a suspension of 1 g. of III in 20 ml. of chloroform or benzene, 40 ml. of 1 N hydrochloric acid was added and the mixture was shaken. The chloroform or benzene layer, after separation, was extracted again with 20 ml. of 1 N hydrochloric acid, washed with water and dried over sodium sulfate. Evaporation of chloroform gave 240 mg. of tetrachlorocatechol, as yellowish crystals, m. p. 185~190°C. The extract with dilute hydrochloric acid was neutralized by addition of sodium hydrogen carbonate, during which orange red crystals separated out. Filtration afforded 400 mg. (90% of yield) of orange crystals (IV), m. p. 143°C (decomp.), which tended to decompose on recrystallization. Purification of IV was done through its hydrochloride as follow: Passing hydrogen chloride gas through a solution of IV in chloroform gave hydrochloride (VI) as yellow crystals, m. p. over 260°C. The hydrochloride could be sublimed at about 200°C and 3 mmHg. Addition of sodium hydrogen carbonate to an aqueous solution of VI gave 3-cyano-1-oxaazulan-2-imine (IV), m. p. 153°C (decomp.). IR (Nujol): 3300, 2207, 1676, 1598, 1498, 1271, 1106, 976, 958, 924, 875, 772, 756 and 720 cm^{-1}.

Found: C, 70.48; H, 3.34; N, 15.90. Calcd. for $C_{10}H_6ON_2$: C, 70.58; H, 3.55; N, 16.46%.

Dehydrogenation of II with Selenium Dioxide (Formation of V).—A solution of 300 mg. (1.7 mmol.) of II and 225 mg. (2.0 mmol.) of selenium dioxide in 5 ml. of methanol was refluxed for 30 min., during which dark brown precipitate separated out. After evaporation of methanol, the residue was washed well with 20 and 10 ml. of 1 N hydrochloric acid. The combined washing was neutralized by adding solid sodium hydrogen carbonate and extracted with chloroform. The extract was washed with water, dried over sodium sulfate and evaporated giving 130 mg. (60% of yield) of brownish orange crystals, m. p. 182°C (decomp.). Infrared spectrum of the product was completely superposed on that of 3-carbamoyl-1-oxaazulan-2-imine (V) (see below).

Sodium Salt (VII) of 1-Hydroxy-8,8-dicyanoheptafulvene.—*a) From IV.*—To a solution of 100 mg. of IV in 2 ml. of chloroform was added the sodium ethoxide, prepared from 30 mg. of sodium and 2 ml. of absolute ethanol, giving 100 mg. of orange yellow crystals (VII), m. p. over 300°C.

Found: N, 13.98. Calcd. for $C_{10}H_5ON_2Na$: N, 14.58%.

b) From Tropolone Methyl Ether.—To a ethanol solution of the sodium salt of malononitrile, prepared from 40 mg. of sodium, 50 mg. of malononitrile and 2 ml. of absolute ethanol, 100 mg. of tropolone methyl ether was added. After being stirred overnight, crystals separated out. Filtration gave 120 mg. of yellow crystals, m. p. over 300°C, infrared spectrum of which was completely the same as that of VII.

c) Regeneration of IV from VII.—Under the coexistence of a chloroform layer, a solution of 200 mg. of VII in 2 ml. of water was neutralized by adding 2 N acetic acid with vigorous stirring. The chloroform layer was separated, washed with water and dried over sodium sulfate. Evaporation of the chloroform afforded 70 mg. of orange red crystals, m. p. 145°C, (decomp.), which was identical with IV (from infrared spectrum).

VII was dissolved in dilute hydrochloric acid and the resulting solution was neutralized by addition of solid sodium hydrogen carbonate giving IV almost quantitatively.

Acylation of Sodium Salt (VII) and 3-Cyano-1-oxaaulan-2-imine (IV)[21].—*a) Acetylation of VII.*—To a suspension of 100 mg. of VII in 2 ml. of pyridine was added 0.3 ml. of acetyl chloride under ice-cooling. The reaction mixture was allowed to stand for 60 min., poured into water and extracted with chloroform. The chloroform extract was washed with water, dried over magnesium sulfate and evaporated to 75 mg. (68% of yield) of yellow crystals, m. p. 144~146°C. Recrystallization from ethanol gave yellow needles (VIII), m. p. 146°C. IR (Nujol): 2164, 1666, 1575, 1493, 1281, 1236, 1224, 1214, 970 and 763 cm^{-1}.

Found: C, 68.20; H, 4.05; N, 12.80. Calcd. for $C_{12}H_8O_2N_2$: C, 67.92; H, 3.80; N, 13.20%.

b) Acetylation of IV.—To a solution of 59 mg. of IV in 0.8 ml. of pyridine was added 0.3 ml. of acetyl chloride under ice-cooling. The same treatment as a) gave 60 mg. of yellow crystals, m. p.

21) This part of the experiment was carried out by Mr. Haruki Tsuruta.

130~137°C, which on recrystallization from ethanol gave VIII, m. p. 145°C.

c) Benzoylation of VII.—To a mixture of 1 g. of VII and 4 ml. of pyridine, 2 ml. of benzoyl chloride was added with stirring under ice-cooling. After being allowed to stand for 1.5 hr., the reaction mixture was poured into water giving some oil, which crystallized on standing. Filtration afforded 1.3 g. of red crystals, m. p. 110~130°C, which on recrystallization from benzene-alcohol mixture gave brown scales (IX), m. p. 155°C. IR (Nujol): 2214, 1645, 1566, 1473, 1296, 1239, 1217, 1046, 960, 897, 715 and 698 cm^{-1}.

Found: C, 74.41; H, 3.59; N, 9.88. Calcd. for $C_{17}H_{10}O_2N_2$: C, 74.44; H, 3.68; N, 10.21%.

Hydrolysis of 3-Cyano-1-oxaazulan-2-imine (IV) with Acid.—*a) With 1N Hydrochloric Acid.*—A solution of 400 mg. of IV dissolved in 100 ml. of 1 N hydrochloric acid was heated on the boiling water bath for 2 hr. After being cooled, the reaction mixture was extracted with ethyl acetate. The extract was evaporated up to give 80 mg. of yellow crystals, which on recrystallization from ethyl acetate afforded 50 mg. of X, m. p. 240°C. It was shown to be identical with 3-cyano-1-oxaazulan-2-one synthesized by Sato[14] by comparing infrared spectra of them and the mixed melting point determination. The acid layer was neutralized by addition of solid sodium hydrogen bicarbonate giving 160 mg. of reddish brown crystals, m. p. 186°C, (decomp.), which were obtained by filtration. The filtrate was extracted with ethyl acetate. After being dried over sodium sulfate, evaporation of the extract gave 100 mg. of brown crystals, m. p. 182°C (decomp.). The combined crystals were recrystallized from ethyl acetate to give reddish orange needles (V), m. p. 192°C (decomp.). IR (Nujol): 3310, 3155, 1650, 1595, 1500, 1408, 1302, 1271, 1143, 1125, 879, 856, 824, 784, 756, 736 and 684 cm^{-1}.

Found: C, 63.65; H, 4.01; N, 14.38. Calcd. for $C_{10}H_8O_2N_2$: C, 63.82; H, 4.29; N, 14.89%.

b) With Ethanolic 4N Hydrochloric Acid Solution.—A solution of 200 mg. of IV in 6 ml. of concentrated hydrochloric acid and 12 ml. of ethanol was refluxed for 2 hr. on a water bath. After addition of 5 ml. of 6N sodium hydroxide, the reaction mixture was extracted with ethyl acetate. The extract was washed with water, dried over sodium sulfate and evaporated to give 15 mg. of brown crystals, m. p. 180~200°C. The aqueous layer was neutralized by adding sodium hydrogen carbonate and extracted with chloroform. The extract was dried over sodium sulfate and evaporated giving 140 mg. of reddish orange crystals, m. p. 180°C (decomp.), which was found to be V contaminated with a little amount of IV by inspection of the infrared spectrum.

Hydrolysis of 3-Carbamoyl-1-oxaazulan-2-one Imine (V) with Acid.—*a) With 1N Hydrochloric Acid.*—Heating of a solution of 230 mg. of V in 20 ml. of 1 N hydrochloric acid on a water bath afforded 110 mg. of brownish crystals, m. p. 270°C, which were filtered off after being cooled. Further heating of the filtrate on a water bath for 10 hr. gave 50 mg. of brown crystals, m. p. 275°C. The combined crystals were recrystallized from acetic acid giving yellow brown needles (XI), m. p. 275°C. IR (Nujol): 3415, 3135, 1740, 1680, 1611, 1544, 1488, 1309, 1277, 1229, 942, 882 and 795 cm^{-1}.

Found: C, 63.73; H, 3.46; N, 7.47. Calcd. for $C_{10}H_7O_3N$: C, 63.49; H, 3.73; N, 7.41%.

b) With Sulfuric Acid.—A solution of 100 mg. of V dissolved in 0.5 ml. of sulfuric acid was heated in a closed vessel on a boiling water bath for 2 hr. The reaction mixture was poured into 10 ml. of water and extracted with chloroform continuously for 6 hr. Evaporation of the extract yielded 40 mg. of yellow brown crystals, m. p. 270°C, which on recrystallization from acetic acid gave XI, m. p. 275°C. The aqueous solution from the chloroform extraction was neutralized by addition of sodium hydrogen carbonate to give orange crystals, which were extracted with ethyl acetate. Evaporation of the extract gave 60 mg. of orange crystals, m. p. 186°C (decomp.), which was identical with the starting material V (from infrared spectrum).

The same treatment of XI as b) with concentrated sulfuric acid resulted in the recovery of XI.

Hydrolysis of the Acylated Compound (VIII and IX) of 3-Cyano-1-oxaazulan-2-imine[21].—a) A solution of 200 mg. of VIII dissolved in a mixture of 1 ml. of concentrated hydrochloric acid and 10 ml. of methanol was refluxed for 30 min., and the methanol was evaporated under reduced pressure. The residual solution was poured into water and extracted with chloroform. The extract was washed, dried over magnesium sulfate and evaporated to 10 mg. of brown crystals, m. p. 167~242°C, which have not been examined. The acidic solution was neutralized by addition of sodium hydrogen carbonate and extracted with chloroform. The same treatment of the extract afforded 100 mg. of reddish orange crystals, m. p. 144~158°C (decomp.), which was found to be a mixture of IV and V by inspection of its infrared spectrum.

b) A solution of 200 mg. of VIII dissolved in a mixture of each 2 ml. of 2 N potassium hydroxide and methanol was refluxed for 2 hr. After being diluted with water and extracted with chloroform, the reaction mixture was neutralized to pH 3 with 2 N hydrochloric acid giving 135 mg. of yellow crystals, m. p. over 250°C. Recrystallization from dimethylformamide gave XII as yellow crystals, m. p. over 280°C, whose infrared spectrum was superimposed on that of the authentic sample[16].

c) To a suspension of 300 mg. of IX in 6 ml. of methanol was added 2 ml. of 2 N potassium hydroxide and the resulting mixture was shaken with ice-cooling for 15 min. By acidification of the solution to pH 3, 145 mg. of dark orange crystals, m. p. over 280°C, were obtained by filtration. The filtration, after being evaporated and diluted with water, afforded 40 mg. of the same crystals, m. p. over 280°C. The combined crystals were identical with the authentic 3-cyano-1-azaazulan-2-one[16] (from infrared spectum).

Condensation of 2-Phenyltropone and Malononitrile (Formation of XIII).—To a solution of 1 g. (5.5 mmol.) of 2-phenyltropone and 400 mg. (6 mmol.) of malononitrile in 4 ml. of absolute ethnol was added 0.2 ml. of piperidine and the

reaction mixture was allowed to stand overnight at room temperature. Filtration of the crystals deposited gave 1.08 g. (80% of yield) of XIII as pale yellow needles, m. p. 150°C. IR (Nujol): 3520, 3380, 2220, 1639, 1601, 1557, 1494, 1100, 837, 789, 743, 728, 698 and 687 cm^{-1}.

Found: C, 77.38; H, 4.77; N, 11.21. Calcd. for $C_{16}H_{12}ON_2$: C, 77.40; H, 4.87; N, 11.28%.

Dehydrogenation of XIII with Tetrachloro-1,2-benzoquinone (Formation of XIV).—To a solution of 400 mg. (1.6 mmol.) of XIII in 20 ml. of benzene was added 480 mg. (1.9 mmol.) of tetrachloro-1,2-benzoquinone and the reaction mixture was allowed to stand at room temperature for 30 min., during which reddish crystals precipitated out. Filtration afforded 850 mg. of dark orange crystals, m. p. 135°C (decomp.), which were difficult to be recrystallized from the usual solvent. The crystals obtained ware added to a mixture of 20 ml. of 2 N hydrochloric acid and 20 ml. of ethanol and the reaction mixture was shaken for 1 hr. and then poured into water. Some resinous matter with dark red separated out, from which the acidic layer was decanted. After being shaken with benzene to remove tetrachlorocatechol, the acidic solution was neutralized by addition of sodium hydrogen carbonate giving 240 mg. (60% of yield) of XIV as orange red crystals, m. p. 183°C (decomp.). IR (Nujol): 3360, 2220, 1658, 1618, 1587, 1538, 1495, 1321, 1285, 1233, 1115, 979, 912, 790, 781, 756, 717 and 692 cm^{-1}.

Found: C, 77.58; H, 3.90; N, 10.94. Calcd. for $C_{16}H_{10}ON_2$: C, 78.03; H, 4.09; N, 11.38%.

Synthesis of 2-Amino-1,3-dicyano-4-phenylazulene (XV) from 3-Cyano-8-phenyl-1-oxaazulan-2-imine (XIV).—A solution of 50 mg. (0.2 mmol.) of XIV and 30 mg. (0.45 mmol.) of malononitrile in 6 ml. of absolute ethanol was stirred overnight in the presence of 60 mg. of *tert*-butylamine giving yellow crystals. Filtration afforded 50 mg. (90% of yield) of yellow crystals (XV), m. p. 296°C, which showed no depression on admixture with the authentic sample synthesized from 2-chloro-7-phenyltropone and malononitrile[18]. The infrared spectrum of XV was superimposed on that of the authentic sample[18].

Hydrolysis of 3-Cyano-8-phenyl-1-oxaazulan-2-imine (XIV) with Acid.—A solution of 400 mg. of XIV dissolved in 35 ml. of 4 N hydrochloric acid was heated on a water bath for 3 hr. and on being cooled dark yellow needles crystallized out. Filtration afforded 150 mg. of yellow needles, m. p. 255°C, which on recrystallization from dimethylformamide gave needles (XVI), m. p. 265°C. IR (Nujol): 2215, 1755, 1613, 1582, 1488, 1312, 1282, 1230, 961, 930, 905, 795, 768, 732 and 699 cm^{-1}.

λ_{Max}^{MeOH} mμ (log ε): 223 (4.40), 255 (4.26), 310 (4.20) and 414 (4.39).

Found: C, 77.25; H, 3.65; N, 5.80. Calcd. for $C_{16}H_9O_2N$: C, 77.72; H, 3.67; N, 5.67%.

The filtrate of XVI was neutralized by addition of solid sodium hydrogen carbonate giving 200 mg. of orange crystals, m. p. 173°C, which were obtained by filtration. The crystals obtained were dissolved in benzene and chromatographed through a column containing 6 g. of alumina. After evaporation, the elute with ether gave 20 mg. of reddish crystals (XIV), m. p. 172~173°C (decomp.), and the elute with ethyl acetate gave 50 mg. of reddish orange crystals (XVII), m. p. 184~185°C (decomp.). IR (Nujol): 3345, 3165, 1660, 1585, 1497, 1357, 1304, 1282, 1107, 1092, 930, 795, 769, 751, 726, 694 and 674 cm^{-1}. λ_{Max}^{MeOH} mμ (log ε): 238 (4.46), 290 (4.18) and 422 (4.38).

Found: C, 72.79; H, 4.46; N, 10.22. Calcd. for $C_{16}H_{12}O_2N_2$: C, 72.71; H, 4.58; N, 10.60%.

Hydrolysis of 3-Cyano-8-phenyl-1-oxaazulan-2-one (XVI) with Sulfuric Acid.—One hundred milligrams of XVI ware dissolved in 0.5 ml. of concentrated sulfuric acid and the solution was heated in a closed vessel in the boiling water bath for 1 hr. The solution was poured into 3 ml. of water to give brownish crystals. Filtration afforded 110 mg. of crystals, m. p. 233~236°C, which on recrystallization from benzene gave yellow crystals (XVIII), m. p. 258~260°C. IR (Nujol): 3400, 3145, 1724, 1672, 1603, 1580, 1490, 1277, 1259, 1217, 804, 781, 754, 735 and 698 cm^{-1}. λ_{Max}^{MeOH} mμ (log ε): 223 (4.37), 253 (4.23), 304 (4.16) and 415 (4.35).

Found: C, 72.49; H, 4.32; N, 4.92. Calcd. for $C_{16}H_{11}O_3N$: C, 72.44; H, 4.18; N, 5.28%.

The authors express their gratitude to Mr. K. Osaka of the Asahi Chemical Industry Co. for his cooperation during the early stage of this experiment and Mr. H. Tsuruta for carrying out some experiment concerning VIII and IX. They also thank Dr. K. Takase for helpful discussion and Mr. K. Takahashi for measurement of the NMR spectrum, and Sankyo Co. for donation of a research fund which covered a part of the expenses for this work.

Department of Chemistry
Faculty of Science
Tohoku University
Katahira-cho, Sendai

The Mannich Base of Troponoid and its Application. IX. Reaction of 3-Bromo-5-formyl-7-isopropyltropolone

By Kyozo OGURA

(Received September 5, 1962)

It has been found that alkaline treatment of 3-bromo-7-isopropyltropolon-5-ylmethylenerhodanine (II) obtained by the reaction of 3-bromo-5-formyl-7-isopropyltropolone (I) and rhodanine resulted in the abnormal intramolecular attack of sulfide anion at the 4-position of the tropolone ring with the liberation of the bromide ion from the 3-position to give thieno [2, 3-d] tropolone derivative III[1].

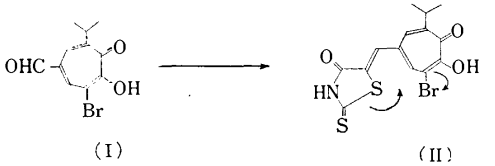

(I) (II)

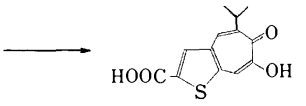

(III)

In order to make further extension of such an abnormal cyclization, some reactions of aldehyde I were studied.

Treatment of I with diethyl acetonedicarboxylate in the presence of piperidine gave colorless needles of m. p. 215°C (IV), corresponding to the molecular formula of $C_{20}H_{22}O_7$. The fact that the bromide ion was liberated in this reaction suggested that IV was not a simple condensation product, but a cyclization product formed by the condensation followed by such an abnormal intramolecular substitution as in the case of thienotropolone derivative III. According to the manner of the intramolecular attack, three structures (A, B and C) are expected for IV, while structure A must be excluded by the analytical values of IV. The ultraviolet absorption spectrum of IV is similar to those of 4, 5-benzotropolone and its derivatives[2], and its infrared spectrum shows absorptions for the hydroxyl group at 3280 cm^{-1} and for the carbonyl group at 1727 and 1680 cm^{-1}. Furthermore it shows absorp-

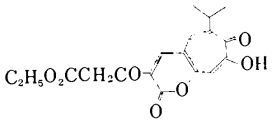

(A)

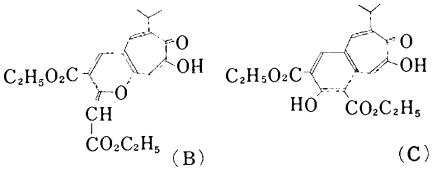

(B) (C)

tions at 1638, 1587, 1538 and 1468 cm^{-1} which agree well with absorption bands of 4, 5-benzotropolone reported by Tarbell et al.[3] These facts show that IV is 1', 3'-diethoxycarbonyl-2'-hydroxy-3-isopropyl-4, 5-benzotropolone (C). Treatment of IV with alkali gave dicarboxylic acid V, whose ultraviolet spectrum was shown in Fig. 1.

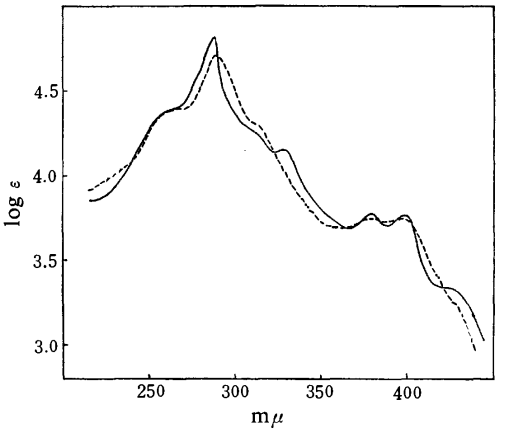

Fig. 1. Ultraviolet spectra of IV (——) and V (·····) in methanol.

Although it was expected that pyrazolotropolone derivative would be obtained by the action of alkali on tosylhydrazone VI, the cyclization did not occur, but 3-bromo-7-isopropyltropolon-5-ylmethyl *p*-tolyl sulfone

1) K. Ogura, This Bulletin, 35, 808 (1962).
2) H. Fernholz, E. Hartwig and J. C. Salfeld, *Ann.*, 576, 131 (1952).
3) D. S. Tarbell, G. P. Scott and A. D. Kemp, *J. Am. Chem. Soc.*, 72, 379 (1950).

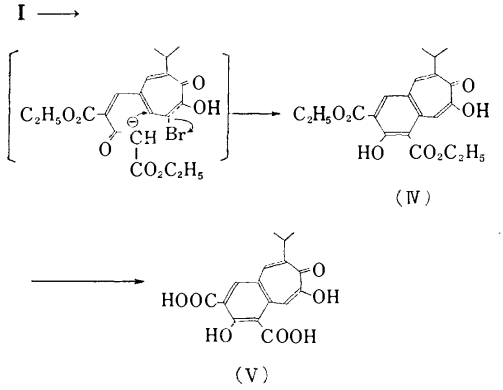

(V)

(VII) was obtained. It seems to have been formed in the same manner as known in the case of benzaldehyde tosylhydrazone[4].

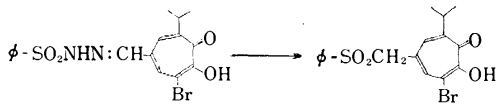

(VI) (VII)

$\phi = p$-tolyl

Finally for the synthesis of thiazinotropolone derivative the reaction of I with thiourea in the presence of pyridine was examined, and the product corresponding to the molecular formula of $C_{11}H_{12}O_3$ (VIII) was obtained. Its infrared spectrum shows an absorption at 1688 cm^{-1} due to a carbonyl group, and other absorptions expect those in the finger print region agree well with those of I. The ultraviolet spectrum is also similar to that of I. These facts suggest that VIII should be 3-isopropyl-5-formyltropolone formed by debromination of I. In order to make this problem more clear the reaction of 3, 7-dibromotropolone with thiourea in the presence of pyridine was examined, and it was found that the

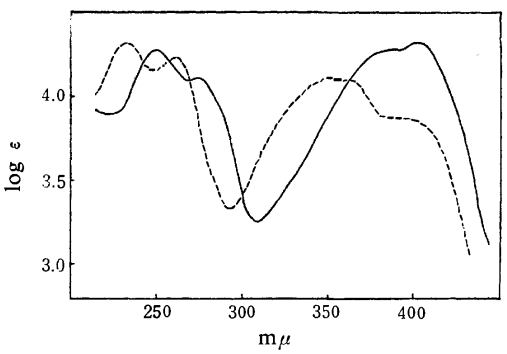

Fig. 2. Ultraviolet spectra of I (——) and VIII (……) in methanol.

4) W. R. Barmford and T. S. Stevens, *J. Chem. Soc.*, 1952, 4735.

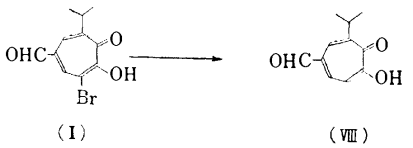

(I) (VIII)

debromination occurred to give 3-bromotropolone in a low yield.

Experimental*

1', 3'-Diethoxycarbonyl-2'-hydroxy-3-isopropyl-4, 5-benzotropolone (IV).—A mixture of I (100 mg.), diethyl acetonedicarboxylate (120 mg.) and piperidine (30 mg.) was refluxed for 7 hr., and then cooled to room temperature. Colorless needles (10 mg.) of IV which precipitated on being cooled were collected. The filtrate was refluxed, with 30 mg. of piperidine further added, for 1 hr., and the solvent was removed to dryness. Addition of a small amount of water and methanol to the resinous residue caused to solidify. The solid thereby formed was collected and recrystallized from ethanol to afford colorless needles of IV (5 mg.), m. p. 213~215°C. λ_{max}^{MeOH} mμ (log ε) : 288 (4.82), 330 (4.16), 380 (3.78), 400 (3.77).

Found : C, 64.15 ; H, 6.19. Calcd. for $C_{20}H_{22}O_7$: C, 64.16 ; H, 5.92%.

1', 3'-Dicarboxy-2'-hydroxy-3-isopropyl-4, 5-benzotropolone (V).—After IV (30 mg.) was heated in aqueous potassium hydroxide solution (potassium hydroxide, 15 mg. ; water, 0.2 ml.) in a water bath for 1 hr., the solution was neutralized with hydrochloric acid (pH, 3~4). The mixture was extracted by ether. The evaporation of the ether from the extract left pale yellow powder, which was collected, washed with water and recrystallized from methanol to afford colorless crystals, m. p. 270~275°C (decomp.). Yield, 10 mg. λ_{max}^{MeOH} mμ (log ε) : 290 (4.72), 380 (3.75), 398 (3.75).

Found : C, 59.39 ; H, 4.71. Calcd. for $C_{16}H_{14}O_7$: C, 60.38 ; H, 4.43%.

3-Bromo-5-formyl-7-isopropyltropolone *p*-Tosylhydrazone (VI).—A solution of I (100 mg.) and *p*-tolylsulfonylhydrazide (60 mg.) in methanol (1 ml.) was refluxed for 15 min., and then cooled to room temperature. Yellow crystals that separated were collected and recrystallized from ethanol to give yellow granular crystals, m. p. 165~166°C. Yield. 120 mg.

Found : C, 47.36 ; H, 4.31 ; N, 6.32. Calcd. for $C_{18}H_{19}O_4N_2$ SBr·H_2O : C, 47.28 ; H, 4.63 ; N, 6.13%.

3-Bromo-7-isopropyltropolon-5-ylmethyl *p*-Tolyl Sulfone (VII).—A solution of VI (100 mg.) and piperidine (30 mg.) in ethanol (1.5 ml.) was refluxed for 4 hr. The evaporation of the ethanol left yellow oily residue, which was solidified by addition of a few drops of 6 N hydrochloric acid and 1 ml. of methanol. The solid was collected and recrystallized from methanol to afford colorless needles,

* All melting points are uncorrected. The microanalyses were carried out by Miss Yoko Endo and Miss Yukiko Endo of this Institute, to whom the present author wishes to express his gratitude.

m. p. 162~164°C. Yield, 20 mg. λ_{max}^{MeOH} mμ (log ε): 277 (4.23), 265 (4.50), 345 (4.00), 413 (3.76).

Found: C, 52.52; H, 4.69. Calcd. for $C_{18}H_{19}O_4SBr$: C, 52.57; H, 4.66%.

3-Isopropyl-5-formyltropolone (VIII).—A mixture of I (130 mg.) and thiourea (40 mg.) in pyridine (1 ml.) was warmed in a water bath for 1.5 hr., by which the whole dissolved to form a black solution. After the removal of pyridine dilute hydrochloric acid was added to the residue and the precipitate was collected, washed with water and recrystallized from benzene to form pale yellow granular crystals, which was further purified by sublimation in reduced pressure, m. p. 107~109°C. Yield, 20 mg. λ_{max}^{MeOH} mμ (log ε): 233 (4.31), 262 (4.23), 351 (4.10), 390 (3.88).

Found: C, 66.55; H, 5.92. Calcd. for $C_{11}H_{12}O_3 \cdot 1/2H_2O$: C, 66.65; H, 6.32%.

Reaction of 3, 7-Dibromotropolone and Thiourea.—A mixture of 3, 7-dibromotropolone (100 mg.) and thiourea (30 mg.) in pyridine (1 ml.) was heated in a water bath for 2 hr., by which the whole dissolved to form a dark red solution. The pyridine was evaporated, 6 N hydrochloric acid (0.5 ml.) was added to the residue, and the brown precipitate so formed was collected. The solid was warmed in benzene and the mixture was filtered. The evaporation of the benzene left pale yellow powder, whose sublimation in reduced pressure afforded a trace of 3-bromotropolone.

The author wishes to express his deep gratitude to Professor Shuichi Seto for his kind guidance and encouragement throughout this work, and to Dr. Yusaku Ikegami and Dr. Shingo Matsumura for their helpful advice. 3-Isopropyltropolone was graciously furnished by the Takasago Perfumery Co., Ltd., and a part of the expenses was defrayed by Sankyo Co., Ltd., to whom the author is deeply indebted.

The Chemical Research Institute of Non-Aqueous Solutions
Tohoku University
Katahira-cho, Sendai

σ Electronic Structures and Some Physicochemical Properties of Halogenated-conjugated Hydrocarbons

By Keiji MOROKUMA, Kenichi FUKUI, Teijiro YONEZAWA and Hiroshi KATO

(Received September 6, 1962)

Researches of the electronic structures of large organic compounds have been carried out, with the molecular orbital and the valence bond methods, almost exclusively on the electronic states of conjugated molecules; these examinations have dealt with electronic spectra, chemical reactivities, π dipole moments and so on. In these discussions no attention has been paid to the behavior of σ electrons in making an unchangeable framework for π electrons to move on. However, some of the physicochemical properties—σ moments, coupling constants *eqQ* in PQR spectra, proton shifts in NMR spectra, etc.—cannot be interpreted theoretically without an explicit consideration on the σ electronic structures.

Recently, in order to discuss the σ electronic structures of conjugated compounds, the present authors have developed a simple molecular orbital method which had previously been successfully adopted for the computation of the electronic structures of saturated hydrocarbons and their derivatives[1-3]; they have published some results of their calculations on the σ electrons of aromatic and olefinic hydrocarbons[4]. In this paper a numerical calculation is performed on the σ electronic structures of halogenated olefins and benzenes, and on this basis the *eqQ* of halogens and the dipole moments of these compounds are discussed.

It would be interesting to compare this paper's calculated results on conjugated halides with those on saturated halides in Refs. 2 and 3.

Method of the Calculation and Evaluation of Parameters

The method of the theoretical calculation of the σ electronic structures of conjugated systems was explained in detail in Ref. 4. In this paper, therefore, it will be repeated only

1) K. Fukui, H. Kato and T. Yonezawa, This Bulletin, **34**, 442, 1111 (1961).
2) K. Fukui, T. Yonezawa and H. Kato, *Progress Reports on Electronic Processes in Chemistry*, 3, 55 (1961).
3) T. Yonezawa, H. Kato, H. Saito and K. Fukui, This Bulletin, **35**, 1814 (1962).
4) K. Fukui, H. Kato, T. Yonezawa, K. Morokuma, A. Imamura and C. Nagata, ibid., **35**, 38 (1962).

briefly. Molecular orbitals are linear combinations of all σ atomic orbitals (LCAO) of all the atoms present—sp^2 hybridized orbitals of carbons, 1s orbitals of hydrogens, and σ atomic orbitals of halogens. Electronic interactions and overlap integrals are completely disregarded. The parameters of the Coulomb and of the resonance integrals employed are given in Table I. Those for carbon atoms and for hydrogen atoms are the same as were given in Ref. 4. The Coulomb integrals for halogen atoms have been chosen so as to fit Mulliken's electronegativity scale and to be consistent with the integrals in saturated compounds, and the resonance integrals between carbon and halogen have been proportionated to the overlap integrals of the bonds.

The effects of the variation of parameters and those of neglecting overlap integrals will be discussed in the following paragraphs.

TABLE I. PARAMETERS OF COULOMB AND RESONANCE INTEGRALS OF σ AO's

Coulomb integral: q_{rr}*		Resonance integral: q_{rs}**	
C_{sp^2}	0	C_{sp^2}–C_{sp^2} (σ bonding)	1
		C_{sp^2}–C_{sp^2} (on the same carbon) m	$\equiv 0.38$
H	−0.2	C_{sp^2}–H	0.94
F	0.7	C_{sp^2}–F	0.45
Cl	0.3	C_{sp^2}–Cl	0.6
Br	0.25	C_{sp^2}–Br	0.5
I	0.2	C_{sp^2}–I	0.45

* Coulomb integral α_r is expressed as follows:

$$\alpha_r = \alpha + q_{rr}\beta$$

where α and β are the standard Coulomb and the standard resonance integrals in sp^2 system.

** Resonance integral β_{rs} is expressed as follows:

$$\beta_{rs} = q_{rs}\beta$$

General Properties of the Results of Calculations

A few examples of the results of our calculations are shown in Tables II and III and in Figs. 1, 2, 3 and 4. The general propeties of these results for halogenated conjugated systems may be summarized as follows:

1) As is seen in Tables I and II and Fig. 1, each orbital has a large distribution on two certain atomic orbitals which form a bond. This tendency seems to reflect the localized nature of the σ electrons.

2) The lowest unoccupied σ orbital of halides lies much lower than that of mother hydrocarbons, and it is localized on carbon-halogen bonds with a negative and large (in magnitude) bond order. Moreover, the lowering of the level becomes more and more notable with the increased number of halogen atoms. This result comes from the electronegativity of the halogen atoms and the small overlap (the small absolute value of the resonance integral) between the carbon and the halogen.

3) The electronegativity of the halogen atoms causes them to attract a considerable amount of electron density to the carbon-halogen (C–X) bonds from other near-by bonds, so that the sum of the σ charge density

TABLE II. CALCULATED σ ELECTRONIC STRUCTURE OF VINYLIDENE CHLORIDE

	Symmetry*	Energy** λ_j	Electron distribution on each AO***					
			H_1	C_2	C_3	C_4	C_5	Cl_6
Unoccupied	10 S	−1.2765	0.05763	0.07558	0.36551	0.31672	0.02242	0.00325
	9 A	−1.2143	0.22617	0.27383	0	0	0	0
	8 S	−0.8173	0.24699	0.10654	0.04037	0.16999	0.03205	0.00924
	7 A	−0.7296	0	0	0	0	0.37325	0.12675
	6 S	−0.2285	0.02004	0.00002	0.11787	0.00668	0.18248	0.23519
Occupied	5 S	+0.6387	0.05870	0.04673	0.20443	0.20529	0.04585	0.14386
	4 A	+0.6496	0	0	0	0	0.12675	0.37325
	3 A	+0.6543	0.27383	0.22617	0	0	0	0
	2 S	+1.0866	0.07398	0.13858	0.00037	0.06859	0.15991	0.09305
	1 S	+1.4570	0.04266	0.13255	0.27145	0.23274	0.05729	0.01541

* Symmetry about the C–C axis

** λ_j is the coefficient in $\varepsilon_j = \alpha + \lambda_j\beta$, where ε_j is the jth molecular orbital energy.

*** Nomenclature of AO's:

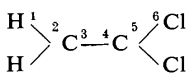

And $(C_{ir})^2$ is given in the table.

on the bond (the σ bond density) exceeds 2 and the net charge on the bond becomes negative.

4) Because of the polarity of a C–X bond, X being negative and C being positive, a similar but weakened polarity is caused in adjacent

TABLE III. CALCULATED σ ELECTRONIC STRUCTURE OF TETRACHLOROETHYLENE

	Symmetry	Energy λ_i	Electron distribution on each AO**		
			Cl_1	C_2	C_3
Unoccupied	A	−1.2131	0.00523	0.03326	0.42302
	AA	−0.7296*	0.12675	0.37325	0
	S	−0.3690	0.10267	0.12766	0.03934
	A	−0.1286	0.14669	0.07484	0.05693
Occupied	S	+0.6395	0.12307	0.03939	0.17506
	AA	+0.6496*	0.37325	0.12675	0
	A	+1.0217	0.09808	0.14189	0.02005
	S	+1.4096	0.02425	0.08295	0.28560

* Doubly degenerate orbital being localized on C-Cl bonds

** Nomenclature of AO's:

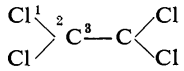

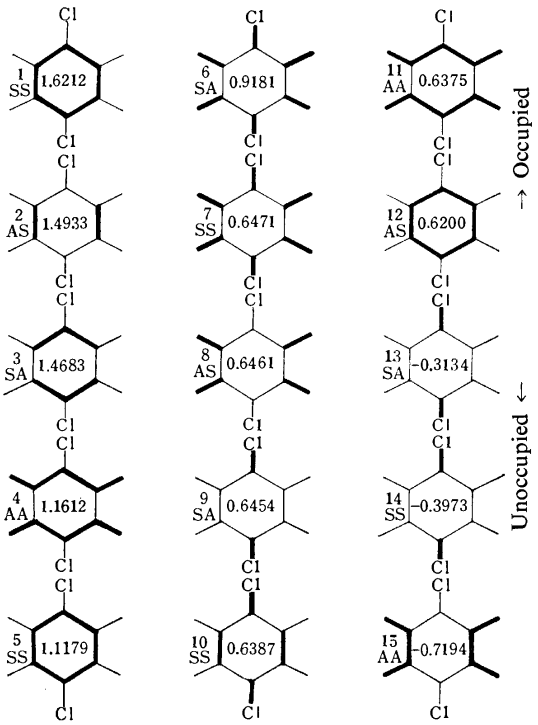

Fig. 1. The σ electron distribution and energy λ_i of some MO's in *p*-dichlorobenzenes (thick lines denote the most densely populated bonds).

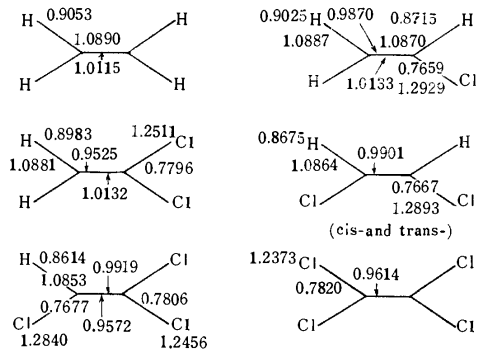

(a) σ Electron density on each AO

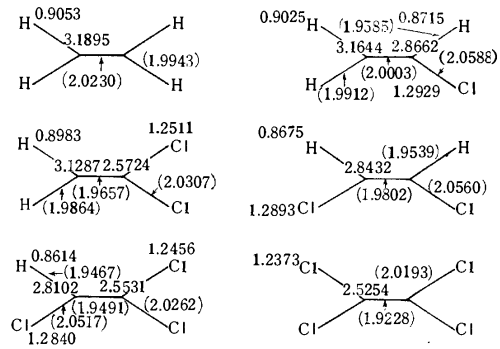

(b) Total σ electron density on each atom and bond σ density (in parentheses)

Fig. 2. Electron distributions of ethylene and chloroethylenes.

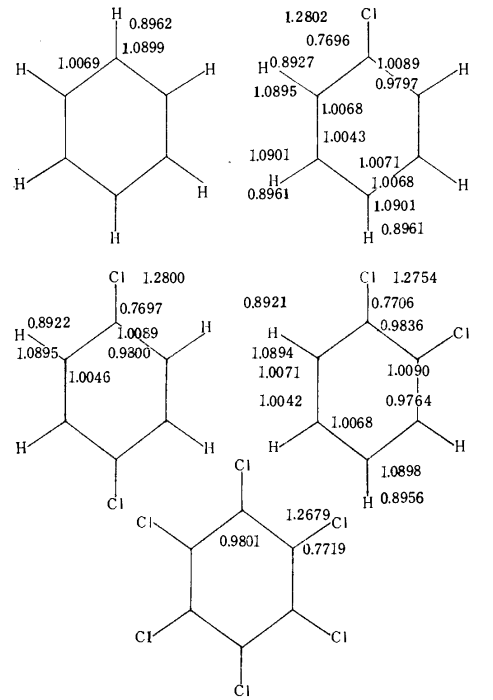

Fig. 3. Total σ electron density of benzene and chlorobenzenes.

TABLE IV. CALCULATED σ ELECTRONIC STRUCTURE OF HEXACHLOROBENZENE

	j	Symmetry xy	Energy λ_j	Electron distribution on each AO		
				Cl_1	C_2	C_3(ring)
Unoccupied	24	AA	−1.38000	0	0	0.08333
	22, 23	SA, AS	−1.27825	0.00209	0.01448	0.15838
	20, 21	SS, AA	−1.08869	0.01299	0.06956	0.12539
	19	SA	−1.01172	0.01128	0.05391	0.05074
	18	SS	−0.56479	0.05150	0.10699	0.00408
	16, 17	SA, AS	−0.52114	0.10496	0.19659	0.01589
	14, 15	SS, AA	−0.34699	0.11312	0.13154	0.04434
	13	SA	−0.15872	0.07009	0.04097	0.02780
Occupied	12	AS	+0.62000	0	0	0.08333
	10, 11	SS, AA	+0.63931	0.16148	0.05164	0.06011
	8, 9	SA, AS	+0.64524	0.21223	0.07026	0.02542
	7	SS	+0.64622	0.11026	0.03671	0.00985
	6	SA	+0.85044	0.08529	0.07178	0.00479
	4, 5	SS, AA	+1.09637	0.04575	0.08059	0.10350
	2, 3	SA, AS	+1.45415	0.01405	0.05200	0.13364
	1	SS	+1.59857	0.00490	0.02296	0.06940

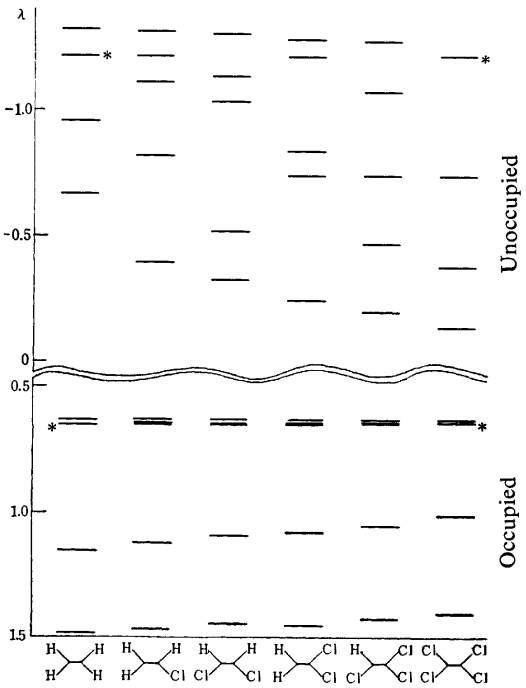

Fig. 4. σ Energy levels of ethylene and chloroethylenes. (*: Doubly degenerate)

C–C bonds and is transmitted to farther bonds with, however, a rapid decrement.

Results 3 and 4 seem to correspond to the so-called inductive effect in organic chemistry.

Effects of Parameters.—In order to see the effects of parameters on the results, some calculations on various compounds have been carried out with varied parameters; a few examples are shown in Tables V and VI. For the sake of brevity, only a summary of the calculated results will be given here. A change in the Coulomb integral of chlorine atoms causes a change in their σ electron density; the bond moment of the C–Cl bond is well explained with its value near 0.3 (as has been adopted) or less, though its influence is little on the qualitative results of calculation.

Effects of Overlap Integrals.—In σ electron systems where neighboring atomic orbitals are mutually deeply overlapping, the neglect of

TABLE V. VARIATION OF PARAMETERS (1)

1,2-Dichloroethylene

q_{Cl}	q_{Cl}	q_H
0.25	1.2488	0.8721
0.28	1.2733	0.8692
0.30	1.2893	0.8675

Vinyl chloride

q_{Cl}	q_{Cl}	q_{H1}	q_{H2}
0.25	1.2522	0.8754	0.9028
0.28	1.2765	0.8730	0.9027
0.30	1.2929	0.8715	0.9025
0.32	1.3088	0.8699	0.9024

TABLE VI. VARIATION OF PARAMETERS (2): CHANGE OF q_{Cl}

q_{Cl}	m	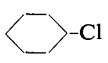	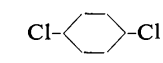	
0.6	0.38	1.2802	1.2800	1.2754
0.6	0.42	1.2914	1.2910	1.2851
0.6	0.45	1.3010	1.3005	1.2935
0.8	0.42	1.2206	1.2205	—

TABLE VII. ELECTRON DISTRIBUTION OF TETRACHLOROETHYLENE WITH OVERLAP INCLUDED

Energy λ_i	Electron distribution (a)**					Electron distribution (b)***		
	Cl_1	C_2Cl_1	C_2	C_3	C_3C_4	Cl_1	C_2	C_3
+0.42935	0.10799	0.03193	0.01115	0.11179	0.17216	0.12395	0.02712	0.19787
+0.47204*	0.30954	0.12796	0.06250	0	0	0.37352	0.12648	0
+0.76116	0.03989	0.06772	0.13586	0.05683	−0.08752	0.07375	0.16972	0.01307
+0.90885	0.00814	0.02505	0.09111	0.14205	0.21875	0.02066	0.10363	0.25143
q	0.93109	0.50531	0.60123	0.62134	0.60678	1.18375	0.85389	0.92473

* Doubly degenerate orbital

** Electron distribution on the atom A is $(C_{iA})^2$, while on the bond AB it is calculated as $2C_{iA}C_{iB}S_{AB}$.

*** In this calculation distribution on the bond AB is divided by two and added to those on the atom A and on the atom B.

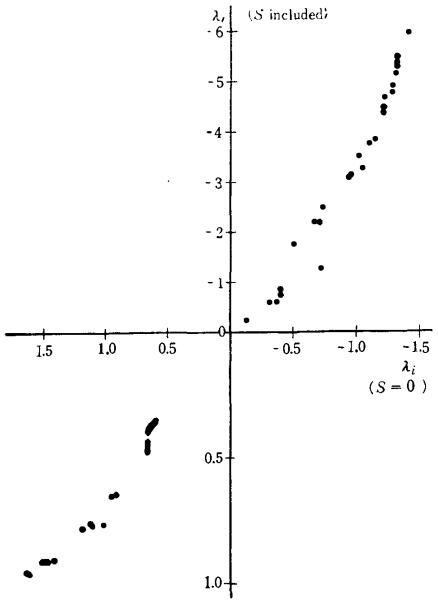

Fig. 5. Energy levels with overlap included and neglected.

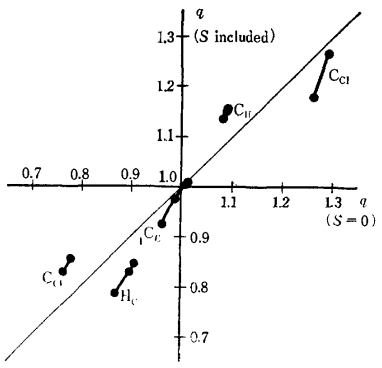

Fig. 6. Total σ electron densities on each kind of AO's with overlap included and neglected (C_H, for example, denotes the carbon AO in a C-H bond.).

the overlap integrals might lead to an erroneous conclusion, even in a qualitative sense. Therefore, some computations have been performed with the inclusion of overlap integrals between adjacent atoms, which have been settled as follows:

$$S_{CH}=0.72$$

$$S_{CC}=0.77$$

$$S_{CCl}=0.46$$

Results with respect to ethylene, 1, 2-dichloroethylene, tetrachloroethylene, benzene and *p*-dichlorobenzene, as shown in Table VII and Figs. 5 and 6, indicate that those energy levels with overlap included are almost completely parallel to those with overlap neglected and that the occupied levels of the former come near to α_σ, while unoccupied levels flee from α_σ. As for the σ electron density, on the basis of Fig. 6, those on similar atomic orbitals on similar bonds (for instance, carbons' AO's on C-Cl bond, as is expressed by C_{Cl} in the figure) very parallel with each other, leading also to an unvaried qualitative conclusion in both calculations.

Dipole Moments

The dipole moment of conjugated compounds is composed of the σ moment and the π moment. Most of the theoretical works have been concerned with only the π moment till now, and in those cases the σ moment was empirically estimated on the basis of bond moments which are assumed to be constant in a series of compounds. In this paragraph, the σ moment of each compound is evaluated by the use of the σ electron distribution given in the tables and the figures. In the evaluation, all the bond angles are assumed to be 120°; the C–Cl bond length, 1.70 Å; C–H, 1.08 Å; C–C (aromatic) 1.40 Å, and C–C (olefinic) 1.34 Å, and the displacement of the center of the charge distribution is taken into

Table VIII. Dipole moments of chloroethylenes (in units of Debye)

Substituent	Calculated			Observed
	σ Moment	π Moment	Total Moment	
Cl	1.84	0.36	1.47	1.44
1,2-di-Cl(cis)	3.20	0.65	2.55	1.74
1,1-di-Cl	1.81	0.34	1.47	1.30
tri-Cl	1.84	0.37	1.47	0.94

Table IX. Dipole moments of chlorobenzenes

Substituent	Calculated			Observed
	σ Moment	π Moment	Total Moment	
Cl	1.69	0.31	1.39	1.57
o-di-Cl	2.96	0.54	2.41	2.25

account by 0.46 Å in an sp^2 hybridized orbital of carbon and by 0.44 Å in a σ orbital (the s character of 15% is tentatively assumed) of chlorine.

The σ moments obtained are tabulated in Tables VIII and IX, together with the π moments calculated in the simple LCAO MO approximation with parameters $\alpha^{\pi}_{Cl}=\alpha_{\pi}+1.8\beta_{\pi}$, $\alpha^{\pi}_{C'}=\alpha+0.18\beta_{\pi}$ and $\beta_{CCl}=0.8\beta_{\pi}$, where α_{π} and β_{π} are the standard Coulomb and the standard resonance integrals in the π electron systems, and with the calculated total moments compared with the observed dipole moments.

Generally speaking, the calculated moments are larger than observed ones; this may be attributed to the choice of parameters and also to a disregard of the σ overlaps. However, a calculated σ moment does not seem to be a simple vector sum of bond moments. A part of the so-called ortho effects—a deviation from the additivity of bond moments in ortho-disubstituted compounds—may be understood on the basis of this result. However, the extremely small moment of trichloroethylene cannot so be explained, probably due to the roughness on the electronic repulsions between the neighboring polar groups. On these problems a theoretical paper would be published in the near future[5].

The Coupling Constant of Halogen in the PQR Spectra

In chlorides, bromides and iodides the coupling constants, eqQ, of halogen nuclei are observed in pure nuclear quadrupole resonance (PQR) spectroscopy. In conjugated chlorides these constants are connected to the σ electron density, q^{σ}_{Cl}, and to the π electron density, q^{π}_{Cl}, on the chlorine atom by the following equation:

$$eqQ=\left(\frac{q^{\pi}_{Cl}+2}{2}-q^{\sigma}_{Cl}\right)eqQ_{atom} \qquad (1)$$

where the eqQ_{atom} is the coupling constant of an atomic chlorine and is set at 109.7 Mc. In Eq. 1 the orbital of chlorine is assumed to be a pure p orbital. If the s character of the orbital is considered to be s%, eqQ is given by Eq. 2 instead of Eq. 1:

$$eqQ=\left[\frac{q^{\pi}_{Cl}+2}{2}-q^{\sigma}_{Cl}-\frac{s}{100}(2-q^{\sigma}_{Cl})\right]eqQ_{atom} \qquad (2)$$

By adopting the π and the σ electron densities calculated in previous paragraphs in Eq. 1, the values of eqQ shown in Tables X and XI are obtained; their parallelism with the experimental values seems to be sufficient.

The difference in the calculated coupling constants among chlorobenzenes is unexpectedly small. As the coupling constants of these compounds were experimentally determined from the resonance spectra in the solid state, a part of this discrepancy may be attributed to the effects of crystal fields, which in some other cases might change the constant by 0.8 Mc[6]. The difference is also probably due in

Table X. Chlorine coupling constants in PQR of chloroethylenes

Substituent	Calculated			Observed eqQ
	q^{π}_{Cl}	$q_{Cl^{\sigma}}$	eqQ	
Cl	1.955	1.298	75.1 Mc	67.2 Mc 70.2(gas)
1,2-di-Cl	1.955	1.289	75.6	70.0(cis) 71.2(trans)
1,1-di-Cl	1.956	1.251	79.8	78.7(gas)
tri-Cl	1.956 1.954	1.246 1.284	80.3 76.0	— —
tetra-Cl	1.955	1.237	81.3	77.2

Table XI. Chlorine coupling constants in PQR of chlorobenzenes

Substituent	Calculated			Observed[a] eqQ
	$q_{Cl^{\pi}}$	$q_{Cl^{\sigma}}$	eqQ	
Cl	1.96200	1.28022	76.9Mc	69.2Mc
p-di-Cl	1.96188	1.28000	76.9	69.6
o-di-Cl	1.96166	1.27540	77.4	71.5
hexa-Cl	1.96126	1.26793	78.2	76.8

a) P. J. Bray, R. G. Barnes and R. Bersohn, *J. Chem. Phys.*, **25**, 813 (1956).

5) K. Fukui and K. Morokuma, to be published.

6) In the case of chloroalkanes: H. O. Hooper and P. J. Bray, *J. Chem. Phys.*, **33**, 334 (1960).

part, however, to the crudeness of our approximation in calculating molecular orbitals. On the approximation of this calculation, some discussions will be published in the future[5].

Other Problems

Interesting relations between the electronic structures and the potential of polarographic reduction of conjugated halides have also been found and will be presented in a separate paper[7].

The proton chemical shifts of these halides in NMR spectra will be discussed in connection with σ electron distributions in another paper[8].

Summary

The simple LCAO MO method previously developed by the present authors has been adopted to the calculation of the σ electronic structures—σ molecular orbitals, their energies, separate and total σ electron densities, etc.—of conjugated halides. The general results of the computation—the so-called inductive effects along σ bonds, the unoccupied levels with the very low energy which is characteristic to halides, and so forth—have been described. Sigma dipole moments and the coupling constants in PQR have been calculated with the σ electron densities obtained and discussed in comparison with the experimental values.

The numerical calculations were carried out on the digital computer KDC-I of Kyoto University.

Faculty of Engineering
Kyoto University
Sakyo-ku, Kyoto

7) K. Fukui, K. Morokuma and H. Kato, This Bulletin in press.
8) T. Tonegawa and K. Fukui, to be published.

The Concentration of Molecular Hydrogen on the Platinum Cathode

By Shigeo SHIBATA

(Received September 6, 1962)

It has previously been shown[1] that the concentration of hydrogen, ${}_0C_{H_2}$, in the immediate vicinity of the cathode during the passage of a current could be estimated by analyzing the potential-time curve which had been obtained when the cathodic current polarizing the electrode was abruptly reversed into a steady anodic one.

In the present work, ${}_0C_{H_2}$ was determined as a function of the cathodic current density by the following two different methods:

1) If the diffusion of hydrogen is the rate-determining stage in the anodic ionization process of the molecular hydrogen in the solution, ${}_0C_{H_2}$ can be estimated by the use of Sand's equation[2]:

$$ {}_0C_{H_2} = i_a \tau^{1/2} / F\pi^{1/2} D^{1/2} \qquad (1) $$

where τ is the transition time of the horizontal portion of the steady potential appearing at the first stage of that potential-time curve, F is a Faraday, D is the diffusion coefficient of the hydrogen molecule in the solution, and i_a is the anodic polarizing current density.

When, in addition to the diffusion, the spontaneous expellant of hydrogen from the solution as bubbles of gas is also contributable, ${}_0C_{H_2}$ can be written as[1]:

$$ {}_0C_{H_2} = \frac{i_a}{2FD^{1/2}k^{1/2}} \exp(k\tau)\,\mathrm{erf}(k^{1/2}\tau^{1/2}) \qquad (2) $$

where k is a expellant rate constant of the hydrogen from the solution. It is assumed that the rate of expellant is proportional to the supersaturation.

2) The polarization, or departure from the reversible potential, observed during the discharge of hydrogen ions at the electrode is generally considered to be due to the following effects[3,4]: a discharge overpotential of hydrogen ions η_D[5]; a recombination overpotential

1) S. Shibata, This Bulletin, **33**, 1635 (1960).
2) H. J. S. Sand, *Phil. Mag.*, **1**, 45 (1901).
3) P. M. Bryant and C. E. Coates, *Discussions Faraday Soc.*, **1**, 115 (1947).
4) R. Clamroth and C. A. Knorr, *Z. Elektrochem.*, **57**, 399 (1953).
5) M. Breiter and R. Clamroth, ibid., **58**, 493 (1954).

of hydrogen atoms, η_R[5-8]; the ohmic fall of resistance between the working electrode and the tip of a fine capillary connecting with the reference electrode, η_Ω[4]; a concentration overpotential of hydrogen ions, η_{H^+}[5,9] and a concentration overpotential of hyrogen molecules, η_{H_2}[5,10]. When the current is cut off, the overpotentials η_D, η_R and η_Ω should disappear at once, while η_{H^+} and η_{H_2} decay only slowly[3,11]. Moreover, in the acidic electrolyte the value of η_{H^+} is so small that it can be disregarded except in the cases of very large electrolytic currents[5,9]. The overpotential which is still contributable after the current of a moderate intensity has been cut off may be η_{H_2} only. Clamroth and Knorr[4] attempted to measure the concentration overpotential ${}_0\eta_{H_2}$ during the passage of current, free from the effect of the other kinds of overpotential, by extrapolating to zero time the decay curve of η_{H_2}, taken after the circuit had been opened. They could also obtain ${}_0\eta_{H_2}$ by means of extrapolating the $m_{H_2}-\eta_{H_2}$ curve to the zero volume of m_{H_2}, where m_{H_2} is the amount of hydrogen gas evolved for the time elapsed since the cut off of the current; it has a linear relation with η_{H_2} observed at the same time. Though their results obtained are reliable for low current experiments, they are not reliable for high current experiments, because the rates of overpotential decay and of H_2 gas evolution are so rapid that their manual potentiometric or microvolumetric technique surely never could follow them. The present author has therefore attempted to obtain a reasonable way of measuring ${}_0\eta_{H_2}$ at high currents, i_k, by means of oscilloscopic observation of the overpotential. The relation of the concentration overpotential, ${}_0\eta_{H_2}$, and the activity, ${}_0a_{H_2}$, of the hydrogen is, according to Nernst's equation, as follows:

$$ {}_0a_{H_2} = a_{H_2}{}^0 \exp\{-(2F/RT)\cdot {}_0\eta_{H_2}\} \qquad (3) $$

where $a_{H_2}{}^0$ is the activity of hydrogen in the solution which is in contact with hydrogen gas at 1 atm. pressure. Since the hydrogen behaves ideally even under high pressure[12,13], the activity can be replaced by the concentration.

Experimental

Measurement of the Potential-time Curve.—The electrical circuit used for reversal of the current through the cell, from cathodic to anodic, is shown in Fig. 1. It is fundamentally the same as that used in the previous work[1], except for modification by the addition of an appropriate switching arrangement. Instead of a mechanical switch, a cyratron was used for the sake of a quick raising of the current following the reversal. The change of the working electrode potential against an S. C. E. was recorded with a cathode-ray oscilloscope (Iwasaki Synchroscope, Model SS-5151) synchronized with the reversal of current direction.

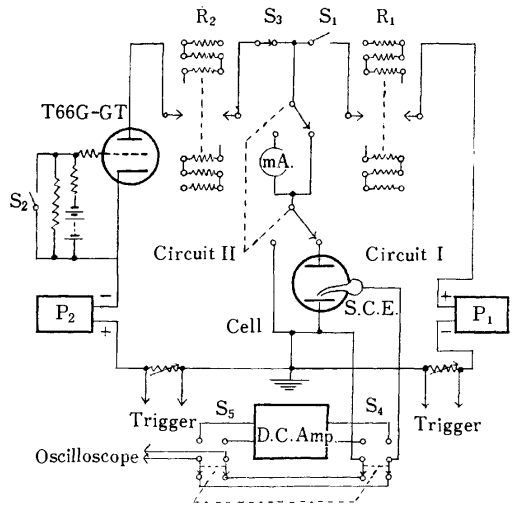

Fig. 1. Circuit diagram.

Measurement of the Decay Curve of η_{H_2}.—In order to measure the decay curves, circuit I was used, circuit II being excluded. A constant cathodic current, i_k, was passed through the cell, sufficient time being allowed for the potential to become constant; the circuit was then opened, and the decay curve was photographed with the cathode-ray oscilloscope synchronized with the cut-off of the current. As the amount of the concentration overpotential was too small for direct oscilloscopic measurement, a d. c. vacuum-tube amplifier was used in order to detect it. The value of ${}_0\eta_{H_2}$ on the cathode was obtained by extrapolating the decay curve to zero time; the constant, k, in Eq. 2 was obtained from the slope of the curve.

The cell used for the experiment is shown in Fig. 2. The working electrode A, bright platinum wire 1 cm. in length and 0.05 cm. in diameter, the end of which had been covered with a small glass ball to prevent edge effect of the discharge, was placed vertically in the solution. B is an auxiliary electrode consisting of a cylindrical platinum foil of a large area, on the center-line of which the working electrode had been fixed in order to ascertain the uniform current density over the surface of the working electrode. A platinized platinum plate C is a hydrogen gas electrode used as a reference electrode immersed in the experimental solution. The difference in potential between A

6) E. Lange, ibid., **58**, 83 (1954).
7) K. J. Vetter, ibid., **56**, 931 (1952).
8) G. Falk and E. Lange, ibid., **54**, 132 (1950).
9) M. Breiter, ibid., **62**, 161 (1958).
10) L. Kandler, C. A. Knorr and M. Schweitzer, *Z. physik. Chem.*, **180A**, 281 (1937).
11) G. Falk and E. Lange, *Z. Elektrochem.*, **54**, 132 (1950); **55** 396 (1951).
12) W. R. Hainsworth, *Science*, **53**, 578 (1921).
13) G. Tammann and H. Dickmann, *Z. anorg. u. allgem. Chem.*, **150**, 129 (1926).

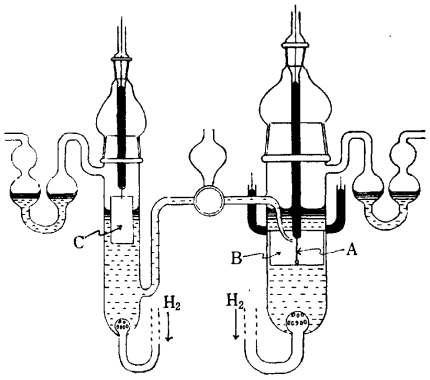

Fig. 2. Electrolysis cell.

and C gives the overpotential directly. The solution was saturated with hydrogen passing through two inlets made at the bottom of each chamber. Prior to use, the working electrode was activated by means of anodic and subsequent cathodic polarizations[14]. The sulfuric acid solution (1 N) used as the electrolyte throughout was prepared with G. R. sulfuric acid and with conductivity water which had been carefully redistilled thrice with a silica still.

All experiments were carried out in a thermostat at a temperature of 25±0.1°C.

Results and Discussion

The Hydrogen Concentration Evaluated from the Transition Time.—Provided that Sand's Eq. 1 is applicable to the anodic process after the reversal of the current, the value of $i_a\tau^{1/2}$ for the given i_k should be constant, independent of i_a. As is seen in Fig. 3, however, the value of $i_a\tau^{1/2}$ was affected considerably by the strength of the anodic polarizing current. Thus, the value of $i_a\tau^{1/2}$ for the given i_a value passed through a maximum at a certain i_k value which is larger because of a higher i_a value. Further, the height of this maximum decreased with the increasing value of i_a untill it vanished when i_a exceeded some definite value. The appearance of such a maximum on the curve may be attributed to the removal of the accumulated hydrogen during τ by the agitation of the solution due to the bubbling of the evolved hydrogen gas. At a low i_k value, the effect of this removal would not be very large, so that the accumulation of deposited hydrogen would be increased with an increasing value of i_k. At a large i_k value, however, the amount of the hydrogen ionized during τ may be rather decreased by increasing stirring. The magnitude of $i_a\tau^{1/2}$ at a given i_k value should grow and finally tend to a limiting value according as the i_a value increases, since the transition time, τ, becomes so short that the effect of stirring is very much diminished during that time. Furthermore, as a cause of the reduction of the transition time, τ, we must call attention to the spontaneous expulsion of hydrogen from the solution due to supersaturation. The curves in Fig. 3 are subject to the influence of both the stirring and the expulsion. For the above-mentioned reason, the correct values of ${}_0C_{H_2}$ at a given i_k value must be evaluated from τ_0, the limiting value of the transition time obtained at a sufficiently large i_a value. Figure 4 shows plots of the concentration of hydrogen, calculated with Eq. 1 and Eq. 2, against i_k for various values of i_a. Since in the range of small i_k values under about 10 mamp./cm² and of large i_a values over about 30 mamp./cm² (cf. Fig. 4.), the value of $i_a\tau^{1/2}$ for a given i_k value is constant, independent of the magnitude of the i_a value, the disturbance, by the expulsion of hydrogen and the agitation, of the solution in relation to the transition time obtained in this range of i_k and i_a values is so small that it can be disregarded. The concentrations calculated with Eq. 2, being little affected by the strength of i_a, may be considered to be the true concentrations of ${}_0C_{H_2}$. These values at higher i_k values were evaluated with a τ_0 value obtained at a large anodic polarization current, i_a=634 mamp./cm².

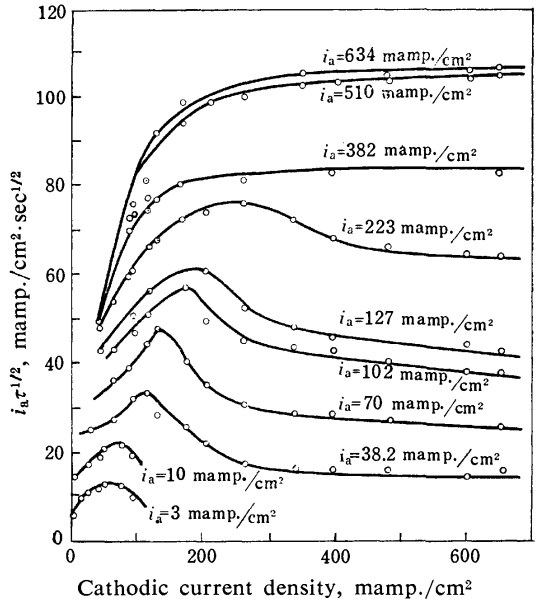

Fig. 3. $i_a\tau^{1/2}$ vs. cathodic current density curves at constant anodic polarizing current densities.

14) J. A. V. Butler and G. Armstrong, *J. Chem. Soc.*, **1934**, 743; E. Wiek and B. Webrus, *Z. Elektrochem.*, **56**, 159 (1952); J. O'M. Bockris, I. A. Ammar and A. K. M. S. Huq, *J. Phys. Chem.*, **61**, 879 (1957); T. Erdey-Gruz and M. Volmer, *Z. physik. Chem.*, **A150**, 203 (1930); J. O'M. Bockris and I. A. Azzam, *Trans. Faraday Soc.*, **48**, 154 (1952); E. Yeager, T. S. Oey and F. Hovorka, *J. Phys. Chem.*, **57**, 268 (1953).

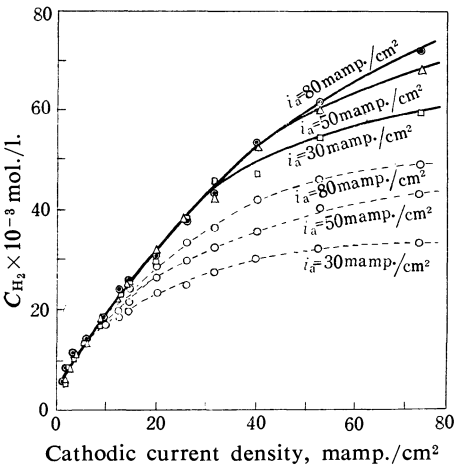

Fig. 4. The hydrogen concentration evaluated with Eq. 1 (dotted line) and with Eq. 2 (solid line).

Relation of the Cathodic Current and the Concentration Overpotential of the Hydrogen.— When, after the cut-off of the cathodic current through the working electrode, the solution in the cell was suddenly stirred with bubbles of hydrogen gas, the overpotential decayed rapidly and settled down on the reversible potential, i. e., on $\eta_{H_2}=0$, as is shown in Fig. 5. This fact is an illustration of how the overpotential is caused by the accumulation of hydrogen and of how the rapid decay, following the bubble agitation, is attributable to the almost

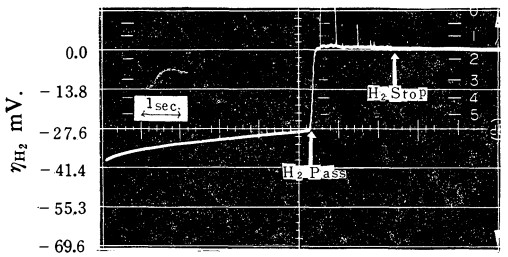

Fig. 5. Oscillogram of the overpotential change when, after the cut off of the cathodic current, $i_k=7.0$ mamp./cm², the solution was stirred with bubbles of hydrogen gas.

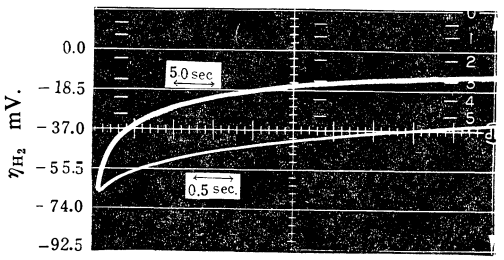

Fig. 6. Oscillograms of the overpotential decaying after the cut off of the cathodic current, $i_k=92.4$ mamp./cm².

complete removal of the accumulated hydrogen. Figures 6 and 7 show oscillograms tracing the decay of η_{H_2} taken after the cut-off of the cathodic current. The potential falls down rapidly at first, but at last tends only slowly to zero. As the initial, short part of the decay curve, as seen in Fig. 7, can be taken to be a straight line, it could be exactly extrapolated to zero time ; ${}_0\eta_{H_2}$ was obtained. As may be seen in Fig. 8, ${}_0\eta_{H_2}$ increases linearly with the logarithm of the cathodic current density, but at last tends to a constant value of 64.5±0.5 mV. as the current density exceeds about 300 mamp./cm².

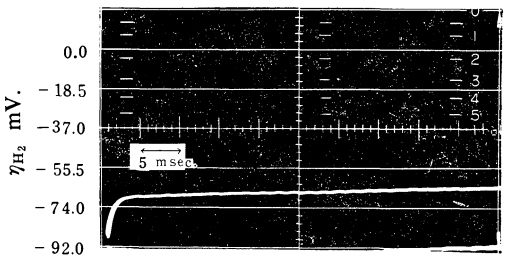

Fig. 7. Oscillogram of the overpotential decaying immediately after the cut off of the cathodic current, $i_k=92.4$ mamp./cm².

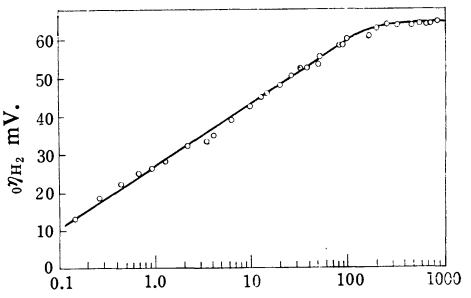

Fig. 8. Relation between the cathodic current density and concentration overpotential of hydrogen.

The concentrations of ${}_0C_{H_2}$ obtained by means of the potential-time curve, together with that obtained from the concentration overpotential, are shown in Fig. 9, the solubility of hydrogen at 1 atm. $C_{H_2}{}^0$ being taken to be 7.24×10^{-4} mol./l.[15] The agreement between the results for ${}_0C_{H_2}$ derived from τ_0 and from ${}_0\eta_{H_2}$ is seen to be satisfactory. The limiting value of ${}_0C_{H_2}$ was 11.6×10^{-2} mol./l. Such a high supersaturation may be ascribed to the fact that the process of the evolution of hydrogen as bubbles of gas may be relatively slow. The rate of the transfer of hydrogen molecules from the solution to the gas phase should be proportional to the product of the

15) A. Seidell, "Solubilities of Organic and Inorganic Compounds", Van Nostrand Co., New York (1940). p. 557.

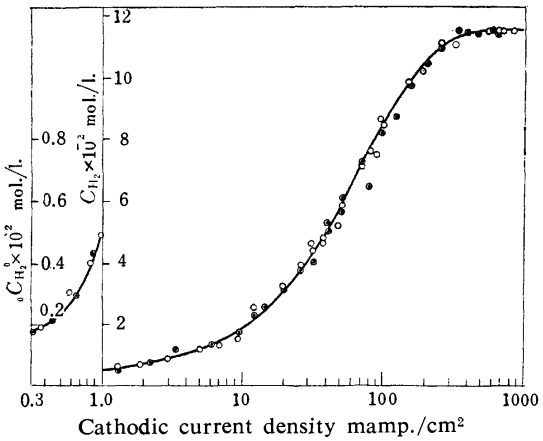

Fig. 9. Relation between the cathodic current density and the concentration of hydrogen in the vicinity of the electrode surface.
—○— from $_0\eta_{H_2}$
—⊙— from τ_0

density of the distribution of bubbles and the rate of growth of each bubble. If the rate of the formation of growth nuclei is represented with the equation described by Hook[16] and if the rate of growth is proportional to $_0C_{H_2}-C_{H_2}^0$, the rate of the transfer of hydrogen, V, may be given by the expression:

$$V=K'C_{H_2}^0(\alpha-1)\cdot K''\exp\left[-\frac{16\pi M^2\sigma^3}{3d^2R^3T^3\ln^2\alpha}\right] \quad (4)$$

where α is the supersaturation as a concentration ratio, $_0C_{H_2}/C_{H_2}^0$; K', a rate constant of the growth; K'', a frequency factor; σ, an interfacial energy between the solution and hydrogen gas; d, the density of the nucleus; M, the molecular weight of hydrogen; R, the gas constant, and T, the absolute temperature. This expression demands an almost explosive increase in the rate of nucleation, as α exceeds the denfinite real value. It has been confirmed that a limiting value of the supersaturation calculated with Eq. 4 for water vapor was in good agreement with that one obtained experimentally, i.e., $\alpha=4.2$ at 275.2°K[17]. Since the d of gaseous nucleus is far smaller than that of the liquid or solid nuclei, the supersaturation of the gas in the solution may be much larger than the above value of the water vapor and also than the result obtained in the present work. However, the irregularity of the electrode surface may accelerate the formation of nuclei, and agitation and convection of the solution may prevent the high increase of α near the electrode.

16) A. V. Hook, "Crystallization", Reinhold Publishing Co., New York (1961), p. 95.

17) M. Volmer and H. Flood, *Z. physik. Chem.*, 170A, 273 (1934); G. M. Pound, *Ind. Eng. Chem.*, 44, 1278 (1952).

Summary

The concentration of molecular hydrogen in the vicinity of the bright platinum cathode during electrolysis was determined as a function of current density by means of two different methods, the potential-time curve on the reversal of current from cathodic to anodic, and the concentration overpotential obtained by extrapolating the decay curve of the overpotential to zero time, free from other overpotentials. The agreement between the results for the concentration derived from the potential-time curve and from the concentration overpotential was satisfactory. It was found that the concentration of hydrogen increased with the increasing i_k value and approached a limiting value of 11.6×10^{-2} mol./l. for cathodic currents exceeding about $i_k=300$ mamp./cm².

The author wishes to express his hearty thanks to Professor Hiroshi Azumi and Professor Nobuyuki Tanaka of Tohoku University, and to Professor Hiroshi Yoshisaki of Yamagata University for their kind guidance and encouragement.

Department of Chemistry
Faculty of Liberal Arts and Science
Yamagata University
Koshirakawa-cho, Yamagata

*Oxidative Degradation of Polyethylene in Nitrogen Dioxide**

By Taeko OGIHARA

(Received September 18, 1962)

The oxidative degradation of polyethylene in the presence of oxygen has been studied by several investigators[1,2]. Oxygen has been reported to react with polyethylene to form hydroperoxide in the early stages of the process. However, the degradation of polymers by reagents other than oxygen has scarcely yet been studied. Only Beachell and Nemphos[3] have studied the degradation of polyethylene in ozone and in fuming nitric acid. They have reported that, at low temperatures, the effect of nitric acid is principally the molecular chain scission, as is seen from the appearance of the C=C stretching band at 1645 cm^{-1} in the infrared region, while at high temperatures nitration becomes the principal reaction. However, it is questionable whether or not it is correct to assign 1645 cm^{-1} to the C=C stretching band as they have done.

The present author's experiments were made on the oxidative degradation of polyethylene in nitrogen dioxide. The oxygenated groups which were produced in polyethylene were identified by the use of infrared absorption spectrometry. Oxidation mechanisms will also be discussed.

Experimental

The sample used was high pressure polyethylene, a relatively highly-branched polyethylene called Yukalon which is produced by the Mitsubishi Yuka Co., Ltd. Its molecular weight has been determined by viscosity measurement to be 34000. The sample contained no antioxidant.

Nitrogen dioxide was prepared by heating mixtures of lead nitrate and sand at 300°C; it was then dried by passing it through phosphorous pentoxide.

The infrared spectra were recorded with a Perkin-Elmer Model 13, a Perkin-Elmer Model 112, or a Hitachi EPI-S infrared spectrometer equipped with either a sodium chloride prism or a potassium bromide prism for the 4000~400 cm^{-1} region.

A film specimen, about 0.015 mm. thick and 20×45 mm. in area was prepared by hot moulding, mounted on a glass plate, and placed in a Pyrex cylindrical reaction vessel, 26 mm. in diameter and 22 cm. in length. One-third of the atmospheric nitrogen dioxide gas, free from air, was put into the reaction vessel, and this vessel was heated in a silicone bath controlled at 100±0.05°C. After heating, a thin polyethylene film was peeled off and its spectrum was recorded at room temperature within 3 min. after it had been taken out from the vessel.

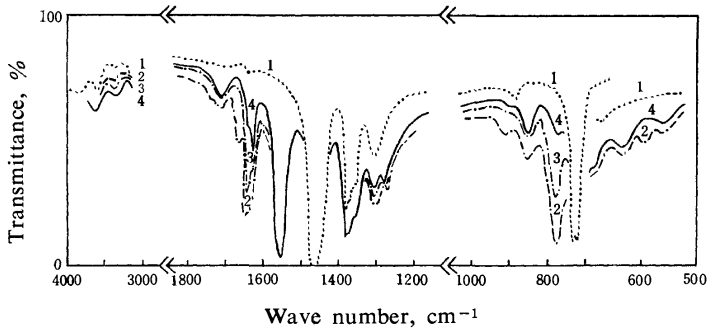

Fig. 1. Infrared spectra of the oxidized polyethylene and their spectral change with the left time in the atmosphere.
1 Original polyethylene
2 Oxidized polyethylene within 3 min. after removal from vessel
3 After 24 hr. in the atmosphere
4 After 2 months in the atmosphere

* Presented at the 15th Annual Meeting of the Chemical Society of Japan, Kyoto, April, 1962.

1) F. M. Rugg, J. J. Smith and R. C. Bacon, *J. Polymer Sci.*, 13, 535 (1954).

2) J. P. Luongo, ibid., 42, 139 (1960).

3) H. C. Beachell and S. P. Nemphos, ibid., 21, 113 (1956).

Results

The experimental results are summarized in Table I, while the characteristic spectra of the oxidized polyethylenes and their spectral changes in accordance with the time they were left in the atmosphere are shown in Fig. 1. According to the spectral changes, the observed bands of oxidized specimens can be divided into four categories, i. e., A, B, C and D.

The bands at 1730, 1300, 900 and 1681 cm^{-1} belong to group A and disappear within 24 hr. when the oxidized film is left in the atmosphere. The bands at 1640, 778 and 600 cm^{-1} belong to group B and disappear within two months. On the other hand, the bands at 3400 and 1713 cm^{-1}, which belong to group C, gradually increase in intensity. The bands at 1554, 1365, 629, 562, 1635, 1280, 852 and 675 cm^{-1}, which fall into group D, did not change. However, when the oxidized film was heated in nitrogen

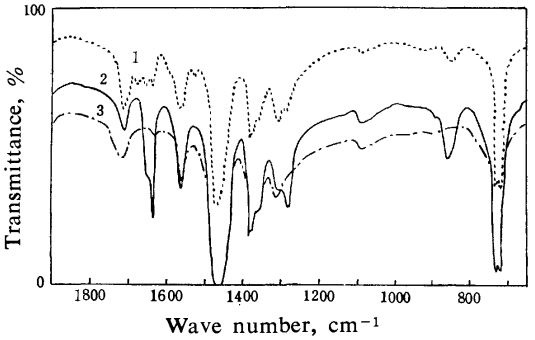

Fig. 2. Infrared spectra of the oxidized polyethylene.

1 Oxidized in fuming nitric acid at room temperature
2 Oxidized in 60% nitric acid at room temperature
3 After the oxidized polyethylene was heated in nitrogen at 200°C.

TABLE I. OXIDATIVE DEGRADATION OF POLYETHYLENE*

Group	Band** cm^{-1}	Spectral change in the atm. at room temp.	Spectral change in N_2 at 200°C	Oxidation in HNO_3 at room temp.	Oxidation in fuming HNO_3 at room temp.	Oxidation in the air at room temp.	Assignment
A	1713	Disap. within 24 hr.	Disap.	—	—	—	HNO_3
	1300						HNO_3
	900						HNO_3
	1681						Nitrite ester group trans N=O str.
B	1640	Disap. within 2 months	Disap.	—	—	—	Nitrite ester group cis N=O str.
	778						Nitrite ester group trans N-O str.
	600						Nitrite ester group cis O-N=O bend.
C	3400	Increase	Increase	App.	App.	App.	Hydrogen bonded O-H str.
	1713						C=O str.
D_1	1554	Stable	Stable	App.	App.	—	Nitro group NO_2 asym. str.
	1365						Nitro group NO_2 sym. str.
	629						Nitro group NO_2 bend.
	562						Nitro group NO_2 bend.
D_2	1635	Stable	Stable	App.	App.	—	Nitrate ester group NO_2 asym. str.
	1280						Nitrate ester group NO_2 sym. str.
	852						Nitrate ester group N-O str.
	675						Nitrate ester group NO_2 bend.

* Abbreviation: atm. atmosphere, tem. temperature, disap. disappear, app. appear, str. stretching vibration, bend. bending vibration, asym. asymmetric, sym. symmetric

** Observed bands in the polyethylene oxidized by nitric dioxide

at 200°C for 20 min., the bands in group A and group B and some of those in group D, namely, 1635, 1280, 852 and 675 cm^{-1}, disappeared. Therefore, group D can be subdivided into group D_1, which did not disappear upon heating, and group D_2, which disappeared upon heating. When polyethylene was aged in nitric acid (more than 60% concentration) at room temperature (Fig. 2), the bands in groups C and D were observed, but those in groups A and B were not.

Assignment

Rigg[4] identified nitroalkanes, alkyl nitrates and alkyl nitrites as reaction products by means of the infrared analysis of an irradiated mixture of *n*-dodecane and nitrogen dioxide. Brand and Stevens[5] also identified nitro alkanes and alkyl nitrates as products in the reactions between nitrogen dioxide and olefins, e. g., cyclohexene and cyclopentene.

As, however, the data obtained above were insufficient for the intended assignment, several compounds were synthesized whose infrared spectra were measured for the assignment. On the basis of these findings, together with changes of observed bands upon various treatments, the assignments of the observed bands were determined as follows:

D_2 Group.—The infrared spectrum of 2-ethylhexyl nitrate, which had been prepared from 2-ethylhexyl alcohol[6], was observed (Fig. 3). The bands other than those due to 2-ethylhexyl alcohol were regarded as bands due to the nitrate group. The locations of the oxygenated groups of polyethylene were compared with those of alkyl nitrate, and it was shown that the bands which belonged to the D_2 group are to be assigned to the nitrate ester group. This assignment is shown in the last column of Table I, with reference to the results on alkyl nitrates given by Brown[7] and by Brand and Cawthon[8].

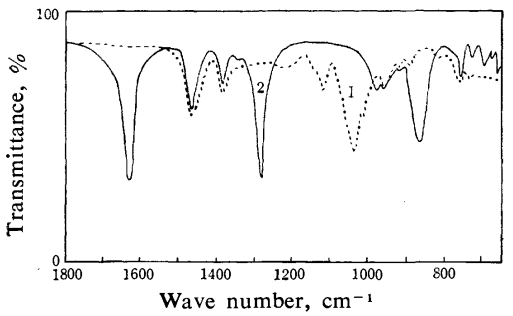

Fig. 3. Infrared spectra of 2-ethylhexyl alcohol (1) and 2-ethylhexyl nitrate (2).

D_1 Group.—By comparison with the data on various types of nitroalkanes reported by Smith et al.[9] and by Pierson et al.[10], the bands in the D_1 group were assigned to the nitro group.

C Group.—The bands at 3400 and 1713 cm^{-1} were also observed when the oxidation of polyethylene was carried out in the presence of oxygen (Fig. 4). The band at 3400 cm^{-1} was assigned to hydrogen-bonded hydroxyl group by reference to the data on low molecular weight compounds[11]. Rugg et al.[1] and Loungo[2] also assigned these bands to the hydroxyl group and carbonyl group respectively.

A and B Groups. — The infrared spectra of low-molecular-weight alkyl nitrites were measured. These compounds had various types of branches, ranging from ethyl nitrite to octyl nitrite. They were prepared by the ordinary synthetic method from alcohols. It was shown that the band at 1681 cm^{-1} in A group and the bands in B group are to be assigned to the nitrite ester group, as may be seen in the last column of Table I, by reference to the data of Tarte[12], Haszeldine and Mattinson[13] and Bellamy et al.[14]

Beachell and Nemphos[3] assigned the band at 1640 cm^{-1} to the C=C stretching band. When the thermal degradation of polyethylene was carried out at 350~370°C for 20 min. in nitrogen, the C=C stretching band was observed at 1640 cm^{-1}. At the same time, four strong bands which were attributable to C–H out of plane vibrations were observed at 900~1000 cm^{-1} (Fig. 4), whereas when the oxidative degradations were carried out in nitrogen dioxide, the bands at 900~1000 cm^{-1} were not observed. Similarly, the bands at 900~1000 cm^{-1} were not observed in the oxidative degradations in fuming nitric acid or in 60% nitric acid at room temperature (Fig. 2). Moreover, when those double bonds of the polyethylene which had been produced by the thermal degradation were brominated, the bands at 1640 cm^{-1} and 900~1000 cm^{-1}

4) T. Rigg, *Nature*, 187, 933 (1960).
5) J. C. D. Brand and I. D. R. Stevens, *J. Chem. Soc.*, 1958, 629.
6) R. L. Shriner and E. A. Parker, *J. Am. Chem. Soc.*, 55, 766 (1933).
7) J. F. Brown, ibid., 77, 6341 (1955).
8) J. C. D. Brand and T. M. Cawthon, ibid., 77, 319 (1955).
9) D. C. Smith, C. Y. Pan and J. R. Nielsen, *J. Chem. Phys.*, 18, 706 (1950).
10) P. H. Pierson, A. N. Fletcher and E. S. C. Cantz, *Anal. Chem.*, 28, 1218 (1956).
11) L. J. Bellamy, "The Infrared Spectra of Complex Molecules", 2nd Ed., John Wiley & Sons, Inc., New York (1958).
12) P. Tarte, *J. Chem. Phys.*, 20, 1570 (1952).
13) R. N. Haszeldine and B. J. Mattinson, *J. Chem. Soc.*, 1954, 691, 4172.
14) L. J. Bellamy, C. P. Conduit, R. J. Pace and R. L. Williams, *Trans. Faraday Soc.*, 55, 1677 (1959).

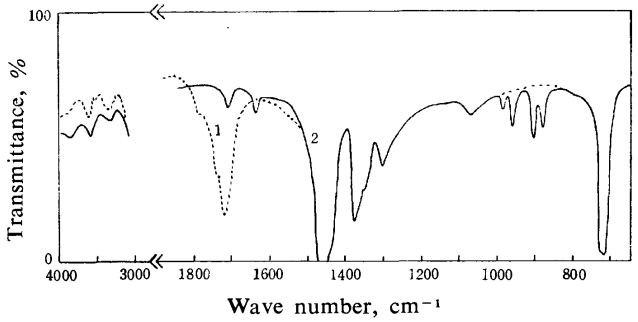

Fig. 4. Infrared spectra of oxidized polyethylene.
1 Thermal oxidation in the air (at 150°C)
2 Thermal degradation in nitrogen (at 350°C)

disappeared and a new band appeared at 573 cm^{-1}. This new one is attributable to the C–Br stretching band[11]. However, when the polyethylene which had been oxidized in nitrogen dioxide was brominated, the band at 1640 cm^{-1} disappeared, but the new band did not appear. Therefore, it would be erroneous to assign the band at 1640 cm^{-1} to the C=C stretching band, as was proposed by Beachell and Nemphos[3].

In the case of low-molecular-weight alkyl nitrites, the intensities of the trans N=O stretching at 1681 cm^{-1} are stronger than those of the cis N=O stretching at 1620 cm^{-1}, as may be seen in Fig. 5, but the reverse is true of the nitrite ester groups in polyethylene (Fig. 1). By preservation of oxidized products in a vessel cooled by a mixture of dry ice and *n*-heptane, the bands at 1730, 1300, 900 and 1681 cm^{-1} in group A could be preserved for more than a week before they disappeared (Fig. 6). When they were kept in a vacuum desiccator with phosphorous pentoxide, the band at 1681 cm^{-1} did not disappear until after more than a week, but the bands at

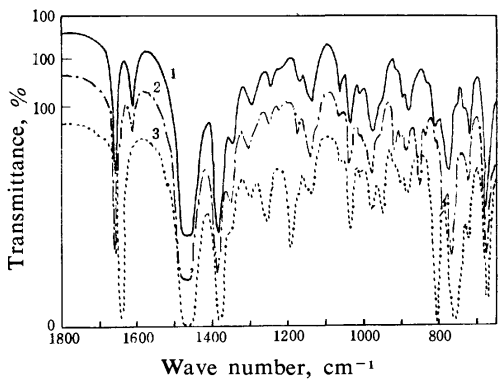

Fig. 5. Infrared spectra of alkyl nitrites.
1 *n*-Butyl nitrite
2 *sec*-Butyl nitrite
3 *tert*-Butyl nitrite

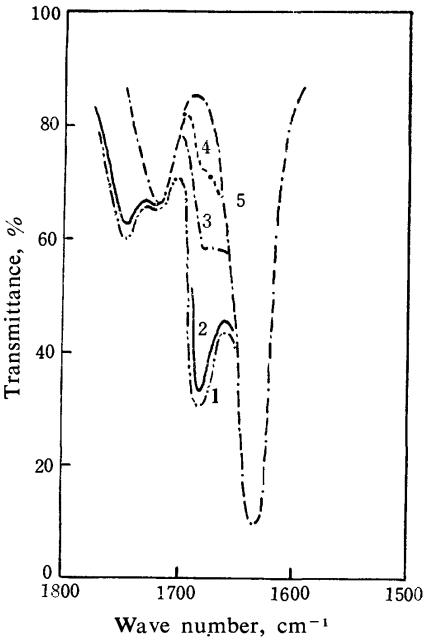

Fig. 6. Spectral change of the band at 1681 cm^{-1}.
1 Oxidized polyethylene
2 Kept 8 days at dry ice-*n*-heptane temperature
3 Kept 8 days in vacuum desiccator with P_2O_5
4 Left 30 min. in the atmosphere
5 Left 3 days in the atmosphere

1730, 1300 and 900 cm^{-1} went away within 24 hr., as when the samples were left in the atmosphere. The prevention of the disappearance of the band at 1681 cm^{-1} was greater in a cool place.

The intensities of bands in the A group decreased as the reaction gas or the produced gas was removed from the polymer. As for the band at 1681 cm^{-1}, it seemed that the above process was not responsible for its disappearance, because when the oxidized films were left in a desiccator, the band did not

disappear. However, the bands at 1730, 1300 and 900 cm^{-1} could be attributed to the production of nitric acid in view of the location of the absorption bands, their relative intensities[15], and the fact that when the products were placed in a desiccator, the bands at 1730, 1300 and 900 cm^{-1} disappeared. It seems that the rate of disappearance of the band at 1681 cm^{-1} depends on the temperature, but it is not clear why the intensity of the trans N=O is weaker than that of the cis N=O in the polymer. This problem should be investigated in the future.

Discussion

The kinetic studies of polyethylene oxidations in nitrogen dioxide were made on the basis of the identification of the groups which were formed in polyethylene during oxidation and of the rates of formation of groups (Fig. 7). The bands used for the studies were 1554 (nitro group), 778 (nitrite ester group), 852 (nitrate ester group) and 1713 cm^{-1} (carbonyl group). As may be seen in Fig. 7, the nitro group and the nitrite ester group were produced in the early stages; the intensity of the nitro group increased constantly, while that of the nitrite ester group reached its maximum point and even began to level off in five hours. On the other hand, the nitrate ester group and the carbonyl group did not appear in the early stages; they appeared after the nitro group and some of the nitrite ester groups had been formed.

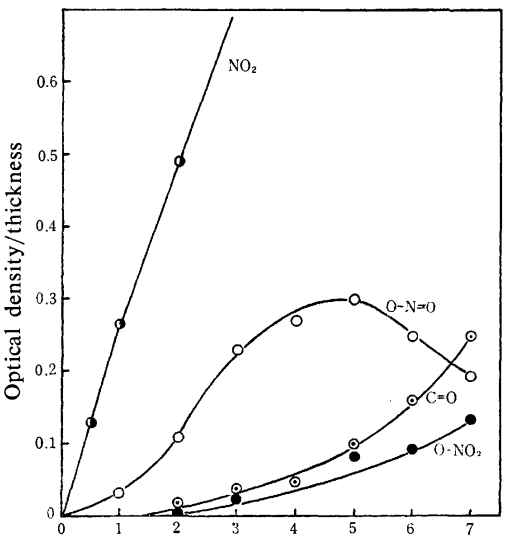

Fig. 7. Rate of formation of oxygenated groups in polyethylene.

15) R. A. Marcus and J. M. Fresco, *J. Chem. Phys.*, **27**, 564 (1957),

As nitrogen dioxide gas has an odd electron structure, it may be expected to combine with radicals easily[4,16]. Therefore, it seems that in the early stages the nitro groups and the nitrite ester groups are produced by the reaction of activated polyethylene with nitrogen dioxide in terms of the $\dot{R} + \dot{N}O_2 \rightarrow RNO_2$ and $\dot{R} + \dot{O}NO \rightarrow RONO$ processes. The carbonyl groups and the nitrate ester groups were produced as decomposition products of the nitro and the nitrite ester groups in the secondary state. Gray et al.[17] have identified aldehyde and ketone as decomposition products of the pyrolyses of alkyl nitro compounds, especially nitroethane, at temperatures between 240 and 800°C. As the intensity of the nitro group did not change when the oxidized products were left in the atmosphere, and as the change in intensity was only a little when the products were heated at 200°C in nitrogen gas, it seems that the nitro group formed in polyethylene is relatively stable. On the other hand, as the intensity of the nitrite ester group decreased when the oxidized products were left in the atmosphere, the nitrite ester group seems to be unstable.

Phillips[18] has identified methyl alcohol, formaldehyde and hydrogen cyanide as the decomposition products of the pyrolysis of methyl nitrite. Levy[19] has identified not only isopropyl alcohol and acetone, but also such chain scission products as acetaldehyde and hydrogen cyanide as the thermal decomposition products of isopropyl nitrite, while for ethyl nitrite he has identified acetaldehyde and ethyl alcohol. Gray and Williams[20] and Pollard et al.[21] have suggested that alkyl nitrate is produced by the pyrolysis of alkyl nitrite in the presence of nitrogen dioxide. From the present analyses of the infrared spectra of the oxidized products, the carbonyl, hydroxyl and nitrate ester groups have been identified and it seems that these are mainly the decomposition products of the nitrite ester group, because the nitrite ester group is unstable, as has been mentioned above.

On the basis of the mechanisms which have been proposed by several investigators for the pyrolyses of alkyl nitrite[18,19,22] and alkyl nitrate[20] and for the photolysis of alkyl

16) A. V. Topchiev, "Nitration of Hydrocarbons", Pergamon Press, London (1959).
17) P. Gray, A. D. Yoffe and L. Roselaar, *Trans. Faraday Soc.*, **51**, 1489 (1955),
18) L. Phillips, *J. Chem. Soc.*, **1961**, 3082.
19) J. B. Levy, *J. Am. Chem. Soc.*, **78**, 1780 (1956); *Ind. Eng. Chem.*, **48**, 762 (1956).
20) P. Gray and A. Williams, *Chem. Revs.*, **59**, 235 (1959).
21) F. H. Pollard, H. S. B. Marchall and A. E. Pedler, *Trans. Faraday Soc.*, **52**, 59 (1956).
22) P. Gray and A. Williams, *Nature*, **188**, 56 (1960).

nitrite[23], the following mechanisms may be considered:

$$RH \xrightarrow{\text{activated}} \dot{R} + \dot{H} \quad RH\text{; polyethylene}$$

In early stages:

$$\dot{R} + \dot{N}O_2 \rightarrow RNO_2\text{; nitro group}$$

$$\dot{R} + \dot{O}NO \rightarrow RONO\text{; nitrite ester group}$$

In secondary stages:

$$RONO \rightarrow R\dot{O} + \dot{N}O\text{; O-N fission}$$

$$R\dot{O} + \dot{N}O_2 \rightarrow RONO_2\text{; nitrate ester group}$$

$$\left.\begin{aligned} R'CH_2\dot{O} &\rightarrow R'CHO + \dot{H} \\ R''R'''CH\dot{O} &\rightarrow R''R'''CO + \dot{H} \\ R''R'''CH\dot{O} &\rightarrow R''CHO + \dot{R}''' \end{aligned}\right\} \text{carbonyl group}$$

$$R\dot{O} + \dot{H} \rightarrow ROH\text{; hydroxyl group}$$

$$RONO_2 \rightarrow R\dot{O} + \dot{N}O_2$$

In our study no decision was made whether the nitro group or the nitrite ester group was produced in the greater amount, for the absolute intensity of the nitrite ester group has not yet been obtained.

23) H. W. Brown and G. C. Pimentel, *J. Chem. Phys.*, **29**, 883 (1958).

Conclusion

From analyses of the infrared spectra of polyethylene oxidized in nitrogen dioxide, the formation of the nitro, nitrite ester, nitrate ester, carbonyl and hydroxyl groups have been identified. In early stages, the nitro group and the nitrite ester group were produced by the addition of nitrogen dioxide to the activated position of polyethylene. The nitrate ester, carbonyl and hydroxyl groups were produced as decomposition products of the two aforementioned groups, mainly the nitrite ester group.

The author wishes to thank Professor Kenji Kuratani and Mr. Soji Tsuchiya of the Aeronautical Research Institute, The University of Tokyo, for their valuable advice in this work.

The Textile Research
Institute of the Japanese Government
Kanagawa-ku, Yokohama

A Study of the Sol-Gel Transformation of Gelatin Solutions

By Nobuo TANAKA and Isamu UTSUMI

(Received August 24, 1962)

Gelatin has been universally used in such pharmaceutical preparations as capsules, tablets and injections. The physical properties of gelatin are important in the production of these pharmaceutical preparations. In recent years, the physical properties of gelatin solutions have been extensively investigated in the field of rheology[1,2], but reports of the sol-gel transformation have been limited to its lower concentrations. Since the productions of pharmaceutical preparations is carried out with gelatin solutions of the higher concentrations, data on the lower concentrations are not useful. Therefore, that sol-gel transformation which is considered to determine the physical nature of the pharmaceutical preparations produced was investigated.

In the study of this transformation, Bourgoin[3] has examined the viscosity and the double refraction of gelatin solutions of the lower concentrations. On the other hand, the method of measuring the solution with a 10% concentration has been described in JIS[4]. In the JIS method for measuring the sol-gel transformation, an apparatus (shown in Fig. 1) is used in which 50 cc. of a hot, 10% gelatin solution is put into an inside vessel. Immediately, the sample is gently stirred with a thermometer, and the flowing behavior of gelatin solution is observed with the naked eye; of the phenomena which the solution shows before the appearance of resistance, some rigidity is called the transformation temperature. The JIS method, however, based as it is on the observation of the human eye, is essentially

1) N. Hirata et al., *J. Chem. Soc. Japan, Pure Chem. Sec.* (*Nippon Kagaku Zassi*), **74**, 347, 441, 810 (1953).
2) K. Nakamura, presented at the 15th Annual Meeting of the Chemical Society of Japan, Kyoto, April, 1962.
3) D. Bourgoin et al., "Gelatin and Glue Research". London Pergamon Press (1958).
4) JIS, K 6503.

inaccurate and is not applicable to solutions of the higher concentrations.

A new measuring method with a Macmichael viscometer is proposed for application to the solutions of necessarily higher concentrations in order to determine their transformation points. On the other hand, a co-axially oscillating rheometer is used for studying the behavior of the sol-gel transformation through the transformation temperature.

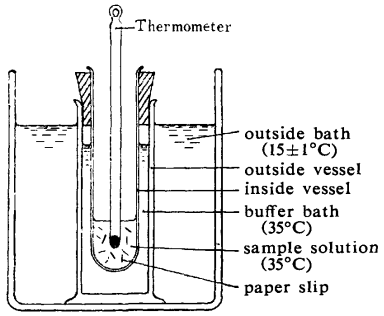

Fig. 1. The apparatus for measuring the transformation temperature. (JIS method).

Experimental

A Macmichael viscometer (I) was used for the observation of viscosity change at the sol-gel transformation, and a co-axially oscillating rheometer (II) was employed to follow the change of viscoelastic behavior through the sol-gel transformation.

Rheometer (I).—The sample was put into the gap between the co-axial internal and external cylinders. The diameters of the internal cylinder, d_1, and of the external cylinder, d_2, were 2.00 and 3.00 cm. respectively. The depth of the immersion of the internal cylinder was 4.00 cm., which was equal to the height of the cylinder. The viscosity is calculated from the following equation:

$$\eta_I = C \cdot (\theta/r) \qquad (1)$$

where η_I is the apparent viscosity, θ is the angle of deflection of the internal cylinder in radian, r is the number of revolutions of the external cylinder (5 r. p. m.), and C is an instrumental constant, which is either 29.0 or 1.79. Both cylinders ware heated previously by circulating water at 52~55°C and by putting the sample into the gap between the cylinders, where it was heated for about five minutes at 52~55°C. Then, the sample was gradually cooled at the rate of 1°C per 5 min. and the viscosity was measured at various temperatures at 5 r. p. m.

Rheometer (II).—A top-drive co-axial rheometer which has previously been described by Nakagawa and Seno[5] was used. The sample was put into the gap between the cylinders. The radius of the internal cylinder, r_1, was 0.6 cm. and that of the external cylinder, r_2, was 0.9 cm. The depth, h, of the immersion of the internal cylinder was about 10 cm. The moment of inertia, I, of the internal cylinder and the wire chuck were 38.07 g. cm. The torsional constants of two wires determined from the period of the free torsional oscillation, $\bar{k}$, were 587.8 and 1313 dyn. cm. To the top of the wire a torsional oscillation was applied, and the oscillation of the internal cylinder was recorded on a paper. A Lissajous figure was obtained by combining perpendicularly the oscillation of the top of the wire and that of the internal cylinder. Since the Lissajous figure thus obtained was an ellipse, the dynamic viscosity, η_{II}, and the dynamic modulus, G, were calculated by the following equations:

$$\eta_{II} = (R/4h) \cdot (1/r_1^2 - 1/r_2^2) \quad \text{(poise)}$$
$$G = (K/4h) \cdot (1/r_1^2 - 1/r_2^2) \quad \text{(dyn./cm}^2\text{)} \qquad (2)$$

where R and K were the quantities to be determined experimentally by using the following equations:

$$R = \bar{k}\ T \sin\phi/2m \text{ and } K = \bar{k} (\cos \phi/m - 1) + (4\pi^2 I/T^2) \qquad (3)$$

Here, the lag angle, ϕ, and the amplitude ratio, m, were obtained by an analysis of the Lissajous' figure, and the period of oscillation, T, was 0.0286 cycl./sec.

Preparation of the Gelatin Solution.—The preparation of the gelatin solution has been generally described in JIS. but here the water content of the gelatin was changed to 16%. The gelatin was then dried for 5 hr. at 105~115°C; after it (X) had been weighed accurately, the amount to be needed was calculated from "$X \times 84/(100-y)$", with y indicating the water concent (%) of gelatin. After water had been added to the gelatin, the solution was kept at room temperature for half an hour in order for the gelatin to be completely swollen and then on a water bath at 55~60°C for 1 hr. for the gelatin to be dissolved. This solution was used for the measurements.

Results and Discussion

The dependnce of the apparent viscosity on the temperature has been shown in Fig. 1. In this figure the sol-gel transformation is shown by a sudden increase in the apparent viscosity. The transformation temperatures obtained by this method are shown in Table I in comparison with the values obtained by the JIS method[4].

The transformation temperature obtained is higher by 1~5°C than that of the JIS method, and the temperature rose with the concentration. The rates of the sol-gel transformation seemed to become slower with the increase in the concentration.

Differences in the behavior of various gelatins could not be observed definitely through the data of the sol-gel transformation. Therefore, the transformation was investigated by rheometer II. From the results of viscoelastic measurement, the dynamic viscosity, η_{II}, and

5) T. Nakagawa and M. Seno, This Bulletin, 29, 471 (1956).

TABLE I. APPARENT VISCOSITY AND SOL-GEL TRANSFORMATION TEMPERATURES OF GELATIN SOLUTION AT VARIOUS CONCENTRATIONS

Sample No.	Viscosity c. p.	JIS method	Sol-gel transformation temp. The present method			
		at 10%	10%	20%	30%	40%
1	22.5	26.4	27.6	30.0	33.3	37.9
2	20.5	24.9	26.8	28.8	32.0	36.5
3	15.4	22.0	25.3	28.2	31.4	34.9
4	21.7	24.2	25.0	28.1	31.4	34.5
5	19.3	22.3	24.6	27.1	30.3	32.8
6	13.4	20.9	24.2	26.9	30.5	33.8
7	19.7	23.8	24.0	27.8	31.3	35.8
8	23.7	23.3	22.4	25.6	28.2	30.4
9	10.7	18.8	19.4	23.1	25.6	28.3
10	23.0	25.7	27.2	29.7	32.5	37.8
11	22.4	25.3	26.4	29.5	32.2	37.3
12	17.5	23.6	24.5	29.0	31.4	35.0
13	15.0	22.0	24.1	26.4	29.1	32.0

the dynamic modulus, G, were calculated by Eq. 2; they are show in Figs. 3—6, where the change of η_{II} or G with time is plotted at several temperatures. Both η_{II} and G at the higher concentration rose rapidly in a shorter time than at the lower concentration at the same temperature.

Further, the kinetic procedure was employed in order to investigate what the nature of the transformation was from sol to gel. From the plot of the logarithm of η_{II} or G against time,

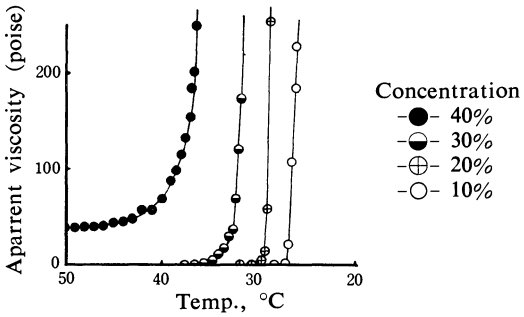

Fig. 2. Dependence of apparent viscosity on temperature.

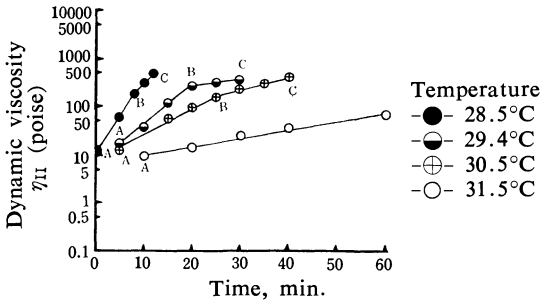

Fig. 3. The change of dynamic viscosity, η_{II}, with time at the concentration of 20%.

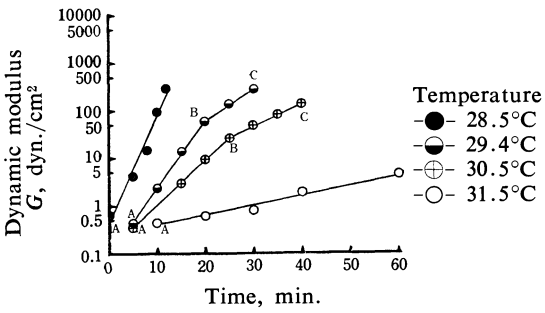

Fig. 4. The change of dynamic modulus, G, with time at the concentration of 20%.

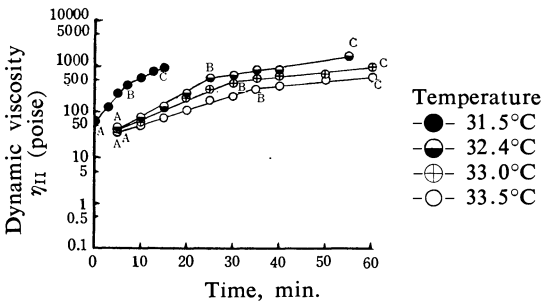

Fig. 5. The change of dynamic viscosity, η_{II}, with time at the concentration of 30%.

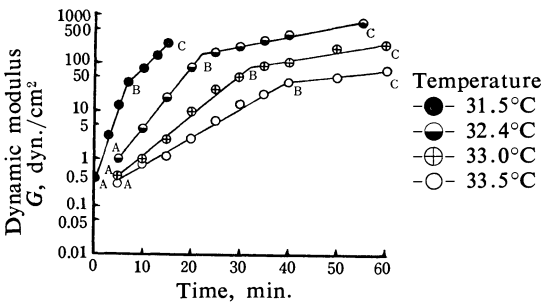

Fig. 6. The change of dynamic modulus, G, with time at the concentration of 30%.

two straight lines, AB and BC, crossing at B were obtained as Figs. 3—6 in most cases. The slope, k, of the initial line, AB, $d \ln \eta_{II}/dt$ or $d \ln G/dt$, was calculated as shown in Table II. On the other hand, the slope, k', of the second line, BC, of the appearance at the 30% solution was calculated by the same method at the initial line, AB.

TABLE II. RELATIONSHIP OF THE INITIAL SLOPE, k, OF THE AB PERIOD TO THE TEMPERATURE

Concn. of sample %	Temp. °C	k	
		η_{II}	G
20	28.5	0.1336	0.2104
	29.4	0.0788	0.1343
	30.5	0.0567	0.0722
	31.5	0.0201	0.0212
30	31.5	0.1095	0.2769
	32.4	0.0490	0.1373
	33.0	0.0422	0.0890
	33.5	0.0326	0.0613

RELATIONSHIP OF THE SECOND SLOPE, k', OF THE BC PERIOD TO THE TEMPERATURE

Concn. of sample %	Temp. °C	k'	
		η_{II}	G
30	31.5	0.04204	0.09933
	32.4	0.02062	0.04027
	33.0	0.01151	0.01918
	33.5	0.00768	0.01148

The values of η_{II} or G at the point of B were lower at the higher temperature than at the lower temperature. The values of k', were lower than that of k. These results are probably due to the increased difficulty of the arrangement of the colloidal particles at the BC period than at the AB period.

Besides, log k was plotted against the inverse temperature, as in Fig. 7. The straight line was obtained within a narrow range at the lower temperatures. Its range decreased in a 20% solution and deviated from the straight line. At the 30% concentration, the relationship of k' and the inverse temperature was similarly obtained as a straight line.

From the relation between the activation energies of k and k', $\Delta E_{K'}^{*}$ and $\Delta E_{K'}^{*}$ were calculated by the Arrhenius equation; they are shown in Table III. $\Delta E_{K'}^{*}$ higher than ΔE_{K}^{*} was obtained.

TABLE III. ACTIVATION ENERGY, ΔE^{*}, OF k AND k'

Concn. of sample %	k		k'	
	η_{II}	G	η_{II}	G
20	77.0	97.3	—	—
30	109	139	159	201

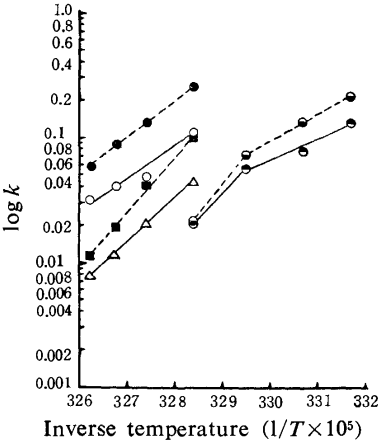

Fig. 7. Relationship of log k of η_{II} or that of G with the inverse temperature.
-◓- η_{II} at the concentration 20% of AB period
-◒- G at the concentration 20% of AB period
-○- η_{II} at the concentration 30% of AB period
-●- G at the concentration 30% of AB period
-△- η_{II} at the concentration 30% of BC period
-■- G at the concentration 30% of BC period

The difference in behavior between the AB and BC periods is probably due to the difference in the interaction of colloidal particles at various temperatures. In other words, the movement of colloidal particles is restricted at the BC period as compared with the AB period.

As has been described above, as the change from sol to gel at the AB period is relatively easy, the aggregation of gelatin particles occurs rapidly in a gelatin solution, but as the gelatin has already started the aggregation at the BC period, it is more difficult for the remaining gelatin particles in sol at the BC period to aggregate than at the AB period, when almost all the gelatin particles are in sol. Accordingly, it is natural that k' should be a smaller quantity than k and that $\Delta E_{K'}^{*}$ should be larger than ΔE_{K}^{*}. The arrangement of colloidal particles at the higher temperature must be more systematical than that at the lower temperature.

The authors wish to express their deep appreciation to Professor M. Nakagaki of Kyoto University and to Dr. M. Fujisawa and Dr. N. Sugimoto of the Tanabe Seiyaku Co., Ltd., for their valuable advice and encouragement, and to Mr. T. Hashimoto for his assistance in this work. Thanks are also due to Nihonhikaku Co., Ltd., which prepared the samples for this work.

Osaka Research Laboratory
Tanabe Seiyaku Co., Ltd.
Higashiyodogawa-ku, Osaka

The Kinetics of Substitution Reactions Involving Metal Complexes. VI. Reaction between Lead(II) and Ethylenediaminetetraacetatocobaltate(II) Complexes in Aqueous Solutions

By Nobuyuki TANAKA, Hisao OSAWA* and Minoru KAMADA

(Received September 21, 1962)

A series of substitution reactions involving metal-ethylenediaminetetraacetate (EDTA) complexes has been studied[1-7]. The reactions were found to proceed through three simultaneous reaction paths in the case of the substitution reactions of lead(II) and copper(II)-EDTA[3,4], lead(II) and zinc(II)-EDTA[2,6] and copper(II) and zinc(II)-EDTA[5], but through four simultaneous reaction paths in the case of the substitution reaction of copper(II) and cadmium(II)-EDTA[1,7].

In the present paper, the kinetic study of the substitution reaction between lead(II) ions and cobalt(II)-EDTA complexes is presented. From the rate constants of substitution of coordinated water[8,9], it was expected that the rate of dissociation of cobalt(II)-EDTA complexes is considerably slower than those of copper(II)-, zinc(II)- and cadmium(II)-EDTA complexes. This expectation was confirmed in the present study by the fact that the dissociation of cobalt(II)-EDTA complexes acts as a rate-determining reaction.

Derivation of the Rate Equation

Let us consider the acetate buffer solution which contains lead(II) ions and cobalt(II)-EDTA complexes. In the solution containing acetate ions less than 0.2 M in concentration, lead(II) forms mono- and diacetato complexes[10] and cobalt(II), monoacetato complex[11]. As for the EDTA complexes, the equilibria

$$CoY^{2-} + H^+ \rightleftarrows CoHY^-,$$
$$PbY^{2-} + H^+ \rightleftarrows PbHY^-$$

must be taken into consideration when pH of the solution is less than 5, where Y^{4-} means a tetravalent EDTA anion. Consequently, the overall substitution reaction is represented by the equations

$$Pb^{2+} + 2OAc^- \rightleftarrows PbOAc^+ + OAc^- \rightleftarrows Pb(OAc)_2 \quad (1)$$

$$Pb^{2+} + \left\{\begin{matrix} CoY^{2-} \\ \downarrow\uparrow \\ CoHY^- \end{matrix}\right\} \rightleftarrows \left\{\begin{matrix} PbY^{2-} \\ \downarrow\uparrow \\ PbHY^- \end{matrix}\right\} + Co^{2+} \quad (2)$$

$$Co^{2+} + OAc^- \rightleftarrows CoOAc^+ \quad (3)$$

As described in the previous papers[6,10], the concentration of simple lead ions that can be determined polarographically is an apparent concentration $[Pb^{2+}]_{app}$ which, under the present experimental conditions, is given by

$$[Pb^{2+}]_{app} = [Pb^{2+}] + [PbOAc^+] + [Pb(OAc)_2] \quad (4)$$

In the preliminary experiments in which the apparent initial rate of the reaction, $-\Delta[Pb^{2+}]_{0,app}/\Delta t$, was determined, the following facts were recognized, where the subscript 0 means the initial state.

(1) At the given pH and the given concentrations of $[Pb^{2+}]_{0,app}$, $[Co^{2+}]_{0,app}$ and $[OAc^-]$, the apparent initial rate was proportional to the initial concentration of cobalt(II)-EDTA complex, $[Co\text{-}EDTA]_0$, given by

$$[Co\text{-}EDTA]_0 = [CoY^{2-}]_0 + [CoHY^-]_0$$

(2) At the given pH and the given concentrations of $[Co\text{-}EDTA]_0$, $[Co^{2+}]_{0,app}$ and $[OAc^-]$, the apparent initial rate varied with the change of $[Pb^{2+}]_{0,app}$ according to the relation

$$-\frac{\Delta[Pb^{2+}]_{0,app}}{\Delta t} \Big/ [Co\text{-}EDTA]_0 = k'[Pb^{2+}]_{0,app} + k'' \quad (5)$$

(3) The relation given by Eq. 5 held at any pH where the experiments were carried

---

* Present Address: Fuji Electric Mfg. Co., Ltd., Kawasaki.

1) H. Ackermann and G. Schwarzenbach, *Helv. Chem. Acta*, **35**, 485 (1952).
2) K. Bril, S. Bril and P. Krumholz, *J. Phys. Chem.*, **59**, 596 (1955); **60**, 251 (1956).
3) N. Tanaka, K. Kato and R. Tamamushi, This Bulletin, **31**, 283 (1958).
4) N. Tanaka and K. Kato, ibid., **32**, 1376 (1959).
5) K. Kato, ibid., **33**, 600 (1960).
6) N. Tanaka and K. Kato, ibid., **33**, 1236 (1960).
7) N. Tanaka and M. Kamada, ibid., **35**, 1596 (1962).
8) M. Eigen, "Advances in the Chemistry of the Coordination Compounds (Proceedings of the Sixth International Conference on Coordination Chemistry)," MacMillan, New York (1961), p. 371.
9) M. Eigen, *Suomen Kemistilehti*, **A 34**, 25 (1961).
10) N. Tanaka and K. Kato, This Bulletin, **33**, 417 (1960).
11) N. Tanaka, M. Kamada, H. Osawa and G. Satô, ibid., **33**, 1412 (1960).

out. In addition, the values of k' and k'' in Eq. 5 which were obtained at various pH's satisfied the relations

$$k' = k_\xi' [H^+] + k_\eta' \quad (6)$$

and

$$k'' = k_\xi'' [H^+] + k_\eta'' \quad (7)$$

These facts, which were analogous to those found in the preliminary study of the substitution reaction between lead(II) and nickel(II)-EDTA complexes[12], suggested that the overall reaction would proceed, under the experimental conditions, through four simultaneous reaction paths,

$$\text{(i)} \quad Pb^{2+} + CoY^{2-} \underset{k_1^-}{\overset{k_1^+}{\rightleftharpoons}} PbY^{2-} + Co^{2+} \quad (8)$$

$$\text{(ii)} \quad Pb^{2+} + CoHY^- \underset{k_2^-}{\overset{k_2^+}{\rightleftharpoons}} PbHY^- + Co^{2+} \quad (9a)$$

$$PbHY^- \rightleftharpoons PbY^{2-} + H^+ \quad (9b)$$

$$\text{(iii)} \quad CoY^{2-} \underset{k_{3a}^-}{\overset{k_{3a}^+}{\rightleftharpoons}} Co^{2+} + Y^{4-} \quad \text{(rate-determining)} \quad (10a)$$

$$Pb^{2+} + Y^{4-} \underset{k_{3b}^-}{\overset{k_{3b}^+}{\rightleftharpoons}} PbY^{2-} \left(\underset{-H^+}{\overset{+H^+}{\rightleftharpoons}} PbHY^- \right) \quad (10b)$$

$$\text{(iv)} \quad CoHY^- \underset{k_{4a}^-}{\overset{k_{4a}^+}{\rightleftharpoons}} Co^{2+} + HY^{3-} \quad \text{(rate-determining)} \quad (11a)$$

$$Pb^{2+} + HY^{3-} \underset{k_{4b}^-}{\overset{k_{4b}^+}{\rightleftharpoons}} PbHY^- \left(\underset{+H^+}{\overset{-H^+}{\rightleftharpoons}} PbY^{2-} \right) \quad (11b)$$

It is assumed that in these reactions only the hydrated lead(II) ion Pb^{2+} is a reactive species. The apparent initial rate for the forward reaction is, then, derived as,

$$-\frac{\Delta [Pb^{2+}]_{0,app}}{\Delta t} = (k_1^+ [CoY^{2-}]_0 + k_2^+ [CoHY^-]_0)[Pb^{2+}]_0 + k_{3a}^+ [CoY^{2-}]_0 + k_{4a}^+ [CoHY^-]_0 \quad (12)$$

Introducing the formation constants of acetatolead(II) complexes $K_{Pb(OAc)_n}$ and the equilibrium constant K_{CoHY}^H ($= [CoHY^-]/([CoY^{2-}][H^+])$), Eq. 13 is obtained for the apparent initial rate of the reaction.

$$-\frac{\Delta [Pb^{2+}]_{0,app}}{\Delta t} = \left[\{k_1^+ + k_2^+ K_{CoHY}^H [H^+]\} \times \frac{[Pb^{2+}]_{0,app}}{1 + \sum_{n=1}^{2} K_{Pb(OAc)_n} [OAc^-]^n} + k_{3a}^+ + k_{4a}^+ K_{CoHY}^H [H^+] \right] \frac{[Co\text{-}EDTA]_0}{1 + K_{CoHY}^H [H^+]} \quad (13)$$

For the sake of convenience, Eq. 13 is rewritten as

$$-\frac{\Delta [Pb^{2+}]_{0,app}}{\Delta t} \cdot \frac{1}{[Co\text{-}EDTA]_0} = \frac{1}{\alpha\beta} \{k_1^+ + k_2^+ K_{CoHY}^H [H^+]\} [Pb^{2+}]_{0,app} + \frac{1}{\alpha} \{k_{3a}^+ + k_{4a}^+ K_{CoHY}^H [H^+]\} \quad (14)$$

$$\alpha = 1 + K_{Co\ Y} [H^+]$$

$$\beta = 1 + \sum_{n=1}^{2} K_{Pb(OAc)_n} [OAc^-]^n$$

Experimental

Reagents.—The solution of disodium ethylenediaminetetraacetate (EDTA) was standardized against the standard copper(II) solution by amperometric titration using a dropping mercury electrode as an indicator electrode[13]. The standard solution of lead(II) nitrate was prepared from the guaranteed grade reagent, and the concentration of lead(II) was determined amperometrically with the standardized EDTA solution[13]. The standard solution of cobalt(II) nitrate was obtained by dissolving cobalt metal in reagent grade nitric acid and standardized against the standardized EDTA solution amperometrically and also volumetrically with murexide[14]. Although the polarographic analysis showed that the cobalt metal contained 0.2% of nickel as impurity, the metal was used without further purification. It was taken into consideration that the substitution reaction between lead(II) and nickel(II)-EDTA complexes proceeds at much slower rate than the reaction between lead(II) and cobalt(II)-EDTA complexes[12], and consequently a small amount of nickel contained in the cobalt metal would not interfere to an appreciable extent in the present experiments. All other chemicals used were of guaranteed reagent grade.

Apparatus and Procedure. — The initial rate of reaction was determined by measuring the change of the polarographic diffusion current of lead ions at −0.60 V. vs. SCE as a function of time in acetate buffer solutions. The current-time curves were recorded with a Shimadzu RP-2 pen-recording polarograph using a dropping mercury electrode. The dropping mercury electrode used had an m value of 2.93 mg./sec. and a drop time of 3.16 sec./drop, being measured in an air-free 0.2 M potassium

12) N. Tanaka, Y. Sakuma and G. Satô, presented at the 12th Annual Meeting of the Chemical Society of Japan, Kyoto, April, 1959, (Lecture No. 1032).

13) N. Tanaka, M. Kodama, M. Sasaki and M. Sugino, *Japan Analyst* (*Bunseki Kagaku*), **6**, 86 (1957).

14) G. Schwarzenbach, "Die Komplexometrische Titration", 2nd Ed., F. Enke Verlag, Stuttgart (1956).

nitrate solution with open circuit at 55 cm. of mercury column at 25°C.

Measurements were made at 5 and 15°C in acetate buffer solutions of pH from 4.75 to 5.66. The ionic strength was adjusted to be 0.2 with potassium nitrate. Gelatin was added as a maximum suppressor by 0.01% in concentration. The pH of the solution was measured with a Hitachi Model EHP-1 pH-meter, within the accuracy of 0.02 pH unit, immediately after the measurement of the current-time curves.

Results

Since α and β in Eq. 14 are constant at the given pH and the given concentration of acetate, a plot of the left-hand side of Eq. 14 versus $[Pb^{2+}]_{0,app}$ should give a straight line with a slope of

$$\frac{1}{\alpha\beta}\{k_1^{+}+k_2^{+}K^{H}_{CoHY}[H^{+}]\} \qquad (15)$$

and the intercept at $[Pb^{2+}]_{0,app}=0$ given by

$$\frac{1}{\alpha}\{k_{3a}^{+}+k_{4a}^{+}K^{H}_{CoHY}[H^{+}]\} \qquad (16)$$

The apparent initial rates were determined at various lead(II) concentrations with the reaction mixtures of the given pH which contained acetate buffer of the given acetate concentration and cobalt(II) ions and cobalt(II)-EDTA complexes in large excess over lead(II) ions. These measurements were carried out at various pH's ranging from 4.75 to 5.66. The plots of the left-hand side of Eq. 14 versus $[Pb^{2+}]_{0,app}$ obtained at 15°C are shown in Fig. 1. The intercepts at $[Pb^{2+}]_{0,app}=0$ and the slopes of these plots were determined by the method of least square. In these measurements at 15°C, the pH of the solutions was varied from 5.04 to 5.66 and consequently the value of α in Eq. 14 changes from 1.00_9 to 1.00_3. In the present calculation α was assumed to be unity, taking into consideration the accuracy of the measurement of the apparent initial rate and the deviations of the plots in Fig. 1. Then, the intercepts at $[Pb^{2+}]_{0,aPp}=0$ in Fig. 1 correspond simply to $\{k_{3a}^{+}+k_{4a}^{+}K^{H}_{CoHY}[H^{+}]\}$ and the slopes to

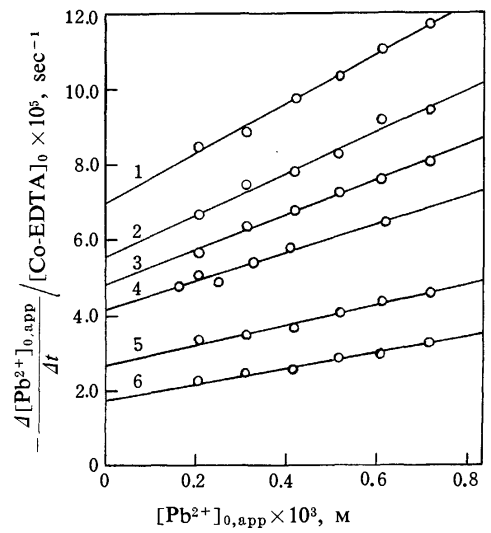

Fig. 1. $(-\Delta[Pb^{2+}]_{0,app}/\Delta t)/[Co\text{-}EDTA]_0$ as a function of the initial concentration of lead(II) ion in acetate buffer-potassium nitrate solutions of ionic strength 0.2 at 15°C. Initial concentrations are: $[Co^{2+}]_{0,app}=5.14\times10^{-3}$; $[Co\text{-}EDTA]_0=4.91\times10^{-3}$ M. pH: (1), 5.04; (2), 5.11; (3), 5.21; (4), 5.30; (5), 5.47; (6), 5.66. Concentration of free acetate is 0.090 M.

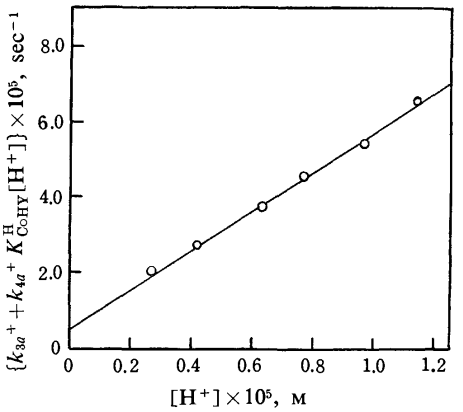

Fig. 2. The observed values for $\{k_{3a}^{+}+k_{4a}^{+}\cdot K^{H}_{CoHY}[H^{+}]\}$ at various hydrogen ion concentrations in acetate buffer-potassium nitrate solutions of ionic strength 0.2 at 15°C. Initial concentrations are: $[Co^{2+}]_{0,app}=5.14\times10^{-3}$ M; $[Co\text{-}EDTA]_0=4.91\times10^{-3}$ M. Concentration of free acetate is 0.090 M.

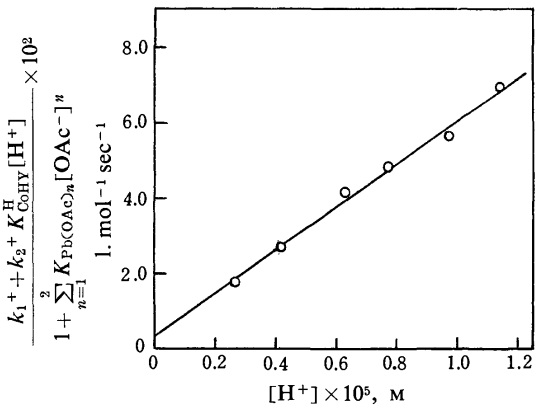

Fig. 3. The observed values for $(k_1^{+}+k_2^{+}\cdot K^{H}_{CoHY}[H^{+}])/(1+\sum_{n=1}^{2}K_{Pb(OAc)_n}[OAc^{-}]^n)$ at various hydrogen ion concentrations. The conditions are the same as Fig. 2.

TABLE I. RATE CONSTANTS FOR REACTIONS (8), (9a), (10a) AND (11a) OBTAINED EXPERIMENTALLY AT IONIC STRENGTH 0.2 AT VARIOUS TEMPERATURES

Temp. °C	k_1^+ l. mol^{-1} sec^{-1}	k_2^+ l. mol^{-1} sec^{-1}	k_{3a}^+ sec^{-1}	k_{4a}^+ sec^{-1}
5	—*	48	—*	4.4×10^{-3}
15	(0.1)**	122	(4×10^{-6})**	7.3×10^{-3}

* The rate constant can not be determined from the plots corresponding to those in Figs. 2 and 3.
** The value is less accurate.

$\{k_1^+ + k_2^+ K^{H}_{CoHY}[H^+]\}/\beta$. The values of $\{k_{3a}^+ + k_{4a}^+ K^{H}_{CoHY}[H^+]\}$ and $\{k_1^+ + k_2^+ K^{H}_{CoHY}[H^+]\}/\beta$ obtained are plotted against the hydrogen ion concentration in Figs. 2 and 3. From these plots, the values of k_1^+, k_2^+, k_{3a}^+ and k_{4a}^+ were determined, when K^{H}_{CoHY} at 15°C was estimated from the value given by Schwarzenbach, Gut and Anderegg[15] and β was calculated with the aid of the formation constant $K_{Pb(OAc)_n}$ reported previously[10]. Similar results were also obtained in the experiments carried out at 5°C. The rate constants k_1^+, k_2^+, k_{3a}^+ and k_{4a}^+ at 5 and 15°C are given in Table I.

Discussion

The assumption that reactions 10a and 11a are rate-determining in reaction paths iii and iv, respectively, should be discussed, though it is confirmed by the experimental results. Let us consider reaction path iii, for example. The initial rate of the reaction (v_3), which is measured by the decrease of $[Pb^{2+}]_{app}$, is given as

$$v_3 = k_{3b}^+ [Pb^{2+}]_0 [Y^{4-}]_0 \qquad (17)$$

Applying the steady state treatment, $[Y^{4-}]_0$ is represented as

$$[Y^{4-}]_0 = \frac{k_{3a}^+ [CoY^{2-}]_0}{k_{3a}^- [Co^{2+}]_0 + k_{3b}^+ [Pb^{2+}]_0} \qquad (18)$$

Introducing Eq. 18 into Eq. 17, v_3 is written as

$$v_3 = \frac{k_{3a}^+ k_{3b}^+ [Pb^{2+}]_0 [CoY^{2-}]_0}{k_{3a}^- [Co^{2+}]_0 + k_{3b}^+ [Pb^{2+}]_0} \qquad (19)$$

In Eq. 19, if the condition,

$$k_{3a}^- [Co^{2+}]_0 \ll k_{3b}^+ [Pb^{2+}]_0$$

is satisfied, Eq. 19 is simplified to

$$v_3 = k_{3a}^+ [CoY^{2-}]_0 \qquad (20)$$

Eq. 20 indicates that the rate of the reaction is independent of the concentration of lead(II) ions present in the solution. A similar treatment is applied to reaction path iv, when the same relation that the reaction rate is independent of the concentration of lead(II) ions is obtained. These results agree with the experimental observations. At this point, the substitution reaction between lead(II) and cobalt(II)-EDTA is entirely different from those reported previously[1-7].

In this study, k_1^+ and k_{3a}^+ at 5°C could not be determined, and those at 15°C were less accurate than other rate constants. This was presumably due to the fact that the reactions through paths i and iii make only a small contribution to the whole reaction. The contribution of the each reaction path was calculated under the appropriate conditions, and is given in Table II, which indicates that the reaction through paths i and iii is less than 10% of the whole reaction.

Equation 13 predicts that the reaction rate decreases with increasing concentration of acetate ion. This has been found and confirmed experimentally with several substitution reactions studied previously. Using Eq. 14, the values of $(-\Delta[Pb^{2+}]_{0,app}/\Delta t)/[Co\text{-}EDTA]_0$ were calculated at various concentrations of acetate ion with the rate constants given in

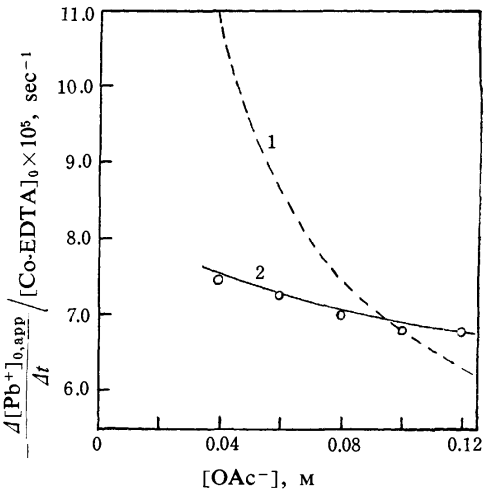

Fig. 4. $(-\Delta[Pb^{2+}]_{0,app}/\Delta t)/[Co\text{-}EDTA]_0$ as a function of the acetate ion concentration in acetate buffer-potassium nitrate solutions of pH 5.22 and ionic strength 0.2 at 15°C. Initial concentrations are: $[Pb^{2+}]_{0,app}=5.00\times10^{-4}$ M; $[Co^{2+}]_{0,app}=5.14\times10^{-3}$ M; $[Co\text{-}EDTA]_0=4.91\times10^{-3}$ M. Curve 1 represents the theoretical values calculated with Eq. 14, while curve 2, that calculated with Eq. 22. ○ indicates the experimental value.

15) G. Schwarzenbach, R. Gut and G. Anderegg, *Helv. Chim. Acta*, 37, 937 (1954).

TABLE II. CONTRIBUTION OF EACH REACTION PATH TO OVERALL SUBSTITUTION REACTION AT pH 5.21, 15°C AND 0.2 IONIC STRENGTH*

Reaction path	Expression for reaction rate**	Reaction rate sec^{-1}	Contribution to total reaction rate %
(i)	$k_1^+[Pb^{2+}]_{0,app}/\alpha\beta$	$2.6_5\times10^{-6}$	2.9
(ii)	$k_2^+K^H_{CoHY}[H^+][Pb^{2+}]_{0,app}/\alpha\beta$	$2.0_6\times10^{-5}$	29.1
(iii)	k_{3a}^+/α	4.0×10^{-6}	5.5
(iv)	$k_{4a}^+K^H_{CoHY}[H^+]/\alpha$	4.5×10^{-5}	62.6

* $[Pb^{2+}]_{0,app}=5.18\times10^{-4}$ M, $[Co^{2+}]_{0,app}=5.14_4\times10^{-3}$ M, $[Co\text{-}EDTA]_0=4.90_5\times10^{-3}$ M, $[OAc^-]=0.090$ M

** $\alpha=1+K^H_{CoHY}[H^+]$; $\beta=1+\sum_{n=1}^{2}K_{Pb(OAc)_n}[OAc^-]^n$

Table I. These values are plotted against acetate ion concentration in Fig. 4 (curve 1), where the experimental values for $(-\Delta\cdot[Pb^{2+}]_{0,app}/\Delta t)/[Co\text{-}EDTA]_0$ obtained at various concentrations of acetate ion are also given. Figure 4 indicates that the values of $(-\Delta[Pb^{2+}]_{0,app}/\Delta t)/[Co\text{-}EDTA]_0$ calculated with Eq. 14 fairly deviate from the experimental ones, as has been noticed in the studies on other substitution reactions[4-7]. The discrepancy apparently arises from the assumption that the reaction proceeds through only hydrated ions.

Then, the reaction was assumed as to proceed through both hydrated ion and monoacetato complex. The rate-determining steps in reaction paths i and ii are as follows:

(i) $Pb^{2+}+CoY^{2-}\overset{k_{1h}^+}{\rightleftharpoons}PbY^{2-}+Co^{2+}$ (8')

$PbOAc^++CoY^{2-}\overset{k_{1c}^+}{\rightleftharpoons}PbY^{2-}+CoOAc^+$ (8'')

(ii) $Pb^{2+}+CoHY^-\overset{k_{2h}^+}{\rightleftharpoons}PbHY^-+Co^{2+}$ (9a')

$PbOAc^++CoHY^-\overset{k_{2c}^+}{\rightleftharpoons}PbHY^-+CoOAc^+$ (9a'')

where k_{ih}^+ and k_{ic}^+ mean the rate constants of the reactions which proceed through the hydrated ion and monoacetato complex, respectively. Reaction paths iii and iv are not concerned with this treatment because the rate-determining steps of these paths are the dissociation of cobalt(II)-EDTA complexes and involve no acetato complex.

Since it seemed extremely difficult, however, to determine all of these rate constants, k_{ih}^+ and k_{ic}^+, separately because of insufficient accuracy in the measurement, a procedure similar to that reported previously[7] was taken up as the first approximation.

In reaction paths i and ii, the ratios of k_{ic}^+ and k_{ih}^+ are assumed to be the same and denoted with x.

$$\frac{k_{ic}^+}{k_{ih}^+}=x \tag{21}$$

Introducing the relation of Eq. 21 into Eq. 13 and rearranging, one obtains Eq. 22.

$$\left\{-\frac{\Delta[Pb^{2+}]_{0,app}}{\Delta t}\cdot\frac{\alpha}{[Co\text{-}EDTA]_0}-k_{3a}^+-k_{4a}^+K^H_{CoHY}[H^+]\right\}\frac{\beta}{[Pb^{2+}]_{0,app}}=\{k_{1h}^++k_{2h}^+K^H_{CoHY}[H^+]\}\times\{1+xK_{PbOAc}[OAc^-]\} \tag{22}$$

Equation 22 indicates that the plot of the left-hand side of the equation against the acetate ion concentration should give a straight line with a slope of $xK_{PbOAc}\{k_{1h}^++k_{2h}^+K^H_{CoHY}[H^+]\}$ and an intercept of $\{[k_{1h}^++k_{2h}^+K^H_{CoHY}[H^+]\}$ at zero acetate concentration.

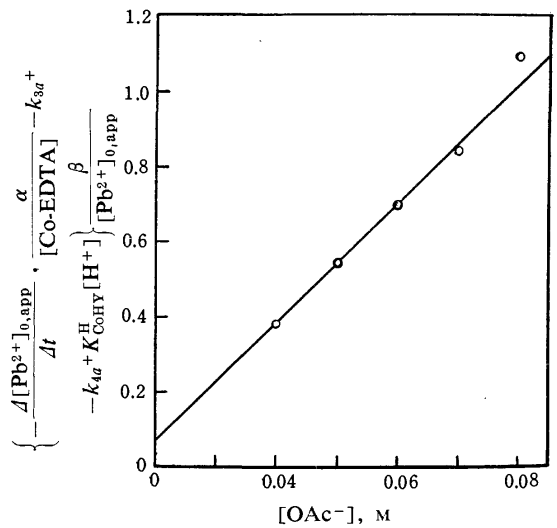

Fig. 5. Left-hand side of Eq. 22 as a function of the acetate ion concentration. The conditions are the same as Fig. 4.

The experimental values obtained at varied acetate concentrations were utilized in a plot given in Fig. 5. A straight line in Fig. 5 shows the validity of the treatment. The values of k_{ih}^{+} and k_{ic}^{+} were calculated with the value of x which was determined from this plot. Using k_{ih}^{+}, k_{ic}^{+}, k_{3a}^{+} and k_{4a}^{+}, $(-\Delta[Pb^{2+}]_{0,app}/\Delta t)/[\text{Co-EDTA}]_0$ was calculated at various concentrations of acetate ion and is given in Fig. 4 (curve 2). It is seen that curve 2 is in satisfactory agreement with the experimental observations. Although this treatment is not strictly rigorous, it proves that the substitution reaction proceeds through both hydrated ions and monoacetato complexes.

Summary

The kinetic study of the substitution reaction of lead(II) and ethylenediaminetetraacetatocobaltate(II) complexes in aqueous solutions has been carried out by a similar method as reported previously[3-7]. The reaction was found to proceed through four simultaneous reaction paths and to be characterized by involving the dissociation of ethylenediaminetetraacetatocobaltate(II) complexes as a rate-determining process. The rate constants of the rate-determining steps of four reaction paths were determined at ionic strength 0.2 at 5 and 15°C. It was confirmed also that this substitution reaction proceeds through both hydrated and monoacetato lead(II) ions.

The authors thank the Ministry of Education for the financial support granted for this research.

Department of Chemistry
Faculty of Science
Tohoku University
Katahira-cho, Sendai

Decomposition of Peroxybenzoic Acid in Solution. IV. Decomposition in Solvents in the Presence of Radical-Generators

By Katsumi TOKUMARU, Naoki INAMOTO and Osamu SIMAMURA

(Received September 22, 1962)

In previous parts of this series, decompositions of peroxybenzoic acid in alcohols[1], hydrocarbons[2] and ethers[3] have been reported, and a radical chain mechanism has been proposed. In this mechanism, the initial radical-forming decomposition of peroxybenzoic acid and its induced decomposition by radicals are essential features. In order to get further information about the induced decomposition, decomposition of peroxybenzoic acid in solvents has been carried out in the presence of radical-generators such as α, α'-azobisisobutyronitrile and isobutyryl peroxide, and the results are described in this part.

Experimental

Materials.—Peroxybenzoic acid was prepared and purified as described previously[1]. α, α'-Azobisisobutyronitrile was recrystallized from ether, m. p. 105~106°C. Isobutyryl peroxide was synthesized from isobutyryl chloride prepared by the usual method[4] and sodium peroxide according to the procedure of Kharasch et al.[5]

Kinetic Measurements.—The rate of decomposition of peroxybenzoic acid was measured by the same method as described previously[1]. The active oxygen of peroxybenzoic acid was determined by the usual method[6]. This method was found not applicable to the case of isobutyryl peroxide, because this peroxide was not easily reduced with iodide under these experimental conditions. Isobutyryl peroxide therefore was assayed according to Wagner, Smith and Peter's[7] procedure.

Product Study.—*Decomposition of Peroxybenzoic Acid in Benzene in the Presence of α, α'-Azobisisobutyronitrile.*—To a solution of peroxybenzoic acid (5.5 g., 40 mmol.) in benzene (20 ml.) heated on a boiling water bath α, α'-azobisisobutyronitrile (6.6 g., 40 mmol.) was added in small portions over 2 hr., and the mixture was heated for a further

1) K. Tokumaru, O. Simamura and M. Fukuyama, This Bulletin, 35, 1673 (1962).
2) K. Tokumaru and O. Simamura, ibid., 35, 1678 (1962).
3) K. Tokumaru and O. Simamura, ibid., 35, 1955 (1962).
4) H. C. Brown, *J. Am. Chem. Soc.*, 60, 1325 (1938).
5) M. S. Kharasch, S. S. Kane and H. C. Brown, ibid., 63, 526 (1941).
6) D. Swern, "Organic Reactions", Vol.7, John Wiley and Sons Inc., New York (1953), p. 378.
7) C. D. Wagner, R. H. Smith and E. D. Peters, *Ind. Eng. Chem., Anal. Ed.*, 19, 976 (1947).

4.5 hr. to complete the reaction. Nitrogen and hydrogen cyanide evolved during the reaction. The reaction mixture, to which sodium hydrogen carbonate was added, was subjected to steam distillation and tetramethylsuccinonitrile was separated from the distillate. On treatment with 2, 4-dinitrophenylhydrazine of the aqueous distillate, 2, 4-dinitrophenylhydrazone of acetone (3.6 mmol.) precipitated. From the residue of the steam distillation benzoic acid (4.3 g., 35 mmol.) was obtained.

In another experiment, peroxybenzoic acid (2.0 g., 14.5 mmol.) and α, α'-azobisisobutyronitrile (2.5 g., 15 mmol.) were similarly allowed to decompose in boiling benzene (20 ml.) for 6.5 hr. The reaction mixture was first distilled on a boiling water bath, chloroform was added to the distilling flask as a carrier to remove low boiling volatile matter completely, and the distillation was continued. The distillate was extracted with water; the aqueous extract, on treatment with 2, 4-dinitrophenylhydrazine, gave 2, 4-dinitrophenylhydrazone of acetone (0.6 mmol.). To the residue from the distillation sodium hydrogen carbonate was added, and the mixture was distilled with steam. The aqueous distillate, on treatment with 2, 4-dinitrophenylhydrazine, gave 2, 4-dinitrophenylhydrazone of acetone (0.6 mmol.).

Decomposition of Benzoyl Peroxide in Benzene in the Presence of α, α'-Azobisisobutyronitrile.—Benzoyl peroxide (5.0 g., 20.6 mmol.) and α, α'-azobisisobutyronitrile (6.6 g., 40 mmol.) were decomposed in boiling benzene (20 ml.) for 7 hr. During the decomposition nitrogen evolved, but hydrogen cyanide was not detected. The reaction mixture was distilled as in the second experiment above, but no acetone was detected in the aqueous extract of the distillate. The residue from the distillation was added with sodium hydrogen carbonate and subjected to steam distillation. Addition of 2, 4-dinitrophenylhydrazine to the aqueous distillate gave 2, 4-dinitrophenylhydrazone of acetone (1.5 mmol.), and the residue from the steam distillation gave benzoic acid (1.5 g., 12.3 mmol.) after the usual working up procedure.

Decomposition of Peroxybenzoic Acid in Benzene in the Presence of Isobntyryl Peroxide.—To a solution of peroxybenzoic acid (4.8 g., 34 mmol.) in benzene (50 ml.) heated at 60°C, a benzene solution of isobutyryl peroxide (17 mmol. in 30 ml.) was added gradually and the heating was continued for a total of 3 hr. The reaction mixture was distilled on a boiling water bath. The distillate was shown to contain isopropyl alcohol and acetone by gas chromatography. It was extracted with water, and the aqueous extract, on treatment with 2, 4-dinitrophenylhydrazine, gave 2, 4-dinitrophenylhydrazone of acetone (4 mmol.). Benzoic acid (3.1 g., 25 mmol.) was obtained from the residue of the distillation.

Decomposition of Peroxybenzoic Acid in Cumene in the Presence of Isobutyryl Peroxide.—A solution of isobutyryl peroxide (4 mmol.) in cumene (20 ml.) was added little by little to a cumene solution (100 ml.) of peroxybenzoic acid (3.0 g., 22 mmol.) heated at 60°C and the heating was continued for a total of 3.5 hr. The reaction mixture was extracted with water, and, on addition of 2, 4-dinitrophenylhydrazine in ethanol to the aqueous extract, 2, 4-dinitrophenylhydrazone of acetone (trace) precipitated. The cumene layer was extracted with aqueous sodium hydrogen carbonate, and the aqueous extract gave benzoic acid (1.7 g., 14 mmol.). Distillation of the cumene solution gave cumyl alcohol (1.2 g., 9 mmol.), m. p. 33°C. The needle shaped crystals (0.2 g.) in the residue from the distillation were filtered off, washed with ethyl alcohol and identified as 2, 3-dimethyl-2, 3-diphenylbutane by m. p. (from ethyl alcohol) and mixed m. p. with an authentic sample, 118~119°C, and by comparing infrared spectra.

Results and Discussion

The results of the analysis of reaction products are summarized in Table I.

The formation of acetone and hydrogen cyanide in the decomposition in the presence of α, α'-azobisisobutyronitrile indicates oxidative attack[8] on the 1-cyano-1-methylethyl radical generated from this azonitrile. The process must be the induced decomposition of peroxybenzoic acid by the 1-cyano-1-methylethyl radical (reaction 1) with formation of the benzoyloxy radical and acetone cyanhydrin, the latter subsequently decomposing to acetone and hydrogen cyanide.

$$PhCO_3H + (CH_3)_2\dot{C}CN \rightarrow PhCO_2\cdot + (CH_3)_2C(OH)CN \quad (1)$$

$$(CH_3)_2C(OH)CN \rightarrow (CH_3)_2CO + HCN \quad (2)$$

Distillation of the reaction mixture gave a distillate containing acetone, and subsequent steam-distillation of the residue after addition of sodium hydrogen carbonate yielded a further crop of acetone in a nearly equal amount (isolated as 2, 4-dinitrophenylhydrazone). The latter acetone must have been produced, in the course of the steam-distillation, from some precursor, probably acetone cyanhydrin benzoate produced by the following reaction:

$$PhCO_2\cdot + (CH_3)_2\dot{C}CN \rightarrow PhCO_2C(CH_3)_2CN \quad (3)$$

A mechanism similar to that suggested by Suehiro[9] for the reaction of peroxybenzoic acid with the triphenylmethyl radical may not be excluded:

$$PhCO_3H + (CH_3)_2\dot{C}CN \rightarrow PhCO_2H + (CH_3)_2C(CN)O\cdot \quad (4)$$

The 1-cyano-1-methylethoxy radical will give rise to acetone and hydrogen cyanide through

8) N. Inamoto and O. Simamura, *J. Org. Chem.*, 23, 408 (1958).
9) T. Suehiro, presented at the 13th Annual Meeting of the Chemical Society of Japan, Tokyo, April, 1960.

TABLE I. PRODUCTS FORMED FROM DECOMPOSITION OF PEROXYBENZOIC ACID IN THE PRESENCE OF RADICAL-GENERATORS

Both the amount of radical-generators and the yields of products are given in percent of the peroxybenzoic acid used.

Radical-Generator	Solvent	Temp. °C	Benzoic acid	Other products
α, α'-Azobisisobutyronitrile 100	Benzene	Under reflux	87	Acetone, 9 Hydrogen cyanide
Isobutyryl peroxide 50	Benzene	60	73	Acetone, 12 Isopropyl alcohol
Isobutyryl peroxide 18	Cumene	60	64	α-Cumyl alcohol, 41 Acetone, trace 2, 3-Dimethyl-2, 3-diphenylbutane, 5

similar paths to those postulated previously in the reaction of α, α'-azobisisobutyronitrile with nitro compounds[8]. If reaction 4 takes place to the complete exclusion of reaction 1, the benzoyloxy radical will not be produced for reaction 3 to occur, and consequently it would be difficult to account for the formation of acetone cyanhydrin benzoate without invoking the improbable reaction 5. It therefore seems that reaction 4 should be only of subordinate importance compared with reaction 1.

The formation of acetone cyanhydrin benzoate would suggest that the following reaction might take place:

$$PhCO_3H + (CH_3)_2\dot{C}CN \rightarrow PhCO_2C(CH_3)_2CN + HO\cdot \quad (5)$$

This possibility, however, seems to be unlikely in view of the evidence discussed previously[2,3], which favours reaction 1 as the more probable one.

In contrast to the case with peroxybenzoic acid, when benzoyl peroxide was decomposed in benzene in the presence of α, α'-azobisisobutyronitrile, no evolution of hydrogen cyanide was detected. Simple distillation of the reaction mixture gave no acetone, but steam-distillation of the residue from the distillation gave acetone, whose source is also attributable to acetone cyanhydrin benzoate.

While peroxybenzoic acid decomposed slowly in *o*-dichlorobenzene at 80°C, addition of α, α'-azobisisobutyronitrile accelerated the decomposition enormously. Thus, while the half life of decomposition of peroxybenzoic acid (the initial concentration, 0.1 mol./l.) was 10.7 hr. in the absence of α, α'-azobisisobutyronitrile, it decreased to 40 min. in its presence (the initial concentration of α, α'-azobisisobutyronitrile, 0.2 mol./l.). On the basis of the rate constant for the unimolecular decomposition of α, α'-azobisisobutyronitrile, 1.53×10^{-4} sec^{-1} at 80°C[10], it is estimated that about 30% of this initiator was decomposed in the course of 40 min., during which 50% of the peroxybenzoic acid originally present had reacted. According to Eqs. 1 and 3, this amount of the acid consumed the 1-cyano-1-methylethyl radical from just an equimolecular quantity of the initiator, that is, 25% of the original amount. This is in rather good agreement with the value of 30% deduced above, indicating that the average efficiency of the 1-cyano-1-methylethyl radical in reaction with peroxybenzoic acid is about 80%. This efficiency of 80% may be too high, because part of peroxybenzoic acid may fairly rapidly be consumed by oxidation of chemical species other than the 1-cyano-1-methylethyl radical, e.g., dimethylketenecyanoisopropylimine produced by dimerization of this radical.

Isobutyryl peroxide decomposes much more rapidly than peroxybenzoic acid in most solvents[11,12]. In the presence of the former, the latter decomposed very rapidly at 60°C. For example, the presence of isobutyryl peroxide (concentration, 0.04 mol./l.) in benzene solution of peroxybenzoic acid (0.1 mol./l.) at 60°C, reduced the half life of peroxybenzoic acid to only 270 sec. Investigation of the products showed the formation of acetone and isopropyl alcohol besides benzoic acid. It therefore was deduced that the isopropyl radical generated thermally from isobutyryl peroxide by way of the isobutyryloxy radical attacks the oxygen atom of peroxybenzoic acid, producing a molecule of isopropyl alcohol and a benzoyloxy radical, and the isopropyl alcohol is further oxidized to acetone (reactions 6 and 7).

$$PhCO_3H + (CH_3)_2HC\cdot \rightarrow (CH_3)_2CHOH + PhCO_2\cdot \quad (6)$$

$$(CH_3)_2CHOH \xrightarrow{\text{oxidation}} (CH_3)_2CO \quad (7)$$

10) F. M. Lewis and M. S. Matheson, *J. Am. Chem. Soc.*, 71, 747 (1949).

11) J. Smid and M. Szwarc, *J. Chem. Phys.*, 29, 432 (1958).

12) K. Tokumaru and O. Simamura, unpublished results.

Obviously, the oxidation of isopropyl alcohol to acetone in accordance with the findings described previously[1] contributes to consumption of peroxybenzoic acid at a rate larger than that corresponding to the straightforward decomposition of isobutyryl peroxide followed by reaction 6 alone.

It was expected that if the reaction was carried out in cumene, which has a hydrogen atom reactive towards radicals, the isopropyl radical generated as well as the benzoyloxy radical from reaction 6 would abstract the hydrogen atom from cumene giving an α-cumyl radical (reactions 8 and 9). This radical then would attack peroxybenzoic acid producing α-cumyl alcohol and a benzoyloxy radical, the latter undergoing reaction 9 leading to the induced decomposition of peroxybenzoic acid as was shown previously[2].

$$(CH_3)_2HC\cdot + PhCH(CH_3)_2 \rightarrow C_3H_8 + Ph(CH_3)_2C\cdot \quad (8)$$

$$PhCO_2\cdot + PhCH(CH_3)_2 \rightarrow PhCO_2H + Ph(CH_3)_2C\cdot \quad (9)$$

$$Ph(CH_3)_2C\cdot + PhCO_3H \rightarrow PhC(CH_3)_2OH + PhCO_2\cdot \quad (10)$$

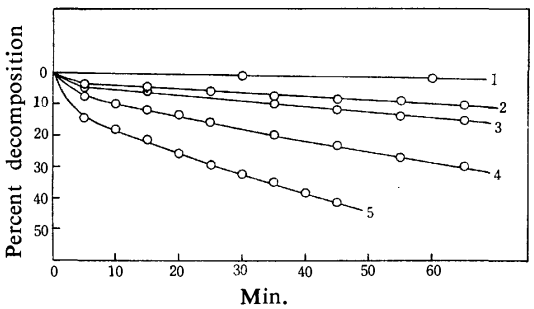

Fig. 1. Decomposition of peroxybenzoic acid in cumene in the presence of isobutyryl peroxide at 40°C. The initial concentration of peroxybenzoic acid, 0.1 mol./l. The initial concentration of isobutyryl peroxide relative to peroxybenzoic acid (in mol. %) : 1, 0%; 2, 5.6%; 3, 13.8%; 4, 22.6%; 5, 46.0%.

In fact, addition of isobutyryl peroxide to a cumene solution of peroxybenzoic acid caused a rapid decomposition of the latter as depicted in Fig. 1, and α-cumyl alcohol and 2, 3-dimethyl-2, 3-diphenylbutane were found among the products. Evidently 2, 3-dimethyl-2, 3-diphenylbutane, which was not detected in the decomposition in cumene in the absence of isobutyryl peroxide[2], was produced by dimerization of the α-cumyl radical, whose stationary concentration was higher owing to rapid supply of radicals by the decomposition of isobutyryl peroxide than that otherwise prevailing.

The rate of decomposition of peroxybenzoic acid became larger according as the initial concentration of isobutyryl peroxide was increased, but further kinetic study was not made, since this reaction was complicated.

Acetyl peroxide, which is known to decompose more slowly than isobutyryl peroxide, was added to a cumene solution of peroxybenzoic acid at 60°C, but the apparent decomposition rate of peroxybenzoic acid was not so much accelerated as when isobutyryl peroxide was added.

The present results indicate that in the presence of an efficient radical-generator a very rapid decomposition of peroxybenzoic acid takes place, and that this is due to the enhanced induced decomposition of the latter by radicals derived from the former.

Summary

The decomposition of peroxybenzoic acid in solvents was accelerated in the presence of radical-generators such as α, α'-azobisisobutyronitrile and isobutyryl peroxide. This acceleration was ascribed to the induced decomposition of peroxybenzoic acid by radicals formed directly or indirectly from these radical-generators.

Department of Chemistry
Faculty of Science
The University of Tokyo
Hongo, Tokyo

Decomposition of Peroxybenzoic Acid in Solution. V. Decomposition of Peroxybenzoic Acid and of Benzoyl Peroxide in Binary Mixtures of Carbon Tetrachloride with Cyclohexane, Toluene, or Diethyl Ether

By Katsumi TOKUMARU and Osamu SIMAMURA

(Received September 22, 1962)

In the course of investigation of the decomposition of peroxybenzoic acid in various organic solvents[1-4], it has become evident that peroxybenzoic acid suffers induced decomposition on the oxygen to oxygen bond by radicals derived from hydrocarbons, alcohols and ethers with great ease. Although a similar induced decomposition also takes place with benzoyl peroxide, the reactivity towards benzoyl peroxide differs widely from radical to radical, decreasing in the order: 1-hydroxyalkyl, 1-alkoxyalkyl>alkyl>chloroalkyl radical[5]. It therefore has seemed of interest to examine the behaviour of chloroalkyl radicals towards peroxybenzoic acid. An account is given in this paper of results of the decomposition of peroxybenzoic acid and of benzoyl peroxide in a binary mixture of carbon tetrachloride with a solvent containing hydrogen, in which the trichloromethyl radical is supposed to be produced by abstraction of a chlorine atom from carbon tetrachloride by radicals.

Experimental

Materials. — Peroxybenzoic acid was prepared according to the procedure described previously[1]. Benzoyl peroxide was purified by precipitation from a solution in chloroform by addition of methyl alcohol. The solvents used were purified as described previously[1-3].

Decomposition of Peroxybenzoic Acid in a Mixture of Cyclohexane and Carbon Tetrachloride. — Peroxybenzoic acid (2.8 g., 20 mmol.) was decomposed in a mixture of cyclohexane (50 ml.) and carbon tetrachloride (25 ml.) at 80°C under an atmosphere of nitrogen. The reaction mixture was extracted with aqueous sodium hydrogen carbonate, and the aqueous extract gave benzoic acid (1.8 g., 15 mmol.) on acidification. Distillation of the organic layer afforded a mixture of carbon tetrachloride and cyclohexane, crude cyclohexyl chloride (ca. 3 g., 25 mmol.) and cyclohexanol (0.2 g., 2 mmol.). Benzene and chloroform were detected in the recovered solvent by gas chromatography. Presence of small amount of chlorobenzene in the crude cyclohexyl chloride was confirmed by infrared spectrum and gas chromatography. Cyclohexanol was identified as 3,5-dinitrobenzoate, m. p. and mixed m. p. with an authentic sample, 112°C. In the residue from the distillation, ε-caprolactone (0.3 g., 3 mmol.) was found and identified as ε-hydroxycaproic acid hydrazide, m. p. 112°C.

Decomposition of Peroxybenzoic Acid in a Mixture of Toluene and Carbon Tetrachloride.—Peroxybenzoic acid (2.8 g., 20 mmol.) was decomposed in a mixture of toluene (50 ml.) and carbon tetrachloride (25 ml.) at 80°C in a stream of nitrogen. The reaction mixture was distilled; after the solvent was recovered, benzyl alcohol distilled over (trace, identified by infrared absorption measurement). Extraction of the residue from the distillation with aqueous sodium hydrogen carbonate gave benzoic acid (2.1 g., 17 mmol.). In the distillate benzene, chlorobenzene and chloroform were detected, but no benzyl chloride was detected by gas chromatography.

Decomposition of Peroxybenzoic Acid in a Mixture of Diethyl Ether and Carbon Tetrachloride.—Peroxybenzoic acid (2.8 g., 20 mmol.) was decomposed in a mixture of diethyl ether (50 ml.) and carbon tetrachloride (25 ml.) at 37°C under an atmosphere of nitrogen. After 30 hr. the reaction mixture was distilled. Acetaldehyde (5 mmol.) was detected in the distillate and characterized as the 2,4-dinitrophenylhydrazone, m. p. 168°C. Chloroform and ethyl alcohol were found by gas chromatography. However, no chloroether was detected in the distillate. Benzoic acid (2.1 g., 17 mmol.) was isolated from the residue from the distillation.

Decomposition of Benzoyl Peroxide in a Mixture of Cyclohexane and Carbon Tetrachloride.—Benzoyl peroxide (3.0 g., 12.4 mmol.) was decomposed in a mixture of cyclohexane (100 ml.) and carbon tetrachloride (50 ml.) at 80°C under an atmosphere of nitrogen until the peroxide was completely decomposed. Distillation of the reaction mixture gave a mixture of carbon tetrachloride and cyclohexane, crude cyclohexyl chloride (ca. 34.4 g., 290 mmol.) and a liquid boiling at higher temperatures (trace). The crude cyclohexyl chloride was shown to contain small amount of chlorobenzene by the infrared spectrum and by gas chromatography, and in the recovered solvent chloroform and benzene were detected by gas chromatography. Extraction

1) K. Tokumaru, O. Simamura and M. Fukuyama, This Bulletin, 35, 1673 (1962).
2) K. Tokumaru and O. Simamura, ibid., 35. 1678 (1962).
3) K. Tokumaru and O. Simamura, ibid., 35, 1955 (1962).
4) K. Tokumaru, N. Inamoto and O. Simamura, ibid., 36, 72 (1963).
5) K. Nozaki and P. D. Bartlett, *J. Am. Chem. Soc.*, 68, 1686 (1946); P. D. Bartlett and K. Nozaki, ibid., 69, 2299 (1947).

of the residue from the distillation with aqueous sodium hydrogen carbonate gave benzoic acid (1.1 g., 9 mmol.). The cyclohexyl chloride was hydrolysed to cyclohexanol and characterized as 3,5-dinitrobenzoate, m. p. 112°C.

Decomposition of Benzoyl Peroxide in a Mixture of Toluene and Carbon Tetrachloride.—Benzoyl peroxide (5.0 g., 20.6 mmol.) was decomposed in a mixture of toluene (100 ml.) and carbon tetrachloride (50 ml.) at 80°C under an atmosphere of nitrogen until the peroxide was completely decomposed. The reaction mixture was distilled, giving carbon tetrachloride, toluene, chlorobenzene (0.9 g., 8 mmol.), b. p. ca. 35°C at 20 mmHg, and benzyl chloride (0.5 g., 4 mmol.), b. p. ca. 72°C at 20 mmHg. Both chlorides were identified by infrared absorption measurement and by gas chromatography, and the benzyl chloride, on treatment with *N*, *N*-dimethylaniline, afforded benzyldimethylanilinium chloride, m. p. 110°C. In the recovered solvent, benzene and chloroform were detected by gas chromatography. The remaining mixture from the distillation was extracted with aqueous sodium hydrogen carbonate, and the aqueous layer gave benzoic acid (0.8 g., 6.5 mmol.) on acidification. Further distillation of the organic mixture gave a distillate (1.8 g.), b. p. 90~120°C at 2 mmHg, which on cooling, gave bibenzyl as needle shaped crystals (0.5 g.), melting point (from ethyl alcohol) and mixed m. p. with an authentic sample, 52°C.

Decomposition of Benzoyl Peroxide in a Mixture of Diethyl Ether and Carbon Tetrachloride.—Benzoyl peroxide (10.0 g., 41.2 mmol.) was allowed to decompose in a mixture of diethyl ether (200 ml.) and carbon tetrachloride (100 ml.) at 37°C for four weeks in a stream of nitrogen. During the reaction volatile product was collected in a trap cooled with dry ice and ethyl alcohol. After the reaction was over, the reaction mixture was distilled below 40°C on a water bath under reduced pressure of a water-jet aspirator. The distillate was subjected to redistillation, giving, after ether and carbon tetrachloride, a fraction (ca. 15 g.), b. p. ca. 25°C at 60 mmHg. This turned out to be 1-chloroethyl ethyl ether, since it afforded, on being allowed to stand in the air, hydrogen chloride and acetaldehyde, which was identified by conversion into the 2,4-dinitrophenylhydrazone, m. p. 168°C. The recovered solvent and the condensate in the trap were combined and extracted with water, and the aqueous extract, on treatment with 2,4-dinitrophenylhydrazine, gave 2,4-dinitrophenylhydrazone of acetaldehyde. The residue from the first distillation was extracted with aqueous sodium hydrogen carbonate, and the aqueous layer yielded benzoic acid (2.2 g., 18 mmol.) on acidification. Addition of methyl alcohol to the organic layer caused precipitation of benzoyl peroxide (0.8 g., 3 mmol.). After it was filtered off, methyl alcohol was removed and the liquid residue was shown to contain chlorobenzene by infrared measurements.

Results and Discussion

The results of the analysis of reaction products are shown in Table I.

The formation of all the products containing no chlorine atom is readily understood on the basis of the free radical mechanism previously postulated for the decomposition of peroxybenzoic acid in solution[1-4], which involves the initial homolysis of the oxygen to oxygen bond:

$$PhCO_3H \rightarrow PhCO_2\cdot + HO\cdot$$

In a mixture of carbon tetrachloride and cyclohexane, the radicals thus generated abstract a hydrogen atom from cyclohexane giving a cyclohexyl radical and benzoic acid or water. The cyclohexyl radical causes the

Table I. Products from decomposition of peroxybenzoic acid or benzoyl peroxide in a mixture of carbon tetrachloride and a solvent (SH) (1 : 2 by volume)

Solvent	Peroxide*	Temp. °C	Product and yield (in % based on peroxide) Benzoic acid	Product of S-Cl type	Products formed by oxidation of solvent	Other products detected
Cyclohexane	PBA	80	75	Cyclohexyl chloride, 125	Cyclohexanol, 10; ε-caprolactone, 15	Benzene, chloroform, chlorobenzene
	BPO	80	73	Cyclohexyl chloride, 2300		Benzene, chloroform, chlorobenzene, ester (trace)
Toluene	PBA	80	85	Benzyl chloride not detected	Benzyl alcohol, trace	Benzene, chloroform, chlorobenzene
	BPO	80	32	Benzyl chloride, 19		Bibenzyl (13), high boiling liquid, chlorobenzene, benzene, chloroform
Diethyl ether	PBA	37	85	1-Chloroethyl ethyl ether not detected	Acetaldehyde, 25; ethyl alcohol	Chloroform
	BPO	37	47	1-Chloroethyl ethyl ether, approximately 330		Benzoyl peroxide recovered (7), acetaldehyde, chlorobenzene

* PBA and BPO stand for peroxybenzoic acid and benzoyl peroxide, respectively.

induced decomposition of peroxybenzoic acid giving a benzoyloxy radical and cyclohexanol, the latter subsequently giving ε-caprolactone as has previously been discussed in detail[2]. For the other solvent mixtures formation of the products containing no chlorine is accounted for in a similar way.

In the presence of carbon tetrachloride besides cyclohexane, the cyclohexyl radical would abstract a chlorine atom from the former yielding cyclohexyl chloride and a trichloromethyl radical. This radical gives chloroform on abstraction of a hydrogen atom from cyclohexane. Chlorobenzene is thought to be formed by attack on carbon tetrachloride by the phenyl radical generated by decomposition of the benzoyloxy radical.

Similarly, benzyl chloride and 1-chloroethyl ethyl ether found in the products from the decomposition of benzoyl peroxide in binary mixtures of carbon tetrachloride with toluene and diethyl ether are formed by abstraction of a chlorine atom from carbon tetrachloride by solvent radicals, namely, the benzyl and the 1-ethoxyethyl radical.

In the decomposition of peroxybenzoic acid in a mixture of cyclohexane and carbon tetrachloride, both cyclohexyl chloride and cyclohexanol were formed, indicating that the two following reactions took place side by side:

$$C_6H_{11}\cdot + PhCO_3H \rightarrow C_6H_{11}OH + PhCO_2\cdot \quad (1)$$

$$C_6H_{11}\cdot + CCl_4 \rightarrow C_6H_{11}Cl + CCl_3\cdot \quad (2)$$

However, in this solvent mixture the yield of cyclohexyl chloride was much higher in the decomposition of benzoyl peroxide than in the case of peroxybenzoic acid. The yield of as much as 23 mol. of cyclohexyl chloride for one mole of the benzoyl peroxide decomposed shows that the chain reaction that produces cyclohexyl chloride is sustained for a considerable number of cycles:

$$C_6H_{11}\cdot + CCl_4 \rightarrow C_6H_{11}Cl + CCl_3\cdot$$
$$CCl_3\cdot + C_6H_{12} \rightarrow CHCl_3 + C_6H_{11}\cdot$$

The difference between the two peroxides undoubtedly lies in greater tendency of peroxybenzoic acid to be attacked by the cyclohexyl radical.

In the decomposition of peroxybenzoic acid in a mixture of toluene and carbon tetrachloride and of diethyl ether and carbon tetrachloride no chlorides derived from the solvents, that is, benzyl chloride and 1-chloroethyl ethyl ether, were found, showing that the reactions corresponding to reaction 2 could not successfully compete with those corresponding to reaction 1 in these cases. The benzyl and the 1-ethoxyethyl radical are accepted as stabilized owing to resonance and therefore rather sluggish in reaction, so that they would abstract a chlorine atom from carbon tetrachloride only slowly, but it is quite remarkable that they attacked peroxybenzoic acid with ease.

On the other hand, the decomposition of benzoyl peroxide in these solvent mixtures gave benzyl chloride and 1-chloroethyl ethyl ether, indicating that the benzyl and the 1-ethoxyethyl radical abstracted a chlorine atom from carbon tetrachloride rather than react exclusively with benzoyl peroxide. Thus it is concluded that peroxybenzoic acid reacts with the cyclohexyl, benzyl and 1-ethoxyethyl radical much more readily than benzoyl peroxide does.

In a mixture of diethyl ether and carbon tetrachloride the decomposition of benzoyl peroxide was not finished in four weeks, whereas it was shown complete in ten days at 37°C in a separate experiment in pure diethyl ether; indeed, the 1-ethoxyethyl radical is known to be highly reactive towards benzoyl peroxide[6]. It is concluded from these findings that the induced decomposition of benzoyl peroxide by the 1-ethoxyethyl radical is suppressed in the presence of carbon tetrachloride, the 1-ethoxyethyl radical readily reacting with carbon tetrachloride instead of reacting with benzoyl peroxide. The change in polarity of the solvent, that is, from pure ether to a mixture of ether and carbon tetrachloride might be another contributing factor.

The formation of bibenzyl in the decomposition of benzoyl peroxide in a mixture of toluene and carbon tetrachloride is accounted for by the comparative inefficiency of the benzyl radical in attacking benzoyl peroxide; thus its stationary concentration would be increased to such an extent that the dimerization giving bibenzyl would become noticeable. The comparative inertness of the benzyl radical towards carbon tetrachloride should be partly responsible for the increased stationary concentration.

The trichloromethyl radical formed from carbon tetrachloride would abstract a hydrogen atom from a molecule of solvent (SH) giving chloroform (reaction 3), and it could attack peroxybenzoic acid, producing phosgene and hydrogen chloride (reactions 4 and 4').

$$CCl_3\cdot + SH \rightarrow CHCl_3 + S\cdot \quad (3)$$

$$CCl_3\cdot + PhCO_3H \rightarrow CCl_3OH + PhCO_2\cdot \quad (4)$$

$$CCl_3OH \rightarrow COCl_2 + HCl \quad (4')$$

Reaction 3 is a well known reaction, and in fact extensive formation of chloroform was

6) W. E. Cass, *J. Am. Chem. Soc.*, **69**, 500 (1947).

observed in all cases examined. Reaction 4, however, does not seem important, since formation of only negligible traces of phosgene and hydrogen chloride was observed. Thus the trichloromethyl radical, in contrast with the other radicals so far examined, appears to be extremely reluctant to attack peroxybenzoic acid. The cause should be ascribed to the electron-accepting property of the trichloromethyl, as will subsequently be discussed.

Summary

Decompositions of peroxybenzoic acid and of benzoyl peroxide were carried out in binary mixtures of carbon tetrachloride with cyclohexane, toluene or diethyl ether. The results of the product study strongly support the radical mechanism established previously and show that the oxygen to oxygen bond of peroxybenzoic acid is attacked by radicals more readily than that of benzoyl peroxide, but even peroxybenzoic acid is hardly attacked by the trichloromethyl radical.

Department of Chemistry
Faculty of Science
The University of Tokyo
Hongo, Tokyo

The Crystal Structure of Phenazine 5, 10-Dioxide

By Yoshiyuki NAMBA, Tsutomu ODA and Tokunosuké WATANABÉ

(Received September 15, 1962)

This paper describes part of an investigation of the structure of the *N*-oxides of heterocyclic compounds. Here we present the results of an analysis of the crystal and molecular structure of phenazine 5, 10-dioxide. In the course of the present investigation, a paper on the structure of the same substance was published[1]. Though the space group and the general scheme of the structure remain the same, the unit cell dimensions, and hence the interatomic distances, are different.

Experimental

Sample.—Phenazine 5, 10-dioxide was synthesized by the oxidation of phenazine 5-oxide using hydrogen peroxide and a acetic acid mixture. Single crystals were obtained from acetic acid solutions. Ethanol solutions of these crystals did not show any trace of absorption lines due to phenazine 5-oxide. Single crystals are elongated needle-like in the direction of the b-axis, are red in color and have predominant faces at {100} and $\{10\bar{2}\}$.

Crystal Data.—The unit cell dimensions were determined from oscillation photographs by recording the same reflections on both sides of the film, while the radius of the camera used was calibrated by superimposing a powder pattern of pure sodium chloride.

The density was measured by the pycnometer method using water as the medium.

Phenazine 5, 10-dioxide, $C_{12}H_8N_2O_2$, M. wt. = 212. D. p. = 190°C

Monoclinic;

$a = 7.83 \pm 0.02$ $\quad b = 3.95 \pm 0.02$

$c = 15.50 \pm 0.05$ Å $\quad \beta = 104°48' \pm 10'$

Volume of the unit cell: 463.47 Å^3

Density: Obs. 1.52 g. cm^{-3}, calcd. (with $z=2$) 1.519 g. cm^{-3}

Linear absorption coefficient for X-ray ($\lambda =$ 1.542 Å): $\mu = 10.1$ cm^{-1}

Total number of electrons per unit cell: $F(000) = 220$

The extinction rules were found to be $(h0l)$ for l odd and $(0kl)$ for k odd. Accordingly, the space group was determined as $P\,2_1/c - C^5_{2h}$.

It may be added here that on extremely long-exposured films there appeared several weak reflections which did not agree with the extinctions mentioned above. However, the shape of these reflections differ from the rest, and their indices (101), (201), $(20\bar{1})$ and (203) can be interpreted as due to double reflections arising from the following combinations of indices whose intensities are all very strong:

$(101) : (0\bar{1}3)$; $(1\bar{1}\bar{2})$ $\quad (201) : (311)$; $(\bar{1}\bar{1}0)$

$(20\bar{1}) : (\bar{1}13)$; $(3\bar{1}\bar{4})$ $\quad (203) : (310)$; $(\bar{1}\bar{1}3)$

It is to be noted that similar double reflections have also been reported in the cases of anthraquinone[2] and other crystals[3] consisting of planar molecule.

Intensity Data.—The intensity data were obtained from equi-inclination Weissenberg photographs

1) R. Curti and V. Riganti, *Rend. it. Lombardo Sci., Pt. I. Classe Sci. mat e nat.*, **94A**, 117 (1960).

2) B. V. Murty, *Acta Cryst.*, **8**, 113 (1955).

3) H. Watase, K. Osaki and I. Nitta, This Bulletin, **30**, 532 (1957).

(*h*0*l*) and (0*kl*) taken by means of CuK_α radiation filtered through nickel foil.

The multiple-film technique was used, and the intensities were estimated visually by comparison with a calibrated scale prepared with the same crystal. The range of intensities measured was 1~6000 for the two zones, and the number of reflections observed were 107 for (*h*0*l*) and 48 for (0*kl*). These figures correspond to 75% and 70% of the total number of reciprocal lattice points included within the sphere of reflection.

The intensities were corrected for Lorentz and polarization factors to obtain the relative values of $|F|^2$.

No absorption corrections were applied, as the cross-sections of the crystals used were 0.2 mm.× 0.2 mm. for *h*0*l* (μr=0.2) and 0.5 mm.×0.5 mm. for 0*kl* (μr=0.5) respectively.

Structure Determination

Since the space group is $P\ 2_1/c$ and since the unit cell contains two molecules, it follows that the center of gravity of the molecules should be placed at one of the following four sets of equivalent positions:

(a) 0, 0, 0; 0, 1/2, 1/2

(b) 1/2, 0, 0; 1/2, 1/2, 1/2

(c) 0, 0, 1/2; 0, 1/2, 0

(d) 1/2, 0, 1/2; 1/2, 1/2, 0

It is immaterial which set is chosen; hence, case (a) was chosen.

The fact that the length of the b-axis of the unit cell is comparable to the van der Waals' contact between condensed rings (3.5Å) suggests that the molecular planes have to be almost parallel to the (010)-plane. Therefore, if we designate the molecular axes by L and M, where L is the longest axis joining the centers of the three hexagons of the phenazine ring and M is the one along the N–O bonds, it is anticipated that the orientations of these molecular axes with respect to the a- and c-axes may be found easily by an optical Fourier transform of a single molecule.

The b-Axis Projection.—With a model of a planar molecule having the bond lengths 1.4 Å, 1.4 Å, 1.3 Å for C–C, C–N and N–O respectively and a bond angles of 120° for all, Fraunhofer diffraction patterns for various inclinations of the molecular axes to the b-plane were prepared. Comparing these Fraunhofer diffraction patterns with the (*h*0*l*) weighted reciprocal lattice, it was found that the molecular axis L points in the [102] direction. Furthermore, using the superposition method proposed by Otsuka and Watanabe[4], signs of the structure factors for several reflections

4) T. Watanabe and M. Otsuka, *Acta Cryst.*, **10**, 377 (1957).

SIGNS FOUND BY THE OPTICAL METHOD

h 0 *l*	Sign	*h* 0 *l*	Sign
1 0 6	−	4 0 10	+
2 0 14	+	5 0 8	+
3 0 2	−	5 0 10	+
3 0 6	−	6 0 4	+
3 0 14	+	7 0 4	+
4 0 0	−	0 0 8	−
4 0 2	−		

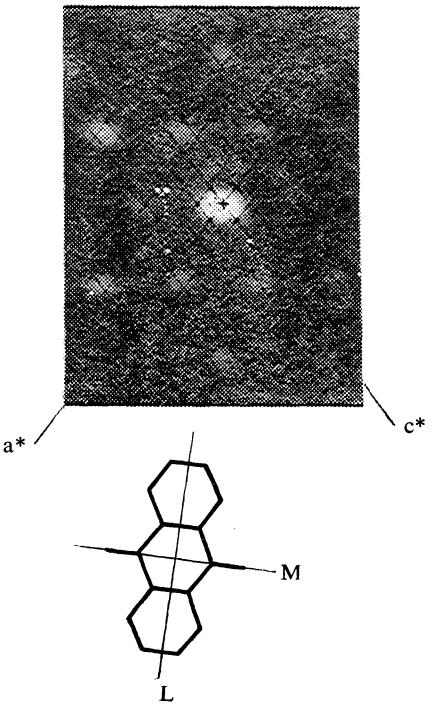

Fig. 1. Optical transform of the (0*l*0) projection and projected molecule giving optical transform.

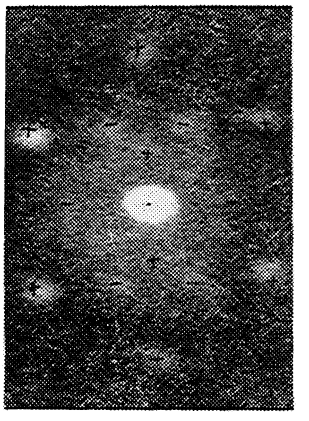

Fig. 2. Optical transform using superposition method, the enhancement of the positive regions are observed.

TABLE I. ATOMIC PARAMETERS WITH STANDARD DEVIATIONS

Atom	x	s. d.	y	s. d.	z	s. d.	B, Å^2
O	−0.229	0.0009	0.061	0.003	0.1053	0.0004	7.1
N	−0.115	0.001	0.030	0.004	0.0545	0.0005	5.1
C	0.048	0.001	0.164	0.004	0.0802	0.0005	5.2
C	0.106	0.001	0.337	0.005	0.1644	0.0005	5.7
C	0.271	0.001	0.473	0.006	0.1891	0.0005	6.3
C	0.393	0.001	0.444	0.006	0.1338	0.0005	6.4
C	0.341	0.001	0.277	0.005	0.0526	0.0005	6.2
C	0.173	0.001	0.136	0.004	0.0244	0.0005	5.4

with strong intensities, as are shown in the following table were obtained.

Signs of the structure factors not determined by the above method were obtained by calculations of structure factors based on the atomic coordinates derived from the molecular orientation found by the optical method.

The first Fourier map $\rho(xz)$ was prepared, by using about 70 terms whose calculated structure factors showed a fairly good agreement with the observed F values. All the atoms were well resolved in this projection. The refinement was made successively by Fourier syntheses and by difference syntheses, which gave a disagreement index R 18 %.

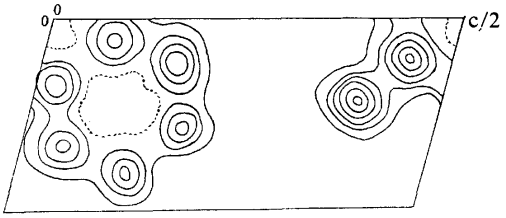

Fig. 3. Electron-density projection along [010].

***y*-Coordinates.**—There remained two possible sets of y-coordinates of all the atoms to be determined. Calculations of the structure factors, $(0kl)$, were carried out for the two structures. It was possible to eliminate one of the two structures from the disagreements between F_c and F_o, even for lower order reflections.

The successive refinement of the y-coordinates was accomplished by the trial and error method with the aid of the structure factor maps[5], while keeping the z-coordinates unchanged from the positions already obtained from the analyses of the (010) projection.

In the calculation of structure factors, the atomic scattering factors given by Berghuis et al.[6] were used throughout.

Final refinements of the positional- and isotropic temperature- parameters of individual atoms were made by least squares calculations[7] for $(h0l)$ and $(0kl)$ zones respectively, the contributions of hydrogen atoms being, however, omitted.

The final positional- and isotropic temperature-parameters with standard deviations, are listed in Table I.

TABLE II. BOND LENGTHS AND BOND ANGLES

Bond length, Å		Bond angle	
O—N	1.34	∠ONC$_1$	121°
N—C$_1$	1.34	∠NC$_1$C$_2$	120°
C$_1$—C$_2$	1.44	∠C$_1$C$_2$C$_3$	120°
C$_2$—C$_3$	1.36	∠C$_2$C$_3$C$_4$	121°
C$_3$—C$_4$	1.44	∠C$_3$C$_4$C$_5$	119°
C$_4$—C$_5$	1.39	∠C$_4$C$_5$C$_6$	119°
C$_5$—C$_6$	1.37	∠C$_5$C$_6$C$_1$	119°
C$_6$—C$_1$	1.45	∠C$_6$C$_1$C$_2$	118°
C$_6$—N	1.39	∠C$_6$C$_1$N	121°
		∠C$_1$N C$_6$′	122°
		∠ONC$_6$′	117°
		∠C$_1$C$_6$N′	117°
		∠C$_5$C$_6$N′	122°

The disagreement index, R, for the final coordinates was 16% for $(h0l)$ and 15% for $(0kl)$. The comparison of the observed structure factors with the calculated ones is shown in Table III.

Discussion of the Structure

Molecular Structure.—The phenazine-ring skeleton found in this investigation is practically the same as those for α-phenazine[8] and phenazine 5-oxide[9]. The bond distances and valency angles found in these three compounds are shown in Table IV.

The value 1.33 Å for the N–O bond indicates that it has some double bond character. In Table V, several N–O bond distances previously

5) W. L. Bragg and H. Lipson, *Z. Krist.*, **95**, 323 (1936).
6) J. Berghuis, I. J. M. Haanappel, M. Potters, B. O. Loopstra, C. H. MacGillavry and A. L. Veenendaal, *Acta Cryst.*, **8**, 478 (1955).
7) K. Osaki, The Programme of Least Squares Calculations in X-Ray Crystallography by the NIAC-2203 Computer (EOI-3330, Nippon Electric Co. (1962)).
8) L. F. Hirshfeld and G. M. Schmidt, *Acta Cryst.*, **7**, 129 (1954); ibid., **9**, 233 (1956); F. H. Herbstein and G. M. Schmidt, ibid., **8**, 399 (1955).
9) R. Curti, V. Riganti and S. Lochi, ibid., **14**, 133 (1961).

TABLE III. OBSERVED AND CALCULATED STRUCTURE FACTORS

$h\,k\,l$	$F_o/4$	$F_c/4$	$h\,k\,l$	$F_o/4$	$F_c/4$	$h\,k\,l$	$F_o/4$	$F_c/4$	$h\,k\,l$	$F_o/4$	$F_c/4$
0 0 2	40.7	44.4	8	8.2	10.0	6	11.1	− 9.2	6	12.2	−12.4
4	27.1	−27.3	10	4.2	6.4	8	4.7	− 6.2	7	14.7	−14.6
6	3.2	− 4.1	12	0.1	0.1	10	9.7	7.5	8	6.7	− 6.0
8	15.6	−14.7	6 0 0	1.9	− 4.9	12	2.5	3.0	9	3.8	3.9
10	4.4	− 4.7	2	1.6	2.3	14	2.5	− 2.6	10	2.9	3.3
12	0.9	− 2.2	4	0.6	− 0.9	16	2.2	− 2.0	11	1.1	− 1.4
14	2.8	− 2.6	6	0.6	− 2.2	18	2.8	− 2.1	12	0.4	0.4
16	0.5	0.5	8	0.3	− 0.5	$\bar{5}$ 0 2	0.5	0.5	13	0.6	− 0.8
18	0.1	0.1	10	0.3	− 1.0	4	10.1	− 9.4	14	1.3	− 1.3
1 0 0	37.9	35.3	7 0 0	2.2	− 2.0	6	1.6	1.9	15	0.5	− 1.1
2	3.5	− 1.4	2	2.2	− 3.6	8	11.5	9.4	16	0.1	0.1
4	22.3	22.7	4	4.7	− 5.9	10	1.3	− 1.8	0 2 0	12.6	12.1
6	26.8	−27.5	6	2.6	− 1.3	12	7.3	− 4.8	1	2.9	3.2
8	29.7	−30.5	8	0.2	0.2	14	2.5	− 0.4	2	5.9	− 5.5
10	0.9	0.9	8 0 0	0.9	1.6	16	0.6	0.7	3	12.6	−12.6
12	3.8	4.4	2	1.9	− 4.0	18	1.3	− 1.4	4	8.0	− 8.5
14	1.6	− 1.2	4	1.3	− 2.6	$\bar{6}$ 0 2	9.0	8.1	5	16.8	−15.6
16	3.5	− 3.9	6	0.5	0.5	4	21.9	21.1	6	0.3	0.3
18	0.6	− 0.8	9 0 0	0.1	0.1	6	8.0	4.8	7	3.8	5.5
2 0 0	27.8	−27.2	2	0.3	0.4	8	0.9	1.3	8	0.8	1.0
2	18.1	15.4	$\bar{1}$ 0 2	39.3	41.7	10	5.7	− 2.7	9	1.3	0.6
4	15.7	18.5	4	22.3	−21.8	12	9.5	− 7.3	10	1.7	1.3
6	0.6	0.9	6	14.3	14.0	14	1.9	− 2.0	11	2.5	− 2.9
8	2.2	− 2.9	8	5.9	6.5	16	1.6	0.8	12	2.9	− 3.4
10	2.2	− 3.0	10	1.9	− 1.3	18	0.1	− 0.1	13	1.7	− 1.9
12	0.9	− 1.4	12	7.6	6.4	$\bar{7}$ 0 2	1.6	0.0	14	0.6	− 1.3
14	4.2	− 3.0	14	1.6	0.1	4	17.7	15.7	15	0.6	− 1.1
16	2.2	− 1.7	16	0.9	1.1	6	12.5	10.7	0 3 1	0.8	1.1
3 0 0	2.8	− 2.3	18	1.3	1.5	8	2.5	− 2.7	2	7.1	− 7.0
2	37.2	−33.2	$\bar{2}$ 0 2	22.3	−21.5	10	1.6	0.1	3	0.8	− 0.6
4	7.6	− 5.7	4	25.4	−26.2	12	0.2	− 0.2	4	0.6	1.0
6	11.8	12.3	6	3.5	− 4.2	14	0.1	− 0.1	5	0.8	− 1.5
8	0.9	0.5	8	0.6	− 1.7	$\bar{8}$ 0 2	1.9	2.0	6	1.7	1.6
10	0.7	− 0.8	10	11.8	−12.1	4	0.8	− 0.8	7	0.5	− 0.5
12	0.1	− 0.1	12	13.6	12.8	6	0.4	0.4	8	0.4	− 0.4
14	1.6	− 0.8	14	21.2	18.4	8	2.5	− 2.5	9	0.8	− 3.5
16	0.6	0.8	16	1.9	2.3	10	0.0	0.0	10	0.8	− 1.8
4 0 0	9.7	−10.9	18	0.3	0.3	12	1.6	0.7	11	2.1	− 2.1
2	19.0	−22.4	$\bar{3}$ 0 2	19.8	18.5	$\bar{9}$ 0 2	0.1	0.1	12	0.8	− 1.3
4	1.9	− 4.9	4	0.4	− 0.4	4	0.4	− 0.4	0 4 0	0.6	0.6
6	2.5	− 3.4	6	36.9	−39.3	6	1.2	− 0.5	1	0.3	− 0.3
8	4.2	7.8	8	15.6	−13.7	8	1.9	− 2.1	2	0.6	0.8
10	10.8	14.6	10	1.9	1.7	10	2.2	− 2.7	3	0.6	− 1.0
12	2.6	2.3	12	3.8	1.4	12	0.9	− 0.7	4	0.2	− 0.2
14	0.3	− 0.8	14	12.3	9.4	0 1 1	23.5	25.6	5	0.6	− 0.6
5 0 0	1.6	− 1.7	19	2.5	3.5	2	43.7	−57.7	6	0.7	− 1.1
2	2.5	5.2	18	1.9	− 0.9	3	39.9	42.1	7	0.7	0.9
4	0.6	0.0	$\bar{4}$ 0 2	2.5	2.8	4	19.3	−22.0	8	1.4	− 1.7
6	1.6	− 3.1	4	3.8	− 4.6	5	21.4	−23.3	9	0.5	− 0.6

reported are given. The value of 1.42Å found for trimethylamine *N*-oxide hydrochloride[15] can be taken as the standard single bond distance. The N–O bond distances in *N*-heteroconjugate ring compounds are shorter than that of trimethylamine *N*-oxide; this indicates that there exists a resonance between lone-pair electrons in the oxygen atom and the π-electron system in conjugate rings. If we assume 1.16 and 1.43 Å for the single and double bonds for N–O, the total bond order N[10] for the N–O bond in phenazine 5, 10-dioxide is

10) W. J. Orville-Thomas, *Chem. Revs.*, **57**, 1179 (1957).

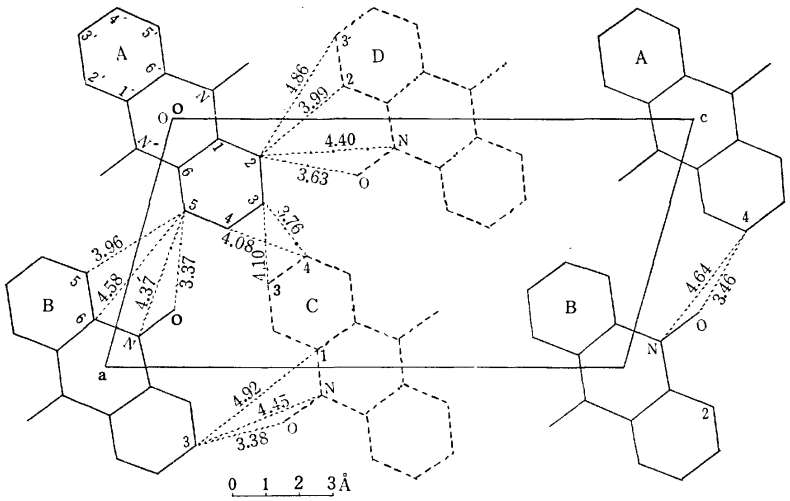

Fig. 4. Projection of the unit-cell contents on (010).

TABLE IV. BOND DISTANCES AND VALENCY ANGLES IN RELATED CRYSTALS

	α-Phenazine	5-Oxide	5, 10-Dioxide
N—C_1	1.355 Å	1.34 Å	1.34 Å
C_1—C_2	1.415 Å	1.40 Å	1.44 Å
C_2—C_3	1.382 Å	1.38 Å	1.36 Å
C_3—C_4	1.412 Å	1.39 Å	1.44 Å
C_4—C_5	1.367 Å	1.36 Å	1.39 Å
C_5—C_6	1.412 Å	1.38 Å	1.37 Å
C_6—C_1	1.433 Å	1.43 Å	1.45 Å
N—O		1.24 Å	1.34 Å
$\angle N C_1C_6$	121.7°	120°	121°
$\angle C_6C_1C_2$	119.4°	119°	118°
$\angle C_1C_2C_3$	120.0°	119°	120°
$\angle C_2C_3C_4$	120.6°	122°	121°
$\angle C_3C_4C_5$	121.0°	120°	119°
$\angle C_4C_5C_6$	120.4°	121°	119°
$\angle C_5C_6C_1$	118.5°	119°	119°
$\angle C_1C_6N$	122.7°	121°	117°
$\angle C N C$	116.6°	119°	122°

calculated to be 1.3, which can be compared to the value $N=1.17$ assigned for the N–O bond in pyridine *N*-oxide hydrochloride[11,12]. The distance, 1.37 Å, found for the N–O bond in pyridine *N*-oxide hydrochloride, which is somewhat longer than that of any other pyridine derivatives, would indicate that the n-π resonance here is weakened by the addition of a proton to oxygen*.

Arrangement of the Molecules.—The arrangement of the molecules and the packing between nearest neighbors are shown in Figs. 4 and 5, which are the b- and c-axes projections of the structure respectively. The packing of the molecules is found to be quite similar to those for α-phenazine[8], phenazine 5-oxide[9] and anthraquinone[16]. It can be said that these are iso-structural.

The shortest intermolecular distance between

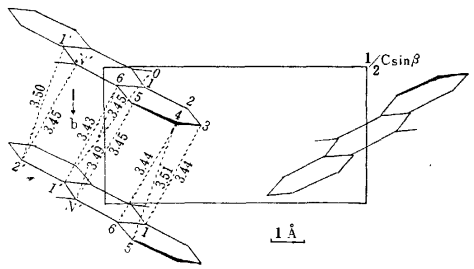

Fig. 5. Projection of the half unit-cell contents down [100].

TABLE V. N–O BOND LENGTHS IN RELATED COMPOUNDS

	N-Oxides	N–O Bond length, Å
	Pyridine *N*-oxide hydrochloride	1.37[11,12]
A	4, 4-*trans*-Azopyridine *N*-oxide	1.28[13]
	4-Nitropyridine *N*-oxide	1.26[14]
	Phenazine 5-oxide	1.24[9]
B	Trimethylaminoxide hydrochloride	1.42[15]

* The crystal structure of pyridine *N*-oxide has not yet been determined. As the result of an infrared absorption study, it was reported by Dr. Kubota et at. of Shionogi Research Laboratory at the 5 th Meeting for Infrared and Raman Spectra that the distance of the N-O bond in it was 1.27~1.29 Å.

11) Y. Namba, T. Oda, H. Ito and T. Watanabe, This Bulletin, 33, 1618 (1960).
12) P. G. Tsoucaris, *Acta Cryst.*, 14, 914 (1961).
13) E. L. Eichhorn, ibid., 12, 746 (1959).
14) F. L. Eichhorn, ibid., 9, 787 (1956).
15) C. Rerat, ibid., 13, 63 (1960).
16) S. N. Sen, *Indian, J. Phys.*, 19, 243 (1945); *Structure Report*, 11.

neighboring molecules related by the translation parallel to the a-axis is 4.04 Å ($C_5\cdots C_{5'}$), while that between molecules related by the glide plane is 3.99 Å ($C_2\cdots C_2$), and that along a diagonal direction, 3.76 Å ($C_3\cdots C_4$).

These intermolecular distances are found to be very close to the corresponding intermolecular distances reported for α-phenazine, as is shown in Table VI.

TABLE VI. THE INTERMOLECULAR DISTANCES OF NEAREST NEIGHBORING MOLECULES

	$C_5\cdots C_{5'}$	$C_2\cdots C_2$	$C_3\cdots C_4$
This crystal	4.04 Å	3.99 Å	3.72 Å
α-Phenazine	4.07 Å	3.88 Å	4.02 Å

It is very interesting to see that in the structures of 5-oxide and 5, 10-dioxide the oxygen atoms can be said to lie in the holes resulting from the packing of the phenazine rings. Such holes, though small in size, can also be found in the structure of α-phenazine. The ratio of the number of oxygen atoms to the number of holes is 1 for 5, 10-dioxide crystal, whereas it is 1/2 for the 5-oxide crystal.

The angle of inclination of the molecule to the (010)-plane is about 30° for the longest molecular axis, L, and about 5° for the shorter one, M.

Let us now compare the structure of the 5, 10-dioxide crystal with those of related crystals. We notice that the unit cell dimensions of these crystals change by degrees with an increase in the number of oxygen atoms in a molecule, as is shown in Table VII.

TABLE VII. UNIT CELL DIMENSIONS OF RELATED CRYSTALS

	a, Å	b, Å	c, Å	β
α-Phenazine	7.088	5.061	13.22	109°13′
5-Oxide	7.37	4.60	14.34	108°59′
5, 10-Dioxide	7.85	3.95	15.50	104°48′
Anthraquinone	7.92	3.98	15.85	102°42′

The differences in the lengths of these b-axes correspond to the different inclinations of the molecular plane to the (010)-plane. However, it is to be emphasized that the interplanar distances between the neighboring molecular planes remain practically the same, about 3.5 Å, for all the compounds listed. The inclination of the molecular plane mentioned above is related to the mutual displacement of the molecular planes in the same stack. These features can well be seen in Fig. 6, where the structures projected onto their molecular planes are shown for α-phenazine and phenazine 5, 10-dioxide. We are now trying to elucidate the different inclinations of the molecular planes in these related structures, taking into account various interactions between molecules.

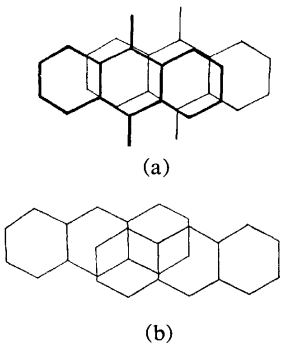

Fig. 6. Normal projection of two molecules in the same stack separated by unit translation along [0/0].
(a) Phenazine-5, 10-dioxide
(b) α-Phenazine (by Herbstein & Schmidt[8])

The authors wish to express their deep thanks to Professor Eizo Matsumura and Mr. Hisao Takeda of Osaka Gakugei University for their kind support in preparing samples, and to Dr. Kenji Osaki of Osaka University for his help in the electronic computer calculations.

Laboratory of Physical Chemistry
Osaka University of Liberal Arts and Education
Tennoji, Osaka (Y. N. and T. O.)

Department of Physics
Osaka University
Osaka (T. W.)

Syntheses of Aliphatic Dibasic Acids from Paraffinic Hydrocarbons by Way of Auto-oxidation in Systems Containing Water[*1]

By Masaru KOBAYASHI[*2], Shiro KUDO[*3] and Kunio SHIMOMURA[*3]

(Received February 5, 1962)

Several attempts have been made to obtain dibasic fatty acids by the direct oxidation of paraffinic hydrocarbons with molecular oxygen; for instance, Zellner and Lister[1] obtained a distillate fraction of succinic acid to sebacic acid in a yield of 20~25% against the amount of reactant consumed in the oxidation of the scale waxes. In this investigation, the oxidation by air or oxygen was carried out at 150°C, employing a catalyst composed mainly of manganese salt; Zellner and Lister have stated that the reaction was inhibited during the course of oxidation due to the lactone-like polymers produced secondarily, leading to the cessation of the reaction at an early stage of oxidation. In order to attain a deep oxidation without a decrease in the reaction velocity in the later stage, many counterplans have been proposed, such as strict control[2] of the reaction temperature and of the depth of oxidation, and employment of effective cocatalysts[3]. However, the yield of the object materials, crystalline dibasic acids (C_4-C_{10}), has been low so far. Recently, however, Tsyskovskii et al.[4] repeated the investigation of Zellner and Lister in an attempt to improve the yield of crystalline dibasic acids; they obtained a fraction of succinic acid—sebacic acid in a yield of 40% against the charged starting material by oxidizing liquid paraffin of a high boiling point and by then hydrolyzing the reaction products at 160°C and 15 atm.

One of the present authors has reported[5] that dibasic acids can be obtained by the auto-oxidation of long chain aliphatic monobasic acids or aliphatic hydrocarbons in the presence also of water. For this paper, this method of reaction has been extended to the oxidation of *n*-decane and solid paraffin; the results obtained are compared with those for the oxidation of anhydrous decane and other former studies, and the effect of water is discussed.

Experimental

Apparatus, Procedure and Materials.—The apparatus used for the oxidation reaction is a vertical autoclave (made of SUS-32) 355 cc. in capacity and with a magnetic stirrer. The reaction temperature was maintained constant within ±0.5°C.

Hydrocarbons and water were charged into the autoclave and, while being stirred, were heated to a desired temperature. Then, after the total pressure had been read, oxygen was introduced until a desired pressure was reached; the depression of the pressure with time was followed at the constant temperature. The rate of the revolution of the stirrer was kept at about 600 r. p. m. to prevent the dissolution of oxygen from becoming a limiting factor for the overall reaction velocity. The total pressure (gauge reading) was kept in a range of 20~80 kg./cm^2 during the reaction.

After the reaction had been stopped by cooling the autoclave, the residual gas, collected in a trap in a dry ice-methanol bath, was subjected to gas analysis. In this experiment, only a trace of condensate was found in the cold trap. The liquid products were taken out, treated according to a method described later, and subjected to analysis.

The *n*-decane used was prepared[6] from commercial *n*-decanol-1; it showed a b. p. of 174~175°C and a purity of 99.5~99.7% (in analysis by gas chromatography). Commercial solid paraffin (m. p., 60°C) and oxygen gas in a cylinder (purity, 99.6~99.7%) were used without further purification.

After-treatment and Method of Analysis.—The carbon dioxide, oxygen, carbon monoxide and unsaturated as well as saturated hydrocarbons in the gaseous product were immediately analyzed according to the usual method employing Hempel's apparatus; in some cases, analysis by gas chromatography was also applied. In order to estimate quantitatively each of the acidic constituents in the liquid product, the reaction product was after-treated according to the scheme summarized in Fig. 1, and gas chromatagraphic analysis[*4] was applied to each fraction.

A liquid reaction product was filtered through a wet filter paper, rinsed with water, and divided

*1 Partly pressented at the 14th Annual Meeting of the Chemical Society of Japan, Tokyo, April, 1961.

*2 Present address, Osaka Municipal Technical Research Institute, Kitaogi-machi, Kita-ku, Osaka.

*3 Present address, Sakai Works, Kyowa Hakko Kogyo Co., Ltd., Takasu-cho, Sakai-shi, Osaka.

1) C. N. Zellner and F. Lister, *Ind. Eng. Chem.*, 48, 1938 (1956).

2) J. P. Buckmann, U. S. Pat. 2729655 (1956).

3) C. N. Zellner and F. Lister, U. S. Pat. 2841603 (1958).

4) V. K. Tsyskovskii, M. I. Levina, B. G. Freidin and V. P. Leont'eva, *Khim. Prom.*, 1960, 272.

5) M. Kobayashi, *Abura Kagaku*, 9, 314 (1960).

6) S. Kudo, K. Shimomura and K. Negishi, *J. Chem. Soc. Japan, Ind. Chem. Sec.* (*Kogyo Kagaku Zasshi*), 65, 1372 (1962).

*4 Perkin-Elmer Model 154 B

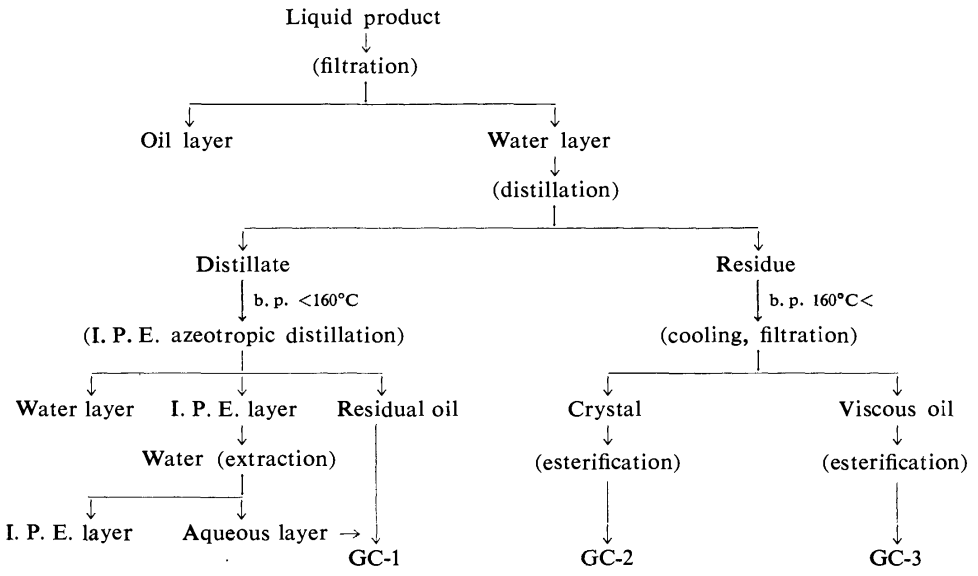

Fig. 1. After-treatment of the liquid product.

into an oily layer and an aqueous layer. While this oily layer consisted of unchanged hydrocarbons containing a few non-acidic oxidation products, the aqueous layer contained, as main ingredients, monobasic fatty acids in addition to the desired dibasic fatty acids, and the existence of a minute amount of carbonyl compound was detected. This aqueous layer was separated by distillation into two fractions, that is, a fraction distilling below 160°C (water and C_1-C_6 monobasic acids) and a residual fraction with a boiling point higher than 160°C (monobasic acids higher than C_7, dibasic acids and other polymerized compounds).

The former fraction was subjected to azeotropic distillation with isopropyl ether (abbreviated as I. P. E. in Fig. 1) and was separated into three portions: water layer, I. P. E. layer, and residual oil. The I. P. E. layer was further extracted with water; a small amount of the acidic ingredients was recovered, added to the residual oil, and subjected directly to gas chromatographic analysis.

The latter high-boiling residue gave crystals of dibasic acids (C_4-C_6) immediately after cooling. These crystals and the highly viscous filtrate were both esterified with *n*-butanol by the aid of sulfuric acid in the usual procedure, using benzene as an accompanying agent for the water formed. Finely powdered sodium carbonate was added to the esterified product to neutralize the acidic contaminant; the solution was then filtered and vacuum distilled; colorless and clear or slightly yellow *n*-butyl esters were used, respectively, as samples for the gas chromatographic analysis.

The GC noted in Fig. 1 indicates the quantitative analysis by gas chromatography.

After-treatment was conducted in the order shown in Fig. 1; the absolute amounts of samples GC-1-GC-3 were calculated from the acid value obtained in the usual way, while the relative amount of each acidic constituent was determined by gas chromatography. The conditions for the gas chromatographic analysis were as follows: for GC-1, column OS 2 m. (dioctyl sebacate+sebacic acid)[7], 150°C, helium as the carrier gas, rate of flow, 47 cc./min.; for GC-2 and GC-3, column O 2 m. (silicon grease), 260°C, helium as the carrier gas, rate of flow, 17 cc./min.

Results

Absorption of Oxygen.—In Fig. 2 are shown examples of the time course of oxygen absoption by *n*-decane (Exp. DX-8, reaction temperature 160°C) and solid paraffin (Exp. DX-14, 150°C). Oxygen is absorbed almost linearly with time after some lapse of the induction period. These curves represent apparent pressure decreases. The true oxygen absoption curves could be almost straight lines if necessary corrections are made for carbon dioxide, carbon monoxide and other gases formed secondarily during the reaction; thus the over-all oxidation reaction may be considered to proceed in a steady state.

With the object of finding the partial pressure of oxygen necessary for maintaining the steady rate in this reaction, the reaction was allowed to proceed without any replenishment of oxygen after the start of the reaction; a gas aliquot was sampled for analysis at the point where the reaction velocity began to decrease, and the partial pressure of oxygen in the gas phase of the reaction system was calculated. The results are shown in Table I. ρ_{max} (maximum rate of oxygen absorption) and θ (induction period) in the table indicate,

7) S. Kudo, K. Shimomura, K. Negishi and K. Fukui, *J. Chem. Soc. Japan, Ind. Chem. Sec.* (*Kogyo Kagaku Zasshi*), 65, 1379 (1962).

TABLE I. EFFECTIVE PARTIAL PRESSURE OF OXYGEN
(Amount of *n*-decane charged, 30 g. water, 70 g., reaction temperature, 160°C)

Experimental No.	θ hr.	ρ_{max} kg·cm^{-2}hr^{-1}	Oxygen pressure when ρ_{max} begins to decline		
			Total pressure kg./cm^2	O_2 Concn. vol. %	O_2 Partial pressure kg./cm^2
DX-4	1.1	9.0	28.0	22.7	5.3
DX-5	0.9	9.0	21.6	26.7	4.6
DX-6	0.9	9.9	16.3	47.1	6.0

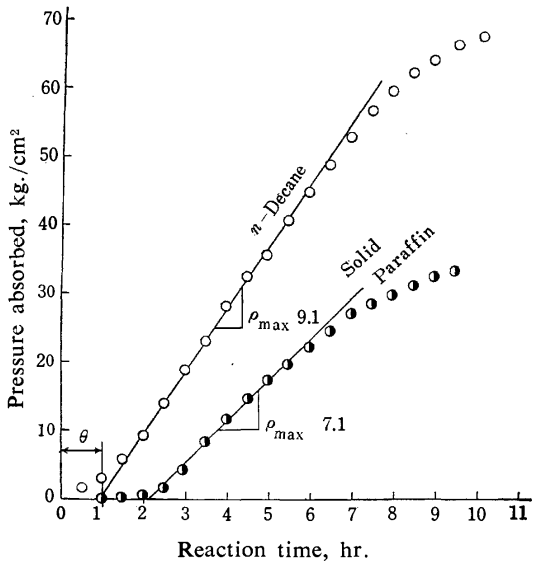

Fig. 2. Rate of oxygen absorption.

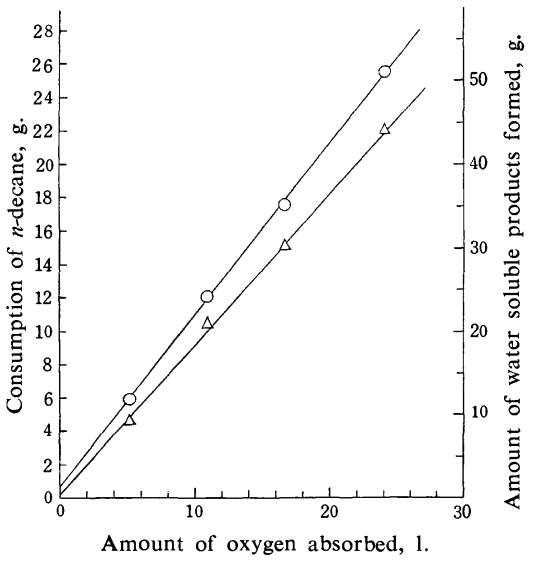

Fig. 3. Consumption of *n*-decane and amount of water-soluble products formed versus depth of oxidation.
○ Consumption of *n*-decane
△ Amount of water soluble products formed

respectively $-d[O_2]/dt$ at the linear portion of the oxygen absorption curve and the time reading at the cross point of this straight line with the abscissa, as is shown in Fig. 2.

It can be infered from the results shown in Table I that ρ_{max} becomes independent of the oxygen pressure when the effective partial pressure of oxygen is higher than 5~6 kg./cm^2 and that $P_{O_2}=5\sim6$ kg./cm^2 may be taken practically as a critical value.

Oxidation Products from *n*-Decane.—*Water-soluble Products and Gaseous Products.*— In Table II are presented the experimental conditions and reaction products in the oxidation of *n*-decane under a pressure at 160°C in the presence also of water. In this table, instances for various depths of oxidation in the case of the oxidation of *n*-decane are given; from these a relation between the amount of oxygen absorbed and the amount of *n*-decane consumed was sought, resulting in a straight line, as shown in Fig. 3. The amount of *n*-decane consumed was calculated by subtracting the amount of the water-insoluble oil layer remaining after the reaction from the amount charged originally. The recovered oil layer consisted mainly of *n*-decane, besides about 10% of *n*-decanone and a small amount of lower fatty acids, as will be described later. Therefore, the oily layer was regarded as the same as the starting material, *n*-decane.

Furthermore, the linear relation between the amount of water-soluble products and that of oxygen absorbed is also illustrated in Fig. 3. From the fact that linear relations were obtained between the depth of oxidation and the consumption of *n*-decane or the amount of water-soluble products respectively, the oxidation reaction in this system containing water may be considered as directly producing water-soluble fatty acid fractions, but not as proceeding step by step via water-insoluble neutral oxidation products.

The water layer separated from the oil layer was clear but slightly yellow, and was subjected to quantitative analysis for each fatty acid in the way cited in Fig. 1; the results are shown in Table II. When the water-soluble products were treated in order of Fig. 1, and the residue of higher boiling point than 160°C was esterified and then vacuum destilled, there

TABLE II. OXIDATION OF *n*-DECANE

Experimental No.	DX-9	DX-7	DX-10	DX-8
Amount of *n*-decane charged, g.	30	30	30	30
Amount of water charged, g.	70	70	70	70
Reaction temp., °C	160	160	160	160
Total reaction press., kg./cm^2	16～40	28～60	22～60	30～60
Reaction time, hr.	2.6	5.0	7.6	10.3
ρ_{max}, kg. cm^{-2} hr^{-1}	9.0	9.0	9.1	9.1
θ, hr.	0.9	1.0	0.8	0.9
Amount of oxygen absorbed, g.	6.9	15.5	23.3	34.6
Amount of *n*-decane consumed, g.	6.9	12.0	17.5	25.5
Products in aqueous layer				
	g. wt. %	g. wt. %	g. wt. %	g. wt. %
Formic acid	0.04 0.5	0.5 4.3	0.85 4.4	0.55 1.9
Acetic acid	2.09 25.5	4.22 36.3	7.31 37.9	14.30 49.4
Propionic acid	1.02 12.4	1.29 11.1	1.92 10.0	2.93 10.1
n-Butyric acid	0.55 6.7	1.08 9.3	1.85 9.6	1.29 4.5
n-Valeric acid	0.21 2.6	0.30 2.6	0.49 2.5	0.90 3.1
Caproic acid	0.06 0.7	0.08 0.7	0.18 0.9	0.19 0.7
Heptanoic acid	1.02 12.4	0.88 7.6	1.72 8.9	1.15 4.0
Caprylic acid	0.62 7.5	0.39 3.3	0.56 2.9	0.17 0.6
Pelargonic acid	0.39 4.7	0.28 2.4	0.26 1.4	0.03 0.1
Succinic acid	1.89 23.0	2.06 17.7	2.91 15.1	5.49 19.0
Glutaric acid	0.28 3.4	0.42 3.6	0.97 5.0	1.59 5.5
Adipic acid	0.05 0.6	0.06 0.5	0.12 0.6	0.26 0.9
Pimelic acid	0 0	0.01 0.1	0.16 0.8	0.02 0.1
Suberic acid	0 0	0.06 0.5	0 0	0.02 0.1
Azelaic acid	0 0	trace	0 0	0 0
Total	8.22 100.0	11.63 100.0	19.3 100.0	28.89 100.0
Gaseous products				
CO_2	1.44 g.	4.19 g.	8.48 g.	17.43 g.
CO	0.15 g.	0.39 g.	0.74 g.	1.36 g.
C=O	0	trace	0	trace
Others	0.24 l.	0.52 l.	0.75 l.	1.31 l.

remained only a small amount (0.2～0.5%) of the residue of distillation (probably polymers of the lactone series) in each experiment listed in Table II. Thus, it can be said that the formation of products which look like polymers of the lactone series is not remarkable in this oxidation procedure.

Furthermore, the gas chromatograms of the samples GC-1-GC-3 obtained by the treatment shown in Fig. 1 were compared precisely, with respect to the retention time, with each standard specimen of the fatty acids, but no peak other than that of the fatty acids was noticed. Thus, the main reaction products in this oxidation reaction can be concluded to be a mixture of fatty acids.

Immediately after the reaction was stopped, both oil and water layers were examined for hydroperoxide (expressed as HPO hereafter), but only a trace was found in each experiment cited in Table II.

As aqueous products, the monobasic fatty acids C_1—C_9 and the dibasic fatty acids C_4—C_7 were obtained; the dibasic acids C_8—C_9 were found only in traces, as is shown in Table II. In order to realized the relation between the depth of oxidation and the formation of each fatty acid, the sum of the monobasic acids C_7—C_9 (cited as higher monobasic acids), the sum of the dibasic acids and the amount of acetic acid formed are plotted against the depth of oxidation in Fig. 4.

The ratio of the amount of dibasic acids consisting mainly of succinic acid to the total acidic ingredients was 22～27%, which can be regarded as nearly constant irrespective of the depth of oxidation. On the other hand, the content of higher monobasic acids decreased, while that of acetic acid increased with the depth of oxidation. Finally it seemed that the aqueous constituents became succinic acid and acetic acid; for instance, in Exp. DX-8

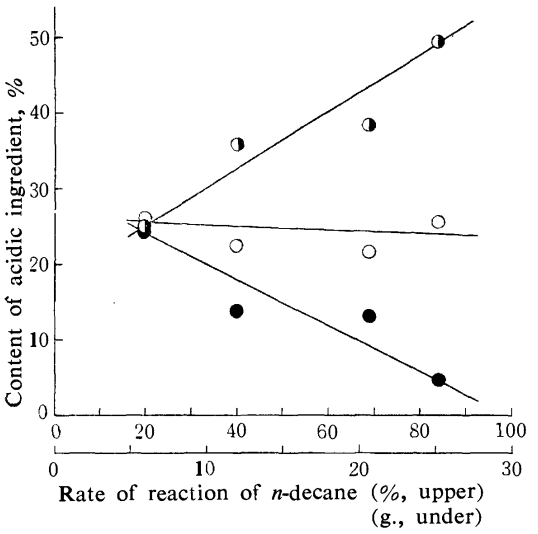

Fig. 4. Depth of oxidation—acidic ingredients.
○ Dibasic acid ◑ Acetic acid
● Higher monobasic acid

of Table II, acetic acid was found to form 49%, succinic acid, 19%, and their sum, 68% at a 85.6% consumption of *n*-decane.

As is shown in Table II, gaseous products consisted mainly of carbon dioxide, together with a small amount of carbon monoxide and a trace of lower olefinic hydrocarbons (shown as C=C in Table II and hereafter).

In order to investigate the other gaseous ingredients, gas chromatographic analysis was conducted on the residual gas in Exp. DX-10 of Table II as an example; the results showed a composition: H_2, 42; CH_4, 4; H_2, 54%. It was also found that hydrogen formed more than 40%. It has not yet been elucidated how this hydrogen is produced, but perhaps it did so in a reaction which can be formulated by the following equation:

$$RCH_2OOH \rightarrow RCOOH + H_2$$

in which prim-HPO is thermally decomposed directly into fatty acids and hydrogen[8]; a mechanism analogous to this may also be interpreted to be operating.

Cleavage of Carbon Chains.—In view of the fact that acetic acid, carbon dioxide and carbon monoxide increase rapidly with the progress of oxidation, as may be seen from the experimental results in Table II, the relation between acetic acid and these gaseous constituents was investigated. As is seen in Fig. 4 and as has been described above, the ratio of the rate forming dibasic acids to the total rates forming all products appears constant, irrespective of the depth of oxidation, whereas the increase in the amount of acetic acid in the range of deep oxidation, contrary to the decrease in the amount of higher monobasic acids, suggests that acetic acid may be formed by a cleavage of the carbon chain of higher monobasic acids. Therefore, the competitive occurrence of the following three elementary steps, A, B_1 and B_2, were assumed to contribute to the overall oxidation reaction:

$$n\text{-Decane} \rightarrow \text{acetic acid} + \text{dibasic acid} + CO_2, CO \quad (A)$$

$$n\text{-Decane} \rightarrow \text{acetic acid} + \text{higher monobasic acid} + CO_2, CO \quad (B_1)$$

$$\text{Higher monobasic acid} \rightarrow \text{acetic acid} + CO_2, CO \quad (B_2)$$

In addition to these steps, other processes, such as the formation of HPO, keto-acid, alcohol and hydroxy-acid as intermediate products, the formation of dibasic acids from higher monobasic acids (perhaps Reaction A proceeds via higher monobasic acids intermediately), and the oxidative decomposition of higher dibasic acids to lower dibasic acids, are also conceivable, but Reactions A, B_1 and B_2 were taken as representative.

Assuming that Reaction A is a normal reaction yielding dibasic acids, and that B_1 and and B_2 represent reactions to shorten carbon chains, it seems probable that B_1 contributes in the early stage of oxidation and that B_2 becomes important in the range of deep oxidation. Thus, if Reaction A actually competes with Reaction B_1, as above, the amount of acetic acid and gaseous constituents found should maintain a constant ratio to the amount of dibasic acids, and the rapid increase of the former in the range of the deeper degree of oxidation is wholly due to reaction B_2. It was established by the experimental results in Table II that this was the case. Experiment DX-9 of shallow oxidation (conversion of *n*-decane, 20.0%) was thought to proceed by way of Reaction A, without any contribution of Reaction B_1 or B_2, until this extent of reaction. Thus, the ratio of each amount of acetic acid (35 mmol.), carbon dioxide (34 mmol.) and carbon monoxide (5.5 mmol.) to the amount of dibasic acids (18 mmol.) obtained in this experiment was assumed to be the normal ratio of production by Reaction A. The increase in the amount of acetic acic and gaseous constituents in experiments of deeper oxidation than this was ascribed to the reaction to shorten the carbon chain and was estimated by calculation. The method of calculation and the results are given in Table III. In

8) H. S. Mosher and C. F. Wurster, *J. Am. Chem. Soc.*, 77, 542 (1955).

TABLE III. RELATION BETWEEN THE AMOUNTS OF ACETIC ACID, DIBASIC ACID, CARBON DIOXIDE AND CARBON MONOXIDE FORMED, AND THE EXTENT OF OXIDATION REACTION

Experimental No.	DX-9	DX-7	DX-10	DX-8
Amount of *n*-decane reacted, g.	6.0	12.0	17.5	25.5
Extent of the reaction of *n*-decane, %	20.0	40.0	58.4	85.0
A. Amount of acetic acid produced, mmol.	35	70	122	238
B. Amount of carbon dioxide formed, mmol.	34	107	211	408
C. Amount of carbon monoxide formed, mmol.[a]	5.5	13.9	26.4	48.7
D. Amount of dibasic acid produced, mmol.	18	19	32	59
Amount of acetic acid formed in the reaction to shorten the carbon chain, mmol. (A−D×35/18)	0	33	64	123
Amount of carbon dioxide formed in the reaction to shorten the carbon chain, mmol. (B−D×34/18)	0	71	151	296
Amount of carbon monoxide formed in the reaction to shorten the carbon chain, mmol. (C−D×5.5/18)	0	8.1	16.6	33.8

a) Sum of carbon dioxide+formic acid

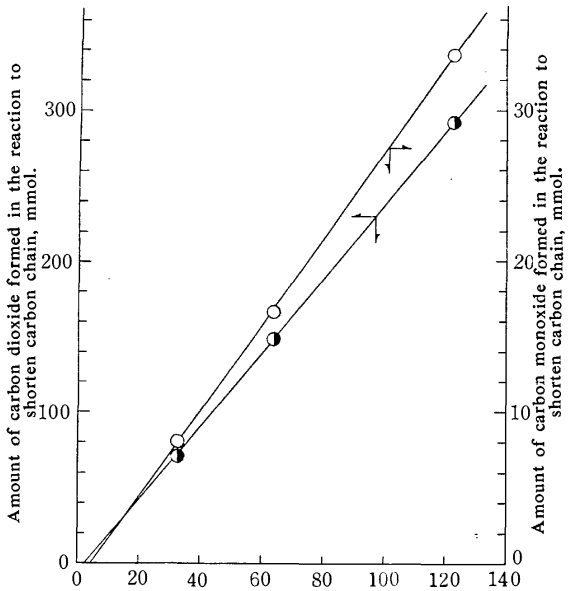

Fig. 5. Formation of acetic acid, carbon dioxide and carbon monoxide in reaction to shorten carbon chain.

the calculations of Table III, formic acid appearing in water-soluble products was regarded as a precursor to carbon dioxide and was so added to the latter.

The amounts of carbon dioxide and carbon monoxide which are thought to have been formed in the reaction to shorten the carbon chain were plotted respectively against the amount of acetic acid, resulting in straight lines, as is shown in Fig. 5. Thus, it is probable that Reactions A and B proceed together, as was presumed afore, and, at least in the reaction of carbon chain shortening, acetic acid and carbon dioxide, together with carbon monoxide, would be formed concurrently.

Ingredients in the Oil Layer.—The oil layer obtained after oxidation constitutes mainly of unchanged *n*-decane, but it also contains a small number of products from shallow oxidation (C_{10} ketone and C_{10} alcohol) and a minute amount of lower fatty acid. These products are estimated, to be from the amount of oxygen absorbed, negligible as compared with products from deep oxidation (water-soluble constituent and gaseous constituent); as no quantitative analysis was conducted, the composition was only roughly examined.

Ten grams of the oil layer from the experiment DX-7 in Table II (carbonyl content, 14.8% as C_{10} ketone, carboxyl content, 15.0% as C_{10} acid) were washed with dilute alkali and water. This sample was applied to the gas chromatography, in a method which has been reported previously[7], and also to the chemical analysis. The results are given in Table IV.

In view of the range of relative retention time,

TABLE IV. COMPOSITION OF OILY MATERIAL

Ingredient	Gas chromatography		Chemical analysis
n-Decane	79.2		
n-Decanone-2	3.3	10.6	10.7
n-Decanone-3	2.1		
n-Decanone-4 + *n*-Decanone-5	5.2		
Others (C_2-C_4 monobasic acid + C_{10} alcohol)	10.2		
	100		

the fraction of C_{10} alcohol seems to be a mixture of isomers having the functional group at different positions, like the *n*-decanone fraction, but the amount was so small that characterization of the constituents was impossible.

On the other hand, the oil layer obtained in the series of experiments in Table II was directly analyzed chemically; the carbonyl content estimated as C_{10} ketone was 9.1% (DX-9), 14.3% (DX-7), 11.4% (DX-10) and 2.8% (DX-8), in the order of degree of oxidation. They were usually about 10% except for the last experiment of the deepest oxidation (the consumption of *n*-decane was 85.6% in DX-8). On the basis of these results, this oxidation reaction is thought to take a course through HPO to ketone and alcohol as the primary process in the same manner as in the oxidation of the system without water; moreover, the composition of the ketone (*n*-decanone) regarded as an intermediate is also identical with that in the thermal auto-oxidation of the system without water. Therefore, the course of this oxidation is thought to be that, initially, *n*-decanone (or *n*-decanol) is formed from *n*-decane, and that it is then subjected continuously to successive oxidation, without accumulating in the oil layer, to give acidic constituents and is then transferred into the aqueous layer.

Oxidation of Solid Paraffin.—Solid paraffin was oxidized in the same way as *n*-decane. The oxygen absorption curve, an example of which is shown in Fig. 2, assumes a straight line after a certain induction period, as does *n*-decane. The experimental results obtained at 150 and 160°C are tabulated in Table V, and an example of an experiment, in which oxidation was continued until the unchanged oil layer disappeared completely at a reaction temperature of 160°C, is presented in Table VI.

In Tables V and VI are shown analytical values for all the acidic ingredients in the aqueous layer, which was treated according to the after-treatment precedure illustrated for *n*-decane in Fig. 1. The unchanged oil layer and the aqueous layer were both distilled, and the residual fraction (b. p. 160°C<) of the latter was esterified in the same way as in Fig. 1. The residue (about 0.3~0.5 g.) remaining after vacuum distillation of esters was not examined in further detail.

As for acidic ingredients, C_1—C_9 monobasic acids and C_4—C_9 dibasic acids were found over the whole range of oxidation, as in the case for *n*-decane. In gas chromatograms of samples GC-2 and GC-3 obtained by the method of treatment in Fig. 1, no peak corresponding to an unidentified substance was found in the range of a lower fraction than that of C_9 monobasic acid, and capric acid could not be detected, even by careful examination while changing the operating conditions for chromatography.

Table V. Oxidation of solid paraffin

Experimental No.	DX-14	DX-17
Solid paraffin charged, g.	15	20
Amount of water charged, g.	85	80
Reaction temp., °C	150	160
Total reaction press., kg./cm²	18~60	17~80
Reaction time., hr.	9.8	8.3
ρ_{max}, kg. cm^{-2} hr^{-1}	7.1	9.2
θ, hr.	2.4	0.6
Amount of oxygen absorbed, g.	19.0	29.7
Solid paraffin consumed, g.	13.0	18.5

Products in the aqueous layer

	g.	wt. %	g.	wt. %
Formic acid	0.27	2.3	0.43	5.2
Acetic acid	3.76	32.5	7.26	37.7
Propionic acid	0.36	3.1	0.50	2.6
n-Butyric acid	0.24	2.1	0.88	4.6
n-Valeric acid	0.06	0.5	0.09	0.5
Caproic acid	0.08	0.7	0.21	1.1
Heptanoic acid	0.74	6.4	1.20	6.2
Caprylic acid	0.28	2.4	0.71	3.7
Pelargonic acid	0.22	1.0	1.13	5.9
Succinic acid	2.71	23.4	3.92	20.4
Glutaric acid	1.73	15.0	1.88	9.8
Adipic acid	0.63	5.4	0.59	3.1
Pimelic acid	0.23	2.0	0.23	1.2
Suberic acid	0.34	2.9	0.19	1.0
Azelaic acid	0.02	0.2	trace	—
Total	11.57	100.0	19.22	100.0

Gaseous products

CO_2	7.52 g.	12.1 g.
CO	0.54 g.	1.0 g.
C=C	0	0.02 g.
Others	0.49 l.	0.55 l.

The effect of the reaction temperature on the product distribution can be seen in Table V. A better yield of dibasic acids and a higher ratio of glutaric acid against succinic acid are obtained at a lower temperature, while the amount of acetic acid produced is greater at a higher temperature, gaseous constituents such as carbon dioxide and carbon monoxide show similar tendencies.

The experiment of complete oxidation of the oil layer (cited as DX-20 in Table VI) was practised as follows: 1.3 g. of the oil layer recovered in the two experiments DX-18 and DX-19 and 18.2 g. of the viscous oily

TABLE VI. OXIDATION OF SOLID PARAFFIN

Experimental No.	DX-18	DX-19	DX-20
Amount of solid paraffin charged, g.	20	20	Recovered oil of DX-18, DX-19
Amount of water charged. g.	80	80	80.5
Reaction temp., °C	160	160	160
Total reaction, press., kg./cm²	18~80	20~80	35~70
Reaction time, hr.	9.5	11.3	5.6
ρ_{max}, kg. cm^{-2} hr^{-1}	8.5	9.0	
θ, hr.	0.62	0.80	
Amount of oxygen absorbed, g.	31.7	30.4	
Amount of solid paraffin consumed, g.	18.0	18.5	

Products in aqueous layer

	g.	wt. %
Formic acid	3.39	9.6
Acetic acid	17.08	48.4
Propionic acid	1.54	4.4
n-Butyric acid	0.70	2.0
n-Valeric acid	0.20	0.6
Caproic acid	0.13	0.40
Heptanoic acid	0.64	1.8
Caprylic acid	0.18	0.5
Pelargonic acid	0.24	0.70
Succinic acid	7.72	21.8
Glutaric acid	2.67	7.6
Adipic acid	0.42	1.2
Pimelic acid	0.08	0.2
Suberic acid	0.01	0.3
Azelaic acid	trace	—
Sebacic acid	0.15	0.4
Higher acid not yet identified	0.05	0.1
Total	35.20	100.0

Gaseous products

CO_2	34.6 g.
CO	2.8 g.
C=C	0
Others	1.39 l.

matter obtained in the treatment of the aqueous layer (of Fig. 1) were joined together and oxidized in experiment DX-20 until the oil layer had completely disappeared. The results reveal that it is possible to convert starting hydrocarbons almost completely into water-soluble products. By comparing these results with those of experiment DX-17, it can be realized that perfectly deep oxidation converts monobasic acids to acetic acid, and dibasic acids to succinic acid. This finding agrees well with that of *n*-decane illustrated in Table II.

In order to compare the results for solid paraffin with those for *n*-decane, Table VII presents the amount of each acidic constituent produced per 1 kg. of hydrocarbon consumed in experiments of roughly the same depth of oxidation (extent of reaction: 85~92%). In summary, the yield of dibasic acids against consumed hydrocarbon is 29% for *n*-decane, poorer than the value of 40% for solid paraffin.

TABLE VII. AMOUNT OF DIBASIC ACID FORMED PER 1 kg. HYDROCARBON CONSUMED

Experimental No.	DX-8	DX-14	DX-17
Original hydrocarbon	*n*-Decane	Solid paraffin	Solid paraffin
Extent of reaction, %	85.1	86.6	92.5
Reaction temp., °C	160	150	160
Dibasic acid			
Succinic acid	215	209	212
Glutaric acid	66	133	102
Adipic acid	10	48	32
Pimelic acid	1	18	12
Suberic acid	1	26	10
Azelaic acid	0	2	0
Total	293	436	368
Monobasic acid			
Acetic acid	560	239	393
C_1, C_3—C_9 acid	283	216	288
Total	843	455	671

The amount of such lower fatty acids as acetic acid and propionic acid is large in the case of *n*-decane, but small, in the case of solid paraffin. It may therefore be concluded that in the case of *n*-decane the yield of dibasic acids is small, while that of lower monobasic acids is large. The discrepancy is probably due to the difference in the carbon chain length of the original hydrocarbons. It seems probable that *n*-decane, owing to its comparatively short carbon chain, has an extremely poor chance to form two moles of dibasic acids of C_4—C_5 by the random attack of a molecular oxygen, but that it has a large possibility to form one mole of dibasic acid and residual fragments of carbon chain, which will then turn into lower monobasic acids. On the contrary, in the case of solid paraffin composed mainly of *n*-paraffins of mean carbon number 26—27, no such restriction is imposed since its yield in dibasic acids is higher.

Comparison with Reactions in the Absence of Water.—In comparing the present oxidation reaction with the reaction without water added in advance[9], some consideration must be given

9) Hereafter we shall call this system the "anhydrous system". A small amount of water is certainly produced in the oxidation reaction, but it is usually carried away from the system together with exhaust gas, by virtue of some suitable apparatus in the works of Zellner[1], Buckmann[2] and Tsyskovskii[4]. Thus the system can be regarded as "anhydrous".

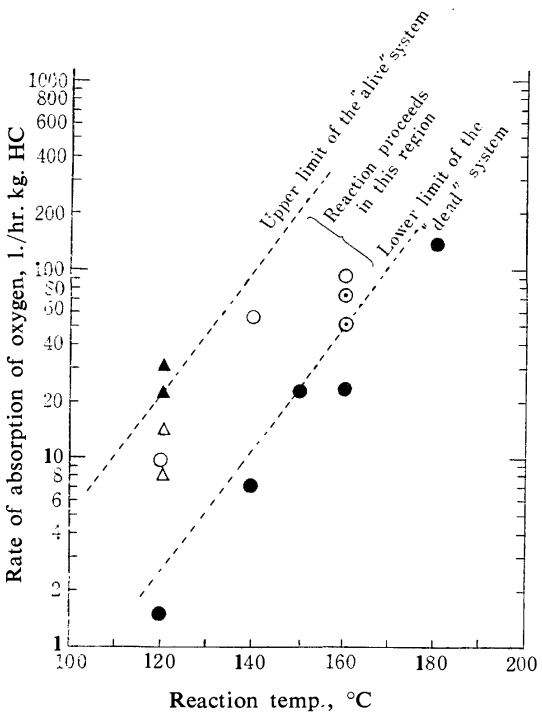

Fig. 6. Rate of oxygen absorption plotted against the reaction temperature.
▲ Instance of dead[2] △ Instance of alive[2]
● Instance of dead[9] ○ Instance of alive[9]
⊙ Instance of this experiment

to the characteristics of the present system, especially the role of water.

In the methods of both Zellner et al.[1] and Buckmann[2], solid paraffin in oxidized under strict control of the reaction temperature as well as of the amount of oxygen absorbed; too large[2] or too small[10] aeration is thought to inhibit the absorption of oxygen on account of the polymerization of reaction products.

For instance, Zellner assumed that the appropriate depth for the oxidation of products would correspond to a saponification value above 400[10], a recent patent has claimed a value of 600[3], and Buckmann considered it to be represented by an acid value above 490[2]; in every case, the main object of study was to realize a rapid and smooth arrival at this line before the reaction was retarded by these polymers. The relation between the reaction temperature and the rate of oxygen absorption observed in these studies, together with data from the present work, are shown in unified units in Fig. 6. (The rate of oxygen absorption is shown in liters of gas absorbed per 1 kg. of original hydrocarbon per hour and is denoted as l./hr. kg. HC). In our experiments, the rates of the oxygen absorption calculated are 56.1 and 78.3 l./hr. kg. HC respectively for DX-8 in Table II (the *n*-decane charged was 30 g., reaction temperature, 160°C; ρ_{max}, 9.1 kg. cm^{-2} hr^{-1}) and for DX-17 in Table V (the solid paraffin charged was 20 g.; reaction temp., 160°C; ρ_{max}, 9.2 kg. cm^{-2} hr^{-1}).

Zellner[10] called a state a "dead system" in which oxidation has been interrupted during the reaction and in which the replenishment of oxygen through aeration does not provoke further oxidation. Figure 6 gives examples of "alive" and "dead" reaction systems. In regions above and below the two dotted lines in the figure, the progress of reaction is stopped owing to the formation of polymers and other retarders.

In 1960 Tsyskovskii et al.[4], improving on the method of Zellner and Lister, oxidized *n*-paraffin with a b. p. of 240~350°C, a by-product of diesel fuel, with oxygen using manganese naphthenate as a catalyst at 135~155°C under ordinary pressure; the reaction product was then hydrolyzed at 160°C under about 15 atm., giving dibasic acids in an yield of 40% against the starting material. The composition of these dibasic acids, including succinic acid through sebacic acid, is almost identical with our results for solid paraffin listed in Table V. The reaction mechanism of hydrolysis at a high temperature in their method has not yet been elucidated, but it seems probable that hydrolysis[11] of a lactone-type compound at a high temperature and pressure was applied to the case of the recovery of fatty acids from oxidized oil.

When the present results of oxidation in systems containing water are compared with the data of previous literature, our method interestingly produces almost no polymers in spite of the small rate of oxidation. Namely, as may be seen from Fig. 6, the rate of oxygen absorption in this experiment lies in the region of "death", if the system were anhydrous, where reaction should cease owing to the formation of polymers. The reason why the reaction is not interrupted in the present system may be attributable to the inhibition of polymerization due to the ring rupture by water (hydrolysis) of lactonic substances during the reaction.

Examinations of the reaction velocity and the distribution of products in comparison with those in the anhydrous system[6] have been perfomed; they are tabulated in Tables VIII-1, 2 and 3,

In these tables are listed, for the sake of comparison, the results of oxidation at the same depth (1 mol. oxygen absorbed per 1

10) C. N. Zellner, U. S. Pat. 2486454 (1949).

11) P. A. Moshkin, U. S. S. R. Pat. 116947 (1959); *Chem. Abstr.*, 53, 17541 (1959).

TABLE VIII-1. OXIDATION IN THE SYSTEM CONTAINING WATER AND THE ANHYDROUS SYSTEM

Exp. No.	Method of oxidation	Sample for oxidation, g.	Amount of water added, g.	Reaction temp., °C	ρ_{max} l./hr. kg. HC	θ, hr.
DX-9	This experiment	*n*-Decane 30	70	160	51.6	0.95
DX-16	Oxidation under ordinary pressure	*n*-Decane 50	0	160	174.2	0.73
DX-12	Same as above	*n*-Decane 50	0	160	78.4	2.20

TABLE VIII-2. OXIDATION IN THE SYSTEM CONTAINING WATER AND THE ANHYDROUS SYSTEM

Exp. No.	System	Depth of oxidation[a] mol./mol.	Extent of reaction of *n*-decane[b], %	Amount of gas formed, ml.			C_{10} Ketone C_{10} Alcohol g.	Water g.
				CO_2	CO	C=C		
DX-9	Containing water	0.99	20.0	2436	406	0	About 6	—
EX-16	Anhydrous	1.00	42.8	814	680	14	12.1	15.2
EX-12	Anhydrous	0.97	38.4	800	294	0	14.0	10.8

a) O_2 mol. absorbed per 1 mol. *n*-decane
b) (Amount charged − Amount recovered)) ÷ Amount charged × 100

TABLE VIII-3. OXIDATION IN THE SYSTEM CONTAINING WATER AND THE ANHYDROUS SYSTEM

Exp. No.	Monobasic acid, g.										Dibasic acid g.	Others g.
	C_1	C_2	C_3	C_4	C_5	C_6	C_7	C_8	C_9	C_{10}	C_4—C_{10}	
DX-9	0.1	7.0	3.4	1.8	0.7	2.0	3.4	2.0	1.3	0	7.4	ca. 0.3
EX-16	1.0	3.8	3.6	3.0	2.6	2.4	2.0	1.2	trace	0.2	0	7.0
EX-12	1.0	4.0	2.4	3.2	3.6	3.4	2.2	1.0	0.2	0.4	0	10.8

mol. decane) in systems both with and without water. The rate of maximum oxygen absorption, ρ_{max}, is shown with a calculated value per 1 kg. of decane in the same way as in Fig. 6, and the amounts of gas produced, C_{10} ketone + C_{10} alcohol and water, and other data listed in Table VIII-3 are all given in terms of weight calculated on the basis of 100 g. of *n*-decane charged. "Other" cited in Table VIII-3 means polymers other than dibasic acids in DX-9, and the sum of lower neutral compounds containing oxygen in EX-16 and EX-12.

As to the effect of water on the reactivity of *n*-decane, a comparison between the data from experiments DX-9 and EX-16 shown in Table VIII-1 indicates that, in the presence of water, the induction period, θ, increases a little, while the maximum rate of oxygen absorption, ρ_{max}, is diminished to about one-third of that in the anhydrous system. That is to say, oxidation is greatly retarded by the addition of water.

As is shown in Table VIII-2, the extent of reaction is equal in these experiments on the basis of the oxygen absorbed, but the extent differs appreciably from experiment to experiment in terms of the *n*-decane consumed; the *n*-decane consumption is twice as much in the anhydrous system as that in water-containing system. Furthermore, the product distribution is also greatly different in these two reaction systems. In the system containing water, the amounts of the fractions of C_{10} ketone and C_{10} alcohol, which are regarded as primary intermediate products in the oxidation, are small, while the amount of acetic acid formed is large. In the case of the anhydrous system, no dibasic acids fraction comes out, whereas oxygen-containing neutral products of a low boiling point (shown as "others" in Table VIII-3) are abundant. Besides, it is interesting to note that caprylic acid is not formed in the system containing water. Monobasic acids of the C_3—C_7 range are continuously richly present in anhydrous systems, while in systems containing water C_3 acid and C_7 are richly present, but C_5 shows only a minimum.

As for gaseous products, carbon dioxide is richly present in the system containing water, while there is far less carbon monoxide than in the anhydrous system.

Thus, the product distribution shown in Tables VIII-2 and VIII-3 suggests that the following two reactions:

n-decane → HPO → C_{10} ketone, C_{10} alcohol

C_{10} ketone, C_{10} alcohol → succeeding oxidation products

proceed with nearly the same velocity in the anhydrous system, whereas in the system containing water, the rate of the succeeding oxidation is so extremely that the C_{10} neutral

fraction of intermediate products (ketone, alcohol) seems not to accumulate in the reaction system.

A comparison of both reactions has also been made from the standpoint of the dependency of the reaction velocity, $-d[O_2]/dt$, on the oxygen pressure. In the system containing water, ρ_{max} becomes independent of the partial pressure of oxygen above $P_{O_2}=6$ kg./cm^2, as has already been shown in Table I, while in the anhydrous system it becomes independent even under ordinary pressure at the same temperature (160°C). The mechanism of this oxidation (including the oxidation of *n*-decane or that of the succeeding C_{10} neutral fractions) seems substantially analogous to the reaction type proposed by Bolland-Gee[12]; hence, the reaction rate may be represented by the well-known equation, (1)[12], where R_i is the rate of chain initiation. The propagation steps are expressed by $R\cdot+O_2 \xrightarrow{k_2} RO_2\cdot$, $RO_2\cdot+RH \xrightarrow{k_3} RO_2H+R\cdot$, and the termination by $2R\cdot \xrightarrow{k_4}$, $R\cdot+RO_2\cdot \xrightarrow{k_5}$, $2RO_2\cdot \xrightarrow{k_6}$, where $k_5^2=k_4k_6$.

$$-d[O_2]/dt = R_i^{1/2}\left(\frac{k_3}{k_6^{1/2}}\right)[RH]\times\left\{\frac{k_2/k_6^{1/2}[O_2]}{k_3/k_4^{1/2}[RH]+k_2/k_6^{1/2}[O_2]}\right\} \quad (1)$$

Assuming that in Eq. 1 the critical values of oxygen pressure, above which the value within the large bracket could be approximated to 1, are $[O_2]=6$ kg./cm^2 (in the system containing water) and $[O_2]=1$ kg./cm^2 (in the anhydrous system), as has been described before, the values of the ratio in the denominator $k_3/k_4^{1/2}$: $k_2/k_6^{1/2}$ are surmised to be fairly different between the two systems.

As the value of [RH] seems equal in both systems, the condition of the oxygen pressure independency can be expressed approximately by Eq. 2, where A_n, B_n (anhydrous system) and A_h, B_h (system containing water) represent $k_2/k_6^{1/2}$ and $k_3/k_4^{1/2}$ respectively.

$$\frac{A_n[1]}{B_n+A_n[1]}=\frac{A_h[6]}{B_h+A_h[6]}=1 \quad (2)$$

In the system containing water, the condition $k_2[R\cdot] \gg k_3[ROO\cdot]$, which makes the content in large bracket 1, can not be established at O_2 pressure below 6 kg./cm^2; that is to say, the applicability of Eq. 1 has been enlarged, namely into the region where ρ_{max} depends upon the oxygen pressure, since the reactivity of RH with molecular oxygen is enhanced as compared with that in anhydrous systems. If RH is presumed to be a C_{10} neutral substance produced during reaction, it is highly probable that these neutral ingredients are attacked preferentially by oxygen to form dibasic acids in the system containing water.

Osaka Municipal Technical Research Institute
Kitaogi-machi, Kita-ku, Osaka
(M. K.)
Research Department
Sakai Works
Kyowa Hakko Kogyo Co., Ltd.
Takasu-cho, Sakai-shi, Osaka
(S. K. & K. S.)

12) J. L. Bolland, *Proc. Roy. Soc.*, **A186**, 218 (1946).

Pyrolysis of Acid Amides. III. Pyrolysis of Cyanoacetamides and 2-Phenylacetamides

By Teruaki MUKAIYAMA, Hisashi TAKEI and Yasuo KOMA

(Received September 13, 1962)

The pyrolyses of acetoacetamides and 2-haloacetamides to give isocyanates and acetone, and nitriles, isocyanates and hydrogen chloride, respectively, have been reported in preceding papers[1,2]. It has been shown there that carboxylic acid amides containing atomic groups which are stable as anion in their acyl groups can produce isocyanates or nitriles by vapor phase decomposition. For the present study, the pyrolyses of cyanoacetamides, 2-phenylacetanilide, 2, 2-diphenylacetanilide and 2, 2, 2-triphenylacetanilide were carried out in order to confirm this finding.

The pyrolysis of cyanoacetamides, which have

1) T. Mukaiyama, M. Tokizawa, H. Nohira and H. Takei, *J. Org. Chem.*, **26**, 4381 (1961).
2) T. Mukaiyama, M. Tokizawa and H. Takei, ibid., **27**, 803 (1962).

TABLE I. PYROLYSIS OF CYANOACETAMIDES

R-NHCOCH$_2$CN R	M. p. °C	Pyrolysis conditions: Charge g.	Temp. °C	Press. mmHg.	Time min.	Products: Aceto-nitrile g.	Iso-cyanate g.	Material recovered g.
C_6H_5-	198~199 (198~199)[d]	5.0	535~540	11.0	20	—	0.06	4.16
C_6H_5-		5.0	590~600	11.0	23	0.30	1.04	2.08
C_6H_5-		5.0	640~645	7.0	78	—	0.17	3.90
C_6H_5-		4.4	630~650	5.0	90	0.33	1.16	1.70
C_6H_5-		5.0	645~650	11.0	55	0.70	1.84	1.17
C_6H_5- [a]		5.0	710~720	7.0	20	—	0.06	about 2
p-$CH_3C_6H_4$-	183~184 (180)[d]	5.0	590~600	7.0	25	0.40	1.22	2.60
p-$CH_3C_6H_4$-		5.0	630~640	5.5~7.0	25	0.36	1.48	1.89
p-$CH_3C_6H_4$-		10.0	640~660	8.0	35	0.56	2.27	4.54
$C_6H_5CH_2$- [b]	122~123 (120)[d]	8.0	640~650	5.0	23	—	trace	2.66
p-$NO_2C_6H_4$- [a,c]	217~218 (decomp.)[e]	5.0	540~550	10.0~11.0	17	—	—	about 2

a) The char deposit in this reaction tube was much larger than in the others.
b) Unidentified by-products were obtained; 0.12 g, b. p., 90~110°C/15 mmHg; 1.29 g., b. p., 130~170°C/0.5~0.8 mmHg.
c) A trace of *sym-p,p'*-dinitrodiphenylurea was obtained.
d) K. G. Naik and Y. N. Baht, *J. Indian Chem. Soc.*, **4**, 547 (1927); *Chem. Abstr.*, **22**, 2353 (1928).
e) Found: C, 52.88; H, 3.50; N, 20.25. Calcd. for $C_9H_7O_3N_3$: C, 52.68; H, 3.44; N, 20.48%.

a structural possibility of forming $NCCH_2^-$ and $RNHCO^+$ ions at an elevated temperature, was tried first by using a quartz column packed with quartz chips; isocyanates and acetonitrile were obtained, as had been expected. The results of the experiments are summarized in Table I.

$$R\text{-}NHCCH_2CN \xrightarrow{\Delta} R\text{-}NCO + CH_3CN$$

The amounts of isocyanate and acetonitrile increase as the temperature rises, but they decrease markedly above 700°C, probably because of side reactions. The amount of undesirable char deposited in the reaction tube was larger than that found in the case of acetoacetamides. In addition, it was shown that the pyrolysis of cyanoacetamides has poor reproducibility, unlike the results obtained in the case of acetoacetamides (see Table I). In the case of 4'-nitrocyanoacetanilide, the char deposit in the reaction tube was much larger and *p*-nitrophenyl isocyanate could not be obtained, although it can be pyrolyzed at a relatively low temperature (550°C).

The results listed in Table I show that the temperature required for the pyrolysis of cyanoacetamides is about 100°C higher than that needed for the pyrolysis of acetoacetamides. This may be attributed to the relative stabilities of the anions[3], $NCCH_2^-$ and $CH_3COCH_2^-$, which determine the ease of the carbon-carbon bond breaking of the acid-amide linkage. Assuming six-membered cyclic intermediates for the pyrolysis, as has been mentioned in the case of acetoacetamides, the result can be explained by the linear nature of the nitrile group, because of which the formation of the cyclic intermediate is more difficult.

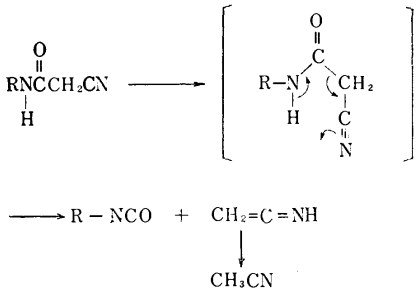

Pyrolyses of 2-phenylacetanilide and 2,2-diphenylacetanilide were next attempted on the assumption that carbon-carbon bond breaking may also be facilitated by the introduction of phenyl groups which stabilize $C_6H_5CH_2^-$ or $(C_6H_5)_2CH^-$ ions by the resonance effect. These amides were expected to produce phenyl isocyanate and toluene, and phenyl isocyanate

3) The pK_a values of acetone and acetonitrile are about 20 and 25 respectively.

TABLE II. PYROLYSIS OF 2-PHENYLACETANILIDES[a]

R-CONHC$_6$H$_5$ R	M. p. °C	Pyrolysis conditions: Charge g.	Temp. °C	Press. mmHg	Time min.	Products: Phenyl isocyanate g.	Aniline g.	R-H g.	*sym*-Diphenylurea g.	Material recovered g.
								(toluene)		
$C_6H_5CH_2$-	115~116 (116)[c]	5.0	500	3.0~4.0	25		trace	—	—	4.26
$C_6H_5CH_2$-		5.0	600	5.0	20	0.03		trace	—	3.31
$C_6H_5CH_2$-		5.0	620	8.0	20	0.76		1.27	0.80	—
$C_6H_5CH_2$- [b]		15.0	680~690	7.0	55		0.94	0.62[f]	1.65	—
$C_6H_5CH_2$- [b]		5.0	700~710	3.0	43		trace	0.39[g]	0.44	—
								(diphenylmethane)		
$(C_6H_5)_2CH$-	179~181 (180)[d]	5.0	490~500	8.0~11.0	30	trace		0.50	0.60	0.80
$(C_6H_5)_2CH$-		5.0	490~520	9.0	20	0.14		0.73	1.01	—
$(C_6H_5)_2CH$-		5.0	550~570	5.0~7.0	37	0.34		1.23	0.34	—
$(C_6H_5)_2CH$-		5.0	600~610	6.0	25	0.54		1.32	0.25	—
$(C_6H_5)_2CH$-		4.2	640~650	7.0	20	0.46		1.20	0.14	—
								(triphenylmethane)		
$(C_6H_5)_3C$- [b]	169~170 (173.5~174.5)[e]	5.0	450~460	3.0	18	—	trace	trace	trace	—
$(C_6H_5)_3C$- [b]		4.0	500~520	12.0	20	—	0.28	—	trace	0.50
$(C_6H_5)_3C$- [b]		5.0	570~600	4.0~11.0	15	—	0.13	0.68	0.02	—

a) The pyrolyses were so complicated that various by-products not listed in this table were also obtained.
b) The char deposit in this reaction tube was much larger than in the others.
c) C. A. Bischoff and P. Walden, *Ann.*, **279**, 125 (1894).
d) F. Klingemann, ibid., **275**, 84 (1893).
e) J. Schmidlin and H. H. Hodgson, *Ber.*, **41**, 446 (1908).
f) Gas chromatographic analysis showed that crude toluene was 15% benzene.
g) Gas chromatographic analysis showed that crude toluene was 11% benzene.

and diphenylmethane, respectively. The reactions, however, were complicated, and the isocyanate and toluene or diphenylmethane formed was accompanied with a considerable amount of by-products. Since the reaction pathway is markedly influenced by even a minor change in the reaction conditions, the pyrolytic reactions also have poor reproducibility in both cases. The results of several runs are listed in Table II.

In the case of 2-phenylacetanilide, generalizations may be made as follows. Below 600°C, most of the starting material was recovered. In temperature range from 600 to 650°C, phenyl isocyanate was obtained along with toluene, benzene and *sym*-diphenylurea. However, it was shown that there was another reaction, the formation of aniline instead of phenyl isocyanate, under nearly the same conditions. At a more elevated temperature (670~680°C), the reaction became more complicated and the char deposit in the reaction tube was much larger. Phenyl isocyanate could not be obtained from the pyrolyzate, although aniline, toluene, benzene and *sym*-diphenylurea were obtained, along with various unidentified by-products.

$$C_6H_5\underset{\underset{H}{|}}{N}\overset{\overset{O}{\|}}{C}CH_2C_6H_5 \xrightarrow{\Delta} C_6H_5NCO + C_6H_5CH_3 + C_6H_6 + C_6H_5NHCONHC_6H_5$$

$$\xrightarrow{\Delta} C_6H_5NH_2 + C_6H_5CH_3 + C_6H_6 + C_6H_5NHCONHC_6H_5$$

When 2, 2-diphenylacetanilide was pyrolyzed with the temperature range from 490 to 650°C, phenyl isocyanate, diphenylmethane and *sym*-diphenylurea were obtained.

$$C_6H_5\underset{\underset{H}{|}}{\overset{\overset{O}{\|}}{N}}CCH(C_6H_5)_2 \xrightarrow{\Delta} C_6H_5NCO + (C_6H_5)_2CH_2$$

$$+ C_6H_5NHCONHC_6H_5$$

As was mentioned in a previous report[2], the percentage of conversion in the pyrolysis of 2-haloacetamides increases in proportion to the number of halogen atoms, with a large electronegativity value being attached to the α-carbon of acid amides. Similarly, the finding that 2, 2-diphenylacetanilide decomposed more easily than 2-phenylacetanilide indicates that the number of phenyl groups attached to the α-carbon of acid amides plays an important role in this type of pyrolysis.

Unexpectedly, phenyl isocyanate could not be obtained by the pyrolysis of 2, 2, 2-triphenylacetanilide, only a large amount of tarry product resulted, although it decomposed at a relatively low temperature (450°C). From the tarry pyrolyzate, traces of aniline, triphenylmethane and *sym*-diphenylurea were obtained. The reason why phenyl isocyanate could not be obtained by the pyrolysis of 2, 2, 2-triphenylacetanilide remains unexplained.

$$C_6H_5\underset{\underset{H}{|}}{\overset{\overset{O}{\|}}{N}}CC(C_6H_5)_3 \xrightarrow{\Delta} C_6H_5NH_2 + (C_6H_5)_3CH$$

$$+ C_6H_5NHCONHC_6H_5$$

Contrary to the cases of the pyrolyses of acetoacetamides and cyanoacetamides, which yield only isocyanates through the cyclic intermediate, the pyrolyses of 2-phenylacetamides gave various products. These results indicate that the pyrolyses of 2-phenylacetamides does not involve cyclic intermediates, but rather proceeds through radical intermediates, benzyl-type radicals, formed by the homolytic breaking of the carbon-carbon bond or the carbon-hydrogen bond.

In conclusion, it can be said of the pyrolysis of acid amides that: 1) The reactivity of amides toward the pyrolytic decomposition depends on the easiness of the carbon-carbon bond breaking of the amide linkage. This suggests that amides containing atomic groups which are stable as anion or free radical in their acyl groups decompose readily.

2) Since acetoacetamides and cyanoacetamides can form the cyclic intermediates, the pyrolytic decomposition takes place in the direction of forming isocyanate. However, such amides as 2-haloacetamides and 2-phenylacetamides, which form the cyclic intermediate only with difficulty, gave a small amount of isocyanate along with various by-products probably through radical intermediates. These results show that the greater the chance of forming cyclic intermediates, the greater the proportion of isocyanate.

Experimental

Materials.—Cyanoacetamides were prepared from corresponding amines and ethyl cyanoacetate. Their melting points are listed in Table I.

2-Phenylacetanilide, 2,2-diphenylacetanilide and 2,2,2-triphenylacetanilide were prepared from aniline and corresponding acid chlorides, and their melting points are listed in Table II.

Pyrolysis of Cyanoacetanilide.—The apparatus used consisted of a vertical quartz tube, 18 mm. in diameter and 120 cm. in length, equipped with a standard taper joint and a side-inlet tube near the top for the replacement of air with nitrogen. This tube was packed with quartz chips and externally heated with an electric furnace. The temperature was measured by a pyrometer with a thermocouple attached to the outside of the pyrolysis tube. During the pyrolysis, a slow stream of dry nitrogen was introduced through the capillary under reduced pressure. By the use of this apparatus, 5.0 g. (0.031 mol.) of cyanoacetanilide was pyrolyzed at 645~650°C over a period of 55 min. under the reduced pressure of 5.0 mm. The pyrolyzate was collected in a flask cooled in a dry ice-ethanol bath, and a 71% (0.70 g.) yield of acetonitrile and a 65% (1.84 g.) yield of phenyl isocyanate were obtained by fractional distillation. From the residue, 1.17 g. (23%) of cyanoacetanilide was recovered; m. p., 196°C.

Pyrolyses of cyanoacetanilide under various conditions and of other derivatives of cyanoacetamides are listed in Table I.

Pyrolysis of 2, 2-Diphenylacetanilide.—With the same apparatus as was employed in the case of cyanoacetamides, 5.0 g. (0.017 mol.) of 2, 2-diphenylacetanilide was pyrolyzed at 550~570° under the reduced pressure of 5.0~7.0 mmHg. The precipitate was collected from the dark brown pyrolyzate and washed with benzene. After recrystallization from ethanol, *sym*-diphenylurea (0.34 g.; m. p., 237°C) was obtained. When the filtrate was distilled, a 42% (1.23 g.) yield of diphenylmethane and a 15% (0.31 g.) yield of phenyl isocyanate were obtained, along with considerable amounts of unidentified by-products.

The results of the pyrolyses of 2,2-diphenylacetanilide under other conditions and of 2-phenylacetanilide and 2,2,2-triphenylacetanilide are listed in Table II.

Summary

The pyrolyses of cyanoacetamides, 2-phenylacetanilide, 2, 2-diphenylacetanilide and 2, 2, 2-triphenylacetanilide have been studied. The pyrolysis of cyanoacetamides gave the corresponding isocyanates and acetonitrile. On the other hand, the pyrolysis of 2-phenylacetanilide and 2, 2-diphenylacetanilide gave a small amount

of phenyl isocyanate, along with various by-products. The pyrolysis of 2, 2, 2-triphenylacetanilide, however, against expectation, did not give isocyanate; only a tarry product resulted.

Laboratory of Organic Chemistry
Tokyo Institute of Technology
Meguro-ku, Tokyo

The Synthesis and Ring-opening Polymerization of N-Substituted 2-Iminotetrahydrofurans

By Teruaki MUKAIYAMA and Kenichiro SATO

(Received September 13, 1962)

A new type of ring-opening polymerization of *N*-substituted iminocarbonates, cyclic ketene acetals and iminooxazolidines, producing polyurethans, polyesters and polyureas respectively, has been shown in previous papers[1,2]. In the present investigation, for the purpose of obtaining polyamides, the synthesis of *N*-substituted 2-iminotetrahydrofurans and their ring-opening polymerization have been studied.

A successful method for the preparation of *N*-substituted iminotetrahydrofurans (II) from 2, 2-diethoxytetrahydrofuran (I) and various amines in the presence of a catalytic amount of acetic acid has been discovered (see Table I).

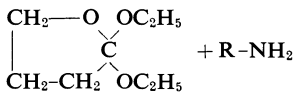

(I)

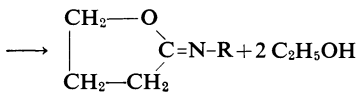

(II)

The highest yield (85%) of 2-phenyliminotetrahydrofuran (V) was obtained when compound I was treated with one equivalent of aniline for 30 min. at 120°C in the presence of a catalytic amount of acetic acid (run 2, Table II). The yield of 2-phenyliminotetrahydrofuran decreased upon prolonged heating because of the polymerization of the tetrahydrofuran produced (run 3, Table II).

It was shown that these tetrahydrofurans were quite sensitive to acidic substances and reacted with hydrogen chloride and benzoic acid to give γ-chlorobutyranilide (IV) and γ-benzoxybutyranilide (V) respectively in good yields.

These reactions seem to proceed through an initial formation of intermediates VI, which in turn decompose to give anilides by ring opening.

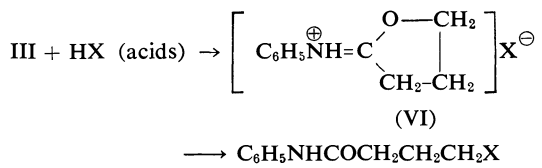

(VI)

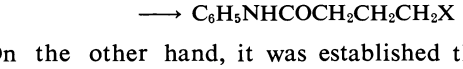

On the other hand, it was established that III was very stable to bases and that III did not react with aniline, even when they were heated for 3 hr. at 120°C and the starting materials were recovered quantitatively.

These behaviors of the tetrahydrofurans toword acids or bases were similar to those of ethylene *N*-phenyliminocarbonate reported in a previons paper[1].

Next, the ring-opening polymerization of *N*-substituted 2-iminotetrahydrofurans was attempted in the presence of a catalytic amount of boron trifluoride etherate. This catalyst

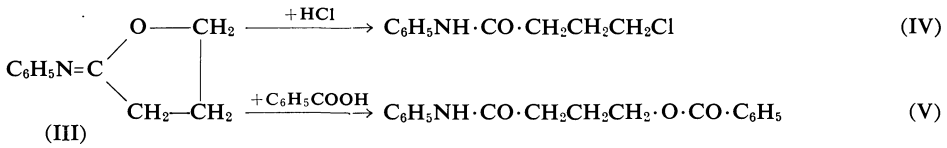

(III)

(IV)

(V)

1) T. Mukaiyama, T. Fujisawa and T. Hyugagi, This Bulletin, **35**, 687 (1962).

2) T. Mukaiyama. T. Fujisawa, H. Nohira and T. Hyugagi, *J. Org. Chem.*, **27**, 3337 (1962).

TABLE I. THE SYNTHESIS OF *N*-SUBSTITUTED 2-IMINOTETRAHYDROFURANS FROM THE REACTION OF 2,2-DIETHOXYTETRAHYDROFURAN WITH VARIOUS AMINES

Run	Amine	Reaction conditions: Time min.	Temp. °C	Catalyst	*N*-Substituted 2-iminotetrahydrofurans: R	Yield, %	B. p., °C	mmHg
1	3,4-Dichloroaniline	10	120	None	3,4-Dichlorophenyl-	70	141～142	0.4
2	*p*-Chloroaniline	20	115	Acetic acid	*p*-Chlorophenyl-	72	124～125	0.4
3	*o*-Chloroaniline	20	115	Acetic acid	*o*-Chlorophenyl-	70	145～146	4
4	Aniline	30	120	Acetic acid	Phenyl-	85	128	2
5	*p*-Anisidine	25	125	Acetic acid	*p*-Methoxyphenyl-	80	155	2
6	*o*-Anisidine	20	115	Acetic acid	*o*-Methoxyphenyl-	70	168	5
7	*p*-Toluidine	15	115	Acetic acid	*p*-Methylphenyl-	65	141	3
8	*o*-Toluidine	15	115	Acetic acid	*o*-Methylphenyl-	70	133	4
9	Cyclohexylamine	420	120	Acetic acid	Cyclohexyl-	45	137	27
10	Benzylamine	30	120	Acetic acid	Benzyl-	75	126～127	3
11	*n*-Hexylamine	680	120	Acetic acid	*n*-Hexyl-	30	65	27

TABLE II. THE EFFECT OF THE REACTION TIME

Run	I g.	Aniline g.	Reaction conditions: Time, min.	Temp., °C	Starting materials recovered, g.	2-Phenylimino-tetrahydrofuran g.	Polymer obtained g.
1	6	3.6	10	120	3	3(50%)	trace
2	6	3.6	30	120	—	5.1(85%)	0.5
3	6	3.6	70	120	—	2.8(47%)	3.0

TABLE III. BULK POLYMERIZATION OF *N*-SUBSTITUTED 2-IMINOTETRAHYDROFURANS

Run	Reactant: R	Polymerization conditions: Time hr.	Temp. °C	Yield %	Properties of polymer: Softening point °C	$[\eta]^{30°}_{\text{chloroform}}$
1	3,4-Dichlorophenyl-	7	60～70	95	60	0.05
2	*o*-Chlorophenyl-	5	60～70	85	90	0.11
3	*p*-Chlorophenyl-	2	80～90	85	65	0.09
4	Phenyl-	72	Room temp.	80	105	0.12
5	*o*-Methylphenyl-	6	65	80	60	0.13
6	*p*-Methylphenyl-	6	65	55	60	0.12
7	Benzyl-	7	90～100	50	40	0.10
8	Cyclohexyl-	7	90～100	50	62	—
9	*n*-Hexyl-	7	90～100	5	—	—

was chosen because it was most effective for the ring-opening polymerization of 2-iminocyclic carbonates, which resemble *N*-substituted 2-iminotetrahydrofurans in structure. The results are listed in Table III.

It is also noted that the polymerization of *N*-substituted 2-iminotetrahydrofurans was promoted by heating, even in the absence of a catalyst.

The polymeric substances obtained by this experiment show a weak N-H absorption at 3350～3450 cm^{-1} and a strong carbonyl absorption at 1650 cm^{-1} but no cyclic ether absorption band at 1170～1180 cm^{-1}, which is present in all the monomers.

A reasonable path by which *N*-substituted 2-iminotetrahydrofurans are converted into polyamides can be the cationic polymerization mechanism proposed in the case of cyclic iminocarbonates[2].

An interesting feature regarding ring-opening polymerization in general is the relationship between ring strain and polymerizability. The successful result for the ring-opening polymerization of tetrahydrofuran suggests that the ring strain considered in tetrahydrofuran facilitates the polymerization[3]. However, no polymerization of γ-butyrolactone has ever

3) E. L. Muetterties, U. S. Pat. 2856370 (Oct. 14, 1958).

Initiation

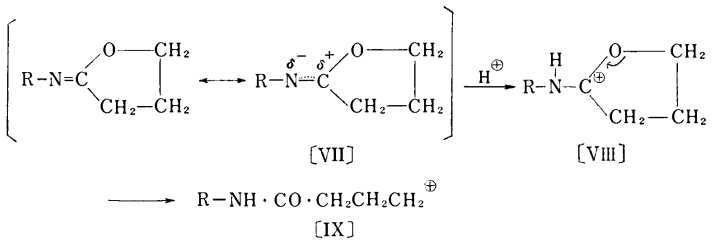

Propagation

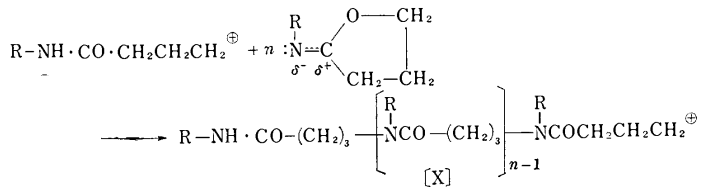

Termination

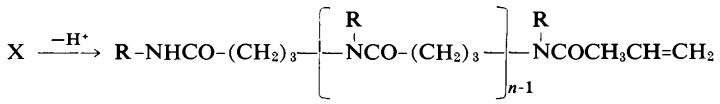

been discovered because the strain is relieved by the introduction of the exo double bond[4].

The fact that *N*-substituted 2-iminotetrahydrofurans which also possess an exo double bond stabilizing the tetrahydrofuran ring are readily polymerized in the presence of cationic catalysts may be because of the basic nature of the imino group, which easily forms a reactive intermediate VIII with the catalyst.

Although *N*-aromatic substituted compounds were readily converted into corresponding polymers, as is indicated in Table III, even under more vigorous conditions, the polymerization of *N*-aliphatic substituted compounds took a long time and their yields were poor. This leads to the conclusion that the step of ring-opening in forming IX from VIII plays a predominant role in this polymerization because the C–O bond fission is facilitated by the introduction of electron-withdrawing aromatic groups.

This type of polymerization was extended further to 2-methylene tetrahydrofuran XII, which also possesses the structural possibility of ring-opening polymerization. When the polymer obtained from the polymerization of XII in the presence of boron trifluoride etherate was examined by means of its infrared spectrum, a strong absorption band attributable to ether linkage (1030 cm^{-1}) was observed. The expected carbonyl band (1700 cm^{-1}) and C=C band (1640 cm^{-1}) were also observed, but they were so weak that the structure of the polymer is assumed to consist of poly cyclic ether, not of poly ketone. This indicates that the polymerization occurs mainly by means of vinyl type ones and that the following mechanism can be suggested:

Initiation

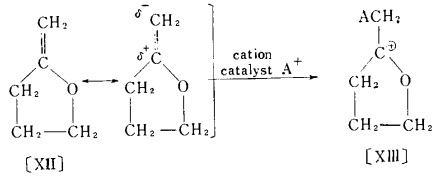

Propagation

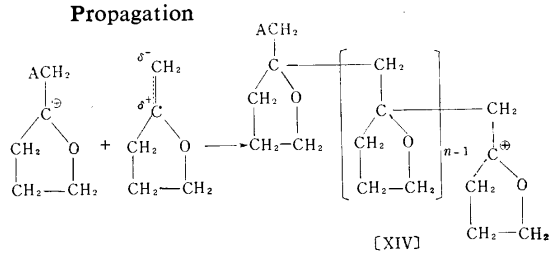

Termination

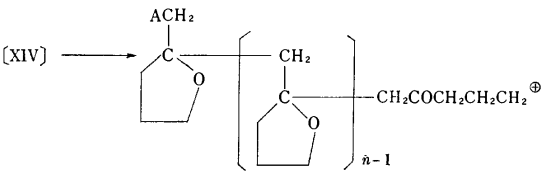

4) H. C. Brown, J. H. Brewstead and H. Shechter, *J. Am. Chem. Soc.*, **76**, 467 (1954).

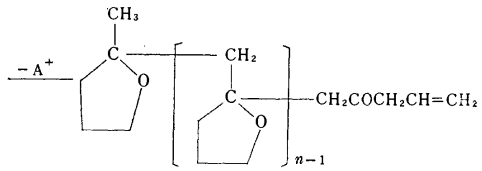

From the results obtained by the polymerizations of those tetrahydrofurans possessing a C=N or C=C exo double bond, it can be said that the ring strain of these tetrahydrofurans is not so large that the compound possessing the structural possibility of vinyl type polymerization does not give raise to ring opening.

In conclusion, ring opening polymerization took place when *N*-substituted 2-iminotetrahydrofurans were treated with acidic catalysts, but this type of ring-opening polymerization was scarcely observed in the case of 2-methylenetetrahydrofuran.

Experimental

2, 2-Diethoxytetrahydrofuran. — This compound was prepared according to the method of Meerwein[5].

Preparation of 2-Phenyliminotetrahydrofuran.— A mixture of 8.0 g. of 2, 2-diethoxytetrahydrofuran, 4.7 g. of aniline, and 2 drops of glacial acetic acid was heated at 120°C for 30 min. After the removal of the alcohol under reduced pressure, 2-phenyliminotetrahydrofuran was distilled as quickly as possible; yield, 6.8 g. (85%); b. p., 128°C/2 mmHg.

In a similar way, 2-(3,4-dichlorophenyl)-, 2-(*p*-chlorophenyl)-, 2-(*o*-chlorophenyl)-, 2-(*p*-methylphenyl)-, 2-(*o*-methylphenyl)-, 2-(*p*-methoxyphenyl)-, 2-(*o*-methoxyphenyl)-, 2-cyclohexyl-, 2-benzyl-, and 2-*n*-hexyliminotetrahydrofuran were prepared from 2, 2-diethoxytetrahydrofuran and corresponding amines.

2-(3,4-Dichlorophenyl)-iminotetrahydrofuran
Found: N, 6.01. Calcd. for $C_{10}H_9ONCl_2$: N, 6.09%.

2-(*p*-Chlorophenyl)-iminotetrahydrofuran
Found: N, 7.32. Calcd. for $C_{10}H_{10}ONCl$: N, 7.19%.

2-(*o*-Chlorophenyl)-iminotetrahydrofuran
Found: N, 7.42. Calcd. for $C_{10}H_{10}ONCl$: N, 7.19%.

2-Phenyliminotetrahydrofuran
Found: N, 8.42. Calcd. for $C_{10}H_{11}ON$: N, 8.69%.

2-(*p*-Methoxyphenyl)-iminotetrahydrofuran
Found: N, 7.21. Calcd. for $C_{11}H_{13}ON$: N, 7.33%.

2-Cyclohexyliminotetrahydrofuran
Found: N, 8.14. Calcd. for $C_{10}H_{16}ON$: N, 8.38%.

2-Benzyliminotetrahydrofuran
Found: N, 7.76. Calcd. for $C_{11}H_{13}ON$: N, 7.99%.

Bulk Polymerization of *N*-Substituted 2-Iminotetrahydrofurans.—About 1.0~2.0 g. of *N*-substituted 2-iminotetrahydrofurans were kept under the condition shown in Table III in the presence of a catalytic amount of boron trifluoride etherate. Polymer obtained were reprecipitated from chloroform-petroleum benzin (boiling range 50~90°C).

Reaction of 2-Phenyliminotetrahydrofuran with Hydrogen Chloride.—Dry hydrogen chloride was passed into a solution of 1.4 g. of 2-phenyliminotetrahydrofuran in 5 ml. of dry benzene at 60~70°C for 15 min. On evaporation of the benzene, crude γ-chlorobutyranilide was obtained and recrystallized from ether-ligloin; yield, 1.2 g. (70%); m. p., 69~70°C. This compound was identical in all respects with the authentic sample.

Reaction of 2-Phenyliminotetrahydrofuran with Benzoic Acid.—A solution of 1.4 g. of 2-phenyliminotetrahydrofuran and 1.0 g. of benzoic acid in 5 ml. of dry benzene was refluxed for 1 hr., and then the benzene was removed. γ-Benzoxybutyranilide was obtained and recrystallized from ether; yield, 60%; m. p., 132~134°C. Found: N, 4.78. Calcd. for $C_{17}H_{17}O_3N$: N, 4.91%.

Preparation of 2-Methylenetetrahydrofuran.— This was prepared according to the method of Paul and Tchelitcheff[6].

Bulk Polymerization of 2-Methylenetetrahydrofuran.—2.0 g. of 2-methylenetetrahydrofuran was kept at 100~110°C for 1 hr. in the presence of a catalytic amount of boron trifluoride etherate. The polymer obtained was reprecipitated from ether-acetone; yield, 40%. Softening point, 62°C (m. p., 62~67°C). $[\eta]^{30°}_{\text{chloroform}}$ 0.1.

Summary

Various *N*-substituted 2-iminotetrahydrofurans are prepared from 2, 2-diethoxytetrahydrofuran and corresponding amines.

N-Substituted 2-iminotetrahydrofurans give *N*-substituted polyamides by ring-opening polymerization when treated with a catalytic amount of boron trifluoride etherate.

On the other hand, 2-methylenetetrahydrofuran undergoes mainly a vinyl-type polymerization.

The authors wish to express their hearty thanks to Mr. Hiroyuki Nohira for his kind advice and to Miss Toshiko Aoyagi for her microanalyses.

Laboratory of Organic Chemistry
Tokyo Institute of Technology
Meguro-ku, Tokyo

5) H. Meerwein, P. Borner et al., *Chem. Ber.*, 89, 2060 (1956).

6) M. R. Paul and S. Tchelitcheff, *Bull. soc. chim. France*, 1950, 520.

Kinetics of the Reaction of N-Arylpyridinium Chloride with Anilines

By Ryohei ODA and Shinji MITA

(Received September 22, 1962)

It is known that some *N*-arylpyridinium salts react with aniline to give glutacondialdehydedianil hydrochloride (I)[1,2]:

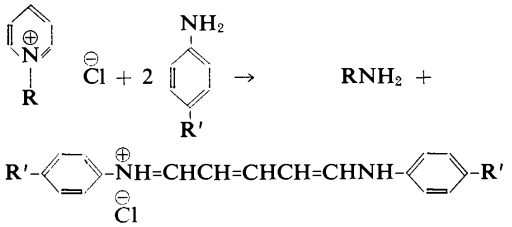

(Here R stands for 2, 4-dinitrophenyl or other electron-withdrawal groups.) Since the mechanism of the reaction had scarcely been studied, for the present paper the rates of the reaction with various R′ and R were measured by the estimation of the dianil produced in order to obtain some information on the mechanism.

Results and Discussion

The rate of the reaction is expressed in terms of the third-order equation:

$$dx/dt = k(a-2x)^2(b-x)$$

or

$$k = \frac{2.30}{t(a-2b)^2}\log\frac{b(a-2x)}{a(b-x)} + \frac{1}{t(a-2b)}\cdot\left\{\frac{1}{a-2x}-\frac{1}{a}\right\}$$

Here, a is the initial concentration of aniline, b, that of pyridinium salts, and x, the concentration of dianil at time t. As an example, a typical run with aniline is shown in Table I. The second-order equation does not agree with the results.

The third-order constants for substituted anilines are listed in Table II, which shows the effect of substituents in aniline.

The Hammett plot of σ: $\log(k/k_0)$ gives a straight line (Fig. 1) which affords the ρ-value of -4.50. This fact suggest a mechanism involving a nucleophilic attack of aniline on the pyridine-aniline complex and a transition state consisting of two molecules of aniline and a molecule of the pyridinium ion:

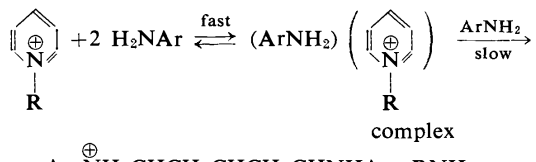

complex

R : 2, 4-dinitrophenyl

The equilibrium for the formation of complex as well as the rate of the nucleophilic attack of aniline should be suppressed by the decreased electrophilicity of the pyridinium salt, i. e., by the smaller electron-withdrawal group. This expectation is supported by the fact that *p*-nitrophenylpyridinium salt (lower electrophilicity) failed to react with aniline.

TABLE I. TYPICAL THIRD-ORDER RATE CONSTANTS FOR THE REACTION OF ANILINE WITH 2, 4-DINITROPHENYLPYRIDINIUM CHLORIDE

Time min.	Conversion %	$k\times10^{-2}$ l. mol^{-2} sec^{-2}
2	2.77	1.89
10	13.1	1.77
20	24.1	1.75
40	39.5	1.77
60	43.5	1.50

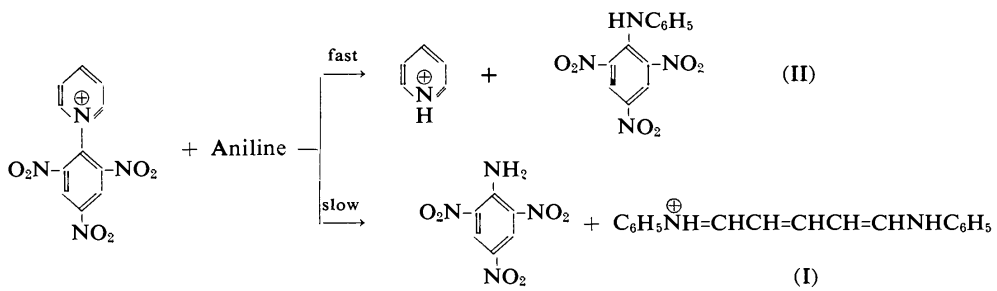

1) T. Zincke, G. Heuser and W. Möller, *Ann.*, 333, 296 (1904).

2) G. E. Ficken and J. D. Kendall, *J. Chem. Soc.*, 1959, 3988.

TABLE II. THE EFFECT OF SUBSTITUENTS IN ANILINE ON THE RATE

R'	*a*, M	*b*, M	*k* (l^2 mol^{-2} sec^{-1})	
			at 30°C	at 50°C
p-OCH_3	0.266×2/5	0.0888×2/5	3.43×10^{-1}	
p-OC_2H_5	0.266×2/5	0.0888×2/5	2.38×10^{-1}	
m-CH_3	0.266×2/3	0.0888×2/3	4.76×10^{-2}	
H	0.266	0.0888	1.75×10^{-2}	2.20×10^{-1}
p-Cl	0.266×5/2	0.0888×5/2	7.80×10^{-4}	
p-NO_2	no reaction			

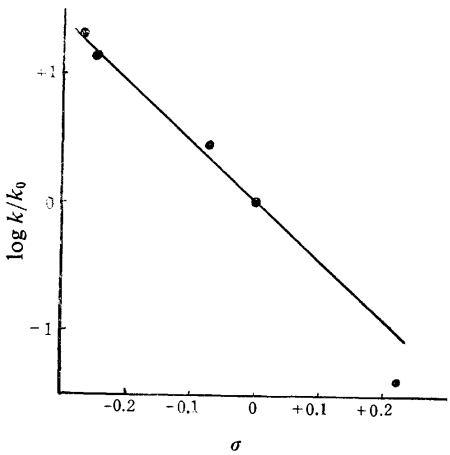

Fig. 1. Hammett's plot of the reaction of pyridinium salt with anilines.

2, 4, 6-Trinitrophenylpyridinium salt reacted very rapidly with aniline, yielding a considerable amount of picrylphenylamine (II) as well as a smaller amount of dianil I.

Experimental

Materials.—2, 4-Dinitrophenylpyridinium chloride was prepared by the reaction of 2, 4-dinitrochlorobenzene and pyridine[1]. *p*-Nitrophenylpyridinium chloride was prepared by the reaction of *p*-nitroaniline, pyridine and cyanogen bromide[2]. 2, 4, 6-Trinitrophenylpyridinium chloride was prepared by the reaction of picryl chloride[2]. The melting points of all these materials agree with those in the literature.

The Rate Measurements.—2, 4-Dinitrophenylpyridinium chloride (2.50 g.) was dissolved in methanol (90 ml.) and 9 ml. of the solution was introduced into test tubes dipped in a thermostat maintained at 30°C. Ten milliliters of a methanolic solution of aniline (2.48 g.) was kept at the same temperature until the temperature equilibrium was reached. One milliliter of the aniline solution was then pipetted out and poured into the pyridinium solution to start the reaction. At appropriate time intervals, the contents of the test tubes were poured into an ice-cooled mixture of acetone (15 ml.) and concentrated hydrochloric acid (15 ml.) to stop the reaction, and the mixture was allowed to stand for about 30 min. while being shaken. The red precipitate, glutacondialdehyde-dianil, was filtered with a glass filter, washed with a small amount of acetone and water, dried at 80~100°C, and weighed. From the amount of the dried product, the third-order rate constant was calculated. Another product, 2, 4-dinitraniline, is soluble in acetone, but is only with difficulty soluble in water, while the dianil is soluble in water, but far less soluble in acetone. From blank tests under the kinetic conditions, the ratios of the produced amount of dianil after a long reaction time vs. the calculated amount were found to be as follows: *p*-anisidine, 1.00; aniline, 1.02; *p*-phenetidine, 1.04; *p*-chloraniline, 1.10; *p*-toluidine, 1.02 and *p*-nitraniline, no reaction. The amount of the obtained precipitate was corrected by the above ratio.

The Reaction of 2, 4, 6-Trinitrophenylpyridinium Chloride.—In a methanolic solution, 2, 4, 6-trinitrophenylpyridinium chloride (0.29 g.) was reacted with aniline (0.248 g.) at 30°C for 5 min. The solution immediately turned red. After filtration of the precipitate of 2, 4, 6-trinitrodiphenylamine (m. p. and mixed m. p. 178°C), diluted aqueous hydrochloric acid was added to the solution. The resulting precipitate, after being filtered and washed with boiling acetone, gave the dianil; 0.011 g. (4.3%); m. p. and mixed m. p., 143°C. 2, 4, 6-Trinitrodiphenylamine was recovered from the acetone solution. The combined yield of this product was 0.213 g. (81%).

Summary

The rates of the reaction of 2, 4-dinitrophenylpyridinium chloride with ring-substituted anilines in methanol have been estimated by the gravimetry of the produced glutacondialdehyde dianil. The rates have been found to be second-order with aniline and first-order with pyridinium salt. The electron-withdrawal groups in pyridine accelerate the reaction. These facts suggest a mechanism involving a nucleophilic attack of the molecules of aniline on a complex consisting of 2 molecules of aniline and a pyridinium ion. The products of the reaction of 2, 4, 6-trinitrophenylpyridinium chloride with aniline were 2, 4, 6-trinitrodiphenylamine and the dianil.

Department of Synthetic Chemistry
Faculty of Engineering
Kyoto University
Sakyo-ku, Kyoto

Charge Carriers in Pyrene Crystals

By Hiroo INOKUCHI and Kenji OHKI

(Received September 25, 1962)

The experimental studies on the electrical behaviours of the organic semiconductors have been carried out by a number of investigators[1]. The work on the determination of signs of charge carriers in molecular crystals have already been reported with association of a several methods. For anthracene, Chynoweth and Schneider[2] found it to be positive by the rectifying behaviour of photoconduction and also Schneider and Waddington[3] found the identical result by means of a charge carrier generation in the crystal by absorption of gases.

Applying the rectifying effect of the photoconduction, on the other hand, the predominant charge carrier in violanthrene ($C_{34}H_{18}$) was found to be negative by the present author[1]. Further, the charge carrier in pentacene, hexacene, ovalene or violanthrene was negative one and in anthracene, pyrene, chrysene, naphthacene or anthanthrene was found to be positive by Northrop and Simpson[4]. Recently, Kepler[5] and LeBlanc[6] reported that positive charge carriers are more mobile than negative ones in anthracene single crystals from an observation of the drift mobility.

As is described above, there are some discrepancies among the different investigators concerning the signs of charge carriers. One of the reasons for such discrepancies may be related to the purity of specimen. In this paper, the authors are presenting the effect of impurities on the sign of the charge carriers in pyrene single crystal and in pyrene thin film.

Experimental

Crude pyrene (A) was provided by Rütgerswerke-Aktiengesellschaft A. G., Germany. Among the methods of purifying pyrene crystals, the techniques of recrystallization from xylene or toluene, sublimation in vacuo and chromatography with benzene or benzene-petroleum ether were effectively applied to make specimens for measuring the electronic

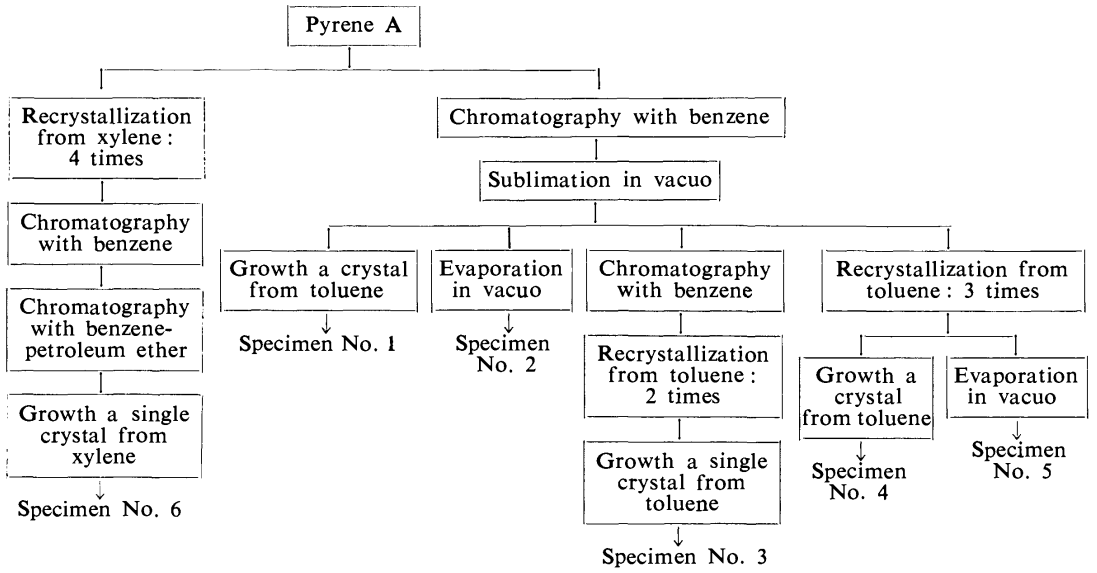

Fig. 1. The purification process of pyrene.

1) H. Inokuchi and H. Akamatu; Electrical Conductivity of Organic Semiconductors in "Solid State Physics", Vol. 12, Academic Press Inc., New York (1961), p. 93.
2) A. G. Chynoweth and W. G. Schneider, *J. Chem. Phys.*, **22**, 1021 (1954).
3) W. G. Schneider and T. C. Waddington, ibid., **25**, 358 (1956).
4) D. C. Northrop and O. Simpson, *Proc. Roy. Soc.*, **A 244**, 377 (1958).
5) R. G. Kepler, *Phys. Rev.* **119**, 1226 (1960).
6) O. H. LeBlanc, Jr., *J. Chem. Phys.*, **33**, 626 (1960).

properties with combination and repeat of the above purification methods six sorts of specimens, single crystals and evaporated thin films, were prepared as shown in the chart, Fig. 1.

The other hydrocarbons applied in this work, violanthrene, dibenzpentacene and quaterrylene, were also purified through the above techniques.

The cell applied in this experiment was prepared by evaporating an organic film on a Pyrex glass which has been coated in advance with a metal film to provide an electrode. For a single crystal specimen, an electrode of metal film was prepared on the crystal directly by means of a vacuum evaporation. The second electrode was formed thereafter by evaporation of a metal onto the surface of the specimen film or single crystal. In order to determine the sign of the predominant charge carrier, the rectifying effects of the photocurrent of the sandwhich-type cells were observed with association of a Cary vibrating-reed electrometer, model-32.

Results and Discussion

It is known that the charge carriers are generated predominately at the thin surface layer closed to the illuminated electrode. Therefore, when the illuminated electrode is charged in negative, the negative charge carriers, electrons, traverse the crystal to reach the other electrode and when the electrode is positive, the positive carriers, holes, will traverse. (It is denoted that the former current is forward one, I_f, and the latter is reverse, I_r.) Therefore, when there is a difference in the mobilities of both signs of charge carriers, the rectifying effects are found.

The variation of the photocurrent (I_p) of the crystal, pyrene, with the applied voltage obeyed the following equation:

$$I_p \propto V^{1.2} \qquad (1)$$

As an example, this variation for specimen No. 1 is illustrated in Fig. 2. When two light sources*, 1000 W tungsten lamp and monochromatic mercury one (3650 Å) were applied no significant difference of the voltage-photocurrent curve was found as shown in the figure. It is suggested that photocarriers are generated only at the surface, even for wavelengths at which it would expect volume generation. For the convenience of understanding, the relation between the photocurrent and the applied voltage is illustrated with logarithmic scale in Fig. 3. Two curves, forward photocurrent and reverse one, are nearly linear except for the highest field applied in the work and are parallel with each other, that is to say, no change of the ratio of these forward and reverse currents, I_f/I_r, is found within the applied electric field.

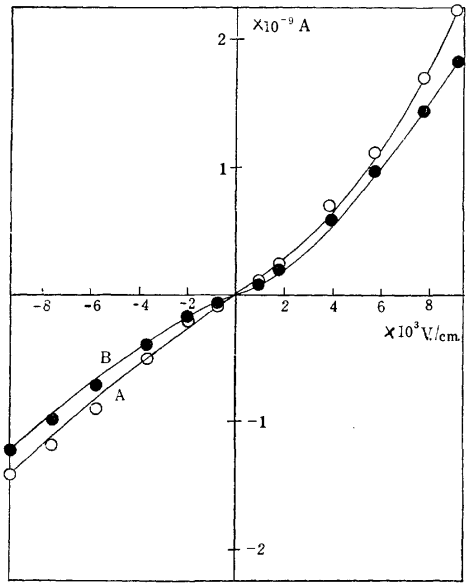

Fig. 2. The variation of the photocurrent with the applied voltage for the pyrene crystal; -●- illuminated with mercury lamp, 3650 Å, and -○- with tungsten lamp.

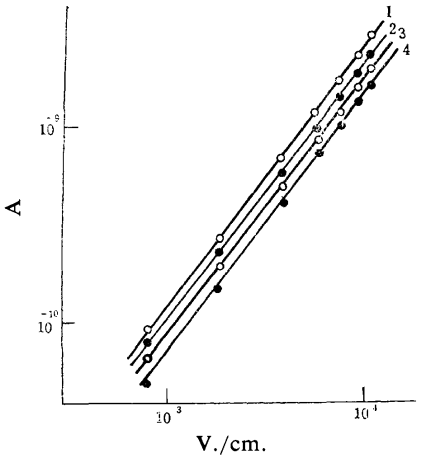

Fig. 3. The photocurrent-voltage curves for pyrene No. 1 with logarithmic scale; -●- illuminated with mercury lamp and -○- with tungsten lamp. Curves 1 and 2 are the reverse photocurrent, 3 and 4 are the forward one.

Following the consideration of transient photoconductivity in ionic crystals, I_f/I_r is described as[7],

* The intensities of these sources were approximately 10^{15}~10^{16} photons/cm² sec.

7) R. S. Van Heyningen and F. C. Brown, *Phys. Rev.*, **111**, 462 (1958).

$$\frac{I_f}{I_r}=\left[\omega_e\left\{1-\frac{e^{-Kl}}{1-K\omega_e}+\frac{K\omega_e}{1-K\omega_e}e^{-l/\omega_e}\right\}+\omega_h\left\{\frac{1}{1+K\omega_h}+\frac{K\omega_h}{1+K\omega_h}e^{-(K+(1/\omega_h))l}-e^{-Kl}\right\}\right]\Big/\left[\omega_e\left\{\frac{1}{1+K\omega_e}+\frac{K\omega_e}{1+K\omega_e}e^{-(K+(1/\omega_e))l}-e^{-Kl}\right\}+\omega_h\left\{1-\frac{e^{-Kl}}{1-K\omega_h}+\frac{K\omega_h}{1-K\omega_h}e^{-l/\omega_h}\right\}\right] \quad (2)$$

where K is an absorption constant ($10^4\,cm^{-1}$ at 365 mμ for pyrene), l is a thickness of crystal, $\omega_e=\mu_e E\tau_e$, $\omega_h=\mu_h E\tau_h$. Furthermore, μ_e and μ_h are the mobilities of electron and hole respectively, τ_e and τ_h are the meantimes for trapping of electron and hole. $E=V/l$, where V is an applied field.

In rough approximation*, this ratio, I_f/I_r, reduces as follows:

$$\frac{I_f}{I_r}\propto\frac{1+K\omega_e}{1+K\omega_h} \quad (3)$$

The ratios for pyrene specimens are summarized in Table I. These results suggests that the ratio reaches over a unity with repeating the purification, that is, the predominant charge carrier is changed from hole to electron with increasing the purity of the crystals. It is expected that the impurities, which may be compounds comprised oxygen**, provide trapping centres for electrons or catch the negative charge carriers. Thereby, it is observed the positive charge carriers in impure crystal are more mobile than the negative one. Recently, Hoesterey has reported the impurity in anthracene acts as an additional dissociation centre capable of trapping the electron component of the exciton[8]. These ratios, I_f/I_r, for violanthrene, dibenzpentacene and quaterrylene were 5~10, 4 and 1.0, respectively. The ratio of pyranthrene ($C_{30}H_{16}$) was found to be 1.5 by Sano[9].

TABLE I. THE RATIOS FOR A NUMBER OF PYRENE CRYSTALS

Sample No.	Form	I_f/I_r
1	Single crystal	0.8
2	Evaporated film	0.9
3	Single crystal	0.6
4	Single crystal	1.3
5	Evaporated film	2.4
6	Single crystal	1.2

To avoid the effect of electrodes and also to estimate the charge mobility in organic crystals, the observation of transient photoconductivity of the organic single crystal sandwiched with two blocking layers is in due course. Further, in comparison with the experimental results, the calculation of overlap integrals between the molecular orbitals of different pyrene molecules in the crystal lattice will be appeared elsewhere.

Summary

From the rectifying behaviour of photoconduction, the sign of charge carriers in molecular crystals is estimated; the ratio of forward photocurrent and reverse one corresponds to the ratio of mobilities μ_e/μ_h, where μ_e is the mobility of electron and μ_h is that of hole. The ratio for pyrene crystal reaches over a unity with repeating the purification, that is, the predominant charge carrier changed from hole to electron with increasing the purity of the crystals. For violanthrene or dibenzpentacene, the ratio is larger than 4 and for quaterrylene, that is almost a unity.

The Institute for Solid State Physics
The University of Tokyo
Azabu, Tokyo

* When we introduce $Kl\gg1$ and $\omega\ll l$, Eq. 2 reduces to Eq. 3.

** The chemical analysis of the contaminants is progressed.

8) D. C. Hoesterey, *J. Chem. Phys.*, **36**, 557 (1962).

9) M. Sano, This Bulletin, **34**, 1668 (1961).

Proton Magnetic Resonance Spectra of Some Thenyl Derivatives[1]

By Kensuke TAKAHASHI, Tyo SONE, Yasuo MATSUKI and Genjiro HAZATO

(Received May 29, 1962)

In the previous works[2,3], we investigated the proton magnetic resonance spectra of some thiophene derivatives. In these studies, the coupling constants and the chemical shifts were measured and discussed in connection with their structures. In the present case we have extended our investigation to some thenyl derivatives.

Experimental

The procedure and apparatus were similar to those described previously[2]. All spectra were observed with a Varian high resolution NMR spectrometer at 40 Mc. The chemical shifts were read directly from the spectra recorded with a Sanborn model 127 recorder. Sweep rate of the magnetic field was calibrated frequently by measuring the displacement between the two peaks for benzene-cyclohexane mixture (1 : 1 by volume). The value assumed for this displacement in the present work is 227 c.p.s. at 40 Mc.[4], although more recent measurements indicate that this value is about 230 c.p.s. at 40 Mc.[5] The small sweep rate was calibrated by running acetaldehyde, with its known splitting of 2.85 c.p.s. The spectra of most of the compounds were measured in cyclohexane solutions and chemical shifts referred to cyclohexane were read in c.p.s., carbon tetrachloride, carbon disulfide, trichloroethylene and acetone were used as solvents in some cases.

All thenyl derivatives and some of the corresponding benzyl derivatives used in the present observations were prepared by the usual method with exception of the commercially available products. The measured conditions and the boiling points or the melting points of the compounds studied are given in Table I.

Results and Discussion

Tables II, III and IV list the results of the chemical shifts and the coupling constants

TABLE I

Compound	B. p. °C/mmHg	Ref.	Measured condition, wt.% Sample	C_6H_{12}	Solvent
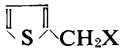					
X = CH_3	133～135	a	80.8	19.2	
CN	115～120/22	b	79.8	20.2	
NH_2	81～83/17	c	80.8	19.2	
C_6H_5	87/8	d	89.3	10.7	
SCN	105～110/3	7	79.5	20.5	
C_4H_3S	125～129/9	e	14.9	4.3	80.8 (CCl_4)
OCH_3	63～64/17	f	85.4	14.6	
Br*	80～85/15	6	80.6	19.4	
Cl	73～75/17	e	83.0	17.0	
OH	94～96/12	c	80.6	19.4	
OAc	92～94.5/11	g	80.5	19.5	
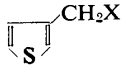					
X = SCN	109～111/3	7	88.0	12.0	
OCH_3**	65～67/17	h	48.4	7.0	44.6 (CCl_4)
Br**	63～80/3	i	83.2	16.8	
CN**	115～120/17	i	83.1	16.9	
COOH	m. p. 79～80	i	11.2	1.7	87.1 (C_2HCl_3)

1) Presented partly at the Meeting of Tohoku District of the Chemical Society of Japan, Yonezawa, October, 1961.
2) K. Takahashi, Y. Matsuki, T. Mashiko and G. Hazato, This Bulletin, 32, 156 (1959).
3) K. Takahashi, Y. Matsuki, Y. Miyake and G. Hazato, ibid., 34, 1599 (1961).
4) B. P. Dailey and J. N. Shoolery, *J. Am. Chem. Soc.*, 77, 3977 (1955).
5) a) B. L. Corio and B. P. Dailey, ibid., 78, 3043 (1956); b) C. M. Huggins and D. R. Carpenter, *J. Phys. Chem.*, 63, 238 (1959).

TABLE I (Continued)

Compound	B. p. °C/mmHg	Ref.	Measured condition, wt.% Sample	C_6H_{12}	Solvent
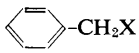					
X = CH_3		j	91.9	8.1	
CN	116~117/20	k	81.1	18.9	
COOH	m. p. 76	l	16.5	4.0	79.5 (C_2HCl_3)
NH_2		j	83.0	17.0	
C_6H_5		j	92.5	7.5	
SCN	102~103/7	h	79.4	20.6	
OCH_3		j	82.7	17.3	
Br		j	82.6	17.4	
Cl		j	82.0	18.0	
OH		j	83.0	17.0	
OAc		j	79.4	20.6	
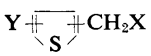					
X Y					
2-CN 5-I	m. p. 58~58.5	h	10.3	1.7	88.0 (CCl_4)
2-SCN 3-NO_2	m. p. 109~110	h	18.3	10.6	71.1 ($(CH_3)_2CO$)
2-SCN 5-CH_2SCN	m. p. 74~75	7	1.5	0.9	97.6 (CS_2)
2-SCN 5-NO_2	m. p. 44.5~45	m	95.7	4.3	
3-SCN 2-NO_2	m. p. 76	h	7.4	15.5	77.1 ($(CH_3)_2CO$)
2-OCH_3 5-Br	91~92/10	f	86.3	13.7	
2-Br 3-NO_2	m. p. 60~61	n	22.0	4.7	73.3 (CCl_4)
2-Br 5-Br	84~86/2	6	84.6	15.4	
3-Br 2-NO_2	m. p. 67	n	7.1	1.4	91.5 (CCl_4)
2-Cl 5-Cl	92~94/15	h	83.6	16.4	
2-Cl 5-Br	72~77/2.5~3	h	79.8	20.2	
2-Cl 5-NO_2	105~107/2	m	80.4	19.6	
2-Cl 3,5-$(NO_2)_2$	m. p. 64	m	82.1	17.9	
2-NCS 5-Br	135~140/3	7	81.7	18.3	
2-OH 5-NO_2	115~118/2	h	92.1	7.9	
2-OAc 5-Br	92~96/2.5~3	h	81.5	18.5	
2-OAc 5-NO_2	m. p. 38~39	h	8.5	3.4	88.1 (CCl_4)

* The sample contains 2-methyl-5-bromothiophene.
** The sample contains 3-methyl-2-bromothiophene.

a W. J. King and F. F. Nord, *J. Org. Chem.*, **14**, 638 (1949).
b F. F. Blicke and F. Leonald, *J. Am. Chem. Soc.*, **68**, 1934 (1946).
c Y. Matsuki and T. Sone, *J. Chem. Soc. Japan, Ind. Chem. Sec. (Kogyo Kagaku Zasshi)*, **63**, 834 (1960).
d W. Steinkopf and W. Hanske, *Ann.*, **541**, 257 (1939).
e F. F. Blicke and J. H. Burckhalter, *J. Am. Chem. Soc.*, **64**, 477 (1942).
f Y. Matsuki and T. Sone, *J. Chem. Soc. Japan, Ind. Chem. Sec. (Kogyo Kagaku Zassi)*, **62**, 1559 (1959).
g W. S. Emerson and T. M. Patrick, Jr., *J. Org. Chem.*, **14**, 790 (1949).
h Y. Matsuki and T. Sone, unpublished work.
i E. Campaigne and W. M. LeSuer, *J. Am. Chem. Soc.*, **70**, 1555 (1948).
j Commercial product.
k "Org. Syntheses", Coll. Vol., **1**, 107 (1948).
l Ibid., **1**, 436 (1948).
m T. Sone and Y. Matsuki, *J. Chem. Soc. Japan, Pure Chem. Sec. (Nippon Kagaku Zasshi)*, **83**, 496 (1962).
n H. R. Snyder et al., *J. Am. Chem. Soc.*, **79**, 2556 (1957).

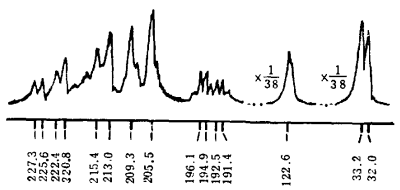

Fig. 1. The proton magnetic resonance spectrum of a mixture of 2-methyl-5-bromothiophene and 2-thenyl bromide at 40 Mc./sec. Applied magnetic field increases from left to right.

which we have obtained. Figure 1 shows the spectrum of a mixture of 2-methyl-5-bromothiophene and 2-thenyl bromide which was obtained by bromination of 2-methylthiophene with *N*-bromosuccinimide in the presence of benzoyl peroxide[6] and cannot be separated easily by distillation. At the highest field, $32._5$ c.p.s. referred to cyclohexane, there is the methyl proton peak of 2-methyl-5-bromothiophene which has the doublet structure with the coupling constant of 1.1_5 c.p.s. The next ill-resolved broad peak at $122._5$ c.p.s. corresponds to the methylene protons of 2-thenyl bromide. The peaks of the ring protons are rather complicated because of the overlapped signals of the two isomers. But it can be partially assigned as follows; two overlapped quartets at the highest field in the ring proton spectrum come from the 3-positioned proton in 2-methyl-5-bromothiophene and four peaks at the lowest field come from the 5-positioned proton in 2-thenyl bromide. The methylene proton peaks in these compounds are distinguished very clearly even with the measurements in the mixture. Chemical shifts of methylene protons in 2-thenyl, 3-thenyl and the corresponding benzyl derivatives are given in Table II. In the course of these studies, we have observed the thermal isomerization of 2-thenyl thiocyanate which easily occurs even at about 150°C[7,8]. But in the case of 3-thenyl thiocyanate, the thermal isomerization could not be observed under the same conditions so that it seems to be sure that 3-thenyl thiocyanate is more stable than 2-thenyl thiocyanate. The chemical shifts of methylene protons given for thenyl and benzyl isothiocyanate in Table II are those obtained from the thermal isomerization of the corresponding thiocyanates. It is seen from Table II that the methylene proton resonance peaks of 2-thenyl derivatives are observed usually at lower field than those of the corresponding 3-thenyl ones. The mean

TABLE II. CHEMICAL SHIFTS OF THE METHYLENE PROTONS IN 2-THENYL, 3-THENYL AND BENZYL COMPOUNDS, REFERRED TO CYCLOHEXANE IN c.p.s. AT 40 Mc./sec.

Group X	Chemical shift, c. p. s. 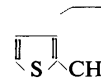	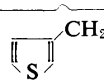	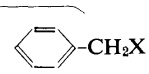
H	$33._5$*1	27*1	$28._5$*2
CH_3	51		43
CN	$89._5$ (0.7*3)	$83._5$	$80._5$
COOH		86	83
NH_2	95 (0.7$_5$*3)		$87._5$
C_6H_5	97		$91._5$
SCN	107	101	95
C_4H_3S	111		97
OCH_3	120 (0.6*3)	$115._5$	113
Br	$122._5$	116	111
Cl	124		113
NCS	125		111
OH	$125._5$		$118._5$
OAc	148		141

*1 The measured condition is given in Ref. 2.
*2 The measurement was made for the solution containing 10 mol.% cyclohexane.
*3 Doublet spacing in c.p.s.

difference between them is about 6 c.p.s. A similar magnitude of the chemical shifts is also observed in thiophene where 3-protons are more shielded than 2-ones by about 6 c.p.s.[9,10,11] From Table II, the methylene protons of benzyl derivatives are more shielded than those of the corresponding 2-thenyl and 3-thenyl derivatives by about 9 and 3 c.p.s. as the mean value, respectively. It is very interesting to note that the ring protons of thiophene are more shielded than those of benzene, while, the methylene protons of thenyl derivatives are less shielded than those of the corresponding benzyl derivatives. This may arise from the difference between the circulating currents of π-electrons in benzene and the thiophene ring. Ring proton spectra of thenyl derivatives studied are rather complex for analyses. But the weighted mean chemical shift for three ring protons in each compound can be estimated from the observed spectrum, the results of which are given in Table III. The ring proton spectrum of each thenyl derivative spreads more widely as compared with the corresponding benzyl derivative. It means that the five ring protons in each benzyl derivative are rather magnetically equivalent, but it is not the case with the three

6) K. Dittmer et al., *J. Am. Chem. Soc.*, 71, 1201 (1949).
7) Y. Matsuki and T. Sone, *J. Chem. Soc. Japan, Ind. Chem. Sec.* (*Kogyo Kagaku Zasshi*), 63, 2171 (1960).
8) K. Takahashi, T. Sone, Y. Matsuki and G. Hazato, This Bulletin, 33, 1465 (1960).
9) S. Gronowitz and R. A. Hoffman, *Arkiv för Kemi*, 15, 45 (1959).
10) R. J. Abraham and H. J. Bernstein, *Can. J. Chem.*, 37, 2095 (1959).
11) T. Isobe, *Bull. Chem. Res. Inst. Non-Aqueous Solutions, Tohoku Univ.*, 9, 115 (1960).

Table III. Mean chemical shifts of the ring protons in 2-thenyl, 3-thenyl and benzyl compounds, referred to cyclohexane in c.p.s. at 40 Mc./sec.

Group X	Mean chemical shift, c.p.s.		
	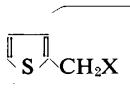	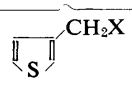	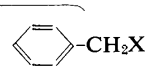
H	210*1	211*1	222
CH_3	210		224
CN	217	225	227.5
COOH		224.5	228.5
NH_2	215.5		227.5
C_6H_5	*2		222
SCN	218	226.5	228.5
C_4H_3S	213.5		*2
OCH_3	217	223	229
Br	218	223.5	226
Cl	215.5		225.5
NCS	*3		*3
OH	216		226.5
OAc	222		229.5

*1 The value was taken from Ref. 2.
*2 Not to be estimated because of overlapping.
*3 Not to be estimated because of the presence of the corresponding thiocyanate.

ring protons in each thenyl derivative. Of the two series of thenyl derivatives, as shown in Table III, the mean chemical shift of the ring protons is mainly affected by the position of the substituent in the ring to which the CH_2X group attached, and in this case, the substituent effect of X in the CH_2X group is unimportant. The Shoolery's method[12] for calculating the alkyl proton frequencies in acyclic systems is highly successful for systems of the type $Y-CH_2-X$[13]. His additivity rule is also applicable to the methylene protons of some benzyl derivatives[13] and the same will be the case with thenyl derivatives. In Table II, acetoxy group, which causes the methylene protons to shift to the lowest field side, is a very distinct one, such a case being not found in Shoolery's or Jackman's table[12,13]. Some of the substituted thenyl derivatives are also investigated and the results are summarized in Table IV. In the case where the signal is split by the indirect spin-spin interaction, the chemical shift given in Table IV is that for the center of the resonance pattern. The observed coupling constants between two ring protons, J_{34}, fall into the range of 3.7~4.2 c.p.s., which are consistent with our previous assumption, $J_{34} \simeq 4.0$

Table IV. Proton magnetic resonace data for the substituted thenyl derivatives, 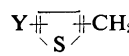 , referred to cyclohexane in c.p.s., at 40 Mc./sec.

Substituents		Chemical shift, c.p.s.					Coupling constant, c.p.s.	
X	Y	CH_3	CH_2	3-H	4-H	5-H	J_{34} or J_{45}	$J_{CH_2 \cdot 3-H}$
2-CN	5-I		94	208.5	223.5	—	$J_{34}=3.7$	1.0
2-SCN	3-NO_2		138.5	—	247.5	247.5		
2-SCN	5-CH_2SCN		114.5	220	220	—		
2-SCN	5-NO_2		126	232.5	258	—	$J_{34}=4.1$	
3-SCN	2-NO_2		129.5	—	233.5	257	$J_{45}=5.5$	
2-OCH_3	5-Br	71.5	117	204	213	—	$J_{34}=3.7$	0.9
2-Br	3-NO_2		141.5	—	243.5	231	$J_{45}=5.5$	
2-Br	5-Br		122.5	210	210	—		
3-Br	2-NO_2		134.5	—	227	239	$J_{45}=5.1$	
2-Cl	5-Cl		122.5	208	203.5	—	$J_{34}=3.7$	0.7
2-Cl	5-Br		123.5	205.5	211.5	—	$J_{34}=3.7$	0.7
2-Cl	5-NO_2		136.5	226	252	—	$J_{34}=4.1_5$	0.8_5
2-Cl	3,5-$(NO_2)_2$		159.5	—	280	—		
2-NCS	5-Br		128.5	208.5	215	—	$J_{34}=3.8$	0.8
2-OH	5-NO_2		144	225.5	256	—	$J_{34}=4.1$	
2-OH	3-NO_2*		*	—	245	237	$J_{45}=5.4$	
2-OAc	5-Br	22	145	211	216	—	$J_{34}=3.9$	0.7
2-OAc	5-NO_2	26.5	148.5	221	249.5	—	$J_{34}=3.9$	

* The measurement was made for a mixture of 5-nitro- and 3-nitro-2-thenyl alcohols. The methylene peak was not observed because of overlapping.

12) J. N. Shoolery, *Tehchnical Information Bulletin, Varian Associates, Palo Alto, California*, 2, No. 3 (1959).

13) L. M. Jackman, "Applications of Nuclear Magnetic Resonance Spectroscopy in Organic Chemistry", Pergamon Press, London (1959), pp. 59, 130.

c.p.s.[2], and also with the others[14]. The coupling constants observed between methylene protons and the 3-positioned ring proton in 2-thenyl derivatives fall into the range of 0.6 ~1.0 c.p.s. This kind of interaction between the ring proton and the methylene protons in thenyl derivative gives us some useful information for the assignments of the spectra, especially in the cases of small internal chemical shifts. For example, in 5-chloro-2-thenyl chloride, the assignment of the two ring protons was made by the observed multiplet structure, but the chemical shift between them is small, then the assignment was also ascertained by taking the spectrum at 56.4 Mc.[15] In all 5-substituted 2-thenyl derivatives tabulated in Table IV, except 5-chloro-2-thenyl chloride, the 3-positioned proton is more shieled than the 4-positioned one, respectively.

TABLE V. DISPLACEMENTS OF THE METHYLENE PROTON PEAKS WHEN THE SAMPLES ARE DILUTED WITH CYCLOHEXANE, CARBON TETRACHLORIDE AND ACETONE, IN c.p.s. AT 40 Mc./sec., REFERRED TO THE VALUES DILUTED WITH CYCLOHEXANE, MINUS SIGN SHOWING THE DISPLACEMENT TOWARD HIGHER FIELD

Compound	Solvent		
	Pure*	CCl_4	Acetone
Benzyl cyanide	−1.0	5.0	16.0
2-Thienylacetonitrile	0.5	5.0	18.0
3-Thienylacetonitrile	1.0	5.0	16.0
Benzyl thiocyanate	−3.5	4.5	15.5
2-Thenyl thiocyanate	−3.5	4.0	15.5
3-Thenyl thiocyanate	−2.5	3.0	13.5
5-Chloro-2-thenyl chloride	1.0	4.5	15.0
Benzyl methyl ether	−1.0	1.5	3.5
2-Thenyl methyl ether	−0.5	1.5	3.5
3-Thenyl methyl ether	0.0	0.5	3.5
Benzyl acetate	1.5	1.0	4.5
2-Thenyl acetate	2.5	1.0	5.0

* The values are estimated from Table II.

The observation of the solvent effects on the chemical shifts for methylene protons of several compounds was also made. Three typical solvents were used. The experiment was carried out with definite dilute solutions of the compounds in each solvent; those are 13.5 wt.% solutions in cyclohexane, 7.5 wt.% solutions in carbon tetrachloride containing 1.5 wt.% cyclohexane and 14 wt.% solutions in acetone containing 14 wt.% cyclohexane. The results are summarized in Table V. The values in pure liquid state in Table V are estimated from the values in Table II. It is seen from Table V that the displacements in question are much affected by the difference of X of the CH_2X groups and not so much by the difference between the corresponding benzyl, 2-thenyl and 3-thenyl derivatives.

The Chemical Research Institute of Non-Aqueous Solutions
Tohoku University
Katahira-cho, Sendai

14) S. Gronowitz and R. A. Hoffman, *Arkiv för Kemi*, **13**, 279 (1958); ibid., **16**, 563 (1960).

15) The authors wish to express their thanks to Dr. N. Hayakawa (Japan Atomic Energy Research Institute) for providing the NMR spectrum of 5-chloro-2-thenyl chloride at 56.4 Mc.

Distribution of Inorganic Impurities in Graphite Electrodes

By Michio INAGAKI and Tokiti NODA

(Received August 10, 1962)

In most domestic graphite electrodes, the ash content is usually less than 0.2%. However, some Acheson 18'' electrodes have been found to contain larger quantities of ash. Moreover, the main component of the ash in the Acheson 18'' electrode was found to be iron. It would be very interesting to know the distribution pattern of inorganic impurities in graphite electrodes. However, the usual method of determining ash content[1] does not serve here.

In the present work, the distribution of inorganic impurities in many graphite electrodes was investigated by means of radiography, ash pattern technique and sulfur print technique.

Experimental and Results

Radiograph. — The arrangement for radiography is illustrated in Fig. 1. Flat specimens

1) JIS (Japan Industrial Standards) R 7202·3·3 (1952).

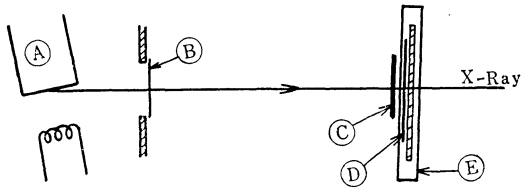

Fig. 1. Arrangement for radiography.
A: Anticathode B: Ni-filter
C: Specimen D: Ni-foil
E: Film cassette

1.0 or 1.5 mm. thick were made from Acheson 14", 18" and 30" graphite electrodes and from six kinds (A—F) of domestic 14" and 18" graphite electrodes. The surface of the specimen was polished with fine sand-paper, although the degree of polishing was found to have no remarkable effect on the radiograph. The distribution of a small amount of iron compound in the graphite product is detectable because the mass absorption coefficient of iron ($\mu/\rho=320$) is far greater than that of carbon ($\mu/\rho=5.50$), while a small amount of sulfur ($\mu/\rho=91.3$) or silicon ($\mu/\rho=60.3$) is very difficult to detect.

The texture of the graphite product, such as the shape and distribution of both grain and pore, can be revealed by a radiograph.

The radiographs of the Acheson electrodes and of some domestic electrodes are represented in Fig. 2a and Fig. 3 respectively. The radiographs for the domestic electrodes were taken from both central and peripheral parts, which are designated as C and P in Fig. 3.

Ash Pattern.—If the specimen was slowly burned out at 750°C on a porcelain plate, an ash pattern consisting of non-volatile impurities was obtained. The ash pattern was very fragile and had to be handled with great caution.

The ash patterns of the Acheson electrodes are shown in Fig. 2b. The ash patterns of these electrodes were found to correspond very closely to the patterns of their radiographs.

Sulfur Print.—The sulfur print technique, which is often used to detect sulfide in steel, was applied to the graphite electrode. The sulfur print of the Acheson 18" electrode is shown in Fig. 4. The pattern of the sulfur print of the electrode does not necessarily correspond to the pattern of the radiograph or to the ash pattern of the same electrode, because the sulfur print only reveals the sulfide distribution on the surface of the specimen plate. As for the Acheson 14" and the domestic electrodes, no sulfur print was obtained of them.

Discussion

The ash pattern of the Acheson 14" electrode consisted of a small amount of white and light ash which was distributed relatively uniformly. Some of the minute black particles in the ash pattern correspond to those on the radiograph, and these particles seem to consist of iron. An appreciable amount of impurities was found in the Acheson 18" and 30" electrodes. The ash content of the Acheson 18" electrode ranged from 0.2 to 2%, varying from place to place even in a single electrode. The main component of the ash was iron oxide (Fe_2O_3), which was identified by the X-ray diffraction method. From both the radiograph and ash pattern, impurities in the Acheson 18" electrode were found to exist in a fibrous

a) Radiograph

b) Ash pattern

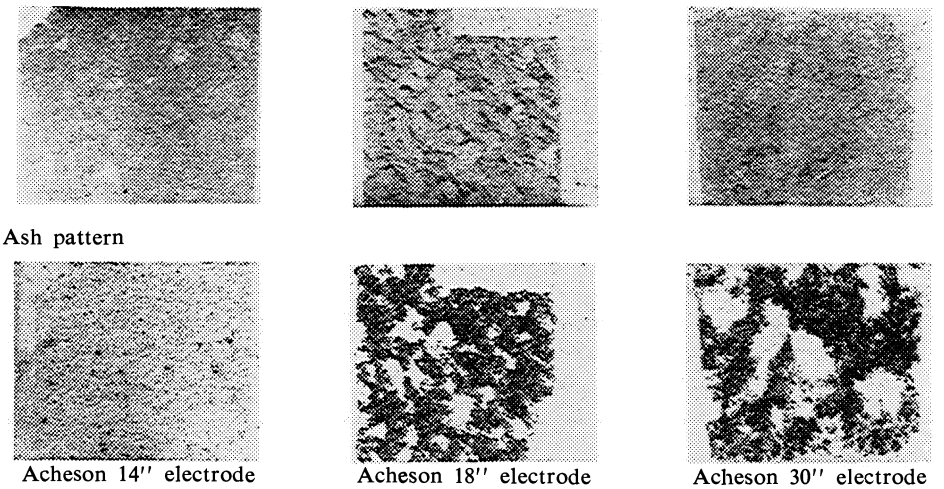

Acheson 14" electrode Acheson 18" electrode Acheson 30" electrode

Fig. 2. Radiograph and ash pattern of Acheson electrodes (×1).

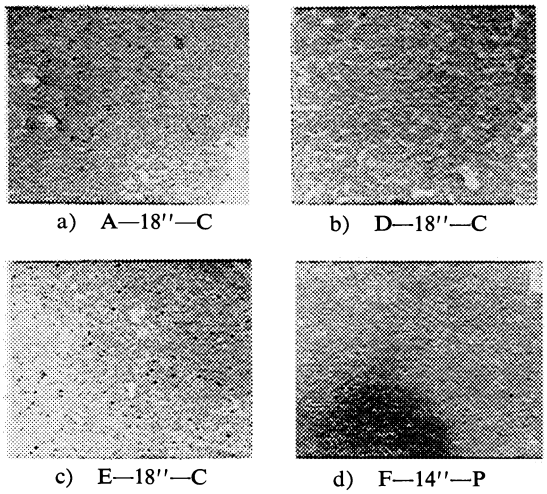

a) A—18″—C b) D—18″—C

c) E—18″—C d) F—14″—P

Fig. 3. Radiographs of domestic electrodes (×1).

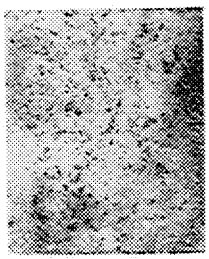

Fig. 4. Sulfur print of Acheson 18″ electrode (×1).

texture intermingled with fine coke powder or with coke derived from binder pitch in the interstices between the coke grains. The fibrous texture of the impurities suggests that they might have condensed from the vapor phase.

The average sulfur content of the Acheson 18″ electrode, which was determined by Eschka's method, was 0.55%, and the average iron content was 1.13%. The impurities in the electrode were gradually dissolved out by dilute sulfuric acid evolving hydrogen sulfide. The mole ratio of sulfur to iron in the electrode, the evolution of hydrogen sulfide, and the development of the sulfur print suggest that the main component of inorganic impurities in the Acheson 18″ electrode is iron sulfide.

In most domestic graphite electrodes, such as E–18″–C and F–14″–P, small black particles of impurities are distributed fairly uniformly all over the electrodes in a way similar to that in the Acheson 14″ electrode. In radiographs of some domestic electrodes such as A–18″–C, however, small clusters of impurities were found to exist in the interstices of the coke grains.

From radiographs of graphite electrodes, one can estimate the shape and the size distribution of coke grains and pores. On the radiographs of A–18″–C and E–18″–C, large coke grains and fairly large pores may be clearly observed. The central part of an eighteen-inch electrode was found to have a less compact texture than the peripheral part of the same electrode. This finding corresponds to the other experimental finding that the bulk density of the peripheral part of graphite electrode is larger than that of its central part[2]. Particularly, the central part of the electrode of D–18″ has an extremely loose texture, as is shown in the radiograph of D–18″–C. Eighteen-inch or larger-sized electrodes contain larger grains and have a less compact texture than 14″ electrodes.

Summary

The distribution of inorganic impurities in graphite electrodes was investigated by means of radiography, ash pattern technique and sulfur print technique. The pattern of the radiograph of an electrode corresponded closely with its ash pattern.

Radiography of graphite electrode was proved to be useful in showing not only the distribution of inorganic impurities in the electrode, but also the texture of the electrode, such as the shape and distribution of both coke grains and pores.

Department of Applied Chemistry
Faculty of Engineering
Nagoya University
Chikusa-ku, Nagoya

2) F. E. Faris, L. Green and C. A. Smith, *J. Appl. Phys.*, 23, 89 (1952).

*Radiation-Induced Addition of Acetaldehyde to Ethylene**

By Kozo HIROTA, Shinji IIZUKA, Hiroshi OCHI and Motoyoshi HATADA

(Received August 13, 1962)

It was found by two of the present authors[1] that several ketones of the type, $CH_3CO\cdot(C_3H_6)_nH$ ($n=1, 2, 3, \cdots\cdots$), can be synthetized by radiation-induced addition of acetaldehyde to propylene at room temperature with a maximum $G(-C_3H_6)$ value of 150. The mechanism could be ascribed to a following chain reaction, where acetyl radical which plays a role of the initiator is produced not only by irradiation but also by a result of chain transfer.

$$CH_3CHO \rightsquigarrow CH_3\dot{C}O + \dot{H} \quad (1)$$

$$CH_3\dot{C}O + C_2H_3R \rightarrow CH_3COCH - \dot{C}HR \quad (2)$$

$$CH_3COCH_2-\dot{C}HR + CH_3CHO \rightarrow CH_3COCH_2CH_2R + CH_3\dot{C}O \quad (3)$$

$$CH_3COCH_2-\dot{C}HR + CH_2=CH_2 \rightarrow CH_3COCH_2CHRCH_2\dot{C}HR \quad (4)$$

etc., where R denotes CH_3.

Such a kind of telomerization was later reported by Stoops and Furrow[2], who investigated the effect of methyl substitution of both telogen and taxogen, but detailed experimental conditions were not described. Radiation-induced telomerizations of similar type have been reported by several authors, who used different telogen (mercaptan[3], carbontetrachloride[4,5], alcohol[6], etc.), though their taxogen were the same and mostly ethylene. Nevertheless, the details of the research have not been described so extensively, except the recent of Takehisa et al.[5]

It was found since then by the present authors that G values of such telomer formation, G(telomer), depend evidently on the temperature and pressure of the irradiated samples and also on the natures of telogens and taxogens. Especially such a dependency was shown when ethylene was adopted as the taxogen instead of higher olefins, and acetaldehyde as the telogen; moreover, G value of ethyl methyl ketone produced, 1 : 1 telomer of ethylene, reached more than 1000 even at room temperature, as reported in the preliminary paper[7]. Therefore, it will be interesting to report the results of this telomerization, the experimental condition of which was varied over the ranges of pressure and temperature up to 50 kg./cm^2 and 110°C, respectively.

Experimental

Materials.—Acetaldehyde was prepared by heating commercial paraaldehyde, which had been purified by distillation at 70°C, with a small amount of concentrated sulfuric acid. The final product was again distilled under vacuum. Ethylene was obtained from the Takachiho Chemicals Co., and was purified by vacuum distillation. Impurities of ethylene thus treated were found to be within 0.5% by mass-spectrometric and gas chromatographic measurements.

Procedure.—Two different procedures were adopted according as the experiments were carried out at low or high pressure. In the first experiment, glass tubes were used as in the former reports. The pressure of ethylene in the tubes could not be determined absolutely. Therefore, a bomb equipped with a pressure gage was used in the second experiment. Both procedures and also the results will be described separately.

Experiment at Lower Pressure.—All the samples were carefully deaerated, and then enclosed in the glass tube, shown in Fig. 1. The following procedure was adopted in order to avoid polymerization of acetaldehyde when it was cooled with liquid nitrogen: 1) A measured amount (0.05 mol.) of acetaldehyde was introduced into A of the glass tube by cooling it at −78°C; 2) the tube was sealed off at B, and connected to the vacuum system at C; 3) a measured amount (0.027$_4$ mol.) of ethylene was introduced into D through C; 4) the tube was sealed off at E; 5) both liquid samples were mixed by opening the break-off tip.

The glass tube was put to irradiation of gamma-rays from the Co-60 source (1000 c.) of our laboratory. If not otherwise described, the irradiation was carried out at 7~15°C. After irradiation, samples were taken out from the tube and their

* Chain Telomerization Induced by Gamma-rays. III.

1) K. Hirota and M. Hatada, This Bulletin, 33, 1682(1960).

2) C. E. Stoops and C. L. Furrow, *J. Org. Chem.*, 26, 3264 (1961).

3) T. D. Nevitt, W. A. Wilson and H. S. Seelig, *Ind. Eng. Chem.*, 51, 311 (1959).

4) E. J. Henley and C. Chang, *J. Polymer Sci.*, 36, 511 (1959).

5) M. Takehisa, M. Yasumoto and Y. Hosaka, *J. Chem. Soc. Japan, Ind. Chem. Sec.* (*Kogyo Kagaku Zasshi*), 65, 531 (1962).

6) K. Hirota and M. Hatada, This Bulletin, 34, 1644 (1961).

7) K. Hirota and H. Ochi, *Isotopes and Radiation*, 3, 509 (1960).

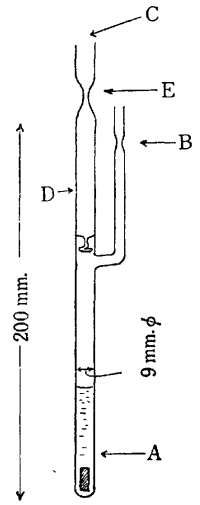

Fig. 1. Irradiation tube for experiments at lower pressure.

liquid part was analyzed by gas chromatography on a Shimadzu G-C 1A instrument by the use of a 3-m. column of dioctyl phthate at the flow rate of 120 ml./min. of helium. For analysis of 1 : 3 telomer, a 5.25-m. column of high vacuum oil was used at an operating temperature of 150°C and at the flow rate of 120 ml./min. of helium.

Experiment at Higher Pressure.—According to the preliminary run, it was found that acetaldehyde reacted with the inner surface of the autoclave made of stainless steel. Therefore, samples were introduced by the following procedures so as to prevent the direct contact of acetaldehyde with the wall:—Acetaldehyde was enclosed under vacuum in a glass ampoule which was then charged in another glass tube which has a small hole A at its side-wall. After the glass ampoule and tube were set up in the autoclave as shown in Fig. 2, an ethylene tank was connected via valves. Ethylene was introduced up to the desired pressure which was measured by a Bourdon gage. The autoclave was rocked and the upper end of the ampoule B was broken by shaking the autoclave upside down. After the time sufficient to reach the dissolution equilibrium of ethylene into acetaldehyde, the sample was irradiated through the wall of the autoclave with Co-60 γ-rays.

After cooling the autoclave down at 5°C and ventilating the unrecacted gas, the liquid product was taken out and put to the gas chromatographic analysis by making methylamyl ketone an internal standard. Operating condition of the gas chromatograph was similar to that of the first experiment.

Gelled part of the product was filtered, dissolved in carbon tetrachloride, and purified by the column chromatography using aluminum oxide as an adsorbent. The result of the elementary analysis is the purified gell was as follows:

Found: C, 81.2; H, 13.47. Calcd. for $C_{21}H_{42}O$: C, 81.21; H, 13.63%.

Mean molecular weight determined by the freezing-point method was found to be 410, though

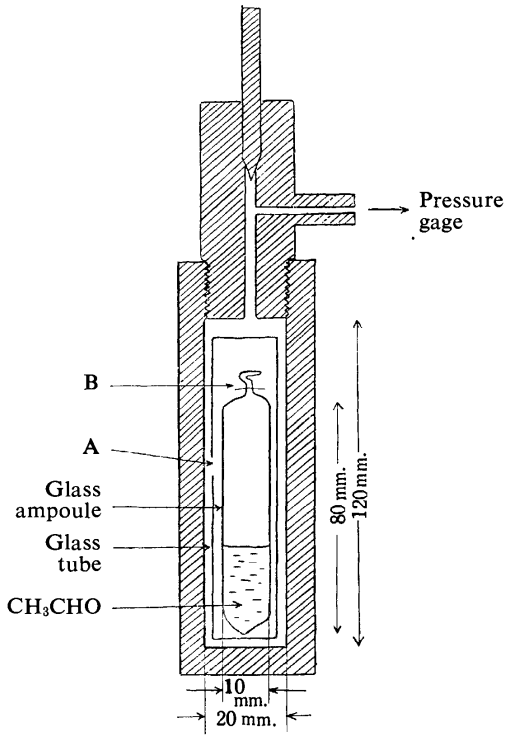

Fig. 2. Irradiation apparatus for experiments at higher pressure.

calculated value was given to be 310 from $C_{21}H_{42}O$.

Results and Discussions of the Experiment at Lower Pressures.—*Identification of the Products.*—Ethyl methyl ketone (EMK) and methyl-*n*-butyl ketone were found to be produced in the irradiated samples. They correspond to

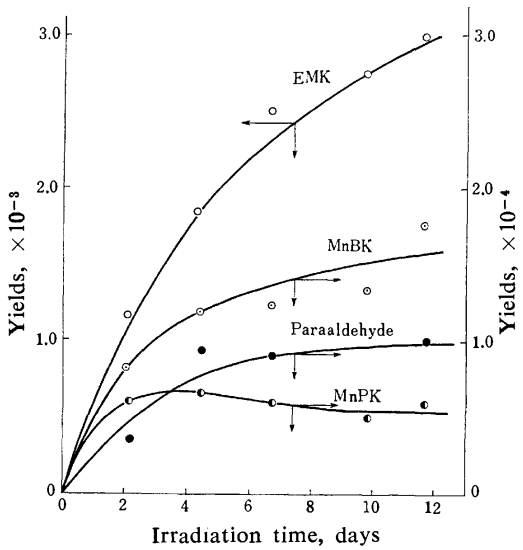

Fig. 3. The yields of EMK, MnBK vs. irradiation time.
Irradiation dose rate 1.3×10^4 r/h.
Ethylene 0.00411 mol.

1 : 1 telomer and 1 : 2 telomer, respectively, of acetaldehyde and ethylene. Both yields increase with irradiation time as shown in Fig. 3*. However, 1 : 3 telomer could not be identified. Besides a small amount of methyl-*n*-propyl ketone was found, which was probably produced by the termination of the following type:

$$CH_3COCH_2-\dot{C}H_2 + \dot{C}H_3 \rightarrow CH_3COCH_2-CH_2-CH_3 \quad (5)$$

The methyl radical in Eq. 5 might be produced by thermal decomposition of acetyl radical, i. e.

$$CH_3\dot{C}O \rightarrow \dot{C}H_3 + CO \quad (6)$$

or directly from acetaldehyde by irradiation, i. e.,

$$CH_3CHO \xrightarrow{h\nu} \dot{C}H_3 + \dot{C}HO \quad (7)$$

Such reactions are very probable from the data of both photochemical and thermal decompositions of acetaldehyde[8].

Effect of Dose Rate on G(Ethyl Methyl Ketone).—The effects of dose rate I on the yield are shown in Figs. 4a and b. The G values were estimated from the initial inclination of the curves in Fig. 4a and logarithms of the G(EMK) are plotted against $\log I$ in Fig. 4b. From this plot, it is clearly shown that EMK is produced in proportion to -0.59 powers of I. This value is slightly smaller than -0.50 which will be derived under the assumption of a bimolecular termination of all the propagating radicals in Eqs. 3 and 4.

Effect of Irradiation Temperature on G(Ethyl Methyl Ketone). — Effect of irradiation temperature on the G(EMK) is shown in Fig. 5. The G values increase gradually with irradiation temperature. From their Arrehnius plots

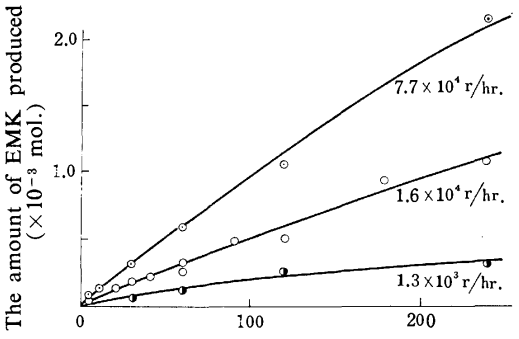

Fig. 4a. The amount of EMK produced vs. irradiation time.

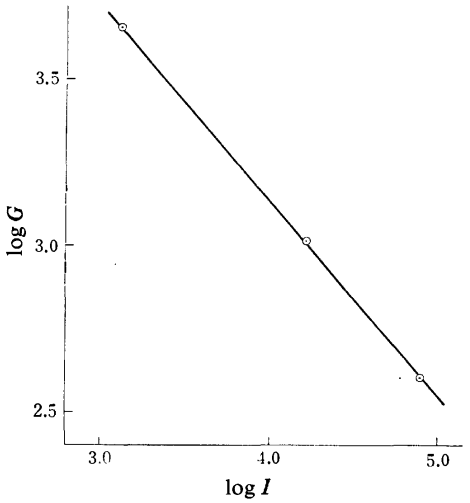

Fig. 4b. Log G vs. log I.

a relatively good straight line was obtained, and an apparent activation energy was determined to be 5.0 kcal./mol. from the inclination of this line. It will be interesting to compare this value with that of the system of ethylene and isopropanol (7.0 kcal./mol.)[7]. Such a smaller value may denote that hydrogen abstraction from acetaldehyde is easier than from isopropanol.

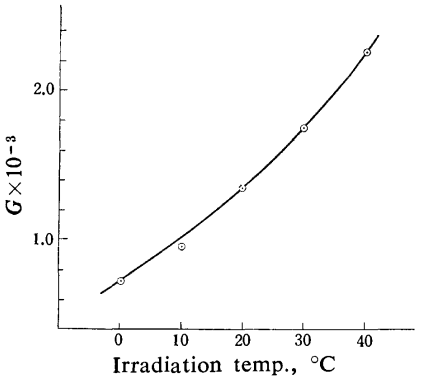

Fig. 5. G(EMK) vs. irradiation temperature.

Because if a bimolecular termination of the propagating radicals is assumed, the apparent activation energy of such a chain polymerization will be given generally by

$$E_a' = E_p - 1/2E_t \quad (8)$$

where E_p and E_t denote the propagating and the terminating steps, respectively. In the present case E_t may be equated practically to zero. The above two values (5.0 and 7.0 kcal./mol.) however do not correspond exactly to E_p of Eq. 8 due to the change of solubility of ethylene into acetaldehyde with the reaction temperature. Nevertheless, since

8) Cf. E. W. R. Steacie, "Atomic and Free Radical Reactions", 2nd ed., Reinhold Publishing Corp., New York (1954), pp. 215—219. pp. 286—294.

* Since the amount of paraaldehyde is not reproducible, it may not be produced by irradiation. The data will therefore be omitted hereafter.

the temperature dependency on solubility of ethylene will be similar in both alcohol and aldehyde, the above conclusion on the difference of activation energy may be drawn.

Effect of Molar Percent of Ethylene in the Feed on G(Ethyl Methyl Ketone).—It is shown in Fig. 6 that the G(EMK) increases with increasing pressure of ethylene, the inclination of the curve decreases gradually. It will be interesting to study the behavior of G values at higher molar per cent. The investigation will be carried out in the higher pressure experiment.

Effect of Additives. — Presence of the air scarcely affected the yield of telomers but rather increased slightly. A small amount of DPPH inhibited the production of telomers perfectly, except that of paraaldehyde. Addition of water reduced the yield markedly; e. g. 20% decrease was found in the telomer formation by the addition of 2% water. Such a reducing effect of water may be ascribed to the hydration of acetaldehyde.

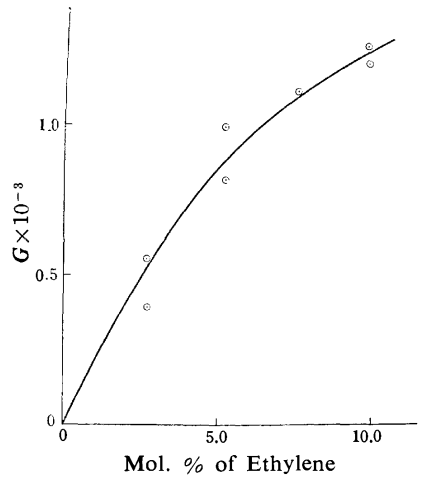

Fig. 6. G(EMK) vs. mol. % of ethylene.
Acetaldehyde 0.05 mol.
Dose rate 1.6×10^4 r/hr.
Irradiation time 1 hr.

Results and Discussion of the Experiments at Higher Pressure*.— *Effects of Irradiation Time on Telomer Yields.*—In addition to the 1 : 1 and 1 : 2 telomers described in the previous section, methyl-*n*-hexyl ketone (1 : 3 telomer) was found to be produced in the experiments at higher pressures. The effects of irradiation time on the yield of each telomer were shown in Figs. 7—9, where ethylene was charged at the initial pressures of 10, 20 and 50 kg./cm², respectively, to 0.05 mol. of acetaldehyde. The yields of 1−1 and 1−2 telomers increase approximately linearly with increasing dose, while tendency of the yield of 1−3 telomer is not so clear, as the value is too small.

Effect of Irradiation Temperature.—As can be shown by the data in Figs. 7—9, it may be clear that the effect of temperature is very small, especially at the pressure range higher than 20 kg./cm², if it ever exist. Such a result

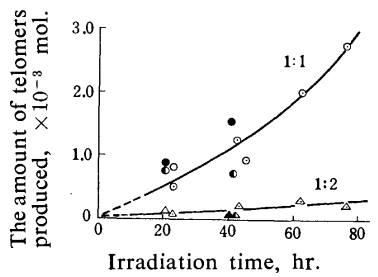

Fig. 7. The amount of telomers produced vs. irradiation time.
CH_3CHO 0.05 mole, C_2H_4 10 kg./cm²
Dose rate: 1.0×10^4 r/hr.
⊙△ room temp., ●▲ 75°C, ◐◭ 103°C

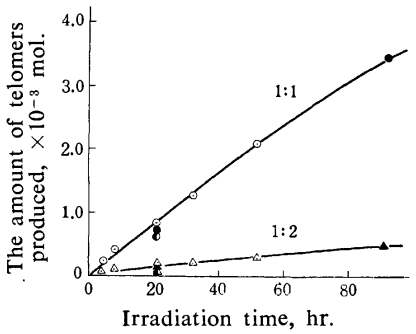

Fig. 8. The amount of telomers produced vs. irradiation time.
CH_3CHO 0.05 mole, C_2H_4 20 kg./cm²
Dose rate: 1.0×10^4 r/hr.
⊙△ room temp., ●▲ 75°C, ◭◑ 103°C

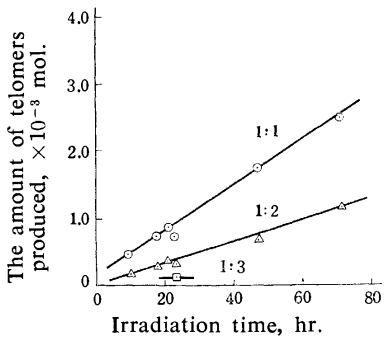

Fig. 9. The amount of telomers produced vs. irradiation time.
CH_3CHO 0.05 mole, C_2H_4 50 kg./cm²
Dose rate: 1.0×10^4 r/hr.
⊙△◉ room temp.

* According to a Germa Pat. 1077662 (Jan. 30, 1957), such telomers are produced without irradiation under the pressures higher than 35 atm. This effect was found to be negligibly small in the present experimental conditions.

is quite different not only from the low pressure experiment but also from the system of isopropanol and ethylene where G(telomers) increases with temperature up to 250°C[9]. These differences may be brought about by the less stability of acetyl radical than that of isopropyl radical, $(CH_3)_2\dot{C}OH$, as already mentioned[8].

Effects of Initial Pressure of Ethylene.—In order to investigate the effect of the initial pressure of ethylene on the yield of telomers, their G values at room temperature and 75°C are plotted against the initial pressure in Fig. 10. It is evident that the total $G(-C_2H_4)$ increases with increasing pressure up to 4000 at 50 kg./cm². However the G(1 : 1 telomer) has an optimum value and decreases above ca. 30 kg./cm² of the initial pressure. This optimum value seems to shift to the region of lower pressure when the irradiation temperature is 75°C. On the other hand, the G(1 : 2 telomer) increases in proportion to the ethylene pressure, and the G(1 : 3 telomer) to its second power. Such results ought to be expected from the reaction mechanism proposed above.

High Molecular Weight Products. — At the highest pressure, a small amount of white gelled product was obtained. This substance is soluble in carbon tetrachloride, benzene, toluene and hot ethanol, and has a melting point of 65～66°C. The infrared spectrum of this substance is shown in Fig. 11. Strong absorption at 1710 cm^{-1} indicates the presence of carbonyl group. Besides, taking the data of elementary analysis of this substance into account, it is considered to be a mixture of telomers differing in n; e.g.

$$CH_3C(-CH_2CH_2-)_nH$$
$$\quad\quad\quad

Molar fractions of $1:i$ telomer, F_i, are plotted against the ratio of acetaldehyde/ethylene(R) as the abscissa in Fig. 12, making both total dose and dose rate constant. In evaluating R, the absorption coefficient of Ostwald was assumed to be five irrespective of pressures. The lines in the figure indicate the calculated curves from the following equation,

$$F_i = \frac{C_i R}{(C_i R + 1)} \qquad (9)$$

where C_i's, chain transfer constants, are assumed to be 1.0, 1.1 and 4.6, respectively as the most probable values. These numerals resemble to those obtained in the system of acetaldehyde and propylene, but are quite different from those obtained in the system of isopropanol and ethylene (cf. Fig. 13). In the latter system, the change of C_i's against i is small as well as their magnitude. This difference, therefore, is a result to be characterized by the nature of the taxogens.

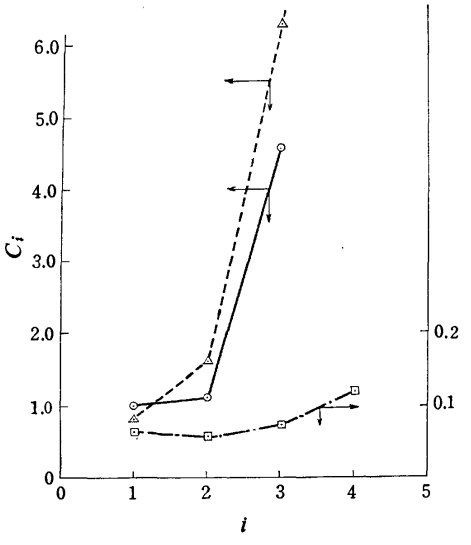

Fig. 13. Chain transfer constant C_i vs. i of the various systems.
⊙ $C_2H_4+CH_3CHO$ △ $C_3H_6+CH_3CHO$
◙ $C_2H_4+(CH_3)_2CHOH$

As mentioned already, the apparent activation energy, 5.0 kcal./mol., obtained between 0 and 40°C seems to correspond approximately to that of the abstraction reaction of hydrogen atom from CHO group of acetaldehyde. However, in the experiment at higher temperature and pressure a smaller temperature dependency or rather independency of temperature was observed on G(telomers). This may probably be ascribed to the increasing occurrence of thermal decomposition of acetyl and/or $CH_3\cdot COCH_2\cdots\cdots\dot{C}H_2$ radicals at higher temperature. Because though telomers of the type as mentioned in Eq. 5 may be produced, the decomposition of acetyl radical, followed by stabilization into CH_4+CO, will contribute to decrease the yield of telomers.

It must be pointed out finally that by the present experiment the acetyl radical seems to be not so unstable as assumed in the photochemical decomposition of acetaldehyde[10]. This conclusion is in agreement with the finding that the activation energy of the decomposition 7 is 9.6 kcal.[11]; i.e., acetyl radical would react with ethylene more easily from the standpoint of the activation energy.

Summary and Conclusions

(1) It has been found that radiation-induced addition of acetaldehyde to ethylene occurs at room temperature with a relatively high $G(-C_2H_4)$, e.g., 4000 at the initial pressure of 50 kg./cm² of ethylene, and that the production of 1:2 telomer is more favorable than that of 1:1 telomer at higher pressure of ethylene. In order to obtain higher G values of 1:1 telomer, it has been shown to be unnecessary to make the initial pressure of ethylene higher than 10 kg./cm², and also to elevate the irradiation temperature much higher than room temperature.

(2) It has been confirmed that a major part of the telomerization proceeds by a chain mechanism, which accompanies a chain-transfer process simultaneously, acetyl radical playing a role of the chain-carrying radical as well as role of initiator. Moreover it has been pointed out that the acetyl radical reacts with ethylene more easily than decomposes, though the decomposition is assumed to occur dominantly in the photochemical and thermal decomposition of acetaldehyde alone[8].

The present research was partly supported by a financial grant from the Ministry of Science and Technology, to which the authors' thanks are due.

Osaka Laboratories
Japanese Association for Radiation Research on Polymers
Neyagawa, Osaka
(K. H., S. I., H. O. & M. H.)

Department of Chemistry
Faculty of Science
Osaka University
Nakanoshima, Osaka
(K. H.)

10) E. I. Akeroyd and R. G. W. Norrish, *J. Chem. Soc.*, 1936, 890; N. Imai and O. Toyama, This Bulletin, 33, 1120 (1960).
11) F. E. Blacet and D. E. Loeffler, *J. Am. Chem. Soc.*, 64, 893 (1942). Older data give also the value between 8.3 and 10 kcal./mol.[8]

Studies of the Photochemical Reactions. V. The Synthesis of Dimethyldioxanylcarbinol and Dimethyl-α-tetrahydrofurylcarbinol[1]

By Kensuke SHIMA and Shigeru TSUTSUMI

(Received September 28, 1962)

In a previous paper[2], it was reported that dimethyl-α-tetralylcarbinol (I) was easily produced by the reaction of photoactivated acetone in tetralin. In order to use the intermediate radical (II) formed from photoactivated acetone for synthetic purposes, dioxane and tetrahydrofuran were chosen as the hydrogen donor solvents in this experiment. New substances, dimethyldioxanylcarbinol (III) and dimethyl-α-tetrahydrofurylcarbinol (IV), were synthesized in fairly high yields.

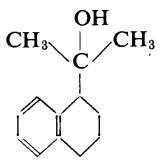

(I)

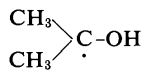

(II)

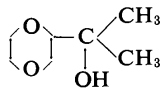

(III)

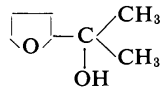

(IV)

A mixture of acetone and dioxane or tetrahydrofuran (mole ratio: 1:4) was irradiated in an atmosphere of nitrogen at room temperature for 10 hr. using a high pressure mercury lamp. The reaction products were then fractionated and analyzed by gas chromatography.

In the photochemical reaction of acetone in dioxane, isopropyl alcohol, dioxanyldioxane and dimethyldioxanylcarbinol (III) were obtained as the reaction products. The new substance, dimethyldioxanylcarbinol (III), which can only with difficulty be prepared by other methods, was easily synthesized.

When acetone was irradiated in tetrahydrofuran, isopropyl alcohol, dimethyl-α-tetrahydrofurylcarbinol (IV) and di-α-tetrahydrofuryl were isolated as the reaction products. The new substance, dimethyl-α-tetrahydrofurylcarbinol (IV), was also easily obtainable by this method. Dimethyl-α-tetrahydrofurylcarbinol was identified by comparison with an authentic sample which had been prepared by the following procedure:

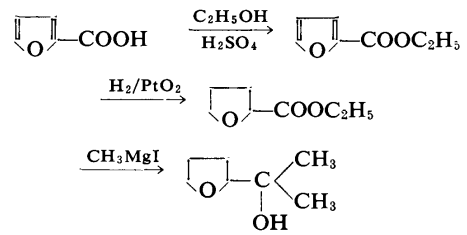

(IV)

The reaction conditions and yields of the products are summarized in Table I.

TABLE I. THE REACTION CONDITIONS AND THE YIELDS OF PRODUCTS

Hydrogen donor solvent	Dioxane	Tetrahydrofuran
Reaction time, hr.	10	10
Acetone used, g.	39.1	40.8
Solvent used, g.	237.2	203.0
Solvent/Acetone, mol. ratio	4	4
Acetone consumed, g.	30.6	31.9
Solvent consumed, g.	29.2	19.8
Isopropyl alcohol, g.	6.8	5.1
R-COH$(CH_3)_2$ g. (A)	12.4	17.8
R—R g.	4.8	7.3
High boiling residue, g.	22.3	12.6
Unidentified product, g.	10.9	8.0
Ultimated yield of (A) based on acetone consumed, mol. %	16.0	24.9
Ultimated yield of (A) based on solvent consumed, mol. %	25.6	49.8

Experimental[3]

Materials.—Dioxane was purified by the following method. The mixture of 900 cc. of commercial dioxane, 11.7 cc. of 37% hydrochloric acid, and 90 cc. of water was refluxed for 10 hr. while nitrogen was bubbled. After the mixture had been cooled, solid potassium hydroxide was added and the separated dioxane layer was fractionated over metallic sodium: b. p., 100~101°C, n_D^{20} 1.4222. Tetrahydrofuran was purified by the fractional distillation over sodium: b. p., 66~67°C, n_D^{20} 1.4052. Acetone was purified by the ordinary method[4]: b. p., 56.5~57°C, n_D^{20} 1.3598.

The Photochemical Reaction of Acetone in Dioxane.—The reaction apparatus used was described in the previous paper[2]. A mixture of

1) Reported at the 15th Annual Meeting of the Chemical Society of Japan, Kyoto, April, 1962.

2) K. Shima, Y. Shigemitsu and S. Tsutsumi, This Bulletin, 35, 1728 (1962).

3) The boiling and melting points are uncorrected.

4) A. Bramley *J.Chem Soc.*, 59, 10 (1916).

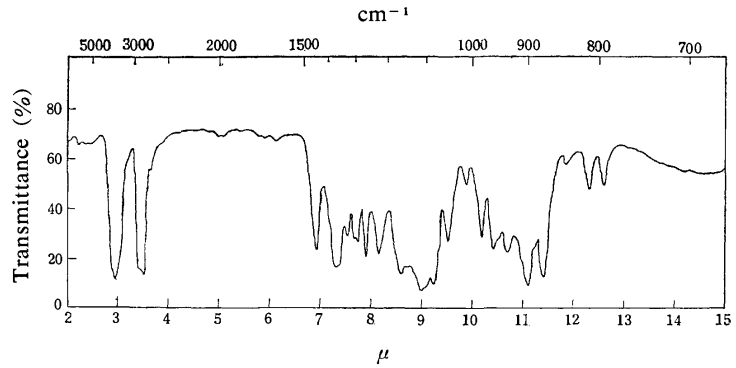

Fig. 1. Infrared spectrum of dimethyldioxanylcarbinol.

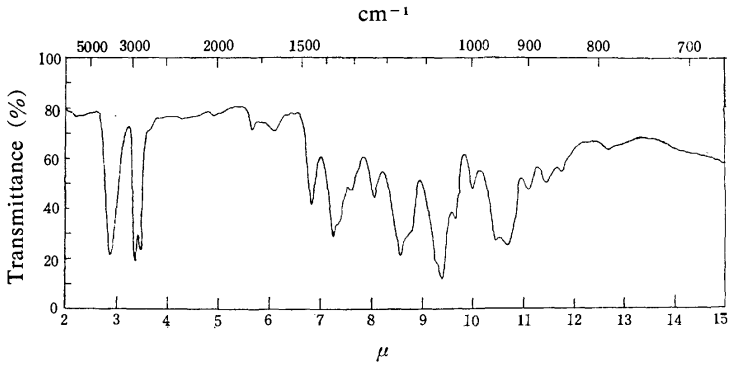

Fig. 2. Infrared spectrum of dimethyl-α-tetrahydrofurylcarbinol.

acetone (39.1 g., 0.675 mol.) and dioxane (237.2 g., 2.69 mol.) was placed in a 300 cc. reaction vessel and irradiated at 11°C in a nitrogen atmosphere for 10 hr. After the irradiation, the reaction product was fractionally distilled to give the following fractions:

b. p., °C	Weight, g.	n_D^{20}
(1) 56～ 63	5.8	1.3572
(2) 63～ 82	4.7	1.3681
(3) 82～ 95	3.4	1.3807
(4) 95～101	13.2	1.4143
(5) 101～103	195.2	1.4199
Residue	53.0	

The presence of isopropyl alcohol was assumed by gas chromatography. 3, 5-Dinitrobenzoate was synthesized from fraction 3 and was identified as the 3, 5-dinitrobenzoate of isopropyl alcohol by the mixed-melting point test. The amounts of acetone, dioxane and isopropyl alcohol were estimated by gas chromatography: column, D. N. P. 3 m.; carrier gas, H_2, 0.32 kg./cm²; bridge current, 160 m amp.; column temp. 50°C; retention time, acetone: 4 min., isopropyl alcohol: 7 min., dioxane: 9.5 min. After the residue had been cooled, the crystalline substance precipitated was filtered and washed with a small amount of cold methanol to give 4.8 g. of dioxanyldioxane, m. p. 155～155.5°C (recrystallized from methanol) (lit[5]. m. p. 157°C). (Found: C, 55.16; H, 7.95. Calcd. for $C_8H_{14}O_4$: C, 55.16; H, 8.10%.)

The filtrate was distilled under reduced pressure to give the following fractions:

b. p., °C/11 mmHg.	Weight, g.	n_D^{20}
(1) ～ 72	1.3	1.4312
(2) 72～ 81	15.1	1.4445
(3) 81～ 87	4.1	1.4497
(4) 87～100	2.2	1.4521
Residue	22.3	

Fractions 2 and 3 were shown by gas chromatography to consist of almost only one component and were purified by using preparative gas chromatography: column, Si D. C. 550; column temp., 150°C; carrier gas, N_2; gas pressure, 1 kg./cm²; b. p. 86～87°C/11 mmHg, n_D^{20} 1.4533. The Denigés test[6] gave a positive result for this fraction. The infrared spectrum is shown in Fig. 1.

Found: C, 57.34; H, 9.42. Calcd. for $C_7H_{14}O_3$: C, 57.51; H, 9.65%.

3, 5-Dinitrobenzoate was synthesized and recrystallized from ethanol; m. p., 158.5～159.4°C.

Found: C, 49.34; H, 4.67. Calcd. for $C_{14}H_{16}O_8N_2$: C, 49.41; H, 4.74%.

From the above results, this fraction was confirmed to be dimethyldioxanylcarbinol.

The Photochemical Reaction of Acetone in Tetrahydrofuran.—A mixture of acetone (40.8 g.,

5) G. Leuschner and K. Pfordt, *Ann.*, **625**, 30 (1959).

6) G. Denigés, *Compt. rend.*, **126**, 1048, 1277 (1898).

0.705 mol.) and tetrahydrofuran (203.0 g., 2.82 mol.) was irradiated at 10~15°C for 10 hr., and the reaction product was fractionally distilled under atmospheric and reduced pressure to give the following fractions:

	b. p., °C	Weight, g.	n_D^{20}
(1)	58~62	11.0	1.3859
(2)	62~66	34.3	1.3980
(3)	66~75	171.6	1.4051
(4)	~30/15 mmHg	5.1	1.3863
(5)	30~57/15 mmHg	2.1	1.4374
(6)	57~78/15 mmHg	21.6	1.4468
(7)	78~85/15 mmHg	9.0	1.4502
	Residue	12.6	

Fraction 4 was assumed to be isopropyl alcohol, and the amounts of acetone, tetrahydrofuran and isopropyl alcohol were estimated by gas chromatography: column, D. N. P. 3 m.; carrier gas, H_2, 0.5 kg./cm²; bridge current, 160 m amp.; column temp. 46°C; retention time, acetone: 3 min., tetrahydrofuran: 7 min.

It was established that fractions 5, 6 and 7 were mainly composed of two components and were separated by preparative gas chromatography.

(A) B. p. 57~59.5°C/10 mmHg, n_D^{20} 1.4468.

Found: C, 64.64; H, 10.83. Calcd. for $C_7H_{14}O_2$: C, 64.58; H, 10.84%.

The infrared spectrum is shown in Fig. 2. 3, 5-Dinitrobenzoate was synthesized and recrystallized from ethanol (m. p., 81~82°C), and no depression was observed in the mixed-melting point test with an authentic sample.

Found: C, 51.95; H, 5.03. Calcd. for $C_{14}H_{16}O_8N_2$: C, 51.85; H, 4.97%.

From the above results, fraction (A) was identified as dimethyl-α-tetrahydrofurylcarbinol.

(B) B. p. 71°C/10 mmHg, n_D^{20} 1.4594

Fraction B was confirmed to be di-α-tetrahydrofuryl from the infrared spectrum and from the elementary analysis described below. Infrared absorption spectrum data: 1070 cm^{-1} (tetrahydrofuran ring), no hydroxy absorption.

Found: C, 67.33, H, 9.66. Calcd. for $C_8H_{14}O_2$: C, 67.57; H, 9.93%.

Synthesis of Dimethyl-α-tetrahydrofurylcarbinol. —Ethyl furan-2-carboxylate[7] was prepared by the reaction of furan-2-carboxlic acid with ethanol in the presence of concentrated sulfuric acid under reflux conditions. B. p. 193~195°C; m. p., 35~36°C (lit[7]. m. p. 34~35°C). Ethyl tetrahydrofuran-2-carboxylate[8] was prepared by the hydrogenation of ethyl furan-2-carboxylate in the presence of an Adams catalyst[9]; b. p., 76~86°C/10 mmHg, n_D^{20} 1.4484 (lit[8]. 82°C/11 mmHg, n_D^{18} 1.4455). Dimethyl-α-tetrahydrofurylcarbinol was prepared by the reaction of methylmagnesium iodide with ethyl tetrahydrofuran-2-carboxylate; b. p., 66~73°C/15 mmHg, n_D^{22} 1.4455, 3,5-dinitrobenzoate; m. p., 82~83°C (from ethanol).

Summary

The photochemical reaction of acetone in dioxane or tetrahydrofuran has been studied, and two new compounds, dimethyldioxanylcarbinol (III) and dimethyl-α-tetrahydrofurylcarbinol (IV), were easily produced by this photoreaction.

Department of Chemical Technology
Faculty of Engineering
Osaka University
Miyakojima-ku, Osaka

7) H. B. Hill and L. L. Jackson, *Am. Chem. J.*, **12**, 24 (1890).

8) W. Kaufmann and R. Adams, *J. Am. Chem. Soc.*, **45**, 3041 (1923).

9) R. Adams, V. Voorhees and R. L. Shriner, "Organic Syntheses," Col. Vol. I. 2nd Ed., (1948) p. 463.

NOTES

2, 2'-Binaphthoxazoline

By Eisuke ISHIDA and Kyoji TÔEI

(Received May 17, 1962)

The reaction between *o*-aminophenol and glyoxal was studied by Bayer[1] and Murase[2]. The condensation product, 2, 2'-bibenzoxazoline, was found to be an organic reagent for various cations and especially selective and specific for calcium. It was used as a metal indicator for calcium in chelatometry[3] and as a colorimetric reagent by extraction[4].

The condensation product of 2-amino-1-naphthol with glyoxal, 2, 2'-binaphthoxazoline, also reacts with calcium to form a deep blue chelate which can be extracted by chloroform;

1) E. Bayer, *Chem. Ber.*, **90**, 2325 (1957).
2) I. Murase, This Bulletin, **32**, 827 (1959); **33**, 59, 607 (1960).
3) D. Goldstein, *Anal. Chim. Acta*, **21**, 339 (1959).
4) K. T. Williams and J. R. Wilson, *Anal. Chem.*, **33**, 244 (1961).

the absorption curve has a maximum at 638 mμ. The chelate is, however, unstable, and the color fades gradually. Therefore, it is usable for the detection but not for the determination of calcium.

Synthesis of 2, 2'-Binaphthoxazoline.—2-Amino-1-naphthol was prepared by the reduction of 2-nitroso-1-naphthol made from α-naphthol. It is very unstable in air, and so its hydrochloride is used for the preparation. Five grams of 2-amino-1-naphthol hydrochloride are dissolved in 1 l. of boiling water containing 10 ml. hydrochloric acid. The solution turns red upon oxidation with air. To reduce the solution, 0.5 g. of tin powder is added and the solution is boiled until it is almost colorless. After cooling quickly, it is filtered. At about 20°C, 3.8 ml. of a 40% glyoxal solution are stirred into it, and then sodium acetate is added until a large volume of a red precipitate is formed (about 20 g. of sodium acetate are needed, and the pH value is 3~4). Three more grams of sodium acetate are added with agitation. The stirring is continued for 1~2 hr. The solution is then allowed to stand for 12 hr., is filtered, and is washed with dilute hydrochloric acid and water. The precipitate is dissolved in 400 ml. of alcohol and decolorized with active carbon. The filtrate is condensed by a rotary evaporator to deposit crystals. They are recrystallized two or three times, affording 100 mg. of pale blue needles which melt at 223°C. The preparation shown above should preferably be done in a dark room, because the compound tends to decompose in daylight.

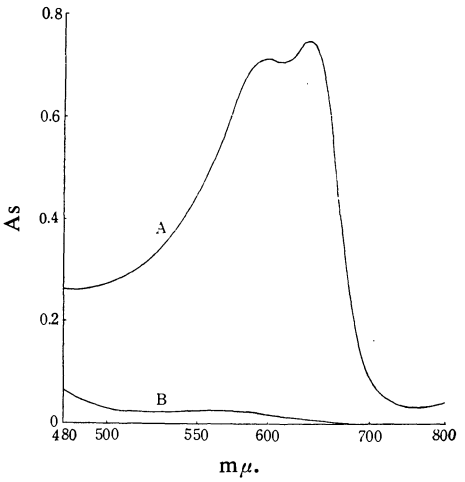

Fig. 1. Absorption curves.
A: 2, 2'-Binaphthoxazoline-Ca complex in chloroform.
B: 2, 2'-Binaphthoxazoline in chloroform (masked a minute amount of Ca in alkaline solution with EDTA).

Found; C, 77.33; H, 4.980; N, 8.280. Calcd. for $C_{22}H_{16}N_2O_2$: C, 77.63; H, 4.74; N, 8.23.

The condensation of 1-amino-2-naphthol with glyoxal was not successful.

Detection of Calcium.—One milliliter of the reagent solution (20 mg. in 100 ml. ethanol), 0.4 ml. of an alkaline solution (10 g. sodium hydroxide and 0.5 g. sodium carbonate in 100 ml. water) and 4 ml. of a calcium solution are mixed together in a 15 ml. stoppered tube and then extracted with 5 ml. of chloroform by vigorous shaking. The absorption curve in chloroform (Fig. 1) has a maximum at 638 mμ. The color change and the extractability are very excellent, and so a micro amount of calcium can be detected. However, the color is not very stable and fades gradually. Therefore, the reproducibility is not so good that the quantitative determination cannot be carried out by this method, though the calibration curve can be roughly drawn.

The authors wish to express their deep gratitude to Dr. Ichiro Murase for his kind suggestion in the course of the preparation of 2, 2'-binaphthoxazoline.

Department of Chemistry
Faculty of Science
Okayama University
Tsushima, Okayama

Products of the Radiolysis of Water Containing Benzene and Nitric Acid

By Ken'ichi SUGIMOTO, Wataru ANDO and Shigeru OAE

(Received August 27, 1962)

Radiolysis of water saturated with benzene and containing dissolved air has been studied by many workers[1-6]. Stein and Weiss[1] reported that phenol and hydrogen peroxide are formed until oxygen is depleted, then, the formation of phenol begins to slow down, while diphenyl starts to appear in increasing yield. The effect of pH on the phenol yield

1) G. Stein and J. Weiss, *J. Chem. Soc.*, **1949**, 3245.
2) T. J. Sworski, *J. Chem. Phys.*, **20**, 1817 (1952).
3) T. J. Sworski, *Radiation Research*, **1**, 231 (1954).
4) J. H. Baxendale and D. Smithies, *J. Chem. Soc.*, **1959**, 779.
5) P. V. Phung and M. Burton, *Radiation Research*, **7**, 199 (1957).
6) E. Collinson and A. J. Swallow, *Chem. Revs.*, **56**, 505 (1956).

is only slight, as might be expected if the mechanism were a free radical one[1,4]. On the other hand, the yield of diphenyl is significantly lower at high pH[4], and this result is difficult to understand. All their experiments were carried out either in aqueous sulfuric acid or in phosphoric acid. No specific influence was observed at the same pH with the two different anions in their experiments. Meanwhile, we found in the irradiation of benzene in nitric acid solution that nitrophenol formed and diphenyl did not appear. The present paper provides data on the radiation induced reaction of water containing benzene and nitric acid at various concentrations.

Experimental

Irradiations.—The γ-radiation was provided by either a 1000 or a 3800 curie cobalt-60 source. The rate of energy absorption in solution was determined with the Fricke ferrous sulfate dosimeter taking G as 15.6[7]. All the irradiations were carried out at ambient temperature between 15 to 25°C.

Preparation of Solutions.—Benzene was purified by an ordinary method. Distilled water and reagent grade nitric acid were used. Actually water shaken with benzene at room temperature is found to dissolve 0.022 mol. per liter. Stock solution of irradiated sample was prepared by mixing standard benzene solution and nitric acid solution to the final desired concentration for both benzene and nitric acid. Solutions used for irradiation were made containing dissolved air.

Determination of *p*-Nitrophenol.—The determination of *p*-nitrophenol was carried out by colorimetry. After adjusting the pH of the irradiation solution, which, if necessary, was filtered off, the absorbance of *p*-nitrophenolate ion was measured spectrophotometrically at 400 mμ, and also determined by pentacyanoammineferroate.

Determination of *o*-Nitrophenol.—The formation of cobalt-chelate compound was used to the determination of *o*-nitrophenol. The *o*-nitrophenol was nitrosated by reduction with calcium chloride and zinc powder and the isolated nitroso compound was treated with a cobalt salt in an acetate buffer solution.

Results and Discussion

Nitric acid solutions of benzene were irradiated with Co-60 gamma rays by a varying dose rate from 2.9×10^3 to 5.6×10^4 r/hr. The yield of *p*-nitrophenol produced is shown in Table I. As is shown in Table I, the yield of *p*-nitrophenol decreases with increasing dose rate. The observed decrease of yield with dose rate may be ascribed to the increased probability of the recombination between generated radicals at the higher dose rate, although its exact nature is not yet clear.

Table I. The yield of *p*-nitrophenol from the irradiated solutions

Dose rate r/hr. $\times10^{-3}$	G-Value
56	0.47
28.2	0.57
16.4	0.71
11.5	0.79
8.1	0.84
5.9	0.86
5.2	0.85
3.8	0.92
2.9	0.96

0.8N HNO_3 saturated benzene solution, 0.022 mol./l. Irradiation time, 18 hr.

Nitric acid concentration dependence for the yield of *p*-nitrophenol at the fixed dose of 3×10^6 r is shown in Table II. The yield of *p*-nitrophenol decreases with increasing nitric acid concentration.

The quantitative results indicate the preferential formation of *p*-nitrophenol to that of *o*-nitrophenol. The formation of *p*-nitrophenol is proportional to the energy absorbed, and the yield depends on dose rate and nitric acid concentration.

Table II. Dependence of nitric acid concentration

Nitric acid concentration	Formation of *p*-nitrophenol	
N	mol./l. $\times10^4$	G-Value
1.7	7.95	0.28
0.86	10.7	0.37
0.43	15.9	0.55
0.23	18.2	0.63

Irradiation time, 6 hr. Dose rate, 5×10^5 r/hr. Benzene concentration, 0.016 mol./l.

The action of ionizing radiations on dilute aqueous solutions results in formation of free radicals according to

$$H_2O \rightsquigarrow H+OH \qquad (1)$$

On the other hand, the gamma radiolysis of nitric acid solutions indicates that nitric acid is decomposed by radical mechanism as given by the following equation[8].

$$HNO_3 \rightsquigarrow HNO^*_3 \rightarrow OH+NO_2 \qquad (2)$$

The radical process is, as direct action effects are generally considered to be, directly proportional to the concentration. The qualitative results are best explained by assuming that the primary reaction 1 and reaction 2, resulting in the formation of hydroxyl radical, which attacks on a benzene molecule.

7) C. J. Hochanadel and J. A. Ghormley, *J. Chem. Phys.*, 21, 880 (1953).

8) H. A. Mahlman, *J. Chem. Phys.*, 35, 936 (1961).

$$C_6H_6+OH\rightarrow C_6H_5+H_2O \quad (3)$$

The phenyl radical formed can reacts with hydroxyl radical, yielding phenol

$$C_6H_5+OH\rightarrow C_6H_5OH \quad (4)$$

or with NO_2 radical, giving nitrobenzene.

$$C_6H_5+NO_2\rightarrow C_6H_5NO_2 \quad (5)$$

In fact, it was found by gas chromatography that the ether extraction from the irradiated solutions contained nitrobenzene. But no phenol was observed in the irradiated solutions. Consequently, the phenol furthermore reacts with hydroxyl radical to forms phenol radical,

$$C_6H_5OH+OH\rightarrow C_6H_4OH+H_2O \quad (6)$$

which is readily scavenged by NO_2 radical.

$$C_6H_4OH+NO_2\rightarrow C_6H_4(OH)NO_2 \quad (7)$$

The phenol is effectively converted to *p*-nitrophenol. While, irradiation of nitrobenzene in nitric acid solution did not give *p*-nitrophenol.

The decrease of *G*-value at higher acid concentration is probably due to the formation of nitrobenzene, which is increases with increasing NO_2 radicals from nitric acid irradiation. This becomes important at higher concentration of nitric acid, and leads to the formation of *p*-nitrophenol in a lower yield.

Department of Chemistry
Radiation Center of Osaka Prefecture
Sakai, Osaka

A Handy Method of Determining Relative Amounts of DL-*Threonine and* DL-*Allothreonine with the Aid of Infrared Absorption Spectroscopy*

By Toshiyuki FURUYAMA and Saburo SENOH

(Received October 2, 1962)

In the preparation of threonine, mixtures of the diastereoisomers, DL-threonine (I) and DL-allothreonine (II), are produced and the selective preparation of one isomer is considered to be difficult. Thus, it is very important to be able to determine the relative amounts of I and II by a simple method.

The authors have found a simplified method to determine the relative amounts of I and II with the aid of infrared absorption spectra in the potassium bromide region. Many quantitative analytical methods for I and II have previously been reported, e. g., paper chromatography[1], ion exchage resin chromatography[2], 2, 4-dinitrophenyl derivative chromatography[3], and microbial assay[4]. Of these, the last one is probably the most reliable[5], but the procedure is still limited in scope.

Concerning the infrared absorption spectra of threonine, there have been some communications[6-8], but they show only the rock salt region.

In the present communication, the infrared absorption spectra of the potassium bromide region are dealt with; also, a simplified calculation method with absorption spectra at 702 cm^{-1} and 619 cm^{-1} by the potassium bromide tablet method is described[9]. The method was found experimentally and was not so much affected by the sizes of the sample granules[10]. Measurements were carried out as usual for qualitative analysis as absorptions appeared in the range between 20 and 80 per cent in transmission[11]. The calculation was

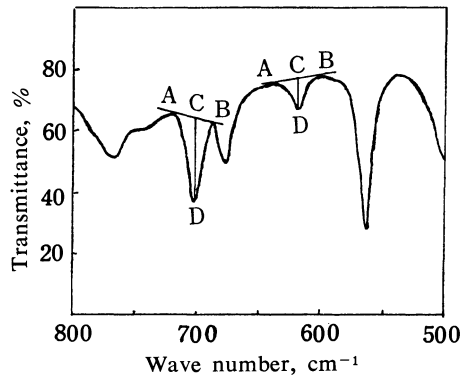

Fig. 1. IR absorption spectra of authentic mixture, No. 5.

1) K. N. F. Shaw and S. W. Fox, *J. Am. Chem. Soc.*, **75**, 3421 (1953).
2) A. T. Shulgin, O. G. Lien, Jr., E. M. Gal and D. M. Greenberg, ibid., **74**, 2427 (1952).
3) T. Seki, *J. Biochem.*, 47, 235 (1960).
4) J. L. Stokes, M. Gunness, I. M. Dwyer and M. C. Caswell, *J. Biol. Chem.*, **160**, 35 (1945); M. Gunness, I. M. Dwyer and J. L. Stokes, ibid., **163**, 159 (1946).
5) K. Pfister, 3rd, E. E. Howe, C. A. Robinson, A. C. Shabica, E. W. Pietrusza and M. Tishler, *J. Am. Chem. Soc.*, **71**, 1096 (1949).
6) R. J. Koegel, J. P. Greenstein, M. Winitz, S. M. Birnbaum and R. A. McCallum, ibid., **77**, 5708 (1955).
7) K. Kodera, Y. Sato and T. Takahashi, *Yakugaku-Kenkyu*, **30**, 38 (1958).
8) K. Kodera, the 7th Infrared and Raman Spectra Conference, Osaka (1960), p. 173; T. Yamazaki and T. Takenishi, ibid. (1960), p. 176. In the above communications, quantitative analytical methods of allo/threo are given with absorption spectra at 14.26μ and 14.83μ, and at 870 cm^{-1} and 835 cm^{-1} respectively. However, the calculation is rather complicated.
9) A double-beam Hitachi infrared spectrophotometer Type EPI-2 was used.
10) S. Tanaka and M. Ogawa, *Japan Analyst*, **6**, 285 (1957). In this paper, Tanaka and Ogawa reported that the size of the sample granules had an effect on the optical density.
11) D. Z. Robinson, *Anal. Chem.*, **23**, 273 (1951).

as follows: In Fig. 1, the base line AB is drawn, and then CD lines are drawn vertically to the zero line at 702 cm^{-1} and 619 cm^{-1}. The CD lines at 702 cm^{-1} and at 619 cm^{-1} are measured with a rule ($\overline{CD}$(702 cm^{-1}) and $\overline{CD}$ (619 cm^{-1}) respectively) and the ratio is calculated.

Thus, the percentages of threonine and allothreonine are obtained:

$$\text{Percentage of threonine} = \frac{\overline{CD}(702\ cm^{-1})}{\overline{CD}(702\ cm^{-1}) + \overline{CD}(619\ cm^{-1})}$$

$$\text{Percentage of allothreonine} = \frac{\overline{CD}(619\ cm^{-1})}{\overline{CD}(702\ cm^{-1}) + \overline{CD}(619\ cm^{-1})}$$

The results obtained for authetic mixtures are presented in Table I. Authentic mixtures of threonine and allothreonine were prepared, using pure DL-threonine and DL-allothreonine. The purity of each substance was examined with infrared absorption spectra in the rock salt region[6], elementary analysis[12], paper chromatography[1] and melting point. From Table I, more favorable results were obtained when the content of DL-allothreonine in relation to DL-threonine was smaller. This method was applied to the synthesized sample. The synthesis was carried out according to the procedure reported by Sato et al.[13] The molar percentages of the threonine and allothreonine synthesized[14] were determined by this method; values of 77.6% of threo and of 22.4% of allo were obtained. The microbial assay method gave values of 78.9% of threo and of 21.1% of allo[15].

TABLE I. RESULTS OBTAINED FOR AUTHENTIC MIXTURES

NO.	A		B	
	threo-	allo-	threo-	allo-
1	95.0	5.0	95.2	4.8
2	93.7	6.3	93.8	6.2
3	84.3	15.7	84.7	15.3
4	83.3	16.7	82.3	17.7
5	74.6	25.4	74.2	25.8
6	53.9	46.1	54.9	45.1
7	48.6	51.4	47.3	52.7
8	35.4	64.6	37.9	62.1
9	11.5	88.5	12.3	87.7

A: Percentages of DL-threonine and DL-allothreonine in authentic mixtures.
B: Percentages determined by infrared absorption spectroscopy.

The bands which appear at 702 cm^{-1} and 619 cm^{-1} also abide by Beer's law in authentic mixtures, so the present authors are also investigating quantitative analysis on the basis of this fact. Details will be presented hereafter.

The authors wish to express their appreciation to Mr. Hideaki Kai for his measurements of infrared spectra.

Technical Research Laboratory
Asahi Chemical Industry Co., Ltd.
Itabashi-ku, Tokyo

12) Found for DL-threonine: C, 40.45; H, 7.84; N, 11.40, for DL-allothreonine: C, 40.48; H, 7.49; N, 11.60. Calcd. for $C_4H_9O_3N$: C, 40.33; H, 7.62; N, 11.76%.

13) M. Sato, K. Okawa and S. Akabori, This Bulletin, **30**, 937 (1957).

14) Found: C, 40.86; H, 7.65; N, 11.63. Calcd. for $C_4H_9O_3N$: C, 40.33; H, 7.62; N, 11.76%.

15) We are indebted to Dr. J. Abe and Miss. Y. Shimojima for their microbial assays with *Streptococcus feacalis* R (ATCC 8043).

SHORT COMMUNICATION

*Synthesis of o-Phosphonobenzeneazochromotropic Acid as a New Reagent and its Thorium Complex**

By Haruo MIYATA

(Received November 15, 1962)

The present paper describes the preparation of *o*-phosphonobenzeneazochromotropic acid, and the spectrochemical properties of the reagent and its thorium complex.

Synthesis of the Reagent.—*o*-Bromobenzenephosphonic acid**,[1] was prepared by the reaction of *o*-bromobenzenediazonium fluoborate with phosphorus trichloride in ethyl acetate, m. p. 198°C.

* Presented in part at the Symposium of the Analytical Chemistry, Tokushima, October, 1962.

** Identification of these samples were made by Doak.

1) G. O. Doak and L. D. Freedman, *J. Am. Chem. Soc.*, **73**, 5658 (1951); **74**, 754 (1952); **75**, 685 (1953).

o-Aminobenzenephosphonic acid** was prepared by the amination of *o*-bromobenzenephosphonic acid with ammonia by the procedure described by Doak and Freedman[2] and by Doak[3] who presented subsequently the following modified methods: Twelve grams of *o*-bromobenzenephosphonic acid, 9 g. of freshly prepared cuprous oxide and 200 ml. of ammonium hydroxide were heated for 18 hr. Nitrogen gas was then passed through the solution in order to remove free ammonia. It is not possible to remove all of the ammonia at this stage. Hydrogen sulfide was then passed into the solution. The precipitated copper sulfide was removed and the pH value of the filtrate was adjusted to 2.1 with concentrated hydrochloric acid. Pure *o*-aminobenzenephosphonic acid (1.1 g.), m.. 185~189°C, precipitated in a crystalline form, free from chloride ion. The mother liquors were evaporated to about 100 ml. and a second crop of 2.8 g. was obtained. This contained a trace of chloride ion.

o - Phsophonobenzeneazochromotropic acid was obtained from the corresponding diazonium salt by coupling with chromotropic acid. *o*-Phosphonobenzeneazochromotropic acid thus obtained was recrystallized from concentrated hydrochloric acid to give reddish brown needles. The reagent being very hygroscopic, it was stored in a phosphrus pentoxide desiccator.

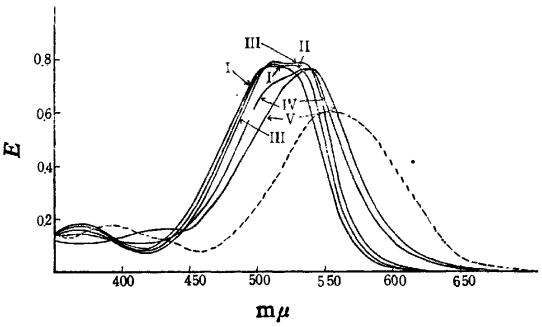

Fig. 1. Absorption curves of *o*-phosphonobenzeneazochromotropic acid (I—V) and its thorium complex (broken line pH 3.3).
I 2.8×10^{-5} mol./l., pH 1.1
II pH 6.3
III pH 8.0
IV pH 6.5
V pH 11.2

Spectrochemical Properties of the Reagent and its Thorium Complex.—Absorption spectra of the reagent solution (2.8×10^{-5} mol./l.) as well as its thorium complex (concentration of the reagent : thorium = 1 : 2) are shown in Fig. 1 over various pH values.

On addition of thorium to the reagent solution, the absorption maxima shifted towards the longer wavelengths. The curve shows an absorption maximum at 555mμ.

Mole ratio of thorium to the reagent was confirmed by the mole ratio method (Fig. 2) and the result obtained indicates the formation of a 1 : 1 complex.

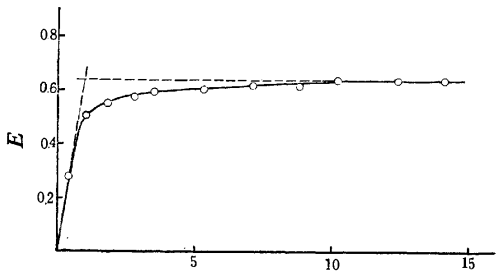

Fig. 2 Mole-ratio method.
pH 3.3, at 580 mμ.
The reagent concn. = 2.8×10^{-5} mol., thorium concn. varied.

Part of the cost of this investigation was degrayed by the Scientific Research Expenditure of the Ministry of Education to which the author's thanks are due. The author also is indebted to Dr. Kyoji Tôei for his guidance, and to Dr. G. O. Doak, Department of Health, Education, and Welfare, Public Health Service, North Carolina, U. S. A., for his kind advice to preparation of the reagent.

Department of Chemistry
Faculty of Science
Okayama University
Tsushima, Okayama

2) G. O. Doak and L. D. Freedman, ibid., 74, 754 (1952).
3) Private communication.

The Chromatographic Separation of Polyoxyethylene Nonylphenyl Ether

By Takashi ISHIWATA, Masuzo NAGAYAMA and Hiroshi ISA*

(Received February 8, 1962)

Studies of the properties of polyoxyethylene derivatives, prepared by the addition of ethylene oxide to molecules already containing active hydrogen, have long been confused by the fact that such preparations have always resulted in mixtures. Mayhew and Hyatt[1] obtained a narrow range of molecular species by distillation in a centrifugal molecular distillation still. Several other workers[2] have studied fractionation by means of molecular distillation. Also, chromatographic separation has been applied by Kelly[3].

In these studies, it has been found that the distribution of molecular weight was close to the theoretical distribution curve proposed by Flory[4]. He assumed that all steps in the reaction of the ethylene oxide sequence are kinetically identical, and his results showed a Poisson's distribution. On the other hand, the products of relatively low molecular weight polyoxyethylene derivatives have been shown by means of vacuum fractional distillation not to agree with Flory's distribution[5].

Regarding the assumption of the kinetic identity of all steps as an oversimplification, Weibull and Nycander[6] have suggested a compromissed treatment for the reaction of an alcohol with ethylene oxide. They have proposed that all hydroxyl groups bound to an oxyethyl group have an equal ability to add ethylene oxide, this ability differing, however, from that of the parent alcohol. This has led to the following equations:

$$v = c \ln\frac{n_{00}}{n_0} - (c-1)\left(1-\frac{n_0}{n_{00}}\right) \qquad (1)$$

$$\frac{n_i}{n_{00}} = \frac{c^{i-1}}{(c-1)^i}\left\{\frac{n_0}{n_{00}} - \left(\frac{n_0}{n_{00}}\right)^c \times \sum_{j=0}^{i-1}\frac{1}{j!}\left[(c-1)\ln\frac{n_{00}}{n_0}\right]^j\right\} \qquad (2)$$

where

N_i=molecule with i added ethylene oxide molecules

m=number of moles of ethylene oxide consumed

n_{00}=number of moles of the starting material

n_0=number of moles of the surviving starting material

n_i=number of moles of N_i in reaction product

k_i=rate constant for the reaction of N_i with ethylene oxide

k_0=rate constant for the reaction of the starting material with ethylene oxide

$c=k_i/k_0$=distribution constant

$v=m/n_{00}$=average number of moles of ethylene oxide per mole of the starting material.

Since the polyoxyethylene derivatives are not thermostable, fractional distillation is not suitable for separation of the products; also, complete separation by distillation is not possible in the presence of many components.

For fractionation of this type, there are several attractive features of column chromatography. This method was used in the present preparation of polyoxyethylene nonylphenyl ether in order to provide data on the distribution of products for comparison with the theoretical equations mentioned above.

Experimental

Materials.—The nonylphenol (produced by the General Aniline and Film Co., Ltd.) was purified by distilling it with a Widmer column at 138~139°C/2.5 mmHg (hydroxyl value 249.8).

Ethylene oxide with a quoted minium purity of 99% was used.

The polyoxyethylene derivatives of nonylphenol were prepared by blowing ethylene oxide gas into nonylphenol in presence of metallic sodium as a catalyst; the amount of sodium was 0.1% by weight of the nonylphenol.

The reaction temperatures of 190, 140 and 100°C (±2°C), were selected. The products were neutralized with sulfuric acid, freed of water under vacuum, and then filtered through filter paper.

The properties of the polymers obtained by the reaction are shown in Table I.

* Present address: Yokkaichi Chemical Company, Yokkaichi, Mie-ken.

1) R. L. Mayhew and R. C. Hyatt, *J. Am. Chemist's Soc.*, **29**, 375 (1952).

2) J. V. Karabinos and E. J. Quinn, ibid., **33**, 223 (1956). L. M. Kushner, W. D. Hubbard and A. S. Doan, *J. Phys. Chem.*, **61**, 371 (1957).

3) J. Kelly and H. L. Greenwald, ibid., **62**, 1096 (1958).

4) P. J. Flory, *J. Am. Chem. Soc.*, **62**, 1561 (1940).

5) K. Nagase and K. Sakaguchi, *J. Chem. Soc. Japan, Ind. Chem. Sec.* (*Kagyo Kagaku Zasshi*), **63**, 588 (1960); A. N. Wrigley, A. J. Stirton and E. Howard, *J. Org. Chem.*, **25**, 439 (1960).

6) B. Weibull and B. Nyoander, *Acta Chem. Scand.*, **8**, 847 (1954).

TABLE I. PROPERTIES OF THE POLYOXYETHYLENE DERIVATIVES OF NONYLPHENOL

Reaction temp., °C	Hydroxyl value	Refractive index n_D^{25}
100	182.5	1.5057
140	179.9	1.5050
190	177.8	1.5050

Apparatus.—The diameter and the length of the column were 3.5 and 75 cm. respectively. The column was packed with silicic acid up to a height of 50 cm. Silicic acid (Mallinckrodt A. R., 100 mesh powder, suitable for chromatographic analysis) was used as supplied. A spectrophotometer (Hitachi Model EPU-2) was used for the spectrophotometric measurements.

Procedure. — The gel ratio was 160 : 1. The development was carried out by applying the mixture of chloroform and acetone (95 : 5, 85 : 15 volume ratio). A solvent system of benzene and methanol was examined for this purpose, but the results were not satisfactory. In each case, 1.000 g. of the sample was used. The flow rate was adjusted to 20 cc. per 13 min., and portions were collected with a volumetric fraction collector. An aliquot of 3 cc. was taken from every 20 cc. fraction, and the solvent was evaporated in a vacuum desiccator. The absorbance of the chloroform solution was measured at the wavelength of 277 mμ by a spectrophotometer.

Results and Discussion

A typical elution curve is plotted in Fig. 1. The figure shows that the chromatographic separation of polyoxyethylene nonylphenyl ether was satisfactory. A very small peak was observed in the fraction, at 26~32 of Fig. 1; this seems to come from a trace of impurity. This will be evident from the following tests.

a) The OCH_2CH_2OH group was not detected.

Following the procedure indicated by Feigl[7], the sample was treated with periodic acid, but no aldehyde was detected.

b) No phenolic OH was detected.

No coloration was observed when a diazonium sulfanilic acid solution was sprayed on filter paper spotted with the samples. The evidence described above suggests that the trace of impurity was not nonylphenol derivatives, but no further investigation was made. The amount of the impurity was at any rate, less than 1%.

The materials eluted from each peak were collected and weighed by microbalance. The molar absorptivities of each peak were calculated from the absorbance of the 0.01% chloroform solution at 277 mμ and were assumed the molecular weight.

If this assumption is right, each molar absorptivity should agree well with that of nonylphenol, because the absorption at 277 mμ originates from the phenyl radical. The numbers of the polymerized oxyethylene radicals for each peak were thereby determined. These results showed no nonylphenol survived in the reaction.

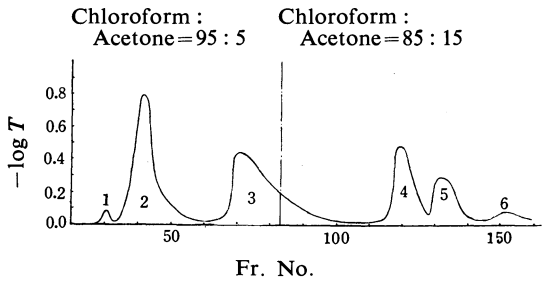

Fig. 1. Chromatogram (reaction temp. 190°C).

This fact shows that the ethylene oxide addition of nonylphenol was selective and that ethylene oxide reacted with nonylphenol completely in the first step.

The weights of all the peaks are shown in Table II. These results show that a high rate

TABLE II. WEIGHT OF THE PEAKS SEPARATED BY THE CHROMATOGRAPHY

Peak No.	Reaction temp. 100°C		Reaction temp. 140°C		Reaction temp. 190°C	
	Wt., g.	Converted total wt.*	Wt., g.	Converted total wt.*	Wt., g.	Converted total wt.*
1	0.00537	0.00634	0.00543	0.00649	0.00858	0.01009
2	0.27230	0.32127	0.21433	0.25597	0.21655	0.25466
3	0.38373	0.45749	0.36016	0.43014	0.33155	0.38990
4	0.13103	0.15466	0.16803	0.20063	0.16730	0.19674
5	0.03544	0.04182	0.05612	0.06702	0.07083	0.08329
6	0.00724	0.00854	0.01424	0.01701	0.01482	0.01728
Acetone elute	0.00103		0.02231		0.04517	
	$\sum$ wt. = 0.99115		$\sum$ wt. = 0.99957		$\sum$ wt. = 0.99713	

* Weight × 20/17

7) F. Feigl, "Spot Tests in Organic Analysis", Elsevier, New York (1956), p. 189.

of recovery should be obtained by adding the fraction eluted with acetone to the separate sample.

The weight percentages of all the peaks are shown in Table III. In this Table, C was calculated by applying Weibull's equation (1). "The number of the starting material" was calculated on the basis of nonylphenyloxyethanol.

TABLE III. DISTRIBUTIONS OF THE WEIGHT PERCENTAGE

Reaction temp.		190°C	140°C	100°C
Oxyethylene, $\bar{P}$		2.04	2.00	1.85
Peak No.	No. of oxyethylene			
2	1	25.5	25.6	32.1
3	2	39.5	43.0	45.8
4	3	20.5	20.1	15.4
5	4	7.1	6.7	4.2
6	5	3.1	1.7	0.9
Acetone elute		3.4	2.3	1.0
Peak No. 1		0.9	0.6	0.6
C		0.66	0.61	0.58

The results of these experiments may be compared with Poisson's and Weibull's distributions.

Poisson's distribution as proposed by Flory[4] (weight):

$$W_x = \frac{M_x}{M+44v} e^{-v} \frac{v^i}{i!} \qquad (3)$$

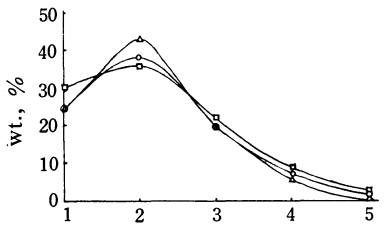

Fig. 2. Weight distribution (reaction temp. 190°C).
-○- Experimental
-△- Weibull's distribution
-□- Poisson's distribution

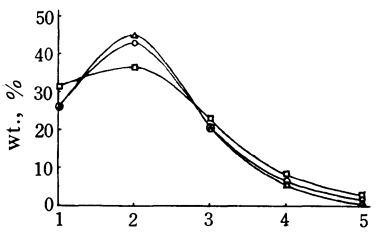

Fig. 3. Weight distribution (reaction temp. 140°C).

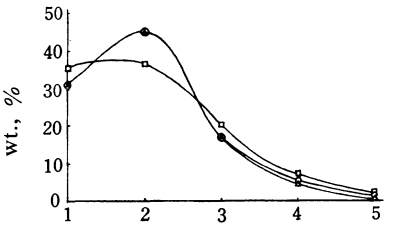

Fig. 4. Weight distribution (reaction temp. 100°C).

Distribution (weight) based on Weibull's formula.

$$W_x = \frac{M_x}{M+44v} \cdot \frac{c^{i-1}}{(c-1)^i} \left\{ \frac{n_0}{n_{00}} - \left(\frac{n_0}{n_{00}}\right)^c \times \sum_{j=0}^{i-1} \frac{1}{j!} \left[(c-1) \ln \frac{n_{00}}{n_0} \right]^j \right\} \qquad (4)$$

where

M=molecular weight of the starting material

M_x=molecular weight of the product of chain length x units.

W_x=weight fraction of the product of chain length x units

The results indicated in Figs. 2, 3 and 4 show that distribution in these cases agreed better with Weibull's distribution than with Poisson's.

With the increase of the reaction temperature, however, a considerable difference was observed.

Also, these figures show that the lower the reaction temperature, the narrower the distribution of molecular weights.

Summary

Polyoxethylene nonylphenyl ether can be separated with respect to the unit of the oxyethylene radical by applying the chromatographic method, using silicic acid as the adsorbent and a chloroform-acetone mixture as the eluent. Nonylphenol was allowed to react with ethylene oxide in the mole ratio of 1:2 in the presence of metallic sodium as a catalyst at the three different temperatures of 190, 140 and 100°C.

The chromatographic method was applied to the reaction products, and it was shown that the distribution became somewhat narrower at the lower reaction temperature.

A comparison of these results with the theoretical distributions proposed by Flory and by Weibull indicated significant agreement with the latter but a discrepancy with the former. However, when the temperature was rather high, the agreement with the Weibull formula was not good.

Similarly, polyoxyethylene nonylphenyl ether having more than two oxyethylene units could be separated by this method. When $\bar{P}=10.3$, 14 peaks was obtained from a chromatogram.

The separation and recovery by this method were considerably better than the distillation method, and a better understanding of the distribution of molecular weights was obtained.

Research Laboratory
Lion Fat and Oil Company
Edogawa-ku, Tokyo

Determination of Sodium, Arsenic, Antimony and Copper in Carbon by Neutron-Activation Analysis

By Yuichiro KAMEMOTO and Shigeru YAMAGISHI

(Received July 17, 1962)

The neutron activation analysis of graphite with or without the chemical separation of impurities after irradiation has been reported by several workers[1-3]. In general, the method with such chemical separation has been more satisfactory than that without in terms of sensitivity and precision of analysis. However, the method involving the chemical processing of the irradiated sample has some problems in the process of the leaching-out of impurities from the irradiated graphite. They are: (1) The burning method for the destruction of graphite has the possibility of the evaporation of a portion of the impurities. (2) The leaching method with concentrated nitric acid has the possibility of the incomplete leaching-out of the impurities from graphite. (3) The destruction of graphite with a nitric acid-perchloric acid mixture is difficult.

The purpose of this investigation was to decide the most desirable method for the separation of impurities from the irradiated graphite. On the basis of the results, the burning method, combined with the treatment of a burning boat (quartz) with a hydrofluoric acid-nitric acid mixture, was found to be the most desirable. This method was applied to the determination of sodium, arsenic, antimony and copper in carbon. The analytical values obtained were compared with those obtained by the non-destructive method.

1) J. V. Jakovlev, Proceedings of the International Conference on the Peaceful Uses of Atomic Energy, Geneva, P/632 (USSR), 15, 54; *Anal. Abstr.*, **4**, 1112 (1957).
2) A. A. Lbov and I. I. Naumova, *Atomnaya Energ.*, **6**, 468 (1959); NSA, **13**, 13335 (1959).
3) T. Nakai, S. Yajima, M. Okada, K. Shiba and T. Moki, *J. Chem. Soc. Japan, Pure Chem. Sec.* (*Nippon Kagaku Zasshi*), **81**, 104 (1960).

Experimental

Sample.—About 1 g. of the amorphous carbon prepared by the Nihon Carbon Co., Ltd., was weighed into a polyethylene pouch.

Standards.—One-tenth of a milliliter of each standard solution, prepared as follows, was infiltrated into a filter paper 2 cm. in diameter and sealed in a polyethylene pouch.

Sodium.—The reagent-grade sodium carbonate was dissolved in water and diluted to 270 μg. of sodium per ml. of solution.

Arsenic.—The reagent-grade arsenious acid was dissolved in hydrochloric acid and diluted to 499.7 μg. of arsenic per ml. of solution.

Antimony.—The 99.998% antimony metal was dissolved in aqua regia and diluted to 210.6 μg. of antimony per ml. of solution.

Copper.—The 99.99% copper metal was dissolved in dilute nitric acid and diluted to 266 μg. of copper per ml. of solution.

Irradiation Conditions.—For the irradiation, the sample and standards were placed side by side in a polyethylene capsule. All irradiations were made in the No. 16 Hole (pneumatic tube) of the JRR-1 reactor. The neutron flux was approximately 10^{11} n/cm^2/sec. Each irradiation was continued for 2 hr.

Radiochemical Separation.—The irradiated sample was placed in a quartz boat and burned for 30 min. at 700°C in an oxygen atmosphere. The apparatus used is outlined in Fig. 1. The sample was completely burned. The boat was then treated twice with a hydrofluoric acid-nitric acid (1 : 1) mixture solution on a hot plate, and the apparatus used was washed with hot nitric acid. The resulting solutions were added to the catching solution. After the addition of 1 ml. each of carrier solutions for sodium, arsenic, antimony and copper (sodium 27.0 mg.; the other cation, 10 mg.), the whole solution was evaporated repeatedly with hydrochloric acid and adjusted to agree with the dilute hydrochloric acid solution.

From this solution, each element mentioned above was isolated as follows. (The flow system of the separation is shown in Fig. 2.)

Arsenic, antimony and copper were precipitated as sulfides with hydrogen sulfide and then separated from the sodium. The filtrate was concentrated to about 3 ml. and then poured into a polyethylene tube, which was mounted on a 3×3 inches sodium iodide scintillator. The sodium content was determined by γ-ray spectrometry.

The precipitate of sulfide was treated with an ammonium polysulfide solution, arsenic and antimony being dissolved in this solution and separated from the copper precipitate. This residual precipitate was then dissolved in aqua regia and reprecipitated as thiocyanate from the dilute sulfuric acid solution. The cuprous thiocyanate was filtered off, washed, dried and weighed to determine the chemical yield, and it was then put in a polyethylene tube; the copper content was determined by γ-ray spectrometry.

The ammonium polysulfide solution of the precipitate sulfide was evaporated with nitric acid and adjusted to agree with the concentrated hydrochloric acid solution. Arsenic was precipitated as sulfide with hydrogen sulfide from the concentrated hydrochloric acid solution and separated from antimony. The precipitate was digested with aqua regia. After the addition of an antimony solution to this solution as the hold-back carrier, the arsenic was reprecipitated as sulfide. The precipitate was filtered off, washed, dried and weighed to determine the chemical yield, and it was then put in a polyethylene tube. The arsenic content was determined by γ-ray spectrometry.

The concentrated hydrochloric acid solution, from which arsenic had been separated, was adjusted to agree with an about 2 N hydrochloric acid solution. Antimony was precipitated as sulfide from this solution. The precipitate was digested with aqua regia. After the addition of an arsenic-carrier solution to this solution, the separation of antimony from arsenic was repeated. The antimony sulfide formed was filtered off, washed, dried and weighed to determine the chemical yield, and it was then put in a polyethylene tube. The antimony content was determined by γ-ray spectrometry.

Counting.—Each isolated element was mounted on 3×3 inch sodium iodide scintillator attached to an RCL-256 channel pulse-height analyzer, and the γ-ray spectrum was measured. The content of each element was determined by comparing the peak height of the photopeak (i. e., at 1.37 MeV. for sodium-24, at 0.56 MeV. for arsenic-76, at 0.57 MeV. for antimony-122, and at 0.51 MeV. for copper-64) with that for the respective standard.

Results

Radiochemical Purity.—From the results of the γ-ray spectra and the decay curves of the photopeaks, it was found that the arsenic, antimony and copper isolated by this method were radiochemically pure.

Although two photopeaks, at 0.82 MeV. and 0.56 MeV., appeared in the γ-ray spectrum of the sodium fraction, the interference of these activities could be disregarded in the determination of sodium by analyzing the decay curve of the sodium-24 photopeak at 1.37 MeV.

Results.—The results obtained are given in Table I.

TABLE I. RESULTS

Element	Content, p. p. m.	Standard deviation
Sodium	170	±11
Copper	35	± 1.3
Arsenic	0.2	± 0.01
Antimony	0.30	± 0.018

Discussion

Leaching-out Methods of Impurities from Irradiated Carbon.—*The Burning Method.*—Irradiated carbon was burned in an oxygen atmosphere at 700°C in the apparatus shown in Fig. 1. After this burning, much activity was found on the quartz-burning boat. This activity could not be completely leached out from the boat by treating it four times with hot aqua regia. It was found, however, that complete leaching is possible when the boat is treated twice with a hydrofluoric acid-nitric acid (1 : 1) mixture solution. The results are shown in Fig. 3.

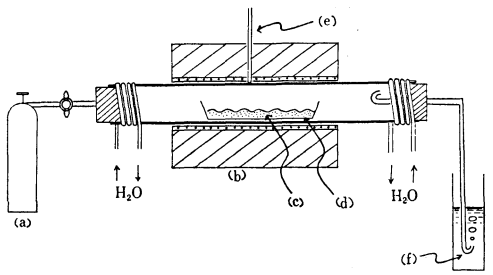

Fig. 1. Apparatus.
(a) O_2 bomb
(b) Heater
(c) Carbon sample
(d) Burning boat
(e) Thermocouple
(f) Catching solution, dil. HNO_3

This solution obtained from the leaching of the quartz boat and from the nitric-acid washing of the apparatus, and the catching solution, together, contained 98~100% of the impurities in carbon.

When a porcelain boat was used, however, the adherring activity could not be leached out from the boat.

The Leaching Method with Concentrated Nitric Acid.—The leaching-out method of impurities from carbon with concentrated nitric acid has

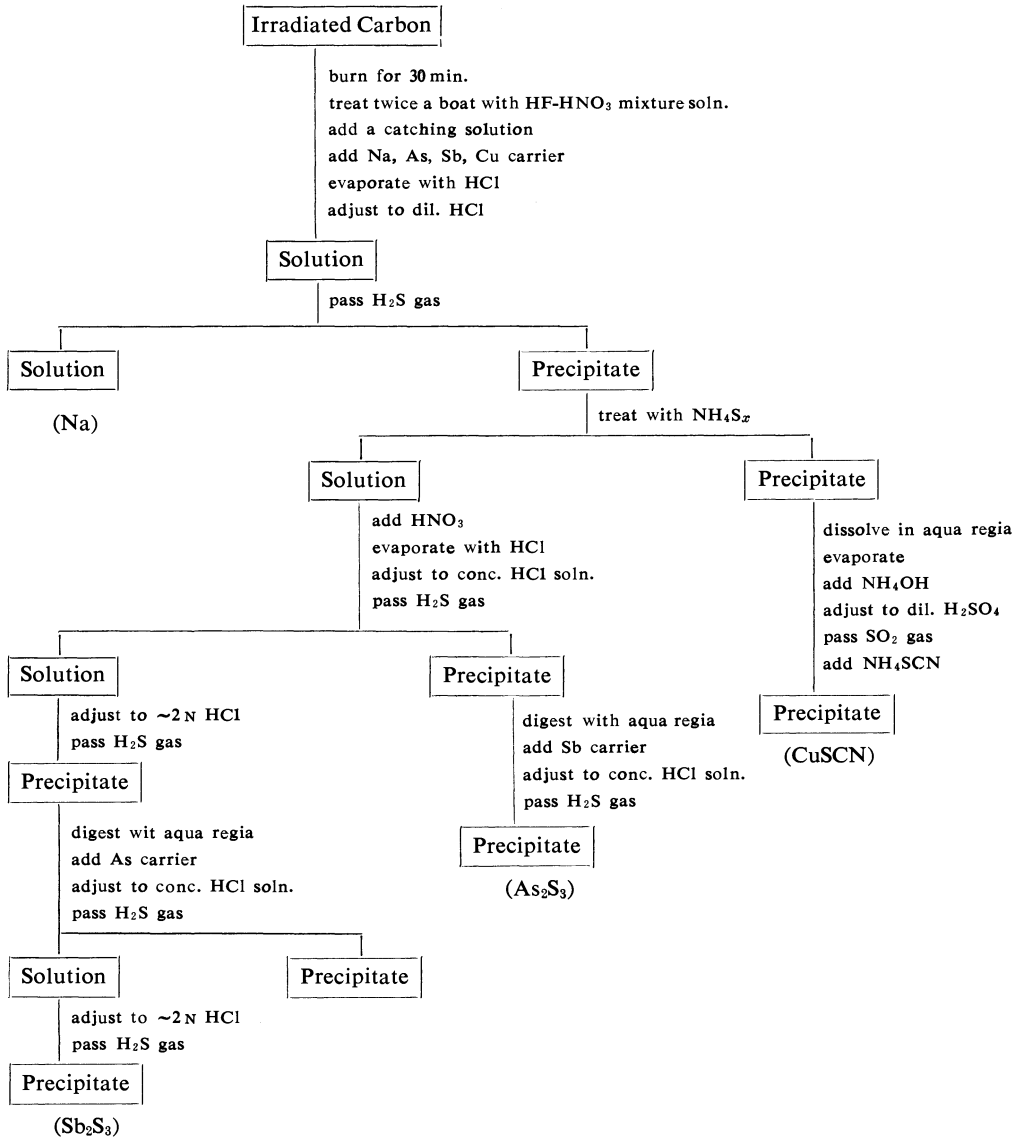

Fig. 2. Flow system of separation.

been reported by several workers[4,5]. However, as it was doubtful that they can be leached out completely by this method, an experiment was made.

About 1 g. of irradiated carbon was treated in a beaker on a hot plate with about 50 ml. of concentrated nitric acid, adding a small volume of nitric acid at some intervals. The γ-ray spectrum of the carbon treated was measured after having been heated for some hours; the results are shown in Fig. 4. The leaching-out of impurities by this method was not complete, however, even when the sample was heated for 7.5 hr. with concentrated nitric acid.

The Carbon-Destruction Method with a Nitric Acid-Perchloric Acid (1:1) Mixture Solution.— The destruction method using a mineral acid-oxidizing agent mixture solution has been reported by some workers[6]; however, the destruction of carbon by this method was not complete. Fifty milliliters of a nitric acid-perchloric acid (1 : 1) mixture solution was added to about 1 g. of the irradiated carbon; the resultant solution was heated on a hot

4) C. D. Susano, H. S. House and M. A. Marler, TID-7555, 208 (1957).
5) T. Sasaki, F. Ichikawa, H. Imai and S. Uruno, 1961 National Nuclear Congress, Tokyo, Japan, Report No. D62 (1961).
6) J. W. Mellor, "A Comprehensive Treatise on Inorganic and Theoretical Chemistry", Vol. V, Longmans, Green and Co., London, (1952), p. 828; A. R. Ubbelohde and F. A. Lewis, "Graphite and its Crystal Compounds", Oxford Univ. Press, London (1960), p. 151.

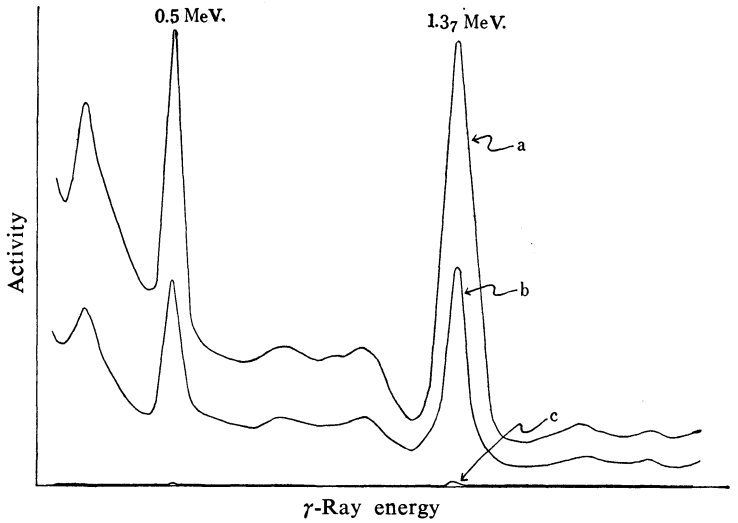

Fig. 3. γ-Ray spectra of adherring activity on the burning quartz boat.
(a) Non-treatment
(b) Treating 4 times with aqua regia
(c) Treating twice with $HF-HNO_3$ (1 : 1) mixture solution

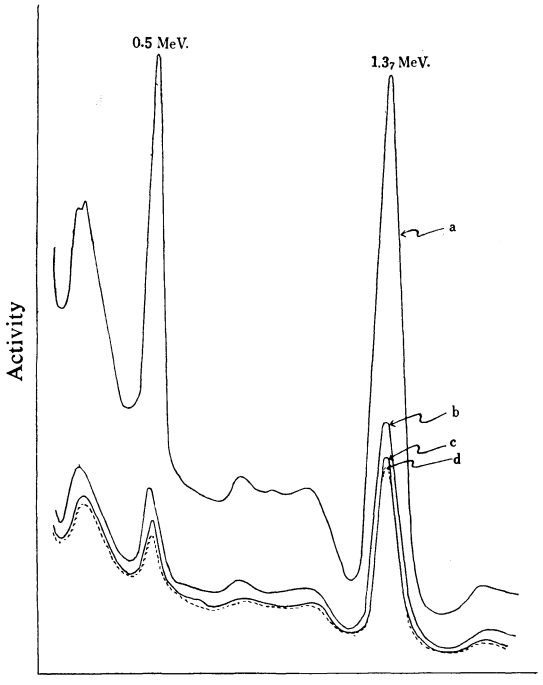

Fig. 4. γ-Ray spectra of carbon after heating for some hours with concn. HNO_3.
(a) Non-treatment
(b) Heating for 2.5 hr.
(c) Heating for 4.5 hr.
(d) Heating for 7.5 hr.

plate for some hours, with a small volume of the same mixture solution being added at some intervals. The γ-ray spectrum of the treated carbon was measured and is shown in Fig. 5. It may be seen from Fig. 5 that some portion of the impurities remained in the carbon even when it had been treated for 5 hr., so this method is not desirable.

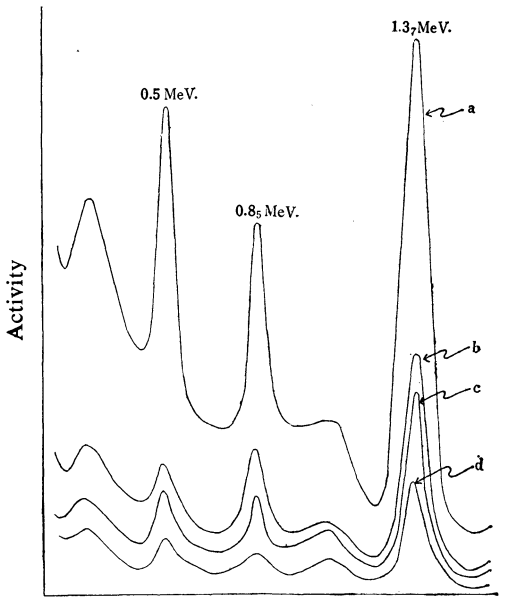

Fig. 5. γ-Ray spectra of carbon after heating for some hours with HNO_3-$HClO_4$ mixture solution.
(a) Non-treatment
(b) Heating for 1.5 hr.
(c) Heating for 2.5 hr.
(d) Heating for 5 hr.

TABLE II. COMPARISON OF THE RESULTS OF THE DESTRUCTIVE AND NON-DESTRUCTIVE METHODS

Element	Destructive method		Non-destructive method	
	Content p. p. m.	Standard deviation	Content p. p. m.	Standard deviation
Sodium	170	±11	230, 220, 180	—
Copper	35	± 1.3	46, 47	—
Arsenic	0.20	± 0.01	2, 3	—
Antimony	0.30	± 0.018	0.4	—
Manganese	—	—	2.2	—

The Sodium Hydroxide-Fusion Method.— About 0.5 g. of irradiated carbon was added to about 3 g. of sodium hydroxide in a nickel crucible. After they had been fused for one or two hours, the melt was leached with water and dilute hydrochloric acid and the carbon which remained undissolved was filtered off.

The activity of the residual carbon was measured with a γ-ray scintillator. The results obtained, which are shown in Fig. 6, indicate that the fusing method did not provide a complete leaching-out of impurities from carbon, even when the fusing lasted for two hours.

Consequently, it was found that the burning method is most satisfactory.

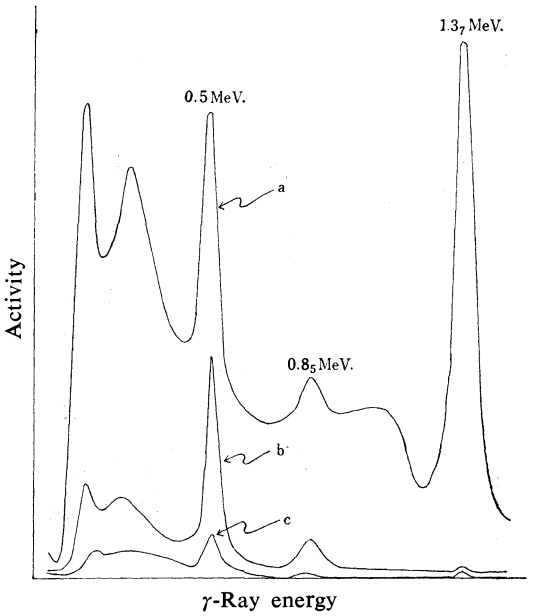

Fig. 6. γ-Ray spectra of carbon after fusing for some hours with NaOH.
(a) Non-treatment
(b) Fusing for 1 hr.
(c) Fusing for 2 hr.

Comparison of the Proposed Method with the Non-destructive One.—Table II compares the results of the destructive and non-destructive methods, which have previously been reported on[7,8].

Not much difference was observed between the results of the two methods, except in the case of arsenic; however, the analytical value of each element in the former was smaller than in the latter. This might be due to the fact that some photopeaks were apparently higher in the latter case, affected by the other peaks near them; this was pointed out in our previous report[9], "Determination of Chlorine and Manganese in Bismuth Metal by Neutron Activation."

The difference between the analytical values of arsenic in the two methods was too large to explain by the effect just mentioned. This large difference may be due to the fact that, in the non-destructive method, the analysis of the decay curve of the photopeak at about 0.5 MeV. into the decay curves of copper-64 (half life: 12.8 hr.), arsenic-76 (half life; 26.8 hr.), and antimony-122 (half life: 2.8 days) was not correct.

The identification of the decay curve for arsenic was difficult in the non-destructive method because its activity was much lower than those of copper and antimony.

The authors wish to thank Dr. Toshio Nakai for the advice he has given during this investigation.

Japan Atomic Energy Research Institute
Tokai-mura, Ibaraki-ken

7) Y. Kamemoto and S. Yamagishi, *J. Chem. Soc. Japan, Pure Chem. Soc. (Nippon Kagaku Zasshi)*, **83**, 572 (1962).
8) Y. Kamemoto and S. Yamagishi, ibid., **83**, 1156 (1962).
9) Y. Kamemoto and S. Yamagishi, ibid., **83**, 463 (1962).

The Spectrophotometric Determination of Vanadium(IV) with Xylenol Orange

By Makoto Otomo

(Received August 22, 1962)

Xylenol orange, in a slightly acidic medium, reacts with vanadyl ion to ~~give a~~ reddish violet complex, and it has widely been used as a metal indicator for vanadium in EDTA titration. Recently this laboratory needed a sensitive method for determining trace amounts of vanadium in uranium compounds. This paper describes the results of a spectrophotometric study of the vanadium-xylenol orange complex and of the application of this reagent to the determination of trace amounts of vanadium. The composition of the colored complex and methods for the elimination of some interfering substances are also discussed.

Experimental

Apparatus.—All absorbance measurements were made with a Hitachi Model EPU-2A spectrophotometer, using 1-cm. cells.

Reagents.—*Vanadyl Chloride Stock Solution.*—Pure vanadium pentoxide was treated with concentrated hydrochloric acid and redistilled ethyl alcohol[2]. The solution was standardized against a standard EDTA solution, using EBT as an indicator[3].

Xylenol Orange Solution.—The same as that used in a previous work[1].

Procedure.—Transfer a sample aliquot, containing 10 to 40 μg. of vanadium, to a 25 ml. Erlenmeyer flask. Add 1 ml. of 5% ascorbic acid and 2 ml. of a xylenol orange solution. Adjust the pH value to 2.8±0.1 with an acetate buffer solution. Mix, and heat the solution on a boiling water bath for 2 to 3 min. Cool the solution, transfer it to a 25 ml. volumetric flask, and dilute it to the mark with small amounts of distilled water. Measure the absorbance of the solution at 562 mμ vs. a reagent blank.

Results and Discussion

Absorption Spectra.—The spectra of xylenol orange and its vanadium(IV) complex are shown in Fig. 1. The maximum absorption of the complex is found at 562 mμ.

Effect of the pH Value. — Figure 2 shows that the optimum pH value range for the color formation of the vanadium-xylenol orange complex is 2.8±0.1.

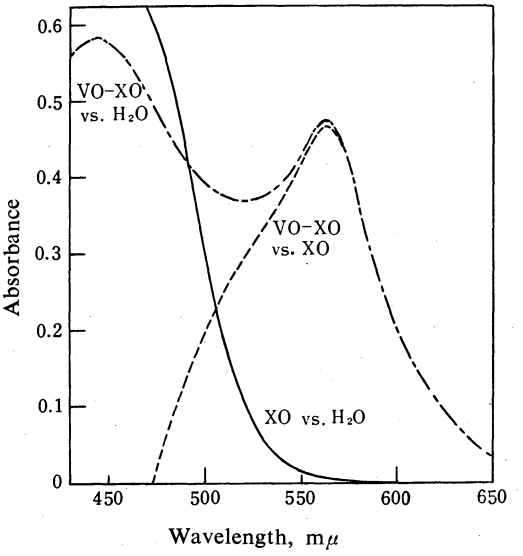

Fig. 1. Absorption spectra of xylenol orange and its vanadium complex.
V: 2×10^{-5} M XO: 9×10^{-5} M

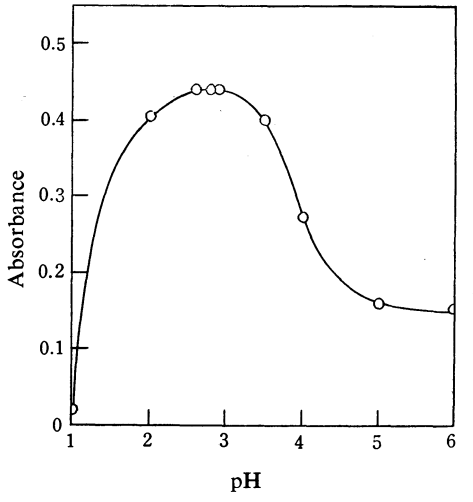

Fig. 2. Effect of pH on color development.
V: 24 μg.

Effect of the Addition of Xylenol Orange.—As is shown in Fig. 3, the absorbance gradually

1) K. Tonosaki and M. Otomo, This Bulletin, 35, 1683 (1962).
2) T. Chitani, "Muki Kagaku (Inorganic Chemistry)" (In Japanese), Sangyo Tosho, Tokyo (1954), p. 497.
3) K. Ueno, "KiretoTekitei (Chelatometric Titration)" (In Japanese), Nankodo, Tokyo (1960), p. 323.

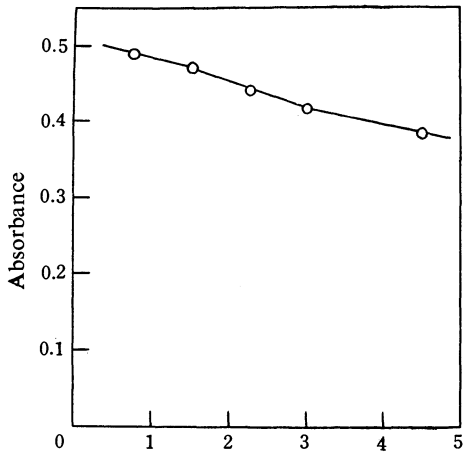

Fig. 3. Effect of addition of xylenol orange.
V: 24 μg.

decreases with the presence of increasing amounts of xylenol orange. However, the use of 1.5ml. of a 1×10^{-3} M xylenol orange solution is recommended for further experiments.

Effect of the Amount of Ascorbic Acid. — Ascorbic acid was used to prevent oxidation of the vanadyl ions to a vanadic state. It is suitable to add 0.2 to 1.5 ml. of a 5% ascorbic acid solution for less than 50 μg. of vanadium.

Effect of the Time of Standing.—Figure 4 shows the curves for the heated and the unheated solutions of the vanadium-xylenol orange complex. Curve I indicates that, for the unheated solution, it requires about 2 hr. for the complete color developement. However, the color formation is greatly accerelated by heating a mixture of vanadium and a xylenol orange solution on a boiling water bath for only 2 to 3 min. The color produced is stable for at least 24 hr.

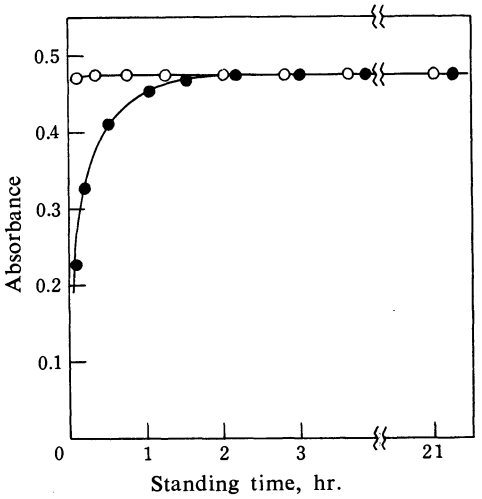

Fig. 4. Effect of time of standing.
V : 24 μg.
-●- : Unheated solution (I)
-○- : Solution heated on a water-bath (II)

Calibration Curve.—A linear concentration-absorbance relationship is obtained in the range between 10 to 40 μg. of vanadium (curve I in Fig. 5). The molar extinction coefficient of the vanadium xylenol orange complex is found to be 24000 at 562 mμ.

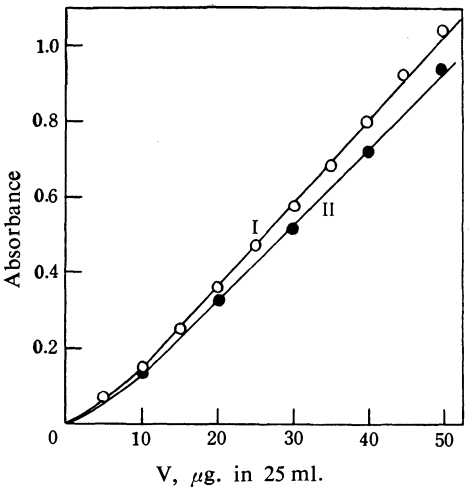

Fig. 5. Calibration curve.
I: In the absence of fluoride
II: In the presence of 50 μmol. of fluoride

Effect of Anions.—No interference is caused by chloride, nitrate, sulfate, thiosulfate, phosphate or tartrate under the conditions studied. As might be expected, such anion as oxalate, citrate, NTA (nitrilotriacetate) and EDTA (ethylenediaminetetraacetate), especially the last two, inhibit the color for mation of the vanadium-xylenol orange complex. A large amount of fluoride also decreases the absorbance moderately. If 1 ml. of a 0.4% fluoride solution is used for masking some interfering cations, the same amount of fluoride must be added in preparing the calibration curve (curve II in Fig. 5).

Effect of Cations.—The effect of foreign elements was studied by preparing solutions containing 0.5 μmol. of vanadium and the same amount of various cations. The results of these tests are presented in Table I. The cations, aluminum(III), bismuth(III), chromium-(III), tin(II), thorium(IV), titanium(IV), yttrium(III) and zirconium(IV), form a colored complexes with xylenol orange to give a positive error in the determination of vanadium. Some of these cations, however, can be completely or partially masked by adding 1 ml. of a 0.4% fluoride solution (Table II). Interference from

TABLE I. EFFECT OF CATIONS ON DETERMINATION OF VANADIUM

Vanadium taken, 25 μg. (0.5 μmol.)

Cations added	Vanadium found μg.
Aluminum(III)	59.8
Barium(II)	24.9
Beryllium(II)	25.4
Bismuth(III)	52.2
Calcium(II)	25.0
Cadmium(II)	25.0
Cerium(III)	25.2
Cobalt(II)	25.1
Chromium(III)	29.8
Copper(II)	24.7
Iron(III)	25.2
Magnesium(II)	24.9
Manganese(II)	25.0
Nickel(II)	25.2
Lead(II)	25.0
Tin(II)	37.3
Strontium(II)	25.0
Thorium(IV)	72.3
Titanium(IV)	38.2
Thallium(III)	25.0
Uranium(VI)	25.4
Yttrium(III)	26.4
Zinc(II)	25.0
Zirconium(IV)	78.8

TABLE II. MASKING ETFECT OF FLUORIDE ON DETERMINATION OF VANADIUM

Vanadium taken, 25 μg. (0.5 μmol.)
Cations added, each 0.5 μmol.
0.4% solution of fluoride added, 1 ml.

Cation	Vanadium found μg.
Aluminum(III)	25.0
Beryllium(II)	25.0
Bismuth(III)	52.3
Chromium(III)	27.3
Tin(II)	27.6
Thorium(IV)	25.0
Titanium(IV)	24.7
Uranium(VI)	25.0
Yttrium(III)	24.8
Zirconium(IV)	25.3

bismuth can also be eliminated by adding thiosulfate. Interference from tin(II) can be avoided by oxidizing it to a stannic state and by adding fluoride before treatment by the recommended procedure*.

Complex Formation.—The mole ratio and the formation constant of the vanadium-xylenol orange complex was determined spectrophotometrically by the same method as that previously reported for the rare earth complex of xylenol orange[1] (Figs. 6 and 7). It is evident that vanadium(IV), like cerium(III) and other rare earths, forms a 1:1 complex with xylenol orange. The formation constant for the

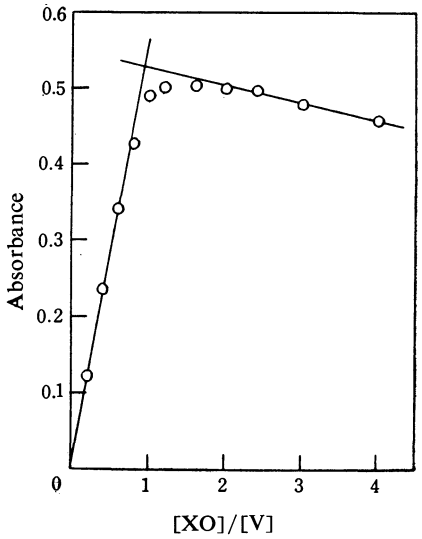

Fig. 6. Mole ratio method.
V: 24 μg.

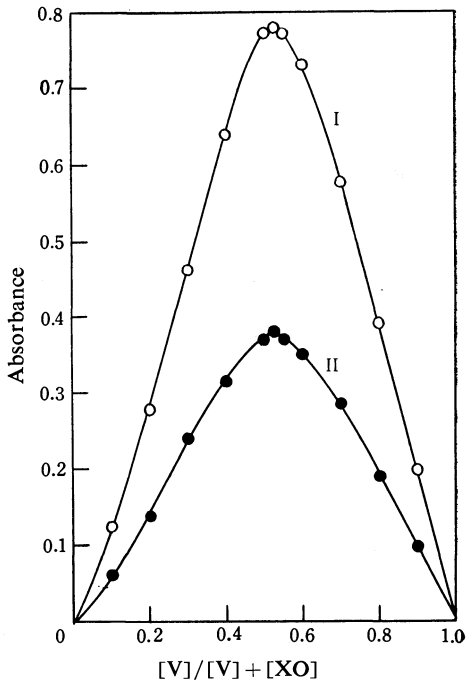

Fig. 7. Continuous variation method.
I: $[V]+[XO]=9.4\times10^{-5}$ M
II: $[V]+[XO]=4.7\times10^{-5}$ M

* As the tin(IV)-fluoride complex is very stable, it is not reduced by zinc or aluminum[4].

4) K. Sone and M. Tanaka "Teisei Bunsekikagaku" Transttd., Charlot, "L'Analyse Qualitative et lesRéaction en Solution" (In Japanese), Kyoritsu Shuppan, Tokyo (1958), p. 333.

complex at a pH value of 2.9 was calculated, from the curves shown in Fig. 7, as 2.8×10^6. It is expected that this dye will find many applications where a highly sensitive reaction for vanadium is desired.

Summary

The reddish-violet complex of vanadium with xylenol orange has been studied spectrophotometrically, and the conditions for using xylenol orange as a reagent for the determination of trace amounts of vanadium have been established. The complex shows a maximum absorption at 562 mμ, and the molar extinction coefficient of the complex is found to be 24000. It is a 1 : 1 complex and has a formation constant of 2.8×10^6 under the conditions studied. Such anions as oxalate, citrate and EDTA inhibit the color formation of the complex. Some of the interfering cations can, however, be completely or partially masked by adding a fluoride solution.

The author wishes to express his deep thanks to Professor Kôichi Tonosaki for his kind guidance and encouragement throughout this work. Thanks are also due to Mr. Tomizô Yamada for his help in the optical measurements.

Department of Chemistry
Faculty of Literature and Science
Hirosaki University
Bunkyo-chô, Hirosaki

The Spectrophotometric Determination of Uranium with Xylenol Orange[1]

By Makoto Otomo

(Received August 27, 1962)

The uranyl ion forms a weak, red chelate with xylenol orange in a slightly acid solution buffered with sodium acetate and acetic acid. The uranium(IV) ion, however, reacts sensitively with this reagent to form a stable, intensely reddish-violet complex, while uranium(VI) is reduced to uranium(IV) by ascorbic acid in an acetate buffer solution in the presence of xylenol orange.

Budĕšínský[2] has recently proposed a method for determining uranium with xylenol orange, using uranium(IV) sulfate as a starting material. He has also indicated that the optimum pH value range for color development is 1.2 to 1.6 and that a complex of 1 to 1 is formed between xylenol orange and uranium.

The present results, however, differ appreciably from those reported by Budĕšínský; the complex has its maximum absorption at 568 mμ, the maximum absorption develops over the pH value range 3.5 to 3.7, and the results of the mole ratio method and the continuous variation method show a complex consisting of two molecules of xylenol orange to one uranium(IV) ion.

1) Presented at the 15th Annual Meeting of the Chemical Society of Japan, Kyoto, April, 1962.

2) B. Budĕšínský, *Collection Czechoslov. Chem. Commun.*, **27**, 226 (1962).

3) K. Ueno, "Kireto Tekitei (Chelatometric Titration)" (In Japanese), Nankodo, Tokyo (1960), p. 320.

Experimental

Reagents.—An approximate 10^{-4} M uranyl nitrate solution was prepared by the dilution of a 10^{-2} M uranyl nitrate solution previously standardized against EDTA by using xylenol orange as an indicator[3].

A pH value 3.6 buffer solution was prepared in the usual manner with sodium acetate and acetic acid.

All the other reagents and apparatus used were the same as those reported previously[4].

Procedure.—Into a 25 ml. Erlenmeyer flask an aliquot of the solution containing up to 120 μg. of uranium was pipetted, after which 10 ml. of the acetate buffer solution and 1 ml. of 5% ascorbic acid were added. The volume was made to about 20 ml. with distilled water, and the flask was covered with a watch-glass. After being boiled gently for about 20 min., the solution was cooled with water to room temperature and transferred to a 25 ml. volumetric flask, and the volume was made up to the mark with distilled water. Within the following 30 min., the absorbance of the solution was then measured at 568 mμ, with reference to a blank solution.

Results and Discussion

Absorption Spectra.—The absorption spectra of xylenol orange and its uranium(IV) chelate are presented in Fig. 1. Inspection of the

4) M. Otomo, This Bulletin, **36**, 137 (1963).

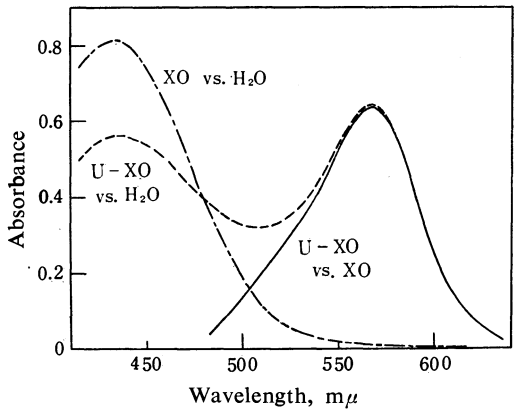

Fig. 1. Absorption spectra of xylenol orange and its uranium complex.
U: 71 μg. XO: 6×10^{-5} M

curves shows that the maximum absorption of red uranium-xylenol orange chelate lies at 568 mμ, at which point the reagent does not absorb appreciably. The spectrum is very similar to that shown by thorium-xylenol orange chelate[5]. The maximum color development was observed over the pH value range from 3.5 to 3.7, the values of which are considerably higher than those reported by Budĕšínský.

Effect of Heating Time.—As in the case of the complexometric titration of uranium with EDTA[3], the chelating reaction of xylenol orange with uranium is made to take place only by boiling a uranium(VI) solution in the presence of ascorbic acid and xylenol orange. The maximum absorbance is attained after about 20 minutes' boiling (Fig. 2). About 1 ml. of 5% ascorbic acid is a sufficient amount to reduce the uranyl ions quantitatively.

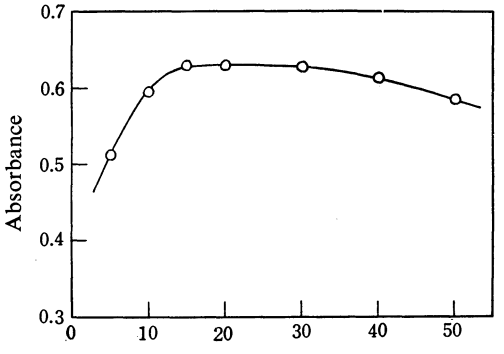

Fig. 2. Effect of heating time.
U: 71 μg. XO: 6×10^{-5} M

5) M. Otomo, unpublished. (Presented at the Tōhoku Branch Meeting of the Chemical Society of Japan, Yonezawa, October, 1961.)

Effect of Excess Reagent.—For 20 to 100 μg. of uranium, 1 to 1.5 ml. of a 1×10^{-3} M xylenol orange solution is required. Much as in the previous cases of the color development of xylenol orange complexes of zirconium[6] and iron[7], large amounts of xylenol orange tend to decrease the absorbance.

Stability of Color. — Figure 3 shows the stability of the color produced with uranium and xylenol orange. The absorbance began to be recorded as soon as the solution was transferred to the volumetric flask. The intensity of the color decreases slowly with time. However, during the first 10 to 30 min. the absorbance remains practically constant.

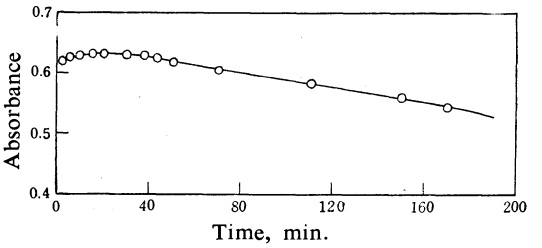

Fig. 3. Stability of color.
U: 71 μg. XO: 6×10^{-5} M

Beer's Law. — Beer's law is obeyed in the range from 20 to 100 μg. (0.8 to 4 p. p. m.) of uranium at 568 mμ. Under the conditions of the spectrophotometric determination, the molar extinction coefficient was found to be 51000.

Effect of Anions. — Chloride, nitrate, sulfate and borate do not interfere. Large amounts of phosphate, fluoride, tartrate and citrate reduce the absorbance considerably. Oxalate, NTA and EDTA interfere with the color reaction because they form more stable complexes with uranium than xylenol orange does.

Effect of Cations.—Of the 26 cations tested, aluminum(III), bismuth(III), chromium(III), copper(II), iron(III), palladium(II), thorium(IV), titanium(IV), vanadium(IV) and zirconium(IV) interfere with the uranium determination. Among the above cations, copper, iron and palladium give large negative errors.

Complex Formation.—Xylenol orange forms 1 to 1 complexes with some bi-, ter- and quadri-valent metals, including zinc(II)[8], iron(III)[7], bismuth(III)[9], rare earths[10], vanadium(IV)[4] and zirconium(IV)[6]. Budĕšínský reported that uranium(IV) and thorium(IV) also form 1 to 1 complexes with this reagent in a slightly acid medium.

6) K. L. Cheng, *Talanta*, 2, 266 (1959).
7) K. L. Cheng, ibid., 3, 147 (1959).
8) K. Studlar and I. Janousek, ibid., 8, 203 (1961).
9) H. Onishi and N. Ishiwatari, This Bulletin, 33, 1581 (1960).
10) K. Tonosaki and M. Otomo, ibid., 35, 1683 (1962).

In this work, the mole ratio of xylenol orange and uranium was studied by the continuous variation method and by the mole ratio method. As is shown in Figs. 4 and 5, both methods indicate clearly that, as with thorium[5], a complex of 1 to 2 between uranium and this reagent is formed under the conditions so far studied.

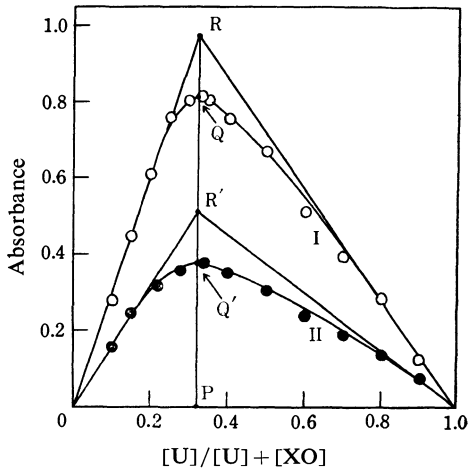

Fig. 4. Continuous variation method.
I: $[U]+[XO]=6\times10^{-5}$ M
II: $[U]+[XO]=3\times10^{-5}$ M

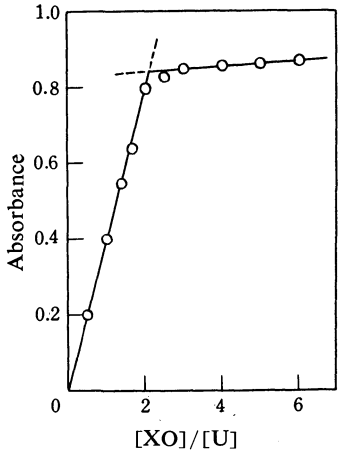

Fig. 5. Mole ratio method.
[U]: 8×10^{-6} M

In the course of spectrophotometric studies of the metal complexes of xylenol orange, it was recently found that such cations as gallium(III)[11], thallium(III)[11] and also iron(III)[12] form 1 to 2 complexes with xylenol orange in a slightly acid or a neutral medium, while they give 1 to 1 complexes in a more acid solution. This is an interesting fact; details of the results will be shown eleswhere. In addition, Leonard and West[13] have suggested that a 1 to 2 complex can be formed between thorium(IV) and alizarin complexan, since thorium adopts an eight co-ordinate configuration. Being capable of adopting a configuration similar to that of thorium, uranium(IV) seems to be considered to form a 1 to 2 complex with alizarin complexan and also with xylenol orange. It seems, therefore, that some differences between the results shown by Budensinsky and those obtained here may be attributed to the differences in the experimental conditions used.

The formation constant, K, was then calculated from the curves shown in Fig. 4, on the basis of the following relationships[14]:

$$K=C(1-\alpha)/(\alpha C)(2\alpha C)^2 \quad (1)$$

$$\alpha=(E_m-E_s)/E_m \quad (2)$$

where C is the total concentration of the complex in moles per liter, assuming no dissociation, α is the degree of dissociation, E_m (PR or PR') is the maximum absorbance obtained from the horizontal portion of the curves, and E_s(PQ or PQ') is the absorbance at the stoichiometric molar ratio of xylenol orange to uranium in the complex. This ratio was found to be 2.9×10^{11}.

Summary

A new spectrophotometric method for determining trace amounts of uranium has been developed. This method is based on the coloration of xylenol orange with uranium(IV) formed by the reduction of uranium(VI) in the presence of ascorbic acid. The effects of the pH value, reagent and boiling time have been thoroughly investigated, and experimental conditions which make possible the determination of 20 to 100 μg. of uranium have been devised. The mole ratio of the complex between uranium and this reagent has also been discussed.

The author gratefully acknowledges the kind guidance and encouragement given him by Professor Kôichi Tonosaki. He thanks also Dr. Shôzô Shibata of the Nagoya Industrial Research Institute for his interest.

Department of Chemistry
Faculty of Literature and Science
Hirosaki University
Bunkyo-chô, Hirosaki

11) M. Otomo, unpubished. (Presented at the 15th Anaual Meeting of the Chemical Society of Japan, Kyoto, April, 1962).
12) M. Otomo, unpublished.
13) M. A. Leonard and T. S. West, *J. Chem. Soc.*, **1960**, 4477.
14) A. E. Harvey, Jr., and D. L. Manning, *J. Am. Chem. Soc.*, **72**, 4488 (1950).

Synthesis of Cyclic Peptide. I.[1] *Preparation of Cyclo-di-β-alanyl from 1,4-Cyclohexanedione*

By Hiroshi WATANABE, Shigeru KUWATA and Sugao KOYAMA*

(Received August 2, 1962)

Since the discovery of such naturally occurring cyclic polypeptides as gramicidines and tyrocidine having strong biological activities, synthetic methods of cyclic polypeptides have been studied. A method used for this purpose is that of cyclizing the corresponding linear peptide in dilute conditions. By this method some of the cyclic peptides having several amino acid residues were prepared successfully, though in some peptides, e.g. tri-α-peptide, cyclization was found difficult.

An alternative method to approach these peptides may be the expansion of a compound already having a cyclic structure. It is well known that cyclic ketone oxime rearranges to lactam by the Beckmann reaction in a good yield. Applying this principle to cyclic diketone compound, Tokura et al.[2] rearranged cyclododecane-1,6-dione dioxime with sulfur trioxide in liquid sulfur dioxide and obtained 1,7-diaza-6,12-dioxocyclododecane. In the same way, from 1,4-cyclohexanedione dioxime, a cyclic dipeptide of β-alanine should be produced. By heating di-*p*-tosylate of 1,4-cyclohexanedione dioxime and hydrolyzing the product, Knunyants and Fabrichnyi[3] obtained β-alanine, succinic acid and ethylenediamine. This result suggests the production of cyclo-di-β-alanyl as well as ethylenesuccinamide as the rearrangement products, and in fact Hall[4] has isolated the former from the rearrangement mixture. On the other hand, Mamlock[5] tried the same reaction using 1,4-cyclohexanedionedioxime monohydrochloride and polyphosphoric acid, but he only isolated 2-chloro-*p*-phenylenediamine as reaction product. Recently, Rothe[6] reported that 1,4-cyclohexanedione dioxime, treated with 8% oleum in a Beckmann rearrangement, gives only cyclo-di-β-alanyl, instead of the mixture of two cyclic amides.

We intended to re-examine these reactions in order to establish a route to obtain cyclo-di-β-alanyl. In the first place, a direct rearrangement was studied. According to Mamlock, 1,4-cyclohexanedione dioxime was treated with polyphosphoric acid at about 120°C for a short time, though the starting material was dioxime itself in order to avoid the complexity caused by chloride ion. The hydrolyzate of the reaction product was studied by paper-chromatography, but the spot corresponding to β-alanine or ethylenediamine could not be found, though the presence of a spot of lower R_f-value was recognized, which was proved to be due to *p*-phenylenediamine by paperchromatography. When such an acid as perchloric acid, sulfuric acid or trifluoroacetic acid, was used under similar conditions (50~100°C), similar results were also obtained. Treatment of the dioxime with polyphosphoric acid in the cold resulted in the mere recovery of the starting material.

Then the indirect method according to Knunyants and Fabrichnyi was examined secondly. Di-*p*-tosylate of the dioxime was heated in methanol at 100°C for 90 min. in an autoclave. In the hydrolyzate of reaction product, the presence of β-alanine and ethylenediamine was confirmed by paperchromatography, as they had observed, though no crystals corresponding to cyclo-di-β-alanyl were isolated after treatment of the syrup with Amberlite IRA-400 and CG-120.

Another reaction which will give the same results with the Beckmann rearrangement is the Schmidt reaction, as has been suggested by Rothe[7]. The latter will be more useful for our purpose, because milder conditions can be chosen. Thus, dry hydrogen chloride was passed into chloroform solution of 1,4-cyclohexanedione and hydrazoic acid at 0~5°C for about 2 hr. From the reaction mixture after removal of hydrogen chloride, a viscous syrup was obtained, containing many fine crystals, from which fine hexagonal plates or granules were isolated, which, after recrystallization

* Present address: Sanken Ka-ko, Ltd., Nakano, Motoyama, Higashinada-ku, Kobe.

1) Previous communication, *Pharm. Bull. Japan*, **9**, 834 (1961).

2) N. Tokura, R. Tada and K. Suzuki, This Bulletin, **32**, 654 (1959).

3) I. L. Knunyants and B. P. Fabrichnyi, *Doklady Akad. Nauk S. S. S. R.*, **68**, 701 (1949) : *Chem. Abstr.*, **44**, 1918 (1950).

4) H. K. Hall, *J. Am. Chem. Soc.*, **80**, 6404 (1958).

5) L. Mamlock, *Bull. soc. chim. France*, **1956**, 1182.

6) M. Rothe, *Acta chim. Akad. Sci. Hung.*, **18**, 449 (1949); *Chem. Abstr.*, **53**, 21693b (1959).

7) M. Rothe and J. Rothe, *Angew. Chem.*, **73**, 769 (1961); after the publication of our previous paper, M. Rothe repoted the experimental result of this reaction: *Chem. Ber.*, **95**, 783 (1962).

from ethanol, showed m. p. of 295~300°C. The elementary analyses and the molecular weight of this substance showed agreement with theoretical values for cyclo-di-β-alanyl. In Fig. 1 its infrared spectrum is shown. It was also confirmed that the paper-chromatogram of the hydrolyzate of this compound shows only one spot, which coincides completely with that of β-alanine itself. From these evidences, it is clear that the compound obtained here is the expected cyclo-di-β-alanyl, formed by the scheme:

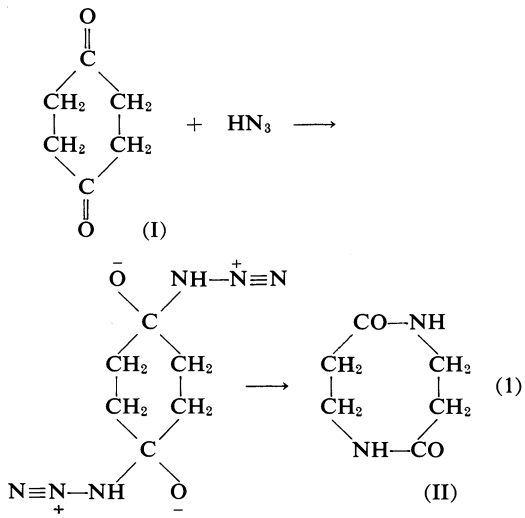

But, the paper-chromatogram of the hydrolyzate of the crude syrupy reaction product shows in addition a different spot which was proved to be due to ethylenediamine, from that of the expected β-alanine. This shows that the reaction by the scheme 2 also occurs simultaneously, though the intermediate cyclic product III could not be isolated.

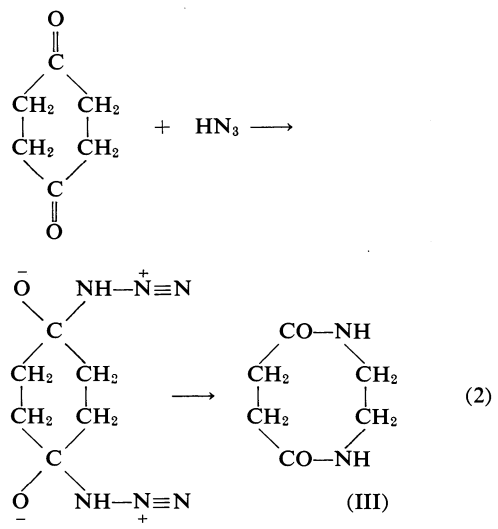

Experimental

Diethyl Succinate (IV).—Succinic acid was esterified with ethanol and sulfuric acid: b. p. 84~85°C/6 mmHg; b. p. 210~214°C.

Diethyl Succinosuccinate (V).—According to the method of Upenski[8], IV was condensed to V by sodium sand: m. p. 126~128°C (lit.[8] 126~127°C).

1, 4-Cyclohexanedione (I).—V was converted to I by the method of Vincent et al.[9]: b. p. 130~131°C/20 mmHg (lit.[9] b. p. 132°C/20 mmHg).

1, 4-Cyclohexanedione Dioxime (VI).—This was derived from I by usual method: m. p. 190~192°C (lit.[10] 192°C).

Attempted Beckmann Rearrangement of VI with Trifluoroacetic Acid.—A mixture of dioxime VI (1 g.) and trifluoroacetic acid (3 g.) was heated in a boiling water-bath for 30 min. After the reaction product was concentrated to dryness, the residue was boiled with 6 N hydrochloric acid for 8 hr. and paper-chromatogrammed. (Method: circular paper-chromatography; developer: *n*-BuOH: AcOH: H_2O=5 : 1 : 4; coloring agent: ninhydrin). Several spots were obtained but no one corresponding to β-alanine could be found. In this chromatogram, a spot having R_f value of ca. 0.29 was identified as that of *p*-phenylenediamine by comparison, after isolation, with an authentic specimen

The same reaction was tried by using polyphosphoric acid, perchloric acid or sulfuric acid, with similar results.

Indirect Beckmann Rearrangement Using Di-*p*-tosylate of VI as an Intermediate.—Dioxime VI in pyridine was added to *p*-tosylchloride in pyridine at −8°C and the mixture was allowed to stand at 0°C overnight[3]. The di-*p*-tosylate was obtained as precipitate by diluting the solution with water. A solution of ditosylate in methanol was heated in an autoclave at 100°C for 90 min. After removal of the solvent, the residue was dissolved in water and passed through Amberlite IRA-400 and CG-120. Viscous syrup was obtained by concentrating the eluate. Crystallization from ethanol did not succeed. From the paper-chromatogram of the hydrolyzate of this syrup, spots corresponding to β-alanine and ethylenediamine were confirmed by the comparison with authentic specimens.

Schmidt Reaction of I.—To a chloroform solution of I (2 g.) and hydrazoic acid (0.6 N chloroform solution, 60 ml.), dry hydrogen chloride was bubbled at 0~5°C for about 2 hr., when a syrupy material containg fine needles was formed. After removal of chloroform, the residual syrup was dissolved in water and treated with silver acetate to remove chloride ion and then hydrogen sulfide to remove excess silver ion. Resulting aqueous solution was concentrated to dryness in vacuo. Syrupy material containing fine crystals was obtained. Paper-chromatogram of the hydrolyzate of this syrup showed the presence of spots corresponding to β-alanine and ethylenediamine. The

8) A. E. Upenski and I. Turin, *Chem. Zentr.*, III, 754 (1923); C. R. Hauser and B. E. Hudson, Jr., "Organic Reactions", Vol. I, 283 (1946).
9) J. R. Vincent, A. F. Thompson, Jr. and L. I. Smith, *J. Org. Chem.*, 3, 606 (1937).
10) A. Baeyer and W. A. Noyes, *Ber.*, 22, 2170 (1889).

syrup was dissolved in hot ethanol and cooled gradually, then hexagonal plates or granules melting at 295~300°C (lit. 298°C[4], 297~299°C[7]) were obtained. Yield was 27%.

Found: C, 50.91; H, 7.39; N, 19.69. Calcd. for $C_6H_{10}N_2O_2$: C, 50.69; H, 7.09; N, 19.71%.

Molecular weight (measured by Schwyzer's method[11]; solvent: CF_3COOH; control: diketopiperazine). Found: 127. Calcd. for $C_6H_{10}N_2O_2$: 142.

Paper-chromatogram of the hydrolyzate of this crystal with hydrogen chloride afforded only one spot corresponding to that of β-alanine.

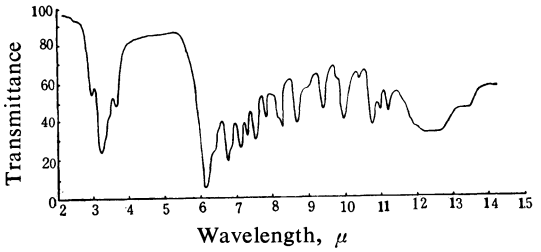

Fig. 1. Infrared absorption spectrum of cyclo-di-β-alanyl.

11) R. Schwyzer, B. Iselin et al., *Helv. Chim. Acta*, **39**, 872 (1956).

Infrared Absorption Spectrum. — The spectrum was recorded with a Perkin-Elmer Infracord, model 137. Phase: KBr disk. The result was shown in Fig. 1.

Summary

1) By the direct Beckmann rearrangement of 1,4-cyclohexanedione dioxime by polyphosphoric acid, trifluoroacetic acid, perchloric acid or sulfuric acid at about 100°C, no expected cyclo-di-β-alanyl but *p*-phenylenediamine was obtained.

2) By indirect Beckmann rearrangement using di-*p*-tosylate of 1,4-cyclohexanedione dioxime as an intermediate, the rearrangement occurs certainly though the isolation of the cyclic dipeptide was not successful.

3) By the Schmidt reaction of 1,4-cyclohexanedione, the expected rearrangement proceeded smoothly and from the reaction products cyclo-di-β-alanyl was easily isolated.

Laboratory of Chemistry
Faculty of Science
Kōnan University
Higashinada-ku, Kobe

Synthesis of 1-Aminocyclobutanecarboxylic Acid

By Rokuro SUDO and Shigehiro ICHIHARA

(Received September 25, 1962)

Some alicyclic amino acids have been known as physiologically interesting compounds. 1-Aminocyclopropanecarboxylic acid (II) was prepared by Ingold and his coworkers[1] and

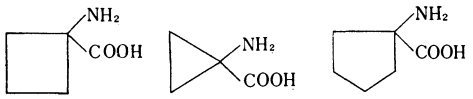

I II III

was recently isolated by Burroughs[2] from apple cider and perry pear juices, and 1-aminocyclopentanecarboxylic acid (III) was reported to show anticancerous action[3,4].

The authors wish to report the synthesis of an additional alicyclic amino acid, 1-aminocyclobutanecarboxylic acid (I) by two methods, the first of which involves reaction of methyl 1-bromocyclobutanecarboxylate (IV) with ammonia and the second involves hydrolysis of 5-cyclobutane-spiro-hydantoin (IX).

The first attempted method did not afford I, but an isomeric unsaturated amino acid, which was produced by a rupture of the cyclobutane-ring. Although IV[5] was easily converted by ammonium hydroxide into 1-bromocyclobutanecarboxamide (V), amination of V by using potassium phthalimide or hexamethylenetetramine was unsuccessful. When V was heated with aqueous ammonia in a sealed tube, a substance of m. p. 163~164°C was obtained and its analytical values corresponded to the molecular formula of $C_5H_{11}ON_2Br$ (VI). Hydrolysis of VI with a solution of barium hydroxide gave a very hygroscopic amino acid (VII). This amino acid was characterized by conversion into its benzoyl derivative VIII

1) C. K. Ingold et al., *J. Chem. Soc.*, **1922**, 1911.
2) L. F. Burroughs, *Nature*, **179**, 360 (1957).
3) R. B. Ross, *J. Chem. Educ.*, **36**, 368 (1959).
4) T. A. Connors and W. C. J. Ross, *J. Chem. Soc.*, **1960**, 2119.
5) A. Campbell and H. N. Rydon, ibid., **1953**, 3002.

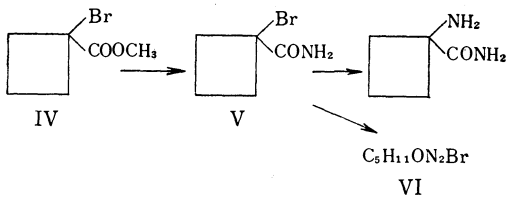

which had the same molecular formula as that of benzoyl derivative of I, but absorbed bromine, indicating the presence of a double-bond.

In the second procedure, partial hydrolysis of 5-cyclobutane-spiro-hydantoin (IX), which was prepared by the method of Ingold[1] et al., afforded 1-uramidocyclobutanecarboxylic acid (X). IX or X was heated with a solution of

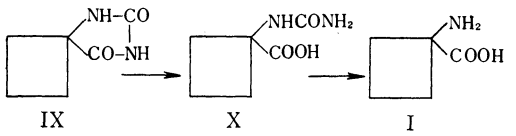

barium hydroxide for 24 hr., affording an amino acid, whose paperchromatograph showed a spot of R_f value 0.5 in *n*-butanol/acetic acid/water; (4 : 1 : 1). This amino acid was confirmed to be 1-aminocyclobutanecarboxylic acid (I) by elementary analysis and conversion into its benzoyl derivative (XII), which saturated against bromine.

Although the structure of VII was thought to be γ-amino-α-methylcrotonic acid from chemical behavior and infrared spectrum of its benzoyl derivative, it could not be confirmed. In addition, paperchromatograph of VII showed a spot of R_f value 0.50 as main-product, whose benzoyl derivative was isolated and some other two spots of R_f value, 0.30 and 0.10 in *n*-butanol/acetic acid/water; (4 : 1 : 1), (Fig. 1). They also seemed to be produced by a rupture of the cyclobutane-ring, but were not isolated.

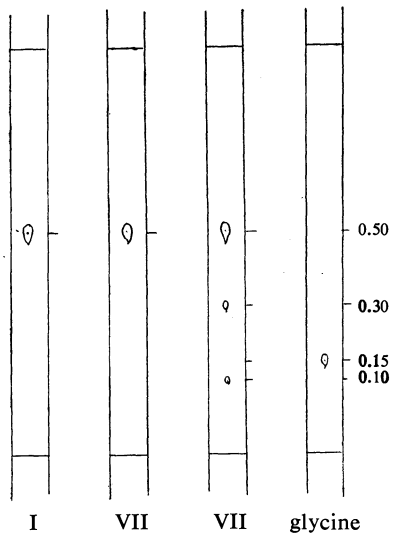

Fig. 1

Experimental

Methyl 1-Bromocyclobutanecarboxylate (IV).—The procedure of Campbell and Rydon[5] was used. Twenty two grams of cyclobutanecarboxylic acid was heated under reflux at 100°C for 1 hr. with 29 g. of thionyl chloride. Red phosphorus (0.25 g.) and 40 g. of bromine were added and heating was continued at 110~120°C for further 3 hr. The reaction mixture was poured into 30 cc. of absolute methanol, and then diluted with water and extracted with ether. After removal of ether, the distillation of the residue gave 30 g. of oil, b. p. 70~75°C/23 mmHg, in a 70% yield.

Found: C, 37.33; H, 4.87; Br, 42.04. Calcd. for $C_6H_9O_2Br$: C, 37.33; H, 4.67; Br, 41.40%.

1-Bromocyclobutanecarboxamide (V).—Twenty six grams of IV was added to 100 cc. of concentrated aqueous ammonia and was continued, stirring for 2 hr. The precipitate was collected and recrystallized from ethanol affording 20 g. of needles, melted at 153~154°C.

Found: C, 33.85; H, 4.64; N, 7.81. Calcd. for C_5H_8ONBr: C, 33.72; H, 4.49; N, 7.87%.

Ammonolysis of V.—Three grams of V was suspended in 30 cc. of concentrated aqueous ammonia and was heated for 6 hr. in a sealed tube. Removal of the solvent from the reaction mixture gave a syrupy residue. When the residue was allowed to stand in an ice bath, a precipitate was formed. After recrystallization from ethanol, 1.5 g. of colorless prisms, m. p. 163~164°C (VI), were obtained.

Found: C, 30.92; H, 5.49; N, 14.11. Calcd. for $C_5H_{11}ON_2Br$: C, 30.77; H, 5.64: N, 14.36%.

Hydrolysis of VI with Barium Hydroxide Solution.—Two grams of VI and 5 g. of barium hydroxide were added to 50 cc. of water and refluxed for 2 hr. The reaction mixture was filtered and to the filtrate was added carbon dioxide gas. After removal of barium carbonate, the solution was concentrated in vacuo resulting a syrupy residue. This syrup was solidified by addition of 30 cc. of absolute ethanol affording a crystalline substance, which was so hygroscopic that its melting point was not determined. The syrup was positive in the ninhydrin-test and its paperchromatograph showed 3 spots of R_f values 0.50, 0.30 and 0.10 in *n*-butanol/acetic acid/water; (4 : 1 : 1). (Fig. 1). The syrup, however, was characterized by conversion into its benzoyl derivative VIII, which melted at 183~185°C and absorbed bromine.

Found: C, 65.19; H, 5.77; N, 6.30. Calcd. for $C_{12}H_{13}O_3N$: C, 65.74; H, 5.98; N, 6.39%.

The infrared spectrum showed strong bands at 3400, 1615, 1545 (-NH-CO-), 1695 (-COOH) and 1425 cm^{-1}.

The carboxyl band, shifting toward a lower wave

number, indicates the presence of C=C bond adjacent to the carboxyl group[6]. The band at 1425 cm^{-1}, seemed to be attributed to the CH_2 deformation frequency of the group of $-C=C-CH_2-$[7].

VIII was hydrolyzed by hydrochloric acid giving an amino acid whose paperchromatograph showed only one spot of R_f value 0.50.

5-Cyclobutane-spiro-hydantoin (IX). — The procedure of Ingold et al.[1] was used. This hydantoin melted at 222~225°C (reported m. p. 225°C).

1-Uramidocyclobutanecarboxylic Acid (X).—Two grams of IV and 4 g. of barium hydroxide were added to 50 cc. of water and refluxed for 2 hr. The reaction mixture was filtered and to the filtrate was added carbon dioxide gas. After removal of barium carbonate, the solution was concentrated in vacuo resulting a residue. The residue was recrystallized from ethanol affording 1 g. of colorless m. p. 200~202°C.

Found; N, 17.25. Calcd. for $C_6H_{10}O_3N_2$: N, 17.71%.

1-Aminocyclobutanecarboxylic Acid (I). — Two grams of IV and 5 g. of barium hydroxide ware added to 50 cc. of water and refluxed for 24 hr. The reaction mixture was filtered and to the filtrate was added carbon dioxide gas. After removal of barium carbonate, the solution was concentrated in vacuo resulting a residue. The residue was recrystallized from ethanol-water affording 1 g. of colorless prisms, m. p. 222~225°C (sublime). Paperchromatograph showed a spot of R_f value 0.50 in *n*-butanol/acetic acid/water; (4:1:1). (Fig. 1). The infrared spectrum showed amino acid bands (2930, 1630, 1520 cm^{-1}).

Found: C, 51.67; H, 7.90; N, 12.15. Calcd. for $C_5H_9O_2N$: C, 52.16; H, 7.88; N, 12.17%.

Benzoyl Derivative of I.—I was converted into a benzoyl derivative by the general method and gave colorless prisms, which melted at 205~206°C and saturated towards bromine. The infrared spectrum showed strong bands at 3280, 1630, 1530 (-CONH-) and 1710 cm^{-1} (-COOH).

Found: C, 65.87; H, 6.18; N, 6.35. Calcd. for $C_{12}H_{13}O_3N$: C, 65.74; H, 5.98; N, 6.39%.

The authors wish to express their deep gratitude to Professor Masaki Ohta for his kind and constant guidance throughout this study and to Dr. Tadashi Sato for the measurement of infrared spectra.

Laboratory of Organic Chemistry
Tokyo Institute of Technology
Meguro-ku, Tokyo

6) L. J. Bellamy, "The Infrared Spectra of Complex Molecules", Methuen & Co., Ltd. London, p. 168.
7) L. J. Bellamy, ibid., p. 22.

*Syntheses and Structures of Acetylformoin and its Related Compounds. I**

By Ryozo GOTO, Yo MIYAGI and Hiromi INOKAWA

(Received May 15, 1962)

Acetylformoin (AF) and benzoylformoin (BF) are synthesized by the acyloin condensation of methyl- and phenyl-glyoxal respectively:

$$2\,RCOCHO \xrightarrow{KCN} RCOCH(OH)COCOR$$

$R=CH_3$: AF

$R=C_6H_5$: BF

The probable structures for these formoins are indicated by I—V in Fig. 1.

The structure of benzoylformoin has been investigated by earlier workers[1,2]. Benzoylformoin has two different kinds of hydroxyl groups, one of which is alkylated with an alcoholic solution of a mineral acid to give an *O*-alkyl derivative. *O*-Methyl derivative (methyl benzoylformoin) is converted to *O*-ethyl derivative (ethyl benzoylformoin) with ethanolic hydrogen chloride and vice versa with methanolic hydrogen chloride.

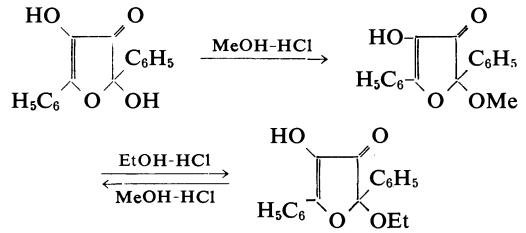

Blatt[2] stated that this type of etherification is characteristic of the glycosidic linkage and has suggested the cyclic structure VI for the

* Partly presented at the 13th Annual Meeting of the Chemical Society of Japan, Tokyo, April, 1959.

1) P. W. Abenius, *Ber.*, 25, 706 (1894).

2) A. H. Blatt, *J. Am. Chem. Soc.*, 57, 1103 (1935); 58, 1894 (1936).

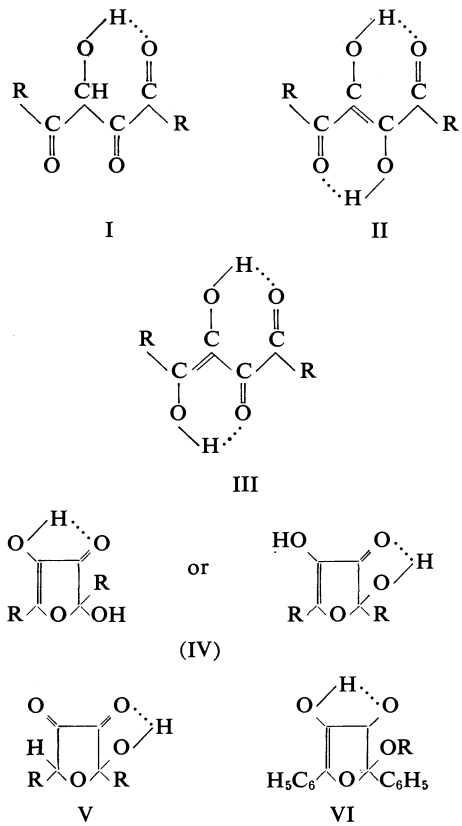

Fig. 1.

O-alkyl derivative. On this basis, he also proposed structure IV for benzoylformoin itself. On the other hand, it has been reported that the reaction with *o*-phenylenediamine and some other chemical behavior supported structure III. Blatt was of opinion that an equilibrium between III and IV occurred in solution. If this is the case, the formation of VI by the etherification can not be considered as an unequivocal evidence for the straightforward structure IV of benzoylformoin, since the equilibrium between the two tautomers could have been shifted due to the removal of IV by the etherification.

Acetylformoin was first synthesized by Nodzu and Kunichika[3] in our laboratory. More recently Steinbauer and Waldmann[4] studied the structure of acetylformoin. The reaction with *o*-phenylenediamine and methanolysis suggest an equilibrium between IV and III or II in solution.

3) R. Nodzu and S. Kunichika, This Bulletin, **15**, 211 (1940).

4) E. Steinbauer and E. Waldmann, *Monat.*, **89**, 570 (1958).

The authors have tried to determine the structure of benzoyl- and acetyl-formoin by the spectrophotometric method.

Results and Discussion

The spectral data obtained by the authors are listed in Tables I and II.

The Structure of Acetylformoin. — Acetylformoin was examined as a solid state in Nujol and as a solution in chloroform. The spectrum of acetylformoin in Nujol is very similar to that of the chloroform solution immediately after dissolving, except that in solution there appears another absorption band of weak intensity, at 1710 cm^{-1}. In both cases, there is an intense absorption at 1620 cm^{-1}. In the chloroform solution, immediately after dissolving a very weak broad absorption band, extending from 2800 cm^{-1} to beyond 3600 cm^{-1}, is observed. In Nujol, acetylformoin shows no distinct absorption over 3000 cm^{-1}, but a weak, broad absorption on both sides of the sides of the strong absorption of Nujol at 2800~3000 cm^{-1}.*

A part of structure II, $-C(OH)=\underset{|}{C}-CO-$, is the enol form of a β-diketone and constitutes the so-called "conjugate chelation". In enolic β-diketones, the C=O stretching absorption band is found to be widely shifted close to 1600 cm^{-1}, with a great enhancement of its intensity, and the OH stretching absorption band becomes very weak and broad. This phenomenon was first reported by Rasmussen, Tunnicliff and Brattain[5], who attributed the anomalies to resonance structures:

This chelation has been termed "conjugate chelation" to distinguish it from the normal hydrogen bonding. Similar observations have been reported for acetylacetone[5,6], benzoylacetone[6], dibenzoylmethane[5,6], α-acetyltetronic acid[7] and many other compounds[8].

Exactly the same type of anomalies was observed with the spectra of acetylformoin: there arise a C=O stretching absorption band at a very low wave number, 1620 cm^{-1}, and a

* The spectum of acetylformoin in hexachlorobutadiene mull also shows this broad absorption band. In this case, however, there arises an additional absorption at 1710 cm^{-1}, as in the chloroform solution. It might be considered that acetylformoin partly dissolves in hexachlorobutadiene. On this point more details are under investigation.

5) R. S. Rasmussen, D. D. Tunnicliff and R. B. Brattain, *J. Am. Chem. Soc.*, **71**, 1068 (1949).

6) S. Batos, D. Hadži and G. Rossmy, *Trans. Faraday Soc.*, **52**, 464 (1956).

7) L. A. Duncanson, *J. Chem. Soc.*, **1953** 1207.

8) L. J. Bellamy, "Infrared Spectra of Complex Molecules", Methuen, London (1958), pp. 104, 142.

weak, broad band of the OH stretching absorption. In structure II, enediol -C(OH)=C(OH)- serves to form conjugate chelation on both sides of the carbonyl group; therefore a stronger chelation may be expected.

In enolic β-diketones, the C=C stretching absorption can not be observed. Rasmussen[5] stated that this is to be accounted for by its being hidden by the very strong C=O band or by its being shifted out of the double-bond region because of its loss of a double-bond character. Furthermore, it is not too difficult to comprehend the disappearance of the C=C stretching absorption band of acetylformoin when due attention is paid to the fact that C=C is fully and symmetrically substituted.

The other structures, I, III, IV and V, are excluded for the following reasons.

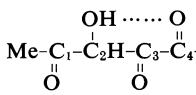

As for structure I, there are three kinds of carbonyl groups: C_1=O is a normal carbonyl group; C_3=O is a carbonyl group in α-diketone, and C_4=O is a hydrogen-bonded carbonyl group. Therefore, their absorption may be expected to split. Among them, the absorption band of C_4=O is expected to arise at the lowest wave number because of the hydrogen bonding, but the so wide shift over to 1620 cm^{-1} as observed can not be expected with the simple hydrogn bonding, which would produce somewhat sharper bands of the OH stretching absorption.

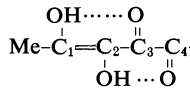

As for structure III, the band at 1620 cm^{-1} is attributable to C_3=O because a part of the structure,

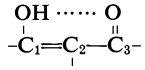

constitutes the conjugate chelation and can result in a large shift, as been observed. C_4=O, however, is simply* a hydrogen-bonded carbonyl group, and its absorption band will arise at a higher wave number, probably close to 1700 cm^{-1}. Since the hydroxyl group attatched to C_2 forms only a simple* hydrogen bonding on C_1=O, there should appear some distinct bands of the OH stretching absorption.

As for structure IV, the value, 1620 cm^{-1}, is too low for the carbonyl group of IV, which is the enol form of α-diketone.

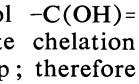

In such enolic α-diketones as phenylbenzylglyoxal $C_6H_5COCOCH_2C_6H_5$, no anomalies arising in enolic β-diketones are observed, and the C=O stretching absorption arises at the position of normal conjugated ketones, around 1670 cm^{-1} [9]. Moreover, in structure IV, the bands of the C=C and C=O stretching absorption may be expected to separate, and weak, broad band of OH stretching absorption can not be explained with structure IV.

As for structure V, the C=O stretching absorption may be expected to arise at a much higher wave number because the α-diketones in 5-membered ring system absorb at 1760~1776 cm^{-1} [10]. In structure V, some distinct bands of OH stretching absorption may be expected to arise.

The absorption band at 1710 cm^{-1}, which is observed in the chloroform solution immediately after dissolving, becomes stronger when the solution is left standing; at the same time there arise very weak but distinct absorption bands at 3600, 3340, 2970, 2880 and 1763 cm^{-1}. Therefore, in the chloroform solution acetylformoin seems to change to another structure than II, but the identity of this new structure has not yet been determined.

The Structure of Benzoylformoin.—Benzoylformoin absorbs at 3500, 3210, 1685, 1608 and 1595 cm^{-1}. An *O*-alkyl derivative, ethyl benzoylformoin (EBF), absorbs at 3270, 1688, 1605 and 1595 cm^{-1}. Structure IV seems to be most compatible with these observations. The reasons are as follows: first of all, in the region of C=O and C=C stretching absorption, the spectrum of benzoylformoin is very similar to that of ethyl benzoylformoin, the structure of which was established to be VI, as mentioned above. The band at 1685 cm^{-1} may be assigned to the carbonyl group, and those at 1608 and 1595 cm^{-1}, to the phenyl and olefin groups. These assignments seem to be appropriate, since enolic α-diketones absorb at around 1670 cm^{-1} [9], as mentioned above in the discussion of acetylformoin. When one of the hydroxyl groups of benzoylformoin is ethylated there occurs an accompanying change in the spectrum: benzoylformoin shows two bands of OH stretching absorption, while ethyl benzoylformoin shows one of OH stretching absorption.

Structures I, II, III and V are excluded for the following reasons.

* Here "simple" or "simply" means hydrogen bondinigs without any involvement in the conjugate chelation.

9) R. P. Barnes and G. E. Pinkney, *J. Am. Chem. Soc.*, 75, 479 (1953).

10) K. Alder, H. K. Schäfer, H. Esser, H. Krieger and R. Reubke, *Ann.*, 593, 23 (1955).

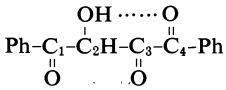

As for structure I, the C=O stretching absorption bands will probably split, because C_4=O is conjugated and hydrogen-bonded, C_3=O is the carbonyl group in α-diketone, and C_1=O is conjugated but not hydrogen-bonded. Above all, the absorption band of C_3=O will arise at around 1710 cm^{-1} [5].

As for structure II, a model compound of II, *trans*-dibenzoylethylene VII, absorbs at 1635 cm^{-1}. The C=O stretching absorption band of structure II may be shifted to a lower wave number than 1635 cm^{-1} by its conjugate chelation*. Furthermore, two distinct bands of OH stretching absorption can not be explained with structure II.

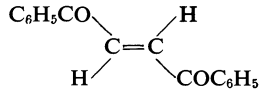

VII

As for structure III, there are two kinds of carbonyl groups: C_4=O is conjugated and simply hydrogen-bonded, while C_3=O is a carbonyl group involved in the conjugate chelation*. Hence, the following assignment

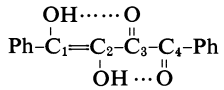

is possible: the absorption band at 1685 cm^{-1} is attributed to C_4=O, and the bands at 1605 and 1595 cm^{-1} are attributed to the overlapping bands of C_3=O and C=C stretching absorptions. If this be the case, the bands at 1605 and 1595 cm^{-1} would have been stronger than the bands at 1685 cm^{-1}, because the band of C_3=O is that of the conjugate chelation, which should have a much stronger intensity and because, moreover, this band of C_3=O is overlapped with the C=C stretching absorption band to enhance the intensity. The intensities of the band at 1685 cm^{-1} and the bands at 1605 and 1595 cm^{-1}, however, are almost equal. Furthermore, the hydroxyl group attatched to C_1 constitutes a conjugate chelation, but the absorption bands of benzoylformoin in the region of the OH stretching absorption are not so weak and broad as that of the conjugate chelation.

As for structure V, structure V is expected to show its C=O stretching absorption bands at a higher wave number, over 1760 cm^{-1}, as mentioned above in the discussion of acetylformoin.

Benzoylformoin is so scarcely soluble in carbon tetrachloride or other desirable solvents for the spectrophotometric measurement that the spectrum of benzoylformoin in solution could not be observed.

More details are under investigation.

* As for the conjugate chelation, see the discussion for acetylformoin.

Table I. Absorption bands of AF (cm^{-1})

Nujol	$CHCl_3$ solution*	$CHCl_3$ solution**
		3600 vw
Weak and broad 3600～2800	Weak and broad 3600～2800	3340 w
		2970 w
		2880 w
	1710 w	1763 m
		1707 s
1620 s	1625 s	1620 s

* 10^{-1} M. immediately after dissolying
** 10^{-1} M. 43 hr. after dissolving
vw: very weak, w: weak, m: medium, s: strong

Table II. Absorption bands of BF and EBF (cm^{-1})

BF (Nujol)	EBF (Nujol)
3500 m	
3210 m	3270 m
1685 s	1688 s
1608 s	1605 s
1595 w	1595 w

Experimental

Synthesis of Acetylformoin[3,4].—The freshly distilled monomer of methylglyoxal was dissolved in cold water (pH value: 2.4) and the solution was stored in a refrigerator overnight. The condensation was effectd according to Steinbauer's method[4], i.e., under a nitrogen stream, a pH-meter being used. An aqueous solution of sodium cyanide (molar ratio to methyl glyoxal: 0.08), previously cooled to 0°C, was added through a dropping funnel to the aqueous methylglyoxal solution; then the pH value rose to 9.5. The temperature of the reaction mixture did not rise above 2°C under cooling with ice-water, though Steinbauer and Waldman stated that it rose up to 5°C under cooling. Sodium bicarbonate was added to keep the pH value of the solution between 7～8. When the aqueous methylglyoxal solution was used soon after dissolving, the pH value did not decrease below 8 even though considerable amount of sodium bicarbonate was added. After 30 min., condensation was stopped by adding phosphoric acid (pH: 5.0). The procedure thereafter was as usual. The solution was concentrated to a syrup, and alcohol was added to it. Inorganic salt was filtered off. The filtrate was concentrated to a syrup which was dissolved in ether, and the inorganic salt was filtered off again. The filtrate was dried over sodium sulfate. The syrup obtained by concentrating the ethereal solution was distilled under a vacuum. The yield was about 10%. The purification was effected by vacuum sublimation at 30～35°C, resulting in yellow crystals, m. p., 82～83°C.

Synthesis of Benzoylformoin. — Phenylglyoxal hydrate (1 g., m. p. 81°C) was dissolved in 35 cc. of water, with slight warming if it was necessary. To this solution was added a solution of 0.04 g. of potasium cyanide (molar ratio to phenylglyoxal hydrate: 0.08) in 10 cc. of water. Immediately the mixture of solution was colored yellow, and crystalline benzoylformoin began to precipitate. After 3 hr, the solution was neutralized with hydrochloric acid. Benzoylformoin was collected by filtration. The yield was about 85%. The recrystallisation was effected from aqueous ethanol. Yellow crystals, m. p., 186~188°C.

Synthesis of Ethyl Benzoylformoin[2].—Benzoylformoin was dissolved in a minimum amount of about 10% ethanolic hydrogen chloride. Ethyl benzoylformoin was deposited when the solution was left standing at room temperature overnight. It was decanted off from the mother liquor, dried in vacuo over potassium hydroxide, and recrystallized from ethanol. The yield was about 90%. Yellow crystals; m. p., 214°C.

Synthesis of *trans*-Dibenzoylethylene. — This was prepared from fumaryl chloride and benzene by the method of Conant and Lutz[11]. Yellow crystals; m. p., 109~110°C.

Spectra. — The infrared spectra were recorded with a Koken model DS-301 spectrophotometer (double-beam type).

Department of Chemistry
Faculty of Science
Kyoto University
Sakyo-ku, Kyoto

11) J. B. Conant and R. E. Lutz, *J. Am. Chem. Soc.*, **45**, 1303 (1923).

The Colorimetric Determination of Traces of Selenium with Dithizone

By Hisao MABUCHI and Hiromichi NAKAHARA*

(Received September 5, 1962)

The composition of selenium is generally determined by reduction to reddish elemental selenium with such reducing agents as sulfur dioxide. This method is, however, not only insensitive but also subject to interference from other elements. Recently, Cheng reported a useful new method of determining traces of selenium colorimetrically by using 3-diaminobenzidine as an organic reagent[1]. Although Cheng's method is more sensitive and simpler than the former one, it still has some difficulties in the color development and involves complicated procedures.

The present authors have recently found that selenium(IV) can be extracted almost quantitatively by dithizone from an acid solution of a fairly high concentration. In carbon tetrachloride the dithizone complex of selenium is yellow in color and shows a maximum absorption at 420 mμ (Fig. 1).

The fact that selenium can be extracted by dithizone from a highly acidic solution, especially a hydrochloric acid solution of as high as 6N, may be regarded as very favorable for the colorimetric determination of selenium, because the high concentration of hydrochloric acid prevents other metals from complexing with dithizone. Taking these points into consideration, the authors studied the colorimetric determination of selenium with dithizone.

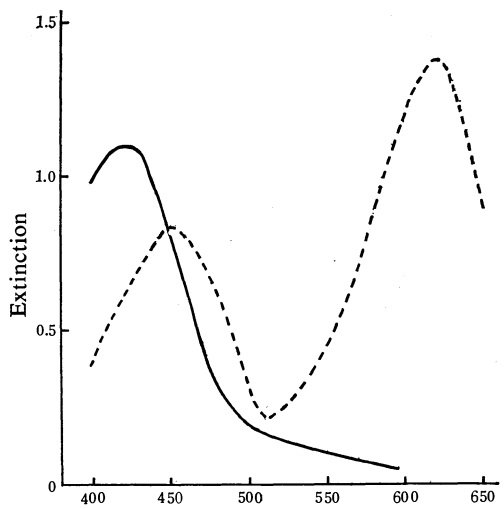

Fig. 1. Absorption curves.
—— Dithizone complex of selenium in carbon tetrachloride
--- Dithizone in carbon tetrachloride

* Present address: Department of Chemistry, Massachusetts Institute of Technology, Cambridge 39, Massachusetts, U. S. A.

1) K. L. Cheng, *Anal. Chem.*, **28**, 1738 (1956).

Experimental

Apparatus and Reagents.—*Spectrophotometer.*—A Beckman model DU spectrophotometer.

Standard Selenium Solution.—Purified metal selenium was first dissolved into a small amount of concentrated nitric acid, and the solution was evaporated to dryness in order to remove any excess nitric acid. Hydrochloric acid was then added to dissolve the residue, and the resulting selenous acid solution was diluted with redistilled water so as to be 0.5~4 μg. selenium per milliliter.

Dithizone Solution.—The concentration of the dithizone-carbon tetrachloride solution was adjusted to be 40~60 μmol./l. As for the purification of dithizone, Iwantscheff's method was employed[2].

Other Reagents.—Redistilled water and distilled ammonium hydroxide were used. The other reagents used were of analytical reagent grade.

Proposed Procedure for Determining Selenium.—Preliminary experiments indicated that selenium can be extracted most favorably from a 6 N hydrochloric acid solution. In general, two ways of colorimetric determination by dithizone are applicable to such metals as can be extracted from acidic media: the so-called mono-color method and the mixed-color method. For the present studies, both methods were examined. The proposed procedures for the mono-color and mixed-color methods will be described separately below. The extraction is carried out from a 6 N hydrochloric acid solution in both cases.

Mono-color Method.—Acidify 5 ml. of a sample solution with the same volume of concentrated hydrochloric acid and shake it thoroughly for two minutes with 5 ml. of a dithizone-carbon tetrachloride solution (60 μmol./l.) in a small separatory funnel. Allow the two phases to separate, and draw off the carbon tetrachloride layer into a 10-ml. measuring flask. Repeat the same extraction procedure with small portions of dithizone until selenium is completely extracted. Finally, wash the aqueous solution with one milliliter of carbon tetrachloride, drawing off the latter into the flask. Dilute the combined extracts in the measuring flask to a definite volume (10 ml.) with carbon tetrachloride, and transfer the solution into a separatory funnel. Wash it with 10 ml. of redistilled water, shaking the funnel for thirty seconds. Draw off the carbon tetrachloride layer into another separatory funnel, and add 10 ml. of dilute ammonium hydroxide (1 : 100) to remove the excess dithizone. Repeat the washing with another portion of ammonium hydroxide, and then determine the extinction of the solution at 420 mμ.

Mixed-color Method.—Acidify 2.5 ml. of a sample solution with the same volume of concentrated hydrochloric acid, and shake it thoroughly in a small separatory funnel for two minutes with 5 ml. of a dithizone solution (45 mol./l.). Allow the two phases to separate, draw off the carbon tetrachloride layer into an absorption cell, and determine the extinction at 410 mμ.

2) G. Iwantscheff, "Das Dithizon und seine Anwendung in der Mikro- und Spurenanalyse", Weinheim/Bergster (1958), p. 60.

Results and Discussion

Absorption Spectra.—The absorption curve of the reagent and the dithizone complex of selenium(IV) in carbon tetrachloride are given in Fig. 1. As may be seen in the figure, the reagent has maximum absorptions at 620 and 450 mμ, while the dithizone complex of selenium has its maximum at 420 mμ. Therefore, extinction measurement may be made at 420 mμ in the mono-color method. As for the mixed-color method, however, it is preferable to measure at 410 mμ, where the absorption by dithizone is rather weak. In fact, in the case of the mixed-color method, it was almost impossible to carry out colorimetric determination at 420 mμ, while good results were obtained at 410 mμ.

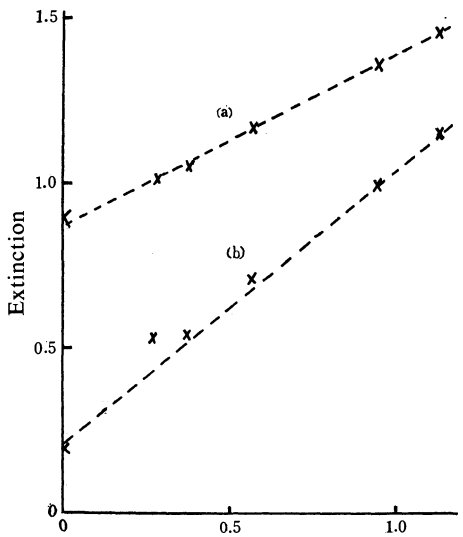

Fig. 2. Calibration curves (referred to carbon tetrachloride)
(a) Mixed-color method (dithizone concentration ~60 μmol./l)
(b) Mono-color method

In the mono-color method, the calibration curve does not cross the origin. This is likely due to some contamination of other metals or decomposition of dithizone during elimination process of excess dithizone.

TABLE I. EXPERIMENTAL ERRORS OF MIXED-COLOR METHOD

Selenium taken μg.	Selenium found μg.	Error %
0.28_2	0.28_4	+ 0.7
0.37_6	0.36_5	− 2.9
0.56_3	0.58_2	+ 3.6
0.93_8	0.93_8	0
1.12_6	1.12_6	0

Table II. Possible interfering metals

Metal	Optimum condition for extraction by dithizone	Metal compounds used in this experiment	λ_{max} of dithizonate in CCl_4, mμ
Cu(II)	pH 2 ~ 4	$CuSO_4$ in H_2O	550
Pd	2 N H_2SO_4	Not tested	640
Ag	pH 2	$AgNO_3$ in H_2O	462
Te(IV)	0.5 N HCl	TeO_2 in HCl	430
Au	2 N H_2SO_4	Not tested	450
Hg(II)	1 N H_2SO_4	$HgSO_4$ in HCl	485
Bi(III)	pH 6	Bi metal in HNO_3	490

Table III. Effect of several interfering metals

Selenium added μg.	Interfering metals present in the aqueous layer	Selenium found under the coexistence of a comparable amount of interfering metal, μg.	Selenium found under the coexistence of a tenfold amount of interfering metal, μg.
0.56_3	Cu(II)	0.70_3	0.91_7
0.56_3	Ag	0.56_3	0.53_9
0.56_3	Te(IV)	0.53_1	0.55_9
0.56_3	Hg(II)	0.68_3	0.53_3
0.56_3	Bi(III)	0.63_7	0.56_9
0.56_3	Cu(II)	0.56_1	—
Preliminary treatment was carried out at pH 7.			
0.56_3	Cu(II), Ag, Te(IV), Hg(II), Bi(III)	0.57_5	—
Preliminary treatment was carried out at pH 2.			

The Calibration Curve and Precision of the Methods.—The calibration curves are given in Fig. 2 for both mono-color and mixed-color methods. Extinction measurements were made at 420 mμ in the mono-color method and at 410 mμ in the mixed-color method. The linearities are good in both cases. The spectrophotometric sensitivity* of the color reaction is, in the mono-color method, 0.001 μg. of selenium in carbon tetrachloride per square centimeters, while it is 0.002 μg. in the mixed-color method.

The experimental errors of the mixed-color method are shown in Table I. From these experimental results, it may safely be said that the proposed mono- and mixed-color methods are both applicable to determining traces of selenium.

Interfering Substances.—The reaction of selenium with dithizone in 6 N hydrochloric acid media is very specific. The substances which would interfere with the determination of selenium with dithizone would include, in the first place, those which oxidize dithizone itself, such

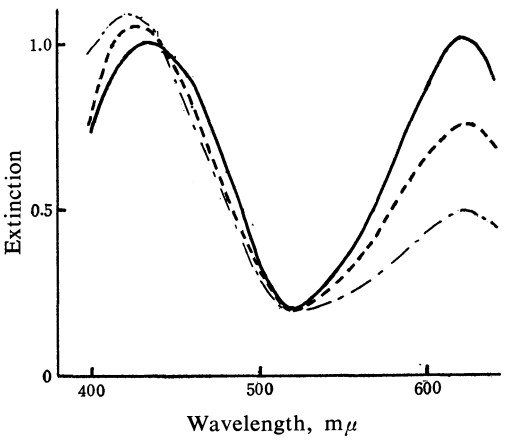

Fig. 3. Changes of absorption curve effected by the presence of copper(II).

—— Absorption curve of dithizone extract of selenium in CCl_4 (0.56 μg. Se/ml. CCl_4).

- - - Absorption curve of dithizone extract when copper(II) is present in the aqueous solution in a comparable amount with selenium.

·—· Absorption curve of dithizone extract when copper(II) is present in the aqueous solution in a tenfold amount of selenium.

* Here, spectrophotometric sensitivity is defined as follows: the number of micrograms of the element, converted to the colored product, which, in a column of solution with a cross section of 1 cm^2, shows an extinction of 0.001. For details, see E. B. Sandell, "Colorimetric Determination of Traces of Metals," Interscience Publishers, New York (1959), p. 83.

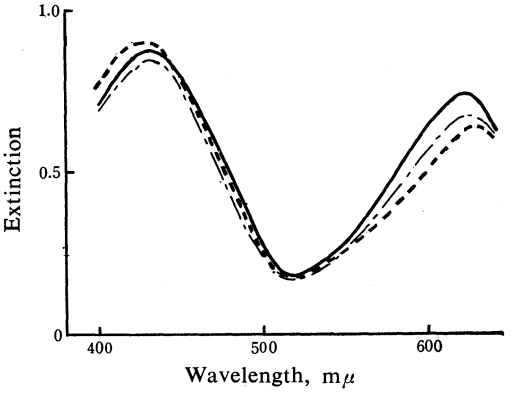

Fig. 4. Changes of absorption curve effected by the presence of mercury(II).

—— Absorption curve of dithizone extract of selenium in CCl_4.
- - - Absorption curve of dithizone extract when mercury(II) is present in the aqueous solution in a comparable amount with selenium.
·—· Absorption curve of dithizone extract when mercury(II) is present in the aqueous solution in a tenfold amount of selenium.

as ferric ion, halogens, nitrous acid, permanganate and so forth. These should be removed, of course, from the reaction system. Some metals which react with dithizone in acidic media, such as copper(II), palladium, silver, tellurium(IV), gold, mercury(II) and bismuth-(III) may possibly be interfering substances (TableII). The interfering action of these metals was investigated expeimentally and is shown in Table III. We paid no attention to palladium and gold, since they are not so abundant in nature.

From Table III we can conclude that tellurium(IV), silver, and bismuth do not essentially interfere with our method even if any of the three exist in amounts of ten times as much as selenium in the sample solution. This seems to be due to the high acidity and/or the high concentration of chloride ions (which may cause the masking effect) in the extraction system. Copper(II) interferes, and mercury(II) may also be considered to interfere. Changes in the absorption curves of the selenium dithizone complex and of dithizone due to the existence of copper(II) or mercury (II) are shown in Figs. 3 and 4.

Separation of Selenium from the Interfering Metals.—We made several tests of selenium extraction with a dithizone solution, using the radioactive isotope ^{75}Se as a tracer, and observed that, for pH values higher than 2, only less than 1.5% of the total amount of selenium is extracted by a 10^{-3} mol./l. dithizone solution. However, a considerable amount of copper(II) is extracted under the same conditions, so it seems probable that we can exclude the interference of copper by extracting it preliminarily from the sample solution. The procedure of selenium determination including such preliminary treatment is as follows:

First, extract copper from the sample solution with dithizone under neutral or slightly acidic media, and then make the aqueous layer approximately 6 N in hydrochloric acid. An example of determining the selenium content in the sample solution, which contains a comparable amount of copper, by such a procedure is shown in Table III. Table III also gives the results obtained from a similar experiment in which the five kinds of interfering metals described above are contained in the sample solution, each in an amount comparable with that of selenium. Both of these examples give good results, and, as we expected, the extraction from 6 N hydrochloric acid solution is found to be really favorable, since even such interfering metals such as copper(II) and mercury(II) can be separated by a simple preliminary treatment.

Molar Extinction Coefficient.—The extinction coefficient of the selenium dithizone complex in carbon tetrachloride was estimated to be about 70×10^3 per mole-centimeter.

Stability of Color.—The stability of color was carefully examined. The experimental results are given in Fig. 5. It may be observed in Fig. 5 that the color of the dithizone extract of selenium is nearly stable when the extract is separated from the aqueous layer (6 N in hydrochloric acid) immediately after shaking, while the color fades away gradually when the organic layer remains in contact with the aqueous one.

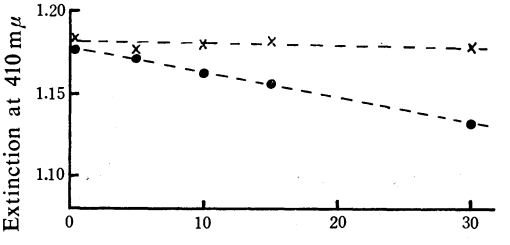

Fig. 5. Stability of color of selenium-dithizone complex in carbon tetrachloride.

×--× Extinction of organic layer which was separated from aqueous layer immediately after shaking.
-•-•-• Extinction of organic layer which has been in contact with aqueous layer after shaking.

Summary

A colorimetric method of determining traces of selenium with dithizone has been studied. Selenium is extracted from a 6 N hydrochloric acid solution with a carbon tetrachloride solution of dithizone almost quantitatively, and the dithizone complex of selenium in carbon tetrachloride has a maximum absorption at the wavelength of 420 mμ. One p. p. m. of selenium can be determined spectrophotometrically, by measuring the extinction at 420 mμ in the mono-color method and at 410 mμ in the mixed-color method.

The errors of these two methods are estimated to be within 3%. Copper(II) and mercury(II) were found to be interfering metals. However, they are easily removed by a preliminary extraction. Finally, attention should be paid to the fact that the color of the dithizone complex of seleium is apt to fade away rapidly when it is left in contact with a 6 N hydrochloric acid solution for some time.

The authors wish to thank Professor Nobufusa Saito, Dr. Yuji Yokoyama and Dr. Hirotoshi Sano for their invaluable advice and comments.

Department of Chemistry
Faculty of Science
The University of Tokyo
Hongo, Tokyo

Asymmetric Hydrogenation with Modified Raney Nickel. II. Studies on Modified Hydrogenation Catalyst. III

By Yoshiharu IZUMI, Masami IMAIDA, Hideaki FUKAWA and Shiro AKABORI

(Received September 24, 1962)

In the previous paper[1], it was reported that R-Ni catalyst treated with L-Glu solution had asymmetric activity on the hydrogenation of some carbonyl compounds to alcohols, and that the activity was much influenced by pH and temperature of Glu solution.

In the present work, asymmetric activity of R-Ni catalyst treated with other sorts of amino acids, that is, *N*-substituted amino acids, hydroxy acids, and L-Glu dissolved in acetate buffer was studied in order to elucidate the mechanism of these asymmetric hydrogenations.

The asymmetric activity of catalyst modified with various amino acids $RCH(NH_2)COOH$ was tested in order to know the effect of substituent (R) on the asymmetric activity of a catalyst. In order to find out the role of the amino residue on the asymmetric activity of a catalyst modified with amino acid, *N*-substituted L-Asp and L-Glu derivatives were used as modifying reagents of the R-Ni catalyst. Since homocysteinic acid is structually analogous to Glu, the asymmetric activity of a catalyst modified with this amino acid was studied for the purpose of elucidating the effect of the structure of a molecule.

In order to elucidate the effect of the carbonyl group on the asymmetric activity of a catalyst modified with Glu, the modification was carried out in the presence of acetic acid. Because, if the asymmetric activity of the catalyst modified with Glu depends on the adsorption of the carbonyl group of Glu, some influence will occur in the presence of the carboxyl group of other acids.

The hydroxy acids were used as a homologue of amino acid used as modifying reagents. Experiments were carried out for the elucidation of the relationship between the absolute configuration of the modifying reagent and that of the hydrogenation product.

Result

In the case of Glu[1], the pH of the modifying solution influenced the asymmetric activity of the catalyst and the great asymmetric activity of the catalyst was obtained near the lower limit of the pH jump of neutralization curve of Glu. The neutralization curve of acidic substances, *N*-substituted L-Asp and L-Glu, D-tartaric acid, L-malic acid et al., were measured with sodium hydroxide solution. The lower and the upper limits of the pH jump of the neutralization curve of these substances

1) H. Fukawa, Y. Izumi, S. Komatsu and S. Akabori, This Bulletin, 35, 1703 (1962); Y. Izumi, M. Imaida, H. Fukawa and S. Akabori, ibid., 36, 21 (1963).

are shown in Table I. Thus the R-Ni catalyst was modified near the neutralization point of each substance and its asymmetric activity was tested.

Treatment with Several Amino Acids.—One and a half unit* of the R-Ni catalyst was treated with solutions of several amino acids as shown in Table II for 1.5 hr.

The asymmetric activity of the catalyst was tested in the hydrogenation of 17.0 g. of methyl acetoacetate to methyl 2-hydroxybutyrate at 60°C. The relationship between the asymmetric activity of the catalyst and modifying temperature is shown in Fig. 1.

From these results, amino acids could be divided into the following two groups.

The catalyst treated with L-Ala, L-Ser, L-Cystine, L-Thr and L-Pro at 0°C produced predominantly methyl D-2-hydroxybutyrate and the L-form contents of the reduced products increased according to the increase of the temperature of treatment. These amino acids

TABLE I. NEUTRAL POINT OF MODIFYING REAGENT

Modifying reagent	pH jump	Lower limit	Upper limit
N-Cyanoethyl-L-Asp.	First step	4.5	5.5
	Second step	9.0	11.0
N-Cyanoethyl-L-Glu.	First step	5.0	6.5
	Second step	9.0	11.0
N, *N*-Dimethyl-L-Glu.		5.5	8.0
N-Acetyl-L-Glu.		6.0	10.5
N-Benzyl-L-Glu.		6.0	10.0
D-Tartaric acid		5.0	11.0
L-Malic acid		6.0	11.0
L-Homocysteinic acid		4.0	8.0

TABLE II. MODIFYING SOLUTION OF AMINO ACID

No.	Amino acid (g.)	Water ml.	pH observed
1	L-Alanine (2.7)	225	7.20
2	L-Serine (3.0)	225	6.60
3	L-Threonine (4.5)	225	6.12
4	L-Proline (3.5)	225	8.10
5	L-Cystine (0.1)	400	7.80
6	L-Tryptophan (6.0)	300	7.00
7	L-Phenylalanine (4.5)	225	7.05
8	L-Aspartic acid (4.5)	225	4.65
9	L-Valine (4.5)	225	6.00
10	L-Isoleucine (4.5)	225	6.30
11	L-Leucine (4.5)	225	7.32
12	L-Methionine (4.5)	225	6.90
13	L-Arginine (5.0)	225	10.80
14	L-Tyrosine (1.0)	225	7.02
15	L-Lysine·HCl (5.0)	225	7.02
16	L-Histidine·HCl (6.0)	225	4.20

* One unit of R-Ni was prepared from 1.0 g. R-Ni alloy by the method described in the previous paper[1].

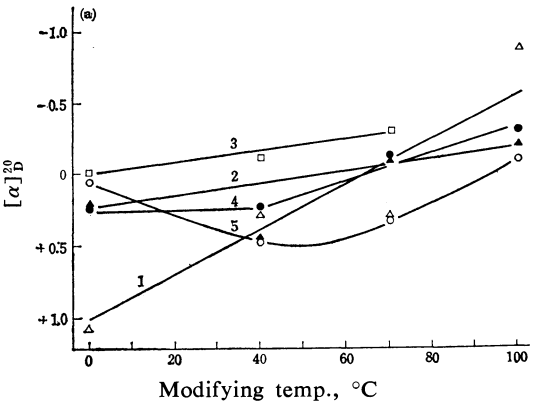

Fig. 1 (a).

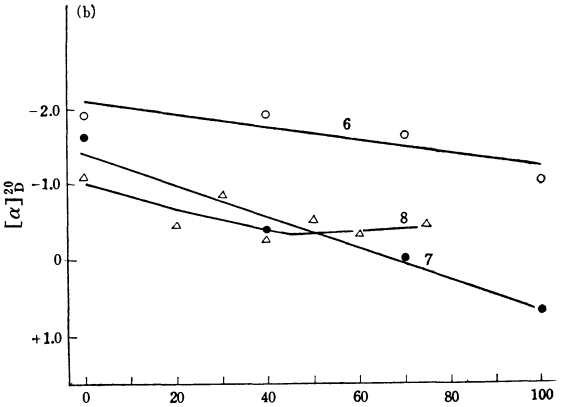

Fig. 1 (b).

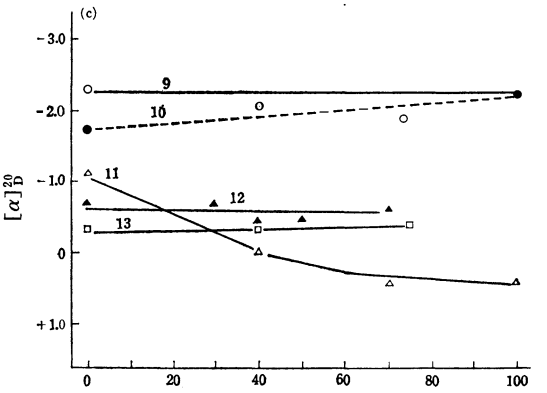

Fig. 1 (c).

1. L-Alanine
2. L-Serine
3. L-Threonine
4. L-Proline
5. L-Cystine
6. L-Tryptophan
7. L-Phenylalanine
8. L-Aspartic acid
9. L-Valine
10. L-Isoleucine
11. L-Leucine
12. L-Methionine
13. L-Arginine
14. L-Tyrosine
15. L-Lysine·HCl
16. L-Histidine·HCl

belong to the amino acids of which the L-form has a sweet taste. Modification by amino acids other than the amino acids mentioned above resulted in giving the catalyst which produces predominantly methyl L-2-hydroxybutyrate at 0°C. Some of the catalysts modified at higher temperature increased the content of the D-form of reduced products as in the case of modification by L-Glu.

L-Met and L-Cys are probably desulfurized by R-Ni during the treatment, so it was omitted from consideration.

The asymemtric activity of the catalyst modified by L-Tyr, L-Lys and L-His are shown in Table III. When the hydrochlorides of L-Lys and L-His were used as the modifying reagents at higher temperature, the chloride anion brought about a remarkable depression of hydrogenation activity of the catalyst; therefore, the asymmetric activity of the catalyst could not be measured.

TABLE III. EFFECT OF THE MODIFYING TEMPERATURE

Modifying reagent	Modifying temp., °C	$[\alpha]_D^{20}$ of Me 2-hydroxybutyrate
L-Tyr	100	−0.50
L-Lys (HCl)	0	−1.45
L-Lys (HCl)	40	−1.42
L-His (HCl)	0	−0.04

(Catalyst modified with amino acid)

Because of the lower solubility of L-Tyr, the effect of temperature on the asymmetric activity could not be measured at a lower modifying temperature.

***N*-Substituted L-Asp and L-Glu Derivatives.**— One and a half unit of the R-Ni catalysts were modified in the neighborhood of the pH jumps of the modifying reagents under the conditions shown in Table IV and the results are shown in this table.

TABLE IV. MODIFYING CONDITION WITH ACIDIC MODIFYING REAGENT

R-Ni (unit)	Modifying reagent, g.	Conditions of treatment				Substrate Me acetoacetate g.	$[\alpha]_D^{20}$ of Me 2-hydroxybutyrate
		pH	Solvent ml.	Temp. °C	Time hr.		
1.5	*N*-Cyanoethyl-L-Asp. (2.0)	3.91	100	0	1.5	17	−0.14
1.5	*N*-Cyanoethyl-L-Asp. (2.0)	4.60	100	0	1.5	17	−0.08
1.5	*N*-Cyanoethyl-L-Asp. (2.0)	6.80	100	0	1.5	17	0
1.5	*N*-Cyanoethyl-L-Asp. (2.0)	8.04	100	0	1.5	17	−0.16
1.5	*N*-Cyanoethyl-L-Asp. (2.0)	8.48	100	0	1.5	17	0
1.5	*N*-Cyanoethyl-L-Asp. (2.0)	10.80	100	0	1.5	17	+0.03
1.5	*N*-Cyanoethyl-L-Asp. (2.0)	8.46	100	100	1.5	17	0
1.5	*N*-Cyanoethyl-L-Glu. (2.0)	4.70	100	0	1.5	17	−0.10
1.5	*N*-Cyanoethyl-L-Glu. (2.0)	6.44	100	0	1.5	17	−0.16
1.5	*N*-Cyanoethyl-L-Glu. (2.0)	8.08	100	0	1.5	17	−0.20
1.5	*N*-Cyanoethyl-L-Glu. (2.0)	9.19	100	0	1.5	17	−0.26
1.5	*N*-Cyanoethyl-L-Glu. (2.0)	9.17	100	100	1.5	17	−0.18
1.5	*N*,*N*-Dimethyl-L-Glu. (2.0)	5.01	100	0	1.5	17	−0.75
1.5	*N*,*N*-Dimethyl-L-Glu. (2.0)	5.59	100	0	1.5	17	−0.72
1.5	*N*,*N*-Dimethyl-L-Glu. (2.0)	5.02	100	100	1.5	17	−0.40
1.5	*N*-Benzoyl-L-Glu. (2.0)	5.60	100	0	1.5	17	+0.15
1.5	*N*-Benzoyl-L-Glu. (2.0)	4.90	100	100	1.5	17	−0.33
1.5	*N*-Benzoyl-L-Glu. (2.0)	5.55	100	100	1.5	17	−0.67
1.5	L-Homocysteinic A. (2.0)	7.10	100	0	1.5	17	−0.15
1.5	L-Homocysteinic A. (2.0)	7.10	100	100	1.5	17	+0.15
1.5	L-Homocysteinic A. (2.0)	3.90	100	0	1.5	17	−0.23
1.5	L-Homocysteinic A. (2.0)	3.90	100	100	1.5	17	+0.19
1.5	L-Malic A. (2.0)	4.08	100	0	1.5	17	+1.85
1.5	L-Malic A. (2.0)	5.22	100	0	1.5	17	+2.35
1.5	L-Malic A. (2.0)	5.52	100	0	1.5	17	+2.20
1.5	L-Malic A. (2.0)	5.70	100	0	1.5	17	+1.95
1.5	L-Malic A. (2.0)	6.30	100	0	1.5	17	+1.68
1.5	L-Malic A. (2.0)	5.39	100	100	1.5	17	+4.57
1.5	L-Malic A. (2.0)	5.61	100	100	1.5	17	+4.70

TABLE V. EFFECT OF ACETIC ACID

No.	R-Ni (unit)	Conditions of modification: 5 M Acetate buffer (pH 5.0) ml.	Temp. °C	2% L-Glu (pH 5.0)	Time hr.	Substrate (Me acetoacetate), g.	$[\alpha]_D^{20}$ of Me 2-hydroxybutyrate
1	1.5	none	0	225	1.5	17	−3.51
2	1.5	5*	0	25	1.5	17	−1.99
3	1.5	5**	0	225	1.5	17	−2.50
4	1.5	50**	0	225	1.5	17	−2.62

* Treated with acetate buffer and then modified with Glu solution.
** Treated with mixture of acetate buffer and Glu solution.

TABLE VI. MODIFYING CONDITION WITH HYDROXY ACID

No.	R-Ni (unit)	Modifying reagents g.	Conditions of treatment: pH	Water ml.[3]	Temp. °C	Time hr.	Substrate (Me Acetoacetate. g.
1	1.5	D-Tartaric A. (2.0)	**2.1～12.3**[1]	100～130	0	1.5	17.0
2	1.5	D-Tartaric A. (2.0)	**4.4～5.9**[1]	130	100	1.5	17.0
3	1.5	D-Tartaric A. (2.0)	5.1～5.2	125	**0～100**[1]	1.5	17.0
4	1.5	D-Tartaric A. (2.0)	5.1～5.2	125	100	**0.1～2.5**[1]	17.0
5	1.5	D-Tartaric A. (**0.015～20.0**)[1]	5.1～5.2	100～360	100	1.5	17.0
6	1.5	L-Malic A. (2.0)	**4.1～6.3**[1]	114～129	0	1.5	17.0
7	1.5	L-Malic A. (2.0)	**5.4～5.6**[1]	127	100	1.5	17.0
8	1.5	Diethyl-L-tartarate (2.0)	—[2]	100[2]	—[4]	1.5	17.0

1) Effect of these conditions is discussed in the other.
2) Ethanol, pH was not measured.
3) pH was adjusted with 1 N NaOH exactly, so total volume of the modifying solution varied with the amount of the modifying reagent.
4) R-Ni was treated under reflux.

These results show that asymmetric activity of the catalyst has no close correlation with basicity of the nitrogen of the modifying reagent, but is much influenced by the steric effect of the substituent.

Homocysteinic Acid $HOOCCH_2CH_2CH(NH_2)\cdot SO_3H$.—The conditions for the preparation of the catalyst and the results are shown in Table IV. Asymmetric activity of this catalyst is much less than that prepared with Glu. But other characteristics of these catalysts resemble each other.

Effect of Acetic Acid on the Modification with Glu.—When the catalyst was prepared by the treatment with Glu in acetate buffer, the asymmetric activity of the catalyst was less, as compared with that treated without acetic acid, as shown in Table V.

Hydroxy-carboxylic Acid.—The modification of the catalsyt with hydroxy carboxylic acid was carried out with the solution shown in Table VI.

1) D-Tartaric Acid. — *Effect of pH (Table VI-No. 1, 2).*—The relation between the pH of the modifying solution and the asymmetric activity of catalyst at 0°C is shown by curve 1 in Fig. 2 and the neutral point is shown in Table I.

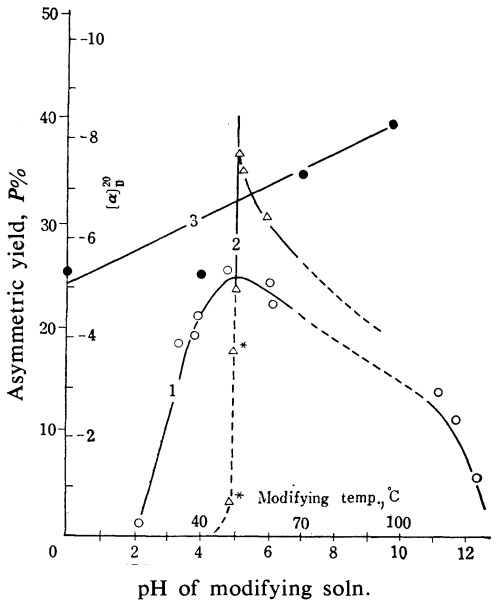

Fig. 2. Effect of modifying pH and temperature.
1 -○- Effect of modifying pH at 0°C
2 -△- Effect of modifying pH at 100°C
3 -●- Effect of modifying temperature
* Calculated value

When the catalyst was treated at 100°C below pH 5.0, the catalyst distinctly decreased its hydrogenating and asymmetric activities as can be seen from curve 2 in Fig. 2.

Effect of Temperature (Table VI-No. 3).— When the temperature of treatment rose, the asymmetric activity increased as shown by curve 3 in Fig. 2. The pH of the modifying solution moved towards alkaline after treatment at higher temperature.

Effect of Temperature (Table VI-No. 4). — The asymmetric activity of catalysts at various immersion time are presented in Fig. 3. The activity became almost constant in 30 min. and one and a half hours is sufficient to gain the constant asymmetric activity.

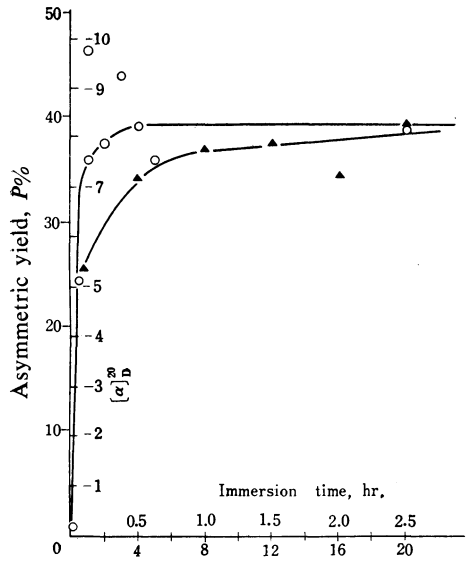

Fig. 3. Effect of concentration of modifying solution and immersion time of catalyst.
-○- Effect of amount of tartaric acid
-▲- Effect of immersion time

Effect of the Concentration of Modifying Solution (Table VI-No. 5).—Effect of the concentration of modifying solution on the asymmetric activity of a catalyst was tested by the treatment with the solution which contained various amounts of tartaric acid. The results are shown in Fig. 3. The constant aymmetric activity was gained when the catalyst was treated with solutions of the concentration above 1.0 per cent. The lowest limit of the concentration is much higher than that of Glu, because tartaric acid has less buffer action than Glu.

2) L-Malic Acid (Table VI-No. 6, 7). — In the case of L-malic acid the greatest asymmetric activity was obtained on the treatment with the solution near its pH jump, as shown in Table I. The asymmetric activity of the catalyst treated at 100°C was greater than that treated at 0°C. The asymmetric activity of this catalyst was about a half of that of the catalyst treated by tartaric acid under the same condition as shown in Table IV.

Discussion

From the results of the three reports of this series[1], it is concluded that asymmetric catalysts are obtained by contacting R-Ni with the solution containing asymmetric compounds.

The modifying reagents used in the experiments must have the substituents of high affinity to nickel, such as $-NH_2$, $-COOH$ and $-OH$ groups at the asymmetric center. With amino acid $RCH(NH_2)COOH$ which have residues (R) possessing higher affinity to nickel gave catalysts of higher asymmetric activity.

Absolute configuration of methyl 2-hydroxybutyrate was affected by the structure of amino acid which was used to modify the R-Ni. The catalysts modified at 0°C with the L-amino acids of small molecular size (sweet taste) predominantly produce the D-form of hydrogenation products, while with L-amino acids of large molecular size (no sweet taste) predominantly produce L-form products.

The *N*-substituted amino acid, acyl, dimethyl or cyanoethyl derivatives, produce much less asymmetric activity of the catalyst. From this evidence, $-NH_2$ residue might greatly participate in making the asymmetric center of the catalyst. From the results described above it could be concluded that the lone pair of nitrogen atom in amino residue must touch on the surface of the catalyst to make asymmetric center.

The treatment with malic acid and tartaric acid cause the powerful asymmetric activity of the catalyst, but the treatment with diethyl tartrate does not. The catalyst treated with Glu dissolved in acetate buffer has much less asymmetric activity than that treated with aqueous Glu solution. These facts show that, with amino or hydroxy acid, the carboxyl group is important to make the asymmetric center on R-Ni. These facts also agree with the results reported by Welch[2] et al. who describe that ester is slightly adsorbed and two different fatty acids are competitively adsorbed by the R-Ni catalyst.

Asp and malic acid resemble each other in the structure, but the asymmetric activity of a catalyst treated with Asp is considerably smaller than that of a catalyst treated with

2) C. M. Welch, H. A. Smith and J. B. Cole, *J. Phys. Chem.*, **65**, 705 (1961).

malic acid. The same relation is found in homocysteinic acid and Glu. The asymmetric activity of a catalyst treated with tartaric acid is much higher than that of a catalyst treated with malic acid. This result corresponds to that tartaric acid and malic acid are 170 and 135 in molecular weight and have two and one active center, respectively. So far as the Stuart's model is used for consideration, it is assumed that these differences depend on whether the molecules on the modifying reagents can attach to the surface of R-Ni without any steric hindrance or not.

Absolute configuration of D-tartaric acid opposed to that of L-malic acid, and the optical rotation of methyl 2-hydroxybutyrate which was produced by the hydrogenation of methyl acetoacetate in the presence of the catalyst treated with these acids, opposed each other. L-Asp and L-malic acid have the same absolute configuration, but the asymmetric activity of a catalyst treated with these reagents have opposit asymmetric activity. From these results, it seems that there are some differences of structure between the asymmetric center of catalysts produced with amino acids and hydroxy acids.

Moreover, the fact that L-Pro produces slightly asymmetric activity is a clear evidence that the asymmetric center of hydrogenation can not be produced by the two-points attachment with carboxyl and amino groups. If this center is produced by the two points-attachment the pyrrolidin ring must stand up outside of the R-Ni surface and a strong steric effect must be produced.

It is concluded that the following two considerations are required for producing the asymmetric activity of R-Ni.

1) R-Ni must adsorb the asymmetric compounds which contain three substituents with affinity to Ni.

2) In order to obtain higher asymmetric activity of the catalyst, it is essential that the molecules of modifying reagents are adsorbed on the R-Ni easily and tightly.

Experimental

Preparation of the catalyst, hydrogenation of methyl acetoacetate and measurement of asymmetric yield were carried out in the same manner as described in the previous paper[1].

Modification of the Catalyst.—The R-Ni catalyst was modified under the conditions shown in Tables IV and VI. The procedure is quite similar to the modification with Glu which was described in the previous paper. The aqueous solution which contained acidic modifying reagent was neutralized with 1 N sodium hydroxide solution and adjusted to a suitable pH.

Effect of Acetic Acid. — *Experiment No. 2 in Table V.* — One and a half unit of R-Ni catalyst treated with 5 M acetate buffer (pH 5.0) at 0°C for 10 min., washed with 50 ml. of cold water, then was modified with 25 ml. of 2% Glu at 0°C for 1.5 hr. as usual method.

Experiment No. 3 and 4 in Table V.—One and a half unit of R-Ni catalyst was modified with the solution containing 225 ml. of 2% Glu which was adjusted to pH 5.02 and 5 ml. (or 50 ml.) of 5 M acetate buffer (pH 5.0) at 0°C for 1.5 hr.

Summary

1) The asymmetric R-Ni catalysts were prepared by the treatment of R-Ni with various asymmetric compounds, and the asymmetric activity of a catalyst was measured by the hydrogenation of methyl acetoacetate

2) Optical rotatory direction and power of the reduced product was affected both by the configuration and molecular size of amino acid which was used as modifying reagent.

3) The asymmetric activity of catalysts treated with *N*-substituted amino acids, *N*-acyl, *N*-dimethyl and *N*-cyanoethyl derivatives of Glu and Asp, were much less than the activity of the catalyst treated with the corresponding amino acids.

4) The asymmetric activity of the catalyst treated with D-tartaric acid and L-malic acid was tested at various conditions. The asymmetric yield in the hydrogenation of methyl acetoacetate in the presence of the catalyst treated with D-tartaric acid solution of pH 5.1 ~5.2 at 100°C was about 45 percent.

This research was made possible through a support of Raney-Nickel alloy by Kawakami Institute Ltd. Co., Tokyo. The authors are indebted to the company for this fellowship.

Division of Organic Chemistry
Institute for Protein Research
Osaka University
Kita-ku, Osaka

*The Absolute Configuration of (−)-N, N-Dimethyl-1, 2-diphenylethylamine and its Analgesic Activity**

By Masao NAKAZAKI, Itaru MITA and Nobuo TOSHIOKA

(Received October 1, 1962)

The (−)-antipode of *N*, *N*-dimethyl-1, 2-diphenylethylamine (Ia) derived from (−)-1, 2-diphenylethylamine (Ib) has been found to possess 1/2∼1/3 the analgesic activity of morphine, whereas the (+)-enantiomer shows negligible activity[1]. This is but one of numerous instances[2,3] in which only one optical active antipode of a compound is physiological efficacious. In this paper, the determination of the absolute configuration of the (−) analgesic Ia is reported.

Acetylation of (−)-1, 2-diphenylethylamine (Ib) gave (+)-*N*-acetyl-1, 2-diphenylethylamine (Ic), which was exhaustively ozonized; the reaction mixture was oxidized with peracetic acid. Upon working up the reaction mixture,

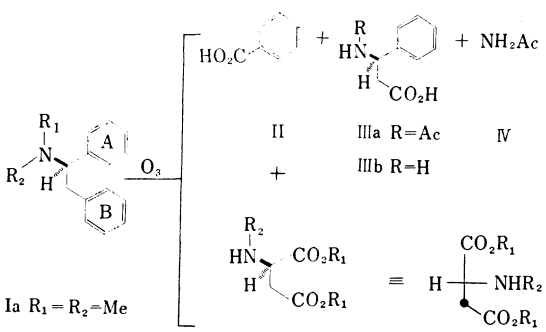

Ia $R_1=R_2=Me$

Ib $R_1=R_2=H$

Ic $R_1=H, R_2=Ac$

Va $R_1=Me, R_2=Ac$

Vb $R_1=R_2=H$

Vc $R_1=H$, $R_2=Bz$

benzoic acid II and (+)-2-acetylamino-2-phenylpropionic acid (IIIa) were isolated and identified, IIIa being then further hydrolyzed to (+)-2-amino-2-phenylpropionic acid (IIIb).

Treatment of the mother liquor of II and IIIa with diazomethane, followed by distillation in vacuo, afforded acetamide IV and dimethyl *N*-acetylaspartate (Va), which was then hydrolyzed with diluted sulfuric acid. The reaction mixture, freed from sulfate ions, was subjected to paper chromatography (methanol: conc. aq. ammonia=3:1). Only a single spot of aspartic acid (R_f 0.24), and no spot corresponding to phenylalanine (R_f 0.63) nor to glycine (R_f 0.46), was detected. This indicates that the carbon atom to which the phenyl and acetamino groups are attached is vulnerable to oxidation and that the B ring is oxidized preferentially to the A ring, probably for steric reasons. The sulfate-free filtrate was concentrated to afford D-aspartic acid (Vb) (decomp. p. 320°C, $[\alpha]_D^{20}$ −23.2° (*c* 1.9 in 1 N hydrochloric acid)), the infrared absorption spectrum of which was superimposable on that of natural L-aspartic acid (decomp. p. 320°C, $[\alpha]_D^{21}$ +23.4° (*c* 2.2 in 1 N hydrochloric acid)).

The identity was further checked by preparing benzoyl-D-aspartic acid (Vc), which gave a racemic compound (with one mole of water of crystallization; m. p., 162∼165°C, after drying at 115°C) with enantiometric benzoyl-L-aspartic acid.

These findings established the (R)-configuration of analgesic active (−)-*N*, *N*-dimethyl-1, 2-diphenylethylamine (Ia)[4]. Inspection of a molecular model of Ia reveals a close stereochemical resemblance with natural (−)-morphine (VI)[5,6].

Since the A and B rings of morphine are almost perpendicular to each other, Ia might be expected to take an analogous eclipsed conformation VII, rather than the energetically favorable conformation VIII, in approaching some reactive surface in the nervous system. A recent observation[7] seems to support this assumption. Neither of the enantiomers of 9-dimethylamino-9, 10-dihydrophenanthrene (IX), in spite of their close resemblance to Ia, show any pronounced analgesic activity.

The reason for this may lie in the fact that

* For a preliminary account of this work, see M. Nakazaki, *Chem. & Ind.*, **1962**, 1577.

1) K. Ogiu, H. Fujimura and Y. Yamakawa, *J. Pharm. Chem. Soc. Japan*, **80**, 283 (1960).

2) H. Brockmann, "Das Biologische Verhalten Stereoisomerer Verbindungen", in K. Freudenberg, "Stereochemie", Franz Deuticke, Leipzig and Wien (1933), p. 920.

3) A. H. Beckett, "Stereochemical Factors in Biological Activity", in E. Jucker, "Progress in Drug Research", Vol. 1, Birkhauser Verlag, Basel and Stuttgart (1959).

4) This correlation also established the (R)-configuration of IIIa and IIIb.

5) K. Kalvoda, P. Buchschacher and O. Jeger, *Helv. Chim. Acta*, **38**, 477 (1955).

6) K. Goto and I. Yamamoto (*Proc. Japan Acad.*, **33**, 477 (1957)) prepared (+)-morphine and showed its analgesic inactivity.

7) M. Hori, Y. Abe, Y. Yamakawa and H. Fujimura, *Ann. Proc. Gifu Pharm. College*, **8**, 65 (1958).

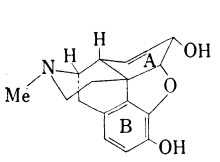

VI

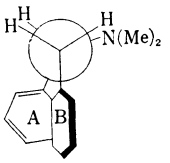

VII

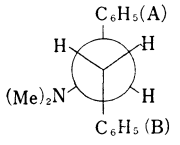

VIII

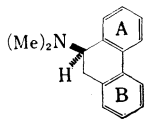

IX

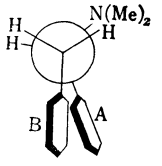

X

IX can not have a conformation in which the A and B rings are perpendicular to each other due to the linkage between two benzene nuclei (projection formula X).

Experimental

(+)-Tartarate of (—)-1, 2-Diphenylethylamine.—The (+)-tartarate of (−)-Ib was recrystallized from diluted acetic acid to give crystals; m. p., 229~230°C (decomp.), $[\alpha]_D^{19}$ −55.3° (*c* 0.92 in water)[8].

(—)-1, 2-Diphenylethylamine (Ib).—Into a solution of 10 g. of sodium hydroxide in 100 cc. of water was added 25 g. of (+)-tartarate of (−)-1,2-diphenylethylamine; the milky emulsion was then extracted with ether. After being washed with a saturated sodium chloride solution and dried over potassium hydroxide pellets, the solvent was removed to afford a pale yellow oil, which distilled at 122~124°C/3 mmHg and weighed 18.1 g. $[\alpha]_D^{19}$ −51.2° (*c* 3.7 in ethanol).

(+)-*N*-Acetyl-1, 2-diphenylethylamine (Ic).—To a solution of 16 g. of Ib in 30 cc. of ether, 10 g. of acetic anhydride in 35 cc. of ether was added. After the crystals which had precipitated were filtered (19 g.) and washed with ether, these were recrystallized from ethanol to give Ic (m. p., 166~167°C), which weighed 16.4 g. $[\alpha]_D^{18}$ +35.7° (*c* 1.5 in acetic acid).

Found: C, 80.5; H, 7.4. Calcd. for $C_{16}H_{17}ON$: C, 80.30; H, 7.16%.

Exhaustive Ozonolysis of (+)-*N*-Acetyl-1, 2-diphenylethylamine (Ic).—A stream of ozone (about 2%) was passed into a solution of 10 g. of Ic in 90 cc. of acetic acid at 19°C for 39 hr., during which time 8.5 cc. of water was added twice. After 10 cc. of 30% hydrogen peroxide had been added, the reaction mixture was allowed to stand for 24 hr. at room temperature. The solution was then warmed on a water bath for 2 hr., and the excess hydrogen peroxide was destroyed by heating the solution with a small amount of palladium on a carbon catalyst.

To remove the acetic acid, 20 cc. of water was added, and the aqueous solution was concentrated at reduced pressure. This process was repeated three times. When the viscous pale yellow residue was dissolved in 20 cc. of water and kept at room temperature, 0.2 g. of leaflets precipitated; these were recrystallized from water to give crystals (m. p., 120~121°C). Their identity with benzoic acid was established by mixed melting point determination with an authentic specimen. When the filtrate from benzoic acid was again concentrated, 0.3 g. of prismatic crystals precipitated; these were identified as (+)-2-acetylamino-2-phenylpropionic acid (IIIa) (vide infra). The filtrate was concentrated again at reduced pressure. The viscous yellow residue (7.5 g.) was dried in a vacuum desiccator over concentrated sulfuric acid overnight to give a glassy solid (7.0 g.), which was then dissolved in 40 cc. of methanol and treated with 140 cc. of an ether solution of diazomethane prepared from 14 g. of nitrosomethylurea. After being kept at room temperature for 3 hr., the excess diazomethane was destroyed with 10 drops of acetic acid, and a small amount of fluffy material was removed by filtration. Removal of the solvent gave a viscous dark red liquid (6 g.) which was distilled at 0.01 mmHg to give 0.1 g. of a sublimate on the wall of the receiver. This sublimate was collected and recrystallized from benzene to give crystals (m. p., 75~78°C) which were identified as acetamid by mixed melting point determination with an authentic specimen.

The main fraction consisted of a viscous yellow oil[9] (b. p., 100~125°C/0.01 mmHg), which weighed 3.5 g. This oil (1.30 g.) was refluxed with 15 cc. of 2.07 N sulfuric acid for 3 hr. and the sulfate ion was removed by adding 82.5 cc. of 0.38 N barium hydroxide (pH 3.4). The barium sulfate was removed by centrifuging and washed with water twice. The filtrate and washings were then combined and filtered through a layer of a Hyflo super cell. The clear solution was concentrated to give 0.199 g. of crystals; further concentration of the mother liquor gave the second crops, 0.27 g. The combined crystals were recrystallized from water to afford 0.405 g. of crystals, which decomposed at 320°C (in a sealed capillary). $[\alpha]_D^{20}$ −23.2° (*c* 1.9 in 1 N hydrochloric acid). Their infrared absorption spectrum in Nujol was found to be superimposable on that of authentic natural L-aspartic acid, $[\alpha]_D^{21}$ +23.4° (*c* 2.2 in 1 N hydrochloric acid).

Found: C, 36.1; H, 5.5; N, 10.5. Calcd. for $C_4H_7O_4N$: C, 36.09; H, 5.30; N, 10.52%.

Benzoyl-D-aspartic Acid (Vc).—The above-mentioned D-aspartic acid (0.198 g.) obtained from Ic was dissolved in 3.3 cc. of water and benzoylated with 1.1 g. of sodium hydrogen carbonate and 0.6 g. of benzoyl chloride, according to Fischer's procedure[10], to give 0.160 g. of needles after recrystallization from water (m. p., 178~179°C, $[\alpha]_D^{18}$

8) R. Söderquist (*J. prakt. Chem.*, (2) **101**, 297 (1921)) reported the following physical constants: (−)-Ib, b. p., 159°C/9 mmHg, $[\alpha]_D^{15}$ −11.80°; (+)-tartarate, m. p., 220~221°C, $[\alpha]_D^{20}$ −43°; the acetyl derivative of (+)-amine prepared by resolution via the (−)-malate, m. p., 168.5°C, $[\alpha]_D^{20}$ −15° (*c* 0.66 in ethanol).

9) E. Hardegger and H. Braunschweiger (*Helv. Chim. Acta*, **41**, 1125 (1961)) obtained dimethyl *N*-acetyl-L-aspartate (b. p., 160~169°C, high vacuum; m. p., 60~61°C, $[\alpha]_D$ −13.4°,) by the exhaustive ozonolysis of *N*-acetyl-L-tryptophane.

$-26.9°$ (c 1.49 in 0.1 N potassium hydroxide)). Their infrared absorption spectrum (in Nujol) was found identical with that of benzoyl-L-aspartic acid (m. p., 180~181°C, $[\alpha]_D^{19}$ $+27.7°$ (c 2.2 in 0.1 N potassium hydroxide)) prepared from natural L-aspartic acid.

Found: C, 55.5; H, 4.9; N, 6.1. Calcd. for $C_{11}H_{11}O_5N$: C, 55.69; H, 4.67; N, 5.91%.

Racemic Benzoyl-aspartic Acid. — A mixture of the same amount (49 mg.) of benzoyl-D-aspartic acid obtained from the ozonolysis of Ic and authentic benzoyl-L-aspartic acid was recrystallized from water to give the racemic compound with one mole of water of recrystallization[10].

Found: C, 52.0; H, 5.0; N, 5.5. Calcd. for $C_{11}H_{13}O_6N$: C, 51.76; H, 5.13; N, 5.49%.

Anhydride obtained by drying at 115°C for 1 hr. at reduced pressure melted at 162~163°C[10].

(+)-2-Acetylamino-2-phenylpropionic Acid (IIIa). —The prismatic crystals obtained from the reaction mixture of ozonolysis of Ic (vide supra) was recrystallized from water to give prisms (m. p., 193~195°C, $[\alpha]_D^{21}$ $+75.0°$ (c 1.48 in 0.1 N potassium hydroxide), $[\alpha]_D^{21}$ $+116.2°$ (c 0.28 in ethanol)) whose infrared absorption spectrum was found to be superimposable on that of racemic 2-acetylamino-2-phenylpropionic acid (m. p. 162~165°C), prepared according to Posner's procedure[11] and recrystallized from diluted aqueous dimethylformamide[11].

Found: C, 63.7; H, 6.6; N, 7.0. Calcd. for $C_{11}H_{13}O_3N$: C, 63.75; H, 6.32; N, 6.76%.

(+)-2-Amino-2-phenylpropionic Acid (IIIb). — A mixture of 0.23 g. of IIIa and 4.2 cc. of 10% hydrochloric acid was refluxed for 2 hr. After 10.90 cc. of 0.1 N potassium hydroxide had been added, the solution was concentrated at reduced pressure to precipitate crystals which were recrystallized from 4 cc. of water to afford 0.09 g. of crystals (m. p., 221°C, $[\alpha]_D^{20}$ $+9.5°$ (c 1.07 in water))[12]. The crystals' infrared absorption spectrum (in Nujol) showed almost the same pattern as racemic 2-amino-2-phenylpropionic acid[13] (decomp. p., 221°C), but a slight discrepancy was observed.

Found: C, 65.3; H, 6.8; N, 8.7. Calcd. for $C_9H_{11}O_2N$: C, 65.44; H, 6.71; N, 8.48%.

A part of the cost of this research was defrayed by a grant-in-aid for Fundamental Scientific Research from the Ministry of Education, to which the authors' thanks are due.

Department of Chemistry
Osaka City University
Kita-ku, Osaka

10) E. Fischer (*Ber.*, **32**, 2451 (1899)) reported for benzoyl-L-aspartic acid: m. p., 180~181°. $[\alpha]_D^{18}$ $-26.9°$ (c 9.56 in the presence of 2 mol. of potassium hydroxide), and for racemic benzoyl-aspartic acid (without water of crystallization): m. p., 161~162°C.

11) T. Posner (*Ber.*, **38**, 2320 (1905)): m. p., 161~162°C from ethanol or acetic aicd.

12) E. Fischer, H. Scheibler and R. Groh (*Ber.*, **43**, 2020 (1910)) resolved racemic 2-formylamino-2-phenylpropionic acid with the aid of its quinine and quinidine salts: (+)-formyl compound (m. p., 142~143°C, $[\alpha]_D^{20}$ $+115.2°$ (c 8.2 in ethanol)) gave (+)-2-amino-2-phenylpropionic acid, m. p., 224~235°C (decomp.), $[\alpha]_D^{20}$ $+6.9°$ (c 1.09 in water). They did not prepare the optical active acetyl derivative.

13) Prepared according to the procedure of R. E. Steiger, "Organic Syntheses", Coll. Vol. III (1955), P. 91.

The Tracer Study of the Reactions of Diphenyl Sulfone and Diphenyl Sulfoxide with Sulfur

By Shigeru OAE and Shunichi KAWAMURA

(Received October 18, 1962)

Many years ago, Krafft and Vorster[1] obtained diphenyl sulfide and sulfur dioxide (Eq. 1) when they heated diphenyl sulfone with sulfur in nitrogen atmosphere. They also performed many other thermal reactions between organic sulfur compounds and sulfur or selenium. Among their observations an especially interesting reaction is that between diphenyl sulfone and selenium as expressed by Eq. 2, because the displacement of SO_2 group in the sulfone with elemental selenium

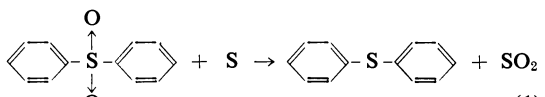

(1)

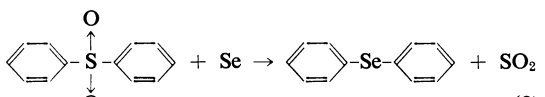

(2)

may imply that a similar replacement of sulfur atom of diphenyl sulfone with elemental sulfur is taking place in the reaction.

1) F. Krafft and Vorster, *Ber.*, **26**, 2813 (1893).

TABLE I. REACTIONS OF ORGANIC SULFUR COMPOUNDS WITH SULFUR

	Original	Sulfide (after converted to sulfone)	Reduction	Replacement	Conditions	Yield
	c.p.m./mg.	c.p.m./mg.	%	%		%
Diphenyl sulfone	2520	673	26.7	73.3	304°C*(30 min.)	80
	2520	641	25.4	74.6	394°C (15 min.)	
Diphenyl sulfoxide	3776	3548	94.0	6.0	280°C (30 min.)	93

* Air-bath temperature

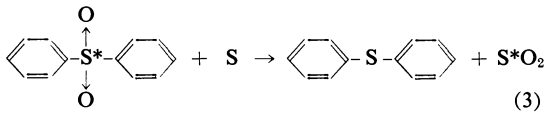

(3)

Years later, Böeseken[2] extended this reaction to *p,p'*-halogeno and *p*-bromo-*p'*-methyl derivatives of diphenyl sulfone but found that they react in entirely different manners; namely, the former gave dihalogen substituted products of benzene and sulfur dioxide and the latter only hydrogen sulfide. However, all the past observations seem to indicate that once C–S bond cleavage takes place, SO_2 group of the sulfone leaves off quite readily. In the case of *p,p'*-halogenated diphenyl sulfones, halogeno-phenyl radical formed in the sulfur-induced cleavage perhaps easily abstracts halogen from other molecule.

It is known that the force constant of S–O bond in sulfone calculated from infrared data, 9.5×10^5 dyn./cm.[3a], is appreciably higher than that of sulfoxide (7×10^5 dyn./cm.)[3a], therefore, unlike those in sulfoxide groups, the sulfur-oxygen links in sulfone groups are not easily cleaved[3b]. In this thermal reaction between diphenyl sulfone and sulfur, it is not unreasonable to consider that SO_2 group in the sulfone may be replaced by sulfur with no cleavage of S–O bonds, while the S–O link in the sulfoxide would be merely reduced with sulfur to sulfide, although the latter reaction has never been reported.

We have investigated the mechanism of these reactions by examining the accompanying exchange of sulfur atom in the reaction of sulfur-35 labeled diphenyl sulfone with ordinary sulfur. Diphenyl sulfide-^{35}S was prepared by Friedel-Crafts reaction of benzene with radioactive sulfur and was converted to the sulfone by oxidation with potassium permanganate. This diphenyl sulfone-^{35}S was treated with ordinary sulfur. The reaction was rather sluggish below 300°C but proceeded nicely at above 300°C giving diphenyl sulfide over 80% yield. The sulfide thus obtained was reoxidized back to the sulfone whose specific activity was compared with that of the original sulfone. These results are tabulated in Table I. Inspection of the data suggests that one-fourth of the over-all reaction proceeded by apparent reduction and the other three-fourths underwent by replacement as one could foresee from the reaction of diphenyl sulfone with selenium.

If one assumes that the over-all reaction is consisted with two simultaneous reactions, i.e., reduction and replacement, and that the reactions have different energies of activation, then one would expect that the ratio of two reactions may change at different temperatures. However, if the two reactions have similar temperature factors, the ratio would remain the same. When the reaction was performed nearly at the boiling temperature of sulfone, 379°C, however, no apparent difference was observed.

In the meantime the over-all reaction could be considered as a combination of two successive reactions, i.e., the initial reduction and the following sulfur exchange reaction between the sulfide and remaining sulfur as shown below:

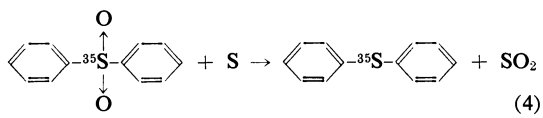

(4)

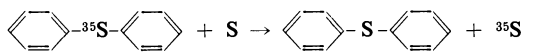

(5)

Incidentally we found that this type of exchange (Eq. 5) actually occured when diphenyl sulfide-^{35}S was refluxed for two hours at 313°C together with natural sulfur.

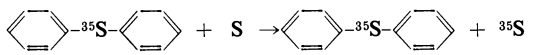

2520 c.p.m./mg.* 1425 c.p.m./mg.* (56.5%) (6)

* Converted to the sulfone

Supposing the exchange rate is much faster than the reduction rate, the amount of radioactivity remained in the sulfide at the end of the reaction will be shown by the following simple equation (see appendix);

2) J. Böeseken, *Rec. trav. chim.*, **30**, 137 (1911).

3a) These values are of alkyl sulfoxides and sulfones, C. C. Price and S. Oae, "Sulfur Bonding", Ranald Press, Inc., New York (1962), p. 66; 3b) ibid., p. 132.

$$\frac{y}{a}=1-\frac{1}{e}=0.632 \qquad (7)$$

where a is the specific activity of the sulfone used and y is the specific activity of the sulfide formed. This indicates that the exchange will transport only 36.8% in total activity from the sulfide to sulfur and major portion of activity, i.e., 63.2% will remain in the sulfide. Therefore, this mechanism also cannot explain the radiochemical results.

The most likely pathway for the main reaction will be the initial cleavage of C–S bond of the sulfone, followed by the formation of diphenyl sulfide, a part of which further undergoes sulfur exchange. It is known that sulfur behaves as biradical chain at high temperature[4] and diphenyl sulfide was obtained together with by-products such as hydrogen sulfide, diphenyl disulfide, etc. when a mixture of benzene and sulfur was heated at 350°C[5]. We also found that a little amount of diphenyl disulfide and polymer-like substance formed in the reaction of diphenyl sulfone with sulfur (Eq. 1). From these facts, it is quite certain that the C–S bond of the sulfone cleaves first, induced by the biradical chain of sulfur, then sulfur dioxide leaves off and the sulfide and a small portion of the disulfide forms in the main reaction. As to the apparent reduction which amounts to about 25%, there are two possibilities, the one is a straight forward reduction that takes place simultaneously with the replacement and the other is the sulfur-exchange reaction between sulfur and diphenyl sulfide. In view of the small percentage, 6%, of replacement reaction in the case of diphenyl sulfoxide, major portion of the apparent reduction reaction of the sulfone would be the real reduction and only several percentage of the apparent reduction originate from the exchange between sulfide formed by the initial replacement and the remaining sulfur.

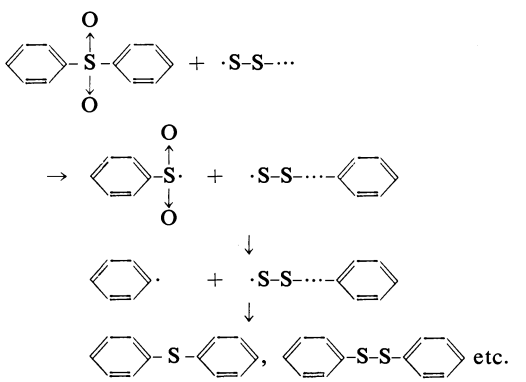

(8)

If the reduction takes place in parallel with the replacement, the sulfide must be formed in the reaction of diphenyl sulfone with selenium, too. In this reaction, however, diphenyl sulfide cannot be separated easily from diphenyl selenide because both the sulfur and the selenium compounds display quite similar chemical properties. To overcome this difficulty, diphenyl sulfone-^{35}S was reacted with selenium for 1 hr. at 305°C and it was found that about one-fifth of the activity of the original diphenyl sulfone-^{35}S remained in the reaction product, apparently the mixture of diphenyl selenide and sulfide. This means that the reduction indeed occured (Eq. 9).

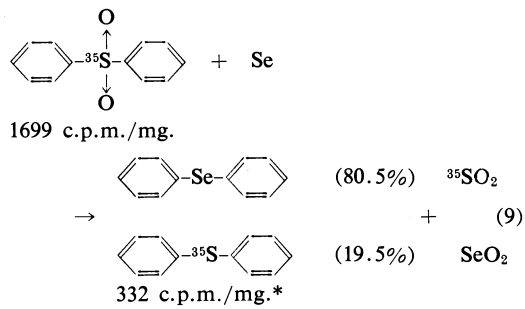

* Converted to the sulfone and selenone

It is interesting to note that benzene or biphenyl was not found among the reaction products of the reaction between diphenyl sulfone and sulfur and biphenyl was not found in the direct reaction of benzene with sulfur[5], while the reaction of p,p'-dihalogeno diphenyl sulfone with sulfur did not give dihalogeno diphenyl sulfide, but did give dihalogeno benzene[2]. We can not offer any satisfactory explanation, however, most of phenyl radicals formed are perhaps immediately caught by sulfur chain before they recombine or abstract hydrogen in the former reaction, while halogen-substituted phenyl radicals easily abstract chlorine in the latter.

Meanwhile we found that diphenyl sulfoxide reacted readily with sulfur at lower temperature than the sulfone giving diphenyl sulfide in quantitative yield if mechanical loss was considered. A similar tracer technique was applied in this reaction, too. Diphenyl sulfoxide-^{35}S was used in this reaction which was prepared by oxidation of diphenyl sulfide-^{35}S with an equivalent amount of hydrogen peroxide and this ^{35}S-labeled sulfoxide was treated with ordinary sulfur. The reaction proceeded quite readily at around 280°C and diphenyl sulfide was obtained in nearly quantitative yield. The sulfide thus obtained was converted

4) W. A. Pryor, "Mechanisms of Sulfur Reactions", McGraw-Hill Book Co., Inc., New York (1962), p. 8.

5) H. B. Glass and E. E. Reid, *J. Am. Chem. Soc.*, **51**, 3428 (1929).

to diphenyl sulfone whose activity was counted. The fact that most of the activity in the original sulfoxide remained in the sulfide formed (as shown in Table I) suggests that simple reduction of sulfoxide to sulfide with elemental sulfur took place by the abstraction of labile oxygen atom with sulfur and only a small portion of the reaction proceeded by replacement contrary to the reaction of the sulfone. This is a clear cut reduction. Similar oxygen-transfer reactions from sulfoxides to divalent sulfur compounds are known. For example, thiacyclopentane-1-oxide was reacted with dibenzyl sulfide in acetic acid to give some dibenzyl sulfoxide[6], and alkyl sulfoxide is known to form when dimethyl sulfoxide and alkyl sulfide are mixed and heated at 160~175°C[7].

A small portion of the apparent replacement reaction can be interpreted either as resulted from the direct exchange between diphenyl sulfide formed and ordinary sulfur during the reaction or as the initial induced cleavage of the C–S link of the sulfoxide followed by the cleavage of S–O bond and the attack of sulfur chain, as in the case of the sulfone. At present, we have very little knowledge to select one from the other.

Experimental

Diphenyl Sulfide-^{35}S was prepared by Friedel-Crafts reaction addopted by Dougherty and Hammond[8]. Diluted and recrystallized active sulfur was added to anhydrous aluminum chloride suspended in refluxing benzene and diphenyl sulfide separated was distilled twice, obtaining oil of b. p. 115°C/2.5 mmHg.

Diphenyl Sulfoxide-^{35}S.—To the solution of 7.7 g. of diphenyl sulfide-^{35}S dissolved in glacial acetic acid containing several drops of concentrated sulfuric acid, was added an equimolar amount of 30% hydrogen peroxide slowly with cooling and stirring. Stirring was continued at room temperature for one hour and then the reaction mixture was kept at 50°C overnight. After a large amount of water added, oil separated was crystallized by adding a small piece of crystalline sulfoxide. White hard crystals was recrystallized from benzene-ligroin, obtaining 4.8 g. (57%) of the sulfoxide, m. p. 69~71°C.

Diphenyl Sulfone-^{35}S was prepared by oxidizing diphenyl sulfide-^{35}S with 1.8 times in mole of potassium permanganate in glacial acetic acid containing a few drops of concentrated sulfuric acid with cooling and stirring. After the addition was over it was warmed at 50°C for 30 min., and then an excess of potassium permanganate was reduced by bubbling sulfur dioxide through the solution. The solution was then poured into a large amount of water, and the precipitate formed was recrystallized from benzene-ligroin, yielding brilliant white crystals, m. p. 122~123.5°C, in 44%.

The Reactions of Diphenyl Sulfone with Sulfur.—Diphenyl sulfone-^{35}S (2520 c.p.m./mg.), 0.01 mol., was thoroughly mixed with 0.01 g. atom of natural sulfur in a Claisen-flask and was put quickly in a pre-heated air-bath, passing nitrogen gas through the reaction flask. Reaction started at about 300°C (air-bath temperature) and sulfur dioxide evolved was trapped in a few traps cooled with dry-ice-acetone. After 15 min. when gas evolution ceased, bath temperature was kept at around 304°C for 15 min. and then diphenyl sulfide was distilled slowly by elevating bath temperatue. When diphenyl sulfide came out, there remained a small amount of sludge insoluble in most organic solvents and water. Crude diphenyl sulfide obtained was redistilled once more, and crystals remained in the distilling flask, m. p. 59°C was found to have the same melting point with diphenyl sulfide when it was mixed with the authentic sample. Diphenyl sulfide was repeatedly distilled untill it became transparent, usually two to three times, then was converted to diphenyl sulfone using the previous method (673 c.p.m./mg.). By the same way as above diphenyl sulfone-^{35}S was treated at 394°C (air-bath temperature), and the activity for the final sulfone was found to be 641 c.p.m./mg.

The Exchange Reaction of Diphenyl Sulfide-^{35}S and Sulfur.—A mixture of diphenyl sulfide-^{35}S (2520 c.p.m./mg. converted to the sulfone), 2.32 g. and 0.39 g. of sulfur was refluxed for 2 hr. at 313°C in nitrogen atmosphere. The sulfide was recovered by distillation. Light yellow oil was redistilled once and converted into sulfone to be subjected to counting analysis (1425 c.p.m./mg.).

The Reaction of Diphenyl Sulfone-^{35}S and Selenium.—Colloidal red selenium was freshly prepared by bubbling sulfur dioxide through the water solution of selenium oxide. Diphenyl sulfone-^{35}S (1699 c.p.m./mg.) and selenium, 0.01 g. atom, respectively, was thoroughly mixed and heated in nitrogen atmosphere. Gas evolved from air-bath temperature of 288°C for 30 min. Bath temperature was kept at 304~306°C for additional 30 min. and then distilled. The oil obtained was redistilled three times, b. p. 300°C, 0.59 g. This oil was oxidized using the previous method. An excess of potassium permanganate was reduced with sulfur dioxide with cooling and it was poured into a large amount of water before oily selenide came out by reduction with excess of sulfur dioxide. After recrystallization from benzene-ligroin, m. p. 135~136°C, 0.3 g. (332 c.p.m./mg.) was obtained.

The Reaction of Diphenyl Sulfoxide with Sulfur.—Diphenyl sulfoxide-^{35}S (3776 c.p.m./mg. converted to the sulfone), 0.01 mol., was mixed with 0.005 g. atom of natural sulfur in a Claisen-flask and treated by the same way as in the reaction of the sulfone. Sulfur dioxide evolved at 280°C (air-bath temperature). The sulfide obtained in quantitative yield was converted to the sulfone (3548 c.p.m./mg.).

6) F. G. Bordwell and B. M. Pitt, ibid., **77**, 572 (1955).
7) S. Searles, Jr. and H. R. Hays, *J. Org. Chem.*, **23**, 2028 (1958).
8) G. Dougherty and P. D. Hammond, *J. Am. Chem. Soc.*, **57**, 117 (1935).

Counting Analysis. — All the compounds was converted into the sulfone or selenone and was counted by Packard, Tri-Carb, liquid scintillation counter, in toluene solution using POPOP as scintilator.

Summary

Diphenyl sulfoxide-^{35}S was reduced to the sulfide-^{35}S nearly quantitatively by heating with sulfur at 280°C, while diphenyl sulfone did not react with sulfur at the same temperature. At around 300°C, diphenyl sulfone-^{35}S started to react with sulfur and gave diphenyl sulfide that lost nearly 75% of the original activity of ^{35}S of the sulfone used. The main reaction of the sulfone was found not to be reduction, but substitution involving induced C–S cleavage and replacement with sulfur chain.

Department of Applied Chemistry
Faculty of Engineering
Osaka City University
Kita-ku, Osaka (S. O.)
Department of Chemistry
Radiation Center of Osaka Prefecture
Sakai, Osaka (S. K.)

Appendix

For convenience in the discussion, the following mechanism and conditions (a—c) will be assumed in the reaction shown below, Eqs. 1 and 2.

$$\mathrm{Ph\text{-}{}^{35}S(\overset{\uparrow}{\underset{\downarrow}{O}})\text{-}Ph + S \rightarrow Ph\text{-}{}^{35}S\text{-}Ph + SO_2} \qquad (1)$$

$$\mathrm{Ph\text{-}{}^{35}S\text{-}Ph + S \rightarrow Ph\text{-}S\text{-}Ph + {}^{35}S} \qquad (2)$$

a) There is no exchange of sulfur atom between diphenyl sulfone and the sulfide or between the sulfone and sulfur.

b) The rate of sulfur exchange shown by Eq. 2 is much faster than the rate of reduction, i. e. Eq. 1.

c) Sulfur dioxide formed will escape from the system so rapidly that there is no time for sulfur dioxide to participate in sulfur-exchange reaction.

Here, let us define x as an amount (in mole) of diphenyl sulfone undergone to the sulfide, y, the specific activity (c.p.m./mol.) of the sulfide when x mol. of the sulfone is converted into the sulfide, v, total amount (in mole) of the sulfone used which is equal to total amount of sulfur or total amount of the sulfide formed in the reaction and a, the specific activity of the sulfone (c.p.m./mol.).

When $(x+\mathrm{d}x)$ mol. of the sulfone is converted to the sulfide, the total activity of the resulting sulfide will be $(xy+a\mathrm{d}x)$; therefore the specific activity will be expressed by $(xy+a\mathrm{d}x)/(x+\mathrm{d}x)$. Meanwhile, the total activity of sulfur at that time will be $[v-(x+\mathrm{d}x)]y$. After an rapid equilibrium is attained between the sulfide and sulfur by exchange, the specific activity will become

$$\frac{[v-(x+\mathrm{d}x)]y+xy+a\mathrm{d}x}{v}$$

Therefore the small variation of specific activity, $\mathrm{d}y$ can be expressed as,

$$\mathrm{d}y=\frac{[v-(x+\mathrm{d}x)]y+xy+a\mathrm{d}x}{v}-y$$

$$=(a-y)\frac{\mathrm{d}x}{v}$$

Integrating this equation, one can get

$$\ln\frac{a}{a-y}=\frac{x}{v}$$

When the reaction is completed, x becomes equal to v; therefore the above equation gives

$$y=a-\frac{a}{e}$$

The ratio of the specific activity of the sulfone and that of the sulfide, y/a, will then be

$$\frac{y}{a}=1-\frac{1}{e}=0.632.$$

The Formation and Reactions of 3, 5, 7-Trinitrotropolone

By Tetsuo NOZOE, Minoru OYAMA* and Katsuo KIKUCHI**

(Received September 26, 1962)

From the result of the molecular orbital calculation on tropone (I) it was predicted that the cationoid substitution reactions would occurr at 2 position of tropone nucleus[1], while the detailed studies of bromination[2] and Diels-Alder reactions[3] of I showed that it has a considerable degree of an unsaturated character compared with tropolone (II).

Recently Buchanan and others[4] obtained a dinitro derivative IV from the reaction of 2,3-benzotropone (III) with concentrated nitric acid, and they thought it must be produced through addition-elimination reaction of III and dinitrogen tetroxide, being produced by mutual oxidation-reduction of III and nitric acid. Doering[5], some years ago, stated in his lecture that the reaction of tropone (I) and nitric acid gave a complex (VI) of 3, 5, 7-trinitrotropolone (V) and I, but the details of which is not available yet. On the other hand, Nozoe, Kitahara and others[6] reported that the action of excess nitric acid on tropolone (II) or on ammonium salt of its 5-sulfonic acid afforded yellow needles (VII), m. p. 238°C (decomp.), and they thought it to be 3, 5, 7-trinitrotropolone, but because of its low yield, the detailed studies on its chemical behavior were not possible.

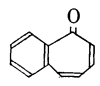

III

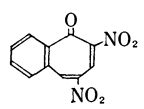

IV

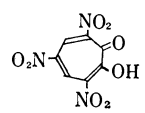

V

As excellent methods for synthesizing tropone (I) from tropilidene were developed recently[7], we attempted to study the action of nitric acid on I as one of the wide range of examination on the properties of I. In this study, we ascertained the formation of 3, 5, 7-trinitrotropolone-tropone complex (VI) as stated by Doering[5], obtained 3, 5, 7-trinitrotropolone (V) therefrom and observed some interesting behaviors of them, and these results will be reported herein.

The reaction condition of tropone (I) and nitric acid to obtain VI is fairly sensitive. Under room temperature, the reaction does not occur practically, while once the reaction started it sometimes proceeds with explosive violence; such a case was already experienced by one[8] of us when hinokitiol was nitrated under variety of conditions. The following procedure is however found to be satisfactory; after the reaction is started by the preliminary addition of a small amount of I into a mixture of fuming nitric acid (4 mol. equiv.) and acetic acid, I (1 mol. equiv.) is added cautiously with stirring while the temperature is maintained at 60~70°C by which the yellow needles (VI), m. p. 228°C (decomp.), of the formula $C_{14}H_9O_9N_3$ are obtained in about a 55% yield.

The compound VI is sparingly soluble in non-polar solvents but very soluble in water and alcohol. With aqueous sodium bicarbonate it gives yellow sodium salt (VIII), $C_{14}H_8O_9N_3Na$, which regenerates original substance by hydrochloric acid. On being left stand at room temperature with aqueous sodium hydroxide or heated with aqueous sodium bicarbonate, VI is converted to colorless crystals (IX), m. p. 132°C (decomp.), which is identified as a 1 : 1-complex of 2, 4, 6-trinitrobenzoic acid (X) and I. VI is not affected with 4 N hydrochloric acid in acetone at refluxing temperature, but gives X when heated with concentrated hydrochloric or hydrobromic acid, and gives 1, 3, 5-trinitrobenzene (XI) when refluxed with aqueous acetic acid (50%). Heating of VI in methanol or ethanol affords methyl ester XII or ethyl ester XIII of X, with the liberation of tropone (I) which is identified as its picrate, m. p. 99~100°C. These facts indicate

* Present address: Research Institute, Toyo-Rayon, Inc., Kamakura, Kanagawa Prefecture.
** Present address: Department of Chemistry, Faculty of Liberal Arts and Science, Yamagata University, Yamagata.

1) R. D. Brown, *J. Chem. Soc.*, **1951**, 2670.
2) T. Nozoe, T. Mukai, K. Takase and T. Nagase, *Proc. Japan Acad.*, **28**, 477 (1952); T. Nozoe, T. Mukai and K. Takase, *Sci. Repts. Tohoku Univ., Ser. I*, **39**, 164 (1956); T. Mukai, This Bulletin, **31**, 846 (1958).
3) T. Nozoe, T. Mukai, T. Nagase and Y. Toyooka, ibid., **33**, 1247 (1960).
4) G. L. Buchanan and D. R. Lockhart, *J. Chem. Soc.*, **1959**, 3586.
5) W. von E. Doering, *Abstracts of XIII, National Organic Symposium (Am. Chem. Soc.)*, p. 1 (1953).
6) T. Nozoe, Y. Kitahara, K. Doi and T. Arai, *Bull. Chem. Research Inst. of Non-Aqueous Solution, Tohoku Univ.*, **7**, 13 (1957).
7) T. Ikemi, T. Nozoe and H. Sugiyama, *Chem. & Ind.*, **1960**, 932; A. P. Ter. Borg, R. van Helden, A. F. Bickel, W. Renold and A. S. Dreiding, *Helv. Chim. Acta*, **43**, 457 (1960).
8) T. Nozoe, *Science of Drugs*, **3**, 174 (1949).

that VI is 1 : 1-complex of 3, 5, 7-trinitrotropolone (V) and tropone (I) and it is thought to be identical with what Doering stated to have obtained[5].

As mentioned above, the treatment of VI with sodium hydroxide or sodium bicarbonate did not yield V, and then the attempt was made to obtain salts of various amines through which V could be obtained as described below.

Treatment of the complex VI with ammonia gives red microcrystals which, when treated with dilute hydrochloric acid, is converted to yellow needles (XIV), m. p. 235°C (decomp.). Similarly, respective treatment of VI with methylamine and pyridine gives yellow needles (XV), m. p. 203°C (decomp.) and yellowish orange needles (XVI), m. p. 201°C (decomp.), respectively. From the fact that the ultraviolet spectra of XIV, XV and XVI resemble that of V (see below) and from the analytical values of them, these are showed to be 1 : 1-salts of V with ammonia, methylamine and pyridine respectively. By the reaction of VI with *p*-toluidine, there are obtained yellow needles (XVII), m. p. 123°C (decomp.) which is thought to be 1 : 1 : 1-complex of V, I and *p*-toluidine from the analytical value and ultraviolet spectrum.

Attempted removal of bases from XIV or from XV with dilute hydrochloric acid does not succeed and heating of XV at 160°C under reduced pressure (4 mmHg) also resulted in the recovery of original substance. But, when pyridinium salt XVI is treated with concentrated hydrochloric acid at room temperature, 3, 5, 7-trinitrotropolone (V) is obtained in about 80% yield with the addition of a small amout of the rearranged product X. Similar treatment of XIV or XV with concentrated hydrochloric acid also gives V but with rather poor yields. Treatment of V and I regenerates VI.

The compound V, yellow needles of m. p. 175°C (decomp.), shows red coloration with ferric chloride in ethanol or dioxane though not colored in water, benzene or chloroform, and gives yellowish orange sodium salt and a yellowish green copper complex. No liberation of nitrogen is observed when treated of V with diazomethane and only a small amount of yellow crystals of unknown structure is obtained. Heating of V with concentrated hydrochloric acid or with sodium hydroxide gives X, and refluxing of V with aqueous acetic acid (50%) gives XI. Treatment of V with methanol or ethanol gives XII or XIII respectively ; these properties are quite similar to those of VI.

The reaction of *o*-phenylenediamine with the compound V or with VI gives dark red crystals (XIX), m. p. over 240°C, soluble in alkaline solution, which is thought to be 6, 8,-

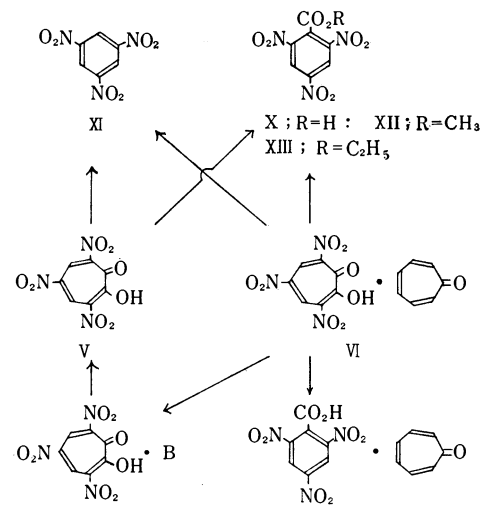

10-trinitrocyclohepta[b]quinoxaline from its analytical value and ultraviolet spectrum[9]. Attempted synthesis of 1, 3-diazaazulene derivative through the reaction of V or VI with guanidine gives only guanidinium salt (XX) of V, yellowish brown needles of m. p. 258°C (decomp.). Heating of V with aniline on a water bath gives colorless scales (XXI), m. p. 245.5°C, the structure of which is not clarified yet.

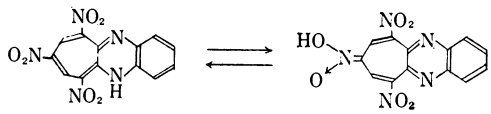

XIX

It seems of interest to note that the compound V, while it is easily rearranged into aromatic compounds on treatment with acid or alkali and on mere heating with alcohols, forms stable salts with various amines.

Ultraviolet spectra of V in methanol and alkaline solution are shown in Fig. 1 ; the absorption curve in methanol resembles those of 5-nitro-[5] and 3, 5-dinitrotropolones[6]. The ultraviolet absorption curve of VI (shown in Fig. 1) corresponds to a superposition of those of V and I. The infrared spectrum of V in Nujol is given in Fig. 2.

Now, the compound VII[6], previously obtained by the nitration of tropolone (II) is considered not to be true 3, 5, 7-trinitrotropolone. We reexamined these experiments and found that

9) S. Ito, *Sci. Repts. Tohoku Univ., Ser. I*, 43. 216 (1959).

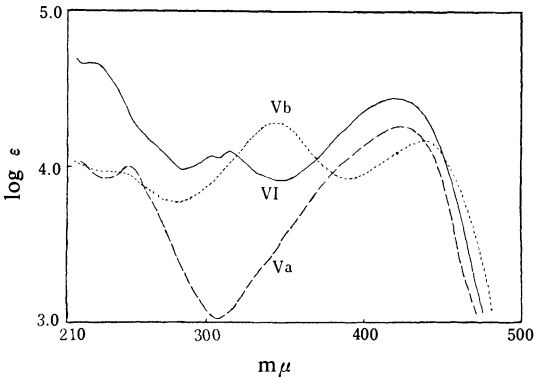

Fig. 1. UV spectra of V in methanol (Va) and in methanolic 0.1 N NaOH (Vb) and of VI in methanol.

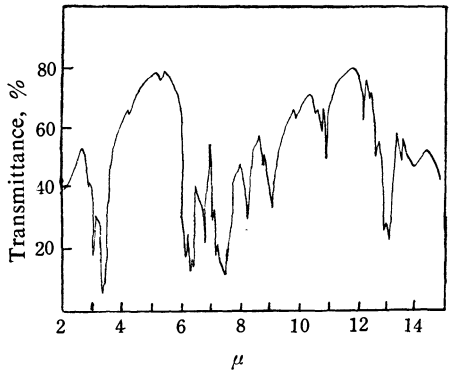

Fig. 2. IR spectrum of V in Nujol.

the fraction, considered to be polynitrotropolone, gave a small amount of the compound VI on adding tropone (I), but the compound VII could not be isolated; in this reaction condition trinitrotropolone once formed must have suffered from further destructive oxidation or rearrangement. On the other hand, the present synthetic procedure for V starting from I is excellent because it is easily isolated as a stable and sparingly soluble complex VI with tropone.

As to the formation of the complex VI from I, two main routes may be considered; one in which VI is formed through the addition-elimination reaction on tropone nucleus and the other in which VI is formed by the preliminary oxidation of I to tropolone (II) followed by the nitration. If the latter is the case, a distinct increasing in the yield of VI may be expected when the mixture of I and II is nitrated under similar conditions, but only slight increasing is actually realized, while the intermediate addition product that might be expected to be formed in the former case is not actually isolated, and the mechanism of its formation remains to be examined.

It is well known from the previous examination that 4-alkyl-5, 7-dinitrotropolones (XXII: R; CH_3[10], C_2H_5[11], *iso*-C_3H_7[12]) are easily rearranged into 3-alkyl-4, 6-dinitrobenzoic acids or their esters by mere warming with various alcohols or with aqueous acetic acid, while 5, 7-dinitrotropolones having substituent at 3 position (XXIII: R; H[6], Br[6], *iso*-C_3H_7[13]) are not rearranged in these conditions as above though they do in alkaline media, and it has been considered that in such rearrangement reactions steric interference between an alkyl group in 4 position and a nitro group in 5 position plays an important role. It seems noteworthy to say that 3, 5, 7-trinitrotropolone (V), having no such substituents at 4 position as to cause steric interaction, is now shown to undergo such a specific rearrangement.

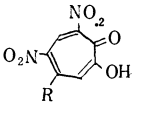

XXII

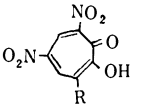

XXIII

Experimental

Reaction of Tropone (I) with Nitric Acid.—After the reaction was induced at 60~70°C by adding several drops of I to a mixture of 14 g. of 94% fuming nitric acid and 15 ml. of acetic acid, a solution of 5 g. of I dissolved in 5 ml. of acetic acid was carefully added to this mixture with stirring while the reaction temperature was maintained at 60~70°C by external cooling. After a violent evolution of nitrogen dioxide ceased, the crystals that formed were collected by filtration to obtain 3.2 g. of yellow crystals, m. p. 218°C (decomp.). Recrystallization from dioxane containing a small amount of water gave yellow needles (VI), m. p. 228°C (decomp.). These crystals showed red coloration in ethanol or dioxane with ferric chloride solution. λ_{max}^{MeOH} mμ (log ε): 225 (4.66), 302 (4.08), 310 (4.09), 420 (4.42); $\lambda_{max}^{H_2O}$ mλ (log ε): 228 (4.49), 313 (3.98), 422 (4.27).

Found: C, 46.22; H, 2.33; N, 11.69. Calcd. for $C_{14}H_9O_9N_3$: C, 46.29; H, 2.50; N, 11.57%.

The filtrate was evaporated under reduced pressure at room temperature and 0.6 g. of colorless crystals, m. p. 97~98°C, was obtained. These crystals were reacted with ethereal diazomethane solution to give colorless crystals, m. p. 54°C., which showed no depression on admixture with dimethyl oxalate.

Nitration of a Mixture of Tropone (I) and Tropolone (II) with Nitric Acid.—To a solution

10) T. Nozoe, T. Mukai, M. Kunori, T. Muroi and K. Matsui, ibid., 35, 242 (1952); T. Muroi, *Bull. Yamagata Univ. Natural Science*, 3, 155 (1954).
11) T. Nozoe, K. Takase and K. Umino, to be published soon.
12) T. Nozoe, Y. Kitahara, K. Yamane and Y. Yamaki, *Proc. Japan Acad.*, 26, (8) 14 (1950).
13) K. Yamane and S. Morosawa, This Bulletin, 27, 18 (1954).

of 4.0 g. of 94% nitric acid (6 mol. equiv. for II) dissolved in 5 ml. of acetic acid was added a mixture of 1.0 g. of I and 1.2 g. of II in 5 ml. of acetic acid in drops under stirring at 30~40°C, and the reaction mixture was allowed to stand for 3 hr. and the yellow crystals were collected by filtration to afford 1.49 g. of VI, m. p. 224°C (decomp.), which showed no depression on admixture with the sample obtained above and the infrared spectra were also identical.

Reaction conditions and the yields of VI were shown in Table I.

Table I. Nitration of mixture of tropone (I) and tropolone (II) with 94% nitric acid

I g.	II g.	Nitric acid g.	React. temp. °C	Yield of VI g.
5.0	0	14	60~70	3.2
1.0	1.2	2.7	40~50	0.63
1.0	1.2	2.7	60~70	0.41
1.0	1.2	4.0	30~40	1.49
1.0	1.2	5.4	30~40	1.27

Reaction of the Compound VI and Aqueous Sodium Bicarbonate or Sodium Hydroxide.—a) Addition of 300 mg. of VI in 2 ml. of saturated aqueous sodium bicarbonate gave deep red solution, and the crystals that precipitated after sometime were collected by filtration and washed with a small amount of water to give 200 mg. of yellow prisms (VIII), m. p. 185°C (decomp.). $\lambda_{max}^{H_2O}$ mμ (log ε): 228 (4.56), 313 (4.08), 420 (4.24), 500 (inf.). $\lambda_{max}^{0.1N\text{-}NaOH}$ mμ (log ε): 224 (4.56), 304 (4.25), 442 (4.27).

Found: C, 43.65; H, 2.35; N, 10.70; Na, 5.54. Calcd. for $C_{14}H_8O_9N_3Na$: C, 43.65; H, 2.09; N, 10.91; Na, 5.97%.

Acidification of an aqueous solution of 50 mg. of VIII with 2 N hydrochloric acid gave 30 mg. of yellow crystals, m. p. 220°C (decomp.). Recrystallization from dioxane containing a small amount of water gave yellow needles, m. p. 228°C (decomp.), which were shown to be identical, by a mixed melting point and the infrared spectra, with VI.

b) A mixture of 200 mg. of VI and 6 ml. of saturated sodium bicarbonate solution was heated for 10 min. on a water bath, and the reaction mixture was acidified with 2 N hydrochloric acid and extracted with ether. The solvent was evaporated from the extract, and 150 mg. of a brown residue thereby obtained was recrystallized from benzene to give 1:1-complex IX of 2, 4, 6-trinitrobenzoic acid and tropone (I) as colorless microneedles, m. p. 132°C (decomp.). The mixed melting point with an authentic sample which was obtained by mixing these two components was not depressed and the infrared spectra were identical. λ_{max}^{MeOH} mμ (log ε): 225 (4.63), 301 (4.10).

Found: C, 46.31; H, 2.43; N, 12.17. Calcd. for $C_{14}H_9O_9N_3$: C, 46.29; H, 2.50; N, 11.57%.

c) A mixture of 200 mg. of VI and 4 ml. of aqueous sodium hydroxide solution was allowed to stand at room temperature for 30 min. The reaction mixture was acidified with 2 N hydrochloric acid, extracted with benzene and the solvent was removed from the extract to give 150 mg. of colorless crystals, m. p. 130°C (decomp.). Recrystallization from a mixture of acetone and benzene gave colorless microneedles, m. p. 132°C (decomp.), identical with IX obtained above.

Reaction of VI and Hydrochloric or Hydrobromic Acid.—a) A mixture of 90 mg. of VI and 2 ml. of concentrated hydrochloric acid was heated at 60~70°C for 30 min., cooled and 40 mg. of colorless crystals, m. p. 195°C (decomp.), that obtained was recrystallized from water to give colorless microneedles (X), m. p. 198°C (decomp.). The mixed melting point with an authentic sample of 2, 4, 6-trinitrobenzoic acid was not depressed and the infrared spectra were identical.

b) Heating of VI and 47% hydrobromic acid at the refluxing temperature for 2 hr. also gave X.

Reaction of VI and Aqueous Acetic Acid.—A mixture of 150 mg. of VI and 2 ml. of 50% aqueous acetic acid was refluxed for 5 hr., cooled and 70 mg. of colorless crystals, m. p. 120°C that obtained was recrystallized from the same solvent to afford colorless microneedles (XI), m. p. 120~121°C. These crystals showed no depression of the melting point on admixture with 1, 3, 5-trinitrobenzene and the infrared spectra were identical.

Reaction of VI and Methanol or Ethanol.—a) A mixture of 50 mg. of VI and 2 ml. of methanol was refluxed for 1 hr., the solution was concentrated and the crystals thereby obtained were collected by filtration to give colorless scales (XII), m. p. 157°C. These crystals showed no depression of the melting point on admixture with methyl 2, 4, 6-trinitrobenzoate and the infrared spectra were also identical.

b) Similar treatment of 30 mg. of VI and 2 ml. of ethanol as in the reaction of VI and methanol gave 15 mg. of colorless scales (XIII), m. p. 154°C, which showed no depression of the melting point on admixture with ethyl 2, 4, 6-trinitrobenzoate and the infrared spectra were identical.

Separation of Tropone (I) from the Complex VI.—A solution of 300 mg. of VI in ethanol was passed through an alumina column and the solvent was evaporated from the elute. The residue was dissolved in a mixture of ether and benzene and the solution was washed with 6 N hydrochloric acid. The aqueous layer was neutralized with sodium bicarbonate, extracted with chloroform and the solvent was removed from the extract to give 45 mg. of pale yellow oil (λ_{max}^{MeOH}: 225, 302 mμ) which afforded a picrate as yellow needles, m. p. 99~100°C. These crystals showed no depression of the melting point on admixture with an authentic sample of tropone picrate.

The solvent was removed from the original benzene-ether solution and the pale yellow crystals that were obtained were recrystallized from ethanol to afford 120 mg. of colorless scales, m. p. 154°C, undepressed on admixture with the authentic sample of XIII.

Reaction of VI and Aqueous Ammonia.—To the suspension of 100 mg. of VI in 1 ml. of ethanol was added 0.2 ml. of 28% aqueous ammonia and the precipitate thereby formed was collected by

filtration and washed with ethanol to give 70 mg. of red crystals which did not show a clear melting point.

The solution of 70 mg. of these red crystals in 1 ml. of water was acidified with concentrated hydrochloric acid and 50 mg. of yellow needles, m. p. 228°C (decomp.), that were obtained was recrystallized from a mixture of acetone and benzene to give 20 mg. of yellow needles (XIV), m. p. 235°C (decomp.). These crystals showed red coloration with ferric chloride in ethanol. λ_{max}^{MeOH} mμ (log ε) : 245 (4.18), 420 (4.40).

Found : C, 30.46; H, 2.25; N, 20.06. Calcd. for $C_7H_6O_8N_4$: C, 30.67; H, 2.21; N, 20.44%.

Reaction of VI and Methylamine Hydrochloride.—A mixture of 40 mg. of methylamine hydrochloride, 200 mg. of VI, 2 ml. of ethanol and 1 ml. of water was refluxed for 30 min., the solution was concentrated and 140 mg. of yellow crystals, m. p. 191°C (decomp.), was obtained. Recrystallization from a mixture of ethanol and benzene gave yellow needles (XV), m. p. 205°C (decomp.). λ_{max}^{MeOM} mμ (log ε) : 243 (4.25), 420 (4.40).

Found : C, 32.64; H, 2.75; N, 18.66. Calcd. for $C_8H_8O_8N_4$: C, 33.34; H, 2.80; N, 19.44%.

Reaction of VI and Pyridine.—A mixture of 50 mg. of VI and 0.2 ml. of pyridine was heated for several minutes on a boiling water bath and benzene was added to the mixture to precipitate orange crystals, m. p. 197~198°C (decomp.). Yield 40 mg. Recrystallization from a mixture of ethanol and pyridine gave yellowish orange needles (XVI), m. p. 201°C (decomp.). λ_{max}^{MeOH} mμ (log ε) : 245 (4.16), 422 (4.36).

Found : C, 43.23; H, 2.36; N, 16.62. Calcd. for $C_{12}H_8O_8N_4$: C, 42.86; H, 2.40; N, 16.67%.

Reaction of VI and *p*-Toluidine.—A mixture of 200 mg. of VI, 60 mg. of *p*-toluidine and 3 ml. of ethanol was refluxed for 30 min., the solvent was removed and a reddish brown oily residue that was obtained was extracted with hot benzene. The benzene extract gave 120 mg. of yellow crystals, m. p. 119~120°C, which was recrystallized from benzene to give yellow needles (XVII), m. p. 123°C. λ_{max}^{MeOH} mμ (log ε) : 232 (4.62), 300 (4.63), 420 (4.40).

Found : C, 53.97; H, 3.97; N, 11.18. Calcd. for $C_{21}H_{18}O_9N_4$: C, 53.62; H, 3.86; N, 11.91%.

Separation of 3, 5, 7-Trinitrotropolone (V) from Amine Salts of V.—a) Trituration of 1.3 g. of pyridinium salt XVI with 20 ml. of concentrated hydrochloric acid at room temperature gave a clear solution from which yellow crystals were reprecipitated. After the mixture was allowed to stand for one hour the crystals were collected by filtration to obtain 0.82 g. of yellow microneedles (V), m. p. 178°C (decomp.). Recrystallization was carried out from benzene but with some difficulty. These crystals showed red coloration in ethanol or dioxane with ferric chloride, but not colored in water, benzene or chloroform. λ_{max}^{MeOH} mμ (log. ε) : 245 (4.20), 420 (4.40).

Found : C, 32.66; H, 1.29; N, 15.63. Calcd. for $C_7H_3O_8N_3$: C, 32.70; H, 1.18; N, 16.34%.

Na Salt.—Yellow microprisms, m. p. 133°C (decomp.).

Cu Complex.—Yellowish green crystals, m. p. over 300°C.

The original filtrate was extracted with ether and the solvent was removed from the extract to give 110 mg. of yellow crystals, m. p. 203~206°C (decomp.). Addition of a solution of 50 mg. of tropone in ether to these crystals, extraction with hot benzene followed by the removal of the solvent gave 80 mg. of IX, m. p. 132°C, and 20 mg. of VI, m. p. 221°C (decomp.).

b) Similar treatment of 30 mg. of ammonium salt XIV with 0.3 ml. of concentrated hydrochloric acid as in the case of a) gave 10 mg. of yellow needles (V), m. p. 178°C (decomp.).

c) Similar treatment of 150 mg. of salt (XV) with 1 ml. of concentrated hydrochloric acid gave 95 mg. of yellow needles (V), m. p. 178°C (decomp.).

Reaction of V and I.—To a solution of 50 mg. of V dissolved in 5 ml. of ether was added 30 mg. of I, and the yellow crystals thereby precipitated were collected by filtration and washed with benzene to give 68 mg. of yellow needles, m. p. 227°C (decomp.). The mixed melting point with authentic sample of VI was not depressed and the infrared spectra were identical.

Reaction of V and Diazomethane.—To a solution of 100 mg. of V in 15 ml. of ether was added an equivalent amount of ethereal diazomethane. No evolution of nitrogen gas occurred though transient red coloration was observed on mixing both solutions. Yellow crystals which precipitated were collected by filtration to give 30 mg. of yellow needles which sintered at about 80°C and decomposed at 170°C, but the purification was not possible.

Reactions of V with Acids, Alkali and Alcohols.—*a) Hydrochloric Acid.*—A mixture of 50 mg. of V and 2 ml. of concentrated hydrochloric acid was refluxed for one hour to give 40 mg. of colorless needles (X), m. p. 204~205°C (decomp.).

b) Aqueous Acetic Acid.—Similar treatment of 50 mg. of V and 2 ml. of 50% aqueous acetic acid as in the reaction of VI and the same acid gave colorless needles (XI), m. p. 120~121°C.

c) *Sodium Hydroxide Solution.*—A mixture of 100 mg. of V and 1 ml. of 2 N sodium hydroxide solution was heated for 2 min. on a water bath and acidified with 2 N hydrochloric acid to obtain 90 mg. of orange crystals, m. p. 188°C (decomp.). Recrystallization from a mixture of benzene and ethanol gave colorless crystals (X), m. p. 194°C (decomp.).

d) Methanol.—Similar treatment of 50 mg. of V with 2 ml. of methanol as in the case of VI gave 25 mg. of colorless scales (XII), m. p. 157°C.

e) Ethanol.—Similar treatment of 30 mg. of V with 2 ml. of ethanol as in the case of VI afforded 25 mg. of colorless scales (XIII), m. p. 154°C.

Reaction of V and VI with *o*-Phenylenediamine.—a) A mixture of 200 mg. of VI, 60 mg. of *o*-phenylenediamine and 2 ml. of ethanol was refluxed for 10 min. and the precipitates thereby formed were collected by filtration and washed with ethanol to afford 140 mg. of a dark reddish violet amorphous solid (XIX), m. p. over 240°C. These

crystals were sparingly soluble in usual organic solvents, but soluble in aqueous sodium hydroxide solution. λ_{max}^{MeOH} mμ (log ε) : 236 (4.54), 321 (3.92), 480 (4.35).

Found : C, 47.73 ; H, 2.35. Calcd. for $C_{13}H_7O_6N_5$: C, 47.42 ; H, 2.14%.

b) Similar treatment of 100 mg. of V as in the case of a) gave 100 mg. of XIX, m. p. over 240°C.

Reaction of V and VI with Guanidine Sulfate.—a) To a mixture of 65 mg. of guanidine sulfate and 50 mg. of sodium methoxide in 2 ml. of methanol was added 200 mg. of VI. The mixture was refluxed for one hour, diluted with 10 ml. of water and 150 mg. of yellow crystals, m. p. 253°C (decomp.), that was obtained, was recrystallized from methanol to give 120 mg. of yellowish brown needles (XX), m. p. 258°C (decomp.). λ_{max}^{MeOH} mμ (log ε) : 245 (4.18), 423 (4.43).

Found : C, 30.73 ; H, 2.41 ; N, 26.51. Calcd. for $C_8H_8O_8N_6$: C, 30.39 ; H, 2.55 ; N, 26.58%.

b) Similar treatment of 100 mg. of V as in the case of a) afforded 110 mg. of XX, m. p. 258°C (decomp.).

Reaction of V and Aniline.—A mixture of 100 mg. of V and 0.5 ml. of aniline was heated for one hour on a water bath and the crystals that precipitated were collected by filtration to afford 55 mg. of pale yellow scales, m. p. 244°C. Recrystallization from acetone gave colorless scales, m. p. 245.5°C. λ_{max}^{MeOH} 275 mμ.

Found : C, 70.29 ; H, 4.69 ; N, 11.31%.

One of us (K. Kikuchi) wishes to express his thanks to the "Japan Society for the Promotion of Science" for the Fellowship which enabled him to carry out this work during his stay in Tohoku University as a visiting research associate.

Department of Chemistry
Faculty of Science
Tohoku University
Katahira-cho, Sendai

Cycloheptathiazole Derivatives. II. Synthesis of a Seven-membered Analog of Firefly Luciferin

By Shuichi SETO, Kyozo OGURA and Yukio NISHIYAMA

(Received November 17, 1962)

In the preceding paper of this series[1], syntheses of cyclohepta[d]thiazole derivatives from 3-bromo-5-aminotropolone were described. As a further investigation of this series, the synthesis of a seven-membered analog of firefly luciferin[2] was reported. Since tropolone is similar to phenol in their chemical properties, it would be interesting from the point of biological actions to synthesize such a compound as II which has a tropolone ring in place of the phenol ring in luciferin (I).

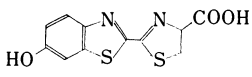

I

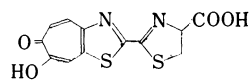

II

For this purpose the preparation of 2-cyano-7-hydroxycyclohepta[d]thiazol-6-one (III) is desirable, for it can be expected that III reacts with cysteine to afford II in the same manner described in the synthesis of I [2,3]. 2-Amino-7-hydroxycyclohepta[d]thiazol-6-one (IV) which has been easily obtained[1] seems apparently suitable for the starting material, but application of Sandmeyer reaction on IV was not successful. As the authors found a convenient method of carbamoylthiocarbonylation of aromatic amines by using carbamoylthiocarbonylthioacetic acid (V), this method was applied to 3-bromo-5-aminotropolone (VI). The reagent V reacted with VI in alkaline solution at room temperature, and *N*-(3-bromotropolon-5-ylthiocarbamoyl)carbamide (VII) was obtained. It shows absorption bands at 3390, 3240 and 1706 cm^{-1} due to its amide group.

Treatment of VII with pyridine resulted in intramolecular nucleophilic reaction[1] to give 2-carbamoyl-7-hydroxycyclohepta[d]thiazol-6-one (VIII). The structure of VIII was confirmed by comparison of its infrared and ultraviolet absorption spectra with those of

1) S. Seto, Y. Nishiyama and K. Ogura, This Bulletin, 35, 1998 (1962).
2) E. H. White, F. McCapra, G. F. Field and W. D. McElroy, *J. Am. Chem. Soc.*, 83, 2402 (1961).
3) S. Seto, K. Ogura and Y. Nishiyama, This Bulletin, in press.

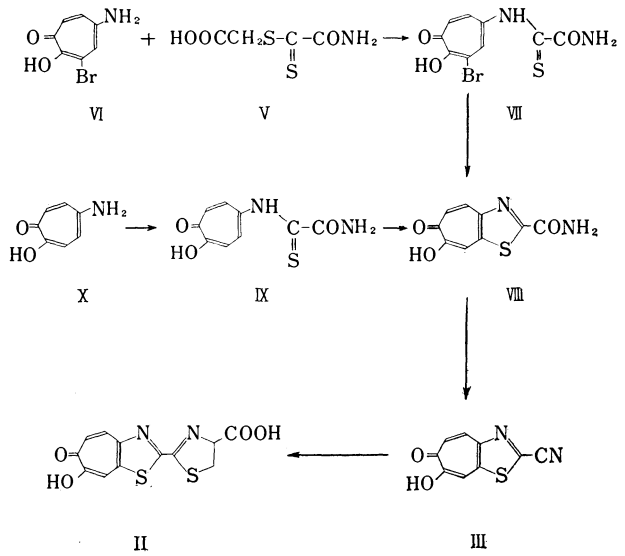

cycloheptathiazole derivatives obtained previously[1]. The amide VIII could be also prepared by the action of bromine to a pyridine solution of *N*-(tropolon-5-ylthiocarbamoyl)carbamide (IX) which was obtained by the reaction of 5-aminotropolone (X) and the reagent V. Infrared spectrum of VIII exhibits absorption at 3370, 1690 and 1665 cm^{-1} for its amide residue, and other absorption bands correspond to those of the known cycloheptathiazole derivatives[1]. Reaction of VIII with phosphorus oxychloride gave 2-cyano-7-hydroxycyclohepta-[d]thiazol-6-one (III), which showed absorptions at 3190 and 2230 cm^{-1} due to a hydroxyl group on tropolone nucleus and a cyano group respectively. The reaction of III with D-cysteine proceeded smoothly in the same way as in the case of 2-cyano-6-hydroxybenzothiazole[2,3], and the analog II was obtained as pale yellow granular crystals. II shows absorption bands at 3200 cm^{-1} for a hydroxyl group in tropolone ring and at 2600 (broad) and 1734 cm^{-1} for a carboxyl group. Ultraviolet spectrum of II is similar to those of III, VIII and other cycloheptathiazoles obtained previously[1].

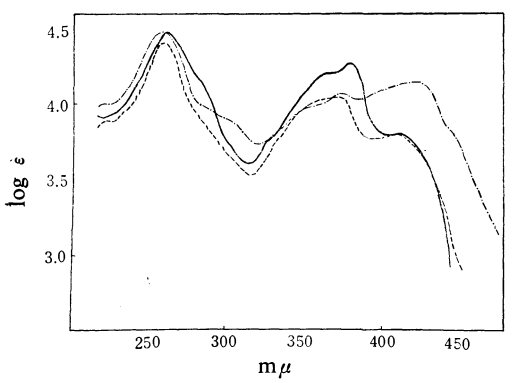

Fig. 1. Ultraviolet spectra of II(——), III(·-·-) and VIII(----) in methanol.

Alkaline solutions of 2-cyano-6-hydroxybenzothiazole and luciferin exhibit greenish blue luminescence on exposure to ultraviolet light[3], while neither II nor III shows such property.

Experimental*

***N*-(3-Bromotropolon-5-ylthiocarbamoyl)carbamide (VII).**—To a solution of VI (500 mg.) in aqueous potassium hydroxide (potassium hydroxide, 130 mg.; water, 2 ml.), the reagent V prepared from 800 mg. of trichloroacetamide was added, and the mixed solution was allowed to stand at room temperature overnight. Orange crystals that formed was collected, and it was acidified with 6 N sulfuric acid to give yellow powder, which was collected, washed well with hot methanol, 200°C (darken). Yield, 270 mg. Evaporation of the methanol filtrate gave 130 mg. of the starting material VI. λ_{max}^{MeOH} mμ (log ε) : 253 (4.34), 420 (4.23).

Found: C, 35.52; H, 2.46; N, 8.56. Calcd. for $C_9H_7O_3N_2SBr$: C, 35.62; H, 2.31; N, 9.24%.

2-Carbamoyl-7-hydroxycyclohepta[d]thiazol-6-one (VIII).—a) When a solution of VII (270 mg.) in pyridine (4.2 ml.) was allowed to stand at room temperature for two days, yellow crystals deposited. The crystals were collected, washed with pyridine, water and hot methanol to afford pale yellow prisms, m. p. 317~325°C (decomp.). Yield, 100 mg. λ_{max}^{MeOH} mμ (log ε) : 258 (4.41), 370 (4.05), 410 (3.80).

Found: C, 48.19; H, 2.96; N, 12.13: Calcd. for $C_9H_6O_3N_2S$: C, 48.66; H, 2.72; N, 12.61%.

b) When a solution of bromine (30 mg.) in pyridine (0.5 ml.) was added to a suspension of IX (40 mg.) in pyridine (3 ml.), the whole was dissolved to form

* All melting points were uncorrected. The microanalyses were carried out by misses Yôko Endô and Yukiko Endô of this Institute, to whom the authors are indebted.

a dark red solution. After the solution was allowed to stand at room temperature for 3 days, pale yellow crystals separated out. The crystals were collected, washed with pyridine, water and hot methanol. Yield, ca. 5 mg.

***N*-(Tropolon-5-ylthiocarbamoyl) carbamide (IX).** —To a solution of X (100 mg.) was added, and the mixed solution was allowed to stand at room temperature for two days. The crystals that formed were collected and acidified with 6 N hydrochloric acid to give yellow powder. Recrystallization from ethanol afforded yellow needles, m. p. 215~220°C (decomp.). λ_{max}^{MeOH} mμ (logε) : 228 (4.36), 305 (3.95), 380 (4.07). IR 3370, 3270, 1692 cm^{-1} (KBr).

Found : C, 48.88 ; H, 3.57 ; N, 12.24. Calcd. for $C_9H_8O_3N_2S$: C, 48.22 ; H, 3.60 ; N, 12.50%.

2-Cyano-7-hydroxycyclohepta[d]thiazol-6-one (III).—A mixture of VIII (50 mg.) in phosphorus oxychloride (2 ml.) was refluxed for 2 hr. During this time the mixture turned dark brown. After removal of an excess of phosphorus oxychloride under a reduced pressure, cracked ice was added to the residue and the precipitate was collected. It was sublimed in reduced pressure (4 mmHg) at 140°C and the sublimate was recrystallized from ethanol to afford pale yellow needles, m. p. 211~215°C (decomp.) Yield, 20 mg. λ_{max}^{MeOH} mμ (logε) : 255 (4.48), 375 (4.07), 420 (4.15).

Found : C, 52,98 ; H, 2.33 ; N, 13.90. Calcd for $C_9H_4O_2N_2S$: C, 52.92 ; H, 1.97 ; N, 13.72%.

2-(4'-Carboxy-2'-thiazolin-2'-yl)-7-hydroxycyclohepta[d]thiazol-6-one (II). — A mixture of III (40 mg.), potassium carbonate (30 mg.), D-cysteine hydrochloride (40 mg.) in 50% aqueous methanol (2 ml.) was stirred under nitrogen stream for 1.5 hr. After removal of methanol in a reduced pressure the mixture was filtered to remove a small amount of insoluble substance. The precipitate which was formed by neutralization with dilute hydrochloric acid was collected, washed with hot benzene and recrystallized from ethanol to afford pale yellow crystals, m. p. 198~201°C (decomp.). Yield, ca. 5 mg. λ_{max}^{MeOH} mμ (logε) : 260 (4.48), 370(4.20), 380 (4.27).

Found : C, 46.23 ; H, 3.08 ; N, 9.35. Calcd. for $C_{12}H_8O_4N_2S$: C, 46.76 ; H, 2.62 ; N, 9.09%.

A part of the expense for this work was defrayed by Sankyo Co., Ltd., to whom the present authors wish to express their sincere gratitude.

The Chemical Research Institute of Non-Aqueous Solutions
Tohoku University
Katahira-cho, Sendai

The Kinetics of Substitution Reactions Involving Metal Complexes. VII. Effect of Acetate Ions on the Reaction between Lead(II) and Zinc-Ethylenediaminetetraacetate Complexes

By Nobuyuki TANAKA and Hiroshi OGINO

(Received September 28, 1962)

Recent studies on a series of substitution reactions between metal ions and metal-ethylenediaminetetraacetate (EDTA) complexes in acetate buffer solutions[1-5] have revealed that these reactions proceed through both the hydrated metal ions and the metal acetato complexes. The reaction through acetato complexes was suggested in some of the previous papers[1-3], while in the others it was treated somewhat quantitatively by the approximate method[4,5].

In this study, a rigorous treatment of the effect of acetate ions on the substitution reaction has been developed and applied to the reaction between lead(II) ions and zinc-EDTA complexes. The reaction mechanisms which involve reaction paths through hydrated ions and those through acetato complexes have been assumed and the rate constants for the rate-determining steps in those reaction paths have been determined.

Experimental

Reagents.—The preparation of the solutions of lead(II) nitrate and disodium ethylenediaminetetraacetate was described in the previous papers[2,6]. A solution of zinc nitrate was prepared by dissolving an appropriate amount of pure zinc metal in nitric acid, and standardized amperometrically against

1) N. Tanaka and K. Kato, This Bulletin, **32**, 1376 (1959).
2) K. Kato, ibid., **33**, 600 (1960).
3) N. Tanaka and K. Kato, ibid., **33**, 1236 (1960).
4) N. Tanaka and M. Kamada, ibid., **35**, 1596 (1962).
5) N. Tanaka, H. Osawa and M. Kamada, ibid., **36**, 67 (1963).
6) N. Tanaka, K. Kato and R. Tamamushi, ibid., **31**, 283 (1958).

the standardized EDTA solution. All other chemicals used were of analytical reagent grade.

Apparatus and Procedure.—The rate of the reaction between lead(II) ions and zinc-EDTA complexes was followed by measuring the decrease of the polarographic diffusion current of lead(II) ions with time in acetate buffer solutions. For the measurements of the current-time curves, a Yanagimoto PB-4 pen-recording polarograph was used. A dropping mercury electrode used had an m value of 2.12 mg./sec. and a drop time t_d of 3.92 sec., being measured at −0.60 V. vs. SCE in an air-free 0.2 M potassium nitrate solution containing 0.01% gelatin at 25.0°C. The pH of the solution was measured accurately with a Hitachi EHP-1 pH meter, after the measurement of the current-time curves. Ionic strength of the solution was adjusted to be 0.2 with potassium nitrate, and gelatin was added as a maximum suppressor by 0.01% in concentration. All measurements were carried out at 25.0°C.

Results and Discussion

In the solution containing acetate ions up to 0.2M in concentration, lead(II) forms mono- and diacetato complexes, whereas zinc(II) forms only a monoacetato complex[7]. The overall substitution reaction between lead(II) and zinc-EDTA complexes is written as the following:

$$\left\{\begin{matrix}Pb^{2+}\\ \downarrow\uparrow\\ PbOAc^{+}\\ \downarrow\uparrow\\ Pb(OAc)_2\end{matrix}\right\} + ZnY^{2-} \rightleftharpoons PbY^{2-} + \left\{\begin{matrix}Zn^{2+}\\ \downarrow\uparrow\\ ZnOAc^{+}\end{matrix}\right\} \quad (1)$$

where Y^{4-} denotes a tetravalent EDTA anion.

When both zinc ions and zinc-EDTA complexes are present in a large excess over lead ions, the substitution reaction 1 can be treated as a pseudo-first-order reaction,

$$\left\{\begin{matrix}Pb^{2+}\\ \downarrow\uparrow\\ PbOAc^{+}\\ \downarrow\uparrow\\ Pb(OAc)_2\end{matrix}\right\} \underset{k^-}{\overset{k^+}{\rightleftharpoons}} PbY^{2-} \quad (2)$$

The rate equation for the reaction 2 is expressed as[1]

$$-\frac{d[Pb^{2+}]_{app}}{dt} = k^+[Pb^{2+}]_{app} - k^-[PbY^{2-}] \quad (3)$$

where $[Pb^{2+}]_{app}$ is the concentration of lead(II) that can be determined polarogaphically as the simple ion, and given by the equation

$$[Pb^{2+}]_{app} = [Pb^{2+}] + [PbOAc^{+}] + [Pb(OAc)_2] \quad (4)$$

Integrating Eq. 3,

$$\ln\{[Pb^{2+}]_{app} - [Pb^{2+}]_{e,app}\} = -(k^+ + k^-)t + \ln\{[Pb^{2+}]_{0,app} - [Pb^{2+}]_{e,app}\} \quad (5)$$

is obtained, where subscripts 0 and e represent the initial and the equilibrium conditions, respectively. The left-hand side of Eq. 5 is plotted against time and from the slope the value of $(k^+ + k^-)$ is determined. At the equilibrium of the reaction, the relation

$$\frac{k^+}{k^-} = \frac{[PbY^{2-}]_e}{[Pb^{2+}]_{e,app}} \fallingdotseq K^{Pb}_{Zn,app}\frac{[ZnY^{2-}]_0}{[Zn^{2+}]_{0,app}}$$

may be satisfied, where $K^{Pb}_{Zn,app}$ represents the apparent equilibrium constant for reaction 1 expressed as

$$K^{Pb}_{Zn,app} = \frac{[Zn^{2+}]_{e,app}[PbY^{2-}]_e}{[Pb^{2+}]_{e,app}[ZnY^{2-}]_e}$$

The values of $K^{Pb}_{Zn,app}$ were determined polarographically to be 10.3 and 5.0 in acetate buffer solutions which contain 0.05M and 0.1M of acetate ions, respectively.

The apparent rate constants of the forward reaction 1, $k^+/[ZnY^{2-}]_0$, were obtained at various pH's and at two different concentrations of Zn(II) and acetate ions. The plots of $k^+/[ZnY^{2-}]_0$ versus $[H^+]$ gave straight lines as shown in Fig. 1.

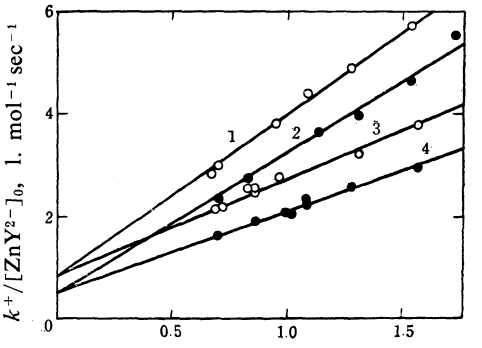

Fig. 1. $k^+/[ZnY^{2-}]_0$ as a function of the hydrogen ion concentration in acetate buffer-potassium nitrate solutions of ionic strength 0.2 at 25°C. Initial concentrations are: $[Pb^{2+}]_{0,app}=2.06\times10^{-4}$ M; $[ZnY^{2-}]_0=5.25\times10^{-3}$ M; $[Zn^{2+}]_{0,app}=5.05\times10^{-3}$ M (curves 1 and 2) and 1.02×10^{-2} M (curves 3 and 4). Concentrations of free acetate are 0.049 M for curves 1 and 3 and 0.098 M for curves 2 and 4.

Bril, Bril and Krumholz[8] found that the reaction proceeds simultaneously through three different reaction paths. This was confirmed by Tanaka and Kato[3], who presumed that the reaction proceeds not only through hydrated metal ions but also through acetato complexes. Considering these facts, the following mechanisms were set down for reaction 1.

7) N. Tanaka and K. Kato, ibid., 33, 417 (1960).

8) K. Bril, S. Bril and P. Krumholz, *J. Phys. Chem.*, 59, 596 (1955); 60, 251 (1956).

$$\text{(i)}\quad Pb^{2+}+ZnY^{2-} \overset{k^{+}_{1h}}{\rightleftharpoons} PbY^{2-}+Zn^{2+} \qquad (6)$$

$$PbOAc^{+}+ZnY^{2-} \overset{k^{+}_{1c}}{\rightleftharpoons} PbY^{2-}+ZnOAc^{+} \qquad (6')$$

$$\text{(ii)}\quad ZnY^{2-}+H^{+} \rightleftharpoons ZnHY^{-} \qquad (7)$$

$$Pb^{2+}+ZnHY^{-} \overset{k^{+}_{IIh}}{\rightleftharpoons} PbHY^{-}+Zn^{2+} \qquad (8)$$

$$PbOAc^{+}+ZnHY^{-} \overset{k^{+}_{IIc}}{\rightleftharpoons} PbHY^{-}+ZnOAc^{+} \qquad (8')$$

$$PbHY^{-} \rightleftharpoons PbY^{2-}+H^{+} \qquad (9)$$

$$\text{(iii)}\quad ZnY^{2-}+H^{+} \underset{k_a^{-}}{\rightleftharpoons} Zn^{2+}+HY^{3-} \qquad (10)$$

$$Pb^{2+}+HY^{3-} \overset{k^{+}_{IIIh}}{\rightleftharpoons} PbY^{2-}+H^{+} \qquad (11)$$

$$PbOAc^{+}+HY^{3-} \overset{k^{+}_{IIIc}}{\rightleftharpoons} PbY^{2-}+H^{+}+OAc^{-} \qquad (11')$$

In reaction paths (iii), the concentration of HY^{3-} is expected to be extremely small during the reaction, and the steady state approximation may be applied. In addition, the condition,

$$k_a^{-}[Zn^{2+}] \gg k^{+}_{IIIh}[Pb^{2+}]+k^{+}_{IIIc}[PbOAc^{+}]$$

is satisfied, as was justified by Bril et al.[8]

In the present treatment, it is assumed that the equilibria between hydrated ions and acetato complexes are maintained while the substitution reaction takes place. This assumption seems to be reasonable from the results in Table II given below. From these assumptions one obtains Eq. 12 for the rate equation for reaction 1, where

$$k^{+}_{1c}=k^{+}_{1c}K_{PbOAc},\quad k^{+}_{2h}=k^{+}_{IIh}K^{H}_{ZnHY},$$

$$k^{+}_{2c}=k^{+}_{IIc}K^{H}_{ZnHY}K_{PbOAc},\quad k^{+}_{3h}=\frac{k^{+}_{IIIh}}{K_{ZnY}K_{HY}},$$

$$k^{+}_{3c}=\frac{k^{+}_{IIIc}}{K_{ZnY}K_{HY}}K_{PbOAc} \qquad (13)$$

$$-\frac{d[Pb^{2+}]_{app}}{dt}=$$

$$\frac{k^{+}_{1h}+k^{+}_{1c}[OAc^{-}]+(k^{+}_{2h}+k^{+}_{2c}[OAc^{-}])[H^{+}]+(k^{+}_{3h}+k^{+}_{3c}[OAc^{-}])\dfrac{1+K_{ZnOAc}[OAc^{-}]}{[Zn^{2+}]_{app}}[H^{+}]}{1+\sum_{n=1}^{2}K_{Pb(OAc)_n}[OAc^{-}]^{n}}$$

$$\times[Pb^{2+}]_{app}[ZnY^{2-}] \qquad (12)$$

$$\frac{k^{+}}{[ZnY^{2-}]_0}=$$

$$\frac{k^{+}_{1h}+k^{+}_{1c}[OAc^{-}]+(k^{+}_{2h}+k^{+}_{2c}[OAc^{-}])[H^{+}]+(k^{+}_{3h}+k^{+}_{3c}[OAc^{-}])\dfrac{1+K_{ZnOAc}[OAc^{-}]}{[Zn^{2+}]_{o,app}}[H^{+}]}{1+\sum_{n=1}^{2}K_{Pb(OAc)_n}[OAc^{-}]^{n}} \qquad (14)$$

Table I. Rate constants in Eq. 14 obtained experimentally at ionic strength 0.2 at 25°C

Rate constant		
k^{+}_{1h}	5	$l.mol^{-1}sec^{-1}$
k^{+}_{1c}	4×10	$l^2mol^{-2}sec^{-1}$
k^{+}_{2h}	$\sim2\times10^5$	$l^2mol^{-2}sec^{-1}$
k^{+}_{2c}	$\sim7\times10^6$	$l^3mol^{-3}sec^{-1}$
k^{+}_{3h}	4×10^3	$l.mol^{-1}sec^{-1}$
k^{+}_{3c}	1×10^5	$l^2mol^{-2}sec^{-1}$

$K_{Pb(OAc)_n}$ and K_{ZnOAc} represent the overall formation constants of acetato lead(II) and acetatozinc(II) complexes, respectively. K^{H}_{ZnHY} represents the equilibrium constant of reaction 7, K_{ZnY}, the formation constant of ZnY^{2-} and K_{HY}, the fourth dissociation constant of ethylenediaminetetraacetic acid.

From Eqs. 3 and 12, Eq. 14 is obtained, where the initial concentrations, $[Zn^{2+}]_0$ and $[ZnY^{2-}]_0$, are substituted for $[Zn^{2+}]$ and $[ZnY^{2-}]$, respectively. Since both Zn^{2+} and ZnY^{2-} are present in the solution in a large excess over lead ions, the change of their concentrations during the reaction can be neglected.

The rate constants in Eq. 14 were obtained from the analysis of plots in Fig. 1, and are given in Table I. The formation constants of acetatolead(II) and acetatozinc(II) complexes which were used in the calculation are reported in the previous paper[7]. The concentration of uncomplexed acetate in the solution was calculated by successive approximation.

The rate constants for reactions 6, 6', 8, 8', 11 and 11' were calculated from the relations given in Eqs. 13. The values of K^{H}_{ZnHY}, K_{ZnY} and K_{HY} which were used in the calculation were reported previously[3]. The obtained rate constants for reactions 6, 6', 8, 8', 11 and 11' are given in Table II. The values in Table II indicate that the all reactions proceeding

TABLE II. RATE CONSTANTS FOR REACTIONS 6, 6', 8, 8', 11 AND 11' AT IONIC STRENGTH 0.2 AT 25°C

Rate constant, l. mol^{-1} sec^{-1}					
k^+_{1h}	k^+_{1c}	k^+_{IIh}	k^+_{IIc}	k^+_{IIIh}	k^+_{IIIc}
5	0.3	$\sim 3\times10^2$	$\sim 7\times10$	3×10^9	6×10^8

through Pb^{2+} are faster than the corresponding reactions through $PbOAc^+$. It is considered to be mainly due to the difference in charge of the reacting species.

From Eq. 12, it is predicted that the reaction rate decreases with the increase of acetate ion concentration. With Eq. 14, $k^+/[ZnY^{2-}]_0$ was calculated as a function of the concentration of acetate ion, using the rate constants given in Table I and the formation constants of acetato complexes. Two sets of calculations which were made at two different hydrogen ion concentrations are shown in Fig. 2, where the experimental values of $k^+/[ZnY^{2-}]_0$ measured at various acetate concentrations are also given. These are in satisfactory agreement with the calculated curves. This fact leads to a definite conclusion that the reaction proceeds not only through hydrated metal ions but also through acetato complexes. It also suggests that the contribution of the reaction through diacetato complexes is of least significance.

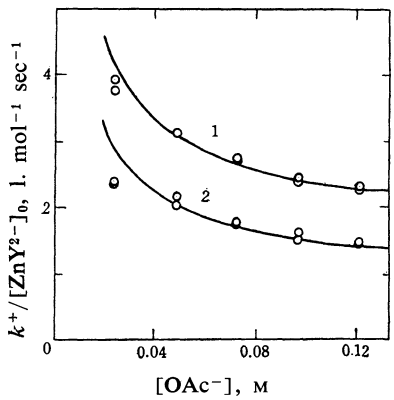

Fig. 2. $k^+/[ZnY^{2-}]_0$ as a function of the acetate concentration in acetate buffer-potassium nitrate solutions of $[H^+]=1.17\times10^{-5}$ M (curve 1) and $[H^+]=0.63\times10^{-5}$ M (curve 2). Initial concentrations are: $[Pb^{2+}]_{0,app}=1.65\times10^{-4}$ M; $[ZnY^{2-}]_0=5.00\times10^{-3}$; $[Zn^{2+}]_{0,app}=1.00\times10^{-2}$ M.
— indicates the theoretical curve and ○, the experimental value.

Summary

The effect of acetate ions on the substitution reaction between lead(II) and zinc-EDTA complexes has been investigated. The reaction was treated as to proceed through both hydrated metal ions and monoacetato complexes, and the rate equation was derived. The rate constants for six elementary reactions of which three involve the hydrated lead(II) ion and the others involve the monoacetatolead-(II) complex were determined at ionic strength 0.2 at 25.0°C. The values indicate that all the reactions proceeding through hydrated lead ions are faster than the corresponding reactions through monoacetato lead complexes. The results also suggest that the rate of the reaction through diacetatolead(II) complexes is much slower than those of the reactions through hydrated ions and monoacetato complexes.

The authors thank the Ministry of Education for the financial support granted for this research. A part of the experimental work was carried out with the assistance of Dr. Gen Satô.

Department of Chemistry
Faculty of Science
Tohoku University
Katahira-cho, Sendai

*Synthesis and Pyrolysis of N-Substituted γ-Aminobutyrates and N-Substituted Bis(β-ethoxycarbonylethyl)amines**

By Shiro MOROSAWA and Akira YOKOO

(Received October 31, 1962)

Some *N*-substituted γ-aminobutyrates and *N*-substituted bis(β-ethoxycarbonylethyl)amines were synthesized and their behaviors upon pyrolysis were investigated. Ethyl *N*-benzoyl-γ-(β-ethoxycarbonylamino)butyrate (III) and ethyl γ-[bis(β-ethoxycarbonylethyl)amino]-butyrate (II) were obtained from the reaction mixture of ethyl γ-aminobutyrate and ethyl acrylate by benzoylation. Direct distillation of the mixture did not give ethyl γ-(β-ethoxycarbonylethylamino)butyrate (I), but gave *N*-(β-ethoxycarbonylethyl)-2-pyrrolidone (V). III was also derived from II by heating with benzoyl chloride as McElvain[1] did about tris-(β-ethoxycarbonylethyl)amine (XIII). V was also obtained by heating II. Both III and V gave γ-(β-carboxyethylamino)butyric acid (IV) on hydrolysis. On heating IV above its melting point, *N*-(β-carboxyethyl)-2-pyrrolidone (VI) was formed, which returned to IV by hydrolysis. IV gave ethyl *N*-ethoxycarbonyl-γ-(β-ethoxycarbonylethylamino)butyrate (VII). Reaction of ethyl β-benzylaminopropionate[2] and ethyl γ-bromobutyrate afforded ethyl *N*-benzyl-γ-(β-ethoxycarbonylethylamino)butyrate (VIII) along with a small amount of *N*-benzyl-2-pyrrolidone (IX)[3]. IX also formed on heating VIII. IX was hydrolyzed to γ-benzylaminobutyric acid (X), which reformed IX by heating. Ethyl *N*, *N*-dibenzyl-γ-aminobutyrate (XI), which was synthesized from ethyl γ-aminobutyrate and benzyl chloride, cleaved into IX and benzyl ethyl ether on heating at about 280°C. When XI was heated in acetic anhydride, it was recovered unchanged. Hydrochloride XII of XI, on the other hand, decomposed readily at about 170°C to yield IX, benzyl chloride and ethanol. Tris(β-ethoxycarbonylethyl)amine (XIII) began to decompose at about 200°C and gave ethyl acrylate, ethanol and a substance which probably could be a condensation product of β-alanine. *N*-Benzyl-bis(β-ethoxycarbonylethyl)amine (XIV)[2,4] also split ethyl acrylate at about 197°C, but the composition of the residual substance was so complicated and could not be determined. *N*-Benzoyl-bis(β-ethoxycarbonylethyl)amine (XV)[1] resisted to decompose, and gave ethyl acrylate and ethyl *N*-benzoyl-γ-aminopropionate at a higher temperature, about 304°C. (Figs. 1 and 2).

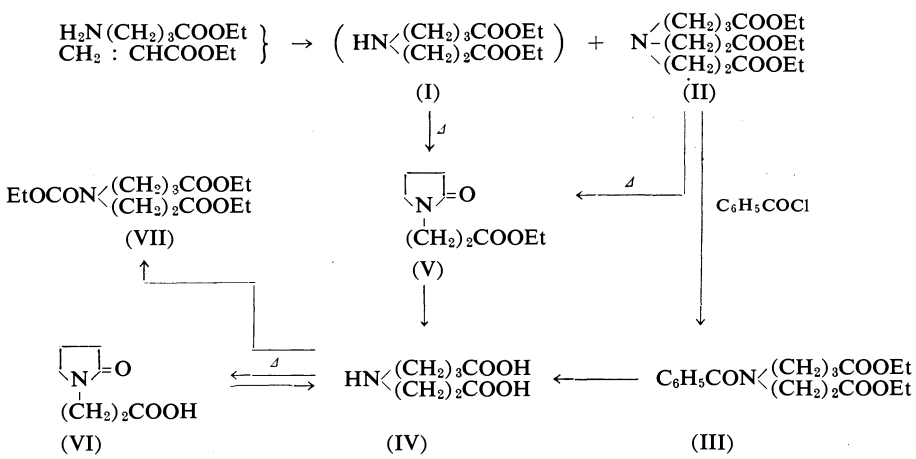

Fig. 1

* Arranged from "Syntheses of Some Amino Acids and Amino Aldehydes", II and III (*J. Chem. Soc. Japan, Pure Chem. Sec.* (*Nippon Kagaku Zassi*), **77**, 599 (1956); ibid., **79**, 1269 (1958)).

1) S. M. McElvain and G. Stork, *J. Am. Chem. Soc.*, **68**, 1049 (1946).

2) G. Stork and S. M. McElvain, ibid., **69**, 971 (1947).

3) E. Späth and J. Lintner, *Ber.*, **69**, 2730 (1936); M. W. Gittos and W. Wilson, *J. Chem. Soc.*, **1955**, 2375.

4) J. R. Thayer and S. M. McElvain, *J. Am. Chem. Soc.*, **49**, 2862 (1927).

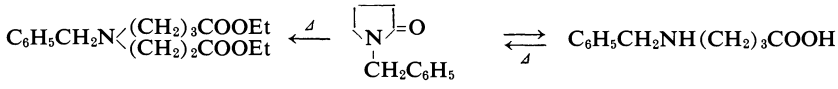

(VIII) (IX) (X)

Fig. 2

Consideration of the Pyrolytic Mechanism.—The ring formation of II during the heating may be driven by the intramolecular nucleophillic attack of nitrogen to carbonyl carbon to split ethyl acrylate and form the stable five-membered ring. (Fig. 3). Likewise, in the case of VIII, XI and XII, the same mechanism was considered. Especially the pyrolysis of XII took place more readily, and this was certainly assumed to be resulted from the positively charged nitrogen, which splits benzyl cation. (Fig. 4).

The decomposition of XIII, XIV and XV was, on the other hand, considered to proceed through an ammonium compound, reversely to the additive reaction between an amino compound and ethyl acrylate. The resistance observed in the pyrolysis of XV may be due to the decrease in electron density at the nitrogen by the neighboring carbonyl group.

The liberation of ethyl acrylate in the reaction between II and benzoyl chloride, on the contrary, will proceed like Hofmann's degradative reaction as shown in Fig. 5.

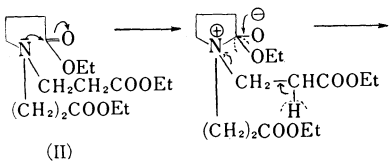

(II)

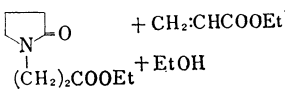

(V)

Fig. 3

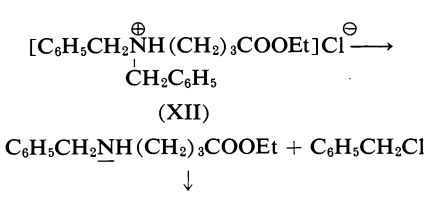

(XII)

(IX)

Fig. 4

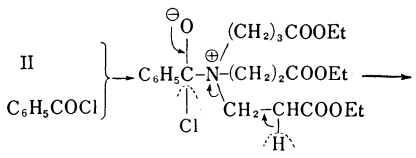

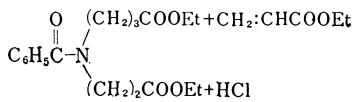

(III)

Fig. 5

Experimental

Ethyl γ-[Bis(β-ethoxycarbonylethyl)amino]butyrate (II) and Ethyl *N*-Benzoyl-γ-(β-ethoxycarbonylethylamino)butyrate (III).—To an ice-cold solution of 26.4 g. of sodium in 1 l. of absolute ethanol was added 190 g. of ethyl γ-aminobutyrate hydrochloride under stirring, followed, after 1 hr., by the addition of a solution of 115.6 g. of ethyl acrylate in 300 cc. of the same solvent. After stirring for 7 hr., the mixture was heated at 70~73°C with stirring. The solvent was removed under reduced pressure, and 100 cc. of dry benzene was added and distilled to expel completely any of the ethanol present. A solution of 160 g. of benzoyl chloride in 250 cc. of dry benzene was added to the residue and refluxed for 20 hr. Then 100 cc. of absolute ethanol was added and refluxed for 1.5 hr. After cooling, ice was added, and the benzene layer was washed successively with cold 10% sodium hydroxide solution, water, 10% hydrochloric acid, water and 5% sodium carbonate solution, and dried over calcium chloride. Removal of benzene and distillation of the residue gave 26 g. of III as a colorless viscous oil of b. p. 200~205°C/0.3 mmHg.

Found: C, 63.95; H, 7.46; N, 4.16. Calcd. for $C_{18}H_{25}O_5N$: C, 64.46; H, 7.51; N, 4.18%.

The above-mentioned acidic washes were united and made alkaline with sodium hydroxide solution. An oil liberated was taken up in ether and dried over calcium chloride. After removal of ether, vacuum distillation gave 129 g. of II as a colorless oil of b. p. 178~183°C/3.0 mmHg.

Found: N, 4.17. Calcd. for $C_{16}H_{29}O_6N$: N, 4.23%.

Reaction of II with Benzoyl Chloride.—A mixture of 66.3 g. of II and 34 g. of benzoyl chloride was heated in a round-bottomed flask attached to a fractionating column in an oil bath. At about 180°C (bath temp.), ethyl acrylate began to distil, and hydrogen chloride evolved vigorously. After 5 hr. at 185~195°C (bath temp.), 30 cc. of absolute ethanol was added to the remainder and refluxed for 1 hr. After cooling, sodium hydroxide solution

was added and extracted with ether. The ethereal solution was washed successively with 2 N hydrochloric acid, water, 5% potassium carbonate solution and water. Drying with calcium chloride and distillation gave 61 g. of III, boiling at 200~205°C/0.3 mmHg. III was not obtained from II and benzoyl chloride in xylene.

***N*-(β-Ethoxycarbonylethyl)-2-pyrrolidone (V).**—a) On heating 2 g. of II in an oil bath, ethyl acrylate and ethanol began to distil at about 190°C (bath temp.). The pyrolysis completed in about 1 hr. at 195~200°C (bath temp.), and 0.7 g. of a distillate was obtained. Distillation of the remainder gave 0.9 g. of V as a colorless oil of b. p. 130~131°C/3.0 mmHg.

Found: N, 7.52. Calcd. for $C_9H_{15}O_3N$: N, 7.56%.

b) By the same procedure in the preparation of II, 60 g. of ethyl γ-aminobutyrate hydrochloride and 35.8 g. of ethyl acrylate, using 8.2 g. of sodium, were allowed to react and directly vacuum-distilled to yield 25.6 g. of V, b. p. 129~131°C/2.5 mmHg (Found: N, 7.60%).

γ-(β-Carboxyethylamino)butyric Acid (IV).—a) After a mixture of 5 g. of III and 30 cc. of 6 N hydrochloric acid was refluxed for 4 hr., it was evaporated under reduced pressure. Water was added to the residue and again evaporated. The residue was taken up in a small amount of ethanol, and acetone was added until turbidity occurred. After standing, crystals formed were collected, washed with a little ethanol. The crystals were dissolved in hot ethanol, and ether was added until the solution became turbid to afford 1.6 g. of hydrochloride of IV as hygroscopic colorless crystals of m. p. 105~106°C.

Found: N, 6.64. Calcd. for $C_7H_{13}O_4N \cdot HCl$: N, 6.63%.

A solution of 1.2 g. of the hydrochloride in 30 cc. of water was treated with an excess of silver oxide, hydrogen sulfide and was evaporated under reduced pressure. The residue was dissolved in a small amount of water, and ethanol was added. Crystals which formed on being left to stand were recrystallized as before to give 0.9 g. of free IV as colorless needles of m. p. 151~152°C (decomp.).

Found: C, 47.85; H, 7.31; N, 8.20. Calcd. for $C_7H_{13}O_4N$: C, 47.99; H, 7.48; N, 8.00%.

b) A mixture of 5 g. of V and 50 cc. of 30% barium hydroxide solution was refluxed for 5 hr. The mixture was treated with carbon dioxide and filtered. The filtrate was adjusted at pH 4.0 with sulfuric acid, filtered and evaporated under reduced pressure. The residue was dissolved in a small amount of water, and ethanol was added. The resulting solution, on standing, gave 3.7 g. of colorless crystals, melting at 151~152°C under decomposition. These did not depress their melting point on admixture with the crystals obtained in a).

c) A mixture of 0.5 g. of VI and 5 cc. of 30% barium hydroxide solution was refluxed for 5 hr. and treated as mentioned in b) to give 0.35 g. of colorless crystals of m. p. 151~152°C (decomp.). These were found to be identical with the crystals in a) by mixed fusion.

***N*-Tosyl Derivative.**—A mixture of 0.1 g. of the hydrochloride of IV and 0.2 g. of *p*-toluenesulfonylchloride in sodium hydroxide solution was stirred for 4 hr. After removal of an excessive unreacted substance by extracting with ether, the solution was acidified by hydrochloric acid and taken up in ether. Ether was expelled, and the residue was recrystallized twice from dilute ethanol to give colorless crystals of m. p. 138~139°C.

Found: N, 4.45. Calcd. for $C_{14}H_{19}O_6NS$: N, 4.24%.

***N*-(β-Carboxyethyl)-2-pyrrolidone (VI).**—a) On heating 0.2 g. of IV in an oil bath at 160~165°C for 10 min., water was lost under melting. The cooled mass was dissolved in ethanol, and ether was added until turbidity took place. Crystals which formed were recrystallized as before to afford 0.15 g. of colorless crystals of m. p. 108~109°C.

Found: N, 9.04. Calcd. for $C_7H_{11}O_3N$: N, 8.91%. Found: equivalent to sodium hydroxide (phenolphthalein as an indicator), 158.5. Calcd. 157.17.

b) The filtrate of the hydrochloride of IV, which was mentioned in a) of preparation of IV, was evaporated, and water was added. The solution was treated with silver oxide and hydrogen sulfide, and was evaporated under reduced pressure to leave a viscous oily substance. Distillation of the oily substance gave an oil of b. p. 190~195°C/0.5 mmHg, which crystallized on standing. Recrystallization from ethanol gave 0.8 g. of colorless crystals of m. p. 108~109°C. These were identified with the crystals in a) by mixed fusion.

Ethyl *N*-Ethoxycarbonyl-γ-(β-ethoxycarbonylethylamino)butyrate (VII).—To a solution of 4 g. of sodium hydroxide in 50 cc. of water was added 11 g. of ethyl chlorocarbonate under stirring and cooling with water. After stirring for 5 hr, the solution was acidified with hydrochloric acid, and extracted twice with 50 cc. of benzene and twice with 50 cc. of ether. The extracts were combined, washed with water and dried over calcium chloride. The solvent was removed completely under reduced pressure. The residue was heated on a water bath (at 60~70°C) with 5 g. of thionyl chloride for 1.5 hr., and the whole was further heated for 1 hr. with 15 cc. of absolute ethanol. Removal of ethanol and distillation of the residue gave 4 g. of a colorless oil of b. p. 163~165°C/2.0 mmHg.

Found: N, 4.60. Calcd. for $C_{14}H_{25}O_6N$: N, 4.62%.

Ethyl *N*-Benzyl-γ-(β-ethoxycarbonylethylamino)-butyrate (VIII).—A mixture of 107 g. of ethyl β-benzylaminopropionate and 50 g. of ethyl γ-bromobutyrate was left to stand for 5 days at room temperature. Ethyl γ-benzylaminopropionate hydrobromide formed was separated by filtration and washed with ether. The filtrate and the ether washings were united, and ether was removed under reduced pressure. The residue was heated on a water bath for 3 hr. and left to stand overnight. The hydrobromide again formed was treated as above. The filtrate and ether washings were united, washed with 10% sodium carbonate solution and water, and dried over calcium chloride. Evaporation of ether and vacuum distillation gave 60 g. of an

oil of b. p. 171~173°C/0.1 mmHg.

Found: N, 4.42. Calcd. for $C_{18}H_{27}O_4N$: N, 4.36%.

***N*-Benzyl-2-pyrrolidone (IX).**—On heating 0.8 g. of VIII in an oil bath at 200°C, ethyl acrylate began to smell. After holding the temperature of the bath at 265~270°C for 2 hr., the remainder was vacuum-distilled to give 0.3 g. of an oil of b. p. 142~144°C/3.0 mmHg.

Found: N, 7.83. Calcd. for $C_{11}H_{13}ON$: N, 7.99%.

γ-Benzylaminobutyric Acid (X).—A mixture of 0.3 g. of IX and 10 cc. of 30% barium hydroxide solution was refluxed for 5 hr. to cause solution of the former. The mixture was diluted with 30 cc. of water, treated with carbon dioxide while hot, and filtered. The filtrate was evaporated to dryness and taken up in absolute ethanol. Ether was added to the ethanolic solution until turbidity took place. Crystals which formed on standing were collected and recrystallized in the same way to yield 0.2 g. of colorless crystals of m. p. 139~140°C (decomp.).

Found: C, 68.10; H, 7.72; N, 7.20. Calcd. for $C_{11}H_{15}O_2N$: C, 68.37; H, 7.82; N, 7.25%.

On fractional distillation of the foreruns in the distillation of VIII, 1.5 g. of an oil of b. p. 141~142°C/3.0 mmHg was obtained. Hydrolysis of the oil as above gave colorless crystals of m. p. 139~140°C (decomp.), which did not show any depression of the melting point on adimixture with the above crystals.

Ethyl *N*, *N*-Dibenzyl-γ-aminobutyrate (XI).—To a solution of 5 g. of sodium in 200 cc. of absolute ethanol was added 37.5 g. of ethyl γ-aminobutyrate hydrochloride. After 30 min., 56.5 g. of benzyl chloride was added and the resulting mixture was refluxed for 2 hr., followed by the further heating for 20 hr. with 61 g. of anhydrous potassium carbonate. The insoluble matters were separated and washed with absolute ethanol. The filtrate and the washings were combined, and ethanol was removed. Vacuum distillation of the residue gave 13.5 g. of a colorless viscous oil of b. p. 175~177°C/1.0 mmHg.

Found: N, 4.65. Calcd. for $C_{20}H_{25}O_2N$: N, 4.50%.

Pyrolysis of XI.—a) On heating 2.8 g. of XI in an oil bath, the decomposition began at about 280°C. The distillate, which was obtained during the heating for 3 hr., was taken up in ether, washed with water and dried over calcium chloride. Evaporation of ether and distillation of the residue gave 0.7 g. of a colorless oil of b. p. 184~187°C. The oil was found to be identical with benzyl ethyl ether by infrared spectrum.

Found: C, 79.65; H, 8.59. Calcd, for $C_9H_{12}O$: C, 79.37; H, 8.83%.

The residue of the pyrolysis gave, on vacuum distillation, 0.9 g. of an oil of b. p. 142~144°C/3.0 mmHg, corresponding to IX. Crystals of m. p. 139~140°C (decomp.) were derived from the oil by the same treatment as described in the preparation of XI, and were identified with XI by mixed fusion.

b) A solution of 3 g. of XI in 25 cc. of acetic anhydride was refluxed for 4 hr. The solvent was removed under reduced pressure, and the residue was vacuum-distilled to recover 2.7 g. of an oil of b. p. 175~177°C/1.0 mmHg. The formation of benzyl ethyl ether was not appreciated thereby.

Ethyl *N*, *N*-Dibenzyl-γ-aminobutyrate Hydrochloride (XII).—Dry hydrogen chloride was passed through a solution of 7 g. of XI in absolute ethanol. The solution was evaporated to dryness under reduced pressure. The residue was dissolved in the same solvent and again evaporated. After two repetitions of this treatment, the residue was dried over potassium hydroxide in a vacuum desiccator. On being left to stand in a refrigerator, the residue became crystalline. A small amount of benzene was added, and the crystalline substances were collected. These were dissolved in a small amount of absolute ethanol, diluted by adding twice the volume of benzene, and the solution was filtered from any undissolved matter present. Addition of ether and seeding caused crystallization. The formed crystals were collected and washed with benzene to yield 6.5 g. of colorless crystals, which began to soften at 146°C with effervescence and melted clearly at 160°C.

Found: N, 3.95. Calcd. for $C_{20}H_{25}O_2N \cdot HCl$: N, 4.02%.

Pyrolysis of XII.—On heating 5 g. of XII in an oil bath at 190~200°C for 1 hr., a fraction running over at 75~78°C was collected. This was assumed to be ethanol. Then 1.6 g. of a distillate was collected during the heating at 220°C. After washing the distillate with sodium carbonate solution and water, followed by drying over calcium chloride, distillation gave 1.1 g. of a colorless oil of b. p. 176~177°C.

Found: C, 66.60; H, 5.82. Calcd. for C_7H_7Cl: C, 66.42; H, 5.54%.

The oil was found to be benzyl chloride by the following procedure. That is, a mixture of 1 g. of the oil, 1.2 g. of anhydrous potassium carbonate and 1 g. of aniline was heated at 180°C for 3 hr. Water was added to the mixture and extracted with ether. After drying over anhydrous potassium carbonate, ether was expelled, and the residue was vacuum-distilled to give an oil of b. p. 180°C/14 mmHg, which crystallized to colorless crystals of m. p. 36°C by recrystallization from ligroin. These did not depress their melting point on admixture with the specimen prepared from benzyl chloride and aniline in the same way. Both hydrochlorides, on recrystallization from ethanol and ether, gave the same crystals which softened at 201°C in green and melted at 202~203°C, turning clear light brown.

On vacuum distillation of the residue in the above pyrolysis, 1.9 g. of IX of b. p. 140~142°C/3.0 mmHg was obtained. (Found: N, 7.80%). This was converted to *N*-benzyl-γ-aminobutyric acid by hydrolysis as before and identified by mixed fusion with the authentic sample.

Pyrolysis of Tris(β-ethoxycarbonylethyl)amine (XIII).—On heating 10 g. of XIII in an oil bath, decomposition began to occur at about 200°C. The bath temperature was held at 210~215°C until no distillate came out. Thereby 6.9 g. of a distillate was collected, which was fractionated into four parts: b. p. 79~85°C (0.5 g.), b. p. 85~90°C (0.4 g.), b. p. 90~96°C (0.4 g.) and b. p. 96~99°C (5.1 g.) (ethyl acrylate). The residue was impossible

to be distilled at 280°C (bath temp.) and 3 mmHg, but solidified on standing. A mixture of 1 g. of the residue and 6 N hydrochloric acid was refluxed for 5 hr. and evaporated under reduced pressure. The remainder was dissolved in water, treated with silver oxide and hydrogen sulfide. The resulting solution was evaporated to a smaller volume, and ethanol was added to cause crystallization. Crystals formed were collected and recrystallized from water and ethanol as before to yield 0.65 g. of colorless crystals of m. p. 197~198°C (decomp.). These were not depressed on admixture with the authentic β-alanine.

Pyrolysis of *N*-Benzyl-bis(β-ethoxycarbonylethyl)amine (XV).—On heating 5 g. of XV in an oil bath, decomposition began to occure at about 307°C. During the heating for 2 hr. at 310~320°C, 1.1 g. of a distillate of b. p. 95~98°C which was assumed to be ethyl acrylate was obtained. The remainder, on vacuum distillation, gave 1.8 g. of an oil of b. p. 157~158°C/2.5 mmHg. This was considered to be ethyl *N*-benzoyl-β-aminopropionate from the analytical values and the experiment below.

Found: C, 69.93; H, 8.42; N, 6.91. Calcd. for $C_{12}H_{17}O_2N$: C, 69.54; H, 8.27; N, 6.77%.

A mixture of 1 g. of the oil and 15 cc. of 6 N hydrochloric acid was refluxed for 4 hr. Benzoic acid which formed overnight was separated, and the filtrate was evaporated under reduced pressure. The residue was dissolved in water, treated with silver oxide and hydrogen sulfide, and again evaporated as before. The final residue was dissolved in a small amount of water, and ethanol was added to form 0.3 g. of β-alanine, melting at 197~198°C.

Chemical Institute
Faculty of Science
Okayama University
Tsushima, Okayama

Studies on Antibiotics and Related Substances. XVI. Syntheses of β-Acetochloro Derivatives of 3-Amino-3-deoxyglucose and 6-Amino-6-deoxyglucose

By Sumio UMEZAWA, Shinkiti KOTO and Yukio ITO

(Received November 10, 1962)

Acetohalogeno derivatives of sugars are important intermediates for the synthesis of glycosides. However, the corresponding derivatives of aminosugars represent a relatively unexplored territory. In the preceding paper in this series, the syntheses of α-acetobromo derivatives of 3-carbobenzoxyamino-3-deoxy- and 6-carbobenzoxyamino-6-deoxy-glucose have been developed. This paper reports the synthesis of 2, 4, 6-tri-*O*-acetyl-3-carbobenzoxyamino-β-1-chloro-1,3-dideoxy-D-glucopyranose (III) and 2,3,4-tri-*O*-acetyl-6-carbobenzoxyamino-β-1-chloro-1, 6-dideoxy-D-glucopyranose (VII). These β-acetochloro derivatives are significant for preparing α-glycoside of aminosugars, as shown here in the prepartion of methyl 2, 4, 6-tri-*O*-acetyl-3-carbobenzoxyamino-3-deoxy-α-D-glucopyranoside (IV) and methyl 2, 3, 4-tri-*O*-acetyl-6-carbobenzoxyamino-6-deoxy-α-D-glucopyranoside (VIII).

The synthesis of III and IV are outlined in the following Chart A:

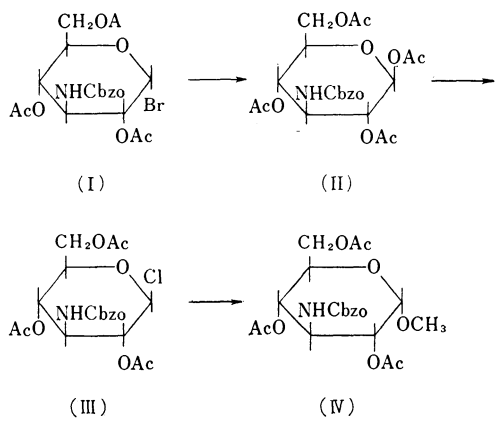

Chart A

2, 4, 6-Tri-*O*-acetyl-1-α-bromo-3-carbobenzoxyamino-1, 3-dideoxy-D-glucopyranose (I) prepared by our method[1] was acetylated by refluxing with silver acetate in dried benzene to give 1, 2, 4, 6-tetra-*O*-acetyl-3-carbobenzoxyamino-3-deoxy-β-D-glucopyranose (II) in 77% yield.

1) Y. Ito, S. Koto and S. Umezawa, This Bulletin, 35, 1618 (1962).

TABLE I

Compound	Specific rotation: Observed in $CHCl_3$	Specific rotation: Calcd.	IR-Absorption, cm^{-1}
II	$[\alpha]_D^{7.5}$ +17.5° (*c* 0.87)	+ 14.8°	898 (Nujol)
III	$[\alpha]_D^{15}$ − 3.5° (*c* 0.85)*	+ 6.3°	890 (KBr)
IV	$[\alpha]_D^{15}$ +75.6° (*c* 0.91)	+116°	847 ($CHCl_3$)
VI	$[\alpha]_D^{12}$ +10.2° (*c* 1.6)	+ 14.8°	892 (Nujol)
VII	$[\alpha]_D^{15}$ + 0.17° (*c* 1.7)**	+ 6.3°	901 (KBr)
VIII	$[\alpha]_D^{15}$ +81° (*c* 0.91)	+116°	847 ($CHCl_3$)

* A rotation change from −3.5 to +55° (192 hr.) was observed.
** A rotation change from +0.17 to +56.3° (144 hr.) was observed.

Zemplén and Mester[2], and Korytnyk and Mills[3] reported on the preparation of so called "unstable chlorides" from fully acetylated aldopyranoses by treatment with aluminum chloride in cold chloroform. When a similar procedure was applied to II at room temperature, a 92.7% yield of 2, 4, 6-tri-*O*-acetyl-1-β-chloro-3-carbobenzoxyamino-3-deoxy-D-glucose (III) was obtained. As detailed below, the specific rotation of III changed very slowly from −3.5 to +55° in dried chloroform during 192 hr.

An attempt to prepare an α-glycoside from III proved to be practical. When shaken with methanol in the presence of silver carbonate and anhydrous calcium carbonate by the procedure of Wolfrom[4], methyl 2, 4, 6-tri-*O*-acetyl-3-carbobenzoxyamino-3-deoxy-α-D-glucopyranoside (IV) was obtained in 67.3% yield.

2, 3, 4-Tri-*O*-acetyl-6-carbobenzoxyamino-1-β-chloro-1, 6-dideoxy-D-glucopyranose (VII) and the corresponding methyl α-glycoside (VIII) have been synthesized by an analogous route outlined in the following Chart B:

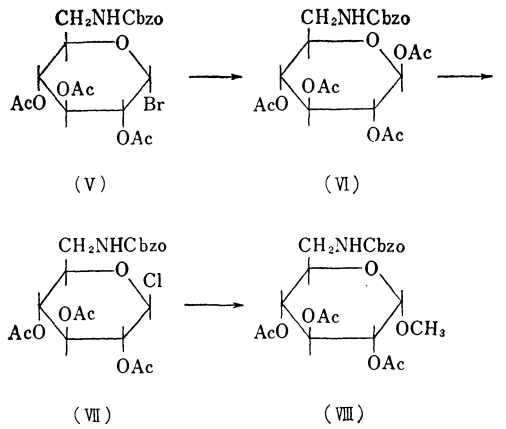

Chart B

2, 3, 4-Tri-*O*-acetyl-6-carbobenzoxyamino-1-β-chloro-1, 6-dideoxy-D-glucopyranose (VII) was obtained in an 89.5% yield and, when subjected to the procedure of Wolfrom mentioned above, VII gave an α-glycoside, methyl 2, 3, 4-tri-*O*-acetyl-6-carbobenzoxyamino-1, 6-dideoxy-D-glucopyranoside (VIII) in 61% yield.

Infrared spectra of the acetochloro derivatives (III, VII) showed absorption near 890 cm^{-1} which is characteristic of β-configuration, while the methylglycosides (IV, VIII) showed absorptions near 840 cm^{-1}, indicating that the methylglycosides have α-configuration as expected from the solvolytic mechanism. Moreover, determination of specific rotation of the above-mentioned derivatives consisted with the spectroscopic results, as shown in Table I, where these data are shown together with the calculated values using Hudson's rules modified by Korytnyk[5].

The agreement between the observed and calculated values of the glycosides (IV, VIII) is not so good, but the results seem to be allowable. The observed differences probably are to be ascribed to concomitance of β-anomer and an orthoester derivative, which are rather often the main product of the Koenigs-Knorr reaction. When the glycoside (IV) was deacetylated with methanolic ammonia and then catalytically reduced to remove the carbobenzoxyl group, there was obtained a mixture of methyl 3-amino-3-deoxy-α-D-glucoside and 3-amino-3-deoxy-D-glucose, which were identified by paper chromatography. The former was a main product and identified by comparison with an authentic specimen obtained by methanolysis of kanamycin. The formation of 3-amino-3-deoxy-D-glucose probably indicates the concomitance of orthoester derivative in the glycoside (IV), provided that the glycosidic linkage is stable enough in the above-mentioned series of reactions. Since the methyl α-glycoside was obtained as a main product, it is probable that, in the case of acetochloro derivatives of

2) G. Zemplén and L. Mester, *Acta Chim. Acad. Sci., Hungary*, **4**, 73 (1954).
3) W. Korytnyk and J. A. Mills, *J. Chem. Soc.*, **1959**, 636.
4) M. L. Wolfrom, A. O. Pittet and I. C. Gillam, *Proc. Nat. Acad. Sci.*, **47**, 700 (1961).
5) W. Korytnyk, *J. Chem. Soc.*, **1959**, 650.

3-carbobenzoxyamino-3-deoxyglucose and 6-carbobenzoxyamino-6-deoxyglucose, the replacement reaction[6] took place more rapidly than the interconversion of isomeric halides.

It should be noted also that the reaction of 1, 3, 4, 6-tetra-*O*-acetyl-2-carbobenzoxyamino-2-deoxy-D-glucose (IX) with aluminum chloride by a similar procedure to that used for the preparation of III and VII afforded 4, 5-(3, 4, 6-tri-*O*-acetyl-D-glucopyrano)-2-oxazolone which had been described by Konstas et al.[7]

Experimental

1, 2, 4, 6-Tetra-*O*-acetyl-3-carbobenzoxyamino-3-deoxy-β-D-glucopyranose (II).—A mixture of 3.0 g. of 2, 4, 6-tri-*O*-acetyl-1-α-bromo-3-carbobenzoxyamino-1, 3-dideoxy-D-glucopyranose (I) prepared by our method[1] and 2.0 g. of well dried silver acetate in 100 ml. of benzene was refluxed for 8 hr. and cooled. A small quantity of active charcoal was added to the resulting mixture, followed by filtration. The filtrate was concentrated under reduced pressure and the residue was recrystallized from isopropanol to yield 2.17 g. (77%) of 1, 2, 4, 6-tetra-*O*-acetyl-3-carbobenzoxyamino-3-deoxy-β-D-glucopyranose, m. p. 165.5~166°C, $[\alpha]_D^{7.5}$ +17.5° (*c* 0.87, $CHCl_3$). The infrared spectrum of the product in Nujol contains absorption bands at 3350 (νNH), 1757 (νC=O in OAc), 1713 (νC=O in Cbzo), 1550 (δNH), 1231, 1215 (νC-O in OAc), 898 (type 2b of pyranose ring), 775, 738, 696 (phenyl).

Found: C, 54.46; H, 5.64; N, 3.08. Calcd. for $C_{22}H_{27}NO_{11}$ (481.5): C, 54.88; H, 5.67; N, 2.91%.

2, 4, 6-Tri-*O*-acetyl-1-β-chloro-3-carbobenzoxyamino-1, 3-dideoxy-D-glucopyranose (III).—A mixture of 0.25 g. of 1, 2, 4, 6-tetra-*O*-acetyl-3-carbobenzoxyamino-3-deoxy-β-D-glucopyranose (II) and 0.3 g. of freshly prepared aluminum chloride in 5 ml. of chloroform was shaken at room temperature for 40 min. After addition of 60 ml. of benzene, the resulting mixture was washed with each 8 ml. of ice water thrice. The benzene-layer was dried over sodium sulfate and evaporated to dryness under reduced pressure and the residue was recrystallized from ether-petroleum ether and then ether to yield 0.22 g. (92.7%) of colorless crystals of 2, 4, 6-tri-*O*-acetyl-1-β-chloro-3-carbobenzoxyamino-1, 3-dideoxy-D-glucopyranose, m. p. 151~151.5°C, $[\alpha]_D^{15}$ −3.5° (initial) → +55° (final, 192 hr.) (*c* 0.85, $CHCl_3$). The infrared spectrum of the product in potassium bromide contains absorption bands at 3160 (νNH), 1763 (νC=O in OAc), 1715 (νC=O in Cbzo), 1545 (δNH), 1228 (νC-O in OAc), 890 (type 2b of pyranose ring), 774, 738, 696 (phenyl).

Found: C, 52.50; H, 5.04; N, 3.08; Cl, 7.30. Calcd. for $C_{20}H_{24}NO_9Cl$ (458.0): C, 52.35; H, 5.27; N, 3.08; Cl, 7.76%.

Methyl 2, 4, 6-Tri-*O*-acetyl-3-carbobenzoxyamino-3-deoxy-α-D-glucoside (IV).—A mixture of 60 mg. of silver carbonate prepared by the procedure of Wolfrom et al.[4] and 400 mg. of anhydrous calcium sulfate in 4 ml. of anhydrous methanol was shaken in dim light for 15 min. at room temperature. To the suspension were added 0.15 g. of 2, 3, 4-tri-*O*-acetyl-1-β-chloro-3-carbobenzoxyamino-1, 3-dideoxy-D-glucopyranose (III), 10 mg. of silver perchlorate and a small quantity of anhydrous calcium sulfate and the mixture was shaken in dim light for 3.5 hr. at room temperature. After removal of silver salts by filtration, the solvent was removed by evaporation under reduced pressure and the residue was dissolved in chloroform and allowed to stand overnight. After removal of an insoluble matter by filtration the filtrate was evaporated to give a crystalline residue, which was recrystallized from isopropanol-hexane to yield 0.1 g. (67.3%) of crystals of methyl 2, 4, 6-tri-*O*-acetyl-3-carbobenzoxyamino-3-deoxy-α-D-glucopyranoside, m. p. 129~130°C, $[\alpha]_D^{15}$ +75.6° (*c* 0.91, $CHCl_3$). The infrared spectrum of the product in chloroform contains absorption bands at 3350 (νNH), 1753 (νC=O in OAc), 1730 (shoulder) 1523 (δNH), 1210 (νC-O in OAc), 847 (type 2a pyranose ring), 695 cm^{-1} (phenyl).

Found: C, 55.83; H, 5.76; N, 3.15. Calcd. for $C_{21}H_{27}NO_{10}$ (453.5): C, 55.77; H, 5.76; N, 3.07%.

A sample of 20 mg. of the above product was dissolved in 4 ml. of methanol saturated with ammonia and allowed to stand overnight in a refrigerator and evaporated to dryness under reduced pressure. The residue was taken up in about 4 ml. of aqueous methanol and 40 mg. of paladium chloride-charcoal catalyst was added to the solution. pH of the mixture was adjusted to about 2 with dilute hydrochloric acid and hydrogenated at room temperature for 3 hr. As the reaction mixture gradually became alkaline, a small quantity of dilute hydrochloric acid was repeatedly added to adjust pH to about 2. After removal of the catalyst by filtration, the solution was evaporated to dryness under reduced pressure. The residue was dissolved in 0.4 ml. of water and subjected to paper chromatography, using two solvent systems. The spots were identified by coloration with ninhydrin and silver-ammonia. The solvent system butanol-pyridine-acetic acid-water (6 : 4 : 1 : 3) gave two spots of R_f 0.43 and 0.30 which were identical with the spots of authentic specimen of methyl 3-amino-3-deoxy-D-α-glucoside (R_f 0.43) obtained by methanolysis of kanamycin and a synthetic specimen of 3-amino-3-deoxy-D-glucose[8] (R_f 0.30). The solvent system butanol-acetic acid-water (10 : 2 : 5) gave two spots of R_f 0.23 and 0.14, which were identical with the spots of the above-mentioned specimens (R_f 0.23, 0.15).

1, 2, 3, 4-Tetra-*O*-acetyl-6-carbobenzoxyamino-6-deoxy-β-D-glucopyranose (VI).—A mixture of 0.3 g. of 2, 3, 4-tri-*O*-acetyl-1-bromo-6-carbobenzoxyamino-1, 6-dideoxy-D-glucopyranose (V) prepared by our method[1] and 0.2 g. of silver acetate in 10 ml. of benzene was refluxed for 8 hr. and then worked up

6) The anomeric replacement by the Koenigs-Knorr reaction was discussed in detail by H. L. Frush and H. S. Isbell, *J. Research Natl. Bur. Standards*, **27**, 413 (1941); E. Pascu, *Advances in Carbohydrates Chemistry*, **1**, 78 (1945); and R. U. Lemieux, ibid., **9**, 1 (1954).

7) S. Konstas, A. I. Photake and L. Zervas, *Chem. Ber.*, **92**, 1288 (1959).

8) Y. Ito, S. Koto and S. Umezawa, This Bulletin, **35**, 16 (1962).

in a similar manner to that used for the compound II. The crude product was recrystallized from ethanol repeatedly to yield 0.18 g. (63.6%) of 1,2,3,4-tetra-*O*-acetyl-6-carbobenzoxyamino-6-deoxy-β-D-glucopyranose, m. p. 144~145°C, $[\alpha]_D^{12}$ +10.2° (*c* 1.6, $CHCl_3$). The infrared spectrum of the product in Nujol contains absorption bands at 3385, 1760, 1745, 1550, 1240, 1212, 892, 774, 736, 700 cm^{-1}.

Found: C, 55.22; H, 5.75; N, 3.18. Calcd. for $C_{22}H_{27}NO_{11}$ (481.5): C, 54.88; H, 5.67; N, 2.91%.

2,3,4-Tri-*O*-acetyl-6-carbobenzoxyamino-1-β-chloro-1,6-dideoxy-D-glucopyranose (VII). — This material was prepared from 0.33 g. of 1,2,3,4-tetra-*O*-acetyl-6-carbobenzoxyamino-6-deoxy-β-D-glucopyranose and 0.42 g. of aluminum chloride by the method used for the preparation of compound III. The crude product was recrystallized from ether-petroleum ether and then from benzene-ether to yield 0.28 g. (89.5%) of colorless crystals of 2,3,4-tri-*O*-acetyl-6-carbobenzoxyamino-1-β-chloro-1,6-dideoxy-D-glucopyranose, m. p. 158~158.5°C (decomp.), $[\alpha]_D^{15}$ +0.17° (initial) → +56.3° (final, 144 hr.) (*c* 1.7, $CHCl_3$). The infrared spectrum of the product in potassium bromide contains absorption bands at 3235, 1753, 1728, 1520, 1252, 1220, 901, 772 751, 696 cm^{-1}.

Found: C, 52.58; H, 5.29; N, 2.95; Cl, 7.36. Calcd. for $C_{20}H_{24}NO_9Cl$ (458.0): C, 52.35; H, 5.27; N, 3.08; Cl, 7.76%.

Methyl 2,3,4-Tri-*O*-acetyl-6-carbobenzoxyamino-6-deoxy-α-D-glucopyranoside (VIII). — A mixture of 60 mg. of silver carbonate prepared by the method of Wolfrom et al.[4] and 300 mg. anhydrous calcium sulfate in 4 ml. of anhydrous methanol was shaken in dim light for 15 min. at room temperature. To the suspension was added 0.124 g. of 2,3,4-tri-*O*-acetyl-6-carbobenzoxyamino-1-β-chloro-1,6-dideoxy-D-glucopyranose and 10 mg. of silver perchlorate and the mixture was shaken in dim light for 2 hr. and then worked up in a similar manner to that used for the compound IV. The crude product was dissolved in isopropanol and *n*-hexane was added to the solution to yield a syrup, which was triturated with *n*-hexane to yield 0.075 g. (61%) of a crystalline powder of methyl 2,3,4-tri-*O*-acetyl-6-carbobenzoxyamino-6-deoxy-α-D-glucopyranoside, $[\alpha]_D^{15}$ +81° (*c* 0.91, $CHCl_3$). The infrared spectrum of the product in chloroform contains absorption bands at 3460, 1758, 1735, 1520, 1233, 1213, 847, 697 cm^{-1}.

Found: C, 55.30; H, 6.22; N, 3.10. Calcd. for $C_{21}H_{27}NO_{10}$ (453.5): C, 55.77; H, 5.76; N, 3.07%.

1,3,4,6-Tetra-*O*-acetyl-2-carbobenzoxyamino-2-deoxy-D-β-glucose (IX).—A mixture of 350 mg. of 2,4,6-tri-*O*-acetyl-1-bromo-2-carbobenzoxyamino-1,2-dideoxy-α-D-glucopyranose[9] and 245 mg. of silver acetate in 25 ml. of benzene was refluxed for 7 hr. and then worked up in a similar manner to that used for the compound II. The crude product was recrystallized from isopropanol-hexane to yield 250 mg. of the title compound, m. p. 147~148°C. Repeated recrystallization raised the m. p. to 150~150.5°C[10], $[\alpha]_D^{23}$ +28.1° (*c* 1.4, $CHCl_3$).

Found: C, 54.98; H, 5.70; N, 2.96. Calcd. for $C_{22}H_{27}NO_{11}$ (481.2): C, 54.88; H, 5.67; N, 2.91%.

Formation of Oxazolone Derivative from Tetra-acetyl Derivative of 2-Carbobenzoxyamino-2-deoxy-D-glucose.—A mixture of 630 mg. of 1,3,4,6-tetra-*O*-acetyl-2-carbobenzoxyamino-2-deoxy-D-glucose and 630 mg. of freshly prepared aluminum chloride in 9.5 ml. of chloroform was shaken at room temperature for 40 min. After addition of 150 ml. of benzene, the resulting mixture was washed with water and the benzene-layer was dried over sodium sulfate and evaporated to dryness under reduced pressure. Trituration of the residue with ether-petroleum ether yielded crystals of 4,5-(3,4,6-tri-*O*-acetyl-D-glucopyrano)-2-oxazolone; yield 450 mg. (75%). Recrystallization from benzene gave m. p. 170.5~174°C[11].

Found: N, 4.08. Calcd. for $C_{13}H_{17}NO_9$ (331.3): N, 4.02%.

The authors wish to express their appreciation for stimulating advice and interest in this research to Dr. Horace S. Isbell of the Organic Chemistry Section, National Bureau of Standards, U. S. A. The authors are also grateful to Mr. Saburo Nakada for microanalysis and Mr. Shin-ichi Nakamura and Mr. Yoshiaki Ito for helping their experiments.

Department of Applied Chemistry
Faculty of Engineering
Keio University
Koganei, Tokyo

9) L. Zervas and S. Konstans, *Chem. Ber.*, **93**, 435 (1960).
10) Reported m. p. 151.5~152°C. W. H. Bromund and R. M. Herbst, *J. Org. Chem.*, **10**, 267 (1945).
11) Reported m. p. 174~175°C. S. Konstas, A. I. Photake and L. Zervas, loc. cit.

*Permeability of Acidic Amino Acid through Anion Exchange Membrane**

By Yujiro HARA*

(Received January 22, 1962)

In order to obtain necessary information on the applicability of an ion-exchange membrane to the separation and purification of amino acids, experiments were carried out to study the permeability of an acidic amino acid through an anion exchange membrane comprised of a styrene-butadiene copolymer, and also to find membranes suitable for the separation of amino acids from chloride ions, conditions for electrolysis, and under what conditions acidic amino acids might or might not permeate through the membrane.

It was found that the permselectivity coefficient, T, of an acidic amino acid through an anion exchange membrane varied according to the current density, the total concentration of acidic amino acid and of chloride ions in the mixed solution used, the hydrogen ion concentration of the mixed solution and of the adjacent solution, separated by a membrane, and the character of the ion-exchange membrane used.

The permeability of ions through an ion-exchange membrane is very complicated, for it is affected by many factors. When an ion dialyzes through an ion-exchange membrane, the permeability of the ion is affected by the equilibrium according to the adsorption of ions by the ion-exchange membrane if the size of the ion is sufficiently smaller than that of the pores of the ion-exchange membrane. However, the permeability of an acidic amino acid through an ion-exchange membrane becomes more complicated when the size of the ion is approximately the same as that of the pore. Also, the hydrogen ion concentration in the membrane may have a very marked effect on the mobility of the amino acid in the membrane as acidic amino acid is an amphoteric electrolyte.

An experiment was carried out with a mixed solution of acidic amino acid and of a chloride ion system in order to examine the permeability of an acidic amino acid through an anion exchange membrane; the permselectivity coefficient, T, was also defined.

$$T=\frac{[A]_t}{[Cl]_t}\cdot\frac{[Cl]_s}{[A]_s} \quad (1)$$

where

$[A]_t$: Moles of acidic amino acid permeated
$[Cl]_t$: Moles of chloride ion permeated
$[A]_s$: Moles of acidic amino acid in the mixed solution
$[Cl]_s$: Moles of chloride ion in the mixed solution

Consequently, the value, T, is a criterion of the permeability of amino acid, with chloride as the standard.

Experimental

Properties of the Anion Exchange Membranes Used.—Membranes A-1 to A-3 were prepared by forming a styrene-butadiene copolymer with a styrene content of 50% into a thin membrane with heating rolls; cross-linkage was carried out by a Friedel-Crafts type catalyst such as the aluminum chloride-ether complex or titanium tetrachloride, followed by chloromethylation and quartenarization[1]. The pore size of the membrane can be changed to any desired size during this process by adjusting the cross-linkage of the resin component of the membrane[2]. The pore size of these membranes is in the decreasing order of A-1, A-2 and A-3

Membranes A-4 to A-6 were prepared by coating the A-3 membrane with a thin layer of such high-molecular substances as styrenesulfonic acid-butadiene copolymer, polyvinylbutyral polymer, and phenolsulfonic acid-formaldehyde condensate to form a porous net. The cation exchange membrane was prepared by sulfonating the above-mentioned thin membrane of styrene-butadiene copolymer with concentrated sulfuric acid[1]. Table I summarizes the properties of these anion and cation exchange membranes. The pore sizes of anion exchange membranes derived from styrene-butadiene copolymer were compared according to the values of water content, W (the amount of water per unit weight of the dry resin), the water penetration ratio[3] (K) of the membrane, and the specific

* This article reports on part of a long-run research program on ion-exchange membranes being conducted by Professor T. Kuwata and Assistant Professor S. Yoshikawa of The University of Tokyo. Part of the data given in this article were presented at the 12th Annual Meeting of the Chemical Society of Japan, Kyoto, April, 1959.

1) T. Kuwata and S. Yoshikawa, Japanese Pat. 239596, 239724, 248669; Brit. Pat. 793212, 804176.
2) S. Yoshikawa, Y. Uchida, A. Yamamoto and T. Kuwata, Presented at the 13th Annual Meeting of the Chemical Society of Japan, Tokyo, April, 1960; T. Kuwata and S. Yoshikawa, Japanese Pat. 248669.
3) Kogyo Butsurikagaku Kenkyu-kai, "Kogyo Butsurikagaku", 2nd Ed., Korona-sha, Tokyo, p. 111.

TABLE I. PROPERTIES OF ION-EXCHANGE MEMBRANES USED

Type	Notation	Capacity of ion-exchange radical in membrane meq./g.	Concn. of ion-exchange radical in membrane meq./g.	Water content of membrane W, %	Water penetration ratio[a] K, $\times 10^{-16}$ cm^3	Specific resistance Ω-cm.	Ion permselectivity (0.1 N NaCl)	Thickness mm.
Anion exchange membrane	A-1	1.78	1.84	54.8	0.45	120	0.85	0.45
	A-2	1.69	3.16	47.2	0.23	250	0.91	0.26
	A-3	1.68	3.91	31.2	0.18	—	0.90	0.23
Fabric coated anion exchange membrane[b]	A-4					125		
	A-5					61		
	A-6					—		
Cation exchange membrane	C-1	1.32	2.13	50.1	0.32	100	0.92	0.28

a) Degree of permeation of a diaphragm is a value indicating the size and distribution of pores derived from Poiseville's law on the assumption that the cross-section of pores of diaphragm is round. This is ordinarily indicated by the quantity (cc.) which transfer through 1 cm^2 of diaphragm having a thickness of 1 cm. in one hour under a static pressure of 1 cm. of water column when 0.5 M sucrose solution and water are placed on the opposite sides of the diaphragm.

b) See Table II.

TABLE II. METHOD FOR PRODUCING AN ION-EXCHANGE MEMBRANE COATED WITH HIGH MOLECULAR SUBSTANCES

Notation	Method for producing coated membrane
A-4	A benzene solution of styrene-butadiene copolymer with a styrene content of 50% is coated on one surface of the A-3 membrane and then sulfonated by dipping it in a 96% sulfuric acid solution for 6 hr.
A-5	One surface of the A-3 membrane is coated 3 times with an ethyl acetate solution of a 3% polyvinylbutyral solution with a brush.
A-6	A solution composed of 4 mol. of phenol, 1 mol. of *p*-phenolsulfonic acid, 3 mol. of sodium hydroxide, and 7 mol. of formaldehyde solution is left standing overnight and then heated to 70~80°C, by which means a viscous solution is obtained. The methanol solution of this is coated on one surface of the A-3 membrane, air-dried at 60°C, and cured by heating it at 120°C for 3~4 hr.

resistance (Ω-cm.). Although these values are the products of the size and number of pores of the membranes and do not indicate the size of the pores themselves, these were used as approximate comparative values.

Apparatus and Procedure.—An electrolytic cell*1, separated by 4 sheets of 7.5 cm. × 7.5 cm. anion and cation exchange membranes, as illustrated in Fig. 1, was used, with carbon (7 cm. × 14 cm. × 0.8 cm.) as the anode and nickel plate (7 cm. × 7 cm. × 0.3 mm.) as the cathode. In the intermediate compartments A and C, a 0.2% sodium sulfate solution was placed, a definite quantity of the mixed solution containing acidic amino acid and chloride ion (a quantity such that the reduction of acidic amino acid and chloride ions before and after the experiment is below 1%) is circulated in the direction of the arrow in compartment B, and a 3% sodium sulfate solution was circulated as the electrode solution in the direction of the arrow at a rate of 0.1~11./hr. in order to neutralyze the hydrogen ions and hydroxide ions produced in the electrode solution at all times and thus to prevent any effect of pH value fluctuation in the intermediate solution. A current of 5000~10000 coulombs was passed through each time. The solution in compartment C was removed after the current had been passed through, a quantitative analysis of the chloride

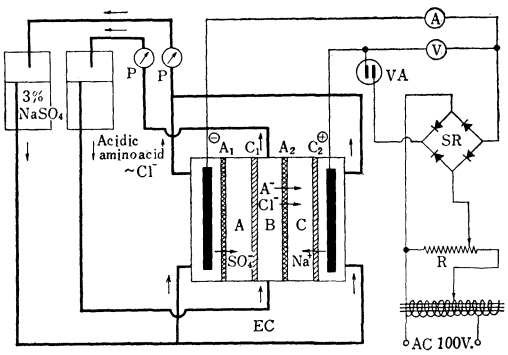

Fig. 1. Apparatus.
A Ammeter
EC Electrolytic cell
P Pump
SR Selenium rectifier
V Voltmeter
VA Copper voltameter

*1 The electrolytic cell was made by assembling the various compartments in the form indicated in Fig. 3 (for intermediate compartments) and in Fig. 4 (for electrode compartments) of a previous paper[4]. The same electrodes as used in this previous work were used.

4) Y. Hara, *J. Chem. Soc. Japan, Ind. Chem. Sec.* (*Kogyo Kagaku Zasshi*), 65, 885 (1962).

ions was made by the Volhard or Mohr method, the acidic amino acid was analyzed by colorimetry[5], and then the T values were determined from these values by using Eq. 1. The transport numbers of the acidic amino acid and of the chloride ions (t_G or t_A*2 and t_{Cl}) were calculated from the following equations from the quantity of electricity Q (coulomb), which had been determined by the use of a copper voltameter:

$$t_G \text{ or } t_A = \frac{Q[A]_t}{96496} \times 100 \quad (2)$$

$$t_{Cl} = \frac{Q[Cl]_t}{96496} \times 100 \quad (3)$$

The experiment was carried out in the temperature range of 15~25°C, but no temperature correction of the T value was made as it was assumed that the relative change in mobility between the acidic amino acid and the chloride ions could be ignored within this temperature range. The electrolytic cell was provided with two pairs of anion and cation exchange membranes, A_1 and C_1, and A_2 and C_2, as is illustrated in Fig. 1, of which, the A_1, C_1 and C_2 membranes were fixed throughout the experiment; only the anion exchange membrane A_2 was changed. Thus, the A-2 membrane was used for the A_1 membrane in Fig. 1, and the C-1 membrane for the C_1 and C_2 membranes.

Results and Discussion

Tables III and IV and Figs. 2—1~2—11 show the experimental conditions and results.

Effect of Current Density.—The permselectivity coefficient, T, should be little affected by varying the current density if the ion-exchange resin pores are sufficiently larger than the size of the acidic amino acid molecules; if this T value changes considerably with the current density, this indicates that the ion-exchange membrane is obstructing the permeation of the ions. Figure 2-1 shows the case of A-2 membrane-glutamic acid (neutral solution). It can be seen that there is a tendency for the ion-exchange membrane to obstruct the

Table III. Experimental conditions

Runs No.	Anion exchange membrane (A_2)	Acidic amino acid*2	Acidic amino acid chrolide ion system		
			pH	$[A]_s$, M	$[Cl]_s$, M
1	A-2	G	6.8	0.10	0.10
2	A-2	G	6.8	0.20	0.20
3	A-2	G	6.8	0.05	0.05
4	A-2	G	6.8	0.09	0.10
5	A-2	G	6.8	0.09	0.08
6	A-2	G	6.8	0.09	0.05
7	A-2	G	6.8	0.09	0.03
8	A-2	G	6.8	0.15	0.05
9	A-2	G	6.8	0.05	0.15
10	A-1	G	6.8	0.10	0.10
11	A-1	G	6.8	0.20	0.20
12	A-2	G	11.6	0.09	0.10
13	A-2	G	3.6	0.09	0.10
14	A-2	G	1.85	0.09	0.10
15	A-1	G	11.6	0.10	0.10
16[a]	A-2	G	6.8	0.10	0.10
17[b]	A-2	G	6.8	0.10	0.10
18[a]	A-1	G	6.8	0.10	0.10
19[b]	A-1	G	6.8	0.10	0.10
20	A-3	G	6.8	0.10	0.10
21	A-4	G	6.8	0.10	0.10
22	A-5	G	6.8	0.10	0.10
23	A-6	G	6.8	0.10	0.10
24	A-2	A	6.8	0.10	0.10
25	A-2	A	6.8	0.20	0.20
26	A-2	A	6.8	0.05	0.05
27	A-1	A	6.8	0.10	0.10
28	A-1	A	11.4	0.10	0.10

Adjacent solution; a) 1 N sulfuric acid solution; b) 0.1 N sulfuric acid solution

5) M. Yamagishi and T. Yoshida, *Yakugaku Zasshi*, **73**, 673 (1954).

*2 G stands for glutamic acid and A, for aspartic acid.

TABLE IV. TRANSPORT NUMBER OF ACIDIC AMINO ACID AND CHLORIDE ION

Runs No.	t_G or t_A Currrent density, amp./dm²						t_{Cl} Current density, amp./dm²					
	1.50	1.00	0.75	0.50	0.25	0.10	1.50	1.00	0.75	0.50	0.25	0.10
1	11.3	8.0	8.2	4.6	7.7	2.1	88.8	92.6	100.1	95.9	92.1	94.9
10	24.1	28.1	20.6	15.3	11.9	13.8	65.5	77.6	76.7	84.6	90.4	97.4
11	—	16.0	9.8	10.3	10.1	11.7	—	84.2	84.9	84.2	91.1	103.0
13	—	1.6 (2.7)	—	—	—	—	—	53.5	—	—	—	—
14	1.0 (6.2)	1.1 (4.5)	—	2.9 (8.4)	—	—	50.7	52.0	—	95.9	—	—
16	1.4	0.8	0.3	0.1	—	0.2	71.5	44.3	43.6	37.5	—	31.3
17	1.7	2.0	1.9	1.6	—	1.7	71.4	82.8	81.9	84.1	—	78.7
18	1.3	1.0	1.2	—	—	2.1	26.9	24.2	20.5	—	—	16.2
19	2.7	6.2	9.2	7.3	—	12.1	75.9	76.7	72.1	70.6	—	60.9
20	—	3.4	—	2.3	1.7	2.2	—	100.0	—	100.7	100.4	104.9
21	1.7	—	2.7	—	3.3	—	76.5	—	75.4	—	71.3	—
22	1.9	—	1.1	1.3	2.0	5.5	48.1	—	43.2	40.8	46.1	62.4
23	1.4	1.2	—	2.2	—	5.5	37.8	33.1	—	38.3	—	34.4

Number in parentheses indicates the transport number of glutamic acid which migrated toward the cathode by passing through cation exchange membrane (C_1).

permeation of acidic amino acid and also that the T value is very low at a low current density but increases with a rise in the current density, irrespective of the concentration. Figure 2–2 shows the relationship between the T value and the current density when the concentration of glutamic acid is fixed and when the molar ratio of chloride ion and glutamic acid is changed variously; almost the same tendency can always be observed despite the changes. This may be assumed as being due to the sieve effect of ions which can be observed when two kinds of ions having different sizes permeate through the ion-exchange membrane. Such a sieve effect is weakened by an increase in the current density, and larger ions will then also begin to permeate. Consequently, the sieve effect of glutamic acid and chloride ions on the ion-exchange membrane increased as the current density becomes lower.

As can be seen in Figs. 2–1 and 2–2, a horizontal movement or a lowering of the T value appears when the current density is increased to a range of 1.0~1.5 amp./dm² in the case of a low-concentration solution. This is due to the participation of hydrogen ions and hydroxide ions arising from the dissociation of water within the membrane as a result of insufficient supplies of glutamic acid and chloride ions resulting from the flow of electric current when the current density is increased more than necessary. Besides this, the relationship between the T value and the current density is affected by the kind and concentration of acidic amino acid, the properties of the membrane, and the hydrogen ion concentration of the mixed solution and of the solution in intermediate compartment C (referred to as the adjacent solution hereafter).

Effect of the Composition of the Mixed Solution.—A change in the composition of the mixed solution should naturally affect the T value due to the change in the ion concentration in the membrane, according to Donnan's membrane equilibrium theory. Figure 2–2 shows the relationship between the current density and the T value with the A-2 membrane when the concentration of glutamic acid is fixed and when the concentration of chloride ions is changed; the increase of the ratio of glutamic acid is accompanied by an increase in the T value when the current density is below 1.5 amp./dm². When the current density is 1.5 amp./dm², dissociation of water takes place above $[G]_S/[G]_S+[Cl]_S=0.65$ and there is a tendency toward a lowering of the T value. On the other hand, if the sum of the concentration of glutamic acid and chloride ions is made constant, the T value does not change very much, even when the solution composition is changed, as is shown in Fig. 2–3. It appears from the above results that the T value has a close relationship with the sum of the concentrations of glutamic acid and chloride ions; and this was also found to be true when comparing the experiments (Runs No. 8 and 9) when the sum of the concentrations of glutamic acid and chloride ions is the same but the concentration of each is reversed, there being almost the same tendencies in the relationship between the T value and the current density of both.

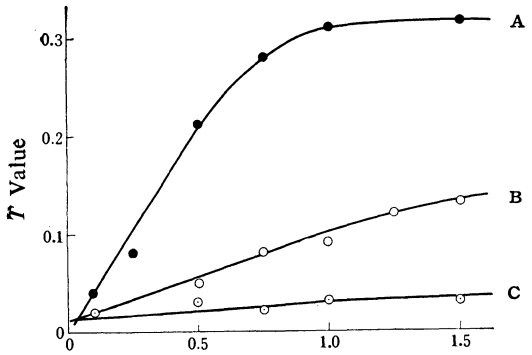

Fig. 2-1. Effect of current density.
Runs No. 3: (A), No. 1: (B), No. 2: (C)

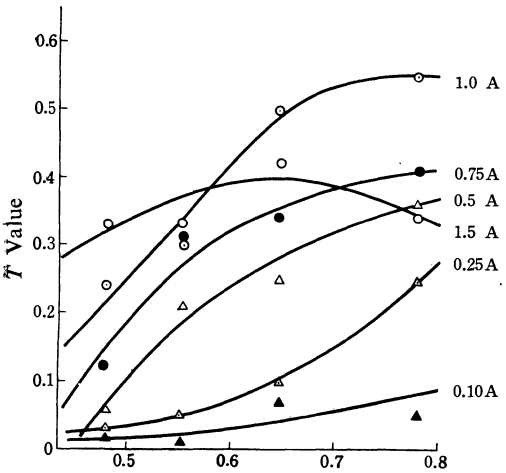

Fig. 2-2. Effect of soltion composition of mixed solution.
Runs No. 4-7, $[A]_s$=const.

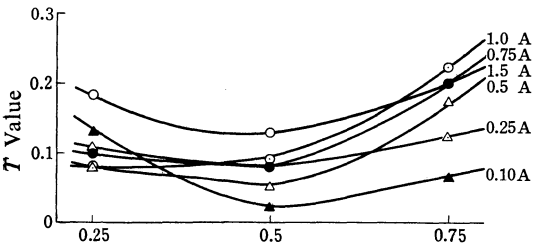

Fig. 2-3. Effect of solution composition of mixed solution.
Runs No. 1, 8 and 9, $[A]_s+[Cl]_s$=const.

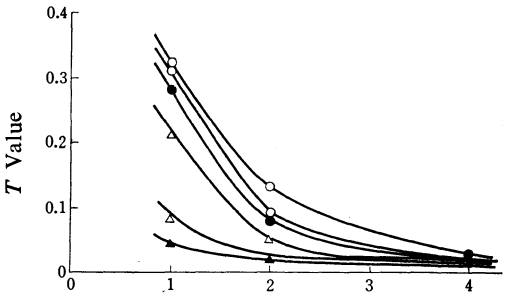

Fig. 2-4. Effect of concentration.
Runs No. 1-3, A-2 membrane, glutamic acid
-○- 1.5 amp. -⊙- 1.0 amp.
-●- 0.75 amp. -△- 0.5 amp.
-△- 0.25 amp. -▲- 0.10 amp.

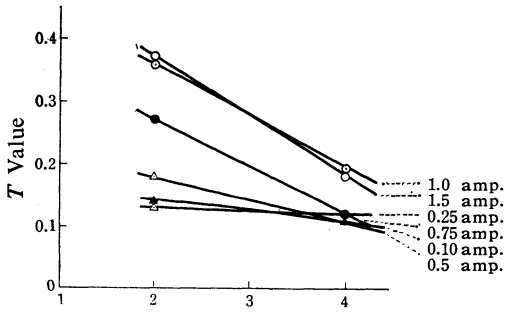

Fig. 2-5. Effect of concentration.
Runs No. 10-11, A-1 membrane, glutamic acid

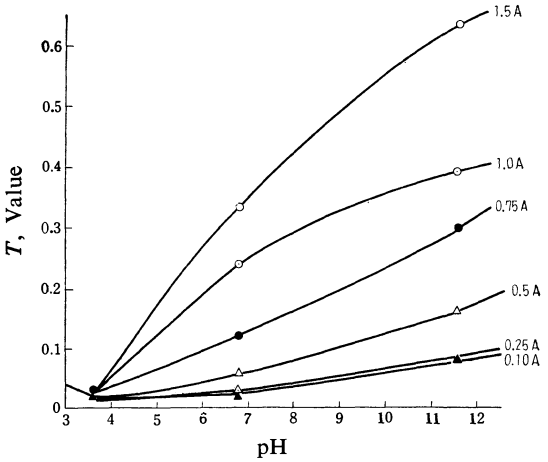

Fig. 2-6. Effect of pH.
Runs No. 4 and 12-14

Effect of Concentration.—The effect of concentration on the permeability of glutamic acid through the A-2 membrane is shown in Fig. 2-4. There is a tendency for the T value to decrease as the concentration increase, and there is almost no permeation of glutamic acid when the concentration of the mixed solution is over 4×10^{-1} M, even if the current density is increased. The permeability of glutamic acid increases in a dilute solution,

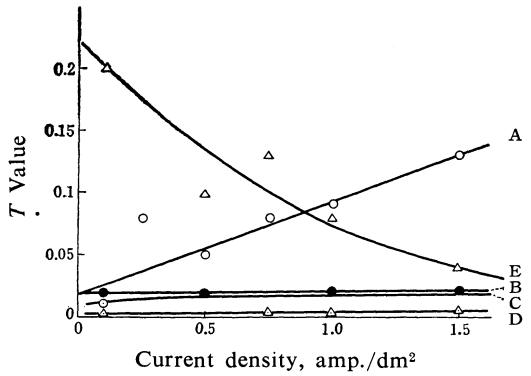

Fig. 2-7. Effect of adjacent solution.
Runs No. 1: (A), No. 16: (B), No. 17: (C), No. 18: (E), No. 19: (D)

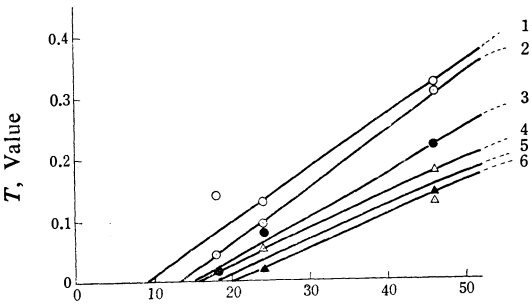

Fig. 2-8. Relation between water penetration ratio (K) of membrane and T value.
Runs No. 1, 10 and 20
1 1.5 amp. 2 1.0 amp. 3 0.75 amp.
4 0.5 amp. 5 0.25 amp. 6 0.10 amp.

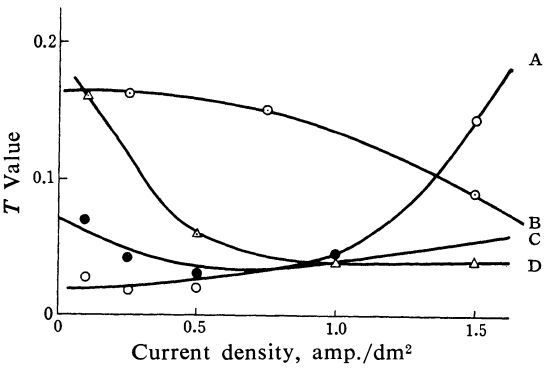

Fig. 2-9. Permeability of glutamic acid through coated membrane.
Runs No. 20: (A), No. 21: (B), No. 22: (C), No. 23: (D)

but water dissociation starts at a high-current density. It was observed from these results that the conditions which make the permeation of glutamic acid through A-2 membrane easiest are the concentration of the mixed solution at 1×10^{-1} M and a current density in the neighborhood of 1.0 amp./dm², and that

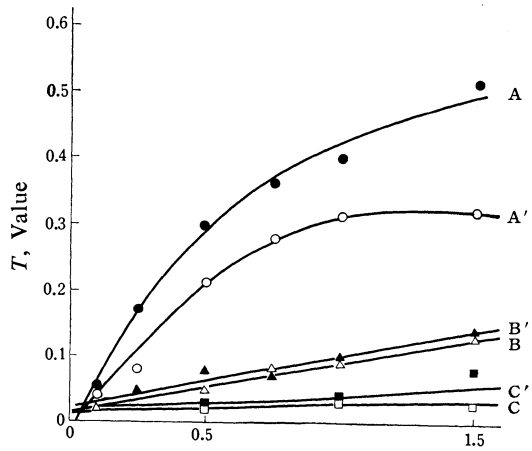

Fig. 2-10. Comparison of permeability of glutamic acid and aspartic acid (through A-2 membrane).
Runs No. 3: (A), No. 26: (A'), No. 1: (B), No. 24: (B'), No. 2: (C), No. 25: (C')
A, B and C: Glutamic acid system
A', B' and C': Aspartic acid system

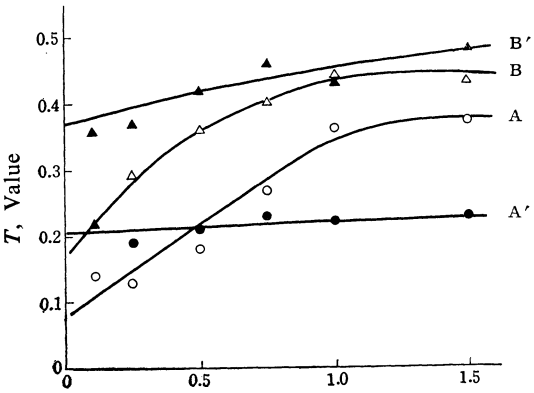

Fig. 2-11. Comparison of permeability of glutamic acid and aspartic acid (through A-1 membrane).
Runs No. 10: (A), No. 27: (A'), No. 15: (B), No. 28: (B')
A and B: Glutamic acid system
A' and B': Aspartic acid system

chloride ions permeate selectively when dialyzed at a high concentration and in a low current density. Figure 2-5 shows the permeability of glutamic acid the A-1 membrane, which has larger pores than the A-2 membrane and in which quite a large T value was found even at a high concentration of over 4×10^{-1} M and in which quite a large penetration of glutamic acid was found through the A-1 membrane. The permeability of aspartic acid through the A-2 membrane was investigated in Run No.

24—26, in which it was observed that the effect of the change in concentration on the T value was more sensitive in the case of aspartic acid than in glutamic acid, since permeability with a dilute solution of below 1×10^{-1} M was good, and also, that it was dialyzed slightly even with a concentrated solution of over 4×10^{-1} M (Fig. 2-10).

Effect of the pH Value.—Amino acids are amphoteric electrolytes, with both anion and cation radicals in the molecule, and naturally their mobilities change according to the pH value when the dissociation condition of these radicals changes. In the present experiment, the permeability of glutamic and aspartic acids was examined under the conditions of hydrogen ion concentration at which the amino radical of acidic amino acid dissociates (near a pH value of 1.8), near the isoelectric point (pH value 3), near the neutral point when the first carboxyl dissociates, and at a pH value of 11.4~11.6 when the second carboxyl dissociates. As a general rule, it can be said that the permeability of an acidic amino acid through an anion exchange membrane is proportional to the degree of the dissociation of its carboxylic radical, which increases as the pH value rises. Consequently, it is advantageous to effect the migration of acidic amino acids in a bivalent state. In looking at the permeability of glutamic acid through the A-2 membrane indicated in Fig. 2-6, it can be observed that the T value increases with a rise in the pH value and that it is advantageous to dialyze glutamic acid in the bivalent rather than in the univalent form. A comparison of Runs No. 10 and 15 indicates that the T value does not increase so much on the weak alkaline side with the A-1 membrane, which has larger pores than the A-2 membrane, and that, consequently, it is not necessarily disadvantageous to dialyze glutamic acid in the univalent state. The same tendency can be observed in the case of aspartic acid (compare Runs No. 27 and 28). Besides the migration of acidic amino acid toward the anode by permeation through the anion exchange membrane (A_2), approximately the same amount migrates toward the cathode by passing through the cation exchange membrane (C_1) within the pH value range near the isoelectric point (Run No. 13). This is proof that amino acid is not in an electrical uncharged state at the isoelectric point but is present as zwitterion, having both negative and positive charges, and is neutral in appearance. It is also of interest to note that in an acid solution (pH value: 1.85) in which the amino radical of acidic amino acid dissociates sufficiently, glutamic acid migrates toward the anode by permeation through the anion exchange membrane (A_2), in addition to its movement toward the cathode through the cation exchange membrane (C_1). (Run No. 14). These results are in accord with those of the report by Yamabe et al.[6], in which they used a heterogeneous ion-exchange membrane, and indicate that amino acid in an aqueous solution is in an equilibrium relations as in the following equation (4);

$$\begin{aligned} NH_3^+\text{-}CH(R)\text{-}COOH &\rightleftharpoons NH_3^+\text{-}CH(R)\text{-}COO^- \\ &\quad + OH^- \qquad\qquad + H_2O \\ &\rightleftharpoons NH_2\text{-}CH(R)\text{-}COO^- \\ &\quad + H_3O^+ \end{aligned} \tag{4}$$

Effect of the Adjacent Solution.—When the anion in the intermediate compartment **B** solution permeates toward the anode through the anion exchange membrane (A_2), the hydrogen ion migrates toward the cathode through A_2 membrane since it can pass through the anion exchange membrane easily from the opposite direction if the hydrogen ion concentration in the adjacent solution (the intermediate compartment C solution) is high; as a result, the transport number of anions (acidic amino acid and chloride ions) in the anion exchange membrane becomes lower. Furthermore, dissociation of the carboxyl radical of acidic amino acid is suppressed and the transport number of acidic amino acid is lowered considerably if the hydrogen ion concentration in the membrane becomes high. Figure 2-7 shows the permeability of glutamic acid through the A-2 membrane when solutions with varying hydrogen ion concentrations (dilute sulfuric acid) were used as the adjacent solution. There was almost no dialysis of glutamic acid when a 0.1 N sulfuric acid solution was used as the adjacent solution, even when the current density was increased. Inhibition of the same degree against glutamic acid was observed when an 1N sulfuric acid solution was used as the adjacent solution with a A-1 membrane, which has a larger pore size. Furthermore, as a general tendency, the transport number (t_G) of glutamic acid becomes higher at a low current density if such an acidic solution is placed as the adjacent solution. It was made clear from these results that the hydrogen ion concentration of the adjacent solution has a great effect on the permeability of acidic amino acid; a hydrogen ion concentration of even about 0.1 N obstructs

6) T. Yamabe, M. Seno and N. Takai, This Bulletin, **32**, 1383 (1959); *J. Chem. Soc. Japan, Ind. Chem. Sec.* (*Kogyo Kagaku Zasshi*), **64**, 556 (1961).

the dialysis of acidic amino acid considerably, and this becomes more marked as the pores of the anion exchange membrane become smaller.

Effect of the Properties of the Anion Exchange Membrane.—Figure 2–8 shows the relationship between the pore size of the membrane and the permeability of glutamic acid. It can be seen from Runs No. 1, 10 and 20 that the permeation of glutamic acid is obstructed considerably with membranes A-2 and A-3, which have small pores, while permeation is not obstructed to such an extent by membrane A-1; a horizontal movement of the T value is observed with a current density of over 1.0 amp./dm^2, and the permselectivity of anions as a whole becomes lower at a high current density. It can, therefore, be seen that A-1 is an appropriate membrane for the permeation of glutamic acid and that A-3 is the most unsuitable membrane of the three for the dialysis of glutamic acid.

Membranes coated with high-molecular substances (A-4 to A-6 membranes) were prepared in order to extend the characteristics of the A-3 membrane to retain the acidic amino acid, pass chloride ions selectively, and increase the mutual-sieving capacity of anions. The permeability of glutamic acid through these coated membranes and the basic A-3 membrane are compared in Fig. 2–9 and Runs No. 21–23, from which it can be seen that, as a common tendency, the permeation of glutamic acid is obstructed over a wide range of current densiy in coated membranes and that there is only a slight dialysis of glutamic acid. However, not only glutamic acid but also the permeation of chloride ions is obstructed by such a coated membrane; a very marked water dissociation takes place over a wide range of current densities in the coated membrane, as is observed from the sum of the transport numbers ($t_G + t_{Cl}$) of glutamic acid and chloride ions. The obstruction of glutamic acid dialysis by membranes coated with high molecular substances is in the decreasing order of A-6, > A-5 and > A-4 membranes; this is assumed to be correlated to the pore size intrinsic to the high molecular substances coated on the membrane. The membrane coated with phenolsulfonic acid-formaldehyde condensate (the A-6 membrane) obstructs the permeation of glutamic acid the most, and this tendency becomes weaker in the order of membranes coated with polyvinylbutyral (the A-5 membrane) and the product of styrenesulfonic acid - butadiene copolymer (the A-4 membrane). An inverse increase in T value is observed in the current density region in all of these coated membranes, but this is due to the fact that the transport number (t_G) of glutamic acid does not lower relative to that (t_{Cl}) of chloride ions.

Comparison of the Permeability of Glutamic Acid and Aspartic Acid.—A comparative study was made of glutamic acid and aspartic acid as representatives of acidic amino acids having a different number of methylene carbons. The permeability of glutamic acid and aspartic acid through the A-2 membrane is shown in Fig. 2–10, from which it can be seen that the permeability of aspartic acid is generally better than that of glutamic acid. The change in T value due to the change in current density with a concentrated solution in the case of aspartic acid is very slight, but the change is more violent with a dilute solution than in the case of glutamic acid. However, in the case of glutamic acid, the dissociation of water takes place with a dilute solution as the current density is increased; this results in a lowering of the T value. It is believed that glutamic acid encounters considerable resistance when permeating through the A-2 membrane. Figure 2–11 compares the permeability of these two acids through the A-1 membrane; it can be seen that the T value of aspartic acid is almost unaffected by the current density in the neutral or weakly alkaline states. In other words, the A-1 membrane does not obstruct the permeation of aspartic acid, but it does obstruct that of glutamic acid slightly. It is clear from this that ions which can permeate perfectly through the A-1 membrane have fewer than four carbon atoms.

The author is deeply indebted to Dr. T. Yawataya and his co-workers of Asahi Glass Co. for the generous supply of ion-exchange membranes used in this work. He is indebted to Mr. K. Tahara for his aid in performing some of the experiments reported on this work.

Research Laboratories
Takeda Chemical Industries, Ltd.
Osaka

Crystal Growth of Magnesium Oxide Prepared by the Thermal Decomposition of Magnesium Hydroxide

By Yoshihide KOTERA, Tatsuo SAITO and Matsuo TERADA*

(Received September 11, 1962)

It is well known that active metallic oxides are prepared by the thermal decomposition of hydroxide or carbonate and that their physicochemical properties are determined by the temperature at which they are formed and by the duration of the calcination. It is, therefore, important to clarify the process which occurs during the decomposition of such a compound as hydroxide or carbonate and the subsequent calcination. We select the crystal growth of magnesium oxide prepared from hydroxide for this purpose, because this process, especially in a relatively low temperature range, has not been studied so much as have its surface properties[1-3]. It is pointed out in our study that the growth is rather complex and that it might nevertheless be possible to clarify that mechanism which is important in the preparation of magnesium oxide.

The present work is an attempt to examine the effect of the temperature of calcination, and of the duration of heating at a fixed temperature, on the crystal growth of magnesium oxide prepared by the dehydration of precipitated magnesium hydroxide and native brucite. The growth is discussed in the light of kinetics, and the activation energy calculated is compared with that for other oxides.

Experimental

Materials.—Two series of magnesium hydroxides have been examined; one of them was prepared by precipitation from a 0.1 N solution of reagent-grade magnesium chloride with a 2.5 N solution of reagent-grade sodium hydroxide, while the other was a piece of native brucite from Nevada, U. S. A.

In the preparation of former series, care was taken to ensure that all air coming in contact with the carbonate-free sodium hydroxide solution and with the mixture of this solution and the magnesium chloride solution had been freed from carbon dioxide. The precipitate obtained by the reaction between the two solutions was washed until a test for chloride ions with a silver nitrate solution gave only a faint milkiness; it was then decanted. Drying of the precipitate was carried out at 60°C for 50 hr. in a vacunm obtained by means of a water pump. The native brucite contains the following impurities: CaO : 0.82%, Fe_2O_3 : 0.79%, Al_2O_3 : 0.23%, SiO_2 : 0.14%.

Apparatus and Procedure.—The samples of magnesium hydroxide were ground into fine powder by a mortar and calcined in air at a definite temperature ranging from 500 to 900°C for varying periods. The fluctuation of the calcination temperature was kept within ± 5°C by means of an automatic temperature controller. After calcination, the products were cooled in a desiccator.

The X-ray specimens of magnesium oxide were smeared on a microscopic slide to give a flat surface approximately 2 cm. square. A Rigaku Denki "Geigerflex" (Geiger counter X-ray diffractometer) was employed to determine the mean apparent crystal sizes of the samples on the basis of the broadening of their X-ray diffraction lines. Measurements were made on the magnesium oxide (200) line using copper radiation. The calculation of particle size was carried out following the procedure of Birks and Friedman[4].

Experimental Results

Calcination at Temperatures Ranging from 500 to 900°C. — Precipitated magnesium hydroxide and brucite were calcined at 500, 600, 700, 800 and 900°C for periods ranging from 5 min. to 24 hr. The mean apparent crystal sizes, d, of the magnesium oxide thus obtained are plotted against the time of calcination, t, in Figs. 1 and 2 for precipitated magnesium hydroxide and for brucite respectively. From these results it can be seen that the crystal growth proceeds during the calcination, its rate being highest immediately after the end of dehydration and decreasing with the increase in the time of heating. In Figs. 3 and 4 the relation between the crystal size and time is plotted on a logarithmic scale. In these figures for all calcination temperatures, the curves are composed of two straight lines intersecting at about 100 min. It is concluded from these results that the calcination process is divided into earlier and later stages for all calcination temperatures. Further, it is possible to divide

* Present address: Hokuriku Salt and Chemical Co., Ltd., 38 Kotohirachō, Minato-ku, Tokyo.

1) S. J. Gregg, R. K. Packer and K. H. Wheatley, *J. Chem. Soc.*, **1955**, 46.

2) D. T. Livey, B. M. Wanklyn, M. Hewitt and P. Murray, *Trans. Brit. Ceram. Soc.*, **56**, 217 (1957).

3) R. I. Razouk and R. Sh. Mikhail, *J. Phys. Chem.*, **61**, 886 (1957); **63**, 1050 (1959).

4) L. S. Birks and H. Friedman, *J. Appl. Phys.*, **17**, 687 (1946).

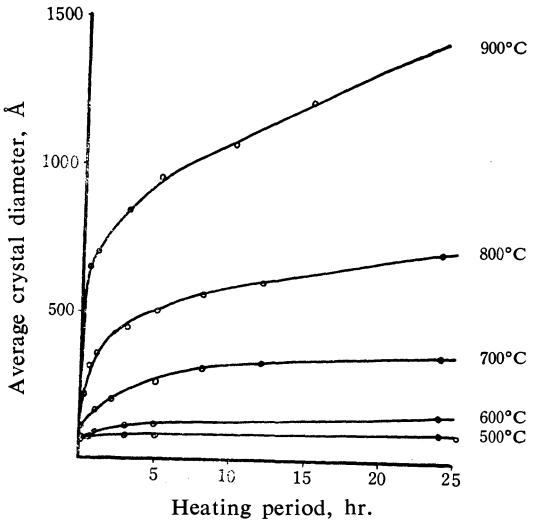

Fig. 1. Diameter change during heating of MgO prepared from ppt. $Mg(OH)_2$ at various temperatures.

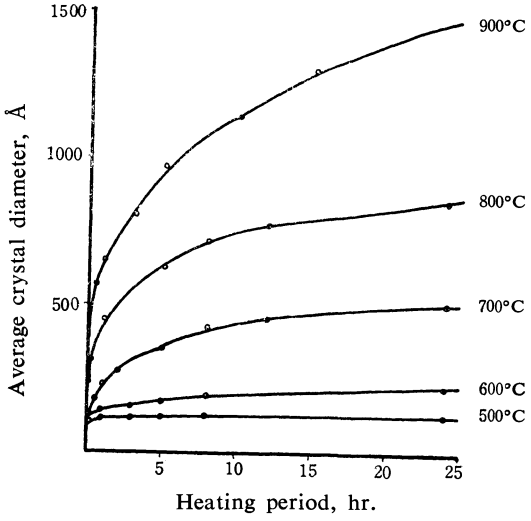

Fig. 2. Diameter change during heating of MgO prepared from brucite at various temperatures.

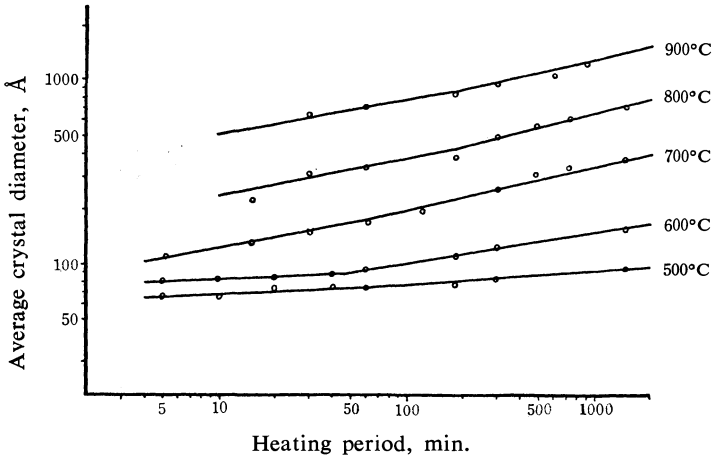

Fig. 3. Logarithmic plot of diameter change during heating of MgO prepared from ppt. $Mg(OH)_2$.

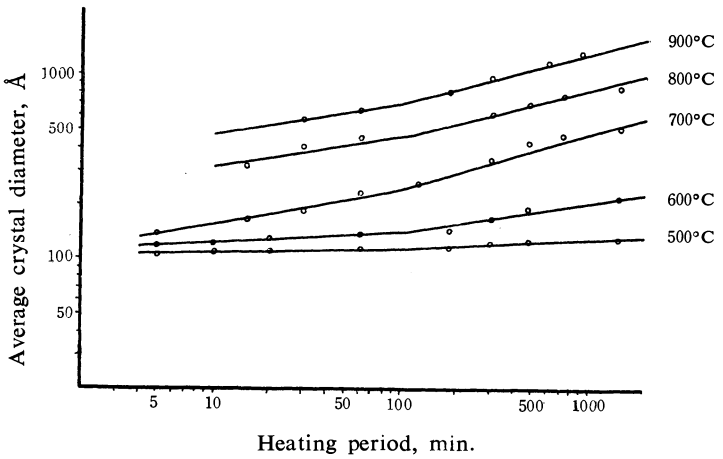

Fig. 4. Logarithmic plot of diameter change during heating of MgO prepared from brucite.

the results into three groups when the slopes of these straight lines are calculated, the first consisting of a whole period at 500°C and an earlier stage at 600°C, the second consisting of a later stage at 600°C and an earlier at a temperature between 700 and 900°C, and the third, of later stages at a temperature between 700 and 900°C.

Calcination at Temperatures Ranging from 700 to 950°C.—Magnesium hydroxide samples were dehydrated at 700°C for 10 hr. and the magnesium oxide samples thus obtained were used as starting materials to clarify the calcination process at a temperature between 700 and 950°C. Magnesium oxide samples were calcined at 800, 850, 900 and 950°C for periods varying from 1 to 8 hr. When the crystal sizes were plotted on logarithmic scale, Fig. 5 was obtained for magnesium oxide from precipitated magnesium hydroxide, and Fig. 6 for magnesium oxide from brucite. Their sizes before the calcination are 350 Å for the former and 530 Å for the latter. It was found that the crystal size increases exponentially with the reciprocal of the calcination temperature, as is implicit for a typical case in Fig. 7.

From the results obtained it is possible to express the crystal sizes as the function of the temperature, T°K, and of the time, t, by the following equations:

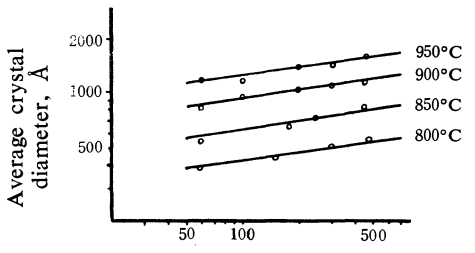

Fig. 5. Logarithmic plot of diameter change during heating between 800 and 950°C for MgO prepared from ppt. $Mg(OH)_2$ at 700°C.

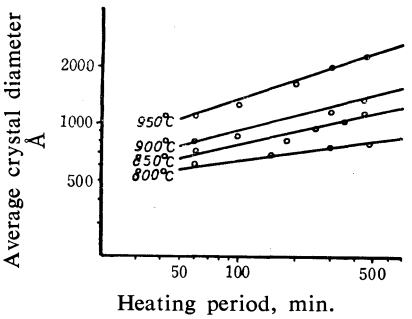

Fig. 6. Logarithmic plot of diameter change during heating between 800 and 950°C for MgO prepared from brucite at 700°C.

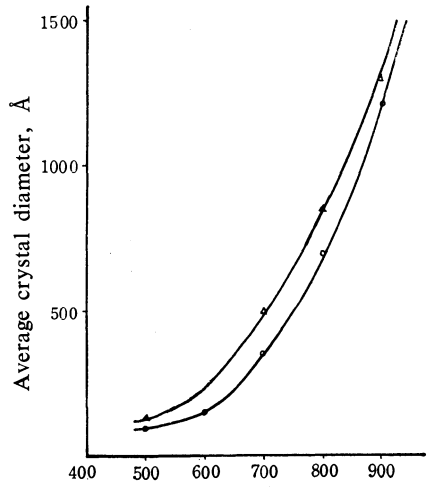

Fig. 7. Average crystal diameter as a function of calcination temperature. (calcination time: 24 hr.)

○—○ MgO prepared from ppt. $Mg(OH)_2$
△—△ MgO prepared from brucite

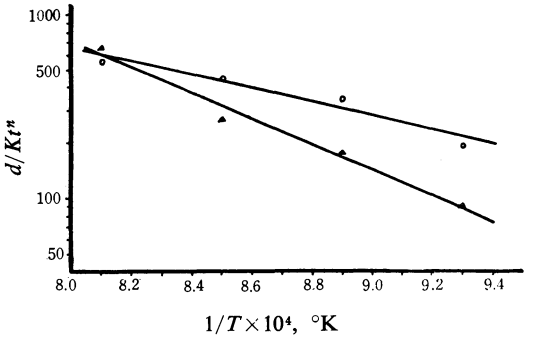

Fig. 8. Arrhenius plot for crystal growth of magnesium oxide samples prepared from ppt. magnesium hydroxide and brucite.

○—○ MgO prepared from ppt. $Mg(OH)_2$
△—△ MgO prepared from brucite

$d=K_1t^{1/6}\exp(-E_1/RT)$ for MgO from precipitated $Mg(OH)_2$ and

$d=K_2t^{1/4}\exp(-E_2/RT)$ for MgO from brucite, where K_1 and K_2 are constans, and E_1 and E_2 are activation energies for the crystal growth of magnesium oxide. It is probable that K_1 or K_2 may depend on the initial value of the crystal size.

In Fig. 8 the relation between $\log(d/Kt^n)$ and $1/T$ is plotted for both magnesium oxide samples; the values of the activation energy calculated from the figure are 17 kcal. for magnesium oxide from precipitated magnesium hydroxide and 32 kcal. for that from brucite.

Discussion

The effect of the conditions of preparation of the active metallic oxide in the thermal decomposition of hydroxide or carbonate upon its physico-chemical properties has been briefly studied. When the surface properties of magnesium oxide prepared from precipitated magnesium hydroxide or from brucite were studied by Gregg et al.[1], Livey et al.[2] and Razouk and Mikhail[3], it was found that these properties depend on the time as well as the temperature of decomposition of a parent substance, viz., precipitated magnesium hydroxide or brucite. Meanwhile, Birks and Friedman[4] studied the particle size determination of magnesium oxide prepared from the carbonate by means of an X-ray line broadening method; they compared the results with direct measurement by means of electron microscopy. They concluded that the results obtained by the two methods agree $\pm$ 10 per cent except for particles smaller than 100 Å. Their results show the dependence of particle size on the time and temperature of calcination, but no explanation was given in their study.

In the present study, precipitated magnesium hydroxide was used as a starting material as well as brucite. It might be necessary to compare the results of the former with those of the latter in order to elucidate the disagreement which seems to be present in the results based on the surface properties of magnesium oxide prepared from precipitated magnesium hydroxide[3]. On the other hand, brucite contains more impurities than precipitated magnesium hydroxide, and this fact may make it impossible to obtain accurate results on crystal growth kinetics which depend upon the purity of a parent substance. The naturally-occuring crystalline brucite chosen was as pure as possible, but it still contains the small amount of impurities described above.

The crystal sizes of magnesium oxide prepared from hydroxide increase with a rise in the calcination temperature and with its duration, a tendency similar to that in the case of carbonate. Comparing Birks' results[4] with ours shows that the increase in crystal size with a rise in the temperature is more prominent for oxide from hydroxide than for that from carbonate. The stages found for oxide from hydroxide are not found in the results by Birks, in which the shortest time of calcination carried out was 2 hr. In the study of the sintering of active magnesium oxide, Gregg et al.[1] found that the micellar length calculated under the assumption that the material exists as equal cubelets increases proportional to the square root of the time between 1 and 350 hr. at temperatures between 400 and 600°C. It is probable that the lowering of the temperature may serve to increase the value of the exponent relative to time in the equation expressing the relation between crystal size and calcination time, such a tendency being seen in our experiments. Nevertheless, it seems to be difficult to compare the micellar length calculated from the surface area with the crystal size obtained by the X-ray broadening method.

According to Hüttig's views[5], which have been verified by others, sintering is caused by three processes, viz., surface adhesion, surface diffusion and lattice diffusion. The first process may occur even at room temperature at the points of contact between neighboring micelles. The shearing stress exerted by the micelles near the region of contact leads to the deformation of the micelles and an increase in the area of contact over which adhesion occurs. As the rise in temperature reduces the rigidity of solids, adhesion will increase with the rise in temperature, and so also will sintering. This process occurs at temperatures above one-fourth of the melting point of the solid. Surface diffusion resulting from the mobility of the ions of the solid at its surface becomes sensible at a temperature about one-third of the melting point of the solid, while lattice diffusion, where the ions can move through the bulk of the micelles, occurs only at temperature above half the melting point. The last effect probably does not play an important part in the present work, as the highest temperature used was 950°C, which corresponds to 40% of the melting point (3100°K). Meanwhile, it has been pointed out[6] that there is a period during which surface roughness is destroyed and which is followed by an adhesion period. In the present study, it was found that there are three groups in the results for the calcination between 500 and 900°C; it may be assumed that they correspond to surface smoothing, surface adhesion and surface diffusion. In the explanation of the results concerning the sintering of magnesium oxide at temperatures between 400 and 600°C, Gregg et al.[1] pointed out that the temperature is so low that both surface diffusion and bulk diffusion seem to be ruled out, leaving adhesion alone, but they also pointed out that simple adhesion cannot represent the whole process. It is probable that surface smoothing remains before an adhesion period in their experiments. This

5) F. Hüttig, *Kolloid-Z.*, **98**, 263 (1942); **99**, 262 (1942).
6) F. S. Stone, "Reactivity of Solids", Elsevier, Amsterdam (1961), p. 15.

idea is supported by the fact that the decreasing rate of surface area is very high, even at such a low temperature as 500 or 600°C[1], while the increase in crystal size is not so rapid at such a low temperature (Figs. 1 and 2). However, the later stage at 600°C may be explained as the beginning of surface adhesion. In the second group, viz., the later stage at 600°C and earlier stages at a temperature between 700 and 900°C, surface adhesion would occur. Furthermore, the crystal growth occurs in the last group, viz., the later stages at a temperature between 700 and 900°C, according to the mechanism associated with surface diffusion.

In the last group, the value of the exponent to time in the equation expressing the relation between crystal size and calcination time, as well as the value of activation energy for the crystal growth, are different in magnesium oxide obtained from precipitated hydroxide and that obtained from brucite. The values of activation energy, 17 kcal. for the former and 32 kcal. for the latter, are nearly the same as those of the surface diffusion in other oxides. Latty[7] studied the crystal growth of rutile-type titanium oxide and obtained a value of 16,68 kcal./mol. for alkali-free oxide in the temperature region between 585° and 750°C, where surface diffusion can be expected to be operative. Further, in their study of the sintering reactions of zinc oxide, Lee and Parravano[8] calculated the activation energy of the diffusion of excess zinc ions through the very thin oxidized layer to be about 18 kcal./mol. in the temperature range between 700 and 900°C. It might be assumed that surface diffusion occurs in this case. The difference in activation energy between precipitated magnesium hydroxide and brucite is difficult to explain in this work, and it is probable that lattice diffusion occurs in the case of brucite. That lattice diffusion occurs at such a low temperature might be due to the presence of impurities.

7) J. E. Latty, *J. Appl. Chem.*, **8**, 96 (1958).
8) V. J. Lee and G. Parravano, *J. Appl. Phys.*, **30**, 1735, (1959).

Summary

The particle size of magnesium oxide crystals prepared by the thermal decompositions of pure precipitated magnesium hydroxide and native brucite at various temperatures between 500 and 900°C has been measured by the X-ray line broadening method, and the effect of the calcination temperature and its duration on the crystal size of magnesium oxide has been examined.

It has been found that the particle size of magnesium oxide crystals increasese with the increase in the calcination temperature and that the rate of crystal growth obeys a different law between the earlier stage of the calcination process at a definite temperature and the later stage. It has also been found that the crystal growth of magnesium oxide proceeds proportional to t^n, (t: time), where n is 1/6 for the later stage of the calcination of magnesium oxide from precipitated magnesium hydroxide at temperatures ranging from 700 to 900°C and 1/4 for the same calcination of that from brucite. The values of the activation energy calculated by Arrhenius plot are 17 and 32 kcal./mol. for magnesium oxide obtained from precipitated hydroxide and from brucite respectively.

Government Chemical Industrial Research Institute, Tokyo
Shibuya-ku, Tokyo

*The Menschutkin Reaction in Liquid Sulfur Dioxide**

By Niichiro TOKURA and Yasuhiko KONDO

(Received September 13, 1962)

Liquid sulfur dioxide has been said to be one of the most ionizing solvents[1]. It has been previously reported that the cationic polymerization[2] and the intramolecular rearrangements such as the Beckmann[3] and Wagner-Meerwein rearrangements[4] in liquid sulfur dioxide are carried out at extraordinarily fast rate. The reasons for such an accelerating effect of sulfur dioxide have also been discussed. Such a conspicuous property of sulfur dioxide perhaps is due to 1) the large ionizing power, 2) the solubility both to organic (olefin and aromatic compounds) and inorganic (aluminum chloride, stannic chloride and so on) materials, 3) the aprotic and protophobic nature with no affinity to proton or carbonium ion.

Among many nucleophilic reactions studied, the Menschutkin reaction is one of the most discussed and well established reaction[5]. Moreover, since the first kinetic study by Menschutkin appeared in 1890[5a], the effect of the solvents on this reaction has been comprehensively studied and summarized in many articles and reviews[5]. Although the rate of solvolysis of alkyl halides depends upon the ionizing power of the solvent, that of the Menschutkin reaction does not. The plot of the specific rates of the latter reaction against the *Z* values[6] of the corresponding solvents does not give a linear correlation.

The object of this investigation has been to study the effect of liquid sulfur dioxide as solvent on the Menschutkin reaction, since no kinetical comparison has been made between the rates in sulfur dioxide and other solvents by this time.

Study of the nucleophilic attack of fluoride anion, amines or pyridine on *m*-chlorobenzhydryl chloride in liquid sulfur dioxide was undertaken by Ingold et al.[7], wherein they observed a peculiar phenomenon, the so-called borderline case, the reaction being classified neither as S_N1 nor S_N2. The aprotic and even protophobic character of liquid sulfur dioxide would be the reason why they performed the reaction in this solvent, though the reaction in liquid sulfur dioxide resulted in more complexity than was expected.

Ingold et al. used electric conductivity measurement of the reaction mixture to trace the kinetics. The organic halides in liquid sulfur dioxide have often been shown to have considerable conductivities[8]. In addition, the presence of a trace of water which could not be eliminated from liquid sulfur dioxide by the ordinary method[9] may perhaps affect largely the results of the kinetic measurement.

The present authors have chosen a reaction, the Menschutkin reaction between methyl or ethyl halide and a base in liquid sulfur dioxide, in which the ionization of the alkyl chloride was surpressed in order to eliminate the S_N1 type reaction as much as possible. The kinetics was followed by a potentiometric titration of iodide ion produced. Dimethylaniline, dimethyl-*o*-toluidine or pyridine was used as a base. The reaction rate in liquid sulfur dioxide has been compared with those in other solvents, such as methanol, nitrobenzene, nitromethane, tetrahydrofuran, acetone, acetonitrile, dimethylformamide and dimethylsulfoxide.

Experimental

Materials. — Methyl, ethyl or isopropyl iodide was washed with sodium thiosulfate solution, water, sodium carbonate solution and water successively, dried and distilled: methyl iodide, b. p. 42.5～43.0°C, ethyl iodide, b. p. 68～72.3°C (impurity was below 1% by V. P. C.), isopropyl iodide, b. p. 88.2～89.0°C. Dimethylaniline or dimethyl-*o*-toluidine was refluxed with acetic anhydride and distilled.

* Substitution in Liquid Sulfur Dioxide, Part II. Preceding paper, N. Tokura, R. Tada and R. Igarashi, This Bulletin, 33, 1176 (1960).

1) S. G. Smith, A. H. Fainberg and S. Winstein, *J. Am. Chem. Soc.*, 83, 618 (1961).

2) a) R. Asami and N. Tokura, *J. Polymer Sci.*, 42, 545 (1960); b) N. Tokura, M. Matsuda and M. Iino, This Bulletin, in press.

3) N. Tokura and K. Shiina, ibid., 35, 1779 (1962).

4) L. P. Hammett, "Physical Organic Chemistry", McGraw-Hill, New York (1940), p. 318.

5) a) N. Menschutkin, *Z. physik. Chem.*, 6, 41 (1890); b) E. A. Moelwyn-Hughes, "Kinetics of Reaction in Solution", Sec. Ed., Oxford Univ. Press., London (1947), p. 207; c) E. L. Eliel, "Steric Effects in Organic Chemistry", Ed. by M. S. Neweman, John Wiley & Sons, New York (1956), Chapter 2, p. 70.

6) E. M. Kosower, *J. Am. Chem. Soc.*, 80, 3253 (1958).

7) a) L. C. Batemean, E. D. Hughes and C. K. Ingold, *J. Chem. Soc.*, 1940, 1017; b) M. L. Bird, E. D. Hughes and C. K. Ingold, ibid., 1954, 634; c) H. Greenstreet, E. D. Hughes and C. K. Ingold, ibid., 1954, 642, 647.

8) Ref. 4, p. 53.

9) D. Murakami and N. Tokura, This Bulletin, 31, 432 (1958).

The distillate was again treated with potassium hydroxide and distilled. Pyridine, rigorously dehydrated and distilled was donated by Ikenoue[10]. Liquid sulfur dioxide was dried with phosphorus pentoxide and distilled. Tetrahydrofuran, acetonitrile, nitromethane, acetone, dimethylformamide and dimethylsulfoxide were purified by known methods[11].

Kinetic Procedure.—The method and the apparatus used were demonstrated elsewhere[12]. An alkyl iodide (0.2~0.6 mol./l.) was reacted with a base (0.2~0.6 mol./l.) in liquid sulfur dioxide in a thermostat. After a definite time, reaction mixture was mixed with petroleum benzine (b. p. 60~80°C) and the iodide ion produced was extracted thrice with water. After evaporation of sulfur dioxide gas from the aqueous extract in vacuo, the iodide ion in the solution was titrated with silver nitrate solution potentiometrically. A typical run of the reaction between methyl iodide and pyridine in liquid sulfur dioxide is listed in Table I. The reaction in acetone or other solvent was also conducted to compare with the result in liquid sulfur dioxide, which is indicated in Table II.

Table I. A typical run of the reaction between methyl iodide and pyridine in liquid sulfur dioxide at 40°C

Methyl iodide 0.399 mol./l.		Pyridine, 0.359 mol./l.	
t, min.	$I^- \times 10^2$ mol. l^{-1}	$k_1 \times 10^3$ min^{-1}	$k_2 \times 10^2$ l. mol^{-1} min^{-1}
20	3.50	4.87	1.50
40	6.75	4.41	1.51
60	9.47	4.16	1.58
80	11.82	3.70	1.53
100	13.76	3.50	1.59
120	15.47	3.18	1.56
			1.55

Table II. The rate constant in acetone at 40°C

Methyl iodide 0.194 mol./l.		Pyridine, 0.292 mol./l.	
t, min.	$I^- \times 10^2$ mol. l^{-1}	$k_1 \times 10^3$ min^{-1}	$k_2 \times 10^2$ l. mol^{-1} min^{-1}
10	1.92	11.10	4.08
20	3.65	10.20	3.98
35	5.75	9.24	3.93
55	7.98	8.51	4.02
75	9.69	8.04	4.12
105	11.65	7.29	4.16
			4.05

10) The present authors are indebted to Assist. Prof. Ikenoue for his courtesy.

11) a) "Technique of Organic Chemistry", VII, "Organic Solvents", Ed. by A. Weissberger, Interscience Publisher, New York (1955); b) F. A. Cotton and R. Francis, *J. Am. Chem. Soc.*, **82**, 2990 (1960).

12) N. Tokura, M. Matsuda and F. Yazaki, *Makromol. Chem.*, **42**, 108 (1960).

Results

Reaction of Alkyl Iodide with Pyridine. — Alkyl iodide (0.2~0.6 mol./l.) was reacted with a base (0.2~0.6 mol./l.) in liquid sulfur dioxide. The reaction followed a second order rate law, being first order both in alkyl iodide and in pyridine. The second order rate constants were calculated according to the equation, $kt = \{1/(b-a)\} \ln [a(b-x)/b(a-x)]$ and the Arrhenius parameters were estimated as is listed in Table III.

Table III. The rate of the reaction between methyl iodide and pyridine*

Reaction temp., °C	$k \times 10^5$ l. mol^{-1} sec^{-1}	$\Delta E^{\ddagger}$ kcal./mol.	$\Delta S^{\ddagger}$ e. u.
20	3.38		
30	9.00	17.8	−22.2(40°C)
40	24.70		

* The concentration of pyridine was equal to that of methyl iodide.

The similar reactions with the concentration range (0.2~0.6 mol./l. of each reactant) have been conducted in acetone (Table II), dimethylformamide, dimethylsulfoxide, nitromethane, acetonitrile or tetrahydrofuran to find out that the reactions were all of the second order. A comparison of the second order rate constants in these solvents is listed in Table IV.

Table IV. Comparison of second order rate constants

Solvent	k, (40°C) l. mol. sec^{-1}	Ratio $k_{solvent}/k_{SO_2}$
Tetrahydrofuran*	1.74×10^{-4}	0.7
Liq. SO_2	2.47×10^{-4}	1
Acetone	6.37×10^{-4}	2.6
Acetonitrile	1.13×10^{-3}	4.6
Nitromethane	1.48×10^{-3}	6.0
Dimethylformamide	3.12×10^{-3}	12.6
Dimethylsulfoxide**	6.85×10^{-3}	27.7

* The reaction was partly heterogeneous.

** However dimethylsulfoxide reacts with methyl iodide as,

$$CH_3I + (CH_3)_2SO = (CH_3)_3SO^+ + I^-$$

the Menschutkin reaction is so fast that the reaction of sulfonium ion formation is not competitive[13].

Reaction of Alkyl Iodide with Dimethylaniline or Dimethyl-*o*-toluidine. — In the series of these experiments, the reaction was also of the second order. The results are listed in Table V.

13) a) S. G. Smith and S. Winstein, *Tetrahedron*, **3**, 317 (1958); b) R. Kuhn and Trischmann, *Ann.*, 611, 117 (1958).

TABLE V. THE RATE CONSTANTS OF THE REACTIONS BETWEEN ALKYL HALIDES AND DIMETHYLANILINES

Reaction temp., °C	k l. mol^{-1} sec^{-1}	$\Delta E^{\ddagger}$ kcal./mol.	$\Delta S^{\ddagger}$ e. u.
(a) Dimethylaniline - methyl iodide			
30	1.72×10^{-5}		
40	4.77	17.2	−27.3(40°C)
50	9.93		
(b) Dimethyl-*o*-toluidine - methyl iodide			
40	1.65×10^{-5}		
50	3.62	15.9	−33.7(50°C)
60	7.81		
(c) Dimethylaniline - ethyl iodide			
40	3.41×10^{-6}		
50	8.63	17.9	−30.4(50°C)
60	21.80		
(d) Dimethylaniline - isopropyl iodide			
50	1.28×10^{-6}		
60	3.14	18.9	−31.0(60°C)
65	4.77		

As is seen in Table III, the reaction rate decreases as the alkyl halides varies from methyl to isopropyl iodide. When dimethyl-*o*-toluidine was reacted with methyl iodide in place of dimethylaniline, the rate depressed slightly. (Table VII).

Comparison of the reaction rate in liquid sulfur dioxide with that in methanol or in nitromethane is listed in Table VI.

TABLE VI

(a) Comparison of the second order rate constants

Dimethyl aniline - methyl iodide

$k_{\text{methanol}}{}^{14)}/k_{SO_2}=4.18$ (50°C)

$k_{\text{nitrobenzene}}{}^{15)}/k_{SO_2}=4.40$ (40°C)

(b) Comparison of the Arrhenius parameter

Solvent	$\Delta E^{\ddagger}$, kcal./mol.	$\Delta S^{\ddagger}$ e. s.
Liq. SO_2	17.2	−27.3
Methanol[14)]	15.2	−31
Nitrobenzene[15)]	12.8	−38

Among the three of the solvents, the rate in liquid sulfur dioxide is the least. The effect of the ortho-methyl group on the benzene ring of aniline derivative on the rate is described in Table VII.

TABLE VII. EFFECT OF *o*-METHYL IN DIMETHYLANILINE

Solvent	k_H/k_{o-Me}
Liq. SO_2	2.74 (50°C)
Methanol[14)]	28.5 (65°C)

k_H/k_{o-Me} is the ratio of the rate constant in the reaction of methyl iodide with dimethylaniline (k_H) against that with dimethyl-*o*-toluidine (k_{o-Me}). However the temperatures in the reaction in comparison are somewhat different, the ortho-effect in liquid sulfur dioxide (2.74) is very small as compared with that in methanol (28.5).

Discussion

In the preceding studies on the cationic reactions, i. e. both in the Beckmann rearrangement[3)] and in the cationic polymerization[2)], the reaction rates were found to be the fastest in liquid sulfur dioxide as compared with the organic solvents generally used. It is, therefore, a question why the Menschutkin reaction in liquid sulfur dioxide is so slow, whereas the rearrangement and the cationic polymerization in the same solvent are so fast.

Here, the role of the solvation as well as the ionizing power of the solvent in the nucleophilic substitution must be considered. A general survey of the solvation is indicated in Chart 1, in which RX may be either a covalent

Chart 1

Classification of the solvation of a solvent on a substrate

$RX=R^+S+X^-S$	(A) Biphilic solvation
$RX=R^++X^-S$	(B) Electrophilic solvation
$RX=R^+S+X^-$	(C) Nucleophilic solvation
$RX=R^++X^-$	(D)

link compound such as alkyl halide or an ionophore[16)] such as tetraethylammonium chloride. In Chart 1, only a general feature of solvation is demonstrated and the detailed discussion on the extent of the ionization or the dissociation may be reserved for further investigation at the present stage. In addition, the number of the solvent molecules solvating on an ion is also not considered. The letter S in Chart 1 thus indicates an indefinite number of the solvent molecules solvating on a cation or an anion. However the strength of each solvation may also be varied as the solvent changes, the four models, A—D, used only to elucidate the role of the solvent on the solvation.

A, (biphilic solvation), is often the case in hydroxylic solvent (a solvent having the OH group) such as water or alcohol, where both ions are solvated by the solvent, the cation being coordinated with the O atom of the solvent and the anion being hydrogen bonded

14) D. P. Evans, H. B. Watson and R. Williams, *J. Chem. Soc.*, **1939**, 1345, 1348.
15) K. Laidler, ibid., **1938**, 1786.
16) R. M. Fuoss, *J. Chem. Educ.*, **32**, 527 (1955).

by the solvent. This is the most popular and the most well established case of the solvation. D, (no solvent solvation) may be the case of no actual existence, but in gaseous state or in extremely inert solvent, a case close to D seems likely to take place. Special attention should be added to the cases, B and C, where either an anion (case B) or a cation (case C) is solvated, the counter ions (a cation in B and an anion in C) being unsolvated by the respective solvents and kept free. B (electrophilic solvation) is the case of liquid sulfur dioxide or sulfuric acid. C (nucleophilic solvation) is the case of the solvent of a basic character such as dimethylformamide, dimethylsulfoxide or acetone. The concept of the *unsolvated ion* or the *bare ion*[17] may be of some importance in the ionic reaction, since such a *bare ion* may be unstable and reactive, and could offer an appropriate driving force for the reaction.

Although sulfur dioxide is a strongly ionizing solvent, the ionizing power is due to the highly selective complexing of the solvent (sulfur dioxide) to the anion, thus the *bare caton* (unsolvated cation) is remaining as an unstable and reactive species. However, since the cation or the carbonium ion is surrounded by the cage of sulfur dioxide molecules which repel the ion, the cation is alive as long as no foreign substance is present in the solution and the counter anion is strongly solvated and supported by liquid sulfur dioxide. The unusual reactivity[2-4] is also consistent with the production of some new types of the nonclassical cations[18] in sulfur dioxide, because in both reactions strong solvation of anions is of utmost necessity.

Since sulfur dioxide is a Lewis acid, the affinity to proton or cation may be extremely small. There have been many evidences which support the denial of the proton affinity of sulfur dioxide[19,20], whereas anion or base is strongly solvated in this solvent. The *bare cation* (carbonium ion or immonium ion) produced in liquid sulfur dioxide as is depicted in Chart 1 may be quite useful to carry out the reactions (rearrangement and polymerization) in unusual speed.

Chart 2

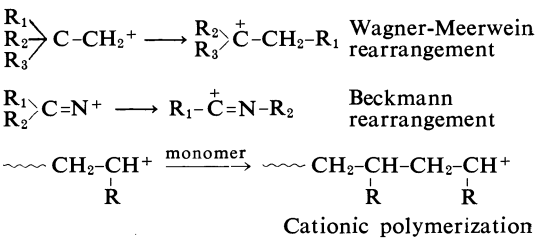

The reverse situation may be found in the Menschutkin reaction. In this case the strong solvation of sulfur dioxide with anion or base may greatly retard the reaction velocity. It is worthy to note that the reaction favored by sulfur dioxide as listed in Chart 2 is a cationic intramolecular reaction or a cationic reaction in which a cation is reacting with a neutral molecule such as a vinyl monomer, the interfering anion being eliminated by complexing with sulfur dioxide.

In a nucleophilic substitution, S_N1 or S_N2, whichever the reaction may be, the attacking reagent, an anion or a base, may be strongly seized by liquid sulfur dioxide. The number of the reacting anion or base available for the reaction must then be reduced greatly. The complexed base may sometimes be able to participate in the reaction, but the reaction rate may be far more depressed. The consideration on the diffusion velocity or on the steric effect of the bulky complexes may also support this view. That a borderline case[7] is observed in a substitution which may otherwise be an S_N1 reaction is accordingly easily understood, since the rate-determining step (the ionization of RX) is not followed by a fast step of the combination of the R^+ (carbonium ion) with an anion or a base. In liquid sulfur dioxide the anion or the base is complexed with sulfur dioxide, so the rate of the second step is not so fast and even a case in which the second step is rate-determining may also be probable. Even if the alkyl halide may be a strong ionizing substrate such as *t*-butyl iodide, the situation that the reaction is very slow will not be improved. In the experimental conditions applied, isopropyl iodide reacted in the slowest rate among the alkyl iodides obeying the second order rate law as is seen in Table VI, which may be attributed to the steric effect[21]. The observed, comparatively small ortho-effect (Table VII) in liquid sulfur dioxide as compared to that in methanol in the reaction of methyl iodide with dimethyl-*o*-toluidine may perhaps due to the smaller solvation of dimethyl-*o*-toluidine by sulfur dioxide.

17) N, Tokura, *Kagaku*, **17**, 575 (1962). The present authors would like to use the term "*bare ion*" instead of the frequently used, "*free ion*", since the latter term has been confusedly adopted both for unsolvated and solvated ions.

18) a) H. Dauben, F. A. Gadecki, K. M. Harmon and D. L. Pearson, *J. Am. Chem. Soc.*, **79**, 4577 (1957); S. Winstein and C. Ordonneau, ibid, **82**, 2084 (1960); c) R. R. Story and M. Saunders, ibid., **82**, 6199 (1960).

19) H. Hart and G. Levitt, *J. Org. Chem.*, **21**, 921 (1956).

20) The view suggested earlier by Sidgwick (W. A. Waters, "Physical Aspect of Organic Chemistry", Routledge and Kogan, London (1950), p. 230.) that liq. SO_2 may have solvations both for cation and anion must be amended.

21) See Ref. 5c), p. 75.

Among the solvents used, the Menschutkin reaction in liquid sulfur dioxide was the slowest (Tables IV and VI). However, the Menschutkin reaction may be greatly favored by the solvent in which a *bare base* is permitted. This is the reason why the reaction in dimethylformamide or in dimethylsulfoxide is very fast. Of course, the quaternization reaction may be facilitated by the ionizing power of the solvent as may be seen by the fact that the rate constant in dimethylformamide is larger than in acetone (Table IV), since the product of the reaction is an ion pair.

Inspection of Table VI reveals that activation energy increases and the activation entropy also increases in liquid sulfur dioxide, the solvation being decreasing in approach to the transition state. The reaction in tetrahydrofuran was slow and comparable to the rate in sulfur dioxide, however, the reaction was heterogeneous owing to the lower solubility of the reactants in this solvent and the rate can not be discussed on the same basis.

The rate in nitromethane was six umes faster as that in liquid sulfur dioxide. No adequate explanation has been prepared for the rate increase except that nitromethane is a very ionizing solvent and the solvation to the base may not be so large by steric reason.

Summary

1) The Menschutkin reaction (reaction of methyl, ethyl or isopropyl iodide with pyridine, dimethylaniline or dimethyl-*o*-toluidine) has been carried out in liquid sulfur dioxide. The reaction rate has been compared with those in other commonly used solvents.

2) The reaction rate in liquid sulfur dioxide is the slowest, whereas the previously performed reactions such as the Beckmann rearrangement and the cationic polymerization in this solvent were the fastest among the solvents ordinarily used.

3) The reason for such a discrepancy has been discussed. Importance of the *bare* (or unsolvated) ion or species in an ionic reaction is presented.

The authors are indebted to the Seitetsu Kakagu K. K. for the denotion of liquid sulfur dioxide. Part of the expensed for this study has been defrayed by the grant-in-aid from the Ministry of Education.

The Chemical Research Institute of Non-Aqueous Solutions
Tohoku University
Katahira-cho, Sendai

The Surface Activities of Bivalent Metal Alkyl Sulfates. I. On the Micelles of Some Metal Alkyl Sulfates

By Iwao SATAKE, Ichiro IWAMATSU, Shizuko HOSOKAWA and Ryohei MATUURA

(Received September 21, 1962)

Innumerable data have been accumulated by a number of authors in the field of surface chemical studies of long chain alkyl sulfates and sulfonates of monovalent metals, especially of sodium. However, only a little work has been performed on the surface chemical properties of water-soluble detergents containing bivalent metals. The first publications on their surface chemical properties were produced by Lottermoser and Stoll[1], and by Lottermoser and Püschel[2] for various bivalent metal dodecyl sulfates, in which the electrical conductivities and the surface tensions of aqueous solutions were reported. Giers and Boide[3] synthesized zinc, calcium and magnesium dodecyl sulfates and measured the viscosities and contact angles of the solutions against solids. Recently Miyamoto[4-6] has determined the solubilities of various bivalent metal dodecyl sulfates in water and the critical micelle concentration (CMC) of the solutions by the surface tension method. He has found that the CMC values of these detergents are

1) A. Lottermoser and F. Stoll, *Kolloid-Z.*, **63**, 49 (1933).
2) A. Lottermoser and F. Püschel, ibid., **63**, 175 (1933).
3) S. Giers and P. Boide, *Soap Chem. Specialties*, **30**, 38, 179 (1954).
4) S. Miyamoto, *Mem. Fac. Sci., Kyushu Univ. Series C, Chem.*, **3**, 93 (1960).
5) S. Miyamoto, This Bulletin, **33**, 371 (1960).
6) S. Miyamoto, ibid., **33**, 375 (1960).

almost independent of the kind of metal ion and are about 1×10^{-3} mol./l. Further discussions on the surface activity of calcium dodecyl sulfate were presented by Lange[7] in connection with the effects of addded electrolytes on the CMC values of detergent solutions, and later by Corkill and Goodman[8] on the micelle formation in an aqueous solution. Tartar and Lelong[9] determined the micellar molecular weight of magnesium dodecyl sulfonate in an aqueous solution. Bone and O'Day[10] have reported the antibacterial activities of various bivalent metal dodecyl sulfates.

It is true that all these works have given us some information on the nature of the surface activity of metal alkyl sulfate, but no deep insight into this surface activity has yet been achieved because of the scarcity of fundamental data on the properties of the solutions of metal alkyl sulfates. The purpose of the present paper is to obtain a knowledge of the micelles of some bivalent metal alkyl sulfates which have not yet been studied fully. As Miyamoto[5] showed, the Krafft point of some metal salts is so high that the determination of the micellar properties is experimentally difficult for them. Therefore, here we have used cobalt, nickel, copper and magnesium salts which had Krafft points near room temperatures.

Experimental

Materials. — The bivalent metal alkyl sulfates were synthesized from pure sodium alkyl sulfate and inorganic salt according to the method used by Lottermoser and Püschel[2]. They were purified by repeated recrystallization. Sodium alkyl sulfate was prepared from the purified fatty alcohol obtained by the fractional distillation of commercial samples, as has been stated earlier[11]. The purity of the metal alkyl sulfates was confirmed by elementary analysis and surface tension measurement. The results of the elementary analysis of these detergents are summarized in Table I.

Method.—The CMC's of the aqueous solutions of bivalent metal dodecyl sulfates were determined by the conductivity method at 30°C using a Yanagimoto conductivity outfit model MY-7. The CMC values of copper tetradecyl and hexadecyl sulfates were determined by the surface tension method at the temperature above each Krafft point; the same surface tension method was adopted for the determination of the CMC's of the detergent solutions with inorganic salts added.

Table I. The elementary analysis of various bivalent metal alkyl sulfates

Detergent		Metal content %	C, %	H, %
$Cu(DS)_2\cdot4H_2O$	Calcd.	9.61	43.23	8.78
	Found	9.55	43.29	8.87
$Co(DS)_2\cdot6H_2O$	Calcd.	8.45	41.29	8.96
	Found	8.62	41.56	9.33
$Ni(DS)_2\cdot6H_2O$	Calcd.	8.41	41.33	8.96
	Found	8.76	41.55	9.16
$Mg(DS)_2\cdot6H_2O$	Calcd.	3.77	43.48	9.35
	Found	3.73	43.45	9.39
$Cu(TS)_2\cdot4H_2O$	Calcd.	8.88	46.66	8.88
	Found	8.58	46.70	9.28
$Cu(HS)_2\cdot4H_2O$	Calcd.	8.24	49.48	9.27
	Found		49.22	9.48

DS: Dodecyl sulfate radical; TS: Tetradecyl sulfate radical; HS: Hexadecyl sulfate radical

The micellar molecular weights were estimated by the light scattering method, using a Shimadzu photoelectric light-scattering photometer and a Brice Phoenix universal light scattering photometer at 436 and 546 mμ with a semi-octagonal cell. The dependence of the refractive indices on the concentration of the detergents were measured by a Brice Phoenix differential refractometer at the same wavelength. The measurements were performed in the salt free and 0.1 M metal sulfate solutions.

The micellar charge was evaluated from the data of conductivity and light scattering using the equation previously reported[12].

Results and Discussion

The CMC's of Various Bivalent Metal Dodecyl Sulfates.—The critical micelle concentration is one of the most fundamental quantities in determining the surface activity of the detergent solution. Table II shows the CMC values of various bivalent metal alkyl sulfates. The CMC values obtained are almost the same within the range of experimental error, and no differences can be observed among various metal dodecyl sulfates. The CMC value of about 1.2×10^{-3} mol./l. obtained for various bivalent metal dodecyl sulfates in the present experiment is in good agreement with the value of 1.7×10^{-3} mol./l. at 40°C obtained by Lottermoser and Püschel[2] and the value of 1×10^{-3} mol./l. at various temperatures obtained by Miyamoto[6].

These CMC values are quite small compared with those of the corresponding monovalent metal dodecyl sulfates, e. g., sodium salt, indicating the increased surface activity of bivalent

7) H. Lange, *Kolloid-Z.*, **121**, 66 (1951).
8) J. M. Corkill and J. F. Goodman, *Trans. Faraday Soc.*, **58**, 206 (1962).
9) H. V. Tartar and A. L. M. Lelong, *J. Phys. Chem.*, **59**, 1185 (1955).
10) J. N. Bone and D. W. O'Day, *J. Am. Pharm. Assoc.*, **47**, 795 (1958).
11) R. Matuura, H. Kimizuka, S. Miyamoto and R. Shimozawa, This Bulletin, **31**, 532 (1958).
12) H. Kimizuka and I. Satake, ibid., **35**, 251 (1962).

TABLE II. THE CRITICAL MICELLE CONCENTRATIONS OF VARIOUS BIVALENT METAL ALKYL SULFATES

Detergent	Temp. °C	CMC mol./l.	Method
$Cu(DS)_2$	30	1.20×10^{-3}	Conductivity
$Mg(DS)_2$	30	1.25×10^{-3}	Conductivity
$Co(DS)_2$	30	1.23×10^{-3}	Conductivity
$Ni(DS)_2$	30	1.24×10^{-3}	Conductivity
$Cu(TS)_2$	47	2.5×10^{-4}	Surface tension
$Cu(HS)_2$	47	5.8×10^{-5}	Surface tension

salts. Miyamoto[5,6] reported that quite similar CMC values are also obtained for calcium, lead and strontium dodecyl sulfates; however, their Krafft points are 50, 53 and 64°C respectively, which are considerably higher than those of copper, cobalt and magnesium salts, which are 24, 23 and 25°C respectively. Also, the solubility of these salts is quite different from each other. Nevertheless, the CMC values are nearly identical for all these bivalent metal dodecyl sulfates. This means that the fundamental factor responsible for determining the CMC value of a detergent is the valency of the metal ion; varying the kind of metal ion having the same valency has little or no detectable effect on the CMC value, provided that the anionic group is the same.

When the alkyl chain length of the anionic group increases for the same metal salt, copper salt in the present case, the CMC value varies according to the formula:

$$\log(\mathrm{CMC}) = AN + B \qquad (1)$$

as is the case with usual monovalent detergents. Here N is the number of carbon atoms in the alkyl chain, and A and B are constants. Figure 1 shows the relation between log (CMC) and N in the copper alkyl sulfates. The value of -0.32 is obtained for A, which is in good agreement with the value of -0.3 obtained for various alkyl sulfates of sodium.

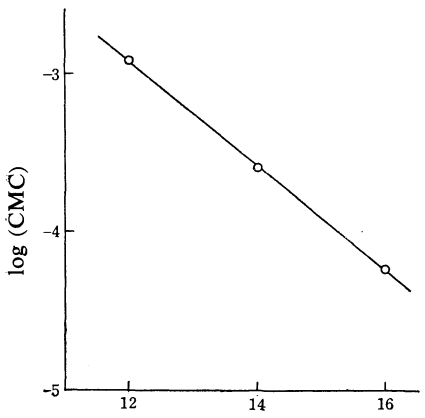

Fig. 1. Relation between log (CMC) and the number of carbon atoms in the chain of copper alkyl sulfates.

Effects of the Added Electrolytes on the CMC Value.—The effects of added electrolytes on the CMC value of the detergent have been widely studied by many authors. Especially, Corrin and Harkins[13] have investigated the effects of added electrolytes on the CMC values of various detergents and have found the following empirical equation between the CMC value and the total gegen-ion concentration:

$$\log(\mathrm{CMC}) = a\log m^+ + b \qquad (2)$$

Here a and b are constants, and $m^+ = (\mathrm{CMC}) + C'$, where C' is the concentration of added electrolytes. Subsequent investigation of this problem was carried out by Lange[7], who obtained the same empirical relation when the valencies of the ion of the added electrolyte and the detergent gegen-ion are identical. However, he pointed out that Eq. 2 is not applicable if the valency of the ion of the added electrolyte is different from that of the gegen-ion, although he suggested that when the concentration of the added electrolytes is higher than that of detergent gegen-ions, a similar type of equation can be applied, one in which the concentration of added electrolytes, C, is substituted for m^+ in Eq. 2:

$$\log(\mathrm{CMC}) = a\log C + b \qquad (3)$$

Theoretical considerations of these empirical relations have been undertaken by Stainsby and Alexander[14], Hobbs[15] and Shinoda[16,17].

The effects of added copper sulfate and sodium sulfate on the CMC values of sodium dodecyl sulfate (SDS) and copper dodecyl sulfate ($Cu(DS)_2$) are shown in Figs. 2 and 3. The general features of the curves shown in Figs. 2 and 3 are quite similar to those obtained by Lange[7] for calcium dodecyl sulfate. At first the CMC value of SDS rapidly decreases with the addition of copper sulfate to about one fourth, and thereafter it gradually decreases as the concentration of copper sulfate increases. In the case of $Cu(DS)_2+Na_2SO_4$, the CMC value of $Cu(DS)_2$ decreases gradually compared with the case of $SDS+CuSO_4$.

In the solutions with the excess salt added, the CMC curve of the $SDS+CuSO_4$ system has a tendency to approach the curve of the $Cu(DS)_2+CuSO_4$ system, and the curve of $Cu(DS)_2+Na_2SO_4$ approaches that of $SDS+Na_2SO_4$. These facts suggest that the nature

13) M. L. Corrin and W. D. Harkins, *J. Am. Chem. Soc.*, **69**, 683 (1947).
14) G. S. Stainsby and A. E. Alexander, *Trans. Faraday Soc.*, **46**, 587 (1950).
15) M. E. Hobbs, *J. Phys. Chem.*, **55**, 675 (1951).
16) K. Shinoda, This Bulletin, **26**, 101 (1953).
17) K. Shinoda, ibid., **28**, 340 (1955).

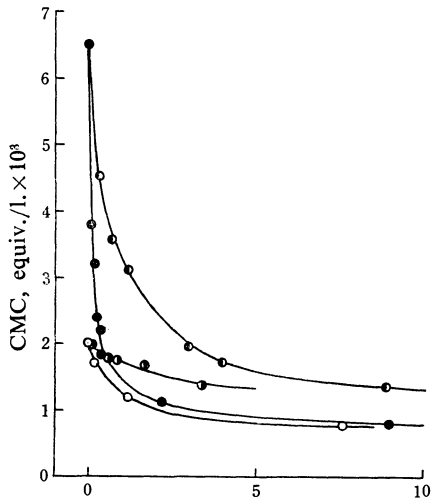

Fig. 2. Effects of the added salts on the CMC's of sodium dodecyl sulfate and copper dodecyl sulfate.
○ : $Cu(DS)_2+CuSO_4$ ◑ : $Cu(DS)_2+Na_2SO_4$
● : $SDS+CuSO_4$ ◐ : $SDS+Na_2SO_4$.
The CMC data of the system $SDS+Na_2SO_4$ was taken from the data reported by Corrin and Harkins[13].

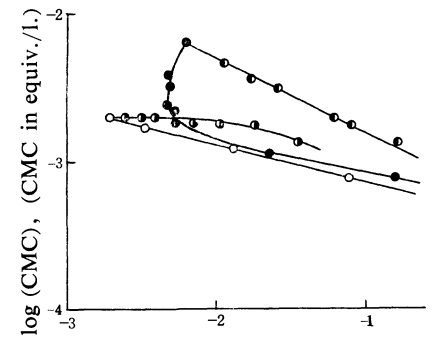

Fig. 3. Effects of the added salts on the CMC's of sodium dodecyl sulfate and copper dodecyl sulfate.
○ : $Cu(DS)_2+CuSO_4$ ◑ : $Cu(DS)_2+Na_2SO_4$
● : $SDS+CuSO_4$ ◐ : $SDS+Na_2SO_4$
The CMC data of the system $SDS+Na_2SO_4$ was taken from the data reported by Corrin and Harkins[13].

of the detergent in excess salt solutions is characterized by the added cations and that there occurs a rearrangement of the detergent micelle, i. e., the variation of the micellar aggregation number and the formation of a new, surface, gegen-ion layer of the micelle caused by the exchange between salt cations and the surface layer gegen-ions of the original detergent micelle. In both cases in which the gegen-ion is different from the added salt cation, there are no linear relationships between log (CMC) and $\log m^+$, as is shown in Fig. 3. On the contrary, for the $Cu(DS)_2+CuSO_4$ system a good linearity is found to exist. Shinoda[17] derived an equation which expresses the effect of added electrolytes on the CMC value of the detergent solution. Using this equation we found that the degree of dissociation of micelle forming ion of copper dodecyl sulfate is 0.52. The degree of dissociation can also be determined by conductivity measurement, as will be described later.

The Determination of Micellar Molecular Weight by the Light-scattering Techinique.— The light-scattering technique is one of the most useful methods of estimating the molecular weight of the colloidal aggregate. However, the effect of micellar charge must be taken into cosideration in the application of this method to the charged system, as has already been pointed out by, for instance, Dosher and Mysels[18] and Hutchinson[19]. Dosher and Mysels[18] pointed out that Eq. 5 should be employed for charged systems in place of the usual scattering formula, Eq. 4.

$$(HC/\tau)_{C\to 0}=1/M \tag{4}$$

$$(HC/\tau)_{C\to 0}=(1+P)/M \tag{5}$$

Here, P is the number of simple ions associated with one charged, colloidal ion, M is the molecular weight of the colloidal particle, τ is the turbidity of the solution, C is the concentration in g./ml., and

$$H=32\pi^3n^2(dn/dc)^2/3N\lambda^4$$

where n is the refractive index of the solution and λ is the wavelength of the incident light. The true molecular weight of the solute particle can be obtained from the scattering experiment in an excess salt solution because P in Eq. 5 tends to zero in this condition. The measurements were conducted at 436 and 546 mμ and at 30°C. The values of micellar molecular weight obtained at 436 and 546 mμ were approximately the same within the range of experimental error. The scattering was observed by using a semi-octagonal cell at the angle of 45 90 and 135° with relation to the incident light, but the dissymmetries of the scattering can not be detected. Thus, the limiting condition in the application of Eqs. 4 or 5, that the dimension of the solute particle must be smaller than $\lambda/20$, is considered to be quite satisfied.

In Fig. 4, the typical scattering curve of copper dodecyl sulfate is given. The abscissa represents the micellar concentration $C-C_o$, where C_o is the CMC value. Table III shows the micellar molecular weights of nickel,

18) T. M. Dosher and K. J. Mysels, *J. Chem. Phys.*, **19**, 254 (1951).
19) E. Hutchinson, *J. Colloid Sci.*, **9**, 191 (1954).

TABLE III. MICELLAR MOLECULAR WEIGHTS OF VARIOUS METAL DODECYL SULFATES AT 30°C

Solute	Solvent	CMC $\times 10^3$ (mol./l.)	MMW	AN	P
$Ni(DS)_2$	H_2O	1.1	24400	92	0.16
	0.1 M $NiSO_4$	0.3	28200	106	
$Co(DS)_2$	H_2O	1.2	27400	103	0.11
	0.1 M $CoSO_4$	0.3	30300	114	
$Cu(DS)_2$	H_2O	1.2	22700	85	0.13
	0.1 M $CuSO_4$	0.3	25600	97	
$Mg(DS)_2$	H_2O	1.2	26300	99	0.19
	0.1 M $MgSO_4$	0.3	31300	118	

MMW: Micellar molecular weight; AN: Aggregation number

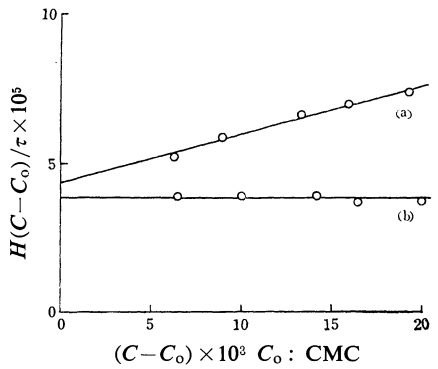

Fig. 4. $H(C-C_0)/\tau\sim(C-C_0)$ curves for copper dodecyl sulfate in H_2O at 436 mμ (a), and in 0.1 M $CuSO_4$ at 546 mμ (b), at 30°C.

cobalt, copper and magnesium dodecyl sulfate in salt free solutions and in corresponding metal sulfate solutions. For the salt free solutions, Eq. 4 was also assumed to hold.

Only small differences are found among the micellar molecular weights of the various bivalent metal dodecyl sulfates studied. The values of the micellar molecular weight in salt free solutions fall in the comparatively narrow range between 23000 and 27000, and those in salt solutions, in the range between 25000 and 31000. The micellar molecular weights of the detergents in salt solutions are slightly larger than those in salt free solutions. The P values calculated from Eq. 5 by using the data of micellar molecular weight in Table III are of the order of 0.1 to 0.2, indicating the almost complete screening action of the bivalent metal ions, even in salt free solutions. The micellar aggregation number, i. e., the number of dodecyl chains in a micelle, of bivalent metal dodecyl sulfates is about 100, which is almost twice the value (41) for SDS[20]. The same order of aggragation number was reported by Tartar and Lelong[9], who obtained the micellar molecular weight of 28500 and the aggregation number of 107 for magnesium dodecyl sulfonate in a salt free solution.

Thus, the marked increase in surface activity, especially the solubilizing power of the bivalent metal dodecyl sulfates, may be expected because of the increased micellar aggregation number of the micelle and their decreased CMC value. The solubilizing power of these detergents will be reported on in another paper.

The Estimation of Micellar Charge from Conductivity Data.—The micellar charge of the detergent can be evaluated from the conductivity of the aqueous solution and from the micellar aggregation number obtained by the light-scattering technique, as has been reported[12].

Using some basic assumptions[12], the following equations can be derived:

$$[(\Lambda_0-\Lambda)/(\Lambda_0-\Lambda_m)]^2=\{(Z_d-Z_c)+(Z_g+Z_c)C/C_m\}/(Z_d+Z_g) \quad (6)$$

$$Z_c=\{Z_m^2-Z_g(nZ_d-Z_m)\}/nZ_d \quad (7)$$

Here, Λ_0 is the equivalent conductivity of the detergent at infinite dilution, Λ_m is the equivalent conductivity at the CMC value, and Z_d and Z_g are the valencies of the detergent ion and gegen-ion respectively. The value of Z_c can be evaluated from the slope of the straight line by plotting the quantity $[(\Lambda_0-\Lambda)/(\Lambda_0-\Lambda_m)]^2$ as the function of the reduced concentration, C/C_m. Moreover, the value of the micellar charge, Z_m, can be calculated from Eq. 7 by using the micellar aggregation number, n, obtained by the light-scattering experiment. Figure 5 shows one of the typical relations between $[(\Lambda_0-\Lambda)/(\Lambda_0-\Lambda_m)]^2$ and C/C_m for copper dodecyl sulfate. The calculated micellar charge, Z_m, and the dissociation degree of the micellar ion, α, are given in Table IV.

The dissociation degrees of the micellar ion, α, obtained in the present experiment are comparatively small, suggesting that about half of the micelle-forming detergent molecules are undissociated. The value of α decreases

20) H. V. Tartar, ibid., **14**, 115 (1959).

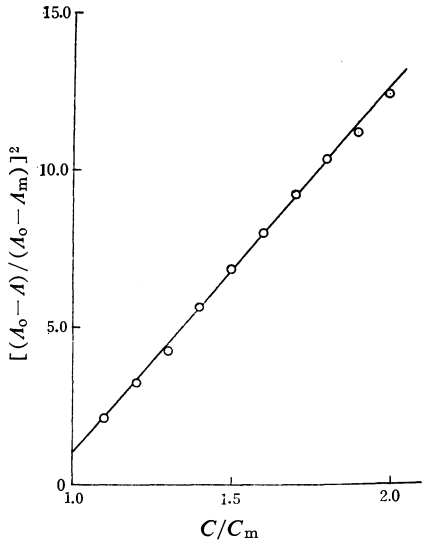

Fig. 5. Typical relation between $[(\Lambda_o-\Lambda)/(\Lambda_o-\Lambda_m)]^2$ and C/C_m for copper dodecyl sulfate at 30°C.

TABLE IV. THE MICELLAR CHARGE AND THE DISSOCIATION DEGREE OF THE MICELLAR ION OF VARIOUS METAL DODECYL SULFATES AT 30°C

Solute	n (In a salt solution	Z_c	Z_m	α
$Co(DS)_2$	114	47	75	0.66
$Cu(DS)_2$	97	34	58	0.60
$Mg(DS)_2$	118	20	50	0.42

Here α equals Z_m/nZ_d.

in the order cobalt>copper>magnesium, but the difference among them is said to be not very large. The value of 0.60 for copper dodecyl sulfate micelle is approximately the same as the value of 0.52 obtained from the effect of the added electrolyte on the CMC value mentioned above.

These experimental results suggest that, above the CMC value, the micelle of the bivalent metal dodecyl sulfate must be treated as a weak electrolyte. The bivalent metal dodecyl sulfates are composed of a weak base and a strong acid; therefore, the effect of the hydrolysis of the bivalent gegen-ion must be considered. This problem will, in the near future, be treated in another paper in connection with the change in the pH value of the detergent solutions with concentration.

Summary

Dodecyl sulfates of bivalent nickel, cobalt, copper and magnesium were synthesized, and studies were carried out on the CMC values of these detergents, the effects of the added electrolytes on these CMC values, on micellar molecular weights, and on micellar charges. The CMC values of the detergents were independent of the kind of metal, and the CMC value of 1.2×10^{-3} mol./l. was obtained. The micellar aggregation numbers of bivalent metal dodecyl sulfates were of the order of 100, which is about twice that of sodium dodecyl sulfate. The dissociation degrees of the micelles were also evaluated from the conductivity data. The α values obtained were 0.66 for cobalt, 0.60 for copper and 0.42 for magnesium. The dissociation degree of the copper dodecyl sulfate micelle was also estimated to be 0.52 from the depression of the CMC value by the added electrolyte; this figure is approximately the same as the value of 0.60 obtained from the conductivity data. These results suggest that the fundamental factor responsible for determining the surface activities of bivalent metal dodecyl sulfates is the valency of the gegen-ion and that the kind of metal has little or no detectable effect on them.

The authors wish to thank to Professor Tomoo Oyama in the Faculty of Technology and to Professor Satoru Akune in the Faculty of Agriculture, both of Kyushu University, for helping in the light-scattering experiment.

Department of Chemistry
Faculty of Science
Kyushu University
Hakozaki, Fukuoka

Infrared Absorption Spectra of Hydrazides. VI. Benzoylhydrazine

By Mitsuo MASHIMA

(Received October 18, 1962)

The infrared absorption spectra of benzoylhydrazine in the solid state and in an acetonitrile solution have previously been observed by the present author[1]. However, the absorption bands observed could not be interpreted with certainty. In the present study, the infrared spectrum of *N*-deuterated benzoylhydrazine is examined in the rock salt region. For the sake of comparison, the infrared spectra of *N*-deuterated benzamide, cyanoacetic acid amide and its *N*-deuterated derivative are also observed. A tentative assignment of the bands of these compounds is described in the present paper. On the basis of results of the assignment, the frequencies characteristic of the $-CONHNH_2$ group are compared with those characteristic of the $-CONH_2$ group.

Experimental

The preparation and purification of benzoylhydrazine and benzamide have been described in a previous paper[1]. Cyanoacetic acid amide was synthesized with cyanoacetic acid ethylester and ammonia and was purified by recrystallization from ethanol, m. p., 119°C. The *N*-deuterated derivatives examined were prepared in sealed tubes in the presence of heavy water (99.8%). The excess heavy water was evaporated in vacuo. The solid spectra of all compounds were studied with potassium bromide disks. The solution spectrum of cyanoacetic acid amide was obtained with acetonitrile as a solvent and with 0.1 mm. cells in the optical path. A double-beam Hitachi infrared spectrophotometer type EPI-2 was used in the rock salt region.

Results and Discussion

Benzoylhydrazine (BH).—The infrared absorption spectra of BH and *N*-deuterated BH (BH-d_3) are illustrated in Fig. 1. The present author has previously investigated the frequencies characteristic of the $-CONHNH_2$ group[2,3]. Cyanoacetylhydrazine[2], for example, has the following bands due to the $-CONHNH_2$ group: NH_2 or NH stretching, 3320, 3180 cm^{-1}; amide I, 1698 cm^{-1}; NH_2 bending, 1625 cm^{-1}; amide II, 1534 cm^{-1}; NH_2 twisting, 1313 cm^{-1}; amide III, 1258 cm^{-1}; NH_2 wagging, 1105 cm^{-1}; NH_2 rocking 1009 cm^{-1}.

The 1664 cm^{-1} band of BH was taken as the amide I band in a previous paper[1]. This assignment is supported by the fact that BH-d_3 has the corresponding band at 1627 cm^{-1}, the ν_H/ν_D ratio being 1.023. BH has an intense band at 1618 cm^{-1}, and this band is displaced by a band at 1209 cm^{-1} on *N*-deuteration, the ν_H/ν_D ratio being 1.338. Therefore, the 1618 cm^{-1} band may surely be assigned to the NH_2 bending vibration, $\beta(NH_2)$. For BH a shoulder band at 1527 cm^{-1}, which is accompanied by the band at 1582 cm^{-1}, vanishes on *N*-deuteration. BH-d_3 has a new band at 1416 cm^{-1}. In cyanoacetylhydrazine the amide II band at 1534 cm^{-1} is displaced by a band at 1451 cm^{-1} on *N*-deuteration. Therefore, the 1527 cm^{-1} band of BH is very probably to be assigned to the amide II band, and the 1416 cm^{-1} band of BH-d_3 may probably be taken as the amide II' band. The 1349 cm^{-1} band of BH has not yet been assigned with certainty. This band vanishes on *N*-deuteration and BH-d_3 has a new band at 1098 cm^{-1}, the ν_H/ν_D ratio being 1.229. Therefore, it seems that the 1349 cm^{-1} band may best be assigned to the NH_2 twisting vibration ($\tau(NH_2)$) because it is close in frequency to the corresponding band at 1313 cm^{-1} of cyanoacetylhydrazine. BH has two additional moderately strong bands, which disappear on *N*-deutration, at 1118 and 987*1 cm^{-1}. These two bands are considered to correspond to the bands at 936 and 897 cm^{-1} for BH-d_3 and are close in frequency to the bands at 1105 and 1009 cm^{-1} of cyanoacetylhydrazine. Therefore, they are considered to be assigned to the NH_2 wagging and rocking vibrations, ($\omega(NH_2)$ and $\gamma(NH_2)$) respectively. BH has a very weak band at 1250 cm^{-1}, which disappears on *N*-deuteration, and BH-d_3 has a new band at 1058 cm^{-1}, the ν_H/ν_D ratio being 1250/1058 (1.182). In consequence, the 1250 cm^{-1} band is can probably best be assigned to an amide III band.

In order to ascertain the assignments above described, the vibrations of a monosubstituted aromatic ring will be considered. Schmid,

1) M. Mashima, This Bulletin, **35**, 332 (1962).
2) M. Mashima, ibid., **35**, 1882 (1962).
3) M. Mashima, ibid., **35**, 2020 (1962).

*1 This is a mean value of the frequencies of the two peaks at 990 and 984 cm^{-1}.

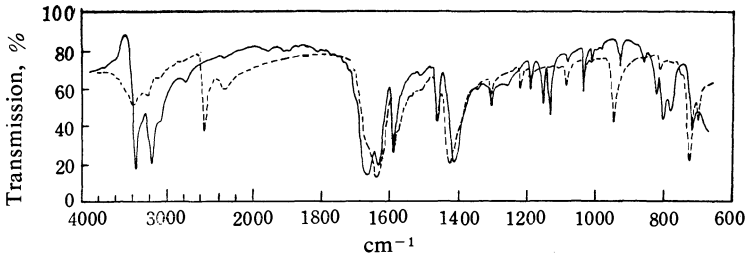

Fig. 1. Infrared spectra of $C_6H_5CONHNH_2$, ——, and $C_6H_5CONDND_2$, ----, in KBr disks.

Brandmeuller and Nonnenmacher[4] have made a calculation of the normal vibrations of the monosubstituted aromatic compounds. On the basis of calculations, they have proposed detailed assignments of the infrared absorption bands and Raman lines for several monosubstituted benzenes. These assignments may be referred to for an interpretation of the bands observed for BH (and also benzamide (BA), infrared spectrum of which is shown in Fig. 3) in the 1600~650 cm^{-1} region. The frequencies of this region due to an aromatic ring are summarized in Table I, in which the corresponding frequencies and their detailed assignments for toluene and chlorobenzene[4] are also represented for the sake of comparison. Four bands (near 1600, 1580, 1500 and 1450 cm^{-1}) of the monosubstituted aromatic compounds are usually used in correlation work[5], and the bands corresponding to them are easily found for BH, BA and their *N*-deuterated derivatives, as is shown in Table I. Four further bands, near 1300, 1180, 1070 and 1020 cm^{-1}, are observed for both BH and BA, and for their *N*-deuterated derivatives also. Those bands can, therefore, very probably be assigned to the in-plane C–H deformation vibrations, δ(C–H). Five of the δ(C–H) vibrations can be reasonably expected to occur, so the 1154 cm^{-1} band of BH (and the 1142 cm^{-1} band BA) is to be taken as another δ(C–H) band. However, this assignment is not certain because no band corresponding to it is found for BH-d_3 (nor for BA-d_2).

Two bands near 1330 and 1000 cm^{-1} are observed for all compounds of BH, BA and their *N*-deuterated derivatives. Therefore, these two bands also are surely assigned to the vibrations of an aromatic ring.

The out-of-plane C–H deformation vibrations (π(C–H)) are expected to occur in the region below 1000 cm^{-1} because they have been obtained in that region for the monosubstituted aromatic compounds[4], as is shown in Table I. The 966 cm^{-1} band of BH, which is observed as a shoulder band at the foot of the more intense band at 987 cm^{-1}, corresponds in frequency to the band at 967 cm^{-1} for BH-d_3. BA also has a very weak band at 987 cm^{-1} which is considered to correspond to the 966 cm^{-1} band of BH. The band near 920 cm^{-1} is observed for BH, BA and all of their *N*-deuterated derivatives. The 863 cm^{-1} band of BH corresponds in frequency to the band at 848 cm^{-1} for BA and 847 cm^{-1} for BA-d_2, while for BH-d_3 the corresponding band can not be ascertained because it is overlapped by the more intense band at 897 cm^{-1} which was already assigned to the $\gamma(ND_2)$ vibration. Thus, the 966, 917 and 863 cm^{-1} bands of BH

TABLE I. INFRARED FREQUENCIES OF AN AROMATIC RING (in the 1600~650 cm^{-1})

Assignment[a]	$C_6H_5CH_3$[a] liq.	C_6H_5Cl[a] liq.	BH solid	BH-d_3 solid	BA solid	BA-d_2 solid
ωB_1	1608	1570	1608	1603	1578	1574
ωA_1	1575	1585	1582	1573		
ωA_1	1497	1477	1492	1490	1497	1497
ωB_1	1452	1455	1450	1450	1451	1452
$\delta_{CH}B_1$	1250	1270	1298	1293	1296	1296
$\delta_{CH}A_1$	1179	1123	1183	1182	1180	1178
$\delta_{CH}B_1$	1157	1156	1154	—	1142	—
$\delta_{CH}B_1$	1082	1068	1070	1070	1073	1074
$\delta_{CH}A_1$	1032	1022	1024	1023	1024	1024
ωB_1	1314	1324	1320	1332	1334	1342
ωA_1	1002	1002	1002	1010	999	1000
$\omega_X A_1$	1211	1086				
$\pi_{CH}B_2$	974	982	966	967	987	987
$\pi_{CH}A_2$	966	963	917	921	917	924
$\pi_{CH}B_2$	895	903	863	—[b]	848	847
$\pi_{CH}B_2$	842	831				
$\pi_{CH}B_2$	729	740	801	797	811	801
$\omega_X A_1$	786	702	747	705	770	713
ΓB_2	694	684	690	674	705	691

a) See Ref. 4.
b) This band could not observe because it is overlapped by a more intense band at 897 cm^{-1}.

4) E. W. Schmid, J. Brandmeuller and G. Nonnenmacher, *Z. Elektrochem.*, **64**, 726 (1960).

5) L. J. Bellamy, "The Infrared Spectra of Complex Molecules", Methuen and Company, Ltd., London (1954).

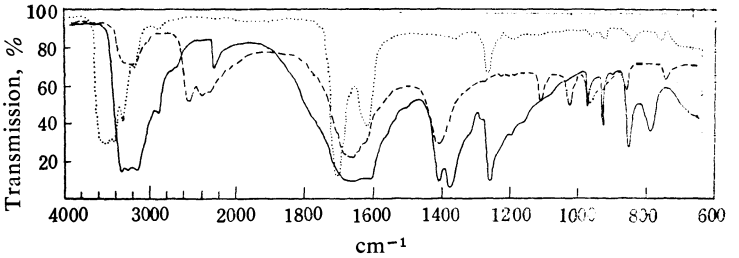

Fig. 2. Infrared spectra of $CNCH_2CONH_2$ in the solid state, ——, and in CH_3CN, ……, and $CNCH_2COND_2$ in the solid state, ----.

TABLE II. INFRARED FREQUENCIES OF BH AND THEIR ASSIGNMENTS

Assignment[a]	BH Solid	BH-d_3 Solid
$\nu(NH_2)$ or ν(NH)	3280 (s)	
	3180 (s)	
	3010 (s)	
	2870 (w)	
		1652 (sh)
Amide I	1664 (vs)	1627 (vs)
$\beta(NH_2)$	1618 (vs)	
ν(C-C)	1608 (sh)	1603 (sh)
ν(C-C)	1582 (s)	1573 (s)
Amide II	1527 (sh)	
		1507 (w)
ν(C-C)	1492 (w)	1490 (w)
ν(C-C)	1450 (w)	1450 (s)
Amide II′		1416 (s)
$\tau(NH_2)$	1349 (s)	
	1320 (sh)	1332 (w)
δ(C-H)	1298 (w)	1293 (w)
Amide III	1250 (vw)	
$\beta(ND_2)$		1209 (m)
δ(C-H)	1183 (w)	1182 (w)
	1154 (vw)	
$\omega(NH_2)$	1118 (m)	
$\tau(ND_2)$		1098 (w)
δ(C-H)	1070 (w)	1072 (w)
Amide III′		1058 (vw)
δ(C-H)	1024 (vw)	1023 (vw)
$\gamma(NH_2)$	990 (m)	
	984 (m)	
π(C-H)	966 (vw)	967 (w)
$\omega(ND_2)$		936 (w)
π(C-H)	917 (w)	921 (w)
$\gamma(ND_2)$		897 (m)
π(C-H)	863 (m)	
	801 (m)	797 (w)
	747 (w)	
	690 (s)	705 (s)
		674 (s)

a) ν; stretching, β; bending, δ; in-plane deformation, π; out-of-plane deformation, τ; twisting, ω; wagging, γ; rocking

are considered to be assigned to the π(C-H) vibrations.

BH has three further bands at 801, 747 and 690 cm^{-1} not yet accounted for. In the region below 800 cm^{-1}, BH-d_3 has also three bands at 797, 705 and 674 cm^{-1}. For monosubstituted aromatic compounds, two bands in the 770～730 and 710～690 cm^{-1} ranges are usually used in correlation work[5]. Although a detailed assignment of the three bands of BH can not be made, it seems certain that they are due to the aromatic ring vibrations.

The infrared frequencies of BH and their assignments are summarized in Table II.

Cyanoacetic Acid Amide (CAA).—The infrared absorption spectra of CAA and CAA-d_2 in the solid state are illustrated in Fig. 2, in which the spectrum of CAA in acetonitrile is also shown. Recently Suzuki[6] studied the infrared spectra of $HCONH_2$ and its three kinds of deuterated derivatives in the 3600～300 cm^{-1} region. He also made a calculation of the normal vibrations for these four kinds of molecules. Suzuki[7] further observed the infrared spectra of CH_3CONH_2 and its three kinds of deuterated derivatives in the 1800～300 cm^{-1} region. He made a calculation of the normal vibrations for those four kinds of molecules and discussed in detail the nature of the absorption bands observed. An assignment of the absorption bands of CAA can, therefore, rather easily be made by a comparison of the spectrum with those of $HCONH_2$ and CH_3CONH_2.

The 3000 cm^{-1} Region. — CAA in the solid state has two strong bands at 3330 and 3140 cm^{-1}. Since these two bands are close in frequency to the 3330 and 3190 cm^{-1} bands of $HCONH_2$[6], they can surely be assigned to the asymmetric and symmetric NH_2 stretching vibrations, $\nu_a(NH_2)$ and $\nu_s(NH_2)$. The fact that they move to higher frequencies in an acetonitrile solution is consistent with the above assignments. CAA-d_2 has $\nu_a(ND_2)$ and $\nu_s(ND_2)$ bands at 2505 and 2350 cm^{-1} respectively. The $\nu(CH_2)$ vibrations are also considered to give rise to bands in this region.

6) I. Suzuki, This Bulletin, 33, 1359 (1960).
7) I. Suzuki, ibid. 35, 1279 (1962).

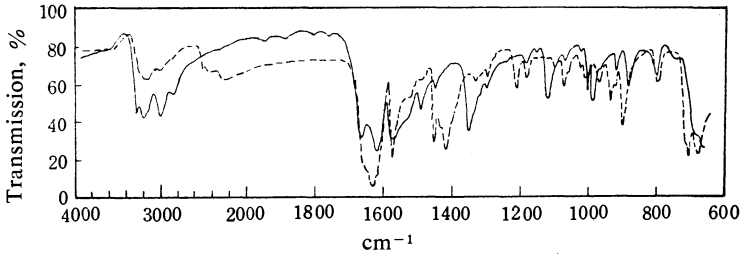

Fig. 3. Infrared spectra of $C_6H_5CONH_2$, ——, and $C_6H_5COND_2$, ----, in KBr disks.

In fact, CAA has two weak bands at 2930 and 2760 cm^{-1} which are probably to be ascribed to the $\nu(CH_2)$ vibrations.

The 2250 cm^{-1} band of CAA is surely to be assigned to the $\nu(C\equiv N)$ vibration because CAA-d_2 has a corresponding band at 2260 cm^{-1}, which is observed as a shoulder band accompanied by the band at 2350 cm^{-1}.

The 1700~700 cm^{-1} Region. — In this region the amide bands and NH_2 deformation bands are expected to appear. In primary amides the amide I band has been obtained near 1650 cm^{-1} [5]. CAA has also the amide I band at 1675 cm^{-1} (solid) and 1703 cm^{-1} (in acetonitrile). The band corresponding to it is shown at 1655 cm^{-1} in CAA-d_2. The 1615 cm^{-1} band of CAA disappears on *N*-deuteration, and CAA in acetonitrile has also a corresponding band at 1618 cm^{-1}. Suzuki[7] has shown that the 1632 cm^{-1} band of CH_3CONH_2 is mainly associated with the NH_2 bending vibration and that the 1189 cm^{-1} band of CH_3COND_2 is to be assigned to an almost pure ND_2 bending vibration. He[6] has also obtained the pure $\beta(NH_2)$ band at 1608 cm^{-1} for $HCONH_2$ and the $\beta(ND_2)$ band at 1118 cm^{-1} for $HCOND_2$. CAA-d_2 has the band at 1100 cm^{-1} instead of the 1615 cm^{-1} band of CAA. Therefore, the 1615 cm^{-1} band is undoubtedly assigned to be to the $\beta(NH_2)$ vibration and the 1100 cm^{-1} band of CAA-d_2, to the $\beta(ND_2)$.

Primary amides usually have a moderately strong band in the 1420~1400 cm^{-1} range[5]. For CH_3CONH_2[7] the 1404 cm^{-1} band was ascribed to the C–N stretching vibration (ν(C–N)) interacting with other kinds of normal vibrations. In CH_3COND_2 the ν(C–N) band moves to a higher frequency and appears at 1427 cm^{-1}. The ν(C–N) band has been obtained at 1309 cm^{-1} for $HCONH_2$ and 1338 cm^{-1} for $HCOND_2$[6]. It is noticeable that a frequency shift of the ν(C–N) band of $HCONH_2$ and CH_3CONH_2 on *N*-deuteration is in the direction shown by the corresponding shift of the ν(C–N) band for urea[8] and oxamide[9], as is summarized in Table III. CAA has two strong bands at 1408 and 1378 (more intense) cm^{-1}. One of them is considered to be due to the CH_2 bending vibration, $\beta(CH_2)$. Cyanoacetylhydrazine[2] has the $\beta(CH_2)$ band at 1396 cm^{-1}, which is rather closer in frequency to the 1408 cm^{-1} band than to the 1378 cm^{-1} band of CAA. Therefore, the 1408 cm^{-1} band is considered to be assigned to the $\beta(CH_2)$ vibration, and the 1378 cm^{-1} band may be assigned to the ν(C–N) vibration. On the other hand, CAA-d_2 has a relatively broad and intense band with its absorption maximum near 1398 cm^{-1}. This band is considered as the ν(C–N) band overlapped by the $\beta(CH_2)$ band near 1400 cm^{-1}. In that case, the 1378 cm^{-1} band of CAA moves to a higher frequency on *N*-deuteration. This frequency shift is in accordance (in direction and value) with those of the ν(C–N) band of compounds containing the $-CONH_2$ group, as may be seen from Table III.

Table III. The frequency shift of the ν(C–N) band on *N*-deuteration

Compound	Frequency	Frequency shift
Urea[a]	1464	+26
Urea-d_4	1490	
Oxamide[b]	1348	+26
Oxamide-d_4	1374	
Formamide[c]	1309	+29
Formamide-d_2	1338	
Acetamide[d]	1404	+23
Acetamide-d_2	1427	
Cyanoacetic acid amide[e]	1378	+20
Cyanoacetic acid amide-d_2	1398	
Benzamide[e]	1408	+12
Benzamide-d_2	1415	

a) See Ref. 8
b) See Ref. 9
c) See Ref. 6
d) See Ref. 7
e) The present observations

8) A. Yamaguchi, *J. Chem. Soc. Japan, Pure Chem. Sec.* (*Nippon Kagaku Zassi*), **78**, (1467 (1957).

9) T. A. Scott Jr. and E. L. Wagner, *J. Chem. Phys.*, **30**, 465 (1959). see also T. Miyazawa, *J. Chem. Soc. Japan, Pure Chem. Sec.* (*Nippon Kagaku Zassi*), **75**, 86 (1954).

CAA has a further intense band at 1259 cm^{-1} which is displaced by a band at 1016 cm^{-1} on *N*-deuteration. In an acetonitrile solution CAA has a corresponding band at 1264 cm^{-1}. For CH_3CONH_2[7] the NH_2 rocking vibration ($\gamma(NH_2)$), which interacts a little with the ν(C–N) vibration, has been found at 1152 cm^{-1}, while for CH_3COND_2 it has been shown that the $\gamma(ND_2)$ vibration takes part in both the 934 and 809 cm^{-1} bands. $HCONH_2$[6] has the $\gamma(NH_2)$ band at 1090 cm^{-1}, while $HCOND_2$ has the $\gamma(ND_2)$ band at 912 cm^{-1}. Therefore, the 1259 cm^{-1} band of CAA is considered to be assigned to the $\gamma(NH_2)$ vibration and the 1016 cm^{-1} band of CAA-d_2, to the $\gamma(ND_2)$ vibration.

Next the CH_2 deformation vibrations, except for the $\beta(CH_2)$ vibration already considered, must be assigned. For cyanoacetylhydrazine[2] the 1347, 1205 and 1009 cm^{-1} bands have been assigned, respectively, to the CH_2 wagging, twisting and rocking vibrations, $\omega(CH_2)$, $\tau(CH_2)$ and $\gamma(CH_2)$. CAA has three weak bands at 1320, 1197 and 972 cm^{-1} which are probably to be assigned, respectively, to the $\omega(CH_2)$, $\tau(CH_2)$ and $\gamma(CH_2)$ vibrations. For CAA-d_2 the $\omega(CH_2)$ and $\tau(CH_2)$ bands can not be observed. However, the $\gamma(CH_2)$ vibration of CAA-d_2 is considered to interact with the $\gamma(ND_2)$ vibration, and two bands appear at 953 and 1016 cm^{-1} assigned above to $\gamma(ND_2)$.

In the region below 930 cm^{-1} CAA has three moderately strong bands at 925, 851 and 787 cm^{-1}, and CAA-d_2 also has three bands, at 913, 848 and 731 cm^{-1}. Of these, two bands may be assigned to the C–C stretching vibrations which are expected to occur in CAA. The ν(C–C) band has been obtained at 874 cm^{-1} for CH_3CONH_2 and at 809 cm^{-1} for CH_3COND_2[7]. In cyanoacetylhydrazine[2] the 924 and 913 cm^{-1} bands were assigned to the ν(C–C) vibrations. The 925 and 851 cm^{-1} bands of CAA can, therefore, be assigned to the ν(C–C) vibrations. These assignments are supported by the fact that those band are little changed in frequency on *N*-deuteration.

The NH_2 wagging and twisting vibrations and skeletal deformation vibrations are not yet accounted for. In CH_3CONH_2[7] a broad band near 700 cm^{-1} was taken as the NH_2 wagging band overlapped with the NH_2 twisting band. $HCONH_2$[6] has the $\omega(NH_2)$ band at 750 cm^{-1}. The 787 cm^{-1} band of CAA is probably to be ascribed to the NH_2 wagging or twisting vibration because no band corresponding to it is observed for CAA-d_2. The 731 cm^{-1} band of CAA-d_2 is tentatively ascribed to the O=C–N deformation vibration, δ(O=C–N). However, this assignment is not certain because the δ(O=C–N) band has been found at 581 cm^{-1} for CH_3CONH_2[7] and 608 cm^{-1} for $HCONH_2$[6].

TABLE IV. INFRARED FREQUENCIES OF CAA AND THEIR ASSIGNMENTS

Assignment[a]	CAA		CAA-d_2
	Solid	in CH_3CN	
$\nu_a(NH_2)$	3330 (s)	3430	
	3260 (sh)	3320	
$\nu_s(NH_2)$	3140 (s)	3180	
$\nu(CH_2)$	2930 (w)	2920	
	2760 (vw)		
$\nu_a(ND_2)$			2505 (m)
$\nu_s(ND_2)$			2350 (m)
$\nu(C\equiv N)$	2250 (w)		2260 (sh)
Amide I	1675 (vs)	1703	1655 (vs)
$\beta(NH_2)$	1615 (s)	1618	
$\beta(CH_2)$	1408 (s)		1398 (s)
ν(C–N)	1378 (s)		
$\omega(CH_2)$	1320 (w)		—
	1284 (vw)		
$\gamma(NH_2)$	1259 (s)	1264	
$\tau(CH_2)$	1197 (w)		—
	1165 (vw)		
	1076 (vw)		
$\beta(ND_2)$			1100 (m)
$\gamma(ND_2)$			1016 (m)
$\gamma(CH_2)$	972 (w)	964	953 (m)
ν(C–C)	925 (m)	920	913 (w)
ν(C–C)	851 (m)	842	848 (w)
$\omega(NH_2)$ or $\tau(NH_2)$	787 (m)	759	
δ(O=C–N)			731 (w)

a) ν; stretching, a; asymmetric, s; symmetric, β; bending, ω; wagging, γ; rocking, δ; in-plane deformation

The observed frequencies of CAA and their assignments are summarized in Table IV.

Benzamide (BA).—Weckherlin and Leuttke[10] observed the infrared spectrum of benzamide containing ^{15}N and aimed at defining the positions of those bands due to vibrations of the $-CONH_2$ group. In the present study the infrared spectrum of BA-d_2 was observed in the rock salt region*2. As has been mentioned already, the $-CONH_2$ vibrations may now be located rather easily.

The infrared spectrum of BA-d_2 is illustrated, along with that of BA, in Fig. 3. An assignment of the vibrations of an aromatic ring has been described already with those of BH (see Table I). In a previous paper[1] the 1656 and 1623 cm^{-1} bands of BA were taken as the amide I and the NH_2 bending bands respectively. These assignments are also supported

10) S. Weckherlin and W. Leuttke, *Z. Elektrochem.*, **64**, 1228 (1960).

*2 The spectrum of BA has been published by the present author (see Ref. 1).

by the present observation for BA-d_2. BA-d_2 shows a very strong band at 1629 cm^{-1} which is surely to be ascribed to the amide I band. On the other hand, the 1623 cm^{-1} band of BH disappears on *N*-deuteration; instead of it, BA-d_2 has a new band at 1209 cm^{-1}, the ν_H/ν_D ratio being 1.342. They correspond in frequency, respectively, to the 1631 cm^{-1} band for CH_3CONH_2[7] and 1189 cm^{-1} band for CH_3COND_2[7]. The 1403 cm^{-1} band of BA shifts to 1415 cm^{-1} on *N*-deuteration. From a consideration similar to the foregoing (see Table III also), they are undoubtedly to be assigned to the ν(C–N) vibration.

BA has two moderately strong bands at 1142 and 1124 cm^{-1}, both of which vanish on *N*-deuteration. Of these, the former band has already been ascribed to the δ(C–H) vibration of an aromatic ring. The latter band may be assigned to the $\gamma(NH_2)$ vibration, because it is close in frequency to the $\gamma(NH_2)$ band at 1152 cm^{-1} for CH_3CONH_2[7]. In BA-d_2 the moderately strong band at 936 cm^{-1} is considered to correspond to the 1124 cm^{-1} band of BA, the ν_H/ν_D ratio being 1.201. The 936 cm^{-1} band of BA-d_2 is very close in frequency to the 934 cm^{-1} band of CH_3COND_2[7], which has been assigned to the $\gamma(ND_2)$ vibration interacting with the ν(C–N) vibration and others. Thus, the 936 cm^{-1} band can probably be assigned to the $\gamma(ND_2)$ vibration. The relatively strong band at 1142 cm^{-1} may be considered to arise from the δ(C–H) vibration resonating with the $\gamma(NH_2)$ vibration. Owing to the fact that the $\gamma(NH_2)$ frequency decreases in value on *N*-deuteration, the δ(C–H) band is considered to be so weakened that we can not define its position.

For BA two moderately strong bands, which vanish on *N*-deuteration, are found at 793 (more intense) and 770 cm^{-1}. One of the two bands may be assigned to the $\omega(NH_2)$ or $\tau(NH_2)$ vibration because the corresponding band has been obtained at 750 cm^{-1} for $HCONH_2$[6] and at 700 cm^{-1} for CH_3CONH_2[7]. Another band is considered to arise from one of the vibrations of an aromatic ring. In the region below 820 cm^{-1}, BA has two further bands at 811 and 705 cm^{-1}. These two bands are very close in frequency to the 801 and 690 cm^{-1} bands of BH; accordingly, they can probably be ascribed to the vibrations of an aromatic ring. In addition to these BH has a band, which is due to an aromatic ring vibration, at 747 cm^{-1}. This band is rather closer in frequency to the 770 cm^{-1} band than to the 793 cm^{-1} band of BA. Therefore, the 793 cm^{-1} band is tentatively taken as the $\omega(NH_2)$ or $\tau(NH_2)$ band. BA-d_2 has three bands, at 801, 713 and 691 cm^{-1}, and BA in an acetonitrile solution*3 has corresponding bands at 805, 720 and 695 cm^{-1}. These three bands can probably be ascribed to the aromatic ring vibrations. BA in acetonitrile has a further band at 755 cm^{-1} which is probably to be assigned to the $\omega(NH_2)$ or $\tau(NH_2)$ vibration. The change in frequency on the change of states (793 to 755 cm^{-1}) is in the right direction for NH_2 deformation vibrations.

In the 3000 cm^{-1} region BA has two intense bands, at 3330 and 3140 cm^{-1}, which are displaced by the bands at 2525 and 2280 cm^{-1} on *N*-deuteration. Therefore, they can surely be assigned to the $\nu_a(NH_2)$ and $\nu_s(NH_2)$ vibrations respectively. A shoulder band at 3050 cm^{-1} and a weak band at 2760 cm^{-1} are scarcely changed in frequency on *N*-deuteration. These two bands are assigned to the aromatic ν(C–H)

Table V. Infrared frequencies of BA and BA-d_2 in the rock salt region

Assignment[a]	BA	BA-d_2
$\nu_a(NH_2)$	3330 (vs)	
$\nu_s(NH_2)$	3140 (vs)	
ν(CH)	3050 (sh)	3050 (w)
	2760 (sh)	2760 (vw)
$\nu_a(ND_2)$		2525 (s)
$\nu_s(ND_2)$		2280 (bw)
Amide I	1656 (vs)	1629 (vs)
$\beta(NH_2)$	1623 (s)	
ν(C-C)	1578 (s)	1574 (s)
		1563 (sh)
ν(C-C)	1497 (vw)	1497 (w)
ν(C-C)	1451 (m)	1452 (m)
	1334 (vw)	1342 (vw)
δ(C-H)	1296 (m)	1296 (w)
	1245 (w)	1237 (vw)
$\beta(ND_2)$		1209 (w)
δ(C-H)	1180 (w)	1178 (w)
δ(C-H)	1142 (m)	—
$\gamma(NH_2)$	1124 (m)	
δ(C-H)	1073 (w)	1074 (w)
δ(C-H)	1024 (m)	1024 (w)
	999 (w)	1000 (vw)
π(C-H)	987 (vw)	987 (vw)
π(C-H)	917 (vw)	924 (vw)
$\gamma(ND_2)$		936 (m)
π(C-H)	848 (w)	847 (vw)
	811 (w)	801 (w)
$\omega(NH_2)$ or $\tau(NH_2)$	793 (m)	
	770 (m)	
		738 (w)
	705 (m)	713 (s)
		691 (m)

a) ν; stretching, a; asymmetric, s; symmetric, β; bending, δ; in-plane deformation, γ; rocking, π; out-of-plane deformation, ω; wagging, τ; twisting

*3 The spectrum of BA in acetonitrile has been published in a previous paper (see Ref. 1).

TABLE VI. FREQUENCIES CHARACTERISTIC TO THE $-CONH_2$ GROUP (in the 1700～700 cm^{-1} region)

Compound	ν(C=O)	$\beta(NH_2)$	ν(C-N)	$\gamma(NH_2)$	$\omega(NH_2)$ or $\tau(NH_2)$
$HCONH_2$[a]	1690	1608	1309	1090	750
CH_3CONH_2[b]	1675	1631	1404	1152	700
$CNCH_2CONH_2$[c]	1675	1615	1378	1259	787
$C_6H_5CONH_2$[c]	1656	1623	1403	1124	793

a) See Ref. 6 b) See Ref. 7 c) Present observations

vibrations. The observed frequencies of BA and their assignments are summarized in Table V.

The present assignments for BA are in conformity with those proposed by Weckherlin and Leuttke[10] except for a few points.

Frequencies Characteristic of the $-CONHNH_2$ and $-CONH_2$ Groups. — For compounds containing the $-CONHNH_2$ group, the present author[2,3] has observed the infrared absorption spectra in the rock salt region and the frequencies characteristic of the group have been proposed. In the 1700～800 cm^{-1} region, a part of the -CONH- in the $-CONHNH_2$ group shows the amide I, II and III bands and a part of the NH_2- shows four bands due to the deformation vibrations. As has already been described in the present paper, BH also has the amide I, II and III bands at 1664, 1527 and 1250 cm^{-1} and the NH_2 deformation bands at 1618, 1349, 1118 and 987 cm^{-1}. These seven frequencies can, with confidence, be taken as characteristic of the $-CONHNH_2$ group. Of these, the amide I, II and III frequencies are within the normal ranges for the corresponding frequencies in secondary amides. On the other hand, four NH_2 deformation frequencies have been found in the 1635～1600, 1365～1260, 1180～1050 and 1050～800 cm^{-1} ranges for the ten compounds hitherto examined by the present author*4.

Spectroscopic investigations of primary amides have been reported by many workers[5], but the vibrations of the $-CONH_2$ group have not yet been located definitely. In recent years, infrared measurements and the calculation of normal vibrations have been made for formamide and acetamide by Suzuki[6,7]. On the basis of the results of Suzuki's studies, the infrared spectra of CAA and BA were rather easily interpreted in the present paper. The frequencies characteristic of the $-CONH_2$ group may now be obtained with certainty. They are summarized in Table VI for frequencies in the 1700～700 cm^{-1} region. It may be seen from the table that the NH_2 deformation frequencies of the $-CONH_2$ group lie in the 1630～1600 (bending), 1150～1090 (rocking) and 800～700 (wagging or twisting) cm^{-1} ranges.

A comparison of the NH_2 deformation frequencies shows that the compounds containing the $-CONHNH_2$ group have a band in the 1365～1260 cm^{-1} range which is not shown by the compounds containing the planar $-CONH_2$ group. This band is close in frequency to the non-planar NH_2 twisting band which has been found at 1320 cm^{-1} for solid hydrazine[11] and at 1455 cm^{-1} for methylamine vapor[12]. Therefore, that band can very probably be ascribed to the NH_2 twisting vibration which is expected for the NH_2 group, being in a pyramidal form. A band observed in the 1635～1600 cm^{-1} range may be ascribed to the NH_2 bending vibration. It is noteworthy that the NH_2 bending band is shown in that region both by compounds containing the non-planar NH_2 group and by those containing the planar NH_2 group.

The author is grateful to Professor Sunao Imanishi of Kyushu University for his generous permission to use the spectrophotometer, and to Dr. Yoshiya Kanda of Kyushu University for his encouragement throughout the work. He is also indebted to the Ministry of Education for financial support.

Department of Literature and Science
Saga University
Saga

*4 For spectroscopic data, see Ref. 2 and Ref. 3.

11) D. A. Giguere and I. D. Liu, *J. Chem. Phys.*, **20**, 136 (1952).
12) A. P. Gray and R. C. Lord, ibid., **26**, 690 (1957); A. Yamaguchi, *J. Chem. Soc. Japan, Pure Chem. Sec.*, (*Nippon Kagaku Zasshi*), **80**, 1105 (1959).

The Polarographic Reduction and Electronic Structures of Organic Halides

By Kenichi FUKUI, Keiji MOROKUMA, Hiroshi KATO and Teijiro YONEZAWA

(Received October 19, 1962)

In the last fifteen years the polarographic reduction of a number of conjugated hydrocarbons has been extensively studied, both experimentally and theoretically. Their pH-independent reversible half-wave reduction potentials, $E_{1/2}$, have been found to be linearly related to the energy, $\varepsilon_{1v}{}^{\pi}$, of their lowest unoccupied π orbital[1,2], the energy which would be needed in order to bring an electron to the orbital, as follows:

$$-E_{1/2}=\lambda_{1v}{}^{\pi}\beta_{\pi}+C$$

where $\lambda_{1v}{}^{\pi}$ is the coefficient of the energy of the level $\varepsilon_{1v}{}^{\pi}=\alpha_{\pi}+\lambda_{1v}{}^{\pi}\beta_{\pi}$ and α_{π} and β_{π} are the standard Coulomb and the standard resonance integrals of the π orbitals. From the inclination of the line the value of the resonance integral, β_{π}, was estimated to be -2.23 eV., which seemed to be reasonable in comparison with the value estimated from other physicochemical sources. The higher the energy of the level, that is, the smaller the value of $\lambda_{1v}{}^{\pi}$, the less reducible the hydrocarbon and, therefore, the more negative the half-wave reduction potential. A similar linear relationship between the lowest unoccupied π levels and the reduction potentials and a similar value of the integral β_{π} have been found for a variety of compounds, such as substituted stilbenes, substituted nitrobenzenes, aromatic ketones and vinyl compounds[3].

Furthermore, the structures of the products of the corresponding controlled potential electrolysis of hydrocarbons have been examined in terms of the π electron distribution of the hydrocarbon anions[2], in which an excess electron is accepted in the lowest unoccupied π levels and from which products will be yielded by protonation. Protons add to those positions which have a large electron density, and a product results in which a double bound or more is reduced. For instance, naphthalene is reduced to give 1, 2-dihydronaphthalene and 1, 4-dihydronaphthalene.

On the other hand, it has been elucidated that halogenated, saturated hydrocarbons are polarographically reducible, showing half-wave potential independent of the pH value and giving products in which carbon-halogen bonds are reduced to carbon-hydrogen bonds[4]. For instance, the half-wave reduction potential of methyl iodide is -1.63 V. vs. S. C. E. (saturated calomel electrode), and it is converted into methane when reduction is performed at that voltage. Further, it is interesting to notice that some of the halogenated, unsaturated hydrocarbons are reduced at a potential less negative than the potential at which the mother hydrocarbons are reducible, and carbon-halogen bonds are reduced in these compounds as well as in saturated halides[4].

With respect to the problems of the polarographic reduction of saturated compounds which have no π conjugated system, theoretical studies have never been carried out in relation to their electronic structure.

The present authors have established a simple molecular orbital method for calculating the σ electronic structure of saturated hydrocarbons and their derivatives[5,6] and have applied this method further to discussing the electronic structure of the σ skeleton in conjugated compounds[7,8]. By the aid of this method, one can calculate the energy levels and charge distribution of σ electrons.

In the present paper, the relations between the half-wave reduction potentials of saturated halides and their lowest unoccupied σ levels, and the connection between the distribution of the lowest unoccupied level and the structures of the reduction products will be discussed first. Then, similar discussions will be made for unsaturated halides and, at the end, a possibility that in polyhalogenated compound the lowest unoccupied σ level may creep below the lowest unoccupied π level will be suggested.

1) A. Maccoll, *Nature*, **163**, 178 (1949).
2) G. J. Hoijtink and J. v. Schooten, *Rec. trav. chim.*, **71**, 1089 (1952).
3) S. Koide and I. Tachi, *J. Electrochem. Soc. Japan*, **23**, 522 (1955); T. Fueno, K. Asada, K. Morokuma and J. Furukawa, *J. Polymer Sci.*, **40**, 511 (1959); T. Fueno, K. Morokuma and J. Furukawa, *Bull. Inst. Chem. Research, Kyoto Univ.*, **36**, 87, 96 (1958).
4) M. v. Stackeberg and W. Stracke, *Z. Elektrochem.*, **53**, 118 (1949).
5) K. Fukui, H. Kato and T. Yonezawa, This Bulletin, **34**, 1111 (1961).
6) K. Fukui, H. Kato, H. Saito and T. Yonezawa, ibid., **35**, 1814 (1962).
7) K. Fukui, T. Yonezawa, H. Kato, K. Morokuma, A, Imamura and C. Nagata, ibid., **35**, 38 (1962).
8) K. Morokuma, K. Fukui, T. Yonezawa and H. Kato, ibid., **36**, 47 (1963).

Method of Calculation

The electronic structures of π and σ electron systems have been calculated by using a simple LCAO MO (linear-combination-of-atomic-orbital molecular orbital) method, disregarding overlap integrals and electronic interactions.

In saturated compounds in which carbon atoms are sp^3-hybridized, molecular orbitals are written as linear combinations of all σ atomic orbitals—hydrogen 1s orbitals, sp^3-hybridized orbitals of carbons, and σ atomic orbitals of halogens. The energy, ε_i, of the ith molecular orbital is expressed as:

$$\varepsilon_i = \alpha_{sp^3} + \lambda_i^{sp^3} \beta_{sp^3-sp^3} \qquad (2)$$

where α_{sp^3} and $\beta_{sp^3-sp^3}$ indicate the Coulomb intergral of a sp^3-hydbridized orbital of carbon and the resonance integral between sp^3 orbitals, making a standard σ bond. The larger value of $\lambda_i^{sp^3}$ corresponds to the lower energy since the resonance integrals is minus in sign. The Coulomb and the resonance integrals of each atom and bond adopted in the calculation are the same as were employed previously[5,6], they will not be repeated for the sake of brevity.

The method can be extended to the calculation of the σ electronic structures of conjugated compounds if, in this case, one regards the π electrons as making a field where σ electrons move. Then the energy of the ith σ molecular orbital, ε_i^{σ}, may be written as:

$$\varepsilon_i^{\sigma} = \alpha_{sp^2} + \lambda_i^{sp^2} \beta_{sp^2-sp^2} \qquad (3)$$

where α_{sp^2} and $\beta_{sp^2-sp^2}$ are the standard Coulomb and the standard resonance integrals of the sp^2 σ orbitals. Similarly, the energy of the jth π molecular orbital calculated by the simple LCAO MO method is given as:

$$\varepsilon_j^{\pi} = \alpha_{\pi} + \lambda_j^{\pi} \beta^{\pi} \qquad (4)$$

Calculated σ electron densities could clearly explain the experimental results of physicochemical properties — for instance, dipole moments, halogen coupling constants in PQR spectra, and proton chemical shifts in NMR spectra — as has been reported previously[7,8].

A no table finding of the calculation in halogenated compounds is that the substitution of hydrogens by halogens, while it does not change the energy of σ occupied levels very seriously, does give rise to a remarkable change in the energy of σ unoccupied levels. There occurs especially a considerable lowering of the lowest unoccupied σ level; this lowering becomes larger as the number of halogen atoms increases.

The Polarographic Reduction and σ Electronic Structures of Haloalkanes

Haloalkanes belong to one of the few groups of compounds which include no conjugated system but which can nevertheless be reduced polarographically. As was pointed out in the previous section, halogen substitution causes a lowering of the lowest unoccupied σ levels.

Imitating Eq. 1, we compared the first half-wave reduction potential of halomethanes with the energy of their lowest unoccupied σ level, obtaining the following relation:

$$-E_{1/2} = \lambda_{1v}^{sp^3} \beta_{sp^3-sp^3} + C' \qquad (5)$$

TABLE I. FIRST HALF-WAVE REDUCTION POTENTIAL AND ENERGY AND ELECTRON DISTRIBUTION OF THE LOWEST UNOCCUPIED LEVEL OF HALOMETHANES

Compound	Half-wave reduction potential[4],*, $E^{1/2}$ V. vs. SCE	Energy of the lowest unoccupied level, $\lambda_{1v}^{sp^3}$	Partial bond order of the lowest unoccupied level on C–X bond	Sum of the distribution of the lowest unoccupied level on C–X bonds
CH_4	NW	−0.848	—	0
CH_3Cl	−2.23	−0.400	−0.369	0.78
CH_2Cl_2	−2.33	−0.229	−0.204	0.82
$CHCl_3$	−1.67	−0.081	−0.147	0.89
CCl_4	−0.78	+0.059	−0.116	1.00
CH_3Br	−1.63	−0.366	−0.375	0.79
CH_2Br_2	−1.48	−0.190	−0.208	0.83
$CHBr_3$	−0.64	−0.045	−0.144	0.87
CBr_4	−0.3	+0.089	−0.112	1.00
CH_3I	−1.63	−0.337	−0.381	0.80
CH_2I_2	−1.12	−0.167	−0.208	0.83
CHI_3	−0.49	−0.027	−0.146	0.90
CI_4	—	+0.095	−0.108	1.00

* NW indicates that the compound gives no reduction wave.

As can be seen in Table I, a parallelism between them was obtained for each series of halomethanes. A similar relation is obtained also in haloethanes. The discrepancy which is observed in comparing bromo- and iodomethanes is probably due to an inappropriate choice of energy parameters for halogen atomic orbitals which have never strictly tested nor improved; it is also perhaps due to the effect of disregarding the overlap integrals.

Although the linear relation represented by Eq. 5 was not precisely adopted to the values in Table I, we roughly estimated the magnitude of $\beta_{sp^3-sp^3}$ by means of Eq. 3 and so obtained a value of ca. -5 eV. This value is very close to that of $\beta_{sp^3-sp^3}$ obtained in the discussion of the NMR chemical shifts of halides (-5.7 eV.)[11] and also in that of the ionization potentials of halides (ca. -5 eV.)[11]. Furthermore, this would be rather rational in comparison with the above cited value of β_π, -2.23 eV.

From these correspondences between $E_{1/2}$ and $\lambda_{1v}^{sp^3}$, it can safely be said that the potential-determining step in the polarographic reduction of haloalkanes is the electron transfer from the electrode to their lowest unoccupied σ level. The fact that methane and other saturated hydrocarbons do not give a reduction wave is clearly because of the high energy of their lowest unoccupied σ levels.

The electron distribution of the lowest unoccupied level is greatly localized on the carbon-halogen bonds, and the bond order of the level on the bond is negative and large in absolute value, as may be seen in the fourth and fifth columns in Table I and Fig. 1. These calculated results suggest that, in a state which has an electron in that level, the carbon-halogen bonds are very easy to break down. The anion, which might be produced at the first step of the polarographic reduction of halides, corresponds to this case. One may consider a second process in which a carbon-halogen bond of the anion breaks and in which the resultant anion, or radical, reacts with a proton, or with a proton and an electron, in the solution (a 75% dioxane and 25% water solution was used as the solvent), as was suggested by Stackelberg and Stracke:

$$\left.\begin{aligned} &R-X+e^- \rightarrow (R-X)^- \\ &(R-X)^- \rightarrow R\cdot + X^- \\ &R\cdot + e^- + H^+ \rightarrow RH \end{aligned}\right\} \quad (6)$$

or

$$\left.\begin{aligned} &R-X+e^- \rightarrow (R-X)^- \\ &(R-X)^- \rightarrow R^- + X\cdot \\ &R^- + H^+ \rightarrow RH \\ &X\cdot + e^- \rightarrow X^- \end{aligned}\right\} \quad (7)$$

Thus, one may clearly explain theoretically such a result of controlled potential reduction as that, for instance, methyl bromide was reduced to give methane, while ethyl bromide gave ethane. This connection seems to support the conclusion derived above that the first reduction potential of saturated halides corresponds to the electron transfer to the lowest unoccupied σ level. It has not yet been decided in which one of the two mechanisms, Eq. 6 or 7 the real breakdown of carbon-halogen bonds occurs. On the basis of the electron affinities of halogen and carbon atoms, however, the first mechanism, Eq. 6, seems to be more probable than the second one. If so, one who carried out the controlled potential electrolysis of halides in an aprotic solvent could observe the ESR spectra of the radical.

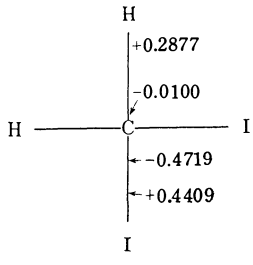

Fig. 1. Coefficient of atomic orbitals in the lowest unoccupied σ MO of diiodomethane.

The Polarographic Reduction and σ and π Electronic Structures of Conjugated Halides

In this section relations between the half-wave reduction potential and the energy of the lowest σ and the lowest π unoccupied levels will be investigated. The experimental $E_{1/2}$ and the calculated height of the lowest unoccupied levels, $\lambda_{1v}^{sp^2}$ and λ_{1v}^{π}, of chlorobenzenes and chloroethylenes, as examples, are tabulated in Table II.

The height of the lowest unoccupied π level hardly varies in these series and seems to have no connection with their half-wave reduction potential, $E_{1/2}$. Even if one forcibly applies Eq. 1 to their relation, one is led to the irrational finding that the absolute value of β must exceed 20 eV. On the other hand, the height of the lowest unoccupied σ levels of these compounds is shown to be parallel to the half-wave potential, as in haloalkanes:

$$-E_{1/2}=\lambda_{1v}^{sp^2}\beta_{sp^2-sp^2}+C'' \quad (8)$$

From the parallelism the magnitude of $\beta_{sp^2-sp^2}$ is estimated to be -6.88 eV. (in the case of chlorobenzene), a value which seems to be appropriate in view of these of β_π and $\beta_{sp^3-sp^3}$.

TABLE II. FIRST HALF-WAVE REDUCTION POTENTIAL AND ENERGY AND ELECTRON DISTRIBUTION OF THE LOWEST UNOCCUPIED σ AND THE π LEVELS OF HALOGENOBENZENES AND HALOGENOETHYLENES

Substituents	Half-wave reduction potential[4]* $E_{1/2}$, V.	Energy of the lowest unoccupied σ level, $\lambda_{1v}^{sp^2}$	Energy of the lowest unoccupied π level, λ_{1v}^{π}	Partial bond order of the lowest unoccupied σ level on C-X	Sum of the distribution of the lowest unoccupied σ level on C-X bonds
1. Chlorobenzenes					
no	NW	−0.501	−1.000	—	0
Cl	NW	−0.345	−0.983	−0.280	0.56
p-diCl	−2.49	−0.313	−0.967	−0.134	0.53
m-diCl	−2.48	−0.305	−0.991	−0.138	0.55
o-diCl	−2.51	−0.274	−0.973	−0.152	0.61
pentaCl	—	−0.187	−0.967	−0.048 −0.070 −0.079	0.64
hexaCl	−1.44	−0.158	−0.951	−0.054	0.67
2. Chloroethylenes					
no	NW	−0.664	−1.000	—	0
Cl	NW	−0.390	−0.975	−0.345	0.70
1,2-diCl	NW	−0.319	−0.951	−0.175	0.70
1,1-diCl	ca. −2.4	−0.229	−0.952	−0.207	0.84
triCl	−2.14	−0.196	−0.928	−0.173 −0.062	0.83
tetraCl	−1.88	−0.129	−0.906	−0.105	0.89

* NW indicates that the compound gives no reduction wave.

Furthermore, as to the reduction products, for instance, naphthalene from α-bromonaphthalene and ethylene from 1,2-diiodoethylene, an explanation similar to that in the case of haloalkanes would be possible based on the localizing and anti-bonding nature of the carbon-halogen bonds of the lowest unoccupied σ level, as is shown in Table II and Fig. 2.

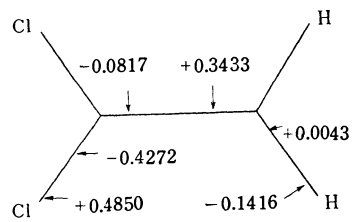

Fig. 2. Coefficient of atomic orbitals in the lowest unoccupied σ MO of 1,1-dichloroethylene.

Thus, the polarographic reduction of conjugated halides would represent the electron transfer process from the cathode to the lowest unoccupied σ, not π, level, in contrast with the case of other conjugated compounds, in which an electron runs into the lowest unoccupied π level, satisfying Eq. 1.

As the entropy change will not be very different between the both processes, that in which the electron transfers to the σ unoccupied level and that in which it transfers to the π unoccupied level, it may be said that the lowest unoccupied σ level would be lower than the lowest unoccupied π level. This conclusion is more certain as the number of halogen atoms in the molecule increases or as the halogen changes in the order $F \rightarrow Cl \rightarrow Br \rightarrow I$.

One may raise the objection that the lowest unoccupied σ level into which an electron jumps may not be the lowest level of all, for, if the selective adsorption of carbon-halogen bonds occurs, an electron will have to run into the level which is localized in the bonds. However, the experimental finding that α-bromonaphthalene is reduced at a voltage (−1.96 V.) less negative than that at which naphthalene can first be reduced (−2.50 V.) renders the objection invalid.

In Fig. 3 is shown the energy diagram of lowest unoccupied levels, which is mainly deduced from the linear relationship (cf. Eqs. 1 and 8) between λ_{1v} and $E_{1/2}$. The value of the energies of the levels might include errors of the order 0.1 to 0.2 eV. The origin of the energy is arbitrary. One can see the inversion of the π and σ lowest unoccupied levels.

It is well-known that the nucleophilic substitution of unsaturated halides takes place exclusively at the halogen atom as follows:

$$Ar-X + Y^- \rightarrow Ar-Y + X^- \qquad (9)$$

where Y^- is a nucleophilic reagent. It seems very interesting to connect this fact with the

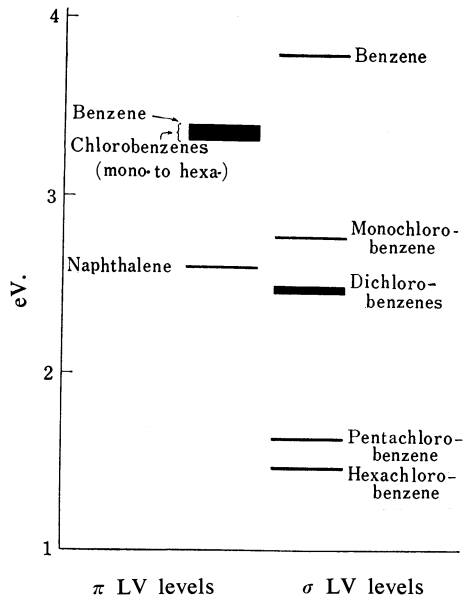

Fig. 3. Estimated lowest vacant π and σ levels.

inversion of energy levels. That is to say, when the reagent comes near the substrate, for instance, electrons on the substrate easily delocalize to the lowest unoccupied level, that is, the lowest unoccupied σ level, which causes a weakening of the carbon-halogen bonds, and so substitution occurs. Therefore, the mechanism of the nucleophilic substitution of unsaturated halides might differ from that of the ordinary substitution reactions of conjugated compounds in which π levels play a dominant role.

Furthermore, the inversion of the lowest unoccupied levels in unsaturated halides would result in a weak and broad transition from the highest occupied π level (the highest occupied of all) to the lowest unoccupied σ level (the lowest unoccupied of all), which would be seen in the range of larger wavelengths; this may be named the $\pi \rightarrow \sigma^*$ transition. An $n \rightarrow \sigma^*$ transition wave observed in saturated halides by Mulliken[9], but the $\pi \rightarrow \sigma^*$ transition in conjugated halides has not yet been observed nor even suggested. A more precise calculation by the LCAO ASMO CI method, which confirms our present conclusion, will be published elsewhere[10].

The Polarographic Reduction of Other Saturated Compounds

It is worth noticing that haloalkanes and alkylperoxides are the only saturated compounds that can be polarographically reduced. Alkylperoxide gives an almost pH value-independent wave at a much less negative potential; for instance, methyl hydroperoxide is reduced at -0.25 V. both in 0.01 N hydrochloric acid and 0.01 N sodium hydroxide. The lowest calculated unoccupied σ level in alkylperoxides, as well as in haloalkanes, is very low. For instance[11],

$$CH_3OOH \quad \lambda_{1v}^{sp^3} = -0.0956^*$$
$$C_2H_5OOH \quad \lambda_{1v}^{sp^3} = -0.0940$$
$$(CH_3)_3COOH \quad \lambda_{1v}^{sp^3} = -0.0898$$

The lowering of the lowest unoccupied σ level in peroxides would have an intimate connection with their polarographic reduction, as one might except from the discussion on saturated halides.

The distribution of the lowest unoccupied level is also very localizing on the oxygen-oxygen bond, and the partial bond order on the bond is negative and large in absolute value (Fig. 4). Thus, after the electron transfer to the level, the breakdown of the bond will follow.

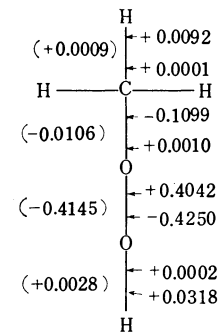

Fig. 4. Coefficient of atomic orbitals and partial bond order (in parentheses) of the lowest unoccupied MO.

Generally speaking, the lowering of the lowest unoccupied level is to be expected if a compound has one or more bonds whose resonance integrals are relatively small and, at the same time, one or both of the atoms constructing it are relatively electronegative. Peroxides and halides are typical examples.

Inversion of the lowest unoccupied σ and the lowest unoccupied π level may occur in the case where the lowering of the lowest unoccupied σ level is large, as has been stated above, and where the lowest unoccupied π level remains rather high. An electronegative atom in the compound necessarily causes a

* The parameters used in the calculation will be published elsewhere[11].

9) R. S. Mulliken., *J. Chem. Phys.*, **8**, 234, 382 (1940).
10) Presented partly at the International Symposium on Molecular Structure and Spectroscopy, Tokyo, September, 1961.
11) K. Fukui and H. Kato, to be published.

lowering of all levels, but when the atom has a lone pair to conjugate with neighboring atoms, the lowest unoccupied π level stays relatively high. The conjugated halides discussed in this paper and some conjugated peroxides seem to be the only examples where inversion may be expected.

Summary

The polarographic reduction potential of haloalkanes is connected with the energy of their lowest unoccupied σ level. Moreover, the reduction products are well explained in terms of the anti-bonding nature of the carbon halogen bond of the level. The polarographic reduction potential of conjugated halides is also correlated to their lowest unoccupied σ, not π, level. It has also been suggested that, in conjugated halides, the lowest unoccupied σ level might be lower than the lowest unoccupied π level and that the $\pi \rightarrow \sigma^*$ transition might be observed.

Most of the calculations have been carried out on the KDC-I digital computer of Kyoto University.

Faculty of Engineering
Kyoto University
Sakyo-ku, Kyoto

The Polymer-like Property of a Non-ionic Detergent Having a Long Polyoxyethylene Chain

By Fumikatsu TOKIWA

(Received August 13, 1962)

Generally, detergent molecule is composed of one large hydrophobic portion and one hydrophilic portion to render the molecule amphipathic. In the case of non-ionic detergents of the polyoxyethylene series, it is possible to start with a substance such as long chain alkyl alcohol and progressively to introduce a controlled number of ether groups by means of ethylene oxide, thereby conferring on it any desired hydrophilic property. The various properties of non-ionic detergent depend, of course, on the number of ethylene oxide groups. In addition, it is possible to consider that the " polymer-like property ", not directly related to the hydrophilic property, will appear in the detergent molecule when the polyoxyethylene chain becomes sufficiently long.

Isemura et al.[1] have shown from the surface tension data of a detergent-like compound, poly-DL-alanine dodecylamide, that at low concentrations the slope of the surface tension vs. concentration curve is the steepest for a certain degree of polymerization and is more gentle when the degree of polymerization is larger than this value; they ascribed this effect to the polymer-like property of poly-DL-alanine dodecylamide. Furthermore, Maruta[2] has observed that the surface tension and foaming power of a non-ionic detergent show, respectively, a minimum and a maximum value at a definite chain-length of polyoxyethylene; he has inferred that these phenomena are also due to the polymer-like behavior of the detergent.

In this paper an attempt is made to interpret tentatively the behavior of a non-ionic detergent with a long polyoxyethylene chain by taking into account the polymer-like property of the detergent. The lengthening of the polyoxyethylene chain of a non-ionic detergent not only increases the hydrophilic property of the molecule but also gives the molecule a polymer-like property. The present paper deals with the nature of the non-ionic detergent with relation to the chain-length of polyoxyethylene. It deals especially with the solubilization and viscosity in connection with the ultracentrifugal data[3] reported previously.

Experimental

Materials.—The detergents studied are polyoxyethylene dodecyl ethers (abbreviated to PODE),

1) T. Isemura, S. Ikeda, F. Tokiwa and J. Noguchi, This Bulletin, **34**, 1236 (1961).

2) I. Maruta, *J. Chem. Soc. Japan, Pure Chem. Sec. (Nippon Kagaku Zasshi)*, **83**, 861, (1962).

$C_{12}H_{25}O(CH_2CH_2O)_nH$, which have been prepared from dodecyl alcohol of a high purity. The samples of PODE used are the same samples as those used in a previous investigation[3]. The degree of the polymerization of ethylene oxide, p, of these samples are listed in Table I, where the number written after PODE represents the value of p, i.e., the average number of oxyethylene groups per molecule. Polyethyleneglycol[3] (abbreviated to PEG) (Carbowax-4000), the molecular weight of which was approximately 4000, was obtained from the Carbide and Carbon Chemicals Co.

Yellow-OB, an oil-soluble dye which was used as a solubilizate, was purchased from the Wako Pure Chemicals Co. and was purified by repeated recrystallization from an ethanol-water mixture.

Measurements of Solubilization. — In order to attain equilibrium, the solubilizations were run in a water bath at a constant temperature of 30±0.1°C for 20 hr. The desired amounts of yellow-OB were taken in test tubes, and then appropriate volumes of detergent solutions of various concentrations were pipetted in. The tubes were sealed and fastened to a revolving drum in the water bath. After equilibrium had been attained, the unsolubilized yellow-OB was filtered off.

This filtration was followed by dilution of an aliquot of the filtrate with ethanol to a final mixture of 7 : 3, by a volume ratio of ethanol to water, ethanol being introduced to prevent precipitation of insoluble matter. Colorimetric measurements were made with a Shimadzu Model B60 spectrophotometer to determine the amount of dye solubilized in terms of optical density at a wavelength of 445 mμ.

Measurements of Viscosity. — The viscosities of detergent solutions were measured with an Ostwald-type viscometer at 25±0.01°C. The efflux time for pure water was 141.2 sec.

Results

Solubilization.—The solubilization of yellow-OB vs. the concentration of PODE curves are illustrated in Figs. 1 and 2, where S is the extent of the solubilization of yellow-OB. The value of S decreases with the increasing length of the polyoxyethylene chain at each concentration of PODE, if an abscissa is expressed in grams per 100 ml. of solution, as is shown in Fig. 1. However, if the abscissa is expressed in moles per liter of solution, as is illustrated in Fig. 2, the value of S is seen to increase with an increasing p value until the maximum value corresponding to PODE of $p \fallingdotseq 27$ is reached while it is seen to decrease beyond this maximum. PEG shows no sign of solubilizing power.

Viscosity. — Figure 3 shows the η_{sp}/c vs. c curves for each PODE in aqueous solutions, where η_{sp}, c and η_{sp}/c represent a specific viscosity, a concentration and a reduced viscosity, respectively. The curves run linearly with c, except for the PODE of the smallest p value, as is shown in Fig. 3. In the case of the PODE where $p=6.2$, its viscosity can not be measured with the viscometer used in the region of higher concentrations because of an extraordinarily high viscosity. This may be attributed to the low cloud-point of this sample. PEG also showed a linear relation.

Intrinsic viscosity, $[\eta]$, was obtained by extrapolating the linear plots of η_{sp}/c to $c=0$. The values of $[\eta]$ for PODE having various polyoxyethylene chains are summarized in Table I. The intrinsic viscosity increases with the increasing chain-length except in PODE in which $p=7.6$. An anomaly found in the value of $[\eta]$ in PODE where $p=7.6$, whose slope of the $\eta_{sp}/c-c$ curve is fairly steep, may also be

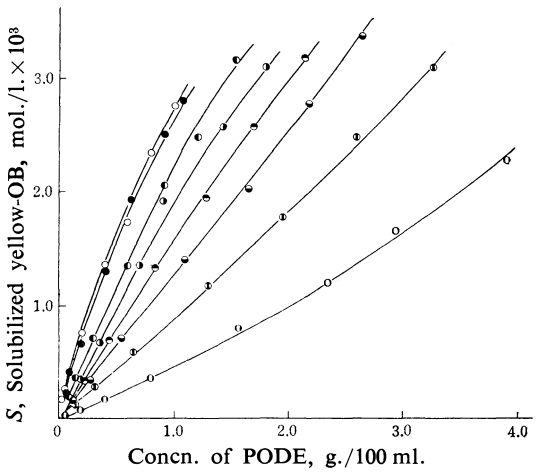

Fig. 1. Solubilization of yellow-OB vs. concentration of PODE curves at 30°C (I).
○ $p=6.2$ ● $p=7.6$ ◐ $p=10.6$
◑ $p=15.8$ ◓ $p=20.4$ ◒ $p=27.1$
◐ $p=38.6$ ◐ $p=67.3$

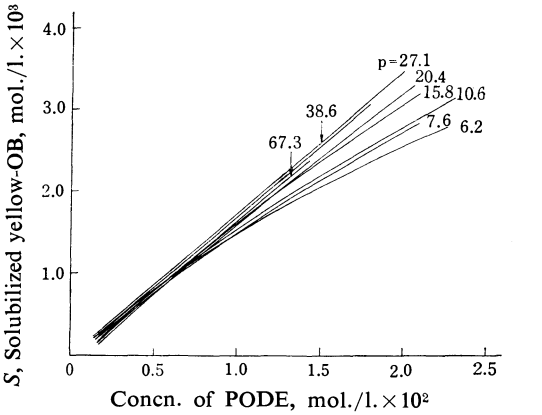

Fig. 2. Solubilization of yellow-OB vs. concentration of PODE curves at 30°C (II).

3) F. Tokiwa and T. Isemura, This Bulletin, 35, 1737 (1962).

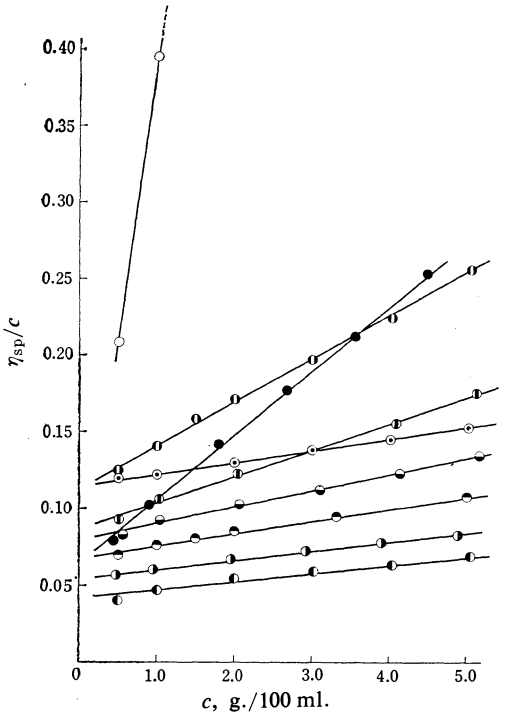

Fig. 3. Reduced viscosity vs. concentration curves of PODE and PEG at 25°C.
○ p= 6.2 ● p= 7.6 ◐ p=10.6
◑ p=15.8 ◓ p=20.4 ◒ p=27.1
◐ p=38.6 ◑ p=67.3 ⊙ PEG

TABLE I. CHARACTERISTICS OF PODE (AND PEG) AS A FUNCTION OF POLYOXYETHYLENE CHAIN-LENGTH

Sample	Cloud-point, °C	n	$[\eta]$	k'	ϕ/c
PODE- 6.2	34.5	0.76	—	—	—
PODE- 7.6	44.6	0.85	(0.065)	(9.88)	—
PODE-10.6	76.5	0.92	0.042	2.95	1.78
PODE-15.8	>100	0.95	0.054	2.05	2.12
PODE-20.4	—	0.98	0.068	1.72	2.61
PODE-27.1	—	1.04	0.080	1.73	3.00
PODE-38.6	—	1.11	0.087	2.25	3.48
PODE-67.3	—	1.20	0.113	2.20	4.52
PEG	—	—	0.114	0.59	—

caused by the relatively low cloud-point of this sample.

Discussion

At a given molar concentration, the number of the molecules per micelle decreases and, at the same time, the number of micelles increases with the increasing length of the polyoxyethylene chain[3-5]. Therefore, the amount of dye solubilized by PODE is expected to increase with the polyoxyethylene chain-length, if the concentration of PODE is expressed by moles per liter of solution. In fact, the polyoxyethylene chain-length is responsible for the solubilizing power up to the PODE where $p \fallingdotseq 27$ at high concentrations, while the amount of dye solubilized decreases as the p value exceeds this value. When the polyoxyethylene chain of PODE becomes quite long, the nature due to the polyoxyethylene chain predominates over that due to the alkyl chain and the characteristics of PEG become obvious; thus the effect of the alkyl chain is reduced and a polymer-like property appears in the molecule. This might be the reason why PODE where $p \fallingdotseq 27$ has the maximum solubilizing power. This is also supported by the observation that PEG shows no solubilization.

Solubilization isotherms above the critical micelle concentration for the oil-soluble dyes can in some instances be fitted to the general form[6,7]:

$$S = Kc^n \qquad (1)$$

where K and n are constants. If the data of the solubilization shown in Fig. 2 are replotted in a logarithmic scale, straight lines are obtained for all cases, irrespective of p value, some of which are illustrated in Fig. 4. We thus confirm that Eq. 1 holds in the present experiment. The values of the constant, n, which can be estimated from the slope of the straight line, are listed in Table I.

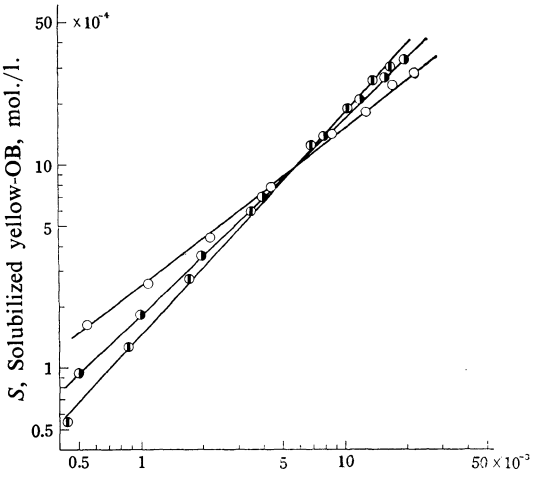

Fig. 4. Log-log plots of solubilization vs. concentration.
○ p=6.2 ◑ p=15.8 ◐ p=38.6

4) T. Nakagawa and K. kuriyama, *J. Chem. Soc. Japan, Pure Chem. Sec.* (*Nipon Kagaku Zassi*), **78**, 1568 (1957).
5) T. Nakagawa and H. Inoue, ibid., **79**, 345, 348 (1958).
6) A. M. Schwartz, J. W. Perry and J. Berch, "Surface Active Agents and Detergents", Interscience Publishers, New York (1958), p. 442.
7) A. M. Mankowich, *J. Colloid Sci.*, **14**, 131 (1959).

As is seen in Table I, the value of n increases with the p value and is greater than unity for PODE of $p>27$. This indicates that solubilization curves plotted in a ordinary scale change from convex to concave upward from around $p=27$. Since the n values are smaller than unity for ordinary detergents[7], the behavior of PODE of $n<1$ in solubilization may also be interpreted as PODE acting as an ordinary detergent[8], though the reason for this action is not clear. On the other hand, the case of an n value larger than unity implies that the solubilizing power increases with acceleration as the concentration of the detergent increases, although the amout of increase is not very much. A similar tendency was observed in the solubilization curve of polysoap[9].

This presumably indicates that there occurs some interaction, which seems to promote the solubilization, among different micelles or aggregates of the detergent, as will be described below. Evidence for some kinds of interaction will be provided by the Huggins' k' and by an effective volume of PODE calculated from the viscosity and other data[10,11], and it is inferred that the interaction might have some relation to the increment of polyoxyethylene chain-length.

As for the interactions among different aggregates of PODE, the initial slopes of the η_{sp}/c against c plots expressing these interactions depend both on the extension of aggregates and on the affinity between aggregate and solvent relative to the aggregate-aggregate and solvent-solvent affinities[11-13]. It has been shown that these two factors can be resolved by expressing the slope as a product of $[\eta]^2$ and a quantity k'[12]. The value of k' can thus be computed by means of Huggins' familiar equation[12]:

$$\eta_{sp}/c=[\eta]+k'[\eta]^2c \qquad (2)$$

Although no completely quantitative theory concerning Huggins' constant k' is available for such colloidal solutions as a PODE solution, the k'-value can be assumed to be a measure of aggregate-solvent affinity[11]. By the use of the k'-value, which leads to a tentative interpretation of some observed effects of the polyoxyethylene chain on the viscosity of PODE solutions, information concerning the interaction among aggregates or the polymer-like behavior of PODE will be obtained.

The fifth column of Table I shows the dependence of the k'-value upon the polyoxyethylene chain-length. The k'-value at first decreases and then somewhat increases with the increasing p value; it then decreases again, finally approaching the k'-value for PEG, with the exception of a high k'-value for PODE in which $p=7.6$, which is caused by an anomalous aggregation. It is noticeable that the increase in k'-value exists in the region of larger p values in spite of increasing hydrophility. This indicates either that the aggregate-aggregate affinity increases more than the hydrophility of PODE, which increases with the p value, or that the affinity increases with the hydrophility, when polyoxyethylene chain becomes sufficiently long. Furthermore, this suggests probably that some interaction occurs among different aggregates by the help of long polyoxyethylene tails, being ascribed to the polymer-like property of the detergent having a long hydrophilic tail.

On the other hand, it is worth while to consider the viscosity data in the light of the theoretical viscosity equation proposed by Guth and Simha[14]:

$$\eta_r=1+2.5\phi+14.1\phi^2 \qquad (3)$$

This equation is applicable to the dispersion systems of spherical particles, where η_r is a relative viscosity and ϕ is a volume fraction of the particle. The use of Eq. 3 in the present experiment involves the assumption that the aggregates of PODE are spherical[5]. From

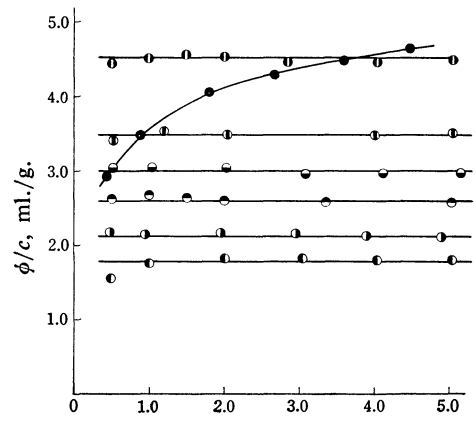

Fig. 5. Effective volume vs. concentration curves of PODE at 25°C.
● $p=7.6$ ◐ $p=10.6$ ◑ $p=15.8$
◓ $p=20.4$ ◒ $p=27.1$ ◑ $p=38.6$
◐ $p=67.3$

8) M. E. L. McBain and E. Hutchinson, "Solubilization", Academic Press, New York (1955), p. 147.
9) U. P. Strauss and E. G. Jackson, *J. Polymer Sci.*, **6**, 649 (1951).
10) U. P. Strauss and N. L. Gershfeld, *J. Phys. Chem.*, **58**, 747 (1954).
11) U. P. Strauss, N. L. Gershfeld and E. H. Crook, ibid., **60**, 577 (1956).
12) M. L. Huggins, *J. Am. Chem. Soc.*, **64**, 2716 (1942).
13) D. A. I. Goring and A. Rezanowich, *J. Colloid Sci.*, **15**, 472 (1960).
14) E. Guth and R. Simha, *Kolloid-Z.*, **74**, 147 (1936).

Eq. 3 the volume fraction, ϕ, was computed, and the effective volume, ϕ/c, shown in Table I denotes the volume occupied by one gram of the detergent in the solution.

The value of ϕ/c is nearly independent of concentration and increases with the increasing polyoxyethylene chain-length, except in the case of PODE in which $p=7.6$, as is shown in Fig. 5. Nakagawa and Inoue[5] have obtained results corresponding to the present ones in the same way, using methoxy polyoxyethylene alkyl ether, in a relatively limited extent of chain-length.

The author has previously shown from the data of ultracentrifugal experiment[3] that the aggregation number, i. e., a number of molecules per aggregate, is highly dependent on the chain-length of polyoxyethylene and decreases with an increase in the chain-length. Considering this result in connection with the values of ϕ/c, therefore, we may say that the number and effective volume of aggregates at a given concentration of PODE increase with the polyoxyethylene chain-length. In concentrated solutions, thus, chances for different aggregates to approach and/or contact each other might be more frequent with the increasing chain-length. The interaction among different aggregates, caused by these chances, is presumably that which results in the polymer-like property of the non-ionic detergent with a long polyoxyethylene tail. From this point of view, the experimental finding that the value of n is slightly greater than unity in the case of PODE with a sufficiently long polyoxyethylene chain, can be attributed to the polymer-like behavior of PODE.

Summary

The solubilization and viscosity of polyoxyethylene dodecyl ether (PODE) solutions were studied as a function of the polyoxyethylene chain-length (p). The solubilization is in accordance with the isotherm $S=Kc^n$, where S is the extent of solubilization, c, the concentration of detergent, and n and K, constants. The value of n increases with the p value and is slightly greater than unity for PODE of $p>27$. The k'-value calculated from Huggins' equation, which is dependent on the p value, decreases at first with the p value and then somewhat increases in spite of the increasingly hydrophilic nature. The effective volume, ϕ/c, of PODE, which is nearly independent of c except for the case of PODE in which $p=7.6$, increases regularly as the p value becomes larger. On the basis of these results, the polymer-like property of PODE of a considerably large p value and the interaction among aggregates of PODE were discussed in connection with ultracentrifugal data reported previously.

The author is much obliged to Professor Toshizo Isemura of Osaka University for his helpful discussion and encouragement during the course of this work. He also wishes to express his appreciation to Mr. Zenichi Miyagawa, Director of this Research Laboratory, for the permission to publish this paper, and to Dr. Iwao Maruta for his advice and encouragement.

Research Laboratory
Kao Soap Co., Ltd.
Sumida-ku, Tokyo

NOTE

The Difference in Free Energy between Equatorial and Axial Isopropyl Groups

By Nobuo MORI and Fumie SUDA

(Received September 11, 1962)

The differences in free energy between equatorial and axial lower alkyl groups are the fundamental quantities on which conformational analysis is based; the values for the methyl and ethyl groups are known to be near -1.8 kcal./mol.[1-4,7,8,10] while those for the isopropyl group are in the wide range of $-2.5\sim-3.55$[3,4] kcal./mol. or are at least often taken[5] to be considerably greater those of methyl and ethyl. Further, an isopropyl group was often assumed to be almost as big as a *t*-butyl group[6].

Recently, however, Lewin and Winstein[7] have given a value of ca. -2.3 kcal./mol. for the isopropyl group from the chemical shifts in the NMR of the 1-proton in isomeric 4-isopropylcyclohexanols. Allinger and his co-workers[8] reported a lower value of -2.1 kcal./mol. from the equilibrium points for the isomerization of *cis*- and *trans*-diisopropylcyclohexanes and of isomeric 4-isopropylcyclohexanecarboxylic acid ethyl esters.

In the present work, the difference in free energy between equatorial and axial isopropyl groups has been determined in the following way. New *cis*- and *trans*-4-isopropylcyclohexylcarbinyl *p*-tosylates have been prepared and acetolyzed, and from the observed rates (k), the difference in free energy (ΔF) between the equatorial and axial isomers* have first been calculated by using the equations[3,9,10]: $K=(k_a-k)/(k-k_e)$ and $\Delta F=-RT\ln K$, where K is the equilibrium constant between equatorial and axial isomers and k_a and k_e are, respectively, the rates for *cis*- and *trans*-4-*t*-butylcyclohexylcarbinyl *p*-tosylates in the same reaction. The calculated values are shown in Table I, along with the relative rates and the mole fractions (N_a) of the axial isomers.

Therefore, the difference in free energy (ΔF_{i-Pr}) between equatorial and axial isopropyl groups may be calculated as follows: The ΔF value of $+0.32$ or 0.42 kcal./mol. for the *cis*-4-isopropyl compound may be regarded as the sum of an energy needed for moving the tosyloxymethyl group from an equatorial to an axial position (i.e., $\Delta F_{Tos}=-1.7$ at 100 and -1.8 kcal./mol. at 110°C[10]) and an energy needed for moving the isopropyl group from an axial to an equatorial position (i.e., $-\Delta F_{i-Pr}$), as illustrated by the relationship: $\Delta F=-\Delta F_{i-Pr}+\Delta F_{Tos}$; thus, the ΔF_{i-Pr} is -2.02 or -2.22 kcal./mol. The averaged value is -2.1 kcal./mol. The good agreement of this value with those obtained by Lewin and Winstein and by Allinger and his co-workers supports the conclusion[8] that the isopropyl group is essentially the same size as a methyl or ethyl group and is in quite a separate class from the *t*-butyl group.

On the basis of the above findings, the energy level of the diaxial conformation of the *trans*-4-isopropyl compound should be $2.1+1.75$ kcal./mol. higher than that of its diequatorial conformation. This corresponds to a K value of about 150 and leads to the prediction, borne out experimentally, that the acetolysis rate for *trans*-4-isopropylcyclohexylcarbinyl *p*-tosylate is identical with k_e within the range of experimental error.

Experimental

***cis*- and *trans*-4-Isopropylcyclohexylcarbinyl *p*-Tosylates** were prepared from the corresponding known carbinols[11] in the usual manner[12], by

1) W. G. Dauben and K. S. Pitzer, in M. S. Newman's "Steric Effects in Organic Chemistry", John Wiley & Sons, New York (1956), p. 1.
2) N. L. Allinger and S. Hu, *J. Am. Chem. Soc.*, **84**, 370 (1962).
3) S. Winstein and N. J. Holness, ibid., **77**, 5562 (1955).
4) D. S. Noyce and L. J. Dolby, *J. Org. Chem.*, **26**, 3619 (1961).
5) A. R. H. Cole and P. R. Jefferies, *J. Chem. Soc.*, **1956**, 4391; W. Takagi and T. Mitsui, *J. Org. Chem.*, **25**, 1476 (1960).
6) For example, W. Klyne, *Experientia*, **12**, 119 (1956); B. C. Lawes, *J. Am. Chem. Soc.*, **84**, 239 (1962).
7) A. H. Lewin and S. Winstein, ibid., **84**, 2464 (1962).
8) N. L. Allinger, L. A. Freiberg and Shih-En Hu, ibid., **84**, 2836 (1962).

* These mean those conformational isomers having, respectively, a tosyloxymethyl group in an equatorial or axial position.
9) E. L. Eliel and C. A. Lukach, *J. Am. Chem. Soc.*, **79**, 5986 (1957).
10) N. Mori, This Bulletin, **35**, 1755 (1962).
11) R. G. Cooke and A. K. Macbeth, *J. Chem. Soc.*, **1936**, 1246.
12) For example, N. Mori, This Bulletin, **34**, 1567 (1961).

TABLE I

4-Substituent	at 99.8±0.1°C				at 110.0±0.1°C			
	Relative rate	K	ΔF kcal./mol.	$N_a \times 100$	Relative rate	K	ΔF kcal./mol.	$N_a \times 100$
cis-t-Bu	4.23	0.00[a]	—	100	4.36	0.00[a]	—	100
cis-i-Pr	2.96	0.65	+0.32	60	3.12	0.58	+0.42	63
trans-i-Pr	1.00	∞	—	0.0	1.00	∞	—	0.0
trans-t-Bu	1.00	∞[a]	—	0.0	1.00	∞[a]	—	0.0

a Assumed

TABLE II. ACETOLYSIS OF *cis*-4-ISOPROPYLCYCLOHEXYLCARBINYL *p*-TOSYLATE AT 110°C

Time, sec.	Tosylate, mol./l.	k, sec^{-1}
0	9.68×10^{-3}	
7200	8.33	$(2.08) \times 10^{-1}$
12000	7.29	2.35
15600	6.68	2.38
19200	6.08	2.42
22800	5.58	2.41
26400	5.12	2.41
30120	4.56	2.41
	Mean	2.40

TABLE III. SUMMARY OF ACETOLYSIS RATES

4-Substituent	Tosylate 10^3 mol./l.	Temp., °C (±0.1°C)	$10^5 k$, sec^{-1}
cis-i-Pr	9.68	99.8	0.860
	9.68	110.0	2.40
trans-i-Pr	9.61	99.8	0.285
	9.61	110.0	0.767
cis-t-Bu[10]	15.5	99.8	1.23
	15.5	110.0	3.35
trans-t-Bu[10]	15.5	99.8	0.290
	15.5	110.0	0.768

treating them with one equivalent proportion of *p*-toluenesulfonyl chloride in pyridine at 0~5°C and recrystallizing from aqueous methanol. The cis-isomer was obtained as plates melting at 44.3~44.6°C, and the trans-isomer, as prisms melting at 54~54.5°C.

Calcd. for $C_{17}H_{26}O_3S$: C, 65.77; H, 8.44. Found: C, 65.69; H. 8.48 for the *cis*-isomer and C, 65.70; H, 8.32% for the trans-isomer.

All reactions and rate measurements were carried out using the same acetic acid without base and following the same procedure as has been previously reported[13] to a 30% completion at 99.8°C and to a 40% completion at 110°C. The calculated first order rate constants were steady to 3%. Table II lists the data for a typical run with *cis*-4-isopropylcyclohexylcarbinyl *p*-tosylate. The rate constants are summarized in Table III.

Tokyo College of Science
Shinjuku-ku, Tokyo

13) N. Mori, ibid., 33, 1144 (1960).

SHORT COMMUNICATIONS

Formation of Paramagnetic Chemical Species of Aromatic Hydrocarbons on Vanadium Pentoxide

By Kozo Hirota and Keiji Kuwata

(Received September 6, 1962)

Recently, formation of radical or radical ion has been demonstrated repeatedly[1,3] by ESR measurement in the chemisorption of anthracene, perylene, 1, 1-diphenylethylene[4], and *p*-phenylenediamine[5] on silica-alumina catalysts in relation to the mechanism of the acid-site of catalysts. It is interesting to find among these researches some contradicted results on the effect of oxygen; i. e., the intensity of the spectrum became larger by the presence of oxygen according to Fogo[3], while the effect is reversed according to Brouwer[2] and Leftin[4]. Such a discrepancy seems not to be explained by the difference of adsorbates, since the results of Brouwer and Fogo are obtained by the same adsorbates, perylene and anthracene.

In order to investigate such an oxygen effect, we measured the ESR spectrum of benzene, naphthalene and anthracene on vanadium pentoxide which would supply oxygen chemically to the adsorbate. These aromatic hydrocarbons were brought about to the oxide surface as a vapor state and/or a *n*-heptane solution*. ESR measurements were carried out using an X-band apparatus as already reported[6], operating with 455 kc. field modulation.

A slightly asymmetric broad line could be observed always in the spectrum of vanadium pentoxide, degassed (less than 10^{-3} mmHg) at 350°C for one hour. According to the data hitherto published[7], this spectrum could be ascribed to V^{4+} or VO_2^{2+} ion, because it is characterized by a *g*-factor of 1.97, its shape and its half-width of 185 gauss. Now, if anthracene and naphthalene were brought into contact with the oxide treated at 350°C, a small but narrow signal appeared at the shoulder of the broad line, especially markedly in the case of anthracene (cf. Fig. 1). By an

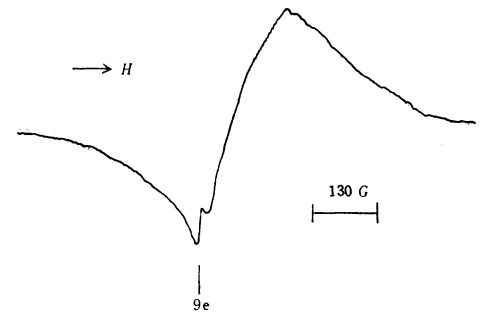

Fig. 1. ESR spectrum of anthracene on vanadium pentoxide.

introduction of air the signals increased their intensity and the corresponding one appeared even in the case of benzene. It is noteworthy that the radicals produced are so stable as can be kept under the atmosphere for a long time. Their half-width and *g*-factor are as follows:

Anthracene	$g=2.0025\pm0.0008$	$H_{msl}=19\pm2$
Naphthalene	2.01 ± 0.005	18.5 ± 3
Benzene	2.00 ± 0.005	18.5 ± 3

In every case no hyperfine structure of the narrower signal could be observed as well as the color change of the adsorbate. These results are not coincident with the systems of anthracene and perylene on silica-alumina[2,4] and on aluminum chloride[8]. However, the effect of oxygen seems to coincide with Fogo's result[3]. Allotting the role of an electron-acceptor to oxygen atom, Fogo ascribed his signal to a hydrocarbon cation-radical formed on Lewis acid site, similarly as Leftin et al.[4] assumed in the chemisorption of 1, 1-diphenylethylene.

It is possible, however, that the same

1) J. J. Rooney and E. C. Pink, *Proc. Chem. Soc.*, **1961**, 70.
2) D. M. Brouwer, *Chem. & Ind.*, **1961**, 77.
3) J. K. Fogo, *J. Phys. Chem.*, **65**, 1919 (1961).
4) H. F. Leftin, ibid., **66**, 1214 (1961).
5) M. Okuda, *J. Chem. Soc. Japan, Pure Chem Sec.* (*Nippon Kagaku Zasshi*), **82**, 1290 (1961); M. Okuda and T. Tachibana, This Bulletin, **33**, 863 (1960).
* Spectroscopic grade of *n*-heptane free from aromatics was used.
6) K. Kuwata and K. Hirota, ibid., **34**, 458 (1961).
7) K. Tarama and S. Teranishi et al., ibid., **34**, 1195 (1961); R. Faber and M. Roggrs, *J. Am. Chem. Soc.*, **81**, 1849 (1959).
8) J. J. Rooney and R. C. Pink, *Proc. Chem. Soc.*, **1961**, 142.

conclusion cannot be applied to the present research, because the paramagnetic species here observed may have a possibility to include some other intermediate species, e. g. semiquinone, formed as the result of oxidation of these aromatic hydrocarbons besides the cation-radical. Such a presumption is in harmony with the oxidative property of the vanadium pentoxide degassed at high temperature. In connection to the above consideration, sample-tube containing anthracene adsorbed on the oxide was heated up to 200°C in the atmosphere, in order to investigate the stability of the radical. Then the shoulder signal disappeared at all; i. e., the radical on the oxide was completely oxidized at higher temperatures.

Added in Proof. In order to investigate the nature of this signal in detail, hydroquinone which is one of the oxidation products of benzene was used as the adsorbate. A signal (g-factor=2.002 $\pm$0.001) appeared also at once, and became very strong at 200°C. The color of the sample became dark-purple, suggesting that quinhydrone is formed, i. e, equimolar complex of quinone and hydroquinone. The signal had no hfs and was narrow as compared to that observed in the case of aromatic hydrocarbons, but it may be allowed to consider that it is due to semiquinone. A similar experiment was carried out, making *p*-phenylenediamine as the adsorbate, and a signal with no hfs could be obtained as reported by Okuda[5] on silica-alumina. This will be another finding to support our viewpoint.

Such being the matter, it will be reasonable to propose that if anthracene, naphthalene or benzene is adsorbed, corresponding semiquinone radical is formed on the degassed vanadium radical.

Details of the study will be published elsewhere.

Science Faculty
Osaka University
Nakanoshima
Osaka

Recoil Reactions in the Irradiated Aquopentamminecobalt(III) Complexes

By Nobufusa SAITO, Takeshi TOMINAGA and Hirotoshi SANO

(Received December 4, 1962)

The present authors previously studied recoil chemistry of various hexamminecobalt(III) complexes and found that outer anions of the

TABLE I. PERCENTAGE DISTRIBUTION OF ^{60}Co-LABELED SPECIES IN IRRADIATED AQUOPENTAMMINECOBALT(III) COMPLEXES

Target	^{60}Co-Labeled species, % *					
	$CoA_5H_2O^{3+}$	CoA_5X^{2+}	$CoA_4X_2^{+}$	Co^{2+}	CoA_3X_3	$CoA_2X_4^{-}$
$[Co(NH_3)_5H_2O](NO_3)_3$	18.6	22.3	5.0	51.1	0.9	0.8
$[Co(NH_3)_5H_2O]_2(SO_4)_3 \cdot 3H_2O$	25.7	3.7	1.9	66.5	0.7	1.5
$[Co(NH_3)_5H_2O]_2(C_2O_4)_3 \cdot 4H_2O$	12.4	2.2	2.4	82.9	0.3	0.0
$[Co(NH_3)_5H_2O]Cl_3$	32.0	9.5	1.5	56.5	0.3	0.1
$[Co(NH_3)_5H_2O]Br_3$	32.9	12.4	2.0	52.3	0.3	0.1
$[Co(NH_3)_5H_2O]I_3$	32.4	7.4	1.8	58.3	0.2	0.0

* $A=NH_3$ (or partly H_2O) ; $X=NO_3$, Cl, Br, I, etc.
Percentage of $^{60}Co(NH_3)_6^{3+}$ was less than 0.4 % and therefore was negligible.

target compound might play an important role in the recoil reactions[1]. In the present work, they have investigated the effects of outer anions on the recoil reactions in the irradiated aquopentamminecobalt(III) complexes.

Six kinds of aquopentamminecobalt(III) complexes listed in Table I were irradiated for one hour at pile temperature in the JRR-1 reactor, at a thermal neutron flux of approximately 3×10^{11} n/cm^2 sec. All irradiations were made in the presence of air. After the bombardments the target salt was stored at dry-ice temperature for one to five days. Then it was dissolved in distilled water and the percentages of ^{60}Co-labeled species present in the aqueous solution were determined by means of separation procedures involving ion exchange, precipitation, or paper electrophoresis (in the acetate buffer)*.

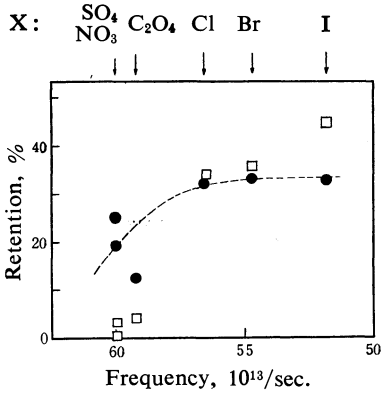

Fig. 1. The relationship between retention and frequency of the maximum in the first absorption band of $Co(NH_3)_5X$.

● Retention of $[Co(NH_3)_5H_2O]X_3$
□ Retention of $[Co(NH_3)_6]X_3$

The results summarized in Table I indicate that the distribution of recoil species in these salts was largely influenced by the kind of outer anions in the target. In Fig. 1 is plotted the retention (percentage of $^{60}CoA_5H_2O^{3+}$) of aquopentamminecobalt(III) complex salts against the frequency of the maximum in the first absorption band of $Co(NH_3)_5X$ (X denotes the outer anion in the target). It appears that the retention is generally increased with the decrease in the frequency of the maximum, or the decrease in stability of the outer anion X as complexed with cobalt. It will be seen that this retention-stability relationship is essentially similar to that already observed for the corresponding hexamminecobalt(III) complexes[1], which are shown together in Fig. 1. Since the corresponding salts in the both series containing the same kind of outer anion may be rather alike in chemical composition except that a ligand NH_3 is replaced by H_2O, and vice versa, such a similarity in the recoil reactions may not be surprising.

In explanation of the results it may be presumed that the recombination process involving NH_3 and H_2O molecules to restore the parent form competes with the substitution processes involving outer anions where the facility of their incorporation into ligands may mainly depend upon the stability of such anions as complexed with cobalt.

Department of Chemistry
Faculty of Science
The University of Tokyo
Hongo, Tokyo

1) N. Saito, T. Tominaga and H. Sano, This Bulletin, 35, 365 (1962).

* Retentions obtained by paper electrophoresis were somewhat lower than those obtained by ion exchange. The latter values were used in Table I.

Effects of Outer Anions on the Recoil Reactions in the Irradiated Nitropentamminecobalt(III) Complexes

By Nobufusa SAITO, Takeshi TOMINAGA, and Hirotoshi SANO

(Received December 4, 1962)

It was already reported that recoil reactions in the irradiated hexammine- and aquopentamminecobalt(III) complex salts were greatly influenced by the kind of outer anions in the target compound[1,2]. In this work, the investigation of the effects of outer anions has been extended to a group of nitropentamminecobalt-(III) complex salts.

Seven kinds of nitropentamminecobalt(III) complex salts (listed in Table I) were irradiated for one hour in the JRR-1 reactor at a thermal neutron flux of approximately 3×10^{11} n/cm^2 sec. All irradiations were made at pile temperature in the presence of air. After irradiation the ^{60}Co-labeled species present in aqueous solutions of the target salt were separated by means of ion exchange, precipitation, or paper electrophoresis*1.

The results are summarized in Table I. For nitropentamminecobalt(III) nitrate, chloride, bromide and iodide (i.e., X=NO_3, Cl Br and I), however, $^{60}CoA_5X^{2+}$ fraction in Table I did not represent real retention but was composed of two divalent complex cations containing different acidic ligands. These two species were further separated by fractional precipitation (recrystallization to constant specific activity), or ion exchange after aquotization*2. Table II shows percentages of the two species: species a represents "retention", whereas species b is a substituted product formed through incorporation of outer anions.

In Fig. 1 are plotted percentages of the species a and b against the frequency of the maximum in the first absorption band of $Co(NH_3)_5X$, where X denotes the outer anion of the target salt*3. It will be seen that, as

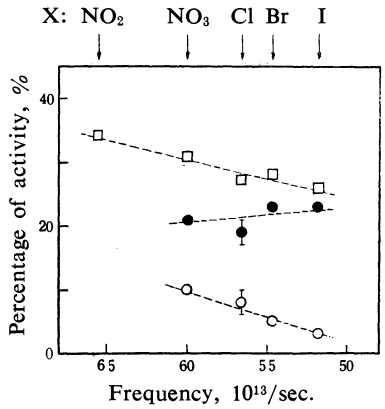

Fig. 1. Relationship between the percentage of $^{60}CoA_5X^{2+}$ fraction (species a and b) and the frequency of the maximum in the first absorption band of $Co(NH_3)_5X$.

● Species a (retention)
○ Species b ($^{60}CoA_5NO_3^{2+}$, $^{60}CoA_5Cl^{2+}$, etc.)
□ a+b

TABLE I. PERCENTAGE DISTRIBUTION OF ^{60}Co-LABELED SPECIES IN IRRADIATED NITROPENTAMMINECOBALT(III) COMPLEXES*

Target	^{60}Co-Labeled species, %**					
	CoA_6^{3+}	CoA_5X^{2+}	$CoA_4X_2^{+}$	Co^{2+}	CoA_3X_3	$CoA_2X_4^{-}$
$[Co(NH_3)_5NO_2](NO_2)_2$	<3.7	34.0	6.1	53.1	1.4	1.7
$[Co(NH_3)_5NO_2](NO_3)_2$	<4.7	30.9	10.0	50.3	2.0	1.9
$[Co(NH_3)_5NO_2]Cl_2$	<3.4	27.3	1.9	67.3	0.1	0.2
$[Co(NH_3)_5NO_2]Br_2$	<3.6	28.1	1.4	66.3	0.6	0.1
$[Co(NH_3)_5NO_2]I_2$	<6.5	25.9	5.9	59.5	1.0	1.2
$[Co(NH_3)_5NO_2]SO_4$	<4.4	25.1	2.3	67.4	0.5	0.4
$[Co(NH_3)_5NO_2]C_2O_4$	<1.9	17.9	2.1	77.8	0.4	0.1

* The irradiated salts were stored at dry-ice temperature for 1~3 days before separation.
** A=NH_3 (or partly H_2O); X=NO_2, NO_3, Cl, Br, I, etc.

1) N. Saito, T. Tominaga and H. Sano, This Bulletin, 35, 365 (1962).
2) N. Saito, T. Tominaga and H. Sano, ibid., 36, 231 (1963).
*1 Sometimes, paper electrophoresis method gave slightly lower retentions than those obtained by ion exchange method. The latter values were used in the present paper.
*2 For example, when the solution containing $CoA_5NO_2^{2+}$ and CoA_5Br^{2+} is warmed in adequate conditions, CoA_5Br^{2+} is rapidly aquotized to give $CoA_5H_2O^{3+}$ whereas $CoA_5NO_2^{2+}$ remains practically unchanged. Then the trivalent and divalent cations can be readily separated by ion exchange method.
*3 Since the oxalate and sulfate containing divalent anions may be different from the other salts as to the crystal structure and the outer anion-to-cobalt ratio, they are not included in Fig. 1.

TABLE II. PERCENTAGES OF ^{60}Co-LABELED SPECIES IN THE FORM OF $^{60}CoA_5X^{2+}$

Target	^{60}Co-Labeled species, %*	
$[Co(NH_3)_5NO_2](NO_3)_2$	a : $CoA_5NO_2^{2+}$	21 ± 1
	b : $CoA_5NO_3^{2+}$	10 ± 1
$[Co(NH_3)_5NO_2]Cl_2$	a : $CoA_5NO_2^{2+}$	19 ± 2
	b : CoA_5Cl^{2+}	8 ± 2
$[Co(NH_3)_5NO_2]Br_2$	a : $CoA_5NO_2^{2+}$	23 ± 1
	b : CoA_5Br^{2+}	5 ± 1
$[Co(NH_3)_5NO_2]I_2$	a : $CoA_5NO_2^{2+}$	23 ± 1
	b : CoA_5I^{2+}	3 ± 1

* Species a represents retention; species b represents a substituted product in each target salt.

the frequency of the maximum decreases, the percentage of species b decreases while the percentage of the parent species a (retention) remains almost unchanged or slightly increases.

As in the preceding works[1,2] the results may be presumably explained by assuming that fragmented NH_3 or NO_2 groups and outer anions compete with each other in the recoil reactions involving complex formation, upon which the stability of the outer anions as complexed with cobalt may be reflected, as indicating the facility of co-ordination.

Department of Chemistry
Faculty of Science
The University of Tokyo
Hongo, Tokyo

A New Spraying Reagent for Ferrous Ion in Paper Chromatography

By Ichiro MORIMOTO

(Received December 5, 1962)

Separation of ferrous and ferric ions from each other, and the detection of these ions are important from the practical point of view. In the previous paper[1], a colorimetric method was described for the determination of iron by making use of its colored complex with 2, 4, 6-pyridinetricarboxylic acid.

2, 4, 6-Pyridinetricarboxylic acid gives a purple complex with ferrous ion and the absorbance of this colored complex increases considerably by the presence of a small amount of pyridine. Therefore, a mixed solution of 2, 4, 6-pyridinetricarboxylic acid and pyridine can be used as a new reagent for ferrous ion in paper chromatography.

One to 2 μg. of ferrous or ferric ion were spotted on a filter paper strip for chromatography (Tôyô Roshi, No. 51, 51 A or No. 53). The paper strips were developed for about 2 hr. by the ascending method in a mixed solvent of 4 N hydrochloric acid-*n*-butanol-acetic acid-acetone[2] (1 : 1 : 1 : 1). The solvent front moved about 15 cm. at 15±2°C. The paper strip was, then, dried and the following solution was sprayed on them: 0.1 g. of 2, 4, 6-pyridinetricarboxylic acid dissolved in 100 ml. of methanol, with the addition of 5 ml. of pyridine. Ferrous ion was detected as a purple spot which did not fade away within about 24 hr. After marking the ferrous ion spot, the paper strip was sprayed with 10% hydroxylamine hydrochloride in methanol. Ferric ion was reduced to ferrous ion and it was clearly detected as a purple band. The detection limit was about 0.1 μg. for ferrous ion. The color reaction is specific for ferrous ion and it does not interfere with other ions.

TABLE I. R_f VALUES OF Fe^{2+} AND Fe^{3+} WITH THE DEVELOPER, 4N HCl-*n*-BUTANOL-ACETIC ACID-ACETONE (1 : 1 : 1 : 1)

Filter paper	R_f	
	Fe^{2+}	Fe^{3+}
No. 51	0.18	0.54
No. 51 A	0.15	0.55
No. 53	0.17	0.57

The results are given in Table I. The separation of ferrous and ferric ions from each other in the mixed solvent gave satisfactory results. Other solvent mixtures were studied, but the results were unsatisfactory in the separation of ferric ion from ferrous ion. This new reagent is much sensitive and more convenient than any other reagents[2] like ammonia or cyanides used frequently in paper chromatography.

Further work is in progress and the results will be published later.

Laboratory of Chemistry
Faculty of Liberal Arts and Education
Gifu University
Nagara, Gifu-shi

1) I. Morimoto and S. Tanaka, *J. Chem. Soc. Japan, Pure Chem. Sec.* (*Nippon Kagaku Zasshi*), **83**, 889 (1962).

2) M. Qureshi and I. Akhtar, *Anal. Chem.*, **34**, 1341 (1962).

Direct Introduction of Ethoxycarbonyl Radical into Hydrocarbons by Photochemical Reactions

By Chyongjin PAC and Shigeru TSUTSUMI

(Received December 11, 1962)

Recently, it has been reported that methoxycarbonyl radical is produced by the abstraction of chlorine atom in methyl chloroformate with methyl radical[1].

It would also be expected that alkoxycarbonyl radical might be produced from alkyl chloroformate by light in the same manner as the photolysis of phosgene[2] and of oxalylchloride[3],

$$Cl-CO_2R \xrightarrow{h\nu} \cdot Cl + \cdot CO_2R$$

being accompanied by the direct introduction of the radical into hydrocarbons.

Therefore, the photochemical reactions of ethyl chloroformate with hydrocarbons were studied, and it was found that the ethoxycarbonyl radical produced by a high pressure mercury arc (600 W) from ethyl chloroformate was introduced into hydrocarbons, such as cyclohexane, benzene and cyclohexene.

The over-all reaction with respect to cyclohexane is shown as follows;

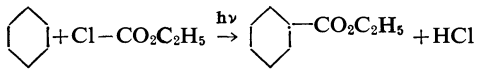

The irradiation of a mixture of cyclohexane (168 g.) and ethyl chloroformate (83 g.) (mole ratio; 3:1) gave the following liquid products at room temperature for 6 hr. in the atmosphere of nitrogen; 1 g. of an ester (b. p. 93~96°C/35 mmHg, n_D^{26} 1.4510) and 1.5 g. of bicyclohexyl (b. p. 65~70°C/3 mmHg, n_D^{25} 1.4743). The above ester was identified as ethyl cyclohexanecarboxylate by infrared absorption spectra, gas chromatographic analyses and the mixed-melting point test of its anilide with an authentic sample (m. p. 143~143.5°C, recrystallized from ligroin). During the irradiation, gases were evolved and analyzed by gas chromatography, which consisted of large amounts of carbon dioxide and ethane, small amounts of ethylene and a trace of ethyl chloride.

In a similar way, a mixture of benzene and ethyl chloroformate afforded only a small amount of ethyl benzoate, without the formation of gaseous products. Ethyl benzoate was confirmed by gas chromatographic analyses.

In the case of cyclohexene, ethyl cyclohexanecarboxylate and 3, 3'-bicyclohexenyl were obtained as major products, although we expected 3-ethoxycarbonylcyclohexene or 1-ethoxycarbonyl-2-chlorocyclohexane as a major product, taking into account the previous experimental results which are shown as bellow;

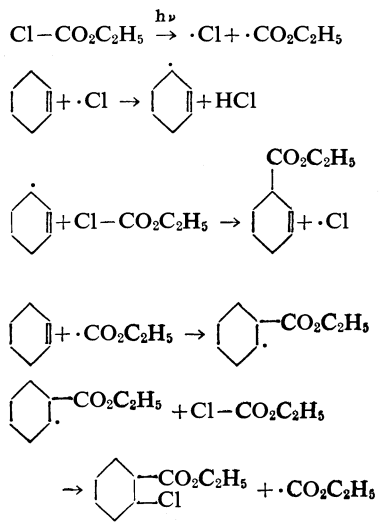

or

In spite of irradiation for a longer time, the amounts of gaseous products were very small compared with those found in the case of cyclohexane. Details of this reaction are now under investigation.

The method of direct carboxylation into hydrocarbons with ethyl chloroformate has never been reported, thus we are intending to carry out further researches in this field.

Department of Chemical Technology
Faculty of Engineering
Osaka University
Miyakojima-ku, Osaka

1) J. C. J. Thynne and P. Gray, *Proc. Chem. Soc.*, **1962**, 141.
2) Bodenstein et al., *Z. physik. Chem.*, **B3**, 459 (1929).
3) Rollefson et al., *J. Am. Chem. Soc.*, **56**, 1089 (1934); **58**, 443 (1935).

The Interpretation of Absorption Spectra of Condensed Polycyclic Aromatic Hydrocarbons by Using a Simple Resonance Theory. I. The Resonance Structure of the Excited State in Correlation with Platt's Theory

By Takashi HANDA

(Received February 25, 1961)

Many theoretical investigations have been made for the purpose of interpreting the absorption spectra of condensed polycyclic aromatic hydrocarbons by such hypotheses as the valence-bond, molecular orbital, and free-electron theories. It is very difficult, however, to understand intuitively the chemical meanings of the upper-state.

With this in mind, the present author has undertaken to learn whether the transition energies of these molecules may be directly related to the differences in empirical resonance energy between the ground and excited states of these molecules. In this case, it is assumed that a chemical resonance structure corresponds to the defined excited state proposed and classified by Platt[1,2].

The estimation of these differences in empirical resonance energy have been carried out by applying Carter's empirical equation to the excited state. We have examined what types of chemical resonance structure correspond to the individual excited states.

The Introduction of the Approximation Formula. — The light-absorption energies of substances can be expressed generally as follows;

$$E_2 - E_1 = \bar{\nu} \qquad (1)$$

where E_2 and E_1 are the total energies of the excited and ground states respectively. These energies, E_2 and E_1, which are caused by the mobile π-electrons in the case of polycyclic aromatic hydrocarbons, can be divided into two pats : bonding-energy (H°) and resonance energy (R), where R means the empirical resonance energy which is the sum of calculated resonance energy and the compression energy. Thus, Eq. 1 can be rewritten into Eq. 2:

$$\bar{\nu} = (H^\circ_E - H^\circ_G) - (R_E - R_G) \qquad (2)$$

where the term $(H^\circ_E - H^\circ_G)$ may be understood to correspond to the light-polarization energies between two polarized carbon atoms on the periphery of the molecule without resonance and to be approximately constant for this series of molecules.

It is assumed that, for the estimation of resonance energies in the excited state, Carter's empirical equation, which is consolidated for the estimation of those in the ground state, can be applied, except for the constant term:

$$R = -20 + 12\,D + 69 \log N \ \text{(kcal./mol.)} \qquad (3)$$

where D is the number of double bonds and N is that of the canonical Kekulé resonance structures in this state. Therefore, Eq. 2 can be rewritten into Eq. 4:

$$\bar{\nu} = A - 69 \log (N^*/N) \quad \text{(kcal./mol.)} \qquad (4)$$

where A is constant and N^* is the number of canonical Kekulé resonance structures of the residual parts of the structure of the molecule defined as an excited state and N is that of a ground state.

An excited state of a molecule in this series may be chemically represented by the resonance among a specified group of an N^* number of elementary polarized-resonance, structures with the same weights, and their symmetrical character probably can not be reduced to a particular, designative symmetry-group. Therefore, it is considered that they include imaginary unit polarizations which cancel each other out finally, in contrast to the irreducible representation which characterizes the discriminative state in other representations. Hence, we must correlate, in some way, the above method of the representation of an excited state with the theoretical method, which pictures a characteristic excited state with a universal designation over all the molecules of this series, irrespective of the different symmetry-characters of their configuration of π-orbitals or electrons, with a few exceptions.

Platt has already classified and assigned the absorption spectra of acenes and phenes into the L_a-, L_b-, B_a-, B_b-, C_a- and C_b-types of polarization by using his free-electron orbital method.

The chemical resonance structures of polycyclic acenes and phenes corresponding to a

1) H. B. Klevens and J. R. Platt, *J. Chem. Phys.*, **17**, 470 (1949).
2) J. R. Platt, ibid., **17**, 484 (1949).

given type of polarization, such as ^1L_a, ^3L_a, ^1L_b, ^3L_b, ^1B_a, ^1B_b, ^1C_a and ^1C_b, are expressed and their numbers of resonance structures (N^*) are estimated in the following section.

As a conclusion, the correctness of the preceding expression of an excited state by resonance structures corresponding to a given type of polarization according to Platt's idea, is judged by plotting $\log(N^*/N)$ versus $\bar{\nu}$ assigned as corresponding to that state, thus determining whether the linear relation prescribed in Eq. 4 is held, and by examining the direction of the resulting electric moment, which is the sum of the elementary moments of each contributing resonance structures, or by examining the oscillator strength due to these structures, as compared to the empirical ones.

Classification of Resonance Structures in Correlation with Platt's Model. — Platt has postulated a convenient diagram for determining the polarizations of transitions from the ground state. The distinctive feature in his theory exists in that he replaces the sign of a free-electron standing-wave to that of a point-charge to picture the transition from the ground state. The polarization of the transition from the ground state will be the same as if we locate + and − point charges at alternate anti-nodes, shrink the perimeter back to its normal shape, and determine the direction of the resulting electric moment. Although it should be emphasized that such a polarization diagram is a device for visualization and not a classical model, it is a very convenient modeling for our purpose in that it pictures an excited state by the resonance of a given type of polarized chemical structures.

For example, the polarization diagrams of each level are illustrated in Fig. 1* for anthracene. The orbital ring quantum number (q) is equal to the ring number (n) in the cata-condensed series, where the number of π-electrons is $2(2n+1)$. Therefore, the total momentum number, Q, is equal to 1 for the B-state and $(2n+1)$ for the L-state.

On the basis of the above considerations, we set resonance structures of a given type of polarization corresponding in our sense to the above polarization diagram of a respective excited state in Platt's sense, as we locate + and − charges along the periphery of the molecule according to the law of alternating polarity. However, the respective transitions from the ground state have been assigned to a simple designation based on the molecular orbital method in the simple and lower molecules. Therefore, it is considered that the above representation of an excited state includes imaginary unit polarizations which cancel each other out finally, in addition to the real representation of an excited state by unit polarizations.

If we separate charges at the cross-linking atoms into $(1-ai)$ and ai in order to eliminate the effect of the cross-linking as we estimate the energy of the ^1L_a and ^3L_a transitions in the following section, and if we select the specified group of polarized structures corresponding to an adequate group designation, the sum of the number of polarized resonance structures of an excited state in this method of computation might be suggested as satisfying Carter's equation in plotting $\log(N^*/N)$ versus the $\bar{\nu}$ value assigned to that excited state.

A Modification of Platt's Idea.—In order to eliminate the effect of cross-linking carbon atoms for the computation of the weights of the resonance structures for the L-state, we will make a little modification of Platt's idea. We will introduce an imaginary point charge vector i to the cross-linking carbon atoms in the ground state in order to divide the corresponding charge-density 1 to $(1-\alpha i)$ and αi; thereby we can divide one cross-linking carbon atom into two imaginary ones with charge-densities of $(1-\alpha i)$ and αi.

It is assumed that that electric current resulting from the motion of the π-electron is not circular on one plane, moving in one direction along the periphery of the molecule, but that it passes through a twisted path imagined to consist of each constituent benzene nuclei as a loop via an imaginary ethylene-linkage formed by cross-linking carbon atoms with the imaginary charges $(1-\alpha i)$ and αi in one direction. In this model, the angular momenta of the π-electrons of each benzene nucleus are not perpendicular to the imaginary twisted orbital plane, but they become parallel as we draw the imaginary atom A with the imaginary charge of αi near to another imaginary atom, A′, with the imaginary charge of $(1-\alpha i)$. The imaginary distance between them may be considered to determine the degree of condensation of the two nuclei. The quantity of the angular momenta is defined as qh where q is the orbital quantum number and the energy is given by q and 1, as in Eq. 5. It is considered that the sum of the orbital ring quantum numbers, q_1 and q_2 of each imaginary twisted path is invariant to the original q, while the sum of each bond-length of the perimeter is increased by an i in an imaginary unit. It is considered in this case that the imaginary bond-length in carbon-atoms is defined as the mean distance multiplied by

* This polarization diagram is just the same as that shown in the paer of Platt. However, for convenience of explanation it is re-illustrated in this paper.

two charge densities at both ends.

When we switch two of the four imaginary atoms, αi, $(1-\alpha i)$, αi, and $(1-\alpha i)$, the imaginary increase in the perimeter-length by imaginary cross-linking ethylene-linkage is equal to $2\alpha i(1-\alpha i)$ and the imaginary decrease in the bonds among cross-linking carbon atoms and their neighbors is 2 for naphthalene. Therefore, each cross-linking ethylene increases $2\alpha i+2(\alpha^2-1)$ in perimeter-length for acenes. The estimated real length of this imaginary path is determined to be $\sqrt{10^2+2^2}$ by vector-synthesis in the case where α is equal to 1 for the naphthalene molecule. For the phenanthrene molecule, it is proposed that the following operations shall be made as illustrated in Fig. 2. We separate each cross-linking carbon atom in the f-position into two imaginary ones with a charge vector of βi on f and $(1-\beta i)$ on f'; then we rotate the i, h, g, and f' atoms upside down to the molecular plane with the $j-k$ bond as an axis, so as to superpose the f' on the carbon atom in the l-position. The charge-rotation vector $\boldsymbol{r}$ is introduced into this operation, and consequently the charge-density of the rotated atoms in the i, h, g, and f'-positions become $\boldsymbol{r}$, $\boldsymbol{r}$, $\boldsymbol{r}$, and $\boldsymbol{r}+1$ by rotation, where $i\times\boldsymbol{r}=0$ and $\boldsymbol{r}\times\boldsymbol{r}=1$. It is also assumed that the ring quantum number which indicates the angular-momentum is invariant in this operation. Therefore, the same procedure is considered as in the case of the anthracene molecule by separating the charge in the $(l+f')$-position into $\{i(\alpha+\beta)+r\}/2$ and $1-\{(\alpha+\beta)i-r\}/2$. The imaginary length of the perimeter l is estimated as $11.68+3.18i+2\boldsymbol{r}$ when α is equal to 1, and the real number of the imaginary perimeter length becomes $\sqrt{11.68^2+2^2+3.18^2}$, treating i and $\boldsymbol{r}$ as orthogonal vectors.

According to Platt's free-electron orbital method, the energy of light-absorption corresponding to that of the center of gravity (E) is given in Eq. 5;

$$E=\frac{q^2h^2}{2ml^2} \tag{5}$$

where q is the ring quantum number of acenes, m is the mass of the electron, and l is the length of the perimeter in the Ångstrom unit. As is illustrated in Fig. 2, the imaginary perimeter lengths of pseudo-anthracene converted from phenanthrene by rotation may be given as follows:

$$\begin{aligned} l_1&=(8.5+3\alpha^2+\alpha\beta)+(3\alpha+\beta)i+2r \\ l_2&=(7.5+3\alpha^2+2\alpha\beta)+(5\alpha+\beta)i+2r \end{aligned} \tag{6}$$

The real values of l_1 and l_2 should be equal. Therefore, the following relations are deduced from Eq. 1:

$$3\alpha^2\beta^2+(27+6\alpha^2)\alpha\beta+10\alpha^2-16=0 \tag{7}$$

When we put $\alpha=0.775$ as the ^1L_a case in Table II, β is estimated to be about 0.4. As a result, we obtain the imaginary perimeter length l corresponding to the ^1L_a-polarization by substituing α and β into Eq. 6. In the same procedure, we obtain β as nearly equal to 0 when we put α as equal to 1.225, which corresponds to the ^3L_a-polarization. When we put α as equal to 1.0, β is estimated to be 0.18, which corresponds to the case of the center of gravity of L_a-polarization. The estimated values of $\bar{\nu}$ from Eq. 5 corresponding to ^1L_a, ^3L_a and $^{c\cdot g}L_a$ polarization are fairly satisfactory. In the same way, we can estimate β in the case of such simpler phenes as 1, 2-benzoanthracene, 1, 2-benzotetracene, chrysene, and 1, 2-5, 6 dibenzoanthracene. The estimated values of $\bar{\nu}$ corresponding to the ^1L_a, ^3L_a and $^{c\cdot g}L_a$ polarizations are considered to be reasonable. The estimated values of the energies of absorptions of the L_a-state of respective compounds are shown in Table I*.

When we switch other two combinations of four imaginary atoms with charges αi and $(1-\alpha i)$, such as αi and αi or $(1-\alpha i)$ and $(1-\alpha i)$, energy-values of the B_a-state are obtained which correspond to the estimated number of resonance structures in the analogous B_a-state, which means that we have imaginarily varied the actual perimeter length or the shape of the potential box of the molecule instead of varying the angular momentum q. The imaginary length of the perimeter of naphthalene with an imaginary increase of $\alpha^2i^2+(1-\alpha i)^2$ in two cross-linking ethylene atoms and a decrease of $2\alpha i+2(1-\alpha i)-4$ in four bonds among cross-linking carbon atoms and their neighbors, is equal to $(9-2\alpha^2)-2\alpha i$. Those of anthracene, naphthacene and phenanthrene are illustrated in Table II. In the case of phenanthrene obtained by being rotated, the residual imaginary charge on the f atom is equal to $(1-\alpha i)$, in contrast to the value of αi in the case of the L_a-state; therefore, the imaginary charge in the $(l+f')$-position is 1, while other elements are equal to those in the above case. The values of $\bar{\nu}$ B_a estimated

* We can empirically obtain satisfactory values of $\bar{\nu}$ in respective polarizations when we put α_1 as equal to 0.775 in the case of the ^1L_a-polarization, α_3 as equal to 1.225 in the case of the ^3L_a-polarization, and $\alpha_{c\cdot g}$ as equal to 1.0 in the case of the $^{c\cdot g}L_a$-polarization in the acene series. The following relations are observed empirically in the case of acenes:

$$\begin{aligned} \bar{\nu}^1L_a+\bar{\nu}^3L_a &\fallingdotseq 2\bar{\nu}^{c\cdot g}L_a \\ \alpha_1+\alpha_3 &\fallingdotseq 2\alpha_{c\cdot g} \end{aligned} \tag{8}$$

where α is considered to determine the degree of the condensation of mutually neighboring benzene nuclei.

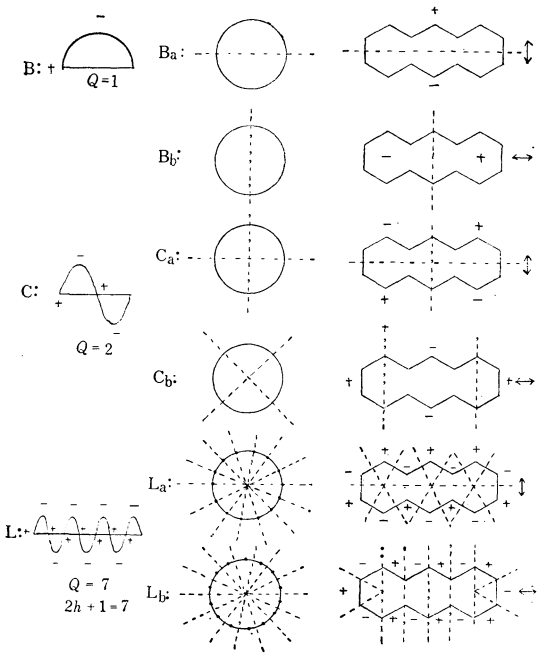

Fig. 1. Polarization diagram of the anthracene molecule according to Platt.

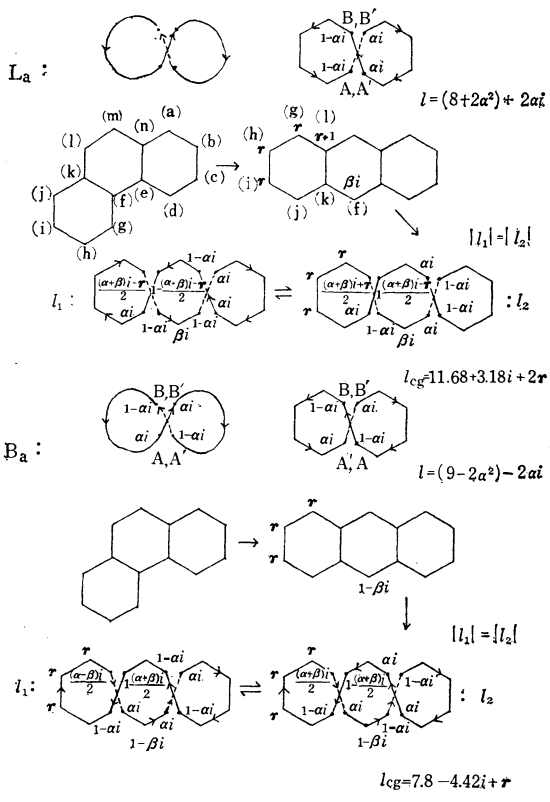

Fig. 2. Imaginary perimeter in the case of L_a- and B_a-polarization.

from the perimeter length are given in Table I. The estimated values corresponding to the ^1L_a- and ^3L_a-excitation illustrated in Table I are considered to be in good agreement, irrespective of their rough estimation.

The above procedure corresponds to the fact that, in the estimation of resonance structures, we put the imaginary charge, i, on the cross-linking atom on the perimeter and separate the imaginary ethylene-linkage with charges $(1-i)$ and $-(1+i)$ at both ends in the representation of the L_a-state, while we put $(1-i)$,

Table I

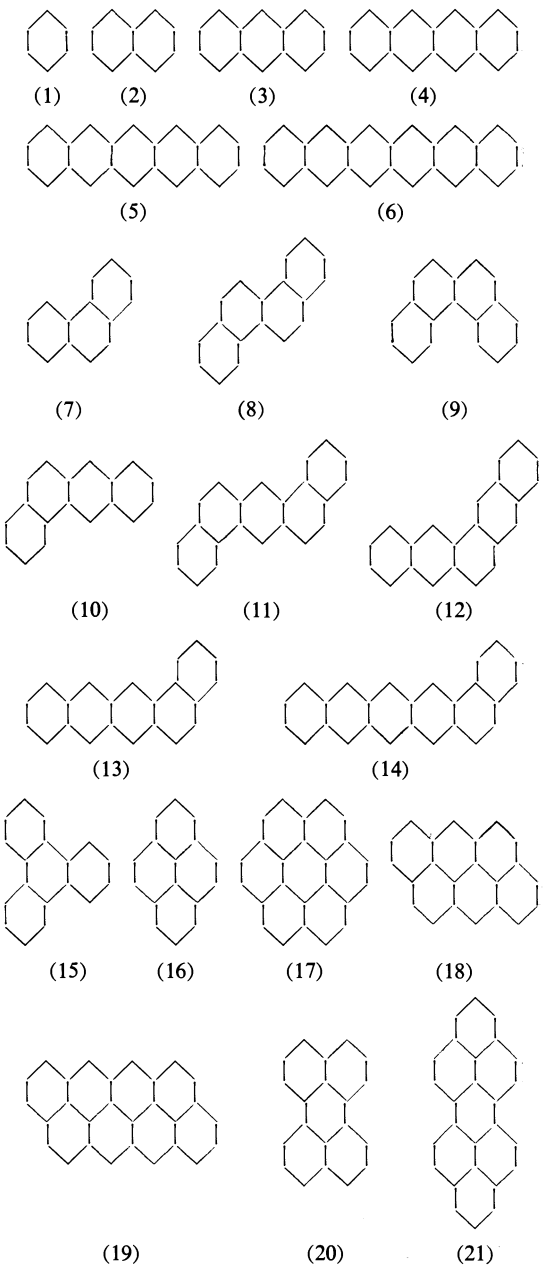

on the perimeter and separate the imaginary ethylene linkage with charges i and i in the case of the B_a-state.

To the problem of the estimation of the number of resonance structures in acenes and phenes, this imaginary point-charge-vector and rotation-vector are also introduced. The correlation with an estimation of their resonance structures will be discussed in the following section. The numbers of Kekulé resonance structures will be given in the analogous form as $a+bi+c\boldsymbol{r}$; their real value is estimated as $\sqrt{a^2+b^2+c^2}$ for phenes and other complex-molecules which are converted into pseudo-acenes, from which we take a given type of resonance structure as corresponding to a given polarization as defined by Platt.

Resonance Structures Corresponding to L_a-type Polarization.—The chemical resonance structures corresponding to the L_a-type polarization of the naphthalene molecule are illustrated in Fig. 3, where + and − point charges are located alternatively on individual elementary carbon atoms on the periphery of the molecule. A combination of one +-labeled atom with all five other −-labeled atoms holding the canonical resonance structures with the residual parts of the molecule produces the 5 or $(2n+1)$ polarized form. The same operation with the four other +-charged atoms produces the 5^2 or $(2n+1)^2$ polarized form, with 32 Kekulé resonance structures.

By superposition of these 5^2 or $(2n+1)^2$ polarized form, Platt's model corresponding to the L-state has been considered to be made. Therefore, the −-charge density on each −-labeled carbon atom in one polarized structure must be $1/4\times1/32$ in estimating the elementary dipole, the 1/4 factor of which will be discussed in a later section. The summation of the elementary dipoles of 32-resonance structures gives only a transversal electric dipole of $11ae'$, where e' is equal to $e/32$. However, it is known intuitively that the weights of the existence of the resonance structures asterisked by * and ** may be different from those asterisked by *** and ****, which include polarization on the cross-linking carbon atoms. The effects of cross-linking are eliminated by introducing the imaginary point charge vector i to the cross-linking carbon atoms, which, positively or negatively, separate the independent ethylene-linkage with the imaginary charges $(1-i)$ and $-(1+i)$, in order to supplement the decrease in total electric dipoles with this polarization, which is illustrated in Fig. 4.

The summation of elementary dipoles with the group asterisked by * gives only a transversal dipole with a magnitude of $12ae'$, while that with the group asterisked by ** gives $2ac'$ dipoles, that with the ***-asterisked group gives a transversal dipole of $-2ae'$, and that with the ****-asterisked group gives $-ae'$ in the same direction. Therefore, the first group asterisked by * possesses a predominant influence for polarization compared with the latter three. The electric dipole of the third group, asterisked by ***, may be substituted by that of the imaginary ethylene-linkage in the above model with charges of $-(1+i)$ and $(1-i)$ at both ends. Both dipoles possess a $-2ae'$ unit of strength. The last group, asterisked by ****, may be equivalent to the polarized structure among imaginary cross-linking carbon atoms with charges of i and i.

As has been mentioned above, the number of resonance structures belonging to the second group (**) may be substituted by those belonging to the imaginary ethylene, in estimating which we may count the resonance structures of the residual benzene nuclei or parts. For example, they are 1, 2, 3, 4 and 5 for naphthalene, anthracene, naphthacene and pentacene, in that order. As for the actual number of resonance structures in the estimation, they are multiplied by $(1+i)\times(1-i)$ or 2. The resonance number for the ***-group is equivalent to that polarized in the i and i position. They are all equal to 1 in one polarized structure. The numbers of polarization among cross-linking atoms mutually with imaginary charges of i are 1 for naphthalene, 4 for anthracene, 6 for naphthacene, etc. This polarization is equivalent to that of the *-type elementary structure in unit strength and hence may be included in the first *-group instead of the **-group, the members of which are mutually canceled. They are also expressed in real number in the above-mentioned imaginary point-charge vector method, while the ***-groups may be expressed in imaginary number and mutually canceled in symmetric acenes.

The second group, asterisked by **, possesses a moment of $2ae'$ in naphthalene and hence takes little part in the main polarization. The members of this group are considered to be caused among two neighboring atoms; hence, in that sense they must include some of the polarization asterisked by *** and ****, which polarizations are substituted for by the effect of the introduced imaginary ethylene-linkage with charges $(1-i)$ and $-(1+i)$. For the convenience of the estimation of the number of resonance structures of the ^1L_a- and ^3L_a-states and of the visualization of the excited states in terms of chemical resonance structures, the polarization among mutually neighboring atoms and imaginary ethylene-linkage are considered to be of the ^3L_a-type judging from their small dipole strength. The polarization

including the *-group and imaginary ethylene-linkage is considered, on the basis of their strong dipoles, to correspond to the ^1L_a-type. The former model of resonance is pictured as if individual dipoles are embedded in combined benzene nuclei independently. The latter model of the ^1L_a-type is pictured as if the electric current flows on the twisted loop along the perimeter of the benzene nuclei and their combining imaginary ethylene-linkage. Their types of polarization are applied to phenes and other higher condensed compounds, where they are developed to be converted into symmetric pseudo-acenes, which process will be referred to in later sections.

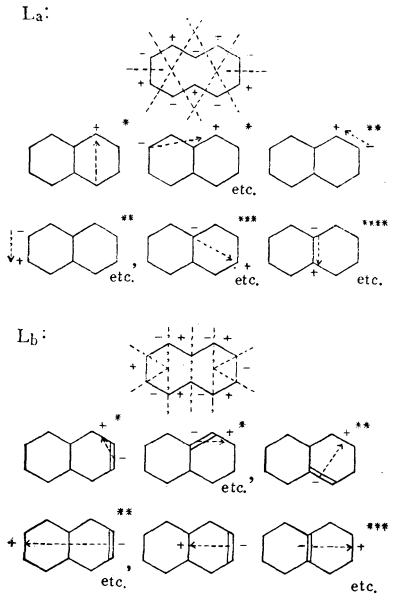

Fig. 3. Resonance structures of naphthalene corresponding to the L_a- and L_b-polarized state.

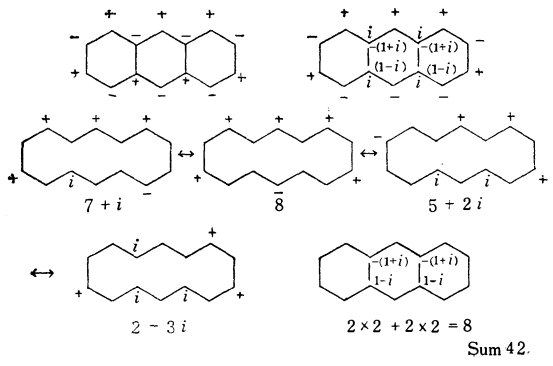

Fig. 4. Resonance structures of anthracene corresponding to the ^1L_a-polarized state, eliminating the effect of cross-linking carbon atoms by introducing the imaginary vector *i*.

Resonance Structures Corresponding to L_b-Levels.—The L_b-state is considered to be the case where the nodal cuts fall on the atoms or where the nodes are located on the middle point of individual bonds in Platt's model. It is pictured by removing charges on the atoms a half bond length along the perimeter in order to locate them on the middle point of the bonds.

In the usual representation of resonance structures, two ways are considered to remove the charge on the cross-linking atoms among the cross-linking bonds and their neighboring bonds. It seems to be a problem of the conjugation of four imaginary atoms which combine in two benzene nuclei. In order to solve this problem, the modified model will be re-examined. We remove unit charges on the atoms in that model corresponding to the ground state a half bond length along the perimeter of the twisted loop in one direction so as to locate them on the middle point of individual bonds, as is illustrated in Fig. 5. The conjugations of four imaginary atoms are then switched as they are in the case of the b-state. For example, an anthracene molecule is used which possesses a meso-position where the charges are considered to be somewhat localized in the ground state. Then, we remove the unit charges which are on the atom in order to locate them on the middle-point of bonds. It is considered that charges flow along the perimeter of the molecule by polarization and that the excitations are caused in the same locations as in the ground state, thus separating the solutions of the b-state from those of original Platt's model. The imaginary path among meso-positions does not alter the path-length compared to the case in which they are not imagined, as with the a-state.

We switch the four imaginary atoms in the b-state to locate them on bonds in one direction in order that, in the switched two-benzene nuclei and in the half-benzene nuclei in the meso-position, the current will flow in the same direction, giving angular momentum with an opposite vector towards the molecular plane that would be mutually cancelled if they are separated. This gives the features of the L_b-state, which is not such a strongly-polarized state. Using this procedure for other acenes, the perimeter-lengths and the $\bar{\nu}$ values of the L_b-state given on Table I are obtained from Eq. 5. We will represent this L_b-polarized state with the chemical resonance structures shown in Fig. 5 and Fig. 6. In Fig. 5, the location of the + and − charges on the bond is interpreted as meaning that if we fix the bond there, we can hold the residual part of the molecule in the canonical Kekulé structure.

TABLE II

Name of substance	Index number	Imaginary perimeter length (l) in unit of mean carbon-carbon distance and estimated values of $\bar{\nu}$ in cm^{-1} unit			
		l_{La}	† $\bar{\nu}^1_{La}$ $\alpha_1=0.775$	$\bar{\nu}_{La}$ $\alpha_{cg}=1.0$	$\bar{\nu}^3_{La}$ $\alpha_3=1.225$
			cm^{-1}	cm^{-1}	cm^{-1}
Naphthalene	2	$(8+2\alpha^2)+2\alpha i$	35460 35000*	29690 28200*	24300 21300*
Anthracene	3	$(10+4\alpha^2)+4\alpha i$	26450 26700*	20920 20700*	15430 14700*
Naphthacene	4	$(12+6\alpha^2)+6\alpha i$	20970 21000	15450 15500*	11200 (10000)* est
Pentacene	5	$(14+8\alpha^2)+8\alpha i$	17330 17300*	12390 11800*	8800 (6300)* est
Phenanthrene	7	$(8.5+3\alpha^2+\alpha\beta)+(3\alpha+\beta)i+2r$ or $(7.5+3\alpha^2+2\alpha\beta)+(5\alpha+2\beta)i+2r$	33000 $\beta\fallingdotseq 0.4$ 33000*	28710 $\beta\fallingdotseq 0.18$	23080 $\beta\fallingdotseq 0$ 21600**
1,2-Benzo-anthracene	10	$(10.5+5\alpha^2+\alpha\beta)+(5\alpha+\beta)i+2r$ or $(9.5+5\alpha^2+2\alpha\beta)+(7\alpha+2\beta)i+2r$	27530 $\beta\fallingdotseq 0.21$ 27300*	20170 $\beta\fallingdotseq 0.065$	15520 $\beta\fallingdotseq 0.016$ 16500**
Chrysene	8	$(8+4\alpha^2+4\alpha\beta)+3(2\alpha+\beta)i+4r$	31200 $\beta\fallingdotseq 0.3$ 30200*		19800**
1,2-5,6-Dibenzo-anthracene	11	$(10+6\alpha^2+4\alpha\beta)+(8\alpha+3\beta)i+4r$ or $(11+6\alpha^2+2\alpha\beta)+(6\alpha+2\beta)i+4r$	26100 $\beta\fallingdotseq 0.15$ 28400***	19920 $\beta\fallingdotseq 0.03$	15870 $\beta\fallingdotseq -0.03$ 18100****

Name of substance	Index number	Imaginary perimeter length (l) in unit of mean carbon-carbon distance and estimated values of $\bar{\nu}$ in cm^{-1} unit			
		l_{Ba}	$\bar{\nu}^1_{Ba}$ $\alpha_1=0.995$	l_{Lb}	$\bar{\nu}^1_{Lb}$ $\alpha=1.05$
			cm^{-1}		cm^{-1}
Naphthalene	2	$(9-2\alpha^2)-2\alpha i$	58060 59800*	$(8+2\alpha^2)+2i$	29400 32200*
Anthracene	3	$(12-4\alpha^2)-4\alpha i$	53700 53700*	$(10+2\alpha^2)+2i$	28000 (28000)*est
Naphthacene	4	$(15-6\alpha^2)-6\alpha i$	47180 47400*	$(12+2\alpha^2)+2i$	26870 (25500)*est
Pentacene	5	$(18-8\alpha^2)-8\alpha i$	41280 —*	$(14+2\alpha^2)+2i$	25390 24000*
Phenanthrene	7	$(11-3\alpha^2-\alpha\beta)-(4\alpha+2\beta)i+r$ $(10-\alpha^2+\alpha\beta)-(2\alpha+\beta)i+r$	53100 $\beta=0.22$ 53400*		

† α_1, α_3 and $\alpha_{c.g}$ are corresponding to the coefficient of imaginary charge-separation at the cross-linking carbon atoms which hold the following mutual relations:

$$\alpha_1+\alpha_3\fallingdotseq 2\alpha_{c.g} \qquad \bar{\nu}^1_{La}+\bar{\nu}^3_{La}\fallingdotseq 2\bar{\nu}_{c.gLa}$$

* H. B. Klevens and J. R. Platt, *J. Chem. Phys.*, **17**, 481 (1949).

** D. S. McClure, ibid., **17**, 905 (1949).

*** E. Clar, "Aromatische Kohlenwasserstoffe", Zweites Band, Springer Verlag, Berlin (1952).

Because the charge is re-located to the neighboring bond through the twisted path, the polarized structures or the position of the bonds that are negatively charged, for instance, become different from those made from the untwisted path along the perimeter. For that reason, the + and − polarizations which occur in ordinary forms are inhibited in order to hold the residual part in the Kekulé canonical form. The polarizations are allowed mainly in the same benzene nucleus or in the neighboring nuclei, and the long-range polarizations among the separate benzene-nuclei are not allowed for the most part, illustrating that, in the L_b-type, the polarizations occur mainly in the same benzene nucleus, so that each

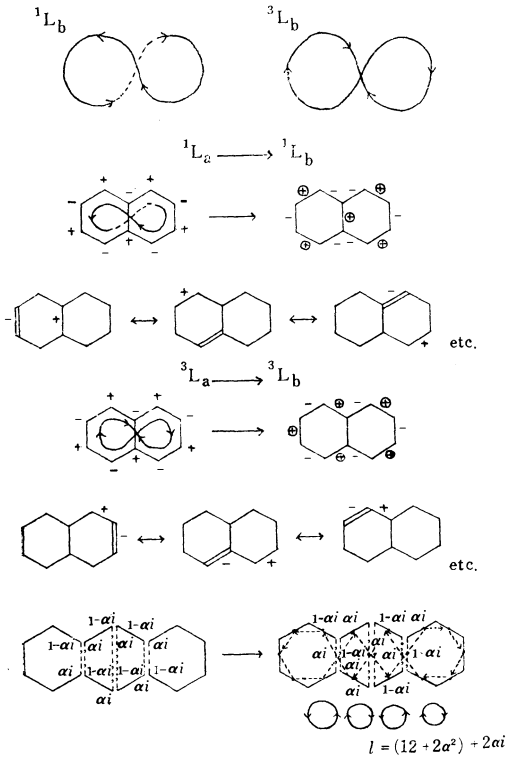

Fig. 5. Resonance structures corresponding to the ^1L_b- and ^3L_b-polarized state of naphthalene.

elementary dipole is canceled in that nucleus. It is suggested that, therefore, the strength of absorption in the position where polarization occurs is very similar to that where ^3L_a-type polarization occurs. Therefore, it is easily supposed that the numbers of resonance structures corresponding to ^3L_b-type polarizations are nearly equal to those corresponding to the ^1L_b-state. The sum of the elementary dipoles of individual structures described in Fig. 3 possesses only a longitudinal component and is small compared to the case of ^1L_a; similarly, each sum of the *-, **- and ***-asterisked groups possess only a longitudinal component and are small.

The general diagram for determining the number of th resonances of ^1L_b- and ^3L_b-structures is shown in Fig. 6. The same relation has been found for phenes and for other circular molecules when they are converted into pseudo-acenes. We can find the numbers of Kekulé resonance structures of the ^1L_b- or ^3L_b-type for acenes and phenes, the estimations of the position of polarization and the method of the estimation of the resonance numbers being like those in the case of ^3L_a.

The Estimation of Resonance Structures Corresponding to the L-State.—In the case of ^1L_a-

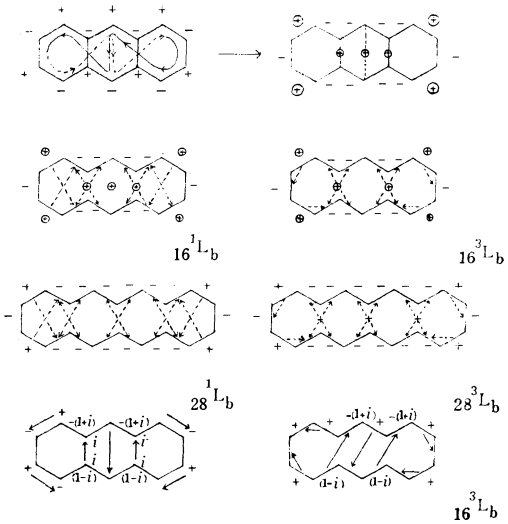

Fig. 6. Resonance structures corresponding to the ^1L_b- and ^3L_b-polarized state of anthracene converted by the half-bond length removal along the perimeter from the polarization diagram corresponding to the ^1L_a-polarization.

polarization, those among neighboring atoms are principally inhibited, except those in the case of imaginary ethylene, as has been stated in a preceding section. The estimated numbers of resonance structures (N_{L_a}) of polyacenes are illustrated in Table III. The correlation of $\log(N_{L_a}/N)$ with $\bar{\nu}_{L_a}$ is illustrated in Fig. 7. They retain the straight-linear relation in Eq. 4 with gradients of 69 kcal./mol. Phenes are transformed into pseudo-polyacene by introducing the charge rotation vector which is illustrated in Fig. 8.

After this procedure, the charges on the (g), (h), and (i) atoms become $-\boldsymbol{r}$, $\boldsymbol{r}$ and $-\boldsymbol{r}$. That on the $(l+f')$ atom becomes $1+\boldsymbol{r}$ where it is assumed that $i\times\boldsymbol{r}$ is equal to zero. Therefore, the separation of the imaginary ethylene-linkage with the charges $(1-i)$ and $-(1+i)$ charges the charge on the superposed cross-linking atoms $(l+f')$ to $(i+\boldsymbol{r})$ and that on atom (k) to i. The number of resonance structures is estimated to be (N), which is enumerated without a vector and multiplied by $\boldsymbol{r}$ or $N\times\boldsymbol{r}$ where one of the two atoms is labeled with vector $\boldsymbol{r}$, and is estimated to be $N\times\boldsymbol{r}^2$ or N where both atoms are labeled with vector $\boldsymbol{r}$. For instance, the numder of resonance structures corresponding to polarization between atoms (g) and (b) is estimated to be $N_{gb}\times\boldsymbol{r}$, while that between (g) and (h) is estimated to be $N_{gh}\times\boldsymbol{r}^2$ or N_{gh} where N_{gb} is the number of resonance structures corresponding to those between atoms (g) and (b) in the ordinary phenanthrene molecule.

TABLE III

Index No.	Name of substance	Number of resonance structures of respective state				
		^1L_a	^3L_a	^1L_a*	^1L_b	^3L_b
1	Benzene	3	3	3	3	3
2	Naphthalene	15	10	15	8	8
3	Anthracene	42	24	42	16	16
4	Naphthacene	93	48	93	28	28
5	Pentacene	178	85	178	41	41
6	Hexacene	—	—	—	—	—
7	Phenanthrene	$22+10i+7r$	$15-2i+3r$	$27+8r$	$18-4i$	$19+i+3r$*
8	Chrysene	$42-3i+19r$	$26-3i+14r$	$56+12r$	$39-9i$	$34+4i+10r$*
9	3,4-Benzo-phenanthrene	$46+2i+23r$	$26+6i+10r$	···	$34+12i$	$34+12i$*
10	1,2-Benzo-anthracene	$69+9i+12r$	$36-3i+8r$	$53+40r$	$34+5i$	$35+i+3r$*
11	1,2-5,6-Dibenzo-anthracene	$84+16i+47r$	$47+10i+13r$			
12	Naphthoanthracene	$97+20i+36r$	$50+3i+8r$			
13	1,2-Benzotetracene	$110+21i+44r$	$74+4i+5r$			
14	1,2-Benzopentacene	$243+17i+70r$	—	$171+80r$		
15	Triphenylene	$35+34i+38r$	$17+9i+13r$		$24+24r$*	
16	Pyrene	$45+18i+21r$	$25+12r$	48	$10+20r$*	
17	Coronene	$118+18i+48r$	$74-6i+34r$		$122+28r$*	
18	Anthanthrene	—	—			
19	Naphtho anthanthrene	—	—			
20	Perylene	$129+11i+48r$	$12-6i+48r$			
21	Peropyrene	—		$260+48r$		

* Number of resonance structures of ^1L_b or ^3L_b obtained by the conversion following Fig. 12.

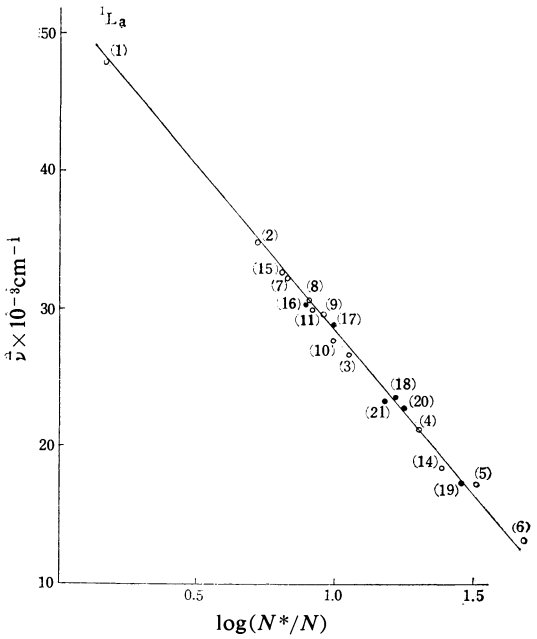

Fig. 7. Correlation of $\bar{\nu}_{^1L_a}$ with $\log(N_{L_a}/N)$, keeping the linear relation with a gradient of about 69 kcal./mol.

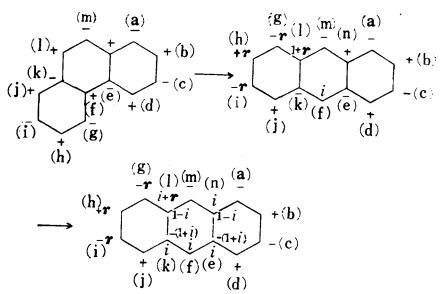

Fig. 8. Estimation of the number of resonance structures of phenanthrene converted by rotation to pseudo-anthracene corresponding to L_a-polarization.

In this way, the numbers of resonance structures corresponding to the ^1L_a-state of phenanthrene, benzoanthracene, benzotetracene, and benzopentacene are estimated in Table III.

As for the chrysene and 1,2-5,6-dibenzoanthracene molecules, which are transformed into pseudo-naphthacene and pseudo-pentacene by separating the charge at the joint of the concaved benzene, the imaginary charge densities on the new joint become $i+r$ and $i-r$

respectively. In the cases of pyrene, perylene, and coronene, the transformations are convert them into pseudo-tetracene, pseudo-pentacene, and pseudo-hexacene. Their numbers of resonance structures are illustrated in Table III. When the $\log(N_{L_a}/N)$ of the above compounds is plotted versus $\bar{\nu}_{L_a}$, they keep the straight-linear relation set forward in Eq. 4 and illustrated in Fig. 7.

The Estimation of the Number of Resonance Structures Corresponding to the ^1L_a-Type Polarization of Acenes and Circular Molecules.— The above procedure for estimating the number of resonance structures corresponding to ^1L_a has been devised for acenes and phenes or for long-shaped hydrocarbons with inner ethylene-linkage. All these molecules have been converted to acenes by imaginary separation and rotation. However, it is very difficult, using the above procedure, to reduce such circular molecules as pyrene, triphenylene, and coronene to pseudo-acenes. They become pseudo-acenes only after complicated trials. Therefore, another approximation method for estimating the number of resonance structures has been devised; it is illustrated in Fig. 9.

The cross-linking carbon atoms of acenes and other molecules are separated into two imaginary atoms with charges of i and $(1-i)$, leaving the inner ethylene-linkage with a charge of $(1-i)$, etc. Then, it is converted into hexagon by rotation. For instance, in the anthracene molecule (A), the imaginary carbon atoms with a charge of i in the cross-linking positions on the perimeter are converted into the structure (B) in Fig. 9 by rotation perpendicular to the molecular plane; after this procedure, the atoms in the meso-position are converted into structure (C) by rotation in the second step. In the first-step rotation, the charges i on the cross-linking position are converted to $i \times \boldsymbol{r}$, which is equal to zero owing to the orthogonality of both vectors defined. In the second-step rotation, the meso-carbon atoms which are rotated in the first-step procedure are afflicated by the second-step rotation. Therefore, the charges of meso-atoms in the converted positions are equal to $\boldsymbol{r}^2$ or 1. Therefore, we select two atoms with alternative + and − signs on the new perimeter to form the polarized resonance structures except for those between neighboring atoms. The number of resonance structures corresponding to the ^1L_a-state is estimated to be the sum of all those mentioned above and of those of two ethylene-linkages.

In the case of phenanthrene as an example of a convex molecule, the charge separations in the concaved positions are different from those in acenes, and the four linked carbon

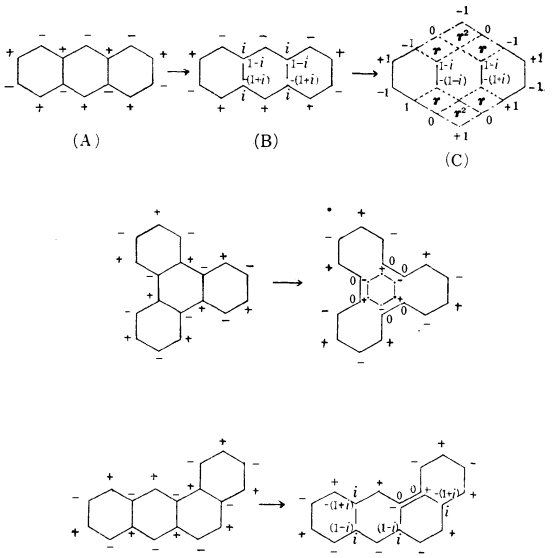

Fig. 9. Estimation of the number of resonance structures of those acenes and phenes corresponding to ^1L_a-polarization by rotation and by imaginary charge separation.

atoms are separated as in butadiene, as is illustrated in Fig. 9. The same example is an instance of a triphenylene molecule. The charge-separation in the concaved positions leaves six carbon atoms linked as a benzene nucleus, with charges alternately signed by $(1-i)$ and $-(1+i)$. The numbers of resonance structures in the case of phenanthrene are the sum of the 26 structures with atoms on the perimeter and of the 8 separated structures with inner butadiene. The number of resonance structures in the case of the triphenylene molecule is the sum of the 51 structures concerning atoms on the perimeter and of the 6 structures concerning atoms on the inner benzene nucleus.

1,2-Benzoanthracene is converted into pseudo-anthanthrene, which is further converted into a hexagon, leaving one imaginary butadiene and one imaginary ethylene inside the molecule. The number of resonance structures concerning the perimeter is equal to $45+18\,\boldsymbol{r}$, while those concerning the inside dienes and ethylene are equal to 20. The pyrene molecule is converted into outer and inner structure. The number of resonance structures concerning atoms on the perimeter is equal to 43 and those concerning the inner conjugation are 5, as has been mentioned above. The total number of resonance structures is equal to 48 in the pyrene molecule. The correlation of $\log(N^*_{L_a}/N)$ versus $\bar{\nu}_{L_a}$ is illustrated in Fig. 7 by the black spot. The values of the absorption

3) P. G. Carter, *Trans. Faraday Soc.*, **45**, 597 (1947).

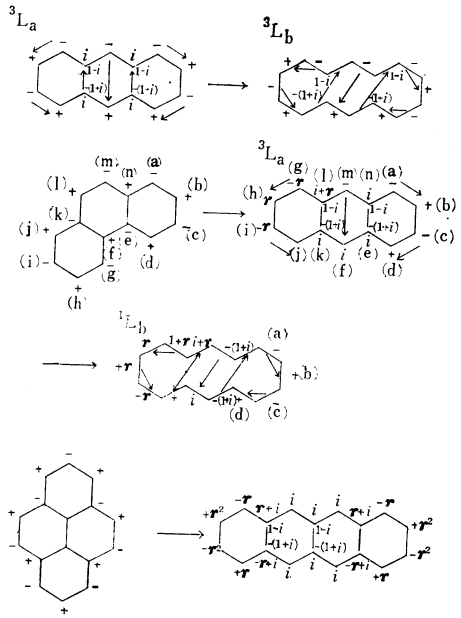

Fig. 10. Estimation of the number of the resonance structures crresponding to ^1L_b- and ^2L_b-polarization from those corresponding to ^3L_a-polarization.

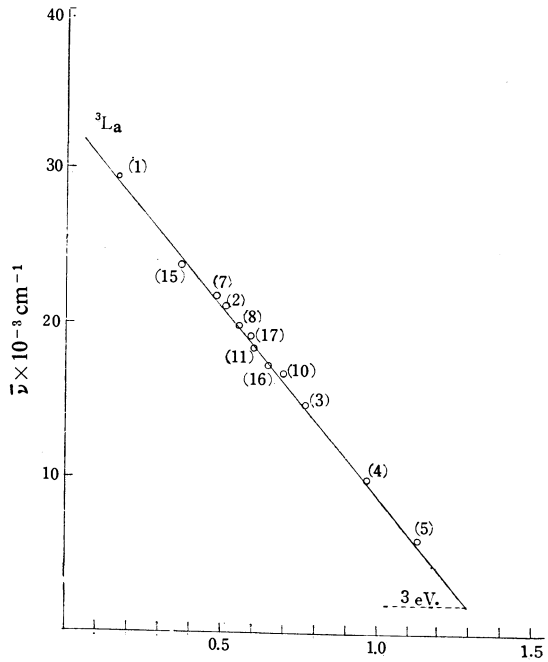

Fig. 11. Correlation of the $\bar{\nu}_{^3La}$ value of the polycyclic aromatic hydrocarbons with their log ($N_{^3La}/N$).

energies $\bar{\nu}_{La}$ are mostly based on the data of Klevens and Platt[1]. Those of coronene, pyrene, peropyrene, etc. are based on the data on p-bands reported by Clar and on those of Matsen[4].

The Estimation of the Number of Resonance Structures Corresponding to the ^3L_a-Polarized State.—The preceding section has discussed how the resonance structures of the naphthalene molecule are classified into groups which possess different sums of elementary dipoles. One of those groups, that whose polarizations are among neighboring atoms and an imaginary ethylene-linkage, possesses too small an electric dipole to be classified as the ^3L_a-state. The ^3L_a-type of polarization is pictured in Fig. 10, where, in the case of anthracene, polarization among meso-positions (9 and 10) is included as the ^3L_a-type.

When the log ($N_{^3La}/N$) of acenes is plotted versus the $\bar{\nu}_{La}$ value assigned in the report of Klevens and Platt, they keep the linear correlation with gradients of 69 kcal./ml. set forth in Eq. 4, which suggests that the above classification of resonance structures corresponding to the ^3L_a-state and the estimation of their number of resonance structures are adequate, as well as the results of oscillator-strength which will be mentioned later.

With a series of phenes, they are transformed into corresponding pseudo-aceness, as in the case of the ^1L_a-state discussed in the preceding section.

Pyrene, coronene, and triphenylene are transformed into pseudo-naphthacene, pseudo-hexacene, and pseudo-naphthacene, as they are in the case of the ^1L_a-state. Their number of resonance structures are given on Table III. The correlation with their log (N_{La}/N) and E_{ST} values given by McClure illustrates the linear relation illustrated in Fig. 11, which is consistent with the same relation in the case of acenes.

The Estimation of the Number of Resonance Structure Corresponding to the ^1L_b-Type Polarization.—The features of chemical resonance structures corresponding to the ^1L_b-level have been mentioned in the preceding section. In these ^1L_b-type resonance structures, + and − polarizations in the separate benzene nuclei do not hold the residual part of molecule in the Kekulé form. Therefore, it seems that there is little difference between ^1L_b- and ^3L_b-type polarizations. The resonance structures corresponding to the L_b-type polarizations of naphthalene and anthracene molecules are illustrated in Figs. 5 and 13. Generally, resonance structures corresponding to ^1L_b-type polarization can be obtained by a half bond-length removal of the charge from atoms to

4) F. A. Matsen, *J. Chem. Phys.*, 24, 602 (1956).

bonds along the perimeter, irrespective of inner ethylene-linkage, from ^3B_a structures.

The number of resonance structures of ^1L_b-type and ^3L_b-type polarizations are approximately equal in acenes, as is illustrated in Table II.

The ^1L_b-type polarization of phenes and other circular-type molecules considered to be in the form of converted pseudo-acenes should be enumerated in such a way as is equal to the number of resonance structures of this polarization in the original molecule multiplied by the charges on polarized atoms in the converted form.

The estimated numbers of resonance structures corresponding to phenanthrene, chrysene, pyrene, etc. are given in Table II. The relation of their $\log(N^1_{Lb}/N)$ and $\log(N^3_{Lb}/N)$ to the

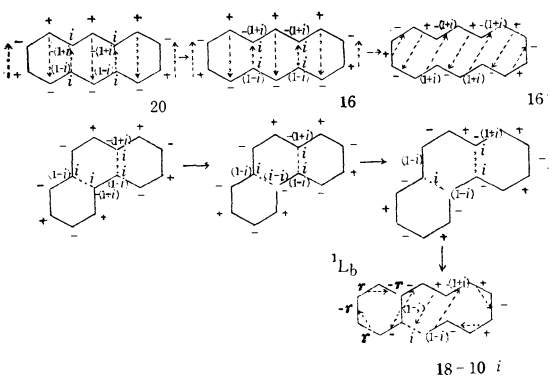

Fig. 12. Relations and estimation of the number of the resonance structures corresponding to ^1L_b, ^1B_b, and other types of resonance structures.

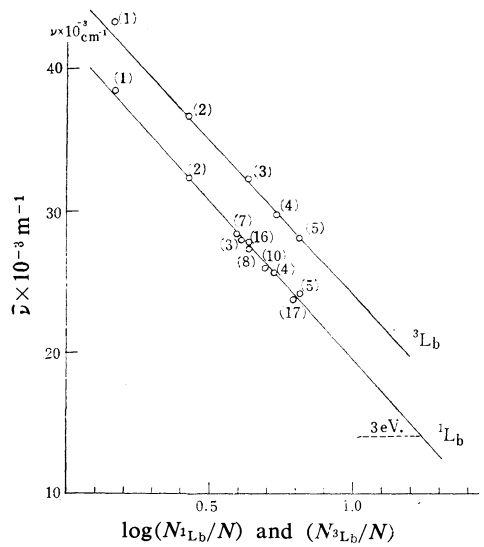

Fig. 13. Correlation of $\bar{\nu}^1_{Lb}$ and $\bar{\nu}^3_{Lb}$ values with their $\log(N^1_{Lb}/N)$ and $\log(N^3_{Lb}/N)$ values respectively.

absorption energies of these levels, $\bar{\nu}_{Lb}$ and $\bar{\nu}_{Lb}$, is illustrated in Fig. 13. They are satisfied by the linear correlations described in Eq. 4. These $\bar{\nu}$ values are mostly based on data of Klevens and Platt[1]. Those of pyrene and coronene are based on the data concerning the energies of α-bands obtained by Clar[5]. The ^1L_b-absorptions of these compounds correspond to those assigned as α-bands by Clar[5], while the p-bands assigned by him correspond to the ^1L_a-absorption.

These results suggest that the assumptions concerning resonance structures of the ^1L_b and ^3L_b states are reasonable.

Results and Discussion

The foregoing results support our assumptions concerning the chemical features of individual excited states, which are represented in terms of hybrid resonance structures corresponding to the characteristic polarization of standing waves of individual excited states, as well as the validity of Carter's empirical equation for the estimation of the empirical resonance energies. There is no mixing or confusion of properties in representing L-excited states in terms of chemical resonance structures.

They are considered to be fairly visualized as corresponding to the motion of mobile π-electrons as currents in interpreting Platt's theory.

The complicated absorption peaks of higher condensed aromatic hydrocarbons can be explained and assigned to their respective levels by this approximation method. In general, the α-bands and p-bands assigned by Clar are considered to correspond to ^1L_b-bands and ^1L_a-bands in this case.

Imaginary charges are introduced in order to eliminate the effect of cross-linking and also in order to visualize easily the hybrid resonance structures corresponding to Platt's theory. We have replaced the sign of the standing wave in his theory to that of the real charge in the above discussion. The differences between the L and B types of polarization may be considered to be reduced to the difference in the method of the conjugation of the switch of four imaginary cross-linking carbon atoms with the charge-densities $(1-i)$, i, $(1-i)$ and i. It is assumed that the angular momenta and other characteristic states, shells and configurations are invariant in this operation. In the above procedure, the perimeter length, which may be interpreted as defining the depth and shape of the constant potential box is given in imaginary units,

5) E. Clar, "Aromatische Kohlenwasserstoffe", Zweites Band, Springer Verlag, Berlin (1952).

which may be expected to include the length to the free end-point of the standing wave.

The difference between a and b types of polarization may be interpreted as having been reduced in this model to the difference in the method of the conjugation of individual benzene nuclei considered as independent closed circuits, in either the parallel (twisted loop) or anti-parallel (perimeter loop) direction, which may be considered as producing the difference in synthesized electric dipole-vector or oscillator strength relating to absorption-intensities in their estimation from corresponding resonance structures.

The estimated number of resonance structures corresponding to L_a, L_b, B_a and B_b states are considered as a result of the above discussions to be fairly consistent with Carter's empirical equation in representing the excitation-energies corresponding to the respective polarization as the difference in empirical resonance energies as well as the absorption intensities estimated from the unit-dipoles in the resonance structures which are described above.

Summary

The chemical resonance structures of the excited states are assumed to correspond to the type of polarization in each state. This theory can explain the absorption energies as the difference in the empirical resonance energies between the ground and excited states by an application of Carter's empirical equations. Imaginary charges are introduced to estimate the number of resonance structures, thus eliminating the influence of cross-linking atoms; the meaning of the resonance hybride corresponding to each levels is easily interpreted in correlation with Platt's theory. As a result, the individual excited state can be represented as a chemical resonance hybride consisting of a group of simple polarized structures; this theory may be said to be adequate from the view-point of absorption energies and of absorption intensities in relation to the direction of electric dipoles.

The author wishes to express his hearty thanks to Professor Hideo Akamatu for his kind guidance and encouragement throughout this study and to Dr. Yoshio Matsunaga and Dr. Hidetsuru Matsushita for their kind abvice and discussions. He also wishes to express thanks to Miss Yayoi Ono, Mr. Konosuke Hayashi, and Miss Masako Ogura for their cooperation in the publication of this report.

Department of Chemistry
Faculty of Science
The University of Tokyo
Hongo, Tokyo

The Electrical Properties of Microcrystalline Selenium. I. Chlorine-doped Selenium

By Tsuneo ARAKI

(Received on May 10, 1962)

Several studies have been made of the electrical properties of micro-crystalline hexagonal selenium[1,2]. Most of them have dealt with pure selenium, iodine-doped selenium or bromine-doped selenium. The present series of studies has been undertaken to inquire into the effect of chlorine and metallic impurities on the electrical properties of selenium.

The conductivity of microcrystalline selenium changes greatly as a result of heat-treatment, because nucleation and the crystal growth occur in it[1,3]. In the present study, the electrical conductivity of chlorine-doped selenium is measured as a function of its crystallinity. The thermoelectric power and the capacity variation with various bias voltages were also measured for this substance, and the carrier concentration was calculated according to Schottky's theory.

Experimental

The selenium used in this investigation was purified from five-nine purity selenium obtained

1) H. W. Henkels, *J. Appl. Phys.*, **22**, 1265 (1951).
2) K. W. Plessner, *Proc. Phys. Soc. London*, **B64**, 681 (1951).
3) H. Rebstock and K. O. Seilier, *Z. Naturforsch.*, **9a**, 49 (1954).

from the Mitsubishi Mining Co. The purification was carried out by the following steps: (1) oxidation with nitric acid, (2) treatment with ion exchange resin, (3) reduction with sulfur dioxide, and (4) distillation in vacuum.

This purified selenium was mixed with various quantities of selenium monochloride at 250°C and then quenched by pouring it onto a cooled marble plate to prepare amorphous selenium. The quantity of chlorine was measured by chemical analysis for each specimen, because some doped chlorine escaped during the heat-treatment.

Specimens used for the measurement of resistivity and thermoelectric power were prepared by the hot press method. Namely, chlorine-doped amorphous selenium was ground into powder of 80~120 μ and was pressed for 5 minutes under a pressure of 250 kg./cm^2. The pressing was done between two thin mica sheets placed on electrically-heated plattens which were thermoelectrically controlled at a temperature of 130°C. The shape of the specimen was a disk. 0.5 mm. thick and 10 mm. in diameter.

The specimen for the capacity measurement was pressed on an iron base plate which had been chemically etched and nickel-plated for the purpose of making ohmic contact. The procedure of the treatment was the same as in the hot press method described above. The thickness of the selenium of this specimen was about 0.1 mm. The specimen was crystallized by heat-treatment at 217°C, and then molten Cd-Sn eutectic alloy (m. p. 177°C) was sprayed onto the selenium surface, which was then used as a counter electrode. The simple barrier layer between the selenium and the counter-electrode alloy was formed by this procedure.

The measurement of electrical resistivity was carried out by the four-point probe method, and the Valdes correction was applied for the thin-sheet selenium[4]. A floating potential difference between inner probes was measured by a vibrating-reed voltmeter (internal resistance was about 10^{15} ohm), while the current through the outer pair of probes was about 5~10 μA.

The measurement of the resistivity of the specimen prepared for the capacity measurement was obtained from the voltage drop due to the current through the selenium layer. Results were in fairly good accord with those obtained from the four-point probe method.

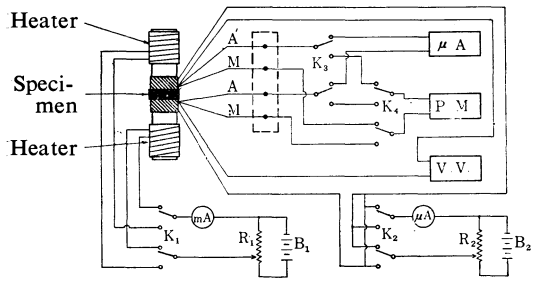

Fig. 1. Experimental arrangements for resistivity and thermoelectric power measurements.

4) L. B. Valdes, *Proc. I. R. E.*, **42**, 420 (1954).

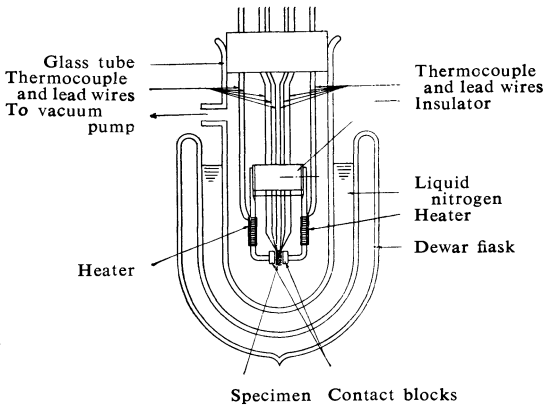

Fig. 2. Experimental arrangements for resistivity and thermoelectric power measurements.

The device used for the measurement of thermoelectric power and resistivity is shown in Figs. 1 and 2. The two points used for the measurement of thermoelectric power were arbitrarily chosen on both sides of the disk. The temperature difference between the two points was measured by an advance and manganin thermocouple. For the thermocouple, a wire homogenous in composition and small in diameter (0.12 mm.) was used, because these conditions reduced the errors due to the thermal conduction. Blocks in contact with the specimen were heated by 0.2-watt coils of of nichrome wire. The surfaces of the blocks were nickel-plated so that their good thermal and electrical contact with the specimen was protected. The temperature difference in a specimen was always maintained within 0.5~1.0°C, and the temperature was measured by a high sensitive potentiometer with an electronic galvanometer (7×10^{-11} A).

The thermoelectric voltage was determined from the measurement of the potential difference between the two advance wires, a high-sensitivity vibrating reed voltmeter being used. All the measurement heads were placed in a vacuum (about 10^{-3} mmHg) in order to reduce the thermal convection and the condensation of water in the measurement at a low temperature. The error in the thermo-electric power measurement was approximately 5 per cent, it was very difficult to maintain the reference junction within 0.02°C even if it was placed in a stirred ice-water bath. Since the resistivity of the specimen became very large at a low temperature, the charge which remained on the surface of the specimen afer the resistivity measurement produced an error in the thermoelectric power measurement. Therefore, these two measurements had to be carried out in different temperature cycles.

The capacity variation due to the bias voltage was measured by the substitution bridge method[5], in which a small AC signal (3 kc./sec., −30 db) was superimposed on the bias voltage.

5) H. Henisch, "Metal Rectifier", Clarendon Press, Oxford (1949), p. 48.

In order to investigate the effect of crystallization time, photomicrographs of the selenium surface were taken. The disk specimen prepared for the resistivity measurement was also used for this investigation.

Results

The results of the resistivity measurement for the specimens containing chlorine in various concentrations are shown in Fig. 3. In this figure, curves a, b, c and d show the resistivity of specimens which were kept for crystallization at 217°C for 0, 20, 60 and 500 min. respectively. The figure shows that there is a resistivity minimum in the curve for each heat treatment. The concentration of chlorine corresponding to the minimum changes with the duration of the heat treatment. The longer the heat treatment the lower the concentration. The observed values for the chlorine-free specimens were smaller than those reported by previous investigators[1,6]. This difference may have been caused by the effect of the atmosphere during the preparation. The specimens in the present experiment were treated in air because they had to be compared with those containing chlorine. Previous investigators had treated them in a vacuum. The present experiment shows that the atmospheric oxygen has some effect on the resistivity of chlorine-free specimens.

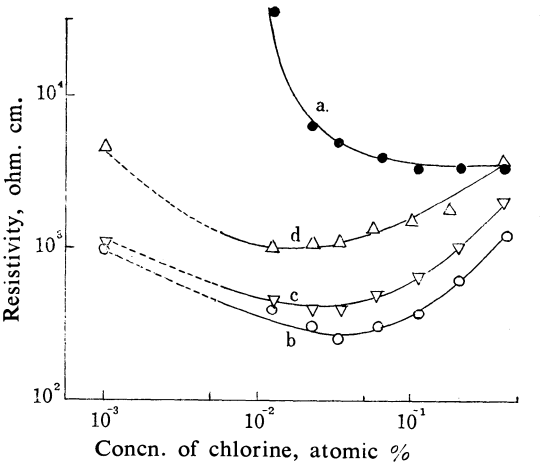

Fig. 3. Resistivity of microcrystalline selenium against chlorine content.

Figures 4 a—d show photographs of the surfaces of specimens which have been kept at 217°C for 20 min. Figures e—f shown photographs of chlorine-free specimens after various durations of heat-treatments, while g

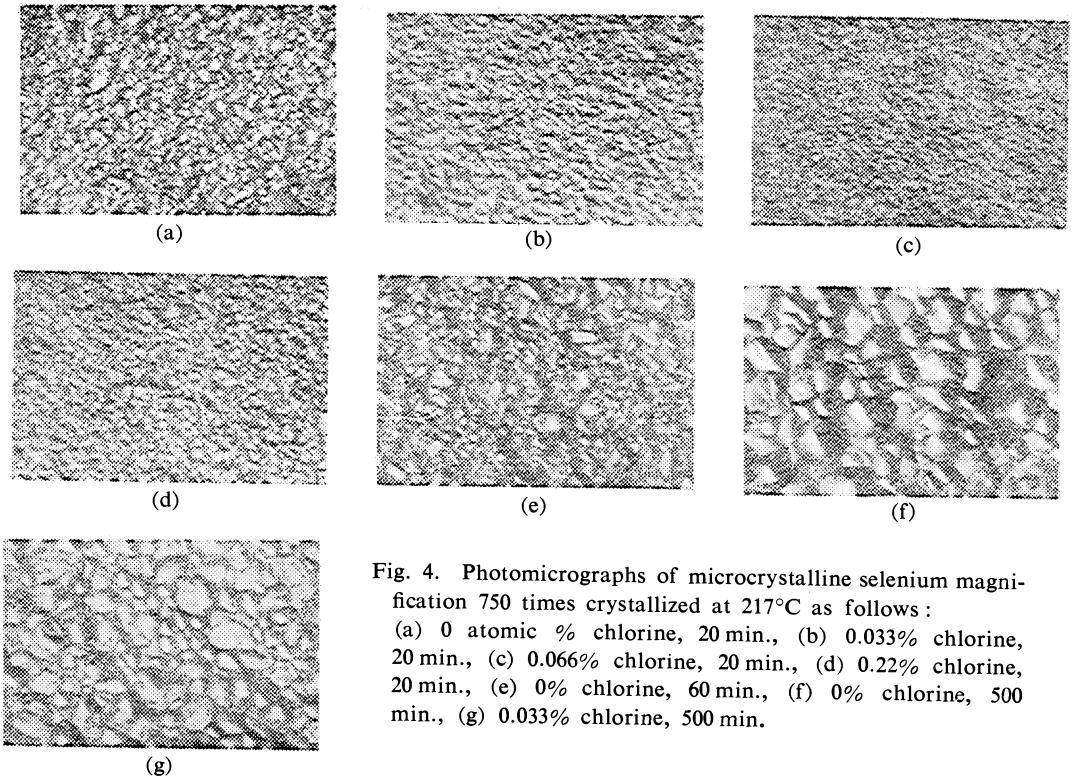

Fig. 4. Photomicrographs of microcrystalline selenium magnification 750 times crystallized at 217°C as follows:
(a) 0 atomic % chlorine, 20 min., (b) 0.033% chlorine, 20 min., (c) 0.066% chlorine, 20 min., (d) 0.22% chlorine, 20 min., (e) 0% chlorine, 60 min., (f) 0% chlorine, 500 min., (g) 0.033% chlorine, 500 min.

6) F. Eckart, *Ann. Phys.*, **14**, 233 (1954); **17**, 84 (1956).

shows a specimen after a 500-min. heat-treatment with the same concentration of chlorine as b. These photographs show that the higher the chlorine concentration, the smaller the grain size, and that the longer the heat treatment, the larger the grain size.

The thermoelectric power for semiconductors of the one-type, non-degenerate carrier is expressed by[7]:

$$Q=Q'+\frac{k}{e}\left[\frac{3}{2}\log T-\log n+\log\left\{\frac{2(2\pi mk)^{3/2}}{h^3}\right\}\right] \quad (1)$$

where k is the Boltzmann constant, n is the carrier concentration, m is the mass of the carrier, and h is the Planck constant. Q' is a number decided by the scattering of the carrier; usually 2 is given for this value for the selenium crystal with simple lattice scattering[8,9]. In the case of selenium containing much impurities, as in this experiment, a larger value of Q' should be used. However, in this report the value 2 was taken for the sake of simplicity. It is well-known that the carrier concentration, calculated from Eq. 1, is in fairly good accord with the results obtained from the Hall effect[9,10].

The carrier concentrations for the specimens were calculated from Eq. 1 and are plotted in Fig. 5. They are scarcely influenced by the chlorine concentration, and their values are in the range of $10^{16}\sim10^{17}/cm^3$.

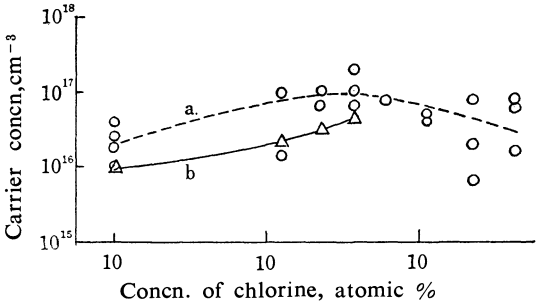

Fig. 5. Carrier concentration against chlorine content.

According to Schottky[11], the carrier concentration near a barrier layer is obtained by the equation:

$$n=2/KeF^2\,dU/d(1/C^2) \quad (2)$$

where $-e$ is the electron charge, F is the surface area, U is the bias voltage, C is the capacity of the barrier layer, and K is the dielectric constant. The dielectric constant for microcrystalline hexagonal selenium at 3 kc. has not yet been reported. In the present calculations, the value of 11 was used for this constant, which is obtained by extrapolation from the data of Hippel[12]. Most of the previous reports[5,13,14] used 6 for this value, but this figure is regarded as that for amorphous selenium.

According to Schottky's[11] theory, the relation between dU and $d(1/C^2)$ is linear for the simple contact between metal and semiconductor. However, it is actually not always linear in the measurement of selenium rectifiers, especially in the neighborhood of zero-bias voltage. Moreover, the relation changes with a lapse of time. The diffusion of the counter-electrode element to the selenium layer or the chemical reaction of these elements has been suggested as the cause of this change[15]. For this reason, the capacity measurement was carried out immediately after the counter electrode was applied.

The carrier concentrations obtained by the capacity measurement are plotted by curve b of Fig. 5. The values are somewhat smaller than those obtained from the thermoelectric power. The variation of specific resistivity with temperature is shown in Fig. 6. Curves, a, b and c, stand for the chlorine-free specimens crystallized by 20-, 60- and 500-min. heat treatments respectively. Each specimen increases

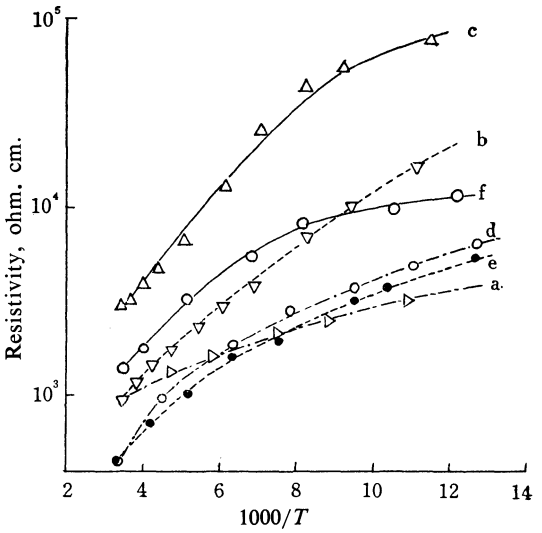

Fig. 6. Resistivity against temperature.

7) V. A. Johnson, "Progress in Semiconductors I", Heywood, London, (1954), p. 68.
8) H. W. Henkels, *J. Appl. Phys.*, **22**, 916 (1951).
9) K. W. Plessner, *Proc. Phys. Soc.*, **B64**, 671 (1951).
10) H. W. Henkels, *Phys., Rew.*, **77**. (1950).
11) W. Schottky, *Z. Phys.*, **118**, 539 (1942).
12) A. R. V. Hippel, "Dielectric Materials and Application", J. Wiley & Sons, New York, 301 (1954).
13) E. Eckart and A. Schmidt, *Ann. Phys.*, **16**, 134 (1955).
14) Y. Moriguchi and A. Okazaki, *Proc. Phys. Soc.*, **B70**, 991 (1957).
15) J. Yamaguchi, *J. Phys. Soc., Japan*, **10**, 234 (1955).

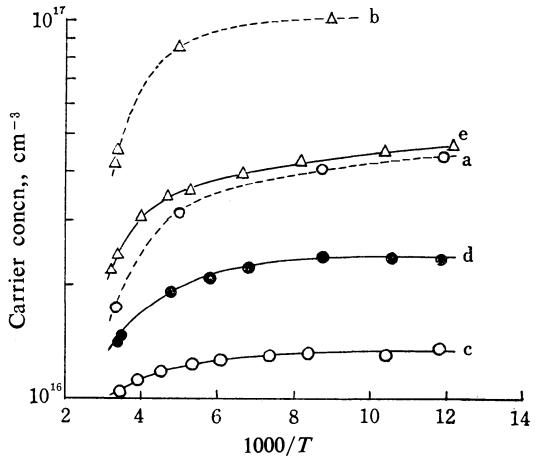

Fig. 7. Carrier concentration against temperature.

its resistivity at a low temperature. The resistivity does not change linearly with $1/T$. The gradient becomes slow at low temperatures. The gradient for the chlorine-free specimen becomes steep with the longer heat treatment, but that for the specimen containing chlorine was not so steep.

The carrier concentrations in the specimens after a 20-min. heat-treatment are shown in Fig. 7. Curves a and b show the results obtained from the thermoelectric power measurement of the chlorine-free and the chlorine-doped specimens respectively.

The temperature variation in carrier concentration obtained from capacity measurements is shown in curves c, d and e of Fig. 7. The results obtained from these two methods show nearly the same tendency. The gradient is steep at room temperature and becomes slow at a low temperature.

Discussion

The resistivity of selenium was at its minimum at a concentration of chlorine. The minimum value varied with the condition of the heat treatment, as is shown in Fig. 3. This fact has been noticed by Schweickert[16], and the results of the present experiment are in good accord with his report.

According to the microscopic observation, the grain size of selenium was affected by the chlorine concentration and by the heat treatment condition, as is shown in Fig. 4. It is well-known that the crystallization usually depends on two factors; (a) the nucleation rate, and (b) the grain-growth rate. The fact that the grain size of the specimen containing chlorine is small shows that the contamination with chlorine promotes the creation of crystalline nuclei. On the other hand, the heat treatment increases the grain-growth rate. The crystallization of selenium from the amorphous to the hexagonal state decreased the resistivity at the beginning of the heat-treatment. However, the resistivity increased gradually again as a result of the long heat treatment. Schweickert has suggested that the chlorine was very loosly bound to the selenium and so was apt to escape from the surface of the specimen during the heat treatment. It was also seen that pure selenium increased its resistivity gradually as a result of the long heat treatment. Henkels[1] suggested that the increase in resistivity is due to the purification process by crystal growth, while Rebstock and Seiler[3] suggested that it is due to the decrease in inter-crystalline volume during the heat treatment.

The addition of chlorine did not increase the carrier concentration in selenium, which remained at an almost constant value in the range of $10^{16}\sim10^{17}/cm^3$. This tendency is similar to that reported in an experiment on selenium containing iodine or bromine performed by Henkels[1] and Plessner[2].

According to the measurements by Henkels[8] and Plessner[9], the selenium single crystal prepared from the liquid or vapor phase had a carrier concentration in the range of $10^{13}\sim10^{14}/cm^3$. Plessner considered that the acceptor centers in selenium did not consist of "impurities" in the form of foreign atoms, but only of imperfections in the selenium crystal lattice. He also considered that most of the chlorine atoms doped in selenium were concentrated in the grain boundary and had an effect on the mobility. However, the mobility calculated from the resistivity and the carrier concentrations is less significant.

According to Nijland[17], the carrier concentration obtained from the Hall coefficient corresponds to the value of a well-conducting phase; on the other hand, that obtained from thermoelectric power corresponds to the value of a low-conducting phase which surrounds the well-conducting phase. Meanwhile, the carrier concentration obtained from the capacity variation due to bias voltage is that near the barrier layer or that in the space-charge transition region itself. Henkels[11] reported that the carrier concentration of selenium obtained from the capacity measurement was not in accord with that obtained from the thermoelectric power or from the Hall coefficient, but details were not reported in his paper.

16) H. Schweickert, *Z. Phys.*, **128**, 47 (1950).

17) L. N. Nijland, *Philips Res. Rep.*, **9**, 259 (1954).

According to Moriguchi[18], the carrier concentration, which was obtained from the capacity measurement for the commercial selenium rectifier, decreased at low temperatures. Therefore, he considered that the mechanism of the barrier layer in the rectifier was very complicated and was not suited for the calculation of its carrier concentration. However, the carrier concentration obtained from the capacity measurement in the present experiment increased at low temperatures, This result was in fairly good accord with that obtained from the thermoelectric power. The present agreement seems to come from the methods of preparing the specimens. Both specimens were prepared from the same selenium material, and the measurement of capacity was carried out immediately after the application of the counter electrode for the purpose of avoiding the formation of other complicated barrier layers.

The resistivity of all the specimens for the present experiment increased at low temperatures. However, it was doubtful whether this resistance was caused by the real bulk resistivity of selenium. The resistance showed departures from Ohm's law at the low fields, and it was supposed that there were some barrier layers. Rebstock and Seiler[3] reported that the resistivity of microcrystalline selenium measured at a high frequency was not so much increased at a low temperature; they considered that the increase of DC resistivity at the low temperature was caused by the grain boundary of microcrystalline selenium. For these reasons, the apparent decrease in mobility calculated from the resistivity and the carrier concentration, especially at a low temperature, might not occur in the bulk phase but might be caused by the intercrystalline structure.

18) Y. Moriguchi, *Kurume Univ. Journal (Nat. Sci.)*, **6**, 9 (1955).

Summary

1. The resistivity of microcrystalline selenium doped with chlorine was changed by heat treatment. The results were in fairly good accord with the measurements obtained by Schweickert. Selenium doped with chlorine had the same characteristics as that doped with iodine or bromine.

2. The results of microscopic observation showed that the grain size became smaller with the higher chlorine concentration. This tendency was similar to that found in iodine- or bromine-doped selenium.

3. The resistivity variation with temperatures below room temperature was affected by the heat treatment of the specimen. The effect was greater for the specimen free from chlorine.

4. Carrier concentrations were obtained from the measurement of capacity and also from the thermoelectric power. These two methods gave results which were in agreement with each other. The concentrations were shown to be increased at low temperatures.

The author wishes to express his thanks to Dr. Takehiko Shimanouchi of The University of Tokyo and to Dr. Juichi Osawa, Dr. Yukimatsu Takeda, Dr. Sueo Hattori, Mr. Yoshinori Mihara and Dr. Yoshiro Moriguchi of his company for their kind advice throughout this work. The author is also grateful to Mr. Shuzaburo Imai and to Mr. Makoto Saito for the preparation of specimens.

Semiconductor Engineering Department
Electronic Components Joint Division
Nippon Electric Company
Kawasaki

The Behavior of Fission Products Captured in Graphite Powder by Nuclear Recoil. VI. The Chemical State of Iodine-131 Diffused out from Graphite, Uranium Dioxide and Thorium Dioxide

By Seishi YAJIMA, Koreyuki SHIBA and Muneo HANDA

(Received June 22, 1962)

A large portion of the enormous energy of nuclear fission is converted into the kinetic energy of nuclear fission fragments. This energy forces the fission fragments to move in the material, in which the kinetic energy is finally absorbed in the form of heat. The range of the fission products is about 5 μ in uranium dioxide and about 12 μ in graphite. Within this short distance, about 0.8 MeV. of the fission fragment energy is imparted to the material, violently disturbing the arrangement of atoms in the material; the fringes of a fragment track are instantly heated to an extremely high temperature. Such a track is called a thermal spike. The chemical behavior of the fission products in the thermal spike belongs to the field of hot atom chemistry. The authors have studied the diffusion of krypton, xenon, tellurium, and iodine trapped in graphite by fission recoil, thus clarifying the following facts. The diffusion rates of the above elements in natural graphite were much larger than in artificial graphite[1]. The diffusion of xenon in graphite was found as not governed by a simple diffusion mechanism, but to depend on the state of imperfection in the graphite crystal[2]. The distribution of the activation energy of xenon diffusion in natural graphite was determined by making a heating curve of xenon-133 or -135 in natural graphite. The distribution of the activation energy shifted to a higher temperature with an increase in the fission product concentration in the graphite[3].

These studies were carried out in connection with the development of a semi-homogeneous fuel in which uranium dioxide or uranium carbide is dispersed in graphite. In the present investigation, the chemical states of the fission fragment iodine-131 diffusing out of uranium dioxide and thorium dioxide and diffusing after being caught by fission recoil in graphite, were studied by means of thermochromatography. The primary fission yield of iodine-131 from uranium-235 (n, f reaction) and thorium-232 (γ, f reaction) is so small that it has little chance to react with the material surrounding the recoiled iodine-131 track in the hot atom state, but it is still of interest to study the diffusion behavior of the iodine-131 generated by its precursor, on account of the high chemical affinity of the iodine-131 and the thermal spike. The results obtained show that the chemical state of the iodine-131 diffusing out of uranium dioxide and graphite was not that of an elementary iodine (I^0) but of iodide (I^-), and that, irrespective of the diffusing matrix concerned, the iodide species were fairly stable at high temperature and deposited on the graphite powder heated to 500~600°C in an argon atmosphere. These facts should be useful in developing an internal trap for the semi-homogeneous fuel element whose features are high burn-up and high temperature.

Experimental Method and Results

Preparation of Samples.—*Sample No. 1 (Uranium Dioxide Powder Containing Fission Products).*— Uranium dioxide powder of a particle size of less than 1 μ was reduced with hydrogen for 5 hr. at 1000°C to obtain a stoichiometric uranium dioxide. About 100 mg. of this uranium dioxide was sealed in a polyethylene bag placed in a glove box filled with nitrogen gas. Then it was neutron-irradiated in the reactor JRR-1 (water-boiler type, thermal neutron flux: about 5×10^{11}n/cm^2·sec.) for 15 hr.

TABLE I. ANALYTICAL DATA OF IMPURITIES IN URANIUM DIOXIDE AND THORIUM DIOXIDE

	Sample	
	Uranium dioxide	Thorium dioxide
Content	99.85%	99.91%
Alkalies and alkaline earths	0.13%	—*
Heavy metals (Pb)	0.005%	—*
Fe_2O_3	0.013%	0.008%
Cl^-	0.004%	0.004%
NO_3^-	Trace	—*
SO_4^{2-}	0.002%	0.07%

* Not analyzed

1) T. Nakai, S. Yajima, K. Shiba, J. Osugi and D. Shinoda, This Bulletin, 33, 497 (1960).
2) S. Yajima, S. Ichiba, Y. Kamemoto, K. Shiba and M. Kori, ibid., 34, 697 (1961).
3) S. Yajima, S. Ichiba, K. Iwamoto and K. Shiba, ibid., 35, 1263 (1962).

After irradiation, the sample was cooled for 5 days to cause the other short-lived isotopes of iodine, as well as the precursor of iodine-131, to decay out. The impurities contained in the uranium dioxide are shown in Table I.

Sample No. 2 (Mixture of Natural Graphite Powder and Uranium Dioxide Containing Fission Products).—Natural graphite powder previously degassed (in vacuum, 1000°C, 24 hr.) was mixed with the stoichiometric uranium dioxide powder in a weight ratio of 2 : 1 in a glove box filled with nitrogen gas. Three handred milligrams of the mixture was sealed in a polyethylene bag, neutron-irradiated and cooled in a way similar to that for sample No. 1. The impurities contained in the graphite are shown in Table II.

TABLE II. ANALYTICAL DATA OF IMPURITIES IN GRAPHITE

Impurities	
Ash	0.8%
SiO_2	3700 p.p.m.
Al_2O_3	3500 p.p.m.
Fe_2O_3	300 p.p.m.
MgO	100 p.p.m.
CaO	300 p.p.m.
V_2O_5	0.5 p.p.m.
Na_2O	25 p.p.m.
K_2O	20 p.p.m.
B_2O_3	0.5 p.p.m.

Sample No. 3 (Natural Graphite Powder Containing Fission Products). — Formbar was dissolved in dioxane, and stoichiometric uranium dioxide powder was suspended in this solution. The suspended solution was then spilled out on a glass plate, and the dioxane was evaporated. The formbar film was removed from the glass plate and cut into chips (500 mg. of chips containing 300 mg. of uranium dioxide). Five hundred milligrams of the formbar chips was mixed with 500 mg. of natural graphite powder, and the mixture was sealed in a polyethylene bag placed in a glove box. The sample was neutron-irradiated and cooled in a way similar to that for samples Nos. 1 and 2. After cooling, the formbar chips were removed from the sample by screening them through a brass sieve. The graphite powder was found to contain sufficient fission products for the experiment.

Sample No. 4 (Natural Graphite Powder Containing Fission Products).—Three hundred milligrams of the same mixture as sample No. 2 was irradiated in JRR-1 and cooled. The mixture was then treated with a nitric acid solution to eliminate uranium dioxide, washed with water, and dried. Most of the fission products were found to be captured in this treated graphite.

Sample No. 5 (Thorium Dioxide Containing Fission Products).—Thorium dioxide powder wrapped in aluminum foil was gamma-irradiated in a linear accelerator for 5 hr. (maximum gamma-energy, 20 MeV.). Fission products were generated in the thorium dioxide by the (γ, f) nuclear reaction, and then the sample was cooled for 5 days. The impurities contained in the thorium dioxide are shown in Table I.

Sample No. 6 (Mixture of Natural Graphite Powder and Thorium Dioxide Containing Fission Products).—Degassed natural graphite powder was mixed with thorium dioxide powder to a weight ratio of 1 : 2. Three hundred milligrams of the mixture was wrapped in aluminum foil, gamma-irradiated, and cooled in a way similar to that for sample No. 5. Most of the fission products were found to have recoiled out of the thorium dioxide powder and to have been captured in the graphite powder.

Sample No. 7 (Elementary Iodine (I_2) Labeled with Iodine-131).—Five hundred milligrams of uranium dioxide powder was irradiated in JRR-1 for 15 hr. and cooled for 5 days. The irradiated uranium dioxide was dissolved in 10 ml. of a 7 M nitric acid solution, to which was added successively 1 ml. of a 0.05 M potassium iodide solution as a carrier and 1 ml. of a 0.1 M sodium nitrite solution as an oxidizing reagent. Iodine-131 was extracted, together with the carrier, with carbon tetrachloride and back-extracted with a mixed solution of sodium hydrogen sulfite and sodium hydroxide. When this procedure was repeated three times, iodine-131 was completely separated from the other fission products, uranium and neptunium.

The Apparatus.—The apparatus used is shown schematically in Fig. 1. The quartz tube seen in the figure (0.6 cm. in inner diameter, 100 cm. long) was packed, in some experiments, with natural graphite powder, and in others with α-alumina powder or copper powder. The sample was placed on the powder. The graphite and α-alumina were degassed (in vacuum, 1000°C, 24 hr.) before use. The atmosphere in the tube was replaced by purified argon after packing. Then the tube was heated with external resistance wires so as to produce a

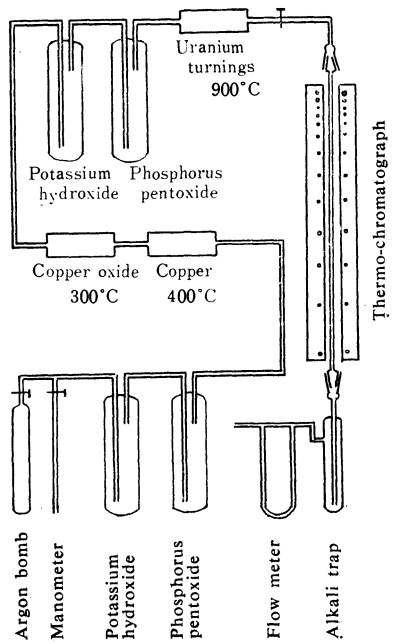

Fig. 1. Apparatus.

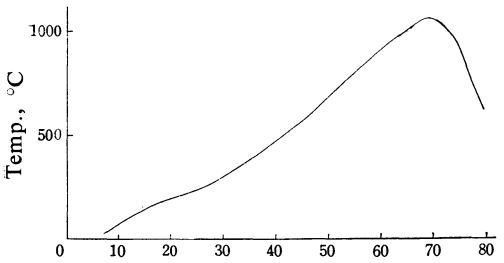

Fig. 2. Condition of the electric furnace when an equilibrium was attained.

linear temperature gradient of about 14°C/cm. ranging from 1000°C to room temperature. This condition, which is shown in Fig. 2, was maintained for 2 hr. after attaining an equilibrium. Then the sample was cooled in a stream of purified argon. After cooling, the specimen tube was surveyed along its whole length in order to locate the iodine-131 activity. An RCL 256 channel gamma-ray scintillation spectrometer connected with a sodium iodide crystal with a lead slit 1 cm. wide was used.

Purification of Argon Gas.—Commercial grade argon was dried over phosphorus pentoxide, and all the carbon dioxide was removed with potassium hydroxide. All the oxygen was removed through a copper net at 300°C. Traces of hydrogen and carbon monoxide were oxidized with copper oxide at 400°C to carbon dioxide and water. After then passing through potassium hydroxide and phosphorus pentoxide tubes, all the gases except argon were removed by passage over uranium turnings at 900°C.

Packing Materials for Quartz Tubes. — *Natural Graphite Powder.*—The natural graphite powder shown in Table II was degassed by heating it in a vacuum at 1000°C for 24 hr. The treated graphite was kept in a helium gas atmosphere until used for the experiment.

α-Alumina Powder. — γ-Alumina commercially available for gas chromatography was heated and kept at 1100°C for 5 hr. By this treatment, the γ-modification was converted into the α-modification, the alumina being degassed.

Copper Powder.—Commercial, triangularly-shaped copper powder was used.

Determination of the Chemical State of Iodine-131.—Iodide (I^-), iodine (I^0), iodate (IO_3^-) and periodate (IO_4^-) states were taken into consideration for the iodine-131 diffusing out of the samples and depositing on the graphite powder. The portion of graphite powder in the quartz tube containing the deposited iodine-131 was removed by cutting the tube, and the graphite powder thus obtained was treated with carbon tetrachloride to determine whether or not iodine-131 (I^0) existed in the graphite powder. The carbon tetrachloride solution was filtered to separate the graphite powder, and the filtrate was assayed with a gamma-ray spectrometer. The separated graphite powder was transferred into an aqueous solution containing 3 mg. of potassium iodide and 8 mg. of potassium iodate and left for 1 hr. to bring about a complete homogeneous mixing of the iodine-131 and its carriers. After 1 hr., the graphite powder was separated by filtration and its radioactivity was measured with a gamma-ray spectrometer. To acidify the filtered solution, small amounts of nitric acid were added. By this treatment the iodide ion (I^-) in the solution was completely

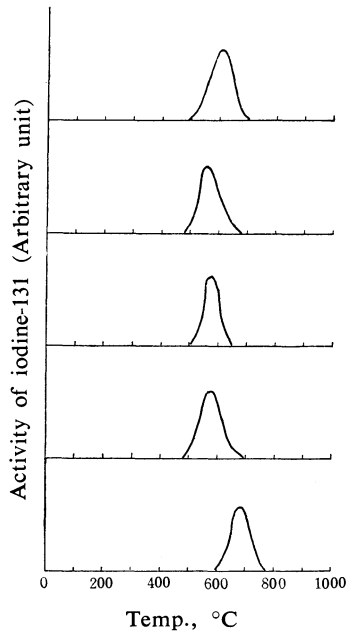

Fig. 3. Sample No. 1 Packing; Natural graphite powder Time; 2 hr.

Fig. 4. Sample No. 2 Packing; Natural graphite powder Time; 2 hr.

Fig. 5. Sample No. 3 Packing; Natural graphite powder Time; 2 hr.

Fig. 6. Sample No. 4 Packing; Natural graphite powder Time; 2 hr.

Fig. 7. Sample No. 2 Packing; Natural graphite powder Time; 0.5 hr.

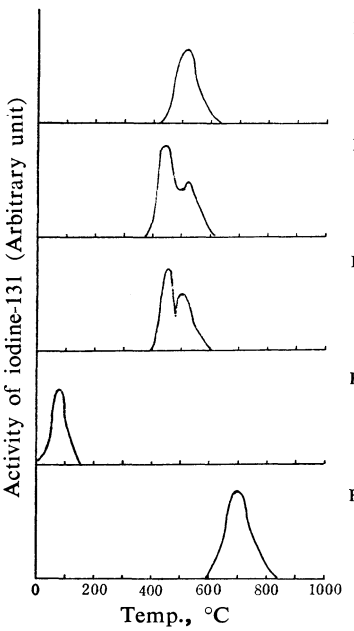

Fig. 8. Sample No. 2 Packing; Natural graphite powder Time; 6 hr.

Fig. 9. Sample No. 5 Packing; Natural graphite powder Time; 2 hr.

Fig. 10. Sample No. 6 Packing; Natural graphite powder Time; 2 hr.

Fig. 11. Sample No. 7 Packing; Natural graphite powder Time; 2 hr.

Fig. 12. Sample No. 2 Packing; Copper powder Time; 2 hr.

TABLE III. CHEMICAL FORMS OF FISSION IODINE-131 DEPOSITED ON THE GRAPHITE POWDER

Chemical form and residue	Iodide (I^-)	Iodine (I^0)	Iodate or periodate (IO_3^-, IO_4^-)	Residue in graphite
Iodine-131 from uranium	62.5	2.0	2.3	33.2
Iodine-131 from thorium deposited at a lower temperature portion	59.8	0	0	40.2
Iodine-131 from thorium deposited at a higher temperature portion	54.2	20.7	12.6	12.6

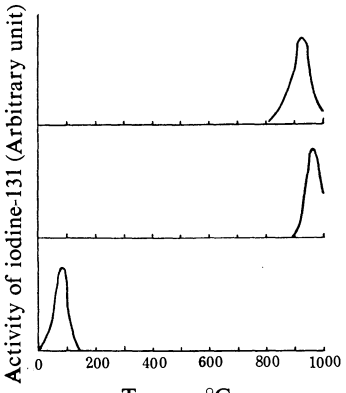

Fig. 13. Sample No. 7
Packing; Copper powder
Time; 2 hr.

Fig. 14. Sample No. 2
Packing; α-Alumina powder
Time; 2 hr.

Fig. 15. Sample No. 7
Packing; α-Alumina powder
Time; 2 hr.

converted into iodine (I^0) The reaction occurring in the solution is as follows:

$$5I^- + IO_3^- + 6H^+ = 6I^0 + 3H_2O$$

The produced iodine (I^0) was extracted and measured with a gamma-ray spectrometer*. The iodate ions (IO_3^-) remaining in the solution was converted into iodine (I^0) by the addition of excess iodide ions (I^-), and the remaining, superfluous iodide ion (I^-) was oxidized into iodine (I^0) by sodium nitrite. The iodine (I^0) thus produced was extracted by carbon tetrachloride, and the radioactivity was measured with a gamma-ray spectrometer**.

As is shown in Figs. 3 to 10, iodine-131 from uranium deposited in only one position, whereas iodine-131 from thorium deposited in two positions on the graphite powder. Experiments were carried out for each portion of the graphite containing the deposited iodine-131. The results obtained are shown in Table III.

The activities of the iodine-131 from uranium and from thorium, which deposited on the lower temperature portion of the graphite powder, were all found to be in iodide fractions. Consequently, the chemical state of the iodine-131 which diffused out of the sample and deposited on the graphite powder should be iodide (I^-). The iodine-131 deposited on the higher temperature portion was in various chemical states. This may be due to the oxygen sensitivity of iodine-131, i. e., the iodide under these conditions may have been decomposed when it was moved into the air from the tube filled with argon. The presence of a considerably large amount of iodine-131 in the graphite may have been caused by the absorption of iodine-131 in the graphite powder or by the intercalation of iodine-131 with graphite.

Thermo-chromatograms.—The results obtained with graphite powder as the packing material are shown in Figs. 3 to 11. A carrier gas of purified argon was made to flow at a rate of 0.5 ml./min., and the sample was heated for 2 hr. at 1000°C. The fission iodine-131 diffusing out was carried by the argon stream and deposited on graphite powder in the tube. The thermo-chromatograms obtained under these conditions with samples of uranium dioxide (sample No. 1), a mixture of uranium dioxide and graphite (sample No. 2), and graphite (sample Nos. 3 and 4) are shown in Figs. 3, 4, 5 and 6 respectively. In each case, the iodide deposisted at the same position of the graphite; the temperature of the position was 580°C. Figures 7 and 8 show the results obtained when the experiments lasted 0.5 and 6.0 hr. respectively; the iodine deposited at 670°C and at 520°C respectively. All the

* It has been shown by W. H. Burgus and T. H. Davies[4] that the exchange reaction between iodide ions (I^-) and iodine (I^0) in an aqueous solution is rapid, but that the reaction between other chemical states is hardly appreciable. The exchange reaction occurs according to the chemical equation:

$$2I^0 + H_2O = HIO + H^+ + I^-$$

In a carbon tetrachloride solution, however, such a reaction cannot occur. In an acid solution, five chemical equivalents of iodide ions (I^-) react with one equivalent of iodate ions (IO_3^-). In the present experiment, the chemical equivalent ratio of iodide ions (I^-) to iodate ions (IO_3^-) was about 13:18, so that if the iodine-131 existed in the iodate state when it diffused out of the sample, about one-seventh of the iodine-131 would be converted into iodine (I^0).

** The iodine (I^0) extracted by the reduction assay of the iodate ions (IO_3^-) contained six-seventh of the indine-131 which had diffused out of the sample as the iodate (IO_3^-). The activity of the iodate fraction was small, so that the fraction of the reduced iodate ions (IO_3^-) did not contribute much to the activty of the iodide fraction. Similarly, no further separation of periodate ions (IO_4^-) from the iodate ions (IO_3^-) was made, because the periodate ions (IO_4^-) behaves in a way very similar to that for the iodate ions (IO_3^-) in the above reactions and, as is shown in Table III, the activity of the iodate fraction was small.

4) W. H. Burgus and T. H. Davies, "National Nuclear Energy Series: Radiochemical Studies: The Fission Products", Book I, Mcgraw-Hill Book Co., Inc., New York (1951), pp. 209—219.

experimental conditions except the time were the same as in the case of Fig. 6. As compared with the results given in Fig. 6, the location of the fission iodine-131 deposited moved toward a lower temperature as the duration of the experiment increased. The experiment which was repeated three times showed that the reproducibility of the deposition temperature was within ±20°C in each case.

The thermo-chromatograms obtained from the thorium dioxide (sample No. 5) and from the mixture of thorium dioxide and graphite (sample No. 6) are shown in Figs. 9 and 10 respectively. It was found that two peaks appeared in both thermo-chromatograms; the corresponding temperatures were 520°C and 430°C in both cases. Figure 11 gives the thermo-chromatogram of the elementary iodine (sample No. 7) obtained under the same conditions as in Figs. 3, 4, etc. The location of radioactivity when using copper powder as the packing material is shown in Figs. 12 and 13. The fission iodine-131 (sample No. 2) was located at 700°C, and the elementary iodine (sample No. 7), at 920°C. When α-alumina was used as the packing material under the same experimental conditions as above, the fission iodine-131 (sample No. 2) deposited at a temperature higher than 950°C, while elementary iodine (sample No. 7) deposited at 80°C.

Conclusion

The data obtained may be summarized as follows:

1) The thermo-chromatograms of the fission iodine-131 were extremely different from that of elementary iodine, whichever packing material was used, i. e., graphite, α-alumina or copper powder.

2) The fission iodine which deposited on graphite at a temperature of 580°C was iodide in terms of its chemical state.

3) Elementary iodine deposited on graphite at 80°C as elementary iodine itself under these experimental conditions. That is, the elementary iodine was not reduced by either graphite, impurities in the graphite, or carrier gas. These results [1), 2) and 3)] indicate that the fission iodine-131 was not diffused out as elementary iodine but as iodide.

4) The displacement of the iodine-131 peak toward a lower temperature, as shown in Figs. 6, 7 and 8, was not the result of the oxidation of iodide to iodine by impurities in the carrier gas. It must be related to the vapor pressure of the fission iodide, since the velocity of the movement tends to decrease sharply with an increase in the diffusion time.

5) The data obtained from samples Nos. 1, 2, 3 and 4, using graphite as the packing material, coincided well with each other. The most reasonable conclusion to be drawn under these circumstances is that the fission iodine-131 exists in the same chemical state and species in all the samples.

6) Since the fission iodine-131 exists as iodide, it should be thought that the fission iodine combines with other fission products, with impurities in uranium dioxide, thorium dioxide, etc., or with the fissionable material, i. e., uranium or thorium.

7) As shown in Figs. 3 and 9, the locations of the fission iodine-131 obtained from uranium on the graphite were different from that of thorium. This eliminates the possibility that the fission iodine-131 combines with the other fission products, even if the fission product-yield curve of uranium is different from that of thorium.

8) The combination of the fission iodine-131 with impurities in uranium dioxide, etc., is not supported by the coincidence of the thermo-chromatograms obtained from samples Nos. 1 and 3, whose impurities are different.

9) Lastly, the combination of fission iodine-131 with fissionable materials, in the present instance, uranium and thorium, may be considered. The fact that the thermo-chromatogram of the fission iodine-131 originating in uranium differs from that of thorium and the results discussed in 7) and 8) lead to the conclusion that the iodine-131 combines with fissionable materials, uranium or thorium. Also, it has been observed by Ershler and Lapteva[5] that, when a foil of uranium metal is neutron-irradiated in high vacuum, a large number of uranium atoms are vaporized from the foil. The present authors cannot help thinking, on the basis of the foregoing data, that a considerable number of uranium or thorium atoms are brought into the graphite crystal by primary fission fragments. The fission iodine-131 would center in the imperfection composed of unstable atoms of uranium or thorium caused by fission, born uranium or thorium iodide, and would diffuse out of the samples.

10) The fission iodine-131 diffusing out of the sample reacts with α-alumina at temperatures higher than 950°C. This finding indicates that α-alumina is a suitable material for use as an internal trap in a semi-homogeneous fuel reactor characterized by high temperature and high burn-up.

11) To determine precisely the chemical species of the iodide, thermo-chromatograms or uranium iodide and thorium iodide must

5) B. V. Ershler and F. S. Lapteva, *J. Nuclear Energy*, **II 4**, 471 (1957).

be studied, and the presence of uranium or thorium in thermal spikes must be confirmed.

The authors wish to express their thanks to Dr. Eizaburo Nishibori, director of the institute, for his valuable advice and discussions, and also to Dr. Toshio Nakai, chief of the division of chemistry, for his encouragement in this work.

Chemistry Division
Japan Atomic Energy Research Institute
Tokai, Ibaraki

The Behavior of Fission Products Captured in Graphite Powder by Nuclear Recoil. VII. The Activation Energy of the Diffusion of Iodine-131 in Graphite

By Seishi YAJIMA, Koreyuki SHIBA and Muneo HANDA

(Received June 22, 1962)

The authors have studied the behavior of fission products captured in graphite by fission recoil and have obtained much interesting information. For example, fission products do not leach out of graphite into nitric acid to any extent, unless the graphite is heated to a high temperature before the leaching assay[1]. Xenon, iodine, and tellurium diffuse more rapidly out of natural graphite than out of artificial graphite[2]. The heating curve and the activation energy of the diffusion of xenon indicate that the diffusion mechanism is not simple, but is related to imperfections in the graphite crystal[3]. The distribution of the activation energy of the diffusion shifts to higher temperatures with an increase in the concentration of fission products in graphite crystal[4]. Iodide is the chemical form of iodine diffusing out of graphite crystal[5].

These studies have been carried out in connection with the development of a semi-homogeneous fuel, that is, a dispersion-type fuel of uranium dioxide or uranium carbide in a graphite base; at the same time, they brought out many facts very interesting from the standpoint of hot atom chemistry.

Taking account of the fact that the iodide is the chemical form of iodine diffusing out of a graphite-uranium dioxide-system fuel, the authors undertook to determine the activation energy of the diffusion of iodine in graphite crystal and to elucidate the mechanism of the diffusion and formation of the iodide.

Experimental

Preparation of Samples.—Natural graphite (NG-1) was used throughout the experiments. The use of natural graphite, which has fewer imperfections than artificial graphite, made analysis of the experimental results clearer and easier; our studies made it clear that the diffusion rates of xenon, iodine, and tellurium in the natural graphite specimen were much larger than those in artificial graphite. Its properties are given in Table I, and those of the uranium dioxide used, in Table II.

A mixture of 1 g. of graphite and 0.5 g. of uranium dioxide powder was irradiated for 15 hr. in a JRR-1 reactor (water boiler type; thermal neutron flux: about 5×10^{11} n/cm^2/sec.) and cooled for 5 days. This cooling time facilitated the analysis of the behavior of iodine-131 by allowing short-lived iodine nuclides and the precursor of iodine-131 to decay out. The cooled sample was then treated with a hot nitric acid solution to separate

TABLE I. ANALYTICAL DATA OF IMPURITIES IN GRAPHITE

Impurities	NG-I
Ash	0.8%
SiO_2	3700 p.p.m.
Al_2O_3	3500 p.p.m.
Fe_2O_3	300 p.p.m.
MgO	100 p.p.m.
CaO	300 p.p.m.
V_2O_5	0.5 p.p.m.
Na_2O	25 p.p.m.
K_2O	20 p.p.m.
B_2O_3	0.5 p.p.m.

1) T. Nakai, S. Yajima, K. Shiba, J. Osugi and D. Shinoda, This Bulletin, 33, 494 (1960).
2) T. Nakai, S. Yajima, K. Shiba, J. Osugi and D. Shinoda, ibid., 33, 497 (1960).
3) S. Yajima, S. Ichiba, Y. Kamemoto, K. Shiba and M. Kori, ibid., 34, 697 (1961).
4) S. Yajima, S. Ichiba, K. Iwamoto and K. Shiba, ibid., 35, 1263 (1962).
5) S. Yajima, K. Shiba and M. Handa, ibid., 36, 253 (1963).

TABLE II. ANALYTICAL DATA OF IMPURITIES IN URANIUM DIOXIDE

	%
Content	99.85
Alkalies and alkaline earths	0.13
Heavy metals (Pb)	0.005
Fe_2O_3	0.013
Cl^-	0.004
NO_3^-	Trace
SO_4^{2-}	0.002

uranium dioxide from the graphite; this was then filtered off, washed with water and acetone, and dried at about 100°C. It was shown that about 60 per cent of the fission products are captured in graphite under these experimental conditions.

Apparatus Used.—The flow system of the apparatus used is shown in Fig. 1. It may be divided broadly into three parts: an argon gas purifier, diffusion equipment, and a trapping device for the diffused iodine.

In the argon gas purifier, carbon dioxide, water, and the major portion of oxygen in the argon gas were eliminated with potassium hydroxide, phosphorus pentoxide, and copper net, heated to 400°C, respectively. Copper oxide heated to 300°C was effective in oxidizing carbon monoxide and hydrogen to carbon dioxide and water, which were then absorbed in potassium hydroxide and phosphorus pentoxide respectively. Finally, nitrogen gas and a trace of oxygen gas were removed with uranium turnings heated to 900°C.

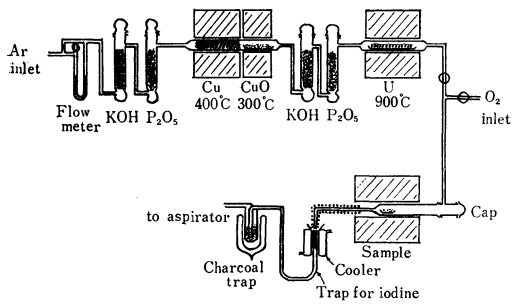

Fig. 1. Apparatus.

A graphite sample placed in a quartz tube was heated in a resistance furnance with nichrome windings. The temperature was controlled with a slide transformer. Diffused iodine-131 was carried by the purified argon gas and introduced into a slender quartz pipe heated to 600°C with a nichrome heater to prevent the iodine-131 from depositing on the wall of the pipe. The absence of such deposits was verified by gamma-assay of a sodium hydroxide solution with which the wall had been rinsed at the end of the experiments.

The trapping of the iodine was given the most careful consideration in setting up the apparatus. It has been established that iodide is the chemical form of iodine diffusing out of graphite into an inert atmosphere and that the iodide deposits on the copper powder surface at about 700°C under certain conditions[5]. Consequently, these facts must be taken into consideration in trapping iodine-131.

A trapping tube for iodine-131 was replaced by a new one at short intervals, whenever a heating curve was obtained or when the activation energy was determined, because a gap was then left between the trap and the pipe. The iodine-131 caught in the trap must be stable in air at room temperature. Such stability was obtained with iodine-131 deposited on copper metal. Before reaching the trap, a portion of the diffused iodine would be oxidized to iodine (I^0) by air entering through the gap. Iodine (I^0) is converted into silver iodide by contact with silver metal at any temperature above that of the room, and the product is stable in air at room temperature. Copper metal also combines with iodine (I^0) at room temperature to form cuprous iodide. The metal, however, is oxidized to copper oxide at a high temperature by air. The authors, therefore, used a trap comprising a glass tube (10 mm. inner diameter; 100 mm. long) stuffed with silver-plated copper netting to a depth of 10 mm. from the end of the tube facing the opening of the pipe, beyond which was copper netting to a depth of 30 mm. The trap was cooled with water circulating through a jacket surrounding the glass tube.

The flow rate of the argon stream through the quartz tube was 150 ml./min.; the narrow opening of the pipe caused the iodine-131 carried with the argon stream to be injected past the gap into the trap. The gas was evacuated through the trapping materials by an aspirator with a capacity of 170 ml./min. With this arrangement, a preliminary experiment showed that all the iodine-131 diffusing out of graphite was in the trap within a depth of 10 mm. from the inlet end.

Making the Heating Curves.—A graphite sample was placed in a quartz boat, which was then inserted through the entrance into the heating part of the diffusion apparatus after taking off the cap. After replacing the cap, the purified argon gas was introduced into the apparatus at a flow rate of 150 ml./min. in order to scavenge the air. At the same time, the slender pipe was set to heat up. As soon as the pipe temperature reached 600°C, the sample was made to start heating, beginning at a temperature of approximately 40°C in all the experiments due to the effect of the slender, highly-preheated pipe. The sample was heated at a rate of 5°C/min., this rate being controlled with a transformer adjusted by hand. The temperature was measured with a platinum-platinum rhodium thermocouple. After reaching 1100°C, the temperature of the sample was lowered to 1000°C, and the argon gas stream was replaced by oxygen gas, flowing at a rate of 150 ml./min., in order to burn out the graphite and to catch remaining iodine-131. Throughout this experiment, the trapping tube was renewed every 10 min. The activity of the iodine-131 caught in each trap was measured with an RCL 256 channel gamma-ray spectrometer equipped with a sodium iodide crystal (3 inch diameter × 3 inch thickness). Errors due to the absorption of gamma-ray from iodine-131 by the glass wall and copper netting of the traps cancelled out, because

the glass tube thickness and diameter, as well as the packing conditions of the trapping materials in the traps, were identical.

The ratio of the iodine-131 counts of each trapping tube to the aggregate count of all the tubes was divided by the temperature increment covering the trap in question, the quotient being plotted against the absolute temperature. The histogram thus obtained was redrawn in the form of a smooth curve equivalent in area, as shown in Fig. 2.

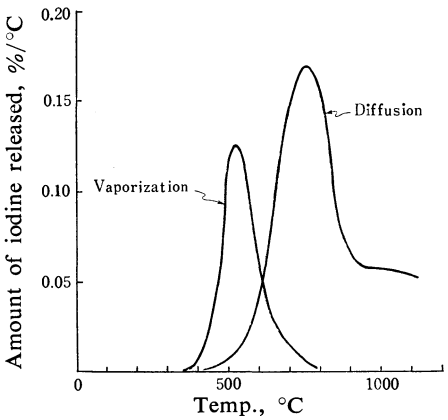

Fig. 2. Heating curves (5°C/min.) of iodine-131.

It is believed that iodine-131, after having diffused, interacts physically or chemically with the graphite crystal on the surface and then leaves the graphite. It would, therefore, be useful to obtain the heating curve of the iodine-131 which, having diffused out of the graphite crystal, has then deposited on the surface of graphite powder of a similar nature. For this purpose, an iodine sample was prepared by means of the thermo-chromatographic method described in a previous report[5]. The heating curve obtained is also shown in Fig. 2.

Determination of Acitivation Energy.—The heating curve of iodine-131 diffusion in graphite crystal has a peak at 750°C, indicating the existence of a mechanism of diffusion predominant at that temperature. Consequently, isotherms for diffusion were determined at 676, 718, 746, and 780°C, temperatures selected in the vicinity of 750°C.

Before putting a sample in the diffusion apparatus, the slender connecting pipe was preheated and kept at 600°C, and the heating section was kept at the designated temperature, while argon gas was allowed to flow at 150 ml./min. through the apparatus. As soon as the graphite sample, placed on a quartz boat, was inserted in the heating section under these conditions, the cap was fastened and the sample heated. The trap was renewed at appropriate intervals. The time of the beginning of diffusion was taken to be the instant the cap was in position.

After being kept at a constant temperature from 2 to 4 hr. in order to get an isotherm, the temperature of the sample was raised to 1000°C and the sample was fired by replacing the argon atmosphere with oxygen gas; the iodine-131 remaining in the graphite was caught in the trap. The trapping tubes were handled and put through spectrometry in the same way as has been described for making heating curves. The amount of diffused iodine-131 is plotted against the diffusion time in Fig. 3.

According to Dienes[6], in the relaxation process, the relaxation time, t, and the activation energy, E, are related by the equation:

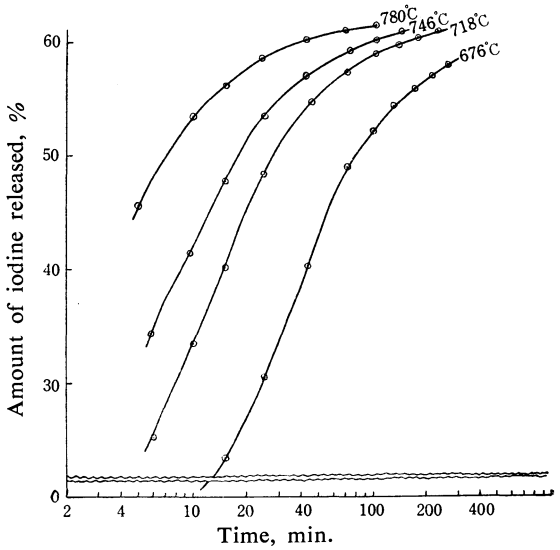

Fig. 3. Isotherms for diffusion of iodine-131.

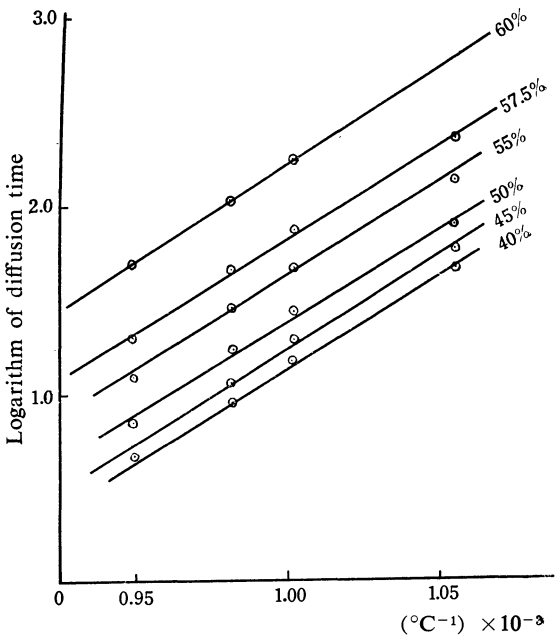

Fig. 4. Activation energies of diffusion of iodine-131.

6) G. J. Dienes and W. E. Parkins, "An Improved Method for Determining Activation Energies of Relaxation Process", NAA-SR-60 (1950).

$$t \times \exp(-E/RT) = \text{constant}$$

where R: gas constant

T: absolute temperature.

In order to apply this to diffusion phenomena and to determine activation energy, the logarithms of diffusion time corresponding to 40, 45, 50, 55, 57.5, and 60 per cent of the total iodine-121 content on each isotherm were plotted against the reciprocal of the absolute temperature, as is shown in Fig. 4. The groups of points stand along lines with the same gradient. This evidently means that the activation energy of the diffusion of iodine-131 is single. The activation energy calculated from each gradient is given in Table III.

TABLE III. ACTIVATION ENERGIES OF DIFFUSION OF IODINE-131

Per cent	Slope, deg.	Activation energy, kcal./mol.
40	1.01×10^4	46.3
45	1.02×10^4	46.7
50	1.00×10^4	45.8
55	1.02×10^4	46.7
57.5	1.02×10^4	46.7
60	1.05×10^4	49.2

Discussion

It has been clarified that iodide is the chemical form of iodine-131 diffusing out of graphite in an inert atmosphere. In the heating curve of the iodide deposited on graphite powder, a peak appears at 530°C, as is shown in Fig. 2. If there should be no chemical interaction between the iodide diffused out of graphite and graphite crystals on the surface, the heating curve is to be related to the vaporization of the iodide. Most compounds have a measurable vapor pressure in the neighborhood of their melting points; therefore, by a first approximation, the iodide can be considered to have its melting point in the range between 400 and 600°C.

The heating curve of deposited iodide has a peak at 530°C, while the peak of the heating curve of "diffusion" is found at 750°C, which is 200°C higher than that of the iodide. This leads to the conclusion that the iodide which had diffused in graphite and had reached the surface did not stay there, but was carried immediately off by the argon gas stream; that is, the peak at 750°C originated in the very diffusion of iodine-131.

Figures 2 and 3 and Table III show that the bulk of the iodine-131 diffusion in graphite at temperatures lower than 1100°C occurs around 750°C, based on a single mechanism with an activation energy of 47 kcal./mol.

In order to compare the diffusion in graphite crystal of iodine with that of xenon, a typical heating curve and the activation energies of the diffusion of xenon have been reproduced from the fourth and fifth papers of this series; they are given in Fig. 5 and Table IV. Whereas, in the heating curve of xenon, peaks appear at 200, 500, 750, 1000 and 1400°C, that of iodine has only one, at 750°C. Attention is drawn to the fact that a peak at 750°C appears also in the xenon diffusion curve and that the activation energies are approximately equal, as is seen in Table IV. This means that the diffusion of xenon and iodine are governed by one and the same mechanism.

It is also interesting to compare the heating curves of volatile fission products, xenon and iodine, diffusing out of graphite, with the annealing curves of graphite irradiated with fast neutrons. To depict the neutron damage to artificial graphite, differential annealing curves of several physical properties are shown in Figs. 5 and 6, based on work carried out by Woods et al.[7] and by Kinchin[8]. In Table

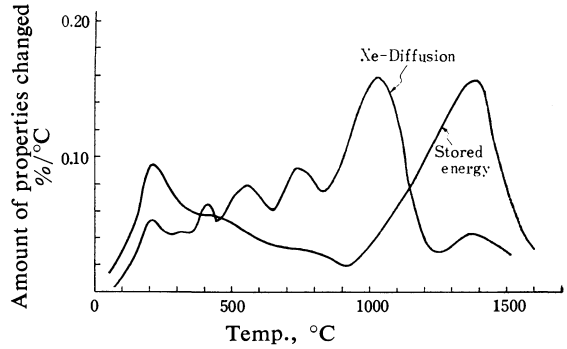

Fig. 5. Heating curve (5°C/min.) of diffusion of xenon and differential annealing curve of neutron damage.

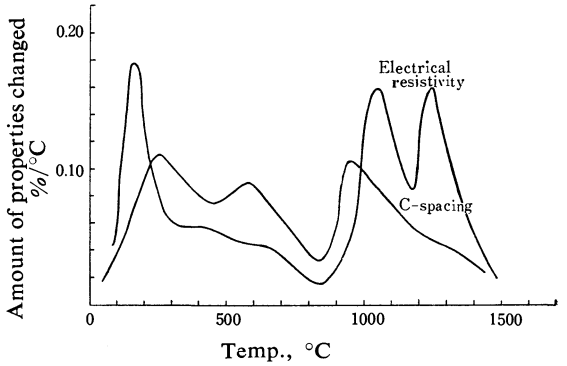

Fig. 6. Differential annealing curves of neutron damage.

7) W. K. Woods, L. P. Bupp and J. F. Fletcher, Geneva Conference Paper, P/746, 7, 455 (1956).
8) G. H. Kinchin, ibid., P/442, 7, 472 (1956).

TABLE IV. ACTIVATION ENERGIES FOR ANNEALING OF DAMAGE (kcal./mol.)

Phenomena	Exposure	Temperature range, °C			Remark
		150~200	650~850	1000~1200	
Electrical resistivity	8.1×10^{18} n/cm^2	23.8		69.5	Woods[7]
	1.5×10^{19} n/cm^2	29.2		58.2	Woods[7]
	5.4×10^{20} n/cm^2	39.6			Woods[7]
	$\sim10^{19}$ n/cm^2	27.6		69	Kinchin[8]
Xenon diffusion	1.4×10^{13} fp/cm^3	23.8	49	68.4	Yajima[3]
	1.4×10^{13} fp/cm^3			65.5	Yajima[4]
Iodine diffusion	2.6×10^{14} fp/cm^3		47		Present work

IV is given the activation energy of the annealing of electrical resistivity determined by using a pulse-annealing technique.

The peaks of the heating curve of the diffusion of xenon and those of the annealing of neutron damage coincide very well with each other except for the one at 750°C; this coincidence is the more remarkable when one considers the differences in such factors as irradiation conditions of the samples, experimental method, and treatment of data. This indicates that the xenon-tracer technique can match other methods with respect to high sensitivity and simplicity when studying the process of the annealing of imperfections in graphite crystal. Furthermore, the activation energies of the diffusion of xenon at 200 and 1000°C are nearly equal to those of the annealing of electrical resistivity. This means that, so far as these peaks are concerned, the damage due to fast neutrons is the same as that due to fission fragments, and that xenon is released on the annealing of these imperfections.

It has been established that fission fragment damage caused by the recoil of fission fragments into graphite crystal is far greater than fast neutron damage[4,9]. The absence of a peak at 750°C in the annealing curves of the neutron damage would indicate either that this damage is characteristic of fission fragment damage or that other methods less sensitive than the xenon-tracer technique obscure the presence of the 750°C-peak caused by fast neutron damage. However, the latter suggestion cannot be easily affirmed. Therefore, the imperfection corresponding to the 750°C-peak may have its origin in the fission fragments themselves or in fissionable materials, in the present instance, uranium atoms brought into the graphite crystal by fission fragments, because the physical interaction of fission fragments with graphite atoms is not considered to be fundamentally different from those of fast neutrons with graphite atoms.

These assumptions lead to the conclusion that iodine-131 was initially distributed evenly over the various imperfections in the graphite crystal, as was the xenon which had recoiled. However, because of the chemical affinity of iodine, iodine-131 caught in the imperfections (C_2, C_3, C_4,—clusters)[10] corresponding to temperatures below 750°C had a very small probability of migrating between layers or of diffusing out of the graphite crystal, and so tended rather to combine successively with clusters corresponding to higher temperatures at the time of the disappearance of the imperfections. Thus, as clusters begin to disappear at lower temperatures, iodine-131 shifts to clusters corresponding to higher temperatures and is trapped there. Consequently, in the case of iodine, no peak is observed at temperatures lower than 750°C. Finally, iodine-131 combines with those foreign atoms which constitute imperfection corresponding to the peak at 750°C to form the iodide species and to diffuse out. This assumption is supported by the fact that, at 2.6×10^{14} fission products per cubic centimeter of graphite, the amounts of iodine and xenon diffusing at temperatures below 900°C are 42 and 44 per cent respectively, which figures are nearly equal. Another evidence is that many halides of metals like UCl_4, UO_2Cl_2 intercalate graphite in the vicinity of 300°C[11]; this quite low temperature facilitates the diffusion of the iodide species in graphite crystal. To confirm the presence of uranium atoms and to determine the concentrations of the atoms along the range of fission fragments in graphite would further consolidate this assumption.

The authors intend further to pursue their studies of the chemical form and diffusion behavior of the iodine-131 remaining in the graphite without diffusing out at temperatures over 900°C.

9) R. J. Harrison, CF-53-3-276 (Del.), Radiation Damage Conference, Part I, 93 (1954).

10) T. Iwata and H. Suzuki, "A Model of Radiation Damage in Graphite", I.A.E.A. Symposium on Radiation Damage in Solid and Reactor Materials, Venice (1962).

11) R. C. Croft, *Aust. J. Chem.*, **9**, 184 (1956).

The authors are grateful to Dr. Eizaburo Nishibori for his helpful abvice and discussions, and to Dr. Toshio Nakai for the encouragement given during this investigation.

Division of Chemistry
Japan Atomic Energy Research Institute
Tokai, Ibaraki

Syntheses of Polyhydroxybenzene Derivatives from Furfural

By Masuo MURAKAMI and Jong-Chen CHEN

(Received June 25, 1962)

It has been impressed that 2-substituted 2, 5-dimethoxydihydrofurans and 2, 5-dimethoxytetrahydrofurans are easily converted into aromatic compounds by hydrolysis in acid solution. For example, Clauson-Kass and co-workers[1] described the hydrolysis and spontaneous recyclization of 2-acetyl-2, 5-dimethoxytetrahydrofuran dimethylketal to catechol and Boehme[2] reported the formation of hydrourushiol (XVII) from the acid hydrolysis of 2-heptadecanoyl-2, 5-dimethoxytetrahydrofuran. Respect of the activated character of hydrogens in the α-position to carbonyl group (such as in the case of the compounds VI and XII) had let to the preparation of polyhydroxybenzenes (Fig. 1) and catechol derivatives including hydrourushiol (Fig. 2).

The compounds VI, VII, VIII and X are new substances. Their structures were determined from the synthetic process, analyses and from the infrared spectra.

The method of synthesis of VII was partly based on a route of its methyl analog developed by Clauson-Kass[1], VII was prepared by hydrolysis of VI at room temperature as well as at 100°C in dilute hydrochloric acid. The reaction at lower temperature produced a larger amount of VII (51.5% yield at room temperature and 21.2% at 100°C). VII showed a green color with ferric chloride and significant infrared

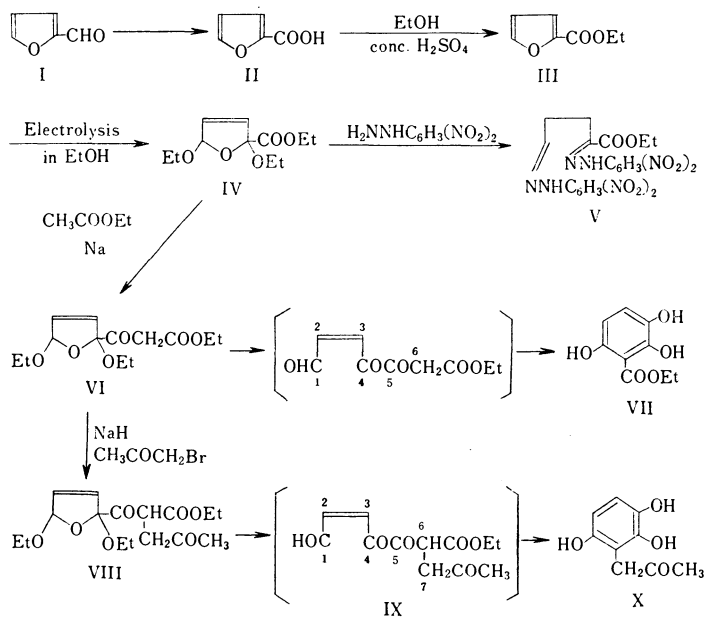

Fig. 1

1) N. Clauson-Kass and P. Nedenskov, *Acta. Chem. Scand.*, **9**, 27 (1955) and preceding papers.

2) W. R. Boehme, *J. Am. Chem. Soc.*, **82**, 498 (1960).

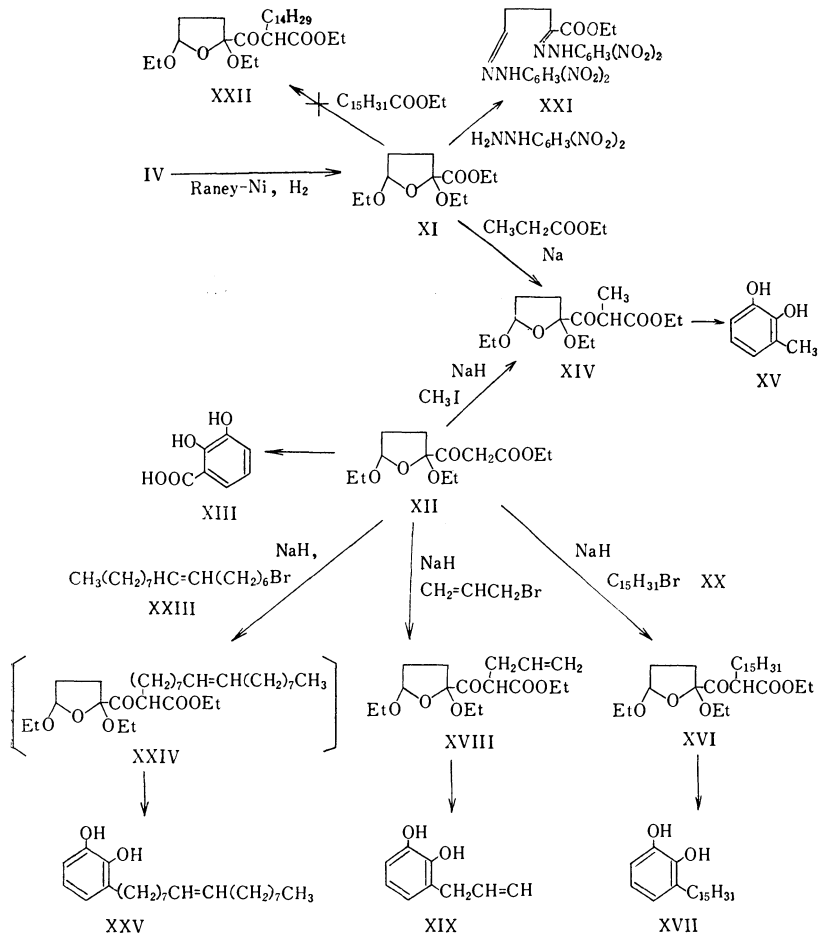

Fig. 2

absorption bands at 2.89~2.94 μ (-OH), and 5.92 μ (ester C=O).

X was obtained through 1,6-intramolecular condensation of the intermediate (IX) which was prepared by acid hydrolysis of VIII. X showed a green color with ferric chloride and gave a red 2,4-dinitrophenylhydrazone. The seven-membered ring compound which was expected from 1,7-intramolecular condensation of IX, was not found in the reaction mixture. The yield of X was 58% and the rest was polymerized in this reaction.

The compounds XII, XIV, XVI, XVIII and XXV are new substances.

XI was prepared by reduction of IV with Raney nickel as a catalyst. IV and XI are distinguished easily by the color of their bishydrazons (V and XXI). V is red and decomposes at 248°C, while XXI is yellow and melts at 194~196°C.

The compound XIII was identified with an authentic sample of commercial 2,3-dihydrobenzoic acid through mixed fusion test and by comparison of infrared spectra.

Pentadecyl bromide (XX) was prepared by the Hunsdiecker reaction[3] from silver salt of palmitic acid.

XVI was prepared (24.6%) by boiling the *n*-butyl ether solution of XII and XX for 5 hr. A large amount of XII and XX was recovered from the reaction mixture. A higher yield of XVI can be expected when the time of reaction is extended. At a lower temperature such as the boiling temperature of a mixture of ether and benzene, only a trace of XVI was obtained.

Very recently Hanafusa and Yukawa[4] have synthesized hydrourushiol (XVII) starting from catechol. Hydrourushiol, one of the Japanese lac urushiol[5] or poison-ivy compound[6], was prepared here by acid hydrolysis of XVI. The

3) H. Hunsdiecker and C. Hunsdiecker, *Ber.*, **75**, 291 (1942); C. V. Wilson, "Organic Reactions," Vol. 9, 332(1957).
4) T. Hanafusa and Y. Yukawa, *Chem. & Ind.*, **1962**, 23.
5) R. Majima and co-workers, *Ber.*, **55**, 172 (1922) and preceding papers.
6) G. A. Holl, V. Mattcotti and W. D. Graham, *J. Am. Chem. Soc.*, **56**, 2736 (1934).

colorless, waxy crystals of synthetic hydrourushiol were identified with an authentic sample[7] by mixed fusion test and comparison of infrared spectra.

On the Claisen condensation of XI with ethyl acetate and ethyl propionate, the yields were 52.3 and 13.0% respectively. Ethyl palmitate failed to condense with XI in the presence of metallic sodium, sodium alkoxide, sodium hydride or triphenylmethyl-sodium using the ether, benzene or *n*-butyl ether as a solvent respectively. The condensation also failed when the timer of reaction was extended,

XVIII was a yellow oil and turned to brown when it was stored in the dark place for a long time. It reacted rapidly with bromine and permanganate. Infrared spectra of XVIII showed terminal double bond at the peaks of 6.06, 10.05, 10.83 μ and carbonyl groups at two peaks of 5.16~5.76 μ.

XIX was obtained by acid hydrolysis of XVIII. 3-Allylcatechol was prepared formerly by the reaction of catechol and allyl bromide through the Claisen rearrangement of monoallyl ether of catechol[9]. XIX was practically colorless just after the distillation and rapidly became golden yellow, but it soon turned to reddish brown on exposure to air. The terminal olefinic bond of XIX was readily detected from the infrared spectra. XIX rapidly decolorized bromine and permanganate and gave an olive green color with ferric chloride.

1-Bromoheptadencen-8 (XXIII) was also prepared by the Hunsdiecker reaction[3] from silver salt of oleic acid. Acid hydrolysis was carried out after the reaction of XII and XXIII had been completed. Lead salt of XXV was isolated from the acid solution with lead acetate. XXV was obtained as a pale yellow oil by means of treating lead salt of XXV with hydrogen sulfide. This manner gave XXV in a high yield (52.4% yield based on reacted XII). When a solution of XXV in alcohol was treated with a drop of aqueous permanganate, the color disappeared after standing for a minute. XXV gave a green color with ferric chloride. Negative Beilstein test of XXX showed that bromine did not add to a double bond of oleic acid under the Hunsdiecker reaction.

It is interesting that application of XIX and XXV to the skin caused a marked blister within a few hours, but on application of hydrourushiol to the skin no blister edema was found. Dawson[9] reported that the 3-(8'-pentadecenyl)catechol caused the marked edema and blister characteristic of poison-ivy dermatitis. It is undoubted that 3-olefinic catechol caused dermatitis. Instead of urushiol, 3-allylcatechol (XIX) may be available for clinical study. Further study of olefinic catechols, some materials which have a characteristic of "Urushi" for paint will be expected. It is believed that the above methods will be available to synthesize the compounds having another substituent in 1-position of 2, 5, 6-trihydroxybenzene (method of Fig. 1) and substituents in 3-position of catechol (method of Fig. 2).

Experimental

2-Furoic Acid (II).—This compound was prepared by the method given earlier[10].

Ethyl 2-Furoate (III).—56.0 g. (0.50 mol.) of II was dissolved in amixture of 300 ml. of ethanol and 56 g. of concentrated sulfuric acid. After the reaction mixture had been heated at a reflux temperature for 6 hr, the ethanol was removed by distillation, the residue was dissolved in ether and a small amount of ice water was added. The ethereal solution was washed with saturated sodium hydrogen carbonate, with water and dried over magnesium sulfate. The ether was removed by distillation, the residue was distilled further, and 67.5 g. (96.5% yield) of III was obtained, b. p. 129~130°C (115 mmHg).

Found: C, 60.01; H, 5.75. Calcd. for $C_7H_8O_3$: C, 59.99; H, 5.75%.

2, 5-Diethoxy-2, 5-dihydrofurancarboxylic Acid Ethyl Ester (IV).—III (55.9 g., 0.40 mol.) was mixed with 230 ml. of methanol and 1.0 ml. of concentrated sulfuric acid. The electrolysis of the solution was carried out by the Clauson-Kaas method[1]. From the fraction at b. p. 115~136°C (11 mmHg), 56.25 g. (61.5%) of IV was obtained as a colorless liquid, n_D^{15} 1.4420.

Found: C, 57.80; H, 7.27. Calcd. for $C_{11}H_{18}O_5$: C, 57.38; H, 7.88%.

V was obtained in a quantitative yield from 1 mol. of IV and 2 mol. of 2, 4-dinitrophenylhydrazine. Crude crystals of V were twice recrystallized from nitrobenzene. V was red crystals, decomp. p. 248°C.

Found: C, 44.18; H, 3.65; N, 21.80. Calcd. for $C_{19}H_{16}O_{18}N_8$: C, 44.19; H, 3.12; N, 21.12%.

Ethyl (2, 5-Diethoxy-2, 5-dihydro)furfuroylacetate (VI).—14.0 g. (0.061 mol.) of IV and 20 ml. of benzene were placed in a three-necked flask fitted with a stirrer, a dropping funnel and a reflux condenser carrying a soda-lime tube and heated with stirring to about 100°C. 21.5 g. (0.244 mol.) of ethyl acetate and 5.6 g. (0.244 mol.) of sodium powder were added at the interval of 30 min. in six portions. After the reaction, ethanol was added dropwise to remove unreacted sodium and the

7) The authors wish to thank the people of Yukawa Laboratory, Osaka University for a gift of the authentic sample.

8) S. Kawai, *Scient. Pap. Inst. Phys. Chem. Res.*, 3, 267 (1926). W. H. Perkin and V. M. Trikojus, *J. Chem. Soc.*, 1927, 1664.

9) B. Loev and C. R. Dawson, *J. Am. Chem. Soc.*, 24, 980 (1959).

10) "Jikken Kagaku Koza" Vol. 17, Maruzen, Tokyo (1957), p. 626.

mixture was left to stand with stirring and heating for 10 hr. The solution was cooled to 0°C and acidified by acetic acid. The dark brown mixture was added to cold water and the benzene layer was separated, washed with saturated sodium hydrogen carbonate then with water, and dried over magnesium sulfate. Benzene was removed by distillation and the residue distilled further, 6.60 g. (40.0%) of VI was obtained as a slightly yellow oil, b. p. 130~140°C/5 mmHg, n_D^{15} 1.4420.

Found: C, 57.02; H, 7.10. Calcd. for $C_{13}H_{20}O_6$: C, 57.34; H, 7.40%.

Ethyl 2, 3, 6-Trihydroxybenzoate (VII).—Two grams of VI was shaken at room temperature for 5 hr. with 20 ml. of 0.1 N hydrochloric acid and left to stand for 2 weeks. A light violet precipitate was collected by filtration, washed with water and dried. The yield of crude VII was 0.82 g. (56.1%), m. p. 149~151°C. Two recrystallizations from 30% ethanol raised the melting point to 154~155°C.

Found: C, 54.26; H, 5.20. Calcd. for $C_9H_{10}O_5$: C, 54.54; H, 5.09%.

VII was also obtained by heating 2.0 g. of VI in 20 ml. of 0.1 N hydrochloric acid at the boiling temperature for an hour. After cooled, a precipitate was removed by filtration, washed with water and dried. The yield of crude VII was 0.31 g. (21.2%). By two recrystallizations of this crude product from 30% ethanol, white crystals of VII, m. p. 154~158°C, were obtained. The product was identified with the sample which was prepared at room temperature by mixed fusion test and comparison of infrared spectra.

Found: C, 54.54; H, 5.20. Calcd. for $C_9H_{10}O_2$: C, 54.54; H, 5.09%.

Ethyl α-(2, 5-Diethoxy-2, 5-dihydro)furfuroyl-γ-oxovalerate (VIII).—Sodium hydride (0.0277 mol.) and 20 ml. of benzene were placed in a three-necked flask fitted with a mechanical stirrer, a dropping funnel and a reflux condenser carrying a soda-lime tube. 7.5 g. (0.0277 mol.) of VI was added dropwise to the stirred contents of the flask at room temperature. 4.56 g. (0.032 mol.) of bromoacetone was added after heating at reflux temperature for an hour, and the reaction mixture was heated for 10 hr. After the reaction, a small amount of ice water was added and acidified with acetic acid. The benzene layer was separated, washed with saturated sodium hydrogen carbonate solution then water, and dried over magnesium sulfate. Benzene and unreacted bromoacetone were removed by distillation, and further fractional distillation of the residue gave 0.7 g. of unreacted compound of VI, and 3.2 g. (45.0%) of VIII boiling at 114~120°C (1.8 mmHg). VIII was redistilled to give a yellow oil, b. p. 118~120°C (1.8 mmHg). n_D^{17} 1.4763. This yellow oil turned to brown when stored.

Found: C, 58.80; H, 6.91. Calcd. for $C_{16}H_{24}O_7$: C, 58.52; H, 7.73%.

2, 3, 6-Trihydroxyphenylacetone (X).—This compound was prepared from 1.90 g. (0.0071 mol.) of VIII as described above for preparation of VII (method of heating at reflux temperature). The yield was 0.80 g. (58.0%) of crude X. After two recrystallizations from water, white crystals of X, m. p. 140~142°C, were obtained. The product gave a green color with ferric chloride.

Found: C, 56.50; H, 6.18. Calcd. for $C_9H_{10}O_4$: C, 56.46; H, 5.92%.

2, 5-Diethoxytetrahydrofurancarboxylic Acid Ethyl Ester (XI).—XI was prepared in a quantitative yield by reduction of IV in ethanol under hydrogen of 50 kg./cm², using the W-6 Raney nickel[11] as a catalyst at room temperature for 7 hr. XI was a colorless liquid, b. p. 109~120°C (11 mmHg), n_D^{15} 0.4378.

XXI (quantitative yield) was prepared by the usual method from XI. Yellow crystals of XXI (m. p. 194~196°C) were obtained by three recrystallizations from nitromethane.

Found: C, 44.92; H, 3.62; N, 21.48. Calcd. for $C_{19}H_{18}O_{10}N_8$: C, 44.02; H, 3.49; N, 21.03%.

Ethyl (2, 5-Diethoxytetrahydro)furfuroylacetate (XII).—This compound was prepared from XI (21.0 g.) and ethyl acetate (23.9 g.) as described above for the preparation of VI. 12.9 g. (52.3%) of XIII was obtained as a light yellow liquid, b. p. 115~124°C (3.5 mmHg), n_D^{17} 1.4612.

Found: C, 57.28; H, 8.21. Calcd. for $C_{13}H_{22}O_6$: C, 56.92; H, 8.08%.

2, 3-Dihydroxybenzoic Acid (XIII).—One gram of XII in a mixture of 36 ml. of 0.1 N hydrochloric acid and 65 ml. of dioxane was heated at reflux temperature for 11 hr. After the reaction, the solvent was removed by distillation and the residue was sublimed under 6 mmHg on an oil bath (120~130°C). The product was identical with an authentic sample of commercial 2, 3-dihydroxybenzoic acid from mixed fusion test and comparison of infrared spectra.

Found: C, 54.73: H, 3.94. Calcd. for $C_7H_6O_4$: C, 54.55; H, 3.92%.

Ethyl α-(2, 5-Diethoxytetrahydro)furfuroyl-α-methylacetate (XIV).—This compound was prepared from 3.1 g. (0.0114 mol.) of XII and 2.61 g. (0.0171 mol.) methyl iodide by heating for 1.5 hr. in the ethereal solution as described above for the preparation of VIII. 2.20 g. (67.5%) of XIV was obtained as a yellow oil which turned to brown after a long time storage. B. p. 105~124°C (3 mmHg). This product was redistilled at 119~124°C (3 mmHg), n_D^{17} 1.4930.

Found: C, 56.25; H, 8.16. Calcd. for $C_{13}H_{24}O_6$: C, 56.56; H, 8.76%.

XIV was also prepared from 2.32 g. (0.01 mol.) of XI and 4.08 g. (0.04 mol.) of ethyl propionate as described above for preparation of VI. The yield of XIV was 0.37 g. (13.0%). Its infrared spectra showed this product was identical with the product which was prepared from XII and methyl iodide by the method described above.

1-Methyl-2, 3-dihydroxybenzene (XV).—0.90 g. of XIV in a mixture of 3.6 ml. of hydrochloric acid (0.1 N) and 6.5 ml. of dioxane was heated at reflux temperature for 3.5 hr. After the reaction, the solvent was distilled off at a reduced pressure. The residue was solidified on cooling. The product was purified by three recrystallizations from benzene to give 0.04 g. (13.0%) of XV which were

11) "Organic Syntheses", Vol. 29, 24 (1949).

colorless crystals, m. p. 46.5~47°C (reported m. p. 47°C). The product gave a green color with ferric chloride.

Found: C, 67.68; H, 6.62. Calcd. for $C_7H_8O_2$: C, 57.63; H, 6.50%.

Ethyl α-(2, 5-Diethoxytetrahydro)furfuroyl-α-heptadecylacetate (XVI).—This compound was prepared from 7.53 g. (0.026 mol.) of XII and 8.3 g (0.0263 mol.) of XX by reflux in *n*-butyl ether for 5 hr. as described above for preparation of VIII. After a fore-run of XII (1.90 g.), 2.0 g. (25.87% yield based on unrecovered XII) of XVI was obtained, b. p. 133~135°C (0.1 mmHg). The product was solidified (colorless) at room temperature, m. p. 46~47°C.

Found: C, 69.60; H, 11.58. Calcd. for $C_{28}H_{52}O_6$: C, 69.38; H, 10.81%.

Hydrourushiol (XVII).—One gram of XVI in a mixture of 10 ml. of 0.1 N hydrochloric acid and 10 ml. of dioxane was heated at reflux temperature for 10 hr. After the reaction, the solvent was distilled off. The residual oil[12] was dissolved in ethanol and treated with an excess of ethanolic solution of lead acetate trihydrate. The dense precipitate of lead salt was filtered off, washed with ether. The lead salt was suspended in ethanol and treated with hydrogen sulfide. The lead sulfide was removed by filtration and the solvent was distilled off from the filtrate, leaving an oil which solidified at room temperature as a colorless wax. The yield was 0.230 g. (34.7%) of XVII, m. p. 57~68.5°C, which was recrystallized from ether. The infrared spectra and melting point of the synthetic product were identical with those of an authentic sample.

Found: C, 78.26; H, 11.21. Calcd. for $C_{21}H_{36}O_2$; C, 78.09; H, 11.32%.

Ethyl α-(2, 5-Diethoxytetrahydro)furfuroyl-α-allylacetate (XVIII).—This compound was prepared from 6.20 g. (0.0228 mol.) of XII and 4.14 g. (0.0342 mol.) of allyl bromide by reflux in benzene for 7 hr. as described above for the preparation of VIII. The yield was 3.2 g. (45.0%) of XVIII, b. p. 125~134°C (3.5 mmHg), n_D^{20} 1.4640. The yellow oil XVIII turned to brown when stored for a few hr. A sample of XVIII reacted with bromine and permanganate.

Fund: C, 61.30; H, 8.72. Calcd. for $C_{16}H_{26}O_6$: C, 61.13; H, 8.34%.

1-Allyl-2, 3-dihydroxybenzene (XIX).—This compound was prepared from 2.70 g. of XVIII in 86 ml. of 0.1 N hydrochloric acid and 50 ml. of dioxane by reflux for 9 hr. After the reaction the solvent was distilled off. The residue was distilled under a reduced pressure to give a colorless liquid of b. p. 140~145°C/15 mmHg. The weight was 0.41 g. (32.0%) of XIX, which reacted rapidly with bromine and with permanganate. A sample of XIX gave an olive color with ferric chloride. The portion, b. p. 144~145°C (15 mmHg.) was analyzed.

Found: C, 72.10; H, 6.65. Calcd. for $C_9H_{10}O_2$: C, 71.98; H, 6.71%.

3-(8'-Heptadecenyl)catachol (XXV).—0.0246 mol. of sodium hydride in 30 ml. of *n*-butyl ether was placed in a three-necked flask with a mechanical stirrer, a dropping funnel and a reflux condenser carrying a soda-lime tube. 6.7 g. (0.0246 mol.) of XII was added dropwise to the stirred contents of the flask at room temperature for an hour, 5.2 g. (0.0164 mol.) of XXIV was added and the reaction mixture was heated for 10 hr. After the reaction, the reaction mixture was acidified with acetic acid and then *n*-butyl ether was removed by vacuum distillation. The residue was added to 30 ml. of 0.1 N hydrochloric acid and 20 ml. of dioxane and heated at reflux temperature for an hour. The reaction mixture was treated as described above for preparation of XVII. 0.298 g. (52.4%) of XXV was obtained as a pale yellow substance, b. p. 215~220°C (0.8 mmHg), m. p. 33~36°C, which gave a green color with ferric chloride and reacted with permanganate.

Found: C, 79.51; H, 11.19. Calcd. for $C_{23}H_{38}O_2$: C, 79.71; H, 11.05%.

The Institute of Scientific and Industrial Research
Osaka University
Sakai-shi, Osaka

12) B. Loev and C. R. Dawson, *J. Am. Chem. Soc.*, **78**, 6095 (1959).

Chelate Formation between Thorium(IV) and Sulfodichlorohydroxydimethylfuchson Dicarboxylic Acid (Trisodium Salt). Studies on the Composition and Stability of the Chelate and Analytical Applications of the Reaction

By Suresh C. SRIVASTAVA*, Surendra Nath SINHA and Arun K. DEY

(Received July 2, 1962)

Several members of the dyes of the hydroxytriphenylmethane group are known to form characteristic colored products with inorganic ions in solution, and due to this property, they are used variously as metallo-chromic indicators in complexometric titrations, as colorimetric reagents for detection and determination of microamounts of metals and as spot reagents.

One of the important members of this group of dyes is sulfodichlorohydroxydimethylfuchson dicarboxylic acid (trisodium salt, commonly known as Chrome Azurol S and abbreviated here as CAS; Color Index 723) represented by the following structure:

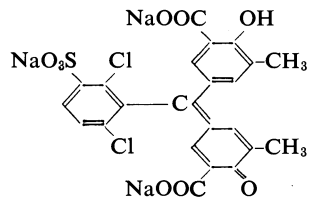

The main use of the reagent, hitherto, has been as a metallochromic indicator in complexometric titrations due to its tendency of forming characteristic colored chelates in solution with certain metal ions. It has been used by Willard and Horton[1] as an indicator in the titration of fluoride with thorium. Theis, and Musil and Theis[2] employed the reagent in the chelatometric determination of aluminum, copper and zinc, and for detecting beryllium in weakly acidic solutions. The utility of Chrome Azurol S as an indicator for zirconium was examined by Fritz and Fulda[3] who found it not to be satisfactory. Under varied specific conditions, Malát and Tenérova[4] used the reagent as an indicator for the complexometric determination of nickel, cerium and lanthanum. The simultaneous determination of iron(III) and aluminum(III) by EDTA titration using Chrome Azurol S as an indicator has also been described by Matsuo[5]. Sangal and Dey[6] have carried out the complexometric determination of thorium using Chrome Azurol S as an indicator.

Few applications of the reagent, except for its use in the determination of fluoride by the bleaching of its colored lakes with metals have been reported in the realm of colorimetric analysis. Ravinson and Harley[7] suggested the spectrophotometric determination of fluoride ion, which prevents the color development of the thorium-Chrome Azurol S lake. Macnulty and Woolard[8] described the use of an aluminum Chrome Azurol S chelate for the micro-determination of fluoride, and also Silverman and Shideler[9] made studies on the spectrophotometric determination of beryllium and fluoride with the reagent.

In view of the interesting chromophoric reactions of Chrome Azurol S, the present investigations were undertaken. It was observed to form very stable colored chelates in aqueous solution with copper(II), beryllium(II), magnesium(II), cadmium(II), aluminum(III), lanthanum(III), cerium(IV), titanium(IV), zirconium(IV), lead(II), thorium(IV), molybdenum(VI), uranium(VI), iron(III), cobalt(II), nickel(II), and palladium(II) under specific experimental conditions. This communication records the investigations with the thorium(IV)-chelate. The composition and stability have been determined by two different methods using absorbance measurements, and the results further corroborated by performing electrical conductance studies.

* Present address: Department of Chemistry, Louisiana State University in New Orleans, New Orleans 22, Louisiana, U. S. A.

1) H. H. Willard and C. A. Horton, *Anal. Chem.*, **22**, 1190 (1950).
2) M. Theis, *Z. anal. Chem.*, **144**, 106, 192, 275 (1955); A. Musil and M. Theis, ibid., **144**, 427 (1955).
3) J. S. Fritz and M. O. Fulda, *Anal. Chem.*, **26**, 1206 (1954).
4) M. Malát and M. Tenérova, *Chem. Listy*, **51**(11), 2135 (1957).
5) T. Matsuo, *Bunseki Kagaku*, **7**, 557 (1958).
6) S. P. Sangal and A. K. Dey, *Z. anal. Chem.*, **178**, 415 (1961).
7) D. Ravinson and J. H. Harley, *Anal. Chem.*, **25**, 795 (1953).
8) B. J. Macnulty and L. D. Woolard, *Anal. Chim. Acta*, **14**, 452 (1956).
9) L. Silverman and M. E. Shideler, U. S. At. Energy Comm. NAA-SR-2686, pp. 21 (1958), *Anal. Chem.*, **31**, 152 (1959).

Experimental

Materials. — *Standara Thorium Solution.* — BDH (AnalaR) sample of thorium chloride was dissolved in double distilled carbon dioxide-free water. The metal was estimated as oxalate in 4% hydrochloric acid and weighed as thorium(IV) oxide after ignition. A 0.1 M stock solution was prepared.

Reagent Solution.—BDH indicator Chrome Azurol S (trisodium salt; Color Index 723) was employed for making the solutions, which were standardized by determining the sulfur content of the compound. Double distilled carbon dioxide-free water was used and always fresh solutions were prepared.

Solutions of Diverse Ions.—These were prepared by dissolving the respective compounds (all reagent grade) in distilled water and made to suitable strengths.

Protective Colloid.—A 0.1% solution of dextrin was prepared in distilled water and filtered. Suitable amounts of this solution were added to the mixtures to avoid any chances of the precipitating out of the lake, as such a tendency was observed at certain concentrations. It was found that although dextrin slowly loses its protective properties with the passing of time, yet, it is by far, the most suitable reagent for the present purpose.

Other Reagents.—All other reagents were of analytical grade and were used without further purification.

Instruments Procedure and Calculations.—*Absorbance Measurements.*—A Unicam SP 500 spectrophotometer was employed for the measurements of absorbance. This was operated by a Doran's Mains unit connected to 220 V./50 cycle a. c. mains, further stabilized by a constant voltage transformer. One centimeter thickness of the solutions was employed by using matched silica cells supplied along with the instrument and distilled water blanks were used. The ultrasensitive phototube was used at wavelengths of 625 mμ or below, and the red sensitive phototube for those above 625 mμ. The phototube circuit was maintained at maximum sensitivity. Under these conditions, the slit width corresponded to very nominal band widths and usually ranged between 0.030 and 0.065 mm.

Colorimetric Measurements.—For these, a Klett Summerson photoelectric colorimeter was employed using the Klett filter No. 54 green (transmission 510~580 mμ). The Klett test tubes in which the solutions were kept for measurements had a uniform diameter of 1 cm.

pH Measurements. — Hydrogen-ion concentration of the solutions was measured with a Leeds and Northrup direct reading pH indicator with a glass calomel electrode system, operated on the aforementioned power mains. The instrument was standardized from time to time with a standard buffer of pH 6.8 supplied along with the same.

Electrical Conductance Measurements.—The measurements of electrical conductance were carried out with a Leeds and Northrup Kohlrausch slidewire with an audio-frequency oscillator in the circuit, operated on the same mains and using a dip type measuring cell having a cell constant 0.580.

Conditions of Study.—All experiments were performed in an air-conditioned room maintained at 30±1°C. The total volume of all the mixtures prepared for the measurements was kept at 50 ml. (variation in the method of continuous variations was done within 25 ml., and the volume then raised to 50 ml. after adding suitable amounts of dextrin and ammonium nitrate, the latter being used for swamping of the system). The individual solutions and mixtures were kept immersed for about an hour, a time which was sufficient for their equilibration and for attaining the temperature of the bath, in a Townson and Mercer's precision thermostat maintaining a temperature of 30±0.01°C. The pH of all the solutions and mixtures was adjusted to 4.5±0.2, by the addition of suitable amounts of sodium hydroxide or perchloric acid. Ionic strength in all the mixtures was also kept constant at 0.15 by the addition of proper amounts of a solution of ammonium nitrate.

Procedure.—The composition of the chelate has been established by employing two different methods viz., (i) the method of continuous variations[10] (using absorbance and electrical conductance measurements) and (ii) the mole ratio method of Yoe and Jones[11] (using absorbance measurements).

Job's method of continuous variations involves the preparation of a series of mixtures with varying mole per cent of the two interactants forming the complex, and the measurement of some physical property of these solutions. A plot of the difference between the observed value and the calculated value of the particular physical property assuming no reaction, should show a maximum or minimum at the mole per cent corresponding to the complex formed.

Despite the various criticisms[12] that have been put against this method, it is still very popular for the study of the composition of complexes in solution, and it is agreed that the results are reliable when absorbance measurements are carried out. In the course of the present studies, electrical conductance was also chosen, besides absorbance, as the index property, and it has been observed that the method yields reliable results not only with absorbance measurements, but with measurements of electrical conductance as well.

In the mole ratio method, a series of solutions is prepared containing a constant amount of the metal ion, but with increasing ratios of reagent to the ion (or vice versa). When the absorbances of these solutions are measured and plotted against the concentration ratios, the plot should be a straight line that rises until the combining ratio of reagent to the metal ion is reached. The curve from this point on should become horizontal unless the reagent itself has some absorbance at the wavelength employed. In such a case the curve should abruptly change slope, but instead of becoming perfectly horizontal, it would have a positive slope, the angle depending upon the degree of absorbance of the reagent solution[13]. No abrupt break in the

10) P. Job, *Compt. rend.*, **180**, 928 (1925); *Ann. Chim.*, (**10**) **9**, 113 (1928).
11) J. H. Yoe and A. L. Jones. *Ind. Eng. Chem., Anal. Ed.*, **16**, 111 (1944).
12) F. Woldbye, *Acta Chem. Scand.*, **9**, 299 (1955).
13) H. P. Holcomb and J. H. Yoe, *Anal. Chem.*, **32**, 612 (1960).

curve occurs, however, in the case of a complex undergoing appreciable dissociation. In such a case, the continuous curve becomes approximately parallel to the molar ratio axis only when an excess of the variable compound is added. Results obtained by extrapolation of this curve are uncertain but it is found in many cases, that such a curve may be made to break sharply at the correct molar ratio by adjusting the ionic strength to a suitable value by the addition of an indifferent electrolyte[14].

Evaluation of the Stability Constant.—The stability constant of the complex has been calculated with the help of absorbance data by two different methods. Anderson and coworkers[15] have described a convenient method for the calculation of the stability of colored complexes in solution based on the composition of mixtures having identical color i.e., the same absorbance values. Their method suffers from a limitation that both the interacting solutions forming the complex should be colorless and should not have any absorbance at the λ_{max} of the complex species. This difficulty has been overcome by a modification of this method by Dey and coworkers[16] who described a procedure for calculating the stability in the case of complexes where one of the interactants may be colored. The method has thus been found to be more useful and applicable under a wider variety of conditions. The method, in precise, is as follows. Continuous variations method is employed using equimolecular solutions and the total volume is kept constant. The absorbances of the mixtures which are noted at the λ_{max} of the complex are plotted against mole fractions of the metal ion i.e., [M]/([M]+[Ke]) ([M] is the concentration of the metal ion and [Ke] that of the chelating agent). The absorbance of the mixtures is due to the color of the chelate and the reagent, since most of the metal ions are colorless at very high dilutions. When the concentration of the metal ions increases progressively (e.g. in the descending portions of the curves), the ligand concentration decreases, and on any point in the descending portions of the curves, a large majority of the reagent may be assumed to be bound up in the complex, and the free chelating agent is negligible to contribute significantly to the total absorbance of the system. The absorbance in these portions is hence, due to the chelate alone, and at the same value of absorbance in a number of such curves, the respective amounts of the complex formed in the individual cases are identical. The concentration of the chelate can be calculated by the following procedure:

In an equilibrium of the type involving a metal ion and a chelating agent in the ratio of 1 : 1,

$$M+Ke \rightleftarrows MKe$$

the stability constant is given by:

$$K=\frac{x}{(a-x)(b-x)} \quad (1)$$

where x is the concentration of the chelate at equilibrium and a and b respectively are the initial concentrations of the metal ion and the chelating agent. Taking two concentrations of the reactants, i.e., two values of a and b, where absorbance is the same, the value of x will also be the same.

Hence

$$K=\frac{x}{(a_1-x)(b_1-x)}=\frac{x}{(a_2-x)(b_2-x)} \quad (2)$$

or

$$x=\frac{a_1b_1-a_2b_2}{(a_1-b_1)(a_2-b_2)} \quad (3)$$

Thus, it is possible to calculate x, and therefrom the value of K with the help of expression 1.

The value of the stability constant, thus calculated, has also been corroborated by the value obtained by the mole ratio method through a calculation of the degree of dissociation, as suggested by Harvey and Manning[17].

Results and Discussion

Rehavior of the Reagent as a Colloidal Electrolyte.—In view of the behavior of a number of dyes as colloidal electrolytes, electrical conductance studies were performed with aqueous solutions of Chrome Azurol S to investigate its colloidal characteristics, if any[18]. The reagent has been found to behave as a colloidal electrolyte and hence, as emphasized by Dey[19] that in the case of colloidal solutions, the characteristics of a true solution are often displayed when extremely dilute solutions are used, very dilute solutions of the order $\approx 10^{-4}$ and 10^{-5} M were employed in the present studies.

Rate of Color Formation and Stability of Color at Room Temperature.—The color formation does not depend upon reaction time and is instantaneous. However, the mixtures were kept for one hour after preparing, to allow for equilibration. A mixture containing 5.0×10^{-5} M thorium chloride and 5.0×10^{-5} Chrome Azurol S at pH 4.5 retained its absorbance value x even after seventy two hours.

TABLE I. INFLUENCE OF TEMPERATURE

Concn. of thorium chloride	5.0×10^{-5} M
Concn. of CAS	5.0×10^{-5} M
pH of the mixture	4.5

Temp., °C	5	10	15	20	30	40	50	60	70	80
Colorimeter reading	268	270	270	270	270	270	280	285	290	295

14) A. E. Harvey and D. L. Manning., *J. Am. Chem. Soc.*, **72**, 4488 (1950).
15) R. C. Anderson and S. E. Turner, ibid., **70**, 1195 (1948); **71**, 909 (1949); R. T. Foley and R. C. Anderson, ibid., **71**, 912 (1949).
16) A. K. Mukherji and A. K. Dey, *J. Inorg. Nucl. Chem.*, **6**, 314 (1958); *Anal. Chim. Acta*, **18**, 324 (1958); S. K. Banerji and A. K. Dey, Proc. Symp. Chem. Coord. Compds., Agra, 1959, **2**, 198 (1960).
17) A. E. Harvey and D. L. Manning, *J. Am. Chem. Soc.*, **72**, 4488 (1950).
18) S. C. Srivastava, R. L. Seth and A. K. Dey, *J. Colloid Sci.*, **17**, 86 (1962).
19) A. K. Dey, ibid., **3**, 473 (1948).

Influence of Temperature.—The color intensity changes slightly above 40°C, as evident from Table I.

Order of Addition of Reagents.—No appreciable change in observations was found to occur when the order of the addition of reagents was alternated. However, a slightly better sensitivity was obtained, when the reagent solution was added to the metallic ion after the pH and ionic strength of the latter were adjusted to the proper values.

Beer's Law.—A calibration curve was prepared in order to determine whether or not the thorium-Chrome Azurol S complex obeys Beer's law. A series of solutions containing varying amounts of thorium ions and excess reagent were prepared. The color intensity was measured against a reagent blank. A plot of the data showed that the complex concentration is proportional to the absorbance between the concentration limits of 0.23 and 8.35 p. p. m. of thorium, as indicated by the straight lines over this range (Figs. 1 and 2).

Nature of the Complex in Solution. — The method of Vosburgh and coworkers[20] was employed to determine the nature of the complexes formed in solution. Mixtures containing thorium chloride and Chrome Azurol S in different stoichiometric ratios (e. g., 3 : 1, 2 : 1, 1 : 1, 1 : 2, 1 : 3, etc.) were prepared and absorbance of each of them was measured at suitable intervals between a range of

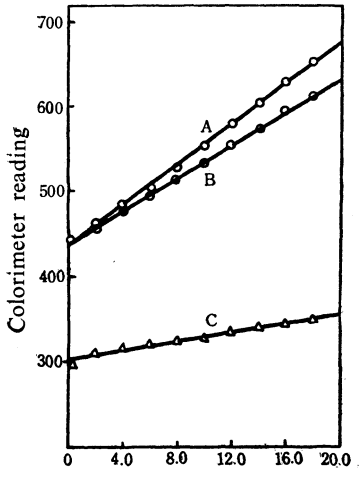

Fig. 1.

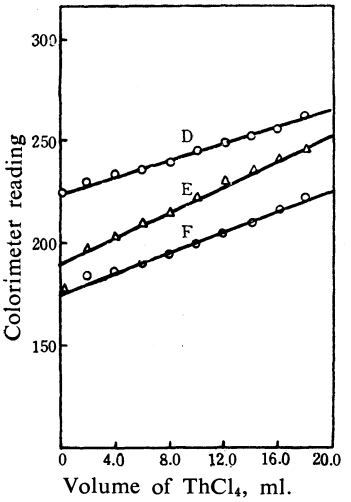

Fig. 2.

Figs. 1 and 2. Adherence to Beer's law.

(Total volume 50 ml.)
20 ml. CAS+x ml. $ThCl_4$+(30−x)ml. H_2O
Concn. of CAS (M×10⁴): Curve A 2.5, B 2.5, C 1.66, D 1.25, E 1.0 and F 1.0
Concn. of $ThCl_4$ (M×10⁴): Curve A 1.0, B 0.5, C 0.33, D 0.25, E 0.4 and F 0.66

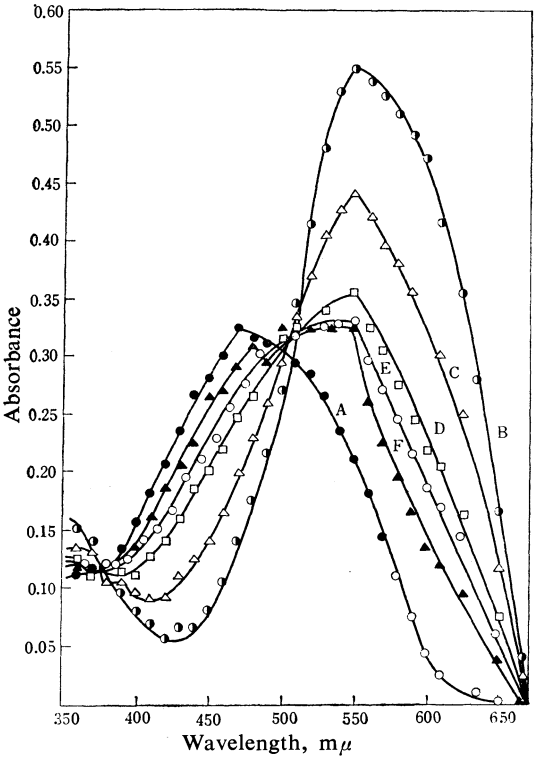

Fig. 3. Absorption spectra studies of mixtures of thorium chloride and Chrome Azurol S, pH 4.5±0.2, μ 0.15 (NH_4NO_3), dextrin 0.1%.

Curve A: Reagent 4.00×10^{-5} M
Curve B: $c=8.00\times10^{-5}$ M, $p=0.5$
Curve C: $c=4.00\times10^{-5}$ M, $p=1.0$
Curve D: $c=2.66\times10^{-5}$ M, $p=1.5$
Curve E: $c=2.00\times10^{-5}$ M, $p=2.0$
Curve F: $c=1.33\times10^{-5}$ M, $p=3.0$

20) W. C. Vosbugh and coworkers, *J. Am. Chem. Soc.*, **63**, 437 (1941); **64**, 1630 (1942).

TABLE II

Fig.	Curve	$c\times10^4$ M	p	mμ	Peak occurs at vol. of $ThCl_4$, ml.	Composition of the chelate Th(IV) : CAS
4	A	4.00	1.00	550	12.5	1 : 1
	B	2.66	1.00	550	12.5	1 : 1
	C	2.00	1.00	550	12.5	1 : 1
5	A	4.00	1.00	530	12.5	1 : 1
	B	2.00	1.00	570	12.5	1 : 1
	C	2.66	1.00	530	12.5	1 : 1
6	A	4.00	0.66	530	10.0	1 : 1
	B	2.66	1.50	530	15.0	1 : 1
7	A	4.00	0.66	550	10.0	1 : 1
	B	2.66	1.50	550	15.0	1 : 1

wavelength from 350 to 750 mμ The results plotted graphically in Fig. 3 show that reagent has its maximum absorption at 470 mμ at pH 4.5 (curve A). In curves B, C, D, E and F, the wavelength of maximum absorbance shifts to 550 mμ. In curves E and F, where Chrome Azurol S is present in excess slight peaks near about 485 mμ may be seen to occur. However, in every case, there is a clear indication of the formation of only one complex in solution under the conditions of study having λ_{max} at 550 mμ. (This fact is further confirmed by the results obtained at different wavelengths of study.)

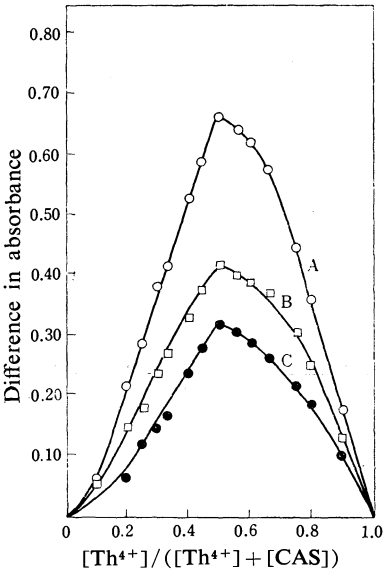

Fig. 4. Determination of the composition from absorption spectra studies of equimolecular solutions at 550 mμ; p=1, pH 4.5±0.2, μ 0.15 (NH_4NO_3), dextrin 0.1%.

Curve A: $c=4.00\times10^{-4}$ M
Curve B: $c=2.66\times10^{-4}$ M
Curve C: $c=2.00\times10^{-4}$ M

Stoichiometry of the Components.—The composition was established by the above-mentioned methods using absorbance as well as electrical conductance measurements. Out of a large number of experiments performed some of the typical results have been represented in Figs. 4—13.

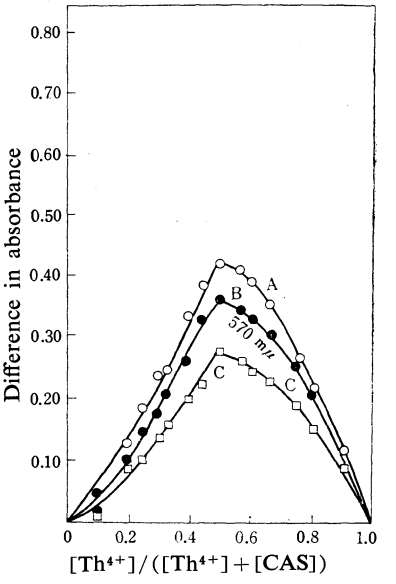

Fig. 5. Determination of the composition from absorption spectra studies of equimolecular solutions at 530 mμ (curve B, 570 mμ); p=1. Concentrations, pH and μ same as in Fig. 4.

TABLE III

Fig.	Curve	$c\times10^4$ M	p	Peak occurs at vol. of $ThCl_4$, ml.	Composition of the chelate Th(IV) : CAS
8	A	6.66	1.00	25.0	1 : 1
	B	5.00	1.00	25.0	1 : 1
	C	3.33	1.00	25.0	1 : 1
9	A	3.33	2.00	33.3	1 : 1
	B	3.33	1.50	30.0	1 : 1

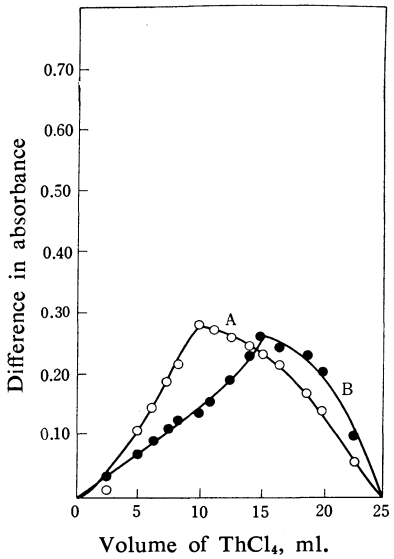

Fig. 6. Determination of the composition from absorption spectra studies of non-equimolecular solutions at 530 mμ; pH 4.5±0.2, μ 0.15 (NH_4NO_3), dextrin 0.1%.

Curve A: $c=4.00\times10^{-4}$ M, $p=0.66$
Curve B: $c=2.66\times10^{-4}$ M, $p=1.50$

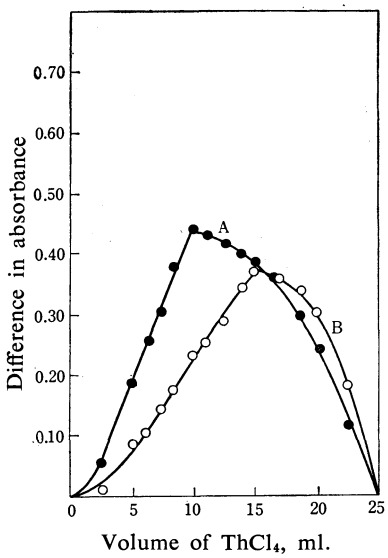

Fig. 7. Determination of the composition from absorption spectra studies of non-equimolecular solutions at 550 mμ. Concentration, pH and μ same as in Fig. 6.

Table II summarizes the results on the composition of the chelate from Figs. 4—7, using the continuous variations method with absorbance measurements. In the legends, c represents the concentration of thorium chloride and p the ratio c'/c, c' being the concentration of Chrome Azurol S.

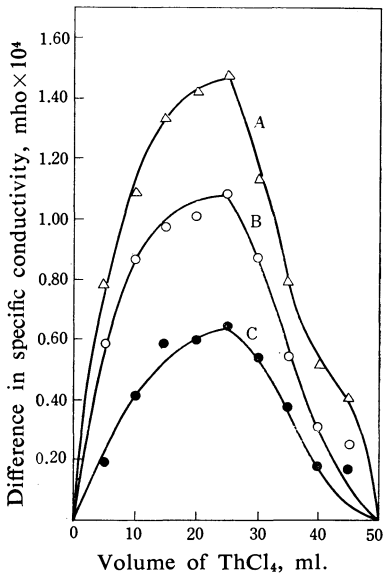

Fig. 8. Determination of the composition from electrical conductance studies of equimolecular solutions ($p=1$).

Curve A: $c=6.66\times10^{-4}$ M
Curve B: $c=5.00\times10^{-4}$ M
Curve C: $c=3.00\times10^{-4}$ M

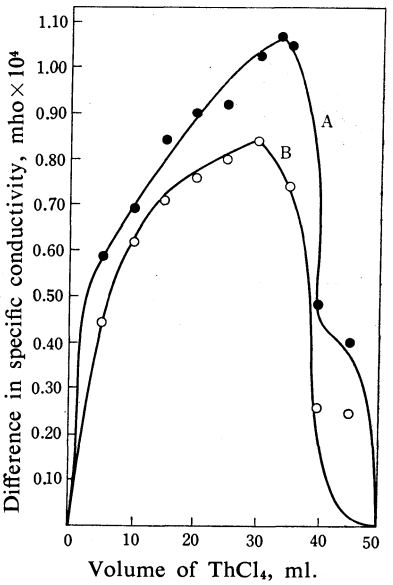

Fig. 9. Determination of the composition from electrical conductance studies of non-equimolecular solutions.

Curve A: $c=3.33\times10^{-4}$ M, $p=2.00$
Curve B: $c=3.33\times10^{-4}$ M, $p=1.50$

The results from the method of continuous variations using electrical conductance measurements (Figs. 8 and 9) are summarized in Table III.

It is perfectly clear from these tables

TABLE IV

Method employed	pH	Ionic strength, μ	Log K	$\Delta F°$ at 30°C, kcal.
Method of Dey et al.	4.5±0.2	0.15 (NH_4NO_3)	4.2±0.1	−5.8±0.1
Mole ratio method	4.5±0.2	0.15	4.8±0.1	−6.7±0.1

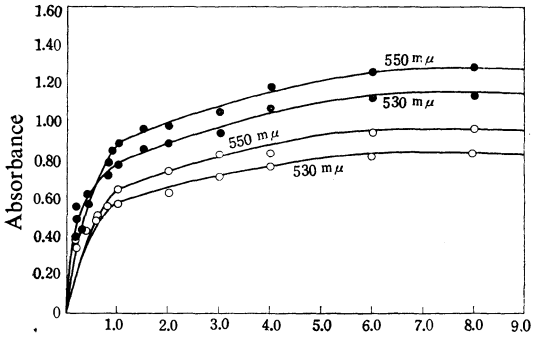

Fig. 10. Determination of the composition from absorbance studies by the mole ratio method; μ not adjusted (Fig. 10), μ 0.15 (NH_4NO_3) (Fig. 11), pH 4.5±0.2, ● concentration of CAS 6.66×10^{-5} M, ○ 5.00×10^{-5} M

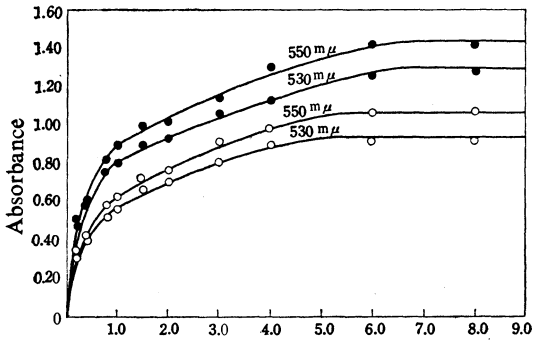

Fig. 11. Determination of the composition from absorbance studies by the mole ratio method; μ not adjusted (Fig. 10). μ 0.15 (NH_4NO_3) (Fig. 11), pH 4.5±0.2, ● concentration of CAS 6.66×10^{-5} M, ○ 5.00×10^{-5} M

that the thorium-Chrome Azurol S chelate consists of one thorium ion to one molecule of reagent, and hence, may be represented as Th (CAS).

Results of the mole ratio method also (Figs. 10 and 11) lend a corroboration for the same composition of chelate.

Calculation of the Stability Constant.—The values of the stability constant (log K), as determined by two different methods outlined earlier, are described in Table IV. The particular values of pH and ionic strength, which were maintained constant, are also mentioned. Also, the free energy change of formation has been calculated with the help of the expression.

$$\Delta F° = -RT\ln K$$

the terms having their usual meaning:

The results obtained by both the methods agree fairly with each other. The values and the methods may, hence, be taken as reliable.

Suggestions on the Structure of the Chelate.—It may be seen from the structure of the reagent Chrome Azurol S, that the trisodium salt is ionizable and in neutral solutions, the compound probably exists as a trivalent anion.

According to the color changes that the compound undergoes with variation in hydrogen-ion concentration of the medium, it may be concluded that it exists in at least three different structural forms. The wavelength of maximum absorbance of the reagent depends upon the pH as follows.

TABLE V

pH	Wavelength of maximum absorbance, λ_{max}, mμ
1.50~5.15	465, 490
6.00~10.15	425
11.65 and above	595

The following structures, therefore, appear to be reasonable for the reagent in the acidic, neutral and alkaline media:

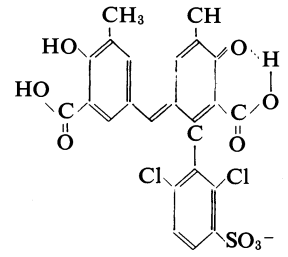

(I) Acidic medium

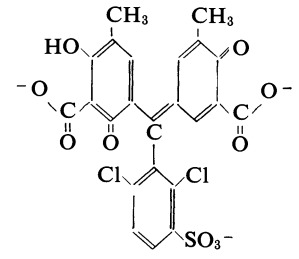

(II) Neutral medium

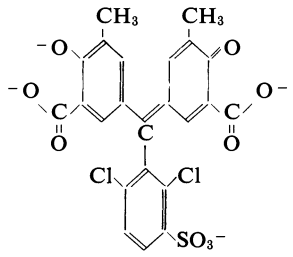

(III) Alkaline medium

It is not possible to obtain definite information on the position of the chelate ring in the thorium-Chrome Azurol S chelate from the experimental results described in the present paper. Still it may be evident that there are two alternative positions where chelation might occur. The metal ion may be coordinated either between the quinoid oxygen and the adjacent oxygen of the carboxylic group, or between the phenolic oxygen and the adjacent carboxylic oxygen. It may be noted that the wavelength of maximum absorbance of the chelate is 550 mμ. The λ_{max} of the reagent alone lies at 595 mμ in a strongly alkaline medium, where the structure seems to suggest the removal of the phenolic hydrogen by ionization. In a neutral medium on the other hand, the reagent is observed to have maximum absorption at 425 mμ. Since the wavelength of maximum absorbance of the chelate is more near to that of structure III, rather than to structures II and I it is very likely that the phenolic hydrogen gets replaced during the process of chelation. Hence, it appears reasonable to suggest that the chelation in this case occurs between the phenolic and the carboxylic oxygens and not between the quinoid oxygen and the adjacent carboxylic oxygen.

Effect of Hydrogen-Ion Concentration.—The absorbances of mixtures containing thorium chloride and Chrome Azurol S in the ratio 1 : 1 (concentration of each 8.0×10^{-5} M) at different pH were measured at various wavelengths. Figure 13 shows the results, where it is clearly seen that the wavelength of maximum absorbance of the chelate is 550 mμ from pH 2.50 to 7.25, indicating thereby that the same is stable within this range of pH. The variation with pH in color intensity of the

Table VI. Tolerance limits for diverse ions

Concn. of thorium chloride	2.0×10^{-5} M
Concn. of CAS	1.0×10^{-4} M
pH of the mixtures	4.5 ± 0.2
Temp.	30°C

Foreign ion	Added as	Concn. of ions p. p. m.	Observed change in absorbance, %	Tolerance limit p. p. m.
Li^+	$LiCl$	140	−4	
		75	−2	75
Ag^+	$AgNO_3$	432	+6	
		162	+2	Large excess
Pb^{2+}	$Pb(NO_3)_2$	246	+3	
		164	+2	Large excess
Hg^{2+}	$HgCl_2$	62	+5	
		28	+2	28
Cu^{2+}	$CuSO_4$	Interferes at all concentrations		0
Bi^{3+}	$Bi(NO_3)_3$	70	+10	15
		15	+2	
Cd^{2+}	$CdSO_4$	112	+4	
		66	+2	66
AsO_3^{3-}	H_3AsO_3	69	+9	
		18	+2	18
Sb^{3+}	$SbCl_3$	49	+3	
		31	+2	31
Pd^{2+}	$PdCl_2$	Interferes at all concentrations		0
Fe^{2+}	$(NH_4)_2Fe(SO_4)_2$	Interferes at all concentrations		0
Fe^{3+}	$FeCl_3$	Interferes at all concentrations		0
Al^{3+}	$Al(NO_3)_3$	Interferes at all concentrations		
Cr^{3+}	$CrCl_3$	36	+4	
		18	+2	18
La^{3+}	$LaCl_3$	Interferes at all concentrations		0
Mn^{2+}	$MnSO_4$	88	+7	
		28	+2	28
Zn^{2+}	$ZnCl_2$	52	+3	
		39	+2	39

TABLE VI (Continued)

Foreign ion	Added as	Concn. of ions p. p. m.	Observed change in absorbance, %	Tolerence limit p. p. m.
Ni^{2+}	$NiSO_4$	40	+4	
		20	+2	20
Co^{2+}	$Co(NO_3)_2$	34	+3	
		22	+2	22
Ba^{2+}	$BaCl_2$	137	+4	
		68	+2	68
Sr^{2+}	$Sr(NO_3)_2$	90	+3	66
		60	+2	
Ca^{2+}	$CaCl_2$	100	+7	
		30	+2	30
Mg^{2+}	$MgSO_4$	45	+6	
		20	+2	20
Be^{2+}	$BeSO_4$	Interferes at all concentrations		0
Zr^{4+}	$ZrOCl_2$	Interferes at all concentrations		0
Ti^{4+}	$TiCl_4$	Interferes at all concentrations		0
Ce^{3+}	$Ce_2(SO_4)_3$	27	+4	
		15	+2	15
Ce^{4+}	$Ce(SO_4)_2$	24	+5	
		10	+2	10
WO_4^{2-}	Na_2WO_4	56	−4	
		28	−2	28
MoO_4^{2-}	$(NH_4)_2NoO_4$	68	+4	
		40	+2	40
CrO_4^{2-}	K_2CrO_4	93	−6	
		36	−2	36
VO_3^-	NH_4VO_3	60	−3	
		45	−2	45
SeO_3^{2-}	H_2SeO_3	72	+3	
		48	+2	48
TeO_3^{2-}	K_2TeO_3	51	−5	
		22	−2	22
UO_2^{2+}	UO_2SO_4	Interferes at all concentrations		0
Au^{3+}	$AuCl_3$	30	+4	
		15	+2	15
F^-	NaF	Interferes at all concentrations		0
Cl^-	KCl	280	−3	
		180	−2	Large excess
I^-	KI	1280	−4	
		640	−2	Large excess
ClO_3^-	$KClO_3$	664	−3	
		451	−2	Large excess
NO_2^-	$NaNO_2$	460	−3	
		293	−2	Large excess
NO_3^-	$NaNO_3$	310	−5	
		165	−2	Large excess
CNS^-	KCNS	Interferes at all concentrations		0
$B_4O_7^{2-}$	$Na_2B_4O_7$	Interferes at all concentrations		0
CO_3^{2-}	Na_2CO_3	Interferes at all concentrations		0
Oxalate	$K_2C_2O_4$	Interferes at all concentrations		0
Tartrate	K_2 tart.	Interferes at all concentrations		0
Citrate	Na_3 cit.	Interferes at all concentrations		0
Acetate	$NaC_2H_3O_2$	280	−6	
		95	−2	95
SO_4^{2-}	K_2SO_4	768	+3	
		576	+2	Large excess
$S_2O_3^{2-}$	$Na_2S_2O_3$	1120	+3	
		784	+2	Large excess
$S_2O_8^{2-}$	$K_2S_2O_8$	960	+8	
		220	+2	Large excess
PO_4^{3-}	NaH_2PO_4	270	−4	
		135	−2	Large excess

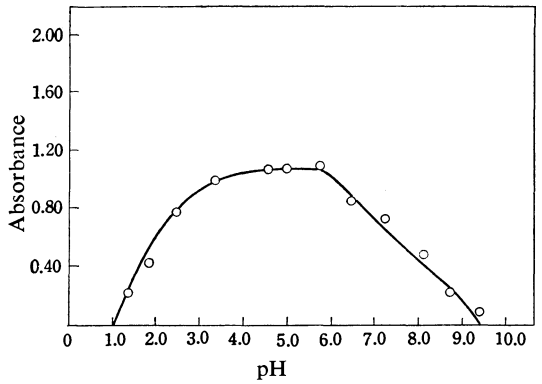

Fig. 12. Variation in color intensity of the chelate with change in pH at 550 mμ.
$c=8.0\times10^{-5}$ M, $p=1.00$

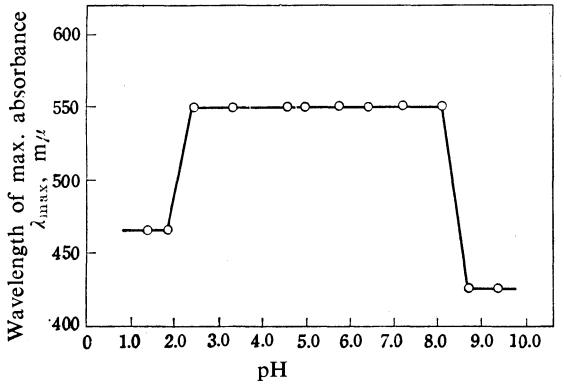

Fig. 13. Variation in the region of maximum absorption of the chelate with change in pH.
$c=8.0\times10^{-5}$ M, $p=1.00$

chelate at its λ_{max} is also represented in Fig. 12.

Sensitivity of the Reaction. — According to Sandell's expression, the sensitivity is 0.0047 γ/cm² at 550 mμ. The practical sensitivity, based on an absorbance of 0.010 unit, is 0.047 γ/cm².

Effect of Diverse Ions.—The effect of a large number of cations and anions has been studied and the tolerance limits calculated out in each case. For tolerance limit, that concentration of foreign ion has been chosen which affects the absorbance of the system by less than ±2%. It has been found that copper(II), beryllium(II), aluminum(III), iron(II), iron-(III), uranium(VI), zirconium(IV), oxalate, borate, citrate, tartrate, carbonate, fluoride and thiocyanate interfere at all concentrations as shown by the results listed in Table VI:

Suggested Procedure for the Colorimetric Determination of Thorium.—For the determination of thorium, using Chrome Azurol S as a reagent, the following procedure may be suggested: The interfering substances should be removed from the sample by the usual methods. The pure solution of thorium ions, thus obtained may directly be treated with a freshly prepared solution of Chrome Azurol S. The reagent should be added in about ten fold molar excess. The temperature should be maintained below 40°C and the pH at 4.5±0.2. The absorbance may be measured with a spectrophotometer and compared with a standard calibration curve to give the amount of thorium.

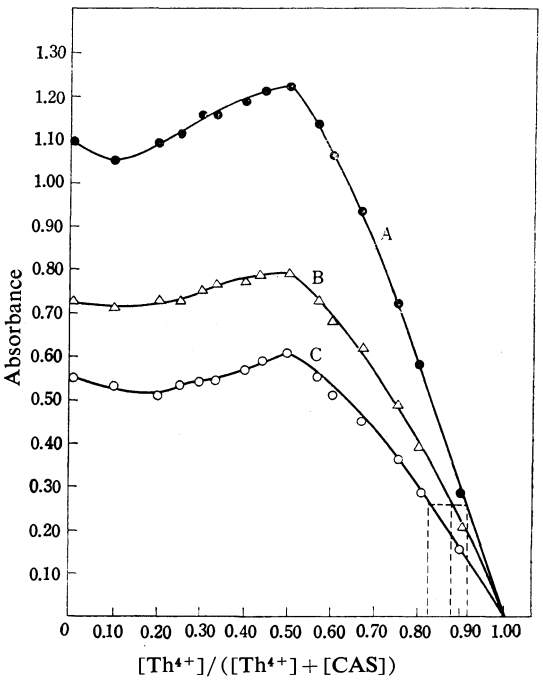

Fig. 14. Determination of the stability constant from absorbance data at 550 mμ. Concentrations, pH and μ same as in Fig. 4.

A grateful acknowledgment is made to the Council of Scientific and Industrial Research, India, for supporting the work, and for the award of research fellowships to two of the authors (S. C. S. and S. N. S.).

Department of Chemistry
University of Allahabad
Allahabad, India

*The Cationic Copolymerization of Styrene and p-Bromostyrene in Liquid Sulfur Dioxide**

By Niichiro TOKURA, Minoru MATSUDA and Masashi IINO

(Received August 11, 1962)

The effect of a solvent on the monomer reactivity ratios in cationic polymerization has been the subject of recent study. Overberger et al., carrying out the cationic copolymerization of styrene and *p*-chlorostyrene in carbon tetrachloride and nitrobenzene respectively, found no appreciable difference in r_1's and r_2's[1a,b]. However, in the cationic polymerization of *p*-chlorostyrene with isobutene, r_1 and r_2 varied as the solvent used was changed[1c]. They therefore suggested that the independence of r_1 and r_2 in the former case was due to the similarity of the structure of the comonomers applied[1b].

Marvel and Dunphy[2] have shown that the cationic copolymerization of 2-chloroethyl vinyl ether with α-methylstyrene and its derivatives resulted in a marked difference in the monomer reactivity ratios according to the solvents applied. Pepper[3] first found that the rate of cationic polymerization is largely dependent on the dielectric constants of the solvents applied. However, other examples have also been shown in which anomalies in the relationship between the dielectric constants of the solvents and the rates have been observed[4,5].

This paper aims at the elucidation of the effect of liquid sulfur dioxide on the cationic polymerization. A cationic copolymerization of styrene and *p*-bromostyrene in liquid sulfur dioxide has been undertaken; the results will be described below. The cationic polymerization in liquid sulfur dioxide differs from that in any other solvent; viz., in liquid sulfur dioxide, (1) the polymerization is much faster than that which would be expected from the dielectric constant of the solvent (liquid sulfur dioxide)[6a], (2) the reaction is assisted by a number of sulfur dioxide molecules in the transition state[6b], and (3) the chain transfers, both to the monomer and the solvent, are very small[6a]. Accordingly, somewhat different results have been expected in this copolymerization.

Experimental

Materials.—Styrene (U.C.C. product) was distilled twice in vacuo in a nitrogen atmosphere. *p*-Bromostyrene was prepared by a known method[7]; b. p., 89°C/13 mmHg, n_D^{20}, 1.5931. Boron trifluoride etherate was distilled twice in a nitrogen atmosphere. Liquid sulfur dioxide was dried over phosphorus pentoxide and distilled. Carbon tetrachloride was refluxed with sodium hydroxide and distilled. Benzene was purified by the ordinary method. Nitrobenzene was washed with a sodium hydroxide solution and with water, dried with phosphorus pentoxide, and distilled in vacuo. Ethylene dichloride was washed with sodium hydroxide and then with water, dehydrated with phosphorus pentoxide, and distilled. *p*-Cymene was washed with concentrated sulfuric acid, an aqueous sodium hydroxide solution, and water successively, dehydrated with calcium chloride, and distilled in vacuo in a nitrogen atmosphere. Cyclohexane was shaken with a mixture of ten per cent of concentrated sulfuric acid and one per cent of fuming sulfuric acid for 24 hr., washed with water, a sodium hydroxide solution, a potassium permanganate solution and water successively, dehydrated with calcium chloride, and distilled over sodium wire.

Method of Polymerization.—Styrene, *p*-bromostyrene and solvent were pipetted into a glass pressure vessel of 20 ml. capacity. The mixture was then, with the catalyst (borontrifluoride etherate), added to liquid sulfur dioxide. The polymerization was started in a constant temperature bath. The reaction was stopped by mixing in a large quantity of methanol. The precipitate was washed with methanol and dried in vacuo. From the weight of the copolymer produced, the rate of the polymerization was calculated. The composition of the copolymer was calculated from the elementary analysis.

* Polymerization in Liquid Sulfur Dioxide, Part XVI.

1) a) C. G. Overberger, L. H. Arond and J. J. Taylor, *J. Am. Chem. Soc.*, **73**, 554 (1951); b) C. G. Overberger, R. J. Ehrig and D. Tanner, ibid., **76**, 772 (1954); c) C. G. Overberger and V. G. Kamath, ibid., **81**, 2910 (1959).

2) C. S. Marvel and J. F. Dunphy, *J. Org. Chem.*, **25**, 2209 (1960).

3) D. C. Pepper, *Nature*, **158**, 789 (1940); *Trans. Faraday Soc.*, **45**, 397 (1949).

4) Y. Imanishi, T. Higashimura and S. Okamura, *Kobunshi Kagaku*, **17**, 236 (1960).

5) D. C. Pepper and P. J. Reilly, *Proc. Chem. Soc.*, **1960**, 200.

6) a) R. Asami and N. Tokura, *J. Polymer Sci.*, **42**, 545 (1960). b) N. Tokura, M. Matsuda and Y. Watanabe, ibid., **62**, 135 (1962).

7) R. H. Boundy and R. Boyer, "Styrene. Its Polymers, Copolymers and Derivatives", Reinhold Pub. Co., New York (1952), p. 788.

Results and Discussion

The Overall Rate of Copolymerization.—To a system consisting of styrene $(St)_0$ (3.0 ml.), *p*-bromostyrene $(BSt)_0$, and liquid sulfur dioxide $(SO_2)_0$ (3.0 ml.) with a catalyst $(BF_3Et_2O)_0$, was added 3.0 ml. of solvent of various dielectric constants. The reaction mixture then consisted of, $(St)_0$ 2.2, $(BSt)_0$ 1.9 and $(BF_3Et_2O)_0$ 5.7×10^{-3} mol./l., respectively. The added solvents were nitrobenzene (dielectric constant at 20°C $D=34.8$), ethylene dichloride ($D=10.4$), carbon tetrachloride ($D=2.3$) and benzene ($D=2.3$). The polymerization was conducted at −15°C.

The relationship between the mixed solvents and the rates of the copolymerization at −15°C is visualized in Fig. 1. As is seen in the figure, the copolymerization in pure liquid sulfur dioxide is the fastest among those in the solvent mixtures. This result is also consistent with the previous finding from the cationic polymerization in liquid sulfur dioxide[6a]. In Fig. 2, similar experiments with added solvents of small dielectric constants are compared: ($(St)_0$, 3.0 ml. (1.9 mol./l.), $(BSt)_0$, 3.0 ml. (1.6 mol./l.), $(BF_3Et_2O)_0$, 3.0×10^{-3} mol./l., $(SO_2)_0$, 3.0 ml., added solvent 5.0 ml., respectively, at −10°C). Although the dielectric constants of the added solvents were very close to each other, it is to be noted that a marked difference among the rates is to be found.

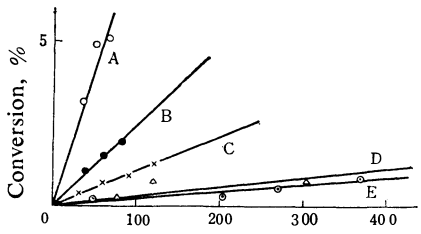

Fig. 1. Conversion vs. time plots.
A liq. SO_2
B Nitrobenzene with liq. SO_2
C Ethylene dichloride with liq. SO_2
D Carbon tetrachloride with liq. SO_2
E Benzene with liq. SO_2

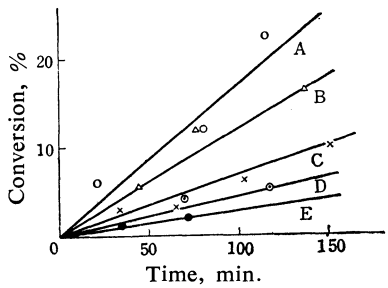

Fig. 2. Conversion vs. time plots.
A Cyclohexane with liq. SO_2
B Carbon tetrachloride with liq. SO_2
C *p*-Cymene with liq. SO_2
D Benzene with liq. SO_2
E Ethylene dichloride with liq. SO_2

The rate of copolymerization may be varied as the interaction of the solvent in this system changes. By the addition of cyclohexane to this system the rate is hardly affected. The order of rate is:

cyclohexane ($D=2.0$) > carbon tetrachloride ($D=2.3$) > *p*-cymene ($D=2.2$) > benzene ($D=2.3$)

and the largest rate drop is brought about by the addition of benzene. Despite the larger dielectric constant of ethylene dichloride ($D=10.4$), its rate ranks among the smallest, as may be seen in Fig. 2. The action of the added solvent on the rate of the cationic polymerization in liquid sulfur dioxide has already been shown and discussed in a previous article[6b], in which aromatic hydrocarbons in the liquid sulfur dioxide-polymerizing system also has a rate retarding effect.

Monomer Reactivity Ratio. — The monomer reactivity ratios were calculated according to

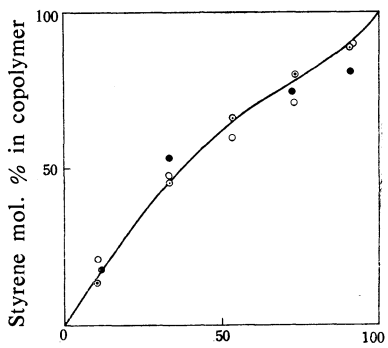

Fig. 3. Feed vs. copolymer composition plots.
○ −20°C ⊙ −15°C ● +10°C

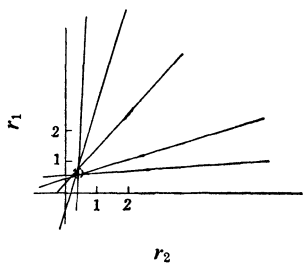

Fig. 4. MRR, r_1-r_2 plots for −20°C copolymerization in liquid sulfur dioxide.

TABLE I

Solvent	Catalyst, $\times 10^3$ mol./l.	Temp., °C	r_1	r_2
liq. SO_2	1.5	10	0.8±0.3	0.4±0.1
liq. SO_2	1.5	−20	0.8±0.3	0.4±0.1
liq. SO_2	5.7	−15	0.8±0.3	0.4±0.1
$C_6H_5NO_2$−liq. SO_2	5.7	−15	0.7±0.3	0.3±0.1[a]
C_6H_6−liq. SO_2	5.7	−15	0.9±0.4	0.4±0.2[a]
CCl_4−liq. SO_2	5.7	−15	1.0±0.5	0.5±0.2[a]
$C_6H_5NO_2$	10[c]	10	1.8±0.3	0.3±0.1[b]
C_6H_6	30	10	1.4±0.4	0.5±0.1[b]
CCl_4	30	10	1.8±0.4	0.3±0.2[b]
$CH_2CH_2Cl_2$	30	10	1.8±0.6	0.3±0.2[b]

a) liq. SO_2 5.0 ml., St-BSt 10.0 ml., solvent 5.0 ml.
b) St-BSt 8.0 ml., solvent 8.0 ml.
c) As the rate of the copolymerization (without liquid sulfur dioxide) was very slow, the catalyst content was increased.

the intersection method of Mayo and Lewis[8]. A typical example is shown in Figs. 3 and 4. In Fig. 3, feed vs. copolymer composition plots for the copolymerization in pure liquid sulfur dioxide at the temperatures of −20, −15 and 10°C with BF_3Et_2O are visualized. In Fig. 4, r_1 and r_2 are plotted to obtain the most suitable value of the monomer reactivity ratio for the result in Fig. 3 (−20°C). The MRR's (monomer reactivity ratios) of styrene (r_1) and *p*-bromostyrene (r_2) in liquid sulfur dioxide were found to be 0.8 and 0.4, respectively. As is shown in Fig. 3, the MRR's in liquid sulfur dioxide were independent both of the temperature of the reaction and of the quantity of the catalyst (BF_3Et_2O) used in the copolymerization.

The r_1's and r_2's were also calculated, by the same method, in the binary mixtures of

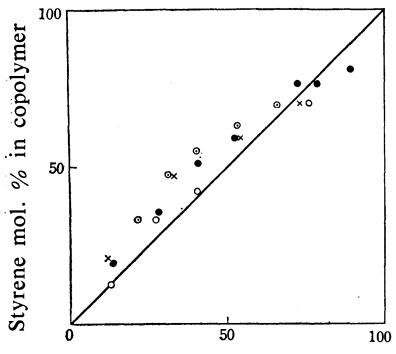

Fig. 5. Feed vs. copolymer composition plots in mixed solvents.
● Benzene+liq. SO_2
⊙ Nitrobenzene+liq. SO_2
○ CCl_4+liq. SO_2
× Liq. SO_2 (alone)

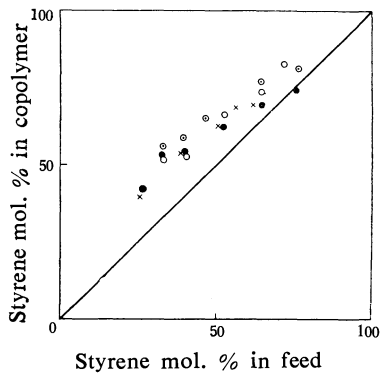

Fig. 6. Feed vs. copolymer composition plots in various solvents.
● Benzene ⊙ Nitrobenzene
○ CCl_4 × Ethylene dichloride

solvent and liquid sulfur dioxide and in pure solvents. The results are summarized in Table I. Figures 5 and 6 are the summarized plots of the feed vs. copolymer composition diagram in various solvents.

The MRR's were measured in equi-volume mixtures of liquid sulfur dioxide and the added solvents at −15°C. In system without liquid sulfur dioxide, since the rate of the copolymerization is too slow to permit the adequate performance of the experiment, the catalyst was increased to 10×10^{-3} in nitrobenzene and to 30×10^{-3} mol./l. in the other solvents respectively, as is described in Table I. The MRR's in the mixture of liquid sulfur dioxide with equi-volumes of *p*-cymene, *p*-xylene and cyclohexane were each also estimated by the same procedures; 0.9 and 0.4 were the values found for r_1, and r_2 respectively, which figures were similar to those of benzene.

The copolymerization in liquid sulfur dioxide is very fast. This fact is consistent with the previous finding that cationic polymerization

8) F. R. Mayo and F. M. Lewis, *J. Am. Chem. Soc.*, **66**, 1594 (1944).

is the fastest in liquid sulfur dioxide[6a] and with the fact that the Beckmann rearrangement in liquid sulfur dioxide is instantaneous[9].

In liquid sulfur dioxide, the monomer reactivity ratios are independent both of the temperatures and of the concentration of the catalyst in the reaction.

It is a very interesting finding that the MRR's in the respective solvents are very similar ($r_1=1.6$ and $r_2=0.3$), whereas by adding liquid sulfur dioxide the MRR's of r_1 drop to 1~0.7, while in liquid sulfur dioxide r_1 is 0.8 in spite of the similarity in the comonomer structure. When sulfur dioxide is added to the system the chain end of the styryl carbonium ion may lose its selectivity to styrene, the reactivity for *p*-bromostyrene being increased. The product of $r_1 \times r_2$ in liquid sulfur dioxide is 0.32, and the composition of the copolymer approaches that of the alternative copolymer. This finding is also in good accordance with the explanation above mentioned.

Summary

1) The cationic copolymerization of styrene and *p*-bromostyrene in liquid sulfur dioxide using boron trifluoride etherate as a catalyst has been carried out; the monomer reactivity ratios (MRR) have been found to be $r_1=0.8$ and $r_2=0.4$. The MRR value was independent of the temperature and of the quantity of the catalyst in the copolymerization.

2) The effect of added solvents in liquid sulfur dioxide has also been examined. However, the MRR's have been little affected by the added solvents, the rates of the copolymerization have largely been depressed, and the rates were not dependent on the dielectric constants of the added solvents, the rate in pure liquid sulfur dioxide being the fastest.

3) The same cationic copolymerization has been conducted in benzene, carbon tetrachloride, nitrobenzene and ethylene dichloride.

The MRR's were almost equal in all ($r_1=1.8$ and $r_2=0.3$).

The authors are indebted to the Seitetsu Kagaku K.K., Ltd., for its donation of liquid sulfur dioxide. A part of the expense for this project has been defrayed by a grant-in-aid by the Ministry of Education.

The Chemical Research Institute of Non-Aqueous Solutions
Tohoku University
Katahira-cho, Sendai

9) N. Tokura, K. Shiina and T. Terashima, This Bulletin, 35, 1986 (1962).

A Study of the Properties of Mixed Solutions of Sodium Dodecyl Sulfate and Dodecyl Alcohol

By Fumikatsu TOKIWA

(Received September 7, 1962)

A number of studies have reported on the effect of long-chain alcohols on such properties of solutions of surface active agents as their electrical conductivity and solubilizing power. Most of these studies have been made with solutions in which the additives have been dissolved completely by solubilization. However, it is also of importance to study the properties of those mixed solutions in which the amount of additives far exceeds that solubilized.

In previous papers[1-4] studying mixed solutions of sodium dodecyl sulfate and dodecyl alcohol, it was established that there exist some complexes composed of sodium dodecyl sulfate and dodecyl alcohol in the mixed solutions. Spectral experiment[2] on the mixed solutions indicated that the metachromatic color of toluidine blue changes abruptly to a normal color at a certain concentration of sodium dodecyl sulfate, the point depending on the amount of dodecyl alcohol. A similar color change has also been observed for the solution in the temperature 37~40°C range[2].

In the present paper electrical conductivity and viscosity measurements have been carried

1) I. Maruta, T. Sakai, F. Tokiwa and T. Saito, *J. Chem. Soc. Japan, Pure Chem. Sec.* (*Nippon Kagaku Zasshi*), **82**, 1512 (1961).

2) I. Maruta and F. Tokiwa, ibid., **82**, 1657 (1961).

3) I. Maruta and F. Tokiwa, ibid., **82**, 1660 (1961).

4) I. Maruta and F. Tokiwa, ibid., **83**, 732 (1962).

out in order to study the properties of the mixed solutions in further detail.

Experimental

Materials.—Dodecyl alcohol (DA) was purified by repeated fractional distillation under reduced pressure. Gas chromatography failed to detect its homologues. The hydroxyl value of DA was found to be 301.0 (calcd. 301.1). Sodium dodecyl sulfate (SDS) was prepared from DA by the method of Dreger et al.[5] and was purified by repeated recrystallization from ethanol, followed by extraction with petroleum ether.

Preparation of Mixed Solutions.—A previously described method[1,2] was used for preparing the mixed solutions of SDS and DA. When a precipitate appeared in the stock solution during storage, it was heated to about 50°C before use, causing the precipitate to disappear.

Electrical Conductivity and Viscosity Measurements.—Electrical conductivity was measured with a conductance bridge, a Yanagimoto Model MY-7. The platinum electrodes were slightly platinized, and the cell constant was 0.482. The water used in preparing the solutions had a specific conductance of $1.0\sim1.5\times10^{-6}$ ohm^{-1} cm^{-1}. The observed values were checked by measuring the equivalent conductances of potassium chloride solutions.

Viscosity was measured with an Ostwald-type viscometer, the flow time for water being 140.5 sec. The measurements were performed at varying temperatures ranging from 20 to 50°C with an accuracy of ±0.01°C.

Results and Discussion

In Fig. 1 the equivalent conductance of an aqueous solution of SDS is plotted against the square root of the SDS concentration with the addition of varying amounts of DA at 30°C. In some cases, the conductance decreased slightly with time in the regions indicated by dotted lines in Fig. 1. Therefore, the reading was taken after the constant value had been attained, which required from 70 to 90 min. Most of the curves represent averages of at least two series of measurements. The addition of DA lowered the conductance, the degree of lowering increasing with an increasing amount of DA for a fixed concentration of SDS.

It has been shown in previous papers that SDS molecules or ions form a complex with DA molecules in the mixed solution, even in the region of a low concentration of SDS. Spectral studies[3,6], furthermore, have suggested that the ion-head of SDS is markedly affected

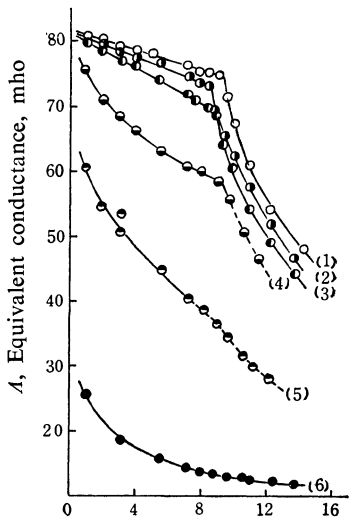

Fig. 1. The equivalent conductance plotted against the square root of the concentration of SDS with the addition of varying amount of DA at 30°C. The relative mole fractions of SDS and DA are; (1) 1.00 : 0.00, (2) 0.94 : 0.06, (3) 0.85 : 0.15, (4) 0.70 : 0.30, (5) 0.50 : 0.50, (6) 0.30 : 0.70.

by the hydroxyl group of DA in the complex formation. Therefore, one may explain the decrease in electrical conductance by the complex formation.

It can been seen in Fig. 1 that, in the mixed solutions, SDS exhibits a conductance behavior typical of ionic detergents up to a 0.3 mol. fraction of DA in SDS-DA. These curves exhibit a break point characteristic of critical concentration at a definite concentration of SDS. It is known that, when DA molecules are present in small amounts, they promote micelle formation and thus lower the critical concentration[7,8]. We can also observe a similar tendency in Fig. 1, though the effect there is not so distinct.

Previous investigation[2] has shown that the metachromatic color of toluidine blue in SDS-DA solutions returns abruptly to a normal color at a certain concentration of SDS, depending on the amount of DA present. The break point of the conductance concentration curve is considered to correspond to the point of this color change. In the present experiment, however, the effect of DA on the critical concentration seems to be not so marked.

5) E. E. Dreger et al., *Ind. Eng. Chem.*, **36**, 610 (1944).
6) I. Maruta, *J. Chem. Soc. Japan, Pure Chem. Sec.* (*Nippon Kagaku Zasshi*), **83**, 788 (1962).
7) B. D. Flockhart and A. R. Ubbelohde, *J. Colloid Sci.*, **8**, 428 (1953).
8) M. Miura and S. Arichi, *J. Sci. Hiroshima Univ., Sec. A*, **22**, 57 (1958).

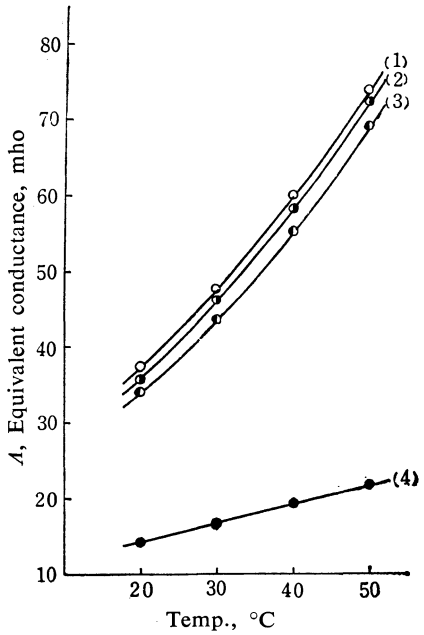

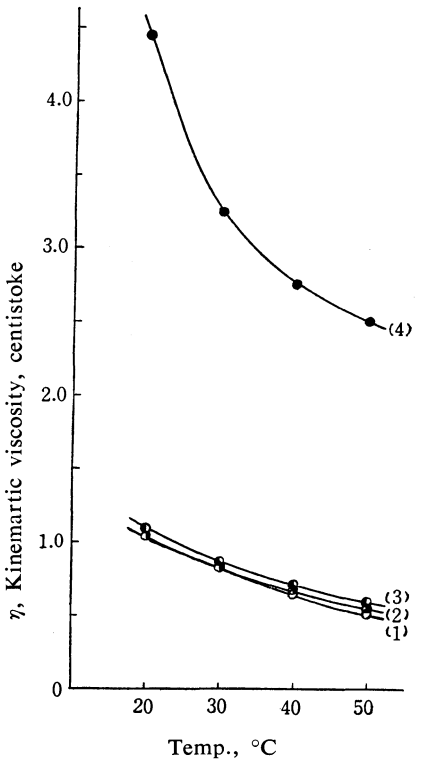

Fig. 2 and Fig. 3. The equivalent conductance and kinematic viscosity plotted against the temperature, for 0.02 molar SDS alone and with DA. The relative mole fractions of SDS and DA are; (1) 1.00 : 0.00, (2) 0.94 : 0.06, (3) 0.85 : 0.15, (4) 0.50 : 0.50.

The variation of the conductance with temperature is shown in Fig. 2 for 0.02 mol. SDS with varying amounts of DA. Figure 3 illustrates the variation of the viscosity for the same solutions. It may be seen in Figs. 2 and 3 that the presence of DA has little effect on the nature of the conductance and viscosity, except for the mixed solution containing a 0.5 mol. fraction of DA in SDS-DA.

In most aqueous solutions the change in conductance with the change in temperature is mainly caused by the change in viscosity, according to Walden's rule[9]. This is true insofar as the solution contains SDS alone, as is shown in Fig. 4, where the product of the conductance and of the viscosity is almost independent of the temperature. However, for mixed solutions with 0.06 and 0.15 mol. fractions of DA in SDS-DA, the product increases slightly with the increasing temperature. This may be explained either by an anomalous increase in conductance or by a decrease in viscosity with the increase in temperature. The results of the present experiment are consistent with the former explanation in that a change in the metachromatic color of toluidine blue in the mixed solutions occurs at relatively high temperatures (37~40°C)[2]. Since this

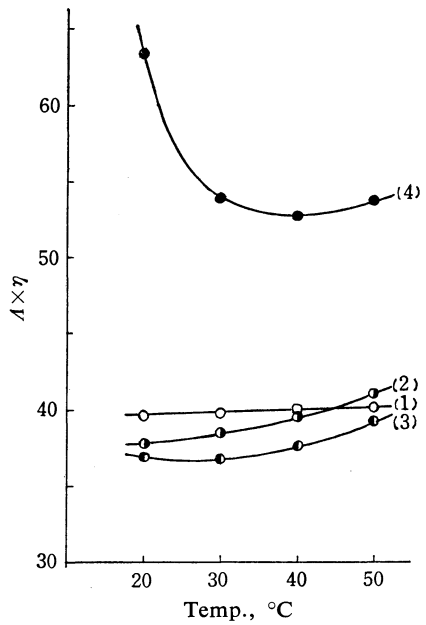

Fig. 4. The product of the equivalent conductance and the kinematic viscosity plotted against the temperature, for 0.02 molar SDS alone and with DA. The relative mole fractions of SDS and DA are; (1) 1.00 : 0.00, (2) 0.94 : 0.06, (3) 0.85 : 0.15, (4) 0.50 : 0.50.

9) A. F. Ward and A. G. Chitale, *Proc. 2nd. Int. Cong. Surface Activity*, 1, 319 (1956).

observation of color change can be interpreted in terms of the decomposition of the SDS-DA complex into SDS and DA, the slight increase in the product may be explained as due to the decomposition of the complex. In the presence of 0.5 mol. fraction of DA, the viscosity behavior somewhat differs. The fact that at low temperatures the mixed solution is very viscous and still shows a relatively good conducting property is an indication of the formation of involved complexes through which the positive ions can easily move.

Summary

Measurements have been made of the electrical conductivity and the viscosity of mixed solutions of sodium dodecyl sulfate (SDS) and dodecyl alcohol (DA). The addition of DA caused a lowering of the conductance, a phenomenon probably related to the formation of a complex composed of SDS and DA, but it did not essentially alter the form of the $\Lambda-\sqrt{c}$ curves up to 0.3 mol. fraction of DA in SDS-DA. The $\Lambda-\sqrt{c}$ curves of the mixed solution exhibit a break point which corresponds to a critical concentration of SDS, up to a 0.3 mol. fraction of DA in SDS-DA; the break point becomes obscure when the amount of DA present is larger than this value. The effect of the amount of DA on the critical concentration was not very large in this experiment.

The variation of the conductance and viscosity with the temperature was measured on the solution of SDS with varying concentrations of DA. For the solution of SDS without DA, the product of the conductance and the viscosity is almost independent of the temperature, while for the mixed solutions the product is dependent on the temperature, especially in the case of the mixed solution containing a considerable amount of DA.

The author wishes to express his hearty thanks to Professor Toshizo Isemura of Osaka University for his kind advice and encouragement throughout this work. Thanks are also due to Mr. Zenichi Miyagawa, Director of this Research Laboratory, for permission to publish this paper, and to Dr. Iwao Maruta for his encouragement.

Research Laboratory
Kao Soap Co., Ltd.
Sumida-ku, Tokyo

Sterically-hindered Organosilicon Compounds Containing Cyclohexyl Groups. II[1]. *Hydrogenation of Phenylsilicon Compounds*

By Michio TAKAKUSA

(Received September 24, 1962)

Since Cusa and Kipping[2] studied the reaction of cyclohexylmagnesium chloride with phenyltrichlorosilane, much effort has been made to overcome the steric hindrance of a cyclohexyl group and prepare highly substituted organosilicon compounds with the cyclohexyl groups. Recently, reactions between fluorosilanes and organolithium compounds[3] were shown to be quite effective ways to obtain those compounds, and preparation of a series of tricyclohexylalkyl- and -aryl-silanes by this method was studied by the present author[1]. Steric hindrance of three cyclohexyl groups attached to one silicon atom does not allow the introduction of a *sec*-alkyl group as the fourth substituent even with this powerful combination of reagents.

The steric hindrance here implies merely that the formation of an intermediate complex is prevented, or simply, attack of the reagent on the silicon atom is obstructed. In these cases, dimensions of both reagents should be naturally considered, as well as their reactivities. It is also quite obvious that magnitude of steric hindrance varies with a type of reaction.

Cyclohexane derivatives are often prepared by hydrogenation of corresponding benzene derivatives, and the method can be applied to the preparation of organosilicon compounds

1) Part I: M. Takakusa, This Bulletin, **36**, 31 (1963).
2) N. W. Cusa and F. S. Kipping, *J. Chem. Soc.*, **1933**, 1040.
3) A. D. Petrov and T. I. Chernysheva, *Zhur. Obshchei Khim.*, **24**, 1189 (1954).

containing cyclohexyl groups[4,5]. As this reaction involves attack on the phenyl group surrounding silicon, not on the silicon atom, by the smallest hydrogen atom[6], the steric hindrance will be much less important. Kanazashi and Takakusa prepared tetracyclohexylsilane[5a], hexacyclohexyldisilane[5b], and some other related compounds in this way.

The present paper reports hydrogenation of several phenylsilicon compounds as a route to cyclohexylsilicon compounds, and the results are compared with those of organolithium compound route obtained in the preceding paper[1]. Attempts were made to prepare tricyclohexyl-isopropylsilane and -*t*-butylsilane through the interactions of triphenylfluorosilane with the corresponding alkyllithiums followed by hydrogenation of the products, since they are expected to be the most hopeful ways for the preparation of these compounds.

Experimental*

Triphenylbutylsilane.—*From Triphenylchlorosilane.* —Triphenylbutylsilane was prepared from the interaction of the chlorosilane with *n*-butyllithium in a yield of 55%. M. p. 87.8~88.5°C (reported[7], 87.5~88°C).

From Butyltrichlorosilane.—A mixture of 9.6 g. of butyltrichlorosilane and 17 g. of chlorobenzene was added dropwise to a mixture of 7 g. of sodium sand and 120 ml. of benzene, the whole mixture refluxed for 2 hr., and then treated with water. Evaporation of the solvent from the benzene layer yielded a crude solid from which 2 g. of triphenylbutylsilane, m. p. 87.5~88°C, was separated. The mixed melting point measurement of both materials did not show any depression.

Triphenylisopropylsilane (Attempted). — Isopropyllithium was prepared in ethyl ether from 0.7 g. of lithium and 5.3 g. of isopropyl bromide in a 300 ml. three-necked round-bottomed flask equipped with a reflux condenser, protected with a calcium chloride tube, a mercury-sealed stirrer and a dropping funnel under nitrogen atmosphere. To the isopropyllithium solution was added 40 ml. of triphenylfluorosilane (6.5 g.) solution in ethyl ether, the mixture refluxed, the solvent replaced by petroleum ether (b. p. 70~90°C), and then the mixture refluxed for 7 hr. From the reaction mixture, 0.2 g. of crude hexaphenyldisiloxane and 1.8 g. of triphenylfluorosilane were recovered.

Triphenyl-*t*-butylsilane (Attempted).—To *t*-butyllithium solution prepared from 4.0 g. of lithium and 22.2 g. of *t*-butyl chloride in petroleum ether (b. p. 30~50°C) was added 7.15 g. of triphenylfluorosilane. The mixture was refluxed with stirring, the solvent gradually replaced by higher boiling petroleum ether, the content of the flask kept refluxing for 16 hr. From the reaction mixture 84% of triphenylfluorosilane and 10% of hexaphenyldisiloxane were recovered. The repeated run using 10.1 g. of lithium and 54.3 g. of *t*-butyl chloride also failed to yield the desired product.

Tricyclohexylphenylsilane. — Prepared in a previous report[1]. M. p. 207~208°C.

Triphenylphenoxysilane. — To sodium phenoxide prepared from 18.6 g. of phenol and 2.5 g. of sodium in benzene 26.7 g. of triphenylchlorosilane dissolved in benzene was added dropwise, and the mixture refluxed for 6 hr. The solvent was distilled off, and 9.2 g. (30%) of triphenylphenoxysilane, m. p. 101~103°C, obtained. Recrystallization from petroleum ether gave 8.4 g. of th material melting at 103~105°C (reported[8], 103~104°C). Found: C, 81.04; H, 5.38. Calcd. for $C_{24}H_{20}OSi$: C, 81.77; H, 5.72%.

Raney Nickel Catalyst. — The catalyst, Adkins' "W-6"[9], was prepared in the same way as that in a previous paper[5a], and stored under absolute alcohol in a refrigerator. The alcohol was replaced by the reaction solvent before being used. Several attempts to obtain more active catalysts showed that lower temperature in development and digestion caused much loss of the catalyst during washing process, though the catalyst appeared to carry higher activity.

Hydrogenation Procedure. — Unless otherwise described, phenylsilanes were dissolved in 40~50 ml. of cyclohexane, and hydrogenated over Raney nickel catalyst. A 100 ml. stainless steel autoclave equipped with a magnetic inner agitator was used, and about 100~110 atm. of hydrogen was charged. Other conditions are listed in Table I.

Tricyclohexylbutylsilane.—(a) (Table I, No. 1) Evaporation of solvent from the hydrogenated mass yielded a crude material melting at about 100°C. Crystallization of the material from ethanol gave 0.35 g. of impure tricyclohexylbutylsilane melting at 149~154°C, and, from its mother liquor, 0.1 g. of another material melting at 86~100°C was obtained. The latter was subjected to chromatography on alumina and separated into two components, one melting at 92~98°C and the other at 111~122°C, but further purifications were not successful. Recrystallization of the impure tricyclohexylbutylsilane raised the melting point to 157~158°C.

(b) From the hydrogenation of 1.6 g. of triphenylbutylsilane was obtained 0.7 g. of a crude material melting at 151~156°C. Three recrystallizations from ethanol-benzene (3 : 1) yielded 0.4 g. of tricyclohexylbutylsilane, m. p. 159~160°C (see the previous paper[1]). (Found: C, 78.87; H, 12.22. Calcd. for $C_{22}H_{42}Si$: C, 78.95; H, 12.65%).

From the mother liquor of the first recrystallization, 0.02 g. of a compound which melts at 97~106°C was obtained, but further purification was not successful.

4) J. L. Speier, *J. Am. Chem. Soc.*, **74**, 1003 (1952).

5) a) M. Kanazashi and M. Takakusa, This Bulletin, **27**, 441 (1954); b) M. Kanazashi and M. Takakusa, ibid., **35**, 1840 (1962).

6) Physico-chemical aspects of catalytic action of Raney nickel catalyst are not considered here.

* All melting points reported here are uncorrected.

7) H. Gilman, R. A. Benkeser and G. E. Dunn, *J. Am. Chem. Soc.*, **72**, 1689 (1950).

8) H. Gilman and G. N. R. Smart, *J. Org. Chem.*, **19**, 441 (1954).

9) H. Adkins and H. R. Billica, *J. Am. Chem. Soc.*, **70**, 695 (1948).

Tetracyclohexylsilane.—*From Tricyclohexylphenylsilane (Table I, No. 2).* — The solvent was distilled off, and 2.2 g. of a solid melting at 271~275°C was obtained. Recrystallization from benzene gave 1.8 g. of tetracyclohexylsilane, m. p. 276~278°C. Mixed melting point with an authentic sample[5a] did not show depression.

From Tetraphenylsilane (Table I, No. 3). — In a similar way, tetracyclohexylsilane was obtained. The concentrated mother liquor was chromatographed on alumina, but no solid but tetracyclohexylsilane was obtained.

Tricyclohexylphenylsilane. — (Table I, No. 4). Products of partial hydrogenation were separated by chromatography on alumina with petroleum ether as an eluent, and 0.4 g. of a solid melting at 200~230°C, 0.2 g. of a solid melting at about 200°C and 0.3 g. of material melting at 120~140°C were obtained. The middle fraction, melting at 200°C, was recrystallized from ethanol and ethanol-benzene to give pure tricyclohexylphenylsilane, m. p. 204~206.5°C. (Found: C, 81.80; H, 10.77. Calcd. for $C_{24}H_{38}Si$: C, 81.28; H, 10.80%.)

Mixed melting point with an authentic sample[1] did not show any depression.

Hydrogenation of Triphenylsilanol at Higher Temperature. — The reaction mixture of the Run No. 8 of Table I was a very sticky viscous liquid, from which neither tricyclohexylsilanol nor hexacyclohexyldisiloxane was separated. Its infrared spectrum does not show an absorption near 4.7 μ of Si-H bond. From another run carried out at about 150°C, a sticky liquid was obtained, from which only a low yield of tricyclohexylsilanol was separated.

Tricyclohexylcyclohexoxysilane (Attempted). — (Table I, No. 10). Hydrogenation of triphenylphenoxysilane gave a material melting at 168~171°C, but not tricyclohexylcyclohexoxysilane. The product was recrystallized twice from petroleum ether to give a compound melting at 175~176.5°C, which was identified as tricyclohexylsilanol by mixed melting point measurement. Cyclohexanol seemed to be also formed.

Results and Discussion

Isopropyltriphenylsilane or *t*-butyltriphenylsilane has not been reported yet in the literature. Incidentally, attempts to prepare them by treating triphenylfluorosilane with the corresponding alkyllithiums were also unsuccessful probably due to steric hindrance, and hence, only tricyclohexylbutylsilane and tetracyclohexylsilane were prepared by hydrogenation as members of a tricyclohexylalkylsilane series. Tricyclohexylphenylsilane was prepared by partial hydrogenation of tetraphenylsilane.

Hydrogenation of hexaphenyldisilane and hexaphenyldisiloxane, which was the subject of a previous paper[5b], was also carried out under similar conditions for comparison. The reaction conditions are shown in Table I. Apparent difference in reaction conditions does not lead to any significant conclusion, since the activity of the catalyst used could not be uniform throughout the series of experiments, and all starting materials were finally converted into the desired products. The greatest difficulty was encountered with hexaphenyldisilane, where the product should have the largest steric requirement among the compounds studied here. With this compound, hydrogen absorption occasionally ceased, but every addition of some fresh catalysts to the system started the reaction again until the calculated amount of hydrogen was completely absorbed. One possible explanation is not steric hindrance but simply low solubility of the product. As the hydrogenated disilane is hardly soluble in the solvent, it probably covered the surface of nickel catalyst, reducing its activity temporarily. It was actually observed that a pretty strong activity had still remained in the used catalyst after completion of the reaction. Furthermore, the difficulty was reduced when a diluted sample was hydrogenated.

The series of studies on hydrogenation of phenylsilicon compounds showed that steric hindrance is not important in hydrogenation process of those compounds and allows the formation of several cyclohexylsilicon compounds that can not be obtained by other

TABLE I. HYDROGENATION CONDITIONS

No.	Material	g.	Ni g.	Temp. °C	Time hr.	Hydrogen, l. Absorbed	Hydrogen, l. Calcd.	Product	%
1	$BuSiPh_3$	1.0	1.4	110~120	2	0.7	0.64	$BuSi(C_6H_{11})_3$	20
2	$(C_6H_{11})_3SiPh$	2.2	1.6	100~140	2.5	0.5	0.42	$(C_6H_{11})_4Si$	80
3	Ph_4Si	1.68	2.0	120~170	2.5	1.4	1.34	$(C_6H_{11})_4Si$	—
4	Ph_4Si	2.1	1.4	90~100	2	1.4	1.26[a]	$(C_6H_{11})_3SiPh$	8
5	$(Ph_3Si)_2$[b]	2.1	4.0	110~160	5	2.1	1.63	$(C_6H_{11})_6Si_2$	
6	$(Ph_3Si)_2O$[b]	2.1	1.6	100~160	1.5	1.6	1.59	$(C_6H_{11})_6Si_2O$	
7	Ph_3SiOH	5.8	1.6	100~120	2	4.2	4.24	$(C_6H_{11})_3SiOH$	85
8	Ph_3SiOH	13.9	4	100~170	—	10.3	10.1	None	
9	Ph_3SiOPh	1.2	1.4	100~120	1.5	1.0	0.91	$(C_6H_{11})_3SiOH$	
10	Ph_3SiOPh	7.04	6	110~160	—	6.0	5.4	$(C_6H_{11})_3SiOH$	

a) Partial hydrogenation b) Methylcyclohexane was used as a solvent.

conventional methods. The steric effects of the residual or pre-existing groups are also small, and limitation of this method for preparation of cyclohexane derivatives in silico-organic chemistry does not lie in steric hindrance.

Si–C and Si–Si bonds are stable enough in the hydrogenation process, and many sterically-hindered cyclohexylsilanes were prepared by hydrogenation without any cleavage of those bonds. The siloxane bond is also stable to hydrogenation, but hydrogenation of triphenylsilanol at higher temperature often yielded a very sticky liquid. The optimum temperature for obtaining tricyclohexylsilanol seems to be 100~120°C, and at a higher temperature a yield of tricyclohexylsilanol was largely reduced. Stability of triphenylsilanol under hydrogen at higher temperature was studied by Dolgov et al.[10], and it was shown that the silanol was converted into hexaphenyldisiloxane at 280°C. Under the present conditions, however, no solid product but tricyclohexylsilanol was obtained, nor any compound with Si–H bond was detected by infrared measurement. An attempt to obtain tricyclohexylcyclohexoxysilane by hydrogenating triphenylphenoxysilane was unsuccessful, and only tricyclohexylsilanol was obtained, probably as a result of hydrolysis.

10) B. N. Dolgov and Yu. N. Volnov, *Zhur. Obshchei Khim., Ser. I*, 91 (1931); *Chem. Abstr.*, **25**, 4535 (1931).

Summary

Tricyclohexylbutylsilane, tetracyclohexylsilane and tricyclohexylphenylsilane were prepared by hydrogenation of triphenylbutylsilane and phenyltricyclohexylsilane and partial hydrogenation of tetraphenylsilane, respectively. Preparation of tricyclohexylisopropylsilane and tricyclohexyl-*t*-butylsilane was unsuccessful due to failure of obtaining corresponding triphenyl derivatives. An attempt to obtain tricyclohexylcyclohexoxysilane by hydrogenating triphenylphenoxysilane was also unsuccessful. In preparation of highly-substituted cyclohexylsilicon compounds, the steric factor is of less importance in the hydrogenation process, while it is very much enhanced in reactions with organolithium compounds.

The author expresses his hearty thanks to Dr. Motonori Kanazashi for kind advice during this work.

Electrotechnical Laboratory
Agency of Industrial Science and Technology
Tanashi-machi, Kitatama-gun, Tokyo

Sterically-hindered Organosilicon Compounds Containing Cyclohexyl Groups. III.[1,2] *Notes on Petrov and Chernysheva's Tetracyclohexylsilane and Tricyclohexyl-n-butylsilane*

By Michio TAKAKUSA

(Received September 24, 1962)

It occasionally happens that two or more melting point values are given to a single compound by separate workers in silico-organic chemistry[3].

The present author[10] obtained tetracyclohexylsilane, m. p. 279~281°C, by hydrogenation of tetraphenylsilane, while Petrov and Chernysheva[11] reported tetracyclohexylsilane melting at 198°C, which was obtained by the reaction of cyclohexyllithium with tetrafluorosilane or dicyclohexyldifluorosilane. The two tetracyclohexylsilanes have been generally

1) Part I: M Takakusa, This Bulletin, **36**, 31 (1963).
2) Part II: M. Takakusa, ibid., **36**, 284 (1963).
3) For example: 172°C by Gilman[4] and 185°C by Petrov[5] for 1-naphthyltriphenylsilane, 161°C by Petrov[6] and 193°C by Gilman[7] for tri-1-naphthylphenylsilane, and 148°C by Gilman[8] and 232°C by Nametkin[9] for triphenylcyclohexylsilane.
4) H. Gilman and C. G. Brannen, *J. Am. Chem. Soc.*, 73, 4640 (1951).
5) A. D. Petrov and V. S. Chugunov, *Doklady Akad. Nauk S. S. S. R.*, **82**, 917 (1952).
6) A. D. Petrov and V. S. Chugunov, ibid., **77**, 815 (1951).
7) H. Gilman, C. G. Brannen and R. K. Ingham, *J. Am. Chem. Soc.*, **77**, 3916 (1955).
8) H. Gilman and D. H. Miles, ibid., **80**, 611 (1958).
9) N. S. Nametkin, A.V. Topchiev and T. I. Chernysheva, *Doklady Akad. Nauk S. S. S. R.*, **111**, 1260 (1956).
10) M. Kanazashi and M. Takakusa, This Bulletin, **27**, 441 (1954).
11) A. D. Petrov and T. I. Chernysheva, *Zhur. Obshchei Khim.*, **24**, 1189 (1954).

thought to be stereoisomers due to steric hindrance[12]. Stereoisomerism in the silane would be possible in the case that free rotation around the Si-C_6H_{11} bond is hindered, but actual existence of isomers, which is the case in tetra-*o*-tolylsilane[13], seems to be less probable in tetracyclohexylsilane because of a squat shape of the cyclohexyl group. Moreover, if there exist some isomers of steric origin, the product of hydrogenation of tetraphenylsilane should be a mixture of the isomers. Our repeated studies on hydrogenation of tetraphenylsilane and phenyltricyclohexylsilane[2] were not successful in an attempt to isolate any other compound than the one melting at 281°C which was previously reported[10]. Interaction of tricyclohexylfluorosilane and cyclohexyllithium was reinvestigated by the present author[1], and the fourth cyclohexyl group could not be introduced under conditions similar to Petrov and Chernysheva's.

Eaborn[14] obtained tricyclohexylcyclohexoxysilane during the reaction of cyclohexylmagnesium bromide with dicyclohexyldifluorosilane at 70°C. A similar example has been reported by Cusa and Kipping[15] who obtained phenyldicyclohexylcyclohexoxysilane from the reaction of cyclohexylmagnesium bromide with phenyltrichlorosilane. The present author separated tricyclohexylcyclohexoxysilane, m. p. 201~203°C, from the reaction mixture of cyclohexyllithium with tetrachlorosilane. The result obtained here seems to be the first example of formation of such a type of compound during the reaction of organolithium compounds with halosilanes. The process seems to involve formation of $C_6H_{11}OLi$ in the reaction system and its successive interaction with tricyclohexylchlorosilane.

$$(C_6H_{11})_3SiCl + C_6H_{11}OLi \rightarrow (C_6H_{11})_3SiOC_6H_{11}$$

Though the cyclohexoxysilane was not obtained in the reaction[1] of tricyclohexylfluorosilane (2.5 g.) with an excess of cyclohexyllithium under a forced condition, about 2~5% (to tetrachlorosilane) of the compound was obtained in every larger scale reaction in which tetrachlorosilane or dicyclohexyldichlorosilane was used. Hence, the compound melting at 198°C, which Petrov and Chernysheva reported as tetracyclohexylsilane, might possibly be tricyclohexylcyclohexoxysilane[16], instead of a stereoisomer.

In addition to the case of tetracyclohexylsilane, tricyclohexylbutylsilane[2] obtained by hydrogenation of triphenylbutylsilane showed a different melting point, 159~160°C, from that of the compound, m. p. 133~135°C, obtained by Petrov and Chernysheva[11] through the substitution reaction with butyllithium. The existence of two isomeric tricyclohexylbutylsilanes can not be accounted for in terms of stereoisomerism due to steric hindrance.

A previous paper[1] reported that the reaction of butyllithium with tricyclohexylfluorosilane gives a compound (41%) identical with that obtained in hydrogenation study, m. p. 159~160°C, instead of Petrov and Chernysheva's tricyclohexylbutylsilane.

Tricyclohexylbutoxysilane was prepared by treating tricyclohexylchlorosilane with sodium butoxide. The butoxysilane was first reported here, but again, its melting point, 132~133°C, is close to that of Petrov and Chernysheva's tricyclohexylbutylsilane[17], 133~135°C; the fact suggests that their compound might be possibly tricyclohexylbutoxysilane.

The infrared spectra of the compounds obtained in our laboratory are shown in Fig. 1, being thought to be of some use for identification.

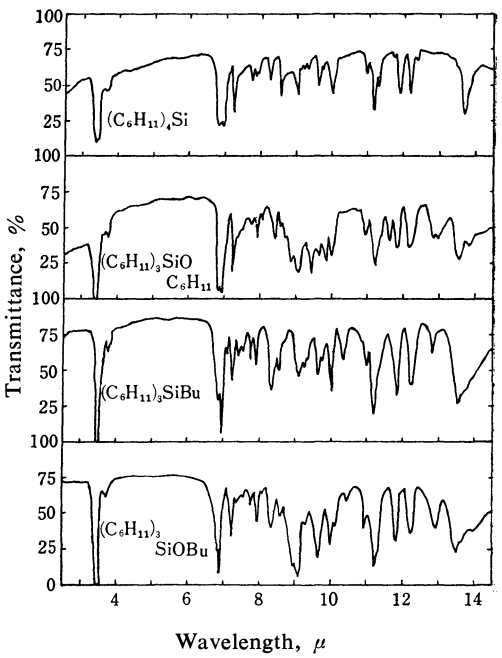

Fig. 1. Infrared spectra.

12) a) H. Gilman and D. H. Miles, *J. Am. Chem. Soc.*, **80**, 611 (1958); b) M. Kumada, A lecture given at Symposium on Organosilicon and Organometallic Compounds, Osaka, October 1958.
13) G. N. R. Smart, H. Gilman and H. W. Otto, *J. Am. Chem. Soc.*, **77**, 5193 (1955).
14) T. Eaborn, *J. Chem. Soc.*, **1952**, 2840.
15) N. W. Cusa and F. S. Kipping, ibid., **1933**, 1040.
16) Calcd. for $C_{24}H_{44}OSi$: C, 76.52; H, 11.77; Si, 7.46. Calcd. for $C_{24}H_{44}Si$ (tetracyclohexylsilane): C, 79.92; H, 12.30; Si, 7.46%. Petrov and Chernysheva reported for their compound: Si, 7.47, 7.87%.
17) No analytical data are shown in their report.

Experimental*

Formation of Tricyclohexylcyclohexoxysilane.— A dry 1 l. three-necked flask equipped with a mercury-sealed stirrer, a reflux condenser and a dropping funnel was flashed with nitrogen, and 400 ml. of petroleum ether was placed in it. Fourteen grams of lithium shots were transfered to the flask under nitrogen atmosphere, and then nitrogen was bubbled through petroleum ether. A long calcium chloride tube connected to a washing bottle containing alkaline pyrogallol solution was attached to the top of the reflux condenser for protection against moisture and oxygen. Ten milliliters of cyclohexyl chloride was added, and the reaction mixture warmed to start the reaction. Over a period of 2 hr., 103 g. of cyclohexyl chloride was added dropwise, and the mixture was kept warm with stirring for an additional 3 hr. Then, 17.6 g. (0.104 mol.) of silicon tetrachloride in 50 ml. of petroleum ether was added slowly, and the mixture refluxed for 5 hr. The reaction mixture was filtered. To the precipitates was added about 400 ml. of petroleum ether, and the mixture treated with diluted hydrochloric acid and fractionated. A fraction boiling at 160~175°C under 6 mmHg gave 3.2 g. (10 %) of tricyclohexylchlorosilane and 4.3 g. (14%) of tricyclohexylsilanol. The distillation residue was subjected to chromatography on alumina, and 1.8 g. of a white solid melting at 192~195°C was obtained. Recrystallization from carbon tetrachloride-ethanol and then from petroleum ether-ethanol raised the melting point to 201~203.5°C.

Found: C, 76.67; H, 11.91. Calcd. for $C_{24}H_{44}OSi$: C, 76.52; H, 11.77%. A mixed melting point measurement with an authentic sample[18] indicated that this compound is tricyclohexylcyclohexoxysilane. Two additional runs also gave about 2~5% of tricyclohexylcyclohexoxysilane, but one case did not give the compound, where treatment with hydrochloric acid solution was so vigorous that cyclohexanol was liberated.

Preparation of Tricyclohexylbutoxysilane.— Sodium butoxide was prepared by dissolving about 0.6 g. of sodium in 50 ml. of dry freshly-distilled *n*-butyl alcohol. The mixture of the solution and 1.7 g. (0.0058 mol.) of tricyclohexylchlorosilane was refluxed for 5 hr. After being cooled, 100 ml. of petroleum ether was added to it, and the solution poured onto cold water. The organic layer was washed and dried over sodium sulfate. The solvent was driven off, and 1.0 g. of crude material obtained, m. p. 117~127°C. Recrystallization twice from ethanol gave pure tricyclohexylbutoxysilane, m. p. 132~133.4°C.

Found: C, 75.31; H, 12.00. Calcd. for $C_{22}H_{42}OSi$: C, 75.35; H, 12.05%.

Summary

Discrepancies among reported melting ponints for tetracyclohexylsilane and tricyclohexylbutylsilane were discussed. Tricyclohexylcyclohexoxysilane was obtained in 2~5% yield in addition to tricyclohexylchlorosilane from the reaction of cyclohexyllithium with silicon tetrachloride. Petrov's compound melting at 198°C is most likely to be tricyclohexylcyclohexoxysilane and not a stereoisomeric tetracyclohexylsilane. Tricyclohexylbutoxysilane, m. p. 133°C, was prepared by treating sodium butoxide with tricyclohexylchlorosilane, and it was pointed out that Petrov's "tricyclohexylbutylsilane" is probably tricyclohexylbutoxysilane.

Electrotechnical Laboratory
Agency of Industrial Science and Technology
Tanashi-machi, Kitatama-gun, Tokyo

* All melting points reported here are uncorrected.

18) The pure sample was kindly granted by Dr. C. Eaborn.

Intramolecular Hydrogen Bonding in α-Keto- and α-Alkoxy-carboxylic Acids. VI. Substituent Effects on the Energy of the Hydrogen Bonding in α-Alkoxy- and α-Aryloxyacetic Acids[1]

By Michinori Ōki and Minoru Hirota

(Received September 25, 1962)

Infrared spectra of various carboxylic acids which are supposed to be capable of hydrogen bonding between the carboxyl group and a substituent at α-position have led to the conclusion that an intramolecular interaction exists between the O–H group and the C=O in a carboxyl group[1-3]. The conclusion is based on the following phenomena. (i) The cis structure I, otherwise less advantageous from the stand point of steric effect than the trans structure II, is exclusively realized when the carboxylic acid has no hydrogen accepting group at the α-position. (ii) The C=O stretching absorption attributed to the cis structure appears at 1760 cm^{-1} region, which is ca. 30 cm^{-1} lower than the C=O stretching frequency of the trans structure (1790 cm^{-1}) in carbon tetrachloride, the fact being reasonably explained from the effect of the increasing polarity of the C=O bond, and more contribution of the polar structure C^+-O^- of less force constant value of the C=O bond. (iii) The intramolecular interaction IIIa of the O–H group with an aromatic nucleus or with a halogen atom at α-position was not observed in phenylacetic acid and chloroacetic acid.

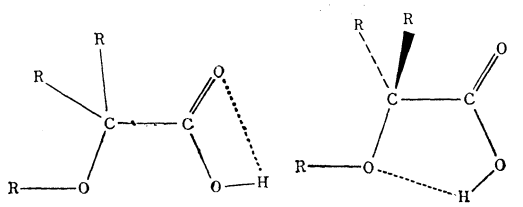

cis
I

trans
II

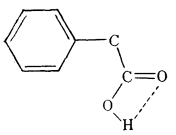

Phenylacetic acid
III

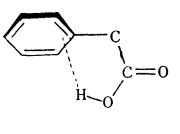

IIIa

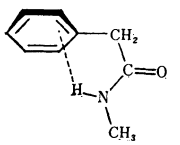

N-Methyl-phenylacetamide
IV

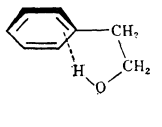

β-Phenylethanol
V

The absence of the interaction in phenylacetic acid would be contradictory with the results obtained with phenylacetamide IV[4] and β-phenylethyl alcohol V[5] which is in the similar steric condition with phenylacetic acid[6].

The temperature dependence of the intensity ratio of the two ν_{O-H} bands was measured in order to determine the energy difference of the cis and trans forms of these acids. This energy difference (ΔH) may give the measure of the relative strength of the hydrogen bond between the carboxylic O–H group and the α-proton acceptor, because the energy of the cis form is thought to be almost unchanged throughout these series. Although the measurement, giving only the energy difference between the cis and the trans forms, cannot be related directly to the stability of the cis form, it may provide an important clue to the energy estimation when compared with the ordinary hydrogen bonding of O–H···O type. Thus the measurements were carried out with the carboxylic acids, ROCR'R''COOH, and the electronic and the steric effects of the substituents will be discussed in this paper in connection with the ΔH values.

Experimental

Preparation of Materials.—Methoxyacetic, ethoxyacetic, isopropoxyacetic and *t*-butoxyacetic acids were prepared from the corresponding alkoxides (2 mol.) and chloroacetic acid (1 mol.) in the corresponding alcohols. This method has been described for ethoxyacetic acid in "Organic Syntheses"[7] and the authors followed this method.

1) Part V of this series: M. Ōki and M. Hirota, *Spectrochim. Acta*, **17**, 583 (1961); Presented at the 14th Annual Meeting of the Chemical Society of Japan, Tokyo, April, 1961.
2) M. Ōki and M. Hirota, This Bulletin, **33**, 119 (1960).
3) M. Ōki and M. Hirota, ibid., **34**, 374, 378 (1961).
4) I. Suzuki, M. Tsuboi and T. Shimanouchi, *Spectrochim. Acta*, **16**, 469 (1960).
5) M. Ōki and H. Iwamura, This Bulletin, **33**, 1135 (1959).
6) M. Ōki and H. Iwamura, ibid., **35**, 283 (1962).
7) R. C. Fuson and B. H. Wojcik, "Organic Syntheses", Col. Vol. II, 260 (1943).

Similarly, α-methoxypropionic and α-methoxyisobutyric acids were prepared from sodium methoxide and the corresponding α-bromo-acids. The analyses and physical constants are reported below with ether new or doubtful compounds.

Isopropoxyacetic acids, b. p. 108°C/25 mmHg. Found: C, 50.73; H, 8.50, Calcd.: C, 50.83; H, 8.53%.

α-Methoxypropionic acid, b. p. 98°C/18 mmHg. Found: C, 45.98; H, 7.91. Calcd.: C, 46.15; H, 7.75%.

α-Methoxyisobutyric acid, b. p. 99.5°C/18 mmHg. Found: C, 51.08; H, 8.78. Calcd.: C, 50.83; H, 8.53%.

Preparation of aryloxyacetic acids and their homologs was already reported[1] in the preceding paper.

Measurement of the Infrared Spectra and Calculation of the Energy Difference (ΔH).—Infrared spectra are determined with a Perkin-Elmer 112 G spectrophotometer as reported previously. The absorption intensities of the two O-H stretching bands attributed to the cis and the trans isomers (ε_c and ε_t, respectively) are measured at various temperatures between 5°C and a temperature near the boiling point of carbon tetrachloride. The temperature of the solution was kept within the range of 1.5° during the measurement and the T (°K) value was obtained as the mean of the temperatures of the solution at the beginning and at the end of the absorption measurement. From these infrared measurements, the intensity ratios ($\varepsilon_t/\varepsilon_c$) were calculated at various temperatures. Assuming that ε-values are proportional to the populations of the cis and the trans isomeric melecules and the linear relation (Eq. 5) is present between the log ($\varepsilon_t/\varepsilon_c$) and $1/T$ values, the energy difference (ΔH) between the cis and the trans isomers are obtained from the gradient of log ($\varepsilon_t/\varepsilon_c$) versus $1/T$ line.

The gradient and the intercept of the line are calculated, by the least square method by the following formulae, where n is the number of the measurement:

$$\sum[\log(\varepsilon_t/\varepsilon_c)] - n\cdot[\Delta S - \boldsymbol{R}\ln a] - [\sum(1/T)]\cdot[\Delta H] = 0 \quad (1)$$

$$\sum\{[\log(\varepsilon_t/\varepsilon_c)]\times[1/T]\} - [\sum(1/T)] \times [\Delta S - \boldsymbol{R}\ln a] - [\sum(1/T^2)]\cdot[\Delta H] = 0 \quad (2)$$

In these formulae, the values $\sum[\log(\varepsilon_t/\varepsilon_c)]$, n, $\sum(1/T)$, $\sum[\log(\varepsilon_t/\varepsilon_c)\cdot 1/T$ and $\sum(1/T^2)$ are known, and ΔH and $(\Delta S - \boldsymbol{R}.\ln a)$ are obtained.

Results and Discussion

Results of the measurement of the O-H stretching absorption intensity of the cis (I) and the trans (II) isomers at various temperatures are shown in Tables I—IX.

Assuming that the absorption intensity of the isomers are proportional to their concentration (x_c and x_t, respectively), the energy difference (ΔH) and the ($\Delta S/\boldsymbol{R} - \ln a$) term are calculated by applying the van't Hoff's equation (Eq.3).

Table I. Methoxyacetic acid

T, °K	$1000/T$	Extinction coefficient ε_c	Extinction coefficient ε_t	Intensity ratio $\varepsilon_t/\varepsilon_c$
278.5	3.60	26.0	27.4	1.054
293.3	3.41	39.6	35.6	0.900
293.8	3.40	38.8	36.4	0.938
298.7	3.35	46.3	40.7	0.880
302.7	3.31	46.1	42.8	0.930
310.2	3.23	52.5	44.6	0.850
319.2	3.14	57.5	48.6	0.847
323.7	3.09	58.8	48.8	0.831
329.2	3.04	60.8	48.6	0.800
332.0	3.02	66.3	54.6	0.824
344.5	2.91	67.3	50.8	0.785

Table II. Ethoxyacetic acid

T, °K	$1000/T$	Extinction coefficient ε_c	Extinction coefficient ε_t	Intensity ratio $\varepsilon_t/\varepsilon_c$
282.2	3.55	26.7	33.4	1.25
294.4	3.40	34.5	38.3	1.11
307.3	3.26	42.5	45.8	1.08
316.8	3.16	46.2	45.5	0.985
331.6	3.02	54.4	49.3	0.907
342.4	2.92	60.0	52.8	0.880
345.7	2.90	64.2	55.3	0.862

Table III. Isopropoxyacetic acid

T, °K	$1000/T$	Extinction coefficient ε_c	Extinction coefficient ε_t	Intensity ratio $\varepsilon_t/\varepsilon_c$
279.9	3.58	22.0	47.7	2.17
298.2	3.36	28.7	53.0	1.85
315.9	3.17	40.2	66.0	1.64
324.4	3.08	43.1	67.4	1.57
337.5	2.96	47.4	68.8	1.45
349.8	2.86	45.8	60.2	1.31

Table IV. α-Methoxypropionic acid

T, °K	$1000/T$	Extinction coefficient ε_c	Extinction coefficient ε_t	Intensity ratio $\varepsilon_t/\varepsilon_c$
280.5	3.57	21.9	22.4	1.02
293.1	3.42	34.9	32.1	0.920
302.5	3.31	39.2	33.0	0.843
315.9	3.17	46.3	38.7	0.804
329.5	3.04	54.8	40.8	0.744
339.7	2.95	59.7	42.0	0.704

Table V. α-Methoxyisobutyric acid

T, °K	$1000/T$	Extinction coefficient ε_c	Extinction coefficient ε_t	Intensity ratio $\varepsilon_t/\varepsilon_c$
280.3	3.57	24.1	35.3	1.46
292.5	3.42	32.2	42.4	1.32
306.4	3.27	34.8	42.7	1.23
314.0	3.19	44.6	50.5	1.13
332.2	3.01	47.8	48.4	1.03
341.3	2.93	51.1	59.1	0.961

TABLE VI. PHENOXYACETIC ACID

T, °K	$1000/T$	Extinction coefficient* ε_c	Extinction coefficient* ε_t	Intensity ratio $\varepsilon_t/\varepsilon_c$
281.6	3.55	26.1	16.7	0.640
296.4	3.38	36.4	21.8	0.599
306.3	3.27	48.7	26.5	0.545
316.7	3.16	57.4	29.0	0.505
330.9	3.02	65.5	31.6	0.483
332.7	3.00	74.5	35.3	0.474
347.5	2.88	76.9	36.5	0.474

* Corrected by Eq. 7.

TAELE VII. α-PHENOXYPROPIONIC ACID

T, °K	$1000/T$	Extinction coefficient* ε_c	Extinction coefficient* ε_t	Intensity ratio $\varepsilon_t/\varepsilon_c$
281.6	3.56	25.7	10.8	0.421
297.3	3.37	38.7	14.8	0.383
305.2	3.28	63.4	22.9	0.361
310.0	3.23	48.9	17.1	0.350
320.6	3.12	57.3	19.3	0.337
341.9	2.93	98.8	31.0	0.314

* Corrected by Eq. 8.

TABLE VIII. α-PHENOXYISOBUTYRIC ACID

T, °K	$1000/T$	Extinction coefficient ε_c	Extinction coefficient ε_t	Intensity ratio $\varepsilon_t/\varepsilon_c$
282.1	3.55	41.5	35.9	0.865
293.3	3.41	50.9	43.3	0.851
306.1	3.27	58.5	45.9	0.785
314.8	3.18	68.6	50.0	0.729
331.4	3.02	77.0	52.8	0.686
340.4	2.94	82.2	51.6	0.628

TABLE IX. α-ARYLOXYISOBUTYRIC ACIDS

A) α-(*p*-Methylphenoxy)isobutyric acid

T, °K	$1000/T$	Extinction coefficient ε_c	Extinction coefficient ε_t	Intensity ratio $\varepsilon_t/\varepsilon_c$
296.3	3.38	48.7	62.1	1.275
307.7	3.25	57.0	66.1	1.160
324.2	3.09	69.3	69.0	0.995
342.5	2.92	71.3	67.4	0.945

B) α-(*p*-Bromophenoxy)isobutyric acid

T, °K	$1000/T$	Extinction coefficient ε_c	Extinction coefficient ε_t	Intensity ratio $\varepsilon_t/\varepsilon_c$
297.1	3.37	64.0	30.2	0.472
313.7	3.19	81.7	35.6	0.436
329.3	3.04	95.2	39.4	0.414
345.4	2.90	107.2	40.9	0.381

$$-\boldsymbol{R}T\cdot\ln K=\Delta F=\Delta H-T\Delta S \qquad (3)$$

The equilibrium constant K can be represented by multiplying the integrated intensity ratio by a constant which is a factor showing the ratio of intensity per molecule due to trans and cis forms and is assumed to be invariable throughout the temperature range in this investigation. Then, Eq. 4 is obtained.

$$K=x_t/x_c=a\,A_t/A_c=a\frac{\varepsilon_t\times(\Delta\nu_{1/2})_t}{\varepsilon_c\times(\Delta\nu_{1/2})_c} \qquad (4)$$

Combining Eq. 3 and Eq. 4 gives

$$\log(\varepsilon_t/\varepsilon_c)=-\frac{\Delta H}{2.30\,\boldsymbol{R}}\times\frac{1}{T}+\frac{1}{2.30}\left(\frac{\Delta S}{\boldsymbol{R}}-\ln a\right)-\log\frac{(\Delta\nu_{1/2})_t}{(\Delta\nu_{1/2})_c} \qquad (5)$$

The authors have found that the separation of two bands due to cis and trans forms are generally good and the half band widths are invariable in the spectra at various temperatures. It is then allowed to use the ratio of apparent molecular extinction coefficients instead of intensities to estimate the enthalpies. An example of these cases is shown with α-methoxyacetic acid in Fig. 1. The absorption spectra of this compound shows two separate O–H stretching bands and the approximation of Eq. 6 holds good, the correction of $\log[(\Delta\nu_{1/2})_t/(\Delta\nu_{1/2})_c]$ being accounted to calculate the entropy term $(\Delta S/\boldsymbol{R}-\ln a)$.

$$\varepsilon^a_{t_{max}}\doteqdot\varepsilon_{t_{max}},\quad \varepsilon^a_{c_{max}}\doteqdot\varepsilon_{c_{max}} \qquad (6)$$

In Eq. 6, $\varepsilon^a_{c_{max}}$ and $\varepsilon^a_{t_{max}}$ are the apparent maximal extinction coefficients of the cis and the trans ν_{O-H} bands.

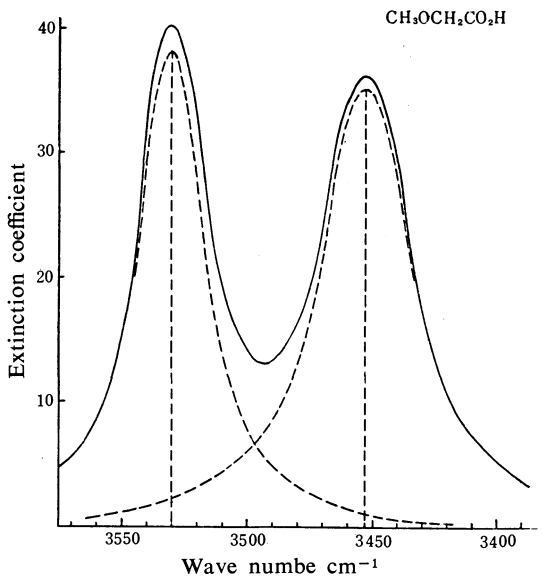

Fig. 1.

A considerable overlap of the two O–H stretching bands was observed in the spectra of phenoxyacetic and α-phenoxypropionic acids and the following corrections (Eq. 7 for phenoxyacetic and Eq. 8 for α-phenoxypropionic acids) were necessary. An example of this correction

is shown in Fig. 2. Coefficients of the correcting terms were calculated from Eq. 9 by assuming the Lorentz envelopes for the two O–H stretching bands.

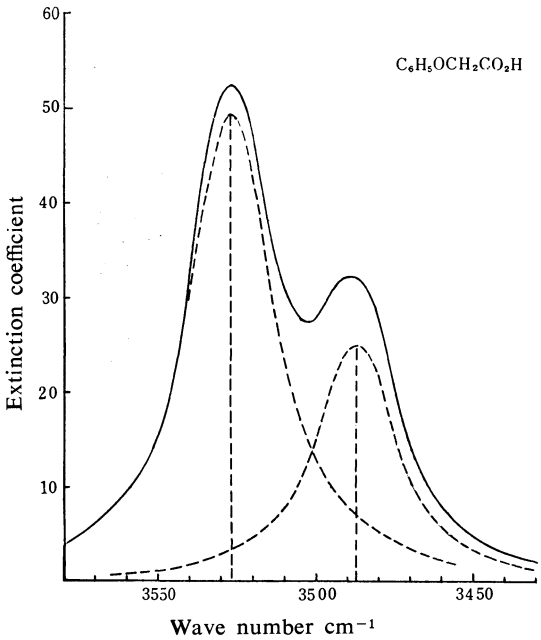

Fig. 2.

$$\left.\begin{aligned}\varepsilon_{c_{max}} &\fallingdotseq \varepsilon^{a}_{c_{max}} - (1/7.9)\,\varepsilon^{a}_{t_{max}} \\ \varepsilon_{t_{max}} &\fallingdotseq \varepsilon^{a}_{t_{max}} - (1/7.2)\,\varepsilon^{a}_{c_{max}}\end{aligned}\right\} \quad (7)$$

$$\left.\begin{aligned}\varepsilon_{c_{max}} &\fallingdotseq \varepsilon^{a}_{c_{max}} - (1/7.3)\,\varepsilon^{a}_{t_{max}} \\ \varepsilon_{t_{max}} &\fallingdotseq \varepsilon^{a}_{t_{max}} - (1/10.7)\,\varepsilon^{a}_{c_{max}}\end{aligned}\right\} \quad (8)$$

$$f(\nu) = a/[(\nu-\nu_{max})^2 + b^2]^{8)} \quad (9)$$

where $\varepsilon_{max} = a/b^2$ and $\Delta\nu_{1/2} = b$.

The $(\varepsilon_t/\varepsilon_c)$ versus $1/T$ relationship is illustrated in Figs. 3, 4, 5 and 6.

In Table X are listed the calculated ΔH and $(\Delta S/R - \ln a)$ values together with the exact band properties of the ν_{O-H} due to the cis and the trans isomers at the ordinary temperature (20~25°C). In Table XI are also summarized the relation between ΔH values and the frequency difference of the two absorption maxima ($\Delta\nu_{max}$). Though the general relationship could not be establishd, monotonous relation is found between the ΔH and $\Delta\nu_{max}$ values within each series of these acids and larger $\Delta\nu_{max}$ generally corresponds to larger ΔH.

From the constancy of the ν_{O-H} frequency of the cis isomer, the energy of the cis-isomer can be considered to be nearly constant in these substituted acetic acids. The ΔH value will, therefore, be a relative value of the energy of the intramolecular hydrogen bonding. The factors which affect the facility of the hydrogen bond formation are i) acidity (hydrogen donating power) of the carboxyl group, ii) basicity (hydrogen accepting power) of the ether oxygen of the alkoxyl or aryloxy group, and iii) steric effects of the alpha and other substituents. The factor i) may be neglected, because the inductive effect of the α-methyl

8) D. A. Ramsay, *J. Am. Chem. Soc.*, **74**, 72 (1952).

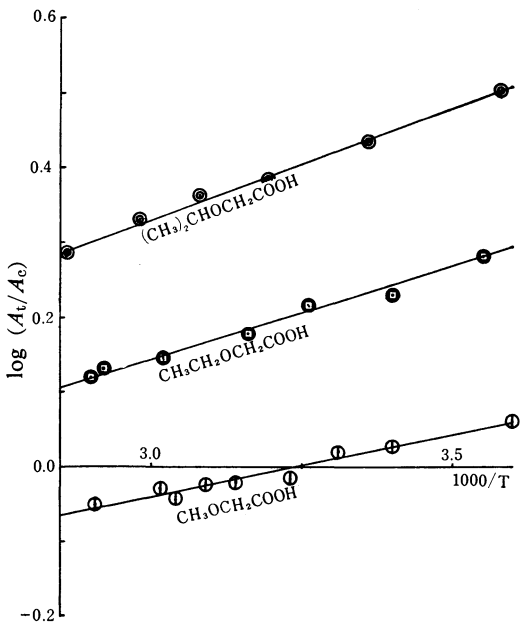

Fig. 3.

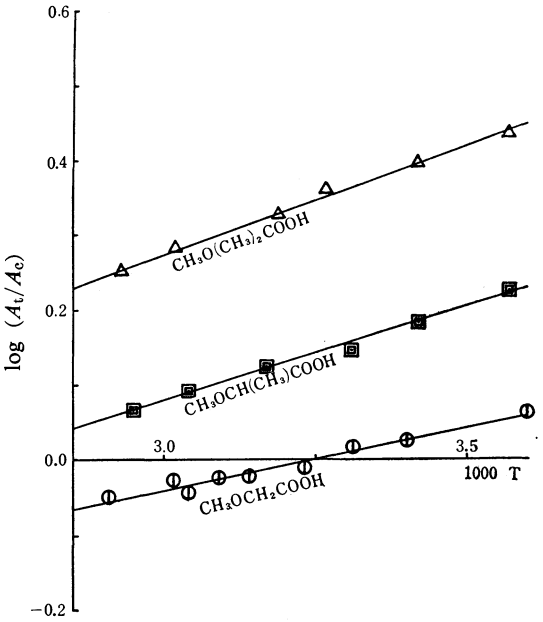

Fig. 4.

Table X. The O-H stretching absorptions and the energy difference values of the "cis" and "trans" forms of various carboxylic acids investigated

Acid	ν_c cm^{-1}	ε_c	$(\Delta\nu_{1/2})_c$	A_b	ν_t cm^{-1}	ε_c	$(\Delta\nu_{1/2})_t$	A_t	A_t/A_c	$\Delta\nu_{max}$ cm^{-1}	ΔH kcal/mol.	$\Delta S/R$ $-\ln a$
CH_3OCH_2COOH	3534.0	38.2	31.2	4.30	3453.4	43.5	35.2	5.52	1.28	77.0	0.76	−1.25
$CH_3CH_2OCH_2COOH$	3531.0	46.7	32.0	5.37	3446.2	47.3	48.5	8.28	1.54	84.8	1.11	−1.34
$(CH_3)_2CHOCH_2COOH$	3531.9	29.9	33.9	3.66	3434.1	54.3	49.9	9.79	2.68	97.8	1.53	−1.56
$(CH_3)_3COCH_2COOH$	3528.0	39.1	28.2	3.98	3424.2	32.8	65.0	7.67	1.93	103.8	—	—
CH_3OCH_2COOH	3534.0	38.2	31.2	4.30	3453.4	43.5	35.2	5.52	1.28	77.0	0.76	−1.25
$CH_3OCH(CH_3)COOH$	3528.5	41.9	32.3	4.87	3431.3	38.6	53.0	7.38	1.51	97.2	1.15	−1.55
$CH_3OC(CH_3)_2COOH$	3528.1	34.4	29.4	3.70	3408.8	45.2	54.7	8.91	2.40	119.3	1.28	−1.30
$C_6H_5OCH_2COOH$	3526.9	49.5	31.7	5.57	3487.5	25.1	29.7	2.69	0.484	39.4	0.98	−2.27
$C_6H_5OCH(CH_3)COOH$	3526.3	37.5	31.6	4.28	3475.1	14.9	41.0	2.20	0.516	51.2	0.94	−2.29
$C_6H_5OC(CH_3)_2COOH$	3526.2	50.3	32.0	6.80	3432.6	41.2	57.6	8.56	1.48	93.9	1.05	−1.47
p-$XC_6H_4OC(CH_3)_2COOH$												
X=CH_3	3526.2	49.4	32.0	5.70	3427.0	63.8	54.1	12.44	2.18	99.2	1.35	—
H	3526.5	50.3	32.0	6.80	3432.6	41.2	57.6	8.56	1.48	93.9	1.05	−1.47
Br	3523.0	55.7	33.9	6.83	3443.5	25.8	52.4	4.88	0.715	79.5	0.88	—

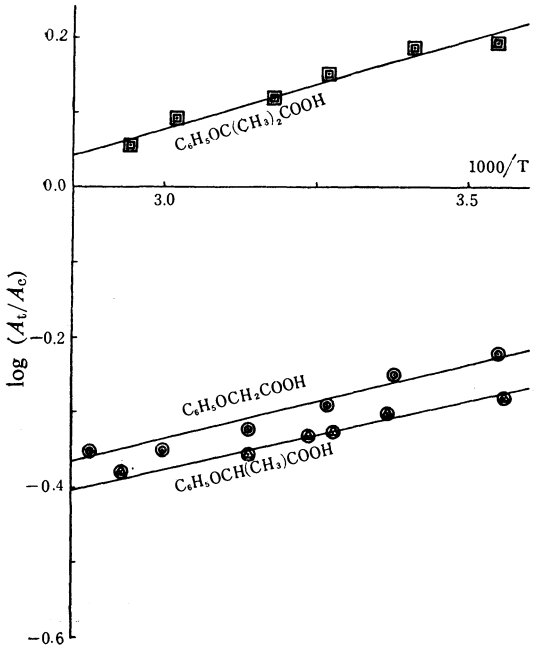

Fig. 5.

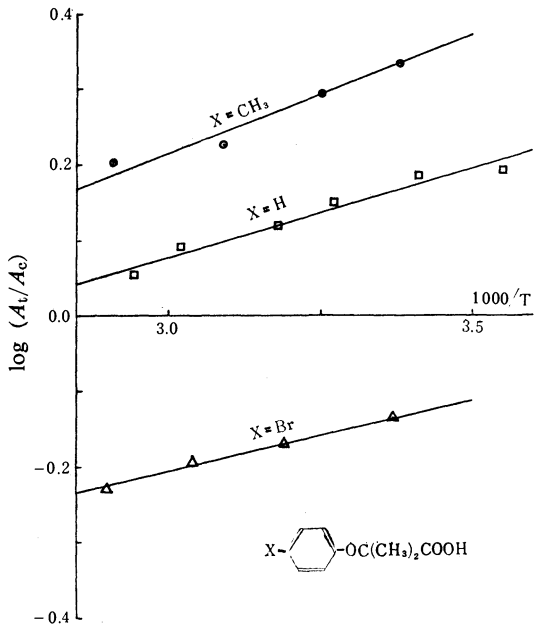

Fig. 6.

substituent does not greatly affect the pK_a values of acetic acids (pK_a values of acetic, propionic and isobutyric acids are known to be 4.76, 4.88 and 4.86[9], respectively), nor the O–H stretching absorption frequencies[10], and the hydrogen donating powers of the acids in the present discussion seem to be nearly the same.

The ΔH value is largely affected by the *O*-substituent and to the lesser extent by the *α*-substituent, though the $\Delta\nu_{max}$ value is affected by both factors in almost the same way. Extreme is the case of phenoxy-acids, in which the ΔH value is nearly equal while the acid changes from phenoxyacetic to phenoxyisobutyric acid. The results may be attributed to the fact that the O–H···O hydrogen bond formation occurs between the carboxylic O–H group and the lone pair electrons of the ether oxygen which conjugates with the aromatic *π*-electrons. The effects of nuclear substitution on the ΔH value also support this hypothesis and the electron-repelling substituent gives higher ΔH value than the electron-attracting substituent.

9) J. F. J. Dippy, *Chem. Revs.*, **25**, 151 (1939).
10) Effects of the acidity on the O–H stretching frequency has been investigated widely by Goulden (J. D. S. Goulden, *Spectrochim. Acta*, **6**, 129 (1954)).

The substituents on oxygen gives the stronger effect than the methyl groups at α-position as shown in Table XI. It is clear that both the steric and the electronic (inductive) effects should be considered to discuss the effect of the α-substituent on the hydrogen bonding.

TABLE XI. THE ΔH AND $\Delta\nu_{max}$ INCREASE BY THE SUBSTITUTION OF ONE ADDITIONAL METHYL GROUP

Acid	ΔH Increase	$\Delta\nu_{max}$ Increase
Methoxyacetic		
Ethoxyacetic	0.35	7.8
Isopropoxyacetic	0.42	13.0
Methoxyacetic		
α-Methoxypropionic	0.39	20.2
α-Methoxyisobutyric	0.13	22.1
Phenoxyacetic		
α-Phenoxypropionic	−0.04	11.8
α-Phenoxyisobutyric	0.11	42.7

The carboxylic acid may include three rotational isomers with respect to the axis between the carboxylic carbon and the alpha carbon ($C_{C=O}-C_{\alpha}$), being represented by VII, VIII and IX. The oxo-groups are omitted in the formulae VII—IX for the sake of simplicity. As is clear from the Newman projections, the methyl group at the α-position increases the steric interaction with the hydroxyl group in the isomer IX in which the hydrogen-bonded structure is impossible, and consequently, the relative stability of the rotational isomers VII and VIII, which have the possibility of existing as hydrogen-bonded structure II, may rise.

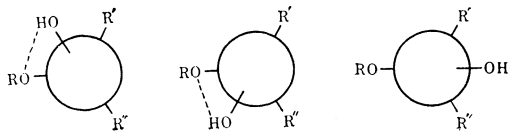

Rotamers of alkoxyacetic acid

VII VIII IX

Therefore, formation of hydrogen-bonding in α-alkoxyisobutyric acid is favored over that in α-alkoxyacetic acid, as far as the steric influence is concerned.

As to the electronic effect of the methyl groups at α-position of the carboxyl group, they will strengthen the basicity of the ether oxygen through the inductive effect, leaving the acidity of the carboxyl group intact as mentioned above. However, the extent of the effects cannot be estimated separately at the present stage. Thus both steric and electronic effects of the methyl groups favor the formation of hydrogen-bonding.

The effect of methyl group substituting methoxyl moiety of methoxyacetic acid seems to be of inductive nature, since the basicity of the corresponding alcohols are in the order; methanol < ethanol < isopropyl alcohol (< *t*-butyl alcohol), and this is the same order as the ΔH and $\Delta\nu_{max}$ values increase, although the ΔH measurement has not been complete with *t*-butoxyacetic acid. The result is in accordance with the fact that no serious steric hindrance is expected from the Fischer's molecular scale models between the alkyl group and *trans*-O–H group.

The order of A_t/A_c ratio (Table X) is not the same as the order of the basicity of oxygen atom. Namely abrupt decrease of A_t/A_c ratio is observed with *t*-butoxyacetic acid in spite of increasing $\Delta\nu_{max}$. The fact may be attributed to the steric effect of bulky *t*-butyl group hindering appoach of the hydroxyl group to ether oxygen, but, even in this compound no serious steric effect was foreseen from the model. Therefore, this phenomenon remains unexplained.

This intramolecular hydrogen bonding forms a five-membered ring and the maximal energy difference (ΔH) is 1.53 kcal./mol. This ΔH value is much smaller than the case of a six-membered intramolecularly hydrogen-bonded system of the same type. The ΔH values for *o*-methoxybenzoic and *o*-phenoxybenzoic acids are 3.3 kcal./mol.[11] and 1.89 kcal./mol.[12], respectively.

In spite of the greater energy, the hydrogen bonding of six-membered ring X has been found only in benzoic acid derivatives which carries an oxygen atom at ortho-position to the carboxyl group and neither β-alkoxy- nor β-aryloxy-propionic acid shows[13] the hydrogen bonding of this type XI.

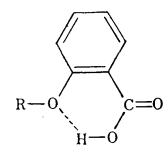

o-Alkoxybenzoic acid

X

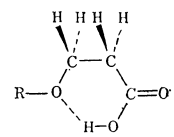

β-Alkoxypropionic acid

XI

These facts may be attributed to the following reasons: i) the six-membered hydrogen-bond system of *o*-alkoxybenzoic acids is a conjugate system, and ii) β-alkoxypropionic acids are enforced to assume the sterically unfavorable

11) M. Davies, "Hydrogen Bonding"—Papers presented at the Symposium on Hydrogen Bonding held at Ljubljana, 29, July 3, August, 1957. (Pergamon Press)
12) M. Ōki and M. Hirota, This Bulletin, **35**, 1948 (1962).
13) M. Ōki and M. Hirota, *J. Chem. Soc. Japan, Pure Chem. Sec.* (*Nippon Kagaku Zasshi*), **81**, 855 (1960).

cis-rotational form (as illustrated by XI) to make a planar six-membered hydrogen-bond system.

Temperature dependence study of the intensities of two ν_{O-H} bands at 3630 cm^{-1} and 3280 cm^{-1} in a ternary system of acetic acid, dibutyl ether and carbon tetrachloride indicates the enthalpy of hydrogen bond be 4.56 ± 0.3 kcal./mol. Provided that this value is applicable for the internal hydrogen bond as in methoxyacetic acid, then it is concluded that the cis form of the carboxyl group is stabilized by 3～4 kcal./mol. over the trans form.

The entropy term has an ambiguity of ($-\ln a$) and no quantitative relation with other physical properties can be fonud, although it increases with the increase of ΔH value.

The authors are indebted to Professor Takehiko Shimanouchi and Professor Ichiro Nakagawa for their valuable discussions throughout this work.

Department of Chemistry
Faculty of Science
The University of Tokyo
Hongo, Tokyo

A Study of Metal Complexes of Analytical Importance. II[1]. *Complexes of Salicylaldoxime and C-Methyl-salicylaldoxime with Vanadium(V)*[2]

By Hiroji NAKAMURA, Yoichi SHIMURA and Ryutaro TSUCHIDA

(Received November 24, 1962)

About the complexes of quinquevalent vanadium, there are few reports, and most of them concern studies of the so-called "solution complexes". Very few vanadium(V) complexes have been isolated. One of the purposes of this work is to isolate new complexes of vanadium(V).

Quinquevalent vanadium has no d-electrons, so its complexes would show no ligand field band, which comes from the d-d transition, and they would be colorless or yellow. Some complexes of vanadium(V), however, have a deep color. One of the examples of these colored complexes is the 8-quinolinol complex, which was reported on in Part I of this series[1]. The strong bands of this complex in the visible region are considered to be electron-transfer bands.

2-Methyl-8-quinolinol was found to form two complexes[1], one of them colored black, due to the charge-transfer bands, and the other, yellow. It was concluded that in the black complex the ligands were coordinated to the central metal as bidentate ligands, while in the yellow complex the ligands were coordinated as unidentate ligands[1].

In order to investigate further the relation between the charge-transfer bands in the visible region and the structure of ligands or the configuration of complexes, we used salicylaldoxime and its methyl derivative, *C*-methyl-salicylaldoxime (*o*-hydroxyacetophenoneoxime), as ligands and investigated the color and the structure of their vanadium(V) complexes.

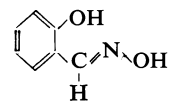

Salicylaldoxime
(symbol: $salmH_2$)

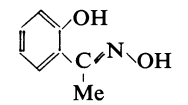

C-Methyl-salicylaldoxime
(symbol: $Me\text{-}salmH_2$)

Results and Discussion

Complexes of Salicylaldoxime with Vanadium(V).—The reaction of vanadate with salicylaldoxime at a pH value of 1 produces a black precipitate. Flagg and Furman[3] reported that in the black precipitate, the ratio of vanadium to salicylaldoxime was 2:3; i.e., the complex had the formula $C_{21}H_{21}N_3O_{10}V_2$. The complex represented by this formula is very queer, because in it vanadium should be quadrivalent. The experiments were, therefore, repeated by us. The complex which was formed under almost

1) Part I of this series: H. Nakamura, Y. Shimura and R. Tsuchida, This Bulletin, **34**, 1143 (1961).

2) A part of this study was presented at the Symposium on Coordination Compounds of the Chemical Society of Japan, Osaka, November, 1961.

3) J. F. Flagg and N. H. Furman, *Anal. Chem.*, **12**, 663 (1940).

the same conditions as mentioned above had the empirical formula approximately represented by $C_{21}H_{21}N_3O_{11}V_2$, and repeated experiments showed that the composition of the precipitate varied with a slight difference in the experimental conditions. As the infrared absorption spectra of the precipitate were not very sharp, it was concluded that the precipitate was not a pure substance. In order to prepare a pure complex having a structure similar to that of the 8-quinolinol vanadium(V) complex (1 : 2-complex), a large excess of the ligand was used, but the attempt was unsuccessful. In aqueous solution, no experiments with different pH values or temperatures were successful in the preparation of the desired complex.

As will be seen below, the recrystallization of the precipitate from benzene containing free salicylaldoxime gave the 1 : 2-complex in a pure crystalline state. The salicylaldoxime-vanadium(V) complex thus obtained may have a structure similar to that of the 8-quinolinol-vanadium(V) complex (Fig. 1a or 1b); its color is black in the crystalline state and violet in benzene and carbon tetrachloride. The absorption spectrum of the complex in benzene is shown in Fig. 2a. The intensity

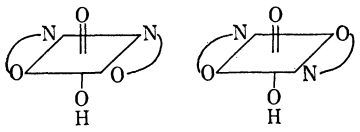

a b

Fig. 1.

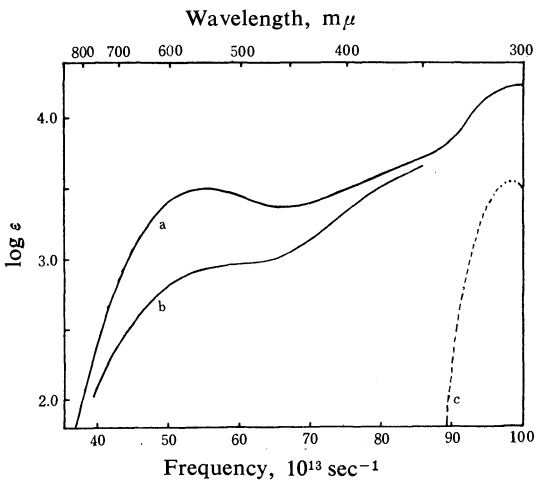

Fig. 2. Absorption spectra of salicylaldoxime-vanadium(V) complex.

a —— [VO(OH)(salmH)$_2$] in benzene
b —— [VO(OH)(salmH)$_2$] in acetone (about fifteen minutes after dissolution)
c --- Free salicylaldoxime in benzene

of the absorption band at 54.6×10^{13} sec^{-1} is as large as that of the corresponding band of the 8-quinolinol complex. The absorption spectrum of [VO(OH)(salmH)$_2$] in carbon tetrachloride coincided with that in benzene. In many other solvents, however, the complex changed its color as time passed after dissolution. In acetone, for example, the complex dissolved immediately after dissolution to show a violet color, which was quite like the color of the benzene solution, but it gradually changed to brown, and finally the color became almost yellow. The absorption spectrum of the complex in acetone about fifteen minutes after dissolution is shown in Fig. 2b. It is considered that the change of color is due to the decomposition of the complex.

The Absorption Spectrum of the Salicylaldoxime Complex in Dimethylformamide.—As was mentioned above, the salicylaldoxime complex dissolved in some solvents to show a violet color immediately after dissolution. This was not the case with dimethylformamide, which formed a solution showing a different color. Although the absorption bands of the complex in dimethylformamide decreased in intensity with time, the color of the solution immediately after dissolution was not violet, but a deep, reddish brown. The absorption curves of the complex in the 460~600 mμ range in dimethylformamide are shown in Fig. 3. In dimethylformamide the complex dissolved very rapidly, so it was possible to measure the change in the absorption intensity with time from the

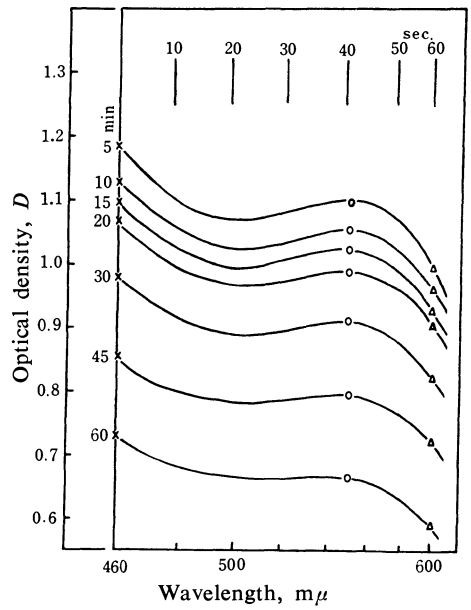

Fig. 3. Absorption spectra of [VO(OH)·(salmH)$_2$] in dimethylformamide.
Concn.: 3.49×10^{-4} M

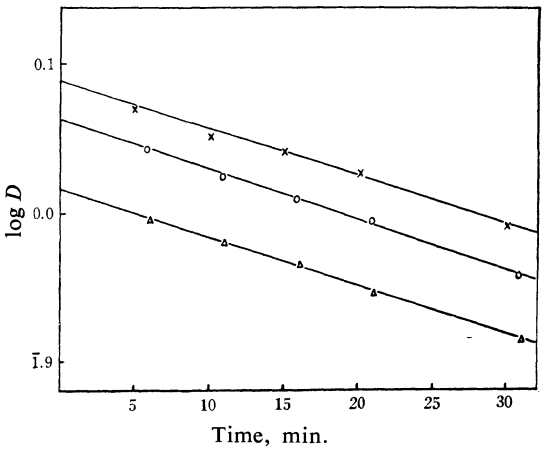

Fig. 4. Plots of log D vs. time after dissolution. ([VO(OH)(salmH)$_2$] in dimethylformamide: concn., 3.49×10^{-4} M)
×: 460 mμ ○: 550 mμ △: 600 mμ

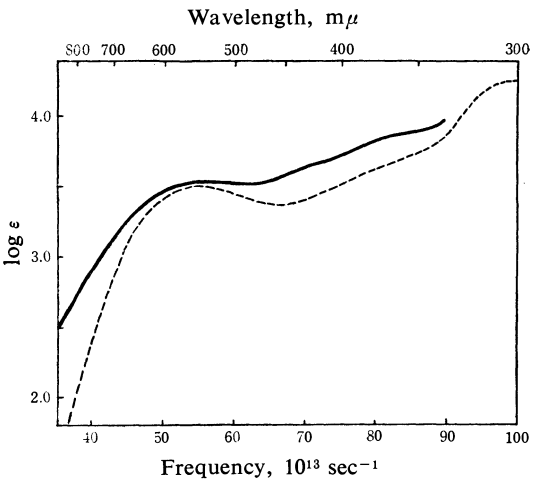

Fig. 5. Absorption spectra of [VO(OH)·(salmH)$_2$].
—— in dimethylformamide
--- in benzene

instant when the complex was dissolved. From Fig. 3, optical densities at 5, 10, 15, 30, 45 and 60 min. after dissolution at 460 mμ were obtained. Similarly, the values at 600 mμ after 6, 11, 16, 31, 46 and 61 min. were obtained. (It took one minute for the curves to be drawn from 460 mμ to 600 mμ). Optical densities at other wavelengths were also obtained. The logarithmic plot of the optical densities vs. time gave straight lines, showing that the decomposition of the complex was of the first order reaction (Fig. 4). By extrapolating the lines to zero, the optical densities of the complex at "zero time" were obtained. Thus, with similar measurements of other ranges, the absorption spectrum of the complex in dimethylformamide was obtained (Fig. 5). A comparison of the absorption spectra of the salicylaldoxime complex in benzene and in dimethylformamide shows a distinct difference which cannot be regarded as the effect of the solvent. In dimethylformamide the bands are broader and are situated at longer wavelengths than in benzene. 8-Quinolinol-vanadium(V) complex has two isomers, the cis and the trans[1] (Fig. 1). The absorption spectra of these isomers are shown in Fig. 6. From a comparison of the spectra of the salicylaldoxime complex with those of 8-quinolinol complexes, it has been concluded that the salicylaldoxime complex has the trans structure (Fig. 1b) in benzene or in carbon tetrachloride and the cis structure (Fig. 1a) in dimethylformamide.

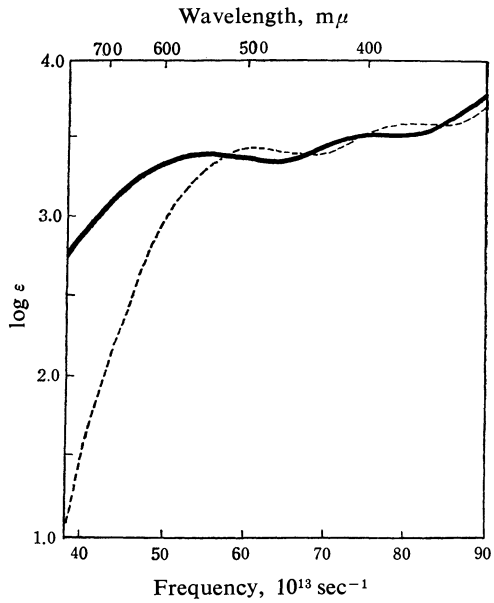

Fig. 6. Absorption spectra of 8-quinolinol-vanadium(V) complexes[1].
—— cis-form --- trans-form

The Esterified Complex of Salicylaldoxime with Vanadium(V). — The 1:2-complex of salicylaldoxime could be recrystallized from ethanol. The complex thus recrystallized from ethanol was esterified in OH, that is, [VO·(O–Et)(salmH)$_2$]. The absorption spectrum of [VO(O–Et)(salmH)$_2$] in benzene is shown in Fig. 7. It has large charge-transfer bands which are quite similar to that of [VO(OH)·(salmH)$_2$], and the esterification does not effect any such remarkable change of color as was reported for 8-quinolinol complexes[1].

The Complex of *C*-Methyl-salicylaldoxime with Vanadium(V).—As was reported in Part I of this series[1], the difference between the reactions of 8-quinolinol and 2-methyl-8-quinolinol

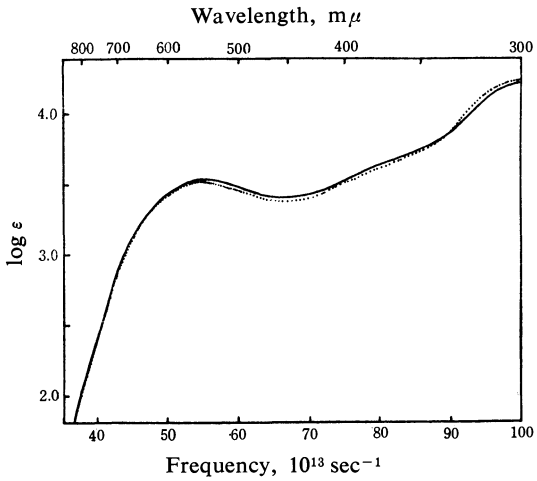

Fig. 7. Absorption spectra of [VO(O-Et)·(salmH)$_2$] (——) and [VO(OH)(salmH)$_2$] (·····) in benzene.

with vanadate is a very interesting problem. At pH values between 3 and 5 the former produced a black complex, whereas the latter gave a yellow complex under the same experimental conditions[1]. Concerning this phenomenon, the color and the structure of the complexes of salicylaldoxime and *C*-methyl-salicylaldoxime with vanadium(V) are problems of great interest.

C-Methyl-salicylaldoxime produced, with vanadate at a pH value of 1, a reddish-brown precipitate, not a black one. It was found that the color of the precipitate depended on the pH value of the solution of vanadate. At a higher pH value, the color of the precipitate was yellow. Contrary to the 2-methyl-8-quinolinol complex, the yellow precipitate did not change in color upon heating or drying. The yellow precipitate has no water of crystallization.

The preparation of a black complex like that of the salicylaldoxime complex was attempted. Lowering of the pH value of the solution of vanadate was effective in producing a rather dark-colored precipitate, but from an aqueous solution it was not possible to obtain a black complex. The precipitate which had been separated from the aqueous solution dissolved in many solvents to show yellow colors. After many attempts, it was found that the precipitate dissolved gradually in boiling benzene and that the color of the solution became violet. Evaporation of the solvent from the violet solution, however, produced a brown precipitate. Therefore, the benzene solution saturated with the complex at the boiling point was cooled rapidly and frozen. After separation of the frozen solvent, brownish-black crystals were obtained. It was observed under a microscope that the crystals were a mixture of yellow and black crystals. As the yellow crystals were soluble in warm alcohol, the black crystals were obtained in a pure state by washing the mixture repeatedly with warm alcohol. The black complex was the 1:2-complex of *C*-methyl-salicylaldoxime corresponding to that of salicylaldoxime. The absorption spectrum in benzene of the former was quite similar to that of the latter (Fig. 8).

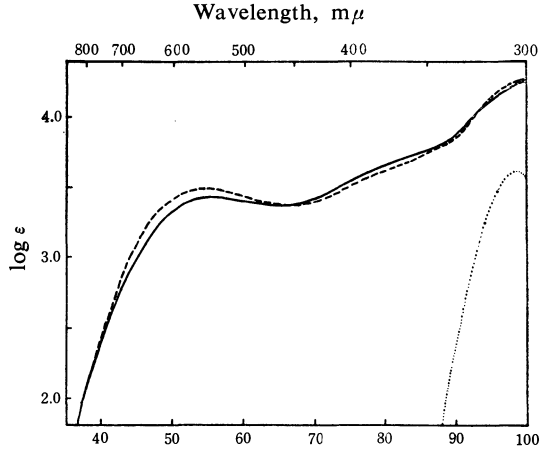

Fig. 8. Absorption spectra of [VO(OH)(Me-salmH)$_2$] (——), [VO(OH)(salmH)$_2$] (- - -) and free *C*-methyl-salicylaldoxime (·····) in benzene.

The Absorption Spectrum of *C*-Methyl-salicylaldoxime in Dimethylformamide. — In a way similar to that used for the salicylaldoxime complex, the absorption spectrum of the *C*-methyl-salicylaldoxime complex in dimethylformamide was determined (Fig. 9a).

By a comparison of Figs. 6 and 9, it can be seen that the *C*-methyl-salicylaldoxime complex has the cis structure in dimethylformamide and the trans structure in benzene, as has the salicylaldoxime complex.

The Yellow Form of the *C*-Methyl-salicylaldoxime Complex. — Recrystallization of the crude complex from toluene gave a yellow complex. The absorption spectrum of the yellow form is shown in Fig. 9c. The great difference between the colors of the black and the yellow forms cannot be ascribed only to the cis-trans isomerization.

The infrared absorption spectra of these black and yellow complexes give us some suggestions about their structures. Although the black form exhibits an O–H stretching band of =N–OH[4] at 3380 cm^{-1}, the yellow form

4) G. Duyckaerts, *Bull. soc. roy. sci. Liège*, **21**, 196 (1952).

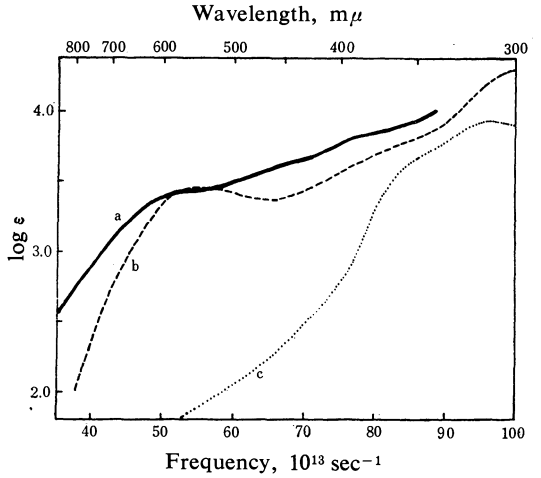

Fig. 9. Absorption spectra of *C*-methyl-salicylaldoxime-vanadium(V) complexes.
a —— [VO(OH)(Me-salmH)$_2$] in dimethylformamide
b - - - [VO(OH)(Me-salmH)$_2$] in benzene
c ····· [V(OH)(Me-salm)$_2$] in dimethylformamide

does not show any band above the 4000~3000 cm^{-1} region. This suggests that in the yellow form the oxygen atoms of a oxime character are bound to the vanadium ion. That is, it is probable that in the yellow form, the ligands are coordinated to the vanadium ion with two oxygen atoms. This view is supported by the elementary analysis of V(OH)(Me-salm)$_2$ and also by the fact that the band at 1620 cm^{-1} of the black form shifts to 1642 cm^{-1} in the yellow form[5].

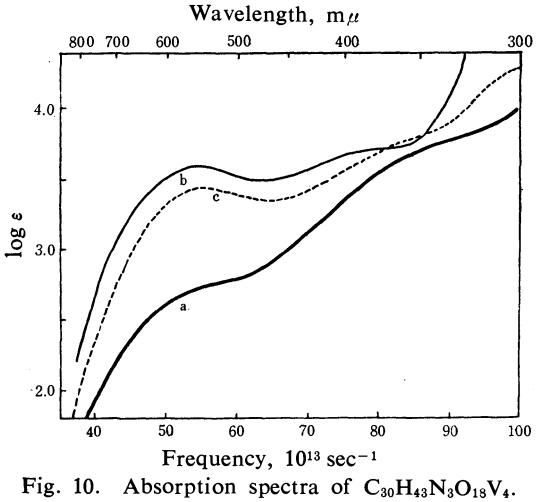

Fig. 10. Absorption spectra of $C_{30}H_{43}N_3O_{18}V_4$.
a —— in benzene
b —— in benzene containing ligand
(c - - - represents [VO(OH)(Me-salmH)$_2$] in benzene)

5) L. J. Bellamy, "The Infrared Spectra of Complex Molecules", 2nd Ed., John Wiley & Sons, Inc., New York (1958).

The Complex Recrystallized from Methanol. —Recrystallization of the yellow form from methanol gave brown planar crystals. The color of the benzene solution of the crystals was also brown (Fig. 10a). Adding *C*-methyl-salicylaldoxime to the solution made its color violet, a color which was similar to that of the black form in the same solvent (Fig. 10b). The composition of the brown crystals was, however, very complicated ($C_{30}H_{43}N_3O_{18}V_4$), and further investigation is nescessary to solve this problem.

Experimental

Preparation of the Salicylaldoxime-Vanadium Complex. — The 1 : 2-complex was prepared as follows : 1.9 g. (1/100 mol.) of sodium metavanadate tetrahydrate ($NaVO_3 \cdot 4H_2O$) was dissolved in 50 ml. of 0.2 N sodium hydroxide. The pH value of the solution was adjusted to about 1 by the use of 2 N sulfuric acid. After the solution had been stirred for thirteen minutes, the black precipitate was filtered, washed and dried in the air. Six hundred milligrams of dried precipitate were refluxed with 200 ml. of benzene containing 500 mg. of salicylaldoxime for one hour. After filtration, the solution was concentrated to about 30 ml. and was left to cool. The black crystals separated were filtered and washed with benzene.

Found : C, 55.38 ; H, 4.24 ; N, 6.75 ; V, 11.80. Calcd. for $C_{20}H_{19}N_2O_6V$=[VO(OH)(salmH)$_2$]·C_6H_6 : C, 55.30 ; H, 4.41 ; N, 6.45 ; V, 11.73%.

The ethyl ester of the complex was prepared by recrystallization from ethanol.

Found : C, 49.70 ; H, 4.13 ; N, 7.59 ; V, 13.42. Calcd. for $C_{16}H_{17}N_2O_6V$=[VO(O-Et)(salmH)$_2$] : C, 49.99 ; H, 4.46 ; N, 7.28 ; V, 13.27%.

Preparation of the *C*-Methyl-salicylaldoxime-Vanadium(V) Complex.—*C*-Methyl-salicylaldoxime was prepared by the method of Poddar[6].

The complex was prepared as follows : 1.9 g. (1/100 mol.) of sodium metavanadate tetrahydrate was dissolved in 50 ml. of 0.2 N sodium hydroxide. The pH value of the solution was adjusted to 1.2 by diluted sulfuric acid. To the solution was added 3.1 g. (2/100 mol.) of *C*-methyl-salicylaldoxime dissolved in 6 ml. of acetone. After three hours, the crude precipitate was filtered and washed with water.

The black form was prepared as follows : 1.0 g. of the crude precipitate was refluxed for three hours with one liter of benzene. After filtration, the solution was cooled with ice and left in a refrigerator. The frozen colorless solvent, which did not contain the complex was removed from the frozen mass with a spoon. The residue was melted at room temperature, and the crystals were separated by filtration. A mixture of yellow and black crystals was thus obtained. The mixture was put into 100 ml. of warm alcohol and stirred. After filtration the crystals were washed several times more with warm alcohol. The crystals thus obtained

6) S. N. Poddar, *Z. anal. Chem.*, **154**, 254 (1957).

were black in color. The absence of yellow crystals was confirmed microscopically.

Found: C, 52.63; H, 4.68; N, 7.10; V, 12.20. Calcd. for $C_{18}H_{19}N_2O_6V$=[VO(OH)(Me-salmH)$_2$]·1/3C_6H_6: C, 52.75; H, 4.67; N, 6.83; V, 12.42%.

The yellow form was prepared as follows: 0.75 g. of the crude complex was dissolved in 500 ml. of toluene at 95°C. After filtration, the solution was left in a refrigerator. The reddish-brown crystals which separated were washed repeatedly with carbon tetrachloride to remove the black form.

Found: C, 52.32; H, 4.16; N, 7.29; V, 13.70. Calcd. for $C_{16}H_{15}N_2O_5V$=[V(OH)(Me-salm)$_2$]: C, 52.47; H, 4.13; N, 7.65; V, 13.91%.

Measurement. — Visible and ultraviolet absorption spectra were determined with a Beckman DU and a Hitachi EPS-2 spectrophotometer using cells with light paths 1.0 and 0.10 cm. in length respectively.

The infrared absorption measurements were made by the KBr pressed-disk technique in a Hitachi EPI-2 infrared spectrophotometer.

Summary

New complexes of salicylaldoxime (symbol: salmH$_2$) and *C*-methyl-salicylaldoxime (symbol: Me-salmH$_2$) with vanadium(V), [VO(OH)·(salmH)$_2$] (A), [VO(O–Et)(salmH)$_2$] (B), [VO·(OH)(Me-salmH)$_2$] (C) and [V(OH)(Me-salm)$_2$] (D) were prepared. A, B and C complexes were dark-colored, while the D complex was light-colored.

The absorption spectra of A and C in dimethylformamide were determined. Based on the measurements of the visible, ultraviolet and infrared absorption spectra of these complexes, the following conclusions were drawn:

1) In benzene complex A has the trans structure, while in dimethylformamide it has the cis structure.

2) Complex C has the same properties as A.

3) The esterification of A does not cause any remarkable change in color.

4) The great difference between the color of C and that of D comes from the difference in the donor atoms of the ligand. In the former the ligands are coordinated as N, O-chelates, and in the latter, as O, O-chelates.

Department of Chemistry
Faculty of Science
Osaka University
Kita-ku, Osaka

The Separation of Trace Amounts of Tellurium from Iron by Solvent Extraction

By Yasumitsu UZUMASA, Kenjiro HAYASHI and Saburo ITO

(Received October 26, 1962)

According to the standard method of the Japan Institute of the Promotion of Science and Techniques[1], when a steel sample containing tellurium is treated with a mixture of ammonium hydrogen fluoride and sulfuric acid, most of iron goes into solution while tellurium, silica, carbon, etc., together with a little iron, are left undissolved. This method of dissolving can be applied to a sample containing as much as 0.1 mg. of tellurium. When we investigated this method in detail, our experiments revealed, however, that when the tellurium content is less than this amount, the separation of tellurium from iron is never complete. It was found that a part of the tellurium passes through the filter paper, the amount of tellurium in the residue being thus reduced. After these studies, therefore, we abandoned this procedure and investigated another method in which tellurium, together with iron, is dissolved in a suitable solvent and the former is separated from the latter by the extraction method.

Experimental and Results

Apparatus.—A Beckman model DU spectrophotometer with 1 cm. silica cells was used.

Procedure.—One gram of solid thiourea is added to 15 ml. of the sample solution; this is equivalent to 2 N of a hydrochloric acid concentration. After the mixed solution is made up to 20 ml. with 2 N hydrochloric acid, it is allowed to stand for 20 min. and absorbance is measured at 350 or 370 mμ[2,3].

1) The Japan Institute of the Promotion of Science and Techniques, "Rapid Analysis of Iron and Steel", Maruzen, Tokyo (1956), p. 247.

2) Kazuo Ota, *J. Japan Inst. Metals*, **23**, 581 (1959).

3) D. F. Boltz, "Colorimetric Determination of Nonmetals", Interscience Pub. Inc., N. Y. (1958), p. 309.

Change in the State of Tellurium During the Dissolution of the Steel Sample. — As to the state of a minute amount of tellurium in steel, very little consideration has been paid it so far. As may be seen from the Fe–Te diagram (Fig. 1)[4], it is quite possible that it exists as $FeTe_{0.90}$. Iron telluride of this niccolite type may produce, by the action of an acid, hydrogen telluride, which may further yield metallic

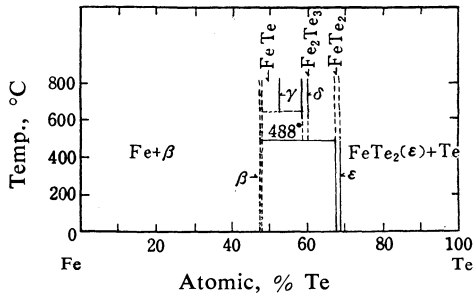

Fig. 1. Fe-Te diagram.
The phase : $FeTe_{0.90}$
The phase : $FeTe_{1.1}$
The phase : $FeTe_{1.4}-FeTe_{1.5}$
The phase : $FeTe_2$

tellurium as indicated by the following equation:

$$H_2Te(aq) = Te + 2H^+ + 2e$$
$$E^\circ_{298} = +0.69\ V.^{5)}$$

It is also possible that a part of the hydrogen telluride thus produced might remain not oxidized and volatilize as gas, since its boiling point is $-1.8 \sim 0°C$ at 1 atm.[6] In order to examine this possibility, 5 g. of the steel sample containing 0.3 mg. Te/g. was dissolved in 6 N hydrochloric or sulfuric acid and the gas evolved was introduced into ammonia. The amount of tellurium absorbed in ammonia was found always to be less than 10 μg. This indicates that the volatilization may be disregarded.

Another possibility is that in acidic media metallic tellurium might be oxidized by ferric iron to tellurium(IV) and dissolve into the solution:

$$Te + 2H_2O \rightleftharpoons TeO_2 + 4H^+ + 4e$$
$$E^\circ_{298} = -0.529\ V.^{5)}$$
$$Fe^{2+} \rightleftharpoons Fe^{3+} + e \qquad E^\circ_{298} = -0.771\ V.$$

Therefore, metallic tellurium suspended in a acidic medium will more or less dissolve in the presence of iron(II) as the latter is oxidized to iron(III) by air. This was confirmed by the following experiment.

The precipitate of metallic tellurium prepared by adding stannous chloride to a hydrochloric acid solution of potassium tellurite was centrifuged and washed with water thoroughly. When this precipitate was suspended in 6 N hydrochloric acid containing ferric chloride, rapid dissolution of the precipitate took place. It is, therefore, possible that, in the practical analysis of steel, the existence of ferric iron brings about the solution of metallic tellurium, if it is present. The time necessary for the complete dissolution of steel samples differs according to type. In cases where it takes a longer time, the partial oxidation of iron(II) to iron(III) occurs, resulting in a partial dissolution of the metallic tellurium. This is illustrated in Table I.

TABLE I. DISSOLUTION OF METALLIC TELLURIUM WITH FERRIC IRON IN HYDROCHLORIC OR SULFURIC ACID

Sample No.	Acid	Dissolving time, min.	Tellurium	
			In the sample, mg.	In the soln., μg.
1	HCl	8	1.03	4.3
2	HCl	18	0.695	7.7
3	HCl	20	0.45	16.5
4	HCl	90	1.35	610.0
1	H_2SO_4	10	1.03	25.3
2	H_2SO_4	17	0.695	12.1
3	H_2SO_4	20	0.45	4.3
4	H_2SO_4	30	1.35	0

Acid concentration : 6 N
Volume of the solution : 25 ml.
Steel sample taken : 1 g.

When sulfuric acid was used, the steel sample dissolved more rapidly and the particles of metallic tellurium coagulated in larger aggregates. Moreover, the oxidation of ferrous iron in sulfuric acid is more difficult.

Reexamination of the Precipitation Method. —There is a conventional method of separation in which the steel sample containing tellurium is dissolved in a suitable solvent and the solution is treated with such a reducing agent as stannous chloride and then the tellurium is reduced and precipitated. The precipitate is filtered off, the tellurium being thus separated from the iron. A critical examination of this method was undertaken.

Ten grams of solid stannous chloride were added to 150 ml. of 3 N hydrochloric acid containing sodium tellurite equivalent to 66 μg. of tellurium. The solution was then boiled

4) M. Hansen and K. Anderko, "Constitution of Binary Alloys", McGraw-Hill Book Co. Inc., N. Y. (1958), p. 722.
5) W. M. Latimer, "The Oxidation State of the Elements and Their Potentials in Aqueous Solutions", 2nd. Ed., Prentice-Hall, N. Y. (1956).
6) "A Comprehensive Treatise on Inorganic and Theoretical Chemistry", XI, Longmans, London (1931), p. 63.

for 5 min. After the liquid had been allowed to stand for one hour at room temperature, the precipitate formed was filtered through Toyo No. 5C filter paper and washed with hydrochloric acid. The precipitate was then brought into solution by nitric acid, and the amount of tellurium was determined spectrophotometrically with thiourea. The results are shown in Table II.

Table II. Fraction of precipitated tellurium

Tellurium, μg.		Recovery %
Taken	Found	
66.0	30	45.5
66.0	26	39.4
66.0	25	37.9
66.0	25	37.9
66.0	24	36.4
66.0	24	36.4
	Ave.	39.0

It is obvious from this table that this precipitation method can not be applied to a sample whose tellurium content is very small.

Extraction of Tellurium with an Organic Solvent. — Ferric iron in highly concentrated hydrochloric acid can be extracted quite efficiently with some organic solvents such as ethyl acetate, *n*-butyl acetate or methyl isobutyl ketone, while the extractability of tellurium under similar conditions has not previously been well known. Tellurium(IV) is oxidized into tellurium(VI) by potassium dichromate. It has already been confirmed by the authors that, in a highly concentrated hydrochloric acid solution, the behavior of the tellurium thus oxidized is remarkably different from that of ordinary tellurate ions[7]. Accordingly, it is expected that the extractability of tellurium-(VI) formed with potassium dichromate into ethyl acetate, *n*-butyl acetate or methyl isobutyl ketone will differ from that of tellurite or tellurate. Therefore, experiments on the extractability of tellurium into the above-mentioned solvents were carried out under various conditions.

Twenty milliliters of a 6 N or 9 N hydrochloric acid solution containing a definite amount of tellurium, together with or without potassium dichromate, was placed in a separatory funnel whose capacity was 100 ml. To this was added 10 ml. of an organic solvent. After 10 sec. shaking, the two layers were separated. The aqueous layer was evaporated to dryness on the water-bath. The tellurium in the organic solvent was extracted back into water, and the aqueous solution thus obtained was also evaporated to dryness. After dissolving each of these two residues, the amount of tellurium in each of them was measured by the spectrophotometric method using thiourea and the extractability of the element was calculated. When potassium dichromate was present, 1 ml. of 30% hydrogen peroxide was added to the aqueous solution, and, after being evaporated to dryness, each residue was dissolved in 6 N hydrochloric acid. When this acid solution was shaken with methyl isobutyl ketone, tellurium went into the organic solvent quantitatively. After the organic layer had been washed twice with 6 N hydrochloric acid, the tellurium in the organic layer was extracted back again into water and determined spectrophotometrically. The extractability is summarized in Table III.

As shown in Table III, of the three solvents used, *n*-butyl acetate seemed to be most suitable since the extractability of tellurium into this

Table III. Extractability of tellurium with various organic solvents

Tellurium taken as	μg.	Concn. of HCl, N	5% $K_2Cr_2O_7$ ml.	Extractability, %		
				Ethyl acetate	*n*-Butyl acetate	Methyl isobutyl ketone
Na_2TeO_3	330	6	0	63	19.4	100
Na_2TeO_3	330	6	0	62	18.4	100
Na_2TeO_3	330	6	1	54	11.0	100
Na_2TeO_3	330	6	1	51	12.7	100
Na_2TeO_3	330	9	0		34.6	
Na_2TeO_3	330	9	0		36.2	
Na_2TeO_3	330	9	1		22.5	
Na_2TeO_3	330	9	1		25.0	
Na_2TeO_4	200	6	0		1.6	2.6
Na_2TeO_4	200	6	0		1.7	2.7
Na_2TeO_4	200	9	0		3.0	
Na_2TeO_4	200	9	0		3.1	

7) Y. Uzumasa, S. Hikime, K. Hayashi and H. Yoshida, *Japan Analyst* (*Bunseki Kagaku*), 11, 78 (1962).

solvent is the smallest. It was also observed that potassium dichromate tends to reduce the extractability of the element. Accordingly, further experiments were carried out to study the extractability in detail, varying the concentration of hydrochloric acid over a wide range. The results are shown in Table IV.

TABLE IV. EFFECTS OF DICHROMATE AND HYDROCHLORIC ACID CONCENTRATION ON THE EXTRACTABILITY OF TELLURIUM WITH *n*-BUTYL ACETATE

Concn. of HCl, N	Extractability of tellurium, %	
	1 ml. of 5% $K_2Cr_2O_7$ added	Without $K_2Cr_2O_7$
3	0.7	2.5
3	1.5	2.7
3	1.8	2.8
6	12.7	18.8
6	12.7	19.0
6		19.4
7.5	19.4	22.4
7.5	20.4	25.0
7.5	20.4	25.6
9	22.5	34.6
9	25.0	36.5
9	26.3	
10.5	41.0	55.8
10.5	44.7	55.2

Tellurium taken: 330 μg.

It has been known that the ferric iron is extracted from a concentrated hydrochloric acid solution into *n*-butyl acetate quite rapidly and quantitatively. When, for example, 20 ml. of 9 N hydrochloric acid containing 1 g. of ferric iron was treated with 10 ml. of *n*-butyl acetate, 99.8% of the iron(III) was found to be removed. Only 1.7 to 2.0 mg. of ferric iron remained in the hydrochloric acid layer after one extraction. Accordingly, this process possibly allows for the separation of a minute amount of tellurium from a large amount of iron.

The extraction of a small quantity of tellurium(IV) with methyl isobutyl ketone was also studied. Table V shows the results, which agree fairely well with those obtained by Goto et al.[8], who investigated the extractability of many metals by this solvent.

When the concentration of hydrochloric acid was adjusted to a normality of 4.5 to 6, tellurium(IV) was extracted into this liquid quantitatively, whereas chromium(III) was not removed at all under the same conditions. This fact suggests that tellurium(IV) and chromium(III) may be separated from each other by this extraction.

8) H. Goto, Y. Kakita and H. Furukawa, *J. Chem. Soc. Japan, Pure Chem. Sec.* (*Nippon Kagaku Zassi*), **79**, 1513 (1959).

TABLE V. EFFECT OF THE HYDROCHLORIC ACID CONCENTRATION ON THE EXTRACTABILITY OF TELLURIUM WITH METHYL ISOBUTYL KETONE

Concn. of HCl, N	Extractability of tellurium, %
3	86.5
3	81.7
4.5	99.3
4.5	99.3
4.5	100.0
6	99.3
6	99.3
6	100.0
6	100.0
7.5	98.2
7.5	98.2

Tellurium taken: 330 μg.

The Separation of Iron and Tellurium with *n*-Butyl Acetate and Methyl Isobutyl Ketone.— It is clear from Table III that tellurium is partly extracted into *n*-butyl acetate when conditions allow a complete extraction of ferric iron. Therefore, further experiments were carried out to find a means of drawing a little tellurium extracted to the aqueous layer back again, leaving ferric iron in the organic layer.

Twenty milliliters of a 9.5 N hydrochloric acid solution containing 330 μg. of tellurium and 1 ml. of 5% potassium dichromate solution was shaken with 10 ml. of *n*-butyl acetate; nearly 30% of the tellurium was extracted into this organic layer. After being separated, the *n*-butyl acetate layer was washed several times with a 5 ml. portion of 9 N hydrochloric acid containing 1 ml. of 5% potassium dichromate. The results are shown in Table VI.

As is evident from Table VI, the tellurium in the organic layer can be shaken completely back to the aqueous layer in three back washings. Another trouble occurred, however, when, by this procedure, ferric iron also turned back, though only slightly, to the aqueous layer. Experiments were repeated, therefore, to find out a means of overcoming this difficulty. Finally the following scheme, by which a fairly satisfactory result was obtained, was obtained.

TABLE VI. BACK WASHING OF TELLURIUM(IV) FROM THE ORGANIC LAYER

No. of back washing	Tellurium remaining in the organic layer, %	
0	33.2	30.0
1	13.0	11.0
2	5.6	4.5
3	1.5	0.0

Back washing solution: 5 ml. of 9 N hydrochloric acid containing 1 ml. of 5% potassium dichromate.

TABLE VII. SCHEME OF THE SEPARATION PROCEDURE FOR TELLURIUM FOR STEEL

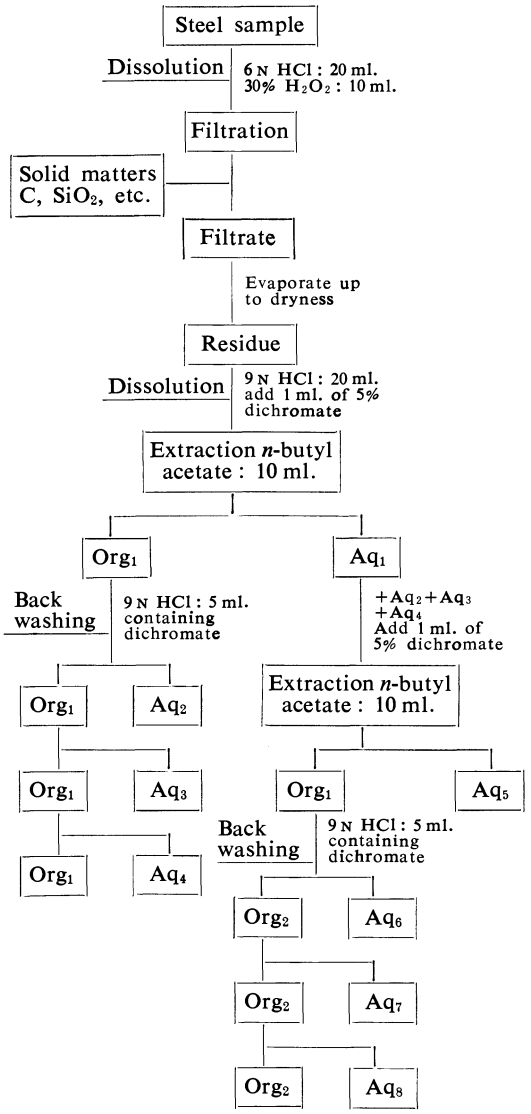

According to this scheme, tellurium is concentrated in the combined aqueous solution ($Aq_5+Aq_6+Aq_7+Aq_8$); the amount of iron in this solution is negligible. Chromium(III) as well as chromium(VI) are enriched in this aqueous layer, so that the removal of this element is necessary prior to the determination of the tellurium. Extraction with methyl isobutyl ketone is recommended for this purpose. The procedure is as follows:

Two milliliters of 30% hydrogen peroxide is added to a hydrochloric acid solution containing tellurium, together with chromium as a dichromate. After chromium(VI) is reduced to chromium(III), the excess of hydrogen peroxide is decomposed by heating and the total volume of the solution is regulated to 20 ml. The acid concentration is adjusted to a normality of 4.5 to 6, and the tellurium is extracted with 10 ml. of methyl isobutyl ketone. One extraction is sufficient for the complete separation of the two elements. The tellurium extracted into the organic layer is successfully transferred back to the aqueous layer by treating it twice with 5 ml. of distilled water. Iron does not interfere in the spectrophotometry since the amount of this metal behaving with tellurium is less than 0.1 mg., even when 1 g. is contained in the original solution. Table VIII shows that a large amount of ferric iron can be separated from tellurium(IV) by this method.

TABLE VIII. SEPARATION OF TELLURIUM FROM IRON

Fe^{3+} Added mg.	Tellurium, μg. Taken	Tellurium, μg. Found	Recovery %
102	33	33.0	100
102	33	33.0	100
102	33	32.5	98.4
510	33	35.5	107.6
510	33	33.0	100
510	33	33.0	100
510	66	63.3	96.0
510	66	65.0	98.4
510	66	65.0	98.4
510	330	329	99.5
510	330	329	99.5
510	330	329	99.5
1020	33	37.5	115
1020	33	34.0	103
1020	66	67.5	102
1020	66	66.0	100
1020	66	65.2	98.8
1020	66	65.0	98.4
1020	330	319.0	96.7
1020	330	310.0	94.0
1020	330	319.0	96.7

Aqueous layer : 20 ml.; organic layer : 10 ml.; when 1.02 g. of iron was taken, aqueous layer : 40 ml.; organic layer : 20 ml.

It has been made clear that our new method furnishes a quantitative means for separating iron and tellurium.

The Determination of Tellurium in Steel. — Since we had no standard sample at hand whose tellurium content was known, the same sample was analyzed both by our method and by the conventional precipitation method and the two results were compared for reference.

In our method, 0.5 g. of the steel sample was heated in a mixture of 20 ml. of 6 N hydrochloric acid and 10 ml. of 30% hydrogen peroxide until it dissolved; the insoluble matters

TABLE IX. COMPARISON BETWEEN THE TWO METHODS

Sample No.	Composition					Tellurium found, %*	
	C	Si	Mn	P	S	By extraction method	By p. p. t. method
1	0	0	0	0	0	0.102***	0.103
2	0	0	0	0	0	0.0695***	0.071
3	0	0	0	0	0	0.045***	0.045
4	0	0	0	0	0	0.135***	0.14
46	3.46	1.43	0.36	0.336	0.08	0.0113	0.0113
113	3.62	1.47	0.34	0.368	0.084	0.0128	0.013
122	3.44	1.38	0.36			0.012	0.0135
144	3.49	1.39	0.40	0.336	0.08	0.007	0.0072**
159	3.52	1.22	0.31	0.544	0.082	0.0077	0.008**

* Mean value of five determinations
** 2 g. of the sample taken
*** 0.1 g. of the sample taken

(carbon, silica, etc.) were then filtered off. After washing the residue with 10 ml. of 6 N hydrochloric acid, the filtrate, together with the washing, was evaporated to dryness on a water bath. The residue obtained was then treated according to the procedure described above.

As was pointed out above, in the precipitation method the amount of tellurium can not be determined accurately unless it is more than 0.1 mg. Therefore, we took many samples of at least 1 g. or more. The samples were dissolved in 20 to 30 ml. of 6 N sulfuric acid. When the solid matter nearly disappeared, 10 g. of stannous chloride was introduced. After having been left standing for 30 min., the solution was filtered and the solid remaining on the filter paper was washed with hydrochloric acid (1 : 10) containing stannous chloride and then with water. The washed precipitate of tellurium was dissolved in hot hydrochloric acid (1 : 2) containing hydrogen peroxide, the excess of which was decomposed by heating. After adjusting the acid concentration and the volume of the solution to about 3 N and 100 ml. respectively, tellurium was precipitated by adding 5 g. of stannous chloride. The results are summarized in Table IX. The two values are in good accord.

Conclusion

1) In the precipitation method, foreign substances existing in the solution tend to coprecipitate and lower results for tellurium are occasionally obtained, especially when the total amount of tellurium is less than 0.1 mg. The authors' method gives better results even when the amount of tellurium falls under this amount.

2) After being separated from iron, tellurium is determined by the spectrophotometric method with thiourea, i. e., by measuring the absorption at 350 and 370 mμ. In this procedure, the variety as well as the quantity of coexisting anions markedly affects the result of analysis, so they must be accurately regulated. When our extraction procedure is applied, however, these troubles are considerably minimized.

3) The amount of the sample to be taken in our method should preferably be not more than 0.5 g. If a larger amount is taken, some time-consuming treatment must be added and the rapidity of the method is lost.

Faculty of Science
Hokkaido University
Sapporo

A Note on the Exchange Interaction between Different Electron Spins in Organic Molecular Complexes

By Minoru KINOSHITA

(Received October 30, 1962)

In a previous paper the electron spin resonance in the complex of 2,2'-dinaphthyl disulfide with antimony pentachloride was presented[1]. It was reported there that the g-value of the complex was found to take two values, depending on the sample chosen; one of these values was 2.0074 ± 0.0001, and the other 2.0051 ± 0.0002 in the powdered state, the origin of which was not clarified. However, yet another g-value, 2.0063 ± 0.0002, has recently been observed in the same complex. This value is a mean of the above values. It is known that such a phenomenon can be interpreted on the basis of the exchange interaction between the species with different g-values.

If there are two electron spins with different g-values, g_1 and g_2, in an external static magetic field, H, and if an exchang interaction is present between them, then the Hamiltonian for this system can be given as:

$$\mathscr{H}=g_1\beta HS_{1z}+g_2\beta HS_{2z}+2J\vec{S}_1\cdot\vec{S}_2 \qquad (1)$$

By the use of the vector model, Hamiltonian (1) can be written as:

$$\mathscr{H}=g_1\beta H(S_z-\gamma S_{2z})+J\{S(S+1)-\frac{3}{2}\} \qquad (2)$$

where S_z is the component of the electron spin operator $\vec{S}=\vec{S}_1+\vec{S}_2$; $S(S+1)$ the eigenvalue of $\vec{S}^2$, and $\gamma=1-g_2/g_1$. Omitting the constant term, the energy levels will be obtained as follows:

$$E_{0,0}=J-(J^2+\frac{1}{4}g_1^2\beta^2H^2\gamma^2)^{1/2} \quad \text{for } S=0,\ M=0$$

$$E_{1,-1}=2J-g_1\beta H(1-\frac{1}{2}\gamma) \quad \text{for } S=1,\ M=-1$$

$$E_{1,0}=J+(J^2+\frac{1}{4}g_1^2\beta^2H^2\gamma^2)^{1/2} \quad \text{for } S=1,\ M=0$$

$$E_{1,1}=2J+g_1\beta H(1-\frac{1}{2}\gamma) \quad \text{for } S=1,\ M=1$$

Now two limited cases will be considered.

In the first case, that of $J\gg g_1\beta H\gamma/2$, the $E_{1,0}$ expression may be given as;

$$E_{1,0}=2J+\frac{1}{2}J(g_1\beta H\gamma/2J)^2$$

According to the selection rule, $\Delta S=0$ and $\Delta M=\pm1$, the two transitions are derived as:

$$h\nu_1=\frac{1}{2}(g_1+g_2)\beta H+\frac{1}{2}J(g_1\beta H\gamma/2J)^2 \text{ and}$$

$$h\nu_2=\frac{1}{2}(g_1+g_2)\beta H-\frac{1}{2}J(g_1\beta H\gamma/2J)^2$$

When J is sufficienty large, only one transition can be observed;

$$h\nu_1=h\nu_2=\frac{1}{2}(g_1+g_2)\beta H$$

In the second case, that of $\frac{1}{2}g_1\beta H\gamma\gg J\approx0$, on the other hand, two absorption lines should be obtained:

$$h\nu_1=g_1\beta H-J, \text{ and } h\nu_2=g_2\beta H+J$$

These circumstances are demonstrated in Figs. 1 and 2.

In the complex of 2,2'-dinaphthyl disulfide with antimony pentachloride, the phenomenon mentioned above may be ascribed to the first

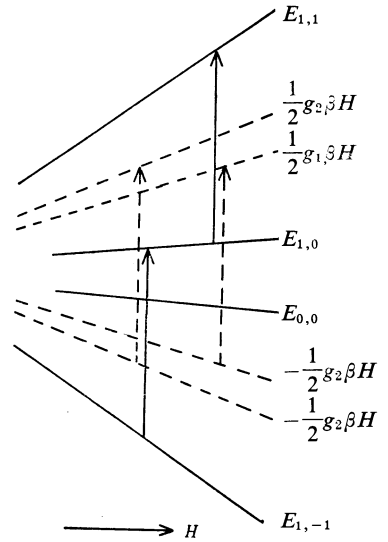

Fig. 1. The Zeeman splittings are shown graphically for the case of $J\ll g_1\beta H\gamma/2$.

—— $g_1\beta H_0 : g_2\beta H_0 : J=4:3:0.1$

- - - $g_1\beta H_0 : g_2\beta H_0 : J=4:3:0$

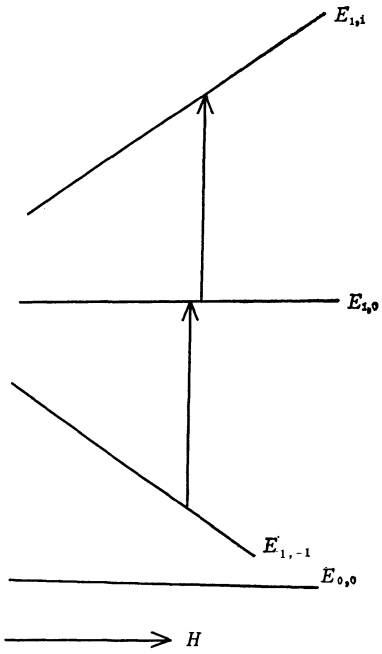

Fig. 2. The Zeeman splittings are shown graphically for the case of $J \gg g_1\beta H\gamma/2$.
$g_1\beta H_0 : g_2\beta H_0 : J = 4 : 3 : 2$

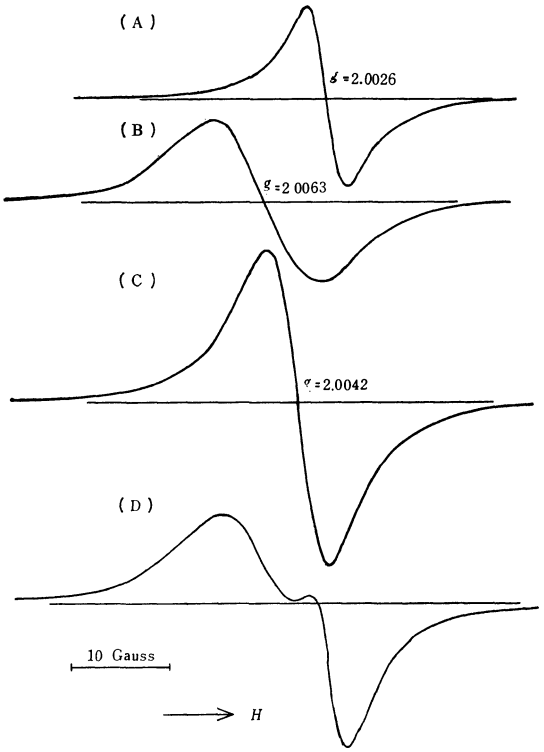

Fig. 3. The ESR absorption (the first derivative) curve of the complexes with antimony pentachloride.
(A) Carbazol
(B) 2, 2'-Dinaphthyl disulfide
(C) The mixed complex of carbazol and 2, 2'-dinaphthyl disulfide
(D) Each complex of (A) and (B) is placed in different capillaries and measured at the same time.

case considered. This assignment is supported by the following experiments. The complex of carbazol with the same reagent gave the resonance line at $g=2.0026\pm0.0003$, while the mixed crystal, which was made by adding the antimony pentachloride solution in chloroform to the mixed solution of carbazol and 2, 2'-dinaphthyl disulfide, gave the line at $g=2.0042\pm0.0002$ (Fig. 3). This value is very near the mean value (2.0045) of 2.0063 for the complex of 2, 2'-dinaphthyl disulfide and 2.0026 for the complex of carbazol, showing that there are sufficiently large exchange interactions between the paramagnetic electron spins produced by the reaction of carbazol and 2, 2'-dinaphthyl disulfide with antimony pentachloride. In this case, the exchange interaction, J, is much greater than $\frac{1}{2}g_1\beta H\gamma \approx 4\times 10^{-8}$ eV.

A similar result was obtained in the mixed complex of carbazol and thio-β-naphthol with antimony pentachloride. The system of thio-β-naphthol with antimony pentachloride has already been reported as giving the spin resonance at $g=2.0076\pm0.0002$ or $g=2.0051\pm0.0002$[1]. The mixed complex showed the resonance at $g=2.0036\pm0.0003$, which was very near the mean of the 2.0051 and 2.0026 values. Again, a sufficiently large exchange interaction between paramagnetic species should be taken into account.

Although antimony pentachloride has been considered to take a diamagnetic form in the complexes[2-4], it is not clarified from this investigation whether the spin exchange between the radicals could occur only in the organic substances, or through the electron-accepting molecules also. It is expected, however, assuming the homogeneous distribution of the radicals in the complex, that the exchange interactions cover over several molecules, since the spin concentration in the complexes studied here was found to be less than 10% of the organic substances.

1) M. Kinoshita and H. Akamatu, This Bulletin, 35, 1040 (1962).

2) H. Kainer and K. H. Hausser, *Chem. Ber.*, 86, 1563 (1953).
3) M. Kinoshita, This Bulletin, 35, 1137 (1962).
4) G. E. Blomgren and J. Kommandeur, *J. Chem. Phys.*, 35, 1636 (1961).

It has been shown that the complex of *p*-phenylenediamine with *p*-chloranil gives two electron spin-resonance absorption lines; they have been assigned to the free radicals produced from the respective components[5]. However, a number of charge transfer complexes, such as aromatic compounds with tetracyanoethylene, haloanils, iodine, etc., have been shown to give only a single resonance line. It is not clear whether the radicals responsible for a single resonance line are formed from only one of the two components or from both components of the complex. If a single resonance line of a complex is due to the radicals generated from both donor and acceptor, it seems very likely that a single resonance line can be explained by the exchange interaction between the radicals.

However, there seems to be no regularity in *g*-values for the aromatics-iodine system. In general, the ESR absorption for the iodine cmplexes is composed of only a single line; in this case, it is supposed, as one of the possibilities, that the strong ESR absorption is due to the strong electron transfer from donor to acceptor molecules. If this is the case, the *g*-values of the iodine complexes are expected to lie at about the average of the *g*-values of an aromatic monopositive ion and of an iodine negative ion (I_2^-). The available data are given in Table I for the iodine complexes, together with the *g*-values of the monopositive ion of aromatic compounds. It seems for the iodine complexes that the observed *g*-values are rather close to, but somewhat higher than, the *g*-value of the monopositive ion of the corresponding aromatic compounds.

The violanthrene-iodine system forms the complex of a non-stoichiometric composition[6,7]; its iodine content can be varied over a very wide range. Uchida and Akamatu[7] have shown that the *g*-value of this system does not depend on the iodine content in the range from a 10^{-4} to a 3-mol. ratio to violanthrene; they have, therefore, concluded, considering the other electronic properties of the system, that the localized charge-transfer state is not the state of paramagnetism and that the free hole, which is produced by the thermal excitation with the activation energy which is correlated with the electrical conduction and that is delocalized over several violanthrene molecules, is responsible for the electrical conductivity and also for the paramagnetism. The coincidence of the activation energy for the

Table I. The *g*-values for the iodine complexes and for the monopositive ions of aromatic compounds

Aromatic compounds	*g*-Values		
	Iodine complex	Positive ion (in conc. H_2SO_4)	Positive ion ($SbCl_5$-complex)
Pyrene	2.0029[8]	2.0031[14]	2.003[4] 2.0022[14]
Perylene	2.0033[8,10] 2.0043[7]	2.00250[12] 2.0026[14] 2.0028[11]	2.003[4] 2.0024[14] 2.004[8]
Pyranthrene	2.0030[10]	2.0022[14]	2.0038[14] 2.004[8]
Violanthrene	2.0025[10] 2.0035[7]	2.0024[14]	2.0028[14]
Phenothiazine	2.0067[14]	2.0057[14]	{2.0064[14] {2.0039

generation of charge carriers with that of unpaired electron spins has been found in the complexes of pyrene-iodine and perylene-iodine by Singer and Kommandeur[8].

If we consider that the spin-orbit coupling constant ($-5060\ cm^{-1}$)[9] of iodine is very large, then the width of the electron spin-resonance of the iodine mononegative ion (I_2^-) might be broadened too much to observe its absorption. In consequence, it may be concluded that the *g*-values of the iodine complex can be expected to be near that of the monopositive ion of the corresponding aromatic compound, as there should be expected no strong interaction between the iodine negative ion and the free hole produced by the scheme which has been proposed by Uchida and Akamatu[7].

The author wishes to express his hearty thanks to Professor Hideo Akamatu for his valuable advice and discussion.

Department of Chemistry
Faculty of Science
The University of Tokyo
Hongo, Tokyo

5) Y. Matsunaga and C. A. McDowell, *Nature*, **185**, 916 (1960).
6) H. Akamatu, Y. Matsunaga and H. Kuroda, This Bulletin, **30**, 618 (1975).
7) T. Uchida and H. Akamatu, ibid., **35**, 981 (1962).
8) L. S. Singer and J. Kommandeur, *J. Chem. Phys.*, **34**, 133 (1961).
9) D. S. McClure, ibid., **17**, 905 (1949).
10) Y. Matsunaga, ibid., **30**, 855 (1959).
11) A. Carrington, F. Dravnieks and M. C. R. Symons, *J. Chem. Soc.*, **1959**, 947.
12) M. S. Blois et al., "Free Radicals in Biological Systems", Academic Press Inc., New York (1961), p. 121.
13) Y. Matsunaga, This Bulletin, **34**, 893 (1961).
14) M. Kinoshita, (unpublished works).

Vinyl Polymerization. LXVII. The Polymerization of Vinyl Acetate in the Presence of Zinc Chloride

By Minoru IMOTO, Takayuki OTSU and Toshio ITO

(Received October 31, 1962)

In the previous paper[1], we have found that photopolymerization of vinyl acetate initiated by azobisisobutyronitrile (AIBN) in the presence of zinc chloride proceeds in the heterogeneous system. The present paper deals with the effect of zinc chloride on the radical polymerization of vinyl acetate and on the properties of the resultant polymers.

Experimental

Materials.—Vinyl acetate was purified as follows: Commercial vinyl acetate was washed successively with 5% sodium thiosulfate solution and dilute sodium hydroxide solution and then dried over calcium chloride. Pure vinyl acetate was obtained by distillation in the presence of 2% azobisisobutyronitrile in a nitrogen atmosphere. Commercial grade zinc chloride was used without further purification and dehydrated according to the method described in a previous paper[1]. Azobisisobutyronitrile and other reagents were purified by the usual method.

Polymerization Procedure.—In a 100 ml. hard glass tube, a given amount of zinc chloride was placed and the tube was heated at about 300°C for 15 min. under vacuum. Pure vinyl acetate was then added and the tube was shaken to make a solution. The resulting solution was rapidly transfered by pipetting into the polymerization tubes. The tubes were then degassed and sealed under vacuum.

Polymerizations were allowed to take place on shaking in a thermostat. Photopolymerizations were carried out in a thermostat, irradiating by the Madzuda SHL type high pressure mercury lamp. After a given time, the tube was removed from the thermostat and the content of the tube was rapidly filtered to separate the monomer-insoluble polymer. Then the filtrate was poured into a large amount of petroleum ether to precipitate the polymer. Both polymers were washed with dilute hydrochloric acid and then purified by the reprecipitation method with petroleum ether from acetone solution. Conversion was calculated from the weight of the dry polymer obtained.

Treatment of the Polymer.—Intrinsic viscosity of polyvinyl acetate was determined by viscosity measurement of its dilute acetone solution at 30°C. Hydrolysis of polyvinyl acetate was performed as follows: 2 g. of polyvinyl acetate was dissolved in 100 ml. of methanol and 3 ml. of 5% aqueous sodium hydroxide solution was added. After standing overnight at room temperature and then refluxing for an hour, polyvinyl alcohol was isolated. Intrinsic viscosity of polyvinyl alcohol was determined from the viscosity measurement in water solution. Reacetylation was carried out by heating polyvinyl alcohol in pyridine-acetic anhydride at 95°C for 3 hr.

Experimental Results

Polymerization of Vinyl Acetate (VAC) with Zinc Chloride.—Results of the polymerization of VAC with zinc chloride are shown in Table I.

As can be seen from Table I, the polymerizations of VAC with zinc chloride proceeded with a slow rate to yield the colored polymer which was insoluble in the VAC monomer. Tho resulting dried polymer melted at 106~108°C and was a low molecular weight polymer. Carbon and hydrogen contents of this polymer were 61.39 and 7.40%, respectively and these values widely differ from those calculated for pure polyvinyl acetate (C, 54.54; H, 9.09%). This polymer was easily soluble in most organic solvents, such as methanol and acetone, to make a colored solution which was decolorized by the addition of bromine. Infrared spectra of this polymer showed the absorption bands of hydroxyl, carbonyl and carbon-carbon double bonds.

It was also found that the polymerization could not be retarded by the addition of hydroquinone. Accordingly, it might be considered that the polymerization of VAC with zinc chloride proceeded with the carbonium ion mechanism and the resulting polymer then reacted with zinc chloride to yield the colored polymer having a complexed structure.

Table II shows the results of the polymerization of VAC by the system AIBN and zinc chloride. Although AIBN is a typical radical initiator, the yields of polymer were approximately equal to those obtained by zinc chloride alone. It was assumed that the polymerization with both initiator and zinc chloride proceeded with carbonium-ion mechanism and the resulted colored polymer served as an inhibitor for the radical polymerization of VAC by AIBN.

1) Part LXVI of this series: M. Imoto, T. Otsu and S. Shimizu, *Makromol. Chem.*, in press.

TABLE I. BULK POLYMERIZATION OF VAC WITH ZINC CHLORIDE FOR 20 hr.

Exp. No.	[$ZnCl_2$] mol./l.	[VAC] ml.	Temp. °C	Conversion %	Color of polymerization mixture
1.1	0.081	10	50	2.19	Blackish-brown
1.2	0.161	10	50	2.28	Blackish-brown
1.3	0.242	10	50	2.92	Blackish-brown
1.4	0.081	10	40	1.20	Reddish-brown
1.5	0.081	10	30	0.33	Reddish-brown

TABLE II. POLYMERIZATION OF VAC INITIATED BY THE SYSTEM AIBN AND ZINC CHLORIDE AT 50°C

Exp. No.	[AIBN] $\times 10^3$ mol./l.	[$ZnCl_2$] mol./l.	[VAC] ml.	Time hr.	Conversion %	Color of polymerization mixture
2.1	0.244	0	10	3	35.60	Colorless
2.2	0.244	0.063	10	20	4.42	Pale-yellow
2.3	0.244	0.126	10	20	3.25	Yellowish-brown
2.4	0.244	0.189	10	20	2.71	Reddish-brown
2.5	0.244	0.252	10	20	2.26	Blackish-brown

TABLE III. PHOTOPOLYMERIZATION OF VAC WITH AIBN-ZINC CHLORIDE [AIBN] = 6.1×10^{-3} mol./l.

Exp. No.	[$ZnCl_2$] mol./l.	[VAC] ml.	Temp. °C	Time hr.	Conversion, %	
					Insolu. Pt.	Solu. Pt.
3.1*	0	10	50	3	0	35.6
3.2*	0.252	10	50	20	0	2.26
3.3	0	10	10	20	0	2.60
3.4	0.218	10	10	20	5.13	1.64
3.5	0	10	−10	20	0	0.59
3.6	0.218	10	−10	20	1.67	0.20
3.7	0	10	−30	20	0	Trace
3.8	0.218	10	−30	20	0.57	Trace
3.9	0	10	−50	20	0	Trace
3.10	0.218	10	−50	20	0.011	Trace

* In these cases, polymerizations were carried out by AIBN (2.44×10^{-3} mol./l.) in the absence of light.

TABLE IV. PHOTOPOLYMERIZATION OF VAC WITH AIBN-ZINC CHLORIDE [AIBN] = 6.1×10^{-3} mol./l.

Exp. No.	$ZnCl_2$	[VAC] ml.	Temp. °C	Time min.	Conversion, %		[η] in C_6H_6	
					Insolu. Pt.	Solu. Pt.	Insolu.	Solu.
4.1	None	10	30	5	0	1.70	—	1.68
4.2	Added*	10	30	5	0.49	1.02	0.88	1.33
4.3	None	10	−30	45	0	Trace	—	—
4.4	Added*	10	−30	45	3.31	Trace	0.98	—

* The concentrations of zinc chloride were about 0.2~0.5 mol./l.

Effect of Zinc Chloride on the Photopolymerization of VAC Sensitized by AIBN.— Results of the photopolymerization of VAC sensitized by AIBN are shown in Tables III and IV.

As can be seen from Tables III and IV, the rates of polymerization of VAC at rather high temperatures (> 30°C) decreased with the addition of zinc chloride. However, at lower temperatures below 10°C, the rates increased with the addition of zinc chloride and the resulting polymer contained the VAC-insoluble polymer which was dissolved in most organic solvents after purification. The amount of the VAC-insoluble polymer increased with decreasing the polymerization temperature. It is also

proved from these tables that at rather high temperatures, cationic and radical polymerizations occured simultaneously and the resulting colored polymer served as inhibitor for the radical polymerization.

Since the low-temperature photopolymerization of VAC sensitized by AIBN in the presence of zinc chloride proceeded in a heterogeneous system, it was difficult to study kinetically this polymerization. As can be seen from Fig. 1, however, the time-conversion curve of the polymerization showed a straight line at the initial stage of the polymerization. Accordingly, it may be possible to investigate kinetically this polymerization.

Figure 1 shows time-conversion curve for the photopolymerization of VAC sensitized by AIBN in the presence of zinc chloride at −30°C. Time-conversion curve shows a straight line up to 2% conversion, but in general the rate decreased with the proceeding of the polymerization. Figure 2 shows the relationship

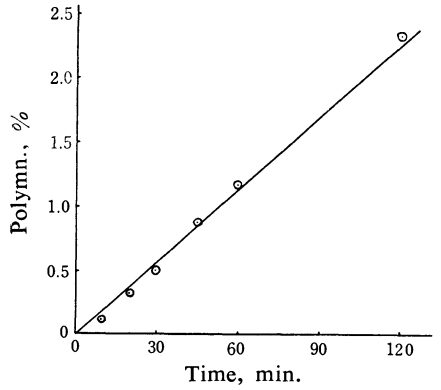

Fig. 1. Time-conversion curve for the photopolymerization of VAC with AIBN-$ZnCl_2$ at −30°C: [AIBN] = 6.1×10^{-3}, [$ZnCl_2$] = 0.215 mol./l.

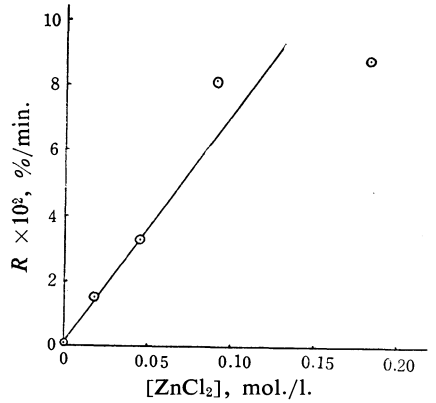

Fig. 2. Relationship between R_p and [$ZnCl_2$] for the photopolymerizations of VAC at −30°C: [AIBN] = 6.1×10^{-3} mol./l.

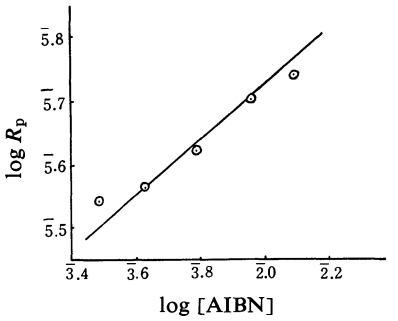

Fig. 3. Relationship between R_p and [AIBN] for the photopolymerizations of VAC at −30°C: [$ZnCl_2$] = 0.341 mol./l.

between the rate of polymerization (R_p) and the concentration of zinc chloride. At lower concentrations of zinc chloride, it was clear that R_p is proportional to the concentration of zinc chloride. Figure 3 shows the relationship between R_p and the concentration of AIBN at constant concentration of zinc chloride. From this figure, it was deduced that R_p was proportional to the square root concentration of AIBN.

Properties of the Resulting Polymer.—A large amount of zinc chloride was detected in the crude VAC-insoluble polymer obtained by the photopolymerization of VAC in the presence of zinc chloride at −30°C. For example, 0.245 mol./l. of zinc chloride was occluded in the polymer isolated at 3.32% conversion, using [$ZnCl_2$] = 0.413 mol./l. This crude polymer was very hygroscopic, but the polymer purified through the reprecipitation method to remove zinc chloride was soluble in VAC, methanol, acetone, ethyl acetate and benzene. Accordingly, it was clear that the formation of the VAC-insoluble polymer was due to a complex formation of PVAC with zinc chloride.

Elementary analysis and infrared spectra also showed that the pure polymer had the structure of ordinary polyvinyl acetate. Intrinsic viscosities of these polymers were lower than those of polymers obtained in the absence of zine chloride, as indicated in Table IV. The result suggested that zinc chloride served as a chain transfer agent for the polymerization.

Experiments of the hydrolysis of this polymer to yield polyvinyl alcohol and of further reacetylation were carried out. During these treatments, it was confirmed by infrared spectra that these reactions proceed completely. Viscosity changes of the polymers are shown in Fig. 4. As understood from this figure, intrinsic viscosities and k'-values of polyvinyl acetates did not change during the hydrolysis and then reacetylation. This fact indicated

that PVAC obtained by the polymerization in the presence of zinc chloride had no long chain branch of the ester type which is capable of scission by hydrolysis. Solubilities in hot water, phenol and dimethyl sulfoxide and the crystallinities by X-ray analysis of these polyvinyl alcohols coincided almost with the ordinary polyvinyl alcohol.

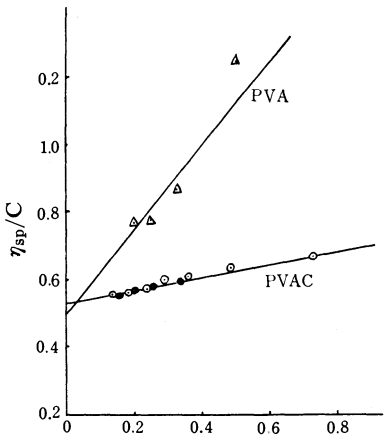

Fig. 4. Relationship between η_{sp}/C and C for polyvinyl acetate (PVAC) and polyvinyl alcohol (PVA) obtained from the photopolymerizations with AIBN-$ZnCl_2$: ⊙ before hydrolysis, ● after hydrolysis and then reacetylation for PVAC.

The Complex Formation of VAC with Zinc Chloride.—In order to isolate the complex of VAC with zinc chloride, a required amount of zinc chloride was dissolved by shaking in an excess of VAC and then the excess of VAC was rapidly removed by vacuum distillation. Pale yellow viscous liquid was obtained. From the weight and chlorine analyses it was proved that the complex was composed of 1 : 1 molar ratio of VAC to zinc chloride.

This complex was very hygroscopic and unstable. When the complex was allowed to stand in a sealed tube at room temperature, the cationic polymerization occured explosively after standing about 20 hr. to produce the colored polymer.

Discussion

It has been generally known that zinc chloride can initiate the cationic polymerization. In polymerization of vinyl acetate, it was observed in the present paper that zinc chloride could also initiate the cationic polymerization. In this case, however, the polymerization was accompanied by side reactions such as hydrolysis, deacetylation or dehydration and the resultant polymer was a yellow or reddish brown powder with a low molecular weight. These results agreed with those obtained by Higashimura and Okamura[2] that tin(II) chloride could initiate the cationic polymerization of vinyl acetate.

The rate of cationic polymerization of vinyl acetate was so slow that it hardly proceeded at rather low temperatures. Therefore, when AIBN as an initiator for radical polymerization was used together with zinc chloride, both radical and cationic polymerizations proceeded at the same time at higher temperatures ($>30°C$).

The polymer obtained in the latter reaction served as an inhibitor for the radical polymerization. At lower temperatures ($<10°C$), however, no inhibition of polymerization was observed, since the cationic polymerization might be retarded and only the polymerization proceeded through the radical mechanism.

The presence of zinc chloride may characterize the photopolymerization of vinyl acetate at lower temperatures using AIBN as photosensitizer, in two respects: acceleration of polymerization and progress of polymerization in a heterogeneous system. Although the rate of decomposition of AIBN could not be affected by the presence of zinc chloride[1], the effect of zinc chloride in the polymerization system might be considered as follows: (1) Complex formation with the monomer (VAC), (2) interaction with the growing radical and the monomer at the transition state of the propagation step, and (3) influences on the transfer and termination reactions. If the interaction of (2) was the most important among them, a stereoregular polymer should be obtained as Kargin et al.[3] pointed out. In fact, this effect of zine chloride could be neglected, since no stereoregular polymers were obtained through radical polymerizations as shown in a previous[1] and in the present paper. As for influences of (3), Table IV showed that smaller values of intrinsic viscosity were obtained in the presence of zinc chloride, indicating that zinc chloride served as a chain transfer agent.

The present authors[4] observed that zinc chloride could readily form a complex with methyl methacrylate or acrylonitrile. It was

2) T. Higashimura and S. Okamura, *Chem. High Polymer, Japan*, **17**, 635 (1960).
3) V. A. Kargin, V. A. Kabanov and V. P. Zubov, *Vysokomol. Soed.*, **2**, 765 (1960).
4) M. Imoto, T. Otsu, Y. Harada and M. Nakabayashi, Presented at the 15th Annual Meeting of the Chemical Society of Japan, Kyoto, April, 1962; *Makromol. Chem.*, in press.

reported by Matsumoto[5] that vinyl acetate made a complex in a molar ratio of 1 : 1 with $Cd(C_2H_5)_2$. A complex of zinc chloride with vinyl acetate in a molar ratio of 1 : 1 could also be isolated in the present work. However, since the complex was so unstable that the cationic polymerization proceeded explosively on standing. Since it was hygroscopic, the present authors could not determined infrared absorption spectra. Nevertheless, both the results of Matsumoto[5] and of the present authors[4] have almost made it clear that the carbonyl group of vinyl acetate might contribute to the complex formation with zinc chloride.

The probable formation of such a complex might cause polarization of double bands. As the *e* value for vinyl acetate was −0.3, the reactivity of uncomplexed vinyl acetate radicals with complexed vinyl acetate was considered to be increased. Therefore, as Bamford et al.[6] pointed out, the acceleration by zinc chloride might be explained in terms of copolymerization of complexed and uncomplexed vinyl acetate. It was confirmed by the fact that a large amount of zinc chloride was detected in the resultant polymer which was insoluble in the monomer, or that polymerization begins in a heterogeneous system.

5) S. Matsumoto, *Chem. High Polymer, Japan*, **16**, 467 (1959).
6) C. H. Bamford, A. D. Jenkins and R. Johnston, *Proc. Royal Soc.*, **A241**, 364 (1957).

Summary

A study of the effect of zinc chloride on the polymerization of vinyl acetate has been made. Zinc chloride can initiate the cationic polymerization of vinyl acetate at above room temperatures to yield the colored low-molecular weight polymer. However, in the low-temperature photopolymerization of vinyl acetate initiated by azobisisobutyronitrile, zinc chloride accelerates the radical polymerization and the colorless polymer which is insoluble in the monomer is obtained. Elementary analysis, infrared spectra and X-ray analyses show that the structure of this polymer after purification does not differ with that of ordinary polyvinyl acetate and polyvinyl alcohol obtained through the hydrolysis of this polymer has no crystallinity superior to that of the ordinary sample.

Faculty of Engineering
Osaka City University
Kita-ku, Osaka

Vinyl Polymerization. LXX. Preparation of 3-(4'-Pentenyl)cyclopentene-1 and its Alternative Copolymerization with Maleic Anhydride*

By Minoru IMOTO, Kazuichi TSUDA and Takayuki OTSU

(Received November 5, 1962)

3-(4'-Pentenyl)cyclopentene-1 (PCP) was prepared from tetrahydrofurfuryl alcohol and cyclopentadiene, by the scheme as shown in Fig. 1.

Tetrahydrofurfuryl alcohol was chlorinated by thionyl chloride into tetrahydrofurfuryl chloride, and the ring cleavage of the chloride formed by metallic sodium led to the formation of 4-penten-1-ol. By the bromination of 4-penten-1-ol with phosphorous tribromide, the unsaturated alcohol was transformed into 5-bromo-1-pentene, which was then converted into its Grignard compound.

3-Chlorocyclopentene-1 was prepared by

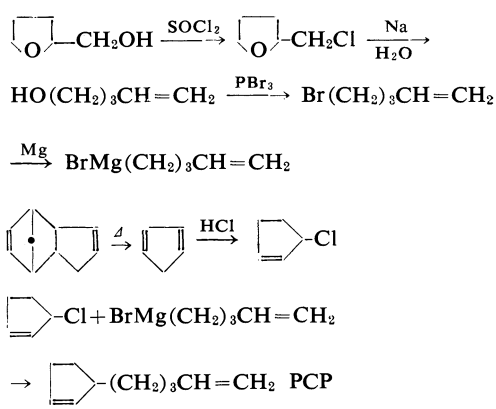

Fig. 1. The process of PCP synthesis.

* Part LXIX of this series: M. Imoto, T. Otsu and M. Nakabayashi, *Makromol. Chem.*, in press.

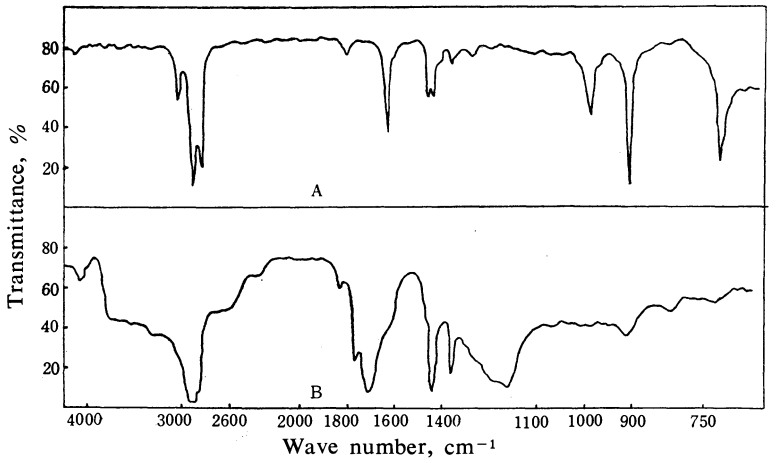

Fig. 2. Infrared absorption spectra.
A PCP (liquid)
B Copolymer (in Nujol)

TABLE I. COPOLYMERIZATION OF PCP WITH MALEIC ANHYDRIDE AT 60°C FOR 3 hr.

Exp. No.	Monomer composition			Copolymer composition*		
	[PCP]	[MA]	[PCP]/[MA]	[PCP]	[MAd]**	[PCP]/[MAd]
	mol. %		mol. ratio	mol. %		mol. ratio
1	50.78	49.22	1.032	35.03	64.97	1/2.004
2	69.07	30.93	2.234	—	—	—
3	33.09	66.91	0.4948	36.07	63.93	1/2.024
4	74.26	25.74	2.7911	34.21	65.79	1/2.011
5	63.91	36.09	1.2912	35.06	64.95	1/2.016

* After hydrolyzed ** [MAd] : Maleic acid

hydrochlorination of cyclopentadiene, which was the pyrolysis product of dicyclopentadiene. A coupling reaction was carried out between the 1-pentenylmagnesium bromide and the 3-chlorocyclopentene-1 at −30∼−35°C. By this reaction, PCP was yielded. The infrared spectrum of PCP is shown in Fig. 2A.

In order to synthesize polyperhydroazulene or poly(methyleneperhydroindene) by intra- and inter-molecular polymerization, radical polymerization was attempted by azobisisobutyronitrile (AIBN) at 60°C for 30 hr. Polymerization by Ziegler catalyst was also tried at 30, 5 and −70°C for 72 and 120 hr., respectively. In the case of using Ziegler catalyst, the Al/Ti molar ratio was changed from 0.93 to 3.39. A little brown methanol-soluble oil was obtained and most of the monomer PCP was recovered in both cases. Cationic polymerization was performed by titanium tetrachloride or boron trifluoride etherate at 30, 5 and −70°C for 72 and 120 hr., respectively, under nitrogen atomosphere. When titanium tetrachloride was employed, the results were the same as in radical and Ziegler polymerization, but by boron trifluoride etherate initiator, a trace of reddish brown gel polymer was obtained. This polymer did not dissolve in common organic solvents, and most of the monomer PCP was recovered. From the above results, it may safely be said that PCP does not homopolymerize under these conditions.

PCP was copolymerized with maleic anhydride (MA) by the use of a radical initiator at 60°C for 3 hr. Under these conditions, neither maleic anhydride nor PCP homopolymerized and the copolymers of PCP with MA were obtained in a good yield.

When the molar ratio in the monomer mixture of PCP to maleic anhydride was varied from 1 : 1 to 1 : 2, 2 : 1 and 2.8 : 1, no change was observed in the copolymer composition (the proportion of PCP to maleic anhydride being 1 to 2), as shown in Table I. The infrared absorptions of vinyl type double bond and unsaturated cyclopentene ring of PCP in copolymer disappeared in the infrared absorption spectrum as shown in Fig. 2B, so it is assumed that both the double bonds participated in the copolymerization and formed glassy gelled pale-yellow copolymer. These

results indicated an alternative copolymerization.

Experimental

Preparation of 4-Penten-1-ol.—Tetrahydrofurfuryl chloride was obtained by Brooks and Snyder's method[1]. Tetrahydrofurfuryl alcohol was chlorinated by thionyl chloride; yield 68~72% (lit. 73~75%); b. p. 40~42°C/11mmHg (lit. 41~42°C/11mmHg).

4-Penten-1-ol was prepared with ring cleavage of tetrahydrofurfuryl chloride by metallic sodium. The yield of b. p. 136~137°C was 71~74% (lit. 76~83%); n_D^{20} 1.4300 (lit. 1.4299). (Found: C, 69.75; H, 12.31. Calcd. for $C_5H_{10}O$: C, 69.77; H, 11.63%.)

Preparation of 5-Bromo-1-pentene.—5-Bromo-1-pentene was prepared by a modification of La Forge's method[2]. 1.6 mol. of 4-penten-1-ol and 0.5 mol. of pyridine were placed in a four-necked flask. The contents of the flask was held, being stirred, at about −30 to −35°C and 0.6 mol. of phosphorus tribromide was added into the flask over a period of about 5 hr. dropwise to prevent vigorous exothermic reaction; stirring was continued one hour more. The reflux condenser was then replaced by a Vigreux column and the product of the reaction was distilled on an oil bath until the temperature in the flask rose to 160~170°C. The distillate was washed with water, dilute sodium hydroxide, and lastly with water. After being dried on calcium chloride, the product was distilled several times. The yield of pure 5-bromo-1-pentene, boiling between 125.5 and 126.0°C at atmospheric pressure, was 55~57%: d_{25}^{25} 1.2595; n_D^{25} 1.4645.

Found: C, 40.55; H, 6.30; Br, 53.60*. Calcd. for C_5H_9Br: C, 40.31; H, 6.08; Br, 53.65%.

3-Chlorocyclopentene-1. — The chlorohydrogenation of cyclopentadiene, which was obtained by the pyrolysis of dicyclopentadiene, yielded 3-chlorocyclopentadiene[3].

Synthesis of PCP.—3.3 g. of magnesium was placed in a four-necked flask, and the mixture of 5-bromo-l-pentene and ether contained in a funnel was added dropwise into the flask which was cooled in a water bath. Stirring was continued two more hours even after the addition was made to complete the reaction. To this 1-pentenylmagnesium bromide, a mixture of 3-chlorocyclopentene-1 (15 g.) and ether (25 g.) was added dropwise, during which time the flask was cooled between −30 to −35°C under nitrogen atmosphere. A vigorous reaction followed immediately and white magnesium halide was precipitated. The addition was made for about 1 hr. and stirring was continued for an additional 2 hr., and then the temperature of the reaction mixture was risen gradually to 25°C. Stirring was carried on for another 2 hr. The reaction product was then poured into a large amount of water and the unreacted compound was decomposed. The ether layer was separated and dried over magnesium sulfate. After the removal of the ether by distillation, the residue was distilled through a Vigreux column. The yield of PCP was 88~91%; b. p. 46.0~47.0°C/7 mmHg. n_D^{25} 1.4582: d_{25}^{25} 0.8267.

Found: C, 88.05; H, 11.91. Calcd. for $C_{10}H_{16}$: C, 88.16; H, 11.84%.

Polymerization of PCP.—*Radical Polymerization.*—AIBN, m. p. 102.0~102.5°C, recrystallized twice from methanol, was used for radical polymerization. The polymerization was carried out in benzene. The benzene solution of PCP (3 ml. of PCP mixed with 7 ml. of benzene or 3 ml. with 3 ml.) and AIBN ($2.303\sim6.911\times10^{-2}$ mol./l. and $1.352\sim3.577\times10^{-1}$ mol./l.) as initiator, were charged into a tube, and sealed in vacuo under cooling in a dry ice-methanol bath. The polymerization was carried out in a thermostat at 60°C under shaking for 30 hr. After polymerization, the content of the tube was poured into methanol.

Anionic Polymerization.—Anionic Polymerization was carried out in *n*-hexane, which was distilled twice over sodium wire. Commercial *n*-butyl lithium was used as initiator which was diluted with *n*-hexane to 0.193~0.385 mol./l. The hexane solution of PCP (2 ml. of PCP in 1 ml. of *n*-hexane) and of *n*-butyl lithium were fed into a tube, and sealed under nitrogen atmosphere. The polymerization was carried out at 30, 5 and −70°C from 72 to 120 hr.

Polymerization by Ziegler Catalyst.—The triisobutylaluminum ($Al(i\text{-}Bu)_3$), supplied by Ethyl Corporation, was diluted with *n*-hexane and titanium tetrachloride was distilled three times and used as *n*-hexane solution. The hexane solution of triisobutylaluminum was charged into a tube and then titanium tetrachloride solution was added under nitrogen atomosphere, and a reddish brown precipitate appeared immediately. An addition of titanium tetrachloride was made and then the tube was stood for 15 min., the monomer, PCP, was added and the tube was sealed under nitrogen atomosphere. The polymerization was carried out at 25, 5 and −70°C for 120 hr. and the tube was shaken at times during the process. In these polymerizations, Al/Ti molar ratio was changed from 0.93 to 1.23, 2.16, 2.47 and 3.39, and the total catalyst concentration to the monomer was varied between 2.04~4.18 wt.%.

After polymerization, the content of the tube was poured into a large amount of methanol, but no polymer was precipitated. In the polymerizations by radical and Ziegler type initiators, a small quantity of brown methanol-soluble oil was obtained, when monomer PCP was recovering.

Cationic Polymerization.—Cationic polymerization was carried out by titanium tetrachloride or boron trifluoride etherate catalysts.

A mixture of 2 ml. of PCP, 2 ml. of *n*-hexane and $6.593\sim13.19\times10^{-2}$ mol./l. of titanium tetrachloride were fed into a tube and sealed under nitrogen atomosphere. The polymerization was carried out at 30 and 50°C for 120 hr. Then the content of the tube was poured into excess methanol. The same results were obtained as both in radical and

1) L. A. Brooks and H. R. Snyder, "Organic Syntheses", Coll. Vol. 3 (1955) p. 698.
2) F. B. La Forge and N. Green et al., *J. Am. Chem. Soc.*, **70**, 3703 (1948).
* By micro Carius method.
3) R. B. Moffett, "Organic Syntheses", Vol. 32 (1952), p. 41.

TABLE II. COPOLYMERIZATION OF PCP WITH MALEIC ANHYDRIDE AT 60°C FOR 3 hr.

Exp. No.	[PCP]	[MA]	Total monomer	AIBN	Polymer Yield	Elementary* analysis		
	g.	g.	g.	g.	g.	C, %	H, %	O, %
1	1.6534	1.1535	2.8069	0.0065	0.6340	58.80	7.43	33.77
2	4.9602	1.5986	6.5588	0.0085	0.6774	—	—	—
3	1.6534	2.4059	4.0593	0.0069	0.6099	59.38	7.44	33.17
4	5.7042	1.4233	7.1275	0.0077	1.2291	59.01	6.76	34.24
5	3.3068	1.3438	4.6506	0.0076	0.8055	59.15	7.10	33.75

* After hydrolyzed by 10% KOH for 50 hr. Theoretical value for 1 : 2 copolymer: C, 58.69%; H, 6.57%; O, 34.75%.

Ziegler catalyst polymerizations and no polymer was formed.

Freshly distilled boron trifluoride etherate was added to a tube containing 2 ml. of PCP and 2 ml. of benzene. The concentration of boron trifluoride etherate was changed between $3.910\sim7.820\times10^{-2}$ mol./l. When the initiator was added to the benzene solution of PCP, the solution immediately turned pale brown. Polymerization was performed at 30, 5°C and room temperature for 72 hr.

After polymerization, when the mixture in the tube was poured into a large excess of methanol, a trace of brown polymer precipitated.

In view of the above results, another polymerization, in which the concentration of boron trifluoride etherate was increased to 1.56×10^{-1} and 7.95×10^{-2} mol./l. was performed at 50°C and room temperature. The results obtained in the secnd series of these polymerizations were the same as those in the first series of the same polymerization of boron trifluoride etherate initiated polymerization. This polymer was swelled a little in tetrahydrofuran only. No double bond being found in infrared absorption spectrum, we assume that PCP is polymerized by boron trifluoride etherate to form a cross-linked polymer. The polymer obtained was a very small quantity.

Copolymerization of PCP with MA.—MA, m. p. 53~54°C, was recrystallized three times from chloroform. AIBN was used as polymerization initiator. Polymerization was carried out as usual, monomers and initiator being charged into a tube and sealed in vacuo, in a thermostat at 60°C under shaking. During the polymerization, a pale yellow waxy polymer precipitated from polymerization system. After 3 hr., the content of the tube was poured into a large amount of methanol. The precipitated polymers were filtered and dried under 40°C in a desiccator. The polymers appeared like a pale yellow glassy substance and swelled a little in tetrahydrofuran, dioxane and dimethylformamide.

The polymers were refluxed in tetrahydrofuran and methanol for 3 hr. to remove as much initiator as possible. Then the polymers were hydrolyzed by 10% potassium hydroxide or hydrochloric acid as catalyst in water for 50 hr. Hydrolyzed polymers by potassium hydroxide catalyst is shown in Table II. The values of carbon % in Table II are somewhat larger than the theoretical value and the values of oxygen % are rather small due to the difficulty in complete hydrolysis: these polymers were gelled and did not dissolve in the solvent.

As Table II shows, PCP and maleic anhydride were copolymerized and when the monomer mixture ratio was changed, the polymer composition was not changed but always kept the constant ratio of 1 to 2. After hydrolysis, the absorption band of carboxyl group appeared in the infrared absorption spectrum.

These results indicate that two unsaturated double bonds of PCP participate in the copolymerization with maleic anhydride to form a glassy gelled alternative copolymer, the ratio of PCP to maleic anhydride being 1 to 2.

Summary

3-(4'-Pentenyl)cyclopentene-1 (PCP) was prepared through the reaction of 1-pentenyl magnesium bromide and 3-chlorocyclopentene-1. An attempt was made for the polymerization and copolymerization of PCP. In the polymerizations by radical (azobisisobutyronitrile) and Ziegler [Al(*i*-Bu)$_3$-TiCl$_4$] initiators, a little brown methanol-soluble oil was obtained. By cationic initiator ($BF_3\cdot OEt_2$), however, a trace of reddish brown polymer which did not dissolve in common organic solvents was formed.

PCP was copolymerized with maleic anhydride by the use of a radical initiator. When the monomer mixture ratio of PCP to maleic anhydride was varied, no change was observed in the copolymer composition (the proportion of PCP to maleic anhydride being 1 to 2). In the infrared spectrum of the copolymer, the absorption bands of the vinyl type double bond and the unsaturated cyclopentene ring of PCP disappeared in the copolymer, so it was to be assumed that both double bonds participated in the copolymerization to form glassy gelled pale-yellow copolymer. These results indicate that an alternative copolymerization took place.

Department of Applied Chemistry
Faculty of Engineering
Osaka City University
Kita-ku, Osaka

Hydrogenation and Hydrogenolysis. VI.[1] *The Stereochemisty of the Catalytic Hydrogenation of Some Allylic Alcohols Related to Cholest-4-ene**

By Shigeo NISHIMURA** and Kazuko MORI

(Received November 5, 1962)

Catalytic hydrogenation of cholest-4-ene-3β,6β-diol with platinum oxide in ethanol gives 5β-cholestane-3β,6β-diol exclusively[2], while in the presence of a trace of hydrochloric acid a much more rapid reduction occurs and 5α-cholestane is obtained as the main product[3] along with 5α-cholestan-3β-ol. The exclusive formation of the 5β-cholestanediol in ethanol seems rather unusual, because it indicates that hydrogen was added preferentially from the β-side which appears to be more hindered than the α-side. A similar phenomenon was observed by Dart and Henbest[4] in hydrogenation of cholest-4-en-3β-ol and other cyclic allylic alcohols, a more β-addition of hydrogen being observed in cholest-4-en-3β-ol than in cholest-4-ene in hydrogenation with platinum oxide in ethanol in the presence of a small amount of sodium nitrite, which depressed hydrogenolysis causing the yield of 5β-cholestanol to increase.

In order to clarify the effects of the accumulative β-hydroxyl groups at C_3 and C_6 carbon atoms and also of solvents on the stereochemistry of the hydrogenation of the 4, 5-double bond, the catalytic hydrogenation of cholest-4-ene, cholest-4-en-3β-ol and cholest-4-ene-3β,6β-diol has been carried out in ethanol and also in acetic acid with (7 : 3)rhodium-platinum oxide[5] as catalyst. This catalyst was used because it can hydrogenate these allylic alcohols with only slight hydrogenolysis in acetic acid[6].

Experimental

Catalysts.—Platinum oxide was prepared by fusion of chloroplatinic acid with sodium nitrate according to the method of Adams et al.[7]

(7 : 3)Rhodium-platinum oxide was prepared by fusion of the mixture of rhodium chloride and chloroplatinic acid in ratio of 7 : 3 by the weights of the metals as described previously[5].

Hydrogenation.—Hydrogenation was carried out at ordinary temperature and pressure. The substrate (0.2~0.5 mmol.) was added after the oxide (20~50 mg.) was reduced to black with hydrogen in the solvent.

Cholest-4-ene.—The hydrogenation of this compound in ethanol proceeded with difficulty and was completed by addition of a new portion of catalyst. The last trace of the starting material remaining in the products was further hydrogenated with addition of a small amount of acetic acid. The hydrogenation in acetic acid proceeded rapidly to completion. The products (5α-cholestane and 5β-cholestane) were analyzed by the method of infrared absorption in carbon disulfide solution. Characteristic bands at 957 and 985 cm^{-1}, respectively, were used for this analysis.

Cholest-4-en-3β-ol.—The hydrogenation products were analyzed by gas-liquid partition chromatography with GC-1B (hydrogen flame detector type) of Shimadzu Seisakusho, Ltd. and a column of 0.1% SE-30 silicone on Chromosorb W (60~80 mesh)*.

The product from ethanol solution consisted of about 36% hydrocarbons (mainly 5α-cholestane) and 64% saturated alcohols (52% 5β-cholestan-3β-ol and 48% 5α-cholestan-3β-ol). The product from acetic acid solution consisted of 13% hydrocarbons (mainly 5α-cholestane) and 87% saturated alcohols (16% 5β-cholestan-3β-ol and 84% 5α-cholestan-3β-ol).

Cholest-4-ene-3β,6β-diol.—The product from hydrogenation in acetic acid was analyzed by gas-liquid partition chromatography as described above and also by elution chromatography. The gas chromatogram indicated that the product consisted of about 2% hydrocarbons (mainly 5α-cholestane), 13% mono-ols (mainly 5α-cholestan-3β-ol) including a very small amount of an unidentified product,

* The authors wish to thank Dr. N. Ikekawa of the Institute of Physical and Chemical Research for gas chromatographic analyses and the discussion of the results.

* Presented at the 15th Annual Meeting of the Chemical Society of Japan, Kyoto, April, 1962.

** Present address: The Institute of physical and Chemical Research, Bunkyo-ku, Tokyo.

1) Part V: S. Nishimura, This Bulletin, 34, 32 (1961).

2) V. Prelog and E. Tagmann, *Helv. Chim. Acta*, 27, 1880 (1944).

3) S. Nishimura and K. Mori, This Bulletin, 32, 103 (1959).

4) M. C. Dart and H. B. Henbest, *J. Chem. Soc.*, 1960, 3563.

5) S. Nishimura, This Bulletin, 34, 1544 (1961).

6) For the behavior of the rhodium-platinum oxide towards hydrogenation and hydrogenolysis, see Refs. 1, 5, and also: S. Nishimura et al., ibid., 33, 566, 1356 (1960).

7) R. Adams, V. Voorhees and R. L. Shriner, "Organic Syntheses", Coll. Vol. I, 2nd Ed. 463, (1941).

and 85% diols (54% 5β-cholestane-3β, 6β-diol and 46% 5α-cholestane-3β, 6β-diol). By elution chromatography 2% hydrocarbons, 10% mono-ols[8] and 85 to 90% diols were obtained. The product from ethanol solution was almost pure 5β-cholestane-3β, 6β-diol. Its infrared spectra showed no absorption due to 5α-cholestane-3β, 6β-diol. The product obtained by hydrogenation with platinum oxide in ethanol in the presence of a trace of hydrochloric acid was chromatographed on silica gel. The product (197 mg.) gave 122 mg. of 5α-cholestane (60%), m. p. and mixed m. p. 80~81°C, by elution with petroleum ether. Further elution with benzene gave 41 mg. of 5α-cholestan-3β-ol (20%), m. p. and mixed m. p. of it sacetate after recrystallization being 108~109°C.

Results and Discussion

Table I summarizes the compositions of products (hydrogenolysis products are excluded) obtained in hydrogenation with (7 : 3)rhodium-platinum oxide along with those obtained with platinum oxide. It shows that in ethanol more 5β-compounds are formed than 5α-compounds and 5β-cholestane-3β, 6β-diol is formed quantitatively in case of cholest-4-ene-3β, 6β-diol. The other two compounds give smaller yields of 5β-compounds not much different from each other. In the presence of sodium nitrite the β-addition of hydrogen is slightly greater in cholest-4-en-3β-ol than in cholest-4-ene[4]. It may be concluded from these results that the 6β-hydroxyl group exerts a definite directing effect to increase the β-addition of hydrogen, but the 3β-hydroxyl group has little effect, if any. Dart and Henbest[4] suggested that the 3β-hydroxyl group of cholest-4-en-3β-ol is likely to be in a quasi-equatorial conformation, from its relatively slight directing effect. In accord with their suggestion, the present results, which show a great difference of the directing effect between the 3β- and 6β-hydroxyl groups, strongly support that cholest-4-ene-3β, 6β-diol is in the conformation shown in Fig. 1a where the 3β-hydroxyl is

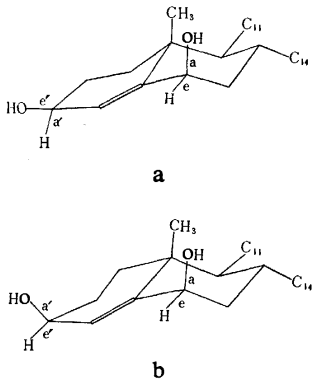

Fig. 1. Conformations of cholest-4-ene-3β, 6β-diol.

quasi-equatorial and the 6β-hydroxyl axial, rather than in the conformation shown in Fig. 1b where the 3β-hydroxyl is quasi-axial. The conformation in Fig. 1a is also consistent with the fact that the 6β-hydroxyl group is more easily hydrogenolyzed than the 3β-hydroxyl group in acidic medium since about 20% of 5α-cholestan-3β-ol was obtained along with 60% of 5α-cholestane, but no 5α-cholestan-6β-ol in hydrogenation of the cholestene-diol with platinum oxide in the presence of hydrochloric acid. The hydrogenolysis of a β-hydroxyl group caused by the α-attack of hydrogen[9] seems to be hindered more at C_3 by the quasi-axial 3α-hydrogen than at C_6 by the equatorial 6α-hydrogen.

In acetic acid the yields of 5α-compounds generally increase. The increase is more pronounced in cholest-4-en-3β-ol (48→84%) and in cholest-4-ene-3β, 6β-diol (0→46%) than in

TABLE I. PROPORTIONS OF 5β- AND 5α-CHOLESTANE DERIVATIVES IN THE PRODUCTS OF HYDROGENATION OF CHOLEST-4-ENE, CHOLEST-4-EN-3β-OL AND CHOLEST-4-ENE-3β, 6β-DIOL[a]

Compound	With (7 : 3)Rh-Pt oxide in EtOH		With (7 : 3)Rh-Pt oxide in AcOH		With Pt oxide in EtOH	
	5β	5α	5β	5α	5β	5α
Cholest-4-ene	73	27	54	46	55[b]	45[b]
Cholest-4-en-3β-ol	52	48	16	84	67[b]	33[b]
Cholest-4-ene-3β, 6β-diol	~100	~0[c]	54	46	~100	~0[c]

a) Hydrogenolysis products are excluded.
b) Dart and Henbest, Ref. 4 (a small amount of sodium nitrite was added).
c) No infrared absorption due to 5α-cholestane-3β, 6β-diol was detected.

8) The infrared absorption spectra showed that this fraction contained a small amount of a carbonyl compound probably resulting from the migration of the 4, 5-double bond during hydrogenation.

9) That the hydrocarbon obtained by hydrogenolysis is always nearly pure 5α-cholestane shows that the hydrogenolysis of a β-hydroxyl group is caused more easily by the α-attack of hydrogen than the β-attack probably by S_{N2} mechanism (cf. Ref. 4).

cholest-4-ene (27→46%). Acetic acid probably weakens the directing effect of the hydroxyl group and increases the steric hindrance to the β-addition of hydrogen. This kind of directing effect of the hydroxyl group probably results from its affinity for the catalyst metals, which may be expected from the theory of catalyst poisons largely developed by Maxted[10].

With platinum oxide in acetic acid as solvent cholest-4-ene-3β, 6β-diol is hydrogenolyzed to an extent of 65% as indicated by hydrogen uptake (Table II). The proportion of hydrogenolysis is further increased in the presence of hydrochloric acid. But, with (7 : 3) rhodium-platinum oxide the cholestenediol and cholest-4-en-3β-ol give good yields of the corresponding saturated alcohols in acetic acid (see Table II and also the experimental part).

TABLE II. MOLES OF HYDROGEN ABSORBED PER MOLE OF CHOLEST-4-ENE-3β, 6β-DIOL IN VARIOUS SOLVENTS

Solvent	Catalyst	
	Pt oxide	(7 : 3) Rh-Pt oxide
Ethanol	1.1	1.1
Acetic acid	2.3	1.2
Ethanol and hydrochloric acid	2.7	—
Acetic acid and hydrochloric acid	2.85	—

10) E. B. Maxted, *J. Chem. Soc.*, **1949**, 1987; "Advances in Catalysis", Vol. III, Academic Press Inc. Publishers, New York (1951), p. 129.

The authors wish to express their hearty thanks to Professor Yoshiyuki Urushibara for his valuable suggestions and encouragement. The authors are also indebted to the Ministry of Education and to Mitsubishi Chemical Industries Co. for financial support. Cholesterol was kindly supplied by Tsurumi Chemical Research Laboratory.

Department of Chemistry
Faculty of Science
The University of Tokyo
Hongo, Tokyo (S. N.)

National Institute of Industrial Health
Kawasaki (K. M.)

The Selective Chelatometry of Calcium in the Presence of Magnesium with Ethylene Glycol-bis(β-aminoethyl ether)-N, N, N′, N′-tetraacetic Acid

By Genkichi NAKAGAWA, Motoharu TANAKA and Hiroko WADA

(Received November 12, 1962)

A difference in the stability constants of ethylene glycol-bis(β-aminoethyl ether)-*N*, *N*,-*N*′, *N*′-tetraacetic acid (EGTA) chelates of calcium and magnesium ($K_{Ca\text{-}EGTA}/K_{Mg\text{-}EGTA} = 10^{5.8}$)[1-3] allows the selective chelatometry of calcium in the presence of magnesium if an appropriate method is available to indicate the equivalence point. Several methods have been reported for this purpose: potentiometric titration using a mercury electrode[2], photometric titration using murexide as an indicator[4], visual titration using Zn-EGTA-zincon system as an indicator[3,5], and visual titration using calcon as an indicator and tartrate to prevent the precipitation of magnesium[6].

In our own previous investigation[7], some theoretical considerations were made of the color change in the vicinity of the equivalence point of chelatometry, using the NY-HA system as an indicator, and more recently a method for the selective chelatometry of calcium has been worked out using the Zn-EGTA-PAN system as an indicator[8]. The choice of an indicator system, the conditions for the titration of calcium with EGTA, and the experimental results from the titration of calcium using the Zn-EGTA-PAN system as an indicator constitute the present paper.

The desirable properties of the metal indicator for the chelatometry of calcium in the

1) G. Schwarzenbach, "Die Komplexometrische Titration", Dritte Auflage, Ferdinand Enke Verlag, Stuttgart (1957), p. 97.
2) R. W. Schmid and C. N. Reilley, *Anal. Chem.*, **29**, 264 (1957).
3) A. Ringbom, G. Pensar and E. Wänninen, *Anal. Chim. Acta*, **19**, 525 (1958).
4) H. Flaschka and J. Ganchoff, *Talanta*, **8**, 720 (1961).
5) F. S. Sadek, R. W. Schmid and C. N. Reilley, ibid., **2**, 38 (1959).
6) R. A. Burg and H. F. Conaghan, *Chemist-Analyst*, **49**, 100 (1960).
7) G. Nakagawa and M. Tanaka, *Talanta*, **9**, 917 (1962).
8) G. Nakagawa, H. Wada and M. Tanaka, ibid., in press.

presence of magnesium may be summarized as follows: the indicator should react with calcium to give a sensitive coloration but should not react with magnesium under the condition where the precipitation of magnesium does not occur, e.g., at pH<10 unless a masking agent such as tartrate is used. No metal indicator having such properties has been reported. Thus an indicator system such as the NY-HA system ought to be used for a successful visual titration of calcium in the presence of magnesium. Even in this case, HA must not react with magnesium; hence, the use of the *o*, *o'*-dihydroxyazo compounds often utilized in chelatometry has to be given up for the present purpose. On the other hand, *o*-hydroxyazo compounds having a pyridine ring[9,10], such as 1-(2-pyridylazo)-2-naphthol (PAN) and 4-(2-pyridylazo)-resorcinol (PAR), or a thiazol ring[11,12], such as 1-(2-thiazolylazo)-2-naphthol, react with neither calcium nor magnesium, but they are known to exhibit a sensitive coloration with copper, zinc, cadmium, nickel, etc. and they are of current use in the chelatometry of these metals[9,10]. Therefore, an appropriate combination of such dyes and these metals would serve as a useful indicator in the chelatometry of calcium in the presence of magnesium. Some theoretical consideration will be given below to the use of the Zn-EGTA-PAN system as an indicator.

The indicator transition in the vicinity of the equivalence point in the chelatometry of M using the NY-HA system as an indicator can be expressed by Eq. 1 according to our previous paper[8]:

$$[Y]_t''/[M]_t = 1 - \frac{[NA_n]}{[A]^n}\cdot\frac{1}{K_1[NY]} + \frac{[A]^n}{[NA_n]}\cdot\frac{K_2[NY]}{[M]_t} \qquad (1)$$

where $K_1 = K_{MY}K_{NA_n}/K_{NY}\beta_{(M)}$, where $K_2 = K_{NA_n}\alpha_{H(Y)}/K_{NY}$[13], and where $[M]_t$ and $[Y]_t''$ denote the total concentrations of M and of the complexan used as a titrant respectively.

The acid-base properties of PAN may be described as follows[14,15];

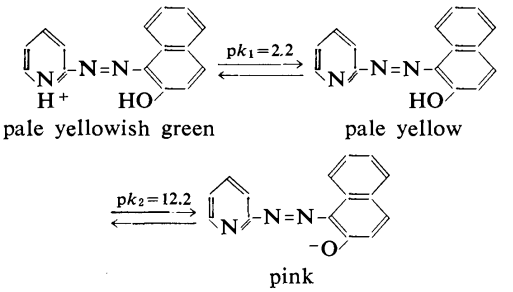

Thus, an aqueous solution of PAN is pale yellow in the pH value range of 3~10.

Since PAN forms a 1:2 chelate with zinc at pH values higher than 6 when its quantity exceeds that of the metal[15], it is certainly $Zn(PAN)_2$ that participates in the indicator transition in the vicinity of the equivalence point of the chelatometry of zinc at pH value higher than 6, using PAN as an indicator. In the absence of the third chelating agent (an auxiliary chelating agent), $\beta_{(Ca)}=1$, $K_{ZnA_2}/(\alpha_{H(A)})^2 = K_{ZnA_2}'$ and $K_{ZnY}/\alpha_{H(Y)} = K_{ZnY}'$. Designating the undissociated PAN as HA, Eq. 1 is transfomed into Eq. 2:

$$[Y]_t''/[Ca]_t = 1 - \frac{[ZnA_2]}{[HA]^2}\cdot\frac{K_{ZnY}}{K_{CaY}K_{ZnA_2}'[ZnY]} + \frac{[HA]^2}{[ZnA_2]}\cdot\frac{K_{ZnA_2}'[ZnY]}{K_{ZnY}'[Ca]_t} \qquad (2)$$

where $[ZnA_2]/[HA]$ is a function of the percentage of color change. The second and third terms on the right side of Eq. 2 mainly concern the color change before and after the equivalence point respectively. From Eq. 2 it may easily be seen that the color change is affected by the pH value, by [ZnY] and, when a 1:2 complex such as ZnA_2 participates, by [HA]. Let

$$K_{ZnY}/K_{CaY}K_{ZnA_2}'[ZnY][HA] = f_1$$

and

$$K_{ZnA_2}'[ZnY][HA]/K_{ZnY}'[Ca]_t = f_2$$

It then follows that the color change in the vicinity of the equivalence point becomes sharper the lower the f_1 and f_2 values. However, it should be remembered that higher values of K_{CaY}' and $[Ca]_t$ are always desirable since $f_1f_2 = 1/K_{CaY}'[Ca]_t$. When dealing with a 10^{-2}~10^{-3} M solution of calcium, the titration has to be carried out at a pH value where K_{CaY}' is higher than 10^8 (see Fig. 1). As is well known, $\alpha_{H(Y)}$ is given by formula 3, in which K_1,.....,K_4 are the formation constants of the proton complexes of the fully dissociated species of EGTA:

$$\alpha_{H(Y)} = 1 + K_1[H] + K_1K_2[H]^2 + K_1K_2K_3[H]^3 + K_1K_2K_3K_4[H]^4 \qquad (3)$$

The conditional stability constants, K_{CaY}', can

9) K. L. Cheng and R. H. Bray, *Anal. Chem.*, **27**, 782 (1955).
10) P. Wehber, *Z. anal. Chem.*, **158**, 10 (1957).
11) B. S. Jensen, *Acta Chem. Scand.*, **14**, 927 (1960).
12) G. Nakagawa and H. Wada, *J. Chem. Soc. Japan, Pure Chem. Sec.* (*Nippon Kagaku Zasshi*), **83**, 1185 (1962).
13) Substituting $\alpha_{H(Y)}$ by $\alpha_{H,M_{II}(Y)}$ the effect of a second metal (M_{II}) as well as pH can be quantitively accounted for by means of the concept "ligand buffer": cf. M. Tanaka, *Anal. Chim. Acta*, in press.
14) B. F. Pease and M. B. Williams, *Anal. Chem.*, **31**, 1044 (1959).
15) G. Nakagawa and H. Wada, *J. Chem. Soc. Japan, Pure Chem. Sec.* (*Nippon Kagaku Zasshi*), submitted for publication.

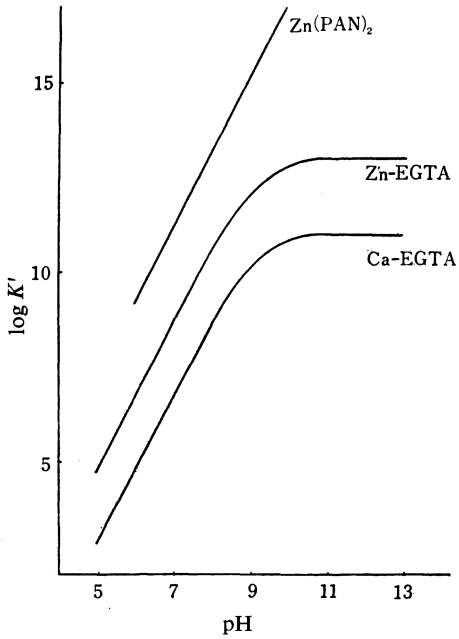

Fig. 1. Conditional stability constants of $Zn(PAN)_2$, Zn-EGTA and Ca-EGTA.

be calculated at various pH values by means of the relationships $K_{CaY'}=K_{CaY}/\alpha_{H(Y)}$ and $\log K_{CaY}=11.0$ (Fig. 1). Similarly, the conditional stability constants of the PAN chelate can be computed for various pH values using the value of $\log K_{ZnA_2}=21.7$ (Fig. 1)[15-17]. For an ordinary condition of chelatometry, viz. $[HA]=10^{-5}$ M and $[ZnY]=10^{-4}$ M, f_1 and f_2 have been computed for various pH values; the results are tabulated in Table I.

From these results it is anticipated that at the pH value of 7 decoloration will occur before the equivalence point, while at the pH value of 10 it will occur gradually after the equivalence point. Therefore, the titration might be successfully carried out in the intermediate pH value range, viz., pH 8~9 (cf. Fig. 1 of Ref. 7).

In the presence of magnesium, the excess EGTA will be bound with magnesium to form MgY. We know that [Y] in equilibrium with Mg and MgY is given by Eq. 4 and that it is a function of $[Mg]_t/[MgY]$ over a considerable range of pH values, viz., pY after the equivalence point is buffered at a higher level by the excess magnesium[13].

$$[Y]=\frac{[MgY]}{([Mg]_t-[MgY])K_{MgY}} \quad (4)$$

Thus the change in pY in the vicinity of the equivalence point is smaller in the presence of magnesium than in its absence, and the indicator transition after the equivalence point becomes sluggish.

TABLE I. f_1 AND f_2 AT VARIOUS pH

Conditions: $[HA]=10^{-5}$ M, $[ZnY]=10^{-4}$ M, $[Ca]_t=10^{-3}$ M

pH	$\log f_1$	$\log f_2$
7.0	−0.3	−3.4
8.0	−2.4	−3.3
9.0	−4.4	−2.9
10.0	−6.4	−1.5

16) Hydrolysis of zinc ions is not taken into account.
17) A. Corsini, I. M. Yih, Q. Fernando and H. Freiser, *Anal. Chem.*, 34, 1090 (1962).

Results and Discussion

All the results summarized in Figs. 2, 3 and 4 were obtained by the trial procedure given in the Experimental section below. $Zn(PAN)_2$ being sparingly soluble in water, it precipitates out near the equivalence point[18]. Therefore, the rate of reaction (5) to the right side is slow and the indicator transition is somewhat irreversible.

$$Zn(PAN)_2 + Y \rightleftharpoons ZnY + 2\,PAN \quad (5)$$

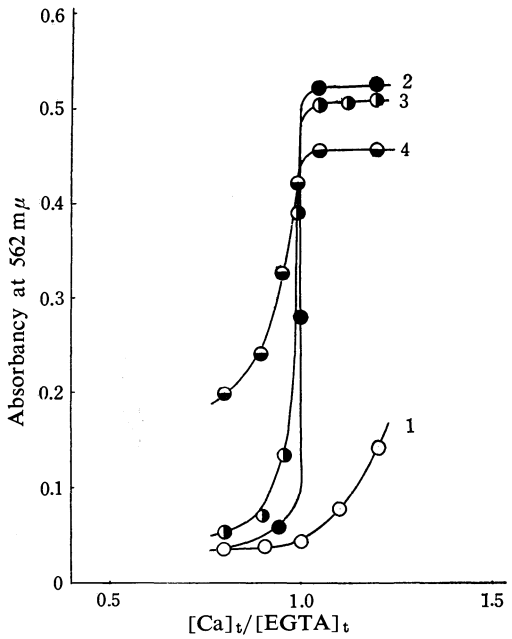

Fig. 2. Effect of pH on the titration of EGTA with calcium standard solution.
Conditions: $[EGTA]_t''=10^{-3}$ M
$[PAN]_t=2\times10^{-5}$ M
$[Zn\text{-}EGTA]_t=4\times10^{-5}$ M
Curve 1: pH 7.0 Curve 2: pH 8.0
Curve 3: pH 9.0 Curve 4: pH 10.0

18) Organic solvents such as dioxane and alcohol have been employed to solubilize Cu(PAN). However, since the solubility of $Zn(PAN)_2$ does not increase appreciably by the addition of such organic solvents, which hardly improves the present situation.

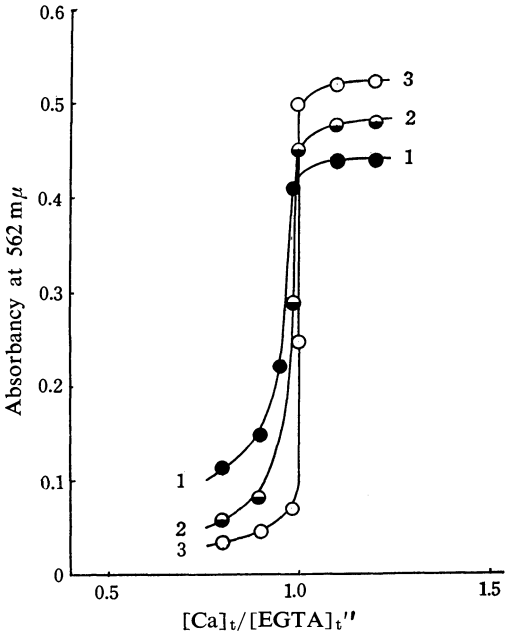

Fig. 3. Effect of Zn-EGTA concentration.
Conditions: $[EGTA]_t'' = 10^{-3}$ M
$[PAN]_t = 2\times10^{-5}$ M, pH 8.0
$[Zn\text{-}EGTA]_t$: Curve 1: 4×10^{-4} M
Curve 2: 8×10^{-5} M
Curve 3: $(2.5\sim5)\times10^{-5}$ M

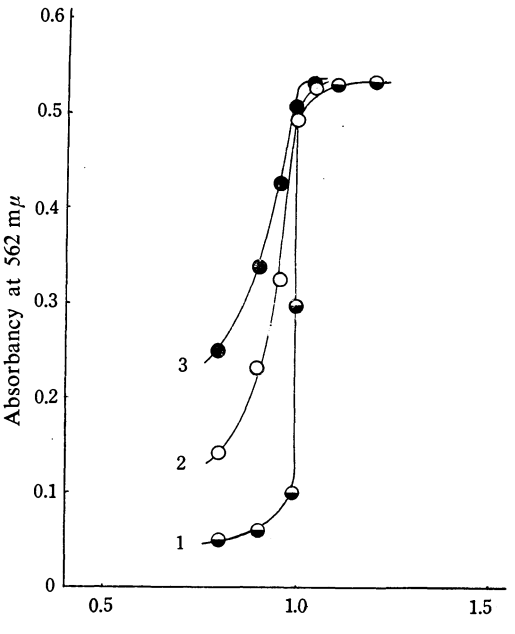

Fig. 4 (a). Effect of magnesium (I).
Conditions: $[EGTA]_t'' = 2.5\times10^{-3}$ M
$[PAN]_t = 2\times10^{-5}$ M
$[Zn\text{-}EGTA]_t = 5\times10^{-5}$ M, pH 8.0
Magnesium present: Curve 1: none
Curve 2: 2.5×10^{-3} M
Curve 3: 5×10^{-3} M

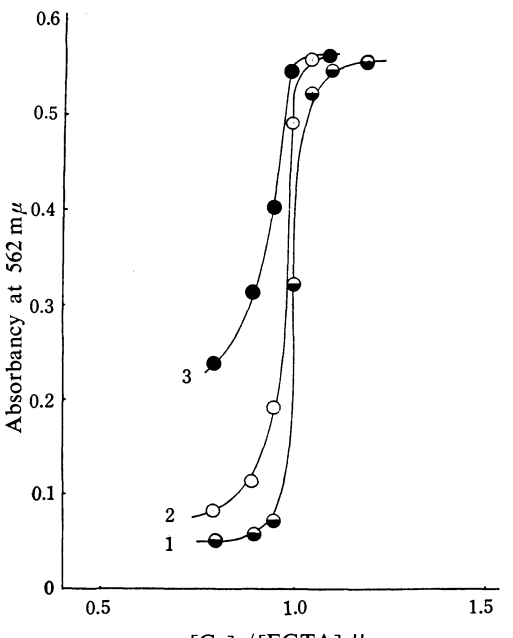

Fig. 4 (b). Effect of magnesium (II).
Conditions: $[EGTA]_t'' = 10^{-3}$ M
$[PAN]_t = 2\times10^{-5}$ M
$[Zn\text{-}EGTA]_t = 2.5\times10^{-5}$ M, pH 8.0
Magnesium present: Curve 1: none
Curve 2: 10^{-3} M
Curve 3: 10^{-2} M

Therefore, it is preferable to titrate the excess EGTA with the calcium standard solution in order to have the reaction 5 proceed from right to left near the equivalence point. Moreover, it is recommended that the solution be heated to about 50~60°C near the equivalence point and that the calcium solution be added drop by drop under vigorous stirring.

Influence of Various Factors.—*The Effect of the pH Value.*—Figure 2 shows the indicator transition in the vicinity of the equivalence point: at a pH value of 7 the color of $Zn(PAN)_2$ is not fully developed even after the equivalence point, while at a pH value of 10 a considerable coloration is observed before the equivalence point. In the intermediate pH range, viz. pH 7.5~9, a very neat color change from pale yellow to pink is realized. Thus within this pH value range the visual titration of calcium will be possible.

The Effect of the Zn-EGTA Concentration.—The effect of the Zn-EGTA concentration is illustrated in Fig. 3: a distinct indicator transition is observed at the optimum concentration of $(2.5\sim5)\times10^{-5}$ M Zn-EGTA.

The Effect of the PAN Concentration.—Theoretically the lower the PAN concentration, the sharper the indicator transition near the equivalence point. However, for the visual

titration the PAN concentration of 2×10^{-5} M is the most satisfactory; a lower concentration of PAN makes the indicator transition obscure because of a faint coloration of $Zn(PAN)_2$.

The Effect of Magnesium. — The effect of magnesium on the calcium determination is shown in Fig. 4. The presence of magnesium gives rise to a pink shade of $Zn(PAN)_2$ before the equivalence point. Thus, in order to secure a distinct indicator transition at the equivalence point in the presence of magnesium, the concentrations of PAN and Zn-EGTA and the pH value of the solution should be kept as low as practical; the most distinct color change is observed under the following conditions: 2×10^{-5} M of PAN, 2.5×10^{-5} M of Zn-EGTA and a pH value of 8 (Fig. 4-b)[19].

In the chelatometry of calcium in the presence of magnesium, the back titration of the excess EGTA with a calcium standard solution is preferable. Denoting the total concentrations of calcium present in the sample and used as a titrant as $[Ca]_{sample}$ and $[Ca]_{titrant}$ respectively, the total concentration of EGTA, $[Y]_t''$, at the equivalence point is given by:

$$[Y]_t'' = [Ca]_t = [Ca]_{sample} + [Ca]_{titrant}$$

Hence, in such a back titration the effect of magnesium on the indicator transition is not determined by $[Mg]_t/[Ca]_{sample}$ but by $[Mg]_t/[Ca]_t$: the color change at the equivalence point becomes less distinct with an increasing $[Mg]_t/[Ca]_t$ ratio (Fig. 4). For a sample with a high $[Mg]_t/[Ca]_{sample}$ ratio, the indicator transition is much improved by the addition of a large excess of EGTA, viz., making the $[Mg]_t/[Ca]_t$ ratio low. As shown in Fig. 4-b, the visual titration of calcium ($[Ca]_t=10^{-3}$ M, $[Ca]_{sample}=0.5\times10^{-3}$ M) in the presence of ten times as much as magnesium ($[Mg]_t=5\times10^{-3}$ M) is possible by the procedure recommended below.

Recommended Procedure.—Fifty milliliters of a buffer solution (pH value: 8) and 5~20 ml. of a 10^{-2} M EGTA solution[20] are added to 25 ml. of a neutral sample solution containing 1~4 mg. of calcium and less than 10 mg. of magnesium[21]. After the addition of 2.5~3 ml. of a 10^{-3} M Zn-EGTA solution and 2 ml. of a 10^{-3} M PAN solution, the excess EGTA is titrated with a 10^{-2} M calcium standard solution. Near the equivalence point, the solution is heated to about 50~60°C and the titration is continued drop by drop while vigorously stirring the solution. A color change from pale yellow to pink is observed at the equivalence point. Titrate to a pink with no yellowish shade.

19) Though the effect of magnesium is less at pH 7.5, appropriate buffer solution of this pH is hardly available.

20) Total concentration of EGTA to be added is preferably more than 1.5 times calcium or 1/2 of magnesium in the sample solution.

21) By means of the photometric titration, presence of about 100 mg. of magnesium is tolerable.

Experimental

Solutions. — *10^{-2} M EGTA Standard Solution.* — 3.8036 g. of EGTA (Dojindo Chemical Co., Kumamoto, Japan) are dissolved in 20 ml. of 1 N sodium hydroxide and the whole is diluted to one liter. The solution is standardized chelatometrically with a 10^{-2} M zinc standard solution using Eriochrome black T as an indicator.

10^{-2} M Calcium Standard Solution.—1.000 g. of calcium carbonate is dissolved in a small amount of hydrochloric acid, the excess of which is expelled completely by evaporation to dryness on a steam bath. The residue is taken up in distilled water and diluted to one liter. The solution is standardized chelatometrically with an EDTA standard solution.

(1~5)$\times10^{-3}$ M Zn-EGTA Solution. — An equivolume mixture of a 10^{-2} M EGTA solution and a 10^{-2} M zinc solution is diluted to an appropriate concentration.

10^{-3} M PAN Solution.—Twenty-five milligrams of PAN (Dojindo Chemical Co., Kumamoto, Japan) are dissolved in 100 ml. of methyl alcohol.

Buffer Solution with a pH Value of 8.—1 N hydrochloric acid is added to a saturated solution of borax until the pH value of the solution is brought to 8.0.

Apparatus.—Filter photometer and conventional titration cell (Hirama Co., Tokyo, Japan).

Trial Procedure.—To a cell for the photometric titration are added 10 ml. of a buffer solution, 2~5 ml. of 10^{-2} M EGTA solution[22] and 0.1~2 ml. of a 5×10^{-3} M Zn-EGTA solution. The solution is then diluted to 20 ml. After the addition of 0.4 ml. of a 10^{-3} M PAN solution, the photometric titration is carried out, using a 10^{-2} M calcium standard solution as the titrant.

Summary

The optimum conditions for the chelatometry of calcium with EGTA have been deduced from the theoretical consideration of the equilibria involved. Some experimental results have been given on the chelatometry of calcium in the presence of magnesium using the Zn-EGTA-PAN system as an indicator. This proposed method seems to be better than earlier ones.

Laboratory of Analytical Chemistry
Nagoya Institute of Technology
Showa-ku, Nagoya (G. N. & H. W.)

Laboratory of Analytical Chemistry
Faculty of Science
Nagoya University
Chikusa-ku, Nagoya (M. T.)

22) Initial concentration of EGTA may be preferably of the order of 10^{-3} M.

The Spectrophotometric Determination of Micro Amounts of Perchlorate by the Solvent-Extraction Method[1]

By Iwaji IWASAKI, Satori UTSUMI and Chisam KANG

(Received November 15, 1962)

It has been reported by Baas Becking, Haldane, and Izard[2] that perchlorate is an important constituent of sea water. If the perchlorate ion is really present in sea water, it is an interesting phenomenon from the geochemical viewpoint. The determination of perchlorate by reducing it to chloride with subsequent titration has been reported[3-5]. Recently, perchlorate has also been determined by the radiochemical method of isotopic dilution[6]. These methods, however, are not suitable for micro quantities of perchlorate.

Nabar and Ramachandran[7] have studied a method for the estimation of perchlorate which is based on the interaction between a known excess of methylene blue and a soluble perchlorate, with a subsequent precipitation of methylene blue perchlorate, and on the photometric estimation of the residual methylene blue. As methylene blue perchlorate is considerably soluble in water, this procedure is subject to serious errors and is also unsuitable for micro amounts of perchlorate Boltz[8] has briefly described a photometric determination of perchlorate depending on the extraction of the complex formed between methylene blue and perchlorate with chloroform; the present authors have investigated this method in greater detail and have reported their findings in a previous paper[9]. However, this method was greatly affected by the temperature upon extraction, owing to the low extration yield, and it did not have a good reproducibility. Lately, it has been found by the present authors that the methylene blue perchlorate is more extractable with dichloroethane than with chloroform. Consequently, the method using extraction with dichloroethane is more sensitive and less affected by temperature than the chloroform method and has a better reproducibility. This improved spectrophotometric method for the determination of perchlorate will be reported on in this paper, and, at the same time, it will be made clear whether or not perchlorate is really present in various sea waters.

Experimental

Apparatus. — The spectrophotometric measurements were made with a Hitachi spectrophotometer, Model EPU-2, with 10.0 mm. cells, at a spectral band width of 1 mμ.

The shaking was done with a Tokiwa shaker, Model TS.

The separation of the organic layer from the aqueous layer was carried out with a separatory funnel approximately 50 ml. fitted in a short leg.

The organic layer was separated from the separatory funnel into a 15 ml. glass tube with a glass stopper.

Materials. — Guaranteed reagent sulfuric acid, 0.1 N.

1,2-Dichloroethane*, guaranteed reagent.

Anhydrous sodium sulfate, guaranteed reagent.

Methylene Blue Solution.—0.030 g. of guaranteed reagent methylene blue ($C_{16}H_{18}N_3ClS \cdot 3H_2O$) was dissolved in distilled water and diluted to 200 ml. with distilled water to give a 4.0×10^{-4} M solution. The solution was stored in a colored bottle and proved to be stable over a period of several months. Recrystallized[7] methylene blue from 50% aqueous alcohol gave the same results as the methylene blue solution mentioned above.

Standard Perchlorate Solution. — Perchloric acid was neutralized with a potassium hydroxide solution to obtain a white precipitate of potassium perchlorate. This was recrystallized and dried at about 130°C for 2 hr. The stock solution which contains 1 mg. of perchlorate ions per ml. was prepared by dissolving 1.393 g. of the potassium perchlorate in distilled water and then diluting it to 1000 ml. The working standard solutions were prepared by diluting the stock solution properly.

Washing Solution.—This was prepared by mixing 10 ml. of 0.1 N sulfuric acid and 20 ml. of the

1) Presented at the Scientific Meeting on Chemistry, Tokyo, Nov., 1961, and at the 11th Annual Meeting of the Japan Society for Analytical Chemistry, Hokkaido, July, 1962.

2) L. G. M. Baas Becking, A. D. Haldane and D. Izard, *Nature*, **182**, 645 (1958).

3) G. P. Haight, *Jr., Anal. Chem.*, **25**, 642 (1953).

4) E. A. Burns and R. F. Muraca, ibid., **32**, 1316 (1960).

5) N. L. Crump and N. C. Johnson, ibid., **27**, 1007 (1955).

6) J. K. Johannesson, ibid., **34**, 1111 (1962).

7) G. M. Nabar and C. R. Ramachandran, ibid., **31**, 263 (1959).

8) D. F. Boltz, "Colorimetric Determination of Nonmetals", Interscience Publishers, New York (1958), p. 176; W. Holland, H. S. Brand and D. F. Boltz, unpublished research.

9) I. Iwasaki, S. Utsumi and C. Kang, *Kogyo Yosui (Industrial Water)*, **37**, 37(1961).

* The dichloroethane already employed once can be used again after purification.

4.0×10^{-4} M methylene blue solution with 200 ml. of distilled water.

Procedure and Calibration Curves.—10.0 ml. of the standard perchlorate solution is placed in a separatory funnel. Then, 0.5 ml. of 0.1 N sulfuric acid, 1.0 ml. of the 4.0×10^{-4} M methylene blue solution and 10.0 ml. of dichloroethane are added. The separatory funnel is shaken for about 30 sec., whereby the complex formed between methylene blue and perchlorate is extracted into the organic layer. When the two layers have clearly separated, the organic layer is transferred to a glass tube with a glass stopper, about 0.5 g. of the anhydrous sodium sulfate is added, and the mixture is shaken vigorously to make it transparent. The absorbance of the clear solution is measured at 655 mμ, using distilled water as a reference.

The calibration curves (I, II, and III) shown in Fig. 1 were obtained by the procedure with standard perchlorate solutions of known concentrations at 15°C, 20°C and 25°C. As can be seen in Fig. 1, the absorbance and the concentration were in a good linear relationship. Though the temperature has a slight effect, this effect is much less than that in the chloroform method[9].

The extracted complex is very stable; even after 24 hr., no measurable change was found when a glass stopper was used to protect against evaporation of the dichloroethane.

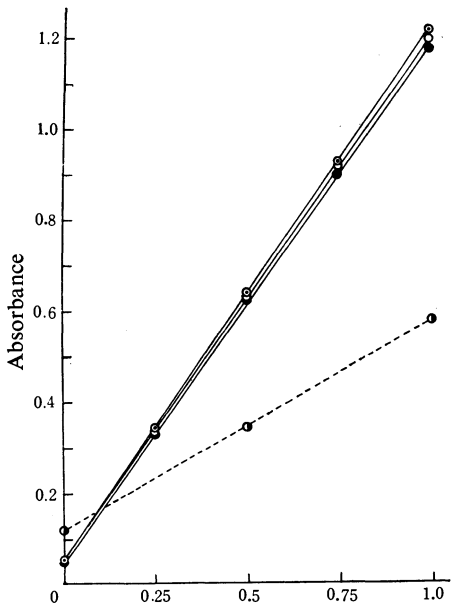

Fig. 1. Calibration curves and effect of temperature.
-⊙- 15°C (I) -○- 20°C (II)
-○- 25°C (III) ---◑--- Chloroform method at 20°C (IV)

Results and Discussion

Spectral Absorbance Curves.—Figure 2 shows the absorbance curves of an aqueous solution

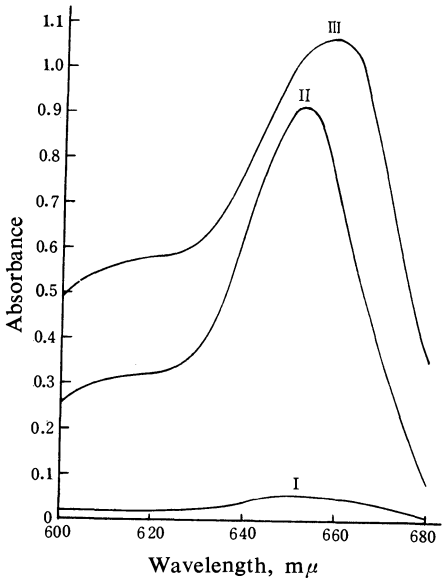

Fig. 2. Spectral absorbance curves.
I Methylene blue in dichloroethane
II Methylene blue perchlorate complex in dichloroethane
III Methylene blue in distilled water

of the methylene blue and dichloroethane solutions of the complex of methylene blue perchlorate and the methylene blue.

The methylene blue perchlorate complex and the reagent blank have a maximum absorbance at 655 mμ (see I and II); on the other hand, the aqueous solution of methylene blue has a maximum at 660 mμ (see III).

The peak at 655 mμ was used in all subsequent measurements because the difference in the absorbance between the complex of methylene blue perchlorate and the reagent blank is greatest at this wavelength.

Extraction by Organic Solvents.—Benzene, carbon tetrachloride, ethyl ether, butyl alcohol, isoamyl alcohol, *n*-hexyl alcohol, tributyl phosphate, chloroform, and 1, 2-dichloroethane were tried as solvent for this extraction. Nonpolar solvents such as benzene and carbon tetrachloride proved not to be useful. Only 1, 2-dichloroethane and chloroform proved useful. The former, being the better extracting agent, was used in this work. It was found most practical to use a one 10 ml. portion of the solvent in the extraction. Figure 3 shows how the complex of methylene blue and perchlorate is extrated with 10 ml. of dichloroethane.

The extraction yield using one 10 ml. portion of dichloroethane is about 95%. Consequently, the sensitivity of this method is much greater than that of the chloroform method, as can be seen in Fig. 1.

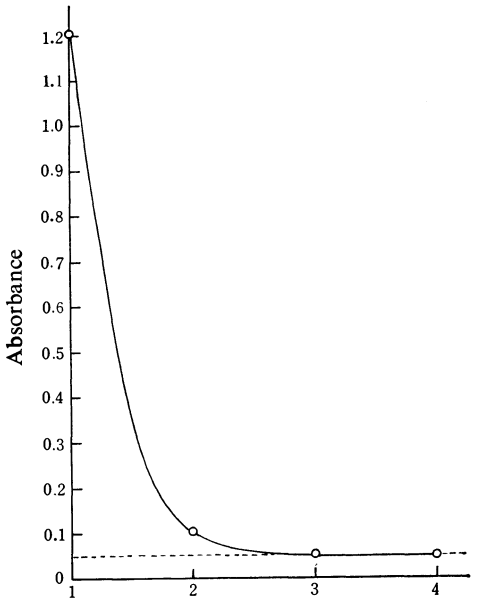

Fig. 3. Experiment for the extraction by dichloroethane.
Concn. of perchlorate: 1 p. p. m.
----: Reagent blank

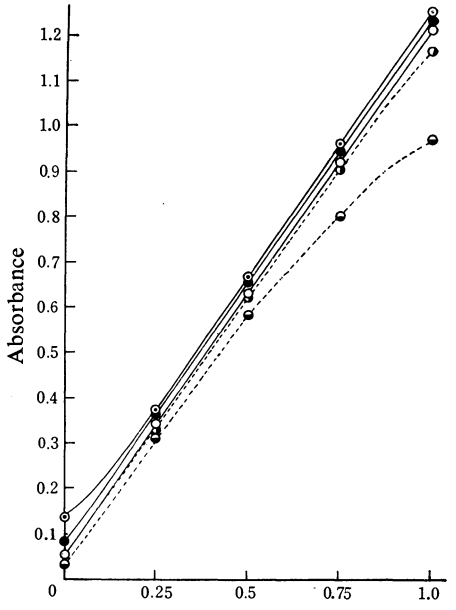

Fig. 4. Effect of concentration of methylene blue. The volume of methylene blue solution added is 1 ml.
---◒--- 1.3×10^{-4} M (I)
---◑--- 2.6×10^{-4} M (II)
—○— 4.0×10^{-4} M (III)
—●— 8.0×10^{-4} M (IV)
—⊙— 1.3×10^{-3} M (V)

The Effect of the Concentration of Methylene Blue Reagent.—The methylene blue perchlorate complex with a 1.3×10^{-4} M methylene blue solution obeyed Beer's law up to about 0.6 p.p.m. of perchlorate, while that with a 2.6×10^{-4} M solution did so up to about 0.8 p.p.m. However, they then showed an increasing deviation from Beer's law for concentrations higher than 0.6 p.p.m. and 0.8 p.p.m. respectively (see I and II in Fig. 4). On the other hand, the higher the concentration of methylene blue was, the higher the absorbance of reagent blank became, and the absorbances, shown in Fig. 4 (see IV and V), did not form a straight line.

Figure 4 shows that the most suitable concentration of the methylene blue solution for the range up to 1 p. p. m. of perchlorate ions is 4.0×10^{-4} M.

The Effect of the Sulfuric Acid Concentration.—When the aqueous solution is alkaline, the dichloroethane extracts become pink, so the procedure should be carried out below a pH value of 6. Sulfuric acid is used for making the aqueous solution acid. The effect of sulfuric acid concentrations on the method is shown in Fig. 5.

The extractability of methylene blue itself increases, while that of the complex does not undergo any measurable change upon an increase in the concentration of sulfuric acid. Therefore, 0.5 ml. of 0.1 N sulfuric acid was added in the present work.

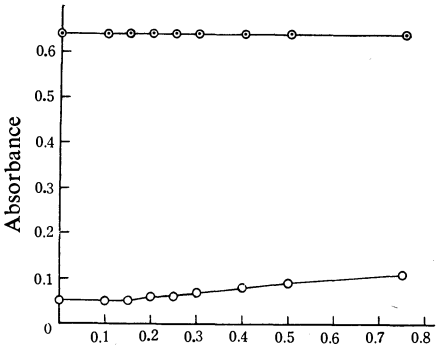

Fig. 5. Effect of sulfuric acid concentration. The volume of sulfuric acid added is 0.5 ml.
—⊙— 0.5 p. p. m. ClO_4^-
—○— Reagent blank

TABLE I. EFFECT OF SHAKING TIME ON EXTRACTION

Time sec.	Absorbance	
	Reagent blank	0.5 p. p. m. ClO_4^-
15	0.060, 0.058	0.635, 0.637
30	0.052, 0.054	0.638, 0.639
60	0.052, 0.051	0.639, 0.639

Table II. Effect of diverse ions

Ion	Added as	Concn. p. p. m.	Absorbance: Reagent blank	Absorbance: 0.5 p. p. m. ClO_4^-	Back washing: Reagent blank	Back washing: 0.5 p. p. m. ClO_4^-	Masking with 50 p. p. m. Hg^{2+}: Reagent blank	Masking with 50 p. p. m. Hg^{2+}: 0.5 p. p. m. ClO_4^-
None		0	0.054	0.630	0.054	0.629	0.052	0.626
Cl^-	NaCl	10	0.129	0.629			0.099	0.633
		10000	0.977	>1.250	0.057	0.594		
		20000	1.226	>1.250	0.068	0.577		
Br^-	KBr	10	0.306	0.721	0.065	0.635	0.080	0.624
		100	0.774	1.094	0.093	0.629	>1.250	>1.250
I^-	KI	0.1	0.118	0.659	0.101	0.655	0.044	0.621
		1	0.510	0.915	0.368	0.812	0.055	0.624
		10	>1.250	>1.250			0.068	0.630
SCN^-	KSCN	0.5	0.660	1.112	0.498	0.921	0.046	0.629
		1	1.005	>1.250	0.708	1.104	0.051	0.623

Table III. Effect of diverse ions

Ion	Added as	Concn. p. p. m.	Absorbance: Reagent blank	Absorbance: 0.5 p. p. m. ClO_4^-	Back washing: Reagent blank	Back washing: 0.5 p. p. m. ClO_4^-
None	None	0	0.054	0.630	0.054	0.629
IO_4^-	$NaIO_4$	1	0.557	1.138	0.476	1.028
ClO_3^-	$KClO_3$	1	0.261	0.720	0.113	0.646
BrO_3^-	$KBrO_3$	100	0.400	0.786	0.063	0.633
IO_3^-	KIO_3	1000	0.069	0.634		
NO_3^-	KNO_3	10	0.749	1.041	0.166	0.645
NO_2^-	$NaNO_2$	10	0.159	0.655	0.103	0.632
SO_4^{2-}	K_2SO_4	5000	0.073	0.630		
SO_3^{2-}	$Na_2SO_3 \cdot 7H_2O$	100	0.135	0.651	0.060	0.631
$S_2O_3^{2-}$	$Na_2S_2O_3 \cdot 5H_2O$	10	0.358	0.743	0.100	0.645
S^{2-}	$Na_2S \cdot 9H_2O$	10	0.060	0.631		
MnO_4^-	$KMnO_4$	10	0.079	0.592		
CrO_4^{2-}	K_2CrO_4	10	0.608	0.974	0.156	0.649
MoO_4^{2-}	Na_2MoO_4	10	0.067	0.644		
WO_4^{2-}	$Na_2WO_4 \cdot 2H_2O$	10	0.111	0.664	0.096	0.665
VO_3^-	KVO_3	10	0.072	0.647		
$Fe(CN)_6^{3-}$	$K_3Fe(CN)_6$	10	0.062	0.615		
$Fe(CN)_6^{4-}$	$K_4Fe(CN)_6 \cdot 3H_2O$	10	0.046	0.621		

The Effect of the Shaking Time on Extraction.—The shaking time on extraction did not change the absorbance. The results listed in Table I show that shaking for 30 sec. is sufficient to extract the complex from the aqueous solution.

The Composition of the Complex between Methylene Blue and Perchlorate.—Application of the continuous variation method[10-13] indicated that only a 1 to 1 complex of methylene blue and perchlorate was formed. The resulting curves, in which the reagent blank was subtracted, are shown in Fig. 6. All the curves have a broad maximum in the vicinity of $x=5$, indicating that the complex is partially dissociated in the aqueous solution and that the extraction yield of the complex by dichloroethane is not 100%.

Effect of Diverse Ions. — In measuring the effect of diverse ions on this method, the experiments were made both in the presence of 0.5 p. p. m. of perchlorate ions and in its absence. The experimental results are given in Tables II, III, IV and V.

10) Y. Shibata, T. Inouye, and Y. Nakatsuka, *J. Chem. Soc. Japan (Nippon Kwagaku Kwaishi)*, **42**, 983 (1921).
11) P. Job, *Ann. chim.*, [10] **9**, 113 (1928).
12) W. C. Vosburgh and G. R. Cooper, *J. Am. Chem. Soc.*, **63**, 437 (1941).
13) R. K. Gould and W. C. Vosburgh, ibid., **64**, 1630 (1942).

TABLE IV. EFFECT OF DIVERSE IONS

Ion	Added as	Concn. p. p. m.	Absorbance	
			Reagent blank	0.5 p. p. m. ClO_4^-
None		0	0.054	0.630
$H_2PO_4^-$	$NaH_2PO_4 \cdot H_2O$	100	0.074	0.639
$HAsO_4^{2-}$	$Na_2HAsO_4 \cdot 7H_2O$	100	0.077	0.635
SeO_4^{2-}	K_2SeO_4	10	0.064	0.627
		100	0.145	0.676
CO_3^{2-}	Na_2CO_3	100	0.072	0.639
CN^-	KCN	10	0.059	0.621
		100	0.126	0.649
F^-	NaF	100	0.079	0.630
Silicate ion	(as SiO_2)	10	0.077	0.639
Borate ion	H_3BO_3	100	0.065	0.625
CH_3COO^-	$CH_3COONa \cdot 3H_2O$	100	0.060	0.645
$C_2O_4^{2-}$	$K_2C_2O_4 \cdot H_2O$	10	0.057	0.621
		100	0.144	0.661

TABLE V. EFFECT OF DIVERSE IONS

Ion	Added as	Concn. p. p. m.	Absorbance			
			Reagent blank	0.5 p. p. m. ClO_4^-	Back washing	
					Reagent blank	0.5 p. p. m. ClO_4^-
None		0	0.054	0.630	0.054	0.629
Na^+	$Na_2SO_4 \cdot 10H_2O$	5000	0.060	0.629		
NH_4^+	$(NH_4)_2SO_4$	5000	0.075	0.626		
Mg^{2+}	$MgSO_4$	1000	0.339	0.762	0.104	0.627
Ca^{2+}	$CaSO_4 \cdot 2H_2O$	280	0.064	0.630		
Sr^{2+}	$SrSO_4$	10	0.267	0.716	0.089	0.631
Al^{3+}	$Al_2(SO_4)_3 \cdot 18H_2O$	100	0.084	0.631		
Cu^{2+}	$CuSO_4 \cdot 5H_2O$	100	0.057	0.631		
Ag^+	Ag_2SO_4	100	0.194	0.673	0.079	0.622
Zn^{2+}	$ZnSO_4 \cdot 7H_2O$	100	0.064	0.630		
Cd^{2+}	$3CdSO_4 + 8H_2O$	100	0.146	0.665	0.077	0.629
Hg^{2+}	$HgSO_4$	50	0.052	0.626		
Pb^{2+}	$PbSO_4 \cdot 7H_2O$	10	0.122	0.641	0.075	0.625
Mn^{2+}	$MnSO_4 \cdot 7H_2O$	100	0.059	0.627		
Fe^{3+}	$Fe(NH_4)(SO_4)_2 \cdot 12H_2O$	100	0.062	0.624		
Fe^{2+}	$Fe(NH_4)_2(SO_4)_2 \cdot 6H_2O$	100	0.078	0.629		
Co^{2+}	$CoSO_4 \cdot 7H_2O$	10	0.063	0.630		
		100	0.103	0.643		
Ni^{2+}	$NiSO_4 \cdot 7H_2O$	10	0.054	0.635		
		100	0.109	0.643		
	H_2O_2	100	0.072	0.628		

There are relatively many anions which cause interference. Sodium, potassium, ammonium, and sulfate do not interfere, however, even when present in amounts of 5000 p. p. m., and the iodate does not interfere at a 1000 p. p. m. It is of interst that halide, when listed in order of increasing interference in this method, are chloride, bromide and iodide, while the oxyacid of the halogens are listed, on the contrary, as iodate, bromate and chlorate. The thiocyanate and iodide, which interfere remarkably even at 0.1 p. p. m., could be masked up to 1 p. p. m. by the addition of 50 p. p. m. of mercuric ion.

The Determination of Perchlorate in the Presence of Other Ions.—Several methods were tried by the present authors to determine the trace amounts of perchlorate in the high concentration of chloride as great as that in sea water. Of these, the back-washing method gave the most satisfactory results for removing chloride and other interfering ions

Table VI. Experiments for the perchlorate ion in sea waters

Sea water	Sample taken, ml.	Diluted twice, absorbance	ClO_4^- found, p. p. m.	ClO_4^- added p. p. m.	ClO_4^- recovered p. p. m.
Artificial sea water	5.0	0.079	0	0.10	0.10
Standard sea water	5.0	0.081	no detected	0.10	0.10
Old sea water* No. 1	5.0	0.072	no detected	0.10	0.10
Fresh sea water** No. 2	5.0	0.072	no detected	0.10	0.10
Fresh sea water** No. 3	5.0	0.074	no detected	0.10	0.09

* Determined after three months since the sample was taken 10 km. apart from the north coast of O-sima, Tokyo, March, 1962.

** Samples from two stations on the coast of the Boso Peninsula, Chiba Prefecture, June, 1962.

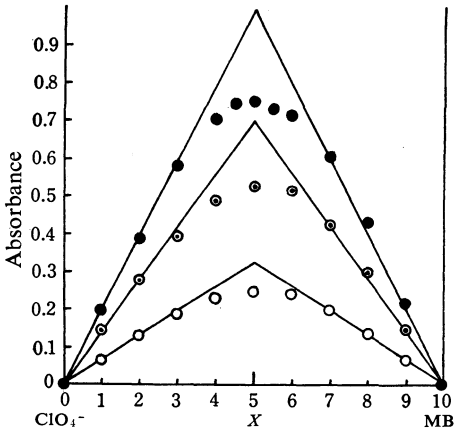

Fig. 6. Method of continuous variation. Concentrations of methylene blue, and perchlorate: 2×10^{-5} M

○ 610 mμ ⊙ 665 mμ ● 655 mμ

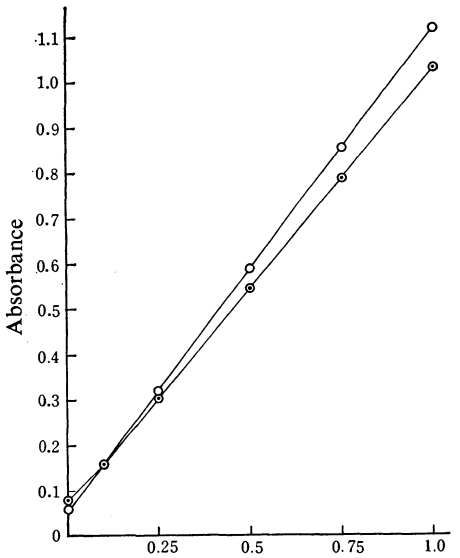

Fig. 7. Calibration curves in the presence of other ions.

-⊙- In artificial sea water diluted twice (I)

-○- In the presence of 10000 p. p. m. Cl^- (II)

to such amounts as are present in sea water.

In order to remove the interfering ions, transfer the organic layer which was separated from the aqueous solution by the procedure mentioned above into another separatory funnel, add 10.0 ml. of the washing solution, and shake for about 30 sec. After the two layers have clearly separated, transfer the organic layer to a glass tube, make it transparent with anhydrous sodium sulfate, and measure the absorbance at 655 mμ.

The results listed in Table II show that one washing is sufficient to eliminate the interference of a 10000 p. p. m. concentration of chloride ions. On the other hand, thiocyanate, periodate, iodide, chlorate, nitrate and nitrite which give remarkably higher results even in small amounts, could not be removed even after two washings. However, most of them are not present in sea water, and the concentration of iodide is too small to consider its interference.

Figure 7 shows the calibration curves of perchlorate ions in the presence of a 10000 p. p. m. of chloride (II) and in artificial sea water[14] diluted twice (I).

The difference between I and II is due in all probability to the fact that there are interfering ions besides chloride in sea water.

The calibration curve (I) was in a good linear relationship for the range from 0.1 to 1.0 p. p. m. of perchlorate ions, but it was not for concentrations lower than 0.1 p. p. m., probably owing to the incomplete removal of magnesium, bromide, and iodide. The concentration of perchlorate in sea water can be readily determined by reference to curve I in

14) J. Lyman and R. H. Fleming, *J. Marine Research*, 3, 134 (1940).

Fig. 7. It was reproducible within the error of ±0.02 p. p. m. of perchlorate ions. It is possible to determine the perchlorate over the range from 0.05 p. p. m. to 2.0 p. p. m. in sea water by this method.

Experiment for the Perchlorate in Various Sea Waters.—Some results of the application of this method to several sea waters are given in Table VI.

As will be seen in Table VI, the experimental results show that the concentration of perchlorate in sea water, if present, is below 0.05 p. p. m., very much less than the figures reported by Baas Becking, Haldane and Izard[2].

Greenhaigh and Riley[15] have investigated the occurrence of perchlorate in sea water by a method they themselves devised, and Johannesson[6] has applied the radiochemical method of isotopic dilution to its determination in sea water. They also detected no perchlorate in natural sea water within the sensitivities of their methods.

Laboratory of Analytical Chemistry and Geochemistry
Tokyo Institute of Technology
Meguro-ku, Tokyo (I. I. & C. K.)

Department of Science and Technology
Nihon University
Chiyoda-ku, Tokyo (S. U.)

15) R. Greenhaigh and J. P. Riley, *Nature*, **187**, 1107 (1960).

A Convenient Synthetic Method of 2-Carbamoyl-6-methoxybenzothiazole, One of Intermediates for the Synthesis of Firefly Luciferin

By Shuichi SETO, Kyozo OGURA and Yukio NISHIYAMA

(Received November 17, 1962)

White et al. reported in their short communication[1] that firefly luciferin (III) was synthesized from *p*-anisidine (I) through eight steps. According to them, the preparation of 2-carbamoyl-6-methoxybenzothiazole (II), which is one of intermediates in this synthetic route, requires five steps from the starting material I.

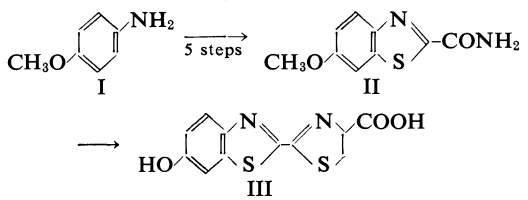

The present authors found a convenient preparative route to II by using carbamoylthiocarbonylthioacetic acid (IV) as a carbamoylthiocarbonylation reagent of *p*-anisidine (I), and II was easily synthesized by two steps from I.

The present paper describes the preparation of the reagent IV and its reactions.

The reagent IV was prepared by the reaction of trichloroacetamide, potassium sulfide and potassium monochloroacetate nearly in the same manner as in the case of thiobenzoylthioacetic acid[2]. Being fairly unstable, IV was freshly prepared and used in alkaline solution without being isolated as free acid. Thus obtained alkaline solution which colored deep red reacted various aromatic amines at room temperature to afford corresponding thioamides. Reaction of aniline, *p*-toluidine, α-naphthylamine and β-naphthylamine gave thiooxanilamide (V), 4-methylthiooxanilamide (VI), α-monothiooxal-α'-amide-α(α-naphthylamide) (VII) and α-monothiooxal-α'-amide-α(β-naphthylamide) (VIII) respectively. Compound V, VI and VII are known substances[3,4]. Application of the reagent IV to I gave 4-methoxythiooxanilamide (IX), which showed absorptions at 3360, 3200 and 1702 cm^{-1} due to its amide residue. Treatment of IX with a large excess of alkaline potassium ferricyanide afforded II in a fairly good yield. It shows amide bands at 3330, 3200, 1689 and 1661 cm^{-1}.

Conversion of the amide II into luciferin (III) by White's method was examined, and 2-cyano-6-methoxy- (X), 2-cyano-6-hydroxybenzothiazole (XI) and III were obtained.

1) E. H. White, F. McCapra, G. F. Field and W. D. McElroy, *J. Am. Chem. Soc.*, **83**, 2402 (1961).

2) J. C. Crawhall et al., *J. Chem. Soc.*, **1951**, 2071.

3) A. Reissert and K. Brugemann, *Ber.*, **57**, 981 (1924).

4) A. Reissert, ibid., **37**, 3708 (1904).

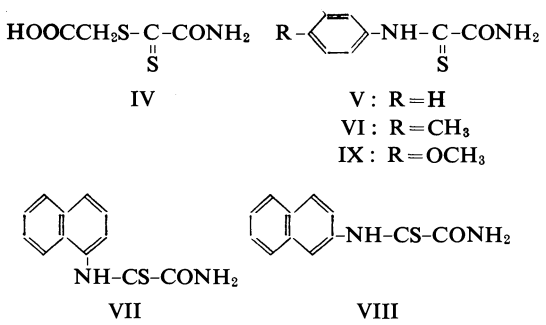

IV V: R=H VI: R=CH_3 IX: R=OCH_3

VII VIII

Experimental*

Carbamoylthiocarbonylthioacetic Acid (IV).—A solution of potassium hydroxide (3.0 g.) in ethanol (20 ml.) was divided into halves and one half was saturated with hydrogen sulfide which had been dried through calcium chloride: the other half was then added to the first portion in a 50 ml. flask fitted with nitrogen inlet and dropping funnel. A slow stream of nitrogen was passed and a solution of trichloroacetamide (1.85 g) in ethanol (10 ml.) was added to the mixture with shaking at room temperature. The mixture gradually turned red and the color change from red to brown occurred. As the temperature was raised during this time, the mixture was occasionally cooled with ice-water. A solution of monochloroacetic acid (1.6 g.) in water (10 ml.), neutralized with potassium carbonate, was added to the mixture under nitrogen stream, and the mixture was well shaken. The mixture immediately turned deep red. After being allowed to stand for a few minutes, the mixture was filtered to remove the precipitate of inorganic salt thereby formed. Thus obtained red solution was quickly used for the reaction.

Thiooxanilamide (V).—To a solution of aniline (200 mg.) in 50% ethanol (1 ml.), the solution IV (2 ml.) was added. After the mixture was allowed to stand at room temperature for 3 days, yellow needles that separated out were collected and recrystallized from ethanol to afford yellow needles, m. p. 168~170°C. Yield, 50 mg.

Found: C, 53.61; H, 3.71; N, 14.61. Calcd. for $C_8H_8ON_2S$: C, 53.33; H, 4.48; N, 15.55%.

4-Methylthiooxanilamide (VI).—To a solution of *p*-toluidine (200 mg.) in 50% ethanol (2 ml.), the solution of IV (2 ml.) was added, and the mixture was allowed to stand at room temperature overnight. Yellow crystals that precipitated were collected and recrystallized from ethanol to form yellow needles, m. p. 166~168°C. Yield, 60 mg.

Found; C, 55.74: H, 5.19; N, 13.94. Calcd. for $C_9H_{10}ON_2S$: C, 55.66; H, 5.19; N, 14.43%.

α-Monothiooxal-α'-amide-α(α-naphthylamide) (VI).—To a solution of α-naphthylamine (100 mg.) in 70% ethanol (1.5 ml.), the solution of IV (2 ml.) was added. After the mixture was allowed to stand at room temperature overnight, crystals that separated were collected and recrystallized from ethanol to give yellow needles, m. p. 198~200°C. Yield, 50 mg.

Found: C, 62.41; H, 4.24; N, 12.18. Calcd for $C_{12}H_{10}ON_2S$: C, 62.60; H, 4.38; N, 12.17%.

α-Monothiooxal-α'-amide-α(β-naphthylamide) (VIII).—The solution of IV (2 ml.) was added to a solution of β-naphthylamine (100 mg.) in ethanol (3 ml.), and the mixture was allowed to stand at room temperature for 4 days. Crystals that separated were collected by filtration, washed well with water to remove a small amount of inorganic salt. Recrystallization from ethanol afforded yellow needles, m. p. 163~166°C. Yield, 40 mg.

Found: C, 62.38; H, 4.38; N, 12.18. Calcd. for $C_{12}HO_{10}N_2S$: C, 62.60; H, 4.38; N, 12.17%.

4-Methoxythiooxanilamide (IX).—To a solution of I (1 g.) in 50% aqueous ethanol (10 ml.), the solution of IV prepared from 1.85 g. of trichloroacetamide was added. After the mixture was allowed to stand at room temperature, yellow crystals that separated out were collected and recrystallized from ethanol to form yellow needles, m. p. 182~185°C. Yield, 0.5 g. λ_{max}^{MeOH} mμ (log ε): 228 (4.14), 270 (3.72), 350 (4.00).

Found: C, 51.42; H, 4.80; N, 13.33. Calcd. for $C_9H_{10}O_2N_2S$: C, 51.16; H, 4.74; N, 13.00%.

2-Carbamoyl-6-methoxybenzothiazole (II).—When a solution of IX (0.5 g) in 10% aqueous sodium hydroxide (40 ml.) was added dropwise into a stirred solution of potassium ferricyanide (9 g.) in water (20 ml.), colorless precipitate separated immediately. After stirring for 30 min., the precipitate was collected by filtration, washed with water and recrystallized from ethanol to form colorless scales, m. p. 246~250°C (decomp.). Yield, 0.4 g. λ_{max}^{MeOH} mμ (log ε): 260 (3.85), 315 (4.20).

Found: C, 51.17; H, 4.06; N, 13.11. Calcd. for $C_9H_8O_2N_2S$: C, 51.92; H, 3.87; N, 13.46%.

2-Cyano-6-methoxybenzothiazole (X).—A suspension of II (100 mg.) in phosphorus oxychloride (1.3 ml.) was refluxed for 30 min., and then an excess of phosphorus oxychloride was distilled off under a reduced pressure. Cold water (0.5 ml.) was added to the residue, and the colorless precipitate thereby formed was collected by filtration. The solid was sublimed under a reduced pressure (4 mmHg) at 100°C, and the sublimate was recrystallized from benzene-petroleum ether to afford colorless needles, m. p. 129~130°C. Yield, 80 mg. λ_{max}^{MeOH} mμ (log ε): 262 (3.87), 320 (4.24). ν_{max}^{KBr} 2230 cm^{-1}.

Found: C, 56.95: H, 3.26; N, 14.91. Calcd. for $C_9H_6ON_2S$: C, 56.84; H, 3.18; N, 14.73%.

2-Cyano-6-hydroxybenzothiazole (XI).—After a mixture of X (120 mg.) and pyridine hydrochloride (240 mg.) was heated in a sealed tube at 150~160°C for 4 hr., water (1 ml.) was added to the reaction mixture. The precipitate thererby formed was collected, washed with benzene and recrystallized from benzene to form pale yellow needles, m. p. 205~207°C (decomp.). Yield, 45 mg. Evaporation of the benzene filtrate gave colorless crystals, which were recrystallized from methanol to give colorless needles of the starting material (X).

* All melting points were uncorrected. The microanalyses were carried out by Misses Yoko Endo and Yukiko Endo of this Institute, to whom the authors are indebted.

λ_{max}^{MeOH} mμ (log ε) : 263 (3.88), 323 (4.19). ν_{max}^{KBr} 3220, 2230 cm^{-1}.

Found : C, 54.60 ; H, 2.14 ; N, 15.76. Calcd. for $C_8H_4ON_2S$: C, 54.55 ; H, 2.29 ; N, 15.91%.

Firefly Luciferin (III).—A mixture of XI (20 mg.), D-cysteine hydrochloride (20 mg.), potassium carbonate (16 mg.) and 50% aqueous methanol (1 ml.) was stirred under nitrogen stream. After being stirred for 1.5 hr., the mixture was neutralized with diluted hydrochloric acid. The precipitate was collected, washed with water and recrystallized from methanol to afford pale yellow prisms, m. p. 200~202°C. Yield, 25 mg. λ_{max}^{MeOH} mμ (log ε) : 268 (3.80), 328 (4.24). ν_{max}^{KBr} 3330, 2550, 1700 cm^{-1}.

Found : C, 47.08 ; H, 3.21 ; N, 9.60. Calcd. for $C_{11}H_8O_3N_2S$: C, 47.14 ; H, 2.85 ; N, 10.00%.

The authors wish to express their sincere gratitude to Sankyo Co., Ltd., which defrayed a part of the expense for the present work.

The Chemical Research Institute of Non-Aqueous Solutions
Tohoku University
Katahira-cho, Sendai

Decomposition of Peroxybenzoic Acid in Solution. VI. Theoretical Consideration of the Induced Decomposition of Peroxides by Radicals

By Katsumi TOKUMARU and Osamu SIMAMURA

(Received October 23, 1962)

In the previous parts of this series[1-5] it has been shown that one of the notable features of the decomposition of peroxybenzoic acid in various solvents is its very facile decomposition, induced by radicals (R·) generated in solution; this takes place according to the following equation:

$$PhCO_3H + R\cdot \rightarrow PhCO_2\cdot + ROH \quad (1)$$

A similar induced decomposition by radicals is generally recognized to occur with various peroxides (POOP')[6,7] with varying degrees of readiness according to the following equation:

$$POOP' + R\cdot \rightarrow ROP + P'O\cdot \quad (2)$$

Thermochemical consideration shows that the induced decomposition takes place exothermically. Thus, since the heat of reaction ($-\Delta H$) is gvien by the difference in bond dissociation energy (D) between the bond formed and the one broken,

$$(-\Delta H) = D(\text{R–OP}) - D(\text{PO–OP}')$$

the heat of reaction for the induced decomposition will be 50~60 kcal./mol., if we assume the generally accepted values of 90[8] and 30~40 kcal./mol.[6] for D(R–OP) and D(PO–OP') respectively. In fact, in accordance with such large exothermicity, the activation energy for the induced decomposition of peroxybenzoic acid by the polymethyl methacrylate radical has been shown to be 6.6 kcal./mol.[9], indicating that this reaction takes place very easily. If the activation energy changes parallel with the heat of reaction, as is usually the case with many reactions, e. g., the abstraction of a hydrogen atom from hydrocarbon by a variety of alkyl radicals[10], the resonance stabilization on the part of the attacking radical would reduce the heat of reaction and would, therefore, be expected to enhance the activation energy thus making the radical the less reactive.

However, the reactivity of a radical in the induced decomposition of peroxides appears to be affected not so much by the resonance stabilization of the radical as by its electron-donating property. Thus, our results[1-5] show that radicals derived from alcohols and ethers, RR'ĊOR'', appear to be the most active; then come the hydrocarbon radicals, e. g., the cyclohexyl radical, and the trichloromethyl radical seems to be least reactive, being unable to cause the induced decomposition of peroxybenzoic acid. This trend suggests that the more electron-donating radical is the more reactive. A similar trend has been observed

1) K. Tokumaru, O. Simamura and M. Fukuyama, This Bulletin, **35**, 1673 (1962).
2) K. Tokumaru and O. Simamura, ibid., **35**, 1678 (1962).
3) K. Tokumaru and O. Simamura, ibid., **35** 1955 (1962).
4) K. Tokumaru, N. Inamoto and O. Simamura, ibid., **36**, 72 (1963).
5) K. Tokumura and O. Simamura, ibid., **36**, 76 (1963).
6) A. V. Tobolsky and R. B. Mesrobian, "Organic Peroxides", Interscience Publishers, New York (1954).
7) C. Walling, "Free Radicals in Solution", John Wiley and Sons Co., New York (1957).
8) M. Szwarc, *Chem. Revs.*, **47**, 75 (1950).
9) H. Terada, *Yuki Gosei Kagaku Kyokaishi*, **20**, 158 (1962).
10) N. N. Tikhomirova and V. V. Voevodski, *Doklady Akad. Nauk S. S. S. R.*, **79**, 993 (1951); *Chem. Abstr.*, **45**, 9940 (1951).

in the induced decomposition of benzoyl peroxide[6,7,11,12]. Mashio and Kato[13] have shown that the reactivity of radicals derived from various alcohols towards benzoyl peroxide decreases in the order: 1-hydroxy-1-methylethyl > 1-hydroxyethyl > hydroxymethyl. Apparently this is the order of decreasing electron-donating property as well as the order of decreasing resonance stabilization. Thus we are led to the conclusion that the more electron-donating radical is more reactive in the induced decomposition of peroxides, even if it is the more resonance-stabilized radical.

The way in which change in the structure of a radical affects its electron-donating property and the extent of resonance stabilization, leading to the above sequence in regard to those two respects, is understood in terms of a molecular orbital theory. A treatment of 1-hydroxyalkyl radicals according to a simple LCAO-MO method with regard to an odd electron on the carbon and two lone-pair electrons on the oxygen atom shows that the radical as a whole is stabilized with respect to the state in which the odd electron and the lone-pair electrons are localized on the carbon and the oxygen atom respectively; that the molecular orbital occupied by the odd electron is located at a higher energy level than the orbital when the odd electron is localized; and that the more stabilized the radical becomes, the higher the level of the odd electron tends to lie. Obviously such results will generally be obtained when a group carrying a lone-pair of electrons or a group capable of hyperconjugation like a methyl is placed in juxtaposition with the radical centre.

The energy level of the highest occupied orbital is related to the ionization potential of this chemical species in such a way that the higher the former is, the smaller is the latter. For lack of appropriate experimental data for hydroxyalkyl radicals for comparison with the theoretical deduction, we quote the values for alkyl radicals in Table I to show the effect on the resonance energy and the ionization potential brought about by the introduction of an increasing number of electron-releasing methyl groups into a methyl radical. The trend which is apparent in the table is in keeping with the foregoing theoretical prediction.

TABLE I. RESONANCE ENERGIES AND IONIZATION POTENTIALS OF ALKYL RADICALS

Radical	Resonance energy[14] in kcal./mol.		Ionization Potential[15] in eV.
	Calcd.	Obs.	
Methyl	—	—	9.85
Ethyl	7.05	7.2	8.66
n-Propyl	8.6	8.1	7.57
Isopropyl	14.1	12.6	7.45
t-Butyl	21.2	16.7	6.90

The view that the electron-donating property is a factor of primary importance in determining the reactivity of radicals in the induced decomposition under consideration suggests that interaction of the charge-transfer type[16] between an attacking radical as a donor and a molecule of a peroxide as an acceptor is important. This charge-transfer interaction is thought to take place, to the first approximation, between the highest occupied orbital on the radical and the vacant antibonding orbital, $2p\sigma_u$, around the oxygen to oxygen bond in the peroxide. Evidently such a low-lying vacant orbital is responsible for the oxidative action in general or for the electron accepting property of peroxides. Thus, the transition state of the induced decomposition may be schematically expressed by the following structures, form II representing the interaction of the charge-transfer type, which contributes to lowering of the energy of the transition state:

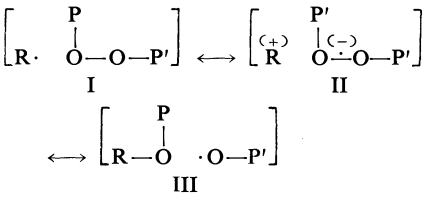

Since such a polar-resonating structure contributes to the structure of the reacting system in charge-transfer interaction, polar solvents like alcohols and ethers would further lower the energy of the system by solvation.

According to the accepted theory[16], the lowering in energy of the reacting system due to the charge-transfer interaction is approximately inversely proportional, other things being equal, to the difference in energy between the highest occupied orbital of the radical and the $2p\sigma_u$ orbital of the peroxide, or to the difference between the ionization potential of the radical and the electron affinity of the $2p\sigma_u$ orbital. Thus, the higher the energy level of the orbital occupied by the odd electron in a radical, the larger is the extent of the charge-transfer, with a corresponding lowering in energy, and, therefore, the more reactive

11) K. Nozaki and P. D. Bartlett, *J. Am. Chem. Soc.*, **68**, 1686 (1946); P. D. Bartlett and K. Nozaki, ibid., **69**, 2299 (1947).
12) W. E. Cass, ibid., **68**, 1976 (1946).
13) S. Kato and F. Mashio, *J. Chem. Soc. Japan, Ind. Chem. Sec.* (*Kogyo Kagaku Zassi*), **59**, 380 (1956); F. Mashio and S. Kato, *Science and Technology* (*Kyoto Tech. Univ.*), **5**, 51 (1958).
14) C. A. Coulson, *Discussions Faraday Soc.*, **2**, 9 (1947).
15) M. Szwarc, ibid., **10**, 336 (1951).
16) R. S. Mulliken, *J. Am. Chem. Soc.*, **74**, 811 (1952).

the radical becomes. This prediction is in agreement with the observed trend in the reactivity of radicals in the induced decomposition.

In the charge-transfer type of interaction, not only the energy difference between the participating orbitals, but also their overlapping, is important. Therefore, the introduction of a bulky group around the radical centre will hinder the overlap sterically, and the introduction of a conjugating group will do so by reducing the electron density at the radical centre of the orbital occupied by the odd electron. In fact, Mashio and Kato[13] have shown that the reactivity towards benzoyl peroxide of radicals derived from primary alcohols decreases as the alkyl chain lengthens. Further, they have shown that the reactivity of the radical derived from benzyl alcohol is twice as large as that from α-tetralol. This difference is probably due to steric hindrance of the overlapping of the relevant orbitals in the charge-transfer interaction, since the energy level of the highest occupied molecular orbital is almost the same for these two radicals. The fact that the reactivity of the radical derived from benzhydrol is lower than that from benzyl alcohol is probably due to the same steric effect as well as to the more extensive delocalization of the odd electron in the former radical.

The rate constant for the chain transfer to a substituted benzoyl peroxide by polymer radicals is known to increase according as the substituent group becomes more electron-attracting[17,18]. This fact is readily understood in light of the fact that an electron-attracting group lowers the energy level of the $2p\sigma_u$ orbital around the oxygen to oxygen bond, resulting in a stronger charge-transfer interaction between the attacking radical and the peroxide, with a corresponding reduction of the activation energy.

The chain transfer constant by the polymer radical generally appears to be larger for hydroperoxides than for benzoyl peroxide[18,19], and as has been previously pointed out[5], peroxybenzoic acid is attacked by radicals more readily than benzoyl peroxide, although benzoyl peroxide might be expected to be more reactive, since the benzoyl group is more electron-attracting than the alkyl group or the hydrogen atom. The disagreement probably is attributable to steric hindrance by the bulky benzoyl group of the overlapping of the two interacting orbitals participating in the charge transfer.

In the induced decomposition of benzoyl peroxide, Swain, Stockmayer, and Clarke[17] have pointed out a contribution of polar resonance structures in which the odd electron is found transferred on the molecule of the peroxide because of the presence of the electron-withdrawing carbonyl group. It is apparent from the foregoing discussion, however, that it is the vacant orbital around the oxygen to oxygen bond that is important in a charge-transfer type interaction in the induced decomposition, and that the role of the carbonyl group, if present in the molecule, is subordinate.

Obviously the charge-transfer concept may readily be applied to the elucidation of the reactions of peroxides with anionoid reagents in general, the nucleophilic attack by the latter being ascribed to the presence in the former of a vacant orbital which is able to accept an electron readily. To cite a few examples, in the reaction of benzoyl peroxides with *N,N*-dimethylanilines, an electron-attracting substituent in the former[20] and an electron-repelling substituent in the latter[21] both accelerate the reaction. This fact can be explained as due to the lowering of the energy level of the antibonding orbital of the oxygen to oxygen bond and to the elevation of that of the lone-pair orbital on the nitrogen atom, the charge-transfer interaction being thus made much easier. It is to be noted in this connection that Imoto and Choe[20] have suggested the coordination of the lone-pair electrons on the nitrogen atom with the peroxidic oxygen. Similarly, reactions of substituted benzoyl peroxides with alkali iodides[22] or with phosphines[23], and reactions of peroxybenzoic acid with olefins[24], sulphides[25] and sulphoxides[26] and the oxidation of sulphides with hydrogen peroxide[27] are to be understood in terms of the charge-transfer interaction.

In the reaction of peroxides with cationoid reagents, e. g., ions of transition metals in the higher oxidation state and Lewis acids, another type of charge-transfer interaction is possible, an interaction in which a lone-pair orbital at

17) C. G. Swain, W. H. Stockmayer and J. T. Clarke, *J. Am. Chem. Soc.*, 72, 5426 (1950).
18) W. Cooper, *J. Chem. Soc.*, 1952, 2408.
19) B. Baysal and A. V. Tobolsky, *J. Polymer Sci.*, 8, 529 (1952).
20) M. Imoto and S. Choe, ibid., 15, 485 (1955).
21) L. Horner and K. Sherf, *Ann.*, 573, 35 (1951).
22) O. Simamura, G. Tsuchihashi and S. Miyajima, presented before the Conference on Organic Reaction Mechanisms, Osaka, October, 1955; O. Simamura, M. Yoshida and R. Okazaki, presented at the 14th Annual Meeting of the Chemical Society of Japan, Tokyo, April, 1961.
23) L. Horner and W. Jurgeleit, *Ann.*, 591, 138 (1955); M. A. Greenbaum, D. B. Denney and A. K. Hoffmann, *J. Am. Chem. Soc.*, 98, 2363 (1956); D. B. Denney and M. A. Greenbaum, ibid., 79, 979 (1957).
24) Y. Nagai, *Yuki Gosei Kagaku Kyokaishi*, 19, 537 (1961).
25) C. G. Overberger and R. W. Cummins, *J. Am. Chem. Soc.*, 75, 4250 (1953); A. Cerniani and G. Modena, *Gazz. chim. ital.*, 89, 843 (1959).
26) O. Simamura, M. Fukuyama and T. Tanigaki, presented at the 12th Annual Meeting of the Chemical Society of Japan, Kyoto, April, 1959.
27) G. Modena and L. Maioli, *Gazz. chim. ital.*, 87, 1306 (1957); G. Modena, ibid., 89, 834 (1959).

a peroxidic oxygen atom will act as an orbital of the donor type.

The polar effect in radical reactions may generally be interpreted as arising from the change in the magnitude of the charge-transfer interaction between radicals and substrates due to the change in energy level of the interacting orbitals.

Summary

On the basis of observations on the induced decomposition of peroxides by radicals, it has been suggested that the interaction of the charge-transfer type, involving the highest occupied molecular orbital in an attacking radical and the $2p\sigma_u$ antibonding orbital around the oxygen to oxygen bond in a molecule of peroxide, contributes to a lowering of the activation energy of reaction. Possible extension of this idea to elucidation of the reactions of peroxides with other reagents has been pointed out.

Department of Chemistry
Facutly of Science
The University of Tokyo
Hongo, Tokyo

*The Synthesis and the Physical Properties of Normal Higher Primary Alcohols. V. Thermal and X-Ray Studies of the Polymorphism of Alcohols of Odd Carbon Numbers from Undecanol to Heptatriacontanol**

BY Akira WATANABE

(Received November 24, 1962)

The transition phenomena in the solid state of normal higher alcohols of the even series from dodecanol ($C_{12}H_{25}OH$) to tetratriacontanol ($C_{34}H_{69}OH$) have already been studied by thermal and X-ray examinatons; the results were reported in a preceding paper[1]. Since it has been known that, in some of the long chain compounds, transition points as well as melting points differ systematically between the odd and even series, it seems important to extend the study to the odd series of the alcohols in order to gain further knowledge on the transition behavior of the compounds. The present paper deals with the thermal analyses and X-ray pattern meaurements of odd alcohols, including the 14 members from undecanol ($C_{11}H_{23}OH$) to heptatriacontanol ($C_{37}H_{75}OH$). It also includes a discussion of the present results of those of the previous studies of the even series, with reference to their relation to the structure analysis data of the selected compounds.

The syntheses of the alcohols investigated here have previously been described in this Bulletin[2-4]. The experimental porcedures used in this study were essentially the same as those used in the previous study of even alcohols. The definition of the terms was given in a previous paper[1] and will be followed in the present paper as well. The crystal modifications will be interpreted briefly. Four modifications, which are called the β, γ_1, γ_2, and α forms, have been known in solid alcohols, the former three modifications being low temperature forms and the latter a high temperature form. When the material is cooled from the melting point, the α form appears at the freezing point, but this form suddenly changes to a low temperature form on further cooling, to either the β, γ_1 or γ_2 form depending upon the carbon number of the compound. This phase change has also been known to occur in some cases on heating the materials. The α form is of interest because of its unique properties. This form is somewhat more transparent than the low temperature forms. It is believed, judging from the X-ray data, that the crystal is nearly hexagonal, that the hydrocarbon chain is

* This study has been carried out at the Department of Physics, Faculty of Science, Kyoto University, as a part of a co-operative research project on "The Synthesis and the Physical Properties of Long Chain Compounds".

1) A. Watanabe, This Bulletin, **34**, 1729 (1961).

2) A. Watanabe, ibid., **32**, 1295 (1959).

3) A. Watanabe, ibid., **33**, 531 (1960).

4) A. Watanabe, ibid., **34**, 398 (1961).

perpendicular to the plane of the end group, and that the molecules are less tightly packed than in the low temperature forms. A high dielectric constant value has been found in the α form, the molecule being assumed to rotate around the long axis. In the β form, the chain is perpendicular to the plane, while in the γ_1 and γ_2 forms the chain inclines at an angle to the plane. In these low temperature forms, no rotational freedom of the molecule has been found.

Since the present author, as well as previous workers, has found that small amounts of impurities influence the transition phenomena of long chain compounds, not only final products but starting materials were purified with great care in this study. The alcohols used in the present measurements were recrystallized several times or were subjected to high vacuum distillation, followed by recrystallizations, until constant melting points and transition points were obtained. The stored materials were recrystallized again before the measurements were undertaken.

Results and Discussion

In Fig. 1 the time is plotted against increasing and decreasing temperature for heptadecanol ($C_{17}H_{35}OH$). The forms of the curves are general for all members of the series. As may be seen in the figure, there is a super cooling at the transition point which could not be avoided even though the sample was cooled very slowly. This made it difficult to determine accurately, the transition temperature on cooling. For undecanol, and Reid[7] found no arrest of the time-temperature curve on cooling. This was confirmed by the present thermal studies, in which it was also indicated that this compound does not show the transition on heating. The transition in tridecanol ($C_{13}H_{27}OH$) is not reversible. The heating curve shows that no phase change occurs until the temperature reaches the melting point, while the cooling curve clearly indicates the existence of the transition. The high temperature form, which was confirmed to be the α form by X-ray[5] and dipolemment[6] measurements, showed such a stability that no tendency to change to a more opaque, low-temperature form was observed in visual examination over a 10 hr. period. In the alcohols from pentadecanol ($C_{15}H_{31}OH$) to hentriacontanol ($C_{31}H_{63}OH$), the transition is reversible, appearing both on cooling and heating. The transitions

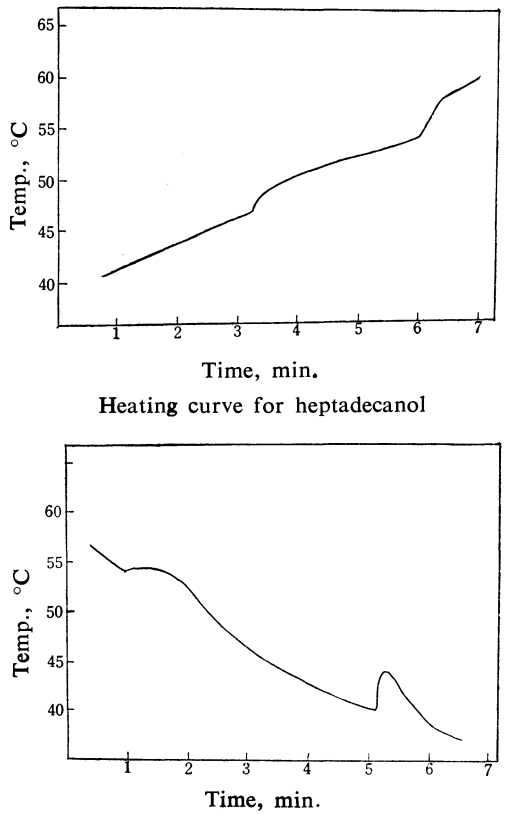

Fig. 1. Cooling curve for heptadecanol.

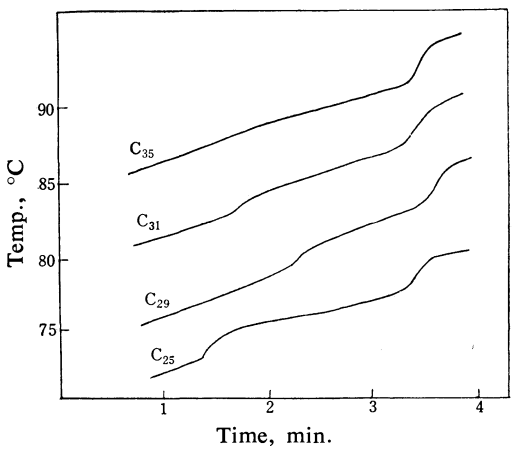

Fig. 2. Heating curves for C_{25}, C_{29}, C_{31} and C_{35} alcohols.

in tritriacontanol ($C_{33}H_{67}OH$) and higher compounds were observed only on cooling. Identification of the phases was made by X-ray pattern measurements, according to which, in the alcohols up to C_{27}, the transition is $\beta \rightleftarrows \alpha$, while in the alcohols above C_{29}, it is $\gamma_2 \rightleftarrows \alpha$. Typical photographs are reproduced in Fig, 3. The data on the transition phenomena for the C_{15}, C_{17} and C_{19} alcohols

5) K. Tanaka, T. Seto and T. Hayashida, *Bull. Inst. Chem. Res., Kyoto. Univ.*, 35, 123 (1957).
6) K. Asai, unpublished.
7) J. D. Meyer and R. E. Reid, *J. Am. Chem. Soc.*, 55, 1574 (1933).

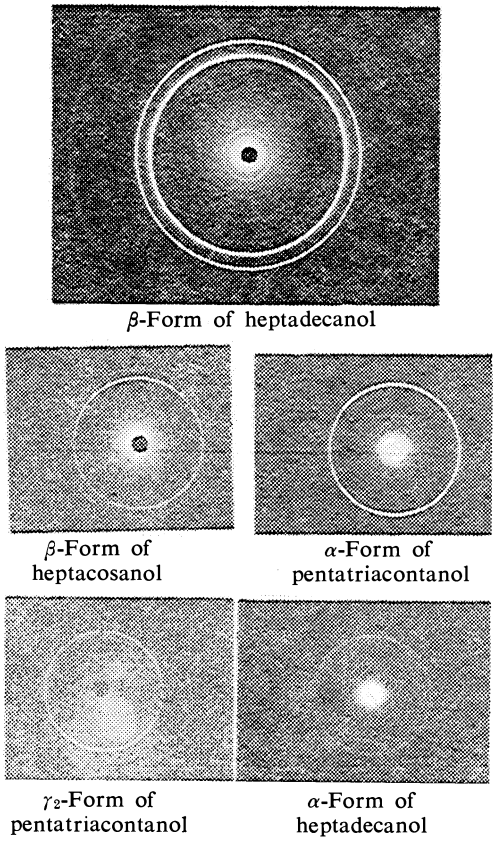

Fig. 3.

were found to agree with those of thermal analyses by Phillips and Mumford[8], while those for other compounds have not yet been reported, except for the X-ray data[9] reported previously from this laboratory. However, some discrepancies were found between the results of the present thermal analyses and those of the X-ray pattern measurements[9]. The X-ray data revealed that the C_{33}, C_{35} and C_{37} alcohols exhibit the transition on heating as well as on cooling. To examine this phenomenon further, pentatriacontanol ($C_{35}H_{71}OH$) was resynthesized and purified, and then the transition was studied with the greatest possible care. The results, however, were identical with those in the previous measurements. It is, therefore, assumed that the appearance of the heating transition can not be ascribed to the presence of impurities. A possible interpretation for the phenomenon is that the γ_2 to α transition is so gradual that it escapes observation in the thermal analyses. This theory is supported by the fact that the inflexion of the heating curve in C_{29} and C_{31} is less sensitive than those in the shorter members, a decrease in the energy barrier at the transition being indicated in the higher members (Fig. 2).

8) J. W. C. Phillips and S. Mumford, *J. Chem. Soc.*, **1931**, 1732.
9) K. Tanaka, T. Seto, A. Watanabe and T. Hayashida, *Bull. Inst. Chem. Res., Kyoto. Univ.*, **37**, 281 (1959).

TABLE I. MELTING POINTS AND TRANSITION POINTS OF *n*-HIGHER ALCOHOLS

C, No.	M. p., °C	Tr. p., °C on heating	Tr. p., °C on cooling
11	14.0	—	—
12	24.0	—	—
13	30.0	—	25.0
14	38.0	36.2	33.5
15	45.5	41.5	36.0
16	49.5	45.7	43.0
17	54.5	47.5	42.0
18	58.5	54.5	52.5
19	62.0	58.0	53.0
20	65.0	63.5	58.2
21	68.5	60.5	54.5
22	70.5	67.6	63.5
23	73.2	66.5	60.5
24	75.5	72.8	71.5
25	77.5	73.0	67.5
26	79.3	78.1	73.5
27	80.5	76.5	72.0
28	82.5	—	77.5
29	83.3	81.0	74.0
31	86.5	82.0	77.0
32	88.5	—	86.2
33	88.5	85.0	81.2
34	91.0	—	—
35	91.0	85.0	82.5
37	91.2	87.5	86.0

The values of C_{30} and C_{36} are omitted because of doubtfulness.

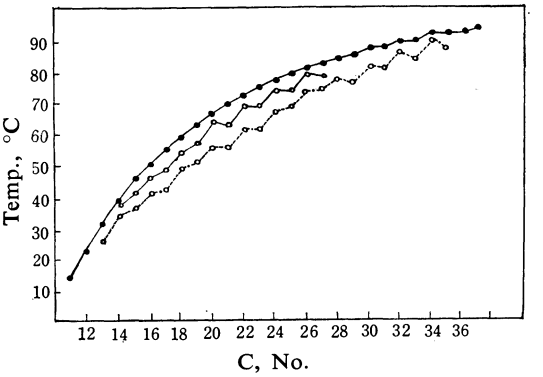

Fig. 4. Melting and transition points of *n*-higher alcohols.
—●— Melting points
—○— Transition point on heating
- -○- - Transition point on cooling

The melting and transition points of the alcohols, including all the odd and even members investigated, are given in Table I and, graphically, in Fig. 4. As may be seen in Fig. 4, the transition points show a definite

alternation in the compounds from C_{13} to C_{37}, the transition points of even members lying on an upper curve. On the contrary, the melting points lie on a smooth curve in the series from C_{11} to C_{29}, but, beginning with C_{29}, the higher series exhibit an alternation relationship.

This melting and transition behavior, with the number of carbon atoms, may be interpreted from the structural point of view. Müller[10] and Malkin[11] interpreted the melting behaviors of normal paraffins with relation to the tilted structure of hydrocarbon chains and to the planes of the end groups. In general, the inclination of the chains to the planes is indicated by the long spacing values, the shorter spacings meaning the more tilted structures, as has already been reported by Malkin[12] for the relatively shorter members of higher alcohols. The series were recently extended in this laboratory with more detailed investigations[9]. The data are represented here in Table II and Fig. 5, from wihch it may be seen that vertical (β) and tilted (γ_1) structures appear alternatively in the series up to C_{29}, the vertical form appearing in odd members and the tilted form in even members. Accordingly, considering the fact that the transition points of even members lie on an upper curve, the tilted structure seems to be more stable than the vertical structure in low temperature forms. This is analogous to the previous observation[1] that, in hexadecanol ($C_{16}H_{33}OH$), the transition point of the γ_1 form was slightly higher than that of the β form. In contrast to the low temperature forms, no difference in structure between the odd and even members seemed to exist in the high temperature forms (Fig. 3). Therefore, it is plausible that the alternation does not appear in the melting points.

Table II. Long spacing of *n*-higher alcohols

C, No.	α-Form	β-Form	γ_1-Form	γ_2-Form
11	28.8 A	32.2 A	— A	— A
12	34.1	34.9	—	—
13	36.1	37.3	—	—
14	38.9	39.63	33.05	—
15	41.3	42.36	—	—
16	43.83	44.90	37.27	—
17	46.34	47.46	—	—
18	48.93	—	41.60	—
19	51.11	52.82	—	—
20	53.13	—	45.67	—
21	55.35	57.95	—	—
22	57.74	—	49.89	—
23	59.82	63.12	—	—
24	61.89	—	54.24	—
25	64.03	68.14	—	—
26	66.08	—	58.02	—
27	68.31	73.29	—	—
28	70.65	—	62.60	—
29	73.5	78.4	—	65.5
31	77.2	—	—	69.7
32	79.4	—	71.0	—
33	81.2	—	—	74.2
34	82.8	—	75.1	—
35	86.6	—	—	78.6
37	90.9	—	—	83.0

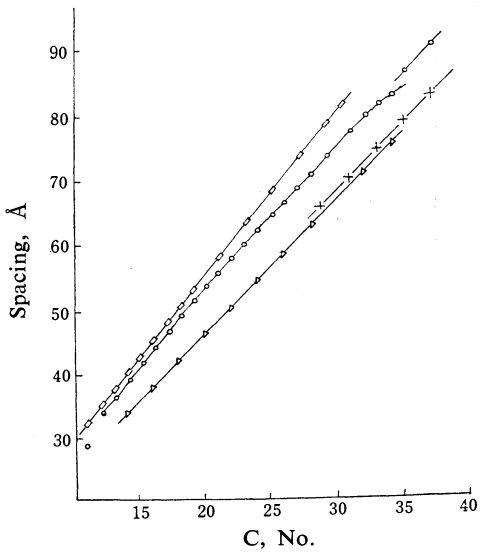

Fig. 5. Long spacing of *n*-higher alcohls.
—○— α-form —△— γ_1-form
—□— β-form —×— γ_2-form

Beyond the interpretation made from the long spacing data, a more elaborate interpretation of the phenomena is possible based on the configurations which were determined by the X-ray structure analysis of heptadecanol by Dr. Seto and of eicosanol synthesized by the present author. (For the use of the data the author is indebted to him.) The structures of two compounds are illustrated in Fig. 6. The alcohols form a monoclinic structure made up of a double layer of molecules. The unit cell contains eight molecules in two layers, in which the chains are parallel to one another. The structure of the β form appears to be somewhat unique. The layer of the hydroxyl groups contains methylene groups adjacent to oxygen atoms as may be seen in the figure, the atoms being packed more compactly than in the γ_1 form. The value of the O–O distance in the β form is slightly shorter than that in the γ_1 form. On the contrary, the distance between adjacent hydrocabon

10) A. Müller, *Proc. Roy. Soc.*, **124**, 317 (1929).
11) T. Malkin, *Nature*, **127**, 126 (1931).
12) T. Malkin, *J. Am. Chem. Soc.*, **47**, 1930 (1930).

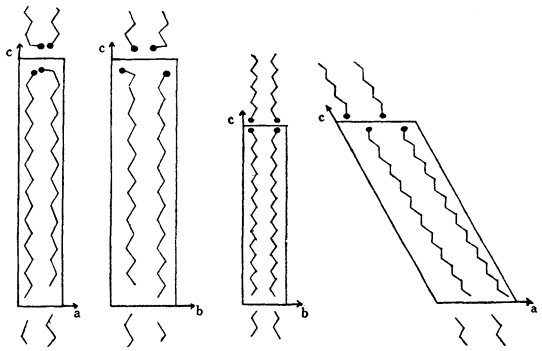

$C_{17}H_{35}OH$ (β-Form) $C_{20}H_{41}OH$ (γ_1-Form)

Fig. 6. Crystal structure of *n*-higher alcohols. Black circles represent O atoms.

chains is greater in the β form than in the γ_1 form. These structures suggest that in the β form the layer of the ends takes the more stable arrangement, while the hydrocarbon chains are arranged more stably in the γ_1-form. Accodingly, it seems reasonable that in those shorter members in which the end groups predominate over the hydrocarbon chains (C_{12} and C_{14}), the β structure proves to be favorable, while in longer members, in which the chains predominate over the end groups, the γ_1 structure tends to be favorable. Presumably, a similar interpretation may be given of the existence of the tilted form (γ_2) in the higher members of the odd alcohols, although the structure of this form has not yet been determined.

The properties of the α form in odd alcohols were found to change gradually with an increase in the chain length, as was observed in even alcohols. For example:

1. The inflexions at the transition points in the time-temperature curves become smaller. (Fig. 2)
2. The opacity of the α phase increases.
3. The spacings of α form split into two lines. (Fig. 3)
4. Long-spacing variations with chain length indicate that the hydrocarbon chains increase their inclination to the planes of the ends. (Fig. 5)

These facts would suggest that, as the chain length increases, the structure of the α form increases its deviation from the hexagonal structure found in shorter members and gradually changes to structures similar to those of the low temperature form.

The alteration in the melting point appearing in the series from nonacosanol ($C_{29}H_{59}OH$) to heptatriacontnol ($C_{35}H_{71}OH$) may be ascribed to the difference in the phases existing just below the melting point.

Summary

On the phase transition of *n*-higher alcohols with odd carbon atoms from undecanol (C_{11}) to heptatriacontanol (C_{37}), thermal analyses and X-ray pattern measurements were made, with the following results:

1. Tridecanol (C_{13}) shows an irreversible transition which appers only on cooling. A reversible transition sets in at pentadecanol (C_{15}) and continues to the end member of the series (C_{37}).
2. X-Ray pattern measurements indicated that, in the alcohols up to nonacosanol (C_{29}), the transtition is β to α, while in the alcohols above C_{29} the transition is γ_2 to α.
3. Presumably, the γ_2 to α transition is gradual.
4. The properties of the α forms change gradually with an increase in the chain length.
5. The results of the present study and those of previous studies with the even series have been discussed from the configurations of the β and γ_1 forms, as determined by X-ray structure analyses.

The author wishes to express his deep thanks to Professor Ryozo Goto and Professor Kenzo Tanaka of Kyoto University for their continual guidance and encouragement. He is also grateful to Dr. Tsuneo Seto of Kyoto University for his kind direction and criticism in the X-ray diffraction measurements. The cost of this work was partly defrayed from a grant (Shigenkagaku Kenkyuhi) from the Ministry of Education.

Faculty of Science and Engineering
Ritumeikan University
Kita-ku, Kyoto

Viscometric Studies of Solutions of Sodium Phosphates, Graham Salts and Vanadium-containing Graham Salts

By Masayuki NAKAGAKI, Shigeru OHASHI* and Fumiko MINATO

(Received November 26, 1962)

Graham salt (amorphous sodium polyphosphate) has often been interested in by many investigators recently[1,2], and it has been made clear that the substance has typical features as a linear-chain polyelectrolyte in a solution. However, the polymer molecules are sometimes decomposed in the solution, especially when the polymer is branched. The points of branching are belived to capable of being hydrolyzed readily.

In the present paper, the degradation of polyphosphate is studied by viscometry. For the sake of the study, it was necessary to know the relation between the intrinsic viscosity and the molecular weight, especially for low molecular weight polyphosphates. Furthermore, vanadium-containing Graham salt (sodium vanadate-phosphate copolymer) was studied, because the –V–O–P– chain was expected to be hydrolyzed much easier than the –P–O–P– chain. Ohashi and Matsumura[3] previously obtained some information on the structures of the glasses and crystals of sodium vanadate-phosphates from paper chromatographic analysis of their solutions.

Experimental

Sodium Phosphates.—Commercial specimens of a guaranteed reagent grade of sodium dihydrogen orthophosphate ($NaH_2PO_4 \cdot 2H_2O$), disodium hydrogen orthophosphate ($Na_2HPO_4 \cdot 12H_2O$), sodium orthophosphate ($Na_3PO_4 \cdot 12H_2O$) and sodium pyrophosphate ($Na_4P_2O_7 \cdot 10H_2O$) were used without further purification. Sodium tripolyphosphate ($Na_5P_3O_{10} \cdot 6H_2O$) of an extra pure reagent grade was recrystallized four times from an alcohol-water mixture. In order to check the purity and the amount of crystallization water, the content of each phosphate was measured by potentiometric titration, using 0.1 N sodium hydroxide for sodium dihydrogen orthophosphate and using 0.1 N hydrochloric acid for the other four phosphates. All results agreed well with the theoretical values within the range of experimental error.

Graham Salts. — Amorphous sodium polyphosphates (Graham salts) of various degrees of polymerization were prepared[4] by heating under the conditions described in Table I; they were then quenched by being pressed between two sheets of copper plate. The degrees of polymerization, $\bar{n}$, as determined by pH-titration[5], are also cited in Table I.

TABLE I. PREPARATION OF GRAHAM SALTS

Sample	Starting material, g.	Heating	$\bar{n}$
A	$NaPO_3$ 29.6, $Na_4P_2O_7$ 25.8	900°C, 1 hr.	4.4
B	$NaPO_3$ 40.3, $Na_4P_2O_7$ 13.5	900°C, 1 hr.	8.6
C	$NaPO_3$ only	900°C, 1 hr.	92
D	$NaPO_3$ only	alternately at 500 and 700°C, 1 week	100
E	$NaPO_3$ 48.1, $Na_4P_2O_7$ 2.6	900°C, 1 hr.	29

Vanadium-containing Graham Salts.—Calculated amounts of Graham salt ($NaPO_3$), vanadium pentoxide (V_2O_5) and sodium carbonate (Na_2CO_3) were mixed and heated at 900°C for 1 hr. and were then quenched by being pressed with copper plates. It was recognized that a part of the vanadium was reduced to V^{4+} during the heating. The amount of V^{4+} was determined by the volumetric method[3]. The per cent of V^{4+} in the total vanadium is given in Table II.

TABLE II. SODIUM VANADATE-PHOSPHATE COPOLYMERS

Sample	Mole ratio P/V	V^{4+}, %	$\bar{n}'$	$\bar{n}$
F	100	40.0	167.7	83.35
G	50	39.4	85.6	42.30
H	10	33.7	21.1	7.62
I	7	30.0	17.1	5.96
J	4	22.9	13.9	3.66
K	1	4.6	28.3	0.98

If it is assumed that all the V^{4+} exists in the solution as gegen ions in the form of VO^{2+}, the average number of residues (both phosphate and

* S. Ohashi: Department of Chemistry, Faculty of Science, Kyushu University, Fukuoka.

1) J. R. Van Wazer, "Phosphorus and its Compounds", Vol. I, Interscience Publishers, New York (1958).

2) C. F. Callis, J. R. Van Wazer and P. G. Arvan, *Chem. Revs.*, **54**, 777 (1954).

3) S. Ohashi and T. Matsumura, This Bulletin, **35**, 501 (1962).

4) Prepared by one of the authors (S. O.) at the Department of Chemistry, Faculty of Science, Kanazawa University, Kanazawa.

5) J. R. Van Wazer, E. J. Griffith and J. F. McCullough, *Anal. Chem.*, **26**, 1755 (1954); E. J. Griffith, ibid., **28**, 525 (1956).

vanadate residues) in one molecule, $\bar{n}'$, may be calculated by the equation:

$$\frac{\bar{n}'+2}{\bar{n}'}=\frac{\mathrm{Na}+2\mathrm{V}^{4+}}{\mathrm{P}+\mathrm{V}^{5+}} \quad (1)$$

where Na, P, V^{4+}, and V^{5+} indicate the atomic ratio of these atoms. The value of $\bar{n}'$ is given in Table II. As will be described in a later section, the value of $\bar{n}'$ is too large to explain the intrinsic viscosity. Therefore, it was further assumed that the molecular chain in the solution was cut off at both sides of V^{5+}, probably due to hydrolysis, remaining as the polymer chains containing PO_3^- only and that no V^{5+} atom had been at the end of the original chain. The degree of polymerization, $\bar{n}$, of the remaining phosphate chains could then be calculated by dividing the $\bar{n}'$ value into the number of P atoms (P) and V atoms (V), and by using the following equation:

$$\bar{n}=\frac{(\mathrm{P})}{(\mathrm{V})+1} \quad (2)$$

The value of $\bar{n}$ is also given in Table II.

Preparation of Solutions.—Samples of a known weight were dissolved in an aqueous 0.035 N or 0.07 N solution of sodium bromide at room temperature and were made up to the required volume. Orthophosphates, pyrophosphate, and tripolyphosphate dissolved immediately in the solvent (a sodium bromide solution). The concentration, c (g./100 ml.), of the solution was expressed as that of anhydride. The Graham salt used was in the form of small transparent pieces about 1~2 mm. thick which took time to dissolve when the molecular weight was high. It was, however, dissolved within 30~40 min. under agitation by a magnetic stirrer. Since Graham salt containing vanadium took a long time to dissolve, it was pulverized by using a mortar of agate and dried over P_2O_5 under reduced pressure. This pulverized sample still took about 0.5~1 hr. to dissolve, however.

Viscometry.—The viscosity of the solutions were measured by Ostwald's viscometer in a thermostat at 25.5°C. The correction term for kinetic energy was determined by using water and ethanol, but the value was so small that it was disregarded in further calculations.

The viscosities of solutions of samples C and D changed for 5~6 hr. after the beginning of dissolution. Thereafter, the viscosities were constant and did not change for more than 24 hr. No change of viscosity with time was observed for the other samples.

Density.—The density of the solutions was measured at 25.5°C by using Ostwald's pycnometer, whose content was about 5~6 ml. The density of solutions was linear to the polymer concentration, so that the density increment, Δ, was calculated by the equation:

$$\Delta=100\left(\frac{d}{d_1}-1\right)\Big/c \quad (3)$$

where d and d_1 are the densities of solution and solvent respectively, and where c is the concentration in g./100 ml.

Results and Discussion

The Intrinsic Viscosities and Molecular Weight of Sodium Phosphates and Graham Salts.—The intrinsic viscosities $[\eta]$ of low molecular weight sodium phosphates and of Graham salts which do not contain vanadium were calculated by extrapolating both η_{sp}/c and $\ln\eta_r/c$ to infinite dilution on the basis of viscosity values measured at the polymer concentrations of 0.1, 0.2, 0.4, 0.8, 1.2 1.6 and 2.0 (g./100 ml). For these calculations, the viscosity values divided by the viscosity of solvent was used as the relative viscosity. Since the Graham salt is a kind of polyelectrolyte, its reduced viscosity (η_{sp}/c) should increase steeply when the polymer concentration is decreased if the concentration of the swamping electrolyte is not sufficiently high. This effect was observed in the case of 0.035 N sodium bromide, so that the intrinsic viscosity was obtained by neglecting the data at low polymer concentrations. In the case of 0.07 N sodium bromide, the effect was not observed and the extrapolation was easy, although in some instances abnormal values were obtained at very low concentrations. The results obtained in a 0.035 N sodium bromide

TABLE III. INTRINSIC VISCOSITY AND DENSITY INCREMENT OF SODIUM PHOSPHATE SOLUTIONS IN 0.035 N NaBr AT 25.5°C

Sample	$\bar{n}$	$[\eta]$	Δ
NaH_2PO_4	1	0.037	0.706
Na_2HPO_4	1	0.044	0.914
Na_3PO_4	1	0.049	1.048
$Na_4P_2O_7$	2	0.035	0.842
$Na_5P_3O_{10}$	3	0.038	0.851
A	4.4	0.043	0.818
B	8.6	0.045	0.819
E	29	0.090	0.788
C	92	0.188	0.812
D	100	0.191	0.782

TABLE IV. INTRINSIC VISCOSITY AND DENSITY INCREMENT OF SODIUM PHOSPHATE SOLUTIONS IN 0.07 N NaBr AT 25.5°C

Sample	$\bar{n}$	$[\eta]$	Δ
NaH_2PO_4	1	0.0313	0.609
Na_2HPO_4	1	0.0500	0.758
Na_3PO_4	1	0.0561	0.936
$Na_4P_2O_7$	2	0.0486	0.767
$Na_5P_3O_{10}$	3	0.0544	0.725
A	4.4	0.040	0.818
B	8.6	0.045	0.784
E	29	0.070	0.722
C	92	0.139	0.701
D	100	0.149	0.713

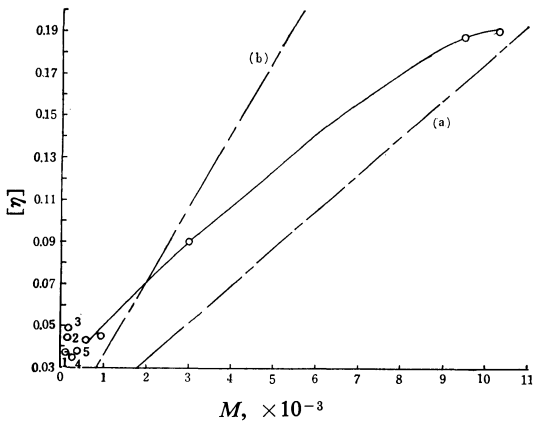

Fig. 1. Relation between $[\eta]$ and M in the solution of 0.035 N NaBr.
1 NaH_2PO_4 2 Na_2HPO_4
3 Na_3PO_4 4 $Na_4P_2O_7$
5 $Na_5P_3O_{10}$

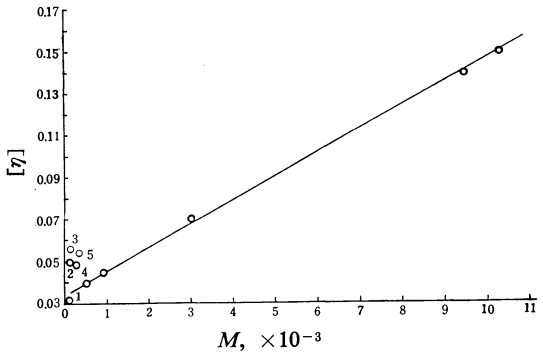

Fig. 2. Relation between $[\eta]$ and M in the solution of 0.07 N NaBr.
1 NaH_2PO_4 2 Na_2HPO_4
3 Na_3PO_4 4 $Na_4P_2O_7$
5 $Na_5P_3O_{10}$

solution and in a 0.07 N sodium bromide solution are given in Table III and Table IV respectively. The value of $[\eta]$ is that for 20~24 hr. after the dissolution, if any time dependency of the viscosity (in the case of sample C and D) was observed. The $[\eta]$ values thus obtained are shown in Fig. 1 and Fig. 2 against the average molecular weight, M, the molecular weight of Graham salts was calculated by:

$$M=(Na_2O)+(NaPO_3)\times\bar{n} \quad (4)$$

Here (Na_2O) and $(NaPO_3)$ indicate their formula weights.

The intrinsic viscosity of Graham salt in a 0.035 N sodium bromide solution had already been measured by Strauss et al.[6], who summarized their results in an empirical equation:

$$[\eta]=1.76\times10^{-5}\times M_w \quad (5)$$

In this equation, the weight average molecular weight, M_w, was used. It has been stated by Van Wazer[7] that the molecular weight of Graham salt shows a Poisson distribution and that the weight average molecular weight is just twice the number average molecular weight, M_n. Therefore, Eq. 5 may be rewritten as:

$$[\eta]=3.52\times10^{-5}\times M_n \quad (6)$$

In Fig. 1, Eqs. 5 and 6 are shown by the straight lines a and b respectively. For the experimental data of Fig. 1, the molecular weight, M, was calculated by Eq. 4, on the basis of $\bar{n}$ values obtained by the determination of the end groups. The experimental molecular weight is, therefore, the number average molecular weight. The experimental data in Fig. 1 are located between the straight lines a and b. This would mean either that the distribution of the molecular weight is not exactly the Poisson distribution, or that the Eq. 5 derived originally for $M_w=7000\sim19000$ has been extrapolated unreasonably to too low a molecular weight.

When 0.035 N sodium bromide is used as the solvent, the experimental values (Fig. 1) showed a linear relationship if $\log[\eta]$ was drawn against $\log M$ at the range of $M=930\sim10300$; the following equation was obtained.

$$[\eta]=6.9\times10^{-4}\times M^{0.61} \quad (7)$$

When 0.07 N sodium bromide was used as the solvent, the experimental data of $[\eta]$ were linear against M, as is shown in Fig. 2. The relation can be expressed for $M=510\sim10300$,

$$[\eta]=0.0348+0.112\times10^{-4}\times M \quad (8)$$

The intrinsic viscosity of sodium phosphates of low molecular weight shows a complicated dependency upon the molecular weight, dependent both on the shape of the molecule and on the degree of hydration. The latter is the greater, the greater the value of the density increment, Δ, because the following equation can be derived readily.

$$\Delta=\Delta V+1/d_1-1/d_2 \quad (9)$$

Here, ΔV (ml./g.) is the volume contraction per 1 g. of solute, and d_1 and d_2 are the densities of the solvent and solute respectively. The value of d_1 is about 1.00 and that of d_2 is pressumed to be about 2.0~2.5, so that the value of the density increment should be equal to 0.5~0.6, if there is no volume contraction, while it should be greater than that value if there is any volume contraction. It

6) U. P. Strauss, E. H. Smith and P. L. Wineman, *J. Am. Chem. Soc.*, **75**, 3935 (1953).

7) J. R. Van Wazer, ibid., **72**, 644, 647 (1950).

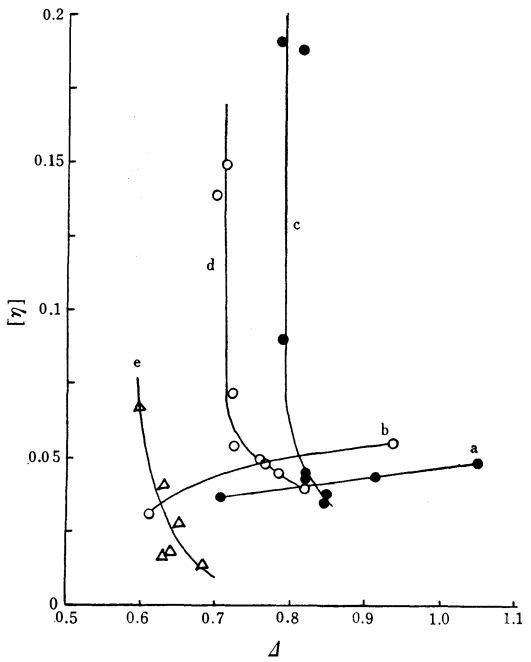

Fig. 3. Relation between $[\eta]$ and Δ of sodium polyphosphate not containing vanadium in 0.035 N NaBr (●) and in 0.07 N NaBr (○), and containing vanadium in 0.07 N NaBr (△).

has been widely accepted that the hydration of ions results in volume contraction.

The relation between the density increment and the intrinsic viscosity is shown in Fig. 3. For the mono-, di- and tri-sodium orthophosphates, the density increment increases in the sequence and the intrinsic viscosity increses according to the increase in the degree of hydration, as is shown by curves a and b. However, the concentration of the swamping electrolyte is the higher, the smaller the degree of hydration, probably because of the dehydrating action of the swamping electrolyte. The value of the intrinstic viscosity, however, does not decrease in accord with the decrease in the density increment, so that the experimental data falls in the different curves a and b in Fig. 3. (Also, compare c and d.)

In the case of the polyphosphates, including pyro- and tripoly-phosphates, the relation between the density increment and the intrinsic viscosity is entirely different from the case with orthophosphates, the data fall on curves c and d. In this case, the shape of the molecule or the value of $\bar{n}$ seems to be more important than the degree of hydration, as has already been described.

The Intrinsic Viscosity of Vanadium Containing Graham Salts.—The intrinsic viscosity of vanadium-containing Graham salts (sodium vanadate-phosphate copolymers) as a function of the average degree of polymerization is shown in Table V and in Fig. 4. No change in viscosity with time was observed, presumably because the rate of hydrolysis at the -V-O-P- junctions was very large and because the vanadium containing specimens took a relatively long time to dissolve. As has already been described, the degree of polymerization, $\bar{n}$, of the copolymer is calculated under the assumptions that the polymer chain has been cut off at both sides of the vanadate residue and that the vanadate residue thus cut off does not contribute to the viscosity. Nevertheless, the intrinsic viscosity of vanadium-containing polyphosphates is smaller than that of polyphosphate of the same degree of polymerization, as is shown in Fig. 4.

The fact that vanadate has a smaller intrinsic viscosity than phosphate is demonstrated further by comparing those of ortho salts. Sodium orthovanadate, Na_3VO_4, cannot be obtained by the usual method, but it can be

TABLE V. INTRINSIC VISCOSITY AND DENSITY INCREMENT OF VANADIUM-CONTAINING GRAHAM SALTS IN 0.07 N NaBr SOLUTION AT 25.5°C

Sample	$\bar{n}$	$[\eta]$	Δ
F	83.35	0.0671	0.597
G	42.30	0.0407	0.631
H	7.62	0.0225	0.630
I	5.96	0.0232	0.641
J	3.66	0.0275	0.653
K	0.98	0.0135	0.683

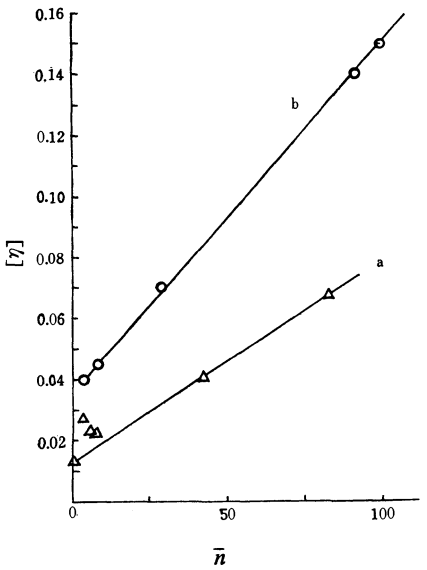

Fig. 4. Relation between $[\eta]$ and $\bar{n}$ of vanadium containing (△) and not containing (○) Graham salt in 0.07 N NaBr.

obtained in solution by dissolving sodium metavanadate ($NaVO_3$) in a strongly alkaline solution. An aqueous solution containing 1 N sodium hydroxide and 0.07 N sodium bromide was used as the solvent to measure the intrinsic viscosity. The result was $[\eta]=0.0118$, which was far smaller than the value of sodium orthophosphate (Na_3PO_4) in the same solvent: $[\eta]=0.0530$.

As for the small intrinsic viscosity of the vanadium-containing Graham salts, there may be several reasons. First, comparing curves d and e of Fig. 3, the hydration of vanadium-containing specimens should be smaller than that of vanadium-free specimens. Secondly, the average degree of the polymerization of vanadium-containing specimens might be smaller than the above-estimated values because of some unknown reasons. According to Fig. 4, curves a and b come together if the real $\bar{n}$ value is one-third of the expected value. Actually, paper chromatographic analysis[3] of solutions of sodium vanadate-phosphate glasses with P/V ratios of 4, 7 and 10 indicated the presence of a relatively large amount of pyrophosphate.

The Time Dependence of Reduced Viscosity. The viscosities of the solutions of samples C and D decreased definitely with time, probably due to the hydrolysis of the branching of the polymer chains[5].

Since the reduced viscosities (η_{sp}/c) of sodium polyphosphate of various molecular weights at various concentrations has been measured, the curves giving the relationship between the molecular weight and the reduced viscosity at a given concentration can be drawn readily. On the basis of these curves, the data on the time dependence of viscosity can be recalculated to the time dependence of the average molecular weight. It may then be assumed that the rate of hydrolysis is proportional to the number of branching B:

$$-dB/dt=kB \qquad (10)$$

It is also assumed that one molecule is produced by the hydrolysis of one branching, so that the decrease in the number of branching is equal to the increase in the number of molecules, N. Therefore, $-dB=dN$ and $B-B_e=N_e-N$, where B_e and N_e are the values of B and N, respectively, at the end of the hydrolysis. (Probably, $B_e=0$). By assuming further that the average molecular weight, M, is reciprocally proportional to the number of molecules, Eq. 10 can be rewritten and integrated to:

$$\ln(1/M_e-1/M)=-kt+\text{const.} \qquad (11)$$

where M_e is the average molecular weight at the end of hydrolysis, which can be obtained from the reduced viscosity of the solution 20 or 24 hr. after the dissolution. The experimental values were obtained in a thermostat at 25.5°C. Experimental data showed the linear relation expected by Eq. 11. The rate constant of the hydrolysis obtained from the slope of the straight lines was 0.39 hr^{-1}, as is shown in Table VI.

TABLE VI. RATE CONSTANT k OF HYDROLYSIS REACTION AT 25.5°C

Samlpe	Polymer concn. g./100 ml.	NaBr concn. N	k hr^{-1}
C	0.8112	0.035	0.39
	0.3703	0.07	0.39
D	1.0436	0.035	0.39
	1.9165	0.07	0.39

Summary

The intrinsic viscosities of sodium orthophosphates, pyrophosphate, tripolyphosphate and Graham salts of relatively low molecular weight (lower than 10300) were measured. The relation between the intrinsic viscosity at 25.5°C and the average molecular weight measured by the end group titration was

$$[\eta]=6.9\times10^{-4}\times M^{0.61}$$

in a 0.035 N sodium bromide solution, and

$$[\eta]=0.0348+0.112\times10^{-4}\times M$$

in a 0.07 N sodium bromide solution.

Vanadium-containing Graham salts (sodium vanadate-phosphate copolymers) seemed to be hydrolyzed immediately by the dissolution. The intrinsic viscosity of the solution was much smaller than that of sodium polyphosphate of the corresponding degree of polymerization.

The rate of the hydrolysis of branched sodium polyphosphate was proportional to the number of branchings, and the rate constant was 0.39 hr^{-1} at 25.5°C.

Faculty of Pharmacy
Kyoto University
Sakyo-ku, Kyoto

Non-Oxygen Exchange Reaction of Sulfone Group of Phenyl Benzenesulfonate in Acid Hydrolysis

By Shigeru OAE, Tsugio FUKUMOTO and Reiko KIRITANI

(Received November 27, 1962)

The hydrolysis of the esters of carboxylic acids has been shown to proceed through reversible addition intermediates both in acid and in alkaline media[1,2]. The alkaline hydrolysis of phenyl benzenesulfonate has been shown by one of us[3] to proceed through a simple S_{N_2} replacement, without involving prior addition of hydroxide ion on the sulfur atom as shown by (A), which was considered earlier as a posibility[4,5].

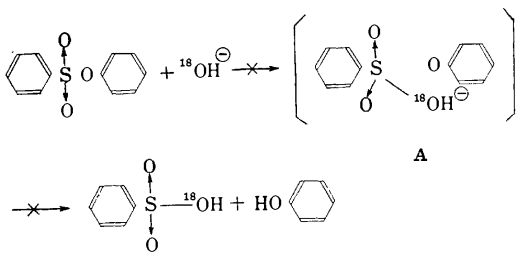

A

Fig. 1.

Similar studies on the neutral and alkaline hydrolysis of alkyl phosphinic chlorides and phosphorochlorides by Dostrovsky and Halmann[6,7] and of alkyl phosphate by Brutcher and Westheimer[8] have also indicated that these reactions do not proceed via pentacovalent phosphorous intermediates. Recently, however, Haake and Westheimer[9] have shown that the acid hydrolysis of alkyl hydrogen phosphates was accompanied by oxygen exchange similar to that of esters of carboxylic acids. This observation has prompted us to extend our ^{18}O tracer study on the acid hydrolysis of the titled compound. The acid hydrolysis of phenyl benzenesulfonate was very sluggish, more so than that of dimethyl hydrogen phosphate and was found to take place only at above 160°C in a sealed tube using 10 N hydrochloric acid.

An aliquot portion of phenyl benzenesulfonate was added on to 10 N hydrochloric acid diluted with ^{18}O enriched water and the mixture was sealed in a sealed tube. After heating the sealed tube at 180°C for 24 hr., the products, phenol and benzenesulfonic acid were separated by extracting with ether. The ether layer, containig phenol, was treated with bromine to derive 2, 4, 6-tribromophenol, while the aqueous layer was treated with *S*-benzylthiuronium chloride to give the sulfonic acid salt. By these reactions, the hydrolysis was found to give both phenol and benzenesulfonic acid in nearly quantitative yields. In a few separate experiments the reaction was stopped when it was half completed in order to see if the hydrolysis reaction proceeds through a reversible addition intermediate, and unchanged phenyl benzenesulfonate was recovered together with the hydrolysis products.

All these compounds were subjected to ^{18}O analysis by the usual method[10], and the results are shown in Table I.

There was no incorporation of ^{18}O in the recovered ester in this reaction, contrary to the acid hydrolysis of alkyl hydrogen phosphate. This excludes clearly any reversible prior addition of water molecule or hydronium ion in the hydrolysis of this compound and appears to suggest that the reaction is either an S_{N_1} reaction involving a slow cleavage of S–O bond followed by rapid solvolysis to form sulfonic acid or a simple S_{N_2} type synchronous one step process initiated by attack of water oxygen on the sulfur atom similar to the alkaline hydrolysis[3] or on the carbon atom of benzene ring bearing phenolic oxygen.

Since the S_{N_1} type cleavage of sulfur-oxygen linkage will leave additional positive charge on the sulfur atom which bears double formal positive charges, this process would require an enormous enorgy and is quite unlikely to occur. A simple S_{N_2} attack of water or hydronium oxygen on the carbon atom of the benzene

1) M. L. Bender, *J. Am. Chem. Soc.*, 73, 1626 (1951).
2) M. L. Bender, H. Landenhein and M. C. Chen, ibid., 83, 123 (1961).
3) D. R. Christman and S. Oae, *Chem. & Ind.*, 1959, 1251.
4) C. A. Bunton and Y. F. Frei, *J. Chem. Soc.*, 1951, 1872.
5) C. A. Bunton and V. A. Welth, ibid., 1956, 3240.
6) I. Dostrovsky and M. M. Halmann, ibid., 1953, 516, 520.
7) M. M. Halmann, ibid., 1959, 305.
8) W. W. Brutcher and F. H. Westheimer, *J. Am. Chem. Soc.*, 72, 2420 (1955).
9) P. C. Haake and F. H. Westheimer, ibid., 83, 1102 (1961).
10) S. Oae, T. Kitao and Y. Kitaoka, ibid., 84, 3359 (1962).

TABLE I. DISTRIBUTION OF THF LABEL IN HYDROLYSIS PRODUCTS

Run	Reaction time, hr.	^{18}O atom % of aq. HCl solution	^{18}O atom % of products		
			Phenol	Benzenesulfonic acid	Recovered ester
1	6	0.42	0.27	0.29 (0.28)*	0.21
2	6	0.80	0.29	0.35 (0.40)	0.21
3	6	1.50	0.78	0.68 (0.64)	0.21
4	24	0.48	0.44	0.35 (0.30)	—
5	24	0.42	0.38	0.29 (0.28)	—
6	24	0.80	0.42	0.41 (0.40)	—

* Numercical values in parrentheses represent theoretical % of ^{18}O atom by the incorporation of one oxygen atom from solvent heavy water.

ring as shown in Fig. 2 also cannot satisfy the results of ^{18}O analysis, because this process will require the phenolic oxygen to be incorporated with the equal amount of ^{18}O to that of the ^{18}O enriched water used, however, this was not the case.

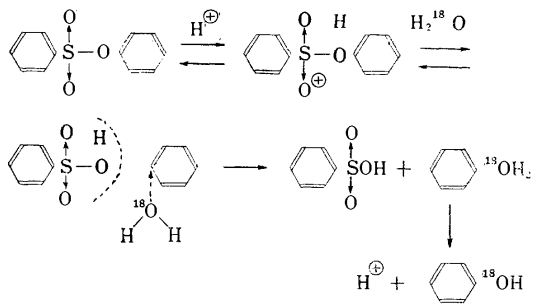

Fig. 2.

Then another, possibly the only, remaining possibility is the S_{N_2} attack of water or hydronium oxygen on the sulfur atom as shown in Fig. 3.

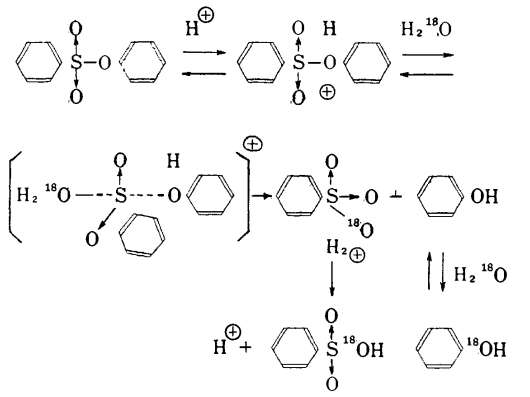

Fig. 3.

If the reaction proceeds through this process, the sulfonic acid will be incorporated with one equivalent amount of ^{18}O and the phenol will remain to be natural just as in the alkaline hydrolysis[3,4,5]. While the sulfonic acid, formed by the hydrolysis, was incorporated with ^{18}O just as much as what is required from this process, phenol was always incorporated with an excess of ^{18}O above the natural concentration and the amount of ^{18}O incorporation appeared to increase with a prolonged heating as shown by Table I.

TABLE II. OXYGEN EXCHANGE REACTION OF PHENOL AND BENZENESULFONIC ACID IN THE ACIDIC SOLUTION

	Reaction time hr.	^{18}O atom % of aq. HCl solution	^{18}O atom % of products
Phenol	5	0.8	0.37
	24	0.77	0.73
Benzene-sulfonic acid	5	0.8	0.23
	24	0.8	0.24

In separate experiments we carried out oxygen exchange reactions of phenol and also benzenesulfonic acid in the same acidic solution. The results are shown in Table II. There was no apparent oxygen exchange in benzenesulfonic acid, even under a prolonged heating, however, all the phenols examined did show rather remarkable oxygen exchange under the condition cited and the amount of ^{18}O incorporation increased with a prolonged heating.

This observation indicates that the phenol formed during the acid hydrolysis of phenyl benzenesulfonate slowly exchange its oxygen with solvent medium.

The overall reaction scheme of this acid-catalyzed hydrolysis of phenyl benzenesulfonate would be the S_{N_2} process in which water molecule attack the sulfur atom, shown by Fig. 3, giving benzene sulfonic acid and phenol that undergoes further slow oxygen exchange with solvent water.

As to the question how phenol exchange its oxygen in acidic medium, we believe that in such a strong acidic medium phenol readily accept a proton at either para or ortho position

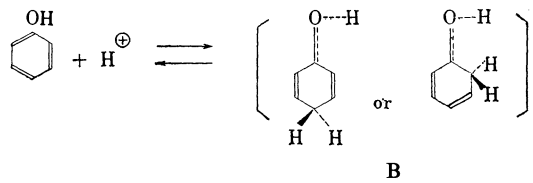

B

Fig. 4.

to form a quasi-stable incipient intermediate, B, in which the original hydroxy function aquires more of carbonyl character and hence facilitates the oxygen exchange with heavy water. Incidentally carbonyl group is known to exchange very readily its oxygen in both acidic and alkaline media[11,12].

The carbonyl character of phenolic compounds has been demonstrated only in the case of β-naphthol[13], where β-naphthyl thioglycollic acid was shown to replace hydroxyl group to form. We have also found that other phenols exchange its oxygen in strong acid media.

More detailed investigations on these oxygen exchange reaction of phenols in both acid and alkaline solutions are in progress in our laboratories and will be reported in future.

Experimental

Analysis for Oxygen-18.—Experimental procedure and calculation were similar to those in the previous paper[10].

Phenyl Benzenesulfonate.—This material was prepared by the Schotten-Baumann method[14], and was purified by repeated distillations. The fraction b. p. 152°C/1 mmHg, m. p. 35°C was used.

Hydrolysis of Phenyl Benzenesulfonate in Hydrochloric Acid.—Phenyl benzenesulfonate 1 g. was mixed with 5 ml. of 10 N hydrochloric acid containing water-^{18}O. The mixture was kept for 24 hr. at 180°C in a sealed tube. Then the sealed tube was broken and the whole content was extracted with ether. The ether extract was treated directly with bromine by the usual method, and 1.4 g. of 2, 4, 6,-tribromophenol (m. p. 96°C) was obtained (97%). In a few experiments, phenol formed by the hydrolysis was repeatedly purified by fractional distillation and subjected directly to ^{18}O analysis.

The aqueous layer was evaporated down to 2 ml.. To this solution was added a few drops of hydrochloric acid and *S*-benzylthiuronium chloride, 0.7 g. and *S*-benzylthiuronium salt of benzenesulfonic acid, 1.2 g. white plate, (m. p. 148.5°C) was obtained. This corresponds to 0.5 g. of benzenesulfonic acid (98% yield).

Partial Hydrolysis of Phenyl Benzenesulfonate in Hydrochloric Acid.—This ester 1 g. was mixed with 5 ml. of 10 N hydrochloric acid containing water-^{18}O. The mixture was heated in a sealed tube for 6 hr. at 180°C. The products were treated as described above. The ether extract was distilled and 0.2 g. of phenol and 0.5 g. of phenyl benzenesulfonate (b. p. 152°C/1 mmHg) were collected.

Isotopic Oxygen Exchange Reaction.—Phenol, 1 g. was mixed with 5 ml. of 10 N hydrochloric acid containing water-^{18}O. An aliquot of the mixture was heated in a sealed tube at 180°C for 5 hr. and the other for 24 hr. Benzenesulfonic acid was also treated in the same way as in the case of phenol.

The exchange products, phenol and benzenesulfonic acid, were derived to 2, 4, 6-tribromophenol and *S*-benzylthiuronium salt, respectively, and these derivatives were subjected to ^{18}O analysis.

Department of Chemistry
Radiation Center of Osaka Prefecture
Sakai, Osaka

11) I. Roberts and L. C. Urey, ibid., **61**, 2580, 2584 (1939).
12) S. C. Datta, J. N. E. Day, and C. K. Ingold, *J. Chem. Soc.*, **1939**, 838.
13) F. M. Furman, J. H. Thelin, D. W. Hein and W. B. Hardy, *J. Am. Chem. Soc.*, **82**, 1450 (1960).
14) "Jikken Kagaku Koza", Vol. 16, Ed. by N. Kubota., Maruzene Book Co., Tokyo (1959), p. 333.

NOTES

A. C. Polarography of Uranium in Non-complexing and Complexing Media

By K. A. KHASGIWALE, S. C. SARAIYA and A. K. SUNDARAM

(Received June 20, 1962)

A. C. polarography of uranium has been studied at 50 c. p. s. by Breyer and Hacobian[1] and the method has been applied for the estimation of uranium[2]. We have observed earlier[3] that the a. c. peak height does not increase with the increase in the concentration of acid or oxalic acid though an increase in the d. c. current is observed. This paper reports a more detailed study of the a. c. polarography of uranium in non-complexing and complexing media.

Experimental

The apparatus and the method of measurement of the alternating current have been described earlier[4]. An H-cell with a saturated calomel electrode as the reference electrode was used but the current was measured across the mercury pool for low cell resistance (300 ohms)[5].

All experiments were carried out at 30±0.5°C with deaerated solutions. Two capillaries [$m^{2/3} \cdot t^{1/6}(mg^{2/3}\,sec^{-1/2}) = 1.75$ (I) and 1.46 (II)] were used for the work. All solutions were made from reagent grade chemicals. Sodium perchlorate was used to maintain the ionic strength and the pH was adjusted with perchloric acid.

Results and Discussion

Non-Complexing Media.—Uranium gives two waves in weakly acid media and the disproportionation reactions are unimportant[6]. An a. c. polarogram of uranium in 0.1 M sodium chloride and 0.01 M hydrochloric acid showed two peaks corresponding to the two d. c. steps. The peak potentials corresponded to the half-wave potentials. Whereas the height of the second d. c. step was nearly double that of the first, the second a. c. peak was smaller than the first.

The peak currents were measured at different salt concentrations (Table I). The current for the first peak reached a constant value but that for the second increased with an increase in the concentration of sodium chloride. The height of the second peak was greater than that of the first at higher salt concentrations, though never double as in the d. c. polarography. The effect of frequency (Table II) showed that the current for the first peak increased upto 200 c. p. s. but that for the second increased only upto 100 c. p. s. Besides, the second peak height was smaller than the first at 500 c. p. s. The results are understandable as the second step is irreversible and the rates of the two electrode processes may be different.

The ratio of the peak current to uranium in 2 M hydrochloric acid (Table III) decreased

TABLE I. EFFECT OF SALT CONCENTRATION ON THE PEAK HEIGHTS OF URANIUM

Supporting electrolyte = NaCl + HCl 0.01 M
A. C. amplitude = 45 mV. at 50 c. p. s.
Capillary I

Sodium chloride M	A. C. peak current μamp.	
	Peak I	Peak II
0.1	14.1	9.3
0.2	15.0	20.9
0.5	15.1	21.5
1.0	15.1	22.9
1.6	15.6	24.3

TABLE II. EFFECT OF FREQUENCY ON THE PEAK HEIGHTS OF URANIUM

U = 1 mM ; NaCl = 1.6 M ; HCl 0.01 M
Capillary I
A. C. amplitude = 45 mV.

Frequency cycl./sec.	A. C. peak current μamp.	
	Peak I	Peak II
50	15.6	24.3
100	19.5	27.5
200	22.5	21.6
500	19.3	12.0

1) B. Breyer and S. Hacobian, *Australian J. Sci. Res.*, **A4**, 604 (1951).
2) B. Breyer and J. R. Beevers, *J. Electroanalyt. Chem.*, **1**, 345 (1959/60).
3) A. K. Sundaram and K. A. Khasgiwale, *Proc. Ind. Sci. Congress Assn.*, **1958**, 54.
4) K. S. G. Doss and A. Kalyanasundaram, *Proc. Ind. Acad. Sci.*, **33**, 298 (1951).
5) H. H. Bauer and P. J. Elving, *Anal. Chem.*, **30**, 334 (1958).
6) W. E. Harris and I. M. Kolthoff, *J. Am. Chem. Soc.*, **67**, 1484 (1945); **68**, 1175 (1946).

TABLE III. EFFECT OF URANIUM CONCENTRATION ON THE FIRST PEAK HEIGHT

Supporting electrolyte = 2.0 M HCl
A. C. amplitude = 14 mV. at 50 c. p. s.
Capillary II

Uranium c, mM	Peak current at −0.18 V. vs. S. C. E. i, μamp.	i/c μamp./mM
0.2	0.95	4.75
0.5	2.2	4.4
1.0	4.3	4.3
2.0	8.5	4.25

with increasing concentration of uranium contrary to that observed in conventional polarography. The increase in the d. c. current for the first step beyond that corresponding to one-electron diffusion controlled reaction is a function of the rate of disproportionation and as the rate in presence of acids in comparatively smaller than that in the presence of complexing agents, the height of the first peak has been studied in complexing media.

Complexing Media.—The polarography of uranium in thiocyanate[7], lactate[8] and oxalate[9] media has been reported. A shift in the half-wave potential to more negative values occurred in lactate and oxalate medium at pH 5 with no change in the limiting current. At this pH the peak potentials of the a. c. polarograms corresponded to the half-wave potentials and the peak currents were the same as that of the simple ion. The limiting current for the first step in these media increased with the concentration of the complexing agent in acidic solutions whereas the a. c. peak currents for low concentration of oxalate, lactate or thiocyanate were nearly the same as for the simple ion and decreased on further increase in the concentration. The peak potentials were the same viz., −0.18 V. vs. S. C. E. whereas the half-wave potentials in the case of oxalate (−0.13 V.) and thiocyanate (−0.11 V.) shifted to more positive potentials at high concentrations.

In explaining these results, the electrode reaction coupled with the chemical reaction will have to be considered. Uranium(V) produced at the electrode by the reduction of uranium(VI) with the half-wave potential at −0.18 V. vs. S. C. E. undergoes disproportionation to produce more of uranium(VI). This is again reduced at the electrode giving rise to an increase in the current. The half-wave potential is for the overall reaction. In a. c. polarography the peak potential of −0.18 V. corresponds to the electrode reaction. But the reversal of the electrode reaction takes place due to the superimposed a. c. and consequently no chemical reaction occurrs. Hence no increase in the a. c. peak current is observed and the peak potential remains same.

The decrease in the peak current at higher concentrations of the complexing agent might be due to the rate of the electrode recation. It was observed that the peak current reduced with the increasing concentration of the complexing agent (Fig. 1).

Thiocyanate was the only system for which a slope of 30 mV. for the log plot of the first wave was obtained whereas a slope of 60 mV. was obtained in the case of oxalate and lactate. Besides, a linear relationship between current and concentration of uranium and a temperature coefficient of less than 2% in the case of thiocyanate would appear to indicate that no kinetic considerations were involved in the reduction. The observations made herein indicated that this was also a case of disproportionation.

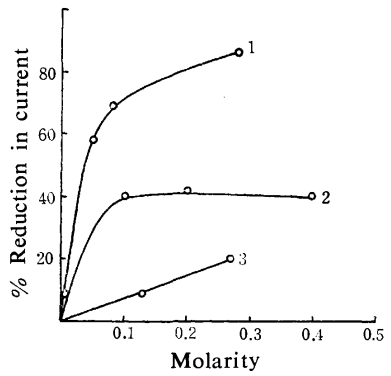

Fig. 1. % Reduction in current at different concentrations of complexing agent.
$U = 1 \cdot 10^{-3}$ $\mu = 1.0$ pH = 1
1, $H_2C_2O_4$ 2, NH_4NCS 3, $CH_3CHOHCOOH$

The authors wish to thank Dr. V. T. Athavale, Head, Analytical Division, for his kind interest.

Analytical Division
Atomic Energy Establishment Trombay
Bombay, India

7) S. C. Saraiya, V. S. Srinivasan and A. K. Sundaram, *Anal. Chem. Acta*, 23, 77 (1960).
8) S. C. Saraiya and A. K. Sundaram, *Anal. Chim. Acta*, to be published.
9) S. C. Saraiya and A. K. Sundaram, unpublished data.

On the Electronic Spectrum of 1, 2-Di-9'-anthrylethane

By Shuzo AKIYAMA and Masazumi NAKAGAWA

(Received November 5, 1962)

The electronic spectrum of 1, 2-di-9'-anthrylethane (III) with unusual low absorption intensity has been reported in a literature[1]. The low absorption intensity is scarcely understandable in view of the presence of two anthracene nuclei in the molecule. The present authors have carried out the synthesis of the hydrocarbon (III) according to the method of Barnett[2] with a modification starting from 10-methyleneanthrone (I)[3], and the spectrum

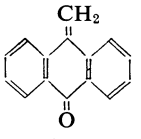

(I)

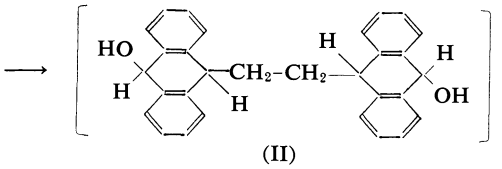

(II)

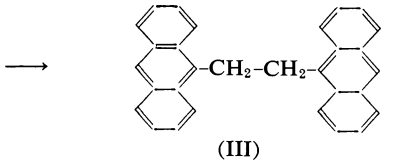

(III)

was measured. Expectedly, the spectrum exhibited much higher absorption intensity as compared with that of the literature value[1] (Fig. 1), and the fact the ε-value of the absorption maximum at the longest wave-length is found to be approximately the double of the corresponding ε-value of 9-methylanthracene[4] is consistent with the additivity principle of absorption intensity of unconjugated chromophores.

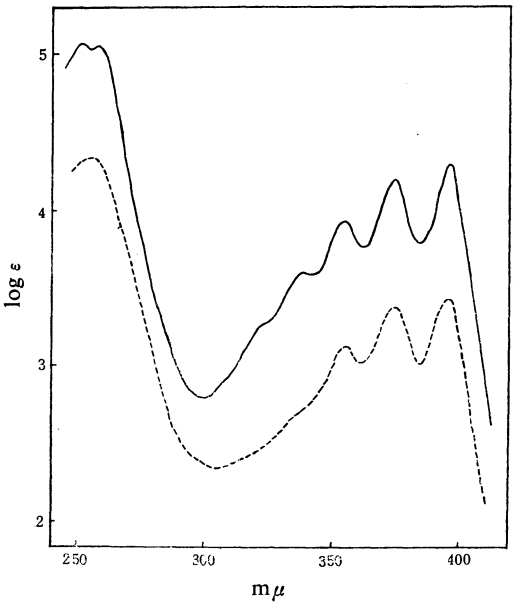

Fig. 1. The electronic spectrum of 1, 2-di-9'-anthrylethane, ——: the result of the present paper, ------: redrawn from Ref. 1).

Experimental*

10-Methyleneanthrone (I). — 10-Methyleneanthrone (I) was prepared according to the procedure of Clar[3] by the reaction of anthrone with formaldehyde. Pale yellow needles, m. p. 148°C (lit. value, m. p. 148°C[3]), 66%.

1, 2-Di-9'-anthrylethane (III).—A mixture of I (3 g., 0.015 mol.), zinc dust (15 g.), 28% aqueous ammonia (35 ml.) and water (35 ml.) was refluxed for 2 hr. After cooling to room temperature, the reaction mixture was washed with water and dried. The dried material (zinc dust, zinc hydroxide and II) was repeatedly digested with boiling ethanol. Five drops of concentrated hydrochloric acid were added to the combined hot alcoholic extract (200 ml.) resulting in the deposition of pale yellow crystals, m. p. 302~307°C (decomp.), 1.4 g., 52%. The crystals were recrystallized three times from toluene yielding pure III, m. p. 314~318°C (decomp.), (lit. values, 310~315°C (decomp.)[1]; 308°C[2]).

Found: C, 93.97; H, 5.97. Calcd. for $C_{30}H_{22}$: C, 94.20; H, 5.80%.

UV spectrum (in chloroform), λ_{max} (log ε); 252.5 (5.07), 259 (5.05), 324 (3.25)†, 339 (3.59), 356 (3.92), 375 (4.20), 397 (4.29). The dagger indicates shoulder.

The infrared spectrum of III was found to be almost identical with that of the reported one[1].

Department of Chemistry
Faculty of Science
Osaka University
Nakanoshima, Osaka

1) I. M. Roitt and W. A. Waters, *J. Chem. Soc.*, 1952, 2695. The spectrum given in this paper was quoted by P. Tardieu without comment on the absorption intensity (*Ann. chim.*, 6, 1445 (1962)).
2) H. Barnett and M. A. Matthews, *Ber.*, 59, 768 (1926).
3) E. Clar, Ber., 69, 1686 (1936).
4) D. D. Phillips and J. Cason, *J. Am. Chem. Soc.*, 74, 2934 (1952).

* All melting points were not corrected. The electronic spectrum was measured with a Hitachi autorecording spectrophotometer, EPS-2. The analysis was performed by Mr. Masakazu Okumiya in the Microanalytical Laboratory of this Department.

Isolation of Carrier-free Tellurium from Antimony Target

By Yuji YOKOYAMA, Hisao MABUCHI, Hitoshi SHOJI and Nobufusa SAITO

(Received November 10, 1962)

On the separation of tellurium from antimony, several different procedures were described in the literature, including coprecipitation method,[1] ion-exchange method[2] and so forth. These methods, however, do not give satisfactory results for the separation of trace amounts of tellurium from several grams of antimony. In a study of the energy level schemes of tin nuclei, it became necessary to separate trace amounts of radioactive tellurium in the state of carrier-free from proton-irradiated antimony targets. The radioactive tellurium thus separated is to be electroplated on a metal foil and to be measured with a β-ray spectrometer.

As reported by one of the present authors,[3] tellurium(IV) is extracted with a carbon tetrachloride solution of dithizone. As to antimony, dithizonate of trivalent antimony was reported,[4] but no definite description on the pentavalent state was made. A simple test showed that antimony(V) is not extracted into a carbon tetrachloride solution of dithizone from acidic solution. Considering such properties, the authors devised the following separation procedure and applied it to bombarded samples.

Separation Procedure

Dissolution of Antimony Target and Extraction of Tellurium.—Several grams of antimony target (metal powder) are dissolved in 30 ml. of aqua regia and the solution is slowly evaporated to dryness. To the residue, another 30 ml. of aqua regia are added and again evaporated to dryness. Such treatment should be repeated at least three times for completion of the oxidation of antimony to pentavalent state. After the treatment with aqua regia, the resulting white residue is dissolved in 20 ml. of 6 M hydrochloric acid and the solution is warmed for a while to ensure the tetravalency of tellurium. Then the solution is diluted with distilled water so as to be 3 M in hydrochloric acid. At lower acidity than 3 M in hydrochloric acid, antimony is hydrolyzed and gives a white precipitate which prevents tellurium from being extracted with dithizone. Extraction of tellurium from the hydrochloric acid solution is carried out in a separatory funnel with an equal volume of concentrated dithizone solution. With a volume ratio of 1 : 1, extractabilities of tellurium under the given condition are 30% with a saturated dithizone-carbon tetrachloride solution and 75% with a saturated dithizone-chloroform solution*1. Therefore, extraction process repeated three times may be enough for essentially complete removal of tellurium from the aqueous layer, when a saturated dithizone-chloroform solution is used.

Back-Extraction of Tellurium.—After combined dithizone extracts are washed with dilute hydrochloric acid, they are transferred into another separatory funnel, together with a suitable amount of distilled water. To this separatory funnel, the aqueous solution of cupric chloride is added until the amount of cupric ion becomes a little in excess to the equivalent amounts combining with dithizone, and then the funnel is thoroughly shaken. When dithizone is saturated with copper, tellurium is liberated from dithizone chelate into the aqueous layer. This is because copper has a greater affinity than tellurium does for dithizone.

Then, the aqueous phase is separated. A small amount of copper contained in it can be removed by repeated extractions with a very dilute carbon tetrachloride solution of dithizone ($\sim 10^{-6}$ M/l.). The loss of tellurium during this operation is negligible, if a sufficiently dilute solution is used for the extraction. By this procedure, more than 90% of radioactive tellurium is brought into the aqueous phase.

Results and Discussion

A preliminary experiment showed that, when trace amouts of ^{129m}Te artificially mixed with 1 g. of antimony were separated by the separation procedure described above, the amount of antimony contaminated in tellurium fraction was less than 60 μg.*2 (0.006% of initial antimony). On the other hand, when carbon tetrachloride was used as a solvent of dithizone instead of chloroform, antimony contamination was less than 30 μg. (0.003%).

As good results were obtained in the preliminary experiment, this method was applied to the separation of a bombarded sample. About 5 g. of antimony were irradiated with 56 MeV. proton (beam current 0.4 μamp.) for 24 hr. After the bombardment, the target was dissolved in aqua regia and treated with a chloroform solution of dithizone as described above. Tellurium fraction thus obtained was again purified with a carbon tetrachloride solution of dithizone in a similar way. Figure 1 shows γ-ray spectra of tellurium and antimony fractions. They are clearly different

1) N. Goldberg and S. Frankel, *Phys. Rev.*, **100**, 1350 (1955).
2) Y. Sasaki, This Bulletin, **28**, 615 (1955).
3) H. Mabuchi, ibid., **29**, 842 (1956).
4) J. K. Carton, W. C. Bradbury and R. Kruh, *Anal. Chim. Acta*, **12**, 101 (1955).

*1 The solubilities of dithizone in carbon tetrachloride and chloroform are 0.64 g. and 17.8 g. per liter at room temperature, respectively.
*2 The amout of antimony was determined by rhodamine B method.

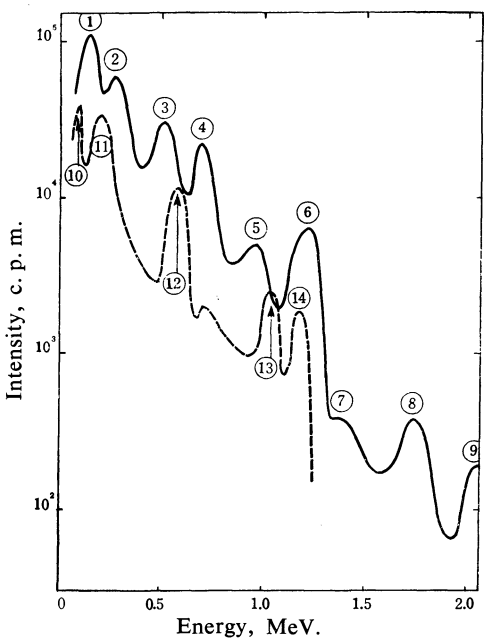

Fig. 1. γ-Ray spectra of tellurium and antimony fractions.
Full line: tellurium fraction one day after the bombardment.
Broken line: antimony fraction two days after the bombardment.

Assignment of the peaks

No. of Peaks	Energy Mev.	Nuclides
1	0.15	^{119}Sb($\leftarrow^{119}$Te)
2	0.27	^{119}Sb($\leftarrow^{119}$Te)
3	0.51	^{118}Sn($\leftarrow^{118}$Sb$\leftarrow^{118}$Te)
4	0.66, 0.71	^{119}Sb($\leftarrow^{119m}$Te)
5	0.92, 0.95, 0.98	^{119}Sb($\leftarrow^{119}$Te)
6	1.22	^{118}Sn($\leftarrow^{118}$Sb$\leftarrow^{118}$Te), ^{119}Sb($\leftarrow^{119}$Te)
7	1.37	^{119}Sb($\leftarrow^{119m}$Te)
8	1.74	^{119}Sb($\leftarrow^{119m}$Te)
9	2.06	^{119}Sb($\leftarrow^{119}$Te)
10	0.09	^{120}Sn($\leftarrow^{120m}$Sb)
11	0.20	^{120}Sn($\leftarrow^{120m}$Sb)
12	0.58	^{122}Sn($\leftarrow^{122}$Sb)
13	1.03	^{120}Sn($\leftarrow^{120m}$Sb)
14	1.17	^{120}Sn($\leftarrow^{120m}$Sb)

from each other, and the peaks in the spectra of antimony fraction were all assigned to those of antimony isotopes.

The important part of this separation method is the oxidation of antimony with aqua regia, because complete oxidation of gram-scale antimony is fairly difficult. Clear-cut separation depends on the completeness of oxidation.

The authors wish to express their hearty thanks to Dr. Hidetsugu Ikegami of the Institute for Nuclear Study of the University of Tokyo for his cordial guidance to physical problems and careful discussions throughout this research.

Department of Chemistry
Faculty of Science
The University of Tokyo
Hongo, Tokyo

Hydrogenation and Hydrogenolysis. VII.[1] *Selective Hydrogenation of Aromatic Compounds Containing C–O Linkages Liable to Hydrogenolysis with a Rhodium-Platinum Oxide under High Pressures*

By Shigeo NISHIMURA and Hisaaki TAGUCHI

(Received November 26, 1962)

In a series of previous papers[1-4], it was shown that (3 : 1) or (7 : 3) rhodium-platinum oxide of Adams' type is not only a highly active catalyst in hydrogenation of various organic compounds, but also very effective for the selective hydrogenation of the compounds having C–O linkages liable to hydrogenolysis[5]. It was also shown that the rhodium-platinum oxides containing 70 to 90% of rhodium by the weight of the metal are even more active and selective than pure rhodium oxide[6]. Subsequently, the use of the rhodium-platinum oxide under high pressures of hydrogen was found to be extremely effective in hydrogenation of various aromatic compounds[7].

This paper describes the high pressure hydrogenation of aromatic compounds containing C–O linkages susceptible to hydrogenolysis with (7 : 3) rhodium-platinum oxide and acetic acid as solvent. As is seen from Table I, most hydrogenations proceed rapidly at room temperature and 100 to 150 kg./cm^2 of hydrogen accompanied with only slight hydrogenolysis.

1) Part VI of this series: S. Nishimura and K. Mori, This Bulletin, **36**, 318 (1963).
2) S. Nishimura, ibid., **33**, 566 (1960).
3) S. Nishimura, T. Onoda and A. Nakamura, ibid., **33**, 1356 (1960).
4) S. Nishimura, ibid., **34**, 32 (1961).
5) Recently, two years after our first publication on this subject[2], Stocker, *J. Org. Chem.*, **27**, 2288 (1962), reported the substantially same results in the hydrogenation of α-substituted benzyl alcohols and benzyl ethers with 5% rhodium-on-alumina and at 3 to 4 atmospheres of hydrogen.
6) S. Nishimura, This Bulletin, **34**, 1544 (1961).
7) S. Nishimura and H. Taguchi, ibid., **35**, 1625 (1962).

TABLE I. CATALYTIC HYDROGENATION OF AROMATIC COMPOUNDS CONTAINING C–O LINKAGES LIABLE TO HYDROGENOLYSIS WITH (7 : 3) RHODIUM-PLATINUM OXIDE

Compound	Amount g.	Catalyst g.	Solvent AcOH ml.	Temp. °C	H_2 press. kg./cm²	Time min.	% Product isolated
Phenol	9.41	0.05	30	23	128～ 99	9	91 Cyclohexanol[a]
Anisole	10.8	0.05	30	20	150～112	6	91 Cyclohexyl methyl ether[b]
Phenyl ether	17.0	0.10	50	22	125～ 87	28	71 Cyclohexyl ether[c] 10 Cyclohexanol
Phenyl ether	8.51	0.20	30	18	1.0	240	51 Cyclohexyl ether[c] 22 Cyclohexanol
p-Hydroxybenzoic acid	13.8	0.10	50	20	140～110	25	82 4-Hydroxycyclohexane-1-carboxylic acids[d] 10 Cyclohexanecarboxylic acid[e]
p-Hydroxybenzoic acid	13.8	0.30	50	19	1.0	480	65 4-Hydroxycyclohexane-1-carboxylic acids[f] 23 Cyclohexanecarboxylic acid[e]
Benzyl acetate	15.0	0.05	15*	25	133～108	15	62 Hexahydrobenzyl acetate[g]
Benzyl acetate	15.0	0.20	50	26	1.0	210	21 Hexahydrobenzyl acetate[g]
Acetophenone	12.0	0.05	30	21	150～115	35	86 Cyclohexylmethylcarbinol[h]
Acetophenone	12.0	0.20	50	25	1.0	210	80 Cyclohexylmethylcarbinol[h]
Benzophenone	9.11	0.05	30	21	148～110	220	93 Dicyclohexylcarbinol[i]
Benzyl ether	9.91	0.10**	30	23	154～123	77	83 Cyclohexylmethyl ether[j]
1-Naphthol	7.21	0.10	50	18	138～110	120	90 1-Decalols[k]
2-Naphthol	7.21	0.10	50	18	142～103	150	90 2-Decalols[l]
Furfuryl alcohol	9.81	0.05	0.5 (+EtOH, 50)	23	125～100	8	88 Tetrahydrofurfuryl alcohol[m]

* With 50 ml. of acetic acid, the yield of hexahydrobenzyl acetate was 50%.

** The catalyst was added in two portions.

a) B. p. 159.0～159.5°C; n_D^{19} 1.4647. b) B. p. 131°C; n_D^{16} 1.4363. c) B. p. 119°C/22 mmHg; n_D^{22} 1.4690. d) M. p. 142～145°C; m. p. after recrystallization twice from chloroform, 149.0～150.5°C: Reported m. p. of the cis isomer, 152°C [N. L. Edison, *J. Soc. Chem. Ind.*, **53**, 138T (1934)]. e) B. p. 127°C/20 mmHg; m. p. 30～31°C. f) M. p. 128～135°C. g) B. p. 89°C/22 mmHg; n_D^{22} 1.4430. h) B. p. 90°C/22 mmHg; n_D^{19} 1.4652. i) B. p. 156～157°C/20 mmHg; m. p. 60～62°C. j) B. p. 150～151°C/22 mmHg; n_D^{20} 1.4703. k) B. p. 126～129°C/20 mmHg; m. p. 84～88°C; m. p. after recrystallization twice from petroleum benzinc, 89.0～90.5°C: Reported m. p. of *cis-cis*-1-decalol, 93°C [W. Hückel et al., *Ann.*, **502**, 99 (1933)]. l) B. p. 133°C/22 mmHg; m. p. 87～94°C; m. p. after recrystallization twice from petroleum benzine, 103～104°C: Reported m. p. of *cis-cis*-2-decalol, 105°C [W. Hückel et al., *Ann*, **451**, 109 (1927)]. m) B. p. 75～76°C/19 mmHg; n_D^{24} 1.4482.

In four compounds in Table I (phenyl ether, *p*-hydroxybenzoic acid, benzyl acetate and acetophenone) which are all liable to hydrogenolysis with great ease, hydrogenations were carried out also at atmospheric pressure and the results compared with those at high pressures (see Table I). In all the cases the proportion of hydrogenolysis at high pressures decreased to about a half of that at atmospheric pressure, and better yields of the corresponding saturated compounds were obtained at high pressures. Under these conditions, phenol, anisole, acetophenone, benzophenone, benzyl ether, 1- and 2-naphthols, and furfuryl alcohol gave in quantitative or nearly quantitative yields the corresponding saturated alcohols or ethers. Benzyl acetate, where the most extensive hydrogenolysis occurred of the compounds investigated, gave a 62% yield of hexahydrobenzyl acetate. At high pressure *p*-hydroxybenzoic acid gave not only 4-hydroxycyclohexane-1-carboxylic acids in a better yield, but also of a higher melting point than at atmospheric pressure, probably the cis isomer being produced more predominantly at high pressure. 1- and 2-Naphthols also gave the

products of melting points not so much lower than those of the corresponding *cis-cis*-decalols. In both cases almost pure cis-cis isomer was obtained in about 50 to 60% yield by recrystallization of the product twice from petroleum benzine[8]. Thus, the results show that the high pressure hydrogenation of aromatic compounds with (7 : 3)rhodium-platinum oxide is a very effective synthetic method where it is desired to avoid the hydrogenolysis concerning C–O linkages. The described method will also be useful for the synthesis of cis compounds by hydrogenation of substituted aromatic compounds[9].

Experimental

Catalyst.—(7 : 3) Rhodium-platinum oxide was prepared as described previously[6].

Hydrogenation.—Hydrogenation was carried out in a 200 ml. autoclave equipped with a magnetic stirrer. The stirrer was driven at the speed of 1000 to 1500 r. p. m.

Isolation of Product.—The hydrogenation product was separated from acetic acid by neutralization with aqueous sodium hydroxide followed by extraction with ether or by distillation at reduced pressure. The product was then distilled at atmospheric or reduced pressure except in case of *p*-hydroxybenzoic acid. In this case, after most of 4-hydroxycyclohexane-1-carboxylic acids was removed as solid, cyclohexanecarboxylic acid was steam-distilled from the residue. Evaporation of water from the residual solution gave a further portion of the hydroxy acid. When the hydrogenation was quantitative, the yield of the product after distillation was usually about 90%.

The authors are indebted to Mitsubishi Chemical Industries Co. for the support of this work.

The Institute of Physical and Chemical Research
Bunkyo-ku, Tokyo

8) Cf. W. G. Dauben et al., *J. Am. Chem. Soc.*, **74**, 5206 (1952); **76**, 4420 (1954).

9) *o*- and *p*-Xylenes also give better yields of *cis*-1, 2- and *cis*-1, 4-dimethylcyclohexanes, respectively, in hydrogenation with (7 : 3)rhodium-platinum oxide at high pressure than at atmospheric pressure or with platinum oxide (S. Nishimura, to be published).

SHORT COMMUNICATIONS

The Electronic Structure of Carbazole in the Fluorescent State

By Noboru MATAGA and
Yoshikazu TORIHASHI

(Received December 14, 1962)

The nature of the electronic states of pyrrole, indole and carbazole seems to be not so well understood as those of benzenoid hydrocarbons, aza-aromatics and their derivatives, although there have been some theoretical studies[1].

We have studied various solvent effects on the absorption and fluorescence spectrum of carbazole, including the effect of hydrogen bonding in a nonpolar solvent and the effect of ionic dissociation in an aqueous alkaline solution[3,1b]. We have also made some quantum mechanical studies of the electronic structure and spectra of this series of molecules by the composite system method[4] and have found a nice agreement with the experimental observations. For example, carbazole was regarded as composed of biphenyl and the >N-H group. Wave functions and energies[5] for the ground state as well as for the excited states of planar biphenyl, which reproduce the observed spectra satisfactorily, were used. For the calculation of the lower excited states, it was sufficient[5] to take into consideration three occupied MO's, ϕ_4, ϕ_5, and ϕ_6, and three vacant MO's, ϕ_7, ϕ_8, and ϕ_9, among the twelve π-MO's of biphenyl. Three charge transfer (CT) configurations from nitrogen to ϕ_7, ϕ_8, and ϕ_9, were taken into consideration. The core resonance integral between nitrogen and the nearest neighbor carbon and the energy of the nitrogen orbital were assumed to be -2.0 and -10.25 eV.[6] respectively.

For the sake of simplicity, only the wave functions for the lowest and the second excited singlet state of carbazole are shown here. $^1\chi_{Nk}$ is the CT configuration, and ^{1}L's and ^{1}B's are locally excited states in biphenyl.

$$^1\Psi_1 = 0.1283\ \chi_0 + 0.7811\ ^1L_b - 0.2575\ ^1B_b - 0.5279\ ^1\chi_{N7} + 0.1684\ ^1\chi_{N9}$$

$$^1\Psi_2 = 0.9961\ ^1L_a - 0.0473\ ^1B_a + 0.0739\ ^1\chi_{N8}$$

The oscillator strengths for these states of carbazole were calculated as: $f(\Psi_0 \rightarrow {}^1\Psi_1) = 0.13$: $f(\Psi_0 \rightarrow {}^1\Psi_2) = 1.02$. These two transitions correspond quite well to the observed band at 3.90 eV. with moderate intensity and the strong band at 4.27 eV. respectively. The form of $^1\Psi_1$ calculated here clearly shows that the very weak " hidden transition "[7] of biphenyl (^1L_b) is modified considerably in carbazole because of the mixing with $^1\chi_{N7}$ and also with ^1B_b. Both the replacement of NH hydrogen by alkyl group and hydrogen bonding of the >N-H···X type cause a large red shift of the 3.90 eV. band, but only a slight shift of the 4.27 eV. band. This fact can be explained quite well on the basis of the calculated results because the contribution from the CT configuration is very small in $^1\Psi_2$ compared with that in $^1\Psi_1$, where it is considerably large, and both the alkyl replacement and the hydrogen bonding lower the energy of the CT configuration and increase the core resonance integral between carbon and nitrogen.

The increase of the dipole moment in the fluorescent state,

$$\Delta\vec{\mu} = \langle {}^1\Psi_1 \mid \sum_i e_i \boldsymbol{r}_i \mid {}^1\Psi_1 \rangle - \langle \Psi_0 \mid \sum_i e_i \boldsymbol{r}_i \mid \Psi_0 \rangle,$$

was calculated to be $\sim 1.96\,D$. The value of $\Delta\vec{\mu}$ was determined experimentally by the method proposed by Lippert[8] and by Mataga[9], using the following equation and assuming $a \sim 4$A.

$$hc(\sigma_a^m - \sigma_f^m) \simeq \text{Const} + 2\left[\frac{D-1}{2D+1} - \frac{n^2-1}{2n^2+1}\right] \cdot \frac{(\Delta\vec{\mu})^2}{a^3}$$

1) For example, a) R. D. Brown and M. L. Heffernan, *Australian J. Chem.*, **12**, 319 (1959); b) H. Kokubun, Summary of the Symposium on the Electronic State, held by the Chem. Soc. Japan, Sept., 1959.
2) N. Mataga, Y. Torihashi and Y. Kaifu, *Z. physk. Chem. N. F.*, in press.
3) N. Mataga and Y. Torihashi, ibid., in press.
4) H. C. Longuet-Higgins and J. N. Murrell, *Proc. Phys. Soc.*, **A68**, 601 (1955); J. N. Murrell, ibid., **68**, 969 (1955).
5) S. Mataga, to be published.
6) The minus value of the observed I. P. of ammonia taken from K. Watanabe, *J. Chem. Phys.*, **22**, 1564 (1954).
7) A. Wenzel, *J. Chem. Phys.*, **21**, 403 (1953); H. Suzuki, This Bulletin, **32**, 1340 (1959).
8) E. Lippert, *Z. Naturforsch.*, **10A**, 541 (1955); *Z. Electrochem.*, **61**, 962 (1957).
9) N. Mataga et al., This Bulletin, **28**, 690 (1955); ibid., **29**, 465 (1956).

The experimental value was estimated to be $\sim$2.2 *D*, which agrees very well with the calculated results.

The $\vec{\Delta\mu}$ values of naphthylamines and naphthols calculated by the ordinary semiempirical ASMO method, with appropriate Hückel MO's delocalized over all cores in the molecule, have been found to be ca. 4$\sim$5 times larger[10] than the observed values. In the present method, however, such a situation does not arise. This fact seems to indicate that the composite system method can give a more reliable charge distribution in the heteroaromatics when appropriate values of semiempirical parameters are chosen.

Faculty of Science
Osaka City University
Sumiyoshi-ku, Osaka

10) N. Mataga, to be published.

The Electronic Spectrum and Structure of the s-Triaminobenzenium Ion

By Noboru MATAGA

(Received December 17, 1962)

A quite interesting example of a kind of aromatic carbonium ion seems to be formed in the aqueous solution of *s*-triaminobenzene (TAB). For the equilibrium TAB+$H^+ \rightleftharpoons$ $TABH^+$ (*s*-triaminobenzenium ion), p$K \sim 5.5$[1]. No such protonation on the ring carbon occurs in the case of aniline or *m*-phenylene diamine, where the amino group is protonated[1]. This is a preliminary report on theoretical calculations on the electronic spectra of TAB and $TABH^+$ and on the stabilities of the protonation products of aminobenzenes, which give a basis for interpretation of the observed results[1].

A semi-empirical ASMO CI method[2] was used. The parameters for Hückel MO calculations were the same as given elesewhere[3]. Pyrrole-type nitrogen was assumed, and the valence state ionization potential and electron affinity were obtained from the table[4]. The value of β_{CN}^{core} was taken to be -2.399 eV. All C–C bond distances were assumed to be 1.39 Å, and all C–N distances, 1.36 Å. The hyperconjugation with the CH_2 group in the case of $TABH^+$ was not taken into account. The calculated results are given in Table I, together with the observed values. D_{3h} and C_{2v} symmetries are assumed for TAB and $TABH^+$ respectively.

The calculated spectra are in satisfactory agreement with the observed values. Although the hyperconjugation was excluded in this calculation, it may be taken into account by some approximate method. In the present case, owing to the presence of the three amino groups, the higher occupied orbitals of the local system I (II is the CH_2 group) should be very much elevated compared with the highest occupied orbital of the corresponding local system of the benzenium ion[5]. Therefore, the excitation energies from the higher occupied orbitals of I to the antibonding π-orbital of II may not be so large, and this charge transfer interaction will increase the stability of the protonated aminobenzenes.

Another measure of the stability of the protonated species is the localization energy. The results of calculation by the Hückel MO method are shown in Table II.

In mode A, the destabilization energy of the π-electrons by protonation becomes considerably smaller from aniline to TAB, whereas it is almost constant or even slightly increases in mode B. This result is in accordance with the observed values. The mode A protonation seems to occur also in the case of tri-O^--benzene (TOB) (phloroglucine trianion)[1], for

TABLE I. CALCULATED ELECTRONIC SPECTRA IN COMPARISON WITH THE OBSERVED VALUES

TAB	Calcd.		Obs.		$TABH^+$	Calcd.		Obs.	
	$h\nu$, eV.	f	$h\nu$, eV.	f		$h\nu$, eV.	f	$h\nu$, eV.	$\log \varepsilon_{max}$
$^1A_2'$	4.27	0	4.4	0	$^1B_1$	3.12	0.39	3.4	3.5
$^1A_1'$	5.21	0	5.0	0	$^1A_1$	4.43	0.65	4.5	3.9
$^1E'$	5.79	2.2	5.6	$\log \varepsilon_{max} \sim 4.3$	$^1A_1$	5.57	1.52	?	?
					$^1B_1$	6.07	0.00	?	?

1) H. Köhler and G. Scheibe, *Z. anorg. u. allgem. Chem.* (*Leipzig*), **285**, 221 (1956).
2) N. Mataga, This Bulletin, **31**, 459, 463 (1958); *Z. physk. Chem. N. F.*, **18**, 285 (1958).
3) H. Baba, This Bulletin, **34**, 76 (1961).
4) H. A. Skinner and H. O. Pritchard, *Chem. Revs.*, **55**, 745 (1955).
5) T. Morita, This Bulletin, **33**, 1486 (1960).

Table II. Localization energies of some aminobenzenes (in unit of β)[a)]

Mode of protonation	A. Carbon	B. Amino group
Aniline	2.2498[b)]	2.8054
m-Phenylenediamine	1.9562[c)]	2.8058
TAB	1.8294	2.8060

a) The localization energies in this table are given by $(m-m^+)$, where the π energy of the neutral molecule is given by $n\alpha+m\beta$ and that of the protonated system, by $(n-2)\alpha+m^+\beta$.
b) Protonation on para-carbon.
c) Protonation on the carbon at the ortho-position in relation to both amino groups.

which we have calculated the localization energy, assuming suitable Hückel MO parameters ($\delta_{o^-}\sim 0.8$, $\beta_{co^-}\sim\beta$) and $(m-m^+)$ being 1.6861.

Mackor et al.[6)] have demonstrated an approximate linear relation between the localization energy and log K in the case of the protonation of many aromatic hydrocarbons. We have observed that the same linear relation holds for TAB and TOB as for aromatic hydrocarbons.

Another possible structure of $TABH^+$ or $TOBH^+$ may be a kind of π-complex in which the proton is situated on the molecular plane. If the proton is situated at the center of the molecule, the lowest energy transition is still forbidden and we cannot interpret the observed strong band. If the proton moves to the periphery of the molecule, the transition becomes possible. This model may finally lead to the localization or hyperconjugation model described above as the most stable equilibrium form.

Faculty of Science
Osaka City University
Sumiyoshi-ku, Osaka

6) E. L. Mackor, A. Hofstra and J. H. van der Waals, *Trans. Faraday Soc.*, **54**, 66 (1958).

Solvent Effects on the Flourescence Spectrum of the Ion-pair (Naphthol-Triethylamine System)

By Noboru MATAGA, Yoshikane KAWASAKI and Yoshikazu TORIHASHI

(Received January 10, 1963)

It has been demonstrated[1] that the strong hydrogen bond between β-naphthol and triethylamine (TEA) in the equilibrium ground state and in the excited Franck-Condon state shifts to the ion-pair in the excited equilibrium state, from which fluorescent transition occurs, in benzene. This phenomenon has been interpreted[1] as due to a strong charge transfer from the nitrogen non-bonding orbital of TEA to the OH antibonding orbital of naphthol in the Franck-Condon excited state, which is followed by an almost complete proton transfer from oxygen to nitrogen in the excited equilibrium state.

We have extended the above work to systems including various solvents of different polarities, thus obtaining results which seem to support the above interpretation. The solvents used here were monochlorobenzene, dichloroethane and acetonitrile. The observed results are summarized in Table I. As one can see from the table, the red shift of the fluorescene band maximum due to the complex formation, ($\Delta\sigma_f$), is larger, the greater the dielectric constant (D) of the solvent, whereas that of the absorption band, ($\Delta\sigma_a$), which is much smaller than $\Delta\sigma_f$, decreases with an increase in the dielectric constant of the solvent.

TABLE I. WAVE NUMBER SHIFTS OF BAND MAXIMA DUE TO COMPLEX FORMATION

Solvent	D	$\Delta\sigma_f$ 10^4 cm^{-1}	$\Delta\sigma_a$ 10^4 cm^{-1}
Benzene	2.284	0.40	0.04
Monochlorobenzene	5.621	0.45	0.03
Dichloroethane	10.36	0.46	0.01
Acetonitrile	37.5	0.58	0.00

As is described elsewhere[2], by using the charge transfer model[3] of the hydrogen bond,

1) N. Mataga and Y. Kaifu, *J. Chem. Phys.*, **36**, 2804 (1962).
2) N. Mataga and Y. Kaifu, to be published.
3) H. Tsubomura, This Bulletin, **27**, 445 (1954); K. Nukasawa, J. Tanaka and S. Nagakura, *J. Phys. Soc. Japan*, **8**, 792 (1953).

the wave function of the proton donor-acceptor pair may be expressed as a superposition of various resonance structures.

$$\Psi = a\Phi(\mathrm{D}-\mathrm{A}) + b\Phi(\mathrm{D}^- - \mathrm{A}^+) + c\Phi(\mathrm{D}^*\mathrm{A}-)$$

where D−A denotes the hydrogen-bonded pair when the proton donor D is in the ground state (no charge transfer), $\mathrm{D}^- - \mathrm{A}^+$, the charge transfer structure, and $\mathrm{D}^*-\mathrm{A}$, the hydrogen-bonded pair when D is in the fluorescent state (on charge transfer).

The energy difference between the charge transfer structure and the infinitely separated D−A pair may be written as:

$$\begin{aligned}\Delta E &= E(\mathrm{D}^- - \mathrm{A}^+) - E(\mathrm{D}-\mathrm{A}) \\ &= I_\mathrm{A} - A_\mathrm{D} + V(\mathrm{D}^- - \mathrm{A}^+) + H_\mathrm{s}\end{aligned}$$

where I_A: the ionization potential of the non-bonding orbital of the proton acceptor, A_D: the electron affinity of the anti-bonding orbital of the O-H bond, $V(\mathrm{D}^- - \mathrm{A}^+)$: interaction energies between the pair, and H_s: the stabilization energy due to the solvation of the ion-pair.

Probably, $\Phi(\mathrm{D}^- - \mathrm{A}^+)$ may interact very strongly with $\Phi(\mathrm{D}^*-\mathrm{A})$, but not so much with $\Phi(\mathrm{D}-\mathrm{A})$, when D and A come close to each other because $E(\mathrm{D}^- - \mathrm{A}^+)$ may be rather small and almost comparable to $E(\mathrm{D}^*-\mathrm{A})$ owing to the quite small I_A value of TEA. Hence, $a \gg b, c$ in the ground state and $b, c \gg a$ in the first excited electronic state of the D−A complex. These circumstances are indicated in Fig. 1,

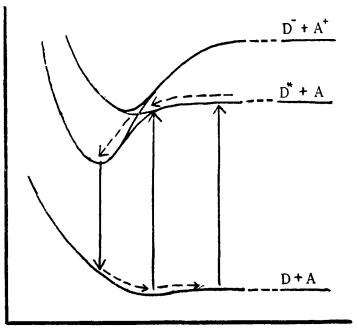

Fig. 1. Potential energy curves for D−A interaction.

where the reaction coordinate represents the D−A distance, the degree of the charge transfer from A to D and the position of the O-H proton.

Furthermore, H_s seems to play an important role in the present case. This quantity seems to be larger in the more polar solvent than in the less polar one, because of the greater dipole-dipole and dipole-polarization forces in the former solvent. The larger H_s value may be a main cause of the greater $\Delta\sigma_\mathrm{f}$ value in the polar solvent. However, hydrogen bonding between D and A may be very weak in the polar solvent, because either D or A may be solvated rather strongly, which seems to result in the very small $\Delta\sigma_\mathrm{a}$ value of this solvent.

Analogous phenomena have been observed when TEA was added to the solution of carbazole in acetonitrile and dichloroethane[4] respectively, and also when a rather large amount of primary or secondary aliphatic amines was added to the cyclohexane or benzene solution of β-naphthol[5]. These phenomena may be interpreted on the basis of similar reasoning.

Faculty of Science
Osaka City University
Sumiyoshi-ku, Osaka

4) N. Mataga and Y. Torihashi, unpublished.
5) N. Mataga and Y. Kawasaki, unpublished.

The ESR Spectrum of the Phthalonitrile Anion Radical

By Kazuo NAKAMURA and
Yasuo DEGUCHI

(Received December 27, 1962)

Though the ESR spectra of many organic anion radicals have been investigated, that of phthalonitrile has not yet been reported on*. When phthalonitrile was reduced in dimethoxyethane (DME) with potassium or sodium, the anion radical was formed.

Thus Fig. 1's ESR hyperfine spectrum of the radical prepared with potassium agrees with the calculated value of Fig. 2, assuming that the coupling constants are $\alpha_{N_{CN}}=1.75$ gauss, $\alpha_{H_5}=\alpha_{H_4}=0.37$ gauss and $\alpha_{H_3}=\alpha_{H_6}=4.11$ gauss respectively.

On the other hand, Fig. 3's ESR spectrum of the same radical reduced with sodium appears to be different from that reduced with potassium, but one can construct a calculated spectrum similar to that of Fig. 2 provided that each line in Fig. 1 will split further into

* The ESR spectra of the electrolytically-generated benzonitrile negative ion have been reported by P. Ludwig and R. N. Adams in *J. Chem. Phys.*, **37**, 828 (1962).

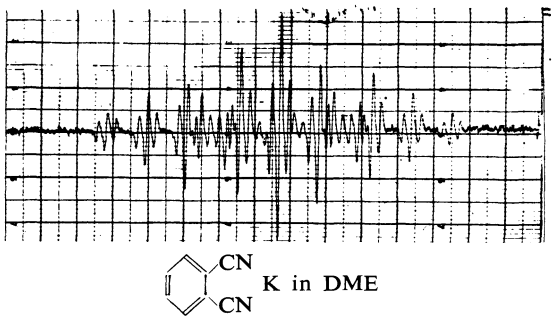

Fig. 1. ESR spectrum of phthalonitrile anion radical reduced with potassium in DME.

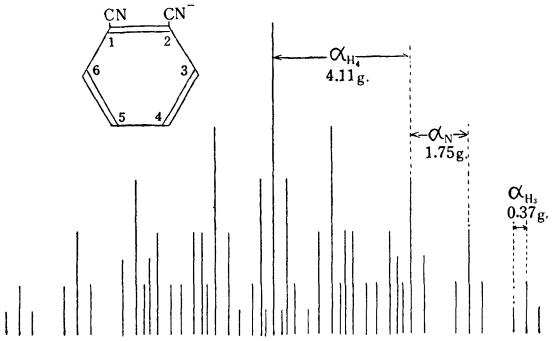

Fig. 2. Calculated spectrum of phthalonitrile anion radical.

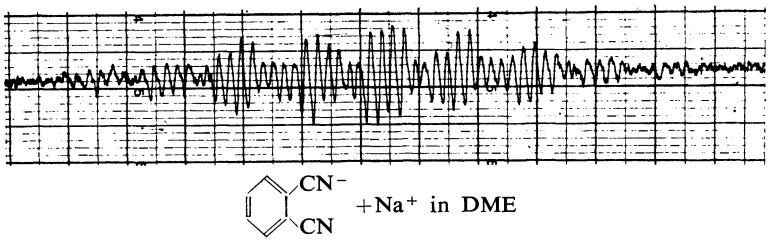

Fig. 3. ESR spectrum of phthalonitrile anion radical reduced with sodium in DME.

four, as is shown in Fig. 3, because of the hyperfine interaction of the unpaired electron spin with the sodium nuclear spin[1], whose coupling constant would be 0.23 gauss.

The ESR spectra of other aromatic nitriles will be reported on soon.

Department of Chemistry
Faculty of Science
Kyoto University
Sakyo-ku, Kyoto

1) N. M. Atherton and S. I. Weissman, *J. Am. Chem. Soc.*, **83**, 1330 (1961).

Studies of Ion Exchange Membranes. XVI. The Preparation of Ion Exchange Membranes by the "Paste Method"

By Yukio MIZUTANI, Reiichi YAMANE, Hirofumi IHARA and Hiroji MOTOMURA

(Received August 23, 1961)

It is generally accepted that the introduction of ion exchange groups into base membranes prepared beforehand is most practically effective for the preparation of ion exchange membranes. Hence, on the preparation of the base membranes many studies have been presented[1-8], and the present author has proposed a "soaking method"[9,10]. The present paper concerns with a method for the preparation of ion exchange membranes in the manner called the "Paste Method".

Fundamental Ideas for the Present Method

The requirements for the base membrane are as follows:

1) It must involve functional groups suitable for the introduction of ion exchange groups and three-dimensional resinous structures in the base membrane; 2) it must possess chemical and mechanical steadiness on the introduction of ion exchange groups; and 3) it must have excellent mechanical strength, that is, a practical reinforcing material in the membrane.

The present work aims to satisfy not only the above requirements but also 4) easy procedures for the preparation and the control of the properties of ion exchange membranes.

The following materials were used as the components of the paste: a) Mf: a monomer containing a functional group suitable for the introduction of an ion exchange group; b) Mc: a monomer copolymerizable with Mf to control the viscosity of the paste, the content of resinous components in the base membrane, and the content of ion exchange groups in the ion exchange membrane; c) DVB: divinylbenzene as a cross-linking agent; d) PVC: the fine powder of poly(vinyl chloride) which endows the base membrane and the ion exchange membrane with flexibility and toughness; e) DOP: dioctyl phthalate as a plasticizer to control the viscosity of the paste; and f) BPO: benzoyl peroxide as a catalyst.

These components were mixed thoroughly and deaerated under reduced pressure. The paste obtained was coated on a reinforcing material and treated in a hot press to prepare the base membrane after having been wrapped with a wrapping material. PVC was not soluble in the paste and dispersed in the swollen state, and the ratio of components was easily controlled. This is a practical merit, since both the resinous component content in the base membranes and the properties of the ion exchange membranes may be easily controlled.

Since PVC was insoluble in the paste, the paste was fairly viscous, but it was not spinnable. Therefore, the paste was easily coated on a reinforcing material, and no pin-hole could be found in the base membrane.

The paste coated on a reinforcing material was heated, and fine particles of PVC in the paste were fused to form a continuous film. Since fine particles of PVC were swollen in the paste, heating at a temperature lower than, say, 175°C, a most suitable temperature for the molding of PVC dispersion[11], would suffice to fuse the particles into a film. The monomers in the continuous film of PVC were polymerized to produce three-dimensional resinous structures.

Under such conditions, the graft copolymer could be produced, as was shown in a previous paper[9], and the homogeneity of the base membrane would be much improved.

If styrene is used as Mf and if the base membrane is a mere mixture of PVC and cross-linked polystyrene, the base membrane would be white or opaque in appearance, because PVC and polystyrene are mutually insoluble. Therefore, the homogeneity of the base membrane, as shown by its transparency, should be ascribed to the very formation of the graft copolymer of styrene, DVB, and PVC.

The use of reinforcing materials may improve

1) H. Hani et al., Japanese Pat. 5388 (1960).
2) T. Kuwata et al., Japanese Pat. 7688 (1960).
3) Y. Tunoda et al., Japanese Pat. 257605-257607.
4) H. Hani et al., Japanese Pat. 13009 (1960).
5) W. K. W. Chen et al., *J. Polymer Sci.*, 23, 903 (1957).
6) H. Hani et al., Japanese Pat. 16036 (1960).
7) F. A. Hazenberg and B. P. Knol, Dutch Pat. 95477 (Sept. 15, 1960).
8) H. Zenftman, Brit. Pat. 863862 (Mar. 29, 1961).
9) Y. Mizutani, *J. Chem. Soc. Japan, Ind. Chem. Sec.* (*Kogyo Kagaku Zasshi*), 65, 118 (1962).
10) Y. Mizutani, ibid., 65, 122 (1962).
11) "Plastics Engineering Handbook", 3rd Ed., Ed. by The Society of the Plastics Industry, Inc., Reinhold Publishing Co., New York (1960), p. 224.

the dimensional stabilities of the base membranes upon treatment to introduce ion exchange groups; it may also provide ion exchange membranes with sufficient mechanical strength for the practical applications.

Finally, ion exchange groups were introduced to the base membranes by various procedures, depending on the nature of the Mf selected.

Experimental

Material.—PVC, Sumilit PX-A, prepared by the Sumitomo Kagaku Co., Ltd., was used. Styrene (St), 2-methyl-5-vinylpyridine (MVP), DOP, and all other reagents were of chemical grade. From the results of the preliminary examinations on various reinforcing materials, Teviron fabrics from the Teijin Co., Ltd., were adopted. As a wrapping material, Vinylon film from the Kurashiki Rayon Co., Ltd., was used.

Preparation of the Base Membranes and the Introduction of Ion Exchange Groups.—To prepare the base membranes, the pastes prepared from St-DVB-DOP-PVC-BPO (I) or MVP-St-DVB-DOP-PVC-BPO (II) were coated on Teviron fabrics, wrapped with a Vinylon film, and heated in a hot press at 100~120°C for 30 min. and then at 70~80°C for 16 hr. Vinylon films were torn off and ion exchange groups were introduced into the base membranes in the following manner:

The base membrane prepared from the paste I was sulfonated with 98% sulfuric acid, or chloromethylated with chloromethyl methyl ether (CME)-stannic chloride-carbon tetrachloride, and then quaternized with an aqueous solution of trimethylamine. The base membrane prepared from the paste II was quaternized with a petroleum ether solution of methyl iodide.

Electrochemical Properties.—Water content, ion exchange capacity, fixed ion concentration, electric resistance, specific conductivity and transport number were measured at 25°C by the same procedure as in previous papers[9,12-15]. Electric resistance and specific conductivity were measured on the membrane dipped in a 0.5 N aqueous solution of sodium chloride at 25°C. The transport number was calculated by Nernst's equation from the membrane potential of a concentration cell composed of 0.5 N and 2.5 N aqueous solutions of sodium chloride, separated from each other by the ion exchange membrane under consideration.

Diffusion.—In a water/membrane/3 N sodium chloride solution system, the amount of electrolytes diffused from a 3 N sodium chloride solution into water was measured at 25°C while the water and the solution phase were being stirred.

Mechanical Strength.—Mullen test-burst strength was measured.

Dimensional Stability.—Before measurement, the samples were treated with 1 N hydrochloric acid and 1 N ammonia water repeatedly.

Test pieces of 2 cm.×100 cm. were examined. Changes in the length of the test pieces immersed in various solutions were measured after they had been left standing for a long time.

Relative Transport Number.—Relative transport numbers were measured at 25°C for the sodium chloride-calcium chloride solution system, the sodium chloride-magnesium chloride solution system, and the sodium chloride-sodium sulfate solution system by the same procedure as in the preceding paper[12]. During the measurements the test solutions used were stirred[16]. The compositions of the test solutions are as follows: $C_{Cl}=0.5$ N, $C_{Na}=0.375$ N and $C_{Ca}=0.125$ N in the sodium chloride-calcium chloride system; $C_{Cl}=0.5$ N, $C_{Na}=0.375$ N and $C_{Mg}=0.125$ N in the sodium chloride-magnesium chloride system; and $C_{Na}=0.5$ N, $C_{Cl}=0.45$ N and $C_{SO_4}=0.05$ N in the sodium chloride-sodium sulfate system.

The relative transport number (P) is shown as follows:

$$P=(t_2/t_1)/(C_2/C_1)$$

where t_1 is the transport number of monovalent ions through the membrane, t_2 is the transport number of bivalent ions through the membrane, C_1 is the concentration of monovalent ions in the test solution, and C_2 is the concentration of bivalent ions in the test solution.

Results and Discussion

The Preparation of the Cation Exchange Membrane.—The composition of the paste seriously affected the ease with which the base membrane was prepared. The following factors were considered:

I) Appropriate viscosity of the paste for coating on a reinforcing material.

II) Ease of the sulfonation of the base membrane.

III) Chemical and mechanical stabilities of the base membrane in the face of sulfonation.

IV) Quality of the resultant ion exchange membrane.

The appropriate compositions of the pastes I were found to be (St+DVB)/PVC=0.7~1.0 (by weight) and DOP/PVC=0.3~0.5 (by weight).

The base membranes were sulfonated with 98% sulfuric acid at 55~60°C for several hours. On prolonged sulfonation, the membranes were deeply colored and might have been degradated.

12) Y. Onoue, Y. Mizutani and R. Yamane, *Denki Kagaku*, **27**, 482 (1959); *J. Electrochem. Soc. Japan (Oversea Ed.)*, **27**, No. 7-9, E182 (1959).
13) Y. Onoue, Y. Mizutani and S. Akiyama, *Denki Kagaku*, **29**, 223 (1961); *J. Electrochem, Soc. Japan (Oversea Ed,)*, **29**, No. 3, E159 (1961),
14) G. Manecke and F. Bonhoeffer, *Z. Elektrochem.*, **55**, 475 (1951).
15) M. Nagasawa and I. Kagawa, *Discussions Faraday Soc.*, **21**, 52 (1956).
16) Y. Onoue, Y. Mizutani, R. Yamane and Y. Takasaki, *Denki Kagaku*, **29**, 187 (1961); *J. Electrochem. Soc. Japan (Oversea Ed.)*, **29**, No. 3, E156 (1961).

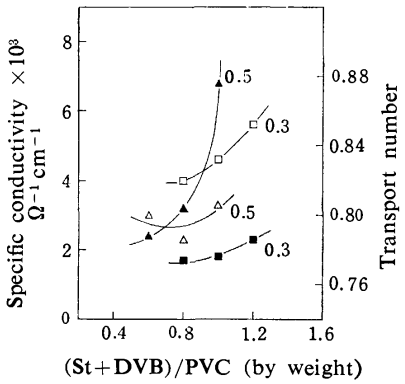

Fig. 1. Monomer contents in the pastes—Properties of cation exchange membranes.
The numbers in the figure are DOP/PVC (by weight).
DVB/(St+DVB)=0.1 (by weight)
□, △: Transport number
■, ▲: Specific conductivity

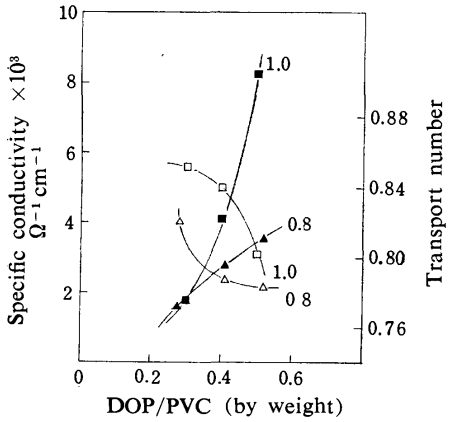

Fig. 2. DOP contents in the pastes—Properties of cation exchange membranes.
The numbers in the figure are (St+DVB)/PVC (by weight).
DVB/(St+DVB)=0.1 (by weight)
□, △: Transport number
■, ▲: Specific conductivity

The relations between the compositions of the pastes and the electrochemical properties of the membranes are shown in Figs. 1 and 2. Figure 1 shows that an increasing (St+DVB)/PVC ratio improves the electrochemical properties of ion exchange membranes by the increase of the density of ion exchange groups per unit volume of the membranes. Figure 2 shows that the increasing DOP content enhances the specific conductivities and depresses the cation transport numbers by the increase of the porosity of the membrane.

The Preparation of Anion Exchange Membranes of the St Type.—The procedures for the preparation of the base membrane were similar to those for cation exchange membranes.

Chloromethylation was considered to be most essential among the treatments to introduce anion exchange groups. The effect of the conditions of chloromethylation, such as temperature, time, and concentration of chloromethyl methyl ether and of stannic chloride, on the quality of the membranes were studied; these factors were found not to be effective enough to change the properties of anion exchange membranes.

These conditions of chloromethylation were considered to be important only for the appearance of anion exchange membranes. In the end, four to eight hours' chloromethylation at room temperature with the solution, $CME/CCl_4=1\sim0.25$ (by volume) and $SnCl_4/(CME+CCl_4)=0.05$ (by volume), was found to be appropriate. Quaternization with trimethylamine was easy, no difficulty being encountered.

The effects of the compositions of the pastes on electrochemical properties are shown in Figs. 3 and 4.

The conditions of chloromethylation and quaternization were as follows:

Chloromethylation: $SnCl_4/(CME+CCl_4)=0.05$ (by volume), $CME/CCl_4=1$ (by volume), at 10°C for 8 hr.

Quaternization with trimethylamine: 30% aqueous solution of trimethylamine, at room temperature, for 16 hr.

With an increasing DVB content in the pastes, the anion transport numbers through the membranes showed only slight changes and specific conductivities were decreased to a greater extent (Fig. 3). This may be attributed to the development of three-dimensional resinous structures.

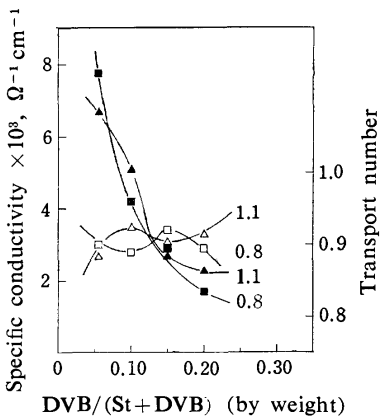

Fig. 3. DVB contents in the pastes—Properties of anion exchange membranes of St type.
The numbers in the figure are (St+DVB)/PVC (by weight).
DOP/PVC=0.2 (by weight)
□, △: Transport number
■, ▲: Specific conductivity

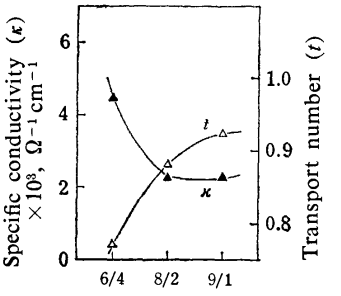

Fig. 4. Composition of the pastes—Properties of anion exchange membranes of St type.
Compositions of the pastes (by weight):
(St+DVB+DOP)/PVC=1.0
DVB/(St+DVB)=0.1

Figure 4 shows the effects of the DOP content of the pastes on the electrochemical properties of the membranes at a fixed (St+DVB)/PVC ratio. With an increasing DOP content, anion transport numbers decreased and specific conductivities increased, since the membranes should become more porous.

The apparent qualities of anion exchange membranes were improved by lowering the DOP content and increasing the DVB content, since the development of the three-dimensional resinous structure depresses the swelling of the base membranes at chloromethylation.

The Preparation of Anion Exchange Membranes of the MVP Type. — Since, at room temperature, PVC was fairly swollen and since the monomers were readily polymerized in paste II, it was recommended that the paste be kept at low temperature.

The following compositions (by weight) of the pastes were found to be appropriate:

when MVP/(MVP+St)=0.8
(St+MVP+DVB)/PVC=1.5～1.8
DVB/(St+MVP+DVB)=0.05～0.1
and DOP/PVC=0.3～0.4 and
when MVP/(MVP+St)=0.6
(St+MVP+DVB)/PVC=1.2～1.4
DVB/(St+MVP+DVB)=0.05～0.1
and DOP/PVC=0.2～0.3

The ratio of methyl iodide to petroleum ether as a solvent does not affect the properties of the membrane very much, but quaternization with methyl iodide by itself injures the appearance of the membrane.

The following conditions were found to be appropriate;

CH_3I/petroleum ether=0.25 (by volume)
at room temperature and for 10～15 hr.

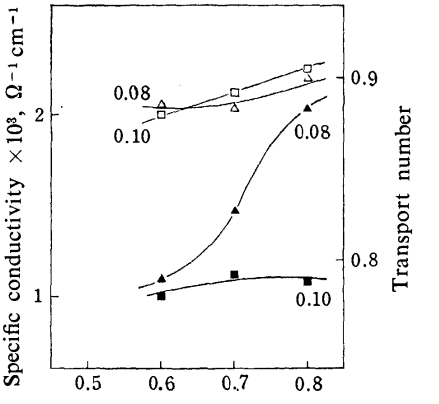

Fig. 5. Ratio of monomers—Properties of anion exchange membranes of MVP type.
The numbers in the figure are DVB/(St+MVP+DVB) (by weight).
Compositions of the paste (by weight):
(St+MVP+DVB)/PVC=1.3, DOP/PVC=0.3
□, △: Specific conductivity
■, ▲: Transport number

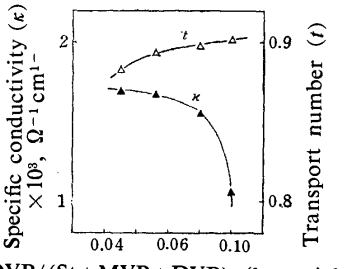

Fig. 6. DVB contents in the pastes—Properties of anion exchange membranes of MVP type.
Compositions of the pastes (by weight):
MVP/(St+MVP)=0.8
(St+MVP+DVB)/PVC=1.3
DOP/PVC=0.3

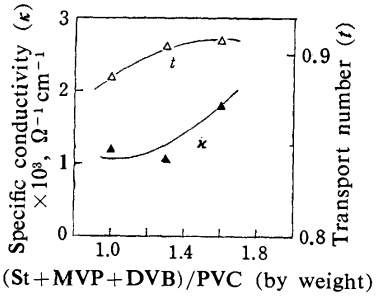

Fig. 7. Monomers contens in the pastes—Properties of anion exchange membranes of MVP type.
Compositions of the pastes (by weight):
MVP/(MVP+St)=0.8
DOP/PVC=0.3
DVB/(MVP+St+DVB)=0.1

TABLE I. RELATIVE DIMENSIONAL CHANGE OF ION EXCHANGE MEMBRANES OF VARIOUS TYPES

Solution	Cation exchange membrane	Anion exchange membrane of St type	Anion exchange membrane of MVP type
0.5 N NaCl	1.000	1.000	1.000
2.5 N NaCl	0.994	0.999	0.999
0.5 N $CaCl_2$	0.997	1.000	1.002
1 N NH_4OH	1.000	1.001	1.004
1 N HCl	0.999	1.000	1.003

TABLE II. PROPERTIES OF THE MEMBRANES

Membrane	Cation exchange membrane	Anion exchange membrane of St type	Anion exchange membrane of MVP type
Water content, g. H_2O/g. dry membrane	0.20~0.22	0.20~0.22	0.28~0.30
Exchange capacity, meq./g. dry membrane	1.1 ~1.2	1.6 ~1.7	1.9 ~2.0
Fixed ion concentration, meq./g. H_2O	5 ~6	5 ~6	6 ~7
Electric resistance, Ω/cm^2	5 ~6	5 ~6	3 ~5
Transport, number	0.86~0.88	0.89~0.91	0.90~0.91
Thickness, mm.	0.23~0.24	0.25~0.26	0.22~0.24
Diffusion constant $\times 10^8$, cm^2/sec.	4 ~5	4 ~5	4 ~5
Burst strength, kg./cm^2	4 ~6	4 ~6.5	6 ~7

TABLE III. RELATIVE TRANSPORT NUMBERS

System	Transport number				
	Total cation or total anion	SO_4^{2-}	Ca^{2+}	Mg^{2+}	P
NaCl-$CaCl_2$-Cation exchange membrane	0.987	—	0.401	—	2.04
NaCl-$MgCl_2$-Cation exchange membrane	0.985	—	—	0.313	1.40
NaCl-Na_2SO_4-Anion exchange membrane of St type	0.971	0.017	—	—	0.16
NaCl-Na_2SO_4-Anion exchange membrane of MVP type	0.986	0.013	—	—	0.12

Figures 5 to 7 show the effects of the compositions of the pastes on the electrochemical properties of the membranes. The higher MVP content improves the properties of the membranes by increasing the content of ion exchange groups in the membranes (Fig. 5). With an increase in the DVB contents, anion transport numbers increased and specific conductivities decreased, because of the development of three-dimensional resinous structures (Fig. 6), and with an increase in the monomer contents, the properties of the membranes were improved (Fig. 7).

Properties of the Membranes. — The various properties of the membranes prepared are shown in Tables I—III. The compositions of the pastes used were as follows: (St+DVB)/PVC=0.75, DOP/PVC=0.35 and DVB/(St+DVB)=0.1 for cation exchange membranes; (St+DVB)/PVC=0.91, DOP/PVC=0.24 and DVB/(St+DVB)=0.1 for anion exchange membranes of the St type; and (St+MVP+DVB)/PVC=1.8, DVB/(St+MVP+DVB)=0.05, MVP/(MVP+St)=0.85 and DOP/PVC=0.3 for anion exchange membranes of the MVP type. The compositions of the pastes are shown by weight.

It was clearly shown that the membranes prepared are excellent in dimensional stabilities, as may be seen in Table I. It was considered from the data shown in Table II that the membranes prepared are useful from the practical point of view. As is shown in Table III, cation exchange membranes were more permselective for calcium ions and magnesium ions than for sodium ions, while anion exchange membranes were less permselective for sulfate ions than for chloride ions. The behavior of sulfate ions through anion exchange membranes is desirable in an electrophoretic concentration of sea water[17], but the behavior of magnesium ions and calcium ions through cation exchange membranes is undesirable[12,16].

The durability of ion exchange membranes prepared by the "paste method" could be considered to be good judging from the results of the electrophoretic concentration of sea water over a long period.

Summary

A method for the preparation of ion exchange membranes, called the "paste method", has

17) Y. Onoue, Y, Mizutani and R. Yamane, *Denki Kagaku*, **29**, 294 (1961); *J. Electrochem. Soc. Japan (Oversea Ed.)*, **29**, No. 4, E220 (1961).

been proposed. The pastes prepared from styrene-divinylbenzene-dioctyl phthalate-poly-(vinyl chloride) powder-benzoyl peroxide or from 2-methyl-5-vinylpyridine-styrene-divinyl benzene-dioctyl phthalate-poly(vinyl chloride) powder-benzoyl peroxide were coated on rein forcing materials of Teviron fabric and were treated in a hot press to prepare the base membranes, to which the ion exchange groups were then introduced. The ion exchange membranes thus prepared were excellent in electrochemical, mechanical and dimensional properties as well as in appearance.

The authors wish to thank Messrs, Wataru Teshima, Sumio Akiyama and Takashi Izuo for their help.

Tokuyama Soda Co., Ltd.
Tokuyama, Yamaguchi

*The A. C. Polarography of Thiamine O-Monophosphate**

By Koichi OKAMOTO

(Received November 22, 1961)

Many investigations of such phosphates of thiamine (B_1) as the monophosphate (TMP), diphosphate (TDP, cocarboxylase) and triphosphate (TTP) of thiamine, have been reported from various points of view because of their importance in the biological and medical fields.

Polarographic studies of such phosphates of B_1 may not yet, however, be considered to have been established. Only a short communication on the polarographic behaviors of TDP has been reported[1], and no precise comparisons to the B_1 findings and no studies of the nature of its electrode process have been carried out.

Among the above three phosphates of B_1, TMP was thought to be the most stable and to have the simplest structure, therefore, it was obtained rather easily as pure crystals.

In this paper, the a. c. polarographic behavior of TMP and a discussion of the differences between the behavior of B_1 reported on in a previous work[2] and that of TMP will be presented.

The d. c. polarographic reduction waves of B_1 and its derivatives were generally ill-defined in the buffer solutions because of the unfavorable influences of hydrogen-discharging currents or pre-sodium waves, while their a. c. polarographic reduction waves were rather well-defined, as was described in the previous paper[2]. Similar results were also obtained in the case of TMP. Therefore, the a. c. method was mainly applied in this investigation.

Experimental

Apparatus and Reagents.—The polarograph used was Yanagimoto model PA-102. (D. C. & A. C.); A. C.: ΔE=15 mV. r.m.s., 50 c.p.s., sinusoidal. The characteristics of the dropping mercury electrode were m=1.003 mg. sec^{-1}, t=4.09 sec. (open circuit), and 3.76 sec. (at −1.273 V.).

The TMP used was prepared by the phosphorisation of B_1[3] and was then hydrolyzed to be monophosphate and purified by the column chromatograph (CG-50) until it gave only one spot on the paper chromatography.

Data for the purified TMP used were as follows: R_f=0.12 (Solvent, acetic acid: *n*-butanol; water=1:4:5); the content of TMP as determined by thiochrome reaction test was 99.1%, m. p.=ca. 200°C (decomp.). Microanalytical data:

Found: C, 31.48; H, 4.01; N, 11.77; H_2O, 8.24. Calcd. for $C_{12}H_{18}N_4O_4PS\cdot HCl\cdot Cl\cdot 2H_2O$: C, 31.80; H, 4.22; N, 12.36; H_2O, 7.95%.

The other reagents used were of reagent grade.

Experiments were carried out two or three times on the same kind of sample at 25±0.5°C, and the values obtained were averaged. All potentials and peak currents were expressed in V. vs. S. C. E. and μamp. r. m. s., respectively.

Results

The Influence of the pH Value on i_s and E_s.—Some of the a. c. polarograms of 5.00×10^{-4} mol./l. TMP in the buffer solutions of pH 0.90~10.65 (their ionic strengths were adjusted

* Polarographic Studies of Some Organo-sulfur Compounds, Part III.

1) I. Tachi, *Kagaku no Ryoiki*, Extra Edition, (Nankōdo), **2**, 37 (1949).

2) K. Okamoto, This Bulletin, **34**, 1063 (1961).

3) P. Karrer and M. Viscontini, *Helv. Chim. Acta*, **29**, 711 (1946).

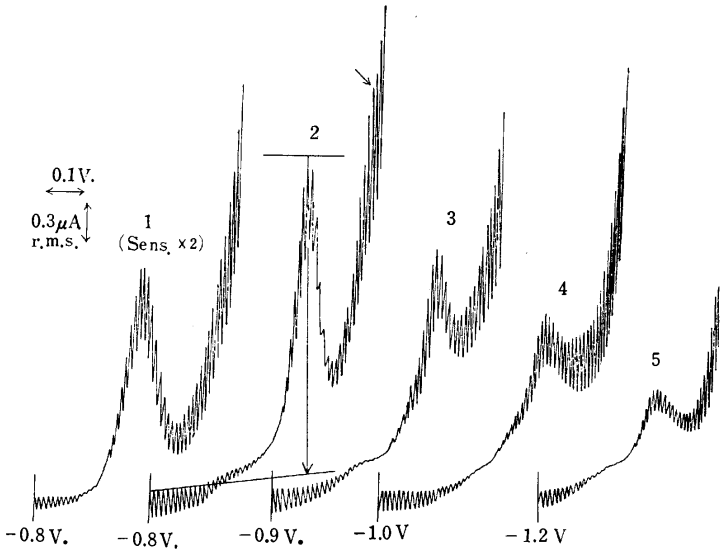

Fig. 1. Some of the A. C. polarograme of TMP.
pH; 1, 0.90; 2, 3.00; 3, 5.00; 4, 6.80; 5, 7.85, [TMP]$=0.500\times10^{-3}$ mol./l., at 25°C, air free, capacitance$=0\mu$F

Table I. The variation of the summit potentials E_s and the peak currents i_s with pH
TMP$=1.00\times10^{-3}$ mol./l., at 25°C

pH	Buffer*	$-E_s$ V. vs. S. C. E.	i_s μamp. r.m.s.
0.90	A	1.090	7.48
1.75	A	1.141	7.48
3.00	B	1.222	5.22
4.00	B	1.270	4.68
5.00	B	1.337	3.78
6.00	C	1.390	3.48
6.80	C	1.440	2.88
7.85	C	1.518	1.08
8.85	C	1.500 1.623	0.87 0.60
9.95	D	ca. 1.517	0.45
10.65	D	NW**	0

A, KCl+HCl
B, 0.25 M acetate buffer
C, 0.25 M phosphate buffer
D, 0.1 M borate buffer
* Ionic strength was adjusted to 0.50 constant by the addition of KCl.
** No wave

to 0.50 by the addition of potassium chloride) and also the method of the measurement of wave height are shown in Fig. 1.

The ralations of the peak currents, i_s, and of the summit potentials, E_s, to the pH value are both summarized in Table I and in Figs. 2 and 3.

One well-defined peaks current was observed at the pH values ca. 2 and ca. 4~8. One peak and an indefinite shoulder (as indicated by an

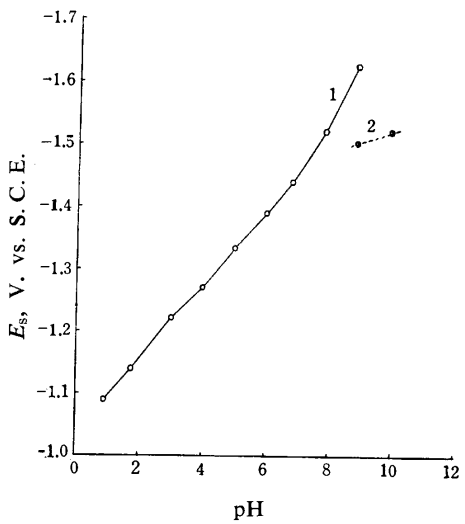

Fig. 2. The relation of pH to E_s.
1, 1st wave 2, pre-wave (indifinite)

arrow in Figs. 1—2.) were observed at the values of pH 1.75 and 3.00.

The behavior of a. c. reduction waves of TMP were not similar to that of B_1[2], as is shown in Fig. 1. Especially the attitude of the second wave of TMP was found to be different from that of B_1; that is, in the case of B_1 a rather definite second peak current was placed at more positive potentials and appeared at the pH value of 4.75, while that of TMP was not observed in the the same pH value region, but at the pH values of 1.75 and 3.00, at more negative potentials.

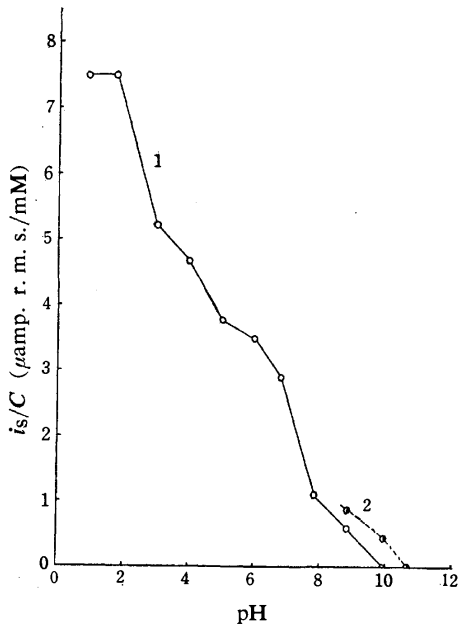

Fig. 3. The relation of pH to i_S.
1 : 1st wave. 2 : pre-wave (indifinite)

The variation of the E_S of TMP was very similar to the E_S of the first wave of B_1 within the pH value range of 4.0~7.0 (Fig. 2).

The peak currents of TMP increased according to the decrease pf pH values, as is shown in Fig. 3, and its heights and that of the first wave of B_1 ware not equivalent, although that of the latter was smaller than the former over all the pH value range studied.

The behavior of the peak current of TMP in basic solutions was almost the same as that of B_1; they both disappeared completely at a pH value of about 10.

The Relation of the Concentration of TMP to i_S and E_S.—In order to learn whether or not the peak current was due to the reduction of TMP itself, the relation between the concentrations and i_S was observed in two kinds of buffer solution, those with pH values of 0.90 and of 4.00. The results obtained are shown in Table II and in Fig. 4.

TABLE II. THE RELATIONS OF THE CONCENTRATIONS TO i_S AT TWO pH VALUES measured at 25°C

Concn. $\times 10^{-3}$ mol./l.	pH=0.90* i_S μamp. r.m.s.	pH=0.90* $-E_S$ V. vs. S.C.E.	pH=4.00** i_S	pH=4.00** $-E_S$
0.05	0.24_5	1.130	0.20_7	1.271
0.10	0.60_5	1.092	0.45_8	1.270
0.25	1.86_5	1.103	1.17_0	1.268
0.50	3.54_8	1.109	2.28_0	1.276
0.75	4.71_0	1.116	3.24_0	1.283
1.00	6.22_5	1.124	4.18_5	1.290

* KCl+HCl (μ=0.50) ** 0.25 M acetate buffer (μ=0.50)

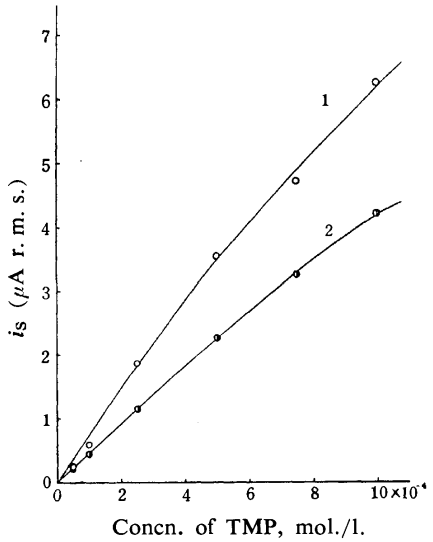

Fig. 4. The relation of the concentrations to i_S.
1, pH 0.90 2, pH 4.00

Almost linear relations between the concentrations and i_S were found for both samples; therefore, the first wave of TMP seemed to be the real reduction wave of TMP itself.

The summit potential, E_S, slightly shifted to negative potentials with the increase in the concentration of TMP.

This variation in of i_S and E_S according to the concentration change was very similar to that of B_1.

The Temperature Coefficients of i_S.—The temperature coefficient of the wave height was obtained as 2.17% between 18~32°C on acetate buffer solutions (μ=0.50) with a pH value of 4.00, containing 5.00×10^{-4} mol./l. of TMP.

The coefficient was larger than the theoretical values, 1.0~1.3%, for a. c. palarographic waves. This was thought to be mainly caused by the irreversible tendency of the electrode process of TMP, not by its kinetic properties.

The Influence of Mercury Heights H to i_S.—The relationship of H to i_S was studied by plotting H (corrected with the reverse pressure of H) against i_S at 25±0.5°C on the acetate buffer solution with a pH value of 4.00, containing 5.00×10^{-4} mol./l. of TMP.

The linear relation obtained may be formulated as follows:

$$i_S = 0.011H + 1.694$$

In the case of a. c. polarography, the i_S values were said to be independent of the H

values. The above relation almost coincided with the theory.

Electrocapillary Curve.—The electrocapillary curve of 5.00×10^{-4} mol./l. of TMP in the acetate buffer with a pH value of 4.00 is drawn in Fig. 5. Over the whole potential range, the drop time, t, in the sample solution was smaller than in the base solution, but at the electrocapillary zero, ca. -0.5 V., the difference was only 0.01 sec. A small step was observed at the potential $-1.25\sim-1.30$ V. corresponding to the summit potential of TMP, -1.273 V. A weak adsorption seemed to take place at the surface of DME over the whole potential range except at electrocapillary zero, but this could not have any remarkable effect upon the apparent a. c. waves.

When the electrocapillary curve of TMP was compared with that of B_1, the adsorption of TMP in the positive side to electrocapillary zero was the most different phenomenon.

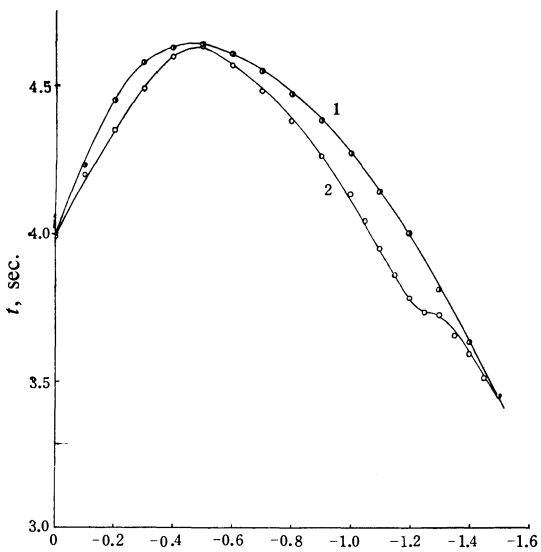

Fig. 5. Electrocapillary curves.
1, Base solution: acetate buffer of pH 4.00, $\mu=0.50$
2, 0.500×10^{-3} mol./l. of TMP in 1

Millicoulometric Determination (D. C. Method) of the *n*-Value.—The electrode reactions of TMP or B_1 have not yet been defined because of their complexity, but comparatively precise investigations of the reduction processes of B_1 have been reported by Asahi[4] recently. Asahi has suggested that B_1 is reduced by DME at the pyrimidine and also that the thiazol ring consumed about 10 electrons.

It was thought that the polarographic reduction process of TMP was similar to that of B_1 considering the reducible groups in a molecule.

Millicoulometric measurement of the n-values, therefore, was employed in order to confirm the number of electrons discharged, but the macro-scale-controlled potential electrolysis with a wide-surface-area mercury cathode was not applied, because the conditions of such a macro-coulometry were thought to be different from those of polarography.

The cell for millicoulometry used was of the Meites type[5], with the external S. C. E. anode separated from the cathodic part by a fine-sintered glass wall and an agar-agar bridge.

The coulometry was carried out on three kinds of bufier solutions, with pH values of 1.45, 3.00 and 4.00. d. c. potentials were applied, and the decrease in the d. c. wave height after electrolysis was measured.

When the pH value of the solution rose above about 4, the d. c. polarogram of TMP came to be very ill-defined, so that in the region with higher pH values than 4, millicoulometric studies could not be carried out.

The results obtained are summarized in Table III.

Table III. The results of millicoulometry

pH	$-E_{applied}$	n-Value
1.45	1.15	9.00
3.00	1.25	8.77
4.00	1.30	7.86

[TMP] $=5.371\times10^{-4}$ mol./l. Volume of solution, 0.25 ml. Electrolysis time, 100 min. Temp., 25 ± 0.5°C. Air was removed by nitrogen gas bubbling.

As is shown in Table III, the n-value of TMP was estimated to be 9 at a pH value of 3.0, but it seemed to decrease at pH values> 4, in accordance with the gradual decrease of the peak current of the a. c. polarogram with the pH value increse (Fig. 3).

The n-values obtained were found nearly to coincide with Asahi's estimation.

Discussion

As has been described in the previous sections, comparatively well-defined a. c. polarographic waves of TMP observed in acidic buffer solutions, were not simple tensammetric waves, but were reduction waves with a few tensammetric properties.

The most remarkable difference between the a. c. polarogram of TMP and that of B_1 was

4) Y. Asahi, *J. Pharm. Soc. Japan* (*Yakugaku Zasshi*), **80**, 1222 (1960).

5) T. Meites and L. Meites, *Anal. Chem.*, **23**, 1893 (1951).

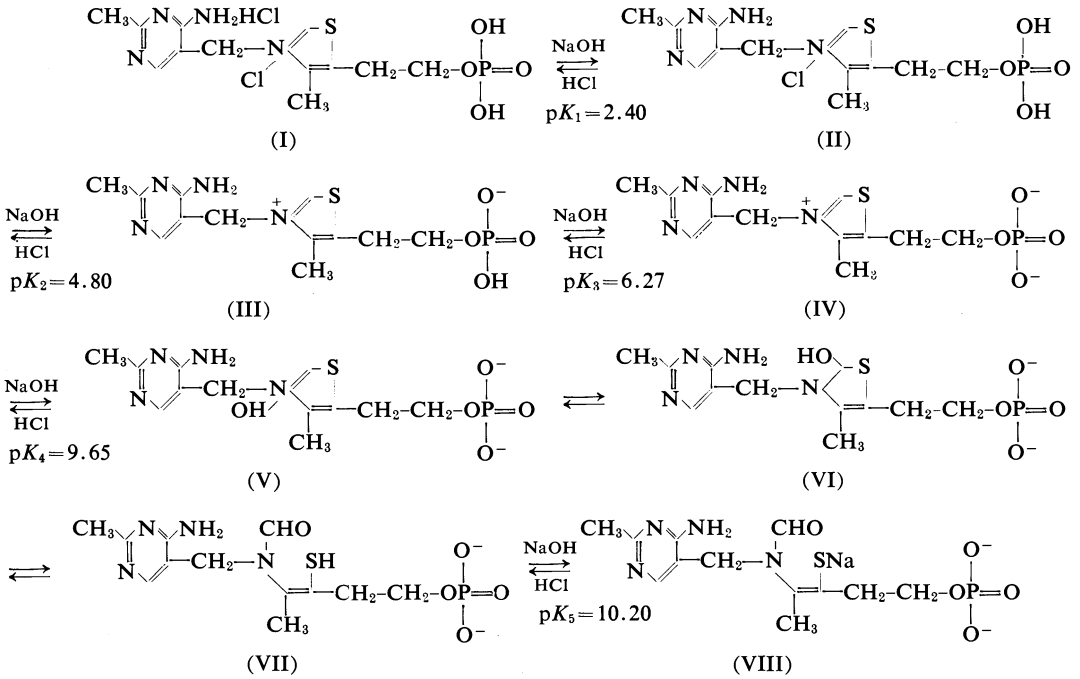

Fig. 6. Acid-base equilibrium of TMP.

the behavior of the second wave, which appeared rather definitely for B_1 at pH values>4.75, while it could not be observed in the same pH value region for TMP, but only as an obscure shoulder in the pH-value region of 1.75~3.

An other different result was the weak adsorption of TMP at the electrocapillary positive range, while the lack of it for B_1 could be observed on the electrocapillary curves.

This different behavior of TMP and of B_1 is thought to be caused by their different acid-base equilibrium processes.

The dissociation equilibrium of TMP when titrated with a sodium hydroxide solution can be shown as in Fig. 6, while its experimental titration curve is as in Fig. 7.

Definite pH-value changes were found at 1 mol. equiv. and at 3 mol. equiv., while an indefinite one was found at about a 5 mol. equiv. of sodium hydroxide.

The pK-values can be approximately estimated on the titration curve as $pK_1=2.4_0$, $pK_2=4.8_0$, $pK_3=6.2_7$, $pK_4=9.6_5$, and $pK_5=10.2_0$.

The obscure shoulder of the a. c. polarograms of TMP which appeared in the region of 1.75 ~3.00 pH values was, therefore, thought to be related to II species, but it could not be defined because of its ill-defined form.

The gradual decrease in the wave height of the a. c. polarograms according to the pH increase was caused by the comparatively continuous transition of the ionic species of

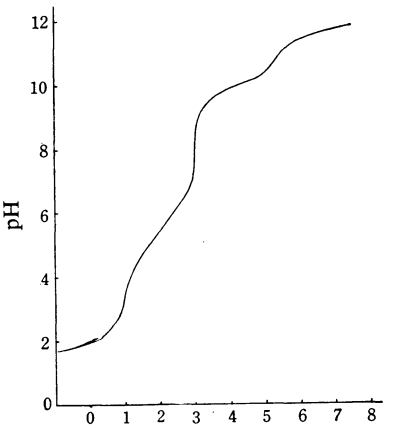

Fig. 7. Potentiometric titration curve of TMP.

TMP and by the complete disappearance of the wave at a pH value of about 10 was due to the disappearance of the thiazol ring as illustrated in Fig. 6.

The electron number discharged was confirmed for I species as 9, and as ca. 8 for II species, but that for other species could not be measured. Such a decrease in the n-values for each ionic species was thought to be mainly due to the reducibility of the pyrimidine rings with or without a proton; the wave height of I species was, therefore, the highest, as is shown in Fig. 3.

When the approximate assignment of the species of TMP in the solution of a certain pH value were made using the titration curve, species I was thought to exist in pH values <2, II in pH values ca. 3.5, III in those ca. 5.5, and IV in those ca. 8.

The comparisons, therefore, of the wave heights at each pH value seemed almost exactly to indicate the reducibility or the distinctive in electrode process of each species. The ratios of i_s at a pH value of 2 and at a pH value of 3.5, and of i_s at a pH value of 3.5 and at a pH value of 5.5 were $i_s^{3.5}/i_s=0.67$ and $i_s^{5.5}/i_s^{3.5}=0.74$ respectively. The apparent reducibility of a pyrimidine ring without hydrogen chloride was lower by about 67% than that of a ring with hydrogen chloride, while that of a thiazol ring without chlorine was also lower by about 74% than that of a ring of with chlorine. The reduction process was considered to be different for each ionic species according to the difference in the state of the amines in them.

The reduction mechanisms of TMP at DME could not be defined in this work, but it was suggested that the reduction may take place at both the pyrimidine ring and the thiazol ring, consuming 8 or 9 electrons.

Summary

A. C. polarographic studies of TMP, as well as a discussion of the polarographic behavior of TMP compared with that of B_1 reported on in a previous paper[1], were carried out.

TMP showed well-defined peak currents of almost the same E_s values as the second peak current of B_1 in the region of pH values <10, and obscure second waves were also observed at pH values between 1.75 and 3.00. The relation of the i_s of the first wave of TMP to the pH value was also similar to the second wave of B_1. The wave corresponding to the first wave of B_1, however, was not recognized for TMP under any of the conditions studied.

The nature of the first wave of TMP was determined to be that of the diffusion currents, not of the adsorption, kinetic, etc.

The number of electrons discharged could be ascertained by the millicoulometric technique as 9 at pH values <3 and 8 at a pH value of 4. The electrode reaction, therefore, of TMP was considered to be the same as that of B_1.

Some explanation of the relation of i_s to the pH value was attempted by reference to the pK values of TMP obtained from its experimental potentiometric titration curve.

The author is very much indebted to Director Munetosi Matsui for affording facilities for this investigation.

Physical Chemistry Section
Takamine Laboratory
Sankyo Co., Ltd.
Shinagawa-ku, Tokyo

*The A. C. Polarography of S-Benzoylthiamine O-Monophosphate**

By Koichi OKAMOTO

(Received November 22, 1961)

One of the new derivatives of thiamine, *S*-benzoylthiamine *O*-monophosphate (BTMP) (I), has been found to have such predominant pharmaceutical effects as the remarkable increase and prolongation of the thiamine blood level in administration. Many pharmaceutical, chemotherapic and physicochemical studies of on BTMP have, therefore, been reported.

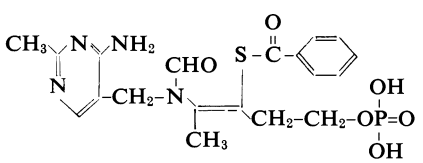

(I)

Some of the polarographic studies of BTMP have been undertaken by the author[1] and by Tachi[2] in order to learn its physicochemical properties.

In a previous work[1] a conventional polarographic study of BTMP was reported, but no theoretical treatment of the d.c. reduction waves of BTMP could be made, because of their irreversibility and ill-defined forms.

Alternating current polarographic techniques were applied in order to make the nature of

* Polarographic Studies of Some Organosulfur Compounds. Part IV.

1) K. Okamoto, *Vitamine (Kyoto)*, **22**, 364 (1961).
2) I. Tachi, ibid., **21**, 423 (1960).

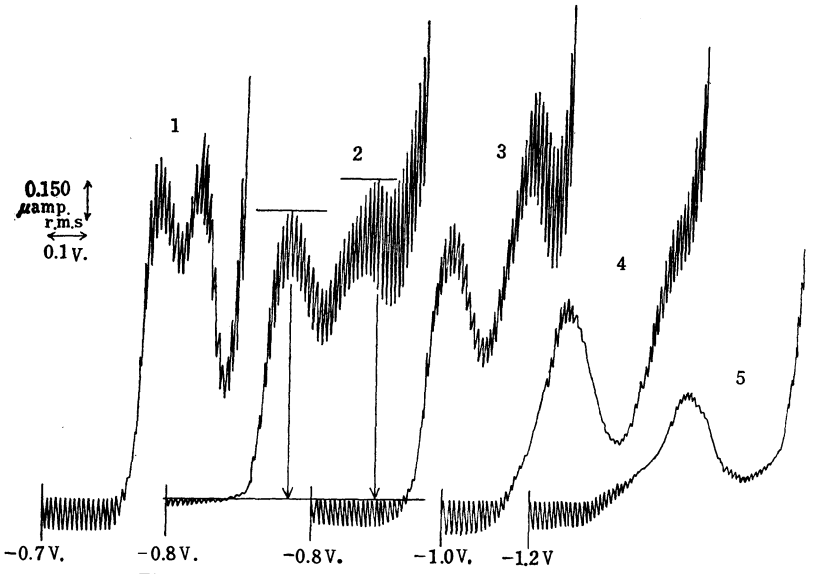

Fig. 1. Some of the a. c. polarograms of BTMP.
pH 1, 1.00 2, 3.00 3, 4.00 4, 7.00 5, 8.55
[BTMP] $=0.40\times10^{-3}$ mol./l., at 25°C, air free, capacitance=0 μF

the reduction waves of BTMP more definite. By the a.c. method, two very definite peak currents could be observed and it became possible to discuss the reversibility of its electrode reaction.

In this paper, the a.c. polarographic behavior of BTMP and some of the theoretical considerations of the reversibilty of its electrode reaction will be presented.

Experimental

Apparatus.—The polarograph used was Yanagimoto model PA-102 (d.c. and a.c.), a.c.; $\Delta E=$ 15 mV. r.m.s., 50 c.p.s., sinusoidal. The characteristics of the dropping mercury electrode were: $m=1.006$ mg. sec^{-1} (open circuit), $t=4.24$ sec. (open circuit), 4.03 sec. (at −1.164 V.) and 3.73 sec. (at −1.377 V.). The thermostat was Yanagimoto's water bath for polarography with an accuracy of ±0.5°C.

Reagents. — The BTMP used was of purified crystal, as in the previous work[1].

The *S*-*p*-nitrobenzoylthiamine *o*-monophosphate (NBTMP) (II) used was that synthesized in our laboratory by the same method as for BTMP; m.p.=154~156°C (decomp.).

Found: C, 41.73; H, 4.70; N, 12.89. Calcd. for $C_{19}H_{22}N_5O_8PS\cdot2H_2O$: C, 41.68; H, 4.79; N, 12.80%.

Results

The Effect of the pH Value on the Summit Potential, E_s, and the Peak Current, i_s.—In the a.c. polarographic technique, the use of comparatively concentrated buffer solutions is

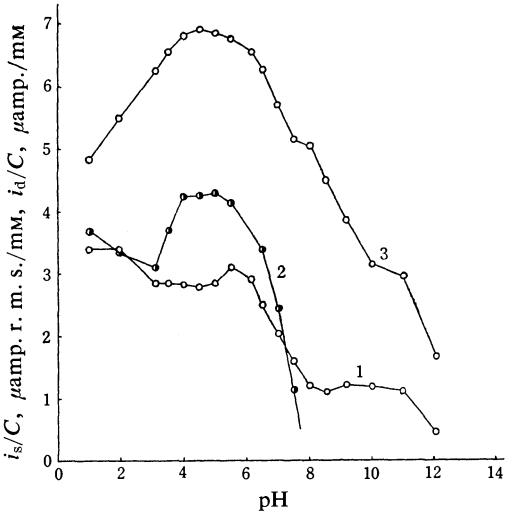

Fig. 2. The relations of pH to i_s^1, i_s^2 and i_d^1.
1, a.c. 1st wave 2, a.c. 2nd wave
3, d.c. 1st wave

preferable in order to reduce the resistance of the electrolyte solution; therefore, 0.2 or 0.25 mol./l. buffer solutions were employed in the following experiments.

No maximum suppressor was used, thus avoiding its unfavorable influences upon the electrode reaction.

All experiments, except for some special studies, were carried out at 25±0.5°C, and air was removed by the bubbling of hydrogen.

All the values of potentials and of currents

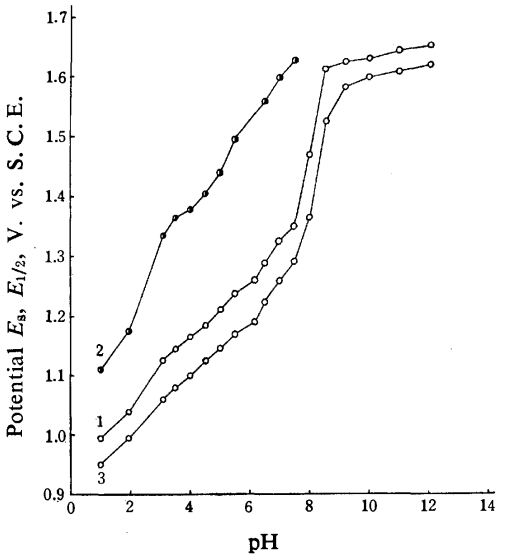

Fig. 3. The relations of pH to E_s^1, E_s^2 and $E_{1/2}^1$.
1: a.c. 1st wave 2: a.c. 2nd wave
3: d.c. 1st wave

TABLE I. THE VARIATION OF THE SUMMIT POTENTIALS E_s AND THE PEAK CURRENTS i_s WITH pH
[BTMP] $=0.40\times10^{-3}$ mol./l., 25°C

pH	Buffer†	i_s^1 μamp. r.m.s.	i_s^2	$-E_s^1$ V. vs. S.C.E.	$-E_s^2$
1.00	A	1.36	1.47	0.994	1.110
1.95	A	1.37	1.34	1.040	1.176
3.10	B	1.13	1.23	1.125	1.335
3.50	B	1.15	1.48	1.143	1.364
4.00	B	1.13	1.70	1.164	1.377
4.50	B	1.11	1.70	1.186	1.404
5.00	B	1.14	1.72	1.212	1.441
5.50	B	1.25	ca. 1.65*	1.237	ca. 1.50*
6.15	C	1.17	NW**	1.262	NW
6.50	C	1.01	ca. 1.35*	1.288	ca. 1.56*
7.00	C	0.81	ca. 0.98*	1.325	ca. 1.60*
7.50	C	0.64	ca. 0.45*	1.350	ca. 1.63*
8.00	C	0.47	NW	1.468	NW
8.55	C	0.43	NW	1.615	NW
9.20	D	0.49	NW	1.627	NW
10.00	D	0.47	NW	1.632	NW
11.00	D	0.45	NW	1.644	NW
12.05	D	0.17	NW	1.653	NW

† Ionic strength was adjusted to 0.50 constant by the addition of KCl.
A, 0.2 M KCl+HCl
B, 0.25 M acetate buffer
C, 0.25 M phosphate buffer
D, 0.1 M borate buffer
* Shoulder
** No wave

are expressed in V. vs. S. C. E. and. μamp. r. m. s. respectively.

On account of the somewhat inferior reproducibility of a. c. polarograms, every measurement was repeated two or three times, and the values obtained were averaged.

Typical polarograms are shown in Fig. 1.

As it was necessary to compare the values obtained under the same conditions by the d. c. and a. c. methods, the d. c. polarograms were observed again.

As is shown in Fig. 2, the effect of the pH value on i_s^1 was very different from that on i_d^1, but the effect on E_s^1 was not different from that on $E_{1/2}^1$, as is shown in Fig. 3.

Fortunately, the second wave, which had not been observed well by the d. c. method, could be obtained clearly by the a. c. method.

As is shown in Fig. 2-2, the behavior of the second wave in various buffer solutions is interesting.

All numerical values are shown in Table I.

The Effect of the Concentration on i_s^1 and i_s^2 and on E_s^1 and E_s^2.—For the theoretical considerations, it seemed to be rather simple to chose that condition in which an ionic form of BTMP in the solution had no charge, namely, the condition at the isoelectric point where the pH value=4.05[3]. For this reason, the following studies were carried out on a 0.25 mol./l. acetate buffer solution with a pH value of 4.0.

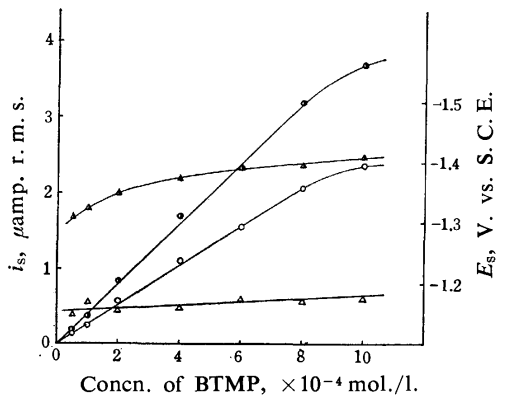

Fig. 4. The relations of the concentrations to i_s and E_s.
1, i_s^1 2, i_s^2 3, E_s^1 4, E_s^2
Base solution: pH 4.00 acetate buffer, 25°C

The relations between the concentrations of BTMP and i_s^1 and i_s^2 were both linear up to 0.8×10^{-3} mol./l. The saturating tendencies were observed over 0.8×10^{-3} mol./l., and they passed exactly through the zero point, as is shown in Fig. 4. Such relationships were

3) A. Ito, ibid, 22, 349 (1961).

considered to indicate that there was no remarkable adsorption or desorption phenomena at the interface of DME and the solution.

The effect of the concentration on E_s^1 and E_s^2 is shown in Fig. 4.

The Effect of the Mercury Reservoir Height on i_s^1 and i_s^2.—In a. c. polarography, the reaction current was not influenced by the height of the mercury reservoir, but it was proportional to the surface area of DME, so that i_s was usually independent of H.

A linear but slight change of i_s for BTMP was observed with these changes in H values:

$$i_s^1 = 0.007H + 0.687$$

$$i_s^2 = 0.004H + 1.404$$

on 0.25 mol./l. acetate buffer solutions of pH 4.0 containing 0.40×10^{-3} mol./l. of BTMP at 25±0.5°C.

The above relations coincide with the theoretical results in a. c. polarography.

Temperature Coefficients of i_s^1 and i_s^2.—In a. c. polarography, the temperature coefficient of i_s was usually smaller than of i_d, so that +1.0~1.3% at about 25°C were considered to be the ordinary values.

When some adsorption-desorption phenomena occur, a negative coefficient was obtained because of the decrease in the number of molecules adsorbed at DME with the rise in temperature. If the measurements of coefficients are carried out at various concentrations of depolarizer, a discontinuous change, such as from positive to negative values, was often observed according to the change in the adsorption state.

TABLE II. TEMPERATURE COEFFICIENTS OF i_s AT VARIOUS CONCENTRATIONS

Base solution: 0.25 M acetate buffer of pH=4.00

Concn. mol./l.	i_s, μamp. r. m. s.		Temp. coeff.
	10°C	25°C	%
8×10^{-5}	$i_s^1=0.16$	0.22	+1.97
	$i_s^2=0.19$	0.30	+2.37
4×10^{-4}	0.79	1.10	+1.85
	0.92	1.64	+2.91
8×10^{-4}	1.40	1.96	+1.89
	1.88	3.05	+2.55
2×10^{-3}	2.55	3.65	+2.01
	4.03	5.88	+2.10

The temperature coefficients of BTMP at various concentrations are summarized in Table II. In the range of concentrations of 8×10^{-5}~2×10^{-3} mol./l., the coefficients of both i_s^1 and and i_s^2 were positive, but they were larger than that of the theoretical one. No discontinuous change was obtained; the coefficient of the first wave was in 1.85~2.01%, and the second was in 2.10~2.91%. The i_s^1 and i_s^2 seemed not to be controlled by the adsorption process but by diffusion, and the values larger than the theoretical ones were attributed to the influence of the irreversibility of the electrode reaction.

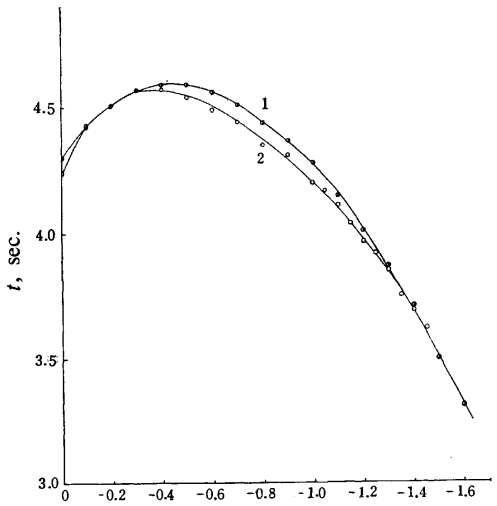

Fig. 5. Electrocapillary curve.
1 Base solution: acetate buffer solution of pH 4.00
2 0.40×10^{-3} mol./l. of BTMP in 1

Electrocapillary Curve.—The electrocapillary curve of 0.40×10^{-3} mol./l. BTMP in a 0.25 mol./l. acetate buffer solution with a pH value of 4.0 and of the base solution are shown in Fig. 5.

Upon the addition of BTMP, a slight decrease of t in the range of potential −0.3~−1.4 V. was observed, and there was no remarkable kink was at any poiential. The values of t were 0.05 sec. and 0.02 sec. smaller than that of the base solution at the potentials corresponding to the first and the second waves.

BTMP was considered to be weakly adsorbed at the positive side of the molecule at the surface of DME in the range of −0.3~−1.4 V., so that there were no predominant influences of adsorption phenomena on i_s^1 and i_s^2.

A Consideration of the Electrode Reaction.—As has been described in previous sections, two definite peak currents of BTMP were considered to be controlled by the electrode reaction, not by the adsorption.

The discussions, therefore, of the reversibility and the mechanism of the electrode reaction were thought to be possible.

The estimations of the diffusion coefficient, D, and the electron number, n, were carried out. Then the calculations of the transfer coefficient, α, and the rate constant, k_G, were also made.

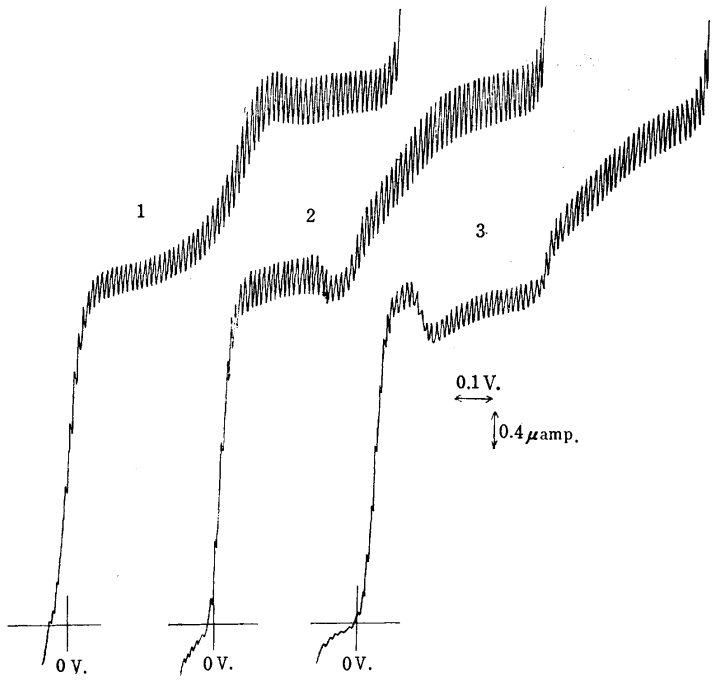

Fig. 6. Some of the d. c. polarograms of NBTMP.
pH 1, 0.81 2, 1.36 3, 1.73 [NBTMP] $=0.477\times10^{-3}$ mol./l., 25°C

The Estimation of the Diffusion Coefficient of BTMP.—The *n*-values and the diffusion coefficient of BTMP could not be obtained because of the irreversibility of the electrode reaction.

When some of the reducible radicals the electrode process of which had already been confirmed were substituted into a suitable position in BTMP, the polarographic diffusion coefficient of the substituted BTMP might be calculated from the reduction wave by the substituted radical.

The nitro radical, therefore, was substituted into the para-position of the phenyl group in BTMP to obtain *S*-*p*-nitrobenzoylthiamine *O*-monophosphate (NBTMP) (II).

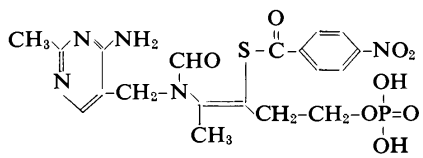

(II)

Some of the d. c. polarographic waves of NBTMP are shown in Fig. 6. The first and the second waves were thought to be reduced to the reduction of the nitro group to hydroxylamine ($n=4$) and to amine ($n=2$) respectively. The third wave, which is not drawn in Fig. 6, was due to the reduction of the *S*-acyl bond, as was observed for BTMP.

A minimum at about −0.25 V. which did not disappear upon the addition of Triton-X-100 was thought to be caused by the strong adsorption of NBTMP to the DME surface.

The values obtained for the first wave of 0.239×10^{-3} mol./l. NBTMP in the buffer solution with a pH value of 1.36 were as follows: $i_d=1.76$ μamp., $n=4$, $C=0.239\times10^{-3}$ mol./l. and $m^{2/3}t^{1/6}=1.330$ mg$^{2/3}$ sec$^{-1/2}$.

The diffusion coefficient D could be obtained by Ilkovic' equation as $D=5.22\times10^{-6}$ cm^2 sec^{-1}.

The molar volumes of BTMP and of NBTMP were thought to be approximately equivalent, so that the D value could be applied to that of BTMP.

The number of electrons discharged for BTMP, therefore, at various pH-value conditions could be calculated using the above D-value. They are summarized in Table III.

The change in *n*-values with the change in pH values was found almost to coincide with the change in the wave height, with the largest value of 4 showing in the pH range of 4.5～5.5. These variations of *n*-values with pH-value change are thought to be due to the differences in the reduction process of the ionic species of BTMP in the solutions of various pH values.

Consideration of the Reversibility of the First Wave.—Theoretical equations for the reversible and irreversible a. c. polarograms have already been given by H. Matsuda[4] as follows:

4) H. Matsuda, *Z. Elektrochem.*, **62**, 977 (1958).

TABLE III. THE COMPARISON OF THE REVERSIBILITIES OF THE ELECTRODE REACTION OF BTMP AT VARIOUS pH VALUES

pH	$-E_{1/2}$	$-E_s$	$E_{1/2}-E_s$	$RT/\alpha nF$	i_d/C	i_s/C	i_s/i_d	n	αn	α	$k_G/D^{1/2}$	k_G
	V. vs. S. C. E.		mV.	mV.	μamp./mmol.	μamp.r.m.s./mmol.					$sec^{-1/2}$	$cm.sec^{-1}\times10^{-4}$
1.00	0.950	0.944	44	25	4.86	3.40	0.70	2.74	2.51	0.91_6	0.25_2	5.7_5
1.95	0.996	1.040	44	26	5.49	3.43	0.63	3.10	2.26	0.72_9	0.38_6	8.8_0
3.10	1.062	1.125	63	36	6.27	2.83	0.45	3.55	1.62	0.45_6	0.34_9	7.9_6
3.50	1.080	1.143	63	35	6.55	2.88	0.44	3.71	1.58	0.42_6	0.38_5	8.7_9
4.00	1.100	1.164	64	37	6.80	2.83	0.42	3.86	1.51	0.39_1	0.43_1	9.8_3
4.50	1.125	1.186	61	43	6.90	2.78	0.40	3.92	1.44	0.36_7	0.60_7	13.8_4
5.00	1.145	1.212	67	46	6.85	2.85	0.44	3.71	1.58	0.42_8	0.30_1	6.8_6
5.50	1.168	1.237	69	50	6.75	3.13	0.46	3.84	1.65	0.43_0	0.22_0	5.0_2
6.15	1.191	1.262	71	52	6.55	2.93	0.45	3.74	1.62	0.43_3	0.21_1	4.8_2
6.50	1.223	1.288	65	67	6.27	2.53	0.40	3.58	1.44	0.40_2	0.48_6	11.0_5
7.00	1.259	1.325	66	63	5.70	2.03	0.36	3.26	1.29	0.39_6	0.67_4	15.3_7
7.50	1.292	1.350	58	63	5.15	1.60	0.31	2.95	1.11	0.37_6	1.51_4	34.5_2
8.00	1.366	1.468	102	77	5.04	1.18	0.23	2.90	0.83	0.28_6	0.68_7	15.6_6
8.55	1.526	1.615	89	100	4.50	1.08	0.24	2.63	0.82	0.31_2	1.00_9	23.0_5
9.20	1.584	1.627	43	50	3.87	1.23	0.32	2.28	1.15	0.50_4	2.70_9	61.7_7
10.00	1.599	1.632	33	35	3.14	1.18	0.38	1.85	1.36	0.73_5	3.23_7	73.8_0
11.00	1.609	1.644	35	41	2.94	1.13	0.38	1.73	1.36	0.78_6	2.91_2	66.3_9
12.05	1.621	1.653	32	55	1.67	0.43	0.26	0.98	0.93	0.94_9	5.83_3	132.9_9

For reversible reaction:

$$[(k_G \cdot f/D^{1/2})/\sqrt{\omega} > 40\alpha^{\alpha}\beta^{\beta}]$$

$$\bar{i}_s = 0.183\bar{i}_d(\tau\omega)^{1/2}(nF\Delta E/2RT) \quad (3)$$

$$E_s = E_{1/2} \quad (4)$$

For irreversible reaction:

$$(k_G \cdot f/D^{1/2})\sqrt{\tau} < 10^{-(1+2\alpha)}$$

$$\bar{i}_s = (2/\pi)\bar{i}_d(\alpha nF/RT)\Delta E[1-1.24(\tau\omega)^{-0.223}] \quad (5)$$

$$E_s = E_{1/2} + (RT/\alpha nF)[\ln k_G f/D^{1/2} - (1/2)\ln\omega - \ln\{1+1.67(\tau\omega)^{-0.490}\}] \quad (6)$$

where: $\bar{i}_d$ = diffusion current (d. c.).

$\bar{i}_s$ = peak current (a. c.).

$\omega = \pi/\theta$, angular frequency of superimposed alternating current

τ = drop time

ΔE = amplitude of superimposed a. c.

α = transfere coefficient ($\alpha+\beta=1$)

k_G = rate constant

D = diffusion coefficient of depolarizer

f = activity coefficient of depolarizer

$E_{1/2}$ = half-wave potential (d. c.)

E_s = summit potential (a. c.)

When the electrode raction is reversible, the half-wave potential $E_{1/2}$ and the summit potential E_s should coincide perfectly, according to Eq. 4, and the rate of $\bar{i}_s/\bar{i}_d$ is 0.183 $(\tau\omega)^{1/2}$ $(nF\Delta E/2RT)$ according to Eq. 3.

The slope of the d. c. wave ($=RT/\alpha nF$) indicates the reversibility of the d. c. electrode reaction. A comparison of the values of $RT/\alpha nF$, $E_{1/2}-E_s$, i_s/i_d, etc. of the first wave at various pH values is shown in Table III and in Fig. 7.

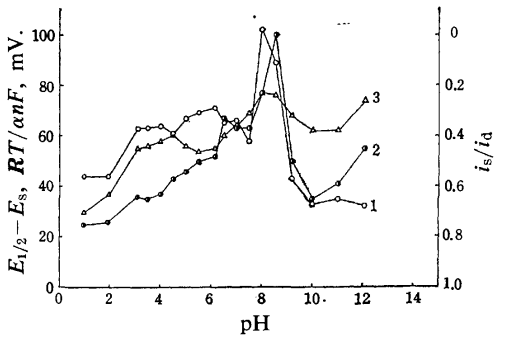

Fig. 7. The relations of pH to $E_{1/2}-E_s$, $RT/\alpha nF$ and i_s/i_d.
1, $E_{1/2}-E_s$ 2, $RT/\alpha nF$ 3, i_s/i_d

As is shown in Fig. 7, the reversibility of the electrode reaction seemed to change in rather a complicated way with the change in the pH-value. The smallest values for $E_{1/2}-E_s$, i_d/i_s and $RT/\alpha nF$ were each obtained at about pH 2~0 and 10 while remarkably large values were obtained at pH 8.0~8.5.

If these three values are taken as indicating the apparent reversibility of the electrode reaction, it is found that the smaller the pH value, the more reversible the electrode reaction in the acidic pH value region.

The stability of the *S*-acyl bond in BTMP was not sufficient in the basic medium, for it therein decomposed to give thiamine *O*-monophosphate, thiamine and other unknown decomposition products. The discussion, therefore, of the electrode reaction of BTMP in the basic medium was thought to be rather impossible. The discontinuous change on the curve in Fig.

7 at pH values 8.0~8.5 seemed to be caused by the decomposition process of BTMP.

In order to calculate the reaction rate constant, Eqs. 5 and 6 were thought to be useful, but they were defined under the condition that the superimposed a. c. amplitude, ΔE, was smaller than 5 mV. r. m. s. In this experiment ΔE=15 mV. r. m. s.; therefore, the accurate value of k_G could not be obtained. However, it seemed possible to estimate k_G and α approximately by the use of the above equations.

The procedure of the calculation may be described in the case of solution with a pH value of 4.00 as follows:

[BTMP] $=1.000\times10^{-3}$ mol./l., T=25°C, ΔE= 15 mV. r. m. s., $i_d=6.80\mu$amp., $i_\lambda=2.83\ \mu$amp. r. m. s., f=1, $\omega=100\pi$ (rad. sec^{-1}), τ=4.03 sec. (at the summit potential of the first wave), $E_{1/2}=-1.100$ V. vs. S. C. E., $E_s=-1.164$ V. vs. S. C. E., n=4.

Equation 6 was rewritten into Eq. 6-1 using the above values:

$$-1.083=1/\alpha n(\log k_G/D^{1/2}-1.2697) \qquad (6\text{-}1)$$

On the other hand, αn was obtained from Eq. 5.

$$\alpha n=1.51;\quad \text{therefore,}\quad \alpha=1.51/4=0.38$$

When αn was introduced into Eq. 6-1, Eq. 6-2 was obtained:

$$k_G/D^{1/2}=4.31_1\times10^{-1} \qquad (6\text{-}2)$$

The $D^{1/2}$ value was obtained, as in the previous section for NBTMP, as 2.284×10^{-3} cm. sec$^{-1/2}$, so that

$$k_G=0.43_1\times2.284\times10^{-3}=9.83\times10^{-4}\ \text{cm. sec}^{-1}$$

The k_G and α-values of the a. c. first wave of BTMP at various pH values calculated by the above procedure are both shown in Table III and Fig. 8.

In the acidic pH value region, the variation of α and k_G with the pH value in Fig. 8 indicates that the more acidic the medium, the larger the transfer coefficient α, but the k_G-values did not change remarkably.

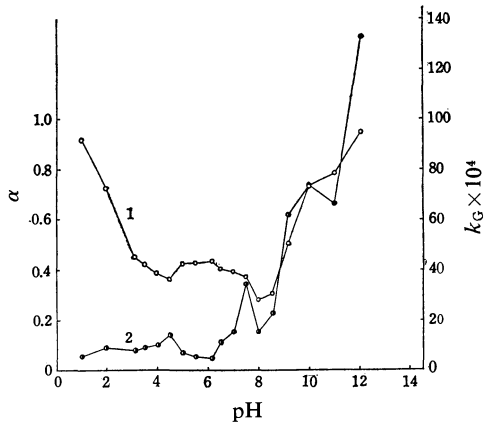

Fig. 8. The relations of pH to α and k_G.
1, α 2, k_G

The Estimation of the Electrode Reaction of BTMP.—The outline of the electrode reaction of BTMP was described in the previous paper[1].

In this paper, the approximation of the D-values of BTMP and the n-values of the electrode reaction at various pH values was carried out, it therefore being thought possible to estimate some of the processes of the electrode reduction.

If the reduction in the acidic solutions take place only at the acyl bond in BTMP and if the reduction at the such other reducible parts of the molecule as the pyrimidine ring is disregarded, the next reactions for the first wave (Fig. 9) may probably be estimated on the basis of the number of electrons, is shown in Table III.

The number of electrons is controlled by the ways in which III split; the alcohol type V is, therefore, produced by a 4-electron discharge, and the pinacol type VI, by a 3-electron discharge.

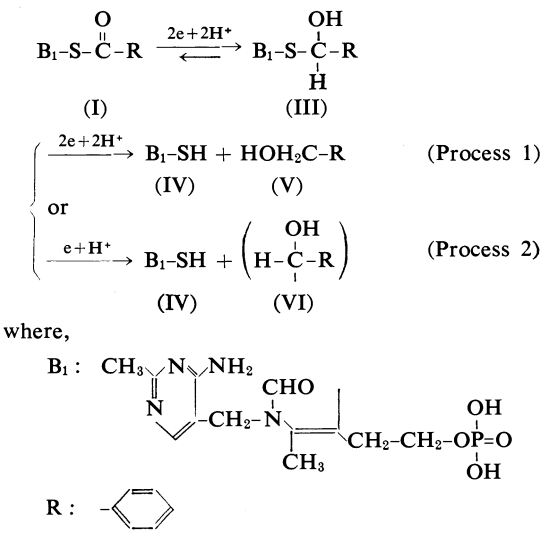

Fig. 9. The reduction processes estimated on BTMP.

Process 1 seemed to take place in the pH range of about 4.5~5.5, and process 2, in the range of pH<2. These two processes were thought to occur at a pH value of about 3.

The decrease of n in pH values higher than 5.5 could not be explained by the chemical splitting of the *S*-acyl bond.

The second wave of BTMP seemed to be due to the reduction of the thiamine *O*-monophosphate (TMP) (IV) that was produced by the reduction of BTMP to give the first wave.

The discontinuous decrease in the wave height was observed for the second wave at pH<4, as is shown in Fig. 2-2, while the first wave of TMP did not show such a decrease[5]. This difference could be explained by a consideration of their species under the same pH value conditions.

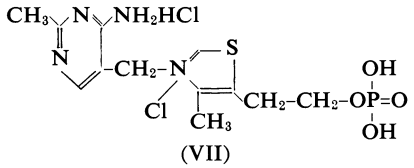

(VII)

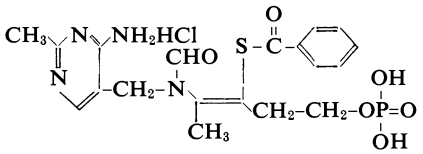

(VIII)

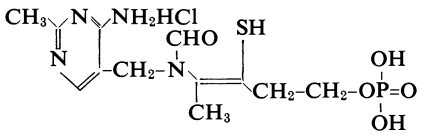

(IX)

At a pH value of about 3, TMP almost existed as VII, and BTMP as VIII. When VIII was reduced at DME, thiol type TMP (IX) was initially produced. Then IX gradually changed to thiazol type VII.

The second reduction process, therefore, was mainly the reduction of the thiol type IX, because the rate of the thiazol-ring formation seemed to be not so sufficiently rapid as to be comparable to or predominant over the potential sweeping rate.

As has been described in the previous paper[5], the a.c. wave heights of TMP without chlorine at the thiazol ring was about 74% that with chlorine.

The approximate ratio of the wave heights of BTMP and TMP[5] at the pH value of 3.0 was $i_s(\text{BTMP})/i_s(\text{TMP})=60\%$, which was thought not to be different from the result obtained for TMP. The second wave of BTMP, therefore, was considered to be due to the reduction of the thiol type TMP, while the first wave of TMP was that of the thiazol type TMP.

Summary

The polarographic behavior of BTMP was studied using the a.c. polarographic method.

The two peak currents of BTMP in a wide pH value range could be observed definitely. Especially, the observation on the second wave, which was not clearly observed by the d.c. method, could be made.

The variations of the two peak current with the change in pH value were not similar to that of the diffusion currents in that the d.c. first wave height gave the largest value at about the pH value of 5, while the a.c. first wave height was largest at the pH value of 2 and then decreased with the increase in pH value.

The second a.c. wave height showed a maximum value at the pH values between 4 and 5, a minimum at a pH value of about 3, and increased at pH values <3.

The two a.c. waves were recognized to be of the diffusion current, not adsorption or kinetic waves.

The approximation of the diffusion coefficient of BTMP was carried out using the d.c. reduction wave of *S*-*p*-nitrobenzoylthiamine *O*-monophosphate (NBTMP) to give $D=5.22\times10^{-6}$ cm^2 sec^{-1}.

The estimation of the electron number, n, at various pH values on the d.c. first wave of BTMP was made using the value of D, so that it was found that 3 or 4 electrons were discharged in the reduction of BTMP in the acidic solutions.

The calculation of the transfer coefficient, α, and the rate constant, k_G, for the first a.c. wave was undertaken by Matsuda's method, giving, $\alpha=0.91_6$, $k_G=5.7_5\times10^{-4}$ cm. sec^{-1} at a pH value of 1.00, and $\alpha=0.43_0$, $k_G=5.0_2\times10^{-4}$ cm. sec^{-1} at a pH value of 5.5, etc.

The reaction processes of BTMP were estimated again according to the results obtained in this work. For the first wave two splitting mechanisms of the *S*-acyl bond which produced benzyl alcohol and benzpinacol consuming 4 and 3 electrons respectively, were considered. For the second wave, as no definite discussion could be undertaken on account of the ill-defined form of the d.c. wave, it can only be suggested that it is the reduction of the reduction products, TMP. Some of the differences between the second wave of BTMP and the first wave of TMP observed in their pH value $-i_s$ curves can be explained by the difference in the wave heights of the thiazol type and of the thiol type of TMP and also by the rather slow rate of the thiazol-ring formation of the latter.

The author is very much indebted to Director Munetoshi Matsui for affording facilities for this investigation.

Physical Chemistry Section
Takamine Laboratory
Sankyo Co., Ltd.
Shinagawa-ku
Tokyo

5) K. Okamoto, This Bulletin, **36**, 366 (1963).

Physico-chemical Studies on the Composition of Complex Arsenates of Metals. I. Thermometric and Conductometric Studies on the Composition of Cupric Arsenate

By Mahendra Singh BHADRAVER

(Received September 24, 1962)

The formation and composition of cupric arsenate complexes has been studied by thermometric and conductometric measurements involving theremometric and conductometric titrations between copper sulfate and sodium arsenate at several concentrations of the reactants both by direct and reverse methods. In the direct thermometric titrations, the curves suggest the formation of $CuNaAsO_4$ as a greenish blue precipitate and in the inverse titrations, the formation of $CuNaAsO_4$ is supported. The intersection of the precipitation line and the titrant line in the curves, both for direct and reverse methods, indicated the equivalence point corresponding to the formation of the complex, $CuNaAsO_4$, where the ratio of Cu : AsO_4 is 1 : 1.

Reference in literature about the study of the composition of copper arsenate complexes by applying physico-chemical methods is scarcely available. Hirsch[1] reported a complex salt of copper and sodium arsenates with different values for the ratios Na_2O : CuO : As_2O_5 : H_2O. Thus the ratios 2 : 24 : 9 : 23 or sodium copper hydro-nona-arsenate, Na_2HAsO_4-$4Cu_3(AsO_4)_2 \cdot 11H_2O$, is obtained by mixing a solution of 4 molecules of cupric nitrate with 7 molecules of sodium hydro-arsenate and washing the precipitate during ten days. The ratios 1 : 12 : 5 : 12 or sodium copper dihydro-penta-arsenate, NaH_2AsO_4-$2Cu_3(AsO_4)_2 \cdot 5H_2O$, were obtained by mixing a dilute solution of 2 molecules of sodium hydro-arsenate, with 4 molecules of cupric sulfate, and washing the precipitate for many days. Salkowsky[2] also made this salt. If in preparing the first of the salts, the precipitate be washed for a shorter time, the product has the ratios 2 : 18 : 7 : 20 or sodium copper bishydro-decatetra-arsenate, $2Na_2HAsO_4 \cdot 6Cu_3(AsO_4)_2 \cdot 19H_2O$; and this salt is made by treating a solution of copper nitrate with an excess of sodium hydroarsenate. The ratios 4 : 36 : 15 : 16 or sodium copper hydrobisdihydrodecapenta-arsenate, $Na_2HAsO_4 \cdot 2NaH_2AsO_4 \cdot 6 \cdot Cu_3(AsO_4)_2 \cdot 16H_2O$ was obtained by mixing solutions of 3 molecules of cupric sulfate and 3 molecules of sodium hydroarsenate, and washing the precipitate for three days; if the precipitate is washed until the runnings are free from sulfuric acid a higher hydrate is produced, viz., $331/2H_2O$. There is nothing here to show that these products do not represent arbitrary stages in a process of hydrolysis. Lefevre[3] obtained sodium copper arsenate, green crystalline mass, $CuNaAsO_4$ by dissolving 7~8% of cupric oxide in sodium metaarsenite melted at a low temperature. He obtained sodium copper tetraorthoarsenate, $2Na_3AsO_4 \cdot Cu_3(AsO_4)_2$, by saturating a fused mixture of sodium metaarsenite and chloride of copper oxide.

In view of the difficulties associated with analytical work and in the absence of any decisive views on the composition of cupric arsenate complexes, it was considered worthwhile to undertake the study of these complexes by physico-chemical methods. The results of thermometric and conductometric titrations have been incorporated and discussed in this paper.

Experimental

A. R. B. D. H. $CuSO_4 \cdot 5H_2O$ was used for the preparation of solution and the solution was standardized against sodium thiosulfate solution of known strength. Merck's sample of Na_3AsO_4 was used and the solution was standardized iodometrically against sodium thiosulfate of known strength.

The thermometric titration arrangement was made according to the proccedings laid down by Haldar[4]. Using different concentrations of two salts in solution, the direct and inverse thermometric and conductometric titrations i. e., when copper sulfate or Na_3AsO_4 solution from a micro-burette was added to solution taken in thermos flask or cell, were carried out. Titrations were also carried out upto total concentration of 20% by volume. Curves were plotted between total rise in temperature or corrected conductance and the volume of the titrant added in ml.

1) A. Hirsch, "Ein Beitrag zur Kenntnis der Arsenate des Kupfers", Halle a. s. (1890).
2) H. Salkowsky, *J. pract. Chem.*, 1, 104, 166 (1868).
3) C. Lefevre. "Sur les Arsenates Cristallises", Paris (1891); *Ann. Chim. Phys.*, 6, 27. 22 (1892).
4) B. C. Haldar, *J. Indian Chem. Soc.*, 23, 147 (1946).

TABLE I. SUMMARY OF OBSERVATIONS OF CONDUCTOMETRIC TITRATIONS

Fig. No.	Curve No.	Conc. $CuSO_4$	Conc. Na_3AsO_4	Med. % Alc.	Points showing breaks Calcd.	Obs.	Formula support
Direct titrations :							
1	1	M/10	M/2	Aq.	2.0	2.0	$CuNaAsO_4$
1	2	M/10	M/2	10	1.8	1.8	$CuNaAsO_4$
1	3	M/10	M/2	20	1.6	1.6	$CuNaAsO_4$
1	4	M/30	M/10	Aq.	3.3	3.25	$CuNaAsO_4$
1	5	M/30	M/10	10	3.0	3.0	$CuNaAsO_4$
1	6	M/30	M/10	20	2.66	2.6	$CuNaAsO_4$
Reverse titrations :							
2	1	M/2	M/2	Aq.	2.0	2.1	$CuNaAsO_4$
2	2	M/2	M/2	10	1.8	1.7	$CuNaAsO_4$
2	3	M/2	M/2	20	1.6	1.6	$CuNaAsO_4$
2	4	M/2	M/8 20 cc.	Aq.	2.5	2.5	$CuNaAsO_4$
2	5	M/2	9 cc.	10	2.25	2.3	$CuNaAsO_4$
2	6	M/2	8 cc.	20	2.0	2.0	$CuNaAsO_4$
SUMMARY OF OBSERVATIONS OF THERMOMETRIC TITRATIONS							
Direct titrations							
3	1	M/5	M/88 20 cc.	Aq.	1.13	1.0	$CuNaAsO_4$
3	2	M/5	18 cc.	10	1.02	1.1	$CuNaAsO_4$
3	3	M/5	16 cc.	20	0.99	1.0	$CuNaAsO_4$
3	4	M/11	M/40	Aq.	5.5	5.5	$CuNaAsO_4$
3	5	M/11	M/40	10	4.95	5.0	$CuNaAsO_4$
3	6	M/11	M/40	20	4.4	4.4	$CuNaAsO_4$
Inverse titrations							
4	1	M/40	M/11 20 cc.	Aq.	5.5	5.5	$CuNaAsO_4$
4	2	M/40	18 cc.	10	4.95	4.7	$CuNaAsO_4$
4	3	M/40	16 cc.	20	4.4	4.3	$CuNaAsO_4$
4	4	M/88 20 cc.	M/5	Aq.	1.13	1.2	$CuNaAsO_4$
4	5	18 cc.	M/5	10	1.02	1.00	$CuNaAsO_4$
4	6	16 cc.	M/5	20	0.99	1.00	$CuNaAsO_4$

The experimental observations of thermometric and conductometric titrations have been given in Table I.

Discussion

The formation of the probable compounds obtained by the interaction of $CuSO_4$ and sodium arsenate can be represented by the following equations:

$$CuSO_4 + Na_3AsO_4 = CuNaAsO_4 + Na_2SO_4 \quad (1)$$

$$2\,CuSO_4 + 3Na_3AsO_4 = Cu_2Na_5(AsO_4)_3 + 2Na_2SO_4 \quad (2)$$

$$3\,CuSO_4 + 2Na_3AsO_4 = Cu_3(AsO_4)_2 + 3Na_2SO_4 \quad (3)$$

$$CuSO_4 + 2Na_3AsO_4 = CuNa_4(AsO_4)_2 + Na_2SO_4 \quad (4)$$

Taking into consideration the strength of solutions of Na_3AsO_4 (pH=8.2) and $CuSO_4$ (pH=4.15), 10 ml. of $CuSO_4$ for the formation of the compounds, $CuNaAsO_4$, $Cu_2Na_5(AsO_4)_3$, $Cu_3(AsO_4)_2$ and $CuNa_4(AsO_4)_2$ will be 2.0, 1.33, 3.0 and 1.0 respectively of Na_3AsO_4 solution. For the inverse titrations and other dilution of reagents, theoretical titer values for the formation of these compounds can be calculated accordingly.

The conductometric titrations curves (Figs. 1 and 2) both in direct and inverse titrations, yield only one point of equivalence at a molecular ratio of reactants $CuSO_4 : Na_3AsO_4$ as 1 : 1, whereas it is much different from the ratios 1 : 2, 2/3 : 1 and 3/2 : 1 as mentioned above (vid. Eqs. 2 to 4) for the formation of probable compounds.

It is observed in direct and inverse titrations that when Na_3AsO_4 solution is added to $CuSO_4$ solution and vice versa, a bluish white precipitate was formed, on adding excess of

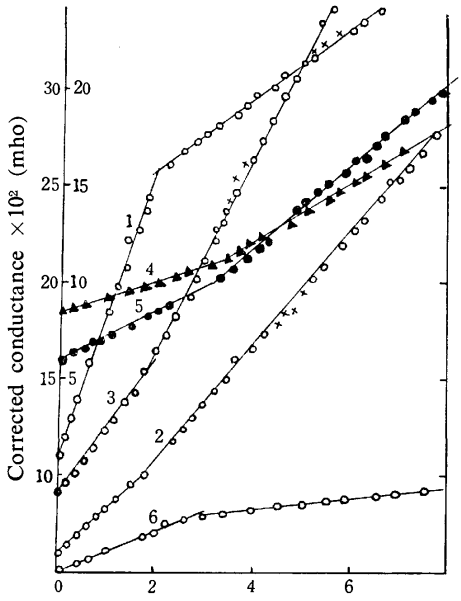

Fig. 1.

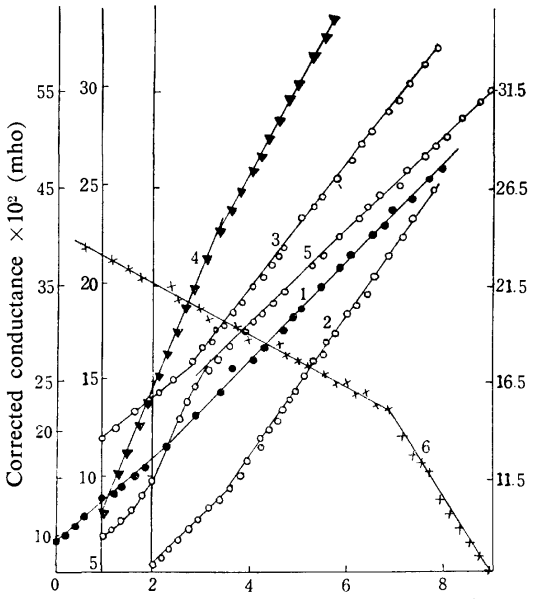

Fig. 2.

either reagent the precipitate in bulk was formed.

The diagrammatic representation of thermometric titrations in Figs. 3—4 reveals that the curves in direct and inverse titrations yield only one point of equivalence corresponding to the formation of the complex, $CuNaAsO_4$, where the ratio of reactants $CuSO_4$: Na_3AsO_4 is 1 : 1. It is evident from the summary of

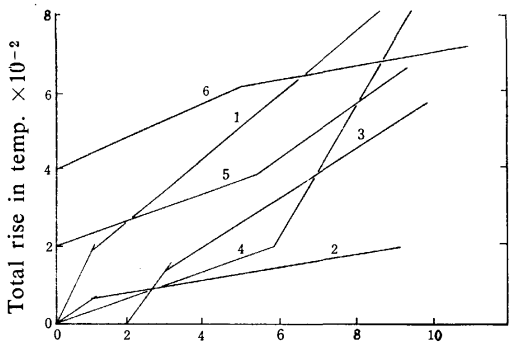

Fig. 3. Direct titrations.

Curves 1, 2, 3; M/5 $CuSO_4$ and M/88 Na_3AsO_4
Curves 4, 5, 6; M/11 $CuSO_4$ and M/40 Na_3AsO_4

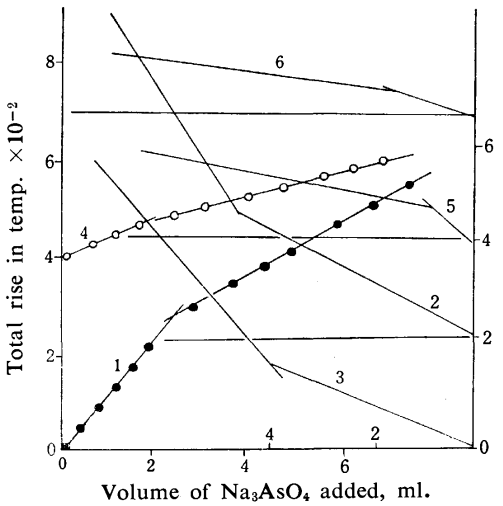

Fig. 4. Reverse titrations.

Curves 1,2,3; M/40 $CuSO_4$ and M/11 Na_3AsO_4
Curves 4,5,6; M/5 Na_3AsO_4 and M/88 $CuSO_4$

observations of thermometric and conductometric titrations that there is close agreement between the values theoretically calculated and observed. In order to show the discrepancy, which is probably due to slight effect of hydrolysis and adsorption, between theoretically calculated on the basis of strength of solutions used and observed values in aqueous and aqueous alcoholic media, the summary of observations have been given above for comparison. There is coordination in the results obtained by conductometry and Dutoit's thermovolumetry.

Lefevre's[3] observations have been supported by my thermovolumetric and conductometric studies. Views and results reported by Hirsch, and Salkowsky (loc. cit.) have not been supported by my studies.

Grateful thanks are due to Dr. J. N. Gaur, University of Rajasthan, Jaipur, for his kind guidance and keen interest in this piece of investigation.

Department of Chemistry
Lohia College
Churu, India

Spectrophotometric Studies of the Complexes of Phenylazochromotropic Acid Formed with Thorium

By Haruo MIYATA

(Received September 22, 1962)

Various *o*-substituted-*o'*-hydroxyazo compounds having functional groups in the ortho position have been synthetized, and their behaviors as analytical reagents have been studied[1-6]. Among these compounds a series of azo compounds coupled with chromotropic acid are most interesting as the reagents for the spectrophotometric determination of various metals.

The present paper describes the basic studies of the reaction of phenylazochromotropic acid with thorium.

Experimental

Reagents.—*Phenylazochromotropic Acid*[6,7]. — Diazotized aniline was coupled with chromotropic acid, and the pure azo compound was obtained in the form of diacid dihydrate after recrystallization from concentrated hydrochloric acid, followed by that from water. Solutions of 2.5×10^{-4} and 3×10^{-4} mol./l. were prepared and stored in the dark.

Thorium Perchlorate Solution. — Purified thorium nitrate[8] was dissolved in water, the hydroxide was precipitated with sodium hydroxide, and then it was dissolved in perchloric acid. The stock solution was standaridized gravimetrically with oxalate[9]. It contained 17.6 mg. of thorium per milliliter and was diluted to an appropriate concentration for each experiment.

Buffer Solution.—The following buffer solutions were prepared from guaranteed reagents:

5.8~7.0 pH values, acetic acid and sodium acetate.

8.0~9.8 pH values, ammonia and ammonium chloride.

1 M Sodium Perchlorate Solution. — This was prepared from twice recrystallized $NaClO_4\cdot H_2O$.

Apparatus.—The absorbance was measured with a Shimadzu spectrophotometer, QR-50 type, and a Hitachi automatic recording spectrophotometer, EPS-2 type, with 1 cm. cells; the pH value was measured with a Horiba glass electrode pH meter, model M-3.

Results and Discussion

Absorption Spectra of the Reagent and its Thorium Complex. — For the measurement of absorption spectra of the reagents and its thorium complex, the following procedure was used. All solutions were prepared in a dark room, for the absorption of the reagent decreases in daylight, especially at higher pH values. Five milliliter of a 2.5×10^{-4} or a 3×10^{-4} mol./l. reagent solution was placed in a 50 ml. volumetric flask, followed by the addition of an adequate volume of 0.2 M perchloric acid in order to adjust the pH value of the solution to 1~5, of a 0.2 M sodium hydroxide solution in order to adjust the pH value of the solution to 11~13, or of 5 ml. of a buffer solution of the pH 5.8~9.8. The ionic strength was maintained at 0.1 by an appropriate addition of a 1 M sodium perchlorate solution, and then the volume was made up to 50 ml. with water.

Thorium complex solutions were prepared similarly: 5 ml. of a 2.5×10^{-4} mol./l. reagent solution was placed in a 50 ml. volumetric flask, followed by the addition of 0.2 M perchloric acid in order to adjust the pH value of the solution to 1~3.2, of a 1 M sodium perchlorate solution to maintain the ionic strength at 0.1, and of 5 ml. of a 2.5×10^{-2} mol./l. thorium perchlorate solution, then the

1) K. Emi, K. Tôei and H. Miyata, *J. Chem. Soc. Japan, Pure Chem. Sec.* (*Nippon Kagaku Zassi*), 78, 736 (1957).
2) K. Emi, K. Tôei and N. Takemoto, ibid., **78**, 741 (1957).
3) K. Emi, K. Tôei and H. Miyata, ibid., **78**, 977 (1957).
4) K. Emi, K. Tôei and H. Miyata, ibid., **78**, 979 (1957).
5) K. Emi, K. Tôei and K. Furukawa, ibid., **79**, 681 (1958).
6) T. Iwachido, H. Miyata and K. Tôei, This Bulletin, **33**, 95 (1960).
7) Color Index 16570, Acid Red 29.
8) R. L. Swan, *J. Chem. Soc.*, **125**, 781 (1924).
9) W. W. Scott, "Standard Methods of Chemical Analysis", D. van Nostrand Co., Inc. (1939), p. 953.

volume was made up to 50 ml. with water. The solutions were allowed to stand for one hour or more at 25°C, after which the absorbance was measured in a 1 cm. cell against water.

In the pH value range higher than 4, thorium hydroxide was precipitated, so absorption measurements were not possible.

In Fig. 1 it is seen that, on the addition of thorium to the reagent solution, the absorption maxima shifted towards the longer wavelengths. Curve VII shows an absorption maximum at 565 mμ.

Dissociation Constant of Phenylazochromotropic Acid. — Judging from the presence of the isosbestic points (348~350, 392~394, 460~462 and 560~562 mμ), two structures (H_2R^{2-} and HR^{3-})[10,11] may be expected to exist (Fig. 1).

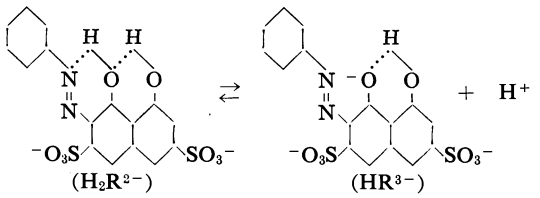

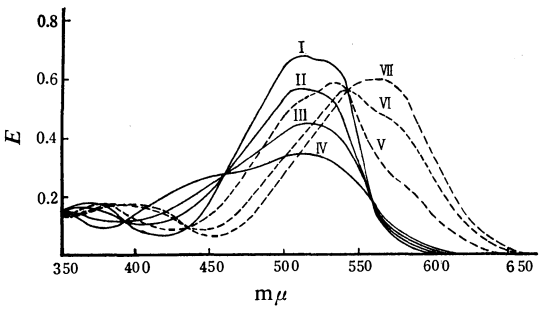

Fig. 1. Absorption spectra of phenylazochromotropic acid (I—IV) and its thorium complex (V—VII).
I 2.5×10^{-5} mol./l., pH 1.8~6, $\mu=0.1$, 25°C; II pH 8.3; III pH 9.3; IV pH 11~12.4; V pH 1.0; VI pH 1.42; VII pH 3.2

The constant of the above dissociation, K_{a_1}, was calculated by the following equation from the absobance vs. the pH value curve at 510 mμ (25°C, $\mu=0.1$) shown in Fig. 2.

In the following equations $[H_2R]$ and $[HR]$ represent the concentrations of H_2R^{2-} and H^{3-} respectively:

$$K_{a_1} = [H][HR]/[H_2R]$$

$$pK_{a_1} = -\log[H] - \log\{[HR]/[H_2R]\}$$

$$= -\log[H] - \log\{(E_{H_2R}-E)/(E-E_{HR})\}$$

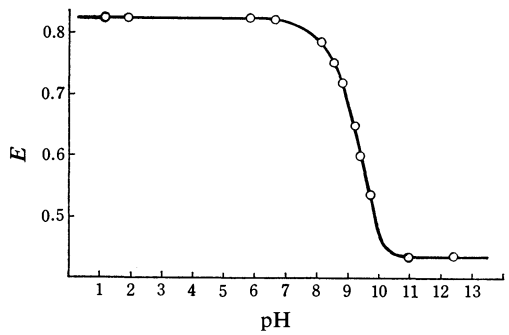

Fig. 2. Absorbance at 510 mμ vs. pH for phenylazochromotropic acid (3×10^{-5} mol./l.).

where E_{H_2R} and E_{HR} represent the absorbance in the 1~6 and 11~12 pH value ranges respectively and E, the absorbance at a pH value of 8~10 (Fig. 2).

In Fig. 3, the values of $\log\{(E_{H_2R}-E)/(E-E_{HR})\}$ were plotted against the pH value, and the value of pK_{a1} was estimated graphically to be 9.30. A value of 9.29 for the same dissociation constant has been reported by Schwarzenbach[12].

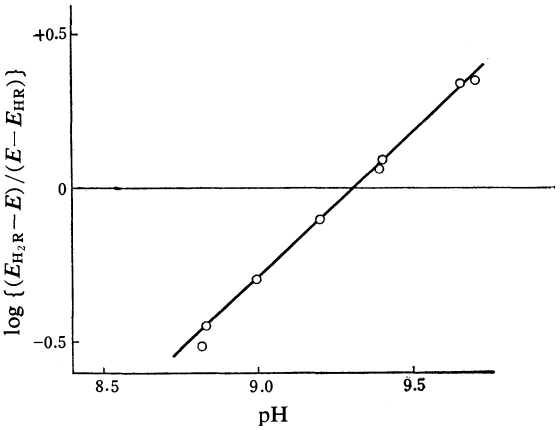

Fig. 3. Relationship between pH and $\log\{(E_{H_2R}-E)/(E-E_{HR})\}$.

Chemical Composition of the Thorium Complex. — *Continuous Variation Method.* — The absorbances at 580 mμ of solutions with various $[Th]/([Th]+[H_2R])$ ratios were measured one hour after the solutions had been prepared; the results indicated the formation of a 1:1 complex of thorium with the reagent (Fig. 4).

Mole Ratio Method. — The results obtained indicate the formation of a 1:1 complex within the range of experimental error. The measurement was made at 580 mμ and at a pH value of 3.1 (Fig. 5).

10) H. Zollinger and W. Büchler, *Helv. Chim. Acta*, **34**, 591 (1951).
11) J. Heller and G. Schwarzenbach, ibid., **34**, 1876 (1951).
12) J. Bjerrum et. al., "Stability Constants Part I: Organic Ligands", The Chemical Soc., London, (1957), p.95.

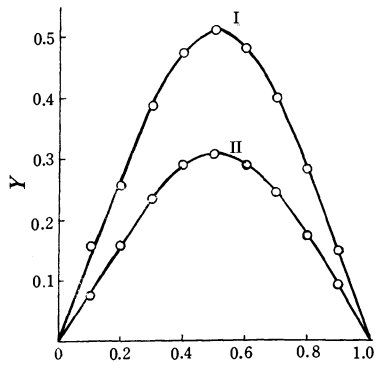

Fig. 4. Continuous variation method.
pH 3.4, μ=0.1, 25°C, 580 mμ
I Th=H_2R=4.5×10^{-5} mol./l.
II Th=H_2R=3.0×10^{-5} mol./l.

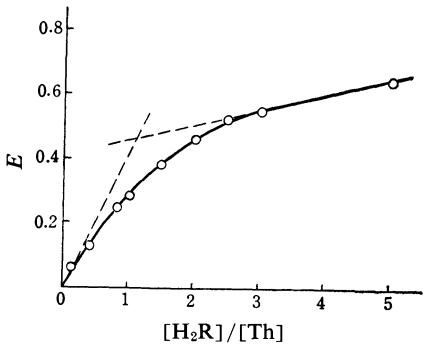

Fig. 5. Mole ratio method.
pH 3.1, μ=0.1, 25°C, 580 mμ
Thorium concn.=3×10^{-5} mol./l., reagent concn. varied.

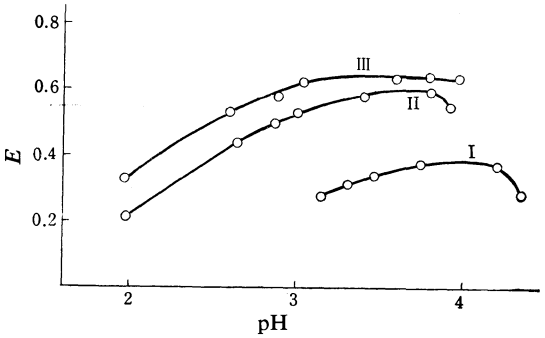

Fig. 6. Effect of pH on absorbance values of the thorium complex.
I H_2R : Th=1 : 1
II H_2R : Th=1 : 5
III H_2R : Th=1 : 10

Both methods show that a 1 : 1 complex is formed between thorium and the reagent in the pH value range studied.

Effect of pH Value on the Color of the Complex.—The pH values of solutions containing thorium and the reagent (3.0×10^{-5} mol./l.) in the molar ratios 1 : 1, 5 : 1 and 10 : 1 were adjusted to 2~4.2 by perchloric acid, and the absorbances were measured (Fig. 6).

The curves in Fig. 6 show that the absorption increases with the increase of the thorium : reagent ratio and that it tends to be constant over a wide pH value range.

Effect of Time. — The relationship between the absorbance at 580 mμ and the lapse of time after the mixing of thorium with the reagent in various pH value ranges is shown in Fig. 7. The color of the thorium complex is fully developed in a few minutes after mixing, and the absorbance remained constant for two hours.

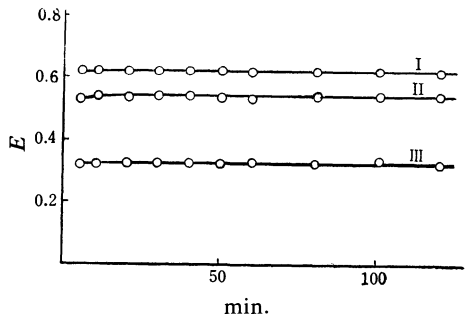

Fig. 7. Effect of reaction time.
I pH 3.5 II 2.59 III 1.95

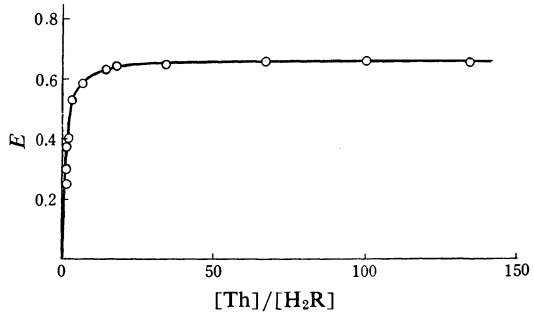

Fig. 8. Effect of excess thorium concentration on the absorbance of the complex.
pH 3.2, μ=0.1, 25°C, 580 mμ
Reagent concn.=3×10^{-5} mol./l.

Effect of an Excess Thorium Concentration. —The effect of an excess thorium concentration on the absorbance is shown in Fig. 8, other experimental conditions being kept constant.

The curve indicates that the absorbance reaches a constant value when the molar ratio of thorium to the reagent exceeds 60.

The Apparent Stability Constant* of the Thorium Complex.—The existence of the isosbestic points (346~347, 436 and 542 mμ) is

* Conditional stability constant suggested by A. Ringbom, *J. Chem. Educ.*, 35, 282 (1958).

TABLE I. APPARENT STABILITY CONSTANT, K', OF THE COMPLEX AT 25°C (μ=0.1)

pH	E	C_R	C_{Th}	[ThHR]	K'
1.98	0.215	3×10^{-5}	15×10^{-5}	0.86×10^{-5}	0.28×10^{4}
2.01	0.203	6×10^{-5}	6×10^{-5}	0.65×10^{-5}	0.23×10^{4}
2.40	0.638	3×10^{-5}	300×10^{-5}	2.87×10^{-5}	0.73×10^{4}
2.50	0.379	12×10^{-5}	2.5×10^{-5}	1.16×10^{-5}	0.80×10^{4}
2.68	0.085	3×10^{-5}	1×10^{-5}	0.24×10^{-5}	1.17×10^{4}
3.0	0.348	2.7×10^{-5}	6.3×10^{-5}	1.51×10^{-5}	2.63×10^{4}
3.1	0.616	3×10^{-5}	40×10^{-5}	2.76×10^{-5}	3.13×10^{4}
3.2	0.274	2.4×10^{-5}	3.6×10^{-5}	1.17×10^{-5}	3.94×10^{4}
3.4	0.317	2.4×10^{-5}	3.6×10^{-5}	1.38×10^{-5}	6.05×10^{4}
3.4	0.428	2.7×10^{-5}	6.3×10^{-5}	1.89×10^{-5}	5.27×10^{4}

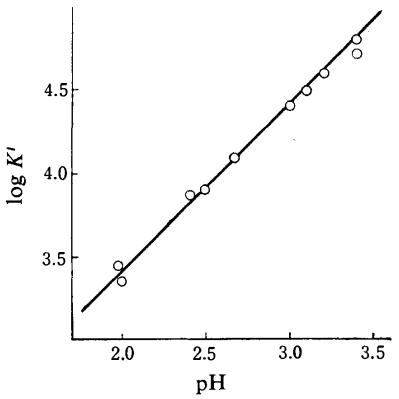

Fig. 9. Relationship between pH and log K'.

excellent evidence that only two structures are present, H_2R and a single complex in the 1.0~3.4 pH value range (Fig. 1).

The value of the apparent stability constant of the thorium complex may be estimated by assuming that the formation of the thorium complex is in accordance with the following equation:

$$Th^{4+} + H_2R^{2-} \rightleftarrows ThHR^{+} + H^{+}$$

The equilibrium constant, K, is given by:

$$K = [ThHR][H]/[Th][H_2R] \quad (1)$$

the ionic charge being neglected for the sake of convenience. The total concentrations of the reagent and thorium are given by:

$$C_R = [H_2R] + [HR] + [R] + [ThHR] \quad (1)$$

$$C_{Th} = [Th] + [ThHR] \quad (2)$$

respectively. At pH values lower than 4, [HR] and [R] can be disregarded. Substitution of Eqs. 2 and 3 into Eq. 1 leads to the following equation:

$$K = [ThHR][H]/(C_{Th} - [ThHR])(C_R - [ThHR]) \quad (4)$$

The absorbance, E, of the thorium complex at 580 mμ may be expressed as:

$$E = \varepsilon_{H_2R}[H_2R] + \varepsilon_{ThHR}[ThHR] \quad (5)$$

The molar absorptivities at 580 mμ, ε_{H_2R} and ε_{ThHR}** were found to be 1.11×10^{3} and 2.33×10^{4} respectively.

From Eqs. 2 and 5.

$$E = \varepsilon_{H_2R}(C_R - [ThHR]) + \varepsilon_{ThHR}[ThHR]$$
$$= \varepsilon_{H_2R}C_R - [ThHR](\varepsilon_{H_2R} - \varepsilon_{ThHR})$$

Hence,

$$[ThHR] = \varepsilon_{H_2R}C_R - E/(\varepsilon_{H_2R} - \varepsilon_{ThHR}) \quad (6)$$

The apparent stability constant, K' (Table I), of the thorium complex was estimated at 2~3.5 pH values using Eqs. 6 and 7:

$$K' = K/[H] = [ThHR]/(C_{Th} - [ThHR])(C_R - [ThHR]) \quad (7)$$

In Fig. 9, the logarithm of the apparent stability constant (log K') is plotted against the pH value. The curve indicates that thorium reacts with the reagent, displacing one hydrogen atom.

Summary

The dissociation constant of phenylazochromotropic acid, pK_a, has been estimated spectrophotometrically to be 9.3_0 (25°C, μ=0.1).

The reagent reacts with thorium in the molar ratio 1:1, displacing one hydrogen atom, and the approximate value of the apparent stability constant of the complex, log K', has been estimated to be 3.4~4.9 in the 2~3.5 pH value range.

The author wishes to express his hearty thanks to Dr. Kyoji Tôei for his guidance in the course of this experiment.

Department of Chemistry
Faculty of Science
Okayama University
Tsushima, Okayama

** The absorbance has reached a constant value when the molar ratio of thorium to the reagent exceeds 60 (Fig. 8). In this case, the formation of the complex was considered to be complete, and the value of ε_{ThHR} was obtained from the absorbance of the solution containing the reagent and thorium in the molar ratio of 1:100.

*Spectrophotometric Studies of the Complexes of o-Sulfobenzeneazochromotropic Acid Formed with Thorium**

By Haruo MIYATA

(Received November 24, 1962)

Azo compounds having arseno, $-AsO_3H_2$[1], or phosphono, $-PO_3H_2$[2], groups in the ortho position have been applied as reagents for the determination of thorium, zirconium and uranium. These groups are most interesting as functional groups for thorium, and the behavior of sulfo group, $-SO_3H$, for thorium is also attractive to the other.

The present paper describes the preparation of *o*-sulfobenzeneazochromotropic acid, and the determination of the first dissociation constant of the reagent by the spectrophotometric method. The complex of the reagent with thorium is studied spectrophotometrically, and the reaction scheme is presented from the relation between the apparent stability constant and the pH value.

Experimental

Reagents.—*o-Sulfobenzeneazochromotropic Acid***. —Diazotized *o*-aminobenzenesulfonic acid was coupled with chromotropic acid, and a pure azo compound was obtained in the form of reddish brown needles of monosodium salt after recrystallization from concentrated hydrochloric acid. A solution of 3×10^{-4} mol./l. was prepared and stored in the dark.

1 M Thorium Perchlorate Solution.—It was prepared by dissolving thorium hydroxide into perchloric acid.

1 M Sodium Perchlorate Solution.—It was prepared from twice-recrystallized $NaClO_4\cdot H_2O$.

Buffer Solutions.—The following buffer solutions were prepared from guaranteed reagents:

5.8~7.0 pH value acetic acid and sodium acetate.

8.0~10.6 pH value aqueous ammonia and ammonium chloride.

Procedure and Apparatus.—All solutions were made in a dark room, for the absorbance of the reagent tended to be decreased in daylight, especially at higher pH values.

Five milliliter of a 3×10^{-4} mol./l. reagent solution was placed in a 50 ml. volumetric flask, after which an adequate volume of 0.2 M perchloric acid, 0.2 M sodium hydroxide or buffer solution was added in order to adjust the pH value to the desired value. Then a 1 M sodium perchlorate solution was added to maintain the ionic strength at 0.1, and the volume was made up to 50 ml. with water. Each of the solutions was used for the determination of the first dissociation constant of the reagent.

To prepare the complex solution, 5 ml. of a 3×10^{-4} mol./l. reagent solution was placed in a 50 ml. volumetric flask, followed by the addition of 0.2 M perchloric acid to adjust the pH value of the solution to 1~3.4 and of a 1 M sodium perchlorate solution to maintain the ionic strength at 0.1. Five milliliter of a 4×10^{-3} mol./l. thorium perchlorate

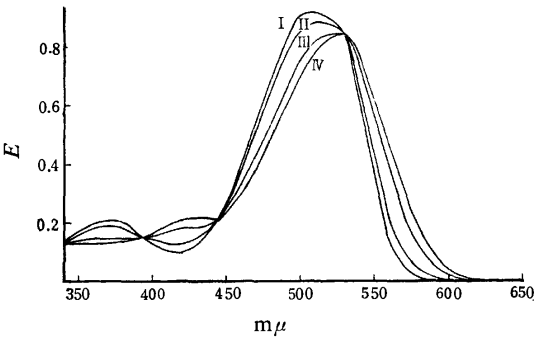

Fig. 1. Absorption curves of *o*-sulfobenzeneazochromotropic acid.
$\mu=0.1$, at 25°C 3×10^{-5} mol./l.
I pH 1~8 II pH 9.2
III pH 10.5 IV pH 11.5~13

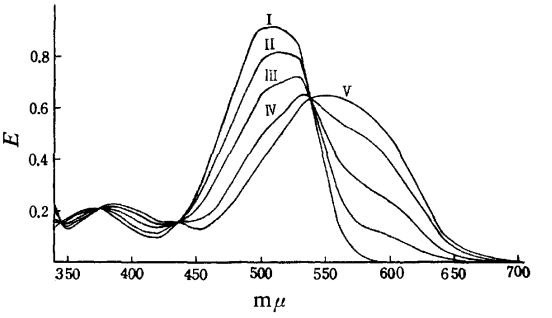

Fig. 2. Absorption curves of the thorium complex.
I Reagent, pH 1~8, $\mu=0.1$ at 25°C
II, III, IV, V Complex, pH 1.9, 2.3, 2.9, 3.4

* Presented at the Symposium of the Analytical Chemical Society of Japan, Tokushima, October, 1962.

1) For example, A. E. Taylor and R. T. Dillon, *Anal. Chem.*, **24**, 1624 (1952).

2) A. A. Nemodruk et al., *J. Anal. Chem. USSR*, **16**, 296 (1961).

** Anal. Found: C, 36.85; H, 2.23; N, 5.20; Na, 4.4. Calcd. for $C_{16}H_{11}O_{11}N_2S_3Na$: C, 36.50; H, 2.11; N, 5.32; Na, 4.36%.

solution was added, and then the volume was made up to 50 ml. with water. The solutions were allowed to stand for one hour or more at 25°C. The absorbance was then measured with a Shimadzu spectrophotometer QR-50 type and a Hitachi automatic recording spectrophotometer EPS-2 type, with 1 cm. cells, while the pH value was measured with a Tôwa-Denpa glass electrode pH meter model HM-5A. Absorption spectra at various pH values are shown in Figs. 1 and 2.

Results and Discussion

Spectral Properties of the Reagent and its First Dissociation Constant.—Between the pH values of 1 and 8, the reagent gives identical absorption spectra, each with one absorption maximum at 507 mμ (Fig. 1). This indicates that the electrolytic dissociation of the naphtholic group does not occur. Above a pH value of 8, the maximum shifts towards another maximum (527 mμ) with an increase in the pH value, and between the pH values of 11.5 and 13 the reagent again gives identical absorption spectra.

Judging from the presence of the isosbestic points (392～394, 442～444 and 528～530 mμ), two structures (H_2R^{3-} and HR^{4-}) are expected to exist.

$$H_2R^{3-} \rightleftarrows HR^{4-} + H^+$$

The constant of the above dissociation, K_{a_1}, was calculated by the following equation[3]:

$$pK_{a_1} = -\log[H] - \log\{(E_{H_2R} - E)/(E - E_{HR})\}$$

where E_{H_2R} and E_{HR} represent the absorbances at $-\log[H] = 1 \sim 8$ and $11.5 \sim 13$ respectively, and E represents the absorbance at $-\log[H] =$ 8～11.5. These absorbances are measured at 560 mμ, because the difference between E_{H_2R} and E_{HR} is the largest.

In Fig. 3, the values of $\log\{(E_{H_2R} - E)/(E - E_{HR})\}$ are plotted against the pH value, and the value of pK_{a_1} is estimated graphically to be 9.7$_6$.

The Chemical Composition of the Complex.—In order to confirm the mole ratio of the complex, two methods were employed, the continuous variation and the mole ratio methods. In the former method, the measurement of the absorbances of a series of solutions containing a varying mole per cent of 6×10^{-5} M reagent and 6×10^{-5} M thorium was undertaken. As is shown in Fig. 4, the maximum absorbance of the complex was obtained when the mole ratio of thorium to the reagent was 1 : 1.

In the latter method, the absorbances of a series of solutions containing a varying concentration of the reagent to a fixed thorium concentration (4×10^{-5} mol./l.) was measured at 580 mμ. The results obtained indicate the formation of a 1 : 1 complex (Fig. 5). The results of these experiments confirm that the mole ratio of thorium to the reagent in the complex formed is 1 : 1.

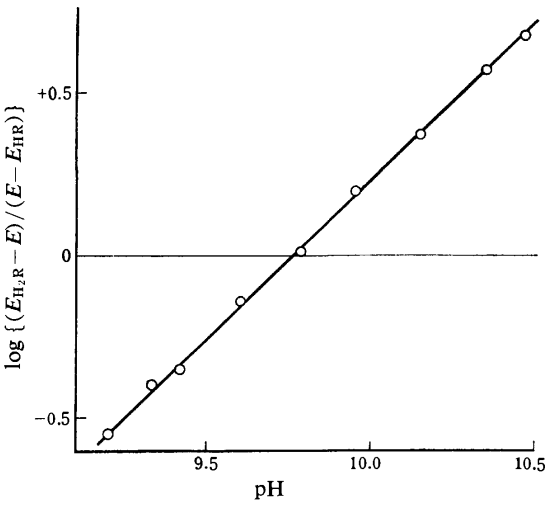

Fig. 3. Relationship between pH and log $\{(E_{H_2R} - E)/(E - E_{HR})\}$.
560 mμ, 25°C, $\mu = 0.1$

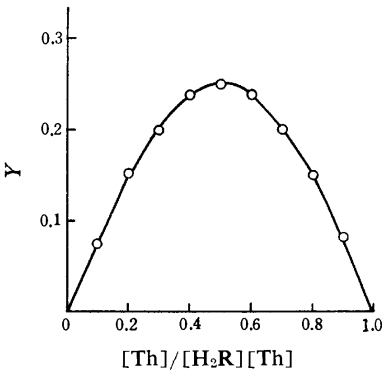

Fig. 4. Continuous variation method.
580 mμ, pH 3.1
$Th = H_2R = 6 \times 10^{-5}$ mol./l.

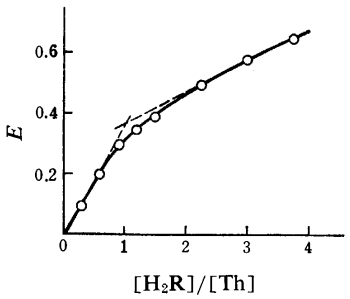

Fig. 5. Mole ratio method.
580 mμ, pH 3.35
Thorium concn. $= 4 \times 10^{-5}$ mol./l.
The reagent concentration varied.

3) H. Miyata, This Bulletin, **36**, 382 (1963).

TABLE I. APPARENT STABILITY CONSTANT OF THE COMPLEX (25°C, $\mu=0.1$)

pH	E	C_R	C_{Th}	[ThHR]	K'
2.3	0.057	3×10^{-5}	4×10^{-5}	0.15×10^{-5}	0.14×10^{4}
2.45	0.062	3×10^{-5}	4×10^{-5}	0.17×10^{-5}	0.16×10^{4}
2.6	0.240	6×10^{-5}	8×10^{-5}	0.89×10^{-5}	0.24×10^{4}
2.9	0.355	6×10^{-5}	8×10^{-5}	1.42×10^{-5}	0.47×10^{4}
2.9	0.119	3×10^{-5}	4×10^{-5}	0.44×10^{-5}	0.48×10^{4}
3.1	0.155	3×10^{-5}	4×10^{-5}	0.60×10^{-5}	0.74×10^{4}
3.1	0.456	6×10^{-5}	8×10^{-5}	1.88×10^{-5}	0.75×10^{4}
3.15	0.154	3×10^{-5}	4×10^{-5}	0.60×10^{-5}	0.74×10^{4}
3.45	0.233	3×10^{-5}	4×10^{-5}	0.96×10^{-5}	1.56×10^{4}
3.5	0.228	3×10^{-5}	4×10^{-5}	0.94×10^{-5}	1.49×10^{4}

The Effet of Time on the Color of the Complex.—The effect of the lapse of time after the mixing of thorium with the reagent at various pH values is shown in Fig. 6. The color of the complex is fully developed in a few minutes after mixing, and the absorbance remained constant for two hours and more.

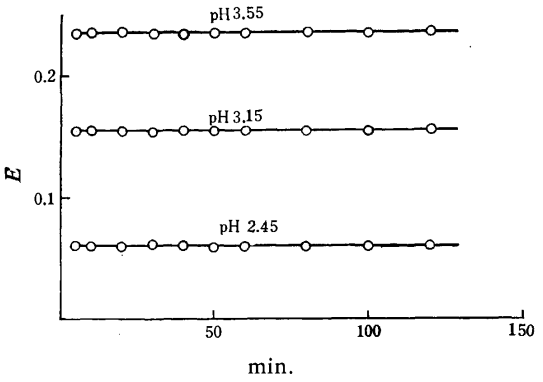

Fig. 6. Effect of reaction time.

The Effect of an Excess Thorium Concentration.—The effect of an excess thorium concentration on the absorbance is shown in Fig. 7, where the curve indicates that the absorbance reaches a constant value when the molar ratio of thorium to the reagent exceeds 110.

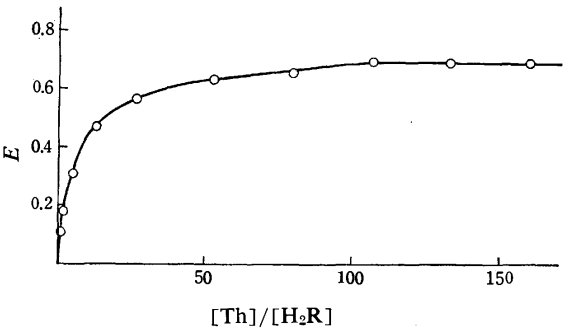

Fig. 7. Effect of excess thorium concentration 580 mμ, pH 2.9, the reagent concentration 3×10^{-5} mol./l.

The Apparent Stability Constant of the Complex. — The existence of the isosbestic points (346～347, 372～374, 435～437 and 540～542 mμ) is excellent evidence that only two structures are present, H_2R^{3-} and a single complex in the pH value range of 2～3.4 (Fig. 2). An approximate value of the apparent stability constant, K', (Table I) of the complex may be obtained by assuming that the formation of the thorium complex is in accordance with the the following equation[3]:

$$Th^{4+}+H_2R^{3-} \rightleftarrows ThHR+H^+$$

The equilibrium constant, K, is given by

$$K=[ThHR][H]/[Th][H_2R]$$

$$K'=K/[H]=[ThHR]/(C_R-[ThHR])\times(C_{Th}-[ThHR])$$

where C_R and C_{Th} represent the total concentration of the reagent and of the thorium respectively, and [ThHR] represents the concentration of the complex.

In Fig. 8, the logarithm of the apparent stability constant ($\log K'$) is plotted against the pH value. The curve indicates that thorium reacts with the reagent, displacing one hydrogen atom.

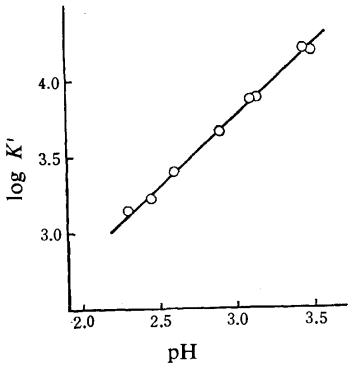

Fig. 8. Relationship between pH and log K'. 580 mμ, 25°C, $\mu=0.1$

Summary

o-Sulfobenzeneazochromotropic acid was prepared in the form of reddish brown needles of monosodium salt, and the value of the first dissociation constant, pK_{a_1}, was estimated spectrophotometrically to be 9.7_6 (25°C, $\mu=0.1$).

The reagent reacts with thorium in the molar ratio 1 : 1, displacing one hydrogen atom, and the approximate value of the apparent stability constant of the complex, $\log K'$, was estimated to be 3.2～4.2 at pH values from 2.5 to 3.5, while the concentration of thorium was about $(4\sim8)\times10^{-5}$.

The author wishes to express his deep thanks to Dr. Kyoji Tôei for his guidance in the course of this experiment.

Department of Chemistry
Faculty of Science
Okayama University
Tsushima, Okayama

A Convenient Synthetic Method of Certain Aromatic Polyiodo Compounds

By Hitomi SUZUKI and Ryozo GOTO

(Received October 16, 1962)

Aromatic polyiodo compounds are usually prepared from the corresponding amines by the lengthy, laborious procedures involving acetylation, nitration, diazotization and reduction. Nevertheless, the authors have found it possible to prepare certain types of polyiodo compounds directly from the readily available, simpler iodo compounds.

This method is based on the migration, in the presence of sulfuric acid, of iodine atoms present in the nucleous of aromatic iodo compound (Jacobsen reaction[1]). The procedure is quite simple and needs only to agitate the starting materials with suitable amount of sulfuric acid for some hours followed by chromatographic separation of the products on an alumina column. The products are sufficiently in high state of purity. Although the yields are, in some cases, not so high by the usual standards, the easy availability of starting materials and the simplicity of the procedure recommend this method over any others previously employed.

Present method is expecially attractive to the synthesis of symmetrically substituted or fully iodinated compounds.

Table I presents the compounds prepared by the authors with the aid of this method. Some examples will demonstrate the ease and mode of preparation.

1) L. I. Smith, "Organic Reactions", Vol. I, 370 (1942).

Experimental

2, 5-Diiodo-*p*-xylene.—A mixture of 17.4 g. of 2-iodo-*p*-xylene and 30 g. of sulfuric acid was agitated vigorously with a magnetic stirrer while the temperature of the reaction mixture was held at 50~55°C for 4 hr. After cooling, the reaction mixture was poured into ice water, and the precipitated crystalline solid was filtered off. Recrystallization from petroleum benzine gave 4.2 g. of white needles, m. p. 103~104°C[2]. Mixed melting point with an authentic specimen showed no depression.

2,4-Diiodotoluene and 2,4,5-Triiodotoluene[3,4].—A mixture of 19.1 g. of *p*-iodotoluene and 35 g. of sulfuric acid was magnetically agitated and heated to 50~60°C for 6 hr. The reaction mixture was poured into ice water and the oily material was removed by ether extraction. The ethereal solution was evaporated and the residual oil was chromatographed on an alumina column with petroleum benzine (b. p. 65~70°C). Each 20 ml. fraction was collected and evaporated. 2,4-Diiodotoluene and 2,4,5-triiodotoluene appeared, respectively, in the early and late fractions. 2,4-Diiodotoluene weighed 4.9 g., b. p. 115~117°/1 mmHg. 2,4,5-Triiodotoluene, recrystallized from ethanol to separate as white needles, weighed 3.4 g. and melted at 119~120°C. Admixture with a sepecimen prepared from *m*-toluidine showed no depression.

2) P. S. Varma and K. S. V. Raman, *J. Indian Chem. Soc.*, **12**, 343 (1935).
3) G. S. Neumann, *Ann.*, **241**, 33 (1887).
4) H. L. Wheeler, *Am. Chem. J.*, **44**, 126, 493 (1910).

TABLE I

Iodo compounds	Sulfuric acid (moles per mole iodo compound)	Experimental condition	Product	M. p. or B. p. °C	Yield %	Iodine, % Found	Iodine, % Calcd.
Iodobenzene	4	6 hr. at 95～100°C	*p*-Diiodobenzene	128	11**	76.90	76.94
			1,2,4-Triiodobenzene	92	～ 5	83.37	83.53
p-Diiodobenzene	8	6 hr. at 120～130°C	1,2,4-Triiodobenzene[7]	92	15**	83.70	83.53
			1,2,4,5-Tetraiodobenzene	253	26	87.51	87.27
o-Iodotoluene	4	6 hr. at 100～110°C	2,4-Diiodotoluene	117/1 mmHg	14**		
			2,4,5-Triiodotoluene	120	26		
p-Iodotoluene	4	6 hr. at 50～60°C	**2,4-Diiodotoluene*** **	117/1 mmHg	33**	73.79	73.79
			2,4,5-Triiodotoluene	120	25	81.07	81.04
p-Iodotoluene	4	6 hr. at 100～110°C	2,4-Diiodotoluene	117/1 mmHg	11**		
			2,4,5-Triiodotoluene	120	28		
o-Iodoethylbenzene	4	6 hr. at 90～100°C	2,4-Diiodoethylbenzene[8]	130/3 mmHg	～ 5**		
			2,4,5-Triiodoethylbenzene	74	24	78.72	78.68
p-Iodoethylbenzene	4	6 hr. at 50～55°C	2,4-Diiodoethylbenzene	130/3 mmHg	53**	70.77	70.90
			2,4,5-Triiodoethylbenzene	74	～ 5		
p-Iodoethylbenzene	4	6 hr. at 90～100°C	2,4-Diiodoethylbenzene	130/3 mmHg	～ 5**		
			2,4,5-Triiodoethylbenzene	74	15		
4-Iodo-*o*-xylene	4	4 hr. at 50～55°C	4,5-Diiodo-*o*-xylene	90	38	70.77	70.90
4-Iodo-*m*-xylene	4	4 hr. at 70～80°C	4,6-Diiodo-*m*-xylene	72	42	70.53	70.90
5-Iodo-*m*-xylene	4	4 hr. at 70～80°C	2,5-Diiodo-*m*-xylene	75	39	70.92	70.90
2-Iodo-*p*-xylene	4	4 hr. at 50～55°C	**2,5-Diiodo-*p*-xylene**	104	32	70.82	70.90
4,5-Diiodo-*o*-xylene	10	4 hr. at 70～80°C	3,4,5,6-Tetraiodo-*o*-xylene	129	72	81.13	83.25
4,6-Diiodo-*m*-xylene	10	4 hr. at 70～80°C	**2,4,5,6-Tetraiodo-*m*-xylene**	127	75	82.84	83.25
2,5-Diiodo-*p*-xylene	10	4 hr. at 65～75°C	2,3,5,6-Tetraiodo-*p*-xylene	247	59	83.33	83.25
5-Iodohemimellitene	4	4 hr. at 55～65°C	Diiodohemimellitene	114	27	68.24	68.23
Iodomesitylene	4	4 hr. at 60～65°C	Diiodomesitylene[9]	82	74	68.37	68.23
2,4-Diiodotoluene	4	6 hr. at 90～100°C	2,4,5-Triiodotoluene	119	65		
2,5-Diiodotoluene	4	6 hr. at 100～110°C	2,4,5-Triiodotoluene	119	42		
3,4-Diiodotoluene	4	6 hr. at 100～110°C	2,4,5-Triiodotoluene	119	55		
3,4,5-Triiodotoluene	5	6 hr. at 90～100°C	2,3,5-Triiodotoluene	68	56	81.06	81.04
2,3,5-Triiodotoluene	15	6 hr. at 120～130°C	2,3,4,5-Tetraiodotoluene[8]	189	74	85.42	85.21
2,3,6-Triiodotoluene	15	6 hr. at 120～130°C	2,3,4,6-Tetraiodotoluene	171	42	85.45	85.21
o-Iodoanisol	2	6 hr. at 20～25°C	2,4-Diiodoanisol	69	76	70.73	70.52
p-Iodoanisol	2	6 hr. at 20～25°C	**2,4-Diiodoanisol**	69	75		
o-Iodophenol	2	6 hr. at 20～25°C	2,4-Diiodophenol	72	59	73.51	73.39
p-Iodophenol	2	6 hr. at 20～25°C	2,4-Diiodophenol	72	～40**		
p-Iodophenol	4	6 hr. at 20～25°C	2,4,6-Triiodophenol	158	～20	80.19	80.70

* Yields based on iodine are not necessarily the best obtainable.
** It is possible to obtain either one of products by proper choice of the experimental conditions.
*** Reaction products in gothic are given as examples in the experimental.

2, 4, 5, 6-Tetraiodo-*m*-xylene[5]. — A mixture of 3.6 g. of 4,6-diiodo-*m*-xylene and 10 g. of sulfuric acid was agitated and heated gradually to 70~80°C. The reaction mixture was kept at this temperature for 4 hr., and then poured over crushed ice. The solid material precipitated was filtered and dissolved in the minimum quantity of cold benzene. Chromatography through a short column packed with alumina gave 2.3 g. of fine, white needles melting at 126~127°C.

2,4-Diiodoanisol[6].—A mixture of 11.7 g. of *p*-iodoanisol and 10 g. of sulfuric acid was stirred at room temperature for 6 hr. The resulting thick mixture was poured into excess water, and the precipitated dark oil was extracted with ether. The ethereal solution was evaporated and the residual oil was chromatographed on alumina. Elution with ether followed by recrystallization from hot petroleum benzine gave colorless large plates of 2,4-diiodoanisol in 70~75% yield, melting point alone or in admixture with an authentic specimen 68~69°C.

Department of Chemistry
Faculty of Science
Kyoto University
Sakyo-ku, Kyoto

5) A. Töhl and E. Bauch, *Ber.*, **26**, 1105 (1893).
6) P. Brenans, *Compt. rend.*, **132**, 831 (1901).
7) M. Boyle, *J. Chem. Soc.*, **95**, 1683 (1909).
8) H. Suzuki and R. Goto, *J. Chem. Soc. Japan, Pure Chem. Sec.* (*Nippon Kagaku Zasshi*), **84**, 167, 284 (1963).
9) A. Töhl and R. Eckel, *Ber.*, **26**, 1099 (1893).

Oligomers and Polymers Containing Triple Bonds. I. Derivatives of Ethynylbiphenyl and Ethynylfluorene

By Hisaya TANI, Fumio TODA and Koreyasu MATSUMIYA

(Received October 18, 1962)

Recently, it has been reported that cupric acetate in pyridine[1] and cuprous chloride in pyridine[2] were effective homogeneous reagents for the oxidative coupling of ethynyl compounds. Using these reagents, the authors synthesized a series of conjugated polyacetylenes from the corresponding diethynyl compounds. Lower homologues of these polymers were also prepared in order to study the influence of phenyl, biphenyl and fluorenyl groups on the conjugated systems.

4-Ethynyl and 4, 4′-diethynyl-biphenyl (II and V) were obtained in moderate yields from the corresponding ketones, 4-acetylbiphenyl (I)[3] and 4, 4′-diacetylbiphenyl (IV)[3], using phosphorus pentachloride followed by sodium amide in liquid ammonia. It was wondered why, in the above reaction to prepare II from I, a small amount of di-(*p*-biphenylyl)diacetylene (III) was produced. From acetophenone, however, a similar treatment did not afford the corresponding diacetylenic compound, but instead produced phenylacetylene, in a 30% yield, together with benzoic acid and a small amount of *meso*-2, 3-diphenylbutane[4]. The cause of these curious reactions is not clear.

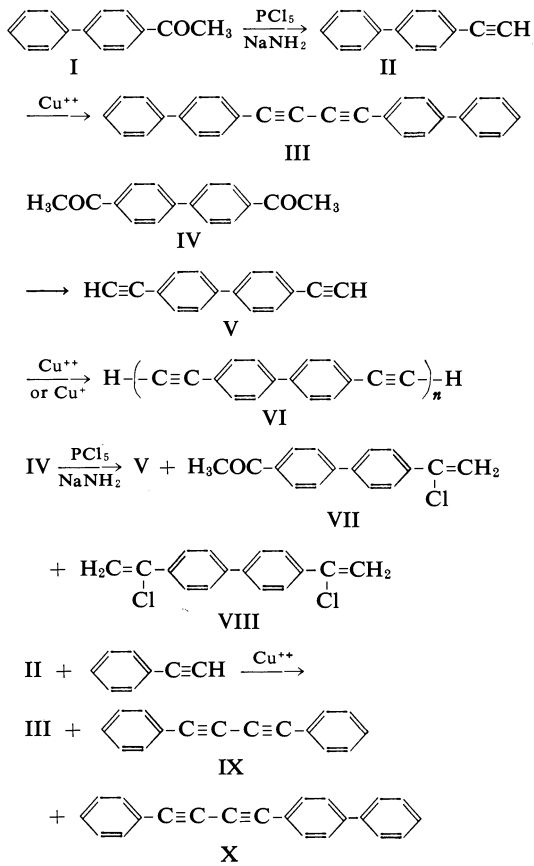

1) G. Eglinton and A. R. Galbraith, *Chem. & Ind.*, **1956**, 937.
2) A. S. Hay, *J. Org. Chem.*, **25**, 1276 (1960).
3) O. V. Ferris and E. E. Turner, *J. Chem. Soc.*, **1920**, 1147.
4) E. Ott, *Ber.*, **61**, 2137 (1928).

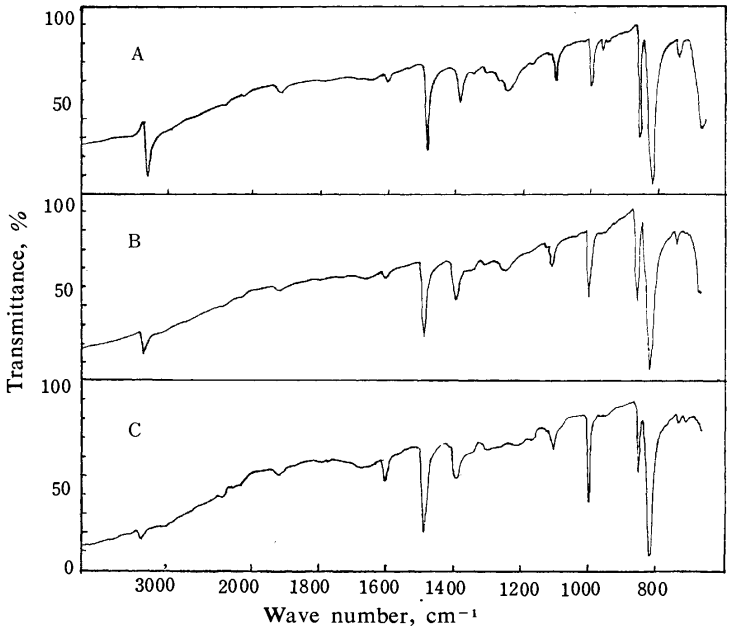

Fig. 1. Infrared absorption spectra.

A, 4,4'-Diethynylbiphenyl (V); B, Di-4-(4'-ethynylbiphenylyl)diacetylene ($VI_{n=2}$); C, Polymer ($VI_{n=4}$); all in KBr disk

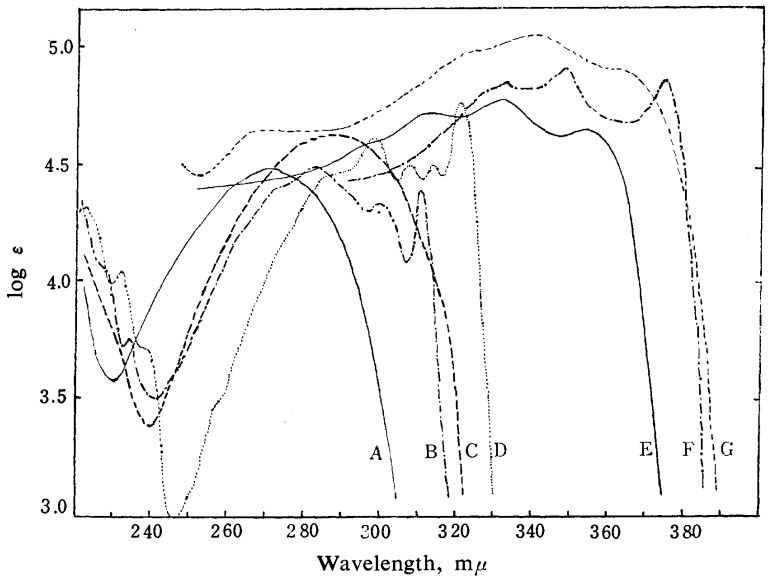

Fig. 2. Ultraviolet absorption spectra.

A, 4-Ethynylbiphenyl (II); B, 2-Ethynylfluorene (XII); C, 4,4'-Diethynylbiphenyl (V); D, 2,7-Diethynylfluorene (XV); all in alcohol, E, Di-(*p*-biphenylyl)diacetylene (III); F, Di-(2-fluorenyl)diacetylene (XIII); G, Di-4-(4'-ethynylbiphenylyl)diacetylene ($VI_{n=2}$); all in dioxane

An attempted synthesis of 4-acetyl-4'-ethynylbiphenyl, a useful compound for the step by step synthesis of conjugated oligomers, failed. Upon the treatment of IV with an equimolecular quantity of phosphorus pentachloride, followed by sodium amide, 4-acetyl-4'-(α-chlorovinyl)biphenyl (VII) and 4,4'-bis-(α-chlorovinyl)biphenyl (VIII) were produced, together with V, but no monoethynylated product was produced.

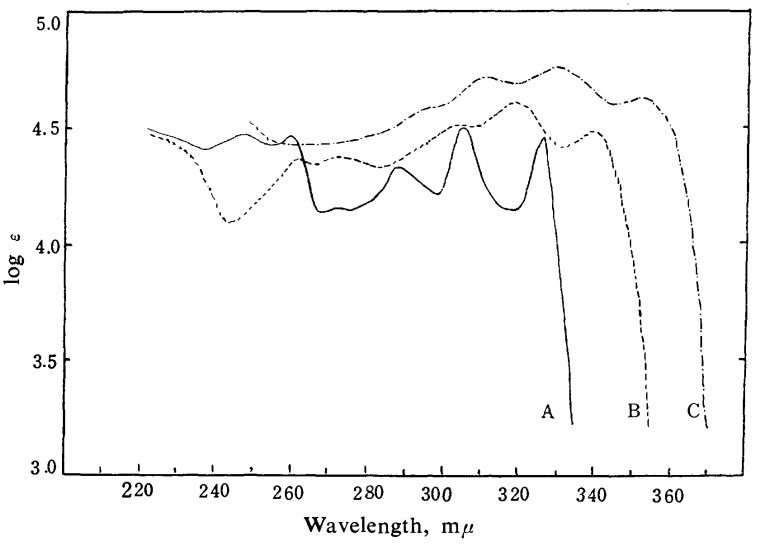

Fig. 3. Ultraviolet absorption spectra.

A, Diphenyldiacetylene (IX); B, 1-Phenyl-4-*p*-biphenylyldiacetylene (X); C, Di-(*p*-biphenylyl)diacetylene (III); all in alcohol

The oxidative coupling of II yielded stable diacetylene III in a quantitative yield. When the oxidative polymerization of V was carried out with cupric acetate in pyridine to which methanol had been added in order to reduce the solubility of the product, the linear dimer of V($VI_{n=2}$) was produced as pale yellow needles in a good yield. The structure of $VI_{n=2}$ was determined by comparing the intensity at the ethynyl maximum in the infrared region of the compound (Fig. 1) with that of V as a standard. This estimation was based on the assumption that the absorbancy of the ethynyl band was not affected by the length of the conjugation system. A comparison of the ultraviolet spectra of $VI_{n=2}$ with that of III, as shown in Fig. 2 and in Table I shows that $VI_{n=2}$ absorbs at ca. 9 mμ longer wavelengths than III. This bathochromic shift may be attributable to the two additional ethynyl substituents.

On the other hand, the shift exhibited when one ethynyl group was introduced into II is 17 mμ (Fig. 2 and Table I). The ultraviolet spectrum of III is similar to that of diphenyldiacetylene (IX), and a bathochromic shift due to two additional phenyl groups is ca. 12 mμ (Fig. 3 and Table I).

In order to study the effects exerted by the addition of one phenyl group on the absorption properties of diphenyldiacetylenes, phenyl-*p*-biphenylyldiacetylene (X) was prepared by the crossed coupling of II and phenylacetylene. As is illustrated in Fig. 3 and in Table I, an increase of one phenyl group in IX and X gave rise to bathochromic shifts of 14 mμ and 12 mμ respectively.

Table I. Ultraviolet absorption spectra at longer wave region

Compound	Solvent*	λ_{max}, mμ ($\varepsilon\times10^{-2}$)	λ_{max}, mμ ($\varepsilon\times10^{-2}$)
II	A	271 (293)	
V	A	288 (410)	
XII	A	299 (209)	310 (241)
XV	A	314 (316)	321 (587)
IX	A	305 (317)	326 (284)
X	A	319 (420)	340 (313)
III	A	330 (592)	352 (436)
$VI_{n=2}$	D	339(1085)	361 (779)
XIII	D	348 (806)	374 (710)

* A, Alcohol D, Dioxane

Further oxidative coupling of $VI_{n=2}$ in boiling pyridine yielded a stable orange solid, the infrared spectrum of which showed that the oxidation of the triple bond to carbonyl had partially occurred during the reaction.

The polymerization of V with the cuprous chloride catalyst in pyridine and in an oxygen atmosphere, as summarized in Table II, resulted in the formation of insoluble and infusible yellow or orange solids. On the basis of the infrared absorption spectra and the elemental analysis, these products were presumed to be linear polymers, the degrees of polymerization of which were about 4~6. The polymers were quite stable, but at a temperature above 300°C they gradually turned to black via brown.

Although all the reactions were carried out

TABLE II. POLYMERIZATION OF 4,4'-DIETHYNYLBIPHENYL (V)

V mg.	Catalyst mg.	Solvent* ml.	Reaction temp., °C	Reaction time, hr.	Atmosphere	Color	Product Degree of polymerization
1000	$Cu(OAc)_2$, 5000	P 30 M 20	50	1.5	Air	Pale yellow	2
500	CuCl, 500	P 100	65	3	O_2	Orange yellow	6
250	CuCl, 20	P 50	65	1	O_2	Yellow	4
250	CuCl, 20	P 50	65	2	Air	Orange yellow	6
150	CuCl, 10	P+PP 15+10	60	1	O_2	Yellow	4

* P, Pyridine M, Methanol PP, Piperidine

at low temperatures, the products showed weak carbonyl absorptions at about the 1675 cm^{-1} region of their infrared spectra, suggesting the partial oxidation of the triple bond to carbonyl.

In the same fashion as with the preparation of II and V, monoethynyl- (XII) and diethynylfluorene (XV) were synthesized from ketones XI[5] and XIV respectively in poor yields. The bathochromic shift (ca. 11 mμ) attributable to an additional ethynyl in XV is comparable to that exhibited by an additional phenyl and described above in the IX-X-III series, but it

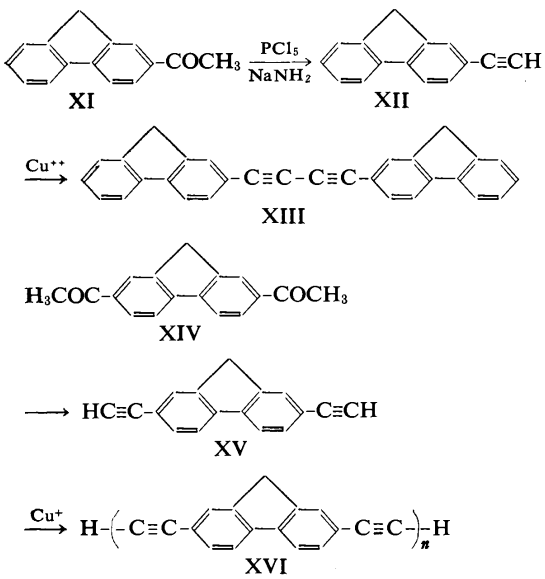

is smaller than that shown in the case of V. The dimerization of XII by oxidative coupling gave XIII as yellow needles quantitatively. The ultraviolet spectra of XIII and related compounds are shown in Fig. 2 and in Table I. The oxidative polymerization of XV resulted in the formation of an orange-brown solid containing a carbonyl group; the intensity at the carbonyl maximum in the infrared spectrum is fairly strong, indicating that the larger the degree of conjugation, the larger the facility of carbonyl formation allowed in the coupling reaction.

Experimental[6]

4-Ethynylbiphenyl (II).—A mixture of 4-acetylbiphenyl (11.8 g., 0.06 mol.), phosphorus pentachloride (16.0 g., 0.078 mol.) and phosphorus oxychloride (25 ml.) was heated at 60°C for 1 hr. After evaporating the phosphorus oxychloride under reduced pressure at a temperature below 30°C, the residue was dissolved in dry tetrahydrofuran (50 ml.) and then stirred drop by drop, over a 20 min. period, into a solution of sodium amide (prepared from sodium 6.5 g., 0.28 g. atom) in liquid ammonia (300 ml.); the stirring was continued for a further 30 min. The residue obtained by the evaporation of ammonia was decomposed with water (100 ml.) and extracted with ether (300 ml.). The ethereal layer was washed with aqueous sodium chloride and dried over anhydrous sodium sulfate. Evaporation of the solvent gave a crude solid which was sublimed at 70°C under 3 mmHg to give II, 7.5 g. (70%) in the form of photo-unstable colorless needles; m. p., 85.5°C (decomp.). IR: KBr disk, 3250 (ethynyl), 2110 (acetylene), 840 (*p*-disubstituted benzene) and 770, 700 cm^{-1} (monosubstituted benzene). UV: λ_{max} in alcohol, 271 mμ (ε, 29300).

Found: C, 93.80; H, 5.52. Calcd. for $C_{14}H_{10}$: C, 93.34; H, 5.66%.

After the sublimation of II, the brownish residue was recrystallized from carbon tetrachloride. Recrystallization of the carbon tetrachloride-insoluble solid from benzene gave pale yellow needles; m. p., 223°C (decomp.). The yield was 200 mg. A mixed melting point with di-(*p*-biphenylyl)-diacetylene (III) showed no depression. The infrared spectrum of this material was identical with that recorded for III.

Di-(*p*-biphenylyl)diacetylene (III).—A mixture of 4-ethynylbiphenyl (II) (2.5 g.), cupric acetate monohydrate (1.5 g.) and pyridine (80 ml.) was stirred for 1.5 hr. at 50°C. After cooling, the crystals formed were collected by filtration, washed with water and alcohol, and then recrystallized from benzene to give III (1.2 g., 48%) as pale yellow needles; m. p., 232° (decomp.). IR: KBr disk, 2150 (acetylene), 840 (*p*-disubstituted benzene) and 766, 700 cm^{-1} (monosubstituted benzene). UV: λ_{max} in alcohol, 294 (shoulder) (ε, 37100), 310.5 (52200), 330 (59200) and 352 mμ (43600).

5) "Organic Syntheses", Coll. Vol. III, 29 (1956).

6) All melting points are uncorrected.

Found: C, 94.73; H, 5.03. Calcd. for $C_{28}H_{18}$: C, 94.88; H, 5.12%.

4, 4'-Diacetylbiphenyl (IV).—Powdered anhydrous aluminum trichloride (2.8 g., 2.1 mol.) was added to a solution of biphenyl (108 g., 0.7 mol.) in carbon disulfide (600 ml.). Acetylchloride (220 g., 2.8 mol.) was stirred into the mixture over a one-hour period at room temperature, and then this stirring was continued for 5 hr. at 55°C. After the removal of the carbon disulfide by distillation, the residue was poured into an ice-cooled, diluted hydrochloric acid to yield a crystalline solid which was then washed with water and alcohol and dried in vacuo. In order to remove both the 4-acetylbiphenyl formed as a by-product and the unchanged biphenyl, the solid thus obtained was washed repeatedly with boiling alcohol. Recrystallization of the alcohol-insoluble solid from benzene yielded IV (60 g., 36%) as pale yellow leaflets; m. p., 189~191°C (lit.[3], 190~191°C). UV: λ_{max} in alcohol, 295 mμ (ε, 32800).

4, 4'-Diethynylbiphenyl (V).—4, 4'-Diacetylbiphenyl (IV) (7.1 g., 0.03 mol.) was treated with phosphorus pentachloride (18.8 g., 0.09 mol.) in phosphorus oxychloride (30 ml.) for 30 min. at 60°C. Evaporation of phosphorus oxychloride under reduced pressure gave chloride as an unstable, bright yellow solid. A solution of the crude chloride in dry tetrahydrofuran (70 ml.) was stirred into a solution of sodium amide (prepared from sodium 7.5 g., 0.32 g. atom) in liquid ammonia (250 ml.) over a 30 min. period, and then this stirring was continued for a further 30 min. The residue obtained by the evaporation of the ammonia was decomposed with water (100 ml.) and extracted with ether (500 ml.). The ethereal layer was washed with aqueous sodium chloride and dried over anhydrous sodium sulfate. After removal of the solvent, the residue was chromatographed on alumina from benzene-carbon tetrachloride (1 : 3) and then crystallized from alcohol to yield V (3.2 g., 53%) as colorless needles; m. p., 165.5~166.5°C. IR: KBr disk, 3260 (ethynyl), 2120 (acetylene) and 860, 825 cm^{-1} (*p*-disubstituted benzene). UV: λ_{max} in alcohol, 288 mμ (41000); dioxane, 290 mμ (ε, 40800).

Found: C, 94.76; H, 5.06. Calcd. for $C_{16}H_{10}$: C, 95.02; H, 4.98%.

***meso*-2, 3-Diphenylbutane.**—The chlorination of acetophenone with phosphorus pentachloride, followed by dehydrochlorination with sodium amide in liquid ammonia, gave an oily product; on distillation this product yielded phenylacetylene (A), (30% b. p. 50°C at 19 mmHg), a high boiling material (B), (b. p. 70~80°C at 19 mmHg) and undistillable resinous material (C). The high boiling material was unstable and solidified after having been left for several weeks. The solid obtained was crystallized from methanol-water to give colorless leaflets (m. p., 114~116°C), which were identified as benzoic acid by mixed melting point determination with the authentic sample and by infrared analysis. The resinous material was chromatographed on alumina from carbon tetrachloride and then crystallized from methanol to afford *meso*-2, 3-diphenylbutane in the form of colorless needles; m. p., 120~122°C (lit[4] m. p. 126°C). IR: KBr disk, 3060, 3010 (aromatic H), 2950 (methyl), 2890 (tertiary H), 1373 (methyl) and 773, 755, 697 cm^{-1} (monosubstituted benzene).

Found: C, 91.31; H, 8.59. Calcd. for $C_{16}H_{18}$: C, 91.37; H, 8.63%.

4, 4'-Bis-(α-chlorovinyl)biphenyl (VIII) and 4-Acetyl-4'-(α-chlorovinyl)biphenyl (VII).—4', 4-Diacetylbiphenyl (IV) (7.1 g., 0.03 mol.) was treated with phosphorus pentachloride (9.4 g., 0.045 mol.) in phosphorus oxychloride (25 ml.) for 30 min. at 80~90°C. The crude chloride obtained in the manner described above was dissolved in dry tetrahydrofuran (50 ml.), and the resulting solution was stirred into a solution of sodium amide (prepared from sodium 3.7 g., 0.16 g. atom) in liquid ammonia (150 ml.) over a one-hour period. After evaporation of the ammonia, water (100 ml.) was added to the residue and then extracted with ether. The ethereal solution was washed with water and dried over anhydrous sodium sulfate. After removal of the solvent, the solid residue was chromatographed on alumina from carbon tetrachloride and benzene. The elute obtained by using carbon tetrachloride gave photosensitive, colorless plates; m. p., 175°C (decomp.). IR: KBr disk, 888 (vinyl) and 825 cm^{-1} (*p*-disubstituted benzene).

Found: C, 69.35; H, 4.34. Calcd. for $C_{16}H_{12}Cl_2$: C, 69.82; H, 4.33%.

The colorless crystals (m. p., 160°C (decomp.)) obtained by elution with benzene were recrystallized from alcohol to yield colorless leaflets; m. p., 160°C (decomp.). IR: KBr disk, 1680 (carbonyl), 890 (vinyl) and 823 cm^{-1} (*p*-disubstituted benzene). UV: λ_{max} in alcohol, 299 mμ (ε, 33500).

Found: C, 74.95; H, 5.12; Cl, 13.54. Calcd. for $C_{16}H_{13}OCl$: C, 74.84; H, 5.06; Cl, 13.84%.

Di-4-(4'-ethynylbiphenyl)diacetylene ($VI_{n=2}$), a Dimer of V.—A mixture of V (1.0 g.), cupric acetate monohydrate (5.0 g.), pyridine (30 ml.) and methanol (20 ml.) was stirred for 1.5 hr. at 50°C. The crude solid obtained in the manner described for III was crystallized twice from dimethylformamide to give pale yellow needles (0.7 g., 70%) showing no clear melting point (>300°C). Upon heating in an air bath, the crystals gradually turned orange, then brown, and finally black. The infrared and ultraviolet spectra showed this compound to be a linear dimer of V. IR: KBr disk, 3260 (ethynyl) and 860, 825 cm^{-1} (*p*-disubstituted benzene). UV: λ_{max} in dioxane, 367 (ε, 43200), 324 (shoulder) (93400), 339 (108500) and 361 mμ (shoulder) (77900).

Found: C, 94.49; H, 4.57. Calcd. for $C_{32}H_{18}$: C, 95.49; H, 4.51%.

1-Phenyl-4-*p*-biphenylyldiacetylene (X).—A mixture of II (0.9 g., 0.005 mol.), phenylacetylene (1.0 g., 0.01 mol.), cupric acetate monohydrate (3.0 g., 0.03 mol.) and pyridine (30 ml.) was stirred for 1 hr. at 50°C. Then alcohol (20 ml.) was added to the reaction mixture to afford pale yellow needles (0.4 g.) after recrystallization from benzene. The crystals (m. p., 230°C (decomp.)) were identified as III by mixed melting point determination with an authentic sample and by the infrared spectrum.

The pyridine-alcohol layer was evaporated to dryness under reduced pressure; the crude material which remained was crystallized from methanol (25 ml.) to give colorless needles (m. p., 85°C, 0.5 g.), which were identified as diphenyldiacetylene by the same methods as have been mentioned above. The methanol-insoluble solid was repeatedly recrystallized from alcohol, resulting in X (0.3 g.) as colorless leaflets; m. p., 148~150°C. IR: Nujol mull, 835 (*p*-disubstituted benzene) and 765, 755, 720 cm^{-1} (monosubstituted benzene). UV: λ_{max} in alcohol, 261 (ε, 23300), 272 (24600), 302.5 (33100), 319 (42000) and 340 mμ (31300).

Found: C, 94.58; H, 5.02. Calcd. for $C_{22}H_{14}$: C, 94.93; H, 5.07%.

2-Ethynylfluorene (XII).—2-Acetylfluorene (XI) (6.42 g., 0.03 mol.) was treated with phosphorus pentachloride (9.37 g., 0.045 mol.) in phosphorus oxychloride (50 ml.) for 3 hr. at 60°C. The mixture was concentrated in vacuo, and the residue was dissolved in dry ether (200 ml.). The ethereal solution was, over a 20 min. period, stirred into a solution of sodium amide (prepared from sodium 3.7 g., 0.16 g. atom) in liquid ammonia (150 ml.); the stirring was then continued for a further 1.5 hr. After the removal of the ammonia, the residue was decomposed with water (150 ml.). Extraction with ether followed by evaporation gave crude crystals, which were chromatographed on alumina from carbon tetrachloride to afford XII (700 mg.) as colorless leaflets; m. p., 85.5°C. IR: KBr disk, 3240 (ethynyl), 2095 (acetylene), 875 (isolated H), 831 (*p*-disubstituted benzene) and 767, 734 cm^{-1} (*o*-disubstituted benzene). UV: λ_{max} in alcohol, 219 (shoulder) (ε, 24600), 228 (shoulder) (10700), 234 (5700), 282 (30100), 299 (20900) and 310 mμ (ε, 24100). λ_{max} in dioxane, 285 (28800), 302 (21800) and 312 mμ (24200).

Found: C, 94.81; H, 5.25. Calcd. for $C_{15}H_{10}$: C, 94.70; H, 5.30%.

Di-(2-fluorenyl)-diacetylene (XIII).—A mixture of 2-ethynylfluorene (XII, 0.5 g.), cupric acetate monohydrate (1.5 g.) and pyridine (15 ml.) was heated at 50°C for 1 hr. while being stirred. The crude crystals deposited were collected by filtration and washed successively with methanol, hot water and methanol. Two recrystallizations of the crystals from benzene gave yellow needles; m. p., 278°C (decomp.) 340 mg. IR: KBr disk, 2120 (acetylene), 870 (isolated H), 326 (*p*-disubstituted benzene) and 764, 733 cm^{-1} (*o*-disubstituted benzene). UV: λ_{max} in dioxane, 832 (67600), 348 (80600) and 374 mμ (ε, 71000).

Found: C, 95.10; H, 4.69. Calcd. for $C_{30}H_{18}$: C, 95.21; H, 4.79%.

2,7-Diacetylfluorene (XIV).—Acetylchloride (19.6 g. 0.25 mol.) was stirred drop by drop into a solution of 2-acetylfluorene (XI) in carbon disulfide over a 30 min. period, and the resulting mixture was then heated under reflux while being stirred for more 3 hr. After the removal of the carbon disulfide under reduced pressure, the residue was decomposed with diluted hydrochloric acid. The crude material collected by filtration was washed with petroleum ether (b. p. 75°C) and alcohol, and recrystallized three times from alcohol to yield XIV 21 g. (33%) as colorless needles; m. p., 178.5~179°C. IR: Nujol mull, 1680, 1359 (ketone), 868 (isolated H) and 841 cm^{-1} (*p*-disubstituted benzene). UV: λ_{max} in alcohol, 320 (ε, 36700) and 326 mμ (36800).

Found: C, 81.13; H, 5.57. Calcd. for $C_{17}H_{14}O_2$: C, 81.58; H, 5.64%.

2,7-Diethynylfluorene (XV).—Crude chloride, obtained by the same treatment of a mixture of 2,7-diacetylfluorene (XIV) (5.5 g., 0.02 mol.), phosphorus pentachloride (12.5 g., 0.06 mol.) and phosphorus oxychloride (60 ml.) as has been described for XII, was treated with sodium amide (sodium 5.5 g., 0.24 g. atom) in liquid ammonia (200 ml.) resulting in crude crystals (800 mg.; m. p., 112~116°C), which were chromatographed on alumina from carbon tetrachloride to give XV (200 mg.) as colorless needles; m. p., 132~132.5°C. IR: Nujol mull, 3290 (ethynyl), 2090 (acetylene), 865 (isolated H) and 845, 825 cm^{-1} (*p*-disubstituted benzene). UV: λ_{max} in alcohol, 222 (ε, 20100), 232 (10200), 240 (shoulder) (4900), 297 (41100), 307 (31600), 314 (31600) and 321 mμ (58700).

Found: C, 95.14; H, 4.73. Calcd. for $C_{17}H_{10}$: C, 95.30; H, 4.70%.

Department of Polymer Science
Faculty of Science
Osaka University
Nakanoshima, Osaka

Synthesis of 7-Hydroxy-2', 4', 5'-trimethoxyisoflavone and Related Compounds

By Kenji FUKUI, Mitsuru NAKAYAMA, Masayuki HATANAKA, Tadao OKAMOTO and Yoshiyuki KAWASE

((Received October 22, 1962)

Little has been reported on isoflavones oxygenated at the 2'-, 4'- and 5'-positions. Caviunin[1] (I) and Harper's phenol (" toxicarol isoflavone ")[2] (II) are the only known instances which occur naturally. We have, therefore, been interested in synthesizing 7-hydroxy-2', 4', 5'-trimethoxyisoflavone (III) and the corresponding 2-methyl derivative (IV) because of their structural resemblance to I and II.

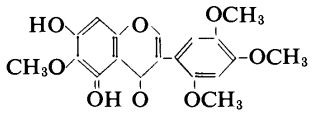

I

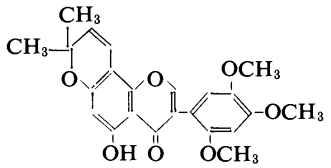

II

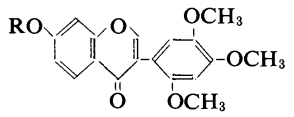

III R=H
X R=CH_3CO
XI R=CH_3

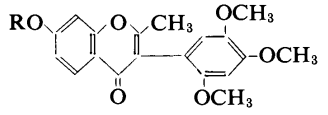

IV R=H
XII R=CH_3CO
XIII R=CH_3

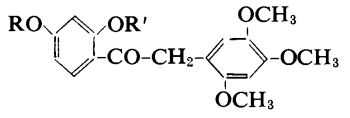

V R=R'=H
VI R=CH_3, R'=H
VII R=R'=CH_3
VIII R=$C_6H_5CH_2$, R'=H
IX R=R'=CH_3CO

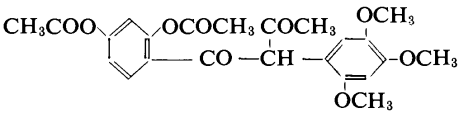

XIV

Hoesch condensation of resorcinol and 2, 4, 5-trimethoxybenzyl cyanide[3] yielded 2, 4-dihydroxyphenyl 2, 4, 5-trimethoxybenzyl ketone (V) in discouraging yields under a variety of reaction conditions. The ketone V could, however, be prepared in a 46% yield by treating a mixture of resorcinol and homoasaronic acid (2, 4, 5-trimethoxyphenylacetic acid)[4] with polyphosphoric acid. Zinc chloride in either the presence[5] or absence of phosphorous oxychloride gave inferior yields of V. Ethers (VI–VIII) and a diacetate (IX) of V were prepared.

When the ketone V was treated with ethyl orthoformate in pyridine[6], the desired isoflavone III was obtained in a 61% yield. An acetate (X) and a methyl ether (XI) of III were prepared.

Reaction of the ketone V with acetic anhydride in the presence of sodium acetate[7] gave a cyclized acetate XII which could easily be hydrolyzed to 7-hydroxy-2', 4', 5'-trimethoxy-2-methylisoflavone (IV). A methyl ether (XIII) of IV was also obtained.

When the acetylation of the ketone V was carried out with acetyl chloride in pyridine at 0°C, a diketone XIV was produced. The alkaline hydrolysis of XIV was accompanied with a simultaneous ring closure to afford the methylisoflavone (IV), which was identical with the above-mentioned product.

1) O. R. Gottlieb and M. T. Magalhaês, *J. Org. Chem.*, **26**, 2449 (1961).
2) S. H. Harper, *J. Chem. Soc.*, **1940**, 1178.
3) J. Harley-Mason and A. H. Jackson, ibid., **1954**, 1165.
4) A. Robertson and G. H. Rusby, ibid., **1935**, 1371.
5) V. R. Shah, J. L. Bose and R. C. Shah, *J. Org. Chem.*, **25**, 677 (1960).
6) V. R. Sathe and K. Venkataraman, *Current Sci. (India)*, 18, 373 (1949); *Chem. Abstr.*, **44**, 8916 (1950).
7) W. Baker and R. Robinson, *J. Chem. Soc.*, **127**, 1981 (1925).

Experimental*

2, 4-Dihydroxyphenyl 2, 4, 5-Trimethoxybenzyl Ketone (V). — *Hoesch Reaction*[8]. — A mixture of resorcinol (1.5 g.) and 2,4,5-trimethoxybenzyl cyanide (m. p., 84~85°C)[3] (1.0 g.) in anhydrous ether (60 ml.) was saturated with dried hydrogen chloride for a 3 hr. period at 0°C and then allowed to stand at room temperature for 4 days. The ethereal solution was decanted from the oily layer of ketimine hydrochloride which had separated. The oily layer was washed twice with dry ether (20 ml.) and then heated on a steam bath with water (30 ml.) for 1 hr. After cooling and standing, the product was collected and recrystallized from ethanol, giving V (m. p., 201~202°C) (reported m. p., 201~202°C[8]) (colorless needles), which showed a reddish-brown ferric chloride reaction in ethanol; yield, 0.2 g. (13%).

Found: C, 64.10; H, 5.82. Calcd. for $C_{17}H_{18}O_6$: C, 64.14; H, 5.70%.

Nencki Reaction. — A mixture of homoasaronic acid (m. p., 102~103°C)[4] (1.0 g.) and freshly fused zinc chloride (0.4 g.) was heated at 130~140°C for 30 min. After resorcinol (1.5 g.) had been added, the mixture was kept at the same temperature for 2 hr. Upon working up the reaction mixture, 0.4 g. (31%) of V was obtained. M. p. and mixed m. p., 199~200°C.

With Phosphorus Oxychloride-Zinc Chloride. — A mixture of resorcinol (2.0 g.), homoasaronic acid (1.5 g.), phosphorus oxychloride (20 ml.) and freshly fused zinc chloride (6.0 g.) was heated at 50~60°C for 2 hr. The product was recrystallized from ethanol, giving V (m. p. and mixed m. p., 197~199°C); yield, 0.6 g. (24%).

With Poly(phosphoric Acid).—A mixture of resorcinol (1.5 g.), homoasaronic acid (1.0 g.) and poly(phosphoric acid) (n=2.5) (10 g.) was warmed on a steam bath for 15 min. The dark red solution was then poured into ice-water. The resulting product was recrystallized from ethanol, giving V (m. p. and mixed m. p., 201~202°C); yield, 0.65 g. (46%).

2-Hydroxy-4-methoxyphenyl 2, 4, 5-Trimethoxybenzyl Ketone (VI). — *With Diazomethane.* — The treatment of V (0.5 g.) in acetone (60 ml.) with an ethereal solution of diazomethane (prepared from 0.5 g. of nitrosomethylurea) gave VI as colorless needles (m. p., 135~136°C (from ethanol)); yield, 0.5 g. (96%).

Found: C, 64.91; H, 6.15. Calcd. for $C_{18}H_{20}O_6$: C, 65.05; H, 6.07%.

With Methyl Iodide.—To a solution of V (1.0 g.) and methyl iodide (0.2 ml.) in acetone (30 ml.) was added potassium carbonate (2.0 g.); the mixture was then refluxed for 70 min. The product was recrystallized from ethanol, giving VI (m. p. and mixed m. p., 135~136°C); yield, 1.0 g. (96%).

2, 4-Dimethoxyphenyl 2, 4, 5-Trimethoxybenzyl Ketone (VII). — To a solution of V (1.0 g.) and dimethyl sulfate (1.0 ml.) in acetone (50 ml.) was added potassium carbonate (5.0 g.); the mixture was then refluxed for 6.5 hr. to provide VII (m. p., 110~111°C) (colorless needles from ethanol); yield, 1.0 g. (91%).

Found: C, 65.89; H, 6.58. Calcd. for $C_{19}H_{22}O_6$: C, 65.88; H, 6.40%.

2-Hydroxy-4-benzyloxyphenyl 2, 4, 5-Trimethoxybenzyl Ketone (VIII).—A mixture of V (1.0 g.), benzyl chloride (1.0 g.) and potassium carbonate (5.0 g.) in acetone (50 ml.) was refluxed for 8 hr. Recrystallization from ethanol gave VIII in the form of colorless needles, (m. p. 149~150°C); yield, 1.2 g. (94%).

Found: C, 70.55; H, 5.99. Calcd. for $C_{24}H_{24}O_6$: C, 70.57; H, 5.92.

2, 4-Diacetoxyphenyl 2, 4, 5-Trimethoxybenzyl Ketone (IX). — The treatment of V (0.1 g.) in pyridine (5.0 ml.) with acetic anhydride (2.0 ml.) at room temperature gave IX as colorless prisms (m. p., 134~135°C (from ethanol)); yield, 0.12 g. (95%).

Found: C, 62.23: H, 5.58. Calcd. for $C_{21}H_{22}O_8$: C, 62.68; H, 5.51.

7-Hydroxy-2', 4', 5'-trimethoxyisoflavone (III).— To a solution of V (0.8 g.) and ethyl orthoformate (2.0 ml.) in pyridine (10 ml.) was added piperidine (0.5 ml.); the mixture was then refluxed for 10 hr. The resulting solution was cooled and acidified with dilute hydrochloric acid. The precipitate was recrystallized from ethanol, giving III (m. p., 244~245°C) (colorless microcrystals), with a negative ferric chloride reaction in ethanol; yield, 0.5 g. (61%). IR: 3320~3200 (broad) (OH), 1640 cm^{-1} (γ-pyrone). UV: λ_{max}^{EtOH} mμ (log ε): 241 (4.35), 249 (4.35), 300 (4.24).

Found: C, 65.62; H, 5.18. Calcd. for $C_{18}H_{16}O_6$: C, 65.85; H, 4.91%.

The acetylation of III with acetic anhydride and pyridine at room temperature gave the acetate (X) (m. p., 156~157°C) (colorless needles from ethanol). IR: 1752 (acetate), 1659 cm^{-1} (γ-pyrone).

Found: C, 64.72; H, 5.11. Calcd. for $C_{20}H_{18}O_7$: C, 64.86; H, 4.90%.

2', 4', 5', 7-Tetramethoxyisoflavone (XI). — This ether XI was prepared from V (0.15 g.) with dimethyl sulfate in acetone. Recrystallization from ethanol yielded colorless plates (m. p., 190~191°C); yield, 0.12 g. (80%). IR: 1639 cm^{-1} (γ-pyrone).

Found: C, 66.62; H, 5.42. Calcd. for $C_{19}H_{18}O_6$: C, 66.66; H, 5.30%.

7-Acetoxy-2', 4', 5'-trimethoxy-2-methylisoflavone (XII).—A mixture of V (1.0 g.) and anhydrous sodium acetate (2.0 g.) in acetic anhydride was refluxed for 18 hr. The cooled mixture was poured into ice-water. An oil separated and solidified on cooling. Recrystallization of the solid from ethyl acetate or ethanol gave XII (m. p., 177~178°C) (colorless needles), with a negative ferric chloride reaction in ethanol; yield, 1.0 g. (83%). IR: 1756 (acetate), 1645 cm^{-1} (γ-pyrone).

Found: C, 65.79; H, 5.31. Calcd. for $C_{21}H_{20}O_7$: C, 65.61; H, 5.24%.

2, 4-Diacetoxyphenyl α-Acetyl-2, 4, 5-trimethoxybenzyl Ketone (XIV).—Into a solution of V (2.0 g.) in pyridine (40 ml.) acetyl chloride (3.0 ml.) was

** All melting points are uncorrected; the infrared spectra were meaured in Nujol.

8) This procedure is based on a private communication from Hiroshi Fukami of the Department of Agricultural Chemistry, Kyoto University.

added with stirring at 0°C. After having been left standing for 24 hr. at 0°C, the reaction mixture was poured into ice-water. The resulting solid mass was collected by filtration and dried. Recrystallization from ethanol gave XIV (m. p., 164~165°C) (colorless prisms), with a negative ferric chloride reaction in ethanol; yield, 2.2 g. (78%).

Found: C, 62.12; H, 5.45. Calcd. for $C_{23}H_{24}O_9$: C, 62.16; H, 5.44%.

2-Hydroxy-2',4',5'-trimethoxy-2-methylisoflavone (IV).—*By Hydrolysis of XII.—i) With Sulfuric Acid:* A solution of XII (0.55 g.) in ethanol (50 ml.) was refluxed with concentrated sulfuric acid (0.3 ml.) for 4 hr. After evaporation of the solvent, the residue was triturated with water. The resulting solid was recrystallized from ethanol giving IV (m. p., 246~247°C) (colorless microcrystals); yield, 0.47 g. (96%). IR: 3248 (OH), 1637 cm^{-1} (γ-pyrone). UV: λ_{max}^{EtOH} mμ (log ε): 242 (4.37), 250 (4.37), 296.5 (4.30).

Found: C, 66.65; H, 5.43. Calcd. for $C_{19}H_{18}O_6$: C, 66.66; H, 5.30%.

The acetylation of IV with acetic anhydride and pyridine gave the acetate (XII) (m. p. and mixed m. p., 177~178°C).

ii) With Sodium Carbonate: A mixture of XII (0.25 g.) and 10% aqueous sodium carbonate (10 ml.) was refluxed for 2 hr. Upon acidification of the hydrolyzate with dilute hydrochloric acid, a precipitate formed. Recrystallization from ethanol gave IV (m. p., 246~248°C, which was identical with that of the above sample); yield, 0.1 g. (48%).

By Hydrolysis of XIV.—XIV (1.0 g.) was treated with sodium carbonate in a manner similar to that described above. Recrystallization from ethanol gave IV (m. p., 246~247°C); yield, 0.5 g. (38%).

2',4',5',7-Tetramethoxy-2-methylisoflavone (XIII).—This ether XIII was prepared from (0.20 g.) with dimethyl sulfate in acetone. Recrystallization from ethanol gave colorless microcrystals (m. p., 189~190°C); yield, 0.20 g. (96%). IR: 1641 cm^{-1} (γ-pyrone).

Found: C, 67.38; H, 5.73. Calcd. for $C_{20}H_{20}O_6$: C, 67.40; H, 5.66%.

The authors are grateful to Professor Minoru Nakajima and Professor Tetsuo Mitsui, Kyoto University, for their measurements of infrared spectra and microanalyses. This work was partially supported by a grant-in-aid for scientific research from the Ministry of Education, which is acknowledged with gratitude.

Department of Chemistry
Faculty of Science
Hiroshima University
Higashi-sendamachi, Hiroshima
(K. F., M. N. & M. H.)

Faculty of Literature and Science
Toyama University
Gofuku, Toyama
(T. O. & Y. K.)

The Preparation of Stereoisomeric α,ω-Diphenylpolyenes and Related Compounds by Means of the Wittig Reaction

By Soichi MISUMI and Masazumi NAKAGAWA

(Received October 29, 1962)

As reported in a previous paper, the authors have found in the synthesis of polystilbenes that the Wittig reaction gave almost the same amount of cis and trans isomers simultaneously with regard to the ethylenic linkage formed by the particular reaction[1]. The method seemed to be promising for the preparation of geometrical isomers of a wide variety of compounds. It is well-known that the cis isomers of α,ω-diphenylpolyene can be obtained by the semihydrogenation[2] of the corresponding acetylenic compounds on Lindlar's catalyst or by the photoisomerization of the all-trans isomer[2a,3]. The fact that the latter method essentially gives a mixture of several cis isomers reduces the practical value of this process for preparative purpose. On the contrary, the Wittig reaction is advantageous in view of the introduction of cis and trans ethylenic linkages at a definite position in the molecule by the reaction of a carbonyl component with an appropriate yield moiety. The present paper deals with the syntheses of stereoisomeric α,ω-diphenylpolyenes and related compounds according to this procedure.

1) S. Misumi, M. Kuwana and M. Nakagawa, This Bulletin, **34**, 1833 (1961); **35**, 135, 143 (1962).

2) a) J. H. Pinckard, B. Wille and L. Zechmeister, *J. Am. Chem. Soc.*, **70**, 1938 (1948); b) M. Akhtar, T. A. Richard and B. C. L. Weedon, *J. Chem. Soc.*, **1959**, 933.

3) L. Zechmeister and A. L. LeRosen, *J. Am. Chem. Soc.*, **64**, 2755 (1942), **76**, 2308, 4144 (1954); *Acta Chem. Scand.*, **8**, 1421 (1954).

The synthesis of *trans, trans*-1, 4-diphenylbutadiene (II) has been reported recently by Campbell employing triphenylcinnamylphosphonium chloride and benzaldehyde[4]. The present authors have confirmed the simultaneous formation of trans, trans and trans, cis isomers (II and III) by the reaction of triphenylcinnamylphosphonium bromide (I) with the aldehyde. The combined yield was found as high as 77%.

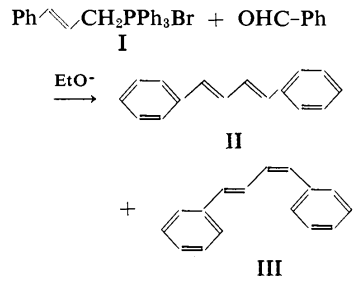

Similarly, the reaction of phosphonium bromide I with cinnamaldehyde afforded two isomers of 1, 6-diphenylhexatriene, trans, trans, trans (IV) and trans, cis, trans (V), in nearly the same yield.

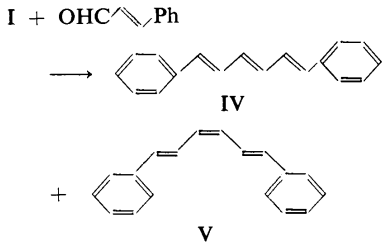

The third isomer, *trans, trans, cis*-diphenylhexatriene (VII) was obtained by the reaction of triphenyl-5-phenyl-2, 4-pentadienylphosphonium bromide (VI) with benzaldehyde and purified by chromatography on alumina. The cis isomer VII, colorless liquid, exhibited the identical electronic spectrum with that of the specimen prepared by Zechmeister and his coworkers[3], and it transformed into an all-trans isomer on exposure to light.

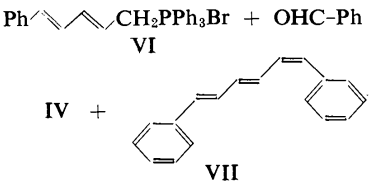

Similarly, the reaction of phosphonium bromide VI with cinnamaldehyde gave two stereoisomers, all-trans (VIII) and trans, cis, trans, trans (IX), of 1,8-diphenyloctatetraene in about the same yield.

4) R. N. McDonald and T. W. Campbell, "Organic Syntheses", **40**, 36 (1960); *J. Org. Chem.*, 24, 1241 (1959).

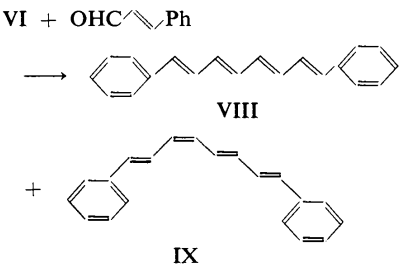

The melting points and the electronic spectra of all above-mentioned stereoisomeric diphenylpolyenes were found to be identical with those of the reported values[3].

The synthesis of phosphonium salt VI was carried out according to the following scheme. 5-Phenyl-2, 4-pentadienol (XII)[5], obtained by semihydrogenation and anionotropic rearrangement of ethynylstyrylcarbinol (X)[6], was treated successively with phosphorus tribromide and triphenylphosphine yielding the phosphonium bromide VI.

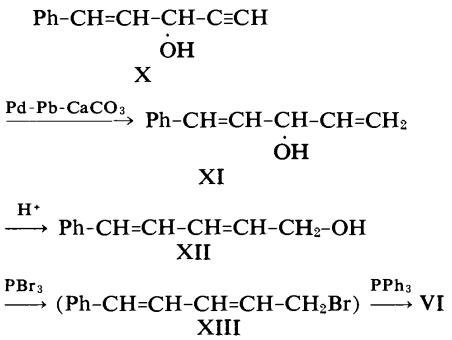

The intermediate, XII and XIII, were used without purification for further reactions owing to their thermal instability. The reduction of ethynylcarbinol X with lithium aluminum hydride afforded unexpectedly 5-phenyl-1-penten-3-ol (XIV) in a 78% yield. The structure of this carbinol XIV was confirmed by elemental analysis, electronic and infrared spectra (Fig. 1). The same type of unusual reduction of $-CH=CH-CH(OH)-C\equiv CH$ grouping by the hydride has been found by Attenburrow in the course of the synthesis of Vitamin A[7].

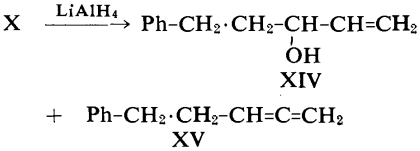

5) G. F. Woods and H. Sanders, *J. Am. Chem. Soc.*, **69**, 2926 (1947).
6) L. Skattebol, E. R. H. Jones and M. C. Whiting, "Organic Syntheses", **39**, 56 (1959).
7) J. Attenburrow, A. F. B. Cameron, J. H. Chapman, R. M. Evans, B. A. Hems, A. B. A. Jansen and T. Walker, *J. Chem. Soc.*, 1952, 1094.

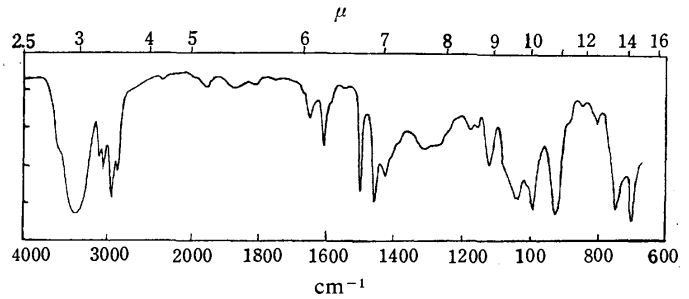

Fig. 1. The infrared spectrum of 5-phenylpent-1-en-3-ol (XIV).

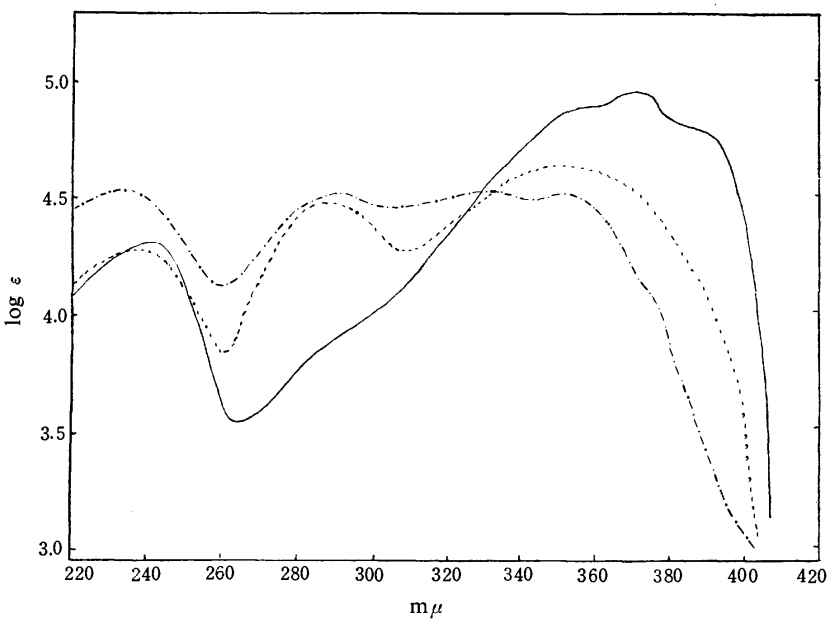

Fig. 2. The electronic spectra of the *p*-styryldiphenylbutadienes (——, all-trans XVI; ------, mono-cis XVII; —·—·—·, Dale's cis compound) (in *n*-hexane).

In addition to the above-mentioned reduction product, a colorless liquid with a lower boiling point was obtained. The formula of an allenic hydrocarbon XV was assigned to this substance on the basis of the absence of hydroxy- and ethynyl-absorptions and the presence of strong peaks of monosubstituted allene in its infrared spectrum.

Dale[8] has obtained a minor amount of a cis isomeric compound by the photoisomerization of *p*-styryldiphenylbutadiene. He suggested the structure of XVII to the minor product by the examination of its electronic spectrum, but there remained an uncertainty on account of its small quantity. We have carried out the synthesis of XVII from stilbenealdehyde in order to ascertain his suggestion. The reaction of phosphonium bromide I with stilbenealdehyde at room temperature resulted in the formation of all-trans (XVI) and mono-cis (XVII) isomers of *p*-styryldiphenylbutadiene in a total yield of 75%. The structure of the cis isomer, pale yellow plates with a green fluorescence, was confirmed by the elemental analysis, the examination of electronic and infrared spectra and the transformation into the all-trans isomer (XVI) on exposure to light.

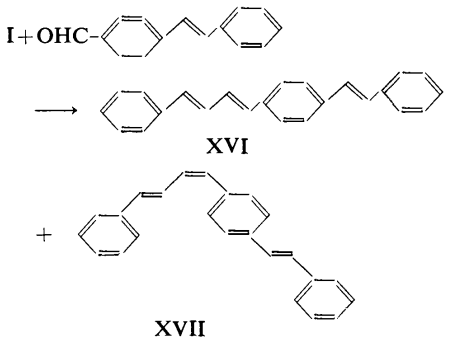

XVI

+

XVII

8) J. Dale, *Acta Chem. Scand.*, 11, 971 (1957).

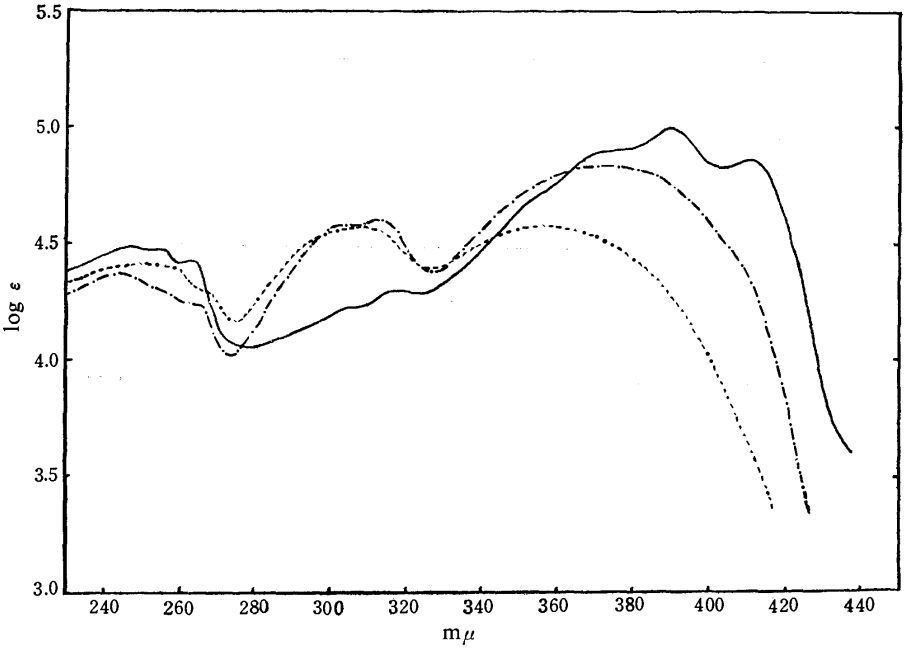

Fig. 3. The electronic spectra of the *p*-bis(phenylbutadienyl)benzenes (——, all-trans XVIII; —·—·, mono-cis XIX; ------, di-cis XX) (in tetrahydrofuran).

As illustrated in Fig. 2, the distinct fine structure in the main band of all-trans isomer XVI disappears in the spectrum of the mono-cis isomer XVII. As the decrease in fine structure in the main band is a general trend in the spectra of sterically hindered cis compounds, the presence of vibrational structure in the main band of the spectrum of Dale's cis compound seems to indicate the contamination of the all-trans isomer XVI.

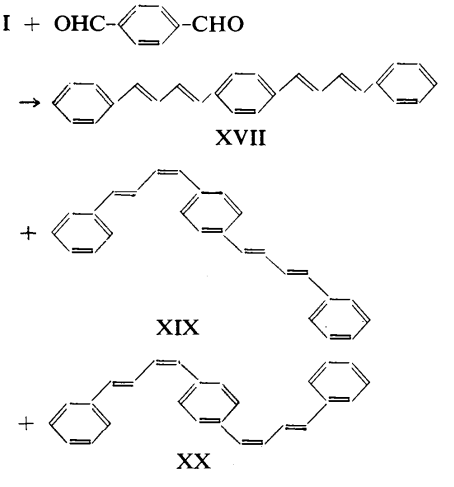

The reaction of phosphonium bromide I with terephthalaldehyde in place of stilbenealdehyde resulted in the formation of three stereoisomeric *p*-bis(phenylbutadienyl)benzenes. One of these isomers, all-trans form has already been synthesized by different authors, especially Campbell and McDonald used the Wittig reaction of *p*-xylenebisphosphonium chloride with cinnamaldehyde[9]. Each isomer, isolated by chromatography, gave correct analysis and could be transformed into the all-trans form by the photoisomerization. The assignment of their structure was performed on the bases of the electronic and infrared spectroscopic evidences. Also in the series of *p*-bis(phenylbutadienyl)benzene, only the all-trans isomer[9] exhibits a distinct fine structure in the absorption curve. The introduction of cis ethylenic linkage to the system caused blue-shifts (mono-cis, 16 mμ; di-cis, 33 mμ) of the main absorption maxima accompanied with the decrease of their absorption intensities and the appearance of new absorption peaks at the wavelength region of ca. 300 mμ in which the all-trans form has only a slight inflexion (Fig. 3).

The cis forms of the above-mentioned diphenylpolyenes seem to contain much less or no steric strain as compared with the previously discussed hindered cis polystilbenes and the related compounds[1]. But from the above-stated observation, it was revealed that the spectroscopic behavior of the geometrical isomers in these two series of conjugate system was

9) G. Drefahl and G. Plotner, *Chem. Ber.*, **91**, 1258 (1958); K. Friedlich and H. Henning, ibid., **92**, 2944 (1959); R. N. McDonald and T. W. Campbell, *J. Org. Chem.*, **24**, 1969 (1959); "Organic Syntheses", **40**, 85 (1960).

similar. This fact indicates that the steric strain in *cis*-polystilbenes are insufficient to exert an influence upon spectroscopic properties.

Experimental*

***trans, trans-* and *trans, cis*-1, 4-Diphenylbutadiene (II and III).**—To a stirred suspension of triphenylcinnamylphosphonium bromide (I, 6.9 g., 0.015 mol.) and benzaldehyde (1.8 g., 0.017 mol.) in anhydrous ethanol (40 ml.) was added a solution of a slight excess of lithium ethoxide (from 0.15 g. of lithium) in anhydrous ethanol (75 ml.) in a dark room. After stirring for ca. 10 hr., water (70 ml.) was added precipitating a solid. This was separated by filtration (filtrate A), dried and dissolved in cyclohexane. The solution was filtered to remove unchanged phosphonium salt. Concentration of the solution gave colorless needles, m. p. 147~150°C (1.46 g., 47%), which were recrystallized from cyclohexane yielding trans, trans isomer (II), m. p. 152~153°C (lit.[4] 152~153°C).

Filtrate A was extracted with light petroleum (200 ml.) and the extract was washed, dried and chromatographed on alumina. The column (2×25 cm.) was eluted with light petroleum to give eight 50 ml. fraction. The fractions 3-8 gave the same electronic spectra with that of Zechmeister's trans, cis isomer (UV λ_{max} mμ: 240, 314. $\lambda_{infl.}$ 247 (in *n*-hexane)) and afforded a colorless liquid, 0.918 g. (30%), which transformed into II, when it was exposed to direct sun light.

***trans, trans, trans-* and *trans, cis, trans*-1,6-Diphenylhexatriene (IV and V).**—The phosphonium bromide (I, 4.6 g., 0.01 mol.) and cinnamaldehyde (1.3 g., 0.01 mol.) in anhydrous ethanol (20 ml.) were treated with lithium ethoxide (from 0.1 g. of lithium) in 70 ml. of anhydrous ethanol as described in the case of diphenylbutadiene. The reaction mixture was stirred for 8 hr. precipitating leaflets (1.3 g.), which were collected by filtration and had m. p. 192~194°C. Recrystallization from ethanol-dioxane (1 : 2) gave pure all-trans isomer (IV), 0.7 g. (30%), m. p. 198~199°C (lit.[3] 203°C). UV λ_{max} mμ (log ε): 242 (3.98), 336 (4.80), 351.5 (4.93), 371 (4.80) (in *n*-hexane).

Found: C, 93.01; H, 6.87. Calcd. for $C_{18}H_{16}$: C, 93.06; H, 6.94%.

The above-mentioned mother liquor was diluted with water (100 ml.) precipitating pale yellow crystals. The crude crystals were collected by filtration, dried and chromatographed on alumina (2×30 cm. column) in a dark place. The column was eluted with light petroleum-benzene (19 : 1, 200 ml. followed by 7 : 3, 600 ml.) to afford ten 50 ml. fractions. The fractions 4-10 gave pale yellow needles, m. p. 103~109°C, 650 mg. (28%); these were recrystallized from water-ethanol (2 : 3) to give central cis isomer (V) as pale yellow long needles, m. p. 109~110°C (lit.[3] 107°C). UV λ_{max} mμ (log ε): 260.5 (4.33), 268.5 (4.33), 336 (4.65), 351 (4.73), 369 (4.55) (in *n*-hexane).

Found: C, 93.04; H, 6.89. Calcd. for $C_{18}H_{16}$: C, 93.06; H, 6.94%.

* All melting points are not corrected.

Reduction of Ethynylstyrylcarbinol (X) with Lithium Aluminum Hydride.—Ethynylstyrylcarbinol (X), colorless needles, m. p. 68~69°C (66%), was prepared according to Campbell and his coworker[4].

To a suspension of lithium aluminum hydride (3.8 g., 0.1 mol.) in anhydrous ether (400 ml.), a solution of the carbinol (X, 6 g., 0.038 mol.) in anhydrous ether (60 ml.) was added dropwise under stirring and the mixture was refluxed for 30 min. to afford a greenish solution. After cooling, a small amount of ethyl acetate was added into the solution to decompose an excess of the metal hydride and then water (200 ml.) was added. The organic layer was separated by decantation and the residue was washed with two 20 ml. portions of ether. The combined organic layer and washings were washed with water and dried over magnesium sulfate in the presence of a minor amount of hydroquinone. The residual colorless oil obtained by evaporating the solvent was distilled in vacuo to yield 5-phenyl-1-penten-3-ol (XIV), b. p. 73~74.5°C/0.2 mmHg, 4.8 g. (78%). UV λ_{max} mμ: 254.5, 259, 261.5, 264.5, 268.5 (in *n*-hexane). IR: 3400, 1040 (OH); 1650, 993, 925 (-CH=CH_2); 760, 710 (Ph-) cm^{-1}.

Found: C, 81.12; H, 8.84. Calcd. for $C_{11}H_{14}O$: C, 81.44; H, 8.70%.

Triphenyl-5-phenyl-2, 4-pentadienylphosphonium Bromide (VI).—The hydrogenation of the ethynylcarbinol (X, 23.6 g., 0.15 mol.) in anhydrous tetrahydrofuran (200 ml.) over Lindlar's catalyst (1 g.) resulted in the uptake of ca. 1.1 mol. of hydrogen. After removal of the catalyst and the solvent, the residue was distilled in vacuo, yielding styrylvinylcarbinol (XI) as colorless oil, b. p. 91~94°C/0.1 mmHg, 21.8 g. (90.8%). A solution of the vinylcarbinol (XI, 21 g.) in aqueous dioxane (70%, 300 ml.) was treated with concentrated sulfuric acid (5 ml.) at 40~50°C for 2 hr. The reaction mixture was poured into water (1 l.) and extracted with ether. The ethereal extract was washed successively with aqueous potassium carbonate and water and dried over magnesium sulfate. The colorless solid obtained by evaporation of ether was recrystallized three times from light petroleum to give 5-phenyl-2, 4-pentadienol (XII), m. p. 73~78°C, 5 g. (24%).

To a solution of the crude pentadienol (XII, 3.2 g.) in chloroform (100 ml.) was added dropwise a solution of phosphorus tribromide (2 g.) in chloroform (30 ml.), and the crude bromide XIII was isolated according to the usual method. A solution of triphenylphosphine (10 g.) in toluene (80 ml.) was added to a solution of the crude bromide in toluene (20 ml.), precipitaing a white phosphonium salt. The reaction was allowed to proceed overnight without external heating and the reaction mixture was then stirred at 40~50°C for 6 hr. After cooling, the light brown oil deposited was immediately crystallized. The crude crystals were filtered and washed with toluene containing a small amount of ethanol to yield slightly brownish white crystals of phosphonium bromide VI, m. p. ca. 236~240°C, in a yield of 5.8 g.

***trans, trans, trans-* and *trans, trans, cis*-1, 6-Diphenylhexatriene (IV and VII).**—A solution of lithium ethoxide in anhydrous ethanol (from 0.05 g. of lithium in 50 ml. of anhydrous ethanol) was

added dropwise to a stirred suspension of the phosphonium bromide (VI, 3 g., 6.2 mmol.) and benzaldehyde (0.8 g., 7.5 mmol.) in anhydrous ethanol (20 ml.) in a dark place. After stirring for 7 hr. at room temperature, a deposition of brownish plates was observed. The reaction mixture was diluted with water and extracted with a mixture of benzene-light petroleum. The crystals, precipitated on standing the mixture, were collected by filtration (filtrate A) and recrystallized from aqueous dioxane yielding all-trans isomer (IV) as yellow plates, m. p. 194~198°C, in a yield of 0.2 g. (14%).

Filtrate A was chromatographed on alumina from benzene-light petroleum (b. p. 60~70°C) (9 : 1 followed by 4 : 1) to afford six 50 ml. fractions. The fractions 4-6 afforded colorless oil, 241 mg. (17%), which exhibited the same electronic spectra with that of Zechmeister's *trans, trans, cis*-1, 6-diphenylhexatriene (VII). UV λ_{max} mμ: 256, 263, 338 (in *n*-hexane).

All-*trans*- and *trans, cis, trans, trans*-1, 8-Diphenyloctatetraene (VIII and IX).—A stirred suspension of phosphonium bromide (VI, 2.5 g., 5.15 mmol.) and cinnamaldehyde (0.8 g., 16 mmol.) in anhydrous ethanol (20 ml.) was mixed with a solution of a small excess of lithium ethoxide in ethanol and stirred at room temperature for 10 hr. After standing overnight, the mixture was diluted with water precipitating a crystalline solid. This solid was separated, dried and digested with a small amount of chloroform. The insoluble part was recrystallized from the same solvent yielding all-trans isomer (VIII) as brownish yellow plates, m. p. 229~233°C, 0.3 g. (23%). This was recrystallized twice from the same solvent to give an analytical sample, m. p. 235~236.5°C (lit.[3] 235°C). UV λ_{max} mμ (log ε): 242 (4.06), 354 (4.89), 372.5 (5.04), 394.5 (4.95) (in *n*-hexane).

Found: C, 92.66; H, 6.59. Calcd. for $C_{20}H_{18}$: C, 92.98; H, 7.02%.

The soluble part obtained by evaporating chloroform was resolved in benzene-light petroleum (b. p. 60~70°C) (1 : 9) and chromatographed on alumina (2×30 cm.). The column was eluted with benzene-light petroleum (1 : 9, 1 : 4 and 1 : 1, successively) and subsequently with benzene to divide into twenty 50 ml. fractions. The fractions 5-14 gave yellow crystals, m. p. 129~136°C, 292 mg. (22%), which was recrystallized from light petroleum (b. p. 60~70°C) yielding pure *trans, cis, trans, trans*-1. 8-diphenyloctatetraene (IX) as yellow needles, m. p. 132.5~133.5°C (lit.[3] 139~141°C). UV λ_{max} mμ (log ε): 236 (4.09), 246.5 (4.06), 274.5 (4.34), 284 (4.39), 353 (4.65), 371 (4.76), 392 (4.61) (in *n*-hexane).

Found: C, 93.00; H, 6.83. Calcd. for $C_{20}H_{18}$: C, 92.98; H, 7.02%.

All-*trans*- and Mono-*cis*-*p*-styryl-1, 4-diphenylbutadiene (XVI and XVII).—A stirred suspension of *p*-stilbenealdehyde (2.1 g., 0.01 mol.) and the phosphonium bromide (I, 4.6 g., 0.01 mol.) in absolute ethanol (30 ml.) was treated with a solution of lithium ethoxide (from 0.1 g. of lithium) in anhydrous ethanol (70 ml.) and the mixture was stirred at room temperature for 18 hr. After standing overnight, the crystals deposited were separated by filtration and digested with benzene (120 ml.). The insoluble product was combined with the other crop which was obtained by the chromatography described below, and recrystallized from chlorobenzene to give all-trans isomer (XVI), m. p. 258~259°C, 1.42 g. (46.1%).

Found: C, 93.41; H, 6.58. Calcd. for $C_{24}H_{20}$: C, 93.46; H, 6.54%.

The above-mentioned soluble part in benzene was chromatographed on alumina (2×30 cm.) and there was obtained a solid, 0.88 g. (28.6%), m. p. 108~115°C, recrystallization of which from aqueous ethanol (90%) gave mono-cis isomer (XVII), m. p. 115~116°C as light yellow plates with a green fluorescence.

Found: C, 93.07; H, 6.50. Calcd. for $C_{24}H_{20}$: C, 93.46; H, 6.54%.

All-*trans*-, Mono-*cis*- and Di-*cis*-*p*-bisphenylbutadienylbenzene (XVIII, XIX and XX).—To a suspension of the phosphonium bromide (VI, 1.8 g., 0.037 mol.) and terephthalaldehyde (2.4 g., 0.018 mol.) in anhydrous ethanol (70 ml.) was added a solution of lithium ethoxide (from 0.3 g. of lithium) in anhydrous ethanol (75 ml.) under stirring at room temperature. After stirring for 3 hr., the mixture was allowed to stand overnight, and then stirred at 40~50°C for 30 min., cooled and diluted with water (150 ml.). The yellow solid precipitated was collected, dried, digested with benzene and filtered (filtrate A). The insoluble solid was recrystallized from chlorobenzene yielding all-trans isomer (XVIII) as yellow plates, m. p. 278~279.5°C, 1.15 g. (18%).

Found: C, 93.06; H, 6.64. Calcd. for $C_{25}H_{22}$: C, 93.37; H, 6.63%.

Filtrate A was chromatographed on alumina. Elution was carried out with light petroleum (b. p. 60~70°C), benzene-light petroleum (b. p. 60~70°C) and finally with benzene. The crude material obtained from the light petroleum eluate (150 ml.) was recrystallized three times from the same solvent to yield di-cis isomer (XX) as pale yellow fine needles, m. p. 120.5~121°C, 0.5 g. (8%).

Found: C, 93.06; H, 6.65. Calcd. for $C_{26}H_{22}$: C, 93.37; H, 6.63%.

Later fractions gave, on recrystallization from benzene-light petroleum, pure mono-cis isomer (XIX), as light yellow plates, m. p. 153~154°C, 1.2 g. (19%).

Found: C, 93.31; H, 6.83. Calcd. for $C_{26}H_{22}$: C, 93.37; H, 6.63%.

The authors are grateful to the Ministry of Education for the financial support. The microanalyses were performed by Messrs. Masakazu Okumiya and Osamu Saiki in the Microanalytical Laboratory of this Department, to whom the authors' thanks are also due.

Department of Chemistry
Faculty of Science
Osaka University
Nakanoshima, Osaka

*The Nuclear Magnetic Resonance Spectra of Olefinic Protons and the Substituent Effects. I. Systems of ω-Substituted trans-Styrenes and 1-Substituted trans-Propenes**

By Hazime KASIWAGI and Jun NIWA

(Received October 31, 1962)

Concerning the dependence of the magnetic resonance of olefinic protons on various features of chemical structures, several investigations have been reported, beginning in 1960[1]. Most of them, however, have failed in their attempts to derive some kind of smooth correlation between shifts and the nature of the substituents. The remaining problems center on the point of inquiring how the deviation of the chemical shifts of olefinic protons from values predictable on the basis of Dailey and Shoolery's proposition, which holds generally in the spectra of protons attached to the SP^3 carbon atom[2], can be elaborated and made consistent with the substituent effects by virtue of Hammett's relationship[3].

The present authors confirmed previously, from an inspection of the proton resonance spectra of series of α- and β-substituted methyl cinnamates, that some trends of correlation exist between the shifts of protons situated in the trans-position to the substituents and Hammett's substituent constants**. This finding may indicate that, if an olefinic part of a series of compounds were constructed in such a way that it might conjugate with another resonating group, such as a benzene ring or a hyperconjugative methyl group, the protons of this part of the structure, even though they were essentially of an olefinic nature, would show a similar nuclear magnetic behavior to that of benzene ring protons[3,4]. Therefore, they would be subject to the controlling effect of the series of terminal substituents in the sense of Hammett's relationship. Taking these considerations into account, the authors have attempted to investigate the proton resonance spectra of series of ω-substituted *trans*-styrenes and 1-substituted *trans*-propenes. This paper reports on the correlation between the chemical shifts of the olefinic protons of the two series of compounds mentioned above and the effect of terminal substituents considered from the viewpoint of Hammett's relationship.

Experimental

The nuclear magnetic resonance spectra of ω-substituted-styrenes were obtained with a Varian 4300-B high resolution spectrometer operating at 56.4 Mc., while a spectrometer operating at 60 Mc. was used for obtaining the spectra of 1-substituted propenes. The sample was dissolved in carbon tetrachloride of a 10 mol. per cent concentration, having been sealed in a glass tube, 5 mm. in outside diameter, which was spun in the magnetic field during the measurement. The absorption lines were measured by relating them with the resonance line of 2 mol. per cent cyclohexane added as an internal reference, while the frequencies of the lines were confirmed by the side band technique of controlled frequencies.

All the compounds are of a trans-configuration, but the spectral inspection has shown that some of them are contaminated by a small amount of cis-isomer. The styrene derivatives are as follows: Styrene, ω-chlorostyrene, ω-bromostyrene, ω-nitrostyrene, cinnamonitrile, 1-phenylpropene, cinnamaldehyde, benzilideneacetone, cinnamoyl chloride, styryl acetate, methyl cinnamate, etc. Free cinnamic acid was also included. The synthesized compounds are of the following nature: ω-Nitrostyrene, m. p., 59~60°C; ω-chlorostyrene (cis), b. p., 199~199.5°C; n_D^{25} 1.5735, 1-phenylpropene, b. p., 73~75°C under 14 mmHg; styryl acetate, b. p., 103~104°C under 6 mmHg. The cinnamonitrile prepared through the dry distillation of a mixture of cinnamic acid and lead rhodanide was fractioned into two parts. Of the products distilled, the first became crystalline upon standing for a long time and melted at 10°C, but the second distillate never did crystallize. The rest of the compounds were commercially obtained and purified***. The examined derivatives of propene are as

* Presented at the 14th Annual Meeting of the Chemical Society of Japan, Tokyo, April, 1961, and at the Symposium on Nuclear Magnetic Resonance, Tokyo, November, 1961.

1) L. M. Jackman and R. H. Wiley, *J. Chem. Soc.*, **1960**, 2881; E. O. Bishop and R. E. Richards, *Mol. Phys.*, **3**, 118 (1960); C. N. Banwell and N. Sheppard, ibid., **3**, 351 (1960); W. Brügel, Th. Ankel and F. Krückeberg, *Z. Elektrochem.*, **64**, 1121 (1960).

2) B. P. Dailey and J. N. Shoorery, *J. Am. Chem. Soc.*, **77**, 3977 (1955).

3) H. S. Gutowsky, D. W. McCall, B. R. McGarvey and L. H. Meyer, *J. Am. Chem. Soc.*, **74**, 4809 (1952); R. W. Taft, Jr., ibid., **79**, 1045 (1957); R. W. Taft, Jr. and I. C. Lewis, ibid., **80**, 2436 (1957).

** Results and discussions are to be discussed in Part II of this series.

4) Y. Yukawa, Y. Sakai and K. Kabazawa, *Memories of Scientific and Industrial Research, Osaka Univ.*, **17**, 185 (1960); Y. Yukawa and H. Yamada, lecture given at the 15th Annual Meeting of the Chemical Society of Japan, Kyoto, April, 1962.

*** Products of Tokyo Kasei Kogyo Co., Ltd., and Wako Pure Chemical Industries, Ltd.

follows : 1-Bromopropene (b. p., 59~60°C), 1-phenylpropene (already mentioned), crotonyl chloride (b. p., 124~125°C), methyl crotonate (b. p., 119~120°C), crotonaldehyde (b. p., 104~105°C), crotonitrile (b. p., 118~119°C) and 1-nitropropene (b. p., 94~95°C under 8 mmHg).

Results

The spectra of olefinic protons with regard to substituted styrenes belong to the simple AB-type, with the exception of those of styrene and cinnamaldehyde. Substituted propenes give the spectra corresponding to the system of 5 nuclei, ABX_3, and crotonaldehyde has a system of ABX_3Y. The chemical shifts obtained by analysis of the spectra are summarized in Table I. The coupling constants will be discussed later.

Discussion

Whipple et al. investigated the substituent effects on the chemical shifts of olefinic protons. They claim that, although the trends of the vinyl proton shifts in 2-substituted propenes are qualitatively consistent with inductive and mesomeric effects attributable to substituents, no precise correlation exists between the shifts and Hammett's constants for substituents[5].

Meanwhile Taft investigated to secure a correlation between the nuclear magnetic resonance shifts of fluorine atoms in mono- and di-substituted fluorobenzenes and Hammett's σ-constants. Taft found that the σ-value leads to a fairly good correlation with the fluorine nuclear shielding constants, $\delta^{F}{}_{m}$ and $\delta^{F}{}_{p}$[3]. The olefinic part in the system examined by Whipple et al. indeed conjugates with the methyl group, but this conjugation will be somewhat disintegrated by the introduction of a second substituent. Therefore, the direct application of the relationship advanced by Taft would not necessarily be suitable for the results obtained for systems of a poorer stabilization due to such cross-conjugation, and any correlations of σ_p would probably be missed. In the case of the compounds here investigated ($RCH_A=CH_BX$, R : C_6H_5 or CH_3), on the other hand, the olefinic bond conjugates not only with the aromatic ring or the methyl

TABLE I. PROTON CHEMICAL SHIFTS OF ω-SUBSTITUTED *trans*-STYRENES AND 1-SUBSTITUTED *trans*-PROPENES, $RCH_A=CH_BX$

Chemical shifts in τ-values, ± 0.05 p. p. m.

Substituent X	R : C_6H_5			R : CH_3		
	δ_{HA}	δ_{HB}	δ_{Ph-H}	δ_{HA}	δ_{HB}	δ_{CH_3-H}
H	3.35	3.36	2.77	4.27[d]	5.04[d]	8.26[e] 8.28[e]
Cl	3.46[a]	3.80[a]	2.79[a]	4.16[d]	4.12[d]	
Br	3.12	3.30	3.79	3.92	4.05	8.16
NO_2	2.08	2.49	2.52	2.78	3.05	
CH_3	3.76	3.76	2.82	4.75[d]	4.75[d]	8.26[d]
CHO	2.57	3.35	2.60	3.21	3.97	7.95
CO_2H	2.28[b]	3.61[b]	2.50[b]	2.93[f]	4.20[f]	
CO_2CH_3	2.43	3.69	2.63	3.13	4.24	8.01
COCl	2.20	3.41	2.64	2.81	3.91	7.98
$COCH_3$	2.55	3.35	2.64			8.00
CN	2.68 2.97[a]	4.23 4.62[a]	2.65	3.32	4.69	8.19[d]
C_6H_5	3.01[c]	3.01[c]	2.73[c]	3.76	3.76	8.12
$OCOCH_3$	2.23 2.65[a]	3.72 4.43[a]	2.80			

a) The values presumably attributable to the cis-isomer.
b) The data were obtained on previous occasions.
c) The values were adopted from Tiers' table (G. van D. Tiers, "Characteristic NMR Shielding Values for Hydrogen in Organic Compounds", Part I, Central Research Department, Minnesota Mining and Manufacturing Co., Minneapolis, Minnesota, 1958).
d) Measurement was performed under the conditions reported by Bothner-By et al. and by Reddy et al. A. A. Bothner-By and C. Naar-Colin, *J. Am. Chem. Soc.*, **83**, 231 (1961). Cf. Ref. 8.
e) Adopted from the monograph: J. A. Pople, W. G. Schneider and H. J. Bernstein, "High Resolution Nuclear Magnetic Resonance", McGraw-Hill, New York (1959).
f) The values were obtained from measurement with the glacial acetic acid solution owing to the low solubility of the compound in carbon tetrachloride.

5) E. B. Whipple, J. H. Goldstein and L. Mandell, *J. Am. Chem. Soc.*, 82, 3010 (1960).

group, but with substituent X in a uniform direction. Consequently, the olefinic proton, H_A, of these compounds seems to be shielded by substituent X in a sharper and more characteristic way than may be the case in the system of Whipple. It may be reasonable, therefore, to apply Hammett's relationship to the τ-values of H_A. It is true, on the other hand, that the influence of substituents on the resonance absorption may be subject also to the anisotropy of the magnetic susceptibility of bonding axes in substituent groups, the diamagnetic anisotropy arising from a long range shielding exerted by the benzene ring and other substituents. Indeed, Spiesecke and Schneider, who studied the resonance spectra of mono-substituted benzenes, assumed that the shifts due to ortho-protons are controlled by the polar nature of substituents as well as by the disturbing factors of the diamagnetic anisotropy of substituents and other magnetic effects[6]. The disturbing factors, however, may be seen as not very considerable from an inspection of Fig. 1, which illustrates that the shifts for ortho-protons correlate practically with those of para-protons, at least so far as the substituents, OCH_3, H, F, Cl, Br, CHO and NO_2, are concerned. This fact implies that the cis-proton chemical shifts in the ω-styrene and 1-propene systems are governed mainly by the polar substituent effects.

Figure 2 shows the relationship between the τ-values of H_A of these compounds and Hammett's constants, σ_p. The value of the resonance line of H_A in stilbene, adopted from Tiers' table, may be lowered by the long-range shielding effect of the benzene ring. As the lowering of the shift by the benzene ring, situated in the cis-position to H_A, is estimated as about 0.05 p. p. m., the τ-value of H_A may be corrected to 3.51 p. p. m.[7] In Fig. 2 the corrected value is used. The value observed with ω-chlorostyrene is tentatively assumed to be attributable to the cis-isomer, but the value may not differ considerably from that of trans-isomer[1]. As for the cinnamo- and crotonitriles, the cyano group exerts on the neighboring cis-proton, H_A, a positive shielding contribution due to the bond anisotropy around its triple bond axis[8]. In the case of crotonitrile, the magnitude of this diamagnetic shielding of the cis-proton has been calculated by Reddy et al. to be as much as +0.287 p. p. m., and that of the geminal proton, as +1.11 p. p. m.[9] In plotting the value of the H_A of cinnamonitrile, it is assumed that a positive shielding of the cyano group would give an exaggeration of about the same order as in the case of crotonitrile. The groups, $COCH_3$ and possibly CO_2CH_3, may have the same kind of anisotropic shielding effect. That an anisotropic shielding effect of some magnitude should not be ignored in computing the substituent effects

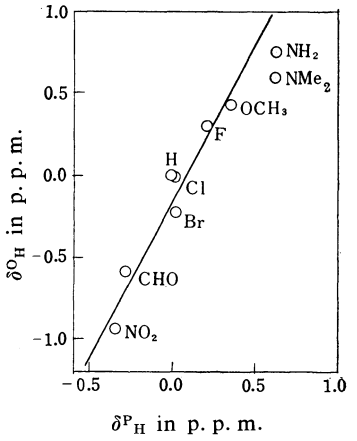

Fig. 1. The correlation between the chemical shifts of ortho- and para-protons in mono-substituted benzenes. The data are cited from Ref. 6 and are accommodated for comparison by taking the benzene proton shift as the point of reference.

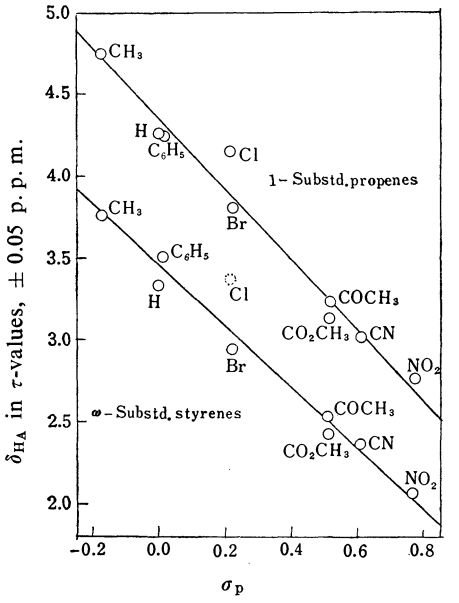

Fig. 2. The cis-proton chemical shifts, plotted vs. Hammett's substituent constants, σ_p.

6) H. Spiesecke and W. G. Schneider, *J. Chem. Phys.*, 35, 731 (1961).

7) C. E. Johnson, Jr. and F. A. Bovey, ibid., 29, 1012 (1958).

8) L. M. Jackman, "Application of Nuclear Magnetic Resonance Spectroscopy in Organic Chemistry", Pergamon, London (1959), p. 59.

9) G. S. Reddy, J. H. Goldstein and L. Mandell, *J. Am. Chem. Soc.*, 83, 1300 (1961).

of halogens, may probably be illustrated from the departure of their plots from the correlation line in Fig. 2.

Generally, the decrease of free energy in the reactions of benzene derivatives changes under the influence of a substituent in such a way that the parameters of the inductive and resonance interactions, σ_I and σ_R, which are inherent to the substituent, may act independently of each other. Since the nuclear magnetic shielding is also supposed to be affected by these two parameters independently, as in the reactions of benzene derivatives, the shielding constants may be expressed by the equation of the general form, $\delta=\alpha\sigma_I+\beta\sigma_R$. The coefficients, α and β, are measures of the susceptibility with which the inductive and resonance influences are called upon to function. Taft has suggested that the relation of the proton shielding might best be described by the equation, $\delta_H=0.40\sigma_I+0.70\sigma_R$[3]. As is shown in Fig. 3, this equation is applicable to the data presented here with regard to styrene and l-propene derivatives. The linearity of its correlation with the observed shifts is a little improved compared with that obtained from σ_p alone. The σ_I and σ_R values and their combination according to Taft's equation are listed in Table II.

From the existence of a certain correlation between the cis-proton shifts of these olefinic compounds and Hammett's σ-values, the same kind of correlation may be expected among the shifts of those protons situated at the

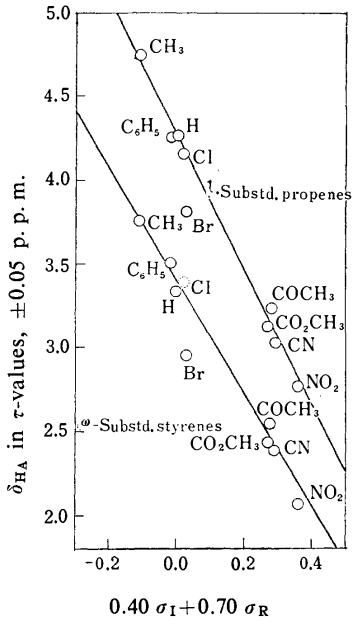

Fig. 3. The cis-proton chemical shifts, plotted vs. substituent parameters, 0.40 σ_I+0.70 σ_R.

TABLE II. THE SUBSTITUENT CONSTANTS

Substituent	σ_I[a]	σ_R[c]	0.40 σ_I +0.70 σ_R
CH_3O	+0.23	−0.50	−0.26
F	+0.50	−0.44	−0.11
CH_3	−0.05	−0.13	−0.11
C_6H_5	+0.10	−0.09	−0.02
H	0.00	0.00	0.00
Cl	+0.47	−0.24	+0.02
Br	+0.45	−0.22	+0.03
I	+0.38	−0.10	+0.08
CO_2R[d]	+0.30[b]	+0.20	+0.26
CN	+0.58[b]	+0.07	+0.29
$COCH_3$	+0.27	+0.25	+0.29
NO_2	+0.63	+0.15	+0.36

a) Evaluated by Taft.
b) Revised by Taft and Lewis, cf. Ref. 3.
c) Calculated from the values of σ_p according to the equation: $\sigma_R=\sigma_p-\sigma_I$. The values of σ_p are cited from the paper of Jaffe's. Cf. *Chem. Revs.*, **53**, 216 (1953).
d) The value is applicable to both H and alkyls.

corresponding positions of the systems which have a similar conjugation structure,—cis-proton shifts, here investigated, ortho-proton shifts of mono-substituted benzenes[6], and β-proton shifts of 4-substituted pyridine l-oxides[10]. In Fig. 4, the fairly clear correlations among them may be observed. This suggests that, in these systems, the modes of the transmittance of substituent effects are essentially similar. These modes would be not only peculiar to the benzene nucleus, but also inherent in the structures of carbon skeltons, which constitute the expanded conjugation systems with certain restricted conditions. To

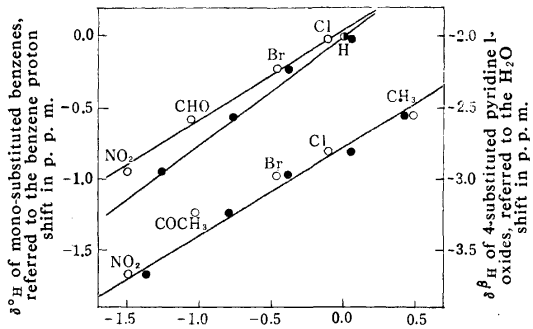

Fig. 4. The chemical shifts of ortho-protons of mono-substituted benzenes (Ref. 6) and of β-protons of 4-substituted pyridine l-oxides (Ref. 10), plotted vs. the cis-proton chemical shifts of l-substituted propenes (○) and ω-substituted styrenes (●) with respect to non-substituted ones respectively.

10) A. R. Katritzky and J. M. Lagowsky, *J. Chem. Soc.*, 1961, 43.

the conditions correspond the constancy of the parameters, α and β.

Figures 5 and 6 illustrate the correlations of the chemical shifts of two sets of protons with each other for styrene and 1-propene derivatives. The former relates with those of cis-protons (H_A), and the latter, with those of geminal protons (H_B). It is clear that the correlation for cis-protons is excellent. Any straightforward correlation of geminal proton shifts has been discernible neither with the electronegativity of the first atom of substituents nor with Hammett's constants. The reasons for this will be clear from an observation of the two figures. It is worthy of brief mention, however, that the geminal proton shifts for compounds, the substituent of which is hydrogen itself, are located in the highest region of the field in both series. This probably arises form the lower electronegativity of hydrogen compared with that of the first atoms in other substituents.

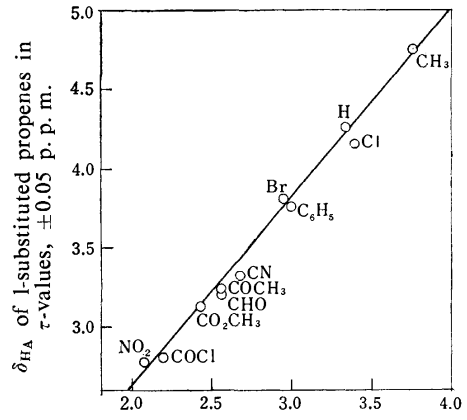

δ_{HA} of ω-substituted styrenes in τ-values, ±0.05 p. p. m.

Fig. 5. The correlation of the cis-proton chemical shifts between ω-substituted styrenes and 1-substituted propenes.

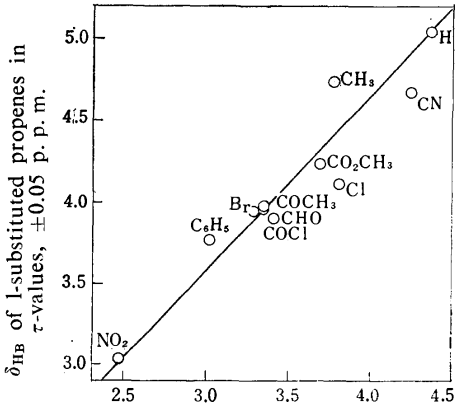

δ_{HB} of ω-substituted styrenes in τ-values, ±0.05 p. p. m.

Fig. 6. A comparison of the chemical shifts of geminal protons for ω-substituted styrenes and 1-substituted propenes.

Summary

High resolution proton magnetic resonance spectra of ω-substituted *tsans*-styrenes and 1-substituted *trans*-propenes have been observed and discussed from the viewpoint of substituent effects. The chemical shifts of protons located at the cis-position to substituents depend roughly upon Hammett's σ_p constants and presumably correlate better with the combination of potential inductive and resonance parameters, namely $0.40\,\sigma_I + 0.70\,\sigma_R$, proposed by Taft.

These results suggest that the chemical shifts of olefinic cis-proton may be computed from the viewpoint of the polar nature of the substituents, though the diamagnetic anisotropy and the long-range shielding effect of the substituents must be carefully considered side by side.

When the chemical shifts of protons situated at corresponding positions of structure in several systems are compared, a fairly good correlation is observed among them. This fact implies that the modes of the transmittance of substituent effects is similar in these systems.

The nature of the substituent effects on the chemical shifts of geminal protons is, however, very complicated and might be out of consonance with both the electronegativity and the available substituent parameters.

The authors wish to take this opportunity to thank Dr. Naoya Nakagawa of the University of Electro-Communications for his helpful discussions. Thanks are also due to Dr. Yô-ichirô Mashiko of the Government Chemical Industrial Research Institute, Professor Shizuo Fujiwara of The University of Tokyo, Dr. Kenkichi Nukada of the Basic Research Laboratories of Tôyô Rayon Co., Ltd., and Dr. Ichirô Yamaguchi of the Japan Atomic Energy Research Institute for kindly giving permission to use the spectrometers of those institutions.

Chemical Laboratory
Department of General Education
Nagoya University
Mizuho-ku, Nagoya

The Nuclear Magnetic Resonance Spectra of Olefinic Systems and the Substituent Effects. II. Methyl Esters of α- or β-Substituted Cinnamic Acids

By Hazime KASIWAGI, Naoya NAKAGAWA* and Jun NIWA

(Received October 31, 1962)

In the preceding paper**, a study of the possibility of Hammett's relationship being applicable to the chemical shifts of olefinic protons in ω-substituted *trans*-styrenes and in 1-substituted *trans*-propenes was reported on. A tentative plotting of the shifts against Hammett's substituent constants showed that such an application was reasonable. In fact, the correlation between the shifts and a certain combination of the potential inductive and resonance parameters for the substituent, that is, $0.40\ \sigma_I + 0.70\ \sigma_R$[1], has been found to fit the purpose even better.

This paper is concerned with the proton magnetic resonance spectra of a series of methyl cinnamates which carry substituents at the α- or β-position. Its main purpose is to examine whether the trends of olefinic proton shifts with regard to these compounds may be represented by the same relationship applied to substituted styrenes and 1-propenes.

Experimental

A Varian 4300-B spectrometer operating at 56.4 Mc. was used for obtaining the spectra. Glass tubes 5 mm. in outside diameter, containing the sample solution of a 10 mol. per cent concentration in carbon tetrachloride, were spun in the magnetic field. The other conditions of measurement were stated in the preceding paper.

Samples. — *Methyl Cinnamate.* — Dry hydrogen chloride gas was passed through a solution of pure cinnamic acid in anhydrous methanol. The product was rectified under reduced pressure. M. p., 33°C.

Methyl α-Chlorocinnamate and Methyl α-Bromocinnamate. — Prior to esterification, each isomer mixture of free acids, which are synthesized from cinnamic acid, is separated into cis- and trans-acids by means of the poorer solubility of the potasium salt of the latter in a buffered ethanol solution[2]. *trans*-α-Chloroester. M.p., 33~34°C; *trans*-α-bromoester: B. p., 150~152°C under 9 mmHg.

Methyl α-Methylcinnamate.—The free acid was prepared through the condensation of benzaldehyde with methylmalonic acid and esterified[3]. M. p., 37~38°C.

Methyl α-Cyanocinnamate.—The free acid, melting at 180.5°C, was obtained by the condensation of benzaldehyde with sodium cyanoacetate. As the ester, melting at 90~90.5°C, is sparingly soluble in carbon tetrachloride, a solution of about a 2 mol. per cent concentration was used for the measurement.

Methyl β-Chlorocinnamate and Methyl β-Bromocinnamate[4]. — From the isomer mixture of free acids, obtained by means of the addition of hydrogen chloride or hydrogen bromide to phenylpropiolic acid, the trans-isomer was separated by means of its poorer solubility[2] and esterified. Chloroester: M. p., 22~4°C; bromoester: 58°C.

Methyl β-Methylcinnamate. — The corresponding acid was converted into its methyl ester. M. p., 27°C; b. p., 109°C under 4.5 mmHg.

Results and Discussion

The signals of olefinic protons in methyl cinnamates, $C_6H_5CH_A{=}CH_BCO_2CH_3$, and the compounds in which H_A or H_B is substituted for by the other substituent, X, are simple and are easily characterized. The estimated values of each signal are summarized in the Table I.

If styrene is assumed to be the reference compound in considering the substituent effects, the resonance of the olefinic proton will take place under the effects of both substituents, i. e., an invariable methoxycarbonyl and a variable X. The correlation of cis-proton shieldings with substituent effects, discussed in Part I, will hold also in the case of the proton situated at the trans-position to the substituent X. The chemical shifts of the trans-proton may be computed from the same data as were applied to the cis-proton and so are governed by the identical combination of inductive and resonance parameters, namely, $0.40\ \sigma_I + 0.70\ \sigma_R$[5]. In Fig. 1, the individual proton shift with regard to the α-compounds is plotted against the combined substituent constants just mentioned. When the trends

* Present address: University of Electro-Communications, Chôfu, Tokyo.

** H. Kasiwagi and J. Niwa, This Bulletin, **36**, 405 (1963).

1) R. W. Taft, Jr., *J. Am. Chem. Soc.*, **79**, 1045 (1957).

2) R. Störmer and P. Heymann, *Ber.*, **46**, 1258 (1913).

3) W. J. Gensler and E. Berman, *J. Am. Chem. Soc.*, **80**, 4949 (1958).

4) H. Kasiwagi, This Bulletin, **31**, 985 (1958).

5) About the used substituent parameters, cf. the preceding paper.

TABLE I. CHEMICAL SHIFTS OF METHYL ESTERS OF α- OR β-SUBSTITUTED CINNAMIC ACIDS
$C_6H_5C(H_A, X)=C(H_B, X)CO_2CH_3$

Substituent X	Chemical shifts in τ-values, $\pm$0.03 p. p. m.				
	δ_{H_A}	δ_{H_B}	δ_{Ph-H}*	δ_{OCH_3-H}	δ_{CH_3-H}
H	2.43	3.69	2.63	6.25	
α-Cl	2.04		2.20 ; 2.60	6.12	
α-Br	1.81		2.16 ; 2.59	6.12	
α-CH_3	2.38		2.67	6.22	7.90
α-CN	1.87		2.10 ; 2.47	6.15	
β-Cl		3.54	2.34 ; 2.62	6.23	
β-Br		3.29	2.34 ; 2.61	6.21	
		(3.41**)		(6.43**)	
β-CH_3		3.92	2.65	6.31	7.44
				(6.48***)	(7.83***)

* The double values are estimated from the principal two peaks of the phenyl proton resonance.
** Presumably attributable to the cis-isomer.
*** It cannot be determined whether these values belong to the cis-isomer or to methanol.

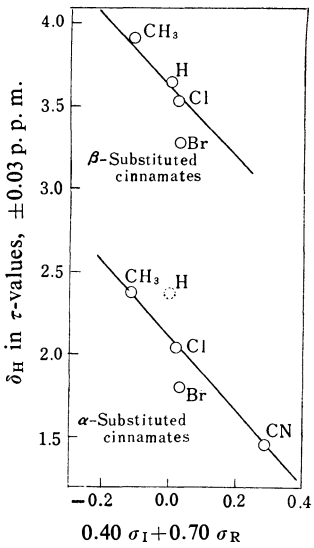

Fig. 1. The plots of the olefinic proton shifts of methyl esters of α- or β-substituted cinnamic acids vs. the substituent parameters, 0.40 σ_I+0.70 σ_R.

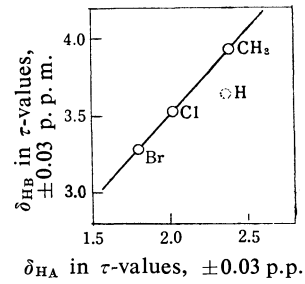

Fig. 2. The correlation of olefinic proton shifts between methyl esters of α- and β-substituted cinnamic acids.

are compared with the correlation line obtained with respect to ω-substituted styrenes, thier regularity, otherwise obscure, may become fairly clear. The introduction of a cyano group causes the proton shifts, here also, to move into a higher region of the field owing to the diamagnetic anisotropy of that group around its triple-bond axis. Reddy et al. have reported that the value of the exaggeration of the trans-proton chemical shift should amount to as much as 0.38 p. p. m. in acrylonitrile[6]. For plotting the proton shift for the cyano substituent, before being used the value is corrected by subtracting this magnitude. From an inspection of Fig. 1, it can be noticed that the plot for H_A in methyl cinnamate keeps a distance from the correlation line. The reason for this can easily be explained. In the case of methyl cinnamates with a substituent at the α-position, the substituent X, interfering with the benzene ring, gives rise to the rotation of the ring. Such a conformation would effectively alter the trends of correlation with substituent parameters originally obtained with the styrene system. Hence, the shift of H_A in methyl cinnamate itself should not be compared directly with proton shifts in other α-derivatives. The δ_{H_A} value for this compound would, then, deviate from the correlation line. This deviation is presumably reflected in Fig. 2, in which the proton chemical shifts for α- and β-substituted cinnamates are shown to correlate with each other, while for the value of hydrogen as the substituent X, the linear correlation does not hold. In β-substituted cinnamates the invariable substituent should be the phenyl group, as

6) G. S. Reddy, J. H. Goldstein and L. Mandell, *J. Am. Chem. Soc.*, **83**, 1300 (1961).

the proton H_B is under the influence of both the phenyl group and the variable substituent X, which are placed in the cis- and the trans-position respectively to the proton under consideration. Here the correlation occurs at a higher part of the figure than that for α-substituted cinnamates, largely because of the diminution of the long-range shielding contribution effected by the benzene ring in β-substituted cinnamates.

Summary

The proton magnetic resonance spectra with regard to methyl esters of α- or β-substituted cinnamic acids have been investigated from the viewpoint of the substituent effect. When the results are compared with the correlation obtained with ω-substituted styrenes, the trends are also explicable as being controlled by the polar nature of the substituents.

The authors wish to take this opportunity to thank Dr. Yô-ichirô Mashiko of the Government Chemical Industrial Research Institute, Professor Shizuo Fujiwara of The University of Tokyo, Dr. Kenkichi Nukada of the Basic Research Laboratories of Tôyô Rayon Co., Ltd. and Dr. Ichiro Yamaguchi of the Japan Atomic Energy Research Institute for kindly affording opportunities for using the spectrometers of their institutions.

Chemical Laboratory
Department of General Education
Nagoya University
Mizuho-ku, Nagoya

*The Distribution Function of Internal Displacement Coordinates in Linear XY_2 Molecules**

By Yonezo MORINO and Takao IIJIMA

(Received November 10, 1962)

Since the motion of atoms in a molecule is dependent on the interatomic force field, it must be of great help for understanding the physical significance of the potential field to consider the probability distribution function of the interatomic displacements. The calculation of the probability function is simple for a diatomic molecule which is treated as a one-dimensional oscillator. In this case the distribution of the interatomic displacements is described by a Gaussian function, if the interatomic potential is assumed to be a simple harmonic one. The effect of the cubic potential constant would be illustrated by resulting asymmetry of the distribution curve. In this work the distribution function is calculated for linear XY_2 molecules, and a schematical interpretation of intramolecular motion is presented by means of a distribution map. Numerical computation of the distribution map is carried out for carbon dioxide and carbon disulfide.

The Probability Distribution Function

The probability distribution function is given in a straight-forward manner by the vibrational wave functions expressed in terms of the normal coordinates,

$$P=\sum_{v} w_v \psi_v^* \psi_v \tag{1}$$

where w_v is the normalized Boltzmann factor of the v-th vibrational state**. The vibrational Hamiltonian of a linear XY_2 molecule consisting of the zeroth- and the first-order terms, is

$$H=H^{(0)}+H^{(1)} \tag{2}$$

where $H^{(0)}$ stands for the terms of the kinetic energy and the harmonic potential energy, while $H^{(1)}$ is given by

$$H^{(1)}=hc\,[k_{111}q_1^3+k_{122}q_1(q_{2a}^2+q_{2b}^2)+k_{133}q_1q_3^2] - \left(\frac{h}{\pi^2 c\omega_1 I}\right)^{1/2}\langle E_{\mathrm{rot}}\rangle q_1 \tag{3}$$

The first term of $H^{(1)}$ is the cubic part of the potential function and the second term is the energy decrease due to the centrifugal stretching, where $\langle E_{\mathrm{rot}}\rangle$ is the mean rotational energy of the molecule[1]. The quartic and higher-order terms of the potential function are ignored in the present treatment. The coordinates q's are dimensionless normal coordinates.

* A preliminary report of this work was presented at the International Conference on Magnetism and Crystallography, Kyoto, 1961.

** A set of quantum numbers designating the vibrational state is symbolically expressed by a single letter v.

1) Y. Morino and E. Hirota, This Bulletin, 31, 423 (1958).

The subscript 1 corresponds to the totally symmetric vibration, $2a$ and $2b$ to the doubly degenerate, and 3 to the antisymmetric vibration, respectively.

The wave function ψ_v is obtained by the first-order perturbation theory according to the equation

$$\psi_v=\psi_v^0-\sum_{v'}{}'\frac{\langle v'|H^{(1)}|v\rangle}{E_{v'}^0-E_v^0}\psi_{v'}^0 \tag{4}$$

as a linear combination of the zeroth-order wave functions ψ_v^0. All non-vanishing coefficients of $\psi_{v'}^0$ are calculated as shown in Appendix I, by substituting Eq. 3 for $H^{(1)}$. By the use of Eq. 4, Eq. 1 is rewritten as

$$P(q_1,q_{2a},q_{2b},q_3)=\sum w_v\psi_v^{0*}\psi_v^0 -\sum_v w_v\sum_{v'}{}'\frac{\langle v'|H^{(1)}|v\rangle}{E_{v'}^0-E_v^0}(\psi_v^{0*}\psi_{v'}^0+\psi_v^0\psi_{v'}^{0*}) \tag{5}$$

Since there hold the relations

$$\psi_v^0=\prod_s\psi_{v_s}^0(q_s), \qquad s=1,\ 2a,\ 2b \text{ and } 3$$

and

$$w_v=\prod_s \chi_s^{v_s}/\sum_{v_s}\chi_s^{v_s}, \left(\chi_s=\exp\left(-\frac{hc\omega_s}{kT}\right)\right)$$

every term of Eq. 5 can be calculated as a product of the summations over single vibrational quantum number. It should be mentioned that this type of calculation was performed by Reitan in his thesis[2], although his method of calculation seems to be a little more tedious than that of the present work. The essential part of the calculation is reported in Appendix II.

As the result of the calculation, we have

$$P(q_1,q_{2a},q_{2b},q_3)=N[1+a_1q_1+a_{111}q_1^3 +a_{122}q_1(q_{2a}^2+q_{2b}^2)+a_{133}q_1q_3^2] \times\exp\left[-\frac{q_1^2}{T_1}-\frac{(q_{2a}^2+q_{2b}^2)}{T_2}-\frac{q_3^2}{T_3}\right] \tag{6}$$

$$T_s=\coth(hc\omega_s/2kT)$$

with the following expressions for the coefficients;

$$a_1=-\frac{2k_{111}}{\omega_1}\left(\frac{1-\chi_1}{1+\chi_1}\right)^2 +\frac{4k_{122}\omega_2\gamma_{122}{}^+}{\omega_1(1+\chi_1)(1-\chi_2)(1+\chi_2)} +\frac{2k_{133}\omega_3\gamma_{133}{}^+}{\omega_1(1+\chi_1)(1-\chi_3)(1+\chi_3)}+\frac{2\langle E_{\rm rot}\rangle}{b_1T_1f_{11}r_e} \tag{7a}$$

$$a_{111}=-\frac{2k_{111}(1-\chi_1)(1+10\chi_1+\chi_1^2)}{3\omega_1(1+\chi_1)^3} \tag{7b}$$

$$a_{122}=-\frac{2k_{122}}{(1+\chi_1)(1+\chi_2)^2}\left\{\frac{2\chi_2(1-\chi_1)}{\omega_1}-\gamma_{122}{}^-\right\} \tag{7c}$$

$$a_{133}=-\frac{2k_{133}}{(1+\chi_1)(1+\chi_3)^2}\left\{\frac{2\chi_3(1-\chi_1)}{\omega_1}-\gamma_{133}{}^-\right\} \tag{7d}$$

and

$$\gamma_{1ss}{}^{\pm}=\left\{\frac{-1+\chi_1\chi_s{}^2}{\omega_1+2\omega_s}\pm\frac{-\chi_1+\chi_s{}^2}{\omega_1-2\omega_s}\right\} \tag{7e}$$

where b_1 is designated by Eq. 9, and f_{11} is the force constant for the symmetric stretching vibration.

Because of the accidental degeneracy of ω_1 and $2\omega_2$, the second term of Eq. 7e would fail to be a good approximation. It will, however, be shown in Appendix III that the same expression can be used without any serious error even in the case of strong degeneracy.

The distribution function in terms of the normal coordinates is converted to the expression in terms of Δz_1, Δz_2 and $\Delta\rho$, the internal Cartesian displacements; Δz denotes the relative displacements of the atom X to Y along the molecular axis and $\Delta\rho$ is the relative displacement perpendicular to the axis. $\Delta\rho^2$ is sometimes written as $\Delta x^2+\Delta y^2$. The displacements of the two X—Y atom-pairs are designated by Δz_1 and Δz_2, respectively.

These internal coordinates are related to the normal coordinates by the following relations,

$$\Delta z_1=b_1q_1+b_3q_3 \tag{8a}$$

$$\Delta z_2=b_1q_1-b_3q_3 \tag{8b}$$

and

$$\Delta\rho^2=b_{22}(q_{2a}{}^2+q_{2b}{}^2) \tag{8c}$$

The coefficients b's are given by

$$b_1=\left(\frac{h\mu_Y}{8\pi^2c\omega_1}\right)^{1/2} \tag{9a}$$

$$b_3=\left[\frac{h}{8\pi^2c\omega_3}(\mu_Y+2\mu_X)\right]^{1/2} \tag{9b}$$

and

$$b_{22}=\frac{h}{8\pi^2c\omega_2}(\mu_Y+2\mu_X) \tag{9c}$$

where μ_X and μ_Y are the reciprocal masses of the atom X and Y, respectively.

By these relations together with the followings,

$$q_{2a}=b_{22}{}^{-1/2}\Delta\rho\cos\varphi \tag{10a}$$

$$q_{2b}=b_{22}{}^{-1/2}\Delta\rho\sin\varphi \tag{10b}$$

where φ is the azimuthal angle, the probability distribution function $P(q_1,q_{2a},q_{2b},q_3)$ is transformed to the expression in terms of Δz_1, Δz_2, $\Delta\rho$ and φ, as

2) A. Reitan, thesis, Institutt for Teoretiske Kjemi, Norges Tekniske Høgskole (1958).

$$P(\Delta z_1, \Delta z_2, \Delta\rho, \varphi) = N\left[1+\frac{a_1}{2b_1}(\Delta z_1+\Delta z_2) + \frac{a_{111}}{(2b_1)^3}(\Delta z_1+\Delta z_2)^3 + \frac{a_{122}}{2b_1b_{22}}\Delta\rho^2(\Delta z_1+\Delta z_2) + \frac{a_{133}}{2b_1(2b_3)^2}(\Delta z_1+\Delta z_2)(\Delta z_1-\Delta z_2)^2\right] \times \Delta\rho \exp\left[-\frac{\Delta\rho^2}{b_{22}T_2}-\frac{(\Delta z_1+\Delta z_2)^2}{(2b_1)^2T_1} - \frac{(\Delta z_1-\Delta z_2)^2}{(2b_3)^2T_3}\right] \quad (11)$$

In order to obtain a two-dimensional probability function $P(\Delta z, \Delta\rho)$, Eq. 11 is integrated over φ and over either one of Δz_1 and Δz_2. The calculation leads to the following result;

$$P(\Delta z, \Delta\rho) = N'\left[1+A_1\Delta z+A_{111}\Delta z^3+A_{122}\Delta z\Delta\rho^2\right] \times \Delta\rho \exp\left[-\frac{\Delta\rho^2}{\langle\Delta\rho^2\rangle}-\frac{\Delta z^2}{2\langle\Delta z^2\rangle}\right] \quad (12)$$

where

$$A_1 = \frac{a_1b_1T_1}{2\langle\Delta z^2\rangle} + \frac{3a_{111}b_1T_1b_3^2T_3}{8\langle\Delta z^2\rangle^2} + \frac{a_{133}b_1T_1T_3(b_1^2T_1-2b_3^2T_3)}{8\langle\Delta z^2\rangle^2} \quad (13a)$$

$$A_{111} = \frac{a_{111}b_1^3T_1^2}{8\langle\Delta z^2\rangle^3} + \frac{a_{133}b_1T_1b_3^2T_3^2}{8\langle\Delta z^2\rangle^3} \quad (13b)$$

$$A_{122} = \frac{a_{122}b_1T_1T_2}{2\langle\Delta z^2\rangle\langle\Delta\rho^2\rangle} \quad (13c)$$

and

$$\langle\Delta z^2\rangle = \frac{b_1^2T_1+b_3^3T_3}{2} \quad (13d)$$

$$\langle\Delta\rho^2\rangle = b_{22}T_2 \quad (13e)$$

It is noted that $P(\Delta z, \Delta\rho)$ describes the relative motion of the end atom Y to the central atom X, the coordinate axes Δz and $\Delta\rho$ being fixed on the rotating plane defined by the triangle Y—X—Y.

The Probability Distribution Function of the Interatomic Distances r_{XY} and r_{YY}

The distribution function $P(\Delta z, \Delta\rho)$ given by Eq. 12 is further transformed to a one-dimensional distribution function in terms of

Δz / $\Delta\rho$																				
A																				
+0.1	00	01	01	02	02	02	02	02	02	01	01	01	01	00	00	00	00	00	00	00
	00	01	02	03	04	04	04	04	04	03	02	02	01	01	01	00	00	00	00	00
	00	02	05	06	08	08	08	08	07	06	05	04	03	02	01	01	01	00	00	00
	00	04	08	11	13	14	14	14	12	10	08	06	05	03	02	02	01	01	00	00
	00	07	14	19	22	24	24	22	20	17	14	11	08	06	04	03	02	01	01	00
	00	11	21	29	34	36	37	34	31	26	21	16	12	09	06	04	03	02	01	01
	00	15	29	40	48	52	52	49	43	37	30	23	17	13	09	06	04	02	01	01
	00	20	38	53	63	68	68	64	57	49	40	31	23	17	12	08	05	03	02	01
	00	24	46	64	76	82	82	78	69	59	48	38	28	21	14	10	06	04	02	01
	00	27	51	71	84	91	92	87	78	67	54	43	32	23	16	11	07	04	03	02
0.0	00	28	53	73	87	94	94	89	80	69	56	44	33	24	17	11	07	05	03	02
	00	26	49	68	82	88	89	85	76	65	54	42	32	23	16	11	07	05	03	02
	00	22	43	59	71	77	77	73	66	57	47	37	28	21	14	10	06	04	02	01
	00	18	34	47	56	61	61	58	53	45	38	30	23	17	12	08	05	03	02	01
	00	13	24	34	40	44	44	42	38	33	27	22	17	12	09	06	04	02	01	01
	00	08	16	22	27	29	29	28	25	22	18	15	11	08	06	04	03	02	01	01
	00	05	10	13	16	17	18	17	15	13	11	09	07	05	04	02	02	01	01	00
	00	03	05	07	09	09	10	09	08	07	06	05	04	03	02	01	01	01	00	00
	00	01	02	03	04	05	05	04	04	04	03	02	02	01	01	01	00	00	00	00
	00	01	01	01	02	02	02	02	02	02	01	01	01	01	00	00	00	00	00	00
A																				
−0.1	00	00	00	01	01	01	01	01	01	01	01	00	00	00	00	00	00	00	00	00

0.2A

Fig. 1a. CO_2

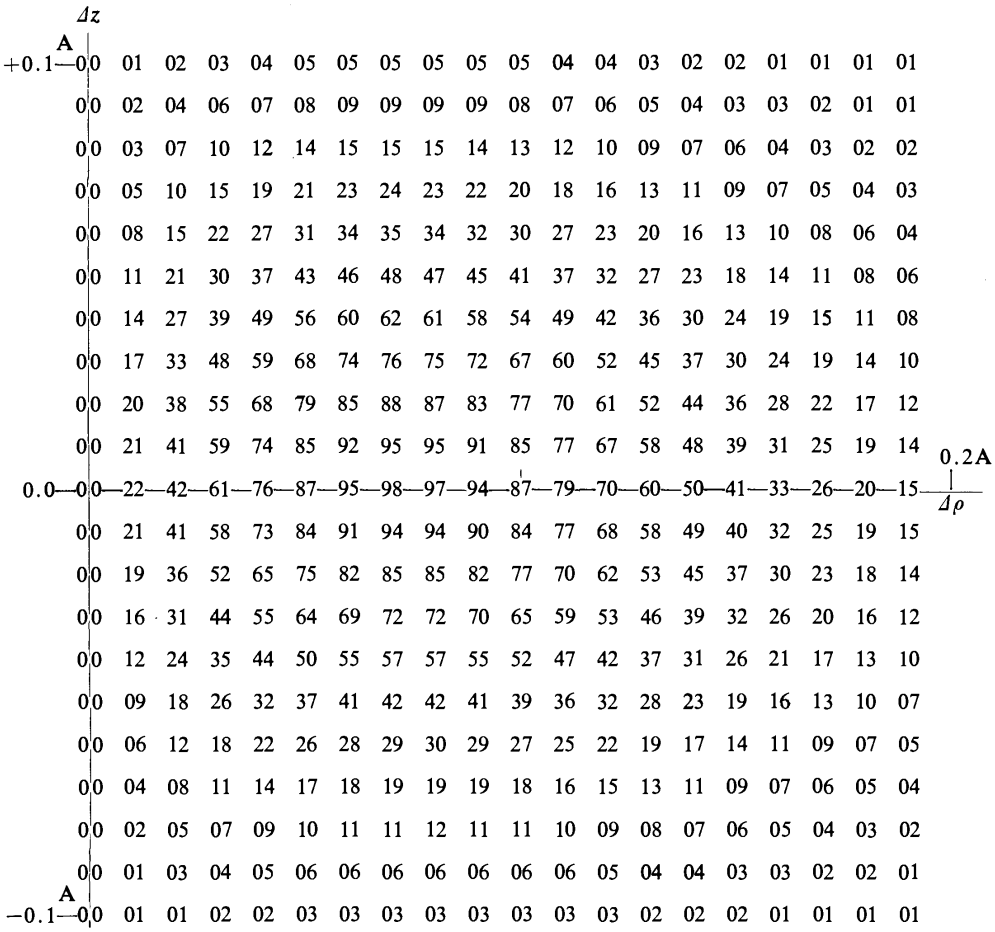

Fig. 1b. CS_2

Fig. 1. Calculated values of the distribution function $P(\Delta z, \Delta\rho)$.

the instantaneous displacement of the interatomic distance δr_{XY}. In this case, the transformation is not linear but it is given by

$$\delta r_{XY} = \Delta z + \Delta\rho^2/2r_e + \cdots\cdots, \quad (\delta r = r - r_e) \qquad (14)$$

to the first-order of approximation. The calculation leads to the result

$$P(r_{XY}) = \frac{1}{(2\pi\langle\delta r^2\rangle)^{1/2}}\left\{1+\left(A_1 + A_{122}\langle\Delta\rho^2\rangle + \frac{\langle\Delta\rho^2\rangle}{2r_e\langle\delta r^2\rangle}\right)\delta r + A_{111}\delta r^3\right\}\exp\left(-\frac{\delta r^2}{2\langle\delta r^2\rangle}\right) \qquad (15)$$

where A's are defined by Eq. 13's.

It is seen that asymmetry is introduced into the Gaussian function by linear and cubic terms of δr. The $P(r)$ function is important in the study of electron diffraction by gaseous molecules, because it is closely connected with the molecular intensity curve and the radial distribution curve obtained by the diffraction study[3]. The empirical asymmetric parameters determined by the analysis of the radial distribution curve will be related to the spectroscopic force constants through this equation. It is accordingly expected that better interpretation of the radial function will be attainable on the basis of intramolecular force field.

The distribution function for the Y—Y distance is calculated more simply, because the transformation is linear as shown below;

$$\delta r_{YY} = \Delta z_1 + \Delta z_2 = 2b_1 q_1 \qquad (16)$$

The $P(r_{YY})$ is therefore obtained from Eq. 6 through integration over q_{2a}, q_{2b} and q_3, as

$$P(r_{YY}) = \frac{1}{(2\pi\langle\delta r^2\rangle)^{1/2}}\{1 + A'_1\delta r + A'_{111}\delta r^3\} \times \exp\left(-\frac{\delta r^2}{2\langle\delta r^2\rangle}\right) \qquad (17)$$

with

3) K. Kuchitsu and L. S. Bartell, *J. Chem. Phys.*, **35**, 1945 (1961).

$$A'_1=\frac{1}{2b_1}\left(a_1+a_{122}T_2+\frac{1}{2}A_{133}T_3\right)$$

and

$$A'_{111}=a_{111}/8b_1^3$$

Numerical Examples: CO_2 and CS_2

The probability distribution function $P(\Delta z, \Delta\rho)$ was numerically calculated for carbon dioxide and for carbon disulfide, respectively. The molecular constants used in the calculation are listed in Table I, together with the

TABLE I. MOLECULAR CONSTANTS OF CO_2 AND CS_2

	CO_2[a]	CS_2[b,c]
ω_1	1354.85 cm^{-1}	671.36 cm^{-1}
ω_2	673.00 cm^{-1}	398.62 cm^{-1}
ω_3	2396.49 cm^{-1}	1551.92 cm^{-1}
α_1	0.00120 cm^{-1}	0.000156 cm^{-1}
α_2	−0.00072 cm^{-1}	−0.000256 cm^{-1}
α_3	0.00309 cm^{-1}	0.000711 cm^{-1}
k_{111}	−45.07 cm^{-1}	−14.90 cm^{-1}
k_{122}	73.81 cm^{-1}	50.10 cm^{-1}
k_{133}	−252.95 cm^{-1}	−129.56 cm^{-1}
A_1	1.8 A^{-1}	1.2 A^{-1}
A_{111}	309 A^{-3}	170 A^{-3}
A_{122}	−114 A^{-3}	−100 A^{-3}

a) C. P. Courtoy, *Ann. Soc. Sci. Bruxelles*, I **73**, 5 (1959).
b) B. P. Stoicheff, *Can. J. Phys.*, **36**, 218 (1958).
c) A. H. Guenther, T. A. Wiggins and D. H. Rank, *J. Chem. Phys.*, **28**, 682 (1958).

cubic potential constants k and the linear and cubic coefficients A of $P(\Delta z, \Delta\rho)$ obtained. The schematic diagrams of $P(\Delta z, \Delta\rho)$ are computed with an arbitrary normalizing-factor and arranged in rows so as to make correspondence to the point specified by the coordinates $(\Delta z, \Delta\rho)$, as seen in Figs. 1a and 1b. The contour lines are drawn on the diagrams, and the distribution maps thus obtained are shown in Fig. 2a for CO_2 and in Fig. 2b for CS_2, respectively.

These maps illustrate the relative motion of the end atom Y to the central atom X. The Δz axis lies on the equilibrium molecular axis. The point specified by $\Delta z=0$ and $\Delta\rho=0$ is the equilibrium position of the Y atom. The location of the atom X is far down out of the figures in the negative direction, specified by $\Delta z=-r_e$ and $\Delta\rho=0$.

It is easily seen in the diagrams of $P(\Delta z, \Delta\rho)$ that in the region of small $\Delta\rho$, the outer region of Δz is more favorable, and the inner region of Δz becomes more favorable as $\Delta\rho$ increases. This is caused by the negative contribution of the coupling term between bending and stretching, or A_{122}, to the distribution function. This general tendency of the probability distribution corresponds to a classical picture of the bending motion that the two X—Y bonds are bent at the central atom and the end atom Y moves along a circular locus which is slightly shifted outwards by the stretching anharmonicity.

It may be accordingly suggested that the intramolecular potential can be described better

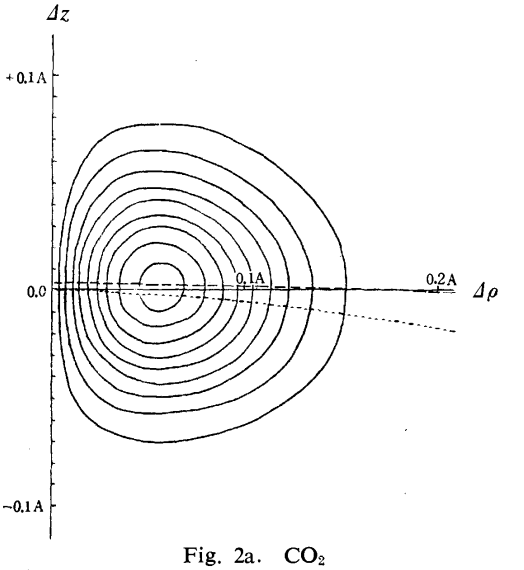

Fig. 2a. CO_2

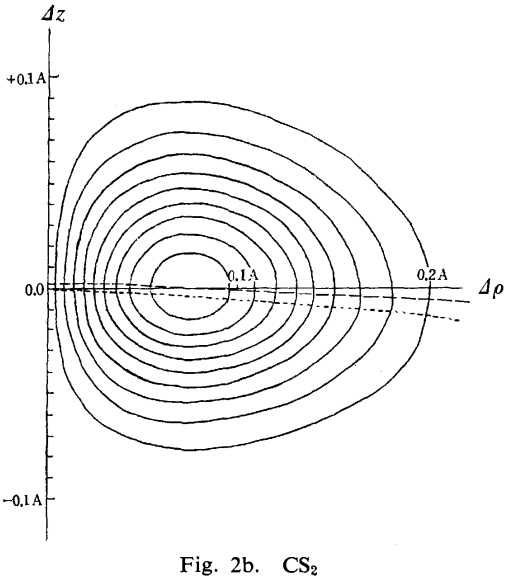

Fig. 2b. CS_2

Fig. 2. Contour map of the probability-distribution.

—— shows the ridge
- - - is the circular locus drawn by keeping the X—Y distance constant

and more simply in terms of internal coordinates, i.e., the bond-stretching δr and the bending angle $\delta\rho$, rather than in terms of Cartesian coordinates. The force constants for the expression of the potential energy in terms of the internal coordinates are expected to have more distinct physical significance and therefore to be transferable among the chemical bonds of the same kind. An extensive study on the anharmonic force constants has been carried out along this line, and it was found that the most part of the constant k_{122} comes from the quadratic stretching force constants through coordinate transformation[4].

A more careful examination of the distribution map reveals that according as $\Delta\rho$ increases, the ridge in the map runs more and more outwards than the circular locus which is drawn by keeping the X—Y distance constant. In other words, it is easier for a bond to stretch when the bending motion takes place. Such an interaction term as $L_3\delta r\delta\alpha^2$ with a negative value of L_3, is therefore expected to improve the description of the intramolecular potential field. As a matter of fact, the predicted value of k_{122} was found to be in complete agreement with the observed value by introducing $L_3=-0.5$ md./A for CO_2, in addition to the main contribution from the quadratic stretching constants; while a smaller value $L_3=-0.1$ md./A is necessary to get the agreement for CS_2[4], corresponding to the fact that the extent of the outward shift is seen to be more appreciable in the case of CO_2 than CS_2.

The authors wish to express their gratitude to Professor Hidetoshi Takahashi and his coworkers, in the Department of Physics, for the use of PC-2 computer. They are indebted to the Ministry of Education of Japan for the research grant.

Department of Chemistry
Faculty of Science
The University of Tokyo
Hongo, Tokyo

Appendix I. Non-vanishing Coefficients of Eq. 4

$(v=v_1,\ v_s,\ v_{s'})$ v'	$\dfrac{\langle v'\lvert H^{(1)}\rvert v\rangle}{E_{v'}^0-E_v^0}$
$v_1+1,\ v_s,\ v_{s'}$	$\dfrac{3k_{111}}{\omega_1}\left(\dfrac{(v_1+1)^3}{8}\right)^{1/2}-\left(\dfrac{h}{\pi^2c\omega_1 I}\right)^{1/2}\times\dfrac{\langle E_{\rm rot}\rangle}{hc\omega_1}\left(\dfrac{v_1+1}{2}\right)^{1/2}+\sum_s\dfrac{k_{1ss}}{\omega_1}\left(\dfrac{v_1+1}{2}\right)^{1/2}\left(v_s+\dfrac{1}{2}\right)$
$v_1+3,\ v_s,\ v_{s'}$	$\dfrac{k_{111}}{3\omega_1}\left[\dfrac{(v_1+1)(v_1+2)(v_1+3)}{8}\right]^{1/2}$
$v_1+1,\ v_s+2,\ v_{s'}$	$\dfrac{k_{1ss}}{\omega_1+2\omega_s}\left(\dfrac{v_1+1}{2}\right)^{1/2}\times\dfrac{[(v_s+1)(v_s+2)]^{1/2}}{2}$
$v_1+1,\ v_s-2,\ v_{s'}$	$\dfrac{k_{1ss}}{\omega_1-2\omega_s}\left(\dfrac{v_1+1}{2}\right)^{1/2}\dfrac{[v_s(v_s-1)]^{1/2}}{2}$
$v_1-1,\ v_s,\ v_{s'}$	$-\dfrac{3k_{111}}{\omega_1}\left(\dfrac{v_1^3}{8}\right)^{1/2}+\left(\dfrac{h}{\pi^2c\omega_1 I}\right)^{1/2}\dfrac{\langle E_{\rm rot}\rangle}{hc\omega_1}\left(\dfrac{v_1}{2}\right)^{1/2}-\sum_s\dfrac{k_{1ss}}{\omega_1}\left(\dfrac{v_1}{2}\right)^{1/2}\left(v_s+\dfrac{1}{2}\right)$
$v_1-3,\ v_s,\ v_{s'}$	$-\dfrac{k_{111}}{3\omega_1}\left[\dfrac{v_1(v_1-1)(v_1-2)}{8}\right]^{1/2}$
$v_1-1,\ v_s+2,\ v_{s'}$	$-\dfrac{k_{1ss}}{\omega_1-2\omega_s}\left(\dfrac{v_1}{2}\right)^{1/2}\times\dfrac{[(v_s+1)(v_s+2)]^{1/2}}{2}$
$v_1-1,\ v_s-2,\ v_{s'}$	$-\dfrac{k_{1ss}}{\omega_1+2\omega_s}\left(\dfrac{v_1}{2}\right)^{1/2}\dfrac{[v_s(v_s-1)]^{1/2}}{2}$

Appendix II. Calculation of the Summation over Vibrational States

It is easily shown that the summations over vibrational states appearing in Eq. 5 can be reduced to the products of some of the following summations:

$$F_0=\sum_v w_v\,|\phi_v^0|^2$$

$$F_1=\sum_v w_v\left(\frac{v+1}{2}\right)^{1/2}\phi_{v+1}^0\phi_v^0$$

$$F_2=\sum_v w_v\left[\frac{(v+1)^3}{8}\right]^{1/2}\phi_{v+1}^0\phi_v^0$$

$$F_3=\sum_v w_v[(v+1)(v+2)]^{1/2}\phi_{v+2}^0\phi_v^0$$

$$F_4=\sum_v w_v\left[\frac{(v+1)(v+2)(v+3)}{8}\right]^{1/2}\phi_{v+3}^0\phi_v^0$$

where ϕ_v^0 is a non-perturbed wave function of a harmonic oscillator with the vibrational quantum number v.

As well known F_0 is given by[5,6],

$$F_0=\pi^{1/2}\left[\tanh\frac{hc\omega}{2kT}\right]^{1/2}\exp\left[-\left(\tanh\frac{hc\omega}{2kT}\right)q^2\right] \qquad \text{(AII-1)}$$

By the use of the recursion formula,

$$\phi_{v+1}^0=\left(\frac{2}{v+1}\right)^{1/2}q\phi_v^0-\left(\frac{v}{v+1}\right)^{1/2}\phi_{v-1}^0$$

F_1 is rewritten as,

4) K. Kuchitsu, T. Iijima and Y. Morino, International Symposium on Molecular Structure and Spectroscopy, Tokyo, Japan, 1962.

5) F. Bloch, *Z. Phys.*, 73, 295 (1932).

6) Series of Modern Physics; "Statistical Mechanics", Iwanami Co., Ltd., Tokyo (1955), p. 212.

$$F_1=q\sum_v w_v\psi_v{}^0\psi_v{}^0-\chi\sum_v w_{v-1}\left(\frac{v}{2}\right)^{1/2}\psi_v{}^0\psi_{v-1}{}^0$$
$$=qF_0-\chi F_1$$

where

$$\chi=\exp\left(-\frac{hc\omega}{kT}\right)$$

Therefore we have,

$$F_1=\frac{1}{1+\chi}qF_0 \qquad \text{(AII-2)}$$

Similarly,

$$F_2=\sum_v w_v\left(\frac{v+1}{2}\right)q\psi_v{}^0\psi_v{}^0-\sum_v w_v\left(\frac{v+1}{2}\right)\left(\frac{v}{2}\right)^{1/2}$$
$$\times\psi_v{}^0\psi_{v-1}{}^0=\frac{q}{2}G+\frac{q}{2}F_0-\chi F_2-\frac{1}{2}\chi F_1$$

Therefore,

$$F_2=\frac{1}{1+\chi}\left(\frac{1}{2}qG+\frac{1}{2}qF_0-\frac{1}{2}\chi F_1\right) \qquad \text{(AII-3)}$$

where

$$G=\sum_v w_v v\psi_v{}^0\psi_v{}^0$$
$$=-\frac{1}{\sum_v\chi^v}\frac{\partial}{\partial\left(\frac{hc\omega}{kT}\right)}[F_0\cdot\sum_v\chi^v]$$
$$=\left\{\frac{\chi^2}{1-\chi^2}+\frac{2\chi}{(1+\chi)^2}q^2\right\}F_0 \qquad \text{(AII-4)}$$

Inserting Eqs. AII-2 and AII-4 into AII-3, we have,

$$F_2=\frac{1}{1+\chi}\left[\frac{1-\chi+\chi^2}{2(1-\chi^2)}q+\frac{\chi}{(1+\chi)^2}q^3\right]F_0$$

and

$$F_3=2qF_1-G-F_0=\left\{-\frac{1}{1-\chi^2}+\frac{2}{(1+\chi)^2}q^2\right\}F_0$$

$$F_4=\frac{1}{2}qF_3-F_2-\frac{1}{2}F_1$$
$$=\frac{1}{1+\chi}\left\{-\frac{3}{2(1-\chi^2)}q+\frac{1}{(1+\chi)^2}q^3\right\}F_0$$

Appendix III. The Effect of Fermi Resonance on the Probability Distribution Function

In order to simplify the discussion, let us consider a resonance between state I ($v_1=1$, $v_2=0$) and state II ($v_1=0$, $v_2=2$), connected by a coupling term $hck_{122}q_1q_2^2$, and calculate the probability distribution function $P=w_1|\psi_I|^2+w_2|\psi_{II}|^2$, both by an ordinary first-order perturbation treatment and more rigorously by solving the secular determinant.

As the result of the first-order treatment, we have the perturbed wave functions as

$$\psi_I=\psi_{10}{}^0-a_{20}\psi_{20}{}^0-a_{22}\psi_{22}{}^0-a_{00}\psi_{00}{}^0-a_{02}\psi_{02}{}^0$$

and

$$\psi_{II}=\psi_{02}{}^0-a_{12}\psi_{12}{}^0-a_{14}\psi_{14}{}^0-a_{10}\psi_{10}{}^0$$

where

$$a_{20}=\frac{k_{122}}{2\omega_1},\qquad a_{12}=\frac{3k_{122}}{2\sqrt{2}\,\omega_1}$$

$$a_{22}=\frac{k_{122}}{\sqrt{2}\,(\omega_1+2\omega_2)},\qquad a_{14}=\frac{\sqrt{3}\,k_{122}}{\sqrt{2}\,(\omega_1+2\omega_2)}$$

$$a_{00}=-\frac{k_{122}}{2\sqrt{2}\,\omega_1},\qquad a_{10}=\frac{k_{122}}{2(\omega_1-2\omega_2)}$$

$$a_{02}=-\frac{k_{122}}{2(\omega_1-2\omega_2)}$$

These wave functions are expressed more simply as

$$\psi_I=\psi_{10}{}^{(1)}-a_{02}\psi_{02}{}^0$$

and

$$\psi_{II}=\psi_{02}{}^{(1)}-a_{10}\psi_{10}{}^0$$

where $\psi^{(1)}$ includes all terms except for the term having a resonance denominator.

Accordingly we have,

$$P=w_1{}^0|\psi_{10}{}^{(1)}|^2+w_2{}^0|\psi_{02}{}^{(1)}|^2+\frac{w_1{}^0-w_2{}^0}{\omega_1-2\omega_2}k_{122}\psi_{10}{}^0\psi_{02}{}^0 \qquad \text{(AIII-1)}$$

$$w_1{}^0=\exp\left(-\frac{hc\omega_1}{kT}\right),\qquad w_2{}^0=\exp\left(-\frac{2hc\omega_2}{kT}\right)$$

On the other hand, in a rigorous treatment, we consider the wave functions ψ_I and ψ_{II} to be expressed as

$$\psi_I=a\psi_{10}{}^{(1)}+b\psi_{02}{}^{(1)}$$
$$\psi_{II}=b\psi_{10}{}^{(1)}-a\psi_{02}{}^{(1)}$$

by the linear combinations of $\psi_{10}{}^{(1)}$ and $\psi_{02}{}^{(1)}$ which include contributions from non-resonant states as defined above. The secular determinant is established as*,

$$\begin{vmatrix}\omega_1-E & k_{122}/2\\ k_{122}/2 & 2\omega_2-E\end{vmatrix}=0$$

As a solution of the determinant, we have,

---

* This secular determinant is not correct for the case of linear XY_2 type molecules, because the ω_2 normal vibration is doubly degenerate. By denoting two degenerate modes as ω_{2a} and ω_{2b}, we have to diagonalyse the energy matrix consisting of the elements among three states, ($v_1=1$, $v_{2a}=0$, $v_{2b}=0$), ($v_1=0$, $v_{2a}=2$, $v_{2b}=0$) and ($v_1=0$, $v_{2a}=0$, $v_{2b}=2$), where the perturbation term is $hck_{122}q_1(q_{2a}{}^2+q_{2b}{}^2)$.

The secular determinant is,

$$\begin{vmatrix}2\omega_2-E, & k_{122}/2, & 0\\ k_{122}/2, & \omega_1-E, & k_{122}/2\\ 0 & k_{122}/2, & 2\omega_2-E\end{vmatrix}=0$$

Therefore we have,

$$E_1=\omega_1+\varepsilon$$
$$E_2=2\omega_2-\varepsilon$$
$$E_3=2\omega_2$$

where

$$\varepsilon=\frac{1}{2}\{-\delta+(\delta^2+2k_{122}{}^2)^{1/2}\}$$

and

$$\psi_1=a\psi_{100}+b\left(\frac{1}{\sqrt{2}}\psi_{020}+\frac{1}{\sqrt{2}}\psi_{002}\right)$$
$$\psi_2=b\psi_{100}-a\left(\frac{1}{\sqrt{2}}\psi_{020}+\frac{1}{\sqrt{2}}\psi_{002}\right)$$
$$\psi_3=\frac{1}{\sqrt{2}}\psi_{020}-\frac{1}{\sqrt{2}}\psi_{002}$$

with

$$a=\frac{k_{122}}{(2\varepsilon^2+k_{122}{}^2)^{1/2}},\qquad b=\frac{\sqrt{2}\,\varepsilon}{(2\varepsilon^2+k_{122}{}^2)^{1/2}}$$

$$E_{\mathrm{I}}=\omega_1+\varepsilon$$

$$E_{\mathrm{II}}=2\omega_2-\varepsilon$$

where

$$\varepsilon=\frac{1}{2}\{-\delta+(\delta^2+k_{122}{}^2)^{1/2}\}$$

and

$$\delta=\omega_1-2\omega_2$$

$$a=\frac{k_{122}}{(4\varepsilon^2+k_{122}{}^2)^{1/2}},\qquad b=\frac{2\varepsilon}{(4\varepsilon^2+k_{122}{}^2)^{1/2}}$$

The probability distribution function is rewritten as

$$P=w_1|\psi_{\mathrm{I}}|^2+w_2|\psi_{\mathrm{II}}|^2$$
$$=(w_1a^2+w_2b^2)\,|\psi_{10}{}^{(1)}|^2+(w_1b^2+w_2a^2)\,|\psi_{02}{}^{(1)}|^2$$
$$+2(w_1-w_2)ab\psi_{10}{}^{(1)}\psi_{02}{}^{(1)}$$

The term $w_1a^2+w_2b^2$ can be replaced by $w_1{}^0$, since $w_1\cong w_2\cong w_1{}^0$ and $a^2+b^2=1$. Similarly we have $w_1b^2+w_2a^2=w_2{}^0$. In the third term, $\psi_{10}{}^{(1)}\psi_{02}{}^{(1)}$ can be approximated by $\psi_{10}{}^0\psi_{02}{}^0$. Thus we have

$$P=w_1{}^0|\psi_{10}{}^{(1)}|^2+w_2{}^0|\psi_{02}{}^{(1)}|^2+2(w_1-w_2)ab\psi_{10}{}^0\psi_{02}{}^0 \qquad \text{(AIII-2)}$$

The zeroth-order term $w_1{}^0|\psi_{10}{}^{(1)}|^2+w_2{}^0|\psi_{02}{}^{(1)}|^2$ is just equal to the corresponding expression in Eq. AIII-1.

In the case of weak resonance, i.e., $|\delta|\gg k_{122}$, we have

$$2(w_1-w_2)ab\cong(w_1{}^0-w_2{}^0)k_{122}/\delta$$

which is equivalent to the resonance-term of Eq. AIII-1.

In the case of strong degeneracy, i.e., $|\delta|\ll k_{122}$,

$$2(w_1-w_2)ab\cong-\frac{hck_{122}}{\boldsymbol{kT}}\exp\left(-\frac{hc\omega_1}{\boldsymbol{kT}}\right) \qquad \text{(AIII-3)}$$

because,

$$2ab=1$$

and

$$w_1-w_2=-\frac{2hc\varepsilon}{\boldsymbol{kT}}\exp\left(-\frac{hc\omega_1}{\boldsymbol{kT}}\right)$$

where $\varepsilon=k_{122}/2$. On the other hand, the resonance term of Eq. AIII-1 yields in the limit of $\delta\to0$,

$$\lim_{\delta\to0}\frac{w_1{}^0-w_2{}^0}{\delta}k_{122}=-\frac{hck_{122}}{\boldsymbol{kT}}\exp\left(-\frac{hc\omega_1}{\boldsymbol{kT}}\right)$$

which is equal to Eq. AIII-3. This result seems to make sure the validity of Eq. AIII-1 even in the case of strong degeneracy.

The ratio of the resonance-term of Eq. AIII-1 to that of Eq. AIII-2 is evaluated at several values of δ, in the case of $k_{122}=50\,\mathrm{cm}^{-1}$. As shown in Table II, no appreciable discrepancy is found between the numerical values of the two expressions throughout the whole region of δ. Therefore, it seems most likely that the probability distribution function obtained in this article holds to a good approximation even in the case of an accidental degeneracy, although complicated manipulation of the summation over upper vibrational states have not been performed in this supplementary note.

TABLE II. RATIO OF THE RESONANCE TERMS CALCULATED BY THE TWO METHODS

δ cm^{-1}	Ratio
5	1.00
10	0.97
20	0.98
50	0.98
100	0.98
150	1.01
250	0.99

Kinetics of the Acid-Catalyzed Decomposition of Trimeric Acetone Peroxide

By Yoshiaki FURUYA and Yoshiro OGATA

(Received November 24, 1962)

Both dimeric and trimeric acetone peroxides explode violently on shock, but they are considerably stable in a solution of organic solvents. In the presence of strong acids, however, these peroxides decompose comparatively fast. Thus far the kinetics of the decomposition of acetone peroxide in solutions have not yet been studied. The present report summarizes our investigation on the kinetics of the sulfuric acid-catalyzed decomposition of trimeric acetone peroxide in acetic acid.

Experimental

Materials. — Trimeric acetone peroxide (abbreviated as TAPO) was prepared by Wolffenstein's method[1] by the reaction of acetone with aqueous hydrogen peroxide containing a small amount of phosphoric acid as catalyst for two or three weeks, and the obtained product was recrystallized from methanol and then from ether, m. p. 97°C, the yield was 80.4%.

1) K. Wolffenstein, *Ber.*, **28**, 2265 (1895).

The Criterion of the Reaction Products.—Trimeric acetone peroxide was dissolved in acetic acid containing a known amount of sulfuric acid. The solution was kept standing at 30°C for 30 min.; the solution of the reaction mixture was developed with a mixture of diethyl ether and ethyl acetate (1 : 4 $^{v}/_{v}$) on Toyo Filter Paper No. 54 which was preliminarily treated with a mixture of acetic acid (300 g.), acetic anhydride (80 g.) and zinc chloride (20 g.)[2]. A pink spot was observed by spraying with methanolic solution of 3% *p*-dimethylaminoaniline dihydrochloride. The value of R_f was found to be 0.77, which corresponded to that of peroxyacetic acid.

Produced peroxyacetic acid liberated iodine from potassium iodide instantaneously, while the acetone peroxide and acetyl peroxide reacted with aqueous potassium iodide very slowly as shown in Table I; hence peroxyacetic acid could be estimated by iodometry. Aliquots (each 5 ml.) of the reaction solution were poured into 100 ml. of an ice-cooled aqueous solution containing ca. 0.1% potassium iodide, iodine liberated by the reaction with peroxyacetic acid being titrated with 0.01 N sodium thiosulfate.

A solution of 0.005 M TAPO in acetic acid containing 0.18 N sulfuric acid was kept standing for one hour and it was confirmed that the reaction was complete after one hour. Acetone formed by decomposition of TAPO was detected and estimated by gas chromatography. The blank test showed that the concentration of acetone in acetic acid was proportional to the corresponding chromatogram area.

TABLE I. THE RATE OF REACTION OF TAPO (5 ml. OF 0.005 M SOLUTION) WITH AQUEOUS POTASSIUM IODIDE EXPRESSED AS THE CONSUMPTION OF 0.01 N SODIUM THIOSULFATE SOLUTION

Time, min.	2	3	7	13	∞
Consumed 0.01 N $Na_2S_2O_3$, ml.	0.03	0.03	0.13	0.20	14.96

The concentrations of peroxyacetic acid and acetone in two samples taken out from a reaction solution at the same time were found to be 0.0138 and 0.0132 M, respectively; hence it is reasonable that the decomposition of TAPO gives the same molar concentrations of peroxyacetic acid and acetone. Therefore, the stoichiometric equation of this acid-catalyzed decomposition may be written as follows:

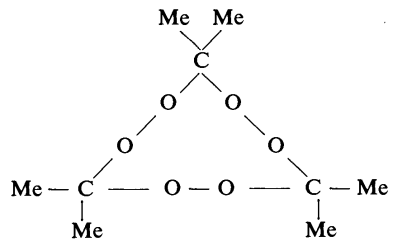

$$+3CH_3CO_2H \xrightarrow{H_2SO_4} 3CH_3COCH_3+3CH_3CO_3H$$

2) J. Janoušek, *Faserforsch. u. Textiltech.*, 8, 339 (1957).

A Typical Run for the Rate Measurements.—After a solution of 49 ml. of 0.0051 M TAPO in acetic acid in a stoppered flask had attained the temperature equilibrium at 20°C, the reaction was started by the addition of 1 ml. of 9 N sulfuric acid in acetic acid. Aliquots (each 5 ml.) were taken out at appropriate time intervals and each aliquot was poured into an ice-cooled 100 ml. solution of ca. 0.1% potassium iodide. Iodine liberated by peroxyacetic acid was quickly titrated with 0.01 N sodium thiosulfate solution to estimate the concentration of peroxyacetic acid.

Results and Discussion

The rate followed the first-order equation with TAPO, although a short induction period was observed, especially when the reaction was slow. The first-order rate constants were shown in Table II. The plot of log k vs. acidity function H_0 gave a straight line with a slope of −1.12 as shown in Fig. 1. The energy of activation was calculated to be 19.14

TABLE II. THE RATE CONSTANTS FOR THE DECOMPOSITION OF TAPO TO PEROXYACETIC ACID IN ACETIC ACID WITH VARYING INITIAL CONCN. OF TAPO AT 20°C WITH ACIDITY FUNCTION OF −1.55

Initial concn. of TAPO, M	3×10^{-3}	5×10^{-3}	7×10^{-3}	10×10^{-3}
$k\times10^4$ sec^{-1}	3.99	3.93	4.05	4.07

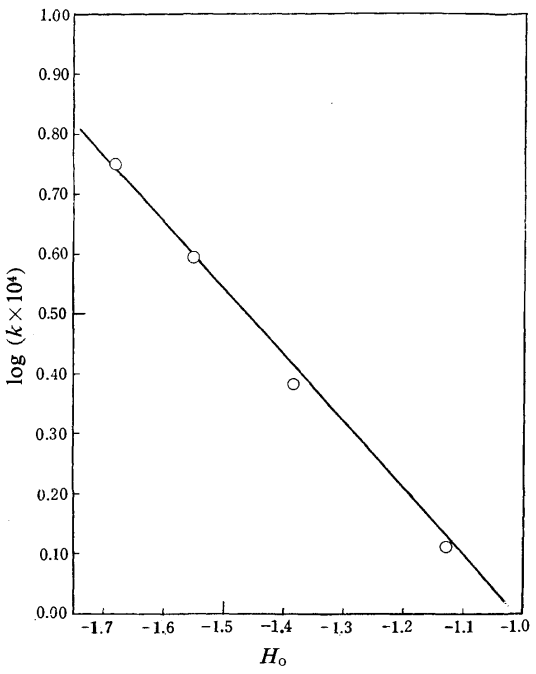

Fig. 1. The plots of log k *vs.* H_0 for the decomposition of TAPO in acetic acid at 20°C.
Initial concn. of TAPO: 5×10^{-3} M

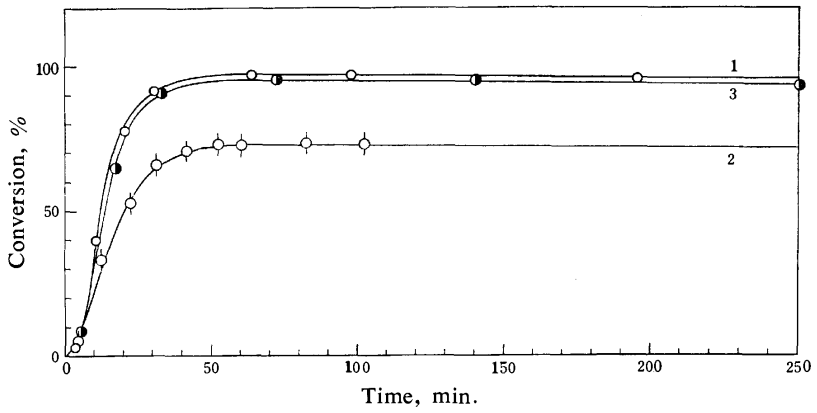

Fig. 2. A typical run for the reaction of TAPO in acetic acid at 30°C.

	Initial concn. of TAPO, M	Concn. of H_2SO_4, N	Concn. of added acetone, M
1	0.005	0.18	—
2	0.05	0.18	—
3	0.005	0.18	0.015

kcal./mol. from the average values of $k\times10^4$ sec^{-1} at 20°C, 1.29; at 25°C, 2.53; at 30°C, 3.88 and at 35°C, 6.99 in a solution with acidity function of −1.13.

Since the reaction has an induction period, it may be autocatalytic or consecutive. If the reaction were autocatalytic, the reaction would be accelerated on addition of the decomposition products or reaction mixture, but this was not observed; i. e., peroxyacetic acid, acetone or reaction mixture did not promote the reaction. Furthermore, the induction period was not affected by the addition of either trinitrobenzene, *p*-benzoquinone or Fenton's reagent. Therefore, these radical sources or radical-trapping agents do not seem to play an important role at least in the early stages of this decomposition reaction, but it is propable that the reaction is consecutive and it may go by way of any metastable intermediate.

It is of interest to note that an increase of the initial concentration of TAPO resulted in a decrease of the ultimate yield of peroxyacetic acid. For example, two solutions with initial concentrations of 0.005 M and 0.05 M TAPO, each containing 0.18 N sulfuric acid, were kept standing for 60~100 min. at 30°C until no production of peroxyacetic acid was observed. The amount of acetone in this resulting solution was estimated by gas chromatography, which showed that the reaction, irrespective of the concentration of TAPO, was 100% complete. But the amount of peroxyacetic acid measured iodometrically was only 74.0% of the theoretical with a solution of 0.05 M TAPO, while a solution of 0.005 M TAPO gave 97.0%. This phenomenon is not due to the reversibility of the reaction, since the "apparent equilibrium constants" calculated varied considerably with the change of the concentration of TAPO and added acetone, as shown in Table III, and the addition of acetone had no effect on the rate as obvious in Fig. 2.

TABLE III. THE VARIATION OF "APPARENT EQUILIBRIUM CONSTANTS" WITH THE CHANGE OF INITIAL CONCENTRATION OF TAPO IN ACETIC ACID SOLUTION WITH 0.18 N H_2SO_4

Concn. of TAPO, M	Concn. of acetone added, M	Equilibrium const.
0.005	None	6.32×10^{-8}
0.05	None	1.43×10^{-9}
0.005	0.015	2.58×10^{-5}

As reported previously[3], the phenomenon may be explained by the transformation of the produced peroxyacetic acid into acetyl peroxide, the extent of the transformation being increased with increasing concentration of peroxyacetic acid.

$$CH_3CO_3H + CH_3CO_2H \rightleftharpoons CH_3CO\text{-}O_2\text{-}COCH_3 + H_2O$$

As shown in Fig. 2, the plot of conversion vs. time gives a slight maximum which suggests the transformation of peroxyacetic acid. Moreover, the paper chromatography of the reaction mixture afforded a spot corresponding to peroxyacetic acid $R_f=0.77$, at 30 min. as stated above, while it gave spots with the R_f values of 0.75 and 0.85, corresponding to peroxyacetic

3) Y. Ogata, Y. Furuya, J. Maekawa and K. Okano, *J. Am. Chem. Soc.*, in press.

acid and acetyl peroxide, respectively[3] at 300 min. The spot corresponding to acetyl peroxide was more remarkable as the concentration of peroxyacetic acid was increased.

Summary

It was confirmed by the iodometry and gas chromatography that one mole of TAPO in acetic acid was decomposed to three moles of acetone and peroxyacetic acid in the presence of sulfuric acid. The rate of the reaction satisfied the first-order equation with a short induction period. The plot of $\log k$ vs. H_0 gave a straight line with a slope of -1.12. When the concentration of TAPO was high, the amount of peroxyacetic acid was not quantitative, probably because of the transformation of peroxyacetic acid into acetyl peroxide.

Department of Applied Chemistry
Faculty of Engineering
Nagoya University
Chikusa-ku, Nagoya

The Crystal Structures of Metal 8-Hydroxyquinolinate. I. Copper 8-Hydroxyquinolinate[*1]

By Fumikazu KANAMARU[*2], Kazuhide OGAWA[*3] and Isamu NITTA

(Received December 1, 1962)

In the course of recent developments in the valency theory and streochemistry of copper, it has been reported by Orgel and Dunitz[1] that there are three types of environment about the cupric ion: (1) distorted octahedral with four short and two long bonds, (2) square coplanar, and (3) tetrahedral. The tetrahedral compounds, such as Cu_2CsCl_4[2], are few in number, but, in the case of the cuprous ion, copper usually makes sp^3 (tetrahedral) bonds with surrounding ligands. A greater number of cupric compounds are of type 1 or 2. These types may be considered together as a single class, since we regard the planar compounds as a limiting case of 1, with the two opposite ligands with long bonds removed completely.

The crystal structure of copper 8-hydroxyquinolinate dihydrate has been determined by Kruh and Dwiggins[3]. It is isomorphous with the corresponding zinc salt, the crystal structure of which has been determined by Meritt et al.[4] Moreover, since Liu and Bailar[5] have found that, in zinc salt of 8-hydroxyquinoline-5-sulfonic acid, the coordination of the zinc is tetrahedral, it may be assumed that the same arrangement of the ligands will be found in the anhydrous zinc 8-hydroxyquinolinate. According to the results of the X-ray analysis of the corresponding anhydrous copper compound by Mundy[6], the copper atoms are not arranged at the centers of symmetry, but in the general positions of the unit cell of the space group $P2_1/a$. Thus, he inferred that there is no reason why the copper complex should not be tetrahedral.

Since copper(II) shows a strong tendency toward a square planar coordination and since Mundy's analysis is not complete, it will be interesting to see which of the two possible structures is the actual arrangement in the anhydrous salt. The present paper deals with the structure analysis of copper 8-hydroxyquinolinate in more detail than Mundy provides. In connection with this substance, it has been determined by Ogawa that the anhydrous zinc 8-hydroxyquinolinate is triclinic, with two formula units in a cell of the dimensions $a=11.1, b=9.20, c=11.1$ Å, $\alpha=114.9°$, $\beta=75.1°$, $\gamma=90.8°$; the details of his research will be published elsewhere.

---

*1 This paper is a portion of a thesis submitted by Fumikazu Kanamaru in partial fulfilment of the requirements for the Degree of Master of Science at Osaka University.

*2 Present address: Institute of Scientific and Industrial Research, Osaka University, Sakai-shi, Osaka.

*3 Present address: Institute of Chemistry, Osaka University, Shibahara, Toyonaka, Osaka.

1) L. E. Orgel and J. D. Dunitz, *Nature*, **179**, 462 (1957).

2) L. Helmholz and R. F. Kruh, *J. Am. Chem. Soc.*, **74**, 1176 (1952).

3) R. Kruh and C. W. Dwiggins, ibid., **77**, 806 (1955).

4) L. L. Meritt, Jr., R. T. Cady and B. W. Mundy, *Acta Cryst.*, **7**, 473 (1954).

5) J. C. I. Liu and J. C. Bailar, *J. Am. Chem. Soc.*, **73**, 5432 (1951).

6) B. W. Mundy, Ph. D. Dissertation, Indiana University (1948).

Experimental

The anhydrous copper 8-hydroxyquinolinate was prepared by heating, on the water bath, the hydrated precipitate obtained by mixing a solution of copper in acetic acid with an alcoholic solution of 8-hydroxyquinoline (oxine). Crystals of anhydrous copper 8-hydroxyquinolinate were grown by slow evaporation at about 45°C from a pyridine solution of the anhydrous compound. The crystals in the shape of rods or of hexagonal plates are colored dark brown. They were not always obtained in the form of rods however, and the axis of the rod was not always parallel to the direction of the b axis. In the present experiment, we used a rod crystal the axis of which was parallel to b, thus obtaining the Weissenberg *h0l* reflections, otherwise we used specimens cut along the b or c direction out of hexagonal tabular crystals with developed (100).

When anhydrous copper 8-hydroxyquinolinate is recrystallized from a pyridine solution, a green pyridine addition compound is also obtained at the same time[7]. In order to ascertain that the specimen is the desired anhydrous salt, we determined the nitrogen content of the specimen and took an X-ray diffraction powder pattern for comparison with the results reported by Sekido[8]. The analysis showed that the chemical formula of the specimen corresponded to $CuC_{18}H_{12}O_2N_2$, while the phase corresponded to the β-form of $Cu(oxine)_2$ designated by Sekido.

Using Ni-filtered Cu-K_α radiation, Weissenberg, Sauter, and oscillation photographs were taken about the b and c axes using the multiple-film technique. These photographs showed that the unit cell was monoclinic and that the cell dimensions were $a=23.66\pm0.04$, $b=8.72\pm0.01$, $c=15.30\pm0.02$Å, $\beta=117.5\pm0.5°$. The systematic absences of *hkl* reflections when $h+l$ is odd, of *h0l* reflections when both h and l are odd, and of $0k0$ reflections when k is odd show that the space group is C_{2h}^5–$B2_1/a$. This space group expression is different from that given by Mundy, but this difference may be due to the difference in the selection of axes between our method and Moundy's. If we adopt the following lattice constants: $a=10.72$, $b=8.72$, $c=15.30$Å, and $\beta=98.0°$, the space group of this crystal becomes $P2_1/c$, but our present investigation is based on the space group $B2_1/a$.

The approximate density measured with a picnometer is 1.5 g. cm^{-3}, so that there are eight molecules in the unit cell (the calculated density 1.66 g. cm^{-3}). The intensities of integrated Weissenberg photographs of *hk*0 and *h0l* layers were estimated visually by comparison with a calibrated scale of time exposures. Corrections for Lorentz and polarization factors were made in the usual way. No absorption corrections were made, since small crystals were used ($\mu=26.1$ cm^{-1} for Cu-K_α).

By the use of Wilson's method, the relative structure amplitudes were converted to the absolute scale by a comparison of the calculated average intensities $\sum f_j^2$ with those observed for five zones of the appropriate reciprocal lattice section; at the same time the values of the temperature factors were calculated to be 4.9Å^2 for (*h0l*) and 3.2Å^2 for (*hk*0).

Determination of Structure

As has been shown by Howells, Phillips and Rogers[9], there are remarkable differences among centric, acentric and hypercentric crystals as regards the distribution of the magnitudes of the structure factors. It is the necessary condition for the application of this method that there should be a sufficiently large number of equal atoms in general positions in the unit cell. In our case, however, there are eight heavy copper atoms in the cell, thus greatly influencing the structure factors, so the statistical method is not strictly applicable. Nevertheless, we applied this method to our crystal and guessed the structure to be a hypercentric one. From this we further inferred that there would be centers of symmetry in the unit cell besides the one in the molecule itself, so that the $Cu(oxine)_2$ molecule will not have a tetrahedral configuration, but a planar one (Fig. 1).

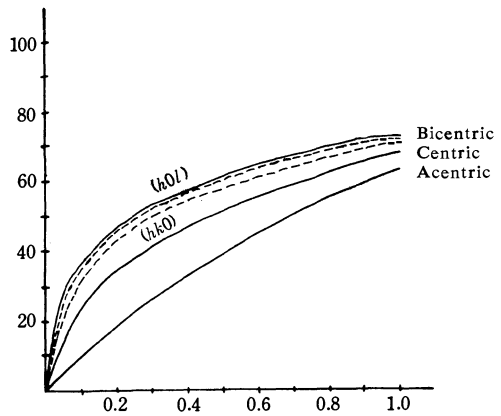

Fig. 1. Comparison of the experimental distribution N(z) for $Cu(oxine)_2$ (marked by dotted lines) with the theoretical distribution curves.

The sharpened Patterson synthesis of (*h0l*) and (*hk*0) projections showed that copper atoms were located at the positions with $x=0.061$, $y=0.118$, and $z=0.010$. In view of the short b axis, this synthesis was considered to proceed first with a projection on (010). On the basis of the above copper parameters, the values of the $F(h0l)$ for the copper atoms only were calculated. From a comparison of

7) Y. Nakatsuka, This Bulletin, **11**, 45 (1936).
8) E. Sekido, *J. Chem. Soc. Japan, Pure Chem. Sec. (Nippon Kagaku Zassi)*, **78**, 1791 (1957).
9) E. R. Howells, D. C. Phillips and Rogers, *Acta Cryst.*, **3**, 210 (1950); D. Rogers and A. J. C. Wilson, ibid., **6**, 439 (1953).

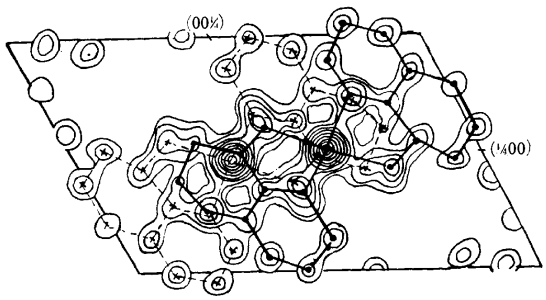

Fig. 2. Electron-density projection along the b axis.

them with the observed structure amplitudes of this compounds, it was possible to deduce the signs of about one-tenth of all the possible reflections $F(h0l)$ within the limiting sphere. In the following calculations, the atomic scattering factors of carbon, nitrogen, and oxygen given by McWeeny and that of copper listed in the Internationale Tabellen were adopted. The expressions for $F(h0l)$ and $F(hk0)$ of the space group $B2_1/a$ are given by:

$$F(h0l) = 8\sum f_j \cos 2\pi(hx_j + lz_j)$$

$$F(hk0) = 8\sum f_j \cos 2\pi hx_j \cdot \cos 2\pi ky_j$$

when k is even,

$$F(hk0) = -8\sum f_j \sin 2\pi hx_j \cdot \sin 2\pi ky_j$$

when k is odd.

Parameters were assigned to all the atoms in the initial projection on (010), using an assumed model of the 8-hydroxyquinoline molecule; these were refined as far as possible by successive Fourier syntheses of electron density. The x parameters finally obtained were incorporated into projections along the c axis. From the information derived from the preceding Patterson projection on (010), and from the fact that the intensity of the (420) reflection is strongest, we could determine the orientation of the 8-hydroxyquinoline molecule in the following way: The calculated copper contribution to the (420) reflection is almost zero, so that the structure factor (420) contributed from 8-hydroxyquinoline molecules must be large. This means that the plane of the oxine molecule must be nearly parallel to (420) or ($\bar{4}$20) through the positions of the copper atoms determined from Patterson projections. In this case, one cannot distinguish between the two-fold axes and the centers of symmetry in the (010) projection, so it was also not possible to decide the two alternatives in the (010) projection. Setting up two kinds of structure models projected on the (00l) plane, in each of which the origin of a unit cell was the two-fold screw axis or the center of symmetry, we found an approximate arrangement of the molecules by spacing the molecules so that they would not be too close together and so that the calculated intensity of the reflection of (420) would be very large in conformity with the obtained one. Then, calculating the three-dimensional structure factors $F(h1l)$, we ascertained that the crystal structure thus obtained gave a satisfactory agreement between the observed and calculated structure factors.

The refinement of the structure was accomplished by using the error synthesis method proposed by Bunn et al.[10] Also we partly adopted Booth's back-shift method as a correction for termination-of-series errors. In order to find the diffraction ripples in a Fourier summation due to copper atoms, which might overlap the positions of light atoms in projection, a Fourier synthesis was carried out using the calculated values of $F(h0l)$ for the copper atoms alone for the reflections included in the original summation; this was then compared with the original Fourier projection. In determining the exact positions of the peaks representing the light atoms, we allowed for these diffraction effects.

The coordinates that gave the best agreement between calculated and observed structure factors were chosen. The results are given in

TABLE I. THE COORDINATES OF THE ATOMS

Atom	x	y	z
Cu	0.0608	0.1200	0.0100
N	0.118	0.007	0.125
C(1)	0.114	−0.022	0.207
C(2)	0.158	−0.127	0.277
C(3)	0.205	−0.193	0.253
C(4)	0.253	−0.230	0.150
C(5)	0.258	−0.197	0.068
C(6)	0.217	−0.105	−0.008
C(7)	0.172	−0.032	0.022
C(8)	0.165	−0.060	0.107
C(9)	0.208	−0.163	0.168
O	0.125	0.063	−0.042
N'	0.004	0.250	−0.092
C'(1)	0.008	0.280	−0.180
C'(2)	−0.031	0.387	−0.245
C'(3)	−0.075	0.460	−0.217
C'(4)	−0.126	0.498	−0.123
C'(5)	−0.130	0.472	−0.028
C'(6)	−0.087	0.362	0.042
C'(7)	−0.043	0.285	0.017
C'(8)	−0.038	0.320	−0.067
C'(9)	−0.078	0.430	−0.130
O'	−0.002	0.180	0.058

10) D. Crowfoot, C. W. Bunn, B. W. Rogers-Low and A. Turner-Jones, "The X-Ray Crystallographic Investigation of the Structure of Penicillin" Princeton Univ. Press, Princeton, N. J. (1949), p. 310.

Table I, where x, y, and z are expressed in fractional coordinates, all referred to the monoclinic axial directions. They are also expressed in orthogonal coordinates x', y', and z' referred to the a, b and c' axes, where c' is an axis perpendicular to the b and a axes. These orthogonal coordinates, not shown here, were used in calculating the interatomic distances and valency angles. They are derived from the monoclinic crystal coordinates by the relations $x'=x+z\cos\beta$, $y'=y$, and $z'=z\sin\beta$.

In electron-density projections on both (*hk*0) and (*h*0*l*), calculations of standard errors by Cruickshank's method were rendered impossible by the overlapping of the maxima which were present in this structure. Therefore, we adopted Luzzati's method as an indication of the accuracy of the given coordinates. The mean errors for *hk*0 and *h*0*l* reflections are 0.07 and 0.06Å respectively. The fact that the values of *R* for *hk*0 reflections do not precisely follow the curve shown by Luzzati may be due to the absorption effect of the crystal. The mean disagreement factors, *R*, were as follows: $R(h0l)=0.18$, $R(hk0)=0.195$

Description and Discussion of the Structure

The interatomic distances and the bond angles calculated on the basis of the above parameter values are shown in Fig. 3. Each copper atom in the lattice is surrounded by two oxygen and two nitrogen atoms in a square configuration. These four atoms are coplanar with the copper atom, and in the direction perpendicular to the plane of this square there are no atoms within a distance of 3.0Å from the copper atom, so that the electronic structure of the copper atom is a typical dsp^2 type.

Each 8-hydroxyquinoline radical is almost flat. Two plane equations for the two crystallographically different radicals coordinated with the same copper atom were determined.

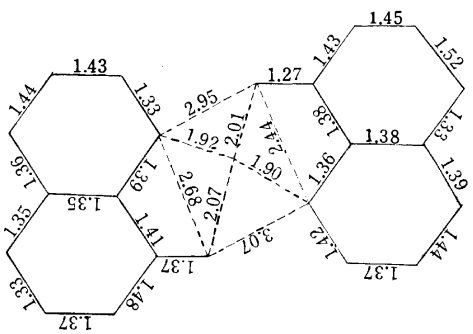

Fig. 3-a. Diagrammatic representation of the Cu(oxine)$_2$, showing bond lengths (in Ångstrom units).

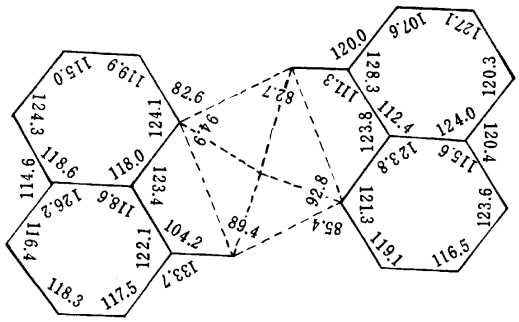

Fig. 3-b. Diagrammatic representation of the Cu(oxine)$_2$, showing bond angles (in degrees).

Within the range of experimental error, they are coplanar with a central copper atom and almost parallel to each other. The mean plane, containing two 8-hydroxyquinoline molecules with a copper atom, was found by the least-squares method to have the following equation:

$$0.268x'+0.465y'+0.256z'=1$$

The orientation of the molecule in the crystal can be expressed by the angles χ, ψ, and ω, which the molecular axes, L, M and their normal, make with the a, b and c axes. Axes L and M are taken to lie in the mean plane of the molecule and to be directed parallel to the C(8)—C(9) line and its normal respectively. The mean values of these angles are listed in Table II. These show also that the inclination of the molecular plane to the (010) plane is about 51.5°. The arrangement of the

Table II. The angles between the molecular axes and the crystal axes

	χ	ψ	ω
L	68.2°	49.3°	49.2°
M	132.7°	58.6°	57.4°

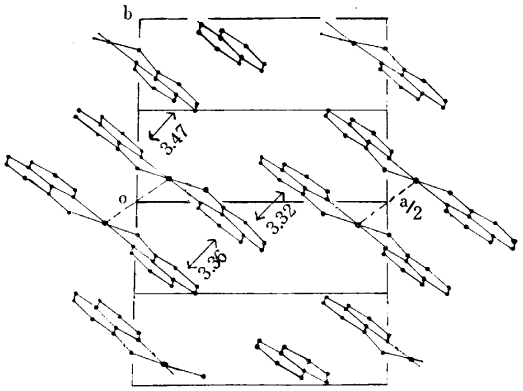

Fig. 4. The c-axis projection of the structure. The adjacent molecules in the direction of the c axis are omitted.

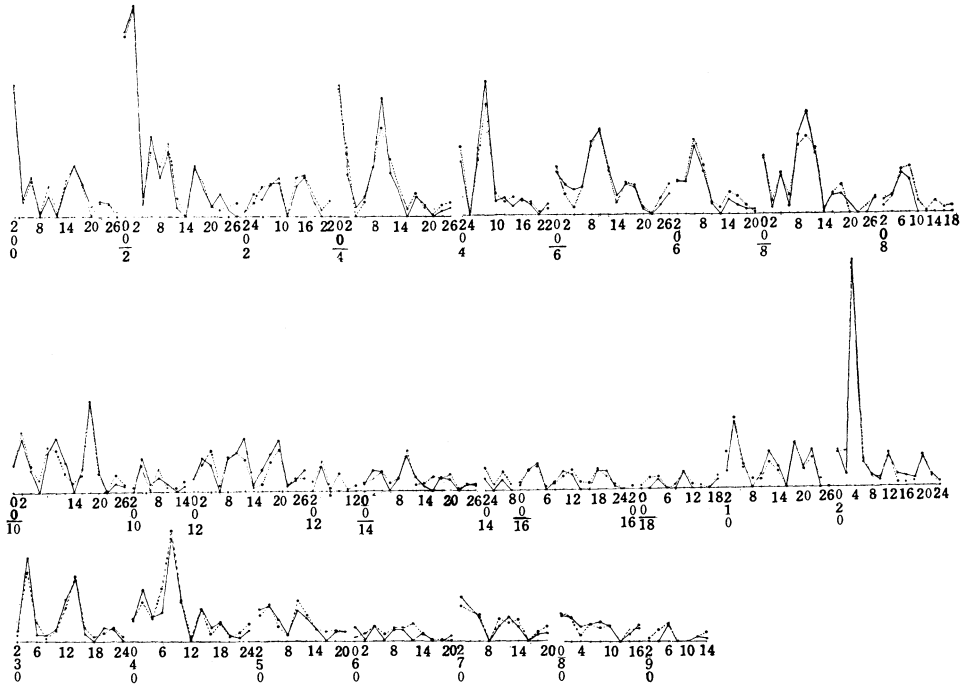

Fig. 5. Comparison of observed (solid lines) and calculated structure factors (dotted lines); $F(h0l)$ and $F(hk0)$.

molecules in the crystal will be clear from the projection in Fig. 4. The perpendicular distances between successive mean molecular planes are 3.36, 3.48 and 3.32Å. These values are to be compared with the interplane spacing in graphite 3.41Å, coronene 3.40Å, or phthalocyanine 3.38Å. The shortest Cu–Cu distance of 3.45Å implies that the Cu–Cu bonds contribute to a union of the two chelate molecules, but not so strongly as in copper acetate dihydrate $Cu_2(CH_3COO)_4 \cdot 2H_2O$[11]. The possibility of the type of metal-metal interaction suggested here has also been shown in nickel dimethylglyoxime[12], in which the metal-metal interaction has been reported to have some relation with the solubility. In the copper 8-hydroxyquinolinate crystal, such dimeric molecules as $Cu_2(oxine)_4$ with the Cu–Cu distance of 3.45Å, are juxtaposed to form layers in the direction of the b and [101] axes like brick walls. The binding forces between these layers may be due to the van der Waals interaction, while within the layers π-bond overlapping will contribute somewhat to the layer formation, as will the metal-metal bond and the van der Waals forces. Such a layer structure, with π-bond overlapping, has been found in quinhydrone[13], phenoquinone[14] and chloranil-hexamethylbenzene complexes[15], while the results of the measurement of the electric conductivity of $Cu(oxine)_2$ powder crystals seems to prove the partial overlap of molecular π-orbitals.

Summary

The crystal structure of anhydrous copper 8-hydroxyquinolinate has been determined by the two-dimensional Fourier method. It is monoclinic and has been shown to belong to the $B2_1/a$ space group, with eight molecules in a cell of the dimensions: $a=23.66$, $b=8.72$, $c=15.30$Å and $\beta=117.5°$. A copper atom is surrounded by four atoms with Cu–N distances of 1.92 and 1.90Å, and Cu–O distances of 2.01 and 2.07Å. Two nitrogen and two oxygen atoms form a square and are coplanar with the copper atom. The closest approach of adjacent chelate molecules occurs along the b axis and in the [101] direction, where the interplanar distances are 3.36, 3.47, and 3.32Å. These chelate molecules are grouped in pairs around the symmetry center at the point of origin with a Cu–Cu bond of 3.45Å. The perpendicular distances between successive dimeric molecules given above are almost the same

11) J. N. van Niekerk and F. R. L. Schoening, *Acta Cryst.*, **6**, 227 (1953).
12) L. E. Godycki and R. E. Rundle, ibid., **6**, 487 (1953).
13) H. Matsuda, K. Osaki and I. Nitta, This Bulletin, **31**, 611 (1958).
14) T. T. Harding and S. C. Wallwork, *Acta Cryst.*, **6**, 791 (1953).
15) T. T. Harding and S. C. Wallwork, ibid., **8**, 787 (1955).

within the range of experimental error. A π-bond overlapping of molecules is considered to be a part of the binding forces between such layers. The metal-metal bond is presumably the same as that in nickel dimethylglyoxime.

The authors wish to express their thanks to Professor Tokunosuke Watanabé for his kind encouragement in the course of this study, to Professor Ryoichi Kiriyama for his continued interest, and to Dr. Kenji Osaki for his helpful discussion.

Department of Chemistry
Faculty of Science
Osaka University
Kita-ku, Osaka

The Normal Vibrations of trans-trans Diacetamide

By Toyozo UNO and Katsunosuke MACHIDA

(Received December 3, 1962)

In a previous report on the infrared spectra and structure of acyclic imides[1], it was concluded that diacetamide takes the trans-cis and the trans-trans configuration in the crystal in A and B forms respectively. With respect to form A, X-ray diffraction study was carried out and the trans-cis configuration was proven to be approximately valid[2]. Such a support from X-ray analysis, however, has not yet been given to form B, for which it is therefore of interest to determine the type of its hydrogen bond in connection with the molecular symmetry in the crystal[3].

The present work has been undertaken to see whether or not the observed infrared frequencies of diacetamide crystals in form B can be reproduced by a reasonable set of force constants based on the assumed trans-trans structure. For this purpose, we have carried out normal vibration calculations for the in-plane vibrations of diacetamide and diacetamide-d in the trans-trans configuration and have obtained satisfactory results, particularly for imide characteristic frequencies.

Calculation

The methyl group was treated as a point mass, and the resulting eight-body problem was treated by Wilson's ***GF*** matrix method[4]. A molecule of diacetamide in the trans-trans configuration has the C_{2v} symmetry. Besides the vibrations arising from the methyl group, there are thirteen inplane vibrations, which are classified into seven A_1 and six B_2 vibrations according to their symmetry[5]. The N–H stretching vibration belonging to the A_1 species was separated from the other A_1 vibrations[4,6], and secular equations of the sixth order were set up for both species A_1 and species B_2. The internal coordinates were defined as shown in Fig. 1, and the symmetry coordinates were constructed as shown in Table I. The bond lengths used in the present calculations are: $r(\mathrm{C{-}N}) = 1.32$ Å, $r(\mathrm{C{=}O}) = 1.21$ Å and $r(\mathrm{CH_3{-}C}) = 1.54$ Å. All the bond angles were assumed to be 120°. These bond lengths and bond angles are the same as those used in the calculations for *N*-methylacetamide by Miyazawa et al.[7]

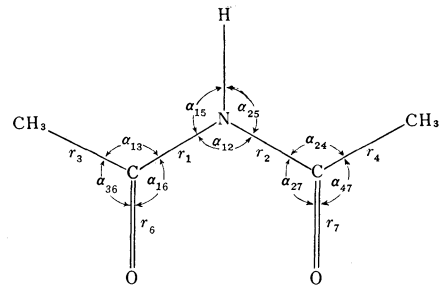

Fig. 1. Internal coordinates of diacetamide.

1) T. Uno and K. Machida, This Bulletin, **34**, 545 (1961).
2) K. Osaki, H. Koizumi and T. Watanabé, Symposium on Molecular Structure, Sapporo, 1960.
3) T. Uno and K. Machida, This Bulletin, **34**, 821 (1961).
4) E. B. Wilson, Jr., *J. Chem. Phys.*, **7**, 1047 (1939); **9**, 76 (1941).
5) The present description of the symmetry species is based on Reports on Notation for the Spectra of Polyatomic Molecules, *J. Chem. Phys.*, **23**, 1997 (1955). The B_2 species in the present work should be compared with the B_1 species of the previous papers[1,3].
6) B. L. Crawford, Jr. and J. T. Edsall, *J. Chem. Phys.*, **7**, 223 (1939).
7) T. Miyazawa, T. Shimanouchi and S. Mizushima, ibid., **29**, 611 (1958).

TABLE I. SYMMETRY COORDINATES

Symmetry species	Symmetry coordinates	Description
A_1	$S_1=(1/2)^{1/2}\Delta(r_1+r_2)$	C-N stretching
	$S_2=(1/2)^{1/2}\Delta(r_3+r_4)$	C-C stretching
	$S_3=(1/2)^{1/2}\Delta(r_6+r_7)$	C=O stretching
	$S_4=(1/6)^{1/2}\Delta(2\alpha_{12}-\alpha_{15}-\alpha_{25})$	C-N-C bending
	$S_5=(1/12)^{1/2}\Delta(2\alpha_{36}-\alpha_{13}-\alpha_{16}+2\alpha_{47}-\alpha_{24}-\alpha_{27})$	CH_3-C=O bending
	$S_6=(1/2)\Delta(\alpha_{13}-\alpha_{16}+\alpha_{24}-\alpha_{27})$	CH_3-C=O rocking
B_2	$S_7=(1/2)^{1/2}\Delta(r_1-r_2)$	C-N stretching
	$S_8=(1/2)^{1/2}\Delta(r_3-r_4)$	C-C stretching
	$S_9=(1/2)^{1/2}\Delta(r_6-r_7)$	C=O stretching
	$S_{10}=(1/2)^{1/2}\Delta(\alpha_{15}-\alpha_{25})$	N-H(N-D) in-plane deformation
	$S_{11}=(1/12)^{1/2}\Delta(2\alpha_{36}-\alpha_{13}-\alpha_{16}-2\alpha_{47}+\alpha_{24}+\alpha_{27})$	CH_3-C=O bending
	$S_{12}=(1/2)\Delta(\alpha_{13}-\alpha_{16}-\alpha_{24}+\alpha_{27})$	CH_3-C=O rocking

Force Constants. — The Urey-Bradley type potential function[8].

$$2V=\sum_i K_i(\Delta r_i)^2+\sum_{i\neq j}\{H_{ij}r_i^0r_j^0(\Delta\alpha_{ij})^2+F_{ij}(\Delta q_{ij})^2\}+\text{linear terms}$$

was assumed. Here, three bond-stretching (K_i), five bond-angle-deformation (H_{ij}), and five non-bonded repulsion (F_{ij}) force constants are necessary. These force constants may be transferred from *N*-methylacetamide[7], which includes all the five pairs of adjacent bonds (H-N-C, C-N-C, C-C-N, O=C-N and C-C=O) included in diacetamide. Diacetamide differs from *N*-methylacetamide, however, in containing a carbonyl carbon atom instead of the methyl carbon atom attached to the nitrogen atom in the latter. This may leave a question about the transferability of the force constants related to the C-N-C linkage. There has been no report, however, on the C-N-C bond angle deformation and the C···C repulsion force constants for the O=C-N-C=O linkage. The calculations were, therefore, started with the initial set of the force constants transferred from *N*-methylacetamide[7,9]. They are listed in the first column of Table II. The refinement of the force constants was made by a comparison of the observed and the calculated frequencies with reference to the Jacobian matrix[10]. Since there are two A_1 and one B_2

TABLE II. FORCE CONSTANTS (md./Å)

	Initial set	Final set
K_{C-N}	5.50	4.00
$K_{C=O}$	8.50	9.80
K_{C-CH_3}	3.40	3.20
H_{H-N-C}	0.35	0.31
H_{C-N-C}	0.20	0.50
H_{N-C-CH_3}	0.30	0.30
$H_{N-C=O}$	0.35	0.20
$H_{CH_3-C=O}$	0.30	0.25
$F_{H\cdots C}$	0.50	0.35
$F_{C\cdots C}$	0.40	1.70
$F_{N\cdots CH_3}$	0.50	0.70
$F_{N\cdots O}$	1.50	1.20
$F_{CH_3\cdots O}$	0.50	0.50

skeletal deformation frequencies which have not yet been observed, it was impossible to adjust the related force constant directly from these frequencies. On the other hand, except for the imide I, II and III frequencies[11], the observed frequencies were found to be not far from the frequencies calculated on the basis of the initial set of the force constants. Considering these facts, adjustment was made particularly with respect to the force constants related mainly to the imide I, II and III frequencies. In the course of this procedure it was found that the difference in the bond orders of C=O and C-N bonds between amides and imides should be taken into account in the refinement of $K_{C=O}$, K_{C-N} and H_{H-N-C}. The conceivable canonical forms in the resonance hybridization of an imide molecule are shown in Fig. 2, from which it may

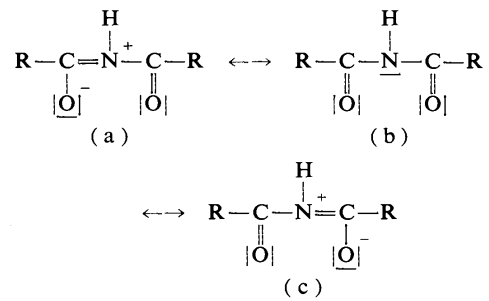

Fig. 2. Resonance structures of imides.

easily be understood that the C=O bond order increases but the C-N bond order decreases with an increase in the contribution of the non-polar form b. The trans-trans configuration may be advantageous for form b since the other two forms should give rise to a strong repulsion between the adjacent oxygen atoms. Thus, it is quite reasonable that

8) T. Shimanouchi, ibid., 17, 245, 734, 848 (1949).
9) The only exception was $F_{C\cdots C}$, which has been chosen to be 0.30 md./Å for *N*-methylacetamide[7].
10) T. Miyazawa, *J. Chem. Soc. Japan, Pure Chem. Sec.* (*Nippon Kagaka Zassi*), 76, 1132 (1955).
11) T. Uno and K. Machida, This Bulletin, 34, 551 (1961).

imides should exceed amides with respect to $K_{C=O}$ and vice versa with respect to K_{C-N} and H_{H-N-C}. In order to compensate for the decrease in the value of K_{C-N}, a marked increase in the value of $F_{C...C}$ was necessary for the frequency fit in the A_1 C-N-C symmetric stretching frequency. As may be seen from Fig. 2, imides have non-localized electrons around the C-N-C linkage. Therefore, a resonance cross term[12] may be implicitly included in the effective value of $F_{C...C}$. In this respect, it is reasonable that the $F_{C...C}$ of diacetamide is comparable to the $F_{O...N}$ rather than to the $F_{C...C}$ of *N*-methylacetamide[7]. The repulsion between the oxygen atoms may also be expected to contribute to the effective value of the $F_{C...C}$ of trans-trans diacetamide. The quantitative treatment of these contributions could not be undertaken without the determination of the lowest three skeletal deformation frequencies. The final set of the force constants obtained in the present calculation is shown in the second column of Table II. They reproduce the observed frequencies with deviations of less than 6%.

Numerical Calculation.—Most of the present calculations were carried out on the KDC-1 digital computer at Kyoto University. A program for the normal vibration calculation was constructed with reference to those of the previous investigators[13,14]. The library subroutines were used for the matrix multiplications and for the solution of the secular equations. These library subroutines were connected to the additional subroutines designed to calculate the $\boldsymbol{F}$ matrix[4], the Jacobian matrix[10], the potential energy distribution[15,16], and the $\boldsymbol{LL'}$ matrix[13]. The $\boldsymbol{F}$ matrix was calculated from the $\boldsymbol{A}_h$ matrices and the force constants, K_h, according to the formula[10]:

$$\boldsymbol{F} = \sum_h \boldsymbol{A}_h K_h$$

The program was designed to be appropriate to such a matrix, including many zero elements as $\boldsymbol{A}_h$. The construction of the $\boldsymbol{F}$ matrix requires the following input for a given matrix $\boldsymbol{A}_h$: (1) the values of the non-zero elements, (2) the indices denoting the locations of the non-zero elements, and (3) the number of the non-zero elements. The same input, together with the $\boldsymbol{L}$ matrix, was used to construct the Jacobian matrix. This method was quite effective in utilizing the memory of the computer and in reducing the computing time. The present calculations, which included four secular equations of the sixth order, the input, and output procedures, could be performed within fifty minutes.

Results and Discussion

In Table III, the final set of the calculated frequencies are listed, together with the potential energy distributions, and are compared with the observed frequencies. The previous assignments[1,11] of the characteristic frequencies are in good agreement with the results of the present calculations.

The calculated values for the imide I frequencies elucidate well the facts that the A_1 frequency (ν_1) is about 40 cm^{-1} higher than the B_2 frequency (ν_7) and that it does not shift on deuteration, while the B_2 frequency undergoes a low-frequency shift by about 15 cm^{-1}. The vibrations responsible for these frequencies are almost all localized at the C=O stretching coordinates (S_3 and S_9). The imide II and III frequencies (ν_8 and ν_9) belonging to the B_2 species are contributed mainly from the C-N stretching and the N-H in-plane deformation vibrations, as was suggested in a previous paper[11]. It may be seen from the present calculations, however, that the energetic contribution of the C-C stretching vibration is also important for the imide III frequency. In contrast with the imide I and II frequencies, the imide III frequency seems to vary with the change of one or both of the frameworks attached to the -CONHCO- group from the methyl to the higher alkyl groups[11]. This fact may reasonably be expected from the present calculations, which show that interaction between the -CONHCO- group and the alkyl framework vibrations is involved in the imide III frequency.

With respect to the imide II' frequency (ν_8'), the contribution of the C-N stretching vibration is three times as energetically important as that of the N-D in-plane deformation vibration. The smallness of the contribution of the C-C stretching vibration seems to be related to the slight dependence of this frequency upon the change of the alkyl group[11]. The imide II, III and II' frequencies of trans-trans diacetamide are quite analogous to, respectively, the amide II, III and II' frequencies of *N*-methylacetamide in the trans configuration[7] in their potential energy distributions. It is of interest that the appreciable difference in the corresponding force constants

12) T. Shimanouchi, International Symposium on Molecular Structure and Spectroscopy, Tokyo (1962); see also S. Califano and B. L. Crawford, Jr., *Spectrochim. Acta*, 16, 889 (1960).
13) T. Shimanouchi and I. Suzuki, *J. Mol. Spectroscopy*, 6, 227 (1961); 8, 222 (1962).
14) J. Overend and J. R. Scherer, *J. Chem. Phys.*, 32, 1289 (1960).
15) Y. Morino and K. Kuchitsu, ibid., 20, 1809 (1953).
16) I. Nakagawa, *J. Chem. Soc. Japan, Pure Chem. Sec.* (*Nippon Kagaku Zassi*), 74, 243 (1953).

TABLE III. FREQUENCIES AND POTENTIAL ENERGY DISTRIBUTIONS

Symmetry species	No.	ν_{calcd}	ν_{obs}	Deviation*1	Assignment*2	P. E. D.*3
			$CH_3CONHCOCH_3$			
A_1	ν_1	1732	1734	0.1	Imide I (sym.)	$S_1(11)$, $S_3(84)$
	ν_2	1289	1295	0.5	ν_{C-N-C} (sym.)	$S_1(61)$, $S_2(39)$
	ν_3	1036	1035	0.1	Skeletal	$S_1(24)$, $S_4(35)$, $S_6(23)$
	ν_4	639	625	2.2	Imide IV	$S_2(51)$, $S_5(18)$, $S_6(8)$
	ν_5	375	—	—		$S_5(69)$
	ν_6	193	—	—		$S_4(52)$, $S_6(55)$
B_2	ν_7	1697	1690	0.4	Imide I (antisym.)	$S_9(85)$, $S_{10}(11)$
	ν_8	1507	1505	0.1	Imide II	$S_7(37)$, $S_{10}(69)$
	ν_9	1203	1236	2.4	Imide III	$S_7(55)$, $S_8(23)$, $S_{10}(20)$
	ν_{10}	896	920	2.3	ν_{C-C}	$S_7(11)$, $S_8(69)$
	ν_{11}	511	523	2.3	Imide IV	$S_{11}(86)$
	ν_{12}	436	—	—		$S_{12}(82)$
			$CH_3CONDCOCH_3$			
A_1	ν_1'	1730	1734	0.2	Imide I (sym.)	$S_1(10)$, $S_3(85)$
	ν_2'	1288	1295	0.6	ν_{C-N-C} (sym.)	$S_1(60)$, $S_2(39)$
	ν_3'	1015	1035	1.8	Skeletal	$S_1(26)$, $S_4(34)$, $S_6(23)$
	ν_4'	637	625	1.9	Imide IV	$S_2(51)$, $S_5(17)$, $S_6(8)$
	ν_5'	375	—	—		$S_5(69)$
	ν_6'	193	—	—		$S_4(52)$, $S_6(55)$
B_2	ν_7'	1681	1675	0.4	Imide I (antisym.)	$S_9(94)$
	ν_8'	1375	1348	2.0	Imide II'	$S_7(78)$, $S_8(10)$, $S_{10}(29)$
	ν_9'	1007	951	5.9	Imide III'	$S_8(42)$, $S_{10}(49)$
	ν_{10}'	861	901	4.4	ν_{C-C}	$S_7(18)$, $S_8(42)$, $S_{10}(19)$
	ν_{11}'	504	523	3.6	Imide IV	$S_{11}(86)$
	ν_{12}'	434	—	—		$S_{12}(84)$

*1 $|\nu_{obs}-\nu_{calcd}|/\nu_{obs}\times 100$
*2 ν : stretching, see also Ref. 11.
*3 $F_{ii}L_{is}^2/\lambda_s\times 100$

between these compounds does not produce any difference in the energetic natures of the corresponding characteristic vibrations. Besides the N–D in-plane deformation vibration, the contribution of the C–C stretching vibration is important for the imide III' frequency (ν_9'), on which it has been revealed that the influence of the alkyl group is also appreciable[11]. The difference between the observed and the calculated values (56 cm^{-1}) for the imide III' frequency may be attributed to the disregard of the interaction with the B_2 CH_3 rocking vibration in the present calculations. This is suggested by the facts that the intensity of the 1035 cm^{-1} band of diacetamide in form B is appreciably reduced on deuteration and that a weak band appears at 1100 cm^{-1} for diacetamide-d in form B[1]. For the undeuterated species, it seems that the absorption due to the B_2 CH_3 rocking vibration is overlapped by the 1035 cm^{-1} band due to the A_1 skeletal vibration. For the deuterated species, however, the B_2 CH_3 rocking vibration seems to couple with the N–D in-plane deformation vibration, thus giving rise to the 1100 cm^{-1} band and pushing the imide III' frequency down from the uncoupled value near the calculated frequency (1007 cm^{-1}) to the observed frequency (951 cm^{-1}). This interpretation may be confirmed by the application of the product rule[4] to the B_2 frequencies. As is shown in Table IV, we have obtained a good agreement between the observed and the theoretical ratios by employing the frequencies ν_i and ν_i' ($i=7$, 8, 9 and 10) which are shown in Table III, together with two additional frequencies: 1035 cm^{-1} for the undeuterated species and 1100 cm^{-1} for the deuterated species.

The present calculations show that the two imide IV frequencies assigned previously to the two C=O in-plane deformation vibrations[1] are essentially different from each other in their vibrational modes. The B_2 frequency (ν_{11}) arises from the almost pure CH_3–C=O bending vibration, while the A_1 frequency (ν_4) has a complicated vibrational mode to which

TABLE IV. PRODUCT RULE RATIOS

Symmetry species	Observed* ratio $\Pi\nu_i/\Pi\nu_i'$	Theoretical ratio $[\|G(H)\|/\|G(D)\|]^{1/2}$
B_2	1.41	1.40

* ν_i : 1690, 1505, 1236, 1035 and 920
ν_i' : 1675, 1348, 1100, 951 and 901

the C–C stretching, CH_3–C=O bending, and CH_3–C=O rocking vibrations contribute. Such a mixing of vibrational modes is also seen for the A_1 skeletal frequency (ν_3). Further discussion of the vibrational modes of ν_3 and ν_4, however, will not be undertaken here since these mixed vibrational modes are probably affected by those force constants related mainly to the unobserved frequencies below 450 cm^{-1}.

Summary

A normal coordinate analysis of the in-plane vibrations of diacetamide and of diacetamide-d taking the trans-trans configuration has been undertaken. The calculated frequencies agree well with the observed frequencies for the crystals in form B. The Urey-Bradley force field has been adopted, and the force constants obtained have been interpreted in terms of the difference in resonance structures between amides and imides. It has been shown that the vibrational modes of the characteristic imide frequencies are closely related to the behavior of the corresponding characteristic bands upon the change in the alkyl frameworks attached to the imide group.

The authors wish to express their thanks to Dr. Kiyoshi Nakamura of the Research Laboratory, Dainippon Pharmaceutical Co., Ltd., and to Dr. Tatsuo Miyazawa of the Institute of Protein Research, Osaka University, for their helpful advice throughout this work.

Faculty of Pharmacy
Kyoto University
Sakyo-ku, Kyoto

*Kinetics of Hydrolytic Reaction Catalyzed by Crystalline Bacterial α-Amylase. II. The Influence of Solvent**

By Sôzaburo ONO, Keitaro HIROMI and Yoshiki SANO**

(Received September 17, 1962)

The electrostatic nature of a chemical reaction in solution can be inferred from the dependence of the reaction rate on the dielectric constant and on the ionic strength of the medium[1-3]. As for enzyme reactions, however, the study of the ionic strength effect is not so useful, because various ions often exert specific effects on enzyme reactions; moreover, the theoretical treatment of this effect is extremely difficult with such large complex ions as protein[4,5]. Thus the study of the dielectric constant effect becomes important in elucidating the electrostatic nature of enzyme reactions, for it would provide information concerning the reaction mechanisms.

There are, however, two difficulties in the study of the dielectric constant effect on enzyme reactions. The first, which is a theoretical one, is that the conventional theories that have been developed for simple ions or molecules[1-3] may no longer be applicable to enzyme reactions because of the complex charge structure of the molecule; the second is that the organic additives used to control the dielectric constant of the medium may possibly influence, directly or indirectly, the reaction rates from various causes other than the electrostatic one.

The effects of solvent on the rates of various enzyme reactions have been studied by several

* Presented at the 8 th Annual Meeting of the Chemical Society of Japan, Tokyo, April, 1955.

** Present Address: Department of Chemical Engineering, College of Engineering, University of Osaka Prefecture, Sakai, Japan.

1) E. A. Moelwyn-Hughes, "The Kinetics of Reactions in Solution", Oxford University Press, London (1947).

2) E. S. Amis, "Kinetics of Chemical Change in Solution", Macmillan Co., New York (1949).

3) S. Glasstone, K. J. Laidler and H. Eyring, "The Theory of Rate Processes", McGraw-Hill, New York (1954).

4) J. G. Kirkwood, *J. Chem. Phys.*, **2**, 351 (1934); J. G. Kirkwood and F. H. Westheimer, ibid., **6**, 506 (1938).

5) C. Tanford and J. G. Kirkwood, *J. Am. Chem. Soc.*, **79**, 5333 (1957).

authors[6-16], some of whom have interpreted[6-10] the results in terms of simple electrostatic theories developed for simple ions or dipolar molecules. Recently one of us developed a theory of the influence of the dielectric constant of solvent on equilibria and reaction rates[17,18], using the Kirkwood model of a spherical solute molecule having an arbitrary charge distribution[4], which is most probably an appropriate model for a protein molecule in solution[5]. The theory is essentially applicable to the dielectric constant effect on reactions in solution, including enzyme reactions, in which any rearrangement of charges occurs within the spherical solute molecules involved. The applicability of the theory was tested for certain enzyme reactions[18], as well as for some simple organic reactions[17], and the results were considered satisfactory. Hosoya has also applied the theory to the interpretation of his data on the peroxidase reaction[15].

As for the second difficulty, we have tried in this paper to find some general kinetic procedures by which we can distinguish the true dielectric constant effect from the other non-electrostatic effects caused by the organic additives.

In Part I of this paper[19], the influence of pH upon the α-amylase-catalyzed hydrolysis of amylose was investigated, and the properties of the ionizable groups essential for the reaction were elucidated. In this paper, the influence of solvent upon the reaction rates will be studied kinetically, and the results will be interpreted on the basis of the theory developed by one of us[17,18]. The possible effects of the addition of the organic solvent will also be examined.

Experimental

Enzyme.—Six times-recrystallized bacterial amyloclastic α-amylase of *Bac. amyloliquefaciens* Fukumoto was kindly provided by Prof. J. Fukumoto and Dr. T. Yamamoto of Osaka City University. An aqueous solution of the crystalline enzyme was used as a stock solution. The enzyme activity of the stock solution was checked before each experiment.

Substrate.—Since amylose is precipitated from an aqueous solution by the addition of even a small volume of such an organic solvent as methanol, it can not be used as the substrate for the present purpose. Therefore, potato soluble starch, washed with cold water and with methanol and dried, was used as the substrate.

Solvent.—Water or a methanol-water mixture was used as the solvent. The methanol was purified with alkaline silver nitrate and twice redistilled.

Reaction Mixture.—The composition of the reaction mixture was as follows: Aqueous solution of soluble starch, 20 ml.; methanol, x ml,; water, $(8-x)$ ml.; diluted-enzyme stock solution, 2 ml. The final concentration of the substrate varied from 0.075% to 0.5%. The methanol concentration ranged from zero to 22.3 per cent by weight. In order to minimize the ionic strength of the medium[17,18] no buffer solution was used. The pH value of the reaction mixture, however, was maintained at 6.0 $\pm$ 0.1, sufficiently close to the optimum pH value of 5.85[19]. The reaction was carried out at 25.0°C throughout the experiments.

Procedure.—Two milliliters of the reaction mixture was pipetted into 1 ml. of 0.5 N sodium hydroxide to stop the reaction every minute during the first five minutes; 1 ml. of a 3, 5-dinitrosalicylate reagent[20] was then added, and the mixture was heated at 65°C for one hour and diluted to 20 ml., and the red color which developed was measured photometrically, using maltose as the standard. Methanol slightly increases the color density, and this effect was calibrated.

Relative Rate-pH Curves. — In the investigation of the effect of methanol on the relative rate-pH curve, a Britton-Robinson buffer was used in its 1/30 concentration to adjust the pH values.

Even at the maximum methanol concentration used, no irreversible inactivation of the enzyme was detected during the reaction period at 25°C and pH 6.0.

Results

The Michaelis constant, K_m, and the first order rate constant for the breakdown of the ES complex, k_3, obtained from the Lineweaver-Burk plot[21] for nine different substrate concentrations at various methanol contents, are listed in Table I. Since the substrate soluble starch contains α-1, 6 linkages, which are not hydrolyzed by this enzyme, the intrinsic substrate concentration cannot be

6) Y. Ogura, A. Hattori, Y. Tonomura and S. Hino, *Symposia on Enzyme Chem.* (*Kôso Kagaku Shinpojiumu*), **5**, 28 (1950).
7) Y. Ogura and H. Hasegawa, ibid., **7**, 79 (1952).
8) Y. Tonomura, *J. Japan. Biochem. Soc.* (*Seikagaku*), **25**, 175 (1953).
9) M. L. Barnard and K. J. Laidler, *J. Am. Chem. Soc.*, **74**, 6099 (1952).
10) K. J. Laidler and M. C. Ethier, *Arch. Biochem. Biophys.*, **44**, 338 (1953).
11) R. Lumry and E. L. Smith, *Discussions Faraday Soc.*, **20**, 105 (1955).
12) A. Stockell and E. L. Smith, *J. Biol. Chem.*, **227**, 1 (1957).
13) M. Castañeda-Agulló and L. M. Del Castillo, *J. Gen. Physiol.*, **42**, 617 (1959).
14) M. Castañeda-Agulló and L. M. Del Castillo, ibid., **43**, 127 (1959).
15) T. Hosoya, *J. Biochem.* (*Tokyo*), **48**, 803 (1960).
16) T. Inagami and J. M. Sturtevant, *Biochim. Biophys. Acta*, **38**, 64 (1960).
17) K. Hiromi, This Bulletin, **33**, 1251 (1960).
18) K. Hiromi, ibid., **33**, 1264 (1960).
19) S. Ono, K. Hiromi and Y. Yoshikawa, ibid., **31**, 957 (1958).
20) G. N. Smith and C. Stocker, *Arch. Biochem.*, **21**, 95 (1949).
21) H. Lineweaver and D. Burk, *J. Am. Chem. Soc.*, **56**, 658 (1934).

TABLE I. THE VALUES OF K_m AND k_3 AT VARIOUS METHANOL CONCENTRATIONS AT 25°C AND pH 6.0

Methanol concn. % by wt.	Water concn. M	D[a]	K_m %	k_3 sec^{-1}
0	55.5	78.5	0.043	1750
5.34	51.9	76.3	0.043	1480
10.84	48.3	74.0	0.042	1210
16.50	44.8	71.6	0.040	970
22.33	41.3	69.1	0.042	750

a) Dielectric constant of the solvent. Interpolated from the values of Davis and Jones[22].

defined accurately. The Michaelis constants, therefore, is conveniently expressed in per cent units.

It is clearly indicated that K_m is constant over the range studied, while k_3 decreases with an increase in the methanol concentration, or with a decrease in the dielectric constant of the medium.

The relationship between pH and the relative rate, v/v_{max}, the ratio of the initial rate at a given pH value to that at the optimum pH value, is influenced by the addition of methanol, as is shown in Fig. 1. The curve is shifted towards the alkaline side by the addition of methanol (22.3 per cent by weight), which is probably due in part to the fact that the pK values of the essential ionizable groups of the enzyme have been influenced by the addition of methanol. It may be seen from Fig. 1 that the velocity is remarkably influenced by the addition of methanol at pH's remote from the optimum pH while the rate at the optimum pH is changed only insignificantly. In order to study the dielectric constant effect on the reaction rates, therefore, the reaction should be observed in the vicinity of the optimum pH. In the present case, in which the reactions were carried out at pH 6.0, the discrepancy between the curves is so small that the observed decreases in k_3 cannot be attributed to the shift of the pH optimum.

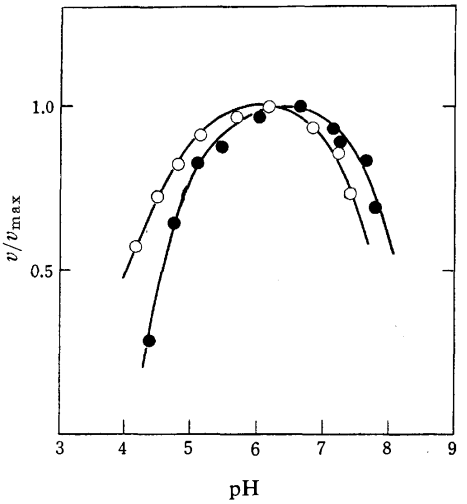

Fig. 1. Plots of v/v_{max} vs. pH.
○: without methanol
●: in 22.3 wt. % methanol
Substrate concn. 0.2%

Analysis of the Results

In the interpretation of the effect of a solvent upon the rate of enzyme reaction special caution is required, since the addition of an organic solvent may give rise to changes in reaction rates for various reasons. Six factors which may influence the rate on the addition of organic solvents and which are considered to be important in the present case are as follows: 1) a change in the dielectric constant of the solvent, which may directly influence the rate; 2) a decrease in the water concentration; 3) an inhibitory action of the organic additive; 4) an irreversible or reversible denaturation of the enzyme; 5) an aggregation of the substrate, and 6) a shift in the relative rate-pH curve. The first factor is the electrostatic one at which the present study is aimed. However, there may possibly exist influences from the other factors. In fact, for the enolase reaction[23] it was observed that the rate is the same function of the water concentration, irrespective of the nature of the organic additives used. In the myosine- and α-chymotrypsin-catalyzed reactions, it has been reported that methanol acts as a "water analogue" to yield methanolysis products, and the existence of the specific water site in these enzymes has been suggested [24,25]. The hydroxylaminolysis of methyl hyppurate catalyzed by α-chymotrypsin has also been observed[26]. On the other hand, by using a variety of organic substances as solvent additives, Castañeda-Agulló and Del Castillo [13,14] have shown that in α-chymotrypsin- and trypsin-catalyzed hydrolyses there is an obvious relationship between the rates and the dielectric constant. Thus, how to distinguish these possible factors is a general and important problem in the interpretation of solvent effects on enzyme reactions. The kinetic procedure for it will be worked out below.

22) R. Davis and T. Jones, *Phil. Mag.*, 28, 307 (1939).

23) E. W. Westhead and B. G. Malmstrom, *J. Biol. Chem.*, 228, 655 (1957).
24) D. E. Koshland, Jr. and E. B. Herr, Jr., ibid., 228, 1021 (1957).
25) M. L. Bender and W. A. Glasson, *J. Am. Chem. Soc.*, 82, 3336 (1960).

Kinetic Treatment Considering the Participation of the Water Molecule.—With respect to the role of water in enzyme-catalyzed hydrolytic reactions, two cases may be considered, based on the usual Michaelis-Menten-Briggs-Haldane mechanism, which includes a single intermediate enzyme-substrate complex[27].

Case 1. Water reacts with the ES complex directly from the bulk of the solvent.

The reaction scheme should be written as follows:

$$E+S \underset{k_2}{\overset{k_1}{\rightleftharpoons}} ES \tag{1}$$

$$ES+H_2O \xrightarrow{k_3'} E+P \tag{2}$$

instead of the ordinary scheme:

$$E+S \underset{k_2}{\overset{k_1}{\rightleftharpoons}} ES \xrightarrow{k_3} E+P \tag{3}$$

Obviously the apparent rate constant, k_3, is proportional to the water concentration $[H_2O]$:

$$k_3=k_3'\,[H_2O] \tag{4}$$

The k_3 values obtained are tentatively plotted against the water concentration in Fig. 2. It is apparent that the observed change in k_3 is too large to be accounted for by Eq. 4.

Case 2. The case in which there is competition between the water molecule and the organic solvent molecule for the water site on the enzyme.

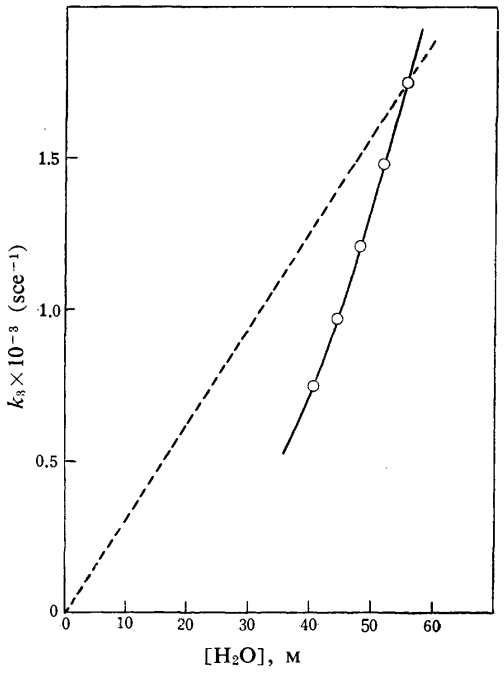

Fig. 2. Plot of k_3 vs. molar concentration of water. The dotted line represents the proportionality between them.

Since evidence has been obtained for the existence of a specific water site in some hydrolytic enzymes[24,26], it is possible that there is a specific water site on this enzyme for which the water molecule competes with the organic solvent molecule. The reaction scheme may then be written as follows:

$$\begin{array}{ccccc} & & \overset{K_M}{\rightleftharpoons} & \overset{K_W}{\rightleftharpoons} & \\ EM & & E & & EW \\ {\scriptstyle K_S''}\downarrow\uparrow & & {\scriptstyle K_S}\downarrow\uparrow & {\scriptstyle K_S'}\downarrow\uparrow & \\ & & \underset{K_M'}{\rightleftharpoons} & \underset{K_W'}{\rightleftharpoons} & \\ EMS & & ES & & EWS \end{array} \xrightarrow{k_o} E+P \tag{5}$$

where W and M represent water molecule and organic solvent molecule, respectively, and where only the ternary complex EWS is assumed to break down into the hydrolytic product P with the rate constant k_o. The K_S' are the association constants for the binding of S, W and M to E, as is indicated in the scheme; five of these are independent. A quasi-equilibrium treatment leads to the equation:

$$v=\frac{k_oK_S'K_wswe}{(1+K_ww+K_Mm)+(K_S+K_S'K_ww+K_S''K_Mm)s} \tag{6}$$

where w, m, s and e are the molar concentration of water, the organic solvent, the substrate and the total enzyme, respectively. The K_m and k_3 obtained from the Lineweaver-Burk plot are now represented by:

$$K_m=\frac{1+K_ww+K_Mm}{K_S+K_S'K_ww+K_S''K_Mm} \tag{7}$$

$$k_3=\frac{k_oK_S'K_ww}{K_S+K_S'K_ww+K_S''K_Mm} \tag{8}$$

If the substrate binding is not affected by the binding of water and that of the organic solvent molecule (it may be true with water and an organic solvent molecule of a small size, such as methanol), i.e., if $K_S=K_S'=K_S''$, K_m reduces to $1/K_S$, which is independent of the solvent composition. The density of a mixed aqueous solvent relative to pure water, ρ, is approximately expressed by $\rho=1+bm$, where b is a constant characteristic of the organic solvent for not so large an organic solvent content (e.g., up to ca. 30% by volume for methanol and ethanol). Using this relation we have:

$$w+pm=55.5 \tag{9}$$

26) S. A. Bernhard, W. C. Coles and J. F. Nowell, ibid., 82, 3043 (1960).

27) Similar treatments have been worked out by Inagami and Sturtevant[15] in the case of two intermediate complexes; according to them, the ratio of the apparent k_3 value to the apparent K_m value should be independent of the water concentration, although each of them is dependent on it. These features are obviously inconsistent with our results.

p is a constant expressed by $p=(M_M-1000b)/M_W$, where M_M and M_W are the molecular weights of the organic solvent and water respectively. (For a methanol-water mixture, $b=-0.0059$ and $p=2.10$.)

From Eqs. 8 and 9 we derive the following equation:

$$\frac{1}{k_3}=\left(\frac{K_S+55.5K_S''K_M/p}{k_OK_S'K_W}\right)\frac{1}{w}+\left(\frac{K_S'K_W-K_S''K_M/p}{k_OK_S'K_W}\right) \quad (10)$$

which predicts a linear relationship between $1/k_3$ and $1/w$. As may clearly be seen from Fig. 3, however, the linearity does not hold for the present case. Thus, this mechanism is not consistent with the observed results.

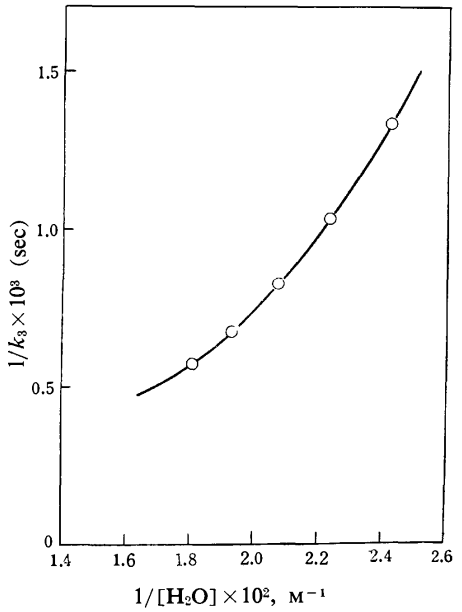

Fig. 3. Plot of $1/k_3$ vs. $1/[H_2O]$.

The Inhibitory Action of the Organic Additive.—Apart from the inhibitory action of the organic additive as a water analogue discussed above, there is a possibility that the organic additive may act as a simple inhibitor, either competitive, or non-competitive. At least qualitatively, the results obtained in this study are not inconsistent with a possible interpretation that methanol acts as a non-competitive inhibitor. If this is the case, k_3 may be written as:

$$k_3=\left(\frac{K_I}{K_I+m^n}\right)\cdot k_3^\circ \quad (11)$$

where m and K_I denote the methanol concentration and the dissociation constant of the inactive complex EM_n (or ESM_n) according to the scheme:

$$E\ (\text{or } ES)+nM \overset{K_I}{\rightleftharpoons} EM_n\ (\text{or } ESM_n) \quad (12)$$

where n is the number of methanol molecules combined with the enzyme molecule to form the inactive enzyme-methanol complex, and k_3° is k_3 at $m=0$. If we define α as the ratio k_3/k_3°, we have:

$$\frac{1-\alpha}{\alpha}=\frac{m^n}{K_I} \quad (13)$$

Thus, a plot of $\log\left(\frac{1-\alpha}{\alpha}\right)$ versus $\log m$ should give a straight line of slope n. This plot is shown in Fig. 4, which does not give a straight line of an integral number of slope, but does give a concave curve with an average slope of ca. 1.4. Thus, the results are not consistent with a typical non-competitive inhibitory mechanism involving the stoichiometric binding of the organic solvent molecule to the enzyme molecule.

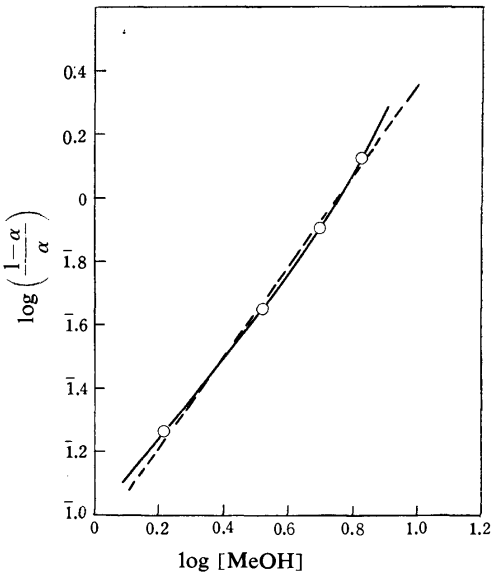

Fig. 4. Plot of $\log\left(\frac{1-\alpha}{\alpha}\right)$ vs. log [MeOH].
The dotted line represents a straight line whose slope is equal to 1.42.

Denaturation of the Enzyme.—Although an irreversible denaturation of the enzyme caused by the addition of the organic solvent could easily be found out experimentally, a rapid, reversible denaturation would be difficult to detect. If the enzyme undergoes a reversible denaturation in the presence of the organic solvent, the scheme may be written as follows:

$$\left.\begin{aligned} &E+S \underset{k_2}{\overset{k_1}{\rightleftharpoons}} ES \overset{k_3}{\rightarrow} E+P \\ &E \overset{K}{\rightleftharpoons} E' \\ &E'+S \overset{K_m'}{\rightleftharpoons} E'S \end{aligned}\right\} \quad (14)$$

where E' denotes the reversibly denatured form of the enzyme, which may (or may not) combine with the substrate to form an inactive complex E'S, where K_m' is the dissociation constant of this complex, and where K represents the equilibrium constant for the denaturation of the enzyme, which, in general, may increase with an increase in the concentration of the organic solvent. Then the initial rate v becomes

$$v=\frac{k_3es}{K_m(K+1)+(K_mK/K_m'+1)s} \quad (15)$$

where $K_m=(k_2+k_3)/k_1$. The apparent Michaelis constant, K_{ma}, and the apparent breakdown rate constant, k_{3a} which are obtained from the Lineweaver-Burk plot, are expressed as follows:

$$K_{ma}=\frac{K_mK_m'(K+1)}{K_mK+K_m'} \quad (16)$$

$$k_{3a}=\frac{k_3K_m'}{K_mK+K_m'} \quad (17)$$

K_{ma} will be independent of the solvent composition if $K_m=K_m'$. Assuming that k_{3a} and K_{ma} in water (or in the absence of the organic additive) are equal to k_3 and K_m, respectively, at a given concentration of organic solvent can be calculated from k_{3a}/K_{ma} (or directly from k_{3a} if $K_m=K_m'$). The K' values were tentatively calculated from the data on the assumption of this mechanism. There is, however, no linear relationship between K and the methanol concentration nor between $\log K$ and $1/D$, as may be seen from Figs. 5 and 6. Thus, the experimental results are inconsistent with this assumption.

Aggregation of the Substrate.—If the addition of the organic solvent gives rise to aggregation of the substrate, the effective concentration of the substrate will be reduced from s to γs, where γ is a positive number less than unity. The initial rate, v, becomes

$$v=\frac{k_3es}{K_m/\gamma+s} \quad (18)$$

Thus, in the presence of the organic solvent, the apparent Michaelis constant will be increased by a factor of $1/\gamma$, while k_3 will remain constant. Obviously this is not consistent with our results.

As was mentioned earlier, it was experimentally confirmed that neither the irreversible inactivation of the enzyme (one of factor 4) nor the shift of pH curve (factor 6) can be the cause of the present results.

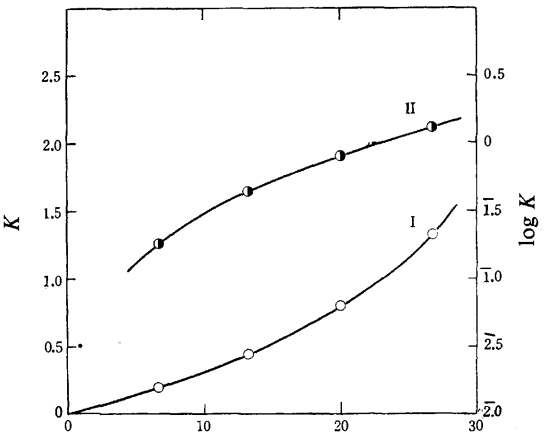

Fig. 5. Plots of K (Curve I) and $\log K$ (Curve II) vs. methanol concentration.

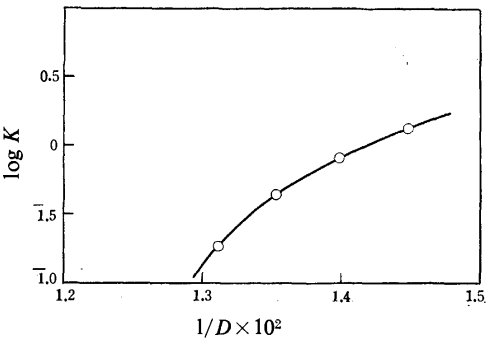

Fig. 6. Plot of $\log K$ vs. $1/D$.

Analysis of the Results by the Electrostatic Theory.—The above arguments have shown that no reasonable interpretation of the results can be obtained on the basis of factors 2 to 6 mentioned above. We will next, examine the possibility of the factor 1, i. e., the electrostatic influence of the dielectric constant of the medium. According to the theory of the dielectric constant effect on enzyme reactions which has been developed by one of the present authors [17,18], the variation of the rate parameters, K_m and k_3, with the dielectric constant, D, of the solvent can be expressed in the following equations:

$$-\frac{d\log K_m}{d(1/D)}=\frac{\varepsilon^2}{2.303(2kT)}\left[\frac{L_S}{b_S}+\frac{1}{b_E}(L_E-L_{ES})\right] \quad (19)$$

$$=\frac{\varepsilon^2}{2.303(2kT)}\left[\frac{L_S}{b_S}+\frac{1}{b_E}(L^o_E-L^o_{ES})\right] \quad (20)$$

$$\frac{d \log k_3}{d(1/D)} = \frac{\varepsilon^2}{2.303(2kT)} \cdot \frac{1}{b_{ES}}(L_{ES} - L_{ES^{\neq}}) \quad (21)$$

$$= \frac{\varepsilon^2}{2.303(2kT)} \cdot \frac{1}{b_{ES}}(L^{o}_{ES} - L^{o}_{ES^{\neq}}) \quad (22)$$

where ε is the protonic charge, k the Boltzmann constant, T, the absolute temperature, b's are the radii of the species denoted by the suffixes, and L's are their "charge configuration functions" as defined elsewhere[17]. L is a dimensionless quantity which is determined by the radius and the charge state of the molecule; it is calculated by the aid of Tables I and II of Ref. 17, provided the charge configuration within the molecule is given. Although the spatial distribution of every charge in E, ES or $ES^{\neq}$ is not yet known, and the exact evaluation of the L values of these species is impossible, it can be shown that under certain conditions we may use the "effective charge configuration function"[18] denoted by L^o instead of the complete charge configuration function, L. L^o is the charge configuration function constructed with respect only to the small number of charges within the local region of the enzyme or the enzyme-substrate complex in which the catalytic reaction is considered to occur, neglecting all the other charges, which are considered to be unimportant for the reaction and to be fixed during the course of the reaction. The radii of E, ES and $ES^{\neq}$ may be equated for small substrates. Thus, Eqs. 20 and 22 are the approximate equations to be used in treating enzyme reactions. These equations predict that the plot of $\log K_m$ or $\log k_3$ against $1/D$ will give a straight line, the slope of which will be determined by the radii and the effective charge configuration functions of the species involved. In Fig. 7 are shown the plots of $\log K_m$ and $\log k_3$ versus $1/D$. The linearity of the plots is in accordance with the theory.

Since L is usually small for a neutral molecule unless it is largely polarized, the contribution of the L_S/b_S term in Eq. 20 to the slope may be no more than the experimental error of the slope. (For example, this contribution has been found to be negligibly small for several uncharged organic acids[17]). Thus, the fact that the slope $d \log K_m/d(1/D)$ is zero implies that L^o_{ES} is equal to L^o_E (or $L_{ES}=L_E$); i. e., there is no appreciable change in charge state during the formation of the ES complex because a change in the charge state would be reflected in a change in L^o. The force operating in the ES complex formation, therefore, is supposed to be non-electrostatic in origin, i. e., van der Waals force or hydrogen bonding, or both.

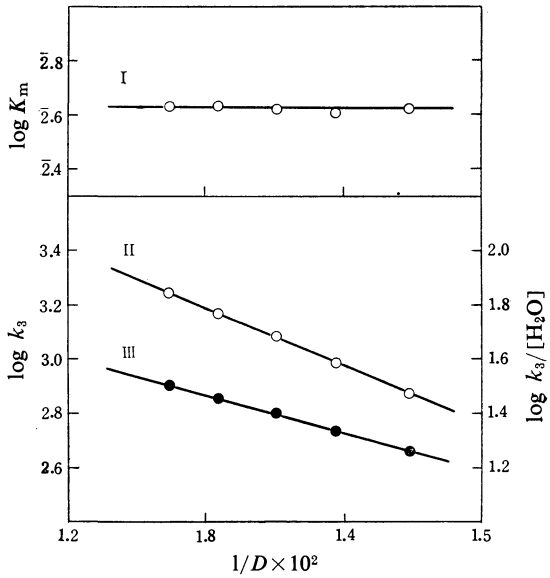

Fig. 7. Plots of log K_m (Curve I), log k_3 (Curve II) and log $k_3/[H_2O]$ (Curve III) vs. $1/D$.

On the other hand, the plot of log k_3 versus $1/D$ gives a straight line of negative slope, indicating that the effective charge configuration function of the activated state of the ES complex ($L^o_{ES^{\neq}}$) is larger than that of the normal ES complex (L^o_{ES}). If we calculate L^o_{ES} and $L^o_{ES^{\neq}}$, assuming certain charge configurations of ES and $ES^{\neq}$, and compare the slope $d \log k_3/d(1/D)$ thus calculated with that observed experimentally, we can pick up some of the charge configurations as plausible; this may give information about the reaction mechanism.

The theoretical estimation of the slope, $d \log k_3/d(1/D)$, will be made on the basis of the following assumptions, all of which are considered plausible: 1) In the activated state of ES, designated by $ES^{\neq}$, the C_1 atom and the glucosidic oxygen atom of the substrate molecule are located near the surface of the sphere of $ES^{\neq}$, with their centers situated d Å below the surface (d was taken to be 0.3 Å to 1.0 Å). The bond length between these atoms is assumed to be ca. 50% stretched over the normal value. (For convenience of calculation, the angle between the lines adjoining the center of the sphere to the C_1 atom and the oxygen atom was kept constant at 5°26'40''. This angle corresponds to the bond length of 2.15 Å when d is 0.5 Å. The bond length ranges form 2.10 Å to 2.17 Å depending on the value of d[28].) As a consequence of the

28) This minor change in the bond length scarely affects the value of the slope.

charge separation in ES‡, two charges of equal magnitude but of opposite signs are produced on the C_1 atom and the glucosidic oxygen atom between which the linkage is to be split. In the ground state of ES, however, no such charge separation is assumed to occur. 2) The essential dissociable groups of the enzyme, the carboxylate and the imidazolium (or ammonium) group, which are considered essential in the breakdown process of ES[19], are assumed to be located below the glucosidic bond and to attack the bond simultaneously as a base and as an acid, respectively[19]. The water molecule is considered to be situated between the carboxylate group and the C_1 atom. The positions of these essential groups are assumed to be kept fixed in ES and ES‡. The geometrical disposition of the atoms assumed in the calculation is shown in Fig. 8. The C_1

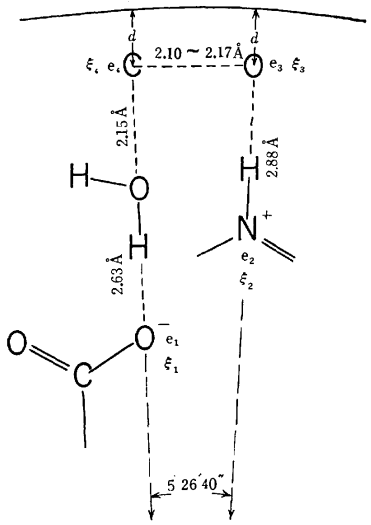

Fig. 8. Model of ES‡.
e_1 and e_2 represent the charges of the essential ionizable groups of the enzyme, and e_3 and e_4 represent the charges produced in the glucosidic linkage in the activated state.

atom, the O–H bond of the water molecule and the carboxylate oxygen atom are assumed to lie on one radius, and the glucosidic oxygen and the N–H bond of the imidazolium group on another radius. The hydrogen-bonded distances of O–H···O and N–H···O are taken as 2.63 Å and 2.88 Å respectively[29]. The charges to be considered (or to be involved in the effective charge configuration functions) are those on carboxylate oxygen, imidazolium nitrogen, glucosidic oxygen, and the C_1 atom; they are designated by $e_1, e_2, \ldots, e_4$, respectively, as is shown in Fig. 8. ξ's are the valences of the charges. In ES, it was assumed that $\xi_1=-1$ and $\xi_2=+1$ and $\xi_3=\xi_4=0$. In ES‡, calculations were carried out for several cases, i.e., $\xi_3=-\xi_4=\pm 1$ and $\pm 1/2$; $-\xi_1=+\xi_2=1$, 1/2 or 0, and $d=0.3$, 0.5, 0.7 and 1.0 Å.

The expressions for L°_{ES} and $L^{\circ}_{ES^{\ddagger}}$ are as follows[18,19]:

$$L^{\circ}_{ES}=\xi_1^2 f_{11}+\xi_2^2 f_{22}+2\xi_1\xi_2 g_{12} \tag{23}$$

$$L^{\circ}_{ES^{\ddagger}}=\sum_{k=1}^{4}\xi_k^2 f_{kk}+\sum_{k=1,l\neq k}^{4}\sum\xi_k\xi_l g_{kl}=\xi_1^2 f_{11}+\xi_2^2 f_{22}+\xi_3^2 f_{33}+\xi_4^3 f_{44}+2\xi_1\xi_2 g_{12}+2\xi_1\xi_3 g_{13}+2\xi_1\xi_4 g_{14}+2\xi_2\xi_3 g_{23}+2\xi_2\xi_4 g_{24}+2\xi_3\xi_4 g_{34} \tag{24}$$

f_{kk} is a function of $(r_k/b)^2$, where r_k is the distance of the charge, e_k, from the center of the molecule. g_{kl} is a function of $(r_k r_l/b^2)$ and $\cos\theta_{kl}$, where θ_{kl} is the angle between r_k and r_l. The values of f_{kk} and g_{kl} may be readily obtained from the tables[17] if r_k's and θ_{kl}'s are calculated from Fig. 8.

The results of the calculation are summarized in Table II, in which the slopes theoretically predicted for various cases are presented. The theoretical slopes are negative in all the cases considered, the magnitude depending primarily upon the valences of the charges produced on the glucosidic linkage (ξ_3 and ξ_4) and on the depth of the charges, d, and being relatively insensitive to the situation of the neighboring charges, e_1 and e_2. The experimentally observed magnitude of the slope, -210, may reasonably be accounted for if $d=0.6$ Å and $-\xi_3=+\xi_4=\pm 1$, i.e., if a considerably large separation of charges occurs in the glucosidic linkage in the activated state, ES‡. The value of d is not of an unreasonable order of magnitude, although it appears to be somewhat smaller than that of the carboxylic oxygen atom (ca. 1.0 Å)[17], calculated from the dependence of the pK values of carboxylic acids on the dielectric constant of the medium.

Discussion

The above calculations have revealed that the observed results can reasonably be explained in terms of the electrostatic effect of the dielectric constant of the solvent on the reaction rates only, although slightly smaller values had to be assigned for d. However, it may also be possible that, in addition to the dielectric constant effect, some non-electrostatic effects, e.g., a decrease in the water concentration or an inhibitory effect of the organic solvent, might have been involved in the observed results. Although it is not a simple matter to determine the magnitude of the effect which is really due to the dielectric

29) G. C. Pimentel and A. L. McClellan, "The Hydrogen Bond", Freeman & Co., San Francisco (1960), pp. 284, 289. These are the average values for carboxylic acids and for ammonium, respectively. A minor change in these values does not affect the resultant slopes seriously.

TABLE II. THE THEORETICALLY PREDICTED SLOPES $d \log k_3/d(1/D)$

No.	Charge state	Schematic representation of the charge state[a]	$-d \log k_3/d(1/D)$ for $d=$ 0.3 Å	0.5 Å	0.7 Å	1.0 Å
1	$\begin{cases}\xi_3=-\xi_4=+1\\ \xi_1=-\xi_2=-1\end{cases}$	● ○ ● ○	656.5	290.2	160.6	85.6
2	$\begin{cases}\xi_3=-\xi_4=-1\\ \xi_1=-\xi_2=+1\end{cases}$	○ ● ● ○	504.9	256.8	136.9	66.9
3	$\begin{cases}\xi_3=-\xi_4=+1\\ \xi_1=-\xi_2=-1/2\end{cases}$	● ○ • ◦	615.5	279.5	152.6	79.3
4	$\begin{cases}\xi_3=-\xi_4=-1\\ \xi_1=-\xi_2=-1/2\end{cases}$	○ ● • ◦	539.7	262.7	140.7	70.0
5	$\begin{cases}\xi_3=-\xi_4=\pm1\\ \xi_1=-\xi_2=0\end{cases}$	○ ●	576.5	270.3	145.9	74.1
6	$\begin{cases}\xi_3=-\xi_4=+1/2\\ \xi_1=-\xi_2=-1\end{cases}$	• ◦ ● ○	183.1	76.7	43.1	23.7
7	$\begin{cases}\xi_3=-\xi_4=-1/2\\ \xi_1=-\xi_2=-1\end{cases}$	◦ • ● ○	107.2	60.0	31.2	14.3
8	$\begin{cases}\xi_3=-\xi_4=+1/2\\ \xi_1=-\xi_2=-1/2\end{cases}$	• ◦ • ◦	161.0	70.1	38.0	19.8
9	$\begin{cases}\xi_3=-\xi_4=+1/2\\ \xi_1=-\xi_2=-1/2\end{cases}$	◦ • • ◦	123.0	61.8	32.1	15.0
10	$\begin{cases}\xi_3=-\xi_4=\pm1/2\\ \xi_1=-\xi_2=0\end{cases}$	◦ •	141.0	65.1	34.3	16.9

a) The large white or black circle represents a positive or a negative unit charge, and the small white or black circle a positive or a negative half unit charge, respectively.

constant of the solvent itself, we may be able to take the non-electrostatic effect to some extent into consideration by plotting the logarithms of $k_3/[H_2O]$ instead of k_3 versus $1/D$. This case corresponds to case 1 considered above, where water reacts with the ES complex directly from the bulk of solvent (see Eq. 4), or to a special case of case 2 (the case in which $K_W=K_M/p$ in Eq. 8), where methanol competes for the water site with the water molecule. This plot is shown in curve III of Fig. 7, where a straight line with a slope of -124 is obtained. Table II shows that this order of magnitude of the slope is reasonably accounted for if $-\xi_3=+\xi_4=\pm1$ and $d=0.75\sim0.8$ Å.

Although there is a little ambiguity in the value of d to be assigned, it may be reasonable to conclude that the main effect operating in the present case is the electrostatic one, i. e., the effect of the dielectric constant on the rate, and the results of calculation are consistent with the hypothesis that the charge separation occurs at the glucosidic linkage of the substrate molecule to be hydrolyzed in the activated state of the ES complex.

Electrostatic Entropy.—Electrostatic entropy is often discussed in relation to the dielectric constant effect on reaction rates[1-3,9,10]. As will be shown in the Appendix, we can estimate the electrostatic part of the entropy change involved in the formation of the ES complex, $\Delta S_{e.s.}$, and of the entropy of activation involved in the breakdown of the ES complex, $\Delta S_{e.s.\neq}$, if we assume that the temperature dependence of the internal dielectric constant of the cavity is much smaller than that of the solvent. From Eqs. A-13 and A-14 in the Appendix, with water as the solvent and at 25°C, we obtain:

$$\Delta S_{e.s.} \fallingdotseq -0.159 \times \frac{d \log K_m}{d(1/D)} \tag{25}$$

$$\Delta S_{e.s.\neq} \fallingdotseq 0.159 \times \frac{d \log k_3}{d(1/D)} \tag{26}$$

Since $d \log K_m/d(1/D)=0$, and $d \log k_3/d(1/D)=-210$ or -124 according as the non-electrostatic effect of the solvent is disregarded or not, we can estimate the electrostatic entropies to be:

$\Delta S_{e.s.} \fallingdotseq 0$

$\Delta S_{e.s.\neq} \fallingdotseq -33$ or -20 cal. deg^{-1} mol^{-1}

The negative entropy of activation suggests that the electrostriction of the solvent is caused by the charge separation in ES$_{\neq}$.

Summary

The influence of methanol on the rate of the hydrolytic reaction of soluble starch catalyzed by crystalline bacterial amyloclastic α-amylase has been studied at 25°C and pH 6.0, over the methanol concentration of 0～22.6% by weight.

The apparent Michaelis constant, K_m, is independent of the methanol concentration,

while the breakdown rate constant of the ES complex, k_3, decreases with an increase in the methanol concentration.

The plot of log k_3 versus the reciprocal dielectric constant of the solvent gives a straight line with a negative slope.

Various possible effects on the reaction rates caused by the addition of methanol have been examind, and it has been concluded that the dielectric constant effect is predominantly operative.

The results have been interpreted quantitatively on the basis of the electrostatic theory previously developed by one of the present authors. The results of calculation have been found to be consistent with the hypothesis that charge separation occurs in the glucosidic linkage to be hydrolyzed in the activated state of the ES complex.

The electrostatic entropy of activation in the breakdown of the ES complex has also been estimated.

The authors wish to express their appreciation to Professor Juichiro Fukumoto and Dr. Takehiko Yamamoto of Osaka City University for their gift of the crystalline enzyme.

Laboratory of Biophysical Chemistry
College of Agriculture
University of Osaka Prefecture
Sakai, Osaka

Appendix

The Evaluation of the Electrostatic Entropy.— The electrostatic part of the entropy of reaction and that of the entropy of activation may be estimated from the variation of the equilibrium constant and of the rate constant with the dielectric constant of the medium respectively, in the following manner. For example, consider an equilibrium:

$$A+B=C+D \tag{A-1}$$

with an equilibrium constant of K. We have:

$$\Delta G=-\boldsymbol{R}T\ln K \tag{A-2}$$

where ΔG is the standard free energy change, which is divided into the non-electrostatic part, $\Delta G_{n.e.s.}$, and the electrostatic part, $\Delta G_{e.s.}$. Thus

$$\Delta G=\Delta G_{n.e.s.}+\Delta G_{e.s.} \tag{A-3}$$

The electrostatic free energy, $\Delta G_{e.s.}$, is expressed in terms of the work of the charging, W, of each species, in the following equation:

$$\Delta G_{e.s.}=\boldsymbol{N}\Delta W=\boldsymbol{N}(W_C+W_D-W_A-W_B) \tag{A-4}$$

where $\boldsymbol{N}$ is the Avogadro number. ΔW of a species for zero ionic strength, designated as W_0, is expressed in the form:

$$W_0=\frac{\varepsilon^2}{2b}\left(\frac{L'}{D_1}+\frac{L}{D}\right) \tag{A-5}$$

where ε is the protonic charge, b, the radius of the species, L, the charge configuration function, and L', a parameter also dependent on the charge configuration of the species. (The full expressions of L and L' will be found in Eq. 3 of Ref. 17.) D_1, the internal dielectric constant of the spherical cavity formed by the solute species, was taken by Kirkwood to be 2 for all the molecules or ions. D is the dielectric constant of the solvent.

The electrostatic part of the entropy change, $\Delta S_{e.s.}$, is obtained by differentiating $\Delta G_{e.s.}$ with respect to the absolute temperature, T. Thus we have:

$$\Delta S_{e.s.}=-\frac{\partial(\Delta G_{e.s.})}{\partial T}=-N\cdot\frac{\partial(\Delta W)}{\partial T}$$
$$=-\frac{N\varepsilon^2}{2}\left[\frac{\partial(1/D_1)}{\partial T}\cdot\Delta\left(\frac{L'}{b}\right)+\frac{\partial(1/D)}{\partial T}\cdot\Delta\left(\frac{L}{b}\right)\right] \tag{A-6}$$

where $\Delta(L'/b)$ and $\Delta(L/b)$ stand for:

$$\Delta\left(\frac{L'}{b}\right)=\frac{L'_C}{b_C}+\frac{L'_D}{b_D}-\frac{L'_A}{b_A}-\frac{L'_B}{b_B} \tag{A-7}$$

$$\Delta\left(\frac{L}{b}\right)=\frac{L_C}{b_C}+\frac{L_D}{b_D}-\frac{L_A}{b_A}-\frac{L_B}{b_B} \tag{A-8}$$

The dielectric constant of a liquid can be expressed as a function of temperature by the empirical formula[30]:

$$D=D^0e^{-T/\theta} \tag{A-9}$$

where D^0 and θ are the constants characteristic of the liquid. Since L and L' are considered to be independent of temperature, if we assume that $\partial(1/D_1)/\partial T$ is much smaller than $\partial(1/D)/\partial T$, i.e., the temperature coefficient of the reciprocal dielectric constant of the cavity is negligibly smaller than that of the solvent, Eq. A-6 becomes:

$$\Delta S_{e.s.}=-\frac{\varepsilon^2\boldsymbol{N}}{D\theta}\cdot\Delta\left(\frac{L}{b}\right)$$
$$=\frac{\varepsilon^2\boldsymbol{N}}{D\theta}\left(\frac{L_A}{b_A}+\frac{L_B}{b_B}-\frac{L_C}{b_C}-\frac{L_D}{b_D}\right)$$
$$=\frac{4.606\,\boldsymbol{R}T}{D\theta}\cdot\frac{\mathrm{d}\log K}{\mathrm{d}(1/D)} \tag{A-10}$$

since

$$\frac{\mathrm{d}\log K}{\mathrm{d}(1/D)}=\frac{\varepsilon}{4.606\,kT}\left(\frac{L_A}{b_A}+\frac{L_B}{b_B}-\frac{L_C}{b_C}-\frac{L_D}{b_D}\right) \tag{A-11}$$

Thus, the electrostatic entropy, $\Delta S_{e.s.}$, is expressed in terms of the slope, $\mathrm{d}\log K/\mathrm{d}(1/D)$, which can be obtained experimentally. Quite similarly, for a rate process, we have:

$$\Delta S_{e.s.\neq}=\frac{4.606\,\boldsymbol{R}T}{D\theta}\cdot\frac{\mathrm{d}\log k}{\mathrm{d}(1/D)} \tag{A-12}$$

where $\Delta S_{e.s.\neq}$ and k are the electrostatic entropy of activation and the rate constant, respectively.

With water as solvent and at 25°C, $\theta=219$[30], $D=78.5$ and $T=298$; therefore, we have

$$\Delta S_{e.s.}\fallingdotseq 0.159\times\frac{\mathrm{d}\log K}{\mathrm{d}(1/D)} \tag{A-13}$$

$$\Delta S_{e.s.\neq}\fallingdotseq 0.159\times\frac{\mathrm{d}\log k}{\mathrm{d}(/1D)} \tag{A-14}$$

30) R. W. Gurney, "Ionic Processes in Solution", McGraw-Hill, New York (1953), p. 16.

Syntheses of Some Derivatives of 7-Hydroxydecahydroisoquinoline

By Tatsuo TOMIOKA, Toshio NAKAMURA and Yasuo HOSHIDE

(Received December 4, 1962)

The syntheses described in this paper were undertaken to prepare some compounds related to reserpine, an important alkaloid found in *Rauwolfia* species. Sastry and Lasslo[1] and Miller and Weinberg[2] have reported syntheses and significant reserpine-like activities of the 3-(*N*, *N*-diethylaminopropyl) and 4-(*N*, *N*-diethylaminobutyl) esters of 3, 4, 5-trimethoxybenzoic acid, and a considerable number of compounds in which the alcohol moiety of the carboxylic ester and the acyl moiety of the trimethoxybenzoic acid ester functions vary have been reported in the patent literature. However, little information is available regarding the related derivatives of decahydroisoquinoline. Of special interest were decahydroisoquinoline derivatives, which contain a peripheral *N*-alkyl group simulating the cut-away indole portion of reserpine. Such a derivative corresponds to that part of reserpine shown by solid line in Formula 1. The present paper is concerned with the synthesis of methyl quaternary bromides of 7-methoxybenzoyloxy-2-methyldecahydroisoquinolines and of 7-methoxybenzoyloxy-2-ethyldecahydroisoquinolines[3].

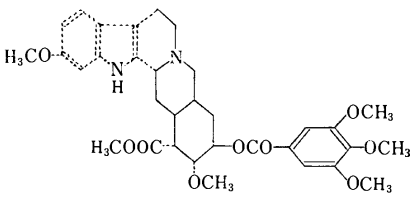

Chart 1

7-Hydroxy-2-methyl- and 7-hydroxy-2-ethyl decahydroisoquinoline and their derivatives were prepared by the general scheme outlined in Chart 2:

Methiodide (I) of 7-hydroxyisoquinoline was reduced with sodium borohydride to yield 7-hydroxy-2-methyl-1, 2, 3, 4-tetrahydroisoquinoline (II) in a 76.5% yield. The catalytic hydrogenation of II with Raney nickel proceeded smoothly, affording an 84.2% yield of 7-hydroxy-2-methyldecahydroisoquinoline (III), an oily product with a b. p. of 110~115°C (2 mmHg). The structure of III was confirmed by elemental analysis and by the formation of a methiodide derivative. Ochiai and Nakagome[4] reported a b. p. of 105~115°C (3 mmHg, bath temperature) for the material obtained on the catalytic hydrogenation of 2-methyl-7-oxo-Δ^8-octahydroisoquinoline with platinum oxide; moreover, they reported a m. p. of 257~258°C for its methiodide. It was found that the melting point of our sample varied with the nature of the solvent used for recrystallization. Repeated recrystallization from alcohol gave a m. p. of 277.5~278.5°C, and recrystallization from alcohol-petroleum ether gave a m. p. of 253~257°C, substantially the same melting point as that described by Ochiai and Nakagome. Although stereoisomeric separation was not attempted, III can be assumed to be a mixture of stereoisomers.

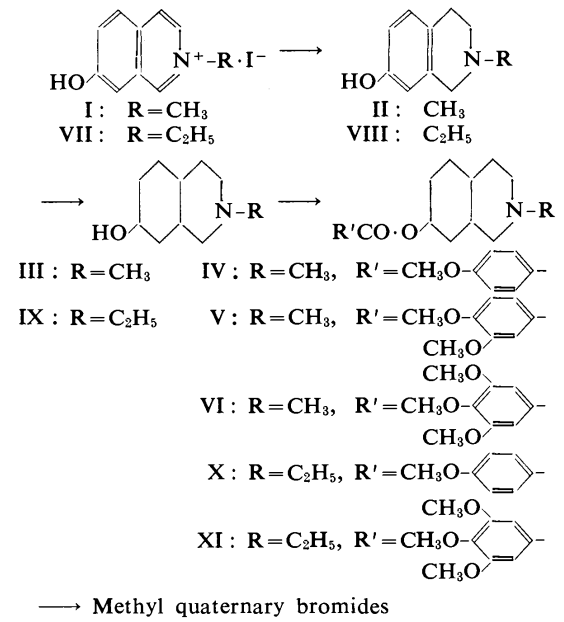

Chart 2

Compounds of Formulas IV, V and VI were prepared by the treatment of 7-hydroxy-2-methyldecahydroisoquinoline (III) with anisoyl

1) B. V. R. Sastry and A. Lasslo, *J. Org. Chem.*, **23**, 1577 (1958).

2) F. M. Miller and M. S. Weinberg, *Chem. Eng. News*, **34**, 4760 (1956); *Chem. Abstr.*, **53**, 18079 (1959).

3) Recently, syntheses of 5-hydroxy-2-methyldecahydroisoquinoline and 6-hydroxy-2-methyldecahydroisoquinoline have been reported by S. Kimoto and M. Okamoto, *Chem. & Pharm. Bull.*, **9**, 480 (1961); **10**, 368 (1962).

4) E. Ochiai and T. Nakagome, *J. Pharm. Soc. Japan*, **78**, 1438 (1958).

chloride, veratroyl chloride and tri-*O*-methylgalloyl chloride respectively in benzene at 45°C for 6 hr. After removal of the solvent, each of the reaction mixtures was treated with water, each giving an insoluble part which was confirmed to be anisic anhydride, veratric anhydride or tri-*O*-methylgallic anhydride respectively. The water-layers were evaporated under reduced pressure, and the viscous products were treated with silver carbonate in acetone-methanol. Each of the resulting free bases was chromatographed on alumina and eluted with ether to give two fractions, namely, the first and second fractions. The second fractions were 7-hydroxy-2-methyldecahydroisoquinoline, unchanged and converted to its crystalline methiodide, which was identified by comparison with the methiodide of III. After removal of ether from the first fractions, each of the resulting syrups was treated with an excess of methyl bromide to yield a crystalline mixture of stereoisomers of methyl 7-aroyloxy-2-methyldecahydroisoquinolinium bromide. Extraction of each of the stereoisomeric mixtures with a large quantity of acetone left a relatively insoluble isomer (A), while evaporation of the acetone-extract gave a soluble isomer (B). Thus, each of the methiodides of 7-anisoyloxy-2-methyldecahydroisoquinoline, 7-veratroyloxy-2-methyldecahydroisoquinoline and 7-tri-*O*-methylgalloyloxydecahydroisoquinoline was separated into two corresponding isomers, A and B.

The synthesis of 7-hydroxy-2-ethyldecahydroisoquinoline (IX) was carried out by procedures analogous to those used for the preparation of the 2-methyl derivative III. The condensation products of 7-hydroxy-2-ethyldecahydroisoquinoline (IX) with anisoyl chloride and tri-*O*-methylgalloyl chloride were treated with water, giving again anisic anhydride and tri-*O*-methylgallic anhydride respectively. The viscous products obtained from the water-layers by evaporation were treated with silver carbonate in acetone, and the resulting free bases were subjected to alumina chromatography to yield again two fractions, the second fraction being unchanged IX. Evaporation of each of the first fractions gave an oily mixture of stereoisomers of 7-aroyloxy-2-ethyldecahydroisoquinoline. The oily product of 7-anisoyloxy-2-ethyldecahydroisoquinoline was treated with an excess of methyl bromide to yield a crystalline product of methyl 7-anisoyloxy-2-ethyldecahydroisoquinolinium bromide (XV). The treatment of this product with acetone again gave two fractions, one soluble and one relatively insoluble; however, only one isomer could be obtained from the soluble fraction.

The oily product of 7-(tri-*O*-methylgalloyloxy)-2-ethyldecahydroisoquinoline was also treated with an excess of methyl bromide, producing a crystalline product of methyl 7-(tri-*O*-methylgalloyloxy)-2-ethyldecahydroisoquinolinium bromide (XVI). Treatment of the product with acetone also gave two fractions, one soluble and one relatively insoluble, from which one isomer could be obtained.

Although stereochemical assignments for the above-mentioned isomers have not yet been made, material differences have been discerned between the biological properties of the stereoisomeric derivatives of methyl quaternary bromide, and some of them look promising for clinical use. Details of the studies of the hypotensive activity and toxicity of the above-mentioned stereoisomeric derivatives will be published elsewhere in the near future.

Experimental

7-Hydroxy-2-methyl-1, 2, 3, 4-tetrahydroisoquinoline (II).—A solution of 1.19 g. of 7-hydroxyisoquinoline methiodide (I) in 25 ml. of 10% aqueous methanol was added to 0.66 g. of sodium borohydride and refluxed for 5 min. After the addition of 10 ml. of acetone, the reaction mixture was allowed to cool to room temperature. After removal of the solvent, the residue was mixed with 15 ml. of a 3.5% sodium carbonate solution to give colorless crystals of the title compound; m. p., 169~170°C, 0.52 g. (76.5%). Repeated recrystallizations from acetone raised the m. p. to 171~172°C (reported[5]: 171~172°C).

7-Hydroxy-2-methyldecahydroisoquinoline (III).—A solution of 2.99 g. of 7-hydroxy-2-methyl-1,2,3,4-tetrahydroisoquinoline (II) in 330 ml. of absolute ethanol was hydrogenated with 3.5 g. of Raney nickel at 155~160°C for 16 hr. at a pressure of 200~202 kg./cm^2. After removal of the catalyst by filtration, the reaction mixture was evaporated to give an oily residue, which was then distilled under reduced pressure to give 2.61 g. (84.2%) of 7-hydroxy-2-methyldecahydroisoquinoline; b. p., 110~115°C (2 mmHg). The b. p. reported by Ochiai and Nakagome[4] is 105~115°C (3 mmHg, bath temperature).

Methiodide of III.—A mixture of 7-hydroxy-2-methyldecahydroisoquinoline and of an excess of methyl iodide in ethyl acetate, when warmed for a while and then allowed to cool to room temperature, gave colorless crystals of methyl iodide; m. p., 229~253°C. Repeated recrystallizations from ethanol raised the m. p. to 277.5~278.5°C.

Found: C, 42.28; H, 7.23; N, 4.76. Calcd. for $C_{11}H_{22}ONI$: C, 42.44; H, 7.07; N, 4.50%.

Recrystallizations of the crude methiodide from ethanol-petroleum ether gave a m. p. of 253~257°C (reported[4] 257~258°C).

Found: C, 42.17; H, 7.15%.

7-Anisoyloxy-2-methyldecahydroisoquinoline (IV).—A solution of 1.29 g. of anisoyl chloride in 15 ml.

5) F. L. Pyman and F. G. P. Remfry, *J. Chem. Soc.*, 101, 1595 (1912).

of dried benzene was stirred drop by drop into a solution of 1.28 g. of 7-hydroxy-2-methyldecahydroisoquinoline (III) in dried benzene. This solution was warmed at 45°C for 6 hr. and then distilled under reduced pressure to give 2.80 g. of a viscous residue. This residue was triturated with 50 ml. of water, and the aqueous layer was separated from the insoluble part by filtration. Recrystallization of the insoluble part (0.66 g.) from ethanol-water gave colorless crystals of anisic anhydride; m. p., 98~99°C (reported m. p., 99°C)[6].

Found: C, 67.12; H, 4.69. Calcd. for $C_{16}H_{14}O_5$: C, 67.13; H, 4.93%.

The above-mentioned aqueous layer was treated with a small quantity of active charcoal and evaporated under reduced pressure. The viscous residue was then dissolved in a mixture of 50 ml. of acetone and 20 ml. of methanol and mixed thoroughly with 3.0 g. of silver carbonate. After removal of the precipitate by filtration, the solution was evaporated under reduced pressure, and the residue was taken up in a small quantity of ether. The ether solution was evaporated to give an oily product (1.56 g.). This product was chromatographed on alumina and then developed and eluted with ether to give two fractions. The second fraction was treated with methyl iodide to yield a methiodide with a m. p. of 266~269°C, which was identical with the methiodide of 7-hydroxy-2-methyldecahydroisoquinoline.

The first fraction was evaporated to give an oily product of 7-anisoyloxy-2-methyldecahydroisoquinoline (IV) (0.75 g.) (32.8%).

Stereoisomers (XII-A, XII-B) of Methyl 7-Anisoyloxy-2-methyldecahydroisoquinolinium Bromide.—A mixture of 0.75 g. of the crude product of 7-anisoyloxy-2-methyldecahydroisoquinoline (IV) and an excess of methyl bromide in 20 ml. of ether was sealed in a test tube and allowed to stand at room temperature for 2 days. Removal of the solvent from the reaction mixture gave 0.97 g. of crude crystals of quaternary ammonium salt. This crude product was thoroughly triturated with 110 ml. of acetone, and the acetone-layer was separated from the insoluble part by filtration. The insoluble part weighed 0.32 g. (33.0%) and melted at 262.5~265.5°C. Repeated recrystallizations from ethanol-petroleum ether gave colorless needles with a m. p. of 281~282°C. Elemental analysis indicated the product to be a stereoisomer (XII-A) of methyl 7-anisoyloxy-2-methyldecahydroisoquinolinium bromide.

Found: C, 57.60; H, 7.32; N, 3.67. Calcd. for $C_{19}H_{28}O_3NBr$: C, 57.29; H, 7.08; N, 3.52%.

The above-mentioned acetone-layer was evaporated, and the residue was again dissolved in 60 ml. of acetone, leaving a small insoluble part. The acetone solution was concentrated to 20 ml., and the separated crystals were collected; 0.25 g. (25.8%); m. p., 216~221°C. Recrystallizations from acetone-ethyl acetate gave colorless needles with a m. p. of 220~223°C. Elemental analysis indicated the product to be another isomer (XII-B) of methyl 7-anisoyloxy-2-methyldecahydroisoquinolinium bromide.

Found: C, 57.63; H, 7.28; N, 3.79. Calcd. for $C_{19}H_{28}O_3NBr$: C, 57.29; H, 7.08; N, 3.52%.

The mixed melting point of the two above-mentioned isomers showed considerable depression and a wide range.

Evaporation of the mother-liquor from the isomer (XII-B) left 0.33 g. of a viscous residue.

7-Veratroyloxy-2-methyldecahydroisoquinoline (V). — In a manner similar to that used for the preparation of IV, 1.47 g. of 7-hydroxy-2-methyldecahydroisoquinoline (III) was treated with 1.78 g. of veratroyl chloride in benzene to give 3.49 g. of a viscous product. Trituration of the product with 250 ml. of water left an insoluble part (0.60 g.), which was recrystallized from ethanol to give colorless needles of veratric anhydride; m. p., 118~120°C (reported m. p., 124~125°C)[7]. The aqueous layer was treated with active charcoal and evaporated. The viscous residue was dissolved in a mixture of 50 ml. of acetone and 20 ml. of methanol and mixed thoroughly with 3.8 g. of silver carbonate. After removal of the precipitate, the solution was evaporated and the residue was taken up in a small quantity of ether. The oily product obtained by the evaporation of the ether solution was chromatographed on alumina and then developed and eluted with ether to give two fractions. The first fraction was evaporated to give 1.05 g. (36.2%) of an oily product of 7-veratroyloxy-2-methyldecahydroisoquinoline (V).

The Stereoisomers (XIII-A, XIII-B) of Methyl 7-Veratroyloxy-2-methyldecahydroisoquinolinium Bromide. — In a manner similar to that used for the preparation of XII-A and XII-B, 1.05 g. of the crude product of 7-veratroyl-2-methyldecahydroisoquinoline was treated with an excess of methyl bromide to give 1.31 g. of crude crystals of quaternary ammonium salt. The crude product was thoroughly triturated with 350 ml. of acetone, and the acetone-layer was separated from the insoluble part. The insoluble part weighed 0.30 g. (22.0%) and melted at 252~255°C. Repeated recrystallizations from ethanol-petroleum ether gave colorless needles; m. p., 263~264°C. Elemental analysis indicated the product to be a stereoisomer (XIII-A) of methyl 7-veratroyloxy-2-methyldecahydroisoquinolinium bromide.

Found: C, 56.08; H, 7.03; N, 3.32. Calcd. for $C_{20}H_{30}O_4NBr$: C, 56.08; H, 7.06; N, 3.27%.

The acetone-layer was evaporated, and the residue was again dissolved in 130 ml. of acetone, leaving a small insoluble part. Concentration of the acetone solution to 17 ml. separated 0.58 g. (43.0%) of crystals; m. p., 157~162°C. Recrystallizations from acetone gave colorless hygroscopic needles with a m. p. of 169~170°C. Elemental analysis indicated the product to be another stereoisomer (XIII-B) of methyl 7-veratroyloxy-2-methyldecahydroisoquinolinium bromide.

Found: C, 55.14; H, 6.93; N, 2.93. Calcd. for $C_{20}H_{30}O_4NBr \cdot 1/2H_2O$: C, 54.93; H, 7.14; N, 3.20%.

The mixed melting point of the two above-mentioned isomers showed considerable depression and

6) F. Pisani, *Ann.*, **102**, 284 (1857).

7) J. Shinoda and S. Sato, *J. Pharm. Soc. Japan* (*Yakugaku Zasshi*), No. 540, 24 (1927).

wide range.

7-(Tri-*O*-methylgalloyloxy)-2-methyldecahydroisoquinoline (VI). — In a manner similar to that used for the preparation of IV, 1.50 g. of 7-hydroxy-2-methyldecahydroisoquinoline (III) was treated with 2.06 g. of tri-*O*-methylgalloyl chloride in benzene to give 3.56 g. of a viscous product. Trituration of the product with 320 ml. of water left an insoluble part (0.93 g.), which was then recrystallized from acetone to give colorless needles of tri-*O*-methylgallic anhydride with a m. p. of 159~160°C (reported m. p., 159~160°C)[8].

Found: C, 59.32; H, 5.53. Calcd. for $C_{20}H_{22}O_9$: C, 59.11; H, 5.46%.

After the aqueous layer had been processed, an oily product (1.86 g.) was chromatographed on alumina by a similar procedure to give two fractions. The oily product from the second fraction gave methiodide (m. p., 261~266°C) which was identical with the methiodide of the starting substance III. The first fraction gave 1.04 g. (32.2%) of an oily product of 7-(tri-*O*-methylgalloyloxy)-2-methyldecahydroisoquinoline.

The Stereoisomers (XIV-A, XIV-B) of Methyl 7-(Tri-*O*-methylgalloyloxy)-2-methyldecahydroisoquinolinium Bromide.—In a manner similar to that used for the preparation of XII-A and XII-B, 1.04 g. of 7-(tri-*O*-methylgalloyloxy)-2-methyldecahydroisoquinoline was reacted with an excess of methyl bromide to give 1.29 g. of crude crystals of quaternary ammonium salt. Fractionation of the product with acetone gave two fractions. The more insoluble fraction weighed 0.29 g. (21.9%) and melted at 260~263°C. Recrystallizations from ethanol-petroleum ether gave colorless needles with a m. p. of 262.5~264.0°C. Elemental analysis indicated the product to be a stereoisomer (XIV-A) of methyl 7-(tri-*O*-methylgalloyloxy)-2-methyldecahydroisoquinolinium bromide.

Found: C, 54.58; H, 7.37; N, 3.36. Calcd. for $C_{21}H_{32}O_5NBr$: C, 55.02; H, 7.04; N, 3.06%.

The soluble fraction weighed 0.47 g. (36.3%) and melted at 192~198°C. Recrystallizations from acetone gave colorless hygroscopic plates with a m. p. of 201.5~203.5°C. Elemental analysis indicated the product to be another isomer (XIV-B) of methyl 7-(tri-*O*-methylgalloyloxy)-2-methyldecahydroisoquinolinium bromide.

Found: C, 55.01; H, 7.04; N, 3.27. Calcd. for $C_{21}H_{32}O_5NBr$: C, 55.02; H, 7.04; N, 3.06%.

7-Hydroxy-2-ethyl-1,2,3,4-tetrahydroisoquinoline (VIII).—The reduction of 7.08 g. of 7-hydroxyisoquinoline methiodide with 3.57 g. of sodium borohydride in 10% aqueous methanol gave 4.08 g. (97.8%) of crude crystals. Recrystallization from acetone-petroleum ether gave colorless needles with a m. p. of 144~147°C.

Found: C, 74.13; H, 8.48. Calcd. for $C_{11}H_{15}ON$: C, 74.53; H, 8.53%.

7-Hydroxy-2-ethyldecahydroisoquinoline (IX).—A sample of 3.22 g. of 7-hydroxy-2-ethyl-1,2,3,4-tetrahydroisoquinoline was hydrogenated with 4.0 g. of Raney nickel in absolute ethanol at about 165°C for 16 hr. at a pressure of 191 kg./cm^2. After processing, the colorless oil of 7-hydroxy-2-ethyldecahydroisoquinoline with a b. p. of 122.5~126.5°C (3 mmHg) was obtained; 2.59 g. (77.8%). The product gave methiodide with a m. p. of 214~219°C.

Found: C, 44.61; H, 7.31; N, 4.64. Calcd. for $C_{12}H_{24}ONI$: C, 44.31; H, 7.44; N, 4.31%.

7-Anisoyloxy-2-ethyldecahydroisoquinoline (X).—The reaction of 1.20 g. of 7-hydroxy-2-ethyldecahydroisoquinoline (IX) with 1.12 g. of anisoyl chloride in dried benzene gave 2.04 g. of a viscous product. The trituration of the product with 100 ml. of water left an insoluble part (0.48 g.) which, after recrystallization from ethanol-water, melted at 98~99°C and which was identical with anisic anhydride. The aqueous layer was processed in a manner similar to that described for the preparation of IV, and the viscous product was chromatographed on alumina to give two fractions. The second fraction gave methiodide (m. p., 216~218°C) which was identical with the methiodide of 7-hydroxy-2-ethyldecahydroisoquinoline. The first fraction gave an oily product (0.68 g., 32.9%) of 7-anisoyloxy-2-ethyldecahydroisoquinoline.

Methyl 7-Anisoyloxy-2-ethyldecahydroisoquinolinium Bromide (XV). — In a manner similar to that used for preparation of XII-A and XII-B, 0.68 g. of 7-anisoyloxy-2-ethyldecahydroisoquinoline was reacted with an excess of methyl bromide to give 0.87 g. of crude crystals of quaternary ammonium salt. Fractionation of the product with 150 ml. of acetone gave two fractions. The more insoluble fraction weighed 0.054 g. (6.1%) and melted at 243.5~245°C. The soluble fraction was concentrated to 12 ml. to give 0.26 g. (29.1%) of colorless crystals with a m. p. of 224.5~228°C. Recrystallization from acetone raised the m. p. to 234~237.5°C.

Found: C, 58.33; H, 7.42; N, 3.25. Calcd. for $C_{20}H_{30}O_3NBr$: C, 58.25; H, 7.33; N, 3.40%.

7-(Tri-*O*-methylgalloyloxy)-2-ethyldecahydroisoquinoline (XI). — The treatment of 1.21 g. of 7-hydroxy-2-ethyldecahydroisoquinoline with 1.52 g. of tri-*O*-methylgalloyl chloride in dried benzene gave 2.94 g. of a viscous product. The trituration of the product with 250 ml. of water left an insoluble part (1.21 g.) which, after recrystallization from ethanol, melted at 159~160°C and was identical with tri-*O*-methylgallic anhydride. The aqueous extract was processed to give a viscous product, which was then chromatographed on alumina to give two fractions. The first fraction gave 0.50 g. (20.0%) of an oily product of 7-(tri-*O*-methylgalloyloxy)-2-ethyldecahydroisoquinoline.

Methyl 7-(Tri-*O*-methylgalloyloxy)-2-ethyldecahydroisoquinolinium Bromide (XVI). — The treatment of 0.50 g. of 7-(tri-*O*-methylgalloyloxy)-2-ethyldecahydroisoquinoline with an excess of methyl bromide gave 0.61 g. of crude crystals of quaternary ammonium salt. Trituration with 16 ml. of acetone left 0.087 g. (14.0%) of an insoluble solid with a m. p. of 241~243.5°C. Recrystallization from ethanol-petroleum ether gave colorless needles with a m. p. of 244.5~245.0°C.

Found: C, 55.89; H, 7.37. Calcd. for $C_{22}H_{34}O_5NBr$: C, 55.93; H, 7.25%.

Evaporation of the acetone solution gave 0.52 g.

8) T. Heap and R. Robinson, *J. Chem. Soc.*, **1929**, 69.

of a viscous product which could not be caused to crystallize.

The authors are indebted to Mr. Saburo Nakada, of Keio University, for his micro-analysis. It is a pleasure also to acknowledge their helpful discussions with Professor Sumio Umezawa, of Keio University, and Dr. Masujiro Ooka, Chairman of the Board of Directors, Nikken Chemicals Co.

Research Laboratories
Nikken Chemicals Co., Ltd.
Oomiya, Saitama-ken

The Wetting of Paraffin by Aqueous Solutions of Fatty Alcohol Homologues

By Teruo TSUNODA*

(Received December 12, 1962)

The relation between the wetting of a solid by solutions and the adsorption of the solute has been studied by various authors. Rehbinder[1] and Cook[2] have proposed formulas expressing the relation between contact angle and adsorption, but these are largely empirical in nature and lack theoretical foundation. On the other hand, Doss[3] and Wada[4] have derived theoretical formulas, but these are not always applicable to all of the practical cases. Recently, Bartell[5] has given a wetting isotherm which predicted fairly well the relation between the solute adsorption and the adhesion tension in the case of the wetting of platinum by water. His formula, however, concerns hydrophilic surfaces and is not applicable to hydrophobic surfaces such as paraffin, which, according to his formula, should have a portion of the surface free from any adsorption, at least in the case of wetting by pure water, which is different from the adsorption model he assumed.

We have also attempted to derive an equation based on the molecular structure of the adsorbed layer which was valid both for the wetting and the anti-wetting of a solid surface by aqueous ethyl alcohol and xanthate solutions respectively[6]. The present investigation was undertaken further to check our wetting isotherm for the case of the wetting of paraffin by aqueous solutions of alcohol homologues and to obtain further knowledge concerning adsorbed films on solid surfaces.

Experimental

The alcohols used were *n*-propyl, *n*-butyl, *n*-amyl and *n*-octyl alcohols, which had been refluxed over calcium oxide for several hours and then distilled twice before use. Their boiling points were within the range of 1°C of the published data. The paraffin used was purified by treating it with concentrated sulfuric acid, then with sodium hydroxide, and finally by vacuum distillation. For the wettability measurement, the paraffin surface was prepared by dipping a glass rod of a uniform diameter into molten paraffin, withdrawing it, and then solidifying the paraffin film on the rod in air. The surface thus obtained was sufficiently smooth for the measurement of contact angle not to obscure the conclusion obtained. The contact angle and surface tension were measured using the Wilhelmy balance. The temperature was controlled to 25 ± 0.3°C throughout the experiments.

Results and Discussion

Contact Angles.—The changes in contact angle with time of immersion in an alcohol solution are shown in Table I, which shows a nearly constant value of the angle after an hour. As the time dependence of the surface tension of aqueous alcohol solutions was not perceptible in this experiment, the observed change in the contact angle may be ascribed mainly to a slow change in the solid/solution interfacial tension with time. In the present experiment, contact angles were measured for paraffin soon after it had been immersed in solution for one hour. The advancing and receding contact angles thus obtained were

* Present address: Hitachi Central Research Laboratory, Hitachi, Ltd., Kokubunji, Kitatama-gun, Tokyo.

1) P. A. Rehbinder et al., *Kolloid-Z.*, **65**, 268 (1933).
2) M. A. Cook et al., *J. Phys. Colloid Chem.*, **55**, 1219 (1951).
3) K. S. Doss et al., *Proc. Ind. Acad. Sci.*, **7A**, 117 (1938).
4) M. Wada, *Nippon Kogyo Kaishi*, **59**, 681 (1943).
5) L. S. Bartell et al., *J. Phys. Chem.*, **64**, 513 (1960).
6) T. Sasaki, H. Kumanomido and T. Tsunoda, 2nd International Congress of Surface Activity, III, Butterworths, London (1957), p. 153.

TABLE I. THE CHANGES OF CONTACT ANGLE WITH TIME OF IMMERSION IN ALCOHOL SOLUTIONS

Alcohol	σ dyn./cm.	$t=0$		$t=30$		$t=60$	
		θ_a	θ_r	θ_a	θ_r	θ_a	θ_r
n-Propyl alc.	60.4	109.8	101.4	110.4	110.6	109.6	98.6
n-Butyl alc.	62.0	112.7	91.8	109.2	90.5	108.9	90.0
n-Amyl alc.	62.0	110.7	97.1	96.2	95.5	95.5	94.8
n-Octyl alc.	60.4	109.7	98.2	110.0	97.8	109.2	97.1

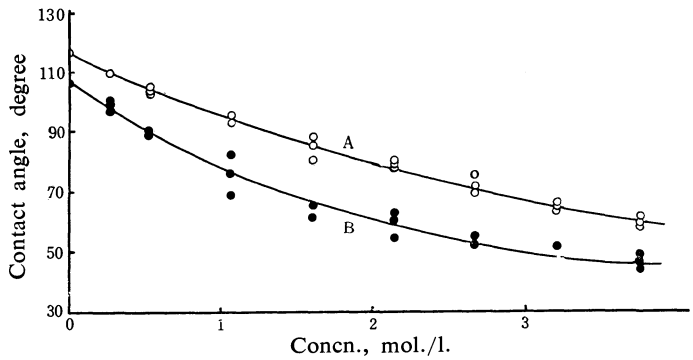

Fig. 1. Contact angle vs. concentration of *n*-propyl alcohol.
A, advancing B, receding

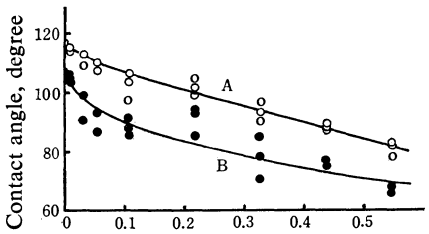

Fig. 2. Contact angle vs. concentration of *n*-butyl alcohol.
A, advancing B, receding

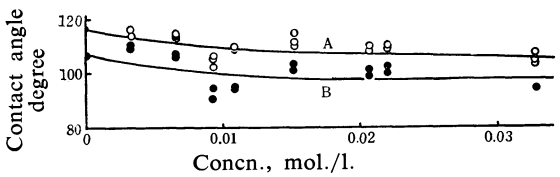

Fig. 3. Contact angle vs. concentration of *n*-amyl alcohol.
A, advancing B, receding

plotted against the concentration of solutions, as is shown in Figs. 1, 2, 3 and 4. It was found that the hysteresis of the contact angles was at most about 10 degrees throughout the experiments.

Wetting Isotherm.—As for the wetting isotherms, Doss[3] proposed an equation which gave the relation between the contact angle and the liquid adsorption as:

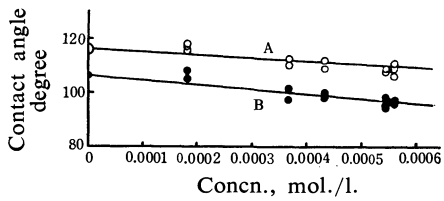

Fig. 4. Contact angle vs. concentration of *n*-octyl alcohol.
A, advancing B, receding

$$\cos\theta = 2\phi - 1 \qquad (1)$$

where θ denotes the contact angles of pure liquid and ϕ, the fractional area of liquid adsorption. By a similar reasoning we derived a more general isotherm[6] for the wetting of a solid by solution:

$$\cos\theta_r = \frac{\sigma_1 + \sigma_w}{\sigma_1}(\phi + aX) - 1 \qquad (2)$$

where θ_r denotes a receding contact angle, σ_1 and σ_w the surface tension of the wetting solution and solvent (water) respectively, ϕ and a, constants depending on the nature of the wetting solution (namely solvent and solute), and X, the fraction of the surface covered with the solute molecules. In deriving Eq. 2 we used θ_r for the contact angles which corresponded to the work of adhesion, $W_a = \sigma_1(\cos\theta_r + 1)$, instead of $W'_a = \pi + \sigma_1(\cos\theta_a + 1)$ for the advancing contact angle, θ_a, where π denotes the spreading pressure of the adsorbed film on the

solid. Equation 2 can be reduced to the Doss Eq. 1 in the case of a pure liquid where $X=0$, $\sigma_1=\sigma_w$. Now in Eq. 2, we can put $X=\Gamma\lambda$, where Γ denotes the amount of adsorption in mol./cm^2, and λ the area occupied by a mole of an adsorbed substance in a closely packed state in cm^2/mol. Equation 2 then takes the form:

$$\cos\theta_r=\frac{\sigma_1+\sigma_w}{\sigma_1}(\phi+K\Gamma)-1 \qquad (3)$$

where K is a new constant equal to $a\lambda$. We checked our wetting isotherm Eq. 3 using the experimental values of σ_r, σ_w, σ_1 and Γ. Γ is calculated from the Gibbs' adsorption isotherm:

$$\Gamma=\frac{d(\sigma_1\cos\sigma_a)}{RT\,d\ln c} \qquad (4)$$

where c expresses the concentration in mol./l. of alcohol in the wetting solution. We used the advancing contact angle, θ_a, for the calculation of Γ, because in the advancing liquid state the solid surface is considered to be practically free from adsorbed solute, which is also assumed to be the case in the derivation of Eq. 4. The adsorption isotherms thus obtained for the paraffin/aqueous solution interface, together with those for the aqueous solution surface, are shown in Figs. 5 and 6. We can see in these figures that the amount of adsorption is somewhat larger for the paraffin/solution interface than for the aqueous surface, while it is nealy equal for both surfaces in the case of butyl and amyl alcohols and is a little larger for the paraffin/solution interface in the case of octyl alcohol. Davies[7] reported that the proportionality between Γ and the concentration of solute is better for the oil/solution interface than for the aqueous surface. However, we can observe no such differences.

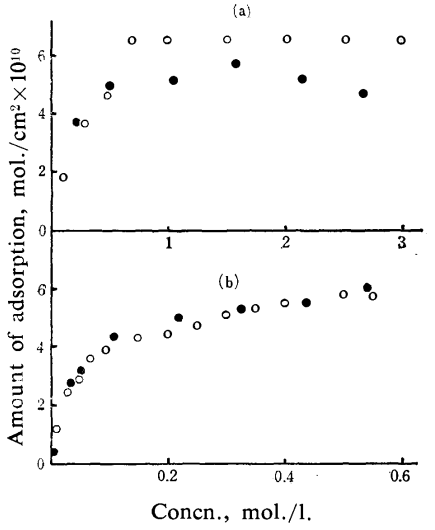

Fig. 5. Adsorption isotherms of (a) *n*-propyl and (b) *n*-butyl alcohol on paraffin/solution (○) and air/solution (●) interfaces.

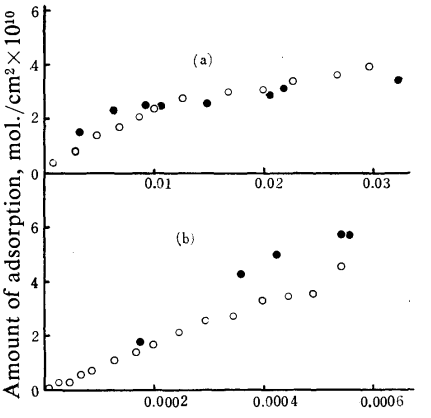

Fig. 6. Adsorption isotherms of (a) *n*-amyl and (b) *n*-octyl alcohol on paraffin/solution (○) and air/solution (●) interfaces.

In order to check Eq. 3, it was transformed into

$$\frac{\sigma_1(\cos\theta_r+1)}{\sigma_1+\sigma_w}=\phi+k\Gamma \qquad (5)$$

and $\sigma_1(\cos\theta_r+1)/(\sigma_1+\sigma_w)$ was plotted against Γ. The results are shown in Fig. 7. The

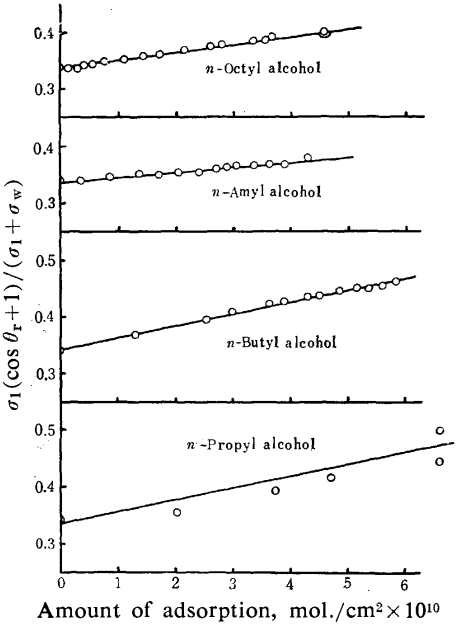

Fig. 7. Validity of Eq. 3.

7) J. T. Davies, *Proc. Roy. Soc.*, **A245**, 415 (1958).

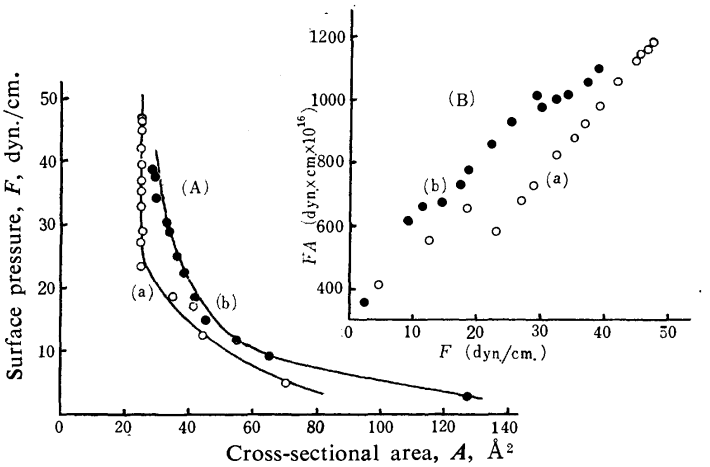

Fig. 8. (A) Pressure~area and (B) $FA \sim F$ relations for adsorbed films of (a) *n*-propyl and (b) *n*-butyl alcohol on paraffin surface.

linearity obtained in these figures lends support to the validity of Eqs. 2 and 3. From the linearity, we calculated the ϕ and K constants which are shown in Table II. We can see in Table II that the calculated value of ϕ is constant, regardless of the alcohol used, while the values of K decrease with an increase in molecular weight with the exception of the irregular value for amyl alcohol. The value of ϕ, which is the proportion of polar part to the total area of the solid surface, should be practically independent of the nature of alcohol used. That the value of ϕ is 0.34 means that the polar part of the surface is about one-third of the total area of the solid surface. The K value, on the other hand, may be expected to decrease with an increase in the molecular weight of the solute, since it depends on the relative polarity of solute and is expected to decrease with an increase in the molecular weight. This requirement is also satisfied as a whole. Using the adsorption isotherm of the Langmuir type, c was substituted for Γ in Eq. 3. We thus obtained, for *n*-propyl alcohol:

$$\cos\theta_r = \frac{\sigma_l + \sigma_w}{\sigma_l}\left(0.346 + \frac{c}{1+6.82c}\right) - 1$$

for *n*-butyl alcohol

$$\cos\theta_r = \frac{\sigma_l + \sigma_w}{\sigma_l}\left(0.347 + \frac{c}{0.536+8.11c}\right) - 1$$

for *n*-amyl alcohol

$$\cos\theta_r = \frac{\sigma_l + \sigma_w}{\sigma_l}\left(0.339 + \frac{c}{0.34+19.6c}\right) - 1 \qquad (6)$$

for *n*-octyl alcohol

$$\cos\theta_r = \frac{\sigma_l + \sigma_w}{\sigma_l}\left(0.342 + \frac{c}{7.88\times10^{-3}+5.58c}\right) - 1$$

TABLE II. CONSTANTS ϕ AND K IN WETTING ISOTHERM 3

Alcohol	ϕ	K, cm²/mol.
n-Propyl alc.	0.346	2.2×10^{8}
n-Butyl alc.	0.347	1.9×10^{8}
n-Amyl alc.	0.339	0.8×10^{8}
n-Octyl alc.	0.342	1.2×10^{8}

The Eqs. 6 are shown as solid lines in Figs. 1—4. We can further express the surface tension, σ_l of the Eqs. 6 in terms of the concentration, c, using an equation, for instance, of the Szyzkowski type, and express the contact angle as a function of the solute concentration alone, but we did not attempt to do so. It should be noted that the wetting phenomena is characterized both by the wetting power (K) of the liquid and the wettability (ϕ) of the solid surface, besides the surface tension of the liquid and the amount of solute adsorption.

The Equation of State for the Film at the Solid/Solution Interface.—Although a number of studies have been undertaken concerning the equation of the state of the film at the liquid/air interface[8], only a few have been reported on the solid/liquid interface[9]. The surface pressure, F, of the adsorbed film at the aqueous solution/solid interface can be expressed by:

$$F \equiv \sigma_{l_0} - \sigma_l = \sigma\cos\theta_a - \sigma_0\cos\theta_{a_0} \qquad (7)$$

where σ_{l_0} and σ_l denote the solid/water and solid/solution interfacial tensions, σ_0 and σ, the surface tensions of water and the aqueous solution, and θ_{a_0} and θ_a, the advancing contact angles of water and the aqueous solution on

8) N. K. Adam, "Physics and Chemistry of Surfaces", Oxford University Press, London (1938), p. 115.
9) W. D. Harkins et al., *J. Am. Chem. Soc.*, **62**, 3377 (1940).

TABLE III. CROSS-SECTIONAL AREA OF ALCOHOL MOLECULE

Alcohol	from Volmer Eq.	from Langmuir Eq.
n-Propyl alc.	25.0 (Å²/mol.)	24.9 (Å²/mol.)
n-Butyl alc.	24.0 (Å²/mol.)	25.0 (Å²/mol.)
n-Amyl alc.	24.0 (Å²/mol.)	26.6 (Å²/mol.)
n-Octyl alc.	—	11.6 (Å²/mol.)

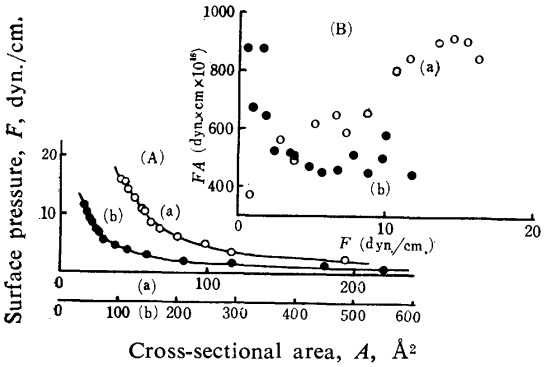

Fig. 9. (A) Pressure~area and (B) $FA \sim F$ relations for adsorbed films of (a) *n*-amyl and (b) *n*-octyl alcohol on paraffin surface.

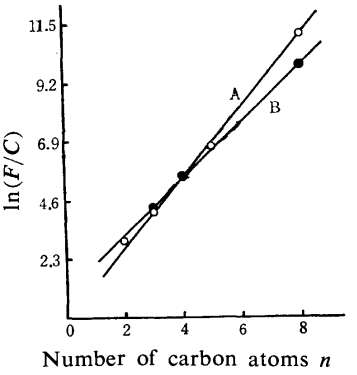

Fig. 10. $\ln(F/c)_n$ vs. number of carbon atoms of fatty alcohol homologues.
A, Paraffin/solution interface
B, Air/solution interface

the solid respectively. Thus, we can calculate the surface pressure of the film at the solid/liquid interface from the measurement of the surface tension and contact angle. Further, the area occupied by a molecule in the film is given by

$$A = 1/\Gamma N \qquad (8)$$

where N denotes the Avogadro number. The $F \sim A$ diagrams were then constructed as shown in Figs. 8 and 9, with $FA \sim F$ curves inserted. The $FA \sim F$ curves of *n*-propyl, *n*-butyl and *n*-amyl alcohols can then be expressed by Volmer's equation as:

$$FA = ikT + A_0F \quad \text{or} \quad F(A - A_0) = ikT \qquad (9)$$

where i and the co-area A_0 are constants. The slope of the straight line of $FA \sim F$ gives the co-area of the adsorbed molecule which corresponds to the saturation amount of adsorption obtained from Langmuir's formula. These values are shown in Table III. The two values coincide and are also equal to the corresponding values of the air/water interface.

Traube's Rule for the Solid Solution Interface.—Traube's rule[10] predicts that

$$\ln(F/c)_n = E + \frac{\Delta W}{RT}n \qquad (10)$$

where $(F/c)_n$ denotes the slope of $F \sim c$ curve at its origin for aqueous C_n-alcohol, ΔW, the work per mol. of CH_2 chain of the alcohol molecules required to bring it from the adsorbed layer to the interior of the solution, and E, a constant. To check Eq. 10, the value of $(F/c)_n$ was calculated from the slope of the $F \sim c$ curve (not shown) at the origin for each solution of alcohol homologues. The diagram of $\ln(F/c)_n$ thus obtained against n is shown in Fig. 10, together with the diagram for an aqueous solution for purposes of comparison. In this figure the plot for ethanol was taken from a preceding report[6]. As is shown in Fig. 10, the linear relation of Eq. 10 holds for both paraffin/solution and air/solution interfaces. We evaluated ΔW from this slope, obtaining the values of 824 cal./mol. CH_2 for the paraffin/solution interface and 656 cal./mol. CH_2 for the aqueous solution surface respectively. As for the ΔW of the paraffin/solution interface, we obtained 774 cal./mol. CH_2 for saturated fatty acid adsorbed on paraffin[11], 1000 cal./mol. CH_2 from the experiment of monolayer penetration[12], 800 cal./mol. CH_2 from the adsorption of benzylamine on the α-bromopalmitic acid monolayer[13], and 810 cal./mol. CH_2 for the oil/solution interface[14], while for the ΔW of the air/solution interface, values of 630 cal./mol.[14] and 640 cal./mol.[12] are given. Our ΔW values may be considered to be of the right order of magnitude as compared with these published

10) J. T. Davies and E. K. Rideal, "Interfacial Phenomena", Academic Press, New York (1961), p. 155.

11) H. Gastalla, *Compt. rend.*, 235, 941 (1952).
12) K. G. A. Pankhurst, *Proc. Roy. Soc.*, A179, 393 (1942).
13) D. J. Crisp, "Surface Chemistry", Butterworths, London (1949), p. 65.
14) J. T. Davies, *Trans. Faraday Soc.*, 48, 1052 (1952).

data. As is seen, the value of ΔW for the paraffin/solution interface is somewhat larger than that for the air/solution interface. This is consistent with the view of a larger affinity of the hydrocarbon chain of the alcohol molecule for the paraffin/solution interface than for the air/solution interface[14].

Here we may add that, in the present case, Eq. 4 or its integrated form,

$$\sigma_1 \cos\theta_a = RT\int_0^c \Gamma \, d\ln c$$

can also be considered as a wetting isotherm which, if we put Γ as a Langmuir-type adsorption isotherm, can be integrated to give an adsorption isotherm similar to that of Eq. 3. However, we should like to emphasize that Eq. 3 is more useful than Eq. 4 because (i) Eq. 3 is an integrated formula with respect to Γ, while the integration of Eq. 4 is not always possible, (ii) Eq. 4 is limited only to cases of physical adsorption, as in the present case, while Eq. 3 fits the wetting data even when Eq. 4 fails to explain the adsorption, as in the case of the chemisorption of xanthate on a mineral surface[6] or the surface attack of polystyrene by sulfuric acid[15], and (iii) Eq. 3 offers the more distinct molecular explanation of the effect of surface film on wetting. It should also be added that Eqs. 3 and 4 cannot be applied to the cases of polymolecular adsorption or deep surface chemical attack where the wetting property cannot be considered as a simple function of the adsorption amount.

15) T. Tsunoda, T. Seimiya and T. Sasaki, This Bulletin, 35, 1570 (1962).

Summary

The wettability of paraffin towards aqueous solutions of *n*-propyl, *n*-butyl, *n*-amyl and *n*-octyl alcohols has been studied. It has been found that the wetting isotherm which had been proposed by the present author and had been valid for the wetting of paraffin by an aqueous ethyl alcohol solution, could also be applied successfully to the present systems. The equations of state for the adsorbed films of these alcohols at the paraffin/aqueous solution interface were obtained. It was further shown that Traube's rule holds for the paraffin/aqueous alcohol solution interface as well as for the air/solution interface. The adsorption energies found were 824 cal./mol.·CH_2 for the paraffin/solution interface and 656 cal./mol. CH_2 for the aqueous surface.

The author wishes to express his hearty thanks to Professor Tsunetaka Sasaki for his helpful guidance throughout this experiment. The cost of this research has been defrayed by a Scientific Research Grant of the Ministry of Education given to Professor Sasaki.

Department of Chemistry
Faculty of Science
Tokyo Metropolitan University
Setagaya-ku, Tokyo

The Wetting of Paraffin by Aqueous Solutions of Sodium Decyl, Dodecyl and Tetradecyl Sulfates

By Teruo TSUNODA* and Tsunetaka SASAKI

(Received December 12, 1962)

The wetting of the surface of such solids as metals, plastics, and fibers by wetting agents and detergent solutions has offered many fundamental problems[1]. However, studies upon the theory underlying the phenomena have hitherto been rather unsatisfactory, especially regarding the relation between the wetting and the solute adsorption[2].

In a previous paper we reported on the relation between the wetting of paraffin by aqueous solutions of fatty alcohol homologues and the solute adsorption[3]. In the present paper we will attempt to study further the relation between the wetting of the paraffin surface by aqueous solutions of sodium decyl, dodecyl and tetradecyl sulfates, and their adsorption.

* Present address: Hitachi Central Research Laboratory, Hitachi, Ltd., Kokubunji, Kitatama-gun, Tokyo.

1) A. M. Schwartz, J. M. Perry and J. Berch, "Surface Active Agents and Detergents", Vol. 2, Interscience Publications, New York (1957), p. 543.

2) K. S. Doss et al., *Proc. Ind. Acad. Sci.*, **7A**, 117 (1938); P. A. Rehbinder et al., *Kolloid-Z.*, **65**, 268 (1933); M. Wada, *Nippon Kogyo Kaishi*, **59**, 681 (1943).

3) T. Tsunoda, This Bulletin, **36**, 445 (1963).

Experimental

The detergents used were sodium decyl (SDeS), dodecyl (SDoS) and tetradecyl (STS) sulfates. They were prepared by the reaction of corresponding alcohols with chlorosulfonic acid in ether. In order to purify them, the alkyl sulfates obtained were dissolved in ethyl alcohol, treated with charcoal, and then recrystallized. The disappearance of the minimum in surface tension concentration curves, as is shown in Fig. 1, proved their purity. The paraffin used was purified by treating it with concentrated sulfuric acid, then with sodium hydroxide, and finally by vacuum distillation. For the wettability measurement, the paraffin surface was

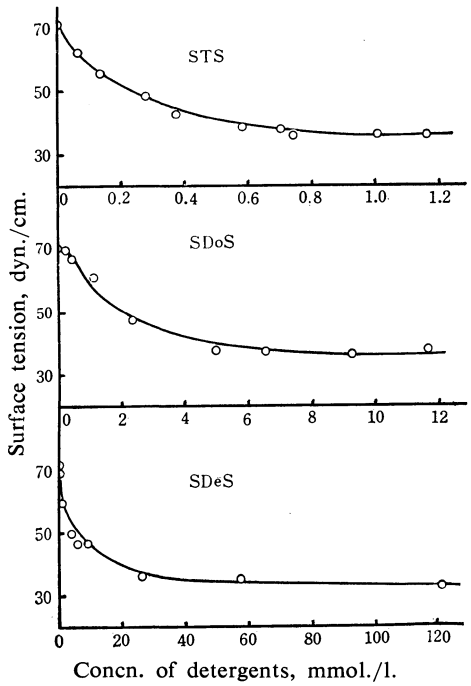

Fig. 1. Surface tension vs. concentration of detergents.

prepared as a thin layer on a glass rod of a uniform diameter. The measurements of wettability and surface tension were made in the same manner as was reported in a preceding paper[3]. The temperature was controlled at 30±0.3°C throughout the experiments. No particular control of the pH was made for the solution used. It was about 6.

Results and Discussion

The changes in the wetting tension of paraffin towards aqueous solutions of detergents with the time of immersion in those solutions are shown in Fig. 2, for instance, for SDoS solution, where $\sigma_1 \cos\theta_r$ is the wetting tensinon, σ_1, the surface tension of the solution, and θ_r, the receding contact angle of the solution on paraffin. The equilibrium values of the wettability were attained within 60 min. after the immersion of the paraffin into the detergent solutions. The equilibrium advancing and receding contact angles thus obtained were plotted against the concentration of detergent solutions as shown in Figs. 3, 4 and 5. The hysteresis of the contact angles was at

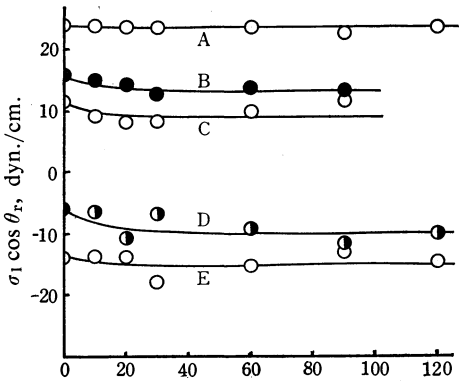

Fig. 2. $\sigma_1 \cos\theta_r$ vs. time of immersion into SDoS solution.

A 2.36×10^{-3} mol./l. B 9.32×10^{-3}
C 1.57×10^{-2} D 1.15×10^{-3}
E 2.70×10^{-4}

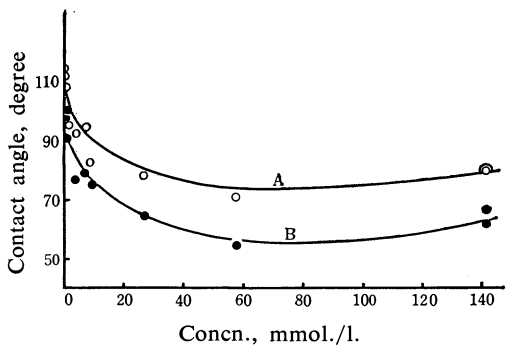

Fig. 3. Contact angle vs. concentration of SDeS.

A, advancing B, receding

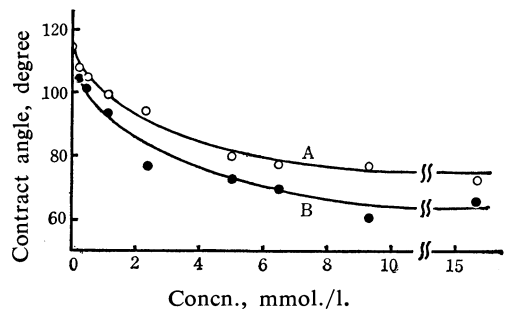

Fig. 4. Contact angle vs. concentration of SDoS.

A, advancing B, receding

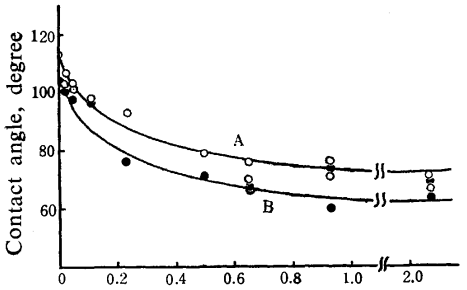

Fig. 5. Contact angle vs. concentration of STS.
A, advancing B, receding

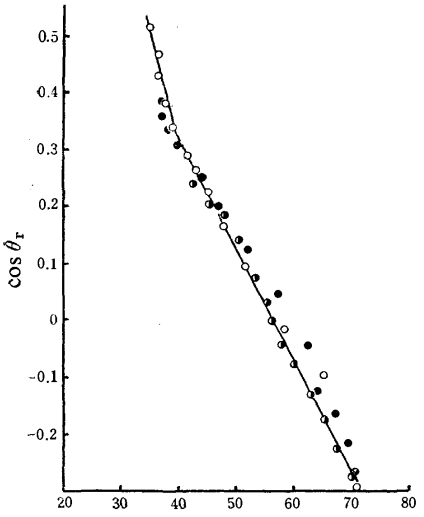

Fig. 6. $\cos\theta_r$ vs. surface tension.
○ Sodium decyl sulfate
● Sodium dodecyl sulfate
◑ Sodium tetradecyl sulfate

most 10 degrees in these experiments. Figure 6 shows the relation between the cosine of the receding contact angles and the surface tension of the detergent solutions. We can observe in this figure that the curves tend to show a discontinuity in slope at about 40 dyn./cm. A similar phenomenon was observed for the wetting of teflon and polyethylene by several detergent solutions[4]. We calculated the Zisman critical surface tension, γ_c[5], by the extrapolation of the σ_l vs. $\cos\theta_r$ plot to $\cos\theta_r=1$ and thus found γ_c to be 26 dyn./cm.

Now we shall refer to the wetting isotherm. As in a preceding paper[6] we used the following wetting isotherm;

$$\cos\theta_r=\frac{\sigma_l+\sigma_w}{\sigma_l}(\phi+K\Gamma)-1 \qquad (1)$$

where θ_r denotes the receding contact angles, σ_l and σ_w, the surface tension of the solution and solvent (water) respectively, Γ, the amounts of solute adsorption in mol./cm^2, and ϕ and K constants. In order to check our wetting isotherm 1, we calculated Γ using Gibbs' adsorption isotherm:

$$\Gamma=\frac{d(\sigma_l\cos\theta_a)}{RT\,d\ln c} \qquad (2)$$

and made plots between the Γ thus obtained and $\sigma_l(\cos\theta_r+1)/(\sigma_l+\sigma_w)$, as in the preceding paper[3]. Figures 7, 8 and 9 show the adsorption isotherm $\Gamma\sim c$. In the region of concentration lower than the CMC of the detergents, the apparent maximum in the adsorption isotherm is observed in these curves. It is, however, hard to interpret these maxima in the adsorption isotherm, since the $\sigma_l\cos\theta_a\sim\ln c$ plot is not generally so accurate in the concentrated region of saturated adsorption. Figure 10 shows the $\sigma_l(\cos\theta_r+1)/(\sigma_l+\sigma_w))\sim\Gamma$ plots. The plots indicate a linear relation in the

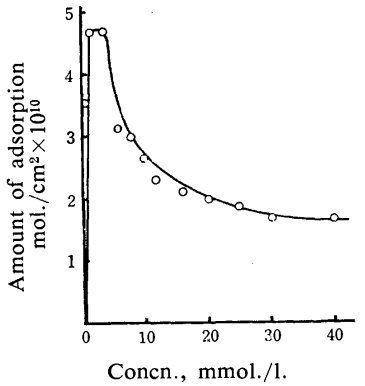

Fig. 7. Adsorption isotherm of SDeS for paraffin/solution interface.

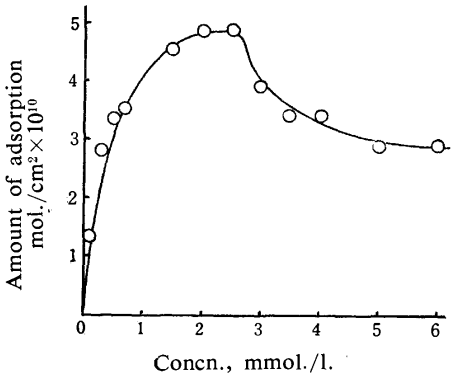

Fig. 8. Adsorption isotherm of SDoS for paraffin/solution interface.

4) W. A. Zisman et al., *J. Phys. Chem.*, 63, 1241 (1959).
5) W. A. Zisman et al., *J. Colloid Sci.*, 47, 428 (1952).
6) T. Sasaki, H. Kumanomido and T. Tsunoda, 2nd International Congress of Surface Activity, III, Butterworths, London (1957), p. 153.

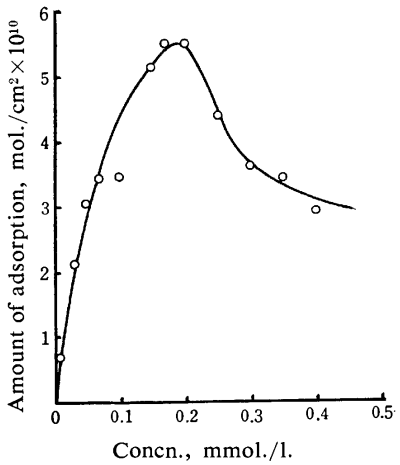

Fig. 9. Adsorption isotherm of STS for paraffin/solution interface.

region of concentration less than that of the maximum adsorption. From this linearity we calculated the constants ϕ and K, which are shown in Table I. In this table we may notice, that the calculated values of ϕ are constant, regardless of the detergents used, while the K values decrease with the increasing molecular weight. These results are similar with the values of ϕ and K obtained for fatty alcohols on paraffin[3]. Inserting the values of ϕ and K into Eq. 1, we obtained:

for SDeS

$$\cos\theta_r=\frac{\sigma_1+\sigma_w}{\sigma_1}(0.353+0.026\times10^{10}\Gamma)-1$$

for SDoS

$$\cos\theta_r=\frac{\sigma_1+\sigma_w}{\sigma_1}(0.347+0.025\times10^{10}\Gamma)-1 \qquad (3)$$

for STS

$$\cos\theta_r=\frac{\sigma_1+\sigma_w}{\sigma_1}(0.347+0.016\times10^{10}\Gamma)-1$$

Figure 11 shows the comparison between the values obtained from Eq. 3 (solid line) and the observed values (circles). Beyond the concentration of maximum adsorption of detergents, the discrepancies between the calculated and observed contact angle values are marked in all cases, partly because of the inevitable inacuracy in observation already mentioned.

TABLE I. CONSTANTS ϕ AND K IN WETTING ISOTHERM 1

Detergent	ϕ	K, cm²/mol.
Sodium decyl sulfate	0.353	2.6×10^5
Sodium dodecyl sulfate	0.347	2.5×10^8
Sodium tetradecyl sulfate	0.347	1.6×10^8

In Figs. 12, 13 and 14, we show $F\sim A$ diagram, together with the $FA\sim A$ curves inserted. The surface pressure of the adsorbed film on the solid/solution interface, F, and the area occupied by molecules in the film, A, is obtained in a manner similar to that used in a preceding paper[6]. Applying Volmer's equation, $FA=ikT+A_0F$ to the $FA\sim F$ curves, as shown by solid lines in Figs. 12, 13 and 14, the co-area A_0's are obtained as 30, 23, 30Å²/molec. for SDeS, SDoS and STS respectively.

We further examined the validity of Traube's rule, which is expressed by:

$$\ln(F/c)_n=\ln(F/c)_1+\Delta w(n-1)/RT \qquad (4)$$

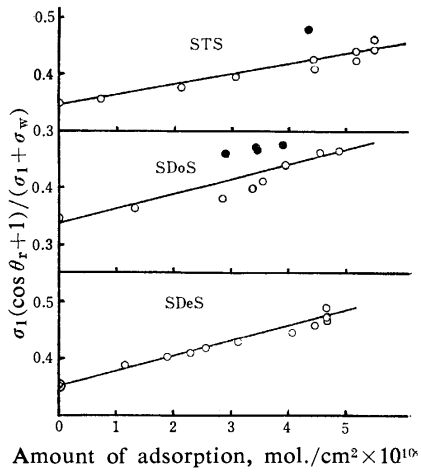

Fig. 10. Validity of Eq. 1.
○ Concn. less than max. adsorption
● Concn. beyond max. adsorption

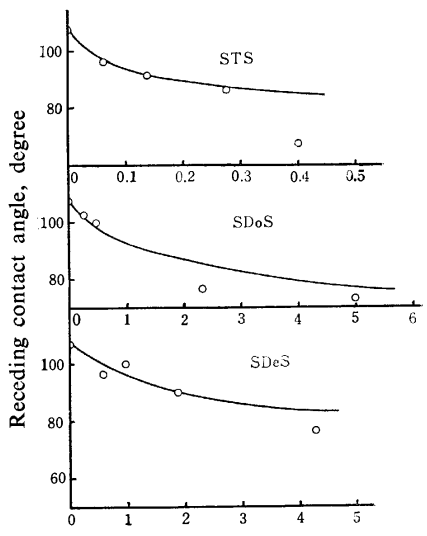

Fig. 11. Comparison between calculated (solid line) and observed (circle) contact angles.

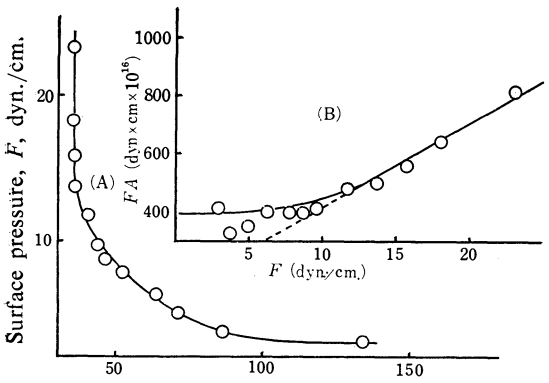

Fig. 12. (A) Pressure~area and (B) $FA \sim F$ relations for adsorbed film of SDeS for paraffin/solution interface.

where F/c denotes the slope of the $F \sim c$ curve at $c=0$, n, the number of carbon atoms in the alkyl sulfate molecules, and Δw, the work per CH_2 of adsorbed solute molecule required to bring it from the paraffin surface back into the interior of the solution. Figure 15 shows the lineality between $\ln(F/c)$ and n. From these figures, we obtained 588.9 cal./mol. CH_2 as the Δw for the paraffin/solution interface. This figure is smaller than 824 cal./mol. CH_2 obtained for the fatty alcohol at the solution/paraffin interface[3]. For the air/solution interface, we obtained 534.7 cal./mol. CH_2 as the Δw value. This value is also smaller than that of 656 cal./mol. CH_2 for fatty alcohols at the aqueous alcohol solution surface[3].

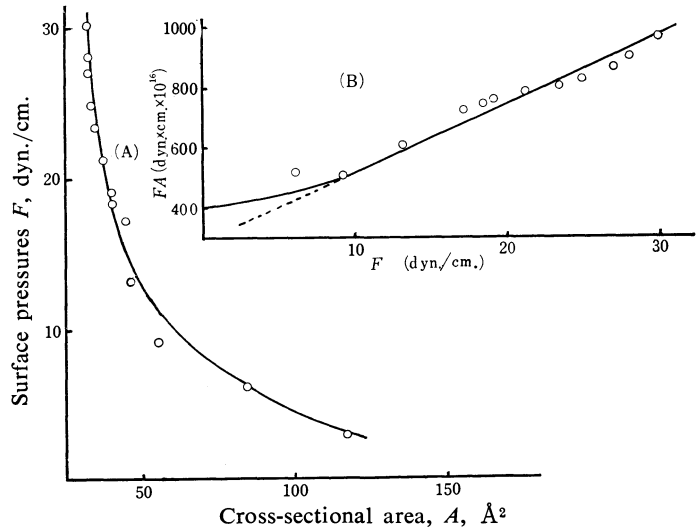

Fig. 13. (A) Pressure~area and (B) $FA \sim F$ relations for adsorbed film of SDoS for paraffin/solution interface.

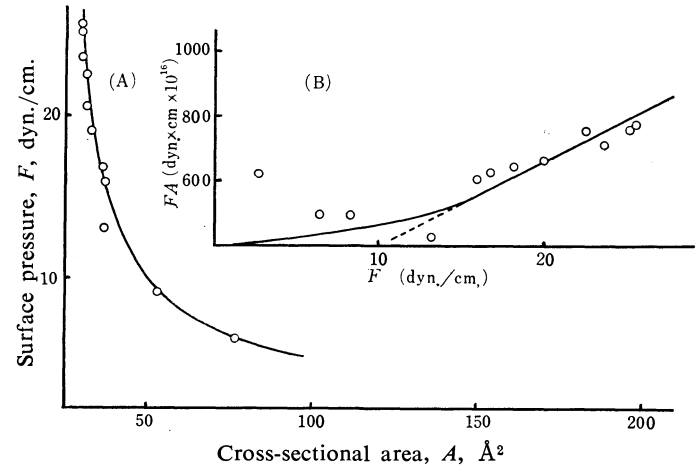

Fig. 14. (A) Pressure~area and (B) $FA \sim F$ relations for adsorbed film of STS for paraffin/solution interface.

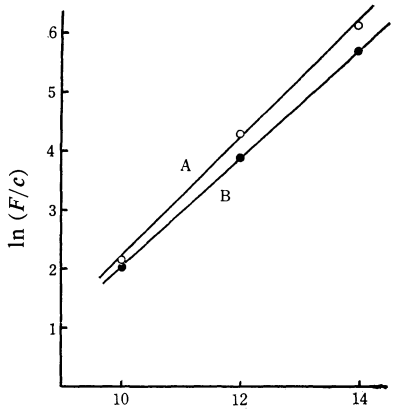

Fig. 15. ln (F/c) vs. number of carbon atoms of detergent molecules

A Paraffin/solution interface
B Air/solution interface

Summary

The wettability of the paraffin by aqueous solutions of sodium decyl, dodecyl and tetradecyl sulfate have been studied. A slight but distinct discontinuity of the slope in the curve of the cosine of the receding contact angle vs. the surface tension of the solution was observed for the solution of sodium decyl, dodecyl and tetradecyl sulfate. The discontinuity of the slope appeared at the surface tension of about 40 dyn./cm. It was found that the wetting isotherm which had been proposed by the present author, and which had been found valid for the wetting of paraffin by the aqueous solution of fatty alcohol homologues, was also valid for this experiment in the dilute aqueous solution of sodium alkyl sulfates. The adsorption energy was 588.9 cal./mol. CH_2 and 534.7 cal./mol. for the paraffin/solution and air/solution interfaces respectively.

The cost of this research has been defrayed by a Scientific Research Grant of the Ministry of Education given to Tsunetaka Sasaki.

Department of Chemistry
Faculty of Scince
Tokyo Metropolitan University
Setagaya-ku, Tokyo

The Stereoregularity-Fractionation of Polyvinyl Alcohol by Foaming

By Kiyokazu IMAI and Masakazu MATSUMOTO

(Received December 17, 1962)

It has been found that several properties of polyvinyl alcohol (PVA), probably related to its stereoregularity, vary with the polymerization conditions of the polyvinyl acetate from which PVA is derived[1]. Therefore, one method to obtain PVA differing in regularity is to control the conditions of the polymerization. As a complementary method, we have evolved a method for separating PVA into fractions differing in regularity. Besides being interesting for its own sake, such a fractionation procedure should give a method for determining the stereoregularity distribution of PVA. We found that PVA can be separated into fractions of different stereoregularity by foaming an aqueous solution of the polymer. Although it is well known that foams can serve to separate substances of different chemical structures[2], the foam method seems not yet to have been applied in the stereoregularity fractionation of polymers. The present report may, therefore, be the first communication about it.

Experimental

Three samples of PVA of differing stereoregularity were used. These samples are listed in Table I.

The fractionation procedure was as follows: a 1~2% aqueous solution of fully hydrolyzed PVA derived from polyvinyl acetate was placed in a 1~5 l. wide-mouthed bottle. The bottle was then shaken at a frequency of 100 cycl. per minute with an amplitude of 6.7 or 10.8 cm. on a horizontal shaker; a foam layer was thus created. After being shaken for a certain time, the solution was allowed to stand for more than 15 hr. In the course of this standing, part of the foam usually disintegrated and drained down, but the remaining layer was separated and the PVA contained in the foam was collected. The residual solution usually became cloudy, and a slight amount of gel precipitated at the bottom of the bottle. To obtain successive fractions, the cloudy solution was heated until it became a completely clear and uniform solution

1) Reference to literature appeared in *J. Polymer Sci.*, 55, 335 (1961).

2) J. J. Bikermann, "Foams", Reinhold, New York (1953), p. 171; T. Sasaki, "Zikken Kagaku Koza", Vol. 7 Maruzen, Tokyo (1956), p. 215.

TABLE I. POLYMERIZATION CONDITIONS OF ORIGINAL POLYVINYL ACETATE FOR PVA SAMPLES

No.	Polymerization temp., °C	Polymerization medium		Initiator	Conversion %	PVA	
		Form	Concn. wt. %			$[\eta]$[a] dl./g.	Degree of polymerization
L-O-43	0	Methyl alcohol	40	Photosensitized with azobis compound	13	0.811	1510
W-6	60	Methyl alcohol	20	AIBN[b]	50	0.866	1680
DM32-2,3	80	Dimethyl sulfoxide	50	AIBN[b]	63	0.878	1710

a) Measured in water at 30°C b) 2,2'-Azobis-isobutyronitrile

TABLE II. D_{620} AND 1,2-GLYCOL CONTENT OF PVA OBTAINED FROM THE FOAM LAYER

Fraction No.	Concn. of PVA g./l.	Amount of solution kg.	Capacity of bottle l.	Amplitude of shaking cm.	Shaking time day	PVA				
						Yield %	$[\eta]$ dl./g.	Degree of polymerization	D_{620}	1,2-Glycol structure mol. %
S1-F1	19.8	2.5	5	6.7	1	5.3	0.895	1760	0.96	1.02
S4-F1	20.2	2.5	5	6.7	1	2.5	0.878	1710	0.73[a]	—
S5-F1	18.9	2.7	5	6.5	1	3.7	0.870	1690	0.83	—
S2-F1	20.1	2.5	5	6.7	3	15	0.927	1860	0.83	1.06
S3-F1	10.4	2.5	5	6.7	1	6.5	0.949	1930	0.91	1.04
S7-F1	10.2	1.0	2	10.8	1	11	1.00	2100	0.81	—
S8-F1	10.2	0.5	2	10.8	1	44	0.986	2050	0.48	—
S6-F1	9.8	0.5	1	10.8	1	14	0.952	1940	0.73	—
W-6[b]	—	—	—	—	—	—	0.866	1680	0.23	1.13

a) Standing time from cessation of shaking to separation of foam was only 2 hr.
b) Original unfractionated PVA

and then the procedure involving shaking, standing, separation and heating was repeated.

We have found that the color reaction of PVA with iodine-iodide in an aqueous solution can be used as a measure of the stereoregularity of PVA[3]. An absorption peak is produced at 620 mμ by the iodine-PVA complex when it is prepared under specified conditions, and the absorbance at this wavelength, D_{620}, is used as a quantitative index of the color reaction. According to some unpublished data of the authors and of K. Fujii, the color reaction does not occur for isotactic PVA, but since it appears to depend on the degree of syndiotacticity of PVA, the D_{620} value may be used as a parameter of the syndiotacticity for PVA samples having the same degree of polymerization. Strictly speaking, it is not certain whether the color reaction is due simply to the existence of the fraction of syndiotactic linkage or to their regular sequence length.

Results and Discussion

The D_{620} values of PVA contained in the foam layers are illustrated in Table II in comparison with that of the original PVA. The degree of the polymerization of the PVA contained in the foam layers is approximately the same as that of the original PVA, but the D_{620} value of the former is quite different from that of the original. In general, the values of the former exceed that of the latter.

Since the D_{620} value depends on the degree of polymerization, a difference in molecular weight distribution between the original PVA and the sample obtained from the foam layer could theoretically explain the observed color-test difference. However, the dependence of the D_{620} value upon the degree of polymerization is not strong enough to make this likely. For example, if the PVA sample is fractionated by a precipitation method from a solvent (water)-non-solvent (*n*-propyl alcohol)-mixture, the D_{620} values range from 0.08 for DP=639 up to only 0.31 for DP=3960. Even at this latter value, the sample lies well below the 0.5 to 1.0 range found in the foam layer in Table II.

The 1,2-glycol content of the PVA from the foam layer is slightly less than that of the original, this also might be a cause of the different D_{620} value. However, since the difference in content of the 1,2-glycol structure is quite small, the predominant cause of the different D_{620} value was considered to be the tacticity of the sample. From the results of Table II, it may be concluded that the stereoregularity, probably the syndiotacticity, of the PVA obtained from the foam layer is larger than that of the original PVA.

3) K. Imai and M. Matsumoto, *J. Polymer Sci.*, **55**, 355 (1961).

TABLE III. SUCCESSIVE FRACTIONATION OF PVA L-O-43 BY REGULARITY
(Capacity of bottle, 2 l.; amplitude of shaking, 10.8 cm.)

Fraction No.	Concn. of PVA g./l.	Amount of solution l.	Shaking time hr.	Foam volume l.	PVA			
					Yield %	$[\eta]$ dl./g.	Degree of polymerization	D_{620}
F1	9.54	1.0	2	1.7	2.7	8.46	1620	3.05
F2	—	1.0	4	1.4	5.3	8.84	1730	2.94
F3	—	1.0	8	1.3	10.9	9.06	1800	2.51
F4	—	0.9	24	1.5	34.3	9.57	1960	1.66
F5	—	—	24	0.6	7.1	8.92	1750	0.54
F6	—	0.8	24	0.5	2.2	8.25	1550	0.38
F7	4.55	0.8	50	0.4	2.1	7.48	1330	0.23
F8[a]	11.0[a]	0.3[a]	24	0.1	1.3	7.14	1410	0.10
F9	—	—	—	—	34.1	5.94	928	0.02
F0[b]	—	—	—	—	—	8.11	1510	1.11

a) Shaken with 1 l. bottle after concentration
b) Original unfractionated PVA, L-O-43

TABLE IV. SUCCESSIVE FRACTIONATION OF PVA W-6 BY REGULARITY
(Capacity of bottle, 5 l.; amplitude of shaking, 6.7 cm.)

Fraction No.	Concn. of PVA g./l.	Amount of solution l.	Shaking time day	Foam volume l.	PVA					
					Yield %	$[\eta]$ dl./g.	Degree of polymerization	D_{620}	Swelling degree	Solubility %
F1	18.88	2.7	1	3.5	3.67	0.870	1690	0.83	1.74	7.5
F2	18.64	2.5	1	3.1	5.21	0.858	1650	0.74	1.97	8.1
F3	—	2.4	1	3.5	6.25	0.899	1770	0.49	—	—
F4	—	2.3	1	3.5	6.19	0.908	1800	0.41	—	—
F5	16.16	2.2	1	3.5	6.97	0.938	1900	0.53	—	—
F6	—	2.2	1	3.3	6.35	0.938	1900	0.42	2.04	9.8
F7	—	2.1	1	3.4	5.50	0.941	1910	0.41	—	—
F8	—	1.9_5	1	2.8	3.80	0.929	1870	0.27	—	—
F9	—	1.9_5	1	2.0	5.44	0.949	1930	0.23	—	—
F10	12.60	1.9	1	2.5	3.86	0.939	1900	0.19	2.24	10.8
F11	—	1.8	1	3.0	3.33	0.955	1950	0.19	—	—
F12	—	1.7	1	3.0	2.41	0.923	1840	0.15	—	—
F13	—	1.7	1	3.0	4.02	0.921	1840	0.12	—	—
F14	—	1.6	1	2.5	3.01	0.926	1860	0.10	—	—
F15	11.14	1.5_5	2	1.1	8.64	0.882	1720	0.04	2.26	12.0
F16	—	1.5	2	0.8	5.94	0.850	1630	0.02	—	—
F17	—	1.3_5	2	0.6_5	2.89	0.835	1580	0.01	—	—
F18	—	1.1	2	0.6	1.37	0.809	1500	0.01	3.27	19.3
F19	—	1.1	2	0.4	0.78	0.784	1430	0.00	—	—
F20	6.80	1.1	1	0.4	0.75	0.809	1500	0.01	—	—
F21	—	1.0_5	2	0.3	0.52	0.728	1280	0.00	—	—
F22	—	0.9_5	2	0.3	1.00	0.733	1290	0.00	—	—
F23	6.10	0.9	—	—	12.08	0.570	870	0.00 (0.00)[a]	3.37 (3.68)[a]	27.4 (30.4)[a]
F0[b]	—	—	—	—	—	0.866	1680	0.23	2.2	—

a) For the sample performed a further treatment to decrease any residual acetyl group of PVA.
b) Original unfractionated PVA, W-6

TABLE V. SUCCESSIVE FRACTIONATION OF PVA DM32-2,3 BY REGULARITY
(Capacity of bottle, 2 l.; amplitude of shaking, 10.8 cm.)

Fraction No.	Concn. of PVA g./l.	Amount of solution l.	Shaking time hr.	Foam volume l.	PVA			
					Yield %	$[\eta]$ dl./g.	Degree of polymerization	D_{620}
F1	9.53	1.0	4.5	0.9	2.8	0.938	1900	0.07
F2	—	1.0	48	0.7	6.3	1.02	2150	0.03
F3	—	1.0	72	0.6	5.4	1.02	2160	0.03
F4	—	1.0	72	0.4_5	3.9	1.01	2120	0.02
F5	8.17	1.0	72	0.3	4.6	0.945	1920	0.01
F6	—	0.9	72	0.2	2.1	0.992	2070	0.00
F7	—	0.9	—	—	74.4	0.824	1550	0.00
F0[a]	—	—	—	—	—	0.878	1710	0.00

a) Original unfractionated PVA, DM32-2,3

Tables III, IV and V show the results of three successive fractionations of PVA by foaming. From the properties and polymerization conditions, the stereoregularity order of the PVA used is as follows:

L-O-43 (Table III) > W-6 (Table IV) > DM32-2,3 (Table V)

Polyvinyl alcohol W-6 is an ordinary one and the same as the original PVA in Table II.

As may be seen in every table, the degree of the polymerization of PVA in each fraction is not constant, but increases slightly with an increase in the fraction number and then decreases again. On the other hand, as the fractionation progresses, the D_{620} value decreases and the swelling degree and solubility increase, suggesting that the sample is being separated according to regularity, i. e., syndiotacticity.

It is well-established that the lower the polymerization temperature of vinyl acetate, the more stereoregular the PVA obtained. Therefore, when PVA prepared by a low temperature polymerization is fractionated by the foam method, it is to be expected that the first fraction will furnish an extremely stereoregular PVA. Such a result is illustrated in Table III. The D_{620} value for PVA F1 in this table is 3.05, much larger than the 0.23 of an ordinary PVA W-6. This indicates that the F1 fraction is highly regular.

According to unpublished data collected by the present authors, the regularity of PVA is responsible for the foaminess of its aqueous solution; the foaminess of the solution increases with an increase in the regularity. This behavior seems to relate more closely to foam stability than to foaming capacity because the foam volume formed by a blowing method remains nearly constant, independent of the polymerization conditions of the parent ester polymer of PVA[4]. On the other hand, it is known that the aging of a concentrated aqueous solution of PVA depends upon such polymerization conditions as the temperature[5] and the solvent[4] used; it has also been observed that the regular polymer shows greater aging.

Furthermore, aqueous solutions of PVA have a tendency to gel at an air-water interface[6]. It is, therefore, believed that foam stabilization due to aging is a basic factor in the performance of fractionation according to regularity. When a blowing method is applied in the foam formation, PVA is not separated in regularity[4]. This is considered to be due to the fact that foam formation occurs more easily in the blowing method than in the shaking method, but foam rupture occurs more easily in the latter than in the former. To fractionate effectively, foaming alone is not sufficient; a proper breaking of the foam seems also to be required.

Research Laboratory
Kurashiki Rayon Co., Ltd.
Kurashiki, Okayama

4) K. Imai and M. Matsumoto, unpublished data.
5) M. Matsumoto and Y. Ohyanagi, *J. Polymer Sci.*, **26**, 389 (1957).
6) D. J. Crisp, *J. Colloid Sci.*, 1, 49, 161 (1946); H. L. Frisch and S. Al-Madfai, *J. Am. Chem. Soc.*, **80**, 3561 (1958); T. Tachibana, K. Inokuchi and T. Inokuchi, *Kolloid Z.*, **167**, 141 (1959); H. Dieu, *Makromol. Chem.*, **35A**, 78 (1960); K. Fukawa, T. Asakura and H. Daimon, *Kobunshi Kagaku*, 18, 596 (1961).

Studies on Antibiotics and Related Substances. XVII. Syntheses of trans-2-Aminocyclohexyl-D-glucosaminides

By Tetsuo SUAMI, Seiichiro OGAWA and Sumio UMEZAWA

(Received December 25, 1962)

As a model compound of simpler structure of kanamycin[1], 2-aminocyclohexyl-D-glucosaminides has been studied in our laboratory[2]. In the present report a further investigation has been accomplished to characterize *l*- and *d-trans*-2-aminocyclohexyl-D-glucosaminides.

d,l-trans-2-Aminocyclohexanol was prepared by the method of Osterberg and Kendal[3]. A literature method[4] for a resolution of *d,l-trans*-2-aminocyclohexanol with L-(+)-tartaric acid by a fractional recrystallization in 80% ethanol proved to be good for the preparation of *l-trans* isomer. Then, by applying 95% aqueous methanol for a fractional recrystallization, a better result for isolating *d-trans* isomer was obtained.

By treatments of L-(+)-tartrates of *l*- and *d-trans*-2-aminocyclohexanol with alkali, *l*- and *d-trans*-2-aminocyclohexanol were obtained respectively in the optically active forms.

N-Carbobenzoxy-*l-trans*-2-aminocyclohexanol (I) and *N*-carbobenzoxy-*d-trans*-2-aminocyclohexanol (V) were prepared directly by carbobenzoxylation of L-(+)-tartrate of *l*- and *d-trans*-2-aminocyclohexanol respectively in good yields.

The condensation of I with α-1-bromo-3, 4, 6-triacetyl-*N*-carbobenzoxy-D-glucosamine[5] in the presence of mercuric cyanide gave β-(*N*-carbobenzoxy-*l-trans*-2-aminocyclohexyl)-3, 4, 6-triacetyl-*N*-carbobenzoxy-D-glucosaminide (II) melting at 217~217.5°C in 37% yield. Also it was noticed that a considerable amount of 4, 5-(3, 4, 6-triacetyl-D-glucopyranosyl)oxazolone-2[10] was formed which was recovered from the mother liquor of II as a by-product.

Deacetylation of II with methanol saturated with ammonia gave β-(*N*-carbobenzoxy-*l-trans*-2-aminocyclohexyl)-*N*-carbobenzoxy-D-glucosaminide (III) melting at 224~225.5°C in 81% yield.

A catalytic hydrogenolysis of III yielde β-(*l- trans*-2-aminocyclohexyl)-D-glucosaminide (IV) melting at 159~161°C (decomp.) in 60% yield.

The reaction sequences employed in the synthesis of β-(*d-trans*-2-aminocyclohexyl)-D-glucosaminide (VIII) were similar to those of IV.

The optical rotations of the products were listed on Table I.

TABLE I. SPECIFIC ROTATION OF *trans*-2-AMINOCYCLOHEXANOLS AND THEIR DERIVATIVES

Derivative	$[\alpha]_D$ *l*	$[\alpha]_D$ *d*
trans-2-Aminocyclohexanol	−37.6°	+38.4°
N-Benzoyl-*trans*-2-aminocyclohexanol	−39.8°	+41.1°
N-Carbobenzoxy-*trans*-2-aminocyclohexanol	−20.1°	+20.3°
β-(*N*-Carbobenzoxy-*trans*-2-aminocyclohexyl)-3, 4, 6-triacety-*N*-carbobenzoxy-D-glucosaminide	+5.6°	+22.9°
β-(*N*-Carbobenzoxy-*trans*-2-aminocyclohexyl)-*N*-carbobenzoxy-D-glucosaminide	−28.1°	+10.3°
β-(*trans*-2-Aminocyclohexyl)-D-glucosaminide	−72.6°	+4.6°

Designation of IV and VIII as β-anomers was based on their optical rotations and infrared spectra. The optical rotations of IV and VIII were less dextrorotatory, compared with that of (α-D-6-amino-6-deoxyglucopyranosyl)deoxystreptamine[6] and paromamine[7]. The infrared spectra of IV and VIII showed characteristic absorption bands for derivatives of β-glucopyranose at 895 cm^{-1} (type 2b)[8], and for cyclohexane ring deformation at 975 and 1044 cm^{-1} [9] in agreement with the assigned structures.

1) H. Umezawa, M. Ueda, K. Maeda, K. Yagishita, S. Kondo, Y. Okami, R. Utahara, Y. Osato, K. Nitta and T. Takeuchi, *J. Antibiotics, Ser. A*, **10**, 181 (1957).
2) T. Suami, S. Ogawa and S. Umezawa, This Bulletin, **35**, 474 (1962).
3) A. E. Osterberg and E. C. Kendall, *J. Am. Chem. Soc.*, **42**, 2616 (1920).
4) R. M. Godchot and M. Mousseron, *Compt. rend.*, **194**, 981 (1932).
5) J. C. Irvine, D. McNicoll and A. Hynd, *J. Chem. Soc.*, **1911**, 250; L. Zervas and S. Konstas, *Chem. Ber.*, **93**, 435 (1960).
6) S. Umezawa and T. Tsuchiya, *J. Antibiotics, Ser. A*, **15**, 51 (1962).
7) T. H. Haskell, T. C. French and Q. R. Bartz, *J. Am. Chem. Soc.*, **81**, 3481 (1959).
8) S. A. Barker, E. J. Bourne, M. Stacey and D. H. Whiffen, *Chem. & Ind.*, **1953**, 196; *J. Chem. Soc.*, **1954**, 171.
9) L. W. Morrison, *J. Chem. Soc.*, **1951**, 1614.

Considering from the optical rotation of *trans*-2-aminocyclohexyl-D-glucosaminides in Table I, β-(d, *l-trans*-2-aminocyclohexyl)-D-glucosaminide in the previous paper[2] had to be corrected to β-(*l-trans*-2-aminocyclohexyl)-D-glucosaminide and *d,l-tsans*-2-aminocyclohexyl-D-glucosaminide must be a crude product of β-(*d-trans*-2-aminocyclohexyl)-D-glucosaminide.

In addition to the above mentioned syntheses of *l-* and *d-trans*-2-aminocyclohexyl-D-glucosaminides, the attempt to prepare glucosaminides via trityl derivative of aminocyclohexanol was made. *N*-Carbobenzoxy-*d,l-trans*-2-aminocyclohexanol was tritylated with trityl chloride in anhydrous pyridine to give *N*-carbobenzoxy-*O*-trityl-*d, l-trans*-2-aminocyclohexanol (IX) melting at 126.5~128°C in 37% yield. Then, IX was condensed with α-l-bromo-3, 4, 6-triacetyl-*N*-carbobenzoxy-D-glucosamine in the presence of silver perchlorate to obtain a mixture of II and VI. The recrystallization of the mixture resulted in obtaining II in a considerably pure state, but VI was not obtained in a pure state.

Experimental

***l-trans*-2-Aminocyclohexanol.**—According to the procedure of Godchot and Mousseron[4], *l-trans*-2-aminocyclohexanol L-(+)-tartrate melting at 175~176°C, $[\alpha]_D^{22}$ −4.8° (*c* 3.2, water) [lit.[4] m. p. 177~178°C, $[\alpha]_D$ −2.73°] was obtained in 10% yield from *d, l-trans*-2-aminocyclohexanol L-(+)-tartrate. A mixture of *l-trans*-2-aminocyclohexanol L-(+)-tartrate and 10% potassium hydroxide solution was extracted with ether. The ethereal solution was dried over anhydrous sodium sulfate and the solvent was removed under reduced pressure to yield *l-trans*-2-aminocyclohexanol melting at 84~86°C, $[\alpha]_D^{22}$ −37.6° (*c* 1.30, water) [lit.[4] m. p. 83~84°C, $[\alpha]_D$ −40.2°].

N-Benzoyl derivative was prepared by shaking 1.0 g. of *l-trans*-2-aminocyclohexanol L-(+)-tartrate with 0.8 g. of benzoyl chloride in 11 ml. of 6.5% sodium hydroxide solution. The amide separating from the reaction mixture was collected by filtration. After three recrystallizations from benzene, the product melted at 168~169°C, $[\alpha]_D^{11}$ −39.8° (*c* 2.9, ethanol).

Fonud: C, 71.33; H, 7.61; N, 6.24. Calcd. for $C_{13}H_{17}NO_2$ (219.3): C, 71.20; H, 7.82; N, 6.39%.

***N*-Carbobenzoxy-*l-trans*-2-aminocyclohexanol (I).**—A solution of 4.3 g. of *l-trans*-2-aminocyclohexanol L-(+)-tartrate and 5.5 g. of sodium bicarbonate in 30 ml. of water was vigorously agitated and 5.3 g. of carbobenzoxy chloride was added to it in toluene (78% solution) in twenty minutes at room temperature. After agitation for two hours, the mixture was kept in a refrigerator overnight. The crystalline precipitate was collected and washed with cold water. The crude product weighed 4.3 g. (98%). The product was recrystallized repeatedly from a water-methanol mixture (3 : 2) to yield 2.8 g. (66%) of *N*-carbobenzoxy-*l-trans*-2-aminocyclohexanol melting at 115.5~116.5°C, $[\alpha]_D^{15}$ −20.1° (*c* 1.2, ethanol).

Found: C, 67.44; H, 7.75; N, 5.66. Calcd. for $C_{14}H_{19}NO_3$ (249.3): C, 67.44; H, 7.68; N, 5.62%.

β-(*N*-Carbobenzoxy-*l-trans*-2-aminocyclohexyl)-3, 4, 6-triacetyl-*N*-carbobenzoxy-D-glucosaminide (II).—A mixture of 1.9 g. of α-l-bromo-3, 4, 6-triacetyl-*N*-carbobenzoxy-D-glucosamine and 1.0 g. of I in 22 ml. of dry benzene was heated under reflux for 2 hr. with 1.7 g. of mercuric cyanide. The mixture was cooled and filtered to remove an insoluble substance. The filtrate was diluted with 70 ml. of chloroform and then washed twice with 10% sodium chloride solution and three times with cold water. After drying over anhydrous sodium sulfate, the solvent was removed under reduced pressure to give a crystalline residue. The residue was washed with anhydrous ether to obtain 1.75 g. of the product. The crude product was recrystallized from absolute ethanol to yield 0.95 g. (37%) of crystals melting at 217~217.5°C, $[\alpha]_D^{25}$ +5.6° (*c* 2, chloroform). A further recrystallization did not raise its melting point.

Found: C, 61.25; H, 6.44; N, 4.06. Calcd. for $C_{34}H_{42}N_2O_{12}$ (670.7): C, 60.88; H, 6.31; N, 4.18%.

The infrared spectrum (KBr) of the product showed absorption at 1751 (ester carbonyl); 1708, 1542, 1294 (amide); 975, 1049 (cyclohexane); 902 (type 2b of β-D-glucopyranose) and 752, 695 cm^{-1} (monosubstituted benzene).

The mother liquor of the above product was evaporated under reduced pressure to half the volume and placed in a refrigerator to yield 0.28 g. of a crystalline product. The product was recrystallized from ethyl acetate to obtain fine crystals melting at 170~170.5°C.

Mixed with an authentic sample of 4, 5-(3,4,6-triacetyl-D-glucopyranosyl)oxazolone-2[10], this product did not show a depression of the melting point. The infrared spectrum of the product was superimposable with that of an authentic sample.

4, 5-(3, 4, 6-Triacetyl-D-glucopyranosyl)oxazolone-2.—According to the procedure of Konstas et al.[10], 1, 3, 4, 6-tetraacetyl-*N*-carbobenzoxy-D-glucosamine, m. p. 148.5~149°C, $[\alpha]_D^{12}$ +20.4° (*c* 1.2, pyridine) [lit.[11] m.p. 150~151°C, $[\alpha]_D$ +21.5°], was treated with aluminum chloride and phosphorus pentachloride in dry chloroform to obtain 4, 5-(3, 4, 6-triacetyl-D-glucopyranosyl)oxazolone-2 melting at 170.5~171°C, $[\alpha]_D^{24}$ +23.7° (*c* 2, chloroform) in 36% yield. [lit.[10] m. p. 174~176°C, $[\alpha]_D$ +50.3° (*c* 2, chloroform)].

Found: C, 47.53; H, 5.21; N, 4.17. Calcd. for $C_{13}H_{17}O_9$ (331.3): C. 47.11; H, 5.18; N, 4.23%.

β-(*N*-Carbobenzoxy-*l-trans*-2-aminocyclohexyl)-*N*-carbobenzoxy-D-glucosaminide (III).—A mixture of 1.31 g. of II and 50 ml. of methanol saturated with ammonia was kept below 5°C for 3 hr. to obtain a clear solution. After it was placed in a refrigerator overnight, the solution was evaporated under reduced pressure to dryness. The residue was washed with 20 ml. of ethyl aceteate and

10) S. Konstas, I. Photaki and L. Zervas, *Chem. Ber.*, **92**, 1288 (1959): see also S. Umezawa, Y. Ito and S. Koto, This Bulletin, **36**, 186 (1963).

11) A. Neuberger and R. P. Rivers, *J. Chem. Soc.*, **1939**, 122.

recrystallized from isopropanol to yield 0.87 g. (81%) of the product melting at 224~225.5°C. A further recrystallization did not show any change in the melting point. $[\alpha]_D^{27}$ −28.1° (*c* 1.8, pyridine).

Found: C, 61.60; H, 6.58; N, 5.28. Calcd. for $C_{28}H_{36}N_2O_9$ (544.6): C, 61.75; H, 6.66; N, 5.14%.

The infrared spectrum (KBr) of the product showed absorption at 3400 broad (OH); 1690, 1553, 1260 (amide); 975, 1049 (cyclohexane); 896 (type 2b of β-D-glucopyranose) and 775, 696 cm^{-1} (mono-substituted benzene).

β-(*l-trans*-2-aminocyclohexyl)-D-glucosaminide (IV).—A suspension of 0.72 g. of III in 30 ml. of dioxane- water mixture (1 : 1) was added to a prehydrogenated suspension of 0.2 g. of palladium black in 10 ml. of the same solvent. The mixture was hydrogenated for 3 hr. at room temperature (31~32°C) with mechanical shaking. At the end of the reaction, 53 ml. of hydrogen was absorbed. The mixture was filtered to remove the catalyzer and the filtrate was evaporated under reduced pressure to dryness. The residue was dissolved in 7 ml. of hot absolute methanol and added with 5 ml. of anhydrous ether. The solution was placed in a refrigerator for a few days to obtain crystals. The crystals were collected by filtration and dried in a vacuum desiccator to yield 0.22 g. (60%) of the product melting at 159~161°C (decomp.). $[\alpha]_D^{30}$ −72.6° (*c* 1.3, water).

Found: C, 51.90; H, 8.77: N, 10.27. Calcd. for $C_{12}H_{24}N_2O_5$ (276.3): C, 52.16; H, 8.75; N, 10.14%.

The infrared spectrum (KBr) of the product showed absoption at 3590 (OH); 3355, 3300, 1593 (amine); 975, 1044 (cyclohexane) and 895 cm^{-1} (type 2b of β-D-glucopyranose).

***d-trans*-2-Aminocyclohexanol.**—From the mother liquor of *l-trans*-2-aminocyclohexanol L-(+)-tartrate, an attempt to isolate *d-trans*-2-aminocyclohexanol L-(+)-tartrate with 80% ethanol was not successful. The suitable solvent for separating *d-trans*-2-amino-cyclohexanol L-(+)-tartrate was found to be 95% methanol. The mother liquor of *l-trans*-2-amino-cyclohexanol L-(+)-tartrate was evaporated under reduced pressure to dryness. The residue was recrystallized repeatedly from 95% methanol to obtain the crystals melting at 169.5~170°C in 30% yield. $[\alpha]_D^{28}$ +36.5° (*c* 2.3, water). (Found: C, 45.33; H, 7.23, N, 5.26%). [lit.[4] m. p. 170~171°C, $[\alpha]_D$ +31.2°].

A further recrystallization did not show any change in the melting point and the specific rotation.

d-trans-2-Aminocyclohexanol was obtained by the same procedue of *l-trans* aminoalcohol from the corresponding tartrate. The *d-trans* aminoalcohol melted at 84~86°C. $[\alpha]_D^{10}$ +38.4° (*c* 1.8, water). [lit[4]. m. p. 83~84°C, $[\alpha]_D$ +40.2°].

N-Benzoyl derivative melting at 168~169°C was obtained by the Schotten-Baumann technique. $[\alpha]_D^{12}$ +43.5° (*c* 2.0, ethanol). Found: C, 71.33; H, 7.61; N, 6.25. Calcd. for $C_{13}H_{17}NO_2$ (219.3): C, 71.20; H, 7.82; N, 6.39%.

***N*-Carbobenzoxy-*d-trans*-2-aminocyclohexanol (V).**—To 5.3 g. portion of *d-trans*-2-aminocyclo-hexanol L-(+)-tartrate in 30 ml. of water was added 6.7 g. of sodium bicarbonate. To the mixture 6.6 g. of carbobenzoxy chloride (80% toluene solution) was added under mechanical agitation. The precipitate was treated similarly as I to obtain 3.3 g. (66%) of the crystals melting at 115.5~116.5°C. $[\alpha]_D^{14}$ +20.3° (*c* 1.1, ethanol).

Found: C, 67.30; H, 7.68; N, 5.68. Calcd. for $C_{14}H_{19}NO_3$ (249.3): C, 67.44; H, 7.68; N, 5.62%.

β-(*N*-Carbobenzoxy-*d-trans*-2-aminocyclohexyl)-3, 4, 6, -triacetyl-*N*-carbobenzoxy-D-glucosaminide (VI).—A mixture of 2.2 g. of α-l-bromo-3, 4, 6-triacetyl-*N*-carbobenzoxy-D-glucosamine and 1.1 g. of V in 25 ml. of anhydrous benzene was refluxed for 2 hr. with 1.9 g. of mercuric cyanide. Then the mixture was treated similarly to a corresponding derivative of *l*-form, II, to obtain 1.1 g. (38%) of the crystalline product melting at 191~192°C. $[\alpha]_D^{17}$ +22.9° (*c* 1.4, chloroform).

Found: C, 60.94; H, 6.19; N, 4.30. Calcd. for $C_{34}H_{42}N_2O_{12}$ (670.7): C, 60.88; H, 6.31; N, 4.18%.

The infrared spectrum of the product showed the same pattern as that of II.

β-(*N*-Carbobenzoxy-*d-trans*-2-aminocyclohexyl)-*N*-carbobenzoxy-D-glucosaminide (VII).—Upon treatment of 2.7 g. of VI with 130 ml. of methanol saturated with ammonia in a refrigerator overnight, the clear solution was obtained. The solution was treated similarly to III to yield 1.6 g. (76%) of crystals melting at 199~200°C. $[\alpha]_D^{11}$ +10.30 (*c* 3.1, pyridine).

Found: C, 61.42; H, 6.66; N, 4.91. Calcd. for $C_{28}H_{36}N_2O_9$ (544.6): C, 61.75; H, 6.66; N, 5.14%.

The infrared spectrum of the product was superimposable with that of III.

β-(*d-trans*-2-Aminocyclohexyl)-D-glucosaminide (VIII).—A 1.39 g. portion of VII was hydrogenated with 0.4 g. of palladium black in 65 ml. of dioxane-water mixture (1 : 1). The mixture was treated similarly to IV to yield 0.35 g. (57%) of the crystalline product melting at 195.5~196.5°C (decomp.). $[\alpha]_D^{11}$ +4.9° (*c* 1.4, water).

Found: C, 52.21; N, 8.57; N, 10.12. Calcd. for $C_{12}H_{24}N_2O_5$ (276.3): C, 52.16; H, 8.75; N, 10.14%.

The infrared spectrum of the product was superimposable with that of IV.

***N*-Carbobenzoxy-*O*-trityl-*d, l-trans*-2-amino-cyclohexanol (IX).**—To a solution of 6.0 g. of *N*-carbobenzoxy-*d, l-trans*-2-aminocyclohexanol in 43 ml. of dry pyridine was added 7.4 g. of trityl chloride. The mixture was heated on a boiling water bath for 20 hr. After placed overnight at room temperature, the mixture was filtered to remove a precipitate.

The filtrate was poured into 180 ml. of ice cold water to give an oily product, which began to crystallize by scratching a wall of the vessel with a glass rod under ice cooling.

The crystals were collected by filtration and then dissolved in ether. The ethereal solution was dried over anhydrous sodium sulfate and evaporated under reduced pressure to yield a crystalline residue. The residue was recrystallized from methanol to yield 6.29 g. (53%) of the product melting at 111~115°C. The crude product was recystallized again

from absolute ethanol to yield 4.36 g. (37%) of crystals melting at 126.5~128°C.

Found: C, 80.52; H, 6.56; N, 2.68. Calcd. for $C_{33}H_{33}NO_3$ (491.6): C, 80.62; H, 6.77; N, 2.85%.

The second crop of the product (0.15 g.) melting at 126~128°C was recovered from the mother liquor.

β-(*N*-Carbobenzoxy-*l-trans*-2-aminocyclohexyl)-3, 4, 6-triacetyl-*N*-carbobenzoxy-D-glucosaminide.—A solution of 1.1 g. of silver perchlorate and 18 ml. of anhydrous nitromethane was added with 1.5 g. of anhydrous calcium sulfate. Then, 2.4 g. of IX and 2.9 g. of α-l-bromo-3, 4, 6-triacetyl-*N*-carbobenzoxy-D-glucosamine were added to the mixture under ice cooling. The mixture was vigorously shaken at room temperature for 2 hr. After standing overnigth at room temperature, the mixture was filtered to remove a precipitate. The filtrate was washed twice with saturated sodium bicarbonate solution and five times with cold water. The organic solvent layer was filtered again to remove triphenylcarbinol and then diluted with 50 ml. of chloroform. The solution was dried over anhydrous sodium sulfate and evaporated under reduced pressure to yield 5.1 g. of a crystalline residue. The residue was washed with anhydrous ether to obtain 2.6 g. of a crude mixture of II and VI melting at 107~167°C. The crude product was repeatedly recrystallized from absolute ethanol to yield 230 mg. (7.0%) of the product melting at 215~216°C. The mixed melting point with II did not show any depression.

From the mother liquor, VI was not obtained in a pure state.

Bioassays.—IV and VIII showed almost no antimicrobial activity against *E. coli* in a paper disk method.

The authors were indebted to Mr. Saburo Nakada for microanalyses and to Mrs. Setsuko Iriyama for bioassays. A part of this research was supported by the Asahi Glass Foundation for the Contribution to Industrial Technology.

Department of Applied Chemistry
Faculty of Engineering
Keio University
Koganei-shi, Tokyo

*The Electronic Spectrum of Cumene Adsorbed on the Silica-Alumina Catalyst Surface during the Cracking Reaction**

By Taro TACHIBANA and Michio OKUDA

(Received December 11, 1962)

It is generally assumed that cumene dealkylation over silica-alumina catalyst involves, as an intermediate, the protonated cumene formed by the addition of a proton to cumene[1]. However, the existence of this intermediate has not yet been proven, although it is considered to form on the surface of catalyst during cracking. Since chemical species such as hydrocarbon ions or radicals often show a characteristic electronic spectrum, it is interesting, in studying the cracking mechanism, to investigate those species adsorbed on the catalyst by measuring their electronic spectra. Recently such studies have been reported by Leftin and Hall[2a-c], who have demonstrated the formation of dimethylphenyl-carbonium ions in the chemisorption of cumene. However, these ions are inconsistent with the generally accepted mechanism for the dealkylation reaction. It should be noted that Leftin's spectral measurement was carried out at room temperature. In order to detect an unstable intermediate on a catalyst, the spectra should be measured on the catalyst during cracking. Such a study, which will be reported on here, should contribute substantially to establishing the reaction mechanism.

Experimental

Cumene was washed with concentrated sulfuric acid and then dried and distilled. The distillate was percolated through columns of silica gel to remove the peroxide.

The silica-alumina catalyst, which had been prepared by the coprecipitation method and which had been calcinated at 500°C in air for 2 hr., was kindly supplied by Prof. Shiba of the Tokyo Institute of Technology and was said to contain approximately 10% alumina. This catalyst was prepared for optical measurement in the form of a semitransparent thin disk (0.1 mm. thick) by pressing its powder at a pressure of 8 ton./cm^2. This disk was placed in an optical cell similar to that described

* Presented at the 14th Annual Meeting of the Chemical Sosiety of Japan, Tokyo, April, 1961.

1) M. F. L. Johnson and J. S. Melik, *J. Phys. Chem.*, **65**, 1146 (1961).

2 a) H. P. Leftin and W. K. Hall, Proceedings of the 2nd International Congress on Catalysis, Paris, France, July, 1950. b) H. P. Leftin, *J. Phys. Chem.*, **64**, 1714 (1960). c) H. P. Leftin and W. K. Hall, ibid., **66**, 1457 (1962).

previously[3]. Heating was provided by a winding of nichrom wire around the outside of the cell; thus the spectrum during reaction at an elevated temperature was obtained. This cell was connected directly to the vacuum system, evacuated for one hour at 300°C, and then sealed off under vacuum. The pure cumene sample to be adsorbed was sealed in a separate compartment, one separated from the cell by a break-off seal. Exposure of the catalyst disk to cumene vapor was carried out by rupturing this break off seal. Exposure times of several hours were allowed to make an equilibrium condition at room temperature. The optical spectra were measured with a Hitachi EPS-2 recording spectrophotometer and were determined by measuring the transmission through this disk. Another disk, pretreated identically in a separate cell, was used as a blank in the reference beam.

Results and Consideration

At first, the absorption spectrum of the material adsorbed on the catalyst disk was measured at room temperature. As is shown by curve A of Fig. 1, the spectrum obtained is characterized by a double peak absorption band in the 258~265 mμ region and is almost identical with the spectrum of an alcoholic solution of cumene, indicating that cumene is physically adsorbed on the catalyst.

The cell was then heated to 150°C, and the absorption spectra at this temperature were taken at various intervals of time. The results are shown by curves B–E of Fig. 1. On heating at 150°C for 30 min., a new band appeared at 335 mμ. With further heating, another band appeared at 430 mμ; this finally proved to be the most intense band.

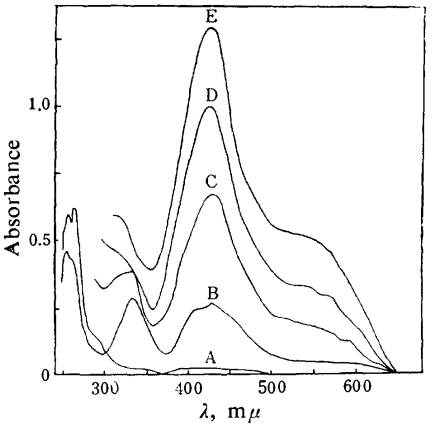

Fig. 1. Spectra of cumene on silica-alumina.
A : Room temperature
B : Heated 150°C for 1 hr.
C : Heated 150°C for 3 hr.
D : Heated 150°C for 6 hr.
E : Heated 150°C for 17 hr.

3) M. Okuda, *J. Chem. Soc. Japan, Pure Chem Sec.* (*Nippon Kagaku Zasshi*), **82**, 1115 (1961).

After heating for 17 hr., the gases in the cell were spectrophotometrically analyzed. The liquid product was mainly benzene, with a small amount of di-isopropylbenzene. This shows that the cracking dealkylation reaction took place mainly in the cell, though the reaction was followed at a lower temperature than that for catalytic cracking in usual (350~450°C). The 430 and 335 mμ bands were not found with the reaction product. Therefore, the bands at both 430 and 335 mμ are ascribed to chemisorbed molecules formed on the catalyst during the cracking reaction.

Recently, Leftin and Hall[2a] have shown, by spectrophotometric studies, that when triphenylmethane and related compounds, including cumene, are adsorbed on the surface of thoroughly dried silica-alumina catalysts, carbonium ions are formed which have an absorption band at about 400 mμ. With reference to their results, the 430 mμ band indicated by curves B–E of Fig. 1 can be assigned to a stable dimethylphenylcarbonium ion produced between cumene and the Lewis acid site on the silica-alumina surface. After the catalyst had been heated at 150°C for 17 hr., it was exposed to air at room temperature. In this case, the 430 mμ band was still observed, and the catalyst developed a brown color. When the catalyst was treated with an aqueous solution of ammonia, the brown color was lost and the 430 mμ band completely disappeared. This indicates that the carbonium ion is displaced from the acid center by the ammonia molecule, which forms a stronger base.

On the other hand, when the 335 mμ band was superimposed on the absorption in the ultraviolet region, which developed gradually with time, it became quite obscure after 6 hr. By reducing the effect of the absorption of the background at the ultraviolet region, it was found that the absorbance at 355 mμ after one hour is almost the same as that after three hours. In order to investigate in more detail the behavior of this band in relation to the time, measurements were made in an earlier stage of reaction. The results are shown by curves A and B of Fig. 2. It may be seen that, immediately after the temperature of cell reached 150°C, an absorption band appeared 327 mμ and that, thereafter, it increased in absorbance with a shift to 335 mμ. In this period the 430 mμ band had not yet appeared. After 13 min., heating was stopped and the spectrum was measured at room temperature. As is shown by curve C of Fig. 2, the 335 mμ absorption was considerably decreased, though absorbance around this peak increased. This fact indicates that the surface

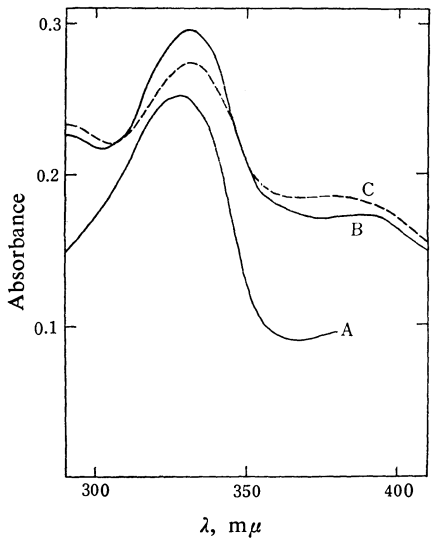

Fig. 2. Spectra of cumene on silica-alumina.
A : Immediately after heating at 150°C
B : Heated 150°C for 13 min.
C : At room temperature after heating for 13 min.

species contributing to the formation of this band ceased to be formed at room temperature.

On the basis of these results, it is suggested that the 335 mμ band could be due to an intermediate in the cracking reaction. A similar spectrum, with a peak at 327.5 mμ, was obtained from a solution of cumene in concentrated sulfuric acid. This absorption disappeared after 20 hr.; therefore, it is due to an unstable chemical species, probably protonated cumene, since it is well known that such hydrocarbon acts as a base in concentrated sulfuric acid and forms a proton adduct[4]. It seems probable that the unstable intermediate on the catalyst is also a protonated cumene produced by the reaction of cumene with the Brönsted acid site of the catalyst.

In summary, under the experimental conditions used, there exist both a Lewis acid site and a Brönsted acid site on the surface of the silica-alumina catalyst; the latter contributes to the cracking reaction through the formation of a chemisorbed intermediate.

This work was made possible by a grant from the Ministry of Education of Japan. The authors wish to thank Professor Tadao Shiba and Professor Tominaga Keii of the Tokyo Institute of Technology for their kind advice throughout the course of this work. Thanks are also due to Miss Fumie Hashimoto and Miss Yaeko Ide for their technical assistance.

Chemical Laboratory
Ochanomizu University
Bunkyo-ku, Tokyo

4) C. K. Ingold, C. G. Raisin and C. L. Wilson, *J. Chem. Soc.*, **1936**, 1637.

The Infrared Spectra of O-Deuterated and O-Methylated Derivatives of Diacetyl Monoxime and Isonitrosoacetone

By Yoko KURODA and Masao KIMURA

(Received December 4, 1962)

In a previous study the assignement of the absorption bands of diacetyl monoxime and isonitrosoacetone was carried out to determine the characteristic frequencies of the O=C–C=N system and also those of the functional group of oximes, –C=N–OH[1]. We have found that (1) these oximes take not a nitroso form but an oxime form in solutions; (2) the C=N stretching vibration appears in a lower frequency range than that of unconjugated oximes; (3) the oximes in solutions make intermolecular hydrogen bonds of an –O–H···O=C*1 type, while unconjugated oximes in solutions or in the solid state make intermolecular hydrogen bonds of an –O–H···N=C type, and (4) the bond character of an O=C–C=N–OH system changes with the hydrogen bonding so that molecules in the free and in the associated state have two sets of frequencies corresponding to these states. The characteristic frequencies of C=N bonds have been observed for some kinds of compounds, such as unconjugated imines[2], unconjugated

1) M. Kimura, Y. Kuroda, H. Takagi and M. Kubo, This Bulletin, 33, 1086 (1960).

*1 Measurements of the dipole moments also rule out intramolecular association (unpublished work).

2) P. L. Pickard and G. W. Polly, *J. Am. Chem. Soc.*, 76, 5169 (1954).

oximes[3-7], conjugated imines[8], conjugated oximes containing phenyl groups[9,10], azines[11], glyoximes[12] and so on[13]. It is worth noting that the frequencies of the bands scatter over a very wide range of wave numbers, 1520~1680 cm^{-1}, depending on the kinds of compounds or the existence of hydrogen bonding. Moreover, absorption intensity is affected to a considerable extent by the environment around a C=N bond[13,14]. Now that the assignment of bands has been made for diacetyl monoxime and isonitrosoacetone, it is quite interesting to observe the effect of environments on the infrared spectra of the O=C-C=N-OH system. Therefore, the *O*-deuterated and *O*-methylated derivatives of diacetyl monoxime and isonitrosoacetone have been dealt with in the present study in order to investigate the effect of substituents on the positions and intensities of bands of the O=C-C=N-O system. This study will also serve to confirm the previous assignment. When the Raman and infrared spectra of these oximes were reported on by Kahovec and Kohlrausch[15], Matsui[16] and Milone and Borello[17], they were not completely analyzed.

Experimental

Deuterated samples were prepared from the same purified samples as used in the previous study[1] by exchanging the hydrogen in OH groups with deuterium in heavy water. These samples were dried before use.

Commercial preparations of diacetyl monoxime-*O*-methyl ether and isonitrosoacetone-*O*-methyl ether were purified by distillation under atmospheric and reduced pressure respectively.

The spectra were taken with the optical system of a Hilger H-800 spectrophotometer equipped with interchangeable fluorite and rock-salt prisms. Solutions of various concentrations in carbon tetrachloride, carbon disulfide and chloroform were

Table I. Observed frequencies (cm^{-1}) of diacetyl monoxime and diacetyl monoxime-*d**

-C=N-OH		-C=N-OD		Intensity change on dilution	Assignment**
Solution	Solid	Solution	Solid		
3577				Increase	$\nu(OH)_{free}$
3345	~3250 (s,b)			Decrease	$\nu(OH)_{assoc}$
		2630		Increase	$\nu(OD)_{free}$
		~2420	2425 (s,b)	Decrease	$\nu(OD)_{assoc}$
1698		1696		Increase	$\nu(C=O)_{free}$
1686	1665 (vs)	1688	1664 (vs)	Decrease	$\nu(C=O)_{assoc}$
1630 (w)		1619 (m)	1610 (m)		$\nu(C=N)$
	~1450 (m)			Decrease	$\delta(OH)_{in\text{-}plane,\ assoc}$
1424 (m)	~1420 (m)	1424 (m)	1418 (m)		$\delta(CH_3)_{deg}$
1365 (s)	1365 (s)	1362 (s)	1366 (s)		$\delta(CH_3)_{sym}$
1355				Increase	$\delta(OH)_{in\text{-}plane,\ free}$
1301 (w)	1313 (w)	1306 (w)	1313 (w)		$\nu(C\text{-}C)_{central}$
1124 (s)	1125 (s)	1124 (s)	1134 (m)		$\rho(N{=}C\text{-}CH_3)_{in\text{-}plane}$
		~1080	1090 (m)	Decrease	$\delta(OD)_{in\text{-}plane,\ assoc}$
1022 (s)	~1020 (s)	1017 (s)	~1015 (s)		$\rho(O{=}C\text{-}CH_3)_{in\text{-}plane}$
		995		Increase	$\delta(OD)_{in\text{-}plane,\ free}$
970	980 (m)	970	~ 975 (m)	Decrease	$\nu(N\text{-}O)_{assoc}$
963				Increase	$\nu(N\text{-}O)_{free}$
933 (w)	933 (w)	930 (w)	933 (w)		$\nu(C\text{-}CH_3)$

* Frequencies to be assigned to the C-H stretching vibrations are not listed in this table.
** ν, stretching; δ, bending; ρ, rocking

3) S. Califano and W. Lüttke, *Z. physik. Chem.* (*Neue Folge*), **6**, 83 (1956).
4) H. Bredereck, A. Wagner, D. Hummel and H. Kreiselmeier, *Ber.*, **89**, 1532 (1956).
5) L. H. Cross and A. C. Rolfe, *Trans. Faraday Soc.*, **47**, 354 (1951)
6) C. N. Caughlan, H. V. Tartar and E. C. Lingafelter, *J. Am. Chem. Soc.*, **73**, 1180 (1951).
7) M. Kimura, Y. Kuroda, O. Yamamoto and M. Kubo, This Bulletin, **34**, 1081 (1961).
8) J. Fabian, M. Legrand and P. Poirer, *Bull. soc. chim. France*, **1956**, 1499.
9) A. Palm and H. Werbin, *Can. J. Chem.*, **31**, 1004 (1953).
10) D. Hadži, *J. Chem. Soc.*, **1956**, 2725.
11) E. R. Blout, M. Fields and R. Karplus, *J. Am. Chem. Soc.*, **70**, 194 (1948).
12) R. E. Rundle and M. Parasol, *J. Chem. Phys.*, **20**, 1487 (1952).
13) L. J. Bellamy, "The Infra-fed Spectra of Complex Molecules", 2nd Ed., Methuen, London (1958); R. N. Jones and C. Sandorfy, "Chemical Applications of Spectroscopy," Interscience, New York (1956).
14) J. Fabian and M. Legrand, *Bull. soc. chim. France*, **1956**, 1461.
15) L. Kahovec and K. W. F. Kohlrausch, *Ber.*, **75** 1541 (1942).
16) Y. Matsui and T. Kubota, *J. Chem. Soc. Japan, Pure Chem. Sec.* (*Nippon Kagaku Zasshi*), **83**, 985 (1962), and private communication.
17) M. Milone and E. Borello, *Gazz. chim. ital.*, **85**, 500 (1955).

TABLE II. OBSERVED FREQUENCIES (cm^{-1}) OF ISONITROSOACETONE AND ISONITROSOACETONE-*d**

-C=N-OH		-C=N-OD		Intensity change on dilution	Assignment
Solution	Solid	Solution	Solid		
3574				Increase	$\nu(OH)_{free}$
3325				Decrease	$\nu(OH)_{assoc}$
		2620		Increase	$\nu(OD)_{free}$
		~2440		Decrease	$\nu(OD)_{assoc}$
1703		1696		Increase	$\nu(C=O)_{free}$
1674	1658 (vs)	1673	~1652 (vs)	Decrease	$\nu(C=O)_{assoc}$
1614 (w)	1620 (w)	1599 (m)	1581 (m)		$\nu(C=N)$
~1450	~1445 (m,b)	~1454	1447 (m,b)	Decrease	$\delta(OH)_{in\text{-}plane,\ assoc}$
(1427)$_{estimated}$					$\delta(CH_3)_{deg}$
1398				Increase	$\delta(OH)_{in\text{-}plane,\ free}$
1366 (s)	1372 (s)	1372 (s)	1377 (s)		$\delta(CH_3)_{sym}$
1320 (vw)	1307 (vw)	1321 (m)	1327 (m)		$\nu(C\text{-}C)_{central}$
1226 (m)	1240 (m)	1223 (m)	1245 (m)		$\delta(CH)_{in\text{-}plane}$
			1062	Decrease	$\delta(OD)_{in\text{-}plane,\ assoc}$
1016	1015 (s)	1015	1017 (s)	Increase	$\delta(OD)_{in\text{-}plane,\ free}$ / $\rho(O=C\text{-}CH_3)_{in\text{-}plane}$
990	991 (m)	990	988 (m)	Decrease	$\nu(N\text{-}O)_{assoc}$
972		971		Increase	$\nu(N\text{-}O)_{free}$
920 (m)	~ 929 (m)	918 (m)	921 (m)		$\nu(C\text{-}CH_3)$
835 (w)	850 (w)	831 (w)	848 (w)		$\delta(CH)_{out\text{-}of\text{-}plane}$

* Frequencies to be assigned to the C-H stretching vibrations are not listed in this table.

TABLE III. OBSERVED FREQUENCIES (cm^{-1}) OF DIACETYL MONOXIME- AND ISONITROSOACETONE-*O*-METHYL ETHERS*

Diacetyl monoxime-*O*-methyl ether	Isonitrosoacetone-*O*-methyl ether	Assignment
1695 (vs)	1696 (vs)	$\nu(C=O)$
1610 (s)	1588 (m)	$\nu(C=N)$
1463 (m)	1465 (m)	$\delta(O\text{-}CH_3)_{deg}$
1442 (m)	1446 (m)	$\delta(O\text{-}CH_3)_{sym}$
1428 (m)	1427 (m)	$\delta(C\text{-}CH_3)_{deg}$
1361 (vs)	1367 (s)	$\delta(C\text{-}CH_3)_{sym}$
1311 (s)	1318 (m)	$\nu(C\text{-}C)_{central}$
	1236 (m)	$\delta(CH)_{in\text{-}plane}$
1190 (vw)	1180 (w)	$\rho(N\text{-}O\text{-}CH_3)_{in\text{-}plane}$
1124 (vs)		$\rho(N=C\text{-}CH_3)_{in\text{-}plane}$
1049 (vs)	1052 (s)	$\nu(N\text{-}O\text{-}C)_{antisym}$
1011 (sh)	1007 (m)	$\rho(O=C\text{-}CH_3)_{in\text{-}plane}$
945 (sh) / 917 (s)	918 (m)	$\nu(C\text{-}CH_3)$ / $\nu(N\text{-}O\text{-}C)_{sym}$
	830 (w)	$\delta(CH)_{out\text{-}of\text{-}plane}$

* Frequencies to be assigned to the C-H stretching vibrations are not listed in this table.

used in order to observe changes in the absorption intensity with changes in the concentration. Isonitrosoacetone-*d* was used only in dilute solutions, since it has only a limited solubility in the solvents used. The deuterated oximes in the solid state were examined as mulls in Nujol and hexachlorobutadiene. The methylated oximes in the liquid state were also examined. However, no additional data were obtained.

The observed frequencies of absorption bands are listed in Tables I, II and III. For the sake of comparison, the observed frequencies of the original oximes are also included in Tables I and II. These values are reproduced from the previous paper[1]. However, the C-H stretching frequencies are omitted from the tables, because they are not necessary for later discussion. Some portions of the spectra are shown in Figs. 1 to 9.

Assignment and Discussion

The Stretching Frequencies of O=C-C=N.— The bands previously assigned to the C=O stretching vibrations, $\nu(C=O)$, of diacetyl monoxime and isonitrosoacetone show no appreciable change in their positions and intensities on deuteration. The general behavior of the concentration dependence of the intensity is also unaltered by replacing hydrogen with deuterium. However, the $\nu(C=O)$ bands of associated molecules at 1686 cm^{-1} for diacetyl monoxime and at 1674 cm^{-1} for isonitrosoacetone not only become weak on dilution but also disappear on methylation (Figs. 1 and 2). These facts confirm the previous assignment. The vibrational mode in the solid state absorbs at a frequency lower by about 20 cm^{-1} than that in solution. The low-frequency shift is a quite general phenomenon observed in condensed phases.

For the C=N stretching vibration, $\nu(C=N)$, distinct variations in intensity and position are observed on deuteration and methylation.

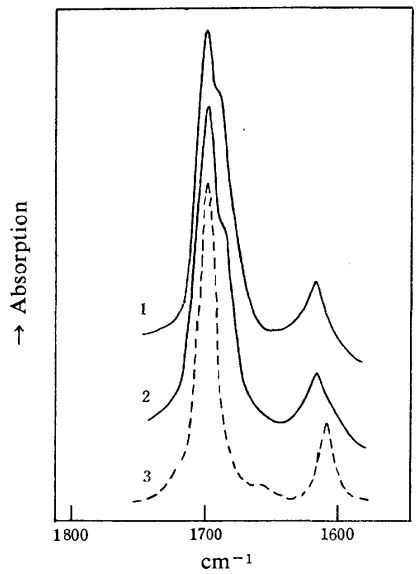

Fig. 1. Infrared spectra of diacetyl monoxime-*d* in CCl_4 solutions: (1) 0.148 mol./l., 0.2 mm. cell; (2) 0.059 mol./l., 0.5 mm. cell, and (3) diacetyl monoxime-*O*-methyl ether (liq.).

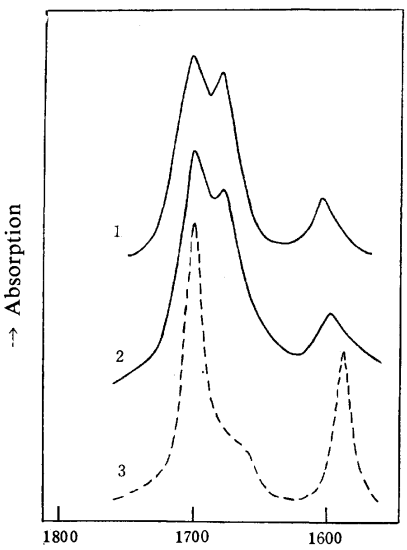

Fig. 2. Infrared spectra of isonitrosoacetone-*d* in $CHCl_3$ solutions: (1) 0.515 mol./l., 0.05 mm. cell; (2) 0.130 mol./l., 0.2 mm. cell, and (3) isonitrosoacetone-*O*-methyl ether (liq.).

Deuteration gives rise to a lowering in frequency along with a slight but perceptible increase in intensity. Methylation causes a similar frequency shift and an intensity change, the magnitude of which is, however, much greater than that on deuteration (Figs. 1 and 2). As a result, the methylated oximes have rather strong and sharp ν(C=N) bands, unlike the original oximes. The doubling of the ν(C=N) bands attributable to free and associated molecules could not be detected for either the deuterated compounds or the original compounds. This fact suggests that the influence of association does not practically extend to the C=N bonds. The ν(C=N) band of diacetyl monoxime in the solid state is masked by the strong band of ν(C=O).

For all compounds treated in the present study, the C=O stretching vibrations appear in a region of lower frequency than that of unconjugated ketones (1705～1725 cm^{-1})[13], while the frequencies of the C=N stretching vibrations are lower than those of unconjugated oximes or imines (1660～1680 cm^{-1}). Conjugation in an O=C-C=N system is considered to be the cause of the lowering in the ν(C=O) and ν(C=N) frequencies. We can find the following absorption ranges for ν(C=O)[13,18]: α-diketones, 1710～1730 cm^{-1}; α,β-unsaturated ketones, 1665～1685 cm^{-1}; and for ν(C=N): azines[11], about 1660 cm^{-1}; benzaldoximes[8,13], 1620～1660 cm^{-1}. Thus, ν(C=O) in an O=C-C=N system can be considered to absorb in a wave number range between those of saturated ketones and of α,β-unsaturated ketones. The ν(C=N) is in a wave number range still lower than that of a C=N group conjugated with a phenyl group*2. *vic*-Dioximes appear to have very weak absorptions near 1620 cm^{-1} originating from an N=C-C=N system[19]*3. This value is very close to the ν(C=N) wave number in an O=C-C=N system.

Deuteration and methylation result in an increase in absorption intensity and a decrease in frequency for ν(C=N), but not for ν(C=O). The frequency shift of ν(C=N) is probably a natural consequence of substitution. The fact that there is no significant change in ν(C=O) implies that the substitution does not affect the C=O bond.

As Cross and Rolfe have pointed out[5], the C=N absorption intensities of oximes are generally weak, while those of other kinds of compounds are not necessarily so. Once the hydrogen atom of an OH group is replaced by another atom or group, the C=N absorption band is intensified. Matsui also made a similar

18) See also M. L. Josien, J. Lascombe, J. Lecomte and J. P. Mathieu, *Compt. rend.*, 240, 1982 (1955).

*2 Palm and Werbin reported the value of about 1620 cm^{-1} for the ν(C=N) of α-benzaldoxime[9]. As the value was observed in the solid state, the frequency for a free state is possibly higher than this.

*3 The frequency was estimated from the spectra given by Voter et al. in their paper[19].

19) R. C. Voter, C. V. Banks, V. A. Fassel and P. W. Kehres, *Anal. Chem.*, 23, 1730 (1951).

finding in his studies of oximes[16]. This seems to be characteristic of the spectra of oximes.

Hydrogen bonding gives rise to a shift towards a frequency lower by about 10 cm^{-1} for the ν(C=O) of diacetyl monoxime and by about 25 cm^{-1} for that of isonitrosoacetone. In general, a frequency shift caused by hydrogen bonding does not exceed 10 cm^{-1} in unconjugated ketones[20,21]. The frequency shift in diacetyl monoxime is of the same order as that in unconjugated ketones. On the other hand, the frequency shift in isonitrosoacetone is greater than that in unconjugated ketones.

In the previous paper, the bands due to the C–C stretching vibrations, $\nu(C-C)_{central}$, in the system discussed here were placed near 1300 cm^{-1} for diacetyl monoxime and at 1320 cm^{-1} for isonitrosoacetone. The corresponding bands of deuterated oximes are at 1306 and 1321 cm^{-1}, while those of methylated oximes are at 1311 and 1318 cm^{-1}. The bands of these oximes become intense on deuteration and more intense on methylation (Figs. 3—6). This property of $\nu(C-C)_{central}$ is analogous to that of ν(C=N). The bands of the deuterated oximes look like single bands rather than composite ones. Reexamination of diacetyl monoxime revealed that two well-defined bands and their concentration dependence could not always be observed. Accordingly, only one frequency is shown in Table I for the $\nu(C-C)_{central}$ of diacetyl monoxime.

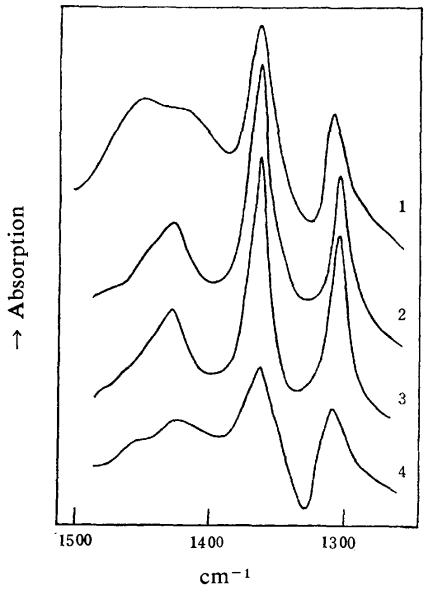

Fig. 3. Infrared spectra of (1) diacetyl monoxime in hexachlorobutadiene mull; and the spectra of diacetyl monoxime-*d* (2) in CCl_4, 0.059 mol./l., 0.5 mm. cell; (3) in CCl_4, 0.148 mol./l., 0.2 mm. cell, and (4) in hexachlorobutadiene mull.

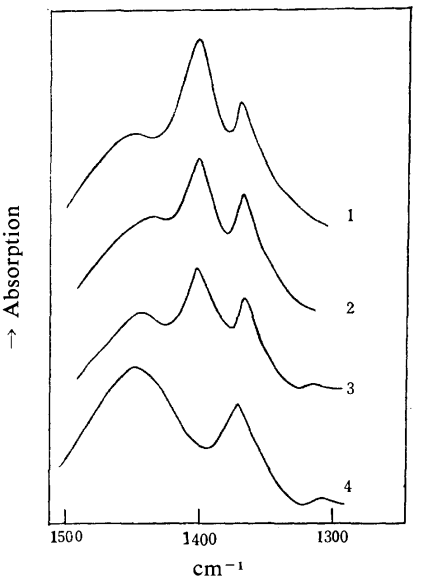

Fig. 4. Infrared spectra of isonitrosoacetone (1) in $CHCl_3$, 0.125 mol./l., 0.2 mm. cell; (2) in $CHCl_3$, 0.250 mol./l., 0.1 mm. cell; (3) in $CHCl_3$, 0.500 mol./l., 0.05 mm. cell, and (4) in KBr disk.

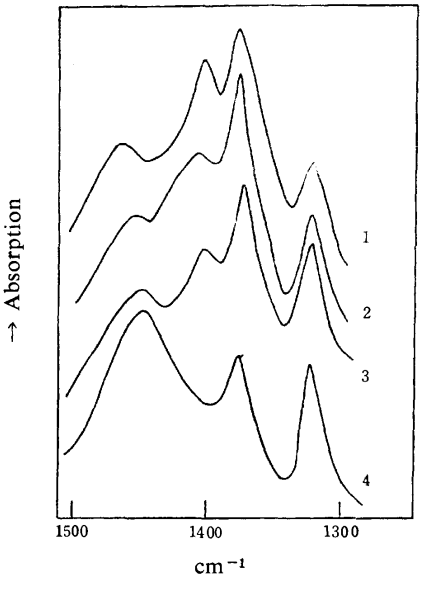

Fig. 5. Infrared spectra of isonitrosoacetone-*d* (1) in $CHCl_3$, 0.125 mol./l., 0.2 mm. cell; (2) in $CHCl_3$, 0.250 mol./l., 0.1 mm. cell; (3) in $CHCl_3$, 0.500 mol./l., 0.05 mm. cell, and (4) in hexachlorobutadiene mull.

20) R. S. Rasmussen, D. D, Tunnicliff and R. R. Brattain, *J. Am. Chem. Soc.*, 71, 1068 (1949).
21) J. F. Grove and H. A. Willis, *J. Chem. Soc.*, 1951, 877.

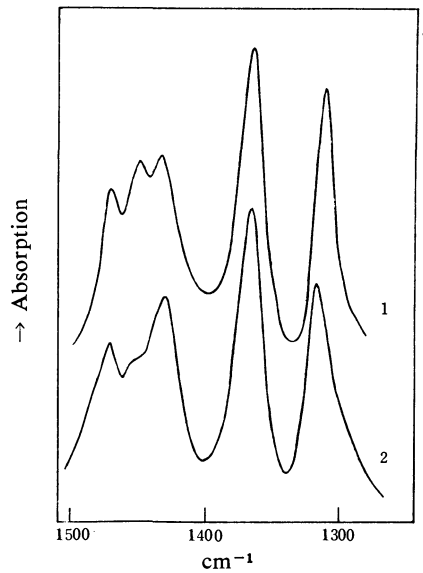

Fig. 6. Infrared spectra of (1) diacetyl monoxime-*O*-methyl ether (liq.), and (2) isonitrosoacetone-*O*-methyl ether (liq.).

The Stretching Frequencies of N–O and N–O–C.—In the previous study, the bands of diacetyl monoxime at 970 and 963 cm^{-1} and of isonitrosoacetone at 990 and 972 cm^{-1} were assigned to the N–O stretching vibrations, ν(N–O).

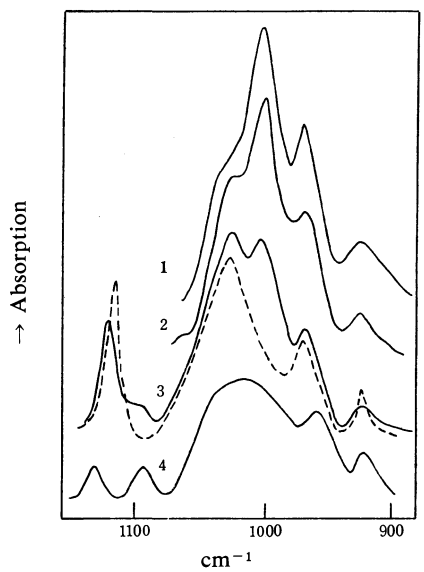

Fig. 7. Infrared spectra of diacetyl monoxime-*d* (1) in CS_2, 0.02 mol./l., 1.5 mm. cell; (2) in CS_2, 0.059 mol./l., 0.5 mm. cell; (3) in CCl_4, 0.345 mol./l., 0.085 mm. cell, and (4) in hexachlorobutadiene mull. The dotted line indicates the spectrum of diacetyl monoxime in CCl_4 at the same concentration as (3).

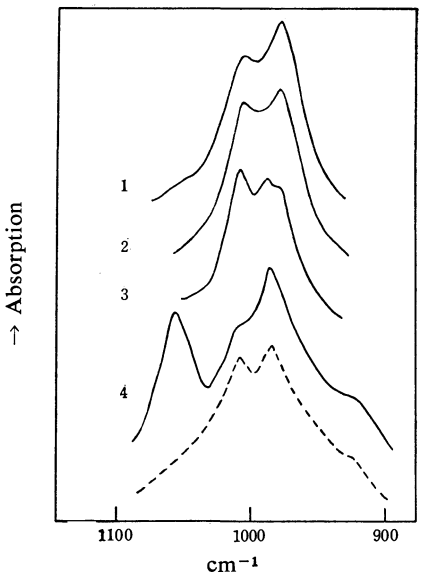

Fig. 8. Infrared spectra of isonitrosoacetone-*d* (1) in $CHCl_3$, 0.13 mol./l., 0.2 mm. cell; (2) in $CHCl_3$, 0.26 mol./l., 0.1 mm. cell; (3) in $CHCl_3$, 0.52 mol./l., 0.05 mm. cell, and (4) in Nujol mull. The dotted line indicates the spectrum of isonitrosoacetone in Nujol mull.

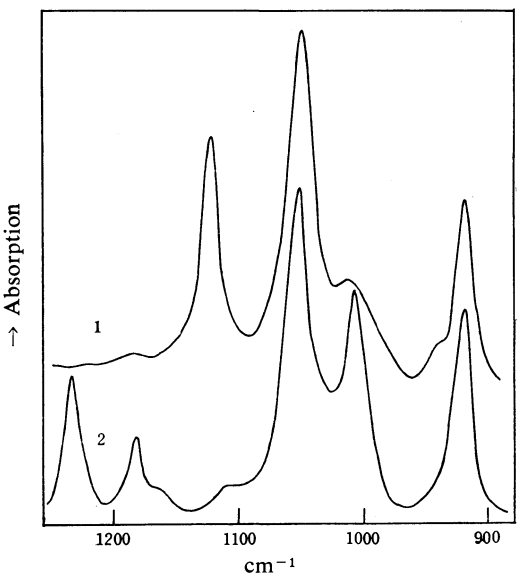

Fig. 9. Infrared spectra of (1) diacetyl monoxime-*O*-methyl ether (liq.), and (2) isonitrosoacetone-*O*-methyl ether (liq.).

On deuteration, no appreciable changes can be observed in the absorption frequencies and in the concentration dependence of the intensity (Figs. 7 and 8). The N–O stretching frequencies of this type of oximes are higher than those of unconjugated oximes[3,7-9] or

benzaldoxime[22], but lower than that of benzoquinone monoxime[10]. This difference in characteristic frequencies is possibly due to the double-bond characters of N–O bonds in conjugation with adjacent bonds or groups as has been stated above.

The bands mentioned above, however, must be turned into an entirely different pattern by methylation, because an N–O system is replaced by a system of three atoms, N–O–C. As expected, all the N–O stretching bands of oximes are missing in the spectra of methyl ethers. Instead, new bands appear at 1190, 1049 and 917 cm^{-1} for diacetyl monoxime-*O*-methyl ether and 1180 and 1052 cm^{-1} for isonitrosoacetone-*O*-methyl ether (Fig. 9). Strong bands are to be assigned to the N–O–C stretching vibration, ν(N–O–C), while weak bands are to be assigned to the CH_3 rocking vibration, as is described below. The stretching vibration of a C–O–C system in alkyl ethers[13] absorbs in the 1060~1150 cm^{-1} range. Analyzing the spectra of dimethyl ether, Kanazawa and Nukada assigned a band at 928 cm^{-1} to the symmetric stretching vibration and a band at 1102 cm^{-1} to the antisymmetric vibration of C–O–C[23]. Accordingly, two strong bands at 1049 and 917 cm^{-1} for diacetyl monoxime-*O*-methyl ether can be assigned to ν(N–O–C). The corresponding bands of isonitrosoacetone-*O*-methyl ether are a band at 1052 cm^{-1} and perhaps a band at 918 cm^{-1} (Figs. 8 and 9). Although the band at 918 cm^{-1} is not a band appearing only in the case of *O*-methylated isonitrosoacetone, it is strengthened by substituting a methyl group for hydrogen. Therefore, it seems to be much more reasonable to assign the band at 918 cm^{-1} rather than a weak band at 1180 cm^{-1} to ν(N–O–C). A value of 918 cm^{-1} for *O*-methylated isonitrosoacetone is practically equal to the value of 917 cm^{-1} for *O*-methylated diacetyl monoxime. The bands near 1050 cm^{-1} are stronger than those near 918 cm^{-1}. The formers belong to the antisymmetric vibration, and the latters, to the symmetric vibration of the N–O–C.

The Stretching and Bending Frequencies of OH and OD.—The bands representing the OD stretching vibration, ν(OD), are evidently those at 2630 and 2420 cm^{-1} for diacetyl monoxime-*d* and those at 2620 and 2440 cm^{-1} for isonitrosoacetone-*d*. In the solid state only bands near 2400 cm^{-1} appear. The observed frequencies of these bands were roughly estimated because of the disturbance caused by the absorption of carbon dioxide. The ν(OD) bands completely disappear from the spectra of the methylated oximes. The bands near 2600 cm^{-1} should be assigned to the ν(OD) of free molecules, and the bands near 2400 cm^{-1}, to that of associated molecules. The values of the ν(OH) : ν(OD) frequency ratio are 1.36 and 1.38 for the free and the associated state of diacetyl monoxime and 1.36 for both states of isonitrosoacetone.

In the previous study, the band of diacetyl monoxime at 1355 cm^{-1} and that of isonitrosoacetone at 1398 cm^{-1} were assigned to the OH in-plane bending vibration, $\delta(OH)_{in\text{-}plane}$, of free molecules. These bands disappear on deuteration (Figs. 3—6). Therefore, the assignment made in the previous study is justified. New bands of free molecules attributable to the OD in-plane bending vibration, $\delta(OD)_{in\text{-}plane}$, appear at 995 cm^{-1} for diacetyl monoxime-*d* and near 1015 cm^{-1} for isonitrosoacetone-*d* in solution. The former band becomes strong with a decrease in the concentration. The concentration dependence of the latter is not simple (Figs. 7 and 8). Judging from the complicated appearance of the band, it can hardly be regarded as a single absorption band. The band changes into a sharp band on methylation (Fig. 9). Therefore, it can be considered to be a composite band of $\delta(OD)_{in\text{-}plane}$ and the rocking vibration of CH_3 attached to the C=O group of isonitrosoacetone-*d*. The values of the δ(OH) : δ(OD) frequency ratio are 1.36 and 1.38 for diacetyl monoxime and isonitrosoacetone respectively.

The $\delta(OH)_{in\text{-}plane}$ band of diacetyl monoxime in the associated state could not be determined definitely in the previous study owing to an overlap with a band at 1424 cm^{-1}. The present study revealed that in solutions a band in this region becomes relatively sharp on deuteration and even sharper on methylation. The corresponding band in the solid state is a broad one at 1450 cm^{-1} which disappears on deuteration (Fig. 3). From these facts, the band at 1450 cm^{-1} can be considered to represent the $\delta(OH)_{in\text{-}plane}$ of diacetyl monoxime in the associated state. Even in solutions, the band should be considered to be present near 1450 cm^{-1}, although it cannot be located precisely because of the presence of a band at 1424 cm^{-1}.

For isonitrosoacetone, no definite conclusion could be drawn in the present study about the exact position of the $\delta(OH)_{in\text{-}plane}$ in the associated state. Nevertheless, it is most likely that the band near 1450 cm^{-1} arises from the δ(OH) of isonitrosoacetone in the associated state and that the CH_3 degenerate deformation band overlaps the band (Fig. 4).

22) A. Palm and H. Werbin, *Can. J. Chem.*, **32**, 858 (1954).
23) Y. Kanazawa and K. Nukada, This Bulletin, **35**, 612 (1962). See also Y. Masiko, *J. Chem. Soc. Japan, Pure Chem. Sec.* (*Nippon Kagaku Zassi*), **79**, 470 (1958).

A very weak band at about 1080 cm^{-1} can be assigned to the $\delta(OD)_{in\text{-}plane}$ of associated diacetyl monoxime-*d*, since it becomes more intense at higher concentrations. In the solid state, two bands appear at 1090 and 1134 cm^{-1} in place of a very weak band at about 1080 cm^{-1} and a strong band at 1124 cm^{-1} in solution (Fig. 7). A band at 1124 cm^{-1} is assigned to the CH_3 rocking vibration in N=C-CH_3, ρ(N=C-CH_3), below. The two bands in the spectrum of the solid have nearly equal intensities and are only half as intense as the band at 1124 cm^{-1} in solution. The frequency shifts and the intensity changes arise probably from a coupling between δ(OD) and ρ(N=C-CH_3) in the associated state. In solution it seems that the band at 1134 cm^{-1}, due to relatively few associated molecules, is poorly defined because of the existence of the strong band at 1124 cm^{-1} due to free molecules (Fig. 7).

The band of solid isonitrosoacetone-*d* at 1062 cm^{-1} can be assigned to the δ(OD) in association, although no distinct band was detected near 1062 cm^{-1} in the spectra of solutions since concentrated solutions could not be prepared. The values of the δ(OH) : δ(OD) frequency ratio are 1.33 for diacetyl monoxime and 1.36 for isonitrosoacetone.

The Bending and Rocking Vibrations of CH_3 and CH.—The bands at 1424 and 1365 cm^{-1} and those at 1450 and 1366 cm^{-1} were assigned previously to the CH_3 deformation vibrations of diacetyl monoxime and isonitrosoacetone respectively[1]. The assignment of the 1450 cm^{-1} band, however, was somewhat ambiguous. The corresponding bands of the deuterated oximes are the bands at 1424 and 1362 cm^{-1} for diacetyl monoxime-*d* and those at about 1465 and 1372 cm^{-1} for isonitrosoacetone-*d*.

Their methyl ethers show bands at 1463, 1442, 1428 and 1361 cm^{-1} for diacetyl monoxime-*O*-methyl ether and bands at 1465, 1446, 1427 and 1367 cm^{-1} for isonitrosoacetone-*O*-methyl ether (Fig. 6). Two new bands observed in the spectra of the methyl ethers do not show the concentration dependence of the intensity. Among the four bands of diacetyl monoxime-*O*-methyl ether, the bands at 1424 and 1365 cm^{-1} can readily be assigned to the CH_3 deformation vibrations of C-CH_3, δ(C-CH_3), because they are present in the spectra of both the original and deuterated oximes. Therefore, the bands at 1463 and 1442 cm^{-1} should be attributed to the CH_3 deformation vibrations of O-CH_3, δ(O-CH_3). The band at 1463 cm^{-1} is stronger than that at 1442 cm^{-1}. The former represents the antisymmetric vibration, and the latter, the symmetric one.

For diacetyl monoxime no substantial change in the positions and intensities of the CH_3 deformation bands is produced by *O*-methylation. A band at about 1365 cm^{-1} is characteristic of all the compounds under investigation. Therefore, it is a natural inference that the CH_3 degenerate deformation vibrations of isonitrosoacetone and its deuterated compound will also give rise to bands at about 1427 cm^{-1}, corresponding to the band observed for the methyl ether, although the band was not identified on the spectrum of the oxime itself because of a broad band due to the $\delta(OH)_{in\text{-}plane}$. The remaining bands of isonitrosoacetone-*O*-methyl ether, at 1465 and 1446 cm^{-1}, should be assigned to $\delta(O\text{-}CH_3)_{degenerate}$ and $\delta(O\text{-}CH_3)_{symmetric}$ respectively. Thus, a consistent interpretation can be achieved for the CH_3 deformation bands. The values of 1465 and 1446 cm^{-1} for δ(O-CH_3) lie in the same range as that observed for dimethyl ether by Kanazawa and Nukada[23], these values being higher than those of δ(C-CH_3) in alkanes.

The band of isonitrosoacetone at 1226 cm^{-1} was assigned previously to the CH in-plane bending vibration, $\delta(CH)_{in\text{-}plane}$. The corresponding bands are present at 1223 cm^{-1} for its deuterated oxime and at 1236 cm^{-1} for its methyl ether. A band at 831 cm^{-1} for the deuterated and methylated isonitrosoacetone can be attributed to the CH out-of-plane bending vibration, $\delta(CH)_{out\text{-}of\text{-}plane}$. None of the bands discussed in this paragraph appear in the spectra of diacetyl monoxime and its derivatives.

There are bands at 1017 and at 1011 cm^{-1} for deuterated and methylated diacetyl monoxime respectively. Similarly, there are bands at 1015 and at 1007 cm^{-1} for deuterated and methylated isonitrosoacetone respectively. These bands are unequivocally due to the CH_3 in-plane rocking vibrations, ρ(O=C-CH_3), of O=C-CH_3, which have bands at 1022 and 1016 cm^{-1} for the original oximes.

In addition, diacetyl monoxime and its derivatives have bands at exactly the same frequency, 1124 cm^{-1}. These bands must be due to the CH_3 in-plane rocking vibrations, ρ(N=C-CH_3), of N=C-CH_3. These facts convince us of the correctness of the assignments made in the previous study. For the solid of diacetyl monoxime-*d*, the band at 1134 cm^{-1} may be interpreted as ρ(N=C-CH_3). The position can be considered to shift in the solid state through a coupling with δ(OD), as has already been mentioned.

In methyl ethers, the CH_3 rocking vibration, ρ(O-CH_3), of O-CH_3 should appear in the rock-salt region. With a methyl group in place of hydrogen, a new additional weak band

appeared at 1190 cm^{-1} for diacetyl monoxime-*O*-methyl ether and at 1180 cm^{-1} for isonitrosoacetone-*O*-methyl ether. The weak band near 1190 cm^{-1} is assigned to $\rho(O-CH_3)$.

The bands of the deuterated diacetyl monoxime at 930 cm^{-1} and of the methylated one at 945 cm^{-1} correspond to the weak band of the original oxime at 933 cm^{-1} which was previously assigned to $\nu(C-CH_3)$. However, the band of the methyl ether at 945 cm^{-1} is detectable merely as a shoulder on the higher frequency side of a strong band at 917 cm^{-1}. Consequently, the observed frequency can only roughly be estimated. For isonitrosoacetone and its derivatives, the corresponding bands are weak ones at 920 cm^{-1} in the oxime and at 918 cm^{-1} in the deuterated and methylated oximes. It is most probable that these bands are due to the stretching vibrations of $C-CH_3$ bonds, $\nu(C-CH_3)$, because the C–C stretching bands cannot be considered to shift substantially on deuteration and methylation and also because no other bands could be found in the spectra of isonitrosoacetone.

Summary

The infrared absorption bands due to the O=C–C=N–OH system have been investigated by the use of diacetyl monoxime, isonitrosoacetone, and their *O*-deuterated and *O*-methylated derivatives. All the bands observed have been reasonably assigned. So far as the infrared spectra are concerned, the degree of conjugation in the C=O bonds is between those of saturated ketones and α,β-unsaturated ketones. The degree of conjugation in the C=N bonds is greater than those of conjugated imines and of aldoximes containing a C=C–C=N group and is approximately equal to those of *vic*-dioximes containing an N=C–C=N group. Under the influence of conjugation, the N–O bonds have a greater double-bond character than those of unconjugated oximes. The bond character varies with the hydrogen bonding, the type of which is not –O–H···N=C, but –O–H···O=C. In general, the bands due to the C=N bonds of oximes are weak. However, they are intensified by deuteration and are intensified remarkably by methylation.

The authors wish to express their gratitude to Professor Masaji Kubo of the Department of Chemistry, Nagoya University, for his helpful advice.

Department of Chemistry
Nagoya University
Chikusa-ku, Nagoya

NOTES

Molecular Rotations of Glucides in Relation to their Structures. XI[1]. *β-D-Allomethylose*

By Shukichi YAMANA

(Received October 29, 1962)

Micheel observed the mutarotation of β-D-allomethylose and obtained the following data[2]: $[M]_D^{18}(W) = -19.7°$ (30 sec. after the time of resolution) $\rightarrow -1.6°$ (85 min. after the time of resolution)

Therefore, it can be expected that the initial $[M]_D^{20}(W)$ of β-D-allomethylose is more laevorotatory than $-19.7°$. However, by using his own method of calculation, Whiffen obtained 2° as the $[M]_D(W)$ of β-D-allomethylose[3]. It is apparent that Whiffen's calculated value is incompatible with the values observed by Micheel. The present author will try to apply the PM-method in this case. The names of the carbohydrates to which the calculations are applied, with the unit groups in their molecules, are given in Table I.

TABLE I

Name	Unit group	$[M]_D(W)$	Ref.
β-D-Allomethylose	$[(OH)^{1\beta}, (OH)^{2\alpha}, (OH)^{3\alpha}, (OH)^{4\alpha}, (CH_3)^{5\beta}$, Ring]		
β-D-Gulomethylose	$[(OH)^{1\beta}, (OH)^{2\alpha}, (OH)^{3\alpha}, (OH)^{4\beta}, (CH_3)^{5\beta}$, Ring]	−69.4°[4]	5

Referring to Table I, if the orientation of $(OH)^4$ changes from β to α in β-D-gulomethylose, β-D-allomethylose is obtained. By using the PM-method, $\sum [\mu]_{D\,obs}^{20}$, caused by this orientation change of $(OH)^4$ (that is to say, $[\mu]_{D\,obs}^{20}$ of Yo. Diff. <β-D-allomethylose − β-D-gulomethylose>[6]), is calculated as below:

$$\{(4\alpha)-(4\beta)\}\chi\{(1\beta)+(2\alpha)+(3\alpha)+(CH_3)^{5\beta}+R\}^{7)}=(4\alpha)\chi(1\beta)+(4\alpha)\chi(2\alpha)+(4\alpha)\chi(3\alpha)+(4\alpha)\chi(CH_3)^{5\beta}+(4\alpha)\chi R-\{(4\beta)\chi(1\beta)+(4\beta)\chi(2\alpha)+(4\beta)\chi(3\alpha)+(4\beta)\chi(CH_3)^{5\beta}+(4\beta)\chi R\}=0.0-0.5+45.4+37.9+(4\alpha)\chi R-\{-0.6+7.1+0.6-37.6+(4\beta)\chi R\}^{8)}=113.3+(4\alpha)\chi R-(4\beta)\chi R=43.8^{9)}$$

The corresponding observed value in given by: $\{[M]_D^{20}(W)$ of β-D-allomethylose$\}$ minus $\{[M]_D^{20}(W)$ of β-D-gulomethylose$\}$. Therefore, if the $[M]_D^{20}(W)$ of β-D-allomethylose is x, the observed value of Yo. Diff. <β-D-allomethylose − β-D-gulomethylose> is $(x-(-69.4))$. This observed value should be equal to the above calculated $[\mu]_{D\,obs}^{20}$.
Therefore,

$$x-(-69.4)\equiv 43.8$$
$$\therefore \quad x=-25.6$$

This expected value of $[M]_D^{20}(W)$ of β-D-allomethylose, −25.6, is compatible with Micheel's data already mentioned. This fact may indicate the suitability of the PM-method in this case.

Department of Chemistry
Kyoto Gakugei University
Fushimi-ku, Kyoto

1) Part X: S. Yamana, This Bulletin, 35, 1950 (1962).
2) F. Micheel, *Ber.*, 63, 347 (1930).
3) D. H. Whiffen, *Chem. & Ind.*, 1956, 964.
4) This is the observed value at 29°C.
5) P. A. Levene and J. Compton, *J. Biol. Chem.*, 111, 335 (1935).
6) Cf. Ref. 17 in a previous paper, S. Yamana, This Bulletin, 35, 1269 (1962).
7) Cf. Ref. *12 in a previous paper, S. Yamana, This Bulletin, 31, 564 (1958).
8) Table II of the preceding paper[1] was used.
9) Equation 15 of the preceding paper[1] was used.

Some Observations on the Calcination Process of Precipitated Magnesium Hydroxide

By Tatsuo SAITO and Yoshihide KOTERA

(Received November 22, 1962)

It has previously been reported[1] that the particle size of magnesium oxide crystals prepared by the thermal decomposition of pure precipitated magnesium hydroxide and of native brucite increases with the calcination temperature and the duration of heating at a fixed temperature according to the equation: $d=Kt^n \exp(-E/RT)$, where d is the average crystal diameter determined from the broadening of the X-ray diffraction line, t is time, E is the activation energy, R is the gas constant, T is the absolute temperature, and K and n are constants. The present paper presents microscopic and atomic observations on the calcination process of precipitated magnesium hydroxide.

Experimental

The materials used were the same as those described in a previous paper[1]. Their NMR spectra were obtained by means of a Varian DP 60 spectrometer equipped with an RF unit of 40 Mc., the modulation frequency and width on operation being 40 c. p. s. and 1.1 gauss respectively. The electron microscopic photographs were taken by means of a Nippon Denshi electron microscope TEM-5G.

Experimental Results and Discussion

NMR spectra were obtained for samples which had been dehydrated in a vacuum from precipitated magnesium hydroxide and brucite for 3 hr. at 100, 200, 280, 300, 310, 330, 400 and 500°C. The results are shown in Fig. 1, where the (a)'s are the spectra of precipitated magnesium hydroxide and the (b)'s, those of brucite. It may be seen in Fig. 1 that there is a great difference between (a) and (b) below 280°C. The spectra of precipitated magnesium hydroxide are rather complex, having the central peak, while those of brucite have the typical two-proton shape. Figure 2 shows the variations in line width of the NMR spectra with the change in calcination temperature. The decrease in line width began at a lower temperature (at about 200°C) for precipitated magnesium hydroxide than for

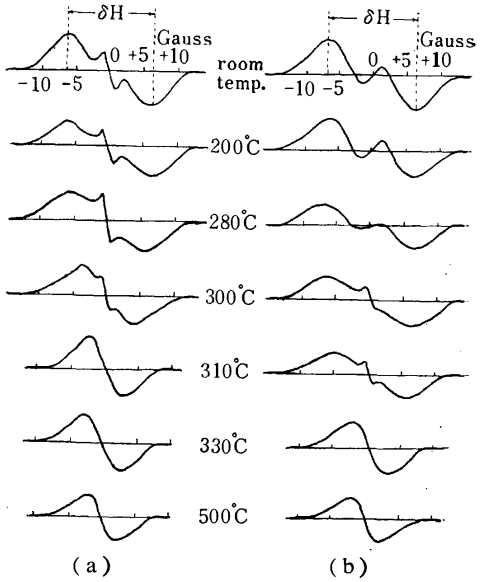

Fig. 1. NMR spectra of proton in the thermally dehydrated products in vacuo.
(a) Samples of precipitated $Mg(OH)_2$ series
(b) Samples of brucite series

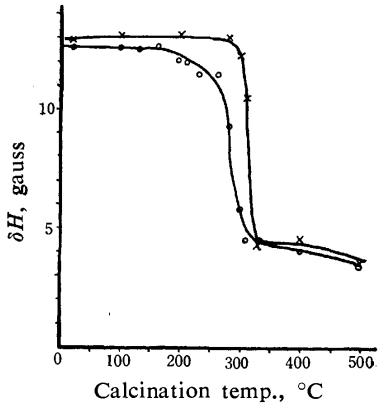

Fig. 2. Variations of line width (δH) of NMR spectra in Fig. 1.
○—○, Precipitated $Mg(OH)_2$ series
×—×, Brucite series

brucite. To clarify the effect of water vapor on dehydrated samples, these samples were prepared from brucite by means of calcination in a vacuum for 3 hr. at 200, 300, 330, 360, 400 and 500°C, and then reacted with water vapor by succesive exposure to an atmosphere saturated with this vapor at room temperature. After the exposure, rehydrated samples were evacuated at room temperature for 12 hr. in order to remove any excess adsorbed water. In Fig. 3 NMR spectra are shown for dehydrated (a) and rehydrated (b) samples. The central peaks seen in Fig. 3 (b) may be a result of the presence of a trace of movable water adsorbed by the samples and not re-

1) Y. Kotera, T. Saito and M. Terada, This Bulletin, 36, 195 (1963).

moved by evacuating the samples at room temperature. It was possible to remove it, however, by heating the samples to 110°C and by then evacuating them at this temperature. It is interesting that the spectra of (b) are similar to those of precipitated magnesium hydroxide (Fig. 1 (a)).

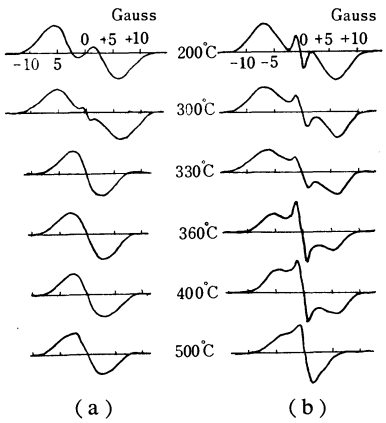

Fig. 3. NMR spectra of proton in the thermally dehydrated products of brucite in vacuo and their rehydrated products.
(a) Samples of dehydration series
(b) Samples of rehydration series

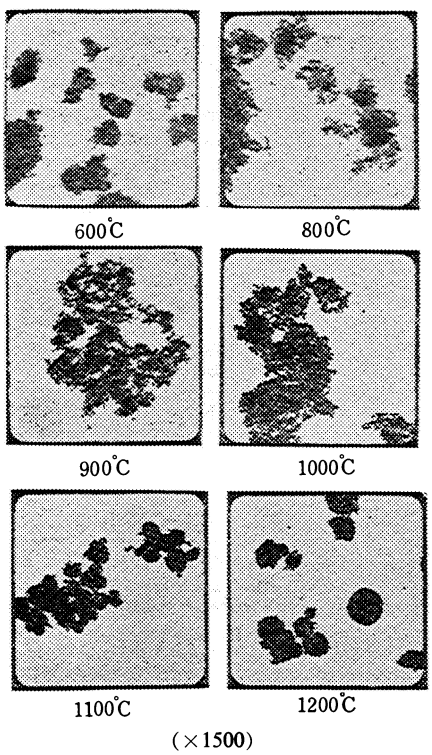

Fig. 4. Electron micrographs of MgO prepared from precipitated $Mg(OH)_2$.

The samples for the electron micrograph were prepared by the calcination of precipitated magnesium hydroxide at 600, 700, 800, 900, 1000, 1100 and 1200°C for durations ranging from 30 min. to 24 hr. The duration had a smaller effect upon the crystal size and the crystal form than the temperature. The effect of the calcination temperature upon the crystal figure is shown in Fig. 4, the rate of magnification being ×1500. From Fig. 4 it may be seen how crystals aggregate with each other until the temperature of 900°C is reached and how they grow to sphere-like particles, the particle size being about 0.1, 1 and 3 μ for the products at 1000, 1100 and 1200°C respectively.

From the results obtained it may be concluded that the precipitated magnesium hydroxide holds the movable water in the interstices between crystal lattice layers or between fine particles and that the structure water is removed only partially from the precipitated magnesium hydroxide by calcination below 280°C. It may also be concluded that the rehydration process is not the reverse reaction of dehydration but proceeds according to the thermal history of the samples. Such a tendency was seen in our experiment, where the water contents of the samples rehydrated by saturated water vapor were measured gravimetrically with the change of storage time; it has also been reported in adsorption experiments carried out for magnesium oxide[2]. The crystal growth of magnesium oxide shown in Fig. 4 would support the conclusion of the preceding paper[1]. A detalied study of these and other aspects will be published elsewhere in due course.

The authors are indebted to Dr. Matsuo Terada for his helpful discussions.

Government Chemical Industrial Research Institute, Tokyo
Shibuya-ku, Tokyo

2) S. J. Gregg and R. K. Packer, *J. Chem. Soc.*, **1955**, 51; R. I. Razouk and R. Sh. Mikhail, *J. Phys. Chem.*, **59**, 636 (1955); **61**, 886 (1957); **62**, 920 (1958); D. T. Livey et al., *Trans. Brit. Ceram. Soc.*, **56**, 217 (1957).

New Addition Reactions. V. Dimerization of Diketene

By Ryohei ODA, Shunichi TAKASHIMA and Masaya OKANO

(Received December 8, 1962)

It is well known that diketene easily dimerizes to give dehydroacetic acid in the presence of a basic catalyst such as sodium ethoxide, sodium phenolate, triethylamine, or pyridine[1]. We now wish to report the formation of two isomeric diketene dimers by the use of aluminum tribromide as a catalyst. This result is in contrast to other Lewis acid-catalyzed reactions, where polymerizations of diketene to a polyketone[2] (by boron trifluoride and aluminum trichloride) or a polyester[3] (by mercuric chloride) were achieved.

When diketene was treated with 5~10 mol. % of aluminum tribromide in ethylene dichloride at 10~20°C for about thirty hours, a mixture of two dimers, 2,6-dimethyl-γ-pyrone-3-carboxylic acid (I) and dehydroacetic acid (II), was obtained in a fair yield without any formation of a polymeric byproduct. Compound I was separated from II by fractional crystallization using a ligroin-chloroform mixture, and their yields were 20 and 35% respectively. Both structures were confirmed by mixed melting point determinations with respective authentic samples. Here, the authentic material of I was prepared from II by the method of Feist[4]. It is interesting to note that the exclusive formation of II was observed (in ca. 20~25% yields) when chloroform or carbon disulfide was used as a solvent, but no plausible explanation for this solvent effect can be offered.

Collie and Hilditch[5] reported that II could be converted to I in hot 85% sulfuric acid. However, when II was treated with aluminum tribromide in cold ethylene dichloride, no isomeric I was found, rather a small amount of an unidentified product (m. p. 230°C) resulted. Therefore, both dimers would be directly produced from diketene as shown in the following scheme. The formation of the anion III (or its protonated form) as a common intermediate seems probable in view of the fact that, in the presence of aluminum trichloride, a similar acylation of benzene with diketene has been achieved with ease[1a].

Experimental

Dimerization of Diketene.—To a stirred mixture of 30 g. (0.11 mol.) of aluminum tribromide and 300 ml. of dry ethylene dichloride, 100 g. (1.20 mol.) of diketene was added dropwise at the rate of 30 g./hr. The temperature was maintained below 10°C by means of an ice-bath. On the completion of the addition, the mixture was held at that temperature for 5 hr., and allowed to stand at room temperature for additional ca. 20 hr. (until the odor of diketene almost disappeared). Then 250~300 ml. of ca. 5 N hydrochloric acid was gradually added to the reaction mixture to destroy the catalyst. The organic layer separated was washed with water, dried over anhydrous sodium sulfate, and the solvent was removed in vacuo. The residue which solidified on cooling was washed with cold ethanol, dried, and weighed 62 g. By recrystallization from ca. 500 ml. of ligroin-chloroform (3 : 2), 20 g. (20%) of light-brown crystals separated. Concentration of the

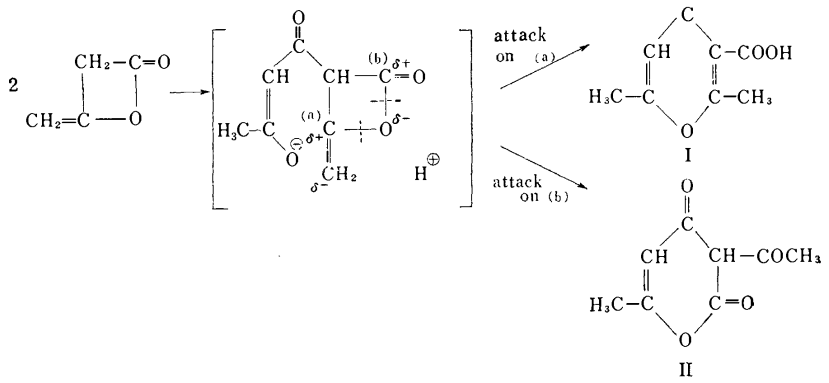

1) a) A. B. Boese, Jr., *Ind. Eng. Chem.*, **32**, 21 (1940); b) A. B. Steele et al., *J. Org. Chem.*, **14**, 460 (1949); c) T. Isozima, *J. Chem. Soc. Japan, Ind. Chem. Sec.* (*Kōgyō Kagaku Zassi*), **57**, 773 (1954).

2) a) R. Oda et al., *Makromol. Chem.*, **43**, 149 (1961); b) J. Furukawa et al., *J. Chem. Soc. Japan, Ind. Chem. Sec.* (*Kogyo Kagaku Zasshi*), **65**, 254 (1962).

3) J. Furukawa et al., *Makromol. Chem.*, **39**, 243 (1960).

4) F. Feist, *Ann.*, **257**, 253 (1890).

5) J. N. Collie and T. P. Hilditch, *J. Chem. Soc.*, **91**, 787 (1907).

filtrate gave 35 g. (35%) of other crystals. The first compound, after two recrystallizations from chloroform or ethanol, showed m. p. 96~98°C. Based on its analytical data, spectral (infrared and ultraviolet) data and chemical reactivities (neutralization with aqueous alkaline, decarboxylation, reaction with amine etc.), formula I was proposed for this compound. The structure was further confirmed by a mixed melting point determination with an authentic material, which was prepared from II, by chlorination with phosphorus pentachloride, and by treatment with concentrated sulfuric acid[4]. The second substance melted at 108~109°C after recrystallization from aqueous ethanol. This compound showed an infrared spectrum identical with that of authentic II, and no mixed melting point depression was observed.

The authors wish to thank Mr. Masahiko Miyanoki for his helpful and stimulating discussions, and Dainippon Celluloid Co., Ltd., for the gift of diketene.

Department of Synthetic Chemistry
Faculty of Engineering
Kyoto University
Sakyo-ku, Kyoto (R. O. & S. T.)

Institute for Chemical Research
Kyoto University
Takatsuki, Osaka (M. O.)

The Quantitative Determinations of High-boiling Divalent Organo Sulfur Compounds by Copper —Determinations of Divalent Sulfur Compounds Formed in the Reaction between Benzene and Sulfur—*

By Wataru ANDO, Ken'ichi SUGIMOTO and Shigeru OAE

(Received December 27, 1962)

Determinations of aromatic mercaptans, sulfides and disulfides dissolved in hydrocarbon are of considerable importance both in industrial and fundamental investigations. Separation of these high-boiling aromatic sulfur compounds into individual components[1,2] is usually difficult because of the similar chemical behaviors toward many reagents. Especially analysis is more difficult when sulfur is present in samples that are to be distilled.

Heavy metals, such as copper, silver and mercury[3-6], are known to form complexes with divalent sulfur compounds and could be used for the analysis of these sulfur compounds. Such a procedure would have an advantage of great rapidity and simplicity in handling at room temperature over other methods. In this investigation, we have chosen metallic copper and studied in detail the behaviors of copper metal toward various divalent sulfur groups and the scope of application of this procedure for the analysis of various divalent sulfur compounds.

Preparation of spongy active copper powder has been reported by Blumer[7]. Actually, we found that we could make two kinds of copper powders, i. e., red-brown and black copper powders depending upon two different procedures we used. These two different copper powders showed different affinities toward various divalent sulfur compounds. Therefore, these different affinities could be utilized for the separation of divalent sulfur compounds. Divalent sulfur compounds used for this work were benzenethiol, diphenyl sulfide, diphenyl disulfide and thianthrene, which are considered to be present in the products mixture of the reaction between benzene and sulfur. Our results indicate that elemental sulfur and benzenethiol can be eliminated from benzene solution of divalent sulfur compounds by precipitation with red-copper, whereas diphenyl sulfide, disulfide, and thianthrene remained in the solution. When the remaining solution was treated with black copper, the disulfide was found to be eliminated leaving other components in the solution.

Experimental

Preparation of Spongy Active Copper Powder. — *Red-brown Copper.*—Copper sulfate, 45 g., was dissolved into 500 ml. of distilled water containing 50 ml. of 2 N hydrochloric acid and slowly stirred. Fifteen grams of thick slurry zinc was added to this solution at once. Stirring was continued until copper which precipitate turns from black to red-brown color. This copper was washed with distilled water, which was replaced with acetone and then with ether. Red-brown copper was kept in vacuum in dried condition. Completely dried copper

* Presented at the 11th Annual Meeting of the Japan Society for Analytical Chemistry, Sapporo, July, 1962.

1) M. W. Tamele and L. B. Ryeand, *Ind. Eng. Chem.*, **8**, 16 (1931).

2) C. R. Stahl and S. Siggia, *Anal. Chem.*, **29**, 154 (1957).

3) C. Ellis, "Chemistry of Petroleum Derivatives", Vol. I and II, Reinhold, N. Y. (1937).

4) A. F. Hardman and H. E. Barbeheun, *Ind. Eng. Chem., Anal. Ed.*, **7**, 103 (1935).

5) J. S. Ball, *U. S. Bur. Mines Rept. Invest.*, 3591 (1941).

6) J. M. Hunt and G. W. Jamieson, *Bull. Am. Assoc. Petroleum Geol.*, **40**, 477 (1956).

7) M. Blumer, *Anal. Chem.*, **29**, 1039 (1957).

powder are quite stable in air. But in the presence of even a trace amount of water, copper reacts with oxygen and carbon dioxide in air to form black copper oxide and green $CuCO_3Cu(OH)_2$.

Black Copper.—When about 20 g. of zinc was added to the copper sulfate solution at several time intervals and the mixture was continued to stir, black colored copper precipitated. It was washed with distilled water and was kept in cold.

Preparation of Copper Column.—In this work, a column with bed volume of 20 ml. of copper powder in a glass tube having the diameter of 2 cm. and length of 25 cm. was used. The size of the column could be adjusted depending on the amounts of sulfur compounds. The copper column was soaked with benzene before a benzene solution containing sulfur compounds were passed through.

Preparation of Standard Sulfur Compounds.—Benzenethiol was purchased from Maruwaka Kagaku, Osaka, and diphenyl sulfide was K and K Lab. Inc., Long Island, N. Y., respectively, and both were used after careful distillations. Diphenyl disulfide was prepared by oxidizing benzenethiol with hydrogen peroxide and recrystallized from ethanol.

Results

The divalent sulfur compounds in benzene were characterized by measuring the intensities of ultraviolet absorption at 280 mμ against benzene blank. Benzenethiol, diphenyl disulfide, diphenyl sulfide, thianthrene, thiophene and elemental sulfur, all have the absorption at around 280 mμ. At this absorption spectra, Beer's law was obeyed at concentration around 5×10^{-5} mol./l. for diphenyl disulfide and thianthrene, 2×10^{-5} mol./l. for diphenyl sulfide, 2×10^{-4} mol./l. for benzenethiol and 0.2 mol./l. for thiophene. Molar extinction coefficients of these compounds at 280 mμ was shown in Table I.

Table I. Molar extinction coefficients of organo sulfur compounds

Compound	Molar extinction coefficient
Benzenethiol	593
Diphenyl disulfide	2500
Diphenyl sulfide	5700
Thianthrene	2400
Thiophene	0.79

Benzene solution containing benzenethiol or diphenyl disulfide was slowly passed through the red-brown copper column. By this procedure, benzenethiol was removed as can be observed from Table II, but diphenyl disulfide was not effected at room temperature. Benzenethiol apparently reacted with copper to form cuprous phenyl mercaptide, which has yellow

$$C_6H_5SH+Cu \rightarrow Cu_2(C_6H_5S)_2$$

brown color and is not soluble in benzene, water, dilute hydrochloric acid or in ammonia. These chemical properties of this compound suggest a formation of cuprous mercaptide[8].

Table II. Removal of benzenethiol from benzene

Initial amount of thiol mM	Residual thiol in elute mM
0.80	0.09
1.06	0.14
2.11	0.15

Meanwhile diphenyl disulfide did not form any compound with copper in this condition. Therefore, when both the mercaptan and the disulfide are present in the solution, at first the total absorbancy of the solution at 280 mμ was measured, and then the solution was passed through the red-brown copper column and the absorbancy of the filtrate was measured again. The absorbancy of the filtrate corresponds to the amount of the disulfide. The amount of benzenethiol can be calculated by subtracting the absorbancy of the disulfide from the total absorbancy of the original solution at 280 mμ. Table III shows their analytical data.

Table III. Determination of benzenethiol and diphenyl disulfide in benzene

Initial concn.		Found	
Thiol mM	Disulfide mM	Thiol mM	Disulfide mM
0.56	0.33	0.55	0.34
0.56	0.24	0.57	0.22
0.93	0.42	0.93	0.34
0.93	0.28	0.93	0.26
0.93	0.14	0.91	0.14
1.34	0.42	1.38	0.40
1.34	0.28	1.38	0.28
1.34	0.14	1.22	0.16

Detection of the disulfide and the sulfide in the presence of elemental sulfur in benzene solution was also tried by the same procedure. Elemental sulfur often presented in these organic sulfur compounds is a serious hazzard in the analysis of these sulfur compounds. To remove elemental sulfur from these divalent sulfur compounds, red-brown copper column was used. Elemental sulfur, the disulfide and the sulfide were dissolved in benzene and this solution was passed through the red-brown copper column. By this procedure only elemental sulfur was removed from the original solution.

In order to determine the amount of the sulfide, the filtrate solution was passed once

8) F. Feigl, "Chemistry of Specific, Selective and Sensitive Reactions", Elsevier Pub. Co., Amsterdam (1949), p. 326.

TABLE IV. DETERMINATION OF DIPHENYL DISULFIDE AND DIPHENYL SULFIDE IN THE PRESENCE OF SMALL AMOUNTS OF ELEMENTAL SULFUR

Elemental sulfur per 100 ml. of benzene	Taken		Found	
	Sulfide	Disulfide	Sulfide	Disulfide
mg.	mM	mM	mM	mM
0	0.33	0.21	0.33	0.21
1	0.071	0.32	0.071	0.32
2.5	0.042	0.16	0.047	0.17
	0.063	0.16	0.068	0.17
	0.072	0.34	0.072	0.34
	0.110	0.12	0.091	0.12
5.0	0.042	0.155	0.047	0.17
	0.063	0.16	0.070	0.16
	0.063	0.28	0.053	0.28
	0.0945	0.28	0.110	0.25
	0.126	0.28	0.140	0.26
10.0	0.042	0.31	0.044	0.265
	0.063	0.28	0.073	0.28

more through the black copper column. By this procedure the disulfide was removed, and the filtrate solution contained only the sulfide. The amount of each sulfur compound was determined by ultraviolet absorption at 280 mμ. Analytical results for the determination of their sulfur compounds were shown in Table IV. Agreement was quite satisfactory. The mechanism of the separation of the disulfide by black copper and the disulfide may produce a similar compound which was obtained by the reaction between the mercaptan and red-brown copper.

A benzene solution containing thianthrene was treated through these copper columns to see how these sulfur compounds behave toward active copper. We found that thianthrene was a little effected by these copper columns. Therefore, active copper is not applicable for quantitative separation of diphenyl disulfide and thianthrene. They were determined by the reaction with concentrate sulfuric acid[9].

These results indicated that the affinities of these divalent sulfur compounds toward active copper depends on the nature of sulfur group. Experimentally determined order of affinities of these sulfur compounds to copper are elemental sulfur>benzenethiol>diphenyl disulfide>thianthrene>diphenyl sulfide.

Department of Chemistry
Radiation Center of Osaka Prefecture
Sakai, Osaka

9) K. Sugimoto, W. Ando and S. Oae, *Japan Analyst (Bunseki Kagaku)*, **12**, 38 (1963).

SHORT COMMUNICATIONS

Photoconductivity in an Organic Liquid Solution

By Mizuka SANO and Hideo AKAMATU

(Received December 17, 1962)

Semi- and photo-conductivity in organic substances have been studied for several years, but most of the experiments have been concerned with the crystalline state[1]. Recently, however, the electronic conduction has been investigated in liquid benzene[2], pyrene[3] and *n*-hexane[4]. The electronic mobility in the liquid was samller by three orders of magnitude than that in the solid[3]. However, the conductivity itself rose sharply at the melting point[5,6]. The rise in the conductivity could not be attributed to the increase in the mobility at the melting point, but it might be due to the enormous increase in the number of charge carriers. In the present experiment the photoconductivity of solutions was investigated preliminarily in relation to the intermolecular energy transfer.

Measurement was made with benzene solutions of pyranthrene (3.3×10^{-5} mol./l.), tetracene (2.0×10^{-5} mol./l.), and pyrene (1.3×10^{-1} mol./l.), all of which show intense absorption spectra in the range of 370~500 mμ. A photocell was made of Teflon, with two parallel Nesa-glass electrodes (1.3 cm^2 in area), forming a sandwich-type cell. The distance between the electrodes was fixed at 3 mm. Through one of the electrodes the solution was illuminated by monochromatized light. The currents were measured by a d.c. method.

The dark currents through the solutions, as well as the benzene, followed Ohm's law below the electric field of 10^2 V./cm. The specific conductivity of benzene was $6.4\times10^{-14}\Omega^{-1}\cdot cm^{-1}$, judging from the observed current in this ohmic range. Beyond the electric field of the above value, the current increased non-

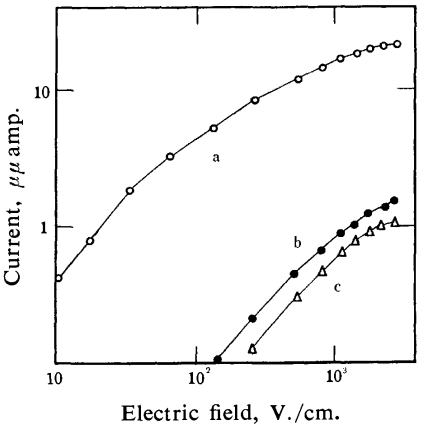

Fig. 1. The relation between current and electric field for the benzene solution of pyranthrene; (a) dark current, (b), (c) photocurrents produced by 450 and 403mμ illuminations, respectively.

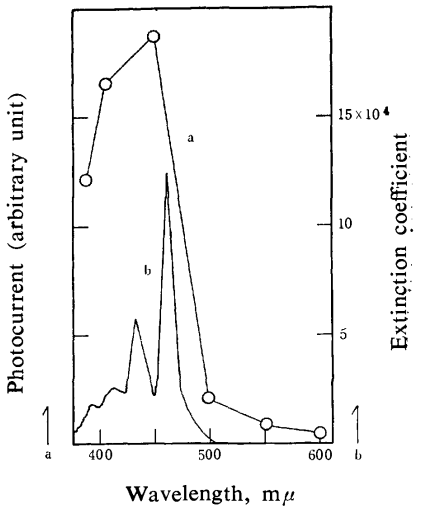

Fig. 2. The spectral responses of (a) photocurrent and (b) extinction coefficient for the benzene solution of pyranthrene.

linearly and showed a tendency to saturate in accordance with an applied voltage. Similar behavior was found in the photocurrent in the solutions, as is shown in Fig. 1.

Benzene itself did not show any response to illumination in the visible spectral region. However, when benzene dissolved pyranthrene, for instance, the solution was found to be

1) M. Sano and H. Akamatu, This Bulletin, 35, 587 (1962).
2) E. Forster, *J. Chem. Phys.*, 37, 1001 (1962).
3) O. H. LeBlanc, Jr., ibid., 37, 916 (1962).
4) O. H. LeBlanc, Jr., ibid., 30, 1443 (1959).
5) J. Kommandeur, G. J. Korinek and W. G. Schneider, *Can. J. Chem.*, 36, 513 (1958).
6) J. A. Bornmann, *J. Chem. Phys.*, 36, 1691 (1962).

photosensitive in the spectral region. As is shown in Fig. 2, the benzene solution of pyranthrene exhibited a remarkable photocurrent in the spectral region between 400 and 500 mμ. The spectral response of photocurrent is located in the absorption region of the pyranthrene molecule. Therefore, the result indicates the contribution of the solute molecules in the first singlet excited state to the photoconduction. The photocurrent depended linearly on the light intensity below 3×10^{17} photons/sec. cm^2. The linearity was independent of the wavelength of the illumination and of the applied voltage, even if the measurement was made outside the ohmic range.

It is uncertain whether the solute molecules facilitate an injection of charge carriers from the electrode, or whether charge carriers are produced by the interaction between the excited solute molecules and the solvent. The presence of solute molecules at the surface of electrode may, however, reduce the work of emitting electrons from the elecrode. This reduction of the work function is probably induced by the excited molecules. It must also be considered that the conducting state of the solvent is located below the first singlet excited state of the solute, and that the excitation energy is transferred from the excited solute molecule to the solvent by interaction, generating the charge carriers. These different patterns of behavior could not, however, be separated in this preliminary experiment.

Department of Chemistry
Faculty of Science
The University of Tokyo
Hongo, Tokyo

The Stereoselective Synthesis of trans-Chrysanthemum Monocarboxylic Acid

By Takeshi MATSUMOTO, Akira NAGAI and Yutaro TAKAHASHI

(Received December 28, 1962)

Chrysanthemum monocarboxylic acid ethyl ester (I) has been synthesized from ethyl diazoacetate and 2, 5-dimethyl-2, 4-hexadiene[1]. However, the product was a mixture of cis and trans esters in a ratio of about 1 : 1[2].

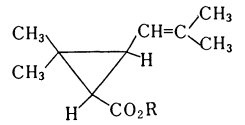

I R=C_2H_5
II R=*t*-C_4H_9
III R=H

The present authors wish to report a stereoselective formation of *trans*-chrysanthemum monocarboxylic acid *t*-butyl ester (II) achieved by treatment of the diene with *t*-butyl diazoacetate.

t-Butyl diazoacetate (1.42 g., 0.010 mol.)[3] was added slowly to a mixture of the diene 2.5 g., 0.022 mol.) and copper powder (0.05 g.) at 120~130°C. The reaction product was distilled to yield 0.95 g. of II (b. p., 120~125°C/14 mmHg; Found: C, 74.82; H, 10.81. Calcd. for $C_{14}H_{24}O_2$: C, 74.95; H, 10.78%; ν_{max} 1720 cm^{-1}; δ (c. p. s.)'s are shown in Table I), the infrared spectrum of which was identical with that of the ester prepared form the silver salt of authentic trans acid III and *t*-butyl iodide. Complete hydrolysis of the ester II was effected in a 1 N hydrochloric acid solution at 100°C, affording a single crystalline acid whose infrared spectrum and m. p. (53~54°C) were identical with those of *trans*-III.

Data of the NMR spectra of I, II and III are summarized in Table I. A quantitative analysis of the cis and trans ratio is especially possible by drawing a comparison between the intensity of the signals due to the olefin proton of each isomer. The fact that the synthetic II exhibited only one detectable

TABLE I. NMR SPECTRA OF CHRYSANTHEMUM MONOCARBOXYLIC ACID DERIVATIVES IN CARBON TETRACHLORIDE SOLUTION AT 56.4 Mc.

	cis-Acid III	*trans*-Acid III	*t*-Bu ester II
CH_3(ring)	0*(6H)	0*(3H) 8.6(3H)	0*(3H) 5.6(3H)
CH (side chain)	25(3H) 29(3H)	27(6H)	31(6H)
CH (olefin)	226 234 (1H)	200 208 (1H)	202.5 211.5 (1H)

* The chemical shifts (c. p. s. unit) were determined relative to the peak at the highest magnetic field.

1) H. Staudinger, O. Muntwyler, L. Ruzicka and S. Seibt, *Helv. Chim. Acta*, **7**, 390 (1924); I. G. M. Campbell and S. H. Harper, *J. Chem. Soc.*, **1945**, 283. The natural chrysathemum moncarboxylic acid has the trans configuration.

2) The ratio of cis and trans isomers can be conveniently determined by measurement of the NMR spectum (cf. Table I).

3) H. Reimlinger and L. Skatteböll, *Chem. Ber.*, **93**, 2116 (1960). In the present work, the *t*-butyl aceturate was prepared by the reaction of isobutylene with aceturic acid in the presence of sulfuric acid in a dioxane solution.

doublet peak in the low magnetic field confirmed the selective formation of the trans ester.

The steric course of this reaction seems to be controlled by the bulkiness of the *t*-butyl group.

Department of Chemistry
Faculty of Science
Hokkaido University
Sapporo

The Importance of NMR in Determining Structure and Electrical Effects in Substituted Ferrocenes[1)]

By Robert A. BENKESER, Yoichiro NAGAI and John HOOZ

(Received December 24, 1962)

The determination of the structure of polysubstituted ferrocenes has proved to be a vexing problem. Classic methods of structure proof based upon unequivocal syntheses or degradations are not often feasible in the case of substituted ferrocenes. The ferrocene moiety is quite stable, and, while degradation of the molecule is possible, generally rather drastic conditions must be employed[2)]. The result is usually a mixture of products which contains substituted cyclopentadienes and cyclopentanes, the structures of which are also frequently in doubt. Likewise the unequivocal synthesis

TABLE I. CHEMICAL SHIFTS FOR THE RING PROTONS OF SUBSTITUTED FERROCENES[1,2)]

Substituent	*a*[3)]	*b*[4)]	*c*[5)]	*d*[6)]
H (ferrocene)	—	—	5.94	—
Me	—	—	6.01(7)	6.06(2)
Et	—	—	5.99(5)	6.03(4)
i-Pr	—	—	5.98(5)	6.04(4)
t-Bu	—	—	5.98(5)	6.08(4)
Ac (acetyl)	5.33(2)	5.64(2)	5.88(5)	—
1-Ac-1'-Me	5.42(2)	5.70(2)	—	6.01(4)
1-Ac-2-Me	5.56(1)	5.72(1) ; 5.82(1)	5.95(5)	—
1-Ac-3-Me	5.40(2)	5.69(1)	5.92(5)	—
1-Ac-1'-Et	5.41(2)	5.69(2)	—	5.99(4)
1-Ac-2-Et	5.53(1)	5.69(1) ; 5.79(1)	5.93(5)	—
1-Ac-3-Et	5.37(2)	5.69(1)	5.91(5)	—
1-Ac-1'-*i*-Pr	5.39(2)	5.66(2)	—	5.98(4)
1-Ac-2-*i*-Pr	5.51(1)	5.64(1) ; 5.76(1)	5.92(5)	—
1-Ac-3-*i*-Pr	5.41(2)	5.71(1)	5.91(5)	—
1-Ac-1'-*t*-Bu	5.32(2)	5.61(2)	—	5.98(4)
1-Ac-2-*t*-Bu	5.46(1)	5.71(1) ; 5.79(1)	5.85(5)	—
1-Ac-3-*t*-Bu	5.43(2)	5.72(1)	5.90(5)	—

1) The data listed are "tau" values using tetramethylsilane as an internal standard.
2) The values in parentheses are relative intensities. All measurements were made on a Varian A-60 analytical spectrometer.
3) Column "*a*" values refer to the H in the 2- and 5-position relative to the acetyl group.
4) Column "*b*" values refer to the H in the 3- and 4-position relative to the acetyl group.
5) Column "*c*" values refer to the H on an unsubstituted ring.
6) Column "*d*" values refer to H on an alkylated ring.

1) This research was supported by the United States Air Force through the Air Force Office of Scientific Research of the Air Research and Development Command under contract No. A. F. 49 (638)-297. Reproduction in whole or in part is permitted for any purpose of the United States Government.

2) A. N. Nesmeyanov, E. G. Perevalova and R. V. Galovnya, *Bull. Acad. Sci. U. S. S. R., Div. Chem. Sci.*, 749 (1956); D. S. Trifan and L. Nicholas, *J. Am. Chem. Soc.*, 79, 2746 (1957).

of a polysubstituted ferrocene is not easily accomplished. Isomeric mixtures are almost invariably encountered which are difficult and tedious to separate[3].

As a result of the synthetic problems associated with structure proofs in this field, considerable reliance has been placed upon infrared spectroscopy[4] for determining the structure of substituted ferrocenes. While infrared is extremely useful in determining the structure of certain ferrocene compounds, there is considerable need for a more unequivocal and universal structural probe. It is the purpose of this paper to report that NMR spectroscopy will provide such a probe in many instances.

Table I lists the chemical shifts and relative intensities for the ring protons of seventeen substituted ferrocene compounds. It is immediately apparent from this table that the structure of the mono-, as well as the disubstituted ferrocenes (1, 1'- as well as 1, 2- and 1, 3-) are clearly pinpointed by the chemical shifts of the ring protons. In addition to establishing the ferrocene structures, the values in Table I can be used also as a measure of the electrical effects of substituent groups at various positions in the ferrocene ring system, a topic of considerable current interest[5].

TABLE II. CHEMICAL SHIFTS FOR α-PROTONS[1] OF ALKYL GROUPS ON FERROCENE RINGS[2-4]

Substituent	α-H(Me)	α-H(Et)	α-H(*i*-Pr)
R(alkyl)	8.04	7.71	7.41
1-Ac-1'-R	8.09	7.73	7.43
1-Ac-2-R	7.67	7.28	6.59
1-Ac-3-R	7.97	7.62	7.34

1) The α-protons referred to in this Table are those located on the carbon atom of the alkyl group which is attached to the ferrocene ring.
2) The data listed are "tau" values using tetramethylsilane as an internal standard. A Varian A-60 analytical spectrometer was used for all the measurements.
3) Ac in the Table refers to the acetyl group.
4) The spectra of all the compounds listed in this table as well as in Table I were obtained in a solvent of carbon tetrachloride.

The structural assignments for the acetylalkylferrocenes listed in Table I are further supported by the trend of the chemical shifts for the α-protons of the various alkyl groups attached to the ferrocene ring (see Table II).

Thus the α-protons in 1-acetyl-1'-alkylferrocenes are at higher field than the 1, 3-isomers. The latter, in turn, are at higher field than the 1, 2-isomers. This trend can be rationalized in terms of the shielding effect on the α-protons induced by their proximity to the electron withdrawing acetyl group.

Department of Chemistry
Purdue University
W. Lafayette, Ind.
U. S. A.

3) Indicative of the problems in this area is a recent article (M. Rosenblum, *J. Am. Chem. Soc.*, **81**, 4530 (1959)) which reports the relative adsorbabilities of certain isomeric disubstituted ferrocenes on alumina. This was offered (and rightly so) as a useful primary indication of structure.

4) M. Rosenblum, *Chem. & Ind.*, **1958**, 953; *J. Am. Chem. Soc.*, **81**, 4530 (1959); K. L. Rinehart, K. L. Motz and S. Moon, ibid., **79**, 2749 (1957).

5) A. N. Nesmeyanov and O. A. Reutov, *Doklady Akad. Nauk., S. S. S. R.*, **115**, 518 (1957); W. F. Little and R. Eisenthal, *J. Org. Chem.*, **26**, 3609 (1961); *J. Am. Chem. Soc.*, **83**, 4936 (1961); M. Rosenblum and W. G. Howells, ibid., **84**, 1167 (1962).

Palladium(II)- and Platinum(II)-complexes of Schiff Bases Derived from Salicylaldehyde and Alkylamines

By Shoichiro YAMADA, Hiroaki NISHIKAWA and Kayo YAMASAKI*

(Received February 7, 1963)

Previous studies of metallic complexes with Schiff bases of a type shown in Fig 1 have

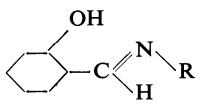

Fig. 1. *N*-Alkylsalicylideneimine.

revealed that it depends much upon the nature of the metal ion as well as upon that of the ligand whether the quadri-co-ordinate complex of a transition element takes a squareplanar configuration or a configuration distorted from it. Thus, the stability of the tetrahedral co-ordination around the metal ion, as compared with that of the square-planar one, is higher for cobalt(II)[1], a little lower for nickel(II)[2], and much lower for copper(II)[3].

* Present address: Department of Chemistry, Osaka City University, Sugimoto-cho, Osaka.

1) H. Nishikawa, S. Yamada and R. Tsuchida, *Z. Naturforsch.*, **17b**, 78 (1962); H. Nishikawa and S. Yamada, This Bulletin, **35**, 1430 (1962); B. O. West, *J. Chem. Soc.*, **1962**, 1374; L. Sacconi, M. Ciampolini, F. Maggio and F. P. Cavasino, *J. Am. Chem. Soc.*, **84**, 3246 (1962).

2) H. Nishikawa and S. Yamada, unpublished. Cf. R. H. Holm, *J. Am. Chem. Soc.*, **83**, 4683 (1961).

3) S. Yamada and H. Nishikawa, unpublished.

A similar study has now been extended to palladium(II) and platinum(II) in order to examine the stereochemistry of these compounds and to explore the possibility of obtaining complexes of palladium(II) and platinum(II) with a configuration distorted from the square-plane, a configuration which is quite rare for these metal ions. For example, in the complexes with R=*t*-butyl the square-planar configuration of the complex is impossible because of serious steric hindrance, so that these complexes, if prepared at all, are expected to have a configuration distorted from the square-plane. Platinum(II) complexes with neither *N-n-* nor isoalkyl-salicylideneimines have been reported previously, nor has the preparation of the corresponding *N*-isopropyl or *t*-butyl derivative been described, although *N-n*-alkylsalicylideneimines of palladium(II) were reported[4]. The present communication reports on the successful preparation of palladium(II)- and platinum(II)-complexes of these Schiff bases, including those complexes with a configuration distorted from the square-plane.

The platinum(II)-complexes were prepared by the following two methods: (1) To an aqueous solution of potassium tetrachloroplatinate(II) were added solutions of potassium hydroxide in water, salicylaldehyde in ethanol, and one of the alkylamines in ethanol, the molar ratio being 1 : 2 : 2 : 2. After the solution had been left at room temperature for a few days, a black mass containing a small orange-colored part was precipitated. By treating the mass with a suitable solvent, such as chloroform, benzene, ethanol and ether, the platinum(II)-complex with the Schiff base was obtained as orange crystals. (2) To a solution of [Pt(*salal*)$_2$] in ethanol was added a solution of an alkylamine in ethanol in the molar ratio of 1 : 4; the solution was then warmed gently[5]. In a few hours, the platinum(II)-complex with the Schiff base separated out.

The second method was adopted in the preparation of the *t*-butyl and the isopropyl derivative. The platinum(II)-compounds with R=methyl, ethyl, *n*-propyl and *n*-butyl were obtained in either way, while the palladium-complexes with R=methyl, ethyl, *n*- and isopropyl, and *n*- and *t*-butyl were prepaerd by the first method. The elemental analyses for carbon, hydrogen and nitrogen agree with the calculated values for the bis(*N*-alkylsalicylideneimine) complexes.

Since palladium(II) and platinum(II) strongly demand the square-planar co-ordination, the configuration of $Pt(N)_2(O)_2$ or $Pd(N)_2(O)_2$ in the *n*-alkyl complexes is most likely to be planar. The co-ordination around the palladium(II) was reported to be trans-planar with the methyl derivative[6]. In general, the cis configuration is very difficult sterically with complexes of this series, and it is usually regarded as unlikely for the modification obtained under ordinary conditions.

When *t*-butyl groups are substituted for the *n*-alkyl groups in the complex, the square-planar co-ordination around the metal ion is completely prevented by the serious steric hindrance, so that the configuration around the metal ion is distorted from the plane. The ultraviolet spectra of the *t*-butyl complex of palladium(II) and platinum(II) differ significantly from the spectra of the corresponding *n*-alkyl complexes of the same central ion, whereas the spectra of the Schiff bases of the type examined in the present work are quite similar to one another both in the frequency of maxima and minima and in band intensity. This is in agreement with the conclusion based on the steric condition that the co-ordination around the palladium(II) or the platinum(II) in the *t*-butyl complex is distorted from the square-plane.

In the case of the isopropyl group, the steric hindrance seems to be considerable, but it may not be as serious as in the case of the *t*-butyl group. The present measurements indicate that the ultraviolet spectra of the isopropyl derivatives of palladium(II) and platinum(II) are nearly identical with the spectra of the corresponding compounds of the *n*-alkyl groups. This fact is taken as showing that the co-ordination around the palladium(II) or platinum(II) in the isopropyl derivative is similar to that of the corresponding complexes of the *n*-alkyl groups, which are most probably planar. In this connection, it is worth noting that bis(*N*-isopropylsalicylidene)-nickel(II)[2], cobalt(II)[1] and copper(II)[3] were found to be distorted from the square-planar co-ordination. The comparison clearly indicates that the stability of the square-planar co-ordination, as compared with that of the tetrahedral one, is higher for palladium(II) and platinum(II) than for cobalt(II), nickel(II) and copper(II).

The present measurements also indicate that the spectra of these complexes of palladium(II) and platinum(II) in pyridine show very little difference from the spectra of the same complexes in chloroform, ethanol or benzene.

4) L. Sacconi, M. Ciampolini, F. Maggio and G. Del Re, *J. Am. Chem. Soc.*, 82, 815 (1960).

5) The notation, *salal*, represents an anion derived when a molecule of salicylaldehyde loses a proton. The preparation of the complex will be reported shortly by the present authors.

6) B. Meuthen and M. V. Stackelberg, *Z. anorg. u. allgem. Chem.*, 305, 279 (1960).

This shows that the pyridine molecules are not co-ordinated with the palladium(II) or platinum(II), whereas it is well-known that the nickel(II) ions in all these complexes except the *t*-butyl complex[2] do take up pyridine molecules to form a sexa-co-ordinate complex. This is also in agreement with the current view that it is much more difficult for the palladium(II) and platinum(II) ions to take sexa-co-ordination than for the nickel(II) ions, for which sexa-co-ordination is quite common.

Department of Chemistry
Faculty of Science
Osaka University
Nakanoshima, Osaka

*The Partial Resolution of Racemic α-Alanine through the Cobalt(III) Complex of L-Aspartic Acid**

By Muraji SHIBATA, Yoshiho FUJITA, Miho NAITO and Kuniko HORI

(Received February 9, 1963)

Studies of the resolution of racemic organic acids and amine have been reported by Bailar and his co-workers[1-3]. As far as alanine is concerned, the percentages of resolutions attained through the L-tartratocopper(II) complex and copper(II) L-glutamate were 3.8 and 3.3 respectively[3]. Attempting to resolve the same racemic mixture by using a cobalt(III) complex of L-aspartic acid, we have succeeded in effecting a much higher resolution.

The reaction path which we adopted for the resolution was as follows:

$$[Co(CO_3)_3]^{-3} \xrightarrow{2\,asp} [Co(asp)_2]^- \xrightarrow{6\,ala} [Co(ala)_3]$$

where "asp" stands for an aspartate ion, and "ala" for an alaninate ion. The starting material, a green solution of potassium tricarbonatocobaltate(III), was prepared by our method[4]. An exactly equivalent amount of L-aspartic acid was introduced into the green solution, and the mixture was stirred in the presence of active charcoal at temperatures not exceeding 15°C. The color of the solution gradually changed to violet with the formation of the asparato-complex. A hundred per cent excess of racemic alanine was added to the above solution, and the resulting mixture was adjusted to pH 9.5~10 with potassium hydroxide and warmed to 30~40°C. When the stirring was continued, *cis-cis-tris*-alaninatocobalt(III), $[Co(ala)_3]\cdot H_2O$ separated out. This was filtered and washed thoroughly with hot water and then with ethanol and ether.

The dried *tris*-alaninatocobalt(III) was suspended in hot dilute aqueous ammonia, and hydrogen sulfide was passed into the suspension. After the removal of the cobalt sulfide by filtration with charcoal, the filtrate was concentrated to a small volume on a water-bath. The solution was once more treated with charcoal for purification, and then acetone was added to precipitate the alanine. A 5% solution of this alanine in 1N hydrochloric acid was prepared, and its optical rotation was measured. The percentage of resolution was calculated by dividing the measured specific rotation with the specific rotation of pure L-alanine, $[\alpha]_D = +14.47°$[5].

In the course of the above experiments, we have discovered the very interesting fact that the co-existence of the cellulose powder

TABLE I. PARTIAL RESOLUTION OF ALANINE

Exp. No.	$CoCl_2\cdot 6H_2O$ used g.	Asp used g.	Ala used	pH	Active charcoal g.	Cellulose g.	$[Co(ala)_3]\cdot H_2O$ g.	Ala recovered g.	Measured deg.	Resolution %
1	6	6.7	13.6	9.5	0.4	none	3.3	2.3	−1.99	13.8
2	6	6.7	13.6	10.8	1	3	5.6	4.1	−4.6	31.8
3	6	6.7	13.6	9.9	2	3	5.6	4.3	−4.9	33.9
4	6	6.7	13.6	9.4	2	6	5.2	4.1	−5.1	35.2

Asp, Asparitc acid; Ala, Alanine

* Presented at the Symposium on Coordination Compounds, Tokyo, November 1962.

1) J. C. Bailar, Jr., H. B. Jonassen and A. D. Gott, *J. Am. Chem. Soc.*, **74**, 3131 (1952).
2) A. D. Gott and J. C. Bailar, Jr., ibid., **74**, 4820 (1952).
3) D. Sarma and J. C. Bailar, Jr., ibid., **78**, 895 (1956).
4) M. Mori, M. Shibata, E. Kyuno and T. Adachi, This Bulletin, **29**, 883 (1956).
5) S. Akabori and S. Mizushima, "Proteine Chemistry", ("Tanpakushitsu-Kagaku"), 1, Kyoritsu Shuppan K. K., Tokyo (1952), p. 527.

intended for chromatography in the reaction system of $[Co(asp)_2]^-$ and racemic alaninate ion effectively increases the resolution of alanine. Some of the data for these experiments are given in Table I. In the absence of the cellulose powder, the resolution was about 13%, while in its presence a resolution over 30% was achieved. In the reaction system used here, the D-form of alanine was preferentially coordinated.

We are continuing our investigations in our attempt to find the conditions giving the highest yield of the alaninatocomplex and to discover some material more effective than the cellulose for a higher resolution.

Department of Chemistry
Faculty of Science
Kanazawa University
Sengoku-machi, Kanazawa

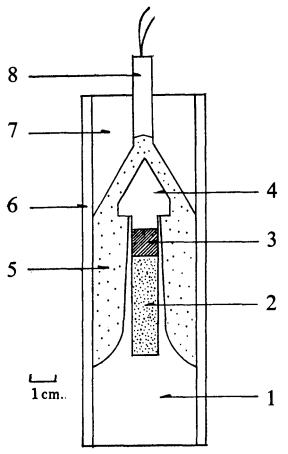

Fig. 1. Schematic diagram of an arrangement for explosive synthesis of titanium carbide.
1 : Mild steel container 2 : Mixture of titanium metal powder and acetylene black 3 : Mild steel plug 4 : Plastic cone 5 : Tetryl powder 6 : Plastic tube 7 : Plastic plug with a small hole 8 : Electric detonator

An Explosive Synthesis of Titanium Carbide

By Yoshikazu HORIGUCHI and
Yōkan NOMURA

(Received February 9, 1963)

Titanium carbides were explosively synthesized from a mixture of titanium metal powder and carbon black by using the arrangement illustrated in Fig. 1. The eight grams of a stoichiometric mixture of titanium metal powder (Osaka Titanium Co., Ltd.) and acetylene black (Denki Kagaku Kogyo Kabushiki Kaisha) to be compacted were put in a mild steel container; this container was then sealed at its open end by a mild steel plug. The arrangement was completed by filling an annulus between the neck of the container and a plastic tube with about 65 g. of a high explosive, tetryl, and by setting up an electric detonator along a prolongation of the central axis of the container. Upon the detonation of the explosive charge, the original mixture, black in color, could be satisfactorily compacted into a grayish white, very hard, cylindrical shape. The X-ray diffraction pattern for the compact agreed well with that of titanium carbide. No additional lines could be observed.

In the same way, direct carburizations of aluminum and tungsten by carbon black have been achieved by the explosive compaction.

Further details of this work will appear in *J. Chem. Soc. Japan, Ind. Chem. Sec. (Kogyo Kagaku Zasshi)*.

Inorganic Chemistry Laboratory
The Institute of Physical and Chemical Research
Bunkyo-ku, Tokyo (Y. H.)

Department of Chemistry
The Defense Academy
Yokosuka, Kanagawa (Y. N.)

Studies of the Absorption Spectra of Azo Dyes and their Metal-complexes. I[*1]. *The Absorption Spectra of Phenylazo-acetoacetanilide and its Related Compounds*

By Yoshiharu YAGI

(Received June 12, 1962)

Although the recent development of neutral-dyeing metal-complex azo dyes has been remarkable[1], the chemical properties of the metal complexes of azo dyes, particularly of *o*, *o'*-disubstituted monoazo dyes, have not been fully investigated. It has, therefore, been considered important for the further progress of these complex dyes to study the structures of ligand azo dyes and their metal-complexes.

In this connection, the author tried to make clear the structure of phenolazoacetoacetanilides, which form yellow-dyeing metal-complexes. As the first step, the electronic and infrared absorption spectra of α-phenylazoacetoacetanilide[*2] and its related compounds were studied.

Results and Discussion

The Electronic Absorption Spectra of Phenylazoacetoacetanilide in Various Solvents.—It had long been studied whether *o*- and *p*-hydroxy azo compounds have the azo form or the hydrazone form[2]. For example, 1-phenylazo-2-naphthol in solution was found[3] to be in a

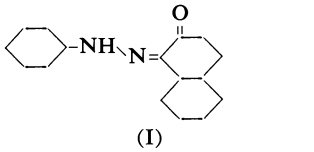

(I)

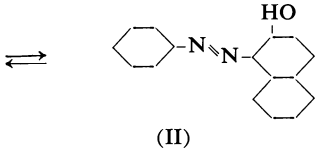

(II)

tautomeric equilibrium between azo- and quinonehydrazone-forms, as is shown in I and II.

An electronic absorption spectrum of phenylazoacetoacetanilide in *n*-hexane shows three bands in the region of 200~400 mμ (Fig. 1).

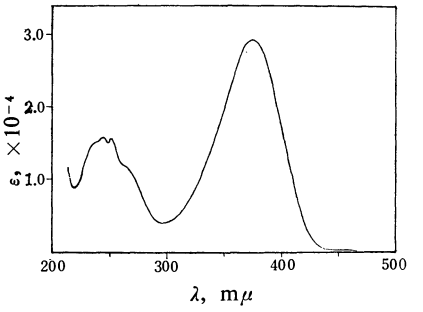

Fig. 1. Phenylazoacetoacetanilide in *n*-hexane.

These bands are referred to as A, B and C—D from the longer wavelength side. Band A is considered to arise from a transition involving electron migration along the whole conjugate system of the molecule. In Table I are shown the absorption spectra of this compound in various solvents. The absorption maxima of band A shift toward a shorter wavelength in the following order: pyridine>chloroform>acetic acid>*n*-hexane>standard solvent[*3]. The relatively small differences in λ_{max} suggest that the displacement of band A is due to the polarity change of the absorbing system caused by solute-solvent interaction; that is, it is due to the general solvent effect.

Burawoy[3] investigated the absorption spectra of 1-phenylazo-2-naphthol in the above-mentioned solvents and concluded that the tautomeric equilibrium of azo ⇌ quinonehydrazone depends upon the polarity of the solvent.

With respect to phenylazoacetoacetanilide, however, the locations of each absorption band in *n*-hexane and in the standard solvent almost coincide. This indicates that the compound is not in a tautomeric equilibrium but may

1) H. Pfitzner, *Melliand Textilber.*, **35**, 649 (1954); *Angew. Chem.*, **62**, 242 (1950); C. Schetty, *J. Soc. Dyers Colourists*, **71**, 705 (1955).

*1 Presented at the 15th Annual Meeting of the Chemical Society of Japan, Kyoto, April, 1962.

*2 For the sake of convenience, the compounds in this study are named as azo compounds; α-phenylazoacetoacetanilide, for example, is abbreviated as phenylazoacetoacetanilide.

2) K. Auwers et al., *Ann.*, **378**, 210 (1911); **487**, 79 (1931); A. Burawoy et al., ibid., **503**, 180 (1933); **504**, 71 (1933); **509**, 60 (1934); H. Shingu, *J. Chem. Soc. Japan, (Nippon Kwagaku Kwaishi)*, **60**, 542, 595 (1939); A. Burawoy et al., *J. Chem. Soc.*, **1953**, 1443; **1952**, 3734.

3) A. Burawoy, A. G. Salem and A. R. Thompson, ibid., **1952**, 4793.

*3 The term "standard solvent" denotes 80% aqueous methanol containing 0.1 g. of acetic acid per liter.

TABLE I. ABSORPTION SPECTRA OF PHENYLAZOACETOACETANILIDE

Solvent	A	B	C-D		
n-Hexane	373.7 (2.93)	270.0* (1.04)	251.2(1.57),	243.3(1.58),	231.7*(1.44)
Standard solvent	373.4 (3.03)	271.5* (1.00)	251.2(1.40),	243.5(1.45),	231.5*(1.34)
Chloroform	379.8 (2.62)	273.5* (0.92)	254.1(1.38)	—	—
Acetic acid	376.2 (2.86)	274.6* (0.88)	—	—	—
Pyridine	380.9 (2.73)	—	—	—	—

Wavelengths (λ) in mμ; Molar extinction coefficients (ε)$\times 10^{-4}$ in parenthesis
* Inflection

exist as a hydrazone form, as is shown in a, irrespective of the nature of the solvents.

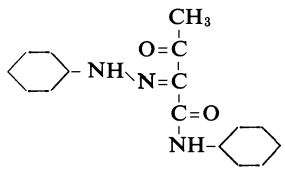

(a)

The Infrared Absorption Spectra of Phenylazoacetoacetanilide and its Related Compounds.— In order to confirm the presumption derived in the preceding paragraph, the following analogous compounds were synthesized: Phenylazocyanoacetanilide (b), phenylazocyanoacetic acid ethylester (c), phenylazomalonic dinitrile (d), phenylazoacetoacetic acid ethylester (e), phenylazomalonic acid dimethylester (f), *p*-chlorophenylazomalonic acid diethylester (g), α-ketopropionaldehydephenylhydrazone (h), and propionaldehyde-*p*-nitrophenylhydrazone (i). Table II shows the carbonyl stretching vibrations, and Table III, the NH stretching vibrations of hydrazone groups:

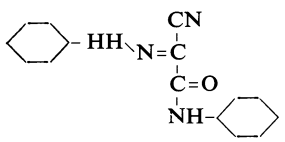

(b)

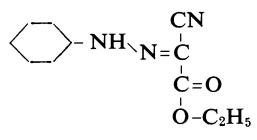

(c)

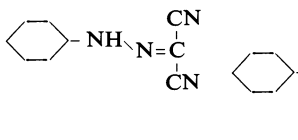

(d)

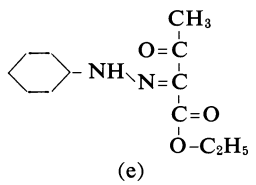

(e)

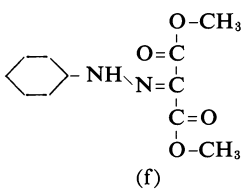

(f)

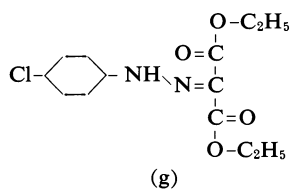

(g)

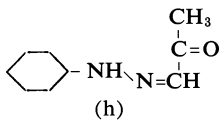

(h)

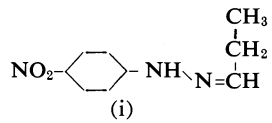

(i)

TABLE II. THE CARBONYL STRETCHING VIBRATIONS (cm^{-1})

Compound	Ketone	Ester	Amide I
a	1623(1633)*	—	1667(1665)
b	—	—	1652(1655)
c	—	1750(1757)	—
e	1620(1630)	1718(1720)	—
f	—	1653(1676) 1728(1733)	—
g	—	1675(1678) 1723(1733)	—
h	1649(1670)	—	—

Values in paraffin-oil and in CCl_4 (in parenthesis) were tabulated.

TABLE III. THE NH STRETCHING VIBRATIONS (cm^{-1})

Compound	Nujol mull	CCl_4
c	3250	3320
d	3240	3333
h	3310	3390
e	not detected	3200
f	3115	3210
g	3160	3195
i	3280	3370

Compounds, a—i, exhibit strong bands in the region of 1590~1600 cm^{-1} (in paraffin-oil) or 1585~1600 cm^{-1} (in a carbon tetrachloride solution). These are considered to be due to C=C skeletal in-plane vibrations of phenyl rings. Although it is generally known that the NH deformation vibration of the secondary amine shows a weak band in the 1550~1650 cm^{-1} region[4], compounds d and i have no band in this region. This suggests that bands due to the NH vibration of the hydrazone group do not appear at frequencies higher than 1600 cm^{-1}. In the region of 1640~1690 cm^{-1} also, the C=N stretching vibration may be expected to appear[5], but, as will be seen in d and i, this band seems to be too weak to detect. Consequently, the bands in the 1620~1760 cm^{-1} region in this study are ascribed to the carbonyl stretching vibration.

4) L. J. Bellamy, "The Infra-red Spectra of Complex Molecules", John Wiley & Sons, Inc., New York (1958), p. 251.
5) Ibid., p. 263.

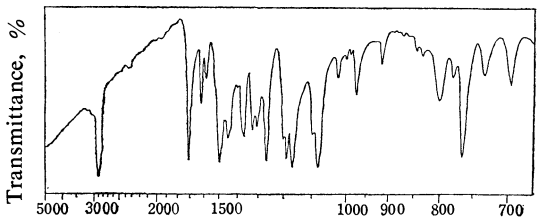

Fig. 2. Infrared spectrum of e (Nujol mull).

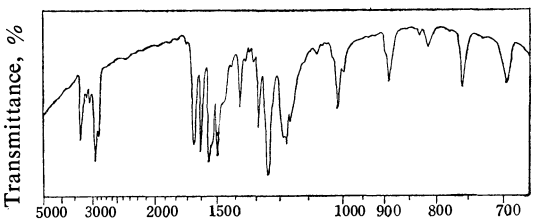

Fig. 3. Infrared spectrum of h (Nujol mull).

Solid 2-hydroxyazobenzene[6] and 3-methyl-1-phenyl-4-phenylazo-5-pyrazolone[7] were found to exhibit $\nu_{C=O}$ at 1610 and 1650 cm^{-1} respectively. The azo compounds in this study also exhibit the C=O absorption in the same region.

As to the acetyl derivatives in Table II, h shows $\nu_{C=O}$ at 1649 cm^{-1}, and a and e, at lower frequencies of about 1620 cm^{-1}. In these cases, a band at about 1665 cm^{-1} in the spectrum of a is assigned to the amide I band, while a strong absorption at 1720 cm^{-1} in the spectrum of e is attributed to the ester carbonyl. The derivatives of alkylmalonates, f and g, have two absorption bands in this region. It is evident that either of these two bands arises from the C=O stretchings of ester carbonyls.

The C=O stretching vibration of the acetyl derivative and that of one ester group in the alkylmalonate derivative are markedly lower in frequency than those of ordinary α,β-unsaturated carbonyl systems. This indicates that the compounds, a, e, f and g, form intramolecular hydrogen bonds in the solid state and in a non-polar solvent, as is shown in V.

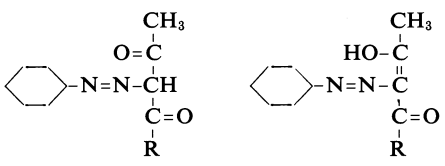

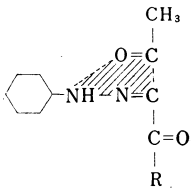

(V)
(R=$-OC_2H_5$, -NHPh, etc.)

In Table III are illustrated the NH stretching vibrations of the hydrazone group belonging to the group of compounds having no acid amide group. Compounds i and d have a sharp absorption at 3370 and 3333 cm^{-1} respectively. These agree with Ramirez and Kirby's value reported[8] for the NH stretching vibrations of hydrazone groups.

The compounds in Table III are classified into two groups, one showing relatively broad bands in the 3195~3210 cm^{-1} region, such as e, f and g (Fig. 4) and the other having sharp bands at higher frequencies in the 3320~3390 cm^{-1} region such as c, d and i. The former group consists of the compounds which have been deduced from the $\nu_{C=O}$ values to have an intramolecular hydrogen bond. It is considered that the ν_{NH} and $\nu_{C=O}$ markedly decrease, owing to the chelate ring formation between a carbonyl oxygen and a hydrazone hydrogen atom. Randall[9] investigated the infrared absorption bands of e and found the ketone and ester carbonyls (1706 cm^{-1}), the azo group (1626 cm^{-1}) and the C=C stretching (1511 cm^{-1}) in an enolized form, as is shown in IV. However, α,α-dimethyl ethylacetoacetate, which is not enolizable, was reported to have a ketonic carbonyl band (1718 cm^{-1}) and an ester carbonyl band (1742 cm^{-1})[10]. The azo

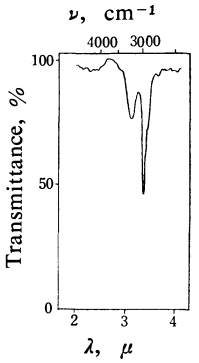

Fig. 4. Infrared spectrum of g in CCl_4.

6) K. Ueno, *J. Am. Chem. Soc.*, **79**, 3066 (1957).
7) S. Toda, *J. Chem. Soc. Japan, Pure Chem. Sec.* (*Nippon Kagaku Zasshi*), **80**, 402 (1959).
8) F. Ramirez and A. F. Kirby, *J. Am. Chem. Soc.*, **76**, 1037 (1954).
9) H. M. Randall et al., "Infrared Determination of Organic Structures", van Nostrand Co., New York (1949), p. 231.
10) R. S. Rasmussen and R. R. Brattain, *J. Am. Chem. Soc.*, **71**, 1073 (1949).

TABLE IV. ELECTRONIC ABSORPTION SPECTRA

Compound	Solvent	A	B	C-D
a	S	373.4(3.03)	271.5*(1.00)	251.2 (1.40), 243.5 (1.45), 231.5*(1.34)
	H	373.7(2.93)	270.0*(1.04)	251.2 (1.57), 243.3 (1.58), 231.7*(1.44)
b	S	370.2(2.13)	285.5*(0.39)	239.0 (1.98)
	H	361.5(1.74)	294.5*(0.45), 284.5*(0.39), 276.0*(0.32)	251.5*(0.74), 243.9*(1.52), 235.7 (2.00)
j	S	356.0(1.95)	—	251.3*(0.67), 237.7 (1.02)
c	S	357.4(2.19)	281.5*(0.14)	251.8*(0.63), 241.5 (0.82)
	H	347.8(2.02)	294.5*(0.28), 285.1 (0.21), 275.2*(0.15)	250.3*(0.60), 243.0*(0.83), 235.2 (0.89)
d	S	357.3(2.12)	—	252.0*(0.65), 243.5 (0.78)
	H	353.2(1.90)	—	252.5*(0.64), 244.0 (0.76), 238.5*(0.71)
e	S	355.7(2.12)	—	249.2*(0.89), 239.8 (1.19)
	H	354.5(1.99)	295.8*(0.24), 286.5 (0.21)	251.6*(0.78), 238.0 (1.34)
f	S	350.6(2.16)	285.5 (0.24)	233.6 (1.09)
	H	348.4(2.12)	294.5*(0.29), 284.8 (0.27), 275.0*(0.21)	246.6*(0.58), 231.1 (1.04)
g	S	350.3(2.33)	301.8 (0.57), 291.5 (0.50)	241.7*(1.28)
	H	350.6(2.29)	303.1 (0.61), 293.1 (0.50)	235.1 (1.10)
h	S	348.8(2.32)	296.0 (0.44), 285.5*(0.36)	237.3 (1.12)
	H	326.5(1.89)	292.5 (0.82), 282.2*(0.62)	232.0 (1.13)
i	S	393.1(2.22)	—	249.9 (0.90)
	H	341.4(0.68)	—	274.2 (1.19)

S, Standard solvent; H, *n*-Hexane

group usually does not exhibit distinct absorption[11]. Further, the author was unable to detect the OH stretching vibration in this study. Consequently, it can not be considered that e has such a structure as III or IV.

In the latter group, the ν_{NH} values do not differ from that of i. It is conceivable that the intramolecular hydrogen bond between the cyano nitrogen and the hydrazone hydrogen atom is almost negligible or does not exist at all. This is supported by the fact that the proton-accepting power of the cyano group is generally weak[12].

The Electronic Absorption Spectra of Phenylazoacetoacetanilide and its Related Compounds. —The electronic absorption spectra of the series of compounds in *n*-hexane and the standard solvent are tabulated in Table IV. The three groups of characteristic bands in the 200~400 mμ region are abbreviated as A, B and C—D.

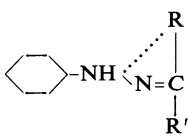

(R, R′ : Substituents)

(VI)

Generally a >C=N linkage was reported[13] to have properties spectrally analogous to an ethylenic linkage. Hence, an electronic effect of R or R′ in VI will be transmitted to the whole conjugate system through the π-p conjugation between a nitrogen atom and a phenyl nucleus in Ph–NH–N=, exerting a considerable influence upon band A. As will be seen in Table IV, every substituent, such as $-COCH_3$, $-CONH_2$, etc., when introduced as R or R′, has a bathochromic effect on the bands A.

The intensity and the maximum wavelength of band A in the spectra of a are the most notable in Table IV, and a comparison of b with phenylazocyanoacetamide (j) indicates that the introduction of a phenyl ring into the carboxylic acid amide group causes a marked red-shift of band A. This suggests that the π-p conjugation at a carboxylic acid anilide group contributes much to the transition along the whole conjugate system.

In the compounds a, e, f and g, the absorption maxima of the bands A are almost equal in *n*-hexane and in the standard solvent. On the other hand, in the compounds b, c, d and h, the bands A in *n*-hexane are at appreciably shorter wavelengths. The former are the compounds having the internal hydrogen bond in the solid state and in non-polar solvents.

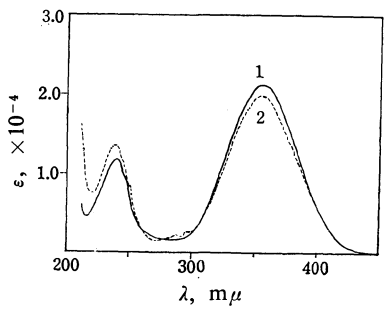

Fig. 5. Absorption spectra of e in the standard solvent (1) and in *n*-hexane (2).

11) Cf. Ref. 4, p. 272.
12) S. Seki et al., "Hydrogen-bond" (Suiso-Ketsugo), Iwanami-Shoten, Tokyo (1956), p. 24.
13) E. A. Braude and E. R. H. Jones *J. Chem. Soc.*, **1945**, 498; **1946**, 948; **1949**, 1898; **1952**, 1068.

It is considered that the six-membered chelate ring in *n*-hexane, as shown in V, stabilizes the excited state and decreases the electronic transition energy[3,8,14].

In the ultraviolet region, the bands B are usually situated in the region of 270~300 mμ, and their intensities are generally small. In some cases, these consist of three peaks in *n*-hexane, but they are apt to disappear in polar solvents. Undoubtedly, the bands B are thought to originate from the carbonyl group, since d and i exhibit no absorption in this region. The true molar extinction coefficients of the B bands seem rather small (10^2~10^3), taking into account the fact that these are superposed by the slopes of the bands A or C-D. These B bands are tentatively ascribed to the $n \rightarrow \pi$ transition (R-band)[15] of carbonyl. However, the band B of a alone absorbs at a shorter wavelength and has a relatively high intensity. This may be a conjugation band (K-band)[16] of another origin.

The bands C-D are located in the 230~250 mμ region. Some of them show fine structures. It is not possible, however, to make a full examination of these bands on the basis of the present knowledge alone.

Experimental

Preparation of Azo Compounds.—*Phenylazoacetoacetanilide (a).*—This was prepared from diazotized aniline and acetoacetanilide. Recrystallization from ethanol gave green-yellow needles; m. p., 107~108°C. (reported 107~108°C)[17].

Phenylazocyanoacetanilide (b).—Cyanoacetanilide was prepared according to the method described in the literature[18]. Compound b was obtained by the treatment of cyanoacetanilide with diazotized aniline. Recrystallization from ethanol gave rectangular yellow plates; m. p., 199~200°C.

Found: C, 68.35; H, 4.18; N, 21.01. Calcd. for $C_{15}H_{12}ON_4$: C, 68.18; H, 4.58; N, 21.19%.

Phenylazocyanoacetic Acid Ethylester (c).—An aqueous alcoholic solution containing ethyl cyanoacetate and an excess of sodium acetate was treated with diazotized aniline to yield yellow needles. This was recrystallized from ligroin, giving yellow needles with an m. p. of 126°C (reported 125°C)[19].

Phenylazomalonic Dinitrile (d).—This was obtained in the same manner as c and was recrystallized from ethanol, giving orange-yellow plates; m. p., 145°C (decomp.) (reported 146~147°C (decomp.))[19].

Phenylazoacetoacetic Acid Ethylester (e).—This was obtained in the manner described in c. Recrystallization from ligroin gave pale-yellow rectangular plates; m. p., 82~83.5°C (reported 82~83°C)[20].

Phenylazomalonic Acid Dimethylester (f).—This was obtained in the same manner as c. Recrystallization from ligroin gave yellow prisms; m. p., 62~63°C (reported 63.5°C)[19].

p-Chlorophenylazomalonic Acid Diethylester (g).—This was obtained in a manner similar to that above. Recrystallization from ligroin yielded pale-yellow rectangular plates; m. p., 59~61°C.

Found: C, 52.39; H, 4.85; N, 9.09. Calcd. for $C_{13}H_{15}O_4N_2Cl$: C, 52.36; H, 5.06; N, 9.37%.

α-Ketopropionaldehydephenylhydrazone (h).—Acetoacetic acid prepared by the method of Schechter et al.[21] was treated with diazotized aniline. An orange precipitate was recrystallized from benzene, affording pale-yellow rectangular plates; m.p., 151~152°C (reported 149~150°C)[22].

Propionaldehyde-p-nitrophenylhydrazone (i).—This was prepared by the treatment of *p*-nitrophenylhydrazine with propionaldehyde in ethanol. Recrystallization from 50% ethanol gave orange-yellow needles; m. p., 124°C (reported 124°C)[23].

Phenylazocyanoacetamide (j)—Cyanoacetamide was prepared by the method described in the literature[24]. Compound j was obtained in the same manner as c and was recrystallized from ethylacetoacetate, giving rectangular yellow plates; m. p., 249~251°C (decomp.).

Found: C, 57.88; H, 4.23; N, 29.46. Calcd. for $C_9H_8ON_4$: C, 57.44; H, 4.30; N, 29.76%.

Measurements of the Spectra.—The infrared spectra were measured by two infrared spectrophotometers, a Perkin-Elmer model 21 and a Shimadzu model IR-27, equipped with NaCl optics. In the case of the solution measurements, the spectra were determined at concentration of 10^{-3}~10^{-4} M.

Visible and ultraviolet absorptions were carried out using two recording spectrophotometers, a Beckman model DK-2 and a Shimadzu model RS-27. The concentration of samples was 2.5×10^{-5} M.

Summary

Phenylazoacetoacetanilide and its related compounds have the hydrazone structure. The phenylazoacetoacetic acid ethylester, for example, forms an intramolecular hydrogen bond between a ketone group and a hydrazone group in the solid state and in non-polar solvents.

The electronic absorption spectra exhibit three groups of bands—A, B and C-D. The effects upon the spectra of the intramolecular hydrogen bond and of the π-p conjugation at

14) P. H. Gore and O. H. Wheeler, *J. Am. Chem. Soc.*, 78, 2160 (1956).
15) A. Burawoy et al., *J. Chem. Soc.*, 1952, 2310; 1955, 3721.
16) A. E. Gillam and E. S. Stern, "An Introduction to Electronic Absorption Spectroscopy in Organic Chemistry", Edward Arnold and Co., London (1954), p. 111.
17) W. F. Whitmore and S. Zuckerman, *Am. Ink Maker*, 34, 28 (1959).
18) K. G. Naik and Y. N. Bhat, *J. Indian Chem. Soc.*, 4, 547 (1927); *Chem. Zentr.*, 1928 I, 1759.
19) A. Hantzsch and K. J. Thompson, *Ber.*, 38, 2266 (1905).
20) C. Kjellin, ibid., 30, 1966 (1897).
21) N. S. Schechter et al., *J. Am. Chem. Soc.*, 71, 3165 (1949).
22) F. R. Japp and F. Klingemann, *Ann.*, 247, 217 (1888).
23) C. D. Harris and K. Oppenheim, *Chem. Zentr.*, 1916 II, 991.
24) H. Gilman (Editor-in-Chief),, "Organic Syntheses", Coll. Vol. I., 179 (1932).

the carboxylic acid amide group have been discussed.

The author wishes to express his deep gratitude to the late Professor Ryutaro Tsuchida for his kindness in participating in discussions throughout this work. The author is also indebted to Sumitomo Chemical Co., Ltd., for its permission to publish this work and to Mr. Kikuo Kimura for his assistance in this study. The reading of the manuscript by Professor Shoichiro Yamada is also gratefully acknowledged.

Sumitomo Chemical Co., Ltd.
Osaka Works
Konohana-ku, Osaka

Studies of the Absorption Spectra of Azo Dyes and their Metal-complexes. II. The Absorption Spectra of Phenolazoacetoacetamide and its Derivatives[*1]

By Yoshiharu YAGI

(Received June 20, 1962)

Phenolazoacetoacetamides[*2] can be used as yellow-dyeing metal-complex dyes and have valuable dyeing properties[1]. The relationships between the chemical structure and the absorption spectra of phenolazoacetoacetamides were investigated in this paper.

Results and Discussion

The Chemical Structure of Phenolazoacetoacetanilides and the Assignments of the A and C Bands.—It was concluded in the preceding paper[2] that phenylazoacetoacetanilide (I) and its related compounds have the hydrazone structure and from a hydrogen bond between a carbonyl oxygen and a hydrazone nitrogen atom in the solid state and in non-polar solvents.

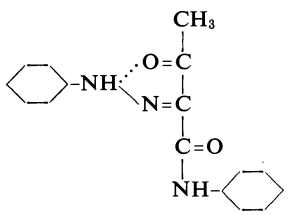

(I)

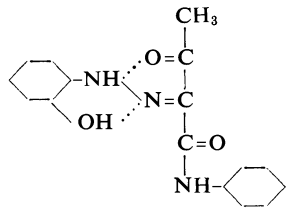

(II)

The infrared spectra of phenylazoacetoacetanilide (I), its 2-hydroxy derivative (II) and 2-methoxy derivative in liquid paraffin are given in Table I. The C=O stretching vibrations of the three compounds are at lower frequencies than those of the strong amide I bands, indicating a marked decrease in frequency compared with ordinary α,β-unsaturated carbonyl systems[3]. Since these frequencies agree with those of phenylazoacetoacetanilide cited in the previous paper, the azo compounds in this paper are also considered to have the hydrazone form. The three compounds show a broad band in the 3000~3500 cm^{-1} region. It is difficult to investigate the exact nature of this band, owing to the superposition of other band systems. In the 2-hydroxy derivative, however, the band is very broad and intense, as is shown in Fig. 1. This band can possibly be attributed to the stretching vibration of the hydroxyl, which forms an intramolecular hydrogen bond

*1 Presented at the 15th Annual Meeting of the Chemical Society of Japan, Kyoto, April, 1962.

*2 The compounds in this study are named as azo compounds; α-(2-hydroxyphenylazo)-acetoacetanilide, for example, is abbreviated as phenolazoacetoacetanilide.

1) Ciba Ltd., U. S. Pat. 2565898 (1951); Brit. Pat. 716753 (1954); J. R. Geigy A.-G., Brit. Pat., 736034 (1955); E. Koike and Y. Yagi, Japanese Pat. Announced No. 36-8730.

2) Part I, This Bulletin, 36, 487 (1963).

3) L. J. Bellamy, "The Infra-red Spectra of Complex Molecules", John Wiley & Sons, Inc., New York (1954), p. 153.

TABLE I. INFRARED ABSORPTION SPECTRA OF PHENOLAZOACETOACETANILIDE ETC. (IN SOLID STATE)

Compound	C=O	Amide I	Bands in 3000~3500 cm^{-1}
Phenylazoacetoacetanilide	1623 (w)	1667 (s)	3170 (m)
2-Methoxyphenylazoactoacetanilide	1630 (w)	1665 (s)	3170 (w)
2-Hydroxyphenylazoacetoacetanilide	1620 (w)	1640 (s)	3200 (b, s)

w, weak; m, medium; s, strong; b, broad

TABLE II. ELECTRONIC ABSORPTION SPECTRA OF 2-HYDROXY-5-(*N*-ETHYLSULFAMOYL)-PHENYLAZOACETOACETANILIDE

Solvent	A	B	C	D
Standard solvent	387.6 (2.96)	302.6*(0.71)	258.5 (1.85)	231.2 (2.03)
Aqueous 0.01 N NaOH	431.0 (2.20)	323.0*(1.02)	283.3 (2.18)	234.5 (1.96)

Wavelengths (λ) in mμ; Molar extinction coefficients (ε)$\times 10^{-4}$ in parenthesis
* Inflection

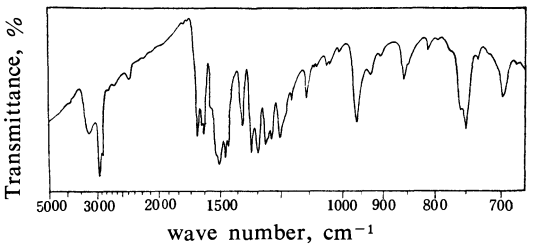

Fig. 1. Infrared absorption spectrum of II (in Nujol mull).

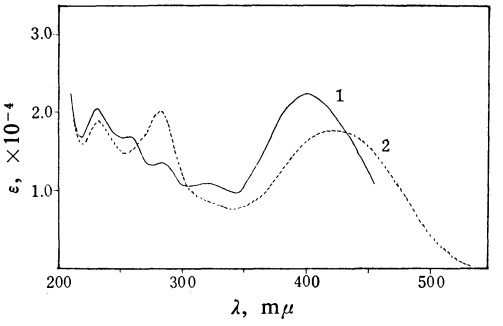

Fig. 2. Absorption spectra of III in anhydrous methanol (1) and 95% methanol (2).

with a hydrazone nitrogen atom, as is shown in II.

The electronic absorption spectra of II in the 200~500 mμ region show four groups of bands, which will subsequently be referred to as A, B, C and D counting from the longer wavelength side. The absorption spectrum of 2-hydroxy-5-(*N*-ethylsulfamoyl)-phenylazoacetoacetanilide (III) in anhydrous methanol (Fig. 2) shows five bands: D, 232; C, 258 and 281: B, 320; A, 400 mμ. In 95% methanol, however, only four bands (D, 231; C, 282; B, 325 as an inflection; A, 426 mμ) are observed; the band at 258 mμ disappears.

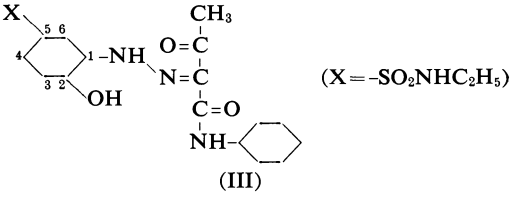

The latter spectrum resembles that in an aqueous 0.01 N sodium hydroxide solution (Table II, Fig. 3). In the standard solvent*3, there is no band at about 280 mμ, and the band C appears distinctly at 258.3 mμ.

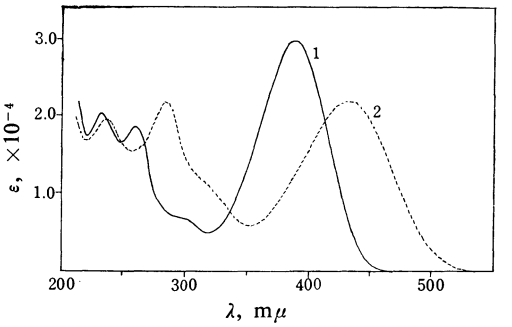

Fig. 3. Absorption spectra of III in the standard solvent (1) and in aqueous 0.01 N NaOH (2).

The above results may be interpreted as follows: The phenolic hydroxyl group is released from the hydrogen-bonded state in polar solvents. This hydroxyl, retaining an equilibrium between a dissociated and an undissociated states in anhydrous methanol (probably due to the absorption of a trace of water while being measured), dissociates in aqueous methanol.

*3 The term "standard solvent" denotes 80% aqueous methanol containing 0.1 g. of acetic acid per liter.

TABLE III. ELECTRONIC ABSORPTION SPECTRA OF II AND ITS METHOXY-ANALOGUE

Compound	Solvent	A	B	C	D
II	S	396.0 (2.81)	(279.0)*(1.00)	258.0 (1.14)	234.0 (1.36)
	H	395.0 (2.59)	319.0* (0.57)	271.0 (1.60) 263.8*(1.48)	243.0*(0.98) 235.7*(1.14) 224.0 (1.20)
Methoxy-analogue of II	S	392.0 (2.88)	277.4* (0.97)	258.5*(1.24)	247.8 (1.33) 237.0 (1.39)
	H	387.4 (2.83)	273.8* (0.95)	253.3 (1.49)	242.5 (1.50) 233.5*(1.43)

Wavelength in parenthesis denotes an indistinct location.
S, Standard solvent; H, *n*-Hexane

The C bands are assigned to a conjugation band (K band)[4] arising from an electronic transition within a partial chromophore[5] consisting of a phenolic nucleus and a hydrazone group. Benzene derivatives usually show B band[6], this band would, however, be submerged by such high intensity K bands as the C bands. Consequently, the absorbing positions and intensities of the C bands alter in accordance with the electronic state of the hydroxyl group. In the standard solvent, the hydroxyl group is fixed in an undissociated state, resulting in a clear-cut formation of the C band.

The A bands are considered to be the absorptions due to a transition involving electron migration along the whole conjugate system of the respective molecule. There also undergo band-shifts according to the polarity of the phenolic hydroxyl, parallel with the shifts of the C bands.

The absorption spectra of II and the 2-methoxy derivative of phenylazoacetoacetamide in the standard solvent and *n*-hexane are shown in Table III. Each band of the 2-methoxy compound in *n*-hexane undergoes a hypsochromic displacement compared with that in the standard solvent. In compound II, λ_{max} of the A band is almost equal in both solvents. However the C band in *n*-hexane is longer in wavelength and higher in intensity than that in the standard solvent, as is shown in Fig. 4. This indicates that the formation of a hydrogen bond ring raises the polar character of the O–H linkage and stabilizes the excited state[7]. Thus, the formation of two internal hydrogen bond rings in a non-polar solvent as shown in II, displaces

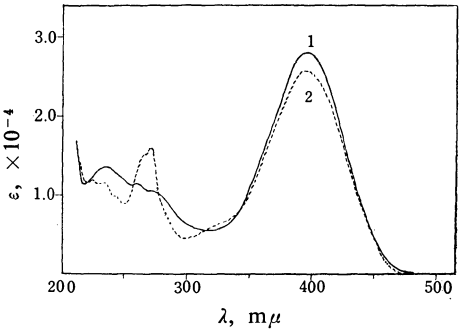

Fig. 4. Absorption spectra of 2-hydroxyphenylazoacetoacetanilide (II) in the standard solvent (1) and in *n*-hexane (2).

the A band towards the longer wavelength region.

It has generally been found[8] that the methylation of a hydroxyl group attached to the conjugate systems causes a small red-shift of the K band. In Table III, however, the A band in both the solvents blue-shifts rather upon methylation. This confirms the view that the hydroxyl group forms the internal or external hydrogen bond in *n*-hexane or in the standard solvent respectively.

The Effects of Substituents in Phenolic Nuclei upon the A and C Bands. — Table IV illustrates the variation of four characteristic bands caused by the introduction of substituents into the phenolic nucleus of II.

The displacements of the C bands by substitution in the 5-position are the most notable and exhibit this decreasing order of λ_{max}: $CH_3 > Cl > H$, $SO_2NH_2 > NO_2$. Such shifts of the C bands suggest that an absorption band due to the electronic transition expected for a partial chromophore is generally very susceptible to the effects of substituents in its chromophore, as has been pointed out by Braude[9]. The maxima of the A bands run

4) A. E. Gillam and E. S. Stern, "An Introduction to Electronic Absorption Spectroscopy", Edward Arnold Publishers Ltd., Lnodon (1954), p. 111; A. Burawoy, *J. Chem. Soc.*, **1937**, 1865; **1939**, 1177.
5) E. A. Braude et al., ibid., **1945**, 490; **1947**, 1104.
6) A. Burawoy et al., ibid., **1955**, 3721.
7) F. Ramirez and A. F. Kirby, *J. Am. Chem. Soc.*, **76**, 1037 (1954); A. Burawoy et al., *J. Chem. Soc.*, **1955**, 3727.
8) E. A. Braude et al., ibid., **1945**, 498; A. Burawoy et al., ibid., **1952**, 3734.
9) E. A. Braude, ibid., **1949**, 1902.

TABLE IV. ABSORPTION SPECTRA OF MONOSUBSTITUTED DERIVATIVES OF II IN THE STANDARD SOLVENT

Substituent	A	B	C	D
5-CH_3	401.5 (2.72)	317.0 (0.64)	268.0 (1.14)	231.4 (1.44)
None	396.0 (2.81)	279.0*(1.00)	258.0 (1.14)	234.0 (1.36)
5-Cl	396.0 (2.76)	311.0 (0.68)	262.5 (1.29)	231.5 (1.64)
5-SO_2NH_2	389.5 (2.81)	303.0*(0.63)	258.0 (1.74)	232.5 (1.84)
5-NO_2	391.0 (2.72)	303.0 (1.38)	246.0 (1.56)	231.0 (1.66)
4-SO_2NH_2	394.4 (3.16)	305.6*(0.54)	258.3 (1.37)	231.9 (1.32)
4-NO_2	415.5 (3.94)	325.0 (0.79)	259.8*(1.21)	238.4 (1.46)

TABLE V. SPECTRA OF DISUBSTITUTED DERIVATIVES (IN THE AMIDE PHENYL RING) OF 2-HYDROXY-5-SULFAMOYLPHENYLAZOACETOACETANILIDE IN THE STANDARD SOLVENT

Substituent	A	B	C	D
None	389.5 (2.81)	303.0*(0.63)	258.0 (1.74)	232.5 (1.84)
2-Cl-6-CH_3-	383.5 (2.63)	296.0 (0.56)	254.5 (1.59)	239.0 (1.56)
5-Cl-2-OCH_3-	393.2 (3.09)	300.5*(0.84)	261.0 (1.69)	236.5 (2.38)
2-OCH_3-5-CH_3-	394.0 (2.92)	290.0*(1.03)	259.0 (1.60)	232.5 (2.06)

almost parallel with the C bands, though the degrees of displacement are smaller. With regard to sulfamoyl and nitro derivatives in the 4-position, the A bands of both the derivatives are higher in intensity and longer in wavelength than those of corresponding 5-substituted derivatives. However, the λ_{max} values of the C bands are almost equal to that to the non-substituted compound II.

It is interesting that the absorption intensity of the C band in a 5-nitro or 5-sulfamoyl derivative, particularly in the latter, is markedly high.

From the results outlined above, it is considered that the substituent in the 5-position—meta to the hydrazone group; i. e., para to the hydroxyl—affects the auxochromic property of the hydroxyl group; e. g., a substitution by methyl emphasizes the auxochromic nature of the hydroxyl group, resulting in the red-shifts of the C and A bands.

On the other hand, the substituent in the 4-position—para to the hydrazone group; i. e., meta to the hydroxyl—is considered to have a mesomeric effect upon the whole absorbing system[10]. However this has little effect upon the auxochromic property of the hydroxyl, because the C band undergoes almost no shift upon the introduction of this substituent.

The Steric Inhibition of the π-p Conjugation and the Assignment of the D Bands.—It seems probable that the amide group participates in the origin of the D bands. In 2-hydroxy-5-sulfamoylphenylazoacetoacet-2-chloro-6-methylanilide (IV-a), a steric conformation of the amide-moiety is shown in a projection (IV-b), exhibiting a steric repulsion between the substituent and the carbonyl oxygen. In the above projection, the covalent radius is conveniently taken for the dimension of the methyl and carbonyl radii. Since the covalent radius represents a minimum measure of the interference radii between non-bonded atoms[11], a true overlap would be larger than that in IV-b.

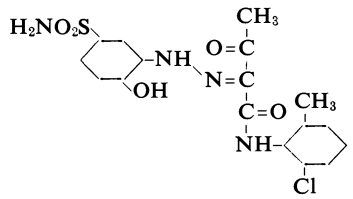

(IV-a)

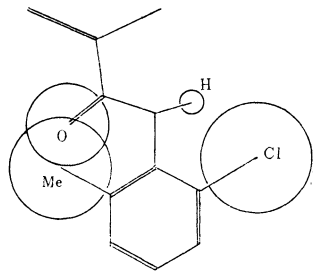

(IV-b)

N.B. Dimensions used: Bond lengths are Pauling's values[12]. H, covalent bond radius 0.31 Å; Me, covalent bond radius 1.39 Å; =O, covalent bond radius 1.10 Å[13]; Cl, radius 1.50 Å.

In Table V (Fig. 5), the A, B and C bands blue-shifts with substitution in the 2- and 6-positions are shown. On the other hand, the D

10) P. H. Gore and O. H. Wheeler, *J. Am. Chem. Soc.*, **78**, 2160, 3363 (1956).

11) E. A. Braude and F. Sondheimer, *J. Chem. Soc.*, **1955**, 3754.

12) W. Klyne, ed., "Progress in Stereochemistry", Vol. I, Butterworths Sci. Publ., London (1954), p. 361.

13) E. A. Braude et al., *J. Chem. Soc.*, **1949**, 1890.

TABLE VI. VISIBLE BANDS OF MONO-SUBSTITUTED (IN THE AMIDE PHENYL RING) OF 2-HYDROXY-5-SULFAMOYLPHENYLAZOACETOACETANILIDE IN THE STANDARD SOLVENT

Substituent		A		Substituent		A	
$-OCH_3$	*o*-	392.5	(3.04)	-Cl	*o*-	390.3	(2.89)
	m-	389.7	(2.94)		*m*-	389.0	(3.02)
	p-	392.0	(2.76)		*p*-	389.5	(3.00)
$-CH_3$	*o*-	388.5	(2.76)	$-NO_2$	*m*-	388.5	(2.91)
	m-	388.0	(2.53)		*p*-	396.0	(3.52)
	p-	389.5	(2.96)				

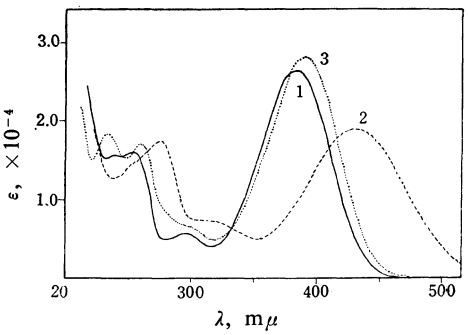

Fig. 5. Absorption spectra of IV-a in the standard solvent (1) and in aqueous 0.01 N NaOH (2). Curve 3 represents the spectrum of 2-hydroxy-5-sulfamoylphenylazoacetoacetanilide in the standard solvent.

band undergoes a reverse shift and a marked intensity-decrease. Consequently, the effect caused by the di-substitution is considered to correspond to Braude's type (2)[14] steric hindrance to uniplanarity; i. e., a phenyl ring within the amide-moiety of the molecule is distorted out of a plane containing -NHCO- and a hydrazone group in the ground state and can not become coplanar or nearly coplanar, even in the excited state. Thus, the A band shows a hypsochromic and a hypochromic displacement, accompanying identical behaviors of the B and C bands.

From the peculiar change of the D band, the following assignment is possible: The D bands are conjugation bands arising from an electronic transition along a partial chromophore V. A phenyl ring within the amide-moiety predominates over a conjugate system involving -NHCO- and the hydrazone group by the π-p conjugation between the phenyl ring and the amide nitrogen atom. When the electronic interaction of the phenyl ring is completely inhibited, these D bands occur in the region of about 240 mμ.

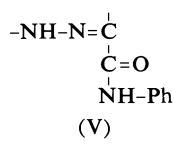

(V)

With regard to 2, 5-disubstituted derivatives, e. g., the 5-chloro-2-methoxy compound, it is considered that such disubstitution in the 2- and 5-positions strengthens the π-p conjugation and causes the small hyper- and bathochromic shifts of the D band, resulting in the same displacements of the A band.

The Effects of Substituents (in the Phenyl Ring of the Amide-moiety) upon the A Bands. —On 2-hydroxy-5-sulfamoylphenylazoacetoacetanilide, a variety of substituents was introduced into the phenyl ring of the amide group. The A bands in the standard solvent are shown in Table VI.

As to each substituent, the absorption maxima of *o*- and *p*-derivatives are larger than those of *m*-derivatives. It may be concluded that the substituent exerts a weak mesomeric effect upon the whole absorbing system by the π-p conjugation between the amide nitrogen atom and the phenyl nucleus, resulting in a decrease in the energy of a transition along the system, i. e., λ_{max} increase in the A bands.

Effects of Substituents Adjacent to the Hydroxyl Group upon the Spectra.—The substitution in the 3- or 3, 5-positions in the phenolic nucleus of II is expected to have a marked effect upon the electronic state of the hydroxyl. In Table VII, the A bands mostly split into two peaks. In the case of the (X, Y = NO_2) compound a single A band is located at a fairly long wavelength in the standard solvent and in an aqueous alkaline solution (Fig. 6).

It is considered that the substituent in the 3-position exerts an inductive effect upon the adjacent hydroxyl rather than upon the whole conjugate system; e. g., the introduction of an electron-withdrawing group causes a polarization of the O-H linkage. This is emphasized by the further introduction of such a group in the 5-position. Consequently, the longer wavelength maxima or inflections of the A bands is considered to be due to an electronic transition along the whole conjugate system of the molecule in which the hydroxyl is dissociated. The complete or almost complete disappearance of this band in the

14) Cf. Ref. 11; G. M. Gray, ed, "Steric Effects in Conjugated Systems", Butterworths Sci. Publ., London (1958), p. 73.

TABLE VII. SPECTRA OF 3- OR 3,5-SUBSTITUTED DERIVATIVES OF II IN THE STANDARD SOLVENT

Substituent	Solvent	A	B	C	D
3-NO_2-5-H	S	406.5 (1.87)	355.5*(1.53)	262.7 (1.64)	234.0 (1.60)
	N	472.6 (1.01)	375.8 (0.85)	279.7 (1.12)	236.7 (1.38)
3-NO_2-5-CH_3	S	410.0 (1.81)	364.0 (1.66)	265.8 (1.61)	234.5 (1.72)
3-NO_2-5-Cl	S	500.0* (0.54), 413.5 (1.68)	350.3 (1.27)	262.5 (1.86)	245.8 (1.96)
	A	410.0 (1.96)	—	—	—
3-NO_2-5-NO_2	S	447.5 (2.70)	313.0 (1.30)	273.0 (1.80)	231.6 (1.94)
	N	446.0 (1.96)	366.0 (1.39)	280.0 (1.61)	230.5 (1.77)
	A	(471.0*)(1.00), 410.0 (2.11)	—	—	—
3-Cl-5-NO_2	S	471.0* (1.32), 396.0 (2.37)	319.0*(1.32)	270.0*(1.12)	233.0 (1.53)
	N	468.6* (1.50), 415.0 (1.84)	332.0 (0.92)	265.7*(0.92)	242.5*(1.03)
	A	382.0 (2.76)	305.2*(1.21)	247.7 (1.56)	231.6 (1.52)

N, Aqueous 0.01 N NaOH; A, Aqueous 80% methanol containing 0.002 mol. of HCl per liter.

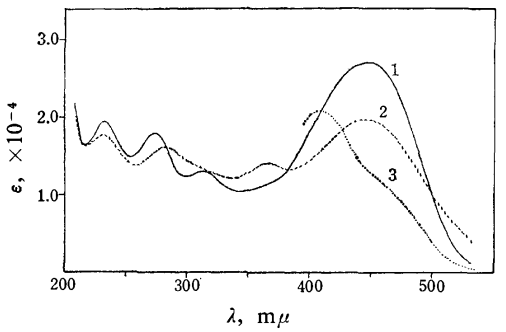

Fig. 6. Absorption spectra of 2-hydroxy-3,5-dinitrophenylazoacetoacetanilide in the standard solvent (1), in aqueous 0.01 N NaOH (2) and in aqueous 80% methanol containing 0.002 mol. of hydrochloric acid per liter (3).

hydrochloric acid-methanol solvent system confirms the above view.

When the splitting of the A band occurs, the C band is located at a longer wavelength than that in the hydrochloric acid-methanol medium and becomes a broad inflection, as is shown in the (X=Cl, Y=NO_2) compound. This is possibly because the molecules of the monoazo compound are in an equilibrium between a dissociated and an undissociated state in this medium.

The Absorption Characteristics of Phenolazoacetoacetbenzylamides and the Assignment of the B Bands. — It has been found[15] that phenolazoacetoacetbenzylamides (VI) form fast-dyeing cobalt(III)-complexes which dye proteinic fibers in clear-yellow shades. It seems reasonable that the four absorption bands in the spectra of phenolazoacetoacetanilides also appear in the series of VI.

15) Y. Yagi and K. Kimura, Japanese Pat., Announced No. 36-11975.

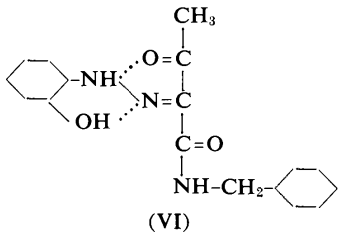

(VI)

Further, the C and D bands are expected to approach to and overlap each other, since the π-p conjugation is intercepted by a methylene bridge. In Table VIII, the spectra of phenylazoacetoacetbenzylamide, its 2-hydroxy derivative VI and related compounds are illustrated. The C bands of the former are superposed upon the D band and appear to be a single band. A similar band system is also observed in the spectra of the derivatives of VI (Table IX, Figs. 7 and 8). The spectroscopic behavior of the C band of VI in *n*-hexane is similar to that of II.

The absorption spectra of the 5-substituted derivatives of VI are illustrated in Table IX. The B bands appear more distinctly than those of the II series. The maximum wavelengths of the C bands, as well as those of the A

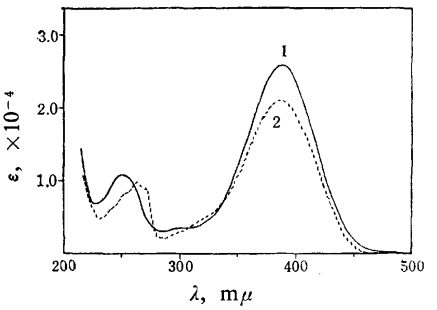

Fig. 7. Phenolazoacetoacetbenzylamide (VI) in the standard solvent (1) and in *n*-hexane (2).

TABLE VIII. ELECTRONIC ABSORPTION SPECTRA OF PHENYL- AND PHENOLAZOACETOACETBENZYLAMIDE

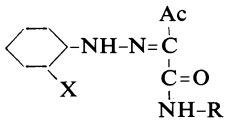

X	R	Solvent	A	B	C–D or C	D
H	Benzyl-	S	365.9 (2.67)	287.5 (0.27)	250.8* (1.20) 244.0 (1.33)	
		H	364.6 (2.65)	297.7*(0.30) 288.0 (0.28)	249.2* (1.17) 241.3 (1.37)	
OH	Benzyl-	S	386.8 (2.60)	302.0*(0.34)	(259.7)*(0.95)	249.5 (1.08)
		H	386.1 (2.11)	(310.0) (0.37)	271.5* (0.85) 262.4 (0.98) 253.3* (0.84)	(247.5)*(0.74)
	n-Hexyl-	S	386.1 (2.56)	301.0*(0.31)	259.3* (0.90)	248.7 (1.05)
		H	385.6 (2.13)	—	271.1* (0.90) 261.3 (0.96) 254.9* (0.85)	248.8*(0.75)

TABLE IX. ABSORPTION SPECTRA OF 5-SUBSTITUED DERIVATIVES OF III IN THE STANDARD SOLVENT

Substituent	A	B	C	D
5-CH_3	393.0 (2.46)	308.3*(0.47)	266.5* (0.81)	247.5 (1.02)
None	386.8 (2.60)	302.0*(0.34)	(259.7)*(0.95)	249.5 (1.08)
5-Cl	387.0 (2.42)	306.0 (0.53)	264.0* (0.79)	245.0 (1.15)
5-SO_2NH_2	380.0 (2.60)	296.0 (0.56)	251.7 (1.43)	239.0 (1.43)
5-NO_2	376.0 (2.46)	302.0 (1.18)	246.0 (1.38)	(232.3)*(1.21)

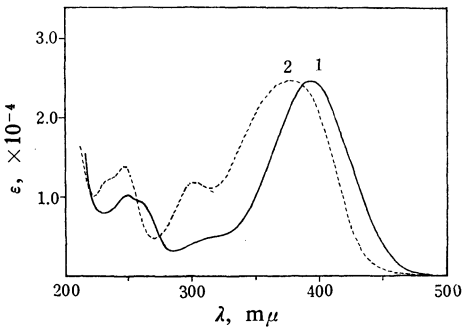

Fig. 8. Absorption spectra of 2-hydroxy-5-methyl- (1) and 2-hydroxy-5-nitrophenylazoacetoacetbenzylamide (2) in the standard solvent.

bands, are displaced towards shorter wavelengths in the order: $CH_3>Cl>H>SO_2NH_2>NO_2$. The range of such wavelength variation of the A bands is wider than that in the II series, so suggesting that the electronic transitions along the whole conjugate systems are liable to suffer the effect of the substituent, because the conjugate systems are shorter in this series.

The origin of the B bands has not yet been explored. When X=H in Table VIII, the benzyl derivative shows a very weak B band, one which splits into two peaks in *n*-hexane. This resembles those of such azo compounds as phenylazoacetoacetic acid ethylester in Part I. It has been considered that these bands are due to the $n\rightarrow\pi$ transition (R band)[4] of a ketonic carbonyl or of an amide carbonyl, because saturated ketones and α,β-unsaturated ketones usually absorb in the region near 300 mμ[16].

On the other hand, those of the hydroxy derivatives have higher intensities. In Table IX, the more electronegative the substituent in the phenolic nucleus, the higher the intensity of the B band. A similar intensity change was observed in the II series. Table IX also indicates that a compound showing the A band at a relatively longer wavelength similarly exhibits the B band at a longer wavelength position. When measured in an aqueous alkaline solution, both the A and B bands of 2-hydroxy-5-sulfamoylphenylazoacetoacetbenzylamide undergo bathochromic displacement, about 45 and 20 mμ respectively, as compared with those in the standard solvent in Table IX.

If the B bands in the hydroxy derivatives are R bands, they should undergo hypsochromic displacement[4] upon any alteration of the electronic configuration of the system, which

16) Cf. Ref. 4, pp. 48 and 95.

would cause a bathochromic shift of the K band. Therefore, these bands can not be attributed to the intensified R bands, nor can they be considered to be B bands, because of the high absorption intensities.

1-Phenylazo-2-naphthol[17], 4-phenylazo-1-naphthol[18] and other hydroxyazo compounds[19] are known to exist in a solvent-dependent tautomeric equilibrium between a hydroxyazo- and a *o*-quinonephenylhydrazone form. In such cases, the introduction of an electronegative group into the phenyl ring has been reported to cause an increased contribution of the hydrazone form in equilibrium[17]. It has also been found in 3-methyl-1-phenyl-4-phenylazo-5-pyrazolone as well as in its 2-hydroxyphenylazo-analogue[20], both of which have the hydrazone form, that the greater the Hammett[21] substituent-constant of a substituent in the phenyl ring attached to the hydrazone group, the weaker the hydrogen bond between a carbonyl oxygen and a hydrazone hydrogen atom and, thus, the higher the frequency of the C=O stretching vibration.

Consequently, the B bands are assigned to a conjugation band, which arises from a conjugative transition within a partial chromophore consisting of the acetyl carbonyl and the hydrazone group. The electronegative substituent in the phenyl ring of VII stabilizes the hydrazone form; i. e., it

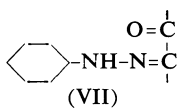

(VII)

increases the double-bond character of >C=N– and >C=O, resulting in the intensity-increase of the B bands. Thus, both 2-hydroxy-5-nitrophenylazoacetoacetanilide and its benzyl analogue exhibit high-intensity B bands in the 302~303 mμ region.

Experimental

Preparations of 2-Aminophenols.—*2-Amino-4-(N-ethylsulfamoyl)phenol.* — This was obtained in the same manner as were the 4-sulfamoyl derivatives[22], pale gray plates; m. p., 128°C.

Found: C, 44.25; H, 5.38; N, 12.85. Calcd. for $C_8H_{12}O_3N_2S$: C, 44.43; H, 5.59; N, 12.94%.

The other 2-aminophenol derivatives were prepared according to the methods in the literature. Their melting points agree with those in the literature.

Preparation of Acetoacetamides.—*1-Acetoacetylamino-2-methoxy-5-methylbenzene.*—Treatment of *p*-cresidine (m. p. 50.5°C) with diketene in solvent naphtha gave cubic crystals. They were recrystallized from ethanol, giving colorless plates; m. p., 82°C.

Found: C, 65.05; H, 6.69; N, 6.28. Calcd. for $C_{12}H_{15}O_3N$: C, 65.14; H, 6.83; N, 6.33%.

1-Acetoacetylamino-2-chloro-6-methylbenzene.—This was obtained from 2-chloro-6-methylaniline (b. p. 120~121°C) and diketene. Recrystallization from 50% ethanol gave colorless needles; m. p., 123~124°C.

Found: C, 58.35; H, 5.05; N, 6.28. Calcd. for $C_{11}H_{12}O_2NCl$: C, 58.53; H, 5.36; N, 6.20%.

Acetoacetbenzylamide. — Colorless plates. Recrystallization from 50% ethanol gave rectangular plates; m. p., 102~103°C.

Found: C, 68.88; H, 6.72; N, 7.47. Calcd. for $C_{11}H_{13}O_2N$: C, 69.09; H, 6.85; N, 7.35%.

Acetoacet-n-hexylamide. — This was obtained as paraffin-like flakes; m. p., 52.0°C.

Found: C, 64.58; H, 10.25; N, 7.25. Calcd. for $C_{10}H_{19}O_2N$: C, 64.90; H, 10.30; N, 7.56%.

The other acetoacetylamino derivatives were obtained in the same manner. The purities were checked by elemental analysis.

Preparations of Phenolazoacetoacetamides. — *2-Methoxyphenylazoacetoacetanilide.* — This was obtained by the treatment of acetoacetanilide with diazotized *o*-anisidine in an aqueous solution. It was recrystallized from ethanol, giving yellow needles.

Found: C, 63.37; H, 5.83; N, 13.65. Calcd. for $C_{17}H_{17}O_3N_3$: C, 65.58; H, 5.50; N, 13.50%.

2-Hydroxy-5-sulfamoylphenylazoacetoacet-2-methoxy-5-methylanilide.—An aqueous solution of diazotized 2-amino-4-sulfamoylphenol was added to a solution containing 1-acetoacetylamino-2-methoxy-5-methylbenzene, sodium carbonate and sodium hydroxide. An orange precipitate was obtained. After an aqueous suspension of this was treated with hydrochloric acid, the precipitate was recrystallized from *n*-butanol, giving yellow needles.

Found: C, 51.49; H, 5.41; N, 13.21. Calcd. for $C_{18}H_{20}O_6N_4S$: C, 51.42; H, 4.80; N, 13.33%.

The Other Phenolazoacetoacetamides.—All of these were synthesized in the above manner. They were recrystallized from ethanol, dioxane, acetoacetic ester, ethylcellosolve or higher alcohols. The purities were checked by elemental analysis.

Measurments of the Absorption Spectra. — Infrared measurements were made by a Shimadzu model IR-27 infrared spectrophotometer equipped with NaCl optics. The Nujol mull method was employed for the preparation of samples. The visible and ultraviolet spectra were measured using a Beckman model DK-2 and a Shimadzu model RS-27 recording spectrophotometers. The spectra were determined at a sufficient dilution, (0.5~2.5) $\times 10^{-5}$ M, Beer's law being valid within these limits except in hydrous methanol. The solvents used were of spectral grades.

17) A. Burawoy et al., *J. Chem. Soc.*, **1952**, 4793.
18) R. Kuhn and F. Bär, *Ann.*, **516**, 143 (1935); A. Burawoy et al., *J. Chem. Soc.*, **1953**, 1443; E. Fischer and Y. F. Frel, ibid., **1959**, 3159.
19) a) G. M. Badger et al., ibid., **1956**, 614; J. B. Müller et al., *Helv. Chim. Acta*, **35**, 2579 (1952); b) H. Singu, *J. Chem. Soc. Japan (Nippon Kwagaku Kwaishi)* **60**, 542 (1939).
20) S. Toda, ibid., **80**, 402 (1959); **81**, 1292 (1960).
21) L. P. Hammett, *Chem. Revs.*, **17**, 125 (1935).
22) W. O. Kermack et al., *J. Chem. Soc.*, **1939**, 608.

Summary

Phenolazoacetoacetamides take the hydrazone form. The phenolic hydroxyl group forms an intramolecular hydrogen bond with a hydrazone nitrogen atom in the solid state and in non-polar solvents.

The electronic absorption spectra of these compounds exhibit four groups of characteristic bands: The A bands arise from a transition involving electron migration along the whole conjugate system of the respective compound; the C bands originate in a conjugative electronic transition between a phenolic nucleus and a hydrazone group, and the D bands, in a conjugative electronic transition between a carboxylic acid anilide group and a hydrazone group.

From the investigation of the series of spectra in phenolazoacetoacetbenzylamides, the B bands have been assigned to the conjugation band; they arise from a conjugative electronic transition within a partial chromophore consisting of an acetyl carbonyl and a hydrazone group.

The author owes gratitude to the late Professor Ryutaro Tsuchida of Osaka University for his encouragement and kindness in participating in discussions throughout this work. The author also wishes to express his gratitude to Sumitomo Chemical Co., Ltd., for its permission to publish this work, and to Mr. Kikuo Kimura for his assistance in this study. The reading of the manuscript by Professor Shoichiro Yamada is also gratefully acknowledged.

Sumitomo Chemical Co., Ltd.
Osaka Works
Konohana-ku, Osaka

Studies of the Absorption Spectra of Azo Dyes and their Metal-complexes. III. The Electronic Absorption Spectra of Metal-complexes Derived from Phenolazoacetoacetanilides[*1]

By Yoshiharu YAGI

(Received July 5, 1962)

Metal-complex dyes, having two molecules of such ligand dyes as *o,o'*-dihydroxymonoazo dyes per atom of chromium(III) or cobalt(III), are recognized to have superior dyeing-properties[1] and are expected to develop progressively. The absorption spectra of such ligand dyes generally undego marked changes by coordination with metal atoms[2].

In previous papers[3] the author investigated the electronic absorption spectra of phenolazoacetoacetamides[*2] in order to assign the four characteristic groups of bands. With respect to the metal-complexes of these azo compounds, there are many problems deserving of further study; e.g., the cobalt(III)-complexes ordinarily have a higher fastness to light than the chromium(III)-complexes[4]. The author supposed that an investigation of the spectral variations of the four characteristic bands with the complex formation would give useful information about the metal-ligand linkage. This paper deals with the absorption spectra of the metal-complexed phenolazoacetoacetanilides.

Results and Discussion

A General Survey of the Electronic Absorption Spectra of the Metal-containing Phenolazoacetoacetanilides and the Assignments of the Four Groups of Bands.—The structure of 2 : 1-metal-complexes of phenolazoacetoacetanilides has up to the present been represented as in I[5]. Two molecules of such terdentate ligand-dyes are known to have a octahedral

*1 Presented at the 15th Annual Meeting of the Chemical Society of Japan, April, 1962.

*2 The compounds in this paper have hydrazone forms but are, for convenience, named as azo compounds. α-(2-Hydroxyphenylazo)acetoacetanilide, for example, is abbreviated as phenolazoacetoacetanilide.

1) H. Pfitzner, *Melliand Textilber.*, **35**, 649 (1954); R. Casty, *Textil-Rundschau*, **11**, 328 (1956).

2) H. Zollinger, "Chemie der Azofarbstoffe", Birkhäuser Verlag, Basel (1958), p. 245.

3) Parts I and II, This Bulletin, **36**, 487, 492 (1963).

4) K. Venkataraman, *Review of Textile Progress*, **7**, 337 (1955); J. R. Geigy A.-G., Brit. Pat. 736034; E. Koike and Y. Yagi, Japanese Pat. Announced No. 36-8730.

5) H. D. K. Drew et al., *J. Chem. Soc.*, **1939**, 823.

TABLE I. ABSORPTION SPECTRA OF THE CHROMIUM(III)-COMPLEX OF 2-HYDROXY-5-(*N*-ETHYLSULFAMOYL)PHENYLAZOACETOACETANILIDE IN A VARIETY OF SOLVENTS

Solvent	A	B	C	D
Anhydrous methanol	460.8(3.67)	322.5*(2.48)	292.9(3.88)	235.0(4.72)
95% Methanol	461.0(3.64)	322.4*(2.42)	292.5(3.86)	235.2(4.64)
Standard solvent	461.0(3.74)	322.3*(2.51)	292.5(3.99)	235.0(4.81)
Aqueous 0.01N NaOH	455.0(3.53)	316.5*(2.49)	288.4(3.63)	234.0(3.56)

Wavelengths (λ) in mμ; Molar extinction coefficients (ε)$\times 10^{-4}$ in parenthesis.
* Inflection

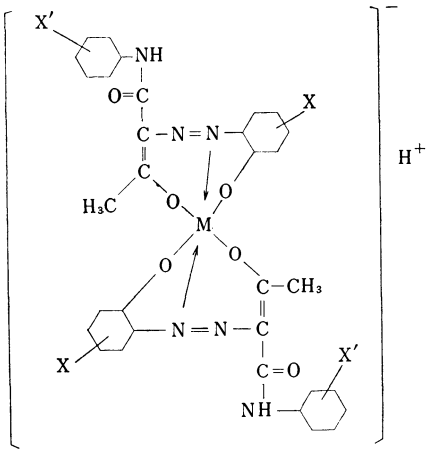

(I)

X, X': Substituents
M: Tervalent metal

conformation around the central metal atom[6] and to form the penetration complex by sp^3d^2 hybridization[7]. It is also known[8] that the metal-complex molecule is a monobasic acid.

The electronic absorption spectra of chromium(III)-, cobalt(III)-, iron(III)-, and aluminum-compexes of 2-hydroxy-5-(*N*-ethylsulfamoyl)phenylazoacetoacetanilide (II) in the standard solvent*3 are shown in Fig. 2. Four

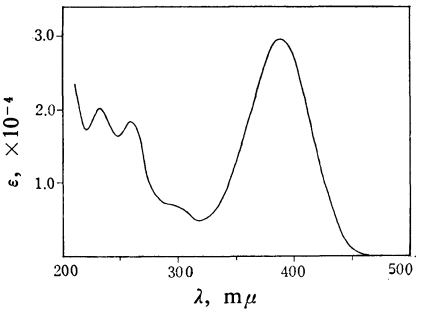

Fig. 1. Absorption spectrum of 2-hydroxy-5-(*N*-ethylsulfamoyl)-phenylazoacetoacetanilide (II) in the standard solvent.

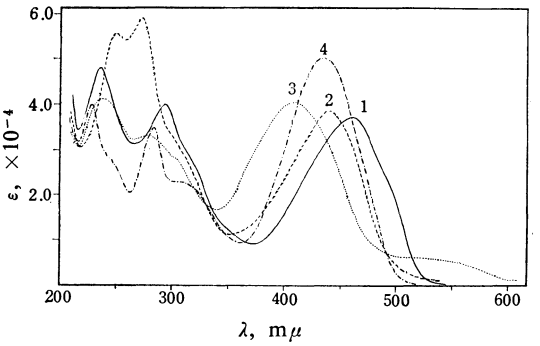

Fig. 2. Absorption spectra of the chromium-(1), cobalt- (2), iron- (3) and aluminum-(4) complexes of II in the standard solvent.

groups of bands are generally observed in the visible and ultraviolet region. These bands will hereafter be referred to as A, B, C and D counting from the longer wavelength side. The absorption spectra of the chromium(III)-complex*4 of II in a variety of solvents are illustrated in Table I. A slight intensity decrease and a small hypsochromic displacement of each band in an aqueous sodium hydroxide solution are probably due to the electrostatic interaction between inorganic ions and solvent molecules around the absorbing system, as was discussed by Klotz[9]. However, the relative positions of the four bands in each solvent are almost invariable. Provided that an anionic charge, which is generated with the ionization of the free complex-acid in a polar solvent, as in an aqueous alkaline solution, is localized in the complex-molecule, there should be appreciable band-shifts in the ultraviolet region, as has been reported in the case of ligand-dyes in Part II. Consequently, the anionic charge is considered to have a non-localized character.

In Part II, the four characteristic groups of bands in the spectra of the ligand-dyes were assigned: the ligand-band A arises from a transition involving electron migration along the whole conjugate system. The ligand-band

6) Pfeiffer and S. Saure, *Ber.*, **74**, 935 (1941).
7) J. C. Bailar, Jr., and C. F. Callis, *J. Am. Chem. Soc.*, **74**, 6018 (1952).
8) H. Zollinger, *Texti-Rundschau*, **13**, 217 (1958).
*3 The term "standard solvent" denotes aqueous 80% methanol containing 0.1 g. of acetic acid per liter.
*4 The term "metal-complex" in this paper denotes the 2:1-metal-complex.
9) I. M. Klotz, *Chem. Revs.*, **41**, 373 (1947).

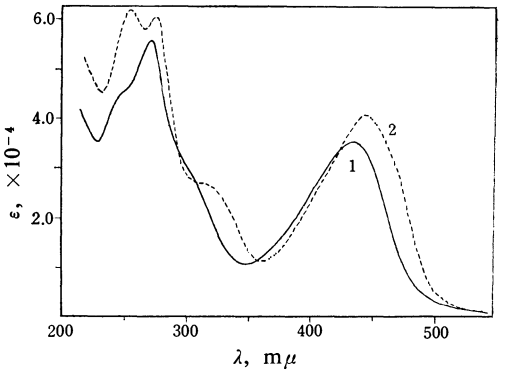

Fig. 3. The cobalt-complexes of 2-hydroxy-5-sulfamoylphenylazoacetoacet-2-chloro-6-methylanilide (1) and 2-hydroxy-5-sulfamoylphenylazoacetoacet-5-chloro-2-methoxyanilide (2) in the standard solvent.

B originates in a conjugative electronic transition between the acetyl carbonyl and the hydrazone group; the ligand-band C, in a conjugative electronic transition between the phenolic nucleus and the hydrazone group, and the ligand-band D, in a conjugative electronic transition between the carboxylic acid anilide group and the hydrazone group.

From the investigation of the wavelength variations and the intensity changes as a result of substitutions, the four groups of bands in the spectra of the metal-complexes are considered to originate in the four bands of the respective ligand-molecule. For example, a marked intensity decrease of the D band in the spectrum of the 2-chloro-6-methyl derivative (Fig. 3) is similar to that of the ligand-dye itself, as has been reported in Part II. The first and the second bands[10] are thought to be submerged in these four bands. That is, these bands are the special bands[11].

The Electronic Absorption Spectra of the Chromium(III)-, Cobalt(III)-, Iron(III)- and Aluminum-complexes.—Metal-complexes of four ligand-dyes were prepared: II, 2-hydroxy-5-sulfamoylphenylazoacetoacet-2-methylanilide (III), 2-hydroxy-5-(*N*-methylsulfamoyl)-phenylazoacetoacet-2-chloranilide (IV), and 5-chloro-2-hydroxyphenylazoacetoacetanilide (V). The electronic absorption spectra of these azo compounds and their metal-complexes are illustrated in Table II.

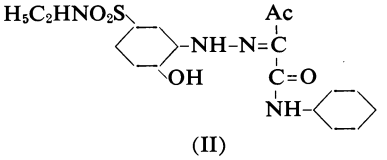

(II)

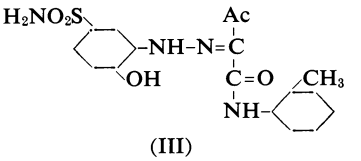

(III)

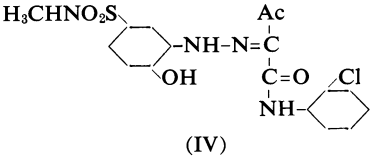

(IV)

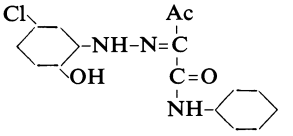

(V)

All the A ligand-bands show red-shifts with complex-formation in the order: Cr> Co> Al > Fe. The A bands of the aluminum-complexes are sharper in shape and higher in intensity,

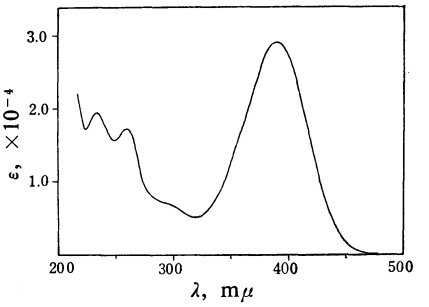

Fig. 4. Absorption spectrum of 2-hydroxy-5-(*N*-methylsulfamoyl) phenylazoacetoacet-2-chloranilide (IV) in the standard solvent.

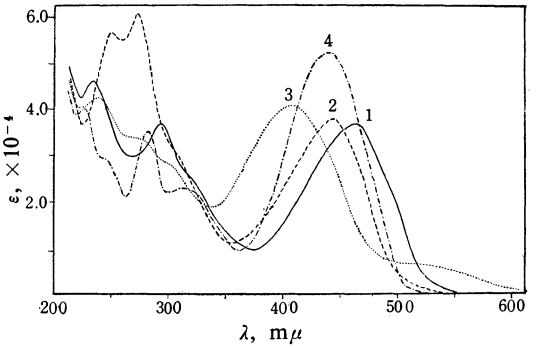

Fig. 5. Absorption spectra of the chromium- (1), cobalt- (2), iron- (3) and aluminum- (4) complexes of IV in the standard solvent.

10) R. Tsuchida, This Bulletin, **13**, 388, 436 (1938); *J. Chem. Soc. Japan, (Nippon Kwagaku Kwaishi)*, **59**, 731,819 (1938): K. Sone, ibid., **71**, 270, 316 (1950).

11) a) R. Tsuchida et al., This Bulletin, **13**, 436, 471 (1938); *J. Chem. Soc. Japan, Pure Chem. Sec., (Nippon Kagaku Zassi)*, **77**, 734 (1956).
b) J. C. Bailar, Jr., ed., "The Chemistry of the Coordination Compounds", Reinhold Publishing Corp., New York (1956), p. 568.

TABLE II. ABSORPTION SPECTRA OF THE CHROMIUM-, COBALT-, IRON- AND ALUMINUM-COMPLEXES OF PHENOLAZOACETOACETANILIDES IN THE STANDARD SOLVENT

Ligand	Metal	A	B	C	D	l	δ
II	None	387.6 (2.96)	302.6* (0.71)	258.5 (1.85)	231.2 (2.03)	4.50	0.35
	Cr	461.0 (3.74)	322.3* (2.51)	292.5 (3.99)	235.0 (4.81)	4.60	0.62
	Co	440.0 (3.88)	314.5* (2.75)	272.9 (5.93)	249.5 (5.56)	4.59	0.65
	Fe	546.0* (0.56) 408.4 (4.10)	306.2* (2.69)	273.5 (3.33)	238.0 (4.19)	6.32	0.65
	Al	435.2 (5.11)	323.2* (2.08)	283.0 (3.53)	248.6*(2.71) 227.9 (4.04)	4.26	0.24
III	None	388.5 (2.76)	302.3* (0.59)	257.0 (1.63)	233.5 (1.72)	4.66	0.31
	Cr	459.0 (3.53)	321.5* (2.19)	291.7 (3.48)	232.5 (4.30)	4.50	0.58
	Co	440.4 (3.54)	317.0* (2.29)	271.5 (5.23)	251.0 (5.00)	4.55	0.81
	Fe	540.0* (0.41) 404.2 (3.79)	304.7* (2.46)	274.0*(3.07)	238.6 (4.08)	6.23	0.52
	Al	433.3 (4.71)	307.3 (2.04)	280.0 (3.01)	247.5*(2.58) 227.6*(3.89)	4.39	0.27
IV	None	389.5 (2.92)	302.3* (0.65)	259.0 (1.74)	233.2 (1.95)	4.57	0.36
	Cr	462.5 (3.68)	325.0* (2.33)	293.8 (3.69)	233.7 (4.63)	4.60	0.64
	Co	442.5 (3.78)	318.5* (2.47)	274.3 (6.09)	249.7 (5.67)	4.65	0.75
	Fe	(540.0)*(0.56) 407.2 (4.06)	305.3* (2.73)	276.0*(3.33)	240.0 (4.20)	6.73	0.77
	Al	437.0 (5.22)	312.2 (2.27)	282.9 (3.52)	248.9*(2.83) 227.6 (3.99)	4.21	0.19
V	None	396.0 (2.76)	311.0 (0.68)	262.5 (1.29)	231.5 (1.64)	4.63	0.31
	Cr	473.3 (3.43)	(365.0)*(1.39) 315.0 (2.59)	289.5 (2.72)	230.4 (4.28)	4.77	0.55
	Co	450.2 (3.19)	313.0 (2.36)	270.3 (4.49)	242.7 (4.72)	5.85	1.10
	Fe	(535.0)*(0.53) 407.2 (3.49)	309.0 (2.14)	266.5*(2.43)	235.2 (3.36)	—	—
	Al	440.0 (3.70)	325.8 (2.04)	264.8*(1.86)	239.0*(2.50)	5.55	0.49

Wavelengths in parenthesis denotes an indistinct location.
The letters, l and δ, are the half-value widths and the inclination parameters of the A bands (in $cm^{-1} \times 10^{-3}$) respectively.

indicating that these are essentially ionic complexes, as was reported by Freeman and White[12].

Shifts of the C ligand-bands with complex-formation are characteristic of the central metal atom used. Generally, red-shifts of the ligand-bands C ($\Delta\lambda_C$) with complex-formation are in the order: Cr> Al> Fe> Co.

Chromium(III)-complexes.—In the series of phenolazoacetoacetamides, it was found that the polarity increase of the phenolic O–H linkage, as in the case of the dissociation or formation of the intramolecular hydrogen bond, causes a red-shift and an intensity increase of the C band. Generally the bond formed between the phenolic oxygen and the tervalent metal is considered to be based on ion-dipole interaction, because the hydroxyl group has a strong dissociative ability[3]. The M–O (M, tervalent metal; O, phenolic oxygen) bond, therefore, is considered to have an essentially polar character. This presumably causes a displacement of the C band towards a longer wavelength. Indeed, such red-shifts of the C bands ($\Delta\lambda_C$) are the largest in the chromium(III)-complexes, indicating that the Cr–O bonds are the most ionic among the four sorts of metal-complexes.

The maintenance of the B ligand-bands, even in the coordinated state, suggests that the double bond character of >C=O in the acetyl group is not eliminated with the complex-formation. The lone pair electrons of the carbonyl oxygen will coordinate with the metal atom to form a σ bond. When the same ligand is used, the B bands of the four metal-complexes are almost equal in intensity and show only small displacements. The shifted order of the B bands as shown in Fig. 6 is probably due to the effect of an electronic transition along the whole conjugate system of the respective ligand-molecule.

12) D. C. Freeman, Jr., and C. E. White, *J. Am. Chem. Soc.*, 78, 2678 (1956).

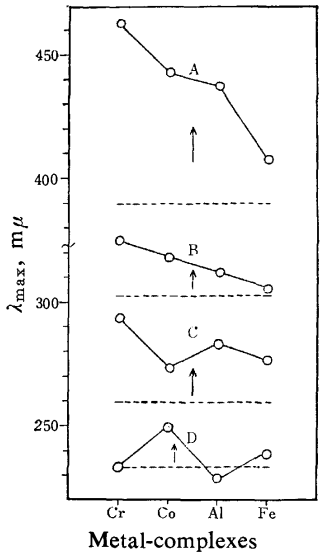

Fig. 6. Absorption maxima of the four bands in the spectra of metallized IV; dotted lines show absorption maxima of the four ligand-bands.

Therefore, the nature of the M–O (O, carbonyl oxygen) bonds are thought to be independent of the central metal used.

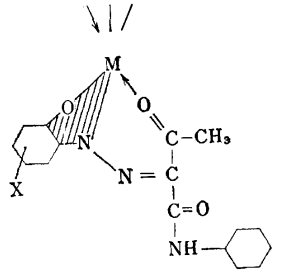

(VI)

(X, Substituent)

The above explanations lead to the conclusion that the structure shown in VI contributes much to the matal-ligand linkage. An imino group in the hydrazone group will coordinate with a metal atom, with a splitting off of a proton. Craig and his co-workers[13] suggested that the nitrogen lone pair has the ability to enter the π-electron orbital and that, therefore, the π-electrons of the system will be distributed over the whole conjugate system of the ligand. Thus, the overlap of the dπ-orbitals[13] of the metal with the nitrogen π-orbital will form the dπ-pπ bonding.

Cobalt(III)-complexes.—The maximum wavelengths of the A bands are always about 20 mμ shorter than those of the chromium(III)-complexes. Generally the values of $\Delta\lambda_C$ are the smallest among the four kinds of the metal-complexes, indicating the highly covalent character of the Co–O (O, phenolic oxygen) bonds.

Since the chromium(III)- and the cobalt(III)-complexes in this study are formed by d^2sp^3 hybridized orbitals, their electronic configurations are:

	3d				4s	4p
Cr:	d^1	d^1	d^1	D^2	S	P^3
Co:	d^2	d^2	d^2	D^2	S	P^3

Such completely filled or half-filled dπ-orbitals are known to be the most stable electronic configurations[14]. Consequently, the dπ-pπ bonds are considered to be almost equally operative in the chromium(III)- and the cobalt(III)-complexes. In such a case, the bathochromic shifts of the A bands with complex-formation are ascribed mainly to two causes: (i) the polarity of the M–O (O, phenolic oxygen) bond, and (ii) the perturbation of the π-electron system by the dπ-pπ interaction, serving to increase the electronic polarizability of the system. The shorter wavelength positions of the A bands in the cobalt(III)-complexes are attributed to the highly covalent character of the Co–O bonds. Thus, a chelate ring (the shaded portion in VI) is stabilized, resulting in a facilitation of an electronic transition which will increase the intensity of the C band.

In the ligand-dye V, $\Delta\lambda_C$ decreases in the order: Cr≫Co> Fe> Al. An electronegative subsutituent in the para position with regard to the hydroxyl will increase the polarity of the M–O (O, phenolic oxygen) bond. Thus, the polarity order of the bond may be somewhat different from those of the metallized II, III and IV.

Iron Compexes.—The absorption spectra of the iron(III)-complexes have some peculiarity. If the penetration complexes (a) are formed, the contribution of the dπ-pπ interaction upon the metal-ligand linkage will be small.

	3d				4s	4p	4d
(a)	d^2	d^2	d^1	D^2	S	P^3	
(b)	d^1	d^1	d^1	d^1d^1	D^2	S	P^3

If the iron(III)-complexes formed are the normal complexes (b), the distribution of the bonding electrons will be biased in the direction of the ligand in order to increase the metal-ligand

13) D. P. Craig et al., *J. Chem. Soc.*, **1954**, 332.

14) Cf. Ref. 11b, p. 185.

distance.[15] The relatively small shifts of the C bands with the complex-formation may indicate the covalent charactr of the Fe–O (O, phenolic oxygen) bonds. However, the A bands are broader than those of the chromium(III)- and cobalt(III)-complexes, in which the $d\pi$-$p\pi$ bondings are effectively operative. Moreover, the C bands of the iron(III)-complexes are also broadened, mostly as shoulders. It may consequently be postulated that the iron(III)-cmplexes are a mixture of different bond types, as is shown in a and b.

The weak shoulders are located in the 535~545 mμ region. Their true absorption intensities are about $(2\sim3)\times10^3$, since these shoulders are superposed by the slopes of the A bands. These may probably be ascribed to the first absorption bands[16] due to the iron(III)-ion, because similar weak bands in the spectra of copper- and nickel-chelates of salicylaldoxime were reported[17] to be due to the metal ions.

Aluminum-complexes. — Aluminum-complexes are ordinarily recognized to be essentially ion-dipole aggregates, as was pointed out by Craig et al.[13]

As is shown in Fig. 6, the values of $\Delta\lambda_C$ are next larger to those of the chromium(III)-complexes, indicating the high polarity of the Al–O (O, phenolic oxygen) bonds. The A bands are sharp and symmetrical; i. e., both the half-value widths (l) and the inclination parameters (δ) are smaller than those of the respective ligand-dye. This indicates that the aluminum-complexes are ionic complexes. The shifts of the A ligand-bands with complex-formation are mainly to be attributed to the polarity of the Al–O (O, phenolic oxygen) bonds.

Experimental

Syntheses of the Metal-complexes of Phenolazoacetoacetanilides.—*Metal-complexes of 2-Hydroxy-5-(N-ethylsulfamoyl)-phenylazoacetoacetanilide (II).*—(*i*) *Chromium(III)-complex.*—The ligand-dye (0.02 mol.) in formamide was treated with chromium(III) formate (0.01 mol.) at 120°C for 10 hr. The reaction mixture was poured into a dilute solution of hydrochloric acid to yield a yellow-brown precipitate of the complex-acid. A small portion of the crude product was dissolved in 95% ethanol, added to a column of activated alumina, and developed with 95% ethanol. A yellow-brown zone was separated and eluted with the same solvent.

After evaporation of the eluted solution to dryness under reduced pressure, a residue was dissolved in dry acetone, filtered, and diluted with hot benzene. Orange-brown needles were obtained.

Found: C, 50.15; H, 4.56; N, 13.33. Calcd. for $C_{36}H_{37}O_{10}N_8S_2Cr$: C, 50.04; H, 4.34; N, 13.06%.

(*ii*) *Cobalt(III)-complex.*—The ligand-dye (0.02 mol.) was suspended in a dilute solution of sodium hydroxide and treated at 80°C with cobalt(II) sulfate (0.01 mol.) to yield a brown precipitate. This precipitate was dissolved in aqueous ethanol containing sodium hydroxide, and the solution was then acidified with hydrochloric acid to precipitate the complex-acid. Purification was performed in the same manner as the chromium(III)-complex. A yellow-brown precipitate was obtained.

Found: C, 49.36; H, 4.51; N, 12.68. Calcd. for $C_{36}H_{37}O_{10}N_8S_2Co$: C, 49.90; H, 4.30; N, 12.98%.

(*iii*) *Iron(III)-complex.*—The ligand was treated with iron(III) chloride in formamide. The reaction mixture was poured into a dilute aqueous solution of acetic acid to yield a brown precipitate. After an aqueous ethanolic solution of the precipitate had been acidified with acetic acid, the complex-acid obtained was purified by chromatographic adsorption, as has been shown above. After removal of the solvent from an eluted solution, a residue was dissolved in dry ethanol and diluted with hot benzene to crystallize brown needles.

Found: C, 49.83; H, 4.45; N, 12.93. Calcd. for $C_{36}H_{37}O_{10}N_8S_2Fe$: C, 50.19; H, 4.30; N, 13.01%.

(*iv*) *Aluminum-complex.*—Reaction was carried out in the same manner as with the iron(III)-complex, except that aluminum sulfate was used instead of iron(III) chloride. The purification procedures were the same as that for the iron(III)-complex. Yellow needles were obtained.

Found: C, 51.38; H, 4.39; N,13.28. Calcd. for $C_{36}H_{37}O_{10}N_8S_2Al$: C, 51.91; H, 4.38; N, 13.46%.

Metal-complexes of 5-Chloro-2-hydroxyphenylazoacetoacetanilide(V). — (*i*) *Chromium(III)-complex.*—The reaction and the chromatographic separation procedures were the same as have been shown for the *N*-ethylsulfamoyl derivative. A residue obtained by the evaporation of an eluted solution was dissolved in aqueous ethanol containing sodium hydroxide. Neutralization of the solution with hydrochloric acid and the addition of sodium chloride to this gave red-brown prisms.

Found: C, 54.09; H, 3.63; N, 11.74. Calcd. for $C_{32}H_{25}O_6N_6Cl_2Cr$: C, 53.94; H, 3.54; N, 11.78%.

(*ii*) *Cobalt(III)-complex.*—Purification was carried out in the same way as with the above-mentioned chromium(III)-complex.

Found: C, 52.92; H, 3.73; N, 11.39. Calcd. for $C_{32}H_{25}O_6N_6Cl_2Co$: C, 53.42; H, 3.50; N, 11.68%.

(*iii*) *Iron(III)-complex.*—A mixture of 95% ethanol and pyridine was used as a developer liquid in chromatographic adsorption. The dilution of a dry-ethanolic solution of the separated complex-acid with hot *n*-hexane gave red-brown needles.

Found: C, 53.24; H, 3.38; 11.58. Calcd. for $C_{32}H_{25}O_6N_6Cl_2Fe$: C, 53.65; H, 3.52; N, 11.73%.

(*iv*) *Aluminum-complex.*—Yellow needles were obtained in the same manner as has been described

15) E. Cartmell and G. W. A. Fowles, "Valency and Molecular Structure", Butterworths Scientific Publications, London (1956).
16) L. E. Orgel, *J. Chem. Soc.*, **1952**, 4756; *J. Chem. Phys.*, **23**, 1004 (1955).
17) K. Sone, *J. Am. Chem. Soc.*, **75**, 5207 (1953).

in the case of *N*-ethylsulfamoyl derivative.

Found: C, 55.38; H, 3.81; N, 12.49. Calcd. for $C_{32}H_{25}O_6N_6Cl_2Al$: C, 55.90; H, 3.67; N, 12.22%.

Metal-complexes of the Other Ligand-dyes.—These were also prepared in the manner described above. The purities were checked by elemental analysis.

Measurements of the Electronic Absorption Spectra.—The absorption spectra were measured by two recording spectrophotometers, a Beckman model DK-2 and a Shimadzu model RS-27. All the spectra were determined at a concentration of 1.6×10^{-5} M. The solvents used had the qualities of spectral grades.

Summary

1) The electronic absorption spectra of metallized phenolazoacetoacetanilides exhibit four characteristic groups of bands—A, B, C and D. These groups of bands originate in the band of the respective ligand-dye.

2) The metal-complexes have the structure shown in formula VI.

3) The bathochromic shifts of the A ligand-bands with complex-formation are ascribed to two causes: (i) the polarity of the M–O (M, tervalent metal; O, phenolic oxygen) bond, and (ii) the perturbation of the π-electron system by the $d\pi$-$p\pi$ interaction. The shifts of the C ligand bands with the complex-formation are closely related to the polarity of the above-mentioned M–O bond. The cobalt(III)-complex has the covalent M–O bond with which to form a stable chelate ring, whereas the chromium(III)-complex has the ionic M–O bond.

4) The absorption characteristics of the iron(III)- and the aluminum-complexes have been discussed.

The author owes his deep gratitude to the late Professor Ryutaro Tsuchida of Osaka University for his encouragement and kindess in participating in discussions throughout this work. The author is also indebted to Sumitomo Chemical Co., Ltd., for its permission to publish this work, and to Mr. Kikuo Kimura for his assistance in this study.

Sumitomo Chemical Co., Ltd.
Osaka Works
Konohana-ku, Osaka

Studies of the Absorption Spectra of Azo Dyes and their Metal-complexes. IV. The Effects of Substituents on the Absorption Spectra of Chromium(III)- and Cobalt(III)-complexes of Phenolazoacetoacetanilides[*1]

By Yoshiharu YAGI

(Received July 9, 1962)

Studies of the relationships between substituents and electronic absorption spectra or stabilities have been reported[1] on metal-complex azo-dyes containing functional groups ortho and ortho' to the azo linkage. Little is known, however, with respect to the 2 : 1-metal-complex monoazo dyes, for example, the chromium(III)- or cobalt(III)-complexes of phenolazoacetoacetamides[*2].

Since the chelate ring involving a phenolic oxygen, a central metal, and a hydrazone nitrogen contributes much toward the metal-ligand linkage, as has been shown in Part III[2], the influence of substituents in the phenolic nucleus upon the electronic absorption spectra will be characteristic of the central metal used. Therefore, the author has investigated the metal-complexes[*3] of substituted phenolazoacetoacetanilides.

Results and Discussion

The Effects of Substituents in the Phenolic Nuclei upon the Electronic Absorption Spectra of Metallized Phenolazoacetoacetanilides.—It has been reported in this series of studies[3]

[*1] Presented at the 15th Annual Meeting of the Chemical Society of Japan, Kyoto, April, 1962.

[*2] The compounds in this paper have hydrazone forms but are, for convenience, named as azo forms. α-(2-Hydroxyphenylazo)-acetoacetanilide, for example, is abbreviated as phenolazoacetoacetanilide.

1) F. A. Snavely et al., *J. Soc. Dyers Colourists*, **73**, 491 (1957); Z. Yoshida et al., *J. Chem. Soc. Japan, Ind. Chem. Sec.* (*Kogyo Kagaku Zassi*), **60**, 1413 (1957).

[*3] The term "metal-complex" in this paper denotes the 2 : 1-metal-complex.

2) Part III, This Bulletin **36**, 500 (1963).

3) Part I, II and III, This Bulletin, **36**, 487, 492, 500 (1963).

that the electronic absorption spectra of phenolazoacetoacetanilides exhibit four groups of conjugation bands (K bands)[4] and that these bands undergo characteristic changes with complex-formation. The A ligand-band arises from a transition involving electron migration along the whole conjugate system of the ligand. The B ligand-band originates in a conjugative electronic transition between the acetyl carbonyl and the hydrazone group, the C ligand-band in a conjugative electronic transition between the phenolic nucleus and the hydrazone group and, the D ligand-band, in a conjugative electronic transition between the carboxylic acid anilide group and the hydrazone group.

Since the degree of modification of the bands expected for the partial chromophores is regarded as an indication of the extent of the electronic interaction therein[5], an investigation of the four characteristic bands of the metal-complexes will reveal useful information about the metal-ligand linkage.

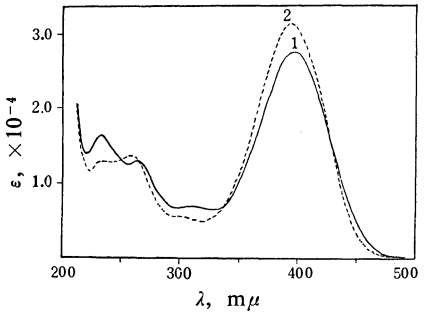

Fig. 1. Absorption spectra of 5-chloro-2-hydroxyphenylazoacetoacetanilide (1) and 2-hydroxy-4-sulfamoylphenylazoacetoacetanilide (2) in the standard solvent.

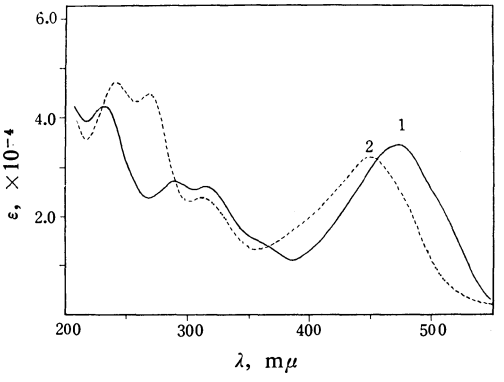

Fig. 2. Absorption spectra of chromium-(1) and cobalt-(2) complexes of 5-chloro-2-hydroxyphenylazoacetoacetanilide in the standard solvent.

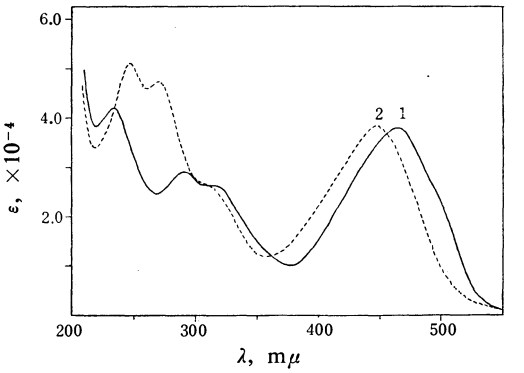

Fig. 3. Absorption spectra of chromium-(1) and cobalt-(2) complexes of 2-hydroxy-4-sulfamoylphenylazoacetoacetanilide in the standard solvent.

The electronic absorption spectra of the chromium(III)- and cobalt(III)-complexes II derived from phenolazoacetoacetanilides I in the standard solvent*4 are illustrated in Table I (Figs. 1—3). This table shows the shift of each ligand-band with the complex-formation, i. e., $\Delta\nu$ (in cm^{-1}) = (ν_{max} of a ligand-band) − (ν_{max} of the corresponding complex-band). The shifts of the bands vary according to the substituent, as is shown in Fig. 4, in which the substituents at abscissa are conveniently

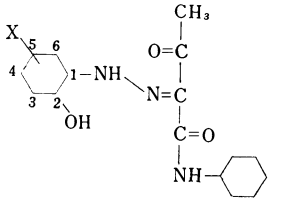

(I)

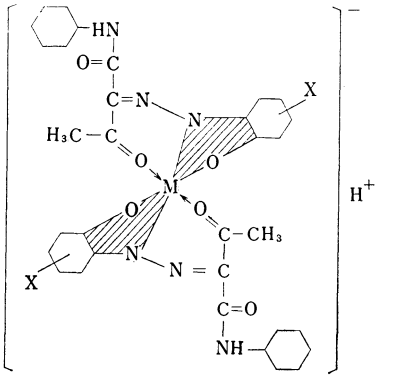

(II)

(X, Substituent; M, Tervalent metal)

4) A. Brawoy, *J. Chem. Soc.*, **1937**, 1865; **1939**, 1177; A. E. Gillam and E. S. Stern, "An Introduction to Electronic Absorption Spectroscopy", Edward Arnold Publishers, Ltd., London (1954), p. 111.

5) E. A. Braude, *J. Chem. Soc.*, **1945**, 490.

*4 "Standard solvent" denotes aqueous 80% methanol containing 0.1 g. of acetic acid per liter.

TABLE I. ELECTRONIC ABSORPTION SPECTRA OF THE METAL-COMPLEXES DERIVED FROM PHENOLAZOACETOACETANILIDES IN THE STANDARD SOLVENT

Substituent	Metal	A					B			C			D		
		λ_{max}	ε_{max}	$\Delta\nu_A$	l	δ	λ_{max}	ε_{max}	$\Delta\nu_B$	λ_{max}	ε_{max}	$\Delta\nu_C$	λ_{max}	ε_{max}	$\Delta\nu_D$
5-CH_3	None	401.5	2.72	—	4.75	0.31	317.0	0.64	—	268.0	1.14	—	231.4	1.44	—
	Cr	474.0	3.27	3.81	5.13	0.62	314.0 (368.8*)	2.69 1.61	−0.30	292.5*	2.58	3.12	228.8	4.19	−0.49
	Co	447.2	2.79	2.55	—	—	318.2	2.33	0.12	270.3	3.92	0.31	244.9	3.83	2.39
H	None	396.0	2.81	—	4.70	0.37	279.0*	1.00	—	258.0	1.14	—	234.0	1.36	—
	Cr	466.9	3.23	3.83	5.13	0.69	310.0	2.63	3.58	(292.3*)	2.50	4.55	232.5	3.81	−0.28
	Co	442.5	3.02	2.65	6.01	1.15	315.2	2.38	4.11	269.5	4.13	1.65	241.0	3.93	1.24
5-Cl	None	396.0	2.76	—	4.63	0.31	311.0	0.68	—	262.5	1.29	—	231.5	1.64	—
	Cr	473.3	3.43	4.12	4.77	0.55	315.0 (365.0*)	2.59 1.39	0.40	289.5	2.72	3.56	230.4	4.28	−0.20
	Co	450.2	3.19	3.04	5.85	1.10	313.0	2.36	0.20	270.3	4.49	1.10	242.7	4.72	2.00
5-SO_2NH_2	None	389.5	2.81	—	4.59	0.36	303.0*	0.63	—	258.0	1.74	—	232.5	1.84	—
	Cr	460.4	3.78	3.95	4.63	0.59	319.6*	2.61	1.71	291.9	3.80	4.50	234.3	4.69	0.33
	Co	440.0	3.79	2.94	4.64	0.69	315.5*	2.58	1.30	272.5	5.95	2.06	249.0	5.57	2.85
5-NO_2	None	391.0	2.72	—	6.81	1.43	303.0	1.38	—	246.0	1.56	—	231.0	1.66	—
	Cr	463.0	4.50	3.98	5.95	1.33	—	—	1.30	315.5	3.89	8.95	241.7	3.27	1.92
	Co	449.1 401.6*	4.66 3.55	3.31	6.35	1.47	309.3	3.68	0.67	263.5	4.44	2.70	(251.0*)	4.18	3.45
4-SO_2NH_2	None	394.4	3.16	—	4.44	0.28	305.6*	0.54	—	258.3	1.37	—	231.9*	1.32	—
	Cr	463.8	3.77	3.80	4.68	0.52	322.2*	2.54	1.68	290.0	2.89	4.23	233.8	4.19	0.35
	Co	448.3	3.81	3.05	4.86	0.73	317.6*	2.48	1.23	269.3	4.74	1.58	246.6	5.11	2.57
4-NO_2	None	415.5	3.94	—	3.88	0.24	325.0	0.79	—	259.8*	1.21	—	238.4	1.46	—
	Cr	490.5	4.70	3.68	4.13	0.33	364.5	2.06	3.34	284.8*	2.63	3.38	255.0	3.14	2.72
	Co	481.2	4.23	3.29	4.86	0.53	303.7	2.83	−2.15	267.5	4.94	1.11	242.7*	4.08	0.74
3-NO_2	None	406.5	1.87	—	—	—	355.5*	1.53	—	262.7	1.64	—	234.0	1.60	—
	Cr	479.0	4.06	3.72	4.42	0.49	—	—	−5.23	299.8	3.21	4.71	237.3*	3.61	0.59
	Co	471.5	3.88	3.39	4.39	0.46	(307.0*)	3.22	−4.44	289.4*	3.76	3.52	249.9	4.86	2.71

N. B. a) Absorotion maxima (λ_{max}) in mμ, molar extinction coefficients (ε_{max}) in 10^{-4}, red-shifts of the ligand-bands with complex-formation ($\Delta\nu$) in $10^{-3}\times cm^{-1}$, half-value widths (l) and inclination parameters (δ) of the A bands in $10^{-3}\times cm^{-1}$.

b) * Inflection.

c) Absorption maximum in parenthesis denotes an indistinct location.

d) In the chromium-complexes of the 3-nitro and 5-nitro derivatives, the C band is superposed by the B band.

e) Inflections near the four main bands are shown under the respective main band.

arranged in the generally accepted order[6] of electronegativity at regular intervals.

Cobalt(III)-complexes.—Band-shifts with substitution are the most notable in the C bands. The degree of the shifts ($\Delta\nu_C$ in cm^{-1}) with complex-formation varies according to the substituent, as is shown in Fig. 4b. Generally an electronegative substituent in para to the M–O (M, tervalent metal; O, phenolic oxygen) bond increases the red-shift of the C band in the chromium(III)- and the cobalt(III)-complexes.

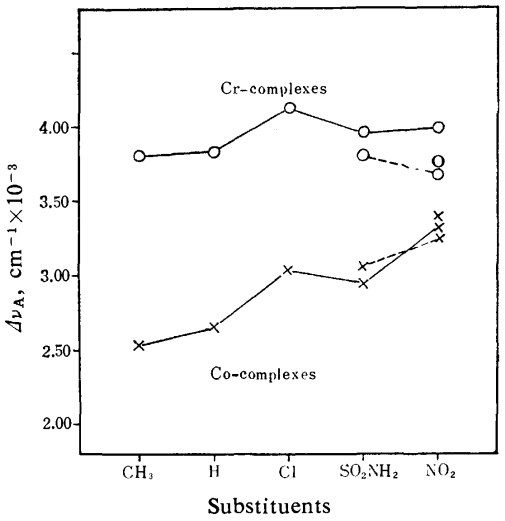

Fig. 4a. Relation between the substituents and the shifts of the A ligand-bands with complex-formation ($\Delta\nu_A$) (full lines, 5-substituted derivatives; dotted lines, 4-substituted derivatives; single marks, 3-substituted derivatives.)

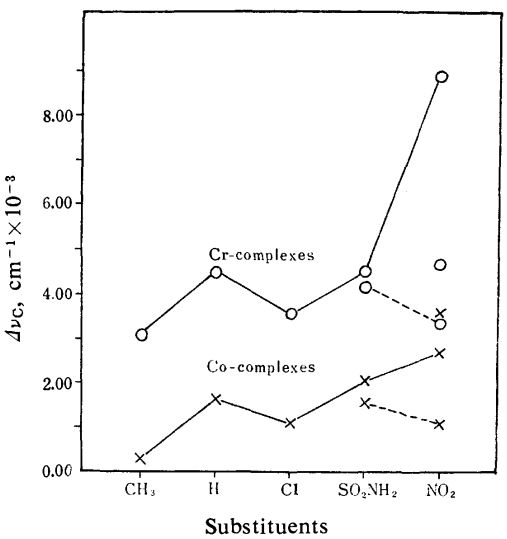

Fig. 4b. Relation between the substituents and the shifts of the C ligand-bands with complex-formation ($\Delta\nu_C$).

In Part II it was noticed how, in the spectra of phenolazoacetoacetamides, the C ligand bands are sensitive to any alteration of the electronic configuration of the system. In the metal-complexes also, the values of $\Delta\nu_C$ are considered to indicate the polarity of the M–O (O, phenolic oxygen) bond. The relatively small $\Delta\nu_C$ value of the cobalt(III)-complexes as compared with those of the chromium(III)-complexes indicate the covalent character of the Co–O (O, phenolic oxygen) bond.

Since the chromium(III)- and the cobalt(III)-complexes in this study are formed by d^2sp^3 hybridized orbitals and since their $d\pi$-orbitals[7a] have stable electronic configurations[2,7b], the $d\pi$-$p\pi$ bondings in both the complexes are considered to contribute equally to the ligand-metal linkage. A five-membered chelate ring (the shaded portions in II) is stabilized in the cobalt(III)-complexes to facilitate the transition expected for a partial chromophore involving the phenolic nucleus, i. e., to increase the intensities of the C bands. Both the half-value widths (l) and the inclination parameters (δ) of the cobalt(III)-complexes are somewhat larger than those of the corresponding chromium(III)-complex, indicating that the stable chelate ring emphasizes the perturbation of the π-electron system.

The bathochromic shift of the A ligand-bands with the complex-formation may be ascribed mainly to two factors; (i) the polarity of the M–O (O, phenolic oxygen) bond, and (ii) the perturbation of the π-electron system by the $d\pi$-$p\pi$ interaction. Generally, influences increasing the polarity of the absorbing system displace the K band to longer wavelengths[8]. Therefore, a substituent increasing the polarity of the above mentioned M–O bond displaces the A band as well as the C band towards longer wavelengths, as is shown in Fig. 4 (i. e., factor i). That is, the more electronegative the substitutent in the 5-position, the larger the values of $\Delta\lambda_A$ and $\Delta\nu_C$. In the metal-complexes, which have larger $\Delta\lambda_A$ and $\Delta\nu_C$ values, the A bands are generally higher in intensity and smaller in l and δ (except those of the 5-nitro derivative). This suggests shat the contribution of the five-membered chelate ring slightly decreases because of the polarity increase of the M–O bond.

6) L. P. Hammett, *Chem. Revs.*, 17, 125 (1935); H. H. Jaffé, ibid., 53, 191 (1953); H. C. Brown and Y. Okamoto, *J. Am. Chem. Soc.*, 80, 4979 (1958).

7) a) D. P. Craig et at., *J. Chem. Soc.*, 1954, 332.; b) "The Chemistry of the Coordination Compounds", Ed. by J. C. Bailar, Jr., Reinhold Publishing Corp., New York (1956), p. 185.

8) A. Burawoy and E. Spinner, *J. Chem. Soc.*, 1955, 2557.

TABLE II. ABSORPTION SPECTRA OF THE METAL-COMPLEXES DERIVED FROM 3, 5-DISUBSTITUTED PHENOLAZOACETOACETANILIDES

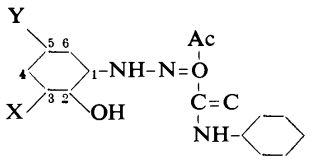

Substituent 3-X	Substituent 5-Y	Metal	Band A λ_{max}	ε_{max}	$\Delta\nu_A$	l	δ
NO_2	CH_3	None	410.0	1.81	—	—	—
		Cr	485.7	4.03	3.80	4.18	0.35
		Co	483.0	3.54	3.68	4.16	0.32
NO_2	Cl	None	410.0	1.96	—	—	—
		Cr	487.7	4.19	3.88	4.05	0.29
		Co	484.2	3.95	3.73	3.93	0.21
NO_2	NO_2	None	410.0	2.11	—	—	—
			471.0*	1.00			
		Cr	468.3	3.18	3.03	6.83	1.58
		Co	461.8	4.35	2.73	5.00	1.95
Cl	NO_2	None	382.0	2.76	—	6.52	1.22
		Cr	461.3	3.63	4.50	—	—
		Co	448.9	4.49	3.90	6.52	1.51
			412.7*	3.78			

All the spectra were measured in the standard solvent. But those of the ligand-dyes, except the dye ($X=NO_2$, $Y=CH_3$), were determined in aqueous 80% methanol containing 0.002 mol. of hydrochloric acid per liter.

In case of the 4-nitro and 4-sulfamoyl derivatives, the polarization of the M–O bond is not so large as those of the 5-substituted derivatives (Fig. 4b). However, the values of $\Delta\nu_A$ are almost equal to those of the 5-substituted derivatives (Fig. 4a). It is considered that an elongation[9] and a planarity increase[10] of the conjugate system upon the introduction of the substituent in the 4-position, i. e., para to the hydrazone group, result in an enhancement of the $d\pi-p\pi$ bonding (i. e., factor ii).

With regard to the 3-nitro derivative, the nitro-group in the 3-position fairly polarizes the M–O bond, resulting in the increase of both $\Delta\nu_A$ and $\Delta\nu_C$ values.

The relatively large $\Delta\nu_D$ values in the cobalt(III)-complexes indicate that the stable chelate ring emphasizes the planarity of the ligand-molecule to reduce the energy of the transition expected for the partial chromophore involving the amide group.

Since most of the B bands are superposed by the C bands and present themselves as inflections, exact evaluations of them are difficult. However, the intensities of the B bands in the spectra of 3-nitro and 5-nitro derivatives are higher than those of the other derivatives. Such intensity increases agree with the finding, reported in Part II, that the electron-withdrawing group stabilizes the hydrazone structure[3,11], resulting in an enhancement of the conjugation B band.

Chromium(III)-complexes.—In the chromium(III)-complexes, the $\Delta\nu_C$ values are larger than that of the corresponding cobalt(III)-complex. That is, the Cr–O (O, phenolic oxygen) bonds have a highly ionic character. The larger shifts of the A bands as compared with those of the coblt(III)-complexes are mainly to be attributed to the ionic Cr–O bond.

In the series of 5-substituted derivatives, the $\Delta\nu_C$ values in Fig. 4b show that an electronegative group increases the polarity of the Cr–O bond. On the other hand, a variation of $\Delta\nu_A$ in Fig. 4a exhibits a gentler slope than that of the chromium(III)-complexes. Consequently, it is concluded that the influence of the i factor on the A bands is not so effectively operative as in the case of the cobalt(III)-complexes, because the Cr–O bonds originally have a highly ionic character.

In the series of 4-substituted derivatives, both $\Delta\nu_A$ and $\Delta\nu_C$ values are smaller than those of the corresponding 5-substituted derivative.

9) H. P. Koch, ibid., **1949**, 408; H. H. Szmant and H. J. Planinsek, *J. Am. Chem. Soc.*, **72**, 4042 (1950).
10) W. R. Brode, "The Roger Adams Symposium", John Wiley & Sons, Inc., New York (1955), p. 29.
11) A. Burawoy, A. G. Salem and A. R. Thompson, *J. Chem. Soc.*, **1952**, 4793; H. Shingu, *J. Chem. Soc. Japan, (Nippon Kwagaku Kwaishi)*, **60**, 542 (1939).

It is considered that the substituent in the 4-position, i. e., meta to the M–O bond, scarcely participates in the polarization of the M–O bond (smaller $\Delta\nu_C$) and that the $d\pi$-$p\pi$ interaction also is not effectively operative, because the five-membered chelate ring is weaker than that of the 4-substitued cobalt(III)-complex (smaller $\Delta\nu_A$).

A small $\Delta\nu_A$ value in the spectrum of the 3-nitro derivative also is attributed to the same reason.

Further Observation of 3, 5-Disubstituted Derivatives.—The bathochromic displacements of the A bands due to the polarization of the M–O (O, phenolic oxygen) bond are pronounced in the cobalt(III)-complexes. As will seen in the series of 5-substituted derivatives in Table I, the A band of the cobalt(III)-complex approaches that of the corresponding chromium(III)-complex in accordance with the polarization of the Co–O bond.

In Table II are shown the visible absorption bands of the chromium(III)- and cobalt(III)-complexes of 3, 5-disubstituted phenolazoacetoacetanilides. Remarkable proximities of the absorption maxima in the two complexes produced by the introduction of electron-withdrawing groups in the 3- and 5-positions are to be seen. That is, the polarization of the Co–O bonds results in the displacement of the A bands to longer wavelengths.

In Table II, the A bands of those metal-complexes having a nitro group in the 5-position are broader than those of the other derivatives. Moreover, the cobalt(III)-complex of the 3-chloro-5-nitro derivative, as well as of the 5-nitro derivative in Table I, exhibits a weak inflection at a shorter wavelength than that of the A band. An assignment of this band will be made in the next paper.

Experimental

Syntheses and Purifications of Metal-complexes Derived from Phenolazoacetoacetanilides.—*Metal-complexes of Phenolazoacetoacetanilide.*—*(i) Chromium(III)-complex.*—The ligand-dye (0.02 mol.) was treated with chromium(III) formate (0.01 mol.) in formamide at 120°C for 12 hr. The reaction mixture was poured into a dilute aqueous solution of hydrochloric acid to yield a precipitate of the complex-acid. This complex-acid was then filtered off, washed with water, and dried in vacuo. Purification was carried out by column-chromatography. The crude complex-acid (200 mg.) was dissolved in 95% ethanol, added to an adsorption-column of activated alumina, and developed with 95% ethanol. A brown zone of the metal-complex was extruded, separated, and eluted with 95% ethanol. The eluted solution was evaporated to dryness under reduced pressure. The residue obtained was dissolved in aqueous ethanol containing sodium hydroxide. The neutralization of the solution with dilute hydrochloric acid at 50°C and the successive addition of sodium chloride to this gave a brown-yellow precipitate. The precipitate was filtered off, washed with water, and dried in vacuo, yielding 140 mg. of the pure chromium(III)-complex.

Found: C, 59.56; H, 4.26; N, 13.09. Calcd. for $C_{32}H_{27}O_6N_6Cr$: C, 59.71; H, 4.23; N, 13.05%.

(ii) Cobalt(III)-complex.—A suspension of the ligand-dye (0.02 mol.) in a dilute aqueous solution of sodium hydroxide was treated at 80°C with cobalt(II) sulfate (0.01 mol.). The sodium-salt of the cobalt-complex crystallized out as fine flakes in the reaction mixture. The reaction mixture was made into a solution by adding ethanol and then acidified (pH 2.40) by the addition of hydrochloric acid. The precipitated complex-acid was filtered off, washed with water, and dried in vacuo. Chromatographic purification of the crude product (200 mg.) was performed in the same manner as with the chromium(III)-complex to yield 150 mg. of a brown-yellow precipitate.

Found: C, 58.86; H, 4.32; N, 12.62. Calcd. for $C_{32}H_{27}O_6N_6Co$: C, 59.08; H, 4.18; N, 12.91%.

Metal-complexes of 2-Hydroxy-5-methylphenylazoacetoacetanilide.—*(i) Chromium(III)-complex.*—The pure chromium-complex was obtained as yellow-brown precipitate.

Found: C, 60.94; H, 4.83; N, 12.49. Calcd. for $C_{34}H_{31}O_6N_6Cr$: C, 60.80; H, 4.65; N, 12.51%.

(ii) Cobalt(III)-complex.—The purified product was in the form of yellow-brown needles.

Found: C, 59.85; H, 4.59; N, 12.25. Calcd. for $C_{34}H_{31}O_6N_6Co$: C, 60.19; H, 4.60; N, 12.38%.

Metal-complexes of the Other Phenolazoacetoacetanilides.—These also wese prepared in the manner described above. Their purities were checked by elemental analysis.

Measurements of the Electronic Absorption Spectra.—The absorption spectra were measured by two recording spectrophotometers, a Beckman model DK-2 and a Shimadzu model RS-27. All the spectra were determined at a concentration of 1.6×10^{-5} M. Beer's law is valid in this dilution. The qualities of the solvents were of spectral grades.

Summary

The electronic absorption spectra of the series of metallized phenolazoacetoacetanilides have been investigated.

The substituent, in the *o*- or *p*- position to the M–O (M, central metal; O, phenolic oxygen) bond, generally alters the polarity of the M–O bond. On the other hand, the substituent, in the *m*-position to the M–O bond, i. e., the *p*-position to the hydrazone group, mainly contributes to the $d\pi$-$p\pi$ interaction between the hydrazone group and the central metal atom.

The effects of such substituents upon the shifts of the A bands are more pronounced in the cobalt(III)-complexes than in the chromium-(III)-complexes, because the former complexes have the stable five-membered chelate rings

involving the highly covalent Co–O (O, phenolic oxygen) bonds.

The author owes his gratitude to the late Professor Ryutaro Tsuchida of Osaka University for his valuable discussions and criticism. Thanks are also to be accorded to Sumitomo Chemical Co., Ltd., for permission to publish this work and to Mr. Kikuo Kimura for his assistance throughout this study.

Sumitomo Chemical Co., Ltd.
Osaka Works
Konohana-ku, Osaka

Studies of the Absorption Spectra of Azo Dyes and their Metal-complexes. V. The Electronic Absorption Spectra of Metal-complexed Phenolazoacetoacetbenzylamides

By Yoshiharu YAGI

(Received July 16, 1962)

Previous studies[1] of the electronic absorption spectra of phenolazoacetoacetanilides*1 have shown that four groups of bands are to be expected for partial or total chromophoric systems[2] of the respective molecules and that the interception of the π-p conjugation between the amide nitrogen and the amide aryl group, as in case of phenolazoacetoacetbenzylamide (I), causes the hypsochromic displacement of the A, B and C bands. The author has also investigated the metal-ligand linkage of the 2 : 1-complexes consisting of two molecules of phenolazoacetoacetanilides (II)[3a] and a tervalent metal atom. The work described in the present paper was first undertaken to study the absorption characteristics and the metal-ligand linkage with respect to the metallized phenolazoacetoacetbenzylamides[3b].

In the series of metallized phenolazoacetoacetanilides, the A band of the cobalt(III)-complex*2 having a nitro group in the para-position to the Co–O (O, phenolic oxygen) bond has been observed to split into two peaks. The cause of such anomalous band-splitting will be investigated, together with the above-mentioned problems.

Results and Discussion

The Electronic Absorption Spectra of Chromium(III)- and Cobalt(III)-complexes Derived from Phenolazoacetoacetbenzylamides. — The electronic absorption spectra of chromium(III)- and cobalt(III)-complexes derived from 5-sulfamoyl- and 5-chloro derivatives of I in the standard solvent*3 are illustrated in Table I (Figs. 1–3), together with the corresponding derivatives of II.

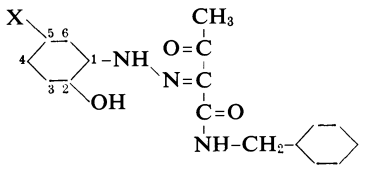

(I)

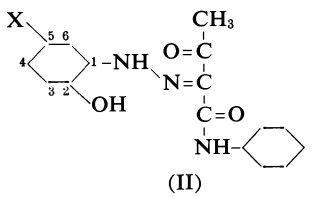

(II)

(X, Substituent)

The spectra of the metal-complexed I in the near ultraviolet and visible regions show four groups of bands, which will be identified as A, B, C and D counting from the longer

*1 The compounds in this paper have hydrazone forms but are, for convenience, named as azo compounds. α-(2-Hydroxyphenylazo)-acetoacetanilide, for example, is abbreviated as phenolazoacetoacetanilide,

1) Parts II, III and IV, This Bulletin, **36**, 492, 500, 506 (1963).

2) E. A. Braude, *J. Chem. Soc.*, **1945**, 490.

*2 The term "metal-complex" in this paper denotes the 2 : 1-metal-complex.

3) a) Such metal-complexes are known as acid dyes. For example: Ciba Ltd., U. S. Pat. 2565898 (1951); Brit. Pat. 716753 (1954); J. R. Geigy A.-G., Brit. Pat. 736034 (1955); E. Koike and Y. Yagi, Japanese Pat., Announced No. 36-8730 (1961).

b) Y. Yagi and K. Kmura, Japanese Pat., Announced No. 36-11975 (1961).

*3 The term "standared solvent" denotes aqueous 80% methanol containing 0.1 g. of acetic acid per liter.

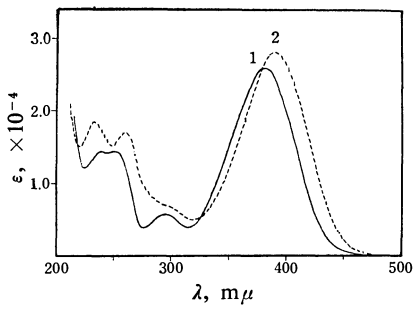

Fig. 1. Absorption spectra of 2-hydroxy-5-sulfamoylphenylazoacetoacetbenzylamide (1) and 2-hydroxy-5-sulfamoylphenylazoacetoacetanilide (2) in the standard solvent.

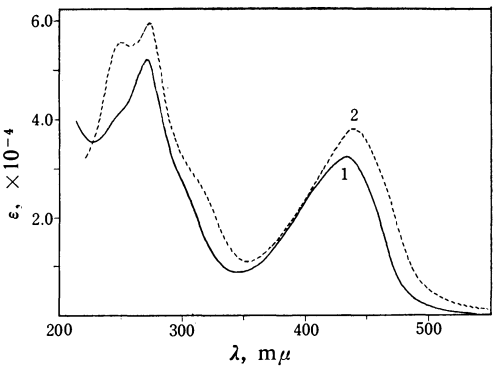

Fig. 2. Absorption spectra of cobalt-complexes derived from the ligand-dyes shown in Fig. 1 in the standard solvent; the numbering of the curves corresponds to those in Fig. 1.

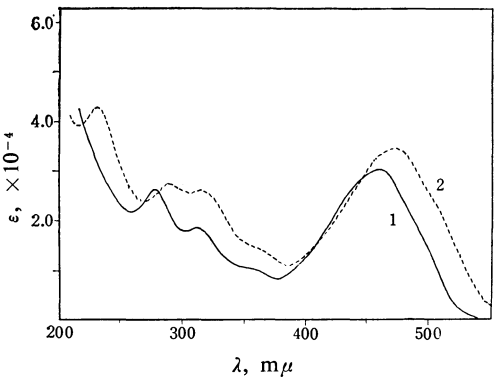

Fig. 3. Absorption spectra of chromium-complexes derived from 5-chloro-2-hydroxyphenylazoacetoacetbenzylamide (1) and 5-chloro-2-hydroxyphenylazoacetoacetanilide (2) in the standard solvent.

wavelength side. As was pointed out in Part III, these bands originate in the four conjugation bands (K bands)[4] of the respective ligand-dye. The A ligand-band arises from a transition involving electron migration along the whole conjugate system of the ligand-molecule. The B ligand-band originates in a conjugative electronic transition between the acetyl carbonyl and the hydrazone group, the C ligand-band, in one between the phenolic nucleus and the hydrazone group, and the D ligand-band, in one between the carboxylic acid amide group and the hydrazone group.

With regard to absorption spectra of the ligand-dye I, the interception of the π-p conjugation by the insertion of a methylene bridge caused a decrease in the intensity and the red-shift of the D band, resulting in the hypsochromic and hypochromic displacement of the A, B and C bands. In the spectra of metal-complexed II also, the D bands markedly decrease in intensity, as is shown in Figs. 2 and 3. For example, the D band in the chromium(III)-complex of the 5-chloro derivative is completely submerged in the other band-system and can not be detected. An absorption band due to a forbidden transition within the phenyl or the phenol nucleus (B-band)[5] should appear near the D bands, but this is considered to be submerged in such conjugation bands as the D or C bands.

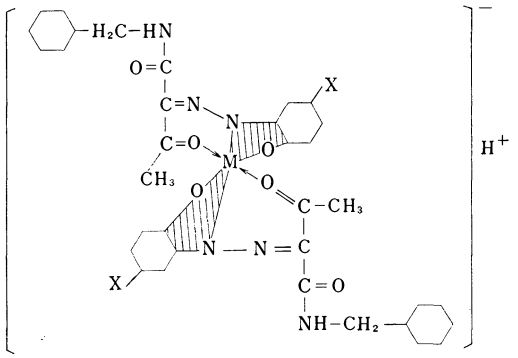

(III)

A comparison of the A bands between the I and II series indicates that the elimination of the π-p conjugation causes a hypsochromic displacement of about 7 mμ in the cobalt(III)-complexes and one of 10~14 mμ in the chromium(III)-complexes, In Table I, the $\Delta\nu_A$ values (the red-shifts of A ligand-bands with complex-formation, i. e., the absorption maximum of the ligand-band A−absorption maximum of the corresponding complex-band, in cm^{-1}) of the chromium(III)-complexes are almost equal in the two series. However, the $\Delta\nu_A$ values of the cobalt(III)-complexes are larger in the I series.

4) A. Burawoy, *J. Chem. Soc.*, **1937**, 1865; **1939**, 1177; A. E. Gillam and E. S. Stern, "An Introduction to Electronic Absorption Spectroscopy", Edward Arnold Publishers, Ltd., London (1954), p. 111.

5) A. Burawoy and J. T. Chamberlain, *J. Chem. Soc.*, **1952**, 2310, 3734.

TABLE I. ELECTRONIC ABSORPTION SPECTRA OF CHROMIUM(III)- AND COBALT(III)-COMPLEXES

Substituent (X)	Series of ligand	Metal	A				
			λ_{max}	ε_{max}	$\Delta\nu_A$	l	δ
$-SO_2NH_2$	I	None	380.0	2.60	—	4.57	0.31
		Cr	449.0	3.26	4.05	4.58	0.58
		Co	433.1	3.23	3.23	4.68	0.68
	II	None	389.5	2.81	—	4.59	0.36
		Cr	460.4	3.78	3.95	4.63	0.59
		Co	440.0	3.79	2.94	4.64	0.69
-Cl	I	None	387.0	2.42	—	4.70	0.27
		Cr	459.3	3.02	4.07	4.55	0.52
		Co	443.5	3.13	3.29	5.06	0.90
	II	None	396.0	2.76	—	4.63	0.31
		Cr	473.3	3.43	4.12	4.77	0.55
		Co	450.2	3.19	3.04	5.85	1.10

N.B. a) Absorption maxima (λ_{max}) in mμ, molar extinction coefficients (ε_{max}) in 10^{-4}, red-shifts of the ligand-bands with complex-formation ($\Delta\nu$) in $10^{-3}\times cm^{-1}$, half-value widths (l) and inclination parameters (δ) of the A bands in $10^{-3}\times cm^{-1}$.

The bathochromic shifts of the A ligand-bands with the complex-formation are ascribed mainly to two factors: (i) the polarity of the M–O (M, tervalent metal; O, phenolic oxygen) bond; i.e., any alteration of the electronic configuration, which polarizes the bond, causes a red-shift of the A band, and (ii) the perturbation of the π-electron system by the $d\pi$-$p\pi$ interaction between the hydrazone group and the central metal. The $d\pi$-$p\pi$ interaction in the chromium(III)- and the cobalt(III)-complexes are considered to be equally effectively operative, because the $d\pi$-orbitals in both the complexes by d^2sp^3 hybridization have stable electronic configurations[6]. Consequently, the different degrees of the bathochromic shifts of the A ligand-bands with the cobalt-complex formation are considered to depend mainly upon the polarities of the M–O bonds. The larger values of $\Delta\nu_A$ in the cobalt(III)-complexs of the I series indicate that the Co–O (O, phenolic oxygen) bond increases its ionic character. This is probably due to the stronger basicity of the phenolic hydroxyl in the I series. Further, since the substituents in the phenolic nuclei of the I series have more pronounced effects upon the absorbing systems, as was pointed out in Part II, the electronegative substituent, such as the 5-chloro or 5-sulfamoyl group, will emphasize the polarity-increase of the Co–O bond.

Since the Cr–O (O, phenolic oxygen) bond originally has a highly ionic character, the values of $\Delta\nu_A$ in the I and II series do not differ from each other.

The half-value widths (l) and the inclination parameters (δ) are generally larger in the cobalt(III)-complexes than in the chromium-(III)-complexes. This suggests that the stable five-membered chelate-ring in the cobalt(III)-complexes, as shown in III (the shaded portions), emphasizes the perturbation of the π-electron system by the $d\pi$-$p\pi$ interaction.

The C bands are closely related to the polarities of the M–O (O, phenolic oxygen) bonds, as was reported in Parts III and IV. That is, the highly ionic character of the Cr–O (O, phenolic oxygen) bond resulted in the appearance of the C bands at markedly longer wavelengths, while the highly covalent character of the Co–O (O, phenolic oxygen) bond caused the slight red-shift and the intensity increase of the C band. Such characteristic band-shifts are also observed in the I series. It is noteworthy that the $\Delta\nu_C$ values of the cobalt(III)-complexes in the I series are relatively larger than those of the corresponding chromium(III)-complexes. This confirms that the Co–O bond increases its ionic character in the I series.

The B bands run parallel to the shifts of the A bands, indicating that this group of bands is influenced by an electronic transition involving electron migration along the whole conjugate system of the molecule. The absorption intensities are almost equal in the chromium(III)- and the cobalt(III)-complexes.

6) "The Chemistry of the Coordination Compounds", Ed. by J. C. Bailar, Jr., Reinhold Publishing Corp., New York (1956), p. 185.

OF PHENOLAZOACETOACETBENZYLAMIDES AND RELATED COMPOUNDS IN THE STANDARD SOLVENT

B			C			D		
λ_{max}	ε_{max}	$\Delta\nu_B$	λ_{max}	ε_{max}	$\Delta\nu_C$	λ_{max}	ε_{max}	$\Delta\nu_D$
296.0	0.56	—	251.7	1.43	—	239.0	1.43	—
317.0*	1.84	2.23	282.5 (264.0*)	3.39 3.07	4.33	232.8	3.60	−1.12
305.5*	2.37	1.05	271.0	5.21	2.83	243.4*	3.99	0.76
303.0*	0.63	—	258.0	1.74	—	232.5	1.84	—
319.6*	2.61	1.71	291.9	3.80	4.50	234.3	4.69	0.33
315.5*	2.58	1.30	272.5	5.95	2.06	249.0	5.57	2.85
306.0	0.53	—	264.0*	0.79	—	245.0	1.15	—
312.0 (359.0*)	1.86 0.99	0.63	278.9	2.62	2.02	—	—	—
307.5*	2.08	0.16	270.3	3.94	0.88	(236.0*)	3.96	−1.55
311.0	0.68	—	262.5	1.29	—	231.5	1.64	—
315.0 (365.0)*	2.59 1.39	0.40	289.5	2.72	3.56	230.4	4.28	−0.20
313.0	2.36	0.20	270.3	4.49	1.10	242.7	4.72	2.00

b) * Inflection
c) Absorption maximum in parenthesis denotes an indistinct location.
d) Inflections near the four main bands are shown under the corresponding main band.

However, exact evaluation is difficult, because most of these bands appear as inflection.

The D bands in the I series also often appear as inflection, because their intensities are generally low because of the interception of the π-p conjugation. Relatively longer wavelength positions and higher intensities of the D bands in the spectra of the cobalt(III)-complexes are observed than in those of the chromium(III)-complexes. This is in accord with the explanation given in the previous paper that the stable chelate ring emphasizes the planarity of the coordinated ligand-molecule, facilitating the electronic transition expected for a partial chromophore involving the amide group and resulting in an approach of the D band to the high-intensity C band.

The Splitting of the A Bands in the Spectra of Metallized 2-Hydroxy-5-nitrophenylazoacetoacetbenzylamide.—The absorption spectra of chromium(III)-, cobalt(III)-, iron(III)- and aluminum-complex of 2-hydroxy-5-nitrophenylazoacetoacetbenzylamide (IV) in a variety of solvents are shown in Table II (Figs. 4 and 5).

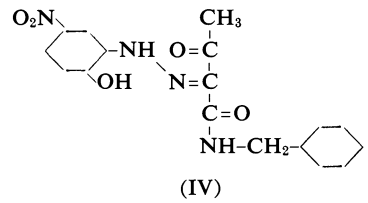

(IV)

Two peaks of the split A band are, for convenience, named as A_1 and A_2 counting from the longer wavelength side.

The splitting of the A bands is observed in every solvents. The D bands of these complexes decrease their intensities in a manner similar to those in Table I. For example, the D band of the cobalt(III)-complex can not be detected, as is shown in Fig. 4. Weak inflections at about 550 mμ in the spectra of the iron(III)-complex are considered to be the first absorption band[7], that due to the iron(III)-ion, as was reported in Part III. The results in Part III also showed that the aluminum-complex generally shows a sharp and symmetric A band. However, all the metal-complexes of IV have broadly split A bands.

It has been reported that the absorption band of salicylaldoxime tends to split with the Ni-chelate formation[8] and that such band-splitting probably arises from different bond-types, such as dsp^2 and sp^3 hybridizations. It can not, however, be thought that the A_1 and A_2 bands originate in two different bond-types, for the 2:1-chromium(III)- or cobalt(III)-complexes, such as the metal-complexes in this studies, are known to be stable penetration complexes by d^2sp^3 hybridization[9]; the results in the preceding papers[1] also confirm the above view. Nor can it be considered that the band-splitting is due to the vibrational

7) R. Tsuchida, This Bulletin, **13**, 388, 436 (1938); *J. Chem. Soc. Japan (Nippon Kwagaku Kwaishi)*, **59**, 731, 819 (1938); K. Sone, ibid., **71**, 270, 316 (1950).
8) K. Sone, *J. Am. Chem. Soc.*, **75**, 5207 (1953).
9) J. C. Bailar, Jr., and C. F. Callis, ibid., **74**, 6018 (1952); P. Pfeiffer and S. Saure, *Ber.*, **74**, 935 (1941).

TABLE II. ABSORPTION SPECTRA OF METALLIZED 2-HYDROXY-5-NITROPHENYLAZOACETOACETBENZYLAMIDE IN A VARIETY OF SOLVENTS

Metal	Solvent	A		B	C	D
		A_1	A_2			
None	S		376.0 (2.46)	302.0 (1.18)	246.0 (1.38)	(232.3*) (1.21)
Cr	S	451.8(4.05)	(424.7*) (3.78)	—	307.7 (3.06)	246.0 (2.48)
	N	452.8(4.13)	(425.0*) (3.88)	—	307.4 (2.84) (267.2*) (2.22)	245.0 (2.42)
	P	466.6(4.39)	(432.4*) (4.11)	—	315.3 (2.75) (351.7*) (1.80)	—
Co	S	439.5(4.10)	414.2 (3.99)	297.6* (3.13)	266.5 (3.81)	not detected
	M	440.9(4.04)	414.6 (4.02)	296.2* (2.94)	265.9 (3.52)	not detected
	N	442.7(4.04)	416.5 (4.06)	295.0* (2.96)	266.5 (3.53)	not detected
	P	457.2(4.61)	421.7 (4.34)	(341.7*) (2.08)	—	not detected
Fe	S	(544.5*) (0.47) 418.1(3.96)	(376.0*) (3.52)	305.5 (2.51)	382.3 (2.49)	254.0* (2.33)
	P	(552.4*) (0.53) 438.4(4.48)	(407.5*) (3.92) (377.0*) (3.26)	312.5 (2.36)	—	—
Al	S	437.0(4.56)	(408.0*) (4.34)	318.8 (2.53)	267.0 (1.63)	248.2 (1.64)
	P	453.0(4.91)	417.1 (4.61)	323.0 (2.48)	—	—

N.B. a) Wavelengths (λ_{max}) in mμ, molar extinction coefficients (ε_{max}) $\times 10^{-4}$ in parenthesis.
b) S, Standard solvent; N, Aqueous 50% methanol containing 0.01 mol. of NaOH per liter; M, Aqueous 50% methanol; P, Pyridine
c) In the chromium-complex, the B band is superposed by the C band.

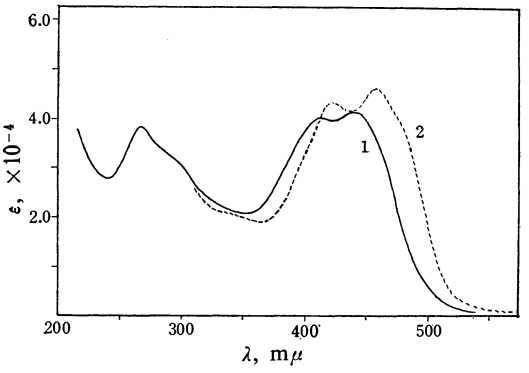

Fig. 4. Cobalt-complex of IV in the standard solvent (1) and in pyridine (2).

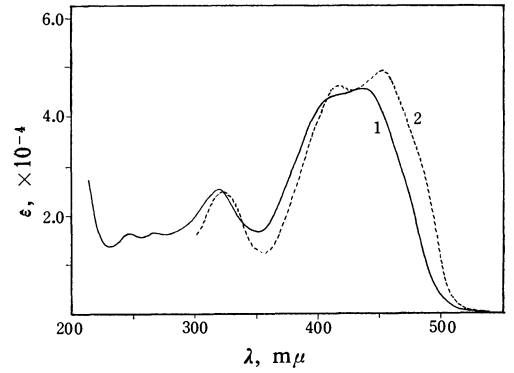

Fig. 5. Aluminum-complex of IV in the standard solvent (1) and in pyridine (2).

structure, as has been reported on metal-chelates of α, α'-dipyridyl[10].

In the cobalt(III)-complex of IV, a comparison of the absorption maxima of the A_1 and A_2 bands in pyridine with those in the standard solvent shows that the A_1 and A_2 bands undergo bathochromic shifts of 0.89×10^3 and 0.42×10^3 (in cm^{-1}) respectively when measured in pyridine. The batho- and hyperchromic displacement is more pronounced in the A_1 band (Fig. 4). Such a tendency is also observed in the other metal-complexes of IV, as is shown in Fig. 5. Generally, the increase in the polarity due to the solute-solvent interaction, and thus the magnitude of the solvent effect, is enhanced with the polar character of the absorbing molecules[11]. Although various causes are conceivable for such band-splitting, the following explanation is thought to be the most reasonable; one of the two M–O (O, phenolic oxygen) bonds which form the chelate-rings of the 2 : 1-metal-complex III is markedly polarized by the *p*-substituted nitro group, and thus an electronic transition along the conjugate system of the coordinated ligand-molecule involving the polarized M–O bond exhibits the A_1 band.

10) K. Sone, P. Krumholz and H. Stammreich, *J. Am. Chem. Soc.*, **77**, 777 (1955).
11) A. Burawoy, M. Cais., J. T. Chamberlain, F. Liversedge and A. R. Thompson, *J. Chem., Soc.*, **1955**, 3721.

Though an anionic charge of the 2:1-complex is generally considered to have a non-localized character, as has been pointed out in Part III, this will be localized at the polarized M–O bond in the metal-complexed IV. To confirm this explanation on other metal-complex systems, further studies are now in progress.

If the metal-complex molecule of IV involves the two M–O bonds of different polarities as explained above, the C bands expected for the partial chromophore involving the phenolic nucleus will split to two peaks. In fact, the C band of the chromium(III)-complex in an alkaline solution splits and forms an inflection near 267 mμ. No such band-splitting, however, can be detected in the other complexes of IV.

That the A_2 band of the cobalt(III)-complex has a relatively higher intensity as compared with that of the A_1 band, as is shown in Table II, agrees with the finding in Parts III and IV that the metal-ligand linkage is the most stable in the cobalt(III)-complexes. Since the M–O bonds of the chromium(III)-, iron(III), and aluminum-complexes are essentially ionic, the A_2 bands of these complexes are low in intensity. A fine structure of the A_2 band in the spectrum of the iron(III)-complex in pyridine may support the deduction in Part III that the iron(III)-complex is a mixture of different bond types.

Experimental

The Preparation of Metal-complexes of Phenolazoacetoacetbenzylamides.—*Metal-complexes of 5-Chloro-2-hydroxyphenylazoacetoacetbenzylamide.* — *(i) Chromium(III)-complex.*—The ligand-dye (0.02 mol.) was treated with chromium(III) formate (0.01 mol.) in formamide at 120°C for 10 hr. The reaction mixture was poured into a dilute aqueous solution of hydrochloric acid to yield a yellow-brown precipitate. This complex-acid was filtered off, washed with water, and dried in vacuo. The crude complex-acid (300 mg.) was dissolved in 95% ethanol, added to an adsorption-column of activated alumina, and developed with 95% ethanol. The brown zone of the complex was separated and eluted with ethanol. The eluted solution was evaporated to dryness under reduced pressure. The residue obtained was dissolved in aqueous ethanol containing sodium hydroxide. The neutralization of the solution with dilute hydrochloric acid and the successive addition of sodium chloride to this gave reddish brown prisms. This product was filtered off, washed with water, and dried in vacuo, yielding 230 mg. of the pure chromium(III)-complex.

Found: C, 54.70; H, 4.02; N, 11.41. Calcd. for $C_{34}H_{29}O_6N_6Cl_2Cr$: C, 55.14; H, 3.94; N, 11.34%.

(ii) Cobalt(III)-complex. — The ligand-dye (0.02 mol.) was suspended in an aqueous alkaline solution containing sodium hydroxide (0.05 mol.) and tartaric acid (0.005 mol.) and treated with cobalt(II) sulfate (0.01 mol.) at 60°C for 1 hr. The reaction mixture was made into a solution by the addition of ethanol and was acidified (pH 2.70) with hydrochloric acid. The precipitated complex-acid was filtered off, washed with water, and dried in vacuo. The chromatographic purification of the product (200 mg.) was carried out in the same manner as with the chromium(III)-complex, giving yellow-brown needles (150 mg.).

Found: C, 54.23; H, 4.18; N, 10.98. Calcd. for $C_{34}H_{29}O_6N_6Cl_2Co$: C, 54.64; H, 3.91; N, 11.24%.

Metal-complexes of the Other Phenolazoacetoacetbenzylamides.—These complexes were also prepared in the manner described above. The iron(III)- and aluminum-complexes of IV were prepared in a method similar to that described in Part III. The purities were checked by elemental analysis.

Measurements of the Electronic Absorption Spectra.—The absorption spectra were measured by two recording spectrophotometers, a Beckman model DK-2 and a Shimadzu model RS-27. All the spectra were determined at concentrations of 1.6×10^{-5} M (metal-complexes) and 2.5×10^{-5} M (ligand-dyes).

Summary

The absorption spectra of metallized phenolazoacetoacetbenzylamides were investigated.

The isolation of the electronic effect of the amide phenyl ring by the insertion of the methylene bridge decreases the intensity of the D band, resulting in the hypso- and hypochromic displacement of the A, B and C bands.

The red-shifts of the A and C ligand-bands with the complex-formation indicate that the Co–O (O, phenolic oxygen) bonds increase their ionic character as compared with those of the metallized phenolazoacetoacetanilides.

The splitting of the A band in the spectra of metallized 2-hydroxy-5-nitrophenylazoacetoacetbenzylamide is possibly to be attributed to the polarization of the M–O (O, phenolic oxygen) bond by the electron-withdrawing nitro group.

The author owes thanks to the late Professor Ryutaro Tsuchida of Osaka University for his valuable discussions and encouragement. Thanks are also to be accorded to Sumitomo Chemical Co., Ltd., for permission to publish this work and to Mr. Kikuo Kimura for his assistance throughout this study.

Sumitomo Chemical Co., Ltd.
Osaka Works
Konohana-ku, Osaka

The Selective Titrations of Calcium in the Presence of Magnesium

By Yoshiko DATE and Kyoji TÔEI

(Received August 18, 1962)

The chelometric determination of calcium in the presence of magnesium is carried out by using ethylenediaminetetraacetic acid (EDTA) as a titrant at pH 12~13. Magnesium is precipitated as the hydroxide, and murexide, thymolphthalein complexone (TPC), Calcon or Patton-Reeder's reagent[1] (NN) is used as an indicator. However, the presence of precipitated magnesium hydroxide causes a coprecipitation of calcium and an adsorption of the metal indicator on the precipitate, and these behaviors interfere to find an end-point of reaction accurately. Some attempts to overcome them have been reported. For example, to prevent the precipitation, tartrate[2] or sucrose[3,4] was added. Although the precipitate was thereby avoided, the end-point was indefinite. This is because of the small difference in the stability constants of calcium- and magnesium-EDTA complexes ($\log K_{CaZ}=10.70$, $\log K_{MgZ}=8.69$).

Instead of using EDTA as a titrant for calcium in the presence of magnesium, glycoletherdiaminetetraacetic acid (GEDTA) could be introduced; the difference between the stability constants of calcium- and magnesium-GEDTA complexes is 5.8 in $\log K$ units ($\log K_{CaZ}=11.0$, $\log K_{MgZ}=5.2$), and therefore the selective titration of calcium in the presence of magnesium would be possible at pH 10 where magnesium remains in the solution. However, a selective indicator for calcium at pH 10 has not yet been found. A potentiometric end-point detection by the mercury electrode[5], and an indirect end-point indication using the zinc-zincon system[6] have been proposed. Unfortunately both methods somewhat restrict the use of certain important masking agents which are often employed in practical analyses.

Burg and Conaghan[7] achieved the selective titration of calcium in the presence of magnesium with GEDTA, using tartrate as a masking agent for magnesium and Calcon as an indicator at pH 13 and at about 40°C.

In this paper, the work of masking agents and indicators on the chelometric determination of calcium in the presence of magnesium is reported. Some applications for limestone, dromite and magnesite will be presented.

Experimental and Results

Reagents.—A 0.01 M EDTA solution was prepared by dissolving 3.73 g. of EDTA (disodium salt) in 1 l. of distilled water. A 0.01 M GEDTA solution was prepared by dissolving 3.8 g. of glycoletherdiaminetetraacetic acid in 20 ml. of 1 N sodium hydroxide and then by diluting this solution with redistilled water to 1 l. A 0.01 M calcium solution; dissolve 1.0009 g. of calcium carbonate in hydrochloric acid, add distilled water, and heat to remove the carbon dioxide. After cooling, dilute with distilled water to 1 l. The 0.01 M EDTA and GEDTA solutions were standardized with this solution. The 0.1 M magnesium solution was prepared by dissolving 24.65 g. of magnesium sulfate heptahydrate in a small volume of distilled water and by diluting this solution. to 1 l.

The BT solution was prepared by dissolving 0.5 g. of Eriochrome Black T and 4.5 g. of hydroxylamine hydrochloride in 100 ml. of methanol. The Dotite NN solution was prepared by dissolving 2-hydroxy-1-(2-hydroxy-4-sulfo-1-naphthylazo)-3-naphthoic acid (Patton-Reeder's reagent) in methanol. For the buffer solution, 7 g. of ammonium chloride and 57 ml. of concentrated aqueous ammonia were dissolved in 100 ml. of distilled water. The tartrate solution was prepared by dissolving 10 g. of potassium sodium tartrate in 100 ml. of distilled water.

Indicators.—The optimum pH ranges for several indicators were studied. Various pH solutions were prepared using aqueous ammonia or potassium and sodium hydroxide. A small amount of an indicator was added to each of them, and the stability of the color was examined. Further, the color of the free indicator was compared with that of the calcium complex. The indicators, their optimum pH ranges, and the methods of preparation are shown in Table I.

It was tested whether or not, in the calcium titration, these indicators indicated the accurate quantitative value, with sharp color changes. These tests were carried out in the following

1) J. Patton and W. Reeder, *Anal. Chem.*, **28**, 1026 (1956).
2) V. Tikkomirova and O. Simackova, *Collection*, **22**, 982 (1957).
3) R. D. Bond and B. M. Tuker, *Chem. & Ind.*, **1954**, 1236.
4) B. M. Tuker, *Analyst*, 82, 284 (1957).
5) R. W. Schmid and C. N. Reilly, *Anal. Chem.*, **29**, 264 (1957).
6) F. S. Sadek, R. W. Schmid and C. N. Reilly, *Talanta*, **2**, 38 (1959).
7) R. A. Burg and H. F. Conaghan, *Chemist-Analyst*, **49**, 100 (1960).

TABLE I

Indicator	Optimum pH range	Preparation
Calcein (Fluorescein complexone)	12.9~13.1	Diluted 1 : 100 with KNO_3
MTB (Methylthymolblue)	11.9~12.5	Diluted 1 : 100 with KNO_3
TPC (Thymolphthalein complexone)	10.4~12.0	Diluted 1 : 100 with K_2SO_4
PC (*o*-Cresolphthalein complexone)	10.5~11.0	0.1% PC in methanol
Calcon (1-(2-Hydroxy-1-naphthylazo)-2-naphthol-4-sulfonic acid)	11.8~12.2	0.5% Calcon in methanol
NN	13.3~13.5	Dotite NN solution

way: Take 10 ml. of a 0.01 M calcium solution and dilute to about 50 ml. with distilled water. Adjust pH and add a small amount of an indicator. Titrate with 0.01 M GEDTA.

The results of these analyses are given in Table II.

TABLE II

Indicator	ca. 0.01 M GEDTA required (ml.)	Nature of end-point
Calcein	10.66±0.01	Sharp
MTB	10.67±0.01	Very sharp
TPC	10.64±0.01	Sharp
PC	10.65±0.06	Fairly sharp*
Calcon	—	Indefinite**
NN	10.67±0.01	Sharp

* Influenced by the amount of the indicator.
** Needs the presence of magnesium.

In the presence of tartrate to prevent the precipitation of magnesium hydroxide, it was investigated whether or not these indicators changed their colors at the end-point and also whether the color changes indicated the accurate quantitative value by this method: Take 10 ml. of a 0.01 M calcium solution and dilute to about 50 ml. with distilled water. Add 2 ml. of a 0.1 M magnesium solution and 2 ml. of a tartrate solution. Adjust pH and add a small amount of an indicator. Titrate with 0.01 M GEDTA.

For Calcein, MTB, TPC and PC, these color changes at the end-point were indefinite. These indicators could, therefore, not be used for this titration.

Calcon was tested according to the procedure proposed by Burg and Conaghan. It changed the color sharply at the end-point. However, because of warming the sample up to about 40°C before the titration, magnesium tended to precipitate. NN was also used in this titration at room temperature, but it took some time for the color to change completely. Both Calcon and NN indicated the correct end-point by MTB in the absence of magnesium.

Masking Agents.—Because many magnesium complexes are the O, O co-ordinated chelates, the suitable masking agents for magnesium at pH 12~13 would be expected to be found among organic substances having oxygen atoms capable of co-ordinating with magnesium. Several masking agents for magnesium were tested; the results were shown in Table III. The test solution was prepared by diluting 10 ml. of 0.01 M calcium and 5 ml. of a 0.01 M magnesium solution to 50 ml. with distilled water and by adding one of the masking agents. The pH value of the solution was adjusted to 13 and 13.5 by potassium and sodium hydroxide. Then we investigated to see whether or not the precipitate was formed at pH 13 and 13.5.

Among the masking agents shown in Table III, tartrate and gluconic acid were found to be the most suitable masking agents for magnesium at pH 13.5.

TABLE III. MASKING AGENTS FOR MAGNESIUM

Masking agent		Precipitation*	
Name	Amount	pH 13	pH 13.5
Glycolic acid (70%)	0.5 ml.	×	×
Lactic acid (75%)	0.5 ml.	○	×
Maleic acid	0.1~0.5 g.	×	×
Potassium sodium tartrate 4 aq. (10%)	2 ml.	○	○
Sodium citrate 2 aq. (10%)	2 ml.	○	×
Aconitic acid	0.1~0.5 g.	×	×
Glucronic acid	0.1 g.	×	×
Glucose (20%)	1 ml.	×	×
Potassium *d*-saccharate	0.1~0.5 g.	×	×
Potassium manno-saccharate	0.1~0.5 g.	×	×
Gluconic acid (50%)	1 ml.	○	○
Mucic acid	0.1 g.	×	×
Sucrose (20%)	1 ml.	×	×
Sodium alginate	0.1~0.5 g.	×	×
Sulfosalicylic acid	0.2 g.	×	×

*×: As soon as the alkaline solution was added, the precipitation occured.
○: The precipitate had not formed after more than about 10 min.

To compare tartrate with gluconic acid, the following experiment was carried out.

A test solution was prepared by diluting 10 ml. of 0.01 M calcium and 2 ml. of 0.1 M magnesium to 50 ml. with distilled water. Then

TABLE IV. TITRATION OF CALCIUM IN THE PRESENCE OF MAGNESIUM WITH GEDTA USING NN INDICATOR

0.01 M Ca taken ml.	0.1 M Mg taken ml.	0.35 M Tartrate taken ml.	ca. 0.01 M GEDTA required ml.	Nature of end-point
10.00	0.0	0.0	10.67±0.01	Very sharp (MTB as an indicator)
10.00	0.0	1.0	—	Indefinite
10.00	0.5	1.0	10.75±0.07	Indefinite (pptd)
10.00	1.0	1.0	10.68±0.01	Sharp
10.00	2.0	1.0	10.69±0.02	Fairly sharp
10.00	0.0	2.0	—	Indefinite
10.00	0.5	2.0	10.72±0.03	Fairly sharp (pptd)
10.00	1.0	2.0	10.67±0.02	Fairly sharp
10.00	2.0	2.0	10.66±0.01	Sharp
10.00	3.0	2.0	10.66±0.01	Sharp
10.00	4.0	2.0	10.67±0.02	Fairly sharp
10.00	5.0	2.0	10.67±0.10	Indefinite (pptd)
10.00	3.0	3.0	10.66±0.05	Sharp
10.00	4.0	3.0	—	Indefinite (pptd)
10.00	4.0	4.0	10.69±0.01	Sharp
10.00	5.0	4.0	10.84±0.15	Indefinite (pptd)
10.00	5.0	5.0	10.67±0.03	Sharp
10.00	6.0	5.0	10.67±0.02	Sharp
10.00	7.0	5.0	10.66±0.03	Fairly sharp
10.00	8.0	5.0	10.71±0.40	Indefinite (pptd)
10.00	8.0	6.0	10.94±0.40	Indefinite (pptd)
10.00	10.0	10.0	—	Indefinite (pptd)
10.00	10.0	12.0	—	Indefinite (pptd)
2.00	7.0	5.0	2.14±0.02	Sharp

2 ml. of a tartrate solution or 2.5 ml. of 5% gluconic acid, 2 ml. of 8 N potassium hydroxide, and a few drops of NN solution were added, and the solution was titrated with 0.01 M GEDTA.

In the presence of gluconic acid, the color change from red to blue at the end-point was proceeding slowly, and the amount of 0.01 M GEDTA was 0.2 ml. smaller than that of the correct end-point as indicated by MTB in the absence of magnesium. On using tartrate, there was a clearer difference than with gluconic acid between the color just before and after the end-point, and the amount of 0.01 M GEDTA consumed was the same as the correct equivalent value.

Magnesium Amount and Tartrate Amount. — With an increase in the concentration of magnesium, the concentration of tartrate should also be increased. The relation between the amounts of magnesium and of tartrate is shown in Fig. 1 and Table IV.

It was found that the maximum concentrations of magnesium and tartrate were 7 ml. of a 0.1 M magnesium solution (about 7×10^{-4} mol.) and 5 ml. of a tartrate solution (about 1.7×10^{-3} mol.).

The color at the end-point upon using the NN solution is light blue and somewhat differs from that of the calcium titration in the absence of tartrate and magnesium.

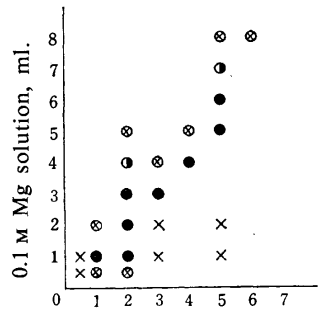

Fig. 1. The relation of magnesium and tartrate amounts.
×: Precipitated.
⊗: Precipitated during the titration and the end-point was indefinite.
●: Given the accurate end-point indicated by MTB in the absence of magnesium.
◑: Given the approximately accurate end-point.

Procedure for Limestone, Dromite and Magnesite.—Pulverize and dry samples for 2 hr. at 110°C and cool in a desiccator. Weigh out 1.0000 g. of each sample and dissolve it in a

TABLE V. DETERMINATION OF CALCIUM AND MAGNESIUM IN LIMESTONE, DROMITE AND MAGNESITE

Sample	Test solution (5 ml.)		Sample (1.0000 g.)	
	0.01 M EDTA* required ml.	0.01 M GEDTA** required ml.	CaO g.	MgO g.
Limestone (Sampo Kozan, Kawakami-gun, Okayama)	19.96±0.01	21.09±0.02	0.5538	0.0044
Limestone (Bisei-cho, Okayama)	19.83±0.01	21.01±0.03	0.5516	0.0034
Dromite (Ikura, Niimi-shi, Okayama)	19.62±0.01	14.83±0.02	0.3894	0.1154
Dromite (Ikura, Niimi-shi, Okayama)	19.21±0.01	18.17±0.02	0.4771	0.0444
Magnesite (Karube, Atetsu-gun, Okayama)	21.90±0.02	0.70±0.05***	0.0092	0.4352

* Factor=1.0007
** Factor=0.9363
*** Test solution: 10 ml.

small amount of dilute hydrochloric acid by heating. If the solution is turbid, leave it to stand for about 12 hours, filter and wash the precipitate with water. Dilute the filtrate in a 250 ml. measuring flask with distilled water. The solution is used as a test solution.

Determination of the Total Amount of Calcium and Magnesium.—Take 5 ml. of the test solution and dilute to about 50 ml. with distilled water. Add 1 ml. of 0.1 M Mg-EDTA, 1 ml. of a buffer solution, 3 drops of a 10% potassium cyanide solution (and triethanolamine, if necessary), and a few drops of a BT solution. Titrate with 0.01 M EDTA.

Determination of Calcium.—For limestone and dromite, take 5 ml. of the test solution and dilute to about 50 ml. with distilled water. Add 2 ml. of a 0.1 M Mg solution, 2 ml. of a tartrate solution, 2 ml. of 8 N potassium hydroxide, 3 drops of 10% potassium cyanide (and triethanolamine, if necessary), and a few drops of an NN solution, and titrate with 0.01 M GEDTA. For magnesite, take 10 ml. of the test solution and dilute to about 50 ml. with distilled water. Add 5 ml. of a tartrate solution and titrate with the procedure mentioned above, or titrate it after adding a known amount of calcium to the aliquot. Calculate by deducting the known amount of calcium. In this paper, the amount of calcium in magnesite was analysed by both two procedures and the two values were averaged.

Determination of Magnesium.—Magnesium is calculated by deducing the calcium from the calcium and the magnesium. The results of the analyses of limestone, dromite and magnesite are given in Table V.

Department of Chemistry
Faculty of Science
Okayama University
Tsushima, Okayama

Studies of Organic Peroxides. VII. The Decomposition of Symmetrically Substituted Benzoyl Peroxides by Iron(II)

By Shigeo HASEGAWA, Norio NISHIMURA, Seiichi MITSUMOTO and Ken'ichi YOKOYAMA

(Received October 10, 1962)

In previous papers[1,2], the rate of the decomposition of benzoyl peroxide catalysed by ferrous ion has been followed by means of analytical and thermal analysis methods. A mechanism involving free radicals has been proposed for the reaction, and the effect of the solvent on the reaction rate has been discussed.

The next step of the study, which seems to be of special interest from the point of view of chemical kinetics, is to investigate the effect of substituents on the peroxide concerning the reaction rate. In this field, some investigators[3,4] have studied the thermal decomposition of many symmetrically-substituted benzoyl peroxides. On the other hand, Orr and Williams[5] and Imoto and Suckon[6] have studied the catalysed decomposition of substituted benzoyl peroxides.

In this report, the rates of decomposition of symmetrically-parasubstituted benzoyl peroxides by ferrous ions will be followed by means of the thermal analysis method. It is confirmed that all the reaction are apparently of the first order, as was the case for the unsubstituted peroxide.

Experimental

All the experiments were carried out in ethanol. In preliminary studies, the presence of water in the reaction system was found to retard the reaction rate to a great extent. One percent of water decreases the reaction rate about half and ten percent of it decreases the rate by a factor of ten. Hence, ethanol was refluxed with calcium oxide for a day, and the water in it was removed with great care.

Ferrous chloride crystals ($FeCl_2 \cdot 4H_2O$) were prepared by the method reported previously[7].

All peroxides were prepared according to the method of Pechmann and Vanino[8] or that of Price and Krebs[9].

Table I lists the peroxides studied, together with pertinent data.

The experimental details were the same as in the previous report[2].

Owing to the poor solubilities of the peroxides in ethanol, the concentration ranges of the peroxides were limited between 0.15 and 0.6 mmol. per liter. The concentrations of ferrous ions in each experiment were taken to be larger than those of the peroxides by a factor of about ten.

Results and Discussion

In the case when a reaction is of the first order, the fundamental equation of the thermal analysis may be given by:

$$\log\left(\frac{dT}{dt}+K\Delta T\right)=\log\frac{Q}{W}\cdot ka-\frac{kt}{2.303} \qquad (1)$$

where dT/dt is the rate of temperature change in the solution, $K\Delta T$ is a correction term for Newtonian cooling, Q and W denote the heat of reaction and the water equivalent of the

TABLE I. SUBSTITUTED BENZOYL PEROXIDES

Peroxide	M. p., °C	Recrystallized by
Benzoyl	106	Chloroform-methanol
Bis-*p*-nitrobenzoyl	156~157	Toluene
Bis-*p*-methoxybenzoyl	126	Ethyl acetate
Bis-*p*-chlorobenzoyl	137~138	Chloroform-methanol
Bis-*p*-methylbenzoyl	129	Chloroform-methanol

1) S. Hasegawa and N. Nishimura, This Bulletin, **33**, 775 (1960).
2) S. Hasegawa, N. Nishimura and K. Miura, ibid., **33**, 1323 (1960).
3) A. T. Blomquist and A. J. Buselli, *J. Am. Chem. Soc.*, **73**, 3883 (1951).
4) C. G. Swain, W. H. Stockmayer and J. T. Clarke, ibid., **72**, 5426 (1950).
5) R. J. Orr and H. L. Williams, *J. Phys. Chem.*, **57**, 925 (1953).
6) M. Imoto and C. Suckon, *Chem. High Polymers (Kôbunshi Kagaku)*, **11**, 396 (1954).
7) S. Hasegawa, N. Hirai, N. Nishimura and T. Kawano, This Bulletin, **31**, 696 (1958).
8) H. V. Pechmann and L. Vanino, *Ber.*, **27**, 1511 (1894).
9) C. C. Price and E. Krebs, "Organic Syntheses", **23**, 65 (1943).

TABLE II. RATE CONSTANT k'* FOR SYMMETRICALLY PARASUBSTITUTED BENZOYL PEROXIDES-IRON(II) REACTIONS IN ETHANOL

Substituent	17°C	22°C	27°C
Bis-*p*-methoxy	2.89±0.10	3.70±0.05	5.04±0.12
Bis-*p*-methyl	2.73±0.03	3.66±0.06	4.76±0.09
Unsubstituted	1.84±0.04 (15°C)	2.49±0.05 (20°C)	3.64±0.06 (25°C)
Bis-*p*-chloro	1.59±0.06	2.40±0.10	3.71±0.06
Bis-*p*-nitro	1.46±0.11	2.15±0.10	3.27±0.17

* Average value in 1. mol^{-1} sec^{-1}

reaction vessel respectively, and a denotes the initial concentration of a reactant concerned.

For the reaction of benzoyl peroxide with ferrous ions, the apparent first order rate constant, k, in Eq. 1 was found to be proportional to the initial concentration of ferrous ions:

$$k = k' [Fe^{2+}]_0 \qquad (2)$$

in which k' is, as was discussed in the previous paper[2], the rate constant of the bimolecular reaction between ferrous ions and benzoyl peroxide. It has also been proposed that the reaction consists of several steps; that is, the primary radical-producing step is followed by radical-induced reactions.

In Table II the values of k' are listed for the reactions between symmetrically parasubstituted benzoyl peroxides and ferrous ions at three temperatures. Using the data in Table II, $\log k'$ was plotted against $1/T$, as is shown in Fig. 1. Straight lines were drawn by means of the least squares method.

The estimated values of the energy and entropy of activation are listed in Table III, together with the values of Hammett's substituent constants[10].

An inspection of Tables II and III will show that there are some relationships between these substituents and the rate of reaction.

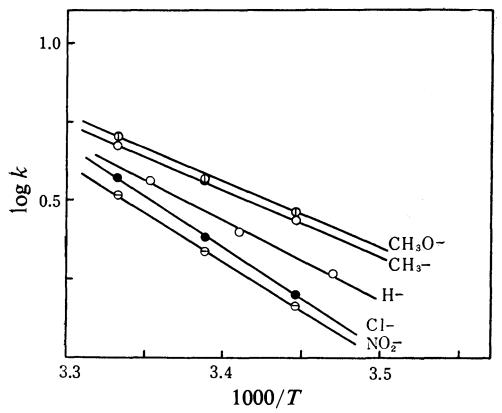

Fig. 1. Arrhenius plot of $\log k'$ against $1/T$.

10) D. H. McDaniel and H. C. Brown, *J. Org. Chem.*, **23**, 420 (1958).

TABLE III. ENERGY AND ENTROPY OF ACTIVATION OF THE FERROUS ION-CATALYSED DECOMPOSITION OF SUBSTITUTED BENZOYL PEROXIDE IN ETHANOL

Substituent	E, kcal./mol.	ΔS^*, e. u. (300°K)	σ
CH_3O-	9.66	−25.2	−0.268
CH_3-	9.70	−25.1	−0.170
H-	11.58	−19.2	0
Cl-	14.77	− 8.7	0.227
NO_2-	14.09	−11.3	0.778

It may be seen that the introduction of an electropositive group at the para position in the benzene nucleus increased the reaction rate, and that an electronegative group caused it to decrease over the range of experimental temperatures. However, it seems more reasonable to discuss the problem in relation to the energy and entropy of activation rather than the reaction rate.

In view of the fact that the activation energies for the spontaneous decomposition of benzoyl peroxides are around 30 kcal. per mole, whereas those for the ferrous ion-catalysed decomposition are around 12 kcal. per mole, there must be a strong interaction between a ferrous ion and the peroxides.

As a ferrous ion approaches a peroxide molecule, there should be interconversion of the translational into vibrational energy, resulting in an activated complex.

Regarding the activated complex, which consists of a ferrous ion and a hydroperoxide, Orr and Williams[5] suggested that the formation of the activated complex would be by coördination and that it would be analogous to an addition reaction.

In our case, a similar formation of an activated complex would be expected to occur. It is quite natural to consider that an electron-attracting group will decrease the availability of the coördinating electrons to which a ferrous ion bonds. Conversely, an electron-repelling group will shift the electrons to the central oxygen atoms, permitting an O-Fe(II) bond to be formed easily; this would lower the activation energy.

According to Rollefson[11], the formation of

11) G. K. Rollefson, *J. Phys. Chem.*, **56**, 976 (1952).

a new normal bond is accompanied by an entropy loss of 30 e. u. in an addition reaction, but if there is only a simple collision process without bond formation, then the entropy loss in activation is 10 e. u. which corresponds to a loss of only one degree of translational freedom.

Therefore, it may reasonably be expected that there would be a range of the entropy of activation between -10 and -30 e. u. in the present reaction series, corresponding to bonds of varying strength formed in the activated complexes. This is in accordance with our data.

For *p*-methyl- and *p*-methoxy-substituted benzoyl peroxide, the entropies of activation have large negative values, indicating the formation of rigid complexes. On the other hand, the small values of the loss in the entropy of activation for *p*-chloro- and *p*-nitro-substituted benzoyl peroxide may indicate weak bond formation in these complexes.

As may be seen in Table III, there also exists a correlation between the entropy of activation and the energy of activation. In Fig. 2, the values for the reaction between benzoyl peroxide and iron(II) are chosen as the standard, and the difference, $\Delta\Delta S^{\neq}$, in the entropy of activation is plotted against the difference, ΔE, in the energy of activation. It may be seen in Fig. 2 that those two quantities are linearly related to each other. From the slope of the best linear line, the isokinetic temperature, β, where all the reaction rates should become identical, is calculated to be 313°K.

In a previous paper[2], the linear enthalpy-entropy relationship has already been discussed, especially in relation to the solvent effect.

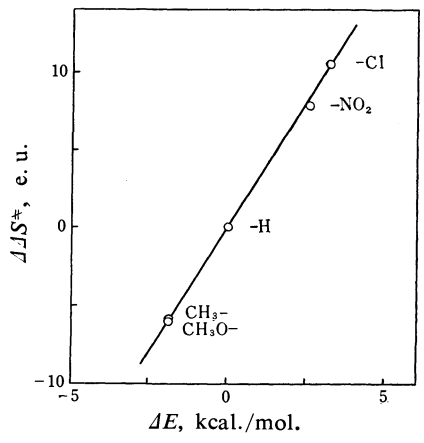

Fig. 2. Relationship between ΔE and $\Delta\Delta S^{\neq}$.

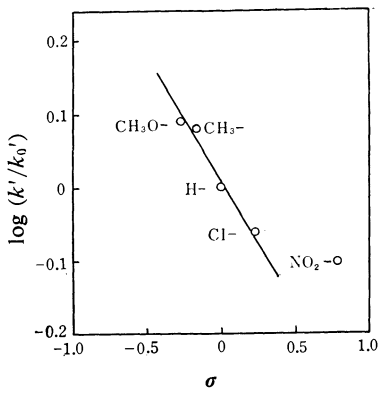

Fig. 3. Hammett's plot of log (k/k_0) against σ.

In Fig. 3, log (k'/k_0') at 27°C is experimentally plotted against σ, where k_0' is the rate constant for the reaction between unsubstituted benzoyl peroxide and iron(II), and the values of k' are those which were estimated from Fig. 1. Allowing for experimental errors, each value seems to fall on a straight line. However, for nitrosubstituted benzoyl peroxide, the deviation is too great to be ascribed to experimental errors.

Blomquist and Ruselli[3], reporting similar results, suggested the possibilities of induced decomposition and a change in the dipole direction. However, further experimental and theoretical information is needed in this field.

Summary

An investigation of the reactions between symmetrically-parasubstituted benzoyl peroxides and iron(II) has been made. From the apparent first order specific reaction rates, which were obtained from the data of the thermal analysis method, the energy and entropy of activation have been estimated. In this reaction series, the linear enthalpy-entropy relationship was observed.

Williams' concept of the coördination of iron(II) to the peroxide molecule was assumed, and the effects of substituents on both the enthalpy of activation and the entropy of activation were discussed. It was also found that the Hammett's equation is approximately applicable, except for nitrosubstituted benzoyl peroxide.

Department of Chemistry
Faculty of Science
Okayama University
Tsushima, Okayama

The Activation of Platinum Electrodes by Preoxidation

By Shigeo SHIBATA

(Received October 15, 1962)

It is well-known[1-11] that the activity of a bright platinum electrode is markedly increased by anodic polarization followed by cathodic polarization. To account for the mechanism of this phenomenon, two theories, the impurity theory[4-7] and the oxidation theory[3,8-12], have been proposed. According to the former theory, the activation is due to the removal of the impurities which have been poisoning the electrode. Indeed, some kinds of impurities, even in very small amounts, poison the platinum electrode considerably[13]. On the other hand, the latter theory attributes the increase in activity to the change of nature of the surface itself caused by the successive formation and reduction of superficial oxide layers.

The present work attemps to elucidate this phenomenon by studying the effects of the conditions of the preoxidation on the decay of the activity.

Experimental

As the test electrodes, a number of square-shaped pieces having an apparent area of 1 cm^2 were cut out of one large plate of bright platinum. Each piece was welded to one end of a fine platinum wire, and the other end of this wire was sealed into a glass tube. The electrodes were cleaned successively with hot concentrated hydrochloric acid, hot concentrated nitric acid, and hot chromic acid and washed with distilled water. Then, after being reduced by cathodic polarization in a sulfuric acid solution, they were aged in a hydrogen atomosphere at room temperature for two weeks.

The electrolyte was 1 N hydrochloric acid for the measurement of the hydrogen overpotential and 1 N sulfuric acid for that of the anodic activation. These electrolytes were prepared from, respectively, water and hydrochloric acid, each distilled carefully several times with a quartz still, and from sulfuric acid distilled twice under reduced pressure. Hydrogen gas was prepared by the electrolysis of a sodium hydroxide solution, and it was freed from oxygen by passage through a column of palladium asbestos. The electrodes were activated by either of the two methods, i. e, the anodic polarization with a 0.1 amp./cm^2 current for 0.25, 1 or 28 hr. or soaking in a chromic acid solution at 80±2°C for 1, 15 or 60 min. The electrodes thus oxidized were washed repeatedly with conductivity water, reduced by cathodic polarization with a 20 mamp./cm^2 current for 200 sec., and then introduced into the cell containing the electrolyte saturated with the hydrogen. After the electrode had thus been let alone for a definite time at open circuit, the hydrogen overpotential was measured in the usual manner against the c. d. in order to determine the activity.

The amount of platinum oxide formed by the anodic polarization or by the soaking in the chromic acid was determined by means of chronopotentiometry with another cell with the electrolyte which was freed from oxyen by passing nitrogen gas of 99.99% purity.

The cells for the measurement of the overpotential and for the chronopotentiometry were of all-glass construction, with anode and cathode compartments separated by a fritted-glass disk, and each was equipped with a gas inlet tube. The reference electrode was a saturated calomel electrode in both cases.

All measurements were carried out in a thermostat of 15±0.1°C. All potentials quoted are on the hydrogen scale.

Results and Discussion

The relation between the c. d., i, and the hydrogen overpotential, η, may be expressed as follows[8,13]:

$$i = i_k - i_a = k' e^{-b'\eta} - k' e^{+b''\eta}$$

where i_k is the cathodic c. d. and i_a, the anodic c. d.

When the value of η is sufficiently small,

$$i = -k'(b' + b'')\eta$$

Since k', b' and b'' are constants for a given electrode, a linear relation should then hold between η and i. The slope, $di/d\eta$, of this straight line is proportional to k' and may be

1) L. P. Hammett, *J. Am. Chem. Soc.*, **46**, 7 (1924).
2) H. T. Beans and L. P. Hammett, ibid., **47**, 1215 (1925).
3) F. P. Bowden, *Proc. Roy. Soc.*, **125A**, 446 (1929).
4) J. O'M. Bockris and I. A. Azzam, *Trans. Faraday Soc.*, **48**, 154 (1952).
5) E. Wieke and B. Weblus, *Z. Elektrochem.*, **56**, 159 (1952).
6) E. Yeager, T. S. Oey and F. Hovorka, *J. Phys. Chem.*, **57**, 268 (1953).
7) J. O'M. Bockris, I. A. Ammer and A. K. M. S. Huq, ibid., **61**, 879 (1957).
8) J. A. V. Butler and G. Armstrong, *J. Chem. Soc.*, **1934**, 743.
9) F. G. Will and C. A. Knorr, *Z. Elektrochem.*, **64**, 258 (1960).
10) F. C. Anson, *Anal. Chem.*, **33**, 934 (1961).
11) F. C. Anson and P. M. King, ibid., **34**, 362 (1962).
12) L. P. Hammett and A. E. Lorch, *J. Chem. Soc.*, **55**, 70 (1933).
13) M. Volmer and H. Wiek, *Z. physik. Chem.*, **175A**, 429 (1935).

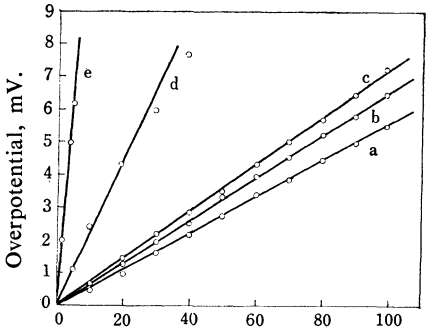

Fig. 1. Hydrogen overpotential against c. d. curves of the electrode activated by anodic prepolarization with 0.1 amp./cm² for 1 hr.

a: Immediatly after the activation
b: After standing for 3 hr.
c: 4 hr. d: 7.5 hr. e: 10 hr.

taken as a measure of the activity of the electrode[8,13]. Typical overpotential-c. d. curves for the electrode activated by means of the anodic polarization are shown in Fig. 1. It may be seen in this figure that the activity decreases with an increase in the aging time. The electrodes have almost identical activity immediately after the activation, irrespective of the pretreatment. However the rate of decay of the activity differed according to the method of pretreatment. Furthermore, in both cases the longer the pretreatment, the slower the decay, as is seen in Fig. 2. If the deactivation or the activation was caused only by either the adsorption or the desorption of the trace of impurities contained in the electrolyte, the rate of decay of the activity would be the same, irrespective of the method of activation. At any rate, it may be inferred from the above experimental facts that the surface texture, depending on the condition of preoxidation, is one of the most important factors determining the behavior of the electrode with regard to the activity. It would be reasonable to postulate that the surface texture of the electrode should be changed by the preoxidation, since the electrode surface is visibly "coarsened" when it is repeatedly oxidized and subsequently reduced, as in the case of the alternating current electrolysis[14,15].

When the electrodes were treated with the chromic acid solution, the amount of platinum oxide formed on the surfaces increased with an increase in the periods of soaking in the solution, as may be seen in Fig. 3. The electrode pretreated anoidically reveals, on the other hand, two rests on the chronopotentiogram (Fig. 4.). The amount of oxide reduced at the potential of the first rest is slightly more than that on the electrode pretreated with the chromic acid. The second rest did not appear until the electrode had beeen preliminarily anodically polarized for a sufficiently long time,

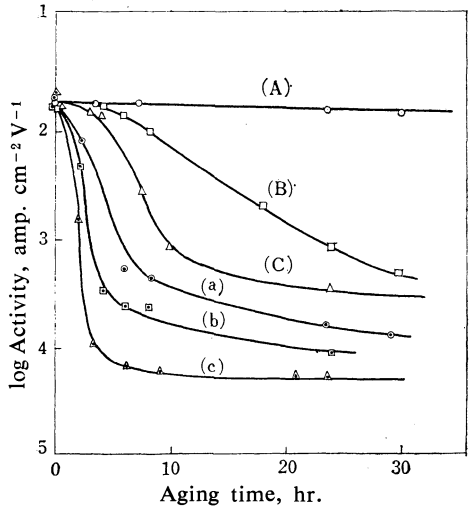

Fig. 2. Time-decay curves of activity.

(A), (B) and (C). For the electrode activated by anodic prepolarization with 0.1 amp./cm² current in 1 N H_2SO_4 for 28, 1 and 0.25 hr. respectively.

(a), (b) and (c). For the electrode activated by pretreatment of chromic acid for 60, 15 and 1 min. respectively.

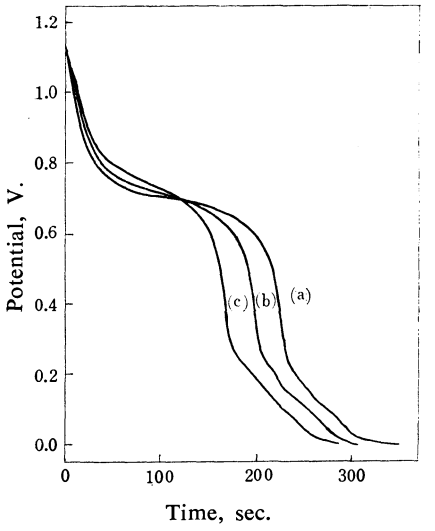

Fig. 3. Cathodic chronopotentiograms for the pretreated with chromic acid for (a) 60, (b) 15 and (c) 1 min. respectively.
i=10 μamp./cm².

14) S. Shibata, *J. Chem. Soc. Japan, Pure Chem. Sec.* (*Nippon Kagaku Zassi*), **79**, 239 (1958).
15) S. Shibata, ibid., **80**, 453 (1959).

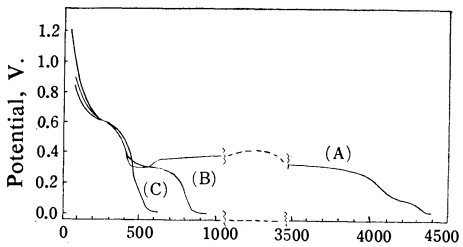

Fig. 4. Cathodic chronopotentiograms for the electrode anodically polarized with 0.1 amp./cm² current in 1 N H_2SO_4 for (A) 28, (B) 1 and (C) 0.25 hr. respectively, $i=10$ μamp./cm².

and the amount of oxide reduced at the potential increased steeply with an increase in the time of the anodic polarization.

The above experimental facts lead the present author to the following hypothesis: as the electrode is oxidized and then reduced, there is formed a very thin layer of unstable atoms, such as a freshly electrodeposited platinum, a layer which has high activity associated with a small crystallization rate[12,16]. The activity decays as the unstable active structure gradually settles down into a more stable state or as, in other words, a sort of recovery takes place in the superficial portion. It would take a long time for a thick activated layer resulting from a thick oxidized layer to recover. It is possible that the electrode is turned so as to be scarcely poisoned at all by the structure change resulting from the preoxidation. In any case, however, it is a reasonable to assume that the structural change itself plays an important part in the activation process.

16) M. Bonnemay, *Z. Elektrochem.*, **59**, 798 (1955).

Summary

The decay of the activity of bright platinum electrodes activated by means both of electrolytic and chemical preoxidations have been studied under a hydrogen atmosphere.

The life of the activity has been shown to depend upon the extent of the oxidation of the surface in the pretreatment. The structural change of surfare caused by the preoxidation appears to be responsibe for the enhanced activity.

Department of Chemistry
Faculty of Liberal Arts and Science
Yamagata University
Koshirakawa-cho, Yamagata

Redox Reaction of Tetrahydrofuran Hydroperoxide

By Shinji MURAI, Noboru SONODA and Shigeru TSUTSUMI

(Received November 24, 1962)

The hydroperoxides of various ethers have been synthesized and their decomposition reactions have been reported by several workers[1]. There have been little reports, however, on the redox reaction of the ether hydroperoxide[2,3]. This investigation was carried out to clarify the nature of the reaction of an ether hydroperoxide, and tetrahydrofuran hydroperoxide (THF-HPO) was used as a starting material since it is readily available by the autoxidation of tetrahydrofuran[4] and can be handled without any explosion. The decomposition reaction of THF-HPO was carried out by using some metal ions such as ferrous or cuprous ion.

1) a) A. V. Tobolsky and R. B. Mesrobian, "Organic Peroxides", Intersicence Pub. Inc., New York, N. Y. (1954); b) A. G. Davies, "Organic Peroxides", Butterworths Pub. Inc. London (1961). There are many other books and reviews.
2) J. Kumamoto, H. E. De La Mare and F. F. Rust, *J. Am. Chem. Soc.*, **82**, 1935 (1960).
3) D. B. Sahrp and T. M. Patrick, *J. Org. Chem.*, **26**, 1389 (1961).
4) H. Rein and R. Criegee, *Angew. Chem.*, **62**, 120 (1950).

Results

THF-HPO was decomposed in the presence of ferrous sulfate at $-2\sim3$°C, and hexane-1,6-diol-diformate (I) and γ-butyrolactone (II) were obtained as the main products, and a small amount of 4-hydroxybutanal (III) was isolated as its 2,4-dinitrophenylhydrazone derivative. Hexane-1,6-diol-diformate (I) might be formed by the dimerization of 3-formoxypropyl radical (IV) produced through the β-fission of the carbon-carbon bond of 2-tetrahydrofuranoxy radical (V).

TABLE I. REACTION OF THF-HPO WITH FERROUS SULFATE

Exp. No.	Reagent		Product[a]		
	THF-HPO g.(mol.)	$FeSO_4 \cdot 7H_2O$ g. (mol.)	Hexane-1, 6-diol-diformate(I) g.(mol.), yield, %	γ-Butyrolactone-(II) g.(mol.), yield, %	4-Hydroxy-butanal(III)[b]
1	10.4(0.10)	27.8(0.10)	1.2(0.007) 13.8	2.7(0.031) 31.4	trace

TABLE II. REACTION OF THF-HPO WITH METAL HALIDES

Exp. No.	Reagent				Product[a]		
	THF-HPO g.(mol.)	CuCl g.(mol.)	$CuCl_2 \cdot 2H_2O$ g.(mol.)	NaCl g.(mol.)	3-Formoxypropyl-chloride(VI) g.(mol.), yield, %	γ-Butyro-lactone(II) g.(mol.), yield, %	4-Hydroxy-butanal (III)[b]
2	13.6(0.13)	12.9(0.13)	22.1(0.13)	—	6.7(0.0055) 42.3	1.9(0.0022) 16.9	trace
3	6.0(0.058)	5.7(0.058)	—	3.4(0.058)	1.7(0.0014) 24.6	1.8(0.0021) 36.8	trace
4	9.0(0.087)	8.6(0.087)	—	—	2.3(0.0019) 21.8	0.7(0.0008) 9.2	trace

a) The yields were calculated from the gas chromatographic analysis of crude products[9].
b) The yields of this product was estimated as less than 1.0 wt. % by the gravimetric determination of its 2, 4-dinitrophenylhydrazone derivative.

In the presence of metal halide, the dimerization of 3-formoxypropyl radical (IV) was not observed, and halogen derivative, trapped by halogen, was obtained as the main product instead of the dimer. For example, when THF-HPO was added to the suspension mixture of cuprous chloride and cupric chloride in water at 0~5°C, 3-formoxypropyl chloride (VI) was produced in a yield of 42.3% being accompanied by γ-butyrolactone (II) (16.9%) and a trace amount of 4-hydroxybutanal (III). The results obtained are summerized in Tables I and II.

Discussion

A hydroperoxide may decompose in a number of different ways when treated with metal ions having variable oxidation numbers. Equations 1 and 2 would be possible in the reaction of hydroperoxide with ferrous (or cuprous) and ferric (or cupric) ions respectively as the first step of the redox reaction.

$$ROOH + Fe^{2+}(\text{or } Cu^{+}) \rightarrow RO\cdot + OH^{-} + Fe^{3+}(\text{or } Cu^{2+}) \quad (1)$$

$$ROOH + Fe^{3+}(\text{or } Cu^{2+}) \rightarrow ROO\cdot + H^{+} + Fe^{2+}(\text{or } Cu^{+}) \quad (2)$$

Equation 1 shows a reaction of a hydroperoxide with a metal ion in its lower oxidation state, such as ferrous (or cuprous) ion, and Eq. 2 shows the reaction with a metal ion in its higher oxidation state. At the reaction temperature of −3~5°C, used in these experiments, the reaction 1 may be preferable from the fact that no reaction was observed between THF-HPO and cupric chloride in water solution below 5°C. Thus, 2-tetrahydrofuranoxy radical (V) seems to be produced as the first step of these reactions.

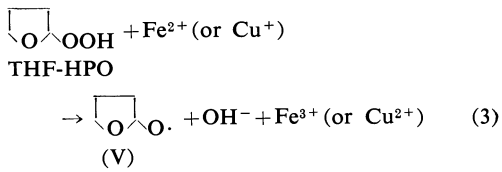

(3)

Several reactions of the radical V would be probable as shown below.

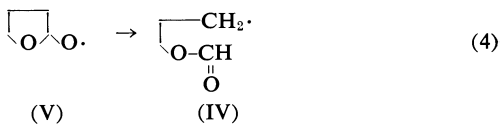

(4)

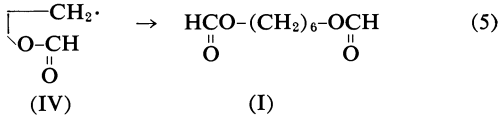

(5)

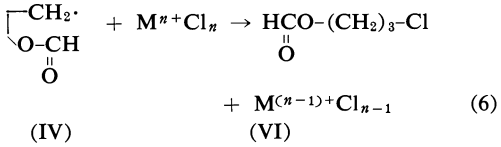

(6)

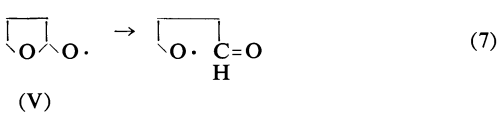

(7)

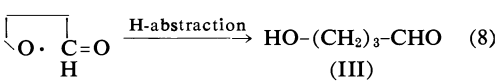

(8)

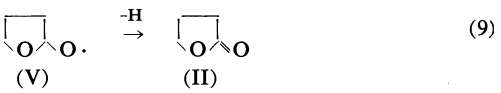

(9)

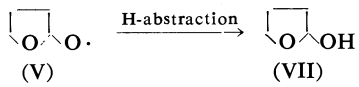

(10)

Equations 4, 7 and 9 show the β-fission of the carbon-carbon, carbon-oxygen and carbon-hydrogen bonds of the 2-tetrahydrofuranoxy radical (V) respectively. Equation 10 is the hydrogen abstraction of the 2-tetrahydrofuranoxy radical (V), giving 2-tetrahydrofuranol (VII).

The 3-formoxypropyl radical (IV) produced in the reaction 4 would dimerize to hexane-1, 6-diol-diformate (I) as shown by Eq. 5. On the other hand, in the presence of additives such as copper chloride, the 3-formoxypropyl radical (IV) gave 3-formoxypropyl chloride (VI) through the path of Eq. 6.

There may be some plausible explanations for such chlorination process. Kumamoto and his coworkers[2] have suggested that the chlorination process is best explicable by chlorine-bridged transition state in which chlorine is transferred to an alkyl radical.

$$R\cdot + M^{n+}Cl_n \rightarrow [R\cdots Cl\cdots M^{n+}Cl_{n-1}]$$
$$\rightarrow RCl + M^{(n-1)+}Cl_{n-1}$$

Recently Minisci[5] has reported the reaction of carbon free radical with some metallic salts and pointed out that such a process may be interpreted by the analogous to that of Sandmeyer's reaction presented by Waters[6]. Kochi[7] has postulated that such a transition state for redox reaction can be well represented as a resonance hybrid between ligand transfer and electron transfer contribution.

$$[R{-}ClM^{+(n-1)} \leftrightarrow R\cdot Cl{-}M^{+n}$$
$$\leftrightarrow R^{\oplus}Cl{-}M^{+(n-1)}]$$

It is considered that the reaction of 3-formoxypropyl radical (IV) would also proceed via the reaction process described above, and dimerization would be inhibited by the more favorable chlorine transfer process.

The reaction 9 gave γ-butyrolactone (II). It might be possible, however, that II was produced through a rather ionic process.

As shown in Eqs. 7 and 8, the product obtained by carbon-oxygen bond fission of 2-tetrahydrofuranoxy radical (V) is 4-hydroxybutanal (III) which is under equilibrium with 2-tetrahydrofuranol (VII). As mentioned above 2-tetrahydrofuranol is also obtained by Eq. 10. The yield of this product is very low and estimated to be less than 1.0 wt. % by 2, 4-dinitrophenylhydrazone gravimetric method. It seems to us from these results that carbon-oxygen bond fission or hydrogen abstraction is more difficult to occur than carbon-carbon or carbon-hydrogen bond fission under these experimental conditions.

From the results of experiments 3 and 4, it is inferred that the addition of chlorine anion has no apparent effect on the yield of 3-formoxypropyl chloride (VI).

Experimental

Material.—THF-HPO[4] used was synthesized by autoxydation of THF at 45°C according to Rein's method. About 20 g. of THF-HPO was obtained from 400 ml. of THF and was purified by distillation, b. p. 40°C/0.2 mmHg. The amount of active oxygen was determined by iodometry, 15.3~15.4% (Calcd. for $C_4H_8O_3$: 15.4%).

Reaction of THF-HPO with Ferrous Sulfate (Exp.1).—To a solution of 27.8 g. of ferrous sulfate heptahydrate in 100 ml. of water was added 10.4 g. of THF-HPO dropwise over the period of 30 min. at −2~3°C under vigorous stirring. The reaction mixture was extracted with ether, and then the extract was dried over anhydrous magnesium sulfate. After the ether was evaporated, the residue was devided into the following two fractions, fraction 1, 2.7 g. of colorless oily liquid: b. p. 102~105°C/27 mmHg, fraction 2, 1.2 g. of colorless oily liquid: b. p. 137~139°C/27 mmHg.

The infrared spectrum of the fraction 1 showed strong bands at 1771 (C=O of lactone) and 1169 cm^{-1} (C-O-C), and was identical with that of γ-butyrolactone (II). This fraction 1 was also identified as II by gas chromatography: column, Silicone DC-550, DNP and PEG; column temperature, 140°C; carrier gas, H_2. The fraction 1 contained 3.7 wt. % of 4-hydroxybutanal (III) identified and determined as its 2, 4-dinitrophenylhydrazone derivative: m. p. 114~115°C (lit.[8] m. p. 116~117°C).

Found: C, 45.44; H, 4.86. Calcd. for $C_{10}H_{12}O_5N_4$: C, 44.78; H, 4.51%.

The fraction 2, b. p. 137~139°C/27 mmHg, was purified by redistillation and showed an identical infrared spectrum with that of an authentic sample of hexane-1, 6-diol-diformate (I): 1720 (C=O) and 1180 cm^{-1} (C-O-C).

Found: C, 55.10; H, 8.12. Calcd. for $C_8H_{14}O_4$: C, 55.16; H, 8.10%.

Reaction of THF-HPO with Cuprous Chloride and Cupric Chloride (Exp. 2).—To the suspension mixture of 12.9 g. of cuprous chloride and 22.1 g. of cupric chloride dihydrate in 100 ml. of water was added dropwise 13.6 g. of THF-HPO over the period of 30 min. under vigorous stirring at 0~5°C. After the reaction mixture was extracted with ether, the ether extract was dried over anhydrous magnesium sulfate, and the ether was removed, and then the residue was separated into two components by the preparative gas chromatography: type, Yanagimoto G. C. G-2, No. 214; column, Silicone DC-550; column temperature, 141.5°C; carrier gas, N_2. The two components were redistilled respectively, fraction 3 of b. p. 65~66°C/27 mmHg and fraction

5) F. Minisci, R. Galli, *Tetrahedron Letters*, p. 533 (1962).
6) D. C. Nonhebel and W. A. Waters, *Proc. Roy. Soc.*, **A242**, 16 (1957).
7) J. K. Kochi, *Tetrahedron*, **18**, 483 (1962).
8) C. L. Wilson, *J. Chem. Soc.*, **1945**, 52.

4 of b. p. 100~105°C/27 mmHg. The fraction 4 was identified as II by gas chromatographic analysis[9]. The infrared spectrum of fraction 3 showed strong absorption bands at 1718 (C=O) and 1180 cm^{-1} (C-O-C) and was identical with that of an authentic sample of 3-formoxypropyl chloride (VI). It shows the same retention time as that of an authentic sample in the gas chromatographic analysis[9]. α-Naphthylurethan derivative of its hydrolysis product, 3-hydroxypropyl chloride, was prepared and mixed melting point with an authentic sample was not depressed, m. p. 76.2~77.2°C.

Found : C, 63.46; H, 5.28. Calcd. for $C_{14}H_{14}O_2 \cdot NCl$: C, 63.76; H, 5.35%.

From the gas chromatographic analysis[9], 8.4 g. of the crude distillate of b. p. 65~102°C/27 mmHg was estimated to contain 6.7 g. of VI and 1.9 g. of II. Compound III was identified and estimated as less than 1.0 wt. % of the crude fraction in the same manner as used in Exp. 1.

Reaction of THF-HPO with Cuprous Chloride and Sodium Chloride (Exp. 3).—To the suspension mixture of 5.7 g. of cuprous chloride and 3.4 g. of sodium chloride in 50 ml. of water was added 6.0 g of THF-HPO at 3~5°C over the period of 25 min. The reaction mixture was treated in the same manner as used above and 3.5 g. of a fraction of b. p. 65~120°C/23 mmHg was obtained. This fraction was estimated to contain 1.7 g. of VI and 1.8 g. of II from the gas chromatographic analysis[9], and also contained a trace of III estimated as less than 1.0 wt. % of this fraction.

Reaction of THF-HPO with Cuprous Chloride (Exp. 4).—To the 8.6 g. of cuprous chloride in 70 ml. of water was added 9.0 g. of THF-HPO at 0~5°C. From the reaction mixture, 3.0 g. of a fraction of b. p. 59~95°C/19 mmHg was obtained. From the gas chromatographic analysis[9], this fraction included 2.3 g. of VI and 0.7 g. of II, and also contained a trace of III identified as its 2, 4-dinitrophenylhydrazone (less than 1.0 wt. % of this fraction).

9) The qualitative and quantative estimations were carried out under the following condition; column, Silicon DC-550; column temperature, 140°C; carrier gas, H_2.

Summary

1) Reaction of tetrahydrofuran hydroperoxide with ferrous sulfate produced hexane-1, 6-diol-diformate (13.8%), which was formed by the dimerization of 3-formoxypropyl radical generated from 2-tetrahydrofuranoxy radical, and γ-butyrolactone (31.4%) and 4-hydroxybutanal (trace).

2) In the presence of metal halide, the dimerization of the 3-formoxypropyl radical did not occur and halogenation of the 3-formoxypropyl radical was observed. For example, when tetrahydrofuran hydroperoxide was reacted with cuprous chloride and cupric chloride, 3-formoxypropyl chloride was obtained in a yield of 42.3%.

3) It is worth nothing that under suitable experimental condition the chloro compound was obtained in a good yield.

4) Probable reaction process was discussed.

The authors wish to thank Dr. Yoshinobu Odaira for his helpful suggestion and encouragement.

Department af Chemical Technology
Faculty of Engineering
Osaka University
Miyakojima-ku, Osaka

The Kinetics of Substitution Reactions Involving Metal Complexes. VIII. Reaction between Copper(II) and Ethylenediaminetetraacetatocobaltate(II) Complexes in Aqueous Solutions

By Nobuyuki TANAKA, Hisao OSAWA* and Minoru KAMADA

(Received November 29, 1962)

In the previous paper[1] the kinetics of the substitution reaction of lead(II) ions and ethylenediaminetetraacetatocobaltate(II) complexes (cabalt(II)-EDTA) was dealt with. The reaction was found to proceed through four simultaneous reaction paths including the reaction paths in which the dissociation of cobalt(II)-EDTA complexes is rate-determining. This kind of rate-determining step was not observed in other substitution reactions[2-8] except the

* Present address: Fuji Electric Mfg. Co., Ltd., Kawasaki.

1) N. Tanaka, H. Osawa, and M. Kamada, This Bulletin, **36**, 67 (1963).

2) H. Ackermann and G. Schwarzenbach, *Helv. Chim. Acta*, **35**, 485 (1952).

3) K. Bril, S. Bril and P. Krumholz, *J. Phys. Chem.*, **59**, 596 (1955); **60**, 251 (1956).

4) N. Tanaka, K. Kato and R. Tamamushi, This Bulletin, **31**, 283 (1958).

5) N. Tanaka and K. Kato, ibid., **32**, 1376 (1959).

6) K. Kato, ibid., **33**, 600 (1960).

7) N. Tanaka and K. Kato, ibid., **33**, 1236 (1960).

8) N. Tanaka and M. Kamada, ibid., **35**, 1596 (1962).

substitution reaction involving nickel(II)-EDTA complexes[9].

In this paper, the kinetic study of the reaction between copper(II) ions and cobalt(II)-EDTA complexes

$$Cu^{2+}+CoY^{2-} \rightleftarrows CuY^{2-}+Co^{2+} \quad (1)$$

is presented.

Derivation of the Rate Equation

In the preliminary experiments that were carried out in the presence of large excess of cobalt(II) ions and cobalt(II)-EDTA complexes over copper(II) ions, the following facts were found out.

(1) In the solutions of the given pH and the given concentrations of $[Co^{2+}]_{0,app}$, $[Cu^{2+}]_{0,app}$ and $[OAc^-]$, the apparent reaction rate of the forward reaction is proportional to the initial concentration of Co(II)-EDTA ($[CoY^{2-}]_0$), and $k^+/[CoY^{2-}]_0$ is independent of $[CoY^{2-}]_0$, where k^+ means the apparent rate constant of the forward reaction, the subscript 0 means zero time, and $[Cu^{2+}]_{app}$ and $[Co^{2+}]_{app}$ represent the apparent concentrations that can be determined polarographically[10]. In the solutions that contain less than 0.2 M of acetate ions, $[Cu^{2+}]_{app}$ and $[Co^{2+}]_{app}$ are given by

$$[Cu^{2+}]_{app}=[Cu^{2+}]+[CuOAc^+]+[Cu(OAc)_2]$$
$$[Co^{2+}]_{app}=[Co^{2+}]+[CoOAc^+] \quad (2)$$

(2) In the solutions of the given pH and the given concentrations of $[Co^{2+}]_{0,app}$, $[CoY^{2-}]_0$ and $[OAc^-]$, the apparent reaction rate is proportional to $[Cu^{2+}]_{0,app}$, and $k^+/[CoY^{2-}]_0$ is independent of $[Cu^{2+}]_{0,app}$.

(3) In the solutions of the given concentrations of $[Co^{2+}]_{0,app}$, $[CoY^{2-}]_0$, $[Cu^{2+}]_{0,app}$ and $[OAc^-]$, $k^+/[CoY^{2-}]_0$ is a linear function of the hydrogen ion concentration, and given by the equation

$$k^+/[CoY^{2-}]_0=k_\xi+k_\eta[H^+] \quad (3)$$

where k_η is dependent on the value of $[Co^{2+}]_{0,app}$.

(4) In the solutions of the given pH and the given concentrations of $[CoY^{2-}]_0$, $[Cu^{2+}]_{0,app}$ and $[OAc^-]$, $k^+/[CoY^{2-}]_0$ is a linear function of the reciprocal of $[Co^{2+}]_{0,app}$ and given by the equation,

$$k^+/[CoY^{2-}]_0=k_\varepsilon+k_\gamma/[Co^{2+}]_{0,app} \quad (4)$$

These observed facts clearly indicate that the mechanism of the reaction between copper(II) ions and cobalt(II)-EDTA complexes would be the same as the reaction between copper(II) ions and lead(II)-EDTA complexes[5] but not the reaction between lead(II) ions and cobalt(II)-EDTA complexes[1].

After the analogy of the reaction between copper(II) ions and lead(II)-EDTA complexes, the present reaction is considered to proceed through three simultaneous reaction paths.

$$\text{(i)}\quad Cu^{2+}+CoY^{2-} \underset{k_1^-}{\overset{k_1^+}{\rightleftharpoons}} CuY^{2-}+Co^{2+} \quad (5)$$

$$\text{(ii)}\quad CoY^{2-}+H^+ \rightleftharpoons CoHY^- \quad (6a)$$

$$Cu^{2+}+CoHY^- \underset{k_{II}^-}{\overset{k_{II}^+}{\rightleftharpoons}} CuHY^-+Co^{2+} \quad (6b)$$

$$CuHY^- \rightleftharpoons CuY^{2-}+H^+ \quad (6c)$$

$$\text{(iii)}\quad CoY^{2-}+H^+ \underset{k_a^-}{\overset{k_a^+}{\rightleftharpoons}} Co^{2+}+HY^{3-} \quad (7a)$$

$$Cu^{2+}+HY^{3-} \underset{k_{III}^-}{\overset{k_{III}^+}{\rightleftharpoons}} CuY^{2-}+H^+ \quad (7b)$$

Assuming that the reaction proceeds through the hydrated ions, the apparent rate of the forward reaction v^+ is expressed as Eq. 8.

$$v^+=k^+[Cu^{2+}]_{app}=\left\{\frac{k_1^++k_2^+[H^+]+k_3^+[H^+]\dfrac{1+K_{CoOAc}[OAc^-]}{[Co^{2+}]_{app}}}{1+\sum_{n=1}^{2}K_{Cu(OAc)_n}[OAc^-]^n}\right\}\times[Cu^{2+}]_{app}[CoY^{2-}] \quad (8)$$

where

$$k_2^+=k_{II}^+K_{CoHY}^H,\quad k_3^+=k_{III}^+/(K_{CoY}K_{HY}) \quad (9)$$

$K_{Cu(OAc)_n}$, K_{CoOAc} and K_{CoY} represent the formation constants of acetatocopper(II), acetatocobalt(II) and cobalt(II)-EDTA complexes, respectively, K_{HY}, the fourth dissociation constant of ethylenediaminetetraacetic acid, and K_{CoHY}^H, the equilibrium constant of Eq. 6a.

Experimental

The preparation of the solutions of copper(II) nitrate, cobalt(II) nitrate, disodium ethylenediaminetetraacetate and sodium acetate-acetic acid buffers was described in the previous paper[10]. Sodium carbonate, acetic acid and other reagents used for the supporting electrolyte were of guaranteed reagent grade and used without further purification.

The rate of the reaction between copper(II) ions and cobalt(II)-EDTA complexes was followed by measuring the change of the polarographic diffusion current of copper(II) ions with time in acetate buffer solutions at 5 and 15°C. The apparatus used was the same as described in the previous

9) N. Tanaka, Y. Sakuma and G. Satô, presented at the 12th Annual Meeting of the Chemical Society of Japan, Kyoto (1959), Lecture No. 1032.

10) N. Tanaka, M. Kamada, H. Osawa and G. Satô, This Bulletin, 33, 1412 (1960).

paper[1]. The experimental procedure was also given previously[4,6,8].

Results

Since the kinetic measurements are carried out in the solutions that contain cobalt(II) ions and cobalt(II)-EDTA complexes in excess over copper(II) ions, the substitution reaction can be treated as a pseudo first-order reaction, and the apparent reaction rate is expressed as

$$-\frac{d[Cu^{2+}]_{app}}{dt}=k^{+}[Cu^{2+}]_{app}-k^{-}[CuY^{2-}] \tag{10}$$

where k^{+} and k^{-} are the apparent rate constants for the forward and the reverse reaction, respectively.

Comparing Eq. 8 with Eq. 10, Eq. 11 is obtained

$$\frac{k^{+}}{[CoY^{2-}]_0}=\left\{\frac{k_1^{+}+k_2^{+}[H^{+}]+k_3^{+}[H^{+}]\dfrac{1+K_{CoOAc}[OAc^{-}]}{[Co^{2+}]_{0,app}}}{1+\sum_{n=1}^{2}K_{Cu(OAc)_n}[OAc^{-}]^{n}}\right\} \tag{11}$$

where the initial concentrations, $[Co^{2+}]_{0,app}$ and $[CoY^{2-}]_0$, are substituted for $[Co^{2+}]_{app}$ and $[CoY^{2-}]$, respectively.

The values of $k^{+}/[CoY^{2-}]_0$ were obtained at various pH's at two different concentrations of cobalt(II) ions but at the same concentrations of other species, and plotted against the hydrogen ion concentration. The plots for 15°C are given in Fig. 1, which indicate linear relations existing between $k^{+}/[CoY^{2-}]_0$ and $[H^{+}]$. Similar relations were observed also at 5°C.

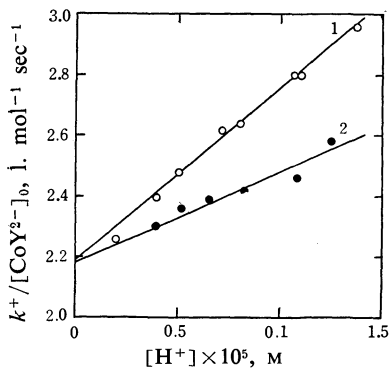

Fig. 1. $k^{+}/[CoY^{2-}]_0$ as a function of the hydrogen ion concentration in acetate buffer-potassium nitrate solutions of ionic strength 0.2 at 15°C. Initial concentrations are: $[Cu^{2+}]_{0,app}=2.0\times10^{-4}$ M; $[CoY^{2-}]_0=5.00\times10^{-3}$ M; $[Co^{2+}]_{0,app}=5.00\times10^{-3}$ M (curve 1) and 15.00×10^{-3} M (curve 2). Concentration of free acetate is 0.10 M.

The rate constants in Eq. 8 were calculated from the plots in Fig. 1, when $K_{Cu(OAc)_n}$ and K_{CoOAc} that were reported in the previous papers[10,11] were employed. With these constants, the rate constants for both elementary reactions 6b and 7b were calculated using Eqs. 9 and the values of K^{H}_{CoHY}, K_{CoY} and K_{HY} which were evaluated with the same procedure as described previously[4,6]. The results were given in Table I.

TABLE I. RATE CONSTANTS FOR REACTIONS 5, 6b AND 7b AT IONIC STRENGTH 0.2

Temp. °C	Rate constant, l. mol^{-1} sec^{-1}		
	k_1^{+}	k_{II}^{+}	k_{III}^{+}
5	7.0	(1.2×10^{2}) a)	(3.1×10^{8}) a)
15	15.3	(1.5×10^{2}) a)	(6.2×10^{8}) a)

a) Values in parentheses are less accurate.

Discussion

The rate constant k_{III}^{+} for the reaction

$$Cu^{2+}+HY^{3-}\xrightarrow{k_{III}^{+}}CuY^{2-}+H^{+}$$

has been determined in the studies of other substitution reactions. These are given in Table II with the value obtained in this study, where it is seen that the value obtained with the substitution reaction between copper(II) ions and cobalt(II)-EDTA complexes is considerably smaller than those obtained with other substitution reactions.

In reaction path iii, the concentration of HY^{3-} is given by

$$[HY^{3-}]=\frac{k_a^{+}[CoY^{2-}]+k_{III}^{-}[CuY^{2-}]}{k_a^{-}[Co^{2+}]+K_{III}^{+}[Cu^{2+}]}[H^{+}] \tag{12}$$

The rate of reaction path iii, therefore, is expressed as Eq. 13, where v_3^{+} and v_3^{-} are the rates of the forward and the reverse reaction of path iii, respectively. When the condition

$$k_{III}^{+}[Cu^{2+}]\ll k_a^{-}[Co^{2+}] \tag{14}$$

is assumed, Eq. 13 can be reduced to a simpler

$$v_3=v_3^{+}-v_3^{-}=\frac{k_a^{+}k_{III}^{+}[CoY^{2-}][Cu^{2+}]-k_a^{-}k_{III}^{-}[CuY^{2-}][Co^{2+}]}{k_a^{-}[Co^{2+}]+k_{III}^{+}[Cu^{2+}]}[H^{+}] \tag{13}$$

11) N. Tanaka and K. Kato, This Bulletin, 33, 417 (1960).

TABLE II. RATE CONSTANT k_{III}^{+} FOR THE REACTION $Cu^{2+}+HY^{3-} \rightarrow CuY^{2-}+H^{+}$ OBTAINED WITH VARIOUS SUBSTITUTION REACTIONS

Substitution reaction	k_{III}^{+}, l. mol^{-1} sec^{-1} 5°C	15°C	Ref.
$Cu^{2+}+PbY^{2-} \rightleftarrows CuY^{2-}+Pb^{2+}$	—	1.7×10^{9}	(5)
$Cu^{2+}+ZnY^{2-} \rightleftarrows CuY^{2-}+Zn^{2+}$	—	2.0×10^{9}	(6)
$Cu^{2+}+CdY^{2-} \rightleftarrows CuY^{2-}+Cd^{2+}$	5.7×10^{8}	1.3×10^{9}	(8)
$Cu^{2+}+CoY^{2-} \rightleftarrows CuY^{2-}+Co^{2+}$	3.1×10^{8}	6.2×10^{8}	This study

TABLE III. CONTRIBUTION OF EACH REACTION PATH TO THE OVERALL REACTION $[Cu^{2+}]_{0,app}=2.0\times10^{-4}$ M, $[CoY^{2-}]_0=5.00\times10^{-3}$ M

$[Co^{2+}]_{0,app}\times10^{3}$ M	Reaction path	A[a] Rate$\times10^{6}$, mol. l^{-1} sec^{-1}	A[a] %	B[b] Rate$\times10^{6}$, mol. l^{-1} sec^{-1}	B[b] %
5.00	i	2.1_9	90	2.1_9	78
	ii	0.0_7	3	0.1_8	6
	iii	0.1_6	7	0.4_3	16
	Total	2.4_2		2.8_0	
15.00	i	2.1_9	95	2.1_9	88
	ii	0.0_7	3	0.1_8	7
	iii	0.0_4	2	0.1_3	5
	Total	2.3_0		2.5_0	

a) $[H^{+}]=3.95\times10^{-6}$ M
b) $[H^{+}]=1.06\times10^{-5}$ M

form and the apparent rate of the forward reaction v_3^{+} is given by

$$v_3^{+}=k_3^{+}\frac{[H^{+}]}{[Co^{2+}]}[Cu^{2+}][CoY^{2-}]$$
$$=k_3^{+}\frac{1+K_{CoOAc}[OAc^{-}]}{1+\sum_{n=1}^{2}K_{Cu(OAc)_n}[OAc^{-}]^{n}}\frac{[H^{+}]}{[Co^{2+}]_{app}}\times[Cu^{2+}]_{app}[CoY^{2-}] \quad (15)$$

In the substitution reaction between copper(II) ions and cobalt(II)-EDTA complexes, the condition given in Eq. 14 was found not to be satisfied. The ratio of $k_a^{-}[Co^{2+}]$ to $k_{III}^{+}[Cu^{2+}]$ $(=(k_a^{-}[Co^{2+}])/(k_{III}^{+}[Cu^{2+}]))$ that was calculated with k_{III}^{+} and k_a^{-} obtained in this and the previous[1] studies respectively ranged from 0.7 to 4 under the experimental condition. When Ep. 14 is not fulfilled, $k^{+}/[CoY^{2-}]_0$ can not be a linear function of $1/[Co^{2+}]_{0,app}$.

The experimental results, however, showed that $k^{+}/[CoY^{2-}]_0$ was proportional to the reciprocal of $[Co^{2+}]_{0,app}$ and independent of $[Cu^{2+}]_{0,app}$. This discrepancy may arise from a small contribution of reaction path iii to the overall reaction. Percentage of the contribution of each reaction path to the overall reaction is given in Table III, which clearly shows that the reaction proceeding through reaction path iii gives only minor contribution to the whole reaction. This fact supports the linearity between $k^{+}/[CoY^{2-}]_0$ vs. $1/[Co^{2+}]_{0,app}$ obtained in the experiments. Consequently, it seems reasonable to consider that the rate constant of reaction path i, k_1^{+}, obtained in this study is acceptable.

It is interesting to compare the substitution reaction between copper(II) ions and cobalt(II)-EDTA complexes with that between lead(II) ions and cobalt(II)-EDTA complexes. In the former the contribution of the reaction path i to the whole reaction is approximately 90%, whereas in the latter it is only several per cents. In reaction path iii, the dissociation of cobalt(II)-EDTA complexes is rate-determining in the reaction between lead (II) ions and cobalt(II)-EDTA complexes but not in the reaction between copper(II) ions and cobalt(II)-EDTA complexes. This suggests that the dissociation of cobalt(II)-EDTA complex is not so slow.

Summary

The kinetic study of the substitution reaction of copper(II) ions and cobalt(II)-EDTA complexes in acetate buffer solutions has been carried out with the same procedure as that reported previously. The reaction was found to proceed, under the experimental conditions, through three simultaneous reaction paths similar to those found in the substitution

reaction of copper(II) ions and lead(II)-EDTA complexes. The rate constants for three elementary reactions of those reaction paths were determined at ionic strength 0.2 at 5 and 15°C. A reaction path in which the dissociation of cobalt(II)-EDTA complex is rate-determining was not observed in this substitution reaction.

The authors thank the Ministry of Education for the financial support granted for this research.

Department of Chemistry
Faculty of Science
Tohoku University
Katahira-cho, Sendai

The Angular Dependency of the ESR Proton Hyperfine Coupling Constant of the CH_2 Group

By Keiji MOROKUMA and Kenichi FUKUI

(Received November 29, 1962)

Recent ESR studies of organic radicals in the solid state have revealed several interesting facts on the structures of these radicals. One of these facts is that, in some radicals, the β protons--the protons in the methyl or methylene groups adjacent to the carbon atom which brings an odd electron—are chemically distinct from each other.

Heller and McConnell[1] have studied the ESR spectra of a γ irradiated single crystal of succinic acid, analyzing them to show that the radical produced was identified as in Fig. 1a and that the coupling constants (nearly isotropic) of the two protons, H_1 and H_2, were

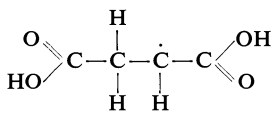

Fig. 1a

not equal. They concluded that the distinction was caused by a kind of deformation of the CH_2 group: the H-C-H angle was no longer bisected by the molecular plane. They assumed the following equation for the angular dependency of the coupling constant of β-protons:

$$a_H(\theta) = \rho_\alpha{}^0 K\cos^2\theta \qquad (1)$$

In the equation, $a_H(\theta)$ is the isotropic hyperfine coupling constant of β protons, $\rho_\alpha{}^0$ is the spin density on the carbon (α carbon) adjacent to the methylene group, and θ is the angle between the carbon pπ orbital on the α carbon and each of the C-H bonds, both

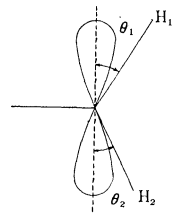

Fig. 2. Projection angles θ_1 and θ_2.

projected to a plane perpendicular to the $C_\alpha-C_\beta$ bond, as is shown in Fig. 2. In this equation they seem to have assumed that the type of deformation would be the rotation of the alkyl group around the $C_\alpha-C_\beta$ axis.

Kurita and Gordy[2] then found a similar distinction between the two protons in a CH_2 group in studying the ESR of the γ irradiated single crystal of L-glycine hydrochloride. In this case the radical was identified as that shown in Fig. 1b, and the coupling constants

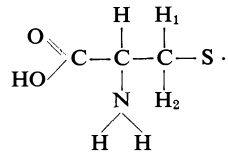

Fig. 1b

were $a_{H_1}=9$ gauss and $a_{H_2}=2$ gauss. If we simply applied Eq. 1 to the discussion of the a_{H_1}/a_{H_2} ratio, the deformation would have to be very large. Pooley and Whiffen[3] have also observed different coupling constants of β protons in the $HOOCCH_2\dot{C}HCOOH$ radical

1) C. Heller and H. M. McConnell, *J. Chem. Phys.*, **32**, 1535 (1960).

2) Y. Kurita and W. Gordy, ibid., **34**, 282 (1961).

3) D. Pooley and D. H. Whiffen, *Mol. Phys.*, **4**, 81 (1961).

from succinic acid (100 Mc and 80 Mc). Jasejà and Anderson[4] have obtained a different pair of unequal coupling constants (115 Mc and 18 Mc) in the same $HOOCCH_2\dot{C}HCOOH$ radical from aspartic acid, attributing the cause of the deformation to intermolecular forces. In both of the papers the deformation angle was discussed by the $\cos^2\theta$ rule.

Recently Ohnishi, Sugimoto and Nitta[5] have carefully studied the temperature dependency of the ESR spectra of the radical in γ-irradiated stretched polyethylene which had been assigned to the allyl-type radical shown in Fig. 1c; they have found that, at a low temperature ($-180°C$), the protons in CH_2 groups adjacent to the allyl group, H_1 and H_2 in the figure, give different isotropic hyperfine coupling constants, that is, 30 and 11 gauss respectively, while at a high temperature

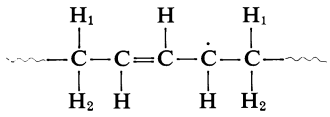

Fig. 1c

($+142°C$) the distinction disappears and the both constants become 21.3 gauss. By using Eq. 1, the calculated θ values of H_1 and H_2 are obtained as 55°02′ and 18°52′. The deviation from the normal angle, 30°, seems irrationally large.

As the mechanism of deformation, the rotation would be more difficult in the case of a methylene group, CH_2R, than in the case of a methyl group, CH_3, because of the bulky group—COOH, alkyl and so forth—attached to the former. Especially in polymeric solids like stretched polyethylene, the R group being a very long chain, the rotation around the $C_\alpha-C_\beta$ axis would be almost entirely hindered. In this case the deformation would be performed by rocking, twisting, or in other ways.

In the present paper considering two typical mechanisms of deformation: one is the rotation around the $C_\alpha-C_\beta$ axis, and the other is the rocking of the CH_2 group on a plane on which normally the two C–H bonds of the CH_2 group exist, we make a valence bond calculation on the spin density on CH_2 protons for their various conformations caused by the rotation and the rocking, in order to see what angular dependency proton hyperfine coupling constants on CH_2 groups obey.

The fact that we assumed rotation and rocking as a source of non-equivalent coupling constants does not necessarily mean that the energy minimum is accomplished by these kinds of deformation. The possibility that one hydrogen is attracted to the odd p orbital, making a bent bond, might be considered, as well as a possibility of twisting. It would be very interesting to study theoretically what is the most stable conformation and why such a deformed conformation could be stable, but the calculation needed in order to explain such a slight difference in conformational energy seems to be excessively complicated, and hence this problem will not be discussed in this paper.

Method of Calculation

In calculating the ground state wave function and the spin density in the state we employed the hypothetical system, consisting of five valence electrons on the five atomic orbitals, as is shown in Fig. 3: the $2p\pi$ orbital (designated by P) on the carbon α in which an odd electron is situated, the two hybridized

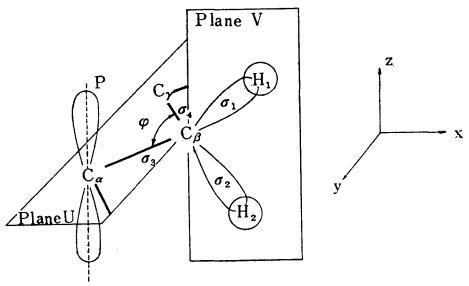

Fig. 3. The model of calculation and the notation used.

orbitals (σ_1 and σ_2) on the carbon β, and the two 1s orbitals (H_1 and H_2) on the two hydrogens which are bonding with the hybridized orbitals, σ_1 and σ_2 respectively. In their normal conformation, the $C_\alpha C_\beta C_\gamma$ chain is situated on the U plane and the two CH bonds are on the V plane, which is perpendicular to the U plane and which bisects the $C_\alpha C_\beta C_\gamma$ angle.

All canonical structures that have the maximum bondings, that is, five structures, are taken as the bases of the valence bond calculation, but all ionic structures were disregarded. This disregard would result in a larger spin density on hydrogen atoms, but we are going to discuss only the relative change of the spin distribution caused by the variation in conformation because of an uncertainty involved in evaluating atomic integrals that will be mentioned later, and in this the disregard does not affect the conclusion.

4) T. S. Jasejà and R. S. Anderson, *J. Chem. Phys.*, **36**, 2727 (1962).
5) S. Ohnishi, S. Sugimoto and I. Nitta, ibid., **37**, 1283 (1962).

Throughout the calculations the deformation is considered to cause the corresponding change in the hybridization of the carbon orbitals making the deformed bonds, and the hydrogen atoms are always regarded as in the direction of the hybridized orbitals, with a CH bond length which is not changed by the deformation.

In treating rotating conformations, the four hybridized orbitals, σ_1, σ_2, σ_3 and σ_4, remain sp^3 hybridized. The calculation of the spin density was made for various rotated angles around the $C_\alpha-C_\beta$ axis.

In treating the rocking conformation, the hybridized orbitals on the carbon β are written with the two parameters a and b. Parameter a corresponds to the variation in the $C_\alpha C_\beta C_\gamma$ angle. The reason why we considered this kind of deformation is that, for instance, regarding the allyl type radical in oriented polyethylene mentioned above, the polyethylene main chain would be fixed, and in order to decrease the strain the allyl radical might change the angle, φ, of $C_\alpha C_\beta C_\gamma$. In our calculations the angle φ is expressed in terms of parameter a, which designates the hybrization of the orbitals, σ_3 and σ_4; a^2 is the s nature of the orbitals σ_3 and σ_4, as can be seen in the following:

$$\varphi=\cos^{-1}[a^2/(a^2-1)] \tag{2}$$

$$\left.\begin{aligned}\sigma_3&=a\psi_{\beta 2s}-\sqrt{(1-2a^2)/2}\ \psi_{\beta 2px}\\&\quad+(\sqrt{2})\ \psi_{\beta 2py}\\\sigma_4&=a\psi_{\beta 2s}-\sqrt{(1-2a^2)/2}\ \psi_{\beta 2px}\\&\quad-(1\sqrt{2})\ \psi_{\beta 2py}\end{aligned}\right\} \tag{3}$$

where $\psi_{\beta 2s}$, $\psi_{\beta 2px}$ and $\psi_{\beta 2py}$ are 2s, 2px and 2py orbitals respectively on the β carbon, the coordinates being taken as in Fig. 3.

In any conformation with a varied a value and with various magnitudes of rocking of the two CH bonds, it is assumed that the $C_\alpha C_\beta C_\gamma$ chain and, consequently, the σ_3 and σ_4 orbitals are always on the U plane, which is perpendicular to the odd p orbital, P, and that the σ_1, σ_2, H_1 and H_2 orbitals are on the V plane, parallel to P and bisecting angle φ. The other parameter, b, is utilized to stand for the hybridization of the σ_1 orbital: b^2 being the s nature of the orbital σ_1, the s nature of the orbital σ_2 is $1-2a^2-b^2$. The exact form of the σ_1 and σ_2 orbitals is written as follows:

$$\left.\begin{aligned}\sigma_1&=b\psi_{\beta 2s}+(\sqrt{2}\,ab/\sqrt{1-2a^2})\psi_{\beta 2px}\\&\quad+(\sqrt{1-2a^2-b^2}/\sqrt{1-2a^2})\psi_{\beta 2pz}\\\sigma_2&=\sqrt{1-2a^2-b^2}\ \psi_{\beta 2s}+(\sqrt{2}a\sqrt{1-2a^2-b^2}\\&\quad/\sqrt{1-2a^2})\ \psi_{\beta 2px}-(b/\sqrt{1-2a^2})\psi_{\beta 2pz}\end{aligned}\right\} \tag{4}$$

Calculations were carried out for the following three values of a:

Series 1: $a=1/2$, i.e., σ_3 and σ_4 are both sp^3 hybridized (s nature: 25%), and, consequently, the $C_\alpha C_\beta C_\gamma$ angle is 109°28′ (normal). The hybridization of σ_1 is varied from sp^3 to p, at the same time as that of σ_2 is varied from sp^3 to sp.

Series 2: $a=1/\sqrt{5}$: σ_3 and σ_4 are both sp^4 hybridized (s nature: 20%), and, consequently, the $C_\alpha C_\beta C_\gamma$ angle is 104°29′, narrower than normal.

Series 3: $a=\sqrt{3/10}$: σ_3 and σ_4 are both s^3p^7 hybridized (s nature: 30%), and the $C_\alpha C_\beta C_\gamma$ angle is 114°23′, more obtuse than normal.

The angles, θ_1 and θ_2, defined in Fig. 2 are easily connected with the parameters, a and b, as follows:

$$\left.\begin{aligned}\tan\theta_1&=ab/\sqrt{1-2a^2-b^2}\sqrt{1-a^2}\\\tan\theta_2&=a\sqrt{1-2a^2-b^2}/b\sqrt{1-a^2}\end{aligned}\right\} \tag{5}$$

The following relationship between the θ_1 and θ_2 angles as a function of parameter a but independent of parameter b will be used in the following section in checking the calculated results:

$$\tan\theta_1\tan\theta_2=a^2/(1-a^2) \tag{6}$$

Matrix elements between the canonical structures are reduced to those between hybridized orbitals by the usual method; they are also reduced to those between atomic orbitals by Eqs. 3 and 4.

The atomic exchange integrals requisite to the calculation are evaluated according to the methods proposed by van Vleck[6] and by

TABLE I. VALUES OF EXCHANGE INTEGRALS EMPLOYED (in unit of eV.)

Exchange integrals between C_β and H	
N_{ss}	2.00
$N_{s\sigma}$	1.82
$N_{\sigma\sigma}$	2.30
$N_{\pi\pi}$	−0.60
Exchange integrals in C_β	
$F_0(2s, 2s)-2F_0(2s, 2p)+F_0(2p, 2p)$	0.430
F_2	0.231
G_1	2.415
Exchange integrals between H_1 and H_2	
$[H_1, H_2]$	Morse function
Exchange integrals between C_β and P	
$N_{\pi ss\pi}$	0.207
$N_{\pi\sigma s\pi}$	−0.253
$N_{\pi\sigma\sigma\pi}$	0.348
$N_{\pi\pi\pi\pi}$	−1.240
$N_{\pi\pi'\pi'\pi}$	0.026

6) J. H. van Vleck, ibid., 1, 219 (1933); 2, 20 (1934).

Karplus et al.[7] The values of the integrals employed are collected in Table I. The N_{rs}'s in the Table are the following exchange integrals between C_β and H_1 or H_2:

$$N_{rs}=-\int\psi_{\beta r}(1)\psi_{H1s}(2)\cdots H\psi_{H1s}(1)\psi_{\beta s}(2)\cdots d\tau \quad (7)$$

H: Total Hamiltonian

and are evaluated from the dissociation energy of methane and the heat of the sublimation of graphite. All N_{rs}'s between C_α and H_1 are neglected because they are small. The F_0's and F_2 and G_1 are the usual one-center atomic integrals of C_β, whose values are deduced from the spectroscopic data of a carbon atom. The exchange integral $[H_1, H_2]$ between H_1 and H_2 is calculated on the Morse function as a function of their interatomic distance. There seems no reliable method available for evaluating the exchange integrals N_{rstu} between C_α and C_β:

$$N_{rstu}=\int\psi_{\alpha r}(1)\psi_{\beta s}(2)\cdots H\psi_{\beta t}(1)\psi_{\alpha u}(2)\cdots d\tau \quad (8)$$

In this paper, except for $N_{\pi\pi\pi\pi}$, the effective two-electron Hamiltonian approximation by Karplus[7] is used, giving the following results:

$$N_{rstu}=\int\psi_{\alpha r}(1)\psi_{\beta s}(2)e^2/r_{12}\psi_{\beta t}(1)\psi_{\alpha u}(2)d\tau_1 d\tau_2 \quad (9)$$

$$\left(\begin{array}{l}\text{for } (r,u)=(2p\pi,\ 2p\pi)\\ \quad\ s,t=2s,\ 2p\sigma,\ 2p\pi'\end{array}\right)$$

As to $N_{\pi\pi\pi\pi}$, Altman's result[8] is adopted.

The overlap integrals between atomic orbitals are entirely disregarded in order to simplify the calculations.

Results and Discussion

The calculated spin densities on protons for rotating conformations of various angles are tabulated in Table II, together with the spin densities on β carbon hybridized orbitals. From the spin density, ρ_H, on the proton, one can calculate the coupling constant, a_H, by the following equation:

$$a_H=Q\rho_H \quad (10)$$

Q being the coupling constant of the proton when ρ_H is unity. In the normal conformation, both θ_1 and θ_2 are 30°. The spin density on a proton does not seem to be dependent only on its own projection angle, θ_1 for instance, but also on the angle of the other proton, for instance θ_2, which one can see by comparing Calculation Nos. 1 and 4, where ρ_H is different for the same θ, 30°. The situation is the same in Calculation Nos. 3 and 5. Roughly speaking, however, it varies in accord with $\cos^2\theta$, as one may see in Fig. 4. In Fig. 4 the $\rho_H=\text{const}\times\cos^2\theta$ curve is drawn so as to fit the calculated result (Calcd. No. 1) at $\theta=30°$. Accordingly, it may be said that the $\cos^2\theta$ rule may be utilized for the hyperfine coupling of CH_2 protons in the rotating conformation.

The spin density on the hybridized orbitals increases with the increased spin density on the proton of the CH bond, as is seen in Table II. Thus, as the isotropic coupling constant of the methylenic proton (deformed by rotation) becomes large, the anisotropy of the coupling will also grow large, though the magnitude of anisotropy seems to be negligibly small.

The results of the calculations for rocking

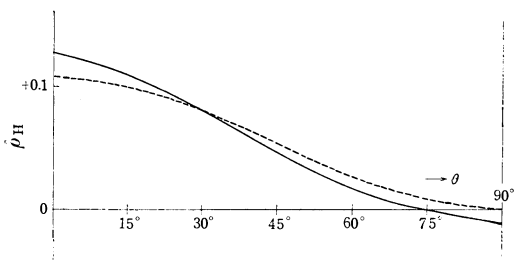

Fig. 4. Angular dependency of proton spin density for rotation.
—: Calculated; ---: const.$\times\cos^2\theta$

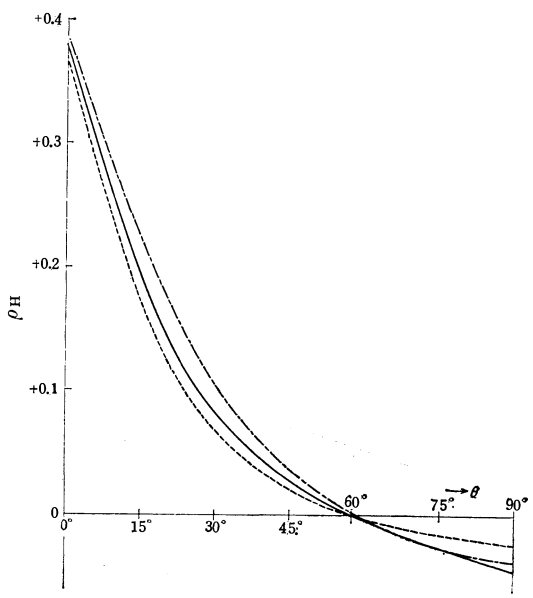

Fig. 5. Angular dependency of proton spin density for rocking.
—: Series 1; -----: Series 2; —·—: Series 3

7) M. Karplus and D. H. Anderson, ibid., **30**, 6 (1959); M. Karplus, ibid., **30**, 11 (1959); H. S. Gutowsky, M. Karplus and D. M. Grant, ibid., **31**, 1278 (1959).
8) S. L. Altman, *Proc. Roy. Soc.*, **A210**, 327, 343 (1951-2).

TABLE II. CALCULATED SPIN DENSITY FOR VARIOUS ROTATING CONFORMATIONS

Calcd. No.	Rotation from normal site	Projection angle		Proton spin density		β Carbon spin density	
		θ_1	θ_2	ρ_{H1}	ρ_{H2}	$\rho_{\sigma 1}$	$\rho_{\sigma 2}$
1	0°	30°	30°	+0.0817	+0.0817	−0.0753	−0.0753
2	10°	20°	40°	+0.1039	+0.0565	−0.0941	−0.0530
3	30°	0°	60°	+0.1262	+0.0108	−0.1124	−0.0098
4	60°	30°	90°	+0.0734	−0.0108	−0.0687	+0.0113
5	90°	60°	60°	+0.0233	+0.0233	−0.0228	−0.0228

TABLE III. CALCULATED SPIN DENSITY FOR VARIOUS ROCKING CONFORMATIONS
(Series 1 : $a^2=1/4$, $\varphi=109°28'$)

Calcd. No.	Parameter b	s Nature of hybridized orbital		Projection angle		Proton spin density		β Carbon spin density	
		σ_1	σ_2	θ_1	θ_2	ρ_{H1}	ρ_{H2}	$\rho_{\sigma 1}$	$\rho_{\sigma 2}$
1	1/2	0.250	0.250	30°00′	30°00′	+0.0817	+0.0817	−0.0753	−0.0753
2	$1/\sqrt{5}$	0.200	0.300	25°14′	35°16′	+0.1097	+0.0567	−0.0988	−0.0531
3	$1/\sqrt{6}$	0.167	0.333	22°13′	39°14′	+0.1273	+0.0422	−0.1129	−0.0399
4	1/3	0.111	0.389	17°09′	47°12′	+0.1719	+0.0178	−0.1465	−0.0167
5	$1/\sqrt{14}$	0.071	0.429	13°16′	54°44′	+0.2094	+0.0017	−0.1723	−0.0009
6	1/5	0.040	0.460	9°40′	62°57′	+0.2491	−0.0119	−0.1975	+0.0129
7	0	0	0.500	0°	90°00′	+0.3829	−0.0459	−0.2662	+0.0497

TABLE IV. CALCULATED SPIN DENSITY FOR VARIOUS ROCKING CONFORMATIONS
(Series 2 : $a^2=1/5$, $\varphi=104°29'$)

Calcd. No.	Parameter b	s Nature of hybridized orbital		Projection angle		Proton spin density		β Carbon spin density	
		σ_1	σ_2	θ_1	θ_2	ρ_{H1}	ρ_{H2}	$\rho_{\sigma 1}$	$\rho_{\sigma 2}$
1	$\sqrt{3/10}$	0.333	0.333	26°34′	26°34′	+0.0816	+0.0816	−0.0752	−0.0752
2	1/2	0.250	0.350	22°54′	30°37′	+0.1035	+0.0626	−0.0936	−0.0586
3	$1/\sqrt{5}$	0.200	0.400	19°28′	35°16′	+0.1280	+0.0453	−0.1133	−0.0430
4	$1/\sqrt{6}$	0.167	0.433	17°14′	38°55′	+0.1455	+0.0348	−0.1268	−0.0333
5	1/3	0.111	0.489	13°24′	46°22′	+0.1827	+0.0182	−0.1538	−0.0177
6	$1/\sqrt{15}$	0.067	0.535	10°01′	54°44′	+0.2207	+0.0058	−0.1792	−0.0058
7	1/5	0.040	0.560	7°37′	61°52′	+0.2529	−0.0048	−0.1991	+0.0049
8	0	0	0.600	0°	90°00′	+0.3786	−0.0277	−0.2631	+0.0280

TABLE V. CALCULATED SPIN DENSITY FOR VARIOUS ROCKING CONFORMATIONS
(Series 3 : $a^2=3/10$, $\varphi=114°23'$)

Calcd. No.	Paramater b	s Nature of hybridized orbital		Projection angle		Proton spin density		β Carbon spin density	
		σ_1	σ_2	θ_1	θ_2	ρ_{H1}	ρ_{H2}	$\rho_{\sigma 1}$	$\rho_{\sigma 2}$
1	$1/\sqrt{5}$	0.200	0.200	33°13′	33°13′	+0.0819	+0.0819	−0.0753	−0.0753
2	$1/\sqrt{6}$	0.167	0.233	28°57′	37°46′	+0.1063	+0.0584	−0.0960	−0.0544
3	1/3	0.111	0.289	22°06′	46°35′	+0.1541	+0.0219	−0.1339	−0.0199
4	$1/\sqrt{15}$	0.067	0.333	16°19′	55°40′	+0.2040	−0.0031	−0.1694	+0.0050
5	1/5	0.040	0.360	12°18′	63°01′	+0.2433	−0.0197	−0.1948	+0.0222
6	0	0	0.400	0°	90°00′	+0.3858	−0.0371	−0.2679	+0.0403

conformations are collected in Tables III, IV and V, together with the spin densities on β carbon hybridized orbitals and the s nature of the latter. The angular dependency of proton spin densities in the case of rocking conformations is entirely different from that in the case of rotating conformations, as is illustrated in Fig. 5. It should be stressed that the $\cos^2\theta$ rule by no means applies to the proton coupling of the methylene group in the rocking conformation; the proton coupling constant varies more rapidly with the projection angle, θ. If one tries to use the $\cos^2\theta$ rule for the rocking methylene group, one will be led to a larger deformation from the normal sites than is really the case. Actually, the rotation,

TABLE VI. OBSERVED HYPERFINE COUPLING CONSTANT AND ESTIMATED PROJECTION ANGLE θ BY SEVERAL METHODS

		H_1 (−180°C)*	H_2 (−180°C)*	H_1 and H_2 (+142°C)*
Observed coupling constant[5]		30 gauss	11 gauss	21.3 gauss
Projection angle θ	$\cos^2\theta$ rule (21.3 gauss is assigned to 30°00′)	impossible	51°32′	30°00′ (assumed)
	$\cos^2\theta$ rule ($K=58$ gauss)	18°52′	55°02′	37°06′
	Rocking deformation ($a^2=1/4$)	24°20′	39°10′	30°00′
	Rocking deformation ($a^2=1/3$)	27°30′	41°49′	33°13′

* Observation temperature

the rocking and other kinds of deformation would take place in the methylene group, which gives unequal proton coupling constants for the two protons. Therefore, minute care should be taken in discussing the deformation angle of the methylene group on the basis of its proton coupling constants.

The proton spin density in the case of this deformation is not simply a function of θ. For instance, the negative spin density on the proton nearly on plane U (for example, −0.0459 in Calcd. No. 7 in Table III) does not seem to originate from the direct interaction of the CH bond with the odd orbital, P, but from the mixing of the interaction of the CH bond with the other CH bond and of the interaction of the latter with orbital P. This is shown by a valence bond calculation of the system consisting of the three atomic orbitals (P, σ and H orbitals of the bond in plane U): the proton spin density in this case is calculated to be −0.0036, which is ten times smaller in magnitude than the spin density shown above.

Actually, there may occur other kinds of deformation than rotation and rocking. So far as the spin density is concerned, other deformations, twisting for instance, might be derived as a mixing of rotation and rocking in the first approximation.

The effect of the $C_\alpha C_\beta C_\gamma$ angle, φ, on the proton spin density may be seen by comparing Table III with Tables IV and V, or in Fig. 5. Generally speaking, the larger value of φ results in the larger (in absolute value) proton spin density for the same hybridization or the same b value, though the difference is relatively small. In a minute discussion this difference should be taken into consideration, but for a rough estimation of the rocking angle, the calculated spin density and its interpolation for the normal φ value (Table III) may safely be used.

The spin density on β carbon hybridized orbitals varies almost in parallel with that on the proton in the bond, as can also be seen in Tables III, IV and V. Thus, the anisotropy of the proton coupling constant becomes important for protons whose projection angle is smaller than 20°.

Application to the Allyl-Type Radical in Oriented Polyethylene

We would like to apply the results of the preceding section to the coupling constants of the two non-equivalent protons in the methylene group adjacent to the allyl-type radical in oriented polyethylene, which were observed by Ohnishi et al.[5] Application to this problem would be appropriate and rational because, as has been mentioned previously, the allyl radical, which is produced midway in an oriented polyethylene molecule, would not be able to rotate because of the long main chain of the molecule, but it would be able to rock, because rocking needs no motion of the main chain.

The coupling constants they observed are given in Table VI, where −180°C is the temperature at which the deformation of the methylene group seems to be entirely frozen to the minima of the potential energy (probably double minima on either side of the normal conformation) and +142°C is the one at which the transformation from one minimum to the other is perfectly free.

At first, for comparison, the $\cos^2\theta$ rule is employed to estimate the projection angle. If 21.3 gauss at +142°C is assumed to correspond to $\theta=30°$, 30 gauss at −182°C cannot be achieved by any θ value (Table VI). On the other hand, if an empirically deduced $K=58$ gauss and the SCF π spin density on the α carbon of allyl radical $\rho_\alpha^0=0.622$ are used for Eq. 1, an unexpectedly large deformation from the normal angle (30°) is obtained (Table VI).

In our valence bond calculation, an odd electron on the π carbon orbital (P) interacting with β CH bonds is treated. However,

in the allyl radical, which is a conjugated system, the number of odd electrons on P is not unity but ρ_α^0. Therefore, instead of Eq. 10, Eq. 11 may be used in the first approximation:

$$a_H = \rho_\alpha^0 \rho_H Q \tag{11}$$

Q is theoretically given as 507 gauss and $\rho_\alpha^0 = 0.622$, as stated above, while a_H is observed, ρ_H can then be calculated, and, consequently, the θ angle will be deduced. However, as the numerical value of the calculated proton spin density, ρ_H, may include some error caused by the approximations employed, e. g., disregard of overlap integrals or of ionic structures, it seems more rational to take ρ_H as compared in its relative value. That is to say, regarding the product, $\rho_\alpha^0 Q$, as a parameter to be decided experimentally, we connect the observed a_H to ρ_H and θ and use one more relation, Eq. 6, to check the consistency of the assignment.

First we assume that the radical has the conformation where $a^2 = 0.250$, that is, $\varphi = 109°28'$. Then the coupling 21.3 gauss at +142°C will correspond to the normal site, $b^2 = 1/4$ and $\theta_1 = \theta_2 = 30°00'$, and from the calculated $\rho_H = +0.0817$ of this case, $Q\rho_\alpha^0$ is obtained as 261 gauss.* Using this, and interpolating the calculated spin density in Series 1 (Table III), the values of θ in Table VI, 24°20' and 39°10', are obtained. This set of θ_1 and θ_2 comes to the relation $\tan\theta_1 \tan\theta_2 = 0.368$ and, with the aid of Eq. 6, $a^2 = 0.269$, which is larger than the assumed value, $a^2 = 0.250$.

Secondly, if the conformation of the radical is assumed to be the case, $a^2 = 0.333$, i. e., $\varphi = 114°23'$; hence we obtain the results in the last line of Table VI and $a^2 = 0.317$, which is smaller than the assumed value.

Thus, the value of a^2 in the allyl radical obtained is between 1/4 and 1/3, and therefore φ lies between 109°28' and 114°23'; a widening of the $C_\alpha C_\beta C_\gamma$ angle from the tetrahedral angle seems to take place in this allyl-type radical. The deformation from the equivalent sites derived by our rocking model is 6° to 9°, which is much smaller and more probable than 18° or more obtained by the $\cos^2\theta$ rule.

By considering the difference of the bond length between the CC single bond and the allyl CC bond, the widening of the $C_\alpha C C_\gamma$ angle is proved to be probable for the radical as a means of reducing the strain[5].

In the present paper we applied our calculations based on the rocking conformations only to the allyl-type radical in polyethylene, but the unequal couplings of some organic radicals in single crystals and in rigid glass also seem to have to be partly reexamined in the light of this finding.

Summary

Valence-bond calculations of the angular dependency of the proton coupling constants of the methylene group in the ESR spectra have been carried out. If the rotation of the group is the only type of deformation, the $\cos^2\theta$ rule by McConnell seems to be valid. If the rocking of the group takes place, however, the angular dependency is entirely different from the $\cos^2\theta$ rule, and the deformation angle based on the rocking model is much smaller than that derived by the $\cos^2\theta$ rule. This finding has been applied to the unequal coupling constants of the two methylene protons of the allyl-type radical in polyethylene.

The authors are much indebted to Dr. Shun-ichi Ohnishi for his showing them his experimental results on the allyl-type radical in polyethylene before publication. Numerical calculations were carried out by means of the KDC-I Digital Computer of Kyoto University.

Faculty of Engineering
Kyoto University
Sakyo-ku, Kyoto

* Here if $\rho_\alpha^0 = 0.622$ is applied, $Q = 420$ gauss is obtained. When we compare this with the theoretical value, 507 gauss, we recognize some effect of disregarding ionic structures, like $C^- H^+$, which makes the calculated spin density on protons larger than it is.

The Electronic Structures and Antioxidizing Activities of Substituted Phenols

By Keiji Morokuma, Hiroshi Kato and Kenichi Fukui

(Received January 7, 1963)

The autooxidation of several organic substance-for instance, petroleum hydrocarbons, rubber and oil-has long been studied by many authors and has been well recognized as a radical chain reaction. Such antioxidants as substituted phenols and anilines work as chain-breaking inhibitors of the peroxy radical:

$$RO_2\cdot + IH \rightarrow ROOH + I\cdot \qquad (1)$$

while the radical I· from the inhibitor is less reactive and can initiate a new chain reaction only with difficulty, as was first discovered by Bolland and ten Haave[1].

From the theoretical point of view, Fueno et al.[2] studied, in the simple LCAO MO approximation of π electronic systems, the relation between the highest occupied π electronic level and the oxidation potential of various hydroxy derivatives of aromatic hydrocarbons, and also the relation between the highest occupied level or the stabilization energy of the transition complex and the antioxidizing efficiency.

In the present paper the antioxidizing activity of substituted phenols is discussed in connection with their σ electronic structure as well as with their π electronic structure.

The π Electronic Structure and Antioxidizing Activity of Substituted Phenols

According to Boozer, Hammond et al.[3-5], the overall inhibition reaction, Eq. 1, does not necessarily mean that the rate determining step of the inhibition is the hydrogen abstraction reaction, for *N*-methylaniline-*N*-*d* and diphenylamine-*N*-*d* showed the same efficiency as the undeuterated compounds. They therefore proposed the following mechanism:

$$\left.\begin{aligned} &RO_2\cdot + IH \rightarrow [RO_2\cdot \leftarrow IH] \\ &\qquad\text{(rate-determining)} \\ &RO_2\cdot + [RO_2\cdot \leftarrow IH] \rightarrow \\ &\qquad\text{inactive product} \end{aligned}\right\} \qquad (2)$$

$[RO_2\cdot \leftarrow HI]$ is a molecular complex between the inhibitor and the radical, and the first complex-formation step is rate-determining. On the nature or structure of the complex no decisive fact seems to have been revealed.

In this section π molecular orbital calculations will be given, and the complex will be discussed. The parameters of the Coulomb and the resonance integrals are as follows: $\alpha_O = \alpha + 0.51\beta$, $\beta_{O-C'} = 0.57\beta$, $\alpha_{C'} = \alpha + 0.05\beta$[6]; $\alpha_{CH_3} = \alpha + 3\beta$, $\beta_{C''-CH_3} = 0.7\beta$, $\alpha_{C''} = \alpha - 0.1\beta$; and $\alpha_{C(adj.\ to\ t\text{-butyl})} = \alpha - 0.2\beta$.

The *t*-butyl group is taken as a purely inductive group, while the methyl group as partly inductive and partly hyperconjugative, hyperconjugation being treated by the well-known one-atom model[7].

The Highest Occupied π Level.—It has often been thought that, no matter what the structure of a molecular complex, the ionization potential of the electron donor and the electron affinity of the acceptor decide the ease of complex formation[8-10]. Some comparisons[11] of the oxidation potential and the antioxidizing efficiency (induction period) have supported this probability. In the molecular orbital sense, the ionization potential is the absolute value of the energy of the highest occupied π orbital. We compared the calculated energy of the highest occupied π level with the relative value of the molecular antioxidizing potency of the 2, 4, 6-substituted phenols measured by Rossenwald et al.[12], as is shown in the third and the

1) J. L. Bolland and P. ten Haave, *Trans. Faraday Soc.*, **2**, 252 (1947).
2) T. Fueno, T. Ree and H. Eyring, *J. Phys. Chem.*, **63**, 1940 (1959).
3) C. E. Boozer and G. S. Hammond, *J. Am. Chem. Soc.*, **76**, 3861 (1954).
4) C. E. Boozer, G. S. Hammond, C. E. Hamilton and J. N. Sen, ibid., **77**, 3233 (1955).
5) G. S. Hammond, C. E. Boozer, C. E. Hamilton and J. N. Sen, ibid., **77**, 3238 (1955).
6) H. H. Jaffé, *J. Chem. Phys.*, **20**, 279 (1952).
7) A. Streitwieser, Jr. and P. M. Nair, "Conference of Hyperconjugation", Pergamon Press, London (1959).
8) R. S. Mulliken, *J. Am. Chem. Soc.*, **74**, 811 (1952).
9) K. Fukui, A. Imamura, T. Yonezawa and C. Nagata, This Bulletin, **34**, 1076 (1961).
10) K. Fukui, A. Imamura, T. Yonezawa and C. Nagata, ibid., **35**, 33 (1962).
11) C. D. Lowry, G. Egloff, J. C. Morrell and C. G. Dryer, *Ind. Eng. Chem.*, **25**, 804 (1933).
12) R. H. Rossenwald, J. R. Hoatson and J. A. Chenicek, ibid., **42**, 162 (1950).

Table I. Antioxidizing potency and π molecular orbital indexes of 2,4,6-substituted phenols

Class	Substituents[a] at position 2	4	6	Relative molecular potency P	Energy of the highest occupied level[b] λ_{ho}	Stabilization energy of the model in Fig. 1 ΔE_1[c]	Stabilization energy of the model in Fig. 2 $S_O^{(R)}$[d]	Total π electron density on oxygen q_O
A	*t*-Bu	Me	*t*-Bu	76.0	0.343	—	2.257	1.9155
	t-Bu	*t*-Bu	*t*-Bu	39.5	0.351	—	2.234	1.9145
B	*t*-Bu	Me	Me	100.0	0.337	3.384	2.281	1.9162
	t-Bu	*t*-Bu	Me	42.5	0.344	3.378	2.258	1.9151
	t-Bu	Me	H	37.5	0.357	3.270	2.190	1.9094
	t-Bu	*t*-Bu	H	33.0	0.365	3.262	2.168	1.9083
	t-Bu	H	H	10.5	0.383	3.235	2.109	1.9018
C	Me	Me	Me	57.0	0.331	—	2.305	1.9169
	Me	Me	H	20.5	0.350	—	2.209	1.9100
	Me	*t*-Bu	Me	18.5	0.338	—	2.282	1.9159
	Me	H	Me	15.0	0.355	—	2.215	1.9095
	Me	*t*-Bu	H	14.5	0.358	—	2.190	1.9089
	H	Me	H	4.0	0.372	—	2.125	1.9039
	H	*t*-Bu	H	3.5	0.380	—	2.106	1.9027
	Me	H	H	3.0	0.375	—	2.130	1.9024
	H	H	H	1.5	0.398	—	2.049	1.8960

a) Me and *t*-Bu stand for methyl and *t*-butyl groups, respectively.
b) λ_{ho} is the coefficient of the energy of the highest occupied level: $\varepsilon_{ho}=\alpha+\lambda_{ho}\beta$
c) In unit of $\gamma^2\beta$
d) In unit of $\gamma^2\beta$

fourth columns of Table I. In the table, the methyl and/or *t*-butyl substituted phenols are divided into three classes—one consisting of 2, 2-di-*t*-butyl phenols (class A), another of 2-*t*-butyl phenols (class B), and the third consisting of phenols with no *t*-butyl group at the 2 and 6 positions (class C). A parallelism between the potency and the energy of the highest occupied π level is observed within each class of compounds, suggesting that the smaller ionization potential will result in an easier formation of the complex and, therefore, in a larger potency. Fueno et al.[2] also compared the highest occupied level and antioxidizing efficiency of some hydroxy derivatives of aromatic hydrocarbons, but they interpreted a similar parallelism in a little different sense. Assuming that the efficiency is fully controlled by the dissociation reaction, ROH$\rightarrow$ RO$\cdot$ + $\cdot$H, and dividing the heat of dissociation into the constant σ electronic contribution and the variable π electronic contribution, ΔH_π(RO–H), they found that, in a simple approximation, ΔH_π(RO–H) is nothing but the energy of the highest occupied level. In this connection, the σ electronic structure and the antioxidizing efficiency will be discussed in the next section. Pederson's ionic model[13] also seems to be certified by this parallelism:

$$RO_2\cdot + IH \rightarrow RO_2^- + IH^+ \qquad (3)$$

13) C. J. Pederson, *Ind. Eng. Chem.*, **48**, 1881 (1956).

but a complete one-electron transfer would be more difficult than a partial electron transfer, which is accomplished in the molecular complex.

The Delocalization Energy of the Complex.— In a more concrete model of the complex proposed by Russel[14,15] and by Walling and Mayahi[16], it is assumed that the peroxy radical will probably approach the inhibitor from the direction perpendicular to the aromatic ring in order to interact with the π electrons on it. If this is true, the delocalization calculation of the molecular complexes[9,10] will be appropriate. Assuming that the radical stays on the axis which stands from the center of the benzene ring and which is perpendicular to the ring and that it interacts with the six π atomic orbitals on it to the same extent (cf. the assumed model of the complex shown in Fig. 1), we obtain the following stabilization energy, ΔE_1, of this model by the perturbation treatment:

$$\Delta E_1=\left(\sum_i^{occ}-\sum_i^{unocc}\right)\frac{(\sum_r C_{ir})^2}{\lambda_i}\gamma^2\beta \qquad (4)$$

where $\gamma\beta$ is the resonance integral between the half-occupied orbital of peroxide and a π AO

14) G. A. Russel, *J. Am. Chem. Soc.*, **79**, 2977 (1957); **80**, 4987, 4997, 5002 (1958).
15) G. A. Russel, *Tetrahedron*, **8**, 101 (1960).
16) C. Walling and M. F. Mayahi, *J. Am. Chem. Soc.*, **81**, 1485 (1959).

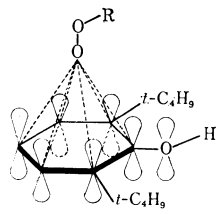

Fig. 1

on the ring, and $\sum_r$ should cover all the AO's on the benzene ring of the compound. The results shown in the fifth column of Table I seem to allow this possibility, too. The charge is transferred from the inhibitor to the peroxy radical in this model.

Another model of the complex would be such as is illustrated in Fig. 2, in which the peroxy

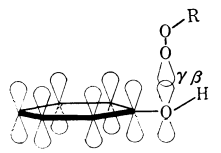

Fig. 2

radical approaches the phenol oxygen so as to interact with the pπ orbital on it. If the peroxy radical is assumed to have one atomic orbital and one electron available to conjugation with the inhibitor, the stabilization energy of the interaction by the second order perturbation treatment is nothing but the superdelocalizability of the oxygen for the radical reaction, $S_O^{(R)}$ *,[17]:

$$S_O^{(R)} = \left(\sum_i^{occ} - \sum_i^{unocc}\right) \frac{(C_{iO})^2}{\lambda_i} \qquad (5)$$

Setting this model, Fueno et al.[2] found a good linear relationship between the logarithm of relative antioxidizing efficiency proposed by Bolland and ten Haave[1] and the superdelocalizability for several unsubstituted phenols**.

We calculated the superdelocalizability, $S_O^{(R)}$, for this series of compounds, obtaining a good parallelism with the potency in each class, as is shown in the sixth column of Table I. Thus, the model in Fig. 2 may be one of the possible structures of the complex in Eq. 2.

Some inhibitor radicals produced by the reaction, Eq. 1 or 2, may sometimes initiate a new chain reaction as follows[19,20]:

$$I\cdot + RH \rightarrow IH + R\cdot \qquad (6)$$

or

$$IO_2\cdot + RH \rightarrow IOOH + R\cdot \qquad (7)$$

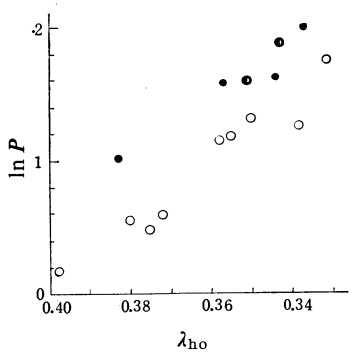

a) The highest occupied level

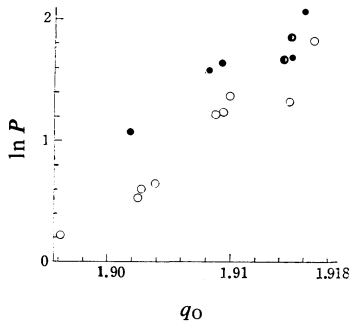

b) Total π electron density on oxygen atom

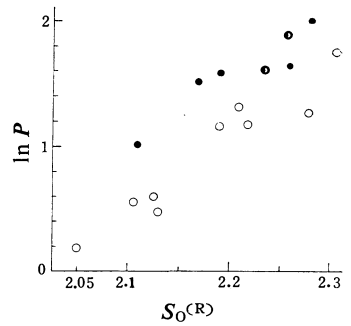

c) Superdelocalizability on oxygen atom for radical attack

Fig. 3. Linear relationship between logarithm of antioxidizing potency and reactivity indexes.
(◐, group A; ●, group B; ○, group C)

17) K. Fukui, T. Yonezawa and C. Nagata, This Bulletin, **27**, 423 (1954).

* As the interacting orbital is not the pseudo-π orbital but the half-occupied orbital of the peroxy radical, the quantity should be rather named "delocalizability" instead of "superdelocalizability".

** In their paper the formula for the transferred charge includes a part of the fourth-order terms mixed with the following correct second order term[18]:

$$\Delta q(\text{second order}) = \left(\sum_i^{occ} - \sum_i^{unocc}\right) \frac{(C_{iO})^2}{(\lambda_i)^2} \gamma^2$$

18) K. Fukui, T. Yonezawa and C. Nagata, *J. Chem. Phys.*, **27**, 1247 (1957).

19) A. F. Bickel and E. C. Kooyman, *J. Chem. Soc.*, **1956**, 2215; **1957**, 2415.

20) W. A. Waters and C. Wickham-Jones, ibid., **1951**, 812.

Ingold[21] has recently proposed to classify the inhibitors into two groups: one, "strong" inhibitors which react very rapidly with the peroxy radical to break the chain reaction, and the other, "efficient" inhibitors each of whose phenoxy radical produced by the reaction (Eq. 1 or 2) is stable enough not to initiate any new chain reaction. Sterically hindered inhibitors are "efficient" inhibitors, for their phenoxy radical is protected from the reactions to follow.

It would be interesting here to discuss the difference in potency among the classes. In Fig. 3 are plotted the calculated indexes against the logarithm of potency. With regard to each index the plots of class A and of class B fall on one line, while those of class C fall on another line. Compounds of classes A and B are both restricted with the bulky *t*-butyl group. The linear relationship found in both these two classes seems to suggest that the restriction would be enough by one *t*-butyl substitution. Judging from the models, the calculated indexes seem to represent only the "strength" of the inhibitors; therefore, the difference, which is estimated from Fig. 3 to be of the order of $\Delta \log P = 0.4$, should probably be attributed to the difference in the "efficiency".

The Total π Electron Density on the Oxygen Atom. — The total π electron density on the oxygen atom, q_O, has also been calculated; as given in the last column of Table I and in Fig. 3b, it is found to possess a good parallelism with the antioxidizing potency. Since, in a radical reaction such as the attack of the peroxy radical, the total π electron density can no longer be the reactivity index, this parallelism would have to be interpreted as indicating that the electron density may affect some other quantity which in turn, has a direct influence upon the reaction. In the next section the total electron density will be taken as affecting the σ electronic structure of the O-H bond.

The σ Electronic Structure and Antioxidizing Activity of Phenols

In this section σ molecular orbital calculations on phenol will first be presented, and then the antioxidizing activity will be discussed in connection with the σ electronic structure.

LCAO MO calculations of the σ electronic structure of conjugated molecules have been carried out with respect to hydrocarbons[22], halides[23] and aldehydes[24], while the parameters of the Coulomb and the resonance integrals of hydrogen and carbon atoms had been determined already[22]. The parameters for phenolic oxygen have been determined to be as follows*: the Coulomb integral of oxygen is settled to be $\alpha_\sigma + 0.3\beta_\sigma$ in accord with that of aldehyde oxygen, β_{O-O} (one center) $= 0.29\beta_\sigma$ from the σ MO treatment of alcohols and peroxides[25], $\beta_{C-O} = 0.6\beta_\sigma$, in accord with the small overlap integral $S(C_{sp^2} - O_p,\ 1.43\text{Å}) = 0.37$, in comparison with $S(C_{sp^2} - C_{sp^2},\ 1.34\text{Å}) = 0.77$ and $\beta_{OH} = 0.7\beta_\sigma$, also with reference to $S(O_p - H_s,\ 0.96\text{Å}) = 0.35$. To make the results more reliable, a calculation with another parameter, $\beta_{OH} = 1.1\beta_\sigma$, has also been made.

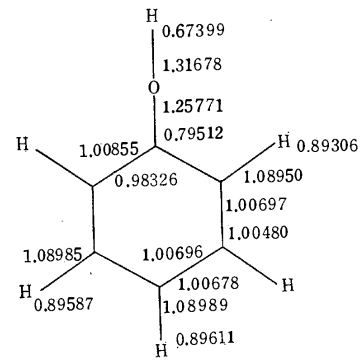

Fig. 4. Total σ electron density of phenol ($\alpha_O = \alpha_\sigma + 0.3\beta_\sigma$, $\beta_{OH} = 0.7\beta_\sigma$).

Figure 4 gives the calculated total σ electron density of phenol, where we can see a clear inductive effect of the oxygen atom. The small σ electron density and, accordingly, the large net positive charge on phenolic hydrogen seem to correspond to its strong acidity. In Table II are gathered the reactivity indexes—delocalizabilities, $D_H^{(N)}$, $D_H^{(E)}$ and $D_H^{(R)}$, for

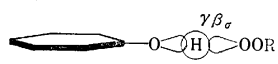

Fig. 5

nucleophilic, electrophilic and radical abstractions of phenolic and para hydrogens, corresponding to the model in Fig. 5. The definition of D_H is as follows[29]:

$$D_H = \sum_i^{\text{all}} (\nu_i - k) \frac{(C_{iH}^\sigma)^2}{\lambda_i^\sigma} \qquad (8)$$

21) K. U. Ingold, *Chem. Revs.*, 61, 563 (1961).
22) K. Fukui, H. Kato, T. Yonezawa, K. Morokuma, A. Imamura and C. Nagata, This Bulletin, 35, 38 (1962).
23) K. Morokuma, K. Fukui, T. Yonezawa and H. Kato, ibid., 36, 47 (1963).
24) K. Fukui, K. Morokuma, H. Kato and T. Yonezawa, ibid., 36, 217 (1963).
25) K. Fukui and H. Kato, to be published.
* α_σ and β_σ are the standard Coulomb and the standard resonance integrals of carbon sp^2 orbitals[22].

TABLE II. DEPENDENCY OF σ DELOCALIZABILITY OF HYDROGEN ON PARAMETER

β_{OH}		$0.7\beta_\sigma$		$1.1\beta_\sigma$	
Position of hydrogen		para	phenolic	para	phenolic
Total σ electron density q_H^σ		0.8961	0.6740	0.8961	0.7852
Delocalizabilities[a]	$D_H^{(E)}$	1.2058	0.9529	1.2058	0.7271
	$D_H^{(R)}$	1.1967	1.4949	1.1968	0.9618
	$D_H^{(N)}$	1.1876	2.0369	1.1877	1.1964

a) In unit of $\gamma^2\beta_\sigma$

TABLE III. CHANGE OF σ REACTIVITY INDEXES OF HYDROGEN ABSTRACTION

α_O		$\alpha_\sigma+0.3\beta_\sigma$		$\alpha_\sigma+0.25\beta_\sigma$	
Delocalizability[a]		$D_H^{(R)}$	$D_H^{(R)}(0.3)$	$D_H^{(R)}$	$D_H^{(R)}(0.3)$
Positions	phenolic	1.4949	1.5955	1.4952	1.6992
	ortho	1.2112	1.5050	1.2098	1.5084
	meta	1.1982	1.5041	1.2120	1.5046
	para	1.1967	1.5067	1.1966	1.5069

a) In unit of $\gamma^2\beta_\sigma$

where ν_i is the number of electrons on the ith σ MO, λ_i^σ is the coefficient of the energy, ε_i^σ, of the ith σ MO, $\varepsilon_i^\sigma=\alpha_\sigma+\lambda_i^\sigma\beta_\sigma$ and $k=0, 1, 2$, according to electrophilic, radical, nucleophilic reactions respectively, and the energy of the reagent X is assumed to be equal to α_σ. If we assume that the change in the reactivity index will be proportional to the square of β_{OH}, as in Fig. 6, $(\beta_{OH})^2$ must be smaller than $0.9(\beta_\sigma)^2$ in order to agree with the experimental findings that phenolic hydrogen is more liable than *p*-hydrogen to radical abstraction reactions. Our choice, $\beta_{OH}=0.7\beta_\sigma$, is supported by this finding.

Now we are going to discuss the relation between the σ electronic structure and antioxidizing activity. Experimentally, either no isotope effect or only a small one on activities have been observed between substituted phenols and their *O*-deuterated species[21] more than between aromatic amines and their *N*-deuterated derivatives[3-5]. Therefore, the molecular complex formation has been considered to be rate-determining. However, there are also some reports which have reported some isotope effects[26,27]. Furthermore, if the earlier stage of the hydrogen abstruction reaction is the transition state of antioxidation, there would naturally be little isotope effect. It would be worth while to study the possibility of such a mechanism. The delocalizability would be capable of being a measure of this mechanism, since this index is derived from a model in Fig. 5 composed of a molecule and a reagent weakly interacting with each other, upon perturbation treatment.

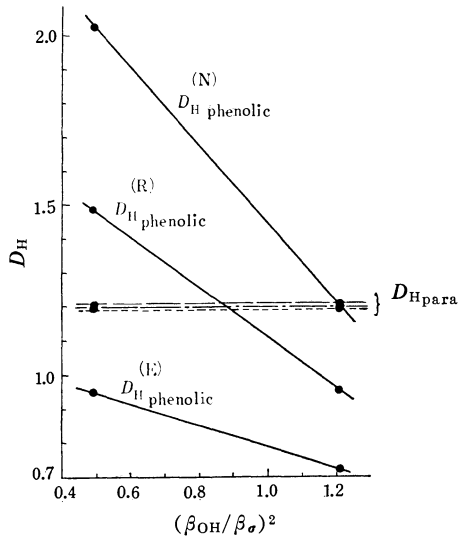

Fig. 6. Crossing of delocalizability of phenolic and para hydrogens.

For an attack of the peroxy radical, a quantity named $D_H^{(R)}(0.3)$ would be more appropriate than $D_H^{(R)}$;

$$D_H^{(R)}(0.3)=\left(\sum_i^{occ}-\sum_i^{unocc}\right)\frac{(C_{iH}^\sigma)^2}{\lambda_i^\sigma-0.3} \qquad (9)$$

This index fits the model in Fig. 5 if the Coulomb integral of the orbital X is equal not to α_σ (in the case of $D_H^{(R)}$) but to $\alpha_\sigma+0.3\beta_\sigma$, the Coulomb integral of the oxygen atom. As is shown in Table III, the high reactivity of phenolic oxygen is indicated also by $D_H^{(R)}(0.3)$. Although all ring hydrogens have almost the same reactivities, the relative reactivity of each position seems to show a slight

26) J. R. Shelton and E. T. McDonel, *J. Polymer Sci.*, 32, 75 (1958).
27) J. R. Shelton, E. T. McDonel and J. C. Crano, ibid., 42, 289 (1960).

difference according to the index, $D_H^{(R)}$ or $D_H^{(R)}$ (0.3).

The parallelism between the total π electron density on oxygen and the antioxidizing activity, which we demonstrated in the previous section, might be interpreted as follows: the total π electron density on the oxygen atom, increased by methyl and *t*-butyl substitutions, will necessarily decrease the electronegativity of the oxygen and make the Coulomb integral of the σ orbitals on oxygen more positive. This change in the Coulomb integral then causes the changes in the σ electronic structure of phenol, especially at the O–H bond. Tentatively putting the Coulomb integral of the oxygen σ orbital as equal to $\alpha_\sigma+0.25\beta_\sigma$, instead of its normal value $\alpha_\sigma + 0.3\beta_\sigma$, we obtain the values of the indexes $D_H^{(R)}$ and $D_H^{(R)}$ (0.3) shown in Table III. As one can clearly see in the table, for an ordinary radical attack, in which $D_H^{(R)}$ would be the index, the reactivity of phenolic hydrogen would hardly be influenced by the change in the total π electron density of oxygen, while for an electronegative radical (such as the peroxy radical) attack, in which $D_H^{(R)}(0.3)$ would be the index, the reactivity is much elevated by an increased π electron density on oxygen.

In order to discuss the change in reactivity, the difference in the calculated total π electron density in Table I should be translated into the difference in $D_H^{(R)}(0.3)$. The change in the Coulomb integral $\Delta\alpha$ caused by the change in the electron density, Δq, on the atom is often estimated by the equation:

$$\Delta\alpha=\omega\Delta q \qquad (10)$$

where ω is a proportionality constant and would have a value ranging from $0.2\beta_\sigma\sim2\beta_\sigma$*. The difference in the total π electron density between the largest and the smallest (phenol) ones in Table I, 0.02, would make the change in the Coulomb integral $\Delta\alpha=0.004\beta_\sigma\sim0.04\beta_\sigma$. Since the change in $D_H^{(R)}$ (0.3) would be proportional to the change in the Coulomb integral, the difference in $D_H^{(R)}$ (0.3), 0.1037, for $\Delta\alpha_0=0.05\beta_\sigma$ (in Table III) would make $\Delta D_H^{(R)}(0.3)=0.0083\sim0.0830$ between the most reactive and the least reactive compounds. These magnitudes of the difference seem to be almost sufficient to explain the experimental differences in antioxidizing activity.

Summary

We have tested several models and their molecular orbital indexes of the rate-determining step of antioxidization by substituted phenols. Some molecular complex models have been found to be rational, though the problem of which of them is actually the true mechanism of the chain-breaking inhibition of autooxidation cannot yet be settled. Another possibility, that the earlier stage of the hydrogen abstraction reaction may be the rate-determining step, cannot yet be abandoned.

The numerical calculations have been carried out on the KDC-I digital computer of Kyoto University.

Faculty of Engineering
Kyoto University
Sakyo-ku, Kyoto

* ω is the difference in the Coulomb integral between the two states, one of which has one more electron than the other. The difference, which is interpreted as being that between the ionization potential and the electron affinity of oxygen in its valence state, would be about 15 eV.[28] As the unit $\beta\sigma$ is estimated to be ca. -7 eV.[23], ω would be ca. $2\beta\sigma$. On the other hand, the ω value, which is often used in π electronic calculations is $0.5\beta\pi\sim2\beta\pi$, and, referring to the ratio $\beta\pi/\beta\sigma\sim1/3$[23], $\omega=0.2\beta\sigma\sim0.7\beta\sigma$ seems to be rational.

28) H. O. Pritchard and H. A. Skinner, *Chem. Revs.*, 55, 745 (1955).
29) K. Fukui, H. Kato and T. Yonezawa, This Bulletin, 34, 1111 (1961).

Magnetic Study of the Amino Group

By S. SRIRAMAN and D. SHANMUGASUNDARAM

(Received November 29, 1962)

The theoretical evaluation of the magnetic susceptibility may be done in two different ways (1) either by considering the atomic contribution of the constituent atoms of the molecule together with suitable constitutive correction or (2) by taking the compound as ionic and adding the contribution of ions. The former one has had wider applications than the latter. In the additive method the process suggested by Ingold[1] seems to be preferable due to the fact that it allows for the calculation, the contribution of atoms and multiple bonds as if there were no interactions. The difference between such calculated value and the experimental value is attributed as due to the interaction or conjugation involved in the system. The method suggested by Yang[2] on the other hand treats the shared electron in the covalent bond as ionic and the structures of molecules of covalent compounds are explained accordingly. But the method has got its own limitations as Yang himself pointed out that it requires, for example, different sets of paramagnetic susceptibilities for carbon ion. Still the method enables one to evaluate the contribution of different ions to the magnetic susceptibility.

In the present investigation, an attempt is made to evaluate the contribution due to NH_2^{1+}. Using this data, the χ_M of different compounds are calculated and compared with the experimental values and with theoretical values calculated by using the atomic and bond values suggested by Ingold. Any difference found from the experimental value has been explained as arising due to conjugation and interaction involved in the system. The contribution due to NH_2^{1+} can be found either from primary amines or from amino acids. In this investigation primary amines both aliphatic and aromatic have been studied.

Experimental

The substances used were mostly Merck G. R. or B. D. H.; A. R. The liquids were all distilled and collected exactly at the corresponding boiling

TABLE I*

S. No.	Substance	χ_S		χ_M Exptl.	χ_M Calcd.	$\Delta\chi_M$	χ_M-Others
1	Ethylenediamine	0.775	±0.002	46.58	46.40	+0.18	
2	1, 2-Propylenediamine	0.780	±0.002	57.82	58.20	−0.38	
3	Amylamine	0.834	±0.001	72.73	73.30	−0.57	69.4[3]
4	Benzylamine	0.699	±0.001	74.91	74.80	+0.11	72.01[4]
5	Ethanolamine	0.689	±0.002	42.08	42.50	−0.42	
6	*o*-Chloroaniline	0.623	±0.002	79.49	77.70	+1.79	
7	*m*-Chloroaniline	0.600	±0.002	76.56	77.70	−1.14	
8	*p*-Chloroaniline	0.609	±0.002	77.69	77.70	−0.01	
9	*o*-Ethylaniline	0.713	±0.002	86.42	87.00	−0.58	
10	*p*-Ethylaniline	0.700	±0.002	84.84	87.00	−2.16	
11	*o*-Anisidine	0.644	±0.001	79.34	79.80	−0.46	80.56[5]
12	*m*-Anisidine	0.625	±0.001	77.00	79.80	−2.80	
13	*p*-Anisidine	0.629	±0.001	77.50	79.80	−2.30	
14	*o*-Nitroaniline	0.482	±0.002	66.56	69.30	−2.74	66.47[6], 66.37[7], 68.42[8]
15	*m*-Nitroaniline	0.506	±0.001	69.88	69.30	+0.58	70.19[6], 67.76[7], 68.96[8]
16	*p*-Nitroaniline	0.479	±0.002	66.15	69.30	−3.15	60.42[6], 66.24[7], 66.82[8]

* All susceptibility values in this paper refer to diamagnetic susceptibility in 10^{-6} c. g. s. units.

1) C. K. Ingold, "Structure and Mechanism in Organic Chemistry", Cornell University Press, New York (1953), p. 193.
2) Tai-Yuan Yang, *J. Chem. Phys.*, **16**, 865 (1948).
3) H. Francois and J. Hoarau, *Compt. rend.*, **240**, 1220 (1955).
4) S. B. Khatavkar, *Journal of C. S. I. R.*, **21B**, 83 (1962).
5) I. C. T. Vol. 6.
6) H. Mikhail, *J. Chem. Phys.*, **21**, 1004 (1935).
7) S. M. Shah et al., *Current Sci.*, **30**, 455 (1961).
8) F. G. Baddar and Sugden, *J. Chem. Soc.*, **1949**, 2927.

TABLE II. DIAMAGNETIC SUSCEPTIBILITY CONTRIBUTION OF THE $(NH_2)^{1+}$ ION

Substance	Experimental value	Neutralization of ions*	Contribution of NH_2^{1+}
Ethylenediamine	46.58	$M_2^{2-}+2(NH_2)^{1+}$	8.99
Benzylamine	74.91	$B^{1+}+M_1^{2-}+(NH_2)^{1+}$	8.25
1, 2-Propylenediamine	57.82	$M_3^{2-}+2(NH_2)^{1+}$	8.68
Ethanolamine	42.08	$NH_2^{1+}+M_1^{2-}+(CH_2OH)^{1+}$	8.19
n-Amylamine	72.73	$M_5^{1-}+(NH_2)^{1+}$	8.55

* The symbols used in column 3 are based on Yang's[2] paper.

TABLE III

S. No.	Substance	Neutralization of ions	χ_M Calcd. (Yang)	χ_M Exptl.	$\Delta\chi_M$
1	*o*-Ethylaniline	$M_2^{1+}+B_{1,2}^{2-}+NH_2^{1+}$	87.02	86.42	−0.60
2	*p*-Ethylaniline	$M_2^{1+}+B_{1,4}^{2-}+NH_2^{1+}$	87.02	84.84	−2.18
3	*o*-Chloroaniline	$Cl^{1+}+B_{1,2}^{2-}+NH_2^{1+}$	77.49	79.49	+2.00
4	*m*-Chloroaniline	$Cl^{1+}+B_{1,3}^{2-}+NH_2^{1+}$	77.49	76.56	−0.93
5	*p*-Chloroaniline	$Cl^{1+}+B_{1,4}^{2-}+NH_2^{1+}$	77.49	77.69	+0.20
6	*o*-Anisidine	$B_{1,2}^{2+}+(O^{2-}M_1^{1+})^{1-}+\theta+NH_2^{1+}$	80.45	79.34	−1.11
7	*m*-Anisidine	$B_{1,3}^{2+}+(O^{2-}M_1^{1+})^{1-}+\theta+NH_2^{1+}$	80.45	77.00	−3.45
8	*p*-Anisidine	$B_{1,4}^{2+}+(O^{2-}M_1^{1+})^{1-}+\theta+NH_2^{1+}$	80.45	77.50	−2.95
9	*o*-Nitroaniline	$(NO_2)^{1+}+B_{1,2}^{2-}+NH_2^{1+}$	70.00	66.56	−3.44
10	*m*-Nitroaniline	$(NO_2)^{1+}+B_{1,3}^{2-}+NH_2^{1+}$	70.00	69.88	−0.12
11	*p*-Nitroaniline	$(NO_2)^{1+}+B_{1,4}^{2-}+NH_2^{1+}$	70.00	66.15	−3.85

point. The solids were all purified by standard methods and the purification was continued till specimens of constant susceptibility were obtained. Great care was taken to prevent absorption of atmospheric moisture.

Measurement of susceptibilities of the liquids were made with a Guoy[9] balance. A correction has been applied for the residual air above the liquid surface. Since uniformity of packing is difficult to achieve in the case of solids the Curie[10] retorsion method was preferred. A.R. benzene dried over sodium wire and distilled over phosphorus pentoxide was used as standard and its specific susceptibility was taken as -0.702×10^{-6} units.

Results

The results obtained for the amines are recorded in Table I, the observed values were the mean of six very closely agreeing values. The theoretical values (column 4) were calculated by taking atomic and bond values as given by Ingold[1].

Evaluation of $(NH_2)^{1+}$ Contribution.—It is well known that in the aliphatic primary amines, the unshared electrons are in the tetrahedral orbital of non-interacting type. Hence the contribution of the $(NH_2)^{1+}$ has been derived from the experimental values of five such amines. In this evaluation the modified ionic values of Angus[11] has been used wherever necessary. It has been further assumed that the removal of a proton does not affect the ionic susceptibilities. This evaluation from these amines gives fairly consistent values for the $(NH_2)^{1+}$ ion, and the values thus obtained are recorded in Table II. The average value of $(NH_2)^{1+}$ works out to be 8.50.

Discussion

The $(NH_2)^{1+}$ value thus obtained has been utilized to calculate χ_M by Yang's method for aromatic compounds. The values are given in Table III.

The last column gives the exaltations observed in the aromatic amines and these can be explained on the basis of molecular orbital theory. The exaltations that are observed is the result of two interactions arising due to the transfer of tetrahedral orbital of the 'N' atom to the p orbital which results in a negative exaltation and the intermingling of the p orbital of the substituting NH_2 group with the π orbital of the benzene ring which yields a positive exaltation. The NH_2^{1+} value was obtained from the aliphatic amines in which the 'N' atom is in the tetrahydral orbital and so the $\Delta\chi_M$ observed is due to the above mentioned interactions. The $\Delta\chi_M$ is negative in all the cases except in *o*-chloroaniline where it is +2.00. In ortho chloroaniline the intramolecular hydrogen bond keeps the molecule in plane and so the full effect of the p orbital with the aromatic π orbital results in a rather positive exaltation.

9) S. R. Rao and A. S. Narayanasamy, *Proc. Ind. Acad. Sci.*, **9**, 35 (1939).
10) S. R. Rao, ibid., **A1**, 123 (1934).
11) W. R. Angus, *Proc. Roy. Soc.*, **A136**, 569 (1932).

Paramagnetic Contribution of N^{3+} Ion.—The close agreement among the calculated values by Yang's method and that of Ingold's additive method shows that the derived value of $(NH_2)^{1+}$ from aliphatic amines is consistent. Hence this value can be conveniently used for the derivation of the ionic susceptibility of the nitrogen ion N^{3+}.

$$(NH_2)^{1+} = -8.50$$

$$\chi_{N^{3+}} + 2\chi_{\theta} + 2\chi_{H^{1+}} = -8.50$$

Using the value of χ_{θ} as -4.88

$$\therefore \chi_{N^{3+}} = +1.26$$

Thus we are led to the conclusion that the ion N^{3+} posseses a paramagnetic susceptibility value. But Angus[11] gives a value of -2.09. The paramagnetic value that is obtained by Yang's method for the ion N^{3+} has been utilized and calculated for triethylamine.

$$\chi_{(C_2H_5)_3N} = \chi_{N^{3+}} + 3\chi_{M_2{}^{1-}} = -84.54$$

The additive method based on Ingold's value gives χ_M as 85.1 which is in fair agreement with that of the value obtained by Yang's method.

Summary

The diamagnetic susceptibilities of several aliphatic and aromatic amines have been determined. The susceptibility contribution, of $NH_2{}^{1+}$ is evaluated from the noninteracting aliphatic amines, and this value is used for calculation of χ_M of aromatic amines. The exaltations are attributed to the interactions in the system. An anomalous value for N^{3+} ion is obtained.

Department of Physics
Annamalai University
Annamalainagar, S. India

The Dissolution and Anion Exchange Behavior of Rare Earth and Other Metallic Elements in Potassium Bicarbonate, Potassium Carbonate and Ammonium Carbonate Solutions

By Tomitsugu TAKETATSU

(Received December 8, 1962)

In a previous paper[1] the present author reported that rare earth ions dissolved in potassium and ammonium carbonate solutions were adsorbed on an anion exchange resin and that the amounts both dissolved and adsorbed increase with the increase in atomic number, except for cerium and yttrium.

In this paper, the state of the dissolution and anion exchange behavior of rare earth ions in a potassium bicarbonate solution, as well as that of other metallic ions (thorim, zirconium, aluminum, gallium, indium, uranyl, beryllium, zinc, cadmium, copper, nickel, cobalt and lead ions) in potassium bicarbonate, potassium carbonate and ammonium carbonate solutions, will be studied. By using the results, the application for analytical separations will be discussed.

Experimental

Standard solutions of the metallic ions investigated were prepared by dissolving the reagent grade oxides (lanthanum, prasodymium, neodymium, samarium, gadolinium, dysprosium, erbium, yttrium and gallium), the chlorides (indium, zinc, cadmium, copper, nickel and cobalt) and the nitrates (zirconium, thorium, aluminum, cerium(III), beryllium and uranium(VI)) in dilute chloric or nitric acid. The concentrations of these ions, except for beryllium, were volumetrically determined with EDTA by using xylenol orange (XO), pyrocatechol violet (PV), eriochrome black T (EBT), PAN and murexide (MX) as indicators[2]. The concentration of beryllium was determined gravimetrically as the oxide.

As the anion exchange resins, Dowex 1, X-8 in carbonate and bicarbonate forms, of 50~100 mesh, were used.

All the other chemicals used were of a analytical reagent grade.

The measurement of the amounts of metallic ions dissolved in potassium bicarbonate, potassium carbonate and ammonium carbonate solutions, and of the distribution coefficient, K_d, of the metallic ions between an anion exchange resin and their solutions were carried out by a previously reported procedure[1]. All the experiments were

1) T. Taketatsu, This Bulletin, 35, 1573 (1962).

2) K. Ueno, "Chelate Titration", Nankodo, Tokyo (1960), pp. 205-330.

carried out at room temperature, which was about 20°C.

Results and Discussion

The determination methods and the quantities of metallic ions used in this experiments are shown in Table I.

The Relation between the Concentration of Potassium Bicarbonate Added and the Amount of Rare Earth Bicarbonate Dissolved. — When an excessive amount of potassium bicarbonate in a solution was added to the rare earth chloride or nitrate, first the rare earth bicarbonate was precipitated, and then the precipitate was dissolved partially or completely by shaking. Figure 1 plots the amounts of the rare earth ions dissolved against various concentrations of potassium bicarbonate. It can be seen that the amounts of rare earth ions dissolved increase with the increase in the concentration of bicarbonate, and also with the increase in atomic number, except for cerium and yttrium. Since cerium is partially oxidized to the tetrapositive state in the bicarbonate solution, its behavior differs from that of other rare earth elements. This finding is similar to that

TABLE I. THE DETERMINATION METHODS AND THE QUANTITIES OF METALLIC IONS USED

Ion	Titration method	Indicator	pH	Taken mg.	Concn. 10^{-4} mol./l.
Th^{4+}	Direct	XO	2.5~3.5	14.797	6.377
Zr^{4+}	Indirect (Bi^{3+})	XO	1 ~2	4.392	4.815
La^{3+}	Direct	XO	4.5~6	7.452	5.363
Ce^{3+}	Direct	XO	4.5~6	7.546	5.385
Pr^{3+}	Direct	XO	4.5~6	7.169	5.087
Nd^{3+}	Direct	XO	4.5~6	7.056	4.891
Sm^{3+}	Direct	XO	4.5~6	7.214	4.798
Gd^{3+}	Direct	XO	4.5~6	7.772	4.942
Dy^{3+}	Direct	XO	4.5~6	5.495	3.382
Er^{3+}	Direct	XO	4.5~6	10.424	6.232
Y^{3+}	Direct	XO	4.5~6	4.208	4.732
Ga^{3+}	Direct	PV	3.8	2.014	2.889
In^{3+}	Direct	XO	3 ~4.5	6.814	5.933
Al^{3+}	Indirect (Zn^{2+})	XO	5 ~6	1.854	6.870
Zn^{2+}	Direct	EBT	10	3.387	5.182
Cd^{2+}	Direct	EBT	10	6.854	6.098
Cu^{2+}	Direct	MX	8	3.241	5.101
Ni^{2+}	Direct	MX	10	2.891	4.924
Co^{2+}	Direct	XO	5 ~6	3.092	5.246
Pb^{2+}	Direct	XO	5	11.039	5.328
UO_2^{2+}	Direct	PAN	4	18.145	6.703
Be^{2+}	Gravimetry			3.21	3.56 10^{-3}

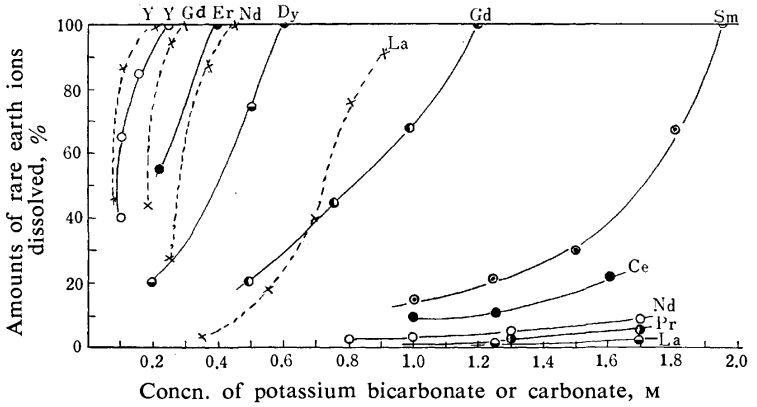

Fig. 1. Relation between the concentration of potassium bicarbonate or carbonate and the amounts of rare earth ions dissolved.
-○- Potassium bicarbonate -×- Potassium carbonate

obtained by using potassium carbonate. However, the precipitates of the light lanthanons (lanthanum, praseodymium and neodymium) can scarcely be dissolved, even in 1.8 M. On the other hand, the heavy lanthanons (dysprosium, erbium and yttrium) can easily be dissolved in a bicarbonate solution of even lower concentrations. For example, the precipitates of samarium, gadolinum, dysprosium, erbium and yttrium bicarbonates are dissolved completely in a bicarbonate solution more concentrated than about 1.95, 1.20, 0.60, 0.40 and 0.25 M respectively. For comparison, the results for several rare earth ions obtained by using potassium carbonate are also plotted in Fig. 1. The variation in the amounts of rare earth ions dissolved in a potassium bicarbonate solution of a certain concentration is more remarkable than in a potassium carbonate solution. Therefore, it is expected that the separation of rare earth elements from each other can be carried out by a fractional separation using the distinct difference.

The Relation between the Adsorbabilities of the Rare Earth Ions and the Concentration of Potassium Bicarbonate.—When the precipitates of rare earth ions were dissolved completely, the anion exchange behavior of these rare earth ions was studied by the batch operation. The distribution coefficient, K_d, is given by

$$K_d = [M_r] / [M_s] \quad (\text{ml./g.})$$

where M_r and M_s are the amount of rare earth ions in one gram of the resin and in one milliliter of the solution respectively. The plot of the distribution coefficient of rare earth ions against various concentrations of potassium bicarbonate is shown in Fig. 2. It can there be seen that the adsorbability of rare earth ions decreases as the concentration of the potassium bicarbonate increases and that the order of the K_d values is yttrium > erbium > dysprosium. However, the differences in these values are very small. Although gadolinium and samarium are dissolved completely in the bicarbonate solution, these ions can only with difficulty be adsorbed on the resin because of the high concentration of the bicarbonate.

When the logarithmic diagram of the K_d value of the rare earth ions against the concentrations of potassium bicarbonate is plotted, the slope of the $\log K_d$ vs. $\log(HCO_3^-)$ curve shows linearity and the lines are parallel to one another with a negative slope. Therefore, it may be concluded, according to a method developed by Kraus et al.[3], that each rare earth ion dissolved in a bicarbonate solution is in a state of identical negative charge.

The Dissolution and Anion Exchange Behavior of the Various Metallic Ions in a Potassium Bicarbonate Solution. — The relation between the amounts of the various metallic ions dissolved and the concentration of potassium bicarbonate was investigated. The results are shown in Fig. 3. The precipitates of thorium, zirconium, gallium and uranyl ions were dissolved at once, while those of beryllium, copper, nickel and cobalt ions were dissolved gradually in those bicarbonate solutions more concentrated than about 0.2 M.

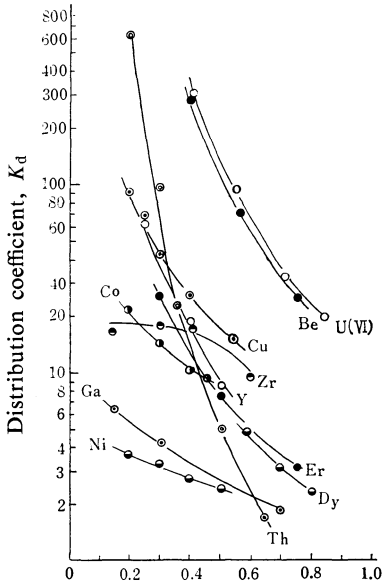

Fig. 2. Distribution coefficient of rare earth and other metallic ions between Dowex 1 and potassium bicarbonate solution.

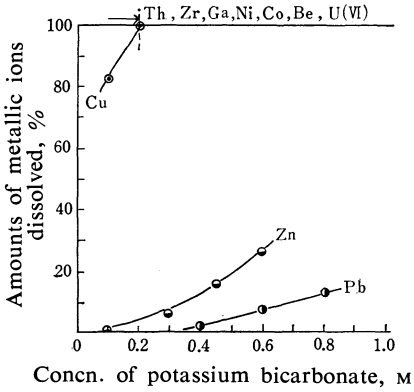

Fig. 3. Relation between the concentration of potassium bicarbonate and the amounts of various metallic ions dissolved.

3) K. A. Kraus and F. Nelson, "Anion Exchange Studies of the Fission Products", in "Peaceful Uses of Atomic Energy", Vol. VII, Proceedings of the International Conference in Geneva (United Nations) (1955), p. 113.

However, the precipitates of lead, zinc and indium could not be dissolved completely, even in 1.0 M.

The plot of the K_d values of the metallic ions dissolved completely in the bicarbonate solution against the concentration of potassium bicarbonate is given in Fig. 2. The K_d values of these metallic ions decrease with the increase in the concentration of potassium bicarbonate. Uranyl and beryllium ions are adsorbed firmly on an anion exchange resin, while copper and cobalt ions are adsorbed less firmly. On the other hand, gallium and nickel ions are adsorbed weakly. The K_d value of zirconium ions is different at different time intervals in the measurement, and so it is difficult to obtain a constant value. This fact is also found in the case of using a potassium carbonate solution, as is described below. It seems that this behavior is a result of the complicated state of the soluble zirconium ion. From the distinct differences in the K_d values, it is expected that uranyl and beryllium ions can be effectively separated from other metallic ions, as well as can copper ions from cobalt and nickel ions, by an anion exchange resin, with the potassium bicarbonate solution as the eluting agent.

The Dissolution and Anion Exchange Behavior of the Various Metallic Ions in a Potassium Carbonate Solution.—The plot of the amounts of the various metallic ions dissolved against the concentration of potassium carbonate is in Fig. 4. It can be seen that uranyl, thorium, zirconium and aluminum ions are dissolved completely in a potassium carbonate solution more concentrated than about 0.2 M, while beryllium, zinc, copper and indium ions can not be dissolved completely, even in 1.0 M.

The relation between the K_d values of the metallic ions dissolved completely in a potassium carbonate solution and the concentration of the carbonate is shown in Fig. 5. Figure 5 shows that the K_d values of uranyl, rare earth and thorium ions depend upon the concentration of potassium carbonate to a remarkable extent, while, on the other hand, those of gallium and aluminum ions are scarcely affected. It is thought that the dissolution and anion exchange behavior of gallium and aluminum ions are related to the amphoteric property rather than to the formation of their carbonate complex ions. Zirconium ion did not give a constant value under these experimental conditions. Although lead ions were dissolved completely in a potassium carbonate solution more concentrated than 0.8 M, their adsorbability for an anion exchange resin is weakly. The distinct difference in K_d values between uranyl and other metallic ions will be applied to their analytical separation by a column operation.

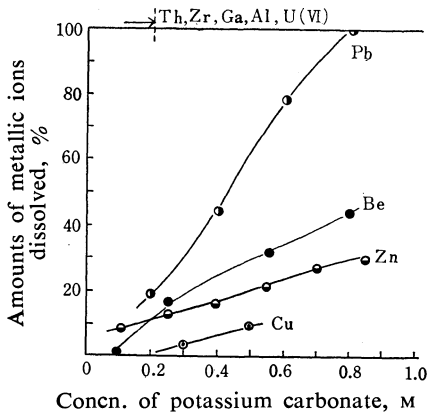

Fig. 4. Relation between the concentration of potassium carbonate and the amounts of various metallic ions dissolved.

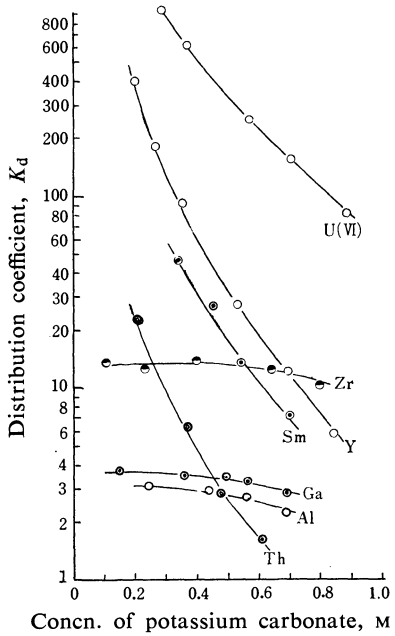

Fig. 5. Distribution coefficient of various metallic ions between Dowex 1 and potassium carbonate solution.

The Dissolution and Anion Exchange Behavior of Various Metallic Ions in an Ammonium Carbonate Solution.—The molar concentration of ammonium carbonate may be represented by a molar formula of $NH_4CO_2NH_2 \cdot NH_4HCO_3$, but this formula is not accurate because of the unstable property of ammonium carbonate. The plot of the amounts of the various metallic ions dissolved against the concentration of ammonium carbonate is given in Fig. 6. Figure 6 shows that uranyl, thorium, gallium, berylliun, zinc, cadmium,

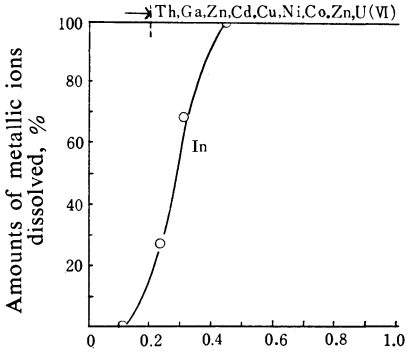

Fig. 6. Relation between the concentration of ammonium carbonate and the amounts of various metallic ions dissolved.

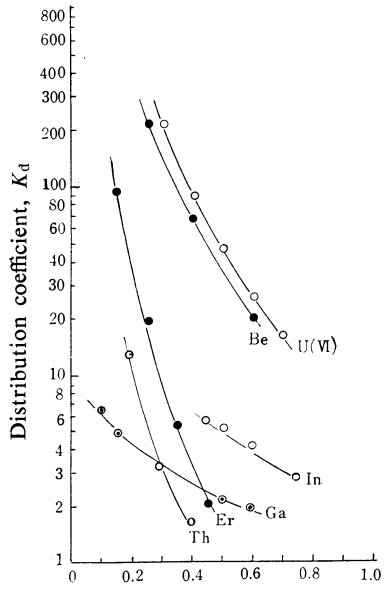

Fig. 7. Distribution coefficient of various metallic ions between Dowex 1 and ammonium carbonate.

copper, nickel and cobalt ions are dissolved completely in an ammonium carbonate solution more concentrated than about 0.2 M. Because of the formation of the ammine complexes, the macro amounts of zinc, cadmium, copper, nickel and cobalt ions are easily dissolved in an ammonium carbonate solution. Indium ions are dissolved completely in a carbonate solution more concentrated than about 0.45 M.

The relation between the K_d values of these metallic ions dissolved completely and the concentration of ammonium carbonate is shown in Fig. 7. The K_d values decrease with the increase in the concentration of ammonium carbonate. Uranyl and beryllium ions are adsorbed firmly on an anion exchange resin, while gallium, indium, thorium and rare earth ions are adsorbed less firmly. On the other hand, zinc, nickel, cobalt, cadmium and copper ions are scarcely adsorbed at all. The differences in K_d values among the metallic ions will be applied to an analytical separation; it is especially expected that the micro amounts of uranyl and beryllium ions may be separated from the macro amounts of nickel, cobalt, zinc, cadmium and copper ions.

Summary

The amounts of rare earth ions dissolved in a potassium bicarbonate solution, as well as those of other metallic ions dissolved in potassium bicarbonate, potassium carbonate and ammonium carbonate solutions, have been measured. Moreover, the minimum concentrations of potassium bicarbonate, potassium carbonate and ammonium carbonate required to dissolve the precipitates of the metallic bicarbonate and carbonate completely has been determined, and the distribution coefficients, K_d, of the completely dissolved metallic ions between an anion exchange resin and a potassium bicarbonate, potassium carbonate or ammonium carbonate solution had been measured. On the basis of those findings, the dissolution and anion exchange behavior of the metallic ions has been discussed, and the applicability to an analytical separation has been described.

The author wishes to express his gratitude to Professor Shozo Misumi for his valuable discussions and encouragement.

General Education Department
Kyushu University
Otsubo-machi, Fukuoka

*Formation of Ion-pair Cr^{3+}—SO_4^{2-} in Aqueous Solution**

By Ryokichi TSUCHIYA and Akira UMAYAHARA

(Received December 20, 1962)

The measurement of coagulation value has, in general, been used for a long time to determine the charge of electrolytes in aqueous solutions. This method has also been applied to complexes. However, it is a rough method. A much more definite and exact methods for determining the charge of salt depends on electrical conductivity.

The molecular conductivity of a solution decreases, as a rule, as its concentration increases. The rate of decrease of the molecular conductivity with the increase in concentration is relatively small in the case of such chlorides as potassium and magnesium chloride and such nitrates as silver nitrate. In such cases, it is comparatively easy to determine the proper charge of the electrolytes, even in a relatively high concentration, by measuring the electrical conductivity.

On the other hand, the decrease in molecular conductivity accompanying an increase in concentration is much greater in the case of the sulfates of such bivalent metals as magnesium, copper and cadmium. The same relation is expected for the sulfate of tervalent chromium. In these cases, the proper charge of the electrolytes can not always be determined from the conductivity as easily as in the former cases.

However, the ionic state of the solution can be inferred from the conductivity.

The formation constants of the ion-pairs of tervalent cobalt, iron or chromium ions and its counter-anions have already been reported for $[Co(NH_3)_6]Cl^{2+}$ [1], $[Co(NH_3)_6]SO_4^+$ [2], $[Co(NH_3)_5H_2O]SO_4^+$ [2], $[Fe(H_2O)_6]Cl^{2+}$ [3], $[Cr(H_2O)_6]SCN^{2+}$ [4], $[Cr(H_2O)_6]Cl^{2+}$ [4] and so on, but not for $[Cr(H_2O)_6]SO_4^+$. It is known that chrome alum, which is often used as the raw material for chromium complexes, has the ion, $[Cr(H_2O)_6]^{3+}$ [5], and the formation of $[Cr(H_2O)_6]SO_4^+$ in its solution is thought to be a matter of course. The formation constant of the ion-pair, $[Cr(H_2O)_6]SO_4^+$, must be known when the properties of chromium(III) ions in the presence of sulfate ions in an aqueous solution are to be investigated. In this study the formation constant concerning chromium sulfate and chrome alum in solution will be determined through the electrical conductivity measurement.

Experimental

Hexa-aquochromium(III) Sulfate. $[Cr(H_2O)_6]_2(SO_4)_3 \cdot nH_2O$ (Violet form).—The salt was crystallized by cooling a mixture of a solution of potassium chrome alum and concentrated sulfuric acid [6]. The value of n was found to be 3.19 by chemical analysis.

Potassium Chrome Alum.—The salt of the "special" commercial grade was further purified by recrystallization. The dehydration curve of the alum was obtained with a Shimadzu thermobalance of the torsion type.

The measurement of the electrical conductivity of the solution was made with a Yokokawa Universal Bridge BV-Z-13A, and its pH was obtained with a Horiba HRL Model M-3 pH meter, both at 25°C.

Two resins, Amberlite IR-120 and Dowex 1×8, were used for the ion exchange.

Calculation and Results

Calculation of the Formation Constant of the Ion-pair in a Hexa-aquochromium(III) Sulfate Solution.—The cation $[Cr(H_2O)_6]^{3+}$ contained in the solution is presumed to produce the hydroxopenta-aquochromium(III) ion, $[Cr(H_2O)_5OH]^{2+}$, by hydrolysis, because the pH of the solution is found to be in the acid range. The experimental finding that the molecular conductivity exceedingly decreases as the concentration of the solution increases indicated the formation of the ion-pair, $[Cr(H_2O)_6]SO_4^+$, between hexa-aquochromium(III) and sulfate ions.

Consequently, the following equilibria are thought to be established in an aqueous solution:

* Read at the 15th Annual Meeting of the Chemical Society of Japan, Kyoto, April, 1962.

1) M. G. Evans and G. H. Nancollas, *Trans. Faraday Soc.*, **46**, 363 (1953).

2) F. A. Posey and H. Taube, *J. Am. Chem. Soc.*, **78**, 15 (1956).

3) M. J. M. Woods, O. P. Patrick, K. Gallagher and E. L. King, *Inorg. Chem.*, **1**, 55 (1962).

4) C. Potmus and E. L. King, *J. Phys. Chem.*, **59**. 1208 (1955).

5) R. Tsuchida and M. Kobayashi, *J. Chem. Soc. Japan (Nippon Kwagaku Kwaisi)*, **64**, 1268 (1943).

6) R. F. Weinland and R. Krebs, *Z. anorg. Chem.*, **49**, 157 (1906).

$$[Cr(H_2O)_6]^{3+} + SO_4^{2-} \overset{K}{\rightleftharpoons} [Cr(H_2O)_6]SO_4^{+} \quad (1)$$

$$[Cr(H_2O)_6]^{3+} \overset{K_h}{\rightleftharpoons} [Cr(H_2O)_5OH]^{2+} + H^{+} \quad (2)$$

$$[Cr(H_2O)_6]SO_4^{+} \overset{K_h}{\rightleftharpoons} [Cr(H_2O)_5OH]SO_4 + H^{+} \quad (3)$$

where the hydrolysis constants of reactions 2 and 3 are assumed to be equal.

When the total concentration of chromium(III) contained in the aqueous solution of hexa-aquochromium(III) sulfate is expressed by a, the total concentration of sulfate is $3/2\ a$. If, in the state of equilibrium, the concentration of sulfate ions spent for the formation of the ion-pairs is expressed by x, that of $[Cr(H_2O)_5OH]^{2+}$ produced by the hydrolysis 2, by y, and that of $[Cr(H_2O)_5OH]SO_4$ produced by the hydrolysis 3 by z, the concentrations of the ionic species are:

$$\left.\begin{array}{ll} [Cr(H_2O)_6]^{3+} & a-x-y \\ SO_4^{2-} & 3/2\,a-x \\ [Cr(H_2O)_6]SO_4^{+} & x-z \\ [Cr(H_2O)_5OH]^{2+} & y \\ [Cr(H_2O)_5OH]SO_4 & z \\ H^{+} & y+z \end{array}\right\} \quad (4)$$

The equilibrium constants of reactions 1, 2 and 3 are given by the equations:

$$K=(x-z)/(a-x-y)(3/2\,a-x) \quad (5)$$

$$K_h=y(y+z)/(a-x-y)=z(y+z)(x-z) \quad (6)$$

By eliminating y and z from Eqs. 5 and 6, the formation constant of the ion-pair $[Cr(H_2O)_6]SO^{+4}$ is obtained as:

$$K=2x/(a-x)(3a-2x) \quad (7)$$

When the molecular conductivities of $[Cr(H_2O)_6]^{3+}$, sulfate, $[Cr(H_2O)_6]SO_4^{+}$, $[Cr(H_2O)_5OH]^{2+}$ and hydrogen ions are expressed by Λ_1, Λ_2, Λ_3, Λ_4 and Λ_H respectively, and the observed conductivity of hexa-aquochromium(III) sulfate in solution, by Λ_0, we have

$$1/2\ a\Lambda_0=\{(a-x-y)\Lambda_1+(3/2\,a-x)\Lambda_2+(x-z)\Lambda_3+y\Lambda_4+(y+z)\Lambda_H\}/\eta \quad (8)$$

where η is the specific viscosity of the solution. This equation was deduced on the basis of Walden's law $\eta\Lambda=$const., which has been established between η and the electrical conductivity Λ.

Since the ionic radii of hexa-aquochromium(III) and sulfate ions are 2.33 Å and 2.30 Å respectively, the ionic volume of $[Cr(H_2O)_6]SO_4^{+}$ is assumed to be approximately twice the size of the hexa-aquochromium(III) ion; therefore, the molecular conductivity of $[Cr(H_2O)_6]SO_4^{+}$ is a half of that of the hexa-aquochromium(III) ion if only the ratio of the ionic radius is considered. On the basis of the ratio of the charges, 1 to, 3 for $[Cr(H_2O)_6]SO_4^{+}$ and the hexa-aquochromium(III) ion, the molecular conductivity of the former is assumed to be one-third of that of the latter. By taking both the ratios of the ionic radii and of the charges into consideration, the molecular conductivity of $[Cr(H_2O)_6]SO_4^{+}$ is reduced to one-sixth of that of the hexa-aquochromium(III) ion. The ionic radius of $[Cr(H_2O)_5OH]^{2+}$ is assumed to be approximately equal to that of the hexa-aquochromium(III) ion, and, therefore, the molecular conductivity of the former is assumed to be two-thirds of that of the latter, allowance being made only for the ratio of their charges.

Solving Eqs. 6, 7 and 8 for x, we get

$$x=\{2a(3a-C_H)\Lambda_1+9a^2\Lambda_2+6aC_H\Lambda_H-3a^2\Lambda_0\eta\}/(5a-C_H)\Lambda_1+6a\Lambda_2 \quad (9)$$

where C_H is the hydrogen ion concentration. By substituting the value calculated by Eq. 9 into 7, the formation constant of the ion-pair, $[Cr(H_2O)_6]SO_4^{+}$, can be obtained.

The ionic strength μ is calculated by the following:

$$\mu=15/2\,a-6x-2y \quad (10)$$

Results of Calculation.—The observed values of electrical conductivity and pH of the solution of hexa-aquochromium(III) sulfate at 25°C are shown in Table I, together with the values of the formation constants of the ion-pair and the ionic strengths calculated from them.

In these calculations, the ionic conductivities of the chromium(III), sulfate and hydrogen ions were taken as $\Lambda_1=201$[7], $\Lambda_2=161.98$[8] and $\Lambda_H=348$[9] respectively. The plot of the measured conductivity against the square root of the concentration is given in Fig. 1.

The observed value of pH is not the hydrogen ion concentration itself, but its activity. Therefore, x was at first calculated by putting the activity, instead of C_H, in Eq. 9, and then the ionic strength was calculated by 10. The activity coefficient of the hydrogen ion corresponding to the ionic strength was then obtained from Kielland's table[10] and employed for finding the hydrogen ion concentration,

7) Landolt-Börnstein, "Phys. Chem. Tabellen", III Erg. 2059 (1936).
8) Ibid., II Erg. 1063 (1931).
9) G. H. Jeffrey and A. I. Vogel, *Phil. Mag.*, **15**, 395 (1933).
10) J. Kielland, *J. Am. Chem. Soc.*, **59**, 1675 (1937).

Table I. The observed values of conductivity and pH of the solution of hexa-aquochromium-(III) sulfate and the calculated values of the formation constant of ion-pair and their hydrolysis constant and the ionic strength of the solution at 25°C

a	Λ_{obs}	pH	η	$K\times10^{-3}$	log$K$	$K_h\times10^5$	logK_h	$\mu\times10^3$	$\sqrt{\mu}$
0.0005	706.76	3.88	1.001	2.275	3.357	5.279	$\bar{5}$.723	2.042	0.04519
0.001	632.26	3.77	1.002	1.304	3.115	4.005	$\bar{5}$.603	4.022	0.06342
0.002	508.59	3.63	1.003	1.397	3.145	3.680	$\bar{5}$.566	6.531	0.08082
0.004	406.58	3.49	1.005	1.587	3.201	3.462	$\bar{5}$.539	10.35	0.1017
0.01	303.54	3.28	1.014	2.952	3.470	3.684	$\bar{5}$.566	18.38	0.1356
0.02	249.18	3.20	1.025	8.514	3.930	2.706	$\bar{5}$.432	31.35	0.1771

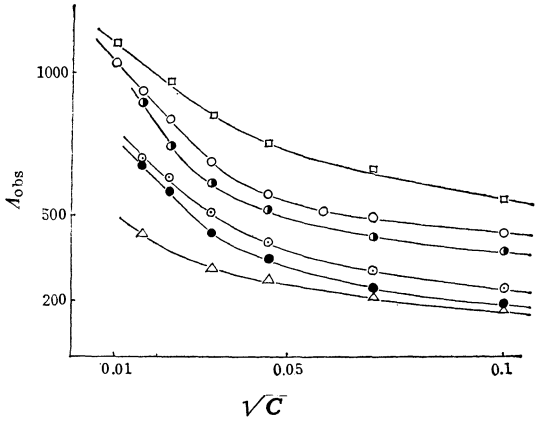

Fig. 1. The plottings of the molecular conductivities at 25°C vs. the square root of the concentrations of the following various solutions:
-⊙- The violet solution of hexa-aquochromium(III) sulfate
-●- The green solution produced by heating the solution at 55°C of hexa-aquochromium(III) sulfate
-○- The violet solution of potassium-chrome alum and that of the solid alum deprived of a half of the water of crystallization.
-◑- The green solution produced by heating the solution at 55°C of potassium-chrome alum
-△- The green solution of $Cr_2(SO_4)_3\cdot6.23H_2O$
-□- The green solution produced by heating the solid potassium-chrome alum at 150°C

C_H, which, substituted in 9 and 10, gave the corrected values of x and μ.

The formation constant of the ion-pair was computed by Eq. 7. The logarithm of the constant is plotted against the square root of the corresponding ionic strength in Fig. 2. By extrapolating the smoothed curve formed by the observed points up to zero ionic strength, the thermodynamic formation constant of the ion-pair, $[Cr(H_2O)_6]SO_4^+$, at 25°C was obtained as $K=6.2\times10^4$.

In addition, the hydrolysis constant of $[Cr(H_2O)_6]^{3+}$ at 25°C was obtained as p$K=3.95$ at $\mu=0$ by Eq. 6.

Calculation of the Formation Constant of the Ion-pair $Cr^{3+}-SO^{2-}$ in Potassium-Chrome Alum in an Aqueous Solution.—An aqueous solution of potassium-chrome alum contains hexa-aquochromium(III), $[Cr(H_2O]_5OH]^{2+}$, $[Cr(H_2O)_6]SO_4^+$, potassium, sulfate and $K\text{-}SO_4^-$ ions. In addition to Eqs. 1, 2 and 3, the following equilibrium is thought to be present in the solution:

$$K^+ + SO_4^{2-} \overset{K'}{\rightleftharpoons} K\text{-}SO_4^- \qquad (11)$$

In this case, if the total molar concentration of chromium(III) is expressed by a, that of the sulfate ion is given by $2a$. When the concentration of the sulfate ion contributing to the formation of the ion-pair $K\text{-}SO_4^-$ in 11 is expressed by x', the concentration of potassium, sulfate and $K\text{-}SO_4^-$ ions at equilibrium are given by $a-x'$, $2a-x-x'$ and x' respectively. The concentrations of the other ionic species are the same as have been given in 4. By considering Eq. 6 at the same time, the formation constant of the ion-pair $[Cr(H_2O)_6]SO_4^+$ in the aqueous solution of chrome alum is obtained as:

$$K=x/(a-x)(2a-x-x') \qquad (12)$$

Since the ionic radii of potassium and sulfate ions are 1.33Å and 2.30Å respectively, the

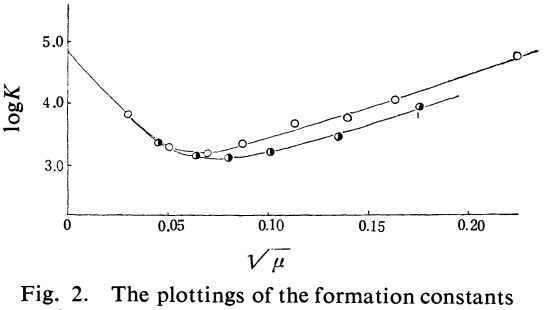

Fig. 2. The plottings of the formation constants of the ion-pair, $[Cr(H_2O)_6]-SO_4^+$, in the aqueous solution of hexa-aquochromium(III) sulfate (◑) and potassium-chrome alum (○) vs. the square root of the ionic strength at 25°C.

TABLE II. THE OBSERVED VALUES OF CONDUCTIVITY AND pH OF THE SOLUTION OF POTASSIUM-CHROME ALUM AND THE CALCULATED VALUES OF THE FORMATION CONSTANT OF ION-PAIR Cr^{3+}-SO_4^{2-} AND THE HYDROLYSIS CONSTANT OF HEXA-AQUOCHROMIUM(III) ION AND THE IONIC STRENGTH OF THE SOLUTION AT 25°C

a	Λ_{obs}	pH	η	$K\times10^{-3}$	log$K$	$K_h\times10^5$	logK_h	$\mu\times10^3$	$\sqrt{\mu}$
0.0002	1029.44	4.08	1.000	6.818	3.834	6.538	$\bar{5}$.815	0.9563	0.03093
0.0005	935.14	3.88	1.001	2.094	3.321	5.352	$\bar{5}$.729	2.513	0.05013
0.001	837.57	3.84	1.002	1.513	3.180	2.847	$\bar{5}$.454	4.813	0.06938
0.002	686.13	3.68	1.004	2.400	3.380	2.909	$\bar{5}$.464	7.514	0.08669
0.004	581.64	3.59	1.007	3.918	3.593	2.175	$\bar{5}$.338	12.59	0.1122
0.0067	519.67	3.53	1.010	5.348	3.728	1.730	$\bar{5}$.238	19.58	0.1399
0.01	489.32	3.45	1.018	11.78	3.071	1.697	$\bar{5}$.230	26.78	0.1636
0.02	441.62	3.36	1.032	58.23	3.765	1.329	$\bar{5}$.124	50.66	0.2251

ionic volume of $K\text{-}SO_4^-$ is assumed to be approximately one-and-a-half times that of the sulfate ion. In addition, by considering that the charge of $K\text{-}SO_4^-$ is a half of that of the sulfate ion, the molecular conductivity of $K\text{-}SO_4^-$ is presumed to be one-third of that of the sulfate ion. By a procedure similar to that used in the case of hexa-aquochromium-(III) salt, the equation corresponding to 9 is introduced as:

$$(5a\Lambda_1+C_H\Lambda_1+6a\Lambda_2)x+(6a\Lambda_5+4a\Lambda_2)x' = 6a^2(\Lambda_5+\Lambda_1+2\Lambda_2)-2aC_H\Lambda_1 + 6aC_H\Lambda_H-3a^2\Lambda_0\eta \quad (13)$$

where Λ_5 is the molecular conductivity of the potassium ion and Λ_0 is the observed conductivity of the potassium-chrome alum in solution.

In order to obtain the x' value, the conductivity of pure potassium sulfate in an aqueous solution was measured. Where the total molar concentration of the potassium ion and that of the ion-pair $K\text{-}SO_4^-$ formed at equilibrium are expressed by a and x' respectively, the concentration of potassium and sulfate ions at equilibrium are given by $a-x'$ and $a/2-x'$. The equilibrium constant for Eq. 11 is given by:

$$K'=2x'/(a-x')(a-2x') \quad (14)$$

When the observed conductivity is expressed by Λ_0' in a solution of potassium sulfate, by using the assumption concerning the ionic conductivity of $K\text{-}SO_4^-$ mentioned above, the equation corresponding to 9 is given by:

$$x'=3a(2\Lambda_5+\Lambda_2-\Lambda_0'\eta)/(6\Lambda_5+4\Lambda_2) \quad (15)$$

The value of x' was obtained by inserting the observed conductivity of potassium sulfate in various concentrations and the ionic conductivities of each species concerned, $\Lambda_5=75.63$[11] and $\Lambda_2=161.98$[8], into Eq. 15, while the value of K' was calculated by Eq. 14. The logarithm of K' by Eq. 14 was plotted against the ionic strengths. The value of K' at each ionic strength where the conductivity of chrome alum had been measured was obtained by interpolation or extrapolation of the above plots.

On the other hand, the formation constant of the ion-pair of $K\text{-}SO_4^-$ in the solution of chrome alum is given by:

$$K'=x'/(a-x')(2a-x-x') \quad (16)$$

By inserting the value of K' obtained above into Eq. 16 and combining it with Eq. 13, the values of x and x' were obtained. By introducing these values of x and x' into Eq. 12, the formation constant of the ion-pair $[Cr(H_2O)_6]SO_4^+$ was calculated. The results of this calculation are listed in Table II. The measured conductivity of chrome alum in the solution at 25°C against the square root of the concentration is given in Fig. 1, while the formation constant is plotted against the ionic strength in Fig 2, together with the case of hexa-aquochromium(III) salt. By extrapolating the latter plot to zero ionic strength, the thermodynamic formation constant at 25°C was obtained as $K=6.4\times10^4$, which is in good agreement with the corresponding constant in the case of hexa-aquochromium(III) sulfate. The mean value is log $K=6.3\times10^4$.

Electrical Conductivity and the Result of the Ion Exchange of the Solution of Heated Potassium-Chrome Alum and That of Chromium-(III) Sulfate in the Green Form.—The loss in weight of solid potassium-chrome alum due to heating is shown in Fig. 3. One-half of the water of crystallization, i. e., 12 H_2O, was lost at 80°C. The product is a violet powder, and the conductivity of its aqueous solution was found to be identical with that of the original alum, as is shown in Fig. 1. At 150°C another eight moles of water of the crystallization of the solid alum are lost. Under this condition

11) Landolt-Börnstein, "Phys. Chem. Tabellen", II Erg. 1062 (1931).

Table III. The values of pH and the percentages of the quantities of ionic species in the aqueous solution of chrome alum and chromium sulfate

Concn.	1/1000 mol./l.	(a)	(b)	(c)	(d)	(e)	(f)
	pH	3.68	3.63	3.45	3.53	3.30	3.23
Concn.	1/1000 mol./l.	(a)	(b)	(c)	(d)	(e)	(f)
	pH	3.36	3.20	3.12	2.27	2.48	2.31
Ionic species (%)	cation	100	100	81.2	—	32.9	47.6
	anion	0	0	17.6	—	31.7	30.3
	non-electrolytes	0	0	1.2	—	35.4	22.1

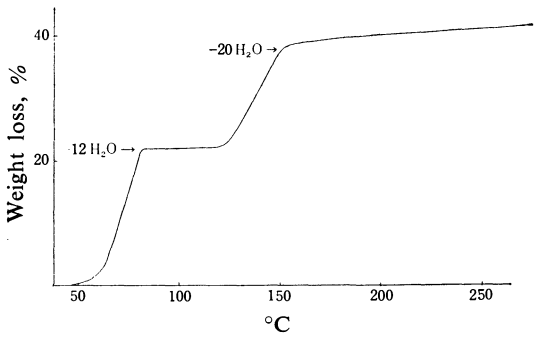

Fig. 3. The curve of the weight loss of potassium chrome alum upon heating.

the salt has lost four of the six moles of water combined with chromium. The conductivity of its solution is remarkably larger than that of the original alum, as is shown in Fig. 1.

The solution of chrome alum was warmed at 55°C for three hours, and the electrical conductivity was measured at the same temperature. By using the equation: $\kappa_t = \kappa_{18}\{1 + 235\times10^{-4}(t-18) + 95\times10^{-6}(t-18)^2\}$[12] where κ_t and κ_{18} are the specific conductivity of salt at t°C and 18°C respectively, the observed conductivity at 55°C was converted into that at 25°C, as is shown in Fig. 1. The molecular conductivity of the chromium(III) sulfate $Cr_2(SO_4)_3\cdot6.35H_2O$ in the green form was also measured; its value is shown in Fig. 1 together with those of hexa-aquochromium(III) sulfate (chromium(III) sulfate in the violet form) and potassium-chrome alum.

The pH values and the percentages of the quantities of cation, anion and non-electrolytes expected to be contained from the ion exchange using Amberlite IR-120 and Dowex 1×8 in the following solutions are listed in Table III:

(a) An M/100 aqueous solution of potassium-chrome alum.

(b) An M/100 solution of the violet form of chromium sulfate (hexa-aquochromium(III) sulfate).

(c) An M/100 solution of chrome alum heated at 55°C for about 3 hr.

(d) An M/100 solution of chrome alum heated at 80°C for 10 min.

(e) An M/100 solution of chrome alum deprived of 20 H_2O in the solid state.

(f) An M/100 solution of the green form of chromium(III) sulfate.

Discussion

On the Formation Constant of the Ion-pair between the Hexa-aquochromium(III) Ion and the Sulfate Ion.—The formation constant of the ion-pair between hexa-aquochromium(III) and sulfate ions is shown in Table IV. The formation constants of the ion-pairs in an aqueous solution of chromium(III) chloride and thiocyanate, iron(III) chloride and several cobalt(III) salts are also listed in this table for comparison.

The power of the sulfate ion to form an ion-pair was found to be exceedingly larger than that of the chloride ion in chromium(III), iron(III) and cobalt(III) salts. This is attributable to the fact that, in the solution, the sulfate ion combines more easily with the hydrogen in H_2O or NH_3 coordinated to the metal than the chloride ion does. It was also found that the hexa-aquochromium(III) ion had a little stronger tendency to form the ion-pair with the sulfate ion than did the hexa-amminecobalt(III) ion. This may be attributed to the fact that the O–H–O bond in the chromium-hexa-aquo ion-pair is stronger than the N–H–O bond in the cobalt-hexa-ammine ion-pair. This result is in good agreement with the study presented at the symposium[13] showing that the force constant between chromium and oxygen in the hexa-aquochromium(III) ion is larger than that between cobalt and nitrogen in the hexa-amminecobalt(III) ion.

Change of the Ionic Species of Chrome-Alum upon Heating in the Solid State and in the Aqueous Solution.—When the aqueous solution of chrome alum was heated, it was found that its color changed from violet to green, that

12) F. Kohlrausch, *Berl. Sitzber*, **1902**, 572.

13) T. Shimanouchi, I. Nakagawa and J. Hiraishi, 12th Symposium of Coordination Compounds, Tokyo, November, 1962.

TABLE IV. THE FORMATION CONSTANTS OF ION-PAIRS IN AQUEOUS SOLUTION OF COBALT(III), IRON(III) AND CHROMIUM(III) SALTS AT 25°C

$[Co(NH_3)_6]^{3+}$	+	Cl^-	=	$[Co(NH_3)_6]Cl^{2+}$	K	=	74 [1]
$[Co(NH_3)_6]^{3+}$	+	SO_4^{2-}	=	$[Co(NH_3)_6]SO_4^+$	K	=	2.2×10^3 [2]
$[Co(NH_3)_5H_2O]^{3+}$	+	SO_4^{2-}	=	$[Co(NH_3)_5H_2O]SO_4^+$	K	=	1.9×10^3 [2]
$[Fe(H_2O)_6]^{3+}$	+	Cl^-	=	$[Fe(H_2O)_6]Cl^{2+}$	K	=	2.9 [3]
$[Cr(H_2O)_6]^{3+}$	+	SCN^-	=	$[Cr(H_2O)_6]SCN^{2+}$	K	=	7 [4]
$[Cr(H_2O)_6]^{3+}$	+	Cl^-	=	$[Cr(H_2O)_6]Cl^{2+}$	K	=	13 [4]
$[Cr(H_2O)_6]^{3+}$	+	SO_4^{2-}	=	$[Cr((H_2O)_6]SO_4^+$	K	=	6.3×10^4 *

* Present study by authors

Data of K are those at zero ionic strength except for that at $\mu = 1.0$ from Ref. 3.

the value of pH fell, that anionic species appeared and that the electrical conductivity of the solution decreased a little. There have been reports[14] that the conductivities of the green solution of chromium(III) sulfate and potassium-chrome alum are greater than those of the respective violet solutions, but the results of the present study are quite the opposite. This suggests that hydrolysis and sulfation take place and that a binuclear complex which contains hydroxy and sulfate ions in the coordination sphere is formed.

In the aqueous solution of chrome alum deprived of $20H_2O$ in the solid state, the quantity of anionic species was larger and the conductivity higher than in the heated solution. It may be inferred from these facts that there are among the complex ions, some species with a higher negative charge due to the possession of more than one sulfate ion group in the coordination sphere.

It may be presumed from the pH values and ion exchange that the composition of species in the aqueous solution of chromium(III) sulfate in the green form is almost the same as that in the solution of chrome alum dehydrated in the solid state mentioned above.

14) V. Monti, *Nuovo Cimento* (4), **43**, 212 (1896).

Summary

1) By measuring the conductivity of the solution of hexa-aquochromium(III) sulfate and potassium-chrome alum, the formation constant of the ion-pair $[Cr(H_2O)_6]SO_4^+$ has been calculated.

2) By measuring the pH, ion exchange separation and electrical conductivity of the heated solution of potassium-chrome alum and of the solution of the alum heated in the solid state, their ion compositions have been deduced.

Appreciation is expressed to Messrs. Teruyoshi Fujishima and Tosuke Imamura for their help in the determination of the electrical conductivity.

Department of Chemistry
Faculty of Science
Kanazawa University
Kanazawa

Electron Spin Resonance Hyperfine Spectra of Di-p-anisyl Nitric Oxide

By Kisaburo UMEMOTO, Yasuo DEGUCHI and Hideo TAKAKI

(Received December 20, 1962)

One of the present authors has previously reported the ESR study of diphenyl nitric oxide (DPNO) in the solid state[1] and in a liquid solution[2]. Similarly, the ESR study of di-*p*-anisyl nitric oxide, one of the derivatives of DPNO, has been reported by some authors[3-7]. Bijl and Rose-Innes[5], for instance, observed the ^{14}N hyperfine structure in a liquid solution for the first time. Roggen et al.[6] also observed the triplet hyperfine structure due to the ^{14}N nucleus; they interpreted it by assuming that the odd electron is associated mainly with the NO group. However, they did not find any evidence for the splitting or significant broadening of the lines by the proton moments. We have now observed the proton hyperfine spectra of di-*p*-anisyl nitric oxide in liquid solutions and have studied the effect of solvents on the spectra and on the width of nitrogen and proton hyperfine splittings.

Experimental

Following the method of Meyer et al.[8,9], we synthesized di-*p*-anisyl nitric oxide. This radical is very stable; it remains unchanged even six months after preparation. Solutions of di-*p*-anisyl nitric oxide were made in various kinds of solvent, i. e., benzene, toluene, cyclohexane, carbon tetrachloride, carbon disulfide, dimethoxyethane, tetrahydrofuran, acetone, acetonitrile, *n*-butyl alcohol, isopropyl alcohol, ethyl alcohol, methyl alcohol and water. These samples were contained in vacuum-sealed glass tubes. The solvents were completely dehydrated, degassed[2] and purified just before the preparation of the sample solutions. In order to determine the nitrogen and proton hyperfine coupling constants, an aqueous solution of peroxylamine disulfonate was used as a reference in the same manner as in the case of DPNO[2]. The ESR spectrometer employed was a JES-3B-type instrument of the Japan Electron Optics Co. This spectrometer is an X-band apparatus employing a cylindrical reflection cavity operated in the TE_{001} mode. The static magnetic field was generated by a JES electro-magnet with 300 mmϕ pole pieces, with a homogeneity of 10^{-6} gauss/sample volume. The magnetic field was modulated in 100 kilocycle/sec.

Results and Discussion

We observed the ESR spectra of di-*p*-anisyl nitric oxide in various kinds of solvent, thus determining a suitable concentration for obtaining a well-resolved hyperfine spectrum. In a properly diluted solution, a well-resolved hyperfine spectrum was obtained. Figure 1a* shows the ESR hyperfine spectrum of di-*p*-anisyl nitric oxide in the carbon tetrachloride solution. There are three large groups in the spectrum, and each of them splits further into many, about 160, fine absorption lines. These three groups arise from the interaction of the unpaired electron spin with the nuclear spin of ^{14}N, as has been suggested by Bijl and Rose-Innes[5] and by others[6,7], while the further splittings may be caused by the interaction with the proton moments. In Fig. 1a, the absorption lines show the effect of the anisotropy of molecular motion in solution, which results in a different line width for each line[10,11], as in the case of DPNO[2].

The measured *g*-value is 2.0054, and the ^{14}N hyperfine coupling constant is 10.20 gauss for the tetrahydrofuran (THF) solution. This coupling constant is a little larger than that of DPNO. This is perhaps because the electron-repelling effect of methoxy groups at the para position in the molecule of di-*p*-anisyl nitric oxide may enhance the unpaired-electron spin density at the nitrogen nucleus more than in the case of DPNO.

The structure of di-*p*-anisyl nitric oxide is shown in Fig. 1c. As the unpaired-electron spin density in this molecule has not yet been calculated, we can not compare the obtained spin density with the theoretically-calculated spin density. In order to explain the obtained

1) Y. Deguchi, This Bulletin, **34**, 910 (1961).
2) Y. Deguchi, ibid., **35**, 260 (1962).
3) A. N. Holden, C. Kittel, F. R. Merrit and W. A. Yager, *Phys. Rev.*, **77**, 147 (1950).
4) A. N. Holden, *J. Chem. Phys.*, **19**, 1319 (1951).
5) D. Bijl and A. C. Rose-Innes, *Phil. Mag.*, **44**, 1187 (1953).
6) A. V. Roggen, L. V. Roggen and W. Gordy, *Phys. Rev.*, **105**, 50 (1957).
7) H. G. Thom and B. E. Wahler, *Z. Naturforsch.*, **13a**, 552 (1958).
8) K. H. Meyer and G. Brilloth, *Ber.*, **52**, 1480 (1919).
9) K. H. Meyer and W. Reppe, ibid., **54**, 330 (1921).

* In all figures of the observed ESR spectra, the magnetic field was swept from the left hand side of a figure to the right.

10) H. M. McConnell, *J. Chem. Phys.*, **25**, 709 (1956).
11) D. Kivelson, ibid., **33**, 1094 (1960).

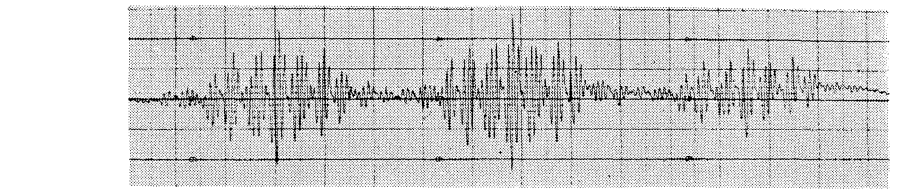

(a)

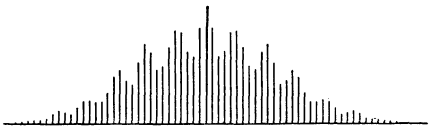

(b)

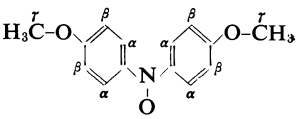

(c)

Fig. 1. (a) ESR spectrum of di-*p*-anisyl nitric oxide in CCl_4.
(b) Spectrum calculated based upon our assumption.
(c) The structure of di-*p*-anisyl nitric oxide.

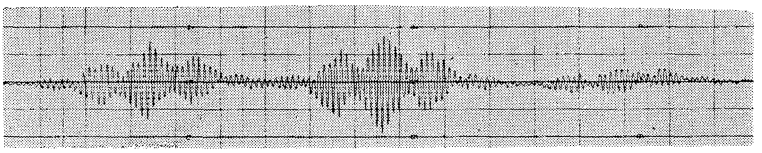

(a)

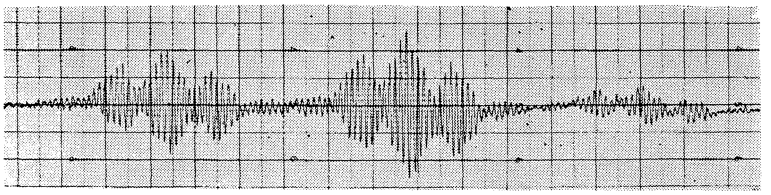

(b)

Fig. 2. (a) The ESR spectrum of di-*p*-anisyl nitric oxide in *n*-butanol.
(b) The one in water solution.

ESR spectrum in Fig. 1a, however, one can assume that the ratios of the unpaired-electron spin densities at the α, β and γ positions of the molecule shown in Fig. 1c are 10 : 4 : 1; according to this assumption one can then construct such a spectrum as is shown in Fig. 1b. In this figure only one of the three groups is shown. Although, in Fig. 1a, the groups overlap with each other at the tails and although the outermost absorption lines are too weak to be distinguished from the noise level, it can be seen that the calculated spectrum in Fig. 1b shows a very good agreement with the observed ESR spectrum in Fig. 1a.

Spectra of a type similar to that obtained in the carbon tetrachloride solution were observed in relatively non-polar solvents, such as benzene, cyclohexane, dimethoxyethane and tetrahydrofuran. The resolution of the proton hyperfine splittings slightly changed from one solvent to another. However, in relatively strong polar solvents, such as acetone, acetonitrile, alcohols and water, a broadening of the line width is clearly observed and the number of proton hyperfine splittings decreases as compared with those in the cases of non-polar solvents. The spectra of the *n*-butanol solution and the aqueous solution are illustrated in Figs. 2a and 2b. In the case of alcohols and water, both of which have a hydroxyl group, the ESR spectra showed another remarkable change in that the absorption lines of the higher magnetic field group are strongly broadened compared with those of the lower one. This phenomenon can be considered to be a result of the strong anisotropic effect[2,11]; it may be illustrated qualitatively as follows. The alcoholic hydroxyl group has a very large affinity to the lone pair electrons of oxygen atoms in the molecule of di-*p*-anisyl nitric oxide, so that alcohol molecules will strongly solvate to the molecule of di-*p*-anisyl nitric oxide in solution.

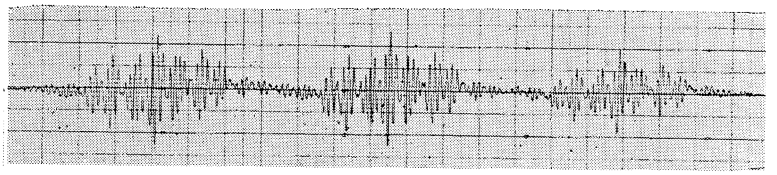

(a)

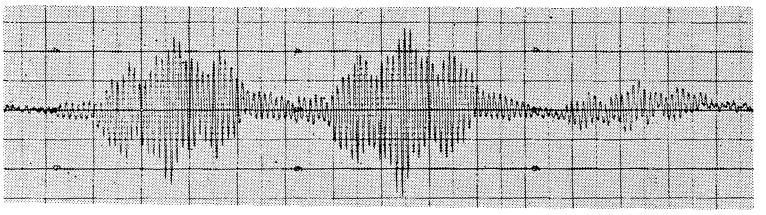

(b)

Fig. 3. (a) The ESR spectrum of di-*p*-anisyl nitric oxide in THF solution at room temperature 20°C.
(b) The one at −55°C.

Therefore, the motion of the solute radical will be reduced, and, consequently, the anisotropic effect will appear, causing a different set of relaxation times, T_2 and T_1, for each hyperfine line[2,10,11]. Thus we may explain this phenomenon, taking into account both the line-width calculation for DPNO[2], which revealed that the absorption lines of the higher magnetic field group were broader than those of the lower one, and the molecular similarity between DPNO and di-*p*-anisyl nitric oxide. For the quantitative varification of the above explanation, an experiment is expected to determine the *g*-tensor of di-*p*-anisyl nitric oxide.

To check the above explanation further, measurements were performed at low temperatures, since the viscosity of a solvent would increase at low temperatures. As an example, the ESR spectra of the THF solution are shown in Figs. 3a and 3b, where the former was measured at room temperature and the latter at −55°C. The latter spectrum is very similar to those shown in Fig. 2a and 2b. At a low temperature the free motion of the solute molecule is reduced and may be hindered as the viscosity of the solvent increases. The anisotropic effect, as a result, becomes appreciably large; it will broaden the width of each absorption line, especially those in the higher magnetic field group as compared with those in the lower magnetic field group, as is shown in Fig. 3b. This effect was not so remarkable in the case of DPNO. This is perhaps because DPNO has no methoxy group and because the free motion of the molecule of DPNO is not so strongly hindered by strong solvation or by the high viscosity of the solvent at a low temperature, as in the case of di-*p*-anisyl nitric oxide.

The effect of solvents on the widths of nitrogen and proton hyperfine splittings, which was first found in DPNO[2], was also found in di-*p*-anisyl nitric oxide. The results obtained are shown in Fig. 4 where the magnitudes of the dielectric constants of the solvents are conveniently taken as an abscissa scale. In this figure the alcoholic and aqueous solutions exhibit remarkably greater values than the others. This solvent effect will be explained qualitatively if one will consider

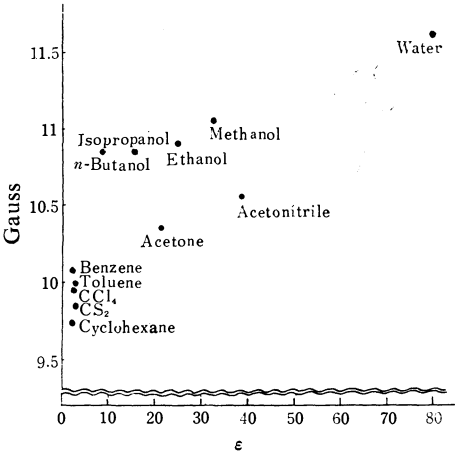

Fig. 4. Solvent effect on the nitrogen isotropic hyperfine coupling constant.

that the ionic structures of the radical molecule in the valence bond theory will be favored by the presence of polar solvents, as in the case of DPNO[2], so that the spin densities at the nitrogen and the ring carbons will be enhanced. Especially in the case of the alcoholic solution, these ionic structures may be much more favored by the effect of strong solvation. However, this explanation is not conclusive and further investigation is required to provide a rigorous theoretical basis.

Department of Chemistry
Faculty of Science
Kyoto University
Kyoto

*Kinetics of Hydrolytic Reaction Catalyzed by Crystalline Bacterial α-Amylase. III. The Influence of Temperature**

By Keitaro HIROMI, Yoshiyuki TAKASAKI** and Sôzaburo ONO

(Received December 22, 1962)

In previous publications[1,2] we have studied the influence of pH[1] and of solvent[2] upon the rates of hydrolytic reactions catalyzed by α-amylase of *Bacillus subtilis*, and obtained information about the nature of the essential ionizable groups of the enzyme and the electrostatic character of the reaction processes. The present paper deals with the influence of temperature upon the kinetic constants of this enzyme reaction; this study will provide information about the reaction mechanism, especially in connection with the results obtained in the previous studies[1,2].

Experimental

Enzyme.—The six times-recrystallyzed bacterial amyloclastic α-amylase of *Bacillus subtilis* (*Bac. amyloliquefacience* Fukumoto), furnished by Prof. J. Fukumoto and Dr. T. Yamamoto of Osaka City University, was dissolved in 1/50 M calcium acetate and was then kept in a refrigerator as a stock solution. This solution was diluted with a 1/300 M calcium acetate solution before use to avoid the inactivation of the enzyme, the enzymic activity of which was checked before each experiment.

Substrate.—Thrice-recrystallized potato amylose provided by the Nagase Sangyo Co., Ltd., was dissolved with a small amount of 1 N sodium hydroxide (to give a ca. 5% solution), kept overnight in a refrigerator, diluted with water and finally neutralized with 1 N acetic acid to pH 5.85 to give a 0.25% amylose solution in a 0.05 M acetate buffer. Substrate solutions of various concentrations were prepared by diluting this solution with a 0.05 M acetate buffer of the same pH.

Procedure.—Reaction was commenced by introducing 1 ml. of the diluted enzyme solution into 25 ml. of the substrate solution placed in a reaction vessel equipped with a glass stirrer. At certain time intervals (usually one minute) 2 ml. of the reaction mixture was pipetted out and poured into 2 ml. of Somogyi's reagent (see below), and the reaction was stopped. The number of reducing ends produced was determined by means of Somogyi-Nelson's photometrical method[3,4] with this slight modification: the amount of anhydrous sodium bisulfate in Somogyi's reagent[3] was reduced to 1/10 of its original amount (18 g. instead of 180 g. per l.), and nitrogen gas was passed through the solution containing Somogyi's reagent and the reaction mixture for 10 min. before boiling it to remove the dissolved oxygen. This latter procedure is especially important in determining a small number of reducing ends, because without this procedure reducing ends less than ca. 30 μmol./l. (or equivalently 5 μg./ml. of glucose) cannot be detected, probably due to the oxidation of the reducing material. The mixture was heated for 30 min. in a boiling water bath and cooled in ice water, into which 2 ml. of Nelson's reagent[4] was added. After 30 min. the colored solution was diluted to 10 ml., and the optical density was measured at 600 mμ with a Shimadzu QB 50 spectrophotometer using glucose as the reference reducing substance.

The reaction conditions were as follows: pH: 5.85 (optimum[1]) with a 0.05 M acetate buffer; substrate concentration: 0.24~0.0096%; enzyme

* Presented in part at the 12th Annual Meeting of the Chemical Society of Japan, Kyoto, April, 1959.

** Present address: Fermentation Research Institute, Agency of Industrial Science and Technology, Ministry of International Trade and Industry, Chiba.

1) S. Ono, K. Hiromi and Y. Yoshikawa, This Bulletin, **31**, 957 (1958).

2) S. Ono, K. Hiromi and Y. Sano, ibid., **36**, 431 (1963).

3) M. Somogyi, *J. Biol. Chem.*, **195**, 19 (1952).

4) N. Nelson, ibid., **153**, 375 (1944).

concentration: 3.0×10^{-9} M unless otherwise described (the molecular weight of this enzyme is 48200[5]); calcium acetate: 1.3×10^{-4} M, and the temperature was in the range from 6 to 40°C.

The concentration of the substrate or product was usually expressed in units of "mole of bond per l." (per cent unit multiplied by 10/162), which means the number of mole of glucosidic linkage per l. present or hydrolyzed.

Results

Typical examples of the reaction time curve are shown in Fig. 1. Each curve was found to have a small break in the earliest phase of the reaction (about 30 seconds after commencement). As is shown in Fig. 2, except for the initial break, the reaction follows an apparent first order kinetics until about 30% hydrolysis is attained (or until 15% of the total linkages is broken). Such a break had not been observed in previous studies[1,2], in which the determination of the reducing ends had been carried out using 3, 5-dinitrosalicylate (DNS)[6]. In Fig. 3, the reaction time curve followed by the DNS method (curve I) is compared with that of the Somogyi-Nelson (SN) method (curve II), glucose being used as the reference in both cases. The discrepancy between the two curves is quite serious, and besides the initial break, the velocity (which is represented by the slope

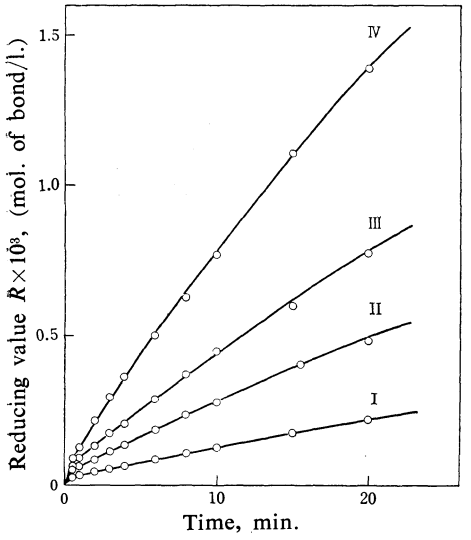

Fig. 1. Reaction time curves. Substrate concentration: 1.50×10^{-2} mol. of bond/l., 12.0°C. Enzyme concentration ($\times10^9$ M): I 0.94, II 2.82, III 4.70, IV 9.40.

5) K. Kakiuchi, S. Kato and T. Isemura, lecture delivered at the Symposium on Protein Structure, Maebashi, November, 1962.

6) G. N. Smith and C. Stocker, *Arch. Biochem.*, **21**, 95 (1949).

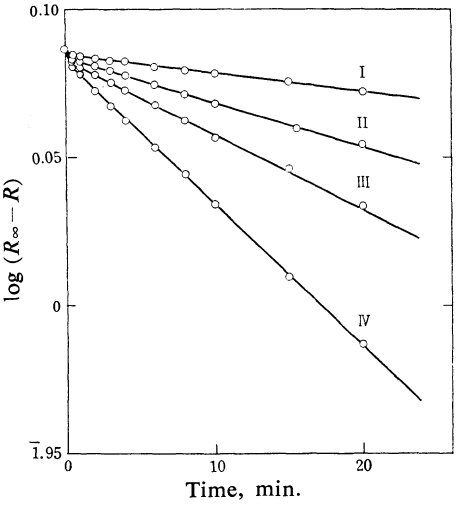

Fig. 2. The first-order plots. The numbers correspond to those in Fig. 1.

of the apparently linear part of the curve) in the SN method is about 1/14 as large as that of the DNS method. This phenomenon, though not yet fully understood, is presumed to be due to the different sensitivity of these two methods for reducing ends of different chain lengths. In fact, it has been found that the ratio of the reducing value (per mole) of maltose to that of glucose is 0.85 in the DNS method, while the ratio in the SN method is 0.50. The latter value is exactly equal to the reciprocal ratio of their molecular weights[7].

The initial velocity, v, was estimated according to the following equation, disregarding the initial break:

$$v=k_a(R_\infty-R_0) \qquad (1)$$

where R_0 and R_∞ are the reducing values at zero time and at complete hydrolysis (the theoretical limit at which 50% of the total linkage is broken) respectively, and where k_a is the apparent first order rate constant determined from the slope of the plot of log $(R_\infty-R)$ versus time (see Fig. 2). The initial velocity, v, thus obtained is in good proportionality with the enzyme concentration, [E], as is shown in Fig. 4.

The Michaelis constant, K_m, and the maximal velocity, V, were obtained from the plot of s/v versus s according to the equation:

7) According to our unpublished data, it has been proved for the SN method that the reduing value (per mole) of malto-oligosaccharide is independent of its chain length, at least up to maltopentaose. Since this relationship has not been proved to hold for amylose, it might be possible that the observed velocity does not reflect the true magnitude of the hydrolysis rate. However, the relative magnitude of rate obtained is correct, as far as initial rates are concerned.

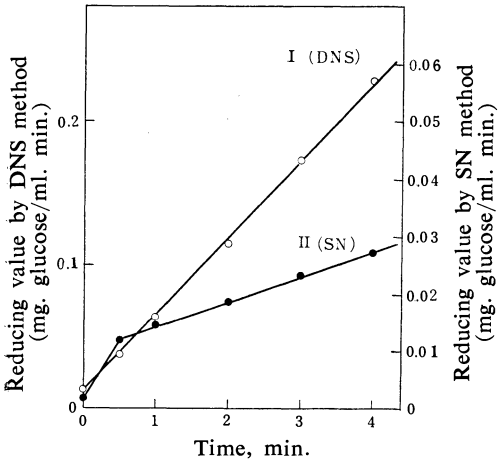

Fig. 3. Comparison of reducing values obtained by DNS and SN methods. Substrate concentration: 1.48×10^{-2} mol. of bond/l., 12.0°C.

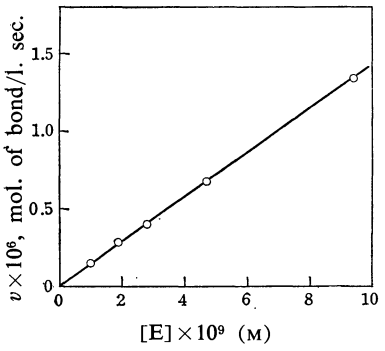

Fig. 4. Relationship between v and [E]. Substrate concentration: 1.50×10^{-2} mol. of bond/l. 12.0°C.

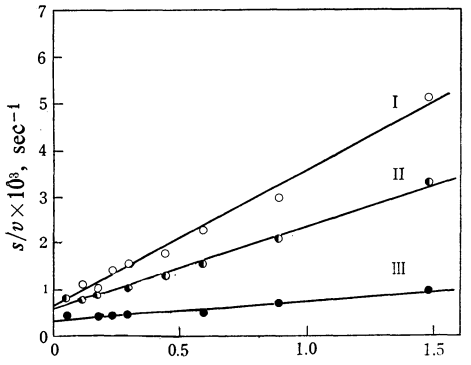

Fig. 5. Plots of s/v versus s. Temperature: I 6°C, II 12°C, III 40°C. [E]= 3.0×10^{-9} M.

$$s/v=K_m/V+s/V \qquad (2)$$

where v is the initial velocity at substrate concentration s. Fig. 5 shows some typical plots of s/v versus s. Let k_3 be a rate constant obtained by dividing V by the enzyme concentration [E]:

$$k_3=V/[E] \qquad (3)$$

According to the Michaelis-Menten-Briggs-Haldane mechanism[8]:

$$E+S \underset{k_2}{\overset{k_1}{\rightleftharpoons}} ES \xrightarrow{k_3} E+P \qquad (4)$$

from which Eq. 2 is derived, k_3 corresponding to the breakdown rate constant of the ES complex. K_m is expressed as

$$K_m=(k_2+k_3)/k_1 \qquad (5)$$

where k_1, k_2 and k_3 are the rate constants designated in Eq. 4.

TABLE I. VALUES OF THE RATE PARAMETERS AT VARIOUS TEMPERATURES

Temp. °C	K_m (mol. of bond/l.)×10³	k_3 sec⁻¹	k_3/K_m (sec⁻¹/mol. of bond/l.)×10⁻⁴
6.0	2.13±0.32	114.5± 4.6	5.38±0.78
12.0	3.22±0.29	187.3± 7.4	5.82±0.48
18.0	4.33±0.49	293.2±17.9	6.77±0.64
25.0	6.15±0.70	460.8±32.1[a]	7.50±0.67
32.0	7.11±0.90	656.8±60.5	9.23±0.80
40.0	8.01±1.13	818.5±88.6	10.21±0.93

a) This value is 1/8.5 as large as the previous value[1], which was obtained by DNS method using maltose as reference. This discrepancy is due to the difference in the analytical method employed and to that in the reference sugar. (See text)

The values of K_m, k_3 and k_3/K_m obtained from Eqs. 2 and 3 using the least square method are listed in Table I, along with their standard deviations[9]. In Fig. 6, the logarithms of K_m, k_3 and k_3/K_m are plotted against the reciprocal of the absolute temperature, T, in which standard deviations are also indicated. It was found that the plots of $\log K_m$ and $\log k_3$ are almost linear below 25°C, but above that point they tend to flatten out. On the other hand, the $\log k_3/K_m$ versus $1/T$ plot was found to give a straight line over the whole temperature range studied.

Apparent Thermodynamic Quantities. — The non-linearity of $\log k_3$ vs. $1/T$ plot suggests that the reaction may be more complicated than is represented by Eq. 4. In this case, the rate parameters, K_m and k_3, should be regarded as empirical and apparent ones. Leaving their meanings to later consideration, however, we will define several apparent

8) L. Michaelis and M. L. Menten, *Biochem. Z.*, **49**, 333 (1913); G. E. Briggs and J. B. S. Haldane, *Biochem. J.*, **19**, 383 (1925).

9) W. J. Youden, "Statistical Methods for Chemists", John Wiley & Sons, Inc., New York (1951), p. 40.

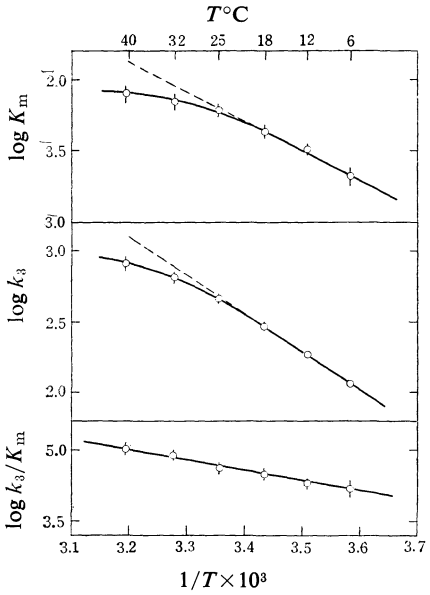

Fig. 6. Plots of $\log K_m$, $\log k_3$ and $\log k_3/K_m$ versus $1/T$.

thermodynamic quantities which are derived from K_m and k_3.

First, we define Δg_m, Δh_m and Δs_m as follows[10]:

$$\Delta g_m = \boldsymbol{R}T \ln K_m \quad (6)$$

$$\Delta h_m = \boldsymbol{R}\mathrm{d}\ln K_m/\mathrm{d}(1/T) \quad (7)$$

$$= \boldsymbol{R}\Delta \ln K_m/(1/T_1 - 1/T_2) \quad (8)$$

$$\Delta s_m = (\Delta h_m - \Delta g_m)/T \quad (9)$$

where $\boldsymbol{R}$ is the gas constant, and $\Delta \ln K_m$ designates the difference between $\ln K_m$ at temperature T_1 and that at temperature T_2.

Similarly, let $\Delta g_3^{\ddagger}$, $\Delta h_3^{\ddagger}$ and $\Delta s_3^{\ddagger}$ be defined by:

$$\Delta g_3^{\ddagger} = \boldsymbol{R}T(\ln \boldsymbol{k}T/\boldsymbol{h} - \ln k_3) \quad (10)$$

$$\Delta h_3^{\ddagger} = E - \boldsymbol{R}T \quad (11)$$

$$E = -\boldsymbol{R}\mathrm{d}\ln k_3/\mathrm{d}(1/T) \quad (12)$$

$$= -\boldsymbol{R}\Delta \ln k_3/(1/T_1 - 1/T_2) \quad (13)$$

$$\Delta s_3^{\ddagger} = (\Delta h_3^{\ddagger} - \Delta g_3^{\ddagger})/T \quad (14)$$

where $\boldsymbol{k}$, $\boldsymbol{h}$ and E are the Boltzmann constant, the Planck constant and the Arrhenius activation energy obtained from k_3, respectively, and where $\Delta \ln k_3$ represents the difference between $\ln k_3$ at T_1 and that at T_2.

Moreover, let the thermodynamic quantities, $\Delta g^{\ddagger}$, $\Delta h^{\ddagger}$ and $\Delta s^{\ddagger}$, be defined as follows:

$$\Delta g^{\ddagger} = \Delta g_m + \Delta g_3^{\ddagger}$$

$$= \boldsymbol{R}T(\ln \boldsymbol{k}T/\boldsymbol{h} - \ln k_3/K_m) \quad (15)$$

$$\Delta h^{\ddagger} = \Delta h_m + \Delta h_3^{\ddagger} = E' - \boldsymbol{R}T \quad (16)$$

$$E' = -\boldsymbol{R}\mathrm{d}\ln (k_3/K_m)/\mathrm{d}(1/T) \quad (17)$$

$$\Delta s^{\ddagger} = \Delta s_m + \Delta s_3^{\ddagger} \quad (18)$$

If the simple Michaelis-Menten scheme is valid, and, further, if K_m is a dissociation constant of ES complex (i.e., $k_2 \gg k_3$), Δg_m, Δh_m and Δs_m would be the standard free energy, enthalpy and entropy change accompanied by the ES complex formation, respectively, and $\Delta g_3^{\ddagger}$, $\Delta h_3^{\ddagger}$ and $\Delta s_3^{\ddagger}$ would stand for the free energy, enthalpy and entropy of activation for the breakdown process of ES complex, respectively.

The values of the apparent thermodynamic quantities calculated by means of least square method, are listed in Table II, which also includes their standard deviations. $\Delta h^{\ddagger}$ was obtained for the whole temperature range studied by using Eqs. 16 and 17. The values of Δh_m and $\Delta h_3^{\ddagger}$ below 25°C were obtained from the linear part of the log plots in Fig. 6, while those values above 25°C, where linearity fails, were obtained by using Eqs. 8, 11 and 13.

Discussion

The non-linearity of $\log K_m$ and $\log k_3$ versus $1/T$ plots, which is often encountered in enzyme reactions, may be attributed to several factors[11]. Possibilities relevant to the present case include: first, the reaction may consist of three steps, including two types of ES complex[12-16], and, second, the reaction may be accompanied by the rapid and reversible denaturation of the enzyme molecule[17-19].

If it is a three-step mechanism, the reaction scheme may be written as follows:

$$E + S \underset{\tilde{k}_2}{\overset{\tilde{k}_1}{\rightleftharpoons}} ES_1 \overset{\tilde{k}_3}{\rightarrow} ES_2 \overset{\tilde{k}_4}{\rightarrow} E + P \quad (19)$$

where ES_1 and ES_2 represent the two types of intermediate complex[20]. The rate parameters, k_3 and K_m, obtained experimentally using Eqs. 2 and 3 are given by:

10) The apparent thermodynamic quantities are designated by small letters in order to distinguish them from the true thermodynamic quantities, which will be designated by large letters (see below).

11) Cf., for example, M. Dixon and E. C. Webb, "Enzymes", Academic Press, New York (1958), p. 62.

12) B. S. Hartley and B. A. Kilby, *Biochem. J.*, **56**, 288 (1954).

13) H. Gutfreund and J. M. Sturtevant, ibid., **63**, 656 (1956).

14) T. Spencer and J. M. Sturtevant, *J. Am. Chem. Soc.*, **81**, 1874 (1959).

15) I. B. Wilson and E. Cabib, ibid., **78**, 202 (1956).

16) R. M. Krupka and K. J. Laidler, *Trans. Faraday Soc.*, **56**, 1477 (1960).

17) G. Kalmitsky and H. Resnick, *J. Biol. Chem.*, **234**, 1714 (1959).

18) W. B. Neely, *J. Am. Chem. Soc.*, **81**, 4416 (1959).

19) G. B. Kistiakowsky and R. Lumry, ibid., **71**, 2006 (1949).

20) On analogy with α-chymotrypsin, it may be supposed, for example, that ES_1 and ES_2 correspond to the Michaelis complex and the glycosyl enzyme, respectively.

TABLE II. VALUES OF THE APPARENT THERMODYNAMIC QUANTITIES AT VARIOUS TEMPERATURES

Temp. °C	6.0	12.0	18.0	25.0	32.0	40.0
$-\Delta g_m$ kcal. mol^{-1}	3.42±0.08	3.24±0.05	3.15±0.07	3.01±0.07	2.99±0.08	3.00±0.08
$-\Delta h_m$ kcal. mol^{-1}	←	9.25±1.38	→	3.7±4.7	2.8±4.5	
$-T\Delta s_m$ kcal. mol^{-1}	5.83±1.40	6.01±1.40	6.10±1.40	6.24±1.40	0.7 ±4.7	−0.2 ±4.5
$-\Delta s_m$ cal. deg^{-1} mol^{-1}	20.9 ±5.0	21.1 ±5.0	21.0 ±4.8	20.9 ±4.7	2.5 ±15.5	−0.5 ±14.5
Δg_3^* kcal. mol^{-1}	13.68±0.02	13.66±0.02	13.73±0.03	13.81±0.04	13.91±0.05	14.16±0.06
E kcal. mol^{-1}	←	12.56±0.61	→	9.1±3.0	5.2±3.4	
Δh_3^* kcal. mol^{-1}	←	12.0 ±0.6	→	8.5±3.0	4.6±3.4	
$-T\Delta s_3^*$ kcal. mol^{-1}	1.7 ±0.6	1.7 ±0.6	1.7 ±0.6	1.8 ±0.6	5.4 ±3.0	9.5 ±3.4
$-\Delta s_3^*$ cal. deg^{-1} mol^{-1}	6.1 ±2.2	6.0 ±2.1	5.8 ±2.1	6.0 ±2.0	18±10	31±11
Δg^* kcal. mol^{-1}	10.27±0.08	10.43±0.04	10.58±0.05	10.80±0.04	10.92±0.05	11.16±0.06
E' kcal. mol^{-1}	←		3.31±0.62		→	
Δh^* kcal. mol^{-1}	←		2.7 ±0.6		→	
$-T\Delta s^*$ kcal. mol^{-1}	7.6 ±0.6	7.7 ±0.6	7.9 ±0.6	8.1 ±0.6	8.2 ±0.6	8.5 ±0.6
$-\Delta s^*$ cal. deg^{-1} mol^{-1}	27.1 ±2.2	27.1 ±2.1	27.1 ±2.1	27.2 ±2.0	27.0 ±2.0	27.0 ±2.0

TABLE III. PHYSICAL MEANINGS OF THE APPARENT THERMODYNAMIC QUANTITIES AT THE LOWER TEMPERATURE RANGE BELOW 25°C

Apparent thermodynamic quantities	Physical meanings: Case a $\tilde{k}_4 \gg \tilde{k}_3$	Physical meanings: Case b $\tilde{k}_3 \gg \tilde{k}_4$	Numerical values at 18°C
Δg_m	ΔG_1	$\Delta G_1+\Delta G_1^*-\Delta G_2^*$	− 3.2 kcal. mol^{-1}
Δh_m	ΔH_1	$\Delta H_1+\Delta H_1^*-\Delta H_2^*$	− 9.3 kcal. mol^{-1}
Δs_m	ΔS_1	$\Delta S_1+\Delta S_1^*-\Delta S_2^*$	−21.0 cal. deg^{-1} mol^{-1}
Δg_3^*	ΔG_1^*	ΔG_2^*	13.7 kcal. mol^{-1}
Δh_3^*	ΔH_1^*	ΔH_2^*	12.0 kcal. mol^{-1}
Δs_3^*	ΔS_1^*	ΔS_2^*	− 5.8 cal. deg^{-1} mol^{-1}
Δg^*	$\Delta G_1+\Delta G_1^*$	$\Delta G_1+\Delta G_1^*$	10.6 kcal. mol^{-1}
Δh^*	$\Delta H_1+\Delta H_1^*$	$\Delta H_1+\Delta H_1^*$	2.7 kcal. mol^{-1}
Δs^*	$\Delta S_1+\Delta S_1^*$	$\Delta S_1+\Delta S_1^*$	−27.1 cal. deg^{-1} mol^{-1}

$$k_3=\tilde{k}_3\tilde{k}_4/(\tilde{k}_3+\tilde{k}_4) \quad (20)$$

$$K_m=\tilde{k}_4(\tilde{k}_2+\tilde{k}_3)/\tilde{k}_1(\tilde{k}_3+\tilde{k}_4) \quad (21)$$

$$k_3/K_m=\tilde{k}_3\tilde{k}_1/(\tilde{k}_2+\tilde{k}_3) \quad (22)$$

where the $\tilde{k}$'s are the rate constants indicated in Eq. 19. Previous study of the pH effect[1] has suggested that $\tilde{k}_2 \gg \tilde{k}_3$ in the present case. Eqs. 21 and 22, therefore, reduce to:

$$K_m=\tilde{k}_4/K_s(\tilde{k}_3+\tilde{k}_4) \quad (23)$$

$$k_3/K_m=\tilde{k}_3K_s \quad (24)$$

where K_s is the equilibrium constant for the process $E+S \rightleftarrows ES_1$ and is given by $K_s=\tilde{k}_1/\tilde{k}_2$.

Eq. 24 suggests that the $\log k_3/K_m$ versus $1/T$ plot should be linear. Eqs. 20 and 23 predict that the $\log k_3$ and $\log K_m$ versus $1/T$ plots will be linear at lower temperatures, where $\tilde{k}_3 \ll \tilde{k}_4$ (case a) or $\tilde{k}_4 \ll \tilde{k}_3$ (case b), but they will be concave in a higher temperature range, where $\tilde{k}_3$ and $\tilde{k}_4$ become comparable. Thus, the present findings may most reasonably be accounted for by considering that the $\tilde{k}_3$ step and the $\tilde{k}_4$ step have different activation energies and that either one of them becomes rate-limiting in the lower temperature range (below 25°C). In the lower temperature range, the rate parameters become as follows:

$$k_3=\tilde{k}_3 \text{ (case a)} \qquad k_3=\tilde{k}_4 \text{ (case b)} \quad (25)$$

$$K_m=1/K_s \text{ (case a)} \qquad K_m=\tilde{k}_4/\tilde{k}_3K_s \text{ (case b)} \quad (26)$$

$$k_3/K_m=\tilde{k}_3K_s \text{ (in both cases)} \quad (27)$$

Accepting this mechanism, we can express the apparent thermodynamic quantities in terms of the true thermodynamic quantities concerned with each step in Eq. 19. Let the true thermodynamic quantities be defined as follows: ΔG_1, ΔH_1 and ΔS_1 represent the standard free energy, enthalpy and entropy change, respectively, accompanied by the K_s step, $E+S \rightleftarrows ES_1$; let ΔG_1^*, ΔH_1^* and ΔS_1^*

represent the free energy, enthalpy and entropy of activation, respectively, of the $\tilde{k}_3$ step, $ES_1 \rightarrow ES_2$, and let $\Delta G_2^{\neq}$, $\Delta H_2^{\neq}$ and $\Delta S_2^{\neq}$ represent the free energy, enthalpy and entropy of activation, respectively, of the $\tilde{k}_4$ step, $ES_2 \rightarrow E+P$. The physical meanings of the apparent thermodynamic quantities in the lower temperature range are given in Table III in terms of these true thermodynamic quantities.

Although at present we have no other evidence which strongly supports the three-step mechanism of this enzyme reaction, the kinetic features which have been observed hitherto are by no means inconsistent with this mechanism. For instance, the fact that pH and solvent both affect k_3 but do not affect K_m[1,2] may reasonably be expected in case a; it may also reasonably be expected in case b if these extrinsic factors influence both the $\tilde{k}_3$ and the $\tilde{k}_4$ steps in the same manner.

The second possibility, that the reaction is accompanied by the reversible denaturation of the enzyme molecule, was also examined kinetically. It was found that, in order to interpret the results in terms of this mechanism, we are forced to assume that the substrate binding greatly facilitates the reversible denaturation. This is obviously contrary to what is expected from the well-known phenomenon that substrates protect enzymes from their thermal denaturation. Thus, this mechanism is poorly consistent with the experimental results.

Entropy change, ΔS, of a reaction in general, as well as other thermodynamic quantities, can be expressed as a sum of the electrostatic part, $\Delta S_{e.s.}$, and the non-electrostatic part, $\Delta S_{n.e.s.}$, the former of which may be estimated from the study of the dielectric constant effect[2,21] The entropy values obtained in the present study being the total entropy change, ΔS, the non-electrostatic entropy, $\Delta S_{n.e.s.}$, can be obtained by subtracting $\Delta S_{e.s.}$ previously obtained from the solvent effect[2] from ΔS. Using the values at 25°C, $\Delta s_m = -21$ cal. deg^{-1} mol^{-1} and $\Delta s_3^{\neq} = -6$ cal. deg^{-1} mol^{-1}, which were obtained in this study and $\Delta s_{m_{e.s.}} = 0$ and $\Delta s_{3\,e.s.}^{\neq} = -33$ (or -20)[22] cal. deg^{-1} mol^{-1}, which were obtained in the previous study[2], we have:

$$\Delta s_{m_{n.e.s.}} = \Delta s_m - \Delta s_{m_{e.s.}} = -21 - 0 = -21 \text{ cal. deg}^{-1} \text{ mol}^{-1}$$

$$\Delta s_{3\,n.e.s.}^{\neq} = \Delta s_3^{\neq} - \Delta s_{3\,e.s.}^{\neq} = -6 - (-33) = 27 \text{ cal. deg}^{-1} \text{ mol}^{-1}$$

$$(\text{or } -6 - (-20) = 14 \text{ cal. deg}^{-1} \text{ mol}^{-1})^{22}$$

The negative value of $\Delta s_{m_{n.e.s.}}$ may be due in part to the loss of freedom by the complex formation. The loss of the electrostatic entropy of activation, $\Delta s_{3\,e.s.}^{\neq}$, which may probably be due to charge separation in the activated complex[2], seems to be compensated for by the gain in the non-electrostatic entropy of activation, $\Delta s_{3\,n.e.s.}^{\neq}$, which may be due to a loosening of the linkage to be broken and/or to some conformation change in the enzyme protein[23].

It may be of interest to note that the value of Δh_m (-9.3 kcal. mol^{-1} in the present case) is of the same sign as, and of a magnitude similar to, those reported with other α-amylases, i. e., the swine pancreatic α-amylase-maxy maize starch system[24] (-7.1 kcal. mol^{-1}) and the Taka-amylase A-phenyl-α-maltoside system[25] ($-12 \sim -13$ kcal. mol^{-1}). The value of Δh_m, together with that of Δs_m, suggests that the binding force between substrate and enzyme may be hydrogen bonding and/or van der Waals force[26]. The results of solvent effect are also consistent with this view[2].

Summary

The influence of temperature upon the Michaelis constant, K_m, and on the breakdown rate constant, k_3, has been investigated for the hydrolytic reaction of amylose catalyzed by crystalline *Bacillus subtilis* α-amylase at pH 5.85 (the optimum pH) over the temperature range from 6 to 40°C.

It has been found that $\log K_m$ and $\log k_3$ increase linearly with a decreasing reciprocal absolute temperature $1/T$ in the lower temperature range below 25°C, while above that point they tend to flatten out. On the other hand, the plot of $\log k_3/K_m$ versus $1/T$ has been found to be linear over the whole temperature range studied. Apparent thermodynamic quantities have been calculated from K_m, k_3 and k_3/K_m and their temperature dependences.

The results have been examined kinetically in terms of two different mechanisms, the first assuming a three-step mechanism, and the

21) M. L. Barnard and K. J. Laidler, *J. Am. Chem. Soc.*, **74**, 6099 (1952); K. J. Laidler, *Discussions Faraday Soc.*, **20**, 83 (1955).

22) The value of the electrostatic entropy in the bracket is obtained based on the assumption that the observed solvent effect is partly due to the non-electrostatic effect caused by the change in solvent composition (see Ref. 2).

23) K. J. Laidler, "The Chemical Kinetics of Enzyme Action", Oxford University Press, London (1958), p. 187.

24) J. W. Van Dyk and M. L. Caldwell, *J. Am. Chem. Soc.*, **78**, 3345 (1956).

25) H. Toda, I. Kato, S. Matsubara and S. Akabori, *Symposia on Enzyme Chemistry (Kôso Kagaku Shinpojiumu)*, **15**, 43 (1961).

26) R. Lumry, "The Enzymes", Ed. by P. D. Boyer, H. Lardy and K. Myrbäck, Academic Press, New York (1959), p. 157.

second assuming the reversible denaturation of the enzyme molecule. It has been found that the former is reasonably consistent, but the latter is poorly consistent with the results.

By combining these findings with the previous data of solvent effect, the non-electrostatic part of the entropies for the reaction processes has been estimated.

The meanings of thermodynamic quantities obtained have been discussed.

The authors are very grateful to Professor Juichiro Fukumoto and Dr. Takehiko Yamamoto of Osaka City University for their gift of the crystalline enzyme, and to Nagase Sangyo Co., Ltd., for supplying the crystalline amylose.

Laboratory of Biophysical Chemistry
College of Agriculture
University of Osaka Prefecture
Sakai

The Diffusion of Barium in a Rutile Single Crystal

By Takashi NAKAYAMA* and Tsunetaka SASAKI

(Received December 22, 1962)

There have been many studies of diffusion in such solids as metals[1], metal halides[2,3] and metal oxides[4]. Little attention has, however, been paid, except in a few cases[5], to mutual diffusion between two metal oxides at higher temperature; this neglect has partly been due to the experimental difficulties and partly due to the chemical and/or crystallographic change taking place. We have studied the diffusion phenomena in the system of titanium dioxide and barium oxide in order to obtain some information concerning the chemical reaction of barium titanate formation and its sintering at higher temperatures. Our investigation is rather microscopic in nature, compared with the published reports of macroscopic observation[6,7]. In the present report, the change of state of the system is first observed qualitatively by means of an optical microscope. The diffusion of barium into a rutile single crystal is then measured by the radiotracer technique.

Experimental

Materials. — A rutile single crystal was obtained from the Tokyo Hoseki Co. The crystal was prepared by the flame fusion method[8] and was then annealed in oxygen gas at 1000°C[9]. Spectroscopic analysis revealed traces of silicon and iron as impurities. It seemed very likely that a minute amount of silicon would contaminate the rutile crystal, as it was ground in a mortar in the preparation of the spectroscopic specimens. Since the rutile crystal is optically anisotropic, the c-axis of the crystal was readily determined by a polarizing microscope. We obtained two kinds of rutile single-crystal plates by cutting, the one having a normal of the plate parallel to, and the other, one perpendicular to the c-axis. The direction of a normal of the crystal plate used for diffusion measurements was determined by X-ray Laue patterns. In most cases, the deviations of the X-ray resulting from the optical determination of the crystal axis were less than 2°. The barium carbonate powder for microscopic observations was of a Merk's reagent, the impurities being listed as calcium and alkali<0.1%, iron<0.001%, lead< 0.001% and barium hydroxide<0.03%. It was used without further purification. The barium carbonate used for the diffusion measurement was of a Johnson-Mathy's "specqure" grade, the impurities being listed as calcium 2 p. p. m., magnesium 1 p. p. m., and copper and sodium 1 p. p. m. Radioisotope ^{133}Ba was obtained as barium chloride in 1 N hydrochloric acid. It was mixed with the non-radioactive barium carbonate dissolved in hydrochloric acid. Sodium carbonate was then added to this mixture, and the labeled barium carbonate was obtained as a precipitate. The specific activity of the barium carbonate thus obtained was 4500 c.p.m./mg.

Microscopic Observations. — As it was difficult to observe a cross-section of the contact plane between the rutile single crystal and the barium carbonate powder, the barium carbonate powder was placed

* Present address: Research Center, Tokyo-Denki-kagaku-Kogyo Co., Ltd., Ichikawa, Chiba.

1) D. Lazarus, "Solid State Physics", Vol. 10, Academic Press, New York (1960).

2) F. Seitz, "Phase Transformation in Solids", Wiley, New York (1951).

3) W. Jost, "Diffusion in Solids, Liquids, Gases", Academic Press, New York (1960).

4) N. S. Gorbunov and V. I. Izvekov, *Soviet Phys. USPKHI*, 3, 778 (1961).

5) Chaudron, "Colloque sur la Diffusion a l'État Solid", North Holland Pub. Co., Holland (1959).

6) D. E. Rose and R. Roy, *J. Am. Ceram. Soc.*, **38**, 102 (1955).

7) L. K. Templeton and J. A. Pask, ibid., **42**, 212 (1959).

8) M. Kunitomi, *Metal Physics*, (*Kinzoku Butsuri*), **4**, 221 (1958).

9) F. Grant, *Rev. Mod. Phys.*, **31**, 646 (1959).

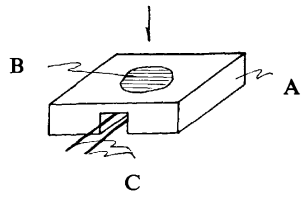

Fig. 1. Microscopic observation of diffusion system at high temperature.
A Rutile single crystal
B Powder of barium carbonate
C Thermocouple
Arrow shows the direction of the observation.

on the rutile crystal and the changes of the state were observed from above at a high reaction temperature, as is shown in Fig. 1. The temperature of the system was measured by inserting a Pt/Pt-Rh hot-junction (C in Fig. 1) into the rutile single crystal. It was reported that rutile is reduced when it is heated in vacuo (10^{-5}~10^{-4} mmHg) at a high temperature[10]. Therefore, the phenomenon we observed was the phase change of the system consisting of a single crystal of rutile with small oxygen vacancies and the powder of barium carbonate at a high temperature. However, as we kept the system at a high temperature for rather a short time (30 to 60 min.), such a reduction of rutile, if any, seemed not to influence the results obtained. After allowing the diffusion to take place at a high temperature (1100~1400°C) for two hours in oxygen gas to avoid reduction, it was cooled; the cross-section of the diffusion layer was then observed at room temperature. To enlarge the cross-section of the reaction layer, the sample plate was cut out obliquely, as may be seen in Fig. 2.

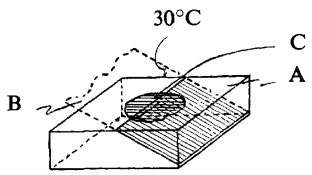

Fig. 2. Cross section of diffusion layer for microscopic observation.
A Rutile single crystal B Cross-section
C Reacted area

Measurement of the Diffusion Coefficient of Barium. — For the diffusion experiment at a high temperature, oxygen gas was led into the furnace at the rate of 2~3 l./hr. under 1 atm. to avoid the back reaction of the carbon dioxide and barium oxide produced by the decomposition of barium carbonate forming barium carbonate again, and to prevent the reduction of rutile at the high temperature. Prior to the introduction of oxygen, the furnace was evacuated by a vacuum pump. The rate-controlled oxygen gas was then passed through a heated platinum black to change the hydrogen impurity into water, which was then cooled and removed by a potassium hydroxide solution and silica gel. The carbon dioxide in the oxygen was also removed by means of an alkaline solution. As is shown in detail in Fig. 3, the oxygen current was preheated before it reached the diffusion system. The rutile crystal sample was cut to about 10×10×1 mm., and a few milligrams of ^{133}Ba-labeled barium carbonate powder were put on the crystal. The whole system was mounted on the ceramic boat, A, and was heated to a desired temperature under the oxygen current. The Pt/Pt-Rh thermocouple was set outside the alumina sheath, C, close to the sample. The actual temperature of the sample inside the alumina sheath was 5°C lower than the value indicated by the thermocouple.

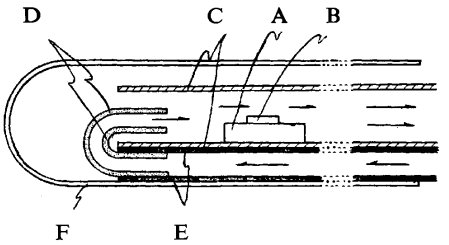

Fig. 3. Sketch of sample mounting in the muffle tube.
A Ceramic boat B Sample
C Alumina sheath D Fused-quartz pipe
E Preheating gas guide tube
F Muffle tube
Arrow shows the direction of gas flow.

After the radioactive material had been heated, utmost care was taken of the waste gas, which was passed through concentrated sulfuric acid and through glass fiber filters to catch the radioactive barium oxide. Actually, however, the radioactivity was not detectable in either the sulfuric acid or in the filters. After the barium had diffused into a single crystal of rutile at a high temperature, the surface of the specimen was abraded successively with powder of carborundum, keeping it flat; the decrement of the thickness was measured by an electromicrometer, the precision of which was checked with a block-gauge to be 0.2 μ/div. The residual radioactivity of the abraded surface due to ^{133}Ba diffusion was measured by a G-M counter. The G-M tube used was equipped with a mica window 27 mm. in diameter and 3.4 mg./cm^2 thick. The specimen was placed 32 mm. below the window. To avoid the edge effect of the diffusion area, we masked the surface of the specimen with a lead plate (12 mm. thick) which had a circular hole 3 mm. in diameter in its center, through which the γ-radiation of ^{133}Ba (half life: 7.2 years) free from self-absorption was measured.

Results and Discussion

Microscopic Observations.—Two processes of diffusion can occur when a single crystal of rutile is in contact with barium oxide at a high temperature, namely: the diffusion of barium into the rutile crystal, the diffusion layer being formed inside the rutile crystal, and the

10) M. E. Straumanis et al., *Acta Cryst.*, **14**, 493 (1961).

diffusion of titanium into barium oxide, the diffusion layer being formed outside the single crystal of rutile. The two processes are illustrated in Figs. 4 (a) and (b) respectively, assuming that the volume does not change on diffusion. To confirm which process really happened, the diffusion layer was cut as shown in Fig. 2 after diffusion had taken place at a high temperature (1300°C, 1 hr.) and was then observed by a microscope (Fig. 5). In this specimen, the c-axis of the rutile crystal was at right angles to the diffusion layer. In Fig. 6, the diffusion front, F, was seen to advance across the reference plane, B, into the rutile crystal region. Therefore, it is clear that barium diffused into the rutile crystal and that the diffusion phenomenon observed was the case of Fig. 5 (a). The diffusion layer was seen to be polycrystalline, and observation by a polarization microscope showed that the optical anisotropy of the crystal grains was random in its direction. This suggests that the crystal grains of the diffusion product did not grow epitaxially. It is likely for the diffusion mechanism that barium diffuses into the rutile single crystal, destroys the crystal structure of rutile, and creates a new crystal structure consisting of titanium, barium and oxygen. A sufficient number of new crystal nuclei are created to result in the polycrystalline diffusion layer.

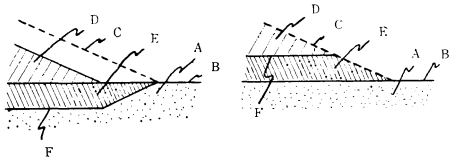

(a) (b)

Fig. 4. Diffusion layer model. (a) is the case where barium diffuses into the rutile single crystal, and (b) titanium diffuses into barium oxide.
A Rutile single crystal
B Surface of rutile
C Barium oxide before diffusion
D Residual barium oxide after diffusion
E Diffusion layer F Diffusion front

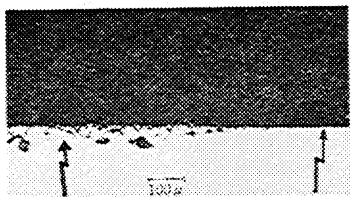

Fig. 5. Microphotograph of the cross-section of diffusion layer. B shows rutile crystal surface, white region being rutile crystal. F is diffusion front.

Since the diffusion of an atom is considered to take place more rapidly in the liquid state than in the solid state, the rate of reaction is expected to be affected profoundly by the liquefaction of the diffusion layer. Microscopic observation of the diffusion system of Fig. 1 at a high temperature revealed two kinds of liquid state. The first liquefaction occurred at 900~1050°C. At the lower temperature of 650°C, the barium carbonate in the single crystal of rutile seemed to remain in a solid state, as is shown in Fig. 6 (a). It was liquefied at 950°C, as is shown in Fig. 6 (b). The fluidity was seemingly increased at 1000°C, as is indicated in Fig. 6 (c). The accuracy of the temperature measurement depended on the position of the hot-junction placed beneath the rutile crystal, as may be understood from Fig. 1. The accuracy of the temperature measurement was ±25°C. Accordingly, the liquid state is considered to be a eutectic mixture of $2BaCO_3 \cdot BaO$, the eutectic point of which is 1030±3°C[11]. This liquid

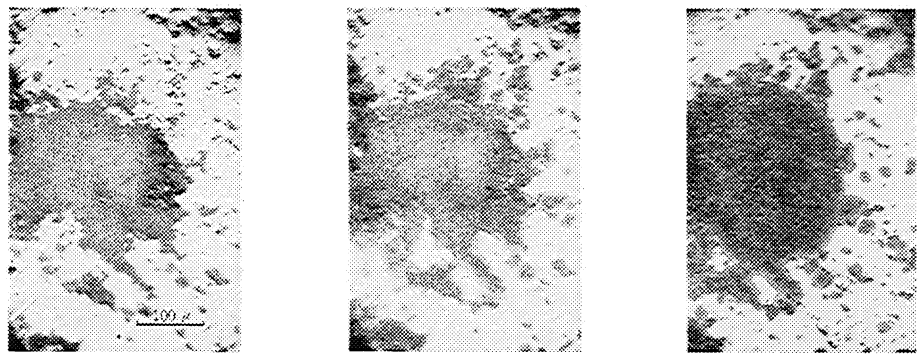

(a) 650°C (b) 950°C (c) 1000°C

Fig. 6. The first liquefaction. White region is rutile crystal, while black region is barium carbonate.

11) J. J. Lander, *J. Am. Chem. Soc.*, 73, 5893 (1951).

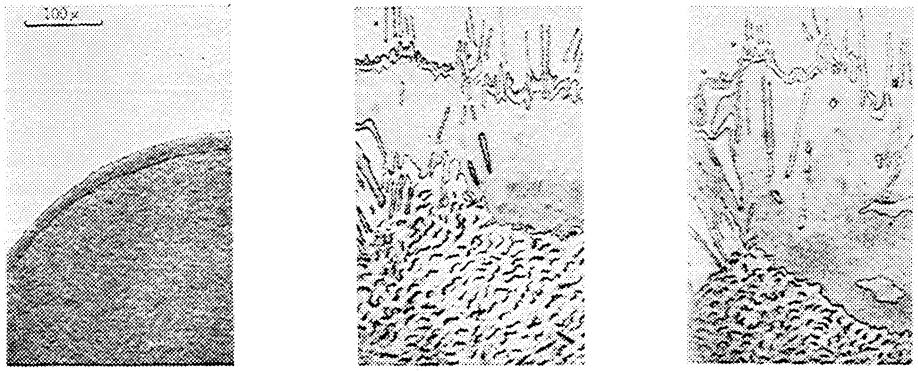

(a) 1200°C (b) 1290°C (c) 1300°C

Fig. 7. The second liquefaction. White region is rutile crystal, while black region is barium carbonate.
Lines are drawn to emphasize the contours and the details of the figures.

state can also be identified with the one observed by Hirota et al.[12], who studied the thermal decomposition of barium carbonate with an electron microscope. Therefore, the liquefaction in the temperature range of 900~1050°C may be considered to be related to barium carbonate and oxide, which may affect the diffusion of barium into a rutile crystal very little.

The second liquefaction occurs at about 1300°C. This is shown in Fig. 7(c). As will be mentioned later, this liquefaction is exclusively concerned with barium oxide and titanium dioxide, not with barium carbonate. To confirm this, barium oxide film was made by evaporation in vacuo on a single crystal of rutile, and barium was diffused into the rutile crystal at a high temperature in vacuo ($5\sim7\times10^{-5}$ mmHg). At 1200°C (Fig. 7 (a)) no liquid state was observed, but at 1290°C (Fig. 7 (b)) the liquefaction was recognized from the interference fringes caused by a relatively uniform liquid film. According to the phase diagram of barium oxide~titanium dioxide proposed by Rose and Rey[6], a eutectic mixture exists at the mole ratio of $BaO : TiO_2$ 68 : 32 (eutectic point 1317°C). Therefore, the liquid phase observed is considered to be the eutectic mixture of this composition produced by the diffusion of barium. This liquefaction explains the marked change in reaction velocity, namely, above 1317°C barium diffusion is rapid, since it takes place in the liquid state, while below 1317°C it is rather slow, owing to the solid state diffusion. This is confirmed further by the following quantitative experiment.

Radiotracer Observation.—After the diffusion was allowed to take place at high temperatures,

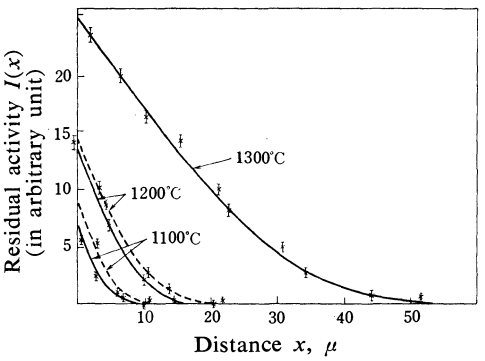

Fig. 8. Relation between diffusion distance and residual activity $I(x)$.
—— Diffusion parallel to c-axis of rutile single crystal
---- Diffusion perpendicular to c-axis of rutile single crystal

the reacted surface was abraded by successive thin layers. After each abrasion the residual radioactivity of the surface was measured. Figure 8 shows the residual radioactivity curve $I(x)$, denoting, in an arbitrary unit, the concentration of barium remaining after the abrasion to the depth x, measured from the plane of contact between the rutile single crystal and ^{133}Ba carbonate. Then, we obtain:

$$I(x)=\int_x^\infty c(x')\cdot A(x'-x)\,dx' \qquad (1)$$

where $A(x'-x)$ is the factor due to the self-absorption of radioactivity through the reacted rutile crystal of the thickness of $x'-x$, and $c(x')$ is the barium concentration per unit thickness at x' for $x'\geqq x$. Differentiating with respect to x, we get

$$dI(x)/dx=[-c(x')\cdot A(x'-x)]_{x'=x}$$
$$=-c(x)\cdot A(0) \qquad (2)$$

12) S. Hirota et al., *J. Phys. Soc. (Japan)*, **15**, 137 (1960).

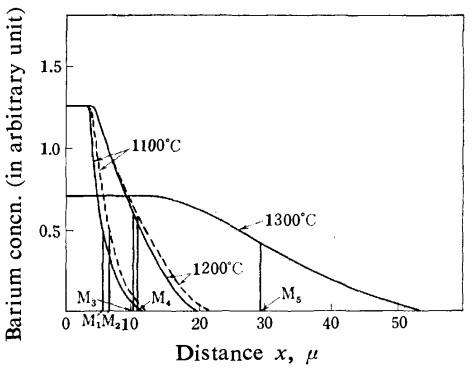

Fig. 9. Relation between diffusion distance and barium concentration $c(x)$.
—— Diffusion parallel to c-axis of rutile single crystal
---- Diffusion perpendicular to c-axis of rutile single crystal

However, since

$$A(0)=1$$

Equation 2 becomes

$$dI(x)/dx=-c(x) \qquad (3)$$

That is, the barium concentration $c(x)$ is given by the negative of the tangent of $I(x)$.

Figure 8 shows the diffusion systems of barium carbonate on the rutile single crystal, systems which were heated to 1100, 1200 and 1300°C under the oxygen current for two hours. As the ionic configuration along the c-axis of the rutile is quite different from that perpendicular to the c-axis[9], the $I(x)$'s along both directions were determined. We can see in Fig. 8 that barium diffuses more rapidly at 1300°C than at 1100 and 1200°C, which may be explained by the formation of liquefied eutectic mixture at 1300°C mentioned above. The $c(x)$ curves in Fig. 9 were obtained by the differentiations of the curves of Fig. 8. Small differences are seen between the $c(x)$ curves parallel to and those perpendicular to the c-axis, but the anisotropic diffusion of barium is not conclusive from these data alone. Above 1300°C, liquefaction occurred and the volume of the diffusion layer slightly decreased, so that the accuracy of $I(x)$ beyond 1300°C is rather low. Actually, no quantitative result could be obtained at 1400°C.

For the calculation of the diffusion coefficient from the concentrations distribution curve, initial and boundary conditions should be given; in our experiments these were:

$$\begin{aligned} &c(x)=\text{const.} \quad \text{for } x<0, \quad t=0 \\ &c(x)=0, \quad \text{for } x>0, \quad t=0 \end{aligned} \qquad (4)$$

where t denotes time.

As a diffusion coefficient is assumed to be dependent on the concentration, the diffusion equation takes the form:

$$\frac{\partial c}{\partial t}=\frac{\partial}{\partial x}\left(D(c)\cdot\frac{\partial c}{\partial x}\right) \qquad (5)$$

Using the Matano interface[14], $D(c)$ can be calculated readily under the conditions of 4. Let c_M be the concentration on the Matano interface, then the diffusion coefficient at c_M is[13]:

$$D(c_M)=-\frac{1}{2t}\left(\frac{dx}{dc}\right)_{c=c_M}\cdot\int_0^{c_M}x\,dc \qquad (6)$$

The Matano interfaces M_1, M_2, M_3,..., M_5 are shown in Fig. 9 for each concentration curve. $D(c_M)$ was calculated using Eq. 6.

The values of $D(c_M)$ obtained were 3.6×10^{-14} (1100°C) and 1×10^{-13} (1200°C) (both parallel to the c-axis), 5×10^{-14} (1100°C) and 2.4×10^{-13} (1200°C) (both perpendicular to the c-axis), and 2.5×10^{-12} (1300°C), expressed in cm^2/sec. As for the self-diffusion coefficient of barium in barium titanate, Verduch and Linder[14] gave about 10^{-14} cm^2/sec. at 1150°C, which is in reasonable agreement with our result of about 3×10^{-14} cm^2/sec. at 1100°C.

Assuming that the activation energy, E, for diffusion is independent of the temperature, T, it can be calculated from:

$$D(c_M)=D_0(c_M)\cdot\exp(-E/RT)$$

by plotting $D(c_M)$ against $1/T$. The rough estimation of E in the of 1100~1200°C range gives 59 kcal./mol. (perpendicular to the c-axis) and 43 kcal./mol. (parallel to the c-axis).

With regard to the state of barium during diffusion, no conclusive statement can be made from our results. However, the experimental results of barium self-diffusion in barium oxide by Redington[15] show, that both charged and neutral barium constituents diffuse in the temperature range from 1077 to 1227°C, whereas only the neutral barium diffuses in the lower temperature range (327~1027°C). Thus we may expect that the barium diffusing in our experiments (1100°C and above) is partly charged and partly neutral.

In these experiments, the average concentration was determined over a circular area 3 mm. in diameter, assuming that the diffusion proceeds vertically to the rutile surface and that the diffusion front is flat. Actually, however, as is shown in Fig. 5, the photomicrograph reveals, that the diffusion front is not completely flat over the area observed. In addition,

13) Cf., for instance, J. Crank, "The Mathematics of Diffusion", Oxford Univ. Press, London (1956).
14) A. G. Verduch and R. Linder, "Proc., Intern. Symposium on Reactivity of Solids, Gothenberg, 1952", (1954), p. 207.
15) R. W. Redington, *Phys. Rev.*, 87, 1066 (1952).

barium is considered to diffuse rather rapidly along such imperfections of the rutile single crystal as the subgrain boundaries. It may be possible to obtain a more exact concentration curve without being disturbed by crystal imperfections if the diffusion is studied by the X-ray microanalyzer. The chemical composition and the crystal structure may also be identified by the X-ray microanalyzer and microdiffraction methods. The details, however, require further study.

Summary

1) Microscopic and radiotracer studies have been made upon the diffusion of barium into a rutile single crystal.

2) In the microscopic observation, the diffusion layer of barium oxide in the rutile single crystal was confirmed to liquefy above 1300°C due to the formation of a eutectic mixture between both constituents. Below 1300°C solid phase diffusion prevails, and the diffusion layer consists of polycrystalline of a random orientation.

3) The diffusion coefficients of barium oxide in a rutile single crystal were measured by means of the radiotracer method using ^{133}Ba. The diffusion coefficients obtained were $3.5\times10^{-14}\sim2.4\times10^{-13}$ cm^2/sec. in the range of 1100~1200°C and 1.1×10^{-12} cm^2/sec. at 1300°C. Between 1100°C and 1200°C, small differences seemed to be observed for the values obtained according to the direction of the diffusion in the crystal, but this is not conclusive. The large value of the diffusion coefficient at 1300°C was considered to be due to the liquefaction of the diffusion layer. The energy of activation was calculated to be 43 kcal./mol. (parallel to the c-axis) and 59 kcal./mol. (perpendicular to the c-axis).

The authors wish to thank Mr. Tsutomu Seimiya of our laboratory for his help in this study, and they also thank the Ministry of Education for the Scientific Research Grant given to Tsunetaka Sasaki.

Department of Chemistry
Faculty of Science
Tokyo Metropolitan University
Setagaya-ku, Tokyo

Nuclear Magnetic Resonance Study of Acetaldehyde Aqueous Solution

By Yuzuru FUJIWARA and Shizuo FUJIWARA

(Received December 28, 1962)

Acetaldehyde in aqueous solution has been the subject of spectroscopic and calorimetric investigations in regards to the equilibrium with hydrated molecules.

$$CH_3CHO + H_2O \rightleftarrows CH_3CH(OH)_2 \qquad (1)$$

In spectroscopic studies, the absorption band due to C=O double bond is the measure of concentration of aldehyde and its disappearance by formation of hydrated molecules has been investigated. Nuclear magnetic resonance (NMR) technique has the merit to measure all kinds of protons in both sides of Eq. 1 and enables us to investigate it more precisely than the spectroscopic method. From the view point of NMR, acetaldehyde shows characteristic features, for instance, aldehyde hydrogen gives the NMR signal in a very low field, and the spin coupling constant between methyl and aldehyde hydrogens is very small. These features of NMR spectra may be interpreted in correlation with the chemical activity of aldehyde hydrogen. Since NMR data such as chemical shift, spin coupling constant, and relaxation time can be interpreted in terms of electronic and structural configurations, and of motion of molecules, we planned to make an NMR investigation of acetaldehyde in aqueous solution.

Experimental

NMR spectra were obtained at 56.445 Mc./sec., using a Varian Associates spectrometer. Chemical shifts were measured by the side band method from the methyl proton signal of free acetaldehyde. Concentrations of various species of hydrogen were measured as the areas of the spectra obtained. This was actually practised by setting the condition that line width was so large that the transverse

1) R. P. Bell and J. C. Clunie, *Trans. Faraday Soc.*, **48**, 439 (1952); R. P. Bell and B. B. Darwent, ibid., **46**, 34 (1950).

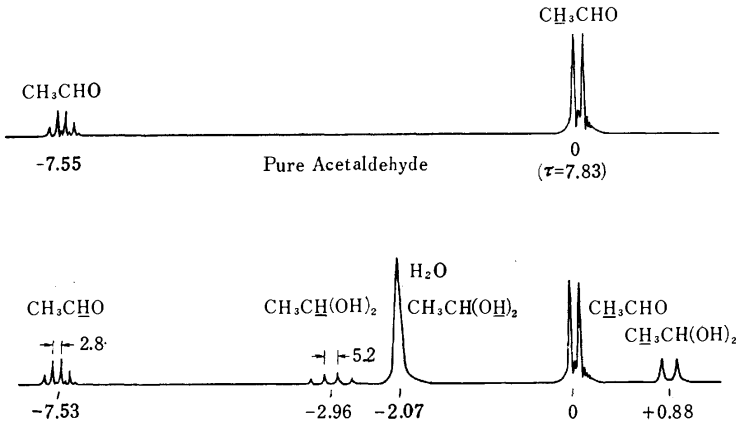

Fig. 1. NMR Spectra of acetaldehyde 42 mol. % aqueous solution.

relaxation times, T_2's, were predominated by the inhomogeneity of the external magnetic field. This method to determine the concentration is helpful to avoid the change of concentration on sealing the sample in the tubes, since acetaldehyde with boiling point 20.8°C volatilizes easily at room temperature. Acetaldehyde was prepared by the decomposition of commercial paraaldehyde using sulfuric acid as catalyst and was redistilled.

Results and Discussion

NMR spectra of acetaldehyde are shown in Fig. 1. Each component of the spectra is easily assigned unambiguously as shown in Fig. 1 with the consideration of the line shape and the intensity[3]. The hydrogens of water and OH radicals of hydrated aldehyde form a single broad line, and its position depends upon concentration (cf. Fig. 2). The width of this line increases as the temperature is lowered or as the concentration of acetaldehyde is increased. This suggests the existence of proton exchange between water and hydrated aldehyde and that of the rate of exchange is rather rapid. The magnitudes of chemical shift and spin-spin coupling constant, J, of all components except water coincide well with those in the literatures[2,3].

The methyl proton signal for the hydrated molecule shows smaller value of chemical

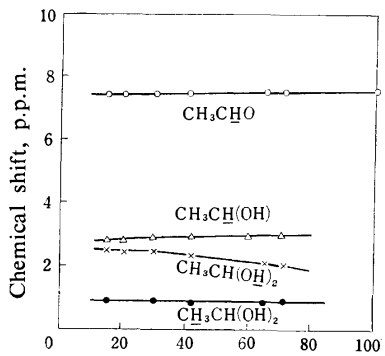

Concn. of acetaldehyde aqueous solution, mol. %
Reference CH_3CHO.

Fig. 2.

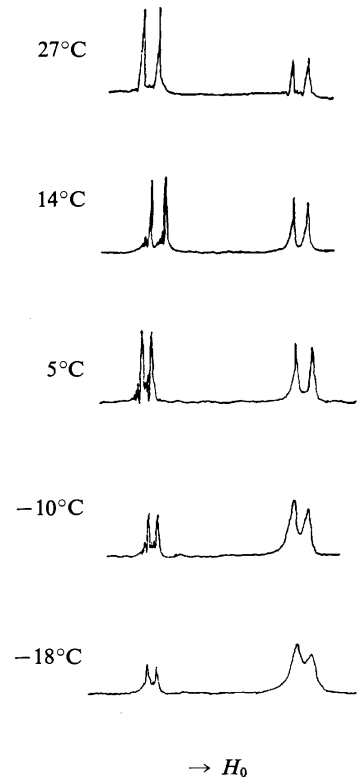

Fig. 3. Acetaldehyde 30 mol. % aqueous solution.

2) G. V. D. Tiers, Private communication "Characteristic NMR Shielding Values for Hydrogen Organic Structures" (1958).

3) E. Lombardi and P. B. Sogo, *J. Chem. Phys.* 32, 635 (1960); M. Matsushima. Abstructs of the 15th Annual Meeting of The Chemical Society of Japan (1961).

shift and a larger coupling constant as compared with that for the free molecule. Moreover, the difference between the two J's as well as that between the two shift is conspicuous; $J=5.2$ and 2.8 c. p. s. and $\delta=2.96$ and 7.53 p. p. m. for hydrated and free molecules, respectively. Resonance positions of all hydrogens other than that in OH are almost constant and independent of the concentration. The spectra are temperature dependent as shown in Fig. 3. The line width of hydrated acetaldehyde increases as the solution becomes viscous in a lower temperature range, while that of free molecules does not vary so much. The intensity of the latter is much reduced at lower temperatures as the result of drift of the chemical equilibrium. Saturation curves for methyl protons in both hydrated and free molecules at two temperatures, 27°C and −14°C, are shown in Figs. 4 and 5, respectively. As seen in Fig. 4, the behaviors of the two lines are almost the same for both species of molecules at 27°C, whereas very different from each other at −14°C. In Table I, the relative relaxation times are shown, where T_1

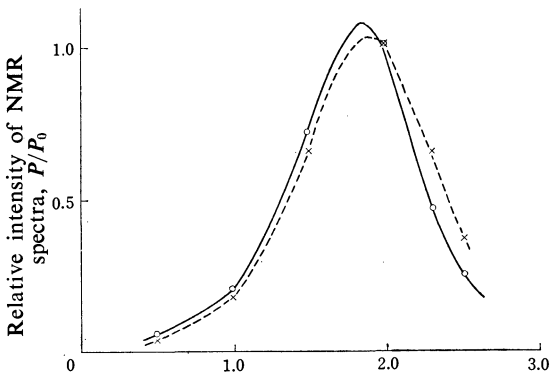

Fig. 4. Saturation carves of CH_3CHO at 27°C.

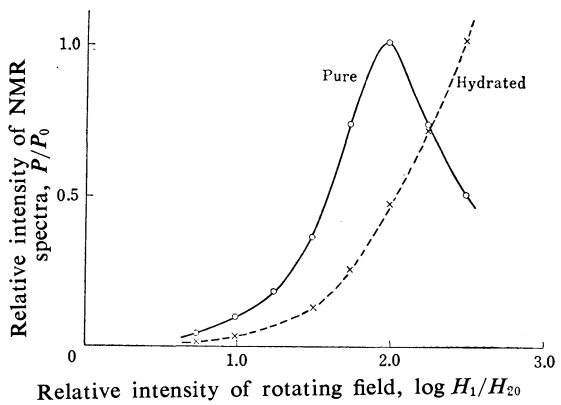

Fig. 5. Saturation curves of CH_3CHO at −14°C.

TABLE I. RELATIVE RELAXATION TIME

Temp., °C		CH_3CHO	$CH_3CH(OH)_2$
27	T_1/T_{20}	1.00	0.771
	T_1/T_{10}	1.0	0.91
−14	T_1/T_{10}	0.724	0.115
	T_2/T_{10}	0.715	0.22

for free molecule at room temperature was taken as unit. The T_1's obtained from saturation curves with the assumption that T_1 is equal to T_2, coincide fairly well with the T_2's which were obtained from the line width. Small discrepancies between the two sets of relaxation times may have been caused by the neglect of field inhomogeneity. T_1 diffrence between the two kinds of molecules at −14°C is due to the difference in correlation times for the Brownian motion of molecules. It is interesting that the correlation times are different between the free and the hydrated acetaldehyde molecules, namely, the molecules of similar size in homogeneous medium of liquid. T_1's of free molecules are almost equal to each other at 27°C and at −14°C inspite of a large difference in viscosity of the solution. This fact suggests that translational motion of the molecule does not effectively contribute to relaxation. On the other hand, T_1 of the hydrated molecule is much smaller than that of free molecule at the lower temperature and this may be attributed to the difference of rotational motions, since hydrated molecules are strongly hydrogen-bonded with surrounding water, receiving hindrance in both translational and rotational motions, whereas unhydrated ones are comparatively speaking, free and rotational motion remains. Measurements of T_1 values in two different temperature ranges made it possible to calculate the apparent activation energy as 7.1 and 1.3 kcal./mol. for the rotational motions of hydrated and unhydrated molecules, respectively. The strength of the hydrogen bond ranges around 5 kcal./mol. for water or ethanol. The fact that the value obtained here (3.5 kcal./mol.) is a little smaller than this value may be due to its structure which has two adjacent OH's, unfavorable to form hydrogen bonds.

Configurations of hydrated and free acetaldehyde will be discussed in regard to the large difference of J's. The value of J, 5.2 c. p. s., for the hydrated molecule may be interpreted by simple application of the electronegativity $-J$ rule which was empirically obtained by Glick et al. for isopropyl derivatives[4]. Equation 2 correlates the coupling constants with

4) R. E. Glick and A. A. Bothner-By, *J. Chem. Phys.*, 25, 362 (1956).

the Huggins' electronegativity scale, E[5], of the substituent, X for $(CH_3)_2CHX$.

$$J(\text{c. p. s.}) = 8.0 - 0.55 \times E \qquad (2)$$

If we modify this relation to replace the methyl radical in isopropyl by OH, Eq. 2 leads to 5.6 c. p. s. as J value for hydrated acetaldehyde, which is a fairly good approximation. This result suggests that the electron density around protons is reduced by this replacement. Provided that this substitution only affects the electron density in such a way that it is reduced homogeneously throughout the molecule, the electron density of aldehyde hydrogen is reduced by 16% from that of propane, by using Karplus calculation of J by the valence bond method[6] and by comparing the J, 5.2 c. p. s. with the J for propane which has been reported as 7.26 c. p. s.[7] If we assume that the electron densities around C–H protons in pure and hydrated molecules are mainly determined by the polarization of C–O bonds, then the electron densities of C–H protons should be very different between the two molecules, since J's are different. Pure aldehyde has one C=O bond and the hydrated molecule has two C–OH bonds. The ionicity of C–O single bond has been reported as about 22%[8] and that of C=O double bond of acetaldehyde as 47%[9] by the measurement of the electric dipole moment[10]. In so far as the polarization is concerned the aldehyde hydrogen can not make any sizable difference between the two molecules. This result contradicts the observed difference of J's for pure and hydrated acetaldehyde, since Glick's rule stands for linear relationship between J and electron density which is determined by the electronegativity of the substituent. The observed difference may be attributed partly to that of hybridization of carbon orbitals; sp^3 and sp^2 structures for hydrated and pure aldehyde, respectively. Comparing propane (J=7.26) with propylene (J=6.4)[7] the orbital effect can be estimated and the expected value for pure acetaldehyde should be 4.6 c. p. s. which is still larger than the experimental value of 2.8 c. p. s. In order to analyze the results more precisely, further investigations would be necessary for many other factors such as difference of excitation energy, bond length[11], and angle[11,12], and electronic configurations. The low value of aldehyde-hydrogen shift could be interpreted in terms of (1) the effect of electric field due to the dipole moment of C=O, (2) the anisotropic magnetic screening of C=O double bond and (3) the reduction of electronic screening associated with the decrease of electron density. The magnetic effect 2 will be of the order of 4.57 p. p. m. which was obtained as the difference between the hydrated and the unhydrated aldehyde. The electronic effect is calculated as 2.8 p. p. m. by using the Lamb's screening constant for hydrogen atom[15] and the electron density obtained from the discussion of J. The electric field effect was estimated to be 4.4 p. p. m. comparing the shifts of ethane and acetaldehyde[2]. The sum of these effects is 11.77 p. p. m. which is reasonable and proves that the above estimations are correct.

The equilibrium constant K for 1, defined as

$$K = (H)/(A-H)(W-H)$$

where W, A and H refer to concentrations of water, free, and hydrated acetaldehyde, respectively. K is plotted against the concentration of acetaldehyde in Fig. 6. The equilibrium constant decreases with the increase of concentration. This may be attributed partly to the experimental error in the measurements of concentration where we neglected effects of relaxation times and activities. For dilute solutions, however, the errors mentioned above are small and K approaches to 0.021 l./mol. This value coincides well with the UV and NMR results by other authors[1,3]. The temperature dependence of the equilibrium constant is also shown in Fig. 7 and the heat of hydration was calculeted as 4.9 kcal./mol., which also agrees well with the data already reported[1], within the experimental errors.

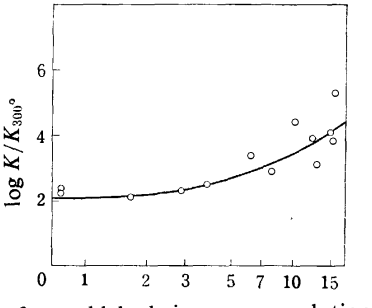

Concn. of acetaldehyde in aqueous solution, mol./l.

Fig. 6.

5) M. L. Huggins, *J. Am. Chem. Soc.*, **75**, 4123 (1953).
6) M. Karplus, *J. Chem., Phys.*, **30**, 11 (1959).
7) D. R. Whitman, ibid., **32**, 67 (1960).
8) C. A. Coulson, "Valence", Oxford Univ. Press, (1951).
9) L. Pauling, "The Nature of Chemical Bond", Cornell Univ. Press, N. Y. (1940).
10) L. G. Wesson, "Tables of Electric Dipole Moments", The Technology Press, M. I. T., Mass. (1948).
11) L. E. Sutton, "Tables of Interatomic Distances and Configuration in Molecules and Ions", The Chem. Soc., London (1958).
12) H. S. Gutowsky, M. Karplus and D. M. Grant, *J. Chem. Phys.*, **31**, 1278 (1959).
13) A. L. Bothner-By and C. Naar-Colin, *J. Am. Chem. Soc.*, **83**, 231 (1961).
14) S. Fujiwara, N. Nakagawa and H. Shimizu, "High Resolution NMR", Maruzen, Tokyo (1962).
15) W. E. Lamb, *Phys. Rev.*, **60**, 817 (1941).

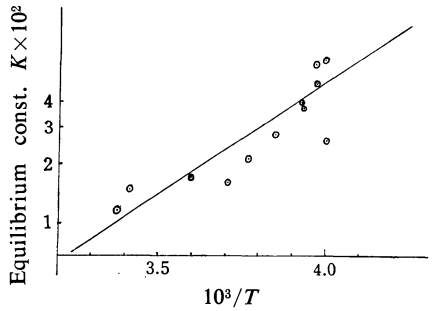

Fig. 7. Temperature dependence of the equilibrium constants.

Conclusion

In aqueous solution of acetaldehyde the hydrated and unhydrated molecules have different relaxation times, since the interaction with the solvent, mainly the formation of hydrogen bonding, is different. Relaxation is dominated mainly by rotational motion of the molecule. The hydrogen bond between the hydrated acetaldehyde and water has the energy about 3.6 kcal./mol. and these hydrogens exchange with each other rapidly.

Small J of acetaldehyde may be attributed to the smallness of electron density around protons and also to the bond angle, the bond length, and the cxcitation energy. The NMR signal of aldehyde hydrogen locates in a low field because of the electron density, the anisotropic magnetic screening of the C=O and the electric field produced by the dipole moment of the C=O and these effects were estimated to be 2.8, 4.6 and 4.4 p. p. m., respectively.

The equilibrim constant and the heat of hydration are determined by the NMR method more accurately than by other conventional methods and the obtained values are in good agreement with the values in the literatures.

The authors thank Mr. Naohiro Hayakawa of the Japan Atomic Energy Research Institute for the help to obtain the NMR spectra. They are grateful to Dr. Hiroshi Shimizu of Chiba University for valuable discussions.

Department of Chemistry
Faculty of Science
The University of Tokyo
Hongo, Tokyo

*Nuclear Magnetic Resonance Spectra of Amino Acids and their Derivatives. II. Analyses of NMR Spectra of Amino Acids**

By Shizuo FUJIWARA and Yoji ARATA

(Receied January 19, 1963)

Investigations of proton resonance in amino acids have so far been restricted to those of the over-all features of the spectra[1-3]. This situation led us to make more detailed study of the spectra.

We will summarize here the results of precise analyses of the spectra of methylene and methine protons of amino acids of the type,

$$R-CH_2-\underset{\displaystyle NH_2}{\underset{|}{CH}}-COOH$$

where R has no protons interacting with those under invesitigation.

* Presented at the International Symposium on Molecular Spectroscopy, Tokyo, 1962.

1) M. Takeda and O. Jardetzky, *J. Chem. Phys.*, **26**, 1346 (1957).

2) O. Jardetzky and C. D. Jardetzky, *J. Biol. Chem.*, **233**, 383 (1958).

3) F. A. Bovey and G. V. D. Tiers, *J. Am. Chem. Soc.*, **81**, 2870 (1959).

Experimental

Materials.—The amino acids studied were all commercial materials (Ajinomoto Co.). They were dissolved in heavy water, 2N HCl, and 2N NaOD at the concentration of 1 mol.%. 2N HCl was prepared by diluting concentrated hydrochloric acid with heavy water. 2N NaOD was prepared by adding sodium peroxide powder to heavy water under cooling.

Spectrometer.—A Varian Associates model V4301C NMR spectrometer operating at 60.00 Mc./sec. was employed for all measurements.

Results

Cysteine dissolved in diluted hydrochloric acid gives a simple spectrum as shown in Fig. 1d. The spectrum tells that the two protons attached to the beta-carbon atom are equivalent to each other. Serine and aspartic acid also

TABLE I. RESULTS OF ANALYSES IN C. P. S. FOR THE SPECTRA MEASURED AT 60.00 Mc./sec.

		$\nu_A-\nu_C$	$\nu_B-\nu_C$	J_{AC}	J_{BC}	J_{CA}
(B) (A)						
H H	Phenylalanine {2N HCl	67.4	3.7	3.2	14.6	10.0
R—C—C—COOH	Phenylalanine {2N NaOD	42.1	14.5	4.0	13.3	8.9
H NH_2	Cystine 2N HCl	68.3	4.3	2.0	15.1	9.8
(C)	Cysteine {2N HCl	74.2	0	5.0	—	5.0
	Cysteine { D_2O	55.5	0	4.9	—	4.9

give the spectra of three protons, two of which are equivalent.

Chemical shifts between alpha and beta protons vary from one amino acid to others. When the chemical shift is large compared to the spin coupling constant between these protons, the spectrum can easily be analyzed by means of the first-order perturbation theory. Cysteine in an acid medium shows a spectrum of this type.

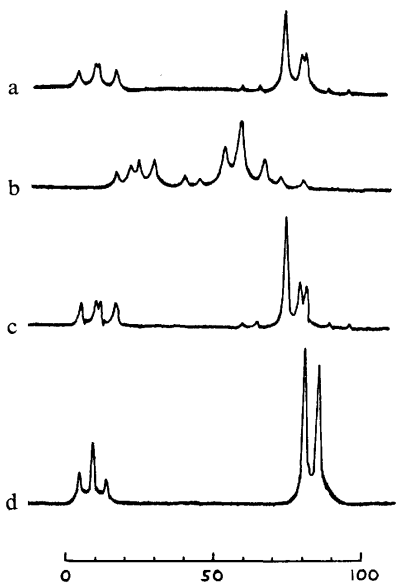

Fig. 1. NMR Spectra of amino acids measured at 60.00 Mc./sec.
(a) Phenylalanine in 2N HCl
(b) Phenylalanine in 2N NaOD
(c) Cystine in 2N HCl
(d) Cysteine in 2N HCl
In these spectra magnetic field increases from left to right.

When cysteine is dissolved in diluted NaOD solution, the spectrum changes to a complex one of a non-equivalent three spin system.

When R is bulky as in the cases of phenylalanine, tryptophane, tyrosine, hystidine and cystine, the spectra take the features of a nonequivalent three spin system even in acid media as well as in basic media.

For the analyses of these spectra we used the method of the least-squares reported by Shimizu and the present authors[4]. This method is useful in the present case, where we have relatively fewer than those theoretically expected. Some examples of the spectra are shown in Fig. 1a—1c and the results of the analyses are summarized in Table I.

The molecular constants shown in the table may be considered to be the weighted averages of chemical shifts and of spin-coupling constants over rotational isomers[5]. The relative population of each rotational isomer depends upon the acidity of the solution. This situation is more clearly seen in the spectra of valine for several kinds of solutions with different pH. The results are summarized in Table II.

TABLE II. CHEMICAL SHIFTS AND SPIN SPIN COUPLING CONSTANTS IN C. P. S. OBTAINED FROM THE SPECTRA OF VALINE AT A SERIES OF pH VALUES

	pH	J_{23}	$\lvert \nu_4-\nu_{4'} \rvert$
(4) CH_3 (4') CH_3 >CH-CH< $\overset{COOH}{NH_2}$ (3) (2)	14	5.1	4.2
	13.0	5.1	4.2
	7.0	4.2	3.0
	2.6	4.4	3.0
	1.0	4.3	1.9
	1	4.3	2.1

The spectra were measured at 60.00 Mc./sec.

The autheors wish to thank Dr. Hironao Momoi of The University of Tokyo for his valuable discussions and Mr. Osamu Yamamoto of Government Chemical Industrial Research Institute for giving us facilities to use the NMR spectrometer.

Department of Chemistry
Faculty of Science
The University of Tokyo
Hongo, Tokyo (S. F.)
Univeresity of Electro-communication
Chofu, Tokyo (Y. A.)

4) Y. Arata, H. Shimizu and S. Fujiwara, *J. Chem. Phys.*, 36, 1951 (1962).
5) J. A. Pople, *Mol. Phys.*, 1, 3 (1958).

Formaldehyde Resins. LXXV. Novolak Resin from p-Chlorophenol and Formaldehyde*

By Minoru IMOTO and Shin-ichi NAKADE

(Received January 5, 1963)

In 1956, Burke et al. obtained some novolak resins of a high molecular weight by the reaction of *p*- or *o*-chlorophenol with *s*-trioxane at 150°C in a sealed tube[1]. They reported that, after fractionation and acetylation of the resin, a fraction of a lower molecular weight showed the molecular weight of 2090, which was determined by the cryoscopic method using benzil as the solvent. This result attracted our attention, as it had previously been believed that the molecular weight of novolak was below 1000. In a foregoing paper of this series, Imoto and Tanigaki[2] repeated Burke's experiments, using *p*-chlorophenol and *α*-polyoxymethylene, but the molecular weight of the resin obtained was below 1000.

In the present study, we followed Burke's experiment accurately and determined the molecular weight distribution of the resin. The molecular weight of the resin obtained here was 400 to 1000. No novolak resin of a high molecular weight, such as those described by Burke, could be obtained. The molecular weight distribution of the resins obtained at the early stage of the reaction showed rather a good agreement with the theoretical equation submitted by one of the present authors (M. I.)[3], but as a general rule, they did not agree. This lack of agreement was due to a reaction of the "reformation" of the novolak-molecules[4]. Therefore, it was considered that the distribution should be ruled by Poisson's distribution equation, as was proved to be true.

Experimental

Materials.—*p*-Chlorophenol was of a commercial grade and was used after distillation (b. p., 79~80°C/5 mmHg). *p*-Toluenesulfonic acid was refined by recrystallization from water; m. p., 103~104°C. *s*-Trioxane was of a purity of over 99%. The solvent, bis(2-ethoxyethyl) ether, was synthesized according to the method given in the literature[5]; b. p., 77~80°C/11 mmHg.

The Formation of the Resin.—A solution composed of 12.86 g. (0.1 mol.) of *p*-chlorophenol, 3.03 g. (corresponding to 0.101 mol. of formaldehyde) of *s*-trioxane, 0.200 g. of *p*-toluenesulfonic acid and 15 ml. of bis(2-ethoxyethyl) ether was placed in a sealed tube and heated at 150°C for 2~24 hr. in an oil bath. After cooling the reaction mixture, it was added slowly with vigorous stirring into about 500 ml. of water containing a small amount of hydrochloric acid. The resin precipitated here was dissolved in about 50 ml. of acetone to purify it. When the reaction was carried out at 150°C over for 11 hr., a small amount of the insoluble resin in acetone was obtained. The acetone solution was poured into one liter of water to precipitate the novolak resin. After the resin had been filtered, it was dried at about 60°C under reduced pressure (1 mmHg).

The Acetylation of the Resin.—After 1 g. of the resin had been dissolved in 10 ml. of pyridine, 2~3 ml. of acetic anhydride was added and left standing for several days at room temperature. The reaction mixture was poured into water to yield an acetylated resin. The purification was carried out by the reprecipitation method, using acetone and water. The completion of the acetylation was comfirmed by the disappearance of the OH bands in the infrared absorption spectra.

The Saponification of the Acetylated Resin.—One gram of caustic potassium was dissolved in 15 ml. of methanol, and the solution was maintained at 5°C, Then, 1 g. of acetylated resin was dissolved in 25 ml. of acetone, and the afore-mentioned solution was added and cooled at 5°C for 24 hr. The reaction mixture was poured into water to yield a saponified resin. The completion of the saponification reaction was comfirmed by the disappearance of the CO absorption bands in the infrared spectra.

The Fractionation of the Resin.—Fractionational precipitation was carried out by the successive addition of a poor solvent to the resin solution or by removing the solvent from the resin solution. Acetone, tetrahydrofuran or dimethylformamide was used as the solvent, and water or 33% ethanol-water as the poor solvent. Five to seven fractions were obtained from an about 5% resin solution by the successive addition of the poor solvent at 30.0 ±0.1°C and by removing the solvent.

* LXXIV: M. Imoto, T. Tanigaki and A. Fukui, *Memoirs of the Faculty of Engineering, Osaka City University*, **4**, 181 (1962).

1) a) W. J. Burke et al., *J. Polymer Sci.*, **20**, 75 (1955). b) W. J. Burke et al., ibid., **32**, 221 (1958).

2) M. Imoto and T. Tanigaki, *Memoirs of the Faculty of Engineering, Osaka City University*, **1**, 1 (1959).

3) M. Imoto, *Textile World (Japan)*, **35**, 589, 634 (1944).

4) a) M. Imoto, H. Kakiuchi and T. Otsu, *Chem. High Polymers, Japan*, **8**, 497 (1951); b) H. Horiuchi, *J. Chem. Soc. Japan, Ind. Chem. Sec. (Kogyo Kagaku Zasshi)*, **63**, 1651 (1960); c) cf. also Ref. 2.

5) L. H. Cretcher and W. H. Pittenger, *J. Am. Chem. Soc.*, **47**, 164 (1925).

The Molecular Weight Determination of the Resin.—The molecular weight of the resin was determined by the cryoscopic method, using camphor as solvents. It was shown by Imoto and Tanigaki[2] in the previous paper that camphor was suitable for the molecular weight determination of the novolak resin. When the molecular weight reached over 1000, however, the determination of molecular weight became difficult, because of the coloring of the camphor solution. Moreover, the acetylated resin is only with difficulty soluble in camphor. Therefore, we used benzil for the resin which could not be determined with camphor, as was described in Burke's papers.

Results

The Yield and Molecular Weight of the Resin. — The yield of the resin reached about 90% at 150°C for 2 hr. The maximum of the yield was seen at 8 hr. With the reduction in yield after that time, a small quantity of the insoluble resin was observed. The molecular weight of the soluble resin became larger with an increase in the yield at the initial stage, but it had the tendency to drop once when the formation of the insoluble resin had taken place and then to increase again (Fig. 1).

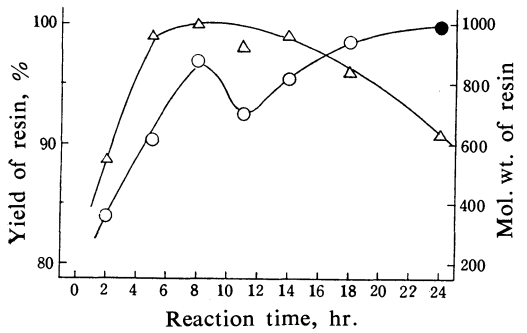

Fig. 1. The process of the formation of resin at 150°C.
△ Yield of resin ○ Mol. wt. of resin
● Mol. wt. calculated from mol. wt. of acetate

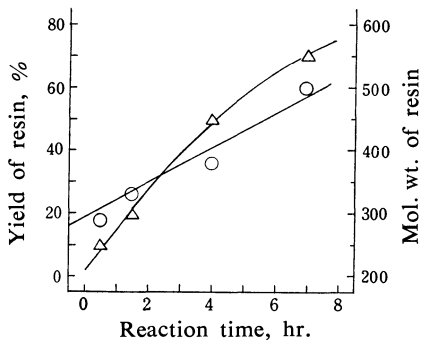

Fig. 2. The process of the formation of resin at 120°C.
△ Yield of resin ○ Mol. wt. of resin

The yields and the molecular weights of the resins obtained at 120°C increased with the reaction time (Fig. 2).

The Viscosity of the Resin. — The viscosity of the resin was determined at 25°C in a solution of 10 ml. of *N*, *N*-dimethylformamide containing 0.05 g. of the sample. Changes of the solution viscosity with reaction time showed the same tendency as that of the molecular weight (Fig. 3). No definite relationship between the molecular weight and the viscosity could be obtained.

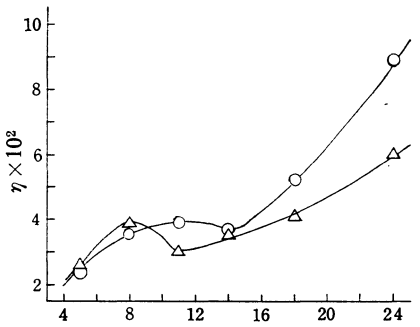

Fig. 3. The changes of specific viscosity of resins with reaction time.
△ Viscosity of acetate
○ Viscosity of resin

TABLE I. FRACTIONATION OF THE RESIN OBTAINED BY THE REACTION AT 120°C FOR 4 hr.

Fraction	Yield*, g.	Differential weight, %	Mol. wt.
1	0.762	15.72	910
2	1.078	22.25	600
3	0.652	13.45	510
4	0.750	15.48	340
5	1.604	33.18	280
Total	4.846	100.0	

* Sample weight: 5.02 g.

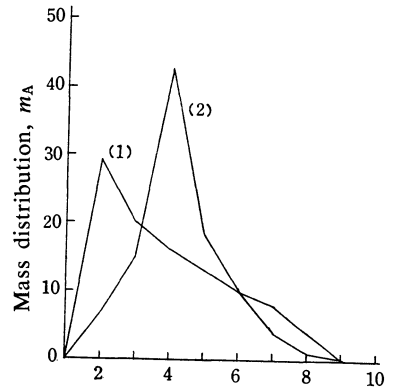

Fig. 4. Mass distribution curves of the resins reacted at 120°C.
(1) 120°C, 4 hr. (2) 120°C, 7 hr.

Fractionation.—Five fractions were obtained from a 100 ml. solution of acetone containing 5 g. of the resin, which was obtained by reacting for 4 hr. at 120°C, by removing the acetone, and by the addition of water. The yield was 96.5% (Table I).

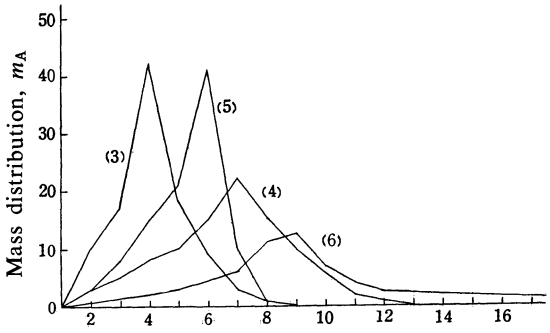

Fig. 5. Mass distribution curves of the resins reacted at 150°C.
(3) 150°C, 2 hr. (4) 150°C, 8 hr.
(5) 150°C, 14 hr. (6) 150°C, 24 hr.

TABLE II. REFORMATION OF THE RESIN

Original resin			Reformed resin		
Conditions of preparations		Mol. wt.	Conditions of reformation		Mol. wt.
hr.	°C		hr.	°C	
1.5	120	330	3	150	460
2	150	360	3	150	620
5	150	610	3	150	920*
8	150	870	3	150	840*
8	150	870	10	150	770*
11	150	700	3	150	930*

* The insoluble product was obtained in a small yield.

The distribution curves are shown in Figs. 4 and 5.

The Reformation of the Resin.—1.3 g. of the resin and 0.020 g. of *p*-toluenesulfonic acid were dissolved in 1.5 ml. of bis(2-ethoxyethyl) ether and then heated in a sealed tube for 3 hr. at 150°C. The reaction product was purified by reprecipitation from acetone with water. The results obtained may be seen in Table II. The yields in all runs were about 75%.

Discussion

A Comparison of Burke's and the Present Author's Results. — The results obtained by Burke and by us are shown in Tables III and IV.

As can be seen from these tables, our results agreed well with Burke's results with regard to the viscosity and elementary analysis. Also, the infrared spectra of the resins show a good agreement (Fig. 6). Consequently, it is believed that the resins obtained by both are the same; only the molecular weights are quite different.

The Molecular Weight Distribution of the Resin.—While the distribution curves of the resins obtained at 150°C did not agree at all with Imoto's equation, a tendency for agreement in Poisson's distribution was observed for the resin obtained by reaction for 8 hr. at 150°C (Fig. 7). It is believed that this was because the reaction was so violent that the yield reached 90% in only 2 hr. and that "a reformation reaction" had already occurred. We, therefore, carried out the reaction under milder conditions, at 120°C, and thus obtained a distribution curve of the resin at the early

TABLE III. COMPARISON OF ELEMENTARY ANALYSIS OF BURKE'S AND OUR RFSINS (150°C for 24 hr.)

	Burke et al.				Imoto and Nakade				
	$[\eta]$	C, %	H, %	Cl, %	$[\eta]$	C, %	H, %	Cl, %	Mol. wt.
Resin	0.095	60.55	3.96		0.088	60.85	4.49	20.88	—
Acetate	0.057	60.75	3.86	18.55	0.059	60.23	3.93	18.64	1250
Resin after saponification	0.097	61.00	3.80		0.080	60.38	4.03		—

TABLE IV. COMPARISON OF THE FRACTIONAL DATA

No. of fraction	Burke et al.			Imoto and Nakade		
	Wt. of resin recovered, g.	$[\eta]$	Mol. wt. of acetate	Wt. of resin recovered, g.	$[\eta]$	Mol. wt. of acetate
1	1.6	0.503	—	0.89	—	—
2	2.0	0.136	—	1.62	0.150	1250
3	1.7	0.089	—	0.52	0.068	1210
4	1.3	0.054	4260	0.85	0.035	1260
5	2.0	0.036	2090	0.76	0.035	720
6	1.0	0.017	—	0.30	0.023	380

TABLE V. ELEMENTARY ANALYSIS DATA OF RESIN

Reaction temp., °C	Reaction time, hr.	Mol. wt. of resin	Obs. C, %	Obs. H, %	Obs. Cl[a], %	Formula	Calcd. C, %	Calcd. H, %	Calcd. Cl, %
120	0.5	290	59.10	4.06	23.05, 23.01	$C_{13}H_{10}O_2Cl_2$	58.01	3.75	26.35
120	1.5	330	59.05	4.39	23.27, 23.00	$C_{20}H_{15}O_3Cl_3$	58.63	3.69	25.96
120	4.0	380	59.12	4.41	24.52	$C_{27}H_{20}O_4Cl_4$	58.93	3.66	25.76
120	7.0	500	59.42	3.59	24.36	$(C_7H_5OCl)_n$	58.81	3.59	25.22
150	2.0	360	59.64	4.65	24.21				
150	5.0	610	59.19	4.39	21.29, 21.21*				
150	8.0	870	59.90	4.35	21.04, 21.28, 22.57*				
150	11.0	700	61.21	4.41	22.64				
150	14.0	820	60.19	4.37	21.17, 21.36, 22.68*				
150	18.0	940	60.64	4.59	21.78*				
150	24.0	1250**	60.85	4.49	20.88*				

a) Determined by macro Carius method
* Observed values by micro analysis
** The mol. wt. of the acetate

TABLE VI. DEVIATIONS OF THE OBSERVED Cl% FROM THE CALCULATED VALUES FOR THE LINEAR NOVOLAK STRUCTURE

Conditions of preparation	Novolak mol. wt.	Obs. Cl, %	Deviation, %	Acetylated resin: Obs. Cl, %	Acetylated resin: Deviation
150°C, 2 hr.	360	24.21	1.07*1	15.59	0.26*3
150°C, 14 hr.	820	21.36	4.23*2	17.68	1.97*4

*1 Calcd. Cl% for $C_{20}H_{15}O_3Cl_3$ (mol. wt. 410), 25.96
*2 Calcd. Cl% for $C_{41}H_{30}O_6Cl_6$ (mol. wt. 830), 25.59
*3 Calcd. Cl% for $C_{26}H_{21}O_6Cl_3$, 19.85
*4 Calcd. Cl% for $C_{53}H_{42}O_{12}Cl_6$, 19.65

TABLE VII. CALCULATED VALUES OF ELEMENTARY ANALYSIS OF THE RESIN CONTAINING THE STRUCTURE CAUSED BY DEHYDROCHLORINATION

Structure	Mol. wt.	C, %	H, %	Cl, %
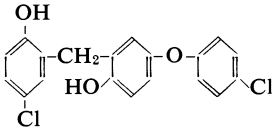	370	63.17	3.91	19.63
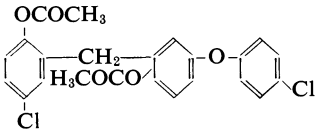	450	62.60	3.20	16.07
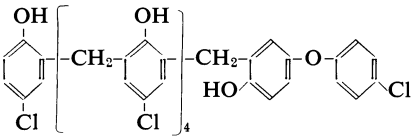	830	61.15	3.67	23.07
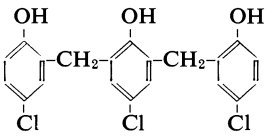	410	58.63	3.69	25.96
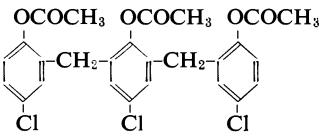	550	58.28	3.95	19.85

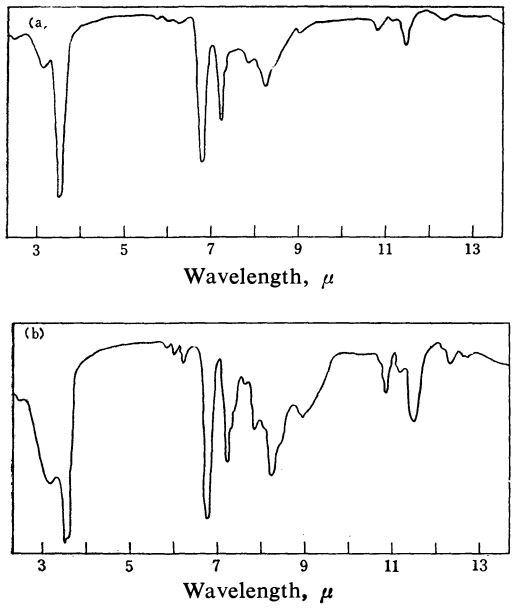

Fig. 6. Infrared absorption spectra of Burke's resin and the present author's resin in Nujol.
a) Burke's resin
b) The present author's resin

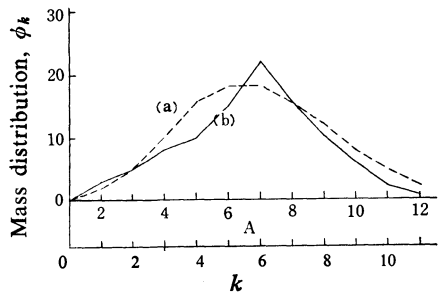

Fig. 7. Comparison between the experimental curve and Poisson's distribution curve.
(a) Theoretical curve calcurated from Poisson's equation $\left(\phi(k)=\frac{e^{-\lambda}\lambda^k}{k!},\ \lambda=6\right)$
(b) Experimental curve (150°C, 8 hr.)

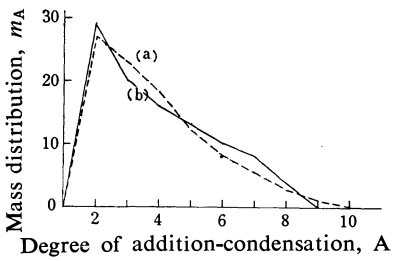

Fig. 8. Comparison between experimental curve and Imoto's theoretical curve.
(a) Theoretical curve ($\alpha=0.60-0.01$ A)
(b) Experimental curve (120°C, 4 hr.)

stage of the reaction. This curve, which agreed with Imoto's equation, is shown in Fig. 8.

Elementary Analysis of the Resin.—From the elementary analysis of the resins, it was made clear that another reaction, one differing from the usual novolak formation, took place. The results obtained are shown in Table V. The determined value of C% was larger than the calculated value, and the difference became lagrer as the reaction proceeded. Moreover, not only was the observed value of Cl% smaller than the calculated value, but the difference became larger with the reaction time and with the increase in the molecular weight, as is shown in Fig. 9. The values of Cl% of the acetylated resin, however, approached the theoretical values (Table VI).

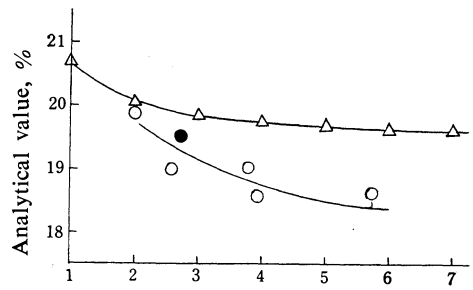

Fig. 9. Analytical values of Cl observed in the resin before and after fractionation. Acetate of the resin (150°C, 2 hr.) was used as sample.
△ Calculated values for acetate
● Observed value of acetate of resin
○ Observed values after fractionation on the acetate

From these facts it may be considered that the reaction of dehydrochlorination occurred, yielding the structure shown in Table VII.

Summary

A novolak resin of a higher molecular weight, as described by Burke et al., was not obtained. It was considered that the reaction of *p*-chlorophenol with *s*-trioxane proceeded as follows: (1) At first, a normal reaction of novolak formation proceeded. The molecular weight distribution was explained by Imoto's theoretical equation (120°C, 4 hr.). The analytical value of Cl% was rather close to the calculated value. (2) Then "reformation reaction" started (120°C, 7 hr. and 150°C, 2 hr.). (3) Reformation took place rather vigorously, and the molecular weight distribution became close to Poisson's distribution (150°C, 8 hr.). (4) A three-dimensional compound was formed, and the molecular weight of the soluble part was lowered (150°C, 11 hr.). (5)

The molecular weight of the soluble part increased by the decomposition of the three-dimensional compound and by the dehydrochlorination reaction (150°C, 24 hr.).

Department of Applied Chemistry
Faculty of Engineering
Osaka City University
Kita-ku, Osaka

The Crystal Structure of Bistetramethyldisilanilenedioxide $((CH_3)_4Si_2O)_2$

By Tsunehiro TAKANO, Nobutami KASAI and Masao KAKUDO

(Received January 5, 1963)

There have been many structural investigations of the bond angle and bond length of the Si–O–Si skeleton in various types of inorganic silicates. It would be of interest to extend these investigations in the field of organic silicon compounds. The crystal structures of various types of siloxanes have been studied by Frevel and Hunter[1], Roth and Harker[2], Peyronel[3] and Steinfink, Post and Fankuchen[4]. These structure analyses have shown that cyclic siloxanes have two configurations in the Si–O–Si rings, one planar and one puckered.

There has, however, been no study of the crystal structure of an organic silicon compound containing the Si–Si bond. It would be interesting, for instance, to determine the crystal structure of bistetramethyldisilanilenedioxide, which has a cyclic member which includes the Si–Si bond. From the results of chemical analysis, it was supposed that the molecule had following constitutional formula:

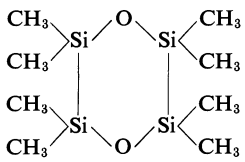

Experimental

Crystals recrystallized several times from petroleum ether at 10°C are colorless, plate-like, and have no cleavage. The crystals very quickly sublime at room temperature, and are soluble in most organic solvents.

To prevent such sublimation of the specimen, the crystal was sealed in a thin-walled glass capillary. The quick sublimation and the low melting point made it impossible cut the crystal into a cylindrical specimen suitable for a X-ray photograph.

Oscillation and Weissenberg photographs were taken using Cu-K_α radiation filtered by nickel foil.

The cell dimensions and physical constants were determined to be as follows;

$a=7.67\pm0.02$ Å	$D_{obs}=1.04$ g. cm^{-3}
$b=6.64\pm0.02$ Å	$D_{calcd}=1.05$ g. cm^{-3}
$c=17.39\pm0.03$ Å	m. p. $=42$°C
$\beta=111.0\pm0.2$°	mol. wt. $=264$
$V=826.8$ Å^3	$Z=2$

The reflections $(0\,k\,0)$ with k odd and $(h\,0\,l)$ with l odd were absent, the $(h\,k\,l)$ reflections showed no extinction rule. These extinction rules show that the corresponding space group is $C_{2h}^5-P2_1/c$. The oscillation photographs taken at -50°C did not show any transition within the temperature range, unlike that taken at room temperature. The exposure time was limited by the sublimation of the crystal, so it was very difficult to obtain three-dimentional intensity data. The equatorial Weissenberg photographs around the a and b axes were taken by using the multiple-film technique. The relative intensities of the observed reflections were estimated in terms of an arbitrary scale by visual comparison with an intensity scale. The observed structure factors were brought to an absolute scale by means of Wilson's method[5].

Determination of the Configuration

The intensities of $(0\,k\,l)$ and $(h\,0\,l)$ reflections were corrected with the Lorentz and polarization factors. For the space group $P2_1/c$, two molecules in a unit cell have to be placed on the center of symmetry. This means that the molecule has a center of symmetry in itself. Therefore the asymmetric unit is a half of the molecule; two silicon atoms, one oxygen atom and four methyl groups. Consequently, twenty-one parameters, except for those of hydrogen atoms, should be determined in this structure analysis.

1) L. K. Frevel and M. J. Hunter, *J. Am. Chem. Soc.*, **67**, 2275 (1945).
2) W. L. Roth and D. Harker, *Acta Cryst.*, **1**, 34 (1948).
3) G, Peyronel, *Chem. Industr.*, **36**, 441 (1954).
4) H. Steinfink, B. Post and I. Fankuchen, *Acta Cryst.*, **8**, 420 (1956).
5) A. J. C. Wilson, *Nature*, **150**, 152 (1942).

First, an attempt was made to locate the silicon atoms by the Patterson function $P(xz)$ projection of the $(0\,l\,0)$ plane, because it is considered that overlapping of atoms were minimized in this projection (Fig. 1). All $(h\,0\,l)$ reflections which formed about two-thirds of the total number of unique $(h\,0\,l)$ reflections, were used to calculate the Patterson function. In the Patterson projection $P(xz)$, the silicon-silicon and silicon-oxygen vectors of adjacent molecules were fairly distinguishable. Thus, the coordinates of silicon and oxygen atoms could be approximately determined. The carbon atoms were not fixed by this Patterson projection. A probable structure model was made from the positions of the silicon and oxygen atoms derived from the Patterson projection and was corrected by structure factor refinements, referring to the covalent radii and tetrahedral angles about the silicon atoms[6].

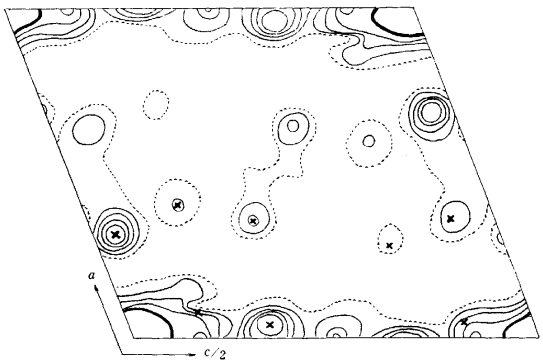

Fig. 1. Patterson function P(xz) projected on the $(0\,l\,0)$ plane. Contours show equal intervals in an arbitrary scale. The intermolecular vectors between ring members are marked with crosses.

Although the results of the calculation of structure factors on the first model did not show a good agreement with the observed structure factors $F(h\,0\,l)$, even for the reflections with low indices, a two-dimensional Fourier synthesis on the $(h\,0\,l)$ plane was tried, using lower order reflections. The electron density map obtained here, however, indicated not only the outline of the molecule but also two silicon atoms, an oxygen atom and two carbon atoms. The structure factors were calculated, and several Fourier syntheses were made. After these procedures, the (F_o-F_c) syntheses were applied for correcting the coordinates and temperature factors. The isotropic temperature factors for carbon atoms, oxygen atom and silicon atoms were $B_C=3.5$, $B_O=3.5$ and $B_{SI}=2.5$ Å^2 respectively at this step of the refinement.

6) L. C. Pauling, "The Nature of the Chemical Bond", Cornell University Rress, Ithaca, N. Y. (1960), p. 246.

On the other hand, an attempt to locate the y parameters was calculating the Patterson function, $P(yz)$. The intensities of the $(0\,k\,l)$ reflections were generally weak because of the limitation of exposure time. The intensities of about one-third of the $(0\,k\,l)$ reflections observed were too weak to be measured. As has been mentioned before, no peaks corresponding to the intramolecular vectors could be resolved in this Patterson projection. Therefore, a special type of modified Patterson function[7] was calculated:

$$P'(yz)=\sum\sum|F(0\,k\,l)|^2(1-\exp(-\xi^2))\times\cos 2\pi ky\cos 2\pi lz$$

where $\xi=2\sin\theta$. This modified Patterson map was particularly effective in distinguishing the intramolecular vectors, as is shown in Fig. 2.

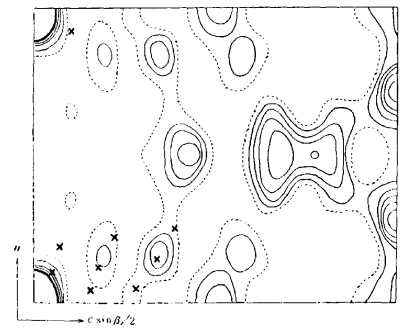

Fig. 2. A modified Patterson function projected on the $(l\,0\,0)$ plane. Contours are at equal intervals in an arbitrary scale. The intermolecular vectors between ring members are marked by crosses.

Using the y parameters derived from this modified Patterson projection and the z parameters obtained from the (0 1 0) projection, the structure factors of $(0\,k\,l)$ reflections were calculated. The usual successive refinements of atomic parameters were carried out. The isotropic temperature factors $B_C=9.0$ for carbon, $B_O=9.0$ for oxygen and $B_{SI}=5.0$ Å^2 were used in the calculations of $F(0\,k\,l)$. At this step of refinement, including the (F_o-F_c) syntheses, the reliability factors, $R=\sum||F_o|-|F_c||/\sum|F_o|$, were 24.6% for $(0\,k\,l)$ and 21.2% for $(h\,0\,l)$.

The least square method was used in the next step of the refinement. Ten cycles of the refinement of positional and isotropic temperature factor parameters reduced the R factor from 24.6% to 20.1% for $(0\,k\,l)$ and from 21.2% to 13.5% for $(h\,0\,l)$, non-observed reflections being excluded.

The calculations of the structure factors and the least square refinements were carried

7) T. Watanabé and Y. Takaki, to be published.

TABLE I. ATOMIC PARAMETERS

	x	y	z	$B(\text{A}^2)$ $(h\,0\,l)$	$B(\text{A}^2)$ $(0\,k\,l)$
Si(1)	0.1700	0.1262	0.0986	2.5	5.5
(2)	0.1400	−0.0233	−0.0716	3.1	6.6
O	0.2170	0.0845	0.0170	7.1	12.1
C(1)	0.2000	0.4000	0.1179	9.0	6.0
(2)	0.3397	−0.0135	0.1894	4.6	6.5
(3)	0.1472	0.1500	−0.1534	5.8	9.0
(4)	0.2800	−0.2590	−0.0777	8.4	6.4

out with a NEAC-2203 electronic computer, and the Fourier and Patterson functions, with a NEAC-2101 electronic computer. The least square calculations were performed using the program of Osaki[8]. The Hartree-Fock atomic scattering curves for carbon and oxygen atoms and Slater's for silicon atoms were employed throughout the calculations of the structure factors. In the computations of the structure factors, the contribution of hydrogen atoms was disregarded. The final atomic coordinates and isotropic temperature factors of each atom as obtained by the least square method are listed in Table I. The final electron density projections upon (1 0 0) and (0 1 0) are shown in Fig. 3 and Fig. 4 respectively. The observed and calculated structure factors are tabulated in Table II.

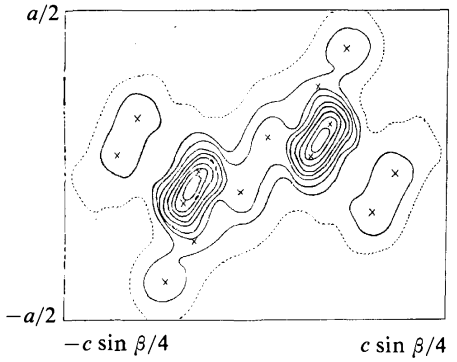

Fig. 3. Electron density projection of one molecule on the (1 0 0) plane. Atomic positions are marked by crosses. Contour intervals are 2 eÅ^{-2}, the lowest contour (broken line) being at 2 eÅ^{-2}.

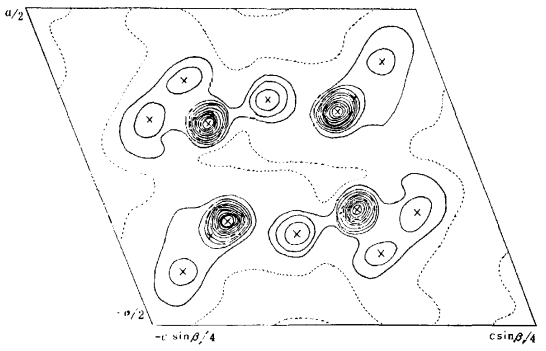

Fig. 4. Electron density projection of one molecule on the (0 1 0) plane. Atomic positions are marked by crosses. Contour intervals are 2 eÅ^{-2}, the lowest contour (broken line) being at 2 eÅ^{-2}.

8) K. Osaki, N3LSIMC (1961).

Results and Discussion

Bond lengths and angles were obtained as given in Table III, and the arrangement of molecules in the unit cell, together with the

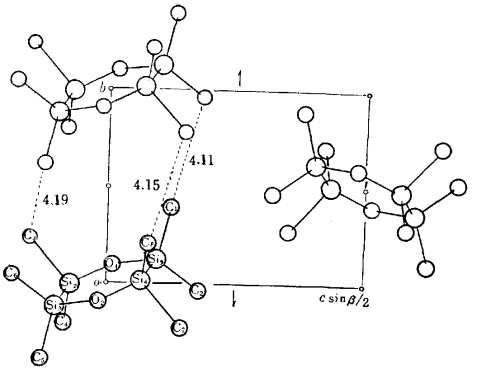

Fig. 5. Arrangement of the molecules projected on the (1 0 0) plane.

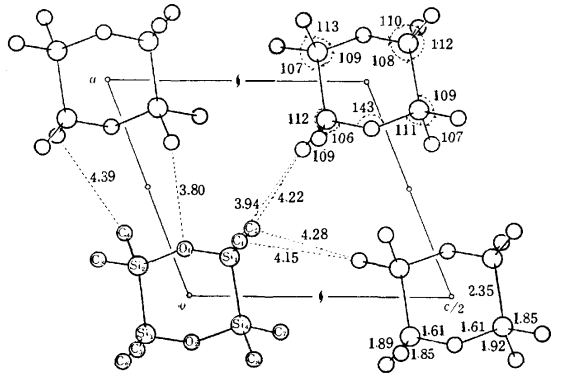

Fig. 6. Arrangement of the molecules projected on the (0 1 0) plane.

TABLE II. OBSERVED AND CALCULATED STRUCTURE FACTORS

0 k l	$\|F_o\|\times10$	$F_c\times10$	0 k l	$\|F_o\|\times10$	$F_c\times10$	0 k l	$\|F_o\|\times10$	$F_c\times10$	0 k l	$\|F_o\|\times10$	$F_c\times10$
002	703	685	024	42	38	0312	48	− 67	052	46	− 6
4	550	−573	5	294	−266	13	34	38	3	0	− 20
6	389	−412	6	69	− 62	14	34	− 20	4	46	− 41
8	163	−147	7	137	137	15	95	88	5	0	27
10	262	236	8	139	−133	16	66	19	6	71	− 64
12	191	153	9	198	133	17	40	24	7	48	− 36
14	0	11	10	0	20	040	60	− 82	8	48	− 46
011	1046	962	11	32	− 46	1	60	− 37	9	48	− 60
2	468	−512	12	32	24	2	0	− 21	10	48	42
3	0	27	13	109	−107	3	88	−108	11	34	− 26
4	510	−520	14	71	35	4	105	127	12	67	69
5	48	− 93	15	48	− 31	5	85	− 91	13	44	7
6	0	66	16	48	42	6	0	− 9	14	42	9
7	298	−292	17	42	31	7	44	− 32	15	0	38
8	276	268	18	40	− 5	8	149	−199	060	0	32
9	38	− 39	031	0	74	9	0	26	1	0	26
10	71	13	2	286	−261	10	99	− 97	2	0	− 6
11	196	180	3	71	78	11	48	59	3	0	22
12	101	− 97	4	212	−215	12	34	20	5	0	− 3
13	105	80	5	93	73	13	48	9	6	0	− 20
14	71	− 46	6	55	54	14	69	80	7	0	− 7
15	0	5	7	125	−166	15	46	− 22	9	0	− 39
020	425	444	8	123	100	16	38	50	10	0	− 24
1	26	− 44	9	131	−141	17	40	− 11	11	0	− 6
2	69	132	10	0	− 30	18	32	− 17	12	38	39
3	306	−332	11	46	− 24	051	0	12	13	36	10

0 h l	$\|F_o\|\times10$	$F_c\times10$	0 h l	$\|F_o\|\times10$	$F_c\times10$	0 h l	$\|F_o\|\times10$	$F_c\times10$	0 h l	$\|F_o\|\times10$	$F_c\times10$
002	648	692	18	118	128	−4	0	5	−10	0	41
4	582	−575	−2	479	−448	−6	456	471	−12	94	52
6	397	−427	−4	471	364	−8	477	443	−14	93	− 13
8	158	−177	−6	172	−209	−10	153	−165	−16	65	19
10	278	300	−8	244	−240	−12	469	−400	−18	107	64
12	259	248	−10	107	109	−12	265	−231	−20	94	86
14	50	35	−12	252	262	−16	65	76	700	145	163
16	0	− 40	−14	139	163	−18	132	154	2	65	− 57
100	675	675	−16	132	−125	−20	59	26	4	113	−140
2	118	173	−18	185	−189	500	132	105	6	59	− 70
4	126	−121	−20	86	− 69	2	118	63	−2	252	260
6	126	−103	300	629	−736	4	166	−136	−4	0	− 17
8	88	44	2	212	−198	6	145	−132	−6	284	−268
10	158	−215	4	404	423	8	0	− 5	−8	332	−285
12	225	−255	6	364	374	10	113	144	−10	93	− 55
14	0	− 23	8	0	8	12	113	143	−12	231	240
16	94	86	10	153	−145	−2	107	71	−14	206	159
18	99	125	12	132	−162	−4	93	85	−16	0	− 40
−2	536	530	14	0	1	−6	183	187	−18	80	− 74
−4	490	−495	16	99	84	−8	364	368	800	0	− 5
−6	450	−485	−2	656	−624	−10	59	43	2	0	11
−8	166	−144	−4	244	248	−12	341	−318	4	0	25
−10	418	433	−6	370	382	−14	172	−170	−2	0	21
−12	603	603	−8	86	−125	−16	94	52	−4	0	46
−14	166	140	−10	198	−226	−18	206	194	−6	132	−100
−16	158	−178	−12	219	−192	−20	113	134	−8	172	−165
−18	132	−148	−14	126	− 70	600	337	316	−10	0	− 37
−20	0	− 40	−16	0	51	2	132	−102	−12	126	134
200	868	−898	−18	65	− 64	4	298	−274	−14	118	164
2	278	−238	−20	61	− 61	6	172	−174	−16	0	− 8
4	0	55	400	311	−315	8	0	7	−18	172	−123
6	383	367	2	158	171	10	113	140	900	46	− 71
8	107	88	4	364	336	−2	319	282	−2	73	−107
10	305	−361	6	59	52	−4	0	− 30	−4	0	− 3
12	279	−326	8	0	4	−6	158	−156	−6	99	79
14	0	− 56	−2	244	−228	−8	158	−131	−8	59	19
16	126	150									

TABLE III. BOND LENGTHS AND ANGLES

Si(1)	Si(2)	2.35 Å	∠C(1)Si(1)Si(4)	111.9°
	O(1)	1.61	∠C(2)Si(1)Si(4)	111.6
	C(1)	1.85	∠C(3)Si(2)Si(3)	109.5
	C(2)	1.89	∠C(4)Si(2)Si(3)	107.3
Si(2)	O(1)	1.61	∠C(1)Si(1)O(1)	106.1
	C(3)	1.85	∠C(2)Si(1)O(1)	110.4
	C(4)	1.92	∠C(3)Si(2)O(1)	111.0
			∠C(4)Si(2)O(1)	113.3
∠O(1)Si(1)Si(4)		107.7°		
∠O(1)Si(2)Si(3)		108.6	∠C(1)Si(1)C(2)	109.1
			∠C(1)Si(2)C(4)	107.0
∠Si(1)O(1)Si(2)		143.2		

TABLE IV. BOND LENGTHS AND ANGLES

Molecule	Si-Si	Si-O	Si-C	∠Si-O-Si	∠O-Si-O	∠C-Si-C	∠O-Si-Si
Bistetramethyl-disilanilenedioxide	2.35	1.61	1.88	143	—	108	109
Octamethylcyclo-tetrasiloxane	—	1.65	1.92	142.5	109	106	—
Hexamethylcyclo-trisiloxane	—	1.614	1.929	136	104	106	—
Spirosiloxane	—	1.64	1.88	130	106	106	—
Diethylsilanediol	—	1.63	1.90	—	110	111	—
Diallylsilanediol	—	1.63	1.90	—	110	110	—

intermolecular bond lengths and angles as well as the intramolecular distances, are illustrated in Figs. 5 and 6.

The equation of a plane including the Si-O-Si triangle the ring member is:

$$6.63x-3.06y+z-62.5=0$$

and that including the four silicon atoms is:

$$3.06x-2.93y+z=0.$$

These two planes form an angle of 170°. Thus, the skeleton of the ring has a chair form. This shows that the configuration of the skeleton compensates for the energy of strain which may exist in the ring if it has a planar form.

The Si-Si bond distance, 2.35 Å, in the molecule is almost the same as that found in metallic silicon (2.34 Å). The Si-O bond length, 1.61 Å, is considerably shorter than the value (1.83 Å) which is the sum of the covalent radii of the silicon and oxygen atoms. This shrinkage of the bond length as known in silicates has already been reported also in organic silicon compounds[9-14]. The bond angle of Si-O-Si (143°) is greater than either the covalent p orbital bond angle or the sp^2 and sp^3 hybrid orbital bond angle. This finding and the shrinkage of the Si-O bond length may indicate the presence of an ionic character in the Si-O-Si configuration, as was been suggested by Pauling[15]. The average bond length of the Si-C bond (1.88 Å) is almost in agreement with those of spirosiloxane, diethylsilanediol and diallylsilanediol. However, the deviations of the Si-C bond lengths from the average bond length are not small in this case. This may be caused by the overlapping of carbon atoms in the two-dimensional projections. The bond angles around the silicon atoms are almost regularly tetrahedral; their values agree with those of spirosiloxane, octamethylcyclotetrasiloxane and hexamethylcyclotrisiloxane, as is shown in Table IV. The intermolecular interaction seems to be somewhat weaker than the ordinary methyl-methyl interaction, because the crystal has an extremely large sublimation nature and a low melting point. In fact, the intermolecular distances of the crystal obtained in this study (Figs. 5 and 6) are longer than the ordinary van der Waals distance (4.0 Å) between methyl groups.

The authors wish to express their gratitude to Professor Makoto Kumada* of Osaka City

9) L. K. Frevel and M. J. Hunter, *J. Am. Chem. Soc.*, 67, 2275 (1945).
10) W. L. Roth and D. Harker, *Acta Cryst.*, 1, 34 (1948).
11) G. Peyronel, *Chem.. Industr.*, 36, 441 (1954).
12) H. Steinfink, B. Post and I. Fankuchen, *Acta Cryst.*, 8, 420 (1956).
13) M. Kakudo and T. Watase, *Tech. Rept. of Osaka Univ.*, 2, 247 (1952).
14) M. Kakudo and N. Kasai. This Bulletin, 27, 605 (1954).
15) L. C. Pauling, "The Nature of the Chemical Bond", Cornell University Press, (1960), p. 321; *J. Phys. Chem.*, 56, 361 (1952).

* Present address: Faculty of Engineering, Kyoto University, Sakyo-ku, Kyoto.

University for kindly supplying the sample for this study. Thanks are also due to Mr. Yukiteru Katsube of Himeji Technical College, who joined in this work in its early stages, and to Mr. Yoshito Takaki of Osaka University of Liberal Arts and Education for his kind advice on the modified Patterson synthesis.

Institute for Protein Research
Osaka University
Kita-ku, Osaka

Faculty of Engineering
Osaka University
Miyakojima-ku, Osaka (N. K.)

The Radiolysis and Photolysis of Cycloheptatriene

By Shigeyoshi ARAI, Michio MAEMORI, Kenji YAMAGUCHI and Shoji SHIDA

(Received January 5, 1963)

Previously we reported[1] that cyclooctatetraene is one of the most radiation-stable organic liquids. Henglein's experiment[2], in which the *G* value of the radical formation was determined by the addition of sulfur dioxide as the radical scavenger, also supports this conclusion. Although cyclooctatetraene resembles benzene in chemical structure, its chemical properties rather belong to the cycloolefins. Therefore, it would be interesting to investigate the radiolysis of cycloheptatriene C_7H_8, which is a cycloolefin with three alternant double bonds and one methylene group. There has been, to the author's knowledge, only one paper dealing with the radiolysis of cycloheptatriene. Juppe and Wolf[3] carried out the irradiation of carbon-14 labeled cycloheptatriene and found that randomly-labeled bitropyl is produced from specifically-labeled cycloheptatriene. They therefore suggested that a symmetrical intermediate is formed as a precursor of the dimer.

It is known that in many cases reactions in the radiation chemistry are similar to those involved in the photochemistry. The photochemical study of cycloheptatriene in the vapor phase is of considerable value for understanding the mechanism in the radiolysis. Recently Srinivasan[4] has found that toluene is mainly formed in its direct photolysis.

A more detailed study of the radiolysis and electron resonace study are presented here. Moreover, the mercury-photosensitized reaction of cycloheptatriene has been investigated in the expectation of elucidating the mechanism of the radiolysis.

1) S. Shida, Y. Yamazaki and S. Arai, *J. Chem. Phys.*, **29**, 245 (1958).
2) A. Henglein, A/Conf., Vol. 29, 206 (1958).
3) G. Juppe and A. P. Wolf, *J. Am. Chem. Soc.*, **83**, 337 (1961).
4) R. Srinivasan, ibid., **84**, 3432 (1962).
5) W. G. Woods, *J. Org. Chem.* **23**. 110 (1958).

Experimental

Material.—Cycloheptatriene was prepared by the thermal isomerization of bicycloheptadiene in the method described by Woods[5]. Repeated distillations were carried out to remove the by-products, especially toluene, from the raw material. However, the sample used here was shown to be 95 to 97% cycloheptatriene and 3 to 5% toluene by gas chromatography.

Irradiation.—The radiation employed in the radiolysis of liquid cycloheptatriene utilized γ rays from 200C ^{60}Co. The sample was degassed on a vacuum line by freezing and pumping, and then sealed off in a glass cell. Irradiations were made at room temperature for 3 to 14 days. The dose rate was about 3.9×10^3 r/min.

Analysis.—After irradiation the non-condensables at -196°C (a mixture of hydrogen and methane) were transferred to a gas-buret by the use of a Toepler pump. Then the hydrogen and methane were analyzed by using a copper oxide furnace. The condensables were divided at -120°C into two fractions, (a) $C_2\sim C_4$ hydrocarbons, and (b) C_7 hydrocarbons. Quantitative analysis of each fraction was accomplished by gas chromatography. The columns, consisting of benzyl ether and silicon oil on crushed firebrick support, enabled the complete separation of the compounds for fractions a and b respectively. After distillation of the volatile products in vacuo at 100°C, a viscous yellow residue was found on the wall of the glass cell. This substance was determined gravimetrically as the polymer.

ESR Experiments.—In the ESR experiments the radiation used was the electron beam from a 1.5MeV. Van de Graaff generator. The sample in an open vessel, which was kept at the temperature of liquid nitrogen, was irradiated with a dose of 1×10^8 rad. The spectra were observed also at -196°C using a Nihon Denshikogaku ESR spectrometer.

Photochemical Experiments.—Cycloheptatriene vapor in a cylindrical quartz cell (diameter, 50 mm., length, 50 mm.), which contained a drop of

mercury, was irradiated by a neon-gas-filled mercury lamp. The light shorter than 2200A was cut off with a filter. The analytical procedures were the same as in the radiolysis.

Results and Discussion

Mercury Photosensitized Reaction in the Vapor Phase.—Owing to the presence of impurities it was not possible to obtain the absorption intensity of cycloheptatriene at the wavelength of 2537A. However, the large absorption coefficient of mercury vapor for the radiation of 2537A led the authors to assume that it is predominantly the mercury photosensitized reaction which takes place.

Figure 1 shows the changes in total pressure as a function of the reaction time. Curves A and B are obtained for the initial pressures

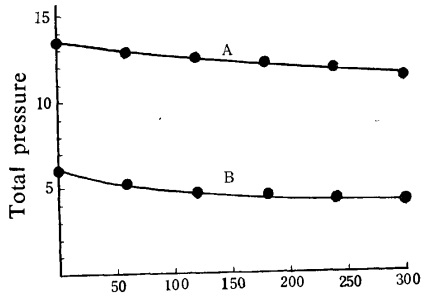

Fig. 1. Variation of total pressure as reaction time proceeds.
A Initial pressure, 13.5 mmHg
B Initial pressure, 6 mmHg

of 13.5 mmHg and 6 mmHg respectively. In run A a decrease in pressure of 2.2 mmHg was observed after the irradiation time of 300 sec., at which time the gas compositions were 30% toluene and 70% cyclcheptatriene. In run B a decrease of 2.0 mmHg was observed after 300 sec. The gas compositions were 75% toluene and 25% cycloheptatriene. In both cases the decomposition products were scarcely detectable. These results indicate that the major reaction is the isomerization of cycloheptatriene into toluene. The small decrease in total pressure may be attributed to the polymerization initiated by some radical decomposition of the cycloheptatriene.

Figure 2 shows the amounts of toluene formed as the irradiation time proceeds. The initial pressure of cycloheptatriene is 7 mmHg. The amount of toluene increases as a linear function of the irradiation time.

In Fig. 3 the amounts of toluene for the irradiation time of a half minute are plotted for the various initial pressures of cycloheptatriene. It may be clearly seen that the rates

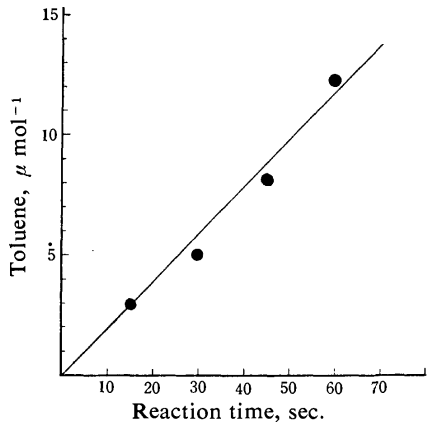

Fig. 2. Amounts of toluene formation as reaction time proceeds. The initial pressure of cycloheptatriene, 7 mmHg.

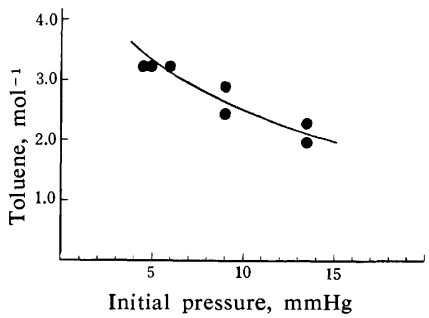

Fig. 3. Variation of toluene formation as a function of the initial pressure of cycloheptatriene. Irradiation time, 30 sec.

of toluene formation are strongly pressure-dependent. Thus, the present authors have concluded that, in the same manner as in cyclooctatetraene[6,7], an excited molecule of cycloheptatriene, which may either isomerize into toluene or be collisionally deactivated, is formed at the initial step. The experimental results may be explained by the following reaction mechanism:

$$C_7H_8 + Hg^* \rightarrow C_7H_8^* + Hg \quad (1)$$

$$C_7H_8^* \rightarrow CH_3C_6H_5 \quad (2)$$

$$C_7H_8^* + C_7H_8 \rightarrow 2C_7H_8 \quad (3)$$

$$C_7H_8 + Hg^* \rightarrow \text{Polymerization initiated by radicals} \quad (4)$$

The steady-state treatment leads to Eq. A:

$$\frac{I_o}{R_t} = 1 + \frac{k_3}{k_2}[C_7H_8] \quad (A)$$

where R_t is the rate of toluene formation, I_o

6) H. Yamazaki and S. Shida, *J. Chem. Phys.*, **24**, 1278 (1956).
7) H. Yamazaki, This Bulletin, **31**, 677 (1958).

is the absorbed intensity of the 2537A resonance line, $[C_7H_8]$ is the pressure of cycloheptatriene, and k_2 and k_3 are the rate constants of reactions 2 and 3 respectively. Thus, there has to be a linear relationship between $1/R_t$ and $[C_7H_8]$. As may be seen in Fig. 4, a satisfactory straight line is given. A slope-to-intercept ratio corresponds to k_3/k_2 in Eq. A. The numerical value is 0.11 $mmHg^{-1}$.

Srinivasan[4] has recently studied the direct photolysis of cycloheptatriene in the vapor phase and has found that the formation of toluene decreases with the total pressure. He suggested that isomerization to toluene occurs not from an electronically-excited molecule of cycloheptatriene but from a vibrationally-excited ground state molecule that is formed

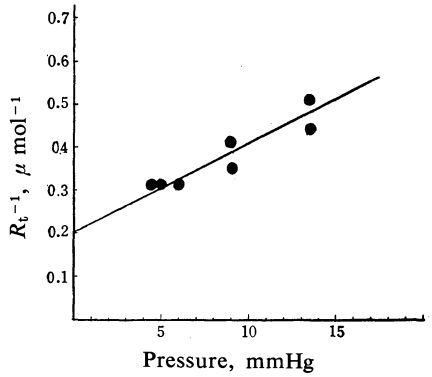

Fig. 4 Relationship between R_t^{-1} and $[C_7H_8]$. R_t is amount of toluene formation for the irradiation time of 30 sec. $[C_7H_8]$ is the pressure of cycloheptatriene.

by the internal conversion of the electronic energy. Generally speaking, however, a triplet state lies at a lower energy than a singlet state formd from the same orbital, and such large molecules as cycloheptatriene and cyclooctatetraene may easily undergo transitions from the initially-excited singlet to the lower triplet level. Further, in the present case, when an excited mercury atom (^3P) reacts with cycloheptatriene, the triplet-excited molecule is considered to be produced according to the spin conservation rule[8]. Hence, in both cases the isomerization reaction to toluene is likely to arise from the triplet excited molecule. The results in the present experiments are very similar to those obtained by Srinivasan from the direct photolysis at 2600A. Moreover, the value of k_3/k_2 nearly agrees with that calculated from his data[9].

Srinivasan pointed out that the formation of toluene was not totally quenched by the addition of even considerable amounts of oxygen or nitric oxide. However, it has been reported[10,11] that in the mercury photosensitized reaction of ethylene nitric oxide has no effect on the decomposition reaction of the triplet-excited ethylene. Therefore, the above experimental finding does not necessarily lead to the exclusion of the triplet-excited molecule.

The Electron Spin Resonance of Irradiated Cycloheptatriene[12].—It has been known that when frozen hydrocarbons are irradiated by ionizing radiations, the free radicals produced can be stabilized. A survey of the their ESR spectra gives valuable information concerning the primary act of ionizing radiations. Therefore, we carried out the ESR measurements of electron-irradiated cycloheptatriene frozen at −196°C.

As is shown in Fig. 5, eight equally-spaced

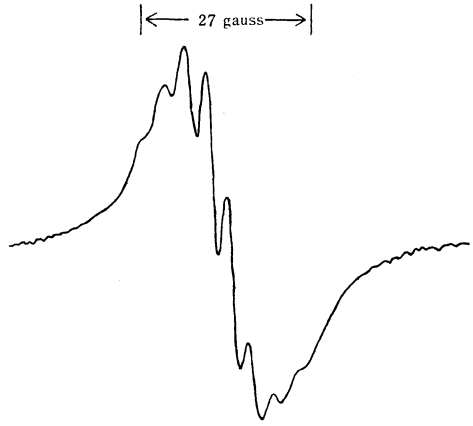

Fig. 5. First derivative ESR spectra of electron irradiated cycloheptatriene. Dose 1×10^8 rad, temperature of irradiation and ESR measurement is −196°C.

lines are observed in the spectrum. This fact clearly indicates that the seven equivalent protons interact on the unpaired electron. That is, the cycloheptatrienyl radical C_7H_7, which has a symmetric conjugated plane frame, is produced by the electron irradiation. On the basis of the simple LCAO MO method, it is to be expected that cycloheptatrienyl radical will have a large delocalization energy, as a

8) K. J. Laidler, "The Chemical Kinetics of Excited States", Oxford University Press, London (1955).

9) He also observed that the formation of toluene at 3130A shows a different pressure dependency from that at 2600A. However, this may be explained as follows. At a shorter wavelength the more vibrationally-excited molecule in the triplet state would be produced as the result of internal conversion. This results in the increase of the rate constant of reaction 2. Consequently, k_3/k_2 at 2600A gets larger than k_2/k_3 at 3130A in Eq. A.

10) S. Arai and S. Shida, *J. Chem. Phys.*, **38**, 694 (1963).

11) D. J. Le Roy and S. W. R. Steacie, ibid., **9**, 839 (1941).

12) S. Arai, S. Shida, K. Yamaguchi and Z. Kuri, ibid., **37**, 1885 (1962).

TABLE I. THE *G* VALUE OF THE PRODUCTS IN THE RADIOLYSIS OF LIQUID CYCLOHEPTATRIENE. Irradiation was made at room temperature. Dose rate was 3900 r/min.

Irradiation time, hr.	Sample g.	*G* Value				Polymer
		H_2 $\times 10^{-2}$	CH_4 $\times 10^{-3}$	C_2H_2 $\times 10^{-3}$	C_2H_4 $\times 10^{-3}$	
24	7.594	5.9	1.6	—	—	3.0
72	3.556	6.8	1.1	—	—	3.2
72	4.805	6.0	1.4	1.6	6.4	3.0
120	5.299	6.2	0.9	3.9	8.6	3.3
120	5.975	7.0	1.2	—	—	3.4
	C_8H_8	2.0				0.66

result of which the bond dissociation energy of the parent molecule, $H\text{-}C_7H_7$, will be much smaller than the other C–H bonds. Lossing et al.[13] reported 74±7 kcal./mol. for this bond. Generally speaking, in the reaction of radiation chemistry the C–H bonds with lower bond energies are preferentially fractured. This principle leads to the conclusion that the formation of the cycloheptatrienyl radical is one of the major reactions in the radiolysis. In order to obtain a rough estimate of the relative yield of the radical formation, the ESR signal intensity of irradiated cycloheptatriene was compared with that of irradiated benzene under the same experimental conditions. The near equality of the signals shows that cycloheptatriene is as stable as benzene with respect to the radical formation by ionizing radiations. During irradiation and the procedures which followed the sample was open to the air. However, the result with a degassed cycloheptatriene sample was the same as that obtained in air. Therefore, oxygen has no effect on the cycloheptatrienyl radical at −196°C.

The Radiolysis of Liquid Cycloheptatriene.— The *G* value of the products in the radiolysis of liquid cycloheptatriene at room temperature are shown in Table I; they are there also compared with the corresponding values for cyclooctatetraene.

The cycloheptatriene used contained 3 to 5% of toluene as an impurity. Judging from the findings about the irradiation of pure toluene[14], however, the direct effect of radiation on toluene is entirely negligible, even when a maximum is present.

The *G* values of the gaseous products found here are very small. Since cycloheptatriene itself is a reactive scavenger for free radical, those products appear to be produced by a molecular process, a hot atom process being included, or by an ion-molecule reaction. In discussing the radiolytic process, electron impact studies of cycloheptatriene will provide interesting information. In the mass spectra of cycloheptatriene obtained by Meyerson and Rylander[15] the most abundant ion ocurrs at mass 91, and the second most abundant ion, at 92. Other peaks of relative intensity greater than 10% occur at 65 and 39. Accordingly, the following reactions may take place:

$$C_7H_8 + e = C_7H_8^+ + 2e$$

$$C_7H_8 + e = C_7H_7^+ + H + 2e$$

$$C_7H_7^+ = C_5H_5^+ + C_2H_2$$

It is very interesting that the $C_7H_7^+$ ion is produced in a large amount. The results of the ESR experiments show that cycloheptatrienyl radicals are formed by electron irradiation. Juppe et al. suggested a cycloheptatrienyl radical as a precursor of the dimer which was isolated in their experiments. This radical may arise from the recombination of $C_7H_7^+$ with the electron, along with the split of a hydrogen atom from a highly-excited neutral molecule of cycloheptatriene. The formation of the hydrogen molecule may be explained by the abstraction reaction of a hot hydrogen atom, which comes from the energetic fragmentation in these processes. According to Meyerson and Rylander, the cyclic $C_7H_7^+$ ion decomposes into the $C_5H_5^+$ ion and acetylene. Thus, the formation of acetylene may be attributed to this reaction. However, the formation of ethylene can not be explained from the mass spectra of cycloheptatriene, because the ions corresponding to the loss of ethylene from $C_7H_7^+$ and $C_7H_8^+$ are relatively small. Probably in this case more complex reactions take place.

The polymer in Table I contains the C_{14} products, of course, together with the heavier hydrocarbons. Cycloheptatriene has a remarkable reactivity to the radicals, and the polymerization reaction gradually takes place even in the presence of air. Judging from this fact, the *G* value found here may be said

13) A. G. Harrison, L. R. Honnen, H. J. Dauben and F. P. Lossing, *J. Am. Chem. Soc.*, **82**, 5593 (1960).
14) J. P. Manion and M. Burton, *J. Phys. Chem.*, **56**, 560 (1952).
15) S. Meyerson and P. N. Rylander, *J. Chem. Phys.*, **27**, 901 (1957).

to be rather small. That is, the yield of the radical formation in the initial step may be low.

Owing to the presence of toluene in the sample used, the precise G value of the toluene formation was not obtained. However, there was no difference between the gas chromatographic check of toluene before and after irradiation. If the experimental error is taken into account, the G value of toluene will be small, not larger than 0.5.

From these experimental results we concluded that, in the radiation chemistry of liquid cycloheptatriene the major part of the absorbed energy results in the formation of the excited molecule, the electronic energy of which is readily converted to thermal energy. In the case of cyclooctatetraene, its high stability against ionizing radiations was attributed to the collisional deactivation of the excited molecule. The life time of 2×10^{-8} sec. is obtained for the excited cycloheptatriene molecule from the above-mentioned photochemical experiment, assuming that k_3 is about 1×10^{11} l./mol. sec.; that is, every collision leads to deactivation. Consequently, it may be considered that in the liquid phase the excited molecule is deactivated prior to its decomposition or its isomerization.

The over-all reaction mechanism of the radiolysis of cycloheptatriene is:

$$C_7H_8 \rightsquigarrow C_7H_8^*$$

$$C_7H_8^* + C_7H_8 \longrightarrow 2C_7H_8$$

The latter process plays a leading role. In addition,

$$C_7H_8 \rightsquigarrow C_7H_7 + H$$

$$C_7H_8 \rightsquigarrow H(\text{hot}), C_2H_2, C_7H_7, \text{ etc.}$$

$$H(\text{hot}) + C_7H_8 \longrightarrow H_2 + C_7H_7$$

$$2C_7H_7 \longrightarrow C_{14}H_{14}$$

$$H \text{ (or the other radicals)} \xrightarrow{C_7H_8} \text{Polymer}$$

As has been stated above, Juppe et al. found ditropyl as the product in the radiolysis of cycloheptatriene. The other reactions have not been considered here because there is no definite evidence for their occurrences.

Summary

1) In the photosensitized reaction of cycloheptatriene vapor, toluene was produced as the result of isomerization. The amount of toluene formation decreases as the pressure of cycloheptatriene increases. Isomerization to toluene proceeds through the excited molecule, which may be collisionally deactivated.

2) The ESR experiments at low temperatures show that cycloheptatrienyl radicals are formed by electron irradiation. However, the yield of the radical formation is low, nearly equal to that of benzene.

3) In the radiolysis of liquid cycloheptatriene the G values of the gaseous products and toluene are very small. The G value of the polymer seems to suggest the low yield of the radical formation at the initial step. We concluded that the major part of the absorbed energy results in the formation of the excited molecule, the electronic energy of which is readily converted to thermal energy.

The anthors wish to thank Professor Zenichiro Kuri and Dr. Shin Sato for their helpful discussions. The bicycloheptadiene was kindly given by Dr. Katsundo Matsuzawa.

Laboratory of Physical Chemistry
Tokyo Institute of Technology
Meguro-ku, Tokyo

The Polymerization Reaction of Sodium Phosphate

By Masayuki NAKAGAKI, Hiroshi INOUE, Tadao FUJIE and Shigeru OHASHI*

(Received January 5, 1963)

The amorphous polymer of sodium phosphate is called by several names, such as Graham's salt, glassy phosphate, sodium metaphosphate glass, sodium polymetaphosphate, and sodium hexametaphosphate[1]. Although the chemical formula of this substance is the same as that of a metaphosphate $(NaPO_3)_n$, it is not a ring-phosphate but a kind of chain polymer[2-4] and so may be called a sodium polyphosphate. The polyphosphate usually prepared is, however, a branched polymer, and it is partly depolymerized within several hours after dissolution in water or in an aqueous sodium bromide solution[5-7]. It has been concluded that the depolymerization is mainly due to the hydrolysis at the point of branching[5,6]. Therefore, it is interesting to polymer chemists[5] that the solution obtained at the end of the hydrolysis contains unbranched molecules only, and that the distribution function of the molecular weight has been determined both theoretically and experimentally[8].

In the present paper, polymerization reaction of sodium phosphate will be studied. Generally speaking, polymerization reactions are classified into two types: (1) condensation polymerization, and (2) addition polymerization, the latter including ring-opening polymerization. In the case of the preparation of amorphous sodium polyphosphate, a reaction starting from sodium hydrogen orthophosphate:

$$n\mathrm{NaH_2PO_4} = (\mathrm{NaPO_3})_n + n\mathrm{H_2O} \qquad (1)$$

is a kind of condensation polymerization, while a reaction starting from sodium trimetaphosphate (a ring-phosphate):

$$(n/3)(\mathrm{NaPO_3})_3 = (\mathrm{NaPO_3})_n \qquad (2)$$

is a kind of ring-opening (addition) polymerization. In this paper, these two reactions will be compared on the basis of viscometry of the products.

Experimental

Material. — The sodium dihydrogen orthophosphate dihydrate ($NaH_2PO_4 \cdot 2H_2O$) used was the same specimen as was used in a previous study[7]. The dihydrate was changed into an anhydrate by heating it at 110°C under a reduced pressure for about 15 hr.; thus it reached a constant weight and could be used for further experiments.

Sodium trimetaphosphate $(NaPO_3)_3$ was prepared by heating the above-described sodium dihydrogen orthophosphate anhydrate in a platinum crucible at 530°C for 5 hr.[1,3] and was then kept in a desiccator.

Polymerization Reaction. — The polymerization reaction was effected by heating about 7 g. of the starting material in a platinum crucible about 35 mm. in diameter, 37 mm. in height and about 30 ml. in capacity. For the heating, a Siliconit electric furnace BH-1020, equipped with a thermoelectric automatic regulator P-400 with a platinum platinum-rhodium thermocouple, was used. It took the furnace about 1.2, 1.8 and 3.5 hr. to reach 530, 700 and 900°C respectively from room temperature. At the end of the polymerization reaction, the content of the crucible was poured on a copper plate and pressed with another copper plate in order to cool the product rapidly.

Viscometry.—The product of the polymerization reaction was dissolved in a 0.07 N sodium bromide solution at the polymer concentration of 1 g./100 ml. It took about 1 hr. to dissolve. Solutions of other concentrations were prepared by the dilution of the above-prepared solution. Viscosity was measured by an Ostwald viscometer, while density was measured by an Ostwald pycnometer in a thermostat at 25.5°C.

Results and Discussion

Polymerization Equilibrium.—As the theory of reorganization[9] suggests, the polymerization reaction of phosphate will reach an equilibrium state if the reaction time is sufficiently long. The state of the equilibrium, however, may depend on the temperature. For a relatively long reaction time, therefore, the average molecular weight of the reaction product will

* S. Ohashi: Department of Chemistry, Faculty of Science, Kyushu University, Fukuoka.

1) Chem. Soc. of Japan, "Synthesis and Purification of Inorganic Compounds", Tokyo, Maruzen (1959), p. 80.
2) K. Karbe and G. Jamder, *Kolloid-Beih.*, 54, 1 (1943).
3) J. R. Van Wazer, "Phosphorus and its Compounds", Vol. I, Interscience Publishers, New York (1958).
4) C. F. Callis, J. R. Van Wazer and P. G. Arvan, *Chem. Revs.*, 54, 777 (1954).
5) U. P. Strauss, E. H. Smith and P. L. Wineman, *J. Am. Chem. Soc.*, 75, 3935 (1953).
6) U. P. Strauss and T. L. Treitler, ibid., 78, 3553 (1956).
7) M. Nakagaki, S. Ohashi and F. Minato, This Bulletin, 36, 341 (1963).
8) J. R. Van Wazer et al., *J. Am. Chem. Soc.*, 72, 639, 644, 647, 655, 906 (1950).
9) J. R. Parks and J. R. Van Wazer, ibid., 79, 4890 (1957).

depend more on the temperature than on the reaction time[10].

Setting the reaction time at 5 hr., the polymerization reaction was effected at various temperatures, and the average degree of polymerization, $\bar{n}$, of the product was determined by end-group titration. On the basis of the results shown in Fig. 1, it may be concluded that the degree of polymerization increases with the reaction temperature, and that the degrees of polymerization are equal for the products both by condensation polymerization and by ring-opening polymerization[11].

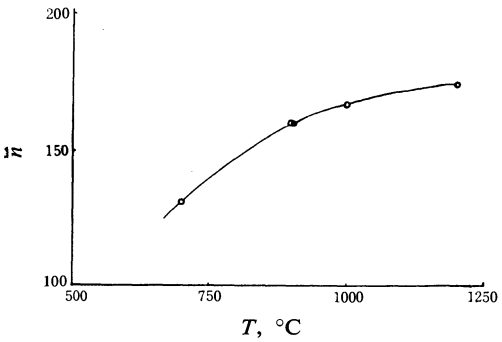

Fig. 1. Relation between polymerization temperature and average degree of polymerization for heating time of 5 hr.
○ Condensation polymerization of orthophosphate
● Ring opening polymerization of trimetaphosphate

Time Dependence of Solution Viscosity.—The viscosity of solutions of the polymerization products decreases with time because of the depolymerization of the polyphosphate, and it has already been shown in a previous paper[7] that the reaction is of the first order. As the examples in Fig. 2 show, the viscosity, η, of the solution relative to that of the solvent (a 0.07 N sodium bromide solution) changes with time, τ, according to the following empirical equation:

$$\log(\eta-\eta_\infty)=\log(\eta_0-\eta_\infty)-K\tau \qquad (3)$$

where the constants, η_0, η_∞ and K, are the relative viscosities at $\tau=0$, $\tau=\infty$, and the rate constant respectively. As for the value of η_∞, the relative viscosity at $\tau=24$ hr. was used,

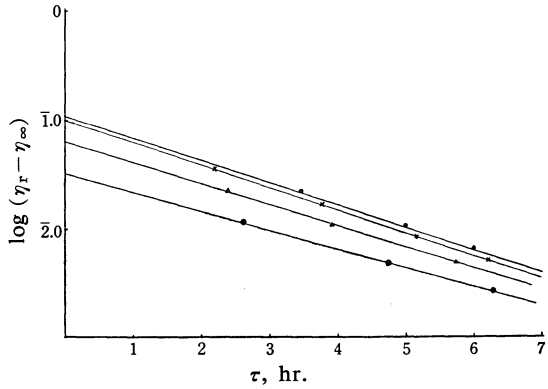

Fig. 2. Examples of decrease of solution viscosity with time in 0.07 N NaBr solution at 25.5°C for the product polymerized by heating of orthophosphate at 900°C for 6 hr.
Concentration of solution: (○) 1, (×) 0.8, (△) 0.4 and (◎) 0.2 (g./100 ml.)

and the value of η_0 was determined on the basis of Eq. 3.

It was widely been known that the intrinsic viscosity of a solution is directly related to the average polymerization degree of the solute. In the case of solutions of sodium polyphosphate in the solvent 0.07 N sodium bromide, the relation between the intrinsic viscosity and the average molecular weight derived in the previous paper[7] can be rewritten as:

$$\bar{n}=877[\eta]-30.5 \qquad (4)$$

where $\bar{n}$ is the average polymerization degree.

The values of $[\eta_0]$ and $[\eta_\infty]$ were obtained on the basis of the values of η_0 and η_∞ respectively, measured at polymer concentrations of 0.1, 0.2, 0.4, 0.6, 0.8 and 1.0 g./100 ml. For the extrapolation to the infinite dilution, two equations,

$$\left.\begin{aligned}(\eta-1)/c&=[\eta]+k[\eta]^2c\\(\ln\eta)/c&=[\eta]-k'[\eta]^2c\end{aligned}\right\} \qquad (5)$$

together with the equation,

$$k+k'=0.5 \qquad (6)$$

were used to confirm the extrapolation[12,13].

As has already been stated in earlier in this paper, it has been concluded that the depolymerization is mainly due to the hydrolysis at the point of branching[5,6]. Therefore, $[\eta_0]$ should be related to the average polymerization degree of the whole molecule before the hydrolysis, that is, the branched molecule formed by the polymerization reaction. On the other hand, $[\eta_\infty]$ should be related to the average polymerization degree of hydrolyzed

10) A. C. Chatterji, *J. Polymer Sci.*, 35, 235 (1959).

11) The data shown in Fig. 1 were obtained by one of the authors (S. O.) at Kyushu University. The end group titration was made about 24h. after dissolution, and the P-O-H end group generated by the hydrolysis of a branching point was believed to be titrated as an end-group[6]. The values of $\bar{n}$ in Fig. 1, therefore, correspond to $\bar{n}_\infty$ of Figs. 3 and 4. The inexact agreement between the numerical values in these figures is probably due to the difference in the methods of $\bar{n}$ determination and also to a minor difference in the experimental techniques of the polymerization.

12) W. Heller, *J. Colloid Sci.*, 9, 547 (1954).

13) M. Nakagaki and H. Nishibayashi, This Bulletin, 31, 477 (1958).

molecules, that is, the average length of each branch.

The Condensation Polymerization of Sodium Dihydrogen Orthophosphate.—Sodium dihydrogen orthophosphate anhydrate (NaH_2PO_4) was put in a platinum crucible and heated in an electric furnace. After the furnace reached the polymerization temperature, the heating was further continued for 1/2, 3 and 6 hr. at that temperature (700°C or 900°C). The intrinsic viscosities, $[\eta_0]$ and $[\eta_\infty]$, of the polymerization products were measured. The results are shown in Table I. The $[\eta_0]$ and $[\eta_\infty]$ values of the products polymerized at 900°C were greater than those polymerized at 700°C. The $[\eta_0]$ value for 900°C reaches a maximum value (0.298) at about 3 hr. and then decreases, but the $[\eta_\infty]$ value for 900°C and the $[\eta_0]$ and $[\eta_\infty]$ values for 700°C are the greater, the longer the polymerization time. The $[\eta_\infty]$ value approaches 0.198 for 900°C and 0.140 for 700°C.

Table I. Condensation polymerization of sodium dihydrogen orthophosphate

Preheating time* hr.	Polymerization condition		Intrinsic viscosity	
	Temp. °C	Time hr.	$[\eta_0]$	$[\eta_\infty]$
1.9	700	1/2	0.164	0.132
1.7	700	3	0.184	0.134
1.7	700	6	0.182	0.140
3.6	900	1/2	0.253	0.168
3.4	900	3	0.298	0.188
3.5	900	6	0.283	0.198
0	—	0	0.0313**	0.0313**

* The time required to reach the polymerization temperature.
** Sodium dihydrogen orthophosphate itself.

The Ring-opening Polymerization of Sodium Trimetaphosphate. — Sodium trimetaphosphate kept in a platinum crucible at room temperature was put in an electric furnace. The furnace had been heated, in advance, to the polymerization temperature. When the heating of 5 min.~2 hr. for the polymerization was over, the product was taken out and the $[\eta_0]$ and $[\eta_\infty]$ values were measured. The results are shown in Table II. The relation between the intrinsic viscosities and the polymerization time is entirely different from the case of condensation polymerization. The maximum points of $[\eta_0]$ and $[\eta_\infty]$ are located at the reaction time shorter than 5 min. for 900°C and 11 min. for 700°C. Five or eleven minutes is required to melt the contents of the crucible. In the case of ring-opening polymerization, therefore, the polymerization is finished almost immediately after the material is melted. The

Table II. Ring-opening polymerization of sodium trimetaphosphate

Polymerization condition		Intrinsic viscosity	
Temp. °C	Time min.	$[\eta_0]$	$[\eta_\infty]$
700	11	0.878	0.318
700	15	0.832	0.332
700	30	0.724	0.314
700	60	0.311	0.181
700	120	0.198	0.145
900	5	0.729	0.356
900	15	0.509	0.273
900	30	0.384	0.235
900	60	0.289	0.190
900	120	0.211	0.166
—	0	0.016*	0.016*

* Sodium trimetaphosphate itself

$[\eta_0]$ value is greater for 700°C than for 900°C, and decreases rapidly when the polymerization time becomes longer. The $[\eta_\infty]$ value decreases gradually and approaches 0.166 for 900°C and 0.145 for 700°C.

A Comparison of Condensation Polymerization and Ring-opening Polymerization.—The intrinsic viscosities, $[\eta_0]$ and $[\eta_\infty]$, were recalculated to the average degrees of polymerization, $\bar{n}_0$ and $\bar{n}_\infty$ respectively, according to Eq. 4, where $\bar{n}_0$ is the polymerization degree of the whole molecule[14] and $\bar{n}_\infty$ is the average polymerization degree of each branch in the molecule. Therefore, the apparent number of branches in one molecule, B, may be obtained by;

$$B=\bar{n}_0/\bar{n}_\infty \qquad (7)$$

The results of the calculation are shown in Figs. 3, 4 and 5.

On the basis of these results, the following points may be emphasized. In the case of the condensation polymerization, both $\bar{n}_0$ and $\bar{n}_\infty$ are the greater, the higher the temperature. This would mean that the polymerization due to the separation of water proceeds the further, the higher the temperature. When the reaction time is longer than 3 hr., the thermal separation of branches occurs simultaneously, so that B and $\bar{n}_0$ decrease to some extent, especially at a high temperature (900°C). The length of each branch, $\bar{n}_\infty$, however, shows no appreciable decrease. In the case of the ring-opening polymerization, on the contrary, the

14) In this case, the molecules are branched. The relation between $[\eta]$ and $\bar{n}$ for branched polymer should be different from that for unbranched polymer. The correction factor for the branching is not known in the case of a sodium polyphosphate solution, but it is not large in the case of an organic polymer. Therefore, Eq. 4 was used to obtain an apparent value of $\bar{n}$. The value thus obtained may be expected to be correct in its order of magnitude.

TABLE III. TEMPERATURE DEPENDENCE OF THE AVERAGE DEGREE OF POLYMERIZATION OF EACH BRANCH AT RELATIVELY LONG POLYMERIZATION TIME

Ref.	Polymerization		Polymerization degree		
	Time, hr.	Starting material	700°	900°	Method
Fig. 1	5	Ortho	126	160	End group titration
Fig. 1	5	Trimeta	—	160	End group titration
Fig. 3	6	Ortho	92	143	Viscometry
Fig. 4	2	Trimeta	97	115	Viscometry

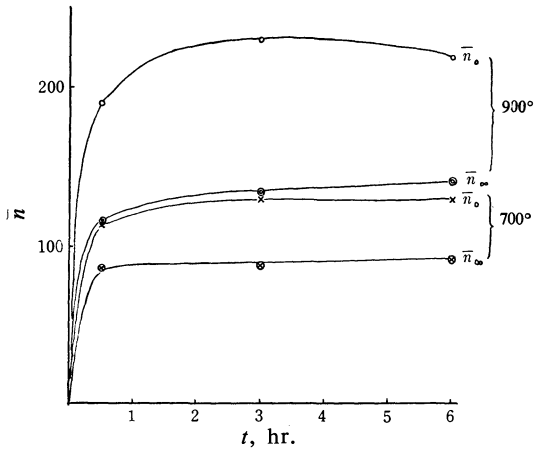

Fig. 3. Dependence of degree of polymerization on the time of polymerization of orthophosphate.

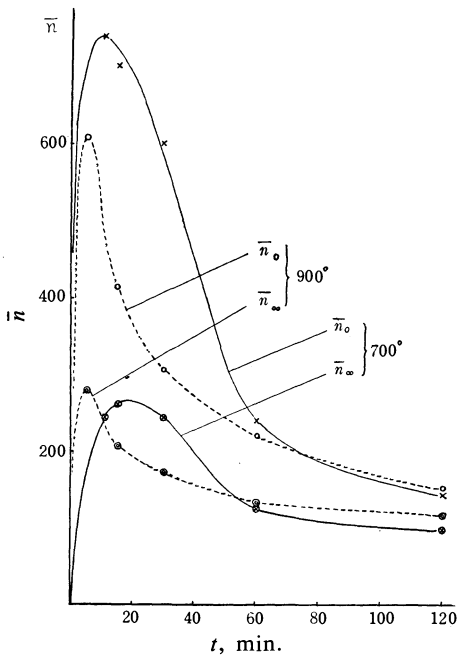

Fig. 4. Dependence of degree of polymerization on the time of polymerization of trimetaphosphate.

$\bar{n}_0$ and $\bar{n}_\infty$ values are the greater, the lower the temperature, if the reaction time is shorter than 1 hr., and they do not depend too much on the temperature if the reaction time is longer than 1 hr. This would mean that the polymerization is completed within 5~11 min., so that the thermal depolymerization is more important in this case. The higher the temperature, the more the separation of the branches proceeds and the more the degree of polymerization, $\bar{n}_0$, decreases. In this case, the thermal break-up of each polymer chain occurs within at least 1 hr., in addition to the separation of the branches at the branching points. After 2 hr., the $\bar{n}_\infty$ value becomes the larger, the higher the temperature. As is shown in Table III, these findings tend to accord with the results of Figs. 1 and 3, although the numerical values do not exactly coincide with each other, probably because of the differences in experimental methods, as has already pointed out[11].

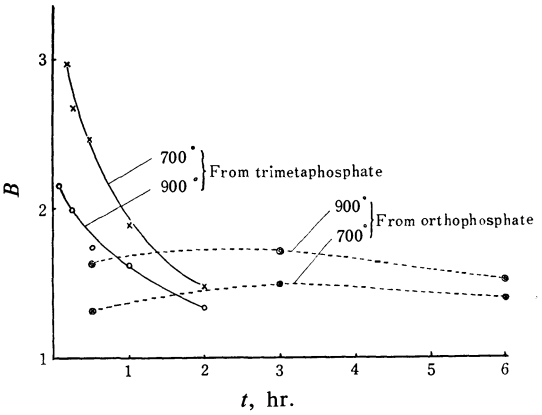

Fig. 5. Relation between the number of branching and the polymerization time.

Thus, the remarkable difference between the condensation polymerization and the ring-opening polymerization can be explained by considering that both the polymerization and depolymerization occur during the heating, and that the process of polymerization is more important in the case of the condensation polymerization because the removal of water needs much heating, while the process of depolymerization is more important in the case of the ring-opening polymerization because in

this case the polymerization is completed almost immediately after the material is melted.

Summary

Two kinds of polymerization reactions, the condensation polymerization of sodium dihydrogen orthophosphate anhydrate (NaH_2PO_4) and the ring-opening polymerization of sodium trimetaphosphate, have been compared by determining the average degree of polymerization of the whole molecule, $\bar{n}_0$, and of each branch, $\bar{n}_\infty$, and the average number of branches, B, per molecule.

As a result, it has been concluded that the remarkable difference between these two reactions can be explained by simultaneous polymerization and depolymerization during the heating. In the case of the condensation polymerization, the polymerization process is more important because the removal of water needs much heating, while, in the case of the ring-opening polymerization, the depolymerization process is more important because the polymerization is completed almost immediately after the material is melted.

Faculty of Pharmacy
Kyoto University
Sakyo-ku, Kyoto

Studies on Seven-membered Heterocyclic Compounds Containing Nitrogen. VII. Thiazolocyanine Dyes

By Akira Yokoo and Shiro Morosawa

(Received January 28, 1963)

No such thiazolocyanine dyes as condensed with the nitrogen-containing seven-membered ring have been synthesized. The present authors report here about the syntheses of these dyes.

Ethiodide (II) of 5-ethoxycarbonyl-2-methyl-5, 6, 7, 8-tetrahydro-4(*H*)-azepino[4, 3-d]thiazole (I)[1] was converted to 2-phenylaminoethenyl derivative (III). II and III reacted to yield 5, 5'-diethoxycarbonyl-1, 1-diethyl-(5, 6, 7, 8-tetrahydro-4(*H*)-azepino[4, 3-d]thiazolo)-carbocyanine iodide (IV), m. p. 193~195°C (decomp.). 2-Phenylaminoethenyl derivative (VII) was derived likewise from 2-methyl-5, 6, 7, 8-tetrahydro-4(*H*)-azepino[4, 3-d]thiazole (V)[1] via its methiodide (VI). VI and VII gave a dye assumed to be 1, 1', 5, 5'-tetramethyl-(5, 6, 7, 8-tetrahydro-4(*H*)-azepino[4, 3-d]-thiazolo)carbocyanine iodide dimethiodide (VIII), m. p. 230~234°C (decomp.).

Another cyanine dye, 11-bromo-5, 5'-diethoxycarbonyl-1, 1'-diethyl-(5, 6, 7, 8-tetrahydro-4(*H*)-azepino[4, 3-d]thiazolo)-pentamethinecarbocyanine iodide (X) was also obtained from II and 2-bromo-3-anilino-2-propen-1-ylidenaniline (IX), m. p. 162~165°C (decomp.).

1) A. Yokoo and S. Morosawa, This Bulletin, **33**, 1118 (1960).

Experimental

5-Ethoxycarbonyl-2-methyl-5, 6, 7, 8-tetrahydro-4(*H*)-azepino[4, 3-d]thiazole Ethiodide (II). — A mixture of 2 g. of I and 4 g. of ethyl iodide was heated under reflux for 4 hr. in a thick, round-bottomed flask. The flask was then stoppered tightly and heated for 5 hr. in a water bath. Precipitates, which formed on adding ether to the reaction mixture, were separated by decantation, and recrystallized from a small amount of ethanol to give 1.3 g. of light yellow crystals, m. p. 157~159°C.

Found: N, 6.94. Calcd. for $C_{13}H_{21}O_2N_2SI$: N, 7.07%.

2-Phenylaminoethenyl-5-ethoxycarbonyl-5, 6, 7, 8-tetrahydro-4(*H*)-azepino[4, 3-d]thiazole Ethiodide (III). — A mixture of 0.5 g. of II and 0.3 g. of diphenylformamidine was heated at 165°C for 20 min. The reaction mixture was dissolved in 2 cc. of absolute ethanol, and 2 cc. of ether was added. Crystals deposited were separated and recrystallized from ethanol to give 0.41 g. of orange crystals, m. p. 185~187°C.

Found: N, 8.15. Calcd. for $C_{20}H_{26}O_2N_3SI$: N, 8.42%.

5, 5'-Diethoxycarbonyl-1, 1'-diethyl-(5, 6, 7, 8-tetrahydro-4(*H*)-azepino[4, 3-d]thiazolo)carbocyanine Iodide (IV). — A mixture of 180 mg. of II, 170 mg. of III, 250 mg. of anhydrous potassium acetate and 1.5 g. of acetic anhydride was heated at 63~65°C for 3 hr. The solid reaction mixture was washed with ether and then with water by decantation, and

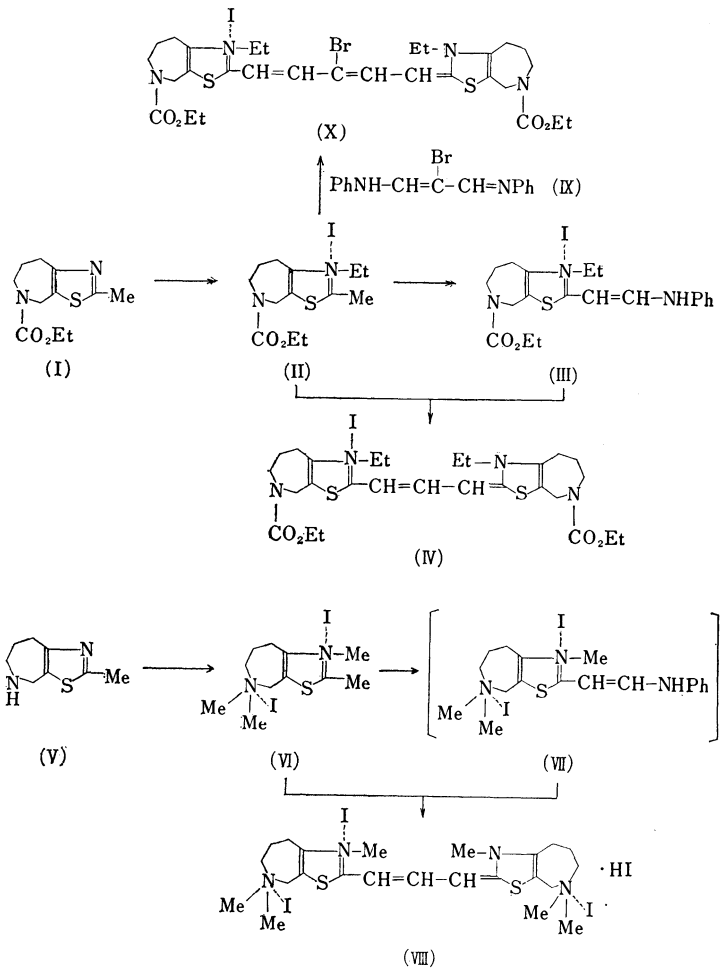

dried in a vacuum desiccator. The solid was dissolved in 1 cc. of absolute ethanol and 1.5 cc. of ether was added to the solution. The solution was left to stand in a refrigerator to cause crystallization. The crystals were collected and dissolved in 0.5 cc. of methanol, followed by the addition of 1 cc. of ether. The resulted solution was filtered and left to stand in a refrigerator. The crystals thus obtained were again crystallized as above to give 18 mg. of dark purple crystals, m.p. 193~195°C (decomp.). UV λ_{max}^{MeOH} mμ(log ε) : 575 (4.99).

Found: C, 47.74; H, 5.81; N, 8.19. Calcd. for $C_{27}H_{39}O_4N_4S_2I$: C, 48.08; H, 5.84; N, 8.31%.

2, 5-Dimethyl-5, 6, 7, 8-tetrahydro-4(*H*)-azepino-[4, 3-d]thiazole Dimethiodide (VI).—To a solution of 2.1 g. of V in 5 cc. of methanol was added 9 g. of methyl iodide. After having been left to stand overnight, methanol was removed and the residue was heated with 5 g. of methyl iodide in a sealed tube for 3 hr. on a water bath. The excessive methyl iodide was removed and the remainder was recrystallized twice from methanol to yield 2.9 g. of light yellow crystals, m. p. 245~248°C (decomp.).

Found: C, 28.30; H, 4.19; N, 6.08. Calcd. for $C_{11}H_{20}N_2SI_2$: C, 28.32; H, 4.33; N, 6.01%.

2-Phenylaminoethenyl Derivative (VII) of V, and 1, 1', 5, 5'-Tetramethyl-(5, 6, 7, 8-tetrahydro4-(*H*)-azepino[4, 3-d]thiazolo)carbocyanine Iodide Dimethiodide (VIII).—A mixture of 300 mg. of VI and 300 mg. of diphenylformamidine was heated at 155°C for 10 min. The reaction mixture was dissolved in methanol and a large amount of ether was added. The resulting precipitates were collected, washed with ether and dried well in a vacuum desiccator to give 380 mg. of VII as an amorphous powder. A mixture of 300 mg. of VII, 230 mg. of VI, 230 mg. of anhydrous potassium acetate and 1.5 g. of acetic anhydride was heated at 70°C for 5 hr. The reaction mixture was washed three times with each 5 cc. portion of ether and dissolved in 1.3 cc. of water. To the solution were added 5 cc. of ethanol and 15 cc. of ether, and decanted after having been left to stand. The remaining crystals, after drying, were dissolved in 4 cc. of methanol and recrystallized by adding 6 cc. of benzene and leaving to stand in a refrigerator for 5 days. After collecting and washing with a mixture of methanol and benzene (1 : 1), the crystals were dissolved in 6 cc. of methanol and 6 cc. of benzene was added. The solution was left

to stand in a refrigerator for 2 days and the crystals formed were collected, dissolved in 3 cc. of methanol and filtered. The solution was left to stand as above and the resulted crystals were further recrystallized twice from methanol to give 18 mg. of dark purple crystals which turn light brown at about 220°C, m. p. 230~234°C (decomp.). UV λ_{max}^{MeOH} mμ (log ε): 575 (4.58).

Found: C, 29.53; H, 4.69; N, 6.02; S, 6.68; I, 52.38. Calcd. for $C_{23}H_{37}N_4S_2I_3 \cdot HI$: C, 29.30; H, 4.07; N, 5.95; S, 6.81; I, 53.85%

11-Bromo-5, 5'-diethoxycarbonyl-1, 1'-diethyl-(5,6, 7, 8-tetrahydro-4(*H*)-azepino[4, 3-d]thiazolo)pentamethinecarbocyanine Iodide (X). — A mixture of 200 mg. of II, 80 mg. of IX, 100 mg. of piperidine and 2.5 g. of pyridine was heated at 50°C for 2.5 hr. After cooling, a large amount of ether was added and decanted. This was repeated three times, followed by further washing with 2 cc. of water (twice) and with 1 cc. of hot water (twice). After drying in a vacuum desiccator, the crude product was dissolved in 1.5 cc. of methanol and the solution was left to stand in a refrigerator for 2 days. The crystals formed were collected and washed with methanol. Recrystallization (twice) as above gave 60 mg. of green crystals, m. p. 162~165°C (decomp.). UV λ_{max}^{MeOH} mμ (log ε): 635 (5.12).

Found: C, 44.05; H, 5.48; N, 7.13. Calcd. for $C_{29}H_{40}O_4N_4S_2BrI$: C, 44.64; H, 5.17; N, 7.18%.

Chemical Institute
Faculty of Science
Okayama University
Tsushima, Okayama

Mechanisms of the Wallach Rearrangement[1]

By Shigeru OAE*, Tsugio FUKUMOTO and Masayuki YAMAGAMI

(Received February 1, 1963)

Recently, Shemyakin, Maimind and Vaichunaite[2] have shown, using ^{15}N-labeled azoxybenzene (I) that the rearrangement of the azoxybenzene (I) gave 4-hydroxyazobenzenes (III) and IV under various condition[3,4], where the two benzene rings were attacked with equal ease. They also observed that azoxybenzene recovered from these reactions remained practically unchanged in isotope distribution, and suggested that the rearrangement proceeds through a symmetrical intermediate II.

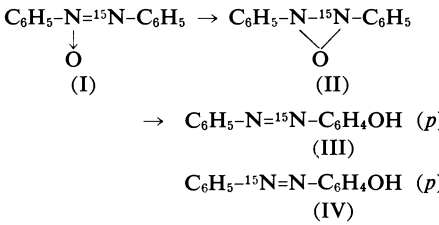

The prior formation of the *N*, *N*-oxide intermediate, II, in the rearrangement was further emphasized by the Russian workers[5] from their observations that there was no incorporation of ^{18}O into *p*-nitroazoxybenzene from ^{18}O-labeled sulfuric acid in the isomerization of *β*-*p*-nitroazoxybenzene (V) to *α*-*p*-nitroazoxybenzene (VI).

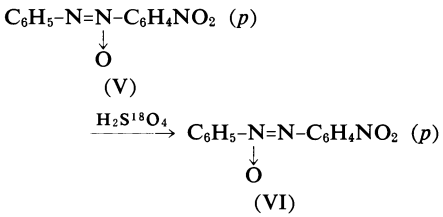

Meanwhile, two mechanisms have been suggested[6]. The one is similar to that of the Bamberger reaction[7] and proceeds via monocation VII in which nucleophilic attack by either water or $-OSO_3H$ group is restricted to the far ring, while the other was suggested

* Present address: Department of Applied Chemistry, Faculty of Engineering, Osaka City University, Kita-ku, Osaka.

1) Paper VII on "Rearrangements of Tertiary Amine Oxides". III—V, S. Oae, T. Kitao and Y. Kitaoka, *J. Am. Chem. Soc.*, **84**, 3359, 3362, 3366 (1962). VI, *Tetrahedron* in press.

2) M. M. Shemyakin, V. I. Maimind and B. K. Vaichunaite, *Chem. & Ind.*, **1958**, 775; *Zhur. Obshchei Khim.*, **28**, 1708 (1958); *Chem Abstr.*, **53**, 1201 (1959); *Izvestia Akad. Nauk. S. S. S. R. Otdel. Khim. Nauk.*, 866 (1960).

3) P. H. Gore and G. K. Hughes, *Austral. J. Sci. Research*, **3A**, 136 (1950); *Chem. Abstr.*, **45**, 2889 (1951).

4) V. O. Lukashurish and T. N. Khurdyumova, *Zhur. Obshchei Khim.*, **18**, 1961 (1948).

5) M. M. Shemyakin, V. I. Maimind and Ts. E. Agadzhanyan, *Chem. & Ind.*, **1961**, 1223.

6) P. H. Gore, ibid., **1961**, 191.

7) a) "Name Reaction in Organic Chemistry" (Jinmei-Yuki-Hannoshu), Vol. II, Ed. by M. Murakami and Y. Yukawa, Asakura Book Publ. Co., Tokyo (1954), p. 228; b) C. K. Ingold, "Structure and Mechanism in Organic Chemistry", Cornell Univ. Press, New York (1953), p. 621.

to involve the symmetrical dication VIII, which may be attacked at either ring.

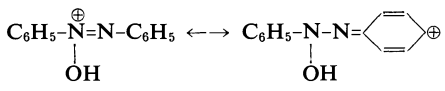

(VII)

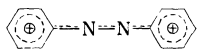

(VIII)

We have reported in the earlier communication[8] that no excess of ^{18}O was incorporated from the medium in *p*-hydroxyazobenzene obtained when the rearrangement of azoxybenzene was carried out with 83% sulfuric acid, labeled by 0.67 atom % of ^{18}O. However, we have found later that a part of our experiments were in error and hence presented a new interpretation with a new set of data[9]. Since then, we have learned that the Russian workers[10] have also worked out a similar problem and presented much the same interpretation from the Wallach rearrangement.

In this paper, we would like to correct a part of the published results and to summarize all the results of our studies hitherto being made on the Wallach rearrangement.

Azoxybenzene-^{18}O was prepared from ^{18}O-labeled nitrobenzene which was made by reacting benzene with the mixture of ^{18}O-labeled potassium nitrate and ^{18}O-labeled sulfuric acid. Then the rearrangement of this ^{18}O-labeled azoxybenzene was performed in 83% ordinary sulfuric acid. The resulting *p*-hydroxyazobenzene was found to have lost almost all the excess of ^{18}O, and only very small amount of excess of ^{18}O (about 10%) was found to be remaining. When an equivalent mixture of azoxybenzene-^{18}O and *o*-methylazoxybenzene was treated in the same medium, both *p*-hydroxyazobenzene and 4-hydroxy-2'-methylazobenzene obtained were also found to have lost most of the excess ^{18}O originally present in the starting azoxybenzene-^{18}O.

We also repeated the rearrangement of azoxybenzene in 83% sulfuric acid enriched with ^{18}O and found that the resulting *p*-hydroxyazobenzene was incorporated with ^{18}O from the medium, but the ^{18}O value was roughly 15~20% less than that of the medium used.

These observations suggest that the main portion of the Wallach rearrangement is an intermolecular process similar to Bamberger type where solvent water attack nucleophilically para position of benzene ring.

Combining with the observations of Russian workers on the prior isomerization, the overall mechanism of the main reaction may be depicted as follows;

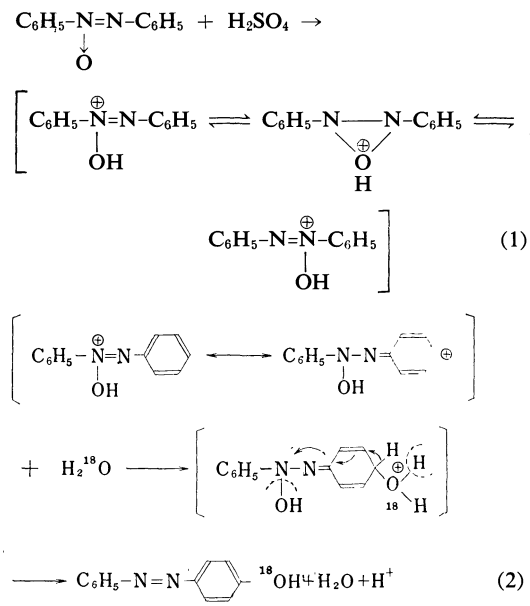

(1)

(2)

Recently, Bunnet, Buncel and Nahahedian[11] have shown that the phenolic products of hydrolysis of 4-(*p*-sulfophenylazo)-1-naphthyl methyl ether (A) and 4-(*p*-sulfophenylazo)-anisole (B) in oxygen-18 labeled water carry the oxygen-18 labeled in the phenolic hydroxy

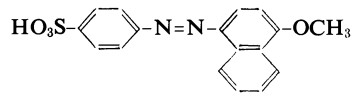

(A)

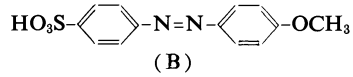

(B)

group, and they suggested the following similar mechanism.

Okazaki and Okumura also have shown that the rearrangement of ^{18}O-labeled hydroxylamine in aqueous acid media gave *p*-aminophenol which have lost almost all the excess ^{18}O originally present in the starting material[12].

8) S. Oae, T. Fukumoto and M. Yamagami, This Bulletin, **34**, 1873 (1961).

9) S. Oae, T. Fukumoto and M. Yamagami, the 15th Annual Meeting of The Chemical Society of Japan, Kyoto, April, 1962.

10) M. M. Shemyakin, Ts. E. Agadzhanyan, V. I. Maimind, R. V. Kudryavtsev and D. N. Kursanov (Inst. Heteroörg. Compds., Moscow). *Doklady Akad. Nauk. S. S. S. R.*, **135**, 346-349 (1960); *Chem. Abstr.*, **55**, 11337 (1961).

11) J. F. Bunnet, E. Buncel and K. V. Nahahedian, *J. Am. Chem. Soc.*, **84**, 4136 (1962).

12) S. Okazaki and M. Okumura, the 15th Annual Meeting of The Chemical Society of Japan, Kyoto, April, 1962.

TABLE I. ^{18}O STUDY OF REARRANGEMENT OF AZOXY COMPOUNDS

No.	Azoxy compound	Rearrangement conditions	Resultant hydroxyazo compound	Excess ^{18}O (at %)		
				Initial azoxy compound	Medium	Hydroxyl of hydroxyazo compound
1	Azoxybenzene (1 g.)	83% H_2SO_4 (90°C, 10 min.)	*p*-Hydroxyazobenzene (0.5 g.)	0	0.32	0.25
2	Azoxybenzene (1 g.)	83% H_2SO_4 (90°C, 10 min.)	*p*-Hydroxyazobenzene (0.5 g.)	0.49	0	0.06
3	α-4-Methylazoxybenzene (20 g.)	83% H_2SO_4 (90°C, 2 min.)	4-Hydroxy-4'-methylazobenzene (14 g.)	0	0.38	0.27
			+			
			2-Hydroxy-4'-methylazobenzene (80 mg.)			0.05
4	Azoxybenzene (0.5 g.)	83% H_2SO_4 (90°C, 10 min.)	*p*-Hydroxyazobenzene (0.15 g.)	0.28	0	0.03
	+		+			
	α-2-Methylazoxybenzene (0.5 g.)		4-Hydroxy-2'-methylazobenzene (0.15 g.)	0		0.04
5	Azoxybenzene (1 g.)	UV light (40~45°C, 65 hr.)	*o*-Hydroxyazobenzene (0.45 g.)	0	0.47	0.01
6	Azoxybenzene (1 g.)	UV light (40~45°C, 25 days)	*o*-Hydroxyazobenzene (0.92 g.)	0.38	0	0.35
7	α-4-Methylazoxybenzene (3 g.)	UV light (40~45°C, 7 days)	2-Hydroxy-4'-methylazobenzene (1.6 g.)	—	—	—
8	*p*-Hydroxyazobenzene (1 g.)	83% H_2SO_4 (90°C, 10 min.)	*p*-Hydroxyazobenzene (0.9 g.)	0	0.30	0

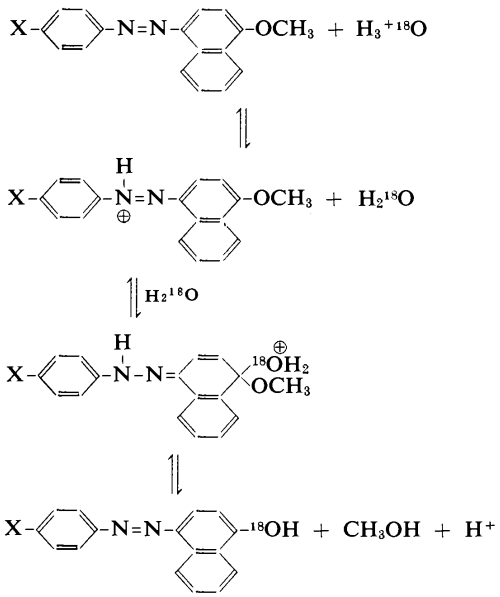

In both our experiments and the Russians, one finds that a small, but noticeable amount of oxygen appeared to be coming directly from the original azoxy-oxygen. Whether or not this is due to the direct oxidation we proposed earlier, one needs further experiments with a little higher concentration of ^{18}O before making any final comment.

Hahn and Jaffé[13] have recently shown that the rearrangement of 4-substituted azoxybenzene gives 2-hydroxy-4'-methylazobenzene as by-product of 4-hydroxy-4'-methylazobenzene. We have allowed 4-methylazoxybenzene to react in 83% sulfuric acid, labeled by 0.58 atom % of ^{18}O at 60~70°C for 10 min. and found that resulting 4-hydroxy-4'-methylazobenzene, the main product, incorporated ^{18}O in 80~90% from the medium, while 2-hydroxy-4'-methylazobenzene obtained as red crystals, m. p. 100~101°C, in a very small yield, incorporated very little excess ^{18}O from the medium.

While the rearrangement to para position followed the Bamberger type intermolecular process, the rearrangement to ortho position apparently proceeded via intramolecular oxygen shift.

Since the oxygen migrated to the far ring in this case just as was shown by the Russian workers previously by the ^{15}N tracer studies[2], they adopted following Badger and Buttery's scheme[16] for the ortho rearrangement. Another alternative and probably more likely

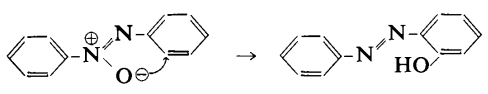

13) Chi-Sun Hahn and H. H. Jaffé, *J. Am. Chem. Soc.*, **84**, 946 (1962).

path for the ortho rearrangement is via the following "intimate ion pair", similar to the one suggested for the formation of 4-tosyloxyisoquinoline by the reaction of isoquinoline *N*-oxide and *p*-toluenesulfonyl chloride[14].

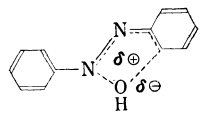

A similar rearrangement of azoxybenzene to *o*-hydroxyazobenzene by ultraviolet light has been known[15,16]. The Russian workers[2] found that the original excess of ^{15}N was in the nitrogen group attached to the hydroxylated benzene when carried out the reaction in 85% ethanol for 65 hr. at 30~40°C. We have performed the reaction in 85% ethanol containing 15% $H_2{}^{18}O$ (enriched by 0.67 atom % of ^{18}O) and found that the resulting *o*-hydroxyazobenzene incorporated very little excess ^{18}O from the medium. We favor that the reaction proceed through an intramolecular oxygen radical shift from *N*-oxide. A similar free radical shift is known in the reaction of dimethylaniline-*N*-oxide with acetic anhydride[17a]. 2-Picoline *N*-oxide was also known to rearrange to 2-pyridinemethanol by ultraviolet irradiation[17b].

Experimental

Azoxybenzene was prepared by refluxing methanol solution containing both nitrobenzene and sodium hydroxide; m. p. 35~36°C.

^{18}O-Labeled Sulfuric Acid.—This preparation was described elsewhere[18].

^{18}O-Labeled Potassium Nitrate was prepared by Anbar's method[19].

^{18}O-Labeled Nitrobenzene was prepared by first dissolving ^{18}O-labeled potassium nitrate (5 g.) in $H_2S^{18}O_4$ (5 g., 0.75 atom % of ^{18}O) and then adding benzene (2 g.) dropwise in the mixture with vigorous stirring. Stirring was continued for 20 min. at 50~55°C after the benzene was added. The reaction mixture was then poured into water (20 ml.) and oily precipitate separated out was extracted with 30 ml. benzene. After drying and removing benzene, the remaining oil was distilled and the fraction of b. p. 93~95°C/17 mmHg was collected. The yield was 2.7 g. (83%).

^{18}O-Labeled Azoxybenzene was prepared by heating ^{18}O-labeled nitrobenzene (8 g., 0.84 atom % of ^{18}O) with sodium hydroxide (8 g.) in methanol (8 g.), m. p. 35~36°C, 0.69 atom % of ^{18}O.

Found: C, 72.60; H, 4.99. Calcd. for $C_{12}H_{10}N_2O$: C, 72.73; H, 5.05%.

2-Methylazoxybenzene was prepared by an improved method. Five grams of 2-methylazobenzene prepared by Parsons's method[20] was dissolved in 40 ml. of glacial acetic acid then, 15 ml. of 30% hydrogen peroxide was added and the mixture was heated for 1 hr. at 85~90°C. As the reaction progressed, the color of reaction mixture changed from brown to orange-yellow finally giving clear yellow solution. Then, the reaction mixture was poured into water. Oily layer separated was washed several times with water and was distilled and the fraction of b. p. 127~129°C/2 mmHg was collected. The yield was 5.2 g. (97%).

Found: C, 73.94; H, 5.77. Calcd. for $C_{13}H_{12}N_2O$: C, 73.58; H, 5.66%.

4-Methylazoxybenzene was prepared from 4-methylazobenzene by similar method as 2-methylazoxybenzene, m. p. 46~47°C.

Found: C, 73.80; H, 5.49. Calcd. for $C_{13}H_{12}N_2O$: C, 73.58; H, 5.66%.

Rearrangement Reaction of Azoxybenzene in ^{18}O-Labeled Sulfuric Acid.—A mixture of 1 g. of azoxybenzene and 4 g. of 83% sulfuric acid (0.50 atom % of ^{18}O) was heated for 10 min. at 90°C and then the reaction mixture was poured into ice water. A tarry product appeared was collected by filtration and this was refluxed for 10 min. with 50 ml. 3% potassium hydroxide solution. Insoluble material was removed by filtration and the black colored filtrate was refluxed with charcoal for 5 min. and filtered while hot. The filtrate was neutralized with 6 N hydrochloric acid solution. The precipitate appeared was collected by filtration and recrystallized from benzene. *p*-Hydroxyazobenzene was thus obtained, m. p. 151~152°C (lit.[21] 152°C), 0.45 atom % of ^{18}O. The yield was 0.5 g. (50%).

Found: C, 72.08; H, 4.96. Calcd. for $C_{12}H_{10}N_2O$: C, 72.73; H, 5.05%.

Rearrangement Reaction of ^{18}O-Labeled Azoxybenzene in Sulfuric Acid.—A mixture of 1 g. of ^{18}O-labeled azoxybenzene (0.69 atom % of ^{18}O) and 4 g. of 83% sulfuric acid was heated for 10 min. at 90°C and treated similarly as described above. *p*-Hydroxyazobenzene was obtained, m. p. 151~152°C, 0.26 atom % of ^{18}O. The yield was 0.5 g. (50%).

Reaction of a Mixture of ^{18}O-Labeled Azoxybenzene and 2-Methylazoxybenzene in Sulfuric Acid.—A mixture of 0.5 g. of ^{18}O-labeled azoxybenzene (0.69 atom % of ^{18}O) and 0.5 g. of 2-methylazoxybenzene was heated in 4 g. of 83% sulfuric acid for 10 min. at 90°C and treated similarly as described above. Crude product (0.5 g.) obtained was recrystallized from 2 ml. benzene. Crystalline powder appeared rapidly was collected by filtration and the filtrate was kept standing overnight. Rhombic crystals came out from the filtrate. The former crystals were recrystallized from benzene and the

14) S. Oae, T. Kitao and Y. Kitaoka, *Tetrahedron*, in press.
15) W. M. Cumming and C. S. Ferier, *J. Chem. Soc.*, **127**, 2374 (1925).
16) G. M. Badger and R. G. Buttery, ibid., **1954**, 2243.
17) a) S. Oae, T. Kitao and Y. Kitaoka, *J. Am. Chem. Soc.*, **84**, 3366 (1962); b) N. Hata, This Bulletin, **34**, 1440 (1961).
18) S. Oae, T. Kitao and Y. Kitaoka, Annual Report of the Radiation Center of Osaka Prefecture, Vol. I, 33 (1960).
19) M. Anbar, M. Halman and S. Pinchas, *J. Chem. Soc.*, **1960**, 1242.
20) T. Parsons, Jr., and J. Ballar, Jr., *J. Am. Chem. Soc.*, **58**, 268 (1936).
21) R. Paganini, *Ber.*, **24**, 366 (1891).

latter were recrystallized from ligroin several times, respectively. The former, m. p. 150~151°C, 0.23 atom % of ^{18}O, 0.15 g. and the latter, m. p. 99~100°C, 0.24 atom % of ^{18}O, 0.15 g. were obtained. Both crystals did not depress the melting point of the two authentic samples, 4-hydroxyazobenzene and 4'-hydroxy-2-methylazobenzene[21] upon admixture.

Rearrangement Reaction of Azoxybenzene under Ultraviolet Irradiation.—In a sealed tube is placed a mixture of 1 g. of azoxybenzene and 20 ml. of 85% ethanol (consisted of 3 ml. of ^{18}O enriched water (0.67 atom % of ^{18}O) and 17 ml. absolute ethanol), and the mixture was irradiated for 65 hr. at 40~45°C under ultraviolet. After removing water and ethanol under reduced pressure, the remaining solid was added 50 ml. 3% potassium hydroxide aquous solution and was refluxed for 10 min. After cooling and removing unreacted azoxybenzene by filtration, the filtrate was neutralized with hydrchloric acid. Brown crystals appeared were recrystallized from ethanol and violet needles, m. p. 82.5°C, 0.21 atom % of ^{18}O, was obtained. The yield was 0.45 g. (45%). (*o*-Hydroxyazobenzene (lit.[22] m. p. 82.5°C)).

Rearrangement Reaction of ^{18}O-Labeled Azoxybenzene under Ultraviolet Irradiation.—In a sealed tube is placed a mixture of 1 g. of ^{18}O-labeled azoxybenzene (0.58 atom % of ^{18}O) and 20 ml. of absolute ethanol, and the mixture was irradiated for 25 days at 40~45°C and was treated similarly as described above. The product, m. p. 82.5°C, 0.55 atom % of ^{18}O, was obtained. The yield was 0.92 g. (92%).

Rearrangement Reaction of *α*-4-Methylazoxybenzene.—In a three-necked flask was placed a mixture of 20 g. of *α*-4-methylazoxybenzene and 80 g. of 83% ^{18}O-labeled sulfuric acid (0.58 atom % of ^{18}O) and the mixture was heated at 60~70°C for 10 min. and was treated similarly. The crude product, m. p. 147~150°C, 14 g. was obtained (70%). The separation of the *o*-isomer, 2-hydroxy-4'-methylazobenzene from the *p*-isomer was achieved by the following method. The product (14 g.) was dissolved in 20 ml. hot benzene and then allowed to stand for 5~6 hr. at room temperature. Yellow needles formed were separated and were recrystallized from benzene repeatedly. 4-Hydroxy-4'-methylazobenzene, m. p. 150~151°C, 0.54 atom % of ^{18}O, was thus obtained.

Found: C, 72.61; H, 5.78. Calcd. for $C_{13}H_{12}N_2O$: C, 73.58; H, 5.66%.

The filtrate was evaporated under reduced pressure, and the residue (ca. 5 g.) was distilled by steam distillation, then red crystals, m. p. 98~101°C, 80 mg. were obtained. The red crystals were converted to copper salt by precipitation with 50% alcoholic copper acetate solution. This copper salt contained 0.25 atom % of ^{18}O and was identified with authentic sample, which was prepared by ultraviolet irradiation of *α*-4-methylazoxybenzene, by infrared spectrophotometric method.

Found: C, 57.53; H, 3.99. Calcd. for $C_{13}H_{11}N_2 \cdot OCu$: C, 56.83; H, 4.01%.

2-Hydroxy-4'-methylazobenzene.—In a sealed tube is placed a mixture of 3 g. of *α*-4-methylazoxybenzene and 20 ml. of ethanol, and the mixture was irradiated under ultraviolet light for 7 days at 40~45°C. After removing ethanol, the solid was distilled by steam distillation and red crystals, m. p.; 100~101°C (1.6 g.) was obtained in 54% yield.

Found: C, 72.80; H, 5.11. Calcd. for $C_{12}H_{12}N_2O$: C, 73.58; H, 5.66%.

Determination of ^{18}O is described elsewhere[15].

The results of ^{18}O distribution of all the ^{18}O tracer experiments for this rearrangement are tabulated in Table. I.

Department of Chemistry
Radiation Center of Osaka Prefecture
Sakai, Osaka

22) E. Bamberger, ibid., **33**, 1950 (1900).

Spectrophotometric Studies of the Nature of Several Iron-Pyridinecarboxylic Acid Complexes

By Ichirô MORIMOTO and Taijun SATÔ

(Received February 2, 1963)

Weidel[1] and Skraup[2] first studied the coloring reaction between iron and pyridinecarboxylic acids. The determination of iron based on this reaction has since been reported by several workers[3-7]. We ourselves have previously reported[5-7] on the 1 : 2 complex formed in the solution by the interaction of metal

1) H. Weidel, *Ber.*, **12**, 1989 (1886).
2) Z. H. Skraup, *Monatsh. Chem.*, **7**, 212 (1886).
3) K. Shinra, K. Yoshikawa, T. Kato and Y. Nomizo, *J. Chem. Soc. Japan, Pure Chem. Sec.* (*Nippon Kagaku Zassi*), **75**, 44 (1954).
4) A. K. Majumdar and S. P. Bag, *Anal. Chim. Acta*, **21**, 324 (1959); **22**, 549 (1960).
5) I. Morimoto, H. Oida and T. Hayashi, *J. Chem. Soc. Japan, Pure Chem. Sec.* (*Nippon Kagaku Zasshi*), **82**, 203 (1961).
6) I. Morimoto and S. Tanaka, ibid., **83**, 889 (1962).
7) I. Morimoto and S. Tanaka, *Anal. Chim.*, **35**, 141 (1963).

ions with 2, 6-pyridinedicarboxylic acid or 2, 4, 6-pyridinetricarboxylic acid. Shinra et al.[3] and Rây and Banerjee[8] have suggested the formation of a 1 : 3 complex between the metal ions and 2-pyridinecarboxylic acid, while Majumder and Bag[4] have found a ratio of 1 : 2 for 2-pyridinecarboxylic acid or 2, 3-pyridinedicarboxylic acid. These are also some discrepancies among the conclusions reached by various workers on the composition of the complexes formed in solution by ferrous ions and pyridinecarboxylic acid. Also, the composition of the complexes formed by the iron with 2, 4-pyridinedicarboxylic acid or 2, 5-pyridinedicarboxylic acid is still obscure. For the present work, studies were made of the composition of the complexes formed in solution by the reaction between ferrous ions and several pyridine-2-carboxylic acids in the presence or absence of potassium cyanide and pyridine.

Experimental

Apparatus.—A Hirama photoelectric colorimeter was employed with 1 cm. cells for optical density measurement at room temperature. A Horiba-Hitachi model 3 pH meter was used for all pH determinations.

Iron Solution.—A standard solution was prepared by dissolving ferrous ammonium sulfate in twice-distilled water. Weaker solutions were prepared by diluting the standard solution.

Buffer Solution.—A Michaelis buffer solution and a 35% sodium acetate solution were used for the regulation of the pH value.

Hydroxylamine Hydrochloride Solution. — Ten grams of hydroxylamine hydrochloride were dissolved in 100 ml. of distilled water.

Reagent Solution. — 2-Pyridinecarboxylic acid, 2, 3-pyridinedicarboxylic acid, 2, 4-pyridinedicarboxylic acid, 2, 5-pyridinedicarboxylic acid, 2, 6-pyridinedicarboxylic acid, and 2, 4, 6-pyridinetricarboxylic acid were used. A 1/100 molar solution of each pyridinecarboxylic acid was used. 2, 5-Pyridinedicarboxylic acid was dissolved in 1 ml. of ammoniac water, and the solution was diluted with aliquots of water. Pyridine and a 0.1 N solution of potassium cyanide were used.

Procedure.—Aliquots of a standard ferrous solution were taken in 25 ml. flasks. To each flask, 1 ml. of the hydroxylamine hydrochloride solution, several milliliters of the reagent solution, a potassium cyanide solution or pyridine, a buffer solution, and water were added to make up the volume. The absorbance of the solution was measured at 420 and 460 mμ respectively.

Results and Discussion

Absorbance Curves. — The absorbance curves for the iron complexes in the ultraviolet range and in the visible range are shown in Figs. 1 and 2. In Fig. 1, curves 1, 2, 2', 3, 4 and 4' represent the absorbance of the colored complexes formed by 16 p. p. m. of iron in the absence of potassium cyanide; curve 5 represents the value with 8 p. p. m. of iron in the absence of potassium cyanide. Each of the solution of the complexes of pyridinecarboxylic acids has a maximum at 265~280 mμ. These maxima of absorption may be the absorption of pyridinecarboxylic acids. In Fig. 2, curves

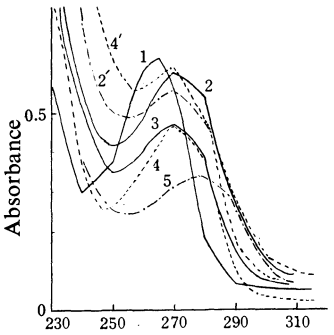

Fig. 1. The ultraviolet absorption spectra of the iron complexes.
1 2-Pyridinecarboxylic acid (pH 5.3)
2, 2' 2, 4-Pyridinedicarboxylic acid (pH 3.9, pH 2.6)
3 2, 3-Pyridinedicarboxylic acid (pH 5.1)
4, 4' 2, 5-Pyridinedicarboxylic acid (pH 5.2, pH 2.9)
5 2, 4, 6-Pyridinetricarboxylic acid (pH 5.3)

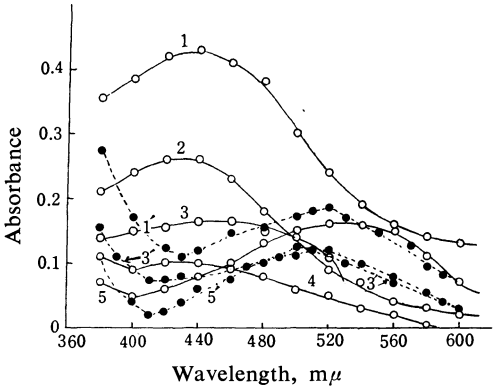

Fig. 2. The visible absorption spectra of the iron complexes.
---- In the presence of potassium cyanide
—— Without potassium cyanide
1, 1' 2-Pyridinecarboxylic acid (pH 5.3, pH 6.5)
2 2, 3-Pyridinedicarboxylic acid (pH 5.1)
3, 3' 2, 4-Pyridinedicarboxylic acid (pH 6.8, pH 6.4)
4 2, 5-Pyridinedicarboxylic acid (pH 5.2)
5, 5' 2, 4, 6-Pyridinetricarboxylic acid (pH 5.3, pH 6.4)

8) P. Rây and B. Banerjee, *J. Indian Chem. Soc.*, **35**, 297, 493 (1958).

1, 2 and 3 represent the absorbance, in the absence of potassium cyanide, of the colored complexes formed by 16 p.p.m. of iron; curves 1', 3' and 5' represent the values obtained in the presence of potassium cyanide with 11 p.p.m. of iron. The complexes of pyridinecarboxylic acid have a maximum at 430~530 mμ. In the presence of potassium cyanide, these complexes have a maximum at 500~520 mμ.

Effect of Pyridine.—The authors frequently observed that the absorbance of the iron complexes was increased considerably by the addition of a small drop of pyridine[9]. The results are shown in Fig. 3. In Fig. 3, curves 1, 2, 3 and 4 show the values obtained at pH 5.9 in the presence of 2 ml. of pyridine and 11 p. p. m. of iron.

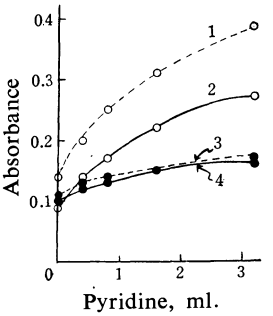

Fig. 3. The effect of pyridine on the iron complexes.
---- 2,5-Pyridinedicarboxylic acid
—— 2,4-Pyridinedicarboxylic acid
1, 2 at 372 mμ 3, 4 at 460 mμ

Nature of the Complexes in Solution. — The empirical formulas of the ferrous iron complexes were established by three independent methods: the continuous variation method of Job[10] modified by Vosburgh and Cooper[11], the mole ratio method of Yoe and Jones[12], and the slope ratio method of Harvey and Manning[13]. The results of these experiments are shown in Figs. 4—12. For Job's method, an equimolar solution (1/200 mol.) of iron and the reagent were taken in different quantities (total, 4 ml.) in 25 ml. flasks. The iron solution was mixed with 1 ml. of hydroxylamine hydrochloride, and the necessary amount of the reagent, 5 ml. of potassium cyanide, a buffer solution (pH 6.2~6.3), and water were added to make up the volume. Curves 1 and 1' in Figs. 4, 5 and 6 represent the results on the 2-pyridinecarboxylic acid and 2, 3-pyridinedicarboxylic acid, 2, 4-pyridinedicarboxylic acid, 2, 5-pyridinedicarboxylic acid, 2, 6-pyridinedicarboxylic acid and 2, 4, 6-pyridinetricarboxylic acid complexes systems respectively. Curves 3 and 3' represent the results on each pyridinecarboxylic acid complex system without potassium cyanide. Curves 2 and 2' represent those

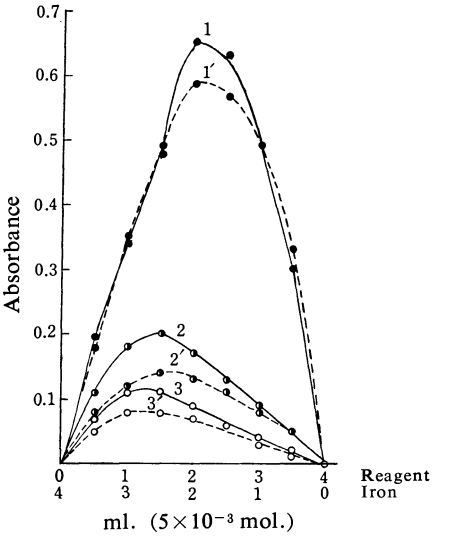

Fig. 4. The continuous variation method applied to the iron complexes at 460 mμ.
—— 2-Pyridinecarboxylic acid
---- 2, 3-Pyridinedicarboxylic acid
1, 1' In the presence of potassium cyanide
2, 2' In the presence of pyridine
3, 3' In the absence of potassium cyanide

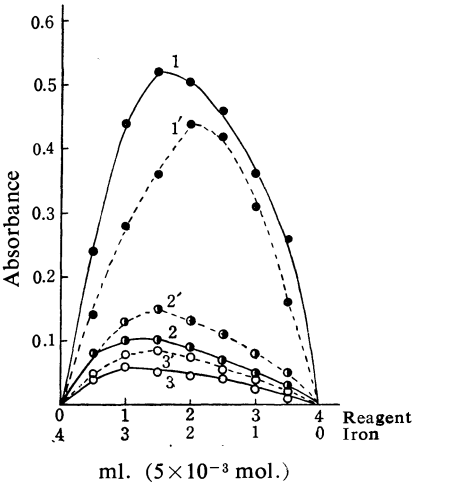

Fig. 5. The continuous variation method applied to the iron complexes at 460 mμ.
—— 2,4-Pyridinedicarboxylic acid
---- 2,5-Pyridinedicarboxylic acid
1, 1' In the presence of potassium cyanide
2, 2' In the presence of pyridine
3, 3' In the absence of potassium cyanide

9) I. Morimoto and K. Furuta, *Anal. Chem.*, **34**' 1033 (1962).
10) P. Job, *Compt rend.*, **180**, 928 (1925).
11) W. C. Vosburgh and G. R. Cooper, *J. Am. Chem. Soc.*, **63**, 437 (1941).
12) J. H. Yoe and A. L. Jones, *Ind. & Eng. Chem., Anal. Ed.*, **16**, 111 (1944).
13) A. E. Harvey and D. I. Manning, *J. Am. Chem. Soc.*, **72**, 4488 (1950).

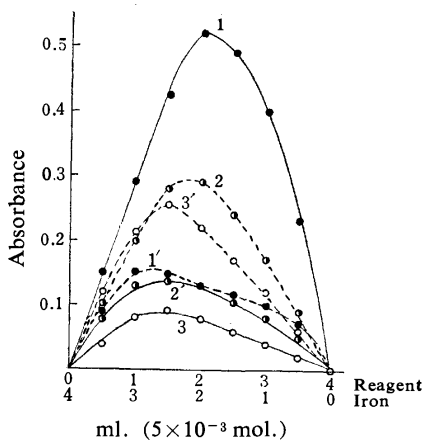

Fig. 6. The continuous variation method applied to the iron complexes at 460 mμ.
—— 2,6-Pyridinedicarboxylic acid
---- 2,4,6-Pyridinetricarboxylic acid
1, 1′ In the presence of potassium cyanide
2, 2′ In the presence of pyridine
3, 3′ In the absence of potassium cyanide

of pyridinecarboxylic acid in the presence of pyridine (2 ml.). 2,4-Pyridinedicarboxylic acid is an exception. From the curves it can easily be inferred that, in the presence of potassium cyanide, the metal forms a 1 : 1 complex with these acids, whereas without cyanide and in the presence of pyridine, the ratio is always 1 : 2.

For the mole ratio method, the absorbance of the solution was obtained by adding various amounts of the organic acids and a fixed amount of potassium cyanide to a constant amount of iron ; the results are shown in Figs. 7 and 8. Curves 4 and 5 in Fig. 7 and curves 3 and 4 in Fig. 8 were obtained by adding different amounts of the reagent (5×10^{-3} mol.) to 2 ml. of an iron solution of the same molarity and by adjusting the pH to 6.2, without adding cyanide. Curves 1, 2 and 3 in Fig. 7, and 1 and 2 in Fig. 8 were obtained by adding different amounts of the reagent (5×10^{-3} mol.) to 2 ml. of an iron solution of the same molarity and to 5 ml. of potassium

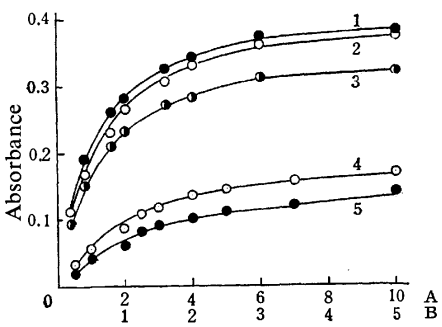

Fig. 7. The mole ratio method applied to the iron complexes.
Axis A Without potassium cyanide
Axis B In the presence of potassium cyanide
2, 4 2-Pyridine carboxylic acid
1, 5 2,3-Pyridinedicarboxylic acid
3 2,6-Pyridinedicarboxylic acid
1,2,3 In the presence of potassium cyanide

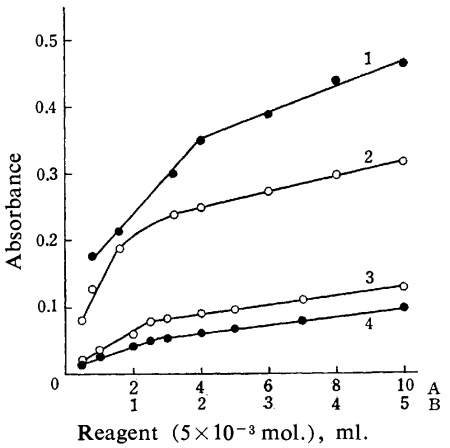

Fig. 8. The mole ratio method applied to the iron complexes.
Axis A Without potassium cyanide
Axis B In the presence of potassium cyanide
1, 4 2,4-Pyridinedicarboxylic acid
2, 3 2,5-Pyridinedicarboxylic acid
1, 2 In the presence of potassium cyanide
3, 4 Without potassium cyanide

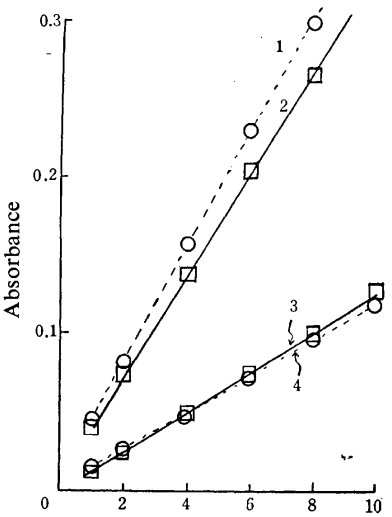

Fig. 9. The slope-ratio method applied to the iron complexes at 420 mμ.
---- 2-Pyridinecarboxylic acid
—— 2,3-Pyridinedicarboxylic acid
1, 2 Excess reagent
3, 4 Excess iron

cyanide and by adjusting the pH to 6.2~6.3. From these curves it can easily be inferred that, in the presence of potassium cyanide, the metal forms a 1 : 1 complex with 2-pyridinecarboxylic acid, 2, 3-pyridinedicarboxylic acid, 2, 5-pyridinedicarboxylic acid, and 2, 6-pyridinedicarboxylic acid, whereas without cyanide the ratio is always 1 : 2.

For the slope ratio method, two series of solution were used. In one series various amounts of a 5×10^{-4} mol. reagent solution were added to a constant amount of iron solution (2 ml. of 5×10^{-3} mol.), while in the other series, the amount of iron solution (5×10^{-4} mol.) was varied and that of the reagent solution was kept constant (5 ml. of 5×10^{-3} mol.). The results are shown in Figs. 9—12. The ratio of the slope of two straight lines supports the view that the complex formed without potassium cyanide contains the metal and the reagent in the ratio of 1 : 2. In the presence of potassium cyanide, the complex contained the metal and the reagent in the ratio of 1 : 1. In the case of 2, 4-pyridinedicarboxylic acid, the complex formed in the presence of potassium cyanide contains the metal and the reagent in the ratio of 1 : 2, while without potassium cyanide, it contains the metal and the reagent in the ratio of 1 : 3.

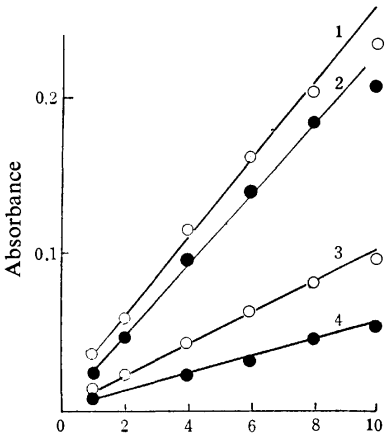

Fig. 10. The slope-ratio method applied to the iron complexes at 420 mμ.
1, 3 2,5-Pyridinedicarboxylic acid
2, 4 2,4-Pyridinedicarboxylic acid
1, 2 Excess reagent
3, 4 Excess iron

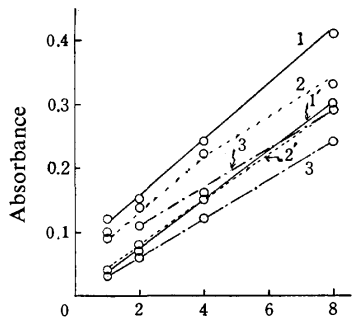

Fig. 11. The slope-ratio method applied to the iron complexes at 460 mμ.
—— 2-Pyridinecarboxylic acid
---- 2,3-Pyridinedicarboxylic acid
•—• 2,6-Pyridinedicarboxylic acid
1,2,3 Excess iron (2 ml. of 5×10^{-3} mol.)
1',2',3' Excess reagent (5 ml. of 5×10^{-3} mol.)

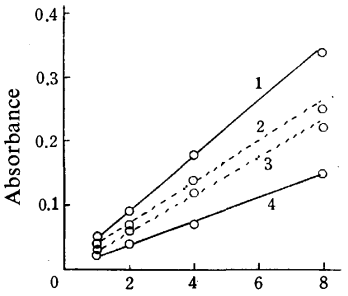

Fig. 12. The slope-ratio method applied to the iron complexes.
—— 2,4-Pyridinedicarboxylic acid
---- 2,5-Pyridinedicarboxylic acid
1, 3 Excess reagent (5 ml. of 5×10^{-3} mol.)
2, 4 Excess iron (2 ml. of 5×10^{-3} mol.)

With the exception of 2, 4-pyridinedicarboxylic acid, it was shown that, in the absence of potassium cyanide, iron in solution is associated with pyridine-2-carboxylic acids in a ratio of 1 : 2, while, in the presence of cyanide, the ratio is 1 : 1. The structure of the complexes, therefore, must be as shown in Fig. 13.

The degree of dissociation, α, and the stability constant, K, were calculated according to the equations of Harvey and Manning[12]. The degree of dissociation is given by $\alpha=(E_m-E_s)/E_m$, where E_m is the absorbance at

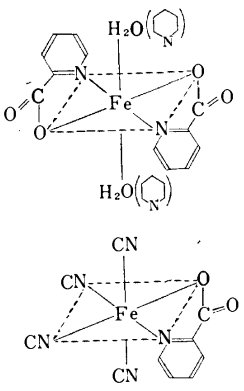

Fig. 13

TABLE I

Complex with	log K		
	With potassium cyanide (1/200 mol.)	Without potassium cyanide (1/200 mol.)	(1/100 mol.)
2-Pyridinecarboxylic acid	3.3	3.8	3.4
2,3-Pyridinedicarboxylic acid	3.2	3.8	3.4
2,4-Pyridinedicarboxylic acid	5.0	4.9	4.5
2,5-Pyridinedicarboxylic acid	3.4	3.8	3.4
2,6-Pyridinedicarboxylic acid	3.3	3.6	3.0
2,4,6-Pyridinetricarboxylic acid	2.2	3.7	4.2

15±2°C, μ=0.1

460 mμ due to a given amount of metal ions being completely complexed with an excess of the reagent, and where E_s is the absorbance calculated for the same amount of the metal ions complexed with a stoichiometric amount of the reagent.

For 2-pyridinecarboxylic acid, the values for E_m and E_s are 0.377 and 0.276 for the complex with cyanide, and α is equal to 0.268 ; without cyanide, E_m and E_s are 0.197 and 0.055 respectively, and α is equal to 0.723.

The stability constant, K, of the complex is obtained by substituting the value of α in the equation $K=C(1-\alpha)/\alpha C(n\alpha C)^n$, where C is the concentration of the metal ions in moles per liter and n is the number of moles of the reagent required for complex formation with 1 mol. of the metal ions. Thus, for the complex with cyanide, $K=2.0\times10^3$, and for the complex without cyanide, $K=7.9\times10^3$. The results are given in Table I. From Table I, the value of log K for iron-pyridinecarboxylic acid complexes are concluded to be 3~5. When pyridinecarboxylic acids are used for the spectrophotometric determination of iron, it should be noted that the absorbance of the iron complexes is increased considerably by the presence of potassium cyanide.

The authors are greatly indebted to Professors Yoshimasa Hirata and Yoshito Kishi of Nagoya University and to Mr. Katushi Furuta of the Sanyo Denki Co., Ltd., for their measurement of the ultraviolet or visible range spectral absorbance of iron complexes. They also acknowledge the valuable advice of Dr. Keinosuke Suzuki of Nagoya University.

Laboratory of Chemistry
Faculty of Liberal Arts and Education
Gifu University
Nagara, Gifu

The Redetermination of the Crystal and Molecular Structure of Chloral Hydrate

By Kazuhide OGAWA*

(Received February 11, 1963)

From a chemical point of view, aldehyde hydrate in the form of the gem-dihydroxy compound is usually said to be unstable and seldom isolable. However, when the electon cloud of the carbon atom of a carbonyl group is attracted towards a strongly electron-attracting group by the inductive effect, giving rise to a positive charge on the carbon atom, the hydrate, with its two gem-C–OH bonds, often becomes stable. In this sense, the crystal of chloral hydrate may not contain the water of crystallization, as is shown by its name, but it may form a part of the molecule, as is evidenced upon its solution by its inability to react with Schiff's reagent.

As for the molecular structure of chloral hydrate, Davies[1] has shown from his infrared study of its carbon tetrachloride solution that there is considerable interaction between the

* Present address: Institute of Chemistry, College of General Education, Osaka University, Toyonaka, Osaka.

1) M. M. Davies, *Trans. Faraday Soc.*, **36**, 333, 1114 (1940).

OH groups and the adjacent CCl_3 radical, and that the OH groups are locked in the cis-position. Novak and Whalley[2] have obtained almost the same results from their infrared study of crystalline chloral hydrate and its solution. They inferred that in solutions of chloral hydrate one of the hydrogen bonds due to the two OH groups might be relatively weakly bonded to one, and the other relatively strongly bonded to the remaining one, of the two chlorine atoms in the same molecule.

According to the quadrupole spectra of chloral hydrate reported by Allen[3], there are three split lines, of which the two with a higher frequency make a pair, while the third is almost 1.25 Mc. lower. It was suggested that two of the three C–Cl bonds are nearly the same, while the third is somewhat different. Theoretical considerations indicated that the hydrogen-bonded chlorine should have a lower C–Cl frequency.

The crystal structure of this substance has been reported by Kondo and Nitta[4] using the X-ray method. However, it was later found by the present author that their results were in error. In view of these circumstances it was felt necessary to determine a new, correct structure for this substance.

Experimental

Chloral hydrate could be recrystallized from a chloroform solution by the evaporation method. At the first stage of crystallization, needle crystals are rapidly formed, but upon repeating recrystallization hexagonal tabular crystals come to grow slowly. The crystals grown along the monoclinic b axes and specimens cut out of hexagonal tabular crystals parallel to the a and c axes respectively were sealed in thin-walled glass capillary tubes to protect the specimens from sublimation by X-rays and from the humidity in the air.

Using Ni-filtered copper K_α radiation, oscillation and Weissenberg photographs were taken of the b and a axes. The photographs were indexed on the basis of a monoclinic unit cell of these dimensions:

$a=11.50\pm0.03$ $\quad b=6.04\pm0.02$

$c=9.60\pm0.03$ Å $\quad \beta=120\pm0.5°$

These dimensions agreed with values determined by Elliot[5] and by Kondo and Nitta within the range of experimental error. The well-developed face referred to by Groth as the c-face was taken here as (1 0 0), and the a, b and c axes designated by Groth agreed with the directions of the −c, b and [1 0 1] axes respectively in the present work. Reflections of the $0k0$ type with k odd and of the $h0l$ type with l odd were systematically absent from all single crystal photographs. The space group is therefore $P2_1/c$, which finding is different from that reported by previous workers[4,5]. The density of chloral hydrate is 1.91, so there are four molecules in the unit cell.

Intensity data were obtained from multiple film photographs using a Nonius-integrating Weissenberg goniometer for $(hk0)$, $(h0l)$, $(h1l)$, $(h2l)$, $(h3l)$ and $(h4l)$. MoK_α radiation was used for precession photographs of $(hk0)$ and $(0kl)$ around the b axis. Several precession photographs were taken under various exposures in order to correlate all reflections with a linear scale. Intensities were estimated visually by comparison with a calibrated scale of time exposures. The usual Lorentz and polarization corrections were applied. The linear absorption coefficients of this crystal are 15.0 and 132.6 for MoK_α and CuK_α respectively. Thin-walled glass capillary tubes prevented the precise determination of the crystal size, however, so that corrections for the absorption of CuK_α could be applied only roughly and those for MoK_α were not be applied.

Determination of Structure

Sharpened Patterson projections on $(0kl)$, $(hk0)$, and $(h0l)$ were computed. The predominant peaks were considered to be due to the intra- or inter-molecular Cl–Cl interactions. The intra-molecular Cl–Cl vectors were sought, at first, within a radius of 2.95 Å from the origin based on a model given by electron diffraction[6]. These vectors must be constructed from a projected figure of the planar regular hexagon with a side length of 2.95 Å. It was expected that the Patterson projection on $(h0l)$ along the short b axis would show a more or less satisfactory resolution of the Cl–Cl vectors. Thus, four possible orientations of the projected hexagon around the point of origin were found in the Patterson projection on $(h0l)$. With these orientations, the Patterson projection on $(hk0)$ was also allowed for. The Patterson projection on $(0kl)$ was not useful, because the number of predominant peaks which could be considered Cl–Cl vectors was so few. Each case of the eight possible molecular arrangements in the unit cell, consistent with the Patterson projections on $(h0l)$ and $(hk0)$, was tried on the basis of the orientations of the projected hexagons mentioned above. After several false starts, electron-density projections along [0 1 0] were computed which showed fairly good agreement with the assumed model. The several starting false models were the so-called false or pseudo structures, which show a convergence to some extent in the R factors. With the correct

2) A. Novak and E. Whalley, *Spectrochim. Acta*, **16**, 521 (1960).
3) H. C. Allen, Jr., *J. Am. Chem. Soc.*, **74**, 6074 (1952); *J. Phys. Chem.*, **57**, 501 (1953).
4) S. Kondo and I. Nitta, *X-Rays*, **6**, 53 (1950).
5) N. Elliot, *Z. Krist.*, **98**, 180 (1937).
6) C. Degard, *Bull. soc. roy. sci. Liége*, **7**, 36 (1938).

TABLE I. ATOMIC COORDINATES AND ISOTROPIC TEMPERATURE FACTORS

	x	y	z	B($h0l$)	B($hk0$)	B($0kl$)
Cl(1)	0.2323	0.0378	−0.2289	3.71	2.51	3.11
Cl(2)	0.3139	−0.3547	−0.0267	4.22	2.80	3.19
Cl(3)	0.4051	0.0844	0.1146	4.14	2.44	3.50
O(1)	0.105	0.178	−0.035	3.4	2.7	2.8
O(2)	0.038	−0.200	−0.126	4.2	2.9	2.5
C(1)	0.256	−0.061	−0.048	3.4	2.4	3.4
C(2)	0.145	−0.065	−0.008	3.5	2.6	1.7

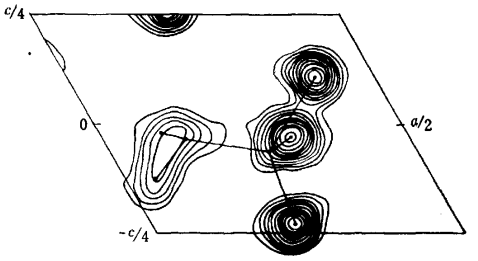

Fig. 1. The b-axis projection of electron density. Contours are at equal arbitrary intervals.

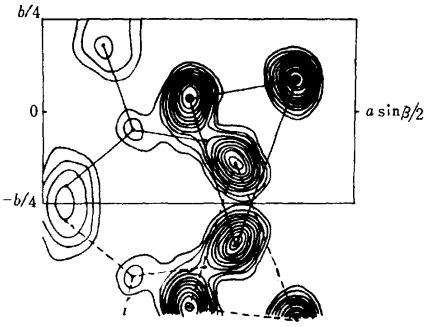

Fig. 2. The c-axis projection of electron density. Contours are at equal arbitrary intervals.

structure mentioned above, the electron-density projection along the b axis was refined by the usual Fourier successive approximations. The final electron-density projection along [0 1 0] showed clearly the molecule of chloral hydrate as a whole (Fig. 1), but the electron-density peaks of the two carbon atoms did not show clear resolution owing to the overlapping with those of the oxygen or chlorine atoms. The Fourier projection along [0 0 1] was then computed on the basis both of approximate y parameters as determined from the molecules in the unit cell and of x parameters as known from the ($h0l$) projection. The Fourier projection along the c axis was also refined in the usual way. The final findings are shown in Fig. 2. The electron-density projection along the a axis was computed on the basis of y and z parameters determined from the Fourier projections along [0 1 0] and [1 0 0]. The results are shown in Fig. 3.

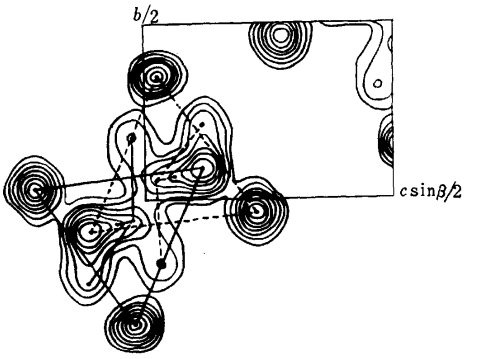

Fig. 3. The a-axis projection of electron density. Contours are at equal arbitrary intervals.

TABLE II. BOND LENGTHS AND BOND ANGLES

	Å		Degree
C(1)-Cl(1)	1.72	C(2)-C(1)-Cl(1)	122.4
C(1)-Cl(2)	1.87	C(2)-C(1)-Cl(2)	104.9
C(1)-Cl(3)	1.86	C(2)-C(1)-Cl(3)	109.5
C(1)-C(2)	1.51	Cl(1)-C(1)-Cl(2)	108.0
C(2)-O(1)	1.53	Cl(1)-C(1)-Cl(3)	107.3
C(2)-O(2)	1.44	Cl(2)-C(1)-Cl(3)	103.2
Cl(1)-Cl(2)	2.91	C(1)-C(2)-O(1)	99.6
Cl(2)-Cl(3)	2.92	C(1)-C(2)-O(2)	108.0
Cl(3)-Cl(1)	2.89	O(1)-C(2)-O(2)	109.8
O(1)···Cl''(1)	3.07	Cl(1)-Cl(2)-Cl(3)	59.4
O(1)···O'(2)	2.76	Cl(2)-Cl(3)-Cl(1)	60.0
O'(2)···Cl''(1)	3.12	Cl(3)-Cl(1)-Cl(2)	60.6
O'(2)···O''(1)	2.91	C(2)-O(1)···Cl''(1)	114.5
		C'(2)-O'(2)···Cl''(1)	156.8
		C(2)-O(1)···O'(2)	99.5
		C(2)-O(2)···O'(1)	94.0

The atomic parameters indicated by the final electron-density map projected along [0 1 0], [1 0 0] and [0 0 1] were further refined by the method of least squares. This least-squares refinement was calculated on the NEAC-2203 computer. In this case, off-diagonal terms were neglected except for those for x and z parameters and those for the scale and overall temperature factors. These results, with the values of the temperature factors for each atom, are listed in Table I. Bond lengths and bond angles calculated from the atomic parameters as determined by the least-squares

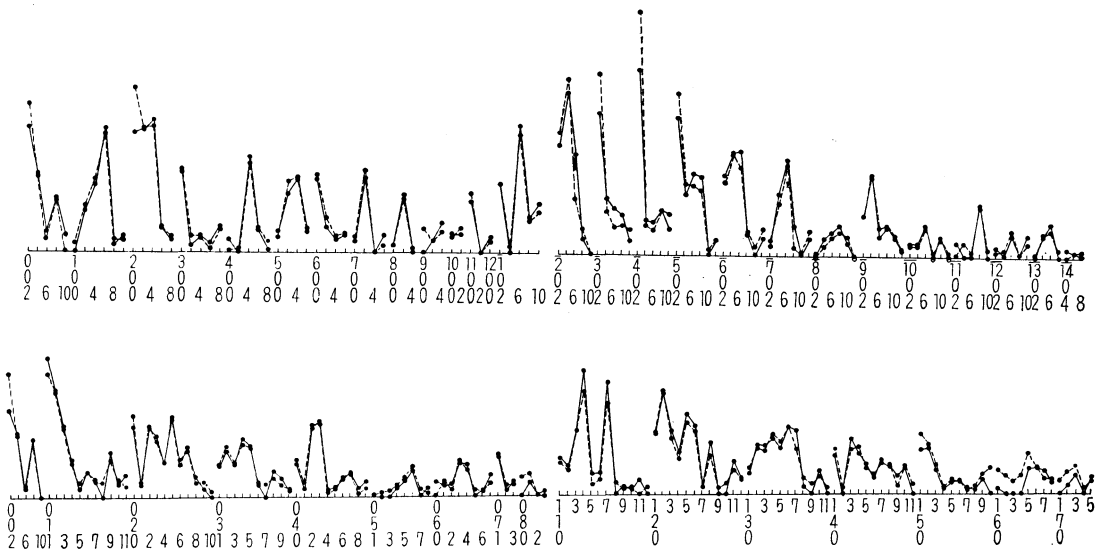

Fig. 4. Comparison between the observed F-values (solid lines) and calculated F-values (dotted lines).

method are listed in Table II. The observed and calculated values of the structure factors are shown in Fig. 4. Isotropic temperature corrections were included in the above calculated values. The R factors for the final coordinates are: $R(h0l)=18.3\%$, $R(0kl)=17.7\%$, $R(hk0)=25.5\%$. In this calculation, only observed structure factors were used.

Discussion and Description of the Structure

As shown in the electron-density maps of Figs. 1, 2 and 3, there is found no existence of the independent molecule of water, as in crystallization, but instead two OH groups attached to one of the two carbon atoms, as given by $CH(OH)_2CCl_3$. The conformation of these OH groups can be described as the staggered gauche referred to as the C–Cl_3 group. It is interesting to note that Davies[1] proposed a cis-conformation for this substance on the basis of his infrared study of its solution. Whether these different conclusion are due to the difference in states of aggregation will be an interesting point for further study.

The molecular arrangement in the crystal is shown in Fig. 5. For the sake of a description of the structure, let us first consider those layers of molecules in the structure parallel to the (0 1 0) plane. In each layer, a molecule is surrounded by six molecules. Such layers are juxtaposed in the direction of the b axis, the spacing of these layers being 6.04Å. The three chlorine atoms of a CCl_3 radical make a nearly regular triangle and face another triangle of chlorine atoms of the neighboring molecule related by a center of symmetry, but

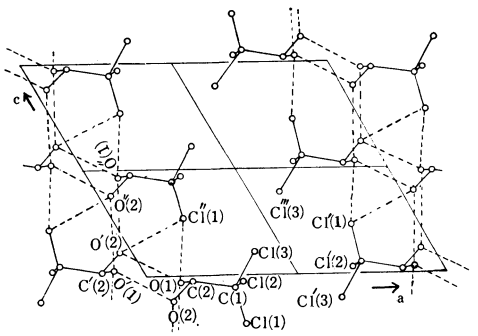

Fig. 5. Projection of the unit cell of chloral hydrate along the b-axis. Hydrogen bonds are shown by dotted lines.

the line joining the two centers of gravity of these triangles is not perpendicular to their triangular planes. The shorter Cl···Cl contracts between these triangles are of the lengths of 3.81, 4.08 and 4.92Å for Cl(1)···Cl′(3), Cl(2)···Cl′(3) and Cl(1)···Cl′(2) respectively, all of which values are greater than the sum of Pauling's van der Waals radius, 3.60Å. Around the Cl(1) atom the shortest approach to another Cl atom is 3.60Å, between Cl(1) and Cl(2) of the next layer above. Around the Cl(3) atom, the separation of 3.79Å is found between the Cl(3) and Cl‴(3) atoms of the molecule approaching diagonally in the same (0 1 0) layer. These circumstances, together with the hydrogen bond formation discussed below, explain the easy cleavage of the crystals parallel to (1 0 0).

In view of the difficulty, for several reasons, in obtaining sufficiently accurate intensity data, the atomic arrangement in the crystal, especially

that of carbon and oxygen, can not be discussed with sufficient precision. In addition to this, the position of the carbon atom bonded with the chlorine atom was still less accurately determined because of the overlapping in the three projected planes seen in Figs. 1, 2 and 3. The discrepancy between C–Cl values, therefore, may not be significant. The C–Cl, C–C and C–O bond lengths may roughly be supposed to be within the range of normal single bond distances.

Hydrogen bond formation is usually determined, in X-ray analysis, from the values of bond lengths and angles. In the crystal of chloral hydrate, the possible hydrogen bonds and angles are:

O(1)···O'(2)	2.8 Å	C(2)-O(1)-O'(2)	100°
O(2)···O'(1)	2.8	C(2)-O(2)-O'(1)	94
O(1)···Cl''(1)	3.1	C(2)-O(1)-Cl''(1)	115
O'(2)···Cl''(1)	3.1	C'(2)-O'(2)-Cl''(1)	157
O'(2)···O''(1)	2.9	C'(2)-O'(2)-O''(1)	143

There seem to be two kinds of bifurcated hydrogen bonds between O(1) and O'(2) or Cl''(1), and between O'(2) and O''(1) or Cl''(1). Such a bifurcated hydrogen bond of the O–H:$\begin{matrix}\cdot\cdot O\\ \cdot\cdot Cl\end{matrix}$ type has been found in the crystal of tetrachlorohydroquinone[7] and pentachlorophenol[8] by Sakurai. In the case of chloral hydrate crystal, the existence of one hydrogen-bonded chlorine atom is consistent with the results of the quadrupole study of Allen[3].

Some Further Structural Studies of Chloral Hydrate

Though the crystal structure of chloral hydrate at room temperature has been determined as stated above, it seemed necessary to examine further whether there is another phase in the crystal. A thermal differential analysis of this substance from room temperature to about 70°C was carried out*. The results thus obtained show that it is transformed into a high-temperature form at 52.6°C on heating and melts at 55.0~64.5°C. The staggered curve shown at a temperature above the melting point appears to suggest the complex nature of chloral hydrate in the molten state. It could be seen with chemical reagents that the decomposition into chloral and water partially took place.

The structure of a possible high-temperature phase could not be determined, but the Norelco

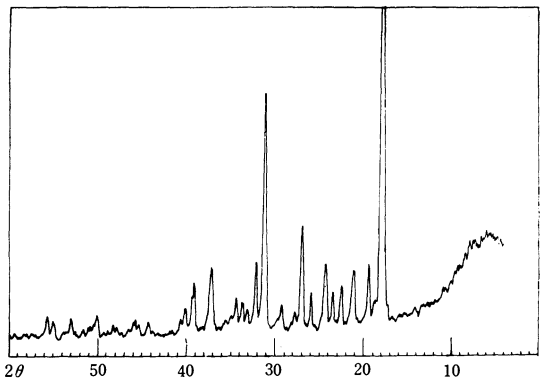

Fig. 6-a. Norelco diffraction powder pattern of chloral hydrate of room-temperature phase.

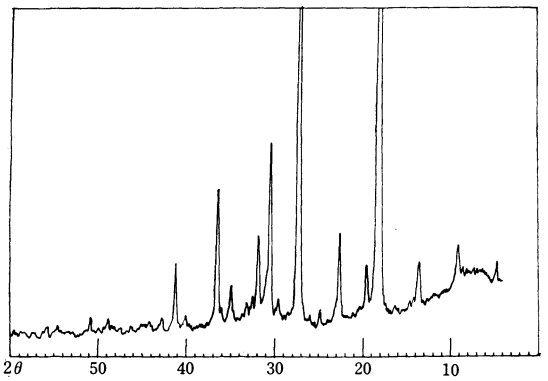

Fig. 6-b. Norelco diffraction powder pattern of chloral hydrate of high-temperature phase which may contain that of room-temperature phase.

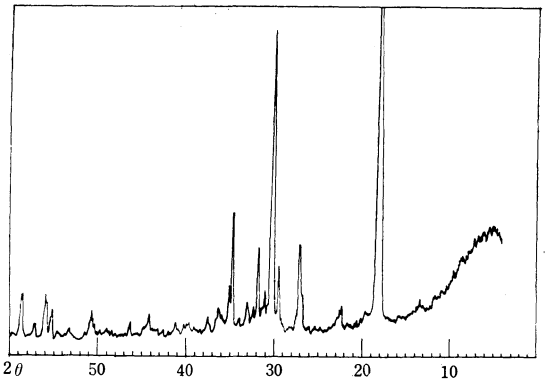

Fig. 6-c. Norelco diffraction powder pattern of chloral hydrate of high-temperature phase after 36 hr. passed from the experiment of Fig. 6-b.

diffraction powder patterns at different times after crystallization from the molten state appear to show that the high-temperature phase changes slowly and partially towards the room-temperature phase. (Fig. 6) The unit cell of the high-temperature phase seems to

7) T. Sakurai, *Acta Cryst.*, **15**, 443 (1962).
8) T. Sakurai, ibid., **15**, 1164 (1962).
* The author is indebted to Professor S. Seki and Dr. H. Suga for the measurements.

be large compared with that of the room-temperature phase, because the spacings of the former cell contain 19.19, 9.71 and 6.51 Å, which correspond to those of (0 0 1/2), (0 0 1) and (010) of the latter cell; these later values are absent because of the limitations of the space group and of the size of the latter cell.

To obtain further information on the molecular structure and on the nature of the intermolecular hydrogen bonds, the infrared spectra of chloral hydrate in a solid and in solutions of several kinds of solvents (benzene, chloroform, carbon tetrachloride and carbon disulfide) have been taken. The measurements were made with a Hitachi model EPI-2 spectrometer equipped with a NaCl or LiF prism. The chief absorption bands noticed are:

	O-H cm^{-1}	C=O cm^{-1}	H_2O cm^{-1}
Solid (KBr disk)	3360 (broad)	—	—
Benzene solution	3617, 3525	1770	1605

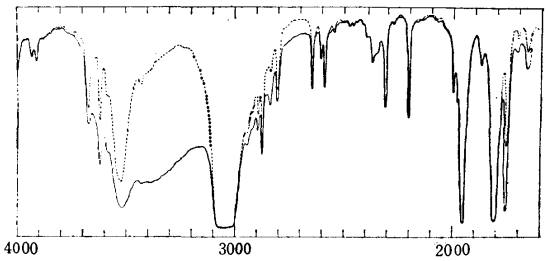

Fig. 7-a. Infrared spectra: (a) solid line, chloral hydrate in benzene solution; (b) dotted line, about one-third of concentration of a.

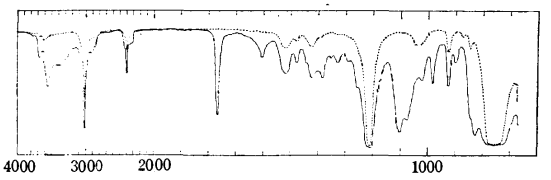

Fig. 7-b. Infrared spectra: (a) solid line, chloral hydrate in chloroform solution; (b) dotted line, pure chloroform.

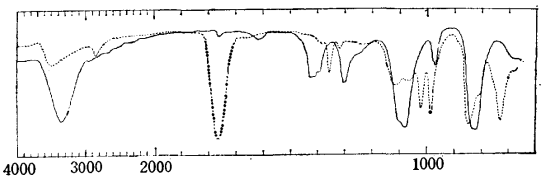

Fig. 7-c. Infrared spectra: (a) solid line, solid chloral hydrate as KBr disk; (b) dotted line, pure chloral.

As has been indicated by previous workers[3,9,10], there are two sharp absorption bands due to two kinds of OH groups in solutions of chloral hydrate, of which the one with the higher frequency is due to the relatively weakly hydrogen-bonded groups and the other, to the relatively strongly hydrogen-bonded groups, whereas the crystalline chloral hydrate has a broad band which is of a lower frequency than the two bands in solutions and which is due to the intermolecular-bonded OH, as is shown in Fig. 7. The solution spectra of chloral hydrate show a strong absorption band at 1770 cm^{-1} and a weak broad band near 1605 cm^{-1}. The former band appears also in chloral, while the latter band often appears in substances containing water molecules, so that it can be considered that the former is due to carbonyl-stretching vibration and the latter, to the in-plane OH deformation vibration of a water molecule. Though the 1770 and 1605 cm^{-1} absorption bands appear very faintly in the solid state, they are caused by the dissociation of crystalline chloral hydrate into chloral and water, because a small part of the solid will dissolve either in moisture within a KBr disk or in Nujol.

On the one hand, chloral hydrate fails to show color with Schiff's reagent and reacts with Tollen's reagent or Fehling's solution, while these three reagents are said to be specific to aldehydes. On the other hand, it is to be noticed that aldose, in general, reduces Fehling's solution and Tollen's reagent, while it does not react with the Schiff reagent. It is said that this is due to the cyclic hemiacetal structure of aldose. From the characteristic chemical reactivity and the interpretation of the infrared absorption bands, it might be inferred that the following dissociation equilibrium would take place in a solution of chloral hydrate as seen in ordinary aliphatic aldehyde. Then, the water and chloral molecules produced by dissociation would re-combine without delay, as shown in the following equilibrium schemes:

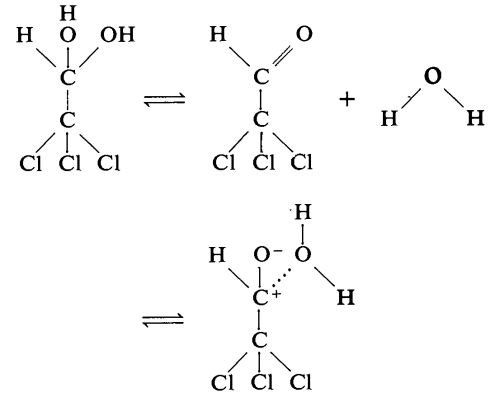

9) D. M. W. Anderson, L. J. Bellamy and R. L. Williams, *Spectrochim. Acta*, 12, 233 (1958).
10) L. P. Kuhn, *J. Am. Chem. Soc.*, 74, 2492 (1952).

This water molecule would be combined with a chloral molecule by a weak bond, but it would be loosened upon being heated more or less, so that chloral hydrate might react differently with the Schiff reagent upon being heated according to the degree of dehydration in the solvents employed, and the color produced by the combination with the Schiff reagent would fade away sooner or later on cooling. At any rate, the molecular structure of chloral hydrate in a solution or liquid state seems to be different from that of a solid state and is so complex that other equilibrium schemes should be considered. Of these possible equilibria, the most predominant one would have the structure cited above.

Summary

The crystal structure of chloral hydrate has been redetermined by the two-dimensional Fourier method and the least-squares method on the NEAC-2203 computer. It is monoclinic and belongs to the $P2_1/c$ space group, with four molecules in a cell of the dimensions $a=11.50$, $b=6.04$, $c=9.60$ Å and $\beta=120.0°$. The molecular structure of chloral hydrate is of the gem-dihydroxy compound type with the two OH groups in the staggered gauche-position referred to the adjacent C–Cl_3 group. The molecules of chloral hydrate in the crystal are held together mainly by the van der Waals attraction of Cl···Cl and by the bifurcated hydrogen bonds of O–H:$\begin{matrix}\cdot\cdot\text{Cl}\\ \cdot\cdot\text{O}\end{matrix}$. As a result of differential thermal analysis, a high-temperature phase has been found between 53.6° and the melting point, which was ascertained by X-ray diffraction powder patterns. Some of the molecules of chloral hydrate appear to dissociate into water and chloral and attain equilibrium with them. This is inferred from infrared study and from the chemical reactivity with the Schiff reagent.

I wish to express my sincere thanks to Professors Isamu Nitta and Tokunosuké Watanabé for their continuous encouragement and helpful discussions in the course of this study. I am also indebted to Dr. Kenji Osaki for the use of his least-squares programs for the NEAC-2203 computer, to Mr. Hiroshi Okuto of Takeda Chemical Industry Co., to Mr. Kiyoaki Tatsuka of the Appraisal Division of the Osaka Custom House, and to Dr. Hiroyuki Tadokoro for providing infrared spectra and for their helpful discussions, and to Dr. Hiroshi Suga for providing differential thermal analysis data.

Recently, according to a private communication from Dr. George Marshall Brown of the Oak Ridge National Laboratory to Professor Isamu Nitta, he is now analyzing the structure of this crystal by the neutron diffraction method.

Department of Chemistry
Faculty of Science
Osaka University
Nakanoshima, Osaka

NOTES

Reaction of Dichlorocarbene and Primary Amines—Preparation of Aromatic Isocyanides

By Tadao SHINGAKI and Matsuji TAKEBAYASHI

(Received November 28, 1962)

It has been established that dichlorocarbene is formed by the reaction of haloform and bases, such as potassium *t*-butoxide[1], sodium hydroxide[2] and alkyl lithium[3], and the existence of carbene has been confirmed by Doering[1] with the formation of an adduct of carbene to cyclohexene. These facts might suggest that the so-called carbylamine reaction is a reaction involving dichlorocarbene as an intermediate, as has been suggested by Hine[4].

In order to confirm this speculation the present authors have studied the reaction using sodium *t*-butoxide in place of potassium or sodium hydroxide. To a hexane solution (or toluene-hexane solution) of an aromatic primary amine and sodium *t*-butoxide was added chloroform drop by drop at 0~5°C. The reaction took place immediately. After the addition of chloroform was over, the reaction mixture was left to stand at 0°C for thirty minutes, and then at 25°C for thirty minutes. The isocyanide was fractionated in the atmosphere of nitrogen or separated by the formation of silver complex compound[5].

$$ArNH_2 + CHCl_3 + 3(CH_3)_3CONa \longrightarrow ArNC + 3NaCl + 3(CH_3)_3COH$$

The results obtained are summarized in the following table.

As shown in the table, it is recognized that the reaction takes place also in the system of chloroform and *t*-butoxide, which has been recognized as a typical system to produce dichlorocarbene, and that the yield of isocyanides is increased according to increase of the concentration of chloroform (compare Expt. 3 with Expts. 4 and 5). Moreover, the yield of isocyanides in this case was much higher than that in the cases of sodium hydroxide.

TABLE I. YIELD OF ISOCYANIDES FROM PRIMARY AMINES

Primary amine, 0.2 mol. Chloroform, 0.2 mol. Sodium *t*-butoxide, 0.6 mol. Reaction time, 5 hr.

Expt. No.	Primary amine	Isocyanide (yield)
1	Aniline	Phenyl isocyanide (73%)
2	*o*-Toluidine	*o*-Tolyl isocyanide (71%)
3	*p*-Toluidine[a]	*p*-Tolyl isocyanide (72%)
4	*p*-Toluidine	*p*-Tolyl isocyanide (86%)
5	*p*-Toluidine[b]	*p*-Tolyl isocyanide (98%)
6	*o*-Chloraniline	*o*-Chlorophenyl isocyanide (93%)
7	*p*-Chloraniline	*p*-Chlorophenyl isocyanide (94%)

a) 0.1 mol. of chloroform was added.
b) 0.4 mol. of chloroform was added.

The results mentioned above indicate that the carbylamine reaction is a reaction involving dichlorocarbene as an intermediate.

We would like to suggest the following reaction mechanism for this reaction.

$$CHCl_3 + t\text{-}BuO^- \longrightarrow t\text{-}BuOH + Cl^- + :CCl_2 \quad (1)$$

$$Ar\text{-}\overset{\overset{H}{|}}{N}: + :CCl_2 \longrightarrow Ar\text{-}\overset{\overset{H}{|}}{N}\overset{(+)\ (-)}{-C-Cl} \quad (2)$$

$$Ar\text{-}\overset{\overset{H}{|}}{N}\overset{(+)\ (-)}{-C-Cl} \longrightarrow Ar\text{-}\overset{\overset{H}{|}}{N}\text{-}C\text{-}Cl \longrightarrow Ar\text{-}\overset{\overset{H}{|}}{\overset{+}{N}}{=}C + Cl^- \quad (3)$$

$$Ar\text{-}\overset{\overset{H}{|}}{\overset{+}{N}}{=}C + t\text{-}BuO^- \longrightarrow Ar\text{-}N{=}C + t\text{-}BuOH \quad (4)$$

$$Ar\text{-}N{=}\overset{\overset{H}{|}}{C} \longrightarrow Ar\text{-}\overset{+}{N}{\equiv}CH + Cl^- \quad (5)$$

$$Ar\text{-}\overset{+}{N}{\equiv}CH + t\text{-}BuO^- \longrightarrow Ar\text{-}\overset{(+)(-)}{N{\equiv}C} + t\text{-}BuOH \quad (6)$$

Department of Chemistry
College of General Education
Osaka University
Toyonaka, Osaka

1) W. Von E. Doering and A. H. Hoffmann, *J. Am. Chem. Soc.*, **76**, 6162 (1954).
2) L. L. McCoy, ibid., **80**, 6568 (1958).
3) G. L. Closs and L. E. Closs, ibid., **81**, 4996 (1959); W. T. Miller, Jr., and C. S. Y. Kim, ibid., **81**, 5008 (1959).
4) J. Hine, ibid., **72**, 2438 (1950).
5) D. L. Hammick et al., *J. Chem. Soc.*, **1930**, 1876.

Abnormal Oxidation of 3-Nitro-2-thenyl Bromide by Cupric Nitrate

By Tyo SONE and Yasuo MATSUKI

(Received December 27, 1962)

The present authors have reported the synthesis of 3-nitro-2-thiophenealdehyde (I): Oxidation of 3-nitro-2-methylthiophene by chromic trioxide in acetic anhydride followed by hydrolysis gave I (m. p. 52~53°C), but the yield was poor[1].

It has been found that oxidation of some aralkyl halides of benzyl halide type substituted by an electronwithdrawing group on the aromatic ring by cupric or lead nitrate, affords corresponding aromatic aldehydes[2] and also that this method is applicable to the thiophene series[1,3]. Therefore, an attempt was made for the synthesis of I by this method starting from 3-nitro-2-thenyl bromide (II).

When II was heated in about 10% cupric nitrate solution (0.75 mol.) for 50 hr., two crystalline products melting at 78.5~79.5°C, and 81~82°C, respectively, were obtained. The low melting material (III) can be considered as an aldehyde from the method of separation of the products as described in the Experimental, but the infrared spectrum (Fig. 1) and the melting point of III are evidently different from those of I. The NMR spectrum of III (in acetone) shows a band of the aromatic hydrogen at 255.5 c. p. s., and a band due to the aldehyde hydrogen at 352.5 c. p. s., referred to cyclohexane. Gronowitz and Hoffman observed that the aldehyde hydrogen of thiophenealdehydes not substituted at the 5-position in the thiophene ring interacted with the hydrogen at the 5-position to split into two lines separated by about 1 c. p. s.[4], and this is also the case in some nitrothiophenealdehydes[1]. The splitting was not observed in the aldehyde hydrogen of III. In addition, III gave a positive test for the Beilstein test. These facts suggest that III is 5-bromo-3-nitro-2-thiophenealdehyde. Elemental analysis, in fact, gave corresponding values. III reacts with ordinary ketonic reagents, and with *p*-toluidine to yield the Schiff base.

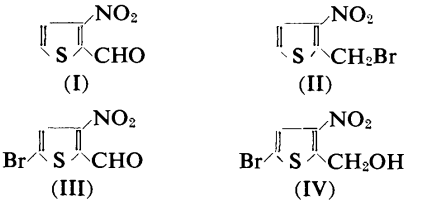

The high melting material (IV) has infrared bands for OH group in the region of 3300~3100 cm^{-1} (Fig. 2). In the NMR spectrum of

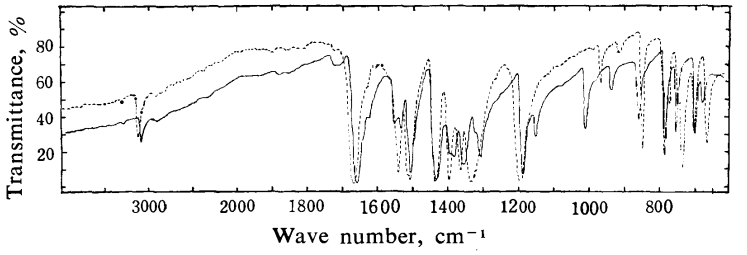

Fig. 1. Infrared spectra of I (----) and III (——) in KBr disk.

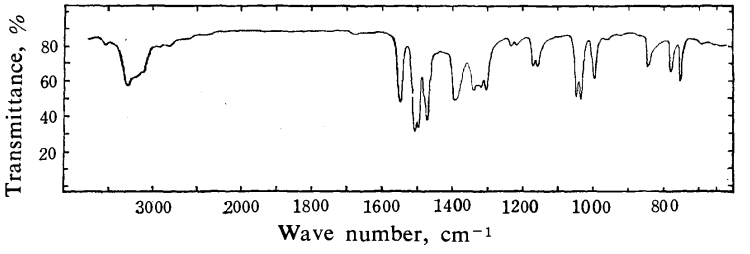

Fig. 2. Infrared spectrum of IV in KBr disk.

1) T. Sone and Y. Matsuki, *J. Chem. Soc. Japan, Pure Chem. Sec.* (*Nippon Kagaku Zasshi*), 83, 496 (1962).
2) Houben-Weyl, "Methoden der Organischen Chemie", Band VII, Teil 1, Georg Thieme Verlag, Stuttgart (1954), p. 193.
3) E. Profft and H. Wolf, *Ann.*, 628, 96 (1959).
4) S. Gronowitz and R. A. Hoffman, *Acta Chem. Scand.*, 13, 1687 (1959).

IV (in carbon tetrachloride), the chemical shifts (69, 145 and 240 c. p. s.) and the relative peak areas (approximately 1 : 2 : 1) of the bands suggest that they are due to a hydroxyl group, a methylene group and a ring hydrogen of trisubstituted thiophene, respectively. IV gave also a positive test for halogen. From these facts, it may be presumed that IV is 5-bromo-3-nitro-2-thenyl alcohol. Elementary analysis and the formation of the benzoate support this assumption. An attempt to synthesize the alcohol by nitration of 5-bromo-2-thenyl acetate followed by hydrolysis was unsuccessful, because the nitration product could not be hydrolyzed by either acid or alkaline solution. Starting material, II, is entirely free from other substances such as 5-bromo-3-nitro-2-thenyl bromide, for the coupling constant (J=5.5 c. p. s.) in the NMR spectrum indicates that II is a 2, 3-disubstituted thiophene[5], and the reaction of II with potassium thiocyanate gave 3-nitro-2-thenyl thiocyanate in 70% yield.

Such an abnormal oxidation of aralkyl halides by a heavy metal nitrate, giving halogenated aldehyde and alcohol, has not been observed as far as the authors know. As it has been suggested that the normal oxidation involves the formation of a nitrate[6] as an intermediate and cupric halide[2] which can be used as a halogenating agent[7], the mechanism of the reaction presented here probably consists in the bromination of intermediate nitrate by cupric bromide to yield 5-bromo-3-nitro-2-thenyl nitrate, which subsequently gives III by elimination and IV by nucleophilic substitution.

Experimental

All melting points are uncorrected. The infrared spectra were measured with a Perkin-Elmer model 21 infrared spectrometer. The NMR spectra were obtained with a Varian Associates Model V-4300B spectrometer at 40 Mc. and cyclohexane was used as an internal reference.

3-Nitro-2-theyl Bromide (II).—Prepared according to the procedure described by Snyder et al.[8], m. p. 60~61°C (reported m. p. 60~62°C; Found: C, 27.04; H, 1.77; N, 6.18%). The chemical shifts are 141.5 (methylene protones), 231 (doublet) and 243.5 c. p. s. (doublet) (ring protons) and the coupling constant is J=5.5 c. p. s., characteristic of 2,3-disubstituted thiophenes (J_{23}=5.4±0.6[5a], 5.4 c. p. s.[5b]).

Reaction of II with Potassium Thiocyanate.—A mixture of II (0.22 g.) and potassium thiocyanate (0.15 g.) in ethanol was warmed at 60~65°C for 30 min. The resulting solution was poured into water and the precipitates were collected and recrystallized from ethanol to form 3-nitro-2-thenyl thiocyanate as pale yellow needles, m. p. 109~110°C. Yield 0.14 g.

Found: C, 36.20; H, 1.73; N, 13.79. Calcd. for $C_6H_4N_2O_2S_2$: C, 35.98; H, 2.01; N, 13.99%.

Oxidation of II by Cupric Nitrate.—A mixture of II (4.4 g.) and a cupric nitrate solution ($Cu(NO_3)_2 \cdot 3H_2O$, 3.6 g.; H_2O, 30 ml.) was gently refluxed for 50 hr. After cooling, the reaction products were extracted with ether and the ether extracts were washed with water and then shaken with excess of saturated sodium bisulfite solution to form the addition product; this was collected and dissolved in water, and the solution was acidified with hydrochloric acid and steam-distilled. The crystals precipitated in the distillate amounted to 1.23 g., m. p. 67~72°C, which, after recrystallization from petroleum ether, gave 5-bromo-3-nitro-2-thiophenealdehyde (III) as pale yellow needles, m. p. 78.5~79.5°C.

Found: C, 25.63; H, 0.89; N, 6.01; Br, 32.92. Calcd. for $C_5H_2BrNO_3S$: C, 25.44; H, 0.85; N, 5.93; Br, 33.85%.

The infrared spectrum showed absorption for the carbonyl group at 1658 cm^{-1}.

Semicarbazone.—Yellow crystals, m. p. 269°C (decomp.) (from dioxane).

Found: N, 18.98. Calcd. for $C_6H_5BrN_4O_3S$: N, 19.11%.

2, 4-Dinitrophenylhydrazone.—Orange needles, m. p. 252~253°C (from ethyl acetate).

Found: C, 31.59; H, 1.28; N, 16.46. Calcd. for $C_{11}H_6BrN_5O_6S$: C, 31.74; H, 1.45; N, 16.82%.

Reaction of III with p-Toluidine.—A mixture of III (0.1 g.) and *p*-toluidine (0.1 g.) in methanol (5 ml.) was left on standing at room temperature for two days. The yellow crystals precipitated were collected and recrystallized from ethanol to form the Schiff base as yellow needles, m. p. 129°C. Yield, 0.13 g.

Found: N, 8.44. Calcd. for $C_{12}H_9BrN_2O_2S$: N, 8.61%.

The ether solution, after separation of the addition product, was washed with water and dried. Evaporation of ether yielded 0.87 g. of crystals, m. p. 80.5~82°C, which were recrystallized from a mixture of ether and petroleum ether to give 5-brom-3-nitro-2-thenyl alcohol (IV) as colorless needles, m. p. 81~82°C.

Found: C, 25.25; H, 1.61; N, 6.01; Br, 33.73. Calcd. for $C_5H_4BrNO_3S$: C, 25.22; H, 1.69; N, 5.88; Br, 33.56%.

Benzoate.—Pale brown needles, m. p. 119~120°C (from ethanol).

Found: C, 42.18; H, 2.51; N, 4.01. Calcd. for $C_{12}H_8BrNO_4S$: C, 42.12; H, 2.35; N, 4.09%.

The authors wish to thank Mr. Kensuke Takahashi for his measurements and helpful advice on NMR spectra, Mr. Shuji Aono for

5) a) S. Gronowitz and R. A. Hoffman, *Arkiv Kemi*, 13, 279 (1958); b) K. Takahashi, Y. Matsuki, T. Mashiko and G. Hazato, This Bulletin, 32, 156 (1959).

6) D. J. Cram and G. S. Hammond, "Organic Chemistry", McGraw-Hill, New York (1959), p. 384.

7) For example, Fort brominated β-naphthol by using cupric bromide in methanol-water at room temperature. A. W. Fort, *J. Org. Chem.*, 26, 765 (1961).

8) H. R. Snyder, L. A. Carpino, J. F. Zack., Jr, and J. F. Mills, *J. Am. Chem. Soc.*, 79, 2556 (1957).

his infrared spectral measurements and Miss Yoko Endo and Miss Yukiko Endo for micro-analyses.

The Chemical Research Institute
of Non-Aqueous Solutions
Tohoku University
Katahira-cho, Sendai

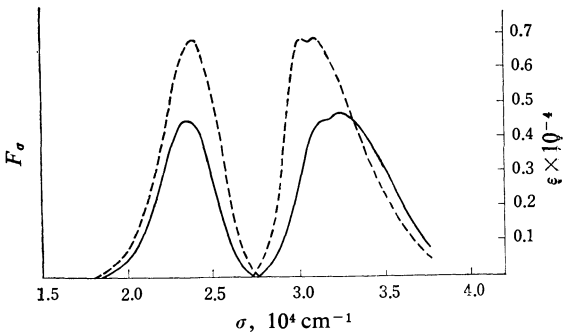

Fig. 1. Absorption and fluorescence spectra of DMNA (——) and NA (----) in acetonitrile. Concentrations of the solute: DMNA, 0.875×10^{-4} mol./l., NA, 0.8×10^{-4} mol./l.

The Electronic Structure of Excited N, N-Dimethyl-α-naphthylamine

By Noboru MATAGA

(Received January 10, 1963)

In the course of studying the effects of solvents on the electronic spectra of naphthalene derivatives, we have found that the solvent shifts of the first absorption band of *N, N*-dimethyl-α-naphthylamine (DMNA) are much smaller than those of α-naphthylamine (NA), whereas those of the fluorescence spectrum are quite large and are almost comparable to the shifts of NA.

On the other hand, Smith[1] has studied the dipole moments of various aromatic amines and their *N, N*-dimethyl derivatives. His results indicate that, in DMNA as compared with NA, the steric repression of the resonance effect of the substituent is very strong. This argument is in accordance with the fact that, as is shown in Table I, the wave numbers of the absorption band maximum (σ_a^m) of DMNA in several solvents are considerably larger than those of NA. The apparent first absorption bands of both NA and DMNA are composed of two electronic bands, ^1L_a and ^1L_b[2,3]. In Table I, the σ_a^m values given for NA are those of ^1L_a, while for DMNA the σ_a^m values of both ^1L_a and ^1L_b are given. In the case of NA, the fluorescent state seems to be ^1L_a[3], although the lowest absorbing singlet state is ^1L_b. It is quite probable that the lowest absorbing state of DMNA is ^1L_b. However, it is not quite clear whether the fluorenscent state of this molecule is ^1L_a or ^1L_b. Nevertheless, this circumstance will not affect the essential conclusion of the present study.

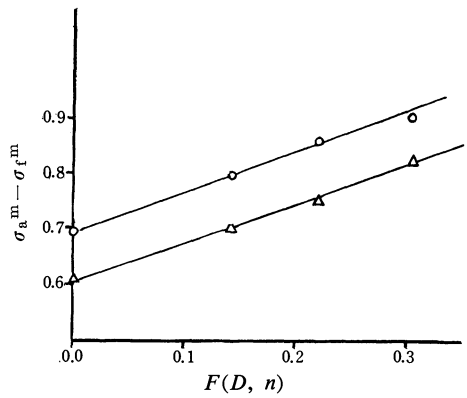

Fig. 2. $(\sigma_a^m - \sigma_f^m) \sim F(D, n)$ relations for DMNA.
○ $\sigma_a^m(^1L_a) - \sigma_f^m$ △ $\sigma_a^m(^1L_b) - \sigma_f^m$

As an example of the difference between the absorption and fluorescence spectra of DMNA and NA, the spectra in acetonitrile are indicated in Fig. 1. The smaller absorption intensity of DMNA compared with NA is also in accordance with the findings of Smith[1].

Thus, the resonance interaction between the substituent and the naphthalene ring in DMNA is rather small in the ground state and in the excited Franck-Condon state. Moreover, the interaction energy between DMNA and the surrounding solvent molecules is not very differemt in the ground state and in the Franck-Condon excited state respectively. However, the very large solvent shift of the fluorescence spectra indicate a rather large difference between the solute-solvents interaction energies in the Franck-Condon state and in the equilibrium excited state of DMNA, and, consequently, a large difference between the electronic structures of DMNA in the ground and in the fluorescent states respectively.

We can now roughly estimate the change of electronic structure in the fluorescent state, as

1) J. W. Smith, *J. Chem. Soc.*, **1961**, 81.
2) H. Baba and S. Suzuki, This Bulletin, **34**, 82 (1961).
3) N. Mataga, to be published.

TABLE I. WAVE NUMBERS OF BAND MAXIMA IN SEVERAL SOLVENTS
(in unit of $10^4\,cm^{-1}$)

Solvent	$F(D, n)$	DMNA			NA	
		$\sigma_a^m(^1L_a)$	$\sigma_a^m(^1L_b)$	σ_f^m	$\sigma_a^m(^1L_a)$	σ_f^m
n-Hexane	0	—	—	—	3.14	2.66
Cyclohexane	0	3.28	3.20	2.59	—	—
Monochlorobenzene	0.1429	3.27	3.17	2.47	3.10	2.51
Dichloroethane	0.2199	3.27	3.16	2.41	—	—
Acetonitrile	0.3054	3.25	3.17	2.35	3.07	2.38

compared with the ground state, by the following equation[4,5]:

$$hc(\sigma_a^m - \sigma_f^m) = \text{const} + 2\cdot F(D, n)\cdot\delta$$

$$F(D, n) = \left[\frac{D-1}{2D+1} - \frac{n^2-1}{2n^2+1}\right],\quad \delta = (\vec{\mu}_e - \vec{\mu}_g)^2/a^3$$

where D and n: the dielectric constant and the refractive index of the solvent, $\vec{\mu}_e$ and $\vec{\mu}_g$: the dipole moments of the solute molecule in the excited and ground states respectively, and a: the cavity radius in Onsager's theory of the reaction field.

The approximate linear relations between $(\sigma_a^m - \sigma_f^m)$ and $F(D, n)$ are satisfied for DMNA, as is shown in Fig. 2. From the linear relations, the δ value can be estimated to be $7500\,cm^{-1}$ for either value of $\sigma_a^m(\sigma_a^m(^1L_a)$ or $\sigma_a^m(^1L_b))$. This δ value is very close to and a little larger than the δ value of NA ($7300\,cm^{-1}$). Thus the change of the electronic structure of DMNA in the fluorescent state is quite large in spite of the steric repression of the resonance effect of the substituent in the ground state. The ionization potential of the nitrogen lone pair orbital of the dimethylamino group may be much smaller than that of the amino group. (The difference between the ionization potentials of methylamine and trimethylamine and the difference between those of ammonia and dimethylamine are both ca. 1 eV.[6]) Therefore, the energy of the CT (charge transfer) configuration, where one electron is transfered from the nitrogen lone pair orbital to a vacant orbital of naphthalene, is much smaller in DMNA than in NA. Accordingly, the interaction between the CT configurations and the locally excited states of naphthalene may be very strong if the core resonance integral between the nitrogen lone pair orbital and the carbon $2p\pi$AO's of naphthalene is not so small.

The large value of δ for DMNA observed in the present study indicates the structural change, i. e., the rotation of the dimethylamino group around the C–N bond during the life time of the excited state, leading to an increase in the overlap between the lone pair orbital and the π-orbital of naphthalene. This structural change is perhaps possible because the considerable increase of CT interaction in the excited state compensates for the increase in the steric repulsion.

Faculty of Science
Osaka City University
Sumiyoshi-ku, Osaka

4) E. Lippert, *Z. Naturforsch.*, **10a**, 541 (1955); *Z. Elektrochem.*, **61**, 962 (1957).
5) N. Mataga et al., This Bulletin, **28**, 690 (1955); ibid., **29**, 465 (1956).
6) K. Watanabe and J. R. Mottle, *J. Chem. Phys.*, **26**, 1773 (1957).

SHORT COMMUNICATIONS

The Catalytic Polymerization of Vinyl Monomers by the Cobalt Cyanide Complex

By Mitsumi TAKAHASHI

(Received January 22, 1963)

In this study of the catalytic activity of the cobalt cyanide complex-hydrogen system, the author found that this complex has the ability to polymerize such vinyl monomers as methyl methacrylate, styrene, acrylonitrile and butadiene.

The polymerization was carried out as follows: 5 ml. of the monomer, 1 ml. of a potassium cyanide solution (3×10^{-1} mol./l.), 1 ml. of a 5% surfactant (non-ionic surfactant "Tween 80" aqueous solution and 2 ml. of water were placed in the main chamber of a Thunberg tube, and the air in the system was replaced with hydrogen. Then 1 ml. of the cobalt(II) chloride solution (5×10^{-2} mol./l.), which had been placed in the side chamber of the tube, was mixed with other components in the main chamber by tilting the side chamber, and the tube was shaken continuously at 25°C.

During the first stage of the reaction, small gel-like polymer particles separate out from the initial white emulsion. As the reaction proceeds, these particles coagulate to larger and harder particles or a mass.

The extent of polymerization on polymethyl methacrylate at various reaction times (in hours) is shown in Fig. 1.

As may be seen in the figure, an induction period was observed in the course of the polymerization of methyl methacrylate. While the surfactant was added to this system, the induction period was not observed (Curve A in the figure) and the reaction rate was accelerated remarkably. The highest yield in the polymerization reactions was 83% in the presence of the surfactant. It was noticed that, in the absence of the surfactant, the polymerization rate was slow (Curve B in the figure). It is recognized also that the intrinsic viscosity of the final product of polymethylmethacrylate was affected by the addition of the surfactant; when the surfactant was added to the polymerization system, the value of 2.75 was obtained for the intrinsic viscosity

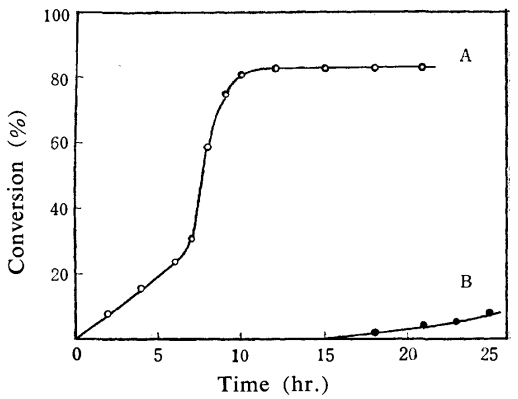

Fig. 1. Process of the polymerization of methyl methacrylate.

determined in benzene at 25°C, whereas it was 9.05 when the surfactant was not added.

Several results obtained for the other monomers are listed in Table I. Generally speaking, it appeared that the use of a surfactant yielded the higher conversion.

TABLE I. POLYMERIZATION* OF VINYL MONOMER BY COBALT CYANIDE COMPLEX POLYMERIZATION CONDITION

Vinyl monomers	Surfactant[a] wt. %	Time hr.	Conversion hr.	Intrinsic viscosity
Methyl methacrylate	1	10	83	2.75[b]
	0	24	12	7.05[b]
Styrene	1	30	90	1.75[b]
Acrylonitril	1	48	25	0.89[c]
Butadiene	1	48	13	—

a) Tween 80 was used as a surfactant.
b) Determined in benzene solution at 25°C.
c) Determined in dimethylformamide solution at 25°C.
* 5 ml. of monomer was polymerized with 5 ml. of cobalt cyanide complex solution (1×10^{-2} ml./l.) as a catalyst under 1 atm. pressure of hydrogen atmosphere at 25°C.

The polymerization rate and yield were depressed when nitrogen gas was used instead of hydrogen gas. When molecular oxygen was present in the reaction systems, the polymerization of these monomers did not occur at all.

From these results, it is deduced that the cobalt cyanide complex-hydrogen system posseses an activity as a polymerization catalyst.

Further details of such catalytic effects of the complex will be published elsewhere.

The author is especially indebted to Professor Masatami Takeda, Professor Masaakira Iguchi and Mr. Kazuyoshi Iimura for their kind and helpful suggestions in this work. Partial support by the Yawata Chemical Industry Co., Ltd., is also gratefully acknowledged.

Department of Chemistry
Tokyo College of Science
Kagurazaka, Shinjuku-ku
Tokyo

The Absolute Configuration of Nupharamine

By Ichiro KAWASAKI, Shigeru MATSUTANI and Takeo KANEKO

(Received February 15, 1963)

The chlorination and subsequent dehydrochlorination of nupharamine (I)[1-3] gave olefins, which were separated into two isomers of anhydronupharamine, IIA and IIB, by alumina chromatography. IIA showed an infrared absorption at 880 cm^{-1} identified as an endomethylene group. The hydroboration-oxidation of IIA gave isonupharamine (III) (perchlorate m. p., 164~166°C ; Found: C, 51.35 ; H, 7.47 ; Cl, 10.07%). III was converted by chlorination and subsequent cyclization to quinolizidine derivatives, which were separated into two diastereoisomers, IVA and IVB, by alumina chromatography. The infrared spectrum of the isomer, IVA (eluted by 10% ether in petroleum ether, $[\alpha]_D$ −76.8°) was identical with that of natural l-deoxynupharidine[4], while the infrared spectrum of the other isomer, IVB (eluted by 15% ether in petroleum ether), was identical with that of rac-7-epi-deoxynupharidine[5]. Therefore, the absolute configuration of nupharamine should be represented by Formula I.

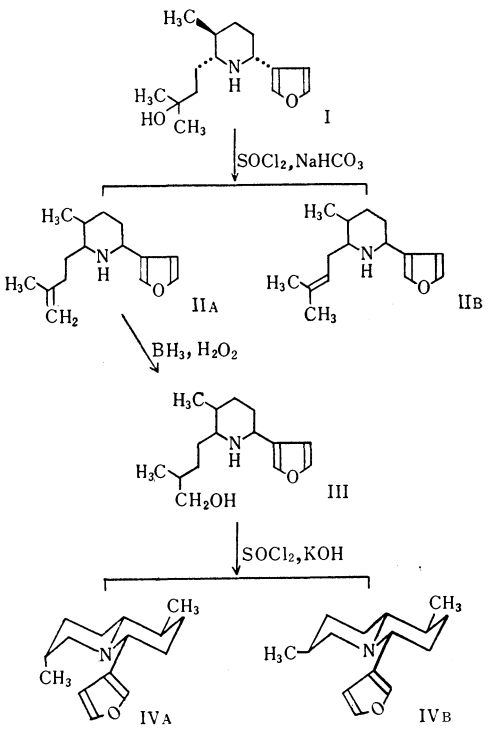

Department of Chemistry
Faculty of Science
Osaka University
Nakanoshima, Osaka

1) Y. Arata and T. Ohashi, *J. Pharmac. Soc. Japan*, **77**, 792 (1957).
2) T. Ohashi, ibid., **79**, 729, 734 (1959).
3) M. Kotake, I. Kawasaki, S. Matsutani, S. Kusumoto and T. Kaneko, *J. Chem. Soc. Japan, Pure Chem. Sec.* (*Nippon Kagaku Zasshi*), **84**, 169 (1963).
4) M. Kotake, I. Kawasaki, T. Okamoto, S. Matsutani, S. Kusumoto and T. Kaneko, This Bulletin, **35**, 1335 (1962).
5) F. Bohlmann, E. Winterfeld, P. Studt, H. Laurent, G. Boroshewoki and K-M. Kleine, *Chem. Ber.*, **94**, 3151 (1961).

*The Activation Energy of Bromine Absorption by Carbonaceous Materials**

By Takashi MUKAIBO and Yoichi TAKAHASHI

(Received September 20, 1962)

The object of the present work, which forms a part of the investigation of the transfer of substances in and through carbonaceous materials, is to study the rate of absorption of bromine by carbonaceous materials, especially its temperature dependence.

It is well known that graphite absorbs several substances such as bromine or metal halides, forming so-called lamellar compounds[1]. The rate of the absorption is known to be rather rapid. It has been reported that, in the case of bromine absorption, equilibrium was established within several hours, even at room temperature[2]. As the absorption by carbonaceous materials contains a process by which the reactant molecules are taken up into the crystal structure of graphite, these experimental results suggest that the reactant molecules may diffuse or move rather easily through graphite layers in the lamellar compounds. Thus, a study of the rate of absorption (viz., the rate of the formation of lamellar compounds) will give useful information on the behavior of the reactant molecules in the lamellar compounds.

Preliminary experiments on this subject which have been reported on previously[3] show that the fractional absorption, plotted against the square root of time, gives a characteristic S-form, and that the rate and the saturation concentration of the absorbed bromine depend strongly upon the degree of graphitization of the materials. All the experiments were carried out at 0°C.

In the present paper, a study of the temperature dependence of the rate and the apparent energies of activation of the reactions at temperatures ranging from 0 to 50°C is described. The results and their relationship to the degree of graphitization of the carbonaceous materials are discussed.

Experimental

In the process of determining the apparent energy of the activation of the bromine absorption by carbonaceous materials, there are several problems to be considered.

The first of them is how to estimate the relative rate of the reaction from the absorption curve at different temperatures. As has been discussed previously[3], the bromine absorption is supposed to be the formation of a solid solution, and the saturation concentration of the absorbed bromine varies by changing such conditions as the temperature or the vapor pressure of bromine. In this case, the relative absorption rate could not be determined so simply. It was shown[3], however, that the bromine absorption curves of almost all samples, which were drawn by plotting the measured fractional absorption against the square root of the time, fell into a single curve by merely adjusting the time scale. The adjustment was done by multipling the time scale by a suitable factor.

The inverse of the multipling factor is considered to give the relative absorption rate. In practical estimations, any of the measured points of fractional absorption may be used for the adjustment of the time scale. For the present study, the fractional absorption of 0.3 was found to be most suitable for the estimation. The reason for this choice will be discussed later.

The second problem was the variation of the saturation concentration of bromine with the reaction conditions. It was desirable to carry out the absorption experiments while the saturation concentration of bromine in carbon samples were kept constant, even at different temperatures, because a difference in the saturation concentrations might affect the rate of absorption. It was expected from a previous work by Hennig[4] that this condition would be satisfied by keeping the vapor pressure of bromine saturated throughout the experiment.

In the course of experiments, however, the saturation concentration of absorbed bromine in carbonaceous materials was found to decrease with an increase in the temperature, even when the vapor pressure of bromine was kept saturated.

Thus, the Arrhenius plot might require some modification on this temperature dependence of the saturation concentration. In spite of this supposition, the Arrhenius plots obtained by the present experiments showed rather good linearities in all samples without any correction or modification of data. Therefore, the values of the apparent

* Presented at the 14th Annual Meeting of the Chemical Society of Japan, Tokyo, April, 1961.

1) G. R. Hennig, "Progress in Inorganic Chemistry", Vol. I, Interscience Pub., New York (1959), p. 125.

2) W. Rüdorff, *Z. anorg. u. allgem. Chem.*, **245**, 383 (1941).

3) T. Mukaibo and Y. Takahashi, *J. Chem. Soc. Japan, Ind. Chem. Sec.* (*Kogyo Kagaku Zasshi*), **65**, 754 (1962).

4) G. R. Hennig, "Progress in Inorganic Chemistry", Vol. I, Interscience Pub., New York (1959), p. 159.

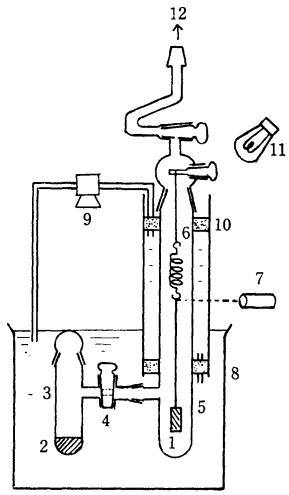

Fig. 1. Apparatus for the measurement of the rate of bromine absorption.
1. Specimen of carbonaceous materials
2. Liquid bromine
3. Bromine container
4. Stop cock
5. Reaction tube
6. Quartz spring balance
7. Running microscope
8. Water bath
9. Stroke pump
10. Cork
11. Infrared heater
12. To vacuum line

energy of activation obtained below were estimated by the conventional method mentioned above.

Apparatus.—The apparatus is shown in Fig. 1. The rate of absorption of bromine was measured by means of a quartz spring balance. The reaction tube and the bromine container were kept at the same temperature, thus keeping the vapor pressure of bromine saturated at the reaction temperature. To avoid the condensation of bromine on the walls of the reaction tube or on the spring balance, the upper part of the reaction tube above the surface of the water bath was kept at the same temperature as the reaction part by circulating the water of the bath. The top of the tube was warmed by an infrared lamp for the same reason.

Nevertheless, a small quantity of bromine condensation on the specimen or on the spring balance was inevitable at the last period of a run lasting for a few hours. A little experimental error was supposed to be caused by the condensed bromine in the measurement of the last stage of absorption and of the saturation concentration of the bromine. This experimental error, however, was estimated to be negligible in calculating the activation energies, as will be described later.

Materials. — The samples of carbonaceous materials were supplied by the Nippon Carbon K. K. The carbon source, the temperature of heat treatment, the density, and the porosity of samples are listed in Table I.

The specimen for each run was cut into a plate, $30\times10\times1$ mm. in size, and weighed.

GR grade bromine was redistilled and passed over through concentrated sulfuric acid before use.

Procedure.—Redistilled bromine was introduced into the evacuated bromine container in a separate vacuum line. After closing the stop cock (shown in Fig. 1) to prevent contamination by the air, the container was removed from the vacuum line and was set to the reaction tube. After keeping both of them in a water bath for a while, a specimen was suspended by a quartz spring balance in the reaction tube. Then the tube was evacuated to 10^{-3} mmHg by a diffusion pump.

The reaction was started by opening the stop cock. The weight gain of the specimen by the absorption of bromine was measured with a running microscope, following the elongation of the spring balance. The sensitivity of the reading was about 0.5 mg. wt. change per division.

The temperature of the water bath was kept constant within ±0.1°C of the setting temperature.

Results

The Saturation Concentration of Absorbed Bromine.—It was found that the saturation concentration, C_s, of absorbed bromine by carbonaceous materials under the saturated vapor pressure of bromine had a tendency to decrease with an increase in the temperature. The findings are shown in Fig. 2, in which $C_s(T)$ values at different temperatures are presented as the ratio to $C_s(0)$ at 0°C. These results showed a definite tendency for C_s to decrease with an increase in the temperature, although there were a few deviations from a monotonic curve. These deviations might be caused by bromine condensation on the specimen or on the spring balance, or by some inconstancy of the reaction temperature. Even a small defference in temperature between the specimen and the bromine container was found to cause rather a large deviation.

TABLE I. CHARACTERISTICS OF THE SAMPLES OF CARBONACEOUS MATERIALS

Sample	Carbon source	Temp. of heat treatment, °C	Apparent density	True density	Porosity %
1—4	Oil cokes	2000	1.64	2.109	22.6
1—6	Oil cokes	2660	1.67	2.163	23.8
5	Oil cokes	2660	1.56_5	2.174	28.0
8	Natural graphite	2660	1.78	2.216	19.6

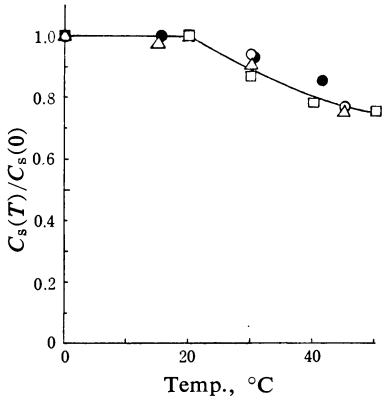

Fig. 2. Temperature dependence of bromine saturation concentration, under the saturated vapor pressure of bromine.
-○- Sample 1—4 -△- Sample 1—5
-●- Sample 5 -□- Sample 8

The Rate of Bromine Absorption and its Temperature Dependence. — The absorption rate curves obtained by one of the samples are shown in Fig. 3, plotting the fractional absorption against the square root of the time. In order to determine the relative absorption rate, the fractional absorption of 0.3 was chosen as a standard in finding out the multipling factor for the adjustment of the time scale. The value of 0.3 was chosen because the experimental error caused by bromine condensation, mentioned earlier, was supposed to be relatively small at the beginning of the absorption, and because the time corresponding to the standard fractional absorption was supposed to be determined most accurately in this region according to the shape of the absorption curve.

Using the multipling factor for adjustment

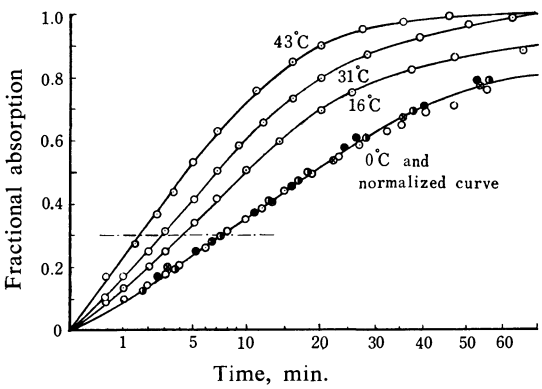

Fig. 3. The rate of bromine absorption by sample 5 and the normalized plots.
On the normalized curve: ○ 0°C, ◑ 16°C, ● 31°C, ⊗ 43°C

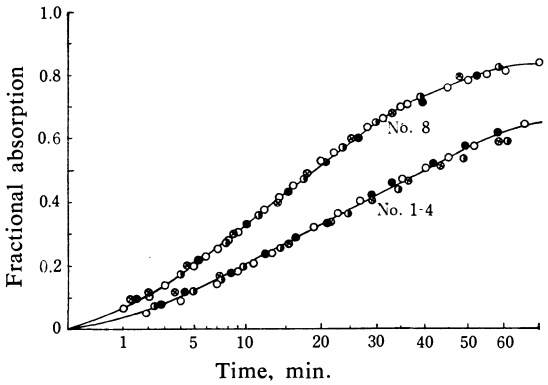

Fig. 4. The normalized rate curves of bromine absorption.
Sample 8 ; ○ 0°C ◑ 20°C
● 30°C ⊗ 40°C
Sample 1-4 ; ○ 0°C ◑ 15°C
● 30°C ⊗ 45°C

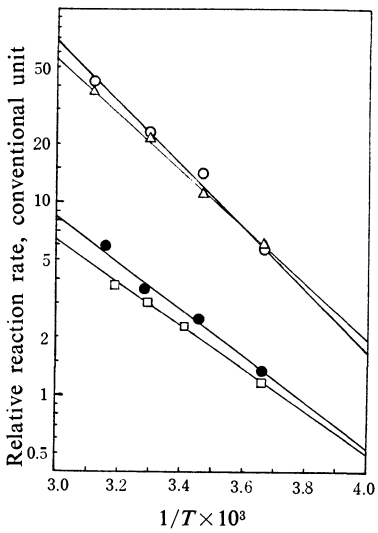

Fig. 5. Arrhenius plots of the rate of bromine absorption by carbonaceous materials.
-○- Sample 1—4
-△- Sample 1—6
-●- Sample 5
-□- Sample 8

thus obtained, the plots normalized to the curve obtained at 0°C are shown in Fig. 3, and in Fig. 4 for other samples. These plots fell into one line, as expected, indicating that the above-mentioned procedure was acceptable.

The relative rate of bromine absorption at different temperatures was the inverse of the multipling factor of each run. From the Arrhenius plotting in Fig. 5, the apparent energies of activation were calculated; they are shown in Table II.

TABLE II. APPARENT ENERGIES OF ACTIVATION OF THE BROMINE ABSORPTION BY CARBONACEOUS MATERIALS

Sample	Apparent energy of activation kcal./mol.
1—4	7.4_5
1—6	6.7
5	5.5_5
8	5.1

Discussion

The Temperature Dependence of the Saturation Concentration of Absorbed Bromine in Carbonaceous Materials. — The fact that the C_s value of bromine in carbonaceous materials under the saturated vapor pressure of bromine decreases with an increase in the temperature has not yet hitherto been reported. Juza[5] predicted that this tendency to decrease might occur on the analogy of the decrease in the reactivity of chlorine gas to carbonaceous materials with an increase in the temperature. The saturation content of chlorine was found to decrease markedly at the temperature 100°C above the melting point of chlorine.

The present results show, however, that the decrease in the saturation concentration of bromine occurs gradually, even at temperatures as low as 30°C, which is only 37.3°C higher than the melting point of bromine.

At the present stage, the data are not numerous enough to enable us to discuss further the significance of the tendency to decrease. A more precise investigation of this problem is now being carried out, however, and will be reported on later.

The Activation Energies and their Relation to the Degree of Graphitization of Carbonaceous Materials.—The Arrhenius plots of the rate of bromine absorption gave good linearities for all samples, indicating that the rate of absorption was not very much affected by a small difference in the saturation concentration of bromine in the lamellar compounds. This fact may support the view that the bromine absorption is a kind of formation of a solid solution.

From the results presented in Table II, the apparent energies of activation are supposed to be dependent upon the degree of graphitization of the carbonaceous materials. To make this clear, the values of the true density of the samples were taken as the measure of the degree of graphitization. The results of X-ray diffraction measurement were not used for this purpose, because the samples were mixed with some binding materials in the course of production. The relation between the activation energies and the values of the true density of the samples is shown in Fig. 6. The plots show clearly that the apparent energies of activation decrease with an increase in the degree of graphitization.

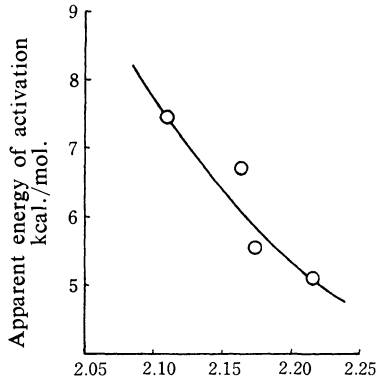

Fig. 6. Relation between the apparent energy of activation and the true density of carbonaceous materials.

The results indicate that the bromine absorption, followed by the diffusion or migration of absorbed bromine into the interior of graphite crystals, proceeds more easily with an increase in the degree of graphitization of the samples. This means that, with the growth of the net plane of graphite crystals, the movements of the molecules intercalated between the net planes of graphite crystals became easier.

Iwata et al.[6], in calculating the activation energy for the migration of Xe in the interlamellar positions of graphite crystal, have obtained the value of 0.69 kcal./mol. It should be noted that the self-energy of Xe interstitial atoms in graphite was also calculated to be 347 kcal./mol., in contrast to the small value of the migration energy. In the case of the bromine absorption, as bromine molecules have some interactions and are stabilized energetically in the lamellar compounds, the uptake of bromine molecules proceeds very easily. On the other hand, the activation energy for the migration of bromine molecules seems to be rather higher in comparison with that of inert Xe molecules. The present finding, the activation energy of 5～7 kcal./mol. for bromine absorption, revealed, however, that the migration of bromine molecules also proceeds very easily, even at room temperatures.

5) R. Juza and A. Schmeckenbecher, *Z. anorg. u. allgem. Chem.*, **292**, 16 (1957).

6) T. Iwata, F. E. Fujita and H. Suzuki, *J. Phys. Soc. Japan*, **16**, 197 (1961).

Summary

In the present paper, the temperature dependence of the rate of bromine absorption by the carbonaceous materials has been studied. The apparent energies of activation of the reaction have been found to be 5～7 kcal./mol. and had a dependence upon the degree of graphitization of carbonaceous materials. The value of the activation energy became smaller with an increase in the degree of graphitization. The results indicate that the mobilities of reactant molecules of the interlamellar compounds increase with the growth of the net plane of graphite crystals.

The saturation concentration of bromine in carbonaceous materials, under a saturated vapor pressure of bromine, was found to decrease with an increase in the temperature at temperatures above 30°C.

The authors wish to express their gratitude to Nippon Carbon K. K., which kindly provided them with the carbon samples. The authors are also indebted to Miss Chiyoko Tanabe for her assistance in the experiments.

Department of Industrial Chemistry
Faculty of Engineering
The University of Tokyo
Hongo, Tokyo

*On the Permeation of Iodine through Graphite**

By Takashi MUKAIBO and Yoichi TAKAHASHI

(Received March 7, 1963)

Gas permeation through artificial graphite can occur, because of its porous nature, via three paths: through the pore volumes, along pore surfaces, and through the graphite structure. The relative importance of these paths depends on the pore structure of the graphite bodies and on the chemical nature of the diffusing substances.

We have previously reported on the permeation of inert gases through graphite[1] and also on the absorption of bromine to carbonaceous materials[2]; each report was concerned with a limiting case of the gas permeation processes through graphite.

In the present paper, the behavior of iodine permeating through graphite is discussed. It is known that iodine is non-reactive with graphite at any temperature and that it does not form a lamellar compound[3], in contrast to the well-known case of bromine.

Nevertheless, iodine possibly has some such weak interaction with graphite as chemisorption[4], and it is expected to show some interesting behavior upon its permeation through graphite because of its condensable character. Moreover, as one of the main fission products of uranium, the behavior of iodine in graphite neutron moderators has attracted recent attention[5,6].

The purpose of the present paper is to discuss the character of the iodine diffusion through graphite at temperatures ranging from 90 to 160°C on the basis of its dependence on temperature and pressure. The effect of the presence of inert gas on the rate of iodine permeation is also investigated.

Experimental

Preparation of the Graphite Specimens.—Samples of graphite were cut to disks, 3 mm. thick and 15 mm. in diameter, which had a ring-shaped depression on one side. As is shown in Fig. 1, glass tubes were cemented to the graphite specimens with silver chloride. The procedure of the cementing was as follows: The surface of the depression on the graphite specimens was electroplated with silver, using the electrolyte of a silver cyanide aqueous solution with which the depresssion was filled. After being washed and dried thoroughly, silver chloride powder was mounted on the electroplated silver and heated indirectly and slowly, until it melted. Then, a moderately preheated glass tube was immersed in the melt and cooled very slowly.

The glass-to-graphite seal was verified to be leak-proof by preliminary experiments, in which the values of the air permeability of the same graphite

* Presented at the 15th Annual Meeting of the Chemical Society of Japan, Kyoto, April, 1962.

1) T. Mukaibo and Y. Takahashi, *J. Chem. Soc. Japan, Ind. Chem. Sec.* (*Kogyo Kagaku Zasshi*), **64**, 835 (1961).

2) T. Mukaibo and Y. Takahashi, ibid., **65**, 754 (1962); This Bulletin, **36**, 625 (1963).

3) G. R. Hennig, "Progress in Iorganic Chemistry", Vol. 1, Interscience Publishers, New York (1959), p. 187.

4) P. Connor, J. B. Lewis and W. J. Thomas, "Proceedings of the 5th Conference on Carbon", Vol. 1, Pergamon, New York (1962), p. 120.

5) S. Yajima, S. Ichiba, Y. Kamemoto and K. Shiba, This Bulletin, **34**, 493 (1962).

6) L. B. Doyle, NAA-SR-255 (1953).

TABLE I. CHARACTERISTICS OF THE GRAPHITE SAMPLES AND A COMPARISON OF THE FLOW RATES FOR AIR AND IODINE

Graphite sample	Characteristics of the sample: Apparent density g./cm³	Porosity %	Permeability at stand. condition K, cm²/sec.	Flow rate (NTP. cc./sec.): Air Q_{air}	Iodine Q_{I_2}	Ratio $\frac{Q_{air}}{Q_{I_2}}$
A	1.49	32.2	6.5×10^{-1}	4.35×10^{-2}	1.57×10^{-2}	2.77
$B_{\parallel}$*	1.78	19.6	1.5×10^{-1}	1.17×10^{-1}	3.34×10^{-2}	2.85
$B_{\perp}$*	1.78	19.6	8.4×10^{-2}	4.75×10^{-2}	1.77×10^{-2}	2.68
D**	1.82	11.8	3.2×10^{-3}	7.5×10^{-4}	$(\sim2\times10^{-4})$†	(~3.5)†

* The subscripts ∥ and ⊥ designate directions of the flow parallel and perpendicular, respectively, to the plane pressed on molding.
** This sample was doubly impregnated.
† This value includes an experimental error of ±50% because of the difficulties of measuring the flow rate of such a small order.

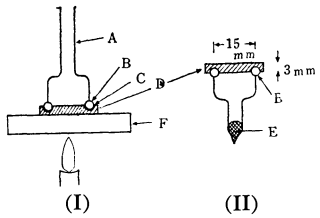

Fig. 1. The sample capsule. The preparation of the glass-to-graphite seal (I) and the complete form of the capsule (II).
A : Glass tube
B : AgCl binder
C : Electroplated silver
D : Graphite specimen
E : Iodine
F : Graphite plate for indirect heating

specimen were compared between two cases with different seals, silver chloride and Araldite†. The results of the two cases agreed very well*.

Measurement of the Rate of Iodine Permeation.—About 1 g. of GR-grade iodine was sealed in a glass tube fitted to the graphite specimen. The capsule thus prepared (as shown in Fig. 2) was suspended by a quartz-spring balance in a reaction tube. The reaction tube was evacuated for about one hour, until the air in the capsule had also been evacuated through the graphite specimen.

The capsule was then heated in vacuo or in argon flow, and the rate of the weight loss of the capsule, which was caused by the iodine permeation through the graphite specimen, was measured at controlled temperatures. The whole apparatus is shown in Fig. 2.

The air permeability of each specimen was also measured by the method described in a previous report[2].

Samples.—Graphite samples were ordinary artificial graphite and high-density nuclear graphite,

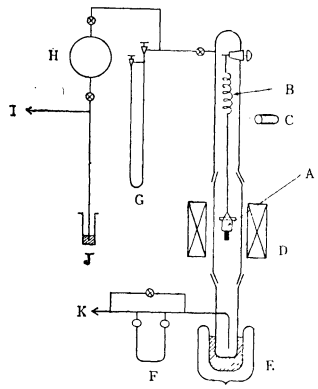

Fig. 2. Apparatus for iodine permeation experiments.
A : Sample capsule
B : Quartz-spring balance
C : Running microscope
D : Electric furnace
E : Dewer vessel
F : Flow meter
G : Manometer
H : Gas reservior
I : To argon bomb
J : Manostat
K : To vacuum line

produced by the Nippon Carbon K. K. and the Tokai Denkyoku Seizo K. K.*

The characteristics of the samples are listed in Table I.

Results and Discussion

Iodine Permeation into a Vacuum.—The rate of iodine permeation was determined from the gradient of a plot of the weight change of the sample capsule vs. time. The plots were found to be linear in a steady state for every run of the experiments.

The results are summarized in Fig. 3, which

† Epoxy resin produced by Ciba, Ltd.

* Typical results of the preliminary experiments were as follows:

Graphite sample	Air permeability, cm²/sec. AgCl seal	Araldite seal
A	1.93	1.88
B	3.51×10^{-2}	3.52×10^{-2}

* The authors wish to express their gratitude to the Nippon Carbon K. K, and the Tokai Denkyoku Seizo K. K. for kindly providing us with the samples.

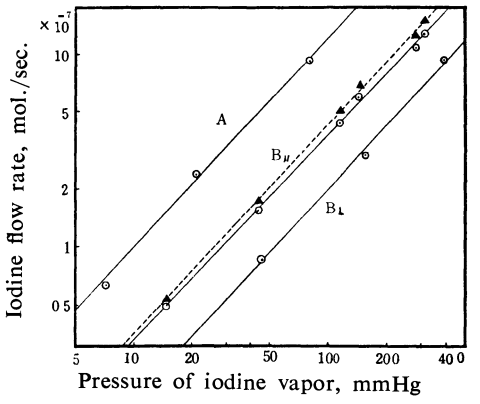

Fig. 3. Iodine flow rate as a function of the pressure of iodine vapor in log-log plot. The broken line is modified with respect to temperatures.
A, $B_{\parallel}$ and $B_{\perp}$ designate the graphite sample, characteristics of which are listed in Table I.

is a log-log plot of the rate of iodine permeation and the pressure of iodine vapor, which was equilibrated with solid or liquid iodine at each temperature of the experiments. The gradients of the plots in Fig. 3 have the same value, 1.06, for all samples. Accordingly, it was concluded that the rate of iodine permeation increased roughly proportionally to the pressure of iodine vapor at pressures lower than 400 mmHg.

It is natural to suppose, as a first appoximation, that the iodine permeation through graphite consists mainly of gas flow through the pore volumes of the media. When a single gas flows isothermally and in a steady state through the pore volumes of the media, the flow is usually considered to consist of two types, namely viscous and Knudsen flows; at any rate, it is known that it can be expressed by the following equation[1]:

$$q_m P_m = vRT = \frac{A}{L}(B_o P_m + K_o)\Delta P \qquad (1)$$

In Eq. 1, the viscous flow rate is expressed by the first term, characterized with the coefficient B_o, and the Knudsen flow by the second term, involving the coefficient K_o. q_m means the volume flow rate, cm³/sec., at a pressure of P_m, and v means the molar flow rate, mol./sec., A and L are the cross-section and the thickness of the specimen respectively.

For the present experiments, where the flowing gas consisted of the iodine gas only, P_m and ΔP in Eq. 1 were replaced by $P_{I_2}/2$ and P_{I_2} respectively. Thereby Eq. 1 becomes:

$$v = \frac{1}{RT} \cdot \frac{A}{L}\left(\frac{1}{2} B_o P_{I_2} + K_o\right) P_{I_2} \qquad (2)$$

Two limiting cases are derived from Eq. 2, pure viscous flow and pure Knudsen flow. In the case of the pure viscous flow, at a definite temperature, v increases with $(P_{I_2})^2$. On the contrary, v increases with P_{I_2} for the pure Knudsen flow.

The experimental resuls of Fig. 3, showing that v increased almost linearly with P_{I_2}, lead to the plausible conclusion that, for the iodine permeation through graphite, the Knudsen flow is predominant. This conclusion was further examined by considering the temperature dependence of the flow rate in Eq. 2. As the coefficient, K_o, for the Knudsen flow is also proportional to the spuare root of T, the values of v, which were measured at different temperatures, ought to be normalized as follows:

$$v_o = v\left(\frac{T}{T_o}\right)^{1/2} \qquad (3)$$

where v_o is the normalized molar flow rate at the temperature of T_o.

The re-plot of v_o normalized at $T_o = 300°K$ is presented in Fig. 3 as a broken line, which gives the gradient of 1.09. This result revealed that the conclusion mentioned above was appropriate.

The Knudsen model for iodine permeation was also supported by the comparison of the flow rates for air and iodine. The obtained values of the flow rates, which are normalized to the same condition of temperature and pressure for both air and iodine, are tabulated in Table I. It was also confirmed experimentally that the air flow at the normalized condition consisted mainly of the Knudsen flow.

Provided that the flows of both air and iodine are those of the Knudsen type, the ratio of the flow rates, (Q_{air}/Q_{I_2}), ought to be equal to the square root of (M_{I_2}/M_{air}), namely, 2.96 (where M means the molecular weight of the gases). The experimental values obtained were 2.68~2.85. The values of theory and experiments agree fairly well. The small discrepancies are possibly due to the small contributions of the viscous part to the total flow, since the mean free path of air is about 1.5 times longer than that of iodine at the same pressure and so the contribution of the viscous part of the air flow is probably smaller than that of the iodine flow.

Iodine Permeation in Argon Gas.—The rate of iodine permeation was measured also in an argon gas flow of controlled pressure in order to clarify the effects of inert gases on the behavior of gas permeation through porous media such as graphite. The apparatus used and the method of measurements were just the same as above, except that argon gas

streamed at the mean flow rate of 1 cm./sec. in the reaction tube shown in Fig. 2.

It was found that the rate of iodine permeation was depressed markedly in the stream of argon gas. As is clear from Fig. 4, in which a plot of $1/v$ vs. mean gas pressure ($P_{I_2}/2 + P_{Ar}$) is presented, even at the mean pressure of the Knudsen diffusion region (at pressure below 400 mmHg), the rate of iodine permeation decreased with an increase in argon gas pressure. This fact seems to be rather curious, because in the Knudsen region the flow rate of one species might not be affected by the presence of the other species.

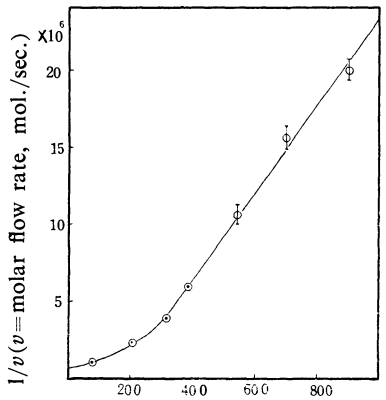

Fig. 4. The dependence of iodine flow rate on the pressure of argon gas.

It has been reported by Korsmeyer[7] and Evans et al.[8], however, that the same phenomena as have been described above were observed in the measurement of the counter-current mutual permeation of helium and argon through graphite septum. They pointed out that, for the gas flow through porous media such as graphite, even at the pressure of the Knudsen region, a pure Knudsen flow is not realized and that the mutual diffusion effect must be taken into account. The Knudsen coefficient, K_o, in Eqs. 1 and 2 is, therefore, replaced by a total diffusion coefficient, $(K_1)_{eff}$, and is represented by the Bosanquet type of an equation[9] as follows:

$$(K_1)_{eff}^{-1} = (D_{12})_{eff}^{-1} + K_o^{-1} \qquad (4)$$

where $(D_{12})_{eff}$ is the effective mutual diffusion coefficient proportional to D_{12}, the usual diffusion coefficient of the gases. The constant of proportionality is charcteristic of the internal geometry of the porous medium. Evans et al.[8] have theoretically derived just the same formula as Eq. 4, applying the "dusty gas model" for the diffusion of gases in porous media.

Since D_{12} in Eq. 4 is roughly inversely proportional to the mean pressure of gases, the relationship of $1/v$ vs. P_m obtained in the present study (as shown in Fig. 4), especially at the linear part of the figure, is explained reasonably by this model. The reason for the discrepancy in the lower pressure region is not clear, but it is likely that this is due to the character of the flow in this region, which is supposed to be intermediate between the capillary model and the "dusty gas model".

Summary

The rate of iodine permeation through graphite has been studied and the following results were obtained:

(1) The process of iodine permeation through graphite has been found to consist mainly of a simple gas flow through the pore volumes, just as in the case of inert gases. The chemical interaction between iodine and graphite has been observed to be negligibly small.

(2) At tempeatures ranging from 90 to 160°C, and under a corresponding pressure of iodine vapor below 400 mmHg the rate of iodine permeation has been observed to be almost linearly proportional to the pressure of iodine. It has been concluded that the Knudsen flow was the predominant element of the total flow.

(3) The ratio of the flow rates for air and iodine, which were interpolated to the value under the same conditions, has been calculated to be 2.68~2.85, close to the value 2.96, namely $(M_{I_2}/M_{air})^{1/2}$, as was expected from the Knudsen flow model.

(4) The rate of iodine permeation has been observed to decrease in the presence of argon gas, even in the region of Knudsen flow. It has been found that the rate is roughly inversely proportional to the pressure of argon gas. The "dusty gas model" discussed by Evans et al. has been adapted to give a reasonable explanation of this phenomena.

The authors are indebted to Mr. O. Lee for help in a part of the measurements.

Department of Industrial Chemistry
Faculty of Engineering
The University of Tokyo
Hongo, Tokyo

7) R. B. Korsmeyer, ORNL-61-3-75 (1961).
8) R. B. Evans, III, G. M. Watson and E. A. Mason, *J. Chem. Phys.*, **35**, 2076 (1961); ibid., **36**, 1894 (1962).
9) W. G. Pollard and R. D. Present, *Phys. Rev.*, **73**, 762 (1948).

The Synthesis of Azuleno[2, 1-b]pyridine Derivatives

By Tetsuo NOZOE and Katsuo KIKUCHI*

(Received November 8, 1962)

Among the azulenes fused with heterocyclic rings, azuleno[6, 5-b]furans (furo[3, 2-f]azulenes)[1], azuleno[6, 5-b]pyrroles (pyrrolo[3, 2-f]-azulenes)[1], azuleno[2, 1-b]thiophenes (thieno-[3, 2-a]azulenes)[2] and azuleno[6, 5-c]pyrazoles (pyrazolo[4, 3-f]azulenes)[3] have already been synthesized. The present writers have synthesized azuleno[2, 1-b]pyridines (pyrido[3, 2-a]-azulenes) by the application of Friedeländer's method to 2-amino-1-formylazulene (I) and its acetate (II); their results have been described briefly elsewhere[4]. In the present paper we wish to report those results in some detail.

Treatment of 2-acetamidoazulene[5] in dimethylformamide with one equivalent of phosphorus oxychloride gave an immonium salt which, without purification, was then treated with aqueous sodium carbonate to afforded 2-acetamido-1-formylazulene (II) and a small amount of 2-acetamido-1, 3-diformylazulene (III). Hydrolysis of II with alcoholic sodium hydroxide afforded 2-amino-1-formylazulene (I). Similar treatment of III afforded 2-amino-1, 3-diformylazulene (IV).

The heating of compound I with acetylacetone in the presence of a small amount of piperidine gave dark greenish brown feathery crystals (V) in about a 50% yield. V easily afforded several kinds of complexes such as hydrochloride, trinitrobenzene complex and picrate, and it gave an oxime. V also showed positive iodoform reaction. The infrared spectrum of V in Nujol showed absorption at 1665 cm^{-1} (conjugated carbonyl). These facts reveal that compound V is 3-acetyl-2-methylazuleno-[2, 1-b]pyridine, as was expected.

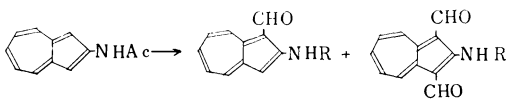

I: R=H III: R=$COCH_3$
II: R=$COCH_3$ IV: R=H

A similar treatment of I with ethyl acetoacetate gave ethyl 2-methylazuleno[2, 1-b]pyridine-3-carboxylate (VI) and I with diethyl acetonedicarboxylate gave ethyl 3-ethoxycarbonylazuleno[2, 1-b]pyridine-2-acetate (VII). The compounds V, VI and VII have quite similar absorptions in the ultraviolet region (Fig. 1).

Prolonged heating of acetate II with diethyl malonate in the presence of piperidine at 50~60°C gave dark brown needles (VIII) in a 50% yield, instead of the expected 2-acetamido-1-(β, β-diethoxycarbonyl)azulene being isolated. The ultraviolet spectrum of VIII is shown in Fig. 2. Judging from the analysis of VIII and the following experimental facts, VIII is thought to be ethyl 1, 2-dihydro-2-oxoazuleno[2, 1-b]-pyridine-3-carboxylate. Compound VIII was not affected by aqueous sodium carbonate, but it gives a brown sodium salt with aqueous sodium hydroxide from which the original substance was regenerated with acetic acid. The prolonged heating of VIII with aqueous sodium hydroxide afforded the acid IX.

When heated with phosphorus oxychloride, VIII was converted to ethyl 2-chloroazuleno-[2, 1-b]pyridine-3-carboxylate (X). The heating of X with sodium methoxide or with sodium ethoxide afforded a 2-methoxy compound XI,

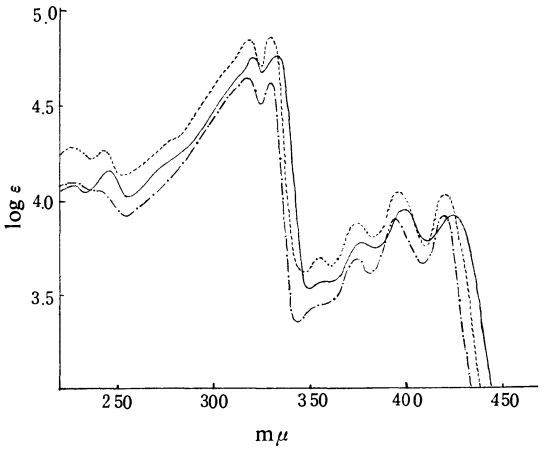

Fig. 1. The ultraviolet spectra of V (——), VI (----) and VII (—·—·) in methanol.

* Present address: Department of Chemistry, Faculty of Liberal Arts and Science, Yamagata University, Yamagata.

1) T. Nozoe, S. Seto and S. Matsumura, *Chem & Ind.*, **1961**, 1715.

2) K. Matsui and T. Nozoe, ibid., **1960**, 1302; K, Matsui, *J. Chem. Soc. Japan, Pure Chem. Sec.* (*Nippon Kagaku Zasshi*), **82**, 1517, 1520, 1522, 1665, 1667 (1961).

3) T. Nozoe, K. Takase and M. Tada, to be published.

4) T. Nozoe and K. Kikuchi, *Chem. & Ind.*, **1962**, 358.

5) T. Nozoe, S. Matsumura, Y. Murase and S. Seto, ibid., **1955**, 1257,

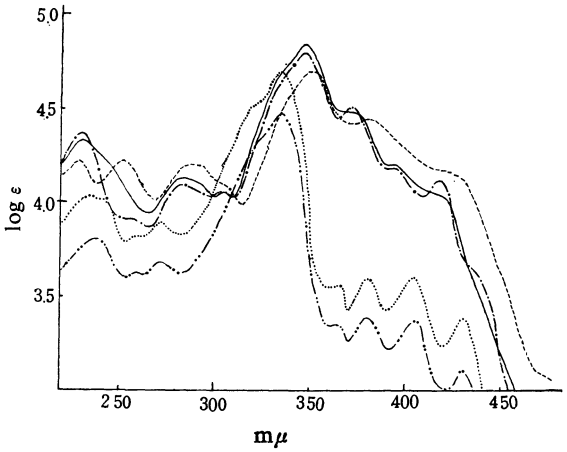

Fig. 2. The ultraviolet spectra of VIII (——), XV (----), XVI (—·—·), XI (·····, log ε−0.2) and XII (—··—, log ε−0.4) in methanol.

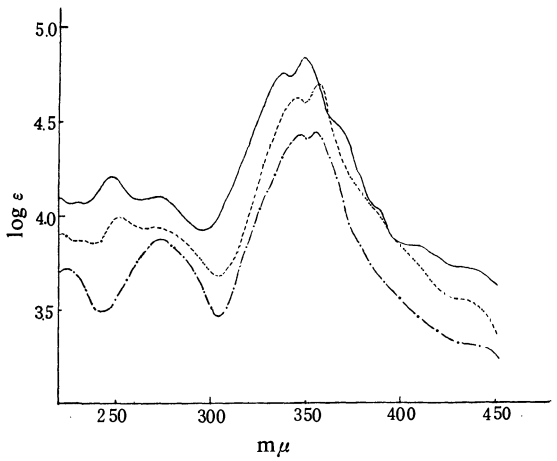

Fig. 3. The ultraviolet spectra of XVII (——), XIII (----, log ε−0.2) and XIV (—·—·, log ε−0.4) in methanol.

or a 2-ethoxy compound XII, respectively. The ultraviolet absorption curves of XI and XII (Fig. 2) are markedly different from that of VIII but rather similar to these of V, VI and VII. The infrared spectrum of VIII in Nujol exhibits a band at 1630 cm^{-1} (pyridone carbonyl) which is absent in those of compounds XI and XII. These fact indicate that compound VIII exists in the 2-pyridone form rather than in the tautomeric 2-hydroxypyridine form VIIIa.

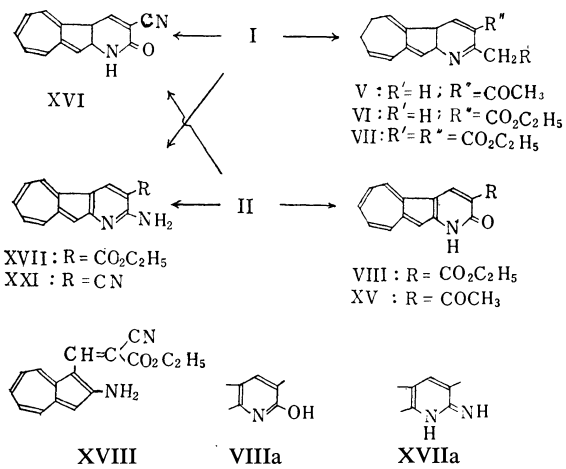

Compound X also reacted with methylamine to give a 2-methylamino compound XIII, and with dimethylamine to give a 2-dimethylamino compound XIV, but the heating of X with alcoholic ammonia resulted in the recovery of the starting material. The ultraviolet spectra of XIII and XIV are shown in Fig. 3.

A similar reaction of compound II with ethyl acetoacetate gave brown crystals (XV) (m. p., 288°C) (decomp.), though in poor yield, compound VI not being isolated. From its analytical values and the resemblance of its ultraviolet absorption curve (Fig. 2) to that of compound VIII, XV is through to be 3-acetyl-1, 2-dihydro-2-oxoauzleno [2, 1-b] pyridine, formed by a mode of cyclization different from that of compound I and the same reagent.

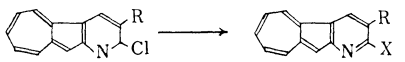

X : R=$CO_2C_2H_5$ XI : R=$CO_2C_2H_5$; X=OCH_3
XIX : R=CN XII : R=$CO_2C_2H_5$; X=OC_2H_5
XIII : R=$CO_2C_2H_5$; X=$NHCH_3$
XIV : R=$CO_2C_2H_5$; X=$N(CH_3)_2$
XX : R=CN ; X=OCH_3

The reaction of I or II with ethyl cyanoacetate was next examined. When I has heated with this reagent reddish brown needles of $C_{14}H_8O_2N_2$ (XVI) (m. p., above 29°C) and a small amount of reddish brown needles (C_{16}·$H_{14}O_2N_2$) (XVIII) (m. p., 141°C) were also obtained. The ultraviolet spectrum of XVI (Fig. 2) resembles these of VIII and XV, and the infrared spectrum shows bands at 1655 cm^{-1} (pyridone carbonyl) and at 2210 cm^{-1} (cyano), indicating XVI to be 3-cyano-1, 2-dihydro-2-oxoazuleno [2, 1-b] pyridine. The infrared spectrum of XVII in Nujol shows bands at 3440, 3300 (amino) and 1680 cm^{-1} (ester carbonyl) thus XVII is thought to be ethyl 2-aminoazuleno-[2, 1-b] pyridine-3-carboxylate. XVIII, isomeric with XVII, shows a band at 2190 cm^{-1} (cyano) besides those at 3490, 3340, 3250 (amino) and 1670 cm^{-1} (ester carbonyl) in its infrared region and is thought to be 2-amino-1-(β-cyano-β-ethoxycarbonylvinyl)azulene. The reaction of II and ethyl cyanoacetate also gave XVI and XVII, with the latter predominating. The

ultraviolet spectrum of XVII (Fig. 3) resembles those of XIII and XIV, indicating that XVII has the 2-aminopyridine structure rather than the tautomeric 2-pyridone imine form XVIIa.

Reaction XVI with phosphorus oxychloride gave 2-chloro compound XIX which when treated with sodium methoxide, was converted to the 2-methoxy compound XX.

Malononitrile reacted with I or II smoothly to give 2-amino-3-cyanoazuleno [2, 1-b] pyridine (XXI).

Experimental

2-Acetamido-1-formylazulene (II) and 2-Acetamido-1, 3-diformylazulene (III). — To a solution of 800 mg. of 2-acetamidoazulene in 2.5 ml. of dimethylformamide was added a solution of 650 mg. of phosphorus oxychloride in 2.5 ml. of dimethylformamide with continuous ice cooling. After the reaction mixture had been left standing for 4 hr. at room temperature, the immonium salt that separated was collected by filtration. This salt was then dissolved in water and neutralized with dilute sodium carbonate solution, and II which crystallized out, was collected and washed with water. Yield; 595 mg; m. p., 148~150°C.

The original filtrate was diluted with water and neutralized with a dilute sodium carbonate solution to give 290 mg. of reddish brown crystals; m. p., 135~180°C. This solid was recrystallized from ethanol to give 70 mg. of III as brown crystals (m. p., 205~220°C) (decomp.) and 75 mg. of II as red crystals.

II was recrystallized from a mixture of benzene and cyclohexane to give red prisms, m. p. 150~115°C.

Found: C, 73.40; H, 5.10; N, 6.23. Calcd. for $C_{13}H_{11}O_2N$: C, 73.22; H, 5.20; N, 6.57%.

III was recrystallized from dimethylformamide to give brown feathery csystals; m. p. 225~235°C (decomp.).

Found: C, 69.76; H, 4.57; N, 5.67. Calcd. for $C_{14}H_{11}O_3N$: C, 69.70; H, 4.59; N, 5.80%.

2-Amino-1-formylazulene (I).—To a solution of 550 mg. of compound II in 20 ml. of ethanol was added 4.5 ml. of a 2 N sodium hydroxide solution and permitted to stand for 1 hr. The acidification of the reaction mixture with acetic acid and the evaporation of the ethanol under reduced pressure gave 420 mg. of a crystalline solid; m. p, 138~140°C. Recrystallization from a mixture of benzene and cyclohexane gave orange scales, m. p., 138~139°C.

Found: C, 77.46; H, 5.08; N, 7.93. Calcd. for $C_{11}H_9ON$: C, 77.17; H, 5.30; N, 8.18%.

Oxime.—Brown scale; m. p., 158~159°C.

Found: C, 70.91; H, 5.11; N, 15.05. Calcd. for $C_{11}H_{10}ON_2$: C, 70.95; H, 5.41; N, 15.05%.

Trinitrobenzene Complex.—Red scales; m.p, 146~147°C.

Found: C, 53.32; H, 2.95; N, 14.58. Calcd. for $C_{17}H_{12}O_7N_4$: C, 53.13; H, 3.15; N, 14.58%.

2-Amino-1, 3-diformylazulene (IV). — Treatment of 400 mg. of III similar to that given II gave 210 mg. of IV; m. p., 196~210°C. Recrystallization from dimethylformamide gave brownish orange needles; m. p., 213~215°C (decomp.).

Found: C, 72.52; H, 4.30; N, 6.89. Calcd. for $C_{12}H_9O_2N$: C, 72.35; H, 4.55; N, 7.03%.

3-Acetyl-2-methylazuleno[2, 1-b]pyridine (V). — A mixture of 150 mg. of I, 300 mg. of acetylacetone and a small amount of piperidine was heated on a water bath for 6 hr., and the crystals which separated out were collected by filtration. These crystals were dissolved in benzene and passed through an alumina column to give 7 mg. of V as greenish brown crystals; m. p., 143~145°C. The original filtrate was washed with petroleum ether and the insoluble portion was dissolved in benzene, and chromatographed on an alumina column giving 35 mg. of V, m. p., 141~143°C, and 35 mg. of I. Recrystallization from dilute ethanol gave dark greenish brown feathery crystals, m. p., 144~145°C.

Found: C, 81.50; H, 5.17; N, 5.88. Calcd. for $C_{16}H_{13}ON$: C, 81.68; H, 5.57; N, 5.95%.

A solution of 30 mg. of V in dioxane was treated with iodine in the usual manner to give approximately 5 mg. of iodoform.

Hydrochloride.—Deep brown crystals, m. p. over 280°C.

Found: C, 66.08; H, 5.24; N, 4.37. Calcd. for $C_{16}H_{14}ONCl \cdot H_2O$: C, 66.32; H, 5.57; N, 4.83%.

Trinitrobenzene Complex. — Dark violet needles, m. p. 119.5~121°C.

Found: N, 12.08. Calcd. for $C_{22}H_{16}O_7N_4$: N, 12.50%.

Picrate. — Yellowish brown microcrystals which showed no definite melting point (they gradually blackened around 190°C and completely carbonized 280°C).

Found: C, 57.48; H, 3.21; N, 12.04. Calcd. for $C_{22}H_{16}O_8N_4$: C, 56.90; H, 3.47; N, 12.07%.

Oxime. — Greenish brown microneedles, m. p. 250~260°C (carbonized).

Found: C, 76.52; H, 5.44; N, 10.83. Calcd. for $C_{16}H_{14}ON_2$: C, 76.77; H, 5.64; N, 11.19%.

Ethyl 2-methylazuleno[2, 1-b]pyridine-3-carboxylate (VI).—A mixture of 150 mg. of I, 170 mg. of ethyl acetoacetate and about 30 mg. of piperidine was heated on a water bath for 7 hr. The crystals which separated were collected by filtration, dissolved in benzene and passed through an alumina column in which manner 40 mg. of VI was thereby obtained as dark violet crystal; m. p., 137~138°C. The original filtrate was dissolved in a mixture of benzene and petroleum ether (1 : 1) and chromatographed on an alumina column giving an additional 40 mg. of VI; m. p., 137~138°C. Recrystallization from a mixture of benzene and petroleum ether gave dark greenish violet plates; m. p., 137~138°C.

Found: C, 77.04; H, 5.36. Calcd. for $C_{17}H_{15}O_2N$: C, 76.96; H, 5.70%.

Hydrochloride.—Dark brown microcrystals, m. p. 217°C (decomp.).

Found: C, 60.10; H, 5.73. Calcd. for $C_{17}H_{16}O_2NCl \cdot 2H_2O$: C, 60.44; H, 5.97%.

Picrate.—Greenish brown crystals, which gradually blackened at around 215°C but which showed no definite melting point.

Found: C, 56.64; H, 3.62; N, 10.98. Calcd.

for $C_{23}H_{18}O_9N_4$: C, 55.87; H, 3.67; N, 11.23%.

Ethyl 3-Ethoxycarbonylazuleno[2, 1-b]pyridine-2-acetate (VII).—A mixture of 150 mg. of I, 300 mg. of diethyl acetonedicarboxylate and a small amount of piperidine was treated as in the case of VI. Chromatographic separation on an alumina column giving an additional 40 mg. of VI; m. p., 137~138°C. Recrystallization from a mixture of benzene and petroleum ether gave dark greenish violet plates; m. p., 137~138°C.

Found: C, 77.04; H, 5.36. Calcd. for $C_{17}H_{15}O_2N$: C, 76.96; H, 5.70%.

Hydrochloride.—Dark brown microcrystals; m. p., 217°C (decomp.).

Found: C, 60.10; H, 5.73. Calcd. for $C_{17}H_{16}O_2NCl \cdot 2H_2O$: C, 60.44; H, 5.97%.

Picrate.—Greenish brown crystals, gradually blackened at around 215°C and showed no definite melting point.

Found: C, 56.64; H, 3.62; N, 10.98. Calcd. for $C_{23}H_{18}O_9N_4$: C, 55.87; H, 3.67; N, 11.23%.

Ethyl 3-Ethoxycarbonylazuleno[2,1-b]pyridine-2-acetate (VII).—A mixture of 150 mg. of I, 300 mg. of diethyl acetonedicarboxylate and a small amount of piperidine was treated as in the case of VI. Chromatographic separation on an alumina column gave 115 mg. of VII as deep violet crystals; m. p., 107~111°C. Recrystallization from ethanol gave dark violet needles; m. p., 116~117°C.

Found: C, 71.08; H, 5.64; N, 4.08. Calcd. for $C_{20}H_{19}O_4N$: C, 71.20; H, 5.68; N, 4.15%.

Hydrochloride.—Dark violet needles; m. p., 200°C (decomp., gradually blackened around 192°C).

Found: N, 3.26. Calcd. for $C_{20}H_{20}O_4NCl \cdot H_2O$: N, 3.57%.

Picrate.—Dark reddish violet crystals; m. p., 216°C (decomp., gradually blackened around 205°C).

Found: C, 54.97; H, 3.86; N, 9.62. Calcd. for $C_{26}H_{22}O_{11}N_4$: C, 55.12; H, 3.91; N, 9.89%.

Ethyl 1, 2-Dihydro-2-oxoazuleno[2, 1-b]pyridine-3-carboxylate (VIII).—To a solution of 300 mg. of II in 6 ml. of ethanol was added 400 mg. of diethyl malonate and 200 mg. of piperidine, and the whole was heated at 50~60°C for about 30 hr. in which manner 185 mg. of VIII was obtained as brown needles, m. p. 208~215°C (decomp.). Recrystallization from dioxane raised the melting point to 212~217°C (decomp.).

Found: C, 72.14; H, 4.77; N, 5.48. Calcd. for $C_{16}H_{13}O_3N$: C, 71.90; H, 4.90; N, 5.24%.

Picrate.—Orange microcrystals; m. p., 186~188°C (decomp.).

Found: C, 54.00; H, 3.25; N, 11.00. Calcd. for $C_{22}H_{16}O_{10}N_4$: C, 53.23; H, 3.25; N, 11.29%.

The addition of a dilute sodium hydroxide solution to a solution of VIII in dimethylformamide or the heating of VIII in a sodium hydroxide solution gave a brown sodium salt, which on acidification with acetic acid gave the original material.

1,2-Dihydro-2-oxoazuleno[2,1-b]pyridine-3-carboxylic Acid (IX).—The heating of 70 mg. of VIII, with the addition of 1 ml. of a 1 N sodium hydroxide solution on a water bath for 1.5 hr., gave a dark greenish-brown sodium salt. Acidification with acetic acid gave 55 mg. of acid as reddish brown crystals; m. p., above 280°C. Recrystallization from dimethylformamide gave reddish brown microneedles.

Found: C, 70.71; H, 3.47; N, 6.27. Calcd. for $C_{14}H_9O_3N$: C, 70.29; H, 3.79; N, 5.86%.

Ethyl 2-Chloroazuleno[2, 1-b]pyridine-3-carboxylate (X).—A mixture of 150 mg. of VIII and 0.8 ml. of phosphorus oxychloride in a sealed tube was heated on a water bath for 1.5 hr. The crystals which separated were collected, suspended in water, treated with aqueous sodium acetate, and extracted with chloroform. The chloroform solution was washed with water and passed through an alumina column. The solvent was evaporated from the effluent, and the crystalline residue was recrystallized from a mixture of benzene and petroleum ether to give 80 mg. of dark greenish violet needles, (m. p., 155~157°C). The original filtrate was poured onto ice to decompose any excess phosphorus oxychloride, treated with aqueous sodium acetate, and extracted with chloroform. The chloroform solution was passed through an alumina column to give 25 mg. of a second crop; m. p., 150~153°C. Recrystallization from a mixture of benzene and petroleum ether gave dark violet needles; m. p., 156~157°C.

Found: C, 67.30; H, 4.06; N, 4.62. Calcd. for $C_{16}H_{12}O_2NCl$: C, 67.25; H, 4.23; N, 4.90%.

Ethyl 2-Methoxyazuleno[2, 1-b]pyridine-3-carboxylate (XI).—To a solution of 40 mg. of sodium in 2 ml. of methanol was added 100 mg. of X; the mixture was then heated on a water bath for 10 min., cooled, diluted with water and extracted with chloroform, The chloroform solution was washed with water and passed through an alumina column. The crystalline residue which was obtained after the evaporation of the solvent from the elute was recrystallized from a mixture of benzene and petroleum ether to give 35 mg. of XI as dark violet crystals, m. p. 161~163°C. Further recrystallization from the same solvent gave dark violet needles; m. p., 162~163°C.

Found: C, 72.17; H, 4.78; N, 5.13.Cal cd. for $C_{17}H_{15}O_3N$: C, 72.58; H, 5.38; N, 4.98%.

Ethyl 2-Ethoxyazuleno[2, 1-b]pyridine-3-carboxylate (XII).—A similar treatment of 100 mg. of X with sodium ethoxide in ethanol gave 30 mg. of XII; m. p. 146~148°C. Recrystallization from ethanol gave dark greenish violet microneedles; m. p., 147.5~149°C.

Found: C, 73.37; H, 5.62; N, 4.59. Calcd. for $C_{18}H_{17}O_3N$: C, 73.20; H, 5.80; N, 4.74%.

Ethyl 2-Methylaminoazuleno[2, 1-b]pyridine-3-carboxylate (XIII).—A mixture of 50 mg. of X and 50 mg. of aqueous methylamine (40%) in 0.4 ml. of ethanol was heated on a water bath for 1 hr. in a sealed tube; it was then cooled, and the crystals which separated were collected to give 38 mg. of XIII (m. p., 146~147°C). Recrystallization from ethanol gave wine red needles.

Found: C, 72.97; H, 5.69; N, 9.61. Calcd. for $C_{17}H_{16}O_2N_2$: C, 72.83; H, 5.75; N, 9.99%.

Ethyl 2-Dimethylaminoazuleno[2, 1-b]pyridine-3-carboxylate (XIV).—The treatment of 50 mg. of X with aqueous dimethylamine (40%) in ethanol in a manner similar to that used in the case of XIII

gave 48 mg. of XIV; m. p., 133~135°C. Recrystallization from ethanol gave wine red plates; m. p., 134~135°C.

Found: C, 73.60; H, 5.85; N, 9.12. Calcd. for $C_{18}H_{18}O_2N_2$: C, 73.45; H, 6.16; N, 9.52%.

3-Acetyl-1, 2-dihydro-2-oxoazuleno[2, 1-b]pyridine (XV).—A solution of 200 mg. of II, 200 mg. of ethyl acetoacetate and 100 mg. of piperidine in 4 ml. of ethanol was heated on a water bath for 5 hr. The crystals which separated were collected and recrystallized from ethanol to give 50 mg. of crystals; m. p., 190~230°C. Repeated recrystallization from dimethylformamide gave brown microcrystals; m. p., 287~288°C (decomp.).

Found: C, 75.77; H, 4.49; N, 6.16. Calcd. for $C_{15}H_{11}O_2N$: N, 75.93; H, 4.67; N, 5.90%.

The Reaction of Compound I and Ethyl Cyanoacetate.—A solution of 400 mg. of I, 400 mg. of ethyl cyanoacetate and 50 mg. of piperidine in 1 ml. of ethanol was heated on a water bath for 2 hr. On cooling of the reaction mixture gave 95 mg. of 3-cyano-1,2-dihydro-2-oxoazuleno[2,1]pyridine (XVI) (m. p., above 290°C) as brown crystals. Evaporation of the solvent from the filtrate, followed by the addition of a small amount of benzene separated 25 mg. of ethyl 2-aminoazuleno[2,1-b]-pyridine-3-carboxylate (XVII) (m. p. 167~187°C). The filtrate was passed through an alumina column giving 35 mg. of 2-amino-1-(β-cyano-β-ethoxycarbonylvinyl)azulene (XVIII) as red crystals, (m. p., 135~139°C).

XVI was recrystallized from dimethylformamide to give reddish brown needles; m. p., above 290°C.

Found: C, 76.17; H, 3.74; N, 12.63. Calcd. for $C_{14}H_8ON_2$: C, 76.36; H, 3.66; N, 12.72%.

XVII was recrystallized from *n*-butanol to give reddish brown needles; m. p., 189~190°C.

Found: C, 72.52; H, 4.99; N, 10.46. Calcd. for $C_{16}H_{14}O_2N_2$: C, 72.16; H, 5.30; N, 10.52%.

XVIII was recrystallized from ethanol to give red prisms; m. p., 139.5~141°C.

Found: C, 71.96; H, 5.02; N, 10.58. Calcd. for $C_{15}H_{14}O_2N_2$: C, 72.16; H, 5.30; N, 10.52%.

The Reaction of Compound II and Ethyl Cyanoacetate.—A similar treatment of 300 mg. of II with ethyl cyanoacetate gave 305 mg. of brownish purple crystals (m. p., 190~230°C). The sparingly soluble portion of these crystals in chloroform afforded 75 mg. of XVI (m. p. over 290°C), while the easily soluble part gave 170 mg. of XVII (m. p., 188~189°C).

2-Chloro-3-cyanoazuleno[2, 1-b]pyridine (XIX).—A mixture of 90 mg. of XVI and 0.5 ml of phosphorus oxychloride in a sealed tube was heated on a water bath for 1.5 hr.; it was then cooled, and the crystals which separated were collected by filtration. Treatment of these crystals with a dilute sodium carbonate solution afforded 72 mg. of dark violet crystals (m. p., 256~261°C). Recrystallization from dimethylformamide gave dark greenish violet needles; m. p., 264~265°C.

Found: C, 70.24; H, 2.78; N, 11.60. Calcd. for $C_{14}H_7N_2Cl$: C, 70.45; H, 2.96; N, 11.74%.

3-Cyano-2-methoxyazuleno[2, 1-b]pyridine (XX).—To a solution of 20 mg. of sodium in 0.6 ml. of methanol was added 40 mg. of XIX; the solution was then heated on a water bath for 20 min. The crystals which were obtained were then dissolved in chloroform, passed through an alumina column, and the solvent was evaporated from the effluent. The residue was recrystallized from a mixture of ethanol and *n*-butanol to give 25 mg. of brownish violet needles; m. p., 229~230°C.

Found: C, 76.86; H, 4.17; N, 11.80. Calcd. for $C_{15}H_{10}ON_2$: C, 76.91; H, 4.30; N, 11.96%.

2-Amino-3-cyanoazuleno[2, 1-b]pyridine (XXI).—a) A solution of 70 mg. of I, 70 mg. of malononitrile and a small amount of piperidine in 0.3 ml. of ethanol was heated for 1 hr. on a water bath, and the resulting crystals (80 mg., m. p. 245~268°C) were recrystallized from dimethylformamide to give brownish violet needles (m. p., 266~268°C) (decomp.).

Found: C, 77.03; H, 3.92; N, 18.61. Calcd. for $C_{14}H_9N_3$: C, 76.69; H, 4.14; N, 19.17%.

Hydrochloride.—Reddish orange microneedles, m. p. over 280°C.

Found: C, 61.62; H, 4.09. Calcd. for $C_{14}H_{10}N_3Cl \cdot H_2O$: C, 61.43; H, 4.42%.

b) The treatment of a solution of 100 mg. of II, 50 mg. of malononitrile and 30 mg. of piperidine in 1 ml. of ethanol in a manner similar to that used in the case of a) afforded 75 mg. of XXI; m. p., 260~265°C. (decomp.). Recrystallization from dimethylformamide raised the melting point 266~268°C (decomp.); these crystals were shown to be identical with those obtained by a).

One of the authors, Katsuo Kikuchi, wishes to express his thanks to Japan Society for the Promotion of Science for the fellowship which has enabled him to carry out this work during his stay at Tohoku University as a visiting research associate.

Department of Chemistry
Faculty of Science
Tohoku University
Katahira-cho, Sendai

Studies of the Electrolytic Conductance of a Dye Solution. I. Complex Formation in an Aqueous Solution of the Mixture of Chlorazol Sky Blue FF and Chrysophenine G

By Kinko SHINZAWA, Yoshié TANIZAKI and Noboru ANDO

(Received December 10, 1962)

As is commonly known, the McBain effect[1] caused by the aggregation of dye ions is observed in most direct dyes in an aqueous solution[2]. A typical McBain effect has been found in Methylene Blue[3], the basic dye, and later it was confirmed by a change in the absorption spectrum that this dye forms an aggregate with an increase of its own concentration[4].

Recently, studies have come to be made, by means of spectrophotometry, of the complex formation of unlike dye molecules in mixtures in an aqueous solution[5-7]. These studies have discovered the important fact that Chlorazol Sky Blue FF and Chrysophenine G form complexes in definite mole ratios[6,7]. In the case of Methylene Blue in water mentioned above, the evidence of its aggregation was found in the measurements of conductance[2] as well as in those of the absorpsion spectrum[8]. In the same way, it may be expected that a proof of complex formation between Chlorazol Sky Blue FF and Chrysophenine G will also be derived from the conductance measurement.

In the present paper, the authors will investigate the complex formation of a two-component dye mixture in an aqueous solution from the view point of electrolytic conductance. Unfortunately, however, in the field of conductance study, there is no rule such as Beer's law in the field of light absorption. Though a theoretical treatment of the conductance of a mixed electrolyte solution has been attempted by Onsager and his co-workers[9], no application of the theory to experimental results has yet been made. Considering that we can not yet analyze quantitatively the conductance of dyes, even in a single solution, much less can we expect to perform a satisfactory analysis of dye mixtures. Accordingly, as a first step towards a preliminary investigation, attention is directed to the examination of how the complex formation of Chlorazol Sky Blue FF and Chrysophenine G is reflected in the conductance of a mixed system. Also, we will examine how the complex formation is to be understood in relation both to the conductance characters of the mixture and to those of its components.

Experimental

The dye samples used were Chlorazol Sky Blue FF and Chrysophenine G, both of which had already been used in other reports by the present authors[7]. Potassium chloride (the extra pure grade of the Japan Pharmacopeia) was once recrystallized from distilled water. Sodium chloride (the extra pure grade of the Japan Pharmacopeia) was purified once by recrystallization from a water-alcohol solution. Conductance water was prepared from a specially-designed distilling apparatus; its specific conductance upon measurement was $(5\sim10)\times10^{-7}$ mho/cm. at 30°C.

Conductance measurement was carried out by means of the usual Wheatstone bridge. The frequency of the oscillator was 800 cycle/sec. A null point was determined with a cathode ray oscilloscope. Waves on the oscilloscope vanished in the cases of resistance under 10^5 ohm. In the other cases, however, the minimum point was regarded as a null point. The volumes of the four conductance cells employed were from 15 to 20 ml. The electrodes of two of the cells were square platinum plates $19\times13\times0.3$ mm^3, while those of the other two were $15\times13\times0.3$ mm^3; all of them had been platinized beforehand. The cell constants were determined by measuring the conductance of a 0.01 D aqueous potassium chloride solution[10] at 30°C. All the cell constants were redetermined every one or two months.

During the preparation and measurement of solutions, attention was paid to avoid the effect of the carbon dioxide in air. For this purpose,

1) J. W. McBain, *Kolloid Z.*, **12**, 256 (1913).
2) N. Ando, *J. Chem. Soc. Japan (Nippon Kwagaku Kwaisi)*, **64**, 1305, 1431 (1943); F. H. Holmes and H. A. Standing, *Trans. Faraday Soc.*, **41**, 568 (1945).
3) C. Robinson, ibid., **31**, 245 (1935).
4) E. Rabinowitch and L. F. Epstein, *J. Am. Chem. Soc.*, **63**, 69 (1941); D. R. Lenin and R. Vickerstaff, *Trans. Faraday Soc.*, **43**, 491 (1947).
5) S. M. Neale and W. A. Stringfellow, *J. Soc. Dyers Colourists*. **59**, 241 (1943); Y. Tanizaki T. Kobayashi and N. Ando, This Bulletin, **32**, 119 (1959); T. Kobayashi, Y. Tanizaki and N. Ando, ibid., **32**, 675, 680 (1959).
6) A. N. Derbyshire and R. H. Peters, *J. Soc. Dyers Colourists*, **72**, 268 (1956).
7) T. Kobayashi Y. Tanizaki and N. Ando, This Bulletin, **33**, 661 (1960).
8) Y. Tanizaki and N. Ando, *J. Chem. Soc. Japan, Pure Chem. Sec. (Nippon Kagaku Zassi)*, **78**, 343 (1957).
9) H. S. Harned and B. B. Owen, "The Physical Chemistry of Electrolytic Solutions", 3rd. Ed., Reinhold, New York (1958), pp. 105-117.
10) International Critical Tables, **6**, 230, Table 2, Parker Solution.

desired volumes of distilled water or solutions were measured out in flasks through burettes under the carbon dioxide-free conditions by the use of a particular device; thus, the sample liquids were prepared without being exposed directly to the open air. The mother solution and distilled water were stored once in each stock bottle, and then sample solutions were prepared from them within 24 hr. All of the concentrations were determined by weight. Each series of solutions in concentrations was prepared by diluting a mother solution. All solution measurements prepared were carried out within two days. The three thermostated water bath were adjusted at 30, 40 and 60°C and were constant within ±0.02°C. The resistance of a cell containing a solution became constant over 10 min. after it had been soaked in a bath. In this report, the observed values are of 20 min. after. The resistance of water as a solvent approached a constant value in about 10 min., but it did not give a stationary value, showing an inclination to decrease slightly with the lapse of time. However, in this case the resistance after 20 min. was employed as an observed value of the water used.

Results and Discussion

Concerning the two series of binary mixtures at the respective constant ratios of Blue (Chlorazol Sky Blue FF) and Yellow (Chrysophenine G), the values of the observed specific conductance, κ_{obs}, divided by the total equivalent concentration of the dyes involved have been plotted against the square root of the total concentration. This provides the white and the half black circles in Fig. 1. A black circle in this figure represents the value, $\kappa_{sum}/(C_F+C_G)$, calculated by the following expressions, using the specific conductances of the components in a single solution:

$$\kappa_{sum}=k_F+\kappa_G=(C_F\Lambda_F+C_G\Lambda_G)\times 1/1000 \quad (1)$$

$$\kappa_{sum}/(C_F+C_G)=(f_F\Lambda_F+f_G\Lambda_G)\times 1/1000 \quad (2)$$

Here, C_F and C_G are the equivalent concentrations, Λ_F and Λ_G, the equivalent conductances, and $f_F=C_F/(C_F+C_G)$ and $f_G=C_G/(C_F+C_G)$, the equivalent fractions of Blue and Yellow respectively. The "sum" value defined here may give a standard for deciding whether or not the observed conductance is abnormally increased in a mixed system. This is because the value of κ_{sum} implies the conductance of mixture when no interaction is produced by mixing between ion species; therefore, κ_{sum} should be larger than κ_{obs}, according to the general tendency of electrolyte solutions for the mobility to decrease with an increase in the concentration. In the comparison of "sum" and "obs" conductances in the mixture, it may be convenient to express the conductance in the very form of κ divided by the total equivalent concentration at which κ was observed (Eq. 2). This form is considered to have the physical meaning that it is the mean conductance applied to a one-gram equivalent of the cations and anions in the solution.

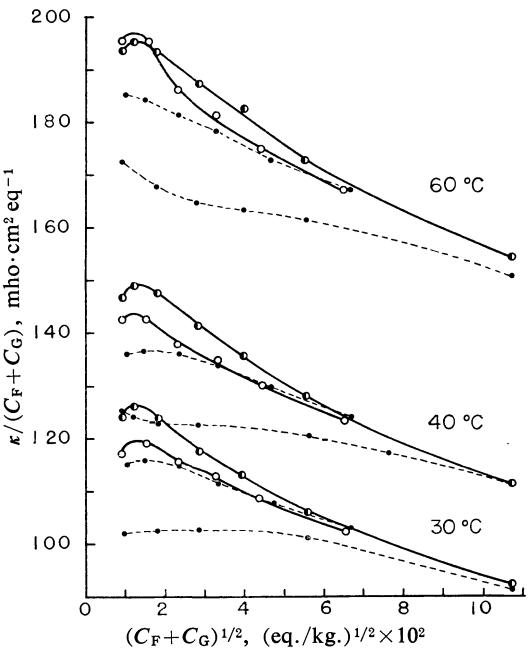

Fig. 1. Relation of conductance of the mixture of Blue and Yellow to square root of its total equivalent concentration.
In each series the concentration ratio of Blue and Yellow is constant.
○: $C_G/C_F=0.1034$ ◐: $C_G/C_F=1.1716$
●: sum

The conductance curves in Fig. 1 indicate the relation,

$$\kappa_{obs}/\sum C \geqq \kappa_{sum}/\sum C \quad (3)$$

in the greater part in the concentration region observed here. In Eq. 3, $\sum C$ means (C_F+C_G). This fact indicates that new ion species having a larger mobility per charge than any respective component are produced in this system. Considering the fact, already clarified by absorption spectra, that in such a system Blue (F) and Yellow (G) form the (FG and FG_2) complexes[6,7], the new ion species mentioned above may be regarded as such complexes.

In the two series of constant mixing ratios shown in Fig. 1, the differences between the corresponding conductances, $\kappa/\sum C$, of "obs" and "sum" are greater at the lower concentrations and decrease with an increase in the concentration. This tendency appears more remarkably in the case of $C_G/C_F=1.716$ than when the values is 0.1034. The correlations of "obs" and "sum" in the other series, which are not illustrated here, showed a similar tendency, but only in the case of the especially

large ratio of $C_G/C_F=4.811$ did the correlation at higher concentration go into the reverse tendency, i.e. $(\kappa_{obs}/\sum C)<(\kappa_{sum}/\sum C)$. In a series of constant ratios of mixing, the concentration ratio of the complexes formed to the respective residual components is considered to be nearly constant. Consequently, it may be said that the above fact indicates that the decreasing conductance rate of the complexes with its increasing concentration is greater than those of components. Moreover, this can easily be accepted because the ionic charges of complexs FG and FG_2 are 6 and 8 respectively.

Thus, in the series of constant mixing ratios, the correlation between $\kappa_{obs}/\sum C$ and $\kappa_{sum}/\sum C$ varied with the total concentration, even when the concentration ratio of the complex to the residual components is constant. However, the system in which the total equivalent concentration is kept constant will be give rise to the following advantage over the above system: the changes in the respective equivalent conductances of the complexes formed and in the residual dye components with the mixing ratio may be considered to be not very large*1. If the $\kappa_{obs}/\sum C$ curve agaist f reveals a marked bend point, with a system involving ion species of respective constant equivalent conductances, the fraction value for this point could be closely related to the composition of a complex formed (see Appendix). In the present case, it can be considered that each conductance value is constant in the neighborhood of the central part of f, so that a conclusion will be derived in the way just mentioned.

The $\kappa_{obs}/\sum C$ values for the total concentration of 2.25×10^{-4} eq./kg. in several mixture-compositions, obtained from Fig. 1 and from other, unshown ones, against the equivalent fraction of the component are expressed by white circles in Fig. 2. Here, black circles represent $\kappa_{sum}/\sum C$ values. The $\kappa_{obs}/\sum C$ and $\kappa_{sum}/\sum C$ values are connected by broad lines and broken ones respectively. This figure shows that $(\kappa_{obs}/\sum C)>(\kappa_{sum}/\sum C)$ in the whole region and that the differences between them are largest at about $f_G=0.5$. Inspecting in more detail, $\kappa_{obs}/\sum C$ at first increases rapidly, forms a shoulder, and then comes to a maximum value with an increase in f_G from 0.

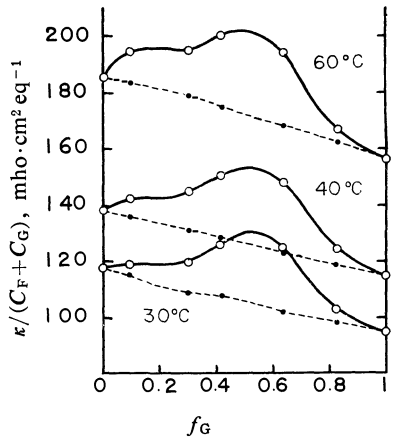

Fig. 2. Relation of conductance of the mixture of Blue and Yellow to equivalent fraction of its components.
The total equivalent concentration is kept at 2.25×10^{-4} eq./kg.
○: obs. ●: sum

This tendency appears more clearly at higher temperatures.

The same relation at six different concentrations of $(1\sim25)\times10^{-4}$ eq./kg. are shown in Fig. 3. Roughly speaking, the $\kappa_{obs}/\sum C$ curves at the several concentrations are similar

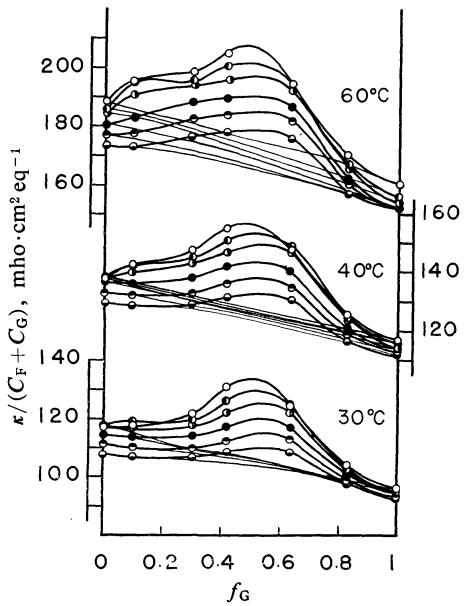

Fig. 3. Relation of conductance of the mixture of Blue and Yellow in six different total equivalent concentrations to equivalent fraction of its components.
The total equivalent concentrations are as follows; ($\times10^{-4}$ eq./kg.)
○: 1 ◐: 2.25 ◑: 4, ●: 9
◓: 16 ◒: 25 —: sum

*1 This concept is based on the fact that, in this series, the equivalent concentration of sodium ions and the sum of those of dye ions are constant. That the electrical effect on an ion due tothe other ions in a solution is constant, however, can be said of the systm in which the constant is not the total concentration but the ionic strength I', i.e., $\sum n_i z_i^2$ (n_i and z_i: the number and the charge of the i-th ion respectively). Since the value in this series changes because of the different charges of the two dye anions, the above assumption can not be exactly true. (See Ref. 9, p.117, Eq. 4-3-69).

to one another and show that $(\kappa_{obs}/\sum C) > (\kappa_{sum}/\sum C)$. However, the maximum points of the curves show a slight tendency to deviate from 0.5 to a large value in f_G with an increase in the total concentration. The shoulders of the curves observed at about $f_G=0.15$ in Fig. 2 disappear with an increase in the concentration.

On the other hand, as is well known, the aggregation of many dye anions is promoted by the presence of another electrolyte[8]. Thus, in this case each Blue or Yellow anion might be promoted in its aggregation by the effect of the partner dye. Consequently, the McBain effect caused by this effect must be taken into account. The promotion effect of the self-aggregation of the dye anion will be produced mainly by the co-existing electrolyte. Therefore, the magnitude of this effect is supposed to be estimated from that produced by the equivalent amount of sodium chloride. From this viewpoint, measurements of the binary system of Blue and sodium chloride were carried out in the first place. In Fig. 4 are shown the $\kappa/\sum C$ values, where $\sum C$ means (C_F+C_{NaCl}), versus the square roots of the total equivalent concentrations of two cases in these results. The solid and broken lines represent $\kappa_{obs}/\sum C$ and $\kappa_{sum}/\sum C$ respectively. This figure

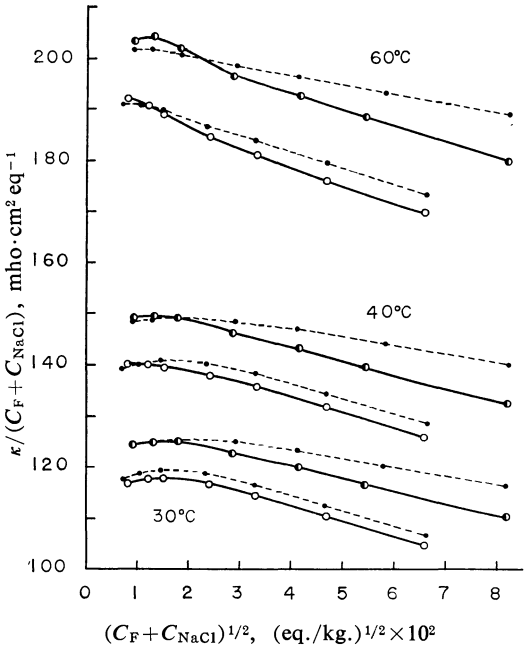

Fig. 4. Relation of conductance of the mixture of Blue and sodium chloride to square root of its total equivalent concentration.
In each series the concentration ratio of Blue and sodium chloride is constant.
◐: $C_{NaCl}/C_F=0.6970$
○: $C_{NaCl}/C_F=0.1015$ ●: sum

indicates that $(\kappa_{obs}/\sum C) < (\kappa_{sum}/\sum C)$ in the greater part, but that at a very low concentration a slight inverse relation appears. This would suggest that the aggregation of Blue anions is promoted more or less by the effect of sodium chloride. The $\kappa/\sum C$ values versus equivalent fractions for the binary mixture of Blue and sodium chloride, corresponding to the dye mixture in Fig. 3, are shown in Fig. 5. The

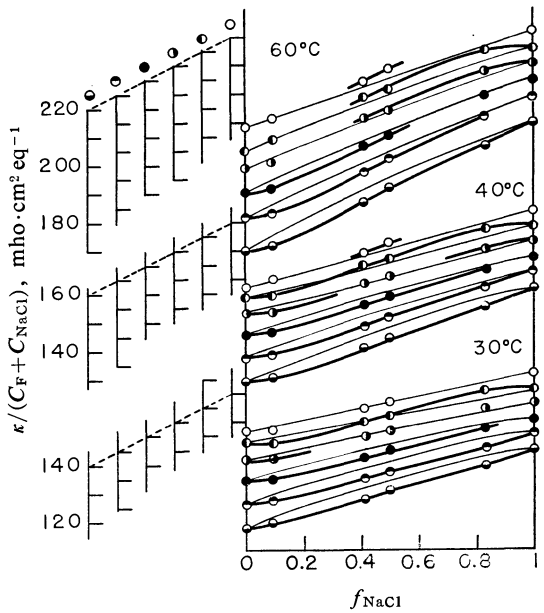

Fig. 5. Relation of conductance of the mixture of Blue and sodium chloride in six different equivalent concentrations to equivalent fraction of its components.
The total equivalent concentrations are as follows; ($\times10^{-4}$ eq./kg.)
○: 1 ◐: 2.25 ◑: 4 ●: 9
◓: 16 ◒: 25 —: sum

circles represent the observed values and are connected by broad lines. In order to avoid superposition of plots, the $\kappa/\sum C$ axes for respective concentrations are shifted from one another. This figure shows that the "obs" value is larger than the "sum" value when the total concentration is below 4×10^{-4} eq./kg. This tendency is clearer at a larger f_{NaCl} (or at a smaller f_F) value. On the other hand, when the total concentration is above 4×10^{-4} eq./kg., the "obs" value is smaller than the "sum" value over the whole region. A similar tendency appears for three different temperatures, though slightly clearer for higher temperatures. In short, the promotion of the self-aggregation of Blue anions in mixture with sodium chloride is certainly recognized by the increase of $\kappa_{obs}/\sum C$ in low concentrations, as has been shown above, but its increase is too

small to be compared with that in mixture with Yellow; further, the $\kappa_{obs}/\sum C$ curves in Fig. 5 do not show a tendency to have their maxima at $f=0.5$ as do these in Fig. 3.

Next, the results obtained in the same way with the binary mixture of sodium chloride and Yellow are shown in Fig. 6. From Fig. 6

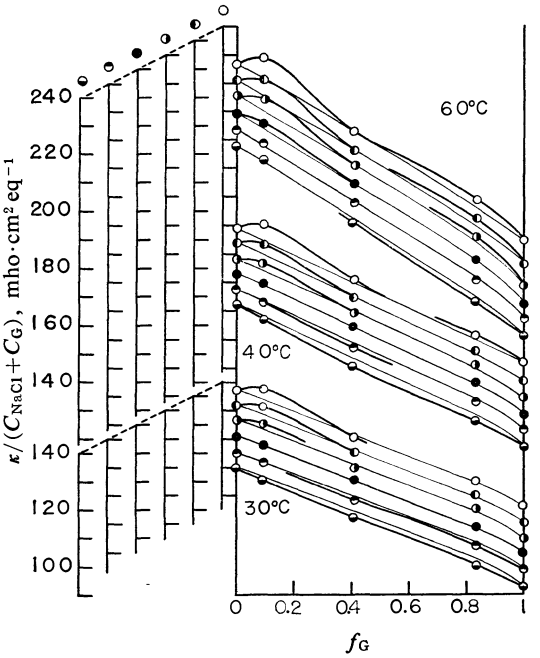

Fig. 6. Relation of conductance of the mixture of Yellow and sodium chloride in six different equivalent concentrations to equivalent fraction of its components.
The total equivalent concentrations are as follows; ($\times 10^{-4}$ eq./kg.)

○: 1 ◐: 2.25 ◑: 4 ●: 9
◓: 16 ◒: 25 —: sum

it is clear that, in the region where the total concentration is below 9×10^{-4} eq./kg., the relation $(\kappa_{obs}/\sum C)>(\kappa_{sum}/\sum C)$, where $\sum C$ indicates $(C_{NaCl}+C_G)$, appears for all equivalent fractions more clearly in the case of smaller f, and that in the region above this concentration the relation is reversed. As a whole, the results of this figure are similar to those of Blue and sodium chloride.

To sum up these results, we can certainly say that the conductance of Blue or Yellow is affected by sodium chloride, and also that the difference in "obs" and "sum" values in a mixture of the dye and sodium chloride is not so large as that in the combination of Blue and Yellow. Accordingly, it may probably be considered that the largest difference in "obs" and "sum" at about the same equivalent fraction of Blue and Yellow in Fig. 3 is due to the complex formation of FG_2. Thus, the formation of FG_2 is concluded from the above discussion, while the formation of another complex, namely FG, is found spectrophotometrically. According to the above argument, an abnormal feature responsible for FG is to appear at $f_G=1/3$, but Fig. 3 does not show any distinctive peak or shoulder at this part of the curve. Comparing the two parts into which a curve of Fig. 3 is divided at a maximum, the difference between $\kappa_{obs}/\sum C$ and $\kappa_{sum}/\sum C$ is greater in the region richer in F than in G. This seems to correspond to the formation of FG.

The shoulder of the $\kappa_{obs}/(C_F+C_G)$ curve at about $f_G=0.15$ in Fig. 3 may be explained by the fact that Yellow is accelerated in its aggregation by the presence of Blue, since the shoulder corresponds to the abnormal increase of $\kappa_{obs}/(C_{NaCl}+C_G)$ obtained with the same fraction of a mixture of sodium chloride and Yellow (Fig. 6).

In Figs. 2 and 3, it must be noticed that the relative increase in conductance due to the complex formation becomes larger with the temperature. If the complex formation is only considered in the system, this does not agree

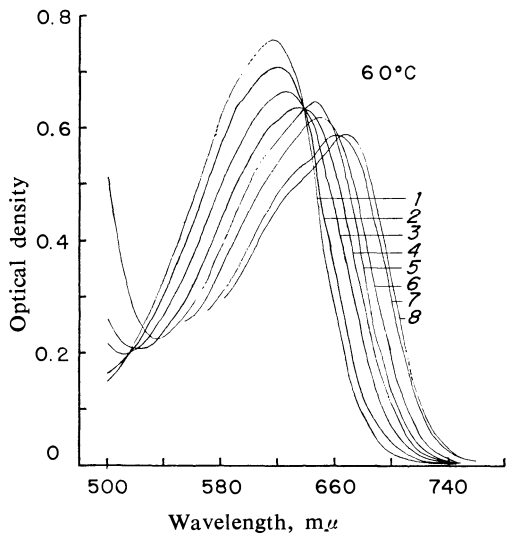

Fig. 7. The visible absorption spectra of Chrysophenine G-Sky Blue FF aqueous solution: temperature, 60°C; cell, 2 cm.

	Chrysophenine G mol./l.	Sky Blue FF mol./l.
1	0	4.000×10^{-6}
2	1.016×10^{-6}	4.000×10^{-6}
3	4.000×10^{-6}	4.000×10^{-6}
4	8.072×10^{-6}	4.000×10^{-6}
5	3.412×10^{-5}	4.000×10^{-6}
6	1.211×10^{-4}	4.000×10^{-6}
7	3.998×10^{-4}	4.000×10^{-6}
8	8.023×10^{-4}	4.000×10^{-6}

with the general rule that the amount of complex formed should decrease with the temperature. This will be understood by taking into account the self-aggregation which competes with the complex in decomposing by raising the temperature. In this case the self-aggregation should be considered to be more unstable than the complex. However, at the present stage, thermodynamic values of the self-aggregation which can be compared with those of the complex have not yet been obtained.

Some results, however, may support the above consideration. It has been reported that Blue and Yellow in an aqueous solution form a 1:1 and a 1:2 complex at room temperature[7]. According to further investigation[11], it may be concluded that even at 60°C the same complexes are formed, as is shown by the well-defined isosbestic points illustrated in Fig. 7. The estimated enthalpy changes show in this case -24 kcal./mol. for $F + G \rightarrow FG$ and -20 kcal./mol. for $FG + G \rightarrow FG_2$. These values are larger than the adsoption energies obtained for the respective components of the cellulose.

Next, the conductance curve of Blue in the single aqueous solution is shown in Fig. 8. It indicates that the McBain effect, which is due to the aggregation considered, comes to disappear with an increase in the temperature; the curve becomes nearly a straight line at 60°C, and then at 80°C it is bent conversely*2. In this case it must be said that at 80°C, the highest temperature observed, the dye anion is closest to the single and that at 30°C the aggregation number is largest.

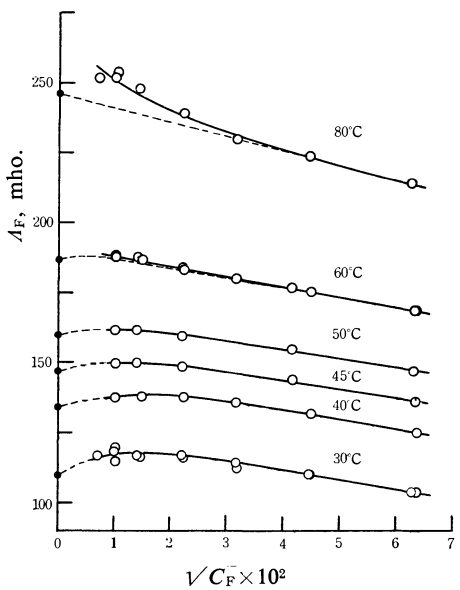

Fig. 8. Conductance of Chlorazol Sky Blue FF in aqueous solution. C_F stands for the equivalent concentration.

Assuming that the straight line of the higher concentration region at 80°C is due to the single dye ion species, the line is extraporated to obtain Λ_0. The Walden product, $\Lambda_0\eta_0$ (η_0: viscosity coefficient of water), is evaluated; then the correspoding Λ_0's at the respective temperatures are estimated by the Walden rule. The results are indicated in black circles in Fig. 8. When the black circles are connected with the corresponding observed curves, the broken lines shown in Fig. 8 are obtained. These curves evidently reveal the change in aggregation against the temperature. It may be supposed from the above discussion that Blue is nearly a single-dye ion species, though not quite a single one.

From the above interpretation, it is proper to consider that the compactness of the complexes in the system under consideration is stronger than that of the self-aggregates and that, for this reason, the higher the temperature, the larger the difference between the $\kappa_{obs}/(C_F+C_G)$ value and the corresponding $\kappa_{sum}/(C_F+C_G)$ value.

Summary

The conductances of aqueous solutions of Chlorazol Sky Blue FF (Blue), Chrysophenine G (Yellow), sodium chloride and their binary mixtures at various constant ratios have been measured. The conductance observed with a mixture of Blue and Yellow increased abnormally compared with that obtained by the sum of individual dye conductances; the difference between the observed and the sum values reached a maximum at about the same fraction of the equivalent concentration of component dyes. A similar relation of the conductance against the fraction of the equivalent concentration of components, obtained with mixtures in which component dye was substituted by sodium chloride, did not always show a coincidence between the observed value and the sum one. The difference, however, was much smaller than that obtained with dye mixtures. Thus, the abnormal increase described above may be attributed to the formation of complexes of Blue and Yellow;

11) T. Hoshi, Y. Tanizaki and N. Ando, to be published.

*2 The increase of conductance at the very low concentration is interpreted as due to the dissociation of the OH group. (cf. C. Robinson and H. E. Garrett, *Trans. Faraday Soc.*, **35**, 771 (1939).) Because, comparing the Walden products for the low concentration region at 80 and 60°C, that of the former is considerably larger than that of the latter, indicating the iecrease of charge per species.

a 1 : 1 complex and a 1 : 2 complex, consisting of Blue and Yellow already known, were sufficiently reflected in the conductance curve, especially in a 1 : 2 complex.

Laboratory of Physical Chemistry
Tokyo Institute of Technology
Meguro-ku Tokyo

Appendix

A general theory of the relationship between the composition of the complex and that of the solution has been set forth by Eaton[12]. This theory will be applied to conductance as follows. Here we assume that the conductance of an electrolyte is linear to its concentration, C, with a gradient $\Lambda/1000$. For a binary mixture of A and B, whose total equivalent concentration is fixed, the Λ curve against the equivalent fraction f_A (or f_B) becomes a line connecting Λ_A and Λ_B, provided that no interaction exists between A and B, as follows:

$$\Lambda \equiv 1000\kappa_{sum}/(C_A+C_B) = \{f_A\Lambda_A + (1-f_A)\Lambda_B\}$$

When p mol. of A react with q mol. of B to form r mol. of complex AB: $pA+qB=rAB$, then

$$1000\kappa_{obs}/(C_A+C_B) = \{f_A\Lambda_A + (1-f_A)\Lambda_B\} + \{\Lambda_C - ap\Lambda_A/(ap+bq) - bq\Lambda_B/(ap+bq)\}f_C$$

where f_C is the equivalent fraction of the complex formed and a and b the charges of A and B respectively. Therefore, $\kappa_{obs}/(C_A+C_B)$ is linear to f_C. f_C reaches its maximum at $f_A=ap/(ap+pq)$ in the case of $a=b$. Accordingly, we can calculate p/q from the f_A value of $\kappa_{obs}/(C_A+C_B)$ at its maximum. However, when $a \neq b$, $f_{A(f_C=max)}$ is dependent on the equilibrium constant, K, and $f_{A(f_C=max)}=ap/(ap+bq)$ only when $K=\infty$. Though in the present case of the combination of Blue and Yellow, the charges are 4 and 2 respectively, namely $a \neq b$, it may safely be said that the above relation is applicable to this combination, as, for instance, the equilibrium constant of $F+2G=FG_2$ is 3×10^{10}.

12) J. C. Eaton, Appendix to F. M. Arshid et al., *J. Chem. Soc.*, **1955**, 67.

The Photochemical Decomposition of α, α-Diphenyl-β-picrylhydrazyl (DPPH) in Solution. I. A Kinetic Study of the Reaction

By Atuo SUZUKI*, Makoto TAKAHASI and Kengo SHIOMI

(Received December 24, 1962)

α, α - Diphenyl - β - picrylhydrazyl (DPPH), which was first prepared by Goldschmidt and Renn[1], has been well known to be a stable radical both in the crystalline state and in solution, and it has been submitted to many studies of electron spin resonance. The chemical behavior of this compound, which was studied first by Goldschmidt and Renn, has recently been of interest because the compound serves as a scavenger of the reactive free radicals. Since there is a noticeable color change from violet to light yellow upon the reaction with other free radicals, the rate of the free radical formation can be followed colorimetrically. On the basis of this principle, Bawn and Mellish[2] measured the rate of the thermal decomposition of benzoyl peroxide and 2, 2-azobisisobutyronitrile in several solvents. In these measurements there was a tacit assumption that DPPH reacts quantitatively with a radical to produce stable products.

However, Hammond[3] and most recently Verdin[4] have observed that the reaction of DPPH with the radicals produced in the thermal decomposition of azobisisobutyronitrile is non-stoichiometric and is sensitive to oxygen.

Although as yet the stability of DPPH itself has scarcely come into quesion, some doubt about its stability has been aroused in the present authors, because they have observed that the solution of DPPH fades gradually on standing in diffused light at room temperature, indicating the photochemical decomposition of DPPH.

In order to investigate the mechanism of this phenomenon, an experiment has been undertaken by the present authors. The experiment is divided into two parts, the first being a kinetic investigation of the reaction, and the second consisting of the identification of the products, the determination of the ratio of the amount of the products, and the structure investigation of an unknown reaction product..

* Present address: Central Research Institute, Teijin Limited, Hirayama Hino-machi, Minamitama-gun, Tokyo.

1) S. Goldschmidt and K. Renn, *Ber.*, **55**, 628 (1922).

2) C. H. E. Bawn and S. F. Mellish, *Trans. Faraday Soc.*, **47**, 1216 (1951).

3) G. S. Hammond, J. M. Sen and C. E. Boozer, *J. Am. Chem. Soc.*, **72**, 3244 (1955).

4) D. Verdin, *Trans. Faraday Soc.*, **56**, 823 (1960).

The first part of the experiment will be described in the present paper, while the second will be treated in a succeeding paper.

Results

Influence of the Wavelength of the Irradiating Light.—As is shown in Fig. 1, DPPH has two absorption maxima, at 520 and 330 mμ. The rates of reaction obtained with different filters are shown in Fig. 2.

Characteristic curves of transmission of the filters used are shown in Fig. 3. As the intensities of the light in the three runs with different filters are not the same, the absolute rates of decomposition cannot be compared with one another; however, since it is observed that the reaction proceeds fairly fast when a Corning (Cd)-filter, which completely cuts the light below 460 mμ, is used, it may be concluded that the decomposition of DPPH can proceed in the light at the first absorption band of DPPH ($\lambda_{max}=520$ mμ, $\varepsilon=1.23\times10^4$ $mol^{-1}cm^{-1}l.$). The rest of the kinetic experiments were carried out using a Corning (Cd)-filter.

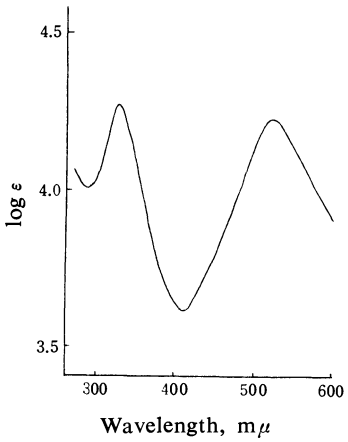

Fig. 1. Absorption spectra of DPPH in carbon tetrachloride.

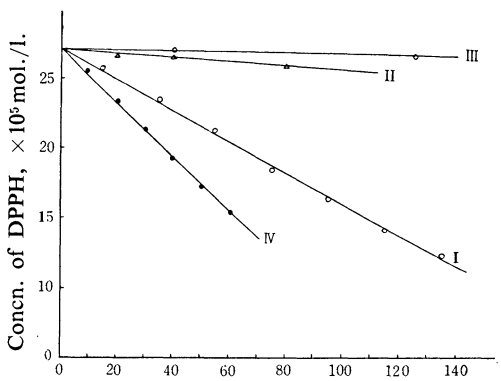

Fig. 2. Rate of decomposition of DPPH at 10°C in carbon tetrachloride with various kinds of filters.
I: Corning (Cd), II: Madzuda VB2, III: Madzuda VG1, IV: without filter. Concentration of DPPH was calculated from the optical density at 520 mμ using $\varepsilon=1.23\times10^4$ l./mol., and assuming $\varepsilon=0$ for the decomposition products.

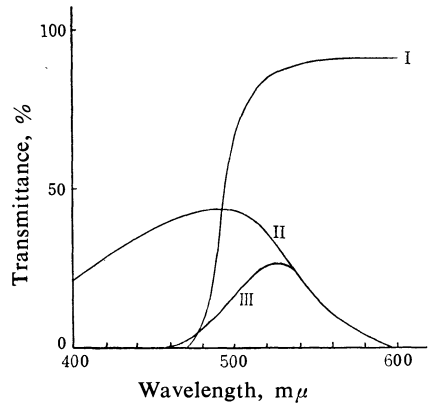

Fig. 3. Characteristic absorption curves of filters.
I: Corning (Cd), II: Madzuda VB2, III: Madzuda VG1.

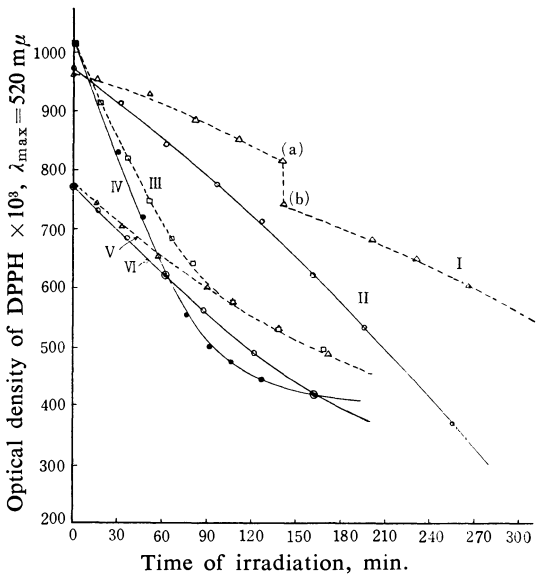

Fig. 4. Rate of decomposition of DPPH at 25°C in various solvents in the absence or in the presence of air.
I: in the absence of air in *n*-heptane, II: in the presence of air in *n*-heptane, (a)—(b) without irradiation for 12 hr. in the dark, showing after effect, III: in the absence of air in benzene, IV: in the presence of air in benzene, V: in the absence of air in carbon tetrachloride, VI: in the presence of air in carbon tetrachloride.

Influence of the Solvent and of Oxygen on the Reaction Rate. — The kinetic features of the decomposition in carbon tetrachloride and in benzene are almost identical, but in *n*-heptane it is different, as is shown in Fig. 4. A remarkable after-effect was observed in *n*-heptane, indicating the interaction of DPPH with the solvent. No further experiment in *n*-heptane was, however, undertaken in the present work. Oxygen slightly accelerates the decomposition, both in carbon tetrachloride and in benzene, but it does not seem to change the main features of the kinetics or of the reaction products, and the nature of its effect is not clear at present.

The Reaction Products. — The recation products were separated and identified by the paper chromatographic method. α, α-Diphenyl-β-picrylhydrazine, α-phenyl-α-(*p*-nitrophenyl)-β-picrylhydrazine and the third, unknown compound were separated on a paper chromatograph.

The details of the separation of these compounds, the determination of their molar ratio after different periods of reaction time, and the discussion of the structure of the third component will be given in the succeeding paper.

Influence of Light Intensity on the Decomposition Rate. — The experiment was carried out using the carbon tetrachloride solution of DPPH, changing the light intensity with copper nets. The plots of the optical densities of DPPH against the time of irradiation at various intensities of irradiating light are shown in Fig. 5.

The decompsition rate for each run was calculated from the slope of the initial part of the decomposition.

The experiments described here were carried out at a lower concentration (3.5×10^{-5} mol./l.) for convenience in determining the concentration of DPPH in the course of the reaction by photometry in vacuo without dilution*. In such a low concentration of DPPH, the amount of light absorbed could not be approximated as I_0, but it is expressed as $I_0(1-10^{-\varepsilon x l})$. However, since the initial concentrations of DPPH in these four runs are identical, the initial rate of the disappearance of DPPH is plotted against the relative intensities of the incident light instead of against the amount of light absorbed in Fig. 6, but this method is considered an approximation sufficient for obtaining a linear relationship between the rate and the amount of light.

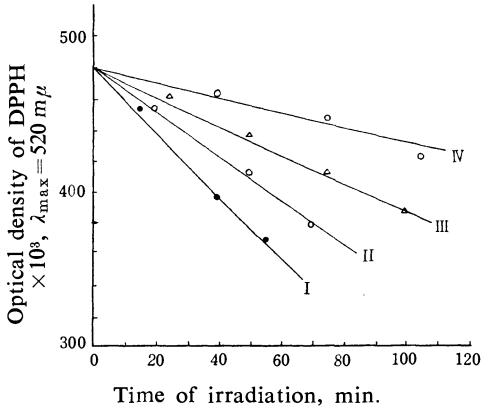

Fig. 5. Plot of the optical density of DPPH solution in carbon tetrachloride against time under the irradiations of various light intensities ranging 100 to 27% at 10°C.
I: 100%, II: 70%, III: 47%, IV: 27%. The initial concentration of DPPH is 3.10×10^{-5} mol./l.

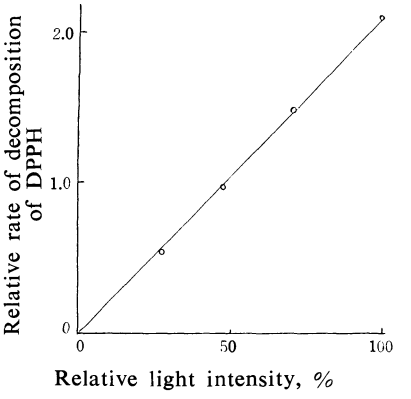

Fig. 6. Relationship between the relative intensity of the irradiating light and the relative rate of the decomposition of DPPH at 10°C.

The extrapolation of the correlation line passes through the origin; this is consistent with the fact that DPPH does not decompose in the dark.

Kinetic Expression of the Experimental Results.—As is shown in Fig. 7, a plot of the concentration against the time hardly shows any departure from linearity in the early stage of the reaction in any run of the experiments in a carbon tetrachloride solution, and the slope might be used as a measure of the observed zero-order rate constant.

This apparent zero-order rate constans was, however, found to be dependent upon the initial concentration of DPPH, and further

* The experiments of photolysis, except for the four runs shown in Fig. 5, were carried out at relatively high concentrations of DPPH (more than 10^{-4} mol./l. in order to keep the absorption of light close to one hundred per cent throughut course of the reaction except in the very late stage.

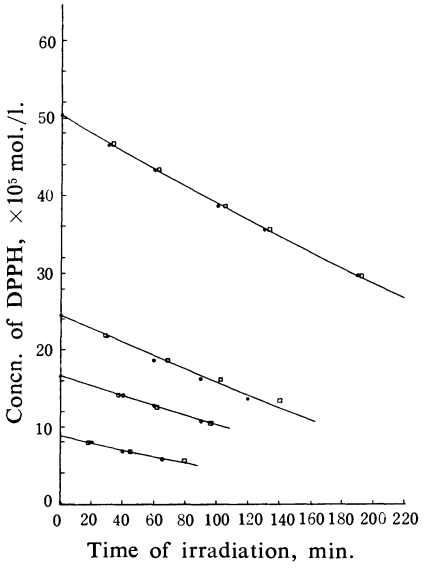

Fig. 7. Rate of decomposition of DPPH at various initial concentrations in carbon tetrachloride at 25°C. Marks of square □ show the calculated values from Eq. 3.

careful inspection of the plots of the concentration of DPPH against the time revealed their slight deviation from linearity, showing that more complicated processes are involved. The initial rate increases with the initial concentration of DPPH up to a limiting value at a higher concentration of 5.0×10^{-4} mol./l. of DPPH.

In order to obtain the appropriate kinetic expression for these experimental results, a plot of $1/(dx/dt)$ against $1/x$ is given in Fig. 8, which shows a fairly good linear relationship. Taking this result into consideration, the following empirical rate equation is introduced;

$$-dx/dt = KI_a x/(x+\alpha) \qquad (1)$$

or

$$-1/(dx/dt) = 1/KI_a + (\alpha/KI_a)/x \qquad (1')$$

where K and α are constants. I_a, the average rate of light absorption is kept constant through

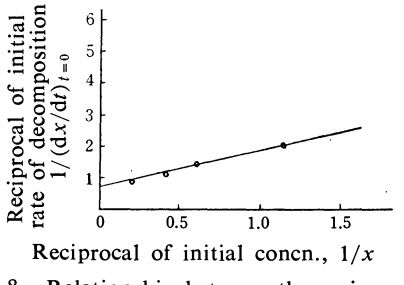

Fig. 8. Relationship between the reciprocal of initial concentration ($1/x$) and that of the initial rate of decomposition ($1/(dx/dt)_{t=0}$) obtained from Fig. 7.

the each series of experiments, though there is some variation between the different series of experiments. The determination of the amount of light absorbed has not been carried out, so that the quantum yield of this experiment is not known at present. As is shown in Fig. 7, the initial concentration of DPPH ranged from 10^{-4} to 5×10^{-4} mol./l., insuring a nearly complete absorption of light. In Table I, the values of α/KI_a and $1/KI_a$ as slope and as its intercept in the ordinate axis, calculated by the least square method from each run of I, II, III, IV in Fig. 7, are given. In addition the values of the slope and the intercept obtained by plotting $1/(dx/dt)_{t=0}$ against $1/x$ in the four runs in Fig. 7 are given in the last column.

TABLE I

	I	II	III	IV	
$\alpha/KI_a\times10^{-2}$	1.63	0.19	0.69	0.61	1.41
$1/KI_a\times10^{-5}$	4.88	10.21	10.10	14.05	5.65

The values of α and KI_a calculated from the figures in the last column are 1.8×10^{-4} mol./l. and 2.5×10^{-6} mol./l. min. respectively*.

As may be seen, the variations in the values of the slope and of the intercept in four runs seem to be fairly large, but the following procedure of the recalculation of x at the various intervals of the reaction time, using the values in the last column, shows that these values are actually within the range of experimental error.

Integrating Eq. 1, Eq. 2 is obtained,

$$(x_0-x)+2.303\ \alpha\log(x_0/x) = KI_a t \qquad (2)$$

where x_0 is the initial concentration of DPPH. Using $\alpha=1.8\times10^{-4}$ mol./l. and $KI_a=2.5\times10^{-6}$ mol./l. min., a relation between x and t was obtained. The calculated values of x from Eq. 2 at various time intervals are plotted in Fig. 7, with a square mark showing that the agreement between observed and calculated values is satisfactory.

The Influence of Temperature on the Decomposition Rate.—The rate of the decomposition of DPPH in carbon tetrachloride was measured at 10, 30 and 50°C. The results are shown in Fig. 9.

The increase in the reaction rate with the temperature indicates that some temperature-dependent processes are involved in the reaction. The plots of $1/(dx/dt)$ against $1/x$ for the curves in Fig. 9 are shown in Fig. 10; KI_a and α in Eq. 1′ at 10, 30 and 50°C were determined from each line. From the values of the

* The probable ranges of KI_a and α with 95% reliability are $3.7\times10^{-6}>KI_a>1.2\times10^{-6}$ and $6.8\times10^{-4}>\alpha>1.2\times10^{-4}$ respectively.

usual Arrhenius plot, the activation energy and frequency factor were evaluated. The results are listed in Table II.

TABLE II. KI_a AND α AT 10, 30 AND 50°C, AND THE CALCULATED ACTIVATION ENERGY (E) AND FREQUENCY FACTORS (A)

	10°C	30°C	50°C	ΔE	A
KI_a	1.27 $\times 10^{-6}$ a)	2.00 $\times 10^{-6}$	2.93 $\times 10^{-6}$	3.8 $\times 10^{3}$ c)	1.2 $\times 10^{-3}$
α	0.34 $\times 10^{-4}$ b)	0.58 $\times 10^{-4}$	0.84 $\times 10^{-4}$	4.1 $\times 10^{3}$	5.2 $\times 10^{-2}$

a) mol./l. min.
b) mol./l.
c) cal.

In addition to these experiments, the induction period and the after effect were investigated, but neither of them was noticeable in the carbon tetrachloride solution, as is shown in Fig. 9.

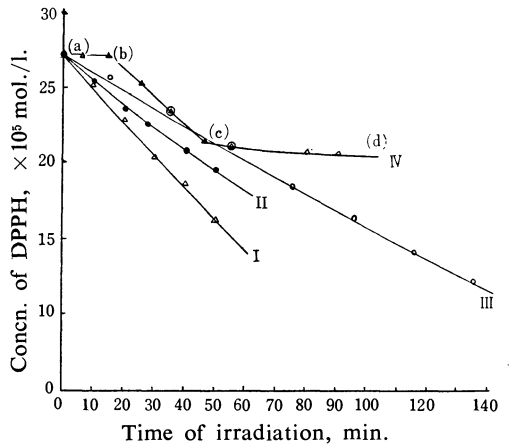

Fig. 9. Influence of temperature on the decomposition rate of DPPH in carbon tetrachloride measured at 520 mμ.
I, IV: 50°C, II: 30°C, III: 10°C, (a)—(b): in the dark, (b)—(c): light on, (c)—(d): light off.

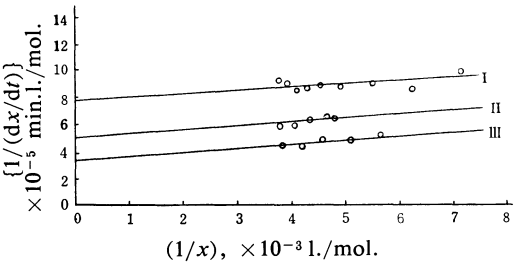

Fig. 10. Plot of $1/(dx/dt)$ against $1/x$ in Eq. 1'.
I: 10°C, II: 30°C and III: 50°C

Discussion of the Reaction Mechanism

The kinetic data obtained above are not enough to establish a unique and overall reaction mechanism, but some possible mechanisms will be discussed. As in most photochemical reactions, the process of this reaction may consist of excitation, quenching (deactivation), and chemical reaction. No fluorescence of DPPH in solution is observed. The deactivation of excited DPPH may proceed by solvent or by another DPPH. As the primary process of chemical reaction, the three different mechanisms, (I) the spontaneous decomposition of excited DPPH, (II) the bimolecular decomposition of the excited DPPH with normal DPPH, and (II') the complex formation of excited DPPH with other molecules of DPPH and the successive decomposition of the complex, are considered, and the expression of the rate of disappearance of DPPH in terms of the concentration of DPPH is derived from each mechanism. The succeeding process of the reaction seems to be complicated, but it may be reasonably assumed that it does not modify the main character of the kinetic expression of the rate of disappearance of DPPH, because the relative ratio of the products is almost constant throughout the course of the reaction, as the succeeding paper will show.

Mechanism I

$$\begin{aligned} &D+h\nu &&\longrightarrow D^* && I_a \\ &D^*(+\text{Solvent}) &&\longrightarrow D && k_1 \text{ (I-1)} \\ &D^*+D &&\longrightarrow 2D && k_2 \text{ (I-2)} \\ &D^* &&\longrightarrow A+B && k_3 \text{ (I-3)} \end{aligned}$$

$$-dx/dt = I_a k_3/(k_1+k_3+xk_2) \qquad (3)$$

Mechanism II

$$\begin{aligned} &D+h\nu &&\longrightarrow D^* && I_a \\ &D^*(+\text{Solvent}) &&\longrightarrow D && k_1 \text{ (II-1)} \\ &D^*+D &&\longrightarrow 2D && k_3 \text{ (II-3)} \\ &D^*+D &&\longrightarrow A+B && k_4 \text{ (II-4)} \end{aligned}$$

$$-dx/dt = 2I_a k_4 x/\{k_1+(k_3+k_4)x\} \qquad (4)$$

Mechanism II'

$$\begin{aligned} &D+h\nu &&\longrightarrow D^* && I_a \\ &D^*(+\text{Solvent}) &&\longrightarrow D && k_{1'} \text{ (II'-1)} \\ &D^*+D &&\longrightarrow D^*D && k_{2'} \text{ (II'-2)} \\ &D^*D(+\text{Solvent}) &&\longrightarrow 2D && k_{3'} \text{ (II'-3)} \\ &D^*D &&\longrightarrow A+B && k_{4'} \text{ (II'-4)} \end{aligned}$$

$$-dx/dt = 2I_a\{xk_{2'}/(xk_{2'}+k_{1'})\}\{k_{4'}/(k_{3'}+k_{4'})\} \qquad (5)$$

where D is a molecule of DPPH, D* is an excited DPPH. The structures of A and B are not known, but it may be reasonably assumed that they are free radicals or reactive molecules, such as NO_2. Mechanism 1, which assumes the

spontaneous decomposition of excited DPPH, does not agree with the experimental results, because the rate expression derived from this mechanism requires a decrease in the rate with a decrease in the concentration of DPPH. The second and third mechanisms have similar kinetic characteristics of rate expression; that is, the rate increases with the concentration. Both satisfy the requirement of kinetic expression (1)*, making it impossible to choose a mechanism on the basis of the present experimental results only. These two mechanisms differ in the point that the complex has some definable lifetime in the latter. The authors are slightly in favor of the latter mechanism, considering similar experimental evidence. Förster and Kasper[5] presumed a complex formation of excited pyrene with normal pyrene from their observation of fluorescence. It is likely that excited DPPH forms a complex with normal DPPH, for many aromatic polynitro compounds tend to form a complex, even at the ground state. If the flash photolysis technique could be applied to the present case, it would be possible to determine whether or not a dimer complex of DPPH is present. According to the proposed reaction mechanisms II and II', the experimental constants, KI_a, in Eq. 1 are related to the rate constants of Eqs. 4 and 5.

According to mechanism II,

$$K=2k_4/(k_3+k_4)$$

and

$$\alpha=k_1/(k_3+k_4)$$

Considering the fact that K increases with the temperature, we might assume that $k_3 \gg k_4$, since otherwise K would actually be independent of the reaction temperature. Assuming $k_3 \gg k_4$, the relation

$$K \fallingdotseq 2k_4/k_3$$

would be derived; this also gives an interpretation of the experimental activation energy:

$$E_4-E_3 \fallingdotseq E_K=3.8 \text{ kcal./mol.}$$

and

$$2I_aA_4/A_3 \fallingdotseq A_{KI_a}=1.2\times10^{-3}$$

It is reasonable that reaction 4 has a larger activation energy than reaction II-3, because the latter is a simple deactivation process.

A similar treatment may be applied to the temperature dependence of α. Assuming $k_3 \gg k_4$, we might also derive the relation

$$\alpha \fallingdotseq k_1/k_3$$

$$E_1-E_3 \fallingdotseq E_\alpha=4.1 \text{ kcal./mol.}$$

and

$$A_1/A_3=A_\alpha=5.2\times10^{-2} \text{ l./mol.}*$$

The finding that reaction II-1 has an appreciable amount of activation energy is not well understood, since the reaction is a simple deactivation process of an excited DPPH with a solvent.

Since the value of I_a is not known, no further discussion of the frequency term will be attempted at this stage.

In mechanism II', a similar argument may be applied, giving the relations:

$$E_K=E_{4'}-E_{3'}, \quad A_{KI_a}=2I_aA_{4'}/A_{3'}$$

and

$$E_\alpha=E_{1'}-E_{2'}, \quad A_\alpha=A_{1'}/A_{2'}$$

Experimental

Material.—DPPH was prepared by the method of Porier[6], recrystallized from a chloroform-ether mixture (1 : 1 by volume), and dried in vacuo at 80°C for more than 10 hr.[7] The solvents used were purified by ordinary methods[8].

Procedure.—A solution of DPPH was irradiated in a thermostat with a light of a constant intensity, and after various periods of time the concentration of DPPH was determined with a spectrophotometer at its maximum absorption ($\lambda_{max}=520 \text{ m}\mu$). The light source was a tungsten lamp (100 V. 150 W), and variations of the source voltage were compensated for by a manual setting of a transformer. The range of wavelengths of the irradiating light was varied by choosing a proper filter.

The light intensity was varied with copper nets of several different meshes, blackened with ammonium sulfide.

In order to study the effect of oxygen on the photolysis of DPPH, the experiments were carried out both in the presence of air and in the absence of air. The solution in the latter experiment was prepared by the following procedure, using the apparatus shown in Fig. 11.

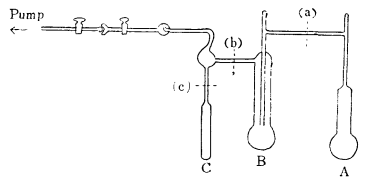

Fig. 11. Shematic diagram of the apparatus of preparing the sample in vacuo.
C: Reaction cell

* For convenince in comparing reaction mechanisms II and II', the rate constants are numbered k_1, k_3 and k_4 in the reaction II instead of k_1, k_2 and k_3. The following relation is easily derived by a comparison of the two mechanisms: $k_3=k_2'k_3'/(k_3'+k_4')$ and $k_4=k_2'k_4'/(k_3'+k_4')$.

5) T. Förster and K. Kasper, *Z. Elektrochem.*, **59**, 976 (1955).

* It is to be noted that k_1 is a pseudo-first-order rate constant and that the second-order rate constant, k_1*, is obtained by dividing k_1 by the number of moles of solvent (10.2 mol.) in one liter, giving the relation $A_\alpha/10.2=A_1*/A_3=5.1\times10^{-3}$.

6) R. H. Porier, E. J. Kahler and F. Benington, *J. Org. Chem.*, **17**, 1437 (1952).

7) J. A. Lyons and W. F. Watson, *J. Polymer Sci.*, **18**, 141 (1955).

8) A. Weisberger and E. S. Proskauer, "Technique of Organic Chemistry", Vol. VII, Interscience Publishers, Inc., New York (1955).

DPPH was placed in B, and a purified solvent was distilled into B from A after degassing. Then A was sealed at (a), a part of the solution in B was poured into C, and B was sealed at (b). The rest of the solution in B was used for the comparative experiments in the presence of air. The solution in C was degassed on a high vacuum line with several repetitions of freezing in liquid nitrogen (−196°C) and melting to remove the residual gas. A reaction cell C was then sealed at (c), and the concentration of the solution was determined photometrically, without contact of the solution with air.

Summary

Studies of the photochemical decomposition of DPPH in solution have been made by the kinetic method.

1) The decomposition proceeds by means of the light in the region of the first absorption band of DPPH ($\lambda_{max}=520\,m\mu$), and the decomposition rate has a linear dependence on the amount of light absorbed.

2) A rate expression fitting the kinetic experiment has been obtained, and this expression has been compared with the rate expession derived on the basis of the possible reaction mechanism, which includes the process of the reaction of an excited DPPH with another, normal DPPH.

3) An increase in the rate with the reaction temperature has been observed in the temperature range 10～50°C, and the two constants determined in the experiment have been related to the rate constants of the elementary processes in the proposed reaction mechanism.

The authors wish to express their thanks to Dr. Hiroshi Suzuki of The University of Tokyo for reading the manuscript and for his invaluable advice. Thanks are also due to Mrs. Robert Back of the National Research Council, Canada, for reading the manuscript.

Department of Chemistry
College of General Education
The University of Tokyo
Meguro-ku, Tokyo

*Syntheses and Structures of Acetylformoin and its Related Compounds. II. Neopentoylformoin**

By Yō MIYAGI and Ryozo GOTO

(Received December 27, 1962)

It is well known that the condensation of ketoaldehydes in the presence of alkali cyanide yields formoins:

$$2\ \mathrm{RCOCHO} \xrightarrow{CN^-} \mathrm{RCOCH(OH)COCOR}$$

Condensation products of phenyl-[1], *p*-methoxyphenyl-[2], *p*-chlorophenyl-[3], *p*-bromophenyl-[3], mesitoyl-[4] and methylglyoxal[5,6] have been reported. Benzoylformoin was synthesized by Abenius[7] in a totally different way.

For these formoins, the following five structures are possible. Structure IV was suggested for benzoylformoin on the basis of the fact

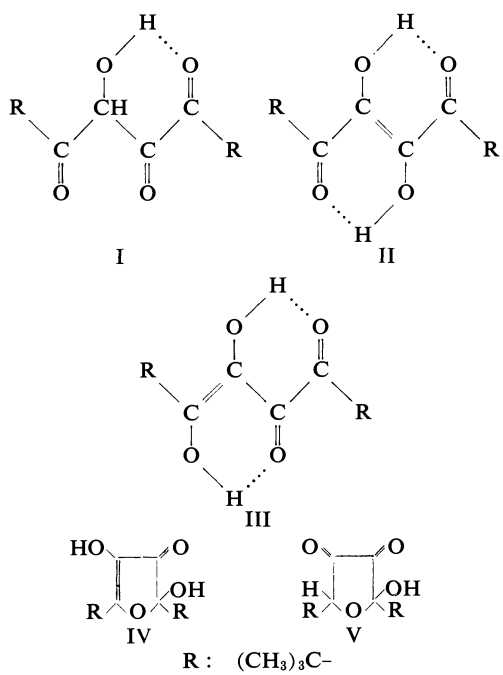

* Presented in part at the 13th Annual Meeting of the Chemical Society of Japan, Tokyo, April, 1960.

1) R. Goto, Y. Miyagi and H. Inokawa, This Bulletin, **36**, 147 (1963).
2) P. Karrer and A. v. Segesser, *Helv. Chim. Acta*, **18**, 273 (1935).
3) P. Karrer and C. Musante, ibid., **18**, 1140 (1935).
4) A. R. Gray and R. C. Fuson, *J. Am. Chem. Soc.*, **56**, 1367 (1934).
5) R. Nodzu and S. Kunichika, This Bulletin, **15**, 211 (1940).
6) E. Steinbauer and E. Waldman, *Monat.*, **89**, 569 (1958).
7) P. W. Abenius and H. G. Söderbaum, *Ber.*, **24**, 3033 (1891); **25**, 3468 (1892); P. W. Abenius, ibid., **27**, 706 (1894).

that it undergoes alcoholysis with an alcoholic solution of an acid to give an alkoxy compound[8]. This fact, however, can not afford a straight foreward deduction of structure IV

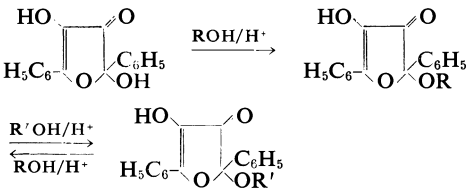

for benzoylformoin itself. The formation of a quinoxaline derivative suggested structure III.

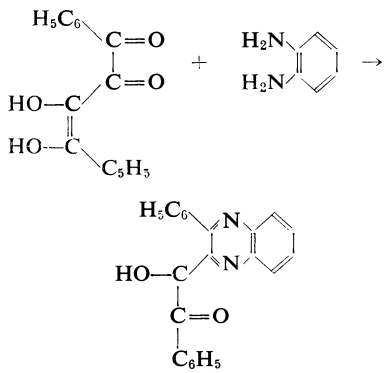

On these bases, an equilibrium between III and IV in solution was proposed[8].

Steinbauer and Waldman[6] also studied the reaction of acetylformoin with *o*-phenyleneamine:

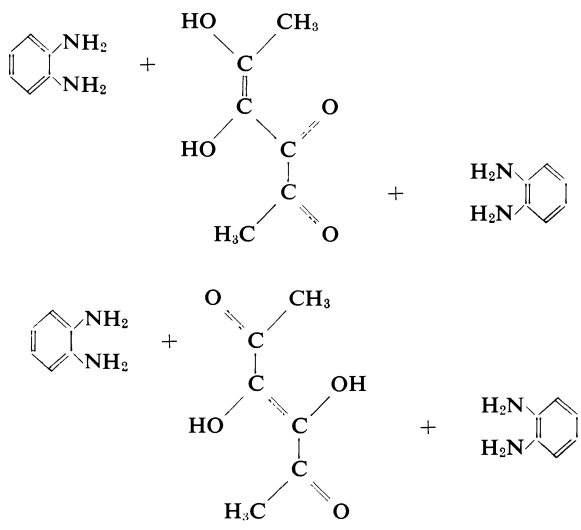

In a previous paper[1], the authors reported that the crystal of acetylformoin has the enediol structure II (R=CH_3) while that of benzoylformoin does the furanone structure IV (R=C_6H_5). In the present paper, the structure of neopentoylformoin and its properties are being reported.

Results and Discussion

Neopentoylformoin is prepared by the action of an alkali cyanide on an aqueous alcoholic solution of *t*-butylglyoxal. The chemical behaviors of neopentoylformoin are rather like those of benzoylformoin[8]. Neopentoylformoin suffers methanolysis with methanolic hydrogen chloride to give a mono-*O*-methyl derivative and ethanolysis with ethanolic hydrogen chloride to give a mono-*O*-ethyl derivative. Furthermore, the mono-*O*-methyl derivative is converted to the *O*-ethyl derivative and vice

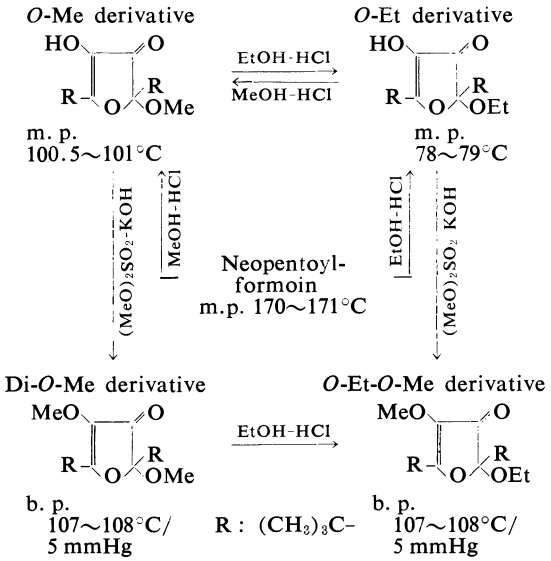

Fig. 1

8) A. H. Blatt, *J. Am. Chem. Soc.*, **57**, 1103 (1935); **58**, 1894 (1936).

versa. Another methoxy group was introduced into the *O*-alkyl derivatives by the methylation with dimethyl sulfate or methyl iodide. It was also tried to convert the di-*O*-methyl derivative to an *O*-ethyl-*O*-methyl derivative, ethanolic hydrogen chloride being used as reagent. Though the boiling point of the product is the same as that of the starting di-*O*-methyl derivative, the completion of the conversion was proved by the fact that the alkoxyl group content and elementary analysis coincided quite well with the values calculated for the *O*-ethyl-*O*-methyl derivative.

This sequence of reactions may be illustrated as in Fig. 1, since the etherification with an alcoholic solution of an acid is characteristic of the glycosidic linkage. Therefore, the structure of the mono-*O*-alkyl derivatives and that of the di-*O*-alkyl derivatives are established as VI, 2, 5-di-*t*-butyl-2-alkoxy-4-oxy-furanone-3 and VII, 2, 5-di-*t*-butyl-2, 4-dialkoxy-furanone-3, respectively.

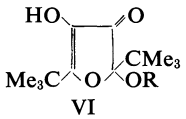

VI

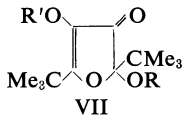

VII

The above sequence of reactions, however, can not suggest structure IV for neopentoylformoin itself, because the equilibrium could be shifted to produce VI in the presence of acids:

$$\text{III} \rightleftharpoons \text{IV} \xrightarrow{H^+} \text{VI}$$

The structure of neopentoylformoin must be determined by another method.

The data of infrared spectra are listed in Table I.

Table I. Absorption bands of infrared spectra (cm^{-1})

Neopentoyl-formoin	Mono-*O*-Me deriv.		Di-*O*-Me deriv.	Benzoyl-formoin
Nujol	Nujol	CCl_4 soln.	CCl_4 soln.	Nujol
3330	3310	3290	—	3500
3180	—	—	—	3210
1690	1690	1693	1705	1688
1600	1600	1610	1615	1605
				1595

Neopentoylformoin and the mono-*O*-methyl derivative were examined as a solid state in Nujol*, then the latter and the di-*O*-methyl derivative as the solution in carbon tetrachloride.

In the regions of the C=O and C=C stretching absorption, there are found very little changes between the spectrum of neopentoylformoin and those of derivatives: neopentoylformoin and the mono-*O*-methyl derivative absorb at 1690 and 1600 cm^{-1}; the latter compound shows similar spectra both in Nujol and in solution; in the di-*O*-methyl derivative, the corresponding absorption bands arise at 1705 and 1615 cm^{-1}.

Since the spectrum of neopentoylformoin is very similar to those of its derivatives**, structure IV, 2, 5-di-*t*-butyl-2, 4-dioxy-furanone-3, may be assigned to neopentoylformoin. This assignment is further supported by the fact that the spectrum of neopentoylformoin is very similar to that of benzoylformoin, the structure of which was established as IV ($R=C_6H_5$)[1].

The absorption band at 1690 cm^{-1} and that at 1600 cm^{-1} may be assigned to the C=O and C=C stretching absorption, respectively. Other structures I, II, III and V seem to be unreasonable on the basis of similar reasons as seen in a previous paper[1].

In the region of the OH stretching absorption, neopentoylformoin shows two distinct bands at 3330 and 3180 cm^{-1} in Nujol. The mono-*O*-methyl derivative shows a distinct band at 3310 cm^{-1} in Nujol and broad one at 3290 cm^{-1} in solution. With *O*-alkylation there occurs a similar change of the spectra of neopentoylformoin and benzoylformoin in Nujol: both formoins show two OH stretching absorption bands while their mono-*O*-alkyl derivatives do only one of the OH stretching absorption. However, nothing conclusive can be deduced from these data of the OH stretching absorption bands, since the OH stretching absorption bands are easily shifted by the strength of hydrogen bondings.

On melting the color of neopentoylformoin turned to red. It is very interesting benzoylformoin changes its color from yellow to red on melting. Blatt considered, without striking evidence, that the reddish distillate of benzoylformoin was enediol II. The authors are also of opinion that the structure of melted neopentoylformoin is an enediol, II or III. However no evidece has been found.

Experimental

Synthesis of Neopentoylformoin.—In 100 ml. of 70% aqueous alcohol, *t*-butylglyoxal hydrate[9] (4 g.) was dissolved. The solution was cooled to 0°C. To this solution, a solution of 0.25 g. of sodium cyanide in 10 ml. of 50% aqueous alcohol was added with stirring. The solution immediately colored yellow. After stirring for 30 min.,

* Neopentoylformoin is insoluble in carbon tetrachloride or other desirable solvents for the spectrophotometric measurement.

** The structures of the derivatives are established as VI and VII, as mentioned above.

9) R. C. Fuson, H. Gray and J. J. Gouza, *J. Am. Chem. Soc.*, **61**, 1937 (1939).

alcohol was evaporated under reduced pressure. White crystals were collected by filtration and washed with water and dried in vacuo over phosphorus pentoxide. Yield, 2.3 g. (73%). Recrystallization was effected from isopropanol. Yield, 1 8 g. (56%). M. p. 170~171°C. Insoluble in ordinary organic solvent except alcohols.

Found: C, 63.04; H, 8.86; mol. wt. (Rast) 219. Calcd. for $C_{12}H_{10}O_4$: C, 63.16; H, 8.77%; mol. wt., 228.

When a crude glyoxal monomer[9] was used, the procedure was the same except for purification; crude formoin was dissolved in a minimum amount of alcohol and precipitated with addition of water.

Mono-*O*-methyl Derivative.—In about 10 ml. of 12% methanolic hydrogen chloride, 2 g. of neopentoylformoin was dissolved. After standing overnight at room temperature, alcohol and acid were evaporated under reduced pressure. The residue, dried in vacuo over potassium hydroxide, was washed quickly with cold water and dried in vacuo over phosphorus pentoxide. M. p. 100.5~101°C.

Found: C, 64.64; H, 9.25; MeO, 12.75. Calcd. for $C_{13}H_{22}O_4$: C, 64.64; H, 9.07; MeO, 12.81%.

Mono-*O*-ethyl Derivative.—The procedure was the same as in methanolysis. M. p. 77~78°C.

Found: C, 65.41; H, 9.43. Calcd. for $C_{14}H_{24}O_4$: C, 65.52; H, 9.38.

Di-*O*-methyl Derivative.—*Method A.*—In 20 ml. of water containing 1 g. of potassium hydroxide, mono-*O*-methyl derivative (4 g.) was dissolved. The solution was brilliant yellow. Into this solution, 2 g. of dimethyl sulfate was added during 30 min. with stirring, and stirring was continued for additional 30 min. After addition of 0.5 g. of potassium hydroxide, the dropping of 1 g. of dimethyl sulfate was continued during 30 min. and then the solution was stirred for additional 30 min. at 50°C. During the reaction, the yellow color of the solution was diminished and colorless oil separated. The whole solution was extracted with carbon tetrachloride. The extract was dried over anhydrous sodium sulfate. The solvent was evaporated and the residue of colorless liquid was distilled under reduced pressure. Fraction boiling at 107~108°C/5 mmHg was collected. Yield, 2.3 g. (53%).

Found: C, 65.51; H, 9.40; MeO, 24.12. Calcd. for $C_{14}H_{24}O_4$: C, 65.52; H, 9.38; MeO, 24.22%.

Method B.—In 30 ml. of absolute methanol containing 0.6 g. of sodium, mono-*O*-derivative (3.6 g.) was dissolved. The solution colored yellow. After addition of 20 g. of methyl iodide, the solution was refluxed for 4 hr. During this period, the color of solution was diminished as in method A. The solution was stood overnight at room temperature. After the addition of 10 ml. of water, methanol was evaporated under reduced pressure. The residue was extracted with ether. The extract was dried over anhydrous sodium sulfate. Ether was evaporated off. The residue of pale yellow liquid was distilled under reduced pressure. Fraction boiling at 107~108°C/5 mmHg was collected. Yield, 2.1 g. (58%).

Found: C, 65.51; H, 9.40%.

The infrared spectrum of the product in carbon tetrachloride solution was coincident with that of the product obtained in the method A even in details.

***O*-Ethyl-*O*-methyl Derivative.**—This compound was prepared as in the method A and boiling at 107~108°C/5 mmHg.

Found: C, 66.74; H, 9.41; RO, 27.94. Calcd. for $C_{15}H_{26}O_4$: C, 66.66; H, 9.63; RO, 28.14%.

The Conversion of the Mono-*O*-methyl Derivative to the Mono-*O*-ethyl Derivative and Vice Versa.—About 0.1 g. of mono-*O*-methyl derivative was dissolved in 1 ml. of 8% ethanolic hydrogen chloride and the procedure was the same as above. M. p. 78~79°C. Mixed melting point with the authentic *O*-ethyl derivative showed not any depression. The procedure was the same in the case of the conversion of the *O*-ethyl derivative to the *O*-methyl derivative. M. p. 100~101°C. Not any depression of the melting point was observed at a mixed melting point.

The Conversion of the Di-*O*-methyl Derivative to the *O*-Ethyl-*O*-methyl Derivative.—A solution of 3 g. of di-*O*-methyl derivative in 15 ml. of 12% ethanolic hydrogen chloride was stood overnight at room temperature. The solvent and the acid were evaporated under reduced pressure and evaporation was repeated with addition of absolute ethanol and the residue of liquid was dissolved in carbon tetrachloride. The solution was washed with cold water, then dried over anhydrous sodium sulfate. Removal of the solvent, followed by distillation, gave 2.2 g. of liquid; boiling at 105~109°C/5 mmHg.

Found: C, 66.65; H, 9.36; RO, 28.01%.

Spectra and Alkoxy Group.—The infrared spectra were recorded with a Koken model DS-301 spectrophotometer.

The alkoxy group content was determined by the method of Hoffman and Wolfrom[10].

Department of Chemistry
Faculty of Science
Kyoto University
Sakyo-ku, Kyoto

10) D. O. Hoffman and M. L. Wolfrom, *Anal. Chem.*, **19**, 225 (1947).

Solvent Effects on the Absorption and Fluorescence Spectra of Naphthylamines and Isomeric Aminobenzoic Acids

By Noboru MATAGA

(Received January 10, 1963)

The solvent effects upon the absorption spectra and those upon the fluorescence spectra are different from each other.

From the study of this difference one may derive some information concerning the nature of the electronically-excited state in contrast to the ground state and also the nature of the interactions between solute and solvent molecules in the excited as well as the ground state.

On the other hand, the nature of the electronic states of such substituted aromatic hydrocarbons as hydroxy and amino derivatives seems to be not so well understood as that of the parent hydrocarbons[1-4] and their aza-derivatives[5-9].

Recently, a number of studies[10,11] have been carried out to elucidate the electronic structures and spectra of the former. Baba[10] has made comparative studies of the mono-substituted hydroxy and amino derivatives of benzene and naphthalene and has made the assignment of the electronic absorption bands of these molecules.

We present here a somewhat different approach to the electronic structures of naphthylamines. We are mainly interested in the electronically excited states and in the difference between the electronic structure in the excited state and that in the ground state. We shall demonstrate in the following the remarkable difference between the conjugation power of the hydroxy and that of the amino group by measuring the solvent effects on the electronic spectra.

Further, the results of similar measurements on isomeric aminobenzoic acids (ABA) will be described, with some discussion of the electronic structure of these molecules.

Experimental

Apparatus.—The absorption spectra were measured with a Beckman spectrophotometer model DU. Details of the fluorescence spectrophotometer have been described elsewhere[12]. The light source for *p*-ABA was a 300 W xenon discharge tube with a stabilizer. For other compounds used in the present study, a high-pressure mercury discharge tube was used as a light source.

The fluorescence of *p*-ABA was excited at 290 mμ, the monochromatic exciting light from the xenon discharge tube being taken out by a quartz prism monochromater. Doublet lines at 313 mμ, taken out from the high-pressure mercury discharge tube by the monochromator, were used for exciting the other compounds.

All measurements were carried out at room temperature ($\sim$20°C).

Materials. — The naphthylamines were recrystallized from ligroin and sublimated in a vacuum. The ABA's were purified by sublimation in a vacuum. Special grade benzene was dried over metallic sodium and distilled fractionally. Cyclohexane was dried over metallic sodium, distilled fractionally and the distillate was then passed through a column of activated silica gel for chromatographic use. *n*-Hexane was shaken with fuming sulfuric acid diluted with concentrated sulfuric acid, washed with water several times, dried over calcium chloride and distilled carefully. The acetic acid esters were dried over potassium carbonate and distilled fractionally. Acetonitrile was refluxed repeatedly over phosphorus pentoxide, distilled into potassium carbonate and fractionally distilled from it. Chloroform was shaken with concentrated sulfuric acid, washed with water, and after being dried over phosphorus pentoxide, distilled carefully. Methanol and ethanol were refluxed with silver nitrate, and after being refluxed with calcium-carbonate, fractionally distilled. Normal butanol was washed with dilute sulfuric acid and with a sodium bisulfate solution. The treated alcohol was then dried with potassium carbonate and fractionally distilled. Monochlorobenzene was dried with phosphorus pentoxide and fractionally distilled. Dioxane was refluxed with dilute hydrochloric acid, treated with potassium hydroxide, dried over metallic sodium and then fractionally distilled from it.

1) J. R. Platt, *J. Chem. Phys.*, **17**, 484 (1949).
2) J. A. Pople, *Proc. Phys. Soc.*, **A68**, 881 (1955).
3) R. Pariser, *J. Chem. Phys.*, **24**, 250 (1956).
4) N. Mataga, K. Nishimoto and S. Mataga, This Bulletin, **32**, 395 (1959).
5) R. Mcweeny, *Proc. Phys. Soc.*, **A70**, 593 (1957).
6) T. E. Peacock, ibid., **A70**, 654 (1957).
7) N. Mataga and K. Nishimoto, *Z. Phys. Chem. N. F.*, **13**, 140 (1957).
8) N. Mataga, ibid., **18**, 285 (1958); This Bulletin, **31**, 453, 459, 463 (1958).
9) R. D. Brown and M. L. Heffernan, *Australian J. Chem.*, **12**, 554 (1959).
10) H. Baba. This Bulletin, **34**, 76 (1961); H. Baba and S. Suzuki, ibid., **34**, 82 (1961).
11) K. Nishimoto and R. Fujishiro, ibid., **31**, 1036 (1958); **35**, 905 (1962).
12) N. Mataga, Y. Torihashi and Y. Kaifu, *Z. Phys. Chem. N. F.*, **34**, 379 (1962).

Experimental Results

Naphthylamines. — Some examples of the solvent shifts of the absorption and fluorescence spectra of naphthylamines are shown in Figs. 1 and 2. In these figures, the intensity of the maximum of each fluorescence band is brought to the same value as that of the corresponding absorption band.

One may observe from Figs. 1 and 2 that the red shift of the absorption and fluorescence spectra becomes larger, the greater the dielectric constant of the solvent, and that the shift of the fluorescence band is much larger than that of the absorption band. This anomalous Stokes red shift can be ascribed to the change in solute-solvent interaction during the lifetime of the excited solute molecule[14-15].

In other words, according to the Franck-Condon principle, the configuration of the solvent molecules surrounding the solute molecule does not change during the light absorption. The momentary excited state (Franck-Condon excited state) is, in general, not the most stable equilibrium state appropriate to the excited solute molecule. The equilibrium-excited state can be reached completely or partially by reorganization of the configurations of the surrounding molecules during the lifetimes of the excited solute molecule.

We can use this difference between the solvent shifts of absorption and fluorescence spectra in order to get experimental information on the electronic structure of the excited molecule[13-15].

In the present study, we have used the method (Eq. 1) proposed by Lippert[14] and by the present author[15], for the evaluation of $\vec{\Delta\mu}$, the difference between the excited state dipole moment, $\vec{\mu_e}$, and that in the ground state, $\vec{\mu_g}$, i.e., $\vec{\Delta\mu}=\vec{\mu_e}-\vec{\mu_g}$, where the excited state is the fluorescent state.

$$hc\Delta\sigma \simeq \text{Const.} + 2\cdot F(D,n)\cdot(\vec{\Delta\mu})^2/a^3$$

$$\Delta\sigma = \sigma_a{}^m - \sigma_f{}^m$$

$$F(D,n) = \left(\frac{D+1}{2D+1} + \frac{n^2+1}{2n^2+1}\right) \qquad (1)$$

In Eq. 1, $\sigma_a{}^m$ and $\sigma_f{}^m$: the wave number of a peak of the fluorescence band and that of the corresponding absorption band respectively; D and n: the dielectric constant and refractive index of the solvent and a: the cavity radius in Onsager's theory of the reaction field. The observed values of $\sigma_a{}^m$, $\sigma_f{}^m$ and $\Delta\sigma$ are given in Table I, together with the values of $F(D,n)$.

Thus, the observed values of $\Delta\sigma$ are plotted against the values of $F(D,n)$, in Fig. 3. As one can see from this figure, Eq. 1 is approximately satisfied, that is, an approximate linear

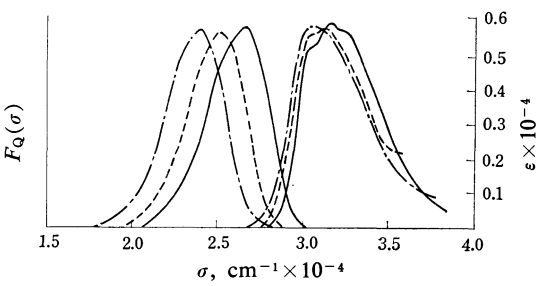

Fig. 1. Absorption and fluorescence spectra of α-naphthylamine.
Solvent: ——— *n*-Hexane
– – – Monochlorobenzene
—·—· Acetonitrile
Concn. of the naphthylamine $\sim0.8\times10^{-4}$ mol./l.

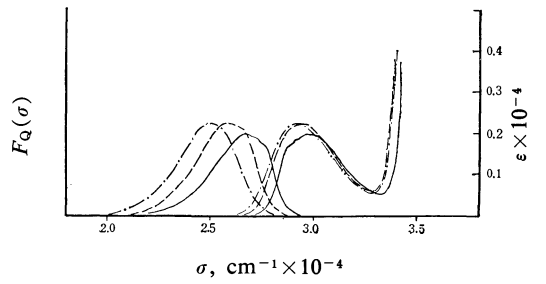

Fig. 2. Absorption and fluorescence spectra of β-naphthylamine.
Solvent: ——— *n*-Hexane
– – – Monochlorobenzene
—·—· Acetonitrile
Concn. of the naphthylamine $\sim2.0\times10^{-4}$ mol./l.

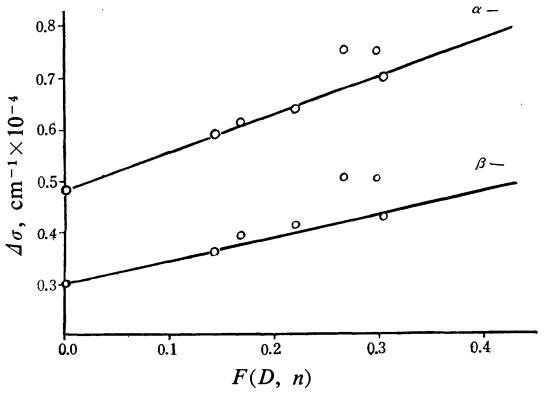

Fig. 3. $\Delta\sigma$ vs. $F(D, n)$ relation for naphthylamines.

13) N. S. Bayliss and E. G. McRae, *J. Phys. Chem.*, **58**, 1002 (1954); E. G. McRae, ibid., **61**, 562 (1957).
14) E. Lippert, *Z. Naturforsch.*, **10a**, 541 (1955); *Z. Elektrochem.*, **61**, 962 (1957).
15) N. Mataga et al., This Bulletin, **28**, 690 (1955); ibid., **29**, 465 (1956).

TABLE I*. THE WAVE NUMBERS OF THE BAND MAXIMA OF NAPHTHYLAMINES IN VARIOUS SOLVENTS

Solvent	$F(D, n)$	α-Naphthylamine			β-Naphthylamine		
		σ_a^m	σ_f^m	$\Delta\sigma$	σ_a^m	σ_f^m	$\Delta\sigma$
n-Hexane	0	3.14	2.66	0.48	2.96	2.66	0.30
Monochlorobenzene	0.143	3.10	2.51	0.59	2.93	2.58	0.35
n-Butyl acetate	0.171	3.07	2.46	0.61	2.90	2.51	0.39
Methyl acetate	0.220	3.06	2.43	0.63	2.92	2.51	0.41
n-Butanol	0.267	3.13	2.31	0.82	2.96	2.46	0.50
Ethanol	0.298	3.13	2.31	0.82	2.96	2.46	0.50
Acetonitrile	0.304	3.07	2.38	0.69	2.91	2.49	0.42

relation between $\Delta\sigma$ and $F(D, n)$ holds, although the $\Delta\sigma$ values of alcohol solutions deviate considerably from the linear relation.

Among the solvents used here, acetic acid esters and alcohols can form hydrogen bonds with naphthylamines of the types,

$$\mathrm{R{-}\underset{\underset{H}{|}}{N}{-}H\cdots O{=}C\langle^{R'}_{R''}},$$

and $\mathrm{R{-}\underset{\underset{H_2}{|}}{N}\cdots H{-}O{-}R'}$ or $\mathrm{R{-}\underset{\underset{H}{|}}{N}{-}H\cdots \underset{\underset{H}{|}}{O}{-}R'}$

or both, respectively. These hydrogen bonding interactions may somewhat complicate the interpretation of the observed results because only the long range dipolar interactions are taken into account in Eq. 1, and actually the values of alcohol solutions do not satisfy the linear relations. However, the hydrogen-bonding interactions with monochlorobenzene and acetonitrile are certainly very weak, and the $\Delta\sigma$ values for these solvents, together with that for *n*-hexane, well satisfy the approximate linear relation.

Equation 1 for naphthylamines can be written approximately as follows:

$$\beta\text{-}, \quad \Delta\sigma = 2900 + 4800\, F(D, n)$$
$$\alpha\text{-}, \quad \Delta\sigma = 4800 + 7300\, F(D, n)$$

From these equations, $\Delta\vec{\mu}$ values for naphthylamines can be evaluated as follows, assuming $a \sim 3$ Å: α-, 4.4 D, β-, 3.5 D. By the same method and with the same value of the cavity radius, the $\Delta\vec{\mu}$ values for naphthols were estimated to be 0.5D~1D[15]. In the latter case, the $\Delta\vec{\mu}$ value of the β-derivative was evidently greater than the $\Delta\vec{\mu}$ value of the α-derivative, in contrast with the former case.

At any rate, it is quite certain that the $\Delta\vec{\mu}$ values of naphthylamines are much larger than those of naphthols and that the relative order of magnitude of this value for α- and β-derivatives is reversed in naphthylamines when compared with naphthols.

ABA's. — The absorption and fluorescence spectra of *o*- and *m*-isomers in a benzene solution are shown in Fig. 4, while those of *p*-isomer in benzene and methyl acetate are given in Fig. 5.

The values of σ_a^m, σ_f^m, $\Delta\sigma$ and $F(D, n)$ for isomeric ABA's are collected in Table II. The relations between the $\Delta\sigma$ values and $F(D, n)$ are shown in Fig. 6.

It appeares, from Fig. 6, that Eq. 1 is not so well satisfied in these cases as in the case of naphthylamines. In particular, the deviations of the $\Delta\sigma$ values of alcohol solutions from the linear relation is quite remarkable.

We have not attempted to evaluate the $\Delta\vec{\mu}$

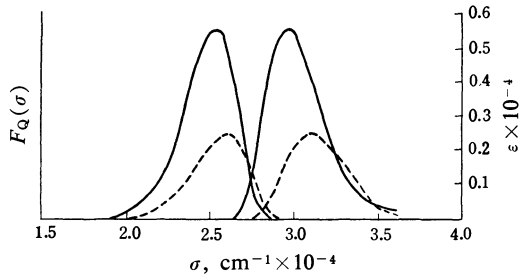

Fig. 4. Absorption and fluorescence spectra of *o*- and *m*-ABA in benzene.
——— *o*- — — — *m*-
Concn. of the solutes:
o-, 1×10^{-4} mol./l. *m*-, 2×10^{-4} mol./l.

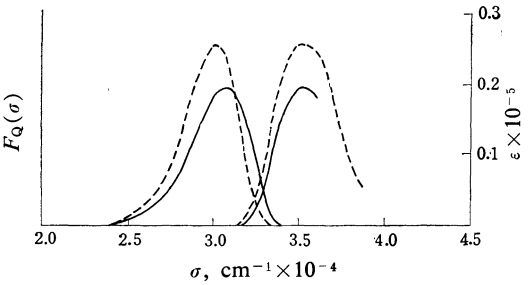

Fig. 5. Absorption and fluorescence spectra of *p*-ABA.
Solvent: ——— Benzene
— — — Methyl acetate
Concn. of *p*-ABA in benzene ~3.4×10^{-5} mol./l. and 2.5×10^{-5} mol./l. in methyl acetate.

TABLE II*. THE WAVE NUMBERS OF THE BAND MAXIMA OF ISOMERIC AMINOBENZOIC ACIDS IN VARIOUS SOLVENTS

Solvent	$F(D, n)$	*o*-ABA			*m*-ABA			*p*-ABA		
		σ_a^m	σ_f^m	$\Delta\sigma$	σ_a^m	σ_f^m	$\Delta\sigma$	σ_a^m	σ_f^m	$\sigma\Delta$
Cyclohexane	0	2.98	2.58	0.40	—	—	—	—	—	—
Benzene	0.002	2.96	2.52	0.44	3.10	2.60	0.50	3.51	3.07	0.44
Monochlorobenzene	0.143	2.96	2.51	0.45	3.08	2.56	0.52	3.47	3.04	0.43
Chloroform	0.185	—	—	—	—	—	—	3.53	3.04	0.49
Acetonitrile	0.304	2.99	2.50	0.49	3.10	2.46	0.64	3.51	2.99	0.52
Dioxane	0.028	2.97	2.51	0.46	3.09	2.57	0.52	3.54	3.01	0.53
n-Butyl acetate	0.171	2.97	2.52	0.45	3.10	2.54	0.56	3.56	3.02	0.54
Ethyl acetate	0.202	2.98	2.51	0.47	3.10	2.52	0.58	3.55	3.01	0.54
Methyl acetate	0.220	2.98	2.50	0.48	3.11	2.46	0.65	3.53	3.00	0.53
n-Butanol	0.267	2.99	2.45	0.54	3.13	2.27	0.87	3.47	2.92	0.55
Ethanol	0.298	2.98	2.42	0.56	3.13	2.27	0.86	3.46	2.90	0.56
Methanol	0.308	3.00	2.42	0.58	3.15	2.25	0.90	3.46	2.90	0.56

* σ's and $\Delta\sigma$'s are in unit of $10^4\,cm^{-1}$.

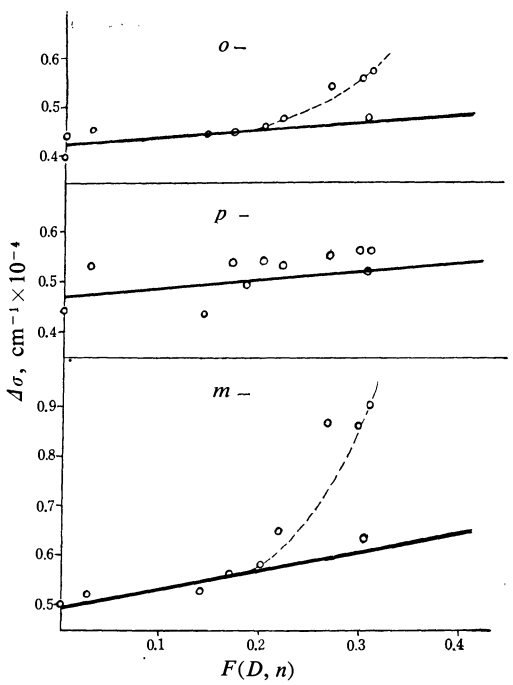

Fig. 6. $\Delta\sigma$ vs. $F(D, n)$ relation for aminobenzoic acids.

values of ABA's because the points are rather scattered and the more specific short-range interactions between solute and solvent molecules seem to be rather dominant. However, the inclinations of the full lines in Fig. 6 may give an approximate measure of th $\Delta\vec{\mu}$ values for these compounds, because the $\Delta\sigma$ values involved here mainly correspond to solvent molecules which make very weak hydrogen bond with solute molecules. The observed inclination is the largest for the *m*-isomer and the smallest for the *o*-isomer.

We can get only a rough estimate of the inclination for the *p*-isomer because the points in this case are scattered considerably. However, the inclination for the *p*-isomer is certainly rather close to that of the *o*-isomer.

Discussion

Deviations of $\Delta\sigma$ Values from the Linear Relation and Hydrogen Bonding Effects. — The lowest excited electronic state of naphthalene is ^1L_b, and the next one is ^1L_a[1-4]. Owing to the substitution by the hydroxy and amino groups, the electronic spectrum of naphthalene is modified considerably. Nevertheless, the lowest excited electronic states of naphthols and naphthylamines can be assigned to modified ^1L_b's and next ones to modified ^1L_a's[10].

It is well known that the electron migration or the charge transfer interaction between the substituent and the aromatic hydrocarbon is the most important factor which affects and determines the electronic spectra of aromatic derivatives[10,11,16-25].

In general, the extent of electron migration or the charge transfer interaction is greater in the excited electronic state than in the ground state. The observed $\Delta\vec{\mu}$ values presumably arise mainly from this difference.

16) A. L. Sklar, *J. Chem. Phys.*, **7**, 984 (1959).
17) K. F. Herzfeld, *Chem. Revs.*, **41**, 233 (1947).
18) F. A. Matsen, *J. Am. Chem. Soc.*, **72**, 5243 (1950).
19) S. Nagakura and H. Baba, ibid., **74**, 5693 (1952).
20) L. Goodman and H. Shull, *J. Chem. Phys.*, **27**, 1388 (1957).
21) S. Nagakura and J. Tanaka, ibid., **22**, 236 (1954); S. Nagakura, ibid., **23**, 1441 (1955); J. Tanaka, S. Nagakura and M. Kobayashi, ibid., **24**, 311 (1956); J. Tanaka and S. Nagakura, ibid., **24**, 1274 (1956).
22) J. N. Murrell, *Proc. Phys. Soc.*, **A68**, 969 (1955).
23) N. Mataga and S. Mataga, This Bulletin, **32**, 600 (1959).
24) I. Fischer-Hjalmars, *Ark. för Fys.*, **21**, 123 (1962).
25) K. Nishimoto, to be published.

Baba[10] calculated the changes (decrease) in π-electron density on the substituent of naphthols and naphthylamines accompanying electronic transitions by a semiempirical ASMO CI method. The calculated results show that this decrease is much larger for naphthylamines than for naphthols, which is in accordance with the observed $\Delta\vec{\mu}$ values of these compounds, at least qualitatively.

This decrease of π-electron density on the substituent in the excited state is probably responsible also for the observed deviations of the $\Delta\sigma$ values of alcohol solutions in Fig. 3.

The hydrogen-bonding interaction in alcohol solutions probably involves both the types of hydrogen bonds indicated in Experimental Results, simultaneously, i. e., a bonding of the type:

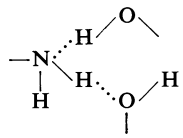

The hydrogen bonding of the type, $H\rangle N\text{-}H\cdots O\langle$, causes a red shift of the absorption spectrum, whereas the other type of hydrogen-bonding interaction cause a blue shift of the absorption spectrum, because the former is favorable but the latter is unfavorable for the charge migration from the substituent to the aromatic ring.

As one can see from the tables, the $\sigma_a{}^m$ values of alcohol solutions are almost the same as or even larger than those in non-polar solvents.

This fact indicates that the effect of the latter type of hydrogen-bonding interaction on the spectral shift is rather important.

As is indicated in Fig. 7, the hydrogen-bonding interaction of the type, $-N\cdots H\text{-}O-$, is certainly very weak in the excited state of naphthylamines, and the other type of hydrogen-bonding interaction is a little stronger in the excited state than in the ground state.

The broken lines in Fig. 7 represent radiationless processes, which are reorganizations of hydrogen-bonding interactions. This sort of radiationless process may cause a large value of $\Delta\sigma$, leading to considerable deviations from the linear relation between $\Delta\sigma$ and $F(D, n)$.

The effect of hydrogen-bonding interaction of this type may be much stronger in the case of ABA's than in the case of naphthylamines because of the existence of the carboxyl group in the former. The near-ultraviolet absorption spectra of the ABA molecule have been interpreted as being due to the

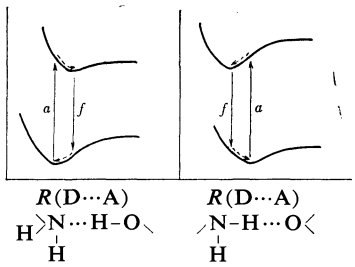

Fig. 7. Potential energy curves for the hydrogen bondings of the types: $-N\cdots H\text{-}O-$ and $-N\text{-}H\cdots O\langle$, respectively. $R(D\cdots A)$ is the distance between the proton donor and the acceptor. a and f indicate the light absorption and fluorescent transitions, respectively, and broken lines represent radiationless processes due to the reorganization of the hydrogen bond.

intramolecular charge-transfer transition from the aniline residue to the antibonding orbital of the carboxyl group[20]. Thus, the electron-accepting character of the carboxyl group results in a stronger decrease in the π-electron density on the amino group in the excited electronic state. This circumstance is probably responsible for the remarkable deviations in the $\Delta\sigma$ values of alcohol solutions in the case of *m*-ABA.

In the case of *o*-ABA, however, the circumstance may be somewhat different because of the existence of an intramolecular hydrogen bond between the amino group and the carbonyl group. Because electronic delocalization through the hydrogen bond is possible[26-29], the charge separation between the two substituents may be smaller in this molecule than in the other isomers. This delocalization is certainly stronger in the excited state than in the ground state because the electronic orbital is more extended, the ionization potential of the carbonyl becomes smaller, and the electron affinity of the amino group becomes larger in the excited electronic state than in the ground state.

In this way, the electronic delocalization through the intramolecular hydrogen bond may result in smaller deviations in the $\Delta\sigma$ values of *o*-ABA in alcohol solutions than is the case with *m*-isomer.

The same factor may be responsible also for

26) H. Tsubomura, This Bulletin, **27**, 445 (1954); *J. Chem. Phys.*, **23**, 2130 (1955); ibid., **24**, 927 (1956).
27) K. Nukasawa, J. Tanaka and S. Nagakura, *J. Phys. Soc. Japan*, **8**, 792 (1953).
28) S. Nagakura and M. Gouterman, *J. Chem. Phys.*, **26**, 881 (1957).
29) N. Mataga and Y. Kaifu, ibid., **36**, 2804 (1962); N. Mataga and S. Tsuno, This Bulletin, **30**, 711 (1957).

the small inclination of *o*-ABA in Fig. 6. However, the distance between the two substituents is the smallest for this isomer, and this may be the main cause for the small inclination. Because the distance between the two substituents is the largest for the *p*-isomer, one may expect the largest inclination for this compound. However, this expectation is not in agreement with the observed result.

As shown in Fig. 5, the absorption intensity of the *p*-isomer is much stronger than those of other isomers and naphthylamines. This very strong absorption intensity indicates a short life time of the fluorescent state, although the observed value of the life time is not available for this molecule. During the very short life time of the fluorescent state, the rearrangement of the solvent molecules surrounding the excited solute molecule may be reached only partially or it may be almost impossible. Such a circumstance has already been observed in the case of *p*-dimethylaminocinnamic-nitrile[30].

It is quite probable that the rearrangement of the solvent molecules during the life time of the excited state occurs only incompletely for *p*-ABA and that, accordingly, the observed inclination is so small as shown in Fig. 6.

Theoretical Calculation of the $\vec{\Delta\mu}$ Values of Naphthylamines and Naphthols. — As has been mentioned in Experimental Results, the observed $\vec{\Delta\mu}$ value for α-naphthylamine was larger than that for β-naphthylamine, contrary to the case of naphthols.

To interpret these facts, the observed results may be compared with the results of theoretical calculation as follows.

The Method of Calculation. — The semiempirical ASMO CI method[3] was used. In this treatment, an electronic state function, Ψ, for the π-electrons is approximated by a linear combination of the ground configuration function, χ_0, and singly excited configuration functions, χ_{ik}'s, where one electron is excited from an occupied MO ϕ_i to an unoccupied MO ϕ_k.

The orthonormal MO's are themselves linear combinations of 2pπAO's, ϕ_μ's:

$$\phi_i=\sum_\mu c_{i\mu}\phi_\mu \tag{2}$$

The theoretical expression for $\vec{\Delta\mu}$ in terms of the state function, Ψ, is given by:

$$\vec{\Delta\mu}=\langle\Psi_e|M|\Psi_e\rangle-\langle\Psi_g|M|\Psi_g\rangle \tag{3}$$

where

$$M=\sum_t e_t r_t \tag{4}$$

e_t and r_t are the charge and the position vector of t-th particle, respectively. In the π-electron approximation, M can be separated into two parts:

$$M=e\sum_\mu r_\mu+\sum_s e_s r_s \tag{5}$$

e is the electronic charge, the first summation being over the π-electrons and the second over the cores. The necessary formulas for the expansion of 3 in terms of integrals over MO's are given as follows:

$$\left.\begin{aligned}
&\langle\chi_0|M|\chi_0\rangle=2\sum_i^{\mathrm{occ}} M_{ii}+\sum_s e_s r_s\\
&\langle{}^1\chi_{ik}|M|{}^1\chi_{ik}\rangle=2\sum_i^{\mathrm{occ}} M_{ii}-M_{ii}\\
&\qquad\qquad +M_{kk}+\sum_s e_s r_s\\
&\langle\chi_0|M|{}^1\chi_{ik}\rangle=\sqrt{2}M_{ik}\\
&\langle{}^1\chi_{ik}|M|{}^1\chi_{jk}\rangle=-M_{ij}\\
&\langle{}^1\chi_{ik}|M|{}^1\chi_{il}\rangle=M_{kl}\\
&\langle{}^1\chi_{ik}|M|{}^1\chi_{jl}\rangle=0\\
&M_{ik}=\langle\psi_i|M|\psi_k\rangle
\end{aligned}\right\} \tag{6}$$

In Eq. 6, occ means the summation over the occupied MO's in χ_0.

In the present calculations, the wave functions calculated by Baba[31] were used. In his treatment, $\Psi_g\sim\chi_0$ and $\Psi_e\sim a^1\chi_{ik}+b^1\chi_{jl}$; therefore Eq. 3 reduces to the following:

$$\vec{\Delta\mu}=a^2(M_{kk}-M_{ii})+b^2(M_{ll}-M_{jj}) \tag{7}$$

In the expansion of M_{ii}'s in terms of integrals over AO's, the following approximation was used:

$$M_{ll}=\sum_{\mu,\nu} c_{i\mu}c_{i\nu}\langle\phi_\mu|M|\phi_\nu\rangle\simeq e[\textstyle\sum c^2_{i\mu}R_\mu] \tag{8}$$

where R_μ is the position vector of the μ-th atom.

All bond distances in naphthylamines and naphthols are assumed to be 1.39Å.

Calculated Results. — The $\vec{\Delta\mu}$ values for the ^1L_b state of naphthols were calculated as follows: α-, 1.63 D and β-, 2.75 D, which are much larger than the observed values.

The usual MO method seems to overestimate the values of dipole moments and also $\vec{\Delta\mu}$ values. Thus, the calculated $\vec{\Delta\mu}$ values for the ^1L_b state of naphthols were four times as large as the observed values.

Because we are concerned here with only the relative values of $\vec{\Delta\mu}$ for these molecules, the calculated values were divided by this factor. Then, one quarter of the $\vec{\Delta\mu}$ values for the ^1L_b state of naphthols was calculated

30) E. Lippert, *Angew. Chem.*, **73**, 695 (1961).

31) H. Baba, private communication; see also Ref. 10.

as: α-, 0.41 D and β-, 0.69 D. The same quantities (i. e., one quarter of the theoretical values) for the ^1L_b state of naphthylamines were: α-, 0.92 D and β-, 1.16 D. These values are considerably smaller than the observed values. However, a more serious disagreement with the experimental results is that the $\vec{\Delta\mu}$ value of the α-isomer is smaller than that of the β-isomer.

One-quarter of the theoretical value of $\vec{\Delta\mu}$ for the ^1L_a state of α-naphthylamine (abbreviated as $\vec{\Delta\mu}(^1L_a{}^{\alpha})$) was 1.35 D, which was larger than $\vec{\Delta\mu}(^1L_b{}^{\beta})$. Moreover, the ratio $\vec{\Delta\mu}(^1L_b{}^{\beta})/\vec{\Delta\mu}(^1L_a{}^{\alpha})$ is 0.86 for the calculated values, which is very close to the observed ratio, 0.80. These facts seems to indicate rather strongly that the fluorescent state of α-naphthylamine is not the ^1L_b but the ^1L_a state.

If all of the structures of the absorption band in *n*-hexane as shown in Fig. 1 belong to the same electronic band, the fluorescence band should have the corresponding structures and the absorption and fluorescence bands should present the "mirror image" appearance*. However, this seems not to be the case in the observed spectrum, because the shortest wavelength shoulder in the fluorescence band, which corresponds to the longest wavelength shoulder in the absorption band, seems to be missing. The latter shoulder was assigned[10] to ^1L_b, which seems to be quite reasonable. These facts also appear to support the above interpretation. Thus, the ^1L_a state of α-naphthylamine may probably become the lowest excited singlet state during the radiationless process from the Franck-Condon to the equilibrium excited state.

The Mechanism of the Level Reversal during the Life Time of the Excited State.—There is a noticeable difference between spectral changes caused by substitutions at the α- and β-positions of naphthalene. Several explanations have been already given for this interesting phenomenon[10,25,32,33].

The reversal of the ^1L_b and the ^1L_a states of α-naphthylamine during the life time of the excited state may be closely related to the factor which determine the spectral characteristics of the α- and β-isomers respectively.

The characteristic difference between the α- and β-isomers may be understood well if we write down the matrix elements of the interactions between the locally excited states of naphthalene and the charge transfer (CT) configurations which arise from the transfer of one electron from the occupied orbital of the substituent to the vacant orbitals of naphthalene.

Using the method developed by Longuet-Higgins and Murrell[22,34], the necessary matrix elements can easily be calculated as follows.

If the SCF MO's of naphthalene are written $\psi_1 \cdots \psi_n$ and those of the substitutent, $\theta_1 \cdots \theta_m$, then the energy of the CT configuration, $^1\chi_{sk}$, where one electron is transferred from an occupied orbital, θ_s, to a vacant MO, ψ_k, is given by:

$$\langle {}^1\chi_{sk} | \mathscr{H} | {}^1\chi_k \rangle = \varepsilon_k - \varepsilon_s - \langle \theta_s(1)\psi_k(2) | G_{12} | \theta_s(1)\psi_k(2) \rangle \quad (9)$$

where ε_k and ε_s are linear combinations of ψ_k and θ_s respectively, and ψ_k's are linear combinations of $2p\pi$AO's $\phi_1 \cdots \phi_n$,

$$\psi_k = \sum_{\mu} c_{k\mu}\phi_{\mu} \quad (10)$$

G_{12} is the two-electron operator, e^2/r_{12}, r_{12} being the inter-electronic distance.

For naphthylamines, ε_s will be given, to a good approximation, by the observed ionization potential of ammonia, i. e., $\varepsilon_s = -10.154$ eV.[35] The difference between the observed and calculated values of the electron affinity of benzene, $\Delta A = A_B{}^{obs} - A_B{}^{calc}$ [4], has been added to the calculated values of ε_k.

With neglect of differential overlap,

$$\langle \theta_s(1)\psi_k(2) | G_{12} | \theta_s(1)\psi_k(2) \rangle = \sum_{\mu} c^2{}_{k\mu}\gamma_{s\mu} \quad (11)$$

$$\gamma_{s\mu} = \langle \theta_s(1)\phi_{\mu}(2) | G_{12} | \theta_s(1)\phi_{\mu}(2) \rangle$$

For the evaluation of $\gamma_{s\mu}$, the equation[4,7,8], $\gamma_{s\mu} = e^2/(\rho + R_{s\mu})$, was used, where $\rho = 1.197$ Å. The value of ρ is the harmonic mean of the ρ for carbon[4,7,8] and that for nitrogen. The latter value was obtained from the one center value of γ for nitrogen calculated by Brown[36] using the VESCF method.

The matrix elements of the interactions between the CT configurations and various local configurations in naphthalene can be evaluated from the following formulas:

$$\langle {}^1\chi_{sk} | \mathscr{H} | {}^1\chi_{jl} \rangle = -\delta_{kl} \langle \theta_s(1) | H(1) | \psi_j(1) \rangle \quad (12)$$

where δ_{kl} is Kronecker's delta.

$$\langle {}^1\chi_{sk} | \mathscr{H} | \chi_0 \rangle = \sqrt{2} \langle \theta_s(1) | H(1) | \psi_k(1) \rangle \quad (13)$$

where χ_0 is the ground configuration.

* See, for example, Th. Förster, "Fluoreszenz organischer Verbindungen", Vandenhoeck and Ruprecht Göttingen (1951).

32) D. Peters, *J. Chem. Soc.*, **1957**, 646, 1993, 4182.

33) E. Döller, Th. Förster and H. Renner, *Z. Phys. Chem. N. F.*, **15**, 34 (1958).

34) H. C. Longuet-Higgins and J. N. Murrell, *Proc. Phys. Soc.*, **A68**, 601 (1955).

35) K. Watanabe and J. R. Mottle, *J. Chem. Phys.*, **26**, 1773 (1957).

36) R. D. Brown and M. L. Heffernan, *Australian J. Chem.*, **12**, 319 (1959).

$$\langle {}^1\chi_{sk}|\mathscr{H}|{}^1\chi_{sl}\rangle = -\langle\theta_s(1)\phi_k(2)|G_{12}|\theta_s(1)\phi_l(2)\rangle = -\sum_{\mu} c_{k\mu}c_{l\mu}\langle\theta(1)\phi_\mu(2)|G_{12}|\theta_s(1)\phi_\mu(2)\rangle \quad (14)$$

The integral $\langle\theta_s(1)|H(1)|\phi_j(1)\rangle$ can be reduced to $c_{jr}\langle\theta_s(1)|H(1)|\phi_r(1)\rangle = c_{jr}\beta^c$, the substituent being attached to the carbon atom 'r'.

Now, by means of these formulas and the SCF MO's and state functions of naphthalene[4], the energy matrices for naphthylamines are calculated as follows (in units of eV.):

α-Naphthylamine

χ_0	${}^1B_{3u}^-$	${}^1B_{2u}^+$	${}^1B_{3u}^+$	${}^1B_{2u}^-$	${}^1\chi_{s6}$	${}^1\chi_{s7}$
0					$0.5995\beta^c$	$-0.3749\beta^c$
	3.99				$0.0023\beta^c$	$-0.2997\beta^c$
		4.51			$-0.4081\beta^c$	$-0.0009\beta^c$
			5.61		$-0.0023\beta^c$	$-0.2997\beta^c$
				7.30	$-0.1145\beta^c$	$0.0032\beta^c$
					6.1679	$-0.0734\beta^c$
						7.3736

β-Naphthylamine

χ_0	${}^1B_{3u}^-$	${}^1B_{2u}^+$	${}^1B_{3u}^+$	${}^1B_{2u}^-$	${}^1\chi_{s6}$	${}^1\chi_{s7}$
0					$-0.3749\beta^c$	$-0.5602\beta^c$
	3.99				$0.2801\beta^c$	$-0.1875\beta^c$
		4.51			$-0.2553\beta^c$	$-0.1069\beta^c$
			5.61		$-0.2801\beta^c$	$-0.1875\beta^c$
				7.30	$-0.0716\beta^c$	$0.3814\beta^c$
					6.5635	$-0.1573\beta^c$
						7.3829

In these matrices, observed values are used for the locally excited states of naphthalene.

The calculated matrix elements correspond quite well to the observed characteristics of the electronic spectra of α- and β-derivatives respectively. That is, there are weak interactions between the ${}^1B_{3u}^-$ and CT configurations and strong interactions between the ${}^1B_{2u}^+$ and CT configurations for the α-isomer, whereas either ${}^1B_{3u}^-$ or ${}^1B_{2u}^+$ interacts moderately with the CT configurations and the interactions of the ${}^1B_{3u}^-$ with CT configurations are a little stronger than those of ${}^1B_{2u}^+$, in the β-isomer. In the case of naphthylamines, the energies of CT configurations are considerably smaller than those of naphthols*. Moreover, the core resonance integral, β^c, for naphthylamines may be a little larger than that for naphthols**.

Therefore, only in the case of α-naphthylamine, the ${}^1L_a$ state will be very close to the ${}^1L_b$ state.

Now, in the excited state of naphthylamine, the more flattened structure of the amino group and the more stretched form of the N–H bond compared with those in the ground state may probably be favored because the gain of the CT interaction energy due to these changes in the structure of the amino group is much larger in the excited electronic state than in the ground state. In other words, these structural changes result in the lowering of the ionization potential of the lone-pair orbital of the amino group and the increase of β^c.

Thus, the excitation energies of the CT configurations becomes smaller and the CT interactions becomes stronger. Because the energy differences between the lower excited states of naphthalene and the CT configurations are much smaller than those between the ground configuration and CT configurations, the CT interactions are considerably larger in the excited electronic state.

Because of these circumstances, ${}^1B_{2u}^+$ mixed with ${}^1\chi_{s6}$ is lowered rather strongly, but the lowering of ${}^1B_{3u}^-$ may be small because of the very small interaction with ${}^1\chi_{s6}$ in the case of α-naphthylamine. Thus, the order of the ${}^1L_b$ and ${}^1L_a$ states may be reversed during the radiationless process in the excited state. This level reversal may be demonstrated by calculations using a simplified model, which are similar to those of an earlier treatment by Nagakura and Tanaka[21] but which take into account the inter-electronic interactions to some extent. In this treatment, we discuss the case of the structural change of the amino group from the pure sp^3 hydride to the pure sp_2 hydrid without a stretching of the N–H bond, and take into consideration only interactions among ${}^1B_{3u}^-$, ${}^1B_{2u}^+$ and ${}^1\chi_{s6}$.

We assume the proportionality of β^c to the corresponding overlap integral, S. Then we must evaluate the overlap integrals for the tetrahedral and trigonal hybrids respectively.

The lone-pair orbital used in this calculation for tetrahedral nitrogen is of the form:

$$\zeta = (1/2)s + (2/3)^{1/2}p_x - (1/12)^{1/2}p_z \quad (15)$$

where the x axis is taken perpendicular to the

* Calculations using similar approximations give for naphthols:

α-, $\langle {}^1\chi_{s6}|\mathscr{H}|{}^1\chi_{s6}\rangle = 8.3435$ eV.
$\langle {}^1\chi_{s7}|\mathscr{H}|{}^1\chi_{s7}\rangle = 9.6003$ eV.

β-, $\langle {}^1\chi_{s6}|\mathscr{H}|{}^1\chi_{s6}\rangle = 8.7971$ eV.
$\langle {}^1\chi_{s7}|\mathscr{H}|{}^1\chi_{s7}\rangle = 9.5860$ eV.

** If we assume the proportionality of the core resonance integral to the corresponding overlap integral, taking $\beta_c(-2.388$ eV.) and $S(0.25)$ between the nearest neighbor $2p\pi$AO's of benzene as a reference, then the β_c for naphthylamines is calculated to be -1.7 eV., whereas it is -1.4 eV. for naphthols. In this calculation, the AO's on the substituents are assumed to be pure $2p\pi$AO's perpendicular to the molecular plane, and the orbital exponent in the Slater AO of the heteroatom is the simple arithmetic mean of the values for the neutral atom and the singly ionized one respectively.

molecular plane. Taking the simple arithmetical mean of the values of neutral and singly ionized atoms for the orbital exponent in the Slater AO of nitrogen, the overlap integrals have been calculated, and from these the core reasonance integrals have been evaluated by the same procedure as described before**: β^c (tetrahedral)~ -1.43 eV., β^c (trigonal)~ -1.75 eV.

The change of the ionization potential of the lone pair orbital on nitrogen caused by this structural change was estimated by means of the following equation:

$$I(\mathrm{tr})/I(\mathrm{tet}) = I/I(\mathrm{NH_3})$$

where I(tr) and I(tet) are the ionization potentials of lone pair orbitals in the trigonal and tetrahedral valence states respectively. These values are evaluated from the valence state quantities given by Hinze and Jaffé[37]: $I(\mathrm{tr}) = 11.958$ eV., $I(\mathrm{tet}) = 14.157$ eV. $I(\mathrm{NH_3})$ is the observed ionization potential of ammonia. Thus, $I = 8.5768$ eV. Using these values of β^c's and I's, the relevant energy matrices can be written as follows:

(a) Tetrahedral $-NH_2$ (b) Trigonal $-NH_2$

$$\begin{array}{c} {}^1B_{3u}^- \quad {}^1B_{2u}^+ \quad {}^1\chi_{s6} \\ \begin{pmatrix} 3.99 & 0 & -0.0033 \\ & 4.51 & 0.5836 \\ & & 6.1679 \end{pmatrix} \end{array} \qquad \begin{array}{c} {}^1B_{3u}^- \quad {}^1B_{2u}^+ \quad {}^1\chi_{s6} \\ \begin{pmatrix} 3.99 & 0 & -0.0040 \\ & 4.51 & 0.7142 \\ & & 4.5909 \end{pmatrix} \end{array}$$

The interaction between ${}^1B_{3u}^-$ and ${}^1\chi_{s6}$ is very small and can be neglected practically. The lower energies and state functions for the interaction of ${}^1B_{2u}^+$ with ${}^1\chi_{s6}$ may then be given as follows:

(a) 4.325 eV. $\Psi = 0.953\,{}^1B_{2u}^+ - 0.302\,{}^1\chi_{s6}$

(b) 3.835 eV. $\Psi = 0.727\,{}^1B_{2u}^+ - 0.687\,{}^1\chi_{s6}$

Thus, the level is reversed and the ${}^1L_a$ state in the latter case contains a large amount of the CT configuration.

Of course, the above calculations are too simplified and the transformation from the tetrahedral to the trigonal structure may be realized only partially. However, the stretching of the N–H bond may also contribute to the level reversal, and the occurence of the latter seems to be plausible.

This change in the structure of the amino group, leading to the stronger CT interaction, may be responsible for the large difference between the theoretical $\vec{\Delta\mu}$ values (one-quarter of the calculated values) and the observed $\vec{\Delta\mu}$ values of the fluorescent state.

In the case of naphthols, such effects may not be important because the CT configurations are considerably higher and β^c is smaller than in naphthylamines.

37) J. Hinze and H. H. Jaffe, *J. Am. Chem. Soc.*, **84**, 540 (1962).

Summary

The absorption and fluorescence spectra of naphthylamines and isomeric aminobenzoic acids in various solvents have been measured.

From the observed results, the difference in the dipole moments in the fluorescent and ground states respectively, i. e., $\vec{\Delta\mu} = \vec{\mu}_e - \vec{\mu}_g$, has been estimated for naphthylamines.

The effect of hydrogen bonding between solute and solvent molecules on the spectral shifts has been discussed. The hydrogen bonding between alcohol and amino nitrogen exerts a especially remarkable influence on the spectra, and the reorganization of this hydrogen bond during the life time of the excited solute molecule has been concluded from the observed results.

The intramolecular hydrogen bond of *o*-aminobenzoic acid considerably decreases the $\vec{\Delta\mu}$ value and the effect of the intermolecular hydrogen bonding on the spectra. This result has been explained as due to the charge transfer through the intramolecular hydrogen bond.

The $\vec{\Delta\mu}$ values for naphthylamines and naphthols have been calculated using the ASMO CI method and compared with the observed results.

This comparison, together with the theoretical interpretation of the characteristics in the spectra of α- and β-isomers, respectively, has indicated that the lowest excited singlet state in the light absorption is ${}^1L_b$, whereas the fluorescent state is ${}^1L_a$ in the case of α-naphthylamine and ${}^1L_b$ is the relevant excited state for both light absorption and fluorescence in the case of β-naphthylamine and naphthols.

The mechanism of this level reversal has been discussed as being due to the change in the structure of the amino group during the life time of the excited state.

The author wishes to express his deep gratitude to Professor Hiroaki Baba of Hokkaido University for sending us his unpublished results of ASMO CI calculations on naphthylamines and naphthols and for his fruitful discussions. The author also wishes to express his hearty thanks to Dr. Yozô Kaifu and Mr. Yoshikazu Torihashi for their help in the experimental measurements.

Faculty of Science
Osaka City University
Sumiyoshi-ku, Osaka

The Separation and Determination of Ruthenium in Fission Products by Liquid-Liquid Extraction with Pyridine

By Toshiyasu KIBA, Akiko MIURA and Yasuyuki SUGIOKA

(Received January 14, 1963)

When a fission product which contains ruthenium is dissolved in nitric acid, the element goes into the solution as the nitrosylruthenium radical (RuNO) III, complexed with nitrato, nitro, hydroxo and aquo ligands[1-3]. The element may have any oxidation number between 0 and +8, according to the composition and other conditions of the solution containing its compounds. The element may exist in various ion-species, polymers and compounds in intermediate states of oxidation[4], and it has been recognized that the separation of radioactive ruthenium from an aqueous solution containing other fission products requires the use of very difficult techniques.

Various methods have been proposed for this separation by many investigators; a summary of the methods intended for practical use has been given by Wyatt and Rickard[5]. According to their description, the isolation of radioactive ruthenium is generally accomplished by electrodeposition, ion exchange, distillation, liquid-liquid extraction or reduction by light metals. All isolation procedures naturally should consist of two steps: the first, to make the oxidation number of the element in all the compounds the same, preferably the lowest or the highest (that is, to convert the element to metallic ruthenium or the tetraoxide), and the second, to separate the compounds obtained by the first step. For separating the ruthenium tetraoxide, in which the element possesses its highest oxidation number, +8, distillation is usually adopted because of the volatility of the compound from an acidic solution containing a strong oxidizing agent, such as permanganate, silver peroxide, sodium bismuthate or periodic acid[6,7]. On the other hand, separation without distillation has been attempted by liquid-liquid extraction, in which ruthenium tetraoxide in an acidic solution is transferred into carbon tetrachloride by agitating the two phases in the presence of a strong oxidant in the aqueous phase. The tetraoxide transferred into the organic phase can be stripped again into another aqueous solution containing a reducing or chelating agent, and the colored, lower oxide is estimated colorimetrically. In both distillation and liquid-liquid extraction, however, some of the ruthenium tetraoxide is easily lost during the operations because of its volatility at moderately high temperatures. It has therefore been found desirable that the tetraoxide be treated in an alkaline rather than an acidic solution. It has already been known that all ruthenium oxide can be easily oxidized by sodium hypochlorite to perruthenate in an alkaline solution[8], and that the spectrophotometric measurement of the ruthenium content of the resulting solution can be made at 385 mμ[9]. This colored solution can also be obtained by passing the gaseous tetraoxide into a solution containing 6 N sodium hydroxide and 0.05 N sodium hypochlorite. Stoner[10] and Larson and Ross[11] employed this reaction for the photometric determination of ruthenium through distillation of the tetraoxide. Although as little as 200 μg. of the element can be determined by this method, however, it cannot be employed for the minute amounts of the element that are ordinarily met with in the radiochemical separation; moreover, accurate measurement of the radioactivity of the separated nuclide is impossible on account of the self-absorption of the radiation by the large amounts of alkaline salts present in the solution.

1) J. M. Fletcher and F. S. Martin, A. E. R. E. Report No. C/M 256, 6 p. p.; Proceedings of the International Conference on the Peaceful Uses of Atomic Energy, Geneva, 1955, Vol. 7, United Nations (1956), p. 141.
2) P. G. M. Brown, J. M. Fletcher et al., ibid., Vol. 17, United Nations (1959), p. 118; P. G. M. Brown, *J. Inorg. Nucl. Chem.*, **13**, 73 (1960); P. G. M. Brown and A. Naylor, *J. Appl. Chem.*, **10**, 422 (1960).
3) G. Rudstam, *Acta Chim. Scand.*, **13**, 1481 (1959).
4) H. H. Cady and R. E. Connick, *J. Am. Chem. Soc.*, **79**, 4242 (1959),
5) E. I. Wyatt and R. R. Rickard, "The Radiochemistry of Ruthenium", Nuclear Science Series NAS-NS 3029. U. S. A. E. C. (1961).
6) T. Kambara, *Japan Analyst*, **6**, 270 (1957), **7**, 89 (1958).
7) R. R. Rickard and E. I. Wyatt, *Anal. Chem.*, **31**, 50 (1959).
8) Gmelins Handbuch der Anorganische Chemie, "Ruthenium", P. P. 1-124, System 63, Verlag. Chem. G. M. B. H. Berlin (1938).
9) G. A. Stoner, *Anal. Chem.*, **27**, 1166 (1955).
10) R. P. Larson and L. E. Ross, U. S. A. E. C. **TID**-7568, Part 1, 9 (1958); *Anal. Chem.*, **31**, 176 (1959).
11) M. S. Tribalat, "Rhenium et Technetium", Gauthier-Villars, Paris (1957), p. 45.

The present authors have found that the perruthenate ion formed in an alkaline solution, as described above, can be easily extracted by pyridine, just as the permanganate, perrhenate and pertechnetate ions can be[9,11]. The present paper describes a method for the rapid determination of radioactive ruthenium by liquid-liquid extraction.

Experimental

Radioactive Ruthenium.—Ruthenium-106 as nitrosylruthenium trinitrate in 8 M nitric acid was purchased from the Radiochemical Centre, Amersham, England, The original solution, containing 0.937 mc./ml. (assayed, 27th, Nov. 1957), was diluted with 3 M nitric acid to make its radioactivity about 1000 c. p. m. per 0.05 ml. The radiochemical purity of the ruthenium-106 was estimated to be above 99% and the radioactivity attributable to ruthenium-103, negligible.

Ruthenium Carrier.—Ruthenium red, that is, ruthenium oxychloride ammoniated $Ru_2(OH)_2Cl_4 \cdot 7NH_3 \cdot 3H_2O$, being regarded as a pure substance, was dissolved in water to prepare a solution containing a definite amount of ruthenium. On the other hand, 0.50084 g. of pure metallic ruthenium (Yokokawa Chem. Co., purity; over 99%) was dissolved in a small quantity of 10% "Antiformin" solution and kept for a time at 40°C. The solution was then filtered through a sintered glass G-4 into a 100 ml. measuring flask, after which the volume was adjusted to the mark with "Antiformin". This dark-brownish solution contains 5 mg. of ruthenium in one milliliter.

Chemical Reagents.—The reagents and solvents employed were all of the chemical pure grade. Among them, the solution of sodium hypochlorite was prepared from the commercial "Antiformin" with or without diluting the original solution. The "Antiformin" contains about 6 g. of active chlorine, 7.8 g. of sodium hydroxide and 32 g. of sodium carbonate per 100 ml.

Filter Paper for Chromatographic Use.—Toyo No. 53 paper (2 cm. by 40 cm.) was employed.

Spectrophotometer.—A Hitachi spectrophotometer, model EPU-2, was employed.

Measurement of Radioactivity.—A G-M counting set of the Kobe Kogyo Co., consisting of a No. 131 G-M tube (mica window; 2.8 mg./cm^2, counting efficiency for $^{90}Sr(^{90}Y)$: 11.7%) and a "100". scalor, was used for the β-counting, and a γ-ray spectrometer of the same company, Model-101 with a single-channel pulse height analyzer AN-105, was used for the γ-counting to identify the nuclide.

Separating Funnel.—A 30 ml. spindle-shaped separating funnel with a stout, short stem was used for the good separation of the two phases.

Shaking Machine.—The shaking of the separating funnel was effected by a vertical electric oscillator operating at 230 double strokes per minute.

The other utensils were of the ordinary laboratory type.

Experimental Results and Discussion

Paper Chromatographic Investigation.—One milliliter of a 3 N nitric acid solution of nitrosylruthenium (Ru-106) trinitrate was treated with 5 ml. of 6 M sodium hydroxide and a few drops of bromine water, and the test tube was held in a boiling water for a while till the brown color of the bromine vanished. The same quantity of the alkaline solution of radioactive ruthenium was prepared in another test tube, but instead of bromine water, 3 ml. of an "Antiformin" solution was added to it, and the mixture was left alone for a day. Paper chromatography was carried out on these two solutions and the original nitrosylruthenium (Ru-106) trinitrate solution as follows: one drop of the solution was placed on each of four strips of the chromatographic filter paper at a point 3 cm. from one end, allowed to dry in the air, and then developed chromatographically by the ascending method with four different solvents: ethanol-buthanol-NH_4CNS (50:50:50), glacial acetic acid-water (9:1), pyridine-water (3:2) and methylisopropyl ketone.

The solvent was allowed to rise about 20 cm. above the spot where the drop of the solution had been placed, and then the paper strip was dried and cut transversally into 1 cm. segments, in such a way that one of the segments included the location of the original drop. This segment was called No. 1, and the numbers from 2 to 20 were assigned to the 19 segments located higher up. Each segment was placed at the center of a counting sample pan, and its radioactivity was measured with an end-window counter. The results revealed that the pyridine-water mixture was the best for the purpose in view. Figure 1 gives the histograms obtained with this solvent.

From the figure it may be inferred that various ion species are present in the original

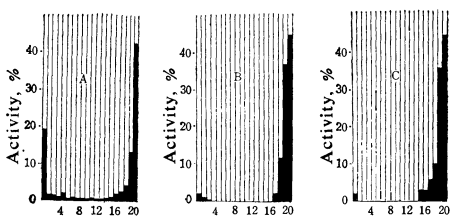

Fig. 1. Chromatograms of Ru-106 developed by pyridine-water (3:2).
A Original solution of nitrosylruthenium trinitrate in 3 N HNO_3
B After oxidation with bromine in sodium hydroxide solution
C After oxidation with hypochlorite in alkaline solution

solution of ruthenium nitrosyltrinitrate, but when it has been made alkaline and oxidized by bromine or chlorine, almost all the ruthenium exists in a single ion species readily distributable in pyridine. Ruthenate ions, RuO_4^{2-}, are obtained by oxidation with bromine and perruthenate ions, RuO_4^-, with hypochlorite. However, the latter may be reduced to ruthenate ions by the cellulose during the chromatographic development. The experiments with the four solvents showed that a more complete separation was effected by pyridine than by any of the others, almost all that element being carried to the solvent front, as is shown in the figure. Therefore, pyridine was adopted as the most choice solvent in the liquid-liquid extraction.

Solvent Extraction Investigation.—To separate the perruthenate in the alkaline solution by liquid-liquid extraction, pyridine was first preferred for the above reason. In a separating funnel, 9 ml. of a sodium hydroxide solution and 1 ml. of a sodium hypochlorite solution were mixed well, and 1 ml. of a nitric acid solution of radioactive nitrosylruthenium trinitrate was added. The concentrations of sodium hydroxide and hypochlorite were so chosen as to make the final aqueous phase of predetermined concentrations. Milliliters of pyridine which had been pre-equilibrated with sodium hydroxide solutions of the corresponding working concentrations were poured into the funnel. The vessel was then tightly stoppered and shaken for five minutes with a shaking machine. After the phases had been disengaged, 1 ml. of the solution from each phase was pipetted out into a porcelain counting pan 1 inch in diameter and evaporated to dryness under an infrared lamp. The radioactivity of each sample was measured by an end-window G-M counter. The ratio of the counting rates of the two samples give the distribution coefficient of the extraction carried out under the given conditions. The dependence of the per cent extraction on the concentration of the reagents in the aqueous phase is summarily illustrated in Fig. 2. It is revealed that, at various concentrations of hypochlorite, the per cent extraction of perruthenate in pyridine is noticeably higher between three and four moles of sodium hydroxide in the aqueous phase. Next, the same experiments were carried out with varying concentrations of hypochlorite, while that of sodium hydroxide was kept constant at 4 M. The pyridine used in these experiments had been pre-equilibrated with 4 M sodium hydroxide. Figure 3 shows the increase in the per cent extraction with the increase in the concentration of hypochlorite, but even under the most favorable conditions,

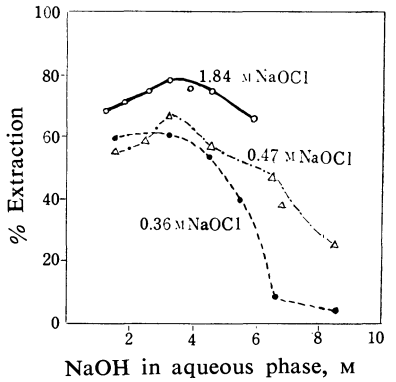

Fig. 2. Relation between % extraction of ruthenium and the concentration of sodium hydroxide and sodium hypochlorite.

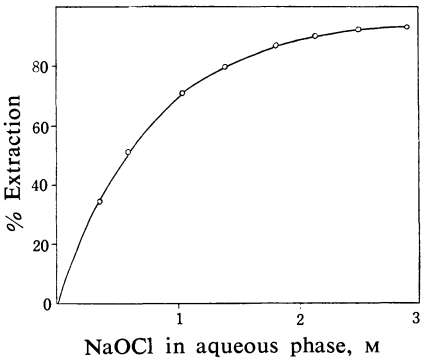

Fig. 3. Effect of concentration of sodium hypochlorite in 4 M sodium hydroxide aqueous solution.

in which the hypochlorite increases nearly to 3 M, the per cent extraction does not exceed 92%. This seems to be due to the incomplete oxidation of ruthenium(III) to perruthenate at room temperatures, so in the next experiment the aqueous phase was kept at 100°C for two hours before the extraction, but the recovery rose only to 95.1%. It was found that when the aqueous phase was left for 24 hr. at room temperature, the recovery percentage reached 100%. Therefore, the following procedure was finally adopted. One gram of sodium hydroxide was dissolved in 10 ml. of an "Antiformin" solution and then a small volume of nitrosylruthenium trinitrate solution was added to it, after which the whole mixture was allowed to stand for a day. Thereafter, extraction was carried out with 10 ml. of pyridine pre-equilibrated with a 4 M sodium hydroxide solution.

Another problem occurred in the estimation of the radioactivity of the separated radioruthenium in the pyridine and aqueous phases. In this case the pyridine contained a small amount of sodium hydroxide, which separated

TABLE I. AMOUNTS OF SODIUM HYDROXIDE WHICH CAN REMAIN IN THE ORGANIC PHASE AFTER EQUILIBRATION

Aqueous phase		Organic phase		Maximum amount of NaOH in the organic, phase, mg./ml.
2 N NaOH	10 ml.	Pyridine 10 ml.		2.3
4 N NaOH	10 ml.	Pyridine 10 ml.		1.07
8 N NaOH	10 ml.	Pyridine 10 ml.		0.4
4 N NaOH	25 ml.	Pyridine 25 ml.		0.74
4 N NaOH	25 ml.	Pyridine 15 ml.		0.73
4 N NaOH	25 ml.	Pyridine 10 ml.		0.79
12 N NaOH 7 ml. / 10% NaClO 18 ml.	25 ml.	Pyridine 25 ml.		7.93 / 7.89
4 N NaOH	25 ml.	Pyridine 7 : *n*-Butyl acetate 3	25 ml.	0.32
4 N NaOH	25 ml.	Pyridine 1 : *n*-Butyl acetate 1	25 ml.	0.09
12 N NaOH 7 ml. / 10% NaClO 18 ml.	25 ml.	Pyridine 7 : *n*-Butyl acetate 3	25 ml.	2.85
12 N NaOH 7 ml. / 10% NaClO 18 ml.	25 ml.	Pyridine 1 : *n*-Butyl acetate 1	25 ml.	0.6
12 N NaOH 7 ml. / 10% NaClO 18 ml.	25 ml.	Pyridine 3 : *n*-Butyl acetate 7	25 ml.	0.06

out during the evaporation, mostly as sodium carbonate. The solidified salt affected the accuracy of the β-counting because of its self-absorption of the β-rays. However, it was proved that the effect was negligible if the sodium hydroxide in the sample pan did not exceed 0.2 mg./cm^2. Therefore, it was thought desirable to make the amount of sodium hydroxide in pyridine as small as possible. The amounts of sodium hydroxide present in pyridine after equilibration with aqueous solutions containing hydroxide and hypochlorite in various concentrations are shown in Table I. In order to minimize the amount of sodium hydroxide in the pyridine, it was attempted to put into it various diluents. Figure 4 shows the results obtained with *n*-butylacetate, toluene, benzene, xylene and *t*-amylalcohol as the diluent in the ratio by volume as indicated on the abscissa. The amount of ruthenium recovered was greatest when pyridine was used as the extracting solvent by itself, but a mixture of pyridine and *n*-butyl acetate was thought promising, even though only 93% of the ruthenium is recovered by it, because at a 1:1 volume composition it dissolved very little sodium hydroxide.

Spectrophotometric Investigation.—The absorption spectrum of the pyridine phase containing perruthenate was measured by a spectrophotometer. In this experiment a carrier ruthenium of 3.4×10^{-4} mol./l. was employed to develop the red-brownish color of the perruthenate. The wavelength-absorbancy curve of the pyridine solution, as well as the curve for pure pyridine, pre-equilibrated with 4 M

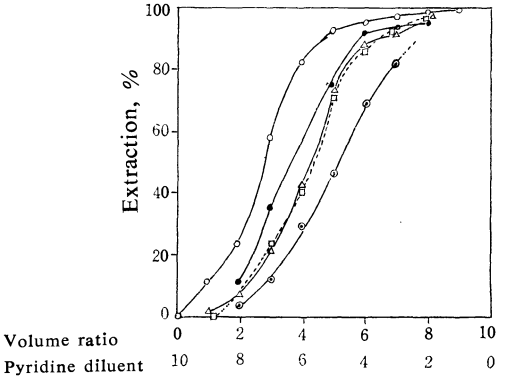

Fig. 4. Effect of diluents of pyridine on the extraction of ruthenium.
○ *n*-Butyl acetate △ Toluene
□ Benzene ● Xylene
⊙ *t*-Amylalcohol

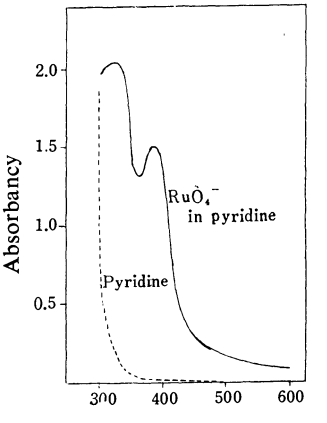

Fig. 5. Absorption spectrum of perruthenate extracted in pyridine.

sodium hydroxide is shown in Fig. 5, which agrees well with that of perruthenate in an alkaline solution obtained by Stoner[10], by Larson and Ross[9] and by Koyama[12]. Therefore, it may be concluded that the perruthenate extracted into pyridine has the same constitution as that in the alkaline aqueous solution.

The Separation of Radioactive Ruthenium from Fission Products.—In this study of the fission products, those nuclides were considered which would account for more than one per cent of the total radioactivity after the products had been aged for one year. The nuclides which fall in this category are zirconium-niobium-95, cerium-praseodymium-144, promethium-147, strontium-yttrium-90, cesium-137-barium-137^{m}, strontium-89 and yttrium-91. Since the chemical behavior of strontium-89 and yttrium-91 are just the same as those of strontium-90 and yttrium-90 respectively, these were excluded from the scope of the present investigation. The short-lived daughters, praseodymium-144, rhodium-106 and barium-137^{m}, are not considered in this study either.

In a separating funnel 1 ml. of a nitric acid solution of the individual radioisotope, 3 ml. of a 10 M sodium hydroxide solution and 7 ml. of "Antiformin" were well mixed, kept on a water-bath at 80°C for three hours, and then kept standing for several hours. Next, 10 ml. of pyridine, which had been pre-equilibrated with 4 M sodium hydroxide, was added, and the vessel was shaken by an electric oscillator for five minutes. Then the aqueous phase was drained into another separating funnel. From the organic phase retained in the first funnel, 1 ml. of the solution was pipetted out and its radioactivity was measured. The residual organic phase was back-washed with a washing liquid consisting of 3 ml. of 10 M sodium hydroxide and 7 ml. of "Antiformin". The washing liquid was rejected, and the organic phase was pipetted out in order to measure the radioactivity. The results obtained for each nuclide are given in Table II, which shows that the radioactive ruthenium can be extracted satisfactorily into the pyridine phase. Only cesium has a tendency to migrate into the pyridine phase, since it behaves like the sodium contained as the sodium hydroxide in the pre-equilibrated pyridine. However, it can be removed from the pyridine phase by a

TABLE II. RECOVERY AND PARTITION COEFFICIENT OF INDIVIDUAL CARRIER-FREE NUCLIDE IN SOLVENT EXTRACTION WITH PYRIDINE

Nuclide	In the first org. phase %	In the first aq. phase %	Partition coefficient
Ru-106	96.2	3.7	26.0
Cs-137	1.54	98.46	1.5×10^{-2}
Sr-90(Y-90)	0.14	99.86	1.4×10^{-3}
Pm-147	0.01	99.99	$<10^{-4}$
Ce-144	0.01	99.99	$<10^{-4}$

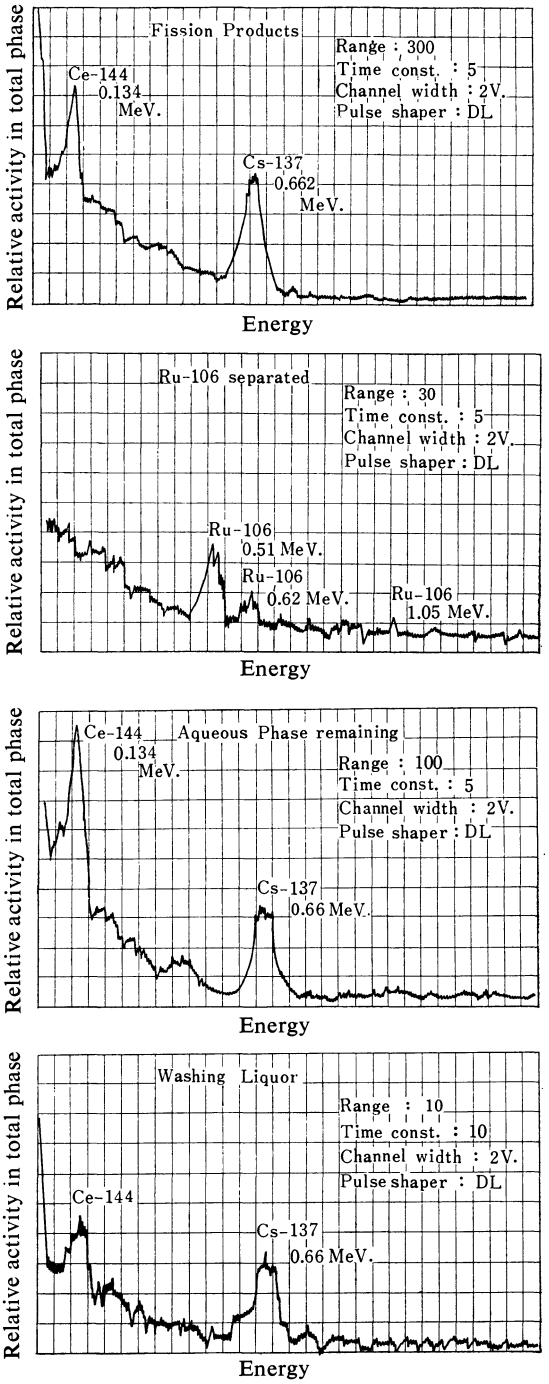

Fig. 6. Distribution of activities due to different fission products in each stage of liquid-liquid extraction.

12) M. Koyama, *J. Chem. Soc. Japan, Pure. Chem. Sec.* (*Nippon Kagaku Zasshi*), **82**, 1182 (1961).

single back-washing. The greater part of the last pyridine phase was evaporated under an infrared lamp, and its radioactivity was measured by a G-M counter. To make sure of the completion of the separation, γ-ray spectra were taken of the mixed fission products before the separation, of the residual aqueous phase, of the last organic phase after the extraction, and of the back-washing liquid, which might contain cesium-137 and cerium-144. These spectra are shown in Fig. 6. It is found that a satisfactory separation of ruthenium has been effected with little contamination by other fission products.

The Separation of Radioactive Ruthenium in the Presence of Ruthenium Carrier.—As has been described above, a perruthenate solution can also be prepared by dissolving metallic ruthenium in "Antiformin", and when this solution is treated with pyridine, the brownish-red color of the solution is completely transferred to the pyridine layer and the residual aqueous layer becomes colorless. The partition coefficient of ruthenium, by a preliminary experiment, was found to be 10^4 in the presence of 10 mg. of ruthenium between 10 ml. each of the organic and aqueous phases. Therefore, an experiment was carried out in a hope of getting a higher partition coefficient in the separation of radioactive ruthenium with a small amount of ruthenium carrier. In this experiment a definite amount of carrier ruthenium was added as perruthenate in "Antiformin" to the aqueous phase before the extraction. In the presence of 0.091 mg. to 2 mg. of ruthenium carrier per ml. of the aqueous phase, the results given in Table III were obtained; this table shows that the per cent extraction could be increased markedly by the presence of the carrier, but that the efficiency of the extraction is almost independent of the amounts of the carrier in this range. The per cent extraction was calculated as the ratio of the radioactivities of the two phases.

TABLE III. EXTRACTION OF RADIOACTIVE RUTHENIUM IN THE PRESENCE OF CARRIER

Ruthenium carrier taken in the initial aq. phase mg.	Ru-106 extracted in pyridine %	Ru-106 remaining in the aq. phase %	Partition coefficient
1.0	99.1	0.9	110
3.0	99.4	0.6	165
5.0	99.3	0.7	141
10.0	99.7	0.3	332

It was thought desirable to diminish the amount of pyridine employed so that less sodium hydroxide might accompany the dried ruthenium salt; some experiments were, therefore, carried out with smaller quantities of the solvent. The results are shown in Table IV, in which it can be seen that as much as 91.2% of the ruthenium present in 11 ml. of the aqueous phase could be extracted with as little as 2 ml. of pyridine, with the resulting presence of only 15 mg. of sodium hydroxide as an impurity.

TABLE IV. EXTRACTION OF RADIOACTIVE RUTHENIUM WITH SMALL VOLUME OF PYRIDINE IN THE PRESENCE OF 10 mg. RUTHENIUM CARRIER

Volume of pyridine used ml.	Volume of aq. phase ml.	Recovery of Ru-106 in pyridine %
11	11	99.7
6	11	96.6
4	11	95.5
3	11	91.1
2	11	91.2

The Separation of Technetium and Ruthenium by Pyridine Extraction.—Technetium can easily be extracted by pyridine[11] because it can exist in an alkaline solution as pertechnetate as its most stable form, but ruthenium can be extracted only when the perruthenate is in an alkaline solution with excess enough of a strong oxidizing agent; otherwise it is very unstable. This difference in chemical behavior between the elements was taken advantage of in effecting their separation.

Technetium-99 as potassium pertechnetate in a 0.1 M sodium hydroxide solution was taken by pipetting 0.5 ml. of the stock solution and mixing it well with 0.5 ml. of a solution of ruthenium-106 as nitrosylruthenium trinitrate in 3 M nitric acid in a separating funnel; then 4 ml. of 12 M sodium hydroxide was added, the total volume thus becoming 5 ml. To this solution was added 5 ml. of pyridine preequilibrated with 4 M sodium hydroxide. The funnel was shaken well for five minutes, and after the two layers had been disengaged, the lower aqueous layer was drained out through the stem into another funnel. One milliliter of the organic phase was pipetted into a counting pan and evaporated to dryness, and its radioactivity was measured by a G-M counter. Here the observed value was corrected for the self-absorption of the radioactivity by the sample. This count must be due to the technetium-99 separated by pyridine, for a Harley plot of the sample with a reference of calcium-45 agreed well with that of a pure technetium-99 within the range of permissible errors, showing its radiochemical purity to be above 99.5%. To the aqueous phase in the second separating funnel, 10 ml. of "Antiformin" and 5 ml. of pyridine were added, and

the funnel was shaken well for five minutes. In this case there was 15 ml. of the aqueous phase and only 5 ml. of the organic phase. After separating the two phases, 1 ml. of the organic layer was pipetted and its radioactivity was measured as above. This radioactivity is presumed to be due to ruthenium-106 separated into pyridine as perruthenate. As the per cent extraction of technetium in the first step could not reach 100%, but only about 94%, some residual technetium might be present in this sample. However, the energy of the β-ray of technetium-99 is so weak that it can be eliminated by an aluminum absorber of about 40 mg./cm^2, while the β-ray of ruthenium-106 has higher energy and is scarcely absorbed by the same absorber. Technetium and ruthenium can be almost completely separated by this procedure.

Summary

The present paper has described a method of separating, by liquid-liquid extraction with pyridine, radioactive ruthenium from fission products and technetium in an aqueous solution containing sodium hydroxide and hypochlorite. In the process, ruthenium in various ionic forms and various oxidation states is oxidized to perruthenate with the hypochlorite, and the perruthenate is transferred into pyridine from the aqueous solution. The partition coefficient of perruthenate was estimated for the carrier-free and the carrier-containing cases, as well as for the case where other fission products were present. Good separation of radioactive ruthenium from other fission products was achieved by this method, with a large decontamination factor. The results were examined by a γ-ray spectrum measured at each step of the extraction process.

The authors wish to express their thanks to Dr. Shigeru Ohashi and Dr. Kikuo Terada for their advice and criticism. A part of the expenses for this study was defrayed by a grant from the Ministry of Education, to which the authors' thanks are due.

Department of Chemistry
Faculty of Science
Kanazawa University
Kanazawa

*Stability Order in Metal Chelate Compounds. I. 4-Carboxy- and 4-Sulfocatechol Complexes**

By Yukito MURAKAMI, Katsuyuki NAKAMURA and Masasuke TOKUNAGA

(Received January 16, 1963)

Irving and Williams[1] collected and examined the stability data of complexes formed with bivalent metal ions of the first transition series and put forward the stability order, manganese < iron < cobalt < nickel < copper > zinc. This order has been shown to hold substantially for nitrogen-type, nitrogen-oxygen-type and oxygen-type ligands. On the other hand, it is of much interest to find a place for the bivalent zinc in the stability order ranging from bivalent manganese through bivalent copper, since the Irving-Williams order does not provide any knowledge about the stability of zinc complexes in comparison with the other transition metal complexes.

Meanwhile, Mellor and Maley demonstrated the stability order for bivalent metal chelates with salicylaldehyde[2] and ethylenediamine[3] and placed zinc between iron and cobalt in the first transition series, i. e., copper > nickel > cobalt > zinc > iron > manganese. However, the general applicability of the Mellor-Maley order has not yet been established, and the higher stability of bivalent zinc complexes than the corresponding bivalent cobalt complexes has been frequently observed. It seems, therefore, that the stability of a zinc complex is quite dependent on the ligand properties and the character of the resulting coordinate bonds. In this connection, the catechol derivatives were selected in this investigation as ligands for the first transition metals as well as for

* Contribution No. 37 from the Department of Organic Synthesis, Faculty of Engineering, Kyushu University.

1) H. Irving and R. J. P. Williams, *Nature*, **162**, 746 (1948); *J. Chem. Soc.*, **1953**, 3192.

2) D. P. Mellor and L. Maley, *Nature*, **159**, 370 (1947).

3) D. P. Mellor and L. Maley, ibid., **161**, 436 (1948).

alkaline earth metals, and the stability order was studied.

Experimental

Materials.—The bivalent metal nitrates, $Zn(NO_3)_2 \cdot 6H_2O$, $Cu(NO_3)_2 \cdot 3H_2O$, $Ni(NO_3)_2 \cdot 6H_2O$, $Co(NO_3)_2 \cdot 6H_2O$, $Mg(NO_3)_2 \cdot 6H_2O$, $Ca(NO_3)_2 \cdot 4H_2O$ and $Sr(NO_3)_2$, and manganese sulfate, $MnSO_4 \cdot nH_2O$, are analytical reagents produced by the Wako Pure Chemical Industries, Ltd.

Reagent grade catechol of the Wako Pure Chemical Industries, Ltd. was purified by means of repeated recrystallization from benzene. Dotite Tiron (analytical grade) was used without further purification.

Preparation of Ligands.—*4-Carboxycatechol (Protocatechuic Acid).*—This catechol derivative was prepared from vaniline following the standard method reported by Pearl and Beyer[4] and was recrystallized from water. M. p. found, 203~204°C; reported, 199~200°C[4].

Found: C, 54.48; H, 4.00. Calcd. for $C_7H_6O_4$: C, 54.55; H, 3.92%.

Potassium Catechol-4-sulfonate.—This material was synthesized by the sulfonation of catechol[5] and was recrystallized from water as white platelets.

Found: C, 31.58; H, 2.39; K, 16.91. Calcd. for $C_6H_5O_5SK$: C, 31.57; H, 2.21; K, 17.13%.

Reagent Solutions.—Aqueous stock solutions of metal ions were standardized by the usual procedures of chelatometric titration[6]. Aqueous stock solutions of all the ligands were standardized by potentiometric titration with a standard base.

Potentiometric Measurements.—The apparatus and procedures for potentiometric titrations have been mentioned elsewhere[7].

Spectral Measurements.—The infrared spectra were measured by the KBr disk method with a Koken model DS-301 spectrophotometer equipped with sodium chloride optics.

Mathematical Treatment

Acid Dissociation Constants.—The equilibria and the dissociation constants involved in the dissociation process of catechol protons are:

$$H_2L \rightleftharpoons HL^- + H^+ \quad K_{H,L}=\frac{[HL^-]\,[H^+]}{[H_2L]} \tag{1}$$

$$HL^- \rightleftharpoons L^{2-} + H^+ \quad K_{HL}=\frac{[L^{2-}]\,[H^+]}{[HL^-]} \tag{2}$$

If T_L represents the total concentration of ligand species and T_{OH} represents the total concentration of base added to the system, the following stoichiometric relations may hold:

$$T_L=[H_2L]+[HL^-]+[L^{2-}] \tag{3}$$

$$T_{OH}+[H^+]-[OH^-]=[HL^-]+2[L^{2-}] \tag{4}$$

Combination of Eqs. 1 through 4 results in:

$$1/K_{H\,L}=A\,K_{HL}+B \tag{5}$$

where

$$A=\frac{\{2T_L-T_{OH}-[H^+]+[OH^-]\}}{\{T_{OH}+[H^+]-[OH^-]\}[H^+]^2}$$

$$B=\frac{\{T_L-T_{OH}-[H^+]+[OH^-]\}}{\{T_{OH}+[H^+]-[OH^-]\}[H^+]}$$

Thus, when $1/K_{H_2L}$ is plotted graphically as a function of K_{HL} with values of A and B corresponding to experimental values of T_L, T_{OH}, and $[H^+]$, straight lines obtained from a number of experimental points are found to intersect at one point, which represents the simultaneous solution of K_{H_2L} and K_{HL} for the dibasic acid.

Chelate Stability Constants.—If the pH value of the system is maintained in an appropriate range so that the metal chelates formed are the 1:1 (ligand to metal) and the 2:1 chelates in significant concentrations, the equilibria involved in metal chelate formation may be expressed as:

$$M^{2+}+L^{2-} \rightleftharpoons ML \quad K_1=\frac{[ML]}{[M^{2+}]\,[L^{2-}]} \tag{6}$$

$$ML+L^{2-} \rightleftharpoons ML_2^{2-} \quad K_2=\frac{[ML_2^{2-}]}{[ML]\,[L^{2-}]} \tag{7}$$

The stoichiometric relationships involved in this system are represented as:

$$T_M=[M^{2+}]+[ML]+[ML_2^{2-}] \tag{8}$$

$$T_L=[H_2L]+[HL^-]+[L^{2-}]+[ML]+2[ML_2^{2-}] \tag{9}$$

$$T_{OH}+[H^+]-[OH^-]=[HL]+2[L^{2-}]+2[ML]+4[ML_2^{2-}] \tag{10}$$

where T_M indicates the total concentration of all the metal species. Equations 6 through 10 may by combined to give an equation for the evaluation of K_1 and K_2:

$$(F-1)K_1[L^{2-}]+(2F-1)K_1K_2[L^{2-}]^2=1 \tag{11}$$

where

$$F=T_M/\{T_L-[H_2L]-[HL^-]-[L^{2-}]\}$$

and

$$[L^{2-}]=\frac{\{2T_L-T_{OH}-[H^+]+[OH^-]\}K_{H_2L}K_{HL}}{\{2[H^+]^2+[H^+]K_{H_2L}\}}$$

Therefore, K_1 may be plotted as a function of K_1K_2, and one straight line may be drawn for each experimental point on the titration curve; the lines thus obtained are to intersect at one point if the metal chelate formations expressed by Eqs. 6 and 7 predominantly hold in the system. This method of evaluation is quite

4) I. A. Pearl, "Organic Syntheses", Vol. 29, 85 (1949); I. A. Pearl and D. L. Beyer, *Ind. Eng. Chem.*, **42**, 376 (1950).
5) J. N. Rây and M. L. Dey, *J. Chem. Soc.*, **117**, 1407 (1920).
6) K. Ueno, "Chelatometric Titration" (in Japanese), Nankodo, Ltd., Tokyo (1960).
7) Y. Murakami, This Bulletin, **35**, 52 (1962).

similar to those mentioned for the determination of acid dissociation constants in the preceding section and for chelate stability constants elsewhere[7], and the intersect of the family of straight lines may provide the chelate stability constants, K_1 and K_2.

When more than three moles of ligand per gram-ion of metal are added to the titrating system and when an appropriate pH range is selected, the 3:1 (ligand to metal) chelate may be formed in a significant concentration, depending upon the coordination ability of the metal ion. Under such conditions, it was found in this investigation that reaction 6 was nearly completed and that reactions 7 and 12 are to be taken into consideration.

$$ML_2^{2-} + L^{2-} \rightleftarrows ML_3^{4-} \quad K_3 = \frac{[ML_3^{4-}]}{[ML_2^{2-}]\,[L^{2-}]} \qquad (12)$$

Then, an adequately modified form of Eq. 11 may be employed for the evaluation of the third stability constant, K_3.

Results and Discussion

Acid Dissociation Constants.—As the electron-withdrawing effect of a substituent group or groups in the catechol derivatives decreases in the order: Tiron, catechol-4-sulfonate, 4-carboxycatechol, catechol, an inflection region for the neutralization of the first catechol proton in their potentiometric titration curves becomes increasingly insignificant. Thus, the first and the second dissociation processes for Tiron do not overlap each other to any significant extent. On the other hand, those processes for catechol do overlap to a great extent, so the inflection region was not noticed.

A carboxy proton of 4-carboxycatechol is very acidic in comparison with other catechol protons, so the first dissociation process was separated clearly from the others in this case.

The acid dissociation constants of the catechol derivatives other than Tiron were calculated with the aid of Eq. 5 and are summarized in Table I.

Table I. Acid dissociation constants of the catechol derivatives

30±0.1°C, μ=0.10 M (KNO_3)

Ligand	pK_{H_3L}	pK_{H_2L}	pK_{HL}
Catechol		9.13	11.59
4-Carboxycatechol	4.38	8.67	11.94
Catechol-4-sulfonate		8.26	12.16
Tiron		7.54	12.26

It is of interest to consider the effect of electron-withdrawing substituents on the dissociation process of catechol protons among these four catechols. The two processes are

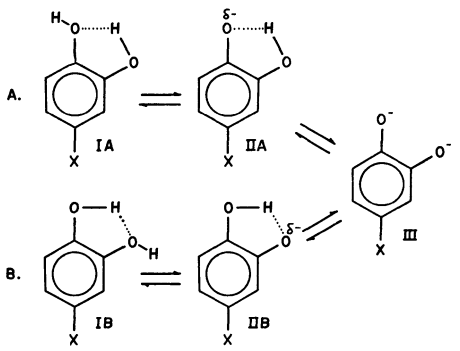

Chart 1. Dissociation processes of catechol-protons.

conceivable in this case, as is shown in Chart 1. A sulfonate and a carboxylate substituent in the benzene ring introduce a pronounced electron-withdrawing effect at their para position. For example, a dissociation constant of the phenol proton of hydroxybenzoic acid has a very close connection with the position of a carboxy group, as may be seen in Table II[8].

Table II. Acid dissociation constants of phenol derivatives[8]

20°C, μ=0.1 M

Acid	pK_{H_2A}	pK_{HA}
Phenol		9.80
m-Hydroxybenzoic acid	3.96	9.61
p-Hydroxybenzoic acid	4.36	8.985

The carboxylate group transmits its strong electronic effect to its para position in the benzene ring through such resonance interaction as is indicated by structure IV, while this

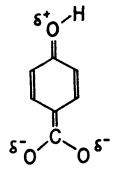

IV

group shows only a weak inductive effect at its meta position, as may be understood from the data in Table II.

As the pK_{HL} values in Table I indicate, the intramolecular hydrogen bond is strengthened as a ligand varies from catechol to Tiron in the order shown in the table. Because of the electrostatic nature of hydrogen bonding, the electrostatic potential ought to be increased in order to raise the strength of bonding. X being an electron-withdrawing group, an intramolecular hydrogen bond in IIA should be weakened

8) A. V. Willi and J. F. Stocker, *Helv. Chim. Acta*, **38**, 1279 (1955).

in comparison with catechol itself. This is, however, contrary to what is observed in this work. Therefore, IIB must be taken instead as a more favorable structure. As a result, process B in Chart 1 may be employed to elucidate the dissociation steps of the catechol protons. Meanwhile, the OH stretching vibrations involved in inter- and intramolecular hydrogen bonds were assigned, as Table III shows. The tendency of the OH frequency shift is in agreement with the change in pK_{HL} value except in the case of Tiron. The reason for the unexpected frequency shift in Tiron is not quite obvious at this moment.

TABLE III. STRETCHING VIBRATIONS OF CATECHOL-HYDROXY GROUPS

Frequency cm^{-1}	Ligand			
	Catechol	4-Carboxy-catechol	Catechol-4-sulfonate	Tiron
ν_{OH}	3320	3300	3165	3260
ν'_{OH}	3435	3440	3245	3475

ν_{OH}: Assignment of intramolecular hydrogen bonded OH vibration.
ν'_{OH}: Assignment of intermolecular hydrogen bonded OH vibration.

Interaction of Metal Ions with 4-Carboxycatechol. — Titration curves are illustrated in Fig. 1 for the 4-carboxycatechol chelates of magnesium(II), manganese(II), cobalt(II), nickel(II), copper(II) and zinc(II) for a 2:1 ratio of ligand to metal ion. The titration curve for the calcium(II) chelate is not shown in the figure because higher concentrations of ligand and metal ion were employed. The drifting behavior of the pH value was noticed for the manganese(II) chelate system during the measurement in the region of $-\log[H^+]$ value ranging from 7.2 to 8.1. A similar phenomenon was observed for the manganese(II) kojate chelate system[7].

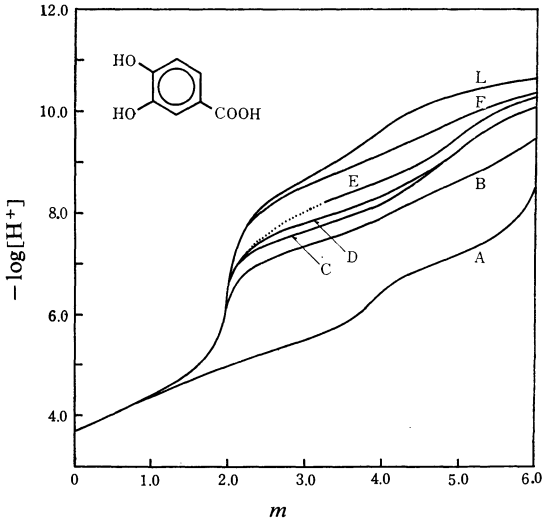

Fig. 1. Potentiometric titration of divalent metal chelates of 4-carboxycatechol in 0.10 M KNO_3 at 30°C, with 2:1 molar ratio of ligand to metal ion: A, Cu; B, Zn; C, Ni; D, Co; E, Mn; F, Mg; L, ligand alone; $T_M = 5.01 \times 10^{-4}$ M; m=moles of base added per gram-ion of metal. Dotted line indicates non-equilibrated region.

Potentiometric titrations for the 1:1 ratio of ligand to metal ion for calcium(II), magnesium(II), cobalt(II), nickel(II), copper(II), and zinc(II) were also performed at the same ligand concentration. Precipitations were found at the end of the titrations of the cobalt(II), nickel(II) and zinc(II) chelate systems where all the protons of the catechols were nearly neutralized. These precipitations were probably caused either by disproportionation to the corresponding 2:1 chelate and metal hydroxide or by further hydrolysis reactions of the 1:1 chelate. The addition of a base to the copper(II) chelate system resulted in neither drifting of the pH values nor precipitation in the range of m values of up to 3.1 ($-\log[H^+] \approx 7.5$). This phenomenon is ascribed to the profound stability of the copper(II) chelate; this chelate could not undergo disproportionation reaction with the ease of other metal chelates.

In the case where more than two moles of ligand were present per gram-ion of metal, no precipitation was observed over the whole pH range of the titration.

As may be seen in Fig. 1, no obvious depression of pH was observed in the lower buffer region (m=0~2.0), where the dissociation of a carboxy proton occurs predominantly, while only the titration curve of the copper(II) chelate system demonstrates such a depression to some extent in the last part of this region. On the basis of these experimental facts, no appreciable chelation was expected in such a pH region expect for the copper(II) chelate system, and the carboxy group was not involved in complex formation with metal ions. It is also obvious from Fig. 1 that stability with respect to the metal ions increases in the order: magnesium(II) < manganese(II) < cobalt(II) ~ nickel(II) < zinc(II) < copper(II). A small inflection at m=4 corresponding to the formation of the 1:1 chelate species and a rather steep inflection at m=6, which corresponds to the formation of the 2:1 chelate species, were observed only for the copper(II) system. The absence of such an inflection at m=4 suggests an appreciable overlapping of the two reactions producing the 1:1 and the 2:1 chelale species.

TABLE IV. STABILITY CONSTANTS OF THE METAL CHELATES OF CATECHOL DERIVATIVES

$30\pm0.1°C$, $\mu=0.10$ M (KNO_3)

Ligand	Catechol		4-Carboxycatechol			Catechol-4-sulfonate			Tiron	
	$\log K_1$	$\log K_2$	$\log K_1$	$\log K_2$	$\log K_3$	$\log K_1$	$\log K_2$	$\log K_3$	$\log K_1$	$\log K_2$
Zn(II)	8.46	6.78	8.91	6.71		9.40	7.20		10.19	8.33
Cu(II)	12.52	9.66	12.79	9.81		13.29	10.23		13.99	11.17
Ni(II)			8.27	4.71	3.89	8.85	5.56	4.73		
Co(II)			7.96	5.40	4.06	8.54	5.86	3.08		
Mn(II)			7.22	5.06		7.87	4.66			
Mg(II)			5.67	4.17		6.27	4.14			
Ca(II)			3.71	2.65		4.40	3.59			
Sr(II)						3.61	—			

Interaction of Metal Ions With Catechol-4-sulfonate.—In Fig. 2 are shown titration curves for solutions containing a 2:1 ratio of ligand to metal ion. The metal ions employed in these measurements were strontium(II), calcium(II), magnesium(II), manganese(II), cobalt(II), nickel(II), copper(II) and zinc(II). No precipitates were observed throughout those titrations where ligand concentration exceeded two moles per gram-ion of metal. A drifting of the pH reading was also realized in the titration of the manganese(II) chelate system in the lower pH region ($-\log[H^+]<8.2$). The stability order is obviously understood from these titration curves and arranged in the increasing order as: calcium(II) < magnesium(II) < cobalt(II) ~ nickel(II) < zinc(II) < copper(II). Again, a titration curve for the copper(II) system exhibits a significant inflection at $m=2$ and a steep one at $m=4$, corresponding to the formation of the 1:1 and 2:1 chelates respectively.

In titrations of solutions containing a 1:1 ratio of ligand to metal ion, pH drifting was observed to start for the transition metal chelate systems in the region where nearly all the catechol protons were neutralized ($m>1.8$ in most cases). This drifting may be ascribed either to disproportionation to the 2:1 chelate and metal hydroxide or to the hydrolysis reaction of the 1:1 chelate in the same manner as has been mentioned for the 4-carboxycatechol chelates.

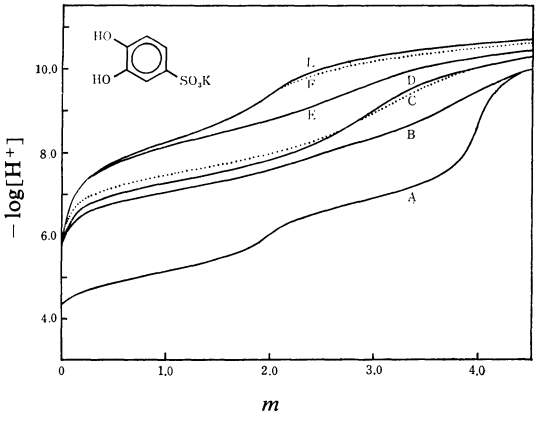

Fig. 2. Potentiometric titration of bivalent metal chelates of catechol-4-sulfonate in 0.10 M KNO_3 at 30°C, with 2:1 molar ratio of ligand to metal ion: A, Cu; B, Zn; C, Co; D, Ni; E, Mg; F, Ca; L, ligand alone; $T_M=5.00\times10^{-4}$ M; m=moles of base added per gram-ion of metal.

Stability Constants.—The stabilty constants for the metal chelate compounds with catechol and its derivatives as ligands have been calculated by the aid of Eq. 11 and its modified forms. The constants thus estimated are listed in Table IV.

For the bivalent transition metal series, the stability order for the metal chelates with 4-carboxycatechol and catechol-4-sulfonate follows the sequence: manganese < cobalt ~ nichel < zinc < copper. The stability order, nickel(II) < zinc(II), seems to be rather unusual. This order has, however, been found occasionally in the literature in the past and may be ascribed to the following two main effects involved in chelation:

Structural Effects.—In most instances where the stability of metal chelates follows the sequence, nickel(II) > zinc(II), a lone pair of valence electrons in a donor atom is directed toward the metal ion, with which coordination is performed, thus forming a stable coordinate bond. However, the perturbation effect may be introduced if such a lone pair is located in a direction unfavorable for a coordinate bond formation, in which case the above sequence is reversed (zinc(II) > nickel(II)). In such a case the ionic size of the metal ion seems to be another factor controlling the stability order. 4-Hydroxybenzimidazole and its analogous compounds (V)[9] may be taken as ligands to elucidate this effect.

9) T. J. Lane, C. S. C., A. Sam and A. J. Kandathil, *J. Am. Chem. Soc.*, **82**, 4462 (1960); T. J. Lane, C. S. C. and A. Sam, ibid., **83**, 2223 (1961).

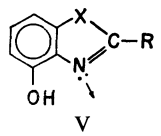

X=NH, O, S

V

A lone pair of the donor nitrogen atoms in this case seems to have the greatest angular distribution toward external direction with respect to the coordinate bond. As a result this electron pair would have less overlapping with the bonding atomic orbital of a metal ion of smaller size.

Electronic Effects.—The stability of a metal chelate compound is certainly dependent on the electronic state of the donor atom. Thus, when a sulfur atom is involved in chelate ring formation as a donor atom, the stability is in favor of zinc chelates. For example, mercaptoacetic acid[10] and mercaptosuccinic acid[11] yielded the corresponding zinc chelates which were more stable than those of nickel.

Even if the ligand species are limited to the nitrogen type, the oxygen type and the nitrogen-oxygen type, such a reversed order of stability for zinc and nickel chelates has been observed. However, such examples are found quite rarely to the best knowledge of the present authors. Tropolones (VI)[12] and kojic acid (VII)[13], as well as 2-hydroxynaphthoquinones (VIII)[13], were observed to form zinc

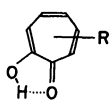

VI

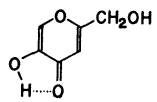

VII

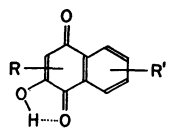

VIII

chelates with a favorable stability. It is of much interest to find that all these ligand species accommodate the same chelating site, as is shown by structure IX:

IX

The electronic configuration of whole ligand molecule and of the central ion, in addition to the electron delocalization effect through the coordinate bond formation, may come into play in these cases to control the stability of metal chelates thus produced.

10) D. L. Leussing, ibid., **80**, 4180 (1958).
11) G. E. Cheney, Q. Fernando and H. Freiser, *J. Phys. Chem.*, **63**, 2055 (1959).
12) J. Bjerrum, G. Schwarzenbach and L. G. Sillén, "Stability Constants, Part I. Organic Ligands", The Chemical Society, London (1956).
13) H. Kido, W. C. Fernelius and C. G. Haas, Jr., *Anal. Chim. Acta*, **23**, 116 (1960).

The unusally high stability of zinc chelates in comparison with that of nickel chelates formed with 4-carboxy- and 4-sulfocatechol as well as with Tiron[12] must be associated to some extent with the electron delocalization through the interaction among zinc 3d orbitals, oxygen-orbitals not involved in σ-bonding, and π orbitals of the benzene ring. The configuration of these orbitals is depicted in Fig. 3.

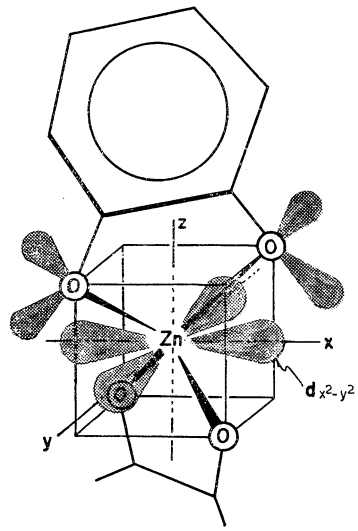

Fig. 3. Probable structure of the Zn(II)-catechol chelate with indication of metal d orbital and lone pair orbitals of oxygens.

The linear relationship between the basicity of the donor group (pK_{HL}) and the chelate stability (log K_n) has been found to hold in a large portion of the literature reported so far. Thus, the weaker the acidity of the donor group, the more stable the chelate compound would be. In this investigation the stability constants for copper(II) and zinc(II) chelates with the four catechols were obtained, as is shown in Table IV. These data obviously prove the parallel relationship between the ligand basicity and the stability constant in agreement with the past observation only if the second pK value (pK_{HL}) is taken. In the opinion of the present authors, the basicity of both hydroxy groups in the ligand molecule should be taken into consideration, since both groups are involved in chelate ring formation. The value of ($pK_{H_2L}+pK_{HL}$), as a measure of ligand basicity, decreases in the order:

Catechol > 4-carboxycatechol > catechol-4-sulfonate > Tiron.

The stability order, however, is antiparallel to this order and is found in the sequence:

Tiron > catechol-4-sulfonate > 4-carboxycatechol > catechol.

In spite of the fact that the second catechol proton is involved in the intramolecular hydrogen bonding, the catechol group (two phenolate groups) certainly lowers its electron density as the 4-substituent group demonstrates a greater electron-withdrawing effect, thus indicating less basicity. The relationship between ligand basicity and chelate stability found in this study is certainly due to ligand nature. It seems that these ligand molecules introduced a more covalent character to the coordinate bonds, and that the resonance contribution of the substituent group made electron delocalization through the coordinate bonds more effective.

For alkaline earth metal ions, no peculiar stability order was observed in this work, and these chelates demonstrate much less stability than the corresponding transition metal chelates, as is shown in Table IV. The stability order, magnesium(II) > calcium(II) > strontium(II), is parallel to the reciprocal of the ionic size of the metal ions.

Meanwhile, the formation of such a hydrogen complex as MHL was noticed in this investigation in the region of relatively low pH value, as has also been observed elsewhere for the Tiron chelates in an aqueous system[12]. A thorough investigation on this behavior has not yet been carried out. Investigations with other catechol derivatives, containing various 4-substituent groups, are under progress in these laboratories.

Summary

The stability constants of 4-carboxy- and 4-sulfocatechol chelates with bivalent transition metals and alkaline earth metals have been evaluated in aqueous media at 30.0±0.1°C and 0.10 M of ionic strength. The stability orders, manganese < cobalt ~ nickel < zinc < copper for transition metal chelates and strontium < calcium < magnesium for alkaline earth metal chelates, have been found to hold in these catechol chelate systems. A unique stability sequence, nickel < zinc, has been discussed in terms of the electron delocalization effect, in which metal d orbitals, lone pair orbitals of catechol oxygens and π orbitals of the benzene ring are involved. A reverse relationship for ligand basicity and chelate stability was observed for copper(II) and zinc(II) chelates, and the stability of metal chelates was found to increase in the sequence; catechol < 4-carboxycatechol < catechol-4-sulfonate < Tiron. Substituent groups were considered to play an important role in this case.

Department of Organic Synthesis
Faculty of Engineering
Kyushu University
Hakozaki, Fukuoka

Studies of the Drawing of Polyamide Fibers. II. The Drawing of Heat-treated Nylon Monofilaments

By Hiroshi HATTORI and Yasuo TAKAGI

(Received January 22, 1963)

In a previous paper, the present authors reported that the tensile strength of nylon 6 filament showed a minimum value at a draw ratio near 2 and that, therefore, the structure seemed to become unstable at the intermediate stage of drawing[1]. For this paper, the authors have investigated the dependences on the draw ratio of some physical properties of nylon monofilaments drawn to various draw ratios after they had been heat-treated at various temperatures from 90 to 180°C; this has been undertaken in order to investigate how the change in the structure, especially the crystallinity, of an undrawn sample influences the behavior of the drawing. Althogh the effect of the heat-treating temperature of the undrawn nylon filament on the load-elongation curve has been studied by Yumoto[2], the change in the physical properties during the drawing of heat-treated samples has not yet been studied.

Experimental

Samples.—The undrawn nlyon monofilament (about 1300 denier), prepared under the same

1) H. Hattori, Y. Takagi and T. Kawaguchi, This Bulletin, **35**, 1163 (1962).

2) H. Yumoto, ibid., **29**, 353 (1956).

conditions as that in the previous paper[1], was heat-treated, more than a week after it had been meltspun, at the temperatures of 90, 110, 114, 150, 160, 170 and 180°C, in an air-bath for 30 sec. Each heat-treated undrawn sample was drawn in water of 90°C, at the feeding speed of 5 m./min.

Measurement. — Various physical properties (strength, shrinkage in boiling water, specific gravity and birefringence) of these variously-drawn samples were measured under the same conditions as those in the previous paper[1].

Results and Discussion

Tensile Strength.—If the decrease in strength observed near the draw ratio of 2 is caused by the flow phenomenon, which is called "super drawing", the decrease in strength will stop, because heat-treatment strengthens the interaction between the polymer molecules and, therefore, it becomes more difficult for the flow during drawing to occur. The experimental results, shown in Fig. 1, indicate that

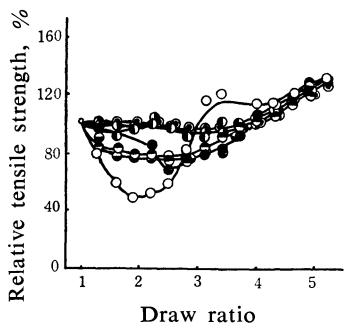

Fig. 1. Dependence of thensile strength on draw ratio.
○, Drawn immediately after spinning
●, Drawn many days after spinning
◓, Drawn after being heat-treated at 90°C
◒, Drawn after being heat-treated at 110°C
◐, Drawn after being heat-treated at 150°C
◑, Drawn after being heat-treated at 160°C
⊙, Drawn after being heat-treated at 170°C

the higher the heat-treating temperature, the less the decrease in strength at the minimum. Though a minimum point was observed near the draw ratio of 2 in the draw ratio-strength curve when the heat-treating temperature is below 110°C, no minimum point was observed when the heat-treating temperature was above 150°C. This fact suggests that the flow occurs during the drawing, and it can be one of the reasons for the minimum strength observed on the drawing of the less crystalline sample, but it seems unsatisfactory to explain this fact completely in terms of flow phenomenon, because even in case of samples which have no minimum in the draw ratio-strength curves, the strength does not increase but is kept nearly constant until it increases with the draw ratio from the ratio of 3~3.5.

Birefringence.—It is thought that the degree of molecular orientation due to the drawing will be lower when the flow occurs during the drawing than when it does not occur. Therefore, the degree of flow can be roughly estimated by comparing the draw ratio-birefringence curves. In the previous paper. the authors noticed the difference observed between the draw ratio-birefringence curve of samples drawn immediately after spinning (I) and that of samples drawn many days after spinning (II). For this paper, we have also compared the curves of samples drawn after the heat-treatment at various temperatures. The results are shown in Fig. 2. All curves,

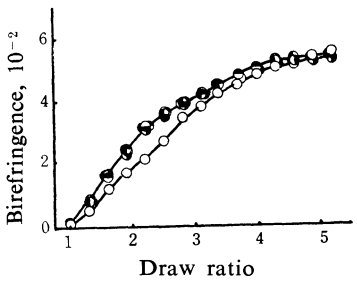

Fig. 2. Dependence of birefringence on draw ratio.
○, Drawn immediately after spinning
●, Drawn many days after spinning
◓, Drawn after being heat-treated at 90°C
◒, Drawn after being heat-treated at 150°C
◐, Drawn after being heat-treated at 160°C
◑, Drawn after being heat-treated at 170°C

except the curve for the samples of group I quite overlap with each other, regardless of whether the minimum strength was observed or not. In consideration of the fact, it is obvious that the phenomenon of minimum strength observed in certain samples is due not only to the flow but also to some other reasons. It is thought that, even if the apparent degree of orientation is equal, the change in internal structure depends on the structure of the undrawn sample and that the difference in the change among heat-treated samples appears most remarkably at the draw ratio near 2, where the polymer structure becomes most unstable.

Shrinkage in Boiling Water.—In the previous part of this paper, the authors chiefly discussed the influence of the heat-treatment of an undrawn sample on the change of strength with the draw ratio, but it is thought that strength data are not precise or reliable

enough to be discussed in detail. From this point of view, the data of shrinkage in boiling water seem to be better as the basis for a discussion of the change of structure during drawing.

The shrinkage in boiling water of heat-treated samples, shown in Fig. 3, changed very peculiarly with the heat-treating temperature and draw ratio. In the case of samples drawn after heat-treatment, the degree of shrinkage rapidly increased in the initial stage of drawing, passed a maximum, and then decreased as the draw ratio increased. At the extreme draw ratio, the degree of shrinkage for all the

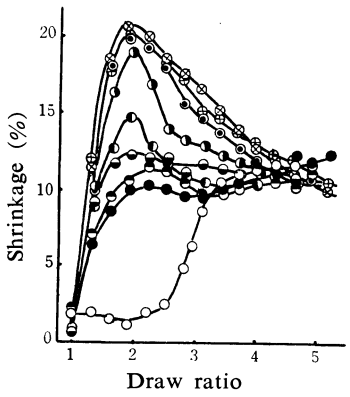

Fig 3. Dependence of shrinkage in boiling water on draw ratio.
○, Drawn immediately after spinning
●, Drawn many days after apinning
◓, Drawn after being heat-treated at 90°C
◒, Drawn after being heat-treated at 110°C
◐, Drawn after being heat-treated at 114°C
◑, Drawn after being heat-treated at 150°C
⊙, Drawn after being heat-treated at 160°C
⊗, Drawn after being heat-treated at 170°C
⊕, Drawn after being heat-treated at 180°C

samples seems to converge to the same value, regardless of the heat-treating condition. The maximum value always appeared near the draw ratio of 2 and increased as the heat-treating temperature of the undrawn sample was raised. It seems very important that the maximum point always appears at a draw ratio near 2. This implies that the internal structure of a nearly 100% drawn sample becomes most unstable and that some unknown change in the drawing mechanism occurs at a draw ratio near 2.

It is known that polyethylene terephthalate fiber also shows a maximum of heat-shrinkage near this draw ratio, but the mechanism seems quite different in polyethylene terephthalate and in nylon; in the former case[3], the undrawn polymer is almost perfectly amorphous and becomes partially crystalline when it is drawn, while in the latter case the higher the crystallinity of the undrawn polymer, the more remarkable the maximum of heat-shrinkage and the decrease of crystallinity due to drawing.

Though some possible reasons will be considered later in further detail, it is natural to think that the polymer structure becomes most unstable when the shrinkage is at its maximum.

Specific Gravity.—The change in specific gravity with the draw ratio is shown in Fig. 4. The specific gravity of a untreated sample or of a sample which had beed heat-treated at a lower temperature increased with the draw ratio, while that of a sample which had been heat-treated at a higher temperature decreased with the draw ratio. This fact indicates that when the crystallinity of an undrawn sample is low, it is increased by orientation, but when it is rather high, the orientation-induced crystallization is exceeded by the decrease of crystallinity due to the rupture of crystallites during drawing.

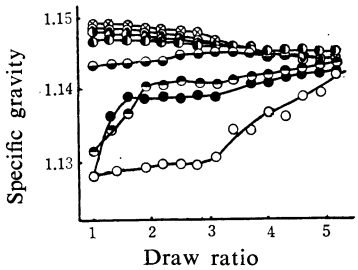

Fig. 4. Dependence of specific gravity on draw ratio.
○, Drawn immediately after spinnirg
●, Drawn many days after spinning
◓, Drawn after being heat-treated at 90°C
◒, Drawn after being heat-treated at 110°C
◐, Drawn after being heat-treated at 150°C
◑, Drawn after being heat-treated at 160°C
⊙, Drawn after being heat-treated at 170°C
⊗, Drawn after being heat-treated at 180°C

Similarly to such properties as strength and shrinkage in boiling water, specific gravity seems to converge to the same value at the extreme draw ratio, regardless of the kind of sample.

Therefore, we can deduce that the structure of highly-oriented nylon filaments is same, whether the crystallinity of an undrawn sample is low or high.

Further Discussion of the Change of Structure with the Drawing.—From the results mentioned above, especially of the shrinkage in boiling water, we believe that there is a certain difference between the mechanism of drawing

3) T. Kawaguchi, unpublished.

in the initial stage (of a lower draw ratio) and that in the later stage of drawing (of a higher draw ratio); in the former, the unstabilization of the polymer structure is predominant, while in the latter a stable structure of drawn polymer is constructed. In other words, a mechanism of drawing is proposed that consists of the unstabilization and stabilization of the polymer by orientation. The former is predominant in the initial stage of drawing, while the latter is predominant in the later stage of drawing.

Therefore, let us further discuss the results of shrinkage in boiling water, because the effect of heat-treatment is most pronounced in these results. It is considered that heat-shrinkage occurs because molecules become more labile upon a rise in the temperature and move in such a direction that the latent strain in the polymer is eliminated; the shrinkage is, then, a measure of the internal strain of polymer. Therefore, it is thought that the internal structure becomes most unstable when the heat-shrinkage becomes greatest.

In the case of ployethylene terephthalate fiber[3], the plot of heat-shrinkage against specific gravity falls on a single curve, in which the shrinkage decreases as the crystallinity increases, regardless of the condition of drawing. This fact implies that the orientation is fixed by the crystallization which occurred during the drawing. In case of nylon, however, this is not true, because the curve of shrinkage in boiling water against specific gravity, as shown in Fig. 5, depends on the heat-treating temperature of the undrawn sample. These facts indicate that, in addition to the degree of orientation and the crystallinity, some unknown factors contribute to the appearance of a maximum near the draw ratio of 2 in the draw ratio-shrinkage curve.

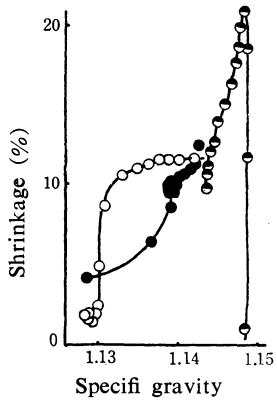

Fig. 5. Relation between specific gravity and shrinkage in boiling water.
○, Drawn immediately after spinning
●, Drawn many days after spinning
◓, Drawn after being heat-treated at 170°C

The curve of shrinkage against the heat-treating temperature of undrawm sample shown in Fig. 6 has an inflection near the temperature of 120°C. According to Yumoto[2], this temperature is a kind of transition, because inflection points are observed near this temperature in the curves of both specific gravity and yield load in the load-extension curve against the heat-treating temperature of undrawn nylon 6 filament. The heat-treating of undrawn nylon filament at a temperature above 120°C seems to tighten its structure much more than treating below this temperature. Therefore, the maximum value of shrinkage in boiling water is thought to be qualitatively proportional to the tightness of the structure of an undrawn filament.

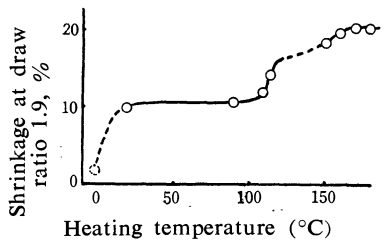

Fig. 6. Relation between heat-treating temperature and the shrinkage at the draw ratio of 1.9.

Now we will discuss the change in shrinkage in connection with that of specific gravity. When the crystallinity of an undrawn sample is low, its specific gravity increases with the draw ratio, but when the crystallinity of an undrawn sample is high, its specific gravity decreases as the draw ratio increases and a maximum of shrinkage is observed. Therefore, it is suggested that a transition from crystalline parts to amorphous parts occurs because of the destruction of crystallites during drawing as well as of a reverse transition owing to strain-induced crystallization, and that the higher the crystallinity of an undrawn sample, the more the destruction of crystallites and the acccumulation of internal strain, as a result of which the shrinkage in boiling water shows a maximum near the draw ratio of 2, where the structure becomes most unstable, though the authors cannot completely explain why it becomes most unstable.

In the case of isotactic polypropylene monofilaments which had been quenched and drawn to various draw ratios, a similar relationship to that of heat-treated and drawn nylon monofilament was also observed between the draw

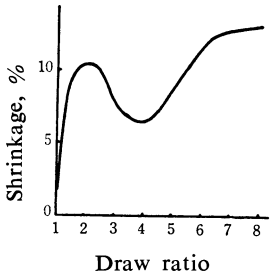

Fig. 7. Change of shrinkage in boiling water of polypropylene monofilament with draw ratio.

ratio and shrinkage in boiling water; that is, a maximum of shrinkage appeared at a draw ratio near 2 (Fig. 7). This phenomenon to seems to be due to the same reason as that for nylon 6, because the crystallinity of undrawn polypropyrene is thought to be rather high even when it is quenched.

Conclusion

Some physical properties have been measured on nylon monofilaments which had been drawn to various draw ratios after the heat-treatment of undrawn samples at various temperatures. The authors found that the shrinkage of a sample in boiling water changes very peculiarly with the draw ratio, showing a maximum, and suggested that the polymer structure becomes, unstable in the intermediate stage of drawing, though no satisfactory explanation of the unstabilization effect has been given. Further effort will be made to make sure of the "unstabilization" during drawing and to elucidate the mechanism of the drawing.

Summary

In order to investigate the influence of the structure of an undrawn sample on the change in physical properties upon drawing, undrawn nylon monofilaments were drawn to various draw ratios after having been heat-treated at several temperatures; some properties, such as tensile strength, shrinkage in boiling water and specific gravity, were then measured on these drawn samples. Although the minimum of tensile strength observed at the draw ratio near 2 had a tendency to disappear upon the heat-treatment of an undrawn sample, the strength did not increase in the range of a low draw ratio. When an undrawn sample was heat-treated above 150°C, a maximum appeared at a draw ratio near 2 in the plot of shrinkage in boiling water against the draw ratio. The higher the heat-treating temperature of an undrawn sample, the greater the maximum of shrinkage. The specific gravity decreased during drawing when the undrawn sample was of a rather high crystallinity, but it increased when the undrawn sample was of a low crystallinity. These results have been discussed, and it has been suggested that the polymer structure becomes most unstable at the intermediate stage of drawing.

The authors wish to express their gratitude to Dr. Haruo Kobayashi, the manager of the research department of Toyo Rayon Company, for permitting them to contribute this paper to this journal.

Nagoya Laboratory
Research Department
Toyo Rayon Co., Ltd.
Minato-ku, Nagoya

Spectrochemical Study of Microscopic Crystals. XXIII[1]. *The Structure and Light Absorption of Red Cupric Complexes with Succinimide*[2]

By Shoichiro YAMADA and Seiko MIKI

(Received February 1, 1963)

Succinimide readily loses a proton and is combined, in the anionic form, with various metal ions. There have been reported a number of cupric compounds with succinimidate anions, which are red or violet in the solid state and many of which change their color from red in the crystalline state to deep-blue in some solvents. On one hand, the formation of the red compounds of copper(II) is interesting, since it is well known that most quadri-co-ordinate cupric complexes are blue, green or violet; red cupric complexes, therefore, are

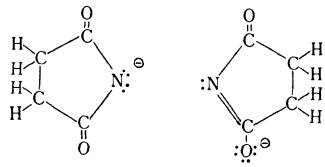

Fig. 1. Succinimidate ion.

rather unusual examples. On the other hand, the color change from the solid to the solution, as observed with these complexes, is so remarkable that the study of this phenomenon is thought to be interesting from the viewpoint of the co-ordination chemistry of cupric complexes. The present work was undertaken both in order to elucidate the structure of these and relevant compounds and in order to discuss the origin of the red color of the cupric compounds in terms of the stereochemistry and bonding involved.

Experimental

Materials.—Bis(succinimidato)diammine-copper-(II) was obtained as pink crystals from copper powder, succinimide and aqueous ammonia by the method of Tschugaeff[3], using ethanol as a solvent. The compound is insoluble in organic solvents.

Bis(succinimidato)bis(alkylamine)-copper(II) complexes with methyl, ethyl, *n*-propyl, isopropyl, *n*-butyl and *n*-amyl amines, which had also been reported previously by Tschugaeff, were prepared as pink crystals according to the directions in the original report. Purification of the compounds was carried out by recrystallization from ethanol containing an excess amount of the free amines, as had also been reported in a previous paper[3].

All these compounds have the formula of Cu·(*sucim*)$_2$(amine)$_2$, except for the compound with ethyl amine, which contains two water molecules of crystallization[4]. The crystals are stable in the air at room temperature when completely free from the solvent. The crystals are not stable in water, methanol, ethanol, dioxan or pyridine. It has been found in the present work that the red crystals of the compounds are soluble and stable enough in non-co-ordinating solvents, such as chloroform, methylene chloride and benzene, to form a dark-blue solution; an exception is the compound with methyl amine, which is readily soluble in chloroform but sparingly soluble in methylene chloride and benzene. The stability of the red complexes seems to increase as the chain of the alkyl group becomes longer.

Potassium tetrakis(succinimidato)copper(II) hexahydrate was prepared as pink crystals according to the method of Tschugaeff[5].

The sample of bis(*N*,*N*-diethylethylenediamine)-copper(II) perchlorate, which is colored pink in the crystalline state and deep-blue in an aqueous solution, was kindly supplied by Dr. Hisao Ito of the medical department, to whom the present authors are grateful.

Measurements.—The dichroism in the visible and ultraviolet regions was determined by Tsuchida and Kobayashi's microscopic method[6] using polarized light on the well-developed faces, which are shown in the figures. The ultraviolet absorption spectra of the compounds in solution were determined with a Beckman DU spectrophotometer. The notations in the present paper are the same as those used in the former papers of this series.

Results and Discussion

The Absorption Spectrum of Potassium Tetrakis(succinimidato)cuprate(II) Hexahydrate.—It is possible that the succinimidate ion in $K_2Cu\cdot(sucim)_4\cdot 6H_2O$ is co-ordinated to the cupric ion through either the nitrogen or the oxygen

1) Part XXII of this series; S. Yamada, H. Nishikawa and R. Tsuchida, This Bulletin, **33**, 1278 (1960).
2) Presented in part at the Symposium of Co-ordination Chemistry, Osaka, November, 1961.
3) L. Tschugaeff, *Ber.*, **39**, 2897 (1905).
4) The notation, *sucim*, represents an anion which is derived when a succinimide molecule loses a proton.
5) L. Tschugaeff, *Ber.*, **40**, 1976 (1907).
6) R. Tsuchida and M. Kobayashi, This Bulletin, **13**, 619 (1938); "The Color and the Structure of Metallic Compounds" (Kinzokukagōbutsu no Iro to Kōzō), Zoshindo, Osaka (1944), p. 180.

atom (Fig. 1). The co-ordination of *sucim* with a copper(II) ion, however, is most probably, through the nitrogen atom, since the oxygen atom of the carbonyl group in the ion is capable of being linked only weakly with the cupric ion. The co-ordination of *sucim* as a chelated ligand using both the nitrogen and the oxygen atoms may not be impossible. In any case, the bonding is mainly through the nitrogen atom, judging from the steric condition and the weak bonding ability of the oxygen atom in the carbonyl group.

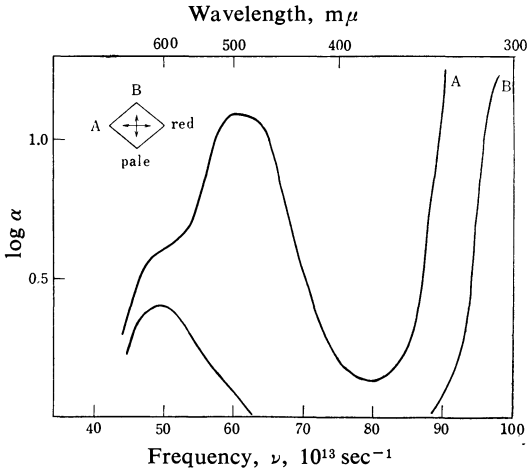

Fig. 2. Polarized absorption spectra of $K_2Cu(sucim)_4 \cdot 6H_2O$ in the crystalline state.

TABLE I. ABSORPTION MAXIMA OF $K_2Cu(sucim)_4 \cdot 6H_2O$ IN THE CRYSTALLINE STATE

	ν_{max}	log α	Half width	Assignment
A-abs.	61.2	1.08	12.5	ν_2
	ca. 50	—	—	ν_1
B-abs.	ca. 50	0.40	ca 11	ν_1

ν; 10^{13} sec^{-1}

The polarized absorption spectra of $K_2Cu(sucim)_4 \cdot 6H_2O$ in the crystalline state are shown in Fig. 2, and the data are given in Table I. The free succinimide shows no absorption in the neighborhood of the ligand field bands of the cupric complexes[7]. Since the crystal structure analysis is not available, it is not possible to determine exactly the components of the absorption coefficient of the planar cupric complex. For the purposes of the present study, however, it is sufficient to find the qualitative characteristics of these absorption components. It is known empirically from dichroism measurements[8] that, for the ligand field absorption band of cupric complexes with the D_{4h} symmetry, the xy-absorption, the absorption with the electric vector along the $Cu(N)_4$-plane, has a much larger oscillator strength than the z-absorption, the absorption with the electric vector perpendicular to the complex-plane. On the basis of this empirical rule, it is found that the A-absorption in Fig. 2 is richer with the xy-absorption than with the z-absorption of the planar complex, and that the B-absorption is richer with the z-absorption. The difference between the A- and the B-absorption on this crystal-face is so remarkable, compared with the dichroism of other cupric complexes, that one may assume that the $Cu(N)_4$-planes are nearly parallel to each other and perpendicular to the B-direction of the crystal.

The compound shows its main ligand field band at about 61×10^{13} sec^{-1}, which corresponds to a much higher frequency than the values reported for an ordinary type of cupric complex with amines, such as ammonia and ethylenediamine. An inspection of data with nickel(II)-succinimidato complexes having the same configuration reveals[9] that the position of *sucim* in the spectrochemical series is as follows[10]: *en* > NH_3 > biguanide > *sucim* > OH_2. This order, in which *en* stands higher than *sucim*, is regarded as applicable to many metal ions, such as chromium(III), nickel(II), cobalt(II), cobalt(III), and copper(II), provided that the complexes have the same configuration. Hence, the fact that the tetrakis(succinimidato)-copper(II) ion shows its absorption band at such a high frequency is not understandable if $K_2Cu(sucim)_4 \cdot 6H_2O$ has a complex-ion with a configuration identical with that of the bis(ethylenediamine)copper(II) complexes. Bjerrum[11] et al. and Ito[12] concluded that the ligand field band of copper(II) suffered bathochromic shift as the cupric complex with a square-planar configuration took additional ligands to form a sexa-co-ordinate complex with a pseudo-octahedral configuration. Taking this and the spectrochemical series into consideration, a comparison of the maxima of the ligand field bands indicates that the co-ordination of the four nitrogen atoms around the cupric ion in $K_2Cu(sucim)_4 \cdot 6H_2O$ is square-planar, the fifth and sixth positions of the complex being unoccupied, whereas the ethylenediamine complex has a sexa-co-ordinate configuration, represented

7) L. J. Saidel, *Nature*, **172**, 955 (1953).
8) S. Yamada and R. Tsuchida, *Ann. Reports Faculty of Sci., Osaka Univ.*, **4**, 79 (1956); This Bulletin, **29**, 289, 694 (1957).
9) S. Yamada and H. Nishikawa, to be published.
10) The notation, *en*, represents a molecule of ethylenediamine.
11) J. Bjerrum, C. J. Ballhausen and C. K. Jørgensen, *Acta Chem. Scand.*, **8**, 1275 (1954).
12) H. Ito, *J. Chem. Soc. Japan, Pure Chem. Sec.* (*Nippon Kagaku Zassi*), **77**, 1395 (1956).

by $[Cu\,en_2\,(OH_2)_2]^{2+}$. In other words, it is concluded that $K_2Cu(sucim)_4 \cdot 6H_2O$ contains a square-planar complex-ion, $[Cu(N)_4]^{2-}$, which leaves the fifth and sixth co-ordination sites empty, the water molecules in this compound being unbound with the cupric ion.

Some of the reasons why the complex-ion, $[Cu(sucim)_4]^{2-}$, leaves the fifth and sixth sites unoccupied seem to be (1) that the steric condition more or less, though not absolutely, prevents other ligands from coming close to the cupric ion and (2) that the oxygen atom in the carbonyl group has only a weak ability to be bound with the cupric ion. Another factor is the electronic state of the ligands, which will be discussed in the later part of this paper.

A similar discussion applies to the corresponding complex of biuret, which involves a chemical bond resembling the bond in the complex of succinimide. It seems to be significant that the position of the biuret ion in the spectrochemical series is close to that of *sucim*. The absorption maximum (505 mμ)[13] of the crystal of $K_2Cu(biuret)_4 \cdot 4H_2O$ also lies at a much higher frequency than that of the ethylenediamine-complex of copper(II). In the same way as in the case of $K_2Cu(sucim)_4 \cdot 6H_2O$, the inspection of the absorption maxima shows that the crystal consists of $[Cu(biuret)_2]^{2-}$ ions which have a square-planar co-ordination around the cupric ion, with the fifth and sixth co-ordination sites left empty, the water molecules being unbound with the cupric ion. This is in agreement with the crystal structure analysis[13] of the compound, which shows that the cupric ion is surrounded by four nitrogen atoms at a distance of about 1.93Å and by two nitrogen atoms of the neighboring complex at about 3.33Å.

It is theoretically predicted that the quadri-co-ordinate cupric complex of the D_{4h} field symmetry will display three ligand field bands, as shown in Fig. 3. There are two ways of assigning these vibronic transitions. According to one of them, the three transitions all fall in a rather narrow frequency range and the superposition of the three usually appears as apparently one absorption band in the visible or near-infrared region. According to the other way of assignment[14], the ν_3 band is assumed to lie at a much higher frequency than ν_1 and ν_2, and usually far from the visible region, covered by a much stronger absorption of a charge transfer type. The present authors regard the latter assignment as more likely on grounds, a detailed discussion of which will be reported shortly. The present dichroism measurements also seem to support this assignment.

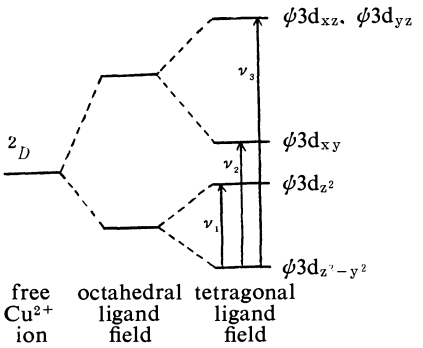

Fig. 3. Energy level scheme model for cupric complexes: (A) sexa-co-ordinate complexes with octahedral symmetry and (B) square-planar complexes of a [Cu A_4] type. In the figure, $\phi 3d_{z^2}$, for example, refers to the state, in which the d_{z^2} orbital is not completely filled.

As may be seen in Fig. 2, $K_2Cu(sucim)_4 \cdot 6H_2O$ shows two maxima, corresponding to the ligand field bands, at about 50 and 61×10^{13} sec^{-1}, for both of which the xy-absorption is more intense than z-absorption. An unambiguous assignment of the observed transitions seems to be difficult for the present, but a tentative assignment is given in Table I on the basis of the dichroism measurement and in terms of the second standpoint described above. Simple theoretical consideration, in terms of the ligand field theory, predicts that both the transitions, ν_1 and ν_2, will take place more readily along the xy-direction than along the z-direction, if it is assumed that the vibrations of the E_u symmetry are more effective in making allowed the originally forbidden electronic transitions than the other vibrations in the complex (Table II). The energy levels of the d_{z^2} and d_{xy} orbitals are usually close to each other, and the order of one with respect to the other

TABLE II. THE TRANSITIONS CORRESPONDING TO THE LIGAND FIELD BANDS OF SQUARE-PLANAR COMPLEXES OF [Cu A_4]-TYPE AND THE SYMMETRIES OF THE VIBRATIONS MAKING THE TRIPLET-TRIPLET TRANSITIONS ALLOWED

Transition	Polariz. of transition predicted from symmetry consideration
ν_1 $d_{z^2} \rightarrow d_{x^2-y^2}$	$x,y(E_u)$; $z(B_{2u})$
ν_2 $d_{xy} \rightarrow d_{x^2-y^2}$	$x,y(E_u)$; $z(B_{2u})$
ν_3 $\left.\begin{matrix} d_{xz} \\ d_{yz} \end{matrix}\right\} \rightarrow d_{x^2-y^2}$	$x,y(A_{2u}, B_{2u})$; $z(E_u)$

In the parentheses are shown the vibrations of the complex making the transition allowed.

13) H. C. Freeman, J. E. W. L. Smith and J. C. Taylor, *Acta Cryst.*, **14**, 407 (1961).
14) D. P. Graddon, *J. Inorg. Nucl. Chem.*, **7**, 73 (1958).

possibly changes from one compound to another. The assignment, as given in the present work, is based upon the order of the d-orbitals assumed in Fig. 3. Irrespective of the order of the two levels, the polarization which has been determined in the present work is found to agree with the prediction from the theory, at least qualitatively.

The Absorption Spectrum of Bis(*N*, *N*-diethylethylenediamine)copper(II) Perchlorate. — The compound consists of complex-ions of a $[Cu(N)_4]$-type with a square-planar configuration. The two ethyl groups attached to a nitrogen atom prevent, to a greater or lesser extent, additional ligands from occupying the fifth and sixth co-ordination sites, although in an aqueous solution the complex takes up two molecules of water to form a sexa-co-ordinate complex. The polarized absorption spectra of the compound in the crystalline state are shown in Fig. 4. The crystal structure analysis

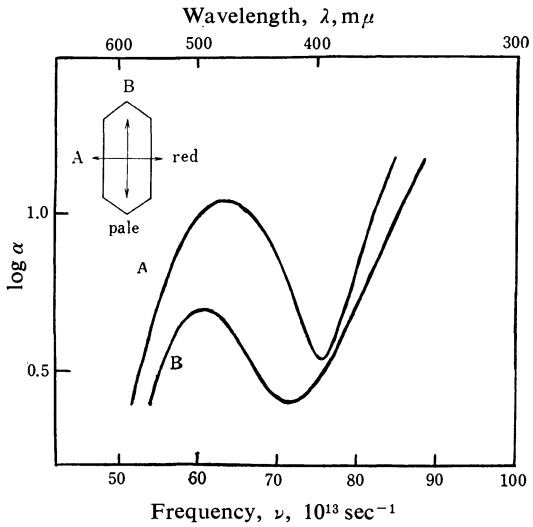

Fig. 4. Polarized absorption spectra of $[Cu(deen)_2](ClO_4)_2$ in the crystalline state.

of the complex salt is not available so far, and usually the planes of the complexes in the crystal are not exactly parallel to each other. However, it is readily found that the A- and B-absorptions in Fig. 4 represent the main features of the xy-absorption and the z-absorption respectively of the square-planar complex, since previous studies have shown that, for the ligand field absorption band, the xy-absorption has a larger oscillator strength than the z-absorption[8]. Strictly speaking, the symmetry of the complex deviates from D_{4h}, but the spectra may be discussed approximately in the scheme of the D_{4h} field symmetry. The absorption bands in the visible region in Fig. 4 probably represent a superposition of the

Table III. Absorption maxima of $[Cu(deen)_2](ClO_4)_2$

Crystal	ν_{max}	log ε	Half width	Assignment
A-abs.	63.4	1.04	18.8	ν_1, ν_2
B-abs.	60.0	0.70	13.6	ν_1
Solution[a]	ν_{max}	log ε		
	50.6	1.18		

ν; 10^{13} sec^{-1}

a) H. Ojima and K. Sone, This Bulletin, **35**, 298 (1962).

two kinds of electronic transitons, ν_1 and ν_2. A tentative assignment of the band which is shown in Table III is made in such a way that the assignment for the compound is consistent with the assignment for the $[Cu(sucim)_4]^{2-}$ ion and other square-planar cupric complexes.

An absorption band in the visible region in the A-absorption is assumed to consist of two electronic transitions, since the band is comparatively broad. The B-absorption shows only one ligand field band at about 61×10^{13} sec^{-1}, which probably arises from the electronic transition, ν_1. As is seen in Table III, the polarization observed for these transitions is found to agree with the prediction from the theory.

It is to be noted that the absorption maximum of the square planar ion of $[Cu(deen)_2]^{2+}$ lies at a much higher frequency than the maximum of $[Cu\,en_2(OH_2)_2](NO_3)_2$ in the crystalline state (57.2×10^{13} sec^{-1}) and that of $Cu\,en_2^{2+}$ (54.0×10^{13} sec^{-1}) and $Cu(NH_3)_4^{2+}$ (49.2×10^{13} sec^{-1}) ions in an aqueous solution. The difference in the maximum frequency between the crystalline $[Cu(deen)_2](ClO_4)_2$ and the latter type of complex is too large to be expected if the two contain complexes of a similar configuration, since the position of *deen* in the spectrochemical series is close to, and even lower than, en. This fact is understood if it is assumed (1) that the co-ordination of ligands at the fifth or the sixth site causes a bathochromic shift of the ligand field band, and (2) that bis(ethylenediamine)- or tetrammine-copper(II) ions in solution and in the crystalline state consist of complex-ions of copper(II), with the fifth and the sixth co-ordination sites occupied by some ligands.

The ligand field band of bis(*N*, *N*-diethylethylenediamine)-copper(II) perchlorate exhibits a great bathochromic shift on going from the square-planar complex, $[Cu(N)_4]^{2+}$, in the solid state to the trans-octahedral complex, $[Cu(N)_4(OH_2)_2]^{2+}$, in an aqueous solution. The following ratio obtains in this case:

$$\nu(\text{trans-octahedr.})/\nu(\text{square-plan.}) = 0.80$$

This value is nearly comparable with the values previously reportd for some cupric complexes[15]. In this connection, it is to be noted that bis(ethylenediamine)copper(II) perchlorate in the crystalline state shows a ligand field band at a comparatively long wavelength[16]. One may assume that the perchlorate ions come rather close to the copper(II) ion to form a sexa-co-ordinate complex, giving rise to the bathochromic shift of the band. The study of this is now in progress and will be reported elsewhere in more detail.

The Origins of the Red Color of Cupric Complexes.—There seem to be largely two kinds of origins of the red or orange color of some cupric compounds. On one hand, the red color results mainly from the charge transfer between the cupric ion and a ligand, and, on the other hand, it originates from the ligand field bands of the cupric ion. Red halide-complexes of copper(II) belong to the former group, owing their red color to a charge transfer between cupric and halide ions. The orange-color of Cs_2CuCl_4 and the red-color of $CsCuCl_3$, for example, are regarded as due to the charge transfer band in the visible region, which is much more intense than the ligand field band. In addition to the charge transfer band, the ligand field band due to the tetrahedral copper(II)-complex is expected to appear in the infrared region.

There are red cupric complexes of the other type, such as cupric complexes with succinimide, biuret, biguanide, phenylbiguanide, and *N*, *N*-diethylethylenediamine (Table IV). The quadri-co-ordinate, planar complex of copper(II) tends to take additional ligands, forming a sexa-co-ordinate complex with a pseudo-octahedral configuration and at the same time causing a bathochromic shift of the ligand field bands. Hence, if the sexa-co-ordination is not possible for one reason or another, the complex is expected to keep the quadri-co-ordinate, planar configuration, displaying the ligand field band in a frequency region much higher than when the sexa-co-ordination is allowed. An example is bis(*N*, *N*-diethylethylenediamine)copper(II) perchlorate in the crystalline state, which owes its red color to the steric condition of the ligands. In this case, the steric condition makes it more or less difficult for other ions or molecules to occupy the fifth and sixth positions of co-ordination around the cupric ion, although it does not completely exclude the sexa-co-ordination, so that the complex takes up two water molecules in an aqueous solution. This ligand has no nitrogen atom which is capable of participating in π-bonding with the cupric ion, excepting through hyperconjugation. The pink color of this compound, therefore, is due not to the π-bonding, but to the special steric condition of the ligand.

TABLE IV. MAIN ABSORPTION MAXIMA OF SQUARE-PLANAR COMPLEXES OF COPPER(II), [Cu A_4] OR [Cu B_2]

A or B	ν_{max}	Sample	Ref.
deen	63.4	Crystal	a
Biguanide	61.9	Powder	b
sucim	61.2	Crystal	a
Dicyandiamidine	58.8	Powder	b
Phenylbiguanide	58.4	Powder	b
Biuret	59.4	Crystal	c

ν: 10^{13} sec^{-1}

a) The present measurement

b) M. Kato, Y. Komuro and K. Sone, *J. Chem. Soc. Japan, Pure Chem. Sec. (Nippon Kagaku Zassi)*, **78**, 896 (1957).

c) Quoted in Ref. 13 of the text.

On the contrary, the steric condition does not seem to be the main reason for the formation of the red cupric complexes of succinimide, biuret, biguanide and phenylbiguanide with a square-planar co-ordination. In these cases, there is little steric hindrance which might prevent other ligands from coming closer to the cupric ion in the direction perpendicular to the $Cu(N)_4$-plane. It is readily found that these ligands all involve a similar kind of linkage around the nitrogen atom, which is capable of entering into π-bonding with the cupric ion. It is likely that, in the cupric complexes of this sort, the π-bonding plays a part in leaving the fifth and sixth co-ordination sites unoccupied. It seems that π-bonding of this sort decreases the effective charge on the cupric ion, weakening the possible copper(II)-to-oxygen bond, which is probably strongly ionic.

The Crystal Absorption Spectra of Bis(succinimidato)bis(alkylamine) copper (II) Complexes.—The compounds with a composition of Cu·(*sucim*)$_2$(amine)$_2$, the amine being methyl, ethyl, *n*-propyl, isopropyl, *n*-butyl or *n*-amyl amine as well as ammonia, are all red in the crystalline state. In order to examine the origin of the unusual color of these compounds, one of the compounds has been chosen. Thus, the dichroism of Cu(*sucim*)$_2$(isopropylamine)$_2$ has been determined by the microscopic method; the results of the measurements are shown in Fig. 5 and in Table V.

The succinimidate ion can be combined with the cupric ion through either the nitrogen or the oxygen atom. The co-ordination in this compound, however, is most probably through

15) See, for example, C. K. Jørgensen, Proceedings of Tenth Solvay Conference, Brussels, May, 1956.

16) S. Yamada and R. Tsuchida, This Bulletin, **29**, 289 (1956).

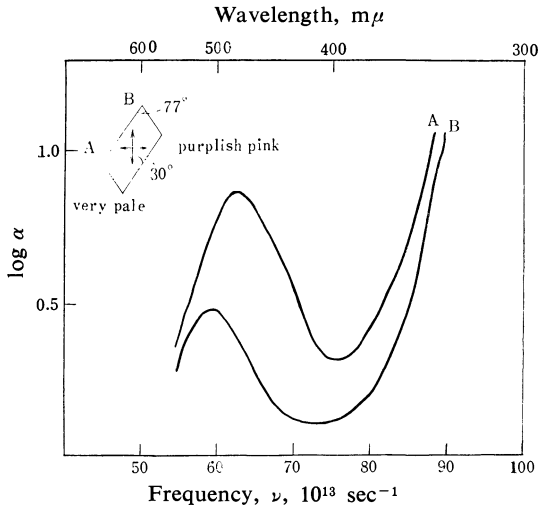

Fig. 5. Polarized absorption spectra of [Cu·(*sucim*)$_2$(*iso*-$C_3H_7NH_2$)$_2$].

TABLE V. ABSORPTION MAXIMA OF [Cu·(*sucim*)$_2$(*iso*-$C_3H_7NH_2$)$_2$] IN THE CRYSTALLINE STATE

	ν_{max}	log α	Half width	Assignment	K
A-abs.	62.6	1.38	12.0	ν_1, ν_2	54.5×10^3
B-abs.	59.1	0.99	11	ν_1	22.2×10^3

ν: 10^{13} sec^{-1}

In the calculation of K, the value of 1.38 was used for the density of the crystal, which was determined with a picnometer. $K=10\alpha M/\rho$ where M and ρ denote molecular weight and density, respectively.

the nitrogen atom, and not through the oxygen atom, as has been discussed in the earlier part of the present paper. There is very little doubt that the amine molecules, besides the unidentate succinimidate ions, are linked with the cupric ion.

The present measurement indicates that the red crystal of Cu(*sucim*)$_2$(*iso*-$C_3H_7NH_2$)$_2$ shows a ligand field absorption band, with its maximum at about 61×10^{13} sec^{-1}, in addition to a strong absorption in the far higher frequency. The absorption maximum of the ligand field band of this compound lies at a much higher frequency than that of most cupric complexes with nitrogen-co-ordinating ligands of an ordinary type, such as ammonia, ethylenediamine and related compounds. This fact shows that there is an essential difference in configuration between Cu(*sucim*)$_2$(*iso*-$C_3H_7NH_2$)$_2$ and [Cu en$_2$ $(OH_2)_2$] $(NO_3)_2$, since *sucim* stands much lower in the spectrochemical series than en, *deen* or ammonia. It was formerly assumed that an absorption maximum of the ligand field band is displaced bathochromically, when a square-planar complex of copper(II) takes up two more ligands to form a sexa-co-ordinate, pseudo-octahedral complex[11,12,15]. It is, therefore, concluded that Cu(*sucim*)$_2$(amine)$_2$ in the crystalline state consists of quadri-co-ordinate, planar cupric complexes, with the two co-ordination sites, perpendicular to the complex-plane, kept unoccupied. It has not been determined in the present study whether the complex belongs to a cis- or a trans-series.

Since the crystal structure analysis is not available and usually the complex-planes are not all parallel to each other, it is not possible to determine exactly the component absorption coefficients of the planar complex. From the empirical rules, however, one can readily find the main characteristics of the z- and xy-absorptions by using the polarization measurements, which are shown in Table V along with a tentative assignment of the absorption bands. It is found, from the intensity of the ligand field band, that the A- and B-absorptions represent the main features of the xy- and z-absorptions of the complex respectively. For Cu(*sucim*)$_2$(*iso*-$C_3H_7NH_2$)$_2$, the z-absorption shows one component band at about 59×10^{13} sec^{-1}, whereas the xy-absorption, having a much larger oscillator strength than the z-absorption, is assumed to represent the superposition of two component absorption bands, with the main maximum at about 62.7×10^{13} sec^{-1}. The observed polarization property of the absorption bands of this complex is quite similar to that of the other cupric complexes with a square-planar configuration, such as $[Cu(sucim)_4]^{2-}$ and $[Cu(deen)_2]^{2+}$, and agrees with the theoretical prediction. Strictly speaking, the symmetry of the complex, Cu·(*sucim*)$_2$(*iso*-$C_3H_7NH_2$)$_2$, deviates from D_{4h}, but it is assumed that the spectrum may be treated approximately in the scheme of D_{4h} field symmetry.

The corresponding compounds of the bis-(succinimidato)-copper(II) complexes with other amines are colored quite similarly to Cu(*sucim*)$_2$(*iso*-$C_3H_7NH_2$)$_2$. Although they are rather unstable in the atmosphere and undergo slow decomposition during the prolonged dichroism measurements, it was possible to determine, by quick measurements, the approximate band maxima of the compounds (about 60×10^{13} sec^{-1}); these lie in the neighborhood of the ligand field band of the corresponding compound with isopropyl amine, but they are at a much higher frequency than the maximum of [Cu en$_2$$(OH_2)_2$] $(NO_3)_2$. It is concluded that all these homologues consist of quadri-co-ordinate, square-planar complexes, with the fifth and sixth site kept empty. With ethyl amine, the compound has two water molecules

of crystallization, but these water molecules are presumed to have nothing to do with the linkage to the copper(II) ion.

There are violet complexes, in addition to the red ones, for ammonia and methyl amine. The examination of the violet form is now progress, and the results will be reported on elsewhere.

The Structure of Bis(succinimidato)bis(alkylamine)copper(II) in Solvents.—The red crystals of Cu(*sucim*)$_2$(amine)$_2$, in general, are unstable in water, ethanol and pyridine. In water, they apparently undergo decomposition and form a pale-blue precipitate upon standing in this solvent for a sufficiently long time. In ethanol and pyridine, the decomposition was not so fast as in water, but the replacement of one of the ligands by a molecule of the solvent seems to take place, along with the addition of the solvent molecules to the cupric complex. On the contrary, the red crystals of the compounds are dissolved in chloroform to form a stable solution with a dark-blue color, which is quite different from the color of the compound in the crystalline states.

The absorption spectra of these compounds in chloroform have been determined in the present work. As may be seen in Fig. 6 and Table VI, the compounds with a formula of Cu(*sucim*)$_2$(amine)$_2$ in chloroform exhibit, in the visible region, one ligand field band with a maximum at about 48 to 50×10^{13} sec^{-1} (625 to 600 mμ), which is far lower than the frequency of the absorption band of the same compounds in the crystalline state. The shift of the band on going from the crystal to the solution is found to be about 11×10^{13} sec^{-1} for the *n*-alkyl amines and about 13×10^{13} sec^{-1} for the isopropyl amine. The shift observed in the present study is much larger than would be expected for typical solvent effects upon the ligand field band with no change in the configuration of the complex. It seems to be evident that, when the crystals are brought into chloroform, some remarkable change in the configuration occurs to the complex-molecules existing in the crystals, in which the complex-molecules have a square-planar coordination of the four nitrogen atoms around the cupric ion.

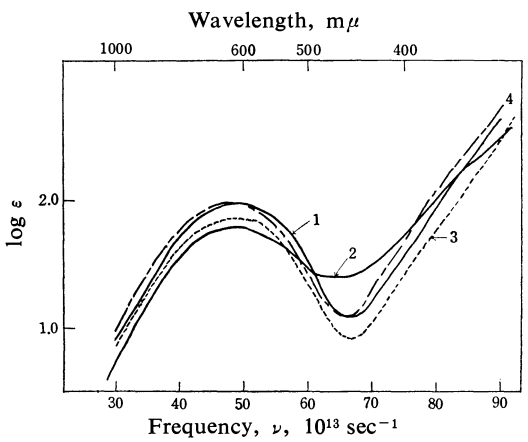

Fig. 6. UV-absorption spectra of [Cu(*sucim*)$_2$·(R·NH$_2$)$_2$] in chloroform 1, R=C_2H_5; 2, R=CH_3; 3, R=*n*-C_3H_7; 4, R=*iso*-C_3H_7

The dissociation of one of the four ligands is quite unlikely, since Beer's law is generally obeyed in the concentration range examined. The present study also reveals that no decomposition of the complexes takes place; at least none takes place at a concentration between 4×10^{-3} and 2×10^{-4} M. The replacement of one of the amine molecules seems to be improbable, since, though chloroform might be bound to a metallic ion, it could only be so very weakly, and since the linkage between the cupric ion and chloroform, if formed at all, would be far weaker than the linkage between the cupric ion and the amine or succinimidate.

It might also be assumed that the chloroform molecules would be co-ordinated, though very weakly, with the cupric ion slightly farther in the direction perpendicular to the complex-plane formed by the cupric ion and the four nitrogen atoms. Judging from the weak perturbing power of the chloroform molecule, this assumption does not seem to explain the enormously large shift of the band maximum on going from the crystal to the solution.

TABLE VI. ABSORPTION MAXIMA OF [Cu(*sucim*)$_2$(R·NH$_2$)$_2$] IN NON-CO-ORDINATING SOLVENTS

R	in $CHCl_3$		in CH_2Cl_2		in C_6H_6	
	ν_{max}(log ε)	h. w.	ν_{max}(log ε)	h. w.	ν_{max}(log ε)	h. w.
CH_3	49.6 (1.79)	21.8	50.4 (1.90)	18.7	insoluble	
C_2H_5	49.4 (1.98)	18.7	49.6 (1.85)	19.2	47.1 (1.71)	18.3
n-C_3H_7	48.9 (1.86)	19.0	50.0 (1.98)	18.6	48.3 (1.86)	18.8
iso-C_3H_7	48.6 (1.97)	18.9	49.8 (1.96)	18.9	48.8 (1.93)	18.8
n-C_4H_9	49.2 (2.02)	18.8	50.2 (1.97)	18.8	48.4 (1.96)	18.2

ν: 10^{13} sec^{-1} h. w.: half width in 10^{13} sec^{-1}

It is expected theoretically, and has been confirmed experimentally, that the ligand field band of a cupric complex suffers a more or less bathochromic shift when the square-planar complex takes up ligands to form an octahedral complex. However, the chloroform molecule usually has so slight an ability to be bound to the metallic ion that the band shift on going from the square-planar complex to the chloroform adduct with a pseudo-octahedral configuration would be much smaller than the corresponding effects of water as well as of ammonia molecules. On the contrary, the present measurements show that the difference in the band maximum between the crystal and the chloroform solution is usually great, the ratio of the maximum frequency of the crystal to that of the chloroform solution deviating remarkably from unity. The values ranging from 0.70 to 0.80 for the succinimidato-complex in chloroform are much smaller even than the values expected for the effects of ammonia molecules as the additional ligands as well as for those of water molecules. It is to be recalled that the corresponding ratio of the crystal to the aqueous solution is about 0.80 in the case of the bis(diethylethylenediamine) complex. The observed ratio for the chloroform solution seems to be too small for the octahedral model with the chloroform molecules in trans-positions.

It may be assumed that the ligand field around the cupric ion of the succinimidato complex is determined mainly by the four nitrogen atoms and is affected only very little by such other ligands, like chloroform molecules, as might occupy the remaining co-ordination sites in the compound. In the light of the discussion above, therefore, the enormous band shift on going from the crystal to the chloroform solution indicates that the co-ordination of the four nitrogen atoms around the cupric ion within the Cu(*sucim*)$_2$(amine)$_2$ complexes in chloroform deviates from a square-planar configuration. In this connection, it is to be noted that the ligand field bands of all these compounds in non-co-ordinating solvents have a much higher intensity and a larger half-width than most cupric complexes with a tetragonal field symmetry. This is in agreement with the theory which predicts that a complex of a transition element with no center of inversion will show a ligand field band of a higher intensity than a complex with a center of inversion. According to the crystal field theory, however, the regularly tetrahedral complex will show a ligand field band in a frequency region much lower than that observed in the present study, since the quadri-co-ordinate complex with a regularly tetrahedral configuration would have a ligand field-splitting parameter which is about 4/9 times that of the octahedral complex. The regular or near regular tetrahedral model seems to be less likely.

One may assume that the oxygen atoms of the carbonyl-groups will be bound to the cupric ion to form a pseudo-octahedral complex. This effect alone, however, is not regarded as strong enough to explain the observed remarkable difference in the absorption maximum between the crystal and the chloroform solution, since the oxygen atom of this type is known to be bound only very weakly to the metal ion. However, even so, this probably plays a part in causing the deviation from the square-plane of the co-ordination in such a way that this weak linkage may help and keep the configuration deviated from the square-plane.

The cupric complexes of the Cu(*sucim*)$_2$-(amine)$_2$ type are also soluble in methylene chloride and benzene to give a stable solution, which is colored dark-blue. As is shown in Fig. 7 and Table VI, the absorption spectra of the compounds in these solvents have main features which are similar to those of the compounds in chloroform. All the compounds show a similar spectrum in these solvents; therefore, the absorption spectra of only some of the compounds are shown in Fig. 7. It is found that bis-(succinimidato)bis(ethylamine)-copper(II) in benzene, for example, shows a ligand field band at a frequency nearly equal to that of the chloroform solution. As in the case of the chloroform solution, it is concluded that the co-ordination of the four nitrogen atoms around the cupric ion with the Cu-(*sucim*)$_2$(amine)$_2$ complex in these solvents

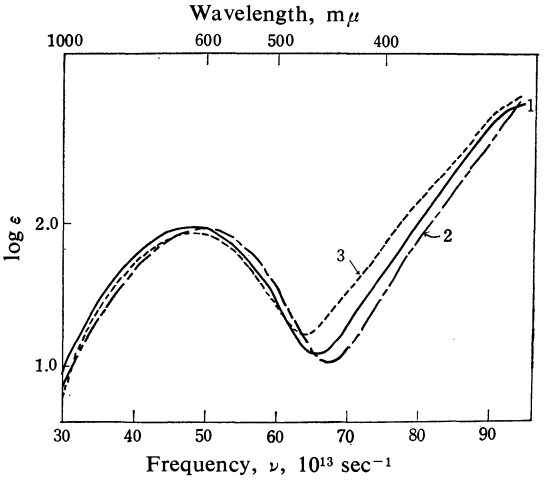

Fig. 7. UV-absorption spectra of [Cu(*sucim*)$_2$-(*iso*-$C_3H_7NH_2$)$_2$] in organic solvents. 1, Chloroform; 2, Methylene chloride; 3, Benzene

probably deviates from the square-planar configuration.

In these non-polar solvents, the oxygen atom of the succinimidate ion of the cupric complex may be subjected to repulsion by the molecules of the solvents, so that the rejected oxygen atom will point toward the cupric ion to form weak linkage with it. When alcohols or water are used as a solvent, however, the oxygen atom in the succinimidate ion is assumed to be associated with the solvent molecule, possibly through hydrogen bonding, since the affinity of this type of the oxygen atom to the cupric ion may be small. Moreover, the molecules of these polar solvents can be co-ordinated to the cupric ion, whereas the molecules of the non-polar solvents, in general, cannot. This probably explains the difference in the configuration of the succinimidato-complexes between the solutions in the polar and in the non-polar solvents. The minor difference in the frequency of the absorption maximum between the solutions in chloroform and the other non-polar solvents is to be ascribed not to the difference in the configuration of the complex in these solvents, but to an ordinary kind of perturbation on the complex by the solvents.

Summary

The dichroism in the visible and ultraviolet region has been determined by the microscopic method with single crystals of $K_2Cu(sucim)_4 \cdot 6H_2O$, $Cu(deen)_2(ClO_4)_2$ and $Cu(sucim)_2(iso\text{-}C_3H_7NH_2)_2$. From a comparison of these spectra with the spectra of most cupric complexes, it has been concluded that these compounds contain square-planar complexes of copper(II), with the fifth and sixth co-ordination sites left empty. It has been concluded, in a similar way, that the compounds with a formula of $Cu(sucim)_2(amine)_2$, the amine being methyl, ethyl, *n*-propyl, isopropyl, *n*-butyl and *n*-amyl amines as well as ammonia, consist of quadri-co-ordinate, square-planar complexes in the crystalline state.

The absorption spectra of bis(succinimidato)-bis(alkylamine)-copper(II) complexes in chloroform, benzene and methylene chloride, in which the compounds are colored dark-blue, have been determined. The enormously large band shift toward a lower frequency, on going from the crystal to the solution, seems to indicate that the configuration in these solvents is not the square-planar or trans-bis-(chloroform) configuration, but deviates from the square-plane.

The present authors are grateful to the late Professor Ryutaro Tsuchida for valuable discussion and to the Ministry of Education for financial support.

Department of Chemistry
Faculty of Science
Osaka University
Nakanoshima, Osaka

The Photoisomerization of cis-Azobenzene in the Presence of Iodine

By Shigeru YAMASHITA, Desmond P. COSGRAVE, Hiroshi ONO and Osamu TOYAMA

(Received February 14, 1963)

We have recently studied the iodine-catalyzed thermal cis → trans isomerization of azobenzene in a *n*-hexane solution at room temperature[1]. The results obtained suggest that the isomerization takes place through an intermediate complex formed between *cis*-azobenzene and iodine. The existence of such a molecular complex in the solution has been shown spectroscopically, and the equilibrium constant and the heat of complex formation have been determined.

The purpose of the present work is to show that the iodine-complex of *cis*-azobenzene yields *trans*-azobenzene when excited by the absorption of light. The reaction can be distinguished from the direct photoisomerization of free *cis*-azobenzene in the solution, which has been studied previously[2]. For purposes of comparison, the isomerization has also been studied in the wavelength region where the only absorbing entity is free iodine in the solution.

1) S. Yamashita, This Bulletin, **34**, 842 (1961).

2) S. Yamashita, H. Ono, and O. Toyama, ibid., **35**, 1849 (1962).

Experimental

Materials.—The preparation or purification of *cis*- and *trans*-azobenzene, iodine and *n*-hexane has already been described in previous papers[1,2].

Apparatus and Procedure.—The absorption bands of the iodine-complex of *cis*-azobenzene and its isomerization under irradiation of light were studied at −78°C, where the equilibrium constant for the complex, estimated from previous data[1] obtained at higher temperatures above 0°C, is as large as 6.62×10^4 l. mol^{-1}, compared to 1.92×10^2 l. mol^{-1} at 10°C. The metal Dewar vessel used for these measurements was similar in design to those described by Ham[3] and Potts[4]. It was set in a brass desiccator box equipped with quartz windows and containing silica gel to protect the cell windows from frosting.

Figure 1 shows the absorption curve for the *cis*-azobenzene-iodine complex thus determined at −78°C. The absorption maximum at 305 mμ has been assigned to a charge-transfer band characteristic of the complex, and the other one at 435 mμ, to a blue-shift of the iodine band due to the complex formation[1].

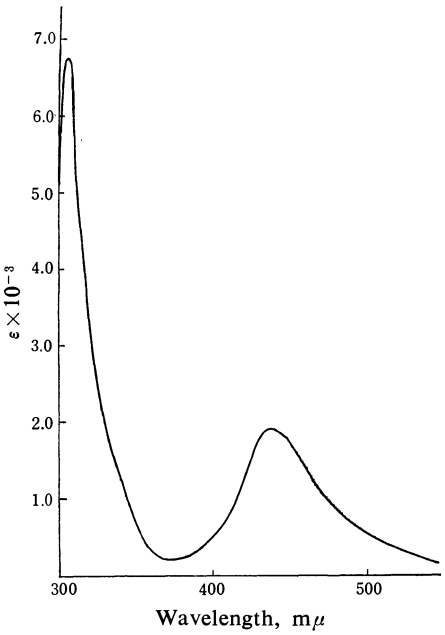

Fig. 1. Absorption curve of *cis*-azobenzene-iodine complex.

The isomerization reaction was studied by the use of the following three different kinds of irradiation: 313 mμ was used to investigate the effect of the charge-transfer absorption of the complex, 436 mμ, for that of the blue-shifted absorption of complexed iodine, and 546 and 577 mμ, for that of the absorption of free iodine in the solution. The filters used for these experiments are given in Table I.

Table I. Mercury lines and filters used for irradiation

Wavelength, mμ	Filter
313	Mazda UV-D2 and K_2CrO_4 aq.
436 (containing small amount of 405 mμ)	Mazda V-V1 and Walz UV
546~577	Walz R-1

Table I. The light source was a Mazda SHL-100 mercury lamp.

The progress of the isomerization reaction in each run was followed spectrophotometrically in a way similar to that described for stilbene in a previous paper[5]. Only the initial rates of conversion were determined in all the experiments; the dependence of the rate on the concentrations of the absorbing entity and other species was obtained from the initial rates determined under varied conditions.

Results and Discussion

Irradiation with Wavelengths of 313 and 436 (Containing a Slight Quantity of 405) mμ.—As may be seen in Fig. 1, 313 mμ approximately corresponds to the charge-transfer absorption maximum of the *cis*-azobenzene-iodine complex, and 436 (containing a small amount of 405) mμ, to the blue-shifted absoption maximum of the complexed iodine. The absorbance of free iodine in this wavelength region is negligible, so its contribution to the isomerization may be neglected. On the other hand, the absorbance of free *cis*-azobenzene in this wavelength range is considerable[1], and its contribution to the isomerization should be taken into account.

Tables II and III show the results obtained with 313 and 436 mμ at −78°C. The contribution of the isomerization of free *cis*-azobenzene was estimated from the extinction coefficients and the quantum yields for free *cis*-azobenzene, both determined previously[1,2], combined with the concentration of free *cis*-azobenzene calculated from the equilibrium constant for the complex at −78°C, 6.62×10^4 l. mol^{-1}.

Tables II and III thus indicate that the *cis*-azobenzene-iodine complex, when excited by 313 or 436 mμ, yields *trans*-azobenzene with a quantum yield which is approximately constant for varied concentrations of *cis*-azobenzene and iodine.

The isomerization caused by the excitation of the molecular complex might be supposed to result from an intermolecular energy transfer between the excited molecular complex and free *cis*-azobenzene. However, the quantum yields, independent of the concentration of

3) J. Ham, *J. Am. Chem. Soc.*, **76**, 3875 (1954).
4) W. J. Potts, *J. Chem. Phys.*, **21**, 191 (1953).
5) S. Yamashita, This Bulletin, **34**, 490 (1961).

TABLE II. QUANTUM YIELD FOR THE cis → trans PHOTOISOMERIZATION OF AZOBENZENE IN THE PRESENCE OF IODINE AT −78°C

Filter, Mazda V-V1 and Walz UV.
Wavelength of exciting light, 436 mμ (containing small amount of 405 mμ).
Absorption band, complexed iodine band having maximum at 435 mμ.

Concn. of the complex ×10⁵ mol./l.	Amount of light quanta absorbed ×10¹⁰ einstein/sec.	Amount of azobenzene converted ×10¹⁰ mol./sec.	Quantum yield
0.31	0.772	0.44	0.57
0.86	2.05	1.16	0.57
1.50	3.46	1.95	0.56
2.18	4.88	2.75	0.56
2.90	6.28	3.53	0.56
3.65	7.66	4.31	0.56
4.42	8.99	5.06	0.56
5.20	10.3	5.76	0.56
5.99	11.5	6.36	0.55
6.79	12.6	6.90	0.55

TABLE III. QUANTUM YIELD FOR THE cis → trans PHOTOISOMERIZATION OF AZOBENZENE IN THE PRESENCE OF IODINE AT −78°C

Filter, Mazda UV-D2 and K_2CrO_4 aq.
Wavelength of exciting light, 313 mμ.
Absorption band, charge-transfer band of the complex having a maximum at 305 mμ.

Concn. of the complex ×10⁵ mol./l.	Amount of light quanta absorbed ×10¹¹ einstein/sec.	Amount of azobenzene converted ×10¹¹ mol./sec.	Quantum yield
8.82	8.50	1.60	0.19
6.79	6.68	1.55	0.23
6.79	6.68	1.51	0.22
5.20	5.84	1.25	0.21
15.2	12.2	2.64	0.22
6.79	9.57	1.80	0.19
3.65	6.81	1.24	0.18

free *cis*-azobenzene, seem to exclude such an intermolecular-energy-transfer mechanism.

There have recently been discovered a number of complex molecules that exhibit intramolecular-energy-transfer processes on light absorption; the molecular complex of trinitrobenzene with anthracene, for instance, when excited by its charge-transfer absorption, dissociates and yields anthrancene in a triplet state which subsequently returns to its ground state by phosphorescence[6]. If a similar mechanism is operative in the present case, the isomerization may be explained by the following reaction scheme:

$$CI_2 + h\nu \rightarrow CI_2^*$$
$$CI_2^* \rightarrow C^* + I_2$$
$$C^* \rightarrow T$$

with appropriate deactivation processes for the excited CI_2^* and C*, where C and T represent *cis*- and *trans*-azobenzene respectively. Table IV shows that the relative magnitudes of the excitation energies and quantum yields for *cis*-azobenzene and its iodine-complex conform to such an interpretation[7].

In the case of the *cis*-stilbene-iodine complex, which has previously been studied[8], the blue-shifted visible absorption band of iodine has a maximum at 420 mμ in *n*-hexane. Although the excitation by this transition is effective for the isomerization, the kinetics is entirely different from that for *cis*-azobenzene reported here and is to be explained by the reactions:

$$CI_2 + h\nu \rightarrow CI_2^*$$
and
$$CI_2^* + C \rightarrow CI + CI$$

followed by the thermal isomerization of the CI complex. The inability of the CI_2^* excited complex to isomerize directly in this case may be explained from the energy relation as follows. Although *cis*-stilbene has π-π^* absorption in the wavelength region shorter

TABLE IV. ABSORPTION BANDS AND QUANTUM YIELDS OF PHOTOISOMERIZATION FOR *cis*-AZBENZENE AND ITS IODINE-COMPLEX

Substance	Absorption band		Isomerization	
	Transition	mμ	Irradiation, mμ	Quantum yield
cis-Azobenzene	π-π^*	<350	313	0.44
	n-π^*	420	405	0.68
cis-Azobenzene -iodine complex	Charge-transfer	305	313	0.20
	Blue-shift of iodine	435	436	0.56

6) S. P. McGlynn and J. D. Boggus, *J. Am. Chem. Soc.*, **80**, 5096 (1958); S. P. McGlynn, *Chem. Revs.*, **58**, 1113 (1958).
7) The intramolecular energy transfer to the donor component might be assumed to take place without dissociation of the complex if the excitation energies for *cis*-azobenzene were not appreciably changed by the complex formation. However, the complex apparently has no absorption to be assigned to the donor in the wavelength region 300 to 500 mμ, where free *cis*-azobenzene has absorption bands.
8) S. Yamashita, This Bulletin, **34**, 972 (1961).

than 350 mμ, it has no n-π^* absorption in the longer wavelength region; the excitation of the complex by the blue-shifted iodine absorption around 420 mμ cannot, therefore, yield the excited molecule of *cis*-stilbene that can isomerize to its trans-form.

Irradiation with 546 and 577 mμ.—These mercury lines are solely absorbed by free iodine in the solution; the absorbance of *cis*-azobenzene, as well as that of *cis*-azobenzene-iodine complex, is negligible in this wavelength range. Figures 2—4, which represent the experimental results obtained at 0°C, show, therefore, that the absorption of light by free iodine in the solution gives rise to the isomerization of *cis*-azobenzene, and that the kinetic data conform to the rate equation:

$$d(T)/dt = kI_0(C)(I_2)^{1/2} \qquad (1)$$

where I_0 is the incident light intensity[9].

Equation 1 is of the same form as the rate equation previously obtained for the iodine-photocatalyzed isomerization of *cis*-stilbene in the same wavelength region[8]. Hence, it may be explained in a similar way:

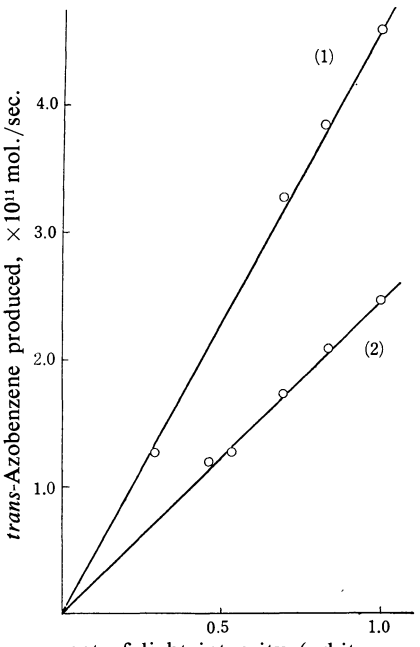

Fig. 2. Experiments with 546 and 577 mμ; dependence of the rate on light intensity. Concentration of iodine, 1.0×10^{-5} mol./l.; initial concentration of *cis*-azobenzene, 2.0×10^{-4} mol./l. for (1); 1.0×10^{-4} mol./l. for (2).

9) The equilibrium concentration of the *cis*-azobenzene-iodine complex at 0°C is so small that the concentrations of free species in the solution are practically equal to the respective initial concentrations.

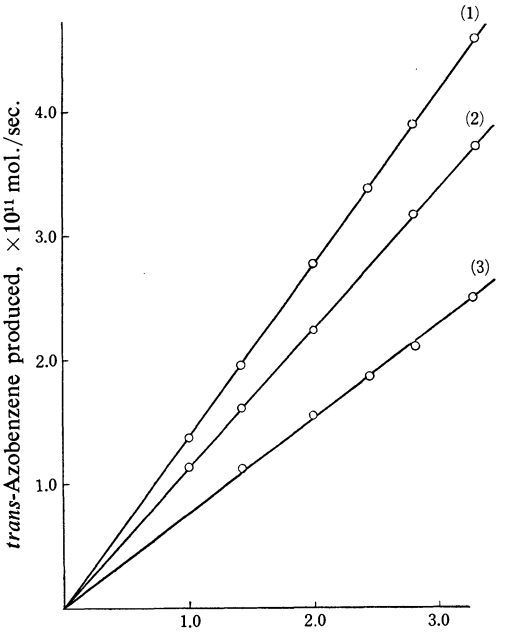

Fig. 3. Experiments with 546 and 577 mμ; dependence of the rate on iodine concentration.
Incident light quanta, 6.63×10^{-8} einstein/sec.; initial concentration of *cis*-azobenzene, 2.0×10^{-4} mol./l. for (1); 1.5×10^{-4} mol./l. for (2); 1.0×10^{-4} mol./l. for (3).

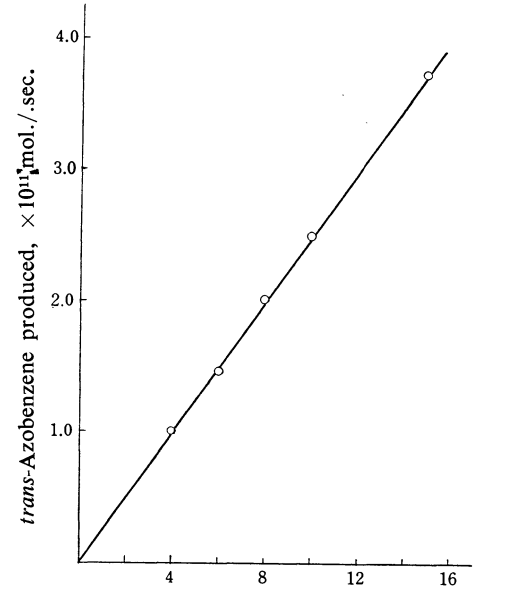

Fig. 4. Experiments with 546 and 577 mμ; dependence of the rate on *cis*-azobenzene concentration.
Incident light quanta, 6.63×10^{-8} einstein/sec.; concentration of iodine, 1.0×10^{-5} mol./l.

$$I_2 + h\nu \rightarrow I + I$$
$$C + I \rightarrow CI$$
$$CI \rightarrow C + I$$
$$CI \rightarrow TI$$
$$TI \rightarrow T + I$$
$$I + I \rightarrow I_2$$

By applying a steady-state treatment to this sequence of reactions, a rate equation that agrees with Eq. 1 is obtained, as has previously been shown for *cis*-stilbene.

For the present, we have no direct evidence for the intermediate complex, CI or TI. However, it is highly probable that atomic iodine forms such complexes, since it has an electron affinity of 3.2 eV.[10], greater than that of molecular iodine, 1.8 eV.[11] By means of a flash technique, Strong[12] and Porter[13] have shown spectroscopically the formation of a number of similar complexes of atomic iodine.

Summary

The conversion of *cis*-azobenzene in a *n*-hexane solution to its trans-isomer in the presence of iodine has been studied by light irradiation. The experiments with wavelengths of 313 and 436 mμ at −78°C have shown that the excitation of the molecular complex formed between *cis*-azobenzene and iodine, by its charge-transfer transition or by the blue-shifted absorption of complexed iodine, yields *trans*-azobenzene with a quantum yield independent of the composition of the solution. By comparing this finding with the results previously obtained for the cis-trans photoisomerization of free azobenzene in *n*-hexane, a probable mechanism has been presented: $CI_2 + h\nu \rightarrow CI_2^*$, $CI_2^* \rightarrow C^* + I_2$ and $C^* \rightarrow T$, where C and T denote *cis*- and *trans*-azobenzene respectively.

The results obtained at 0°C by irradiation at wavelengths of 546 and 577 mμ, which are solely absorbed by free iodine in the solution, are similar to those previously obtained for stilbene; they may, therefore, be explained in a similar way, i. e., by the photochemical dissociation of free iodine, followed by the iodine atom-catalyzed isomerization of *cis*-azobenzene.

The authors are grateful to Professor Teruo Hayakawa for his valuable discussions.

Department of Applied Chemistry
College of Engineering
(O. T., H. O. & D. P. C.)
Department of Chemistry
College of General Education
(S. Y.)
The University of Osaka Prefecture
Sakai, Osaka

10) D. Cubicciotti, *J. Chem. Phys.*, **34**, 2189 (1961); J. D. Morrison, H. Hurzeler, M. G. Inghram and H. E. Stanton, ibid., **33**, 821 (1960).
11) R. S. Mulliken, *J. Am. Chem. Soc.*, **72**, 600 (1950).
12) S. J. Rand and R. L. Strong, ibid., **82**, 5 (1960); R. L. Strong, S. J. Rand and J. A, Britt, ibid., **82**, 5053 (1960).
13) T. A. Gover and G. Porter, *Proc. Roy. Soc.*, **A262**, 476 (1961).

Preparation of Radioactive Antimony-120 of a High Specific Activity by the Irradiation of Tin with Protons

By Kazuo SAITO, Nobuo SUZUKI*, Kunio SETO** and Hidetsugu IKEGAMI

(Received February 15, 1963)

This paper describes the separation of pure radioactive antimony from a tin target irradiated by protons, and the preparation of a radioactivity source suitable for an accurate study of the decay scheme by the measurement of the angular correlation of its γ-rays and of the conversion electron spectrum. Separation of a trace of antimony from tin has been studied by several workers[1-4]. Since solvent extraction from a hydrochloric acid solution[5] and cation exchange in a weakly acid solution containing tartaric acid[2] appeared to be most

* Present address: Institute of Mineral Dressing and Metallurgy, Tohoku University, Nagamachi, Sendai.
** Present address: Faculty of Science, Tohoku University, Katahira-cho, Sendai.

1) R. D. Maxwell, H. R. Haymond, W. M. Garrison and J. G. Hamilton, *J. Chem. Phys.*, **17**, 1340 (1949).
2) F. Mylius and C. Hutter, *Ber.*, **44**, 1315 (1911).
3) C. E. White and H. J. Rose, *Anal. Chem.*, **25**, 351 (1953).
4) K. Kimura, N. Saito, H. Kakihana and T. Ishimori, *J. Chem. Soc. Japan, Pure Chem. Sec.* (*Nippon Kagaku Zassi*), **74**, 305 (1953).
5) G. K. Schweitzer and L. E. Storms, *Anal. Chim. Acta*, **19**, 154 (1958).

suitable for our present purpose, these two methods were examined, with commercially-available radioisotope ^{124}Sb[6]. It was found that both methods require significant modification in order to be applied to the irradiated target, because the amount of irradiated tin is very large.

A great deal of difficulty is involved in the preparation of an activity source which satisfies the following demand. The sample for the measurement of angular correlation of γ-rays must be a liquid less than 0.05 ml. in volume and more than 200 μc. in intensity. Nevertheless, the presence of carrier antimony is permissible. The source for the measurement of the internal conversion electron spectrum, on the other hand, must be practically carrier-free and placed on a thin finlm; the presence of any material brings about confusion in angular correlation. Evaporation of an ethereal or esterial solution of antimony pentachloride and electrolytic deposition provide a useful source for the angular correlation and the conversion electron spectrum measurement, respectively.

Experimental and Results

Materials.—Metallic tin of a high purity (containing less than 8×10^{-4}% Sb) was kindly supplied by Dr. K. Itsuki of Mitsubishi Metal and Mining Co. The organic solvents were purified by the usual method. The other chemicals are of extra pure grade.

Irradiation.—Metallic tin was fused, poured into four square holes in an aluminum slab, which was fixed onto a water-cooled target holder, covered with aluminum foil (20 μ thick), and inserted into the vacuum chamber of INSJ cyclotron (diameter of the magnet polepiece, 165 cm.; maximum proton energy, 15 MeV.; maximum proton current intensity, 1 mamp.). The target was irradiated with 11.5 and 14 MeV. protons with a mean current, 15 μamp. A greater current density caused metallic tin to melt in the shallow hole. With a total bombardment of 120 μamp. hr., about 10 mc. of radioactive substances was produced altogether, including ca. 1 mc. of ^{120}Sb.

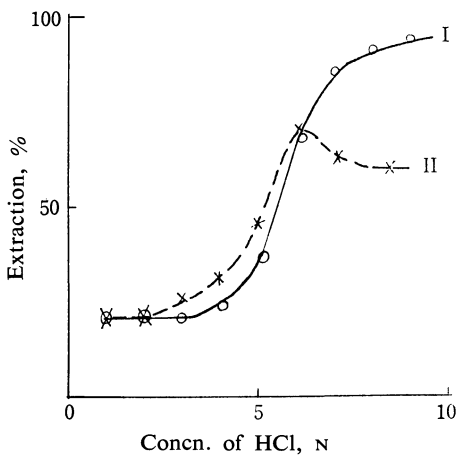

Fig. 1. Extraction of radioactive antimony-(V) from hydrochloric acid solution of irradiated tin.
vol. of the aq. phase, 100 ml.; vol. of org. phase, 30 ml.; I, amylacetate; II, ethylacetate.

The head of the target holder was taken off out of the chamber after a few hours' cooling and subjected to chemical separation.

Dissolution of the Target.—Tin was easily torn off from the aluminum plate, and each piece (2.5 g.) was either dissolved in 6 N hydrochloric acid (150 ml.) or in a mixture (100 ml.) of 6 N hydrochloric acid and concentrated nitric acid (3+1, v/v). In the former case, antimony remained in the tervalent state and was suitable for cation exchange separation from tin, but the time taken for dissolution was about 24 hr. In the latter case, dissolution was completed within 30 min.; the antimony was in the quinqui-valent state and extracted with organic solvent as shown below.

Solvent Extraction. — White et al. stated that the extraction of antimony with ethylacetate was best effected from 1 to 2 N hydrochloric acid solution in the presence of tartaric, acetic or oxalic acid. Our preliminary examination with ^{124}Sb disclosed that the extraction was facilitated by increased concentration of hydrochloric acid[6]. In a concentration greater than 6 N, however, the separation of the organic layer became incomplete, especially by the use of small quantity of the ester as compared with the volume of aqueous phase; hence, the extraction was less effective. By the use of amylacetate, such a defect was eliminated and the antimony, in both ter- and quinqui-valent state, was extracted almost quantitatively from more than 9 N hydrochloric acid. It appears as if the presence of organic acids little affects the extraction, when the antimony is in the quinqui-valent state. Nitric acid, used for the solution of the target, did not cause any interference. Tervalent antimony was extracted with less ease. A small amount of quadrivalent tin was extracted, because its concentration in the aqueous phase was great, but it was extracted back with 8 to 10 N hydrochloric acid. Only a negligible amount of antimony was transferred into the aqueous phase on the back extraction of tin. The amount of tin in the washed organic phase appears to be less than that of antimony coming from the impurity of the target metal. When antimony hydrolysed in too diluted an acid solution, solvent extraction was unsuccessful. Treatment with aqua regia, however, reverted the aged antimony to the ionic state

6) N. Suzuki, *J. Chem. Soc. Japan, Pure Chem. Sec.* (*Nippon Kagaku Zasshi*), 81, 437 (1960).

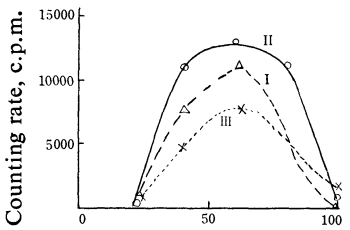

Fig. 2. Elution of radioactive antimony(III) from cation exchange resin with tartaric acid solution.

Resin column, 10 mm. in a diameter, 10 cm. in length, Dowex 50 X8, 100 to 200 mesh; concn. of tartaric acid, 0.4%; pH adjusted with HCl; I, pH, 0.4; II, pH, 0.6; III, pH, 1.6.

extractable with esters. The ester phase was evaporated and used for the γ-ray angular correlation measurement.

Ion Exchange. — Kimura et al. found that tervalent antimony in 0.4% tartaric acid of pH 1 passes through a column of cation exchange resin, bi-valent tin being quantitatively adsorbed on the resin[4]. Our re-examination made it clear that this method may satisfactorily be applied to the separation of radioactive antimony from a large amount of tin. However, it was also elucidated that the behavior of antimony was highly dependent on its state in the acid solution. So far as antimony(III) is not aged, the allowable pH range is rather

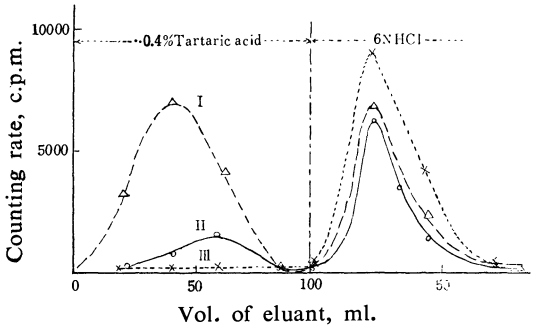

Fig. 3. Elution of radioactive antimony(III) after aging.

I Irradiated Sn (0.3 g.) was dissolved in 6 N HCl (30 ml.) mixed with tartaric acid (0.1 g.), evaporated to ca. 1 ml., set aside overnight and diluted to ca. 25 ml. (pH, 0.6).

II Prepared similarly to I; the tartric acid (1 g.) was added to the condensed soln., which was immediately diluted to ca. 25 ml. for ion exchange (pH, 0.6).

III Prepared similarly to I; the condensed soln. (1 ml.) was set aside overnight, mixed with tartaric acid (0.1 g.) and diluted.

wide, as is shown in Fig. 2. The tervalent antimony is apt to age in a dilute hydrochloric acid solution or in the presence of a less excess of hydrochloric acid. In the presence of tartaric acid, the aging was retarded in the cold, but not on boiling (see Fig. 3). When the antimony(III) was aged (perhaps by hydrolysis), its elution with a 0.4% tartaric acid solution of pH 1 was quite incomplete. It was partly eluted with 6 N hydrochloric acid, together with bivalent tin, but the remainder was eluted with great difficulty by the use of various agents including the following: 3 N hydrochloric acid containing 1% potassium chlorate, 3 N hydrochloric acid containing 5% (by volume) concentrated nitric acid, concentrated hydrochloric acid, 6 N hydrochloric acid containing various amounts of hydrogen iodide, and diluted hydrochloric acid containing various amounts of sodium bisulfite.

Electrolytic Deposition of Antimony.—Since the radioactive antimony consists of several kinds of nuclide, the scintillation spectrum is not resolving enough to enable an accurate study of the decay scheme. For the measurement of the internal conversion spectrum and the electron-gamma directional correlation, a source of a high specific activity is required. In order to minimize the scattering of electrons inside the source, the source thickness must be very small*. The lower the energy of electrons to be measured, the thinner the source should be. For the measurement in a rather high energy region, on the other hand, the influence of the scattering is less marked, and the conversion co-efficient is smaller. Hence, the demand for source thickness is less severe, but the intensity must be stronger.

The electrolysis of antimony is highly dependent on the state in the electrolytic solution. It is essential to avoid hydrolysis and to keep the antimony in an ionic state, either ter- or quinqui-valent. For this purpose, the radioactive antimony must be kept either in an organic solvent or in a hydrochloric acid solution more concentrated than 3 normal. When the organic solution is converted into an aqueous solution, care must be taken to maintain the acid concentration above this level. Aged antimony can be converted into an ionic state by boiling it with dilute aqua regia.

* In this measurement the source should be embedded in a metallic lattice. This condition is imperative in this case, where the nuclear transition occurs through an electron capture or internal conversion. The electronic shell will be excited by these processes, and the excited electronic shell will give a time-dependent perturbation. In a metallic surrounding, however, the recovery time is much shorter than the mean lifetime of the nuclear intermediate state and, consequently, there will be no attenuation.

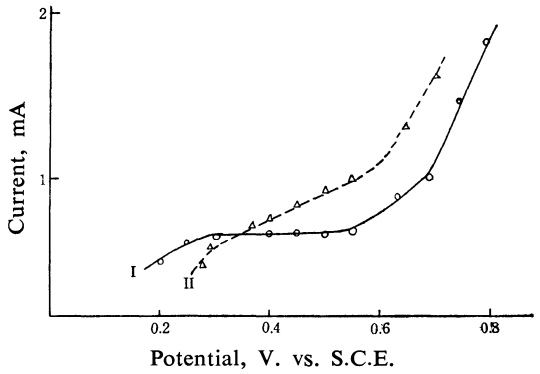

Fig. 4. Potential vs. current diagram for the electrolytic deposition of radioactive antimony in diluted hydrochloric acid.
I, in 1 N HCl; II, in 2.5 N HCl; 1% (w/v) hydroxylamine hydrochloride; 25°C; amount of Sb carrier < 2 μg.

Antimony was electrolytically deposited on a cathode (2×20 mm.) of silver or copper film (10 μg. per cm^2), which was evaporated in vacuo on a rubber hydrochloride film (0.25 mg. per cm^2), with platinum wire as anode. The potential-current diagram is shown in Fig. 4. About 70% of the radioactive antimony in ca. 1 N hydrochloric acid (ca. 10 ml.), containing 1% (w/v) hydroxylamine hydrochloride and less than 2 μg. of carrier antimony coming from the target, was deposited within 3 hr. with a terminal voltage 1.4 V. Under this condition the cathode potential vs. S.C.E. is −0.46 V. When the terminal voltage and the acid concentration were increased, the electrolysis was rather facilitated. However, an amorphous black substance appeared on the cathode surface, and the specific activity decreased. Such a black substance appeared even in the absence of antimony or by the use of pure carbon as anode. Spectrographic analysis indicated no other metal than the cathode metal. It appears as if the cathode is partly dissolved in the electrolytic solution owing to, e.g., local cell formation and then deposited again in the form of a very fine powder.

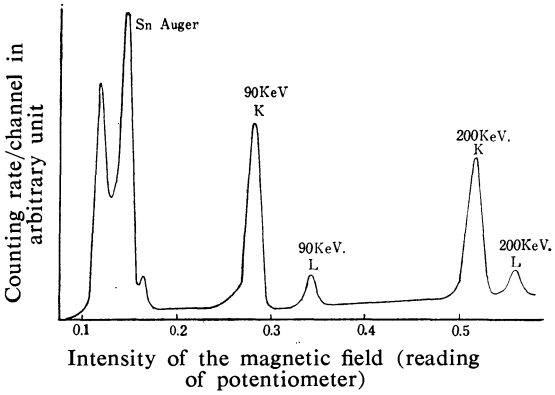

Fig. 5. Internal conversion electron spectrum of ^{120}Sb.

Measurement of the Internal Conversion Electron Spectrum. — Figure 5 illustrates the conversion electron spectrum in the lowest energy region; it clearly indicates that the source is so thin that the peaks corresponding to the Auger electron are distinctly separated. The form of the lines is symmetrical, indicating no source-scattering of low energy electrons.

Discussion

When tin with natural abundance ratio is irradiated with protons, radioactive antimony isotopes of mass numbers 115 to 124 are formed. Among these only Sb-119, 120 m and 124 survive after one day. The first gives only γ-rays of a low energy (23.8 keV.), and the last two are the main components of radioactive antimony. Although Sb-124 gives several γ-rays, they interfere neither with the accurate measurement of γ-ray energies by the conversion electron method nor with that of angular correlation of the γ-rays of Sb-120, because of the low abundance of ^{124}Sn.

Examination of solvent extraction, ion exchange and electrolysis of a micro amount of antimony disclosed that the procedures are satisfactorily effected so far as the antimony is not hydrolysed in the aqueous phase. Hence, care must be taken to avoid the hydrolysis especially in a rather low acid concentration. The recommended procedure is shown below.

The product is of so high a specific activity as to be more than 0.1 mc. per μg. of Sb. (The highest specific activity of Sb-124 produced in a reactor with a neutron flux of 10^{14} per cm^2 per sec. is ca. 0.01 μc. per μg. of Sb.) Figure 5 provides one of the rarest examples of low energy conversion electron spectra ever observed.

Recommended Procedure (*Separation by Solvent Extraction*).—Dissolve the target tin (4 g.) in a mixture (100 ml.) of 6 N hydrochloric and concentrated nitric acids (3+1 v/v), boil to decompose the nitric acid and treat it with concentrated hydrochloric acid to produce ca. 50 ml. of 8 N hydrochloric acid. Shake with amylacetate (25 ml.×2), and wash the ester layer with 8 N hydrochloric acid (20 ml.×2). Evaporate the organic phase almost to dryness with occasional addition of 8 N hydrochloric acid. Use the residual, rather viscous solution (ca. 0.1 ml. in volume) for γ-γ angular correlation study. Convert the residue into a 1 to 3 N hydrochloric acid solution (10 ml.) containing 1% (w/v) hydroxylamine hydrochloride and

electrolyse antimony, using the apparatus illustrated in Fig. 6 of Ref. 7, upon an evaporated film of silver (thickness: 10 μg. per cm^2) on rubber hydrochloride (0.25 mg. per cm^2) with a terminal voltage, 1.4 V.

Summary

1) By irradiation of a tin target (antimony content, less than 8×10^{-4}%) with 15 MeV. protons (120 μ amp. hr.), about 1 mc. of ^{120}Sb was produced, with a specific activity more than 30 μc. per μg. of antimony.

2) The radioactive antimony was either separated by extraction with amylacetate from more than 6 N hydrochloric acid containing tin(IV) or by cation exchange in a 0.4% tartaric acid solution of pH 0.6 to 1.6 containing tin(II).

3) ^{120}Sb is electrolytically deposited on an evaporated film of silver or copper from a 1 to 3 N hydrochloric acid solution containing 1% hydroxylamine hydrochloride with a yield of 70% within 3 hr.

4) Care should be taken to avoid hydrolytic aging of antimony in diluted hydrochloric acid, which vitiates the extraction, the ion exchange, and the electrolysis.

The authors wish to express their thanks to Drs. Mitsuo Sakai and Toshimitsu Yamazaki and the cyclotron crew of the Institute for their co-operation. They are also deeply indebted to Dr. Kamihiko Itsuki of Mitsubishi Metal and Mining Co. for kindly supplying them with very pure tin.

Institute for Nuclear Study
The University of Tokyo
Tanashi, Tokyo

7) K. Saito, Y. Inoue and T. Yamazaki, ibid., **84**, 220 (1963).

The Ultraviolet Spectra of Monohalo-, Mononitro- and Monoamino-p-terphenyls

By Kaoru IGUCHI, Tadashi NOZAKI, Akira IMAMURA and Setsuji TAKAHASHI

(Received February 16, 1963)

The molecule of *p*-terphenyl has a system of eighteen π-electrons and shows ultraviolet absorption with the peak at 276 mμ. When *p*-terphenyl is monosubstituted, the absorption peak shifts to red or blue and sometimes splits into two or three peaks according to the nature and the position of the substituent. These phenomena are due to the perturbation of the π-electronic system caused by the substitution. The perturbation consists principally of the following two factors: (1) interaction between the molecular orbital of *p*-terphenyl and the substituent orbital, and (2) the steric effect caused by the substituent. The ultraviolet absorption spectrum will give useful information concerning these factors.

The ultraviolet spectra of all isomers of monochloro-, monobromo-, monoiodo-, mononitro- and monoamino-*p*-terphenyl were measured, and the wavelength for maximum absorbance, the half-width of the absorption peak, the oscillator strength and the molar extinction coefficient were determined. For halo-*p*-terphenyls, the shift of the absorption peak was qualitatively treated theoretically by a molecular orbital method, which gave rather a good result considering its simplicity.

Experimental

The preparation of the compounds has been reported[1] previously, together with some of their properties. A weighed amount (ca. 1 mg.) of the sample was dissolved in purified *n*-heptane (10 ml.); then a definite volume (ca. 0.3 ml.) of the solution was withdrawn and added to the same solvent (10 ml.) in an absorption cell. The spectrum was measured at room temperature with a Shimadzu SV-50 A spectrophotometer in the range of 210~340 mμ. The oscillator strength (f) was determined by the use of Mulliken and Rieke's formula[2]:

$$f=\frac{mC^2}{\pi e^2 n}\int \gamma k_{\tilde{\nu}}\mathrm{d}\tilde{\nu}=\frac{4.318\times10^{-9}}{\text{mol. density}}\int D\mathrm{d}\tilde{\nu} \qquad (1)$$

1) T. Nozaki and Y. Harada, This Bulletin, 35, 1783 (1962).
2) R. S. Mulliken and C. A. Rieke, *Rep. Prog. Phys.*, 8, 231 (1941).

where n is the number of molecules in 1 ml. of solution; γ, the correction constant (here taken as unity); k_ν, the extinction coefficient, and D, the optical density ($\log_{10} I_0/I$). The integration was performed graphically by means of a planimeter.

Results and Discussion

The Absorption Peak and Oscillator Strength. —The measured spectra are shown in Figs. 1–5, while the numerical results are given in Tables I–V. The wavelength for the absorption peak depends strongly on the position of the substituent but only slightly on its nature. A similar tendency is also seen in the case of the melting point and the solubility[1], though the ultraviolet spectrum of the solution depends principally on the intramolecular state, while

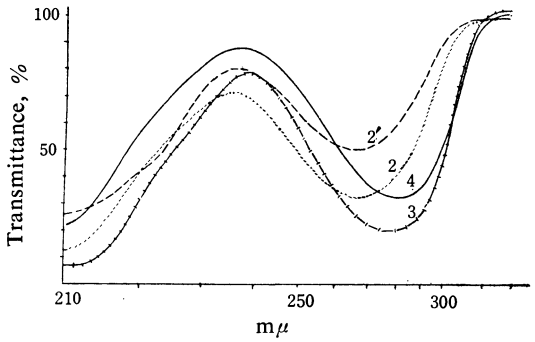

Fig. 1. Absorption spectra of chloro-*p*-terphenyls.
Curve 4 (position of substitution);
$C=1.386\times10^{-5}$
3; $C=1.228\times10^{-5}$
2; $C=1.383\times10^{-5}$
2'; $C=1.042\times10^{-5}$ mol./l.
(C=Conc. of solution)

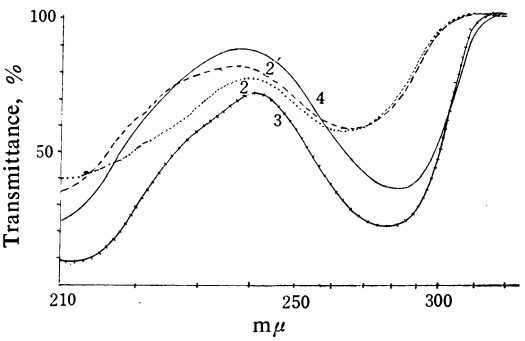

Fig. 2. Absorption spectra of bromo-*p*-terphenyls.
Curve 4; $C=0.922\times10^{-5}$
3; $C=1.236\times10^{-5}$
2; $C=0.927\times10^{-5}$
2'; $C=0.967\times10^{-5}$ mol./l.
(C=Conc. of solution)

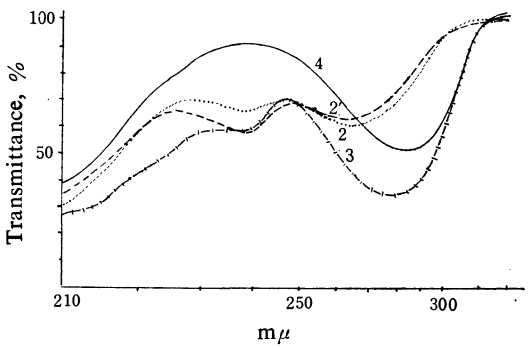

Fig. 3. Absorption spectra of iodo-*p*-terphenyls.
Curve 4; $C=0.707\times10^{-5}$
3; $C=1.317\times10^{-5}$
2; $C=0.736\times10^{-5}$
2'; $C=0.866\times10^{-5}$ mol./l.
(C=Conc. of solution)

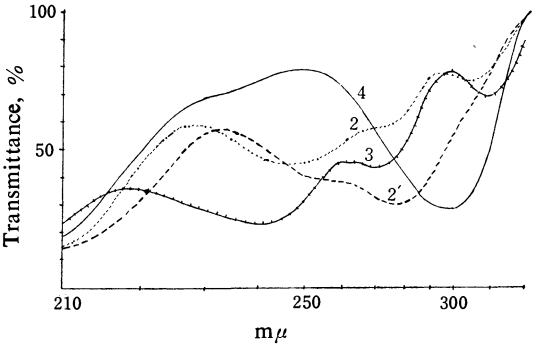

Fig. 4. Absorption spectra of amino-*p*-terphenyls.
Curve 4; $C=1.515\times10^{-5}$
3; $C=1.354\times10^{-5}$
2; $C=1.274\times10^{-5}$
2'; $C=1.667\times10^{-5}$ mol./l.
(C=Conc. of solution)

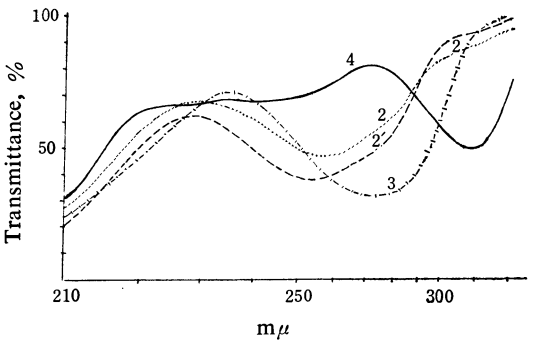

Fig. 5. Absorption spectra of nitro-*p*-terphenyls.
Curve 4; $C=0.992\times10^{-5}$
3; $C=1.424\times10^{-5}$
2; $C=1.233\times10^{-5}$
2'; $C=1.404\times10^{-5}$ mol./l.
(C=Conc. of solution)

TABLE I. CHLORO-*p*-TERPHENYLS

Position of substitution	4	3	2	2′
λ_m mμ	281	278	266	266
$\tilde{\nu}_m$ 10^4 cm^{-1}	3.56	3.60	3.76	3.76
Half width 10^4 cm^{-1}	0.57_5	0.58_5	0.61	0.58
f	0.929	1.256	0.920	0.733
ε 10^4 mol^{-1} l. cm^{-1}	3.50	5.81	3.49	2.87

TABLE II. BROMO-*p*-TERPHENYLS

Position of substitution	4	3	2	2′
λ_m mμ	282.5	278	265	266
$\tilde{\nu}_m$ 10^4 cm^{-1}	3.54	3.60	3.78	3.76
Half width 10^4 cm^{-1}	0.58	0.56	0.57	0.59_5
f	1.253	1.351	0.645	0.626
ε 10^4 mol^{-1} l. cm^{-1}	2.10	5.26	2.62	2.41

TABLE III. IODO-*p*-TERPHENYLS

Position of substitution	4		3		2		2′	
λ_m mμ	284.5	237.5	279	237	265	238	264	238
$\tilde{\nu}_m$ 10^4 cm^{-1}	3.51_5	4.21	3.59	4.20	3.78	4.20	3.79	4.20
Half with 10^4 cm^{-1}	0.58	0.28_5	0.57	0.25	0.61	0.66	0.60	0.67
f	1.135	0.032	0.858	0.095	0.782	0.201	0.645	0.195
ε 10^4 mol^{-1} l. cm^{-1}	4.19	0.26	3.43	0.80	3.01	1.71	2.33	1.66

TABLE IV. AMINO-*p*-TERPHENYLS

Position of substitution	4		3		
λ_m mμ	239	297.5	240	270	317.5
$\tilde{\nu}_m$ 10^4 cm^{-1}	4.18	3.36	4.17	3.70	3.15
Half width 10^4 cm^{-1}	0.39	0.56	0.55	0.38	0.12
f	0.091	0.932	1.095	0.338	0.185
ε 10^4 mol^{-1} l. cm^{-1}	0.53	3.70	4.73	2.67	1.17
Position of substitution	2			2′	
λ_m mμ	245	269	308	245	277	314.5
$\tilde{\nu}_m$ 10^4 cm^{-1}	4.07	3.71_5	3.25	4.07	3.61	3.18
Half width 10^4 cm^{-1}	0.41	0.42	0.38	0.37	0.54	0.34
f	0.459	0.282	0.123	0.260	0.764	0.076
ε 10^4 mol^{-1} l. cm^{-1}	2.77	1.93	1.02	1.66	3.17	0.51

TABLE V. NITRO-*p*-TERPHENYLS

Position of substitution	4		3	2			2′		
λ_m mμ	243	316	272	257	278	323	254	276	319.5
$\tilde{\nu}_m$ 10^4 cm^{-1}	4.12	3.16_5	3.67_5	3.89	3.60	3.10	3.94	3.62	3.13
Half width 10^4 cm^{-1}	0.62	0.63	1.28	0.72	0.15	0.40	0.72	0.33	0.31
f	0.478	0.824	1.425	0.849	0.004	0.571	1.247	0.035	0.043
ε 10^4 mol^{-1} l. cm^{-1}	1.76	3.09	3.50	2.65	0.07	0.18	2.76	0.23	0.29

TABLE VI. LOWEST TRANSITION ENERGIES OF MONOHALO-*p*-TERPHENYLS, ΔE†

Position of substitution	
4	$1.185+0.088 \times \left(\frac{1}{\alpha+0.593}-\frac{1}{\alpha-0.593}\right) \gamma^2$
3	$1.185+0.008 \times \left(\frac{1}{\alpha+0.593}-\frac{1}{\alpha-0.593}\right) \gamma^2$
2	$1.185+0.060 \times \left(\frac{1}{\alpha+0.593}-\frac{1}{\alpha-0.593}\right) \gamma^2-0.328\times(\delta\beta)$
2′	$1.185+0.049 \times \left(\frac{1}{\alpha+0.593}-\frac{1}{\alpha-0.593}\right) \gamma^2-0.328\times(\delta\beta)$

† in units of $(-\beta)$

The values of C^i_r in Eq. 2 are obtained from the following reference: A. and B. Pullman, *J. chim. phys.*, **46**, 212 (1949).

the melting point and solubility should relate strongly to the intermolecular forces.

The ultraviolet spectra of the halo-*p*-terphenyls have the following characteristics; (1) The wavelenthgs of the absorption peaks are in the order 4-halo>3-halo>*p*-terphenyl; (2) Halogenation at 2- or 2'-position, on the other hand, shows a blue shift probably because of the steric effect; (3) The wavelength for the main absorption peak depends only slightly on the nature of the halogen atom; (4) The oscillator strength of a 4- or 3-halo-*p*-terphenyl is usually larger than that of the 2- or 2'-compound. Similar phenomena have also been observed with substituted biphenyl[3] and in more general cases[4]. The 238 mμ peaks of the iodo-*p*-terphenyls may be attributed to the absorption by the iodine atom itself[3].

LCAO MO Perturbation Treatment.—Many authors have tried to elucidate theoretically the effect of a substituent on the ultraviolet spectrum. Matsen[5] gave general formulas for the wavelength and oscillator strength of ultraviolet absorption using the perturbation theory and then applied them to benzene derivatives. Longuet-Higgins and Sowden[6] successfully explained the ultraviolet spectrum of methylated hydrocarbons. I'haya[7] also developed the perturbation theory and treated benzene derivatives.

We intend to explain our experimental results on the basis of a simple LCAO MO perturbation treatment. The substitution has an effect on both the electronic structure and the steric configuration of the *p*-terphenyl molecule. The substitution at the 3- or 4-position has influence only on the electronic structure, while that at the 2- or 2'-position has the further effect of twisting the molecule. The variation in electronic structure is due to the change in the degree of resonance and inductive effects. In the present paper, however, only the resonance effect is considered on the assumption that the difference in the inductive effect is small among the halo-*p*-terphenyls. The steric effect is taken up in the form of a variation in the resonance integral of the carbon-carbon bond between two benzene rings.

For the perturbed system, the energy, λ'_i, is given as follows, with the higher terms being neglected[8];

$$\lambda'_i=\lambda_i+2C^i_rC^i_s(\delta\beta)-\frac{(C^i_t)^2}{\alpha-\lambda_i}\gamma^2 \qquad (2)$$

where λ_i is the energy and C^i_r, the coefficient of the r-th atom in i-th non-perturbed MO; the subscripts r and s denote the atoms binding the two benzene rings being considered, and t is the position of the substituent. Here, α designates the energy of the highest occupied orbital of the substituent, while γ is the resonance integral of the bond between the substituent and *p*-terphenyl, $\delta\beta$ is the change in the resonance integral caused by the twist of *p*-terphenyl and is negative. All these quantities are expressed in units of $(-\beta)$, the resonance integral of the benzene carbon-carbon bond.

The lowest transition of *p*-terphenyl in the simple LCAO MO treatment can be regarded as $A_{1g}\rightarrow B_{3u}$ on the assumption that *p*-terphenyl has a plane structure. The energy differences between the lowest vacant and the highest occupied orbitals, ΔE, are calculated and listed in Table VI. Since the biphenyl molecule twists slightly, the *p*-terphenyl molecule should twist too. Using the above assumptions, however, we probably have not committed any serious errors in drawing our conclusions.

Since the value of any α in Table VI is larger than unity, all the second terms in the formulas are negative. Hence, for 4- and 3-halo-*p*-terphenyls, ΔE becomes smaller and a red shift occurs. Further, it is apparent that 4-substitution gives a larger red-shift than 3-substitution. These results agree well with the experimental data. Substitution at the 2- or 2'-position causes a remarkable blue shift owing to the third term, which is positive and has a larger absolute value than the second. Moreover, the blue shift is of nearly the same degree for 2 and 2' isomers, because the third terms are the same and the second terms differ only slightly between them. All these predictions are supported by the experimental data. The magnitude of the second term varies with the nature of the halogen. However, the change is too small to cause a shift of the peak, as may be seen in the experimental results. It is worth noticing that the all conclusions are derived independently of the values of the parameters in the formulas. In spite of the roughness in our treatment, the qualitative agreement with the experimental results is very good.

For the nitro- and amino-derivatives, however, the situation is too complicated to be treated by such a perturbation method; a more elaborate treatment is required.

The Electrical Communication Laboratory
Musashino, Tokyo

3) E. A. Braude and W. F. Forbes, *J. Chem. Soc.*, **1955**, 3776.
4) E. g., M. S. Newman, "Steric Effects in Organic Chemistry", John Wiley, New York (1956), p. 481.
5) F. A. Matsen, *J. Am. Chem. Soc.*, **72**, 5243 (1950).
6) H. C. Longuet-Higgins and R. G. Sowden, *J. Chem. Soc.*, **1952**, 1404.
7) Y. I'haya, *J. Am. Chem. Soc.*, **81**, 6120, 6127 (1959).
8) K. Fukui, C. Nagata, T. Yonezawa, H. Kato and K. Morokuma, *J. Chem. Phys.*, **31**, 287 (1959).

*Anomalies in the Counting Rate of the Solid Thin Film of Tritiated Lauric Acid in Relation to its Film Structure**

By Kazuo TAJIMA, Tsunetaka SASAKI and Mitsuo MURAMATSU

(Received February 20, 1963)

Recently, increasing attension has been drawn to the special application of tritium as a radiotracer, because of the extremely soft nature of its β-radiation. Especially in the field of surface chemistry, tritium has proved to be very useful for studying the details of adsorption and related surface phenomena[1,2]. For this purpose, several tritiated compounds were prepared in our laboratory, and the condition of their solid counting was examined precisely[3] since the counting rate of tritium is highly dependent on the detailed geometry of each of the solid surface. In the course of this observation, we have found peculiar phenomena with a thin solid film of tritiated lauric acid.

A thin film of this substance deposited from benzene on a stainless steel dish and put in a 2π gas-flow counter gave a counting rate which decreased far more rapidly than was to be expected from the natural decay of tritium β-activity. Moreover, we could observe a distinct break point in the decay curve ten days after the deposition of the film, independent of the amount of sample taken, provided that the film was sufficiently thin. The present paper describes the details of these studies.

Experimental

The α,β-ditritiated lauric acid $CH_3(CH_2)_8(CHT)_2COOH$[4] was dissolved in benzene to give a 5.12×10^{-3} mol./l. solution, which was then spread on the stainless steel dish with a micro-pipette. The solid thin film of tritiated lauric acid left after the evaporation of the solvent was of a mean thickness of about 4~10 μg./cm^2. The β-counting rate of these films was then measured with a 2π gas-flow windowless counter ("Aloka DC-1001", a Nihon Musen Co. product), using propane[5] as a flow gas at the flow rate of 120 bubbles per minute. The results are shown in Fig. 1, where the counting rate is plotted against the time which elapsed after the formation of the thin film. We can notice in this figure that the radioactivity first decreases linearly with time, but its inclination is far steeper than is to be expected from the natural decay rate of tritium (half-life; 12.46 years), and that after ten days, a break point appears and another straight line of a smaller inclination follows. We can confirm that this behavior, especially the time of the appearance of the break point, is fairly reproducible, provided that the thickness of the sample film is sufficiently thin. At first, we presumed that this peculiarity comes from the extremely soft nature of the β-ray of tritium, but precise studies revealed that the phenomena are mainly due to the evaporation of the deposited film of an uneven structure. The following possibilities have been examined experimentally to arrive at the conclusion.

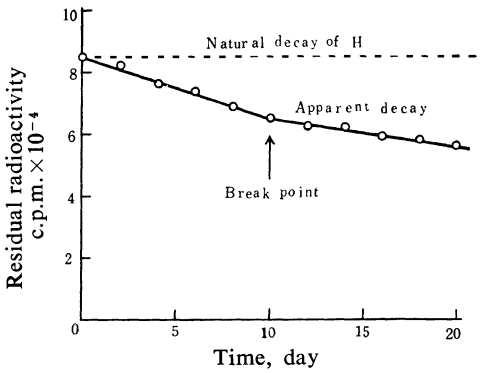

Fig. 1. The decrease in the radioactivity of the thin film of tritiated lauric acid with time.

Exchange with the Hydrogen from the Atmosphere Moisture and the Effect of Flow Gas.— First, as a possible cause of the anomalous rapid decay, we considered the labile position in the lauric acid molecule of the tritium atom, which can be removed by an exchange with a hydrogen atom of water vapor in the flow gas. To examine this possibility three similar tritium samples were prepared, two of which were allowed to come in contact with streams of dry and moist air respectively at the rate of 100 cc. per minute, while the remaining one was kept in a closed vessel without any air current. Changes in the counting rate with time were measured for these samples; the results are shown in Fig. 2. We can see in this figure that, as a whole, the curves are similar. This excludes the possibility that air flow and moisture can remove tritium. The possibility of flow gas itself producing the anomalous phenomena is also

* Paper presented at the 4th International Congress of Radioactivity, Koyto, Japan, 1961; and at the Annual Meeting of Colloid Chemistry, Ueda, Japan, 1961.

1) G. Nilsson, *J. Phys. Chem.*, **61**, 1135 (1957).
2) A. R. G. Lang and S. G. Mason, *Int. J. Appl. Radiation and Isotopes*, **7**, 251 (1960).
3) M. Muramatsu and T. Sasaki, *Science*, **131**, 302 (1960).
4) M. Muramatsu, O. Fujii and T. Sasaki, *Radioisotopes*, **10**, 100 (1961).
5) M. Muramatsu and T. Sasaki, The Proceedings of the 3rd Japan Conference on Radioisotopes (1959), p. 453.

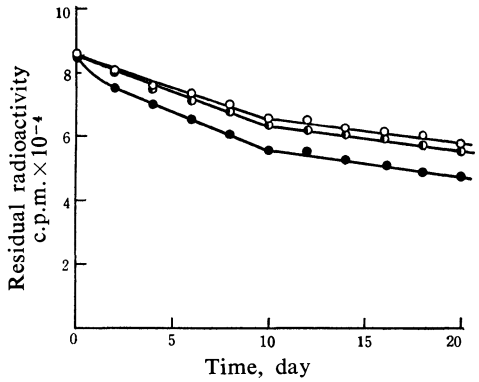

Fig. 2. The effect of the air current on the decrease in the counting rate.
● Dry air flow ◐ Humid air flow
○ Dry air without flow

excluded, since the tritiated stearic acid showed no such anomalies under similar conditions.

The Surface Migration of the Film Substance on the Dish. — If the film substance moves along the surface and clusters, it may decrease the surface area effective for counting. To examine this possibility, two tritium samples were prepared; in one of them tritiated lauric acid was spread in a uniform film, while in the other the substance was mounted as separate twenty-five small spots or clusters. The counting rate-agaist-time curves for these samples, as plotted in Fig. 3, failed to eliminate the anomalies, even for the spotted sample. This excludes the surface migration as an explanation.

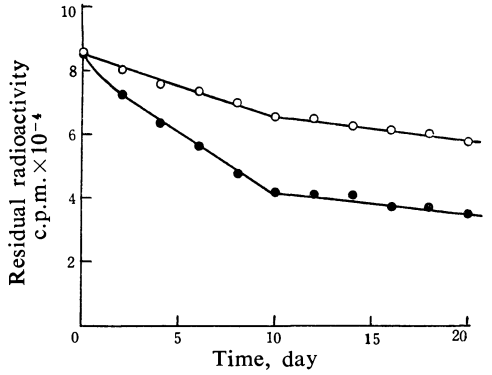

Fig. 3. The effect of the difference in mounting on the counting-rate-versus-time curve.
○ Uniform thin film
● Sample mounted in twenty-five spots

Chemical and Radiochemical Impurities. — Tritiated lauric acid may contain, for instance, other tritiated impurities which give rise to a rapid decrease in counting rate due to its evaporation. Such a possibility can, however, be excluded on the basis of the following experiments.

(1) We prepared at one time twenty samples of the film similar to that of Fig. 1, measured their weights, each on a different day, and constructed a diagram of weight loss due to evaporation versus

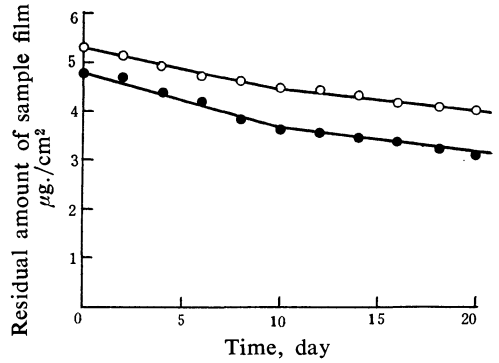

Fig. 4. The measurement of evaporation by radiotracer and surface trough experiment.
○ Surface trough measurement
● Radioactive measurement

time. Here the sample weight was determined by the monolayer method, that is, by dissolving the remaining sample film in 1 cc. of benzene, spreading the aliquot of the solution on a slightly acidified aqueous substrate, and determining, under a constant surface pressure, its limiting area, which is proportional to the amount of the remaining sample film. The results are shown in Fig. 4. We can see a break point on the 10th day similar to that found in Fig. 1. Thus we confirm that the evaporation is the main cause of these phenomena, as will be more precisely established later. Here the question arises as to whether this is exclusively due to the evaporation of the impurity. However, the weight loss during ten days is too large to explain the impurity, considering the m. p. of 43.5°C observed for the lauric acid and that of 75.5°C for the lauryl amide used. The presence of a volatile impurity has also been denied since in such a case we should have a simple horizontal straight line instead of the curve of Fig. 4, on account of the rapid evaporation of any such impurity from a spread monolayer for all samples.

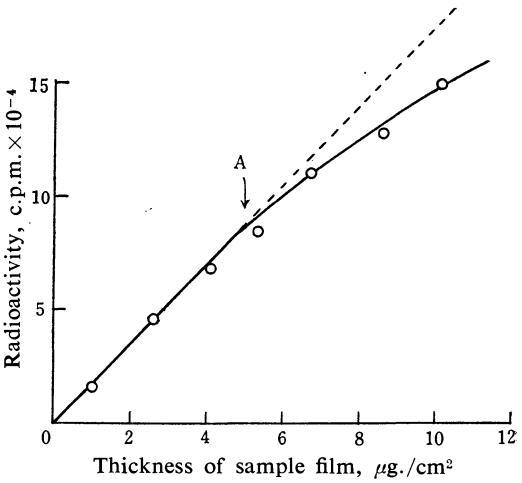

Fig. 5. The counting-rate-versus-sample-thickness curve.
A, Upper limit of linearity

However, the results did not agree with this expectation.

(2) If the phenomena are mainly due to the evaporation of volatile tritiated impurities, the slow decreasing curve attained after ten days, as shown in Fig. 1, is to be explained by the evaporation loss of impurities extending far deep from the solid surface contributing only a little to the actual loss in the β-counting rate. This critical depth roughly corresponds to point A of the counting rate curve shown in Fig. 5. This would indicate that the anomalies shown in Fig. 1 are largely independent of the film thickness, at least for a sufficiently thick film. However, the diagram for the extremely thick film of 530 μg./cm^2 proved to be practically a horizontal line, without a break, even after 10 days or more. These findings are contrary to the above expectation. The possibility of any other short-life radio-nuclide causing these phenomena can be excluded, since the radioactivity of the sample was completely absorbed with a sheet of thin polyethylene or paraffin paper about 3 mg./cm^2 thick.

The Evaporation of Lauric Acid and the Possible Explanation of the Phenomena. — According to the reasoning of the preceding section, the anomalies shown in Fig. 1 can reasonably be explained on the basis of the evaporation of the lauric acid film itself. This is further confirmed by comparing the β-counting rate of the samples of lauric acid films prepared from a benzene solution by evaporating it at 16.5 and 50°C. The marked evaporation at the higher temperature is evident, as may be seen in Fig. 6. As to the detailed explanation of the phenomena in terms of the evaporation of the lauric acid film, the heterogeneity of the deposited film should be pointed out, since a homogeous film and a uniform evaporation result, rather, in a simple straight line of a negative slope, without a break point. In fact, when a drop of lauric acid is put on the dish, most of it spreads as a thin film, while some portion remains as minute droplets. The solvent then evaporates, leaving lauric acid in a thin, uniform film with many clusters scattered upon it. Some of those can even be traced by the naked eyes. This behavior is quite similar to oleic acid on the water surface, which results in a monolayer and liquid droplets.

Therefore, a brief consideration indicates that the radioactive thin film of the thickness of a simple Gaussian-like distribution, as shown by A or B in Fig. 7(II), when exposed to the uniform evaporation, shows a decrease in radioactivity, as is illustrated by A or B in Fig. 7(I), according to whether the thickness is smaller or larger than the critical thickness of the self-absorption of tritium β-radiation, as is shown in Fig. 7(II). Neither of these curves can alone explain the observed curves of Fig. 1.

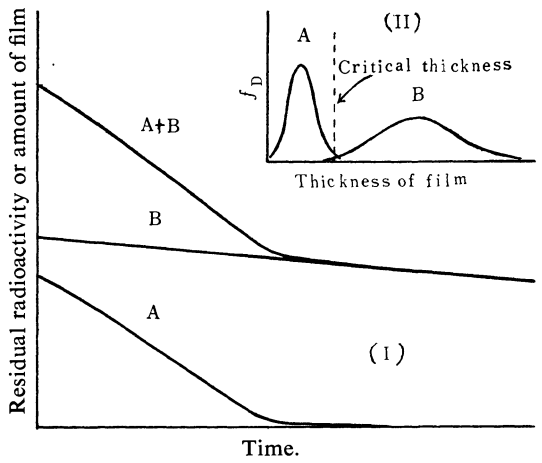

Fig. 7. A diagram showing the decrease in the counting rate depending on the thickness distribution of thin film. (I)A and (I)B indicate the c.p.m.-versus-time curves for the evaporation of films of the f_D thickness-distribution curve shown in (II)A (steep and narrow) and (II)B (flat and broad) respectively. (I)A+B represents c.p.m.-versus-time curve for the film composed of A and B. The dotted line represents the critical thickness for self-absorption.

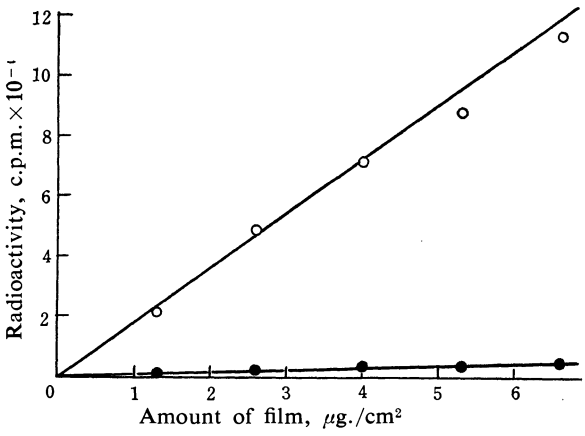

Fig. 6. The effect of the drying temperature on the counting rate of film.
○ Film prepared at 16.5°C
● Film prepared at 50°C

To explain the observed characteristics of the evaporation curve, a film having at least two peaks in the thickness-distribution curve, as in Fig. 7(II), should be taken into account. The composite evaporation curve of such a film is illustrated by curve A+B in Fig. 7(I), which closely resembles the actual evaporation curve. The abrupt decrease with time in surface area and, accordingly, in the slope of the counting-rate-versus-time curve is produced after the complete evaporation of the thinner film, A. The fact that the time of the appearance of the break point is largely independent of the amount of film taken is an indication of the relative constancy of the thickness distribution of the thinner film, which requires about ten days for complete evaporation.

The smaller inclination after the break point

corresponds to the rate of evaporation only from the thicker portion of film B. The disappearance of the break point for the film 530 μg./cm^2 thick may be explained as resulting from the initial deposit being sufficiently thick and consisting exclusively of film B. According to the results of our experiment, the thickness distribution of film A is considered to be constant, at least in the region of apparent thickness from 4 to 10 μg./cm^2. The thickness distribution presumably shifts towards a thinner region for a film of a much smaller apparent thickness, since the break point for the film of, say, 1 μg./cm^2 appeared five days earlier than the above film, as is shown in Fig. 8. It

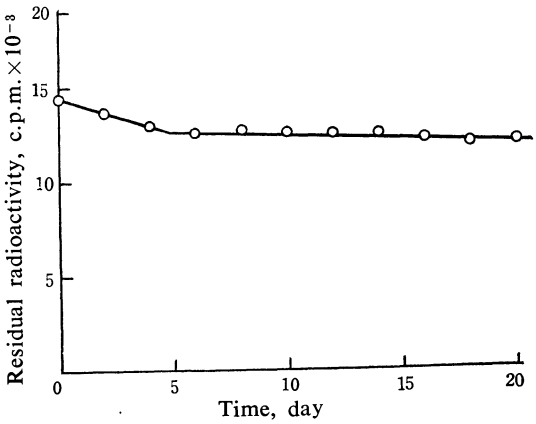

Fig. 8. The counting-rate-versus-time curve for the thinner film of 1 μg./cm^2.

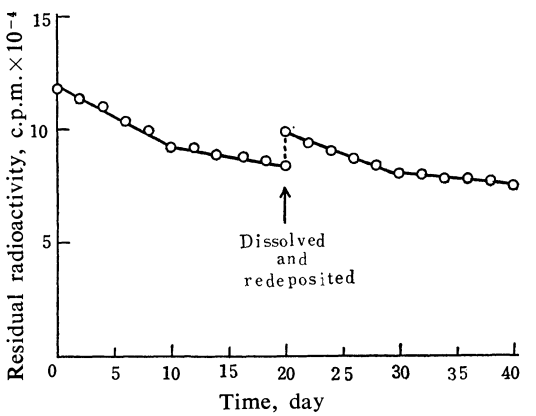

Fig. 9. The effect of the dissolution and redeposition of film on the counting-rate-versus-time curve.

should also be mentioned that the film already in the stage of a slow decrease in counting rate beyond the break point, when dissolved completely with benzene and redeposited by evaporation, again repeats all the changes of the curve of Fig. 1, as is shown in Fig. 9. This can be explained by the fact that the portion of film B still remaining thicker than the critical thickness at this stage and not contributing to the counting rate, when redeposited, produces a considerable amount of film A again, as is shown in Fig. 7(II). The slight increase in the counting rate (shown by the arrow in Fig. 9) when the film is redeposited can also be explained by the appearance of film A. It must be added that the experimental results showing the absence of the gas-flowing effect on the evaporation of the sample (cf. Fig. 2) seems, at first sight, to contradict our conclusion. However, it may be that the air current is insufficient to show the effect of evaporation in any perceptible amount in the case of such a small vapor pressure and rate of evaporation as those of lauric acid.

Summary

A thin film of α,β-ditritiated lauric acid $CH_3(CH_2)_8(CHT)_2COOH$ deposited from benzene on a stainless steel dish and put in a 2π gas-flow windowless counter gave a counting rate which decreased far more rapidly than was expected from the natural decay of the β-activity of tritium. We observed a distinct break point in the decay curve ten days after the deposition of the film, independent of the amount of sample taken, provided that the film was sufficiently thin.

Various factors, such as impurities, surface migration, exchange reaction and evaporation, were considered to explain the phenomena; among these the evaporation of the lauric acid from the deposited surface film of the composite structure was proved to be the main factor responsible for these phenomena.

In conclusion, the authors wish to express their thanks to the Ministry of Education for the Scientific Research Expenditure Grant given to Tsunetaka Sasaki.

Department of Chemistry
Faculty of Science
Tokyo Metropolitan University
Setagaya-ku, Tokyo

The Crystal Structure of Ethylenediammonium Chloride

By Tamaichi ASHIDA and Sakutaro HIROKAWA

(Received February 25, 1963)

Ethylenediamine, as a ligand of the coordination compounds, has been studied by several authors[1-4]. In these crystals, ethylenediamine usually has a gauche-configuration. However, ethylenediamine in other types of compounds has not been sufficiently investigated. In the structure of ethylenediammonium sulfate[5], for instance, though it has not been fully studied, the ethylenediammonium ion has been reported to have a gauche-configuration. On the other hand, in ethylenediammonium adipate, of which only the crystallographic data have been reported[6], a planar and a trans-configuration can be expected on the basis of the data, because the ethylenediammonium ion seems to have a center of symmetry. Thus, the ethylenediammonium ion seems to have either a trans- or a gauche-configuration. Ethylenediammonium chloride was chosen to be investigated in order to add to the data on the trans- and gauche-stereoisomerism of the ethylenediammonium ion. The results of the investigation will be given here.

Recently, tetramethylenediammonium chloride has also been investigated by the present authors from a similar view-point. These results will be published later.

Experimental

The crystals of ethylenediammonium chloride, $H_3N(CH_2)_2NH_3Cl_2$, were grown from an ethylalcohol-water solution. Most of the crystals were obtained as needles elongated along the c axis, while others were obtained as plates, the main face of which was (0 0 1). This difference may be due to slight changes in the conditions of the recrystallizations. A marked cleavage was found perpendicularly to the c axis, as had been reported by Groth[7]. The crystals belong to the monoclinic system. The unit cell dimensions were obtained from the Weissenberg photographs of $(h\,0\,l)$ and $(h\,k\,0)$ by overlapping the powder patterns of aluminum as a standard on the same films; they are;

$$a=9.95\pm0.01 \qquad b=6.89\pm0.01$$
$$c=4.42\pm0.01\text{Å} \qquad \beta=90.7\pm0.3^\circ$$

and $$a:b:c=1.449:1:0.642$$

The axial ratios of the present investigation agree with the values given by Groth[7] to within the stated range of experimental error, though the β-angles differ a little from one other. The values given by Groth are:

$$a:b:c=1.4439:1:0.6439$$

and $$\beta=91^\circ35'$$

The space group of the crystal was found to be $P2_1/a$ from the systematic absences of the $(0\,k\,0)$ spectrum for $k=2n+1$ and the $(h\,0\,l)$ spectrum for $h=2n+1$. The density, 1.46 g. cm^{-3}, observed by the floatation method corresponds to two formula units in a unit cell; the calculated density is 1.46 g. cm^{-3}.

Weissenberg photographs were taken around the b and c axes, using Cu$K\alpha$ radiation. The multiple-film technique was used, and the intensities of the $(h\,0\,l)$, $(h\,k\,0)$ and a part of the $(h\,k\,1)$ reflections were estimated visually, comparing them with a standard scale made by the same crystal. The corrections for polarization and Lorentz factors were made. No absorption corrections were made because the shapes of the crystals used were irregular; they should have been made, however, because the linear absorption coefficient for Cu$K\alpha$ radiation is rather large ($\mu=85.0\,\text{cm}^{-1}$).

Structure Determination

Since the crystal belongs to the $P2_1/a$ space group and the number of formula units in a unit cell is two, the ethylenediammonium ion has to occupy a center of symmetry. The position of the chloride ion was determined from the projections of the Patterson function along the b and c axes. The projections of the electron-density functions along the two principal axes were synthesized using the structure factors whose phases were assigned by the coordinates of the chloride ion. The maps thus obtained showed the positions of the carbon and the nitrogen atoms. The coordinates of the atoms thus obtained were, then, refined by successive (F_o-F_c) syntheses. In these procedures, it was found that the

1) A. Nakahara, Y. Saito and H. Kuroya, This Bulletin, **25**, 331 (1952).
2) Y. Saito, K. Nakatsu, M. Shiro and H. Kuroya, *Acta Cryst.*, **8**, 729 (1955).
3) H. Scouloudi, ibid., **6**, 651 (1953).
4) M. R. Truter and E. G. Cox, *J. Chem. Soc.*, **1956**, 948.
5) Y. Okaya and I. Nitta, *Acta Cryst.*, **5**, 564 (1952).
6) S. Hirokawa, T. Ohashi and I. Nitta, ibid., **7**, 87 (1954).
7) P. Groth, "Chemische Krystallographie", Vol. III, Engelman, Leipzig (1910), p. 52.

contributions of the hydrogen atoms to the structure factors were not negligible (the electrons which belong to the hydrogen atoms amount to 14% of the total number of electrons in the crystal). Therefore, the coordinates of all the hydrogen atoms were calculated geometrically, using the coordinates of the heavier atoms, and the presences of these hydrogen atoms were confirmed on the $(\rho_o-\rho_c)$ maps. They were included in the calculations of the structure factors, which were used in the further refinements of the structure, whereupon the R factors of two zones decreased by about 0.02. The final $(\rho_o-\rho_c)$ maps of $(h\,0\,l)$ are shown in Fig. 1, where significant changes due to the inclusion or exclusion of the hydrogen atoms are observed not only at the positions of the hydrogen atoms but also almost everywhere. The final atomic coordinates of the heavier atoms are listed in Table I. The isotropic temperature factors assigned for the atoms are: 2.66 for all the atoms for $F(h\,0\,l)$, and 1.40, 0.86, 0.91 and 1.00 for C, N, Cl^- and H's respectively for $F(h\,k\,0)$. Each absolute value of these temperature factors may not have significance, because no absorption corrections for the intensities were made. The observed and the calculated structure factors are compared in Table II. The final

Table I. Final atomic coordinates

	x	y	z
C	0.026	0.072	0.118
N	0.083	0.241	0.954
Cl^-	0.1703	0.5803	0.4058

Table II. Observed and calculated structure factors

In each column, the left hand column is the h index, the middle column the observed structure factor, and the right hand column, the calculated structure factor. All structure factors have been multiplied by ten.

$(h\,0\,l)$			−10	174	158	$(h\,k\,0)$			11	87	96	5	89	80
$h\,0\,0$			−12	42	47	$h\,0\,0$			12	39	36	6	0	− 16
2	24	42	$h\,0\,3$			2	40	42	$h\,3\,0$			7	40	40
4	178	−174	0	40	57	4	187	−193	1	0	10	8	111	110
6	241	241	2	196	−213	6	245	275	2*	272	441	9	181	−162
8	160	−151	4	139	144	8	200	−210	3	52	50	10	95	− 87
10	21	− 24	6	61	− 68	10	38	− 43	4	255	−264	$h\,6\,0$		
12	142	116	8	203	−189	12	211	219	5	0	6	0	316	−382
$h\,0\,1$			10	68	58	$h\,1\,0$			6	0	− 6	1	49	− 48
0	75	− 73	− 2	138	133	1	57	− 41	7	18	11	2	52	59
2	220	224	− 4	271	−278	2	33	− 29	8	101	87	3	34	− 34
4	299	297	− 6	33	36	3*	304	564	9	22	14	4	96	96
6	321	−326	− 8	116	117	4*	260	−356	10	308	−297	5	0	− 6
8	12	− 29	−10	53	− 56	5	173	−151	11	0	− 18	6	183	−185
10	102	98	$h\,0\,4$			6	0	2	12	9	16	7	28	− 29
12	111	− 88	0	141	−154	7	91	− 82	$h\,4\,0$			8	147	142
− 2	724	693	2	156	175	8	156	146	0	67	− 57	9	0	6
− 4	58	− 52	4	59	− 60	9	202	223	1	274	−274	$h\,7\,0$		
− 6	246	−232	6	108	−112	10	85	− 74	2	122	117	1	33	34
− 8	220	220	8	61	62	11	141	−135	3	0	5	2	21	− 24
−10	0	9	− 2	93	−101	12	0	11	4	20	− 2	3	230	−245
−12	35	− 28	− 4	78	79	$h\,2\,0$			5	186	172	4	119	121
$h\,0\,2$			− 6	131	−135	0	136	164	6	220	−201	5	104	104
0	249	243	− 8	0	5	1*	191	−425	7	250	−267	6	0	− 10
2	272	282	$h\,0\,5$			2	162	−156	8	29	32	7	50	63
4	313	−335	0	82	96	3	16	− 15	9	17	− 17	$h\,8\,0$		
6	32	19	2	80	− 68	4	45	27	10	60	51	0	123	−115
8	0	1	4	0	− 13	5	221	195	11	75	77	1	156	151
10	170	−158	− 2	90	− 94	6	264	282	$h\,5\,0$			2	56	56
− 2	364	−339	− 4	121	−109	7	245	−280	1	91	96	3	23	21
− 4	152	173				8	62	− 49	2	60	57	4	0	2
− 6	41	47	− 6	61	64	9	0	11	3	272	−283	5	86	− 89
− 8	123	−126				10	55	− 67	4	237	−242			

* These reflections were not used for the refinements because of their marked extinction effects.

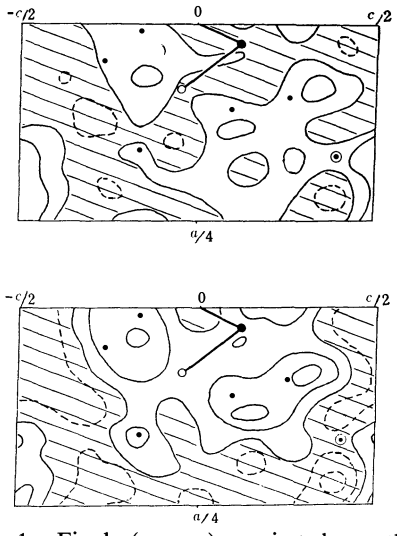

Fig. 1. Final $(\rho_o-\rho_c)$ projected on the (0 1 0). (a) : ρ_c includes all the atoms; (b) : ρ_c does not include any hydrogen atoms. Contours at intervals of 0.4 e. Å^{-3}, broken lines represent negative contours, and negative areas are shaded.
● C ○ N ⊙ Cl • H

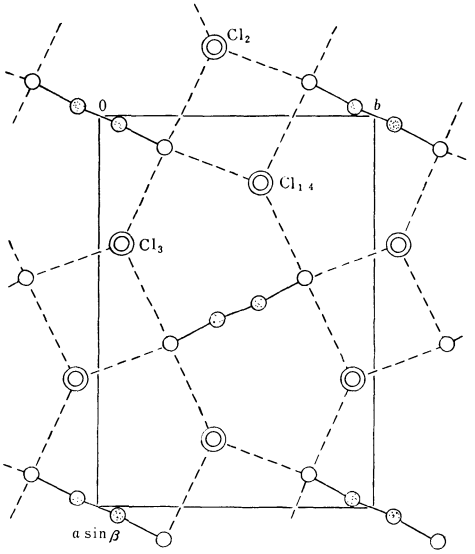

Fig. 2. The structure of ethylenediammonium chloride projected on the (0 0 1). Broken lines represent hydrogen bonds.
◎ C ○ N ◎ Cl

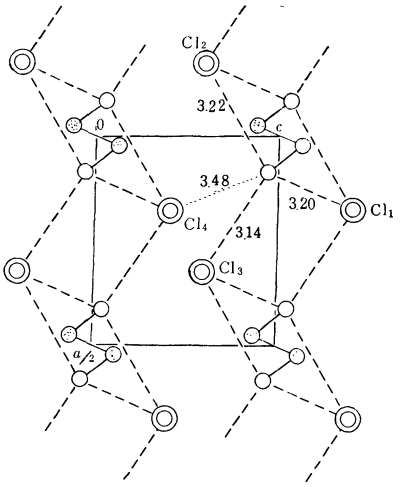

Fig. 3. The structure of ethylenediammonium chloride projected on the (0 1 0). Broken lines represent hydrogen bonds. A dotted line shows another short contact between N and Cl$^-$.
◎ C ○ N ◎ Cl

R factors are 0.065 for all the observed reflections of $(h\,0\,l)$ and 0.081 for $(k\,k\,0)$, excluding four reflections which showed marked extinction effects (these are shown with asterisks in Table II).

Discussion

In Table III, some of the important interatomic distances and bond angles in this crystal are shown. Because the ethylenediammonium ion occupies a center of symmetry, the ion has a trans-configuration and the N-C-C-N chain of the ion is geometrically planar. The equation of the plane is:

$$0.895X-0.448Y-0.020Z=0$$

where $X=ax\sin\beta$, $Y=by$ and $Z=cz+ax\cos\beta$. Thus, in the crystals, the ethylenediammonium ion was found to have either a trans- or a gauche-configuration, depending on the structure of the crystals.

TABLE III. IMPORTANT INTERATOMIC DISTANCES (Å) AND ANGLES (deg.)

C-C	1.53	CCN	109.8
C-N	1.49		
		CNCl(1)	111.5
N-Cl(1)	3.20	CNCl(2)	103.8
N-Cl(2)	3.22	CNCl(3)	106.0
N-Cl(3)	3.14	Cl(1)NCl(2)	103.9
		Cl(1)NCl(3)	111.3
N-Cl(4)	3.48	Cl(2)NCl(3)	120.5
Cl(3)-Cl(4)	3.89		

The crystal structures projected on the (0 1 0) and the (0 0 1) planes are shown in Figs. 2 and 3. The nitrogen atom's three nearest neighbors are chloride ions (Cl(1), Cl(2) and Cl(3), cf. Figs. 2 and 3), the N-Cl distances being 3.20, 3.22 and 3.14 Å respectively. These N-Cl lengths may be compared

to the values 3.11 and 3.24Å found in hexamethylenediammonium chloride[8] and to many others[9]. Thus, these short contacts may be said to be hydrogen bonds, when we consider the $<$CNCl or $<$ClNCl angles shown in Table III and the positions of the hydrogen atoms shown in Fig. 1. One N–Cl contact 3.48Å in length may not have significance, judging from the argument given above, and such a length has also been reported in hexamethylenediammonium chloride[8] (3.37 and 3.58Å). The shortest Cl–Cl distance is 3.88Å, between those chloride ions which are related to each other by a twofold screw axis. Thus, in this crystal, the three N–H···Cl hydrogen bonds binds the organic ions and the chloride ions and make infinite two-dimensional networks perpendicular to the c axis. The forces which combine these layers along the c axis may be van der Waals forces, together with weak electrostatic forces, if any. These facts explain the perfect cleavage along the (0 0 1) plane.

8) W. P. Binnie and J. M. Robertson, *Acta Cryst.*, **2**, 180 (1949).

9) G. C. Pimentel and A. L. McClellan, "The Hydrogen Bond", W. H. Freeman and Co., San Francisco (1960), p. 290.

Summary

The crystal structure of ethylenediammonium chloride has been determined. The crystal belongs to the monoclinic system with $a=9.95$, $b=6.89$, $c=4.42$Å and $\beta=90.7°$; the space group is $P2_1/a$. The unit cell contains two ethylenediammonium ions and four chloride ions. The ethylenediammonium ion occupies a center of symmetry and takes a transform; thus, the ethylenediammonium ion was found to be either a trans- or a gauche-form in the crystals, depending on the structures of the crystals. The bond distances and angles of the ethylenediammonium ion are: C–C 1.53, C–N 1.49Å and $<$CCN 109.8°. Three N–H···Cl hydrogen bonds (3.20, 3.22 and 3.14Å) make two-dimensional networks of the ions perpendicular to the c axis.

Department of Chemistry
Defense Academy
Yokosuka

The Color Reactions of Lower Oxoacids[1] of Phosphorus with Molybdate and their Application to Colorimetric Determinations of $\overset{4}{P}-\overset{3}{P}-\overset{4}{P}-$ and $(-\overset{3}{P}-)_6$-Acid[2]

By Shigeru OHASHI and Norimasa YOZA

(Received February 28, 1963)

In the last ten years a number of salts of new, lower oxoacids of phosphorus have been reported[3]. Blaser and Worms[4,5] have synthesized a series of alkali salts of lower oxoacids by the oxidation of red phosphorus. Some of them, such as $\overset{4}{P}-\overset{3}{P}-\overset{4}{P}-$ and $(-\overset{3}{P}-)_6$-acid, are compounds in which more than two phosphorus atoms are bound directly. The former has a chain structure, while the latter has a ring structure. More recently two compounds, $\overset{4}{P}-\overset{4}{P}-O-\overset{4}{P}-\overset{4}{P}-$ and $(-\overset{4}{P}-\overset{4}{P}-O-)_2$-acid, which are obtained by the polymerization of $\overset{4}{P}-\overset{4}{P}$-acid have been reported[6].

It is well known that the $\overset{5}{P}$-acid reacts with molybdate in a mineral acid solution to produce molybdophosphate and that the resulting yellow salt produces a blue color in the presence of a reducing agent. In this paper the authors describe the color reactions of lower oxoacids of phosphorus with molybdate in

1) In this paper the authors use the term "lower oxoacids of phosphorus" for oxoacids of phosphorus with a lower oxidation number than 5.

2) These acids do not yet have chemical names. The authors use the notations proposed by Blaser and Worms for these two acids as well as for other oxoacids of phosphorus because of their simplicity. The Arabic numerals attached to the phosphorus atoms represent the oxidation numbers of the phosphorus atoms. See B. Blaser and K.-H. Worms, *Z. anorg. u. allgem. Chem.*, **300**, 225 (1959). The structural formulas of lower oxoacids of phosphorus represented by the notations are shown in Table I.

3) Reviewed by S. Ohashi, *Kagaku-no-Ryoiki (Tokyo)*, **15**, 926 (1961).

4) B. Blaser and K.-H. Worms, *Z. anorg. u. allgem. Chem.*, **300**, 250 (1959).

5) Ibid., **300**, 237 (1959).

6) Ibid., **311**, 313 (1961).

TABLE I. COLOR REACTIONS OF OXOACIDS OF PHOSPHORUS WITH MOLYBDATE IN THE NEUTRAL AND THE ACID SOLUTION

Oxoacids		In the neutral solution	In the acid solution	
Abbreviated formulas	Structural formulas		No reducing agent	In the presence of amidol
^{1}P-Acid	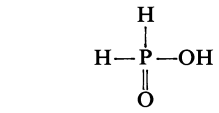	No	No	No
^{3}P-Acid	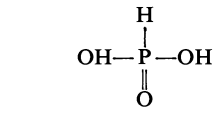	No	No	No
^{5}P-Acid	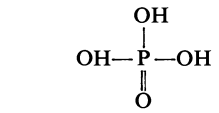	No	Yellow	Blue
^{3}P-O-^{3}P-Acid	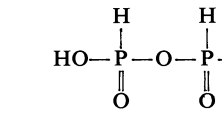	No	No	No
^{3}P-O-^{5}P-Acid	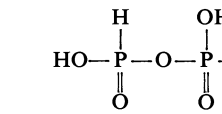	No	Yellow	Blue
^{5}P-O-^{5}P-Acid	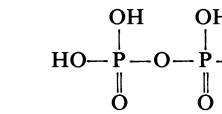	No	No	Blue
^{2}P-^{4}P-Acid	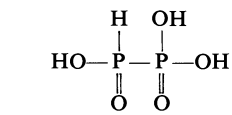	No	Bluish green	Blue
^{4}P-^{4}P-Acid	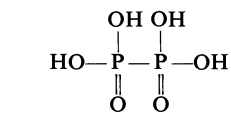	No	No	Blue
^{3}P-O-^{4}P-^{4}P-Acid	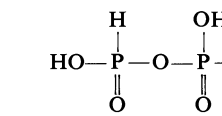	No	No	Blue
^{5}P-O-^{4}P-^{4}P-Acid	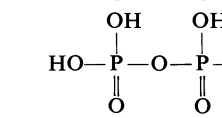	No	Yellow	Blue
^{4}P-^{4}P-O-^{4}P-^{4}P-Acid	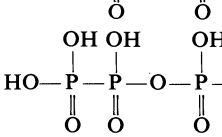	No	No	Blue
$(-^{4}P$-^{4}P-O-$)_2$-Acid	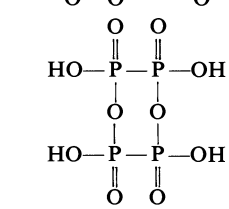	No	No	Blue

Table I. (Continued)

Oxoacids: Abbreviated formulas	Oxoacids: Structural formulas	In the neutral solution	In the acid solution: No reducing agent	In the acid solution: In the presence of amidol
$\overset{4}{P}\text{-}\overset{3}{P}\text{-}\overset{4}{P}$-Acid	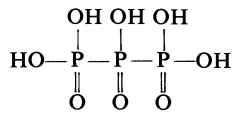	No	Bluish green	Blue
$(\text{-}\overset{3}{P}\text{-})_6$-Acid	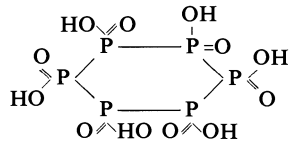	Bluish green (unstable)	Bluish green	Blue

neutral or acid solutions. Samples include twelve lower oxoacids as well as $\overset{5}{P}$- and $\overset{5}{P}\text{-O-}\overset{4}{P}$-acid.

The authors found that three of the fourteen oxoacids, $\overset{2}{P}\text{-}\overset{4}{P}$-, $\overset{4}{P}\text{-}\overset{3}{P}\text{-}\overset{4}{P}$- and $(\text{-}\overset{3}{P}\text{-})_6$-acid, show characteristic color reactions with molybdate; i. e., the three oxoacids react with molybdate in acid solutions to produce a blue color without any reducing agent. These chemical properties give a means for the analysis of these compounds, especially for colorimetric determinations of $\overset{4}{P}\text{-}\overset{3}{P}\text{-}\overset{4}{P}$- and $(\text{-}\overset{3}{P}\text{-})_6$-acid.

Experimental

Materials and Equipment.—An aqueous solution of guaranteed reagent-grade ammonium molybdate tetrahydrate and an amidol (1-amino-2-naphthol-4-sulfonic acid) solution for a reducing agent were prepared by Nakamura's method[7].

Sample solutions of salts of fourteen oxoacids of phosphorus were prepared; $NaPH_2O_2 \cdot H_2O$ was used for $\overset{1}{P}$-acid, $Na_2PHO_3 \cdot 5H_2O$ for $\overset{3}{P}$-acid, $Na_2HPO_4 \cdot 12H_2O$ for $\overset{5}{P}$-acid, $Na_2P_2H_2O_5$ for $\overset{3}{P}\text{-O-}\overset{3}{P}$-acid, $Na_3P_2HO_6 \cdot 4H_2O$ for $\overset{3}{P}\text{-O-}\overset{5}{P}$-acid, $Na_4P_2O_7 \cdot 10H_2O$ for $\overset{5}{P}\text{-O-}\overset{5}{P}$-acid, $Na_3P_2HO_5 \cdot 12H_2O$ for $\overset{2}{P}\text{-}\overset{4}{P}$-acid, $Na_2H_2P_2O_6 \cdot 6H_2O$ for $\overset{4}{P}\text{-}\overset{4}{P}$-acid, $(CN_3H_6)_4P_3HO_8 \cdot$ aq. (guanidinium salt) for $\overset{3}{P}\text{-O-}\overset{4}{P}\text{-}\overset{4}{P}$-acid, $(NH_4)_5P_3O_9 \cdot$aq. for $\overset{5}{P}\text{-O-}\overset{4}{P}\text{-}\overset{4}{P}$-acid, $Na_6P_4O_{11} \cdot$aq. for $\overset{4}{P}\text{-}\overset{4}{P}\text{-O-}\overset{4}{P}\text{-}\overset{4}{P}$-acid, $Na_4P_4O_{10} \cdot 4H_2O$ for $(\text{-}\overset{4}{P}\text{-}\overset{4}{P}\text{-O-})_2$-acid, $Na_5P_3O_8 \cdot 14H_2O$ for $\overset{4}{P}\text{-}\overset{3}{P}\text{-}\overset{4}{P}$-acid, $(K(Na)PO_2)_6 \cdot$aq.[8] for $(\text{-}\overset{3}{P}\text{-})_6$-acid. The salts of $\overset{1}{P}$-, $\overset{3}{P}$-, $\overset{5}{P}$- and $\overset{5}{P}\text{-O-}\overset{5}{P}$-acid were commercial reagents, while the others were supplied by Blaser and Worms. It was confirmed by paper chromatography that all of these compounds were pure.

Measurements of absorbances were carried out with a Shimadzu spectrophotometer QB-50, with glass cells 1.00 cm. in width.

Paper Chromatography.—An ascending technique was employed. A basic solvent recommended by Thilo and Heinz[9] was made by mixing 150 ml. of 2-methyl-1-propanol, 190 ml. of ethanol, 225 ml. of water, and 3 ml. of concentrated aqueous ammonia. A spray reagent was made according to the method of Hanes and Isherwood[10] by mixing 5 ml. of 60% perchloric acid, 1 ml. of concentrated hydrochloric acid, and 1 g. of ammonium molybdate tetrahydrate, and diluting it to 100 ml. with distilled water. Rectangular battery jars and Toyo No. 51A filter papers were used.

Color Reactions and Measurement of Absorbances. — Three series of 10 ml. of 1% ammonium molybdate solutions were prepared. One of them was neutral (only dissolved in distilled water), and the others were 1 N acid solutions in relation to perchloric acid. One milliliter of the respective sample solutions (about 10^{-2} M) was added to each series of the molybdate solutions, and 1 ml. of an amidol solution was added to one of the series of acid solutions. They were shaken well, and the color reactions were observed for an hour at room temperature.

Five milliliters of the 10% ammonium molybdate solution and 10 ml. of a 5 N perchloric acid solution were added to a 50 ml. volumetric flask. It was diluted to 30 ml. with distilled water, and then each sample solution was added. The concentration of the sample, $\overset{4}{P}\text{-}\overset{3}{P}\text{-}\overset{4}{P}$- or $(\text{-}\overset{3}{P}\text{-})_6$-acid, was adjusted to $10^{-3} \sim 10^{-5}$ M. The volume was brought up to the 50 ml. mark with distilled water. The mixture was shaken well and, after 30 min., the absorbances were measured in the range of 400 to 800 mμ wavelength, using a reagent solution as a reference.

Determination of Total Phosphorus.—All the phosphorus in a sample was converted into $\overset{5}{P}$-acid and determined colorimetrically. Five milliliters of aqua regia were added to a 25 ml. flask containing

7) M. Nakamura, *J. Agr. Chem. Soc. Japan (Nippon Nogei Kagaku Kaishi)*, **24**, 1 (1950).

8) This salt is mainly composed of the potassium salt of $(\text{-}\overset{3}{P}\text{-})_6$-acid, but it contains a small amount of the sodium salt of the acid.

9) E. Thilo and D. Heinz, *Z. anorg. u. allgem. Chem.*, **281**, 303 (1955).

10) C. S. Hanes and F. A. Isherwood, *Nature*, **164**, 1107 (1948).

1 ml. of the sample solution. It was evaporated gently on the water bath so as to decompose and oxidize the lower oxoacid. The residue was dissolved and then diluted to 25 ml. with distilled water. An aliquot of the solution was transferred to a 25 ml. volumetric flask, and 10 ml. of the 5 N perchloric acid solution, 5 ml. of the 10% ammonium molybdate solution, 20 ml. of distilled water, and 5 ml. of the amidol solution were added. It was brought up to the mark with distilled water, shaken well and, after 30 min., the absorbance at 780 mμ, using a reagent solution as a reference.

Results and Discussion

The color reactions of fourteen oxoacids of phosphorus with ammonium molybdate were tested. The results are summarized in Table I, $\overset{1}{P}$–, $\overset{3}{P}$– and $\overset{3}{P}$–O–$\overset{3}{P}$–acid give no color reaction in either the neutral or the acid solutions, even in the presence of the reducing agent.

It is well-known that $\overset{5}{P}$–acid does not show any color change in a neutral solution but does give a yellow color in an acid solution, and that the yellow heteropoly acid changes into a blue compound in the presence of a reducing agent such as amidol. $\overset{3}{P}$–O–$\overset{5}{P}$– and $\overset{5}{P}$–O–$\overset{4}{P}$–$\overset{5}{P}$–acid show the same behavior as $\overset{5}{P}$–acid does, because they are readily hydrolyzed in the acid solution to produce $\overset{5}{P}$–acid. $\overset{5}{P}$–O–$\overset{5}{P}$–Acid gives no detectable yollow color in the acid solution because of the slower rate of hydrolysis of the $\overset{5}{P}$–O–$\overset{5}{P}$–acid in comparison with the other compounds containing a $\overset{5}{P}$–unit.

Four compounds which contain a $\overset{4}{P}$–$\overset{4}{P}$–unit and no $\overset{5}{P}$–unit show a blue color only in the presence of amidol. This may be because of the hydrolysis of $\overset{4}{P}$–$\overset{4}{P}$–acid into $\overset{3}{P}$– and $\overset{5}{P}$–acid in the acid solution[11].

$\overset{2}{P}$–$\overset{4}{P}$–Acid produces a faint bluish green color (absorbance, about 0.04) in the acid solution, when the concentration of the $\overset{2}{P}$–$\overset{4}{P}$–acid is 10^{-3} M. In the concentrations more than 10^{-3} M, it colors semiquantitatively, but the reproducibility is not good. It was shown by paper chromatography that a main product of the reaction is $\overset{3}{P}$–acid due to the hydrolytic decomposition of the $\overset{2}{P}$–$\overset{4}{P}$–acid. The bluish-green coloration may be due to the redox reaction between molybdenum(VI) and the $\overset{2}{P}$–$\overset{4}{P}$–acid, where a part of the $\overset{2}{P}$–$\overset{4}{P}$–acid is oxidized into $\overset{4}{P}$–$\overset{4}{P}$–acid and a part of the molybdenum(VI) is reduced to molybdenum(V).

$\overset{4}{P}$–$\overset{3}{P}$–$\overset{4}{P}$–Acid shows a bluish-green color reaction only in the acid solution. $(-\overset{3}{P}-)_6$–Acid produces bluish-green colors in both the neutral and the acid solution. However, the bluish-green color caused by the $(-\overset{3}{P}-)_6$–acid in the neutral solution is very unstable; its intensity diminishes rapidly with time.

By paper chromatography distinct spots of $\overset{3}{P}$– and $\overset{4}{P}$–$\overset{4}{P}$–acid and a faint spot of $\overset{5}{P}$–acid were detected in the reaction products of the $\overset{4}{P}$–$\overset{3}{P}$–$\overset{4}{P}$–acid and molybdate in the acid solution. It appears reasonable to consider the following scheme for this reaction:

$$\overset{4}{P}\text{–}\overset{3}{P}\text{–}\overset{4}{P}\text{–Acid} \begin{cases} \xrightarrow{A} \overset{3}{P}\text{–Acid} + \overset{4}{P}\text{–}\overset{4}{P}\text{–Acid} \\ \xrightarrow{B} \overset{5}{P}\text{–Acid} + \overset{4}{P}\text{–}\overset{4}{P}\text{–Acid} \end{cases}$$

Path A is the hydrolysis of the $\overset{4}{P}$–$\overset{3}{P}$–$\overset{4}{P}$–acid, and path B is the oxidation of the acid by molybdate. The larger part of the $\overset{4}{P}$–$\overset{3}{P}$–$\overset{4}{P}$–acid is decomposed by path A and the smaller part of the acid by path B.

The reaction between $(-\overset{3}{P}-)_6$–acid and molybdate in the acid solution seems to be more complicated. Unfortunately, paper chromatographic identification of the reaction products was not certain. On the paper chromatogram a spot of $\overset{3}{P}$–acid was observed, but spots of other species were spread near the initial point.

The authors found that the bluish-green color produced by the reaction of $\overset{4}{P}$–$\overset{6}{P}$–$\overset{4}{P}$– or $(-\overset{3}{P}-)_6$–acid with molybdate in the acid solution is quite stable, at least in the range of

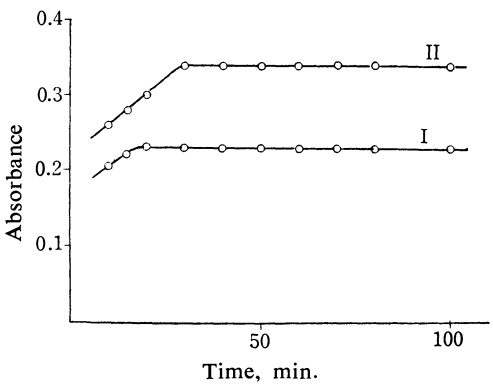

Fig. 1. Stability of bluish green color.
I $\overset{4}{P}$–$\overset{3}{P}$–$\overset{4}{P}$–acid, 4.42×10^{-4} M
II $(-\overset{3}{P}-)_6$–acid, 6.41×10^{-5} M

11) J. R. Van Wazer, "Phosphorus and its Compounds", Interscience Publishers, Inc., New York (1958), p. 410.

TABLE II. SIMULTANEOUS DETERMINATIONS OF $^{4}_{}P\text{-}^{3}_{}P\text{-}^{4}_{}P$- AND $(-^{3}_{}P\text{-})_6$-ACID

No.	Taken, mol./l.		Found, mol./l.			
	$^{4}_{}P\text{-}^{3}_{}P\text{-}^{4}_{}P$-Acid	$(-^{3}_{}P\text{-})_6$-Acid	$^{4}_{}P\text{-}^{3}_{}P\text{-}^{4}_{}P$-Acid	Error, %	$(-^{3}_{}P\text{-})_6$-Acid	Error, %
1	—	4.85×10^{-5}	—	—	4.81×10^{-5}	0.8
2	4.51×10^{-4}	—	4.52×10^{-4}	0.22	—	—
3	1.80×10^{-3}	4.85×10^{-5}	1.83×10^{-3}	1.6	4.20×10^{-5}	13
4	9.02×10^{-4}	4.85×10^{-5}	8.87×10^{-4}	1.4	4.80×10^{-5}	1.0
5	4.51×10^{-4}	4.85×10^{-5}	4.51×10^{-4}	0.00	4.83×10^{-5}	0.41
6	4.51×10^{-4}	9.70×10^{-5}	4.55×10^{-4}	0.89	9.77×10^{-5}	0.72
7	1.50×10^{-4}	1.62×10^{-4}	1.51×10^{-4}	0.66	1.60×10^{-4}	1.2
8	1.50×10^{-5}	1.62×10^{-4}	1.89×10^{-5}	25	1.60×10^{-4}	1.2

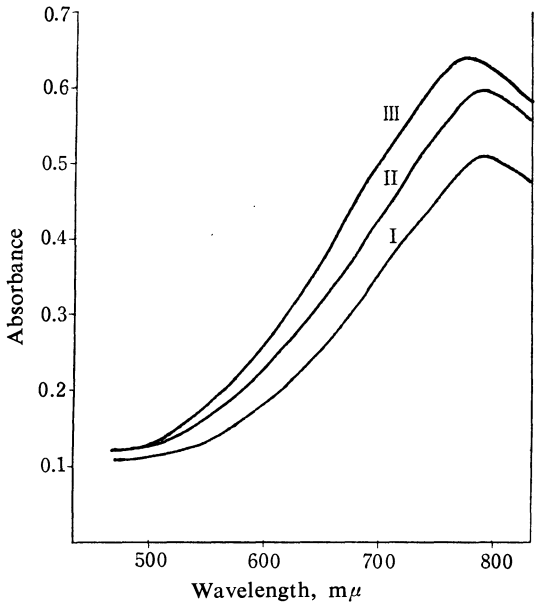

Fig. 2. Absorption curves of bluish green solutions.

I $^{2}_{}P\text{-}^{4}_{}P$-acid, 7.4×10^{-3} M

II $^{4}_{}P\text{-}^{3}_{}P\text{-}^{4}_{}P$-acid, 1.21×10^{-3} M

III $(-^{3}_{}P\text{-})_6$-acid, 1.21×10^{-4} M

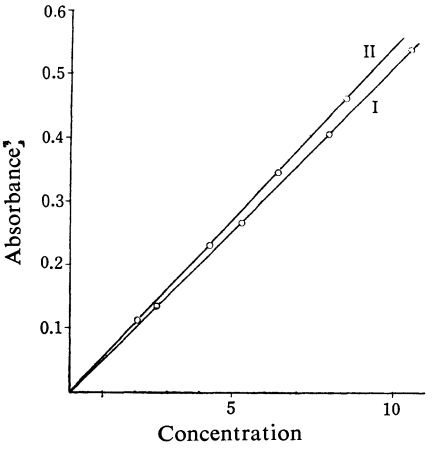

Fig. 3. Calibration curves for $^{4}_{}P\text{-}^{3}_{}P\text{-}^{4}_{}P$- and $(-^{3}_{}P\text{-})_6$-acid at 780 mμ.

10^{-4} M unit for $^{4}_{}P\text{-}^{3}_{}P\text{-}^{4}_{}P$-acid (I)

10^{-5} M unit for $(-^{3}_{}P\text{-})_6$-acid (II)

30~100 min., as is shown in Fig. 1. The absorption curves of the bluish-green colors due to $^{2}_{}P\text{-}^{4}_{}P$-, $^{4}_{}P\text{-}^{3}_{}P\text{-}^{4}_{}P$- and $(-^{3}_{}P\text{-})_6$- acid are shown in Fig. 2. The curves are similar to one another, having their maxima at 780~785 mμ. An absorption curve of so-called heteropoly blue[12] produced by the reduction of molybdophosphate has a shape similar to the curves of Fig. 2, but it has its maximum at 830 mμ.

The molar extinction coefficients for $^{4}_{}P\text{-}^{3}_{}P\text{-}^{4}_{}P$- and $(-^{3}_{}P\text{-})_6$-acid at 780 mμ are 5.09×10^{2} and 5.30×10^{3} respectively. As is shown in Fig. 3, they comform well to Beer's law at 780 mμ.

Experimental results show that $^{1}_{}P$-, $^{3}_{}P$-, $^{5}_{}P$-, $^{4}_{}P\text{-}^{4}_{}P$- (10^{-2} M, respectively),-and $^{2}_{}P\text{-}^{4}_{}P$-acid (less than 5×10^{-4} M) do not inhibit the quantitative color development of $^{4}_{}P\text{-}^{3}_{}P\text{-}^{4}_{}P$- or $(-^{3}_{}P\text{-})_6$-acid in the acid solution. $^{2}_{}P\text{-}^{4}_{}P$-Acids more than 10^{-3} M increase distinctly the absorbance of the bluish-green color.

The methods described above are satisfactory when one component, either $^{4}_{}P\text{-}^{3}_{}P\text{-}^{4}_{}P$- or $(-^{3}_{}P\text{-})_6$-acid, is present, accompanying other oxoacids of phosphorus, in a given sample, but it is not applicable if the two components are both present. When both $^{4}_{}P\text{-}^{3}_{}P\text{-}^{4}_{}P$- and $(-^{3}_{}P\text{-})_6$-acid are present in a given sample, the problem is resolved by combining this method with another procedure in which lower oxoacids are converted into $^{5}_{}P$-acid and the total phosphorus is

12) D. F. Boltz, "Colorimetric Determination of Nonmetals", Interscience Publishers, Inc., New York (1958), p. 33.

determined by the usual heteropoly blue method. The concentrations of $\overset{4}{P}\text{–}\overset{3}{P}\text{–}\overset{4}{P}$– and $(\text{–}\overset{3}{P}\text{–})_6$–acid are obtained by calculating the absorbances measured by both methods. In this case it should be noted that three and six moles of $\overset{5}{P}$–acid are produced by the oxidation of one mole of $\overset{4}{P}\text{–}\overset{3}{P}\text{–}\overset{4}{P}$– and $(\text{–}\overset{3}{P}\text{–})_6$–acid respectively. The experimental results are shown in Table II. The errors for the components of the lower concentrations in Nos. 3 and 8 of Table II are so large that the application of apply this method most be avoided in cases where the differences between the concentrations of the two components are large.

Summary

The color reactions of twelve lower oxoacids of phosphorus, as well as of $\overset{5}{P}$– and $\overset{5}{P}\text{–O–}\overset{5}{P}$–acid with molybdate, have been described. Of these compounds, $\overset{2}{P}\text{–}\overset{4}{P}$–, $\overset{4}{P}\text{–}\overset{3}{P}\text{–}\overset{4}{P}$– and $(\text{–}\overset{3}{P}\text{–})_6$–acid react with molybdate in the acid solution to produce a bluish-green color without any reducing agent.

The bluish-green color caused by $\overset{2}{P}\text{–}\overset{4}{P}$–acid is not reproducible. Since the colors caused by $\overset{4}{P}\text{–}\overset{3}{P}\text{–}\overset{4}{P}$– and $(\text{–}\overset{3}{P}\text{–})_6$–acid are stable and since their intensities are proportional to their concentrations, one can detect and determine minute amounts of $\overset{4}{P}\text{–}\overset{3}{P}\text{–}\overset{4}{P}$– or $(\text{–}\overset{3}{P}\text{–})_6$–acid colorimetrically in the presence of the other oxoacids of phosphorus. When both $\overset{4}{P}\text{–}\overset{3}{P}\text{–}\overset{4}{P}$– and $(\text{–}\overset{3}{P}\text{–})_6$–acid are present in a given sample, one can determine each component by combining the method described above with the usual heteropoly blue method for the total phosphorus.

The authors wish to express their hearty thanks to Professor Jun Yoshimura for his kind suggestions made in the course of this work. The authors also wish to thank Dr. Bruno Blaser and Dr. Karl-Heinz Worms for supplying the samples used in this study.

Department of Chemistry
Faculty of Science
Kyusyu University
Hakozaki, Fukuoka

The Preparation of Trimethylamine Oxide Complexes and Some Infrared Studies

By Sigeo KIDA

(Received March 4, 1963)

Metal complexes of pyridine *N*-oxide have been prepared, and their infrared studies have been recently reported[1-3]. In these investigations, it has been shown that pyridine *N*-oxide readily combines with various metal ions in organic solvents to form metal complexes, and that the infrared frequency of the N–O stretching vibration of pyridine *N*-oxide considerably shifts to lower frequencies upon coordination to metal ions (1265→1220∼1200 cm^{-1}). This shift has been attributed to a change in the contribution of the various resonance structures of pyridine *N*-oxide as a result of the coordination. In other words, the N–O stretching vibration shifts to a lower frequency, as the double bond character of the N–O bond decreases upon coordination A considerable difference in the behavior of the N–O stretching vibration would be expected in the case of trimethylamine oxide, since its N–O bond has no double-bond character. Infrared and Raman studies of trimethylamine oxide have been reported[4-8];

1) J. V. Quagliano, J. Fujita, G. Franz, D. J. Phillips, J. A. Walmsley and S. Y. Tyree, *J. Am. Chem., Soc.*, **83**, 3770 (1961).
2) S. Kida, J. V. Quagliano, J. A. Walmsley and S. Y. Tyree, *Spectrochimica Acta*, **19**, 189 (1963).
3) Y. Kakiuti, S. Kida and J. V. Quagliano, ibid., **19**, 201 (1963).
4) J. Goubeau and I. Fromme, *Z. anorg. u. allgem. Chem.*, **258**, 18 (1949).
5) J. T. Edsall, *J. Chem. Phys.*, **5**, 225 (1937).
6) J. Wagner, *Z. physik. Chem.* **40B**, 36 (1938).
7) R. Matis-Noel, R. Wolf and F. Gallais, *Compt. rend.*, **242**, 1873 (1956).
8) A. Giguere and D. Chin, *Can. J. Chem.*, **39**, 1214 (1961).

however, no investigation of its metal complexes has yet been reported*.

In the present investigation, it was attempted to prepare the metal complexes of trimethylamine oxide by the procedure used in the case of pyridine *N*-oxide, but it was found difficult, with the exception of the cobalt(II) complex, to obtain pure crystals of the products. The zinc(II) and cadmium(II) complexes were prepared as pure crystals by careful dehydration of the starting materials, but other metal ions, such as iron(II), nickel(II), copper(II), aluminum(III), chromium(III) and iron(III), failed to give pure products.

Matis-Noel et al.[7] measured the infrared spectra of trimethylamine oxide and its derivatives and assigned the strong band at 952 cm^{-1} to the N–O stretching vibration. This assignment was based only upon a comparison of the spectrum of trimethylamine oxide with those of its derivatives; it does not seem to be a definite assignment. In fact, in trimethylamine oxide the N–O stretching vibration may probably be coupled with the other mode of vibration. Hence, in the present investigation, the normal coordinate treatment has been carried out on trimethylamine oxide, and the discussion has been extended to the metal complexes.

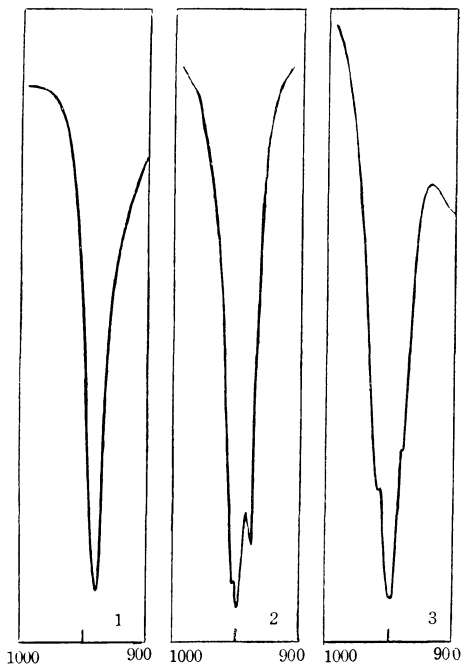

Fig. 1

1; Trimethylamine oxide in bromoform solution
2: Trimethylamine oxide hydrochloride in KBr disk
3: Trimethylamine oxide in KBr disk

While this work was in progress, Giguere and Chin[8] published a paper on the infrared spectra of trimethylamine oxide and its hydrochloride. They assigned the 937 cm^{-1} and 945 cm^{-1} bands to the N–O and the N–C stretching vibrations respectively. However, it appears to the present author that these two bands are due to a splitting of what should appear as a single band in a free molecule. One should be aware of the fact that a single band observed in solution or in a gaseous state may sometimes split into a couple of bands in the solid state. In fact, the frequencies of these two bands are close together, and the present experiment shows that, in a bromoform solution, only one band can be observed in this region; no splitting has ever been observed, as is shown in Fig. 1. Also, no such splitting was observed in the Raman investigation[4].

Experimental

Preparation of the Compounds.—*Trimethylamine Oxide.*—The hydrate, $(CH_3)_3NO \cdot 2H_2O$, was first distilled under reduced pressure, then resublimed twice in vacuo.

Tetrakis (Trimethylamine Oxide) Cobalt(II) Nitrate.—To a solution of 2.0 g. of trimethylamine oxide in 10 ml. of 95% ethanol was added 1.0 g. of cobalt(II) nitrate hexahydrate dissolved in 10 ml. of 95% ethanol. The resulting deep blue-violet solution was evaporated to half volume and cooled in a refrigerator. The blue-violet crystals which were formed were collected on a glass filter, washed with ethanol, and dried in vacuo over phosphoric anhydride.

Found: C, 25.56; H, 6.46; Co, 10.62. Calcd. for $[Co\{(CH_3)_3NO\}_4](NO_3)_2$: C, 25.81; H, 6.50; Co, 10.56%.

Tetrakis (Trimethylamine Oxide) Cobalt(II) Perchlorate.—The compound was prepared as described for the corresponding nitrate from cobalt(II) perchlorate hexahydrate and trimethylamine oxide in ethanol. Deep blue-violet crystals were obtained. The compound melts at 207°C and explodes at 213°C.

Found: C, 25.56; H, 6.46; N, 10.30; Co, 10.62. Calcd. for $[Co\{(CH_3)_3NO\}_4](ClO_4)_2$: C, 25.81; H, 6.50; N, 10.34; Co, 10.56%.

Tetrakis (Trimethylamine Oxide) Zinc(II) Perchlorate.—Eight-tenth grams of zinc(II) perchlorate, previously dried over phosphoric anhydride in vacuo, was dissolved in 15 ml. of absolute ethanol. This solution was added to 1.7 g. of trimethylamine oxide dissolved in 15 ml. of absolute ethanol. The mixture was kept in a refrigerator overnight. The white fine crystals which were

* Recently, the preparation of $CoBr_2L_2$ and $MnBr_2L_2$ (where L denotes trimethylamine oxide) has been reported: K. Isslied and A. Kreibich, *Z. anorg. u. allgem. Chem.*, 313, 338 (1961).

precipitated were separated, washed with absolute ethanol, and desiccated over phosphoric anhydride. All these procedures were carried out in a dry box. The compound decomposes in the presence of moist air or moist solvents and melts at 210~230°C with decomposition.

Found: C, 25.13; H, 6.62; Zn, 11.29; Calcd. for $[Zn\{(CH_3)_3NO\}_4](ClO_4)_2$: C, 25.52; H, 6.62; Zn, 11.58%.

Tetrakis (Trimethylamine Oxide) Zinc(II) Nitrate.—This compound was prepared by the method described above for the corresponding perchlorate, using zinc(II) nitrate instead of zinc(II) perchlorate. The white crystals have properties similar to those of the corresponding nitrate and melt at 169°C with decomposition.

Found: C, 29.43; H, 7.21; Zn, 13.36. Calcd. for $[Zn\{(CH_3)_3NO\}_4](NO_3)_2$: C, 29.42; H, 7.41; Zn, 13.35%.

Tetrakis (Trimethylamine Oxide) Cadmium(II) Nitrate.—One gram of trimethylamine oxide was dissolved in 5 ml. of absolute methanol, and to this solution was added 0.45 g. of cadmium(II) nitrate which had been dried over phosphoric anhydride in vacuo and dissolved in 10 ml. of absolute methanol. The solvent was evaporated in an evacuated desiccator at room temperature. The resulting fine white crystals were collected on a glass funnel, washed with absolute ethanol, and desiccated over phosphoric anhydride. All these procedures were carried out in a dry box. M. p., 172°C.

Found: C, 26.53; H, 6.94; Cd, 20.89. Calcd. for $[Cd\{(CH_3)_3NO\}_4](NO_3)_2$: C, 26.85; H, 6.76; Zn, 20.94%.

Absorption Measurements.—The infrared spectra were obtained using a Perkin-Elmer infrared spectrophotometer model 221 equipped with a grating (4000~1400 cm^{-1}), an NaCl prism (1400~650 cm^{-1}), and a CsBr prism (680~300 cm^{-1}). All the spectra were obtained in Nujol mulls. The spectra in KBr disks were also obtained in the NaCl region and were checked against those in Nujol.

Calculation of Normal Vibrations

Considering the methyl group to be a dynamic unit, the skeletal vibrations of trimethylamine oxide have been treated as those of a five-body model of the point group C_{3v}.

The secular equation was set up according to Wilson's[9] procedure, using a potential function of the Urey-Bradley type[10,11].

The symmetry coordinates for this calculation are the following:

$$S_1 = \Delta r_1$$

$$A_1 \quad S_2 = 1/\sqrt{3} \cdot \Delta(r_2 + r_3 + r_4)$$

$$S_3 = 1/\sqrt{6} \cdot \Delta(\alpha_{12} + \alpha_{13} + \alpha_{14} - \alpha_{34} - \alpha_{42} - \alpha_{23})$$

$$S_{4a} = 1/\sqrt{6} \cdot \Delta(2r_2 - r_3 - r_4)$$

$$E \quad S_{5a} = 1/\sqrt{6} \cdot \Delta(2\alpha_{12} - \alpha_{13} - \alpha_{14})$$

$$S_{6a} = 1/\sqrt{6} \cdot \Delta(2\alpha_{34} - \alpha_{42} - \alpha_{23})$$

$$S_{4b} = 1/\sqrt{2} \cdot \Delta(r_3 - r_4)$$

$$E \quad S_{5b} = 1/\sqrt{2} \cdot \Delta(\alpha_{13} - \alpha_{14})$$

$$S_{6b} = 1/\sqrt{2} \cdot \Delta(\alpha_{42} - \alpha_{23})$$

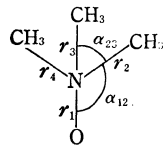

The bond angles are regarded as tetrahedral, 109°28'. For the bond length, the values $r_{NO}=1.44$ and $r_{NC}=1.49$ Å, were used according to Rundle[12]. The force constants and intermolecular tension, κ, used in the calculation are shown in Table I. The values of F', the linear term of the interaction between non-bonded atoms, were determined using the relation, $F' = -1/10 \cdot F$[13].

TABLE I. FORCE CONSTANTS IN 10^5 dyn./cm. AND INTERMOLECULAR TENSION IN 10^{-11} dyn. cm. OF TRIMETHYLAMINE OXIDE

K		H		F		κ
N-O	2.30	O-N-CH_3	0.30	O···CH_3	0.80	0.05
N-CH_3	3.40	CH_3-N-CH_3	0.40	CH_3···CH_3	0.35	

Results and Discussion

The observed infrared frequencies are shown in Table II. They coincide with Giguere and Chins' values within the range of minimum experimental error. The assignment of the bands of the methyl group can be made as shown in the table according to the commonly accepted group frequencies of the methyl group[14]. Regarding the symmetry of the trimethylamine oxide molecule as a point group C_{3v}, there should be 3 non-degenerate vibrations in A_1 and 3 degenerate vibrations in E. Using the force constant values listed in Table I, we have obtained the results shown in Table III, in which each calculated frequency is related to the observed value. The values in Table I have been selected to produce the best agreement between the observed and calculated frequencies, but they also seem to be reasonable if compared with the values used in the calculation of trimethylamine[15] and tetramethylammonium ion[5] ($K=3.63$, $H=0.459$, $F=0.615$, for the former and $K=2.18$, $H=0.43$,

9) E. B. Wilson, Jr., *J. Chem. Phys.*, **7**, 1047 (1939).
10) H. C. Urey and C. A. Bradley, *Phys. Rev.*, **38**, 1963 (1931).
11) T. Shimanouchi, *J. Chem. Phys.*, **17**, 245 (1949).
12) R. E. Rundle, private communication quoted by P. W. Allen and L. E. Sutton in *Acta Cryst.*, **3**, 46 (1950).
13) T. Shimanouchi, *J. Chem. Soc. Japan, Pure Chem. Sec.* (*Nippon Kagaku Zassi*), **74**, 266 (1953).
14) For instance, L. J. Bellamy, "Infrared Spectra of Complex Molecules", 2nd Ed., Methuen, London, (1958); K. Nakanishi, "Infrared Absorption Spectra", Nankodo, Tokyo (1960).
15) K. Shimizu, *J. Chem. Soc. Japan, Pure Chem. Sec.* (*Nippon Kagaku Zassi*), **77**, 1103 (1956).

TABLE II. OBSERVED INFRARED FREQUENCIES (cm^{-1}) OF TRIMETHYLAMINE OXIDE, THE HYDROCHLORIDE AND THE METAL COMPLEXES

Trimethylamine oxide (=L)		Hydrochloride	[Co L_4]-$(ClO_4)_2$	[Zn L_4]-$(ClO_4)_2$	[Zn L_4]-$(NO_3)_2$	[Cd L_4]-$(NO_3)_2$	
**	in $CHBr_3$	*	**	**	*	*	Assignment
1465 s	1470 s	1465 s	1490 s	1490 sh	1490 s	1479 sh	CH_3 deg. def.
	1451 s	1450 s	1470 s	1470 s	1470 s		
1400 m	1395 m	1429 m	1395 m	1395 m	1365 vs, b (NO_3^-)	1365 vs, b (NO_3^-)	CH_3 sym. def.
1245 s	—[1]	1259 s	1240 m	1245 s	1245 m	1245 m	CH_3 rock.
1125 m	—[1]	1124 m			1121 w	1127 m	C-N str. (E)
			1090 vs (ClO_4^-)	1090 vs (ClO_4^-)			
960 vw, sh		953 vw, sh					
948 s	940 s	948 s	947 sh	963 s	960 s	950 s	N-O str. (A_1)
941 w,		939 w	940 s	958 s	950 sh		
892 m, b						894 m, b	
865 m, b							
					827 m (NO_3^-)	835 m (NO_3^-)	
755 s	757 s	750 vs	765 s	770 s	770 s	757 s	C-N str. and N-O str. (A_1)
623 s, b	—[1]	—[3]	621 s (ClO_4^-)	621 s (ClO_4^-)	—[3]	—[3]	
	—[1]	—[3]			—[3]	—[3]	
509 m	536 m[2]	—[3]	563 s	560 s	—[3]	—[3]	C-N-O def. (E)
491 m	492 m	—[3]					
464 s	457 m	—[3]	480 s	478 s	—[3]	—[3]	C-N-O def. and C-N-C def. (A_1)
383 s	379 s	—[3]	405 m	402 m	—[3]	—[3]	C-N-C def. (E)
		—[3]	382 m	382 m	—[3]	—[3]	

* In KBr
** In KBr 1500~650 cm^{-1} and in Nujol 650~300 cm^{-1}
1) Strong solvent absorption
2) Obscure due to the solvent absorption
3) No good spectrum was obtained.
Abbreviations: L=trimethylamine oxide; s=strong; m=medium; w=weak; sh=shoulder; v=very

TABLE III. THE OBSERVED AND THE CALCULATED FREQUENCIES (cm^{-1}) OF THE SKELETAL VIBRATIONS OF TRIMETHYLAMINE OXIDE

Symmetry class	Raman[4]	IR[a]	Calcd.	Vibrational mode (c/o Table IV)
	945	948	961	N-O str.
A_1	759	755	771	$N-CH_3$ str. and N-O str.
	439	464	504	CH_3-N-O def. and CH_3-N-CH_3 def.
	1135	1125	1076	$N-CH_3$ str.
E	494	509 491	528	CH_3-N-O def.
	304	383	431	CH_3-N-CH_3 def.

a) In KBr 1500~650 cm^{-1} and in Nujol 650~300 cm^{-1}

F=0.35, for the latter), considering that the nature of the C-N bond of trimethylamine oxide is intermediate between those of these compounds. Furthermore, no alternative assignments of the vibrations which have been tried so far have given reasonable results. Goubeau and Fromme[4] had calculated the frequencies of trimethylamine oxide using the central force field and had related each calculated frequency to the observed one, although the agreement between the calculated and the observed frequencies were poor compared with that of the present calculcula-tions. Though the present assignment was carried out independently from that of Goubeau and Fromme, the results do not conflict with their results. Thus, the author believes these assignments to be correct.

The assignments of the skeletal vibrations shown in Table III are based on the results of the calculation of the potential energy distributions shown in Table V. The assignment of the band around 950 cm^{-1} does not conflict with that of Matis-Noel et al.[7], in

TABLE IV. POTENTIAL ENERGY DISTRIBUTIONS AMONG SYMMETRY COODINATES ($F_{ii}L^2_{i\lambda}$)

		ν_1	ν_2	ν_3
	S_1	0.3518	0.1434	0.0121
A_1	S_2	0.2685	0.1493	0.0203
	S_3	0.1956	0.0030	0.1063
		ν_4	ν_5	ν_6
	S_4	0.6493	0.0142	0.0021
E	S_5	0.0926	0.0911	0.0393
	S_6	0.0865	0.0362	0.0727

TABLE V. *J*-Matrices $\{\partial\nu/\partial K$ etc.; $\nu(\mathrm{cm}^{-1})$, K $(10^5$ dyn.$\cdot\mathrm{cm}^{-1})\}$

A_1				E			
	ν_1	ν_2	ν_3		ν_4	ν_5	ν_6
K_{NO}	82	42	5	K_{NC}	125	58	62
K_{NC}	49	34	7	H_{ONC}	4	116	55
H_{ONC}	141	3	145	H_{CNC}	0.6	62	128
H_{CNC}	146	3	150				

which the N–O stretching vibration mainly contributes to this band. However, Table IV shows that the N–C stretching and the deformation vibrations also considerably contribute to it. It has also been found that the N–O and the N–C stretching vibrations almost equally contribute to the band at 755 cm^{-1}. In the band at 1125 cm^{-1} a coupling with the deformation vibrations of the methyl group is possible to some degree, although in the present calculation this effect was not taken into consideration.

As may be seen in Table II, the vibrations of trimethylamine oxide do not shift much in the sodium chloride region upon coordination to metal ions. It is notable that the band at ~950 cm^{-1}, which is mainly contributed by the N–O stretching vibration, shows very little shift to the low frequency region. This makes a remarkable contrast to the relatively large shift in the N–O stretching vibration of pyridine *N*-oxide.

The very small shift of the N–O stretching vibration on coordination may be explained as follows: 1) The coordination effect is small because of the weak covalent character of the O-metal bond; 2) unlike pyridine *N*-oxide, trimethylamine oxide can not form π-bonding, and 3) this vibration is affected not only by the force constant K_{NO}, but also by K_{NC}, H_{CNC} and H_{CNO}. Therefore, even if K_{NO} is changed on coordination, the frequency shift of this band could considerably be canceled by the simultaneous change of the other force constants (as is understandable by looking at the *J*-matrix in Table IV). It is not certain at the present stage which of these factors is mainly responsible for the observed spectral behavior.

The skeletal deformation vibrations appear in the cesium bromide region. As is shown in Table II, these bands undergo a large change upon coordination. This may be due to 1) a change in the character of the N–O bond due to the formation of the O-metal bond, or 2) a change in the steric arrangement of the surrounding groups. However, the latter reason seems more plausible to the author, since not only the frequencies but also the contour of the splitting changes upon coordination. However, further investigation is necessary to reach a definite conclusion on this point.

In the pyridine *N*-oxide complexes of cobalt(II) and zinc(II), the O-metal stretching vibration was observed in the 319~331 cm^{-1} region[3]. In the present investigation, however, no crresponding band was found. It is possible that the band appears in a lower frequency region, below 300 cm^{-1}. One may, therefore, assume that the metal-O bonding of trimethylamine oxide complexes has a less covalent character than that of pyridine *N*-oxide complexes.

In addition to the bands mentioned above, broad bands were observed at 892 and 865 cm^{-1}, while a rather intense broad absortion appeared at 623 cm^{-1}. No fundamental vibrations could be assigned to these bands. In the Raman spectrum[4] no corresponding Raman lines were observed; all normal vibrations belonging to A_1 and E are infrared and Raman active in C_{3v} symmetry. They appear to be absorptions specific of the solid state (probably containing water), but no final conclusion can be drawn at present.

Summary

Metal complexes of trimethylamine oxide with cobalt(II), zinc(II) and cadmium(II) have been prepared.

The infrared spectra of trimethylamine oxide and its complexes have been measured in the 1500 to 300 cm^{-1} range. Assignment of the observed bands has been made on the basis of the calculation of the normal vibrations of trimethylamine oxide.

The band at 950 cm^{-1} was found to be mainly contributed by the N–O stretching vibration, as was expected from the former investigations, but it was also considerably contributed to by the other mode of vibrations.

The metal-O stretching band was not found in the region of the present investigation; consequently, a rather weak bond was assumed to exist between trimethylamine oxide and metal ions.

The experiments of this investigation were carried out in the Department of Chemistry,

Florida State University. The author wishes to express sincere thanks to Professor J. V. Quagliano of the Florida State University for his kind help and valuable suggestions throughout this work. He also wishes to thank to Professor Yuzo Kakiuti of Rikkyo St. Paul's University for his helpful advice and discussion.

Department of Chemistry
Wakayama University
Masago-cho, Wakayama

Thermal and Radiation Oxidations of Benzene to Phenol in Aqueous Solutions Containing Metal Ions at Elevated Temperatures. I. The Thermal Behavior of Iron Sulfate and Chloride in Aqueous Solutions without Benzene

By Hiroshi HOTTA and Nobutake SUZUKI

(Received January 9, 1963)

Benzene can be oxidized to phenol in an aerated aqueous solution by cobalt-60 gamma rays at room temperature[1]. The yield is improved in the presence of iron and copper ions[2,3]. It has been reported that the yield also increases somewhat above 130°C, even in the absence of any metal ions[4,5].

This subject has been studied also in this Laboratory in co-operation with a group of researchers at Showa Denko Co., Tokyo. Especially, the effect of metal ions on the oxidation reactions has been studied at elevated temperatures. The experiments were rather troublesome due to the corrosion of the reactor and the precipitation of metal ions. In order to clarify such complicated phenomena, the first problem was to understand the thermal behavior of metal salt aqueous solutions, used for benzene oxidation, without benzene at elevated temperatures. Therefore, the experimental methods employed in benzene oxidation were also used for this purpose. The results for iron sulfate and chloride aqueous solutions will be given in the present paper.

Experimental

Solutions. — G. R. reagents without further purification were dissolved initially by 0.01 M-Fe[6] in 0, 0.01 and 0.1 N sulfuric acid for ferrous and ferric sulfates or in hydrochloric acid of these concentrations for these chlorides.

Apparatus and Procedure.—A hard-glass reaction tube with a stopper, having a small hole for gas, was set tightly in a 50 ml. stainless-steel reactor. Fifteen ml. of the solution was put in the glass tube under oxygen pressure of 30 atm. The temperature was varied in all cases by the same procedure, using an electric controlling-heater, that is, a) the reactor was heated up to the given temperature during 30 min. by the heater (first-stage), b) kept at that temperature within ±1°C for 30 min. (middle-stage), and c) cooled outside the heater by a fan (final-stage). For reference, the same experiments were carried out without the middle stage to find the contribution of reactions during the first and final stages[7]. The temperature was measured by thermocouple set in the wall of the reacter.

Analytical.—The solutions after reaction were analyzed by a spectrophotometer as follows: The concentration of total iron species dissolved was determined from the optical density of ferric-oxine complex in chloroform at 470 mμ at pH=3.5~4.5 (0.0105 for 1 μg. iron species)[8], and the concentration of ferrous species in it from that of ferrous-α,α'-dipyridyl complex in an aqueous solution at 522 mμ at pH 3~9 (ε=8520), adding some potassium fluoride if necessary. The amount of ferric species in the aqueous phase and the amount of precipitated iron species were evaluated from these observed values. The original impurities, ferrous species in ferric solutions and vice versa, were $2\sim4\times10^{-5}$ M respectively.

Results

Ferric Sulfate and Chloride.—The ferric concentrations after experiment in ferric sulfate

1) P. V. Phung and M. Burton, *Radiation Research*, **7**, 199 (1957).
2) J. H. Baxendale and D. Smithies, *J. Chem. Soc.*, **1959**, 779.
3) H. Hotta and A. Terakawa, This Bulletin, **33**, 335 (1960).
4) M. A. Proskurnin and Y. M. Kolotyrkin, Proc. 2nd Conf. Peaceful Uses A. E., Geneva, **29**, 52 (1958).
5) E. J. Henley, J. Goodman and I. Tang, *Trans. Am. Nuclear Soc.*, **3**, No. 2, 387 (1960).
6) All the concentrations of solutions were initially 0.01 M of iron ion.
7) Such experiments are represented by the "reference experiment" in this series.
8) K. Motojima and H. Hashitani, *Japan Analyst* (*Bunseki Kagaku*), 151 (1960).

solutions dissolved by 0.01 M of ferric ion in 0, 0.01 and 0.1 N sulfuric acid respectively, are given by solid marks and solid lines in Fig. 1, with the results of the corresponding reference experiments given by open marks and dotted lines. The corresponding results for ferric chloride dissolved in hydrochloric acid are given in Fig. 2. The low values of the reference experiment at 75°C for the neutral ferric chloride solution was just equal to the value of the filtrate before experiment, namely, the saturated concentration at room temperature. All the ferrous concentrations after experiment for ferric salts were not so different from their initial concentration contained as impurities, namely, $(1\sim4)\times10^{-5}$ M.

The same results of ferric and ferrous concentrations as those in Fig. 1 were obtained within the range of experimental error between 130 and 200°C for the neutral ferric sulfate solution under the following conditions: a) with irradiation by cobalt-60 gamma rays for 25 min. at the middle-stage of the heating procedure (14000 r), and b) with and without the same irradiation under nitrogen pressure of 30 atm. Therefore, the precipitation

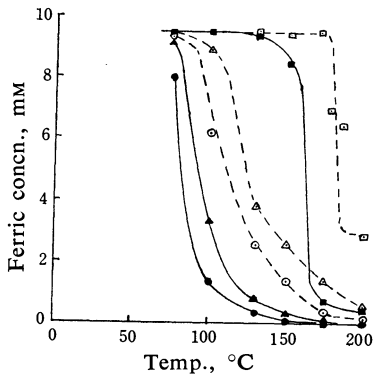

Fig. 1. Ferric concentration in 0.01 M-Fe ferric sulfate solutions after reaction (solid marks) with results of reference experiment (open marks); (⊙ and ●) in neutral, (△ and ▲) in 0.01 N and (▣ and ■) in 0.1 N sulfuric acid.

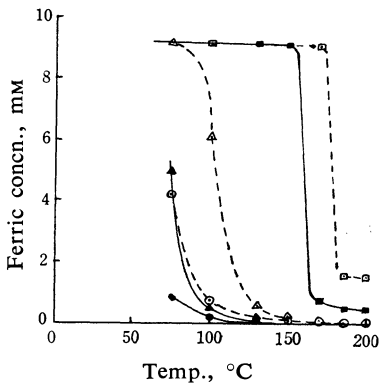

Fig. 2. Ferric concentration in 0.01 M ferric chloride solutions after reaction (solid marks) with results of reference experiment (open marks); (⊙ and ●) in neutral, (△ and ▲) in 0.01 N and (▣ and ■) in 0.1 N hydrochloric acid.

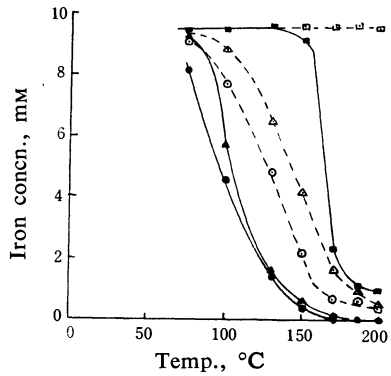

Fig. 3. Iron concentration in 0.01 M ferrous sulfate solutions after reaction with results of reference experiment; marks are the same with Fig. 1.

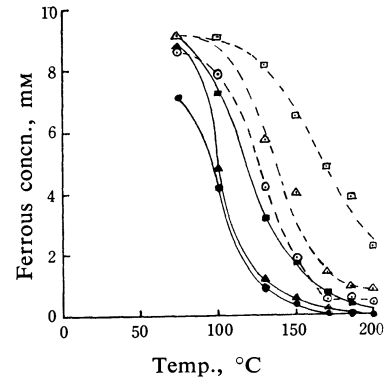

Fig. 4. Ferrous concentration in the results shown in Fig. 3; marks are the same with Fig. 1.

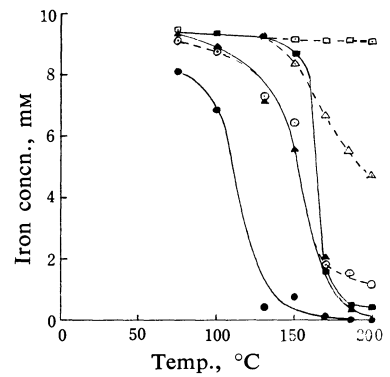

Fig. 5. Iron concentration in 0.01 M ferrous chloride solutions after reaction with results of reference experiment; marks are the same with Fig. 2.

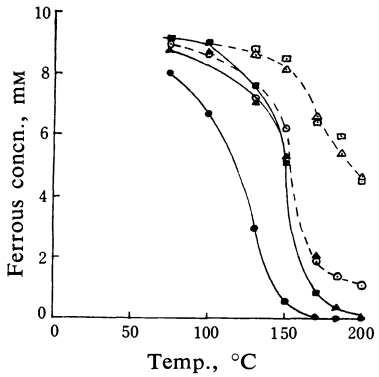

Fig. 6. Ferrous concentration in the results shown in Fig. 5; marks are the same with Fig. 2.

reaction is independent of oxygen and radiation. It is noted that the ferrous concentration dose not increase in all cases over that original impurities.

Ferrous Sulfate and Chloride.—The total iron and ferrous concentrations after experiment are shown in Figs. 3 and 4 for ferrous sulfate, and in Figs. 5 and 6 for ferrous chloride respectively.

Discussion

Oxidation of Ferrous Ions. — The oxidation of ferrous ions by oxygen in an aqueous solution is usualy assumed to be[9,10]

$$Fe^{2+} + O_2 + H^+ = Fe^{3+} + HO_2 \qquad (1)$$

The concentration of hydrogen ion for reaction 1 is supposed to be fairly higher at elevated temperatures than at room temperature due to the higher dissociation of iron salt and water[11].

Since the ferrous sulfate solution in 0.1 N sulfuric acid gave no precipitate at temperatures lower than 150°C (Fig. 3), the rate of ferrous oxidation, k_o, in such a non-precipitated system can be expressed as

$$\frac{dx}{dt} = k_o(a-x)$$

at a given oxygen pressure from reaction 1; that is,

$$k_o = \frac{1}{t} \ln \frac{a}{(a-x)} \qquad (i)$$

where a is the initial ferrous concentration, and x the amount which is oxidized in time t. On putting the observed value of the reference experiments to a and that of the actual experiments to $a-x$ in Eq. i, the oxidation rate, k_o, in 0.1 N sulfuric acid can be estimated as 1.24, 5.17 and 6.10×10^{-4} sec^{-1} at 100, 130 and 150°C respectively. Huffman and Davidson had estimated the rate to be 1.93×10^{-5} atm^{-1} sec^{-1} at 159°C, i. e., 6×10^{-4} sec^{-1} at 30 atm. of oxygen[12]. The activation energy, estimated from the present values is also nearly equal to their value, 13.4 kcal./mol.[12]

Similarly, the oxidation rates of ferrous chloride in 0.1 N hydrochloric acid are estimated as 0.83 and 2.78×10^{-4} sec^{-1} at 130 and 150°C respectively. These rates are slower than the above values of ferrous sulfate. The rate seems to increase as the complexing affinity of the anion for ferric ion increases[12,13]. However, the high oxidation rate in sulfuric acid may be partially due to decomposed products of sulfate ion, which is ignored in Eq. i.

Precipitation of Iron Species.—Milburn concluded, in his study of the hydrolysis of ferric ion at 25°C, that the dimerization of ferric monohydroxide is predominant in a solution more concentrated than 0.001 M[14]. In fact, more precipitate was found in the lower acidic solution. Therefore, it can be assumed that the precipitation reaction is through the dimerization of partially hydrolyzed ferric ions, for the equilibrium constant of ferric hydrolysis is much higher[15] and the stability of ferric hydroxide is lower[16] in comparison with ferrous species.

When the rate-determining step of the precipitation reaction is assumed from these facts to be bimolecular for the formal concentration of iron species in the solution, the precipitation rate, k_p, can be expressed as

$$\frac{dx}{dt} = k_p(a-x)^2$$

That is,

$$k_p = \frac{x}{ta(a-x)} \qquad (ii)$$

where a is the initial iron concentration in the solution, and x the amount of iron precipitate during time t.

The rates of the precipitation reaction, k_p, for ferric sulfate, estimated from Eq. ii like Eq. i, are plotted against the reciprocal of the absolute temperature in Fig. 7. This figure suggests that the ratio of the rates is 1.00 : 0.47 : 0.105 in 0, 0.01 and 0.1 N sulfuric

9) A. M. Posner, *Trans. Faraday Soc.*, **49**, 382 (1953).
10) M. Cher and N. Davidson, *J. Am. Chem. Soc.*, **77**, 793 (1955).
11) Intern. Critical Table, **6**, 152, McGraw-Hill Co. (1926).
12) R. E. Huffman and N. Davidson, *J. Am. Chem. Soc.*, **78**, 4856 (1956).
13) H. Hotta and S. Ohno, This Bulletin, **34**, 1640 (1961).
14) R. M. Milburn, *J. Am. Chem. Soc.*, **77**, 1352 (1955); **79**, 537 (1957).
15) B. O. A. Hedslröm, *Arkiv Kemi*, **5**, 457 (1953); **6**, 1 (1954).
16) W. F. Linke, "Solubilities of Inorganic and Metal-organic Compounds", Vol. 1, D. Van Nostrand Co., New York (1958), pp. 1038-1039.

TABLE I. X-RAY ANALYSIS OF PRECIPITATE

Solute	Solvent	Precipitation temp., °C		
		100	130	200
$Fe_2(SO_4)_3$	Water	Completely amorphous	—	α-Fe_2O_3
	0.1 N H_2SO_4	—	—	α-Fe_2O_3
$FeSO_4$	Water	—	Amorphous α-Fe_2O_3	α-Fe_2O_3
	0.1 N H_2SO_4	—	—	α-Fe_2O_3

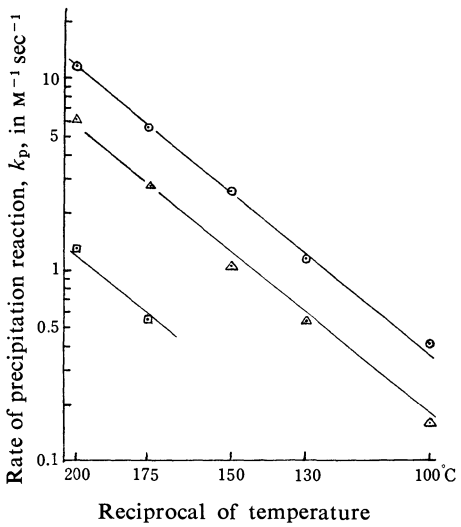

Fig. 7. Rate of precipitation reaction, k_p, from 0.01 M-Fe ferric sulfate aqueous solutions plotted against reciprocals of absolute temperature; (⊙) in neutral, (△) in 0.01 N sulfuric acid and (▣) in 0.1 N sulfuric acid.

acid over a wide range of temperature, and that the activation energy of this reaction is 12.5 kcal./mol. in this range of acid concentration. When the precipitation reaction is assumed as above, this ratio means the ratio of the proportions of hydrolyzed ions at the respective acidities, i. e., the ratio of the true reactants.

The precipitation in the ferrous solution should also be attributed to ferric hydroxide oxidized from ferrous species, for the precipitate is the same from the ferric solution as shown in Table I. (See the next section). When the results for the 0.1 N acid solutions shown in Figs. 1, 2, 3 and 5 are compared, it is noted that precipitation is independent of either sulfate or chloride species, but dependent on either ferric or ferrous species, and that the precipitation is retarded in the ferrous solution compared with the ferric, but there is no difference between ferric and ferrous species in the iron concentration after experimentation. On the other hand, when the ferric solution is heated with benzene, the precipitation is somewhat retarded upon the reduction of ferric ions, as will be shown in detail in the next paper. These facts also support the assumption about the precipitation as mentioned already.

Precipitates. — Since the precipitates, when dried in a vacuum, gave no pattern for X-ray analysis, they were dried for one day at 70°C. The results of their X-ray analysis are given in Table I; the precipitate at 100°C still did not give any pattern, but the one at 130°C gave a weak pattern of α-Fe_2O_3, and all the precipitates at 200°C gave a sharp pattern of α-Fe_2O_3 independent of ferrous and ferric sulfates. Therefore, it is concluded that the precipitate at the lower temperature is completely amorphous. The color varied from orange to brown with rise of the precipitation temperature.

According to Shipko and Douglas[17], the precipitate of ferrous hydroxide containing $Ni(OH)_2$ is decomposed spontaneously in this manner;

$$3Fe(OH)_2 = Fe_3O_4 + H_2 + 2H_2O \qquad (2)$$

with the activation energy of 10.2 kcal./mol. below 100°C, and the pure ferrous hydroxide is more stable, decomposing with the activation energy of 30 kcal./mol. at 150~200°C in the same manner. The former value for the amorphous precipitate is nearly equal to the activation energy from Fig. 7.

Summary

The rate of the ferrous oxidation at 150°C is 6.10×10^{-4} sec^{-1} for sulfate, and 2.78×10^{-4} sec^{-1} for chloride at the oxygen pressure of 30 atm. The precipitation reaction of iron species is through hydrolyzed ferric ions even in the ferrous solution. The rate of precipitation for ferric sulfate is given in Fig. 7, with the activation energy of 12.5 kcal./mol. The precipitate is amorphous at 100°C and completely α-Fe_2O_3 at 200°C.

The authors wish to express their appreciation to Mr. Akira Terakawa and Mr. Mitsuteru Nitto of the Showa Denko Co. for their kind

17) F. J. Shipko and D. L. Douglas, *J. Phys. Chem.*, **60**, 1519 (1956).

about the apparatus, and also to Mr. Toshio Honda of JAERI for his co-operation on the X-ray analysis.

Japan Atomic Energy Research Institute
Tokai, Ibaraki

Thermal and Radiation Oxidations of Benzene to Phenol in Aqueous Solutions Containing Metal Ions at Elevated Temperatures. II. The Effect of Iron Sulfate and Chloride on Phenol Yield

By Hiroshi HOTTA, Akira TERAKAWA[1], Kazuo SHIMADA and Nobutake SUZUKI

(Received January 9, 1963)

The yield of phenol in the thermal oxidation of gaseous benzene has been reported to be at its optimum at about 400°C in the presence of some organic promotors[2,3]. The thermal oxidation of benzene to phenol has usually been made at temperatures higher than 300°C, giving some amount of biphenyl as by-product.

As mentioned in the introduction to Part I of the present series[4], it is expected that benzene can be also oxidized to phenol with a good yield in the aqueous phase at lower temperatures by the use of cobalt-60 gamma rays. However, the irradiation method without metal salt also gives some amount of biphenyl[5]. On the other hand, it is well known that oxidation reaction is usually promoted in the presence of metal ions[6,7]. In fact, benzene is oxidized to phenol without biphenyl production in the presence of iron salts at temperatures lower than 200°C as is shown in the present paper.

Experimental

Apparatus and Procedure.—1 ml. of benzene, purified by the usual method, was put on 15 ml. of an aqueous solution of 0.01M iron ion, as has been mentioned in Part I[4], in a hard-glass tube in the reactor under the oxygen pressure of 30 atm. This system was heated by the controlled procedure mentioned in Part I. Although the reactor had no stirring device, the solution seemed to be agitated spontaneously at elevated temperatures, at least above 150°C. For the irradiation experiments, the solution was irradiated with cobalt-60 gamma rays for 25 min. (about 14000 r by the Fricke dosimeter) at the middle stage of the heating procedure, kept at a given temperature. (Cf. Part I). The reference experiment without the middle stage was also made as in Part I. The heating procedure is shown schematically Fig. 1.

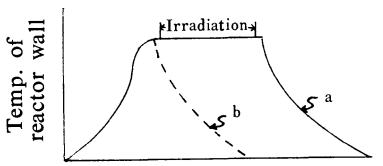

Fig. 1. Schematic heating procedure.
a) Actual experiment
b) Reference experiment

Analytical.—The produced phenol was first extracted from 1 ml. of the aqueous phase as an ether solution after the addition of 2 N hydrochloric acid. After the separation of acidic products from the ether solution by agitating with 5% sodium bicarbonate, phenol was again extracted in 1 N sodium hydroxide, and then, after being acidified by 2 N hydrochloric acid, extracted in ether. The phenol, in the benzene phase and mixed with iron precipites, was extracted together in 2 N sodium hydroxide, and then treated by the above procedure.

The amount of phenol in the above extract was determined from the optical density at 273.5 mμ ($\varepsilon=2167$), because Goodman and Steigman recommended the separation by ether[8]. The absorption curve of the extract was identical with that of pure phenol. In all cases, no biphenyl was found in the ether extract by gas-chromatography through a polyethylene-glycol column at 180°C.

The analytical methods for iron species were the same as in Part I.

1) Present address: Showa Denko Co., Minato-ku, Tokyo.
2) W. I. Denton, H. G. Doberty and R. H. Krieble, *Ind. Eng. Chem.*, **42**, 777 (1950).
3) Y. Hosaka, *J. Chem. Soc. Japan, Ind. Chem. Sec.* (*Kogyo Kagaku Zassi*), **57**, 197, 375 (1954).
4) H. Hotta and N. Suzuki, This Bulletin, **36**, 717 (1963).
5) E. J. Henley, J. Goodman and I. Tang, *Trans. Am. Nuclear Soc.*, 3, No. 2, 387 (1960).
6) G. H. Twigg, *Chem. & Ind.*, **1962**, 4.
7) A. V. Tobolsky and R. B. Mesrobian, "Organic Peroxides", Interscience Pub., Inc., New York (1954).
8) J. Goodman and J. Steigman, *J. Phys. Chem.*, **62**, 1020 (1958).

Preliminary Experiment.—When the reactants were put directly in the reactor using no glass tube, reaction seemed to be promoted considerably above 150°C with corrosion of the stainless-steel wall. Next, the reaction was carried out in a Teflon tube set tightly in the reactor in order to prevent the corrosion effect. The yield of phenol was less in a Teflon tube than in a glass tube. The yield seemed to be the highest for 0.01M salt solutions. The present experimental conditions were decided on the basis of these results.

Results

Phenol Yield in Ferric Solutions.—The total yields of phenol produced in the ferric sulfate solution of 0, 0.01 and 0.1 N sulfuric acid (0.01M of ferric ion) are shown in mg. in Fig. 2 for the cases of irradiation (solid marks and solid lines) and non-irradiation (open marks and

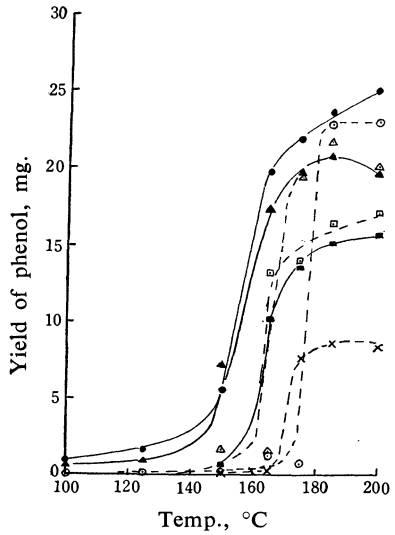

Fig. 2. Yield of phenol in 0.01M-Fe ferric sulfate solutions with radiation (solid marks) and without radiation (open marks) in neutral (● and ⊙), in 0.01N (▲ and △), in 0.1N sulfuric acid (■ and ▣), and in 1.0N sulfuric acid without radiation (×).

dotted lines), and, further, by crosses for the non-irradiated 1.0 N sulfuric acid solution. No phenol was found in any of the reference experiments. In general, as the acidity increases, the maximum yield at higher temperatures decreases, and the difference between the irradiated and non-irradiated systems disappears.

The results for 0.01M ferric chloride solutions in hydrochloric acid are shown in Fig. 3 in the same manner. The tendency of the yield is almost the same, but the yield is considerably suppressed by chloride ions.

The contribution of radiation is shown in

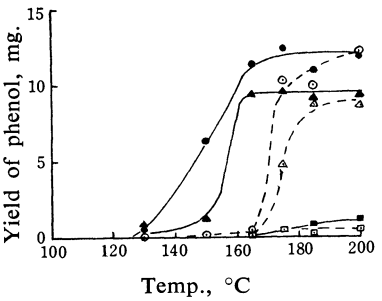

Fig. 3. Yield of phenol in 0.01M ferric chloride solutions with radiation (solid marks) and without radiation (open marks) in neutral (● and ⊙), in 0.01N (▲ and △) and 0.1N hydrochloric acid (■ and ▣).

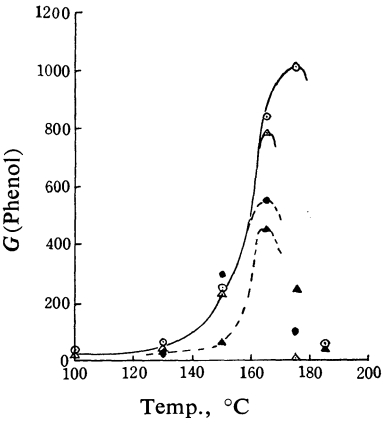

Fig. 4. G(Phenol) in ferric sulfate solutions (open marks) and in ferric chloride solutions (solid marks); in neutral (⊙ and ●) and in 0.01N acid (△ and ▲). G-values are evaluated as mentioned in text.

Fig. 4 by the G-value of phenol, estimated as the number of phenol molecules per 100 eV. of energy absorbed in 15 g. water, from the difference between the values of irradiated and non-irradiated systems plotted in Figs. 2 and 3.

Iron Concentration in Ferric Solutions after Reaction.—The total iron concentrations dissolved in the solutions of ferric sulfate and chloride after experiment, determined by the oxine method, are shown in Figs. 5 and 6 (the same marks as Figs. 2 and 3). The result for the ferric chloride solution in 0.01 N hydrochloric acid was almost the same as for that in the neutral solution. The precipitation reaction of iron salts seems to be somewhat retarded by phenol production as has been pointed out in Part I[4].

The ferrous content of these total iron species in the solutions, determined by the α, α'-dipyridyl method, is shown in Fig. 7 for the non-irradiated ferric sulfate solutions and

in Fig. 8 for the irradiated ones, using the same marks as in Fig. 2; and in Fig. 9 for the non-irradiated and irradiated ferric chloride solutions, using the same marks as in Fig. 3.

The ferrous concentration in these figures has a maximum, and increases with increase of

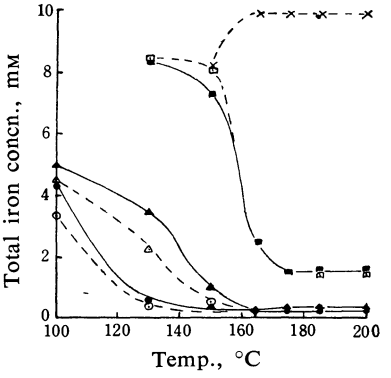

Fig. 5. Total iron concentration in ferric sulfate solutions after experiment shown in Fig. 2; marks are the same with Fig. 2.

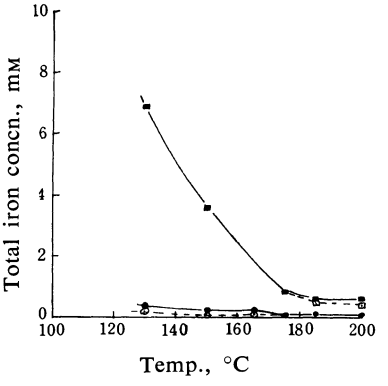

Fig. 6. Total iron concentration in ferric chloride solutions after experiment shown in Fig. 3; marks are the same with Fig. 3.

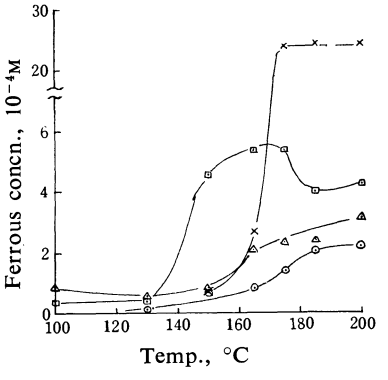

Fig. 7. Ferrous content in total iron concentrations shown in Fig. 5, for non-irradiated ferric sulfate systems; marks are the same with Fig. 2.

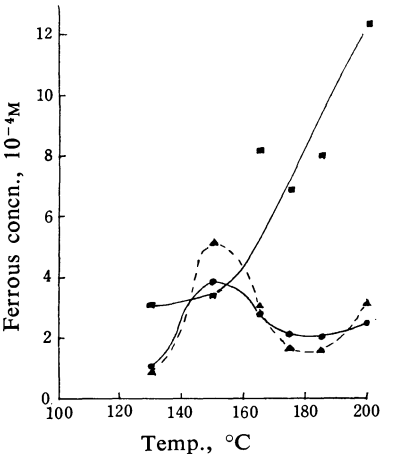

Fig. 8. Ferrous content in total iron concentrations shown in Fig. 5 for irradiated ferric sulfate systems; marks are the same with Fig. 2.

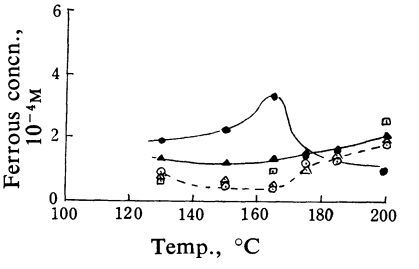

Fig. 9. Ferrous content in total iron concentrations shown in Fig. 6 for ferric chloride systems; marks are the same with Fig. 3.

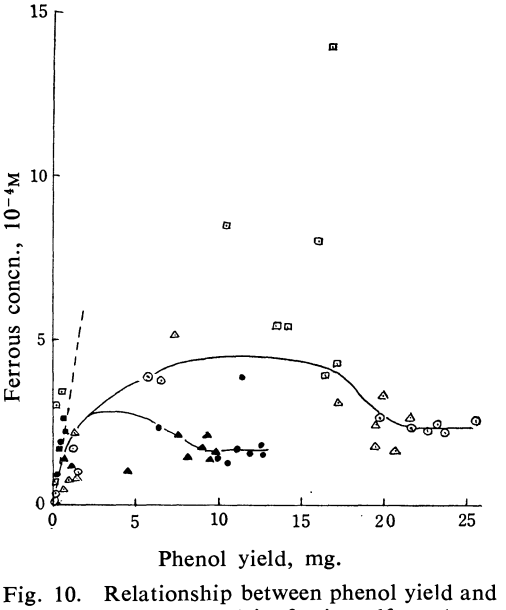

Fig. 10. Relationship between phenol yield and ferrous ion produced in ferric sulfate (open marks) and ferric chloride (solid marks) solutions in neutral (⊙ and ●), 0.01N (△ and ▲) and 0.1N (▣ and ■) acids.

acidity. Moreover, the ferrous proportion of iron species increases as the reaction temperature rises. The iron species is mostly ferrous above 180°C. Such reduction in ferric ions is never found for ferric solutions without benzene, as has been mentioned in the ferric results of Part I[4]. When all the ferrous concentrations observed are plotted against the corresponding phenol yields as in Fig. 10, there is the interesting relationship. The decrease in the ferrous concentration at the high phenol yield is due to thermal precipitation at higher temperatures[4]. In fact, the hardly precipitated systems give the high ferrous yield instead of such a decrease.

Phenol Yield in Ferrous Solutions.—The yields of phenol in 0.01M ferrous sulfate solutions are shown in Fig. 11 using the same marks as in Fig. 2. Since the yield seems to increase with the lapse of time after the preparation of the solution, the values are rather scattered. However, it might be concluded that the yield is larger even without radiation than in the ferric sulfate solution with radiation in Fig. 2; and that the difference between with and without radiation is minor. Even after the deduction of the yield at the reference experiment from the value shown in Fig. 11, the yield is still higher below 175°C but lower above 175°C than the irradiated ferric sulfate solution. This means that the oxidation reaction is promoted by ferrous species and apparently retarded by phenol production as will be discussed later.

The results of the ferrous chloride solution, shown in Fig. 12, indicate more clearly that the yield for the ferrous solution is independent

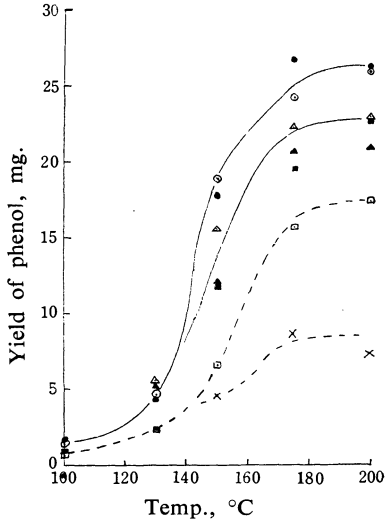

Fig. 11. Yield of phenol in 0.01M ferrous sulfate solutions; marks are the same with Fig. 2.

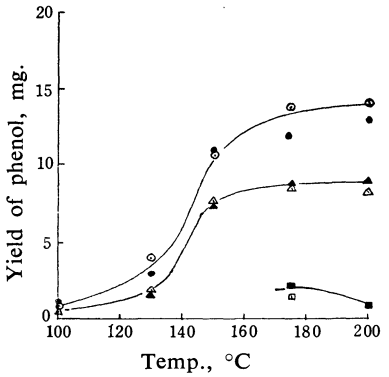

Fig. 12. Yield of phenol in 0.01 M ferrous chloride solutions; marks are the same with Fig. 3.

of radiation. This yield is also suppressed by chloride ions.

Iron Concentration in Ferrous Solutions after Reaction.—The concentrations of the total iron species and ferric species dissolved in the ferrous sulfate solutions after experiment are shown in Figs. 13 and 14 respectively, using

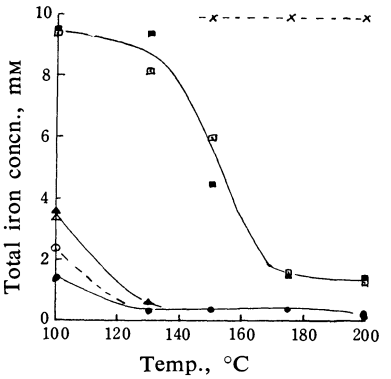

Fig. 13. Total iron concentration in ferrous sulfate solutions after experiment shown in Fig. 11; marks are the same with Fig. 2.

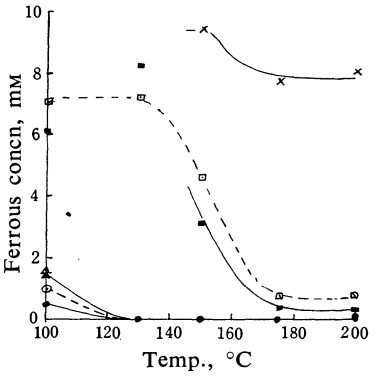

Fig. 14. Ferrous content in total iron concentrations shown in Fig. 13 for ferrous sulfate systems; marks are the same with Fig. 2.

the same marks as in Fig. 2. The results are interesting in comparison with the corresponding ones without benzene in Part I[4]; there is no ferric ion above 130°C in 0 and 0.01 N sulfuric acid even though the present reactions were carried out under the high pressure of oxygen at elevated temperatures.

The results for the ferrous chloride solution were almost the same as those for the ferrous sulfate solution.

Discussion

The Effect of Radiation.—Dorfman et al. concluded, on the basis of electron-pulse radiolysis, that the radiation oxidation of benzene in an oxygenated aqueous solution at room temperature is through the following transient species[9];

$$H_2O \rightsquigarrow H,\ OH,\ H_2,\ H_2O_2 \qquad (1)$$

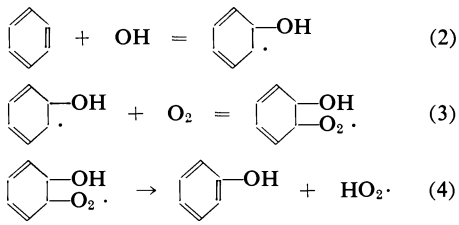

They estimated the rate of these reactions at 23°C to be $(4.3 \pm 0.9)\times10^9 M^{-1}sec^{-1}$ for reaction 2 and $(5.0 \pm 0.6)\times10^8 M^{-1}sec^{-1}$ for reaction 3. According to their observation, this hyroxycyclohexadienyl peroxy radical is fairly stable.

Hydrogen atom from reaction 1 combines with dissolved oxygen;

$$H + O_2 = HO_2 \qquad (5)$$

The rate of this reaction at 25°C is 1.1×10^9 $M^{-1}sec^{-1}$ in acid and $5.5\times10^9 M^{-1}sec^{-1}$ in a neutral solution[10]. The HO_2 radical and hydrogen peroxide is converted to OH radical as discussed in the next section. Ferric ions are not reduced by products of reaction 1 when oxygen exists[11,12]. In fact, the ferrous concentration in the ferric sulfate solution without benzene does not increase upon irradiation, as has been mentioned in the results section of Part I[4].

The suppression of phenol production in the chloride solutions is due to scavenging of the initiator of reaction 2;

$$Cl^- + OH + H^+ = Cl + H_2O \qquad (6)$$

The rate of this reaction at 25°C is supposed to be $1.8\times10^8 M^{-1}sec^{-1}$ at pH 2, and about ten times as fast as in 0.8 N sulfuric acid[13,14]. The effect of chloride ions, shown in Figs. 3 and 12, can be understood qualitatively by comparing these rates with the rates of reaction 2 and of reaction 11 to be discussed in the next section.

Initiation in Ferrous Solutions.—The results obtained by the same procedure in the aqueous phase containing no salt are given in Table I, in which the *G*-value in parentheses is reported by Proskurnin and Kolotyrkin[15]. Since a yield less than 0.04 mg. is unreliable, it can be said that no phenol is produced without any salt and radiation. Therefore, it is certain that the oxidation of benzene shown in Figs. 11 and 12 is neither initiated by the thermal cracking of benzene nor by the hydrogen abstraction of oxygen from benzene.

Table I. Phenol yield without iron salts

Medium	Radiation	Yield	
		mg.	*G*-Value
Water	Yes	0.33	16, (20)[15]
	No	0.02	—
0.1 N H_2SO_4	Yes	0.48	24
	No	0.04	—

As has been mentioned in Part I[4], the autooxidation of ferrous ions in an aqueous solution has usually been interpreted by the reaction

$$Fe^{2+} + O_2 + H^+ = Fe^{3+} + HO_2 \qquad (7)$$

Even if the HO_2 radical can not react directly with benzene, it can be converted to OH radical in the presence of ferrous ions. Therefore, it can be assumed that the oxidation of benzene in the ferrous solution is initiated by OH radical produced through reaction 7 and proceeds like reactions 2 and 3 even without reaction 1.

When the oxidation process is initiated through these reactions, hydroxycyclohexadienyl peroxy radical of reaction 3 is considered to be complexed in the ferrous solution in this manner;

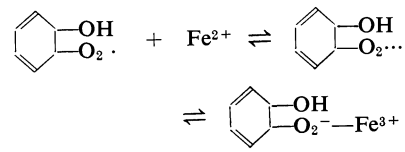

as is usually assumed for the catalytic action

9) L. M. Dorfman, I. A. Taub and R. E. Bühler, *J. Chem. Phys.*, **36**, 3051 (1962).
10) A. R. Anderson and E. J. Hart, *J. Phys. Chem.*, **65**, 804 (1961).
11) H. Hotta and S. Ohno, This Bulletin, **34**, 1640 (1961).
12) G. Dobson and G. Hughes, *Trans. Faraday Soc.*, **57**, 1117 (1961).
13) H. A. Schwarz, *J. Phys. Chem.*, **66**, 255 (1962).
14) C. Ferradini, *Advances in Inorganic and Radiochem.*, **3**, 171 (1961).
15) M. A. Proskurnin and Y. M. Kolotyrkin, Proc. 2nd U. N. Intern. Conf. Geneva, **29**, 52 (1961).

of redox ions[16]. Since such complexing stabilizes further the peroxy radical which has a fairly long life as has been pointed out already[9], the peroxy radical is allowed to react with benzene in this manner[17];

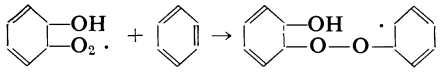
(9)

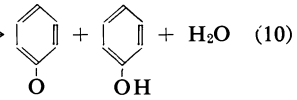
(10)

as well as via reaction 4. However, reaction 9 seems to have a threshold temperature.

The rate of reaction 7 at 150°C is 6×10^{-4} sec^{-1} in 0.1 N sulfuric acid under the present experimental conditions as was estimated in Part I[4]. Although OH radical is scavenged by ferrous ions thus;

$$Fe^{2+} + OH = Fe^{3+} + OH^- \qquad (11)$$

where the rate of this reaction is $2.6\times10^{8}M^{-1}$ sec^{-1} at pH 2 and 25°C[13], the rate of reaction 2 is very fast as has been mentioned already. According to the earlier results[14], the rate of reaction 2 at 25°C is 3.2 times as fast as that of reaction 11.

It may be open to doubt about the stability of the HO_2 radical and of hydrogen peroxide at elevated temperatures, especially in the presence of ferrous ions. The rate of the decomposition reaction

$$Fe^{2+} + H_2O_2 = Fe^{3+} + OH^- + OH \qquad (12)$$

is supposed to be $6.6\times10^{3}M^{-1}sec^{-1}$ at 150°C from extrapolation of the finding of Barb et al.[18], who extensively studied this subject in the room temperature range. The rate of reaction 2 is further faster than this rate. In any case, the present fact of phenol production is a good answer to the doubt.

When Figs. 2 and 11 are compared with Figs. 3 and 12, the yield of phenol in the non-irradiated ferrous solutions is almost the same as that in the irradiated ones, and it is larger than in the irradiated ferric solutions. Therefore, the overall yield of OH radicals by these thermal reactions seems to be considerably higher in spite of reacction 11, than by radiation-induced reaction 1 and reaction 5.

Initiation in Ferric Solutions.—Among the primary products of reaction 1, in the irradiated ferric solution, the OH radicals are not only scavenged like reaction 11, but they can also not be converted from the hydrogen atom and hydrogen peroxide, through reactions 5 and 12, to initiate the oxidation process. Therefore, the high yield of phenol is supposed also to be due to the complexing of the peroxide radical from reaction 3, with a trace amount of ferrous ions being present initially, as has been pointed out in Part I[4].

On the other hand, the oxidation process is also initiated without radiation in the ferric solution above 170°C, as is shown in Fig. 2. It can be understood similarly if ferrous ions are produced by any reaction in the ferric solution. Some reports seem to suggest such a possibility[19-21]. Recently the reaction

$$2Ce^{4+} + H_2O \rightarrow 2Ce^{3+} + \frac{1}{2}O_2 \qquad (13)$$

was assumed to account for the fact that cerric ions are reduced thermally in sulfuric acid at elevated temperatures[22]. Dobson and Hughes also discussed the possibility of ferric reduction in an irradiated ferric aqueous solution[12]. As if suggesting a process like reaction 13, the ferric solution gave an trace amount of ferrous species by about $2\times10^{-5}M$ as pointed out above.

Propagation Processes.—After reaction 10, the oxidation process of benzene is propagated through the following reactions [6,7,23]:

$$PhO + PhH = PhOH + Ph \qquad (14)$$

$$Ph + O_2 = PhO_2 \qquad (15)$$

$$PhO_2 + PhH = PhO_2H + Ph \qquad (16)$$

$$PhO_2H + Fe^{3+} = PhO_2 + H^+ + Fe^{2+} \qquad (17)$$

$$PhO_2H + Fe^{2+} = PhO + OH^- + Fe^{3+} \qquad (18)$$

(Ph: Phenyl radical)

in the iron solution, since ferrous and ferric ions are present together at once even if the reaction starts either with the pure ferrous or ferric solution.

Ferric ions are reduced considerably with phenol production as has been mentioned in the description of Fig. 10. This fact cannot be interpreted without the aid of reactions 10, 14 and 17. In the interpretation of Fig. 10, it should be noticed that some of the ferrous ions produced by reaction 17 are reoxidized by other reactions and precipitated, as has been mentioned already. Among the related reactions, the rate of the precipitation reaction in the neutral ferric sulfate solution is

16) J. K. Kochi, *J. Am. Chem. Soc.*, **83**, 3162 (1961).
17) J. K. Kochi and F. F. Rust, ibid., **83**, 2017 (1961).
18) W. G. Barb, J. H. Baxendale, P. George and K. R. Hargrave, *Trans. Faraday Soc.*, **47**, 462 (1951)
19) J. H. Baxendale and J. Magee, ibid., **51**, 205 (1955).
20) J. H. Baxendale and C. F. Wells, ibid., **53**, 800 (1957).
21) N. K. King and M. E. Winfield, *J. Am. Chem. Soc.*, **80**, 2060 (1958).
22) D. Grant and D. S. Payne, *Anal. Chim. Acta*, **25**, 422 (1961).
23) A. J. Chalk and J. F. Smith, *Trans. Faraday Soc.*, **53**, 1214 (1957).

$2.5 M^{-1}sec^{-1}$ at 150°C, as has been estimated in Part I[4]. The rate of the oxidation reaction 7 is slow as mentioned already. Although no report has been found on the decmposition of phenyl hydroperoxide, the rate of cumene hydroperoxide decomposition, as in reaction 17 in the presence of oxygen, is supposed to be $1.6\times10^{4} M^{-1}sec^{-1}$ at 150°C by extrapolation from the equation of Fordham and Williams[24]. Therefore, the rate of phenyl hydroperoxide decomposition is supposed to be the same order or faster than this rate, due to the high resonance energy of phenoxy radical[25,26]. At any rate, ferrous ions accumulate first with phenol production, as the reaction temperature rises, but the concentration decreases due to the precipitation at higher temperatures.

The mole ratio of the amount of ferrous ions to phenol is 0.46 ± 0.02, judging from the results at 175, 185 and 200°C in the non-irradiated 1.0 N sulfuric acid solution, which gave scarcely any precipitate. This ratio is represented by the dotted line in Fig. 10. Since ferrous ions for reaction 18 are produced only by reaction 17 in the ferric solution, this ratio means that the contribution of reaction 17 is greater than reaction 18, but not necessarily that the rate of the former is faster than that of the latter, when taking account of the difference between the initial concentrations of ferrous and ferric ions. In general, the dissociation energy of the O–O bond in hydroperoxide is smaller than the O–H bond. Especially, the decomposition

$$PhOOH = PhO + OH \qquad (19)$$

should be fast, even without redox ions, as has been discussed above[25].

Termination and Retardation Processes.—The yield of phenol hardly increases with rise of temperature at higher temperatures as at lower temperatures. Such saturation of the phenol yield is mainly attributed to the oxidation decomposition of phenol produced[27] rather than to the self-inhibition effect of phenols on oxidation reactions[28].

The other by-reactions between the reactants of the above reactions are also minor as the termination and retardation processes. For example, the present oxidation process is not terminated, as would usually be expected, by the reaction between phenyl peroxide;

$$2PhO_2 = PhO\text{–}OPh + O_2 \qquad (20)$$

as biphenoxy should be decomposed at least at elevated temperatures thus;

$$PhO\text{–}OPh = 2PhO \qquad (21)$$

due to the repulsion between the high dipoles[7]; that is, the overall reaction can be expressed as

$$2PhO_2 = 2PhO + O_2 \qquad (22)$$

Such a reaction is confirmed for cumene peroxide[6]. However, reaction 20 might play part in the retardation process at higher temperatures, at which phenyl peroxide is concentrated.

Effect of Acid Concentration.—As the acidity increases, the yield of phenol decreases due to the decrease of the concentration for the effective reactants of reactions 8 and 18. The reactivity of ions is very sensitive to the state in a solution, either free or complexed, dependent on the acidity[11].

The other effect of acids is as an anion, as in reaction 11. The decomposed products of sulfate ions might initiate the oxidation process of benzene in the concentrated acid solution.

Summary

In the ferric sulfate solution, benzene can be oxidized to phenol with a good yield above 170°C, when not irradiated, but at lower temperatures, when irradiated. In the ferrous sulfate solution, the yield of phenol is independent of irradiation, and somewhat larger than in the irradiated ferric sulfate solution. Such a high yield of phenol is due to the complexing of hydroxycyclohexadienyl peroxy radical, produced with OH radical and oxygen dissolved, with ferrous ions.

The authors wish to express their appreciation to Dr. Akibumi Danno of JAERI and Dr. Tōru Hirayama of Showa Denko Co. for their interest and kind encouragement, and also to Dr. Hiroshi Itatani of Osaka University and Dr. Akihisa Sakumoto of JAERI for their valuable advice on organic mechanisms.

Japan Atomic Energy Research Institute
Tokai, Ibaraki

24) J. W. L. Fordham and H. L. Williams, *J. Am. Chem. Soc.*, **72**, 4465 (1950); **73**, 1634 (1951).
25) C. Walling, "Free Radicals in Solution", John Wiley & Son, Inc., New York (1957), p. 466.
26) P. D. Bartlett, "Peroxide Reaction Mechanisms", Interscience Pub., New York (1962), p. 1.
27) H. Hotta, K. Shimada and N. Kanazawa, to be published.
28) K. U. Ingold, *Chem. Revs.*, **61**, 563 (1961).

The Mechanism of Azoxybenzene Formation[1]

By Shigeru OAE*, Tsugio FUKUMOTO and Masayuki YAMAGAMI

(Received February 1, 1963)

It has been well known for many years[2] that nitrobenzene is readily reduced to azoxybenzene by refluxing it with sodium alkoxide in alcohol, and the formation of azoxybenzene is generally believed to involve the condensation of phenylhydroxylamine and nitrosobenzene, both of which are produced in the reduction of nitrobenzene. Recently the condensation of phenylhydroxylamine and nitrobenzene has been studied and the formation of azoxy compounds discussed by Ogata, Tsuchida and Takagi[3]. More recently, Ogata and Mibae[4] have studied the kinetics and mechanism of azoxybenzene formation in the reduction of nitrobenzene by sodium methoxide and have suggested that the condensation of phenylhydroxylamine with nitrosobenzene to form azoxybenzene (4) is very fast compared with the reduction step of nitrobenzene with sodium methoxide and that the reduction step ((1) and (2)) is rate-determining. They have also indicated that nitrosobenzene and phenylhydroxylamine can be readily interconverted.

$$PhNO_2 + 2CH_3ONa \rightarrow PhNO + HCHO + NaOH + CH_3ONa \quad (1)$$

$$PhNO_2 + 2CH_3ONa \rightarrow PhNHOH + HCOONa + CH_3ONa \quad (2)$$

$$PhNHOH + PhNO_2 \rightarrow 2PhNO + H_2O \quad (3)$$

$$PhNHOH + PhNO \rightarrow PhN{=}NPh + H_2O \quad (4)$$
$$\downarrow$$
$$O$$

Shemyakin, Maimind and Vaichunaite[5] have studied the azoxy coupling reaction between phenylhydroxylamine and ^{15}N-labeled nitrosobenzene and have shown that the excess ^{15}N originally present in nitrosobenzene was distributed equally in both nitrogens of the azoxybenzene, suggesting the formation of an intermediate compound with an equivalent location of the N atom such as $(Ph\ ^{15}NOH)_2$.

During the course of our study of the Wallach rearrangement, we have also come to be interested in this azoxy-coupling reaction. Here again, our approach to this problem is through ^{18}O. When ^{18}O-labeled nitrobenzene was reacted with sodium methoxide in refluxing aqueous methanol, the resulting azoxybenzene was found to retain 0.69 atom % of ^{18}O; that is, about 22% of the excess ^{18}O was lost during the reaction, and the azoxybenzene retained 77% of the excess ^{18}O originally present in nitrobenzene. This means that a small portion of oxygen exchange is taking place at some stage, either at the reduction or at the azoxy coupling of the reaction.

We then examined the reaction of nitrosobenzene with ^{18}O-labeled phenylhydroxylamine in boiling ethanol containing potassium hydroxide and found that the amount of excess ^{18}O in the resulting azoxybenzene was almost exactly a half of that of the phenylhydroxylamine employed. This is excellent supporting evidence both for Ogata's idea that the azoxy-coupling reaction is a very fast step and for the Russians' mechanism of the prior formation of a symmetrical *N, N'*-diol intermediate in the coupling reaction. However, since we found that the reaction of phenylhydroxylamine alone with sodium methoxide gave azobenzene in a good yield and that of nitrosobenzene alone with sodium methoxide gave azoxybenzene in a superb yield, there remain the other possibility that nitrosobenzene was exchanging oxygen with ^{18}O-enriched water formed from the azoxy coupling of hydroxylamine before self-condensing to form azoxybenzene.

This, however, was not the case, because the reaction of nitrosobenzene alone with ^{18}O-labeled sodium methoxide was found to give azoxybenzene incorporated with no excess ^{18}O. The most likely path for the azoxy-coupling reaction appears to be via an intermediate, *N, N'*-diol before dehydration to give azoxybenzene in a rapid process, regardless of whether one uses both phenylhydroxylamine and nitrosobenzene or nitrosobenzene alone.

* Present address: Department of Applied Chemistry, Faculty of Engineering, Osaka City University, Kita-ku, Osaka.

1) Paper VIII on "The Rearrangements of Tertiary Amine Oxides", Paper VII: S. Oae, T. Fukumoto and M. Yamagami, This Bulletin, **36**, 601 (1963).

2) H. S. Fry and J. L. Cameron, *J. Am. Chem. Soc.*, **49**, 864 (1927); E. Bamberger and E. Renauld, *Ber.*, **30**, 2278 (1897); E. Bamberger and A. Rising, *Ann.*, **316**, 257 (1901).

3) Y. Ogata, M. Tsuchida and Y. Takagi, *J. Am. Chem. Soc.*, **79**, 3397 (1957).

4) Y. Ogata and J. Mibae, *J. Org. Chem.*, **27**, 2048 (1962).

5) M. M. Shemyakin, V. I. Maimind and B. K. Vaichunaite, *Izvest. Akad. Nauk S. S. S. R., Otdel. Khim. Nauk*, 1957, 1260-2; *Chem. Abstr.*, **52**, 6231 (1958).

Since no oxygen exchange was observed in the azoxy-coupling stage, the loss of some of the excess ^{18}O found in the reduction of nitrobenzene to azoxybenzene must be taking place in the slow stage, where nitrobenzene is being reduced to nitrosobenzene. A similar loss of excess ^{18}O was observed in the reduction of ^{18}O-labeled nitrobenzene to phenylhydroxylamine with zinc and ammonium chloride. Here also about 22% of the excess ^{18}O was lost during the reduction. Probably, in both reductions, there is a common step where an incipient intermediate exchanges its oxygen with that of the solvent medium.

Experimental

^{18}O-Labeled Azoxybenzene was prepared by heating ^{18}O-labeled nitrobenzene[6] (8 g., 0.84 atom % of ^{18}O) with sodium hydroxide (8 g.) in methanol (8 g.); m. p., 35~36°C, 0.69 atom % of ^{18}O.

Found: C, 72.60; H, 4.99. Calcd. for $C_{12}H_{10}N_2O$: C, 72.73; H, 5.05%.

^{18}O-Labeled Phenylhydroxylamine.—In a 50 ml., three-necked flask fitted with a stirrer were placed 2.5 g. of ammonium chloride, 5 g. of nitrobenzene (0.66 atom % of ^{18}O) and 50 ml. of water; the mixture was then cooled to 5°C and 7 g. of zinc powder was stirred in over a period of 40 min., keeping the temperature between 5 and 10°C. Stirring was continued for 10 min. The zinc hydroxide formed was removed by filtration and washed with 40 ml. of hot water three times. The filtrate and washing were combined 25 g. of sodium chloride was added, and the mixture was allowed to stand overnight in a refrigerator. The precipitate formed was collected and recrystallized from a mixture of petroleum ether and benzene. Phenylhydroxylamine (m. p., 81°C) (lit.[7] 81°C), 0.56 atom % of ^{18}O) was thus obtained. The yield was 3 g. (70%).

The Condensation Reaction of ^{18}O-Labeled Phenylhydroxylamine and Nitrosobenzene Using Potassium Hydroxide.—In a three-necked flask was placed a mixture of 0.4 g. of ^{18}O-labeled phenylhydroxylamine (0.56 atom % of ^{18}O), 0.4 g. of nitrosobenzene and 10 ml. of ethanol; an ethanol solution which had been saturated with 0.45 g. of potassium hydroxide was stirred in and then allowed to react for 1 hr. at 75~80°C. After ethanol had been removed by evaporation under reduced pressure, the residue was poured into 100 ml. cold water. The yellow solid formed was collected and recrystallized from methanol. Azoxybenzene (m. p., 36°C, 0.38 atom % of ^{18}O) was thus obtained. The yield was 0.5 g. (80%).

The Condensation Reaction of Phenylhydroxylamine and Nitrosobenzene Using ^{18}O-Labeled Potassium Hydroxide.—^{18}O-Labeled potassium hydroxide was prepared by exchange reaction between potassium hydroxide and ^{18}O-enriched water. A mixture of 0.4 g. of phenylhydroxylamine, 0.4 g. of nitrosobenzene and ^{18}O-labeled potassium hydroxide (0.54 atom % of ^{18}O) was allowed to react similarly. The main product, azoxybenzene (m. p., 35°C) contained 0.22 atom % of ^{18}O. The yield was 0.5 g. (80%).

The Condensation Reaction of Phenylhydroxylamine alone with Potassium Hydroxide.—A mixture of 0.8 g. of phenylhydroxylamine and 0.45 g. of potassium hydroxide in 10 ml. of ethanol was allowed to react for 1 hr. at 75~80°C and was then treated similarly. The main product was red crystals (m. p., 66~67°C). The yield was 0.5 g. (75%). It did not depress the melting point of an authentic sample, azobenzene (m. p., 66~67.5°C) on admixture.

The Condensation Reaction of Nitrosobenzene alone with ^{18}O-Labeled Potassium Hydroxide.—A mixture of 0.8 g. of nitrosobenzene and 0.45 g. of ^{18}O-labeled potassium hydroxide (0.54 atom % of ^{18}O) in 10 ml. of ethanol was allowed to react for 1 hr. at 75~80°C and was then treated similarly. Azoxybenzene (m. p., 35~36°C) was the main product obtained, but unreacted nitrosobenzene was not recovered. This azoxybenzene contained 0.21 atom % of ^{18}O. The yield was 0.48 g. (66%).

The Determination of ^{18}O is described elsewhere[8].

Department of Chemistry
Radiation Center of Osaka Prefecture
Sakai, Osaka

6) S. Oae, T. Fukumoto and M. Yamagami, This Bulletin, **36**, 601 (1963).

7) R. Oda, "Organic Preparative Chemistry" (Yuki-Gosei-Kagaku), Kyoritsu Book Co. (1953), p. 123.

8) S. Oae, T. Kitao and Y. Kitaoka, *Ann. Report Radiation Center of Osaka Prefecture*, **1**, 33 (1960).

The Formation of 1,6-Dithia-3a-azonia-2,3,4,5-tetrahydropentalene Salt

By Shuichi SETO and Yusaku IKEGAMI

(Received February 16, 1963)

The reaction of bis(2-chloroethyl)amine hydrochloride with carbon disulfide in hydrous pyridine, under ice cooling, afforded colorless needles (I), (m. p., 95°C). The present paper deals with the structure of I and with some of its reactions.

The analytical values of I correspond to those of $C_5H_8NS_2Cl\cdot 2H_2O$, and the yield of its formation reaction is over 90%. I is quite easily soluble in water, but only sparingly soluble in organic solvents. The infrared spectrum of I indicated absorptions at 3405, 3340, 1643 and 1618 cm^{-1} due to the water of crystallization. When left in dry air or in a vacuum desiccator, I undergoes efflorescence with the loss of a part of the water of crystallization.

The addition of an excess of potassium bromide to the aqueous solution of I results in the precipitation of colorless crystals (II) (m. p., 95°C), $C_5H_8NS_2Br\cdot 2H_2O$, which are slightly more sparingly soluble in water than I. The addition of potassium iodide to the aqueous solution of I precipitates more sparingly soluble colorless cubic crystals (III) (m. p., 220°C) (decomp.), $C_5H_8NS_2I$. I forms a picrate (IV) of yellow needles, (m. p., 154°C), $C_5H_8NS_2\cdot C_6H_2O_7N_3$. It is certain from the foregoing reactions that the atom group, $C_5H_8NS_2$, in I to IV is present as a cation. From these facts and from considerations of NMR, infrared and Raman spectra to be discussed below, the structure of 1, 6-dithia-3a-azonia-2, 3, 4, 5-tetrahydropentalene can be given to this cation.

$$ClCH_2CH_2\diagdown\!\!\diagup NH\cdot HCl + CS_2 \rightarrow C_5H_8NS_2Cl\cdot 2H_2O$$
$$ClCH_2CH_2\diagup\!\!\diagdown$$

I

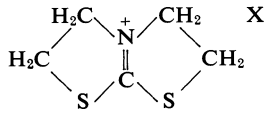

X

I ; X=$Cl^-\cdot 2H_2O$
II ; X=$Br^-\cdot 2H_2O$
III ; X=I^-
IV ; X=Picrate anion

The NMR spectrum of I in heavy water shows only one signal at 5.82τ, excluding that due to water, and only one signal at 5.70τ, in that of the iodide III. These facts indicate that the protons of the two methylene groups on either side of nitrogen atom are in an equivalent shielding state.

For this cation (A), a structure with all eight skeletal atoms in one plane, or a structure similar to it, is suggested. If all the skeletal atoms were included in one plane, this cation should have two symmetrical planes at right angles to each other. Consequently, its vibrational spectrum can be handled as the vibration of the C_{2v} symmetrical group, and the freedom of 42 vibrations can be classified into the following four species:

A_1	A_2	B_1	B_2	(Total)
13	8	12	9	42

Of these, the eight vibrations belonging to the A_2 species are infrared inactive, and the Raman lines due to the 13 vibrations belonging to A_1 species should show polarizability.

Under such assumptions, the infrared and Raman spectra of the chloride I were measured and their spectra were analyzed. The Raman spectrum was measured in an aqueous solution (ca. 32%), and the infrared spectrum, as a potassium bromide disk*1. The results of these measurements are shown in Table I, together with the infrared absorption frequencies of the bromide II and the iodide III.

The data in Table I show the following points:

a) The number of Raman lines of I was not as great as had been expected, but the majority of these Raman lines corresponded to the infrared absorption bands. The infrared spectra of the three compounds show that the absorptions due to the water of crystallization (3405~3220 and 1665~1618 cm^{-1}) are not present in the spectrum of III and that the majority of absorption bands, excluding specially weak ones, appear in all the three compounds, with only a slight difference in frequency and in a similar intensity. This will appear natural if it is assumed that the observed vibrations are virtually all due to the vibration of the cation (A).

b) The Raman line at 1566 cm^{-1}, assigned to the C=N stretching vibration shows an especially small depolarization factor (ρ); this fact, signifying that C=N stretching is a vibration belonging to the A_1 species which does not change the symmetry of a molecule,

*1 The same results were obtained by measurement in Nujol.

TABLE I. OBSERVED FREQUENCIES OF 1,6-DITHIA-3a-AZONIA-2,3,4,5-TETRAHYDROPENTALENE HALIDES

Chloride·$2H_2O$ (I)				Bromide·$2H_2O$ (II)	Iodide (III)
Raman*1			IR*2	IR*2	IR*2
cm^{-1}	Int.	ρ	cm^{-1}	cm^{-1}	cm^{-1}
			3470 sh		
3445	10.5		3405 vs	3335 vs	
3393			3340 vs		
3300				3230 s	
3120	6.8		3220 sh		
3023	4.2	0.78	3010 w	2990 vw	3000 vw
2976	10.0	0.47	2965 w		2965 vw
				2930 vw	
2908	2.3	0.41			2910 vw
2873	2.2	0.48			2840 vw
			2110 w	2140 w	
			1643 s	1655 sh	
			1618 m	1639 s	
1566	8.2	0.33	1571 vs	1571 vs	1574 vs
1486	w			1478 vw	
			1469 w		
1455	6.7	0.60		1449 sh	1451 w
1435	3.8	0.9	1433 m	1435 w	1440 w
					1425 m
				1380 vw	1376 vw
			1375 vw		
				1365 vw	1358 vw
			1334 w	1329 w	1320 w
					1308 m
1310	5.0	0.49	1304 m	1302 m	
					1302 m
1259	4.5	0.46	1260 m	1259 m	1253 m
				1231 w	1216 m
1201	1.0		1201 s	1205 s	1201 vs
1170	1.2	1.0	1186 s	1190 s	1171 s
			1154 w	1150 w	1163 sh
					1134 m
			1072 s	1071 s	1063 s
1070	1.0	0.9			
			1058 s	1057 s	1048 s
1020	w		1021 vw	1021 w	999 s
			997 vw	996 w	
967	1.5	0.8	975 w	970 w	961 m
910	1.2				910 vw
					846 w
827	1.1		825 wb		
					814 m
758	0.7				
674	2.2	0.5	661 sb	707 sb	677 m
649	vw		635 sh		649 vw
			613 sb	598 sh	600 w
605	9.7	0.36			
			592 sb	585 sh	582 m
			492 sb	538 sb	547 m
470	1.9				
			458 sh	458 m	456 w
453	5.8	1			
			425 sh		

*1 Raman spectrum was measured as the aqueous solution; the relative intensities were given taking the peak intensity of the intense line at 2976 cm^{-1} as the standard.

ρ: Depolarization factor

*2 Infrared spectra were measured as the potassium bromide disk.
vs: very strong, s: strong, m: medium, w: weak, vw: very weak, sh: shoulder, b: broad

also indirectly endorses the correctness of the structure of I. Besides the above, the lines at 2976 and 2908 cm^{-1} (CH_2 stretching), 1310 and 1259 cm^{-1} (skeletal stretching or CH_2 wagging), and 674 and 599 cm^{-1} (skeletal stretching?) all have small depolarization factors; these can all be assigned to vibrations of the A_1 species.

c) The observed C=N stretching frequencies (1574~1566 cm^{-1}) are rather lower than those of 2-methylthiazolidine (1635 cm^{-1}; hydrochloride, 1630 cm^{-1})[1] and 2-phenylthiazolidine (1605 cm^{-1})[2]. This is thought to be due to the great contribution of the A′ structure, and it is also considered to be responsible for the appearance of eight signals as a singlet in the proton NMR spectrum of I.

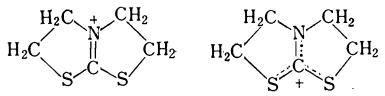

A A′

d) The frequencies in the 1486~1439 cm^{-1} region are assigned to the scissor vibrations of CH_2 groups. The bands in the 1205~1170 and 1072~1048 cm^{-1} regions which are strong in the infrared spectra, may probably be assigned to the CH_2 twisting and skeletal stretching vibrations, respectively.

When the aqueous solution of I is allowed to stand for a long period of time, a liquid (V) sparingly soluble in water separates out. V shows infrared absorptions at 2550 and 1667 cm^{-1}, due to -SH and C=O respectively, and lacks the absorption at 1571 cm^{-1} seen in I. V forms a lead salt (VI) of yellow needles (m. p., 143°C), $(C_5H_8ONS_2)_2Pb$. This lead compound shows an absorption for carbonyl at 1661 cm^{-1}, but it does not show the infrared absorption characteristic of the SH group. From these facts, a structure of *N*-(2′-mercaptoethyl)-2-thiazolidinone can be given to V and its lead sulfide to VI. I changes into V even when its solution is heated on a water bath.

When the mercapto compound V is treated with hydrogen peroxide in ethanol, β-(2-thiazolidinon-3-yl)ethyl disulfide (VII) is obtained as colorless plates (m. p. 94°C). VII is also obtained on treating the picrate IV with dilute alkali. The oxidation of V to VII occurs easily, as is usually the case with mercapto compounds. Therefore, in the case of the preparation of V, the disulfide VII is obtained at times as the crystalline part insoluble in ether.

1) R. B. Martin, S. Lowey, E. L. Elson and J. T. Edsall, *J. Am. Chem. Soc.*, **81**, 5089 (1959).
2) M. G. Ettlinger, ibid., **72**, 4699 (1950).

The drop-by-drop addition of a sodium hydroxide solution into the aqueous solution of I affords colorless crystals (VIII) of m. p., 114°C. The molecular weight of VIII is over 300; its infrared spectrum does not show absorptions characteristic of the C=N and SH groups, but it does show absorption bands in the finger-print region considered to be that due to the thiazolidinone group. The treatment of VIII with 2 N sodium hydroxide in ethanol gives the disulfide VII, and its passage through an alumina column gives a mixture of V and VII. The treatment of VIII with picric acid in ethanol results in the formation of approximately equivalent amounts of the picrate IV of the cation and the mercapto compound V. Similarly, the treatment of VIII with hydrochloric acid gives the chloride I and mercapto compound V. From the foregoing experimental results, the structure of 1a-[β-(2-thiazolidinon-3-yl)ethylthio]-1, 6-dithia-3a-aza-2, 3, 4, 5-tetrahydropentalene can be given to VIII.

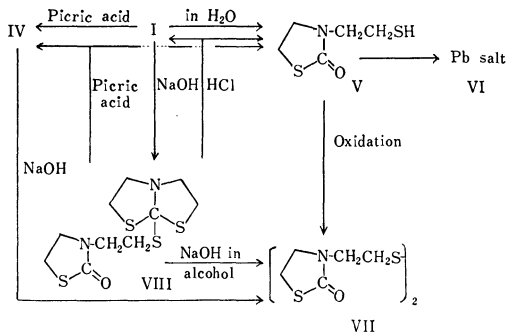

Experimental*2

1,6-Dithia-3a-azonia-2, 3, 4, 5-tetrahydropentalene Chloride (I).—To a solution of 7.14 g. of bis(2-chloroethyl)amine hydrochloride dissolved in 4 ml. of water, with 10 ml. of pyridine added, 2.4 ml. of carbon disulfide was added drop by drop during about a 1 hr. period, during which time the solution was stirred while being cooled with ice. The white turbid solution so formed was stirred at room temperature for 45 min., warmed at 40°C for 20 min., and chilled in ice, after which process colorless crystals precipitated out. By filtration, 7.95 g. of crystals (yield, 91.4%) were obtained; these were then dissolved in a minimum amount of water and recrystallized by the addition of ethanol to colorless needles (I) (m. p., 95°C).

UV λ_{max}^{MeOH} 257 mμ (log ε 4.01).

Found: C, 27.54; H, 5.37; N, 6.30; S, 29.15;

*2 All melting points are uncorrected. Elemental analyses for carbon, hydrogen and nitrogen were carried out by Miss Yoko Endo and Miss Yukiko Endo of this Institute, while that for sulfur was carried out by the Takamine Research Laboratory, Sankyo Co., Ltd., to all of whom the authors thanks are due.

Cl, 16.34. Calcd. for $C_5H_8NS_2Cl \cdot 2H_2O$: C, 27.56; H, 5.56; N, 6.44; S, 29.46; Cl, 16.29%.

The drying of I over phosphorus pentoxide in a vacuum desiccator results in the loss of a part of the water of crystallization, and it effloresces to a white powder (m. p., 115~131°C).

Found: C, 30.28; H, 5.38; N, 7.43. Calcd. for $C_5H_8NS_2Cl \cdot H_2O$: C, 30.07; H, 5.05; N, 7.01%.

1,6-Dithia-3a-azonia-2, 3, 4, 5-tetrahydropentalene Bromide (II), Iodide (III) and Picrate (IV).—A solution of 2.5 g. of potassium bromide dissolved in 3 ml. of water was added to a solution of 1.6 g. of I dissolved in 3 ml. of water; the mixture was then allowed to stand under ice cooling, by which process 0.8 g. of the bromide (II) was obtained as colorless crystals (m. p. 95°C).

Found: C, 22.98; H, 4.99; N, 5.51. Calcd. for $C_5H_8NS_2Br \cdot 2H_2O$: C, 22.89; H, 4.62; N, 5.34%.

A solution of 3 g. of potassium iodide dissolved in 3 ml. of water was added to the solution of 1.6 g. of I dissolved in 3 ml. of water; the mixture was then allowed to stand. The crystals that separated out were collected by filtration (1.7 g. of colorless cubic crystals (III); m. p., 220°C (decomp.). Recrystallization from ethanol containing a small amount of water gave colorless rhombs of the same melting point.

UV λ_{max}^{MeOH} 258 mμ (log ε 4.03).

Found: C, 21.87; H, 2.73; N, 5.15; S, 21.90; I, 46.00. Calcd. for $C_5H_8NS_2I$: C, 21.97; H, 2.95; N, 5.13; S, 23.48; I, 46.47%.

To 114 mg. of I suspended in 3 ml. of ethanol, 2 ml. of a 6% ethanolic solution of picric acid was added; the mixture was then warmed on a water bath until the whole dissolved. When this solution was allowed to stand at room temperature, 194 mg. of yellow needles (IV) (m. p., 154°C) was obtained.

UV λ_{max}^{MeOH} mμ (log ε): 250 (4.29), 355 (4.21).

Found: C, 35.44; H, 2.67; N, 14.93. Calcd. for $C_{11}H_{10}O_7N_4S_2$: C, 35.29; H, 2.69; N, 14.97%.

The picrate IV was also obtained by the treatment of III with picric acid.

***N*-(2'-Mercaptoethyl)-2-thiazolidinone (V) and its Lead Salt (VI).**—A solution of 660 mg. of I dissolved in 3 ml. of water was heated in a sealed tube. After the solution had been heated for 3 hr., a liquid layer separated out; the tube was then heated for a further 15 hr. The separated aqueous layer was evaporated in vacuo to dryness at room temperature, and 5 ml. of benzene was added to its residue. From the insoluble crystals, 70 mg. of I were recovered, while from the benzene soluble part, 85 mg. of liquid mercapto compound V were obtained. The remaining liquid layer was washed with water and dried in a vacuum desiccator to 360 mg. of liquid V which is easily soluble in ether, benzene and alcohols and which vaporizes gradually at 120~140°C/0.1 mmHg.

This mercapto compound V was also obtained when an aqueous solution of I was allowed to stand in a sealed tube at room temperature for 4 months.

IR strong bands (liquid): 2925, 2865, 2550, 1667 (1690 in CCl_4), 1479, 1447, 1412, 1360, 1328, 1293, 1234, 1199, 1147, 935, 698 and 662 cm^{-1}.

The addition of a solution of 530 mg. of basic lead acetate dissolved in 5 ml. of water to a solution of 160 mg. of V dissolved in 5 ml. of ethanol resulted in the precipitation of yellow crystals. The crystals were collected by filtration and washed with water to 330 mg. of the lead salt (VI) as yellow needles (m. p., 143°C). VI is sparingly soluble in water and in organic solvents.

Found: C, 22.23; H, 3.08; N, 4.93; Pb, 39.27. Calcd. for $C_{10}H_{16}O_2N_2S_4Pb$: C, 22.59; H, 3.03; N, 5.27; Pb, 38.97%.

β-(2-Thiazolidinon-3-yl)ethyl Disulfide (VII).—a) A mixture of 100 mg. of V dissolved in 1.5 ml. of ethanol and 1.5 ml. of 10% hydrogen peroxide solution was allowed to stand overnight at room temperature. By the evaporation of the solvent, 90 mg. of crystals (m. p., 93.5~94°C) were obtained. Recrystallization from ethyl acetate gave colorless plates (VII) (m. p., 94°C).

IR strong bands (KBr disk): 1660, 1441, 1411, 1291, 1237, 1201, 923, 815 and 696 cm^{-1}.

Found: C, 37.31; H, 4.99; N, 8.72%; mol. wt. (Rast), 335. Calcd. for $C_{10}H_{16}O_2N_2S_4$: C, 37.01; H, 4.97; N, 8.63%; mol. wt., 324.5.

b) To a solution of 80 mg. of V in 2 ml. of ethanol, 3 drops of ammonia water were added; air was then blown on the mixture for 3 hr. With the evaporation of the solvents, 73 mg. of rhombic crystals (m. p. 91.5~93°C) were obtained. Those crystals showed no depression of the melting point on admixture with the VII obtained by afore-mentioned method a).

The Treatment of IV with Alkali.—To 40 mg. of the picrate IV suspended in 3 ml. of water, 2.2 ml. of 0.05 N sodium hydroxide were added; the mixture was then warmed on a water bath until in solution. This yellow solution was adjusted to pH 8 and allowed to stand; 15 mg. of VII were thereby obtained as colorless plates (m. p., 91~93°C).

1a-[β-(2'-Thiazolidinon-3'-yl)ethylthio]-1,6-dithia-3a-aza-2, 3, 4, 5-tetrahydropentalene (VIII).—Into a solution of 2.18 g. of I dissolved in 20 ml. of water, about 6 ml. of a 2 N sodium hydroxide solution were stirred drop by drop over a 1 hr. period; crystals were thereby precipitated out. The mixture was adjusted to pH 8.0, allowed to stand in an ice box overnight, and filtered to collect 1.40 g. of crystals (m. p., 108~110°C).

The filtrate with a pH value of 4.5 was adjusted to pH 8.0 by the addition of a 2 N sodium hydroxide solution and again allowed to stand in an ice box; 0.13 g. of crystals (m. p., 107~110°C) was thereby obtained.

The two crops of crystals were combined (quantitative yield) and recrystallized from benzene as rhombic crystals with an m. p. of 108.5°C. Further recrystallization from methanol gave colorless needles (VIII) (m. p., 114°C).

UV λ_{max}^{MeOH} 258 mμ (log ε 3.91).

IR strong bands (KBr disk): 1668, 1451, 1447, 1410, 1286, 1229, 1203, 1073, 930, 744, 735, 695 and 689 cm^{-1}.

Found: C, 39.26; H, 5.17; N, 9.15; S, 41.18%; mol. wt., 311. Calcd. for $C_{10}H_{16}ON_2S_4$: C, 38.93; H, 5.23; N, 9.08; S, 41.57%; mol. wt., 308.5.

The Treatment of VIII with Alkali in Ethanol.—A suspension of 50 mg. of VIII in 2.5 ml. of ethanol was stirred, and 0.5 ml. of 2 N sodium hydroxide solution was added. The mixture was stirred at room temperature for one hour until the whole dissolved and then allowed to stand overnight; the ethanol was then evaporated. The residue was acidified with hydrochloric acid and extracted with benzene. The extract was dried over anhydride. sodium sulfate, and the benzene was evaporated, leaving a liquid. A part of this liquid crystallized. A small amount of ether was added to this residue and filtered to collect 20 mg. of colorless crystals (m. p., 87~89°C), which showed the same infrared spectrum as that of VII.

The Reaction of VIII and Picric Acid.—A solution of 69 mg. of picric acid dissolved in 2 ml. of ethanol was added to a solution of 95 mg. of VIII dissolved in 6 ml. of ethanol while being warmed. The crystals that precipitated out were allowed to dissolve by warming, the solution was allowed to stand, and the crystals that precipitated out were collected by filtration (115 mg. of yellow needles; m. p., 154°C). This substance showed no depression of the melting point on admixture with the picrate IV obtained by the afore-mentioned method.

The filtrate was passed through an alumina column to remove the picric acid, and the ethanolic effluent was evaporated to remove the solvent, leaving 50 mg. of a colorless liquid. The infrared spectrum of this liquid agreed completely with that of the mercapto compound V.

The Reaction of VIII and Hydrochloric Acid.—Into a suspension of 120 mg. of VIII in 5 ml. of ethanol, 0.5 ml. of 2 N hydrochloric acid was added under stirring at room temperature, and the solution thus obtained was allowed to stand in an ice box overnight. After the evaporation of the solvent, a small amount of benzene was added to the residue, and it was filtered to collect 80 mg. of colorless crystals which were identified as cation chloride I. The solvent evaporated from the filtrate to 70 mg. of a liquid which showed the same infrared spectrum as the mercapto compound V.

Spectral Measurements.—The NMR spectra were measured in heavy water with a Varian V-4300 spectrometer (60 Mc.). The ultraviolet spectra were taken with a Hitachi model EPS-2 spectrophotometer, and the infrared spectra, with a Perkin-Elmer model 21 infrared spectrophotometer (sodium chloride and potassium bromide prisms) and a Hitachi model EPI-S2 infrared spectrophotometer (sodium chloride prism).

The Raman spectrum of I was measured with a Shimadzu automatic-grating Raman spectrometer, Type GRS-750, using the Hg-e line (4358 Å) from a Toronto-type mercury lamp as the exciting line.

The authors are indebted to Mr. Kensuke Takahashi for the measurement of the NMR spectra, to Mr. Tetsuo Hata for co-operation in the measurement of the Raman spectrum, and to Mr. Humio Sato for that of the ultraviolet spectra. The authors are also grateful to the Sankyo Co., Ltd., for its financial assistance in the present research.

The Chemical Research Institute of Non-Aqueous Solutions
Tohoku University
Katahira-cho, Sendai

Synthetic Resins Catalyzing the Racemization of Amino Acids. I. The Preparation of the Resins

By Koji Toi, Yoshiharu Izumi and Shiro Akabori

(Received February 16, 1963)

In general, optically-active free amino acids racemize only slowly even in a strongly alkaline or acidic solution at a boiling temperature. Heating the solution at a much higher temperature under high pressure accelerates the reaction, but this acceleration is accompanied by an appreciable decomposition of the amino acids. The racemization processes most commonly used involve heating suitable derivatives of optically-active amino acid with alkali or treating free amino acid with acetic anhydride or ketene in the presence of alkali and hydrolyzing the resulting acetyl-DL-amino acid. In the latter method, however, the recovery of the racemized amino acid has been achieved only with some difficult. Thus, it would be useful to prepare a catalyst which would accelerate the racemization of optically-active free amino acids under milder conditions.

In nature the so-called racemase catalyzes the racemization of amino acid under physiological conditions. These enzymes require pyridoxal phosphate as a coenzyme[1-5]. In

1) W. A. Wood and I. C. Gunsalus, *J. Biol. Chem.*, **190**, 403 (1951).
2) P. Ayengar and E. Roberts, ibid., **197**, 453 (1952).
3) W. A. Wood and S. Narrod, *Arch. Biochem. Biophys.*, **35**, 462 (1952).
4) H. T. Huarg, D. A. Kita and J. W. Davidson, *J. Am. Chem. Soc.*, **80**, 1006 (1958).
5) A. Ichihara, S. Furuya and M. Suda, *J. Biochem.*, **48**, 277 (1960).

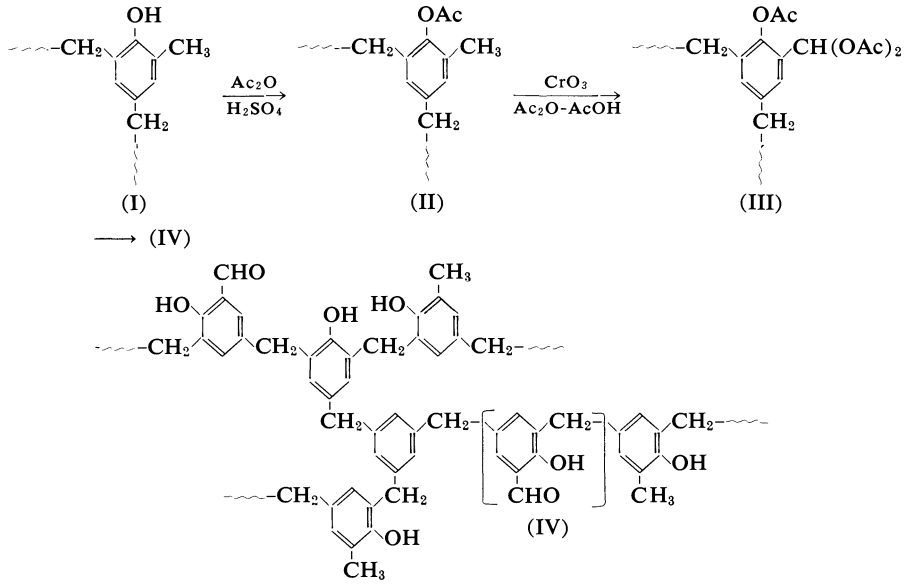

Structure of Resin A

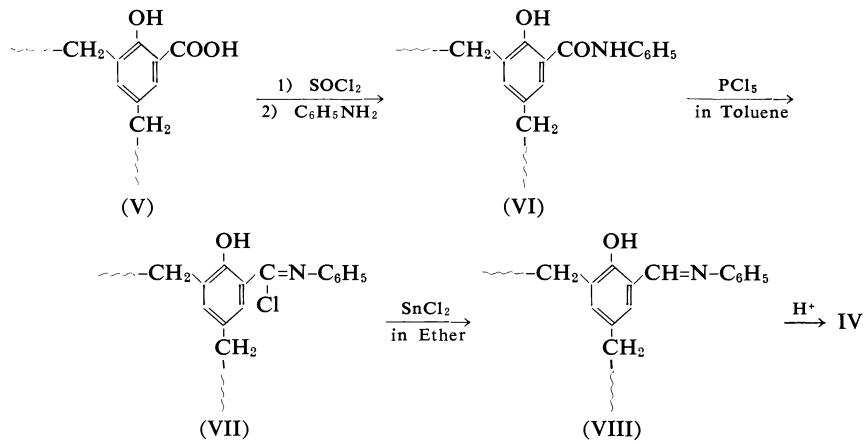

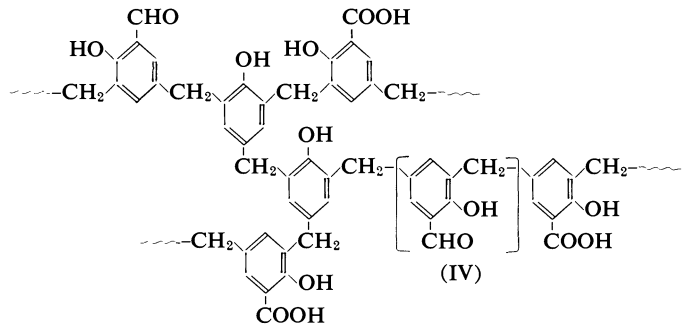

Structure of Resin B

studies of the non-enzymatic reaction between pyridoxal and amino acids, Snell et al. found that pyridoxal itself catalyzes the racemization of amino acids in the presence of some metal ions[6] and proposed a general mechanism for pyridoxal-catalyzed reactions[7].

6) J. Olivard, D. E. Metzler and E. E. Snell, *J. Biol. Chem.*, **199**, 669 (1952).

7) M. Ikawa and E. E. Snell, *J. Am. Chem. Soc.*, **76**, 653 (1954).

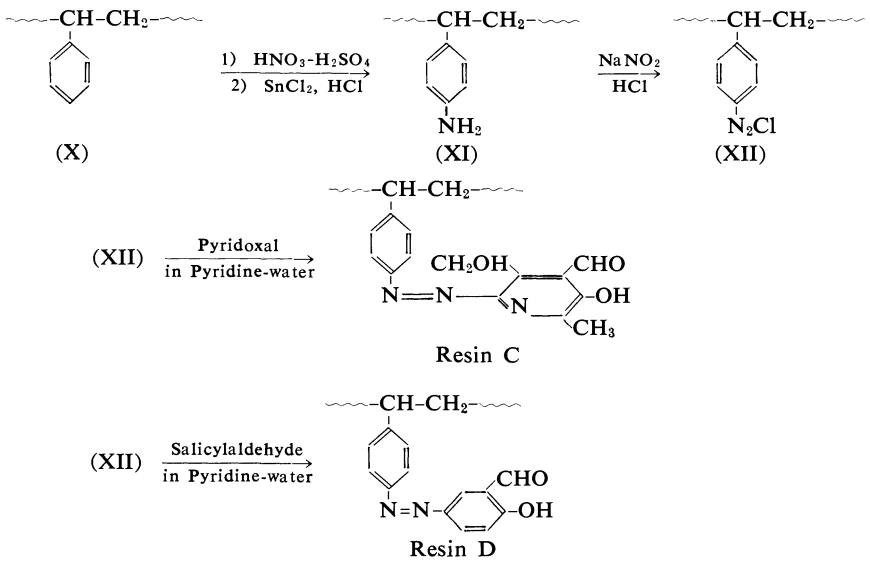

Furthermore, it has been demonstrated that benzene analogues of pyridoxal, such as salicylaldehyde and its derivatives, namely 4- and 6-nitrosalicylaldehyde, also catalyze the racemization of amino acids in the presence of metal ions[8-10].

In a previous paper[11] it was reported that a resin, part of which was structurally similar to salicylaldehyde, namely, a benzene ring with formyl and hydroxy groups at positions ortho to each other (IV), accelerated the racemization of L-alanine, L-aspartic acid and L-glutamic acid in the presence of cupric ions.

In the present work, various methods of preparing such resin were investigated. Thus, four resins (Resins A—D) were prepared. All of them were found to be able to catalyze the racemization of amino acids in the presence of cupric ions.

Resin A, the activity of which has been reported in a previous paper[11], was prepared from *o*-cresol-phenol-formalin resin (I) by converting the methyl groups in the resin to formyl groups. The crushed resin was oxidized with chromium trioxide in a mixture of acetic acid and acetic anhydride, and then the acetal product III was hydrolyzed with 4 N hydrochloric acid to give IV.

Resin B was prepared from salicylic acid-phenol-formalin resin (V) by reducing the carboxy groups in the resin to formyl groups according to the Sonn-Müller method[12]. The crushed resin was treated with thionyl chloride and then with aniline to give the anilides VI in the resin. The anilides were converted to chloroimides VII by treatment with phosphorous pentachloride in toluene, and the chloroimides were then reduced to aldimines VIII with stannous chloride in ether saturated with hydrogen chloride. The aldimines were finally converted to aldehyde groups IV by hydrolysis with N hydrochloric acid.

Resins C and D were obtained from diazotized poly-*p*-amino styrene (XII) by coupling with pyridoxal and salicylaldehyde respectively. A cross-linked polystyrene resin (X) was nitrated with a mixture of nitric acid and sulfuric acid, and then the nitro groupings in the resin were reduced to amino groupings with stannous chloride in hydrochloric acid according to the procedure of D'Alelio[13]. The amino-resin (XI) was then treated with sodium nitrite in hydrochloric acid, and the XII produced was subjected to coupling with pyridoxal or salicylaldehyde. The coupling was carried out in a mixture of pyridine and water. The resins so obtained had the dark red color characteristic of the azo groupings.

The amount of formyl group in the resin was measured by Schultes' procedure[14]. A given amount of the resin was treated with aqueous hydroxylamine sulfuric acid, and the amount of sulfuric acid liberated was determined quantitatively by alkaline titration (Table I).

The racemization experiment was conducted

8) K. Ohno, I. Sasaji and M. Hara, Abstract of the 12th Annual Meeting of the Chemical Society of Japan (1959), p. 27.
9) K. Ohno, I. Sasaji and M. Hara, Japanese Pat. 295110.
10) A. E. Martell and M. Carvin, "Chemistry of the Metal Chelate Compounds", Prentice-Hall, Inc., New York, N. Y. (1952), pp 397-401.
11) K. Toi, Y. Izumi and S. Akabori, This Bulletin, 35, 1422 (1962).
12) A. Sonn and E. Müller, *Ber.*, 52, 1927 (1919).
13) G. F. D'Alelio, U. S. Pat. 2366008.
14) H. Schultes, *Z. Angew. Chem.*, 47, 258 (1934).

TABLE I. ALDEHYDE CONTENTS OF THE RESINS

Resin	Aldehyde content mmol./g.
A	0.24
B	0.31
C	0.10
D	0.20

with L-alanine in the presence of cupric ions. The results are shown in Figs. 1 to 3. Racemization tests with Resin A for L-alanine, L-aspartic acid and L-glutamic acid have already been reported in a previous paper[11]. An aqueous L-alanine solution of pH 10 containing cupric ions and a borate buffer was heated with the resin at 100°C. Aliquots of the reaction mixture were removed at varying intervals and filtered. Each filtrate was diluted with an

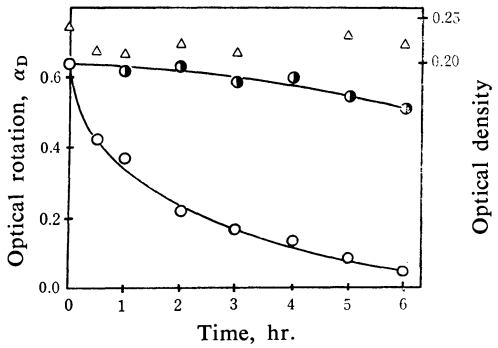

Fig. 1. Racemization of L-alanine by Resin B in the presence of cupric ion.
- ○ Optical rotation in the resin-catalyzed reaction
- ◑ Optical rotation of heated sample without resin
- △ Optical density measured by the ninhydrin method

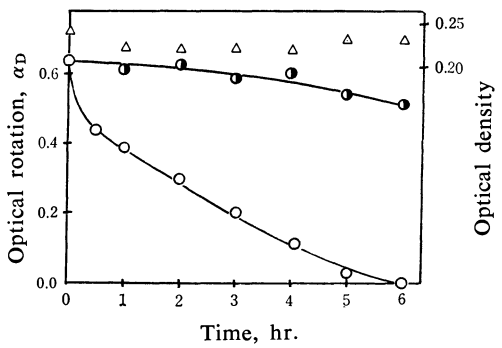

Fig. 2. Racemization of L-alanine by Resin C in the presence of cupric ion.
- ○ Optical rotation in the resin-catalyzed reaction
- ◑ Optical rotation of heated sample without resin
- △ Optical density measured by the ninhydrin method

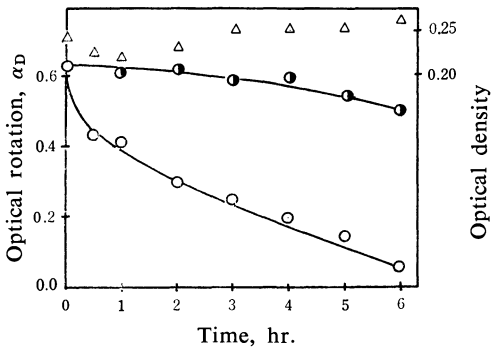

Fig. 3. Racemization of L-alanine by Resin D in the presence of cupric ion.
- ○ Optical rotation in the resin-catalyzed reaction
- ◑ Optical rotation of heated sample without resin
- △ Optical density measured by the ninhydrin method

equal volume of 12 N hydrochloric acid, and its optical rotation was measured. The amino acid contents of the reaction mixtures were checked in order to determine whether or not the simultaneous decomposition of amino acid had occurred. Appropriate aliquots of the acidic solutions, which had been prepared for rotation measurement, were evaporated to dryness. The residues were dissolved in water, and the solutions were made alkaline with sodium hydroxide. Each alkaline solution was evaporated to dryness. The residues was dissolved in water, and the amino acid content of each was determined by the ninhydrin colorimetric method[15]. The values of their optical densities are plotted in Figs. 1 to 3.

It is considered that the reaction conditions under which these catalysts will pass through their maximum activities depend on many factors, such as the pH value of the reaction mixture, the reaction temperature and the nature and concentration of metal ions used.

Experimental

Preparation of Resin A.—A mixture of 108 g. of *o*-cresol, 38 g. of phenol, 160 ml. of 37% formalin and 5 ml. of 50% aqueous sodium hydroxide was stirred at 80~90°C. When the mixture became viscous after 3 hr., stirring was stopped. This mixture was then heated at 100°C for 15 hr. The rigid mass which resulted was crushed to 50~200 mesh, thoroughly washed with water, and dried at 50°C under vacuum. Forty grams of this product were mixed with 240 ml. of acetic anhydride containing 5 ml. of concentrated sulfuric acid for 1 hr., and then 160 ml. of acetic acid were added. Into

15) E. W. Yemm and E. C. Cocking, *Analyst*, **80**, 209 (1955).

this mixture were slowly stirred 16 ml. of concentrated sulfuric acid while it was being externally cooled. When the temperature of the mixture decreased to 0°C, 20 g. of chromium trioxide were added in small portions at such a rate that the temperature did not rise above 5°C. Stirring at 4~5°C was continued for 3 hr. after the addition of the chromium trioxide. The reaction mixture was vigorously stirred into 1.5 l. of water. The product was separated by decantation and washed with water. This material was then hydrolyzed with 300 ml. of 4 N hydrochloric acid under reflux for 3 hr. The final product was filtered with suction, washed with aqueous 5% sodium bicarbonate and then thoroughly with water, and dried at 50°C under vacuum.

Preparation of Resin B.—A mixture of 13.8 g. of salicylic acid, 4.7 g. of phenol, 36 g. of 37% formalin, and 45g. of 20% aqueous sodium hydroxide was stirred at 100°C. When the mixture became viscous, stirring was stopped and the mixture was allowed to stand at 100°C for 12 hr. The resulting rigid mass was crushed to 100~200 mesh, washed thoroughly with dilute hydrochloric acid and then with water, and dried.

Ten grams of this product were swollen with *N*, *N*-dimethylformamide and stirred at 0°C in 65 ml. of thionyl chloride for 3 hr. The resulting resin was filtered, washed with chloroform, and stirred at 0°C for 5 hr. in a mixture of 60 ml. of chloroform, 20 ml. of aniline and 10 ml. of triethylamine. After the mixture had been allowed to stand overnight at room temperature, the product was filtered washed with chloroform and dried. The anilides produced were added to a solution obtained by dissolving 12 g. of phosphorous pentachloride in 100 ml. of toluene and stirred at 90°C for 6 hr. The resulting product, the chloroimides, was filtered, washed with toluene, and then subjected to reduction by stirring it with a solution which was prepared by dissolving 40 g. of stannous chloride dihydrate in 200 ml. of ether saturated with hydrogen chloride. The product obtained was filtered, washed with ether, and then stirred in 200 ml. of N hydrochloric acid at 60°C for 6 hr. The final product was filtered, thoroughly washed with water, and dried under vacuum. Yield, 12 g.

Preparation of Resin C.—A cross-linked polystyrene resin (8% of divinylbenzene, 100~200 mesh) was converted to a poly-*p*-aminostyrene following the procedure of D' Alelio[13]. The polystyrene resin was nitrated with nitric acid and sulfuric acid, and then the nitro groups were reduced to amino groups by stannous chloride in hydrochloric acid. The total capacity of its anion exchange was 1.02 meq. per g.

Ten grams of poly-*p*-aminostyrene resin were stirred in 50 ml. of N hydrochloric acid at 0°C with external cooling. To this suspension 5 ml. of 20% aqueous sodium nitrite were added drop by drop, and stirring was continued for 2 hr. at 0°C. The resulting resin was filtered and washed with cooled aqueous urea and then with cooled water. The diazotized resin was suspended in a solution which was cooled to 0°C and which was prepared by dissolving 3.0 g. of pyridoxal hydrochloride in a mixture of 20 ml. of pyridine and 20 ml. of water. The suspension was stirred at 0°C for 15 hr. The resulting resin was filtered, washed successively with dilute hydrochloric acid, dilute sodium acetate and water, and then dried under vacuum. Yield, 10.3 g.

Preparation of Resin D.—Ten grams of poly-*p*-aminostyrene were diazotized as has been described in the previous paragraph on Resin C. A solution was made of 3.7 g. of salicylaldehyde and 1 g. of sodium carbonate in a mixture of 30 ml. of N sodium hydroxide and 20 ml. of pyridine. This salicylaldehyde solution was cooled to 0°C, and the diazotized resin was added. This mixture was stirred at 0°C for 15 hr. The resulting resin was filtered and washed thoroughly with water. The washed resin was dried under vacuum. Yield, 10.5 g.

Measurement of the Aldehyde Contents of the Resins.—One gram of a resin was shaken for 3 hr. at 60°C with 5 ml. of N hydroxylamine sulfuric acid in a sealed test tube. The mixture was filtered, and an aliquot of the filtrate was titrated with 0.1 N sodium hydroxide, using bromphenol blue as an indicator.

Racemization Test. — An aqueous solution of L-alanine was prepared; it was adjusted to pH 10 with sodium hydroxide and was found to contain 17.8 g. of L-alanine and 0.45 g. of $CuCl_2 \cdot 2H_2O$ in a total volume of 100 ml. Fifteen milliliters of the above solution, 15 ml. of 0.2 M borate buffer of pH 10, and 5 g of the resin were stirred at 100°C.

Summary

1) Four resinous catalysts (Resins A—D) for the racemization of amino acids were prepared. They had structures partially similar to that of salicylaldehyde or pyridoxal. Resins A and B were prepared by the chemical modification of *o*-cresol-phenol-formalin resin and salicylic acid-phenol-formalin resin respectively. Resins C and D were obtained by attaching chemically pyridoxal and salicylaldehyde residues respectively to a styrene-divinylbenzene lattice.

2) These resins catalyzed the racemization of amino acids in the presence of cupric ions at 100°C.

Division of Organic Chemistry
Institute for Protein Research
Osaka University
Kita-ku, Osaka

Synthetic Resins Catalyzing the Racemization of Amino Acids. II. The Activity of the Resins

By Koji Toi

(Received March 5, 1963)

In the previous paper it was reported that some synthetic resins, to which pyridoxal is partially attached or which have a structure partially similar to salicylaldehyde, catalyzed the racemization of amino acids in the presence of cupric ions[1,2]. It was suggested that the conditions under which these catalytic resins are maximally active probably depend on many factors, such as the pH of the reaction mixture, the reaction temperature, the concentration of substrate and the presence of metal ions. Thus, in the present work, a study will be made of the influence of these conditions on the resin-catalyzed racemization.

Studies were made using two typical resins in order to elucidate the general properties of the resins. One (Resin I) is a styrene-divinylbenzene resin, to part of which pyridoxal is attached through azo bondings.

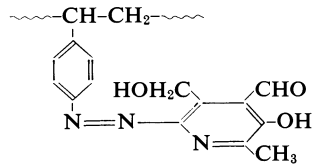

Partial structure of Resin I

The other (Resin II) is chemically-modified *o*-cresol-phenol-formalin resin, part of which is structurally similar to salicylaldehyde, —a benzene ring with formyl and hydroxy groups ortho to each other—

Experimental

Amino Acid Solutions. — These solutions were prepared by dissolving 0.1 mol. of an amino acid and a given amount of a metal salt in a 0.1 M buffer solution and then adjusting it to the desired pH in a final volume of 100 ml. The buffers used were as follows: pH 4 to 5, acetate; pH 6 to 8, phosphate; pH 9 to 12, borate.

Catalytic Resins.—The preparation of Resins I and II was described in the previous paper[2]. Resin I was prepared from a styrene-divinylbenzene resin by nitration, reduction, diazotization, and subsequent coupling with pyridoxal in a mixture of water and pyridine. The formyl content was 0.10 mmol. per g. of dry resin. Resin II was prepared from *o*-cresol-formalin resin by converting the methyl groups in the resin to formyl groups. The crushed resin was oxidized with cromium trioxide in a mixture of acetic acid and acetic anhydride, and the acetal product was hydrolyzed with hydrochloric acid. The formyl content of Resin II was 0.24 mmol. per g. of dry resin.

Racemization Procedure.—A mixture of 5 ml. of an amino acid solution, prepared as described above, and 1 g. of Resin I or II was heated in a sealed test tube while being vigorous shaken in a water bath of the desired temperature. After the reaction, the catalyst was removed by filtration. The filtrate was diluted with a definite volume of 12 N hydrochloric acid, and its optical rotation was measured. For glutamic acid, the measurements were made after this acidic solution had been heated for 2 hr. at 100°C to reconvert the pyroglutamic acid formed during the racemization reaction to glutamic acid[3].

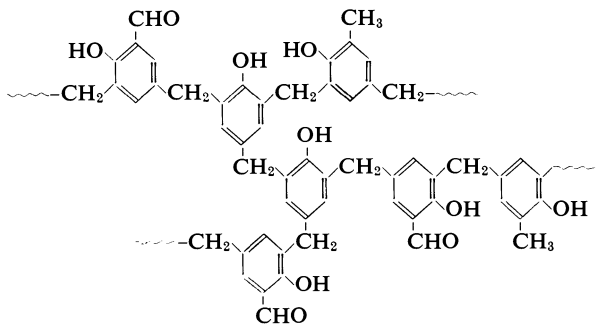

Partial structure of Resin II

1) K. Toi, Y. Izumi and S. Akabori, This Bulletin **35**, 1422 (1962).
2) K. Toi, Y. Izumi and S. Akabori, ibid., **36**, 734 (1963).
3) H. Wilson and R. K. Cannan, *J. Biol. Chem.*, **119**, 309 (1937).

Determination of the Amino Acid Content of the Reaction Mixture.—An aliquot of the solution used for optical rotation measurements was evaporated to dryness. The residue was dissolved in a small amount of water, and the solution was made alkaline. The alkaline solution was evaporated to dryness. The residue was dissolved in water, and the amino acid content of the solution was determined by the ninhydrin colorimetric method[4].

Results and Discussion

Effect of the pH Value of the Reaction Mixture.—The resin-catalyzed racemization of amino acids was tested as a function of pH in the presence of cupric ions. The test was conducted with L-alanine at 98°C. The results are shown in Figs. 1 and 2.

The reaction is influenced by the number of cupric ions, as is shown in Fig. 5. An increase in the concentration of cupric ions accelerates the reaction, but it also causes the racemization of amino acids in the absence of resin on heating in an alkaline medium, especially above pH 11. Therefore, it was undesirable to use much cupric salt in this test.

An aliquot of the L-alanine solution used for the test was simultaneously heated at the same temperature in the absence of resin, as a control for the resin-catalyzed racemization. The degree of racemization of the control was substracted from that of the sample heated with resin.

The results show that the catalysts have

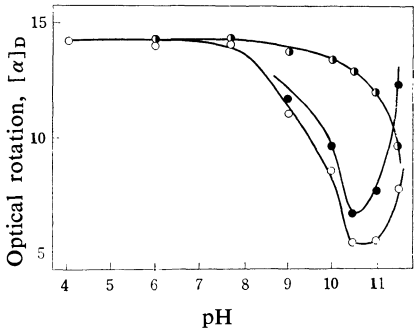

Fig. 1. Effect of pH on racemization of L-alanine by Resin I.

The reaction mixture contained 1 g. of Resin I and 5 ml. of amino acid solution containing 1 M L-alanine, 0.025 M $Cu(CH_3COO)_2 \cdot H_2O$, and 0.1 M concentrations of the following buffers: pH 4 to 5, acetate; pH 6 to 8, phosphate; pH 9 to 12, borate. Reaction time, 1 hr. at 98°C.

○ $[\alpha]_D$ resin-catalyzed racemization
◑ $[\alpha]_D$ recemization in absence of resin
● Difference between ○ and ◑

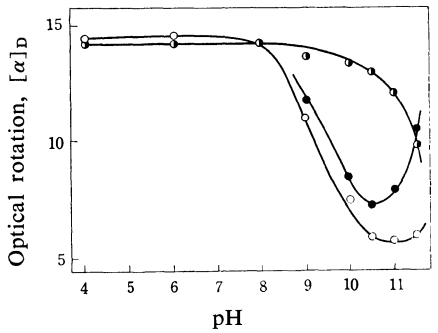

Fig. 2. Effect of pH on racemization of L-alanine by Resin II.

The reaction mixture contained 1 g. of Resin II and 5 ml. of amino acid solution containing 1 M L-alanine, 0.025 M $Cu(CH_3COO)_2 \cdot H_2O$, and 0.1 M concentrations of the following buffers: pH 4 to 5, acetate; pH 6 to 8, phosphate; pH 9 to 12, borate. Reaction time, 1 hr. at 98°C.

○ $[\alpha]_D$ resin-catalyzed racemization
◑ $[\alpha]_D$ racemization in absence of resin
● Difference between ○ and ◑

optima at about pH 10.5. In their work on the pyridoxal-catalyzed racemization of L-alanine in a non-enzymatic system, Snell et al. found that the optimum pH of pyridoxal was between 9 and 10[5]. Thus the two results agree roughly with each other.

Effect of the Reaction Temperature. — The racemization of L-alanine with Resins I and II was carried out at 60, 80 and 97°C. The results are shown in Figs. 3 and 4.

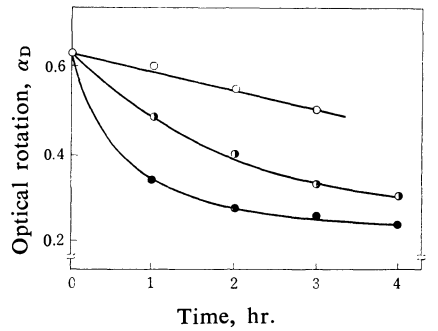

Fig. 3. Apparent racemization of L-alanine by Resin I at 60, 80 and 97°C (pH 10).

The reaction mixture contained 1 g. of Resin I and 5 ml. of amino acid solution containing 1 M L-alanine, 0.025 M $Cu(CH_3COO)_2 \cdot H_2O$ and 0.1 M borate buffer.

○ Optical rotation in reaction at 60°C
◑ Optical rotation in reaction at 80°C
● Optical rotation in reaction at 97°C

4) E. W. Yemm and E. C. Cocking, *Analyst*, **80**, 209 (1955).

5) J. Olivard, D. E. Metzler and E. E. Snell, *J. Biol. Chem.*, **199**, 669 (1952).

TABLE I. COMPAPISON OF ACTIVITIES OF METAL IONS IN THE RESIN-CATALYZED RACEMIZATION OF L-ALANINE

Metal ion	Solution of L-alanine		Racemization with Resin I				Racemization with Resin II			
	α_D	$[\alpha]_D$	α_D	Recovery of L-alanine	$[\alpha]_D$	Racemization yield	α_D	Recovery of L-alanine	$[\alpha]_D$	Racemization yield
Cu^{2+}	0.43	15	0.20	94	7.2	52	0.06	86	2.3	85
Co^{2+}	0.43	15	0.35	90	11	27	0.24	78	10	33
Ni^{2+}	0.44	15	0.40	87	15	0	0.29	73	13	13
Mg^{2+}	0.44	15	0.39	89	15	0	0.28	72	13	13
Zn^{2+}	0.44	15	0.40	94	14	7	0.32	79	14	7

The reaction mixture contained 1 g. of Resin I or II and 5 ml. of amino acid solution (pH 10) containing 1.0 M L-alanine, 0.06 M a metal salt, and 0.1 M borate buffer. The metal salts used were $Cu(CH_3COO)_2 \cdot H_2O$, $CoCl_2 \cdot 6H_2O$, $Ni(CH_3COO)_2 \cdot 4H_2O$, $MgSO_4 \cdot 7H_2O$ and $Zn(CH_3COO)_2 \cdot 2H_2O$. Reaction time, 1 hr. at 98°C. The optical rotation α_D was measured in acidic solution prepared by diluting the reaction mixture with two volumes of 6 N HCl.

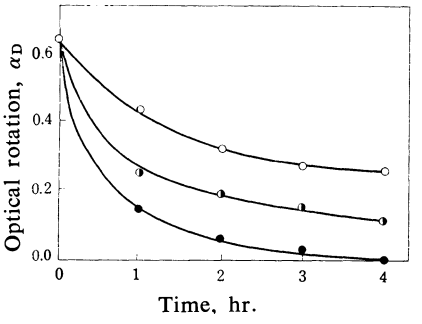

Fig. 4. Apparent racemization of L-alanine by Resin II at 60, 80 and 97°C (pH 10).

The reaction mixture contained 1 g. of Resin II and 5 ml. of amino acid solution containing 1 M L-alanine, 0.06 M $Cu(CH_3 \cdot COO)_2 \cdot H_2O$ and 0.1 M borate buffer.

○ Optical rotation in reaction at 60°C
◑ Optical rotation in reaction at 80°C
● Optical rotation in reaction at 97°C

In the presence of a given amount of cupric ion, the racemization reaction proceeded like an ordinary chemical reaction in that, as the temperature was increased, the rate of the reaction increased.

Effect of the Type of Metal Ion Present.—The racemization of amino acids catalyzed by the resin proceeds well in the presence, but not in the absence, of metal ions. A comparison was made of the effect of fixed concentrations of metal ions on the catalysis of the racemization by the resin. Table I shows the results of this test. Of the metal ions tested, cupric ions were the most effective, while cobaltous ions were quite active. Experiments with ferric and aluminum ions were impossible because these metals precipitated as hydroxides under the conditions used.

The concentration of metal ions in the reaction mixture has a considerable effect on the rate of racemization (Fig. 5). An increase in concentration of metal ions raises the rate of the reaction.

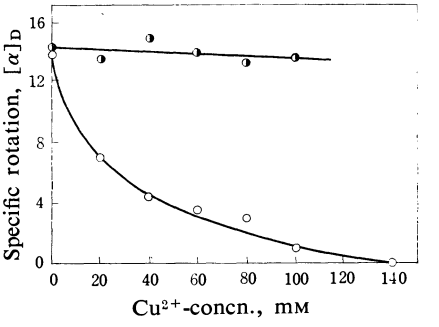

Fig. 5. Effect of the Cu^{2+}-concentration on racemization of L-alanine by Resin II.

The reaction mixture contained 1 g. of Resin II and 5 ml. of amino acid solution (pH 10) containing 1.0 M L-alanine and 0.1 M borate buffer. Reaction time, 1 hr. at 98°C.

○ $[\alpha]_D$ with Resin II
◑ $[\alpha]_D$ in absence of resin

Retention of Resin Activity.—It is desirable that the catalytic resin should retain its activity during the reaction and on repeated use. The activity of Resins I and II on repeated use was, therefore, tested; the results are given in Table II. L-Alanine was tested with the resin for 1 hr. at 98°C in the presence of cupric ions, and the resin was recovered by filtration. After recovery, the catalyst was washed with borate buffer and used for the next run. The activity of the resin was retained for at least seven runs.

The Racemization of Various Amino Acids.—A study was made of the extent of racemization of a series of amino acids. As may be

Table II. Retention of activity

	Apparent racemization, α_D	
	Resin I	Resin II
Before reaction	0.42	0.42
Original resin	0.17	0.08
After 1st recovery	0.16	0.10
After 2nd recovery	0.18	0.09
After 3rd recovery	0.19	0.08
After 4th recovery	0.18	0.12
After 5th recovery	0.11	0.08
After 6th recovery	0.16	0.11

The reaction mixture contained 1 g. of Resin I or II and 5 ml. of amino acid solution (pH 10) containing 1 M L-alanine, 0.06 M $Cu(CH_3COO)_2 \cdot H_2O$ and 0.1 M borate buffer. Reaction time, 1 hr. at 98°C.

seen in Table III, each of the amino acids tested underwent racemization to some extent. In the case of L-phenylalanine, L-tyrosine and L-methionine, cobaltous ions were chosen instead of cupric ions because of the insolubility of the copper complexes of these amino acids under the conditions used. L-Alanine racemized most rapidly, and L-aspartic acid, at quite a high rate. In the course of the reaction, amino acids underwent some spontaneous decomposition. The recovery of amino acid was estimated by the optical density of the ninhydrin colorimetric reaction of the amino acid after its isolation from the reaction mixture on a paper chromatogram.

A Comparison of the Activity of the Resin and of Pyridoxal.—In non-enzymatic systems, pyridoxal may be most effective as a catalyst for amino acid racemization. A comparison was made of the effects of the resin and of pyridoxal on the rate of racemization of L-alanine in the presence of cupric ions at 80 and 98°C, though pyridoxal was dissolved in the reaction systems. Conditions were used under which the catalytic resin passed through its maximum activity at a given temperature. The amount of each catalyst was adjusted to give equal contents of aldehyde.

The resin has no stereospecificity and can simultaneously catalyze the conversion of both the L- to the D-form and the D- to the L-form. Therefore, the racemization of amino acids is,

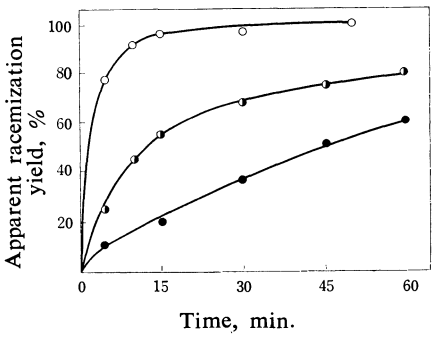

Fig. 6. Comparison of the activities of the resins and pyridoxal in catalysis of the racemization of L-alanine at 98°C.
The reaction system contained 1 g. of Resin I, 0.42 g. of Resin II, or 0.1 mmol. of pyridoxal hydrochloride and 6 ml. of L-alanine solution (pH 10.0) containing 0.83 M L-alanine, 0.083 M $Cu(CH_3COO)_2 \cdot H_2O$ and 0.1 M borate buffer. Reaction time, 1 hr. at 98°C.
○ Pyridoxal ◑ Resin II ● Resin I

Table III. Racemization of various amino acids

Amino acid ($[\alpha]_D$)	Metal ion	pH	Racemization without Resin	Racemization with Resin I			Racemization with Resin II		
			$[\alpha]_D$	$[\alpha]_D$	Racemization yield, %	Recovery of amino acid, %	$[\alpha]_D$	Racemization yield, %	Recovery of amino acid, %
Ala (+15)	Cu^{2+}	10.5	+14	+ 6.4	(57)	99	+ 2.2	(85)	91
Val (+25)	Cu^{2+}	10.5	+25	+25	(0)	99	+19	(24)	98
Asp (+26)	Cu^{2+}	10.0	+25	+23	(11)	95	+ 5.0	(81)	90
Glu (+32)	Cu^{2+}	10.0	+27	+26	(19)	95	+20	(37)	91
Arg (+29)	Cu^{2+}	10.0	+27	+27	(7)	87	+22	(24)	47
Lys (+26)	Cu^{2+}	10.0	+26	+22	(15)	74	+17	(35)	65
Phe (−9.1)	Co^{2+}	10.5	− 8.2	− 8.3	(9)	99	− 5.8	(36)	99
Tyr (−13)	Co^{2+}	10.5	−10	− 9.0	(31)	98	− 6.3	(52)	97
Met (+24)	Co^{2+}	10.5	+22	+20	(17)	100	+15	(38)	98

The reaction mixture contained 1 g. of Resin I or II and 5 ml. of amino acid solution, containing 1 M amino acid, 0.06 M metal salt, and 0.1 M borate. Because of the insolubility of their metal complexes in the case of L-valine, L-tyrosine and L-methionine, the concentration was reduced to 0.5 M amino acid and 0.03 M metal salt.

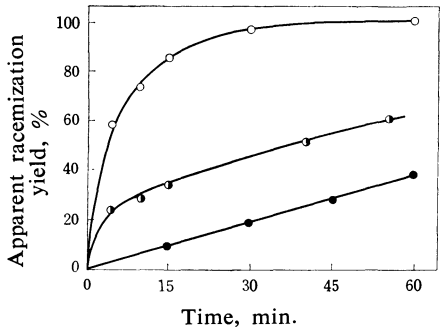

Fig. 7. Comparison of activities of the resins and pyridoxal in catalysis of racemization of L-alanine at 80°C.

The reaction system consisted of 1 g. of Resin I, 0.42 g. of Resin II, or 0.1 mmol. of pyridoxal hydrochloride and 6 ml. of L-alanine solution (pH 10.5) containing 0.83 M L-alanine, 0.033 M $Cu(CH_3COO)_2 \cdot H_2O$ and 0.1 M borate buffer. Reaction time, 1 hr. at 80°C.

○ Pyridoxal ◑ Resin II ● Resin I

in theory, a first-order reaction. The rate of the reaction should be proportional to the concentration of L-alanine at a fixed concentration of cupric ions.

The rate observed in the resin-catalyzed racemization of L-alanine described a curve like a first-order reaction, but it deviated from the theoretical course when the reaction period was long, as may be seen in Figs. 6 and 7. However, after a certain initial period, the rate may be approximately regarded as of the first order.

Thus, the rate constants, k, of the reaction with resin and pyridoxal were compared over the initial five-minute period. The values obtained are summarized in Table IV. At 98°C, the activities of Resins I and II were, respectively, about 8×10^{-2} and 2×10^{-1} of that of pyridoxal.

Table IV. Rate constant

Temp. °C	k, min^{-1}		
	Pyridoxal	Resin I	Resin II
98	3.0×10^{-1}	2.3×10^{-2}	6.4×10^{-2}
80	1.8×10^{-1}	9.2×10^{-3}	5.5×10^{-2}

The values of k were calculated with the formula,

$$k=\frac{2.3}{5}\log\frac{100}{100-x}$$

where x is the apparent racemization yield.

Summary

1) A study has been made of the factors influencing the racemization of amino acids by resinous catalysts with structures partially similar to those of pyridoxal and salicylaldehyde.

2) The optimum pH of the reaction was about 10.5.

3) A rise in temperature resulted in an increase in the rate of the reaction.

4) The racemization reactions catalyzed by the resins required the presence of metal ions, and cupric ions were found to be most effective.

5) Of the amino acids tested, L-alanine was racemized most rapidly.

6) The resinous catalysts retained activity after repeated usage.

7) The racemization-activity of the resins was compared with that of pyridoxal.

The author wishes to express his thanks to Professor Shiro Akabori and Dr. Yoshiharu Izumi for their valuable advice and encouragement throughout this work.

Division of Organic Chemistry
Institute for Protein Research
Osaka, University
Kita-ku, Osaka

Spectrophotometric Study on the Interaction of Chromium(III) with Alizarinsulfonic Acid

By Wahid U. MALIK, Rizwanul HAQUE and Surendra PRATAP

(Received August 13, 1962)

The interaction of metal ions with alizarinsulfonic acid has been studied by a number of workers[1-6], but little seems to have been done as regards the chromium(III) complexes. Preliminary experiments show that chromic chloride does not react with alizarinsulfonic acid at room temperature. However, on heating the mixture at about 80°C for nearly half an hour a red color develops, indicating the probable existence of the complex. The work described here deals with the spectrophotometric studies on the composition of the red product obtained at 80°C.

Chromic chloride (A. R.) was dissolved in redistilled water and the concentration was determined by the usual methods. The solution of alizarinsulfonic acid (sodium salt) was prepared by dissolving a known amount in acetate buffer of pH 3.1. Absorption experiments were carried out with a Bausch and Lomb 'Spectronic 20'. Measurements of pH were made with a Beckman pH-meter model G.

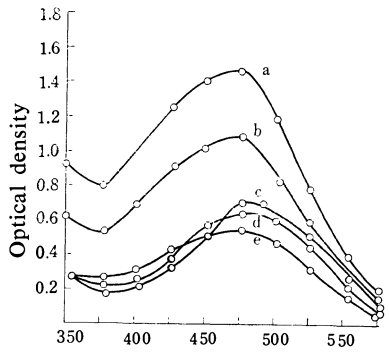

Fig. 1

a) 1 : 1 ratio of the reactants at pH 3.1
b) 1 : 2 ratio of the reactants at pH 3.1
c) 1 : 3 ratio of the reactants at pH 3.1
d) 2 : 1 ratio of the reactants at pH 3.1
e) 3 : 1 ratio of the reactants at pH 3.1

Vosburgh and Cooper's[7] method was employed to determine the number of complexes formed. The reactants were mixed in different molar ratios (1 : 1, 1 : 2, 1 : 3, 2 : 1, 3 : 1), heated on a water bath for about half an hour, cooled to room temperature and their optical densities were measured. All the mixtures gave a maximum at 475 mμ (Fig. 1) showing thereby the formation of only one complex.

The Job's method of continuous variation[8] was followed for determining the composition of the complex. Solutions of chromic chloride and sodium alizarinsulfonic acid of two different concentrations, M/3000 and M/4000, were mixed according to the method of continuous variation and the optical densities measured at 475 mμ. In order to account for the absorption of alizarinsulfonic acid, the mixtures of water (in place of chromic chloride) and alizarinsulfonic acid were taken, heated on a water bath to 80°C, cooled and their optical densities were measured. The chromic chloride solutions prepared under exactly similar conditions showed almost negligible absorption at 475 mμ. A curve was plotted between the

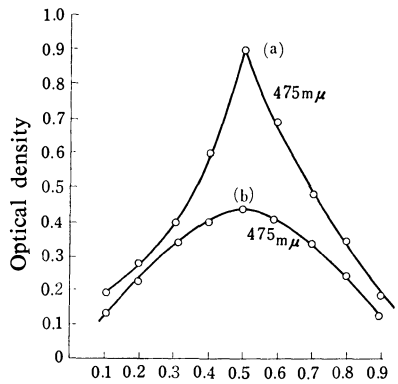

Fig. 2

a) For M/3000 of the reactants at pH 3.1
b) For M/4000 of the reactants at pH 3.1

1) Y. Dorta-Schaeppi, H. Hurzllr and W. D. Treadwell, *Helv. Chim. Acta*, **34**, 797 (1951).
2) D. L. Manning and J. C. White, *Anal. Chim. Acta*, **27**, 1389 (1955).
3) K. S. Venkateswarloo and B. S. V. R. Rao, ibid., **13**, 79 (1950).
4) C. A. Parker and A. P. Goddard, ibid., **4**, 517 (1950).
5) R. W. Reinehart, *Anal. Chim.*, **26**, 1820 (1954).
6) A. K. Dey and A. K. Mukherji, *Proc. Nat. Acad. Sci. (India)*, **26**, 20 (1957).
7) W. C. Vosburgh and G. R. Cooper *J. Am. Chem. Soc.*, **63**, 437 (1941).
8) P. Job, *Ann. Chim.*, **9**, 113 (1928).

difference in optical density of complex and alizarinsulfonic acid and the ratio $Cr^{3+}/(Cr^{3+}+$ alizarinsulfonic acid). The results are depicted in Fig. 2.

The results were also confirmed by the slope ratio[9] and the molar ratio methods[9]. Two sets of experiments were performed for the slope ratio method. In the first set the concentration of sulfonic acid (taken in excess) was kept constant while the concentration of chromic chloride was varied. In the other set the mixtures were prepared by mixing the reagents just in the reverse manner. The optical densities of the mixtures in the two sets were measured under exactly similar conditions as described above and curves drawn between the optical density of the solution and the volume of the reactant (Fig. 3) to be varied. In the

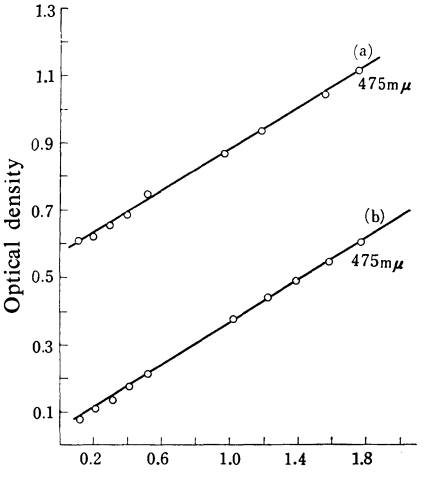

Fig. 3

a) $CrCl_3$ variable
b) Alizarin variable

case of molar ratio method the optical densities of the following two sets of mixtures were measured: (i) 5 cc., alizalinsulfonic acid of 0.5×10^{-3} M mixed with 0.5 cc., to 8.0 cc., chromium(III) chloride 0.5×10^{-3} M, total volume made upto 20 cc. by adding required amount of buffers; (ii) reagent mixed in just the reverse manner as given under (i). The results are shown in Fig. 4.

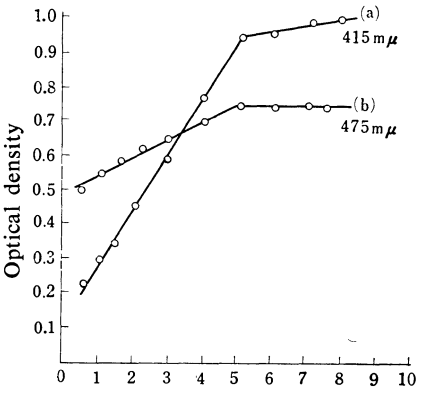

Fig. 4

a) Alizarin variable
b) $CrCl_3$ variable

The Vosburgh and Cooper's method shows the existence of one complex with an absorption maximum at 475 mμ. By applying the Job's method at two different concentrations of the reactants, peaks are obtained corresponding to the molar ratio 1:1 (Fig. 2). The results obtained by the Job's method find support from the slope ratio and molar ratio methods. Hence the probable composition of the complex may be written as:

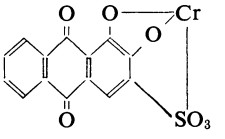

Dey and Mukherji[6] determined the stability constant and free energy of the red alizarinsurfonic acid complex by considering two concentrations of the reactants which gave the same optical density. No such attempt was made here in view of the inert nature of the chromium complex[10] and the slowness with which the reaction is expected to reach equilibrium. The composition put forward here, therefore, refers only to the product formed by the interaction of chromic chloride and alizarinsulfonic acid at 80°C.

Thanks are due to Professor Akhlaq R. Kidwai for providing facilities and C.S.I.R. for the award of a fellowship to one of us (R. H.)

Chemical Laboratories
Aligarh Muslin University
Aligarh, India

9) E. Harvey and D. L. Manning, *J. Am. Chem. Soc.*, **72**, 4488 (1950).
10) H. Taube, *Chem. Revs.*, **50**, 69, (1952).

Polarographic and Spectrophotometric Determination of Zinc in Zinc Stearate

By Wahid U. MALIK, Rizwanul HAQUE and Surendra Pal VERMA

(Received August 13, 1962)

The problem of the estimation of the metal content in heavy metal soaps has been a subject of detailed study in these laboratories for some time. Working with copper, nickel and cobalt soaps, it was found that their property of forming complexes with pyridine base[1] can be advantageously put to use for estimating the metal content by polarography[2] and spectrophotometry[3]. The present communication deals with the estimation of zinc in zinc stearate by the above two methods[2,3].

All the reagents used were either A. R. samples or purified products. Stearic acid (British Drug House) was crystallized with alcohol and finally fractionated under reduced pressure. A. R. pyridine and A. R. mercury (triple distilled) were used.

Zinc stearate was prepard by the precipitation method[4]. The solution was prepared in pyridine and metal content estimated gravimetrically.

Polarographic measurements were carried out with a Fisher Electropode in conjunction with a Multiflex galvanometer model MGF2. Experiments were performed in H-type cell[5] using dropping mercury cathode and a saturated calomel electrode. Lithium chloride and methyl hydrogen sulfate in 1 : 1 benzene-methanol mixture were used as supporting electrolytes[6]. The capillary constants, $m^{2/3}t^{1/6}$, for these supporting electrolytes (0.033 M) were 1.618 and 1.532 respectively in the open circuit. Two sets of experiments were performed: (1) fixed amount of soap (5 cc., approximately 1%) and varying amounts of supporting electrolyte (1.0, 2.0, 3.0, 5.0, 10.0 cc. of 0.165 M), making total volume 30 cc.; (2) fixed amount of supporting electrolyte (5.0 cc. of 0.165 M) and varying amounts of soap (3.0, 5.0, 8.0, 10.0, 12.0 cc. approximately 1%), making total volume 30 cc. Inert atmosphere was maintained in the cell by passing pure nitrogen and experiments were performed at 25±0.1°C in thermostatic water-bath (Townson and Mercer).

The typical polarograms of zinc stearate in lithium chloride and $MeHSO_4$ (concentration 0.005 M) are shown in Fig. 1, the values of

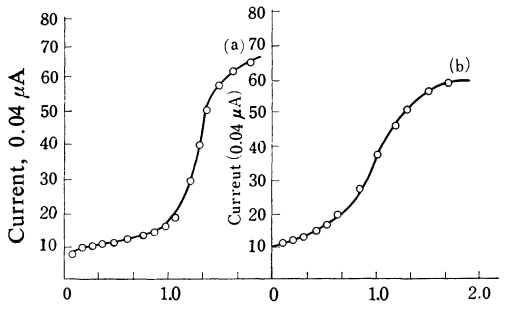

Fig. 1. Polarograms of zinc stearate pyridine complex.

a) 2.5 mM Zn^{2+} in Zn-stearate in 0.055 M LiCl

b) 2.5 mM Zn^{2+} in Zn-stearate in 0.055 M $MeHSO_4$

$E_{1/2}$ in the two supporting electrolytes being −1.4 and −0.9 V. respectively. The values of $E_{3/4}-E_{1/4}$, however, came out to be abnormally high indicating the irreversible nature of the wave. The limiting current was found to increase with increasing concentration of the soap. The values of the concentration of zinc in soap in millimoles per liter (C), the limiting current in microamperes (i_l) and i_l/C are summarized below.

Table I shows that the value of i_l/C remains fairly constant, showing thereby that the estimation of zinc can be made from these results.

TABLE I

C	0.033 M i_l	LiCl i_l/C	0.033 M i_l	$MeHSO_4$ i_l/C
1.5	2.40	1.60	1.20	0.80
2.5	4.16	1.64	2.00	0.80
3.0	4.80	1.60	2.28	0.76
4.0	6.40	1.60	3.12	0.78
5.0	7.68	1.56	3.75	0.75
6.0	9.44	1.56	4.68	0.78

1) C. J. Boner, *Ind. Eng. Chem.*, **29**, 58 (1937).
2) W. U. Malik and R. Haque, *Nature*, in press.
3) W. U. Malik and R. Haque, *Z. Anal. Chem.*, in press.
4) R. G. Bossert, *J. Chem. Educ.*, **27**, 10 (1950).
5) J. J. Lingane and H. A. Laitinen, *Ind. Eng. Chem. Anal. Ed.*, **11**, 504 (1939).
6) W. R. Lewis and coworkers, *Anal. Chem.*, **24**, 762 (1949).

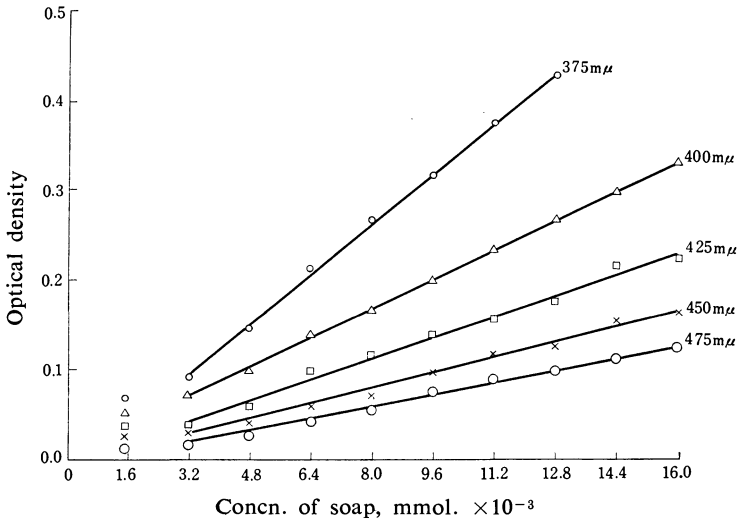

Fig. 2. Optical density as a function of concentration of soap.

Spectrophotometric measurements were carried out with a Bausch and Lomb 'Spectronic 20'. Solutions of zinc stearate of different dilutions were prepared by diluting the stock solution with pyridine. Measurements were carried out in the wavelength region 375 to 475 mμ.

The plot between the optical density and concentration of the metal in the soap gave straight lines upto a certain concentration of the soap solution (Fig. 2). Below this concentration the points did not lie on the straight line, showing thereby that the Beer's law is not obeyed for very dilute solutions and that the zinc ions can be estimated spectrophotometrically in the zinc stearate solution for concentrations higher than 3.2×10^{-3} mM.

Thanks are due to Professor Akhlaq R. Kidwai for providing facilities and C.S.I.R. for the award of a fellowship to one of us (R. H.).

Chemical Laboratories
Aligarh Muslim University
Aligarh, India

*An Improved Synthesis of 1,3,5-Tri-t-butylbenzene**

By Setsuo WATARAI

(Received January 5, 1963)

Various methods of preparing tri-*t*-butylbenzene have been reported in the literature[1], but the first positive mention of 1,3,5-tri-*t*-butylbenzene (I) is to be found in a paper by McCaulay and Lien[2]; the material was obtained by the disproportionation of *t*-butylbenzene with hydrogen fluoride and boron trifluoride at 0°C. The same substance has also been obtained by the Friedel-Crafts alkylation of *p*-di-*t*-butylbenzene (II)[3,4] or by other reactions[3,5,6].

Undoubtedly the procedure of Barclay and Betts[4], who showed that I was obtained from the aluminum chloride-catalyzed alkylation of II with a large excess of *t*-butyl chloride in

* This work was presented at the 13th Annual Meeting of the Chemical Society of Japan, Tokyo, April, 1960.

1) a) M. Senkowski, *Ber.*, **23**, 2412 (1890); b) F. Kunckell and G. Ulex, *J. prakt. Chem.*, **87**, 233 (1913); c) V. N. Ipatieff, B. B. Corson and H. Pines, *J. Am. Chem. Soc.*, **58**, 919 (1936).

2) D. A. McCaulay and A. P. Lien, ibid., **75**, 2411 (1953).

3) P. D. Bartlett, M. Roha and R. M. Stiles, ibid., **76**, 2349 (1954).

4) L. R. C. Barclay and E. E. Betts, *Can. J. Chem.*, **33**, 672 (1955).

5) W. Van Hartingsveldt, P. E. Verkade and B. M. Wepster, *Rec. trav. chim.*, **75**, 349 (1956).

6) U. Krüerke, C. Hoogzand and W. Hübel, *Chem. Ber.*, **94**, 2817 (1961).

TABLE I. *t*-BUTYLATIONS OF *m*-DI-*t*-BUTYLBENZENE

Exp. No.	1*	2	3	4	5	6	7
Reagents (mol.)							
m-Di-*t*-butylbenzene (III)	0.40	0.40	0.37	0.37	0.37	0.37	0.30
t-Butyl chloride	3.20	3.20	0.37	0.37	0.48	0.48	0.15
Aluminum chloride	0.20	0.20	0.022	0.022	0.03	0.03	0.005
($AlCl_3$, mol./mol. *t*-butyl chloride)	0.06	0.06	0.06	0.06	0.06	0.06	0.03
($AlCl_3$, mol./mol. aromatics (III)	0.5	0.5	0.06	0.06	0.08	0.08	0.02
Temp., °C	−8	−8	−8	30	30	30	25
Reaction time, hr.	1.0	1.0	1.0	1.0	2.0	4.0	6.0
Products, mol. %							
m-Di-*t*-butylbenzene (III)	—	—	94	37	35	9.5	67
1,3,5-Tri-*t*-butylbenzene (I)	76	76.5	—	56.5	57	79	21**
Total mol. %	76	76.5	94	93.5	92	88.5	88

* The method described by Barclay and Betts[4], *p*-di-*t*-butylbenzene (II) was used in spite of *m*-di-*t*-butylbenzene (III).
** Theoretical yield; 42%

the cold, is very attractive when large quantities of this compound are to be prepared.

However, *p*-di-*t*-butylbenzene has some undesirable properties for this purpose in comparison with *m*-di-*t*-butylbenzene (III); a large excess of *t*-butyl chloride[4] or of other organic solvents[3], such as carbon disulfide or ethylene dichloride, should be used to dissolve *p*-di-*t*-butylbenzene, while III is misible in *t*-butyl chloride in all proportions. The m. p. (76~77°C) of II is close to that (73.5°C) of I; furthermore, a rearrangement other than alkylation should be involved in the reaction steps.

Some unusual cyclialkylation products, such as IV[7], V[8] and others[3], have been isolated from a complex mixture as by-products of the preparation of I by the aluminum chloride-catalyzed alkylation of II with a large excess of *t*-butyl chloride in the cold. The mechanism of the formation of these by-products has been discussed by several workers[7-10].

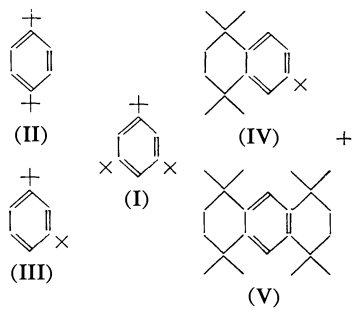

+ ; *t*-Butyl group

7) P. C. Myhre and W. M. Schubert, *J. Org. Chem.*, **25**, 708 (1960).
8) L. R. C. Barclay and E. E. Betts, *J. Am. Chem. Soc.*, **77**, 5735 (1955).
9) L. R. C. Barclay and J. W. Hilchie, *J. Org. Chem.*, **22**, 633 (1957).
10) F. E. Condon, ibid., **21**, 761 (1956).
11) T. Kinugasa and S. Watarai, *J. Chem. Soc. Japan, Pure Chem. Sec. (Nippon Kagaku Zasshi)*, **83**, 333 (1962).

An earlier communication[11] reported the formation of hydrocarbon II through a simple procedure from the alkylation of *t*-butylbenzene with *t*-butyl chloride in the presence of

TABLE II. DISPROPORTIONATIONS OF *m*-DI-*t*-BUTYLBENZENE

Exp. No.	8	9
Reagents (mol.)		
m-Di-*t*-butylbenzene (III)	0.25	0.37
Aluminum chloride	0.004	0.03
$AlCl_3$, mol./mol. III	0.02	0.08
Temp., °C	25	30
Reaction time, hr.	6.0	6.0
Products, mol. %		
t-Butylbenzene	6.0	8.0
m-Di-*t*-butylbenzene (III)	80.5	24.5
p-Di-*t*-butylbenzene (II)	4.0	40.0
1,3,5-Tri-*t*-butylbenzene (I)	2.0	9.0
Total mol. %	92.5	81.5

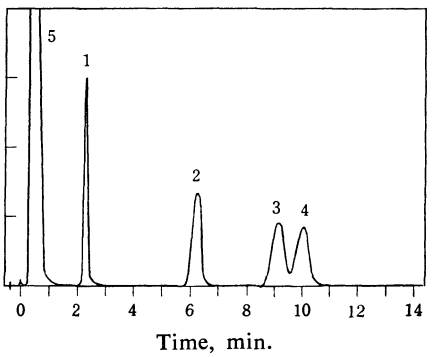

Fig. 1. Gaschromatogram of *t*-butylated benzenes.
1 *t*-Butylbenzene
2 *m*-Di-*t*-butylbenzene (III)
3 *p*-Di-*t*-butylbenzene (II)
4 1, 3, 5-Tri-*t*-butylbenzene (I)
5 Benzene (solvent)

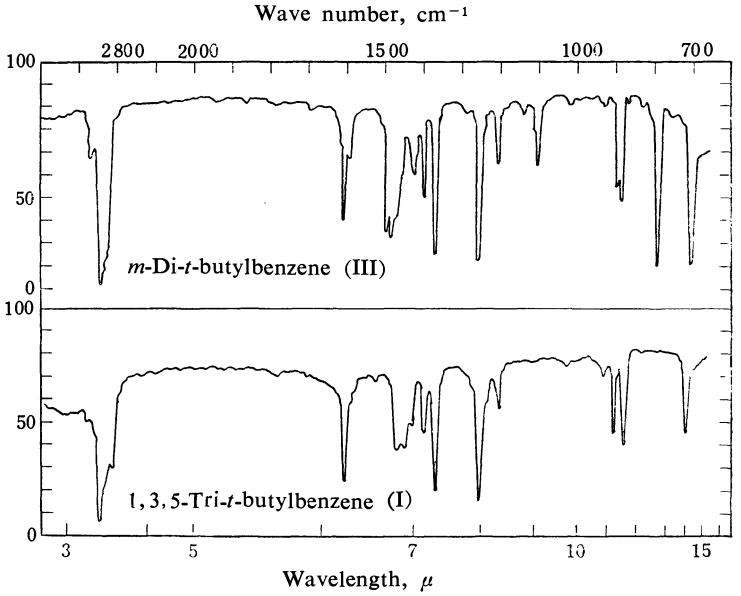

Fig. 2. Infrared spectra of compounds I and III.

rather a little aluminum chloride, and the preparative condition for this hydrocarbon was proposed.

In the present paper, the *t*-butylations of *m*-di-*t*-butylbenzene and an improved method of preparing 1, 3, 5-tri-*t*-butylbenzene are reported.

The experiments shown in Tables I and II were carried out under several conditions, which involved different amounts of the alkylating reagent and the catalyst, reaction times, and temperatures. The reaction products were fractionated, and each fraction was identified by its physical properties by means of gaschromatographic (Fig. 1) and spectrometric analysis (Fig. 2).

In these alkylations with a slight excess or a small amount of *t*-butyl chloride, the remarkable side-reactions previously reported in the literatures could not be observed, even under the influence of a prolonged reaction time at or over room temperature, although few boiling fractions higher than I were isolated.

At −8°C, *m*-di-*t*-butylbenzene (III) treated with the equivalent alkylating reagent was almost entirely recovered; on the other hand, when III was treated with a large excess of *t*-butyl chloride, it was alkylated rapidly into I in the same yield as in the case of II. However, at or over room temperature, I was formed from III using a very small amount of catalyst (Exp. No. 7), and the quantity was increased with the reaction time (Exp. No. 4—6). Thus, 1, 3, 5-tri-*t*-butylbenzene (I) was obtained in a good yield from *m*-di-*t*-butylbenzene (III) without using large excess of an alkylating reagent and a catalyst, which are apt to cause side-reactions.

The disproportionation of III shown in Table II was also examined under the same conditions as in the case of alkylation. From these experiments of alkylation and disproportionation, it was found that alkylation proceeds before the isomerization of III and that too many reaction times should be avoided, even in the case of III in the preparation of I.

The melting point of the 1, 3, 5-tri-*t*-butylbenzene (I) obtained in this manner was identical with that of the hydrocarbon obtained by Barclay's method (Exp. No. 1), and the mixed melting point was not depressed. The infrared spectra of the two materials were also identical.

Experimental*

Materials. — *m*-Di-*t*-butylbenzene[11]; b. p., 132°C (60 mmHg), 116°C (30 mmHg), n_D^{20} 1.4880, n_D^{25} 1.4874.

t-Butyl Chloride.—This was prepared essentially in the manner described in the literature[12], except that it was dried over phosphorus pentachloride and was used directly after filtration without further distillation.

Improved Synthesis of 1, 3, 5-Tri-*t*-butylbenzene. —Finely powdered anhydrous aluminum chloride (4.0 g., 0.03 mol.) was added in small portions to

* The melting points are uncorrected, and the infrared spectra were taken by the liquid film method or the KBr disk method. Gaschromatogaraphic analysis were carried out at 185°C with a Yanagimoto model GCG3D, using a 2m.×5mm.φ stainless steel tube packed with Celite 545, which was coated with Apiezon grease L and H_2-carrier gas; flow rate, 56 ml./min.

12) J. F. Norris and A. W. Olmsted, "Organic Syntheses", Coll. Vol. I, (1948) p. 144.

the stirred reaction mixture of *m*-di-*t*-butylbenzene (III, 70 g.. 0.37 mol.) and *t*-butyl chloride (44.5 g., 0.48 mol.) over a period of 1 hr. between 25 and 30°C. Hydrogen chloride was evolved, and the reaction mixture became brown. While the stirring was continued at 30°C, a crystalline material was obtained in the reaction mixture. After a total reaction time of 4 hr., the brown complex, on decomposition with cold diluted hydrochloric acid, formed a colorless semi-solid. This semi-solid layer was extracted with benzene, and the organic layer was separated, washed with ice-water, and with a 5% sodium carbonate solution. After evaporation of the solvent, the following fractions were obtained by distillation through a fractionating column 75 cm. in length and packed with Helipak No. 3.

Fraction	B. p. °C	Pressure mmHg	Wt. g.	Component
1[a)]	115～117	30	3.0	III
2[b)]	120～134	30	5.0	III, II and I
3	138～142	30	71.0	I
4[c)]	145～	30	—	

a) n_D^{20} 1.4877
b) This fraction, partially solid, was identified as a mixture of I, II and III by gaschromatographic analyses
c) Trace of yellow oil

Fraction 3, melting at 71～73°C, was practically pure, not needing further purification, and its infrared spectrum (Fig. 2) was identical with that of authentic I prepared in this laboratory by Barclay's method[4)] (Exp. No. 1). One recrystallization gave a sample melting at 73.5°C.

Found: C, 87.69; H, 12.33. Calcd. for $C_{18}H_{30}$: C, 87.73; H, 12.27%.

The author wishes to express his thanks to Professor Toshio Kinugasa for his kind advice and encouragement throughout this work, to Mrs. Sachiko Takao of Kobe Women's College of Pharmacy for her elementary analyses, and to Mr. Keiichi Fuzita of Kobe Customs for his infrared spectrum measurements. He is also indebted to Mr. Takeshi Ozima and Mr. Mitsumasa Taniyama for their skillful collaboration.

Department of Chemistry
Facutly of Science
Kobe University
Mikage, Kobe

NOTES

Studies of the Recoil Tritium-labeling Reaction

By Teruhiko MESHI and Yoshishige SATO

(Received January 10, 1963)

In the reaction of the energetic tritium atom produced in the $Li^6(n, \alpha)T$ reaction with organic compounds, radiation-damage products with specific activities higher than the labeled parent molecule have been detected[1-3]. In order to investigate the specificity of the chemical reactions of recoil tritium, studies have been made of the reaction with crystalline glucose, lactose and α-hydroximinopropionic acid.

A finely powdered mixture of 20 g. of each sample and 2 g. of lithium carbonate was irradiated in the JRR-1 reactor for 21 hr. at a flux of $\sim 2.5 \times 10^{11}$ n/cm^2/sec. The irradiated materials were somewhat brownish as a result of radiation decomposition. Sugars were separated from lithium carbonate by hot water extraction and adsorption on Amberlite IR-120 resin. Since Rowland et al.[4] reported that macro amounts of organic acids were separated during the purification of the irradiated galactose, attempts were made to separate the neutral and acidic constituents by the use of ion-exchange resin.

The solution of sugars was passed through a column of Amberlite IR-45, which was washed with water to produce a neutral fraction. Acids were removed from the column with a 2 N ammonia solution, and free acids were liberated by passage of the solution through a column of Amberlite IR-120.

The constituents in both the neutral and the acidic fraction were separated chromatographically on Toyo paper No. 50. The acidic sugars

1) M. A. El-Sayed, P. J. Estrup and R. Wolfgang, *J. Phys. Chem.*, **62**, 1356 (1958).
2) R. M. White and F. S. Rowland, *J. Am. Chem. Soc.*, **82**, 5345 (1960).
3) J. K. Lee, B. Musgrave and F. S. Rowland, ibid., **82**, 3545 (1960).
4) F. S. Rowland, C. N. Turton and R. Wolfgang, ibid., **78**, 2354 (1956).

were developed with *n*-butanol-acetic acid-water (4 : 1 : 5) and detected with bromophenol blue or benzidine hydrochloride. The neutral sugars were irrigated with *n*-butanol-pyridine-water (6 : 4 : 3) and detected with benzidine hydrochloride or ammoniacal silver nitrate.

Paper chromatography of the neutral fraction of lactose showed five spots, but that of glucose showed only one spot. The R_f values of the three spots derived from lactose were identical with those of lactose (0.12), galactose (0.19) and glucose (0.23). The chromatogram of the acidic fraction of lactose revealed three spots which were identified as mucic acid (0.01), gluconic acid (0.12) and saccharic acid (0.20).

The irradiated oxime was extracted with ether, and the residue was chromatographed with *n*-butanol-acetic acid-water (4 : 1 : 1). The two spots produced by spraying ninhydrine corresponded to DL-alanine and glycine. The results obtained with the undegraded samples are summarized in Table I.

Table I. Incorporation of recoil tritium into organic compounds

Sample	Total tritium d.p.m./mg.	Nonlabile tritium incorporated d.p.m./mg.	Entry of tritium %	Recovery %
Glucose	2.2×10^5	5.3×10^4	24	89.0
Lactose	2.2×10^5	2.2×10^4	10	47.4
Oxime	2.2×10^5	2.0×10^4	9	55.0

The total tritium content, which was calculated from the bombardment condition, represents the number of tritons produced by the nuclear reaction. The low recovery of lactose as compared with that of glucose may be attributed to the fact that the glucoside linkage is ready to undergo radiolysis. The amount and the specific activity of the radioactive mucic acid produced by the irradiation of lactose was determined by the double dilution method. For a comparison of the specific activity, the isolated lactose was oxidized with nitric acid to mucic acid. As a result, the radiation-damage mucic acid had a specific activity about ten times higher than the chemically degraded mucic acid, as is shown in Table II.

Table II. Comparison of the specific activity of mucic acid produced by radiation damage and chemical degradation

Sample	Specific activity μc./mM	Yield %
Radiation-damage mucic acid	12.0	0.09
Chemically-degraded mucic acid	1.26	—
Lactose	3.4	—

Table III. The chemical state of tritium produced by the neutron irradiation of α-hydroximinopropionic acid

Sample	Specific activity μc./mM	Yield %
DL-Alanine	169.0	0.34
Glycine	75.0	0.17
Oxime	0.93	55.0

The production of mucic acid of high specific activity from lactose suggests that the initial substitution of T for H on the -CH- carbon leaves an excited molecule which eventually decomposes to the labeled mucic acid.

Table III shows the specific activities and the yields of tritium-labeled products formed by the reaction of recoil tritium with α-hydroximinopropionic acid.

The great difference in the specific activity between DL-alanine and oxime can be explained on the basis of the preferential utilization of the tritium atom for the addition of the double bond. White and Rowland[2] have demonstrated that the addition of recoil tritium to the double bond occurs in fumaric acid and maleic acid.

The radioactive glycine is presumably produced by the substitution of T for CH_3, Hoff and Rowland[5] have already shown the production of labeled acetaldehyde in the reaction of recoil tritium with acetone.

Osaka Research Laboratory
Tanabe Seiyaku Co., Ltd.
Higashiyodogawa-ku, Osaka

5) W. J. Hoff, Jr. and F. S. Rowland, ibid., 79, 4867 (1957).

Detection of the Interaction between an Iron Surface and Organic Molecules by Means of Infrared Absorption

By Kaneko SAKURAI, Naoe HIRAI and Katsuya INOUYE

(Received February 22, 1963)

For the surface treatment of steel with organic substances or polymers to increase corrosion resistance and to improve appearance, the selection of materials with a strong enough interaction with the surface appears to be an increasingly significant problem.

The authors have tried to use an infrared absorption method to observe the anomaly in

the absorption bands which might be due to the interaction of the iron surface with some organic substance.

Examining the reflection of infrared light from organic films covering the surface of the metal plate, the intensity of the infrared light is not sufficient to serve for the present purpose. To increase the intensity, fine iron powders are mixed with organic substances.

The rouge (iron oxide) 0.2 to 0.5 μ in diameter was reduced to iron with pure hydrogen at 500°C for 4 hr., cooled in a flow of hydrogen, and replaced in pure ethyl alcohol. The gradual evaporation of alcohol at room temperature gave iron powders which are stable when exposed in air.

The absorption bands of mixtures of the powders and organic substances, described later, measured by means of an infrared spectrophotometer with an NaCl prism (e.g., Hitachi EPI-2) did not provide data enough on the presence of interaction.

A single-beam spectrophotometer with the grating system (Perkin-Elmer 112G) gave the following results.

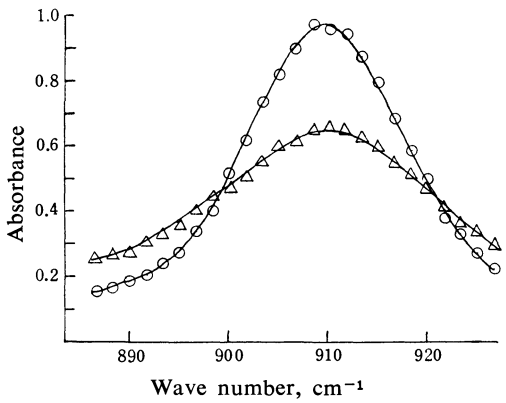

Fig. 1. Infrared absorption of styrene and styrene-iron mixture.

—○— Styrene —△— Styrene+Fe

Figure 1 shows the absorption bands of purified styrene and the reduced iron powders wetted completely with styrene. Table I gives the wave number, calculated from the micrometer readings (GD), of the main absorption bands and the discrepancy of wave number between styrene and the mixed system; no change in the absorption bands has been observed.

TABLE I. INFRARED ABSORPTION OF STYRENE AND STYRENE-IRON MIXTURE

	Wave number, ν (cm^{-1}) and intensity		
Styrene	1629.5(m)	1600.5(w)	908.2(s)
Styrene+Fe	1629.0	1600.2	908.4
$\Delta\nu$ (cm^{-1})	0.5	0.3	0.2

Figure 2 and Table II show similar results for vinylpyridine and the iron-vinylpyridine system. It is recognized that the strong absorption at 832 cm^{-1} for vinylpyridine splits into two bands at 830 and 837 cm^{-1}. The discrepancy of wave number between the mixed system and the vinylpyridine monomer is apparently over the expected experimental error, confirmed by a separate examination for vinylpyridine, of approximately 0.7 cm^{-1} in the region of 830~840 cm^{-1}.

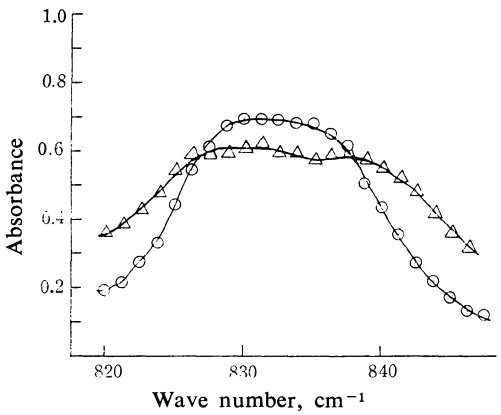

Fig. 2. Infrared absorption of vinylpyridine and vinylpyridine-iron mixture.

—○— Vinylpyridine
—△— Vinylpyridine+Fe

TABLE II. INFRARED ABSORPTION OF VINYLPYRIDINE AND VINYLPYRIDINE-IRON MIXTURE

	Wave number, ν (cm^{-1}) and intensity		
Vinylpyridine	1595.1(s)	1545.6(m)	832.4(s)
Vinylpyridine +Fe	1595.1	1546.2	837.2 830.4
$\Delta\nu$ (cm^{-1})	0	0.6	4.8 2.0

This may be attributed to the fact that the absorption in the region of 832 cm^{-1} corresponds to the out-of-plane bending vibration of the skeletal CH bonds. The splitting of the band might be due to an effect of the interaction between the iron surfaces and, possibly, the pyridine group. However, a doubt still remains because the intensity of the two split bands is almost identical, although it is presumed that only a fraction of the vinylpyridine monomer is affected by the iron surface.

It was purposely confirmed further that the coated film of polystyrene from the polymer solution on the steel plate adheres less than the similar film of the copolymer composed of

styrene and vinylpyridine, on which results a separate report will be published elsewhere.

Tokyo Research Institute
Yawata Iron and Steel Co., Ltd.
Ida, Kawasaki

*Terpenoids. V. A Note on the Diterpene Isolated from the Leaves of "Sugi" (Cryptomeria Japonica D. Don.)**

By Shizuo NAGAHAMA

(Received February 26, 1963)

A diterpene hydrocarbon named α-cryptomerene was first isolated by Uchida[1] from the steam-distillate of "Sugi" leaves. Another diterpene, α-podocarprene[2], has also been found to occur in the same oil[3]. Briggs and Cawley[4] have reported that α-podocarprene is identical with the kaurene** obtained from *Agathis australis*. Kaurene has been isomerized via its hydrochloride to isokaurene, and this isomer has recently been shown to be identical with Uchida's α-cryptomerene[5].

Upon careful re-examination of the "Sugi" diterpene fraction, the present author was able to obtain kaurene (or α-podocarprene) as the sole isolable product. The presence of isokaurene (or α-cryptomerene) could not be confirmed. This deviation from the observations of previous investigators should be ascribed to the changes in isolation procedures. In this investigation, the diterpene fraction was obtained by extracting "Sugi" leaves with acetone; the sesquiterpene alcohols were removed by distillation in vacuo, and the less volatile residue was subjected to chromatography on an alumina column to afford kaurene.

The heating of kaurene in the presence of abietic acid resulted in the formation of isokaurene, no isomerization being observed in the absence of the acid. These findings suggest that the previous isolation of isokaurene was presumably a consequence of the isomerization of kaurene during the isolation procedures.

Experimental

Isolation. — Foliage and terminal twigs of Sugi (6 kg.), collected on Mt. Seburi, near Fukuoka city, were chopped up and extracted twice with hot acetone for 20 hr. The precipitate was filtered off, and the acetone was evaporated. The residue was extracted with petroleum ether (b. p., 40~60°C), and the neutral fraction was steam-distilled. The steam volatile oil (15 g.) was dried over sodium sulfate and distilled under reduced pressure (5 mmHg) with a Claisen flask. When the bath temperature reached to 180°C and the sesquiterpene alcohol fraction had been removed, the heating bath was removed quickly and the distillation residue (about 3 g.) was chromatographed on an alumina column (20 g.). Petroleum ether eluted kaurene (1.5 g.); m. p., 49~50°C (lit.[4] m. p. 50°C) (recrystallized from ethanol), $[\alpha]_D$ −78° (*c* 2.09, chloroform) (lit.[4] $[\alpha]_D$ −75.2°). Mixed m. p. with authentic sample (m. p., 48~51.5°C), 48~51°C.

Isomerization.—A mixture of kaurene (200 mg.) and abietic acid (100 mg.) was heated at 200°C for 1 hr. Distillation under reduced pressure (10 mmHg, bath temp. 230~240°C) gave isokaurene, m. p. and mixed m. p., 62~64°C (lit.[4] m. p., 64°C) (recrystallized from ethanol) $[\alpha]_D$ −30° (*c* 1.27, chloroform) (lit.[4] $[\alpha]_D$ −27.4°C). The infrared spectrum was superimposable on that of an authentic sample. The distillation of kaurene under the same conditions without added abietic acid did not cause isomerization. Authentic isokaurene was obtained by heating kaurene with iodine[6].

The author wishes to express his thanks to Dr. Yoshiyuki Hirose, The University of Tokyo, for his gift of authentic kaurene and to Professor Tamio Kondo of this University for supplying him with abietic acid. He is also indebted to Professor Nobuo Izumiya for permitting him to make the rotation measurements, and to Dr. Tamaki Kubota for "Sugi" leaves.

Department of Organic Synthesis
Faculty of Engineering
Kyushu University
Hakozaki, Fukuoka

* Contribution No. 39 from the Department of Organic Synthesis, Faculty of Engineering, Kyushu University.

** The English authors have pointed out that the so-called "Kaurene" originally recorded by Hosking (*Rec. trav. Chim.*, **47**, 578 (1928)) is probably impure isokaurene. (*J. Chem. Soc.*, **1950**, 407)

1) S. Uchida, *J. Soc. Chem. Ind.* (*Kōgyō Kwagaku Zasshi*), **19**, 610 (1916); *J. Am. Chem. Soc.*, **38**, 687 (1916).

2) K. Nishida and H. Uota, *J. Agr. Chem. Soc. Japan* (*Nippon Nōgei Kagaku Kaishi*), **7**, 157 (1931); *Bull. Agr. Chem. Soc. Japan*, **7**, 1 (1931); J. Kawamura, *Bull. Imp. Forestry Exp. Sta. Tokyo* (*Ringyō Shiken Hōkoku*), No. 31, 77, 93 (1931).

3) T. Nakatsuka, Y. Hirose and M. Matsuda, *J. Japan Wood Research Soc.* (*Mokuzai Gakkaishi*), **3**, 206 (1957).

4) L. H. Briggs and R. W. Cawley, *J. Chem. Soc.*, **1948**, 1888.

5) L. H. Briggs, B. F. Cain, B. R. Davis and J. K. Wilmshurst, *Tetrahedron Letters*, **1959**, No 8, 8.

6) L. H. Briggs, B. F. Cain, R. C. Cambie, B. R. Davis and P. S. Rutledge, *J. Chem. Soc.*, **1962**, 1850.

SHORT COMMUNICATIONS

*The Synthesis of N_ω-Formyl Basic Amino Acid**

By Kenji OKAWA and Satoe HASE

(Received March 6, 1963)

It is a well-known fact that Sheehan's method[1], using formic acid and acetic anhydride, is the most convenient procedure for the formylation of α-amino acid because the reaction proceeds relatively well under mild conditions. This method can, however, be used for the *N*-formyl blocking of the α-amino acid; it can not be used for the selective formylation of one of two amino groups in such basic amino acids as ornithine or lysine.

The authors attempted to introduce a formyl group into the end amino group of ornithine or lysine selectively and found that the *p*-nitrophenyl formate was a useful reagent for this purpose, as is shown in the following scheme:

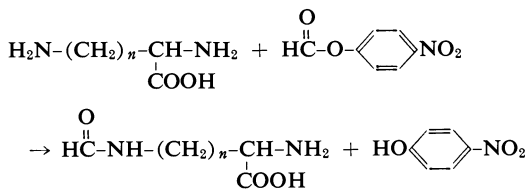

(n=3 or 4)

The formylation of arginine or histidine are now being investigated.

Experimental. — *p-Nitrophenyl Formate.* — A solution of 10.3 g. of *N, N'*-dicyclohexylcarbodiimide[2] in 30 ml. of tetrahydrofuran was added drop by drop into a stirred solution of 6.95 g. of *p*-nitrophenol and 2.76 g. of formic acid in 60 ml. of tetrahydrofuran in an ice bath. After the addition was over, the reaction mixture was allowed to stand for 1 hr. at room temperature. The urea produced was filtered off, and the filtrate was concentrated under reduced pressure until crystals appeared. From the mother solution, other crops of the crystals were obtained. The total yield was 5.3 g. (63.4%). Recrystallization from the mixed solution of tetrahydrofuran and ether gave 4.3 g. (51.4%) of fine crystals; m. p., 72~74°C.

Found: C, 50.48; H, 3.15; N, 8.26. Calcd. for $C_7H_5O_4N$: C, 50.30; H, 3.02; N, 8.38%.

N_δ-Formyl-L-ornithine.—An aqueous solution of 10.1 g. of L-ornithine mono-hydrochloride was neutralized with an equivalent amount of a 1 N aqueous sodium hydroxide solution. Into the above solution was added drop by drop 15.0 g. of *p*-nitrophenyl formate in tetrahydrofuran in an ice bath, while the solution was stirred. The stirring was continued for 6 hr. at room temperature; then the reaction mixture was extracted with ether to remove *p*-nitrophenol, and concentrated in vacuo, and the remaining solution was passed through a column of Amberlite IRC-50 to remove unreacted basic amino acid. The effluent was concentrated in vacuo, and methanol was added until the mixture became a little turbid. The mixture was then allowed to stand in a refrigerator. The crystals produced were filtered and dried. The yield was 5.0 g. (52%). Recrystallization from water methanol gave a pure compound; m. p. 217°C (decomp.); $[\alpha]_D^{15}$ +2.8° (3.97% in water); $[\alpha]_D^{15}$ +17.1° (2.17% in satd. sodium bicarbonate):

Found: C, 44.52; H, 7.64; N, 17.81. Calcd. for $C_6H_{12}O_3N_2$: C, 44.98; H, 7.55; N, 17.49%.

N_ε-Formyl-L-lysine[3].—L-Lysine monohydrochloride was treated with *p*-nitrophenyl formate as above; yield, 35%; m. p., 225~226°C (decomp.); $[\alpha]_D^{15}$ +3.0° (4.27% in water); $[\alpha]_D^{15}$, +17.7° (2.12% in satd. sodium bicarbonate):

Found: C, 48.74; H, 8.22; N, 16.22. Calcd. for $C_7H_{14}O_3N_2$: C, 48.27; H, 8.10; N, 16.08%.

Department of Chemistry
Faculty of Science
Kwansei Gakuin University
Nishinomiya

* Reported in part at the First Peptide Seminar of the Institute for Protein Research (Osaka University), November, 1962.

1) J. C. Sheehan and D-D. H. Yang, *J. Am. Chem. Soc.*, **80**, 1154 (1958).

2) E. Schmidt, F. Hitzler and E. Lahde, *Ber.*, **71**, 1933 (1938).

3) K. Hofmann, E. Stutz, G. Spühler, H. Yajima and E. T. Schwartz, *J. Am. Chem. Soc.*, **82**, 3727 (1960).

Copper(II)-complexes of Schiff Bases Derived from Salicylaldehyde and Alkylamines

By Shoichiro YAMADA and Hiroaki NISHIKAWA

(Received March 8, 1963)

Four-co-ordinate copper(II) usually demands a planar configuration with comparatively strong ligands, and bis(*N*-*n*-alkyl-salicylideneiminato)copper(II)-complexes ($Cu(O\cdot C_6H_4\cdot CH:N\cdot R)_2$) are expected to have a four-co-ordinate, planar configuration. One can, however, expect cupric complexes of the Schiff bases which are distorted from the square-plane, when R denotes a group which causes steric hindrance to the planar co-ordination[1,2]. The present communication deals with the preparation of those anomalous cupric complexes with the Schiff bases which take a co-ordination distorted from the square-plane, it also discusses the stereochemistry of copper(II) in relation to that of cobalt(II) and nickel(II).

Bis(*N*-*n*-alkyl-salicylideneiminato)copper(II)-complexes, which are considered to have a planar configuration of $Cu(N)_2(O)_2$, on the basis of X-ray crystal structure analysis with the methyl-substituted complex[3,4], show almost identical ultraviolet absorption spectra in non-co-ordinating organic solvents and in the crystalline state, regardless of the number of the carbon atoms of the *n*-alkyl groups.

On the contrary, bis(*N*-*t*-butyl-salicylideneiminato)copper(II), which has newly been prepared as dark-red crystals by warming a solution of bis(salicylaldehyde)copper(II) and an excess of *t*-butylamine in ethanol, is expected to be tetrahedral, because of the steric condition imposed by the bulky *t*-butyl group[1,2]. Bis(*N*-*t*-butyl-salicylideneiminato)copper(II) in organic solvents (Fig. 1) displays a ligand field band at a much lower frequency (about $39.0\times10^{13}\,sec^{-1}$) than the *n*-alkyl-substituted complex (about $53\times10^{13}\,sec^{-1}$). This is in agreement with the presumption that the *N*-*t*-butyl-substituted complex has a tetrahedral configuration[5]. The ligands show nearly identical absorption curves, whether they contain for R a normal or a branched alkyl. The maxima in the crystal spectra nearly coincide with those in the solution spectra.

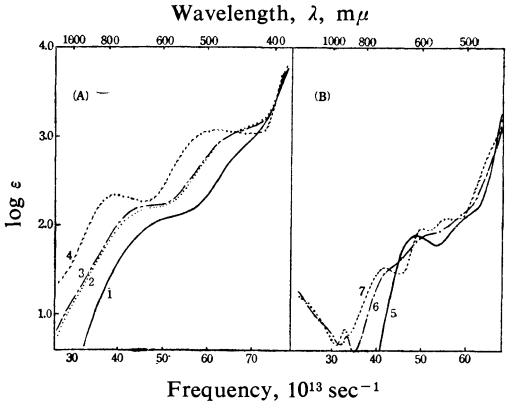

Fig. 1. Visible and near-infrared absorption spectra of (A) $Cu(O\cdot C_6H_4\cdot CH:NR)_2$ in chloroform: 1. R=methyl, 2. cyclohexyl, 3. isopropyl, and 4. *t*-butyl, and (B) $Ni(O\cdot C_6H_4\cdot CH:NR)_2$ in chloroform: 5. R=ethyl, 6. isopropyl and 7. *t*-butyl.

When R represents isopropyl, *sec*-butyl, 1-ethylpropyl or cyclohexyl, steric hindrance to the planar co-ordination may not be as serious as in the case of R=*t*-butyl, but nevertheless it seems significant[1,2]. The copper(II)-complexes with these substituents, which have been prepared in a way similar to that used for the *t*-butyl-substituted complex, show ligand field bands at a much lower frequency (about $47\times10^{13}\,sec^{-1}$) than when R=*n*-alkyl in non-co-ordinating organic solvents, indicating that the configuration of the cupric complexes with these substituents is not planar but tetrahedral. The absorption spectra of these four complexes are almost superposable with one another, so that the distortion from planarity is to a nearly equal degree in these complexes. The distortion is considered to be greater in the *t*-butyl-substituted complex, which shows a ligand field band at an appreciably lower frequency than when R is any of the other branched alkyls.

Quite a similar type of distortion is concluded for bis(salicylideneiminato)nickel(II) from an inspection of the ligand field bands[6]. The absorption spectra of the *N*-*t*-butyl, isopropyl and cyclohexyl-substituted complexes

1) H. Nishikawa, S. Yamada and R. Tsuchida, *Z. Naturforsch.*, **17b**, 78 (1962), etc.

2) H. Nishikawa and S. Yamada, This Bulletin, **35**, 1430 (1962); S. Yamada, H. Nishikawa and K. Yamasaki, ibid., **36**, 483 (1963).

3) B. Meuthen and M. V. Stackelberg, *Z. anorg. u. allgem. Chem.*, **305**, 279 (1960).

4) L. Sacconi, M. Ciampolini, F. Maggio and F. P. Cavasino (*J. Inorg. Nucl. Chem.*, **19**, 73 (1961)) proposed a flattened pyramidal structure.

5) Bis(*N*-*t*-butyl-salicylideneiminato)cobalt(II) was also prepared and was established as having a tetrahedral configuration (H. Nishikawa and S. Yamada, to be submitted shortly).

6) A similar conclusion was reached recently from another kind of data by L. Sacconi, P. L. Orioli, P. Paoletti and M. Ciampolini (*Proc. Chem. Soc. (London)*, **1962**, 255).

in organic solvents (Fig. 1B) have the main features characteristic of tetrahedral nickel(II)-complexes and are quite different from the spectrum of bis(*N*-ethyl-salicylideneiminato)-nickel(II), which is known to be planar in chloroform. Similar by to the case of the cupric complexes, the slight difference in the spectrum between the branched alkyl-substituted complexes seems to be understood on the assumption that the extent of distortion from planarity becomes gradually smaller in the order: R=*t*-butyl, isopropyl, cyclohexyl. The hypothesis of the association of complexes in solution, which has currently been postulated, seems to be superfluous when R is one of the branched alkyls.

Since the bis(*N*-alkyl-salicylideneiminato)-cobalt(II)-complexes take a tetrahedral co-ordination around the cobalt(II) ion, whether the substituent is normal or branched alkyl[1,2,7], the present work indicates that copper(II) and nickel(II) are more inclined to take a planar co-ordination than cobalt(II), in agreement with the prediction from the simple crystal field theory.

Department of Chemistry
Faculty of Science
Osaka University
Nakanoshima, Osaka

7) L. Sacconi, M. Ciampolini and F. Maggio, *J. Am. Chem. Soc.*, **84**, 3246 (1962), etc.

The Polarography of o-Phenanthroline Cobalt(III) and Cobalt(II) Complexes

By Nobufumi MAKI, Taizo HIRANO and Soichiro MUSHA

(Received March 8, 1963)

Vlček[1] and Waind et al.[2] found that the tris(dipyridyl) complex, $[Co^{III}\,dip_3](ClO_4)_3\cdot 3H_2O$, or $[Co^{II}\,dip_3](ClO_4)_2$*, is reversibly reduced to cobalt(I) ions, $[Co^{I}\,dip_3]^+$, at the dropping mercury electrode (DME). In the present communication, the tris(phenanthroline) cobalt(III) and cobalt(II) complexes, $[Co^{III}\,phen_3]Cl_3\cdot 7H_2O$ and $[Co^{II}\,phen_3]Cl_2\cdot 8H_2O$*, are found to be reduced irreversibly to the cobalt(0) state through cobalt(I) complexes in a 0.5 F sodium sulfate aqueous solution.

Figure 1 shows all the waves of the step-by-step reduction of the cobalt(III) complex. The cobalt(II) complex also gave the same waves after the second wave.

The first, the second and the third wave, each corresponding to an acceptance of one electron, represent the reduction of cobalt(III)→cobalt(II), of cobalt(II)→cobalt(I), and of cobalt(I)→cobalt(0) respectively. The limiting current of the waves, except that of the last one, is controlled only by diffusion. The diffusion current and the concentration of the complex are linearly related in the concentration range of $10^{-2}\sim10^{-4}$ F. The third wave disappears into the catalytic maximum one, decreasing the concentration of the complex.

In absolute alcohol, the cobalt(I) ion, $[Co^{I}\,phen_3]^+$, may dissociate into the $[Co^{I}\,phen_2]^+$ ion, and so on. Therefore, without excess ligands, the reduction to the cobalt(I) state is almost irreversible (Table I). In an aqueous solution, the shape of the wave for this system is quite different from that of the usual current-voltage curve of the S-type, and the current-rise at the half-wave potential is almost at right angles to the line of galva zero. This phenomenon is considered to be due to the hydrophobic effect of the phenanthroline ligands or to the adsorption of the complex at the surface of the DME.

The processes of the electrode reaction are as follows:

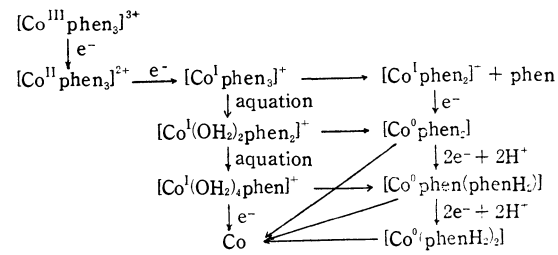

The tris(bathophenanthroline)cobalt(III) chloride**, $[Co^{III}\,bathophen_3]Cl_3$, gave similar polarographic waves.

As for the oscillopolarograms of the $dE/dt\sim E$ (potential) curves, the cut-ins in the cathodic branch are generally larger than those in the anodic branch. This means that the electrode process is irreversible, even in the

1) A. A. Vlček, *Nature*, **180**, 573 (1957); *Z. Elektrochem.*, **61**, 1014 (1957); *Z. physik. Chem. Sonderheft* (Internationales Polarographisches Kolloquium, Dresden) (1958), p. 143.

2) G. M. Waind and B. Martin, *J. Inorg. & Nuclear Chem.*, **8**, 551 (1958).

* dip = 2,2'-dipyridyl, $(C_5H_4N)_2$; phen = 1,10-phenanthroline, $C_{12}H_8N_2$

** bathophen = 4,7-diphenyl-1, 10-phenanthroline, $C_{12}H_8N_2(C_6H_5)_2$

TABLE I. HALF-WAVE POTENTIALS OF THE WAVES FOR THE COBALT(III) COMPLEXES OF THE LUTEO-TYPE (25°C)

Compound	$E_{1/2}$ of 1st wave Co(III)→Co(II)	$E_{1/2}$ of 2nd wave Co(II)→Co(I)	$E_{1/2}$ of 3rd wave Co(I)→Co(0)	Supporting electrolyte
$[Co\ phen_3]Cl_3 \cdot 7H_2O$	−0.08	-1.00_5	−1.34	0.5 F Na_2SO_4
$[Co\ phen_3]Cl_3 \cdot 7H_2O$	—	−1.62	—	1 F LiCl ethanolic soln.
$[Co\ phen_3]Cl_3 \cdot 7H_2O$	—	−0.83	—	1 F LiCl & 0.1 M phen. ethanolic soln.
$[Co\ bathophen_3]Cl_3$	+	−0.80	−1.11	1 F LiCl ethanolic soln.

Concentration of the complex, 10^{-2} F; voltage unit, V. vs. S. C. E.

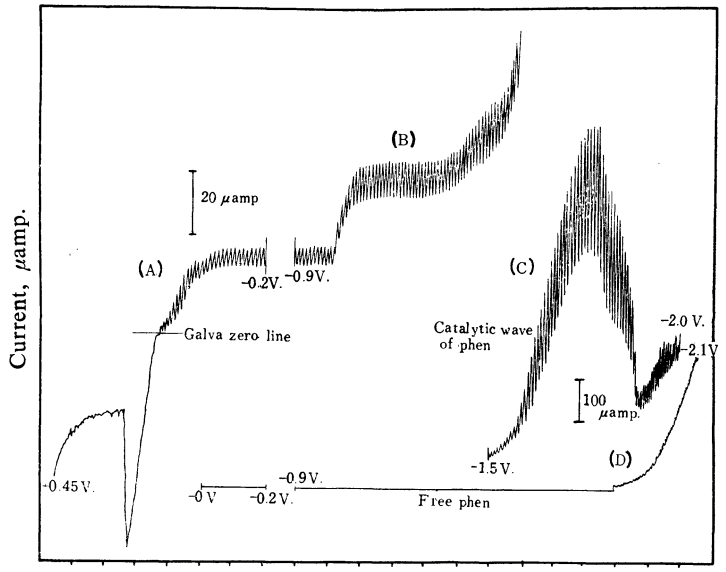

Fig. 1. The polarograms of the complex, $[Co^{III}\ phen_3]Cl_3 \cdot 7H_2O$ obtained at the concentration of 10^{-2} M in 0.5 M Na_2SO_4 aqueous solution (25°C).
(A) Recorded from +0.45 to −0.2 V.; Sensitivity, 1.0 μamp./mm.
(B) Recorded from −0.9 to −1.6 V.; Sensitivity, 1.0 μamp./mm.
(C) Recorded from −1.5 to −2.1 V.; Sensitivity, 6.0 μamp./mm.
(D) The polarogram of 0.5 M Na_2SO_4 aqueous solution saturated with *o*-phenanthroline
$E_{1/2}$ of 1st wave = +0.08 V., $E_{1/2}$ of 2nd wave = -1.00_5 V., $E_{1/2}$ of 3rd wave = −1.34 V., voltage unit: V. vs. S. C. E.

presence of many excess ligands, due to the slower rate of oxidization.

Radiation Center of Osaka Prefecture
Shinke-cho, Sakai
(N. M. & S. M.)

Department of Chemistry
University of Osaka Prefecture
Nakamozu, Sakai
(T. H.)

The Polarography of Bis(dipyridyl)cobalt(III) Complexes. Unstable Univalent Cobalt Complexes

By Nobufumi MAKI and Hiroshi ITATANI

(Received March 14, 1963)

Vlček[1] and Waind et al.[2] found that the tris(dipyridyl) complex ion, $[Co^{III}dip_3]^{3+}$, is reversibly reduced to the cobalt(I) state through cobalt(II) ion, $[Co^{II}dip_3]^{2+}$, the

1) A. A. Vlček, *Nature*, **180**, 573 (1957); *Z. Elektrochem.*, **61**, 1014 (1957); *Z. physki. Chem. Sonderheft* (Internationales Polarographisches Kolloquium, Dresden) (1958), p. 143.

2) G. M. Waind and B. Martin, *J. Inorg. & Nuclear Chem.*, **8**, 551 (1958).

TABLE I. HALF-WAVE POTENTIALS OF THE DIPYRIDYL COBALT(III) COMPLEXES (25°C)

Compound	$E_{1/2}$ of 1st wave Co(III)→Co(II)	$E_{1/2}$ of 2nd wave Co(II)→Co(I)	Supporting electrolyte
[Co gly dip_2]Cl_2	−0.14	ca.−1.4	1 F KCl
[Co ala dip_2]Cl_2	−0.20	ca.−1.4	1 F KCl
[Co tyrosine dip_2]Cl_2	−0.19	−1.36	1 F KCl
[Co leuc dip_2]Cl_2	ca.−0.25	-1.37_8	1 F KCl
[Co $OCOCCH_3$ dip_2]Cl_2 (NO)	-0.37_3	-1.39_5	1 F KCl, 0.0032% Tween 80[2]
[Co dip_3]$(ClO_4)_3 \cdot 3H_2O$	−0.14	−1.32	0.1 F KNO_3, $5 \cdot 10^{-2}$ M dip
	+	-1.10_4	1 F KCl
[Co dip_3]$(ClO_4)_2$		−0.91	1 F LiCl, ethanolic soln.[1]

Concentration of the complex; $2 \cdot 10^{-2}$ F Voltage unit; V. vs. S.C.E.
Tween 80=Polyoxyethylene sorbitan mono-oleate

dropping mercury electrode (DME) in a 1 F lithium chloride ethanolic solution or in a 0.1 F potassium nitrate aqueous solution containing excess dipyridyl. In the present report, the mixed ligand complexes of the [$Co^{III}dip_2Y$] type are examined polarographically. It is found that unstable univalent cobalt complexes are formed during the course of reduction, where the bidentate ligand, Y, expresses the ion, $NH_2CH_2COO^-$ (glycinate), $NH_2CH(CH_3)COO^-$ (alaninate), $NH_2CH(COO^-)CH_2CH(CH_3)_2$ (leucinate), $HOC_6H_4C_2H_3(NH_2)COO^-$ (tyrosinate), or $CH_3C(NO)COO^-$ (α-keto-propionic acid oximate) respectively[3]. All the complexes treated here are new ones which were prepared from the praseo-salt, [Co Cl_2 dip_2]Cl, by the substitution reaction.

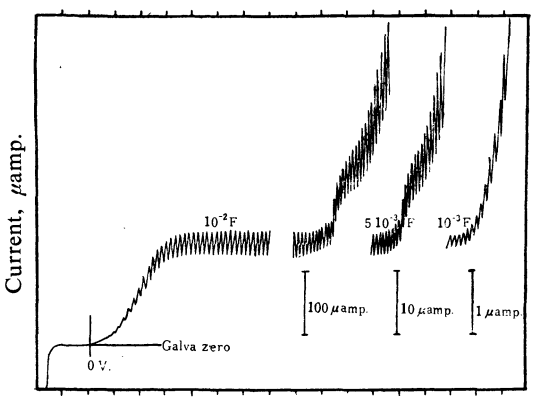

Applied potential, V. vs. S.C.E. 100mV./*absc.*

Fig. 1. Dependence of the second wave for the complex, [Co^{III}gly dip_2]Cl_2, on the concentration of the complex.
Supporting electrolyte; 0.5 F K_2SO_4 aq. soln.
Concn. of the complex; 10^{-2}, $5 \cdot 10^{-3}$, 10^{-3} F/l.
$E_{1/2}$ of 1st wave=−0.11 V. vs. S.C.E.
$E_{1/2}$ of 2nd wave=−1.31 V. vs. S.C.E.

These bis(dipyridyl)cobalt(III) complexes gave irreversible two-step waves at the DME in 1 F potassium chloride or in 0.5 F potassium sulfate supporting electrolyte. The first wave is well-defined, but the second one can be discerned only at a concentration of the complex higher than 10^{-2} F. The first and second waves, each corresponding to an acceptance of one electron, represent the reduction of cobalt(III) → cobalt(II) and of cobalt(II) → cobalt(I) respectively.

Figure 1 shows the polarograms of glycinato-bis(dipyridyl)cobalt(III) chloride at various concentrations. Upon a decrease in the concentration, the second wave disappears into the current-rise of the hydrogen wave because of the glycine partly liberated from the complex on the way of reduction.

The following processes of the electrode reaction are considered to be most plausible:

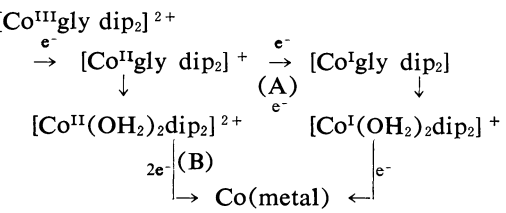

The more the concentration of the original complex increases, the more the electrode reaction proceeds along path A rather than along path B. Thus, such an unstable cobalt(I) complex as [Co^Igly dip_2] can be detected at a high concentration only by means of polarography.

Table I shows the half-wave potentials of the cobalt(III) complexes studied. As most of the second waves were fairly well covered by the hydrogen wave because of the amino acid liberated from the complex, the half-wave potentials could not necessarily be determined exactly. The oscillopolarograms of the $dE/dt \sim E$ (potential) curves also indicated that the

3) M. Murakami, S. Senoh, N. Matsusato, H. Itatani and J. W. Kang, *J. Chem. Soc. Japan, Pure Chem. Sec.* (*Nippon Kagaku Zasshi*), **83**, 734, 737 (1962).
* dip=2,2′-dipyridyl

reduction process takes place in two stages at the DME.

Radiation Center of Osaka Prefecture
Shinke-cho, Sakai

The Dual Effect of a Surface-active Substance on the Polarographic Electron-transfer Process

By Nobuyuki TANAKA, Yasuko KIKUCHI and Yuichi SATO

(Received March 27, 1963)

The deceleration and the acceleration of the polarographic electron-transfer process by the adsorption of a surface-active substance have been studied in connection with the heterogeneous reaction mechanisms at the electrode surface[1-3]. Frumkin and his co-workers reported the dual effect of a surface-active substance on the reduction of $PtCl_4^{2-}$ ions; the $(C_5H_{11})_4N^+$ ion accelerates the reduction at its lower concentration and decelerates at its higher concentration[4].

In the course of our study of the polarographic reduction of manganese(III) in an alkaline tartrate solution, we found a remarkable deceleration and acceleration of the electron-transfer process upon the addition of trimethyloctadecylammonium chloride, $(CH_3)_3(C_{18}H_{37})N^+Cl^-$, (TMOAC). An alkaline tartrate solution of manganese(III), which was obtained by air oxidation of that of manganese(II), gave the peculiar polarogram shown in Fig. 1 (curve 1)[5]. Current-potential curves obtained at various concentrations of TMOAC in alkaline tartrate solutions of pH 11.8 (Fig. 1) indicate that the addition of a small concentration of TMOAC depresses both the first round-shape and the second drawn-out wave, and that, at a higher concentration of TMOAC, the first wave was further depressed but the second, considerably improved. The dual (deceleration and acceleration) effect of a surface-active substance which is of a different type from that reported by Frumkin et al. is more clearly demonstrated by the current-time curves during the life of a mercury drop that were obtained at −0.82 V. vs. S. C. E. at varied concentrations of TMOAC (Fig. 2). In Fig. 2, curve 3 shows that the acceleration of the electron-transfer is controlled by the rate of adsorption of the surface-active cations.

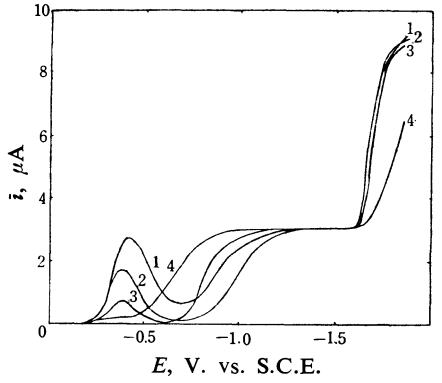

Fig. 1. Current-potential curves of Mn(III) in Britton-Robinson buffer of pH 11.8 containing 0.25 M sodium tartrate in the absence *(curve 1) and in the presence of 0.13 mM* (2), 0.25 mM (3), and 1.2 mM (4) trimethyloctadecylammonium chloride.

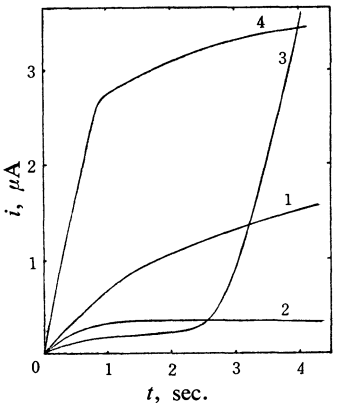

Fig. 2. Current-time curves at −0.82 V. vs. S.C.E. obtained with the same solutions as given in Fig. 1.

Manganese(III) is considered to form negatively-charged hydroxotartrato complexes in an alkaline tartrate solution. The adsorption of a sufficient amount of surface active cations, therefore, apparently lessens the repulsive interaction between the negatively-charged electrode and the electroactive anions, accelerating the electron transfer.

Department of Chemistry
Faculty of Science
Tohoku University
Katahira-cho, Sendai

1) C. N. Reilley and W. Stumm, "Progress in Polarography", Ed. by Zuman and Kolthoff, Interscience Publishers, N. Y. (1962), Chapter V, p. 81.
2) R. Tamamushi, T. Takeuchi and N. Tanaka, 18th International Congress of Pure and Applied Chemistry, Montreal, Canada (1961), No. B3-39.
3) N. Tanaka and R. Tamamushi, 1st Australian Conference on Electrochemistry, Sydney and Hobart (1963).
4) A. N. Frumkin, O. A. Petrii and N. V. Nikolaeva-Fedorovich, *Doklady Akad. Nauk S. S. S. R.*, **136**, 1158 (1961).
5) The details of this study will be published elsewhere.

The Acyl Halide-initiated Polymerization of Styrene in Liquid Sulfur Dioxide

By Niichiro TOKURA, Tetsuyo KAWAHARA and Takeshi WATANABE

(Received April 5, 1963)

The polymerization of styrene in liquid sulfur dioxide initiated by various alkyl and aralkyl chlorides has recently been reported by two of the present authors[1]. We have now examined polymerization of styrene in liquid sulfur dioxide initiated by acyl halides and have found that various acyl halides, such as acetyl, chloroacetyl, propionyl, *n*-butyryl, isobutyryl and benzoyl chlorides, and acetyl and isobutyryl bromides are all effective initiators of the cationic polymerization of styrene in liquid sulfur dioxide. *p*-Toluenesulfonyl chloride is also an excellent initiator.

The polymerizations were performed at 25°C in liquid sulfur dioxide with 0.698 mol./l. of styrene and 0.004~0.34 mol./l. of an acyl halide in a total volume of 175 ml. The initial over-all rates of polymerization, the average degrees of polymerization of the polymer, and the conversion in 3 hr. are listed in Table I. The average molecular weight of the polymer was calculated from the intrinsic viscosity in benzene by Pepper's equation[2] to be:

$$[\eta] = 2.7 \times 10^{-4} M^{0.66}$$

The polymer produced by acyl halides was polystyrene, as was expected; it was identified by the infrared spectra. Sulfur analysis showed the product was not contaminated by polysulfone ruling out a radical nature of this polymerization process.

The results mentioned above and listed in Table I suggest that the polymerization is initiated by an acylium cation, $R\overset{+}{C}O$. which may be derived by the ionization of an acyl halide in liquid sulfur dioxide:

$$RCOCl \rightleftarrows RCO^+ + Cl^-$$

or by an associated ion, such as RCO^+Cl^--RCO^+, which may likely be present in a medium with a low dielectric constant[3]. The characteristic feature of this polymerization is that the over-all rate of polymerization seems to depend on the initiation, because the species of the initiator has a strong influence on the rate of the polymerization, while the counter anion (Cl^- or Br^-) is unchanged throughout the reaction and the nature of the propagation of the polymer chain remains the same.

The evidence for such an assertion is that: (a) Chloroacetyl chloride is a weaker initiator than acetyl chloride; (b) *p*-toluenesulfonyl chloride is an excellent initiator; (c) *p*-nitrobenzoyl chloride cannot initiate the polymerization, whereas benzoyl chloride can initiate the polymerization; (d) the acyl bromide is more reactive than the corresponding chloride; (e) the polymerizations are terminated by the addition of such substances as tetramethylammonium chloride or triphenylmethyl chloride, and (f) the time-conversion curve of the polymerization is flattened as time elapses, the polymerization being terminated at a lower conversion when an initiation is not so strong. These phenomena may partly be elucidated by the mass-law effect[4] on both the ionization of

TABLE I. ACYL HALIDE-INITIATED POLYMERIZATIONS IN LIQUID SULFUR DIOXIDE

Acyl halide, 0.34 mol./l.	Initial rate $-dM/dt \times 10^5$ mol./l. sec. at 25°C	$[\eta]$ dl./g. in benzene	$\bar{P}$	Conversion in 3 hr. %
Isobutyryl bromide	Very large	0.149	136	9.4
Isobutyryl chloride	Very large	0.445	746	9.6
Acetyl bromide	Very large	0.189	197	11.2*
p-Toluenesulfonyl chloride	11.92	0.114	94	84.2*
Acetyl chloride	6.29	0.195	206	18.8
Propionyl chloride	4.46	0.172	170	18.5
Chloroacetyl chloride	0.93	0.161	150	4.7
Benzoyl chloride	0.93	0.205	220	3.9
n-Butyryl chloride	0.56	0.207	226	1.1
p-Nitrobenzoyl chloride	0			0

* Conversion at 2 hr.

1) N. Tokura and T. Kawahara, This Bulletin, **35**, 1902 (1962).
2) D. C. Pepper, *J. Polymer Sci.*, **7**, 345 (1951).
3) D. E. Hughes, C. K. Ingold, S. Patai and Y. Pocker, *J. Chem. Soc.*, **1957**, 1206.
4) C. K. Ingold, "Structure and Mechanism in Organic Chemistry", Cornell Univ. Press, Ithaca, New York (1953), p. 360.

the acyl halide and the growing ion pair in liquid sulfur dioxide. *p*-Toluenesulfonyl chloride is an excellent initiator in the sense that this halide initiates a polymerization which proceeds to over an 80% conversion within 2 hr.

We have not yet been able to identify the terminal acyl group or the carbonyl group in the polymer end; however, the inclusion of a sulfur atom in the polymer initiated by *p*-toluenesulfonyl chloride was verified by elementary analysis. No correlation has been found between the average degrees of polymerization and the initial rates of polymerization. The mechanism of the polymerization will be scrutinized again in a further study.

The Chemical Research Institute
of Non-Aqueous Solutions
Tohoku University
Katahira-cho, Sendai

The Reaction of Olefines with Lead Tetracarboxylates

By Yasuhide YUKAWA and Mitsuru SAKAI

(Received April 18, 1963)

Recently decarboxylative syntheses using lead tetraacetate have been reported by Corey and Casanova[1]. We wish to report on the reaction of olefines with lead tetracarboxylates. Lead tetra-monocarboxylates (I), as well as lead di-dicarboxylates (II), can be prepared by warming the corresponding acid with lead tetraacetate (Table I). Bachman and Wittmann[2] reported recently a similar procedure for the synthesis of lead tetra-monocarboxylates.

$Pb(OCOR)_4$ (I) $Pb(OCORCOO)_2$ (IIa, $R=-(CH_2)_7-$; b, $R=-(CH_2)_8-$)

Lead diazelate (IIa) and lead disebacate (IIb) are colorless stable solids and have high melting points (m. p., 260°C and 233~236°C respectively).

It is well-known that the reaction of styrene with lead tetraacetate gives phenylacetaldehyde diacetate (a rearrangement product) (III) or 1-phenylpropanol acetate (an addition product of the methyl radical) (IV). The reaction of styrene with lead tetrapropionate gave 1-phenylbutanol propionate (an addition product of the ethyl radical) (V). On the other hand, styrene glycol dicarboxylates (VI) were obtained in the reactions with lead tetra-monocarboxylates prepared from higher carboxylic acids than propionic acid. In the case of lead di-dicarboxylates, the reaction proceeds slowly at 70°C in benzene and gives a macrocyclic compound (VII) in a 50% yield. Because the reaction of styrene is accompanied by some polymerization of styrene, the high yield of macrocyclic compound is striking in such a concentrated solution.

Table I. Lead tetra-monocarboxylates (I)

R-	M. p., °C
CH_3CH_2-	133.0~133.5
$CH_3(CH_2)_{10}-$	95~97
$CH_3(CH_2)_{12}-$	104~105
$CH_3(CH_2)_{14}-$	104
$CH_3(CH_2)_{16}-$	103~104
Ph-	180
$PhCH_2-$	170
Ph_2CH-	175~180
Ph_2CHCH_2-	109~113

$PhCH{=}CH_2 + Pb(OAc)_4 \rightarrow PhCH_2CH(OAc)_2$ (III) $+ PhCHCH_2CH_3$ (OAc) (IV)

$+ Pb(OCOCH_2CH_3)_4 \rightarrow PhCHCH_2CH_2CH_3$ ($OCOCH_2CH_3$) (V)

$+ Pb(OCOR)_4 \rightarrow PhCHCH_2OCOR$ ($OCOR$) (VIa, R=Ph; b, R=$PhCH_2$; c, R=Ph_2CH; d, R=Ph_2CHCH_2)

$+ Pb(OCORCOO)_2 \rightarrow$ PhCH——CH_2 ($OCORCOO$) (VIIa, $R=-(CH_2)_7-$; b, $R=-(CH_2)_8-$)

Ethyl vinyl ether, when reacted with lead tetra-monocarboxylate in benzene at room temperature, afforded 1-ethoxyethyleneglycol dicarboxylate (VIII) in a good yield. The hydrolysis of VIII gave glycolaldehyde (2, 4-dinitrophenylhydrazone; m. p., 159°C). No macrocyclic addition products were obtained in the reaction with lead di-dicarboxylate, in contrast to the case of styrene. The major product was IX namely, 1-ethoxyethyleneglycol dicaprylate, obtained from the reaction with lead diazelate. This means the occurrence of

1) E. J. Corey and J. Casanova, *J. Am. Chem. Soc.*, **85**, 165 (1963).
2) G. B. Bachman and J. W. Wittmann, *J. Org. Chem.*, **28**, 65 (1963).

the decarboxylation of a dicarboxylic residue to give a monocarboxylic residue.

$$EtOCH{=}CH_2 + Pb(OCOR)_4 \rightarrow EtOCH(OCOR)\text{-}CH_2OCOR \quad \text{VIII}$$

$$EtOCH{=}CH_2 + Pb(OCO(CH_2)_nCOO)_2 \rightarrow EtOCH(OCO(CH_2)_{n-1}CH_3)\text{-}CH_2OCO(CH_2)_{n-1}CH_3 \quad \text{IX}$$

When *t*-butylethylene was treated with two equivalents of lead di-sebacate in benzene at room temperature, a similar decarboxylated addition product, 3, 3-dimethylbutane-1, 2-diol dipelargonate (b. p., 100~103°C/0.9 mmHg, m. p. 6~8°C) was obtained in a 65% yield.

$$t\text{-}BuCH{=}CH_2 + Pb(OCO(CH_2)_8COO)_2 \rightarrow t\text{-}BuCH(OCO(CH_2)_7CH_3)\text{-}CH_2OCO(CH_2)_7CH_3$$

The infrared spectra of lead tetracarboxylates show that lead tetra-monocarboxylates (I) absorb at 1417 and 1510 cm^{-1}, indicating the presence of a carboxylate anion group, but lead di-dicarboxylates (II) absorb at 1405, 1505 and 1710 cm^{-1}, the last band being assignable to the carbonyl in the carboxyl group.

It is of interest that II has a band of the carbonyl group in addition to those due to the carboxylate anion group. This suggests that there are two types of bonds between the lead and carbonyl groups in II. The one has mainly an ionic character, while the other has mainly a covalent character X.

TABLE II. INFRARED SPECTRA (1400~1800 cm^{-1} REGION) OF I AND II IN KBr

		C=O group	COO^- group	
I	$R=CH_3(CH_2)_{12}-$	—	1417	1511
	$R=CH_3(CH_2)_{14}-$	—	1417	1510
	$R=CH_3(CH_2)_{16}-$	—	1416	1508
	IIa	1718	1403	1500
	IIb	1703	1406	1510

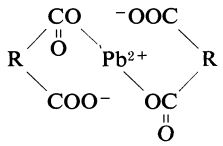

X

The macrocyclic addition to styrene and the decarboxylated addition to ethyl vinyl ether or *t*-butylethylene can be understood from the above structure X of II. The details and mechanism of the reaction will be published elsewhere.

The Institute of Scientific and Industrial Research
Osaka University
Sakai, Osaka

Homogeneous Hydrogenations of Organic Compounds with Cobalt Complex Ions[1]. *VII. Homogeneous Hydrogenations of Organic Compounds with a Cyano Cobalt Complex as a Catalyst*

By Masuo MURAKAMI and Jung-Wong KANG

(Received September 6, 1962)

Previous papers[2] from our laboratory have reported various successful reductions of unsaturated groups combined to with such divalent and trivalent cobalt complexes as bis-(pyruvic acid-oximato)-cobalt(II)[3] and phenylpyruvic acid-oximato-bis(propylenediamine)-cobalt(III) carbonate[4] by hydrogenations in an homogeneous solution. We have also reported[2] that the homogeneous hydrogenations were accomplished most effectively when 5~6 mol. of potassium cyanide were added as a co-catalyst to one mole of cobalt complex ions. In the meantime, Iguchi and his co-workers[5] have reported that, in the presence of sodium hydroxide and potassium chloride, unsaturated compounds (such as cinnamic acid, sorbic acid or nitrobenzene) are successfully reduced by homogeneous hydrogenation with a cyano cobalt(II) complex (pentacyanocobaltate(II)-ion) as a catalyst under atmospheric pressure and at room temperature.

It has been shown by Devries[6] that sorbic acid may be reduced, using pentacyanocobaltate-(II) ions selectively, to γ,δ-hexenoic acid. However, since these reactions were investigated in a small scale, neither the yield nor the separation of the reduction products were clearly shown; therefore, the mechanism of the homogeneous hydrogenations have not been touched upon. Kwiatek and his coworkers[7] reported recently that the homogeneous hydrogenations of unsaturated compounds had been successfully carried out by use of pentacyanocobaltate(II)-ions in an aqueous solution. In an earlier investigation[2], we ourselves reported that the hydrogenation of a cobalt chelate compound, in which the ligand containes unsaturated linkage, in the presence of potassium cyanide and the hydrogenation of an unsaturated compound with pentacyanocobaltate(II)-ions as a catalyst proceed through the entirely different intermediates.

The present paper describes in detail our study on the hydrogenation of an unsaturated compound with a cyano cobalt complex in comparison with other studies; it also presents a new method for the preparation of amino acid from α-keto acid[8].

Results and Discussion

The results of the hydrogenations with a cyano cobalt complex ($CoCl_2 6H_2O + 5KCN$) as a catalyst under the various conditions in an homogeneous medium are summarized in Table I.

The above findings on the hydrogenation of the oxime of phenylpyruvic acid with a cyano cobalt complex can be summarized as follows (runs 1—7).

(1) When the reaction was carried out under atmospheric pressure and at room temperature, phenylalanine could not be detected among the products, even by the paper chromatographic analysis.

(2) At a hydrogen pressure of 100 kg./cm^2 and at 100°C, phenylalanine was obtained in an about 30% yield, but it was found that the cobalt ions originally in the complex were quantitatively reduced to the metal. It has already been demonstrated that the oxime of phenylpyruvic acid was not reduced by the hydrogenation with a metallic cobalt[2] catalyst. We found that the oxime of phenylpyruvic acid was also reduced to phenylalanine in an about 30% yield by using a cyano cobalt complex which had been exposed to air for 72 hr.

(3) The homogeneous hydrogenation of the oxime of phenylpyruvic acid was carried out at 40~70°C under a hydrogen pressure of 100

1) Part VI: M. Murakami, K. Suzuki and J. W. Kang, presented at the 15th Annual Meeting of the Chemical Society of Japan, Kyoto, April, 1962.

2) M. Murakami, J. W. Kang, H. Itatani, S. Senoh and N. Matsusato, presented at the 12th and 14th Annual Meetings of the Chemical Society of Japan, Kyoto, April, 1959 and Tokyo, April, 1961.

3) M. Asymaretto, *Gazz. Chim. ital.*, **57**, 648 (1927).

4) M. Murakami, S. Senoh, N. Matsusato, H. Itatani and J. W. Kang, *J. Chem. Soc. Japan, Pure Chem. Sec. (Nippon Kagaku Zasshi)*, **83**, 747 (1962).

5) M. Iguchi, M. Takahashi et al., presented at the 9-13th Annual Meetings of the Chemical Society of Japan, Tokyo and Kyoto, April, 1956-1960.

6) B. Devries, *Koninkle. Ned Akad. Wetenshap. Proc. Sec.*, **B63**, 443 (1960).

7) J. Kwiatek, I. L. Mador and J. K. Seyler, *J. Am. Chem. Soc.*, **84**, 304 (1962).

8) Part V: M. Murakami and J. W. Kang, This Bulletin, **35**, 1243 (1962).

TABLE I. HOMOGENEOUS HYDROGENATIONS OF THE OXIMES OF α-KETO ACIDS AND KETOXIMES USING A CYANO COBALT COMPLEX[a)]

Compound	Run	Substrate/ $CoCl_2 6H_2O$	Temp. °C	Time hr.	Corresponding product, %	Co deposited
$C_6H_5CH_2C(=NOH)COOH$	1	1	30	8	—[b)]	None
	2	1	40	8	30.0	None
	3	3	60	8	78.3	None
	4	1	70	8	82.0	None
	5	5	70	5	75.2	None
	6	1	100	15	30.0[c)]	Much
	7	1	100	15	30.0[d)]	Much
$CH_3C(=NOH)COOH$	8	2	40	8	20.0	None
	9	2	70	8	63.6	None
$HOOC(CH_2)_2C(=NOH)COOH$	10	1.5	70	8	47.5	None
$CH_3C(=NOH)CH_3$	11	7.1	70	8	40.0	None
$C_6H_5C(=NOH)CH_3$	12	3.5	70	8	57.8	None

a) The reaction was carried out under a hydrogen pressure of 50 kg./cm²
b) Atomospheric pressure
c) A hydrogen pressure of 100 kg./cm²
d) A cyano cobalt(II) complex which had been exposed to air for 72 hr. was employed as a catalyst.

TABLE II. THE REDUCTIVE AMINATIONS OF α-KETO ACIDS AND α- AND β-KETO ESTERS WITH 6% AMMONIUM HYDROXIDE USING A CYANO COBALT COMPLEX AS A CATALYST[a)]

Compound	Run	Substrate/ $CoCl_2 6H_2O$	Temp. °C	Time hr.	Corresponding product, %	Co deposited
$C_6H_5CH_2C(=O)COOH$	13	1	30	8	—[b)]	None
	14	3	40	8	85.6	None
	15	1	70	5	95.0	None
	16	10	70	5	76.5	None
	17	1	70	5	36.3[c)]	None
$CH_3C(=O)COOH$	18	3	70	5	84.6	None
	28	1	40	8	73.2	None
$HOOC(CH_2)_2C(=O)COOH$	19	1	40	8	36.4	None
$CH_3C(=O)COOC_2H_5$	20	1	40	8	68.2	None
$C_6H_5CH_2C(=O)COOC_2H_5$	21	1	40	8	76.7	None
$CH_3C(=O)CH_2COOC_2H_5$	22	1	40	8	—	None

a) Most of the runs were carried out under the hydrogen pressure of 50 kg./cm².
b) The reaction was carried out under a hydrogen pressure of one atmosphere.
c) Potassium cyanide was not added to the reaction mixture.

kg./cm² to give phenylalanine in 33~82% yield.

These results indicate that the appropriate hydrogen pressure and temperature are necessary in homogeneous hydrogenation with a cyano cobalt complex as a catalyst. The oximes of other α-keto acids were also reduced in a similar method; these results are shown in runs 8—10.

It has been known[9)] that reductive amination of an α-keto acid with aqueous ammonia can

9) F. Knoop and H. Oesterlin, *Z. Physio. Chem.*, **148**, 294 (1925); 170, 185 (1927).

be carried out with an active metal such as platinum, palladium or Raney nickel. In the present study, the reductive aminations of the various α-keto acids and their esters with 6% aqueous ammonia could be carried out with a cyano cobalt complex as a catalyst. These results are summarized in Table II. In runs 20 and 21, although esters of α-amino acids were not obtained, free amino acids were obtained in good yields. Perhaps when the ester of α-imino acid is coordinated with cobalt complex ions, the hydrolysis of the ester group takes place more easily than the hydrogenation of the α-imino group. In the reductive amination of α-keto-glutaric acid, a minimum amount of α-hydroxyglutaric acid was obtained as a by-product, together with glutamic acid. This result can be explained by saying that glutamic acid was obtained in a poor yield because α-keto glutaric acid formed the ring structure II in the process of the reductive amination.

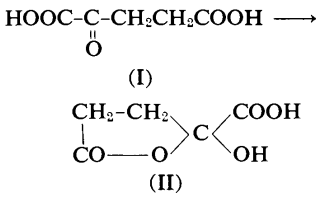

(I)

(II)

In the reductive amination of the ester of a β-keto acid, neither the ester of the β-amino acid nor the β-amino acid was formed. The ester of β-keto acid may be more readily hydrolyzed by the action of the cyano cobalt complex ions to yield a stable, enolized compound before the formation of an imino compound. Consequently it can be concluded that the reductive amination of an α-keto acid is carried out smoothly when an α-imino acid is coordinated with cobalt complex ions.

When the reaction was carried out at room temperature under an atmospheric pressure, phenylalanine was not detected among the products, even by the paper chromatographic analysis of these products.

In the run 17, the reductive amination of phenylpyruvic acid was carried out with cobaltous chloride under similar conditions. A comparison of the runs 15 and 17 indicates that the yield of phenylalanine increases appreciably because of the action of potassium cyanide on the reaction mixtuure.

The above results indicate that a cyano cobalt complex serves as a new catalyst for the hydrogenation of an unsaturated compound and for the reductive amination of an α-keto acid with aqueous ammonia in the synthesis of an amino acid. The mechanism of these reactions seems to be as follows: The unstable intermediate, the α-imino acid or the α-isonitroso carboxylic acid, coordinates with cobalt complex ions, and then the complex is reduced. In the case of the ester of an α-keto

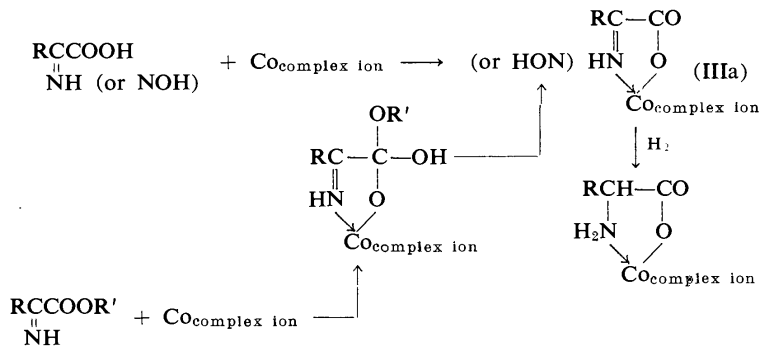

Eq. III

TABLE III. THE REDUCTIVE AMINATIONS OF α-KETO ACIDS WITH $[Co(NH_3)_5Cl]Cl_2$ IN AN ALKALINE SOLUTION

Compound	Run	nKCN	Keto acid/complex	Corresponding amino acid, %	Co deposited
$C_6H_5CH_2CCOOH$ (O)	30	0	1	29.6	Little
	31	5	5	53.0	None
	32	5	2	96.4	None
	33	5	1	94.0	None
CH_3CCOOH (O)	34	5	2	85.0	None

TABLE IV. THE HYDROGENATIONS OF UNSATURATED HYDROCARBONS AND UNSATURATED ACIDS WITH A CYANO COBALT COMPLEX

Compound	Run	Substrate/ $CoCl_26H_2O$	Reduction product, %	Co deposited
$C_6H_5CH{=}CHCOOH$	23	3.2	70.0	None
$CH_3CH{=}CHCH{=}CHCOOH$	24	4.2	60.0	None
Cyclohexene	25	5.8	—	None
Styrene	26	4.6	—	None

acid, the ester group of the α-imino acid is hydrolyzed and then the product is reduced through the intermediate IIIa (Eq. III).

When α-keto acids were treated with chloropentammine cobalt(III) chloride[10] alone or together with potassium cyanide at 70°C under a hydrogen pressure of 50 kg./cm² for five hours in an alkaline solution, α-amino acids were obtained. The results of the reductive aminations with $[Co(NH_3)_5Cl]Cl_2$ are summarized in Table III.

While the reductive amination[8] of phenylpyruvic acid with $[Co(NH_3)_5Cl]Cl_2$ gave phenylalanine in a 29.6% yield, phenylalanine was obtained in a good yield by the addition of five moles of potassium cyanide to the above reaction mixture. The yield of the amino acid decreased with the decrease in the molar ratio of $[Co(NH_3)_5Cl]Cl_2$ to the α-keto acid.

The mechanism of this reaction seems to be similar to that of the reductive amination of an α-keto acid with a cyano cobalt complex.

In the hydrogenations at 70°C under a hydrogen pressure of 50 kg./cm², cinnamic acid and sorbic acid gave dihydrocinnamic acid in a 70% yield and γ,δ-hexenoic acid in a 60% yield respectively. Runs 11 and 12 revealed that acetoxime and acetophenone oxime were hydrogenated under similar conditions. However, cyclohexene and styrene did not give any reduction product in a similar hydrogenation. This was confirmed by the gas chromatographic analysis (runs 25 and 26).

Table IV indicates that unsaturated hydrocarbons which can not coordinate with cobalt ions are not reduced, while the unsaturated compounds containing functional groups which can coordinate with cobalt ions are readily reduced. These results thus indicate that the homogeneous hydrogenation with a cyano cobalt complex proceeds along a different path from that of the heterogeneous hydrogenation with the metal catalyst. Probably, in the former, hydrogenations are taking place within the molecule of the cobalt complex.

While the α-isonitroso carboxylic acids and the α,β-unsaturated acids were readily hydrogenated with a cyano cobalt complex (Table II, runs 23 and 24), the γ,δ-unsaturated acid was not (run 24). We found, in our previous work[2], that the homogeneous hydrogenations of $[Co\,pn_2\,OCOC(NHCOCH_3){=}CHC_6H_5]Cl_2$ and $[Co\,pn_2\text{-}OCOCH(NH_2){=}CHC_6H_5]Cl_2$ with six moles of potassium cyanide gave reduction products in a 45.5% and a 3.5% yield respectively. Thus, the hydrogenations of the unsaturated compounds in both cases seem to be carried out through the transition states in which the reducible double bond is fixed in the chelate ring with the cobalt atom (VI and VII) or can come in the same plane (V).

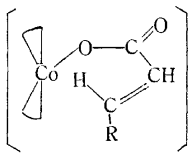

(V)

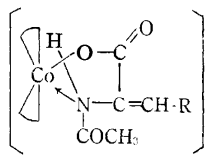

(VI)

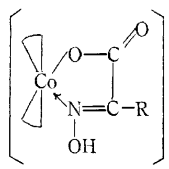

(VII)

A question remains as to the nature of the intermediate in the hydrogenations of the unsaturated compounds with a cyano cobalt complex and in the hydrogenations of the mixed organo-cobalt complexes with potassium cyanide. When the hydrogenation of *N*-acetylaminocinnamic acid with a cyano cobalt complex was carried out at 100°C under a hydrogen pressure of 100 kg./cm², the yield of phenylalanine was small. Also, the metallic cobalt quantitatively separated. In the meantime, the mixture of $[Co\,pn_2\,OCOC(NHCOCH_3){=}CHC_6H_5]Cl_2$ and six moles of potassium cyanide gave phenylalanine in a 45.5% yield under the same conditions. Whereas phenylalanine was obtained in a 55% yield from the hydrogenation of $[Co\,pn_2\,OCOCCH_2C_6H_5(NO)](CO_3)_{1/2}$ with six moles

10) B. Inoue, "Mukikagaku Seizo Jickken", Shokabo Co., Tokyo (1949), p. 358.

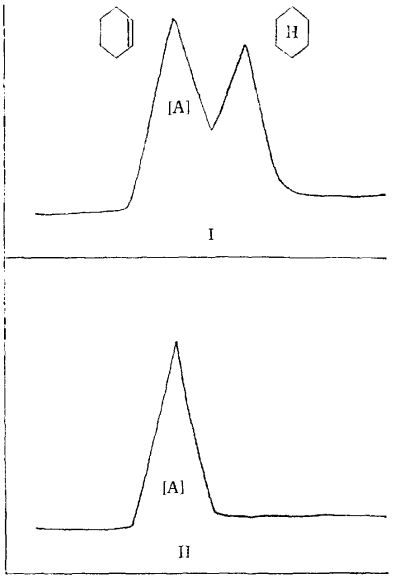

Fig. 1. Gas chromatographic analysis.

I: Standard sample (cyclohexene+cyclohexane), II: The reduction product of cyclohexene. The employed resin is as follows; Silicon grease 30%, Celite 545, 80~100 mesh.

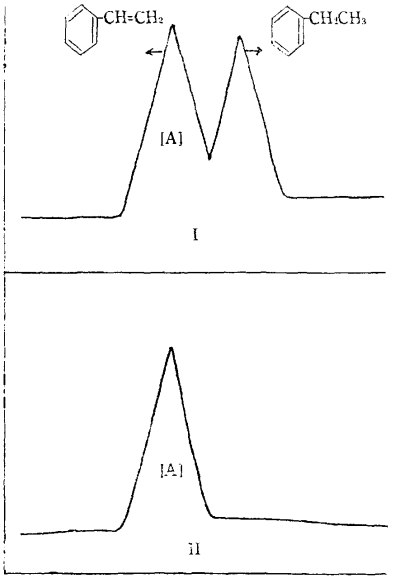

Fig. 2. Gas chromatographic analysis.

I: Standard sample (styrene+ethyl benzene), II: The reduction product of styrene. The employed resin is as follows; Silicon grease 30%, Celite 545, 80~100 mesh.

of potassium cyanide under a hydrogen pressure 100 kg./cm^2 and 100°C, it was also obtained in a 30% yield from the hydrogenation of the oxime of phenylpyruvic acid with a cyano cobalt complex under the same condition together with the metallic cobalt quantitatively deposited. A comparison of the two reaction enables us to conclude the following points: Whereas the yield of hydrogenation of an unsaturated compound with a cyano cobalt complex was high under mild conditions, the yield of the hydrogenation of the mixed organo-complex with potassium cyanide was low under the similar conditions. Under the drastic conditions, the results were contrary to those observed under the mild conditions.

Consequently, although the two hydrogenations do not seem to proceed through the same intermediate, the unsaturated compound and the cyano group should be combined in the same molecule of the cobalt complex. Accordingly, the homogeneous hydrogenations seems to occur very easily when cyanide and the unsaturated compound are combined with a cobalt ion simultaneously. However, at present we do not known the number of cyano groups which coordinate with a cobalt ion.

Experimental

Apparatus.—Hydrogenations were carried out in a stainless steel autoclave with a capacity of 100 ml.

Hydrogenation of the Oxime of Phenylpyruvic Acid.—To a solution of 0.37 g. (0.0021 mol.) of the oxime of phenylpyruvic acid and 0.082 g. (0.0025 mol.) of sodium hydroxide in 25 ml. of distilled water was added 0.685 g. (0.0105 mol.) of potassium cyanide. After the mixture had been poured into an autoclave, fine crystals of 0.5 g. (0.0021 mol.) of cobaltous chloride were added to the mixture and the autoclave was immediately sealed. The reaction completed at 70°C under a hydrogen pressure of 50 kg./cm^2 in eight hours. The reaction mixture was homogeneous. When 2 ml. of the reaction mixture was treated with the hydrochloric acid solution of 2,4-dinitrophenylhydrazine, only a trace of the hydrazone derivative was detected. The mixture was concentrated to dryness under reduced pressure. The residue was dissolved in the minimum amount of water and the solution was filtered. The filtrate was charged on a column of Ion-Exchange Amberite I. R. 120 (washed with 2 N ammonium hydroxide, water, 2 N hydrochloric acid and water) eluted with water until the elute was shown to be free of halide ions. The amino acid was then eluted with 2 N ammonium hydroxide, and the excess ammonia was evapolated to dryness under reduced pressure to give 0.28 g. (82.1%) of phenylalanine (m. p., 242~262°C decomp.). After the recrystallization from water-ethanol, it melted at 267~270°C with decomposition. The identity of the phenylalanine obtained was confirmed by the paper chromatographic analysis and by the mixed melting point determination.

The Reductive Amination of Phenylpyruvic Acid.—To a solution of 1.0 g. (0.0061 mol.) of phenylpyruvic acid in 25 ml. of 6% ammonium hydroxide was added 0.685 g. (0.0105 mol.) of potassium cyanide; the mixture was then poured into an autoclave. Fine crystals of 0.5 g. (0.0021 mol.) of cobaltous chloride were added to the mixture. The

reaction completed at 40°C under a hydrogen pressure of 50 kg./cm² in eight hours. The reaction mixture was homogeneous. When 2 ml. of the cooled reaction mixture was treated with a hydrochloric acid solution of 2,4-dinitrophenylhydrazine, only a trace of hydrazone derivative was detected. The residual solution was treated with hydrogen sulfide to remove the cobalt ion as its sulfide. The filtrate was concentrated to dryness under reduced pressure. After the residue was treated with a minimum amount of water, the mixture was filtered. The filtrate was then treated in a method similar to that of the previous experiment. The phenylalanine obtained was 0.856 g. (a 85.6% yield); m. p., 248~262°C (decomp.). The identity of the phenylalanine obtained was confirmed by the paper chromatographic analysis and by the mixted melting point determination.

The Reductive Amination of Ethyl Phenylpyruvate.—To a solution of 0.38 g. (0.0019 mol.) of ethyl phenylpyruvate in 25 ml. of 6% ammonium hydroxide was added 0.68 g. of potassium cyanide; the mixture was then poured into an autoclave. Fine crystals of 0.5 g. of cobaltous chloride were added to the mixture. The reaction completed at 40°C under a hydrogen pressure of 50 kg./cm² in eight hours. The cooled reaction mixture was repeatedly extracted with ether. When the ether layer was evaporated after dried over anhydrous magnesium sulfate, the ethyl ester of phenylalanine was not obtained. The aqueous layer was treated in a way similar to that above. The phenylalanine obtained was 0.24 g. (a 76.6% yield); m. p., 242~252°C (decomp.). The paper chromatographic analysis of the product proved its identity with the authentic phenylalanine.

The Hydrogenation of Acetoxime.—Into a solution of 1.0 g. (0.0141 mol.) of acetoxime and 0.6 g. (0.0150 mol.) of sodium hydroxide in 25 ml. of water was dissolved 0.685 g. of potassium cyanide. After the mixture had been poured into an autoclave, fine crystals of 0.5 g. of cobaltous chloride were added to the mixture. The reaction was completed under the condition similar to that used in the previous experiment. The cooled reaction mixture was extracted with the ethereal hydrochloric acid solution by means of extraction apparatus. The acidic ether extracts were concentrated to dryness under a reduced pressure, and the residue was dried over sulfuric acid in vacuo. The crude isopropylamine hydrochloride (0.34 g., 40%) melted at 121~138°C. After three additional recrystallizations from ethanol, it was identified with the authentic sample; m. p., 137~139°C.

Found: C, 37.08; H, 10.72; N, 14.05; Cl, 36.89. Calcd. for $C_3H_{10}NCl$: C, 37.48; H, 10.47; N, 14.55; Cl, 37.17%.

The Hydrogenation of Acetophenone Oxime.—A mixture of acetophenone oxime (1.0 g., 0.0074 mol.), sodium hydroxide (0.3 g., 0.0075 mol.), potassium cyanide (0.685 g.) and cobaltous chloride (0.5 g.) in 15 ml. of water was hydrogenated by the method similar to that of the above experiment. The homogeneous solution was repeatedly extracted with ether. After the ethereal extracts had been dried over anhydrous magnesium sulfate, the ether was removed and the product was collected at 81~82°C (16 mmHg). The yield of α-methylbenzylamine was 0.52 g. (57.8%).

Found: C, 79.36; H, 9.01; N, 12.00. Calcd. for $C_8H_{11}N$: C, 79.29; H, 9.15; N, 11.56%.

The Reductive Amination of Phenylpyruvic Acid.—To a solution of 1.0 g. (0.0061 mol.) of phenylpyruvic acid and 0.6 g. (0.015 mol.) of sodium hydroxide in 25 ml. of water was added 0.95 g. (0.0146 mol.) of potassium cyanide. After the mixture had been poured into an autoclave, fine powder of 0.75 g. (0.0030 mol.) of chloro pentammine cobalt(III) chloride was added to the mixture. The reaction completed at 70°C under a hydrogen pressure of 50 kg./cm² in five hours. The cooled reaction mixture was concentrated to dryness under a reduced pressure. To the residue was added the minimum amount of water and the mixture was filtered. The filtrate was charged on a column of Ion-Exchange Amberite I. R. 120 and eluted with water until the elute was shown to be free of halide ions. The amino acid was then eluted with 2 N ammonium hydroxide, and the excess ammonia was concentrated to dryness under a reduced pressure to give 0.94 g. (94%) of phenylalanine (m. p., 245~263°C (decomp.)). The identity of the phenylalanine obtained was confirmed by the paper chromatographic analysis.

The Hydrogenation of Cinnamic Acid.—To a solution of 1.0 g. (0.0067 mol.) of cinnamic acid, 0.3 g. (0.0076 mol.) of sodium hydroxide and 0.685 g. of potassium cyanide in 25 ml. of water, 0.5 g. of cobaltous chloride was added. The reaction completed at 70°C under a hydrogen pressure of 50 kg./cm² in eight hours. The cooled reaction mixture was acidified with 2 N hydrochloric acid and was repeatedly extracted with ether. After the mixture had been dried with anhydrous magnesium sulfate, the ether was removed to give 0.76 g. of the crystalline product (m. p. 43~65°C). The crude product was dissolved in 5 ml. of ethanol, and the insoluble material was filtered. After the ethanol had been removed, the residue was crystallized from 5 ml. of ligroin. The product weighed 0.7 g. (70%) and melted at 45~46°C. The product was identified with an authentic sample of hydrocinnamic acid.

The Hydrogenation of Sorbic Acid.—A mixture of sorbic acid (1.0 g., 0.0089 mol.), sodium hydroxide (0.36 g., 0.0090 mol.) potassium cyanide (0.685 g.) and cobaltous chloride (0.5 g.) in 25 ml. of water was hydrogenated and was treated in a way similar to that above. γ,δ-Hexenoic acid (0.61 g., 60%) was collected, its b. p. being 101~102°C (12 mmHg). The identify of γ,δ-hexenoic acid was confirmed by its infrared spectrum and by the titrimetric determination of the double bond of the product.

The Hydrogenation of Cyclohexene.—A mixture of cyclohexene (1.0 g., 0.0122 mol.), potassium cyanide (0.685 g.) and cobaltous chloride (0.5 g.) in 15 ml. of water was hydrogenated as above. The cooled reaction mixture was then acidified with 2 N hydrochloric acid and repeatedly extracted with ether. After the mixture had been dried with anhydrous magnesium sulfate, the ether layer was

removed and the residue (0.95 g.) was collected at a boiling point of 78~83°C. It was confirmed by the gas chromatographic analysis that cyclohexane was not present in the product obtained.

The Institute of Scientific and Industrial Research
Osaka University
Sakai, Osaka

*The Spectrophotometric Determination of Uranium with Dibenzoylmethane**

By Yoshimi UMEZAKI

(Received October 17, 1962)

Recently, many organic reagents which are very sensitive to uranium, such as dibenzoylmethane[1], PAN[2] and arsenazo[3], have been used for the spectrophotometric determination of uranium. In general, however, these reagents are liable to be affected by diverse ions. Accordingly, it is preferable to separate uranium from diverse ions by extraction prior to its spectrophotometric determination.

Of these chromogenic reagents, dibenzoylmethane can be advantageously used for the direct color development in the organic phase; thus the time for the analysis may be shortened and, at the same time, the possible loss of uranium during stripping may be prevented. From this point of view, several kinds of extractant, such as tetrapropylammonium nitrate (in methyl isobutyl ketone)[4], tri-*n*-octylphosphine oxide (in cyclohexane)[5] and tributyl phosphate (in ethyl acetate[6], or in isooctane[7], or in no diluent[8]), in combination with the use of dibenzoylmethane, have been reported. Some of these, however, involve procedures too complicated for routine use, or are too greatly subject to interference from diverse ions.

This paper describes a simple direct spectrophotometric determination of uranium with dibenzoylmethane in combination with tributyl phosphate, which is selected as the extractant of uranium because of its popularity.

* The main part of this work was done while the writer was at the School of Chemistry, University of Minnesota, U. S. A.

Presented at the 11th Annual Meeting of the Japan Society for Analytical Chemistry, Sapporo, July, 1962.

1) J. H. Yoe, F. Will and R. A. Black, *Anal. Chem.*, **25**, 1200 (1953).
2) K. L. Cheng, ibid., **30**, 1027 (1958).
3) H. P. Holcomb and J. H. Yoe, ibid., **32**, 616 (1960).
4) W. J. Maeck et al., ibid., **31**, 1130 (1959).
5) C. A. Horton and J. C. White, ibid., **30**, 1779 (1958).
6) M. W. Lerner and A. R. Eberle, *U. S. Atomic Energy Comm. Rept.*, **NBL-127**, 8 (1956).
7) C. A. Francois, *Anal. Chem.*, **30**, 50 (1958).
8) J. L. Long and L. F. Gill, *U. S. Atomic Energy Comm. Rept.*, **FP-78** (1957).

Experimental

Apparatus.—Absorbance measurements were made with a Beckman Model B spectrophotometer using 1-cm. glass cells.

Reagents.—*Standard Uranium Solution.*—A stock solution containing 100 μg. of uranium per ml. was prepared by dissolving uranyl nitrate in water. The standardization was made by titration with a standard potassium dichromate solution after the reduction of uranium with zinc amalgam. Dilutions of this solution were made as required.

Dibenzoylmethane Solution.—A 1% solution was prepared by dissolving 1 g. of dibenzoylmethane in 100 ml. of 95% ethyl alcohol.

Tributyl Phosphate Solution.—A 30% tributyl phosphate solution was prepared by mixing 300 ml. of tributyl phosphate with 700 ml. of benzene. This solution was washed first with a 5% sodium hydroxide solution and then with a 1 N nitric acid solution.

Aluminum Salting Agent.—An aluminum salting agent was prepared by dissolving 500 g. of aluminum nitrate nonahydrate and 70 ml. of concentrated nitric acid in enough water to make 1 l. of solution.

The other solvents and reagents were of an analytical reagent grade and were used without further purification.

Procedure.—*Extraction of Uranium.*—*a*) Samples which do not contain interfering ions.—Bring the nitric acid concentration of the sample solution to approximately 1N and then make it up to a definite volume with 1N nitric acid. Transfer 5 ml. of the sample solution to a 50-ml. separatory funnel. Add 5 ml. of a salting agent and 3 ml. of a tributyl phosphate solution. Shake vigorously for about 1 min. After it has settled, discard the aqueous layer and, if necessary, wash the organic layer with 2~3 ml. of a 10% sodium nitrate solution (1 N in acid) and discard the aqueous layer. Run the organic layer through a small plug of filter paper in the stem of the separatory funnel into a dried small vessel (e. g., a weighing bottle).

b) Samples containing chromium(VI) and cerium(IV).—Bring the nitric acid concentration of the sample solution to approximately 1 N in a definite volume. Transfer 5 ml. of the sample

solution to a small beaker. Add 1~2 ml. of a 10% sodium nitrite solution and warm this solution at 80~90°C until small bubbles of colored gas disappear. After cooling, transfer the solution into a 50-ml. separatory funnel and treat this solution as in a).

c) Samples containing thorium (IV) and zirconium (IV).—Bring the nitric acid concentration of the sample solution to approximately 1 N in a definite volume. Transfer 5 ml. of the sample solution to a 50-ml. separatory funnel. Add 3~5 ml. of a 1 M potassium fluoride solution. When 5 ml. of a potassium fluoride solution is used, the amount of salting agent should be doubled. In this case, solid aluminum nitrate nonahydrate is preferable. Treat this solution as in a).

Color Development.—Pipet 2 ml. of the extract into a 10-ml. volumetric flask. Add 1 ml. of a 1% dibenzoylmethane solution and 5 ml. of pyridine, and dilute with ethyl alcohol to the mark. Measure the absorbance at 410~425 mμ against a blank.

Results and Discussion

Effect of Salting Agent.—When uranium is extracted as the tributyl phosphate complex from a nitric acid solution, the optimum acidity is approximately 6 N[9]. However, if salting agents, e. g., sodium nitrate or aluminum nitrate, are used, uranium can be extracted quantitatively, even from a nitric acid solution of a lower acidity. In this case, the amount of pyridine used to neutralize the co-extracted acid may be reduced. The effect of the aluminum salting agent was examined while keeping other factors constant. As is shown in Fig. 1, 5 ml. of an aluminum salting agent is sufficient for the standard procedure.

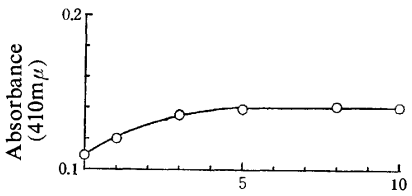

Fig. 1. Effect of salting agent.
2 p. p. m. U, extracted from 1 N nitric acid

Choice of Solvents.—An aliquot of the extract is mixed with dibenzoylmethane, a neutralizer and a diluent. The neutralizer is used to neutralize the acid extracted simultaneously in the organic phase in order to insure the full color development of the complex. Pyridine has been used almost exclusively by previous authors for this purpose.

Several kinds of solvents, such as kerosene, isooctane and ethyl acetate, have been used as a diluent for tributyl phosphate. In this method, benzene was chosen because of its high miscibility with pyridine.

Ethyl alcohol, used as the solvent for dibenzoylmethane, is useful at the same time to prevent the precipitation of a pyridinium compound, which is produced by the addition of pyridine to the extract. These solvents are miscible with each other and can be handled without special consideration because they are not extremely volatile at room temperature.

Pyridine Concentration.—Though it is known that the maximum color intensity is obtained in the "apparent" pH range of 6.5 to 8.5 in alcoholic aqueous media[1], these values can not be applied to the present organic solution because these pH values have no significance here. Therefore, the effect of the pyridine concentration on color development was studied in the extract which was obtained from a 1 N nitric acid solution with a salting agent, and in that obtained from a 6 N nitric acid solution without a salting agent. Other factors were kept constant.

As is shown in Fig. 2, with the former solution a 40~60% pyridine concentration is necessary to insure the full color development; a slight decrease in color intensity is observed with 80% pyridine. With the latter solution, a 60~80% concentration is necessary. The addition of 5 ml. of pyridine was therefore decided for the standard procedure.

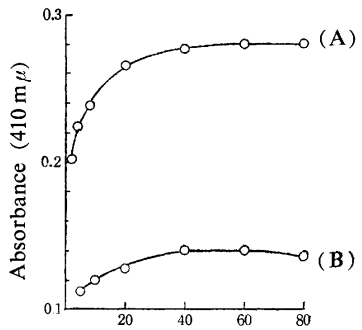

Fig. 2. Effect of pyridine concentration on absorbance.
(A) 4 p. p. m. U, extracted from 6 N nitric acid
(B) 2 p. p. m. U, extracted from 1 N nitric acid

The absorbance of the blank solution increases linearly with the increasing concentration of pyridine.

Dibenzoylmethane Concentration.—As is shown in Fig. 3, 1 ml. of a 1% dibenzoylmethane solution is necessary for full color development with 2 ml. of the 3 ml. extract. However, a

9) H. A. C. McKay, *Proc. Intern. Conf. Peaceful Uses of Atomic Energy*, Geneva, 1955, 7, 314 (1956).

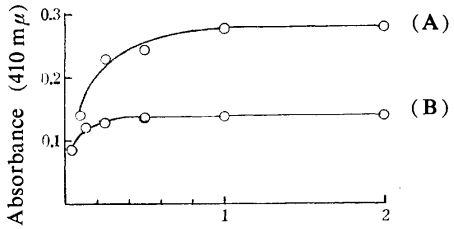

Fig. 3. Effect of dibenzoylmethane conentration on absorbance.
(A) 4 p. p. m. U (60 μg. U in aqueous solution, 2 ml. of 3 ml. extract is used for color development.)
(B) 2 p. p. m. U (60 μg. U in aqueous solution, 1 ml. of 3 ml. extract is used for color development.)

TABLE I. EFFECT OF DIBENZOYLMETHANE CONCENTRATION

U in aqueous solution μg.	Ext. used ml.	Dibenzoylmethane ml.	U found μg.
60	1	0.5	60.0
60	2	0.5	52.1
120	1	0.5	119
120	1	1.0	119
120	1+benzene 1 ml.	0.5	119
120	1+blank ext. 1 ml.	0.5	112

smaller portion of the extract may be used for samples of a higher uranium content. When 1 ml. of the 3 ml. extract is used for color development, which is frequently useful because the blank value is lowerd, 0.5 ml. of 1% dibenzoylmethane is sufficient. This value is independent of the uranium concentration in the sample solution. As summarized in Table I, this is because of the influence of excess tributyl phosphate in the organic phase. There is apparently some competition between tributyl phosphate and dibenzoylmethane in forming a complex with uranium.

Effect of the Acidity of the Sample Solution.—According to previous authors, strict control of the acidity of the aqueous solution is required in order to obtain reproducibility. In this method, where *in situ* color development is adopted, however, the change in acidity does not have any serious influence on the color intensity. This is as expected from Fig. 2. In fact, the change in the acidity of the sample solution within the range of 0.8 N and 2.0 N did not have any influence at all on the absorbance of the uranium complex in the standard procedure. This may be attributed to the fact that the amount of acid extracted simultaneously into the organic phase is not large compared with the pyridine used, while, at the same time, the excess of pyridine has little influence on the color intensity of the complex in the organic solution.

Effect of the Volume of Aqueous Solution.—In the standard procedure, the volume of aqueous solution is 10 ml., including the salting agent. In practice, however, a larger volume of aqueous solution is sometimes necessary, for instance, the complete dissolution of a precipitate. The influence of the volume of aqueous solution was studied while keeping the acidity and salting agent of the sample solution constant and using 3 ml. of tributyl phosphate.

The results reveal that when the volume of the aqueous solution is 20 ml. or 40 ml., the absorbance is 99% or 94% respectively of the absorbance from 10 ml. of the aqueous solution.

Wavelength.—The absorption spectra of the uranium complex, the thorium complex and dibenzoylmethane are shown in Fig. 4. Though

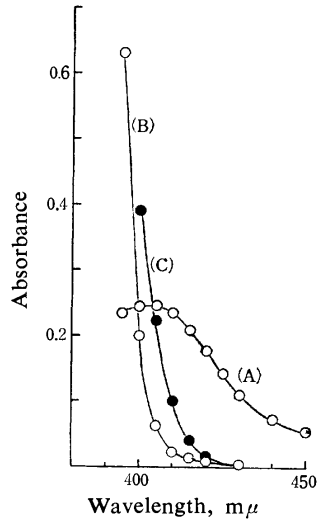

Fig. 4. Absorption spectra.
(A) 3.3 p. p. m. U
(B) Blank solution, 0.1% dibenzoylmethane
(C) 6.7 p. p. m. Th

the maximum absorption of uranium complex is observed at 400~405 mμ, the absorbance of the blank solution is fairly large at this wavelength. Moreover, as the slope of this curve is very sharp in this region, the results are liable to fluctuate when some of the factors are slightly varied. From this point of view, it is preferable to use a wavelength 410 mμ long or longer, even though the absorbance of the uranium complex decreases.

Stability.—The yellow color develops instantaneously on the addition of the reagent and

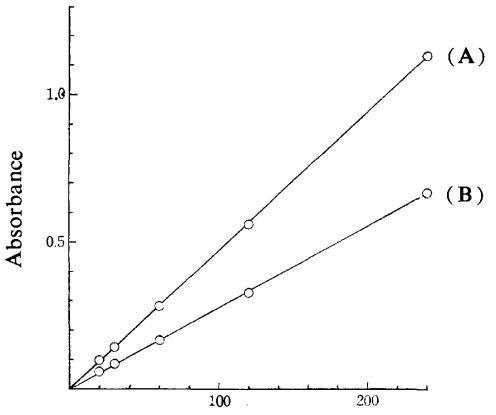

Fig. 5. Calibration curves.
(A) 410 mμ (B) 425 mμ

pyridine and is stable for at least 20 hr. at room temperature, provided the container is sealed.

Beer's Law.—Beer's law is obeyed up to 240 μg. of uranium in the aqueous solution, as Fig. 5 shows.

Diverse Ions.—In order to simplify the method, it is desirable to use the extract directly for color development without any washing procedure. The results obtained by this procedure are shown in Table II. When large amounts of a foreign ion, e.g., iron, are present in the sample solution, it is better to wash the extract with 2~3 ml. of a 10% sodium nitrate solution (1 N nitric acid) in order to reduce the interference, which may be attributed, in part, to the contamination of the extract with the aqueous suspension in the organic phase. The presence of chloride and iron ions in the same solution should be avoided. Bismuth may be present up to 3 mg. when measuring the absorbance at 425 mμ.

The interference of chromium(VI) and cerium(IV) can be minimized or eliminated by reduction with a proper reductant. For this purpose, sodium nitrite and sodium sulfite were each tried. At a low cerium(IV) concentration, sodium sulfite can be used without any difficulty. At a high concentration (e.g., 50 mg. Ce), however, a precipitate, presumably cerium(III) sulfate, is sometimes produced. When sodium nitrite is used as a reductant, caution should be taken to expel the colored gas which is liberated by the addition of nitrite; otherwise it is extracted into the organic phase and produces a positive error. In order to expel this gas completely, the solution is warmed at 80~90°C for several minutes until the fine bubbles disappear.

Thorium and zirconium interfere seriously because they are extracted into the organic phase and react with dibenzoylmethane. The absorption of these complexes decreases rapidly at longer wavelengths (shown in Fig. 4 for thorium). Masking these ions with fluoride is effective to some extent, even in the presence of a large number of aluminum ions, which form a stable complex with fluoride ions. Thus, the interference up to 2 mg. of each of these ions can be minimized. The results of the reduction and the masking experiments are shown in Table III.

Table II. Effect of diverse ion
(50 μg. of U(VI) present)

Ion	Added mg.	Added as	U recovered, μg. 410 mμ	420 mμ	425 mμ
Cd(II)	50	NO_3	50.0	49.9	
Co(II)	50	ClO_4	51.1	50.9	
Cu(II)	50	NO_3	50.4	50.9	
Hg(II)	50	NO_3	49.4	49.2	
Mn(II)	50	SO_4	51.1	50.6	
Ni(II)	50	NO_3	50.5	51.2	
Pb(II)	50	NO_3	51.1	51.0	
Zn(II)	50	NO_3	49.5	49.5	
La(III)	50	NO_3	52.1	51.6	
Bi(III)*1	1.0	NO_3	51.3	50.6	
	3.0	NO_3	56.4	53.1	51.7
Fe(III)	50	NO_3	51.9	53.4	
	100*2	NO_3	51.5	53.4	
Fe(III) + Cl^-	10 + 20	NO_3 + NaCl	54.8	54.3	
Ti(IV)	50	SO_4	48.1	48.5	
V(V)	50	VO_3^-	50.2	50.2	
Mo(VI)	50	MoO_4^{2-}	52.2	51.9	
W(VI)*3	50	WO_4^{2-}	49.8	51.1	
Cl^-	100	NaCl	50.0	50.6	
SO_4^{2-}	100	Na_2SO_4	50.0	50.6	
ClO_4^-	100	$NaClO_4$	49.6	50.3	
OAc^-	100	NaOAc	48.2	48.9	
PO_4^{3-}	100	Na_3PO_4	44.2	45.5	
	100*4	Na_3PO_4	48.6	49.8	
F^-	175	KF	48.5	49.6	
	290*4	KF	49.1	49.8	
F^- + SO_4^{2-}	290*4 + 250	KF + H_2SO_4	47.0		47.2
	290*5 + 250	KF + H_2SO_4	49.4		48.9

*1 Precipitate is produced in organic phase upon standing.
*2 Washed with 2 ml. of 10% sodium nitrate solution.
*3 Precipitate is produced in aqueous phase upon standing.
*4 5 g. of aluminum nitrate nonahydrate was used.
*5 9 g. of aluminum nitrate nonahydrate was used.

TABLE III. REDUCTION AND MASKING OF DIVERSE IONS

(50 μg. of U(VI) present)

Ion	Added mg.	Added as	Reductat or masking agent	U recovered, μg. 410 mμ	425 mμ
Cr(Vl)	50	CrO_4^{2-}	None	Approx.	260
	50	CrO_4^{2-}	$NaNO_2$	50.3	
	50	CrO_4^{2-}	Na_2SO_3	50.2	
Ce(IV)	5.0	SO_4	None	59.4	
	50	SO_4	$NaNO_2$	52.7	51.4
	50*	SO_4	Na_2SO_3	55.1	
Th(IV)	0.1	NO_3	None	67.2	
	1.0	NO_3	KF 3 ml.	70.1	50.7
	2.0	NO_3	KF 5 ml.	73.1	51.4
Zr(IV)	0.1	NO_3	None	76.5	
	1.0	NO_3	KF 3 ml.	60.9	50.3
	2.0	NO_3	KF 5 ml.	67.3	52.9

* Precipitate is produced in aqueous solution upon standing.

The Determination of Uranium in Ores.—The above-mentioned procedure was applied to the determination of uranium in uranium ores and in monazite.

For uanium ore, 1 g. of sample was decomposed with aqua regia. After filtration, uranium was precipitated with ammonium hydroxide. The precipitate was dissolved in enough nitric acid to make exactly 50 ml. or 250 ml. of a 1~1.5 N nitric acid solution.

For monazite, 1 g. of sample was decomposed with 10 ml. of fuming sulfuric acid. After cooling, the solution was poured into cold water. After filtration, the filtrate was transferred to a 250-ml. volumetric flask and made up to volume with water.

Using an aliquot of these stock solutions, uranium was determined according to the above-mentioned procedure. In the case of monazite, 1 ml. of nitric acid (1 : 1), 1 ml. of a 10% sodium nitrite solution*, and 5 ml. of a 1 M potassium fluoride solution for 5 ml. of sample solution were used.

The absorbance measurements were made at 410 mμ and 425 mμ respectively. The results shown in Table IV show good agreement with the values obtained by the authorized method.

TABLE IV. ANALYSIS OF URANIUM ORE AND MONAZITE

Sample	U* Content, U_3O_8, %	U Found, U_3O_8, %	No. of Detns.
Uranium ore (sedimentary) No. 1	0.321	0.344	12
Uranium ore (sedimentary) No. 2	0.057	0.057_2	5
Monazite	0.286	0.300	5

* Results of the co-operative analysis at 11 laboratories.

The author wishes to express his thanks to Professor E. B. Sandell, University of Minnesota, for his helpful suggestions and encouragement throughout this work.

Resources Research Institute
Kawaguchi, Saitama-ken

* When sodium sulfite was used a white precipitate was produced in the organic phase after neutralizing the extracts with pyridine. This could be prevented by expelling the excess of sulfur dioxide before extraction.

*The Volatilization of Chlorine and Fluorine Compounds from Igneous Rocks on Heating**

By Minoru YOSHIDA

(Received November 30, 1962)

It is important for the study of volcanic phenomena to make clear the nature of the volcanic emanation. There are many ways of investigation. Some of the most important information on the problem are provided by analyses of volcanic gases, volcanic sublimates and other products of volcanic activity. An investigation of the chemical composition of volcanic gases from more than 600 fumaroles and hot springs in Japan has, accordingly, been carried out by Iwasaki et al.[1] However, the environmental conditions which affect the chemical composition of volcanic gases are so

* Read at the Symposium on Geochemistry of the Chemical Society of Japan, October, 1961.

1) I. Iwasaki, T. Ozawa, M. Yoshida, T. Katsura, B. Iwasaki, M. Kamada and M. Hirayama, *Bull. Tokyo Inst. Tech.*, No. 47, 1 (1962).

complicated that it is difficult to understand the nature of volcanic emanations satisfactorily on the basis of this information alone.

The second way to investigate the nature of volcanic emanation is to study the equilibrium between the gas phase and the condensed phase represented by the igneous rocks with which the gas phase is thought to be in contact. Some calculations of these gas-solid equilibria have been made by Ellis[2], Krauskopf[3], Matsuo[4], and others. In some cases, a close approach has been made to the chemical composition of natural volcanic gases by theoretical calculations. There remain, however, many difficult problems concerning the maintenance of equilibrium and the insufficiency of thermochemical data on rock-forming minerals.

The third way is to study the nature of the gases obtained by heating igneous rocks. The components of those gases obtained by heating samples of igneous rocks have been studied by many investigators[5-13]. Little work has, however, been done on the halogen compounds evolved from igneous rocks on heating. Shepherd[9-11] studied the amount of chlorine and fluorine compounds evolved at 1200°C. Brun[8] reported that chlorine compounds were evolved from igneous rocks at temperatures higher than "the explosion temperature". Iwasaki et al.[13] reported that the evolution of hydrogen chloride occured when rocks were heated at temperatures above 800°C. However, the exact relationships between the temperature and the amount of evolved halogen compounds, especially that of fluorine, have not yet been established. The objectives of the present paper are to make clear the volatilization of chlorine and fluorine compounds from igneous rocks at various temperatures ranging from 400 to 1200°C.

Experimental

Materials.—The rock samples used in this study are listed in Table I, together with their chlorine and fluorine contents. The chlorine in the rocks was determined by the method of Iwasaki et al.[13] with some improvements, while the fluorine in the rocks was determined by the method of Kamada et al.[14] The main chemical composition of these rocks is also known.

Reagent grade chemicals and redistilled water were used in the preparation of all reagents and in the procedures.

Methods of Collecting Halogens Evolved from Rock Samples.—The apparatus used in this study is shown in Fig. 1. The maximum temperature attained by electric furnace A is about 1300°C, and the temperature can be controlled with an accuracy of ±20°C. A pyrometer with a platinum-platinum, 10% rhodium thermocouple D was used to measure the temperature of the furnace. A silica-glass tube B (1 m. in length, 25 mm. in inside diameter) was connected to the commercial nitrogen gas cylinder and absorption vessels E by taper joints. Two absorption vessels were connected in a series, each of them containing about 75 ml. of a 0.05 N sodium hydroxide solution.

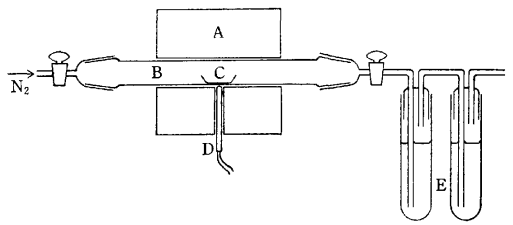

Fig. 1. Apparatus.
A Electric furnace
B Silica-glass tube
C Platinum boat
D Thermocouple
E Absorption vessels

One gram of a finely powdered sample was placed in a platinum boat, which was then inserted in silica-glass tube B and placed in the center of the furnace. The flow of nitrogen gas was then started at the rate of 20~30 l./hr. After the air in the apparatus had been replaced by nitrogen, the sample was heated to a programmed temperature and was maintained at that temperature for one hour. Experiments were carried out at 400, 600, 800, 1000 and 1200°C (in one case, also at 200°C). The acid gas species evolved from the sample in the nitrogen gas were absorbed by the solution in absorption vessels. After the furnace had been cooled, the solutions in each absorption vessel were diluted to 100 ml. in a volumetric flask. An aliquot of the solution was used for the determination of fluoride. Another portion was used for the determination of chloride after oxidizing the sulfide ion by heating the solution with a small amount of sodium peroxide. Sublimates were deposited on the inside surface of the silica-glass tube on outgassing the rocks. These sublimates were dissolved in water by washing the inside of the silica-glass tube three times. All the washings were transferred

2) A. J. Ellis, *Am. J. Sci.*, 255, 416 (1957).
3) K. B. Krauskopf, "Researches in Geochemistry", Ed. by P. H. Abelson, John Wiley and Sons, Inc., New York (1959), p. 260.
4) S. Matsuo, *J. Earth Sci. Nagoya Univ.*, 8, No, 2, 222 (1960); 9, No. 1, 80, 101 (1961).
5) T. Graham, *Proc. Roy. Soc.*, 15, 502 (1867).
6) A. Gautier, *Compt. rend.*, 132, 58, 189 (1901).
7) R. T. Chamberlin, "The Gases in Rocks", Carnegie Inst. Wash. Rubl., Washington, D. C. (1908).
8) A. Brun, "Recherches sur l'Exhalation Volcanique", Libraire Kündig, Genève (1911).
9) E. S. Shepherd, *J. Geol.*, 33, (Supplement to No. 3), 289 (1925).
10) E. S. Shepherd and H. E. Merwin, ibid., 35, 97 (1927).
11) E. S. Shepherd, *Am. J. Sci.*, 35A, 311 (1938).
12) Lord Rayleigh, *Proc. Roy. Soc.*, 170, 451 (1939).
13) I. Iwasaki, T. Katsura and N. Sakato, *J. Chem. Soc. Japan, Pure Chem. Sec.*(*Nippon Kagaku Zassi*), 76, 778, 1116 (1955).
14) The Chemical Society of Japan, "Jikken Kagaku Koza" (Experimental Chemistry), Vol. 14, "Geochemistry" (in Japanese), Maruzen, Tokyo (1958), p. 333.

TABLE I. F AND Cl CONTENTS OF THE ROCK SPECIMENS USED IN THE PRESENT STUDY

No.	Sample	F%	Cl%	F/Cl (atomic ratio)
1	Basalt (lava of 1950 Mt. Mihara Ō-sima volcano, Tokyo Metr.)	0.011	0.031	0.66
2	Basalt (Sakasagawa, Itō, Sizuoka Pref.)	0.025	0.010	4.7
3	Andesite, (Tamagawa hot spring, Akita Pref.)	0.042	0.010	7.9
4	Andesite (lava of 1946 Sakura-zima volcano, Kagoshima Pref.)	0.035	0.033	2.0
5	Dacite (somma lava Akagi volcano, Gumma Pref.)	0.027	0.003	17
6	Liparite (Kōzu-sima volcano, Tkoyo Metr.)	0.025	0.091	0.51
7	Obsidian (Imari, Saga Pref.)	0.049	0.062	1.5
8	Obsidian (Hime-sima, Oita Pref.)	0.049	0.016	5.7
9	Granite (Mt. Tukuba, Ibaragi Pref.)	0.057	0.010	11
10	Granite (Kiuragi, Saga Pref.)	0.028	0.005	10

into a 100 ml.-volumetric flask and diluted to the mark to determine the chlorine and fluorine contents. To minimize the contamination during the procedure, the silica-glass tube and platinum boat were heated and washed in duplicate before being used.

Methods of Determining the Chloride and Fluoride in the Solution.—The chloride was determined by the mercuric thiocyanate method[15] with some improvements. By using this method a difference of 5 μg. of chloride per 100 ml. can be distinguished in the range of 5~200 μg. per 100 ml.

The fluoride was determined by the *p*-dimethylaminoazophenylarsonic acid-zirconium method[16]. A difference of 1 μg. fluoride per 100 ml. can be distinguished in the range of 2~100 μg. per 100 ml. by procedure **A**, while a difference of 10 μg. of fluoride per 100 ml. can be distinguished in the range of 20~1000 μg. per 100 ml. by procedure **B**. The accuracy and precision of the methods are enough for the present purposes.

Results and Discussion

Amount of Chlorine and Fluorine Evolved from Igneous Rocks.—To determine the amounts of chloride and fluoride contaminated from reagents, nitrogen gas, or experimental procedures, blank tests were carried out at 1200°C. 10 μg. of chlorine was found from the solutions in each absorption vessel, and 6 μg. of chlorine was found from the solution washed inside the silica-glass tube. However, fluorine was found in neither of them. The data of chloride were corrected for these blank values.

Two absorption vessels connected in a series were used for absorbing the acid gases, but usually both chlorine and fluorine were absorbed almost completely by the solution in the first vessel.

Very small amounts of chlorine and fluorine were evolved from the sample which had once been heated at 1200°C for one hour on reheating at the same temperature for two hours.

The data obtained are shown in Table II. In this table, "Abs." means the amount of chlorine or fluorine determined from the solution in absorption vessels, "Sub." means the amount of chlorine or fluorine determined from the solution washed inside the silica-glass tube, and "Total" is equal to "Abs." plus "Sub.". In the last two columns of the same table, the atomic ratios F/Cl and $(F/Cl)/(F/Cl)_{original\ rock}$ are given. In these two columns, ( ) means that the amounts of evolved chlorine and fluorine are fairly small and that the F/Cl ratio might, therefore, contain comparatively a larger error, while > means that the exact value of F/Cl can not be calculated, but only a lower limit of the value given, because the amount of evolved chlorine is smaller than the limit of exact determination.

To examine the reproducibility of the processes, the experiments were duplicated by using basalt from Ō-sima. The results are to be seen in Table II-1. The reproducibility is enough to illustrate the releasing tendency of halogen in rocks at different temperatures.

The percentage of X_{max} to the amount of halogen originally contained in 1 g. of rock sample is shown in Table III. X_{max} means the amount of halogen evolved from 1 g. of a certain rock sample at a temperature where the amount reaches its maximum value in each series of experiments. In most cases the temperature was 1200°C. This table shows that, in general, chlorine and fluorine in a rock can not be completely evolved at temperatures at or below 1200°C, as was reported in previous papers[11,13]. As may be seen in Tables II and III, chlorine is generally easier to release by heating than fluorine, so the

15) I. Iwasaki, S. Utsumi and T. Ozawa, This Bulletin, 25, 226 (1952); S. Utsumi, *J. Chem. Soc. Japan, Pure Chem. Sec.* (*Nippon Kagaku Zassi*), 73, 835 (1952).

16) M. Kamada, T. Onishi and M. Ota, This Bulletin, 28, 148 (1955); M. Kamada and T. Onishi, *J. Chem. Soc. Japan, Pure Chem. Sec.* (*Nippon Kagaku Zashhi*), 80, 275 (1959).

TABLE II. THE AMOUNTS OF Cl AND F RELEASED AT VARIOUS TEMPERATURES

Temp., °C		Amounts of evolved halogen, μg. Cl	F	F/Cl (atomic ratio)	$(F/Cl)/(F/Cl)_{rock}$
Sample No. 1 Basalt, Ō-sima volcano					
Abs.	400	10, 0	2	(0.7)	(1)
	600	25, 30	0	(0)	(0)
	800	105, 85	20	0.39	0.59
	1000	185, 155	26	0.29	0.44
	1200	200, 235	25	0.21	0.32
Sub.	400	5, 0	1, 1, 2	(0.7)	(1)
	600	5, 5	3, 2, 5	(1.1)	(2)
	800	5, 5	21, 14, 18	6.7	10
	1000	10, 15	18, 20, 18	2.8	4.2
	1200	25, 25	20, 17, 20	1.4	2.1
Total	400	15, 0	4	(1.0)	(1.5)
	600	30, 35	5	(0.3)	(0.4)
	800	110, 90	38	0.71	1.1
	1000	195, 170	44	0.45	0.68
	1200	220, 260	45	0.35	0.53
Sample No. 2 Basalt, Itō					
Abs.	400	10	1	(0.2)	(0.04)
	600	15	0	(0)	(0)
	800	30	1	0.1	0.02
	1000	70	50	1.3	0.28
	1200	100	86	1.6	0.34
Sub.	400	0	0	—	—
	600	0	1	(>0.4)	(>0.08)
	800	0	8	>3	>0.6
	1000	0	22	>8	>1.7
	1200	0	38	>14	>3
Total	400	10	1	(0.2)	(0.04)
	600	15	1	(0.1)	(0.02)
	800	30	9	0.6	0.13
	1000	70	72	1.9	0.40
	1200	100	124	2.3	0.49
Sample No. 3 Andesite, Tamagawa hot spring					
Abs.	400	10	1	(0.2)	(0.02)
	600	10	1	(0.2)	(0.02)
	800	25	52	3.9	0.49
	1000	55	220	7.5	0.95
	1200	65	220	6.3	0.80
Sub.	400	0	2, 4	(>1)	(>0.1)
	600	0	7, 7	>2.5	>0.3
	800	0	24, 31	>9	>1
	1000	0	49, 55	>18	>2
	1200	0	53, 49	>18	>2
Total	400	10	5	(0.9)	(0.1)
	600	10	8	(1.5)	(0.2)
	800	25	83	6.2	0.78
	1000	55	280	9.5	1.2
	1200	65	270	7.8	0.99

TABLE II (Continued)

Temp., °C		Amounts of evolved halogen, μg. Cl	F	F/Cl (atomic ratio)	$(F/Cl)/(F/Cl)_{rock}$
Sample No. 4 Andesite, Sakura-zima volcano					
Abs.	400	20	0	(0)	(0)
	600	50	2	0.07	0.04
	800	245	150	1.1	0.55
	1000	350	200	1.1	0.55
	1200	340	180	0.99	0.50
Sub.	400	0	1	(>0.4)	(>0.2)
	600	0	5	>2	>1
	800	0	29	>11	>5.5
	1000	0	41	>15	>7.5
	1200	0	36	>13	>6.5
Total	400	20	1	(0.09)	(0.05)
	600	50	7	0.26	0.13
	800	245	180	1.4	0.70
	1000	350	240	1.3	0.65
	1200	340	220	1.2	0.60
Sample No. 5 Dacite, Akagi volcano					
Abs.	400	10	1	(0.2)	(0.01)
	600	10	1	(0.2)	(0.01)
	800	10	1	(0.2)	(0.01)
	1000	15	9	1.1	0.06
	1200	30	98	6.1	0.36
Sub.	400	0	1	(>0.4)	(>0.02)
	600	0	1	(>0.4)	(>0.02)
	800	0	4	>1	>0.08
	1000	0	14	>5	>0.3
	1200	0	31	>11	>0.6
Total	400	10	2	(0.4)	(0.02)
	600	10	2	(0.4)	(0.02)
	800	10	5	(0.9)	(0.05)
	1000	15	23	2.9	0.17
	1200	30	129	8.0	0.47
Sample No. 6. Liparite, Kōzu-sima					
Abs.	200	10	—	—	—
	400	20	0	0	0
	600	125	0	0	0
	800	465	50	0.20	0.39
	1000	705	91	0.24	0.47
	1200	670	72	0.20	0.39
Sub.	200	0	—	—	—
	400	25	4, 4	0.30	0.59
	600	35	6, 6	0.32	0.63
	800	55	31, 25	0.95	1.9
	1000	45	36, 38	1.5	2.9
	1200	55	29, 35	1.1	2.2
Total	200	10	—	—	—
	400	45	4	0.17	0.33
	600	160	6	0.07	0.14
	800	520	75	0.27	0.53
	1000	750	129	0.32	0.63
	1200	725	107	0.28	0.55

TABLE II (Continued)

Temp., °C		Amounts of evolved halogen, μg. Cl	F	F/Cl (atomic ratio)	$(F/Cl)/(F/Cl)_{rock}$
		Sample No. 7 Obsidian, Imari			
Abs.	400	15	1	(0.1)	(0.07)
	600	50	2	0.07	0.05
	800	320	130	0.76	0.51
	1000	515	240	0.87	0.58
	1200	525	180	0.64	0.43
Sub.	400	0	1	(>0.4)	(>0.2)
	600	0	4	>1.5	>1
	800	0	24	>9	>6
	1000	5	49	18	12
	1200	10	42	8	5
Total	400	15	2	(0.2)	(0.1)
	600	50	6	0.22	0.15
	800	320	150	0.87	0.58
	1000	520	290	1.0	0.67
	1200	535	220	0.77	0.51
		Sample No. 8 Obsidian, Hime-sima			
Abs.	400	10	0	(0)	(0)
	600	10	0	(0)	(0)
	800	65	190	5.5	0.96
	1000	120	300	4.7	0.82
	1200	115	270	4.4	0.77
Sub.	400	0	2	>0.7	>0.1
	600	0	5	>2	>0.3
	800	0	33	>12	>2
	1000	0	47	>17	>3
	1200	0	36	>13	>2
Total	400	10	2	(0.4)	(0.07)
	600	10	5	(0.9)	(0.16)
	800	65	220	6.3	1.1
	1000	120	350	5.4	0.95
	1200	115	310	4.9	0.86
		Sample No. 9 Granite, Mt. Tukuba			
Abs.	400	10	1	(0.2)	(0.02)
	600	20	0	(0)	(0)
	800	15	1	(0.1)	(0.01)
	1000	45	280	12	1.1
	1200	35	340	18	1.6
Sub.	400	0	0, 1	—	—
	600	0	4, 1	(>1)	(>0.1)
	800	0	22, 15	>7	>0.6
	1000	0	51, 75	>24	>2
	1200	0	80, 74	>29	>2.5
Total	400	10	2	(0.4)	(0.03)
	600	20	1	(0.1)	(0.01)
	800	15	16	2.0	0.18
	1000	45	360	15	1.4
	1200	35	410	22	2.0

TABLE II (Continued)

Sample No. 10 Granite, Kiuragi

	Temp., °C	Amounts of evolved halogen, μg. Cl	F	F/Cl (atomic ratio)	$(F/Cl)/(F/Cl)_{rock}$
Abs.	400	0	0	—	—
	600	10	1	(0.2)	(0.02)
	800	25	1	0.1	0.01
	1000	40	87	4.1	0.41
	1200	50	137	5.1	0.51
Sub.	400	0	1	(>0.4)	(>0.04)
	600	0	1	(>0.4)	(>0.04)
	800	0	7	>2.5	>0.25
	1000	0	33	>12	>1.2
	1200	0	39	>14	>1.4
Total	400	0	1	(>0.4)	(>0.04)
	600	10	2	(0.4)	(0.04)
	800	25	8	(0.6)	0.06
	1000	40	120	5.6	0.56
	1200	50	176	6.6	0.66

TABLE III

Sample No.	$[X_{max}/(\text{Amount of halogen in the rock})]\times 100$ Cl	F
1	84	41
2	100	50
3	65	66
4	106	69
5	100	48
6	82	52
7	86	59
8	75	71
9	45	72
10	100	63

$(F/Cl)_{evolved,\ total}$ ratio is smaller than the $(F/Cl)_{original\ rock}$ ratio. The $(F/Cl)_{sub}$ ratio is always larger than the corresponding $(F/Cl)_{abs}$ ratio. The results indicate that fluorine is more easily deposited on the surface of the silica-glass tube than chlorine.

$(F/Cl)_{total}$ at 1200°C is plotted against $(F/Cl)_{rock}$ (Fig. 2), and $(F/Cl)_{abs}$ is plotted against $(F/Cl)_{sub}$ (Fig. 3). In these figures, F/Cl values with ( ) or > in Table II are omitted. The almost linear relations, how the F/Cl value of the gas increases as the F/Cl value of the original rock increases, and how the F/Cl value of the sublimate increases as the F/Cl value of the gas from which the sublimate is deposited increases, will be readily seen in these figures.

It has been already stated that 30% or more of the fluorine in the rock is not given off at temperatures at or below 1200°C. However, it can not be decided from the data given in

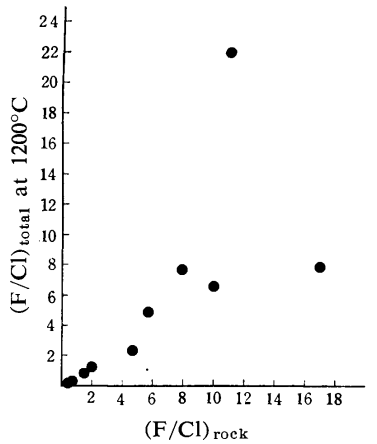

Fig. 2. Relation between $(F/Cl)_{rock}$ and $(F/Cl)_{total}$.

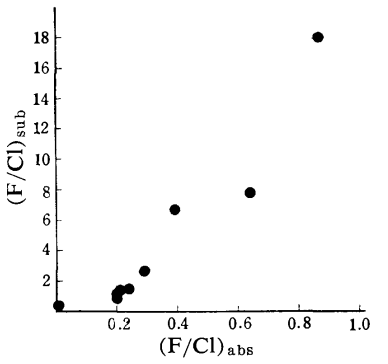

Fig. 3. Relation between $(F/Cl)_{abs}$ and $(F/Cl)_{sub}$.

Table II whether this 30% of the fluorine still remains in the rock or is deposited on the silica-glass tube in a water-insoluble form. In order to make clear the balance of fluorine, rock samples (basalt from Ō-sima and andesite from Tamagawa) which had been heated at 1000°C were analyzed for fluorine and were compared with F_{abs}, F_{sub}, and $F_{original\ rock}$ (Table IV). It may be safely said that the amount of fluorine which deposits on the surface of the silica tube in a water-insoluble form is fairly small compared with that in other forms.

TABLE IV

	F corresponding to 1 g. of original rock (μg.)	
	Basalt Ō-sima	Andesite Tamagawa
Abs.	26± 1	220±10
Sub.	18± 1	55± 1
Residual in the rock	60±20	100±20
Sum	104	375
Original rock	110±20	420±20

The percentage of F_{max} to the amount of fluorine originally contained in the rock sample has a correlation with the fluorine contents of the rock sample, as may be seen in Fig. 4.

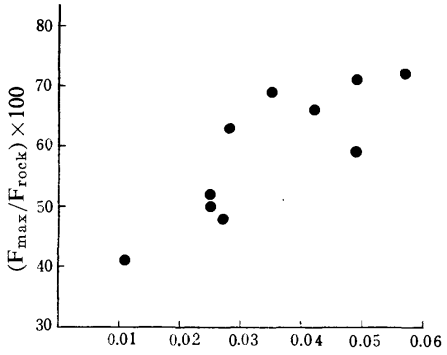

Fig. 4. Relation between F content of original rock and $(F_{max}/F_{rock})\times100$.

To see the change in the amounts of evolved fluorine and chlorine at different temperatures, the value [(the amount of chlorine or fluorine evolved from a certain rock sample at a certain temperature)/X_{max}] $\times$ 100 is plotted against the temperature (Figs. 5 and 6). Using this value, the results of experiments with various rock samples can be compared with each other in the same diagram. Chlorine compounds are evolved at 600°C (in the experiment with liparite from Kōzu-sima at 400°C), and the amount of evolved chlorine compounds increases gradually with the elevating temperature. On the other hand, although fluorine compounds are evolved scarcely at all at temperatures below 800°C, the amount of evolved fluorine increases suddenly at a certain temperature above 800°C. The temperature above which fluorine compounds are evolved varies from 800 to 1200°C with the kind of rocks.

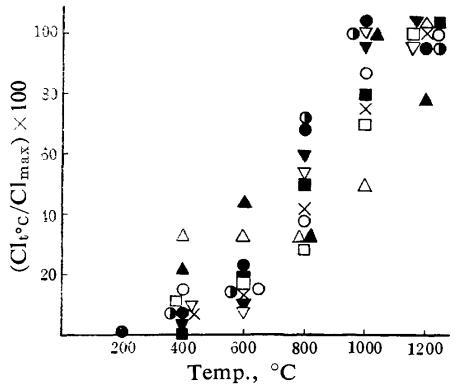

Fig. 5. The change of the amounts of Cl evolved at different temperatures.
× Basalt, Ō-sima
□ Basalt, Itō
○ Andesite, Tamagawa hot spring
◑ Andesite, Sakura-zima
△ Dacite, Mt. Akagi
● Liparite, Kōzu-sima
▼ Obsidian, Imari
▽ Obsidian, Hime-sima
▲ Granite, Mt. Tukuba
■ Granite, Kiuragi

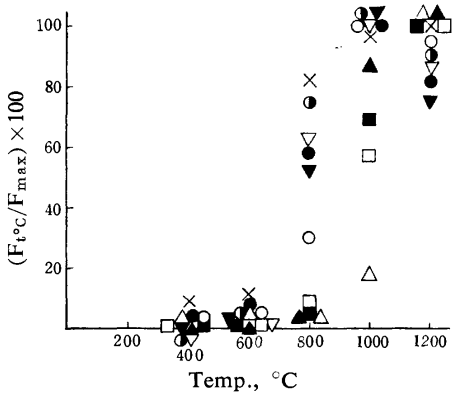

Fig. 6. The change of the amounts of F evolved at different temperatures.
× Basalt, Ō-sima
□ Basalt, Itō
○ Andesite, Tamagawa hot spring
◑ Andesite, Sakura-zima
△ Dacite, Mt. Akagi
● Liparite, Kōzu-sima
▼ Obsidian, Imari
▽ Obsidian, Hime-sima
▲ Granite, Mt. Tukuba
■ Granite, Kiuragi

From these results, it is obvious that the behavior of fluorine and chlorine in the igneous rocks differs markedly when they are heated at high temperatures.

The temperature above which fluorine compounds are evolved must be related to the state of fluorine in rocks. It is interesting to compare this temperature with the various natures of igneous rocks. For this purpose, it is best to determine this temperature by continuous measurement of the amount of evolved fluorine. It is, however, hard to make such experiments, with various kinds of rocks. In this paper, only the values measured at intervals of 200°C are available. The $1/2\cdot[\{(\text{Amount of F evolved at } 800°C)/F_{max}\}\times 100 + \{(\text{Amount of F evolved at } 1000°C)/F_{max}\}\times 100]$ value is used in place of the temperature above which fluorine compounds are evolved. As will be readily understood from the formula mentioned above, the larger the value the lower the temperature above which fluorine compounds are evolved. Comparing this value with the chemical composition of the rocks, it is found that the value has a relation with the fluorine and chlorine contents of the rock. The values mentioned above are plotted against the F/Cl and 1/Cl of the rocks (Figs. 7 and 8). Very good correlations are seen in these figures. The phenomena observed in Figs. 4, 7 and 8 may give interesting suggestions on the distribution of fluorine and chlorine in the igneous rocks.

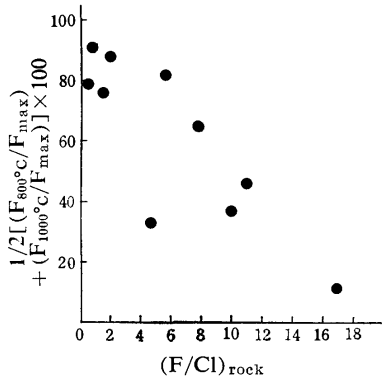

Fig. 7. Relation between $(F/Cl)_{rock}$ and $1/2[(\text{Amount of F evolved at } 800°C/F_{max})\times 100+(\text{Amount of F evolved at } 1000°C/F_{max})\times 100]$.

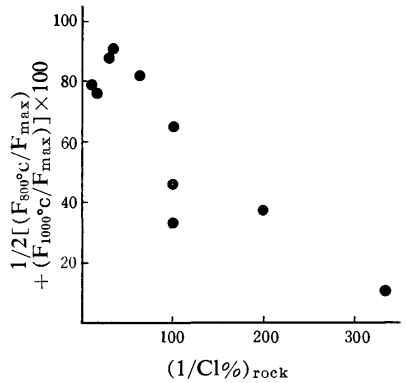

Fig. 8. Relation between $(1/Cl)_{rock}$ and $1/2[(\text{Amount of F evolved at } 800°C/F_{max})\times 100+(\text{Amount of F evolved at } 1000°C/F_{max})\times 100]$.

A Comparison with Natural Volcanic Emanation.—Data on the chlorine and fluorine contents of volcanic gases are rather scarce. Day and Shepherd[17] determined the chlorine and fluorine contents of condensed water from magmatic gases which were exhaled directly from a lava lake of Kilauea volcano, Hawaii, thus obtaining 4 g.Cl/l. and 10 g.F/l. data. Iwasaki et al.[18] obtained condensed water from magmatic gas exhaled from a lava lake of Mt. Mihara, Ō-sima volcano; its chlorine content was 67.7 g./l. The present author has determined the chlorine and fluorine contents of many samples of condensed water from active fumarolic gases in Japan*; their maximum values are 42 g.Cl/l. and 3 g.F/l. (Kamanokuti fumarole, Iwo-zima volcano).

The H_2O (+) content of the basalt from Ō-sima volcano used in the laboratory experiments is 0.3% (analyst: B. Iwasaki). Therefore, 3 mg. (3 μl. as liquid water) of water will be obtained from 1 g. of rock sample on heating. The laboratory experiments in this paper show that 240 μg. of Cl and 45 μg. of F are evolved from 1 g. of basalt from Ō-sima volcano at 1200°C. If we made condensed water from the gas evolved from this rock sample, the concentration of halogen in the water would be 80 g.Cl/l. and 15 g.F/l. respectively. It is interesting that these values agree well with the maximum halogen concentrations in water condensed from natural volcanic gases.

The "$F/Cl_{rock} > F/Cl_{gas}$" and "$F/Cl_{sublimate} > F/Cl_{gas}$" relations were obtained in laboratory experiments. To ascertain whether or not these relations are also true in natural volcanic phenomena, comparisons among the data on natural volcanic products were made. Many data on the fluorine and chlorine contents in igneous rocks are reviewed by Correns[19]. The mean value of the F/Cl (atomic ratio) calculated from those data and from data on

17) A. L. Day and E. S. Shepherd, *Bull. Geol. Soc. Am.*, 24, 573 (1913).

18) I. Iwasaki, T. Katsura, H. Shimojima, T. Ozawa, T. Tarutani and K. Sato, *Bull. Volcanological Soc. Japan*, 2nd Series, 3, 70 (1958).

* Partly reported in Ref. 1. The details of the study will be reported on in another paper.

19) C. W. Correns, *Neues Jb. Mineral. Abh.*, 91, 239 (1957).

Japanese volcanic rocks[20] is 5.3 for igneous rocks. The mean value of F/Cl (atomic ratio) for the volcanic gases in Japan* is about 0.1, and a comparison between the mean values gives the "$F/Cl_{rock} > F/Cl_{gas}$" relation again. It is difficult to find representative data on the F/Cl value of natural volcanic sublimate to be compared with sublimate in laboratory experiments. There are indeed some data on the fluorine and chlorine content of volcanic sublimate. However, in natural conditions, several halogen-bearing minerals are formed by the fractional sublimation from a certain volcanic gas, and the distribution of halogen in these minerals is not uniform. Investigators of the volcanic sublimate usually endeavor to obtain mineral samples of a high purity, but these individual samples represent only a part of the whole sublimate which corresponds to the sublimate in the laboratory experiments. In this paper, the author used the data on the water-soluble component of volcanic ash as a representative of the natural volcanic sublimate, because the volcanic ash is discharged from a volcanic vent with large amounts of volcanic gas and is cooled rather quickly; it is hard, therefore, for fractional separation to occur. The fluorine and chlorine contents of volcanic ash have been studied by Kamada et al.[21] Their study shows that the F/Cl of the water-soluble component of volcanic ash was 0.1~7 (mean value 0.8). The "$F/Cl_{sublimate} > F/Cl_{gas}$" relation is obtained by comparing mean values.

The comparisons of mean values are somewhat ambiguous and may sometimes lead to a wrong conclusion. Therefore, the F/Cl value of the volcanic gas, volcanic rock and water-soluble parts of volcanic ash from the same volcano should be compared with each other. Such data are rather scarce, however; only two sets of data are available, one of Naka-dake Aso volcano[22], and another of Mt. Mihara, Ō-sima volcano. They are shown in Tables V and VI respectively. It may be readily seen in the tables that F/Cl_{rock} is larger than F/Cl_{gas} and that $F/Cl_{sublimate}$ is larger than F/Cl_{gas}.

TABLE V. F/Cl (ATOMIC RATIO) OF VOLCANIC PRODUCTS OF 1958 ACTIVITY OF NAKA-DAKE ASO VOLCANO (BY H. MATSUMOTO and S. TANAKA)[22]

Fumarolic gas	June (231°C)	0.077
Fumarolic gas	July (139°C)	0.0080*
Water soluble component of volcanic ash		0.18
Old lava		0.55
New scoria		0.80

* Determined by the present author

TABLE VI. F/Cl (ATOMIC RATIO) OF VOLCANIC PRODUCTS OF MT. MIHARA Ō-SIMA VOLCANO (BY M. KAMADA)[1,21],etc.

Fumarolic gas	Aug. 1958 (270°C)	0.37
Water soluble component of volcanic ash	Oct. 1957	0.52
	Aug. 1958	1.35
Lava of 1950		0.66*

* Determined by the present author

Conclusion

From the foregoing results, it may be concluded that chlorine and fluorine behave in different ways in the process of the separation of the gas phase from the solid phase. Fluorine compounds are less volatile than that of chlorine and are more liable to be fixed in solid phases as a sublimate.

A comparison between the results of the laboratory experiments and the data on natural volcanic products suggests that the study of the behavior of halogen compounds during heat treatment would be useful in understanding volcanic phenomena.

The author wishes to express his deep thanks to Professor Iwaji Iwasaki, Tokyo Institute of Technology, for his constant guidance throughout this study. He is also much obliged to the members of Laboratory of Analytical Chemistry and Geochemistry, Tokyo Institute of Technology, for their fruitful discussions. In addition, he wishes to express his hearty thanks to Dr. Takashi Katsura, Tokyo Institute of Technology, Dr. Masaakira Kamada, the Laboratory of Analytical Chemistry, Faculty of Liberal Arts, Kagoshima University, and Dr. Hatao Matsumoto, the Institute of Geology, Kumamoto University, for their valuable advice and criticism.

Laboratory of Analytical Chemistry and Geochemistry
Tokyo Institute of Technology
Meguro-ku, Tokyo

20) I. Iwasaki, T. Katsura, N. Sakato and M. Hirayama, *J. Chem. Soc. Japan, Pure Chem. Sec.* (*Nippon Kagaku Zassi*), 78, 164 (1957).

21) M. Kamada et al., read at the Symposium on Geochemistry of the Chemical Society of Japan, July, 1957, and at the Meeting of the Volcanological Society of Japan, October, 1957,

22) H. Matsumoto and S. Tanaka, *Kumamoto J. Sci.*, Series A, 4, No. 2, 151 (1959).

The Urey-Bradley Force Constants of Boron Halides and their Transferability

By Hiroshi TOYUKI, Kazuhiro SHIMIZU and Hachiro HIYAMA

(Received January 21, 1963)

The infrared and Raman spectra of several boron trihalides have been recorded[1-9] and their Urey-Bradley force constants[10], except for those of boron triiodide, have already been calculated.

We have now recalculated the force constants of the boron trihalides BX_3 (X: F, Cl, Br and I) by using the most probable observed values of the fundamental frequencies of ^{10}B and ^{11}B compounds as a means of studying the transferability of force constants from boron trihalides to boron mixed halides.

The force constants for boron mixed halides were estimated by applying the usual additive property[11] to the recalculated values for boron trihalides.

The calculated values of the normal vibrational frequencies of boron mixed halides were obtained by using these constants and were compared with the observed values[7].

Calculations

The boron trihalides have a planar configuration and belong to the point group D_{3h}[12]. These tetraatomic molecules have six normal modes of vibration, of which two are degenerate; $\nu_1(A_1')$, $\nu_2(A_2'')$, $\nu_3(E')$ and $\nu_4(E')$. The A_1' mode is active only in the Raman and the A_2'' only in infrared spectra, while the doubly degenerate E' vibrations are both infrared and Raman active.

Unfortunately we have no configuration data for boron mixed halides. If the boron mixed halides of the BX_2Y type are assumed to have a planar configuration, they belong to the point group C_{2v}. All six normal modes, thus, are nondegenerate; $\nu_1(A_1)$, $\nu_2(A_1)$, $\nu_3(A_1)$, $\nu_4(B_2)$, $\nu_5(B_1)$ and $\nu_6(B_1)$. All the vibrations are both infrared and Raman active.

In this paper, only the in-plane vibrations (BX_3; A_1' and E', BX_2Y; A_1 and B_1) are described.

The following symmetry coordinates are used for the transformation into the factored $\boldsymbol{F}$ and $\boldsymbol{G}$ matrices defined by Wilson[13]:

For BX_3 molecules;

A_1'; $S_1=(\Delta r_1+\Delta r_2+\Delta r_3)/\sqrt{3}$

E'; $S_3=(2\Delta r_1-\Delta r_2-\Delta r_3)/\sqrt{6}$

$S_4=(2\Delta\alpha_{23}-\Delta\alpha_{12}-\Delta\alpha_{13})/\sqrt{6}$

For BX_2Y molecules;

A_1; $S_1=(\Delta R_1+\Delta r_2+\Delta r_3)/\sqrt{3}$

$S_2=(2\Delta R_1-\Delta r_2-\Delta r_3)/\sqrt{6}$

$S_3=(2\Delta\beta_{23}-\Delta\alpha_{12}-\Delta\alpha_{13})/\sqrt{6}$

B_1; $S_5=(\Delta r_2-\Delta r_3)/\sqrt{2}$

$S_6=(\Delta\alpha_{12}-\Delta\alpha_{13})/\sqrt{2}$

The internal coordinates used in boron trihalides and boron mixed halides are shown in Fig. 1.

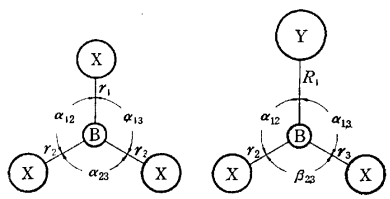

Fig. 1. Definition of internal coordinates for BX_3 and BX_2Y molecules.

The Urey-Bradley force constants of boron trihalides can be calculated uniquely by using the three observed values of fundamental frequencies (ν_1, ν_3 and ν_4) which are listed in Table I.

In the calculation, the force constant F' is

1) S. Venkateswaran, *Indian. J. Phys.*, 6, 275 (1931).
2) T. F. Anderson, E. D. N. Lassettre and D. M. Yost, *J. Chem. Phys.*, 4, 703 (1936).
3) C. R. Bailey, J. B. Hale and J. W. Thompson, *Proc. Roy. Soc.*, A161, 107 (1937).
4) D. M. Gage and E. F. Barker, *J. Chem. Phys.*, 7, 455 (1939).
5) G. Herzberg, "Molecular Spectra and Molecular Structure", Vol II, 299 D. Van. Nostrand Princeton, N. J. (1949).
6) R. E. Scruby, J. R. Lacher and J. D. Park, *J. Chem. Phys.*, 19, 386 (1951).
7) L. P. Lindman and M. K. Wilson, ibid., 24, 242 (1956).
8) D. C. Mckean, ibid., 24, 1002 (1956).
9) T. Wentink and V. H. Tienusuu, ibid., 28, 826 (1958).
10) T. Shimanouchi, Private communication, "Force constants of small molecules", (1962), p. 10. (Department of Chemistry, Faculty of Science, The Universtiy of Tokyo, Tokyo, Japan)
11) T. Shimanouchi, *J. Chem. Phys.*, 17, 245, 734, 848 (1949).
12) J. H. M. Bowen, "Tables of Interatomic Distances and Configuration in Moleculer and Ions", M 17, The Chemical Society, Burlington House, W. 1, London (1958).
13) E. B. Wilson, *J. Chem. Phys.*, 9, 76 (1941).

Table I. Trihalide frequencies used to calculate force constants (cm^{-1})

	ν_1	ν_3	ν_4
$^{10}BF_3$ a)	888	1505	482
$^{11}BF_3$ a)	888	1454	480
$^{10}BCl_3$ a)	471	994	—
$^{11}BCl_3$ a)	471	954	243
$^{10}BBr_3$ b)	278	856	150
$^{11}BBr_3$ b)	278	820	150
$^{10}BI_3$ b)	190	737	100
$^{11}BI_3$ b)	190	704	100

a) From Ref. 7
b) From Ref. 9

assumed to be equal to $-0.1F$, as usual[11], and the following molecular constants which have been previously reported are used; r(B–F) = 1.295 Å[14], r(B–Cl) = 1.73 Å[12], r(B–Br) = 1.87 Å[15] and r(B–I) = 2.10 Å[9], while all bond angles = 120°[12,14,15].

For boron triiodide, the tentative values which had been proposed by Wentink and Tiensuu[9] were used because there are no experimental values.

The force constants calculated for each boron trihalide to fit the most probable fundamental frequencies are shown in Table II.

In Table II, the force constants for the ^{10}B compound of boron trichloride are not given because the frequency ν_4 for this molecule has not been observed, as is shown in Table I.

Table II. Force constants of boron trihalides (10^5 dyn./cm.)

	K	H	F
$^{10}BF_3$	6.032	0.210	0.932
$^{11}BF_3$	6.051	0.212	0.925
$^{10}BCl_3$	—	—	—
$^{11}BCl_3$	3.022	0.055	0.537
$^{10}BBr_3$	2.401	0.058	0.412
$^{11}BBr_3$	2.406	0.059	0.411
$^{10}BI_3$	1.838	0.042	0.287
$^{11}BI_3$	1.838	0.041	0.287

Table III. Estimated force constants for boron mixed halides (10^5 dyn./cm.)

K(B-F)	6.051	H(F-B-F)	0.212	F(F···F)	0.925
K(B-Cl)	3.022	H(F-B-Cl)	0.134	F(F···Cl)	0.731
K(B-Br)	2.406	H(F-B-Br)	0.136	F(F···Br)	0.668
K(B-I)	1.838	H(F-B-I)	0.127	F(F···I)	0.606
		H(Cl-B-Cl)	0.055	F(Cl···Cl)	0.537
		H(Cl-B-Br)	0.057	F(Cl···Br)	0.474
		H(Cl-B-I)	0.048	F(Cl···I)	0.412
		H(Br-B-Br)	0.059	F(Br···Br)	0.411
		H(Br-B-I)	0.050	F(Br···I)	0.349
		H(I-B-I)	0.041	F(I···I)	0.287

14) A. H. Nielsen, ibid., 22, 659 (1954).
15) H. A. Levy and L. O. Brockway, *J. Am. Chem. Soc.*, 59, 2085 (1937).

It may be seen in Table II that the values for ^{10}B and ^{11}B compounds are approximately equal, as was expected. The force constants of boron mixed halides are estimated by applying

Table IV. Observed and calculated frequencies of boron mixed halides (cm^{-1})

		ν_1	ν_2	ν_3	ν_5	ν_6
$^{10}BF_2Cl$	Obs.	1286	701	—	1470	366
	Calcd.	1265	708	428	1485	367
$^{11}BF_2Cl$	Obs.	1242	696	427	1421	366
	Calcd.	1223	703	428	1428	365
$^{10}BF_2Br$	Obs.	1247	637	—	1468	—
	Calcd.	1228	646	363	1483	339
$^{11}BF_2Br$	Obs.	1208	632	—	1417	—
	Calcd.	1188	639	363	1431	337
$^{10}BF_2I$	Obs.	—	—	—	—	—
	Calcd.	1197	615	326	1480	322
$^{11}BF_2I$	Obs.	—	—	—	—	—
	Calcd.	1161	608	325	1428	320
$^{10}BCl_2F$	Obs.	1355	—	—	1031	—
	Calcd.	1360	575	268	1035	376
$^{11}BCl_2F$	Obs.	1312	—	—	993	—
	Calcd.	1315	571	267	993	375
$^{10}BCl_2Br$	Obs.	916	—	—	991	—
	Calcd.	915	409	214	991	208
$^{11}BCl_2Br$	Obs.	878	405	218	951	—
	Calcd.	878	409	213	952	207
$^{10}BCl_2I$	Obs.	—	—	—	—	—
	Calcd.	854	378	196	985	185
$^{11}BCl_2I$	Obs.	—	—	—	—	—
	Calcd.	820	377	196	946	185
$^{10}BBr_2F$	Obs.	1344	—	—	901	—
	Calcd.	1342	442	178	915	324
$^{11}BBr_2F$	Obs.	1302	—	—	862	—
	Calcd.	1298	439	178	876	324
$^{10}BBr_2Cl$	Obs.	954	—	—	864	—
	Calcd.	952	346	166	860	192
$^{11}BBr_2Cl$	Obs.	918	—	—	827	195
	Calcd.	913	346	166	824	192
$^{10}BBr_2I$	Obs.	—	—	—	—	—
	Calcd.	834	230	141	850	128
$^{11}BBr_2I$	Obs.	—	—	—	—	—
	Calcd.	798	230	141	813	128
$^{10}BI_2F$	Obs.	—	—	—	—	—
	Calcd.	1319	378	123	818	302
$^{11}BI_2F$	Obs.	—	—	—	—	—
	Calcd.	1277	374	123	782	302
$^{10}BI_2Cl$	Obs.	—	—	—	—	—
	Calcd.	916	287	118	750	170
$^{11}BI_2Cl$	Obs.	—	—	—	—	—
	Calcd.	880	286	118	717	170
$^{10}BI_2Br$	Obs.	—	—	—	—	—
	Calcd.	812	220	108	746	124
$^{11}BI_2Br$	Obs.	—	—	—	—	—
	Calcd.	777	220	108	713	124

The observed values are cited from the Ref. 7.

the usual additive property to the constants for ^{11}B compounds of boron trihalides.

The bending force constant, H, and the repulsive force constant, F, are evaluated from the following equation;

$$H(X\text{-}B\text{-}Y) = [H(X\text{-}B\text{-}X) + H(Y\text{-}B\text{-}Y)]/2$$

$$F(X\cdots Y) = [F(X\cdots X) + F(Y\cdots Y)]/2$$

The stretching force constant, K, is assumed to be equal to one in boron trihalides.

The values estimated for boron mixed halides are shown in Table III.

The normal vibrational frequencies of boron mixed halides are calculated by using these constants.

The molecular constants for these compounds have not been given. Since it may be assumed that the nature of bonds of these molecules does not differ greatly from that of boron trihalides, their values are taken from those of the boron trihalides.

Results

It has been described how Urey-Bradley potential function is quite suitable for calculating the normal vibrational frequencies of saturated hydrocarbons and their halogen compounds[11].

Making use of this function with reference to boron halides, we have obtained a good agreement between the observed and the calculated values of vibrational frequencies for boron mixed halides, as Table IV shows.

The frequencies for ν_4 corresponding to the out-of-plane bending vibration are omitted in Table IV.

The greatest difference between the observed and the calculated values was about $\pm 2\%$, while the average deviation was about $\pm 1\%$.

It has thus been found that the transferability of Urey-Bradley force constants from boron trihalides to boron mixed halides was reasonable and that the error due to the assumed planar configuration and molecular constants of boron mixed halides had no great effect to the transferability of the force constants.

The authors wish to thank Professor Haruo Shingu of Kyoto University, Professor H. Murata of Hiroshima University, and Dr. K. Kawai of the author's institute for their helpful advice.

Osaka Municipal Technical Research Institute
Kita-ku, Osaka

Formaldehyde Resins. LXXVII. The Synthesis of Some Anthracene Derivatives as a Wavelength Shifter of a Plastic Scintillator*

By Minoru IMOTO and Tadao NAKAYA

(Received February 15, 1963)

A liquid or plastic scintillator generally contains two kinds of organic compounds. One is called the primary solute, and the other, the secondary solute. They disperse themselves in the solute or the plastic to set one of their fluorescent wavelengths by the most sensitive wavelength of a photoelectron amplifier. As the primary solute, terphenyl, tetraphenylbutadiene or quaterphenyl are widely used, while for the second solute, many kinds of aromatic compound are used. POPOP (*p*-di-(5-phenyl-2-oxazol)benzene)[1] is said to be the best second solute.

Recently, one of the present authors synthesized 9, 10-bis(2, 4-dimethylbenzyl)anthracene (I)[2], which was proved to behave excellently as a second solute[3].

The present paper concerns the syntheses of three compounds similar to I and a study of their ultraviolet and fluorescent spectra. The first compound synthesized was 9, 10-di-*m*-xylylanthracene (II), in which the nucleus of benzene is attached directly to the nucleus of anthracene. The two other compounds are derivatives of I with methyl groups in different positions, 9, 10-bis(4-methylbenzyl)anthracene (III) and 9, 10-bis(2, 3, 5, 6-tetramethylbenzyl)anthracene (IV).

* LXXVI: M. Imoto and A. Ninagawa, in preparation.

1) W. C. Kaski and C. O. Jomas, *J. Chem. Phys.*, **79**, 1286 (1951).

2) M. Imoto, K. Ko and F. Sakurai, *J. Chem. Soc. Japan, Ind. Chem. Sec.* (*Kogyo Kagaku Zasshi*), **65**, 622 (1962).

3) K. Osio, private communication.

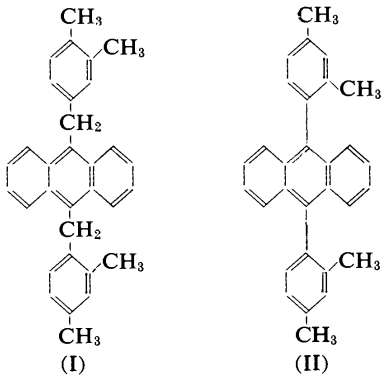
(I)

(II)

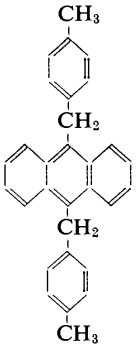
(III)

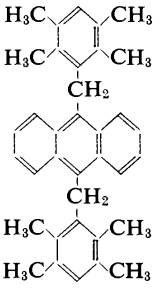
(IV)

These compounds have been little described in literature but have been proved by Osio et al.[3] to be more usable as second solutes than POPOP.

Experimental

9, 10-Bis(2', 4'-dimethylphenyl)anthracene (II).— 4-Iodo-*m*-xylene was obtained by the method described in the literature[4]; b. p., 105°C/12 mmHg; yield, 44%. A mixture of anthraquinone (27 g.) and 200 ml. of tetrahydrofuran was gradually added to a Grignard solution prepared from the mixture of 102 g. of 4-iodo-*m*-xylene, 9.7 g. of magnesium, 200 ml. of tetrahydrofuran and a trace of iodine. After the mixture had been heated under reflux for 4 hr., a saturated solution of ammonium chloride was added to decompose the excess reagent. The solid product, 9,10-dihydroxy-9,10-(2',4'-dimethylphenyl)anthracene, was twice extracted with ethyl acetate. The extract was then concentrated to give crystals. After recrystallization from a mixture of benzene and ethanol (1 : 1 in vol.), white needle crystals melting at 277~288°C were obtained in a 76% yield.

Found: C, 85.22; H, 6.74. Calcd. for $C_{30}H_{28}O_2$: C, 85.72; H, 6.67%. IR: ν-OH 3620 cm^{-1} in Nujol mull.

9,10-Dihydroxy-9,10-(2',4'-dimethylphenyl)anthracene was heated under reflux with 1 g. of zinc dust in 30 ml. of acetic acid for 1 hr. The mixture was then concentrated and cooled, and the crystals separated were extracted with toluene. Recrystallization was performed from a mixture of ethanol and benzene (2 : 1 in vol.). 9,10-Bis(2',4'-dimethylphenyl)anthracene was obtained as pale yellow crystals melting at 289~291°C. In the infrared spectrum, ν-OH was not observed in Nujol mull.

Found: C, 93.01; H, 6.89. Calcd. for $C_{30}H_{26}$: C, 93.21; H, 6.79%. UV absorptions: λ_{max}(mμ): 260, 356, 376, 397 in dioxane, as shown in Fig. 1.

9, 10-Bis(4-methylbenzyl)anthracene (III).— Twenty eight grams of *p*-xylylene chloride was added to 400 ml. of carbon disulfide already containing 17 g. of anthracene and 5 g. of zinc dust. The mixture was heated under reflux for 30 hr. while being stirred and then cooled. The precipitate was collected and recrystallized from benzene. Colorless crystals melting at 288~289°C were obtained in a 22% yield.

Found: C, 93.02; H, 6.98. Calcd. for $C_{30}H_{26}$: C, 93.26; H, 6.74%. λ_{max} (mμ): 260, 357, 378, 400 in dioxane.

9, 10-Bis(2, 3, 5, 6-tetramethylbenzyl)anthracene (IV).— By a method similar to that which gave 9,10-bis(4-methylbenzyl)anthracene, the reaction of 16.9 g. of anthracene with 36.5 g. of tetramethylbenzyl chloride was carried out in 350 ml. of carbon disulfide under refluxing for 30 hr. Colorless powder with a m. p. of 369~370°C was obtained from benzene in a 18% yield.

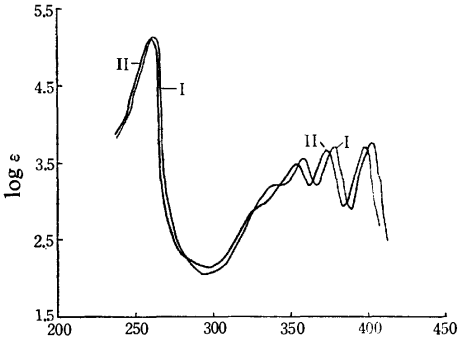

Fig. 1. UV absorption spectra of I and II in dioxane (concn. 2×10^{-4} mol./l.).

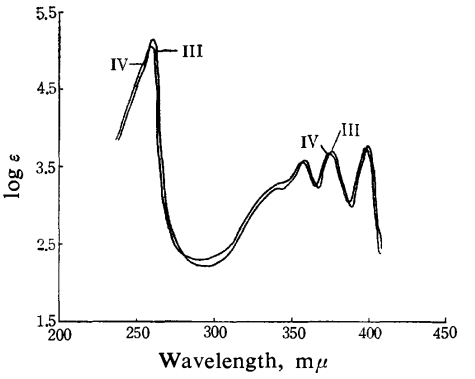

Fig. 2. UV absorption spectra of III and IV in dioxane (concn. 2×10^{-4} mol./l.).

4) R. L. Datta and N. R. Chatterjee, *J. Am. Chem. Soc.*, 39, 438 (1917).

Found: C, 91.96; H, 7.94. Calcd. for $C_{30}H_{38}$: C, 91.92; H, 8.08%. λ_{max} (mμ): 260, 356, 376, 397 in dioxane.

Discussion

Ultraviolet Absorption Spectra. — The ultraviolet absorption spectra of compounds I, II, III and IV are shown in Figs. 1 and 2. The O–O bands of the absorption spectra are tabulated in Table I. The O–O bands may be compared with the B-bands of the phenyl type and with benzyl-type derivatives of anthracene.

TABLE I. THE WAVELENGTHS OF THE O–O BANDS OF ULTRAVIOLET ABSORPTION SPECTRA

Compound	O–O, mμ	Log ε	Solvent
I	403	3.75	Dioxane
II	397	3.73	Dioxane
III	400	3.74	Dioxane
IV	397	3.73	Dioxane
Anthracene[5]	380	3.90	Ethanol

Comparing the absorption wavelengths of compound II with those of compounds I and III, it is clear that the CH_2 group between the anthracene and benzene rings shifts the absorption band toward longer wavelengths. In order to explain the fact that the extent of conjugation is greater when the CH_2-group was present between the nuclei, two interpretations may be possible. One of them is the concept of hyperconjugation by the CH_2-group; the other is the direct conjugation of the rings of anthracene and benzene.

From the identical values of the λ_{max} in compounds II and IV, it can not be possible that the hyperconjugation effect of the CH_2-group plays an important role.

Actually, when the model of 9,10-bis(2',4'-dimethylphenyl)anthracene (II) was constructed by use of Stuart model, it was observed that the benzene and anthracene rings twist by an angle of about 60° to each other; it was therefore considered that the direct conjugation of the two rings may be very small. However, in the case of 9,10-bis(2',4'-dimethylbenzyl)anthracene (I), the rings of anthracene and benzene are situated opposite one another at an angle of about 110°. Accordingly, the molecular orbitals of the anthracene ring and the benzene rings may directly interact; thus, the absorption bands may shift to longer wavelengths.

In 1950, Bartlett[6] considered a direct conjugation in the mode of the following formula:

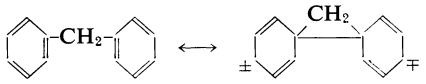

Also, McClure and Coffman[7] and Stewart[8] observed the same phenomenon in polyphenylalkanes and agreed with the idea of direct conjugation.

As for the identical absorption maxima of compounds II and IV, it may be considarable that the 2',6'-dimethyl groups of the durene nucleus prevent the conjugation.

Fluorescence Spectra.—The fluorescence spectra measured are shown in Figs. 3 and 4. The O–O and O–1 bands are tablated in Table II, along with the differences in the wavelengths between the O–O bands of the fluorescence spectra and the O–O bands of the ultraviolet absorption spectra.

The fluorescence O–O bands shifted toward wavelengths longer by 5~7 mμ than those of the ultraviolet absorption spectra. This may be ascribed to the fact that the conjugation between the anthracene and two benzene rings

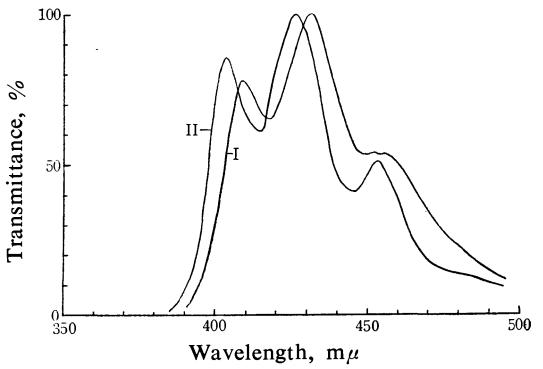

Fig. 3. Fluorescence spectra I and II in dioxane (concn. 2×10^{-4} mol./l.).

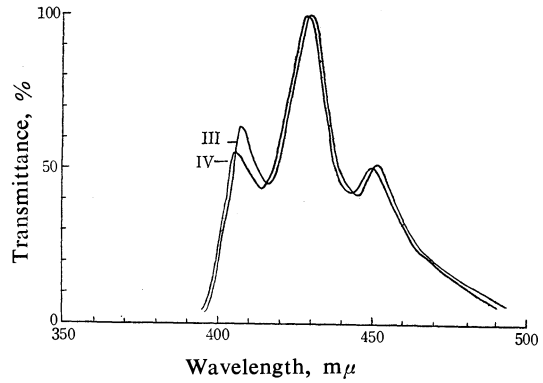

Fig. 4. Fluorescence spectra III and IV in dioxane (concn. 2×10^{-4} mol./l.).

5) E. Clar, *Ber.*, **69**, 607 (1936).
6) P. D. Bartlett and E. S. Lewis., *J. Am. Chem. Soc.*, **72**, 1005 (1950).
7) D. S. McClure and R. Coffman, *Can. J. Chem.*, **36**, 48 (1958).
8) F. H. C. Stewart, *J. Org. Chem.*, **27**, 3374 (1962).

Table II. The wavelengths of the O-O and O-1 bands of the fluorescence spectra

Compound	O-O mμ	O-1 mμ	Differences in O-O bands between fluores. and UV absorption, mμ
I	408	432	5
II	403	427	6
III	407	430	7
IV	404	428	7

occur more easily in the excited state than in the ground state, because the molecule is somewhat less strained in the excited state.

Since the best sensitivity of the photoelectron amplifier exists at the wavelength of about 450 mμ, it is desirable to have the fluorescence also in this region. While the strongest band of the POPOP is 417 mμ, those of compounds II and III are 429 and 430 mμ respectively. The compounds described in the present paper are, therefore, considered to be better second solutes of the plastic scintillator than POPOP[2].

Summary

Three anthracene derivatives, 9, 10-di-*m*-xylyl-anthracene (II), 9, 10-bis(4-methylbenzyl)-anthracene (III), and 9, 10-bis(2, 3. 5, 6-tetramethylbenzyl)anthracene (IV), have been synthesized and their ultraviolet and fluorescence spectra measured. The shift of the spectrum to the longer wavelength by the presence of methylene groups between anthracene and benzene rings may be explained in terms of direct conjugation between three rings.

According to the spectra, these compounds are believed to be better second solutes of the plastic scintillator.

The authors are indebted to Professor K. Osio and his coworkers for measuring the ultraviolet and fluorescence spectra and for their helpful discussions.

Department of Applied Chemistry
Faculty of Engineering
Osaka City University
Kita-ku, Osaka

Crystal Structure of m-Methylbenzamide

By Seiki ORII[*1], Toshio NAKAMURA[*2], Yoshito TAKAKI[*3], Yoshio SASADA and Masao KAKUDO

(Received February 18, 1963)

The crystal structure of *m*-methylbenzamide, C_8H_9NO, has been investigated as a part of a study of the crystal structure of carboxyamide. The main interests of this study have been to determine the molecular configuration and to learn the features of the hydrogen bonding in the crystal.

In recent studies, the molecular configurations of salicylic acid[1], benzoic acid[2], nicotinic acid[3] and α-pyrazinamide[4] have been shown to be approximately planar, while nicotinamide[5] and benzamide[6] are non-planar, with an angle of 25~26° between the amide group and the six-membered ring plane.

It is interesting to compare the crystal structure of *m*-methylbenzamide with the above-mentioned crystal structures.

Experimental

m-Methylbenzamide crystals were obtained from an alcohol-water solution[*4]. They are colorless plates, with the a axis normal to the plates, and have a cleavage plane parallel to (1 0 0).

The crystallographic data obtained were as follows:

$a=8.93\pm0.03$ Å $b=16.02\pm0.03$ Å

$c=5.12\pm0.02$ Å $\beta=95.0\pm0.6°$

Absent spectra: $(h\,0\,l)$ when h is odd
$(0\,k\,0)$ when k is odd

Space group: $P2_1/a$

Four molecules per unit cell

Volume of the unit cell: 729.6 Å^3

Density (flotation): 1.22_5 g. cm^{-3}
(calculation): 1.23_0 g. cm^{-3}

*1 Present address: Tokyo Sanyo Electric Co., Ota, Gunma.

*2 Present address: Medical Department, Kanazawa University, Kanazawa.

*3 Present address: Department of Physics, Osaka University of Liberal Arts and Education, Tennoji, Osaka.

1) W. Cochran, *Acta Cryst.*, **6**, 260 (1953).

2) G. A. Sim, J. M. Robertson and T. H. Goodwin, ibid., **8**, 157 (1955).

3) W. B. Wright and G. S. D. King, ibid., **6**, 305 (1953).

4) Y. Takaki, Y. Sasada and T. Watanabé, ibid., **13**, 693 (1960).

5) W. B. Wright and G. S. D. King, ibid., **7**, 285 (1954).

6) B. R. Penfold and J. C. B. White, ibid., **12**, 130 (1959).

*4 The crystal used was supplied by the Sankyo Co., Ltd.

TABLE I. OBSERVED AND CALCULATED STRUCTURE FACTORS

h k l	F_o	F_c	*h k l*	F_o	F_c	*h k l*	F_o	F_c	*h k l*	F_o	F_c
0 2 0	8.53	− 8.39	3 4 0	6.91	− 7.19	6 0 0	6.66	− 7.48	9 6 0	1.56	− 1.64
4	9.61	− 9.15	5	2.77	2.55	1	3.01	− 2.46	7	1.05	1.16
6	14.02	−13.58	6	3.18	2.86	2	1.12	0.92	8	1.10	0.70
8	0.24	− 0.59	7	5.57	− 5.86	3	1.35	1.45	9	0.36	0.50
10	2.38	2.02	8	2.35	2.50	4	0.61	0.87	10	1.34	− 1.67
12	2.32	1.86	9	0.20	0.08	5	1.24	1.07	11	0.59	− 0.52
14	1.66	1.47	10	3.34	3.17	6	3.23	3.58	12	0.59	0.97
16	0.34	0.43	11	1.58	1.33	7	3.39	− 3.21			
18	0.84	− 0.62	12	3.99	− 4.34	8	1.75	− 1.78	10 0 0	0.37	0.27
20	1.04	− 0.81	13	0.33	− 0.46	9	0.67	0.50	1	0.37	0.17
			14	3.61	3.56	10	1.65	0.89	2	0.91	0.69
1 1 0	5.74	− 5.87	15	0.76	0.82	11	0.39	0.20	3	1.00	1.28
2	2.24	1.65	16	0.92	− 1.21	12	1.52	− 1.61	4	1.42	− 1.41
3	1.08	− 0.88	17	0.42	0.05	13	1.27	1.16	5	0.35	− 0.51
4	6.03	− 6.41	18	0.72	− 0.34	14	0.39	0.52	6	0.29	0.71
5	4.18	3.69	19	0.28	0.10	15	0.37	0.45	7	0.32	− 0.20
6	5.53	− 5.20	20	0.20	− 0.87	16	0.32	− 0.16	8	0.29	0.54
7	4.93	4.96				17	0.25	− 0.08	9	0.55	0.61
8	7.26	7.09	4 0 0	4.44	− 4.87				10	0.18	− 0.79
9	0.79	− 0.71	1	6.11	6.68	7 1 0	0.37	0.47			
10	0.45	− 0.47	2	2.45	− 1.99	2	1.44	1.46	11 1 0	0.28	− 0.16
11	3.08	− 3.14	3	4.71	4.73	3	0.65	0.60	2	0.51	1.08
12	0.77	0.87	4	2.88	2.98	4	2.89	2.92	3	0.26	− 0.56
13	2.13	1.84	5	3.26	3.39	5	0.86	− 1.05	4	0.62	− 0.85
14	0.96	− 0.81	6	0.31	0.46	6	0.39	0.41	5	1.00	1.45
15	1.55	− 1.37	7	2.12	− 1.89	7	0.39	0.18			
16	0.37	− 0.27	8	1.36	1.23	8	2.40	− 2.19	0 2 0	8.35	− 8.37
17	0.37	0.15	9	3.04	− 3.29	9	1.77	− 1.68	4	8.75	− 8.96
18	0.62	0.58	10	0.36	0.47	10	0.37	− 0.01	6	14.00	−13.98
19	0.86	− 0.59	11	2.24	− 2.38	11	2.00	2.66	8	0.25	− 0.84
20	1.00	− 0.87	12	1.22	0.85	12	0.39	− 0.18	10	2.40	1.98
			13	2.75	2.79	13	0.37	0.25	12	2.21	2.13
2 0 0	0.21	0.20	14	2.45	− 2.09	14	0.35	− 0.21	14	1.49	1.66
1	20.66	20.76	15	0.83	0.83	15	0.85	− 0.88	16	0.34	0.41
2	10.84	10.76	16	0.39	0.49	16	0.23	− 0.41	18	0.64	− 0.84
3	12.05	12.15	17	0.37	0.13				20	1.02	− 1.02
4	3.64	− 2.84	18	0.32	− 0.41	8 0 0	2.20	1.73			
5	5.05	5.21	19	0.29	− 0.45	1	0.96	− 0.87	0 0 1	20.14	−19.83
6	7.21	− 7.17				2	1.23	− 1.09	1	6.57	− 6.73
7	6.62	− 6.35	5 1 0	5.98	5.77	3	1.78	− 1.64	2	4.26	4.31
8	0.62	− 0.78	2	2.53	1.90	4	0.39	0.38	3	6.32	6.51
9	1.37	− 1.77	3	1.88	1.89	5	0.39	0.11	4	5.40	5.51
10	1.74	0.98	4	1.65	− 1.37	6	0.39	0.63	5	1.33	1.24
11	0.50	− 0.96	5	6.82	− 7.07	7	2.20	2.36	6	3.26	2.93
12	3.30	3.19	6	2.11	2.17	8	0.37	− 0.02	7	5.17	− 4.60
13	1.62	− 1.57	7	1.67	− 1.73	9	2.39	− 2.49	8	5.07	− 4.72
14	0.55	0.95	8	0.92	− 0.57	10	1.02	− 1.15	9	1.52	− 1.50
15	1.94	1.91	9	1.63	1.46	11	0.84	0.65	10	0.30	− 0.51
16	2.15	− 1.97	10	0.39	− 0.03	12	0.36	− 0.80	11	1.04	− 1.61
17	0.37	0.26	11	1.17	0.91	13	0.44	0.39	12	2.18	1.68
18	0.88	− 0.60	12	0.39	0.58	14	0.72	0.70	13	3.63	3.18
19	0.33	0.13	13	1.66	− 1.10				14	1.35	− 1.03
20	0.74	0.56	14	1.71	− 2.23	9 1 0	0.37	− 0.10	15	2.93	3.28
			15	1.72	1.50	2	0.37	0.06	16	0.35	0.50
3 1 0	3.71	3.93	16	0.84	0.71	3	0.37	− 0.54	17	1.31	− 1.09
2	10.34	−10.54	17	0.33	0.17	4	1.84	2.14	18	0.34	− 0.09
3	1.80	− 0.93	18	0.26	0.40	5	0.39	− 0.32	19	2.58	− 1.97

TABLE I (Continued)

$h\,k\,l$	F_o	F_c	$h\,k\,l$	F_o	F_c	$h\,k\,l$	F_o	F_c	$h\,k\,l$	F_o	F_c
0 20 1	0.22	− 0.13	0 16 3	0.92	− 0.56	0 2 6	1.23	0.84	$\bar{4}$ 0 2	15.49	−14.96
			17	0.28	0.03	3	0.30	− 0.10	3	2.45	2.23
0 0 2	8.80	− 9.15	18	0.82	− 0.61	4	1.35	− 0.91	4	0.35	1.37
1	4.98	− 4.18				5	0.27	0.35	5	0.35	− 0.19
2	4.85	− 4.28	0 0 4	1.68	1.61	6	0.81	0.86	6	1.99	1.36
3	2.58	2.30	1	2.98	2.47	7	0.22	− 0.21			
4	1.57	− 1.05	2	2.36	1.59	8	0.17	0.25	6 0 0	6.66	− 7.50
5	3.17	− 2.84	3	1.08	0.80				1	1.35	− 2.15
6	7.81	7.42	4	0.82	− 0.09	0 0 1	20.12	−19.91	2	1.19	1.71
7	0.62	− 0.33	5	1.26	1.19	2	8.80	− 8.89	3	1.93	1.82
8	4.95	4.61	6	2.08	− 2.00	3	1.10	1.12	4	0.38	0.16
9	0.69	0.77	7	1.23	− 0.58	4	1.68	1.35	5	1.59	− 1.49
10	0.57	− 0.88	8	1.54	− 1.79	5	1.76	2.10			
11	4.15	4.02	9	3.08	− 3.29	6	1.94	− 1.69	$\bar{6}$ 0 1	4.70	7.13
12	4.25	− 4.08	10	0.35	− 0.04				2	3.17	2.64
13	2.96	− 2.96	11	1.74	1.75	2 0 0	0.20	0.21	3	1.57	− 2.94
14	0.50	− 0.42	12	1.21	1.50	1	5.55	− 4.84	4	1.20	− 1.07
15	1.41	− 1.33	13	1.08	0.83	2	1.00	1.45	5	1.19	1.09
16	0.35	− 0.51	14	0.55	0.36	3	2.71	1.93			
17	0.34	0.29	15	0.48	− 0.37	4	0.35	− 0.45	8 0 0	1.87	1.75
18	1.18	1.05	16	0.34	0.09	5	1.28	− 0.55	1	0.71	− 0.73
19	1.10	0.90				6	0.28	− 0.61	2	0.35	0.16
			0 0 5	1.76	2.02				3	0.35	− 0.28
0 0 3	1.10	1.19	1	0.85	− 0.57	$\bar{2}$ 0 1	2.56	− 2.85	4	0.24	− 0.05
1	1.11	1.74	2	3.56	− 3.25	2	1.54	− 0.15			
2	3.86	3.76	3	0.48	0.08	3	4.20	3.72	$\bar{8}$ 0 1	0.70	− 0.26
3	3.55	− 3.56	4	2.16	1.67	4	2.96	1.68	2	0.50	0.57
4	1.85	− 1.72	5	1.93	− 1.90	5	3.95	− 3.45	3	2.57	− 3.71
5	2.52	2.20	6	1.04	0.93	6	0.31	− 0.03	4	1.57	2.96
6	3.33	− 3.23	7	0.49	0.41				5	0.20	0.80
7	1.74	1.52	8	0.48	0.37	4 0 0	4.44	− 4.90			
8	0.33	0.39	9	1.40	1.03	1	2.09	0.53	10 0 0	0.34	0.30
9	3.18	2.82	10	1.22	− 0.62	2	0.81	1.24	1	0.33	0.51
10	0.79	0.47	11	0.10	− 0.36	3	1.69	− 1.24	2	0.27	− 0.79
11	4.19	− 4.13	12	0.52	− 0.53	4	1.12	− 1.16			
12	0.87	0.77	13	0.70	0.18	5	0.84	0.68	$\bar{10}$ 0 1	0.97	− 1.68
13	0.60	0.11				6			2	1.12	2.51
14	0.85	0.87	0 0 6	1.94	− 1.79				3	0.26	− 0.67
15	0.35	− 0.19	1	0.70	− 1.02	$\bar{4}$ 0 1	13.20	13.43			

The unit cell dimensions were determined from oscillation and Weissenberg photographs. The sets of intensities for $(h\,k\,0)$, $(0\,k\,l)$ and $(h\,0\,l)$ were obtained by the multiple-film Weissenberg technique, with CuK_α radiation and using a Ni filter. Intensities were estimated by visual comparison with a calibrated intensity scale.

Corrections for Lorentz and polarization factors were applied in the usual way, while that for absorption was disregarded. Preliminary scaling and temperature factors were determined by Wilson's method[7] and were further improved during the later stages of the refinement.

Structure Determination

Approximate Structure on the (0 0 1) Projection.—It is to be expected from the axial length that an approximate crystal structure should be obtained without serious overlapping of the molecule from the electron-density projection on (0 0 1). A trial molecular model was set up as planar, with conventional bond lengths and angles. The approximate structure on the (0 0 1) projection was obtained by the trial and error method, using the structure factor maps successively. The ordinary Fourier syntheses were followed. In the calculation of structure factors, an isotropic temperature factor $\exp\{-3.0(\sin\theta/\lambda)^2\}$ was applied. After several successive Fourier refinements, the R-value ($R=\sum\{|F_o|-|F_c|\}/\sum|F_o|$) became 0.25.

Approximate Structures on the (1 0 0) and (0 1 0) Projections. — The approximate structures on the (1 0 0) and (0 1 0) projections

7) A. J. C. Wilson, *Nature*, **150**, 152 (1942).

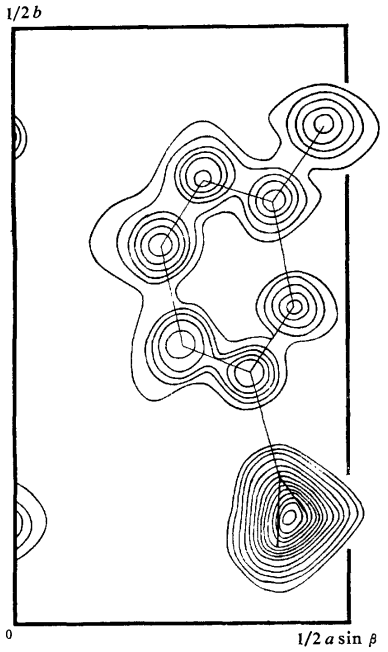

Fig. 1 (a)

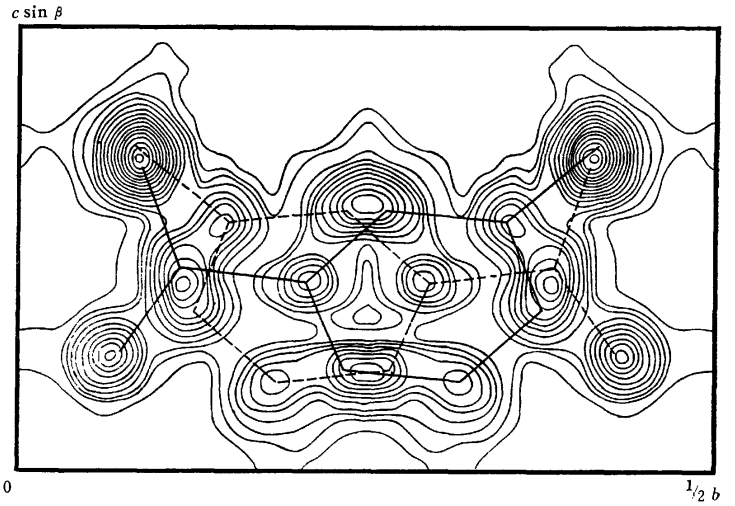

Fig. 1 (b)

Fig. 1. The final electron-density projections (a) along the c axis, (b) along the a axis. Contours are at an interval of 1 e. Å^{-2}, the lowest being at 2.0 e. Å^{-2}.

were given by assuming the planarity of the molecule with x and y coordinates obtained from the (0 0 1) projection. After several successive Fourier syntheses for the (1 0 0) and (0 1 0) projections, the R-values became 0.31 for ($0\,k\,l$) and 0.44 for ($h\,0\,l$). In the calculation of the structure factors, the isotropic temperature factor $\exp\{-3.0(\sin\theta/\lambda)^2\}$ was applied.

Refinement of Structure

Refinements of the structure were made by the method of modified (F_o-F_c) syntheses[8]. Preliminary hydrogen atoms were placed at the distance of 1.0Å from each of the C_2, C_4, C_5 and C_6 atoms, and two hydrogen atoms in the amino group were placed at the distance of 1.0Å from the nitrogen atom of the amino group on the N-O′ and N-O″ lines.

The locations of hydrogen atoms in the methyl group were obtained at the later stage of refinements. The isotropic temperature factor of each atom was corrected in each stage of the refinement. After ten successive (F_o-F_c) syntheses, the R-values reduced down to 0.11, 0.11 and 0.20 for ($h\,k\,0$), ($0\,k\,l$) and ($h\,0\,l$) respectively. The observed and calculated structure factors are listed in Table I. The final atomic parameters are given in Table II, while the final Fourier maps are shown in Fig. 1.

Throughout this study, the calculations of the structure factors were carried out on an NEAC 2101 electronic computer.

8) T. Watanabé and Y. Takaki, to be published.

Table II. Atomic coordinates and isotropic temperature factors

Atom	Coordinates			Temperature factors		
	x/a	y/b	z/c	($h\,k\,0$)	($0\,k\,l$)	($h\,0\,l$)
C_1	0.354	0.207	0.423	2.5	3.0	2.5
C_2	0.418	0.266	0.595	3.0	3.0	3.0
C_3	0.387	0.350	0.565	3.1	3.0	3.1
C_4	0.285	0.375	0.360	3.1	3.0	3.1
C_5	0.219	0.316	0.195	3.1	3.0	3.1
C_6	0.254	0.233	0.224	3.0	3.0	3.0
C_7	0.392	0.116	0.458	3.0	3.0	3.0
C_8	0.464	0.416	0.745	4.2	3.0	4.2
N	0.386	0.068	0.254	3.0	3.0	3.0
O	0.433	0.089	0.681	3.0	3.0	3.0
H_2	0.492	0.248	0.745	3.5	3.5	3.5
H_4	0.267	0.437	0.338	3.5	3.5	3.5
H_5	0.140	0.337	0.049	3.5	3.5	3.5
H_6	0.199	0.187	0.098	3.5	3.5	3.5
H_{M_1}	0.387	0.431	0.910	3.5	3.5	3.5
H_{M_2}	0.567	0.392	0.835	3.5	3.5	3.5
H_{M_3}	0.484	0.470	0.640	3.5	3.5	3.5
H_{N_1}	0.424	0.008	0.294	3.5	3.5	3.5
H_{N_2}	0.395	0.072	0.059	3.5	3.5	3.5

Description of the Structure and Discussion

Molecular Structure.—The bond lengths and angles found in *m*-methylbenzamide are shown in Fig. 2. None of the bond lengths observed in the benzene ring differ significantly from

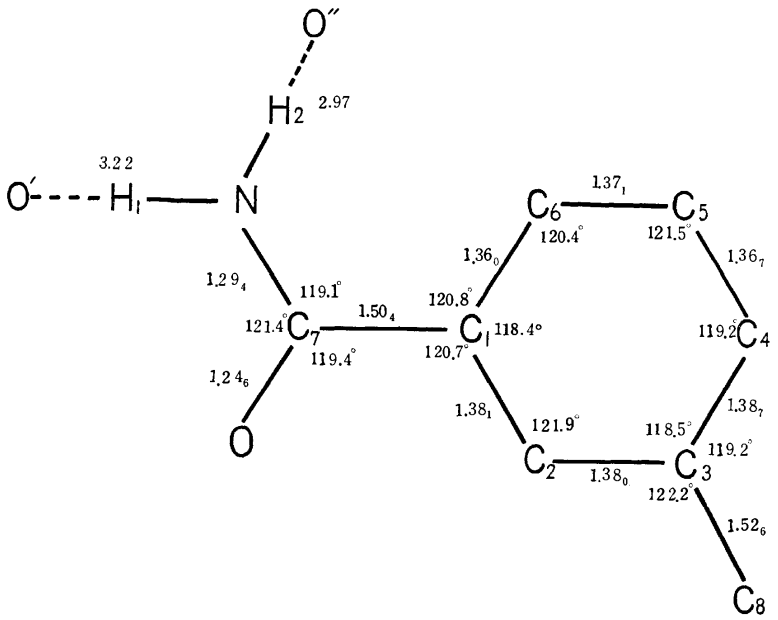

Fig. 2. Bond lengths (Å) and bond angles in *m*-methylbenzamide.

each other or from the mean observed value of 1.37$_5$Å which is in good agreement with the mean C–C bond length, 1.38Å, in the benzamide[6].

The C_1–C_7 bond length (1.50Å) leading to the amide group is somewhat less than 1.54Å, the standard length for a single bond. This value is, however, in good agreement with the 1.50, 1.52, 1.48, 1.48 and 1.48Å observed in α-pyrazinamide[4], nicotinamide[5], benzamide[6], benzoic acid[2] and nicotinic acid[3] respectively, though it is somewhat less than that observed in oxalic acid dihydrate[9] (1.53Å and α-oxalic acid[10] (1.56Å).

The shortening of this C_1–C_7 bond may indicate that there is some double bond character caused by the resonance effect between the amide or acid group and the six-membered ring.

The bond length C_3–C_8 (1.52$_6$Å) is in fairly good agreement with the standard single bond length.

TABLE III. DIMENSIONS OF THE AMIDE GROUP IN THE ANALOGOUS COMPOUNDS

	m-Methylbenzamide	Benzamide[6]	Nicotinamide[5]	α-Pyrazinamide[4]
	Å	Å	Å	Å
C-N	1.29	1.31	1.34	1.31
C-O	1.25	1.24	1.22	1.24

9) F. R. Ahmed and D. W. J. Cruickshank, *Acta Cryst.*, **6**, 385 (1953).
10) E. G. Cox, M. W. Dougill and G. A. Jeffrey, *J. Chem. Soc.*, **1952**, 4854.

The dimensions of the amide group agree closely with those observed in the analogous compounds. Some examples are shown in Table III.

The plane of the benzene ring can be represented by the equation:

$$0.550X' + 0.072Y - 0.403Z' - 1 = 0$$

where X', Y and Z' refer to the orthogonal axes a, b and c*, and the values of the coefficients are determined by means of the least squares. The perpendicular displacements of atoms from the mean plane are shown in Table IV.

TABLE IV. DISPLACEMENT OF EACH ATOM FROM THE MEAN PLANE OF THE BENZENE RING

	Å		Å
C_1	+0.006	C_6	+0.001
C_2	−0.013	C_7	+0.008
C_3	+0.007	C_8	+0.062
C_4	+0.006	N	+0.570
C_5	−0.012	O	−0.487

The mean value of the displacements for atoms in the benzene ring is 0.007$_5$Å, that is, the benzene ring is concluded to be planar. On the other hand, the nitrogen atom and oxygen atom deviate significantly from the mean plane of the benzene ring, and the angle between the ring plane and the amide plane is 28.7°.

It has been shown that the amide planes in nicotinamide[5] and benzamide[6] make an angle

about 25~26° to their ring planes, while in salicylic acid[1], benzoic acid[2], nicotinic acid[3] and α-pyrazinamide[4] the molecules are approximately planar.

The twists of the amide group around the C_1-C_7 axis in *m*-methylbenzamide can be explained by the steric hindrance on the contact of H_6 in the benzene ring and H_{N2} in the amino group, as has been suggested by Penfold and White[6].

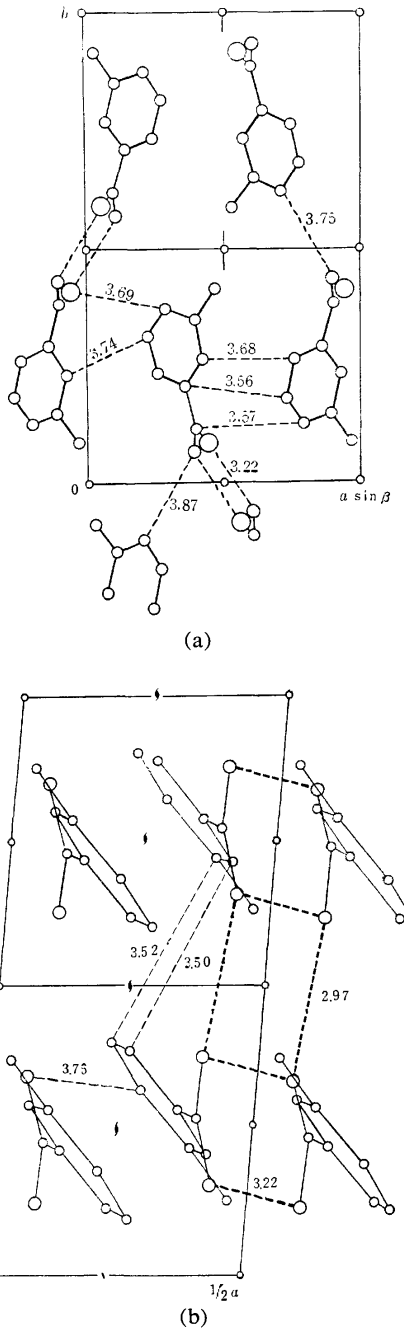

Fig. 3. Views of the arrangement of molecules (a) along the c axis, (b) along the b axis showing hydrogen bond as broken lines.

Crystal Structure. — The projection of the crystal structure along the c and b axes is shown in Fig. 3. The molecules are connected by the two NH-O hydrogen bonds, the first set 3.22Å in length forming a dimer across the center of symmetry, and the second set 2.97Å in length joining such dimers into endless chains extended along the c axis. The linkage of molecules by hydrogen bonding is of a type very similar to that found in the crystals of benzamide[6] and δ-pyrazinamide[12]. The hydrogen bond lengths in *m*-methylbenzamide are in agreement with those found for the NH-O type hydrogen bond, which have values ranging from 2.67 to 3.17 Å[11]. This crystal consists of endless chains linked by the NH-O hydrogen bonds, and the intermolecules between these chains are held in contact by the van der Waals force; such molecular arrangements as shown in Fig. 3 can reasonably explain the existence of the cleavage parallel to the (1 0 0) plane.

Summary

The crystal structure of *m*-methylbenzamide has been determined by two-dimensional X-ray methods. The atomic positions obtained from the trial and error method are refined by the modified $(F_o - F_c)$ synthesis[8].

1. The mean C-C distance in the benzene ring is 1.37_5Å, while C_3-$C_8 = 1.52_6$, C_1-$C_7 = 1.50_4$, C_7-$N = 1.29_4$ and C_7-$O = 1.24_6$Å.
2. The amide group twists around the C_1-C_7 axis with an angle of 28.7° because of the steric hindrance on the contact of H_6 and H_{N2}.
3. The molecules are connected by NH-O hydrogen bonds, 3.22Å, forming dimers which are linked with each other by other NH-O hydrogen bonds, 2.97Å, into endless chains.

The crystal structure is of a type analogous to benzamide[6] and δ-pyrazinamide[12].

The authors wish to thank Mr. Yukiteru Katsube, Mr. Tsunehiro Takano and Miss Yoriko Ogawa for arrangements made for the use of the electronic computer. They wish also to thank the Sankyo Co., Ltd., for supplying the samples.

Institute for Protein Research
Osaka University
Kita-ku, Osaka

11) J. Donohue, *J. Phys. Chem.*, 56, 502 (1952).
12) Y. Takaki, to be published.

Polarographic Determination of the Formation Constants of Sulfato, Acetato and Sulfatoacetato Complexes of Nickel(II) at Ionic Strength 1.0

By Nobuyuki TANAKA, Yu SAITO and Hiroshi OGINO

(Received February 27, 1963)

In the previous study[1], a method for the polarographic determination of the formation constants of weak complexes, $Ni(OAc)_i \cdot (Z)_j^{(2-i-zj)+}$ $(0 \leq i \leq n,\ 0 \leq j \leq p)$, was developed and applied to the nickel(II) complexes in sulfate-acetate media. The results indicated that mixed ligand complexes were not present in appreciable concentrations at ionic strength 0.2.

Because of the increasing interest in the determination of the formation constants of weak complexes with two or more different ligands, it seems worthwhile to apply the method under the conditions favorable for the formation of mixed ligand complexes. In the present paper, the formation of complexes of nickel(II) with sulfate and/or acetate is demonstrated in a solution containing higher concentrations of these anions, and the formation constants of these complexes determined at 25°C and ionic strength 1.0 are presented.

Experimental

The method employed in this study was in principle the same as in the previous paper[1]. However, the ionic strength of the solution was adjusted to 1.0 with sodium perchlorate, and sodium sulfate was used instead of potassium sulfate.

Results and Discussion

The polarograms were recorded with the acetate buffer solutions of pH 3.72 containing 9.90×10^{-4} M nickel nitrate, 1.06×10^{-3} M NTA, and various concentrations of sulfate and acetate. The limiting current of nickel(II) was found to be diffusion-controlled.

The values of $[Ni^{2+}]_{app}$, which is the sum of the concentrations of hydrated nickel ions and nickel(II) complexes with sulfate and/or acetate, were obtained at various concentrations of acetate and the given concentration of sulfate. The F_0 values were calculated according to the left-hand side of Eq. 13 of the previous paper[1] and were plotted against the acetate concentration (Fig. 1). The straight plots

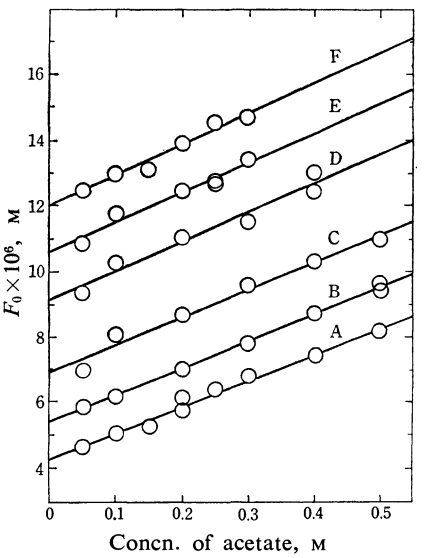

Fig. 1. F_0 as a function of acetate concentration at 25°C. Concentrations of sulfate are: 0 (A), 0.05 M (B), 0.10 M (C), 0.15 M (D), 0.175 M (E) and 0.20 M (F).

clearly indicate that n is equal to 1 and that no appreciable amount of complexes with two acetates or more coordinated is present in the solution investigated. Consequently, the F_0 function is written as follows:

$$F_0 = \frac{\alpha}{\beta K_{NiX}} \times \sum_{i=0}^{1} \sum_{j=0}^{p} K_{Ni(OAc)_i(SO_4)_j} [OAc^-]^i [SO_4^{2-}]^j \quad (1)$$

Next, F_0 was calculated with $[Ni^{2+}]_{app}$ obtained at various concentrations of sulfate and the given concentration of acetate and plotted against the sulfate concentration. A typical example of these F_0 plots is shown in Fig. 2. By extrapolating the F_0 plot as given in Fig. 2 to the zero sulfate concentration, the value of

$$\frac{\alpha}{\beta K_{NiX}} \quad (1 + K_{NiOAc}[OAc^{-1}])$$

was obtained. The F_1 function

1) N. Tanaka and H. Ogino, This Bulletin, 34, 1040 (1961).

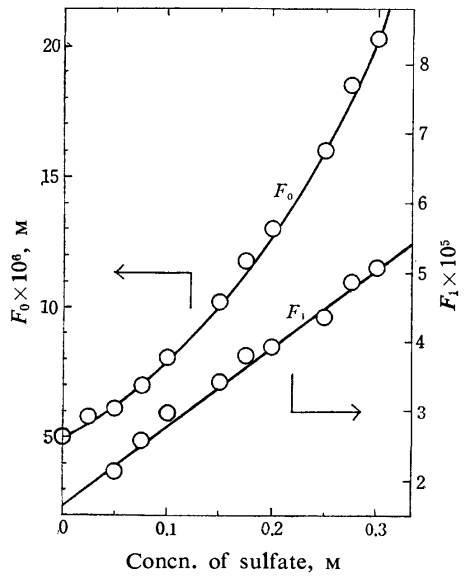

Fig. 2. F_0 (Eq. 1) and F_1 (Eq. 2) as a function of sulfate concentration at 25°C. Acetate concentration is 0.1 M.

$$F_1 \equiv \frac{F_0 - \frac{\alpha}{\beta K_{\mathrm{NiX}}}(1+K_{\mathrm{NiOAc}}[\mathrm{OAc}^-])}{[\mathrm{SO_4}^{2-}]} = \frac{\alpha}{\beta K_{\mathrm{NiX}}} \times \sum_{i=0}^{1}\sum_{j=1}^{p} K_{\mathrm{Ni(OAc)}_i(\mathrm{SO_4})_j}[\mathrm{OAc}^-]^i[\mathrm{SO_4}^{2-}]^{j-1} \quad (2)$$

was calculated from the F_0 plot and plotted against the sulfate concentration, as seen in Fig. 2, where the F_1 plot shows as a straight line. This indicates that p is equal to 2 and that no appreciable amount of complexes with three sulfates or more coordinated is present in the solution investigated. The same result was also obtained with other concentrations of acetate.

The fact that n and p are equal to 1 and 2 respectively suggests that complex species of $NiOAc^+$, $Ni(SO_4)$, $Ni(OAc)(SO_4)^-$, $Ni(SO_4)_2^{2-}$, and $Ni(OAc)(SO_4)_2^{3-}$ may exist in the solution. Therefore, Eq. 1 is written as

$$F_0 = \frac{\alpha}{\beta K_{\mathrm{NiX}}}\{1+K_{\mathrm{NiOAc}}[\mathrm{OAc}^-]+K_{\mathrm{NiSO_4}}[\mathrm{SO_4}^{2-}] + K_{\mathrm{Ni(OAc)(SO_4)}}[\mathrm{OAc}^-][\mathrm{SO_4}^{2-}]+K_{\mathrm{Ni(SO_4)_2}}[\mathrm{SO_4}^{2-}]^2 + K_{\mathrm{Ni(OAc)(SO_4)_2}}[\mathrm{OAc}^-][\mathrm{SO_4}^{2-}]^2\} \quad (3)$$

The formation constants and the value of $\alpha/(\beta K_{\mathrm{NiX}})$ were determined from the plots in Fig. 1 by a graphical treatment similar to that reported previously[1]. The value for $\alpha/(\beta K_{\mathrm{NiX}})$ was obtained to be $4.2_8\times10^{-6}$ mol. l.$^{-1}$ at pH 3.72, and the formation constants obtained are given in Table I. The uncertainties of the

Table I. Formation constants of nickel(II) complexes at 25°C and ionic strength 1.0

K_{NiOAc}	1.9	l. mol^{-1}
$K_{\mathrm{NiSO_4}}$	3.7	l. mol^{-1}
$K_{\mathrm{Ni(SO_4)_2}}$	2.6×10	l.^{2} mol^{-2}
$K_{\mathrm{Ni(OAc)(SO_4)}}$	1	l.^{2} mol^{-2}
$K_{\mathrm{Ni(OAc)(SO_4)_2}}$	~3	l.^{3} mol^{-3}

determined values were examined by a graphical method[2,3].

Using the $\alpha/(\beta K_{\mathrm{NiX}})$ thus obtained and the formation constants given in Table I, the values of F_0 can be calculated at various concentrations of sulfate and acetate. Two sets of F_0 values were calculated as a function of sulfate concentration at two different concentrations of acetate. The solid curves in Fig. 3 indicate

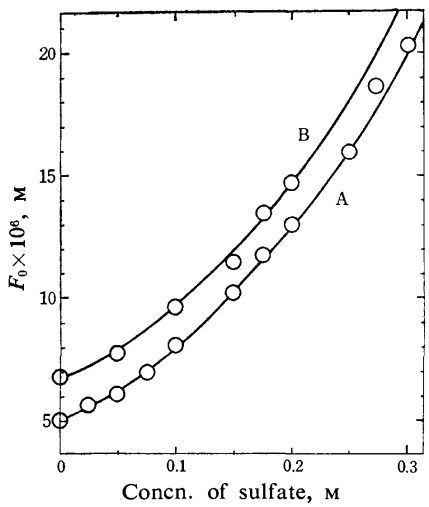

Fig. 3. Calculated and experimental values of F_0 at various concentrations of sulfate in the presence of 0.1 M (A) and 0.3 M (B) of acetate at 25°C: — indicates the calculated, and ○ the experimental value.

these calculated values, which are in satisfactory agreement with the F_0 values obtained experimentally at various sulfate concentrations.

The formation constants of K_{NiOAc} and $K_{\mathrm{NiSO_4}}$ at 25°C and ionic strength 0.2 have been given as 2.5 and 11.6 respectively[1]. The formation constants given in Table I are apparently smaller than these values; especially, $K_{\mathrm{NiSO_4}}$ at ionic strength 1.0 is considerably smaller than that at ionic strength 0.2.

In the previous study, at ionic strength 0.2, complex species, $Ni(SO_4)_2^{2-}$, $Ni(OAc)(SO_4)^-$ and $Ni(OAc)(SO_4)_2^{3-}$, were not found to exist

2) A. E. Martell and M. Calvin, "Chemistry of the Metal Chelate Compounds", Prentice-Hall, Inc., N. J. (1959), p. 91.

3) G. Schwarzenbach, A. Willi and R. O. Bach, *Helv. Chim. Acta*, **30**, 1303 (1947).

in appreciable concentrations, whereas in the present study, at ionic strength 1.0, the existence of these complexes is confirmed. It should be noted that the existence of these complex species was confirmed not because of the increase in ionic strength but because of the increase in the concentrations of sulfate and acetate ions. This obviously suggests that the increase in ligand concentration is one of the most important conditions in the study of weak complexes with two or more different ligands.

Summary

The formation of nickel(II) complexes with sulfate and/or acetate has been studied at 25°C and ionic strength 1.0 by the polarographic method reported previously[1]. The results obtained reveal that complex species, $NiOAc^+$, $NiSO_4$, $Ni(SO_4)_2^{2-}$, $Ni(OAc)(SO_4)^-$ and $Ni(OAc)(SO_4)_2^{3-}$, are present in the solution. The formation constants determined are: $K_{NiOAc}=1.9$, $K_{NiSO_4}=3.7$, $K_{Ni(SO_4)_2}=2.6\times10$, $K_{Ni(OAc)(SO_4)}=1$ and $K_{Ni(OAc)(SO_4)_2}=\sim3$ at 25°C and ionic strength 1.0.

The authors wish to thank the Ministry of Education for its financial support of this research.

Department of Chemistry
Faculty of Science
Tohoku University
Katahira-cho, Sendai

*Brown Nitrosylpentamminechromium(III) Salts and Green Nitrosylpentamminechromium(III) Perchlorate**

By Masayasu MORI, Shigeru UESHIBA and Shinichi KAWAGUCHI

(Received March 5, 1963)

An ammoniacal solution of chromium(II) salt is readily oxidized; the oxidation products vary widely, depending upon the kind of oxidizing agent employed. Thus, when it is allowed to evolve hydrogen at a temperature near 0°C, especially in the presence of iron(II) salt as a catalyst, the main product is hexamminechromium(III) salt[1,2], while a rapid stream of oxygen produces μ-hydroxobis{pentamminechromium(III)} salt as an oxidation product[3]. The present authors have found that the same binuclear complex is also formed by oxidation with ammonium nitrate and that, in this case, brown crystals, however small in quantity, are often found admixed in the red μ-hydroxo salt. Further research has shown that the brown crystals are nitrosylpentamminechromium(III) dichloride, a new type of acidopentamminechromium salt, and that the perchlorate prepared by metathesis is green in contrast to chloride, bromide and nitrate, all of which have been found to be brown; that is to say, the color of crystals is completely changed by a mere substitution of an anion which is not coordinated in the ordinary sense. Such an example seems to be quite rare, though analogous cobalt compounds might be regarded as another example. There are, however, points of considerable difference between these two cases, as will be discussed below. In this paper the method of preparation of and an investigation of infrared absorption spectra pertaining to the new chromium ammines will be described.

Experimental

Preparation.—Although nitrosylpentamminechromium(III) salts were first obtained as described above, the best way of preparing them is by oxidizing an ammoniacal chromium(II) solution with sodium nitrite. The reaction may be represented by the equation:

$$2[Cr(NH_3)_6]Cl_2+NaNO_2+NH_4Cl \rightarrow [CrNO(NH_3)_5]Cl_2+[CrOH(NH_3)_5]Cl_2+NaCl+3NH_3$$

Nitrosylpentamminechromium(III) Chloride. — Fifteen grams of potassium dichromate are mixed in a 1 l. beaker with 20 ml. of ethanol and 40 ml. of 12 N hydrochloric acid. When the violent reaction has ceased somewhat, the mixture is heated on a hot plate until no orange crystals of potassium dichromate are left at the bottom of the beaker.

* Presented at the Symposium on Coordination Chemistry, Osaka, November, 1961.

1) S. M. Jörgensen, *J. prakt. Chem.*, **30**, 1 (1884).

2) M. Mori, *J. Chem. Soc. Japan, Pure Chem. Sec.* (*Nippon Kagaku Zassi*), **74**, 253 (1953).

3) S. M. Jörgensen, *J. prakt. Chem.*, **25**, 321 (1882).

TABLE I. INFRARED ABSORPTION PEAKS OF NITROSYLPENTAMMINECHROMIUM(III) SALTS AND THEIR ASSIGNMENTS (wave number, cm^{-1})

$[CrNO(NH_3)_5]Cl_2$ (brown)		$[CrNO(NH_3)_5](ClO_4)_2$ (green)		Assignments
3300 vs	(broad)	3410 vs 3340 vs	(sharp) (sharp)	NH_3 stretch.
2960 vs 2900 vs	(sharp) (sharp)	2960 vs 2900 vs	(sharp) (sharp)	NH_3 stretch.
2030 vw		2030 vw		?
1690 vs		1730 vs		NO stretch.
1610 s		1625 s		NH_3 deg. def.
1465 m	(sharp)	1465 m	(sharp)	?
1380 m	(sharp)	1380 m	(sharp)	?
1275 vs	(sharp)	1300 vs	(sharp)	NH_3 sym. def.
1240 w	(sharp)	——		
——		1120 1080 vvs	(shoulder) (broad)	ClO_4 deg. stretch.
770 s 730	(broad) (shoulder)	760 730 s	(shoulder)	NH_3 rock.

Abbreviations: v, very; s, strong; w, weak; stretch., stretching; deg., degenerate; def, deformation; sym., symmetric; rock., rocking.

The green solution is then transferred into a smaller beaker and covered with a 3 cm. layer of ligroin or liquid paraffine. It is then kept at 80~90°C, together with 30 g. of pure zinc grains, until the green chromium(III) solution has been completely reduced to the bivalent state with a pure blue color. If the solution has become turbid before the complete reduction, 1~2 ml. of hydrochloric acid may be added and heating continued.

The pure azure-colored solution is cooled in running water to room temperature and quickly poured, together with the mineral oil, into an Erlenmeyer flask containing a mixture of 40 g. of ammonium chloride and 100 ml. of 15 M aqueous ammonia; the whole mixture is then carefully stirred and cooled in an ice bath. To this is then added 15 g. of sodium nitrite dissolved in 25 ml. of 15 M aqueous ammonia; the mixture is stirred vigorously and allowed to stand for several minutes, and the precipitate of crude chloride is separated by filtration. Not only the chloride, but also various other salts may be prepared from this crude product.

In order to prepare pure chloride, the crude product is dissolved in the smallest possible quantity (ca. 1000 ml.) of cold water, and after filtration pure nitrosylpentamminechromium(III) chloride is recrystallized by the slow addition of 200 g. of ammonium chloride and 10 ml. of 12 N hydrochloric acid. The brown crystals are washed with ethanol, air-dried, and kept in a desiccator protected from light. Yield, 9 g.

Found: Cr, 22.69; N (total), 34.85; NH_3, 35.70; Cl, 30.02. Calcd. for $[CrNO(NH_3)_5]Cl_2$: Cr, 22.32; N (total), 36.06; NH_3, 36.53; Cl, 30.42%.

Nitrosylpentamminechromium(III) Nitrate. — The crude precipitate of nitrosylpentamminechromium-(III) chloride is dissolved in ca. 1000 ml. of cold water, and the solution is filtered. The nitrate may be crystallized by slowly adding 300 g. of ammonium nitrate and 10 ml. of 14 N nitric acid. Yield, 3.6 g. The precipitate may be further purified by dissolution in water and recrystallization with ammonium nitrate.

Found: Cr, 18.12; NH_3, 28.76. Calcd. for $[CrNO(NH_3)_5](NO_3)_2$: Cr, 17.86; NH_3, 29.25%.

Nitrosylpentamminechromium(III) Bromide. — The bromide can be obtained by a procedure analogous to that used for preparing the nitrate. The bromide is much less soluble and a better yield is obtained by the use of a somewhat smaller quantity of ammonium bromide. However, special care should be taken to prevent the precipitate from becoming too fine. Thus, ammonium bromide is added little by little while the solution is continuously agitated.

Found: Cr, 15.91; NH_3, 25.62; Br, 49.72. Calcd. for $[CrNO(NH_3)_5]Br_2$: Cr, 15.91; NH_3, 26.04; Br, 48.86%.

Nitrosylpentamminechromium(III) Perchlorate.—The precipitate of crude chloride is dissolved in a mixture of 180 ml. of 6 N sulfuric acid and 220 ml. of water, and the solution is filtered. To the filtrate is added 200 ml. of 60% perchloric acid. The mixture is cooled in an ice bath, and the green precipitate of the perchlorate is collected on a glass filter under suction and washed with ethanol. Yield, 6 g. It may be purified by dissolution in the smallest possible quantity of water and by recrystallization with perchloric acid in an ice bath.

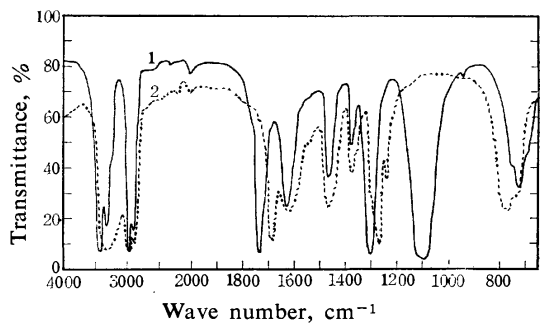

Fig. 1. Infrared absorption spectra of nitrosylpentamminechromium(III) salts.
1: Perchlorate 2: Chloride

Found: Cr, 14.58; NH_3, 22.73; Cl, 19.79. Calcd. for $[CrNO(NH_3)_5](ClO_4)_2$: Cr, 14.21; NH_3, 23.26; Cl, 19.37.

Infrared Absorption Spectra. — The infrared absorption spectra of powder samples of the chloride and the perchlorate were obtained by the Nujol mull technique in the rock salt region with a Hitachi EPI-2 spectrometer. The spectra are given in Fig. 1.

Results and Discussion

The wave numbers of the main infrared absorption peaks and their possible assignments are given in Table I. The assignments were made on analogy with the nitrosylpentamminecobalt(III) salts studied by Bertin, Mizushima, Lane and Quagliano[4]. All the features of the spectra are analogous to those of cobalt compounds, but the rocking frequency of the ligating NH_3 is somewhat lower in chromium ammines and especially so in green perchlorate (chloride: 770; perchlorate: 730; cobaltammines: 800 cm^{-1}). This seems to show indirectly that the coordinate linkage is weaker[5], especially in green nitrosylpentamminechromium(III) perchlorate. The spectra also show that the vibrational frequency of NO is higher in the green perchlorate (1730) than in the brown chloride (1690)*. This would seem to be evidence that in the green form the ligating NO is influenced less by the central ion than in the brown chloride. (Gaseous NO: 1876 cm^{-1})

There is evidence to show that nitrosylpentamminechromium(III) compounds are not simple analogues of similar cobalt compounds[6]. For example, the black series of nitrosylpentamminecobalt(III) salts can be prepared only in the absence of air, the pink series, in the presence of air[7], and the two series are not interchangeable[8]. Moreover, they are reported to behave differently toward acids: the salts of the black series are readily decomposed to give cobalt(II) salts, whereas those of the pink series form acidopentamminecobalt(III) salts[8]. Thus, in cobalt compounds the difference in anions is probably not the only factor causing color change.

On the other hand, both green nitrosylpentamminechromium(III) perchlorate and brown nitrosylpentamminechromium(III) chloride are stable when dissolved in cold water, both solutions presenting exactly the same absorption spectra; from any such solutions, either the perchlorate or the chloride may be crystallized by a mere choice of the precipitant (i.e., perchloric acid or hydrochloric acid). Thus, the environment in the ionic lattices seems to have an effect sufficient to cause a difference in the state of the complex cation, as is evidenced by the difference in color and vibrational frequencies.

A spectroscopic investigation of these chromium compounds is now under way and will shortly be reported. Let us say here, however, that the color of the chloride changes to orange when cooled to the temperature of liquid nitrogen, but that the color of the green perchlorate does not change appreciably down to this temperature.

Summary

A new series of chromium ammines, i.e., nitrosylpentamminechromium(III) salts, were obtained by the reaction of an ammoniacal chromium(II) solution with sodium nitrite. The derivatives are usually reddish brown, but only the perchlorate is bright green. The infrared absorption spectra indicate that in the green perchlorate the rocking frequency of ligating ammonia is lower, while the stretching frequency of the nitrosyl group is higher than in the brown chloride. These results seem to show indirectly that the coordinate linkage is weaker in the green perchlorate.

It is the authors' pleasure to express their gratitude to Professor Tatsuo Miyasawa of Osaka University for his valuable suggestions.

Faculty of Science
Osaka City University
Sumiyoshi-ku, Osaka

4) E. P. Bertin, S. Mizushima, T. J. Lane and J. V. Quagliano, *J. Am. Chem. Soc.*, 81, 3821 (1959).

* In the case of the cobalt compounds, such a frequency overlaps that of the degenerate deformation vibration of NH_3 (1630 cm^{-1}, Ref. 4).

5) J. Fujita, K. Nakamoto and M. Kobayashi, *J. Am. Chem. Soc.*, 78, 3295 (1956).

6) J. Sand and O. Gennsler, *Ann.*, 123, 43 (1862); ibid., 329, 194 (1903); *Ber.*, 36, 2083 (1903).

7) T. Moeller and G. L. King, "Inorganic Syntheses", Vol. 4 (1953), p. 168.

8) T. Moeller and G. L. King, ibid., Vol. 5 (1957), p. 186.

Acetylenic Analogues of Chichibabin Hydrocarbon

By Hirohisa KATAOKA and Masazumi NAKAGAWA

(Received March 14, 1963)

There have been many discussions of the unstable nature of Chichibabin hydrocarbon (I), which was prepared by Chichibabin as early as 1907[1]. Schwab and Agliardi have observed that hydrocarbon I catalyzed the interconversion of ortho- and para-hydrogen; they have attributed this catalytic activity to the presence of the biradical structure (I_b) in the hydrocarbon[2]. On the other hand, Müller and Müller-Rodloff have assigned the quinomethane structure (I_a) on the basis of the diamagnetic behavior of this hydrocarbon[3]. More recently, Huchison has measured the ESR spectrum of a solution of I and concluded that I in the solution contained 4~5% of the biradical (I_b)[4]. However, in a private communication to Ingram, he has pointed out that

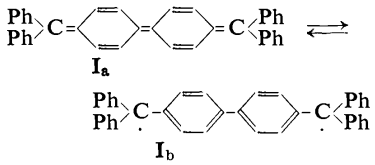

I_a

I_b

there is a distinct possibility of the presence of an impurity to which the observed signal may be attributable*. Also, there have been fairly many investigations concerning the quinomethane or biradical structure of Chichibabin type hydrocarbons[5]. If there exists an equilibrium between the quinomethane and biradical structures, it would be reasonable to conclude that the energy levels corresponding to these two possible structures do not differ appreciably. If Chichibabin hydrocarbon (I) exists mainly in the form of the quinomethane (I_a), the loss of the resonance energy of the central benzene rings should be covered by an increase in the resonance energy of the newly-formed, more extended conjugate system.

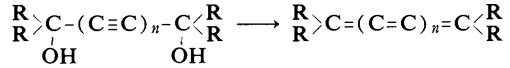

II III

On the other hand, the formation of cumulene (III) from the acetylenic glycol of type II is well-known[6]. Also, the rearrangement of the acetylenic linkage to an allenic system under rather mild conditions has been shown in several instances[7]. Therefore, the insertion of a triple bond to I or a substitution for the central benzene ring in I of a triple bond seems to cause a change in the valence tautomeric equilibria between the quinoid and the biradical structures of these acetylenic analogues of Chichibabin hydrocarbon.

The present paper deals with the synthesis and the properties of the following acetylenic analogues of I:

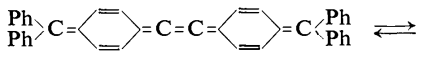

IV_a

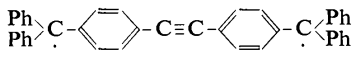

IV_b

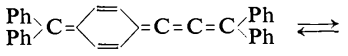

V_a

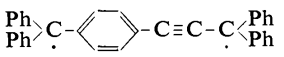

V_b

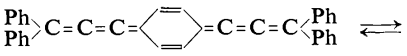

VI_a

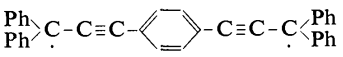

VI_b

The Synthesis of the Precursors of the Acetylenic Analogues of Chichibabin Hydrocarbon

4, 4'-Bis(diphenylchloromethyl)-tolan (VIII). —Dibenzyl was converted to 4, 4'-dibromotolan according to the method of Barber[8].

1) A. E. Chichibabin, *Ber.*, 40, 1810 (1907).
2) G.-M. Schwab and N. Agliardi, ibid., 73, 95 (1940).
3) E. Müller and I. Müller-Rodloff, *Ann.*, 517, 134 (1935).
4) C. A. Huchison, Jr., A. Kowalsky, R. C. Paster and G. W. Wheland, *J. Chem. Phys.*, 20, 1485 (1952).
* D. J. E. Ingram, "Free Radicals as studied by Electron Spin Resonance", Butterworth Scientific Publications, London (1958), p. 229.
5) a) E. Müller and H. Pfanz, *Ber.*, 74, 1051, 1075 (1941); b) G. Sloan and W. R. Vaughan, *J. Org. Chem.*, 22, 750 (1957); c) G. J. Sloan, W. R. Vaughan and H. S. Jarrett, *J. Phys. Chem.*, 25, 697 (1956); d) G. Wittig and W. Wiemer, *Ann.*, 483, 144 (1930); e) W. Theilacker, H. Schulz, U. Baumgarte, H. G. Drössler, W. Rohde, F. Tharter and H. Uffmann, *Angew. Chem.*, 69, 322 (1957).
6) For reviews, see P. Cadiot, W. Chodkiewicz and J. Rauss-Godineau, *Bull. soc. chim. France*, 1961, 2176.
7) E. R. H. Jones, G. H. Whitham and M. C. Whiting, *J. Chem. Soc.*, 1957, 4628; T. L. Jacobs and D. Danker, *J. Org. Chem.*, 22, 1424 (1957).
8) S. Bance, H. J. Barber and A. M. Woolman, *J. Chem. Soc.*, 1943, 1; H. J. Barber and R. Slack, ibid., 1944, 612.

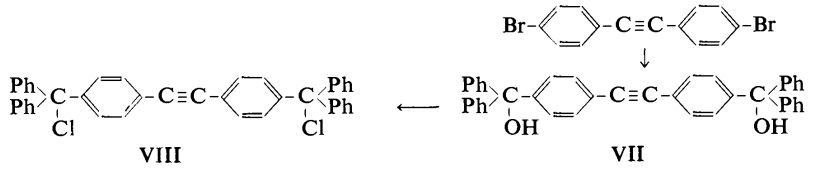

VIII VII

The successive treatment of the tolan with *n*-butyllithium and then with benzophenone yielded 4,4'-bis(diphenylhydroxymethyl)-tolan (VII) in an almost quantitative yield. The reaction of thionyl chloride with the glycol VII resulted in the formation of 4,4'-bis-(diphenylchloromethyl)-tolan (VIII) in a good yield. The dichloride VIII was found to be a fairly unstable compound which decomposed easily upon the heating of the solution or of the crystals. The development of a blue band was obseved when a solution of VIII was passed through a column of activated alumina. The blue-colored material could not be eluted with various kinds of polar solvents, and the blue color disappeared gradually without the movement of the band. From the eluate with ethyl acetate, the glycol VII was obtained as the sole decomposition product.

4,4'-Bis(9''-chloro-9''-fluorenyl)-tolan (XI).—The synthesis and interesting properties of the biphenylene analogue of Chichibabin hydrocarbon (IX) have been reported by Theilacker[5e].

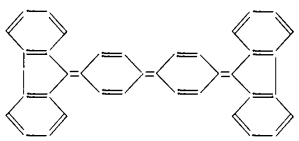

IX

In order to prepare the acetylenic analogue of IX, the corresponding dichloride (XI) was synthesized according to the following scheme. The metalation of 4,4'-dibromotolan by means of *n*-butyllithium, followed by the reaction with fluorenone, afforded the glycol X in a good yield. It was found that the displacement of the hydroxyl groups by chlorine proceeds

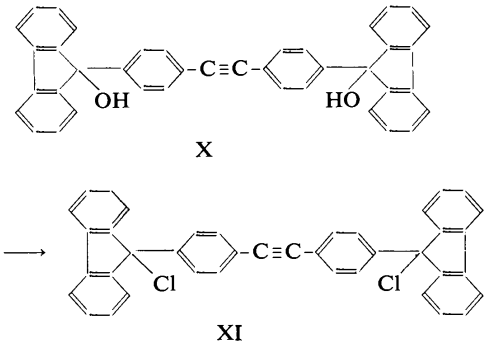

X XI

sluggishly compared with the case of VII. The dichloride XI was obtained in a reasonable yield after refluxing the mixture of X with a large excess of thionyl chloride for over 6 hr.

1-Diphenylchloromethyl-4-(3'-chloro-3',3'-diphenyl-1'-propynyl)-benzene (XVII).—The successive treatment of *p*-bromophenylacetylene with *n*-butyllithium and benzophenone gave the glycol XVI in a poor yield, together with an appreciable amount of 1,1-diphenyl-3-(4'-bromophenyl)-propyn-1-ol (XVIII). It was found that this reaction was scarcely feasible, however, because of the poor yield and the poor reproducibility. *p*-Bromoacetophenone was converted to *p*-acetylbenzonitrile (XIII)[9]. This was hydrolyzed to give the corresponding benzoic acid XIII. Methyl *p*-ethynylbenzoate (XV) derived from XIII via two steps was treated with phenyllithium and benzophenone successively, affording the glycol XVI in a reasonable yield. The glycol XVI thus obtained was heated with a large excess of thionyl chloride in benzene or acetyl chloride in hydrochloric acid[5b], yielding the unstable dichloride XVII.

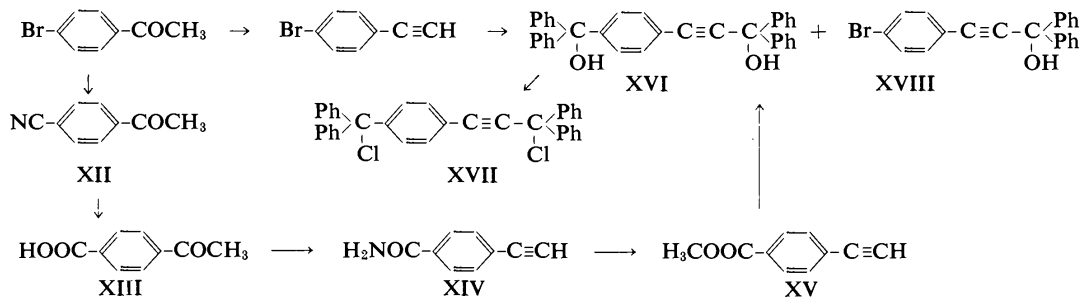

XII XVI XVII XVIII XIII XIV XV

9) T. Mowry, M. Renoll and W. F. Huber, *J. Am. Chem. Soc.*, 68, 1108 (1946) (cf. J. H. Helberger and A. von Rebay, *Ann.*, 531, 279 (1937)).

1, 4-Bis-(3'-chloro-3, 3'-diphenyl-1'-propynyl)-benzene (XX). — 1, 4-Bis(3'-hydroxy-3', 3'-diphenyl-1'-propynyl)-benzene (XIX) was prepared according to the method of Ried[10] by the reaction of the lithium derivative of *p*-diethynylbenzene with benzophenone. The dichloride XX was obtained by treating the glycol XIX with thionyl chloride in benzene or acetyl chloride in hydrochloric acid at a low temperature. XX was found to be extremely unstable in the presence of heat.

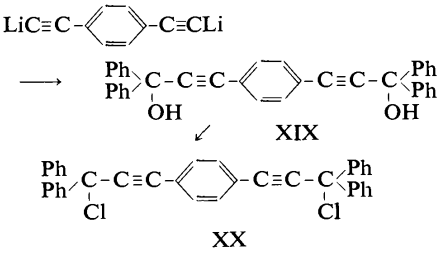

XIX

XX

Results

On 4, 4'-Bis-diphenylmethylyl-tolan (IV).— The rapid development of an intense blue-violet color was observed when a solution of the dichloride VIII in benzene or tetrahydrofuran was shaken with mercury or zinc dust at room temperature in an atmosphere of pure nitrogen. The solution could be kept without change of its color for several hours at the temperature of −70°C. A rapid change of the color to orange was observed when the solution was warmed to room temperature. Also, the exposure to air of the blue-violet solution caused an instant decolorization of the solution. The ultraviolet absorption spectrum of the orange solution exhibits a distinct peak at 465 mμ and the broad absorption, at a shoter wavelength. The ESR spectra were measured to determine the presence of the biradical structure IV_b employing tetrahydrofuran solutions (5.1×10^{-3} mol./l. and 2.0×10^{-2} mol./l. based on the dichloride, VIII) at 21°C. The spectrum is illustrated in Fig. 1, together with that of diphenylpicrylhydrazyl (solid) for purposes of comparison. The shape of the differential absorption curve was found to be a typical one for a carbon radical. Calculation of the concentration of the biradical IV_b, which was carried out by a comparing the integrated differential absorption curve of IV_b with that of diphenylpicrylhydrazyl, showed that 5% and 7% of IV_b should be present in the above-mentioned solution, assuming that the dechlorination of the dichloride VIII by zinc dust proceeds to 100% conversion.

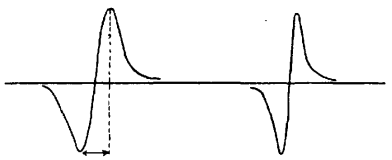

(a) (b)

Fig. 1. The ESR spectra of IV_b (a) and diphenylpicrylhydrazyl (b).

The attempts to isolate the unstable IV in a solid state failed. The concentration of the blue-violet solution in vacuo at a low temperature resulted in the formation of an orange-yellow polymeric substance.

As the structure of a cyclic dimer has been assigned to the peroxide of Chichibabin hydrocarbon by Müller[11], the formation of the same type of cyclic peroxide as XXI was expected in the case of IV_b. An intense blue-violet solution of IV in tetrahydrofuran was exposed to air, resulting in the formation of a light brown solution. The attempts to isolate XXI in a pure state gave unsatisfactory results. The absorption of oxygen by IV was measured using a Warburg manometer. A rapid uptake of oxygen was observed when the dichloride VIII in tetrahydrofuran was shaken with an excess of zinc dust in an atmosphere of pure oxygen. A representative absorption

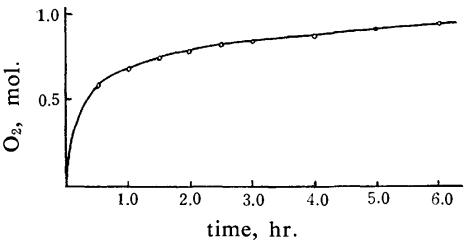

Fig. 2. The absorption of oxygen by IV_b.

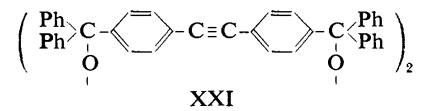

XXI

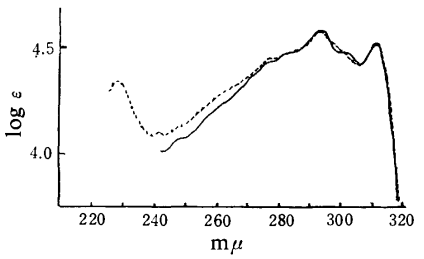

Fig. 3. The ultraviolet spectra of the peroxide (XXI, —) and the glycol (VII, -----).

10) W. Ried and G. Dankert, *Chem. Ber.*, **92**, 1223 (1959).

11) E. Müller and E. Tietz, *Ber.*, **74**, 807 (1941).

curve is presented in Fig. 2. The ultraviolet spectrum of the peroxide was found to be closely related with that of the glycol VIII illustrated in Fig. 3. The peroxide solution was chromatographed on alumina, and colorless needles (m. p., 175~177°C) were isolated; these were proved to be identical with the glycol (VIII; m. p., 179~179.5°C) by a mixed melting point determination (mixed m. p., 173~178°C). The mode of the formation of the glycol VII is not clear, but it seems to arise from the peroxide XXI by a decomposition on the surface of alumina.

The ultravoilet spectrum of IV could not be measured accurately because of the unstable nature of IV. A fairly rapid change in absorption intensity was observed during the course of the measurement. Approximate absorption maxima were found at the wavelengths of 750, 678, 590 (strongest) and 439 mμ.

The Attempted Formation of 4, 4-Bis-(9''-fluorenylyl)-tolan (XXII).—The replacement of the diphenylmethylyl group in IV by a 9-fluorenyl group constitutes an interesting system XXII, which can be regarded as an acetylenic analogue of Theilacker's hydrocarbon IX[5e]. It was hoped that the terminal fluorenyl groups might stabilize the quinomethane structure, but all attempts to remove the chlorine atoms from the dichloride XI or to subtract the hydroxyl groups from the glycol X failed. No developement of an intense color was observed under various reaction conditons.

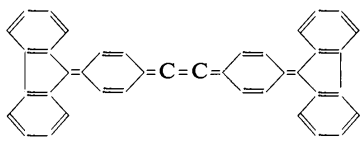

XXII

The Formation of 1-Benzhydryliden-4-(3', 3'-diphenylpropadienyliden)-1, 4-dihydrobenzene (V_a).—Powdered anhydrous stannous chloride was added to a dilute solution of the dichloride XVIII in benzene, and the mixture was shaken for several hours. A small quantity of black-violet needles with a greenish surface luster was isolated from the reaction mixture. It was found that this substance was contaminated with a small amount of chlorine compound, but the impurity could not be removed by chromatography on alumina or by treatment with molecular silver. The ultraviolet spectrum of this substance is illustrated in Fig. 4, together with those of the related compounds. The stability of this substance in the solid state or in a benzene solution suggests the quinomethane structure of the substance V_a. However, it was observed that the reddish-violet color of a benzene solution of V_a rapidly

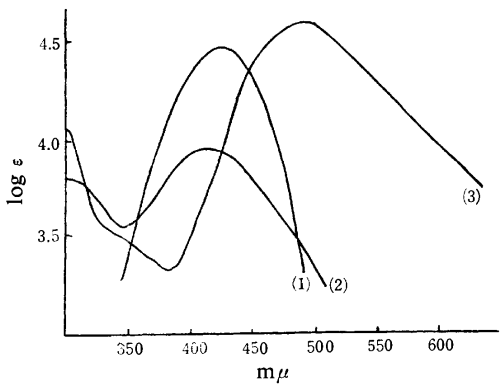

Fig. 4. The ultraviolet spectra of (1) Thiele's hydrocarbon (XXIII), (2) the mono-radical (XXV) and (3) the quino-cumulene (V_a).

changed to light brown on exposure to light. The measurement of the ESR spectrum showed no signal, indicating the absence of the biradical structure V_b.

The characteristic features of the infrared spectrum of V_a are the absence of cumulenic absorption (1900~2050 cm^{-1})[12] and the presence of strong absorptions at 822 and 1365 cm^{-1}. The absorption at about 800 cm^{-1} is usually attributed to the out-of-plane deformations of the two adjacent hydrogen atom in a para-disubstituted benzene derivative. This argument, however, is not consistent with the structure of V_a, in which the disubstituted six-membered ring has a cyclohexadiene structure. The infrared spectrum of Thiel's hydrocarbon[13], which has been regarded as having a quinomethane structure XXIII, also exhibits absorption at 831 cm^{-1}. Quite recently, it was

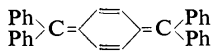

XXIII

found that *cis*-1, 3, 5-hexatriene showed a strong absorption in this region (818 cm^{-1}) which was lacking in the spectrum of the trans-isomer[14]. Therefore, the strong absorption at 822 cm^{-1} in V_a may reasonably be attributed to the out-of-plane deformation of the hydrogen atoms of the conjugated cis-double bonds in the cyclohexadiene structure.

A solution of the dichloride XVII in benzene was treated with molecular silver at 60°C, resulting in a deep brown solution. The solution was passed through a column of alumina, and the filtrate was evaporated, affording a red-brown solid. The free radical nature of

12) R. C. Lord and P. Venkateswarlu, *J. Chem. Phys.*, **20**, 1237 (1952); W. Otting, *Chem. Ber.*, 87, 611 (1954).
13) J. Thiele and H. Balhorn, *Ber.*, 37, 1463 (1904).
14) J. C. H. Hwa, P. L. de Benneville and H. J. Sims, *J. Am. Chem. Soc.*, 82, 2537 (1960).

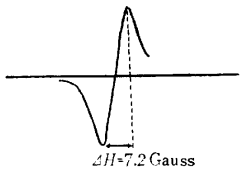

Fig. 5. The ESR spectrum of the mono-radical (XXV).

this substance was revealed by an ESR measurement employing a specimen which had been kept in an evacuated desiccator for two days (Fig. 5). The sharp and highly symmetrical absorption curve suggests that the radical center should not be an oxygen atom, but it concerns a carbon radical. The analytical data ($C_{34}H_{24}OCl$) indicates the presence of chlorine and oxygen in the molecule. From these observations, it seems highly probable that the red-brown solid consists mainly of the peroxide XXVI, containing a small amount of the mono-radical XXV. The remaining chlorine atom seems, in view of its inertness to molecular silver, to attach to an unsaturated carbon atom. There are two possibilities of the formation of such a rearranged product. One of

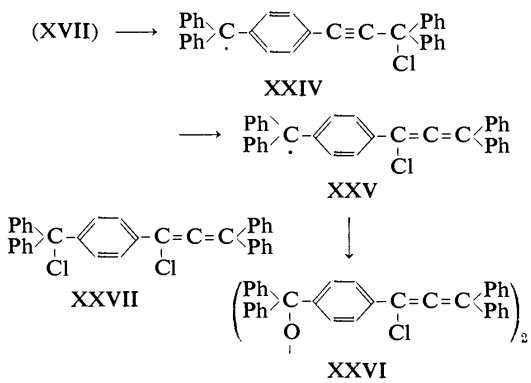

them is that the starting dichloride was already a mixture of XVII and the rearranged dichloride XXVII which had been formed during the course of the displacement of the hydroxyl groups by chlorine atoms. Another is the rearrangement of XXIV to the isomeric radical XXV by the catalytic action of molecular silver.

Attempts to form 1, 4-Bis(3', 3'-diphenyl-1'-propadienyliden)-1, 4-dihydrobenzene (VI_a) or 1, 4-bis(3', 3'-diphenyl-1'-propynylyl)-benzene (VI_b).—Recently, Ried has reported that the treatment of 1, 4-bis(3'-hydroxy-3', 3'-diphenyl-propynyl)-benzene (XIX) with Stephen's reagent resulted in the formation of a dark red solution. He has assigned the biscumulene structure VI_a to the reaction product on the basis of the stable color of the solution[10]. The initially-developed blue color of the reaction mixture rapidly changed to red-violet, then to reddish-brown, and finally to brown. When the glycol XIX in tetrahydrofuran was mixed with Stephen's reagent in the same solvent at −70°C, the immediate development of a transient, deep violet-blue color was observed; this color rapidly changed to red-violet, then to orange-red. The orange-red color of the solution changed to blood-red gradually at −70°C or rapidly at room temperature. The blood-red solution was found to be fairly stable, but it gradually changed to a yellow-brown solution on exposure to air at room temperature. The electronic spectra of the deep violet-blue and the red-violet solutions could not be determined because of their instability. The blood-red and the yellow-brown solutions exhibited the absorption maxima at 284, 482 mμ and 328, 540 mμ respectively. The absorption of the yellow-brown solution coincides with the reported values (333.0 and 539.5 mμ)[10]. Ried has assigned the structure of VI_a to this substance, but, as has been mentioned above, the yellow-brown solution is the ultimate stage of the complex color change in the transformation of the glycol XIX. Therefore, it seems highly probable that the yellow-brown solution consists mainly of a decomposition or a polymerization product. The absorption maximum of the bloodred solution (482 mμ) shifted to a shorter wavelength than that of V_a (492 mμ). In view of the presence of the more extended conjugate system in VI_a, this fact seems to exclude the possibility of the existence of the quinocumulene (VI_a) in the blood-red solution.

The treatment of the dichloride XX with various kinds of dehalogenation reagents, such as zinc dust, mercury, molecular silver, or anhydrous stannous chloride in benzene, tetrahydrofuran or dioxane, gave unsatisfactory results.

It was found from the above-mentioned experiments that the isolation of the reaction product in substantia was difficult, but the extremely unstable nature of the reaction product of the glycol XIX seems to suggest the transient formation of the biradical VI_a.

Discussion

As has already been mentioned, the ESR spectrum of IV showed a strong signal, indicating the presence of the double doublet IV_a[5b], which may be in an equilibrium with the quinocumulene structure IV_a. This finding indicates that the resonance energy of the central benzene nuclei in IV is large enough to prevent the complete interaction of the two unpaired electrons through the conjugate π-electron system which necessarily accompanies

the transformation of benzenoid to the *p*-quinoid structure of the central nuclei. The stable triphenylmethyl structure of the radical center in IV_b may also contribute to the stabilization of IV_b.

In the case of the dechlorination of XVII, the product could be isolated in substantia and the structure of V_a assigned on the basis of analytical and ESR evidence. Although the possibility that this substance exists in a triplet state can not be excluded, the high stability of V to air in a pure state seemed to reflect the singlet state, at least at room temperature.

Recently, various kinds of stable quinocumulenes of type XXVIII bearing anthracene or pentacene nucleus in the center of the molecule have been synthesized[10,15]. VI can be regarded as a parent compound of these quinocumulenes. Therefore, it was expected that VI might

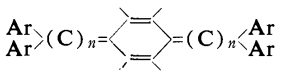

XXVIII

form a more stable quinocumulene (VI_a) than V or IV. In fact, however, the dehydroxylation of the glycol XIX gave an extremely unstable product. Because it has been well recognized that the tendency of polyacene to form a quinoid structure is more pronounced than that of benzene or naphthalene, the marked difference between XXVIII and VI seems to be attributable to the difference in the delocalization energy which accompanies the trasformation of the central aromatic system to the quinoid structure. Also, the instability of the radical seems to be related to the lack of a triphenylmethyl structure in the radical center of VI_b.

Experimental*

4, 4'-Bis(diphenylhydroxymethyl)-tolan (VII).—4, 4'-Dibromotolan was prepared according to the method of Barber[9]. The tolan (5.0 g., 0.015 mol.) in anhydrous ether (50 ml.) was mixed with *n*-butyllithium (0.04 mol.) in the same solvent (35 ml.) in an atmosphere of nitrogen. After the solution had been stirred for 15 min. at room temperature, a solution of benzophenone (6.0 g., 0.033 mol.) in anhydrous ether (50 ml.) was added drop by drop over a one-hour period, resulting in a light yellow solution. The reaction mixture was then refluxed for an hour. After standing overnight, the mixture was stirred a further 2 hr. at room temperature and 1.5 hr. under reflux. A saturated solution of ammonium chloride was added to the reaction mixture, and the organic layer was worked up according to the usual manner, affording a light yellow solid (10.0 g.). The solid was crystallized from benzene-petroleum benzine (1 : 1), yielding colorless grains; m. p., 177~179°C (8.1 g., quantitative). Further recrystallization from the same solvent gave an analytical specimen; m. p., 179~179.5°C.

Found: C, 88.57; H, 5.39. Calcd. for $C_{40}H_{30}O_2$: C, 88.53; H, 5.57%.

4, 4'-Bis(diphenylchloromethyl)-tolan (VIII).—Thionyl chloride (20 ml., 32.8 g.) was added to the suspension of the above-mentioned glycol (VII), (1.6 g., 0.003 mol.) in benzene (40 ml.). The mixture was refluxed for 2 hr., resulting in a brownish pink solution. The volatile material was removed under reduced pressure. The residue was dried over potassium hydroxide in an evacuated desiccator and then dissolved in benzene-petroleum benzine without heating. The solvent was partly removed under reduced pressure at room temperature, yielding crystals. The crystals were treated in the same way, affording pure VIII as light brown cubes; m. p., 198~203°C (1.2 g., 70%).

Found: C, 82.71; H, 4.84; Cl, 12.01. Calcd. for $C_{40}H_{28}Cl_2$: C, 82.89; H, 4.87; Cl, 12.24%.

4, 4'-Bis(9''-hydroxy-9''-fluorenyl)-tolan (X).—In an atmosphere of nitrogen, a solution of *n*-butyllithium in ether (36 ml., 0.042 mol.) was added over a 10-min. period to a solution of 4, 4'-dibromotolan (6.7 g., 0.02 mol.) in ether (60 ml.) and tetrahydrofuran (10 ml.). The blue-white suspension formed was stirred for 15 min., and then fluorenone (7.2 g., 0.04 mol.) in ether (60 ml.) was added drop by drop over a 15-minute period. After being stirred for 1.5 hr. at room temperature, the mixture was left to stand overnight, yielding a yellow brown suspension. The suspension was stirred another hour and then heated under reflux for 1.5 hr. The reaction mixture was decomposed by the addition of a saturated aqueous ammonium chloride. The organic layer was separated, and the aqueous layer was extracted with benzene (300 ml.). The insoluble material was filtered and washed with a small amount of benzene. The solid (8.0 g., m. p., 277~280°C) was recrystallized from aqueous acetone to yield X as colorless needles; m. p., 307~312°C (7.0 g., 64.7%).

Found: C, 89.04; H, 4.61. Calcd. for $C_{40}H_{26}O_2$: C, 89.19; H, 4.87%.

A chromatographic purification of the residue which had been obtained from the combined organic layer afforded a small amount of X.

4, 4'-Bis(9''-chloro-9''-fluorenyl)-tolan (XI).—The glycol (X, 0.5 g.) was added to a mixture of benzene (7 ml.) and thionyl chloride (8 ml.), and the mixture was refluxed for 6.5 hr., resulting in a brown solution. The red brown residue obtained by the evaporation of the volatile material was dried over sodium hydroxide. Recrystallization of the dried material from carbon tetrachloride-petroleum benzine yielded crude XI as brown needles; m. p., 200~226°C (0.3 g.). Further recrystallization from benzene afforded pure XI as brown plates; m. p., 224~226°C (0.2 g., 40%).

15) N. G. Loudet, W. Chodkiewicz, P. Cadiot and A. Willemart, *Compt. rend.*, 250, 366 (1960).

* All melting points are uncorrected. The nitrogen used was purified by passing the gas from a commercial steel cylinder through a Fieser solution. The ESR spectra were measured by Dr. S. Onishi in the Osaka Laboratories of the Japanese Association for Radiation Research on Polymers.

Found: C, 83.36; H, 4.15; Cl, 12.48. Calcd. for $C_{40}H_{24}Cl_2$: C, 83.46; H, 4.20; Cl, 12.32%.

***p*-Bromophenylacetylene.**—The acetylene was prepared from *p*-bromoacetophenone according to the well-known method[16].

***p*-Acetylbenzoic Acid (XIII).**—*p*-Cyanoacetophenone (XII, 4.9 g., 0.034 mol.) which was prepared from *p*-bromoacetophenone[9] was heated with 58% sulfuric acid (7.8 g.) at 150°C for an hour. The yellow crystals deposited were recrystallized from boiling water, yielding XIII as yellow long needles; m. p., 207~209°C (3.8 g., 69%); lit. value[17], m. p., 205°C.

***p*-Ethynylbenzamide (XIV).**—A mixture of the acetylbenzoic acid (XIII, 6.6 g., 0.04 mol.), phosphorus pentachloride (19.0 g., 0.09 mol.) and phosphorus oxychloride (8.0 ml.) was refluxed for 2 hr., and the oxychloride was removed under reduced pressure. The residual viscous brown oil was dissolved in ether (100 ml.) and added drop by drop into a solution of sodium amide (prepared from sodium, 6.6 g., 0.29 g. atom) in liquid ammonia (250 ml.) over a 15-min. period. The mixture was kept overnight at −70°C and was then stirred for 8.5 hr. at −33~−40°C. After evaporation of the ammonia, the reaction mixture was decomposed with a saturated aqueous ammonium chloride. The ethereal layer was separated, and the aqueous layer was extracted with ether (200 ml.×5). The combined ether solution was washed with a saturated solution of sodium chloride and dried (Na_2SO_4). Evaporation of the solvent yielded crude XIV as light yellow powder; m. p., 172~173°C (2.7 g., 46.5%). IR ν_{max}, 3440 (NH); 1662, 1630 (-$CONH_2$); 3235 (≡CH); 2250 cm^{-1} (-C≡C).

This was used without further purification for the following reaction.

Methyl *p*-Ethynylbenzoate (XV).—A mixture of the benzamide (XIV, 2.7 g., 0.017 mol.), methanol (40 ml.) and concentrated sulfuric acid (3 ml.) was refluxed for 5 hr. on an oil-bath (110°C). The reaction mixture was poured into water (100 ml.) and extracted with ether (100 ml.×3). The ethereal extracts were successively washed with saturated aqueous solutions of sodium chloride, sodium hydrogen carbonate and sodium chloride and dried (Na_2SO_4). Evaporation of the solvent yielded brown needles; m. p., 88~94°C (2.9 g., 96.6%). The crude crystals were recrystallized from methanol to give pure XVII; m. p., 93~95°C.

Found: C, 74.92; H, 5.02. Calcd. for $C_{10}H_8O_2$: C, 74.99; H, 5.03%.

1-Diphenylhydroxymethyl-4-(3',3'-diphenylhydroxy-1'-propynyl)-benzene (XVI).—*a) From p-Bromophenylacetylene.*—Into a solution of *p*-bromophenylacetylene (6.0 g., 0.03 mol.) in ether (100 ml.) in an atmosphere of nitrogen was added an ethereal solution of *n*-butyllithium (45 ml., 0.07 mol.) over a 30-min. period. The mixture was stirred another hour at room temperature and then refluxed for an hour. Benzophenone (12.0 g., 0.067 mol.) in ether (100 ml.) was added to the mixture over a 40-min. period. The reaction mixture was kept for 2 days at room temperature and then stirred for 1.5 hr. under reflux, resulting in a pale yellow solution with a white precipitate. After decomposition with aqueous ammonium chloride, the ethereal layer was separated, washed with saturated sodium chloride solution, and dried ($MgSO_4$). Evaporation of the solvent resulted in a brown oily material (17.2 g.). A benzene solution of this substance was passed through a column of alumina and eluted with ether containing 1% of methanol. The eluate was evaporated to give a light yellow liquid. The liquid was treated with benzene-petroleum benzine (1 : 1), yielding colorless needles; m. p., 80~86°C (containing benzene of crystallization), 2.8 g. The crystals were heated at 80°C for 5 hr. in vacuo, affording XVI; m. p., 131~132°C. IR ν_{max}, 3400 cm^{-1} (OH).

Found: C, 87.21; H, 5.72. Calcd. for $C_{34}H_{26}O_2$: C, 87.52; H, 5.62%.

The mother liquor obtained by filtrating XVI was distilled, yielding viscous oil; b. p., 193°C/0.008 mmHg, (6.0 g.). Treatment of this substance with *n*-butyllithium, followed by hydrolysis, afforded a viscous oil. The oil could be crystallized by the addition of a small amount of benzene-petroleum benzine. Recrystallization from the same solvent yielded 1, 1, 3-triphenylpropyn-1-ol. It showed no depression of the melting point on admixture with an authentic specimen*. Also, the infrared spectrum was found to be identical with that of the specimen. On the basis of this evidence, the structure of XVIII was assigned to the viscous oil obtained from the mother liquor.

b) From Methyl p-Ethynylbenzoate (XV).—Methyl *p*-ethynylbenzoate (XV, 1.6 g., 0.01 mol.) in ether (30 ml.) was stirred drop by drop into a solution of phenyllithium (0.033 mol. in 35 ml. of ether) under an atmosphere of nitrogen. The mixture was added for 1.5 hr. at room temperature and then refluxed for another hour. To the cooled mixture, benzophenone (1.8 g., 0.01 mol.) in ether (30 ml.) was added. After being left standing overnight, the mixture was stirred for 2 hr. and mixed with a saturated aqueous ammonium chloride. The aqueous layer was extracted with ether (80 ml.× 3) and combined with the ethereal layer. The combined ethereal solution was washed with a saturated sodium chloride solution and dried (Na_2SO_4). Evaporation of the solvent gave a brown viscous oil. This was dissolved in benzene and chromatographed on alumina. Elution with ether containing 1% of methanol, followed by recrystallization from benzene-petroleum benzine, afforded XVI (2.8 g., 61.4%), which was proved to be identical with the specimen obtained by method a) by mixed melting point determination and infrared spectroscopy.

1-Diphenylchloromethyl-4-(3'-chloro-3', 3'-diphenyl-1'-propynyl)-benzene (XVII).—A mixture of XVI (1.5 g., 0.003 mol.), benzene (15 ml.), and thionyl chloride (15 ml.) was refluxed for 2 hr., and the volatile material was removed under reduced pressure. The residue was dried over sodium hydroxide in vacuo, yielding a yellowish brown solid (XVII, 1.5 g.). XVII was also obtained by treating

16) T. L. Jacobs, "Organic Reactions", Vol. 5, 50 (1949).
17) H. Ingle, *Ber.*, 27, 2527 (1894).

* The authentic specimen was kindly supplied by Dr. G. Nakaminami of this Laboratory.

XVI with a mixture of acetyl chloride and hydrochloric acid[5b]. Further purification of XVII by recrystallization was proved to be difficult owing to its unstable nature in the presence of heat and light. The infrared spectrum of the crude XVII lacks the absorption of the hydroxyl group.

1-Benzhydryliden-4-(3', 3'-diphenylpropadienyliden)-1, 4-dihydrobenzene (V_a).—A mixture of finely powdered anhydrous stannous chloride (2.0 g.), XVII (0.4 g.), and benzene (1500 ml.) was shaken for 2 hr.; then fresh anhydrous stannous chloride (2.0 g.) was added, and the shaking was continued for a further 5 hr. The reaction mixture was filtered, and the filtrate was washed with water and then dried over anhydrous sodium sulfate for 30 min. The dried solution was passed through a column (20 cm.) of alumina (25 g.). The filtrate was concentrated under reduced pressure below 40°C, yielding a partly crystallized solid. Treatment of the solid gave a small amount of deep purple needles with a green metallic surface luster. The melting point (ca. 170°C (decomp.)) could not be determined accurately because of its deep color. A qualitative analysis of this substance revealed the contamination of a chlorine compound.

Found: C, 92.96; H, 5.71; Calcd. for $C_{34}H_{24}$: C, 94.41; H, 5.59%.

Formation of 4-(3', 3'-Diphenyl-1'-chloro-propadienyl)-phenyl-diphenylmethyl (XXV) and its Peroxide (XXVI).—A mixture of molecular silver (4.0 g.) and XVII (1.0 g.) in benzene was stirred at 60°C for 2 hr. in an atmosphere of nitrogen in a dark place, forming a dark brown solution. The molecular silver was removed by filtration, and the filtrate was passed through a column (20 cm.) of alumina (25 g.). The red-violet filtrate thus obtained was concentrated under reduced pressure in a nitrogen atmosphere, yielding a dark brown solid (0.1 g.). The solid gradually changed to a red-brown solid on being kept in an evacuated desiccator.

Found: C, 84.11; H, 4.74; Cl, 7.49. Calcd. for $C_{34}H_{24}ClO$: C, 84.36; H, 4.99; Cl, 7.33%.

After 2 days, the substance was subjected to ESR measurement without further purification.

1, 4-Bis-(3'-hydroxy-3', 3'-diphenyl-1'-propynyl)-benzene (XIX).—This substance was prepared according to the method of Ried[10] by the action of benzophenone (14.5 g.) on the dilithium derivative of *p*-diethynylbenzene (5.0 g.)[18]. Pale yellow plates; m. p., 222~226°C (11 g., 56%) (lit. values, m. p., 226°C, 56%)[10].

1, 4-Bis(3'-chloro-3', 3'-diphenyl-1'-propynyl)-benzene (XX).—Hydrogen chloride was introduced for 30 min. into a mixture of XIX (1.0 g.), ether (80 ml.), tetrahydrofuran (20 ml.) and acetyl chloride (0.5 ml.). The mixture was allowed to stand overnight in an ice-bath. The precipitate formed was filtered and washed repeatedly with cold ether, yielding XX as colorless needles (1.0 g., 91%). This substance decomposed at 130°C, forming a red solid which did not fuse at temperatures over 300°C. Also, the action of thionyl chloride (15 ml.) with a suspension of XIX (0.5 g.) in benzene (15 ml.) at 0.5°C resulted in the formation of XX in a low yield (0.1 g., 18%). Several attempts to purify XX failed, but the absence of a hydroxyl group was proved by infrared spectroscopy.

The authors wish to express their hearty thanks to Dr. Shun'ichi Onishi of the Osaka Laboratories of the Japanese Association for Radiation Research on Polymers for his measurements of the ESR spectra and for his valuable discussions. We are also grateful to Mr. Masakazu Okumiya for his microanalyses.

Department of Chemistry
Faculty of Science
Osaka University
Nakanoshima, Osaka

18) W. Ried, H. J. Schmidt and A. Urschel, *Chem. Ber.*, **91**, 2472 (1958).

Synthetic Studies of the Flavone Derivatives. II[1]. *The Synthesis of Meliternatin and Some 3,5-Dimethoxy-6,7-methylenedioxyflavones*[*1]

By Kenji FUKUI and Takashi MATSUMOTO

(Received March 15, 1963)

Meliternatin was first isolated from the bark of *Melicope ternata* by Briggs and Locker[2], together with wharangin, meliternin and ternatin, in 1949; it has also been recently isolated from the bark of *M. mantelli* by Cambie[3]. It has been shown to contain two methoxy groups and two methylenedioxy groups; up to now it has been only known naturally-occurring 3-methoxyflavone containing two methylenedioxy groups. From degradative experiments, Briggs and Locker first identified

[*1] Presented at the Ube Local Meeting of the Chemical Society of Japan, November, 1962.

1) Part I: K. Fukui and T. Matsumoto, This Bulletin, **35**, 1931 (1962).

2) L. H. Briggs and R. H. Locker, *J. Chem. Soc.*, **1949**, 2157.

3) R. C. Cambie, ibid., **1960**, 2376.

it as 3, 5-dimethoxy-7, 8 ; 3', 4'-bismethylenedioxyflavone (I)[2]. On the basis of further experiments[4], however, they proposed the revised formula of 3, 5-dimethoxy-6, 7 ; 3', 4'-bismethylenedioxyflavone (II). It would be interesting to confirm the structure of meliternatin by synthesis.

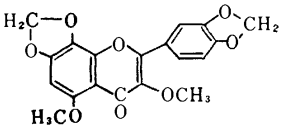

(I)

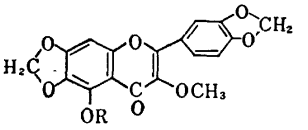

(II) R=CH_3
(VIII) R=H
(IX) R=$COCH_3$

The present report describes the synthesis of meliternatin and some related compounds. The Hoesch condensation of 3-methoxy-4, 5-methylenedioxyphenol (III)[5] and methoxyacetonitrile yielded a ketone, $C_{11}H_{12}O_6$. Two structures (IV and V) were expected for this ketone. Since Folkers et al.[6] have demonstrated that III is condensed with *o*-acetoxybenzylcyanide to given 2'-(6-hydroxy-2-methoxy-3, 4-methylenedioxyphenyl)-benzofuran (VI), it seems probable that III is substituted not at the 6-position but at the 2-position in the Hoesch condensation. Therefore, IV was formed from the reaction with methoxyacetonitrile. In order to elucidate the structure of the ketone, a flavone was prepared with piperonylic anhydride from the ketone. This product did not agree in its properties with 3, 7-dimethoxy-5, 6 ; 3', 4'-bismethylenedioxyflavone (VII) (cf. our succeeding paper). On the basis of this evidence, IV, 6-hydroxy-2, ω-dimethoxy-3, 4-methylenedioxyacetophenone is postulated as the structure for the ketone. Judging from its physical and chemical properties, IV was identical with the ketone which was obtained as the main phenolic product[2] of the action of alcoholic potassium hydroxide on meliternatin. According to Allan and Robinson's flavone synthesis[7], the condensation of IV with piperonylic anhydride in the presence of potassium piperonylate, followed by treatment with alcoholic potassium hydroxide, afforded the desired flavone II, whose identity with natural meliternatin was confirmed by mixed melting point, infrared and ultraviolet spectral comparison (Table I, Fig. 1 and Fig. 2). Synthetic meliternatin was also characterized as 5-demethyl compound VIII and its acetate IX (Table I).

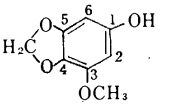

(III)

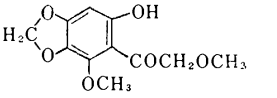

(IV)

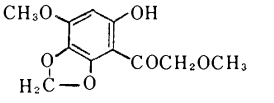

(V)

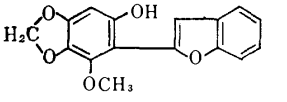

(VI)

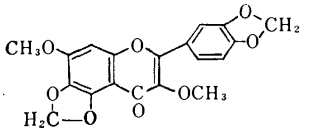

(VII)

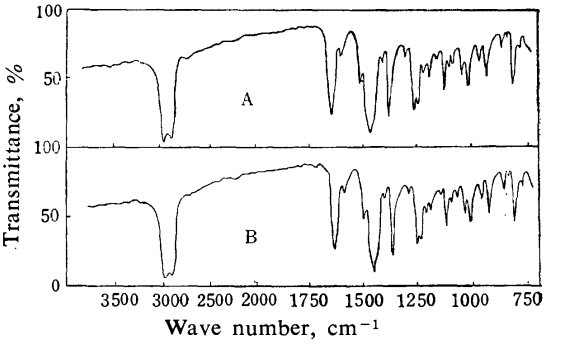

Fig. 1. IR spectra of synthetic (A) and natural meliternatin (B) in Nujol.

By a similar method, the condensation of the ketone IV with acid anhydrides (benzoic anhydride, anisic anhydride, veratric anhydride and trimethylgallic anhydride) in the presence of the potassium salt of the corresponding acids gave 3, 5-dimethoxy-6, 7-methylenedioxyflavone (X), 3, 5, 4'-trimethoxy-6, 7-methylenedioxyflavone (XI), 3, 5, 3', 4'-tetramethoxy-6, 7-methylenedioxyflavone (XII) and 3, 5, 3', 4', 5'-pentamethoxy-6, 7-methylenedioxyflavone(XIII) respectively. These flavones gave a negative ferric chloride reaction and were soluble in concentrated sulfuric acid to a yellow solution.

4) L. H. Briggs and R. H. Locker, ibid., **1951**, 3131.
5) A. F. Wagner, E. Walton, A. N. Wilson, J. O. Rodin and F. W. Holly, *J. Am. Chem. Soc.*, **81**, 4983 (1959).
6) A. F. Wagner, A. N. Wilson and K. Folkers, ibid., **81**, 5441 (1959).
7) J. Allan and R. Robinson, *J. Chem. Soc.*, **1924**, 2192.

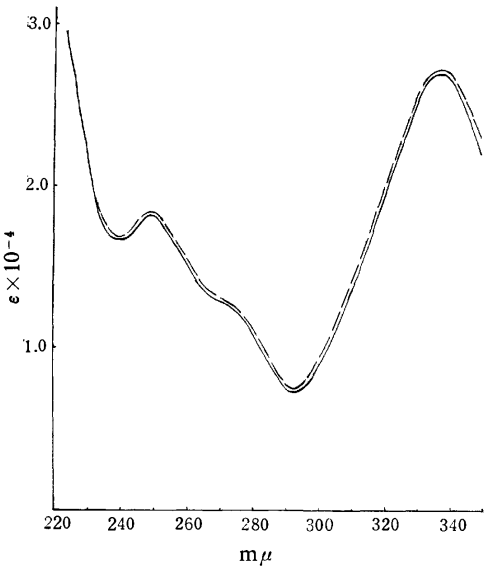

Fig. 2. UV spectra of natural (——) and synthetic meliternatin (----) in ethanol.

TABLE I. THE MELTING POINTS OF MELITERNATIN AND ITS DERIVATIVES (°C)

	Synthetic compound	Natural compound[2,4]*
Meliternatin (II)	196～197	198～198.5
5-Demethylmeliternatin (VIII)	256～257	258～258.5
Acetate (IX) of VIII	205～206	208.5～210

* Melting points are corrected.

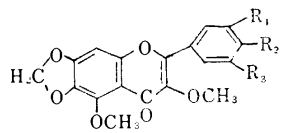

(X) $R_1=R_2=R_3=H$
(XI) $R_1=R_3=H$, $R_2=OCH_3$
(XII) $R_1=R_2=OCH_3$, $R_3=H$
(XIII) $R_1=R_2=R_3=OCH_3$

Experimental[*2]

6-Hydroxy-2, ω-dimethoxy-3, 4-methylenedioxyacetophenone (IV).—A mixture of 3-methoxy-4, 5-methylenedioxyphenol (III) (790 mg.)[5], methoxyacetonitrile (0.4 g.) and anhydrous zinc chloride (0.7 g.) in anhydrous ether (40 ml.) was saturated with dried hydrogen chloride at 0°C and allowed to stand overnight. The ethereal solution was decanted from the oily layer of ketimine hydrochloride, which had separated. The oily layer was washed twice with dry ether and heated on a steam bath with water (40 ml.) for 30 min. After cooling and standing, the product was collected and recrystallized from ethanol giving IV (m. p., 140～142°C) (reported m. p., 142～144°C[2]) (golden yellow prisms), which showed a dark green ferric chloride reaction in ethanol; yield, 460 mg.

IR 1640～1606 (broad) (C=O), 1046 (=C-O-C), 930 (O-CH_2-O) cm^{-1}.

Found: C, 55.15; H, 5.13. Calcd. for $C_{11}H_{12}O_6$: C, 55.00; H, 5.04%.

Meliternatin (3,5-Dimethoxy-6,7;3',4'-bismethylenedioxyflavone) (II).—Ketone IV (240 mg.), piperonylic anhydride (780 mg.) and potassium piperonylate (300 mg.) were ground together and heated at 170～180°C under reduced pressure for 3.5 hr. The reaction mixture was then ground and boiled with 10% aqueous alcoholic (1 : 9) potassium hydroxide (20 ml.) for 7 min. After the removal of the solvent in vacuo, water (10 ml.) was added to the pasty mass. The precipitated solid was collected, washed with water, and recrystallized from ethanol, giving II (m. p., 196～197°C) (colorless needles), which gave a negative ferric chloride reaction in ethanol; yield, 120 mg. The melting point was undepressed on admixture with natural meliternatin kindly supplied by Dr. Cebalo.

IR 1640 (C=O), 1033 (=C-O-C), 921 (O-CH_2-O) cm^{-1}. UV λ_{max}^{EtOH} mμ (ε×10^{-4}); 248 (1.86), 270[*3] (1.31), 337 (2.73).

Found: C, 61.98; H, 3.90. Calcd. for $C_{19}H_{14}O_8$: C, 61.62; H, 3.81%.

According to the method of Briggs and Locker[4], II was demethylated with aluminum chloride to the 5-demethyl derivative VIII (m. p., 256～257°C) (reported m. p., 258～258.5°C[3]) (slender yellow needles). IR 1678 (C=O), 1026 (=C-O-C), 929 919 (O-CH_2-O) cm^{-1}.

Found: C, 60.42; H, 3.50. Calcd. for $C_{18}H_{12}O_8$: C, 60.68; H, 3.40%.

With acetic anhydride and pyridine, VIII gave the acetate IX (m. p., 205～206°C) (reported m. p., 208.5～210°C[4]) (pale yellow needles).

Found: C, 60.33; H, 3.76. Calcd. for $C_{20}H_{14}O_9$: C, 60.30; H, 3.56%.

3, 5-Dimethoxy-6, 7-methylenedioxyflavone (X).—From ketone IV (360 mg.), benzoic anhydride (700 mg.) and potassium benzoate (400 mg.), synthesis was carried out by a method similar to that used for II. Recrystallization from ethanol gave X (m. p. 192.5～193.5°C) (colorless needles); yield, 180 mg. IR 1624 (C=O), 1013 (=C-O-C), 920 (O-CH_2O) cm^{-1}. UV λ_{max}^{EtOH} mμ (ε×10^{-4}); 251[*3] (1.63), 268.5 (1.99), 314 (1.98).

Found: C, 66.06; H, 4.36. Calcd. for $C_{18}H_{14}O_6$: C, 66.25; H, 4.32%.

3, 5, 4' - Trimethoxy - 6, 7 - methylenedioxyflavone (XI).—Ketone IV (360 mg.), anisic anhydride (860 mg.) and potassium anisate (430 mg.) were treated with the same procedure as has been described for II. Recrystallization from ethanol gave XI (m. p., 184～185°C) (colorless needles); yield, 150 mg. IR 1638 (C=O), 1034 (=C-O-C), 925 (O-CH_2-O) cm^{-1}. UV λ_{max}^{EtOH} mμ (ε×10^{-4}); 272 (1.70), 328 (2.85).

Found: C, 64.04; H, 4.57. Calcd. for $C_{19}H_{16}O_7$: C, 64.04; H, 4.53%.

[*2] All melting points are uncocrrected; the infrared spectra were measured in Nujol.

[*3] Inflection point.

3, 5, 3′, 4′ - Tetramethoxy - 6, 7 - methylenedioxyflavone (XII). — Ketone IV (360 mg.), veratric anhydride (1.00 g.) and potassium veratrate (500 mg.) were treated with the above method. Recrystallization from ethanol gave XII (m. p.. 172~173°C (dried at 100°C)) (pale yellow needles); yield, 110 mg. IR 1621 (C=O), 1016 (=C-O-C), 930 cm^{-1} ($O-CH_2-O$). UV λ_{max}^{EtOH} $m\mu$ ($\varepsilon \times 10^{-4}$); 247 (1.87), 269*[3] (1.48), 335 (2.69).

Found: C, 62.03; H, 4.69. Calcd. for $C_{20}H_{18}O_8$: C, 62.17; H, 4.70%.

3, 5, 3′, 4′, 5′-Pentamethoxy - 6, 7-methylenedioxyflavone (XIII).—Ketone IV (360 mg.) trimethylgallic anhydride (1.20 g.) and potassium trimethylgallate (600 mg.) were treated with the above method. Recrystallization from acetone gave XIII (m. p., 226~227°C) (colorless needles); yield, 150 mg. IR 1635 (C=O), 1018 (=C-O-C), 925 ($O-CH_2-O$) cm^{-1}. UV λ_{max}^{EtOH} $m\mu$ ($\varepsilon \times 10^{-4}$); 244 (1.57), 275 (1.37).

Found: C, 60.42; H, 4.95. Calcd. for $C_{21}H_{20}O_9$: C, 60.57; H, 4.84%.

The authors are grateful to Dr. T. P. Cebalo, the University of Auckland, for his gift of a specimen of natural meliternatin. Grateful acknowledgement is also made to the members of the Microanalytical Center of Kyoto University, and to Mr. Ichiro Nitta for his technical cooperation. The cost of this research was partly defrayed by the Scientific Research Expenditure Found of the Ministry of Education, to which the author's thanks are due.

Department of Chemistry
Faculty of Science
Hiroshima University
Higashi-Sendamachi, Hiroshima

The Spectrophotometric Determination of Aluminum with Xylenol Orange[1]

By Makoto Otomo

(Received November 5, 1962)

Various workers have proposed a variety of reagents for aluminum determination, including aluminon[2], hematoxylin[3], pontachrome blue black R[4], oxine[5], eriochrome cyanine R[6,7], quinalizarin[8], alizarin S[9], arsenoazo[10], cupferron[11], stilbazo[12], quercetin[13] and morin[14]. Of these reagents, the most promising one appears to be eriochrome cyanine R[15], which is sensitive for 0.004 μg. of aluminum per cm^2 for log $I_0/I=0.001$.

The present paper describes a new spectrophotometric method for the determination of aluminum, based on the highly sensitive color reaction of xylenol orange with aluminum in an acetate buffer solution. The development of the method includes a study of the effects of pH value, reagent concentration and foreign ions. The composition of the complex is also discussed.

It is found that, for aluminum, xylenol orange is a more sensible reagent than eriochrome cyanine R.

Experimental

Reagents. — An aluminum stock solution was prepared by dissolving aluminum nitrate crystals of analytical grade in dilute nitric acid; it was then standardized against a standard EDTA solution[16]. It was diluted with water to desired concentrations.

Acetic acid and sodium acetate solutions were used for all pH adjustments.

Apparatus. — Spectrophotometric measurements

1) Presented at the Tohoku Branch Meeting of the Chemical Society of Japan, Yonezawa, October, 1961.
2) F. D. Snell and C. T. Snell, "Colorimetric Methods of Analysis", D. Van Nostrand Company, Inc., New York (1949), p. 248.
3) H. W. Knudson, V. W. Meloche and C. Juday, *Ind. Eng. Chem., Anal. Ed.*, **12**, 715 (1940).
4) A. Weissler and C. E. White, ibid., **18**, 530 (1946).
5) C. H. R. Gentry and L. G. Sherrington, *Analyst*, **71**, 432 (1946).
6) F. Alten, W. Weiland and E. Knippenberg, *Z. anal. Chem.*, **96**, 91 (1934).
7) U. T. Hill, *Anal. Chem.*, **20**, 1117 (1948); **31**, 429 (1959).
8) I. M. Kolthoff, *Chem. Week-blad*, **24**, 447 (1927).
9) J. H. Yoe and W. L. Hill, *J. Am. Chem. Soc.*, **50**, 748 (1928).
10) V. I. Kuznetsov and R. B. Golubstova, *Zavodskaya Lab.*, **72**, 406 (1956).
11) L. de Brouckere and E. Belche, *Bull. soc. chim. Belg.*, **36**, 288 (1927).
12) M. Jean, *Anal. Chim. Acta*, **10**, 526 (1954).
13) A. L. Daxydov and U. S. Devekki, *Zavodskaya Lab.*, **57**, 134 (1941).
14) C. E. White and C. S. Lowe, *Ind. End. Chem., Anal. Ed.*, **12**, 229 (1940).
15) D. Blair, K. Power, D. L. Griffiths and J. H. Wood, *Talanta*, **7**, 80 (1960).
16) K. Ueno, "Chelatometric Titration", (in Japanese), Nankodo, Tokyo (1960), p. 207.

were made with a Hitachi Model EPV-2 spectrophotometer, using 1 cm. glass transmission cells.

All experiments were carried out at 25±0.5°C.

Procedure. — To an aliquot portion of the aluminum nitrate solution in a 50 ml. Erlenmeyer flask, 10 ml. of a pH 3.4 buffer solution and 2 ml. of a 1×10^{-3} M xylenol orange solution were added. The solution was heated on a boiling water bath for a few minutes, cooled with water to room temperature, and transferred to a 25 ml. volumetric flask. The volume of the content was then made up to the mark with water. After the solution had been kept for about 15 min. in a 25°C thermostat, the absorbance of the solution was measured at 536 mμ using a reagent blank.

Results and Discussion

Absorption Spectra. — Figure 1 shows the absorption spectra of solutions containing 6.2 μg. of aluminum with xylenol orange added in various amounts up to 6×10^{-5} M. These spectra show an isosbestic point at 536 mμ. The absorption maximum at about 555 mμ shifted slightly towards a shorter wavelength,

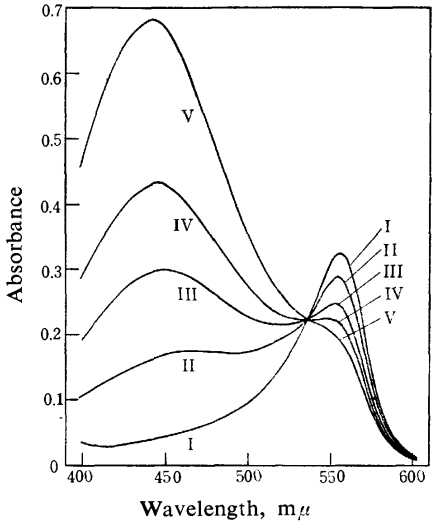

Fig. 1. Absorption spectra of aluminum-xylenol orange at pH 3.4.
Al: 6.2 μg.
XO concn.: I, 1×10^{-5} M; II, 2×10^{-5} M; III, 3×10^{-5} M; IV, 4×10^{-5} M; V, 6×10^{-5} M

and the extinction coefficient at this wavelength decreased, with increasing amounts of xylenol orange. From these observations it is expected that, by adding an xylenol orange solution in excess, a new complex other than one with an absorption maximum at about 555 mμ may be formed. The optimum pH range for the color development was found to be 3.4±0.1.

Effect of Heating. — As in the case of the titration of aluminum with EDTA[17], the color reaction of xylenol orange with aluminum was very slow at room temperature. About 4 hr. were required for complete color development. When a solution containing xylenol orange and aluminum was heated on a boiling water bath, however, the reaction was greatly accelerated, and the maximum color development was obtained within only a few minutes.

Stability of Color.—The absorbance of the solution of the aluminum-xylenol orange complex at 555 mμ decreased gradually with the time of standing. About 10% of its intensity was diminished within the first 2 hr., and about 2% within an additional 2 hr. However, the absorbance at the isosbestic point of 536 mμ remained constant for several hr.

The Effect of Reagent Concentration. — In order to study the effect of the concentration of xylenol orange, a series of absorbances was measured under various concentrations of xylenol orange, using water and reagent blanks of the same concentration as points of reference. At 555 mμ, as is shown in Fig. 2, the maximum absorbance is obtained with a molar ratio of the reagent to aluminum of 1 : 1. Above this ratio, the additional reagent decreases the absorbance greatly, showing that a complex other than a 1 : 1 complex may be formed in this region. However, the absorbance at the isosbestic point of 536 mμ is not affected by the amounts of xylenol orange. In the actual aluminum determination, therefore, 2 ml. of a 1×10^{-3} M reagent solution were used, and the absorbance measurements were made at 536 mμ.

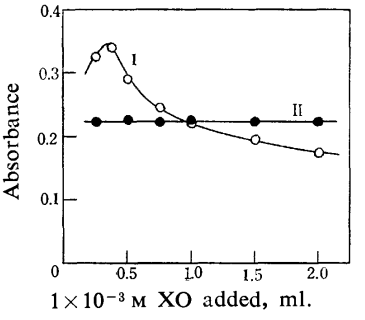

Fig. 2. Effect of reagent concentration.
Al: 6.2 μg. I: 555 mμ II: 536 mμ

Calibration.—Measurements of the absorbance were made with a number of colored solutions containing varying amounts of aluminum. Figure 3 shows that Beer's law is obeyed over the range 5 to 25 μg. of aluminum. The sensitivity is 0.001 μg. of aluminum per cm² for $\log I_0/I=0.001$. The molar extinction

17) K. Ueno, ibid., p. 205.

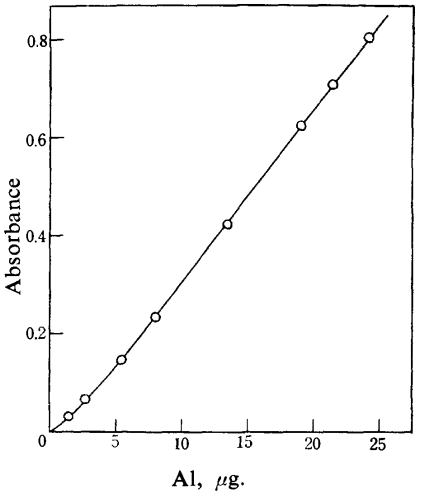

Fig. 3. Calibration curve at 536 mμ.

coefficient is 21100. Of the reagents proposed for aluminum determination, xylenol orange seems to be the most sentitve.

The Effect of Anions.—The effect of 15 cations was studied, along with that of the corresponding sodium salts. Chloride and nitrate ions did not interfere. Large amounts of sulfate, phosphate, tartrate and citrate reduced the absorbance considerably. Such anions as fluoride, nitrilotriacetic acid (NTA) and EDTA could form more stable complexes with aluminum than xylenol orange, giving very low results.

The Effect of Cations.—In order to test the effect of diverse cations upon the aluminum determination, absorbance measurements were made for the solutions containing 13.0 μg. of aluminum and 0.5 μmol. of several cations. The results are presented in Table I. Some of cations tested produce a red color, giving too high results. This is the only weak point in applying the present method to aluminum determination. However, the interferences from some cations such as chromium and nickel can be tolerably eliminated by shortenning the time of heating for color development and prolonging the time of standing.

The Composition of the Complex.—As has been suggested above, two complexes which differ in composition are probably in equilibrium with each other. From Fig. 2, one of them seems to be a 1 : 1 complex.

In order to observe the spectral changes on varying pH values, absorption curves for the aluminum complex were prepared at various pH values, using the reagent blanks of the same concentration and pH value. The results are shown in Fig. 4. The absorption maximum at 555 mμ arising at pH 2 to 2.5 is shifted towards a shorter wavelength with an increase

Table I. Effect of cations on aluminum determination

Aluminum taken, 13.0 μg.
Cation added, 0.5 μmol.

Cation	Al found, μg.	Deviation, μg.
Barium(II)	12.7	−0.3
Bismuth(III)	21.7	+8.7
Calcium(II)	12.6	−0.4
Cadmium(II)	12.8	−0.2
Cerium(III)	14.1	+1.1
Cobalt(II)	13.5	+0.5
Chromium(III)	18.2	+5.2
Copper(II)	13.2	+0.2
Iron(III)	31	+18
Mercury(II)	13.2	+0.2
Lanthanum(III)	14.0	+1.0
Magnesium(II)	12.8	−0.2
Manganese(II)	13.1	+0.1
Neodymium(III)	15.7	+2.7
Nickel(II)	16.0	+3.0
Lead(II)	12.8	−0.2
Palladium(II)	13.7	+0.7
Tin(II)	14.9	+1.9
Thorium(IV)	33	+20
Titanium(IV)	20.7	+7.7
Thallium(III)	13.3	+0.3
Uranium(VI)	12.8	−0.2
Vanadium(IV)	21.7	+8.7
Yttrium(III)	20.6	+7.6
Zinc(II)	13.9	+0.9
Zirconium(IV)	20.5	+7.5

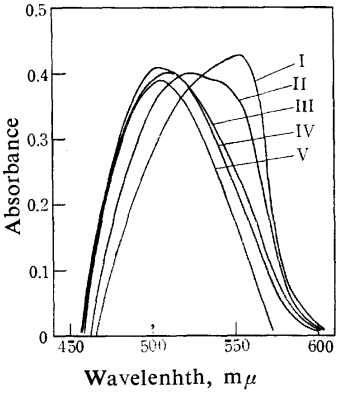

Fig. 4. Absorption spectra at various pH values.
Al: 13 μg. I, pH 2.0~2.5; II, pH 3.0; III, pH 4.0; IV, pH 4.5; V, pH 5.5

in the pH value; at pHs 3.0, 4.0 and 4.5 to 5.5, the maxima are found at about 520, 510 and 505 mμ respectively. These shifts in absorption maximum mean that probably two species of absorbing entity are involved; the one is a complex having an absorption maximum at about 555 mμ, which is formed at pH

below 3, while the other is one having a maximum at about 505 mμ, which is formed at pH above 4.5.

Figures 5 and 6 indicate the absorption spectra at pHs 2.0 and 5.0 respectively. In both cases, the spectra were prepared with solutions containing 0.5, 1 and 2 parts of xylenol orange to one part of aluminum, using

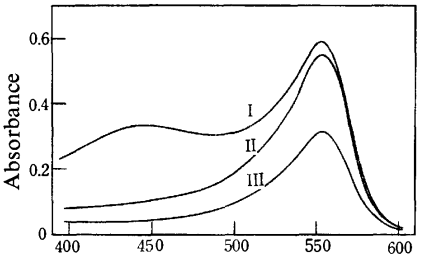

Fig. 5. Absorption spectra at pH 2.0.
I: XO : Al=2 : 1
II: XO : Al=1 : 1
III: XO : Al=1 : 2

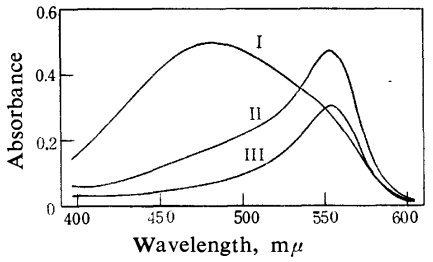

Fig. 6. Absorption spectra at pH 5.0.
I: XO : Al=2 : 1
II: XO : Al=1 : 1
III: XO : Al=1 : 2

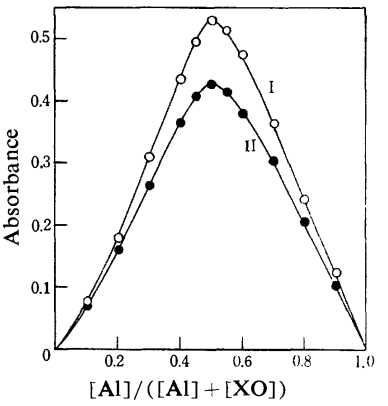

Fig. 7. Method of continuous variations at pH 2.0.
[Al]+[XO]=4×10⁻⁵ M
I: 545 mμ, II: 535 mμ

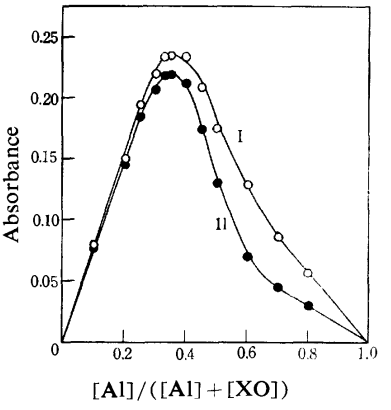

Fig. 8. Method of continuous variations at pH 5.
[Al]+[XO]=4×10⁻⁵ M
I: 505 mμ, II: 495 mμ

water as a reference. No change in the position of the absorption maximum is observed, when 1 : 2 and 1 : 1 are the molar ratios of xylenol orange to aluminum. Almost the same position of the absorption maximum is obtained at pH 2.0, even if the ratio is changed to 2 : 1. At pH 5.0, however, as is shown in Fig. 6, the absorption maximum at 555 mμ fades away to give a new maximum at a shorter wavelength when the ratio is changed to 2 : 1. The appearance of this new band means that, in a higher pH region, a new complex is also formed by adding xylenol orange in a slight excess.

Figures 7 and 8 show plots of the results obtained by applying the method of continuous variations. These results indicate that only a 1 : 1 complex is formed at pH 2.0 and a 1 : 2 complex at pH 5.0. Although the data are not, because of the large corrections for the absorption of xylenol orange, precise enough to permit a further interpretation of the plots in Fig. 8, it is possible to consider that a small amount of 1 : 1 complex is also formed, even at pH 5.0.

From Figs. 5 to 8, it may be concluded that the complex formed at pH less than 3 has a different composition from one formed in a higher pH region. Namely, one of them has 1 : 1 as the ratio of the reagent to aluminum, and the other is a mixture of 1 : 1 and 1 : 2 complexes. It seems that formation of the 1 : 1 complex gradually diminishes with increasing pH value, whereas the 2 : 1 complex increases with pH. Similar relations were also observed for gallium- and thallium-xylenol orange complexes[18].

18) M. otomo, unpublished. (Presented at the 15th Annual Meeting of the Chemical Society of Japan, Kyoto, April, 1962.)

Summary

Aluminum reacts with xylenol orange in a slightly acidic solution to form two red complexes which are in equilibrium with each other. At pH 3.4±0.1, Beer's law is obeyed up to an aluminum concentration of 1.0 p.p.m. in 1 cm. absorption cells. The absorbance was measured at the isosbestic point of 536 mμ. The molar extinction coefficient was found to be 21100. This method seems to be the most favorable one for aluminum determination if the aluminum is first separated from any interfering ions. The composition of the complexes has also been discussed.

The author wishes to express his hearty thanks to Professor Kôichi Tonosaki for his kind guidance, to Mr. Yasuo Watanabe for his assistance, and to Dr. Kengo Uchida of the Faculty of Science, Tohoku University, for his helpful discussion.

Department of Chemistry
Faculty of Literature and Science
Hirosaki University
Bunkyo-chô, Hirosaki

The Surface Activities of Bivalent Metal Alkyl Sulfates. II. The Solubilization of Some Hydrocarbons in Aqueous Solutions of Bivalent Metal Alkyl Sulfates

By Iwao SATAKE and Ryohei MATUURA

(Received February 25, 1963)

In a previous paper[1], we studied some basic surface chemical properties of bivalent metal alkyl sulfate detergents in aqueous solutions. It was found that the critical micelle concentrations (CMC) of bivalent metal alkyl sulfates are nearly independent of the kind of bivalent metals and considerably smaller than that of corresponding monovalent metal alkyl sulfates; light-scattering experiments indicated that the micellar aggregation number of various bivalent metal dodecyl sulfates lies in the comparatively narrow range from 100 to 120, about 2 to 3 times higher than that of sodium dodecyl sulfate (SDS) reported by some authors[2-4]. In this connection it seemed interesting to study the solubilizing power of the bivalent metal alkyl sulfates, since the phenomenon of solubilization is generally considered to have much to do with the micelle formation in the detergent solution. The solubilization of substances by various detergents has widely been studied by a number of authors, and the general features of the phenomena have been summarized, for example, in the critical reviews of Klevens[5] and Hutchinson[6]. However, no data have been published on the solubilization by the solutions of ionic detergents containing bivalent metals. The purpose of the present paper is to determine the solubilizing powers of some bivalent metal alkyl sulfates towards some typical hydrocarbons, and to discuss the differences, if any, among them.

Experimental

Materials.—The detergents used in the present experiment are copper(II), cobalt(II), magnesium-(II) and nickel(II) dodecyl sulfates, and copper(II) tetradecyl sulfate. The preparation and the results of elementary analysis have previously been reported[1]. The values of CMC are 1.2×10^{-3} mol./l. at 30°C for all the bivalent metal dodecyl sulfates used and 2.5×10^{-4} mol./l. at 47°C for copper tetradecyl sulfate. For the sake of comparison, the solubilizing power of sodium dodecyl sulfate (CMC, 7.2×10^{-3} mol./l.) was also measured. Benzene, toluene, *m*-xylene and *n*-hexane were used as solubilizates. They were purified by distillation.

Method.—The maximum amounts of hydrocarbons solubilized at any given temperature and the detergent concentration were determined optically as follows: a series of vessels, each containing

1) I. Satake, I. Iwamatu, S. Hosokawa and R. Matuura, This Bulletin, **36**, 204 (1963).
2) L. M. Kushner and W. D. Hubbard, *J. Colloid Sci.*, **10**, 429 (1955).
3) H. V. Tartar and A. L. M. Lelong, *J. Phys. Chem.*, **59**, 1185 (1955).
4) H. V. Tartar, *J. Colloid Sci.*, **14**, 115 (1959).
5) H. B. Klevens, *Chem. Revs.*, **47**, 1 (1950).
6) M. E. L. McBain and E. Hutchinson, "Solubilization", Academic Press, New York (1955).

10 ml. of a detergent solution of a fixed concentration with an increasing amount of the hydrocarbon added, is shaken at a constant temperature for several hours. It took about six hours for the solubilization to reach an equilibrium. Then the turbidities of the solutions were measured using a Hitachi Photoelectric Photometer EPO-B at 430 mμ for copper and magnesium salts, at 610 mμ for cobalt salt, and at 500 mμ for nickel salt. The turbidity of the solution rose sharply when a definite amount of the hydrocarbon was added. Figure 1 shows the typical turbidity curve of

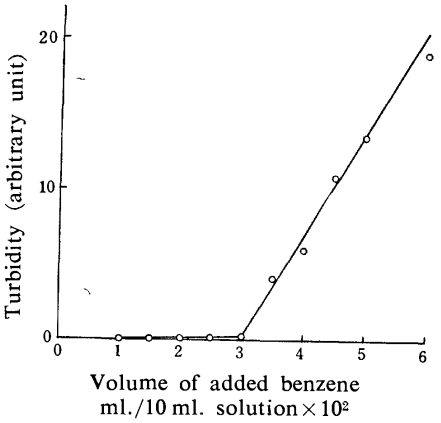

Fig. 1. Typical turbidity curve for benzene in 3×10^{-3} mol./l. copper dodecyl sulfate solution at 30°C.

benzene in 3×10^{-3} ml./l. copper dodecyl sulfate at 30°C. The apparent amount of hydrocarbon solubilized can be determined by the interpolation of the two linear portions of the turbidity curve. Then the net amount of hydrocarbon solubilized is obtained by subtracting the solubility of hydrocarbon in pure water from the apparent amount of solubilization.

The measurements were conducted at 30°C or above for bivalent metal dodecyl sulfates and at 40°C for copper tetradecyl sulfate in order to make experiments above the Krafft point of each detergent[1,7].

Results and Discussion

In Figs. 2 and 3, the amount of benzene solubilized in grams per liter of solution is plotted against the detergent concentration at 30 and 40°C respectively. For the sake of comparison, the amount of benzene solubilized by the SDS solution is also shown. The amount of benzene solubilized by bivalent metal dodecyl sulfates is found to be much larger than that by SDS, and only small differences in solubilizing power can be observed among the different bivalent salts. As has previously been reported[1], the nature of bivalent metal

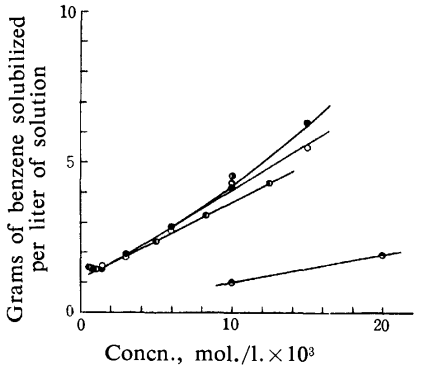

Fig. 2. Solubilization of benzene in aqueous solutions of bivalent metal dodecyl sulfates at 30°C.
○ ; Copper ● ; Cobalt ◐ ; Magnesium
◑ ; Nickel ◓ ; Sodium

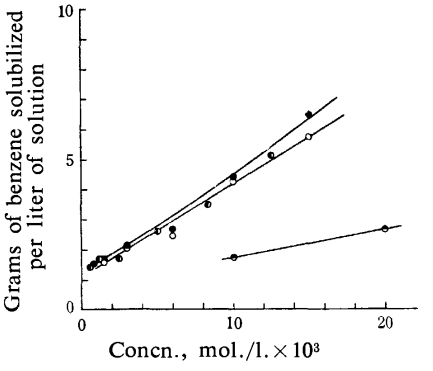

Fig. 3. Solubilization of benzene in aqueous solutions of bivalent metal dodecyl sulfates at 40°C.
○ ; Copper ● ; Cobalt ◐ ; Magnesium
◓ ; Sodium

has no detectable effect on CMC. Thus, all the bivalent salts used had the identical CMC value of 1.2×10^{-3} mol./l., which is quite small compared with the value of 8×10^{-3} mol./l. for SDS. In addition, the micellar aggregation numbers of bivalent salts determined by a light-scattering experiment[1] are 97 for copper, 114 for cobalt, 118 for magnesium and 106 for nickel, aggregation numbers which are 2 to 3 times those for SDS[2-4]. The marked increase in the solubilizing power of bivalent metal dodecyl sulfates may reasonably be explained in terms of the increased micellar aggregation numbers.

A nearly linear relation is observed between the amount of benzene solubilized and the detergent concentration. Mankowich[8] has pointed out that there are linear relations between log of solubilized amount and log of concentration for dye solubilization by various detergents,

7) S. Miyamoto, This Bulletin, 33, 371 (1960).

8) A. M. Mankowich, *J. Colloid Sci.*, 14, 131 (1959).

but he has given no theoretical considerations. In a narrow concentration range as in the present experiment, the micellar aggregation number and the micellar size may be assumed to be independent of the detergent concentration, as is shown by the light-scattering experiment[1]. If this is true, a linear relation between the amount of benzene solubilized and the detergent concentration is most probable. The slope of these lines indicates the amount of benzene solubilized per mole of micelle-forming detergent molecules. The available volume, v, for the solubilization in a micelle of a solubilized state can be evaluated from the micellar aggregation number, n, and the slope of these lines, provided that the partial molar volume of the solubilizate is assumed to be nearly identical with the molar volume of its pure state. The value of v is given by nmV/ZN, in which V is the molar volume of benzene; m, the number of moles of benzene solubilized per mole of micelle-forming detergent molecules; Z, the valency of gegen ions, and N, the Avogadro number. The values of v thus calculated are about $(3\sim4)\times10^4$ Å^3 for bivalent metal dodecyl sulfates and about $(7\sim9)\times10^3$ Å^3 for SDS, when we use the values of m taken from Figs. 2 and 3. In the calculation of the v for the SDS micelle, we take the micellar aggregation number of 40. Then the available volume for solubilization in a micelle of bivalent metal dodecyl sulfates is about four times that of the SDS micelle.

Now, we assume the spherical micellar models for both SDS and bivalent metal dodecyl sulfates; further, the area, s, which is occupied at the micellar surface by a polar head of a micelle-forming detergent molecule is assmed to be nearly independent of the micellar aggregation number and the nature of gegen ion. Therefore, the geometrical volume of a spherical micelle is given by $(ns)^{3/2}/6\pi^{1/2}$. If, therefore, the micellar aggregation number, n, is increased, the volume of the spherical micelle will be increased being proportional to $n^{3/2}$. Thus, the ratio of the available volume for solubilization in a micelle may be expected to be proportional to $(n_1/n_2)^{3/2}$, because the available volume for solubilization would be proportional to the total micellar volume. Here n_1 and n_2 are the micellar aggregation numbers of SDS and of bivalent salt respectively. In the present case, the ratio of the micellar aggregation number is taken to be about 2.5 to 3.0, from which the ratio of the micellar volume may be estimated to be 4 to 5. Thus, the experimental results obtained above may approximately be explained by the simple spherical micellar model of the detergent.

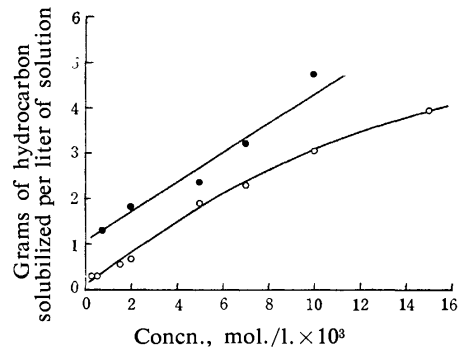

Fig. 4. Solubilization of toluene and n-hexane in aqueous solution of coopper dodecyl sulfate at 40°C.
○; Toluene ●; n-Hexane

The increase in the molar volume of the solubilizate has the normal effect of decreasing the solubilization. Figure 4 shows the amounts of toluene and n-hexane solubilized by copper dodecyl sulfate at 40°C. Table I gives the effect of the size of the solubilizate on the solubilization by metal dodecyl sulfates at 30°C. The effect of the molar volume of the solubilizates on the extent of solubilization has been investigated by several authors[5,9,10]. Especially, Harkins et al.[9] pointed out, on the basis of their solubilization experiments on a number of hydrocarbons using potassium laurate and myristate, that the amount of hydrocabon solubilized is inversely proportional to the molar volume of the solubilizate so far as the same homologous series is concerned. In the present experiment, however, one can find no such simple relationships between the molar volume and the amount of hydrocarbon

TABLE I. THE EFFECT OF THE SIZE OF THE SOLUBILIZATE ON THE SOLUBILIZATION OF HYDROCARBONS BY VARIOUS METAL DODECYL SULFATES AT 30°C

Detergent	Concn. mol./l.	Grams of hydrocarbon solubilized per litre of solution		
		Benzene	Toluene	*m*-Xylene
$Cu(DS^*)_2$	1×10^{-2}	4.31	2.94	2.30
$Co(DS)_2$	1×10^{-2}	4.15	3.13	2.82
$Ni(DS)_2$	1×10^{-2}	4.55	2.95	2.22
$Mg(DS)_2$	8.3×10^{-3}	3.22	2.07	2.22**
NaDS	2×10^{-2}	1.93	1.46	

* DS; Abbreviation of the dodecyl sulfate radical.
** By 10^{-2} mol./l. solution

9) R. S. Stearns, H. Oppenheimer, E. Simon and W. D. Harkins, *J. Chem. Phys.*, 15, 496 (1947).
10) J. W. McBain and P. H. Richards, *Ind. Eng. Chem.*, 38, 642 (1946).

TABLE II. THE EFFECT OF TEMPERATURE ON THE SOLUBILIZATION OF HYDROCARBONS IN GRAMS PER LITER OF SOLUTION OF BLVALENT METAL DODECYL SULFATES

Solubilizate	Detergent	Concn., mol./l.	Temp., °C			
			30	40	45	50
Benzene	$Cu(DS)_2$	1.5×10^{-2}	5.48	5.72	5.92	6.63
	$Mg(DS)_2$	1.25×10^{-2}	4.34	5.10	4.78	4.87
Toluene	$Cu(DS)_2$	1.0×10^{-2}	2.94	2.80		2.77
	$Co(DS)_2$	1.0×10^{-2}	3.13	3.16		2.78

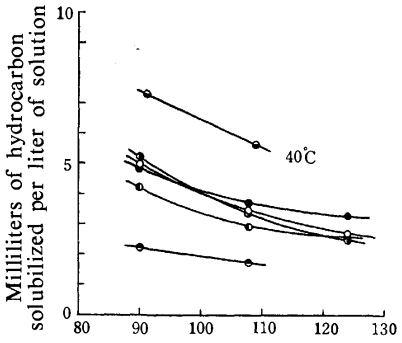

Fig. 5. Relation between the molar volume of solubilizate and the amount of hydrocarbon solubilized by 10^{-2} mol./l. metal alkyl sulfates at 30°C.
○; $Cu(DS)_2$ ●; $Co(DS)_2$ ◐; $Mg(DS)_2$ ◑; $Ni(DS)_2$ ◒; $Cu(TS)_2$ ◓; NaDS(2×10^{-2} mol/l.).

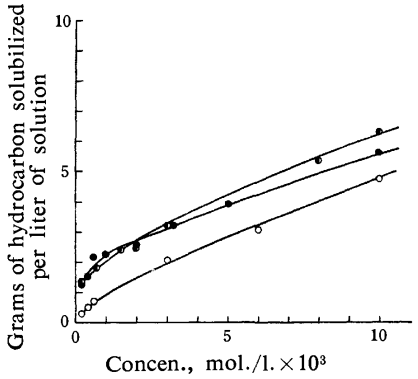

Fig. 6. Solubilization of hydrocarbons in aqueous solution of copper tetradecyl sulfate at 40°C.
◐; Benzene ○; Toluene ●; *n*-Hexane

solubilized, as is shown in Fig. 5. It can only be said that the extent of solubilization decreases as the molar volume of the solubilizate increases; no unique and quantitative relation has been found between them.

Table II shows the effect of temperature on the solubilization of benzene and toluene by bivalent metal dodecyl sulfates. The temperature change has no appreciable effect on the extent of the solubilization of benzene or toluene, as may be seen from Table II, suggesting that the heat of the solubilization of benzene or toluene in these detergent micelles is negligibly small. This is not unreasonable if the micellar interior is assumed to be of a liquid hydrocarbon-like structure.

In Fig. 6 the solubilization of benzene, toluene and *n*-hexane by copper tetradecyl sulfate is plotted against the concentration at 40°C. The considerable increase in the solubilizing power of copper teradecyl sulfate is to be noted. At the same detergent concentration, say at 10^{-2} mol./l., the ratio of the amount of hydrocarbons solubilized by copper tetradecyl sulfate to that by copper dodecyl sulfate is found to be 1.5 for benzene, 1.6 for toluene and 1.4 for *n*-hexane. The effect of chain length on the solubilizing power of the detergent has already been studiend by several authors. Harkins et al[9], for example, have shown in their study of the solubilization of benzene and *n*-hexane that the solubilizing power of potassium myristate is about twice that of potassium laurate. The same order of increase in solubilizing power was reported by Klevens[5] for the solubilization of ethylbenzene by the same detergents as above. If the above-mentioned spherical micellar model can also be applied to the copper tetradecyl sulfate micelle, meaning that the increase in the solubilizing power of copper tetradecyl sulfate may be ascribed to the increase in micellar volume caused by the change in micellar aggregation number, we can estimate the micellar aggregation number of this detergent to be 127.

It is to be noted that a small number of hydrocarbons can be solubilized at quite low concentrations of the detergents, as may be seen in Figs. 2, 3, 4 and 6. It is really a well-known fact that the CMC value of the detergent solution decreases with the solubilization of hydrocarbons[11,12], but, for example, the depression of the CMC value caused by the addition of hydrocarbons has been found to lie only within the range of 10 to 30 per cent for sodium alkyl sulfonate[11]. If this is the case with the metal dodecyl sulfates, the

11) H. B. Klevens, *J. Phys. & Colloid Chem.*, 54, 1012 (1950).
12) W. C. Lin, This Bulletin, 28, 227 (1955).

solubilization of hydrocarbons at very low concentrations of these detergents could not be due to their micelles. It seems that a small amount of some hydrocarbons is bound with singly-dispersed detergent molecules or ions in order to be soluble in the solution. The scheme of this binding is a problem to be examined in the future.

Summary

The solubilizing power of the bivalent copper, cobalt, nickel and magnesium dodecyl sulfates, and of copper tetradecyl sulfate towards benzene, toluene, *m*-xylene and *n*-hexane has been determined over the concentration range from 10^{-3} to 1.5×10^{-2} mol./l. at various temperatures. There were approximately linear relationships between the amounts of hydrocarbons solubilized and the detergent concentration. No fundamental difference could be observed among the solubilizing powers of the various bivalent salts studied, in accordance with such other micellar properties as CMC or micellar aggregation number. The solubilizing power, in moles of hydrocarbon solubilized per equivalent detergent, was found to be about 2.0 for the solubilization of benzene by bivalent metal dodecyl sulfates, which is about 1.5 times that by sodium dodecyl sulfate. This increased solubilizing power of bivalent salts was ascribed to the increased micellar volume and to the increased micellar aggregation number compared with that of sodium dodecyl sulfate. The increasing chain length causes a normal increase in solubilizing power. The ratio of the amount of hydrocabons solubilized by copper tetradecyl sulfate to that solubilized by copper dodecyl sulfate was about 1.5.

Department of Chemistry
Faculty of Science
Kyushu University
Hakozaki, Fukuoka

*The Radiation-Induced Addition of Acetaldehyde to Isobutylene**

By Shinji IIZUKA, Motoyoshi HATADA and Kozo HIROTA

(Received March 2, 1963)

It has been found by the present authors that several ketones of the $CH_3CO(CH_2)_nH$ ($n=1, 2, 3, \cdots$) type can be synthetized by the radiation-induced telomerization of acetaldehyde to olefins, propylene[1] and ethylene[2] at room temperature with high G values. The mechanism can be ascribed to a chain telomerization reaction as follows,

$$CH_3CHO \rightsquigarrow CH_3\dot{C}O + H\cdot \quad (1)$$

$$CH_3\dot{C}O + RCHCH_2 \longrightarrow CH_3COCH_2\dot{R}CH \quad (2)$$

$$CH_3COCH_2\dot{R}CH + CH_3CHO \xrightarrow{k_d} CH_3COCH_2RCH_2 + CH_3\dot{C}O \quad (3)$$

$$\text{or } CH_3COCH\dot{R}CH + RCHCH_2 \xrightarrow{k_p} CH_3COCH_2RCHCH_2\dot{R}CH \quad (4)$$

and so on.

The first purpose of the present paper is to investigate the effect of the structure of taxogens on such a telomerization reaction, making isobutylene a taxogen of branched olefins. The second purpose is to analyze the products in detail so as to investigate the radical mechanism described above, because this monomer is easily polymerizable by a cationic mechanism.

Experimental

Materials.—Acetaldehyde was prepared by heating commercial paraldehyde, which had been purified by distillation at 70°C, with a small amount of concentrated sulfuric acid. The final product was again distilled in vacuo. Isobutylene was prepared by dehydrating commercial *t*-butyl alcohol with concentrated sulfuric acid at 70°C. Impurities were found to be less than 0.5% by the gas chromatographic method.

Procedure.—The sample was carefully deaerated by evacuation; then, while being kept at −80°C, it was enclosed and irradiated in a glass ampoule. Irradiation was carried out in the ampoule with a gamma-ray source (ca. 1000 curie Co-60) installed in the present laboratory. The dose rate was determined with a Fricke dosimeter.

* Chain Telomerization Induced by Radiation. IV.

1) K. Hirota and M. Hatada, This Bulletin, **33**, 1682 (1960).

2) K. Hirota, S. Iizuka, H. Ochi and M. Hatada, ibid., **36**, 115 (1963).

For the detailed analysis of the irradiation products, a large amount of the sample (acetaldehyde/isobutylene=1.6; 200 g.) was irradiated at the dose rate of 4×10^4 r/hr. and the total dose of 5×10^7 r. After the irradiation, unreacted acetaldehyde and isobutylene were separated by distillation, and the residue obtained was fractionally distilled. Each fraction was analyzed by the use of a gas chromatograph (apparatus: Shimadzu GC-1A), an infrared spectrometer (Shimadzu AR-275), and a nuclear magnetic resonance spectrometer (Varian V-4300 B; field modulation, 40 Mc./sec.). In some cases they were derived to 2, 4-dinitrophenylhydrazone, whose melting point was determined. However, in most cases, 10 g. of the sample was irradiated in an ampoule (1.2 cm. in diameter; 15 cm. in length), and the products were analyzed. In the case of irradiation at a higher temperature, 5 g. of the sample was used in an ampoule (1.2 cm. in diameter; 5 cm. in length), the ampoule being get up in a small autoclave. After irradiation, each ampoule was opened, and unreacted acetaldehyde and isobutylene were carefully distilled out. The residue obtained was quantitatively analyzed by gas chromatography.

The effects of catalysts on the reaction were investigated, enclosing the catalysts prepared as follows; a) Nickel: nickel, prepared by decomposing commercial nickel formate (12 g.) for 2 hr. at 380°C, was evacuated for 2 hr. at the same temperature. b) Zinc oxide: commercial zinc oxide (5 g.) was evacuated for 2 hr. at 250~300°C. c) Alumina for chromatography (8 g.) was evacuated for 2 hr. at 350~400°C. d) Silica gel: silica gel for chromatography (8 g.) was evacuated for 2 hr. at 350~400°C. After irradiation, the ampoule was opened, and the catalyst was filtered off by a glass filter (G-4). The filtrate was analyzed by the method described above.

Results and Discussion

Identification of the Irradiation Products.— Figure 1 shows the gas chromatograms of the irradiation products. The large peak, P_1, was easily assigned to acetaldehyde. The P_2 peak was separated into two peaks, P_{2-1} and P_{2-2}, by the use of a 3.0-m. column of dioctylphthalate at 120°C instead of a 5.3 m. column of high vacuum oil. The retention times of P_{2-1} and P_{2-2} agreed with those of methyl *t*-butyl ketone and methyl isobutyl ketone, which in turn correspond to two isomeric 1:1 telomers. The formation of two types of telomers had been found previously in the acetaldehyde and propylene system[1].

From a large irradiated sample, two fractions were obtained by distillation. The first fraction (b. p., 114~117°C at 760 mmHg) corresponds to P_{2-2} and was identified as methyl isobutyl ketone, 1:1 telomer, by the retention time of the gas chromatogram, the boiling point and the melting point of its 2, 4-dinitrophenylhydrazone. The second fraction (96~101°C at 37~38 mmHg) corresponds to the P_4 peak. The reaction of this fraction with 2, 4-dinitrophenylhydrazine gave a red brown oily substance. The infrared spectrum of the second fraction showed a carbonyl band at 1720 cm^{-1} and isopropyl bands at 1150 and 1170 cm^{-1}.

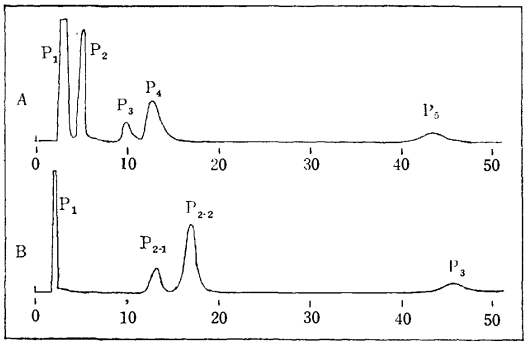

Fig. 1. Gas chromatograms of the irradiation products.
Curve A was obtained by using a high vacuum oil 5.3 m. column, and He as carrier gas (120 ml./min.) at 180°C.
Curve B was obtained by using a dioctyl phthalate 3.0 m. column, and He as carrier gas (120 ml./min.) at 120°C.

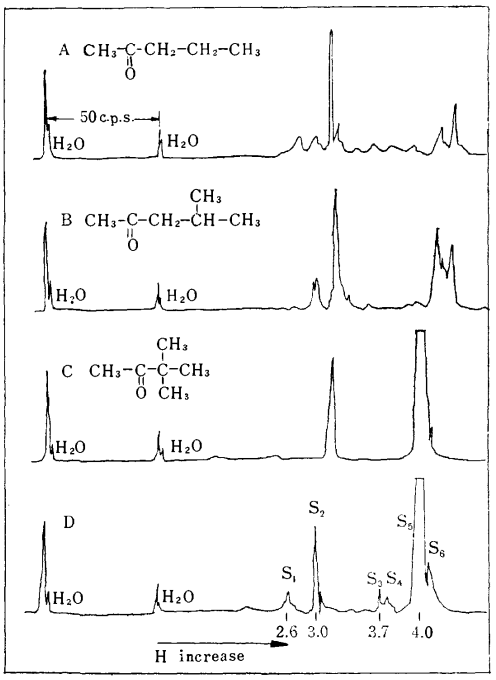

Fig. 2. NMR spectra of the second fraction of irradiation product and related compounds (40 Mc./sec.).
A Methyl *n*-propyl ketone
B Methyl isobutyl ketone
C Methyl *t*-butyl ketone
D The second fraction of irradiation product

TABLE I. CHEMICAL SHIFT (δ) AND RELATIVE AREAS OF THE NMR SIGNALS*

	$-CH_2-(\alpha)$		CH_3-CO		$-CH_2-(\beta)$		$-C-CH_3$	
	δ	Ratio	δ	Ratio	δ	Ratio	δ	Ratio
A	2.8 2.9	1.5	3.2	3.0	3.4 3.6 3.8 3.9	1.0	4.1 4.3	2.3
B	2.9 2.9	1.6	3.2	3.0			4.2 4.2	5.4
C			3.1	3.0			4.0	8.0
D	2.6	1.8	3.0	3.0	3.7 3.8	1.3	4.0 4.1	11.6

A: Methyl *n*-propyl ketons
B: Methyl isobutyl ketone
C: Methyl *t*-butyl ketone
D: The second fraction

$$\delta = \frac{H_{\text{sample}} - H_{\text{reference}}}{H_{\text{reference}}} \times 10^6$$

* One third of the area of the CH_3CO signal was taken as the unit of relative areas.

The NMR spectra (D, A, B and C) in Fig. 2 are that of this fraction and those of its related compounds, i. e., methyl *n*-propyl ketone, methyl isobutyl ketone and methyl *t*-butyl ketone. When one compares the D spectrum with the A, B and C spectra, it is apparent that each signal from S_1 to S_6 in D relates to the proton of the following groups; S_1 to $-CH_2-CO-$ (α-position), S_2 to CH_3-CO, S_3 and S_4 to $-CH_2-$ (β- and more portions) and/or $-CH-$, S_5 and S_6 to CH_3-C. Table I shows the chemical shift δ, taking water as the reference and with the relative areas of the signals making one-third of the area of the CH_3-CO signal as a unit. It can be estimated, therefore, that the second fraction contains substances of one CH_3CO-, one $-CH_2C$ (α) and four CH_3-C groups as well as a few $-CH_2-$ (β- and more positions) and/or $-\underset{|}{C}H-$groups. The mean molecular weight of these substances was determined to be 155 from the freezing point depression of benzene. On the basis of the results described above, the structure of the main substance in the fraction was reasonably estimated to be the 1 : 2 telomer; i. e.,

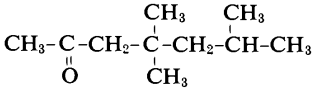

(molecular weight : 156)

Although the minor products corresponding to the other peaks of the gas chromatogram were not isolated, it may be estimated that two peaks, P_3 and P_5, are due to the isomeric 1 : 2 telomer and 1 : 3 telomer respectively. It is possible, however, that the amount of isomeric 1 : 4 telomer was too small to be detected because of steric hindrance.

The Effect of the Dose on Yields.—The effect of the total dose on the yields of each telomer is shown in Fig. 3 where the dose rate was kept constant at 4.0×10^4 r/hr., while the molar ratio in the feed R, as defined by acetaldehyde/isobutylene, was kept constant at 1.5. After an induction period observed in the initial part of the curves, the amount of each telomer increased linearly. It is interesting to note that similar induction periods had been also observed in the gamma-ray-induced addition of acetaldehyde to ethylene[2] and of propanol-2 to ethylene[3]. It is not certain whether

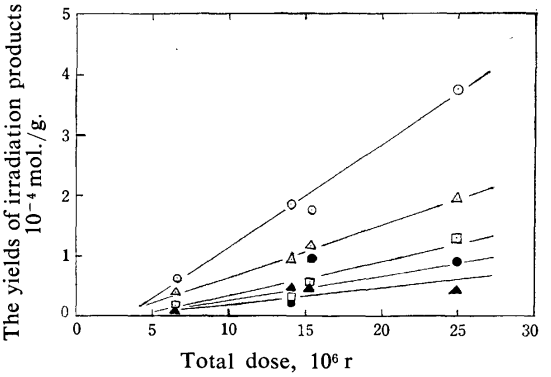

Fig. 3. Amounts of the irradiation products *vs.* total dose.
[acetaldehyde]/[isobutylene] ≒ 1.5
Dose rate 4.0×10^4 r/hr.
⊙, 1 : 1; ●, 1 : 1_{iso}; △, 1 : 2; ▲, 1 : 2_{iso}; ⊡, 1 : 3 telomer

3) K. Hirota and M. Hatada, ibid., 34, 1644 (1961).

or not this tendency is due to the presence of some undetectable impurities, e. g., oxygen or other radical-scavengers.

Generally speaking, the yields decreased by one or two orders of magnitude upon the substitution of isobutylene for propylene or ethylene as the taxogen. The reason for such a smaller reactivity of isobutylene will be discussed later.

The Effect of the Dose Rate on *G* Values.—In Fig. 4, the logarithms of the *G* values of the telomers, $G(1:n)$, are plotted against the logarithm of the dose rate. It is shown that in the cases of $G(1:1)$, $G(1:2)$ and $G(1:3)$, linear relations were otained, their inclination being nearly equal to −0.50, i. e., −0.47, −0.47 and −0.52 respectively. Since −0.50 is expected to occur in the case of the bimolecular termination of radicals, this finding seems to indicate a radical chain mechanism. However, $G(1:1_{iso})$ and $G(1:2_{iso})$ were not affected by the dose rate; thus suggesting a contrary thesis that these telomers were produced according to a mechanism different from that of the major telomers.

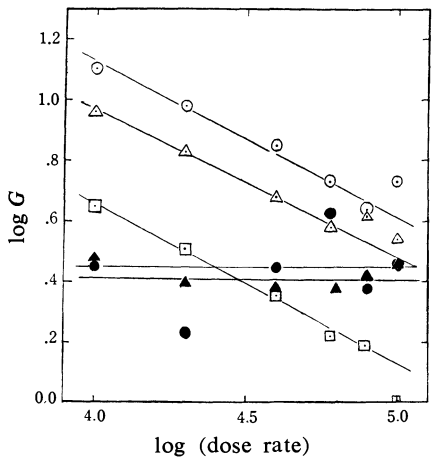

Fig. 4. log *G* vs. log (dose rate).
[acetaldehyde]/[isobutylene] ≒ 1.5
Total dose; 1.5×10^7 r
⊙, 1 : 1; ●, 1 : 1_{iso}; △, 1 : 2;
▲, 1 : 2_{iso}; ◙, 1 : 3 telomer

The Effect of the Molar Ratio in the Feed on *G* Values.—In Fig. 5, the *G* values of the telomers produced at 15°C are plotted against the molar ratio in the feed, taking both total dose and dose rate at constant values, i. e., at 2.2×10^7 r and 4.0×10^4 r/hr. respectively. It is shown that $G(1:1)$ was larger than the other *G*'s and that it increases markedly with the molar per cent of acetaldehyde, but that even its maximum value was smaller by one or two factors than the corresponding one when ethylene or propylene was adopted as the taxogen.

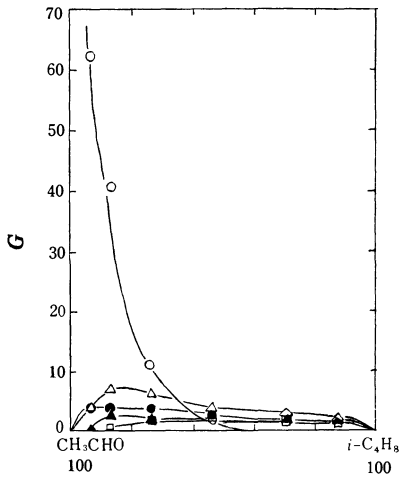

Fig. 5. *G* vs. molar percent.
Dose rate 4.0×10^4 r/hr.
Total dose 2.1×10^7 r
Irradiation temp., 15°C
⊙, 1 : 1; ●, 1 : 1_{iso}; △, 1 : 2;
▲, 1 : 2_{iso}; ◙, 1 : 3 telomer

Another point to be mentioned is the finding that $G(1:1_{iso})$ and $G(1:2_{iso})$ did not depend on the molar ratio so markedly; this is the second fact which seems to be related to the mechanism of these products.

The Effect of the Irradiation Temperature on *G* Values.—The *G* values of telomers are plotted against the irradiation temperature in Figs. 6 and 7, where the R's are very different (1.5 and 15 respectively). The *G* values of the 1 : 1, 1 : 2 and 1 : 3 telomers markedly increased with the temperature below 100°C and show a maximum at a temperature between 110 and 150°C. The decrease in the *G* values of these products at higher temperatures may result from the decomposition of the acetaldehyde molecule, the acetyl radical and/or other intermediate radicals.

By plotting the logarithm of these values at a low temperature against $1/T$, relatively good straight lines were obtained. The apparent activation energies of formation were thus determined to be 6.5, 5.8 and 7.0 kcal./mol. for 1 : 1, 1 : 2 and 1 : 3 telomer respectively. These values are slightly larger than those observed in the case of acetaldehyde and ethylene[2], i. e., 5.0 kcal. for the 1 : 1 telomer. However, it seems that $G(1:1_{iso})$ and $G(1:2_{iso})$ remained constant in relation to the temperature, suggesting a low activation energy. This point will be taken up again below.

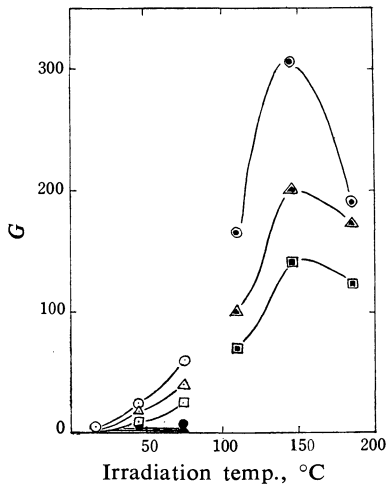

Fig. 6. G-values vs. irradiation temperature.
($R \fallingdotseq 1.5$)
⊙, 1 : 1; ●, 1 : 1_{iso}; △, 1 : 2; ▲, 1 : 2_{iso}; ▣, 1 : 3 telomer
Dose rate 1.8×10^4 r/hr.
Total dose 7.4×10^6 r
⊙, 1 : 1; △, 1 : 2; ▣, 1 : 3 telomer
Dose rate 1.0×10^4 r/hr.
Total dose 1.0×10^6 r

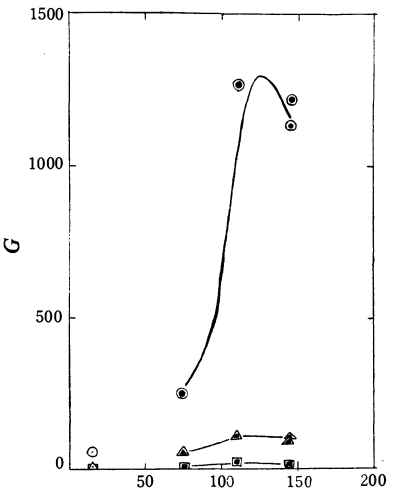

Fig. 7. G-values vs. irradiation temperature.
($R \fallingdotseq 15$)
⊙, 1 : 1; △, 1 : 2; ▣, 1 : 3 telomer
Dose rate 4×10^4 r/hr.
Total dose 2.1×10^7 r
⊙, 1 : 1; △, 1 : 3 telomer
Dose rate 1.0×10^4 r/hr.
Total dose 1.0×10^6 r/hr.

Reaction Mechanism.—Considering the effects on the G(telomers) described above, it may be said that the major parts of the telomers are produced by the following chain schemes, which have been proposed by the present authors[1,2] or by others[4].

$$CH_3CHO \rightsquigarrow CH_3\dot{C}O + H$$

$$CH_3\dot{C}O + CH_2{=}C(CH_3)_2 \xrightarrow{k_{po}} CH_3COCH_2\dot{C}(CH_3)_2$$

$$CH_3COCH_2\dot{C}(CH_3)_2 + CH_3CHO \xrightarrow{k_{dl}} CH_3COCH_2CH(CH_3)_2 + CH_3\dot{C}O$$

or

$$CH_3COCH_2\dot{C}(CH_3)_2 + CH_2{=}C(CH_3)_2 \xrightarrow{k_{pl}} CH_3COCH_2C(CH_3)_2CH_2\dot{C}(CH_3)_2$$

and so on.

On the basis of the data in Fig. 5, the molar fractions F_n's, of the 1 : n telomers to the total telomers were calculated; they are plotted against R in Fig. 6. The lines in the figure indicate the theoretical curves based on the following equation;

$$F_n = \frac{C_n R}{\prod_{i=1}^{n}(C_i R + 1)} \qquad (C = k_{dn}/k_{pn})$$

which was derived by assuming the above scheme[5]. The chain transfer constants, C_n's, 0.6_0, 1.2_7 and 2.0 were selected as the most

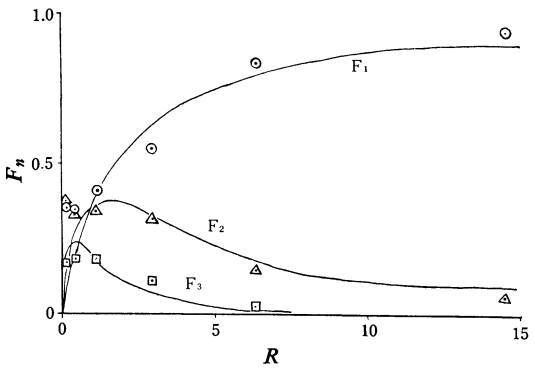

Fig. 8. Molar fractions of 1 : n telomers vs. molar ratio of acetaldehyde/isobutylene in the feed.

4) C. E. Stoops and C. L. Furrow, *J. Org. Chem.*, **26**, 3264 (1961).
5) Cf. C. Walling, "Free Radicals in Solution", John Wiley and Sons, New York (1957), p. 245.

TABLE II. CHAIN TRANSFER CONSTANTS OF RADIATION-INDUCED TELOMERIZATION

Telogen	Taxogen	C_1	C_2	C_3	Literature
CH_3CHO	C_2H_4	1.0	1.1	4.6	(2)
CH_3CHO	C_3H_6	0.86	1.64	6.1	(1)
CH_3CHO	i-C_4H_8	0.6	1.2_7	2.0	Present paper
$(CH_3)_2CHOH$	C_2H_4	0.062	0.073	0.12	(3)
CCl_4	C_2H_4		— 0.12(mean) —		γ-Ray initiation (6)
CCl_4	C_2H_4	0.08	0.9	3.2(?)	Peroxide-initiation at 70°C (7)

TABLE III. THE EFFECT OF THE PRESENCE OF CATALYSTS ON THE G VALUES OF TELOMERS

Dose rate: 4×10^4 r/hr.; total dose: 1.5×10^7 r

	Absence	Nickel	Zinc oxide	Alumina	Silica gel
1 : 1	17	7.4	2.5	3.1	5.7
1 : $1_{iso.}$	3	—	—	—	—
1 : 2	13	1.9	0.9	7.0	3.4
1 : $2_{iso.}$	3	0.2	0.1	1.3	0.6
1 : 3	7.5	0	1.0	5.7	2.1

probable values. However, the observed values at a smaller R value do not lie on the calculated curves. This may be due to the errors caused by the use of $G(1:1)+G(1:1_{iso})$ instead of $G(1:1)$ in this region*, and also to the approximation where the amounts of higher telomers ($n\geq4$) were assumed. For the sake of comparison, chain transfer constants of similar reactions are shown in Table II. As ought to be expected, they are much larger than those in the case of polymerization and take values of an order of magnitude similar to those of peroxide initiation.

However, to summarize the effects of the dose rate, the molar ratio and the irradiation temperature on G values, the mechanism of producing the isomeric 1 : 1 and isomeric 1 : 2 telomers will be different from the above scheme, as has already been suggested. It is natural for the reaction to assume another mechanism; e. g., isomeric 1 : 1 telomer will be produced in accordance with the Markownikoff rule on the addition to a double bond as follows:

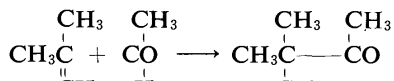

However, the production of the isomeric 1 : 2 telomer is difficult to explain by this mechanism. Therefore, the following ionic mechanism is more reasonable:

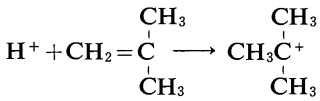

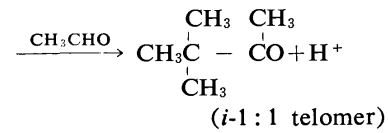

(*i*-1 : 1 telomer)

or

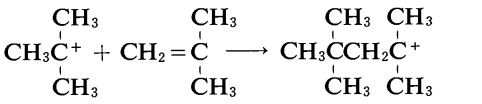

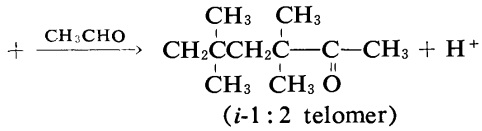

(*i*-1 : 2 telomer)

Such an ionic mechanism may be allowed, because isobutylene can be cationically polymerized by gamma-rays, according to Dainton et al.[8] Moreover, it may be explained on the basis of this ionic nature of isobutylene and on the basis of steric hindrance why the G values of this system are much lower than those when ethylene or propylene was used as the taxogen.

The Effect of the Presence of Catalysts on G Values.—Table III shows the effects of the presence of catalysts, i. e., nickel, zinc oxide, alumina and silica gel, on the G values of telomers to be produced at room temperature. The G values of all the telomers decreased whenever the catalysts were present. This finding suggests the possibility of the catalytic decomposition of acetyl and other intermediate radicals, but since several by-products were detected in the gas chromatogram, it can be concluded that aldehyde was also decomposed by the contact with these catalysts and was turned into the by-products.

* Due to experimental reasons, these $G(1:1_{iso.})$ and $G(1:1_{iso.})$ values could not be determined separately.

6) M. Takehisa et al., *J. Chem. Soc. Japan, Ind. Chem. Sec.* (*Kogyo Kagaku Zasshi*), **65**, 531 (1962).

7) Ref. 5, p. 257.

8) E. Collinson, F. S. Dainton and H. A. A. Gills, *J. Phys. Chem.*, **63**, 909 (1959).

Summary

The radiation-induced addition of acetaldehyde to isobutylene has been found to proceed at room temperature; the G(telomer)'s are smaller by one or two orders of magnitude than those when ethylene or propylene is adopted as the taxogen, and they increase markedly with the temperature, reaching a maximum at 110~150°C.

It has been shown from the gas chromatographic and NMR analyses of the telomer produced that the radical chain mechanism proposed in former papers by the present authors is reasonable, although minor products seem to be formed in accordance to an ionic mechanism.

It has been found that the G values of all the telomers decrease in the presence of several solid materials, suggesting the catalytic decomposition of acetyl and other intermediate radicals.

The authors wish to express their sincere thanks to Dr. Hazime Kusumoto of the Research Institute of Industry and Science, Osaka University, for his measurement of NMR spectra.

A part of the expense has been defrayed by a grant given by the Ministry of Science and Technology, to which the authors' thanks are due.

Japanese Association for Radiation Research on Polymers
Osaka Laboratory
Neyagawa City, Osaka
(S. I., M. H. & K. H.)

Department of Chemistry
Faculty of Science
Osaka University
Kita-ku, Osaka (K. H.)

Terpenoids. VI. The Structure of Thunbergene[*,1]

By Hiroshi KOBAYASHI and Saburo AKIYOSHI[**]

(Received March 4, 1963)

Thunbergene (I) $C_{20}H_{32}$; m. p., 60°C, $[\alpha]_D$ +233°, is a monocyclic diterpene hydrocarbon which was first isolated from the wood turpentine oil of *Pinus thunbergii, Parl.* by one (S. A.) of the present authors[2]. The compounds which are identical with thunbergene or which are considered to be so have been found to occur in the exudates of many other *Pinus* species[3].

In their studies of the structure of this compound, the authors have arrived at the conclusion that thunbergene has the structure shown in Fig. 1. At almost the same time

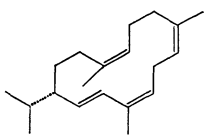

Fig. 1. Thunbergene (I)

Professor Dauben proposed that the structure of cembrene is 1-isopropyl-4, 8, 12-trimethylcyclotetradeca-2, 4, 7, 11-tetraene[4]; direct comparison of cembrene with thunbergene proved them to be the same[5].

The present paper describes the author's own work on this compound. A preliminary communication proposing the structure I (Fig. 1) has already appeared[6]. This structure was assigned to thunbergene (I) on the basis of the following evidence.

* Contribution No. 40 from the Department of Organic Synthesis, Faculty of Engineering, Kyushu University, Fukuoka.

** Professor Emeritus of the Department of Organic Synthesis. Present position: Executive Director of the Central Research Laboratory, the Teijin Co., Ltd., Hinomachi, Minamitama-gun, Tokyo.

1) Presented before the Sixth Symposium on Organic Chemistry of Natural Products, Sapporo, Japan, July, 1962.

2) S. Akiyoshi, *Rep. Osaka Ind. Res. Inst.*, **17**, No. 10 (1937).

3) a) Y. Sebe, *J. Chem. Soc. Japan (Nippon Kwagaku Kwaishi)*, **56**, 1118 (1935); b) H. Wienhaus, *Nord Kemistmötet* (1926) 211; *Chem. Abstr.*, **24**, 1635 (1930); c) A. J. Haagen-Smit, T. H. Wang and N. T. Mirov, *J. Am. Pharm. Assoc.*, **40**, 557 (1951); d) N. T. Mirov and P. M. Illof, Jr., ibid., **44**, 424 (1955); e) P. M. Illof, Jr. and N. T. Mirov, ibid., **45**, 77 (1956); f) V. A. Pentegova, O. Motl and V. Herout, *Collection Czechoslov. Chem. Commun.*, **26**, 1362 (1961).

4) W. G. Dauben, W. E. Thiessen and P. R. Resnick, *J. Am. Chem. Soc.*, **84**, 2015 (1962).

5) The authors are indebted to Professor William G. Dauben of the Department of Chemistry, University of California, Berkeley, for identifying thunbergene with cembrene. For the systematic index of this compound, the authors suggest employing the single name, thnnbergene, which was given to the compound by its first reporter.

6) H. Kobayashi and S. Akiyoshi, This Bulletin, **35**, 1044 (1962).

The hydrogenation of I gives an octahydro-derivative (II), $C_{20}H_{40}$, $[\alpha]_D \pm 0°$; thus I contains four double bonds and one ring. The infrared spectrum of I shows the strong band at 963 cm^{-1} characteristic of a trans-disubstituted double bond. Its ultraviolet absorption spectrum shows a band at 246 mμ (ε, 17100) indicative of a conjugated diene. The partial hydrogenation of I gives a dihydro-derivative (III) which shows no infrared band near 963 cm^{-1} and a weakened ultraviolet band at 246 mμ (ε, 355). The trans-disubstituted double bond is, therefore, a part of the conjugated diene system.

The ozonolysis of I gives levulinic acid (IV) and 2-isopropyl-5-oxohexanoic acid (V). The latter V, $[\alpha]_D -30°$, is the only optically active product of the ozonolysis and affords a semicarbazone melting at 140°C[7]. The hypobromite oxidation of V furnishes an optically active 2-isopropylglutaric acid (VI), $[\alpha]_D -20°$. Formaldehyde, acetaldehyde and acetone are not found to occur among the ozonolysis products, in contrast to the findings of previous reports[3a,b].

The presence of an isopropyl group is suggested by the infrared doublet band at 1368 and 1387 cm^{-1} of I; it is confirmed by the NMR study (two doublets centered at 9.20 and 9.10 p.p.m.[8], both J, 2.3 c.p.s.) and by the occurrence of V upon the ozonolysis of I. In connection with the conformation of I, it is noted that the NMR bands associated to the methyl of the isopropyl group split to two doublets indicative of the hindered rotation of the isopropyl group.

The lack of infrared bands characteristic of terminal methylene and of vinyl group is consistent with the absence of formaldehyde among the ozonolysis products. The NMR spectrum indicates the presence of two methyl groups attached to ethylenic carbons (8.52 and 8.42 p.p.m.) and of one methyl group on a conjugated diene (8.22 p.p.m); these are concidered to be on double bonds which are in the midst of carbon chains. If this were not the case, I would give acetaldehyde upon ozonolysis.

The groupings of seventeen carbon atoms are now clarified, namely, those corresponding to two ozonolysis products, IV and V, and the conjugated diene bearing a methyl group. The three remaining carbon atoms must belong together to a single group, which cannot be trifunctional or vicinal bifunctional; therefore, the C_3-group must be a propanediylidene-type one. Thus, the groupings of all the carbon atoms are known to be bifunctional, and consequently, the ring structure of I must consist of fourteen carbon atoms and four double bonds.

Consistent with the fourteen-membered ring structure of I is its dehydrogenation with selenium to give an aromatic hydrocarbon (VII) ($C_{19}H_{20}$; m. p., 78°C[9]) which has an ultraviolet spectrum indicative of alkylphenanthrene. Its NMR spectrum can be explained by formula VII (Fig. 2); it reveals the presence of two methyls of an isopropyl group

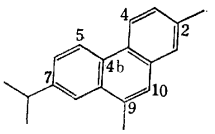

Fig. 2. (VII)

(9.0 p.p.m.), two methyl groups attached to a phenanthrene nucleus (8.0 p.p.m.) and seven hydrogens on a phenanthrene nucleus (2.5 and 1.5 p.p.m), two of them at a lower field position being at the 4- and 5-positions of the nucleus[10].

As known already, phenanthrene, if its 9- and 10- positions are both unsubstituted, is readily oxidized, giving an *o*-quinone which shows a characteristic visible absorption above 400 mμ[11]. The oxidation of VII brings about no change in the visible absorption of this region, indicating that VII resists the oxidation and that, consequently, either the 9- or 10-position should be substituted.

For the first maximum of the *p*-group[12] of the ultraviolet spectrum of VII occurring at 299 mμ, assignment of the three substituted positions can be made on the basis of the known relationship[13]. Provided that the parent cyclic system is fourteen-membered, an application of the isoprene rule indicates the unique structure of VII as 7-isopropyl-2, 9-dimethylphenanthrene (Fig. 2); this presumption has been confirmed synthetically[14]. A methyl group lost upon the dehydrogenation would have attached to the 4b-position, and the structure II is given to the octahydro-derivative (II) (Fig. 3).

Together with the preceding structural data regarding to the groupings of the carbon atoms,

7) O. Wallach, *Ann.*, **379**, 182 (1911).

8) All chemical shifts are quoted in reference to the τ-scale.

9) This aromatic hydrocarbon is presumably identical with the C_{20}-dehydrogenation product reported by Sebe, Ref. 3.

10) J. A. Pople, W. G. Schneider and H. J. Bernstein, "High-Resolution Nuclear Magnetic Resonance", McGraw-Hill Inc., New York (1959), p. 247.

11) T. Sugasawa, *Chem. Pharm. Bull.* (*Tokyo*), **9**, 894 (1961).

12) Clar's notation. E. Clar, *Spectrochim. Acta*, **4**, 116 (1950).

13) a) E. Heilbronner, H. U. Däniker and Pl. A. Plattner, *Helv. Chim. Acta*, **32**, 1723 (1949); b) E. Ochiai, T. Okamoto, S. Sakai and M. Natsume, *Pharm. Bull.* (*Tokyo*), **5**, 113 (1957).

14) H. Kobayashi, This Bulletin, **35**, 1970 (1962).

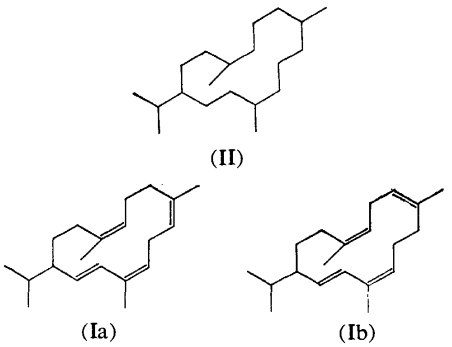

Fig. 3.

structure II gives two equally probable structures, Ia and Ib, for I (Fig. 3). From the biogenetic point of view, structure Ia is rather preferable since this diterpene hydrocarbon I is considered to be derived from geranylgeraniol in a manner analogous to the formation of the ten-membered monocyclic sesquiterpenoids from farnesol[15] (Fig. 4).

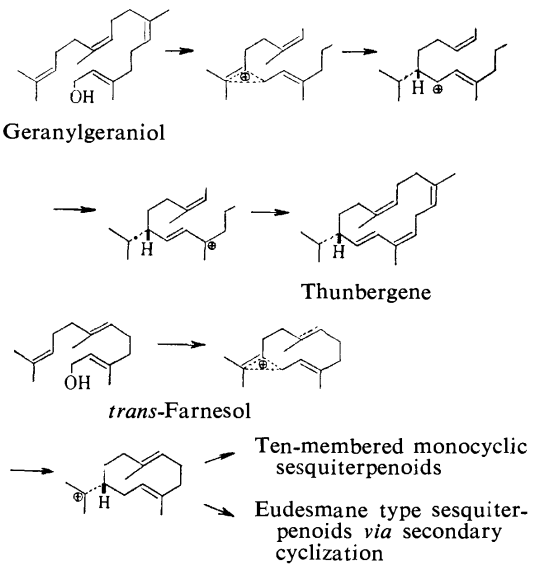

Fig. 4. Hypothetic biogenesis of thunbergene. Comparison with that of sesquiterpenoids proposed by Hendrickson[15].

Structure Ia coincides with that proposed by Dauben[4].

The absolute configuration of the only asymmetric carbon can be directly related to that of (−)-VI, which was confirmed by Fredga[16]. The configuration should be retained throughout the degradation sequence from I to (−)-VI since all the degradation reaction would not affect the asymmetric center.

15) J. B. Hendrickson, *Tetrahedron*, **7**, 82 (1959).
16) A. Fredga and J. Miettinen, *Acta Chem. Scand.*, **1**, 137 (1947).

Thus, Fig. 1 represents the structue of thunbergene (I). This compound is a novel type of diterpene and is the first characterized naturally- occurring fourteen-membered carbon ring compound. It is interesting in connection with the hypothetic biogenesis of I that the absolute configuration of the isopropyl group of I is quite analogous to these found in ten-membered monocyclic sesquiterpenoids or related compounds (Fig. 4).

The stereochemistry of the three trisubstituted double bonds remains to be elucidated. The results of the NMR studies of the stereochemistry of ethylenic double bonds[17] are not considered to be applicable to the elucidation of this problem, because the long-range shielding effect of the double bonds on the methyl groups is difficult to ascertain. Probably the only final solution to the problem will be obtained by the X-ray analysis of a suitable derivative of I.

Experimental[18]

Isolation of Thunbergene (I). — A neutral turpentine oil from the root of *Pinus thunbergii*, *Parl.* was fractionated by distillation under reduced pressure. Thunbergene (I) was separated as a crystalline mass from the fraction boiling at 135～155°C/3 mmHg. The minimum content of I found in the wood turpentine oil was 1% by weight. Repeated recrystallizations from ethanol gave colorless needles melting at 59～60°C, $[\alpha]_D$ +233° (*c* 0.70 in chloroform); molecular weight, 272 (from a parent peak of the mass spectrum of I[19]).

Found: C, 88.14; H, 11.77. Calcd. for $C_{20}H_{32}$: C, 88.16; H, 11.84%.

C-Methyl number: 2.61, 2.64 and 2.54. IR $\tilde{\nu}_{max}$ 1667(w), 1387(s), 1368(s), 963(s), 938, 907 and 837 cm^{-1} (in carbon tetrachloride): UV λ_{max}: 246 mμ (ε, 17100) (in hexane). NMR spectrum[20]: 9.20(3) (doublet, *J* 2.3 c.p.s.) 9.10(3) (doublet, *J* 2.3 c.p.s.), 8.52(3), 8.42(3), 8.22(3), 8.15～7.80 (broad band), 5.30～4.30 (broad band), and 3.95 p.p.m.(1) (doublet, *J* 15 c.p.s.).

17) a) R. B. Bates and D. M. Gale, *J. Am. Chem. Soc.*, **82**, 5749 (1960); b) L. M. Jackman and R. H. Wiley, *J. Am. Chem. Soc.*, **1960**, 2881; c) R. B. Bates, R. H. Carnighan, R. O. Rakutis and J. H. Schauble, *Chem. Ind. (London)*, **1962**, 1020.

18) All melting points were uncorrected and were measured on a Koffer micro hot stage. Elementary analyses were performed by the Service Center of Elementary Analysis of Organic Compounds, Department of Chemistry, Kyushu University. All spectra in the ultraviolet and visible regions were recorded on a Hitachi model EPS-2 spectrophotometer, and in infrared region on a Nippon Koken model DS-301 double-beam spectrophotometer. The authors wish to thank Miss Yasuko Ikejiri for measuring the ultraviolet and visible spectra, and Miss Yuko Tomita for measuring the infrared spectra.

19) The authors are indebted to Dr. Curt Enzell of the Royal Institute of Technology, Stockholm, for the mass spectral datum.

20) The authors are indebted to the staff of the Japan Electron Optics Laboratory, Tokyo, for the NMR spectrum of I. The spectrum was measured in deutrochloroform (an about 20% solution) on a JNM C-60 instrument.

Hydrogenation of I. — Upon catalytic hydrogenation in an ethyl acetate solution (25 ml.) over platinum black, I (1.15 g.) absorbed 502 ml. of hydrogen in the standard state (the calculated amount for 4 mol. of hydrogen, 497 ml.), giving an oily octahydro-derivative (II), n_4^{29} 0.8632, n_D^{29} 1.4730, $[\alpha]_D \pm 0°$ (*c* 7.84 in chloroform), C-methyl number: 2.62.

Found: C, 85.48, 85.35; H, 14.10, 14.30. Calcd. for $C_{20}H_{40}$: C, 85.63; H, 14.37%.

Thunbergene (I) (500 mg.) in ethyl acetate (15 ml.) was hydrogenated with palladium black (100 mg.) until one mole of hydrogen (41 ml. in the standard state) was absorbed. Dihydro-derivative (III) was an oil with the following properties: d_4^{22} 0.890, n_D^{22} 1.5020, $[\alpha]_D$ −2.2° (*c* 8.13 chloroform). UV, λ_{max}: 246 mμ (ε, 355) (in hexane).

Ozonolysis of I. — Ozone was passed through a solution of I (9.8 g.) in methylene chloride (200 ml.) at −70°C until the solution turned purple. The resulting ozonide in methylene chloride was added drop by drop into hot 30% hydrogen peroxide (15 ml.). The solvent was taken off by distillation. After the ozonide in hydrogen peroxide had been refluxed for an hour, manganese dioxide was added to decompose the excess hydrogen peroxide. The resulting mixture was steam-distilled. The residue was acidified and extracted with ether, the ethereal extract giving a non-volatile acid (4.85 g.). The aqueous layer was further extracted with ether for 3 hr. by means of an Asahina continuous extraction apparatus[21]. From the second ethereal extract, levulinic acid (IV) (0.91 g.) was obtained; this gave succinic acid upon being treated with sodium hypobromite at 0°C for 3 hr. The semicarbazone of levulinic acid (IV) melting at 184°C was identified by the comparison of the infrared spectra and the mixed melting point determination with an authentic sample.

The non-volatile acid (2.60 g.) was partition-chromatographed on silica-gel (60 g.) holding 0.5 N sulfuric acid (30 ml.). Eluant was wet ether saturated with 0.5 N sulfuric acid. A keto-acid was isolated from the middle fractions and was purified via semicarbazone (m. p., 138~140°C), which was prepared according to Asahina and Kuwata[22] and was recrystallized from water.

Found: C, 52.30; H, 8.55; N, 18.14. Calcd. for $C_{10}H_{19}N_3O_3$: C, 52.38; H, 8.35; N, 18.33%.

The keto-acid (V) (96 mg.) ($[\alpha]_D$ −30° (*c* 0.56 in chloroform)) was regenerated from the semicarbazone (200 mg.) by heating it together with 25% sulfuric acid (10 ml.) for an hour.

The keto-acid (V) (123 mg.) was oxidized to a dicarboxylic acid (VI) (117 mg.) by treating it for 3 hr. at 0°C with a sodium hypobromite solution. Recrystallization from dilute hydrochloric acid gave a sample (VI) (27 mg.) melting at 92~95°C. Repeated recrystallizations from benzene raised the melting point to 94~95°C, $[\alpha]_D$ −20° (*c* 1.64 in chloroform).

The dicarboxylic acid (VI) was dehydrated by heating it together with acetic anhydride for one and a half hour. The anhydride was separated by distillation under reduced pressure and recrystallized from petroleum ether (b. p. 50~70°C); m. p., 72°C. IR $\bar{\nu}_{max}$ 1810 and 1770 cm^{-1} in carbon tetrachloride.

The degradation products, V, VI and their derivatives, were identified by infrared spectral comparisons in solution with corresponding racemic authentic samples derived from diosphenol[23].

Dehydrogenation of I.—A mixture of I (2.00 g.) and selenium (3.00 g.) was heated at about 300°C for 3 hr. The resulting mixture was washed with 20% aqueous potassium hydroxide and was fractionated by distillation under reduced pressure. Fractions boiling above 180°C/1.5 mmHg (n_D above 1.6025) were combined and chromatographed on alumina. Elution with petroleum ether (b. p. 30~50°C) afforded a fluorescent oil, which gave a picrate (350 mg.) upon treatment with a 6% ethanol solution of picric acid. Repeated recrystallizations from ethanol gave a picrate as orange needles melting at 133.5~134.7°C. From the lower boiling fraction (n_D 1.5832), 50 mg. of the same picrate was obtained.

The aromatic hydrocarbon (VII) was regenerated from the picrate by eluting it from an alumina column using petroleum ether (b. p., 30~50°C)-ethyl ether (1 : 1) as an eluant. The evaporation residue crystallized upon treatment with a small amount of ethanol to give the hydrocarbon (VII) (190 mg.), which was then recrystallized from ethanol; m. p., 77.0~77.8°C. Infrared and ultraviolet spectra were superimposable on these of the authentic sample[14], and the mixed melting point was undepressed.

Found: C, 91.90; H, 8.19. Calcd. for $C_{19}H_{20}$: C, 91.88; H, 8.12%.

UV λ_{max} mμ (log ε): 224 (4.44), 249 (4.48), 257 (5.00), 274 (4.41), 281 (4.37), 288 (4.19), 299 (4.08), 319 (2.46), 328 (2.40), 335 (2.45) (in hexane). NMR spectrum[24]: 1.5, 2.5, 8.0 and 9.0 p.p.m., relative intensities: 2, 5, 6 and 6 respectively.

The chromic acid oxidation of VII and the visible absorption spectroscopy of the oxidation product were performed according to Sugasawa[11].

The authors are indebted to Dr. Shizuo Nagahama for his valuable advice and assistance in the laboratory work.

They also gratefully acknowledge the use of the facilities to obtain the turpentine oil afforded by the Messrs Ogawa Perfumery Co., Ltd., Osaka.

Departmen of Organic Synthesis
Faculty of Engineering
Kyushu University
Fukuoka

21) Y. Asahina, *J. Pharm. Soc. Japan* (*Yakugaku Zasshi*), No. 533, 531 (1926).
22) Y. Asahina and S. Kuwata, ibid., No. 491, 3 (1923).
23) F. W. Semmler and Mc. Kenzie, *Ber.*, **39**, 1164 (1906).
24) The proton chemical shifts were measured in a carbon tetrachloride solution in reference to water as an external standard on a Nippon Electron Optics Laboratory model JNM-1 NMR spectroscope, and were converted to the τ-value above quoted (±0.2 p. p. m. accurate), assuming the proton chemical shift of 5.0 p. p. m. for the water reference. The authors wish to thank Mr. Ganzo Kawano for his technical assistance with the NMR spectroscopy.

The Structure of Bis(dithizonato)-zinc(II) and -Cadmium(II)

By Yasuo YAMAMOTO, Tetsuo YOSHINAGA* and Shoichiro YAMADA

(Received March 27, 1963)

One of the present authors, (T. Y.) devised a new method for dyeing the zinc ion in tissues[1]. In order to analyze this dyeing mechanism[2], some information about the structure of bis-(dithizonato)zinc(II) became necessary. Though dithizone has been used widely in the field of analytical chemistry and many investigations of the complex compounds with various metals have been carried out[3], information about the structure of metal complexes with dithizone has been very scarce[4,5]. It was thought be interesting and significant to examine various metal complexes with dithizone.

The present paper deals with the preparation methods and structure of bis(dithizonato)-zinc(II) and bis(dithizonato)cadmium(II), in comparison with bis(dithizonato)mercury-(II), whose structure has recently been determined by the X-ray method[5].

Experimental

Preparation of Bis(dithizonato)zinc(II). — Bis-(dithizonato)zinc(II) was prepared according to the method of Pariaud and Archinard[6]. To a solution of zinc acetate (0.5 g.) in aqueous ammonia was added a solution of dithizone (1.7 g.). A dark red precipitate, which formed instantaneously, was filtered off. This precipitate was then dissolved in 30 cc. of chloroform and filtered. The filtrate was evaporated until its volume was reduced by half; then 50 cc. of ethanol was added, and it was evaporated again until crystals began to appear in the solution. This solution was allowed to stand for 3 to 4 hr. Thin plate-like crystals with a green fluorescence were obtained. Recrystallization was made from chloroform-ethanol.

Found: C, 53.16; H, 3.77; N, 19.47. Calcd. for $C_{26}H_{22}N_8S_2Zn$: C, 54.21; H, 3.85; N, 19.43%.

Preparation of Bis(dithizonato)cadmium(II).— Bis(dithizonato)cadmium(II), which had not been isolated as crystals, was prepared by almost the same method as the zinc compound. Here, however, one of two forms of the compound was obtained, depending upon the conditions of the reaction. When a solution of cadmium acetate in aqueous ammonia was poured into a solution of dithizone, a dark red precipitate, which was easily dissolved in chloroform, was formed. By vacuum evaporation of the chloroform solution of this precipitate, however, violet needles which were only slightly soluble in chloroform were obtained. On the other hand, when a solution of dithizone was poured into a solution of cadmium acetate, a dark brown precipitate which was insoluble in chloroform was formed. After this precipitate was thoroughly washed with chloroform, brown powder was obtained. Both forms, the violet and the brown, are soluble in pyridine to give a solution with a strawberry color. After recrystallization from pyridine, both forms yielded a dark red crystalline powder of the same composition.

Found: C, 50.20; H, 3.70; N, 17.69. Calcd. for $C_{26}H_{22}N_8S_2Cd$: C, 50.12; H, 3.56; N, 17.99%.

Elementary analyses of the brown powder and violet needles were also carried out. The results were quite identical with those of the dark red crystalline powder.

Preparation of Bis(dithizonato)mercury(II).—Bis(dithizonato)mercury(II) was prepared by the same method as the zinc compound.

Found: N, 16.02. Calcd. for $C_{26}H_{22}N_8S_2Hg$: N, 15.76%.

Results and Discussion

The analytical results of these metal complexes of dithizone show that the zinc(II) and cadmium(II) compounds, as well as the mercury(II) compound, are composed of one metal ion and two dithizonate ions. The structures of bis(dithizonato)zinc(II) and bis-(dithizonato)cadmium(II) have not yet been determined, but the coordination around these metal ions is regarded as tetrahedral, judging from the stereochemistry of these metal ions and the configuration of dithizone. In the molecules of these metal complexes of dithizone, it may be presumed that dithizonate ions are capable of being coordinated to the metal in eight ways, i. e., in four ways through two nitrogen atoms which do not adjoin each other, and in the other four ways through a

* Permanent address: Second Department of Internal Medicine, Osaka University Medical School, Kita-ku, Osaka.

1) T. Yoshinaga and Y. Shinji, *Acta. Histochemica*, to be published.
2) T. Yoshinaga, Y. Yamamoto, Y. Shinji, T. Katayama and I. Nakajima, *J. Histochemica Japan*, to be published.
3) E. B. Sandell, "Colorimetric Determination of Trace of Metals", Interscience Publishers, New York (1959), p. 163; H. Mabuchi and H. Nakahara, This Bulletin, 36, 151 (1963); T. Ashizawa, *Japan, Analyst* (*Bunsekikagaku*), 10, 354, 443, 449 (1961); H. Irving and J. J. Cox, *Proc. Chem. Soc.* 1959, 324.
4) R. F. Bryan and R. M. Knopf, ibid., 1961, 203.
5) M. H. Hardig, *J. Chem. Soc.*, 1958, 4136.
6) J. C. Pariaud and P. Archinard, *Rec. Trav. Chim.*, 71, 634 (1952).

sulfur atom and one of the four nitrogen atoms. The posibility of behaving as a tridentate may be ruled out because of the steric condition.

According to the crystal structure analysis[5], the dithizonate ions in the bis(dithizonato)-mercury(II) molecule are coordinated through its sulfur atoms and nitrogen atoms of the azo radicals to the central metal, as shown in Fig. 1. In fact, the crystal structure analysis was carried out with a pyridinated compound. The nitrogen atoms of the pyridine molecules, however, are not linked with the mercury(II) ions but are connected with nitrogen atoms of imino groups of the dithizonate ion by hydrogen bonds. Therefore, the configurations around the mercury(II) ion in the non-solvated crystals, prepared in the present work, may be assumed to be the same as that in the pyridinated compound.

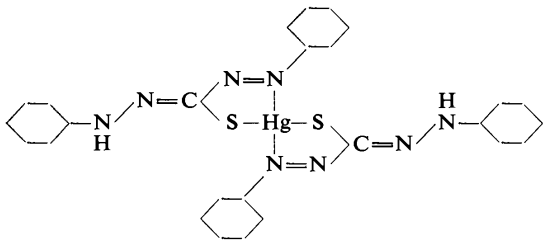

Fig. 1. The structure of bis(dithizonato)-mercury(II).

The infrared spectra of these metal dithizonates and of dithizone itself are shown in Fig. 2. Because the dithizonate ion is coordinated through its sulfur and nitrogen atoms to the mercury(II) ion, the C-S streching and -N=N- stretching absorptions may be shifted to lower frequencies. The N-H stretching vibration was observed by Duncan and Thomas[7] at 3272 cm^{-1} for the mercury(II) compound in carbon tetrachloride. The present measurement, using the KBr method, reveals that the corresponding absorption band appears at 3260, 3235 and 3232 cm^{-1}, respectively, for the mercury(II), cadmium(II) and zinc(II) compounds. However, these characteristic bands of dithizone have not yet been assigned; it is difficult, therefore, to discuss the coordination from these stretching vibrations at the present stage. Nevertheless, some conclusion may be derived by comparing these spectra. If the coordination type of bis(dithizonato)zinc(II) and bis(dithizonato)cadmium(II) is different from that of bis(dithizonato)mercury(II), the configuration of the dithizonate ion in th zinc(II) or cadmium(II) compound is not the same as in the mercury(II) compound. Accordingly, the skeletal vibrations of zinc(II) or cadmium-(II) complexes of dithizone should vary considerably compared with those of the mercury-(II) compound. However, as can be seen in Fig. 2, patterns of skeletal vibrations which are

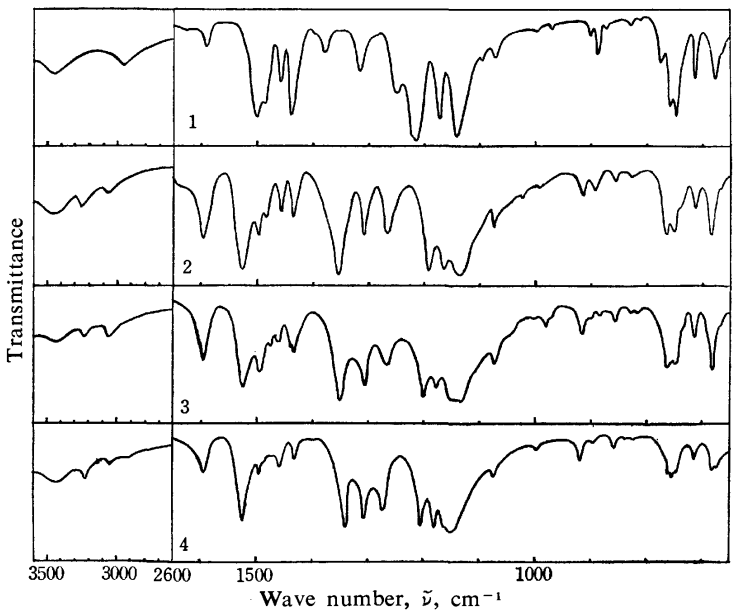

Fig. 2. Infrared spectra in KBr disk.

1 Dithizone
2 Bis(dithizonato)mercury(II)
3 Bis(dithizonato)cadmium(II)
4 Bis(dithizonato)zinc(II)

7) J. F. Duncan and F. G. Thomas, *J. Chem. Soc.*, **1960**, 2823.

expected to appear from 1000 cm^{-1} to 1300 cm^{-1}, are very similar, and the peaks for the corresponding vibrations are found to be shifted regularly in the order of the atomic number. It may, therefore, be concluded that the configurations and the mode of the coordination of dithizonate ions are all identical in these metal complexes of dithizone. Consequently dithizonate ions are presumed to be coordinated through the sulfur atom and nitrogen atom of the azo radical to the zinc(II) or the cadmium(II) ion as well as to the mercury(II) ion.

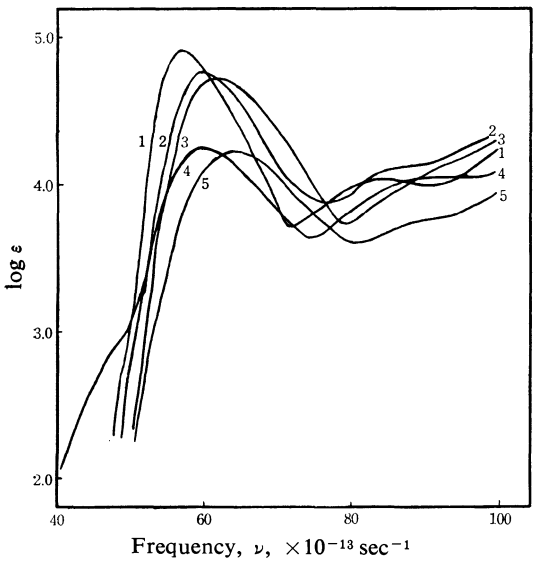

Fig. 3. Absorption spectra in pyridine.
1 Bis(dithizonato)zinc(II)
2 Bis(dithizonato)cadmium(II)
3 Bis(dithizonato)mercury(II)
4 Dithizone
5 Dithizone in aqueous ammonia

The visible and ultraviolet absorption spectra of these complexes in pyridine were determined and are shown in Fig. 3. The spectra of the zinc(II) and mercury(II) complexes in chloroform were found to be almost identical with the spectra of the same complexes in pyridine. As may be seen in Fig. 3, these curves are essentially similar, and maxima of the corresponding bands are shifted to a higher frequency in the order: zinc(II)<cadmium(II)<mercury(II). The order agrees with the current view about the strength of the perturbing effect of the metal ions on the ligand. The rather close similarity of the spectra and the regular shift of the absorption bands seem to be in agreement with the above-mentioned conclusion that the mode of the coordination of dithizonate ions is quite similar among the complexes of the three metal ions.

Summary

Two forms of bis(dithizonato)cadmium(II) have newly been isolated. Upon recrystallization from pyridine, both the forms yielded the same dark red crystalline powder. A comparison of their infrared and ultraviolet spectra shows that the mode of coordination and the configuration of zinc(II) and cadmium(II) are the same as in the mercury(II) complex.

Department of Chemistry
Faculty of Science
Osaka University
Nakanoshima, Osaka

Synthetic Resins Catalyzing the Racemization of Amino Acids. III. Racemization by the Column Procedure

By Koji Toi, Yoshiharu Izumi and Shiro Akabori

(Received March 27, 1963)

In previous papers[1-3], the preparation and activity of the resins catalyzing the racemization of amino acids were described. In the present research, it was found that, on the continuous flow of an amino acid solution containing cupric ion through a column of the resin, racemization of the amino acid was achieved to a degree which was determined by or was dependent on the flow rate. The catalytic resin used was prepared, as has been described in a previous paper[2], by chemical modification of *o*-cresol-phenol-formalin resin. Powdered *o*-cresol-phenol-formalin resin was oxidized with chromium trioxide in a mixture of acetic

1) K. Toi, Y. Izumi and S. Akabori, This Bulletin, **35**, 1422 (1962).
2) K. Toi, Y. Izumi and S. Akabori, ibid., **36**, 734 (1963).
3) K. Toi, ibid., **36**, 739 (1963).

anhydride and acetic acid, and the acetal produced was hydrolyzed with 4 N hydrochloric acid. The aldehyde content of the resin was 0.24 mmol. per gram of dry resin.

A column 30 cm. long and 2 cm. in diameter was made with 40 g. of the resin, which had been previously buffered to pH 10.0~10.5 with a borate buffer. The column was fitted with a glass jacket, through which water at 80°C was circulated, and operated at a constant temperature. An aqueous solution of 1.0 M L-alanine containing 0.1 M cupric acetate monohydrate was adjusted to pH 10.0~10.5 with sodium hydroxide. This solution was run through the column, and the effluent was fractionated every 5 ml. Each fraction of five intervals was diluted with two volumes of 6 N hydrochloric acid, and its optical rotation was measured. The racemization reaction during the passage through the column proceeded well, with the decrease in the flow rate shown in Fig. 1. L-Alanine racemized completely at a flow rate of 5 ml. per 13 min.

The amino acid content in the solution used for the optical rotation measurement was determined by the ninhydrin colorimetric method[4]. The loss of the alanine during the passage through the column was below 10%.

Fractions 80 to 120 were combined and made acidic with hydrochloric acid. The acidic solution was treated with hydrogen sulfide to remove the cupric ion. After subsequent treatment of the solution with ion exchange columns to remove the sodium salt, alanine was obtained in a yield of 14 g., which corresponded to 80% recovery. The alanine which recovered was optically inactive. $[\alpha]_D^{15}$ 0.00 (*c* 3, 6 N hydrochloric acid).

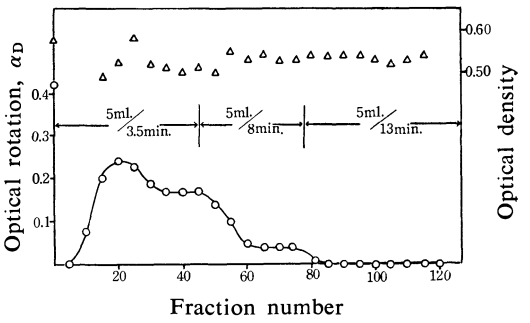

Fig. 1. Racemization of L-alanine by column procedure.
○ Optical rotation of the effluent.
△ Optical density measured by the ninhydrin method.

Division of Organic Chemistry
Institute for Protein Research
Osaka University
Kita-ku, Osaka

4) E. W. Yemm and E. C. Cocking, *Analyst*, **80**, 209 (1955).

*A Simple Digestion Method for the Quantitative Analysis of Metal in Some Organometallic Compounds**

By Shigemi KOHAMA

(Received March 28, 1963)

Metal in organometallic compound can be quantitatively determined as metallic oxide by either the combustion method or the digestion method. Since the latter procedure is simpler than the former, the digestion method has been extensively applied in various ways through the years by many workers[1]. In this digestion, generally, the complete decomposition of organometallic compounds can be achieved by treatment with concentrated sulfuric acid alone or with an accompanying oxidizing agent, such as nitric acid, perchloric acid and hydrogen peroxide.

In a preceding paper[2], the present author has proposed an analytical method in which organosilicon compounds were completely decomposed in a mixture of concentrated sulfuric acid and perchloric acid, silica being left. However, this method was unsuitable for the determination of tin in organotin compounds, since lower analytical values were

* Added in proof: This study was presented at the 16th Annual Meeting of the Chemical Society of Japan, Tokyo, April, 1963.

1) Cf. R. W. Leeper, L. Summers and H. Gilman, *Chem. Revs.*, **54**, 158 (1954); T. W. Campbell, H. G. Walker and G. M. Coppineer, ibid., **50**, 282 (1952); C. A. Burkhard, E. G. Rochow, H. S. Booth and J. Hartt, ibid., **41**, 138 (1947); R. K. Ingham, S. D. Rosenberg and H. Gilman, ibid., **60**, 519 (1960).

2) S. Kohama and S. Fukukawa, *Sci. and Ind.* (*Kagaku to Kogyo*), **32**, 113 (1958).

Table I. Changes of tribenzyltin chloride in various reagent mixtures
Sample 0.5 g. Temp. 150~200°C

No.	Reagent solution		Observation
	Conc. H_2SO_4 cc.	Oxidizing reagent	
1	5	None	Required long time for digestion
2	—	Fuming HNO_3 5cc. alone	Difficult to dissolve and carbonize
3	5	Fuming HNO_3 2cc.	By adding HNO_3, separation of sample and then carbonization occured
4	5	Conc. $HClO_4$ 2cc.	Volatilization of tin chloride
5	—	Conc. $HClO_4$ 2cc. + Fuming HNO_3 2cc.	Vigorous oxidation and frequent explosion
6	5	NH_4NO_3 crystal 1.4 g.	Moderate and complete Decomposition

Table II. Results of analysis
Sample 100~200 mg. Conc. H_2SO_4 3cc.

Compound	NH_4NO_3 g.	Metal Calcd. %	Metal Found %	Daviation %
$(C_4H_9)_3SnCl$	0.8	36.46	36.42	−0.10
$(C_4H_9)_2SnCl_2$	0.8	39.06	38.98	−0.20
$(C_8H_{17})_2SnCl_2$	1.0	28.52	28.50	−0.07
$(C_8H_{17})_2SnO$	1.0	32.86	32.86	±0.00
$(C_6H_5CH_2)_3SnCl$	1.0	27.76	27.75	−0.03
$(C_6H_5CH_2)_2SnCl_2$	1.0	31.92	31.86	−0.19
$(C_6H_5)_3SnOOCCH_3$	1.0	29.02	29.23	+0.72
$(C_6H_5)_4Sn$	1.0	27.79	27.67	−0.43
$(i\text{-}C_3H_7O)_4Ti$	0.4	16.85	16.79	−0.36
$(n\text{-}C_4H_9O)_4Ti$	0.4	14.07	14.05	−0.14
$(C_6H_5)_2SiCl_2$	0.8	11.08	11.02	−0.54
$(C_6H_5)_2Si(OOCCH_3)_2$	0.8	9.35	9.39	+0.43
$C_6H_5Si(OOCCH_3)_3$	0.8	0.95	10.01	+0.60
$(C_6H_5)_2Si(OC_2H_5)_2$	0.8	10.31	10.34	+0.29
$C_6H_5Si(OCH_2CH{=}CH_2)_3$	0.6	10.16	10.20	+0.39
$(CH_3)_3SiOC_3H_7{}^i$	0.6	21.24	21.23	−0.04
$(CH_3)_2Si(OC_3H_7{}^i)_2$	0.6	15.93	15.88	−0.31
$CH_3C_2H_5Si(OH)_2$	0.6	26.45	26.28	−0.64
$CH_3(CH_2{=}CH)Si(OH)_2$	0.6	26.96	26.88	−0.29
$CH_3(C_6H_5CH_2)Si(OH)_2$	0.8	16.69	16.65	−0.24
$(C_6H_5)_2Si(OH)_2$	0.8	12.99	12.93	−0.46
$(CH_3)_2(p\text{-}ClC_6H_4)SiOH$	0.8	15.04	15.06	+0.13
$((CH_3)_2SiO)_4$	0.8	37.87	38.05	+0.48
$((C_6H_5)_2SiO)_3$	1.0	14.16	14.27	+0.78
$((C_6H_5)_2SiO)_4$	1.0	14.16	14.11	−0.35
$(p\text{-}BrC_6H_4)_2Si(CH_3)_2$	1.0	7.58	7.61	+0.33
$1,4\text{-}(CH_3)_3SiC_6H_4Si(CH_3)_3$	1.0	12.62	12.57	−0.39

always obtained because of the volatilization of some tin compounds.

For the quantitative analysis of tin in organotin compounds, a procedure[3] has recently been recommended in which the tin compound was first converted into less volatile bromide with bromine in carbon tetrachloride and then digested by the usual way; however, this method disadvantageously requires a long time (about six hours) for a run of analysis.

In order to select a suitable oxidizing agent for tribenzyltin chloride, which is known to be difficult to decompose, digestions were carried out in concentrated sulfuric acid with the usual oxidizing reagents and with ammonium nitrate. The results are shown in Table I.

It is found that ammonium nitrate is superior to other oxidizing reagents in digesting the tin compound. Hence, the author carried out

3) H. Gilman and W. B. King, *J. Am. Chem. Soc.*, **51**, 1213 (1929).

the quantitative estimation of the metal in some organometallic compounds, using ammonium nitrate as an oxidizing reagent. The results on a number of organosilicon compounds, organotin compounds and organotitanium compounds are indicated in Table II; it has thus been found that almost all of the metal in these compounds could be determined accurately.

The values given in Table II are the average of three determinations in most cases.

Thus, the method seems to be a convenient procedure for the determination of the metal in various organometallic compounds. By using ammonium nitrate as a reagent, the loss of the metal salt owing to the volatilization can be completely avoided. There are two further advantages as well; solid ammonium nitrate dissolves uniformly in the solution without forming a separate phase, as in the case of liquid oxidizing agents, and the colorless solution can be obtained by about 30 min. of heating, without any spattering of the sample.

Experimental

All the reagents used were of analytical grade. The organometallic compounds subjected to the tests were partly commercial products and partly compounds which had been synthesized in this Institute. Most of them were further purified according to the methods of the literature.

The Observation of Changes of Tribenzyltin Chloride in Digesting a Solution Containing Perchloric Acid.—A small amount of tribenzyltin chloride was placed in concentrated sulfuric acid containing perchloric acid and then heated to 150~200°C for 5 min., at which time a vigorous reaction started, accompanied with white vapor; this vapor was then passed into dilute aqueous ammonia through a delivery tube. The white precipitate formed in the absorbing solution was identified as tin oxide after ignition.

Analytical Procedure.—About 0.2 g. of a sample is placed in previously-weighed platinum crucible (40 ml.). Then 3 ml. of concentrated sulfuric acid is added, and the mixture is carefully warmed to dissolve the sample. After the mixture has then been cooled somewhat, a spoonful of crystalline ammonium nitrate (about 0.2 g.) is added, with gentle shaking. Gradual oxidation begins as the crystal dissolves into the solution, and the mixture is kept standing for 5 min. In many cases, the content is not yet decolorized, and another spoonful of ammonium nitrate is added, the mixture is then heated carefully so as to avoid spattering. When the mixture is difficult to decolorized, the above procedure is repeated until a colorless solution is obtained. The maximum weight of ammonium nitrate required for the completion of the reaction is about one gram. The contents of the platinum crucible are heated moderately during evaporation and finally ignited intensively until the constant weight of the metallic oxide is attained. The metal is weighed as metallic oxide. The whole procedure takes about 50 min.

Summary

A new, modified digestion method for the quantitative analysis of metal in various organometallic compounds containing silicon, tin and titanium has been developed by the use of ammonium nitrate as a new oxidizing reagent. It has been shown that this method can be carried out more rapidly and more accurately than the other known methods.

The author wishes to express his gratitude to Dr. Sadaomi Fukukawa of this Institute for his advice, and to Professor Shunsuke Murahashi of Osaka University for his kind encouragement and advice throughout this work. He is also grateful to Mr. Toyoji Nakajima, Mr. Manabu Morimoto and Mr. Shoji Suzuki for checking the analysis.

The Osaka Municipal Technical Research Institute
Kita-ku, Osaka

The Electronic Spectra of Aromatic Molecular Crystals. I. Substitued Benzene Molecules

By Jiro TANAKA

(Received February 11, 1963)

Considerable progress has recently been made in the interpretation of the electronic spectra of benzene and the polyacenes[1]. The effect of substituents on the spectrum of benzene has been studied by Nagakura and Tanaka[2], Longuet-Higgins and Murrell[3] and many others[4]. The best way of confirming the theoretical assignments is to measure the polarization of the single crystal absorption band. One such investigation is the study of *p*-dimethoxybenzene by Albrecht and Simpson[5]. They measured the polarization of crystalline absorption and showed that the 280 mμ band of the molecule is polarized perpendicular to the two-fold symmetry axis; hence, the symmetry of the excited level corresponding to the 260 mμ band of benzene is confirmed to be $^1B_{2u}$. In general, monosubstituted benzene molecules have an absorption band corresponding to the 260 mμ band of benzene. When electron-donating substituent groups (such as amino, hydroxyl, methyl and others) are introduced, the 260 mμ band of benzene shifts to the red and increases in intensity. When electron-accepting groups (such as nitro, carbonyl and carboxyl) are substituted, a conspicuous strong, new absorption band appears in the region of 230~360 mμ; this has been interpreted as an intramolecular charge transfer band on the basis of relative energy level locations of benzene and substituent[2]. The direction of the transition moment (polarization) of the latter type of band should be quite different from the former; it may lie on the line connecting the center of the benzene ring and the substituent group.

The primary purpose of this paper is to present a sound basis for the intramolecular charge transfer theory of the spectra of monosubstituted benzenes by measuring the polarization of bands with single crystals. The crystal structures of durene, *p*-nitroaniline, benzoic acid, acetanilide and *trans*-cinnamic acid are known, so the directions of the transition moments can be determined easily by measuring the crystal spectra on the assumption that an oriented gas model is applicable. Owing to a mixing of different excited states and an electron exchange interaction between neighboring molecules, some crystals show noticeable deviations from an oriented gas model, but the crystals of the present investigation show little of this. For this reason it is safe to deduce the direction of the transition moment from the polarization measurement. The possibility of Davydov splitting and of intermolecular charge transfer bands in the crystal has also to be taken into account[6-10].

Experimental

The Spectra of Solutions.—Ultraviolet absorption spectra measurements have been made with a Cary recording spectrophotometer model 14. The spectrophotometer was flushed with dry nitrogen for recording between 220~185 mμ.

Ultraviolet Microspectrophotometer. — For the transmission measurement of aromatic molecular crystals, very thin crystals less than one micron thick are needed because the molar extinction coefficients are 10^4 to 10^5. An ultraviolet microspectrophotometer was used for measuring the spectra of very thin and small crystals.

A schematic diagram of the apparatus is shown in Fig. 1. A double monochromator of the Olympus Optical Co. (A), equipped with synthetic silica prisms and a hydrogen discharge lamp or tungsten lamp (L), has been used. The small diaphragm (B) is set to eliminate the stray light at the exit slit. The light beam is reflected by a mirror (C), is polarized by a Rochon-type polarizer (D) made of natural quartz, and is condensed by

1) M. G. Mayer and A. L. Sklar, *J. Chem. Phys.*, **6**, 645 (1938); R. Pariser and R. G. Parr, ibid., **21**, 466, 767 (1953); M. J. S. Dewar and H. C. Longuet-Higgins, *Proc. Phys. Soc.*, **A67**, 795 (1954); R. Pariser, *J. Chem. Phys.*, **24**, 250 (1956); **25**, 1112 (1957).

2) S. Nagakura and J. Tanaka, ibid., **22**, 236 (1954); S. Nagakura, ibid., **23**, 1441 (1955); J. Tanaka, S. Nagakura and M. Kobayashi, ibid., **24**, 311 (1956); J. Tanaka and S. Nagakura, ibid., **24**, 1274 (1956).

3) H. C. Longuet-Higgins and J. N. Murrell, *Proc. Phys. Soc.*, **A68**, 601 (1955); J. N. Murrel, ibid., **A68**, 969 (1955).

4) A. L. Sklar, *J. Chem. Phys.*, **7**, 984 (1939); ibid., 10, 135 (1942); F. A. Matsen, *J. Am. Chem. Soc.*, **72**, 5243 (1950); J. R. Platt, *J. Chem. Phys.*, **19**, 263 (1951); L. Goodman, I. G. Ross and E. Shull, ibid., **26**, 474 (1957).

5) A. C. Albrecht and W. T. Simpson, ibid., **23**, 1480 (1955).

6) D. P. Craig, *Rev. Pure and Appl. Chem.* (*Australia*), **3**, 207 (1953).

7) D. S. McClure, *Solid State Physics*, **8**, 1 (1958).

8) H. C. Wolf, ibid., **9**, 1 (1959).

9) J. Tanaka, *Prog. Theoret. Physics* (*Kyoto*), Suppl. **12**, 183 (1959).

10) K. Nakamoto, *J. Am. Chem. Soc.*, **74**, 1739 (1952).

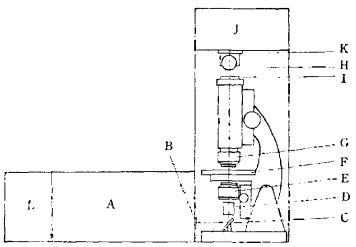

Fig. 1. Ultraviolet microspectrophotometer.

a lens (E) onto the sample. The lenses (E and G) are of Grey's Bausch and Lomb reflecting-refracting type. The numerical aperture of the lens is 0.20~0.72, and the magnification is ×53. The condenser lens (E) is used to collimate the monochromatic light onto the crystal, thereby eliminating the Schwarzschild-Villiger effect[12]. The crystal to be measured is placed between a quartz objective slide 1.0 mm. thick and a 0.18 mm-thick cover glass, and settled on the rotatable table (F). The orientation of the crystal is adjusted, so that one of the crystalline axes is parallel to the direction of the polarization of the light, by the aid of the eyepiece (H) and the cross (I). The iris-diaphragm placed at the top of the microscope is used to cut off the flare light, which disturbs the accurate measurement of the polarization. The shutter (K) is placed in front of an RCA 1p-28 photomultiplier tube, by the use of which, along with that of a direct current amplifier (J), it is possible to measure the light intensity. The effective slit-widths are smaller than 1 mμ, which is sufficient to resolve the broad absorption band of aromatic crystals at room temperature.

The angle of the incident light normal to the plane of the crystal ranges from 12° to 46° because objective and condenser lenses have numerical apertures of 0.20 to 0.72. The polarization of the light is not altered by reflection and refraction at the lens surfaces. In addition, if the transition moments associated with each molecules are parallel to the developed crystalline surface, the intensity of the absorption bands does not depend on the angle of the incident light[13]. However, when the transition moments are vertical to the developed crystalline plane, the absorption may depend greatly on the directional angle of the incident light, and the intensity of absorption has only a qualitative significance.

The stray light of the instrument is estimated to be less than 0.5% of the total light; hence, the measured optical density is reliable up to 2.5. By the use of this microspectrophotometer, the ultraviolet absorption spectra of small single crystals, as small, for example, as $20\mu \times 20\mu \times 0.5\mu$, of aromatic molecules are easily obtained.

p-Nitroaniline

The ultraviolet absorption spectra of *p*-nitroaniline in ethanol and *n*-heptane solutions are shown in Fig. 2. A large solvent effect is observed for this molecule. The first band undergoes a shift from 320 mμ in *n*-heptane to 370 mμ in ethanol. The shift is probably due to a polar solvent effect—the stabilization of the polar-excited state in the polar solvent —or to the hydrogen bonding between the amino group and the oxygen atom of the hydroxyl group of ethanol[14]. One interpretation of this band is that its origin is the 260 mμ band of benzene shifted to the red and intensified by the substituent groups. However, according to Nagakura and Tanaka's theory of intramolecular charge transfer spectra, the 370 mμ band is interpreted by a mechanism

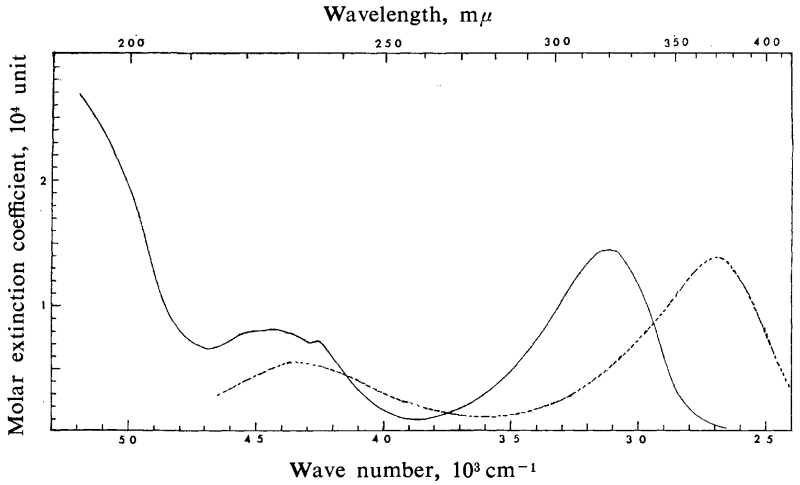

Fig. 2. Electronic absorption spectrum of *p*-nitroaniline.

11) D. S. Grey and P. H. Lee, *J. Opt. Soc. Am.*, 39, 719 (1949).
12) H. Naora, *Science*, 114, 279 (1951).
13) M. F. Perutz, *Acta Cryst.*, 6, 859 (1953).
14) S. Nagakura and H. Baba, *J.Am. Chem. Soc.*, 74, 5693 (1952).

of charge transfer, which takes place from the highest-occupied level of the anilino group to the vacant orbital of the nitro group. Following the former interpretation, the band should be polarized along the short axis of the molecule, while the latter predicts the long axis polarization. By a polarization measurement of the crystalline spectrum, it is easy to eliminate one of these possibilities.

Calculation of the Excited State of *p*-Nitroaniline.—The author[15] has previously calculated the electron affinity of the nitro group and has shown that it behaves as an electron acceptor when conjugated with other π-electron systems, because the group has a large electron affinity. In the present treatment, *p*-nitroaniline is considered to be a composite molecule, consisting of anilino and nitro groups; the electronic interaction between those two groups is calculated by the method of Longuet-Higgins and Murrell[3].

The electronic spectrum of aniline has been studied by Platt and Klevens[16] experimentally and by Murrell[3] theoretically. According to the latter assignment, the ground state and lower excited states configurations are described by a combination of the χ_0, ψ_α, ψ_p, ψ_β, $\psi_{\beta'}$, $\theta^{-1}\varphi_4$ and $\theta^{-1}\varphi_5$ wave functions, where χ_0, ψ_α, ψ_p, ψ_β and $\psi_{\beta'}$ are the wave functions of benzene in its ground state, $^1B_{2u}$, $^1B_{1u}$ and $^1E_{1u}$ are excited states. Functions $\theta^{-1}\varphi_4$ and $\theta^{-1}\varphi_5$ represent, respectively, charge transfer configurations in which a non-bonding electron in the amino nitrogen (denoted by θ) is transferred into the vacant φ_4 and φ_5 orbitals of benzene.

The electron affinity of the nitro group was calculated as -0.40 eV.[15], and the vacant orbital is written as

$$\varphi_w = 0.700\chi_N - 0.502(\chi_0 + \chi_{0'})$$

where χ_N, χ_0 and $\chi_{0'}$ are the $2p\pi$ atomic orbitals of nitrogen and oxygen atoms.

We restrict our attention to the two charge transfer configurations of lowest energy. The highest-occupied orbital of aniline is at -7.70 eV., and the second highest orbital is assumed to be the same as benzene. Next, the configurational interaction between the charge transfer configuration with the locally-excited configurations of aniline is taken into account. The energy of the $\varphi_2{}^{-1}\varphi_w$ and $\varphi_3{}^{-1}\varphi_w$ charge transfer configurations are calculated by the following formula;

$$H_{CT} = I_p - E_A - (\varphi_w\varphi_w \mid \varphi_D\varphi_D) + \sum \delta_{DS}$$

where E_A is the electron affinity of the nitro group, I_p is the ionization potential of the donor orbital in aniline, $(\varphi_w\varphi_w \mid \varphi_D\varphi_D)$ is the electrstatic energy between electrons in φ_w and φ_D orbitals, and the last term, $\sum \delta_{DS}$, denotes the electrostatic energy between the hole in the anilino group with the formal charges on each atom of the substituent nitro group. Taking the numerical values of $E_A = -0.40$ eV., $I_{p_2} = 7.70$ eV., $I_{p_3} = 9.24$ eV., $(\varphi_w\varphi_w \mid \varphi_{D_2}\varphi_{D_2}) = 4.60$ eV., $(\varphi_w\varphi_w \mid \varphi_{D_3}\varphi_{D_3}) = 4.13$ eV., $\sum \delta_{2S} = 0.27$ eV. and $\sum \delta_{3S} = 0.43$ eV., the levels are calculated as 3.77 eV. and 5.94 eV. for the A-type and B-type symmetry states respectively.

The off-diagonal matrix elements are calculated by taking the carbon-nitrogen atom's exchange integral β to fit the calculated value with the observed excitation energies, and the value is selected as -2.30 eV. Then the secular equations for A and B type symmetry levels are given as follows:

A-type symmetry:

$$\begin{array}{c|ccccc} \varphi_0 & -E & 0.93 & 0 & 0 & 0 \\ \varphi_2{}^{-1}\varphi_w & 0.93 & 3.77-E & 0.21 & 0.33 & 0.73 \\ \varphi_{1A} & 0 & 0.21 & 5.27-E & 0 & 0 \\ \varphi_{2A} & 0 & 0.33 & 0 & 6.30-E & 0 \\ \varphi_{3A} & 0 & 0.73 & 0 & 0 & 7.40-E \end{array} \qquad (3)$$

B-type symmetry:

$$\begin{array}{c|cccc} \varphi_{1B} & 4.31-E & 0.51 & 0 & 0 \\ \varphi_3{}^{-1}\varphi_w & 0.51 & 5.94-E & 0.71 & -0.40 \\ \varphi_{2B} & 0 & 0.71 & 6.30-E & 0 \\ \varphi_{3B} & 0 & -0.40 & 0 & 7.40-E \end{array} \qquad (4)$$

15) J. Tanaka, *J. Chem. Soc. Japan, Pure Chem. Sec.* (*Nippon Kagaku Zassi*), 78, 1636 (1957).

16) J. R. Platt and H. B. Klevens, *J. Am. Chem. Soc.*, 71, 1714 (1949).

By solving these equations, the energies of the states are obtained as follows:

Energy	Wave function	Symmetry	
−0.22 eV.	$0.972\varphi_0+0.231\varphi_2{}^{-1}\varphi_w-0.212\varphi_{1A}-0.017\varphi_{2A}-0.025\varphi_{3A}$	A	
+3.78 eV.	$-0.232\varphi_0+0.937\varphi_2{}^{-1}\varphi_w-0.121\varphi_{1A}-0.113\varphi_{2A}-0.201\varphi_{3A}$	A	
+5.30 eV.	$0.089\varphi_0-0.132\varphi_2{}^{-1}\varphi_w-0.991\varphi_{1A}-0.022\varphi_{2A}-0.019\varphi_{3A}$	A	(5)
+6.34 eV.	$0.012\varphi_0-0.123\varphi_2{}^{-1}\varphi_w+0.040\varphi_{1A}-0.990\varphi_{2A}-0.053\varphi_{3A}$	A	
+7.55 eV.	$0.022\varphi_0-0.189\varphi_2{}^{-1}\varphi_w+0.042\varphi_{1A}+0.078\varphi_{2A}-0.978\varphi_{3A}$	A	
+4.15 eV.	$0.947\varphi_{1B}+0.294\varphi_3{}^{-1}\varphi_w+0.126\varphi_{2B}-0.080\varphi_{3B}$	B	
+5.53 eV.	$-0.303\varphi_{1B}+0.702\varphi_3{}^{-1}\varphi_w-0.641\varphi_{2B}+0.068\varphi_{3B}$	B	(6)
+6.90 eV.	$0.100\varphi_{1B}-0.646\varphi_3{}^{-1}\varphi_w-0.756\varphi_{2B}-0.077\varphi_{3B}$	B	
+7.37 eV.	$0.029\varphi_{1B}-0.051\varphi_3{}^{-1}\varphi_w-0.037\varphi_{2B}+0.998\varphi_{2B}$	B	

TABLE I.

Calculated energy Symmetry A	Calculated energy Symmetry B	Observed energy
4.00 eV.		3.88 eV (320 mμ in *n*-heptane solution)
	4.37 eV.	4.60 eV (270 mμ in the crystal)
5.52 eV.	5.75 eV.	5.52 eV (220 mμ in *n*-heptane solution)
6.56 eV.		
	7.12 eV.	
7.77 eV.	7.59 eV.	

where φ_0, φ_{1A}, φ_{2A}, φ_{3A}, φ_{1B}, φ_{2B} and φ_{3B} denote the wave functions of aniline in the ground and excited states as calculated by Murrell, and $\varphi_2{}^{-1}\varphi_w$ and $\varphi_3{}^{-1}\varphi_w$ are the charge transfer configurations described above. The levels belonging to the A-type symmetry group should be active in the long axis, and the B-type symmetry levels, in the short axis of the molecule. The calculated excitation energies are tabulated in Table I, together with the observed values. The agreement between observed and calculated values is generally good, and it is shown that the first strong band at 320mμ in an *n*-heptane solution is predominantly derived from the charge transfer configuration with A-type symmetry. The polarization of this band is deduced to be long-axis, while the next band, at 270 mμ, should be short axis-polarized. The latter band is observed in the crystalline spectrum, but not in *n*-heptane and ethanol solutions, this may be because it borrows intensity from allowed transitions in the crystal. In the region below 220 mμ, there are several transitions belonging to both A- and B-type symmetries; hence, the 220 mμ absorption may consist of two bands, namely, those arising from the transitions between the ground state and the 5.30 eV. and 5.53 eV. states.

The Spectrum of *p*-Nitroaniline Crystal.—The optical properties of *p*-nitroaniline crystal are described by Groth and Winchell as follows[17,18]:

$N_X' = 1.556$, $N_Y = 1.777$, N_Z ?;

Optical plane (010): $2V = 80°(\pm ?)$

The optical axis X is nearly vertical to the (101) plane, and Y=b. This work has been confirmed with the addition of $2V=-80°$. By the use of these values, N_Z is calculated to be 2.005, and the birefringence with (101) plane is estimated to be 0.228. The crystal used for spectral measurement is made by sublimation, and it develops the (101) cleavage plane.

The crystal structure of *p*-nitroaniline has been determined by Abrahams and Robertson and by Donohue and Trueblood[19]. The crystal is monoclinic with the following unit cell dimensions: $a=12.34$, $b=6.02$, $c=8.63$Å and $\beta=91°40'$. The space group is $C_{2h}{}^5-P2_1/n$ with four molecules per unit cell. The projection of the molecules in the unit cell onto the (101) plane, which is the most easily developing face, is shown in Fig. 3(a).

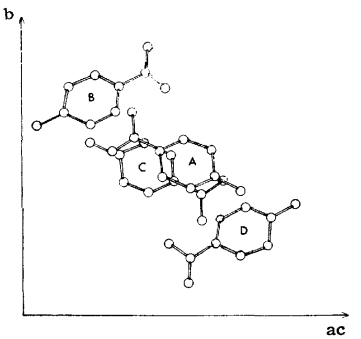

Fig. 3 (a). Projection of *p*-nitroaniline molecules onto the (101) plane.

17) P. Groth, "Chemische Kristallographie", W. Engelmann Leipzig (1906-1919).
18) A. N. Winchell, "The Optical Properties of Organic Compounds", University of Wisconsin Press, Madison. Wisconsin (1943).
19) S. C. Abrahams and J. M. Robertson, *Acta Cryst.*, **1**, 252 (1948); J. Donohue and K. N. Trueblood, ibid, **9**. 960 (1956); K. N. Trueblood, E. Goldish and J. Donohue, ibid., **14**, 1009 (1961).

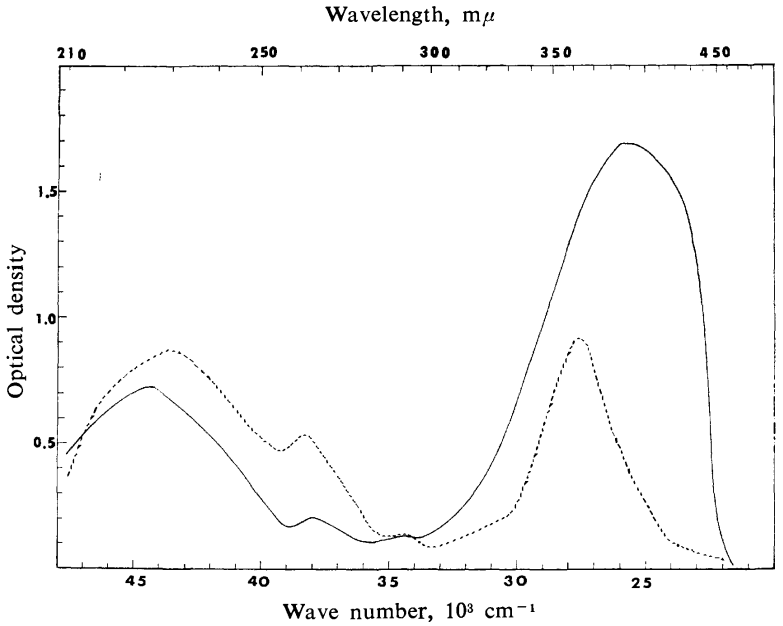

Fig. 3 (b). Polarized absorption spectrum of *p*-nitroaniline crystal.
—— The light polarized parallel to 101 dirrection
---- The light polarized parallel to b-axis

The thickness of the crystal was determined approximately by observing the interference color with a polarizing microscope and by using the relation between the retardation and birefringence; namely $R=d(n_{ac}-n_b)$, where R is the retardation and $n_{ac}-n_b$, the birefringence with the (101) plane, and d, the thickness. For more accurate measurement of crystalline thickness, the "apparent absorption band" in the visible region was measured with the polarized light. This absorption appears as a result of the interference of the beam reflected from the front surface with the beam reflected upon the rear surface[20]. For a wavelength at which the two beams interfere additively upon reflection and at which the transmission is at a maximum, the thickness, d, of the crystal is given by:

$$d=m\lambda/2n, \text{ where } m=3, 4, 5, \cdots\cdots$$

and n is the refractive index at the wavelength of measurement. For a wavelength where the transmission is at a minimum,

$$d=(2m+1)\lambda/4n, \text{ where } m=3, 4, 5, \cdots\cdots$$

In principle we can obtain the crystal thickness accurately by these means, but the dispersion of refractive index is not known, so the accuracy is limited to $\pm 0.03\mu$.

As has been mentioned before, the light falls onto the crystalline surface not at right angles but inclined about 46° to 12°. However, because of the refraction of the light at the crystalline surface, the light passes into the crystal inclined from 22° to 6° normal to the surface plane, and the optical path becomes necessarily large by about 1 to 10 per cent. This correction must be made in considering the optical path and, hence, the intensity of the crystalline absorption. As for the dichroism of the crystal, the transition moments of the molecules are nearly parallel to the (101) plane, so the dichroic ratio may be quite reliable in determining the polarization properties of molecular excited states.

The crystalline spectrum is shown in Fig. 3(b), where the spectrum with the light

Table II. The oscillator strength of the 370 mμ band in crystal

	Observed	Calculated (Oriented gas model)
$b_\perp$	0.127	0.74
$b_\parallel$	0.033	0.19

Table III. The observed and calculated dichroic ratios

	Observed	Calculated	
		Long-axis polarization	Short-axis polarization
$D_{ac}:D_b$	3.90 : 1.00 (370 mμ band) 1.00 : 3.26 (270 mμ band)	3.96 : 1.00	1.00 : 3.32

20) A. Bree and L. E. Lyons, *J. Chem. Soc.*, **1956**, 2658; E. Edser and C. P. Butler, *Phil. Mag.*, **46**, 207 (1898).

polarized parallel and perpendicular to the b-axis is presented. The thickness of this crystal is estimated to be 0.36 μ. Four absorption bands are seen in the spectrum, three are fairly strong and one very weak. Each band shows a conspicuous dichroism. The observed oscillator strength and dichroic ratios for the 370 mμ and 270 mμ bands are given in Tables II and III, together with the calculated values for the oriented gas model. Comparing the calculated dichroic ratio with the observed value, it is unequivocally determined that the 370 mμ band is polarized parallel to the long axis of the molecule, while the 270 mμ band is directed to the short axis of the molecule. This result is in conformity with the above-mentioned theory, and the strong band appearing at 370 mμ (320 mμ in an *n*-heptane solution) is proved to be an intramolecular charge-transfer absorption. The fact that the 270 mμ band is not observed in solution but appears in the crystal may be explained by a perturbation of other allowed transitions or by a lowering of the symmetry of the excited state in the crystal. Anyway, this transition is shown to have the symmetry of the B type, polarized to the short axis of the molecule, while the wave function in Eq. 6 shows that the state is mainly composed of the $^1B_{2u}$ excited state of benzene. In addition to this band, another very weak absorption band is also observed at 295 mμ only in the crystalline spectrum. This band is not seen in the spectrum of the solution, but Wepster[21] had found a corresponding band in the spectrum of 4-nitro-*N*, *N*-dimethylaniline. Since a very weak transition of this kind would not be expected to appear judging from the results of the calculation of the π-electron system mentioned before, it is most probable that this is an n-π^* transition of the nitro group. The polarization of such a weak band cannot retain its own characteristic directional property of n-π^*, because the intensity mainly comes from the mixing with the allowed π-π^*. Therefore, the polarization of this band cannot be perpendicular to plane of the molecule, and the dichroism may be observed according to the mixing with nearby π-π^* transition.

The band at 220 mμ has a much larger intensity in the ac direction than in the b-axis; however, we cannot say anything conclusive about the polarization of this band, because the calculated energy levels are crowded in this region and a mixing with higher excited levels also easily takes place.

The Calculation of Davydov Splitting.—The crystal of *p*-nitroaniline belongs to a space group of $C_{2h}^5-P2_1/n$, and the molecule A in Fig. 3 (a) is transformed into B by a screw axis rotation parallel to the b-axis, into D by a glide plane vertical to the b-axis, and into C by an inversion. Combining the results of this operation with the character table of the C_{2h}^5 group, we obtain the following excited states wave functions:

$$\left.\begin{aligned}
A_g:&\quad \varphi_\alpha=\frac{1}{2}(\varphi_D'+\varphi_C'+\varphi_A'+\varphi_B')\\
A_u:&\quad \varphi_\beta=\frac{1}{2}(\varphi_D'+\varphi_C'-\varphi_A'-\varphi_B')\\
B_u:&\quad \varphi_\gamma=\frac{1}{2}(\varphi_D'-\varphi_C'+\varphi_A'-\varphi_B')\\
B_g:&\quad \varphi_\delta=\frac{1}{2}(\varphi_D'-\varphi_C'-\varphi_A'+\varphi_B')
\end{aligned}\right\} \quad (7)$$

where φ_A', φ_B', φ_C' and φ_D' denote the excited states wave functions of A, B, C and D site molecules respectively.

The selection rule allows a transition to the A_u excited state polarized along the b-axis and to the B_u state polarized along the a, c-axes. The energies of these levels can be shown to be:

$$\Delta E_\beta=\Delta E_m+D+\varepsilon_\beta$$
$$\Delta E_\gamma=\Delta E_m+D+\varepsilon_\gamma$$
$$\varepsilon_\beta=(\lambda_{AB}-\lambda_{AC}-\lambda_{AD})/2$$
$$\varepsilon_\gamma=(-\lambda_{AB}-\lambda_{AC}+\lambda_{AD})/2$$
$$\lambda_{AB}=\sum_B\int \psi_A^{*\prime}(r_1)\psi_B^*(r_2)\times\frac{e^2}{r_{12}}\psi_A(r_1)\psi_B'(r_2)d\tau_1 d\tau_2$$

where ΔE_m is the excitation energy for a free molecule, D is the whole shift of the center of the crystalline level from that of the free molecule, and λ_{AB} represents the interaction between an excited A molecule ψ_A' with all other excited B site molecules in the crystal.

It is the splitting of the band between b and a, c crystalline directions which is important: $\Delta E_\gamma-\Delta E_\beta$. The calculation of the integrals λ_{AB} and λ_{AD} was carried out using the dipole-dipole approximation, and the summation was taken over a 11 Å radius sphere. The results are shown in Table IV. Comparing them with the experimental value of the splitting $E_b-E_{a,c}=1680\,cm^{-1}$, it is evident that an assignment of the band as long axis polarized gives the better result; the agreement

TABLE IV. THE CALCULATED AND OBSERVED VALUES OF DAVYDOV SPLITTING (E_b-E_{ac})

Assumed polarization	Calculated	Observed
Long axis	1484 cm^{-1}	1680 cm^{-1}
Short axis	76 cm^{-1}	

21) B. M. Wepster, *Rec. trav. chim.*, **76**, 357 (1959).

between the observed and the calculated values is remarkably good. The appearance of such a large splitting means that a strong coupling of resonance energy transfer takes place in the crystal of *p*-nitroaniline.

The Intensity of the Crystalline Absorption.— The intensity of the 370 mμ band decreases greatly in the crystal in both crystalline directions, namely about one-sixth of the expected value of the oriented gas model, as is seen in Table II. One of the reason for the reduction in the intensity of the crystal is that the actual electric field acting upon a molecule has a factor of $(n/\varepsilon(E_e/E))$, where n is the refractive index of the crystal, ε is the static dielectric constant, and E_e and E are the effective field and the average field respectively[22]. The numerical estimation of this factor is a difficult problem. However, an approximate values may be $\sim 1/n$. This accounts in part for the reduction of the intensity, because n is in the range of 2.0~2.5.

Recently Tinocco[23] and Rhodes[24] have presented a formula of the hypochromism of polymeric systems. However, it has not yet been established that their formula explains the results in the crystal of *p*-nitroaniline.

In some other aromatic molecular crystals such as naphthalene, McClure and Schnepp[25] and the present author[26] have found a more pronounced decrease in the intensity from the oriented gas values. This phenomenon is not explained by a simple oriented gas model, neglecting the electronic exchange interaction between neighboring molecules. In order to explain it, we must use another approach, taking into consideration the electronic exchange interaction of the electronic levels of the molecules in the crystal. On the contrary, the crystal of *p*-nitroaniline affords a good example of an appearance of the Davydov splitting; it also presents a successful use of the exciton theory of molecular crystals in explaining the features of the crystalline spectrum except for the anomalous reduction of the absorption intensity.

Abrahams and Robertson[19] have proposed the formation of a self-molecular complex of *p*-nitroaniline, but no absorption was found which could be attributed to the intermolecular charge transfer. Probably the intramolecular charge transfer process is predominant in the molecule itself, and the highest occupied orbital (the donor orbital) of aniline is stabilized by the nitro group, so that no intermolecular charge transfer occurs in the *p*-nitroaniline crystal.

Benzoic Acid

The ultraviolet absorption spectrum of benzoic acid has been measured in an *n*-heptane solution and is shown in Fig. 4. Three absorption bands appear in the region of 185~290 mμ; only the one of the longest wavelength shows some vibrational structures. A theoretical interpretation of the spectrum has been given previously[2], and that of benzaldehyde has been investigated more extensively by the present author[27]. The spectrum of benzaldehyde is very much like that of benzoic acid except that it has an n-π^* transition in the 330 mμ region. According to earlier calculations[27], the 280 mμ band of benzoic acid is assigned to the transition between the $^1A_{1g}$ ground state and the excited state, mainly

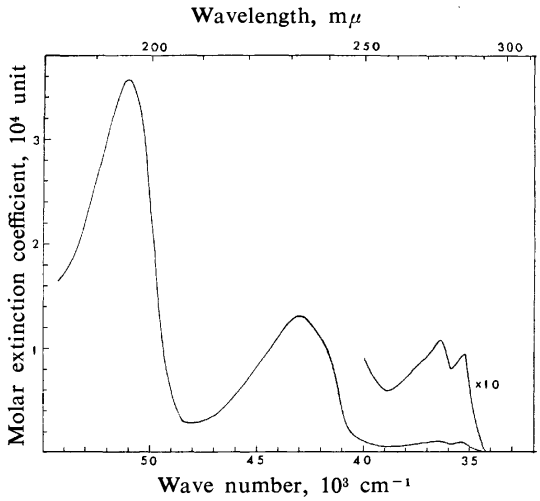

Fig. 4. Ultraviolet absorption spectrum of benzoic acid in *n*-heptane solution.

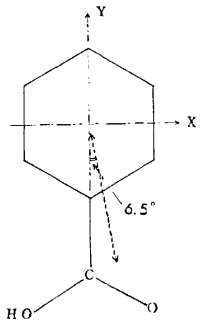

Fig. 5. Direction of the transition moment of the 230 mμ band of benzoic acid.

22) M. Lax, *J. Chem. Phys.*, 20, 1752 (1952).
23) I. Tinocco, Jr., *J. Am. Chem. Soc.*, 82, 4785 (1960); *J. Chem. Phys.*, 33, 1532 (1960); ibid., 34, 1067 (1961).
24) W. Rhodes, *J. Am. Chem. Soc.*, 83, 3609 (1961).
25) D. S. McClure and O. Schnepp, *J. Chem. Phys.*, 23, 1575 (1955).
26) J. Tanaka, unpublished result.
27) J. Tanaka, *J. Chem. Soc. Japan, Pure Chem. Sec. (Nippon Kagaku Zassi)*, 79, 1114 (1958).

composed of the $^1B_{2u}$ excited level of benzene, which has the short-axis polarization. The second excited state, corresponding to the 230 mμ absorption, is assigned to a state having a large component of the intramolecular charge transfer configuration, and the direction of the polarization is calculated to be on the 6.5° line, inclined outward from the Y axis (Fig. 5) to the carbonyl group. Another interpretation of this band is to regard it as derived from the $^1B_{1u}$ excited level of benzene; then the polarization would be along the Y-axis. The measurement of the crystalline spectrum was undertaken in order to decide between the two interpretations.

Spectrum of Benzoic Acid Crystal.—The crystal structure analysis of benzoic acid as carried out by Sim, Robertson and Goodwin[28] showed that the crystal belongs to $C_{2h}^5-P2_1/c$ space group, including four molecules in a unit cell. Based on this finding the projection of molecules onto the (001) plane is pictured in Fig. 6 (a). Thin flakes of crystal are obtained by sublimation and are used for spectral measurement. The developed face is (001). The optical properties of the crystal are as described by Winchell[18], and the axes are easily determined by a polarization microscope. The thickness of the crystal is measured by the interference pattern described in a previous paragraph. The observed crystalline spectrum crystal 0.23 μ thick, is shown in Fig. 6(b). Comparing the integrated intensity of each band when the polarization of light is along the a-axis with that of along the b-axis, the dichroic ratio is estimated to be $D_a : D_b =$ $(10\pm2) : 1$ for the 280 mμ band. In the region between 210~230 mμ there are two bands overlapping each other, and the band near 210 mμ is much stronger along the a-axis than along the b-axis. The 230 mμ band is apparently stronger in the b-axis. In order to estimate the dichroic ratio of the 230 mμ band, we have separated these overlapping bands; the dichroic ratio of the 230 mμ band was thus found to be $D_a : D_b = 1 : (31\pm3)$.

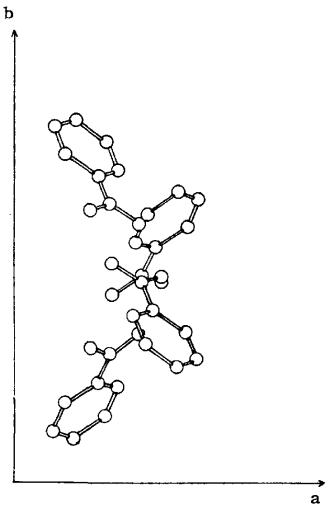

Fig. 6 (a). Projection of benzoic acid molecules onto the (001) plane.

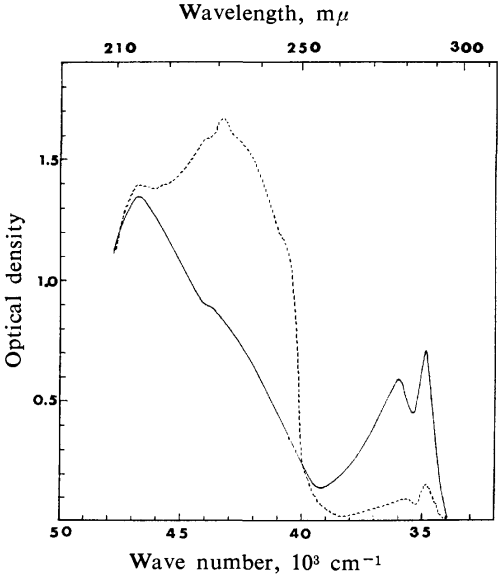

Fig. 6 (b). Polarized absorption spectrum of benzoic acid crystal.
—— The light polarized parallel to the a-axis
---- The light polarized parallel to the b-axis

According to the crystalline structure data, the dichroic ratio is calculated for the short-axis (X-axis in Fig. 5) transition as $D_a : D_b = 12 : 1$; hence, the 280 mμ band is confirmed to be polarized along the X-axis of the molecule, and to be largely a $^1B_{2u}$ transition. As for the 230 mμ band, the ratio is 1 : 30 if we take the direction of the transition moment to lie 6.5° inclined outward to the Y-axis towards the carbonyl group, but it is 1 : 11 if the direction is assumed to be on the Y-axis. Comparing the calculated value with the observed one, it is concluded that the 230 mμ band is polarized 6.5° outward to the Y-axis towards to the carbonyl group. Thus, the 230 mμ band is shown to have a characteristic polarization of an intramolecular charge transfer. The band at 210 mμ is not seen in solution; it may appear as the result of borrowing intensities from the allowed excited states situated in the shorter wavelength region. The polarization of this band seems to be

28) G. A. Sim, J. M. Robertson and T. H. Goodwin, *Acta Cryst.*, 8, 157 (1955).

short-axis, but it cannot be discussed further because the absorption band is not wholly observed.

Finally, as for the intensity of the crystalline absorption bands, the observed value is compared with the calculated value in Table V. The observed intensity of the 278 mμ band is nearly equal to the calculated value, but in the case of the 230 mμ band the observed value is one half the calculated one. In this case the hypochromic effect is again observed in the crystalline spectrum.

Acetanilide

The absorption spectrum of acetanilide measured in an *n*-heptane solution is shown in Fig. 7. Three absorption bands are seen in the region of 290~190 mμ; the long wavelength one is safely regarded by analogy with other substituted benzenes to be an absorption analogous to the 260 mμ band of benzene. In the theoretical interpretation of the spectrum

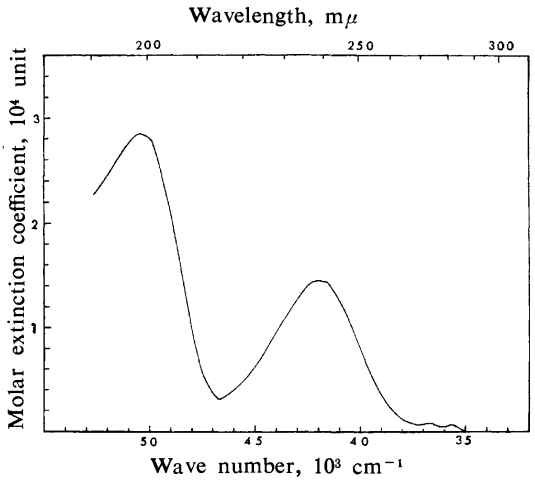

Fig. 7. Ultraviolet absorption spectrum of acetaniline in *n*-heptane solution.

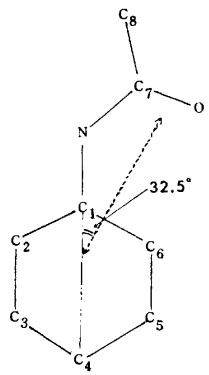

Fig. 8. Direction of the transition moment of the 230 mμ band of acetanilide.

of acetanilide given by Baba and Suzuki[29], it has been shown that the transition moment of the second band at 230 mμ lies 20.5° inclined to the C_1N axis towards the carbonyl group. According to the X-ray crystal structure analysis made by Brown and Corbridge[30], acetanilide is not a planar molecule and the plane of the acetyl group makes an angle of 37°54′ to the plane of the anilino group. The acetyl group can accept electrons from other conjugated systems, and aniline is a good electron donor, so that it is quite probable that an electron transfer takes place from the highest occupied orbital of the anilino group to the vacant orbital of the carbonyl group. If this charge transfer configuration is predominant for the excited state, in this particular transition the polarization should be along the line connecting the center of the highest occupied orbital of the anilino group to that of the vacant orbital of the carbonyl group (the center of the highest occupied orbital is 0.58 Å from the center of the benzene ring in the direction of the amino group, according to the LCAO MO calculations). This direction makes an angle of 32.5° with the C_1C_4 axis (Fig. 8). The 230 mμ band may be considered to have the large character of the charge transfer of this type. However, in order to give an accurate description of the nature of electronic transition, the configurational interaction between the charge transfer state and the locally excited states of aniline and of the carbonyl group must be taken into account. The symmetry of the molecule is less simple than *p*-nitroaniline, and the excited states will be a more complicated mixture of several excited configurations. Anyway, the crystalline spectrum will reveal the direction of the transition moment, and it will be useful for the theoretical assignment of the absorption bands.

The Spectrum of Acetaniline Crystal.—According to Brown and Corbridge[30], the crystal belongs to the space group of Pbca-D_{2h}^{15}, with the unit cell dimensions of $a=19.640$, $b=9.483$ and $c=7.979$ Å, and eight molecules are contained in a unit cell. The crystals for the spectral measurement were made by sublimation, and the (100) or (001) faces develop most easily. Projections of molecules onto these faces are shown in Figs. 9 (a) and 10 (a). The identification of the developed face is made by the use of X-ray rotation photography and the polarization microscope. The crystalline absorption is measured with a (100) face by a light polarized along the b and the

29) H. Baba and S. Suzuki, *J. Chem. Phys.*, **32**, 1706 (1960).
30) C. J. Brown and D. E. C. Corbridge, *Acta Cryst.*, **7**, 711 (1954).

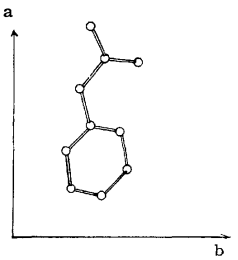

Fig. 9 (a). Projection of acetanilide molecule onto the (001) crystalline plane.

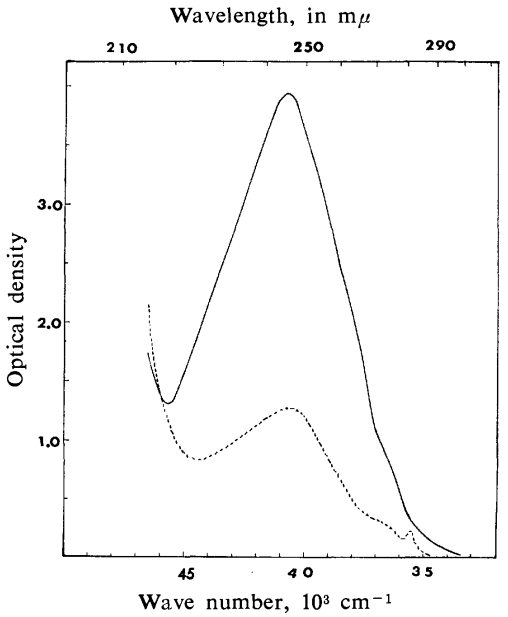

Fig. 9 (b). Polarized absorption spectrum of acetanilide crystal through the (001) plane.
—— The light polarized parallel to the a-axis
---- The light polarized parallel to the b-axis

c axes and with a (001) face by a light polarized along the a and the b axes, are respectively. The results are shown in Figs. 9(b) and 10(b). From Fig. 10(b), the direction of the transition moment of the 284 mμ band is confirmed to be nearly perpendicular to the C_1N axis, because the observed intensity ratio, $D_b : D_c = 2.90 : 1.0$, is almost in agreement with the calculated value of $D_b : D_c = 2.76 : 1.0$. This result is fairly satisfactory, considering the fact that the 284 mμ band overlaps the 230 mμ band which has a much larger intensity.

The polarization of the next 230 mμ band is determined by both (100) and (001) spectra independently. From the (100) spectrum, the observed intensity ratio is $D_b : D_c = 1.0 : 0.76$,

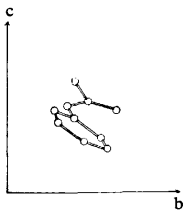

Fig. 10 (a). Projection of acetanilide molecule onto the (100) plane.

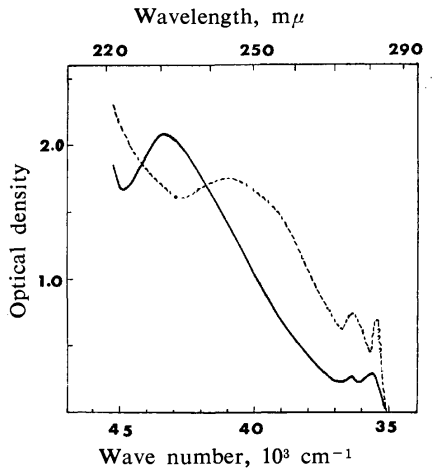

Fig. 10(b). Polarized absorption spectrum of acetanilide crystal through the (100) plane.
—— The light is polarized parallel to the c-axis
---- The light polarized parallel to the b-axis.

while the calculated value is 1.0 : 0.74 if we take the direction of the transition moment on the line inclined 32.1° to the C_1C_4 axis toward the carbonyl group (36.2° to the C_1N axis) (Fig. 8). From the (001) spectrum, the observed intensity ratio $D_a : D_b$ is 4.53 : 1.0, whereas the calculated value is 4.95 : 1.0 if the direction of the transition moment is assumed along the line 33.2° inclined to the C_1C_4 axis (35.4° to the C_1N axis) outward to the carbonyl group. The agreement of these two measurements is quite satisfactory, and the polarization of the 230 mμ band is determined to be along the direction of 32.5±0.5° inclined to the C_1C_4 axis (35.6° to the C_1N axis) outward to the carbonyl group. This direction is the same as the direction of the charge transfer from the highest occupied orbital of the anilino group to the vacant orbital of the carbonyl group, but this coincidence cannot be stressed too much, because the exact description of the excited state must be given by the configurational interaction calculations.

The Davydov splitting of the second absorption is obviously seen in Figs. 9(b) and

10(b); namely, it appears at 243 mμ in the a-axis, at 244 mμ in the b-axis, and at 230 mμ in the c-axis. The splitting was not found with the 282 mμ band, because the dipole-dipole interaction between the excited states is smaller than for the stronger 230 mμ band.

As for the intensity of the 230 mμ band in the crystal, the observed intensity is about one half that of the calculated value, as is shown in Table VI. The hypochromism of crystalline absorption is found again; hence, it seems a common experimental fact that the fairly strong absorption band loses some of its intensity in the crystalline spectrum.

Table V. The oscillator strength of the crystalline absorption of benzoic acid

	Observed	Calculated
287 mμ band (a-axis)	0.032	0.030
230 mμ band (b-axis)	0.17	0.36

Table VI. The oscillator strength of the 230 mμ crystalline absorption of acetanilide

	Observed	Calculated
a-axis	0.290	0.72
b-axis	0.066	0.145

trans-Cinnamic Acid

The electronic absorption spectrum of *trans*-cinnamic acid measured in an *n*-heptane solution is illustrated in Fig. 11. A weak absorption band is seen at 296 mμ as a shoulder of the stronger band at 277 mμ. Another stronger band with vibrational structure is observed near 222 mμ.

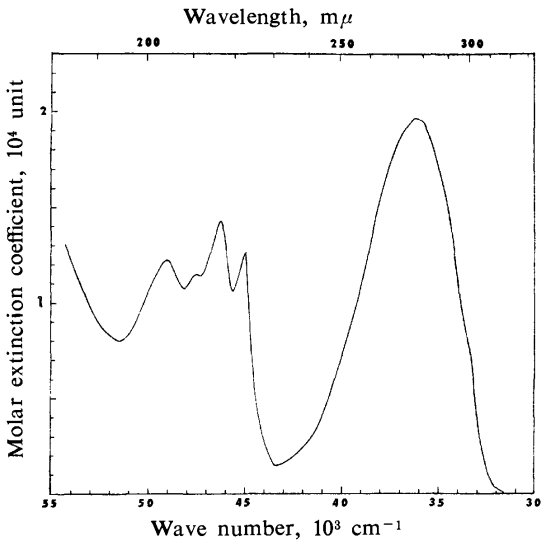

Fig. 11. Ultraviolet absorption spectrum of *trans*-cinnamic acid in *n*-heptane solution.

trans-Cinnamic acid is considered to be a composite, consisting of the electron-donating styryl group and the electron-accepting carboxyl group. The charge transfer from the highest occupied orbital of the styryl group to the vacant orbital of the carboxyl group will take place quite easily, because the ionization potential of styrene is as small as 8.86 eV.[31] and the charge density of the highest occupied orbital of styrene is most dense at the terminal α-carbon atom, where the interaction between the donor and the acceptor group takes place. By this reasoning, the strong absorption band at 277 mμ is regarded as an intramolecular charge transfer band; this is confirmed by a measurement of the crystalline absorption spectrum.

The Crystalline Spectrum of *trans*-Cinnamic Acid.—The crystal structure analysis of *trans*-cinnamic acid is now being carried out by Schmidt and his coworkers[32]. They find two crystalline forms. The α-form belongs to the $P2_1/a$ space group and has lattice constants as follows: $a=8.94$, $b=17.56$, $c=5.51$ Å and $\beta=58°40'$ and $n=4$; the β is found to have cell dimensions of $a=6.05$, $b=4.04$, $c=31.3$ Å, $\beta=90.3°$ and $n=4$. By sublimation, both α and β forms are obtainable, and the α-form develops a (010) face and the β develops a (001) plane. These crystalline faces are confirmed by X-ray rotation photographs. According to the unpublished results of Schmidt et al.[32] the projection of molecules of the α crystal onto a (010) face is shown in Fig. 12(a). The crystalline ultraviolet absorption of the *a*-form as measured through the (010) plane by a light polarized parallel and perpendicular to a-axis is shown in Fig. 12(b). With the β-form, spectrum is taken through the (001) face; the result is shown in Fig. 13. Comparing the spectrum of Fig. 12 (b) with the projections of molecules in Fig. 12 (a), it is easily found that the 270 mμ absorption band

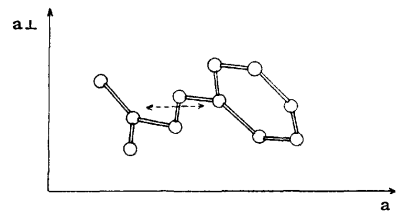

Fig. 12(a). Projection of *trans*-cinnamic acid molecule onto the (010) plane of α-form.

31) J. D. Morrisson and A. J. C. Nicholson, *J. Chem. Phys.*, **20**, 1221 (1952).
32) G. M. J. Schmidt, private communication based on the work by J. Ladell, T. R. R. McDonald and G. M. J. Schmidt, *Acta Cryst.*, **9**, 195 (1956).

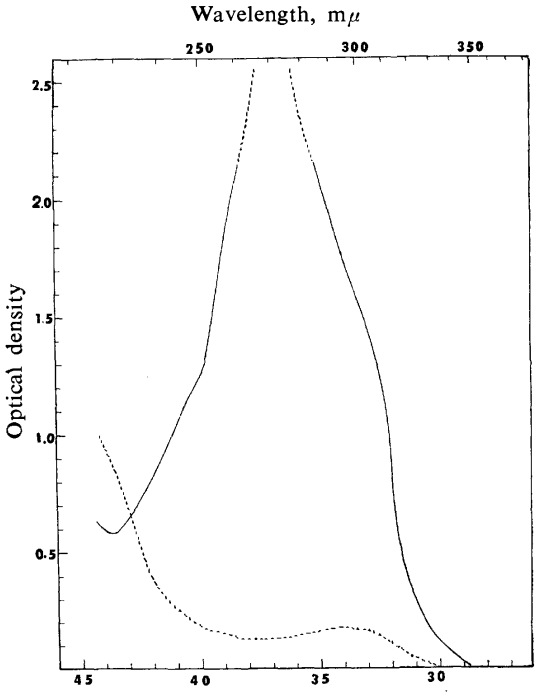

Fig. 12 (b). Polarized absorption spectrum of *trans*-cinnamic acid α-form through the (010) plane.
—— The light polarized parallel to the a-axis
---- The light polarized perpendicular to the a-axis

has a polarization nearly parallel to the a-crystalline axis. The direction of the transition moment is on the line expected from the charge transfer from the styryl group to the vacant orbital of the carboxyl group. In the crystalline spectrum, particularly in the β-form as seen in Fig. 13, the band which is at 277 mμ in an *n*-heptane solution shifts to about 255 mμ. The *trans*-cinnamic acid molecules are supposed to be aligned in pairs by a hydrogen bonding in the crystal. In this situation the transition moments of the pair of molecules are parallel to each other but are in oposite directions, and by a dipole-dipole interaction the excited states split into two, one allowed at a higher energy and the other forbidden at a lower energy. Therefore, the observable band should move to a shorter wavelength region. As a result of this blue shift, the weak absorption band which appears as a little shoulder in a solution at about 296 mμ becomes more evident in the crystalline spectrum. As is seen in Fig. 12 (a), if this absorption corresponds to the 260 mμ band of benzene, it should be observed in directions both parallel and perpendicular to the a-axis

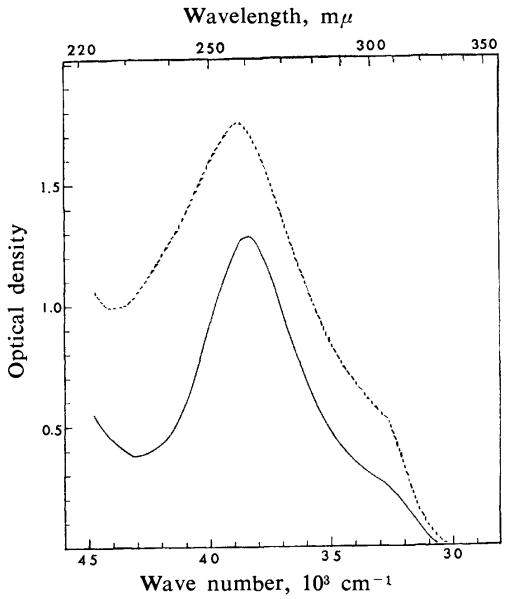

Fig. 13. Polarized absorption spectrum of *trans*-cinnamic acid β-form through the (001) plane.
—— The light polarized parallel to the a-axis
---- The light polarized parallel to the b-axis

because the polarization should be short-axis. In Fig. 12 (b), the 295 mμ band appears both parallel and perpendicular to the a-axis so it is established that the band is derived from the $^1B_{2u}$ excited state of benzene. We cannot discusss further the spectrum shown in Fig. 13 because the crystal structure has not yet been fully analyzed.

Durene

The electronic absorption spectrum of durene is quite similar to that of benzene, and the spectrum in *n*-heptane is illustrated in Fig. 15.

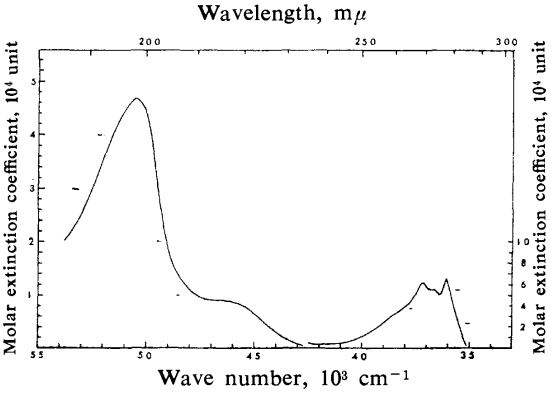

Fig. 14. Ultraviolet absorption spectrum of durene in *n*-heptane solution.

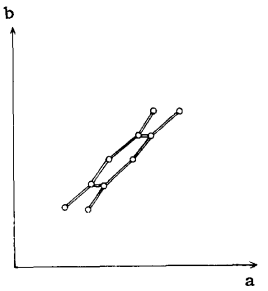

Fig. 15 (a). Projection of durene molecule onto the (001) plane.

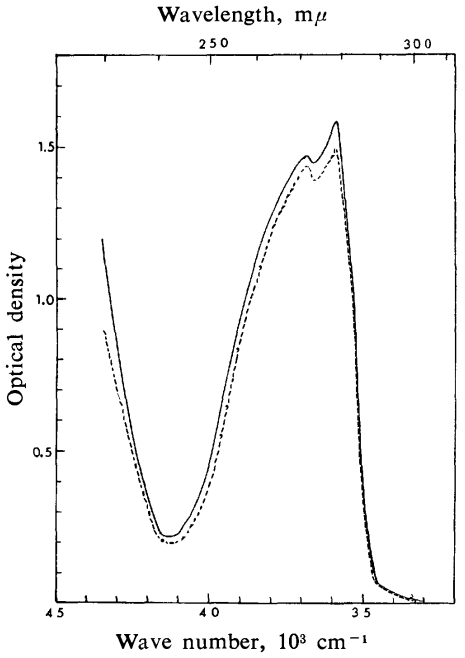

Fig. 15 (b). Polarized absorption spectrum of durene crystal.
—— The light polarized parallel to the a-axis
---- The light polarized parallel to the b-axis

The band near 278 mμ corresponds to the 260 mμ band of benzene ($^1A_{1g} \rightarrow {}^1B_{2u}$), the band around 217 mμ is correlated with 205 mμ band ($^1A_{1g} \rightarrow {}^1B_{1u}$) of benzene, and the strongest one, at 198 mμ, corresponds to the 185 mμ band ($^1A_{1g} \rightarrow {}^1E_{1u}$) of benzene. Following the theory of the spectrum of benzene[1], the first singlet excited state, $^1B_{2u}$, was shown to be polarized perpendicular to the two-fold symmetry axis of the molecule; hence, the polarization of the first band of durene should be perpendicular to the line connecting the two carbon atoms not substituted by methyl groups.

The crystalline absorption spectrum of durene has been studied by Schnepp and McClure[33]. The crystal structure of durene was determined by Robertson[34], and its optical properties were described by Groth[17]. Using Robertson's results, the molecules are projected onto the (001) plane in Fig. 15(a). The crystals measured are obtained by sublimation, and the developed face is easily confirmed as (001) by the aid of a polarization microscope. From Fig. 15(a) it is easy to see that the absorption band should have the same intensity in the a and b axes if the transition moment is parallel to the long axis of the molecule, while it should be stronger along the a-axis than along the b-axis if it is parallel to the short axis. The observed absorption spectrum is shown in Fig. 15 (b). As compared with the results of Schnepp and McClure, the present spectrum is broad and diffuse, because the measuement is made at room temperature. However, the general features of bands are in accordance with their results, and it is confirmed that the intensity ratio of the 280 mμ band is nearly equal in the directions of the a and b crystalline axes. The results show that the polarization of the 278 mμ band is parallel to the long axis of the molecule; hence, the excited level is confirmed to correspond exactly to the $^1B_{2u}$ excited state of benzene. The observed intensity ratio is rather small compared with the oriented gas ratio of $D_a : D_b = 1.0 : 1.3$; this deviation must be explained by the mixing of the $^1B_{2u}$ excited state of a particular molecule with the $^1B_{1u}$ excited state of neighboring molecules[35]. As compared with other substituent groups mentioned before, methyl groups have rather a small influence on the spectrum of benzene, and the polarization of durene's band is in accordance with that of benzene.

Conclusion

The electronic absorption spectra of substituted benzenes are in some way modifications of that of benzene itself. When the substituent group has rather a small influence as in, for instance, the methyl, hydroxyl or chloro groups, the pattern of the benzene spectrum is retained, the absorption peaks being shifted to red and the intensity of the 260 mμ band being strengthened to some extent[4]. A substitution by an amino, *N*, *N*-dimethylamino or ionized hydroxyl group causes the appearance of an additional excited level next to the $^1B_{2u}$

33) O. Schnepp and D. S. McClure, *J. Chem. Phys.*, **30**, 874 (1960).
34) J. M. Robertson, *Proc. Roy. Soc.*, **A141**, 594,; **A142**, 659 (1933).
35) D. P. Craig and J. R. Walsh, *J. Chem. Soc.*, **1958**, 1613.

level of benzene, since a charge transfer takes place in this region because the non-bonding electrons of these groups have relatively low ionization energies[3]. Two charge transfer states are possible, one from the substituent to the vacant orbital symmetrical to the two-fold axis, and the other to the antisymmetrical orbital. The former interacts with the $^1B_{1u}$ state, and the latter mixes with the $^1B_{2u}$ state. However, upon a substitution of the electron-donating groups, there are no serious changes in the polarization properties of each band, because the symmetrical properties of the excited states are not altered in sequence. The $^1B_{2u}$ excited state is the lowest singlet excited state in these substituted benzenes even if the electron-donating power of the substituent is so strong that the lowest state has a large percentage of charge transfer; hence, the longest absorption band is always polarized perpendicular to the two-fold symmetry axis of the molecule. Both the $^1B_{1u}$ excited state and the symmetrical charge transfer state have a polarization parallel to the two-fold axis, so the next band has this polarization in all cases. The results of durene and *p*-dimethoxybenzene[5] confirm the above statement, and such other molecules as aniline and phenol can be treated similarly.

In other substituted benzene molecules, in which the substituents have an electron-accepting property, a different situation arises. Electrophilic substituent groups have vacant orbitals which accept electrons from the benzene ring; as a result of this, new absorption bands often appear in addition to benzen's intrinsic transition[2,19,27]. The 370 mμ band of *p*-nitroaniline, which is the longest absorption band of this molecule, is not an analogous band to the 260 mμ band of benzene but a charge transfer band, and it is polarized along the two-fold symmetry axis of the molecule. In the case of benzoic acid, acetanilide and *trans*-cinnamic acid, charge transfer bands are observed next to the band derived from the $^1B_{2u}$ excited level of benzene. In these molecules, there are also other charge transfer states which interact with the $^1B_{2u}$ state of benzene. In fact, the longest absorption band of nitrosobenzene includes fairly large amounts of this type of charge transfer, together with the $^1B_{2u}$ state of benzene[27]. The sequence of these levels has been determined by the order of the energy levels of the initial states prior to configuration interaction.

Such electrophilic substituent groups as nitro, carbonyl, carboxyl, azo, nitroso are classified by Witt's classical theory as "chromophores"[36]. These groups are characterized by low-lying vacant orbitals which can receive electrons by resonance interaction. When an unsaturated hydrocarbon, which has electronic absorptions in the visible or near-ultraviolet region, is substituted by an electrophilic group, a new strong absorption band is often observed in the visible or the near-ultraviolet region arising from a new charge transfer state in which an electron is transferred from the parent hydrocarbon to the vacant orbital of the substituent. This is a quantum-chemical explanation of Witt's chromophore theory. Witt's "auxochrome" (such substituents as NH_2, NMe_2, OH, OMe, and Cl) may be understood in two ways; it produces bathochromic shifts in the transitions of the parent molecule, and it facilitates the transfer of electrons from the parent system to the electrophilic substituent by decreasing the ionization potential of the parent molecule.

The crystalline ultraviolet absorption spectral measurements are very useful in confirming this theory, because they give information about the directions of the transition moments of the bands and confirm the symmetry properties of excited levels. Moveover, some hidden and ambiguous bands in solution become evident in the crystalline spectra; they are very instructive in ascertaining what kinds of electronic interactions are prevalent in molecular crystals. It turns out that the dipole-dipole interactions of the exciton type are predominant in the case of the crystals studied here.

Summary

The electronic absorption spectra of some substituted benzene molecules *p*-nitroaniline, benzoic acid, acetanilide, *trans*-cinnamic acid, and durene have been measured in ethanol or *n*-heptane solutions and as single crystals, using polarized light. The measurement of the crystalline spectra reveals in many respects the properties of the transitions of substituted benzene molecules. The 277 mμ of durene, which is reasonably regarded as a band analogous to the 260 mμ of benzene, is shown to be polarized perpendicular to the two-fold symmetrical axis of the molecule. Bands of the same type occur at 264 mμ in *p*-nitroaniline (crystal), at 284 mμ in benzoic acid, at 282 mμ in acetanilide and at 299 mμ in *trans*-cinnamic acid. In addition, those molecules in which the benzene ring is substituted by the electron-accepting groups, show a strong band, associated with intramolecular charge transfer, in the near ultraviolet region. The 370 mμ band of *p*-nitroaniline is shown to be

36) A. E. Gilam and E. S. Stern, "Electronic Absorption Spectroscopy", Edward Arnold, Ltd., London (1958).

polarized parallel to the long axis of the molecule, and the 230 mμ band of benzoic acid has a polarization parallel to the line connecting the centers of the benzene ring and the carbonyl group. The directions of the transition moments of the 240 mμ band of acetanilide and the 276 mμ band of *trans*-cinnamic acid are also shown to be on the line connecting the substituents and the benzene ring. Davydov splitting is observed in the crystal of *p*-nitroaniline; this splitting is in good agreement with the values calculated by the exciton theory.

The author thanks Professor Saburo Nagakura for his continued encouragement and Professor Zyun Koana for lending him Bausch and Lomb's lenses. The author's gratitude is also due Dr. G. M. J. Schmidt for his kind communication of his unpublished findings on *trans*-cinnamic acid and also Dr. J. N. Murrell for his valuable discussion and kind hospitality during the author's stay in Sheffield, where some parts of this paper were written.

The Institute for Solid State Physics
The University of Tokyo
Azabu, Tokyo

*The Synthesis of γ,δ-Dimethyl-γ-(2-carboxyethyl)-δ-valerolactone**

By Toshihiro TAKATA, Kazunori SAYAMA, Yukihide FURUTSU and Masahiko TAKIGAWA

(Received March 8, 1963)

The present paper describes a synthesis of γ,δ-dimethyl-γ-(2-carboxyethyl)-δ-valerolactone, through the scheme shown below, from γ-acetyl-γ-methylpimelonitrile derived from ethyl methyl ketone by cyanoethylation with acrylonitrile[1].

The cyanoethylation of ethyl methyl ketone was carried out according to the method of Bruson and Riener[1] to give γ-acetyl-γ-methylpimelonitrile (I), which was then hydrolyzed to γ-acetyl-γ-methyl pimeric acid (II)[1]. Compound II was hydrogenated, in the presence of a Raney-nickel catalyst in an aqueous sodium hydroxide solution, to sodium γ-methyl-γ-(l-hydroxyethyl)-pimelate (III), which was not isolated and which, after treatment with hydrochloric acid, gave γ,δ-dimethyl-γ-(2-carboxyethyl)-δ-valerolactone (IV).

Though δ-valerolactone gives an associated molecule[2], compound IV gives no associated molecule, as was detected by the cryoscopic method.

As another route, compound I was esterified with ethanol, water and sulfuric acid to give diethyl-γ-methyl-γ-acetylpimelate, which was then hydrogenated to γ,δ-dimethyl-γ-(2-carboethoxyethyl)-δ-valerolactone (VII) through diethyl-γ-methyl-γ-(l-hydroxyethyl)-pimelate (VI), which was not isolated.

On the other hand, I was hydrogenated with sodium borohydride to give γ-methyl-γ-(l-hydroxyethyl)-pimelonitrile (VIII). In this procedure the nitrile group was not attacked, but the carbonyl group hydrogenated to the hydroxyl group, as is shown in Fig. 1. The absorption bands at 1095 and 1075 cm^{-1} of compound VII are probably due to the formation of the hydroxyl group, while the absorption band at 1705 cm^{-1}, being due to the carbonyl group of I, is absent in VIII. The band at 2250 cm^{-1}, being due to the nitrile group, is present in both I and VIII.

Then, compound VIII was treated with concentrated sulfuric acid in order to obtain γ-methyl-γ-(l-hydroxyethyl)-pimelic acid diamide

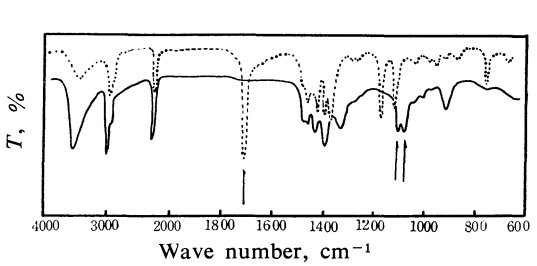

Fig. 1. Infrared absorption spectrum of γ-acetyl-γ-methylpimelonitrile (I) (- - -, KBr disk) and of γ-methyl-γ-(l-hydroxyethyl)-pimelonitrile (VIII) (——, liquid film).

* Reported at the Chūgoku & Shikoku Meeting of the Chemical Society of Japan, Tokushima, August, 1962.

1) H. A. Bruson and T. W. Riener, *J. Am. Chem. Soc.*, **64**, 2850 (1942).

2) K. Sayama, T. Takata and M. Taniyama, *J. Chem. Soc. Japan, Ind. Chem. Sec.* (*Kōgyō Kagaku Zassi*), **58**, 112 (1955).

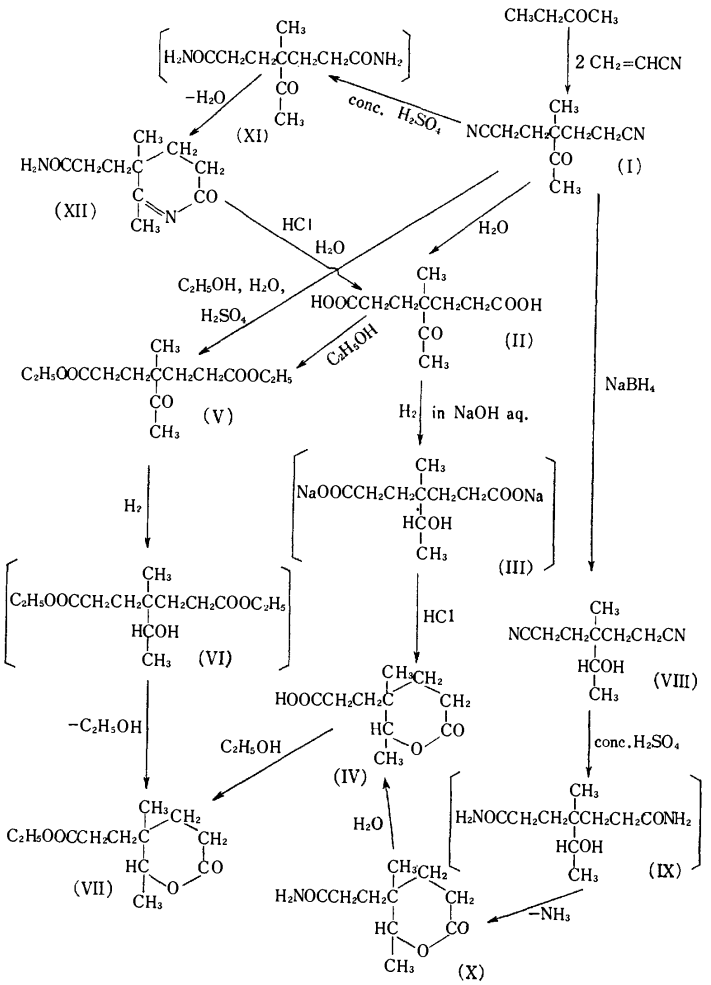

(IX). However, IX was not obtained, and γ,δ-dimethyl-γ-(2-carbamoylethyl)-δ-valerolactone (X) was obtained; it was converted to IV by hydrolysis. The infrared spectrum of X, shown in Fig. 2, has absorption bands at 1730 cm^{-1} and 1675 cm^{-1}, which are, respectively, due to the structures of the six-membered lactone and of the amide group.

Moreover, compound I was treated with concentrated sulfuric acid in order to obtain γ-methyl-γ-acetylpimelic acid diamide (XI). In this case XI was not obtained, but 2-keto-5, 6-dimethyl-5-(2-carbamoylethyl)-2, 3, 4, 5-tetrahydropyridine (XII) was obtained; it was converted to II by hydrolysis, but it could not be hydrogenated under high hydrogen pressure in the presence of a Raney-nickel catalyst nor by sodium borohydride. The infrared absorption spectrum of XII shown in Fig. 3 has absorption bands at 1685, 1660 and 1640 cm^{-1} which are due to the structures of the carbonyl in the ring, of the double bond between C and N in the ring, and of the amide group in the side chain. Moreover, the ultraviolet absorption spectra shown in Fig. 4 has absorption maxima at 201.5 mμ (ε, 11900) and 282.5 mμ (ε, 5) in water, at 210 mμ (ε, 4067) and 280 mμ (ε, 8) in ethanol, at 202.5 mμ (ε, 20810) and 282.5 mμ (ε, 6) in 0.5 N aqueous sulfuric acid, and at 222 mμ (ε, 2165) and 291 mμ (ε, 6) in 0.5 N aqueous sodium hydroxide. Such a shift of ultraviolet absorption bands according to the pH value of the

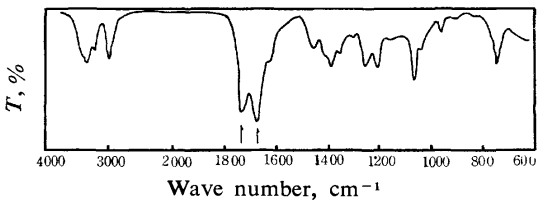

Fig. 2. Infrared absorption spectrum of γ,δ-dimethyl-γ-(2-carbamoyl-ethyl)-δ-valerolactone (X) (liquid film).

medium suggests the possibility of such tautomerism as the following.

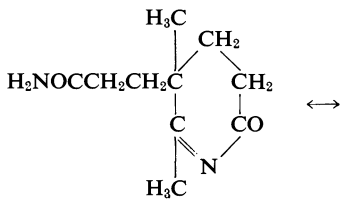

(In an acidic medium or a neutral medium)

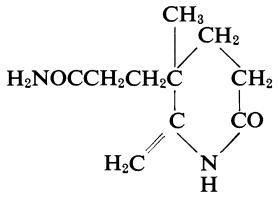

(In an alkaline medium)

Further experiments may be necessary to establish this phenomenon completely.

Experimental

γ, δ-Dimethyl-γ-(2-carboxyethyl)-δ-valerolactone (IV).—In a 220 ml. autoclave, compound II (40 g. in 90 g. of a 20% aqueous sodium hydroxide solution) was hydrogenated under about 80 atm. of hydrogen pressure at 104~120°C in the presence of a Raney-nickel catalyst (from 20 g. of Ni-Al alloy 50 : 50) for 4.3 hr. The reaction mixture was evaporated and acidified with concentrated hydrochloric acid, and extracted with ether. From the ether extract IV was obtained as a viscous liquid (b. p., 200~202°C/1 mmHg), which after standing became crystalline; m. p., 60~62°C; yield, 35.2 g. (95.0%).

Found: C, 59.92; H, 8.15; N, 0.00. Calcd. for $C_{10}H_{14}O_4$: C, 59.98; H, 8.06; N, 0.00%.

Neutralization and saponification equivalent, 100.3. Calcd. for IV, 100.1.

Mol. wt., 196.5 (cryoscopic method in acetic acid). Calcd. for IV, 200.2.

Diethyl γ-Methyl-γ-acetylpimelate (V).—Compound I (17.8 g.) was dissolved in a mixture of ethanol (36.8 g.) and concentrated (96%) sulfuric acid (25 6 g.), and the mixture was heated under reflux at a bath temperature of 140~143°C for 3.5 hr. The reaction mixture was washed with water, and the oily layer was extracted with ether, dried with sodium sulfate, and distilled to give V; b. p., 158°C/2 mmHg, d_4^{20} 1.0522, n_D^{20} 1.4562; yield, 20.9 g. (76.7%).

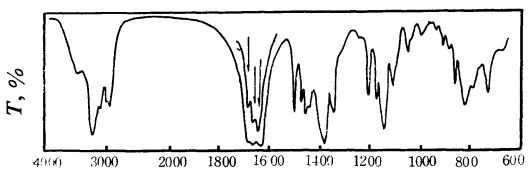

Wave number, cm^{-1}

Fig. 3. Infrared absorption spectrum of 2-keto-5, 6-dimethyl-5-(2-carbamoylethyl)-2, 3, 4, 5-tetrahydropyridine (XII) (KBr-disk).

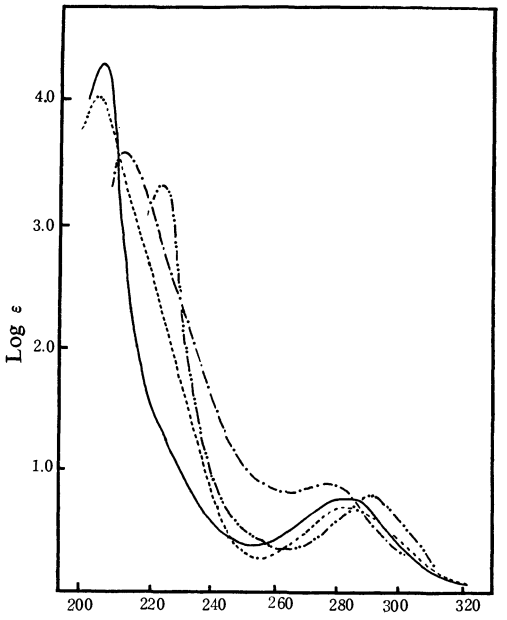

Fig. 4. Ultraviolet absorption spectra of 2-keto-5, 6-dimethyl-5-(2-carbamoylethyl)-2, 3, 4, 5-tetrahydropyridine (XII).

- – – In water
- –·–· In ethanol
- —— In 2 N aqueous sulfuric acid
- –··– In 2 N aqueous sodium hydroxide

Found: C, 61.88; H, 8.83; O, 28.99. Calcd. for $C_{14}H_{24}O_5$: C, 61.74; H, 8.88; O, 29.38%.

Saponification value, 414.4. Calcd. for V, 412.0.

This compound was obtained in an 82.3% yield by the esterification of II (50 g.) with ethanol (200 g.) in the presence of sulfuric acid (9 g.) at a bath temperature of 130~140°C for 5 hr.

γ, δ-Dimethyl-γ-(2-carboethoxyethyl)-δ-valerolactone (VII).—Compound IV (10 g., in 10 ml. of ethanol) was hydrogenated under about 85 atm. of hydrogen pressure at 140~150°C in the presence of a Raney-nickel catalyst (from 5 g. of Ni-Al alloy 50 : 50) for 2hr. From this reaction mixture VII was obtained by distillation; b. p., 155°C/2 mmHg, d_4^{20} 1.0579, n_D^{20} 1.4640; yield, 6.3 g. (75.2%).

Found: C, 63.07; H, 8.90; O, 27.80. Calcd. for $C_{12}H_{20}O_4$: C, 63.13; H, 8.83; O, 28.04%.

Saponification value, 487.2. Calcd. for VII, 491.2.

This compound was obtained in a 76.3% yield by the esterification of IV (5 g.) with ethanol (50 g.) in the presence of sulfuric acid (2 g.) at a bath temperature of 130~140°C for 5 hr.

γ-Methyl-γ-(1-hydroxyethyl)-pimelonitrile (VIII).—Into a solution of I (90 g.) in methanol (500 ml.) sodium borohydride (9.6 g.) was slowly stirred below 30°C; after it had been left standing for 2.5 hr. at room temperature, this mixture was

neutralized with concentrated hydrochloric acid, evaporated, separated from the precipitate by filtration, and dried in vacuum to give a viscous substance which was identified as VIII by the infrared spectrum shown in Fig. 1 and by elementary analysis as follows. Yield, 90 g. (quantitatively), n_D^{20} 1.4800.

Found: N, 15.48. Calcd. for $C_{10}H_{15}N_2O$: N, 15.55%.

γ, δ-Dimethyl-γ-(2-carbamoylethyl)-δ-valerolactone (X).—A mixture of VIII (10 g.) and 90% sulfuric acid (20 g,) was heated at 60°C for 1 hr., neutralized with concentrated aqueous ammonia while being vigorously stirred and externally cooled, and extracted with chloroform. From this extract after evaporating. X was obtained as a viscous liquid, n_D^{20} 1.4945; yield, 11 g. (99.6%). The infrared spectrum of X is shown in Fig. 2.

Found: N, 7.01. Calcd. for $C_{10}H_{17}NO_3$: N, 7.03%.

The Hydrolysis of X.—Compound X was treated with sodium hydroxide (4 g., in 40 g. of water) on a water bath for 3 hr., acidified with hydrochloric acid, evaporated, and extracted with ether. From the ether extracts IV was obtained; yield 2.2 g. (54.7%).

2-Keto-5, 6-dimethyl-5-(2-carbamoylethyl)-2, 3, 4, 5-terahydropyridine (XII).—By a method similar to that described for X, XII was obtained from I (10 g.) and 90% sulfuric acid (20 g.) in the form of colorless crystals; m. p., 237~238°C (from ethanol); yield, 5.1 g (42.4%). The infrared spectrum of XII is shown in Fig. 3, while the ultraviolet absorption spectra are shown in Fig. 4.

Found: C, 61.64; H, 8.26; N, 14.29. Calcd. for $C_{10}H_{16}N_2O_2$: C, 61.20; H, 8.22; N, 14.28%.

The Hydrolysis of XII.—Compound XII was treated with 20% aqueous hydrochloric acid on a boiling water bath for 2.7 hr. and then extracted with ethylene dichloride. From the ethylene dichloride extract II was obtained; yield, 1.85 g. (84.1%); m. p., 124~125°C (from ethylene dichloride), undepressed on admixture with the authentic specimen derived from I.

Found: C, 55.39; H, 7.33; N, 0.00. Calcd. for $C_{10}H_{16}O_5$: C, 55.54; H, 7.46; N, 0.00%.

The authors are grateful to Mr. Masatomo Kusunose (Manager of the Research Institute, Toho Rayon Co., Ltd.), Dr Minoru Imoto (Professor of Osaka City University), and Dr. Torakichi Yosioka (Professor of Tokushima University) for their valuable advice on the experiments; to Mr. Toshikazu Inoue, Miss Keiko Yano and Miss Akiko Hiroshe for helping them with the elementary analyses, and to Mr. Kiyosumi Kubo for helping them with the infrared and ultraviolet spectral work.

The Research Institute, Toho Rayon Co., Ltd.
Itano-gun, Tokushima

Studies of the Solvent Extraction of Zirconium-95 in the Tribenzylamine-Hydrochloric Acid System

By Takashi OMORI and Nobuo SUZUKI*

(Received December 17, 1962)

In a previous paper[1], the mechanism of the amine extraction of niobium-95 was reported on and the niobium species in a hydrochloric acid solution were estimated. If the zirconium species in the same medium were known, the separation of zirconium and niobium could be carried out successfully. Although a number of investigations have been carried out on the zirconium species in a hydrochloric acid solution, the results reported are not in satisfactory agreement with each other[2-4].

In the present paper, the distribution of carrier-free zirconium-95 between hydrochloric acid and tribenzylamine is investigated.

Experimental

Carrier-free zirconium-95 was prepared from zirconium-niobium-95 by the anion-exchange resin method and was stored in 9 N sulfuric acid. Before being used for each experiment, zirconium-95 was extracted with acetylacetone from an aqueous solution containing hydrogen peroxide[5]. The zirconium-95, being free from niobium-95, was then converted

* Present address: Research Institute of Mineral Dressing and Metallurgy, Tohoku University, Nagamachi, Sendai.

1) T. Omori and N. Suzuki, This Bulletin, **35**, 1633 (1962).

2) J. Bjerrum, G. Schwarzenbach and L. G. Sillén, "Stability Constants of Metal Ion Complexes, Part II: Inorganic Ligands", The Chemical Society, London (1958), p. 94.

3) B. A. J. Lister and L. A. McDonald, *J. Chem. Soc.*, **1952**, 4315.

4) D. Naumann, *Z. anorg. u. allgem. Chem.*, **309**, 37 (1961).

5) N. Suzuki and T. Omori, This Bulletin, **35**, 595 (1962).

into the chloride form by back extraction with concentrated hydrochloric acid. The experiments were carried out within four hours to avoid the error due to the growth of niobium-95.

All the other chemicals and the techniques employed were similar to those described in the previous paper[1].

The experiments were carried out at 25±0.5°C unless otherwise stated.

Results and Discussion

The Distribution Mechanism and Some Related Equations.—It has been revealed that the anionic species in the aqueous phase are transferred to the organic phase in the amine extraction through the anion exchange mechanism and that, for the niobium-tribenzylamine system, the metal complexes in the organic phase form the more stable additive compounds with the amine. Thus, the distribution coefficient for zirconium, D_{Zr}, can be represented in terms of activities as follows:

$$D_{Zr}=\frac{\sum_p\sum_q\sum_i(R_{p+q-4}Zr(OH)_pCl_q\cdot iRCl)_o}{\sum_m\sum_n(Zr(OH)_mCl_n^{(4-m-n)+})_a}$$

$$=\frac{(Cl^-)_a^4}{\sum_m\sum_n(\beta_{m,n}(H^+)_a^{-m}(Cl^-)_a^n)}$$

$$\times\sum_p\sum_q\sum_i(K_{p,q}\cdot K_i\cdot\beta_{p,q}(RCl)^{p+q+i-4}$$

$$\times(H^+)_a^{-p}(Cl^-)_a^{-p})$$

$$(5\leq(p+q)\leq8) \qquad (1)$$

where the subscripts a and o denote the aqueous and organic phases respectively, and RCl represent the chloride form of tribenzyl amine (TBA-Cl). $K_{p,q}$, K_i and $\beta_{m,n}$ are defined as follows:

$$K_{p,q}=\frac{(R_{p+q-4}Zr(OH)_pCl_q)_o(Cl^-)_a^{p+q-4}}{(Zr(OH)_pCl_q^{(4-p-q)+})_a(RCl)_o^{p+q-4}} \qquad (2)$$

$$K_i=\frac{(R_{p+q-4}Zr(OH)_pCl_q\cdot iRCl)_o}{(R_{p+q-4}Zr(OH)_pCl_q)_o(RCl_o)^i} \qquad (3)$$

$$\beta_{m,n}=\frac{(Zr(OH)_mCl_n^{(4-m-n)+})_a}{(ZrCl_6^{2-})_a}$$

$$\times(H^+)_a^{-m}(Cl^-)_a^{6-n} \qquad (4)$$

For the sake of simplicity it is assumed in these expressions that only mononuclear complexes exist in solutions. The activities of the species concerned have been employed in a way similar to that reported previously[1].

The Variation of the Distribution Coefficient with Hydrochloric Acid and TBA-Cl Concentrations.—The distribution of zirconium-95 between hydrochloric acid and a TBA-Cl solution in chloroform was determined. As is shown in Fig. 1, the distribution of zirconium-95 increases with an increase in the concentration of hydrochloric acid and TBA-Cl.

The Dependence of the Distribution Coefficient for Zirconium-95 on the Tribenzyl Amine Concentration.—A plot of log D_{Zr} against log$(RCl)_o$ in Fig. 2 gives two straight lines with a slope of 2.8 up to 0.06 M TBA-Cl and of 3.8 above this point, indicating that one molecule of the zirconium complex associates with up to four molecules of TBA-Cl. At a constant acidity and chloride level, Eq. 1 can be written by:

$$D_{Zr}=\frac{\sum K_5\cdot(RCl)_o+\{\sum K_6+\sum(K_5\cdot K_{i=1})\}(RCl)_o^2+\cdots}{F(H,\ Cl)} \qquad (5)$$

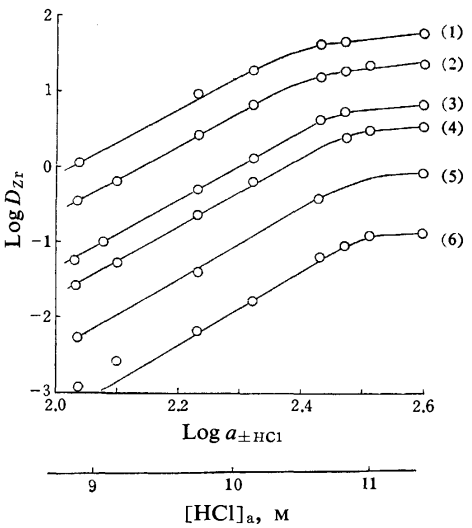

Fig. 1. Distribution of zirconium between hydrochloric acid and TBA-chloroform at 25°C.

	(1)	(2)	(3)	(4)	(5)	(6)
$[RCl]_o$, M:	0.200	0.150	0.100	0.075	0.050	0.025

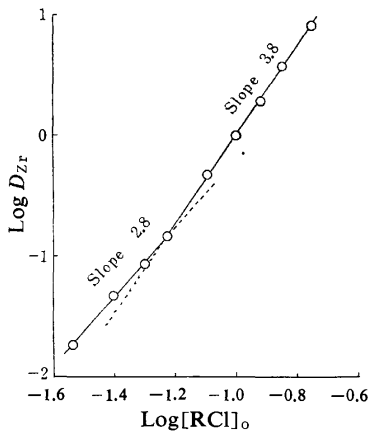

Fig. 2. TBA dependence of D_{Zr} values for zirconium at 25°C.

in which

$$F(\mathrm{H,Cl})=\frac{(\mathrm{Cl^-})_a^4}{\sum\sum\{\beta_{m,n}(\mathrm{H^+})_a^{-m}(\mathrm{Cl^-})_a^{n}\}}$$

$$K_5=K_{p,q(p+q=5)}\beta_{p,q(p+q=5)}\times(\mathrm{H^+})_a^{-p}(\mathrm{Cl^-})_a^{-p} \quad (6)$$

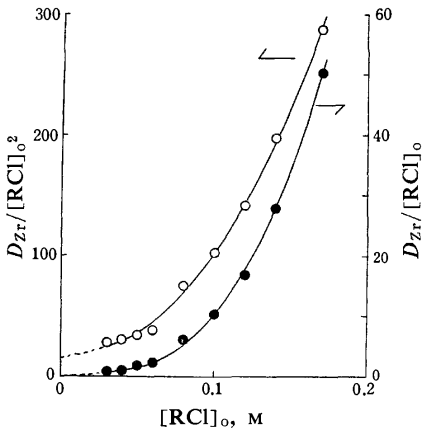

Fig. 3. Plot of $D_{Zr}/[RCl]_o$ and $D_{Zr}/[RCl]_o^2$ vs. $[RCl]_o$ for zirconium.

The plots of $D_{Zr}/(RCl)_o$ and $D_{Zr}/(RCl)_o^2$ against $(RCl)_o$ are given in Fig. 3. The plot of $D_{Zr}/(RCl)_o$ against $(RCl)_o$ provides a curve passing through the point of origin, showing that the values of $K_{p,q(p+q=5)}$ are equal to zero; i.e., the zirconium species with the charge of -1 are not extracted. The value of $\sum K_{p,q(p+q=6)}$ obtained by extrapolation of the plot of $D_{Zr}/(RCl)_o^2$ vs. $(RCl)_o$ to a zero concentration of TBA-Cl is not equal to zero. Thus, one of the charge numbers of the zirconium chloro-complexes extracted is probably -2.

The Dependence on Chloride Ion and Hydrogen Ion Activities.—The dependence of the distribution coefficients on the chloride ion activities is given by the differentiation of Eq. 1 with respect to chloride ion activity at a constant acidity:

$$\frac{\partial \log D_{Zr}}{\partial \log(\mathrm{Cl^-})_a}=4-\bar{p}-\bar{n} \quad (7)$$

In this experiment, the concentration of hydrochloric acid was held at 7.62 M, while the chloride ion activity was varied by the addition of lithium chloride. As is shown in Fig. 4, the distribution coefficients in hydrochloric acid-lithium chloride mixed solutions are lower than those in a hydrochloric acid solution over the range of chloride ion activity investigated, because of the deficiency of the acidity.

The distribution curve has a slope of four at higher chloride ion activities. This suggests,

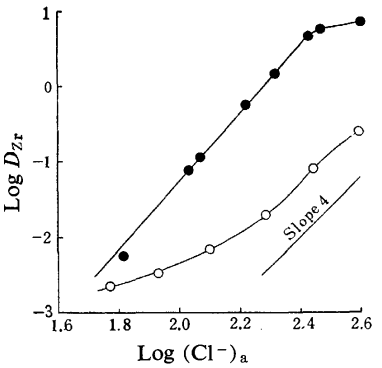

Fig. 4. Chloride dependence of D_{Zr} values for zirconium at 25°C.

○ HCl-LiCl mixture $[H^+]_a=7.62$ M
● Pure HCl

according to Eq. 7, that the zirconium exists as Zr^{4+} in the aqueous phase, i.e., $\bar{p}+\bar{n}=0$, and that $ZrCl_6^{2-}$ (viz., $\bar{p}=0$) is extracted to the organic phase; however, the existence of a zirconyl ion can not be ignored, as will be mentioned later.

Proceeding as above, the following equation can be derived from Eq. 1 at a constant chloride level:

$$\frac{\partial \log D_{Zr}}{\partial \log(\mathrm{H^+})_a}=\bar{m}-\bar{p} \quad (8)$$

By using hydrochloric acid-lithium chloride mixtures, the chloride levels were held at 9.45 and 11.5 M, while the hydrogen ion activity was varied. The plot in Fig. 5 has a slope of ca. 2, i.e., $\bar{m}-\bar{p}=2$, when the chloride level was held at 11.5 M. Since $\bar{p}$ is equal to zero at a high chloride level, even in the region of relatively lower acidity (7.62 M), $\bar{m}$ should be equal to two. These suggest that the extractable species, $ZrCl_6^{2-}$, can be formed by the action of hydrogen ions as follows:

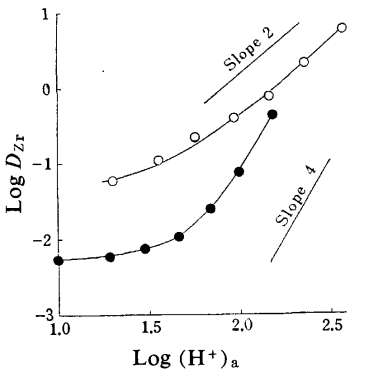

Fig. 5. Acid dependence of D_{Zr} values for zirconium at 25°C.

○ $[Cl^-]_{a,total}=11.5$ M
● $[Cl^-]_{a,total}=9.45$ M

$$Zr(OH)_2Cl_n^{(2-n)+} + 2H^+ + (6-n)Cl^- \rightleftharpoons ZrCl_6^{2-} + 2H_2O \quad (9)$$

Since the slope decreases as the acidity decreases, zirconium-95 may be partly extracted as $Zr(OH)_2Cl_4^{2-}$, which is formed from the zirconyl ion existing predominantly in the aqueous phase.

On the other hand, at a lower chloride level (9.45 M) such a plot shows a curve with a slope of four (Fig. 5), indicating the hydrolysis and/or the polymerization of the zirconium species. Thus, it should be recognized that hydrogen ions play a very important role in the zirconium extraction.

Temperature Effect.—It has been found that the extraction of the niobium with TBA-Cl is fairly much affected by the temperature[1]. Similar studies of the zirconium were carried out at 10±0.5 and 40±0.5°C. These results are shown in Fig. 6. There is an appreciable

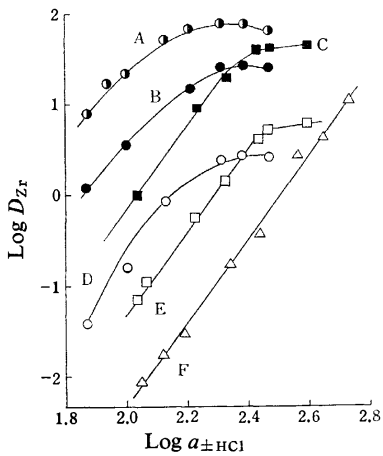

Fig. 6. Temperature dependence of D_{Zr} values for zirconium.

	$[RCl]_0$, M	Temp., °C
A	0.300	40
B	0.200	40
C	0.200	25
D	0.100	40
E	0.100	25
F	0.100	10

difference among the distribution curves obtained at different temperatures. At 40°C the distribution curve has a maximum in the region of higher acidity, whereas at 10°C it shows a straight line over the acidity range investigated. From the slope of the distribution curves in Fig. 6 it is concluded that the reaction expressed in Eq. 9 is promoted with an increase in the temperature.

To judge from the above considerations, the extraction processes of zirconium-95 from hydrochloric acid solutions with tribenzylamine are presumably shown by the following reactions:

$$ZrCl_6^{2-} + 2RCl \rightleftharpoons R_2ZrCl_6 + 2Cl^-$$
$$R_2ZrCl_6 + 2RCl \rightleftharpoons R_2ZrCl_6 \cdot 2RCl \quad (10)$$

and partly

$$Zr(OH)_2Cl_4^{2-} + 2RCl \rightleftharpoons R_2Zr(OH)_2Cl_4 + 2Cl^-$$
$$R_2Zr(OH)_2Cl_4 + 2RCl \rightleftharpoons R_2Zr(OH)_2Cl_4 \cdot 2RCl \quad (11)$$

Although it is considered that the greater part of zirconium is extracted through the process expressed in Eq. 10, the $K_{p=0,q=6}$ value is relatively small in comparison with the $K_{l=2}$ value, as has been shown in the case of the niobium extraction[1]. The formation constants, $\beta_{m,n}$, for the zirconium chloro-complexes and the distribution constants, $k_{p,q}$, can not be obtained because of their complexity, but the authors have drawn up a scheme (Fig. 7) concerning the zirconium species in the chloride system. This includes the most probable species.

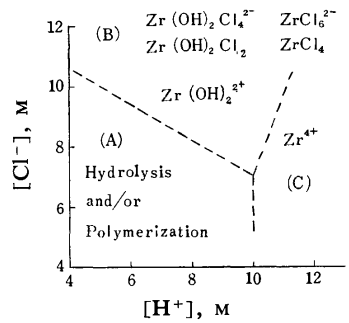

Fig. 7. Zirconium species in hydrochloric acid-lithium chloride solutions at 25°C.

The Possibility of the Mutual Separation of Zirconium-95 and Niobium-95.—In spite of the usefulness of the mutual separation of zirconium-niobium-95 in hydrochloric acid solutions, such a separation has not been carried out completely[6]. However, the more effective separation of zirconium and niobium can be expected, since there is an appreciable difference between the distribution coefficients of the zirconium and niobium with regard to the dependence of the distribution coefficient on the hydrogen ion concentration.

The separation factor, SF, under various conditions of a hydrochloric acid-lithium chloride solution at 25°C are tabulated in Table I. The separation factor increases up to 200 with a 7.6 M hydrochloric acid-0.8 M lithium chloride mixture, whereas it is 110 under optimum conditions for hydrochloric acid alone.

6) E. H. Huffman and R. C. Lilly, *J. Am. Chem. Soc.*, 73, 4474 (1951).

The separation factor as a function of temperature is also given in Table II. The separation factor is remarkably affected by the temperature and, even at 7.6 M hydrochloric acid, has a high value of 400 at 10°C. Since at a lower temperature the reaction expressed in Eq. 9 to zirconium is effectively restricted in comparison with the similar reaction to niobium, the higher separation factor is to be expected at lower temperature under suitable conditions, e.g., 7.5 M hydrochloric acid-1 M lithium chloride.

In the TBA extraction, however, the distribution coefficients for both zirconium and niobium are relatively so small that it is desirable to use other amines, possessing a higher extractability for niobium.

TABLE I. SEPARATION FACTOR, SF*, IN HYDROCHLORIC ACID-LITHIUM CHLORIDE SOLUTION AT 25°C ($[RCl]_o = 0.100$ M)

[HCl] M	[LiCl] M	log D_{Nb}	log D_{Zr}	SF
7.6	—	−0.59	−2.64	110
8.0	—	−0.42	−2.20	62
9.0	—	−0.11	−0.98	7.4
2.5	9.0	0.28	−1.95	170
4.0	7.5	0.28	−1.67	89
7.6	0.3	−0.42	−2.64	166
7.6	0.8	−0.24	−2.54	200

* $SF = D_{Nb}/D_{Zr}$

TABLE II. SEPARATION FACTOR IN HYDROCHLORIC ACID SOLUTION AS A FUNCTION OF TEMPERATURE ($[RCl]_o = 0.100$ M)

[HCl] M	log D_{Nb}	log D_{Zr}	SF	Temp. °C
7.6	−0.50	−2.52	100	40
7.6	−0.59	−2.64	110	25
7.6	−0.68	−3.28	400	10
8.0	−0.35	−2.08	54	40
8.0	−0.42	−2.20	62	25
8.0	−0.51	−2.90	310	10
9.0	−0.06	−0.89	6.8	40
9.0	−0.11	−0.98	7.4	25
9.0	−0.06	−1.58	33	10

Summary

The extraction process of zirconium-95 from hydrochloric acid solutions tribenzylamine is shown by the following reactions:

$$ZrCl_6^{2-} + 2RCl \rightleftharpoons R_2ZrCl_6 + 2Cl^-$$

followed by the reaction of the above species with TBA-Cl in a chloroform solution:

$$R_2ZrCl_6 + 2RCl \rightleftharpoons R_2ZrCl_6 \cdot 2RCl$$

The main extractable species of zirconium, $ZrCl_6^{2-}$, is formed from the zirconyl ions:

$$Zr(OH)_2Cl_n^{(2-n)+} + 2H^+ + (6-n)Cl^- \rightleftharpoons ZrCl_6^{2-} + 2H_2O$$

On the basis of the present results and of previously reported data on niobium extraction, some information with respect to the optimum conditions for the separation of zirconium and niobium have been given.

The authors wish to express their hearty thanks to Professor Takanobu Shiokawa and Assistant Professor Kunio Seto for their kind suggestions made in the course of this work.

Department of Chemistry
Faculty of Science
Tohoku University
Katahira-cho, Sendai

The Stereochemistry and Mechanisms of Catalytic Hydrogenation and Catalytic Hydrogenolysis. II[1]. *The Catalytic Hydrogenolysis of Optically-active Ethyl α-Phenyl-α-aryloxypropionates over Palladium and Nickel Catalysts*[2]

By Sekio MITSUI and Shin IMAIZUMI

(Received March 30, 1963)

In order to clarify the mechanisms of catalytic hydrogenolysis, hydrogenation, and the exchange reaction of hydrogen on the surface of the catalyst, we have carried out an investigation of the catalytic hydrogenolysis over Raney nickel of optically-active ethyl atrolactate and its derivatives[3] and suggested the mechanisms of both catalytic hydrogenolysis and hydrogenation[1,4].

In the catalytic hydrogenolysis of ethyl atrolactate (I) and its alkyl (II) and aryl ethers (III) over Raney nickel, optically-active ethyl α-phenylpropionate (IV) was obtained with a 90% retention of optical activity. While I and II were hydrogenolyzed with retention of their configurations, III, underwent an apparent Walden inversion.

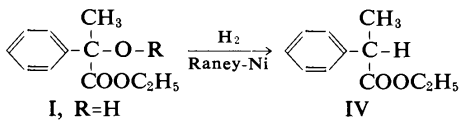

I, R=H
II, R=alkyl

IV

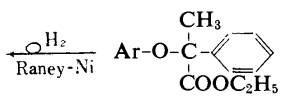

III Ar=aryl
III$_1$ Ar=C_6H_5-
III$_2$ Ar=p-$CH_3C_6H_4$-
III$_3$ Ar=o-$CH_3C_6H_4$-
III$_4$ Ar=p-$CH_3OC_6H_4$-
III$_5$ Ar=o-$CH_3OC_6H_4$-

In view of these results, we have suggested the following explanation[1,4]. In the cases of I and II, the phenyl, carboethoxy and hydroxy (alkoxy) groups, which are the chemisorption groups on Raney nickel, can be easily adsorbed on the catalyst surface without any steric hindrance (Fig. 1), and the electron or electrons and the proton are transferred from the catalyst surface to the asymmetric carbon of the molecule; accordingly, there results a retention of the configuration (S_{NI} type mechanism on the catalyst). However, owing to steric hindrance by a planar structure of the aryloxy group in III, the three chemisorption groups (phenyl, carboethoxy and aryloxy) can not be so easily adsorbed on the same catalyst surface. Therefore, the aryloxy group is adsorbed on one side of the catalyst surface and the carboethoxy and phenyl groups on the other, thus avoiding steric hindrance and allowing adsorption to proceed smoothly on the catalyst surface (Fig. 2). The asymmetric carbon is then drawn near to the catalyst surface and the electron or electrons and the proton are transferred from the latter, pushing out the aryloxy groups to another catalyst surface (that is, there is a concerted reaction), thereupon allowing the Walden inversion to take place (an S_N2 type reaction on the catalyst).

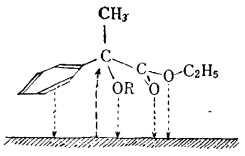

Fig. 1.

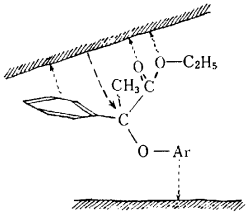

Fig. 2.

Although a molecule has steric hindrance, it can not be chemisorbed on two faces of the catalyst surface unless the catalyst contains suitable pores. It is presumed that the Raney nickel catalyst has a large number of such pores, since it is made by dissolving the aluminum with alkali from the nickel-aluminum alloy.

From the stereochemical viewpoint, it seemed pertinent to investigate hydrogenolysis using a catalyst other than Raney nickel. Therefore, the present paper reports observations on the hydrogenolysis of ethyl α-phenyl-α-aryloxypropionates (III) using palladium and nickel catalysts on some carriers.

1) Part I in this series: S. Mitsui and S. Imaizumi, This Bulletin, 34, 774 (1961).
2) Presented at the 8th and 9th Symposiums on Catalysis of The Chemical Society of Japan, Osaka, March, 1959 and Tokyo, April, 1960.
3) S. Imaizumi, *J. Chem. Soc. Japan, Pure Chem. Sec.* (*Nippon Kagaku Zassi*), 77, 1511 (1956); 78, 1396 (1957); 80, 336 (1959); 81, 627, 631, 633 (1960).
4) S. Mitsui and S. Imaizumi, ibid., 77, 1516 (1956); *Chem. Abstr.*, 53, 5179g (1959).

TABLE I. STEREOCHEMICAL RELATIONSHIPS IN THE CATALYTIC HYDROGENOLYSIS OF ETHYL α-PHENYL-α-ARYLOXYPROPIONATE OVER 5% PALLADIUM ON CHARCOAL AND RANEY NICKEL CATALYSTS

Aryl ether (III) -Ar		Catalyst	Maintained optical activity of IV %	Configuration
$-C_6H_5$	(III_1)	5% Pd-C	47	Retention
$-C_6H_5$	(III_1)	Raney-Ni	90	Inversion
$-C_6H_4CH_3(p)$	(III_2)	5% Pd-C	52	Retention
$-C_6H_4CH_3(p)$	(III_2)	Raney-Ni	92	Inversion
$-C_6H_4CH_3(o)$	(III_3)	5% Pd-C	48	Retention
$-C_6H_4CH_3(o)$	(III_3)	Raney-Ni	88	Inversion
$-C_6H_4OCH_3(p)$	(III_4)	5% Pd-C	64	Inversion
$-C_6H_4OCH_3(p)$	(III_4)	Raney-Ni	94	Inversion
$-C_6H_4OCH_3(o)$	(III_5)	5% Pd-C	49	Inversion
$-C_6H_4OCH_3(o)$	(III_5)	Raney-Ni	95	Inversion

TABLE II. STEREOCHEMICAL RELATIONSHIPS IN THE CATALYTIC HYDROGENOLYSIS OF ETHYL L(+)-α-PHENYL-α-PHENOXYPROPIONATE (III_1) OVER VARIOUS AMOUNTS OF 5% PALLADIUM ON CHARCOAL CATALYST

Weight of III_1 used, 1.4 g.; Optical rotation, absolute configuration and optical purity of III_1, $[\alpha]_D^6$ +6.2° (*c* 9.0, absolute ethanol), L, 44.6%; Solvent, absolute ethanol 50~100 ml.

Weight of catalyst g.	Reaction time hr.	Yield %	IV					
			Optical rotation[a]			A. C.[b]	Optical purity, %[c]	Maintained optical activity %[d]
			$[\alpha]_D^t$	*t*, °C	*c*			
0.1	48	60	−12.5°	12	7.7	L	17.4	39
1.0	5	100	−15.0°	7	8.0	L	20.9	47
7.0	2	100	− 9.7°	8	5.1	L	13.3	30
15.0	4	100	−14.6°	10	10.0	L	20.2	45

a) Solvent is absolute ethanol.
b) Absolute configuration
c) Calculated by (optical rotation of IV/optically pure rotation of IV) ×100. The rotation of optically pure IV is 72.2° (absolute ethanol)[2].
d) Calculated by (optical purity of IV/optical purity of III) ×100.

TABLE III. STEREOCHEMICAL RELATIONSHIPS IN THE CATALYTIC HYDROGENOLYSIS OF ETHYL L(+)-α-PHENYL-α-PHENOXYPROPIONATE (III_1) OVER PALLADIUM ON CHARCOAL CATALYSTS

Weight of III_1 used, 1.4 g.; Optical rotations, absolute configration and optical purity of III_1, $[\alpha]_D^6$ +6.2° (*c* 9.0, absolute ethanol), L, 44.6%; Solvent, absolute ethanol 50 ml.

Catalyst	g.	Reaction time hr.	Yield %	IV					
				Optical rotation[a]			A. C.[b]	Optical purity %[c]	Maintained optical activity %[d]
				$[\alpha]_D^t$	*t*, °C	*c*			
1% Pd-C	3.0	2	100	−20.8°	7	9.4	L	28.8	65
5% Pd-C	1.0	5	100	+15.1°	7	8.0	L	20.9	47
10% Pd-C	1.0	5	90	+ 2.0°	4	9.8	D	2.8	6
25% Pd-C	1.0	6	75	+ 5.9°	4	7.0	D	8.2	18
50% Pd-C	0.5	20	80	+ 9.5°	7	9.2	D	13.2	30
75% Pd-C	0.5	48	80	+15.9°	5	8.5	D	22.0	49
90% Pd-C	0.5	48	50	+24.8°	7	8.5	D	34.3	77
Pd	1.0	48	25	+13.9°	6	5.6	D	19.4	44
5% Pd-$BaSO_4$	1.0	24	75	+14.2°	6	9.0	D	19.7	44

Notation a—d) refer to the footnotes of Table II.

Optically-active ethyl α-phenyl-α-aryloxypropionates (III) were prepared according to the process described in the preceding paper[1] and were shaken with 5% palladium on a charcoal catalyst at an ordinary temperature and under hydrogen pressure. These aryl ethers III were hydrogenolyzed to ethyl α-phenylpropionate (IV) and related phenols. As may be seen in Table I, the retention of optical activity and the configuration of IV varied with the structure of the aryl group attached to III. In another series of experiments, ethyl α-phenyl-α-phenoxypropionate (III_1) was hydrogenated by employing various amounts of 5% palladium on a charcoal catalyst. The effects of various amounts of catalyst did not produce appreciable differences in the results, as is shown in Table II. The phenyl ether, III_1, was then hydrogenated over palladium on charcoal catalyst of different palladium concentrations. The configurations of IV produced in each case are shown in Table III.

It may be seen that, with concentrations of palladium on charcoal of 1 and 5%, the retentions of the optical activity of ethyl α-phenylpropionate (IV) with retention of configuration were 65 and 47% respectively. When the palladium concentration on charcoal was increased to 10, 25, 50, 75 and 90%, the retentions of the optical activity of IV with the inversion of the configuration were 6, 18, 30, 49 and 77% respectively. These results show that the percentage of Walden inversion in catalytic hydrogenolysis increases in an orderly fashion with an increase in the concentration of palladium on charcoal. When palladium was used without a carrier, the amount of Walden inversion in the catalytic hydrogenolysis was about the same as that produced with 5% palladium on barium sulfate, but much less than that produced with 75 and 90% palladium on charcoal.

These results lead to the conclusion that, when the palladium concentration on charcoal is low, the catalytic surfaces on which the phenyl ether III_1 can be chemisorbed on the two faces of the catalyst are comparatively small, because the palladium is deposited thinly on the carrier surface, but with an increase in the palladium concentration, the crystals of palladium are deposited on charcoal in such a manner that they create rugged surfaces so that the phenyl ether III_1 can be chemisorbed on the two faces of the catalyst. Thus, the occurrence of the two face-chemisorption of the phenyl ether III_1 is increased, and the proportion of the inverted product IV is likewise increase, because the palladium catalysts are capable of causing a catalytic hydrogenolysis of the phenyl ether III_1 even in a one face-chemisorption state on the catalysts, the proportion of D- and L-forms of IV is principally determined by the quantity of suitable pores in which phenyl ether III_1 can be chemisorbed on the two faces of the catalysts. Of course, besides this fact, the proportion is also related to the reaction rates of both the one face-chemisorption state and the two face-chemisorption state of phenyl ether III_1.

The palladium catalyst without the carrier acted less stereospecifically than 90% palladium on charcoal. This fact seems to account for the existence of fewer suitable pores on the catalyst because of its massive state. Moreover, 5% palladium on barium sulfate acted in the same manner as the palladium catalyst without the carrier. This result may be because the barium sulfate acted merely as a dispersing agent of the palladium, since the adsorptive power of the carrier is comparatively weak.

When alumina instead of charcoal was used as the carrier of the palladium catalyst, the stereospecific hydrogenolysis of the phenyl ether III_1 gave results qualitatively similar to these observed during the course of hydrogenolysis over the palladium on charcoal catalysts, as is shown in Table IV. In the case of palladium on alumina catalysts, however, the extent of the inverted product IV was high, even when 2% palladium on alumina was employed. The reason for this may be that the surface area of alumina is smaller than that of charcoal.

The *p*-anisyl ether III_4 was hydrogenolyzed in the same manner as the phenyl ether III_1 using palladium on charcoal and palladium on alumina catalysts. In these cases, however, the proportion of inverted IV was high, even when 1% palladium on charcoal and 0.2% palladium on alumina catalysts were used, as Table V shows. Therefore, it may be conceived that the hydrogenolysis of the *p*-anisyl ether III_4 in the one face-chemisorption state on the catalyst surface presents some difficulty, since the steric hindrance of the *p*-anisyl ether III_4 in the one face-chemisorption state is more predominant than the corresponding steric hindrance of the phenyl ether III_1, because of a greater chemisorption of the *p*-methoxy group.

The above results prove that not only a small difference in the chemical structure of a molecule but also in the surface structure of the catalyst alters the steric structure of the hydrogenolyzed product. That is, the steric state of a molecule which is being chemisorbed on the catalyst surface is the most important factor in the stereochemistry of the hydrogenolysis.

TABLE IV. STEREOCHEMICAL RELATIONSHIPS IN THE CATALYTIC HYDROGENOLYSIS OF ETHYL D(−)-α-PHENYL-α-PHENOXYPROPIONATE (III_1) OVER PALLADIUM ON ALUMINA CATALYSTS

Weight of III_1 used, 1.4 g.; Optical rotation, absolute configuration and optical purity of III_1, $[\alpha]_D^{27}$ −7.0° (*c* 9.0, absolute ethanol), D, 49.5%; Solvent, absolute ethanol 50 ml.,

Catalyst	g.	Reaction time hr.	Yield %	IV					
				Optical rotation[a]			A. C.[b]	Optical purity %[c]	Maintained optical activity %[d]
				$[\alpha]_D^t$	*t*, °C	*c*			
0.2% Pd-Al_2O_3	12.5	10	100	+11.2°	28	10.0	D	15.5	31
0.5% Pd-Al_2O_3	10.0	4	100	+ 5.2°	25	9.3	D	7.3	15
1% Pd-Al_2O_3	5.0	10	100	+ 1.1°	25	9.3	D	1.5	3
2% Pd-Al_2O_3	5.0	10	100	− 5.9°	25	11.0	L	8.1	16
5% Pd-Al_2O_3	1.0	24	80	−25.4°	23	5.3	L	35.1	71
10% Pd-Al_2O_3	1.5	24	100	−27.1°	23	9.5	L	37.1	76

Notations a—d) refer to the footnotes of Table II.

TABLE V. STEREOCHEMICAL RELATIONSHIPS IN THE CATALYTIC HYDROGENOLYSIS OF ETHYL L(+)-α-PHENYL-α-(*p*-ANISOXY)PROPIONATE (III_4) OVER PALLADIUM ON CHARCOAL AND PALLADIUM ON ALUMINA CATALYSTS

Weight of III_4 used, 1.5 g.; Optical rotation, absolute configuration and optical purity of III_4, $[\alpha]_D^7$ +10.9° (*c* 8.7, absolute ethanol), L, 50.3%; Solvent, absolute ethanol 50 ml.

Catalyst	g.	Reaction time hr.	Yield %	IV					
				Optical rotation[a]			A. C.[b]	Optical purity %[c]	Maintained optical activity %[d]
				$[\alpha]_D^t$	*t*, °C	*c*			
1% Pd-C	3.0	24	90	+19.3°	6	8.1	D	26.8	53
5% Pd-C	2.0	24	90	+23.2°	9	9.6	D	32.1	64
50% Pd-C	1.0	24	70	+27.8°	5	8.9	D	38.5	77
0.2% Pd-Al_2O_3	12.5	10	40	+29.5°	15	9.5	D	4.09	81
1% Pd-Al_2O_3	10.0	5	50	+28.1°	18	8.5	D	38.9	77
5% Pd-Al_2O_3	3.0	7	50	+27.6°	18	8.9	D	38.2	76

Notations a—d) refer to the footnotes of Table II.

TABLE VI. STEREOCHEMICAL RELATIONSHIPS IN THE CATALYTIC HYDROGENOLYSIS OF ETHYL L(+)-α-PHENYL-α-PHENOXYPROPIONATE (III_1) OVER VARIOUS NICKEL CATALYSTS

Weight of III_1 used, 1.4 g.; Optical rotation, absolute configuration and optical purity of III_1, $[\alpha]_D^6$ +6.2° (*c* 9.0, absolute ethanol), L, 44.6%; Solvent, absolute ethanol 50 ml.

Catalyst	g.	Reaction time hr.	Yield %	IV					
				Optical rotation			A. C.[b]	Optical purity %[c]	Maintained optical activity %[d]
				$[\alpha]_D^t$	*t*, °C	*c*			
Catalyst VI[e]	5.0	48	65	+31.1°	7	7.6	D	43.1	97
Catalyst VIII[f]	2.5	48	65	+31.6°	24	9.0	D	43.8	98
Catalyst X[e]	5.0	48	50	+31.9°	24	9.2	D	44.2	99
Catalyst FC[e]	10.0	24	70	+31.7°	11	8.2	D	43.9	98
Catalyst FD[e]	10.0	24	80	+31.8°	7	8.7	D	44.1	99
U-Ni-B[g]	0.5(Ni)	48	50	+32.1°	9	8.7	D	44.5	100

Notations a—d) refer to the footnotes of Table II.

e) Stabilized nickel on kieselguhr catalyst (Ni, about 50%); cf. T. Yamanaka et al., *J. Sci. Res. Inst.*, **51**, 168 (1957); **52**, 143 (1958).

f) Stabilized Raney nickel catalyst: cf. ibid.

g) Urushibara nickel-B catalyst: cf. Y. Urushibara and S. Nishimura, This Bulletin, **27**, 480 (1954).

Attention was next paid to the hydrogenolysis of the phenyl ether III_1 over nickel catalysts which had been prepared by different methods. In the cases of these catalysts, the retention of the optical activity of the product IV produced with an inversion of the configuration was almost 100%, as is shown in Table VI.

Since it is not likely that these catalysts, have more pores than are found in an ordinary Raney nickel catalyst, it is presumed to be scarcely possible to hydrogenolyze the phenyl ether III_1 in the one face-chemisorption state. This concept is supported by the fact that larger amounts of these catalysts are essential to complete the hydrogenolysis of the phenyl ether III_1.

Experimental

Optically-active Ethyl α-Phenyl-α-aryloxypropionate (III). — The procedure for preparing the aryl ethers III and their optical purities were reported in the experimental part of the preceding paper[1].

The Catalytic Hydrogenation of Optically-active Ethyl α-Phenyl-α-aryloxypropionate (III). — A mixture of the aryl ether III, 50 ml. of absolute ethanol, and a catalyst was shaken under hydrogen at an ordinary temperature and pressure until the catalyst hydrogen was no longer adsorbed. The catalyst was filtered and rinsed with ethanol, and the solvent was distilled. The residual oil was taken up in ether and extracted with a 5% sodium hydroxide solution. The alkaline insoluble material was dried over anhydrous sodium sulfate, and the solvent was removed. The residual oil was distilled at reduced pressure to give ethyl α-phenylpropionate (IV) (b. p., 103～104°C/12 mmHg).

The alkaline extract was acidified with hydrochloric acid. In the case of phenyl ether III_1, bromine was added to the acidified solution to give tribromophenol (m. p., 94～95°C). The yield was calculated from the weight of the tribromophenol. In the cases of other aryl ethers (III_{2-5}), the resulting oil in the acidified solution was taken up in ether and dried; the solvent was removed by distillation, and the residue was converted to a solid derivative.

It has been established in previous papers[1,3] that (+)-III (absolute ethanol solution) and (−)-IV (neat or absolute ethanol solution) have the same L-form.

These results are described in Tables II-VI and are as follows: Ethyl L(+)-α-phenyl-α-phenoxypropionate (III_1) (b. p., 142～143°C/2.5 mmHg, $[\alpha]_D^6$ +6.2° (*c* 9.0, ethanol), 44.6% optical purity) gave ethyl L-(−)-α-phenylpropionate (IV) ($[\alpha]_D^7$ −15.1° (*c* 8.0, ethanol), 20.9% optical purity) and phenol over 5% palladium on a charcoal catalyst[5], while if gave D(+)-IV ($[\alpha]_D^8$ +29.0° (*c* 5.0, ethanol), 40.2% optical purity) and phenol over a Raney nickel catalyst[6].

Ethyl L(+)-α-phenyl-α-(*p*-cresoxy)propionate (III_2) (b. p., 143～145°C/0.5 mmHg, $[\alpha]_D^3$ +3.5° (*c* 5.4, ethanol), 37.5% optical purity) gave L(−)-IV ($[\alpha]_D^5$ −14.3° (*c* 7.6, ethanol), 19.5% optical purity) and *p*-cresol (its tosylate; m. p., 69～70°C) over 5% palladium on a charcoal catalyst, while it gave D(+)-IV ($[\alpha]_D^8$ +23.3° (*c* 8.8, ethanol), 34.5% optical purity) and *p*-cresol over a Raney nickel catalyst.

Ethyl D(−)-α-phenyl-α-(*o*-cresoxy)propionate (III_3) (b. p., 145～146°C/3 mmHg, $[\alpha]_D^5$ −7.3° (*c* 5.6, ethanol), 45.2% optical purity) gave D(+)-IV ($[\alpha]_D^6$ +15.7° (*c* 9.1, ethanol), 21.7% optical purity) and *o*-cresol (its tosylate; m. p., 54～55°C) over 5% palladium on a charcoal catalyst, while it gave L(−)-IV ($[\alpha]_D^7$ −28.7° (*c* 8.7, ethanol), 39.8% optical purity) and *o*-cresol over a Raney nickel catalyst.

Ethyl L(+)-α-phenyl-α-(*p*-anisoxy)propionate (III_4) (b. p., 170～172°C/3 mmHg, $[\alpha]_D^7$ +10.9° (*c* 8.7, ethanol), 50.3% optical purity) gave D(+)-IV ($[\alpha]_D^9$ +23.2° (*c* 9.6, ethanol), 32.1% optical purity) and *p*-methoxyphenol (m. p., 52～53°C) over 5% palladium on a charcoal catalyst, while it gave D(+)-IV ($[\alpha]_D^8$ +34.0° (*c* 7.4, ethanol), 47.2% optical purity) and *p*-methoxyphenol over a Raney nickel catalyst.

Ethyl L(+)-α-phenyl-α-(*o*-anisoxy)propionate (III_5) (b. p., 158～160°C/2 mmHg, $[\alpha]_D^5$ +13.6° (*c* 4.2, ethanol), 52.5% optical purity) gave D(+)-IV ($[\alpha]_D^6$ +18.5° (*c* 8.5, ethanol), 25.7% optical purity) and guaiacol (*o*-anisoxyacetic acid; m. p., 126～127°C) over 5% palladium on a charcoal catalyst, while it gave D(+)-IV ($[\alpha]_D^5$ +36.0° (*c* 9.2, ethanol), 49.8% optical purity) and guaiacol over a Raney nickel catalyst.

The stereochemical results calculated from the above results are shown in Table I.

Department of Applied Science
Faculty of Engineering
Tohoku University
Katahira-cho, Sendai

5) H. Adkins and J. P. Carnahan, "Organic Syntheses", Vol. 26, p. 78, Method C.
6) W-4 Raney nicke; H. Adkins and A. A. Pavlic, *J. Am. Chem. Soc.*, **69**, 3039 (1947).

Studies on Antibiotics and Related Substances. XVIII. The Synthesis of 5-Methyl-2-methylenecyclopentanone-3-carboxylic Acid, an Antitumor Substance, and Related Mannich Bases

By Mitsuhiro KINOSHITA, Saburo NAKADA and Sumio UMEZAWA

(Received April 6, 1963)

Recent publications[1-2] from this laboratory have described the syntheses and antitumor activities of the methylene derivatives of cyclopentanone-3-carboxylic acid, which are related to Sarkomycin[2], an antitumor antibiotic. The present work is concerned with an extension of this work, and the syntheses and activities of 5-methyl-2-methylenecyclopentanone-3-carboxylic acid and related compounds are described. In addition, we here describe a rare example of the Mannich reaction where the formation of geometrical isomers due to the presence of cyclopentanone ring is demonstrated.

5-Methylcyclopentanone-3-carboxylic acid (I) was prepared by the method of Shemyakin and others[3]. A mixture of 5-methylcyclopentanone-3-carboxylic acid, paraformaldehyde and dimethylamine hydrochloride was fused, and the reaction mixture was treated with absolute ethanol to give 5-(dimethylaminomethyl)-5-methylcyclopentanone-3-carboxylic acid hydrochloride (hydrochloride of IIa) with an m. p. of 155°C and an R_f of 0.39 in the solvent system of *n*-butanol-acetic acid-water (4 : 1 : 1); IIa melted at 99~100°C. On being treated with benzaldehyde in the presence of sodium hydroxide, IIa afforded a benzylidene derivative, indicating the presence of an activated methylene group in IIa.

The mother liquor separated from the above product was concentrated and esterified with methanol to give a mixture of Mannich base esters; paper chromatographic study of the mixture (hydrochlorides) showed three spots (R_f 0.54, 0.49 and 0.41) in the solvent system described above. Treatment of the mixture with methyl iodide in ether at about 10°C resulted in the separation of a crystalline methiodide (VIII) of substance with a R_f of 0.54 (VII). The methiodide was hygroscopic and unstable and, when treated with an 10% potassium bicarbonate solution, afforded methyl 5-methyl-2-methylenecyclopentanone-3-carboxylate (IX). The ozonolysis of IX gave formaldehyde (isolated as the methone derivative)

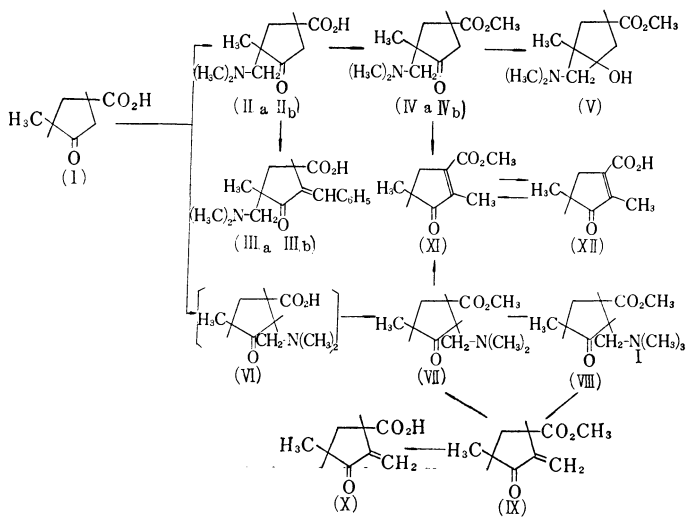

Chart 1

1) S. Umezawa and M. Kinoshita, This Bulletin, **30**, 267 (1957).
2) H. Umezawa, T. Yamamoto, T. Takeuchi, T. Okami, S. Yamaoka, T. Okuda, K. Nitta, K. Yagishita, R. Utahara and S. Umezawa, *Antibiotic & Chemotherapy*, **4**, 514 (1954).
3) M. M. Shemyakin, M. N. Kolosov, M. G. Karapechan and V. Ya. Rodinov *Zhur. Obshchei Khim.*, **28**, 2068 (1958).

and butane-1, 1, 3-tricarboxylic acid, as expected. Methylsuccinic acid was obtained also, suggesting that the sample of IX is accompanied by methyl 2, 5-dimethyl-2-cyclopenten-1-one-3-carboxylate (XI). However, reaction of the methylene compound (IX) with dimethylamine gave, in a 77% yield, methyl 2-(dimethylaminomethyl) -5-methylcyclopentanone-3-carboxylate, which is paper chromatographically identical with VII; this indicated that the sample of IX consists mainly of an exocyclic methylene compound. Additional evidence for this was found in the ultraviolet absorption data; the ultraviolet absorption of a freshly prepared sample of IX showed a strong band at 229 mμ (Fig. 1). However, when the sample was allowed to stand, even at room temperature, the band gradually shifted towards a longer wavelength and also decreased in intensity. On the other hand, we obtained methyl 2, 5-dimethyl-2-cyclopenten-1-one-3-carboxylate (XI) by the thermal decomposition of the hydrochloride of VII; the cyclopentenone derivative (XI) could be purified by the hydrolysis of XI, followed by methylation with diazomethane. The cyclopentenone derivative (XI) showed a strong band at 246 mμ (Fig. 1). Thus, it is evident that the above-mentioned shift of band and decrease in the intensity of the band are due to the gradual shift of the double bond into the cyclopentanone ring and to polymerization respectively. Moreover, a significant difference was observed between the infrared spectra of XI and IX; absorptions at 1357, 1100, 1062, 990 and 761 cm^{-1} were observed in the spectrum of XI, but not in that of IX (Fig. 2).

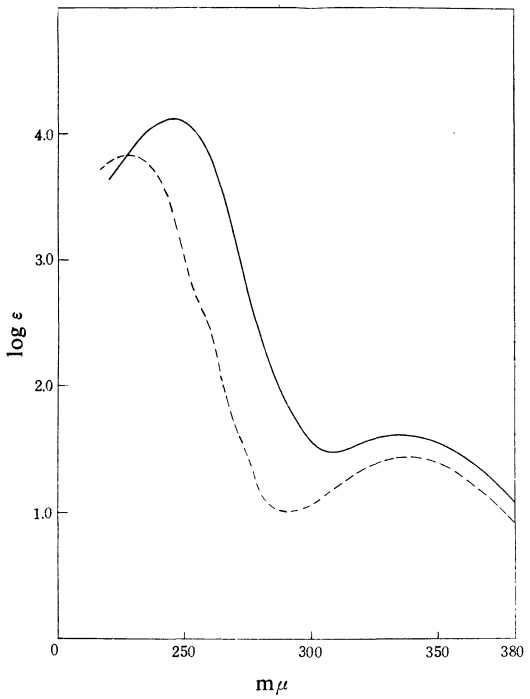

Fig. 1. Ultraviolet absorption spectra of methyl 5-methyl-2-methylenecyclopentanone-3-carboxylate (IX) (----) and methyl 2, 5-dimethyl-2-cyclopenten-1-one-3-carboxylate (XI) (——) in methanol.

The mild hydrolysis of IX with dilute sulfuric acid gave a crude product of 5-methyl-2-methylenecyclopentanone-3-carboxylic acid (X), a viscous liquid which polymerized gradually.

Paper chromatographic study of the mother liquor separated from the above-mentioned unstable methiodide (VIII) indicated the presence of a mixture of unchanged Mannich base esters with an R_f of 0.49* and a small quantity of methylene compound (IX). Fortunately, the oxalate of the unchanged Mannich base esters were crystallized from an absolute ether solution. Recrystallization of the oxalate from methanol, followed by treatment with sodium carbonate, gave a single free Mannich base ester (IVb), a colorless liquid. The hydrochloride of IVb melted at 140~141°C (decomp.). The hydrolysis of IVb with barium hydroxide gave the free Mannich base (IIb) (m. p., 124~125°C (decomp.)). IIb and its hydrochloride coincided in analysis with IIa and its hydrochloride respectively. The mixed m. p. of the

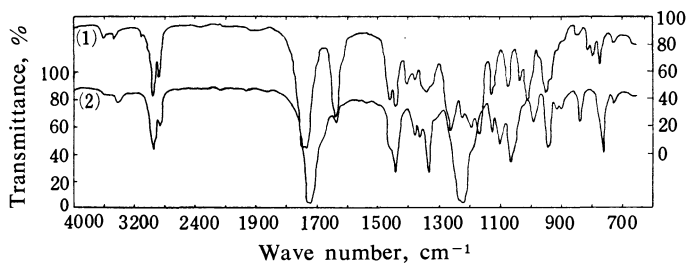

Fig. 2. Infrared absorption spectra of methyl 5-methyl-2-methylenecyclopentanone-3-carboxylate (IX) (1) and methyl 2, 5-dimethyl-2-cyclopenten-1-one-3-carboxylate (XI) (2) in liquid film.

* This spot corresponds to the overlap of the two spots of IVa (R_f, 0.51) and IVb (R_f, 0.47).

hydrochloride (m. p. 155~156°C) of IIb with the hydrochloride of IIa showed depression.

On being treated with benzaldehyde in the presence of sodium hydroxide, IIb afforded a benzylidene derivative (IIIb), indicating the presence of an activated methylene group in IIb. The methiodides of IVa and IVb were resistant to treatment[4] with a potassium bicarbonate solution, indicating the absence of hydrogen at the α-carbon atom to which the dimethylaminomethyl group is attached. Moreover, the hydrogenation of methyl ester (IVa) of IIa with an Adams platinum catalyst afforded methyl 3-hydroxy-4-(dimethylaminomethyl)-4-methylcyclopentane-1-carboxylate (V); the resistance of the C-N linkage of IVa to hydrogenolysis also suggested the absence of hydrogen at the α-carbon atom, because, by hydrogenation of methyl 5-(dimethylaminomethyl)cyclopentanone-3-carboxylate, we had obtained methyl 5-methylcyclopentanone-3-carboxylate[1]. Thus it has been clearly established that IIa and IIb are geometrical isomers of 5-(dimethylaminomethyl)-5-methylcyclopentanone-3-carboxylic acid, although the steric relation therein requires further discussion (vide infra).

Finally, it is noteworthy that the thermal decomposition of the hydrochloride of methyl 5-(dimethylaminomethyl)-5-methylcyclopentanone-3-carboxylate (IVa), followed by hydrolysis, afforded 2,5-dimethyl-2-cyclopenten-1-one-3-carboxylic acid (XII). This finding may be accounted for on the assumption that methyl 2-(dimethylaminomethyl)-5-methylcyclopentanone-3-carboxylate (VII) may conceivably be formed by a rearrangement of the dimethylaminomethyl group through a kind of retrograde Mannich reaction and may then be changed to IX.

Both 5-methyl-2-methylenecyclopentanone-3-carboxylic acid (X) and its methyl ester (IX) were found to possess antitumor and antimicrobial activities; the methyl ester was more potent than the corresponding free acid.

Discussion

On the basis of the data described herein, it is not possible to clearly decide between two structural possibilities for the two racemic geometrical isomers (IIa and IIb) of 5-(dimethylaminomethyl)-5-methylcyclopentanone-3-carboxylic acid. However, the problem is of interest. The infrared absorption study of IIa and IIb or of their hydrochlorides in KBr did not reveal their steric relation. Similarly, no steric relation was observed between the infrared spectra of IVa and IVb or their hydrochlorides. However, infrared absorptions in chloroform (c, 0.028 M) showed small but real differences (Fig. 3): the dimethylamino frequencies at 2830 and 2780 cm^{-1} and the C=O frequency of the carboxyl group at 1720 cm^{-1} were found in IIa, but IIb showed no absorption at these regions; the N^+-H stretching frequency at 2540~2300 cm^{-1} was found in both IIa and IIb, and the frequency of COO^- at 1603 cm^{-1} was found in both IIa and IIb. These observations led us to the conclusion that IIa exists as a mixture of the XIII and XIV forms, whereas IIb exists as a mixture of the XV and XVI forms.

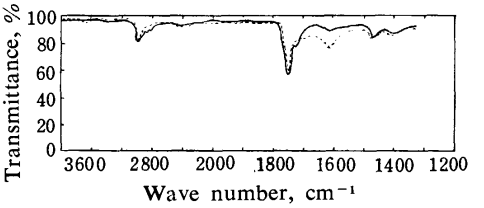

Fig. 3. Infrared absorption spectra of 5-(dimethylaminomethyl)-5-methylcyclopentanone-3-carboxylc acid (IIa) (——) and its geometrical isomer (IIb) (----) in chloroform solutions: 0.028 M, 0.104 mm. cell.

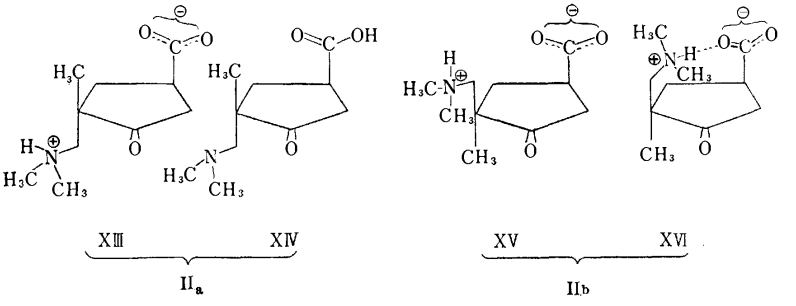

Chart 2

4) G. Büchi, N. C. Yang, S. R. Emerman and J. Meinwald, *Chem. & Ind.*, 1953, 1063; E. E. van Tamelen and S. R. Bach, *J. Am. Chem. Soc.*, 77, 4683 (1955); cf. Ref. 3.

This suggestion has been supported by the determination of pK_a. IIa had pK_{a_1} 3.60 and pK_{a_2} 8.34, whereas IIb had pK_{a_1} 3.49 and pK_{a_2} 8.66. The effect of hydrogen bonding in IIb may decrease the pK_{a_1} and increase the pK_{a_2}. A comparable effect of hydrogen bonding had been shown by the relation of pK_a values between lysergic acid and isolysergic acid[5].

As to racemic 2-(dimethylaminomethyl)-5-methylcyclopentanone-3-carboxylic acid (VI), four geometrical isomers are possible. Recent evidence and discussions[6] have shown that stable conformations of cyclopentanones substituted at the 2- and 3-positions with bulky groups are trans-form. However, it is not possible to state a steric structure in the case of compound VI, which contains acidic and basic groups in ortho-positions.

Experimental

Paper chromatograms of the Mannich bases were run with *n*-butanol-acetic acid-water (4 : 1 : 1) on Toyo Roshi No. 50 papers, using the ascending technique. Spots on paper chromatograms were detected by spraying the chromatograms with Dragendorff's reagent[7]. Paper chromatography of the products obtained by ozonolysis was carried out with xylene-phenol-85% formic acid (7 : 3 : 1)[8], and spots were detected by means of a spray of a 0.1% ethanolic solution of bromophenol blue.

The pK_a values were determined by the method of Parke and Davis[9], except that the titrant was with 0.1 N sodium hydroxide and was delivered by a Gilmont micropipet-buret with a total capacity of 1.0 ml. and with readings to 0.001 ml. on a microgage. The temperature was 22±1°C. The pK_a values were reproducible within a range of ±0.03.

Hydrochloride of 5-(Dimethylaminomethyl)-5-methylcyclopentanone-3-carboxylic Acid (IIa).—A mixture of 5-methylcyclopentanone-3-carboxylic acid[10] (I) (8.52 g.) and dimethylamine hydrochloride (4.96 g.) was heated to 75°C. To the resulting melt was added paraformaldehyde (1.80 g.), and the mixture stirred at 78°C for 2 hr. and evaporated in a vacuum to remove moisture. The resulting sirup, which gave three major spots (R_f 0.50, 0.38 and 0.30) on a paper chromatogram, was dissolved in hot absolute ethanol (13 ml.) and filtered. The cooled filtrate was stored in a refrigerator to give crude crystals of 5-(dimethylaminomethyl)-5-methylcyclopentanone-3-carboxylic acid hydrochloride; yield, 5.40 g. (38.7%); m. p., 150.0~152.5°C (decomp.). Recrystallization from propan-2-ol gave a pure sample of the hydrochloride of IIa as colorless plates, m. p., 155°C (decomp.), R_f 0.39. ν_{max}^{KBr} 2700 ($\overset{+}{N}H$), 1747 (C=O) and 1721 cm^{-1} (COOH). pK_{a_1} 3.60 and pK_{a_2} 8.34.

Found: C, 50.79; H, 7.48; N, 5.74. Calcd. for $C_{10}H_{18}O_3NCl$: C, 50.93; H, 7.70; N, 5.94%.

5-(Dimethylaminomethyl)-5-methylcyclopentanone-3-carboxylic Acid (IIa).—A mixture of 114 mg. of free amine ester (IVa) and a 0.45 N barium hydroxide solution (1.23 ml.) was stirred at 25°C for 2.5 hr. The resulting solution was treated with 2.2 N sulfuric acid, and the barium sulfate was removed by centrifuging. The supernatant layer and washings were then combined and subjected to lyophilization. The resulting colorless glass (102 mg.) was dissolved in a small volume of hot propan-2-ol and cooled in a refrigerator overnight to give colorless plates; yield, 76 mg. (71%); m. p., 99~100°C (decomp.). Recrystallization from propan-2-ol afforded an analytical sample; m. p., 99~100°C (decomp.), R_f 0.42, ν_{max}^{KBr} 1720 (C=O) and 1620 cm^{-1} (COO^-); $\nu_{max}^{ClCH_3}$ 2830, 2789 (dimethylamino group), 2415 ($\overset{+}{N}H$) 1745 (C=O), 1720 (COOH) and 1603 cm^{-1} (COO^-) (0.028 M, 0.104 mm.).

Found: C, 60.10; H, 8.65; N, 6.99. Calcd. for $C_{10}H_{17}O_3N$: C, 60.28; H, 8.60; N, 7.03%.

2-Benzylidene-5-(dimethylaminomethyl)-5-methylcyclopentanone-3-carboxylic Acid (IIIa).—To a solution of IIa (200 mg.) in 2.5 N sodium hydroxide (1.6 ml.) was added benzaldehyde (100 mg.), and the mixture was stirred at 20°C for 1 hr. The resulting yellow solution was adjusted to pH 3 with 3 N hydrochloric acid and shaken with ether. The water-layer was evaporated to dryness in vacuo and then extracted with absolute ethanol. Evaporation of the ethanol solution afforded a crude hydrochloride of IIIa as hygroscopic yellow amorphous powder; yield, 204 mg. (75%); characteristic, strong absorption in the ultraviolet spectrum at λ_{max}^{MeOH} 308~309 mμ ($E_{1cm}^{1\%}$ 558). To a solution of the crude hydrochloride of IIIa (130 mg.) in methanol (1.5 ml.), picric acid (130 mg.) in hot ethanol (1.5 ml.) was added. Short yellow prisms of picrate of IIIa were obtained; yield, 135 mg. (60% based on the crude hydrochloride of IIIa); m. p., 186~187°C (decomp.). Recrystallization from ethanol-methanol (2 : 1) showed no elevation in the melting point.

Found: C, 53.36; H, 4.70; N, 10.96. Calcd. for $C_{23}H_{24}O_{10}N_4$: C, 53.49; H, 4.68; N, 10.85%.

Hydrochloride of Methyl 5-(Dimethylaminomethyl)-5-methylcyclopentanone-3-carboxylate (IVa).—A mixture of hydrochloride of 5-(dimethylaminomethyl)-5-methylcyclopentanone-3-carboxylic acid (IIa) (1.7 g.) and absolute methanol (20 ml.) was saturated with dry hydrogen chloride and allowed to stand overnight. The solvent was removed by

5) J. B. Stenlake, *Chem. & Ind.*, 1953, 1089; A. Stoll, Th. Petrzilka, J. Rutschmann, A. Hofmann and Hs. H. Günthard, *Helv. Chim. Acta*, 37, 2039 (1954).

6) Y. Amiel, A. Loffler and D. Ginsburg, *J. Am. Chem. Soc.*, 76, 3625 (1954); M. M. Shemyakin et al., *Zhur. Obshchel Khim.*, 27, 742 (1957), A. B. Arendaruk et al., ibid., 27, 1398 (1957); L. J. Chinn, E. A. Broun, R. A. Mikulec and R. B. Garland, *J. Org. Chem.*, 27, 1733 (1952); E. Demole, E. Lederer and D. Mercier, *Helv. Chim. Acta*, 45, 685 (1962); E. Demole and M. Stoll, ibid., 45, 692 (1962).

7) T. Kariyone and Y. Hashimoto, *J. Pharm. Soc. Japan*, 71, 436 (1951).

8) N. F. Holyer and B. C. L. Weedon, *Chem. & Ind.*, 1955, 1219; H. Kolbe, *Z. physiol. Chem.*, 297, 19 (1954).

9) T. V. Parke and W. W. Davis, *Anal. Chem.*, 26, 642 (1954).

10) 5-Methylcyclopentanone-3-carboxylic acid (I) was prepared by the method of Shemyakin et al.[3]; m. p., 56~58°C; 2,4-dinitrophenylhydrazone (70% yield); m. p., 142~143°C.

distillation in a vacuum, and the residue was dried over phosphorus pentoxide. The crude hydrochloride of methyl ester thus obtained was recrystallized from butanone; yield, 1.6 g. (89%) of short colorless needles; m. p., 160~161°C (decomp.). R_f 0.51. ν_{max}^{KBr} 2690 ($\overset{+}{N}H$) and 1750 (ketone and ester C=O).

Found: C, 53.12; H, 8.23; N, 5.70. Calcd. for $C_{11}H_{20}O_3NCl$: C, 52.90; H, 8.07; N, 5.61%.

Methyl 5-(Dimethylaminomethyl)-5-methylcyclopentanone-3-carboxylate (IVa).—The hydrochloride of IVa (1.4 g.) in chloroform (10 ml.) was added to a 1.33 N ammonia-methanol solution (4.9 ml.). The chloroform layer was separated from the precipitated ammonium chloride and concentrated under reduced pressure. The resulting yellow oil was distilled without decomposition; b. p., 100~103°C (bath temp.)/0.03 mmHg; yield, 1.03 g. (86%). Repetition of distillation gave an analytical sample as a colorless liquid; b. p., 55°C (bath temp.)/0.001 mmHg, n_D^{27} 1.4609, ν_{max}^{liq} 2870, 2825, 2779 (dimethylamino group), 1747 (ketone and ester C=O) and 1410 cm^{-1} (methylene group in $-CO-CH_2-$).

Found: C, 61.73; H, 9.07; N, 6.70. Calcd. for $C_{11}H_{19}O_3N$: C, 61.94; H, 8.97; N, 6.57%.

The Oxalate of IVa.—To a solution of IVa (214 mg.) in absolute ether was added an ethereal solution of anhydrous oxalic acid (96 mg.), whereupon a thick gum separated; this gum was crystallized by trituration. Filtration followed by washing with ether gave a crude oxalate of IVa (279 mg., 92%) melting at 105~108°C (decomp.). Two recrystallizations from methanol afforded a pure sample as colorless prisms; m. p., 110.5~111°C (decomp.), R_f 0.51.

Found: C, 51.32; H, 7.10; N, 4.72. Calcd. for $C_{11}H_{19}O_3N \cdot C_2H_2O_4$: C, 51.48; H, 6.98; N, 4.62%.

The Methiodide of IVa.—A mixture of IVa and an excess of methyl iodide was allowed to stand for 48 hr. at room temperature. Evaporation of the methyl iodide, followed by washing with ether, gave the methiodide of IVa melting at 213°C (decomp.) in a quantitative yield. Two recrystallizations from methanol gave colorless plates; m. p., 216~217°C (decomp.). ν_{max}^{KBr} 1735 (ketone and ester C=O) and 1412 cm^{-1} (methylene group in $-CO-CH_2-$).

Found: C, 40.54; H, 6.28; N, 4.07. Calcd. for $C_{12}H_{22}O_3NI$: C, 40.57; H, 6.24; N, 3.94%.

Methyl 3-Hydroxy-4-(dimethylaminomethyl)-4-methylcyclopentane-1-carboxylate (V).—A solution of IVa (1.03 g.) in methanol (4 ml.) was shaken with platinum oxide (80 mg.) and hydrogen; 122 ml. (759.2 mmHg, 20.5°C) of hydrogen was absorbed in 1 hr. The reaction mixture was filtered and concentrated in a vacuum and then distilled under reduced pressure to give the title compound (927 mg., 89%) as a colorless viscous oil; b. p., 115~120°C (bath temp.)/0.005 mmHg, $\nu_{max}^{liq.}$ 3400 (OH), 2875, 2823, 2772 (dimethylamino group), and 1737 cm^{-1} (ester C=O).

The Hydrochloride of V.—It was prepared by the addition of a methanolic hydrogen chloride solution to V dissolved in absolute methanol, followed by dilution with absolute ether. Two recrystallizations from absolute methanol-ether gave the specimen with an m. p. of 170~171°C (decomp.).

Found: C, 52.44; H, 9.03; N, 5.88. Calcd. for $C_{11}H_{22}O_3NCl$: C, 52.50; H, 8.81; N, 5.57%.

The 3,5-Dinitrobenzoate of V.—To a solution of V (200 mg.) in chloroform (0.2 ml.) was added a solution of 3,5-dinitrobenzoyl chloride (240 mg.) in chloroform (0.2 ml.), and the mixture was allowed to stand overnight. Dilution with absolute ether gave a viscous oil, which was then triturated with absolute ether to give a crystalline powder (430 mg.). Two recrystallizations from absolute methanol-ether afforded a pure sample of 3,5-dinitrobenzoate hydrochloride of V (273 mg., 66%); m. p., 187~189°C (decomp., sintered at 185°C).

Found: C, 48.35; H, 5.60; N, 9.20. Calcd. for $C_{18}H_{24}O_8N_3Cl$: C, 48.48; H, 5.39; N, 9.22%.

Methyl 5-Methyl-2-methylenecyclopentanone-3-carboxylate (IX).—The mother liquor of 5-(dimethylaminomethyl)-5-methylcyclopentanone-3-carboxylic acid hydrochloride (5.4 g.) described above was concentrated in a vacuum. The oily residue was dissolved in water (20 ml.), and the solution was extracted with four 15 ml. portions of ethyl acetate to recover the unchanged keto acid (crude 1 g.). The aqueous layer was washed with chloroform several times and evaporated in a vacuum at 40°C. The sirupy residue was dried in a vacuum over phosphorus pentoxide to give a yellow glassy solid (7.6 g.). Paper chromatography showed that the solid consisted of two major components (R_f, 0.50 and 0.37), but a small amount of the hydrochloride of IIa (R_f 0.39) was also found. A mixture of the residue (7.5 g.) and absolute methanol (62 ml.) was saturated with dry hydrogen chloride and allowed to stand for 2 days at room temperature. After evaporation of the solvent in a vacuum, the resulting orange-yellow sirup (8.0 g.) was dissolved in water (11 ml.) while beeing cooled in an ice-water bath, and to the solution was added a 50% aqueous potassium carbonate solution (26 ml.) to separate a viscous oil. The oil was extracted with four 20 ml. portions of ether. After being dried over fused potassium acetate, the ethereal extract was evaporated to give a mixture of free amine esters as an orange-yellow liquid (4.1 g.); paper chromatography of its hydrochloride showed R_f values of 0.54, 0.49 and 0.41. The addition of methyl iodide (9.2 g.) to a solution of the free amino ester in absolute ether (16 ml.) immediately resulted in the crystallization of methiodide. The mixture was allowed to stand for 1 hr. at 9°C and then stored in a refrigerator overnight. The precipitate was collected rapidly on a filter and washed with absolute ether. After drying in vacuo over phosphorus pentoxide, there were obtained 3.4 g. of methyl 2-(dimethylaminomethyl)-5-methylcyclopentanone-3-carboxylate methiodide (VIII), which was very hygroscopic and which was gradually decomposed by moisture. The crude methiodide (3.4 g.) was dissolved in water (7 ml.) at 10°C, and to this solution was added a 10% aqueous potassium bicarbonate solution (17 ml.). The resulting solution immediately appeared turbid and

separated a colorless oil with a pungent odor. The oil was extracted with ether (10 ml.) while being occasionally shaken for 20 min. at 10°C. After separating the ether layer, the aqueous layer was again extracted with two 10 ml. portions of ether. The combined ethereal extracts were washed with 0.1 N sulfuric acid and then with water. After being dried over fused potassium acetate. the ethereal extract was evaporated at about 0°C to afford a colorless liquid of methyl 5-methyl-2-methylenecyclopentane-3-carboxylate (IX); yield, 882 mg. (54.7% based on the crude methiodide (VIII)), n_D^{16} 1.4775, λ_{max}^{MeOH} 229 (ε, 6580) and 340 mμ (ε, 28). Distillation gave a pure sample; b. p., 43°C (bath temp.)/0.005 mmHg, n_D^{19} 1.4726, λ_{max}^{MeOH} 229 (ε, 6830) and 338 mμ (ε, 28), $\nu_{max}^{liq.}$ 1747, 1733 (ester and ketone C=O), 1640 (C=C), 1400 and 951 cm^{-1} (=CH_2).

Found: C, 64.30; H, 7.02. Calcd. for $C_9H_{12}O_3$: C, 64.27; H, 7.19%.

The mother liquor of the methiodide (VIII) was concentrated to give an orange oil intermixed with a small amount of solid. The oily residue was dissolved in ether, and the solution was washed with water. The ether layer was extracted with dilute sulfuric acid until the pH of the aqueous layer became 4.3 and was then washed with water. The ethereal layer was dried and then evaporated to afford a light-yellow oil (110 mg.), which was again distilled to give a sample identical to IX in ultraviolet and infrared spectra.

To the diluted sulfuric acid extract a 50% potassium carbonate solution (4 ml.) was added, and the mixture was extracted with three 7 ml. portions of ether. The ethereal extract dried over potassium acetate was evaporated to recover an unchanged amine ester (1.804 g.) as an orange-yellow oil. The paper chromatogram of its hydrochloride showed an intense spot (R_f 0.49) owing to the overlapping of the two spots (R_f 0.51 and 0.47) and another spot (R_f 0.41), but no spot (R_f 0.54) of the hydrochloride of VII. A mixture of the amine ester (200 mg.) and an excess of methyl iodide was allowed to stand for 48 hr. at room temperature. Evaporation of the excess methyl iodide followed by washing with ether yielded a methiodide (330 mg.) melting at 155~180°C (decomp.). It was found that the methiodide was not decomposed by treatment with a 10% aqueous potassium bicarbonate. Fractional crystallization of the crude methiodide from methanol gave two kinds of methiodides. The less soluble methiodide (67 mg., m. p. 216~217°C (decomp.)) and the more soluble one (60 mg. m. p. 169~171°C (decomp.)) were identical to the methiodide of IVa and to the methiodide of IVb respectively, as was shown by mixed melting points and infrared spectra.

The Formation of Methyl 2-(Dimethylaminomethyl)-5-methylcyclopentanone-3-carboxylate (VII) from IX.—The methyl 5-methyl-2-methylenecyclopentanone-3-carboxylate (IX) (834 mg.) was added drop by drop to an ice-cooled 32% dimethylamine-methanol solution (816 mg.) while it was being shaken. The solution was allowed to stand at 18°C for 1 hr. and then placed in a refrigerator. After removing the methanol by distillation in a vacuum, the residue was dissolved in ether. The ethereal solution was neutralized with dilute sulfuric acid until the pH in the aqueous layer became 2.3. The aqueous layer was separated and washed twice with ether. From the combined ethereal extracts, an unchanged methylene compound (IX) was recovered (112 mg., λ_{max}^{MeOH} 231 and 336 mμ. To the aqueous layer was added a 50% potassium carbonate solution (2 ml.), and the mixture was extracted with ether repeatedly. The ethereal extract dried over potassium acetate was evaporated to give the methyl 2-(dimethylaminomethyl)-5-methylcyclopentanone-3-carboxylate (VII) as a light yellow liquid (770 mg., 77.2%). The infrared spectrum of the sample showed no peak near 1410 cm^{-1} (methylene group in -CO-CH_2-). The paper chromatogram of its hydrochloride showed a single spot (R_f 0.54).

The Oxalate of VII.—It was prepared by the addition of an ethereal solution of anhydrous oxalic acid (90 mg.) to VII (200 mg.) in ether. The yield. was 267 mg. (94%): m. p., 105~117°C. Two recrystallizations from methanol gave an analytical sample as colorless needles; m. p., 147°C (decomp., sintered at 122~137°C), R_f 0.54.

Found: C, 51.56; H, 7.18; N, 4.75. Calcd. for $C_{11}H_{19}O_3N \cdot C_2H_2O_4$: C, 51.48; H, 6.98; N, 4.62%.

Methyl 2-(Dimethylaminomethyl)-5-methylcyclopentanone-3-carboxylate Methiodide (VIII).—To a solution of VII (200 mg.) in absolute ether (1 ml.) methyl iodide (800 mg.) was added at 10°C to give methyl 2-(dimethylaminomethyl)-5-methylcyclopentanone-3-carboxylate methiodide (VIII) immediately. After the solution has been left standing for 6 hr. at 10°C, the precipitate was rapidly collected and washed with absolute ether by centrifuging; yield: 306 mg. (91.5%) as pale-yellow crystals. This precipitate was very hygroscopic and was easily decomposed by moisture, but it was stable in a vacuum over phosphorus pentoxide at a lower temperature. This methiodide (158 mg.) was treated with a 10% aqueous potassium bicarbonate solution to afford the methyl 5-methyl-2-methylenecyclopentanone-3-carboxylate (IX); yield, 56 mg. (75%). The product was identical with IX in its ultraviolet and infrared spectra.

The Ozonolysis of IX.—A solution of freshly prepared methyl 5-methyl-2-methylenecyclopentanone-3-carboxylate (IX) (400 mg.) in ethyl acetate (20 ml.) was treated with an approximately 2% (by weight) ozone-oxygen mixture at −10°C at a rate of 500 ml./min. for 3 hr. The volume of the reaction mixture was adjusted to 20 ml. by the addition of ethyl acetate. To a 5 ml. aliquot of this solution were added water (5 ml.) and zinc dust (150 mg.), and the mixture was refluxed for 30 min. The reaction mixture was filtered while hot into a solution of methone (150 mg.) in 5 ml. of ethanol. Dilution with water (10 ml.) afforded the needles of formaldehyde methone; yield, 50 mg. (28.7%); m. p., 187~189.5°C. Admixing with an authentic specimen of formaldehyde methone showed no depression of melting point.

The remaining, ozonized solution (15 ml.) was concentrated in a vacuum at a temperature below

10°C to afford a viscous pale-yellow oil, which was then heated with 30% hydrogen peroxide (1.6 ml.) at about 90°C for 1 hr. The colorless solution was evaporated under reduced pressure. The addition of water to the residue, followed by evaporation, was repeated to remove the excess hydrogen peroxide. The final residue (296 mg.) was refluxed with 1.6 N methanolic potassium hydroxide (3.1 ml.) for 1 hr. After removing methanol, the residue was acidified to pH 2.4 with dilute sulfuric acid, saturated with ammonium sulfate, and extracted with ether continuously for 12 hr. The extract was dried over sodium sulfate and distilled to give a residue which immediately crystallized; yield, 186 mg. The paper chromatogram of the product run with xylene-phenol-85% formic acid[8] showed two spots (R_f 0.45 and 0.10). The crystalline mass was pulverized and placed in a sublimation apparatus. The temperature of the bath was gradually raised to about 95°C under about 3 mmHg. A considerable amount sublimed at the bath temperature from 76 to 95°C; sublimation was continued until the bath temperature reached 105°C. The total sublimate weighed 30 mg., m. p., 97~108°C. The paper chromatogram of this material showed one major spot (R_f 0.45) of methylsuccinic acid, but no spot (R_f 0.59) corresponding to α-methylglutaric acid. The material was purified by repetition of the sublimation to afford pure sample of methylsuccinic acid; m. p. and mixed m. p., 109~110°C. The crystals remaining in the sublimator weighed 57 mg.; m. p., 158~160°C (decomp.). The paper chromatogram of the sample showed a single spot (R_f 0.10). Mixed melting point, infrared spectra and paper chromatography showed that this is identical to butane-1, 1, 3-tricarboxylic acid[11].

2, 5-Dimethyl-2-cyclopenten-1-one-3-carboxylic Acid (XII).—2.2 g. of an orange-yellow, viscous sirup (see the preparation of IX) containing methyl 2-(dimethylaminomethyl)-5-methylcyclopentanone-3-carboxylate hydrochloride was placed in a distillation flask and heated in an oil bath at 150°C for 15 min. The orange-red product was distilled at 150°C (bath temp.)/0.3 mmHg to afford a light-yellow liquid of methyl 2, 5-dimethyl-2-cyclopenten-1-one-3-carboxylate (XI), λ_{max}^{MeOH} 243 mμ ($E_{1cm}^{1\%}$ 567). The crude ester (420 mg.) was mixed with a 10% sodium hydroxide solution (1 ml.) and was stirred at room temperature for 2 hr. The orange-yellow solution was acidified to pH 1.8 by the addition of 6 N hydrochloric acid; whereupon a crystalline precipitate of 2, 5-dimethyl-2-cyclopenten-1-one-3-carboxylic acid (XII) separated; yield, 240 mg.; m. p., 127~130°C. Two recrystallizations from water followed by vacuum sublimation yielded colorless prisms melting 129~130.5°C, λ_{max}^{MeOH} 245 (ε, 12200) and 334 mμ (ε, 41). $\nu_{max}^{CHCl_3}$ 1720 (COOH), 1707 (C=O) and 1645 cm^{-1} (C=C); ν_{max}^{Nujol} 1722, 1681 and 1640 (SH) cm^{-1}.

Found: C, 62.12; H, 6.66; Neut. eq. 155. Calcd. for $C_8H_{10}O_3$: C, 62.32; H, 6.54%; Neut. eq. 154.1.

The VII was also obtained by the destructive distillation of IVa hydrochloride, followed by saponification in the manner described above. The destructive distilation of IVa hydrochloride (2.0 g.) gave methyl 2, 5-dimethyl-2-cyclopenten-1-one-3-carboxylate (563 mg.). The crude ester (490 mg.) was saponificated to afford XII (156 mg.) melting at 117~123°C. Recrystallization from water followed by vacuum sublimation yielded a pure sample of XII; m. p., 129~130.5°C.

The Ozonolysis of XII.—A solution of XII (71 mg.) in ethyl acetate (5 ml.) was ozonized in the manner described above. The resulting ozonide was decomposed with 30% hydrogen peroxide (0.4 ml.) at about 90°C for 1 hr. to afford a crystalline mass (44 mg.); m. p., 82~97°C. The paper chromatography of the product showed one major spot (R_f 0.45) of methylsuccinic acid. Fractional vacuum sublimation yielded a pure sample of methylsuccinic acid; m. p. and mixed m. p., 109~110°C.

Methyl 2, 5-Dimethyl-2-cyclopenten-1-one-3-carboxylate (XI).—A solution of a pure sample of XII (115 mg.) in ether was treated with a ethereal diazomethane soluion at 0°C. Evaporation of ether, followed by vacuum distillation, gave a colorless liquid of the title compound; yield, 103 mg.; b. p., 73°C (bath temp.)/3 mmHg, n_D^{25} 1.4880, λ_{max}^{MeOH} 246 (ε, 13250) and 336 mμ (ε, 42), ν_{max}^{CCl} 1724 (ester and ketone C=O) and 1640 cm^{-1} (C=C).

Found: C, 64.50; H, 7.19. Calcd. for $C_9H_{12}O_3$: C, 64.27; H, 7.19%.

Semicarbazone of XI.—Colorles needles; m. p., 228°C (decomp.)

Found: C, 53.45; H, 6.75; N, 18.63. Calcd. for $C_{10}H_{15}O_3N_3$: C, 53.32; H, 6.71; N, 18.66%.

5-Methyl-2-methylenecyclopentanone-3-carboxylic Acid (X).—A mixture of freshly prepared methyl 5-methyl-2-methylenecyclopentanone-3-carboxylate (IX) (1.0 g.) and 1.5 N sulfuric acid (20 ml.) was stirred at 30°C for 4.5 hr. and then extracted with three 10 ml. portions of ether. The ethereal extracts were netralized while being shaken with an aqueous sodium bicarbonate solution until the pH value in the aqueous layer became 7.5. The aqueous layer was separated, washed with ether, adjusted to pH 1.8 with 1.5 N sulfuric acid, saturated with ammonium sulfate, and extracted with three 10 ml. protions of ethyl acetate. The extract was dried over sodium sulfate and evaporated in a vacuum at about 0°C to afford a crude 5-methyl-2-methylenecyclopentanone-3-carboxylic acid (X) as a pale-yellow viscous oil; 154 mg. (16.9%), λ_{max}^{MeOH} 233 mμ ($E_{1cm}^{1\%}$ 189), ν_{max}^{liq} 2700~2500 (carboxyl OH), 1740 (carboxyl C=O), 1720 (C=O), 1640 (C=C) and 956 cm^{-1} (=CH_2).

The Oxalate of Methyl 5-(Dimethylaminomethyl)-5-methylcyclopentanone-3-carboxylate (IVb).—The unchanged mixed Mannich base ester (1.76 g.) recovered from the mother liquor of the methiodide (VIII) was dissolved in absolute ether. To the solution was added an ether solution of anhydrous oxalic acid (0.80 g.), whereupon a gummy solid separated and was crystallized by rubbing. Filtration, followed by washing with ether, gave a crude oxalate (2.56 g.). The crude oxalate was dissolved in absolute methanol at about 50°C. After the solution had cooled and stood at room temperature for 1 hr., the first crop (the oxalate of IVb) was separated and washed with a small quantity of

11) F. Voche, *Z. physiol. Chem.*, **191**, 83 (1930)

methanol and then with methanol-ether (1 : 1); yield, 0.83 g.; m. p. 132~133°C (decomp.). The paper chromatogram of the first crop (IVb oxalate) showed a single spot (R_f 0.47), but no spot (R_f 0.51) corresponding to the oxalate of IVa. To the mother liquor separated from the first crop was added a small quantity of ether to afford a second crop (0.14 g.); m. p., 128~130°C (decomp.). A third crop was obtained by the further addition of ether to the mother liquor of the second crop; yield, 0.45 g.; m. p., 90~105°C. Recrystallizations of the second and third crop from methanol yielded crystals of IVb oxalate melting at 132~133°C (decomp.); the total yield of IVb oxalate was 1.01 g. Recrystallization of the first crop from methanol gave an analytical sample, a colorless plates; m. p., 133~134°C (decomp.).

Found: C, 51.36; H, 7.11; N, 4.78. Calcd. for $C_{11}H_{19}O_3N \cdot C_2H_2O_4$: C, 51.48; H, 6.98; N, 4.62%.

Methyl 5-(Dimethylaminomethyl)-5-methylcylcopentanone-3-carboxylate (IVb).—The oxalate of IVb (347 mg.) was made alkaline with a 10% aqueous sodium carbonate solution while being ice-cooled, and the reaction mixture was extracted with ether. The ether extracts were dried over potassium acetate and evaporated to give free amine ester (IVb) as a pale-yellow liquid; yield, 232 mg. (90.5%). Vacuum distillation afforded an analytical sample, a colorless liquid; b. p., 55°C (bath temp.)/0.001 mmHg, $n_D^{25.5}$ 1.4635, ν_{max}^{liq} 2870, 2825, 2780, (dimethylamino group), 1750, 1745 (ketone and ester C=O) and 1412 cm^{-1} (methylene group in -CO-CH_2-), R_f 0.47 (as hydrochloride).

Found: C, 62.20; H, 9.12; N, 6.73. Calcd. for $C_{11}H_{19}O_3N$: C, 61.94; H, 8.97; N, 6.57%.

The Methiodide of IVb.—A mixture of IVb (35 mg.) and an excess of methyl iodide was allowed to stand for 24 hr. at room temperature. Evaporation of methyl iodide. followed by washing with ether, yielded the methiodide melting at 163~170°C in a quantitative yield. Recrystallization from methanol-ether gave colorless plates (49 mg.); m. p., 171~172°C (decomp.), ν_{max}^{KBr} 1748, 1735 (ketone and ester C=O), and 1412 cm^{-1} (methylene group in -CO-CH_2-).

Found: C, 40.64; H, 6.01; N, 4.0.3. Calcd. for $C_{12}H_{22}O_3NI$: C, 40.57; H, 6.24; N, 3.94%.

The Hydrochloride of IVb.—A solution of IVb in absolute ether was carefully neutralized by the addition of a methanolic solution of hydrochloric acid to afford the crystalline hydrochloride of IVb. Recrystallization from butanone gave a pure sample as colorless plates; m. p., 140~141°C (decomp.), R_f 0.47, ν_{max}^{KBr} 2700~2400 (broad) ($\overset{+}{N}H$) and 1747 cm^{-1} (ketone and ester C=O).

Found: C, 52.76; H, 7.86; N, 5.70. Calcd. for $C_{11}H_{20}O_3NCl$: C, 52.90; H, 8.07; N, 5.61%.

5-(Dimethylaminomethyl)-5-methylcyclopentanone-3-carboxylic Acid (IIb).—A mixture of the free amine ester (IVb) (98 mg.) and a 0.45 N barium hydroxide solution (1.05 ml.) was shaken at 26°C for 2.5 hr. The resulting solution was treated with 2.2 N sulfuric acid, and barium sulfate was removed by centrifuging. The supernatant layer and washings were combined and subjected to lyophilization to give a pale-yellow glass which became a hygroscopic crystalline powder by rubbing; yield, 84 mg. (91%); m. p., 118~120°C (decomp.). Two recrystallizations from propan-2-ol gave a pure sample of IIb (46 mg.) as colorless prisms; m. p., 124~125°C (decomp.), R_f 0.40, ν_{max}^{KBr} 1718 (C=O) and 1625 cm^{-1} (COO$^-$): $\nu_{max}^{CHCl_3}$ 2410 ($\overset{+}{N}$-H), 1745 (C=O) and 1603 cm^{-1} (COO$^-$) (0.028 M, 0.104 mm.).

Found: C, 60.00; H, 8.83; N, 6.95. Calcd. for $C_{10}H_{17}O_3N$: C, 60.28; H, 8.60; N, 7.03%.

The Hydrochloride of IIb.—It was at first obtained as a viscous oil by the acidification (pH 1.8) of IIb in metanol with methanolic hydrogen chloride, followed by dilution with absolute ether. However, when the oil was dissolved in propan-2-ol for about one month at room temperature, the crystalline hydrochloride separated. Recrystallization from propan-2-ol afforded a pure sample of IIb hydrochloride as hygroscopic colorless prisms; m. p., 155~156°C (decomp.), R_f 0.37. When admixed with IIa, the hydrochloride showed depression of the melting point. ν_{max}^{KBr} 2730 ($\overset{+}{N}H$), 1745 (C=O) and 1720 cm^{-1} (COOH). pK_{a_1} 3.49 and pK_{a_2} 8.66.

Found: C, 51,19; H, 7.96; N, 5.83. Calcd, for $C_{10}H_{18}O_3NCl$: C, 50.93; H, 7.70; N, 5.94%.

2-Benzylidene-5-(dimethylaminomethyl)-5-methylcyclopentanone-3-carboxylic Acid (IIIb).—A mixture of methyl 5-(dimethylaminomethyl)-5-methylcyclopentanone-3-carboxylate (IVb) (90 mg.), benzaldehyde (45 mg.) and 10% sodium hydroxide (0 5 ml.) was stirred at 25°C for 2.5 hr. The orange-yellow solution was processed in the same manner as described in the preparation of IIIa to yield a crude picrate of IIIb (40 mg.) melting at 182°C (decomp.). Recrystallization from methanol afforded a pure sample of the 2-benzylidene-5-(dimethylaminomethyl)-5-methylcyclopentanone-3-carboxylic acid picrate (IIIb) in the form of yellow needles; m. p., 184°C (decomp.). Admixing it with a sample of IIIa picrate melting at 187°C (decomp.) showed a depression of the melting point; mixed m. p., 177°C (decomp.).

Found: C, 53.57; H, 4.87; N, 10.75. Calcd. for $C_{23}H_{24}O_{10}N_4$: C, 53.49; H, 4.68; N, 10.85%.

Bioassays.—Preliminary results indicate that 5-methyl-2-methylenecyclopentanone-3-carboxylic acid (X) and its methyl ester (IX) completely inhibit the growth of *M. pyogenes var. aureus* 209-p in dilutions of 1 : 400 and 1 : 16000 respectively, and inhibit the growth of *Candida albicans* and *Penicillium* 408-701 in dilutions of 1 : 4000 and 1 : 32000 respectively. Moreover, X and IX completely inhibit the growth of *Trichophyton mentagrophytes* in dilutions of 1 : 8000 and 1 : 16000 respectively.

It is interesting that X and IX possess antitumor activity. The minimum necessary concentrations of X and IX for the anti-HeLa cell effect were 125 and 32 mcg./ml.

A detailed report on the biological activity of X and IX will be published elsewhere.

Summary

1) The Mannich reaction of 5-methylcyclopentanone-3-carboxylic acid with formaldehyde

and dimethylamine hydrochloride gave a mixture of 2-(dimethylaminomethyl)-5-methylcyclopentanone-3-carboxylic acid (VI) and two kinds of geometrical isomers of 5-(dimethylaminomethyl)-5-methylcyclopentanone-3-carboxylic acid (IIa and IIb), from which IIa, an unstable methiodide (VII) of methyl ester of VI, and IIb were isolated.

2) Methyl 2-(dimethylaminomethyl)-5-methylcyclopentanone-3-carboxylate methiodide (VIII) was degraded to give methyl 5-methyl-2-methylencylopentanone-3-carboxylate (IX), which was then hydrolyzed to 5-methyl-2-methyleneclycopentanone-3-carboxylic acid (X), a homolog of sarkomycin.

3) The steric relation between IIa and IIb has been discussed.

4) The destructive distillation of methyl 2-(dimethylaminomethyl)-5-methylcyclopentanone-3-carboxylate (VII), followed by hydrolysis, afforded 2,5-dimethylcyclopenten-1-one-3-carboxylic acid (XII), an isomer of X. It was found that the product was obtained also by the thermal decomposition of the methyl ester hydrochloride of IIa. This fiinding may be accounted for on the assumption that a rearrangement of the dimethylaminomethyl group occurred through a kind of retrograde Mannich reaction.

5) Some derivatives of the above-mentioned Mannich bases were described.

6) Both X and its methyl ester were found to possess antitumor and antibacterial activities.

The authors are indebted to Professor Hamao Umezawa, the National Institute of Health, Tokyo, for the antitumor assays. This work has been supported in part by a cancer reserch grant of the Ministry of Education and by a grant from the Research Society of Microbiological Chemistry, Tokyo, to which the authors thanks are due.

Department of Applied Chemistry
Faculty of Engineering
Keio Univerity
Koganei-shi, Tokyo

NOTES

Organoborverbindungen. Über die Synthese der höheren Bortrialkyle und ihre Stabilität gegen die Oxydation

Von Seiji KATO, Moriyasu WADA und Yojiro TSUZUKI

(Eingegangen am 25. December, 1962)

Im Anschluss an die Untersuchungen über die Synthese der hochmolekularen borhaltigen Verbindungen haben die Verfasser seit einigen Jahren versucht, die bisher noch nicht beschriebenen Bortrialkyle mit längeren Ketten herzustellen.

Höhere Homologe als die Hexyl-Verbindungen sind noch nicht beschrieben, obwohl eine grosse Anzahl von Bor-Verbindungen mit der Zusammensetzung BR_3 schon bekannt ist[1].

Für die Synthese von Bortrialkylen sind einige Reaktionen recht bekannt, von denen Folgendes am besten verwendet wird.

$$BF_3(\text{Ätherat}) + 3RMgX = BR_3 + 3MgFX$$

In der letzten Zeit ist das Bortrifluorid-Ätherat leicht zugänglich geworden und daher sind das daraus zu bekommende Triäthyl-, Tripropyl- und Tributyl-bor als Katalysatoren verwendet worden[2].

Nun haben die Verfasser nach der obenerwähnten Reaktion die folgenden Bortrialkyle synthetisiert. Die Ergebnisse sind in der Tabelle I zusammengestellt.

Aus den Infrarotspektren von Bortrialkylen, die im NaCl-Bereich mittels Hitachi-EPI-II aufgenommen wurden, zeigten sich die folgenden Wellenzahlen der B–C Bindung. Die Wellenzahlen des Trimethyl-, Triäthyl- und Tributylbors, die ebenfalls im NaCl-Bereich aufgenommen wurden, sind auch in der Tabelle II gezeigt.

1) M. F. Lappert, *Chem. Revs.*, **56**, 1028 (1956); N. Ashikari, *J. Soc. Org. Synth. Chem. Japan*, **17**, 320 (1959).

2) J. Furukawa und Mitarb., *J. Chem. Soc. Japan, Ind. Chem. Sec. (Kogyo Kagaku Zassi)*, **61**, 728 (1958); J. Furukawa und T. Tsututa, *J. Polymer Sci.*, **40**, 237 (1959).

TABELLE I. BORTRIALKYLE UND ELEMENTARANALYSE

R_3B	Sdp., °C	Schmp. °C	Ausbeute %	Mol. Gew. Gef.	Mol. Gew. Ber.	Elementaranalyse Gef. C	Gef. H	Gef. B	Ber. C	Ber. H	Ber. B
$(C_5H_{11})_3B$	160～162/30.5 mmHg		60								
$(C_8H_{17})_3B$	189～192/12 mmHg		64	369.8	350.5	82.75	14.89	2.36	82.24	14.64	3.09
$(C_{12}H_{25})_3B$		50.0	74	562.3	518.8	85.13	15.11	1.85	83.25	14.55	2.20
$(C_{18}H_{37})_3B$		66.4～70.0	50	803.1	771.3	84.21	14.61	1.18	84.08	14.52	1.40

TABELLE II. WELLENZAHL DER B-C BINDUNG

R	B-C, cm^{-1}	R	B-C, cm^{-1}
Methyl	1150～1180	*n*-Octyl	1065
Äthyl	1130	Dodecyl	1065
n-Butyl	1080	Stearyl	1065
n-Hexyl	1075		

Die Zuordnung der B-C Bindung im Spektrum wurde schon von einigen Forschern studiert. Lehmann und seine Mitarbeiter[3] beobachteten mit Hilfe vom Deuterium die Bände 1130 und 1180 cm^{-1} als die Wellenzahlen der B-C Bindung des Trimethyl- und Triäthylbors, während Catz[4] für *p*-Vinylphenylborsäure die Wellenzahl 1086 cm^{-1} angab.

Unsere Daten liegen auch im Bereich der Wellenzahl 1060～1080 cm^{-1}, und daraus ersieht man von den Bortrialkylen, dass sich die Wellenzahl der Schwingung der B-C Bindung etwa umso mehr nach dem kleineren Bereich verschiebt, je nachdem die Alkylkette verlängert wird.

Die Stabilität der Bortrialkyle gegen die Oxydation.—Im allgemeinen werden die Bortrialkyle mit den kleineren Alkylgruppen als C_4H_9 leicht oxydiert und sind explosiv in der Luft. Aus dieser Eigenschaft geht hervor, dass die Bortrialkyle, besonders das Triäthyl- und Tributyl-bor als Katalysatoren zur Polymerisation der Vinylmonomeren verwendet werden können, wobei der molekulare Sauerstoff zu dieser Radikalketten-polymerisation eine wichtige Rolle spielt.

Der Mechanismus der Oxydation dieser Bortrialkyle wurde bereits von Johnson[5] beschrieben. Er zeigte, dass die Bortrialkyle dabei zwei Mole molekularen Sauerstoffs, aber in Gegenwart von Wasser nur ein Mole desselben aufnehmen. Später wurde der Reaktionmechanismus auch von Parsons[6] mit der Annahme von Peroxyd-Bildung elektronen-theoretisch erklärt.

Ausserdem hat Abraham[7] durch die ausführliche Untersuchung gezeigt, dass die Aufnahme des Sauerstoffs von Bortrialkylen ausserordentlich gross ist, wenn man sie mit organischen Lösungsmitteln verdünnt.

In der letzten Zeit hat Mirviss[8] an einem kinetischen Versuch gezeigt, dass die erste Bindung zwischen Bor- und Kohlenstoffatomen durch Oxydation leicht gespalten wird, aber die zweite sowie die letzte Bindung etwa beständig ist. Er hat aber sowohl die Geschwindigkeit der Reaktion als auch den Einfluss der Alkylkettenlänge nicht studiert.

Die Verfasser haben nun die Oxydation der Bortrialkyle nach der Methode von Abraham untersucht und beobachtet, dass die Reaktion mit einer monomolekularen Geschwindichkeit verläuft, und dass das Volumen des von diesen Bortrialkylen aufgenommenen Sauerstoffs umso kleiner wird, je länger die Alkylkette wird. Die Versuchsdaten von dem Oxydationsverlauf werden in der Abbildung 1 und 2, und in der Tabelle III gezeigt.

TABELLE III. VERSUCHSDATEN ÜBER DEN OXYDATIONSVERLAUF

R (im R_3B)	Aufgenommener Sauerstoff in Hexan* mol.	Hergestelltes Peroxyd** mol.	k*** 10^{-3} Sek^{-1}
C_2H_5	1.32	0.65	8.54
C_4H_9	1.28	0.42	9.26
C_6H_{13}	0.78	0.26	9.78
C_8H_{17}	0.76	0.06	9.00

* Im Falle der Abwesenheit von Lösungsmitteln ergab es keine günstigeren Resultate.

** Diese Werte wurden als Peroxyd R_2BOOR jodometrisch bestimmt.

*** Bestimmt aus folgender Gleichung

$$k=2.5/t_n\{\log V-\log(V-V_n)\}$$

Hier; k: Geschwindigkeitskonstante

V_n: Das Volumen des aufgenommenen Sauerstoffs am t_n

V: Das Maximalvolumen des aufgenommenen Sauerstoffs

Aus diesen Resultaten kann man sagen, dass die Reaktionsfähigkeit der Bortrialkyle gegenüber Sauerstoff je nach der Länge der Alkylkette abnimmt. So versteht man auch dass,

3) W. J. Lehmann und Mitarb., *J. Chem. Phys.*, **28**, 770 (1958).
4) Jöe Catz, *Compt. rend.*, **247**, 2019 (1958).
5) J. R. Johnson und Mitarb., *J. Am. Chem. Soc.*, **60**, 106 (1938).
6) T. D. Parsons und Mitarb., *ebenda*, **79**, 5091 (1957).
7) M. H. Abraham und Mitarb., *J. Chem. Soc.*, **1959**, 429.
8) S. B. Mirviss, *J. Am. Chem. Soc.*, **83**, 3051 (1961).

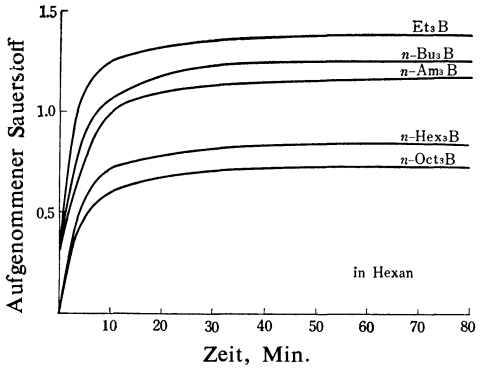

Abb. 1. Oxydationsverlauf.

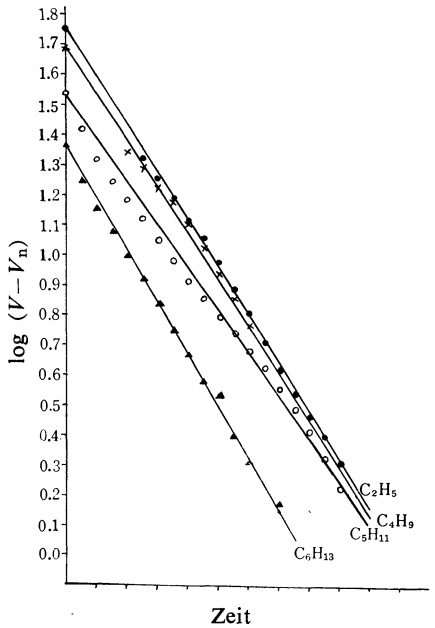

Abb. 2. Verhältnis zwischen der Zeit und Verlauf.

die niedrigen Bortrialkyle tatsächlich als Katalysatoren besser wirken.

Diese Eigenschaften der Bortrialkyle als Polymerisationskatalysator beruhen angeblich auf der Elektronlücke im Boratom, also auf seiner Lewis-Acidität. Daher bilden sie leicht unter Absorption von molekularem Sauerstoff immer Peroxyde, die auch bekanntlich einen Radikal-Charakter zeigen:

$$R_3B + O_2 \rightarrow R_2BOOR \rightarrow R_2BOO\cdot + \cdot R$$

Die Fähigkeit der Peroxydbildung ist umso merklicher, je niedriger die Kettenlänge der Alkylgruppe ist, also hängt die Wirkung der Bortrialkyle als Polymerisationskatalysator namentlich mit der räumlichen Grösse der Alkylgruppe zusammen.

Die wissenschaftliche Hochschule zu Tokyo
(Tokyo Rika Daigaku)
Shinjuku-ku, Tokyo

The Reactions of Nitrosobenzene and Some Methylene Compounds

By Hiroyuki NOHIRA, Kenichiro SATO and Teruaki MUKAIYAMA

(Received March 1, 1963)

As part of a study of the dehydration reactions of primary nitroparaffins[1], aldoximes[2,3], and hydroxamic acids[4] by means of such organic reagents as isocyanates, carbodiimides and iminocarbonates[5], the reactions of iminocompounds having carbonyl groups, such as diethyl phenyliminomalonate (I) and phenyliminoacetylacetone (III), have been studied. Although Walker[6] has reported that diethyl phenyliminomalonate (I) (m. p., 113.5°C) was prepared from the reaction of nitrosobenzene and diethyl malonate, it was found by this experiment that the crystalline product is not the iminomalonate, but diethyl dianilinomalonate (II). This is identical with an authentic sample obtained from the reaction of diethyl dibromomalonate with aniline[7]. Iminomalonate I was obtained as a pale brown liquid by distillation (b. p., 108~109°C/0.15 mmHg) in about a 70% yield, when the same reaction was carried out in absolute ethanol in the presence of a catalytic amount of sodium hydroxide. It was further confirmed that, when I was exposed to the moist air, the liquid material I changed gradually to the crystalline substance II.

In order to examine the effect of the water involved in the solvent on the ratio of the products I and II, the experiments in Table I were carried out in aqueous ethanol.

These results suggest that the reaction of nitrosobenzene with diethyl malonate proceeds through the initial formation of I, which is subsequently hydrolyzed to give II and diethyl oxomalonate, if any excess of water is present.

$$C_6H_5\text{-}N{=}O + CH_2\langle^{COOC_2H_5}_{COOC_2H_5} \rightarrow C_6H_5\text{-}N{=}C\langle^{COOC_2H_5}_{COOC_2H_5} + H_2O$$

(I)

1) T. Mukaiyama and T. Hoshino, *J. Am. Chem. Soc.*, **82**, 5339 (1960).
2) T. Mukaiyama and T. Hata, This Bulletin, **33**, 1712 (1960).
3) T. Mukaiyama, K. Tonooka and K. Inoue, *J. Org. Chem.*, **26**, 2202 (1961).
4) T. Mukaiyama and H. Nohira, ibid., **26**, 782 (1961).
5) T. Mukaiyama, T. Fujisawa and T. Hyugaji, This Bulletin, **35**, 687 (1962).
6) T. K. Walker, *J. Chem. Soc.*, **125**, 1625 (1924).
7) R. Curtiss, *Am. Chem. Journal*, **19**, 695 (1897).

TABLE I. THE REACTION OF NITROSOBENZENE WITH DIETHYL MALONATE

Solvent	Catalyst	Product I, %	Product II, %
50% C_2H_5OH	aq. NaOH	5	60
95% C_2H_5OH	NaOH in 50% C_2H_5OH	30	40
abs. C_2H_5OH	NaOH in abs. C_2H_5OH	72	0

TABLE II. THE ADDUCTS OF DIETHYL PHENYLIMINOMALONATE AND AMINES

Amine	Yield %	M. p. °C	Formula		Analyses Calcd., %	Analyses Found, %
Piperidine	80	84	$C_{18}H_{26}N_2O_4$	C,	64.56	64.94
				H,	7.84	7.96
				N,	8.38	8.03
Aniline	90	117	$C_{19}H_{22}N_2O_4$ = II	C,	66.67	66.25
				H,	6.43	6.11
				N,	8.19	8.20
N, *N*-Dimethyl-*p*-phenylene diamine	80	119	$C_{21}H_{27}N_4O_4$	C,	65.43	65.12
				H,	7.06	6.65
				N,	10.90	10.68
p-Aminoazobenzene	80	142	$C_{25}H_{26}N_4O_4$	C,	67.25	67.07
				H,	5.87	6.04
				N,	12.55	12.52

TABLE III. THE ADDUCTS OF PHENYLIMINOACETYLACETONE AND AMINES

Amine	Yield %	M. p. °C	Formula		Analyses Calcd., %	Analyses Found, %
Aniline	80	147	$C_{17}H_{18}N_2O_2$	C,	72.32	72.11
				H,	6.43	6.70
				N,	9.92	9.79
p-Anisidine	70	121	$C_{18}H_{20}N_2O_3$	C,	69.21	68.82
				H,	6.45	6.35
				N,	8.97	9.08
p-Aminoazobenzene	70	142	$C_{23}H_{22}N_4O_2$	C,	71.48	70.38
				H,	5.74	5.70
				N,	14.50	15.34

$$2I + H_2O \rightarrow \underset{C_6H_5NH}{\overset{C_6H_5NH}{\rangle}}C\langle\overset{COOC_2H_5}{COOC_2H_5} \quad \text{(II)} + O{=}C\langle\overset{COOC_2H_5}{COOC_2H_5}$$

Similarly, phenyliminoacetylacetone (III) and ethyl phenyliminoacetoacetate (IV) were prepared by the reaction of nitrosobenzene with acetylacetone or ethyl acetoacetate respectively in absolute ethanol.

$$C_6H_5{-}N{=}C\langle\overset{COCH_3}{COCH_3} \quad \text{(III)} \qquad C_6H_5{-}N{=}C\langle\overset{COOC_2H_5}{COCH_3} \quad \text{(IV)}$$

Next, the reactions of these imino-compounds with various amines were studied. Diethyl phenyliminomalonate (I) or phenyliminoacetylacetone (III) reacts with various primary and secondary amines to give their addition compounds, *gem*-diaminomalonate (V) or *gem*-diaminoacetylacetone (VI). These reactions are accelerated by a catalytic amount of acetic acid.

$$C_6H_5{-}N{=}C\langle\overset{COR_1}{COR_1} + R_2{-}NH_2 \rightarrow \underset{R_2NH}{\overset{C_6H_5NH}{\rangle}}C\langle\overset{COR_1}{COR_1}$$

$R_1 = -OC_2H_5$: I — $R_1 = -OC_2H_5$: V

$R_1 = -CH_3$: III — $R_1 = -CH_3$: VI

The yields, melting points and analyses for these adducts are listed in Tables II and III.

These adducts are unstable at an elevated temperature, and when pyrolyzed in a Claisen flask at 150~200°C, they decompose into their components, imino-compounds and amines. For example, when the adduct of diethyl phenyliminomalonate and ethyl *p*-aminobenzoate (VII), which is a viscous liquid and does not crystallize, was pyrolyzed, aniline and diethyl *p*-carbethoxyphenyliminomalonate (VIII) were obtained along with ethyl *p*-aminobenzoate and I. Furthermore, it was confirmed that the asymmetrical adducts like VII are not stable at room temperature but easily undergo a disproportionation reaction to give two symmetrical *gem*-diamino compounds. Thus, in the course of attempts to isolate the above-mentioned adduct (VII), II and IX were isolated.

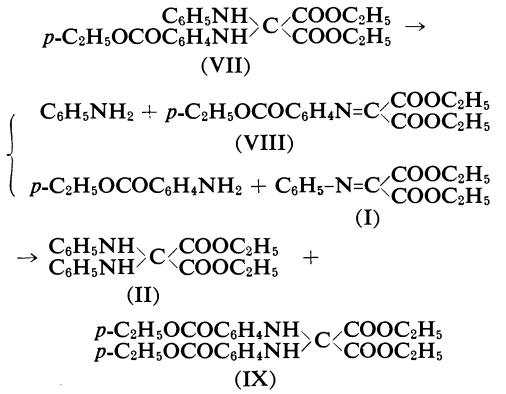

Experimental

Diethyl Phenyliminomalonate (I).—To a solution of diethyl malonate (23 g.) and nitrosobenzene (15 g.) in 30 ml. of absolute ethanol, an absolute ethanol solution of sodium hydroxide was added slowly, until the green solution of nitrosobenzene changed to pale brown. After the removal of the solvent under reduced pressure, the residual liquid was distilled and 26 g. (72%) (b. p., 108~109°C/0.15 mmHg) of diethyl phenyliminomalonate was obtained. Found: C, 62.19; H, 6.39; N, 5.73. Calcd. for $C_{13}H_{15}NO_4$: C, 62.64; H, 6.07; N, 5.62%.

Similarly, phenyliminoacetylacetone (III) (b. p., 82°C/0.28 mmHg) (58%). Found: C, 70.09, H, 6.21; N, 7.24. Calcd. for $C_{11}H_{11}NO_2$; C, 69.82; H, 5.86; N, 7.40%, and ethyl phenyliminoacetoacetate (IV) (b. p., 99°C/0.18 mmHg) (64%). Found: C, 65.62; H, 6.47; N, 6.79. Calcd. for $C_{12}H_{13}NO_3$: C, 65.74; H, 5.98; N, 6.39% were prepared from the reaction of nitrosobenzene with acetylacetone or ethyl acetoacetate in absolute ethanol in the presence of triethylamine instead of sodium hydroxide.

The Reaction of I with Varions Amines.—To a mixture of I (2.5 g.) and aniline (0.9 g.), one drop of acetic acid was added. After an exothermic reaction took place, the mixture solidified gradually. It was recrystallized from 95% ethanol, and 3.1 g. (90%) (m. p., 116.5~117.5°C) of diethyl dianilinomalonate (II) was obtained.

Similarly, I reacted with piperidine, *N*, *N*-dimethyl *p*-phenylenediamine and *p*-aminoazobenzene to give the corresponding adducts of type V (Table II). The adducts of I with *p*-toluidine, *p*-anisidine and ethyl *p*-aminobenzoate were viscous liquids and did not solidify.

The adducts VI of phenyliminoacetylacetone (III) with aniline, *p*-anisidine and *p*-amino azobenzene were prepared analogously from the reactions of III with the corresponding amines (Table III).

The Pyrolytic Decomposition of the Adduct (VII).—A viscous liquid of the adduct VII obtained from 5.0 g. of I and 3.2 g. of ethyl *p*-aminobenzoate was decomposed under a reduced pressure in a Claisen flask, and the following three fractions were obtained: aniline, b. p. 43~50°C/2 mmHg; a mixture of I and ethyl *p*-aminobenzoate, b. p. 130~150°C/2 mmHg, and diethyl *p*-carbethoxyphenyliminomalonate (VIII), b. p. 160~170°C/2 mmHg.

This iminomalonate VIII reacted with ethyl *p*-aminobenzoate to give a symmetrical adduct, diethyl di-(*p*-carboethoxyanilino)malonate (IX) (m. p., 135°C. Found: C, 62.19; H, 6.44; N, 5.71. Calcd. for $C_{25}H_{30}N_2O_8$: C, 61.71; H, 6.22; N, 5.76%.)

The same crystalline substance IX was isolated, along with II, in the course of attempts to crystallize the above-mentioned asymmetrical adduct VII.

Laboratory of Organic Chemistry
Tokyo Institute of Technology
Meguro-ku, Tokyo

The Synthesis of Elliptol Isoflavone

By Kenji FUKUI, Mitsuru NAKAYAMA and Masayuki HATANAKA

(Received March 15, 1963)

In 1942, elliptol isoflavone (furano(2'', 3'' ; 7, 8)-2', 4', 5'-trimethoxyisoflavone) (I) was prepared by Harper[1] from elliptol methyl ether (II)[2], a degradative fragment of elliptone (III)[3]. As I belongs to the same isoflavone type as Harper's phenol (" toxicarol isoflavone ")[4], which has been isolated from the *Derris elliptica* root along with other rotenoids, I has attracted increasing attention. As described in a previous paper[5], 7-hydroxy-2', 4', 5'-trimethoxyisoflavone (IV) was produced from 2, 4-dihydroxyphenyl 2, 4, 5-trimethoxybenzyl ketone. Now we will describe a total

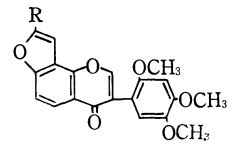

I R=H
VI R=$CO_2C_2H_5$
VII R=CO_2H

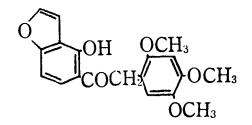

II

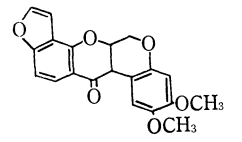

III

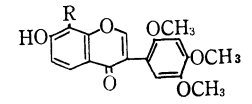

IV R=H
V R=CHO

1) S. H. Harper, *J. Chem. Soc.*, **1942**, 595.
2) S. H. Harper, ibid., **1942**, 587.
3) S. H. Harper, ibid., **1939**, 1099, 1424.
4) S. H. Harper, ibid.. **1940**, 1178.
5) K. Fukui, M. Nakayama, M. Hatanaka, T. Okamoto and Y. Kawase, This Bulletin, **36**, 397 (1963).

synthesis of I from IV by the same procedure as described in the previous papers[6].

The formylation of IV by the hexamine method gave the 8-formyl compound V, which was converted into 5''-ethoxycarbonyl-furano-(2'', 3''; 7,8)-2',4',5'-trimethoxyisoflavone (VI) by the action of ethyl bromomalonate and potassium carbonate. The alkaline hydrolysis of VI furnished the corresponding acid VII, which was decarboxylated in quinoline into I (m. p., 172~173°C) (reported m. p., 175°C[1]) in a good yield. To confirm the structure of I, the alkaline hydrolysis of I was carried out, giving II as colorless needles (m. p., 135~136°C) (reported m. p., 137°C[2]), which gave a brownish green ferric chloride test in ethanol.

Experimental*

8-Formyl-7-hydroxy-2', 4', 5'-trimethoxyisoflavone (V).—A mixture of IV (10 g.), hexamine (53 g.) and acetic acid (860 ml.) was heated on a steam bath for 8 hr. The hot solution obtained was treated with 1 : 1 hydrochloric acid (168 ml.) and again heated for 15 min.; then the solvent was removed in vacuo until ca. 200 ml. remained. After dilution with water (2000 ml.), the precipitates obtained were collected and crystallized from ethanol. The product was recrystallized from benzene to give V in the form of faintly yellow-colored needles (m. p., 190~191°C), which showed a red ferric chloride test in ethanol; yield, 6.3 g. (58%).

Found: C, 63.75; H, 4.58. Calcd. for $C_{19}H_{16}O_7$: C, 64.04; H, 4.53%.

5''-Ethoxycarbonyl-furano(2'', 3''; 7, 8)-2', 4', 5'-trimethoxyisoflavone (VI).—To a solution of V (6.3 g.) and ethyl bromomalonate in methyl ethyl ketone (500 ml.) potassium carbonate (21 g.) was added; the mixture was then refluxed for 10 hr. on a steam bath. The resulting mixture was filtered from precipitates, and the solvent was distilled off. The residual product was recrystallized from ethyl acetate to give VI in the form of colorless needles (m. p., 185~186°C) with a negative ferric chloride test in ethanol; yield, 5.2 g. (71%). IR: 1735 cm^{-1} (ester), 1650 cm^{-1} (γ-pyrone).

Found: C, 65.22; H, 4.82. Calcd. for $C_{23}H_{20}O_8$: C, 65.09; H, 4.75%.

5''-Carboxy-furano(2'', 3''; 7, 8)-2',4',5'-trimethoxyisoflavone (VII).—A mixture of VI (5.2 g.), acetone (600 ml.) and 10% aqueous potassium carbonate (175 ml.) was heated under reflux on a steam bath for 4 hr. After the acetone had been removed in vacuo, the residue was acidified with dilute hydrochloric acid. The resulting precipitate was recrystallized from ethanol to give VII in the form of colorless microcrystals (m. p., 282~283°C (decomp.)); yield, 2.7 g. (56%). IR: 1719 cm^{-1} (acid), 1648 cm^{-1} (γ-pyrone).

Found: C, 63.35; H, 4.36. Calcd. for $C_{21}H_{16}O_8$: C, 63.63; H, 4.07%.

Elliptol Isoflavone (I).—A mixture of VII (1.2 g.), copper powder (0.6 g.) and quinoline (30 ml.) was heated while being stirred in an atmosphere of nitrogen for 30 min. at 190~210°C until the evolution of carbon dioxide ceased. The solvent was then distilled off by steam distillation from the resulting mixture. The cooled mixture was filtered from precipitates and then extracted with ethyl acetate. After being washed successively with dilute hydrochloric acid, aqueous sodium bicabonate and then water, the solution was dried and evaporated. The residue was recystallized from methanol to give I in the form of colorless needles (m. p., 182~183°C) (reported m. p., 185°C[1]); yield, 0.8 g. (75%). IR: 1640 cm^{-1} (γ-pyrone).

Found: C, 68.28; H, 4.39. Calcd. for $C_{20}H_{16}O_6$: C, 68.18; H, 4.58%.

Elliptol Methyl Ether (II).—A mixture of I (0.3 g.), a 5% aqueous sodium hydroxide solution and ethanol (20 ml.) was refluxed for 3 hr. on a steam bath. After the solvent was evaporated, the residue was extracted with ethyl acetate. The resulting precipitate was recrystallized from methanol to give II in the form of colorless prisms (m. p., 135~136°C) (reported m. p., 137°C[2]), which showed a brownish green ferric chloride test in ethanol; yield, 0.2 g. (69%). IR: 1629 cm^{-1} (ketone).

Found: C, 66.70; H, 4.39. Calcd. for $C_{19}H_{18}O_6$: C, 66.66; H, 5.30%.

The authors are grateful to Professor Tetsuo Mitsui of Kyoto University, for the microanalyses. This work was supported in part by a grant-in-aid from the Ministry of Education.

Department of Chemistry
Faculty of Science
Hiroshima University
Higashi-Sendamachi, Hiroshima

6) K. Fukui et al., ibid., **31**, 688, 693 (1958); **33**, 1240 (1960).

* All melting points are uncorrected; the infrared spectra were measured in Nujol.

Rhodium-Platinum Oxide as a Catalyst for Hydrogenation. III[1]*. The Catalytic Hydrogenation of Aniline*

By Shigeo NISHIMURA and
Hisaaki TAGUCHI

(Received April 11, 1963)

It has been reported in previous papers[1-7] that (3 : 1) or (7 : 3) rhodium-platinum oxide,

1) Part II: S. Nishimura, This Bulletin, **34**, 1544 (1961).
2) S. Nishimura, ibid., **33**, 566 (1960).
3) S. Nishimura, T. Onoda and A. Nakamura, ibid., **33**, 1356 (1960).
4) S. Nishimura, ibid., **34**, 32 (1961).
5) S. Nishimura and H. Taguchi, ibid., **35**, 1625 (1962).
6) S. Nishimura and K. Mori, ibid., **36**, 318 (1963).
7) S. Nishimura and H. Taguchi, ibid., **36**, 353 (1963).

prepared by fusion of a mixture of rhodium chloride and chloroplatinic acid with sodium nitrate, is not only highly active, but also very selective as a catalyst in the hydrogenation of various organic compounds. Its high selectivity has already been shown in the hydrogenation of the compounds having C–O linkages liable to hydrogenolysis[1-4,6,7] and in the cis hydrogenation of substituted aromatic compounds[7].

This paper descibes another example of the high selectivity of the rhodium-platinum oxide revealed in the hydrogenation of aniline. Numerous catalysts have been used in the hydrogenation of aniline; of these, cobaltic oxide promoted with calcium oxide and ruthenium dioxide have been shown to give high yields of cyclohexylamine[8,9]. In an acidic medium, platinum catalyzes the hydrogenation even at room temperature, but so much dicyclohexylamine is produced that it is often more dominant than cyclohexylamine[10-12] (see Table I). As has already been reported[5], (7 : 3)rhodium-platinum oxide also catalyzes the hydrogenation in acetic acid at room temperature and gives a better yield of cyclohexylamine than platinum oxide. Table I summarizes the results of further investigations carried out in various solvents at an atmospheric or high pressure of hydrogen. With (7 : 3)rhodium-platinum oxide, aniline is hydrogenated most rapidly in acetic acid, and 16~22% of dicyclohexylamine is obtained with cyclohexylamine as the main product in hydrogenation at room temperature. With ethanol as a solvent, aniline is hydrogenated rather rapidly at 50°C and gives cyclohexylamine exclusively[13]. The addition of a small amount of acetic acid to ethanol causes the formation of dicyclohexylamine to the extent of 12% at 50°C, and a longer time is required for the completion of the hydrogenation than in ethanol. In ethanol and acetic acid in the amount equivalent to that of aniline, the hydrogenation proceeds smoothly at room temperature, and less than half as much dicycloheylamine is formed as in acetic acid. It is obvious from these results that acetic acid greatly promotes the formation of the secondary amine. The high selectivity of cobalt and ruthenium catalysts is probably connected with their use in neutral or alkaline conditions. Figure 1 shows the effect of hydrogen pressure on the rate of the hydrogenation of aniline in

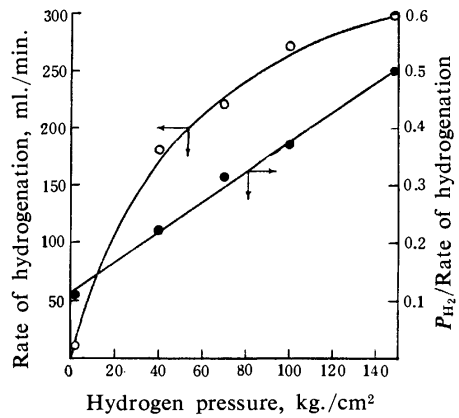

Fig. 1. Effect of hydrogen pressure on the rate of the hydrogenation of aniline with (7 : 3) rhodium-platinum oxide (0.1 g.) in acetic acid at 27°C.

TABLE I. CATALYTIC HYDROGENATION OF ANILINE WITH RHODIUM-PLATINUM AND PLATINUM CATALYSTS

Aniline g.	Catalyst g.	Solvent ml.	Temp. °C	H_2 press. kg./cm²	Time min.	% Product: Cyclohexylamine	% Product: Dicyclohexylamine
9.31	Pt oxide, 0.5	AcOH, 50	25	1.0	600	35	51
9.31	(3 : 1)Rh-Pt oxide, 0.5	AcOH, 50	25	1.0	480	65	20
4.66	(7 : 3)Rh-Pt oxide, 0.3	AcOH, 30	25	1.0	280	65	22
9.31	Pt oxide, 0.1	AcOH, 50	22	100~ 72	55% Reduction/6hr.		
9.31	(7 : 3)Rh-Pt oxide, 0.1	AcOH, 50	26	70~ 20	73	68	20
9.31	(7 : 3)Rh-Pt oxide, 0.1	AcOH, 50	27	149~ 93	40	72	16
9.31	(7 : 3)Rh-Pt oxide, 0.1	EtOH, 50	50	90~ 71	47	92	~0
9.31	(7 : 3)Rh-Pt oxide, 0.1	EtOH, 50 +AcOH, 0.5	50	91~ 78	100	75	12
9.31	(7 : 3)Rh-Pt oxide, 0.1	EtOH, 44 +AcOH, 6.2 g.	26	150~130	60	84	6

8) C. F. Winans, *Ind. Eng. Chem.*, **32**, 1215 (1940).
9) G. M. Whitman, U. S. Pat. 2606925 (1952); *Chem. Abstr.*, **47**, 3874i (1953). Cf. also L. C. Behr et al., *J. Am. Chem. Soc.*, **68**, 1296 (1946); A. E. Barkdoll et al., ibid., **75**, 1156 (1953); M. Freifelder and G. R. Stone, *J. Org. Chem.*, **27**, 3568 (1962).
10) A. Skita and W. Berendt, *Ber.*, **52**, 1519 (1919).
11) G. S. Hier and R. Adams, ibid., **59**, 162 (1926).
12) R. H. Baker and R. D. Schuetz, *J. Am. Chem. Soc.*, **69**, 1250 (1947).
13) Cf. Abbott Laboratories, Brit. Pat. 881512 (1961); *Chem. Abstr.*, **56**, 11465f (1962).

acetic acid. The rate is approximately proportional to $P_{H_2}/(1+bP_{H_2})$, where b is a constant, in the range of 1 to 149 kg./cm^2 of hydrogen pressure, which is indicated by the straight line of P_{H_2}/rate versus P_{H_2} shown in Fig. 1. The rate of the hydrogenation at 149 kg./cm^2 is about thirty times as great as that at atmospheric pressure, but the yield of cyclohexylamine is increased only slightly by increasing the hydrogen pressure. The condensation reaction to give secondary amines seems to be rapid in acetic acid, not a rate-controlling step in the formation of dicyclohexylamine. The use of platinum oxide under high pressures is quite unsatisfatory because of the decrease of the activity during the hydrogenation, as has already been noticed by Baker and Schuetz[12]. The findings on the hydrogenation of various substituted anilines will be published later.

Experimental

The procedure for the preparation of catalysts and the hydrogenation apparatus at high pressure have been described previously[1,7]. Hydrogenations at atmospheric pressure were carried out in a 200 ml. glass bottle shaken at about 300 to 400 oscillations per minute.

The reaction mixture was allowed to stand in order to let most of the catalyst settle, and the upper layer was filtered. The catalyst was washed with acetic acid three times. After the addition of an excess of hydrochloric acid to the filtrate, the solvent was distilled off at reduced pressure. The residual solid was treated with aqueous sodium hydroxide and extracted with ether, and the ethereal solution was dried on solid potassium hydroxide. Distillation at atmospheric pressure followed by distillation at reduced pressure gave cyclohexylamine (b. p., 133~136°C) and dicyclohexylamine (b. p., 129~130°C/20 mmHg).

The authors are indebted to the Mitsubishi Chemical Industries Co. for its support of this work.

The Institute of Physical and Chemical Research
Bunkyo-ku, Tokyo

SHORT COMMUNICATIONS

Paramagnetic Chemical Species of Triphenylmethane and Diphenylamine Formed on the Surface of Several Oxides[1]

By Kozo HIROTA, Yoichi KAGEYAMA and Keiji KUWATA

(Received May 9, 1963)

In a previous communication[2] it was reported that some paramagnetic chemical species were formed if anthracene, naphthalene, benzene and hydroquinone were adsorbed in the presence of air on powdered vanadium pentoxide (V_2O_{5-x}). On the basis of their stabilities and for other reasons, the species were hypothesized to be mainly paramagnetic intermediates in the oxidation process of these aromatic hydrocarbons, e. g. radicals of the semiquinone type, rather than the molecule cations such as have been proposed in the research papers[3] when these hydrocarbons were adsorded on silica-alumina, especially in the absence of air.

In order to confirm the above hypothesis, the research was extended to other adsorbents besides vanadium pentoxide, i. e., cupric oxide, cuprous oxides and alumina. Moreover, instead of aromatic hydrocarbons, triphenylmethane and diphenylamine were used as the adsorbates, because these compounds are known to give radicals by oxidation easily. The experimental procedure and the ESR apparatus used were the same as in the previous paper.

As is shown in Fig. 1, triphenylmethane, when adsorbed on V_2O_{5-x} and heated in air, gave a signal at $g=2.00$ superposed on a broad signal with incompletely resolved hfs of the vanadium ion, in a way similar to that of

1) Paper presented at the 16th Annual Meeting of the Chemical Society of Japan, Tokyo, April, 1963.

2) K. Hirota and K. Kuwata, This Bulletin, **36**, 229 (1963).

3) J. J. Rooney and R. C. Pink, *Proc. Chem. Soc.*, **70**, 70 (1961); J. K. Fogo, *J Phys. Chem.*, **65**, 1919 (1961); D. M. Brouwer, *Chem. & Ind.*, **1961**, 177; *J. Catalysis*, **1**, 372 (1962); H. P. Leftin et al., *J. Phys. Chem.*, **66**, 1214 (1962).

4) Unpublished.

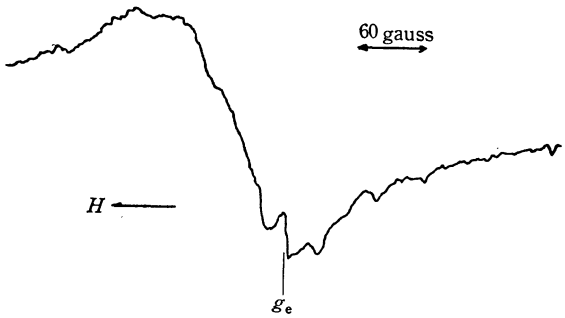

Fig. 1. ESR spectrum of triphenylmethane/V_2O_{5-x} system heated in air for 2.5 hr. at 200°C.

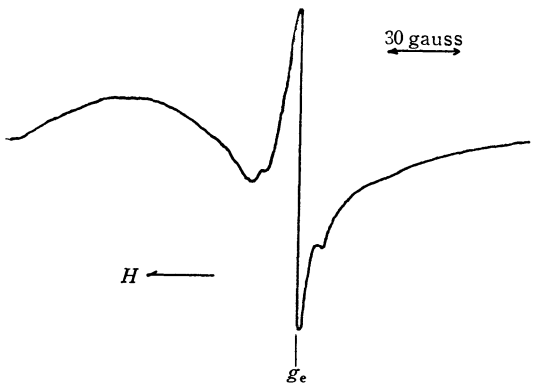

Fig. 2. ESR spectrum of diphenylamine/V_2O_{5-x} system heated in air for 1 hr. at 150°C.

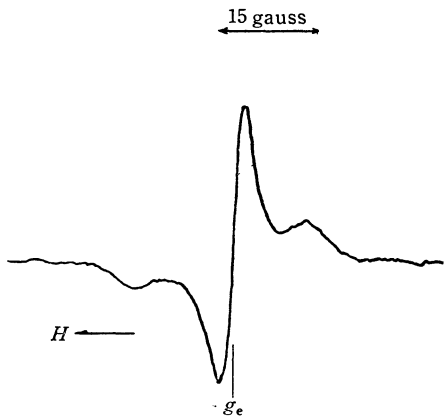

Fig. 3. ESR spectrum of diphenylamine/Cu_2O system heated in air for 15 min. at 200°C.

hydroquinone[4], but it gave no signal when adsorbed on cuprous oxide, cupric oxide, or aluminum oxide. The hfs here observed may be due to the decrease in the number of paramagnetic vanadium ions in the oxide. This finding may be explained by the following process:

$$(C_6H_5)_3CH + 2(\dot{V}) + 2O_2 \rightarrow (C_6H_5)_3C\dot{O}O + (\dot{V})OH + V^{(v)}O \quad (1)$$

occurring in connection with the oxidation of triphenylmethane by air, where $(\dot{V})$ denotes the paramagnetic-valency state of vanadium.

Diphenylamine, however, gave signals at $g=2.00$ for all these oxides. Judging from their shape, all the paramagnetic species produced may not be the same. An interesting point is the splitting of the signal into a triplet of unequal height in the case of cuprous oxide (Fig. 3). This may be brought about by the nuclear spin of ^{14}N of the adsobed species and by the anisotropic effect[5]. A similar tendency was observed, though not so clearly, in the spectrum of diphenylamine adsorbed on V_2O_{5-x} (Fig. 2), while no splitting could be observed in the spectra of cupric oxide and aluminum oxide. From such a difference it may be concluded that the adsorptive power of aluminum oxide is stronger than that of cuprous oxide. The reason why hfs of the adsorbent did not appear can be explained by the constancy in quantity of $(\dot{V})$ during the oxidation, if the following mechanism be assumed in the case of diphenylamine:

$$(C_6H_5)_2NH + (\dot{V}) + O_2 \rightarrow (C_6H_5)_2N\dot{O} + (\dot{V})OH \quad (2)$$

After the ESR measurement had been made, the adsorbates were extracted with carbon disulfide in the cases of triphenylmethane/V_2O_{5-x} and diphenylamine/V_2O_{5-x}. Both extracted substances were found to show ESR signals at $g=2.00$, suggesting the formation of stable radicals by oxidation.

For the sake of comparison, DPPH was similarly adsorbed at room temperature on V_2O_{5-x}; it was found to give no signal. The extract also gave no signal of radicals, suggesting the perfect oxidation of DPPH. Mechanisms (1) and (2) are, therefore, plausible.

Science Faculty
Osaka University
Nakanoshima, Osaka

5) A. van Roggen, L. van Roggen and W. Gordy, *Phys. Rev.*, **105**, 50 (1957).

Anomalous Conduction across Ion-exchange Membranes

By Manabu SENŌ and Takeo YAMABE

(Received June 12, 1963)

It is extensively shown that a constant electric current passes across ion-exchange membranes under normal conditions, when a constant voltage being applied. Sometimes, however, the anomalous conduction phenomena are observed; that is, non-ohmic conduction and pulse generation[1,2]. The aim of the present communication is to clear the conditions under which the anomalous conduction takes place and to propose a mechanism for pulse generation.

Anomalous conduction is observed in the sample arrangement shown in Fig. 1, which is one of the simplest system for pulse generation. Cellophane diaphragms are used to separate the sample solutions from the electrode solutions; sample solution II is a gel solution of sodium chloride containing agar. Ion-exchange membranes used are Selemion CMG-10 (cation-selective) and AMG-10 (anion-selective) manufactured by Asahi Glass Co., Ltd.

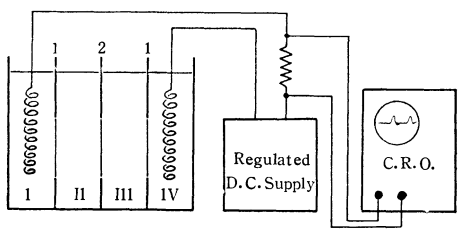

Fig. 1. The sample arrangement for observation of anomalous conduction and the measuring apparatus.
1. Cellophane (Visking) diaphragms
2. Ion-exchange membranes
Electrode solutions I and IV and sample solution III are 0.05 N NaCl solutions and sample solution II is 0.05 N NaCl solution containing agar (1.5 wt%).

The relationship between the voltage applied and the current passed is ohmic at the initial state when the voltage is applied. But, when the membrane is cation-selective and the electrode I is positive, the current decreases with time and reaches a constant value, which is characteristic of the system and independent of the voltage applied. When the polarity of electrode is reversed, such a decrease is not observed.

When higher voltages are applied to the system in the former case, the current no longer decreases and repeated pulses superimposed on the direct current are observed, an example of which is shown in Fig. 2.

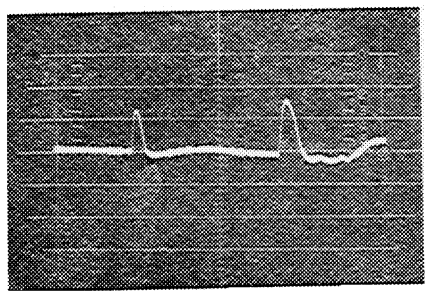

Fig. 2. The pulse train superimposed on the direct current across the ion-exchange membrane in Fig. 1.

The following mechanism is proposed for this anomalous conduction. When the current passes across ion-exchange membranes, the concentration polarization takes place in the diffusion layers (interfaces between solutions and membranes), owing to the difference of transport numbers of ions in the solution and membrane phases. When the limiting current flows, the salt concentration in the salt-depletion diffusion layer, which is built up facing to the anode in the case of cation-selective membranes, becomes zero[3]. When a higher voltage than the critical one is applied to the system, a higher current governed by the ohmic resistance of the system passes initially but, as soon as the salt-depletion layer is built up, a lower and stationary diffusion-controlled current is observed. In this stationary state, the current is independent of the voltage applied, and the electrical potential difference at the salt-depletion layer increases remarkably with the increase of the applied voltage.

When the electrical potential difference becomes higher than a critical value, a sudden increase in current is observed probably because the increasing dissociation of water occurs in the salt-depletion layer. However, such a high current can not pass stationarily, because the salt-depletion layer is built up again in the cource of time. Thus the current passing through this system oscillates along the limit cycle on the voltage-current diagram of the diffusion layer, which is shown in Fig. 3. At the point A the increasing dissociation of water occurs, and the point B is determined by

1) C. Forgacs, *Nature*, **190**, 339 (1961),
2) K. Yamamoto, *Kagaku*, **31**, 265 (1961).
3) T. R. E. Kressman and F. L. Tye, *Discussion Faraday Soc.*, **21**, 185 (1956); N. W. Rosenberg and C. E. Tirrell, *Ind. Eng. Chem.*, **49**, 780 (1957).

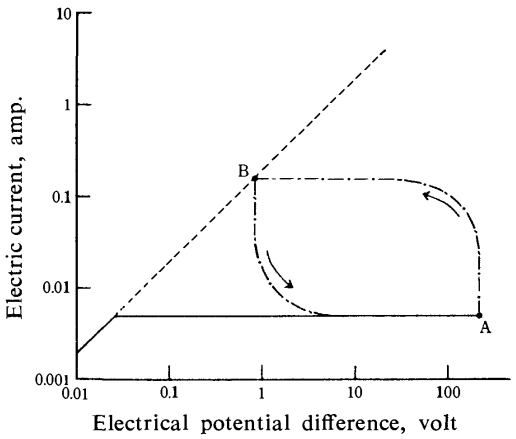

Fig. 3. Log-log plot of electric current against electrical potential difference at the salt-depletion diffusion layer.

the ohmic resistance of the system.

When an aqueous sodium chloride solution is used as the sample solution II, the stationary diffusion-controlled current is not established and the pulse current is not observed. The gel-like structure of agar stabilises mechanically the diffusion layer. Concentrated glycerol-water solutions of sodium chloride can beused as the sample solution for pulse generation.

The same behavior is observed in a double ion-selective membrane, which is made by pressing cation- and anion-selective membranes face to face. In this case, a junction plane between two parts of the membrane plays the same role as the salt-depletion diffusion layer in the case of the single-membrane system.

The rectification effect is also observed in these cases. Further extensive investigations are being made in order to exploire the electric circuit elements with ions as charge carriers and examine its similarity with biological membranes.

The Institute of Industrial Science
The University of Tokyo
Azabu, Tokyo

The Effects of Stationary Liquids on the Separation of the Isomers of Aromatic Hydrocarbons in Gas Chromatography[*1]

By Takeo ARAKI[*2]

(Received October 17, 1962)

The author has continued gas chromatographic studies of stationary liquids with regard to the separation of xylene isomers[1-4]. Such mixed stationary phases as β-naphthylamine/fluorenone (1 : 1) have been proven to be effective for the separation of xylene isomers containing ethylbenzene[3]. When the separating power of this mixed stationary liquid was compared with that of 7,8-benzoquinoline, which was proposed by Desty et al.[5], there was no appreciable difference between these two stationary phases in the case of the xylene isomers, but when ethylbenzene was present in the isomers, the former one seemed to be rather more suitable[*3,*4].

Of the xylene isomers, the para-isomer can be regarded as the most electronically inactive, its dipole moment is zero. Therefore, *p*-xylene was chosen as the standard isomer in the estimation of the separation factors; the relation of the separation factors to the σ_p values (Jaffé[6]) of the substituents in the aromatic stationary liquids was investigated and discussed in a previous paper[4].

It was found that this relation did not coincide entirely with Hammett's rule, but it had a rather closer relationship. More interesting facts were illustrated by smooth curves, which formed what has been called a "separation diagram"[4].

In connection with the preceding works, there remains the question of whether or not the "separation diagram" of xylenes at 88°C can be applied generally to the gas chromatographic separation of other aromatic hydrocarbon isomers in the same isomeric relation. The present work was undertaken to answer this problem.

Experimental

Apparatus.—The apparatus used was constructed in this laboratory. Some glass chromatographic columns (the dimensions of a unit are 1 m.×6 mm. i. d.) were joined together with copper slender tubes (1 mm. i. d.). A thermal conductivity detector with a tungsten filament was then settled in the apparatus.

Samples.—The ethyltoluene isomers, *o*-, *m*- and *p*-ethyltoluenes and *n*-propylbenzene, were prepared in this laboratory by the preparative methods reported in the literature[7].

Stationary Liquids.—The stationary liquids used were restricted to aromatic compounds. α-Naphthylamine, α-naphthol, benzophenone, 1,3-diphenylbenzene, DOP (dioctylphthalate), dichloronaphthalene and *m*-dinitrobenzene were used as typical of those stationary liquids which showed substituent effects in the separation diagram of a previous paper. TCP (tricresylphosphate), 7,8-benzoquinoline fluorenone, fluorene picrate, α-naphthonitrile and 1,4-dichloro-2-nitrobenzene were used as typical of different stationary liquids which gave results which somewhat deviated from the separation diagram. The inert solid support was coated with these compounds and then packed in glass columns.

Experimental Conditions.—Every effort was made to adjust the many conditions so as to be able to compare the results obtained with ethyltoluenes and xylenes with each other. The experimental conditions for the separation of the ethyltoluene series, together with those of the xylene series, are shown in Table I. The column temperature is setteled at 105°C in this work; it may be assumed

---

*1 This article is the fourth paper in the series, "Studies of Gas Liquid Partition Chromatography". The preceding papers are cited below.

*2 Present address: Department of Polymer Science, Faculty of Science, Osaka University, Nakanoshima, Osaka.

1) R. Goto, T. Araki and S. Munemiya, *J. Chem. Soc. Japan, Pure Chem. Sec.* (*Nippon Kagaku Zasshi*), **81**, 1315 (1960).

2) T. Araki and R. Goto, This Bulletin, **33**, 115 (1960).

3) T. Araki, R. Goto and A. Ono, *J. Chem. Soc. Japan, Pure Chem. Sec.* (*Nippon Kagaku Zasshi*), **81**, 1318 (1960).

4) T. Araki, R. Goto and A. Ono, ibid., **82**, 1081 (1961).

*3 Separation factors are determined as follows: $S_{E,p}$= 0.104, $S_{p,m}$=0.077 on the mixed stationary liquid of β-naphthylamine/fluorenone (1 : 1) and 0.072 and 0.075 on 7,8-benzoquinoline respectively, with a 6 mm.×3 m. column, packed with 17 parts of stationary liquid on 100 parts (w/w) of Celite-545 (60~80 mesh), at 80°C. The separation factors are represented in this paper by the term of S_{12}. in which the suffix 1 denotes the first peak and 2, the second peak. Thus, $S_{E,p}$ is the separation factor between the ethylbenzene and *p*-xylene peaks, and $S_{p,m}$ is that between the *p*- and *m*-xylene peaks.

*4 The separation of *m*- and *p*-xylene by gas chromatography has been developed recently by several investigators: a) G. M. Rouayheb, O. F. Folmer and W. C. Hamilton, *Anal. Chim. Acta*, **26**, 378 (1962); b) J. van Rysselberge and M. van der Stricht, *Nature*, **193**, 1281 (1962).

5) D. H. Desty, A. Goldup and W. T. Swanton, *Nature*, **183**, 107 (1959).

6) H. H. Jaffé, *Chem. Revs.*, **53**, 191 (1953).

7) "Organic Syntheses", Coll. Vol. I, pp. 111, 133, 135, 136; E. Bartow and A. W. Sellards, *J. Am. Chem. Soc.*, **27**, 369 (1905); A. Claus and F. Mann, *Ber.*, **18**, 1121 (1885); H. Gilman and W. E. Catlin, "Organic Syntheses", Coll. Vol. I, p. 471.

TABLE I. EXPERIMENTAL CONDITIONS

	Xylene isomers	Et-toluene isomers
Column	3 m.×6 mm.	3 m.×6 mm.
	J. M. Sil-O-Cel C-22	J. M. Sil-O-Cel C-22
Solid support	Firebrick	Firebrick
	(30~50 mesh)	(35~50 mesh)
Ratio of stationary liquids	25 : 100~32 : 100 (w/w)	25 : 100~32 : 100 (w/w)
Column temp.	88°C	105°C
Injection temp.	90°C	110°C
Carrier gas flow	N_2, ca. 50 ml./min.	N_2, ca. 50 ml./min.
Sample size	0.02 ml.	0.02 ml.

TABLE II. VAPOR PRESSURES OF ISOMERIC XYLENES AND ETHYLTOLUENES

Xylene	B. p. °C	Vap. press. mmHg at 88°C	Et-toluene	B. p. °C	Vap. press. mmHg at 105°C
Et-benzene	136.2	168	*n*-Pr-benzene	159.2	149
p-Xylene	138.3	157	*m*-Et-toluene	161.3	139
m-Xylene	139.1	151	*p*-Et-toluene	162.0	135
o-Xylene	144.4	128	*o*-Et-toluene	165.1	124

TABLE III. RELATIVE RETENTION VOLUMES (ETHYLBENZENE=1.000) OF ETHYLTOLUENE ISOMERS AT 105°C

Stationary liquid	Toluene	Et-benzene	*n*-Pr-benzene	*m*-Et-toluene	*p*-Et-toluene	*o*-Et-toluene
α-Naphthylamine	0.53_9	1.000	1.71_1	1.91_1	1.85_2	2.40_0
α-Naphthol	0.52_4	1.000	1.72_4	2.01_5	1.95_5	2.50_3
Benzophenone	0.51_5	1.000	1.80_7	1.98_4	1.97_2	2.38_1
1,3-Diphenylbenzene	0.51_5	1.000	1.86_4	2.03_1	2.03_3	2.44_1
DOP	0.51_7	1.000	1.85_9	2.01_0	2.04_9	2.36_4
Dichloronaphthalene	0.51_1	1.000	1.94_1	2.24_8	2.29_4	2.73_9
m-Dinitrobenzene	0.62_4	1.000	1.55_7	2.00_2	2.08_5	2.58_6
TCP	0.53_4	1.000	1.73_6	1.90_0	1.90_9	2.30_4
7,8-Benzoquinoline	0.51_7	1.000	1.83_7	2.08_7	2.06_2	2.58_5
Fluorenone	0.54_1	1.000	1.78_0	2.07_1	2.04_2	2.56_9
Fluorene picrate	0.61_9	1.000	1.60_7	2.00_0	2.05_1	2.64_3
α-Naphthonitrile	0.53_5	1.000	1.79_5	2.06_7	2.08_5	2.55_9
1,4-Dichloro-2-nitrobenzene	0.55_8	1.000	1.76_2	2.09_6	2.19_3	2.64_3

to be a thermal condition parallel to the previous case of the xylene series at 88°C. The vapor pressures of all these isomers are shown in Table II. The other factors are adjusted so as to be identical in both cases.

Results and Discussion

A Comparison of the Separation Power of Stationary Liquids. — By the separation factor S_{12}*, which was defined by Jones et al.[8], the separation powers of stationary liquids were compared with each other, as had been done in preceding papers. *p*-Ethyltoluene was chosen as a standard isomer for the estimation of the separation factors for the same reasons as *p*-xylene was chosen. It might be interesting to compare the experimental results of the ethyltoluene series directly with those of the xylene series. In the expression of the separation factor given by

$$S_{12}=(t_2-t_1)/t_1 \qquad (1)$$

of either t_1 or t_2, the retention time of the first or the second peak respectively, is always chosen as the retention time of *p*-ethyltoluene.

The relative retention volumes (ethylbenzene=1.000) of the ethyltoluene series on the above-mentioned stationary liquids are tabulated in Table III, while the separation factors estimated from these data are shown in Table IV, in which the separation factors of the xylene series at 88°C on the same stationary liquids are presented for the sake of comparison.

* The $(S_{12}+1)$ value is ordinarily used as the separation factor. In this investigation, however, S_{12} is used as the significant figure of results obtained, because the retention values of these isomers are very close.

8) W. L. Jones and R. Kieselbach, *Anal. Chem.*, **30**, 1590 (1958).

TABLE IV. SEPARATION FACTORS OF ETHYLTOLUENE ISOMERS AT 105°C COMPARED WITH THOSE OF XYLENE ISOMERS AT 88°C

Stationary liquid	Separation factor (S_{12})[a]							
	$S_{E,p'}$	($S_{T,p}$)	$S_{Pr,p'}$	($S_{E,p}$)	$S_{m',p'}$	($S_{p,m}$)	$S_{p',o'}$	($S_{p,o}$)
α-Naphthylamine	0.85	(0.94)	0.082	(0.009)	−0.032[b]	(0.085)	0.296	(0.404)
α-Naphthol	0.96	(1.08)*	0.134	(0.049)*	−0.031[b]	(0.082)*	0.280	(0.41)*
Benzophenone	0.97	(1.10)	0.092	(0.042)	−0.006[b]	(0.056)	0.207	(0.331)
1,3-Diphenylbenzene	1.03	(1.19)	0.090	(0.089)	0.001	(0.033)	0.201	(0.282)
DOP	1.05	(1.17)	0.102	(0.074)	0.019	(0.025)	0.154	(0.253)
Dichloronaphthalene	1.29	(1.46)	0.182	(0.188)	0.021	(0.034)	0.194	(0.293)
m-Dinitrobenzene	1.09	(1.23)**	0.339	(0.364)	0.042	(0.011)	0.240	(0.325)
TCP	0.91	(1.04)	0.100	(0.057)	0.005	(0.035)	0.207	(0.304)
7,8-Benzoquinoline	1.06	(1.22)	0.123	(0.070)	−0.012[b]	(0.070)	0.253	(0.356)
Fluorenone	1.04	(1.22)	0.147	(0.170)	−0.014[b]	(0.056)	0.258	(0.329)
Fluorene picrate	1.06	(1.25)	0.279	(0.334)	0.030	(0.019)	0.288	(0.347)
α-Naphthonitrile	1.09	(1.24)	0.162	(0.147)	0.007	(0.034)	0.227	(0.323)
1,4-Dichloro-2-nitrobenzene	1.19	(1.41)	0.244	(0.290)	0.046	(−0.006)[b]	0.206	(0.281)

a) Suffix T: toluene, E: ethylbenzene, p: *p*-xylene, m: *m*-xylene, Pr: *n*-propylbenzene. p': *p*-ethyltoluene, m': *m*-ethyltoluene, o': *o*-ethyltoluene
For example, $S_{E,p'}$ denotes separation factor between ethylbenzene and *p*-ethyltoluene.
b) Negative sign represents that the order of emergence of two components is inverse to boiling point of these components.
* Values obtained on β-naphthol column (extrapolated from the results of mixed stationary liquid with TCP).
** This value is re-examined; the author reported incorrectly 0.98 in the preceding paper.

Separation Diagrams.—In Fig. 1 of previous paper[4] the separation factors are plotted against the σ_p values (Jaffé) of the substituents in the aromatic stationary liquids. These relationships are interesting, although they are not entirely subject to Hammett's rule. Some discussion of this has already been presented in a previous paper, where the authors pointed out that the diagram of the separation factors against the modified σ_p values of substituents in the stationary liquids was rather effective for practical application to the estimation of the separation of aromatic hydrocarbons in gas chromatography. Figure 2 of this previous paper[4] was obtained when the σ_p values of –OH and $-CO_2R$ radicals were transferred moderately in a negative direction (−0.45 and 0.1 respectively), that of the $-COC_6H_5$ radical, excessively in the same direction (−0.25), and the –X (halogens) radical, in a positive direction (0.35).

Figure 1 illustrates a separation diagram for the ethyltoluene series obtained in a manner analogous to the case of the xylene series; data for the xylene series (88°C) are superposed in broken lines for the sake of comparison. The original points on the horizontal axis indicate the para-isomer.

A parallel relationship between the solid lines and the broken lines is well established in Fig. 1. Only a pair of curves does not show such excellent agreement; they are a solid line for *n*-propylbenzene ($S_{Pr,p'}$) and a broken line for ethylbenzene ($S_{E,p}$). Even in these cases, the inclination of two lines is similar. From the parallel relationship between two series of isomers, it is clear that the results for the xylene series illustrated in Fig. 2 of the previous paper[4] (the separation factors were plotted against the modified σ_p values of the substituents of the aromatic stationary liquids) can be applied to the ethyltoluene series; therefore, the relationship illustrated in Fig. 1 of the previous paper (the separation factors and unmodified σ_p values of the substituents in the aromatic stationary liquids were related to each other by means of Hammett's rule) can also be applied to this series.

It appears certain that the factor which controls the gas chromatographic separation is common in the two isomeric series. For the separation of isomeric aromatic hydrocarbons of *o*-, *m*-, *p*- and *n*-alkylbenzene, these points seem to be important in the selection of the suitable stationary liquids.

A Survey of the Separation Factor, ΔS_{12}.—It can be seen from Fig. 1 that the separation between individual isomers is better in the xylene series than in the ethyltoluene series. The vapor pressures of these isomers at operating column temperature are shown in Table II. The values for the ethyltoluene series (at 105°C) are lower than for the xylene

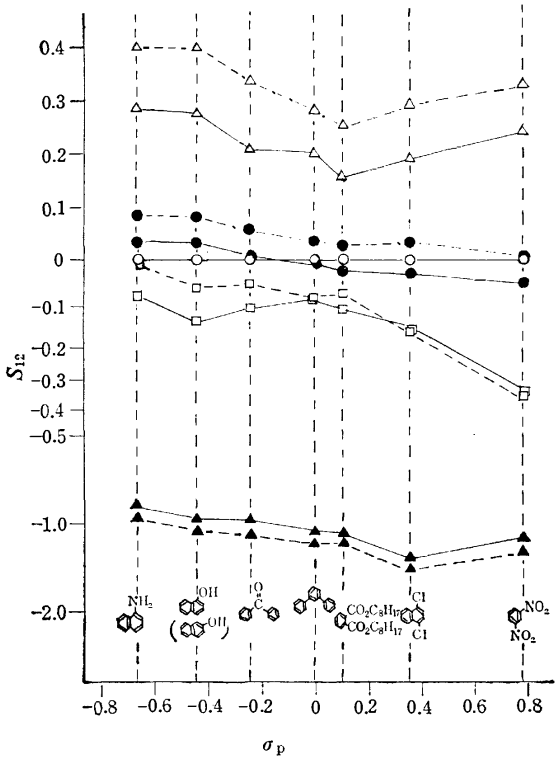

Fig. 1. Comparison of separation diagrams of ethyltoluene series and xylene series.
---- Xylene series (88°C)
—— Ethyltoluene series (105°C)
△ $S_{p,o}$ ● $S_{p,m}$
○ *p*-Xylene and *p*-ethyltoluene
□ $S_{A,p}$ ▲ $S_{A-1,p}$ (cf. Table V)

series (at 88°C). In fact, all ethyltoluenes eluted from the column more rapidly on every stationary liquid used than on corresponding xylenes. This depression of the separation factor (ΔS_{12}) in the ethyltoluene series relative to the xylene series is illustrated in Fig. 1 as roughly uniform on seven liquids, except for the values between $S_{E,p}$ and $S_{Pr,p'}$. ΔS_{12} is defined as follows:

$$\Delta S_{12} = S_{12}(\text{xylenes at } 88°C) - S_{12}(\text{ethyltoluenes at } 105°C) \quad (2)$$

On the other stationary liquids, which show something of a deviation, as has been mentioned above, the ΔS_{12} values likewise fell to roughly constant values (Table V). When an average of thirteen stationary liquids is taken, the values for $\Delta S_{p,o}$, $\Delta S_{p,m}$ and $\Delta S_{A-1,p}$ are 0.094, 0.047 and 0.15 respectively. $\Delta S_{A,p}$ does not, however, show any constant value.

From the other point of view, it is interesting to note that it is possible to predict the separation of these isomeric dialkylbenzenes from the ΔS values, since they do not depend upon sorts of stationary liquids and their polarity character, but rather seem to be dependent only upon the number of carbon atoms in the alkyl groups.

As the S_{12} values of the xylene series are known on many stationary liquids (cf. the literature), if only one set of S_{12} values of given ethyltoluenes is determined on one of these stationary liquids, then the ΔS_{12} value can be readily calculated. It will then be easy to find the suitable stationary liquid by simple

TABLE V. DISCREPANCY OF SEPARATION FACTORS BETWEEN XYLENE ISOMERS AND ETHYLTOLUENE ISOMERS (ΔS_{12})

Stationary liquid	$\Delta S_{A-1,p}$*	$\Delta S_{A,p}$*	$\Delta S_{p,m}$*	$\Delta S_{p,o}$*
α-Naphthylamine	0.086[a)]	−0.073	0.053	0.11
α-Naphthol	0.12	−0.085	0.051	0.13
Benzophenone	0.13	−0.050	0.050	0.12
1,3-Diphenylbenzene	0.16	−0.001	0.034[a)]	0.081
DOP	0.12	−0.028	0.044	0.099
Dichloronaphthalene	0.17	0.006	0.055	0.099
m-Dinitrobenzene	0.15	0.025	0.053	0.085
TCP	0.13	−0.043	0.040	0.097
7,8-Benzoquinoline	0.16	−0.053	0.058	0.10
Fluorenone	0.18	0.023	0.042	0.071
Fluorene picrate	0.19	0.055	0.049	0.059[a)]
α-Naphthonitrile	0.16	−0.015	0.041	0.095
1,4-Dichloro-2-nitrobenzene	0.22	0.046	0.040	0.075
Average value	0.15	—	0.047	0.094

a) The value is seriously deviated from the average.
Suffix p: para-isomers, m: meta-isomers, o: ortho-isomers, A: isomeric *n*-alkylbenzenes, A−1: *n*-alkylbenzenes of lower members than A by one carbon atom.
For example,
$\Delta S_{A,p} = S_{E,p}(88°C) - S_{Pr,p'}(105°C)$ $\Delta S_{A-1,p} = S_{T,p}(88°C) - S_{E,p'}(105°C)$

arithmetic addition or subtraction of the S_{12} value of the xylene series and of the ΔS_{12} values. For example, to separate *m*- and *p*-ethyltoluene isomers, one of the best stationary liquids may be tetrahalogenophthalate, which has been tested for the separation of xylene series by Langer et al.[9] On this stationary liquid, $S_{p,m}$ (xylene) was given as -0.045; therefore, $S_{p',m'}$ (ethyltoluene) will be -0.092 $(-0.045-0.047)$ or in that neighborhood*1.

The Interaction which Controls the Separation Factor Affecting the Gas Chromatographic Separation of Xylene and Ethyltoluene Isomers. —This problem has been considered, but unfortunately, experimental proofs are not satisfactory at present.

In a gas chromatographic column, separation is affected by two sorts of factors. One of these is the vapor pressure of solutes (hydrocarbons), and the other is the solute-solvent interaction of the stationary liquid. This solute-solvent interaction may be represented approximately in the following Eq. 3*2. Because

$$S_{12}(\text{solute-solvent interaction}) = S_{12}(\text{observed}) - S_{12}(\text{vap. press.}) \quad (3)$$

the separation factors of the two series are compared with each other at approximately the same vapor pressures (cf. Table II), and because, furthermore, the operating temperature of each series is kept constant, the inclination of the curves in Fig. 1 may be accepted as the measure of the solute-solvent interaction of the stationary liquids. The absolute value of S_{12} (vap. press.) was calculated from the table of vapor pressures as: $S_{p',o'}$(vap. press. at 105°C) $=0.089$; $S_{m',p'}$(vap. press. at 105°C) $=0.030$; $S_{Pr,p'}$(vap. press. at 105°C) $=0.104$, and $S_{E,p'}$(vap. press. at 105°C) $=1.03$.

In the preceding section, it was shown that the factor which controls the separation is common in both the xylene and the ethyltoluene series. As will be seen in Fig. 1 of a preceding paper[4], $S_{p,m}$ and $S_{A,p}$ curves vary monotonously, while the $S_{p,o}$ curves has a minimum and the $S_{A-1,p}$ curve, a maximum. From the inclination of the $S_{p,m}$ and $S_{A,p}$ curves, the meta-isomer and its isomeric *n*-alkylbenzene (ethylbenzene in the xylene series and *n*-propylbenzene in the ethyltoluene series) appear to interact more weakly with liquids containing electron-withdrawing groups (π-acids) and more strongly with those containing electron-releasing groups (π-bases) than the para-isomer does. The ortho-isomer seems to be independent of the sign of the σ_p values.

The acid strength of the π-acidic stationary liquids will decrease with the σ_p values. Of the stationary liquids used in this study, *m*-dinitrobenzene and 1,4-dichloro-2-nitrobenzene are extremely strong π-acids. These compounds are known as complexing agents, as are picric acid, tetracyanoethylene (TCNE)[10], pyromellitic dianhydride (PMDA)[11] and so on[12], all of which make stable π-complexes (π-π) with xylene isomers.

The order of the relative basicities of the xylene isomers determined from the stabilities of the π-complexes formed with PMDA, for example, was *o*-xylene>*p*-xylene>*m*-xylene〉〉〉ethylbenzene. On gas chromatography, the solute-solvent interaction of *m*-dinitrobenzene was determined at 88°C as follows:

o-Xylene:

$S_{p,o}$(on *m*-dinitrobenzene) $-S_{p,o}$(vap. press. at 88°C)[a] $=0.33-0.23=0.10$

m-Xylene:

$S_{p,m}$(on *m*-dinitrobenzene) $-S_{p,m}$(vap. press. at 88°C) $=0.011-0.040=-0.029$

p-Xylene: 0.000

Ethylbenzene:

$S_{p,E}$[b](on *m*-dinitrobenzene) $-S_{p,E}$ (vap. press. at 88°C) $=-0.36-(-0.07)=-0.29$

9) S. H. Langer, C. Zahn and G. Pantazoplos, *Chem. & Ind.*, **1958**, 1145.

*1 Stronger π-acids appear to be more effective for the separation of these isomers, inverse to the corresponding xylene isomers. The order of boiling points of this pair is opposite to that of the latter; therefore, the stationary liquid of the opposite polarity character will be more effective in this case.

*2 The S_{12} value is represented as follows:

$S_{12} = V_{R2}/V_{R1} - 1 = K_2/K_1 - 1 = \gamma_1^\circ p_1^\circ/\gamma_2^\circ p_2^\circ - 1$

while S_{12}(vap. press.) and S_{12} (solute-solvent interaction) are:

S_{12}(vap. press.) or S_{12} (vap.) $= p_1^\circ/p_2^\circ - 1$

S_{12}(solute-solvent interaction) or S_{12} (int.) $= \gamma_1^\circ/\gamma_2^\circ - 1$

Therefore,

$S_{12} = S_{12}(\text{int.}) \cdot S_{12}(\text{vap.}) + S_{12}(\text{vap.}) + S_{12}(\text{int.})$

In this case, the term $S_{12}(\text{int.}) \cdot S_{12}(\text{vap.})$ is negligibly small and the following approximation is obtained:

$S_{12} \fallingdotseq S_{12}(\text{vap.}) + S_{12}(\text{int.})$

V_R: retention volume corrected by the dead volume of the column; K: partition coefficient; γ°: activity coefficient; p°: vapor pressure of solute at column temperature.

10) R. E. Merrifield and W. D. Phillips, *J. Am. Chem. Soc.*, **80**, 2778 (1958).

11) L. L. Ferstanding, W. G. Toland and C. D. Heaton, ibid., **83**, 1151, 5049 (1961).

12) See, for instance, L. J. Andrews, *Chem. Revs.*, **54**, 713 (1954); R. S. Mulliken, *J. Am. Chem. Soc.*, **74**, 811 (1952); S. P. McGlynn, *Chem. Revs.*, **58**, 1113 (1958).

a) S_{12}(vap. press. at 88°C) is determined from the vapor pressure difference of two isomers at 88°C:

$S_{12}(\text{vap. press.}) = (p_1 - p_2)/p_2$

p_1 denotes a vapor pressure of isomer (i).

b) $S_{p,E} \fallingdotseq -S_{E,p}$

Thus, xylenes are absorbed in *m*-dinitrobenzene in the order of decreasing strength: *o*-xylene > *p*-xylene > *m*-xylene ≫ ethylbenzene, as in the order of the relative basicities in PMDA. This fact suggests a π-complex formation, on gas chromatography, between the aromatic hydrocarbon eluent and π-acidic stationary liquids as Langer et al. and Case have described.

On the other hand, the interaction on the π-basic stationary liquids is ambiguous. Case[13] explained this as dependent upon π-π repulsion between two phases. His interpretation seems to be reasonable, but other theories also appear possible.

When α-naphthylamine was used at 88°C as the stationary liquid of gas chromatographic separation, the following results were obtained:

o-Xylene:

$S_{o,p}$(on α-naphthylamine)
$-S_{p,o}$(vap. press. at 88°C)
$=0.40-0.23=0.17$

m-Xylene:

$S_{p,m}$(on α-naphthylamine)
$-S_{p,m}$(vap. press. at 88°C)
$=0.085-0.040=0.045$

p-Xylene: 0.000

Ethylbenzene:

$S_{p,E}$(on α-naphthylamine)
$-S_{p,E}$(vap. press. at 88°C)
$=-0.011-(-0.071)=0.060$

Thus, the α-naphthylamine absorbs xylenes in the order of decreasing strength: *o*-xylene > ethylbenzene > *m*-xylene > *p*-xylene.

By means of their solubility experiment with hydrogen chloride, Brown and Brady[14] determined the relative basicities of xylenes as follows; *m*-xylene: 1.26; *o*-xylene: 1.13; ethylbenzene: 1.06, and *p*-xylene: 1.00. They concluded that π-complexes were also formed between hydrogen chloride and xylenes. It is generally appreciated that the π-complex formed in this hydrogen chloride system is essentially different from that formed in the π-acid-xylene system, because the orders of the relative basicities of xylenes differ. It may be considered that the π-complex of the former case seems to be largely of the *n*-π type.

13) L. C. Case, *J. Chromatography*, 6, 381 (1961).
14) H. C. Brown and J. D. Brady, *J. Am. Chem. Soc.*, 74, 3570 (1952).

Between the results of our gas chromatographic separation and those obtained by Brown and Brady, no accurate agreement could be observed. However, these two sets of results seem to be essentially identical (*p*-xylene acts as the most acidic compound), and both of them are much different from those of the π-acid system. If π-π repulsion is an effective factor, *o*-xylene should be repulsed most strongly in the π-base system and $S_{p,o}$ curve in Fig. 1 should decline monotonously as the σ_p value decreases.

For the above reason, we may derive a hypothesis that the separation of aromatic hydrocarbons may be affected by π-complex formation with stationary liquids of a π-base as well as of π-acid. In the ethyltoluene series, however, these complex formations will be much weaker than in the xylene series because of the steric effects of the ethyl groups.

Summary

1) The gas chromatographic separation of the isomer of aromatic hydrocarbons has been investigated on the aromatic stationary liquids.

2) It has been established from the experimental results on the xylene series that the $S_{12}-\sigma_p$ diagram of Fig. 1 of the previous paper[4] is applicable to the separation of the ethyltoluene series.

3) ΔS_{12} has been defined, and it has been proven that this value was roughly constant between two series of dialkylbenzenes. Moreover, this value seems to throw a light on the prediction of the separation of the isomers of aromatic hydrocarbons.

4) This separation seems to be affected by π-complex formation between aromatic hydrocarbons and aromatic stationary liquids of both the π-acidic and π-basic types.

The author wishes to thank Professor Ryozo Goto of Kyoto University for many valuable discussions throughout this investigation. He would also like to express his appreciation for the support given his construction of the apparatus by the Yawata Chemical Industry Co. This work was supported in part by a Scientific Research grant-in-aid of the Ministry of Education.

Department of Chemistry
Faculty of Science
Kyoto University
Sakyo-ku, Kyoto

Chromotropic Acid and Its Zirconyl and Thorium Complexes

By Michiaki SAKAGUCHI*, Atsunobu MIZOTE**, Haruo MIYATA and Kyoji TÔEI

(Received November 26, 1962)

Chromotropic acid reacts with some metal ions to form its colored complexes[1], and many kinds of the azo-derivatives are especially sensitive to various metal ions; they are therefore used widely as colorimetric reagents and as metal indicators in chelatometry.

Chromotropic acid has two naphtholic hydroxyl groups, and the first dissociation constant was measured spectrophotometrically.

The composition of zirconyl and thorium chromotropate was determined by the continuous-variation and the mole-ratio methods, while the stability constants of the zirconyl and thorium complexes were measured from their absorbances.

Calculations

The Dissociation Constant of Chromotropic Acid.—Disodium chromotropate (abbr. $H_2Ch\text{-}Na_2$) is dissociated in water as follows:

$$H_2Ch^{2-} \rightleftarrows HCh^{3-} + H^+$$

The first dissociation constant, K_1, is

$$K_1 = [HCh]\,[H] / [H_2Ch]$$

Therefore,

$$pK_1 = pH - \log [HCh] / [H_2Ch]$$

When [HCh] is equal to $[H_2Ch]$, the pH is pK_1. As the concentrations are proportional to the absorbances, pK_1 is obtained by the following equation:

$$pK_1 = pH - \log (E_1 - E)/(E - E_2) \qquad (1)$$

in which E_1 and E_2 are the characteristic absorbances of H_2Ch and HCh respectively at a constant wavelength, and E is an absorbance of their mixed solution at an arbitrary pH value.

The second dissociation constant, however, can not be obtained, because the dissociation occurs above pH 14, and it is too hard to get it under ordinary experimental conditions.

The Stability Constants of the Zirconyl and Thorium Complexes. — K_1 and K_2 are the first and the second dissociation constants of chromotropic acid, and K_{MCh} is the stability constant of the zirconyl or thorium complex.

$$K_1 = [H]\,[HCh] / [H_2Ch] \qquad (2)$$

$$K_2 = [H]\,[Ch] / [HCh] \qquad (3)$$

$$K_{MCh} = [MCh] / [M]\,[Ch] \qquad (4)$$

The total concentration of chromotropic acid C_{Ch}, and the total zirconyl or thorium concentration, C_M, are

$$C_{Ch} = [H_2Ch] + [HCh] + [Ch] + [MCh] \qquad (5)$$

$$C_M = [M] + [MCh] \qquad (6)$$

On the basis of Eqs. 2—6, the stability constant, K_{MCh}, is:

$$K_{MCh} = \frac{[MCh]\{[H]^2/K_1K_2 + [H]/K_2 + 1\}}{\{C_{Ch} - [MCh]\}\{C_M - [MCh]\}} \qquad (7)$$

The apparent stability constant, K'_{MCh}, is:

$$K'_{MCh} = [MCh] / \{C_{Ch} - [MCh]\}\{C_M - [MCh]\} \qquad (8)$$

[MCh] can be obtained from the absorbance of the zirconyl or thorium complex solution.

$$E = \varepsilon_{H_2Ch}[H_2CH] + \varepsilon_{HCh}[HCh] + \varepsilon_{Ch}[Ch] + \varepsilon_{MCh}[MCh]$$

ε_{H_2Ch}, ε_{HCh}, ε_{Ch} and ε_{MCh} are the absorption coefficients of H_2Ch, HCh, Ch and MCh respectively. [Ch] may be neglected below pH 4.

$$E = \varepsilon_{H_2Ch}[H_2Ch] + \varepsilon_{HCh}[HCh] + \varepsilon_{MCh}[MCh] \qquad (9)$$

Therefore, the concentration of [MCh] is

$$[MCh] = \frac{E\{1 + K_1/[H]\} - \varepsilon_{H_2Ch}C_{Ch} - \varepsilon_{HCh}C_{Ch}K_1/[H]}{\varepsilon_{MCh}\{1 + K_1/[H]\} - \varepsilon_{H_2Ch} - \varepsilon_{HCh}K_1/[H]} \qquad (10)$$

By substituting Eq. 10 into Eqs. 7 and 8, K_{MCh} and K'_{MCh} can be calculated.

Experimental and Results

Reagents.—*Disodium Chromotropate.*—The purification of chromotropate is carried out in a dark room. Disodium chromotropate dihydrate (Dôjindo Pharaceutical Co.) is dissolved in water, acidified by concentrated hydrochloric acid, and treated with active carbon by heating. The filtrate is evaporated so as to deposit crystals by a rotary evaporator and

* Present address: Nippon Oil Co., Chita-gun, Aichi-ken.
** Present address: Polymer Science Dept., Kyoto University, Kyoto.

1) K. C. Mathur and A. K. Dey, *Z. anal. Chem.*, **154**, 347 (1957).

then cooled. The crystals are recrystallized again by the same manner, and then dried over phosphorus pentoxide to obtain the anhydrous compound. The sodium content is found to be quantitative by the use of a flame photometer.

Zirconyl Chloride[2]. — When a saturated solution of zirconyl chloride octahydrate (c. p. grade) is added to an acetone-hydrochloric acid mixture, the flocky octahydrate is precipitated and filtered. After the procedure is repeated twice, the precipitate is washed with acetone and dried in air. Cubic colorless crystals were obtained. The zirconyl content is analyzed gravimetrically by the use of cupferron[3].

Found: ZrO_2, 38.23, 38.26. Calcd. for $ZrOCl_2 \cdot 8H_2O$: ZrO_2, 38.24%.

A 5×10^{-4} M zirconyl chloride solution is prepared by dissolving 16.11 mg. of a zirconyl chloride octahydrate with a 0.1 M potassium chloride solution in a 100 ml.-measuring flask, and it should be used within 20 min.

Thorium Perchlorate.—Thorium nitrate is purified through thorium hydroxy peroxide five or six times[5]. Thorium hydroxide prepared from the purified thorium nitrate is disssolved in perchloric acid, and the concentration is measured gravimetrically by oxalate[4].

Procedure.—All experiments are carried out in a dark room, because chromotropate tends to decompose in daylight, especially at higher pH values.

The Dissociation Constant of Chromotropic Acid. — Five milliliters of a 5×10^{-4} M chromotropate solution and a suitable buffer solution are poured into a 50 ml.-measuring flask, which is then filled up to the mark with 0.2 M sodium perchlorate and water to keep the ionic strength (μ) at 0.1. The spectra are measured with a Hitachi EPS-2 automatic recording spectrophotometer (Fig. 1). The pH values are measured with a Horiba Model M-4 glass electrode pH meter. With an increasing pH, a new absorption maximum appears at 361.5 mμ, and the absorbance is determined by a Shimadzu Model QR-50 spectrophotometer with 1 cm. quartz cell. pK_1 is calculated from Eq. 1, and the average value of six runs is shown in Table I.

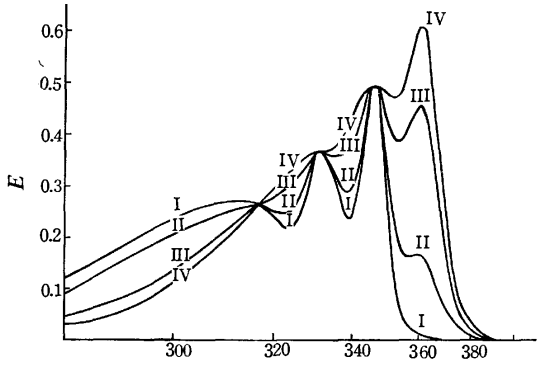

Fig. 1. Absorption curves of chromotropic acid.
5×10^{-5} M, $\mu=0.1$

	I	II	III	IV
pH	1~3	5.0	5.8	10~12

TABLE I. pK_1 OF CHROMOTROPIC ACID

The authors	5.44±0.03	(μ=0.1, 16~23°C)
Schwarzenbach et al.[6]	5.36	(μ=0.1, ~20°C)
Zollinger et al.[7]	5.53	(20°C)

Zirconyl Complex. — Each 5 ml. of a 5×10^{-4} M solution of zirconyl and chromotropate is mixed in a 50 ml.-measuring flask containing a suitable amount of hydrochloric acid; the flask is then filled up to the mark with a potassium chloride solution and water to maintain the ionic strength at 0.1.

A new absorption maximum appears at 356.5 mμ. The absorbance reaches its maximum at pH 2 after standing for one hour.

The composition was determined by the continuous variation method (Fig. 2). The composition should be 1 : 1, but the stability of the complex is not very good.

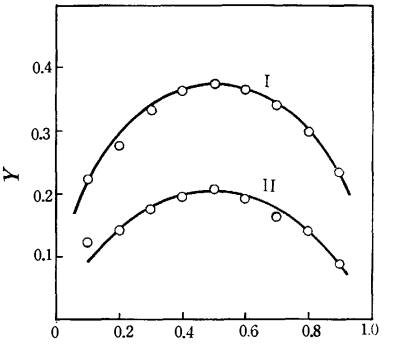

Fig. 2. Continuous variations.
I $[Zr]+[H_2Ch]=2\times10^{-4}$ mol./l.
II $[Zr]+[H_2Ch]=1\times10^{-4}$ mol./l.
pH=2, μ=0.1, at 357.5 mμ

From Eq. 8, the following equation can be obtained.

$$\log K'_{MCh}=\log[MCh]/\{C_{Ch}-[MCh]\} -\log\{C_M-[MCh]\}$$

The values of the first term were plotted against the second term at a constant pH (Fig. 3).

In Fig. 3, straight lines are obtained, and the slope indicates that the ratio of zirconyl to chromotropic acid is 1 to 1; $\log K'_{MCh}$ is 3.6$_3$ at pH 2.0, and 29 at pH 1.2.

Thorium Complex.—Five milliliters of a 5×10^{-4} M chromotropate solution and 5 ml. of a 2.5×10^{-3} M thorium perchlorate solution are poured into a 50 ml.-measuring flask containing a suitable amount

2) A. W. Henderson and K. B. Higbie, *J. Am. Chem. Soc.*, 76, 5857 (1954).
3) W. W. Scott, "Standard Methods of Chemical Analysis", D. van Nostrand Co. Inc., New York (1939), p. 1099.
4) Ibid., p. 953.
5) R. L. Swan, *J. Chem. Soc.*, 125, 781 (1924).
6) J. Heller and G. Schwarzenbach, *Helv. Chim. Acta*, 34, 1876 (1951).
7) H. Zollinger and W. Büchler, ibid., 34, 591 (1951).

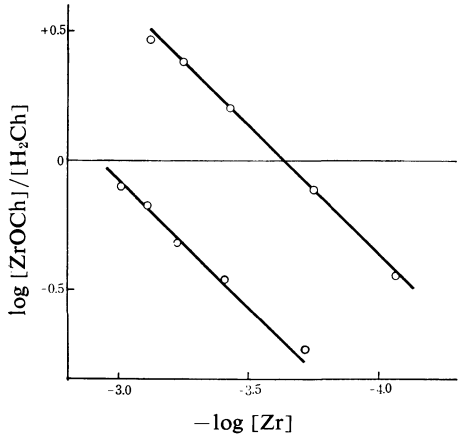

Fig. 3. Plots of log [ZrOCh]/[H_2Ch] against −log [Zr].

$C_{H_2Ch}=5\times10^{-5}$ M/l. $\mu=0.1$ at 357.5 mμ

of perchloric acid and then diluted to the mark by a sodium perchlorate solution and water so that the ionic strength is kept at 0.1. The absorption curve has a maximum at 361 mμ. The absorbance at 361 mμ reached its maximum after standing for 90 min., when it was measured. The absorbance is plotted against pH in Fig. 4. As the absorbance decreased above pH 3.6, the following experiment was carried out at pH 3.3~3.5.

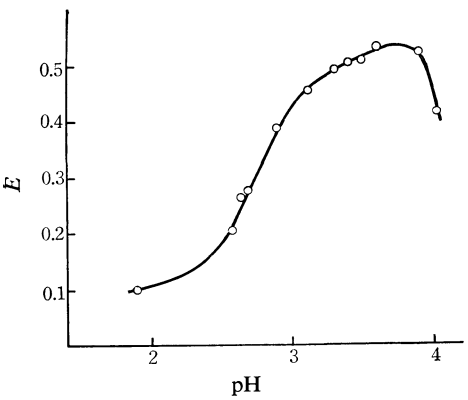

Fig. 4. Effect of pH on the absorbance of the complex.

$\mu=0.1$ at 361 mμ

The Mole-ratio Method.—A plot of the moles of chromotropic acid against the absorbance is given in Fig. 5. The 1 : 1 complex is indicated, being considerably dissociated under the conditions of this experiment.

The Continuous-variation Method.—At pH 3.5, equimolecular solutions of chromotropic acid and thorium perchlorate were mixed in varying proportions, the total number of moles remaining constant. The absorbances of each solution were measured at 361 mμ after they had been left standing for 2.5~3 hr. in a dark room. The values of the absorbances calculated on the assumption of "no reaction" were then substracted from the

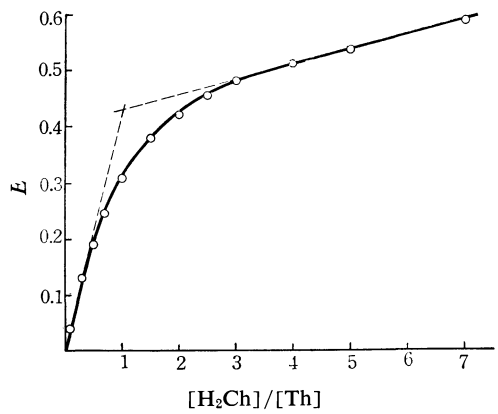

Fig. 5. Mole ratio method.
$C_{Th}=5\times10^{-5}$ M/l. $\mu=0.1$ at 361 mμ

measured absorbances to give what are commonly referred to as Y values (Fig. 6). The ratio of chromotropic acid to thorium was 1 to 1.

Stability Constant.—ε_{H_2Ch}, ε_{HCh} and ε_{MCh} were calculated from the absorbances at 361 mμ; the values were 1.89×10^2, 1.16×10^4 and 1.17×10^4 respectively. The stability constant, K_{MCh}, was calculated from Eqs. 9 and 10 by using $pK_2=15.6$[6]

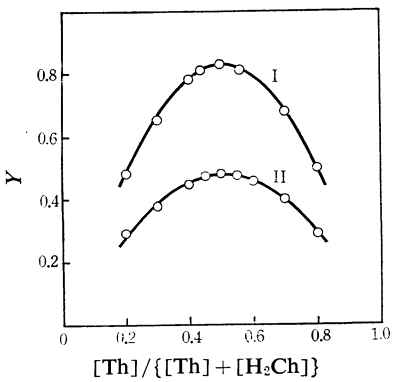

Fig. 6. Continuous variations.
I [Th]+[H_2Ch]=2.5×10^{-4} M/l.
II [Th]+[H_2Ch]=1.5×10^{-4} M/l.
$\mu=0.1$, pH=3.5, at 361 mμ

TABLE II. STABILITY CONSTANTS OF THORIUM CHROMOTROPATE

$C_{Ch}\times10^{-5}$	$C_{Th}\times10^{-5}$	pH	E	[ThCh] $\times10^{-5}$	$K_{ThCh}\times10^{18}$
2	2	3.42	0.0774	0.59	4.80
3	3	3.41	0.1334	1.09	5.05
4	4	3.41	0.2060	1.71	5.44
5	5	3.42	0.2775	2.31	5.11
6	6	3.42	0.3469	2.89	4.80
7	7	3.41	0.4125	3.44	4.56
8	8	3.42	0.4994	4.18	4.59
9	9	3.40	0.5629	4.72	4.51
10	10	3.42	0.6508	5.46	4.24
			The average value		4.79

(Table II). The apparent stability constants (Eq. 8) are shown in Table III. A plot of the apparent stability constants against pH is indicated in Fig. 7.

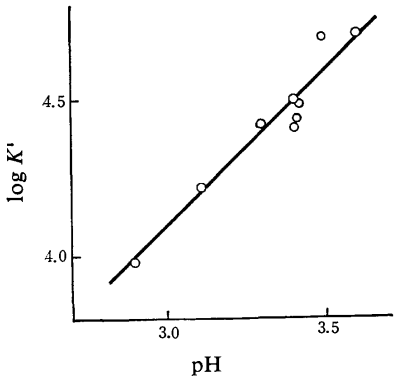

Fig. 7. Relationship between $\log K'_{ThCh}$ and pH.

TABLE III. APPARENT STABILITY CONSTANTS OF THORIUM CHROMOTROPATE

C_{Ch} $\times 10^{-5}$	C_{Th} $\times 10^{-4}$	pH	E	[ThCh] $\times 10^{-5}$	K'_{ThCh} $\times 10^{4}$
5	2.5	2.90	0.3969	3.37	0.955
5	2.5	3.11	0.4559	3.88	1.65
5	2.5	3.30	0.4976	4.25	2.71
5	2.5	3.40	0.5072	4.33	3.15
9	0.9	3.40	0.5629	4.71	2.57
7	0.7	3.41	0.4125	3.44	2.72
6	0.6	3.42	0.3469	2.89	3.00
5	2.5	3.49	0.5331	4.56	5.02
5	2.5	3.60	0.5346	4.57	5.18

Discussion

The first dissociation constant of chromotrophic acid (pK_1) is 5.4[4], and so, below pH 3.5, chromotropic acid exists predominantly in the form of H_2Ch. It reacts with zirconyl or thorium ions to form its complex. Figures 3 and 8 show that the metal ions react with the acid to replace only one hydrogen ion. There are two possibilities:

$$M + H_2Ch \rightleftarrows MHCh + H^+$$

$$M(OH)_n + H_2Ch \rightleftarrows MCh + H^+ + H_2O$$

In the former case, the following structures of the complex are possible:

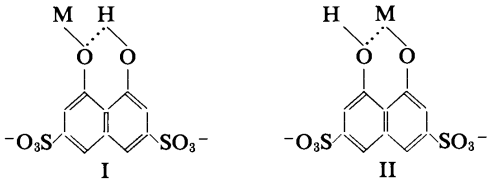

Form I is not a chelate but a salt, and by preliminary experiments, 1-naphthol-4-sulfonic acid does not react with the ions under the conditions of this experiment. Therefore, the complex is unlikely to be of Form I.

The second dissociation constant of acid (pK_2) is 15.6[6], because the second hydrogen atom is bridged between two oxygen atoms. The first hydrogen atom is far more exchangeable by the metal ions than the second one. Therefore, it is difficult to consider Form II.

In the latter case, the reaction species of zirconyl or thorium ion can not be detected directly from the absorbance because they have no absorbance at any wavelength.

Zirconium would exist in the form of $Zr(OH)_2^{2+}$ in acidic solutions, but the species has not yet been exactly confirmed[7].

Kraus and Holmberg[8] stated that the hydrolysis of $2.5\times10^{-4}\sim1.5\times10^{-2}$ M thorium ions was negligible below pH 3 and was influenced by the concentration, but that at about pH 3.5 the number of moles of hydroxide attached to thorium was several tenths of the total and that the equilibrium was rapidly established.

In our experiments, the concentration of zirconyl or thorium ions less than 2.5×10^{-4} M and the pH is about 1~2 in zirconyl and about 2~3.5 in thorium. Although the state of the ions has not been studied under the conditions of our experiments and although the reaction species have not been confirmed, zirconyl or thorium ions should have some $M(OH)_n^{4-n}$ ions in acidic solutions. Therefore, the latter equation seems to hold.

Department of Science
Faculty of Chemistry
Okayama University
Tsushima, Okayama

8) B. A. J. Lister and L. A. McDonald, *J. Chem. Soc.*, **1952**, 4315.
9) K. A. Kraus and R. W. Holmberg, *J. Phys. Chem.*, **58**, 325 (1954).

The Spectrophotometric Determination of Palladium(II) with Xylenol Orange[1]

By Makoto Otomo

(Received December 14, 1962)

The preceding works in this series of publications on the spectrophotometric determination of metal cations with xylenol orange have dealt with such metals as rare earths[2], vanadium[3], uranium[4] and aluminum[5], all of which react with this reagent in a slightly acidic medium to give red or reddish-violet chelates. Because of the low selectivity of xylenol orange, for the practical determinations in slightly acidic media it was necessary either to mask interfering ions with an appropriate masking agent or preliminarily to separate these ions from the object ion.

In a strongly acidic solution of perchloric acid, however, this reagent reacts selectively with palladous ions, even in the presence of many other cations, to give a bright-red complex with an absorption maximum at 518 mμ.

This paper chiefly presents a spectrophotometric study of the reaction between palladous ion and xylenol orange in a perchloric acid solution. The formation constant is also calculated from the results of the mole ratio method and those of the method of continuous variations.

Experimental

Reagents and Apparatus. — A stock solution of palladium was prepared by dissolving 1.927 g. of palladous chloride in a small amount of nitric acid and then diluting it with water to one liter. The standardization was carried out volumetrically by EDTA titration[6]. A standard working solution was prepared by taking an aliquot of the stock solution and diluting it to the desired concentration.

A 2×10^{-3} M solution of xylenol orange and a 1 : 1 solution of perchloric acid were prepared.

Stock solutions of diverse cations, which were prepared from reagent grade salts, contained approximately 0.1 μ mol. of the ions per ml.

All absorbance measurements were made at 25± 0.5°C with a Hitachi spectrophotometer, Model EPV-2, using 1 cm. glass cells.

1) Presented at the Tôhoku-Hokkaidô Branch Meeting of The Chemical Society of Japan, Hakodate, July, 1962.
2) K. Tonosaki and M. Otomo, This Bulletin, 35, 1863 (1962).
3) M. Otomo, ibid., 36, 137 (1963).
4) M. Otomo, ibid., 36, 140 (1963).
5) M. Otomo, ibid., 36, 809 (1963).
6) J. Kinnunen and B. Merikanto, *Chemist-Analyst*, 47, 11 (1958).

Results and Discussion

The Determination of Palladium.—In a preliminary test, it was shown that a red-colored palladium xylenol orange complex was formed in solutions of nitric, sulfuric and perchloric acids, but no color development was obtained in hydrochloric acid or in a solution containing a large number of chloride ions. In a perchloric acid solution, the complex gave the highest absorbance. Perchloric acid was therefore used in further experiments.

Absorption Spectra.—The absorption spectra of xylenol orange and its palladium complex are shown in Fig. 1. The complex has an

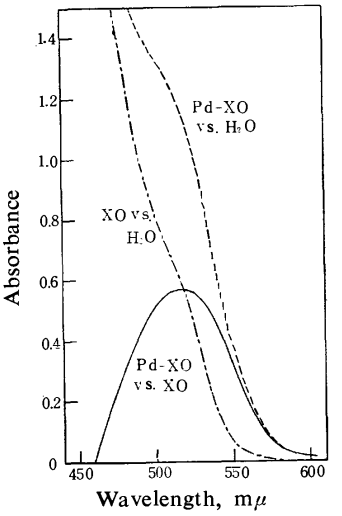

Fig. 1. Absorption spectra of xylenol orange and its palladium complex.
Pd : 57.8 μg. XO : 1.6×10^{-4} M
$HClO_4$: 1.3 N

absorption maximum at 518 mμ. It is of interest to note that the spectrum of xylenol orange has a small shoulder at about 515 mμ and that the position of the absorption peak of the complex is very close to that of the peaks shown by xylenol orange in strongly acidic solutions. For the sake of comparison, the absorption spectra of xylenol orange in sulfuric acid of various concentrations are also shown in Fig. 2.

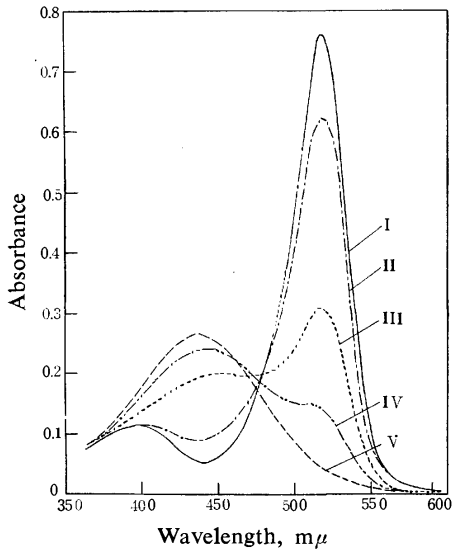

Fig. 2. Absorption spectra of xylenol orange in sulfuric acid of various concentrations.
XO: 2×10^{-5} M
Concentration of sulfuric acid:
I, 21.6 N II, 10.8 N III, 7.2 N
IV, 3.2 N V, 0.7 N

The Effect of the Concentration of Perchloric Acid. — In order to examine the effect of the concentration of perchloric acid, tests were made at varying concentrations of perchloric acid. The maximum and constant absorbance is obtained over the concentration range from 1.1 to 1.7 N in perchloric acid, as is indicated in Fig. 3. Seven to 8 ml. of 1 : 1 perchloric acid in a total volume of 25 ml. is sufficient to maintain the acid concentration within the optimum range.

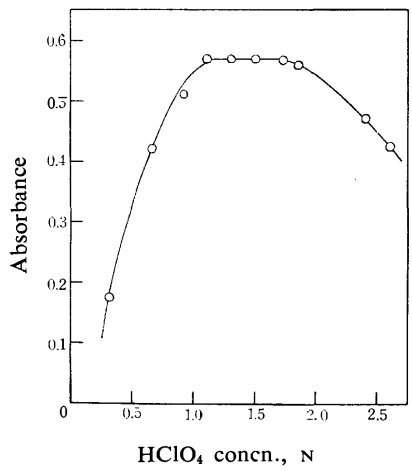

Fig. 3. Effect of concentration of perchloric acid.
Pd: 57.8 μg. XO: 1.6×10^{-4} M
Wavelength: 518 mμ

The Effect of the Concentration of the Reagent. —An excess of xylenol orange must be added, since the absorbance of the complex at 518 mμ is somewhat increased with an increased concentration of the reagent. Two milliliters of a 2×10^{-3} M solution of xylenol orange was found to be a sufficient amount for less than 100 μg. of palladium.

The Effect of Heating Time and the Color Stability. — The maximum color development was reached after about 20 ml. of the sample solution had been kept at boiling temperature for 2 to 3 min. The 20 ml. of solution contained 7 ml. of 1 : 1 perchloric acid and 2 ml. of a 2×10^{-3} M solution of xylenol orange, along with the desired quantity of palladium. After this heating period, the solution was cooled, transferred to a 25 ml. volumetric flask, and diluted to the mark with water. The absorbance of the resultant solution decreased slowly with time for the first 30 min. After this period, however, it remained practically constant for at least 3 hr.

Beer's Law. — Beer's law is obeyed over the concentration range from 0.2 to 4.0 p. p. m. of palladium. The optimum concentration range for the determination of palladium was determined by the method described by Ringbom[7] and was found to be 0.8 to 3.2 p. p. m. The molar extinction coefficient was approximately 26000 at 518 mμ.

Procedure. — To a palladium solution in a 50 ml. Erlenmeyer flask, 7 ml. of 1 : 1 perchloric acid and 2 ml. of a 2×10^{-3} M solution of xylenol orange were added. The volume was made to about 20 ml. with water. After being kept at boiling temperature for 2 to 3 min., the solution was cooled, transferred to a 25 ml. volumetric flask, and diluted to the mark with water. The absorbance of the solution was measured at 518 mμ against the reagent blank. The amount of palladium was then determined from the calibration curve prepared above.

The Effect of Diverse Ions. — The effect of diverse ions on the spectrophotometry was examined. As is shown in Table I, such anions as nitrate, sulfate, oxalate, tartrate and citrate do not interfere, even when as much as 100 μmol. of them are present. However, chloride, nitrilotriacetate and ethylenediaminetetraacetate ions interfere seriously, even when only a small amount is present.

Of the 25 cations which react with xylenol orange in a slightly acidic solution, only zirconium gave a large positive error. However, the interference from less than 200 μg. of zirconium could be effectively removed by

7) A. Ringbom, *Z. anal. Chem.*, 115, 332 (1938/9).

TABLE I. EFFECT OF ANIONS ON PALLADIUM DETERMINATION

Palladium taken, 57.8 μg.

Anion	Taken, μ mol.	Palladium Found μg.	Palladium Deviation μg.
Cl^-	5	56.6	− 1.2
	20	41.3	−16.5
	100	11.0	−46.8
F^-	10	57.6	− 0.2
	25	56.8	− 1.0
NO_3^-	50	57.5	− 0.3
	100	57.0	− 0.8
SO_4^{2-}	100	57.5	− 0.3
	250	57.8	± 0.0
PO_4^{3-}	10	57.5	− 0.3
	50	56.6	− 1.2
$C_2O_4^{2-}$	10	58.4	+ 0.6
	50	57.8	± 0.0
$C_4H_4O_6^{2-}$	20	58.2	+ 0.4
	50	58.7	+ 0.9
$C_6H_5O_7^{3-}$	10	57.6	− 0.2
	50	58.1	+ 0.3
NTA*	1	57.0	− 0.8
	5	55.9	− 1.9
EDTA**	0.2	45.2	−12.6
	1	16.1	−41.7

* Nitrilotriacetate ion
** Ethylenediaminetetraacetate ion

adding 1 to 2 ml. of a 0.01 M fluoride solution. Accordingly, it is possible to say that, in a strongly acidic solution of perchloric acid, xylenol orange is a highly selective color reagent for palladium.

A Comparison with Other Methods. — Several reagents have been used for the spectrophotometric determinations of palladium. The most sensitive reagents have been found to be *p*-nitrosodiphenylamine and *p*-nitrosodimethylaniline, reported by Yoe and Overholser[8,9]. Thioglycolic acid[10], potassium iodide[11], ethylenediaminetetraacetic acid[12] and nitrilotriacetic acid[13] have been used as colorimetric reagents for palladium by König and Cromell, Fraser et al., McNevin and Kriege and Desideri and Pantani respectively. Niesch[14], Cheng[15], Menis and Rains[16] and, recently, Jacobs et al.[17] have described some new reagents for the determination of palladium. The methods using the above reagents, however, in many cases required the extraction of the palladium complexes into such an organic solvent as chloroform or toluene. A method which can be carried out in an aqueous medium and which is rapid, sensitive, selective and relatively free from interference is more desirable.

The present reagent, xylenol orange, has some advantages as a colorimetric reagent for palladium: No extraction of the complex is required, since a palladium-xylenol orange complexes is water soluble; the acid concentration for the maximum color development can easily be controlled; not many cations besides zirconium interfere; and this method is comparable in sensitivity with the β-nitroso-α-naphthol method[15].

Composition and Formation Constant. — The composition of the palladium-xylenol orange complex was determined by the mole ratio method and also by Job's method of continuous variations. The results are presented graphically in Figs. 4 and 5, from which it is evident that only one palladium xylenol orange complex is present and that the mole ratio of xylenol orange to palladium in this complex is 2:1. For the calculation of the formation constant, the absorbance data obtained from the above methods were employed.

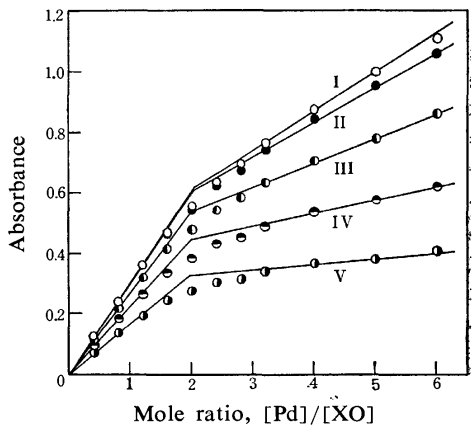

Fig. 4. Mole ratio method.
[Pd] = 2.0×10^{-5} M
Absorbances were measured at:
I, 510 mμ II, 518 mμ III, 530 mμ
IV, 540 mμ V, 550 mμ

Calculation from the Results of the Mole Ratio Method. — Since one part of palladium ions reacts with two parts xylenol orange molecules, the following equilibrium must exist:

$$Pd + 2XO \rightleftarrows Pd(XO)_2$$

$$K = x/(a-x)(b-2x)^2 \qquad (1)$$

8) J. H. Yoe and L. G. Overholser, *J. Am. Chem. Soc.*, **61**, 2058 (1939).
9) J. H. Yoe and L. G. Overholser, ibid., **63**, 3224 (1941).
10) O. König and W. R. Crowell, *Mikrochem. ver. Mikrochim. Acta*, **33**, 298 (1948).
11) J. G. Fraser, F. E. Beamish and W. A. E. McBryde, *Anal. Chem.*, **26**, 495 (1954).
12) M. W. McNevin and O. H. Kriege, ibid., **26**, 1768 (1954).
13) P. Desideri and F. Pantani, *Talanta*, **8**, 235 (1961).
14) W. Niesch, *Z. anal. Chem.*, **142**, 30 (1954).
15) K. L. Cheng, *Anal. Chem.*, **26**, 1894 (1954).
16) O. Menis and T. C. Rains, ibid., **27**, 1932 (1955).
17) W. D. Jacobs, C. M. Wheeler and W. H. Waggoner, *Talanta*, **9**, 243 (1962).

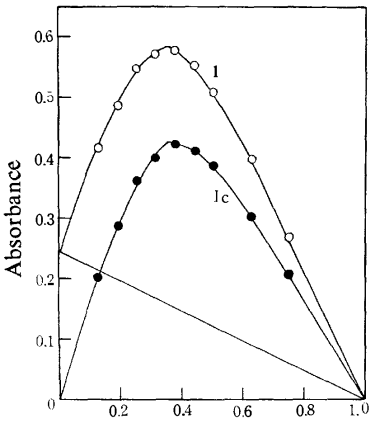

Fig. 5. Method of continuous variations.
[Pd]+[XO]=6.4×10^{-5} M
Wavelength: 518 mμ
I: Uncorrected curve
I_c: Corrected curve

where x is the concentration of the complex at equilibrium, and a and b are the initial concentrations of palladium ion and xylenol orange respectively. In the visible region, the contribution of the palladium ions to the absorbance of the system is negligible. Accordingly, the observed absorbance, D, may be regarded as due to the color of the complex formed and to the free xylenol orange. It is given by:

$$D=\varepsilon_C x+\varepsilon_{XO}(b-2x) \qquad (2)$$

where ε_C and ε_{XO} are the molar extinction coefficients of the complex and xylenol orange respectively. ε_C can be obtained from the equation[18]

$$D'=\varepsilon_C a \qquad (3)$$

where D' is obtained from the absorbance observed by adding xylenol orange in a large excess compared to the concentration of the palladium ions. The values of ε_{XO} and ε_C at various wavelengths are given in Table II. The formation constant, as calculated by combining Eqs. 1, 2 and 3, was found to be 1.4×10^{10} (as an average value at the three wavelengths 510, 518 and 530 mμ).

Table II. Values of ε_{XO} and ε_C at various wavelengths

Wavelength, mμ	ε_{XO}	ε_C
510	5280	36240
518	4660	35320
530	3020	30660
540	1520	23560
550	630	16080
560	250	9440

Calculation from the Results Obtained by Job's Method.—Job's method of continuous variation was then employed for the calculation of the formation constant. At the concentration and the wavelengths investigated, the palladous ion has no absorption. Therefore, the color of the system is due to the free xylenol orange and the complex only. Since xylenol orange has a considerable absorption at the wavelengths investigated, corrections were made. The corrected values are also plotted in Fig. 5. The formation constant, K, was then calculated from the curve, based on the relationships described by Harvey and Manning[19]. It was found to be 2.6×10^{10}.

From the above, therefore, K may reasonably be represented as 2×10^{10}. This value is slightly lower than that of the formation constant for the uranium-xylenol orange complex[4], but it is higher than the values for 1:1 complexes between some metal cations and xylenol orange.

Summary

A new, sensitive spectrophotometric method for the determination of palladium(II) by using xylenol orange as a color reagent has been described. The palladium-xylenol orange complex has an absorption maximum at 518 mμ. The effects of the concentration of perchloric acid and of the reagent have been investigated. In addition, various conditions, including the duration of heating, the stability of the color, and the effect of diverse ions, have been investigated. In a solution of perchloric acid (1.1 to 1.7 N), xylenol orange is a highly selective reagent for palladium, although it reacts with a number of metal cations in a slightly acidic or a neutral solution. Beer's law is obeyed in the range from 0.2 to 4.0 p. p. m. of palladium at 518 mμ. The results of Job's method and of the mole ratio method show a complex consisting of two molecules of the reagent to one palladous ion. The formation constant was calculated to be 2×10^{10}.

The author wishes to express his deep thanks to Professor Kôichi Tonosaki for his kind guidance and encouragement throughout this work. He is also grateful to Dr. Kôyô Aida of Tohoku University for his interest.

Department of Chemistry
Faculty of Literature and Science
Hirosaki University
Bunkyo-chô, Hirosaki

18) L. Newman and D. N. Hume, *J. Am. Chem. Soc.*, **79**, 4571 (1957).

19) A. F. Harvey, Jr. and D. L. Manning, ibid., **72**, 4488 (1950).

*The Radiation-induced Reactions of Benzene with Sulfur and Sulfur Compounds**

By Wataru ANDO, Ken'ichi SUGIMOTO and Shigeru OAE

(Received December 27, 1962)

The radiolysis of the aqueous benzene solution has been studied extensively and is known to give phenol and other minor products[1]. The formation of phenol is known to be increased by the introduction of oxygen into the system. The radiation-induced reaction of benzene has also been studied by many workers[2-6]. According to the reaction mechanisms hitherto suggested, the process of phenol formation involves the initial formation of a hydrogen atom and of a phenyl radical which reacts immediately with dissolved oxygen. We have extended a similar study in the hope of getting thiophenol and other sulfur-containing compounds, since sulfur is also quite an effective radical scavenger[7-9]. Since mercaptans are readily oxidized to their corresponding disulfides under irradiation with X-, beta-, or gamma-rays[10-11], one would expect diphenyl disulfide and hydrogen among the products formed. The present paper deals with the radiation-induced reaction of benzene with sulfur, together with the chemical behavior of thiophenol and hydrogen sulfide in benzene under the irradiation of gamma-rays.

Experimental

Chemicals.— *Benzene.*— Reagent-grade thiophene-free benzene was purified by three successive distillations.

Sulfur.—The sulfur employed was C. P.-grade, large, rhombic crystals, formed from carbon disulfide. The sulfur was again recrystallized from hot, reagent-grade benzene to obtain small, granular, rhombic crystals.

Thiophenol.—C. P.-grade thiophenol was purified by repeated distillations in a nitrogen atmosphere and was vacuum-distilled shortly before use.

The Preparation of the Samples.—Exactly 40 ml. of a benzene solution containing an aliquot amount of sulfur was sealed under vacuum in an ampoule with a glass break-off tip. Air was degassed by freezing and pumping.

The irradiation was carried out with 3800-curie cobalt-60 gamma rays at room temperature. The dosimetry was based on a Fricke dosimeter. The dose rate was approximately 5×10^5 r/hr.

Analysis.—All the analyses of the irradiated samples containing sulfur or thiophenol in benzene were carried out as described below. First, gases were collected from the irradiated samples by the usual repeated freezing evacuation and melting technique[12]. The collected gases were then passed through liquid nitrogen traps. The uncondensed gas was identified as hydrogen, and the gas which passed through a series of dry-ice acetone trap and was condensed at the liquid nitrogen temperature was identified as hydrogen sulfide.

Hydrogen sulfide was absorbed into a solution containing 5% of zinc acetate and 1% sodium acetate. Then, 25 ml. of 10% ammonium molybdate and 5 ml. of phosphoric acid were added to the solution. It was diluted to 50 ml., and the absorption at 670 mμ was observed after one or two days[13].

Thiophenol, which was distilled from irradiated benzene and sulfur at 50°C into a trap cooled by a dry-ice acetone bath, was allowed to react with *p*, *p'*-dinitrodiphenyl disulfide; then, the amount of *p*-nitrobenzenethiol formed was determined by spectrophotometry following the method of Ellman[14]. For each run, 5 ml. of a 0.1 M phosphate buffer at pH 8 and 5 ml. of a saturated acetone solution of *p*, *p'*-dinitrodiphenyl disulfide were added into 20 ml. of the sample and the whole solution was diluted to 100 ml. with acetone. The absorbancy at 470 mμ was measured within one minute after the disulfide had been added.

When a benzene solution of thiophenol was irradiated, both the initial and final amounts of thiophenol was determined by titrating the solution with a solution of silver nitrate in isopropyl

* Presented at the 5th Symposium of Radiation Chemistry, Tokyo, November, 1962.

1) E. Collinson and A. J. Swallow, *Chem. Revs.*, 56, 505 (1956).
2) J. P. Manion and M. Burton, *J. Phys. Chem.*, 56, 560 (1952).
3) G. E. Gibson, N. Blake and M. Kalm, *J. Chem. Phys.*, 21, 1000 (1953).
4) W. N. Patrick and M. Burton, *J. Am. Chem. Soc.*, 76, 2626 (1954).
5) S. Gordon, A. R. VanDyken and J. F. Douman, *J. Phys. Chem.*, 62, 20 (1958).
6) G. Hughes, ibid., 65, 2160 (1961).
7) A. J. Parker and N. Kharasch, *Chem. Revs.*, 59, 583 (1959).
8) C. H. Wang and S. G. Cohen, *J. Am. Chem. Soc.*, 81, 3005 (1959).
9) P. D. Bartlett and D. S. Trifan, *J. Polymer Sci.*, 20, 457 (1956).
10) J. Weiss and H. Fishgold, *Nature*, 137, 71 (1936).
11) E. S. G. Barron and V. Flood, *J. Gen. Phys.*, 33, 229 (1950).
12) R. T. Sanderson, "Vacuum Manipulation of Volatile Compounds", John Wiley & Sons., Inc., New York, N. Y. (1948).
13) F. D. Snell and C. T. Snell, "Colorimetric Methods of Analysis", Vol. IIIA, D. Van Nostrand Co., N. Y. (1961), p. 446.
14) G. L. Ellman, *Arch. Biochem. and Biophys.*, 74, 443 (1958).

alcohol[15]. The break in the potentiometric curve was found to be between approximately −325 and −175 mV. vs. SCE. The amounts of decreased thiophenol were calculated by subtracting the final values from the initial ones.

Results and Discussion

The Radiolysis of a Benzene Solution of Sulfur.—An aliquot amount of sulfur was dissolved in benzene and was irradiated with gamma-rays. The vacuum technique was employed throughout. The thiophenol and hydrogen sulfide formed were measured. The results obtained at varying concentrations of sulfur and radiation doses are shown in Tables I and II.

TABLE I. THE FORMATION OF THIOPHENOL AT VARIOUS SULFUR CONCENTRATIONS

Sulfur concentration	*G*-Value of thiophenol formed Irradiation dose		
g./100 ml.	1.1×10^7 r	2.5×10^7 r	3.6×10^7 r
2.0	0.056	0.039	0.041
1.5	0.027	0.039	0.037
0.8	0.041	—	0.030
0.25	0.017	0.017	0.013

Dose rate: 5×10^5 r/hr.

TABLE II. THE FORMATION OF HYDROGEN SULFIDE AT VARIOUS SULFUR CONCENTRATIONS

Sulfur concentration	*G*-Value of hydrogen sulfide irradiation dose		
g./100 ml.	1.1×10^7 r	2.5×10^7 r	3.6×10^7 r
2.0	0.047	0.049	0.049
1.5	0.058	0.049	0.040
0.8	0.040	0.040	0.026
0.25	0.003	0.011	0.008

Dose rate: 5×10^5 r/hr.

The formation of thiophenol and hydrogen sulfide showed nearly identical *G*-values, and both are independent of the sulfur concentration and the radiation dose except at an extremely low concentration of sulfur. This means that sulfur cleavage is not the initial step in the formation of these substances and that sulfur reacts at a secondary step of the overall reaction. It appears that the formation of the phenyl radical and of hydrogen atoms from a benzene solution and the reactions of these species with sulfur to form thiophenol and hydrogen sulfide follow.

However, thiophenol, being a very strong hydrogen donor, does not remain unchanged in the solution; rather, a portion is oxidized to diphenyl disulfide. Table II shows a little higher *G*-value of hydrogen sulfide formation than that of thiophenol formation. This seems to suggest that hydrogen sulfide is also produced by the radiolysis of thiophenol, along with the reaction of hydrogen atoms and sulfur.

Radiolysis of Thiophenol in Benzene.—The radiolysis of thiophenol in a benzene solution was carried out under various conditions. Figure 1 shows the relation between the *G*-values and the radiation doses.

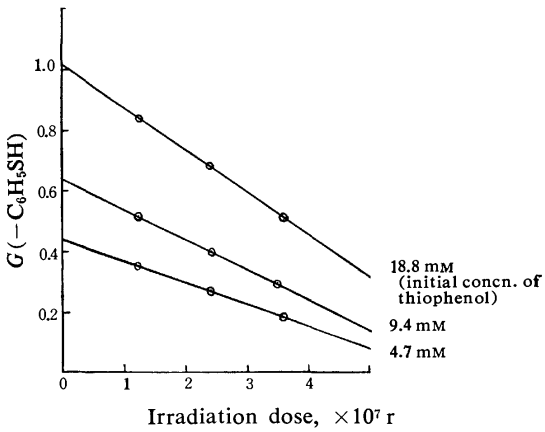

Fig. 1. Relation of *G*-value of decreased thiophenol and irradiation dose on radiolysis of thiophenol in benzene.

The decrease in thiophenol by irradiation was proportional to the initial concentration of thiophenol. This suggests that thiophenol is more susceptible to gamma irradaition than benzene. Therefore, the *G*-value for thiophenol decomposition in benzene could be calculated from the remaining thiophenol concentration.

The variation in *G*-values for different radiation doses and for initial concentrations of thiophenol seems to be caused by the regeneration of thiophenol from the radiolysis of diphenyl disulfide[16], which was found to be the main product in the radiolysis of thiophenol in benzene. In fact, we found that thiophenol was formed by the radiolysis of diphenyl disulfide, as Table III shows.

TABLE III. RADIOLYSIS OF DIPHENYL DISULFIDE IN BENZENE

Disulfide	50 mmol./l.
Irradiation dose	2.8×10^7 r
Found	*G*-Value
Thiophenol	0.024 mM
Hydrogen sulfide	0.001 mM

15) M. W. Tamele and L. B. Ryland, *Ind. Eng. Chem., Anal. Ed.*, **8**, 16 (1936).

16) C. Walling and R. Rabinowitch, *J. Am. Chem. Soc.*, **81**, 1137 (1959).

17) E. C. Truesdale and S. C. Lind, ibid., **54**, 516 (1932).

The formation of hydrogen sulfide increases with an increase in the radiation dose, but at a high radiation dose, the formation of hydrogen sulfide became steady or decreased. This can be explained if one assumes that hydrogen sulfide is slowly decomposed in benzene with an increase in the radiation dose[17].

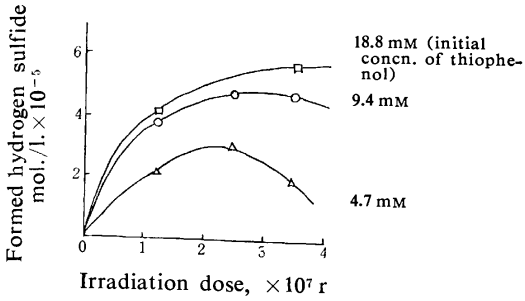

Fig. 2. Relation of hydrogen sulfide formed and irradiation dose on radiolysis of thiophenol in benzene.

This reaction of hydrogen sulfide in a benzene solution will give thiophenol again as a result of the attack of the phenyl radical on hydrogen sulfide. However, this reaction is of minor importance. Therefore, the formation of hydrogen sulfide can probably best be explained as a result of the direct decomposition of thiophenol.

The radiolysis of benzene saturated with hydrogen sulfide was also carried out; the results are shown in Table IV. The amounts of thiophenol formed were similar at various radiation doses, suggesting that more than a certain amount of thiophenol was always converted to diphenyl disulfide.

Table IV. Radiolysis of benzene saturated with hydrogen sulfide

Irradiation dose	Thiophenol formed	*G*-Value
1.2×10^7 r	0.46 mmol./l.	0.046
2.6×10^7 r	0.41 mmol./l.	0.020
3.6×10^7 r	0.42 mmol./l.	0.014

Proposed Mechanisms.—*The Radiolysis of a Benzene Solution of Sulfur.*—The mechanism for the radiolysis of benzene has recently been shown in a number of publications[2-6]. In the formation of the phenyl radical and the hydrogen atom under the irradiation of benzene, they further react with benzene to form polymers :

$$C_6H_6 \xrightarrow{I} C_6H_6^* \quad (1)$$

$$C_6H_6^* \rightarrow C_6H_5 + H \quad (2)$$

However, when elemental sulfur is dissolved in benzene, the phenyl radical and the hydrogen atom formed in the primary step of the radiolysis of benzene react with sulfur to form thiophenol and hydrogen sulfide, as can be seen from the data in Tables I and II.

Since the overall stoichiometry of the *G*-values of the thiophenol and hydrogen sulfide formed is independent both of the radiation dose and the relative concentration of sulfur, the following reaction scheme may be considered :

$$C_6H_5 + S_8 \rightarrow C_6H_5\text{-}S_8 \rightarrow C_6H_5S + S_x \quad (3)$$

$$H + S_8 \rightarrow HS_8 \rightarrow HS + S_x \quad (4)$$

In this case, benzene and sulfur compete for reaction with the phenyl and hydrogen radicals formed in reaction 2. As elemental sulfur is an effective radical scavenger, the phenyl radical and hydrogen atom attack the S-S bonds of sulfur and the open S_8 ring rather than reacting with benzene. Therefore, reactions 3 and 4 take place more readily than the polymer formation.

The incipient open chain polysulfides radicals are quite unstable and immediately decompose to give phenyl, sulfenyl and sulfhydryl radicals[18-20]. These sulfenyl radicals then react with free hydrogen to form the thiophenol. Similarly, the formation of hydrogen sulfide can be written as in reaction 6. Some sulfenyl radicals also recombine to form diphenyl disulfide :

$$C_6H_5S + H \rightarrow C_6H_5SH \quad (5)$$

$$SH + H \rightarrow H_2S \quad (6)$$

$$2C_6H_5S \rightarrow C_6H_5S\text{-}SC_6H_5 \quad (7)$$

The Radiolysis of Thiophenol in Benzene.—The rate of the disappearance of thiophenol was found to depend on the initial concentration of thiophenol and on the radiation dose. This indicates that the main path for the disappearance of thiophenol is not through the following reaction :

$$C_6H_6^* \rightarrow C_6H_5 + H \quad (2)$$

$$C_6H_5 + C_6H_5SH \rightarrow C_6H_6 + C_6H_5S \quad (8)$$

$$2\ C_6H_5S \rightarrow C_6H_5S\text{-}SC_6H_5 \quad (7)$$

Although most of the radiation energy is absorbed into the benzene, the energy absorbed is transferred to thiophenol, which upon the absorption of energy splits into the sulfenyl radical and the hydrogen atom.

$$C_6H_6^* + C_6H_5SH \rightarrow C_6H_6 + C_6H_5SH^* \quad (9)$$

$$C_6H_5SH^* \rightarrow C_6H_5S + H \quad (10)$$

18) P. D. Bartlett and R. E. Davis, ibid., **80**, 2513 (1958).
19) M. Schmidt and C. Talsky, *Ber.*, **90**, 1673 (1957).
20) P. D. Bartlett and G. Maguerian, *J. Am. Chem. Soc.*, **78**, 3710 (1956).

The sulfenyl radicals thus formed mainly recombine, forming diphenyl disulfide, as is shown by 7. Another reaction for the decomposition of thiophenol may be proposed from the formation of hydrogen sulfide[21-23] as follows:

$$C_6H_5SH^* \rightarrow C_6H_5 + SH \quad (11)$$

$$SH + C_6H_5SH \rightarrow C_6H_5S + H_2S \quad (12)$$

$$SH + H \rightarrow H_2S \quad (6)$$

By comparing the yield of hydrogen sulfide with the amount of the decomposition of thiophenol, the relative bond stability of S–H and C–S under the irradiation may be calculated, as is shown in Table V. From these calculations, one finds that reactions 10 and 11 occur in the ratio of about 200 to 1.

TABLE V. THE RATIO OF THE NUMBERS OF BROKEN BONDS S-H/C-S

Irradiation dose	Initial concentration of thiophenol		
	18.8 mM	9.4 mM	4.7 mM
1.2×10^7 r	217	133	189
2.4×10^7 r	—	167	200
3.6×10^7 r	285	175	217
Average	192 S-H/C-S		

The Radiolysis of Diphenyl Disulfide in Benzene.—Sulfenyl radicals are produced from the radiolysis of diphenyl disulfide; these radicals are then converted into thiophenol by reaction with free hydrogen from the radiolysis of benzene:

$$C_6H_5S\text{–}SC_6H_5 \rightarrow 2\ C_6H_5S \quad (13)$$

$$C_6H_5S + H \rightarrow C_6H_5SH \quad (5)$$

The Energy Transfer of Excited Benzene in the Decomposition of Thiophenol.—The *G*-value of decomposition of thiophenol apparently depends on the concentration of thiophenol, the value ranging anywhere 200 to 600 when it is calculated on the basis of the concentration of thiophenol.

The available bond dissociation energy is less than 70 kcal. per mol. for the S–H bond of thiophenol. This means that the *G*-value for the thiophenol decomposition is much larger than the maximum *G*-value obtained when the absorbed energy is used completely for the decomposition of thiophenol.

By assuming the energy transfer from benzene to thiophenol, the overall kinetics for the only favorable conditions of thiophenol decomposition in benzene can be developed by the steady-state approach. Since one may reasonably assume that the direct excitation of thiophenol by gamma rays and the recombination of the sulfenyl radical and the hydrogen atom are small, the *G*-value of the decomposition of thiophenol may be given by the following equation:

$$G(-C_6H_5SH) = \frac{2k_4k_3(M)I}{(k_2+k_4)(k_1+k_3(M))}$$

which may be written in the following convenient form, since k_4 is much larger than k_2:

$$\frac{1}{G} = \frac{1}{2I}\left(1+\frac{k_1}{k_3(M)}\right)$$

where I represents the rate constant for the formation of benzene molecules excited by 100 eV.; k_1 and k_2, the rate constants for the deactivation of excited benzene and thiophenol; k_3 and k_4, the rate constants for Eqs. 9 and 10, and M, the initial concentration of thiophenol.

This equation can be used only for lower concentrations of thoiphenol; at higher concentrations, the direct decomposition of thiophenol by gamma irradiation becomes so large as to obscure the overall assumptions for setting up the equation.

Figure 3 illustrates the relation between the *G*-values at the minimum radiation dose obtained from Fig. 1 and the initial concentrations of thiophenol.

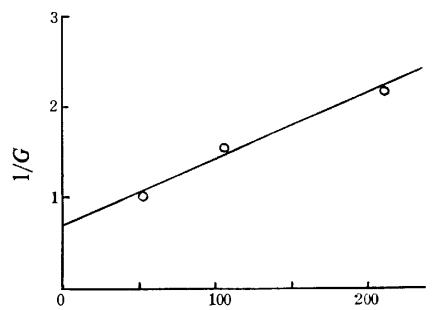

Fig. 3. Relation of *G*-value of decreased thiophenol and its initial concentration on radiolysis thiophenol in benzene.

From Fig. 3, (I) can be obtained by intersecting the slope with the vertical line, and k_1/k_3, from the slope of the line.

The calculation indicates that about 0.7 molecule of excited benzene is formed per 100 eV. of gamma irradiation, and that the ratio of the energy transfer to thiophenol from excited benzene to the deactivation of excited benzene itself is about 100 to 1.

21) E. W. Steacic, "Atomic and Free Reactions", Vol. II, Reinhold, New York (1954).
22) W. M. Malisoff and E. M. Marks, *Ind. Eng. Chem.*, 23, 1114 (1931).
23) K. Araki, T. Hoshino, S. Sida and K. Yamagishi, *Proceedings of the Second Symposium on Atomic Energy of Japan*, 4, 158 (1958).

Summary

The irradiation of a benzene solution of sulfur gave thiophenol, diphenyl disulfide, diphenyl sulfide, hydrogen sulfide, hydrogen and some polymers. The formation of thiophenol and of hydrogen sulfide is considered to be initiated by the radiolysis of benzene, which gives phenyl and hydrogen radicals, which in turn combine with sulfur in succeeding steps.

However, the thiophenol formed is oxidized to the disulfide as the radiation energy absorbed in benzene transfers to thiophenol. The effect of the initial concentration of thiophenol and of the radiation dose has been measured. The relative stability of the S–H and C–S bond for radiation was about 1 : 200. The radiolysis of diphenyl disulfide or hydrogen sulfide in benzene were found to form thiophenol. In a kinetical study of the decomposition of thiophenol in benzene, 0.7 benzene molecule is excited by the 100 eV. of gamma rays absorbed, while the ratio between the energy transfer to thiophenol from excited benzene and the deactivation of excited benzene itself is about 100 to 1.

Department of Chemistry
Radiation Center of Osaka Prefecture
Sakai, Osaka (W. A. & K. S.)

Department of Applied Chemistry
Faculty of Engineering
Osaka City University
Kitaku, Osaka (S. O.)

The Syntheses of Polyhydroxybenzene Derivatives from Furfural. II[1]

By Masuo MURAKAMI and Jong-Chen CHEN

(Received January 5, 1963)

It is well-known that poison ivy and Japanese lac urushiol contain a mixture of four components which have the carbon skeleton of 3-pentadecylcatechol. One of these components has a completely reduced side chain (hydrourushiol). The other three contain one, two and three olefinic bonds respectively[2,3]. A number of investigators[1,2,4-6] have synthesized hydrourushiol. The mono-olefinic compound of urushiol and its homologs have also been synthesized by several investigators[1,8,9].

Because of the absence of a general method for the preparation of 3-alkyl catechol and for the other reasons pointed out by Loev and Dawson[9,10], none of di- or tri-olefinic catechols has heretofore been available, either from natural sources or by synthetic means. Consequently, there has been interest in the development of a method of synthesizing such alkenylcatechols. The present paper's method of the syntheses of di- and tri-olefinic catechols (Fig. 1) is based on a route developed earlier[1] by us for syntheses of 3-alkylcatechols. This paper also describes syntheses of 3-alkynylcatechol, as well as of 3-phenylcathechol, neither of which has ever been synthesized before.

Heptadecyl bromide, 1-bromo-8, 11-heptadecadiene and 1-bromo-8, 11, 14-heptadecatriene were prepared by Hunsdiecker reaction from the silver salts of stearic acid, linoleic acid and linolenic acid respectively. It is noteworthy that Hunsdiecker reaction is useful in the preparation of olefinic bromides.

The structures of I, II, III, IV and V were determined from the synthetic process, from analyses, from infrared spectra, and from their reduced products. All of these compounds gave dark blue color with ferric chloride and turned red when dilute aqueous alkali was added.

Hydrolaccol (I)[2,11], one of the components of the Indochina lac tree (*Rhus succedenea*), was also obtained by the reduction of II and 3-(8'-heptadecenyl)catechol[1].

1) Part I: M. Murakami and J. C. Chen, This Bullettin, **36**, 263 (1963).
2) R. Majima, *Ber.*, **55**, 172 (1922) and preceding papers.
3) W. F. Symes and C. R. Dawson, *J. Am. Chem. Soc.*, **76**, 2959 (1954).
4) H. J. Backer and N. H. Haack, *Rec. trav. chim.*, **57**, 225 (1938).
5) H. S. Mason, *J. Am. Chem. Soc.*, **67**, 1538 (1954).
6) B. Loev and C. R. Dawson, ibid., **78**, 6905 (1956).
7) W. R. Boehme, ibid., **82**, 498 (1960).
8) T. Hanafusa and Y. Yukawa, *Chem. & Ind.*, **1961**, 23.
9) B. Loev and C. R. Dawson, *J. Am. Chem. Soc.*, **81**, 980 (1959).
10) B. Loev and C. R. Dawson, ibid., **78**, 1180 (1956).
11) G. Bertrand, H. J. Backer and N. H. Haack, *Bull. soc. chim. France*, **6**, 1670 (1939).

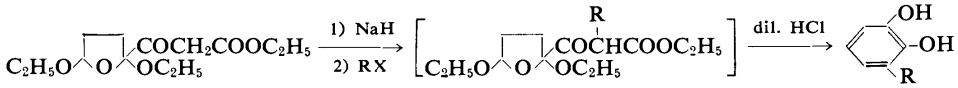

(I) R : $-(CH_2)_{16}CH_3$
(II) R : $-(CH_2)_7CH=CHCH_2CH=CH(CH_2)_4CH_{32}$
(III) R : $-(CH_2)_7CH=CHCH_2CH=CHCH_2CH=CHCH_2CH_3$
(IV) R : $-CH_2C\equiv CH$
(V) R : $-C_6H_5$

Fig. 1

It is known that a latex of the lac tree is polymerized by enzyme laccase on exposure to air at room temperature. A crude laccase, which had a specific activity of 4.1×10^2 at 25°C[12], was isolated from the latex of the Japanese lac tree (*Rhus vernicifera*). To each synthetic 3-alkylcatechol was added a small amount of crude laccase. It was shown that such 3-alkylcatechols as hydrourushiol, hydrolaccol, 3-propylcatechol, and 3-methylcatechol did not solidify as a hard thin film, while 3-olefinic catechol and 3-alkynylcatechol solidified as such a hard thin film when exposed to air at room temperature. The solidification rates are shown in the following comparison:

Latex of the Japanese lac tree<3-allylcatechol<3-(8'-heptadecenyl)catechol< II <III <IV.

Experimental

Heptadecyl Bromide. — This compound was prepared from a pure stearic acid according to the method described in the literature[13].

1-Bromo-8, 11-heptadecadiene.—Into a mixture of 14.0 g. of pure linoleic acid in 300 ml. of hot water and 2.9 g. of potassium hydroxide in 50 ml. of hot water was added 8.5 g. of silver nitrate in 25 ml. of hot water with stirring. The precipitated silver salt was collected on a filter, washed with water and acetone, and dried in a vacuum at room temperature. This material was powdered and then dried in a vacuum at room temperature over phosphorus pentoxide. 37.5 g. (96.6%) of silver linoleate was thus obtained. Into a suspension of 22.8 g. of silver linoleate in 150 ml. of carbon tetrachloride (dried over phosphorus pentoxide) was added dropwise 9.0 g. of dry bromine with stirring at room temperature. After the evolution of carbon dioxide had ceased, the silver bromide was removed by filtration, and the filtrate was washed with a saturated sodium hydrogen carbonate solution and then with water and dried over magnesium sulfate. The carbon tetrachloride was distilled off under reduced pressure. The residue was crude 1-bromo-8, 11-heptadecadiene (a yellowish brown viscous oil) which was pure enough for subsequent purposes. The yield was 9.6 g. (52.0%).

Found: C, 64.03; H, 9.04; Br, 25.00. Calcd. for $C_{17}H_{31}Br$: C, 64.74; H, 9.91; Br, 25.34%.

1-Bromo-8, 11, 14-heptadecatriene. — The silver linoleate (a quantitative yield) was prepared from pure linolenic acid by the method described above for the preparation of the silver linoleate. A yellowish-brown viscous oil of 1-bromo-8, 11, 14-heptadecatriene was prepared from 26.5 g. of silver linoleate and 9.0 g. of dry bromine by the method described above for the preparation of 1-bromo-8, 11-heptadecadiene.

Found: C, 64.40; H, 9.21; Br, 25.78. Calcd. for $C_{17}H_{29}Br$: C, 65.15; H, 9.33; Br, 25.50%.

Hydrolaccol (I), 3-(8', 11'-Heptadecadienyl)-catechol (II), 3-(8', 11', 14'-Heptadecatrienyl)-catechol (III), 3-Propargyl Catechol (IV), and 3-Phenyl Catechol (V). — Each of these compounds was prepared from 1 mol. each of sodium hydride and of *n*-butyl ether in a three-necked flask with a mechanical stirrer, a dropping funnel, and a reflux condenser carrying a soda-lime tube. One mole of ethyl (2, 5-diethoxytetrahydro)-furfuroyl-acetate was added dropwise to the stirred contents of the flask at room temperature for an hour, the corresponding alkyl bromide (iodobenzene was used for the preparation of IV) was added, and the reaction mixture was heated for 8 hr. After the reaction was over, the reaction mixture was acidified with acetic acid, and then *n*-butyl ether was removed by vacuum distillation. The residue was added to 100 ml. of 0.1 N hydrochloric acid and 200 ml. of dioxane and the mixture was allowed to stand at room temperature for a week; the solvent was then removed by vacuum distillation, and the residue was dissolved in ether. The ethereal solution was washed with saturated sodium hydrogen carbonate and with water and dried over magnesium sulfate. The ether was removed by distillation, and the residual oil was dissolved in ethanol and treated with the excess of an ethanolic solution of lead acetate trihydrate. The dense precipitate of lead salt was filtered off and washed with ether. The lead salt was suspended in ethanol and treated with hydrogen sulfide. The lead sulfide was removed by filtration, and the solvent was distilled off from the filtrate. The residual oil was distilled further.

The Reduction of II to Hydrolaccol. — 0.51 g. of II in ethanol was reduced through the use of W-6 Raney nickel[14] at room temperature for 10 hr. The product was then recrystallized from toluene; m. p., 63°C. The yield was 0.505 g. (87% yield).

12) T. Omura, *J. Biochem.*, 50, 246 (1961).
13) J. W. H. Oldham, *J. Chem. Soc.*, 1950, 100.
14) *Organic Syntheses*, 29, 24 (1949).

Compound	Molecular formula	M. p. or b. p.	Yield %	Calcd., %		Found, %	
				C	H	C	H
I	$C_{23}H_{40}O_2$	m. p. 62～63°C	26.4	79.25	11.57	79.28	11.37
II	$C_{23}H_{36}O_2$	212～221°C/0.03 mmHg	15.9	80.18	10.53	80.48	10.64
III	$C_{23}H_{34}O_2$	209～217°C/0.022 mmHg	19.9	80.65	10.01	79.89	9.82
IV	$C_9H_8O_2$	130～136°C/5 mmHg	11.8	72.96	5.44	73.22	5.91
V	$C_{12}H_{10}O_2$	m. p. 57～59°C	7.82	77.40	5.41	77.38	5.40

This product was identified by mixed melting point determination and comparison with the infrared spectra of a sample which had been prepared from ethyl (2,5-diethoxytetrahydro)-furfuroylacetate and heptadecyl bromide.

Laccase. — Crude laccase was isolated from the latex of the Japanese lac tree (*Rhus vernicifera*) according to the method described in the literature[12].

The Action of Laccase. — Into each synthetic 3-alkylcatechol was added a small amount of crude laccase with stirring, the mixture was then spread over a watch glass as thinly as possible at room temperature. A hard thin film adhered to the watch glass when solidification had been completed. The times required for this solidification were then compared.

The Institute of Scientific and Industrial Research
Osaka University
Sakai-shi, Osaka

The Synthesis of Four Optical Isomers of β-Hydroxyaspartic Acid

By Takeo KANEKO and Hakuji KATSURA

(Received January 16, 1963)

In 1904 Skraup[1] suggested that he had found β-hydroxyaspartic acid in the hydrolyzate of casein, but in 1921 Dakin[2] reported that he found none of this amino acid in the hydrolyzate of casein, as compared with the *threo-* and *erythro*-β-hydroxy-DL-aspartic acid synthesized by him. Recently, *erythro*-β-hydroxy-L-aspartic acid ($[\alpha]_D+51°$)[3] has been obtained by the action of a transaminase on dihydroxyfumaric acid and L-glutamic acid. β-Hydroxyaspartic acid has been found in a culture solution of a certain sort of Azotobactor[4], and in a hydrolyzate of Phallicidine[5], a toxic substance isolated from *Amanita phalloides*. Some methods of synthesizing β-hydroxyaspartic acid[6] were reported a few years ago, but the absolute configurations of the optical isomers of this amino acid have never been determined. The present paper deals with the chemical determination of the absolute configurations of these optical isomers by the establishment of the configurational correlation between these isomers and glyceric acid.

Dakin[2] reported that *erythro-* and *threo*-β-hydroxy-DL-aspartic acids (DL-VI and II) were prepared by the ammonolysis of *erythro*-β-chloro-DL-malic acid (DL-IV)*. To determine the stereochemical behavior of this reaction, *cis*-[7] and DL-*trans*-epoxysuccinic acid[8] (I and DL-V) were treated with aqueous ammonia to obtain *threo-* and *erythro*-β-hydroxy-DL-aspartic acids (DL-II and VI) respectively[9]. From D_S-(−)-*trans*-epoxysuccinic acid (D-V)[8] and (−)-*erythro*-β-chloro-D_S-malic acid (D-IV)[8], which were derived from D_S-tartaric acid (III), the same *erythro*-β-hydroxy-L_S-aspartic acid ($[\alpha]_D$ +53°) (L-VI) was obtained. This acid was identical with that given by the enzymatic

1) Zd. H. Skraup, *Ber.*, **37**, 1596 (1904); *Z. physiol. Chem.*, **42**, 274 (1904); *Monatsh.*, **25**, 633 (1904).

2) H. D. Dakin, *J. Biol. Chem.*, **48**, 273 (1921); ibid., **50**, 410 (1922); cf. also E. Erlenmeyer, *Ann.*, **337**, 218 (1904); W. Lossen, *Ann.*, **348**, 306 (1906).

3) a) H. J. Sallach, *Federation Proc.*, **15**, 344 (1956); b) H. J. Sallach and T. H. Peterson, *J. Biol. Chem.*, **223**, 629 (1956); c) H. J. Sallach, ibid., **229**, 437 (1957); d) H. J. Sallach and M. L. Kornguth, *Biochim. Biophys. Acta*, **34**, 582 (1959).

4) N. F. Saris and A. I. Virtanen, *Acta Chem. Scand.*, **11**, 1440 (1957).

5) Th. Wieland, *Helv. Chim. Acta*, **44**, 919 (1961).

6) a) D. E. Metzler, J. B. Longenecker and E. E. Snell, *J. Am. Chem. Soc.*, **76**, 639 (1954); b) M. L. Kornguth and H. J. Sallach, *Arch. Biochem. Biophys.*, **91**, 39 (1960); c) C. S. Franklin, *J. Chem. Soc.*, **1960**, 4709.

* This acid has been named "Chloromalic acid I" by Kuhn[8].

7) E. Weitz, H. Schobbert and H. Seibert, *Ber.*, **68**, 1163 (1935); O. Gawron, A. J. Glaid III, A. Lomont and S. Gray, *J. Am. Chem. Soc.*, **80**, 5856 (1958).

8) R. Kuhn and F. Ebel, *Ber.*, **58**, 919 (1925); R. Kuhn and R. Zell, ibid., **59**, 2514 (1926).

9) Cf. Y. Liwschitz, Y. Rabinsohn and A. Haber, *J. Chem. Soc.*, **1962**, 3589.

method[3]. These results show that epoxy acid (V) is the intermediate in the ammonolysis of chloromalic acid (IV) to amino acid (VI).

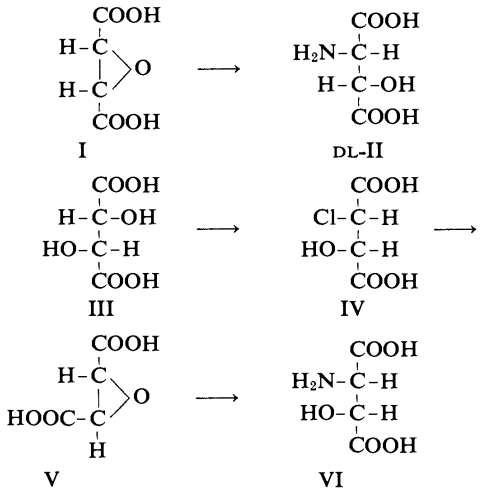

threo-β-Hydroxy-D$_S$-aspartic acid ($[\alpha]_D - 1.2°$) (D-II) was obtained from the oxazolidone derivative (X)[10] of 4, 6-benzylidene-D$_g$-glucosaminic acid hydrochloride (VIII)[11], which was readily derived from D$_g$-glucosamine hydrochloride (VII), by hydrolysis of the benzylidene group and oxidation with periodic acid followed by bromine, and then by the hydrolysis of the oxazolidone ring. From ethyl 4, 6-benzylidene - 2-benzyloxycarbonylamido - 2 - deoxy-D$_g$-gluconate (XI)[11,12], which was derived from VIII, the *threo*-D$_S$-amino acid was also obtained by cyclization to the oxazolidone derivative followed by the oxidation and hydrolysis described above.

TABLE I. THE PHYSICAL AND PHYSIOLOGICAL NATURES OF β-HYDROXYASPARTIC ACID

Configuration	Taste (salty)	Specific rotation $[\alpha]_D$ in N-HCl	Specific rotation $[\alpha]_D$ in water
L-Erythro	Weak	+53.0°	+41.4°
D-Erythro	Very slightly	−49.2°	—
L-Threo	Slightly	+ 1.3°	− 8.9°
D-Threo	Tasteless	− 1.2°	+ 8.9°

threo-β-Hydroxy-L$_S$- and *erythro*-β-hydroxy-D$_S$-aspartic acids (L-II and D-VI) were obtained from *erythro*-β-hydroxy-L$_S$- and *threo*-β-hydroxy-D$_S$-aspartic acids (L-VI and D-II) via their

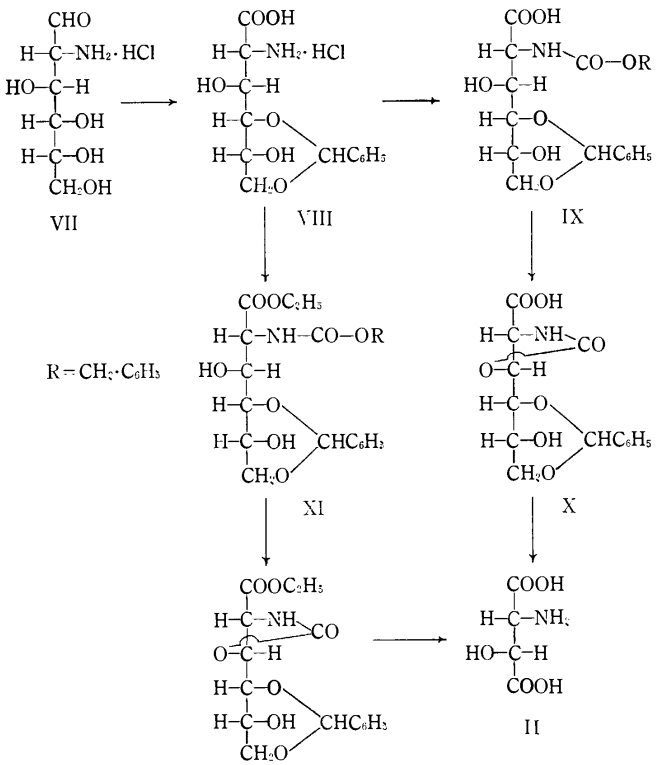

10) T. Kaneko and T. Inui, *J. Chem. Soc. Japan, Pure Chem. Sec.* (*Nippon Kagaku Zasshi*), **82**, 1075 (1961).
11) D. B. Hope and P. W. Kent, *J. Chem. Soc.*, **1962**, 3589.
12) P. A. Levene and F. B. LaForge, *J. Biol. Chem.*, **21**, 345 (1915).

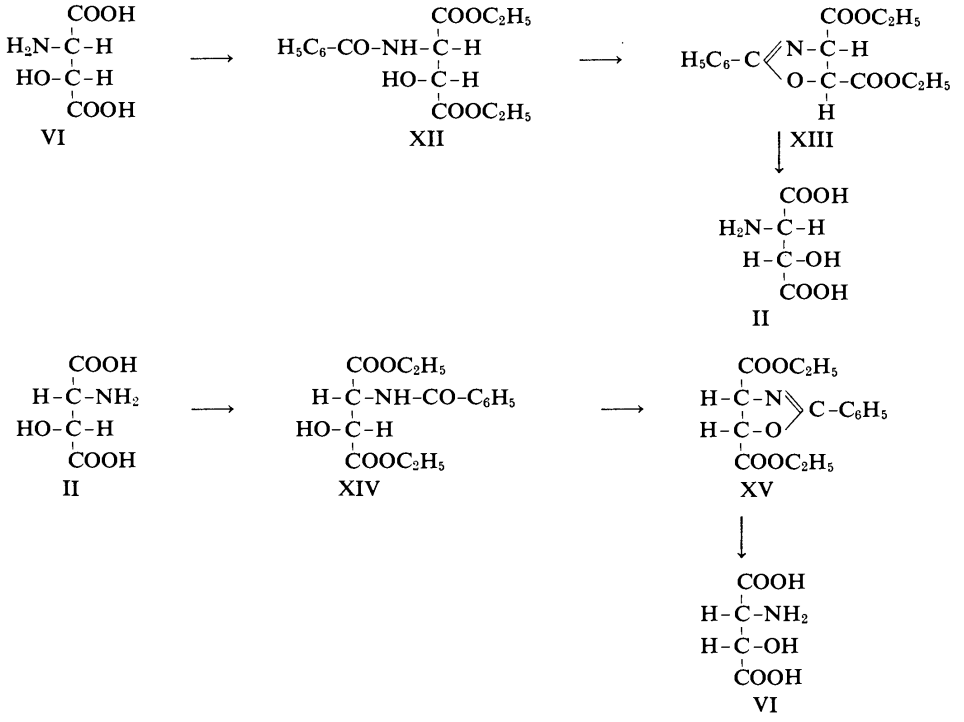

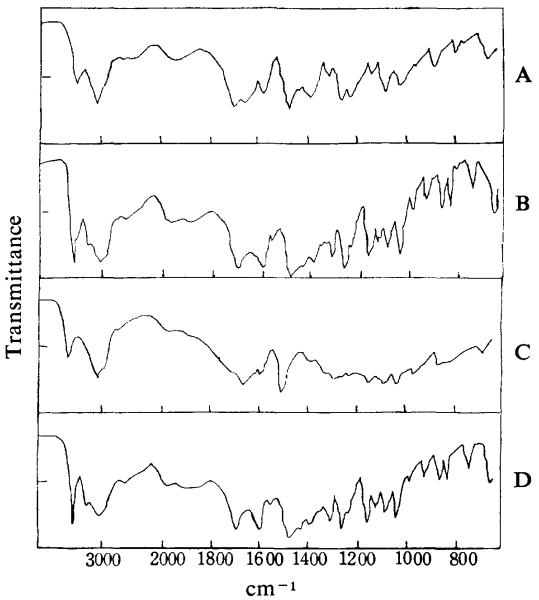

Fig. 1. Infrared spectra of (A) *threo*-β-hydroxy-DL-aspartic acid, (B) *erythro*-β-hydroxy-DL-aspartic acid, (C) *threo*-β-hydroxy-D- and L-aspartic acid and (D) *erythro*-β-hydroxy-D- and L-aspartic acid (in KBr disks).

oxazoline derivatives, XII and XV, respectively[13].

13) D. F. Elliott, *J. Chem. Soc.*, **1949**, 589; ibid., **1950**, 62; K. Pfister 3rd., C. A. Robinson, A. C. Shabica and M. Tishler, *J. Am. Chem. Soc.*, **71**, 1101 (1949).

The physical and physiological natures of optically-active β-hydroxyaspartic acids are summarized in Table I. In this table, it is shown that Lutz-Jirgensons' displacement rule[14] is applicable to these isomers.

The optically active and inactive isomers of β-hydroxyaspartic acid can not be identified by paper chromatography in various solvent systems. The infrared spectra of the isomers prepared in this paper are shown in Fig. 1.

Experimental

***threo*-β-Hydroxy-DL-aspartic Acid (DL-II) from *cis*-Epoxysuccinic Acid (I).**—A solution of 7.0 g. of I[7] in 70 ml. concentrated aqueous ammonia was heated in a sealed tube at 130°C for 18 hr. Crude DL-II was separated from the reaction mixture by concentration and then acidification with acetic acid, and recrystallization from water gave pure amino acid; yield, 8.6 g., 75%.

Found: C, 32.17; H, 4.76; N, 9.66. Calcd. for $C_4H_7O_5N$: C, 32.22; H, 4.73; N, 9.40%.

***erythro*-β-Hydroxy-DL-aspartic acid (DL-VI) from DL-*trans*-Epoxysuccinic Acid (DL-V).**—From 8 g. of DL-V[8], DL-VI was obtained in a similar manner; yield, 5.0 g., 55%.

Found: C, 32.11; H, 4.88; N, 9.03%.

***erythro*-β-Hydroxy-L-aspartic Acid (L-VI).**—*From D-(−)-trans-Epoxysuccinic Acid (D-V).*—From 6.0 g. of D-V[8], L-VI was obtained in a similar manner; yield, 4.9 g., 72%: $[\alpha]_D^{21}$ +53.2° (*c* 2.46,

14) O. Lutz and B. Jirgensons, *Ber.*, **63**, 448 (1930); ibid., **64**, 1221 (1931); ibid., **65**, 784 (1932).

1 N HCl); Found: C, 32.26; H, 4.83; N, 9.46%.

From erythro-β-Chloro-D$_S$-malic Acid (D-IV).—D-Chloromalic acid (D-IV)* was derived from dimethyl *erythro*-β-chloro-D$_S$-malate[15] by hydrolysis with 2.5N hydrochloric acid. A mixture of 10 g. of this acid and aqueous ammonia was heated in a sealed tube for 20 hr. and then concentrated in vacuo. The aqueous solution of this concentrate was treated through a Dowex 2 (OH-form) column and eluted with 2 N acetic acid. Crude L-VI was separated from the concentrate of this eluate and was then recrystallized from water to obtain the pure substance; yield, 5.5 g., 62%: $[\alpha]_D^{21}+53.0°$ (*c* 2.66, 1 N HCl); $[\alpha]_D^{21}+41.4°$ (*c* 2.43, water). Found: C, 32.23; H, 4.73; N, 9.17%. No pure *threo*-amino acid was separated by fractional crystallization from water or by partition chromatography through a Dowex 1 column by elution with 0.03 N formic acid[6b].

4, 6-Benzylidene-2-benzyloxycarbonylamido-2-deoxy-D$_g$-gluconic Acid (IX).—From 3.7 g. of VIII[11], IX was prepared in the usual manner; m. p., 167°C, $[\alpha]_D^{14}-51.0°$ (*c* 3.39, 99% ethanol); yield, 3.4 g., 83%. For analysis, pure substance obtained by recrystallization from ethyl acetate and petroleum ether and dried at 110°C for 22 hr. was used.

Found: C, 60.59; H, 5.52; N, 3.31. Calcd. for $C_{21}H_{23}O_8N$: C, 60.42; H, 5.52; N, 3.36%.

The Oxazolidone Derivative (X) of VIII.—*From IX.*—A mixture of 2.6 g. of IX and 1 g. of sodium hydroxide in 150 ml. of water was stirred continuously below 5°C for 6 hr. After the reaction mixture had been extracted with ether and the aqueous layer acidified with hydrochloric acid, the solution was extracted with ethyl acetate. Crude X (1.2 g., 62%) was separated by concentration of this extract and then recrystallized from ethyl acetate and petroleum ether to obtain the pure substance; m. p. 152°C, $[\alpha]_D^{14}-102.9°$ (*c* 3.15, methanol).

Found: C, 54.25; H, 4.92; N, 4.54. Calcd. for $C_{14}H_{15}O_7N$: C, 54.37; H, 4.89; N, 4.53%.

From VIII.—After a mixture of 25 g. of VIII, 25.5 g. of benzyloxycarbonyl chloride and 25 g. of sodium hydrogen carbonate in 400 ml. of water had been stirred at room temperature for 1 hr., a solution of 5 g. of sodium hydroxide in 20 ml. of water was added to this solution at 5°C and two solutions were stirred continuously together for 6 hr. Crude X (16.4 g., 78%) was obtained from the reaction mixture in a method similar to that described above.

***threo*-β-Hydroxy-D$_s$-aspartic Acid (D-II).**—*From X.*—A mixture of 3.0 g. of X and 30 ml. of 10% aqueous acetic acid was warmed in a boiling water bath for 1 hr.[16], and, on cooling, the reaction mixture was extracted with ether to remove the benzaldehyde. The aqueous layer was evaporated to dryness in vacuo, and the residue was dissolved in water. This solution was treated with 7 g. of a periodic acid dihydrate in 50 ml. of water and allowed to stand overnight at room temperature. The mixture was neutralized with 2 N sodium hydroxide, again set aside overnight, acidified to pH 4 by the addition of hydrochloric acid, and then treated with an aqueous barium chloride solution until no more salts were precipitated. A solution of 10 ml. of bromine in 90 ml. of a 2 N aqueous sodium hydroxide solution was added to the filtered solution. After standing overnight, the reaction mixture was acidified with hydrochloric acid and evaporated to dryness in vacuo. The residue was extracted with 99% ethanol, and the alcoholic extract was concentrated in vacuo. The residual oil was refluxed with 60 ml. of 6 N hydrochloric acid for 6 hr., and the solution was concentrated to dryness in vacuo. When the aqueous solution of the residual oil was treated with a Dowex 2 X8 (OH-form) column, elution with 2 N aqueous acetic acid and subsequent evaporation in vacuo gave crude D-II, yield, 1.1 g., 76%.

From XI.—An ethanolic solution (90 ml.) of 7 g. of XI[11,12] was added dropwise to a solution of 8 g. of sodium hydroxide in 100 ml. of 50% aqueous ethanol in an ice bath, and the mixture was stirred continuously for 7 hr. The reaction mixture was acidified with hydrochloric acid and concentrated to dryness in vacuo, and the residue was extracted with 99% ethanol. The extracts were concentrated in vacuo to a glassy solid (about 5 g.), and this solid was treated with 10% acetic acid, oxidized first with periodic acid, and then with bromine, and then hydrolyzed with hydrochloric acid. The product was isolated by the aid of a Dowex 2 column in the manner described above. The crude D-II weighed 1.5 g. (64%). Recrystallization from water gave the pure substance; $[\alpha]_D^{24}-1.2°$ (*c* 5.16, 1 N HCl), $[\alpha]_D^{28}+8.9°$ (*c* 0.91, water).

Found; C, 31.91; H, 4.71; N, 9.17. Calcd. for $C_4H_7O_5N$; C, 32.22; H, 4.73; N, 9.40%.

Diethyl *erythro*-β-Hydroxy-DL-aspartate Hydrochloride.—A suspension of 4.0 g. of DL-VI in 80 ml. of absolute ethanol was saturated with dry hydrogen chloride, and 125 ml. of dry ether was added. The crude crystals which separated were purified by recrystallization from absolute ethanol; yield, 3.3 g., 51%; m. p., 157~157.5°C (lit.[17]; m. p., 154~156°C).

Found; C, 39.54; H, 6.77; N, 5.52; Cl, 15.14. Calcd. for $C_8H_{16}O_5NCl$; C, 39.76; H, 6.67; N, 5.58; Cl, 14.70%.

Diethyl *N*-Benzoyl-*erythro*-β-hydroxy-DL-aspartate (DL-XII).—From 3.3 g. of the avove-mentioned ester hydrochloride, DL-XII was prepared in the usual manner and recrystallized from benzene and petroleum ether; yield, 3.0 g., 71%; m. p., 84°C.

Found; C, 58.29; H, 6.12; N, 4.46. Calcd. for $C_{15}H_{19}O_6N$: C, 58.24; H, 6.19; N, 4.53%.

Diethyl *N*-Benzoyl-*erythro*-β-hydroxy-L$_s$-aspartate (L-XII).—After 4.1 g. of L-VI had been esterified with absolute ethanol and dry hydrogen chloride, L-XII was obtained from the oily ester in the usual manner and recrystallized from benzene; yield, 5.4 g., 64%; m. p., 99~100°C; $[\alpha]_D^{16}+27.9°$ (*c* 4.52, 99% ethanol). Found: C, 58.52; H, 6.16; N, 4.45%.

Diethyl *N*-Benzoyl-*threo*-β-hydroxy-DL-aspartate (DL-XIV).—From 7.1 g. of DL-II, DL-XIV was

* M. p., 159°C, $[\alpha]_D^{21}$ −28.3° (*c* 3.19, ethyl acetate): literature[8]; m. p., 165~166°C, $[\alpha]_D$ −31°.

15) T. Kaneko and H. Katsura, *Chem. & Ind.*, **1960**, 1188; H. Katsura, *J. Chem. Soc. Japan, Pure Chem. Sec.* (*Nippon Kagaku Zasshi*), **82**, 98 (1961).

16) Cf. L. V. Vargha, *Ber.*, **68**, 18 (1935).

obtained in a similar manner and was recrystallized from benzene and petroleum ether; yield, 8.3 g., 56%; m. p., 101~102°C. Found: C, 58.55; H, 6.29; N, 4.40%.

Diethyl *N*-Benzoyl-*threo*-β-hydroxy-D$_8$-aspartate (D-XIV).—From 4.8 g. of D-II, D-XIV was obtained in a similar manner and was recrystallized from benzene; yield, 6.6 g., 62%; m. p., 121°C; $[\alpha]_D^{25}$ −21.2° (*c* 3.54, 94% ethanol). Found: C, 58.43; H, 6.17; N, 4.55%.

***threo*-β-Hydroxy-DL-aspartic Acid** (DL-II).—An oily oxazoline derivative[13] (DL-XIII) was obtained from 3.0 g. of DL-XII by the aid of 20 ml. of thionyl chloride. The crude oily DL-XIII was hydrolyzed by refluxing it with 6 N hydrochloric acid for 7 hr. The pure DL-II was obtained by a concentration of the hydrolyzate, followed by recrystallization from water; yield, 0.7 g., 48%. Found: C, 32.05; H, 4.79; N, 9.00. Calcd. for $C_4H_7O_5N$: C, 32.22; H, 4.73; N, 9.40%.

***threo*-β-Hydroxy-L$_8$-aspartic Acid** (L-II).—From 9.0 g. of L-XIII, L-II was obtained in a similar manner via a crude oily oxazoline derivative (L-XIII) and purified by passing it through a Dowex 2 column, followed by recrystallization from water; yield, 3.6 g., 83%: $[\alpha]_D^{27}$ +1.3° (*c* 3.12, 1 N HCl); $[\alpha]_D^{27}$ −8.5° (*c* 1.76, water). Found: C, 32.33; H, 4.87; N, 9.43%.

***erythro*-β-Hydroxy-DL-aspartic Acid** (DL-VI).—A crystalline oxazoline derivative (DL-XV) was obtained from 3.0 g. of DL-XIV by the action of 20 ml. of thionyl chloride; it was purified by the same methods as have been described by Hauptmann[17]; m. p., 99°C (lit.; m. p., 97.5~99°C). Found: C, 62.00; H, 5.97; N, 4.48. Calcd. for $C_{15}H_{17}O_5N$: C, 61.84; H, 5.88; N, 4.81%.

From a crude DL-XV derived from 8.3 g. of DL-XIV, DL-VI was obtained in a similar manner and was recrystallized from water; yield, 1.9 g., 39%. Found: C, 32.26; H, 4.84; N, 9.63. Calcd. for $C_4H_7O_5N$: C, 32.22; H, 4.73; N, 9.40%.

***erythro*-β-Hydroxy-D$_8$-aspartic Acid** (D-VI).—From 6.4 g. of D-XIV, D-VI was obtained in a similar manner via an oily oxazoline derivative (D-XV) and was recrystallized from water; yield 0.7 g., 23%: $[\alpha]_D^{27}$ −49.2° (*c* 1.85, 1 N HCl). Found: C, 32.25; H, 4.70; N, 9.45%.

Department of Chemistry
Faculty of Science
Osaka University
Nakanoshima, Osaka

17) H. Hauptmann and H. Berl, *J. Am. Chem. Soc.*, **77**. 7 04 (1955).

An Attempt to Convert Glycine Residues to Threonine Residues in Polyglycine

By Toshiyuki FURUYAMA*, Fumio SAKIYAMA and Kozo NARITA

(Received January 24, 1963)

Some attempts have already been made to introduce side chains into the glycine residues of synthetic or naturally-occurring polypeptides[1,2].

Regarding the "fore-protein" formation, for example, Akabori postulated that polyglycine was produced according to the polymerization of aminoacetonitril and that then various side chains were introduced into the glycine residues of polyglycine, thus leading to the fore-protein[3]. In order to prove his hypothesis, Akabori et al. tried to introduce side chains into polyglycine which had been dispersed on the kaolinite surface by means of aldehydes in the presence of some basic catalysts. It was thus shown that small amounts of serine and threonine were formed from the glycine residues in the polymer by reactions with aqueous formaldehyde and acetaldehyde respectively[2].

The present authors have attempted the conversion of the glycine residues in polyglycine to threonine residues by means of acetaldehyde in a non-aqueous medium. Although they were unsuccessful in obtaining polythreonine from polyglycine in the present study, appreciable amounts of threonine could be isolated from the hydrolyzates of the reaction product of polyglycine with acetaldehyde in liquid ammonia. The spatial configuration of the threonine thus formed was also examined by the aid of infrared absorption spectroscopy.

Experimental

Polyglycine. — Polyglycine was prepared by Leuchs' *N*-carboxylic anhydride method[4]. The

* Present address: Technical Research Laboratory, Asahi Chemical Industry Co., Ltd., Itabashi-ku, Tokyo.

1) T. Wieland and K. Dose, *Angew. Chem.*, **66**, 781 (1954).

2) S. Akabori, K. Okawa and M. Sato, This Bulletin, **29**, 608 (1956).

3) S. Akabori, *Science* (*Kagaku*), **25**, 54 (1955).

4) Y. Go and H. Tani, This Bulletin, **14**, 510 (1939).

average degree of polymerization of the polymer was estimated to be 93~97 by titrating the terminal carboxyl groups[5] with sodium methoxide in dimethylformamide.

The Condensation of Acetaldehyde with Polyglycine and Acid Hydrolysis.—Five hundred milligrams of polyglycine, together with a piece of ferric nitrate crystal, were dispersed in 100 ml. of liquid ammonia in a dry ice-acetone bath. Then, 400 mg. of metallic sodium were added, the mixture was stirred for 80 min., and 50 ml. of freshly distilled acetaldehyde were added dropwise into the above reaction mixture. This was stirred for two hours under cooling and then left overnight at room temperature. During this period, the liquid ammonia evaporated. The residual brown oily substance was dried over concentrated sulfuric acid under reduced pressure. The residue was then hydrolyzed with 6 N hydrochloric acid for 15 hr. at 110°C. The hydrolyzate of the modified polyglycine was evaporated to dryness on a steam bath.

The Isolation of Threonine from the Acid Hydrolyzate of the Modified Polyglycine.—The isolation of threonine was carried out utilizing the O→N acetyl shift reaction[6]. The above-dried hydrolyzate was dissolved in 40 ml. of glacial acetic acid, and dry hydrogen chloride gas was saturated to convert threonine into its *O*-acetyl derivative. The O→N acetyl shift reaction of *O*-acetyl threonine was performed at pH 8 in a pH-stat (Radiometer Co., Demmark) for 4 hr. at 31°C. The reaction mixture was treated with ion exchange resin as in the procedures of Fujiwara et al.[6] One hundred and nine milligrams of crude *N*-acetyl threonine were thus obtained. It was hydrolyzed with 6 N hydrochloric acid. The dried hydrolyzate was dissolved in 5 ml. of methanol, and 0.1 ml. of triethylamine was added; 5.3 mg. of the crystals (m. p., 208~209°C with decomp.) were obtained. The results of paper electrophoresis (500 V., 0.2 mamp./cm., in 1 N acetic acid, pH 2.5) and infrared absorption spectra showed that the material was threonine.

Glycine was recovered from the adsorbed fraction on the resin column, which was used after the O→N acetyl shift reaction for the separation of *N*-acetyl threonine from glycine, by eluting it with 2 N ammonium hydroxide. It was recrystallized from water-ethanol, 410 mg. (m. p., 237°C with decomp. Found: C, 32.08; H, 6.54; N, 18.42. Calcd. for $C_2H_5NO_2$: C, 32.00; H, 6.71; N, 18.66%).

Results and Discussion

As for the formation of the threonine residue from glycine residue in polyglycine, an aldol-type condensation is expected to occur under certain conditions which activate the methylene group in the glycine residue. Akabori et al.[7] found that the formation of a glycine copper chelate complex brought on the activation of the methylene group, and they succeeded in synthesizing threonine by an aldol-type condensation of acetaldehyde. Moreover, they attempted to introduce some side-chain groups into polyglycine which had been dispersed on a clay, kaolinite, and suspended in aqueous alkaline media with formaldehyde or acetaldehyde[2]. In these experiments 0.4~3.1%*1 of glycine residues were shown to be converted to serine and 1.4~1.5%, to threonine residues, but polyglycine which had not been dispersed on kaolinite was not affected under similar conditions.

In the present investigation, it was shown that 7~9%*2 of the glycine residues converted to threonine residues. The analyses were made by means of paper chromatography of their 2,4-dinitrophenyl derivatives after hydrolysis of the modified polymers. Therefore, it seems that the use of liquid ammonia in place of water as a reaction medium is more favorable for this aldol-type condensation reaction[8].

The condensation reaction seemed to occur not only at the *N*- and *C*-terminal glycyl residues in polyglycine but also at the non-terminal residues, since one terminal residue was calculated as being approximately 1% on the basis of the measurement of the average degree of polymerization.

The chromatogram of the 2,4-dinitrophenyl derivatives of the hydrolyzates of the modified polyglycine showed four spots, 2,4-dinitrophenyl (DNP) glycine, DNP-threonine, 2,4-dinitrophenol and one unknown spot which located at the position between threonine and dinitrophenol on a two-dimensional paper chromatogram (*n*-butanol saturated with aqueous ammonia, a 1.5 M phosphate buffer (pH 6)). However, the only amino acids obtained after the isolation procedure are glycine and threonine. Therefore, the amount of an unknown spot on the chromatogram may be insignificant.

It is of interest to examine the spatial configuration of threonine thus obtained from the modified polyglycine. As has already been described, Akabori et al. identified serine and threonine chromatographically from the hydrolyzates of the formaldehyde- and acetaldehyde-treated polyglycine, but they did not isolate the hydroxy amino acids thus formed. In the present studies, liquid ammonia was used as a

5) M. Sela and A. Berger, *J. Am. Chem. Soc.*, **77**, 1893 (1955).
6) S. Fujiwara, S. Morinaga and K. Narita, This Bulletin, **35**, 438 (1962).
7) M. Sato, K. Okawa and S. Akabori, ibid., **30**, 937 (1957).

*1 Molar per cent.
*2 The isolated threonine amounted approximately to only one per cent. This small value probably results from the fairly complex recovering procedure.
8) K. Shimo and R. Asami, *Hisui-Kenkyusho Hokoku (Tohoku University)*, 4, 67 (1954); ibid., 4, 75 (1954). In these papers, Shimo et al. attempted the introduction of side chains into the glycine residues in 2,5-diketopiperazine (glycine anhydride) in liquid ammonia with alkyl halides and they obtained the *N*-substituted compounds.

reaction medium and the threonine formed was isolated by the use of the O→N acetyl shift reaction[6].

The threonine isolated from the modified polyglycine was examined by infrared absorption spectroscopy. The absorption spectra showed the threonine sample to contain appreciable amounts of allothreonine[9]. Estimation of the amount of contaminated allothreonine was made by the use of characteristic bands at 702 and 619 cm^{-1} [10]. The values of 64.4% for threonine and 35.6% for allothreonine were obtained.

9) K. Kodera, Y. Sato and T. Takahashi, *Yakugaku-Kenkyu*, **30**, 38 (1958).
10) T. Furuyama and S. Senoh, This Bulletin, **36**, 126 (1963).

Summary

When polyglycine was reacted with acetaldehyde in liquid ammonia in the presence of metallic sodium, it was observed that 7~9% of the threonine residues were formed from glycine residues. From the hydrolyzate of the modified polyglycine, threonine could be isolated by the aid of the O→N acetyl shift reaction. It was shown that the threonine thus isolated was 35.6% allothreonine.

Institute for Protein Research
Osaka University
Kita-ku, Osaka

Consideration on the Q-e Scheme. III. Q-e Factors in Ionic Polymerization

By Nariyoshi KAWABATA, Teiji TSURUTA and Junji FURUKAWA

(Received February 7, 1963)

The reactivity of vinyl compounds in radical copolymerization has been generalized by the *Q-e* scheme proposed by Alfrey and Price[1]. According to the scheme, the rate constant of propagation step, k_p, is expressed by the following equation:

$$k_p = P_R Q_M \exp(-e_R e_M) \quad (1)$$

where P is the reactivity associated with polymer radical, Q is the general reactivity term characteristic of the monomer and e is the polarity term characteristic of the radical and the monomer. In part I of this series[2], a revised pattern of the scheme by assuming the e-value of styrene to be equal to zero was described and a notation e_{RM} was proposed instead of $e_R e_M$ for the polarity term. In part II of this series[3], we tried to give some theoretical background to the scheme. We tried to divide the conjugation-stabilization energy between monomer and attacking radical[4], E_{RM}, into four terms by the following equation:

$$E_{RM} = E_{RoMo} + E_R + E_M + E'_{RM} \quad (2)$$

where E_{RoMo} is the stabilization energy between polyethylene radical and ethylene monomer, E_R and E_M are the increments in the stabilization energy introduced by the substituent of radical and by that of monomer, respectively, E_{RoMo} as standard. E'_{RM} is the surplus increment in the stabilization energy introduced by the substituents of the radical and the monomer. We proposed the relations 3 to 5 for P-, Q- and e-terms.

$$P_R \propto \exp(E_R/RT) \quad (3)$$

$$\ln Q_1 - \ln Q_2 = (E_{M_1} - E_{M_2})/RT \quad (4)$$

$$e_{RM} = -E'_{RM}/RT \quad (5)$$

For ionic copolymerization, however, no such generalization has been established, although several attempts have been made[5]. The most characteristic feature of ionic copolymerization has long been considered to be that the product of monomer reactivity ratios, $r_1 r_2$, is close to unity. Thus,

1) T. Alfrey, Jr., and C. C. Price, *J. Polymer Sci.*, **2**, 101 (1947); T. Alfrey, Jr., J. J. Bohrer and H. Mark, "Copolymerization", Interscience Publishers, New York (1952).
2) N. Kawabata, T. Tsuruta and J. Furukawa, *Makromol. Chem.*, **51**, 70 (1962).
3) N. Kawabata, T. Tsuruta and J. Furukawa, ibid., **51**, 80 (1962).
4) T. Yonezawa, K. Hayashi, C. Nagata, S. Okamura and K. Fukui, *J. Polymer Sci.*, **14**, 312 (1954); K. Hayashi, T. Yonezawa, C. Nagata, S. Okamura and K. Fukui, ibid., **20**, 537 (1956); G. S. Levinson, ibid., **60**, 43 (1962).
5) a) C. G. Overberger, L. H. Arond, D. Tanner, J. J. Taylor and T. Alfrey, Jr., *J. Am. Chem. Soc.*, **74**, 4848 (1952); b) Y. Landler, *J. Polymer Sci.*, **8**, 63 (1952); G. E. Ham, ibid., **14**, 483 (1954).

TABLE I. CONJUGATION-STABILIZATION ENERGY BETWEEN

Monomer	Styrene	Butadiene	Ethylene	Acrylo-nitrile	Methacrylo-nitrile	Vinylidene cyanide	Methyl vinyl ketone
Styrene	0.860	0.842	1.064	1.165	1.046	1.228	1.289
Butadiene	0.871	0.854	1.079	1.187	1.063	1.255	1.316
Ethylene	0.692	0.680	0.833	0.833	0.778	0.802	0.884
Acrylonitrile	0.688	0.678	0.804	0.836	0.772	0.830	0.893
Methacrylonitrile	0.735	0.722	0.874	0.912	0.838	0.907	0.980
Vinylidene cyanide	0.641	0.632	0.722	0.767	0.706	0.775	0.819
Methyl vinyl ketone	0.658	0.655	0.759	0.785	0.728	0.775	0.835
Methyl acrylate	0.692	0.681	0.815	0.837	0.776	0.823	0.893
Methyl methacrylate	0.743	0.729	0.889	0.917	0.846	0.904	0.983
Vinyl acetate	0.769	0.755	0.942	0.991	0.905	1.003	1.077
Vinyl chloride	0.778	0.765	0.952	0.986	0.907	0.907	1.066
Vinylidene chloride	0.798	0.783	0.993	1.053	0.958	1.064	1.145
α-Methylstyrene	0.916	0.896	1.148	1.266	1.131	1.348	1.409
p-Methylstyrene	0.870	0.854	1.079	1.189	1.064	1.264	1.317
p-Chlorostyrene	0.863	0.849	1.069	1.177	1.054	1.252	1.304
p-Methoxystyrene	0.973	0.952	1.230	1.680	1.361	4.401	2.174

TABLE II. CONJUGATION-STABILIZATION ENERGY BETWEEN

Monomer	Styrene	Butadiene	Ethylene	Acrylo-nitrile	Methacrylo-nitrile	Vinylidene cyanide	Methyl vinyl ketone
Styrene	0.859	0.843	1.064	0.666	0.682	0.552	0.652
Butadiene	0.871	0.854	1.079	0.672	0.688	0.556	0.657
Ethylene	0.692	0.680	0.833	0.571	0.581	0.487	0.562
Acrylonitrile	1.300	1.269	1.710	0.837	0.866	0.654	0.808
Methacrylonitrile	1.234	1.204	1.610	0.807	0.836	0.636	0.781
Vinylidene cyanide	1.866	1.817	2.534	1.042	1.091	0.776	0.996
Methyl vinyl ketone	1.372	1.339	1.816	0.864	0.895	0.670	0.833
Methyl acrylate	1.091	1.066	1.404	0.763	0.785	0.611	0.742
Methyl methacrylate	1.027	1.004	1.309	0.734	0.755	0.593	0.714
Vinyl acetate	0.718	0.705	0.867	0.588	0.599	0.493	0.577
Vinyl chloride	0.779	0.765	0.952	0.627	0.639	0.527	0.615
Vinylidene chloride	0.811	0.796	0.995	0.646	0.659	0.540	0.634
α-Methylstyrene	0.806	0.791	0.984	0.640	0.647	0.536	0.627
p-Methylstyrene	0.851	0.835	1.050	0.662	0.678	0.550	0.649
p-Chlorostyrene	0.862	0.848	1.067	0.667	0.683	0.553	0.671
p-Methoxystyrene	0.814	0.799	0.995	0.647	0.663	0.542	0.634

$$k_{11}/k_{12} \fallingdotseq k_{21}/k_{22} \quad (6)$$

Here, k_{AB} is the propagation rate constant for polymer ion A and monomer B. Landler[5b] and Pepper[6] interpreted the relation 6 in terms of the nearly equal reactivities of polymer ions, i. e.,

$$k_{11} \fallingdotseq k_{21} \quad (7)$$

and

$$k_{12} \fallingdotseq k_{22} \quad (8)$$

However, this assumption has been denied by some experimental results of Okamura et al.[7], who showed that the polymer cation derived from a less reactive monomer had the larger reactivity. The same conclusion was reached in anionic copolymerization by Kuntz and O'Driscoll[8]. The $r_1 r_2 \fallingdotseq 1$ relation was afforded by Okamura et al., who assumed that the rate constant of propagation reaction, k_p, was expressed as a product of the reactivity of ion R_I and that of monomer R_M, i. e.,

6) D. C. Pepper, *Quart. Revs.*, **8**, 88 (1954).

7) S. Okamura, N. Kanoh and T. Higashimura, *Makromol. Chem.*, **47**, 35 (1961).

8) K. F. O'Driscoll and I. Kuntz, *J. Polymer Sci.*, 61, 19 (1962).

MONOMER AND ATTACKING CATION, $E_{CM}(-(\Delta\beta)^2/\beta)$

Polymer cation								
Methyl acrylate	Methyl methacrylate	Vinyl acetate	Vinyl chloride	Vinyliden chloride	α-Methyl-styrene	p-Methyl-styrene	p-Chloro-styrene	p-Methoxy-styrene
1.178	1.050	0.885	0.991	0.927	0.807	0.852	0.860	0.781
1.200	1.067	0.896	1.005	0.940	0.816	0.862	0.867	0.789
0.855	0.793	0.716	0.781	0.734	0.661	0.687	0.690	0.646
0.848	0.777	0.708	0.763	0.724	0.652	0.684	0.687	0.669
0.927	0.846	0.761	0.824	0.779	0.696	0.732	0.734	0.702
0.772	0.705	0.657	0.695	0.667	0.606	0.639	0.642	0.653
0.796	0.733	0.677	0.724	0.690	0.625	0.656	0.658	0.649
0.853	0.784	0.713	0.771	0.731	0.658	0.688	0.691	0.680
0.935	0.856	0.765	0.836	0.788	0.704	0.737	0.741	0.701
1.009	0.916	0.793	0.858	0.810	0.727	0.762	0.760	0.703
1.009	0.917	0.805	0.890	0.835	0.738	0.773	0.777	0.719
1.071	0.967	0.835	0.928	0.870	0.764	0.803	0.807	0.743
1.282	1.136	0.944	1.064	0.992	0.858	0.906	0.912	0.821
1.200	1.067	0.895	1.004	0.939	0.816	0.861	0.867	0.788
1.188	1.057	0.888	0.995	0.931	0.810	0.854	0.860	0.784
1.576	1.300	0.993	1.139	1.061	0.897	0.962	0.968	0.854

MONOMER AND ATTACKING ANION, $E_{AM}(-(\Delta\beta)^2/\beta)$

Polymer anion								
Methyl acrylate	Methyl methacrylate	Vinyl acetate	Vinyl chloride	Vinylidene chloride	α-Methyl-styrene	p-Methyl-stylene	p-Chloro-styrene	p-Methoxy-styrene
0.718	0.750	0.992	0.991	0.927	0.919	0.870	0.857	0.911
0.726	0.757	1.006	1.015	0.940	0.931	0.881	0.867	0.923
0.608	0.627	0.776	0.781	0.735	0.724	0.698	0.690	0.719
0.953	1.016	1.615	1.579	1.466	1.467	1.327	1.293	1.472
0.916	0.972	1.522	1.487	1.393	1.388	1.260	1.206	1.386
1.228	1.338	2.449	2.326	2.149	2.218	1.920	1.853	2.245
0.990	1.059	1.718	1.675	1.554	1.558	1.391	1.364	1.565
0.854	0.899	1.306	1.302	1.213	1.190	1.108	1.085	1.199
0.813	0.855	1.221	1.214	1.132	1.117	1.042	1.022	1.113
0.624	0.646	0.809	0.811	0.748	0.755	0.724	0.715	0.748
0.672	0.695	0.884	0.889	0.835	0.821	0.787	0.777	0.815
0.694	0.720	0.924	0.929	0.871	0.856	0.819	0.808	0.850
0.685	0.712	0.921	0.917	0.858	0.859	0.814	0.803	0.850
0.713	0.744	0.979	0.978	0.916	0.907	0.860	0.848	0.900
0.720	0.751	0.995	0.994	0.940	0.921	0.872	0.858	0.914
0.692	0.720	0.930	0.928	0.869	0.866	0.822	0.810	0.857

$$k_p = R_I R_M \qquad (9)$$

Recently, Szwarc et al.[9,10] have found several anionic copolymerization systems in which the reactivity ratio products determined directly by the use of living polymers are less than unity. Thus, the widely held view that $r_1 r_2$ products for ionic copolymerizations are always nearly equal to unity seems to require some amendment. The authors herewith have tried to give an interpretation of these experimental facts by a logical extention of the Q-e scheme for radical polymerization investigated in previous papers[2,3] to the ionic case. P-, Q- and e-terms were therefore regarded as corresponding to the components of the conjugation-stabilization energy between monomer and attacking ion, much as in the case of radical copolymerization[3].

Method of Calculation

On the basis of Dewar's LCAO MO second-order perturbation method[11], the conjugation-stabilization energy between the attacking

9) C. L. Lee, J. Smid and M. Szwarc, *J. Am. Chem. Soc.*, **83**, 2961 (1961).
10) J. Smid and M. Szwarc, *J. Polymer. Sci.*, **61**, 31 (1962).
11) M. J. S. Dewar, *J. Am. Chem. Soc.*, **74**, 3341 (1952).

polymer ion and the monomer was calculated as the total π-electronic energy difference between the pair of interacting mesomeric systems and the addition product formed by their union. The energy parameters adopted here are those used in the preceding paper[3].

Results and Discussion

***P*-, *Q*- and *e*-Terms in Ionic Polymerization.** —As has been mentioned above, we assume that the activation energy, E_p, in ionic polymerization can be expressed by Eq. 10, as in radical polymerization;

$$E_p = C + \Delta E_\sigma + \Delta E_\pi \qquad (10)$$

where C is a constant, ΔE_σ is the activation energy arising from σ-electrons, and ΔE_π is that arising from π-electrons. We further assume that C and ΔE_σ in Eq. 10 are common throughout all the ion-monomer pairs. According to the view of Fukui et al.[12], ΔE_π is the stabilization energy between the monomer and the attacking polymer ion. Thus,

$$\Delta E_\pi = -E_{CM} \qquad (11)$$

or

$$\Delta E_\pi = -E_{AM} \qquad (12)$$

where E_{CM} is the stabilization energy between monomer and polymer cation and E_{AM} is that between monomer and polymer anion. The stabilization energies recalculated by us are given in Tables I and II*1.

It can be seen in Tables I and II that the relative reactivity of the monomer or the polymer ion is consistent with some experimental results except for the extraordinarily large stabilization energies of the systems of (*p*-methoxystyrene monomer—vinylidene cyanide, acrylonitrile and methyl vinyl ketone cations)*2.

We tried to divide the stabilization energies into four terms by the following equations in

TABLE III. E_M^+- AND E_C-VALUE

Vinyl compound	$E_M^+(-(\Delta\beta)^2/\beta)$	$E_C(-(\Delta\beta)^2/\beta)$
Styrene	0.231	−0.141
Butadiene	0.246	−0.153
Ethylene	0	0
Acrylonitrile	−0.029	0.000
Methacrylonitrile	0.041	−0.055
Vinylidene cyanide	−0.111	−0.031
Methyl vinyl ketone	−0.074	0.051
Methyl acrylate	−0.018	0.022
Methyl methacrylate	0.056	−0.040
Vinyl acetate	0.109	−0.116
Vinyl chloride	0.119	−0.052
Vinylidene chloride	0.160	−0.099
α-Methylstyrene	0.315	−0.172
p-Methylstyrene	0.246	−0.146
p-Chlorostyrene	0.326	−0.143
p-Methoxystyrene	0.397	−0.187
Isobutene	0.255	−0.119

TABLE IV. SURPLUS CONJUGATION-STABILIZATION ENERGY

Monomer	Styrene	Butadiene	Ethylene	Acrylo-nitrile	Methacrylo-nitrile	Vinylidene cyanide	Methyl vinyl ketone
Styrene	−0.063	−0.069	0	+0.101	+0.037	+0.195	+0.174
Butadiene	−0.067	−0.072	0	+0.108	+0.039	+0.207	+0.186
Ethylene	0	0	0	0	0	0	0
Acrylonitrile	+0.025	+0.027	0	+0.032	+0.023	+0.057	+0.038
Methacrylonitrile	+0.002	+0.001	0	+0.038	+0.019	+0.064	+0.055
Vinylidene cyanide	+0.060	+0.063	0	+0.045	+0.039	+0.064	+0.046
Methyl vinyl ketone	+0.040	+0.049	0	+0.026	+0.024	+0.047	+0.025
Methyl acrylate	+0.018	+0.019	0	+0.022	+0.016	+0.039	+0.027
Methyl methacrylate	−0.005	−0.007	0	+0.028	+0.012	+0.046	+0.040
Vinyl acetate	−0.032	−0.034	0	+0.049	+0.018	+0.092	+0.084
Vinyl chloride	−0.033	−0.034	0	+0.034	+0.010	+0.058	+0.063
Vinylidene chloride	−0.054	−0.057	0	+0.060	+0.035	+0.102	+0.101
α-Methylstyrene	−0.091	−0.099	0	+0.118	+0.231	+0.038	+0.210
p-Methylstyrene	−0.068	−0.072	0	+0.110	+0.040	+0.216	+0.187
p-Chlorostyrene	−0.065	−0.067	0	+0.108	+0.040	+0.214	+0.184
p-Methoxystyrene	−0.116	−0.120	0	+0.450	+0.186	+3.202	+0.944

12) T. Yonezawa, T. Higashimura, K. Katagiri, K. Hayashi, S. Okamura and K. Fukui, *J. Polymer Sci.*, 26, 311 (1957).

*1 The conjugation-stabilization energy in ionic copolymerization was calculated by Fukui and others[12]. Our recalculated values of the energy are considerably different from theirs because we used somewhat different values of parameters, the examination of which was described in the preceding paper[3].

*2 In theses, cases, Dewar's second-order perturbation method is inadequate because the energy difference between the lowest vacant level of the polymer cation and highest occupied level of the monomer is too small.

the manner which had been adopted in the preceding paper[3] for radical polymerizations:

$$E_{CM}=E_{CoMo}+E_C+E_M^+ +E'_{CM} \quad (13)$$

$$E_{AM}=E_{AoMo}+E_A+E_M^- +E'_{AM} \quad (14)$$

Here, E_{CoMo} is the stabilization energy between polyethylene cation and ethylene monomer, E_C and E_M^+ are the increments in the stabilization energies of the systems of (substituted polyethylene cation—ethylene monomer) and (polyethylene cation—substituted ethylene monomer) with respect to E_{CoMo} as standard. E'_{CM} is the surplus increment in the stabilization energy of the system of substituted polyethylene cation and substituted ethylene monomer. E_{AoMo}, E_A, E_M^- and E'_{AM} have the significance analogous to E_{CoMo}, E_C, E_M^+ and E'_{CM}, respectively. The values of E_C and E_M^+ are given in Table III; those of E'_{CM}, in Table IV; those of E_A and E_M^-, in Table V; and those of E'_{AM}, in Table VI.

For ionic polymerization, we propose the relations:

$$k_{CM}=P_C^+ Q_M^+ \exp(-e_{CM}^+) \quad (15)$$

$$k_{AM}=P_A^- Q_M^- \exp(-e_{AM}^-) \quad (16)$$

which are just the logical extentions of Eq. 1 to the ionic cases. The terms Q_M^+, P_C^+, e_{CM}^+, Q_M^-, P_A^- and e_{AM}^- will then be given by Eqs. 17 to 22, respectively:

$$\ln Q_{M_1}^+ - \ln Q_{M_2}^+ = (E_{M_1}^+ - E_{M_2}^+)/RT \quad (17)$$

$$P_C^+ \propto \exp(E_C/RT) \quad (18)$$

$$e_{CM}^+ = -E'_{CM}/RT \quad (19)$$

$$\ln Q_{M_1}^- - \ln Q_{M_2}^- = (E_{M_1}^- - E_{M_2}^-)/RT \quad (20)$$

$$P_A^- \propto \exp(E_A/RT) \quad (21)$$

$$e_{AM}^- = -E'_{AM}/RT \quad (22)$$

The Product of Monomer Reactivity Ratios in Ionic Polymerization. — In cationic polymerization, the surplus energy term, E'_{CM}, is negligibly small for most pairs of cations and monomers, as is obvious from Table IV*3. Therefore, Eq. 15 is reduced to Eq. 23.

TABLE V. E_M^-- AND E_A-VALUES

Vinyl compound	$E_M^-(-(\Delta\beta)^2/\beta)$	$E_A(-(\Delta\beta)^2/\beta)$
Styrene	0.231	−0.141
Butadiene	0.246	−0.153
Ethylene	0	0
Acrylonitrile	0.877	−0.262
Methacrylonitrile	0.777	−0.252
Vinylidene cyanide	1.701	−0.346
Methyl vinyl ketone	0.983	−0.271
Methyl acrylate	0.571	−0.225
Methyl methacrylate	0.476	−0.206
Vinyl acetate	0.034	−0.057
Vinyl chloride	0.119	−0.052
Vinylidene chloride	0.162	−0.098
α-Methylstyrene	0.151	−0.109
p-Methylstyrene	0.217	−0.135
p-Chlorostyrene	0.234	−0.143
p-Methoxystyrene	0.162	−0.114

BETWEEN MONOMER AND ATTAKING CATION, $E'_{CM}(-(\Delta\beta)^2/\beta)$

Polymer cation								
Methyl acrylate	Methyl methacrylate	Vinyl acetate	Vinyl chloride	Vinylidene chloride	α-Methyl-styrene	p-Methyl-styrene	p-Chloro-styrene	p-Methoxy-styrene
+0.092	+0.026	−0.062	−0.021	−0.038	−0.085	−0.066	−0.061	−0.096
+0.099	+0.028	−0.066	−0.022	−0.040	−0.091	−0.071	−0.069	−0.103
0	0	0	0	0	0	0	0	0
+0.022	+0.013	+0.021	+0.011	+0.019	+0.020	+0.026	+0.026	+0.052
+0.031	+0.012	+0.004	+0.002	+0.004	−0.006	+0.004	+0.003	+0.015
+0.028	+0.023	+0.052	+0.025	+0.044	+0.056	+0.063	+0.063	+0.118
+0.015	+0.014	+0.034	+0.017	+0.030	+0.038	+0.043	+0.042	+0.077
+0.016	+0.009	+0.015	+0.008	+0.015	+0.015	+0.019	+0.019	+0.052
+0.024	+0.007	−0.007	−0.001	−0.002	−0.013	−0.006	−0.005	−0.001
+0.045	+0.013	−0.032	−0.032	−0.033	−0.043	−0.034	−0.039	−0.052
+0.035	+0.005	−0.030	−0.010	−0.018	−0.042	−0.033	−0.032	−0.046
+0.056	+0.014	−0.041	−0.013	−0.024	−0.057	−0.044	−0.043	−0.063
+0.112	+0.028	−0.087	−0.032	−0.057	−0.118	−0.096	−0.093	−0.140
+0.099	+0.028	−0.067	−0.023	−0.041	−0.090	−0.072	−0.069	−0.104
+0.097	+0.028	−0.064	−0.022	−0.039	−0.087	−0.069	−0.066	−0.098
+0.324	+0.110	−0.120	−0.039	−0.070	−0.161	−0.122	−0.119	−0.189

*3 This seems not to be the essential feature of cationic polymerization, but to be ascribable only to the lack of a strongly electrondonating substituent[13].

13) N. Kawabata, unpublished finding.

TABLE VI. SURPLUS CONJUGATION-STABILIZATION ENERGY

Monomer	Styrene	Butadiene	Ethylene	Acrylo-nitrile	Methacrylo-nitrile	Vinylidene cyanide	Methyl vinyl ketone
Styrene	−0.064	−0.068	0	−0.136	−0.130	−0.166	−0.141
Butadiene	−0.067	−0.072	0	−0.145	−0.139	−0.177	−0.151
Ethylene	0	0	0	0	0	0	0
Acrylonitrile	−0.269	−0.288	0	−0.611	−0.592	−0.710	−0.631
Methacrylonitrile	−0.235	−0.253	0	−0.541	−0.522	−0.628	−0.558
Vinylidene cyanide	−0.527	−0.564	0	−1.230	−1.191	−1.412	−1.267
Methyl vinyl ketone	−0.303	−0.324	0	−0.690	−0.669	−0.800	−0.712
Methyl acrylate	−0.172	−0.185	0	−0.379	−0.367	−0.447	−0.391
Methyl methacrylate	−0.142	−0.152	0	−0.313	−0.302	−0.370	−0.324
Vinyl acetate	−0.008	−0.009	0	−0.017	−0.016	−0.028	−0.019
Vinyl chloride	−0.032	−0.034	0	−0.063	−0.061	−0.079	−0.066
Vinylidene chloride	−0.043	−0.046	0	−0.087	−0.084	−0.109	−0.090
α-Methylstyrene	−0.037	−0.040	0	−0.082	−0.085	−0.102	−0.086
p-Methylstyrene	−0.058	−0.062	0	−0.126	−0.120	−0.154	−0.130
p-Chlorostyrene	−0.064	−0.066	0	−0.138	−0.132	−0.168	−0.125
p-Methoxystyrene	−0.040	−0.043	0	−0.086	−0.080	−0.107	−0.090

$$k_{CM} \fallingdotseq P_C{}^+ Q_M{}^+ \qquad (23)$$

That is, Eq. 23, which does not involve the e-factor, is a good approximation of Eq. 15. This result correlates with the experimental finding that $r_1 r_2 \fallingdotseq 1$ for all the cationic copolymerization systems investigated so far. Thus, the experimental finding that $r_1 r_2 \fallingdotseq 1$ seems to be ascribable to the negligible quantity of the surplus energy term. In anionic polymerization, however, the E'_{AM} term often plays a large part in the stabilization energy, E_{AM} (Table VI). Thus, the usual claim that for ionic polymerization the $r_1 r_2$-products are always very close to unity seems not to be of general validity; it seems necessary to amend the generalization to allow for the cases where E'_{AM} is relatively large. Recent experimental findings by Szwarc et al.[9,10] favor our theoretical consideration.

Relative Reactivity toward Carbonium Ions.— According to the above discussion, the relative reactivity of vinyl compounds toward carbonium ions established by Pepper[6] and by Burnett[14] is considered to correspond to the general reactivity term in cationic polymerization, Q^+. In fact, a good linear relationship holds between the logarithm of the relative reactivity and the $E_M{}^+$-value, as is shown in Fig. 1*4.

Overberger et al.[5a] pointed out that when the logarithm of the relative reactivity of substituted styrenes toward α-methylstyrene carbonium ions was plotted against Hammett's substituent constant σ, large deviations of plots from linearity were observed in the cases of the substituents $-OCH_3$ and $-N(CH_3)_2$. Tsuruta (one of the authors) has suggested that linearity was improved when σ^+ was used instead of σ for these substituents[16]. A linear relationship was also observed between σ^+ and $E_M{}^+$.

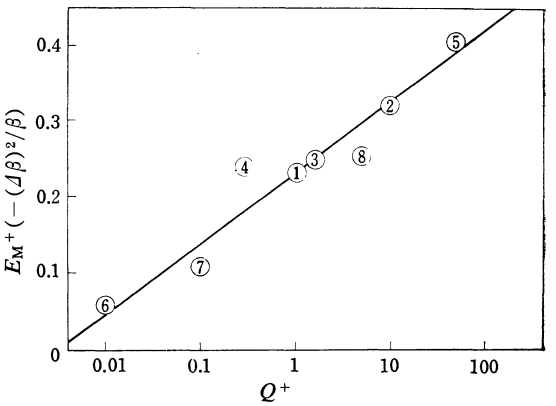

Fig. 1. Plot of $E_M{}^+$ against logarithm of Q^+.
(1) Styrene (5) p-Methoxystyrene
(2) α-Methylstyrene (6) Methyl methacrylate
(3) p-Methylstyrene (7) Vinyl acetate
(4) p-Chlorostyrene (8) Isobutene

Conclusion

The correlation of the monomer reactivity ratios in ionic polymerization with the conjugation-stabilization energy between monomer

14) G. M. Burnett, "Mechanism of Polymer Reactions", Interscience Publishers, New York (1954), p. 418.

*4 Later experimental data[15] are included here.

15) T. Higashimura and S. Okamura, Abstracts of the 13th Meeting of Japan Chemical Society, (1960), p. 361; S. Okamura, T. Higashimura and K. Takeda, *Chem. High Polymers (Kobunshi Kagaku)*, **18**, 389 (1961); A. V. Tobolsky and R. J. Bondreau, *J. Polymer Sci.*, **51**, s 53 (1961).

16) T. Tsuruta, *J. Japanese Chem. (Kagaku no Ryoiki)*, **8**, 209 (1954); *Bull. Inst. Chem. Research, Kyoto Univ.*, **32**, 149 (1954).

BETWEEN MONOMER AND ATTACKING ANION, $E'_{AM}(-(\Delta\beta)^2/\beta)$

Polymer anion								
Methyl acrylate	Methyl methacrylate	Vinyl acetate	Vinyl chloride	Vinylidene chloride	α-Methyl-styrene	p-Methyl-styrene	p-Chloro-styrene	p-Methoxy-styrene
−0.121	−0.108	−0.015	−0.021	−0.039	−0.036	−0.059	−0.064	−0.039
−0.128	−0.116	−0.016	−0.022	−0.041	−0.039	−0.063	−0.069	−0.042
0	0	0	0	0	0	0	0	0
−0.532	−0.488	−0.038	−0.079	−0.146	−0.134	−0.248	−0.274	−0.124
−0.469	−0.432	−0.031	−0.071	−0.119	−0.113	−0.125	−0.261	−0.110
−1.081	−0.990	−0.028	−0.156	−0.287	−0.207	−0.479	−0.538	−0.175
−0.601	−0.551	−0.041	−0.089	−0.164	−0.149	−0.290	−0.309	−0.137
−0.325	−0.299	−0.041	−0.050	−0.093	−0.105	−0.161	−0.176	−0.091
−0.271	−0.248	−0.031	−0.043	−0.079	−0.083	−0.132	−0.144	−0.082
−0.018	−0.015	−0.001	−0.004	−0.021	−0.003	−0.008	−0.009	−0.005
−0.055	−0.051	−0.011	−0.011	−0.019	−0.022	−0.030	−0.032	−0.023
−0.076	−0.069	−0.014	−0.014	−0.026	−0.030	−0.041	−0.044	−0.031
−0.074	−0.066	−0.006	−0.015	−0.028	−0.016	−0.035	−0.038	−0.020
−0.112	−0.100	−0.014	−0.020	−0.036	−0.036	−0.055	−0.059	−0.036
−0.122	−0.110	−0.015	−0.021	−0.039	−0.037	−0.060	−0.066	−0.039
−0.078	−0.069	−0.008	−0.015	−0.028	−0.020	−0.038	−0.041	−0.024

and polymer ions pointed out by Fukui et al.[12] has been re-examined. The reactivity ratios have been satisfactorily explained in terms of the stabilization energy. The authors have also tried to explain the experimental findings that the r_1r_2 products for all the cationic copolymerization systems so far investigated are nearly equal to unity while those for several anionic copolymerization systems are appreciably smaller than unity. The experimental finding that $r_1r_2 \fallingdotseq 1$ seems to be ascribable to the negligible quantity of the surplus energy term.

In the present paper, the authors have assumed an ideally ionic polymerization in which various energy terms other than the stabilization energy are common throughout all ion-monomer pairs. Ionic polymerizations are sometimes largely affected by the nature of the catalyst, the cocatalyst and the solvent as well as by other experimental conditions[17-19]. In the case of radical polymerization, the reactivity of vinyl compounds can be explained satisfactorily on the basis of the stabilization energy[3,4]. In ionic polymerization, other factors than the stabilization energy, especially the electrostatic interaction between monomer and ion, should also be taken into consideration to explain the reactivity. Other factors than the stabilization energy may then be discussed.

17) For example, T. Tsuruta et al., "Kobunshi no Gosei", Kagaku Dojin, Kyoto (1961), p. 53.
18) S. Okamura et al., *Chem. High Polymers (Kobunshi Kagaku)*, **18**, 267, 333, 389, 561 (1961).
19) A. V. Tobolsky, D. J. Keller, K. F. O'Driscoll, C. E. Rogers, *J. Polymer Sci.*, **28**, 425 (1958); K. F. O'Driscoll and A. V. Tobolsky, *J. Am. Chem. Soc.*, **81**, 205 (1959); C. G. Overberger and V. G. Kamath, ibid., **81**, 2910 (1959).

Summary

The authors have tried to divide the conjugation-stabilization energy between monomer and attacking polymer cation, E_{CM}, and that between monomer and attacking polymer anion, E_{AM}, into four terms by means of the equations $E_{CM}=E_{CoMo}+E_C+E_M^+ +E'_{CM}$ and $E_{AM}=E_{AoMo}+E_A+E_M^- +E'_{AM}$, respectively. Here, E_{CoMo} is the stabilization energy between polyethylene cation and ethylene monomer, E_C and E_M^+ are the increments in the stabilization energies of systems of (substituted polyethylene cation —ethylene monomer) and (polyethylene cation —substituted ethylene monomer) with respect to E_{CoMo} as standard. E'_{CM} is the surplus increment in the stabilization energy of the system of substituted polyethylene cation and substituted ethylene monomer. E_{AoMo}, E_A, E_M^- and E'_{AM} have the significance analogous to E_{CoMo}, E_C, E_M^+ and E'_{CM}, respectively. The E'_{CM} values for most cation-monomer pairs have been found to be negligibly small. This result correlates with the experimental findings that the products of r_1r_2 are nearly equal to unity for all the cationic copolymerization systems investigated so far. The equation, $k_{CM}=P_C^+Q_M^+ \exp(-e_{CM}^+)$, is assumed to be applicable to cationic polymerization, the e^+-terms being, however, negligible for any cation-monomer pair. Here, P_C^+ is the reactivity associated with polymer cation, Q_M^+ is the general reactivity term of monomer in cationic polymerization, and e^+ is the corrective term characteristic of polymer cation and monomer. On the other hand, the E'_{AM} values were often found to play a large part in E_{AM}. This result

is consistent with some experimental findings by Szwarc et al. The relative reactivity value of vinyl monomers toward carbonium ions is considered to be the general reactivity term in cationic polymerization, Q^+. A good correspondence of Q^+ with $E_M{}^+$ has been observed.

The authors wish to thank Dr. Takayuki Fueno for his helpful advice and discussion.

Department of Synthetic Chemistry
Faculty of Engineering
Kyoto University
Sakyo-ku, Kyoto

Reduction of Hexamminechromium(III) Ions at the Dropping Mercury Electrode

By Nobuyuki TANAKA, Kazuko EBATA and Gen SATÔ*

(Received February 20, 1963)

It has been found that hexamminechromium(III) ions give no well-defined polarographic wave in unbuffered neutral solutions[1], but that, in acetate buffer solutions, they give a two-step wave, the first a well-defined one-electron reduction wave and the second a two-electron reduction wave[2,3]. The previous paper[2] also demonstrated that the first well-defined wave appears only when the solution contains sufficient hydrogen ions to neutralize the six ammonia molecules that the reduced chromium-(II) species liberates.

Friend and Smith[3] observed the half-wave potential of the first wave at -0.83 to -0.84 V. versus a saturated calomel electrode and presumed a reduction mechanism similar to that of hexamminecobalt(III) ions, i. e., an irreversible electron transfer followed by hydrolysis of the divalent species.

Recently, Ichniowski and Clifford[4] investigated the polarographic behavior of hexamminechromium(III) in Divers' liquids and reported the half-wave potential to be -0.972 V. versus the mercury pool anode. From their experimental results, including the slope of the log-plot, they concluded that the electrode process is a reversible one. These results apparently contradict those obtained by Friend and Smith, but comparison of the two seems unreasonable because of the different solvents and reference electrodes used.

In this paper, extensive studies of the nature of the one-electron reduction wave of hexamminechromium(III) ions in aqueous solutions, both neutral and acid, are presented.

Experimental

Hexamminechromium(III) chloride was prepared according to the method of Mori[5]; the chromium and nitrogen contents were determined by the usual methods.

Found: Cr, 19.74%; N, 31.5%. Calcd. for $[Cr(NH_3)_6]Cl_3$: Cr, 19.96%; N, 32.2%.

As the complex is sensitive to light and not very stable in an aqueous solution[6], precautions were taken when it was used. All other chemicals used were of guaranteed reagent grade.

Direct current (d. c.) polarograms were recorded with a Yanagimoto Model PB-4 pen-recording polarograph. A Yanagimoto Y-GR 2 Galvarecorder with an automatic voltage scanner was used for recording alternating current (a. c.) polarograms. The Kalousek circuit used was the same as that

TABLE I. CHARACTERISTICS OF THE DROPPING MERCURY ELECTRODES AT -0.5 V. VS. SCE AND AT 55 cm. OF THE MERCURY HEIGHT

	Rate of flow of mercury, m mg./sec.	Drop time t_d, sec.
Electrode A*	1.92	4.72
Electrode B**	2.11	4.22

* Measured in deaerated solution containing 0.4 M NH_4Cl, 0.5 M KCl, 0.1 M acetate buffer and 0.005% gelatin.

** Measured in deaerated solution containing 1 M NH_4Cl and 0.005% gelatin.

* Present address: Department of Chemistry, Sophia University, Chiyoda-ku, Tokyo.

1) N. Maki, Y. Shimura and R. Tsuchida, This Bulletin, **31**, 413 (1958).

2) N. Tanaka and G. Satô, *Nature*, **197**, 176 (1963).

3) J. A. Friend and P. W. Smith, *J. Phys. Chem.*, **63**, 314 (1959).

4) T. C. Ichniowski and A. F. Clifford, *J. Inorg. Nucl. Chem.*, **22**, 133 (1961).

5) M. Mori, *J. Chem. Soc. Japan, Pure Chem. Sec.* (*Nippon Kagaku Zassi*), **74**, 253 (1953).

6) D. Jørgensen and J. Bjerrum, *Acta Chem. Scand.*, **12**, 1047 (1958).

described by Tanaka, Tamamushi and Takahashi[7]. The current-time curves were measured with an apparatus similar to that reported by Tamamushi, Momiyama and Tanaka[8].

The characteristics of the dropping mercury electrodes employed in this study are given in Table I. A saturated calomel electrode (SCE) with a large surface area served as the reference electrode. All measurements were carried out at 25°C unless otherwise stated. All the polarograms presented in this paper have been corrected for the residual current. The half-wave potentials and the log-plots are given after the correction for the *iR*-drop across the electrolysis cell.

Results

The current-potential curves of hexammine-chromium(III) ions, in both neutral and acid media, are given in Fig. 1. The nature of the wave in neutral media was investigated in a 0.1 M potassium chloride solution. Polarograms

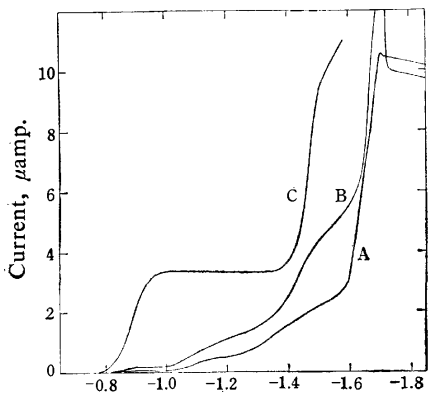

Fig. 1. Polarograms of 1 mM $[Cr(NH_3)_6]Cl_3$, in 0.1 M KCl (A), 0.1 M $NaClO_4$ (B) and in 0.1 M acetate buffer of pH 4.7 (C), in the presence of 0.005% gelatin.

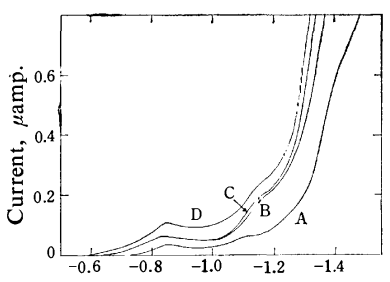

Fig. 2. Polarograms of 0.25 mM (A), 0.5 mM (B), 1 mM (C) and 5 mM (D) of $[Cr(NH_3)_6]Cl_3$ in 0.1 M KCl.

7) N. Tanaka, R. Tamamushi and A. Takahashi, *Collection Czech. Chem. Commun.*, **25**, 3016 (1960).
8) R. Tamamushi, S. Momiyama and N. Tanaka, *Anal. Chim. Acta*, **23**, 585 (1960).

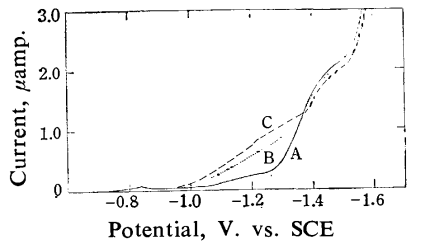

Fig. 3. Polarograms of 1 mM $[Cr(NH_3)_6]Cl_3$ in 0.1 M KCl in the absence (A) and in the presence of 0.001% (B) and 0.005% (C) of gelatin.

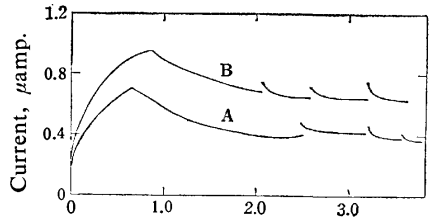

Fig. 4. Current-time curves during the life of a mercury drop measured at −1.25 V. (A) and −1.30 V. (B) in 0.1 M KCl.

Table II. Effect of the height of mercury reservoir on the limiting current of 0.5 mM $[Cr(NH_3)_6]Cl_3$

Supporting electrolyte: 0.1 M acetate buffer +0.4 M NH_4Cl+0.5 M KCl+0.005% gelatin (pH 4.9)

Electrode: A

h_{corr}* cm.	$\bar{i}_{-1.2}$**$/\sqrt{h_{corr}}$ μ amp. $cm^{-1/2}$
63.4	0.260
53.4	0.256
48.4	0.254
43.4	0.254
38.4	0.252

* Height of mercury reservoir corrected for the back pressure

** Current at −1.2 V. vs. SCE.

Table III. Effect of gelatin on the polarogram of 1 mM $[Cr(NH_3)_6]Cl_3$ in acid media

Concn. of gelatin %	$\bar{i}_d$, μ amp.	$E_{1/2}$ V. vs. SCE	Slope of log-plot mV.
A. In 0.1 M acetate buffer +0.9 M NH_4Cl (pH 4.8) (Electrode B)			
0.002	3.57	-0.96_2	66
0.005	3.57	-0.97_8	65
0.01	3.54	-1.01_6	73
B. In 0.012 N HCl+0.984 M NH_4Cl (Electrode A)			
0.001	3.51	-0.96_2	68
0.005	3.51	-0.98_3	68
0.01	3.47	−1.04	79

TABLE IV. EFFECT OF IONIC STRENGTH AND SUPPORTING ELECTROLYTE ON THE POLAROGRAM OF HEXAMMINECHROMIUM(III) IN SOLUTIONS CONTAINING 0.01 N ACID AND 0.005% GELATIN

Ionic strength	NH_4ClO_4			NH_4Cl			$(NH_4)_2SO_4$			$BaCl_2$		
	I*	$E_{1/2}$, V. vs. SCE	Slope** mV.	I*,	$E_{1/2}$, V. vs. SCE	Slope** mV.	I*	$E_{1/2}$, V. vs. SCE	Slope** mV.	I*	$E_{1/2}$, V. vs. SCE	Slope** mV.
0.01				1.81	−0.81							
0.02				1.83	-0.81_5							
0.05				1.85	−0.84		1.62	−0.86				
0.1	1.83	-0.88_3	59 (51)	1.82	-0.87_0	61 (52)	1.62 (1.62_5)	-0.88_5	59 (53)	1.78 (1.79)	-0.88_3	62 (57)
0.2	1.84	-0.91_5	64 (51)	1.82	-0.91_6	61 (53)	1.60 (1.61)	-0.91_7	59	1.78 (1.79_5)	-0.90_7	63
0.4				1.82	-0.94_5	65	1.59 (1.62)	-0.95_4	61			
1.0				1.81 (1.80)	-0.98_3	68	1.56 (1.62)	-0.98_5	62	1.74 (1.80)	-0.96_2	68 (64)

The concentration of the complex was 1 mM when $\mu \geq 0.1$. When $\mu < 0.1$ smaller concentrations were used to prevent the migration current.

* Diffusion current constant. The value in parentheses is that corrected for the viscosity according to Eq. 5.

** Slope of log-plot. The value in parentheses is that of the upper part of the plot corresponding to the part of the wave at more negative potentials.

obtained at various concentrations of the complex are shown in Fig. 2. No linear relation was found between the concentration and the current. The plots of $\log h$ (mercury height) versus $\log \bar{i}$ (average current) gave straight lines whose slopes were close to unity at −1.1 V. and −1.2 V. vs. SCE. In Fig. 3, the effect of gelatin on the current-potential curve of hexamminechromium(III) ions in a 0.1 M potassium chloride solution is shown. The current-time curves during the life of a mercury drop were measured at various potentials; those measured at −1.25 V. and −1.30 V. are reproduced in Fig. 4.

In acetic acid-sodium acetate buffer solutions, well-developed waves were observed (see C in Fig. 1). The limiting current was proportional to the concentration of the complex up to 5 mM and to the square root of the height of the mercury reservoir as seen in Table II. No well-defined wave was obtained in the absence of gelatin, while in the presence of gelatin the shape of the wave was affected considerably by the concentration of gelatin. Table III indicates a parallel shift of the wave toward negative potentials observed at lower gelatin concentrations. Diffusion current constants, half-wave potentials, and slopes of the log-plots obtained in various supporting electrolytes and at varied ionic strength are given in Table IV. Measurements were also made at various concentrations of ammonium and

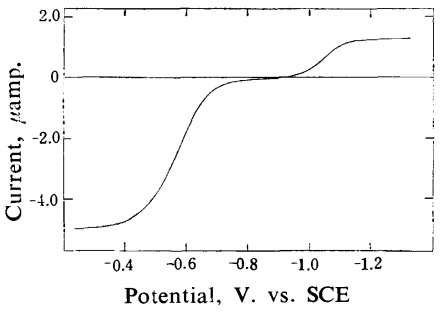

Fig. 5. A Kalousek polarogram of 0.7 mM $[Cr(NH_3)_6]Cl_3$ in 0.1 M acetate buffer +0.9 M NH_4Cl +0.002% gelatin (pH 4.7). The constant potential was set at −1.30 V. vs. SCE.

TABLE V. EFFECT OF AMMONIUM ION ON THE POLAROGRAM OF 1mM $[Cr(NH_3)_6]Cl_3$, IN 0.1 M ACETATE BUFFER+0.005% GELATIN (pH 4.9) AT IONIC STRENGTH 1.0 (KCl)

Concn. of NH_4Cl, M	$E_{1/2}$ V. vs. SCE	Slope of log-plot, mV.
0	-0.97_0	67
0.10	-0.97_0	70
0.40	-0.96_8	66
0.90	-0.97_0	67

TABLE VI. EFFECT OF pH ON THE POLAROGRAM OF 1 mM $[Cr(NH_3)_6]Cl_3$ IN 0.4 M NH_4Cl+ 0.005% GELATIN AT IONIC STRENGTH 1.0 (KCl)

pH or acid concn.	$E_{1/2}$ V. vs. SCE	Slope of log-plot, mV.
pH 5.45*	-0.97_2	64
pH 4.83*	-0.97_7	65
pH 4.51*	-0.97_7	65
pH 3.91*	-0.98_1	64
[HCl] = 0.012 N	-0.98_3	68
[HCl] = 0.024 N	-0.98_7	67

* pH was adjusted with the acetate buffer of 0.1 M in acetate.

TABLE VII. EFFECT OF TEMPERATURE ON THE POLAROGRAM OF 1 mM $[Cr(NH_3)_6]Cl_3$ IN 0.1 M ACETATE BUFFER+0.9 M NH_4Cl+ 0.005% GELATIN (pH 4.56)*

Temp. °C	i_d μ amp.	$E_{1/2}$, V. vs. SCE	Slope of log-plot, mV.	$2.303\frac{RT}{nF}$ mV.
0.5	2.45	-1.02_0	61	54.3
15.0	3.15	-0.99_5	65	57.2
25.0	3.59	-0.97_8	67	59.2
35.0	4.10	-0.96_4	71	61.2

* Electrode B was used.

hydrogen ions at a constant ionic strength of 1.0. The results are presented in Tables V and VI. In Table VII, the results obtained at various temperatures are given.

On the a. c. polarogram, a peak was observed at a little more negative potential than the half-wave potential on the corresponding d. c. polarogram. One of the typical Kalousek polarograms of hexamminechromium(III) ions in an acetate buffer solution is reproduced in Fig. 5, where the anodic wave is clearly separated from the cathodic one.

Discussion

In Unbuffered Neutral Solutions.—In a 0.1 M potassium chloride solution, no well-defined wave of hexamminechromium(III) was observed. Upon the addition of hydrochloric acid, a wave began to appear at -0.89 V.; it attained its full development just when the ratio of the flux of hydrogen ions diffusing toward the electrode to that of the complex ions was equal to six. Further addition of the acid made no essential change in the shape of the developed wave[2]. Hydrogen ions seem to play an essential role in the reduction of hexamminechromium(III) to its divalent state. However, as will be mentioned later, hydrogen ions are considered not to be involved in any chemical reaction prior to the electron transfer; they act rather as a neutralizing agent on the ammonia which the divalent chromium species liberates. In an unbuffered neutral solution, the liberated ammonia will make the solution layer near the electrode surface alkaline; it will also cause the divalent chromium species to precipitate as an insoluble film on the surface of the electrode.

This explanation is supported by the following observations. In a 0.1 M potassium chloride solution, the current in the potential region between -0.6 V. and -1.3 V. was almost independent of the concentration of the complex ions (Fig. 2), and the currents at -1.1 V. and -1.2 V. were nearly proportional to the height of the mercury reservoir. The addition of gelatin increased the current between -1.0 V. and -1.35 V., as can be clearly seen in Fig. 3. In addition, further confirmation was obtained by measuring the current-time curve during the life of a mercury drop. Not only did the instantaneous current reach its highest value in the early life of the drop and then decrease with time, but also several sudden breaks were observed in the current (Fig. 4).

It is, therefore, expected that any reagent that can prevent divalent chromium from precipitating will make the one-electron reduction wave of hexamminechromium(III) appear. Figure 6 shows that the wave of hexamminechromium(III) is nearly complete when 1 mM of disodium dihydrogen ethylenediaminetetraacetate (EDTA) was added to a neutral solution of the complex; the divalent chromium is kept in the solution as its EDTA complex.

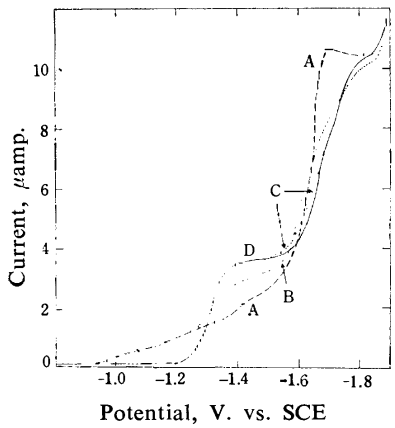

Fig. 6. Polarograms of 1 mM $[Cr(NH_3)_6]Cl_3$ in solutions containing 1 M KCl and 0.005% gelatin without (A) and with 0.52 mM (B), 1.04 mM (C) and 1.56 mM (D) of EDTA. The residual current is not corrected.

That a well-defined one-electron reduction wave does not appear in neutral solutions, though it does in acid media, is a general characteristic of those chromium(III) complexes that have one or more basic ligands, unless the corresponding divalent complexes are stable enough to be maintained in the solution. In fact, the following complex ions gave the one-electron reduction wave in acetate buffer solutions (with 0.005% gelatin added), but not in neutral solutions: $[Cr(H_2O)(NH_3)_5]^{3+}$, $[Cr(en)_3]^{3+}$ (en=ethylenediamine), *trans*-$[Cr(NCS)_2(NH_3)_4]^+$, *trans*-$[Cr(NCS)_2(pn)_2]^+$ (pn=propylenediamine), $[Cr(ox)(en)_2]^+$ (ox=oxalate), and *trans*-$[Cr(NCS)_4(NH_3)_2]^-$. On the other hand, a well-defined reduction wave of chromium(III) to chromium(II) is observed

in potassium chloride or sodium chloride solutions for hexathiocyanatochromate(III), tris-(dipyridyl)chromium(III)[9] and ethylenediaminetetraacetatochromate(III).

In Acid Media.—Every experimental result indicates that the limiting current of the wave in an acetate buffer solution is controlled by diffusion. Assuming the limiting current to correspond to one-electron reduction, the diffusion coefficient of hexamminechromium(III) ions was calculated to be 0.85×10^{-5} cm^2 sec^{-1} at 25°C in an air-free solution containing a 0.1 M acetate buffer, 0.9 M ammonium chloride, and 0.005% gelatin. This value appears to be appropriate for this type of ion[10]. From the change in the limiting current with a change in temperature, the activation energy of diffusion was calculated to be 5.0 kcal./mol.

In most cases, the log-plots gave straight lines whose slopes were 60 to 70 mV. (see Tables IV, V and VI). The values are close to 59 mV. which is to be expected in a reversible one-electron reduction at 25°C. However, as is shown in Fig. 5, the shape of the Kalousek polarogram was that of an irreversible wave, and the peak of an a. c. polarogram was much lower than that expected for a reversible wave. It has been pointed out by Senda, Senda and Tachi[11] that the value of $i_p/(n\,\bar{i}_d\sqrt{t_d})$ represents the degree of polarographic reversibility, where i_p is the peak current in the a. c. polarogram, $\bar{i}_d$, the diffusion current (average) in the corresponding d. c. polarogram, n, the number of electrons involved in the electrode process, and t_d, the drop time. The value for the reduction wave of hexamminechromium(III) ion in acetate buffer solutions was calculated to be 0.009 kΩamp^{-1} sec$^{-1/2}$, which is as small as that for a typical irreversible reduction wave of hydrated nickel(II) ions[12].

The above-mentioned observations can be explained by assuming that the electron transfer between hexamminechromium(III) and the divalent chromium is irreversible with the transfer coefficient close to, or by some chance appearing to be, unity. However, there is the alternative explanation of these observations. The electron transfer process is assumed to proceed reversibly, and the divalent chromium species produced on the surface of the electrode to undergo hydrolysis:

$$[Cr(NH_3)_6]^{3+}+e \rightleftarrows [Cr(NH_3)_6]^{2+} \quad (1)$$

$$[Cr(NH_3)_6]^{2+}+n\,H_2O \rightleftarrows [Cr(H_2O)_n(NH_3)_{6-n}]^{2+}+n\,NH_3 \quad (2)$$

$$NH_3+H^+ \rightleftarrows NH_4^+ \quad (3)$$

If the forward reaction of Reaction 2 is rapid and the backward reaction is extremely slow, the net electrode process will appear to be irreversible in the a. c. and the Kalousek polarogram. Similar mechanisms, viz., mechanisms involving a rapid electron transfer followed by a chemical reaction, have been reported for the oxidation of ascorbic acid[13] and for the reduction of manganese (II) complexes[14]. In these cases, the half-wave potential is dependent on the rate of the following reaction[14,15], as given by

$$E_{1/2}=E_{1/2}^{\circ}+\frac{RT}{nF}\ln 0.89\ (k\,t_d)^{1/2} \quad (4)$$

where $E_{1/2}^{\circ}$ is the half-wave potential with no following reaction and k, the first-order rate constant of the following reaction.

At the moment, it seems impossible to decide, from the experimental results, by which mechanism the reduction of hexamminechromium(III) ions takes place. This is mainly because of insufficient knowledge on the reactivity of chromium(II) complexes.

Table IV shows that in all electrolytes the half-wave potentials shift to more negative potentials with an increase in ionic strength. The shift is much greater than can be expected from the change in the activity coefficients of electroactive species with ionic strength.

The diffusion currents show a slight decrease with increasing ionic strength, but they become almost independent of the ionic strength in the range from 0.1 to 1.0 after the effect of viscosity is corrected for by the equation:

$$I_{corr}=\frac{I}{\sqrt{\eta_{rel}}} \quad (5)$$

where I is the diffusion current constant observed, I_{corr}, that corrected for the viscosity, and η_{rel}, the relative viscosity[16]. The diffusion current constants in ammonium sulfate, however, were found lower by some 10% than those in other electrolytes. This is considered as due to the formation of ion pairs between hexamminechromium(III) ions and anions.

As is seen in Table V, the half-wave potentials vary by no more than a few millivolts when ammonium chloride is replaced by potassium chloride, provided that pH and ionic strength are kept constant. Similarly, the half-wave potential is almost independent of the hydrogen ion concentration of the solution (Table VI). These results indicate definitely

9) A. A. Vlček, *Nature*, **189**, 393 (1961).
10) S. Takamoto, private communication.
11) M. Senda, M. Senda and I. Tachi, *J. Electrochem. Soc. Japan (Denki Kagaku)*, **27**, 83 (1959).
12) N. Tanaka and Y. Sato, unpublished.
13) D. M. H. Kern, *J. Am. Chem. Soc.*, **76**, 1011 (1954).
14) J. Biernat and J. Koryta, *Collection Czech. Chem. Commun.*, **25**, 38 (1960).
15) D. M. H. Kern, *J. Am. Chem. Soc.*, **75**, 2473 (1953).
16) "Landolt-Börnstein, Physikalisch-Chemsiche Tabellen," Verlag von Julius Springer, Berlin (1923).

that there is no chemical reaction involving hydrogen ions, ammonium ions or ammonia preceding the electron transfer.

Summary

The reduction of hexamminechromium(III) ion at the dropping mercury electrode has been studied in neutral and acid aqueous solutions. Hexamminechromium(III) ion gives no well-defined d. c. polarographic wave in an unbuffered neutral solution, whereas in an acid solution it gives a well-defined two-step wave, the first wave corresponding to the reduction of chromium(III) to chromium(II) and the second, to that of chromium(II) to chromium-(0).

The first wave of the d. c. polarogram obtained in an acid solution is diffusion-controlled and gives a slope of the log-plot close to that expected for a reversible wave. The a. c. and the Kalousek polarogram, however, are of the irreversible type. No chemical reaction involving hydrogen ions, ammonium ions or ammonia takes place preceding the electron transfer. Considering these results, the following mechanism is temporarily suggested for the reduction of hexamminechromium(III) ions at the dropping mercury electrode:

$$[Cr(NH_3)_6]^{3+} + e \rightleftarrows [Cr(NH_3)_6]^{2+}$$

$$[Cr(NH_3)_6]^{2+} + n\,H_2O \longrightarrow [Cr(H_2O)_n(NH_3)_{6-n}]^{2+} + n\,NH_3$$

$$NH_3 + H^+ \rightleftarrows NH_4^+$$

The authors wish to thank the Ministry of Education for the financial support granted for this research.

Department of Chemistry
Faculty of Science
Tohoku University
Katahira-cho, Sendai

Ionic Charge Effect on the Reduction Potential of Inert-type Metal Complex

By Nobuyuki TANAKA, Eiki ITABASHI and Eishin KYUNO*

(Received March 19, 1963)

It has been found that there is a relation between the half-wave potentials of polarographic reduction waves and the frequencies of the maxima of the absorption spectra of inert-type metal complexes. In the polarographic study of cobalt(III), chromium(III) and rhodium(III) complexes, Vlček[1] pointed out that the half-wave potentials of the reduction waves of $[MXY_5]$-type complexes were shifted to more positive values with an increasing difference in the position of ligands X and Y in the spectrochemical series, and that the plot of $E_{1/2}$ against $\Delta\nu$ gave a straight line. Maki, Shimura and Tsuchida[2], who studied the polarographic reductions of a number of cobalt(III) complexes, reached the same conclusion.

In the course of our studies of the electrode processes of chromium(III) complexes, we found that the repulsion and attraction between the electrode and the reducible species plays an important role in determining the reduction potential of the species. In contrast with oxalatocobalt(III) complexes[2], the reduction potentials of oxalatochromium(III) complexes were shifted to more negative potentials with an increasing number of oxalates coordinated. In this paper, the study of the polarographic reduction of various oxalatochromium(III) complexes is presented, and the relation of the reduction potential and the ionic charge is discussed.

Experimental

Current-potential curves were obtained with a pen-recording polarograph, Yanagimoto Galvarecorder Model AP-1, with an automatic potential scanner. The dropping mercury electrode used had an m value of 1.499 mg./sec. and a drop time, t_d, of 3.32 sec. as measured in an air-free 1 M potassium nitrate solution at -1.70 V. vs. SCE at 50 cm. of the mercury reservoir. The cell equipment used in this study was the same as has been reported

* Present address: Department of Chemistry, Faculty of Science, Kanazawa University, Kanazawa.

1) A. A. Vlček, *Discussions Faraday Soc.*, **26**, 164 (1958).

2) N. Maki, Y. Shimura and R. Tsuchida, This Bulletin, **30**, 909 (1957).

previously[3]. Potentials were referred to the saturated calomel electrode (SCE). The current-potential curves presented in this paper are corrected for the residual current and the *iR* drop across the electrolysis cell. All measurements were carried out in a thermostat of 25±0.1°C unless otherwise stated.

$K_3[Cr(ox)_3]\cdot 3H_2O$[4] (ox=oxalate), *cis*-$K[Cr(ox)_2(H_2O)_2]\cdot 2H_2O$[5], *trans*-$K[Cr(ox)_2(H_2O)_2]\cdot 3H_2O$[5], *cis*-$(NH_4)_2[Cr(OH)(ox)_2(H_2O)]\cdot H_2O$[5], and *cis*-$K[Cr(ox)_2(NH_3)_2]\cdot H_2O$[5] were prepared with the procedures given in the literature. $K[Cr(ox)_2en]\cdot KI$ (en=ethylenediamine), $[Cr(ox)(NH_3)_4]I$, and $[Cr(ox)(en)_2]I$ were prepared with newly-devised procedures[6]. The analysis of these compounds gave the following results:

$K[Cr(ox)_2en]\cdot KI$
Calcd.: Cr, 10.52; N, 5.69; C, 14.57%
Found: Cr, 10.49; N, 6.01; C, 15.10%

$[Cr(ox)(NH_3)_4]I$
Calcd.: Cr, 16.83; N, 18.13; C, 7.76%
Found: Cr, 16.59; N, 18.20; C, 7.72%

$[Cr(ox)(en)_2]I$
Calcd.: Cr, 13.34; N, 14.47; C, 18.60%
Found: Cr, 13.88; N, 14.61; C, 18.72%

Results and Discussion

Current-potential curves of the oxalatochromium(III) complexes were obtained in various supporting electrolyte solutions. In acid solutions or acetate buffers only the monooxalato complexes gave a polarographic wave; this is considered to be due to the reduction from chromium(III) to chromium(II). One of the current-potential curves of monooxalatobis(ethylenediamine)chromium(III) is reproduced in Fig. 1. Di- and trioxalato complexes of chromium(III) gave no reduction wave at less negative potentials than the potential of the reduction of hydrogen ions. This is in agreement with the findings of Hamm and Davis[7], who reported that dioxalatodiaquochromate(III) gave no wave in the solution with an ionic strength of 0.3 containing potassium nitrate, nitric acid, 0.1 F potassim oxalate, and 0.005% gelatin.

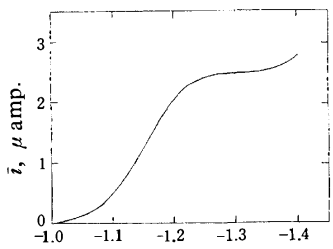

Fig. 1. Current-potential curve of 1.0 mM $[Cr(ox)(en)_2]I$ obtained in the solution containing 0.9 M KCl, 0.1 M acetate buffer and 0.005% gelatin at 25°C.

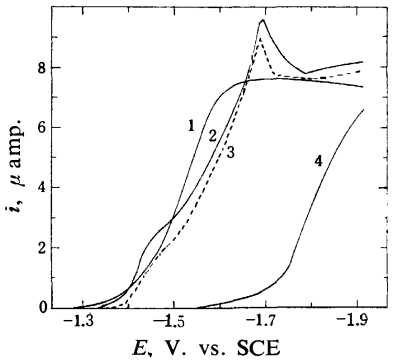

Fig. 2. Current-potential curves of 1.0 mM dioxalatochromate(III) complexes obtained in 0.3 M KCl solutions containing 0.005% gelatin at 25°C: 1, *cis*-$[Cr(ox)_2(H_2O)_2]^-$; 2, *cis*-$[Cr(ox)_2(NH_3)_2]^-$; 3, $[Cr(ox)_2(en)]^-$; 4, *cis*-$[Cr(OH)(ox)_2(H_2O)]^{2-}$.

The reduction waves of dioxalatochromate(III) complexes, therefore, were measured in neutral solutions. The examples shown in Fig. 2 were obtained with 1.0 mM of the complexes in solutions containing 0.3 M potassium chloride and 0.005% gelatin. Dioxalatodiaquochromate(III) gives a well-defined wave, as is shown in Fig. 2.

All attempts to obtain a polarographic wave of trioxalatochromate(III) ions were unsuccessful. No wave was obtained, even in a 0.1 M tetramethylammonium bromide solution. This leads to the conclusion that trioxalatochromate(III) is not reducible at the dropping mercury electrode in the possible range of potential.

Table I gives the potentials at $\bar{i}=\bar{i}_l/10$ (denoted as $\bar{i}_l/10$-potential) on the polarographic waves of mono- and dioxalato complexes. The use of half-wave potentials was avoided because of the irregular polarograms observed with most of the dioxalato complexes. Table I indicates that the monooxalato complexes give the $\bar{i}_l/10$-potential at approximately −1.05 ~ −1.1 V., the dioxalato complexes of univalent anions, at approximately −1.4 ~ −1.45 V., and the dioxalato complexes of divalent anions, at −1.67 V.

In oxalatocobalt(III) complexes, the half-wave potential shifts to more positive potentials with an increasing number of oxalates coordinated[2]; this shift is considered to agree

3) N. Tanaka, K. Ebata and G. Satô, This Bulletin, 36, 912 (1963).
4) A. Rosenheim, *Z. anorg. Chem.*, 11, 196, 225 (1892).
5) A. Werner, W. J. Bowis, A. Hoblik, H. Schwarz and H. Surber, *Ann.*, 406, 261 (1914).
6) The details of the syntheses of these compounds will be published elsewhere.
7) R. E. Hamm and R. E. Davis, *J. Am. Chem. Soc.*, 75, 3085 (1953).

TABLE I. POTENTIALS AT $\bar{i}=\bar{i}_l/10$ OF THE CURRENT-POTENTIAL CURVES OF VARIOUS OXALATOCHROMIUM(III) COMPLEXES (AT 25°C)

Complex ion	Supporting electrolyte	Potential at $\bar{i}=\bar{i}_l/10$ V. vs. SCE
$[Cr(ox)_3]^{3-}$	0.1 M $(CH_3)_4NBr$	—
cis-$[Cr(OH)(ox)_2(H_2O)]^{2-}$	0.3 M KCl	−1.67
cis-$[Cr(ox)_2(H_2O)_2]^-$	0.3 M KCl	−1.44
cis-$[Cr(ox)_2(H_2O)_2]^-$	0.3 M KCl	−1.44*
trans-$[Cr(ox)_2(H_2O)_2]^-$	0.3 M KCl	−1.43*
cis-$[Cr(ox)_2(NH_3)_2]^-$	0.3 M KCl	−1.43
$[Cr(ox)_2(en)]^-$	0.3 M KCl	−1.41
$[Cr(ox)(NH_3)_4]^+$	0.9 M KCl+0.1 M acetate buffer	−1.10
$[Cr(ox)(en)_2]^+$	0.9 M KCl+0.1 M acetate buffer	−1.06

* Measured at 0°C.

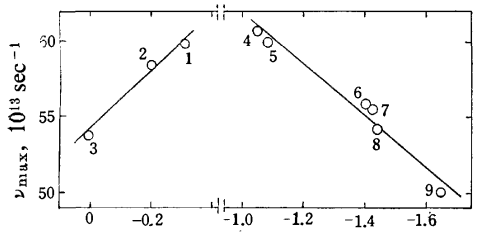

Fig. 3. Relation between the reduction potentials and the frequencies of the first absorption band of oxalatocobalt(III) and oxalatochromium(III) complexes: 1, $[Co(ox)(en)_2]^+$; 2, $[Co(ox)(NH_3)_4]^+$; 3, $[Co(ox)_2(NH_3)_2]^-$; 4, $[Cr(ox)(en)_2]^+$; 5, $[Cr(ox)(NH_3)_4]^+$; 6, $[Cr(ox)_2(en)]^-$; 7, *cis*-$[Cr(ox)_2(NH_3)_2]^-$; 8, *cis*-$[Cr(ox)_2(H_2O)_2]^-$; 9, *cis*-$[Cr(OH)(ox)_2(H_2O)]^{2-}$.

with the order of the spectrochemical series. In Fig. 3, the half-wave potentials of oxalatocobalt(III) complexes and the $\bar{i}_l/10$-potentials of oxalatochromium(III) complexes are plotted against the frequencies of the absorption band of the cobalt(III)[8] and chromium(III) complexes respectively. The absorption spectra of all the chromium(III) complexes were measured in this laboratory[9] except for that of the hydroxodioxalatoaquochromate(III) complex, which was obtained by Grant and Hamm[10].

It is interesting to note that, in the cobalt(III) and chromium(III) complexes, the absorption bands shift in the same direction with an increasing number of oxalates coordinated, whereas the reduction potentials shift in the opposite directions. The oxalatocobalt(III) complexes are reduced at the positively-charged electrode, whereas the oxalatochromium(III) complexes are reduced at the negatively-charged electrode. This indicates that the electrostatic effect between the reacting species and the electrode is one of the important factors in determining the reduction potential. In the case of chromium(III) complexes, the difference in repulsion between the reacting species and the electrode seems to cancel out the difference in ease with which one electron enters into the reacting chromium(III) species. These observations definitely suggest that the relationship between the reduction potential and the structure of the metal complex can be discussed only when the difference in the electrostatic interaction between the reacting species and the electrode can be disregarded or after an appropriate correction is made for the difference.

Summary

Current-potential curves of various oxalato complexes of chromium(III) were obtained at the dropping mercury electrode in acid or neutral aqueous solutions. The reduction potentials that were defined as potentials at $\bar{i}=\bar{i}_l/10$ were found to shift to more negative potentials with an increasing number of oxalates coordinated. The ionic charge effect on the reduction potentials was discussed in connection with the electrostatic interaction between the reacting species and the electrode.

The authors wish to thank the Japan Society for the Promotion of Science for the financial support granted to one of the authors (E. K.) in this research.

8) Y. Shimura and R. Tsuchida, This Bulletin, **28**, 572 (1955).
9) The details will be published elsewhere.
10) D. M. Grant and R. E. Hamm, *J. Am. Chem. Soc.*, **78**, 3006 (1956).

Department of Chemistry
Faculty of Science
Tohoku University
Katahira-cho, Sendai

The Dehydrating Cyclization of S-Carboxymethyl-cysteine and N-Acetyl-S-carboxymethyl-cysteine

By Hitoshi OZAWA

(Received March 2, 1963)

It is well known that acidic amino acids and their peptides form ring compounds by dehydration between their β- or γ-carboxyl group and the α-amino group or adjacent imino group of peptide linkage. For instance, glutamic acid and glutamine can be converted to pyrrolidonecarboxylic acid[1]. Aspartyl-ε-lysine can form ε-(amino succinyl)-lysine when treated with concentrated hydrochloric acid. It is to be expected, therefore, that *S*-carboxymethyl-cysteine (SCMC), a reaction product of cysteine with iodoacetic acid, can cyclize in a similar way by dehydration between its amino group and the carboxyl group of the carboxymethyl moiety. This paper describes the formation of 3-oxo-5-carboxyperhydro-1, 4-thiazine (SCMC-lactam) from SCMC and *N*-Ac-SCMC.

Experimental and Results

The Synthesis of SCMC.—A solution of 1.6 g. of cysteine in 30 ml. of water was neutralized with 1 N ammonium hydroxide. A solution of 2.9 g. of iodoacetic acid in 5.0 ml. of water was adjusted to pH 7.6 with 1 N ammonium hydroxide. Both solutions were mixed and left to stand for one hour. The pH value was kept at 7.6 by adding 1 N ammonium hydroxide occasionally. A small amount of precipitate produced during the reaction was filtered off, and this filtrate was passed through a column (3×15 cm.) of Amberlite IR-120 (hydrogen form) resin which was then washed thoroughly with water. The column was then treated with 1 N ammonium hydroxide. The acidic fraction showing a positive ninhydrin reaction was evaporated to dryness under reduced pressure. About 2 g. of SCMC (free acid) was obtained and recrystallized from water-ethanol. From the last fraction with a positive ninhydrin reaction, about 0.4 g. of the ammonium salt of SCMC was obtained. It was converted to the free acid by absorbing it on a column (4×20 cm.) of Amberlite IR-45 (acetate form) resin and eluting it with 2 N acetic acid. The preparation melted at 196~198°C. The overall yield was 95% of the theoretical.

The Synthesis and Properties of SCMC-lactam.—SCMC (400 mg.) was dissolved in water (5.0 ml.), and the pH brought to 4.8 by the addition of 1 N sodium hydroxide. The solution was then heated in a sealed glass tube at 110°C for 48 hr. and poured onto a column (1.5×15 cm.) of Amberlite IR-120 (hydrogen form) resin which was then washed with water (30 ml.). The filtrate and washings were combined and concentrated under reduced pressure. To a solution of an oily residue in a small amount of glacial acetic acid, ether was added drop by drop. Hexagonal crystals with a melting point of 182~183°C were obtained (about 260 mg., 74% of the theoretical).

Found: C, 37.68; H, 4.65. Calcd. for $C_5H_7O_3NS$: C, 37.26; H, 4.38%.

The compound was acidic and gave a negative ninhydrin reaction. When it was hydrolyzed with 1 N hydrochloric acid at 110°C for 1 hr., SCMC was recovered. The electrophoretic mobility was equal to that of pyrrolidonecarboxylic acid, as is shown in Fig. 3. The infrared absorption spectrum of the preparation is shown in Fig. 1, together with that of SCMC. From these results, it was concluded that SCMC-lactam was obtained as follows:

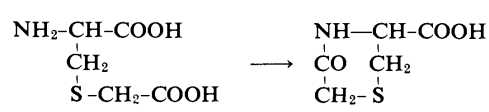

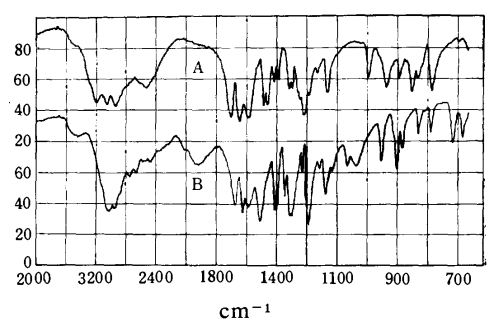

Fig. 1. Infrared absorption spectra of
A *S*-carboxymethyl-cysteine lactam
B *S*-carboxymethyl-cysteine

The Cyclization of SCMC under Various Conditions.—An aqueous solution of SCMC or of its mono sodium salt (1.0 mM) was heated at various temperatures for 1 to 48 hr., and the amount of amino acid remaining was estimated by the ninhydrin method of Yemm and Cocking[3]. The

* The following abbreviations are used: SCMC, *S*-carboxymethyl-cysteine; *N*-Ac-SCMC, *N*-acetyl-*S*-carboxymethyl-cysteine.

1) J. P. Greenstein and M. Winitz, "Chemistry of the Amino Acids", Vol. 3, John Wiley and Sons, Inc., New York (1961), p. 1937.

2) D. L. Swallow and E. P. Abraham, *Biochem. J.*, **70**, 364 (1958).

3) E. W. Yemm and E. C. Cocking, *Analyst*, **80**, 209 (1955).

results are summarized in Fig. 2. When SCMC was heated at 130°C, about 70% of the amino group disappeared in 1 hr., while no measurable reaction occurred at this temperature in the case of glutamic acid, in agreement with the report[4] that the rate of dehydration is very slow under these conditions. The disappearance of the ninhydrin positive substance, however, did not proceed to its completion. The paper chromatogram of the reaction mixture (*n*-butanol : acetic acid : water, 4 : 1 : 2, v/v) gave several ninhydrin positive spots, but no spot of SCMC, indicating that some side-reactions occurred in addition to the main cyclization reaction. When the reaction was carried out at 180°C, only 30% of the amino group disappeared, showing that the side reactions occurred to a larger extent. With SCMC mono sodium salt, the reaction rate was smaller, but the reaction proceeded to its completion. The paper chromatogram of the reaction mixture showed no by-products.

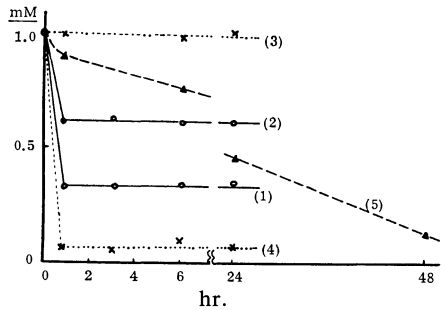

Fig. 2. Disappearance of amino group of *S*-carboxymethyl-cysteine (SCMC) and glutamic acid. Aqueous solution of SCMC (1.0 mM) was heated at (1) 130°C and (2) 180C° for 0 to 24 hr. and tested for ninhydrin reaction. (5) Solution of SCMC-mono sodium salt (1.0 mM) was heated at 110C° for 0 to 48 hr. Solution of glutamic acid (1.0 mM) was treated at (3) 130°C and (4) 180C°.

The Synthesis of *N*-Ac-SCMC.—SCMC (200 mg.) was suspended in water (1 ml.) and dissolved by neutralizing it with sodium hydroxide (4.0 M). Acetic anhydride (0.4 ml.) was added drop by drop to the solution, which was kept about pH 7.0 by adding sodium hydroxide (4.0 M). The reaction mixture, which showed a negative ninhydrin reaction on a filter paper, was diluted with water (20 ml.), passed through a column (1.5×15 cm.) of Amberlite IR-120 (hydrogen form) resin to remove the sodium ion, and evaporated to dryness under reduced pressure. *N*-Ac-SCMC was obtained as an oily residue. The electrophoretic mobility of the compound was similar to that of *N*-acetyl-aspartic acid (Fig. 3). The oily preparation was used as such for further experiments.

The Cyclization Reaction of *N*-Ac-SCMC.—*N*, *N'*-Dicyclohexylcarbodiimide (DCCD) (380 mg.) was added to a suspension of *N*-Ac-SCMC (120 mg.) in ethyl acetate (8.0 ml.) A massy precipitate was produced in ten minutes. After the reaction mixture had been kept at room temperature for two hr., glacial acetic acid (two drops) was added to decompose excess DCCD. Paper chromatography and paper electrophoresis of the reaction mixture showed acidic compounds upon its being sprayed with a 0.05% solution of bromcresol green in ethanol. The spot of the starting material, *N*-Ac-SCMC, was not detected. A large new spot with a somewhat smaller electrophoretic mobility (pyridine : acetic acid : water, 27 : 1 : 142, pH 6.0) and a larger R_f value (0.85 with *n*-butanol : acetic acid : water, 4 : 1 : 2) than SCMC-lactam was detected. Two minor spots with lower electrophoretic mobilities and R_f values were also observed (Fig. 3). The reaction mixture was evaporated to dryness under reduced pressure. The residue was mixed with 2.0 ml. of water, and the pH was adjusted to 9.0 with ammonium hydroxide (1.0 N). After the mixture had been left standing at 37°C for 30 min., the precipitate was centrifuged off and extracted twice with water; then the combined extract was evaporated to dryness in vacuo. The residue gave two spots, together with two other minor spots, by paper chromatography and paper electrophoresis, as is shown in Fig. 3. The main spot had the same electrophoretic mobility and R_f value as SCMC-lactam. The second spot coincided with *N*-Ac-SCMC. The water extract was poured onto a column (1.5×15 cm.) of Amberlite IR-45 (acetate form) resin. After washing with 1.0 N acetic acid (100 ml.), the column was eluted with 0.1 N hydrochloric acid. The crystals of SCMC-lactam were obtained by evaporating the eluate under reduced pressure and were identified by means of the infrared absorption spectrum. The cyclization reaction was also carried out under the following conditions: one mole of *N*-Ac-SCMC was treated (a) with 10 mol. of DCCD at 77°C for 2 hr., (b) with 3 mol. of DCCD at 77°C for 2 hr., or (c) with 10 mol. of DCCD at room temperature for 24 hr. There was no difference in the results.

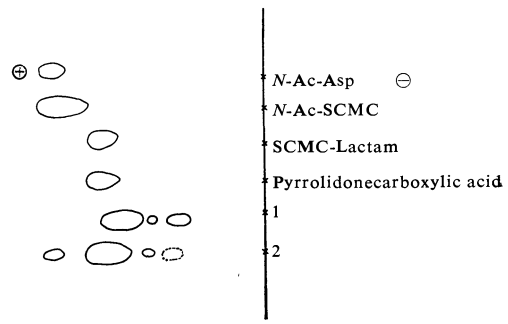

Fig. 3. Drawing of paper electrophoresis of *S*-carboxymethyl-cysteine lactam (SCMC-lactam), *N*-acetyl-SCMC and reaction products of *N*-acetyl-SCMC with *N*, *N'*-dicyclohexylcarbodiimide. 1: Direct dehydration products. 2: After treatment at pH 9.0. Electrophoresis was carried out at pH 6.0, 18 v/cm. for two hr. on Toyo-Roshi filter paper No. 51.

4) H. Wilson and K. Cannan, *J. Biol. Chem.*, **119**, 309 (1937).

SCMC-lactam was not formed when the aqueous solution of *N*-Ac-SCMC was heated at various temperatures (100~180°C) for 10 to 48 hr. Under these conditions, *N*-Ac-SCMC was completely decomposed. No SCMC-lactam was formed either when diethyl ester of *N*-Ac-SCMC was suspended in a 5% sodium hydrogen carbonate solution and heated at 80°C for two hours. The product obtained in this reaction was *N*-Ac-SCMC.

Discussion

SCMC cyclizes easily by dehydration to form 3-oxo-5-carboxy-perhydro-1, 4-thiazine (SCMC-lactam).

The same ring compound was also obtained from *N*-Ac-SCMC when the latter was treated with DCCD at room temperature for two hours and hydrolyzed at pH 9.0. The direct dehydration product of *N*-Ac-SCMC had a larger R_f value and a smaller electrophoretic mobility than SCMC-lactam. The course of the reaction may be explained as follows:

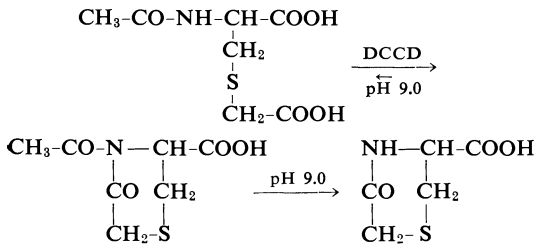

A minor part of the intermediate may be converted to the starting material under hydrolysis at pH 9.0.

An attempt to apply the cyclization reaction to the splitting of cysteine-containing peptides is now in progress.

Summary

S-Carboxymethyl-cysteine (SCMC) cyclizes by dehydration to form 3-oxo-5-carboxy-perhydro-1, 4-thiazine (SCMC-lactam) when the aqueous solution was heated at 110~180°C. SCMC-lactam was also obtained from *N*-acetyl-SCMC when the latter was treated with *N*, *N'*-dicyclohexylcarbodiimide and hydrolyzed subsequently at pH 9.0.

The author wishes to express his gratitude to Professor Nobuo Tamiya of the laboratory for his stimulating discussion and encouragement throughout this work. He is also grateful to Miss Keiko Tanno and Miss Hiroko Arai for their technical assistance.

Institute for Hard Tissue Research
Tokyo Medical and Dental University
Yushima, Bunkyo-ku, Tokyo

Synthese von 3, 6-Disubstituierten 2-Oxopiperazinen

Von Mitsuo MASAKI und Masaki OHTA

(Eingegangen am 8. März, 1963)

Die Derivate des 2-Oxopiperazins sind bekanntlich in der Pharmazeutik[1], z. B. als Anticonvulsiva, Antihistaminica, Ataraktica oder Heilmittel auf das Zentralnervensystem brauchbar.

Während die in 3-Stellung substituierten 2-Oxopiperazine durch Umsetzung von Äthylendiamin mit α-Halo-[2], α-Oxy-[1-c] säureestern oder Cyanhydrin[3] hergestellt werden können, ist über die Synthese von 3, 6-disubstituiertem 2-Oxopiperazin noch nicht berichtet worden, mit Ausnahme von Tetrahydrodeoxyaspergillsäure (IV, $R_1 = s\text{-}C_4H_9$, $R_2 = iso\text{-}C_4H_9$), die bei der Reduktion[4] des Antibiotikums Aspergillsäure erhalten wurde.

In dieser Mitteilung wird eine Synthese von 3,6-disubstituierten 2-Oxopiperazinen (IV), die auf der Reduktivcyclisation von dem durch Umsetzung von α-Halo-oxim (I) mit Aminosäureester leicht erhaltenen *N*-(2-Oximinoalkyl)-aminosäureester (II) beruht, beschrieben.

1) a) J. S. Strong u. a. (Rohm & Hass Co.), A. P. 2700668 vom 25. 1. 1955; *Chem. Abstr.*, **50**, 413 (1956); b) J. W. Cusic u. a, (G. D. Searle), A. P. 2787617 vom 2. 4. 1957; *Chem. Abstr.*, **51**, 12155 (1957); c) J. Bindler u. a. (J. R. Geigy Akt. Ges.), A. P. 2920077 vom 5. 1. 1960; *Chem. Abstr.*, **54**, 8868 (1960); d) A. P. Phillips (Burroughs Wellcome & Co.), A. P. 2958693 vom 1. 11. 1961; *Chem. Abstr.*, **55**, 9438 (1961); e) Lepetit S. p. A. (G. Melone u. a.), E. P. 870888 vom 21. 6. 1961; *Chem. Abstr.*, **56**, 482 (1962).

2) a) S. R. Aspinall, *J. Am. Chem. Soc.*, **62**, 1202 (1940); b) R. L. Hodgson, I. R. C. Bick und D. J. Cram, ebenda, **76**, 1137 (1954); c) T. Kametani, W. Taub und D. Ginsburg, Dieses Bulletin, **31**, 860 (1958).

3) J. S. Strong u. a. (Rohm & Hass Co.), A. P. 2649450 (1953); *Chem. Abstr.*, **48**, 8271 (1954).

4) J. D. Dutcher, *J. Biol. Chem.*, **171**, 321 (1947). vgl. G. T. Newbold u. a., *J. Chem. Soc.*, **1951**, 2679.

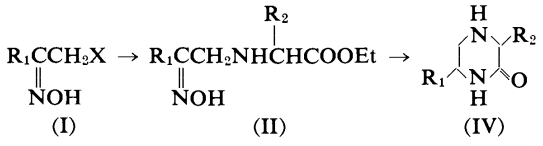

(I) (II) (IV)

	a	b	c	d
R_1	C_3H_7	*iso*-C_4H_9	C_6H_5	C_6H_5
R_2	*iso*-C_4H_9	*iso*-C_4H_9	*iso*-C_4H_9	$CH_2C_6H_5$

Schon sind die Reaktionen[5,6,7] von α-Chloroximen mit Piperidin und mit tertiären Aminen beschrieben worden, dagegen ist über Reaktion von α-Halo-oxim mit primärem Amin noch nichts berichtet worden.

Die Umsetzung von α-Brom- bzw. α-Chloroxim mit Aminosäureester gelang uns jedoch in Äther bei Raumtemperatur und ergab *N*-(2-Oximino-alkyl)-aminosäureester, aus denen 3-Isobutyl-6-propyl-, 3,6-Diisobutyl-, 3-Isobutyl-6-phenyl- und 3-Benzyl-6-phenyl-2-oxopiperazin synthesiert werden konnten.

Durch die Reduktion von 2-Nitro-1-penten mit Zinn(II)-chlorid in ätherischer Lösung[6] wurde 1-Chlor-2-oximinopentan (I-a) dargestellt, das leicht zersetzlich ist und sich als Piperidino-verbindung charakterisieren liess.

Durch Behandlung des Chlor-oxims (I-a) mit 2 Mol Leucinester in absol. Äther bei Raumtemperatur erhielten wir *N*-(2-Oximino-pentyl)-leucinester (II-a), der als die entsprechende Carbonsäure (V-a) charakterisiert wurde.

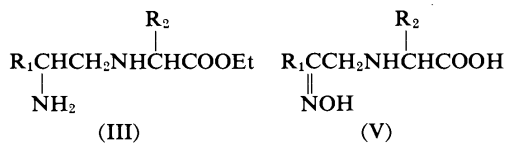

(III) (V)

Wenn man dabei als Chlorwasserstoffabspaltungsmittel *N*-Methylmorpholin benutzte, entstand *N*-Methylmorpholiumsalz des Chloroxims quantitativ und wurde Leucinester zurückerhalten, und beim Benutzen des Triäthylamins als dasjenige konnte kein definiertes Produkt erhalten werden.

Durch Reduktion von II-a unter Druck bei Raumtemperatur in Gegenwart von Raney-Nickel konnten wir 3-Isobutyl-6-propyl-2-oxopiperazin synthesieren, dessen Konstitutionsbeweis durch Elementaranalyse und IR-Spektrum erreicht wurde.

Wenn man Rücksicht auf Cyclisation[8] von δ-Amino-*n*-valeriansäure zum Piperidon nimmt, kann es leicht erwarten, dass sich die spontane Cyclisation des als Zwischenprodukt entstehenden *N*-(2-Aminopentyl)-leucinesters (III-a) ohne Erhitzen vollzieht, obgleich Aspinall[2a] beschrieben hat, dass beim Erhitzen auf 200°C der Ringschluss des bei der Umsetzung von Äthylendiamin mit α-Halo-ester als Zwischenprodukt entstandenen Diamino-esters auftritt.

In analoger Weise wie bei II-a liessen sich die Reaktionen von 1-Chlor-2-oximino-isohexan (I-b), das aus 2-Nitro-1-isohexen dargestellt werden kann, und von Phenacylbromid-oxim (I-c) mit Leucinester oder Phenylalaninester erreichen und ergaben *N*-(2-Oximino-isobutyl)-leucinester (II-b), *N*-(2-Phenyl-2-oximinoäthyl)-leucinester (II-c) und *N*-(2-Phenyl-2-oximinoäthyl)-phenylalaninester (II-d), die jeder für sich als die entsprechende Carbonsäure (V) charakterisiert wurden.

Bei der Reduktion lieferte II-b besonders leicht, wie bei II-a erwähnt wurde, das entsprechende 2-Oxopiperazin(IV-b), die Reduktivcyclisation von II-d zum 3-Benzyl-6-phenyl-2-oxopiperazin vollzog sich dagegen beim Erwärmen auf ca. 100°C. Die Effizienz der Reduktivcyclisierungsreaktion nimmt daher mit Austausch von aliphatischen durch aromatische Substituenten ab.

Über die pharmazeutische Aktivität der oben beschriebenen 3,6-disubstituierten 2-Oxopiperazine werden wir bald zusammen mit diejenige der anderen 2-Oxopiperazine berichten.

Beschreibung der Versuche

1-Chlor-2-oximinopentan (I-a).—Die Lösung des Reduktionsmittels liess sich dadurch erhalten, dass man 45 g krist. Zinn(II)-chlorid-dihydrat (96%) in 220 ccm absol. Äther, der 12 g Chlorwasserstoff enthielt, löste.

Eine Lösung von 17.3 g (ca. 0.15 Mol) 2-Nitro-1-penten[9] und 8 g Chlorwasserstoff in 150 ccm Äther wurde unter kräftigem Rühren und Kühlen im Eis/Kochsalz-Bad mit der oben beschriebenen Zinn(II)-chlorid-Lösung im Laufe von 4 Stdn. tropfenweise versetzt. Nach der Zugabe der Lösung des Reduktionsmittels wurde die Mischung noch 2 Stdn. weiter gerührt, dann mit Wasser im Scheidetrichter durchgeschüttelt. Die abgetrennte Ätherschicht wurde dreimal mit 1 N Salzsäure, einmal mit Weinsäure-lösung und anschliessend fünfmal mit Wasser gewaschen und über Natriumsulfat getrocknet. Der nach dem Abdampfen des Äthers verbliebene Rückstand wurde bei 77~86°C/10 mmHg destilliert. Ausb. 13 g (70%). Das bei 78~82°C/7 mmHg redestillierte α-Chlor-oxim ist leicht zersetzlich und scheidet bald farblosen Niederschlag ab.

Bei der Umsetzung mit Piperidin ergibt das Destillat 2-Oximino-1-piperidino-pentan vom Schmp. 66~67°C (aus Petroläther).

Gef.: N, 15.44. Ber. für $C_{10}H_{20}ON_2$: N, 15.20%.

5) O. Wallach, *Ann.*, 306, 278 (1899).
6) A. Dornow, H. D. Jordan und A. Müller, *Chem. Ber.*, 94, 67 (1961).
7) A. Dornow und H. D. Jordan, ebenda, 94, 76 (1961).
8) E. Fischer und G. Zemplin, *Ber.*, 42, 4884 (1909).
9) M. Masaki und M. Ohta, Dieses Bulletin, 35, 1418 (1962).

***N*-(2-Oximino-pentyl)-*N*-methyl-morpholiumchlorid.**—Dieses wurde bei dem Versuch zur Reaktion von I-a mit Aminosäureester in Gegenwart von *N*-Methylmorpholin als Chlorwasserstoffabspaltungsmittel erhalten.

Eine Lösung von 13.5 g I-a in 40 ccm absol. Äther liess man unter Rühren und Kühlen einer Lösung von 15.9 g L-Leucin-äthylester und 10.1 g *N*-Methylmorpholin in 100 ccm absol. Äther zutropfen, saugte das nach einnächtigem Stehen bei Raumtemperatur ausgeschiedene Salz ab und wusch mit absol. Äther. Farblose Prismen vom Schmp. 169~171°C (aus Äthanol). Ausb. 18 g.

Gef.: N, 11.62. Ber. für $C_{10}H_{21}O_2N_2Cl$: N, 11.89%.

***N*-(2-Oximino-pentyl)-leucin-äthylester (II-a).**—Eine Lösung von 63 g L-Leucin-äthylester in 200 ccm absol. Äther wurde mit einer Lösung von 26 g I-a in 100 ccm absol. Äther unter Kühlen und kräftigem Rühren versetzt und noch 30 min. weitergerührt. Bald begann Leucinesterhydrochlorid langsam sich auszuscheiden, dann wurde die Mischung bei Raumtemperatur (10~20°C) stehengelassen. Nach 8 Tagen filtrierte man das Salz ab, wusch mit absol. Äther, engte die vereinigte ätherische Lösung zu ca. 120 ccm ein, wusch dann mit Wasser und extrahierte dreimal mit je 50 ccm 3 N Salzsäure. Die einmal mit Äther gewaschene und dann mit Kohle behandelte salzsauere Lösung wurde mit Natriumcarbonat neutralisiert und ausgeäthert. Der Ätherextrakt wurde fünfmal mit Wasser gewaschen und über Natriumsulfat getrocknet. Beim Abdampfen des Äthers hinterblieb ein gelbliches Öl, das beim Stehen im Eisschrank erstarrte, doch sich durch weder Umkristallisation noch Destillation reinigen liess. Rohausb. 35 g (70%). Das Produkt wurde durch Verseifung zur freien Carbonsäure (V-c) charakterisiert.

Das Rohprodukt (2 g) wurde in einer Lösung von 2 g Kaliumhydroxyd in 8 ccm Wasser gelöst und über Nacht bei Raumtemperatur belassen. Am anderen Tage wurde die Lösung mit 40~50 ccm Wasser verdünnt, mit Kohle behandelt, filtriert und aus dem Filtrat durch langsames Eintropfen von 20-proz. Essigsäure die Oximino-aminosäure (V-a) in kristalliner Form ausgefällt. Ausb. 1.4 g. Farblose Nädelchen vom Schmp. 192~193°C (aus Methanol).

Gef.: C, 57.43; H, 9.95; N, 12.11. Ber. für $C_{11}H_{22}O_3N_2$: C, 57.36; H, 9.63; N, 12.17%.

3-Isobutyl-6-propyl-2-oxopiperazin (IV-a).—Zur Lösung von 2 g II-a in 60 ccm Äthanol gab man eine Aufschlammung von 1 g Raney-Nickel in 40 ccm Äthanol. Diese Mischung wurde bei Raumtemperatur im Rührautoklav bei 100 atm. Wasserstoff bis zur Druckkonstanz hydriert, dann durch Abfiltrieren vom Katalysator befreit und das Lösungsmittel auf dem Wasserbad unter vermindertem Druck entfernt. Der Rückstand wurde zweimal aus Petroläther umkristallisiert. Ausb. 0.8 g. Farblose Nadeln vom Schmp. 106°C. $[\alpha]_D^{18}$ −50.7° in Äthanol, c=1.06. IR-Spektrum in CCl_4: 3400, 3200, 3080, 1665 und 1470 cm^{-1}.

Gef.: C, 66.70; H, 11.26; N, 14.17. Ber. für $C_{11}H_{22}ON_2$: C, 66.62; H, 11.18; N, 14.13%.

***N*-(2-Oximino-isobutyl)-leucin-äthylester (II-b).**—Eine Lösung von 16.5 g 2-Nitro-1-isohexen[10] und 7 g Chlorwasserstoff in 130 ccm Äther wurde im Laufe von 4 Stdn. mit 38.5 g Zinn(II)-chlorid und 10.5 g Chlorwasserstoff, gelöst in 190 ccm absol. Äther, versetzt und dann analog wie bei I-a aufgearbeitet. 1-Chlor-2-oximino-isohexan (Sdp. 84~89°C/7.5 mmHg) wurde in Ausb. 12.5 g (65%) erhalten, aber nach der Destillation war das Produkt sehr unbeständig und wurde daher direkt weiter verarbeitet.

Die Lösung des erhaltenen Produkts in 80 ccm absol. Äther liess man unter Rühren einer Lösung von 26.5 g L-Leucin-äthylester in 120 ccm absol. Äther zutropfen und bei Raumtemperatur (10~25°C) stehen. Nach 9 Tagen wurde das Gemisch analog wie bei II-a aufgearbeitet und ein gelbliches viskoses Öl erhalten. Rohausb. 12.5 g. Ein Teil des Rohprodukts wurde versuchsweise in Stickstoff-atmosphäre bei 126~128°C/0.02 mmHg destilliert, wobei das gelbe Destillat sofort trübe wurde. IR-Spektrum in CCl_4: 3600, 1650 (-C=N-OH) und 1735, 1180, 1150 cm^{-1} (-$COOC_2H_5$).

Gef.: N, 10.11. Ber. für $C_{14}H_{28}O_3N_2$: N, 10.28%.

Beim analogen Verseifen wie bei II-a lieferte das Rohprodukt (2 g) die entsprechende Carbonsäure (V-b). Ausb. 1.5 g. Farblose Nadeln vom Schmp. 195~197°C.

Gef.: N, 11.42. Ber. für $C_{12}H_{24}O_3N_2$: N, 11.47%.

3,6-Diisobutyl-2-oxopiperazin (IV-b).—Eine Lösung von 4 g II-b in 100 ccm Äthanol wurde unter gleicher Bedingung wie bei IV-a reduziert. Ausb. 1.7 g. Farblose Nadeln vom Schmp. 105.5~106.5°C (aus Petroläther und dann n-Hexan). $[\alpha]_D^{18}$ −50.5° in Äthanol, c=1.00. IR-Spektrum in CCl_4: 3380, 3190, 3070, 1665 und 1465 cm^{-1}.

Gef.: C, 67.83; H, 11.56; N, 13.10. Ber. für $C_{12}H_{24}ON_2$: C, 67.88; H, 11.39; N, 13.19%.

***N*-(2-Phenyl-2-oximinoäthyl)-leucin-äthylester (II-c).**—Zur Lösung von 6.4 g L-Leucin-äthylester in 100 ccm absol. Äther versetzte man mit 4.3 g Phenacylbromid-oxim (Schmp. 85~86°C) und liess bei Raumtemperatur stehen. Nach einer Woche wurde der ausgeschiedene Niederschlag (L-Leucin-äthylester-hydrobromid) abfiltriert, und das Filtrat auf dem Wasserbad auf ca. 50 ccm eingeengt, mit Wasser gewaschen und dreimal mit 3 N Salzsäure extrahiert. Der Extrakt wurde einmal mit Äther gewaschen, mit Kohle behandelt dann mit Natriumcarbonat neutralisiert und ausgeäthert. Der ätherische Extrakt wurde dreimal mit Wasser gewaschen, dann über Natriumsulfat getrocknet und die Lösungsmittel unter vermindertem Druck eingedampft, wobei 4.2 g rohes II-c zurückblieben.

Beim analogen Verseifen des Rohprodukts wie bei II-a erhielt man *N*-(2-Phenyl-2-oximinoäthyl)-leucin (V-c) in 77 proz. Ausb. Schmp. 162°C.

Gef.: N, 10.46. Ber. für $C_{14}H_{20}O_3N_2$: N, 10.60%.

3-Isobutyl-6-phenyl-2-oxopiperazin (IV-c).—Der rohe Oximino-ester II-c (3 g) wurde bei 70~90°C analog wie bei IV-a reduziert. Ausb. 1.2 g. Farblose Nadeln vom Schmp. 117~118°C (aus Ligroin und dann *n*-Hexan). $[\alpha]_D^{18}$ −36.5° in Äthanol, c=1.29. IR-Spektrum in CCl_4: 3380, 3190, 3060, 1664 und 1458 cm^{-1}.

10) M. Masaki und M. Ohta, ebenda, 35, 1808 (1962).

Gef.: C, 72.67; H, 8.43; N, 12.21. Ber. für $C_{14}H_{20}ON_2$: C, 72.38; H, 8.64; N, 12.06%.

***N*-(2-Phenyl-2-oximinoäthyl)-phenylalanin-äthylester (II-d).**—Zur Lösung von 15.4 g DL-Phenylalanin-äthylester in 200 ccm absol. Äther versetzte man unter Rühren mit 8.5 g Phenacylbromid-oxim und liess bei Raumtemperatur stehen. Nach einer Woche wurde die von ausgeschiedenem Niederschlag befreite Lösung auf dem Wasserbad auf ca. 100 ccm eingeengt, zweimal mit Wasser und einmal mit 1 N Salzsäure (10 ccm) gewaschen und dann mit 3 N Salzsäure (20 ccm) geschüttelt, wobei sich ein Öl abschied. Die äther. Schicht wurde noch einmal mit 3 N Salzsäure (20 ccm) extrahiert, dann die vereinigte salzsaure Lösung und das ausgeschiedene Öl einmal mit Äther gewaschen, mit Natriumcarbonat neutralisiert, ausgeäthert und zweimal mit Wasser gewaschen. Die über Natriumsulfat getrocknete äther. Lösung wurde unter vermindertem Druck eingedampft, wobei eine gelbliche Schmiere, rohes II-d, zurückblieb. Ausb. 6.9 g.

Beim Verseifen in üblicher Art lieferte die Schmiere (2 g) die freie Säure V-d (1.7 g) vom Schmp. 210~212°C.

Gef.: N, 9.62. Ber. für $C_{17}H_{18}O_3N_2$: N, 9.39%.

3-Benzyl-6-phenyl-2-oxopiperazin (IV-d).— Der rohe Oximino-ester II-d (4 g), in 100 ccm Äthanol gelöst, wurde bei ca. 100°C analog wie bei IV-a reduziert. Der beim Entfernen des Äthanols hinterbliebene Rückstand erstarrte beim Kühlen zu einem Kristallbrei. Dieser wurde abgesaugt, und mit Tetrachlorkohlenstoff gewaschen. Rohausb. 1.5 g. Zweimalige Umkristallisation aus Methanol gab farblose Prismen vom Schmp. 170~171°C. IR-Spektrum in KBr: 3400, 3275, 3190, 3070, 1660 und 1458 cm^{-1}.

Gef.: C, 76.67; H, 6.95; N, 10.58. Ber. für $C_{17}H_{18}ON_2$: C, 76.66; H, 6.81; N, 10.52%.

Laboratorium für Organische Chemie
Tokyo Institut für Technologie
Meguro-ku, Tokyo

*Steady-state Studies by the ESR Method of the Photopolymerization of Vinyl Acetate and Methyl Methacrylate**

By Keiji KUWATA, Ko-ichi NISHIKIDA, Hiroshi KAWAZURA** and Kozo HIROTA

(Received March 20, 1963)

In the free radical-initiated photopolymerization of vinyl monomers, free radical intermediates paly an important role as chain initiators or chain carriers or both. In the kinetic studies[1] it has already been shown that both the rate and the degree of polymerization are closely related to steady-state concentration of the radical intermediates. It becomes important, therefore, not only to identify the free radical intermediates, but also to determine their concentration in the course of the reaction.

The use of the ESR method in identifying such radical intermediates in nonsteady-state photopolymerization has given us very useful knowledge about the initiating step[1-4], the propagating step[2-4] and the terminating step[3]. The structures of the decomposition products of initiators and those of both initiating and propagating free radicals formed by the reaction of the primary radical fragment of the initiator with monomers have been investigated.

It has now become possible to determine by the ESR method the rates of initiation, propagation, and termination steps on some plausible assumptions and also to determine the steady-state concentration of the radical chain carriers. Therefore, the steady-state study by the ESR method, as abopted by Piette et al.[5] in the photo-dissociation of some alkyl hydroperoxides, should be very effective in a detailed investigation of the kinetic process of the present photopolymerization.

By a comparison of the steady-state concentration determined experimentally with the one derived by a simple steady-state treatment of the polymerization, it will be possible to

* A preliminary report was presented to the 1st Meeting of ESR (Japan), October, 1962, Osaka.

** Present address: The Nippon Synthetic Chem. Ind. Co., Ltd., Kami-Kema, Amagasaki City.

1) Cf. C. H. Bamford et al., "The Kinetics of Vinyl Polymerization by Radical Mechanisms", Butterworths Scientific Publications, London (1958).

2) D. J. E. Ingram, M. C. R. Symons and M. G. Townsend, *Trans. Faraday Soc.*, **54**, 409 (1958).

3) K. Hotta and R. S. Anderson, The 4th International Symposium on Free Radical Stabilization, Washington, D. C., 1959.

4) K. Kuwata and K. Hirota, The 10th Annual Meeting of the Association of Polymer Science of Japan, Tokyo, May, 1961.

5) L. H. Piette and W. C. Landgraf, *J. Chem. Phys.*, **32**, 1107 (1960).

analyze the kinetic data of polymerization. It is particularly important to reconsider the use of an average rate constant for various polymeric chain carriers of different molecular weights. Therefore, we attempted in the present investigation to apply such a steady-state method to the photopolymerization of vinyl acetate and methyl methacrylate, using hydrogen peroxide as the initiator; a reasonable accordance was found to exist between experiment and theory.

Experimental

Materials.—Commercial vinyl acetate and methyl methacrylate were repeatedly distilled and used. Commercial hydrogen peroxide (ca. 30%) was concentrated by vacuum-distillation up to ca. 90%.

Apparatus and Procedure. — To each monomer was added a small amount of enriched hydrogen peroxide so that the latter concentration became ca. 1 mol.%. The sample thus prepared was poured into a quartz tube in which a capillary tube, charged with diphenyl picryl hydrazil (DPPH) or ultramarine of a known spin concentration so as to serve as an analytical internal standard, has been set coaxially. The sample tube thus set up was repeatedly degassed in vacuo and was then sealed off.

Ultraviolet light from a high pressure mercury lamp (1 kW) was focussed with a quartz lens onto the sample tube, which had been inserted into a resonant cavity of a spectrometer. The spectrometer was a high frequency field modulation type, operated at 455 kc. The resonant cavity was a rectangular H_{102} one of the Ingram type and was dipped in a low temperature bath charged with liquid nitrogen as a coolant. The temperature in the cavity was measured with a thermocouple of copper versus constantan, its accuracy being ± 1°K. The temperature in the cavity was adjusted by controlling the level-height of the coolant. The design of this part of the cavity has already been published[6].

The Determination of Rate and Rate Constant. —Before the polymerization reached a steady state, the growth rate of the initiating radical* was measured at such a low temperature (ca. 100°K) that the recombination could be assumed completely quenched. Then, warming the sample up to the temperature where the radical concentration remained constant, i.e., when the steady-state polymerization was realized, the steady-state concentration of the radical was measured, and the rate of decay was determined at the same temperature by cutting off the irradiation source. The temperatures when the steady-state concentration was attained were 115°K for vinyl acetate and 180°K for methyl methacrylate.

The radical concentration was evaluated by comparing the intensity of the absorption of the radical with that of DPPH in the case of vinyl acetate. However, due to the closeness of g-factors between DPPH and the radicals, the two absorption spectra overlapped each other, thus lowering the accuracy of the concentration determination. In the case of methyl methacrylate, therefore, ultramarine ($g=2.030$) was used instead of DPPH.

Results and Discussion

It is shown by Fig. 1 that the initiating radical increases linearly with time in the case of vinyl acetate, though it is not clear if an induction period exists. Similarly, a linear relation was obtained also in the case of methyl methacrylate, as Fig. 2 shows. Assuming the initiation step of the photopolymerization to be of the zeroth order reaction*, the rate of radical growth can be determined from the slope of the curve in Figs. 1 and 2. Stricktly speaking, the radical concentrations

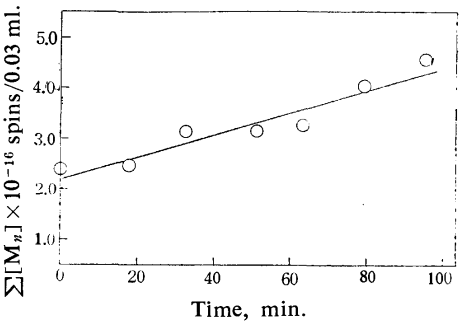

Fig. 1. Radical growth of vinyl acetate against irradiation time at 100°K.

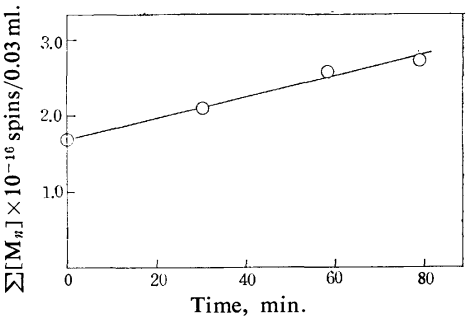

Fig. 2. Radical growth of methyl methacrylate against irradiation at 100°K.

6) K. Kuwata and K. Hirota, This Bulletin, 34, 458 (1961).

* It has been confirmed[4,7] that by irradiating such a system, occluding H_2O_2 at 77°K, an asymmetric signal appears which can be ascribed to the OH or O_2H radical, but if it is kept at 90~100°K, another signal increases its intensity and replaces the first one finally. The initiating radical in the present paper corresponds to the second signal.

7) K. Kuwata, T. Ichikawa and K. Hirota, *J. Chem. Soc. Japan, Pure Chem. Sec.* (*Nippon Kagaku Zasshi*), 83, 652 (1962).

* This is due to the fact that the production of $\dot{M}$ is very fast compared with that of $\dot{X}$ in Eq. 1.

TABLE I. RATE CONSTANTS AND STEADY-STATE RADICAL CONCENTRATIONS

		Vinyl acetate	Methyl methacrylate
Rate of radical growth, v_l		$1.2_2\times10^{-5}$ molec./l./min.	$8.3_1\times10^{-6}$ molec./l./min.
Rate constant of radical decay, k_t		$2.7_1\times10$ l./molec./min.	$1.8_1\times10$ l./molec./min.
Steady-state radical concn. $\sum_n[\dot{M}_n]$	Obs.	$1.1_1\times10^{-3}$ molec./l.	$7.2_2\times10^{-4}$ molec./l.
	Calcd.	$6.7_1\times10^{-4}$ molec./l.	$6.7_8\times10^{-4}$ molec./l.
	% dev.	−40%	−8%

thus determined include that of the propagating radicals, but since their amount equals that of the initiating radical which disappeared, the above procedure to determine the rate of radical growth may be said to be justified. The procedure was applied to both monomers, and the rates of radical growth, v_l, obtained are described in Table I.

Next, the rate of the termination step was that determined in a similar manner by assuming the radical concentration decays only by way of the termination reaction of the second order. The rate constants of radical decay, k_t, thus obtained are shown in Table I. The decay rate is shown for vinyl acetate by Figs. 3 and 4, where the open circles denote the experimental values, while the curve is the calculated value. These rate constants correspond to the ones defined by the following reaction scheme:

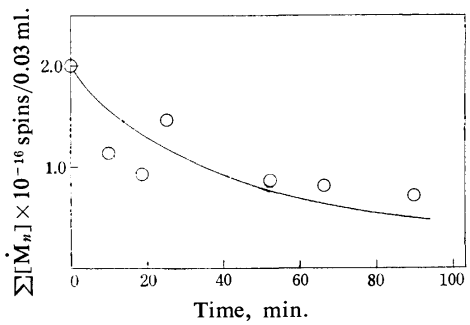

Fig. 3. Radical decay of vinyl acetate at 115°K.

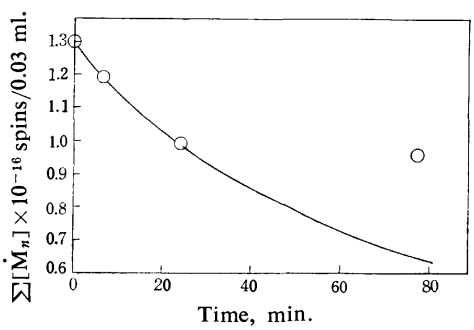

Fig. 4. Radical decay of methyl methacrylate at 180°K.

$$\left.\begin{array}{lll} \text{Initiator} \rightsquigarrow \dot{X} & & v_d=\phi I \\ M+\dot{X} \longrightarrow \dot{M} & & v_l=k_l[M][\dot{X}] \\ \dot{M}_{n-1}+M \longrightarrow \dot{M}_n & & v_p=k_p[M](\sum[\dot{M}_{n-1}]) \\ \dot{M}_n+\dot{M}_m \longrightarrow M_{n+m} & & v_{tc}=k_{tc}(\sum[\dot{M}_n])^2 \\ \dot{M}_n+\dot{M}_m \longrightarrow M_n+M_m & & v_{td}=k_{td}(\sum[\dot{M}_n])^2 \end{array}\right\} \quad (1)$$

Here, I is the light intensity absorbed by the initiator. k_t is defined by a sum of the rate constant of radical recombination, k_{tc}, and that of the disproportionation, k_d, between two propagating radicals $\dot{M}_n$ and $\dot{M}_m$, as shown by reaction scheme 1, i. e.,

$$k_t = k_{td}+k_{tc} \quad (2)$$

In Table I, the steady-state concentrations of the propagating radicals are compared with those calculated by Eq. 3, which employs a simple kinetic treatment[8]:

$$\sum_n[\dot{M}_n] = (v_i/k_t)^{1/2} \quad (3)$$

which exists among the steady-state concentration, $\sum_n[\dot{M}_n]$, of the propagating radical, the rate of radical growth, v_l, and that of termination, k_t.

Table I tells us that the steady-state radical concentrations calculated by Eq. 3 coincide well with those observed in the cases of both vinyl acetate and methyl methacrylate within a factor of two. This agreement seems to be surprisingly good if one considers that the errors occurred in the determination of the radical concentration and the rate of growth. There remains some doubt about the oversimplifications which were worked out in the simple kinetic treatment. In the calculation, only one decay constant is used as an average value for all the polymer radicals of different molecular weights. However, the observed decay curve corresponds to the one superposed by those of individual polymer radicals of different chain lengths. Therefore, the rate constant of radical decay determined on the assumption of simple second order kinetics

8) Cf. Ref. 1, p. 14; J. Laidler, "Chemical Kinetics", McGraw Hill Book Co., Inc., New York (1950), pp. 345—364.

ought not to be used over a wider range of the progress of reaction. Actually, the calculated curve of MMA polymerization (Fig. 4) deviates gradually from the observed values as the polymerization proceeds, i. e., as the chain length of the polymer radical becomes larger. This is probably due to the fact that the reaction rate decreases with the chain length of the polymerizing radicals. A similar tendency seems to occur in the case of VAc as well (Fig. 3), though it cannot be observed so clearly.

There are some modifications of the treatment regarding the direction which will give a more exact feature concerning the radical decay in the case of radical polymerization[9]. However, it can be shown as above that the simple kinetic treatment retains its usefulness in such a limited case of the liquid state photopolymerization at a low temperature as in the present research. One of the reasons why such an accordance was realized seems to be because the error in the determination of the decay rate was canceled out, together with the errors in the determination of the growth rate.

9) G. Gee and H. W. Melville, *Trans. Faraday Soc.*, **40**, 240 (1944).

Summary

It has been attempted, by the ESR technique, to study the steady-state photopolymerization of vinyl acetate and methyl methacrylate, using hydrogen peroxide as the initiating substance. The observed steady-state radical concentration has been found to coincide within a factor of two with the calculated value, Eq. 3, derived under the assumption of a simple kinetic treatment. Although, it has been shown that the calculated decay curve deviates from the observed curve in the later period of decay, especially in the case of methyl methacrylate; such a discrepancy seems to be explainable if the reaction rate decreases with the chain length of the polymerizing radicals.

A part of the expense of this research has been defrayed by a special grant given us by the Ministry of Education to which our thanks are due.

Department of Chemistry
Faculty of Science
Osaka University
Nakanoshima, Osaka

The Thermal Annealing of Phosphorus-32 Formed by the Neutron Irradiation of Several Inorganic Phosphorus Compounds

By Hiroshi BABA, Kichizo TANAKA and Kenji YOSHIHARA

(Received April 6, 1963)

The distribution of chemical forms of phosphorus-32 in neutron-irradiated phosphorus compounds has been reported on by several investigators[1-8]. It has been found that these phenomena are very complicated. It seems important to solve the problem that the proportions of the different chemical species of phosphorus-32 appear to depend on various complicated factors: the effect of thermal annealing, which has proceeded during and after the neutron irradiation, the chemical form of the target materials[9], and the circumstances during neutron irradiation[10]. The change in the distribution of phosphorus-32 in various chemical forms after neutron irradiation of phosphorus compounds has been pointed out by Lindner and Harbottle[11] and also by Yoshihara and Yokoshima[12]. They treated the

1) W. F. Libby, *J. Am. Chem. Soc.*, **62**, 1930 (1940).
2) W. D. E. Thomas and D. J. D. Nicholas, *Nature*, **163**, 719 (1949).
3) I. G. A. Fiskell, *Science*, **113**, 244 (1951).
4) I. G. A. Fiskell, W. A. Delong and W. F. Oliver, *Can. J. Chem.*, **30**, 9 (1952).
5) P. A. Sellors, T. R. Sato and H. H. Strain, *J. Inorg. Nucl. Chem.*, **5**, 31 (1957).
6) T. R. Sato, P. A. Sellors and H. H. Strain, ibid., **7**, 84 (1959).
7) A. H. W. Aten, Jr., H. van der Straaten and P. C. Riesbos, *Science*, **115**, 267 (1952).
8) M. Shima and S. Utsumi, *J. Inorg. Nucl. Chem.*, **20**, 177 (1961).
9) H. Baba, to be published.
10) T. R. Sato and H. H. Strain, "Proceedings of the Symposium on Chemical Effects of Nuclear Transformations", Vol. I, I A E A, Prague (1961), p. 503.
11) L. Lindner and G. Harbottle, ibid., 485 (1961).
12) K. Yoshihara and T. Yokoshima, This Bulletin, **34**, 123 (1961).

irradiated salts at room temperature and suggested a specific interpretation of the change in the proportion of the distributed chemical species. Claridge and Maddock[13] have performed thermal annealing experiments using the precipitation method for the separation of chemical species and have suggested an increase in retention and in the threshold temperature as the result of thermal annealing.

Green and Maddock[14] first found that the retention in the Szilard-Chalmers process was increased by the thermal annealing of heating-irradiated chromates. The activation energy for this process has been shown by Harbottle and Sutin[15] to be the energy of the recombination reaction of fragments formed by recoil phenomena. In their treatment for thermal annealing, the term of the change of the retention meant the composite process of change in all the species chemically distributed. In the case of phosphorus recoil chemistry, however, such a treatment of " retention " may give somewhat ambiguous results in the analysis of the given annealing curves.

In a previous communication[16] the present authors pointed out the different behaviour of the different fractions of phosphorus-32 upon thermal annealing. It should be considered that the activation energy of the thermal annealing process of each fraction differs from that of the retention.

In this paper, the authors will describe a detailed study of the thermal-annealing effect of phosphorus-32 in the distributed chemical species with several anhydrous inorganic phosphates and pyrophosphate in crystal, and will report their findings on the activation energies of separated fractions of phosphorus-32.

Experimental

Target Materials.—The sodium dihydrogen phosphate and sodium dihydrogen phosphite used were guaranteed reagents of the Wako Chemicals Co. while the disodium hydrogen phosphate, potassium dihydrogen phosphate, sodium pyrophosphate, and disodium hydrogen phosphite were guaranteed reagents of the Kanto Chemicals Co. Each of these hydrated salts, except potassium dihydrogen phosphate and sodium pyrophosphate, was dehydrated upon heating in a porcelain dish, and evaporating it to near dryness. All salts were dried in vacuo at 100°C for one night over phosphorus pentoxide. Anhydrous trisodium phosphate was prepared from $Na_3PO_4 \cdot 12H_2O$ in the same way. The content of sodium or potassium ions in these salts was determined by flame photometry using a Perkin-Elmer flame photomater. The purity of anions was tested by activation analysis as follows: a small portion of each salt was dissolved in water and was subjected to paper chromatographic separation. Dried paper strips were irradiated in a nuclear reactor, and were cut to pieces 1 cm. in width. The radioactivity was counted by a GM counter 2 weeks after the end of the neutron irradiation. The purity was calculated from the percentage of the radioactivity of the fraction at the corresponding position on the strips. The results are tabulated in Table I.

Table I. Purity of target materials

Target material	Anionic %	Cationic* %
NaH_2PO_4	96	99
Na_2HPO_4	99	99
Na_3PO_4	99	60
$Na_4P_2O_7$	88	99
Na_2HPO_3	98	—
KH_2PO_4	94	—

* Purity as corresponding molecular form.

Neutron Irradiation.—The irradiations were mainly performed in the irradiation hole No. 12 (a vertical hole; thermal neutron flux 4.8×10^{11} n/cm^2·sec.) of JRR-1 (a water boiler reactor operated at 40 kW) for 15 hr. The salts which had been sealed in polyethylene tube in the presence of air were placed in an ambient reactor temperature. After being stored for 1 week at room temperature, the salts were subjected to thermal-annealing experiments. For irradiation and storage, all of the salts were maintained in as constant a condition as possible in order to avoid a change in the initial distribution of phosphorus-32 species.

Thermal-Annealing and Chemical Separation.—The irradiated salts were heated in a quartz boat (size: $10.5 \times 1.2 \times 1.2$ cm^3) which was placed in a thermostatically-controlled electric furnace (a quartz cylinder 2.4 cm. in diameter was used for heating the samples). The samples were inserted at the center of the cylinder, and a Pt-Rh thermostat was operated at the same time. A small portion of the heated samples in the boat was taken into the small water-cooled glass bottle at definite time intervals and was dissolved in a sufficient volume of water.

The separation and identification of the chemical species of phosphorus-32 were accomplished by paper chromatography. Two methods were tried for separation. One of them was that reported previously by one of the present authors, using the Toyoroshi No. 53 (2 cm. × 40 cm.) to separate the polyphosphates and orthophosphate fractions. One drop of the sample solution was put on filter paper (5 cm. from the end of the strip), dried in air, and developed by the one-dimensional ascending method with 2 N nitric acid-saturated *n*-butanol for about 24 hr. Another method was chosen to separate the fraction in such reduced species as phosphite and

13) R. F. C. Claridge and A. G. Maddock, " Proceedings of the Symposium on Chemical Effects of Nuclear Transformations ", Vol. I, I A E A, Prague (1961), p. 475.
14) I. H. Green and A. G. Maddock, *Nature*, **164**, 788 (1949).
15) G. Harbottle and N. Sutin, " Advances in Inorganic Chemistry and Radiochemistry ", Vol. 1. Ed., by H. J. Emeleus and A. G. Sharpe, Academic Press, New York and London. (1959), p. 305.
16) H. Baba, K. Yoshihara, H. Amano, K. Tanaka and N. Shibata, This Bulletin **34**, 590 (1961).

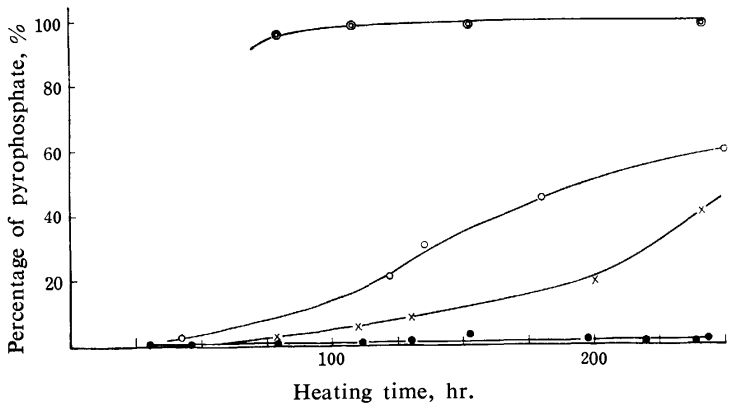

Fig. 1. Formation of pyrophosphate by heating several phosphates.
—×— Sodium dihydrogen phosphate at 150°C
—◎— Sodium dihydrogen phosphate at 200°C
—●— Disodium hydrogen phosphate at 150°C
—○— Disodium hydrogen phosphate at 200°C
For trisodium phosphate, sodium pyrophosphate and disodium hydrogen phosphite no change of chemical species is observed by heating at 200°C for 230 hr.

hypophosphite from the bulk of the neutron-irradiated salts. Pretreated filter paper was used in this case; the paper was preliminarily immersed into a solution of dilute hydrochloric acid for 1 day, soaked with redistilled water for another day, washed repeatedly with water, and dried in air; it was then developed with a mixture of 1 N ammonia, dioxane, and *n*-butanol (1 : 1 : 1 volume ratio) for 20 hr.

Counting Procedure.—After developing and drying, the paper was cut into pieces 1 cm. in width. The radioactivity of the pieces was measured by a thin end window-type GM gas flow counter at a constant geometry. Decay curves were drawn for all salts. Counting was started at least 10 days after the end of neutron irradiation in order to avoid errors besed on the radioactivity of sodium-24 or potassium-42. The gamma ray spectra of salts were measured with a NaI scintillation spectrometer in order to verify the absence of other activities.

A Test of the Pyrolysis of the Target Materials.—The target materials, which had not been neutron-irradiated, were heated under the same conditions as in the thermal-annealing experiments but for a comparatively prolonged time. The heated samples were dissolved in water, and the anions were separated by paper chromatography with 2 N nitric acid-saturated *n*-butanol. The strip of paper was dried in air and was subjected to neutron irradiation in a reactor. The radioactivity on the paper was counted with a GM counter 2 weeks after the end of neutron irradiation, and the percentage of the fraction of polyphosphate was estimated. Figure 1 shows the pyrophosphate formed by heating sodium dihydrogen phosphate and disodium hydrogen phosphate at 150~200°C versus the heating time. The formation of neither such higher polyphosphates as tripolyphosphate, tetrapolyphosphate and Grahams' salt, nor such reduction products as phosphite and hypophosphite was detected in any of the salts used here.

Results and Discussion

Figures 2 and 3 are histograms of paper chromatography showing the distribution of phosphorus-32 in various chemical species. The results obtained by development with nitric acid-saturated *n*-butanol are shown in Fig. 2, while those obtained by development with the mixture of 1 N ammonia, dioxane and *n*-butanol are shown in Fig. 3. The several peaks found in the histograms are noted as A, B, C, etc.

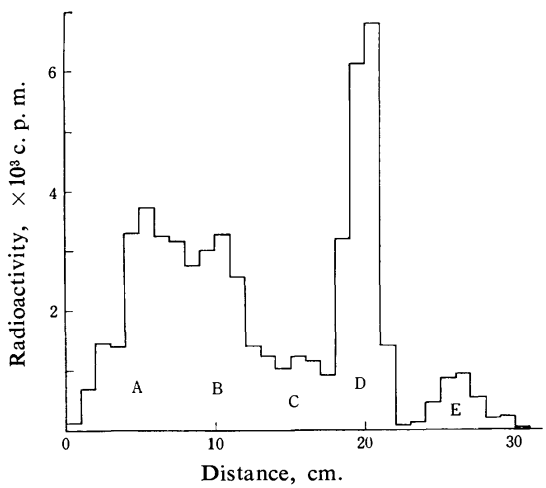

Fig. 2. Chromatographic separation of neutron irradiated disodium hydrogen phosphate with 2 N nitric acid saturated *n*-butanol.

From the R_f value in the chromatograms, it is indicated that the A and B fractions corresponded to the mixture of such higher polyphosphates as tripolyphosphate and polymerized metaphosphates. Pyrophosphate was found in C fractions and orthophosphate, in D fractions. A mixture of phosphite and hypophosphite appeared in E fractions. The separation among A, B and C fractions was not very significant, so the sum of A, B and C was identified as a polyphosphate fraction. In the case of pyrophosphate salt, the sum of the A and B fractions was denoted as a polyphosphate fraction. The E fraction was noted as a reduced species fraction, and D, as an orthophosphate fraction. These assignments were also expected from the results of other experiment[17]. The percentage of the F fraction is equal to the sum of A, B, C and D, the percentage of the E fraction also corresponds to the sum of G and H, while the G fraction can not be identified as phosphite because a low R_f value of the G fraction compared with that of phosphite is obtained. The R_f value of the H fraction is in agreement with that of hypophosphite.

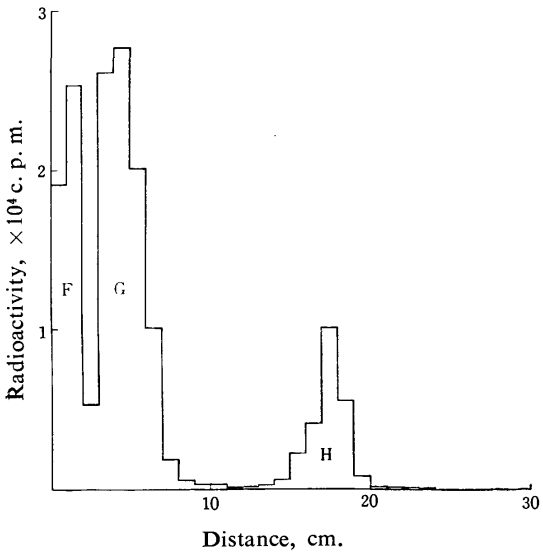

Fig. 3. Chromatographic separation of neutron irradiated disodium hydrogen phosphite with mixed solution (1 : 1 : 1) of 1 N ammonia, dioxane and *n*-butanol.

The samples irradiated in a nuclear reactor were heated in the temperature range of 85~200°C. Similar annealing curves were obtained from all of the orthophosphate salts used. Typical examples of these annealing against the logarithm of time are shown in Figs. 4, 5 and 6. The proportion of phosphorus-32 in the fraction is registered on the ordinate, while on the absissa the heating time is given in minutes. The percentage of the activities in the polyphosphate fraction decreases remarkably, while only a slight decrease is observed in the case of the reduced-species fractions. However, retention as orthophosphate always increases. The annealing curves given from sodium pyrophosphate are very similar to that of orthophosphate salts, but the orthophosphate fraction is a little changed. In the case of sodium phosphite, quite different annealing behavior is observed. Retention as the phosphite fraction increases while an increase in the hypophosphite fraction occurs at the same

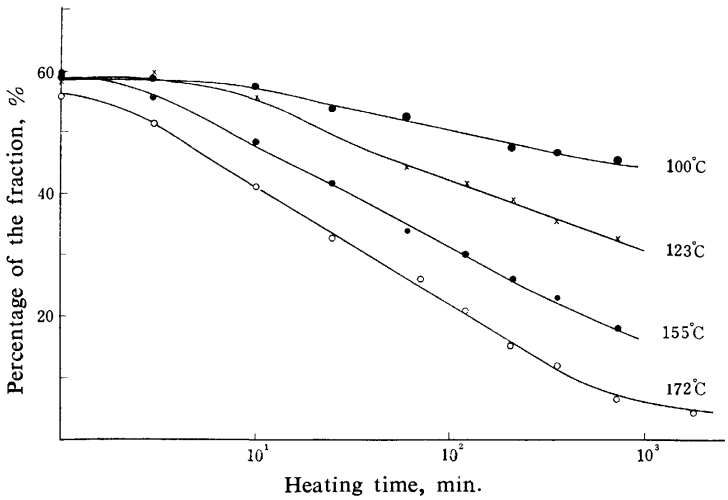

Fig. 4. Isothermal annealing curves for the polyphosphate fraction in irradiated disodium hydrogen phosphate.

17) K. Tanaka, to be published.

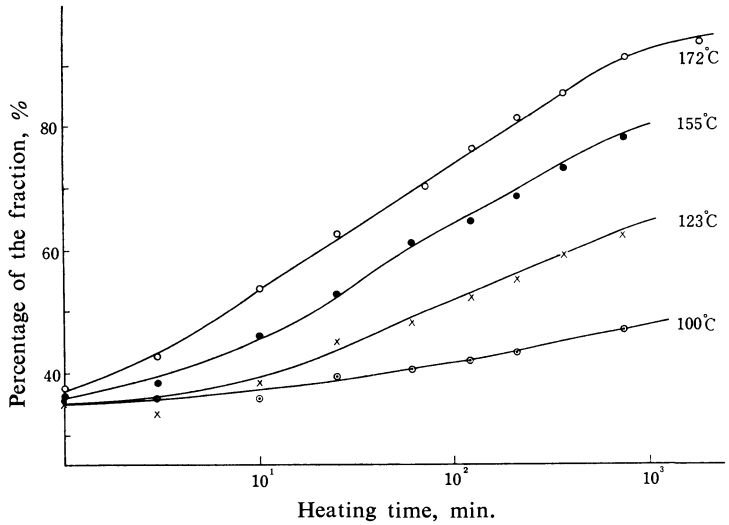

Fig. 5. Isothermal annealing curves for the retention as orthophosphate in irradiated disodium hydrogen phosphate.

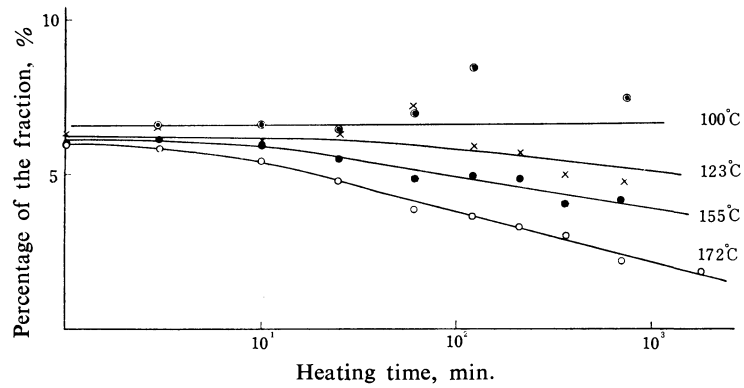

Fig. 6. Isothermal annealing curves for the reduced species fraction in irradiated disodium hydrogen phosphate.

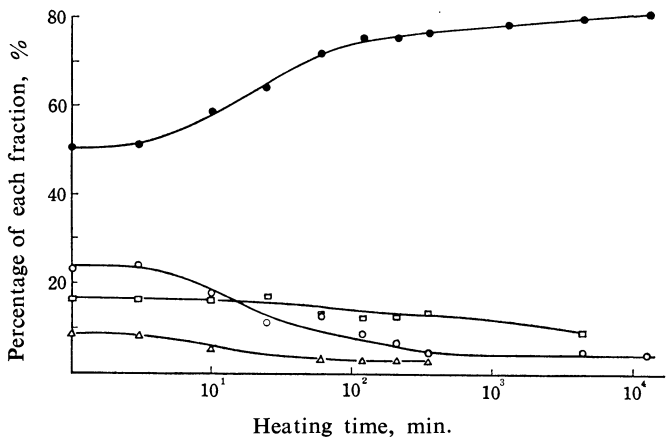

Fig. 7. Isothermal annealing curves for each fraction in irradiated sodium pyrophosphate at 200°C.

—○— The polyphosphate fraction —●— The pyrophosphate fraction (retention)
—△— The orthophosphate fraction —□— The reduced species fraction

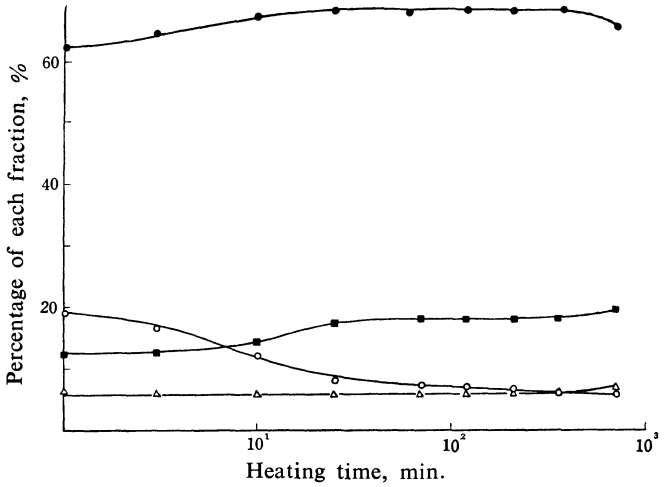

Fig. 8. Isothermal annealing curves for each fraction in irradiated disodium hydrogen phosphite at 172°C.
—○— The polyphosphate fraction —△— The orthophosphate fraction
—●— The phosphite fraction (retention) —■— The hypophosphite fraction

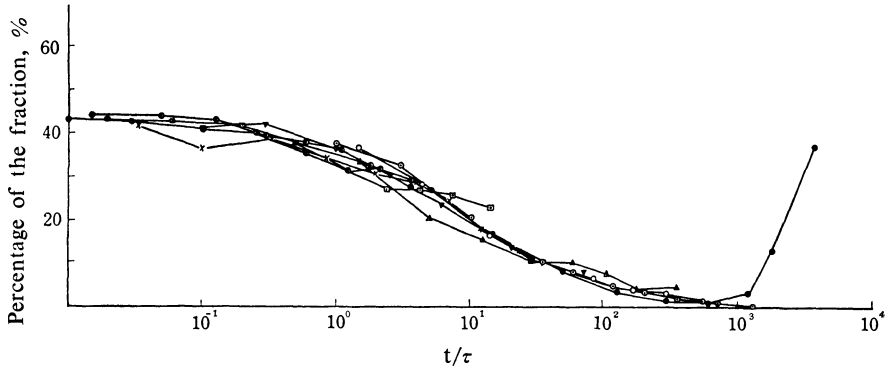

Fig. 9. Composite annealing curves for superposition with respect to the polyphosphate fraction in irradiated potassium dihydrogen phosphate at 165°C.

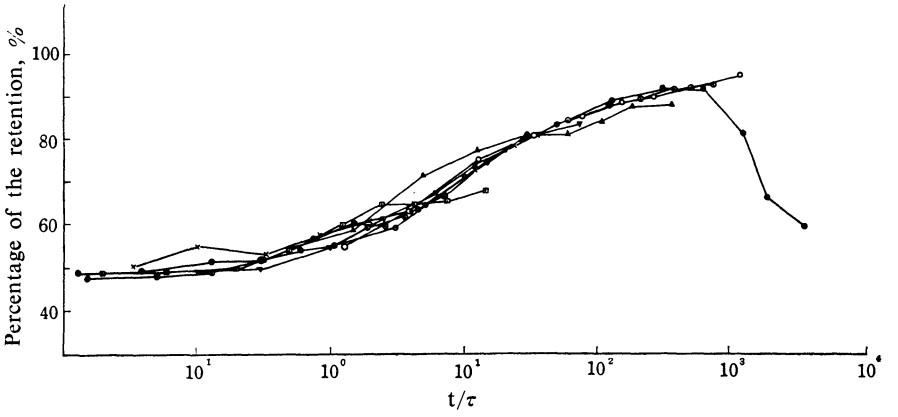

Fig. 10. Composite annealing curves for superposition with respect to the orthophosphate fraction (retention) in irradiated potassium dihydrogen phosphate at 165°C.

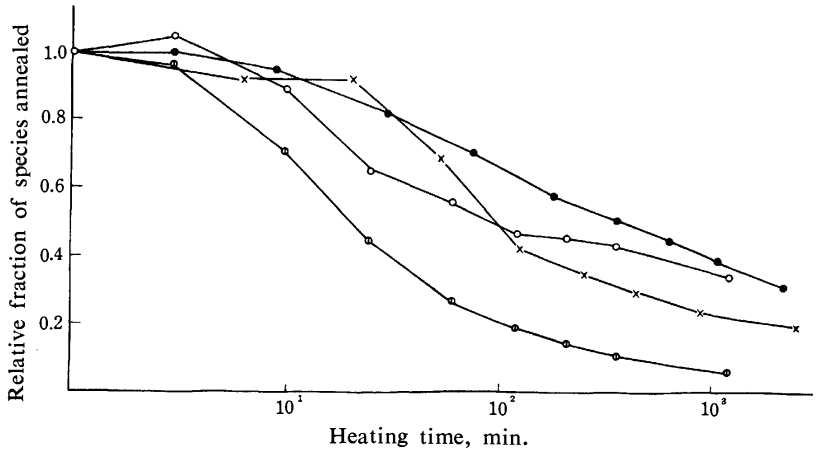

Fig. 11. Isothermal annealing curves for the polyphosphate fraction in irradiated certain phosphates at 140°C.
—○— Sodium dihydrogen phosphate —●— Disodium hydrogen phosphate
—×— Trisodium phosphate —ⓘ— Potassium dihydrogen phosphate

time, and only a decrease in the polyphosphate fraction is shown. The composition of the polyphosphate fraction may differ from that of the polyphosphate fraction in phosphate crystals. The results obtained from each of the irradiated salts are shown in Figs. 7 and 8.

For thermal annealing in every salt used here except sodium dihydrogen phosphite, the amount of the increase in retention corresponded to the sum of the decrease in the other fractions. From the results with orthophosphate and pyrophosphate salts, it is found that there is some difference in the annealing behavior between polyphosphate and reduced species. At the initial step, the majority of annealing reaction consists of the reaction of the polyphosphates fraction. This is also found in the case of the phosphite sample. The annealing effect of the reduced species fraction gradually becomes more predominant on prolonged heating.

Fletcher and Brown[18] assumed that the thermal annealing was represented by an expression in which t/τ was the ultimate variable. In this case τ was arbitrarily chosen. In order to obtain a composite annealing curve, the temperature interval was pursued more precisely that of the above experiments. In this treatment we found, that these curves showed the temperature dependency of the annealing behavior. An equivalent annealing curve for 165°C for potassium dihydrogen phosphate is shown in Figs. 9 and 10. These curves show that there might be little difference in the annealing kinetics in this temperature range since a good overlapping of all the curves is to be seen here. The curves given from the change in the proportions of the polyphosphate fraction are each compared with some of different orthophosphate samples in

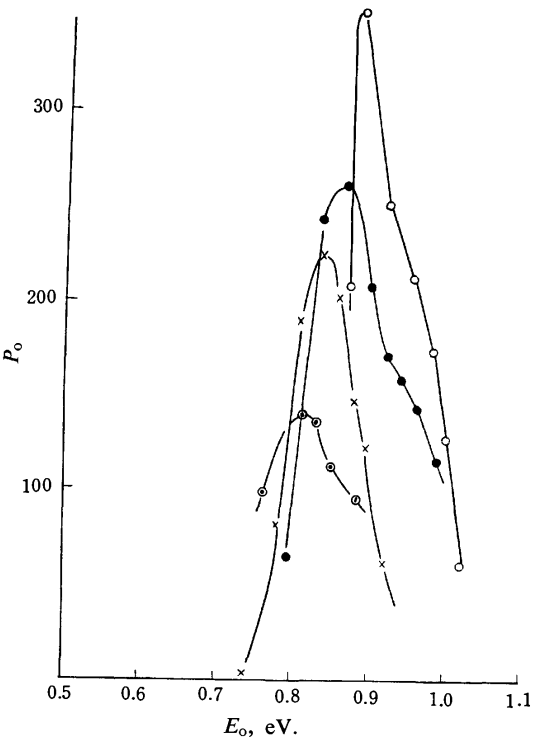

Fig. 12. The initial distribution of activation energy for the polyphosphate fraction in irradiated sodium dihydrogen phosphate.
—⊙— at 90°C —×— at 112°C
—●— at 140°C —○— at 166°C

18) R. C. Fletcher and W. L. Brown, *Phys. Rev.*, **92**, 585, 591 (1953),

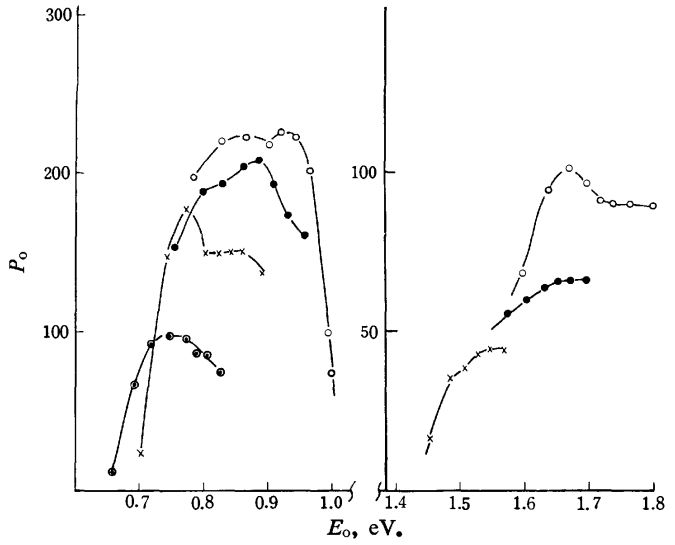

Fig. 13. The initial distribution of activation energy for ^{32}P in irradiated disodium hydrogen phosphate.
Left hand side——the polyphosphate fraction
Right hand side——the reduced species fraction.
—⊙— at 100°C —×— at 123°C —●— at 155°C —○— at 172°C

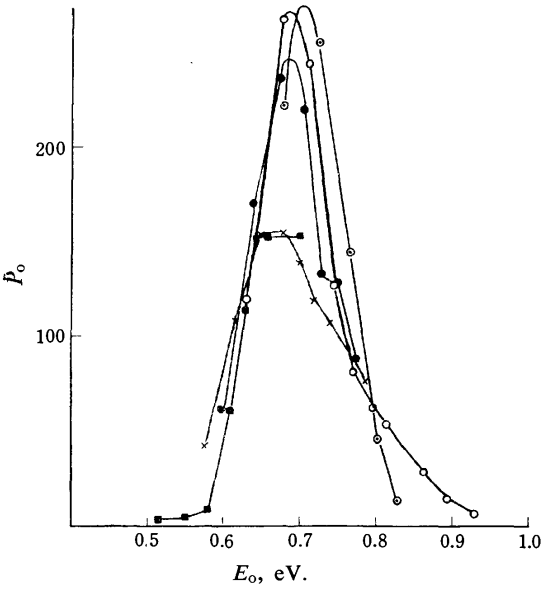

Fig. 14. The initial distribution of activation energy for the polyphosphate fraction in irradiated trisodium phosphate.
—■— at 85°C —×— at 127°C
—●— at 144°C —○— at 167°C
—⊙— at 200°C

Fig. 11. On the ordinate the initial proportions of the polyphosphate fraction in irradiated phosphates are plotted as a unity. There are some differences in the annealing curves given from the orthophosphate samples used. However, no definite dependency on the chemical forms of the target materials is found.

It has been found by many investigators that thermal annealing can be described formally by first order kinetics at the initial step of annealing and then followed by second order kinetics. Our results can not accurately be fitted to a definite order of kinetics. For the determination of the activation energy we have adopted Vands' concept[19] as amplified by Primak[20]. If it is assumed that the kinetics can be explained by processes with distributed activation energies, the approximate initial distribution of the activation energy, P_o, for the percentage changes in fractions are given by $(-1/\boldsymbol{k}T)\mathrm{d}p/\mathrm{d}(\ln t)$ vs. $E_o=\boldsymbol{k}T\ln(B_f\,t)$, where E_o is the activation energy in eV., p is the fraction annealed at the time t, B_f is a constant having the dimension of frequency, $\boldsymbol{k}$ is Boltzman's constant, and T is the absolute temperature. This treatment has already been adopted by several authors[15,21,22]. The B_f factor was taken as the best overlapping of successive annealing curves. The estimated values of B_f are described in Table II. The initial distribution of activation energies is plotted in Figs. 12—17. The activation energies of the annealing of the polyphosphate fraction are mostly distributed between 0.60 and 1.0 eV.,

19) V. Vand, *Proc. Phys. Soc.*, **55**, 222 (1943).
20) W. Primak, *Phys. Rev.*, **100**, 1677 (1955).
21) F. P. Clarke, *Discussions Faraday Soc.*, **23**, 141, 170 (1957).
22) T. Costea, *J. Inorg. Nucl. Chem.*, **19**, 27 (1961).

TABLE II. ESTIMATED VALUE OF FACTOR B_f

Irradiated sample	Retention	log B_f Fraction as polyphosphate	Fraction in reduced species
NaH_2PO_4	7.4	7.4	Uncertain
Na_2HPO_4	7.2	6.6	11.3
Na_3PO_4	8.3	5.0	Uncertain
$Na_4P_2O_7$	8.4	9.2	Uncertain
Na_2HPO_3	—	5.6	Uncertain
KH_2PO_4	6.6	6.5	10.3

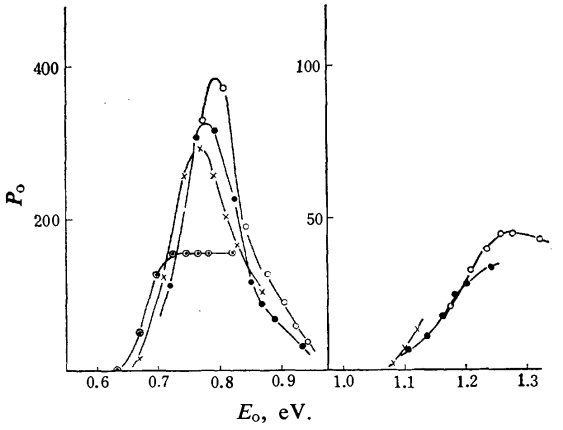

Fig. 15. The initial distribution of activation energy for ^{32}P in irradiated potassium dihydrogen phosphate.
Left hand side——the polyphosphate fraction
Right hand side——the reduced species fraction.
—⊙— at 90°C —×— at 112°C
—●— at 140°C —○— at 166°C

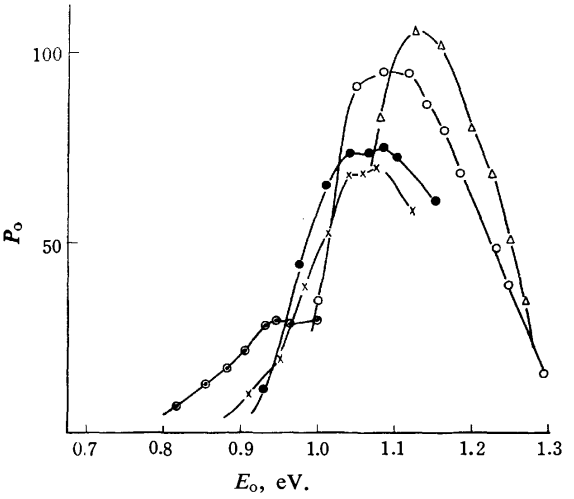

Fig. 16. The initial distribution of activation energy for the polyphosphate fraction in irradiated sodium pyrophosphate.
—⊙— at 85°C —×— at 127°C
—●— at 137°C —○— at 167°C
—△— at 200°C

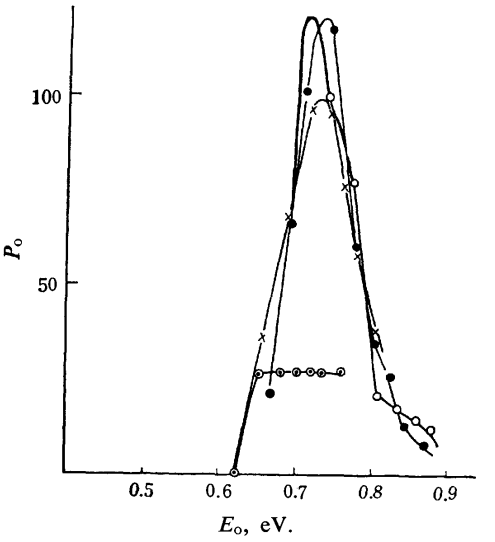

Fig. 17. The initial distribution of activation energy for the polyphosphate fraction in irradiated sodium dihydrogen phosphite.
—⊙— at 100°C —×— at 123°C
—●— at 155°C —○— at 172°C

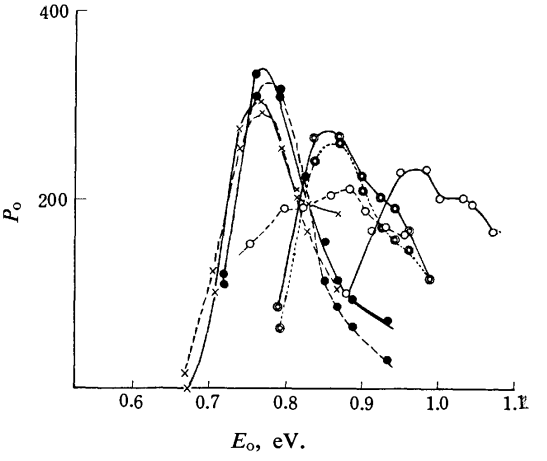

Fig. 18. The initial distribution of activation energy for retention as orthophosphate in irradiated certain phosphates.
---×--- The polyphosphate fraction, at 112°C, KH_2PO_4
---●--- The polyphosphate fraction, at 140°C, KH_2PO_4
—×— Orthophosphate (retention), at 112°C, KH_2PO_4
—●— Orthophosphate, (retention), at 140°C, KH_2PO_4
---◎--- The polyphosphate fraction, at 140°C, NaH_2PO_4
—◎— Orthophosphate (retention), at 140°C, NaH_2PO_4
---○--- The polyphosphate fraction, at 155°C, Na_2HPO_4
—○— Orthophosphate (retention), at 155°C, Na_2HPO_4

except for the pyrophosphate sample, in which the polyphosphate fraction is annealed with the activation energy distributed between 0.78 and 1.3 eV. Much larger errors are found when the B_f factor is obtained from the annealing of the reduced species fraction because the annealing conditions are limited. However, it is clear that the activation energies of these fractions are distributed higher than that of the polyphosphate fraction. These distribution curves are given in Figs. 13 and 15. The distribution curve starts at 1.4 eV. for disodium hydrogen phosphate and 1.1 eV. for potassium dihydrogen phosphate.

In Fig. 19 the distribution of activation energies for the annealing of the polyphosphate fraction is compared with that of retention as orthophosphate in the case of three kinds of orthophosphate samples. It is found that the distribution curves given from the thermal annealing of retention are very similar to those of the polyphosphate fraction. This means that the distribution curve of activation energy given from the thermal annealing in retention shows only the majority of the fractions annealed, so the annealing behavior seems to be quite different from each particular fraction annealed. Therefore, in the annealing of the phosphate samples used it is possible that the results obtained from the thermal annealing of retention indicate a composite of discrete thermal annealing curves. There would be some advantage in separating the species more elaborately.

The proportions of phosphorus-32 in the polyphosphate fraction show an abnormal increase on prolonged heating at 167 and 200°C in the case of the sodium dihydrogen phosphate and disodium hydrogen phosphate samples. This change is attributed to the formation of pyrophosphate by the pyrolysis of salts shown in Fig. 1. This is confirmed by the activation analysis of chromatographically-separated paper strips after the decaying out of phosphorus-32.

Summary

Thermal annealing curves given from the chemically-distributed phosphorus-32 formed by neuton irradiation in a nuclear reactor were obtained by heating several orthophosphates, sodium pyrophosphate, and disodium hydrogen phosphite samples in crystal. The separation was accomplished by one-dimensional paper chromatography. The amounts of phosphorus-32 in the chemical species different from the parent species decreased upon the heating of the salts, except in the case of sodium dihydrogen phosphite, whereas retention always increased.

By the analysis of thermal annealing curves obtained from the initial distribution of activation energies, it was found that there was a difference between the thermal-annealing behavior of the polyphosphate fraction and that of the reduced species fraction. The activation energies of the polyphosphate fractions were in the range of 0.60 to 1.0 eV., but the pyrophosphate sample showed an exceptionally high value, i. e., 0.78 to 1.3 eV. Higher activation energy values were estimated for the annealing of the reduced species fraction than for those of the polyphosphate fractions.

The authors wish to express their deep gratitude to Dr. Kenjiro Kimura, the Director of this Institute, and to Professor Nobufusa Saito of The University of Tokyo, for their guidance and valuable suggestions. Their thanks are also due to Dr. Nagao Shibata and Dr. Hiroshi Amano for their encouragement throughout this work.

Radioisotope Production Laboratory
Japan Atomic Energy Research Institute
Tokai-mura, Ibaraki-ken

ESR Studies on Negative Ions of Biphenyl Derivatives. I. Electron Spin Resonance Hyperfine Spectra of 4-Methyl Biphenyl and p, p'-Bitolyl Mononegative Ions

By Kazuhiko ISHIZU

(Received January 30, 1963)

The electron-spin resonance spectra of biphenyl mononegative ions have been observed by several investigators[1-3], however, those of the derivatives have not yet been studied extensively. In order to study the effect of methyl-group substitution on the spin densities at biphenyl ring carbons, the author synthesized 2-methyl, 3-methyl, 4-methyl, *o*, *o'*-bitolyl, *m*, *m'*-bitolyl and *p*, *p'*-bitolyl and the electron-spin-resonance hyperfine spectra of these mononegative ions were observed. The findings about the ESR spectra of 4-methyl biphenyl and *p*, *p'*-bitolyl will be presented in this paper.

Experimental

Solvents and Reducing Agents.—Each mononegative ion was made in a solution of either tetrahydrofuran (THF) or dimethoxyethane (DME) by reduction with potassium metal. These solvents were purified by the method described by Deguchi[4].

Spectrometer.—The ESR spectrometer employed was a high-resolution apparatus (type JES-3B) constructed by Japan Electron Optics Lab. Co., Ltd; its maximum resolution is about 30 milligauss. The operating frequency of the klystron was about 9470 Mc./sec. The magnetic field was modulated at a frequency of 100 kc./sec. and at a modulation width of about 100 milligauss. An aqueous solution of peroxylamine disulfonate[5] was used as a standard for the *g*-value and the magnetic field.

Overall widths were measured between the points where the resonance signal could just be distinguished from the noise level.

Results

***p, p'*-Bitolyl Mononegative Ion.**—The observed spectra measured in THF and DME are shown in Fig. 1(a) and Fig. 1(b) respectively.

In both cases, the hyperfine structures of these spectra were identical, and the overall width was 46.7 gauss. The *g*-value was 2.0025.

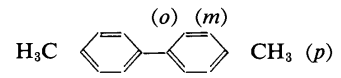

The observed spectra consisted of seventeen groups, each split further into several hyperfine lines. In order to analyze the hyperfine structures of the observed spectrum, we assumed by referring to the spin densities on the carbon atoms of the biphenyl ring as calculated by Hückel's MO treatments (as shown in Fig. 1(d), that the hyperfine splitting coefficients of the six protons in the two methyl groups attached to the para-positions (ΔH_p), these of four-ring protons at the ortho-positions (ΔH_o), and those of four-ring protons at the meta-positions (ΔH_m) were equal to the following values: $\Delta H_p = 5.63$ gauss, $\Delta H_o = 2.66$ gauss, and $\Delta H_m = 0.51$ gauss. Thus, one can explain almost all the hyperfine structures of the observed spectra fairly well. The relative intensities of these hyperfine lines calculated on the basis of this assumption are shown in Fig. 1(c).

The spectra constructed on the basis of calculated spin densities are shown in Fig. 1(d). The observed and calculated spectra were in fairly good agreement in this case.

4-Methyl Biphenyl Mononegative Ion.—The observed spectra measured in THF and DME are shown in Fig. 2(a) and Fig. 2(b) respectively.

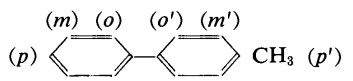

Although the shapes of hyperfine structures observed in THF were different from those in DME, inspite of the concentration having been adjusted in a number of ways, the overall width was 33.6 gauss, and the *g*-value was 2.0024 for both samples.

As shown in Fig. 2(a) and Fig. 2(b), the observed spectra consisted of thirteen groups, each of which split alternately into eight or nine hyperfine lines, while the terminal groups split into only a few hyperfine lines.

The line spacing of these hyperfine lines in each group of the spectra was equal to 0.32 gauss. In order to explain the structures of

1) E. de Boer, *J. Chem. Phys.*, **25**, 190 (1956).
2) E. de Boer and S. I. Weissman, *J. Am. Chem, Soc.*, **80**, 4551 (1958).
3) A. Carrington and J. Dos Santos-Veiga, *Mol. Phys.*, **5**, 21 (1962).
4) Y. Deguchi, *J. Chem. Phys.*, **32**, 1584 (1960).
5) G. E. Pake, J. Townsend and S. I. Weissman, *Phys. Rev.*, **85**, 682 (1952).

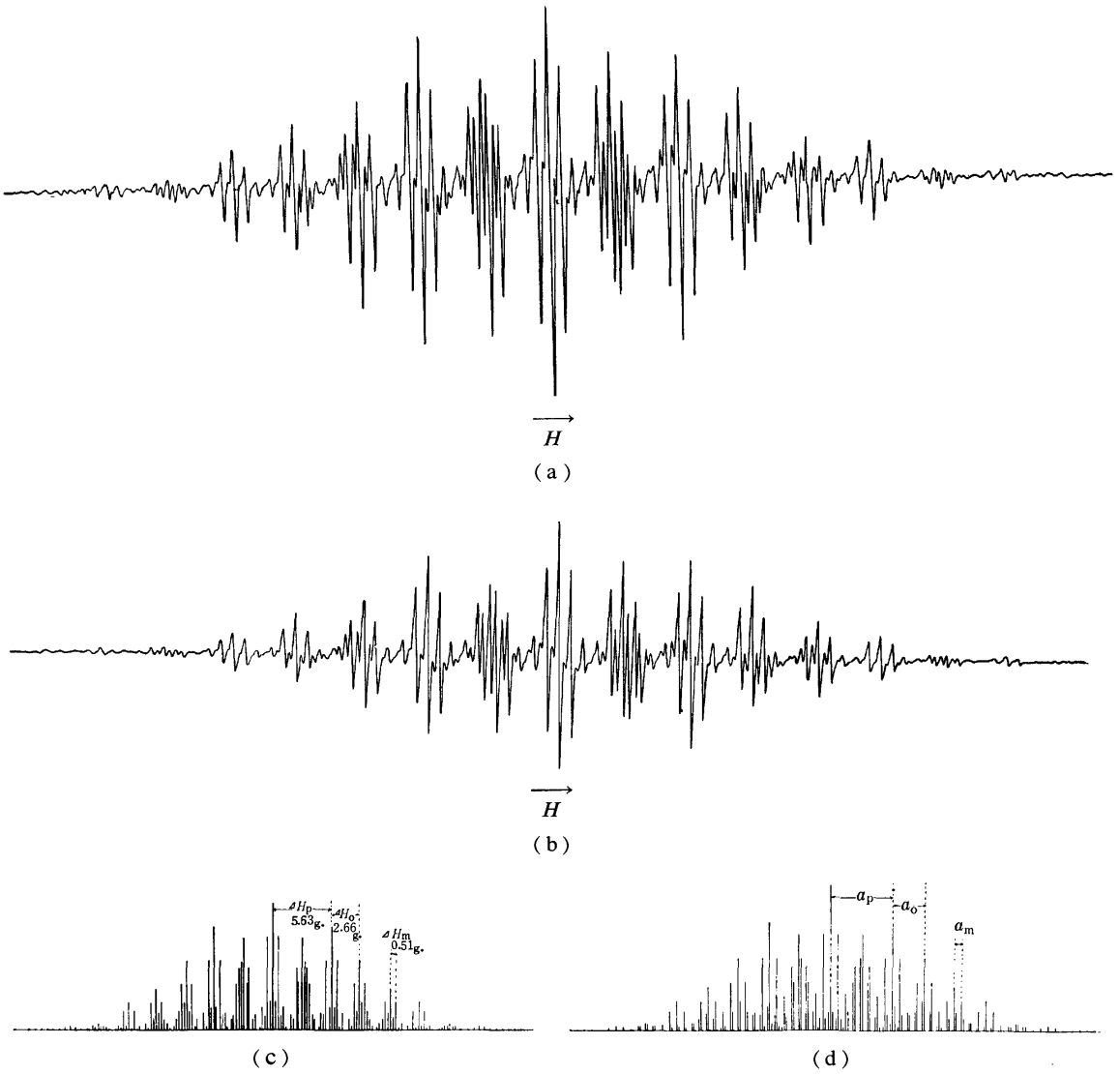

Fig. 1. *p,p'*-Bitolyl mononegative ion.
(a) and (b): ESR spectra in THF and DME
(c) and (d): Intensity diagrams constructed based upon experimentally determined and theoretically calculated spin densities

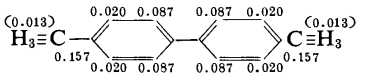

the observed spectra, the author at first assumed, by referring to the spin densities on the carbon atoms of the biphenyl ring as shown in Fig. 2(d) predicted by Hückel's MO calculations, that the splitting coefficients of each methyl proton and of a ring proton at the para-position (ΔH_p, $\Delta H_p'$) were almost equal, and that the splitting coefficient ratios of methyl protons and of each ring proton at the para-, ortho and meta-positions were nearly equal to 8:4:1.

Thus, one can explain that the observed spectra consisted of thirteen groups. In this case, however, it was difficult to explain the details of the hyperfine structures of the observed spectra thoroughly. In order to account for the details of the hyperfine structures, the author paid attention to those of the terminal and the next inner groups of the spectrum, since few overlaps of the hyperfine lines would occur among them. Each of the terminal groups and each of the next inner groups in

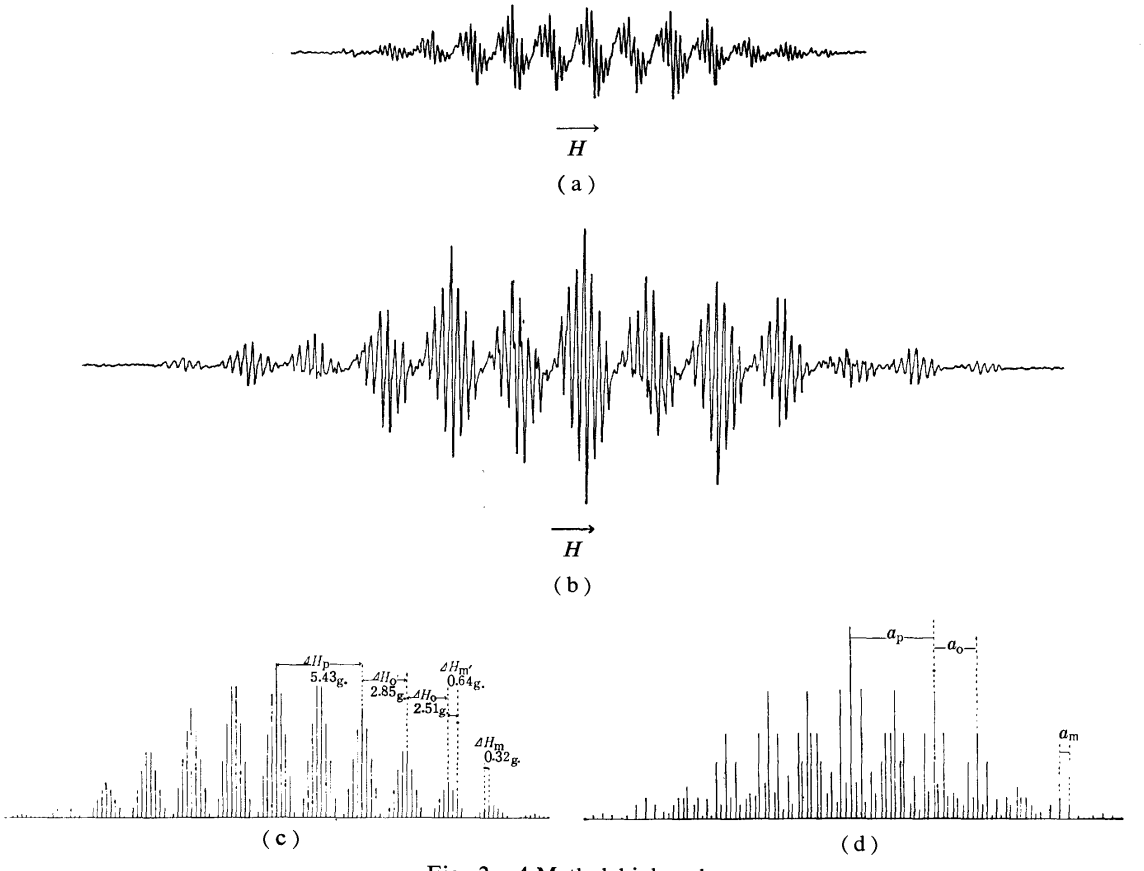

Fig. 2. 4-Methyl biphenyl.
(a) and (b) : ESR spectra in THF and DME
(c) and (d) : Intensity diagrams constructed based upon experimentally determined and theoretically calculated spin densities

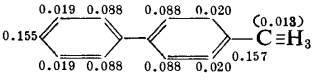

the spectra consisted of seven and eight lines respectively, and their relative intensity ratios were 1 : 2 : 3 : 4 : 3 : 2 : 1 and 1 : 3 : 5 : 7 : 7 : 5 : 3 : 1.

On the basis of these relative intensity ratios of the hyperfine lines in the terminal groups, the author assumed that the splitting-coefficient ratio in both pairs of ring protons at the meta-positions ($\Delta H_m' : \Delta H_m$) was equal to 2 : 1. Moreover, since the hyperfine structures of the terminal groups and the next inner groups were different from each other, we assumed finally that the splitting coefficients of both pairs of ring protons at the ortho-position would have different values ($\Delta H_o'$ and ΔH_o) respectively, and that the difference between these values ($\Delta H_o' \sim \Delta H_o$) was equal to 0.32 gauss. Thus one can explain the hyperfine structures of the next inner groups from one end group by considering it as an overlap of two groups of hyperfine lines which have intensity ratios equal to those of the terminal groups.

In this case, one cannot determine which is larger $\Delta H_m'$ or ΔH_m and $\Delta H_o'$ or ΔH_o, but we assumed that $\Delta H_m'$ is larger than ΔH_m, taking into account the results of Hückel's MO calculations, and that $\Delta H_o'$ is larger than ΔH_o, considering the electron inductive effects due to a methyl group.

Putting together these assumptions in the manner described above, the arithmetic ratios of the splitting coefficients, ΔH_s, of each methyl, para, ortho and meta-protons were determined as follows:

$\Delta H_p : \Delta H_o : \Delta H_m' : \Delta H_o : \Delta H_m = 19 : 10 : 9 : 2 : 1$.

The relative intensities of the hyperfine lines thus constructed are shown in Fig. 2(c). The measured values of the splitting coefficients of each proton were as follows:

$\Delta H_p = 5.43$, $\Delta H_o' = 2.85$, $\Delta H_o = 2.51$, $\Delta H_m' = 0.64$, $\Delta H_m = 0.32$ gauss.

On the other hand, the spectrum calculated

by Hückel's MO theory is given in Fig. 2(d). The observed and calculated spectra were not in satisfactory agreement with each other in this case.

Summary

The electron spin resonances of 4-methyl biphenyl and p,p'-bitolyl mononegative ions were observed in either dimethoxyethane or tetrahydrofuran, using potassium metal as a reducing agent. Well-resolved proton hyperfine spectra were observed in each case, and the g-value, the overall width, and the hyperfine splitting coefficients due to the methyl protons and ring protons were determined.

The theoretical spectra were constructed according to the spin densities calculated by Hückel's MO treatment, and these results were compared with the observed spectra.

The author wishes to express his gratitude to Professors Hideo Takaki and Ryozo Goto for giving him the opportunity to use the ESR apparatus and encouraging him during the course of this work. He is also much obliged to Dr. Yasuo Deguchi for his helpful discussions and for his calculation of Hückel's MO treatment.

Faculty of Literature and Science
Yamaguchi University, Yamaguchi

Studies in the Two Phases System Sodium Formate-Pyridine. Extraction of Nickel and Separation from Chromium

By G. S. DESHMUKH and A. L. J. RAO

(Received February 12, 1963)

Chloroform[1-4] and benzene[5-8] have been widely used for the extraction of nickel and its separation from many elements. A new two phase system sodium formate-pyridine[9] has been reported from these laboratories recently. The behavior of nickel in this system, its quantitative extraction by the batch extraction technique and its estimation in presence of chromium have now been studied.

Experimental

Reagents.—Nickel chloride (B. D. H. AnalaR) sample), sodium formate (Reidel de Haen's recrystallized sample), Baker's analyzed pyridine and sodium chromate (E. Merck's AnalaR sample) are used.

Effect of various factors like the volume of pyridine, molarity of sodium formate, pH and the metal ion concentration on the extraction of nickel have been studied in detail.

Effect of Volume of Pyridine.—Five milliliters of sodium formate containing 1 ml. 0.1 N nickel chloride is taken, various volumes of pyridine are added each time and the amount of nickel extracted into pyridine after equilibration is determined. It is found that with 2 ml. pyridine, both the layers tend to separate but it is not possible to effect a clear separation of the two immiscible phases. The percentage extraction (% E) increased with the volume of pyridine upto 5 ml. and remained constant with a further increase in the volume of pyridine (Fig. 1) and therefore in all the cases 5 ml. of pyridine are used.

Effect of Formate Concentration.—Formate concentration has got very little effect on the amount of metal extracted into the pyridine and its strength need not be rigorously adjusted provided its molarity is above 3 M. At and below 2.3 M formate mixes freely with pyridine and no separation of layers occurs.

Effect of pH.—pH has got a profound influence on the amount of nickel extracted into the pyridine layer. The amount of metal extracted into the organic phase remained constant over a pH range of 7.5~9.2, but on further increase of pH, the percentage extraction decreased markedly. These results are given in Fig. 2.

Effect of Nickel Concentration.—Maintaining optimum conditions of pH, concentration of formate

1) P. G. Butts, A. R. Gahler and M. E. Mellon, *Metal Finishing*, **49**, 50 (1951).
2) G. C. Taylor, *Analyst*, **81**, 369 (1956).
3) Y. Uzumasa and S. Washizuka, This Bulletin, **29**, 403 (1956).
4) W. Nielsch, *Z. anal. Chem.*, **150**, 114 (1956).
5) A. Johnson and E. J. Newmann, *Analyst*, **81**, 318 (1956).
6) D. Mornier and W. Haerdi, *Anal. chim. Acta*, **20**, 444 (1959).
7) M. Mashima, *Japan Analyst.*, **9**, 269 (1960).
8) T. Dono, G. Nakagawa and H. Wada, *J. Chem. Soc. Japan, Pure Chem. Sec.* (*Nippon Kagaku Zasshi*), **82**, 590 (1961).
9) G. S. Deshmukh and A. L. J. Rao, *J. Sci. Ind. Res.* (*India*), **21B**, 141 (1962).

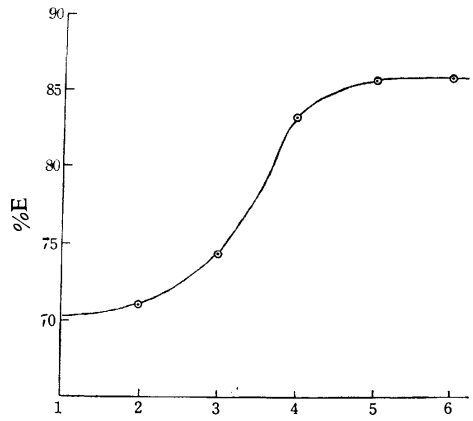

Fig. 1. Effect of volume of pyridine.

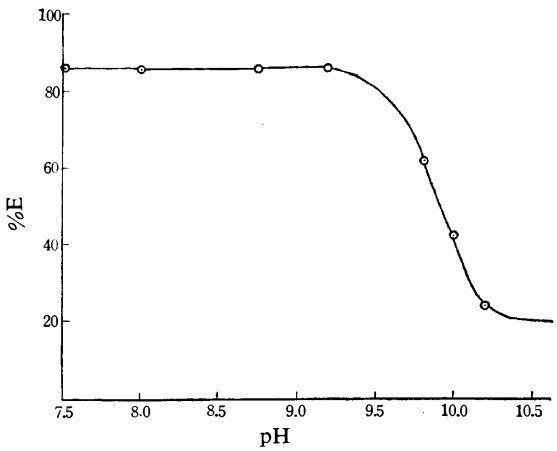

Fig. 2. Effect of pH on nickel extraction.

and pyridine, nickel solution of various concentrations are added each time to the system and the amount extracted into the pyridine is determined in each case. In all the cases the distribution coefficient is found to be constant, thus proving the validity of Nernst's distribution law (Table I).

Table I. Effect of nickel concentration on the extraction

System: 5 ml. of pyridine + 5 ml. 3 M formate containing $NiCl_2$, pH=8

S. No.	Amount of nickel added mg.	Amount of nickel extracted mg.	D
1	0.2	0.172	6.14
2	0.4	0.345	6.27
3	0.6	0.515	6.05
4	0.8	0.690	6.27
5	1.0	0.860	6.14

Procedure for the Extraction of Nickel.—From the study of all the above variables it is concluded that maximum extraction is obtained when the formate concentration is 3 M and 5 ml. of pyridine are used for the extraction, the pH range being 7.5~9.2. To an aliquot of sodium formate (necessary to give 5 ml. of 3 M solution when diluted) nickel chloride solution is added and the volume is made upto 5 ml. in a separating funnel. Five milliliters of pyridine is now added and the whole mixture is equilibrated for 2 min. The formate layer is collected into another separating funnel to which further 5 ml. of pyridine is added to extract some more nickel which remain in the formate during the first extraction. The process is repeated once more so as to get an almost complete extraction of nickel into pyridine. All the pyridine extracts are collected together in 100 ml. conical flask, diluted with a little water and the pyridine is boiled off. The nickel content of this residue is determined polarographically using 1 M ammonium chloride and 0.1 M ammonium hydroxide as the supporting electrolyte[10].

Table II. Analysis of a synthetic mixture of nickel and chromium

Amount of nickel		Amount of chromium	
Taken mg.	Found mg.	Taken mg.	Found mg.
1.45	1.45	1.25	1.243
2.90	2.87	2.50	2.496
4.35	4.34	3.75	3.750
5.80	5.82	5.00	4.926
7.25	7.20	6.25	6.250

Thus a complete extraction of nickel by pyridine from sodium formate is achieved in a three stage batch extraction technique.

Preliminary experiments with chromium under identical experimental conditions showed that it remains completely in the formate layer and is not extracted into pyridine. The observation has been utilized for the separation of nickel and chromium.

Analysis of a Mixture of Nickel and Chromium.—A mixture of nickel and sodium chromate solutions containing various concentrations of nickel and chromium are taken to which the required quantity of sodium formate (necessary to give 5 ml. of 3 M solution) and 5 ml. of pyridine are added and the whole mixture is shaken thoroughly. The formate layer is transferred into another separating funnel and the remaining nickel is re-extracted with a further aliquot of pyridine. For a complete extraction a three stage batch extraction is thus carried out. All the pyridine extracts are mixed together and the nickel content was determined polarographically (vide infra) while the chromium in the formate layer is determined iodometrically[11].

Summary

The distribution of nickel in the two phase system, sodium formate-pyridine is studied in

10) R. G. Menzel and M. L. Jackson, *Anal. Chem.*, 23, 1861 (1951).
11) A. L. Vogel, "A Text Book of Quantitative Inorganic Analysis", Longman Green & Co., New York (1960), p. 350.

detail. The effects of pH, volume of pyridine and molarity of formate are studied and the optimum conditions for the complete extraction are established. The possibility of using this extraction technique for the separation of nickel and chromium has also been worked out and a procedure for the analysis of a synthetic mixture of nickel and chromium is given.

Sincere thanks of the authors are due to Professor G. B. Singh for providing the necessary facilities. The award of a fellowship by the University Grants Commission to one of them (A. L. J. Rao) is also acknowledged.

Division of Analytical Chemistry
Banaras Hindu University
Varanasi-5, India

Oxidation of Alcohols by Cerium(IV). I. Oxidation of Methanol by Ceric Perchlorate

By S. S. MUHAMMAD and K. Vijayachander RAO

(Received March 12, 1963)

The oxidation of alcohols belongs to the category of reactions in which electron transfer is accompanied by the fission of one or more covalent bond:

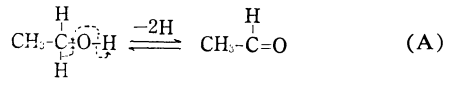

(A)

When the oxidant is a one-electron abstractor such as a ceric or cobaltic ion, these reactions involve the formation of free radicals, as pointed out by Dainton[1] in his Tilden lecture. Thus the work of Bawn and White[2,3] on the oxidation of formic acid, formaldehyde and methanol by cobaltic ions and the work of Mino, Kaizerman and Rasmussen[4] on the oxidation of pinacol by ceric sulfate demonstrated the formation of the free radicals. For example in the oxidation of ethanol by ceric ions the following reactions take place:

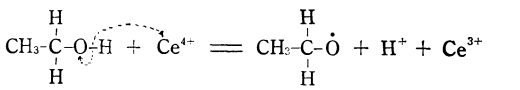

(A1)

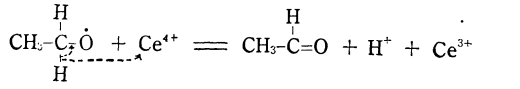

(A2)

which conform to the observed stoichiometry of 2 ceric ions for one alcohol molecule.

On the basis of his kinetic studies on the trivalent manganese-oxalate reaction[5] and the oxidation[6] of acetone by selenious acid, Duke developed the theory of specific oxidation of glycols and related compounds. He assumed that coordination intermediates[7] are first formed through rapidly established equilibrium between the oxidant and the reductant and thence a slow disproportionation of these complexes occurs. The oxidation of 2, 3-butanediol by nitrato cerate was shown by Duke and Forist[8] to proceed through the disproportionation of a monoglycollated coordination intermediate. Similarly, in their study of the oxidation of meso-2, 3-butanediol (G) by ceric perchlorate, Duke and Bremer[9] noticed the formation of complexes such as $\{Ce\,G(H_2O)_4\}^{4+}$, and $\{Ce\,G_2(H_2O)_2\}^{4+}$ which then decomposed unimolecularly. Later Ardon's[10] investigation of the oxidation of ethanol by ceric ions in perchloric acid showed that the reaction occurred in two consecutive steps, similar to the scheme of Duke. He also established the existence of a 1-1 cerate-alcohol complex independently by a spectrophotometric method. Further, Venkatakrishnan and Santappa[11] found that the oxidation of acetone and methylethyl ketone via the formation of a

1) F. S. Dainton, *J. Chem. Soc.*, **1952**, 1537.
2) C. E. H. Bawn and A. C. White, ibid., **1951**, 323, 331, 343.
3) C. E. H. Bawn and A. C. White, *Discussions Faraday. Soc.*, **14**, 181 (1953).
4) G. Mino, S. Kaizerman and E. Rasmussen, *J. Am. Chem. Soc.*, **81**, 1494 (1959).
5) F. R. Duke, ibid., **69**, 2855 (1947).
6) F. R. Duke, ibid., **70**, 419 (1948).
7) Similar views were also expressed by H. Taube: ibid., **70**, 1216 (1948).
8) F. R. Duke and A. A. Forist, ibid., **71**, 2790 (1949).
9) F. R. Duke and R. F. Bremer, ibid., **73**, 5179 (1951).
10) M. Ardon, *J. Chem. Soc.*, **1957**, 1811.
11) S. Venkatakrishnan and M. Santappa, *Z. physik. Chem. (N. F.)*, **16**, 1-2, 93 (1958).

complex between the ceric ions and enolic form of acetone.

On the other hand, several studies[12] using ceric sulfate as oxidant in the oxidation of acetone, formaldehyde, alcohols and hydroxy-acids have given no indication of any intermediate complex formation. Hence it appeared of interest to investigate the divergence of behavior of ceric perchlorate and ceric sulfate, using methanol as the substrate under varying conditions of reagent concentration, acidity and temperature.

The first part contains our data on the oxidation of methanol by ceric perchlorate and this will be followed by the results in presence of ceric sulfate in Part II.

Experimental Method and Results

All the chemicals used were analar and of highest purity. Ceric perchlorate was prepared by the anodic oxidation of cerous perchlorate. This was obtained by dissolving the freshly precipitated ceric hydroxide in perchloric acid and reducing the resulting ceric perchlorate by adding concentrated hydrogen peroxide. The colorless solution of cerous perchlorate was electrolyzed with a current of 3 amp. at 4 V., using a platinum hood as the cathode and a platinum wire as the anode, the temperature of the electrolytic bath being maintained at 0°C. The solution of ceric perchlorate obtained had a strength of 0.01 M approximately and could be diluted to desired extent. For each series of experiments, ceric perchlorate was freshly prepared and it was not allowed to age long, as Vickery[13] asserts that aged solutions develop hydrosols and become less reactive.

Methanol was analar reagent grade. The formaldehyde produced was identified and estimated by Schiff's and Schryver's reagents. In the latter case, a photometric calibration curve was constructed with standard solutions of formaldehyde with the Schryver's reagent. All aqueous solutions were prepared with twice distilled water free from oxidizable impurities.

The reaction study was conducted in an all glass quickfit apparatus, having three jointed necks. Through the middle neck passed mercury seal stirrer, the second allowed nitrogen gas in the reacting system, while the third neck was used for the solutions to be put in or taken out by means of a pipette. During reaction, the latter two were closed by ground glass stoppers.

To maintain temperature, a Gallen Kamp thermostat with a toluene regulator was used, the range of fluctuations being ± 0.1°C. For temperatures lower than the room temperature ice cold water was circulated in lead coils in the bath.

The colorimetric estimation of cerium(IV) or formaldehyde was carried out on a Bosh & Lomb's Spectronic 20 type colorimeter, while the complex study was done on a Unicam spectrophotometer, model Sp 500.

The photochemical and thermal oxidation of water by ceric perchlorate is a well established fact[14]. Hence experiments were conducted in a dark room; the reaction vessel was covered with a black cloth. Blank experiments were also done and corrections were applied wherever necessary.

The rate of oxidation was followed by the rate of disappearance of ceric perchlorate, which was measured by adding excess of standardized ferrous ammonium sulfate solution and titrating the unreacted ferrous ion by standard ceric sulfate in presence of methyl red as indicator. Preliminary experiments showed that the volumetric titration was as accurate as the photometric estimation. Besides it was more suitable than the potentiometric titration which took longer time.

Stoichiometry and Order of Reaction.—The reaction mixture containing different proportions of reactants were analyzed after different intervals both for formaldehyde and for ceric perchlorate. The results are given in Table I.

TABLE I. STOICHIOMETRY OF THE REACTION
Temp., 20°C; 1.0 M perchloric acid

MeOH $\times 10^2$ M	Ce^{4+} $\times 10^{+3}$ M	$-\Delta Ce^{4+}$ $\times 10^3$ M per min.	$+\Delta HCHO$ $\times 10^3$ M per min.
2.0	3.55	0.56	0.26
3.0	3.55	0.82	0.40
5.0	3.55	1.32	0.63
6.0	3.55	1.58	0.75
10.0	3.55	2.48	1.20

In each case formaldehyde formed (or methyl alcohol consumed) is nearly half of the ceric ions disappearing in a given time. Hence the stoichiometry is "2 ceric 1 alcohol".

Using different initial amounts of ceric perchlorate with 0.11 M methanol and 1.0 M perchloric acid, the rate of disappearance of ceric ions was found to be directly proportional to ceric ions concentration. Further log Ce^{4+}-time graph was a straight line, confirming the first order dependence of rate on the ceric ion concentration. The latter graph was generally used to derive the rate constants.

Keeping ceric perchlorate at 3.55×10^{-3} M in a molar perchloric acid at 20°C and changing the concentrations of methanol between 0.01 to 0.50 M, it was found that the rate of oxidation rises with increase of methanol concentration, but tends to reach a limiting value at high concentrations of methanol. This is clear from the plot of rate of oxidation vs. methanol concentration shown in Fig. 1a. Figure 1b is the plot of log relative rate against log

12) See part II: This Bulletin, 36, 949 (1963).

13) R. C. Vickery, "Chemistry of Lanthones", Butterworths, London (1953), p. 233.

14) See for example: a) L. J. Heidt and M. E. Smith, *J. Am. Chem. Soc.*, 70, 2476 (1948); b) Don Kolp and H. C. Thomas, ibid., 71, 3047 (1949); c) F. B. Baker, T. W. Newton and M. Kahn, *J. Phys. Chem.*, 64, 109 (1960).

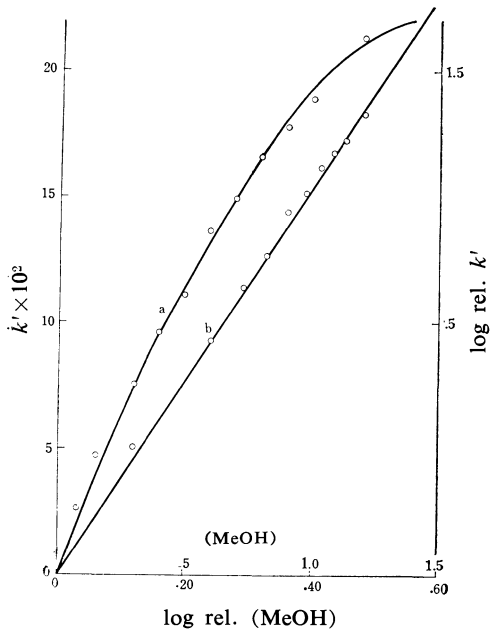

Fig. 1. Effect of methanol concentration.
a k' vs. (MeOH)
b log rel. k' vs. log rel. (MeOH)

relative methanol concentration and has a slope of 0.77.

Effect of Acid and Ionic Strength.—Experiments at constant ionic strength showed that at low acidities the rate is proportional to acid concentration, but at high acidities, it reaches a maximum value (Table II).

Table II. Effect of acid concentration at constant ionic strength
$Ce^{iv} = 3.55 \times 10^{-3}$ M, methanol = 0.11 M, $\mu = 2.504$ M and $T = 20°C$

$HClO_4$ M	$k' \times 10^2$ min^{-1}	$1/HClO_4$	$1/k'$
0.75	7.37	1.33	13.57
1.00	8.64	1.00	11.58
1.25	9.67	0.80	10.39
1.50	10.36	0.67	9.63
2.00	10.70	0.50	9.35
2.50	11.40	0.40	8.77
3.00	11.60	0.33	8.62

If the reciprocals of the rate constants are plotted against the reciprocals of the acid concentration, a straight line results. But keeping the acid concentration the same and varying the amount of added sodium perchlorate (Table III) it was found that the reaction has a normal salt effect.

The variations of the rate constants in the range 7~27°C are shown in Table IV.

The activation plot yields 14.45 kcal./mol. as the apparent activation energy.

Table III. Influence of ionic strength at constant acidity
$Ce^{iv} = 3.55 \times 10^{-3}$ M, methanol = 0.11 M, $HClO_4 = 1.0$ M and $T = 20°C$

Lot of $NaClO_4$ in 50 cc.	Total ionic strength	$k' \times 10^2$ min^{-1}		$\log k' + 2$
0.0000	1.030	8.60	1.015	0.9345
0.2385	1.069	8.94	1.034	0.9513
0.4770	1.108	9.21	1.052	0.9643
0.7200	1.148	9.44	1.072	0.9750
0.9542	1.186	9.81	1.089	0.9917
1.1922	1.226	10.17	1.108	1.0072
1.4298	1.264	10.60	1.124	0.0251

Table IV. Variations of rate constants with temperature
$Ce^{iv} = 3.55 \times 10^{-3}$ M, methanol = 0.11 M, $HClO_4 = 1.0$ M

Temp. °C	First order rate constant (each constant is the mean of three experiments)	Mean $k' \times 10^2$ min^{-1}
7	0.027, 0.026, 0.029	2.73
13	0.050, 0.044, 0.053	4.90
20	0.088, 0.086, 0.087	8.70
27	0.174, 0.188, 0.164	17.53

Discussion

The present data on the oxidation of methanol are directly in line with the findings of Duke and Bremer[9] and Ardon[10] and may be explained on similar lines. Hence we invoke Duke's mechanism and assume that methanol in perchloric acid medium is oxidized by cerium(IV) only after complex formation:

$$MeOH + Ce^{iv} \rightleftharpoons Ce \leftarrow O\begin{matrix}Me\\H\end{matrix} \quad \text{(complex)} \qquad \text{(B1)}$$

$$Ce \leftarrow O\begin{matrix}Me\\H\end{matrix} \longrightarrow Ce^{iii} + H^+ + \dot{MeO} \quad \text{(methoxy free radical)} \qquad \text{(B2)}$$

These reactions are of course followed by a very fast step in which the methoxyl free radical reacts with another ceric ion:

$$\dot{MeO} + Ce^{iv} \longrightarrow Ce^{iii} + HCHO + H^+ \qquad \text{(C)}$$

which accounts for the observed stoichiometry, 2 ceric: 1 methanol. But the last step being very fast is out side the scope of the present study.

State of Ce^{iv} in Perchloric Acid.—In order to elucidate Duke's mechanism we require a knowledge of (1) the state of Ce^{iv} in perchloric acid, (2) the complex or complexes formed and (3) the disproportionation of these complexes. Hardwick and Robertson[15] have shown that

15) T. J. Hardwick and E. Robertson, *Canad. J. Chem.*, **29**, 818 (1951). See also, E. L. Ring and M. L. Pandow, *J. Am. Chem. Soc.*, **74**, 1966 (1952).

in aqueous perchloric acid solutions of ceric perchlorate three ionic species Ce^{4+}, $CeOH^{3+}$, and $(Ce-O-Ce)^{6+}$ can exist, comprising the reactions:

$$Ce^{4+}+H_2O \rightleftharpoons CeOH^{3+}+H^+ \quad (D)$$

$$CeOH^{3+}+CeOH^{3+} \rightleftharpoons Ce\text{-}O\text{-}Ce^{6+}+H_2O \quad (E)$$

High acidity favors the Ce^{4+} ions, though very high acidities (probably above 4 M) have to be avoided, for according to Vickery[13], autoreduction may occur. In low acidity and dilute solutions, the hydrolyzed form predominates. But increase in total ceric concentration helps the dimerization process and if acidity is also low, Ardon and Stein[16] state that irreversible colloidal polymers are also formed. As the ceric concentration in the present work was of the order of 10^{-3} M, the existence of the binuclear species $Ce\text{-}O\text{-}Ce^{6+}$ may be neglected and we take the reactive species to be unhydrolyzed Ce^{4+} as done by Duke and Bremer[9] and Ardon[10]. Our observation that the rate of oxidation increases though slowly, by rise in perchloric acid concentration in the range 1.0 to 3.5 M, is in conformity with the equilibrium D, in which higher acidity should favor the existence of the unhydrolyzed monomeric species Ce^{4+}. This may actually be the hexahydrated ion $Ce(H_2O)_4^{4+}$, for which the symbol Ce^{4+} will be used in later treatment.

Cerium(IV)-Methanol Complexes. — The coordination complexes between ceric perchlorate and methanol may be formed as a result of the displacement of perchlorate or water. Observed positive salt effect rules out any displacement of perchlorate by alcohol molecules. If the latter were correct, increasing addition of perchlorate would have decreased the rate. Hence it may be concluded that the displacement of coordination water by methanol molecules from Ce^{IV} occurs. The possible complexes would be $\{Ce\,X_5\cdot MeOH\}^{4+}$; $\{Ce\,X_4\,(MeOH)_2\}^{4+}$; $\{Ce\,X_3\,(MeOH_3)_3\}^{4+}$; $\{Ce\,X_2\,(MeOH)_4\}^{4+}$; $\{Ce\,X\,(MeOH)_5\}^{4+}$ and $\{Ce\,(MeOH)_6\}^{4+}$. Further since in solution $Ce\,OH^{3+}$ also exists, complexes such as $\{Ce(OH)X_4MeOH\}^{3+}$; $\{Ce(OH)X_3(MeOH)_2\}^{3+}$; $\{Ce(OH)\,X_2\,(MeOH)_3\}^{3+}$; $\{Ce(OH)\,X\,(MeOH)_4\}^{3+}$ and $\{Ce(OH)\,(MeOH)_5\}^{3+}$ are also possible. But according to Duke and Bremer, the latter type of complexes can not exist in appreciable amount in solution, for the hydrolyzed species has been found to be unimportant in the oxidation reaction.

Complex Formation and Disproportionation.— In the reaction:

$$Ce^{4+}+MeOH \rightleftharpoons \left[Ce \leftarrow O\begin{matrix}Me\\H\end{matrix}\right]^{4+} \quad (F)$$

if the equilibrium concentrations are put as $Ce^{4+}=c-x$; (complex) $=x$; $MeOH=B$ (where methanol being in excess, its initial concentration is supposed to remain unchanged) the equilibrium constant

$$K=\frac{x}{(c-x)B} \quad (1)$$

This gives

$$x=\frac{KBc}{1+KB} \quad (2)$$

or $$(\text{complex})=\frac{K(MeOH)(Ce^{4+})}{1+K(MeOH)} \quad (3)$$

The rate of disproportionation of the complex:

$$Ce \leftarrow O\begin{matrix}Me\\H\end{matrix} \longrightarrow Ce^{3+}+R\dot{O}+H^+ \quad (G)$$

$$\frac{-d\,Ce^{4+}}{dt}=k\ (\text{complex}) \quad (4)$$

But using complex concentration from 3,

$$\frac{-d\,Ce^{4+}}{dt}=\frac{kK(MeOH)(Ce^{4+})}{1+K(MeOH)} \quad (5)$$

This may be written as

$$\frac{-2.303\,d\log Ce^{IV}}{dt}=\frac{kK(MeOH)}{1+K(MeOH)} \quad (6)$$

because the concentration of Ce^{4+} directly depends on total cerium(IV), which is the quantity measured experimentally. It shows that in any given experimental condition, the plot of log Ce(IV) vs. time will be a straight line, the slope of which multiplied by 2.303 gives the first order constant k', which varies with methanol concentration in the manner of Eq. 6. Hence

$$k'=\frac{kK(MeOH)}{1+K(MeOH)} \quad (7)$$

or

$$\frac{1}{k'}=\frac{1+K(MeOH)}{kK(MeOH)}=\frac{1}{k}+\frac{1}{kK(MeOH)} \quad (8)$$

It means that the plot of the reciprocal of the apparent rate constant against the reciprocal of methanol concentration is a straight line with an intercept (Fig. 2). This intercept is equal to $1/k$ and the slope $1/kK$, thus enabling us to evaluate the constants of cerate-methanol complex formation and of its disproportionation in different experimental conditions.

Equation 8 may also be used as an evidence for the formation of an intermediate complex in a reaction. It may be noted here that it

16) M. Ardon and G. Stein, *J. Chem. Soc.*, **1956**, 104.

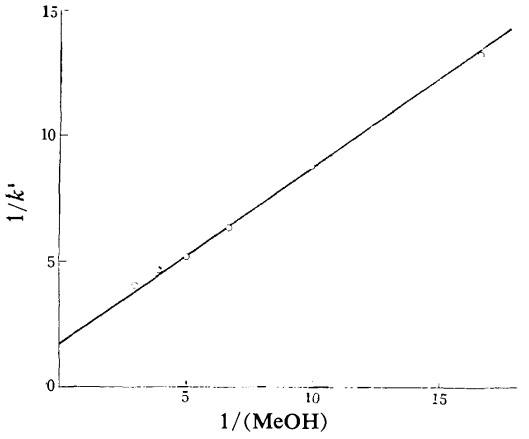

Fig. 2. Evidence for complex formation. Kinetic data.

is similar to Lineweaver and Burke's[17] equation which was a modification of the equation of Michaelis and Menton[18]. In order to explain the widely observed fact that the rate of an enzyme catalyzed reaction increased with the concentration of the substrate as a rectangular hyperbola and eventually levelled off a symptotically (compare Fig. 1), Michaelis and Menton suggested that the substrate combined with the enzyme to form a transient intermediate which then broke down to products:

$$\text{Enzyme}+\text{Substrate} \rightleftarrows \text{Complex} \rightarrow \text{Products}+\text{Enzyme}$$

Hence Lineweaver and Burke showed that in the above case, if the reciprocal of the apparent velocity was plotted against the reciprocal of the concentration of the substrate, then a slope and intercept relation resulted. The graph of Fig. 2 gives 1.36 l. mol^{-1} as the stability constant at 20°C and 1.0 M perchloric acid.

To understand the proposed mechanism, the structure of the cerate-methanol complex should be known. Job's method being unsuitable here, Ardon's optical method based on the spectrophotometric method of Hildebrand and Benesi[20] was employed. In this method the plot of $(1/D-CE_a)$ against 1/(methanol) at 400 mμ gives a straight line with an intercept, provided 1 : 1 complex is formed between ceric and methanol. Here D is the optical density of the equilibrium mixture and C and E_a the concentration and molecular extinction coefficient of the colored species ceric ions. When all the mixtures observed are made to have the same volume, the measured optical density D' of the ceric ions may be used in place of CE_a. Figure 3 shows the graph of $1/(D-D')$ against 1/(methanol). The value of the formation constant is 2.97 at 20°C and 3.0 M acid.

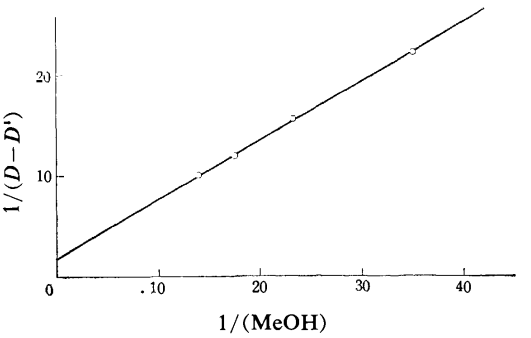

Fig. 3. Spectrophotometric data.

As the method of Ardon is based on the assumption that 1 : 1 complex is formed, it may be concluded that only 1 : 1 cerate-methanol is important in our experimental condition.

Effect of Acid Concentration. — If complex formation is represented by

$$Ce^{IV}+MeOH \rightleftarrows (Ce^{IV}\cdot MeOH)$$

and initial $Ce(IV)=Ce_0(IV)$ and at equilibrium the complex $=X'$, then the equilibrium constant,

$$K=\frac{X'}{(Ce^{IV}-X')(MeOH)} \qquad (10)$$

where it has been assumed that methanol being in excess, its concentration remains unchanged. But the reactive species being Ce^{4+}, the complex formation actually consists of reaction F:

$$Ce^{4+}+MeOH \rightarrow (Ce\cdot MeOH)^{4+} \qquad (F)$$

and the equilibrium constant $\bar{K}$

$$\bar{K}=\frac{X}{(Ce^{4+}-X)(MeOH)} \qquad (11)$$

In this equation Ce^{4+} is not equal to Ce^{IV} and $\bar{K}$ may be called the true stability constant, while K is the apparent stability constant.

In identical conditions of concentrations, acidity and temperature, the quantities X and X' may not be much different and we may assume them to be equal. Hence

$$\frac{\bar{K}}{K}=\frac{Ce^{IV}}{Ce^{4+}} \qquad (12)$$

But $Ce^{IV}(\text{total})=Ce^{4+}+CeOH^{3+}$ in conditions where binuclear species are negligible and

17) H. Lineweaver and D. Burke, *J. Am. Chem. Soc.*, **56**, 81 (1934).
18) L. Michaelis and M. Menton, *Bioch. Zeit.*, **49**, 333 (1913).
19) P. Job, *Ann. chim. (France)*, **9**, 113 (1928).
20) J. H. Hildebrand and H. A. Benesi, *J. Am. Chem. Soc.*, **71**, 2703 (1949).

$$\frac{\bar{K}}{K}=\frac{Ce^{4+}+CeOH^{3+}}{Ce^{4+}}=1+\frac{CeOH^{3+}}{Ce^{4+}}$$

and from equilibrium of Eq. D, $CeOH^{3+}/Ce^{4+}=K_h/H^+$, where K_h is the hydrolysis constant. This gives

$$\frac{\bar{K}}{K}=1+\frac{K_h}{H^+}$$

or

$$\frac{1}{K}=\frac{1}{\bar{K}}+\frac{K_h}{\bar{K}\cdot H^+} \qquad (13)$$

This means that a plot of the reciprocal of the apparent stability constant (derived from Fig. 4) against the reciprocal of the acid concentration, yields a straight line with an intercept $=1/\bar{K}$ and a slope $=K_h/\bar{K}$. Table V incorporates our data on the variation of the rate constants at different acidities by changes of methanol concentration at 20°C and constant cerium(IV) concentration.

TABLE V. VARIATION OF RATE CONSTANTS AT DIFFERENT ACIDITIES BY CHANGING METHANOL AT 20°C

MeOH mol. l.	$k'\times10^2$ min^{-1}	1/MeOH	$1/k'$
		$HClO_4=1.00$ M	
0.03	2.60	33.30	38.42
0.06	4.79	16.67	20.79
0.11	8.68	9.10	11.63
0.24	16.58	4.17	6.03
		$HClO_4=2.00$ M	
0.05	6.70	20.00	14.93
0.06	7.69	16.67	13.00
0.10	11.51	10.00	8.69
0.15	15.76	6.67	6.34
		$HClO_4=3.50$ M	
0.05	9.26	20.00	10.80
0.08	12.74	12.50	7.85
0.15	20.90	6.67	4.79
0.20	26.30	5.00	3.80

The plot of 1/(methanol)-1/(rate constants) is shown in Fig. 4. It is interesting to note from this graph that while apparent stability constants decrease with decreasing acid concentration, the constant of disproportionation remains the same at different hydrogen ion concentrations. This proves that there is only one complex that decomposes.

Figure 5 shows a plot of the reciprocal of the apparent stability constant (as derived from Fig. 4) against the reciprocal of acid concentration. This yields the following values at 20°C:

True stability constant $\bar{K}=6.67$

Hydrolytic constant $K_h=3.75$

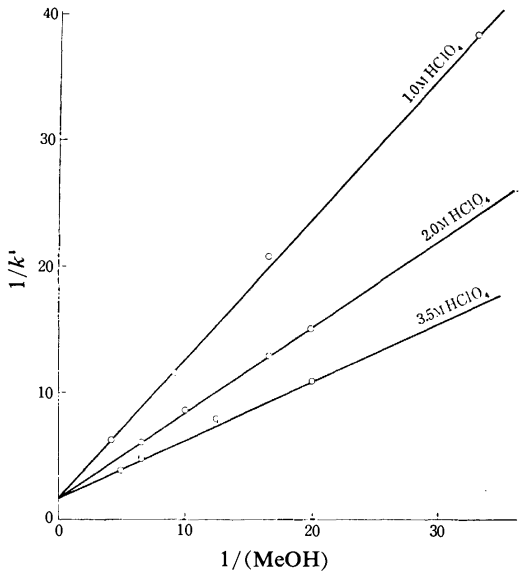

Fig. 4. Rate constants at different acidities at several methanol concentrations.

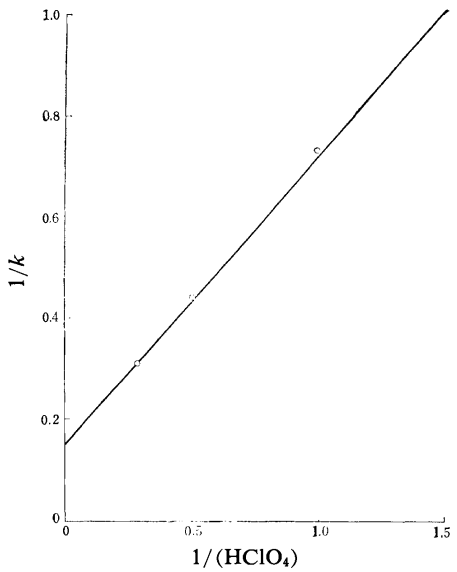

Fig. 5. Evaluation of hydrolytic constant and true formation constant.

The latter value closely agrees with Hardwick and Robertson's value 3.40. It has to be noted that though the apparent formation constant K decreases with decreasing acid concentration, the true formation constant $\bar{K}$ remains unchanged. Measurements at two temperatures yield the following values:

Temp.	K at 2.0 M acid	$\bar{K}$	K_h
13°C	3.74	7.21	1.85
20°C	2.34	6.67	3.57

while the apparent stability constant K has a temperature coefficient of 1.60 (for 7°C rise), that for the true stability constant is only 1.08. The former corresponds to a value of $\Delta H=$ 11.0 kcal. and the latter to about 2.0 kcal. This small heat of formation for the complex $Ce \leftarrow O\begin{matrix}Me\\H\end{matrix}$ again indicates that methanol is replacing only the cordinated water from the hydrated ceric ion, $Ce(H_2O)_6^{4+}$. Similarly the hydrolysis constants derived for 20 and 13°C, indicate the heat of hydrolysis to be 15.6 kcal. in agreement with Hardwick and Robertson's value of 15.3 kcal.

Summary

The oxidation of methyl alcohol by ceric perchlorate in perchloric acid solution was studied at 13, 20 and 26°C. The stoichiometry consisted of two ceric ions for the oxidation of one molecule of methanol. While the rate of disappearance of ceric ions directly depended on the concentration of ceric ions, the dependence on methanol concentration was such as to suggest a 'broken order':

$$\frac{-\mathrm{d}\,Ce^{iv}}{\mathrm{d}t}=\frac{k(Ce^{iv})(MeOH)}{1+k'(MeOH)}$$

This rate also depended on the concentration of perchloric acid in such a way that at high acidity it became independent of it.

These data were explained on the basis of Duke's mechanism for 2, 3-butane diol-ceric perchlorate reaction, i. e. the oxidation of methanol by ceric ions proceeded via an intermediate complex between one Ce^{4+} ion and one methanol molecule. The formation of this complex was also proved independently by a spectrophotometric method. The kinetic data were further used to derive the true heat of formation of the methanol-cerate complex and the heat of hydrolysis of the ceric ions in aqueous perchloric acid.

Department of Chemistry
Osmania University
Hyderabad-7, India

Oxidation of Alcohols by Cerium(IV). II. Oxidation of Methanol by Ceric Sulfate

By S. S. MUHAMMAD and K. Vijayachander RAO

(Received March 12, 1963)

Benrath and Ruland[1] were the earliest to investigate the oxidizing action of ceric sulfate on several substances, while Lejune[2] studied the oxidizability of alcohols, aldehydes and ketones by potassium permanganate and potassium dichromate. Later Willard and Young[3] observed the unreactivity of formic and acetic acids towards ceric sulfate and complicated kinetics and stoichiometry in the case of tartaric, malonic and other acids. Ross and Swain[4] tried to apply the principle of the concentration cells to kinetic studies on the oxidation of oxalic acid by ceric sulfate. The work of Shorter and Hinshelwood[5] concerned the oxidation of acetone[6] by ceric sulfate in dilute sulfuric acid. They assumed direct reaction between trisulfato-hydroxy cerate ion $\{H_2CeOH(SO_4)_3\}^-$ with enolic form of acetone. Hargreaves and Sutcliffe[7], using rather high concentrations of sulfuric acid, found the rate of oxidation of formaldehyde to depend on the cubic exponent of sulfuric acid concentration, indicating tetra-sulfate ceric acid $H_4Ce\cdot(SO_4)_4$ to be the reactive species. Dodson and Black[8] favored the existence of the trisulfato cerate ions $Ce(SO_4)_3^{2-}$ in soulution and assumed the main reductant to be the bioxalate ion $HC_2O_4^-$. Shao Minchzhou and Gorbachev[9]

1) A. Benrath and K. Ruland, *Z. anorg. Chem.*, **114**, 267 (1920).
2) G. Lejune, *Compt. rend.*, **181**, 694 (1926).
3) H. H. Willard and P. Young, *J. Am. Chem. Soc.*, **52**, 132 (1930).
4) S. D. Ross and C. G. Swain, ibid., **69**, 1325 (1947).
5) J. Shorter and C. N. Hinshelwood, *J. Chem. Soc.*, **1950**, 3276,
6) See also J. Shorter, ibid., **1950**, 3425.
7) G. Hargreaves and L. H. Sutcliffe, *Trans. Faraday Soc.*, **51**, 1105 (1955).
8) V. H. Dodson and A. H. Black, *J. Am. Chem. Soc.*, **79**, 3657 (1957).
9) S. Minchzhou and S. V. Gorbachev, *Zhur. Fiz. Khim.*, **32**, 635 (1958).

studied the oxidation of methanol, ethanol, isopropanol, *n*- and iso-butanol and benzyl alcohol with potassium permanganate and ceric sulfate and activation energy of these reactions was correlated with dipole moments of the alcohols. Mino, Kaizerman and Rasmussen[10] studied the oxidation of pinacol by ceric sulfate and found no evidence of complexing between the reactants. They also noticed that in presence of acrylamide the primary radicals are captured by it. Krishna and Tewari[11] studied the oxidation of mandelic, *dl*-malic and lactic acids by ceric sulfate.

The present work concerns the study of the kinetics of the oxidation of methanol by ceric sulfate and activation data for the oxidation of methanol, ethanol and *n*-propanol.

Experimental Results

The ceric ammonium sulfate was of Merck's analar. It was dissolved in standardized sulfuric acid of highest purity and was assayed with ferrous ammonium sulfate. Other experimental details remain the same as given in Part I. Ceric sulfate solutions are much more stable as compared to ceric perchlorate. They do not decompose or undergo dimerization. Hence the rates could be followed in ordinary daylight.

The stoichiometry of reaction proves to be 2 ceric sulfate for each methanol molecule, the same as found with ceric perchlorate-methanol reaction.

Effect of Added Bisulfate Ion on Methanol-Ceric Perchlorate Reaction.—Addition of potassium hydrogen sulfate causes large retardation in the oxidation of methanol by ceric perchlorate. Thus using 3.55×10^{-3} M ceric perchlorate and 0.15 M methanol at 20°C, we get the data of Table I.

TABLE I. EFFECT OF ADDED BISULFATE IONS

$KHSO_4$ added g.	0	0.10	0.20	0.30	0.40	0.50
Apparent rate constant x $\times10^2$ min^{-1}	8.60	5.07	3.80	3.38	3.03	2.82

Methanol-Ceric Sulfate Reaction in Perchloric Acid.—The log-time plots showed the order to be one with respect to cerium(IV). Using differential method, the value of the exponent

$$n=\frac{\log(k_2/k_1)}{\log(C_2/C_1)}$$

was found to be one, where k_2 and k_1 are first order constants with methanol concentrations C_2 and C_1 in identical conditions.

The effect of perchloric acid was similar to ceric perchlorate-methanol reaction and the reciprocals of rates versus reciprocals of acid concentration, gave a straight line. Further the sodium perchlorate added results in a positive salt effect. But the search for complex formation led to negative result as the plot of $1/k'$ against 1/(MeOH) gave a straight line without an intercept (similar to Fig. 4). Hence it may be concluded that methanol and ceric sulfate in perchloric acid react without the prior formation of a complex.

Methanol-Ceric Sulfate Reaction in Sulfuric Acid.—The rate of oxidation depends directly on the concentrations of ceric sulfate and methanol. The plots of log titre value against time gave a straight line. The first order

TABLE II. DEPENDENCE OF OXIDATION ON METHANOL

Ceric sulfate 4.2×10^{-3} M, sulfuric acid 1.0 M, temp. 55°C

MeOH M	$k\times10^3$ min^{-1}	rel. k	rel. (MeOH)	log rel. k	log rel. (MeOH)
1.00	5.68	1.00	1.00	0.000	0.000
1.50	8.15	1.46	1.50	0.158	0.176
2.00	10.45	1.84	2.00	0.265	0.301
2.50	13.51	2.38	2.50	0.376	0.398
3.00	16.67	2.94	3.00	0.468	0.477
4.00	21.68	3.81	4.00	0.582	0.602

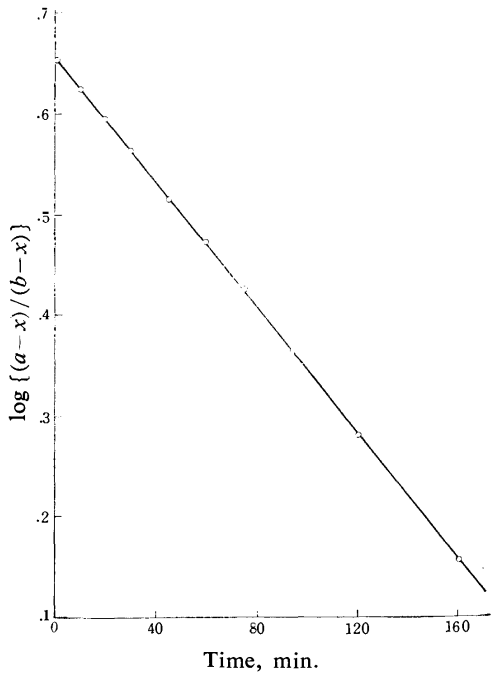

Fig. 1. Verification of order 2.

10) G. Mino, S. Kaizerman and E. Rasmussen, *J. Am. Chem. Soc.*, **81**, 1494 (1959).
11) B. Krishna and K. C. Tewari, *J. Chem. Soc.*, **1961**, 3097.

character with respect to ceric sulfate continues till half of ceric sulfate is consumed, after which the rate falls off. The plot of log rel. (methanol) versus log rel. (first order constant), gave a straight line with a slope of unity. These data are contained in Table II. Hence the dependence of oxidation on methanol is of first order and the overall order of this reaction is two. This was varified by plotting $\log\{(a-x)/(b-x)\}$ against time (Fig. 1), using a = (ceric sulfate) = 6.75×10^{-3} M, b = (methanol) = 1.5 M and (sulfuric acid) = 1.0 M at temperature 55°C.

Effect of Sulfuric Acid and Ionic Strength.—Keeping the ionic strength constant at 2.53 M at 55°C the solutions containing 1.5 M methanol and 4.2×10^{-3} M ceric sulfate were made 0.5 M to 2.0 M with respect to surfuric acid. The plot of initial rate against molarity of sulfuric acid is shown in Fig. 2. This shows direct dependence of rate on the concentration of the

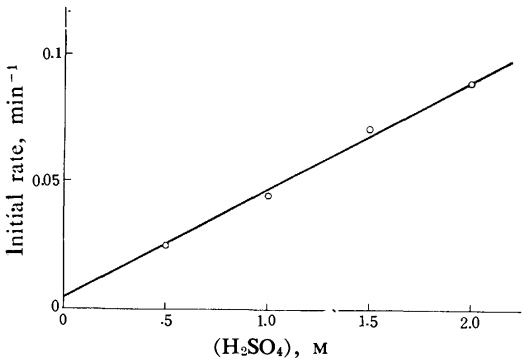

Fig. 2. Effect of acidity.

acid. But when the ionic strength is not maintained constant, the rate decreases directly with increase of sulfuric acid concentration. Besides, when the sulfuric acid concentration is maintained constant the plot of log of initial rate against (ionic strength)$^{1/2}$ shows a negative salt effect (Fig. 3).

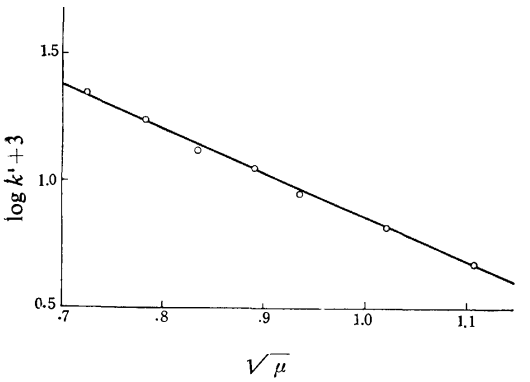

Fig. 3. Effect of ionic strength.

Effect of Temperature.—Using mixtures of 2.0 M methanol, 1.5 M sulfuric acid and 4.2×10^{-3} M ceric sulfate, the first order rate constants were determined at different temperatures and are given in Table III. The Arrhenius plot gives the value of 26300 cal. mol^{-1} for the activation energy.

Table III. Variation of rate constants with temperature

Temp. °K	First order rate constant $\times10^3$ min^{-1} (each is a mean of 3 expts.)	Mean k $\times10^3$ min^{-1}
313.2	2.50, 2.32, 2.61	2.48
318.2	4.64, 4.39, 4.48	4.50
323.2	8.68, 8.47, 8.27	8.47
328.2	14.15, 15.76, 14.76	14.88
333.2	32.53, 32.24, 32.20	32.32
338.2	56.56, 57.01, 55.51	56.36

Search for Complex Formation.—The plot of $1/k'$ against 1/(MeOH) (Fig. 4) is a straight line passing through the origin. Similarly the plot of $1/(D-D')$ against 1/(MeOH) is a straight line passing through the origin. Both facts show that the complex is not formed during oxidation.

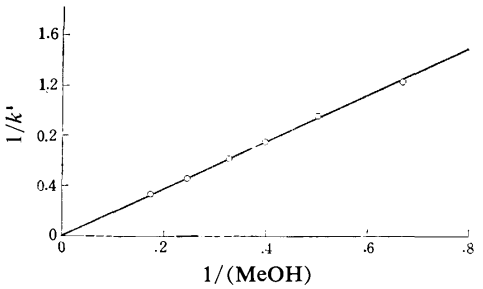

Fig. 4. Search for complex formation.

Discussion

The oxidation of methanol by ceric sulfate exhibits the same stoichiometry as the reaction of alcohols with ceric perchlorate, indicating that this also consists of two stages—the first being the slow reaction:

$$Ce^{IV} + CH_3OH \rightarrow Ce^{III} + CH_3\dot{O} + H^+ \quad (1)$$

followed by the very fast step:

$$Ce^{IV} + CH_3\dot{O} \rightarrow Ce^{III} + HCHO + H^+ \quad (2)$$

But the fact that in sulfuric acid medium, oxidation of alcohols does not involve the formation of a complex implies a difference between the mode of oxidation in the two media. This might be due to the difference in the state of Ce^{IV} in the two media.

The stability of ceric sulfate solutions compared to easy decomposition of ceric perchlorate and the fact that addition of alcohol to ceric sulfate does not change its color[12] are suggestive of covalent bonding between cerium(IV) and sulfate. While ion migration studies by Jones and Soper[13] and spectrophotometric studies by Hardwick and Robertson[14] support this, they do not agree about the species existing in solution[15]. Similarly, as shown in the introduction, different authors have assumed the existence of diffenent complexes to explain their kinetic data. It has to be admitted that in aqueous sulfuric acid solutions of ceric sulfate, several complexes can exist depending on the concentration of ceric sulfate and sulfurid acid such as

$\{Ce(SO_4)\}^{2+}$, $\{Ce(OH)SO_4\}^{1+}$, $\{Ce(SO_4)_2\}$, $\{Ce(SO_4)_3\}^{2-}$, $\{HCe(SO_4)_3\}^{1-}$, $\{H_2Ce(SO_4)_4\}^{2-}$ and $\{Ce(SO_4)_4\}^{4-}$

The choice of the right species is difficult. But our observation that the rate of oxidation of methanol by ceric perchlorate is retarded by added sulfuric acid and also the observation that the oxidation of methanol by ceric sulfate decreases on the addition of sulfuric acid point to the fact that the relative species should be the covalent by bond ceric sulfate $Ce(SO_4)_2$.

Mechanism of Waters.—Admitting that the reactive participants are the neutral ceric sulfate and methanol, the course of reaction may be assumed to be analogous to that proposed by Waters and Levesley[16] for the oxidation of α-hydroxy acids by manganese pyrophosphate. Earlier this mechanism was adopted by Krishna and Tiwari[11] to explain the kinetics of the oxidation of mandelic and *dl*-malic and lactic acids.

Hence we assumed that ceric sulfate and methanol react to form a transition complex which decomposes to produce a free radical, a hydrogen ion and cerous sulfate complex. The free radical then picks up another ceric sulfate (as in the case of ceric perchlorate-methanol reaction) and quickly produces the final products of reaction:

$$Ce(SO_4)_2 + CH_3OH \rightarrow \underset{\text{transition state}}{Ce(SO_4)_2\cdots\cdots CH_3OH} \rightarrow Ce^{III}(SO_4)_2 + H^+ + CH_3\dot{O} \quad (3)$$

$$Ce(SO_4)_2 + CH_3\dot{O} \xrightarrow{\text{very fast}} Ce^{III}(SO_4)_2 + H^+ HCHO \quad (4)$$

The retarding action of bisulfate ions at constant acidity can be explained as due to the removal of ceric sulfate by the reaction

$$Ce(SO_4)_2 + HSO_4^- \rightleftharpoons HCe(SO_4)_3^- \quad (5)$$

while the accelerating effect of hydrogen ions at constant ionic strength might be due to the reactions:

$$Ce(SO_4)_2 \rightleftharpoons Ce(SO_4)^{2+} + SO_4^{2-} \quad (6)$$

$$Ce(SO_4)^{2+} + H_2O \rightleftharpoons Ce(OH)SO_4^- + H^+$$

According to reaction 3, the rate of disappearance of ceric sulfate

$$\frac{-d(Ce(SO_4)_2)}{dt} = k''[Ce(SO_4)_2][CH_3OH] \quad (a)$$

and the rate is first order with respect to both reagents and the overall order is 2. Hence the bimolecular constant can be calculated by

$$k'' = \frac{2.303}{t(a-x)} \log \frac{b(a-x)}{a(b-x)} \quad (b)$$

where $a>b$ and x is the quantity of cerium(IV) disappearing in the time interval t.

From Eq. 5,

$$[C(SO_4)_2] = \frac{[HCe(SO_4)_3^-]}{K[HSO_4^-]}$$

$$\frac{-d\,(Ce(SO_4)_2)}{dt} = \frac{k''[HCe(SO_4)_3^-][MeOH]}{K[HSO_4^-]} \quad (c)$$

Assuming that ceric sulfate in sulfuric acid exists largely as $HCe(SO_4)_3^-$, the concentration of the latter is proportional to that of cerium(IV) and $HSO_4^- \propto H_2SO_4$, we arrive at the rate equation:

$$\frac{-d\,Ce^{IV}}{dt} = \frac{k'[MeOH][Ce^{IV}]}{[H_2SO_4]} \quad (d)$$

Evidence for the Proposed Mechanism.—The proposed mechanism is also supported by the behavior of methanol-ceric sulfate in perchloric acid medium. The reaction between methanol and ceric sulfate is very fast due to the absence of the bisulfate ions which slow down the reaction by removing ceric sulfate in the form of the complex ion $HCe(SO_4)_3^-$. Further the hydrogen ions of the perchloric acid stop the hydrolysis and degradation of the ceric sulfate (as shown in Eqs. 6 and 7).

According to Hinshelwood and Fairclough[17]

12) F. R. Duke and G. F. Smith, *Ind. Eng. Chem. Anal. ed.*, 12, 201 (1940).
13) E. G. Jones and F. G. Soper, *J. Chem. Soc.*, 1930, 802.
14) T. J. Hardwick and E. Robertson, *Can. J. Chem.*, 29, 828 (1951).
15) For example: W. Moore and R. C. Anderson, *J. Am. Chem. Soc.*, 67, 167 (1945), disagree with Ref. 14.
16) W. A. Waters and P. Levesley, *J. Chem. Soc.*, 1955, 217.
17) C. N. Hinshelwood and R. A. Fairclough, *J. Chem. Soc.*, 1937, 538, 1573.

TABLE IV. RELATION BETWEEN $(1/E)^{1/2}$ AND $\log PZ$ FOR OXIDATION OF ALCOHOLS BY Ce^{iv}

	Reaction system	Medium	E, cal. mol^{-1}	$\sqrt{1/E}\times10^3$	$\log PZ$
1	Methanol-ceric sulfate	Sulfuric acid	21850	6.76	10.74
2	Ethanol-ceric sulfate	Sulfuric acid	18800	7.59	9.10
3	*n*-Propanol-ceric sulfate	Sulfuric acid	13860	8.50	6.32
4	Methanol-ceric sulfate	Perchloric acid	12210	9.05	6.08

Data obtained with $Ce^{iv}=3.55\times10^{-3}$ M, $H_2SO_4=1.0$ M and rate constants derived from Eq. d

in a series of related reactions, the relation between $(1/E)^{1/2}$ and $\log PZ$ should be linear. In Table IV are recorded the values of the activation energy E, the square root of its reciprocal $(1/E)^{1/2}$ and the logarithm of the product of steric fator P and the collision number Z for the reactions of the three alcohols, methanol, ethanol and *n*-propanol with ceric sulfate as obtained in the present study:

Figure 5 is the graphical representation of

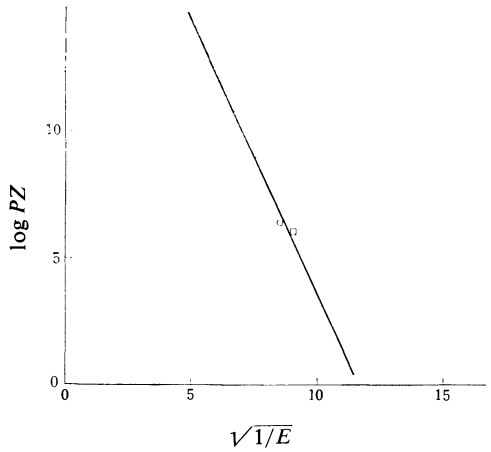

Fig. 5. Relation between $(1/E)^{1/2}$ and $\log PZ$.

$\log PZ$ against $(1/E)^{1/2}$. The four systems lie on a smooth line with a slope -2.16×10^3. This value of slope, according to Hinshelwood, is a characteristic of many bimolecular reactions.

Summary

The oxidation of methanol by ceric sulfate in sulfuric acid solutions was studied in the temperature range 40~70°C. The rate of oxidation depended directly on the concentration of cerium(IV) and methanol. At constant ionic strength the rate was directly dependent on the concentration of sulfuric acid. But when the ionic strength is not maintained, the rate changes inversely with sulfuric acid. At constant acid concentration, a negative salt effect is observed. The reaction occurs without the intermediate formation of a complex. The activation energy was derived to be 26300 cal. mol^{-1}. It has been shown that the mechanism of Waters for the oxidation of α-hydroxy-acids by manganese pyrophosphate can be used to explain the present data.

Department of Chemistry
Osmania University
Hyderabad-7, India

The Hydration of Some Organic Compounds in an Aqueous Solution. I. Studies of Aliphatic Aldehydes by Raman-effect Observation

By Michiko MATSUSHIMA

(Received March 22, 1963)

It has long been recognized that acetaldehyde is partly hydrated in an aqueous solution to the $CH_3CH(OH)_2$ molecule; Bell and his co-workers have summarized this evidence[1] and have reported kinetic measurements[2] of the reversible hydration process. The hydrate in question could not be isolated except for those from chloro-substituted aldehydes, and such a structure as $=C(OH)_2$ is often mentioned as a reactive intermediate in the organic reactions. It is, therefore, of interest to examine the species existing only in solution from the spectral point of view. Moreover, it seems worthwhile to pay attention to the infinite solubility with which formaldehyde and acetaldehyde dissolve, in water as well as in organic solvents. Since the formation of hydrates obviously helps their solubility, to obtain hydration energy is also of interest. The present paper aims at obtaining the molecular vibrational spectra characteristic of the hydrated structure; it also aims at elucidating molecular interactions through measurement of the changes in the relative intensities of suitable Raman lines produced by changes in temperature.

In the case of formaldehyde, an interesting phenomenon was observed by Hibben[3] in the Raman spectrum in an aqueous solution. The spectrum in solution has a relatively close similarity to that of glycol: $CH_2O+H_2O \rightleftharpoons CH_2(OH)_2$. The simplicity of the Raman spectrum of water led us to hope that the Raman effect technique would prove useful in detecting the species existing in an aqueous solution. Further, it seemed reasonable to expect that each spectrum corresponding to aldehyde and its hydrate would change in intensity as the temperature changed. In the present paper, the Raman spectra of acetaldehyde and its solutions in light and heavy water are studied. At the same time, those of dimethylacetal, chloral and chloral hydrate are recorded as related compounds useful for the sake of comparison.

Experimental

Materials.—Pure acetaldehyde was obtained from its trimer compound, which was depolimerized with a drop of concentrated sulfuric acid. The fraction below 27°C of the distillate was redistilled to get acetaldehyde, boiling at 20~20.5°C. The dimethylacetal synthesized[4] was purified by distillation over metallic sodium. Fractional distillation was repeated until the boiling point was constant at 64.3°C. Chloral and the chloral hydrate of E. P. grade (Tokyo Kasei) were used without further purification. Water purified through ion exchange resins was used as a solvent. The isotope content in the deuterium oxide used was 99%.

Measurements.—*The Raman Spectra of Liquids.*— A Cary Raman spectrophotometer, model 81, was used to measure the Raman spectra of pure liquids and solutions. Measurements were usually carried out at ordinary temperatures in a mercury lamp compartment (35~40°C), a sealed glass cell (O. D. 7 mm.) 4.5 ml. in volume being used. For the purpose of recording a spectrum at various points of equilibrium, the temperature of the Raman cell was kept almost constant by circulating water of a desired temperature through the tube jacket. The jacket was specially fitted to the space between the filter cylinder and the cell, as is illustrated in Fig. 1.

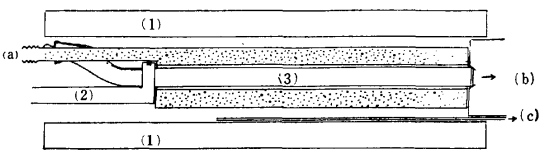

Fig. 1. Illustration of the tube jacket for adjusting temperature in a Raman tube.
(a) To a thermostat and a pump for circulating water
(b) To a monochrometer
(c) To a reference beam entrance
(1) Filter cylinder
(2) Cell holder
(3) Raman tube

The Raman Spectra of Solids.—The Raman spectrum of chloral hydrate, (m. p. 58°C) was

1) R. P. Bell and W. C. E. Higginson, *Proc. Roy. Soc.* **A197**, 141 (1949).
2) R. P. Bell and D. B. Darwent, *Trans. Faraday Soc.*, **46**, 34 (1950).
3) J. H. Hibben, "The Raman Effect and Its Chemical Applications", Reinhold Publishing Corp., New York (1939), p. 187.
4) K. Nukada, *Reports of the Government Chemical Research Institute, Tokyo*, **55**, 99 (1960).

recorded at 60°C in the melted phase by using the tube jacket mentioned above.

The Irradiation of Polarized Lights.—The exciting light was polarized by surrounding a Raman tube with a polaroid cylinder, the transmitted electric vector of which was either parallel or perpendicular to the axis of the Raman tube. Baffles were not used to get a parallel exciting light, nor were the observed depolarization ratios corrected for the convergence error, so the results should be treated only as a measure of the true ratios.

Results (Part I)

The Raman Spectra of Acetaldehyde and Its Solutions in Light and Heavy Water. — The results obtained are summarized in Table I, together with the relative intensities. The spectra shown in Figs. 2, 3, and 4 were recorded at ordinary temperatures; Fig. 5 shows the spectrum of pure water. In a heavy water solution, the exchange reaction of deuterium with hydrogen in aldehyde might occur following the instantaneous hydration process. It was, however, observed that there

TABLE I. OBSERVED FREQUENCIES (cm^{-1})

Acetaldehyde	Aqueous solution (equimolar)	Heavy water solution (equimolar)
	325 W	322 W
	420 w	410 w
	480 w	473 w
513 m	516 m	520 m
	567 w	
770 m (D)	772 m (D)	770 m (D)
	838 w	
	857 s (P)	845 s (P)
895 m (b)	882 m	
916 m (b)	920 m	918 m (b)
	1095 m	
1113 m	1116 m	1118 m
	1156 w	1198 W
1353 m (D)	1353 m (D)	1358 m (D)
1398 s	1400 s	1400 s
1429 S	1430 s	1430 s
	1449 S	1449 S
1720 S	1715 s	1715 s
2696 sh	2688 W	2688 W
2732 m	2741 m (P)	2738 sh
2754 m	2765 m (P)	2766 m
2844 s		
	2874 m	2873 m
2919 S (P)	2919 S (P)	2919 S
	2939 S	2941 S
2962 m		
	2996 s	2995 s
3000 W	3115 w	3118 w

The order of intensities: S, s, m, W and w relatively.

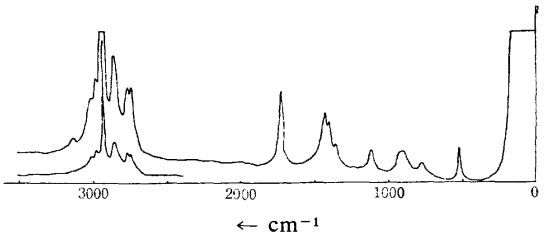

Fig. 2. Raman spectrum of acetaldehyde.

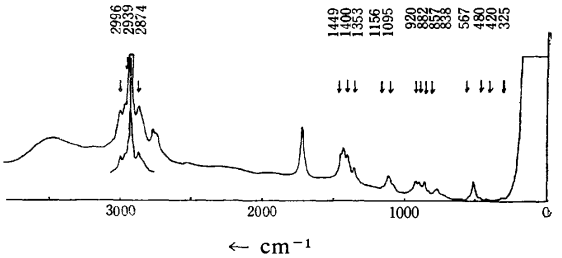

Fig. 3. Raman spectra of acetaldehyde in aqueous solution at ordinary temperature (equimolar solution).

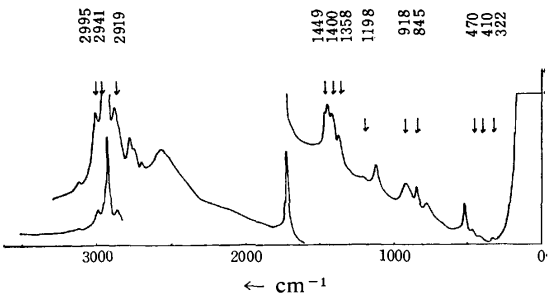

Fig. 4. Raman spectra of acetaldehyde in heavy water solution at ordinary temperature (equimolar solution).

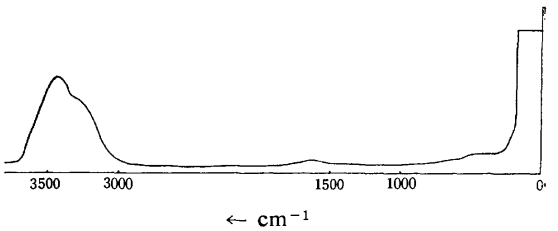

Fig. 5. Raman spectrum of pure water.

are no visible changes in intensity for the lines arising from C–H vibrations, and no visible new lines corresponding to C–D vibrations either. Since the rate of the exchange reaction is much less than that of the hydration process, it is not necessary to take account of the effect of the former reaction within the period of time employed for recording the Raman spectra.

In practice, the spectra of solutions are different from that of pure aldehyde, although in Figs. 3 and 4 the difference is not clearly shown. Arrows are given to show the position of each new line as it was acertained from observations at various temperatures and concentrations. (See Results, Part II.)

The spectra shown below, in Figs. 7 and 8, obviously indicate the effect of the temperature and concentration on the intensities of certain new lines; these factors cause at the same time compensative changes in the intensities of lines for aldehyde. Spectral lines corresponding to the new species may be distinguished from those for the original aldehyde when the lines of the latter are subtracted from all those observed in solution, at least with the exception of some overlapping lines. Generally, lines for aldehyde itself are not substantially shifted, even in solution, nor do they change their shapes except for the line around 900 cm^{-1}. This line is very broad, and its center shifts to a higher frequency in the case of a solution. It seems, however, very reasonable to interpret this change by regarding the broad line as the superposition of a couple of lines which might have their peaks within this range. The decrease in intensity of the lower frequency peak resulted in showing the higher frequency peak to be stronger. The change about 900 cm^{-1} can be interpreted thus, and not as the result of solvent shift of the broad line.

Concerning C–H vibrations, one of the noticeable changes is the appearance of a strong new line at 1449 cm^{-1} with the decrease in intensity of the line at 1430 cm^{-1} for aldehyde. The line at 2919 cm^{-1} (aldehyde) produces a strong line at 2939 cm^{-1} as it decreases. A similar change is observed on the new lines at 2874 and 2996 cm^{-1}.

For the O–H stretching region, it is obvious that the stronger of the two broad peaks, around 3275 and 3425 cm^{-1} in pure water, shifts towards a frequency higher by 50 in the unit of cm^{-1} and that the separation becomes unclear. There may be a new broad line centered about 3400 cm^{-1} which would lead to the general broadening in this region.

The Raman Spectra of Related Compounds.—The results obtained with chloral, chloral hydrate and dimethylacetal are listed in Table II. The difficulty in the purification of chloral hydrate caused the superposing on the spectrum of a main impurity, chloral. The lines showing the same frequencies as Raman lines belonging to chloral are marked with (?) in the Table. The spectrum for dimethylacetal is shown in Fig. 6.

An Analysis of the Spectrum for the Hydrated Molecule.—Since $CH_3CH(OH)_2$ involves ten atoms, twenty-four normal vibrations are expected. Assuming that the hydrate molecule takes a symmetric configuration belonging to the point group C_s, all the modes of normal vibrations expected are listed in Table III.

TABLE II. OBSERVED FREQUENCIES (cm^{-1})

Chloral	Chloral hydrate	Dimethyl-acetal
200 s	194 m	292 W
242 S	242 ?	396 W
266 s	269 S	537 s
313 s	300 m	631 W
	340 w	808 S (P)
	414 S	829 m (P)
444 S (P)	444 ?	869 W
	570 s	988 m
614 s	623 s	1045 W
	686 W	1061 W
728 s (D)	728 ?	1087 W
846 m (D)	830 s	1125 m
983 W (D)	984 ?	1140 m
1018 W (D)	1015 w	1190 m
	1070 W	1362 m (D)
	1105 W	1448 S (D)
	1275 w	
1348 W	1358 m	
1454 w (P)	1388 w	2674 W
1757 S	1757 ?	2768 W
2685 w		2833 m
2860 S	2870 ?	2910 s
	2940 S	2944 S
3110 w	3550 vb	2994 s

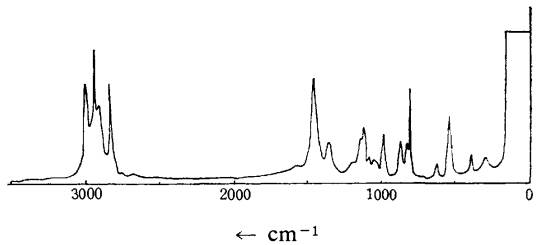

Fig. 6. Raman spectrum of dimethylacetal.

TABLE III. THE NUMBER OF THE NORMAL MODES FOR THE HYDRATE

	A′	A″		A′	A″
C–H stretching	1	0	C–C stretching	1	0
C–H deformation	1	1	$O\diagup C\diagdown O$ stretching (sym. & asym.)	1	1
CH_3 stretching					
symmetric	1	0	$O\diagup C\diagdown O$ scissoring	1	0
degenerate	1	1	$O\diagup C\diagdown O$ skeletal deformation	1	1
CH_3 sym. def.	1	0			
deg. def.	1	1	O–H stretching	2	0
CH_3 rocking	1	1	O–H deformation (in- and out-of-plane)	2	2
CH_3 torsion	0	1			

As both A′ and A″ species of vibrations are active in the Raman effect, all of those modes of vibration are observable. Six of them, such as the C–H and O–H stretching modes, are expected in the region above 2500 cm^{-1}; another six, including skeletal deformation, CH_3 torsion and O–H out-of-plane deformation, are below 700 cm^{-1}, and the remaining twelve are between 700 and 1500 cm^{-1}.

Tentative Assignments.—First, in the region below 700 cm^{-1}, all the lines except 420 cm^{-1} are assigned as follows. The line at 325 cm^{-1} in an aqueous solution is remarkable among new lines. This could be most reliably assigned to the skeletal deformation vibration (A′) in the $C-C\langle^{O}_{O}$ structure. Also, the line at 322 cm^{-1} in a heavy water solution seems to correspond to the mode in its lower frequency and sharpness. This assignment is supported by the fact that the line at 292 cm^{-1} for dimethylacetal is due to the skeletal deformation vibration, which shows a similar property in its shape. Those wave numbers are reasonable, considering their mass difference. The out-of-plane vibrations of O–H are also expected in this region. The line at 567 cm^{-1} in an aqueous solution is attributed to it because no line is observed in a heavy water solution near the frequency and because the line at 410 cm^{-1} in the heavy water solution could be regarded as the corresponding one from the product rule. The rather higher frequency of this vibration is explained by the fact that the hydrogen bonding in water could shift a frequency of this mode to a higher frequency than usual. The line at 480 cm^{-1} in the aqueous solution is assigned to $O\diagup C\diagdown O$ scissoring (A′), the line at 473 cm^{-1} in the heavy water solution corresponding to it. This scissoring mode (A′) is more reasonable than that other skeletal deformation vibration (A″) which is the only mode left among the skeletal deformation vibrations. Since a mode belonging to the A″ species can not usually show a stronger intensity than that for A′ species in a Raman spectrum, we can not attribute the observed line in question to a mode belonging to the A″ species when no suitable line for the remaining mode is observed.

Moreover, such an assignment is unacceptable because the scissoring mode is probable for the frequencies left in this region. All the assignments stated above being relatively consistent with each other, the broad band at 420 cm^{-1} in an aqueous solution is the only line in this region on which no comment can be made at present.

In the region between 700 and 1500 cm^{-1}, skeletal stretching vibrations and $C-H_n$ and O–H (in-plane) deformation vibrations are expected. No clear conclusion on some of them can be obtained at present, mainly because couplings between similar modes should be considered, especially in the region between 700 and 1200 cm^{-1}. The following attempt is focused on the modes of vibration related to the O–H group. The most distinguishable line, at 857 cm^{-1}, was assigned to the symmetric stretching vibration of $C\langle^{O}_{O}$ in the structure of $C-C\langle^{O}_{O}$. At the same time, it was observed that the new line at 845 cm^{-1} in the heavy water solution is also sharp, equivalent in its intensity and with the same order of depolarization ratio. The assignment is decisively supported by the existence of the line at 808 cm^{-1} in dimethylacetal, which has features similar to those mentioned above and has been attributed to the symmetric skeletal stretching vibration. The asymmetric stretching vibration seems to be at 920 cm^{-1} in the aqueous solution and around 918 cm^{-1} in the heavy water solution.

The features of the broad line centered at 918 cm^{-1} imply the superposing of another line, which line may well be assigned to O–D (in-plane) deformation since it is a reasonable position evaluated from the product rule if we suppose either the line at 1095 cm^{-1} or the line at 1156 cm^{-1} to be an O–H (in-plane) deformation vibration. It might be one coupled with a CH_3 rocking vibration. The reasons why we should suppose either of those lines to be an O–H deformation vibration are, one, that no lines are observed in the same frequency region in heavy water, which implies a large frequency shift due to the change of mass from H to D, and, two, that those frequencies are probable for O–H (in-plane) deformations. This assignment, as well as those for such vibrations as C–C stretching, C–H deformation (A′) and CH_3 rocking (A′ and A″), will be discussed elsewhere with extensive further data.

The lines at 1353, 1400 and 1449 cm^{-1} are due to C–H deformation (A″), CH_3 symmetric deformation, and CH_3 degenerate deformation respectively. The assignment for the first one, (A″), is supported by the value of its depolarization ratio and by the existence of the line at 1348 cm^{-1} in the chloral hydrate. The new line at 1449 cm^{-1} changes in intensity in compensation for the intensity at 1430 cm^{-1} for aldehyde. Moreover, it keeps the same frequency in a heavy water solution. The depolarization ratio implies the superposition of the A′ and A″ species of vibration. In

the spectrum of dimethylacetal, the equivalent line is found at 1448 cm^{-1}.

In the region of C–H stretching vibrations, one C–H stretching (A'), one CH_3 symmetric, and one CH_3 degenerate stretching vibration are to be expected. As a result of the investigation of their relative intensities and degrees of depolarization, the line at 2995 cm^{-1} is attributed to the CH_3 degenerate stretching mode, the one at 2940 cm^{-1} to the CH_3 symmetric stretching mode, and the other, at 2874 cm^{-1}, to the C–H stretching vibration. This conclusion is not consistent with that obtained for the CH_3 symmetric stretching frequencies of formals, acetals and related compounds.[4] For these, however, it has been suggested that the CH_3 symmetric stretching frequencies of OCH_3 groups split into two frequencies as a result of the Fermi resonance, with overtones of the CH_3 asymmetric deformation frequencies of OCH_3 groups. The splitting of the symmetric stretching frequency under the influence of an overtone frequency was not introduced here. Those frequencies remain in deuterated compounds, also. The fact that the frequency for a tertiary C–H stretching mode varies rather widely from hydrates to acetals may indicate a strong dependency of this frequency upon the groups attached to the tertiary carbon atom.

Thus, assignments have been carried out tentatively for as many observed lines as possible on the basis of the data presented here. The assignments described above are shown in Table IV.

As has been discussed above, reliable lines characteristic of hydrated molecules which exist only in solution can be used for spectroscopic investigation of reactive intermediates having two hydroxy groups on one and the same carbon atom.

Since changes in an aqueous solution are closely connected with a skeletal structure, further precise analysis of the relative intensities for new and original lines and a complete knowledge of acetaldehyde would provide us with assignments in more detail, especially for the region where complicated lines are produced out of couplings with skeletal vibrations.

TABLE IV. THE ASSIGNMENT OF THE RAMAN LINES FOR THE HYDRATE AND DEUTERATE OF ACETALDEHYDE

$CH_3CH(OH)_2$	$CH_3CH(OD)_2$	Mode
325	322	Skeletal deformation (A')
480	473	$O\diagup C\diagdown O$ scissoring
567	410	O–H or O–D out-of-plane deformation
857	845	$O\diagup C\diagdown O$ sym. stretching
920	918	$O\diagup C\diagdown O$ asym. stretching
1095 or 1156	918~	O–H or O–D in-plane deformation
1353	1358	C–H deformation (A'')
1400	1400	CH_3 sym. deformation
1449	1449	CH_3 deg. deformation
2874	2873	C–H stretching
2939	2941	CH_3 sym. stretching
2996	2996	CH_3 deg. stretching

Results (Part II)

Observation of the Spectra at Various Temperatures and in Various Concentrations.—The spectra for solutions were recorded at various temperatures from 0 through 60°C, some of which are shown in Figs. 7 and 8. The ratios of the intensities for new lines to those of original lines increase as the temperature and

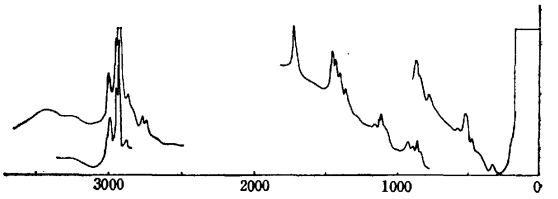

Fig. 7(a). Raman spectra of acetaldehyde in aqueous solution at 0°C (equimolar solution).

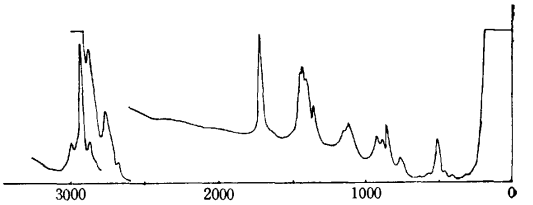

Fig. 7(b). Raman spectra of acetaldehyde in aqueous solution at ordinary temperature (molar ratio, 1 : 2 H_2O).

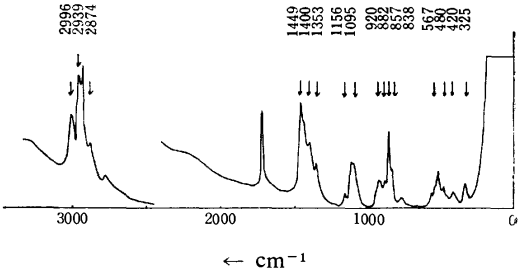

Fig. 7(c). Raman spectra of acetaldehyde in aqueous solution at 0°C (molar ratio, 1 : 2 H_2O).

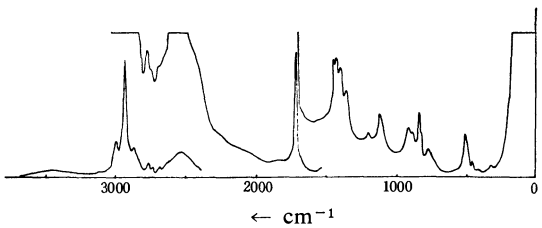

Fig. 8(a). Raman spectra of acetaldehyde in heavy water solution at ordinary temperature (molar ratio, 1 : 2 D_2O).

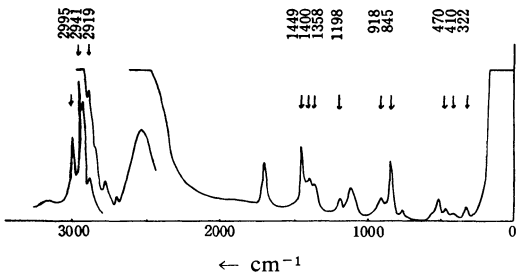

Fig. 8(b). Raman spectra of acetaldehyde in heavy water solution at 0°C (molar ratio, 1 : 2 D_2O).

the concentration of aldehyde decrease. At 60°C only a few stronger lines are observable. Their compensative changes with the lines for aldehyde have been described in Results (Part I) of this paper. This observation was quite helpful in attributing the observed lines to the species present in a solution.

The reproducibility of their intensities upon a change in temperature is good enough to prove this hydration process to be reversible.

Evaluation of Raman Intensities.—For the purpose of quantitative measurements, working curves were drawn for various temperatures by using mixtures of acetaldehyde and *n*-hexane. The carbonyl frequency, 1720 cm^{-1}, in this solution does not undergo any significant changes due to intermolecular interaction, but retains the same shape as in a pure liquid. We have, therefore, used the peak height of this line as a measure of the concentration of acetaldehyde in order to obtain each working curve at different temperatures. Using these working curves, we can eliminate several basic factors which must be taken into account in intensity measurement[5,6]. We, however, have still had trouble in an aqueous solution in estimating the peak heights of a carbonyl frequency at a lower temperature, trouble such as a lifting-up of

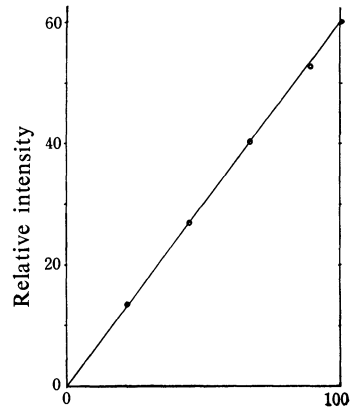

Fig. 9. The working curve for carbonyl band in solution.
$\nu_{C=O}$: 1720 cm^{-1}
at 0°C, in *n*-hexane solution

a base line and a variation in the shape. The specific causes of these phenomena have not yet been elucidated. Therefore, the values calculated of the basis on this observation could give only a measure of the true values. One of the working curves is shown in Fig. 9.

Equilibrium Constants and Calculation of the Hydration Energy. — The equilibrium constant is written as

$$K=\frac{(X)}{(a-X)(b-X)}$$

where a and b denote the initial concentrations of aldehyde and water respectively and X, the concentration of the hydrated species. The concentration of aldehyde remaining at an equilibrium point was determined from the spectrum recorded after keeping the sample tube at a desired temperature for more than one hour[7]. K's were obtained since the values of a and b were known.

The hydration energy can be determined from a plot of $\log K$ against $1/T$, as is obvious in the following equation:

$$K=A\exp(-\Delta H^{h}/RT)$$

The equilibrium constants and the calculated hydration energy are: $K^{273}=0.029$, $K^{313}=0.0040$ (mol^{-1}), and $\Delta H^{h}=-8.7$ kcal./mol., and the initial concentrations: $a=12.1$, and $b=18.5$ mol./l. Fig. 10 shows the experimental results from which the value of the hydration energy was calculated.

Bell and Clunie[7] made an attempt to separate the instantaneous heat of solution from that of the subsequent hydration process, and

5) H. J. Bernstein and G. Allen, *J. Opt. Soc. Amer.*, **45**, 237 (1955).
6) R. Rea, ibid., **50**, 90 (1960).
7) R. P. Bell and J. C. Clunie, *Trans. Faraday Soc.*, **48**, 439 (1952).

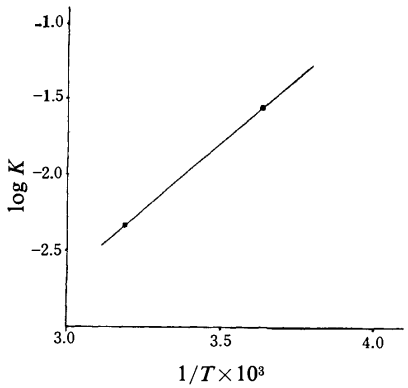

Fig. 10. The plot of $\log K$ against $1/T$.

reported, by combining calorimetric and ultraviolet absorption measurements, that the heat of hydration in question is -5.10 kcal./mol. for a very dilute solution. The value obtained here seems to be a little larger than those given by others. We have to notice, however, that there is confusion in the literature regarding the equilibrium constants and the heat of hydration. Our experiments concerned a very concentrated solution. Most others have investigated rather dilute solutions, and no consideration has been paid to the form of the equation for equilibrium constants. Since water molecules are apt to associate with each other, they are also at an equilibrium between aggregate water and isolated water, in which we should mention various extents of aggregation. Moreover, the isolated form might be a reactive form. Therefore, the effective concentration of water, for instance, must be varied according to the initial concentration as well as to the temperature range investigated. This could be introduced as a correction for use in determining the actual equation for this hydration equilibrium in an effort to obtain constant values. Generally speaking, a very delicate balance between the hydration process and the dissociation of aggregate water molecules might be shown in changes of the value of K depending on the initial concentration of components. This will be discussed elsewhere[8] through the precise measurement of the proton magnetic resonance.

Summary

The Raman spectra of acetaldehyde, its aqueous solution and its heavy water solution have been recorded at various temperatures and in various concentrations in order to find the Raman frequencies characteristic of the hydrated species and in order to investigate the reversible hydration process. Almost all the lines have been assigned tentatively on the assumption that the hydrate molecule has C_s symmetry. The lines at 325, 480, 567, 1353, 1440, 1449, 2874, 2939 and 2996 cm^{-1} can be referred to as the lines characteristic of the hydrate. Supporting data have also been obtained for the related compounds for the sake of comparison. Moreover, through the intensity measurements, equilibrium constants, as well as the heat of hydration, have been evaluated as the basis for a discussion of the hydration process.

The author would like to express her deepest appreciation to Dr. Yo-ichiro Mashiko, Dr. Shinnosuke Saeki, and Dr. Kenkichi Nukada for their helpful discussions.

Government Chemical Industrial Research Institute, Tokyo
Shibuya-ku, Tokyo

8) M. Matsushima, Hydration Studies, II, to be published.

*Syntheses and Structures of Acetylformoin and Its Related Compounds. III. Isobutyrylformoin**

By Yō Miyagi and Ryozo Goto

(Received April 16, 1963)

In previous papers, the chemistry of acetyl-[1], benzoyl-[1] and neopentoyl-formoin[2] was reported on. These formoins were synthesized by the acyloin condensation of methyl-, phenyl- and *t*-butyl-glyoxal; the possible structures for these formoins are I—III. The structures of acetyl-, benzoyl- and neopentoyl-formoin in the crystalline state were established as I (R=CH_3), II (R=C_6H_5) and II (R=$C(CH_3)_3$) respectively.

The present report is concerned with isobutyrylformoin, which was also synthesized by the acyloin condensation of isopropylglyoxal:

$$2\ (CH_3)_2CHCOCHO \rightarrow (CH_3)_2CHCOCH(OH)COCOCH(CH_2)_3$$

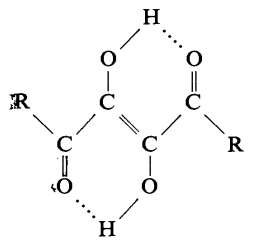

I

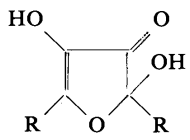

II

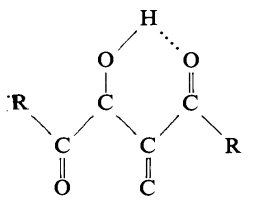

IIIa

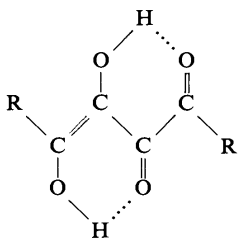

IIIb

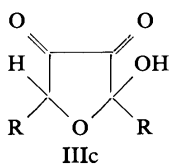

IIIc

Results and Discussion

The Preparation of Isopropylglyoxal.—Conrad and Gast[3] first synthesized isopropylglyoxal by the following sequence of reactions:

$$CH_3COCH_2COOC_2H_5 \xrightarrow[Na]{CH_3I} CH_3COC(CH_3)_2COOC_2H_5 \xrightarrow{Br_2} BrCH_2COC(CH_3)_2COOC_2H_5 \xrightarrow{AcOK} CH_3COOCH_2COC(CH_3)_2COOC_2H_5 \xrightarrow{H_2SO_4}$$

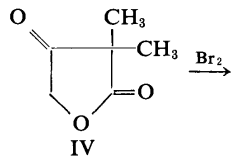

IV

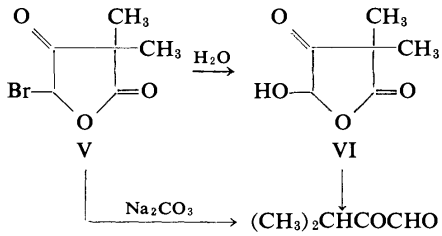

V VI

$$\xrightarrow{Na_2CO_3} (CH_3)_2CHCOCHO$$

They obtained isopropylglyoxal by the decarboxylation of 5-oxy-3, 3-dimethyltetronic acid VI, which had been prepared by the hydrolysis of 5-bromo-3, 3-dimethyltetronic acid V. They isolated the latter compound as an oily products, but we found it a white solid melting at 52.5~54°C. Reid, Fortenbaugh and Patterson[4] prepared isopropylglyoxal by the steam distillation of 5-bromo-3,3-dimethyltetronic acid V in a 20% yield. We are of opinion that the low yield may be due to the decomposition of isopropylglyoxal by hydrogen bromide, which is produced by the hydrolysis of V.

We succeeded in obtaining isopropylglyoxal directly from the bromide V by suspending it in an aqueous solution of enough amount of sodium carbonate to neutralize the acid produced and then by heating the entire mixture.

* Present at the 16th Annual Meeting of the Chemical Society of Japan, Tokyo, April, 1963.

1) R. Goto, Y. Miyagi and H. Inokawa, This Bulletin, **36**, 147 (1963).

2) Y. Miyagi and R. Goto, ibid., **36**, 650 (1963).

3) M. Conrad and R. Gast, *Ber.*, 31, 2726 (1898).

4) E. B. Reid, R. B. Fortenbaugh and H. R. Patterson, *J. Org. Chem.*, **15**, 572 (1950).

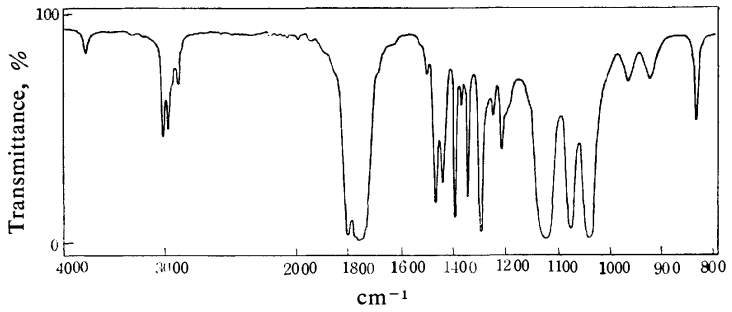

Fig. 1. Infrared spectrum of 3,3-dimethyltetronic acid (IV) in carbon tetrachloride.

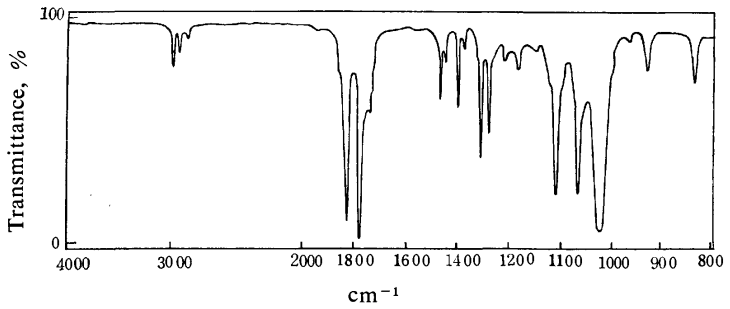

Fig. 2. Infrared spectrum of 5-bromo-3,3-dimethyltetronic acid (V) in carbon tetrachloride.

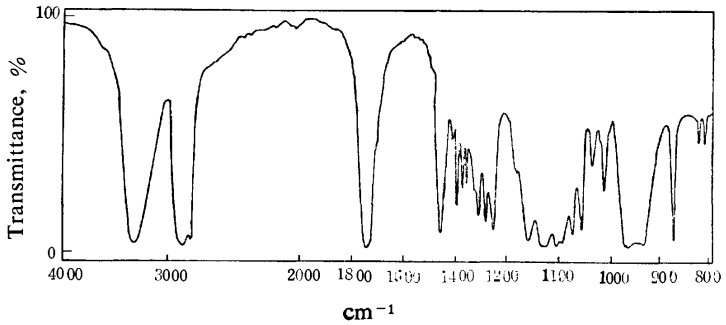

Fig. 3. Infrared spectrum of 5-oxy-3,3-dimethyltetronic acid (VI) in Nujol.

Figures 1, 2 and 3 show the infrared spectra of compounds IV, V and VI respectively. Compound IV shows a broad band of the C=O stretching absorption between 1740 and 1810 cm^{-1} in carbon tetrachloride. Similarly, compound VI absorbs at 1740~1770 cm^{-1} in Nujol. These broad bands may be overlapping bands of ring ketones and γ-lactones; five-membered ketones are said to absorb at around 1750 cm^{-1} [5-7], and γ-lactones absorb at around 1770 cm^{-1} [8,9]. The C=O stretching absorption band of compound VI arises at 1760~1800 cm^{-1} in tetrahydrofuran. Compound V shows two separated bands, at 1825 and 1773 cm^{-1}. The absorption bands of α-bromoketones are usually shifted to a higher frequency by about 20 cm^{-1}. Thus, in compound V, the absorption band of the ring ketone may be considered to arise at a higher frequency, 1825 cm^{-1}, separated from the lactone band at 1773 cm^{-1}.

Isobutyrylformoin.—The reaction product of isopropylglyoxal with sodium cyainde is a white solid, which was proved by elementary analysis and by molecular weight determination to be a condensation product of the two molecules of isopropylglyoxal.

The infrared absorption bands of isobutyrylformoin in the regions of C=O, C=C and OH stretching absorption are listed in Table I. The

5) R. N. Jones, V. Z. Williams, M. J. Whalen and K. Dobriner, *J. Am. Chem. Soc.*, 70, 2024 (1948).
6) E. J. Hartwell, R. E. Richards and H. W. Thompson, *J. Chem. Soc.*, 1948, 1436.
7) J. F. Grove and H. A. Willis, ibid., 1951, 883.
8) R. S. Rasmussen and R. Brattain, *J. Am. Chem. Soc.*, 71, 1073 (1949).
9) D. H. Whiffen and H. W. Thompson, *J. Chem. Soc.*, 1946, 1005.

TABLE I. INFRARED ABSORPTION BANDS, cm^{-1}

Formoin	Phase					
Benzoyl-	Nujol	3500	3270	1685	1608	1595
Neopentoyl-	Nujol	3330	3180	1690	1605	
Isobutyryl-	Nujol	3340	3100	1690	1598	
	Tetrahydrofuran	3290		1705	1635	
	Chloroform	weak and broad 3700~2600		1635		
Acetyl-	Nujol, Chloroform	weak and broad 3600~2800		1625		

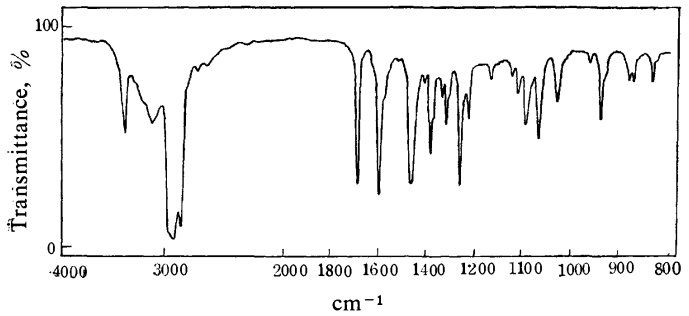

Fig. 4. Infrared spectrum of isobutyrylformoin in Nujol.

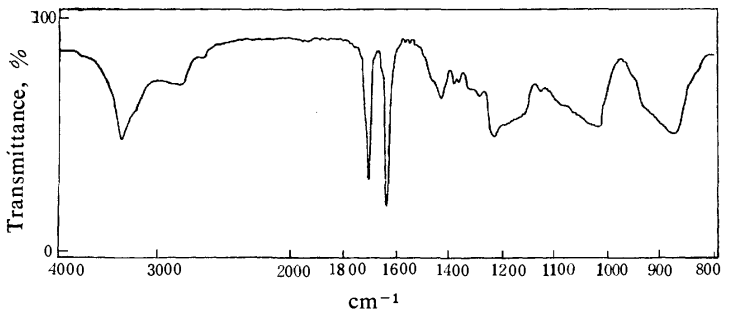

Fig. 5. Infrared spectrum of isobutyrylformoin in tetrahydrofuran.

infrared spectrum of isobutyrylformoin in Nujol (Fig. 4) is very similar to those of benzoylformoin and neopentoylformoin, the structures of which were both established as II ($R=C_6H_5$ and CMe_3)[1,2]. Thus, the structure of isobutyrylformoin also seems to be II ($R=CHMe_2$). The absorption band at 1598 cm^{-1} and that at 1690 cm^{-1} are attributable to the C=C and C=O stretching absorption respectively. This assignment seems probable, in spite of the lack of spectral data on furanones, because conjugated ketones usually absorb at 1690~1680 cm^{-1}, and olefinic linkages do at around 1600 cm^{-1}.

The spectrum in tetrahydrofuran (Fig. 5) resembles that in Nujol, except that the former shows only one band of the OH stretching absorption at 3290 cm^{-1}, while the latter shows two bands, at 3340 and 3100 cm^{-1}. Therefore, isobutyrylformoin may be considered to have structure II in tetrahydrofuran. The difference in the hydroxyl bands between the solid state and the solution does not suggest that isobutyrylformoin would have a structure other than II in tetrahydrofuran, because the position of the OH stretching absorption band is easily shifted with the strength of hydrogen bondings, which may be different in the solid state and in the solution. Moreover, the spectrum can not be explained on the basis of structures I, IIIa, IIIb and IIIc for reasons similar to those discussed in a previous paper[1].

The spectrum of isobutyrylformoin in chloroform (Fig. 6) is remarkably different from those in tetrahydrofuran and Nujol; it is, however, very similar to that of acetylformoin in chloroform or Nujol. There is only a broad, weak absorption band extending from 2600 cm^{-1}

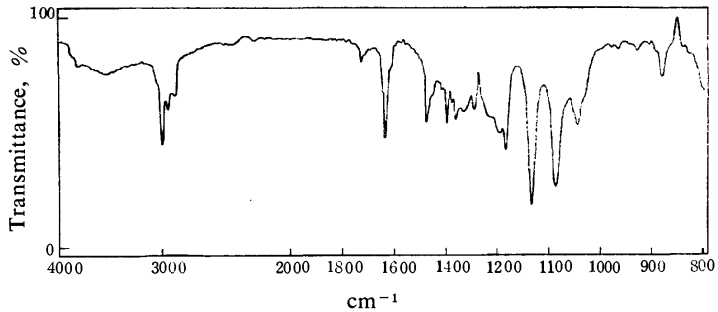

Fig. 6. Infrared spectrum of isobutyrylformoin in chloroform.

beyond over 3700 cm^{-1} instead of distinct bands at 3340 and 3100 cm^{-1} in Nujol or at 3290 cm^{-1} in tetrahydrofuran. The C=O stretching absorption band is widely shifted to 1635 cm^{-1}. This type of spectra has been said to be characteristic of the enol form of β-diketones and has been attributed to the resonance structures[10]:

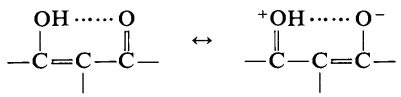

Structure I (R=$CHMe_2$) is most compatible with these observations, as in the case of acetylformoin. Any further explanation and exclusion of the other structures, II, IIIa, IIIb and IIIc, would be the same as have been given in a previous paper[1].

A similar tendency is observed in the ultraviolet absorption spectra. In tetrahydrofuran, the absorption maximum is attained at 305 mμ with ε_{max}, 7350. On the other hand, in chloroform it is shifted to 360 mμ, with a great enhancement of its intensity (ε_{max}=14200). Thus, the absorption at 360 mμ is attributable to the enediol structure I and that at 305 mμ, to the furanone structure II.

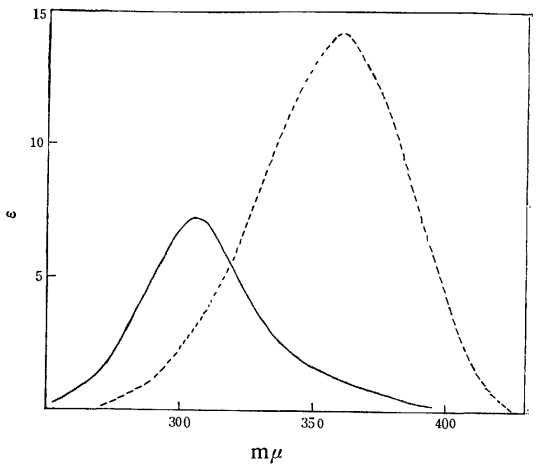

Fig. 7. Ultraviolet spectra of isobutyrylformoin: —— in tetrahydrofuran; ---- in chloroform.

Experimental

Ethyl α,α-Dimethylacetoacetate. — This compound was prepared by the method of Marshall and Cannon[11]; 51%; b. p. 96~98°C/40 mmHg; n_D^{25} 1.4180.

Found: C, 60.99; H, 8.96. Calcd. for $C_8H_{11}O_3$: C, 60.74; H, 8.92%.

Ethyl γ-Bromo-α,α-dimethylacetoacetate.—This compound was prepared by the method of Conrad and Gast[3,12]: 70%; b. p. 109~111°C/10 mmHg; n_D^{25} 1.4682.

Found: C, 40.62; H, 5.50; Br, 33.68. Calcd. for $C_8H_{13}O_3Br$: C, 40.55; H, 5.49; Br, 33.42%.

Ethyl γ-Acetoxy-α,α-dimethylacetoacetate. — This compound was also prepared by the method of Conrad and Ggast[3,12]: 55%; b. p. 91~92°C/1 mmHg; n_D^{25} 1.4339.

Found: C, 55.32; H, 7.22. Calcd. for $C_{10}H_{21}O_5$: C, 55.54; H, 7.46%.

3, 3-Dimethyltetronic Acid.—This compound was prepared by the method of Cannon and Jones[12]: 70%; b. p. 70~72°C/3 mmHg; n_D^{25} 1.4475.

Found: C, 56.30; H, 6.52. Calcd. for $C_6H_8O_3$: C, 56.24; H, 6.29%.

5-Bromo-3, 3-dimethyltetronic Acid.—A solution of 16 g. of 3,3-dimethyltetronic acid in 30 ml. of carbon tetrachloride was warmed at 60°C, and then 20 g. of bromine was added with stirring. The solvent was evaporated off under reduced pressure. Upon the cooling with ice-water, all the residue was solidified. The product was washed with cold water, dried in vacuo over potassium hydroxide, and recrystallized from ether; 92%; m. p. 52.5~54°C (decomp.).

Found: C, 34.75; H, 3.68; Br, 42.02. Calcd. for $C_6H_7O_3Br$: C, 34.78; H, 3.38; Br, 41.88%.

5-Oxy-3, 3-dimethyltetronic Acid[3].—A suspension of 5-bromo-3, 3-dimethyltetronic acid in water was stored in a refrigerator for over a month. The solid product was recrystallized from methanol; m. p. 137°C.

10) R. S. Rasmussen, D. D. Tunnicliff and R. B. Brattain, *J. Am. Chem. Soc.*, 71, 1068 (1949); L. J. Bellamy, "Infrared Spectra of Complex Molecules", Methuen, London (1958), pp. 104, 142.

11) R. J. Marshall and W. N. Cannon, *J. Org. Chem.*, 21, 245 (1956).

12) W. N. Cannon and R. G. Jones, ibid., 23, 126 (1958).

Found: C, 49.89; H, 5.72. Calcd. for $C_6H_8O_4$: C, 50.00; H, 5.60%.

Isopropylglyoxal. — Five grams of pulverized 5-bromo-3,3-dimethyltetronic acid was suspended in an aqueous solution of 1.3 g. of sodium carbonate in 50 ml. of water. The entire mixture was whirled. The evolusion of carbon dioxide began immediately, and after about half an hour the characteristic odor of isopropylglyoxal could be smelled. The entire mixture was stored in a refrigerator. After a few hours, most of the solid disappeared, but after standing overnight many white needles were deposited. The entire mixture was then gradually heated to 90°C. The needles dissolved in the solution, and a steady evolution of gas took place. After its end, the solution was cooled with ice-water. The long white needles which were deposited were collected by filtration. The purification was effected by vacuum sublimation; yield, 85%; m. p. 95~96.5°C.

Found: C, 59.80; H, 8.07. Calcd. for $C_5H_8O_2$: C, 60.00; H, 8.00%.

Isobutyrylformoin.—Into a solution of 4.5 g. of isopropylglyoxal in 150 ml. of 90% aqueous alcohol, a solution of 0.2 g. sodium cyanide in 5 ml. of water was added under a nitrogen stream. The entire solution was then cooled at 0°C for about twenty minutes. After the addition of a few drops of phosphoric acid, the solvent was evaporated off under reduced pressure. The faint-colored crystals which appeared were washed with about 50 ml. of cold water, then dissolved in a minimum amount of alcohol and crystallized by the addition of water: yield, 68%; m. p. 88~93°C.

Found: C, 59.78; H, 7.75; mol. wt. (Rast), 186. Calcd. for $C_{10}H_{16}O_4$: C, 60.00; H, 8.00%; mol. wt., 200.

Spectra. — The infrared spectra were recorded with a Koken model DS-301 spectrophotometer. The ultraviolet spectra were recorded with a Shimadzu model QR-50 spectrophotometer.

Department of Chemistry
Faculty of Science
Kyoto University
Sakyo-ku, Kyoto

The Determination of the Water Content of the Low Polymers of Formaldehyde by the Karl Fischer Method. I. The Determination of the Adsorbed Water and Bound Water Formed by the Pyrolysis of the Polymer

By Kaname MUROI and Kunihiko OGAWA

(Received April 20, 1963)

The difficulty in determining the water content in the low polymers of formaldehyde by the vacuum-drying method is that the content of bound water produced by the pyrolysis of the polymer via the reaction,

$$HO-(CH_2O)_n-H \rightleftharpoons nCH_2O+H_2O \quad (1)$$

and also the content of water physically adsorbed on the polymer are determined at the same time[1]. The determination of the adsorbed water with a high degree of accuracy is, therefore, difficult in this method. The authors have found a new method to determine these two kinds of water separately by using the Karl Fischer method.

Experimental

Materials.—Both commercial grade and a special-class reagent of paraformaldehyde were used without further purification. α-Polyoxymethylene was supplied by our laboratory. Methanol was dried by magnesium metal. Ethylene glycol, butylene glycol and propylene glycol were dried by boiling. The Karl Fischer reagent SS "Mitsubishi", free from methanol supplied by the Mitsubishi Chemical Industries, was used (titer: 0.5 mg. H_2O/ml. and 3.0 mg. H_2O/ml.).

Apparatus.—The Karl Fischer electrometric titration apparatus, operating by the dead stop method, was manufactured by the Tsutsui Chemical Instrument Co. The apparatus is illustrated in Fig. 1. A is the container of anhydrous methanol prepared by adding the Karl Fischer reagent drop by drop to the end point. The methanol was used for the extraction of the adsorbed water. The polyethylene bag, H, filled with dry nitrogen was used to keep the titration flask from moisture in the air. The titration flasks J and K were used for the determination of the adsorbed water, and L, for the bound water, in polymers. Figure 2 illustrates the Ward-type automatic buret which was used as the container and the pipet of dry propylene glycol. Dry propylene glycol was treated

1) J. F. Walker, "Formaldehyde", Reinhold Publishing Co., New York (1953), p. 129.

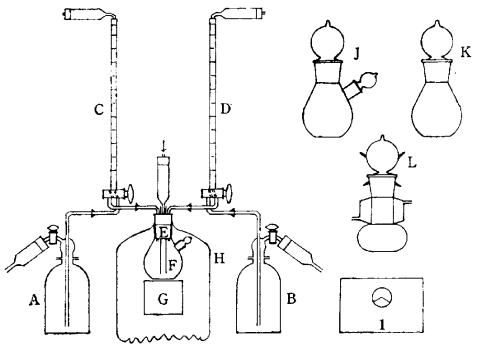

Fig. 1. Apparatus for electrometric titration.

A: Container of methanol
B: Container of the Karl Fischer reagent
C: Buret of methanol, 50 ml., graduated by 0.1 ml.
D: Buret of the Karl Fischer reagent, 10 ml., graduated by 1/50 ml.
E: Ground glass adaptor having two buret inlets, breathing tube and sealed-in electrodes
F: Platinum electrodes
G: Magnetic stirrer
H: Polyethylene bag
I: Indicator of end point
J: Titration flask with a ground glass stopper fitted with a side-arm, 200 ml.
K: Titration flask with a ground glass stopper, 200 ml.
L: Titration flask with a ground glass stopper and a water jacket, 200 ml.

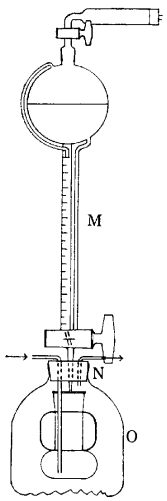

Fig. 2. Automatic buret of propylene glycol.

M: Ward-type automatic buret, 1000 ml.
N: Rubber stopper
O: Polyethylene bag

in the polyethylene bag, O, filled with dry nitrogen.

Procedure.—*The Determination of the Adsorbed Water.—Undried Sample:* The titration flask, J, was attached to E and filled with 25 ml. of anhydrous methanol as exactly measured by the buret, C. After adding the Karl Fischer reagent to the dead stop end point, an exactly-weighed polymer sample was added through a side-arm; the methanol solution was then stored about 10 min. The percentage of adsorbed water, *a* %, is calculated from the titration value of the Karl Fischer reagent (titer 3 mg. H_2O/ml.) for this solution.

Dried Sample: The flask K, containing about 10 g. of a carefully dried sample, was attached to E in bag, H, filled with dried nitrogen. Fifty milliliters of anhydrous methanol was added, and the solution was stored about 10 min. The water content, *a* %, was calculated from the titration value of the Karl Fischer reagent (titer 0.5 mg. H_2O/ml.) for this solution, from which the blank value obtained by the control experiments for a methanol solvent had been subtracted.

The Determination of the Bound Water.—Undried Sample: The titration flask, L, attached to the automatic buret, M, was flushed with dry nitrogen so as to completely remove the adsorbed water from the wall. An exactly weighed sample was added to 25 ml. of propylene glycol in the flask, L, and heated at 160°C about 5 to 10 min., while the jacket around the flask, L, was cooled. The sample was completely dissolved into propylene glycol in this condition. The flask, L, was carefully attached to E so as not to come in contact with moisture in the air by using a dry nitrogen-filled bag, H. The water content in the solution, *b* %, was calculated from the titration value with the Karl Fischer reagent of the titer of 3 mg. H_2O/ml., from which the value for control experiment had been subtracted.

Dried Sample: About 5 g. of a weighed sample in the flask, L, was carefully dried in a vacuum desiccator. The flask, L, was attached to the automatic buret, M, via the joint, N, in a completely dry condition by using the polyethylene bag, O, filled with dry nitrogen. Fifty milliliters of propylene glycol was added to the sample. Again the sample was dissolved into propylene glycol after 5 to 10 min. heating at 160°C. The water content, *b* %, was calculated by the method previously described for the undrid sample. The content of bound water, *c* %, was given by the difference between *b* and *a*; i.e. $c(\%) = b(\%) - a(\%)$.

Results and Discussion

The Elimination of the Effect of Moisture in the Air.—The interference of moisture in the air with the Karl Fischer method and a method of eliminating this interference have been discussed in detail by Bastin et al.[2] and by Loveland and Wester[3]. In the course of the present work, the authors found that the Karl Fischer reagent had a great sensitivity to the moisture in the air and that the water adsorbed on the wall of the flask caused a big error in the determination of a

2) E. L. Bastin. H. Siegel and A. B. Bullock, *Anal. Chem.*, 31, 467 (1959).
3) J. W. Loveland and T. B. Wester, ibid., 31, 30 (1958).

Table I. Comparison of the water contents in the dried sample obtained in a dry nitrogen atmosphere and in air

In dry nitrogen		In air		Difference
H_2O mg.	Error mg.	H_2O mg.	Error mg.	H_2O mg.
0.49	+0.04	5.07	−0.01	
0.42	−0.03	5.18	+0.10	
0.45	0	5.03	−0.05	
0.50	+0.05	5.09	+0.01	
0.48	+0.03	5.13	+0.05	
0.40	−0.05	5.05	−0.03	
0.43	−0.02	4.99	−0.09	
average	0.45±0.05	5.08	±0.10	+4.63

small amount of water. Table I lists the amount of adsorbed water for the dried sample and the range of error in two cases, one, for the experiment carefully conducted in a dry nitrogen atmosphere and the other, in air. It is obvious that, in the latter case, moisture in the air and the water adsorbed on the glass wall yield much larger values and errors. To eliminate this interference, the authors propose the following two methods:

1) To flush dry nitrogen through a titration flask about 20 min.

2) In the case of the determination of a small amount of water adsorbed on a dried sample, in order to eliminate the repetition of control experiments and also to prevent moisture from entering a flask during the sampling, anhydrous methanol which had been prepared by adding a Karl Fischer reagent to the dead stop point was added to the sample from columns A and C. It would be more effective to put the whole apparatus in a dry box or in a low-humidity room, but in the present work the authors have reported a convenient method for use in an ordinary laboratory.

The Determination of the Adsorbed Water.—Various conditions of the extraction of adsorbed water by dry methanol were studied using the special class reagent paraformaldehyde as a sample. Table II lists the experimental conditions and observed values of water content. It is concluded that the adsorbed water was easily extracted by 25 ml. of methanol after storing the solution for 10 min. Table III lists the values of water content in the various dried samples. An excellent reproducibility is obtained.

Table II. Results of determination of adsorbed water on *p*-formaldehyde by methanol extraction

Sample weight g.	Methanol ml.	Time of extraction min.	Water mg.	Content %
0.6539	50	5	4.51	0.69
0.5972	50	10	4.18	0.70
0.8133	50	20	5.62	0.70
0.7156	50	40	5.08	0.71
0.6734	50	60	4.75	0.70
0.9114	50	120	6.65	0.73
0.8227	10	10	5.59	0.68
0.7955	25	10	5.81	0.73
0.8023	50	10	5.62	0.70
0.8154	100	10	5.87	0.72

Table III. Results of the reproducibility test for determination of adsorbed water of dried samples

Sample	Water content, %
Paraformaldehyde	0.098
	0.095
	0.095
α-Polyoxymethylene A	0.025
	0.021
	0.020
α-Polyoxymethylene B	0.019
	0.019
	0.019

The Determination of the Summed Amount of Bound Water and Adsorbed Water.—Iliceto and Bezzi discovered the reaction of formaldehyde with methanol and suggested the use of the Karl Fischer reagent after changing formaldehyde to cyanohydrine by treating it with hydrogen cyanide[4]. The authors have tried to find a better solvent than methanol. Dimethylformamide, *o*-chlorophenol, dioxane, *m*-cresol and ethylene glycol, propylene glycol, and butylene glycol were used as solvents. First, the solubility of samples in these solvents was studied. The samples had low solubility in dimethylformamide, *o*-chlorophenol, *m*-cresol and diethylene glycol, even at 120°C. They had a high solubility in hot dioxane, but a low value at room temperature. It was concluded from the solubility tests that ethylene glycol, propylene glycol and butylene glycol were good solvents. Formaldehyde reacts readily with glycols and yields water in the presence of acid catalysis or at a high temperature via the reaction:

$$\begin{matrix} CH_2OH \\ | \\ CH_2OH \end{matrix} + HCHO \rightarrow \begin{matrix} CH_2O \\ | \\ CH_2O \end{matrix}\!\!>CH_2 + H_2O \quad (2)$$

The water thus formed might interfere with the determination of water by the pyrolysis method.

Table IV lists the variation in water content of paraformaldehyde at various conditions of pyrolysis in dry ethylene glycol. The sample is insoluble below 60°C, when only the

4) A. Iliceto and S. Bezzi, *La Chimica e l'Industria*. 42, 728 (1960).

adsorbed water was extracted. The water content reached a constant value in the temperature region 120~150°C within 10 minutes heating. At 170°C the same constant value was obtained in 3 minutes heating. At 150°C, the water content increased with the heating period, which suggests the occurrence of reaction 2. The reaction of formaldehyde with propylene glycol and butylene glycol was also studied, because it is well known that the rate of esterification decreases in the order of primary, secondary and tertiary alcohols. Figure 3 illustrates the results. It is concluded that propylene glycol is the best solvent because it gives an almost constant value of water content during the heating period studied. The dependence of the value of water content on the ratio of the amount of propylene glycol to that of sample was studied. Table V lists the value of water content with various amounts of sample and solvent. It is suggested that about 5 g. of a sample in 25 ml. of propylene glycol is suitable for conducting experiments. Table VI lists the value of the summed content of adsorbed water and bound water in various types of low polymers of formaldehyde determined by the pyrolysis method in dry propylene glycol. Table VII lists the value of adsorbed water content for the samples determined by the methanol extraction method. The difference in values corresponds to the content of bound water in the polymers. The average degree of polymerization was calculated from the content of bound water.

The determination of the degree of polymerization of the low polymer of formaldehyde is rather difficult, and only a few methods have been reported[5,6]. Recently, Iliceto and Bezzi[4] have determined the degree of polymerization from the water content by the Karl Fischer method, but they have not determined bound water and adsorbed water separately, as the present authors have now done. In the other works, since the calculation was based on the summed amount of bound and adsorbed water, the accuracy of

TABLE IV. RESULTS OF THE DETERMINATION OF WATER FORMED BY PYROLYSIS AT VARIOUS TEMPERATURES

Condition of pyrolysis		Water content
Temperature °C	Time min.	%
20	20	0.57
40	20	0.54
60	20	0.57
80	20	1.37
110	20	2.86
120	20	3.03
130	20	3.08
150	10*	3.08
150	30*	4.03
150	60*	6.14
170	3*	3.05

* The heating time after a sample dissolves completely in solvent.

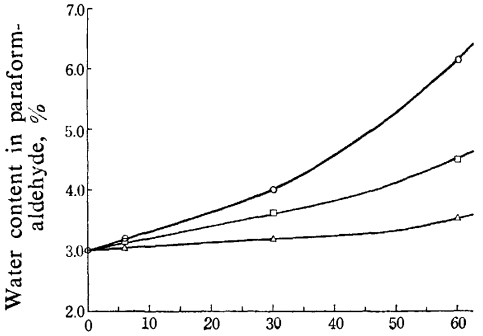

Fig. 3. Variation of the water content with heating period of paraformadehyde in various solvents.

TABLE V. WATER CONTENT IN VARIOUS CONCENTRATIONS OF THE SAMPLE IN PROPYLENE GLYCOL

Weight of sample %	Propylene glycol ml.	Water content %
2.0056	25	0.42
3.1643	25	0.45
4.5315	25	0.41
1.9881	50	0.44
3.0624	50	0.42
5.3211	50	0.40

TABLE VI. RESULTS OF THE DETERMINATION OF THE WATER CONTENTS BY THE PYROLYSIS METHOD FOR VARIOUS TYPES OF THE LOW POLYMERS OF FORMALDEHYDE

Sample	Temperature of dissolution °C	Water content %
Commercial grade paraformaldehyde	150	3.32
	150	3.28
Dried commercial grade paraformaldehyde	150	2.58
	150	2.56
α-Polyoxymethylene	170	1.65
	170	1.66
Dried α-polyoxymethylene	170	0.45
	170	0.45

5) J. Löbering and K. P. Jung, *Monatsh. Chem*, 70, 281 (1939).
6) J. F. Walker, "Formaldehyde", Reinhold Publishing Co., New York (1953), p. 121.

TABLE VII. RESULTS OF CALCULATIONS OF THE DEGREES OF POLYMERIZATION FROM THE CONTENT OF BOUND WATER

Sample	Water content %		Bound water %	Degree of polymerization
	By propylene glycol dissolution method	By methanol extraction method		
Commercial grade paraformaldehyde	3.30	0.60	2.70	22
Dried commercial grade paraformaldehyde	2.57	0.09	2.48	24
α-Polyoxymethylene	1.64	1.05	0.59	102
Dried α-polyoxymethylene A	0.44	0.02	0.42	143
Dried α-polyoxymethylene B	0.45	0.02	0.43	140

TABLE VIII. RESULTS OF THE TOTAL ANALYSIS

Sample	Formaldehyde %	Methanol %	Water %	Total %
85% Paraformaldehyde	87.2	0.70	11.9	99.8
95% Paraformaldehyde	95.8	0.50	3.4	99.7
Paraformaldehyde special-class reagent	96.6	0.30	2.7	99.6
α-Polyoxymethylene	99.2	—	0.6	99.8
Dried α-polyoxymethylene	99.5	—	0.4	99.9

the determination of the degree of polymerization was not very high. The method reported in the present work can be used for the determination of the degree of polymerization of formaldehyde with a high degree of accuracy. To verify the accuracy of the determination of bound water, formaldehyde and methanol in polymer were determined independently. The former was determined by the sodium sulfite method, and the latter, by gas chromatography. Table VIII lists the percentage of formaldehyde and methanol thus determined, together with that of bound water. The sum of these three components is almost 100%, thus establishing the accuracy of this method.

Summary

The adsorbed water of the low polymer of formaldehyde was determined by extraction with dry methanol and Karl Fischer titration. The sum of the adsorbed water and the water formed by the pyrolysis of the sample was determined by titration with the specially prepared Karl Fischer reagent SS, after the sample had been dissolved in propylene glycol by heating. The method of the separation and the determination of the two kinds of water was thus established. When the average numerical degree of polymerization of the polymers was calculated from the content of bound water determined by this method, satisfactory results were obtained. To verify the accuracy of the determination of water content, formaldehyde and methanol were determined independently; their sum was found to be almost 100%.

The authors wish to thank Mr. Daikichiro Nishikawa of the High Polymer Research Department, for the samples used in this study and Mr. Hisakazu Araki, Manager of the Analytical Research Department, for his kind advice.

Central Research Laboratory
Mitsubishi Chemical Industries Ltd.
Kawasaki-shi, Kanagawa

Studies of Acenaphthene Derivatives. IX[1]. *The Reaction of Acenaphthenequinone with Ammonia*

By Otohiko Tsuge and Masashi Tashiro

(Received April 22, 1963)

In the course of the investigation of the reaction of acenaphthenequinone (I) with various amines, the reaction of I with ammonia was studied.

Many years ago, Graebe and Gfeller[2] found that the treatment of I with aqueous ammonia at 100°C in a sealed tube afforded red crystals (II) (m. p. over 300°C) with the formula $C_{24}H_{12}ON_2$, for which acenaphthenequinoneimide anhydride (IIa) was assumed. Later, Schönberg and Nedzati[3] suggested that acenaphthazine (IIb) (m. p. 400°C (decomp.)), with the formula $C_{24}H_{12}N_2$ for II, would be more reasonable than IIa because of its formation by the reduction of acenaphthenequinone dioxime (III) with a very poor yield and its having properties similar to those of phenanthrazine as well as because of the elemental analyses. In a similar manner, Charrier and Ghigi[4] obtained naphthalimide in addition to II, whose structure was not reexamined.

Furthermore, Schiedt[5] reported that IIb (m. p. 438°C) was produced by the heating of I with formamide in the presence of glacial acetic acid at 170°C. However, its structure was not characterized.

Although the structure of acenaphthazine for II seemed to be reasonable, the authors were doubtful about the reduction procedure of III and the purification method of II carried out by Schönberg and Nedzati[3]. They recognized that IIb was formed by the condensation of 1,2-diaminoacenaphthene (IV) and I, which had been produced by the reduction, accompanied by the simultaneous hydrolysis of III, as is depicted in Chart 1. However, it can also be considered that this product was formed by the reaction of I produced by hydrolysis with ammonia, since they treated the reaction mixture with aqueous ammonia for a long time. Further, even if I reacted with IV, IIb was not the only possible product. Furthermore, the purification of II was carried out by sublimation with iron powder.

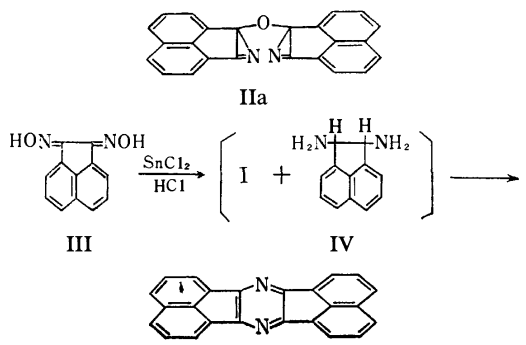

Chart 1

This paper deals with the results of a reexamination of the structure of II and of the reaction of I with ammonia under various conditions.

Results and Discussion

Reaction by Graebe's Procedure.—The reaction of I with 21% aqueous ammonia at 100°C in a sealed tube according to Graebe's procedure afforded red crystals (II) (m. p. 382°C), naphthalimide (V), and a new colorless compound (VI) (m. p. 286~287°C).

The elemental analytical data of II was in agreement with the formula $C_{24}H_{12}ON_2$ given by Graebe and Gfeller[2] but not with Schönberg's formula, $C_{24}H_{12}N_2$[3]. Its infrared spectrum exhibited the sharp bands at 1704 and 1616 cm^{-1} ascribed to the carbonyl group[6] and the C=N bond respectively, but it did not reveal any bands for the amino group (Fig. 1.). Also, the infrared spectrum of the compound purified by sublimation was exactly the same as that of the original substance. As no suitable solvent of II could be found, its molecular weight was not determined.

In order to elucidate the structure of II more clearly, the following experiments were carried out. It is obvious that II contains two acenaphthene rings in the molecule, because the oxidation of II (1 mol. as $C_{24}H_{12}ON_2$) with sodium dichromate in glacial acetic acid

1) Part VIII: H. Saikachi, O. Tsuge and M. Tashiro, *J. Pharm. Soc. Japan* (*Yakugaku Zasshi*), **80**, 584 (1960).
2) C. Graebe and E. Gfeller, *Ann.*, **276**, 1 (1893).
3) A. Schönberg and F. Nedzati, *Ber.*, **54**, 238 (1921).
4) G. Charrier and E. Ghigi, *Atti accad. Lincei*, **16**, 262 (1932).
5) B. Schiedt, *J. prakt. Chem.*, **157**, 203 (1941).
6) The infrared spectra of one acenaphthene or acenaphthenequinone exhibited sharp bands at 1724 or at 1727, 1742 and 1776 cm^{-1} respectively for the carbonyl group.

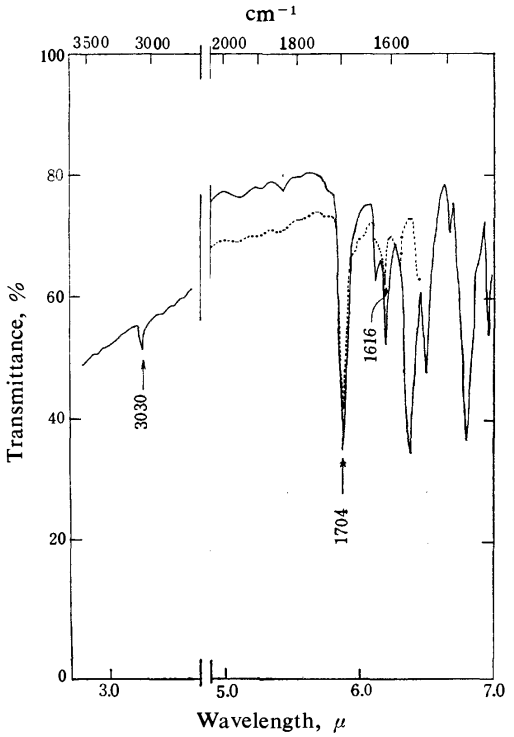

Fig. 1. Infrared spectra of II.
—— In hexachlorobutadiene mull
------ In Nujol mull

afforded naphthalimide (V) (ca. 1.5 mol.) and naphthalic anhydride (VII) (ca. 0.5 mol.) (Chart 2). The reduction of II with zinc dust in acetic acid gave a labile orange substance which was purified as the picrate. In the infrared spectrum of the orange product just after the reduction, there was no band due to the carbonyl group, but there were two bands, at 3120 and 1618 cm^{-1}, which may be ascribed to the hydroxyl group and the C=N bond respectively. However, this compound could not be identified.

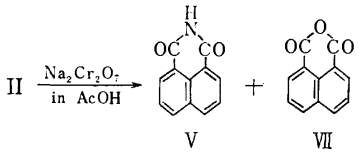

Chart 2

In addition, II was obtained quantitatively by the heating of the acenaphthenequinone monoimine (VIII) which had been obtained by the reaction of I with ammonia in ethanol, as will be described below.

Weiss[7] discovered that the reaction of benzil with ammonium acetate in the presence of acetic acid resulted in isoimidazole derivatives.

7) M. Weiss, *J. Am. Chem. Soc.*, 74, 5193 (1952).

Accordingly, these observations are accommodated much better by the structure of acenaphtho[1,2-b]isoimidazole-2-spiro-2'-acenaphthenone (IIc) than by IIa or IIb. IIc is assumed to be formed by the self-condensation of the VIII which was produced by the dehydration of the ammonia-adduct (IX) of I as depicted in Chart 3.

On the other hand, VI accorded with the formula $C_{24}H_{13}O_3N$, which is the result of the

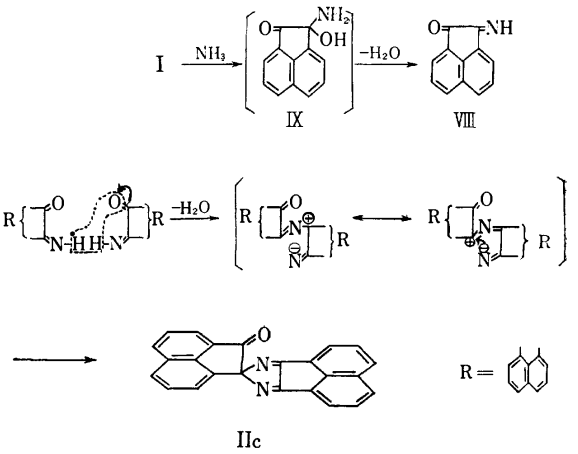

IIc

Chart 3

elemental analysis and the molecular weight measurement. The infrared spectrum of VI showed the absorption bands at 1721 or 1698 and 1658 cm^{-1} assigned to the carbonyl group or the amide I band respectively. The bands at 3077 cm^{-1} for the aromatic C-H bond and at 2933 cm^{-1} ascribed to the aliphatic C-H bond were also observed[8] (Fig. 2.). Its ultraviolet spectrum is very similar to that of *N*-phenylnaphthalimide, as is shown in Fig. 3.

These observations indicate that this compound is *N*-(2-oxo-acenaphthenyl)naphthalimide (VI).

It has previously been well-known that the treatment of I with alkali gives naphthaldehyde and naphthalic acid[9]. Consequently, VI is assumed to be formed by the condensation of the ammonia-adduct (IX) and naphthaldehyde, as is depicted in Chart 4.

Furthermore, the formation of V and VII can be illustrated naturally, as Chart 4 shows. The effect of the reaction time on the yields of these compounds was examined. The results are listed in Table I.

As is shown in Table I, IIc was formed as

8) The infrared spectrum of IIc did not show any absorption due to the aliphatic bonds, but it did show a band at 3030 cm^{-1} for the aromatic C-H bond. Also, *N*-phenylnaphthalimide exhibited the bands at 1701 and 1664 cm^{-1} assigned as the amide I bands in its infrared spectrum.

9) J. Cason and J. D. Wordie, *J. Org. Chem.*, 15, 608 (1950).

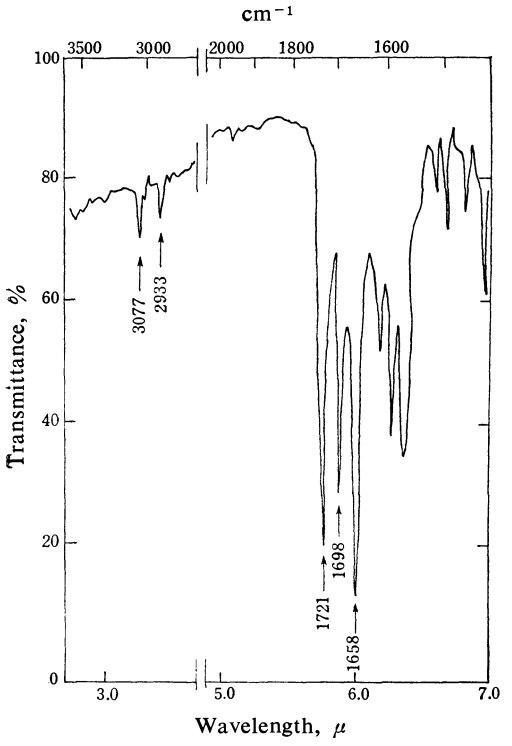

Fig. 2. Infrared spectrum of VI in hexachlorobutadiene mull.

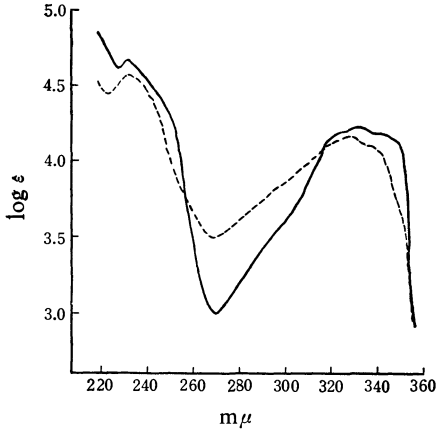

Fig. 3. UV spectra of VI and *N*-phenylnaphthalimide in dioxane.
—— VI
------ *N*-Phenylnaphthalimide

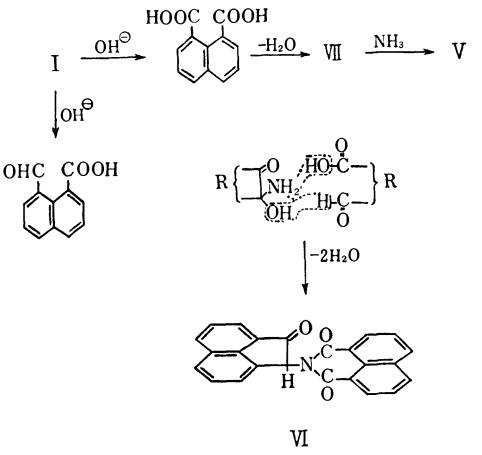

Chart 4

Table I. Reaction of I with aqueous ammonia*

Time	Product IIc	Product V	Product VI	Recovered I
hr.	%		%	%
1.0	37.7	+**	19.0	40.0
2.0	57.2	+	21.0	21.3
3.0	64.6	+	22.2	—
4.0	65.6	+	21.5	—
6.0	65.2	+	21.7	—

* Mixtures of I (5.0 g.) and 21% aqueous ammonia (50 ml.) were heated at 100°C in a sealed tube for the specified periods
**+ : Trace amount

Table II. Reaction of I with ammonia gas in water*

Time	Product IIc	Product V	Product VI	Recovered I
hr.	%	%		%
2.0	11.4	5.0	+	72.0
3.0	11.4	5.9	+	60.4
6.0	37.9	11.8	+	30.0
7.0	51.7	22.1	+	—
10.0	65.2	22.3	+	—

* Ammonia gas was violently passed through the suspension of I (5.0 g.) in water (50 ml.) at 70~80°C for the specified periods.

the main product, accompanied by a considerably large amount of VI. The yields of these compounds were nearly constant, even if the reaction time was longer than 3 hr.

The Reaction with Ammonia in Water or Ethanol.—Ammonia gas was violently passed through the suspension of I in either water or ethanol. The results are shown in Tables II and III.

In the case of the reaction of I with ammonia gas in water, also, IIc, V and VI were obtained, as is shown in Table II. However, more V was formed than VI, and the rate of the formation of IIc was slower than in Graebe's procedure mentioned above.

The reaction of I with ammonia gas in ethanol gave V as the main product, accompanied by IIc and an unknown compound

TABLE III. REACTION OF I WITH AMMONIA GAS IN ETHANOL*

Time	Product			Recovered
	IIc	V	VIII	I
hr.	%	%	%	%
0.5	1.9	22.3	1.6	46.0
1.0	7.0	46.2	5.0	25.0
2.0	14.4	51.7	12.6	20.5
4.0	13.9	49.7	13.4	16.0

* Ammonia gas was violently passed through the suspension of I (5.0 g.) in ethanol (50 ml.) under reflux for the specified periods.

(VIII) (m. p. 343°C (decomp.)) in almost identical yields. As the heating of VIII gave IIc in a quantitative yield, it seems reasonable to assume that VIII is the intermediate of IIc.

Zincke[10] reported long ago that the reaction of phenanthrenequinone with ammonia afforded phenanthrenequinone monoimine, which in turn yields a red substance upon being heated. In addition, the infrared spectrum of VIII, which corresponds to the formula $C_{12}H_7ON$, revealed absorption bands at 3128 and 1605 or 1681 cm^{-1} for the -C=NH or the carbonyl group respectively[11].

On the basis of these facts, this compound is considered to be acenaphthenequinone monoimine (VIII) formed as shown in Chart 3. The observed shifts of these bands to a longer wavelength region seem to be due to the intermolecular chelation of VIII.

TABLE IV. REACTION OF I WITH AMMONIUM CARBONATE IN GLACIAL ACETIC ACID*

Time min.	$(NH_4)_2CO_3$/I**	Product	
		IIc %	V %
30	10	—	—***
30	20	19.0	37.0
30	30	25.4	45.3
30	40	33.8	48.1
30	100	44.4	47.9
15	50	33.8	50.0
30	50	39.1	50.0
45	50	38.6	49.4
60	50	39.1	49.2

* Mixtures of I (1.0 g.) and $(NH_4)_2CO_3$ of the indicated amounts in glacial acetic acid (30 ml.) were heated under reflux for the specified periods.
** Molar ratio
*** Recovery of I was almost quantitative.

10) Th. Zincke, *Ber.*, 12, 1641 (1879).
11) Phenanthrenequinone monoimine prepared by the reaction of phenanthrenequinone with ammonia showed the infrared absorption bands at 3215 and 1605 or 1678 cm^{-1} due to the -C=NH or the carbonyl group respectively.

The reaction of I with ethanolic ammonia in a closed vessel at room temperature for ten days afforded IIc, VI and VIII in about 10, 35 and 45% yields respectively. Another reaction with liquid ammonia gave IIc, VI and naphthalic acid.

The Reaction of I with Ammonium Carbonate in Glacial Acetic Acid.—The treatment of I with ammonium carbonate in boiling glacial acetic acid gave IIc and V. The effect of reaction conditions on the yields of these compounds is summarized in Table IV. As is shown in Table IV, this simple procedure seems to be the most promising route to IIc.

Furthermore, the heating of I with formamide and glacial acetic acid at 170~180°C afforded a red substance which was confirmed to be identical with IIc by a comparison of their infrared spectra. Also, another reaction of 2, 2-dichloroacenaphthenone with ammonium carbonate in glacial acetic acid afforded IIc.

Experimental[12,13]

The infrared spectra of all compounds were measured in hexachlorobutadiene mull. Acenaphthenequinone (I) was prepared by the oxidation of acenaphthene[14] in the form of yellow needles (m. p. 244~245°C).

The Reaction of I with Aqueous Ammonia by Graebe's Procedure.—A mixture of I (5.0 g.) and 21% aqueous ammonia (50 ml.) was heated in a sealed tube at 100°C for 1 hr. After it had cooled, the reaction mixture was poured into water and the precipitate was extracted by boiling acetic acid (100 ml.), leaving red crystals. Those red crystals were washed with ethanol and dried to give 1.78 g. (m. p. 375~376°C). Recrystallization from pyridine or sublimation afforded acenaphtho[1, 2-b]-isoimidazole-2-spiro-2'-acenaphthenone (IIc) as red needles (m. p., 382°C).

Found: C, 83.61; H, 3.56; N, 8.42. Calcd. for $C_{24}H_{12}ON_2$: C, 83.71; H, 3.51; N, 8.13%.

The precipitate obtained by the pouring of the extract and washings into water was heated with 40% sodium bisulfite (200 ml.) for 10 min. The hot solution was then filtered by suction. The filtrate was treated with concentrated sulfuric acid as usual to recover I (2.0 g.). The sodium bisulfite solution-insoluble residue was washed with hot water and ethanol, and then dried to afford 0.95 g. of colorless crystals melting at 260~270°C. On the fractional recrystallization of the colorless crystals from acetic acid, two compounds were obtained: one with an m. p. of 300°C and the other with an m. p. of 286~287°C. The former was in a trace amount and was proved to be identical with naphthalimide (V) by the admixed melting point with an authentic sample. The latter was *N*-(2-oxo-acenaphthenyl)naphthalimide (VI) as colorless prisms in a large amount.

12) All melting points are uncorrected.
13) The microanalyses were carried ont by M. Shidō of Kyushu University, to whom the authors are indebted.
14) "Organic Syntheses", 24, 1 (1944).

Found: C, 79.43; H, 3.69; N, 3.82; mol. wt. (Rast), 362.5. Calcd. for $C_{24}H_{13}O_3N$: C, 79.32; H, 3.61; N, 3.85%; mol. wt., 363.35.

$\lambda_{max}^{Dioxane}$ mμ (log ε): 231 (4.69), 330 (4.23)[15].

The effect of reaction conditions on the yields of these products is shown in Table I.

The Oxidation of IIc.—Sodium dichromate (6.0 g.) was added slowly to a suspension of IIc (2.0 g., 5.8 mmol.) in glacial acetic acid (50 ml.) at 80°C.

After being refluxed for 1 hr., the reaction mixture was poured into water and allowed to stand overnight. The precipitate was then collected and extracted with a 10% aqueous sodium carbonate solution. The insoluble residue was washed with water and dried to afford 1.7 g. (8.6 mmol.) of colorless crystals (m. p. 287~279°C). On recrystallization of these crystals from acetic acid, colorless needles (m. p., 300°C) were obtained and proved to be identical with V. The sodium carbonate-extract was acidified with dilute hydrochloric acid, and the deposited precipitate was collected, washed with water, and dried to give 0.62 g. (3.1 mmol.) of a white solid (m. p. 267~269°C). Recrystallization of this from concentrated nitric acid gave colorless needles (m. p. 274°C) which were identical with naphthalic anhydride.

The Reduction of IIc.—A suspension of IIc (0.5 g.) and zinc dust (1.0 g.) in a mixture of acetic anhydride (20 ml.) and glacial acetic acid (6 ml.) was heated under reflux for 20 min.; additional zinc dust (1.0 g.) was then added to the reaction mixture and it was refluxed for another 30 min. The hot solution was filtered by suction, and the filtrate was poured into water to give a labile orange precipitate which tended to decompose on heating.

Purification of the orange substance was accomplished through its picrate. This picrate was obtained (0.45 g.) as a yellow solid (m. p. 270°C (decomp.)) which, on recrystallization from dioxane, gave a yellow crystalline powder (m. p. 275°C (decomp.)). (Found: C, 63.90; H, 3.73; N, 12.51%). This compound could not be identified.

The Reaction of I with Ammonia Gas in Water.—Ammonia gas was violently passed through a suspension of I (5.0 g.) in water (50 ml.) at 70~80°C for 6 hr. The reaction mixture was poured into water, and the precipitate was collected. The same treatment as in Graebe's procedure gave the starting material, I (1.5 g.), IIc (1.79 g.), V (0.64 g.) and VI in a small amount. The results of other experiments, along with various reaction conditions, are listed in Table II.

The Reaction of I with Ammonia Gas in Ethanol.—a) Ammonia gas was violently passed through a suspension of I (5.0 g.) in boiling ethanol (50 ml.) for 4 hr. The same treatment as in the above-mentioned procedure gave the starting material, I (0.8 g.). The sodium carbonate-insoluble residue was extracted with hot glacial acetic acid and then with hot chloroform[16], (40 ml.×2) remaining a white solid (0.67 g.; m. p. over 300°C). (Recrystallization from pyridine gave acenaphthene monoimine (VIII) as colorless prisms (m. p. 343°C (decomp.)).

Found: C, 79.69; H, 4.16; N, 7.75. Calcd. for $C_{12}H_7ON$: C, 79.54; H, 3.89; N, 7.73%. Hydrochloride of VIII, Found: N, 6.99. Calcd. for $C_{12}H_8ONCl$: N, 6.43%.

The acetic acid-extract was concentrated in vacuo to afford V (2.69 g.), and from the chloroform-extract IIc (0.66 g.) was obtained. The results of other reactions in ethanol are shown in Table III.

b) A mixture of I (2.0 g.) and ethanol (50 ml.) containing ammonia (ca. 0.4 g.) was stirred in a closed vessel at room temperature for ten days.

After the reaction mixture had been poured into water, the precipitate was collected, washed with water, dried, and extracted with hot chloroform (50 ml.×2). The recrystallization of the insoluble white solid (0.9 g.) (m. p. 343°C (decomp.)) whose infrared spectrum was superimposed on that of VIII obtained above was undertaken. The chloroform-extract was evaporated, and the residue was further extracted with hot glacial acetic acid to give insoluble red crystals IIc (0.17 g.) and soluble colorless prisms VI (0.8 g.). The structures of these compounds were confirmed to be as described above.

The Reaction of I with Ammonium Carbonate in Glacial Acetic Acid.—The refluxing of a mixture of (1.0 g.) and ammonium carbonate (13.0 g.) in glacial acetic acid (30 ml.) resulted in the precipitation of red crystals within a few minutes. After the mixture had been refluxed for 1 hr., filtration gave red crystals (0.37 g.) (m. p. 377~378°C), the infrared spectrum of which was exactly the same as that of IIc. The filtrate was poured into water, and the precipitate was treated, as usual, with a 40% sodium bisulfite solution (50 ml.) to give I in a small amount. The sodium bisulfite-insoluble residue was washed with hot water and dried to give colorless crystals (0.53 g.), which were found to be identical with V from the admixed m. p. and infrared spectrum. The findings on the effect of reaction conditions on the yields of these compounds are summarized in Table IV.

The Reaction of I with Liquid Ammonia.—A mixture of I (10.0 g.) and liquid ammonia (120 ml.) was shaken in a dry ice-methanol bath for 7 hr.

After the ammonia had been removed at room temperature, the residue was washed well with water. The washings were acidified with dilute hydrochloric acid and dried to afford white crystals (3.0 g.) (m. p. 268~272°C) which, on recrystallization from concentrated nitric acid, gave colorless needles (m. p., 274°C). This compound was identical with VII. The treatment of the insoluble residue with a 40% sodium bisulfite solution, and then with hot acetic acid, as mentioned above, gave I (3.2 g.), IIc (2.0 g.), and VI (1.0 g.).

The Reaction of I with Formamide in the Presence of Acetic Acid.—A mixture of I (2.5 g.), formamide (40 ml.) and glacial acetic acid (1 ml.) was heated at 170~180°C in an oil bath for 20 min.

After being cooled, the mixture separated out crystals. Filtration gave red crystals (1.5 g.) (m. p.

15) *N*-Phenylnaphthalimide: $\lambda_{max}^{Dioxane}$ mμ (log ε); 231 (4.59), 329 (4.17).

16) IIc was soluble in boiling chloroform.

over 300°C) which, on recrystallization from pyridine, showed an m. p. of 382°C. The infrared spectrum and elemental analytical values were in agreement with those of IIc. (Found: C, 83.83; H, 3.60; N, 8.48%.)

The Reaction of 2, 2-Dichloroacenaphthenone with Ammonium Carbonate in Glacial Acetic Acid. —A mixture of 2, 2-dichloroacenaphthenone[17] (1.0 g.) and ammonium carbonate (26.0 g.) in glacial acetic acid (30 ml.) was refluxed for 30 min. After the mixture had been cooled, filtration afforded red crystals (0.4 g.) (m. p. 360~363°C) which, on recrystallization from pyridine, gave red needles (m. p. 382°C), the infrared spectrum of which was superimposed on that of IIc. The filtrate was not examined.

17) 2, 2-Dichloroacenaphthenone was prepared by the reaction of I with PCl_5. (A. I. Tochilkin, *Zhur. Vsesoynz. Khim., Obshchestva im. D. I. Mendeleeva*, **6**, 591 (1961).)

The authors wish to express their deep gratitude to Dr. Takashi Yoshida of the Yawata Chem. Co. for contributing acenaphthene used in this study.

The Research Institute of Science and Industry
Kyushu University
Hakozaki, Fukuoka

*Ionic Hydration in an Aqueous Electrolyte Solution and Its Parameter**

By Kiyoshi TAMURA** and Tsunetaka SASAKI

(Received April 8, 1963)

It is well-known that ion-solvent interaction in aqueous solutions plays an important rôle in various properties and phenomena[1-4], such as the adsorption, surface tension, mobility, viscosity, diffusion, compressibility and activity coefficient, as well as the swelling, salting-out and other lyotropic phenomena. A concept of ionic hydration has been introduced as an important factor in attempting to explain these phenomena, and the amount or the intensity of hydration has been determined by various methods, such as measurements of the compressibility[5-8], the activity[9-11], the diffusion[12] and the dielectric constant[13,14]. All these quantities measure in some way the ion-solvent interaction or the hydration properties, but each of these different methods measures a different extent of ionic hydration. It is desirable, therefore, to establish a common and basic parameter concerning ionic hydration.

The dissolution of an electrolyte in water causes a volume contraction and a decrease in compressibility due to the interaction between the ions and water molecules. The magnitude of these changes can, therefore, be used as a measure of the hydration. We have already noticed[8,15,16] that the volume contraction is proportional to the amount of hydration water calculated from the compressibility data and that the proportionality constant is independent of the temperature and the nature of the electrolyte. For the explanation of this fact, we can refer to the studies of Webb[17] and Bernal and Fowler[18], who have calculated the mutual interaction between water molecules and ions. However, the lack of data necessary for calculation, especially the lack of knowledge about the hydrostatic pressure in the immediate vicinity of an ion in an aqueous solution, made a similar calculation impossible in the present case. Therefore, we adopted another method of calculation, one similar to

* Presented at the 12th Anual Meeting on Colloid Chemistry, Hiroshima, October, 1959.

** Present address: Department of Chemistry, Defense Academy, Yokosuka.

1) N. Dhar, *Z. Elektrochem.*, **20**, 57 (1914).
2) R. Fricke, ibid., **28**, 161 (1922).
3) M. Rubner, *Abh. preuss. Akad. Wiss Phys. math. Klasse* (1922), p. 3.
4) R. A. Gortner, "Selected Topics in Colloid Chemistry with Especial Reference to Biochemical Problems", Cornell University Press, Ithaca (1937), p. 128.
5) A. Passynski, *Acta Physicochimica USSR*, **8**, 385 (1938).
6) Y. Wada, S. Shimbo, M. Oda and J. Nagumo. *Applied Phys.* (*Oyo Buturi*), **17**, 257 (1948).
7) T. Yasunaga, *J. Chem. Soc. Japan, Pure Chem. Sec.* (*Nippon Kagaku Zassi*), **72**, 87 (1951).
8) T. Sasaki and T. Yasunaga, This Bulletin, **28**. 269 (1955).
9) R. H. Stokes and R. A. Robinson, *J. Am. Chem. Soc.*, 70, 1870 (1948).
10) E. Glueckauf, *Trans. Faraday Soc.*, **51**, 1235 (1955).
11) D. G. Miller, *J. Phys. Chem.*, 60. 1296 (1956).
12) R. A. Robinson and R. H. Stokes, "Electrolyte Solutions", 2nd Ed.. Butteworths Scientific Publications, London (1959). p. 325.
13) R. M. Noyes, *J. Am. Chem. Soc.*, **84**, 513 (1962).
14) G. H. Haggis, J. B. Hasted and T. J. Buchanan, *J. Chem. Phys.*, **20**, 1452 (1952).
15) T. Yasunaga and T. Sasaki, *J. Chem. Soc. Japan, Pure Chem. Sec.* (*Nippon Kagaku Zassi*), **72**, 89 (1951).
16) T. Sasaki, T. Yasunaga and H. Fujihara, ibid., **73**, 181 (1952).
17) T. J. Webb, *J. Am. Chem. Soc.*, **48**, 2589 (1926).
18) J. D. Bernal and R. H. Fowler, *J. Chem. Phys.*, **1**, 515 (1933).

Harned and Owen's[19] and based upon the empirical equation of Tait, which gives the compressibility of water under pressure. Thus we obtained the quantity which may be proposed as a common parameter of hydration.

Tait's Equation and its Applicability to Water. —Tait's equation is applicable to many pure liquids in either of the form:

$$\beta_1^{(p)}V_1^{(p)} \equiv -(\partial V_1^{(p)}/\partial P)_T = 0.4343C/(B+P) \quad (1)$$

or in its integrated form:

$$V_1^{(p_0)} - V_1^{(p)} = C\log\{(B+P)/(B+P_0)\} \quad (2)$$

where β_1 is the isothermal compressibility; V_1, the molar volume of water (solvent); P, the pressure; T, the absolute temperature, and B and C, constants dependent only upon the temperature and the nature of the liquid. The superscript (p) indicates the properties under the external pressure, P, and P_0 is the standard pressure, which may be taken as one bar.

According to Carl[20] and Gibson[21], Eq. 1 is applicable to water up to about $P=10000$ bar; the former author has also shown that the value of $0.4343C/V_1^{(p_0)}$ is independent of the temperature. The values of B, C and $0.4343C/V_1^{(p_0)}$ for water at temperatures ranging from 20 to 50°C, calculated from Bridgman's data[22] by the present authors, are shown in Table I. The average value of $0.4343C/V_1^{(p_0)}$ is somewhat different from the value obtained by Carl (0.1243)[20] and that obtained by Gibson (0.1368)[23].

TABLE I. CONSTANTS OF TAIT'S EQUATION FOR WATER

Temp., °C	B, bar	C, ml./mol.	$0.4343C/V_1^{(p_0)}$
20	2897	2.394	0.1327
25	2978	2.430	0.1345
30	3039	2.459	0.1359
40	2998	2.405	0.1325
50	3019	2.430	0.1333
		Average	0.1338

The Molar Volume of the Solute in a Solution.—The molar volume of the solute was calculated by a method similar to that of Harned and Owen[19]. According to Tammann[24], water in an electrolyte solution behaves like a substance under a constant effective pressure which is higher than the atmospheric one by P_e. This state is called electrostriction by Nernst[25]. The volume contraction and the decrease in the compressibility of a solution produced by the addition of an electrolyte to it are ascribed exclusively to the changes in the respective properties of the solvent water. The volume, $\varphi_1^{(p)}$, occupied by one mole of water in an electrolyte solution under an external pressure, P, is, therefore, the molar volume of pure water under the pressure $(P+P_e)$. Thus, from Eq. 2 we obtain:

$$V_1^{(p)} - \varphi_1^{(p)} = C\log\{(B+P+P_e)/(B+P)\} \quad (3)$$

A solution containing n_1 mol. of water and one mole of solute has the volume

$$V^{(p)} = n_1\varphi_1^{(p)} + \varphi_2^{(p)} \quad (4)$$

where $\varphi_2^{(p)}$ is the contribution to the volume of the solution made by one mole of solute in the state of solution.

From Eqs. 2, 3 and 4, we obtain

$$V^{(p)} = n_1V_1^{(p_0)} - n_1C \times\log\{(B+P+P_e)/(B+P_0)\} + \varphi_2^{(p)} \quad (5)$$

Putting $P=P_0$, we get

$$V^{(p_0)} = n_1V_1^{(p_0)} - n_1C \times\log\{(B+P_0+P_e)/(B+P_0)\} + \varphi_2^{(p_0)} \quad (6)$$

By the differentiation of Eq. 5 with respect to pressure at a constant temperature and composition, we obtain:

$$\beta^{(p)}V^{(p)} \equiv -(\partial V^{(p)}/\partial P)_T = 0.4343Cn_1/(B+P+P_e) - (\partial\varphi_2^{(p)}/\partial P)_T \quad (7)$$

where β is the isothermal compressibility of the solution.

As the last term of Eq. 7 is negligible at moderate pressures and concentrations for an electrolyte solution[21], we obtain from Eqs. 1 and 7:

$$(B+P_0+P_e)/(B+P_0) = n_1\beta_1^{(p_0)}V_1^{(p_0)}/\beta^{(p_0)}V^{(p_0)} \quad (8)$$

and from Eqs. 6 and 8:

$$\varphi_2^{(p_0)} = V^{(p_0)} - n_1V_1^{(p_0)} + n_1C\log(n_1\beta_1^{(p_0)}V_1^{(p_0)}/\beta^{(p_0)}V^{(p_0)}) \quad (9)$$

By Eq. 9 we can calculate $\varphi_2^{(p_0)}$ from the isothermal compressibilities and the densities of both solution and solvent water. The isothermal compressibility can be determined by the sound velocity measurement[7].

19) H. S. Harned and B. B. Owen, "The Physical Chemistry of Electrolytic Solutions", 2nd Ed., Reinhold Publ. Corp., New York (1950), p. 267.
20) H. Carl, *Z. physik. Chem.*, **101**, 238 (1922).
21) R. E. Gibson, *J. Am. Chem. Soc.*, **56**, 4 (1934).
22) P. W. Bridgman, *Proc. Am. Acad. Arts Sci.*, **48**, 309 (1912).
23) H. S. Harned and B. B. Owen, loc. cit., p. 272.
24) G. Tammann, "Über die Beziehungen zwischen den inneren Kräften und Eigenschaften der Lösungen", Voss, Leipzig (1907), p. 36.
25) W. Nernst and P. Drude, *Z. physik. Chem.*, **15**, 79 (1894).

TABLE II. THE MOLAR VOLUME OF ELECTROLYTES IN THE STATE OF SOLUTION AND IN SUPER-COOLED LIQUID STATE

Electrolyte	$[\varphi_2^{(p_0)}]$ ml./mol.	V_2 ml./mol.	Temp. °C	Reference for sound velocity*
LiCl	27.7	24.21	25	C
$LiNO_3$	36.3	36.08	25	C
NaCl	31.2	29.99	20	F
	29.5	30.04	25	C
NaBr	34.9	35.35	20	F
NaI	42.7	43.83	20	F
NaOH	15.7	19.2	25	C
KCl	39.3	38.06	20	F
	38.0	38.12	25	C
KBr	43.3	44.21	20	F
KI	52.3	52.90	20	F
NH_4Cl	40.5	—	25	C
$MgCl_2$	44.9	50.57	20	T-S
	42.9	50.62	25	C
$CaCl_2$	46.2	47.0	20	T-S
$Ca(NO_3)_2$	61.4	—	25	C
$BaCl_2$	56.6	56.2	20	T-S
	55.6	56.2	30	T-S
	56.2	56.2	40	T-S
Na_2CO_3	41.2	46.15	20	T-S
	35.8	46.18	25	C
Na_2SO_4	56.8	57.16	20	T-S
K_2SO_4	70.1	70.89	25	C
$(NH_4)_2SO_4$	76.6	—	25	C
$CuSO_4$	29.5	—	25	C
$MgSO_4$	35.2	—	25	C

* C: Corey[26] F: Freyer[27]
T-S: Present authors

The values of $\varphi_2^{(p)}$ obtained were nearly independent of the concentration. The values at an infinite dilution are shown in Table II as $[\varphi_2^{(p)}]$. According to the view that the solute merely melts on going into a solution and occupies the same volume as that of the super-cooled liquid[21], the molar volume of a molten electrolyte at a high temperature was calculated and was extrapolated to the temperatures corresponding to those at which $[\varphi_2^{(p)}]$ was calculated. The values obtained are listed in the third column of Table II as V_2. The two values, obtained from independent methods, exhibit a satisfactory agreement except for a few cases which require further study. This result strongly supports the view that the solute in a solution behaves as a super-cooled liquid so far as its contribution to the volume of the solution is concerned. This means that the aqueous electolyte solution behaves ideally when we use as the molar volume of water the value under the pressure (P_0+P_e) instead of that under P_0.

26) V. B. Corey, *Phys. Rev.*, **64**, 350 (1943).
27) E. B. Freyer, *J. Am. Chem. Soc.*, **53**, 1313 (1931).

Rosen[28] also calculated the molar volume of alkali halides in the solution state from the density of the solution on a principle similar to, but by using an equation of state different from ours. Thus he obtained the same result as did Scott[29], who actually calculated the value by the extrapolation of the apparent molar volume. Both of these authors have given values slightly smaller than ours.

The Parameter of Hydration

Before we discuss the common parameter of hydration, it is pertinent to list some useful quantities relating to the amount of hydration, which will itself be discussed in a later section.

Effective Pressure. — Following Tammann's principle[24] mentioned above, Eucken[30] has calculated the "Hydratationsdruck" the measure of the intensity of solute-solvent interaction for some electrolytes and non-electrolytes such as alcohol and sugar, by comparing the effects of pressure and solute on the specific volume of the solvent water. However, the effective pressure, P_e, or electrostriction, which can be calculated by Eq. 8, expresses more clearly the intensity of the ionic hydration. P_e is further correlated with the molar concentration of water (C_1) and solute (C_2) in a solution in a manner similar to van der Waals' cohesive pressure in gases as follows[31]:

$$P_e = LC_1C_2 \qquad (10)$$

where L is a constant representing the electrostriction or electrostatic attraction under unit concentration.

Volume Contraction. — A number of investigators have examined the volume change which takes place when a solute dissolves into a solvent[1,2,15,17]. This is also one of the simplest quantities representing the intensity of hydration and is directly related to the effective pressure mentioned above. The present authors define the volume contraction of the system, ΔV, due to the dissolution of one mole of solute by

$$\Delta V \equiv n_1 V_1^{(p_0)} + \varphi_2^{(p_0)} - V^{(p)} \qquad (11)$$

From Eqs. 6 and 11, we obtain

$$\Delta V = n_1 C \log \{(B+P_0+P_e)/(B+P_0)\} \qquad (12)$$

Eq. 12 enables the calculation of ΔV from the value of P_e. Here the volume contraction is ascribed exclusively to the change in the volume of the solvent water.

28) J. S. Rosen, *J. Phys. Chem.*, **60**, 7 (1956).
29) A. F. Scott, ibid., 35, 3379 (1931).
30) A. Eucken, "Lehrbuch der chemischen Physik", Akademische Verlagsgesellschaft M. B. H., Leipzig (1932), p. 459.
31) R. E. Gibson, *J. Am. Chem. Soc.*, **57**, 284 (1935).

The Amount of Hydration Water.—An entirely different method has been adopted to give a parameter of hydration based on the incompressible hydration shell model[5-8].

If we assume, as is usual with inorganic ions, that the hydration shells, together with the central solute ions, are incompressible, the volume of water, V_h, bound to one mole of solute in solution, reduced to the atmosphere pressure of P_0, is given by

$$V_h = (n_1\beta_1^{(p_0)}V_1^{(p)} - \beta^{(p_0)}V^{(p_0)})/\beta_1^{(p_0)} = -K_2/\beta_1^{(p_0)} \quad (13)$$

where K_2 is the apparent molal compressibility of the solute. The value of V_h may be calculated from the compressibility and density data. We can also give the average hydration number of water molecules for a pair of solute ions by

$$h = V_h/V_1^{(p_0)} \quad (14)$$

The evaluation of V_h and h has been attempted by several authors[5-8,15,16].

The Correlation between L, ΔV and V_h, and the Parameter of Hydration

In order to discuss the correlation between the above three quantities, L, ΔV and V_h, the

TABLE III. VARIOUS PARAMETERS FOR HYDRATION OF ELECTROLYTE

Electrolyte	$[\Delta V]$ ml./mol.	$[V_h]$ ml./mol.	$[h]$	$[h^*]$	Temp. °C	Reference for sound velocity*
LiCl	10.3	77	4.24	4.38	25	C
$LiNO_3$	7.25	54	2.98	3.40	25	C
NaCl	14.3	107	5.96	6.41	20	F
	12.1	90	4.98	5.45	25	C
NaBr	11.5	87	4.82	5.46	20	F
NaI	8.06	61	3.37	4.03	20	F
NaOH	20.4	152	8.40	8.90	25	C
KCl	12.4	93	5.17	5.50	20	F
	10.8	80	4.44	4.80	25	C
KBr	9.51	72	3.97	4.39	20	F
KI	6.99	53	2.92	3.40	20	F
KCN	—	—	—	4.23	25	C
$KClO_3$	—	—	—	3.82	25	C
NH_4Cl	3.64	27	1.50	1.83	25	C
$NH_4(CH_3CO_2)$	—	—	—	2.20	25	C
$MgCl_2$	27.6	208	11.5	11.8	20	T-S
	25.2	187	10.4	10.8	25	C
$Mg(NO_3)_2$	20.4	151	8.38	9.32	25	C
$CaCl_2$	27.0	203	11.3	11.8	20	T-S
$Ca(NO_3)_2$	18.5	137	7.60	8.43	25	C
$NiCl_2$	—	—	—	11.5	25	C
$CoCl_2$	—	—	—	11.6	25	C
$Co(NO_3)_2$	—	—	—	9.91	25	C
$Co(CH_3CO_2)_2$	—	—	—	14.7	25	C
$BaCl_2$	30.2	227	12.6	13.3	20	T-S
	28.1	207	11.4	12.4	30	T-S
	26.7	201	11.1	11.7	40	T-S
$Ba(OH)_2$	—	—	—	18.4	25	C
$AlCl_3$	—	—	—	13.6	25	C
$Al(NO_3)_3$	—	—	—	14.4	25	C
Na_2CO_3	45.7	345	19.1	20.3	20	T-S
	38.2	284	15.7	16.9	25	C
Na_2SO_4	43.6	329	18.2	18.8	20	T-S
K_2CO_3	—	—	—	16.7	25	C
K_2SO_4	34.9	259	14.4	15.3	25	C
$K_2Cr_2O_7$	—	—	—	10.8	25	C
$(NH_4)_2SO_4$	22.7	169	9.34	9.90	25	C
$MgSO_4$	35.8	266	14.7	15.4	25	C
$CoSO_4$	—	—	—	15.5	25	C
$CuSO_4$	32.1	239	13.2	14.0	25	C

* Same as in the footnote of Table II.

density, $d^{(p)}$ and the isothermal compressibility, $\beta^{(p)}$, of a dilute solution at atmospheric pressure are expressed as follows:

$$d^{(p_0)}=d_1^{(p_0)}+aC_2 \quad \text{and} \quad \beta^{(p_0)}=\beta_1^{(p_0)}+bC_2$$

where a and b are constants characteristic of the electrolyte and where the higher terms of concentration are disregarded. Putting these relations into Eqs. 10, 12 and 13, and extrapolating C_2 to zero, we get the following relations:

$$[L]=(B+P_0)(V_1^{(p_0)}/1000)^2[h] \quad (15)$$

$$[\Delta V]=0.4343C[h] \quad (16)$$

$$[V_h]=-[K_2]/\beta_1^{(p_0)}=V_1^{(p_0)}[h] \quad (17)$$

where $[L]$, $[\Delta V]$, $[V_h]$, $[K_2]$ and $[h]$ denote L, ΔV, V_h, K_2 and h at an infinite dilution respectively, and

$$[h]=(1000d_1^{(p_0)}/M_1)(a/d_1^{(p_0)}-b/\beta_1^{(p_0)})-M_2/M_1 \quad (18)$$

where M_1 and M_2 are the molecular weights of the solvent and of the solute respectively. It is noticeable that each of the three quantities contains a common factor $[h]$ multiplied by a different coefficient which depends only upon the nature of water. Therefore, they vary proportionally to each other and to $[h]$; namely, they change proportionally with the change in the nature of the solute provided that the solvent and temperature are kept unchanged. It is quite legitimate, therefore, to take the quantity $[h]$ as a common parameter of hydration. The quantities of $[\Delta V]$, $[V_h]$ and $[h]$ for several electrolytes are listed in Table III.

An important conclusion evidently follows from Eqs. 16 and 17; that is,

$$[\Delta V]/[V_h]=0.4343C/V_1^{(p_0)} \quad (19)$$

As is seen in Table I, the values of $0.4343C/V_1^{(p_0)}$ for water are independent of the temperature, their average being 0.1338. This, together with Eq. 19, explains the previously-mentioned facts[8,15,16] that the volume contraction due to the dissolution of the electrolyte is about 10% of the volume of hydration water for the same electrolyte and that this value does not change with the temperature or the nature of the solute. There, the volume of hydration water (called V_h^*) was calculated from the data of adiabatic compressibility instead of from those of isothermal compressibility in Eq. 13, and the volume contraction (called ΔV^*) was calculated by using V_2 instead of $\varphi_2^{(p_0)}$ in Eq. 11. Figure 1 shows the plots of $[\Delta V^*]$ against $[V_h]$, together with the theoretical straight line of Eq. 19. Agreement is satisfactory.

It is further noticed in Table III that the value of $[h]$ decreases with the increase in

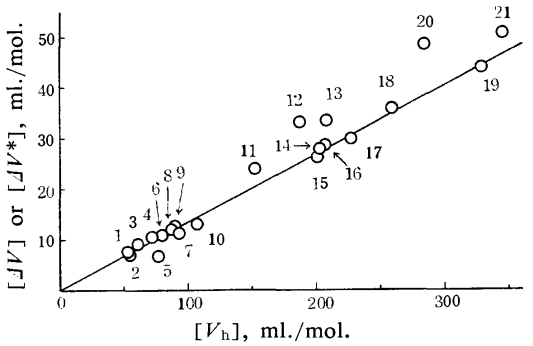

Fig. 1. Correlation between $[\Delta V^*]$ and $[V_h]$.

1	KI (20)	2	$LiNO_3$(25)
3	NaI (20)	4	KBr(20)
5	LiCl (25)	6	KCl(25)
7	KCl (20)	8	NaBr(20)
9	NaCl (25)	10	NaCl(20)
11	NaOH (25)	12	$MgCl_2$(25)
13	$MgCl_2$(20)	14	$CaCl_2$(20)
15	$BaCl_2$(40)	16	$BaCl_2$(30)
17	$BaCl_2$(20)	18	K_2SO_4(25)
19	Na_2SO_4(20)	20	Na_2CO_3(25)
21	Na_2CO_3(20)		

The numbers in bracket indicate temperature (°C) and solid line expresses Eq. 19.

temperature, as can be seen in the case of barium chloride. A similar temperature change was found for sodium chloride in the temperature range from 0 to 60°C[8]. The hydration reaction proves, therefore, to be exothermic in nature.

Stokes and Robinson[9] and Miller[11] modified the Debye-Hückel equation for the activity in a solution of strong electrolytes and expressed the effect of ion-solvent interaction by the term "hydration number". Though their numerical values agree as a whole with ours, their results are not staisfactory in that the hydration numbers increase with the increasing size of the anion and in that the law of the additive contribution of individual ions to the total hydration number does not hold.

Glueckauf[10] calculated hydration numbers with a model similar to that of Stokes and Robinson by means of volume fraction instead of mole fraction statistics; he found values about half as large as those of Stokes and Robinson. In his results, the anomalies of anions are less remarkable, and the additivity law holds fairly well. However, since his hydration numbers for anions are relatively small and since the variation among anions is not so distinct, it does not fully explain the difference in the contribution of each anion to the various phenomena involved in hydration. The superiority of the $[h]$ parameter in comparison with the hydration

numbers cited above is shown by the fact that it varies significantly among ions and is directly proportional to such quantities as $[L]$, $[\Delta V]$ and $[V_h]$.

The values of $[V_h^*]$ are somewhat greater than those of $[V_h]$, and the ratio $[V_h^*]/[V_h]$ is roughly constant, being 1.08 ± 0.14 for the electrolytes listed in Table III. The former can, therefore, be used in place of the latter after due precautions. This is rather fortunate, since the accurate data necessary for the calculation of isothermal from adiabatic compressibility are often lacking. Conventional hydration numbers, $[h^*]$, calculated from the value of $[V_h^*]$ are also listed in the fifth column of Table III.

Summary

Tait's equation for water and Harned and Owen's treatment of an electrolyte solution, together with sound velocity data, enabled the calculation of the molar volume of electrolytes in the solution state. The results agreed fairly well with the molar volume of the super-cooled molten electrolyte extrapolated to room temperature.

The concentration coefficient of electrostrictive pressure, $L=P_e/C_1C_2$, the volume contraction due to the dissolution of one mole of solute, ΔV, and the volume of hydration water per mole of solute, V_h, as an incompressible part of water have been evaluated. We have found a common variable, $[h]$, for L, ΔV and V_h, and it has been proposed that this variable can be used as a parameter of hydration expressing the mole number of hydration water per mole of electrolyte. A conventional hydration number, $[h^*]$, was also proposed.

The authors wish to express their hearty thanks to the Ministry of Education for the Scientific Research Grant given to Tsunetaka Sasaki.

Department of Chemistry
Faculty of Science
Tokyo Metropolitan University
Setagaya-ku, Tokyo

Influence of Substituent Groups on Nuclear Reactivity in the Formation of Substituted Biphenyls by Reaction of Aromatic Diazo and Related Compounds with Aromatic Liquids. VI. p-Chlorophenylation

By Toshihiko MIGITA, Naotake MORIKAWA and Osamu SIMAMURA

(Received May 10, 1963)

In a previous paper[1] the determination has been reported of the partial rate factors of nitrobenzene in *p*-methoxyphenylation by the *p*-methoxyphenyl radical derived from *N*-nitroso-*p*-acetanisidide. In order further to examine the effect of the substituent in the attacking radical in the homolytic arylation, competitive *p*-chlorophenylations of nitrobenzene, chlorobenzene, anisole, and toluene using benzene as a reference substrate have been carried out, with *N*-nitroso-*p*-chloro(^{36}Cl)acetanilide as a source of the *p*-chlorophenyl radical, and the products have been analyzed by isotope dilution analysis. We now report the results of this study.

Table I lists the values for the partial rate factor and the relative rate calculated from the relative amounts in which 4-chlorobiphenyl and the three isomeric substituted 4-chlorobiphenyls were formed in the competitive *p*-chlorophenylation. Because of difficulty in isolating radiochemically pure 3,4′-dichlorobiphenyl from the reaction mixture with chlorobenzene, we could not determine the partial rate factor for the meta position of chlorobenzene by means of isotope dilution analysis. The value of 0.87 given in Table I for this partial rate factor was estimated from the value of the partial rate factor for the ortho position obtained by this method and the molar ratio, as determined by means of infrared-spectrophotometry, in which 2,4′- and 3,4′-dichlorobiphenyl were formed by the reaction of non-labelled *N*-nitroso-*p*-chloroacetanilide with chlorobenzene.

Inspection of the table shows that the ortho- and para positions are more reactive than the meta position for all aromatic compounds,

1) O. Simamura and T. Migita, This Bulletin, **27**, 228 (1954).

TABLE I. PARTIAL RATE FACTORS AND RELATIVE RATES IN *p*-CHLOROPHENYLATION OF MONOSUBSTITUTED BENZENES AT 20.0°C

Compound	Exp. No.	Partial rate factors			Relative rate
		k_o/k	k_m/k	k_p/k	k_x/k_H
$C_6H_5NO_2$	1*	4.53	0.62	5.76	2.68
	2*	4.18	0.60	6.60	2.69
	Mean	4.35	0.61	6.18	2.69
C_6H_5Cl	5	2.69	—	1.30	—
	6	2.70	—	1.35	—
	Mean	2.70	0.87**	1.33	1.41
$C_6H_5OCH_3$	1*	3.81	0.97	1.42	1.83
	2*	4.05	0.90	1.65	1.93
	Mean	3.93	0.94	1.54	1.88
$C_6H_5CH_3$	3	2.97	1.01	1.35	1.55
	4	2.97	1.13	1.29	1.58
	Mean	2.97	1.07	1.32	1.56

* Reaction temperature was 18°C. ** See text.

k, k_o, k_m, and k_p denote the rate constants on one nuclear position of benzene and the ortho, meta, and para position of the substituted benzene, respectively.

$k_x=2k_o+2k_m+k_p$ and $k_H=6k$

and that all substituents, regardless of their polar nature, activate the aromatic ring, especially at the ortho and the para position. This substitution pattern is in keeping with what is already known to be typical of the homolytic aromatic phenylation[2] and is quite different from that found in the electrophilic substitution. Qualitative consideration of the substitution pattern would therefore suggest that the polar influence due to the chlorine atom in the attacking radical is of minor, if any, importance in the chlorophenylation.

It has been reported in Part III[1] that no polar influence has been detected in the *p*-methoxyphenylation of nitrobenzene. The effect of the polarized aryl radical, however, was soon after recognized by Dannley and Sternfeld[3], who examined the isomer distribution of the products from the reactions of *p*-chlorobenzoyl and of *p*-nitrobenzoyl peroxide with benzotrichloride, and by Cadogan, Hey, and Williams[4], who measured the relative rates of the *p*-chlorophenylation of chlorobenzene and of nitrobenzene by means of *p*-chlorobenzoyl peroxide, and subsequently by Chang, Hey and Williams[5], who determined the partial rate factors in the same reaction. In the present study of chlorophenylation, although no simple correlation is apparent between the partial rate factor for the ortho or the para position and the electronic nature of the substituents on the substrates, the partial rate factor of the meta position was found to diminish in the order: toluene>benzene, anisole>chlorobenzene>nitrobenzene, and this order appears to represent the electronic effect of the substituent. Indeed, a plot of the logarithm of the partial rate factor against Hammett's substituent constant for the meta position falls on a straight line with a slope of −0.27, as shown in Fig. 1. This fact, more convincingly than anything else, demonstrates that the *p*-chlorophenyl radical has a measure of electrophilic character due to the polar nature of the chlorine atom.

The homolytic aromatic arylation is considered[2] to proceed through the rate-determining step of the addition of an aryl radical to

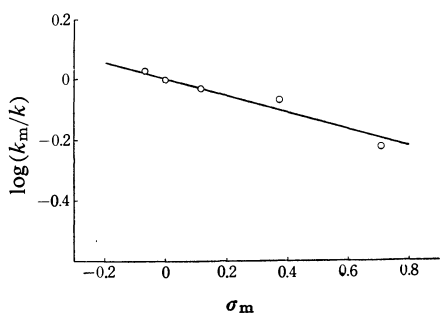

Fig. 1. The Hammett plot for the *p*-chlorophenylation.

2) D. R. Augood and G. H. Williams, *Chem. Revs.*, **57**, 123 (1957); T. Migita, *Yuki Gosei Kagaku Kyokai Shi*, **15**, 74 (1957); G. H. Williams, "Homolytic Aromatic Substitution", Pergamon Press, Oxford (1960).

3) R. L. Dannley and M. Sternfeld, *J. Am. Chem. Soc.*, **76**, 4543 (1954).

4) J. I. G. Cadogan, D. H. Hey and G. H. Williams, *J. Chem. Soc.*, **1955**, 1425.

5) Chang Shih, D. H. Hey and G. H. Williams, ibid., **1958**, 1885.

an aromatic ring, giving an arylcyclohexadienyl radical. The generally observed ortho-para orientation suggests that the major factor controlling the orientation of the entering group is the degree of stabilization of the transition state due to the delocalization of the odd electron. Thus, when the addition occurs at the ortho or the para position to a substituent, the odd electron, in the transition state, can conjugate with the substituent group through the π-electron system of the aromatic nucleus; consequently, the substituent contributes to the stabilization of the transition state. In substitution at the meta position, however, it is obvious that no such conjugation, and hence no such stabilization, is possible, with the result that all substituents direct the homolytic substitution mainly to the ortho and the para position.

In the *p*-chlorophenylation at the ortho and the para position, the subtle influence of the polar character of the radical is masked by the foregoing major factor, that is, the conjugative effect; it is consequently not revealed in the variation of either the partial rate factor or the relative rate. On the other hand, when the addition occurs at the meta position, the odd electron, in the transition state, conjugates only with the π-electrons on the aromatic ring, and the conjugation does not, to the first approximation, extend further into the substituent group. The stabilization due to the conjugative effect therefore will have nearly equal magnitude for every monosubstituted benzene, and the effect of the polar nature of the attacking radical will become significant enough to be reflected in the sequence of the reactivity of the meta position of aromatic compounds, as has actually been observed.

Experimental

Melting points are uncorrected.

Solvents. — Thiophene-free benzene was purified by repeated fractional distillations through a Vigreux column, b. p. 79.5°C. Nitrobenzene was purified by heating commercial material with an aqueous solution of potassium bichromate, distilling it in steam and then under reduced pressure, and finally freezing it fractionally, m. p. 5.9°C. Toluene was purified by shaking it with concentrated sulphuric acid and then fractionating through a Vigreux column, b. p. 109°C. Anisole was prepared from purified phenol and dimethyl sulphate and was purified by distilling it through a Vigreux column, b. p. 153°C. Commercial chlorobenzene was purified by fractionating it through a Vigreux column, b. p. 131°C.

4-Chlorobiphenyls.—A variety of substituted 4-chlorobiphenyls, including several new compounds, which were used as carriers in the isotope dilution analysis were prepared as follows:

4-Chlorobiphenyl was prepared by reaction of *N*-nitroso-*p*-chloroacetanilide with benzene, m. p. 78.5°C (from methanol).

4-Chloro-2'- and -4'-nitrobiphenyl were prepared by the nitration[6] of the above 4-chlorobiphenyl and were purified by chromatography on alumina in petroleum ether-benzene and then by recrystallization from methanol or ethanol; they had the melting points of 69°C and 146°C, respectively.

4-Chloro-3'-nitrobiphenyl was prepared by the chlorination of 3-nitrobiphenyl according to the method described by Blakey and Scarborough[7], m. p. 94°C (from methanol).

4-Chloro-2'- and -4'-methoxybiphenyl were prepared by reaction of *N*-nitroso-*p*-chloroacetanilide with anisole. After removal of anisole from the reaction mixture, the residue was distilled with superheated steam, and the distillate was treated with stannous chloride and concentrated hydrochloric acid in methanol to free it from coloured material. Fractional distillation of the mixture, followed by chromatography on alumina in petroleum ether-benzene, gave the 2'-isomer, m. p. 58°C (from methanol) (Found: Cl, 16.17. Calcd. for $C_{13}H_{11}ClO$: Cl, 16.21%), and the 4'-isomer, m. p. 116°C (from ethanol). The structure of the 2'-isomer was established by demethylation by heating it with pyridine hydrochloride[8] into the known 4-chloro-2'-hydroxybiphenyl[9], m. p. 53°C. The 4'-isomer was also prepared by the Ullmann reaction from *p*-iodoanisole and *p*-chloroiodobenzene.

4-Chloro-3'-methoxybiphenyl was prepared by heating a mixture of *m*-iodoanisole and *p*-chloroiodobenzene with copper powder at 230°C for 11 hr. The oily material extracted from the reaction mixture with benzene was fractionally distilled under reduced pressure. The crystals of 4,4'-dichlorobiphenyl which deposited from the cooled distillate (b. p. 197~212°C/27 mmHg) were filtered off, and then the filtrate was heated with pyridine hydrochloride at 210°C for 7 hr. The phenolic fraction was separated and fractionated by chromatography on alumina in benzene, giving 4-chloro-3'-hydroxybiphenyl[10], m. p. 84°C. This was methylated with dimethyl sulphate and aqueous alkali to yield 4-chloro-3'-methoxybiphenyl, m. p. 36~37°C (from methanol) (Found: Cl, 16.02. Calcd. for $C_{13}H_{11}ClO$: Cl, 16.21%).

4-Chloro-2'-, -3'- and -4'-methylbiphenyl were prepared by the *p*-chlorophenylation of toluene with *N*-nitroso-*p*-chloroacetanilide. After removal of the toluene, distillation with superheated steam gave an oily material, which was then fractionally distilled three times under reduced pressure. In each distillation, some 4-chloro-4'-methylbiphenyl (m. p. 124°C) was separated from the after-run in the

6) C. K. Bradsher and L. J. Wissow, *J. Am. Chem. Soc.*, **68**, 404 (1946).
7) W. Blakey and H. A. Scarborough, *J. Chem. Soc.*, **1927**, 3003.
8) V. Prey, *Ber.*, **74**, 1219 (1941); **75**, 350 (1942).
9) J. C. Colbert and R. M. Lacy, *J. Am. Chem. Soc.*, **68**, 270 (1946).
10) V. Prelog, J. Würsch and K. Königsbacher, *Helv. Chim. Acta*, **34**, 258 (1951).

form of crystals, which were collected and recrystallized from methanol. Cooling a methanolic solution of the first fraction (b. p. 101~105°C/2 mmHg) in a dry ice-ethanol bath yielded crystals (m. p. 27°C), which were purified by chromatography on alumina in petroleum ether to afford 4-chloro-2'-methylbiphenyl (Found: Cl, 17.29. Calcd. for $C_{13}H_{11}Cl$: Cl, 17.48%), m. p. 29.5~30.5°C (from methanol). Similarly, the second fraction (b. p. 105~115°C/2 mmHg) gave 4-chloro-3'-methylbiphenyl (Found: Cl, 17.40. Calcd. for $C_{13}H_{11}Cl$: Cl, 17.48%), m. p. 36~37°C (from methanol). The structure of this compound is evident, since it was found to be identical with the unsymmetrically substituted biphenyl obtained from *p*-chloroiodobenzene and *m*-iodotoluene by the Ullmann reaction, and consequently the structure of the 2'-methyl isomer is also established. Incidentally, Otto and Smith[11] prepared this isomer by a similar method and described it as an oil.

2,4'-Dichlorobiphenyl was prepared by the Sandmeyer reaction from 2-amino-4'-chlorobiphenyl[6]. To a stirred solution of 2-nitro-4'-chlorobiphenyl (5 g.) in benzene (200 ml.), dry iron powder (50 g.) activated by treatment with concentrated hydrochloric acid (10 ml.) was added[12]. After refluxing the mixture for 1 hr., 10 ml. of water was added over a period of 5 hr. under refluxing. The benzene layer was separated from the cooled reaction mixture, and passage of dry hydrogen chloride to the dried benzene solution yielded 4.8 g. of 2-amino-4'-chlorobiphenyl hydrochloride, which was then hydrolysed to 2-amino-4'-chlorobiphenyl (m. p. 43~43.5°C). The amine hydrochloride (14.5 g.) was diazotized by 42 g. of sodium nitrite in aqueous hydrochloric acid. The diazotized solution was filtered quickly and added to a wet precipitate of cuprous chloride prepared from cupric sulphate (19.5 g.) and sodium chloride (6 g.) by reduction with an alkaline solution of sodium bisulphite (4.2 g.). The reaction mixture was left to stand overnight and then distilled with steam. The 2,4'-dichlorobiphenyl thus isolated was purified by chromatography on alumina in petroleum ether, m. p. 44.5°C (from methanol) (Found: Cl, 31.66. Calcd. for $C_{12}H_8Cl_2$: Cl, 31.78%).

3,4'-Dichlorobiphenyl was prepared by a similar method from 4-chloro-3'-nitrobiphenyl. The product was purified by chromatography on alumina in petroleum ether and distillation under reduced pressure, b. p. 125°C/1 mmHg (Found: Cl, 31.55. Calcd. for $C_{12}H_8Cl_2$: Cl, 31.78%).

4,4'-Dichlorobiphenyl was prepared by the Ullmann reaction from *p*-chloroiodobenzene and was purified by chromatography on alumina in benzene, m. p. 147~148°C (from ethanol).

p-Chloro(^{36}Cl)acetanilide.—This was prepared by chlorination of acetanilide with chlorine-36, which had been obtained by oxidation of silver chloride-(^{36}Cl) precipitated from hydrochloric-(^{36}Cl) acid (4.06 mc./mol.). The detailed procedure is described elsewhere[13].

N-Nitroso-p-chloro(^{36}Cl)acetanilide.—To an ice-cooled, stirred mixture of *p*-chloro(^{36}Cl)acetanilide (0.371 g.), fused potassium acetate (0.9 g.), acetic acid (3.2 ml.), acetic anhydride (0.8 ml.), and a trace of phosphorus pentoxide, 4 ml. of an 11.8% solution of nitrosyl chloride in acetic anhydride was added over a period of 18 min. The mixture was kept in ice-water for a further 30 min. and then poured into ice-water to precipitate the *N*-nitroso compound, which was collected, washed with water, and dried in a vacuum desiccator (m. p. 75°C; yield, 0.358 g.).

Decomposition of N-Nitroso-p-chloro(^{36}Cl)acetanilide. — *N*-Nitroso-*p*-chloro(^{36}Cl)acetanilide was allowed to decompose in an equimolar binary or ternary mixture of aromatic solvents, each containing benzene as one component (see Table II). The reaction vessel was immersed in a thermostat kept at 20.0°C and let stand for two days. In experiments 1 and 2, which were carried out at 18°C, at the end of two days the volume of nitrogen evolved reached final values of 77% and 80% of theory, respectively.

General Procedure for Isotope Dilution Analysis.—The reaction mixture was diluted with benzene to a volume of 50 or 100 ml., and the resulting solution was weighed and divided into several weighed portions. To each portion an accurately known amount of each of the biaryls to be assayed was added as a carrier; the solvent was then driven off at atmospheric pressure through a Vigreux column 15 cm. in length and, if necessary, further under reduced pressure. From the residue the labelled biaryl diluted with the carrier was recovered by chromatography on activated alumina in benzene-petroleum ether. The crystalline material thus recovered was purified by repeated crystallization from methanol or ethanol. The purification was considered to be complete when the specific activity of a specimen remained constant on further crystallization.

Since the dilution was made with a large excess of carriers, the molecular ratio in which two labelled biaryls (A and B) were formed in this reaction is given by the ratio $(f_B M_A C_A / f_A M_B C_B)$, where f_A and f_B denote the ratios to the total reaction mixture of the portions used for the determination of A and B, respectively; C_A and C_B, the specific activities in counts per minute of recovered A and B, and M_A and M_B, the amounts of non-labelled A and B added as carriers. All the numerical results are listed in Table II.

Measurement of Radioactivity.—The radioactivity of ^{36}Cl-labelled compounds was determined by a method described elsewhere[14], which comprises decomposition of the labelled compounds with sodium in boiling isopropyl alcohol, precipitation of the liberated chloride ions as mercurous chloride, and counting the radioactivity of the chloride on an "infinitely thick" layer with an end-window Geiger-Müller counter.

Determination of the Partial Rate Factor for the Meta Position of Chlorobenzene.—*N*-Nitroso-*p*-chloroacetanilide (9.86 g.) was dissolved in 509 g.

11) D. G. Otto and G. G. Smith, *J. Am. Chem. Soc.*, **77**, 2325 (1955).
12) S. E. Hazlet and C. A. Dornfeld, ibid., 66, 1781 (1944).
13) N. Morikawa, T. Migita and O. Simamura, *Radioisotopes (Tokyo)*, **10**, 236 (1961).
14) T. Migita, N. Morikawa and O. Simamura, ibid., 5, 28 (1956).

TABLE II. DECOMPOSITION OF *N*-NITROSO-*p*-CHLORO(^{36}Cl)ACETANILIDE AND RESULTS OF ISOTOPE DILUTION ANALYSES OF THE PRODUCTS

Exp. No.	Ratio of the portion taken to the total reaction mixture $f\times10^2$	Carrier added 4-ClC$_6$H$_4$C$_6$H$_4$X: X	*M*, mmol.	Radioactivity of recovered biaryl as counts of HgCl c. p. m.*	Molar yield relative to biphenyl
1	The nitroso compound, 358 mg.; the substrate, an equimolar mixture (16.9 g.) of nitrobenzene, anisole and benzene				
	5.0	H	10.09	131.9±1.8	1.000
	5.0	2'-NO_2	10.07	199.8±2.6	1.51
	30.0	3'-NO_2	10.03	162.2±2.3	0.205
	5.0	4'-NO_2	10.06	128.0±1.9	0.96
	5.0	2'-CH_3O	10.06	167.8±2.3	1.27
	30.0	3'-CH_3O	10.03	255.9±3.0	0.322
	15.0	4'-CH_3O	7.36	128.3±2.1	0.237
2	The nitroso compound, 460 mg.; the substrate, an equimolar mixture (22.4 g.) of nitrobenzene, anisole, and benzene				
	5.00	H	15.02	65.1±1.9	1.000
	4.99	2'-NO_2	15.05	90.5±1.9	1.39
	30.05	3'-NO_2	15.03	77.9±1.2	0.199
	4.99	4'-NO_2	15.03	71.4±1.2	1.10
	5.00	2'-CH_3O	14.97	88.4±1.5	1.35
	19.98	3'-CH_3O	12.83	90.4±4.1	0.30
	24.99	4'-CH_3O	14.94	89.9±1.4	0.275
3	The nitroso compound, 101 mg.; the substrate, an equimolar mixture (3.81 g.) of toluene and benzene				
	9.99	H	19.96	282.3±2.5	1.000
	4.01	2'-CH_3	20.00	111.9±1.9	0.99
	20.03	3'-CH_3	20.00	190.7±2.4	0.338
	20.03	4'-CH_3	10.13	250.9±3.1	0.225
4	The nitroso compound, 97.5 mg.; the substrate, an equimolar mixture (3.71 g.) of toluene and benzene				
	3.97	H	19.98	109.6±1.5	1.000
	3.96	2'-CH_3	19.98	108.4±1.8	0.99
	11.94	3'-CH_3	19.99	123.9±2.0	0.376
	19.89	4'-CH_3	10.02	187.4±2.6	0.214
5	The nitroso compound, 48.0 mg.; the substrate, an equimolar mixture (2.25 g.) of chlorobenzene and benzene				
	10.01	H	20.62	307.8±1.7	1.000
	10.01	2'-Cl	10.00	284.9±3.0	0.90
	39.96	4'-Cl	10.13	271.3±3.0	0.216
6	The nitroso compound, 47.0 mg.; the substrate, an equimolar mixture (2.13 g.) of chlorobenzene and benzene				
	9.90	H	19.98	317.1±2.1	1.000
	9.90	2'-Cl	10.00	287.6±2.6	1.000
	40.01	4'-Cl	10.00	287.6±2.6	0.225

* Indicated deviations are probable errors.

of chlorobenzene and allowed to decompose at 20.0°C. After removal of most of chlorobenzene through a Vigreux column (60 cm.), 2 ml. of nitrobenzene was added to the residue. By fractionating the mixture through a concentric column, all the chlorobenzene retained in the mixture and 0.3 ml. of nitrobenzene were driven off. The residue was dissolved in benzene, and the solution was passed through a column of alumina and then treated with 50 g. of iron activated by treatment with hydrochloric acid[12] and 10 ml. of water for reduction of the nitrobenzene contained in the solution. The benzene layer was washed with diluted hydrochloric acid and then with water and dried over calcium chloride. The reddish-brown material obtained by removal of the benzene was fractionated by chromatography on an alumina column using a mixture of ether and petroleum ether (1 : 1) as an eluant into the following fractions: the first fraction (a light yellow oil and a small amount of a crystalline

material): a mixture of 2,4'- and 3,4'-dichlorobiphenyl; the second fraction (a yellowish crystalline material): 4,4'-dichlorobiphenyl; the third fraction: traces of reddish crystals; and the succeeding fractions: traces of crystals and reddish impurities. The first and the second fraction were combined, and the mixture was analyzed for three isomeric dichlorobiphenyls by infrared spectrophotometry in carbon disulphide with a Perkin Elmer-21 spectrophotometer, using absorptions at 883 cm^{-1}, 730 cm^{-1}, and 810 cm^{-1} for 2,4'-, 3,4'- and 4,4'-dichlorobiphenyl, respectively. It was found that the foregoing mixture consisted of 65, 21 and 12% of the respective isomers, giving 3.1 as the molar ratio of the 2,4'- and the 3,4'-isomer formed. This value, in conjunction with the value of the partial rate factor for the ortho position determined by the isotope dilution analysis, leads to the partial rate factor of 0.87 for the meta position, while the value is 1.16 when the molar ratio of the 4,4'-isomer to the 3,4'-isomer is used. The former value is considered to be more reliable for the following reason. From the spectrophotometric result, the ratio of the reactivity of the *o*-position to that of the *p*-position of chlorobenzene towards *p*-chlorophenylation is calculated to be 2.7, which is rather too large when compared with the corresponding value, 2.0, calculated from the results of the isotope dilution analysis. This discrepancy is most probably due to the method of preparing the sample subjected to the spectrophotometric analysis, in which the third fraction containing a little of the least elutable 4,4'-dichlorobiphenyl was discarded to avoid contamination of the sample by any coloured impurities.

Summary

N-Nitroso-*p*-chloro(^{36}Cl)acetanilide has been decomposed in mixtures of benzene and monosubstituted benzene C_6H_5X (X=NO_2, Cl, OCH_3, and CH_3), and the reaction products have been analyzed for 4-chlorobiphenyl and isomeric 4-$ClC_6H_4C_6H_4X$ by the isotope dilution method. On the basis of these results, the partial rate factors for the *p*-chlorophenylation have been calculated to be, for nitrobenzene: *o*, 4.35; *m*, 0.61; *p*, 6.18; for chlorobenzene: *o*, 2.70; *m*, 0.87; *p*, 1.33; for anisole: *o*, 3.93; *m*, 0.94; *p*, 1.54 and for toluene: *o*, 2.97; *m*, 1.07; *p*, 1.32.

The values of the partial rate factor for the meta position give a satisfactory Hammett plot with a slope of −0.27. This fact demonstrates that the *p*-chlorophenyl radical shows a measure of electrophilic character in the homolytic aromatic substitution.

Department of Chemistry
Faculty of Science
The University of Tokyo
Hongo, Tokyo

Influence of Substituent Groups on Nuclear Reactivity in the Formation of Substituted Biphenyls by Reaction of Aromatic Diazo and Related Compounds with Aromatic Liquids. VII. p-Nitrophenylation and p-Methoxyphenylation

By Ryôichi Itô, Toshihiko Migita, Naotake Morikawa, Morihiko Ōkuni and Osamu Simamura

(Received May 10, 1963)

In the preceding paper[1], the partial rate factors for the *p*-chlorophenylation of monosubstituted benzenes by the *p*-chlorophenyl radical derived from *N*-nitroso-*p*-chloroacetanilide have been reported. The variation of the reactivity of the meta position with the nature of the substituent has suggested that the attacking *p*-chlorophenyl radical has a somewhat electrophilic nature due to the presence of a chlorine atom. The study has now been extended to include *p*-nitrophenylation and *p*-methoxyphenylation, the former being expected to be more electrophilic than *p*-chlorophenylation and the latter to be rather nucleophilic because of the electron-releasing nature of the *p*-methoxy group in the radical.

N-Nitroso-*p*-nitroacet(anilide-^{14}C) and *N*-nitroso-*p*-methoxyacet(anilide-^{14}C) were used as sources of the *p*-nitrophenyl and the *p*-methoxyphenyl radical, respectively, and the arylated products were analyzed by isotope

1) T. Migita, N. Morikawa and O. Simamura, This Bulletin, **36**, 980 (1963).

TABLE I. PARTIAL RATE FACTORS AND RELATIVE RATES IN *p*-NITROPHENYLATION OF MONOSUBSTITUTED BENZENES AT 20.0°C

Compound	Exp. No.	Partial rate factors			Relative rate*
		k_o/k	k_m/k	k_p/k	k_x/k_H
$C_6H_5NO_2$	1	0.90	0.347	1.49	0.66
	2	0.95	0.354	1.57	0.69
	Mean	0.93	0.35	1.53	0.68
C_6H_5Cl	1	1.50	0.650	0.99	0.88
	2	1.55	0.645	1.03	0.90
	Mean	1.53	0.65	1.01	0.89
$C_6H_5OCH_3$	3	5.16	0.83	2.45	2.40
	4	5.18	0.85	2.15	2.37
	Mean	5.17	0.84	2.30	2.39
$C_6H_5CH_3$	5	3.27	1.45	1.48	1.82
	6	3.28	1.27	1.53	1.77
	Mean	3.28	1.36	1.51	1.80

* $k_x = 2k_o + 2k_m + k_p$; $k_H = 6k$

TABLE II. PARTIAL RATE FACTORS AND RELATIVE RATES IN *p*-METHOXYPHENYLATION OF MONOSUBSTITUTED BENZENES AT 20.0°C

Compound	Exp. No.	Partial rate factors			Relative rate
		k_o/k	k_m/k	k_p/k	k_x/k_H
$C_6H_5NO_2$	7	6.53	1.26	8.30	3.98
	8	6.37	1.11	8.42	3.90
	Mean	6.45	1.19	8.36	3.94
C_6H_5Cl	7	3.15	1.83	1.78	1.96
	8	3.00	1.80	1.69	1.88
	Mean	3.08	1.82	1.74	1.92
$C_6H_5OCH_3$	9	3.64	1.06	1.32	1.79
	10	3.71	1.00	1.30	1.79
	Mean	3.68	1.03	1.31	1.79
$C_6H_5CH_3$	11	3.10	1.00	1.19	1.56
	12	3.09	0.99	1.17	1.56
	Mean	3.09	1.00	1.18	1.56

dilution analysis. The results are summarized in Tables I and II.

The partial rate factors for the *p*-methoxyphenylation of nitrobenzene had previously been determined to be 7.24, 0, and 8.95 for the *o*-, *m*-, and *p*-position, respectively, the product analysis being done by means of column chromatography[2]. The more accurate results obtained in the present work have shown that the meta-substituted product is actually formed. Probably the meta isomer could not be separated from the ortho isomer by the chromatographical method used in the previous experiments.

It is apparent from Table I that the relative rate of a monosubstituted benzene in *p*-nitrophenylation decreases in the order: anisole > toluene > benzene > chlorobenzene > nitrobenzene. This trend, which is parallel to the order of reactivity towards electrophilic reagents, has not been observed in the case of *p*-chlorophenylation[1]. This shows that the *p*-nitrophenyl radical is decidedly more electrophilic than the *p*-chlorophenyl radical. It has been shown[1] that in *p*-chlorophenylation the major factor controlling the rate is the stabilization of the transition state due to the delocalization of an odd electron, that is, the conjugative effect, and that the polar character of the attacking radical is of subordinate importance. In the *p*-nitrophenylation, however, it has now turned out that the polar effect of the *p*-nitrophenyl radical is strong enough to compete with the foregoing major

2) O. Simamura and T. Migita, This Bulletin, 27, 228 (1954).

factor, with the result that the relative rate sequence resembles that observed in electrophilic substitutions. The electrophilic nature of the *p*-nitrophenyl radical becomes even more evident when the reactivity is compared at the meta position, where the conjugative effect of the substituent group in the substrate may be regarded as negligible. Thus, the reactivity of the meta position of monosubstituted benzenes in the *p*-nitrophenylation decreases in the order: toluene>benzene> anisole > chlorobenzene > nitrobenzene. The same trend is observed in the *p*-chlorophenylation[1], but the variation is much more conspicuous in the *p*-nitrophenylation. Figure 1 shows the relation between the partial rate factor for the meta position of a substituted benzene and the Hammett substituent constant for the substituent at the meta position. From the slope of the line, the reaction constant for the *p*-nitrophenylation is found to be −0.81, while the corresponding value of the *p*-chlorophenylation is −0.27[1]. It is evident from a comparison of these values that the electrophilic nature of the *p*-nitrophenylation is more pronounced than that of the *p*-chlorophenylation because of the much stronger electron-withdrawing effect of the nitro group.

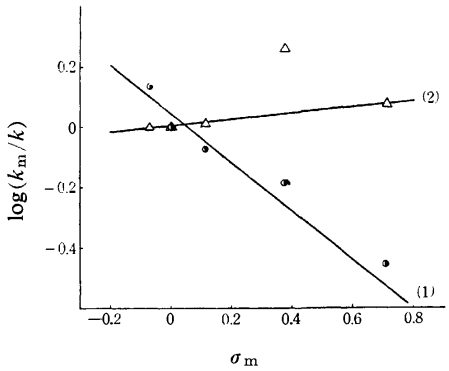

Fig. 1. The Hammett plots for the *p*-nitro-(1) and the *p*-methoxy-(2) phenylation.

In the *p*-methoxyphenylation, on the other hand, Table II shows that all substituents increase the nuclear reactivity of the aromatic nucleus, and that, except for chlorobenzene, the meta position is less reactive than the ortho and the para position, as has been observed in the *p*-chlorophenylation. Except for chlorobenzene, the partial rate factor for the meta position of every compound is approximately unity, so that the reactivity of the meta position of a monosubstituted benzene is close to that of a single position of benzene itself. This finding suggests that the *p*-methoxyphenyl radical has little, if any, polar character. The reaction constant of the Hammett relation between $\log(k_m/k)$ and σ_m is +0.09; this value might indicate a very slight, if any, nucleophilic nature for the *p*-methoxyphenylation. The partial rate factor of 1.82 for the meta position of chlorobenzene seems to be anomalously high; the Hammett plot would predict it to be 1.08. It is not clear whether the value is true or erroneous owing to some unknown experimental difficulty in the analysis of 3-chloro-4′-methoxybiphenyl.

Recently, Hambling, Hey, and Williams[3] have observed that the relative reactivity of nitrobenzene towards the arylations by aroyl peroxides increases in the order: *p*-nitrophenylation < *p*-chlorophenylation < *p*-methoxyphenylation < phenylation. On the basis of this tendency, which has also been recognized in the present study, and of its parallelism to the dipole moment values of the compounds corresponding to the aryl radicals which cause these arylations, they have concluded that the *p*-methoxyphenyl radical has rather an electrophilic character compared with the phenyl radical. The disagreement between their view and ours seems to be attributable to the fact that, in their deduction, a comparison has been made between the relative rates of *p*-methoxyphenylation and of phenylation of nitrobenzene, using benzene as the reference substrate in both cases.

Experimental

Melting points are uncorrected.

Solvents.—Nitrobenzene, chlorobenzene, anisole, toluene and benzene were purified as described in Part VI[1].

Substituted Biphenyls Used as Carriers in Isotope Dilution Analysis. — 4-Nitrobiphenyl was prepared by nitration of biphenyl according to Maki and Ôbayashi's method[4], m. p. 112.8～113°C (from methannol).

4-Methoxybiphenyl was prepared by reaction of *N*-nitrosoaceto-*p*-anisidide[5] with benzene and was purified by recrystallization from methanol, m. p. 90°C.

2,4′- and 4,4′-Dinitrobiphenyl were prepared by the nitration of *p*-nitrobiphenyl according to Maki and Ôbayashi's method[4]. The 2,4′-isomer was recrystallized from ethanol, m. p. 93.5～94°C, and the 4,4′-isomer from acetone, m. p. 237°C.

3,4′-Dinitrobiphenyl was prepared as follows: To a cooled solution of 3-nitrobiphenyl[6] (15 g.) in acetic anhydride (20 ml.), a mixture of fuming nitric acid (*d*, 1.54; 6.8 ml.), acetic anhydride

3) J. K. Hambling, D. H. Hey and G. H. Williams, *J. Chem. Soc.*, **1960**, 3782.
4) T. Maki and K. Ôbayashi, *J. Chem. Soc. Japan, Ind. Chem. Sec.* (*Kōgyō Kagaku Zassi*), **54**, 375 (1951).
5) J. W. Haworth and D. H. Hey, *J. Chem. Soc.*, **1940**, 361.
6) H. France, I. M. Heilbron and D. H. Hey, ibid., **1940**, 369.

(3.4 ml.) and urea (0.2 g.) was added over a period of 15 min., and the mixture was heated on a steam bath. After being cooled, the mixture was poured into water to give a precipitate (17 g.), which was then collected, washed with water, and dried. The product was purified by chromatography on alumina in benzene-acetone (4 : 1) to give 3,4'-dinitrobiphenyl, m. p. 189°C (from ethanol).

2-Chloro-4'-nitrobiphenyl was prepared by reaction of *N*-nitroso-*p*-nitroacetanilide[6] with chlorobenzene. The product, which was isolated by removal of chlorobenzene under reduced pressure followed by distillation with superheated steam, was purified by chromatography on alumina in petroleum ether-benzene (4 : 1), m. p. 79~80°C (from methanol).

3-Chloro-4'-nitrobiphenyl was obtained by nitration of 3-chlorobiphenyl[7]. The procedure for the nitration was analogous to that used for preparation of 3,4'-dinitrobiphenyl. The brown oily product was fractionated by distillation under reduced pressure (b. p. 157~158°C/1 mmHg) and then by chromatography on alumina in petroleum ether-benzene (4 : 1), m. p. 93~94°C (from methanol).

The preparation and purification of 4-chloro-4'-nitrobiphenyl were described in Part VI[1].

2-Methoxy-4'-nitrobiphenyl was prepared from *N*-nitroso-*p*-nitroacetanilide and anisole and was purified by chromatography and recrystallization from methanol, m. p. 63~64°C.

3-Methoxy-4'-nitrobiphenyl was prepared from diazotized *m*-anisidine and nitrobenzene by the Gomberg reaction. After removal of the solvent from the reaction mixture, the residue was distilled with superheated steam to afford a crystalline distillate, which was then fractionated by chromatography on alumina in petroleum ether-benzene (1 : 1), m. p. 90~91°C (from methanol).

4-Methoxy-4'-nitrobiphenyl was prepared as described in Part III[2].

Methyl-4'-nitrobiphenyls were prepared as follows: *N*-Nitroso-*p*-nitroacetanilide (35 g.) was dissolved in 1 l. of toluene and left to stand for two days. After removal of the toluene, the residue was distilled with superheated steam and the distillate was fractionated by chromatography on alumina in petroleum ether-benzene into three parts: (i) an oily material which contained 3-methyl-4'-nitrobiphenyl (see below), (ii) 2-methyl-4'-nitrobiphenyl (6 g.), m. p. 102.5~103°C, and (iii) 4-methyl-4'-nitrobiphenyl (1.5 g.), m. p. 139~140°C. Fraction (ii) was further purified by similar chromatography, m. p. 102.5~103°C (from methanol). Distillation of fraction (i) under reduced pressure gave nitrobenzene (2 g.) and the residue, which chromatographed on alumina in petroleum ether-benzene (10 : 1) yielded, besides a small amount of 2-methyl-4'-nitrobiphenyl, 3-methyl-4'-nitrobiphenyl (0.5 g.), m. p. 60°C. The structure of this compound was established by the following preparation. Nitrosation of *m*-acetotoluidide (33 g.) by nitrous fumes in a mixture of acetic acid and acetic anhydride yielded oily *N*-nitroso-*m*-acetotoluidide, which was allowed to decompose in nitrobenzene. The products were isolated as usual and chromatographed on alumina to give the same methylnitrobiphenyl (2.5 g.), m. p. 60°C. 3-Methyl-4'-nitrobiphenyl was further purified by chromatography, m. p. 61.5°C (from methanol) (Found: C, 73.10; H, 5.21; N, 6.65. Calcd. for $C_{13}H_{11}NO_2$: C, 73.22; H, 5.20; N, 6.57%). 4-Methyl-4'-nitrobiphenyl was also prepared by nitration of 4-methylbiphenyl according to Grieve and Hey's method[8]. The product was combined with fraction (iii) obtained above and purified by recrystallization from ethanol, m. p. 141°C.

4-Methoxy-2'-nitrobiphenyl was prepared as described in Part III[2], m. p. 62.5~63°C.

4-Methoxy-3'-nitrobiphenyl was prepared by reaction of *N*-nitroso-*m*-nitroacetanilide[9] with anisole and was purified by distillation and chromatography on alumina in petroleum ether-benzene (4 : 1), m. p. 78~79°C (from methanol).

2-Chloro-4'-methoxybiphenyl was prepared as follows: 2-Nitro-4'-methoxybiphenyl (5 g.) was reduced with activated iron powder and water[10] to 2-amino-4'-methoxybiphenyl, which was then diazotized and allowed to react with cuprous chloride in a manner similar to the preparation of 2,4'-dichlorobiphenyl described in a previous paper[1], giving 2-chloro-4'-methoxybiphenyl (0.5 g.), m. p. 24~24.5°C. In another preparation *N*-nitroso-*p*-acetoanisidide (50 g.) was allowed to decompose in 700 ml. of chlorobenzene. The isolated product was treated with a little stannous chloride and concentrated hydrochloric acid in methanol and then distilled under reduced pressure. The distillate (b. p. 135~141°C/1 mmHg, 3.1 g.) was purified by chromatography on alumina in petroleum ether, yielding 2-chloro-4'-methoxybiphenyl (3.5 g.), m. p. 24~24.5°C. Specimens from both preparations were combined and purified by recrystallization from methanol, m. p. 24~24.5°C (Found: Cl, 16.18. Calcd. for $C_{13}H_{11}ClO$: Cl, 16.21%).

3-Chloro-4'-methoxybiphenyl was prepared by heating *m*-chloroiodobenzene (25 g.), *p*-iodoanisole (73.3 g.), and copper powder (100 g.) at 250°C for 8 hr. and purified by distillation under reduced pressure (b. p. 130~140°C/1.3 mmHg; yield, 13.1 g.) followed by chromatography on alumina in petroleum ether, m. p. 56~57°C (from methanol) (Found: Cl, 16.08. Calcd. for $C_{13}H_{11}ClO$: Cl, 16.21%).

4-Chloro-4'-methoxybiphenyl was prepared and purified as described in Part VI[1].

2,4'-Dimethoxybiphenyl was prepared by the method described by Dunstan and Hughes[11] and was purified by recrystallization from methanol, m. p. 71.5°C.

3,4'-Dimethoxybiphenyl was prepared by the Ullmann reaction of *p*-iodoanisole (70 g.) and *m*-iodoanisole (25 g.), m. p. 60~61°C (yield, 7 g.) (Found: C, 78.64; H, 6.63. Calcd. for $C_{14}H_{14}O_2$:

7) J. Elks, J. W. Haworth and D. H. Hey, *J. Chem. Soc.*, **1940**, 1284.

8) W. S. M. Grieve and D. H. Hey, ibid., **1932**, 1888.

9) H. France, I. M. Heilbron and D. H. Hey, ibid., **1939**, 1288.

10) S. E. Hazlet and C. A. Dornfeld, *J. Am. Chem. Soc.*, **66**, 1781 (1944).

11) W. J. Dunstan and G. K. Hughes, *J. Proc. Soc. N. S. Wales*, **80**, 77 (1947); *Chem. Abstr.*, **42**, 4160 (1948).

TABLE III. DECOMPOSITION OF *N*-NITROSO-*p*-NITROACET(ANILIDE-^{14}C) AT 20.0°C AND RESULTS OF ISOTOPE DILUTION ANALYSES OF THE PRODUCTS

Exp. No.	Ratio of the portion taken to the total reaction mixture $f\times10^2$	Carrier added 4-$NO_2C_6H_4C_6H_4X$ X	*M*, mmol	Specific activity of biaryl μc./mol.*	Amount of biaryl formed μmol.
1	The nitroso compound (61.2±0.5 mc./mol.), 141 mg.; the substrate, an equimolar mixture (6.21 g.) of nitrobenzene, chlorobenzene, and benzene; nitrogen evolved, 82%				
	2.97	H	2.02	115.4±0.9	128
	8.93	2'-NO_2	2.01	104.6±1.0	38.5
	29.87	3'-NO_2	2.00	135.1±1.1	14.8
	11.96	4'-NO_2	2.01	115.9±1.0	31.8
	8.95	2'-Cl	2.01	174.8±1.4	64.1
	8.94	3'-Cl	2.00	75.9±0.7	27.8
	14.92	4'-Cl	2.00	97.0±0.7	21.3
2	The nitroso compound (61.2±0.5 mc./mol.), 140 mg.; the substrate, an equimolar mixture (6.21 g.) of nitrobenzene, chlorobenzene, and benzene; nitrogen evolved, 78%				
	3.01	H	2.05	108.6±1.2	121
	9.97	2'-NO_2	2.10	110.3±1.1	37.2
	26.79	3'-NO_2	2.06	113.5±1.1	14.3
	11.87	4'-NO_2	2.05	112.4±1.1	31.7
	5.96	2'-Cl	2.07	109.9±1.0	62.4
	12.95	3'-Cl	2.05	100.3±1.1	26.0
	17.93	4'-Cl	2.04	111.3±1.1	20.8
3	The nitroso compound (46.6±0.3 mc./mol.), 192 mg.; the substrate, an equimolar mixture (7.69 g.) of anisole and benzene; nitrogen evolved, 73%				
	9.89	H	2.03	377 ±3	167
	5.91	2'-OCH_3	2.02	390 ±3	288
	29.75	3'-OCH_3	2.03	314 ±3	46.3
	33.76	4'-OCH_3	2.02	530 ±5	68.6
4	The nitroso compound (46.6±0.3 mc./mol.), 192 mg.; the substrate, an equimolar mixture (7.70 g.) of anisole and benzene; nitrogen evolved, 76%				
	9.98	H	2.02	342 ±3	149
	5.89	2'-OCH_3	2.01	349 ±3	257
	19.80	3'-OCH_3	1.89	205 ±2	42.2
	23.95	4'-OCH_3	2.01	294 ±3	53.4
5	The nitroso compound (61.2±0.5 mc./mol.), 185 mg.; the substrate, an equimolar mixture (6.73 g.) of toluene and benzene; nitrogen evolved, 39%				
	5.88	H	1.98	218 ±2	120
	6.10	2'-CH_3	2.02	243 ±2	132
	17.98	3'-CH_3	2.02	317 ±3	58.2
	29.91	4'-CH_3	2.02	270 ±2	29.8
6	The nitroso compound (46.6±0.3 mc./mol.), 193 mg.; the substrate, an equimolar mixture (7.04 g.) of toluene and benzene; nitrogen evolved, 50%				
	8.00	H	2.02	172 ±2	93.5
	7.99	2'-CH_3	2.17	174 ±2	102
	15.95	3'-CH_3	3.10	93.8±0.9	39.3
	31.96	4'-CH_3	2.17	162 ±2	23.7

* Indicated deviations are probable errors.

C, 78.48; H, 6.59%). The structure of this compound was established by the fact that it was different from the possible isomeric products, the 3,3'- (m. p. 35°C)[12] and the 4,4'- (m. p. 173°C)[13] isomer.

12) J. van Alphen, *Rec. trav. chim.*, **50**, 1111 (1931).
13) F. Ullmann, G. M. Meyer, O. Loewenthal and E. Gilli, *Ann.*, **332**, 38 (1904).

4,4'-Dimethoxybiphenyl was prepared by the Ullmann reaction from *p*-iodoanisole and was purified by recrystallization from ethanol, m. p. 173~173.5°C.

4-Methoxy-2'- and -4'-methylbiphenyl were prepared as follows: *N*-Nitroso-*p*-acetoanisidide was allowed to decompose in toluene, and the product was fractionally distilled under reduced pressure to

TABLE IV. DECOMPOSITION OF *N*-NITROSO-*p*-METHOXYACET(ANILIDE-^{14}C) AT 20.0°C AND RESULTS OF ISOTOPE DILUTION ANALYSES OF THE PRODUCTS

Exp. No.	Ratio of the portion taken to the total reaction mixture $f\times10^2$	Carrier added 4-$CH_3OC_6H_4C_6H_4X$ X	*M*, mmol.	Specific activity of biaryl μc./mol.	Amount of biaryl formed μmol.
7	The nitroso compound (27.4±0.2 mc./mol.), 496 mg.; the substrate, an equimolar mixture (24.04 g.) of nitrobenzene, chlorobenzene, and benzene; nitrogen evolved, 85%				
	6.98	H	2.01	154 ±2	163
	3.98	2'-NO_2	2.00	191 ±2	354
	24.98	3'-NO_2	2.00	232 ±2	69
	5.97	4'-NO_2	2.00	182 ±2	225
	6.98	2'-Cl	2.01	162 ±2	171
	19.91	3'-Cl	2.01	267 ±3	99
	24.93	4'-Cl	1.99	164 ±2	48
8	The nitroso compound (27.4±0.2 mc./mol.), 495 mg.; the substrate, an equimolar mixture (24.01 g.) of nitrobenzene, chlorobenzene, and benzene; nitrogen evolved, 84%				
	8.96	H	2.00	213 ±2	176
	3.99	2'-NO_2	2.00	202 ±2	373
	19.95	3'-NO_2	2.01	176 ±2	65
	5.96	4'-NO_2	2.00	200 ±2	247
	7.95	2'-Cl	2.01	190 ±2	176
	15.98	3'-Cl	2.01	228 ±2	105
	29.94	4',Cl	2.00	201 ±2	50
9	The nitroso compound (31.4±0.4 mc./mol.), 145 mg.; the substrate, an equimolar mixture (6.25 g.) of anisole and benzene; nitrogen evolved, 52%				
	7.91	H	2.00	130 ±1	105
	6.98	2'-OCH_3	2.00	139 ±1	128
	19.97	3'-OCH_3	2.00	116 ±1	37.1
	39.94	4'-OCH_3	2.00	144 ±1	23.1
10	The nitroso compound (31.4±0.4 mc./mol.), 145 mg.; the substrate, an equimolar mixture (6.28 g.) of anisole and benzene; nitrogen evolved, 54%				
	7.95	H	2.00	132 ±1	107
	5.96	2'-OCH_3	2.00	123 ±1	132
	23.98	3'-OCH_3	2.00	133 ±1	35.6
	39.94	4'-OCH_3	2.01	144 ±1	23.1
11	The nitroso compound (31.4±0.4 mc./mol.), 145 mg.; the substrate, an equimolar mixture (5.70 g.) of toluene and benzene; nitrogen evolved, 46%				
	6.00	H	2.01	47.7±0.7	51.1
	11.93	2'-CH_3	4.07	48.4±0.6	52.7
	29.97	3'-CH_3	2.03	78.5±1.0	17.0
	19.98	4'-CH_3	1.80	35.3±0.5	10.1
12	The nitroso compound (31.4±0.4 mc./mol.), 145 mg.; the substrate, an equimolar mixture (5.74 g.) of toluene and benzene; nitrogen evolved, 50%				
	7.95	H	2.00	75.9±1.0	60.9
	14.99	2'-CH_3	4.00	73.6±1.0	62.7
	19.98	3'-CH_3	2.00	63.0±0.9	20.2
	39.89	4'-CH_3	2.00	74.2±0.7	11.9

give two main distillates, b. p. 118~128°C/1 mmHg and b. p. 153°C/1 mmHg. The latter solidified to give 4-methoxy-4'-methylbiphenyl, m. p. 111°C (from methanol). The former was chromatographed on alumina in petroleum ether and distilled under reduced pressure to yield an oily material (b. p. 136~138°C/5 mmHg). The oil was heated with picoline hydrochloride at 220~230°C for 8 hr. After being cooled, the reaction mixture was poured into water, and the phenolic product was isolated and purified by chromatography on alumina in benzene to give 4-hydroxy-2'-methylbiphenyl (m. p. 80~81°C). The structure of this compound was evident from its preparation by the Ullmann reaction of *p*-iodoanisole and *o*-iodotoluene in the presence of copper powder at 200~220°C, followed by demethylation with picoline hydrochloride at 220~230°C for 8 hr. 4-Hydroxy-2'-methylbiphenyl

was methylated with dimethyl sulphate in aqueous alkali to afford 4-methoxy-2'-methylbiphenyl, b. p. 140~141.5°C/13 mmHg (Found: C, 85.06; H, 7.28. Calcd. for $C_{14}H_{14}O$: C, 84.81; H, 7.12%).

4-Methoxy-3'-methylbiphenyl was prepared by the Ullmann reaction from *p*-iodoanisole (110 g.) and *m*-iodotoluene (40 g.) and was purified by chromatography on alumina in petroleum ether (yield, 12 g.), m. p. 53~54°C (from methanol) (Found: C, 84.84; H, 7.21. Calcd. for $C_{14}H_{14}O$: C, 84.81; H, 7.12%).

Preparation of Labelled Compounds.—The preparations of *p*-nitroacet(anilide-^{14}C) and *p*-methoxyacet(anilide-^{14}C) from benzene-^{14}C have been described elsewhere[14,15]. The detailed procedure for nitrosation of these substituted acetanilide-^{14}C was analogous to that of *p*-chloro(^{36}Cl)acetanilide described in a previous paper[1]. Nitrosation of *p*-nitroacet(anilide-^{14}C) (specific activity, 61.2±0.5 mc./mol., 0.506 g.) with 7 ml. of a 10% solution of nitrosyl chloride in acetic anhydride in a mixture of acetic acid (5.2 ml.) and acetic anhydride (1.3 ml.) in the presence of fused potassium acetate (1.7 g.) and a trace of phosphorus pentoxide yielded 0.475 g. of *N*-nitroso-*p*-nitroacet(anilide-^{14}C). A mixture of *p*-methoxyacet(anilide-^{14}C) (specific activity, 27.4±0.2 mc./mol., 0.941 g.), fused potassium acetate (1.2 g.), acetic acid (4.5 ml.), acetic anhydride (1.1 ml.) and a trace of phosphorus pentoxide, treated with 4.5 g. of a similar solution of nitrosyl chloride, gave 0.992 g. of *N*-nitroso-*p*-methoxyacet(anilide-^{14}C).

Decomposition of Labelled *N*-Nitroso Compounds and Isotope Dilution Analysis. — The reaction was carried out in an equimolar binary or ternary mixture of aromatic solvents at 20.0°C in a manner similar to the *p*-chlorophenylation[1] (see Table III). The general procedure for the analysis of the products was analogous to that described in a previous paper[1]. The 4-methoxy-2'-methylbiphenyl recovered from the reaction mixture in the *p*-methoxyphenylation was demethylated by heating it with picoline hydrochloride to crystalline 4-hydroxy-2'-methylbiphenyl, which was then chromatographed on alumina in benzene, recrystallized from a mixture of benzene and petroleum ether, and assayed for carbon-14. 4,4'-Dinitrobiphenyl was purified by chromatography in acetone and by recrystallization from a mixture of ethanol and acetone. 3,4'-Dinitrobiphenyl, 4-methoxy-4'-nitrobiphenyl, and 4-methyl-4'-nitrobiphenyl were purified by chromatography in benzene and by recrystallization from ethanol. The other biaryls recovered were normally purified by chromatography on alumina in a mixture of benzene and petroleum ether and by recrystallization from methanol or ethanol. Carbon-14 determination was carried out as described in Part V[16]. The numerical results are summarized in Tables III and IV.

Summary

N-Nitroso-*p*-nitroacet(anilide-^{14}C) and *N*-nitroso-*p*-methoxyacet(anilide-^{14}C) have been decomposed at 20.0°C in mixtures of benzene and monosubstituted benzenes C_6H_5X (X=NO_2, Cl, OCH_3, and CH_3), and the reaction products have been analyzed for 4-nitro-and 4-methoxybiphenyl and isomeric 4-$NO_2C_6H_4C_6H_4X$ and 4-$CH_3OC_6H_4C_6H_4X$ by the isotope dilution method.

From the results of these competitive experiments, the partial rate factors for the *p*-nitrophenylation and *p*-methoxyphenylation have been calculated (Tables I and II).

The values of the partial rate factor for the meta position give a satisfactory Hammett plot with a slope of −0.81 for the *p*-nitrophenylation and one with a slope of +0.09 for the *p*-methoxyphenylation, showing that the *p*-nitrophenyl radical has a pronounced electrophilic character while the *p*-methoxyphenyl radical has little, if any, nucleophilic character.

Department of Chemistry
Faculty of Science
The University of Tokyo
Hongo, Tokyo

14) N. Morikawa, T. Migita and O. Simamura, *Radioisotopes (Tokyo)*, **10**, 236 (1961).
15) N. Morikawa, R. Itô, T. Migita, T. Tanno and O. Simamura, ibid., **8**, 246 (1959).
16) T. Inukai, K. Kobayashi and O. Simamura, This Bulletin, 35, 1576 (1962).

Influence of Substituent Groups on Nuclear Reactivity in the Formation of Substituted Biphenyls by Reaction of Aromatic Diazo and Related Compounds with Aromatic Liquids. VIII. Phenylation and p-Methylphenylation. The Separation of the Polar and the Conjugative Effect

By Ryôichi Itô, Toshihiko Migita, Naotake Morikawa and Osamu Simamura

(Received May 10, 1963)

The results of our study of the influence of some substituent groups, viz., the *p*-methoxy, *p*-chloro, and *p*-nitro group, in the attacking aryl radical on the homolytic arylation of monosubstituted benzenes have been reported in Parts III,[1] VI,[2] and VII[3]. The present paper deals with the phenylation and *p*-methylphenylation, in which *N*-nitrosoacet-(anilide-^{14}C) and *N*-nitroso-(*p*-methyl-^{14}C)-acetanilide have been used as the sources of the phenyl and the *p*-methylphenyl radical, and the arylated products have been analyzed by isotope dilution analysis. The partial rate factors and relative rates are listed in Tables I and II; the values for the phenylation obtained previously[4] by the same method are also included in Table I.

The tables show that all substituents in the aromatic substrate make the aromatic ring more reactive at the ortho and the para than at the meta position or at a nuclear position of benzene itself, and that they consequently direct the phenylation and *p*-methylphenylation preferentially to the ortho and para positions. This observation is in keeping with the already known results[5] concerning the orientation in the homolytic phenylation which were mainly obtained by the study of the decomposition of benzoyl peroxide, and it corroborates the view already adumbrated on the basis of the previous findings[2,3] that the invariable ortho-para orientation is characteristic of the homolytic aromatic arylation, irrespective of the nature of the attacking aryl radical.

As with the *p*-methoxyphenylation[3], the partial rate factors for the phenylation and *p*-methylphenylation of the meta position of aromatic compounds are all very close to unity. This fact suggests that the *p*-methylphenyl radical has little, if any, measure of polar character. Satisfactory Hammett plots are obtained for both the phenylation and *p*-methylphenylation, as shown in Fig. 1, between the logarithm of the partial rate factor for the meta position and the substituent constant, σ_m. The values for the Hammett reaction constant, ρ, together with those for *p*-nitro-[3], *p*-chloro-[2], and *p*-methoxy-phenylation[3], all obtained by the least squares method, are listed in Table III. The negative ρ values for the *p*-chloro- and *p*-nitro-phenylation indicate the electrophilic character of the *p*-chloro- and the *p*-nitrophenyl radical, as has already been discussed in Parts VI and VII. The polar character of these radicals is obviously attributable to the electron-withdrawing nature of their substitituent groups.

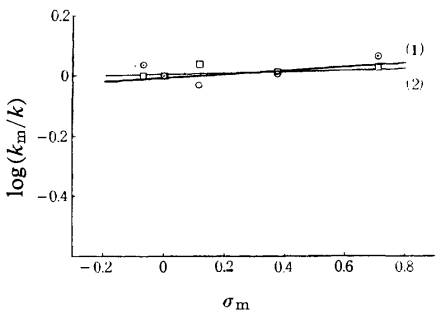

Fig. 1. The Hammett plots for the phenylation (1) and the *p*-methylphenylation (2).

The Hammett substituent constants, σ_p, which are shown in Table III for purposes of comparison, may be taken more or less to represent the electronic influence of the substituent groups in the aryl radicals upon the carbon atom on which the odd electron is located. Therefore, it is plausible to suppose that the σ_p value may show some correlation with the polar nature of arylation. In fact, in the *p*-nitro- and *p*-chloro-phenylation and in phenylation

1) O. Simamura and T. Migita, This Bulletin, **27**, 228 (1954).
2) T. Migita, N. Morikawa and O. Simamura, ibid., **36**, 980, (1963).
3) R. Itô, T. Migita, N. Morikawa, M. Ôkuni and O. Simamura, ibid., **36**, 985 (1963).
4) T. Inukai, K. Kobayashi and O. Simamura, ibid., **35**, 1576 (1962).
5) G. H. Williams, "Homolytic Aromatic Substitution," Pergamon Press, Oxford (1960).

TABLE I. PARTIAL RATE FACTORS AND RELATIVE RATES IN PHENYLATION OF MONOSUBSTITUTED BENZENES AT 20.0°C

Compound	Exp. No.	Partial rate factor			Relative rate
		k_o/k	k_m/k	k_p/k	k_X/k_H
$C_6H_5NO_2$	*	9.38	1.16	9.05	5.02
C_6H_5Cl	1	3.09	1.01	1.48	1.61
$C_6H_5OCH_3$	*	3.56	0.93	1.29	1.71
$C_6H_5CH_3$**	2	3.30	1.09	1.27	1.68

* Results by Inukai, Kobayashi and Simamura[4].

** Simamura and Inukai (This Bulletin, **28**, 445 (1955)) reported the partial rate factors of 3.7, 0.9 and 1.1 for the *o*-, *m*-, and *p*-position, as determined by infrared spectrophotometry.

TABLE II. PARTIAL RATE FACTORS AND RELATIVE RATES IN *p*-METHYLPHENYLATION OF MONOSUBSTITUTED BENZENES AT 20.0°C

Compound	Exp. No.	Partial rate factor			Relative rate
		k_o/k	k_m/k	k_p/k	k_X/k_H
$C_6H_5NO_2$	3	10.73	1.07	8.93	5.50
C_6H_5Cl	3	3.10	1.04	1.16	1.57
$C_6H_5OCH_3$	4	3.69	1.09	1.52	1.85
$C_6H_5CH_3$	5	3.27	1.00	1.33	1.65

TABLE III. POLAR NATURE OF ARYL RADICALS IN ARYLATION

Aryl radical	Hammett's reaction constant, ρ	Substituent constant		
		σ_p	σ_p^n	σ_p^o
p-Nitrophenyl	−0.81	0.778	0.78	0.73
p-Chlorophenyl	−0.27	0.227	0.24	0.27
Phenyl	0.05	0	0	0
p-Methylphenyl	0.03	−0.170	−0.13	−0.15
p-Methoxyphenyl	0.09	−0.268	−0.11	−0.16

the numerical magnitudes of ρ and σ_p approximately coincide with each other. Although no theoretical significance can be attached to this numerical coincidence, if this correlation should hold throughout the entire range of σ_p values, it would predict much larger ρ values for the *p*-methyl- and *p*-methoxy-phenylation than have actually been found. In fact, the values for these arylations are practically indistinguishable from that for the phenylation. If, for purposes of comparison, we take σ_p^n [6] or σ_p^o [7] as a measure of the polar influence of a substituent, the parallelism becomes much better. This fact evidently indicates that the influence on the arylation reaction exerted by a substituent group in the attacking radical is purely inductive in nature, since both σ_p^n and σ_p^o are thought to represent the inductive polar effect for the para-substituted phenyl group, including the conjugative interaction between the substituent and the benzene ring. This view seems quite reasonable in view of the nature of the orbital occupied by the odd electron, for that orbital does not allow the electron to conjugate with the π-elctronic system of the substituted phenyl group.

The value of ρ should be dependent, at least partly, on the reactivity of the attacking radical as well; the more reactive an attacking radical is, the more difficult it is for this radical to discriminate differently substituted substrates, and, consequently, the lower will be the absolute value of ρ. Such an effect ought to be observed in the arylations by substituted phenyl radicals, which simple molecular orbital calculations have shown to be more reactive than the phenyl radical itself. This effect, however, does not seem important in view of the simple correlation between the ρ value and the inductive substituent constant.

No simple correlation can be found of the effect of the polar substituent in the substrate on the partial rate factors of the para and

6) H. van Bekkum, P. E. Verkade and B. M. Wepster, *Rec. trav. chim.*, **78**, 815 (1959).

7) R. W. Taft, *J. Phys. Chem.*, **64**, 1805 (1960).

Table IV. Conjugative effect of a substituent group in the substrate, τ_p

Arylation	Substrate			
	$C_6H_5NO_2$	C_6H_5Cl	C_6H_5OMe	C_6H_5Me
p-Nitrophenylation	0.81	0.19	0.14	0.04
p-Chlorophenylation	1.00	0.19	0.12	0.07
Phenylation	0.92	0.16	0.12	0.11
p-Methylphenylation	0.93	0.06	0.19	0.13
p-Methoxyphenylation	0.85	0.22	0.14	0.09
Mean	0.90	0.16	0.14	0.09

Table V. Estimation of the conjugative effect in the homolytic arylation

X	Extra resonance energy[a]			
	C_6H_5X (I)	ArC_6H_5X (II)	Diff.	τ_p[c]
CH_3	0.24[b]	0.26	0.02	0.09
Cl	0.26[b]	0.29	0.03	0.16
OH	0.32[b]	0.37	0.05	0.14 (CH_3O)
NO_2 $\delta=-0.5$	0.29	0.48	0.19	0.90
NO_2 $\delta=-0.2$	0.35	1.01	0.66	

a) In terms of the usual resonance integral value.
b) See Ref. 11.
c) See Table IV.

ortho position, since the conjugative effect of the substituent is overwhelming at these positions. In fact, the Hammett relation does not hold for the para position. For this position, however, the following equation has now been found to give a very noteworthy correlation with regard to the effect of the substituent:

$$\log (k_p/k) = \rho\sigma_p + \tau_p \qquad (1)$$

where k_p/k is the partial rate factor of the para position of a substituted benzene in an arylation; ρ, the Hammett reaction constant for this arylation as determined from the Hammett plot of the partial rate factors of the meta position; and σ_p, the Hammett substituent constant for the para position. As shown in Table IV, the value for τ_p may be regarded as tolerably constant for each substituted benzene irrespective of the nature of the attacking radical and decreases in the order: $NO_2 \gg Cl$, $MeO > Me$. Since the term $\rho\sigma_p$ obviously represents the polar effect consisting of the inductive and the conjugative or electromeric response in the presence of a polar attacking radical, τ_p may be considered to represent that part of the conjugative effect of the substituent which is independent of the polar nature of the attacking radical. It is therefore natural that τ_p should have been found to be a constant quantity characteristic of the nature of the substituent group, in so far as such a treatment, in which the substituent effect is divided into several independent components, is valid[8]. Thus, τ_p or, expressed in energy term, $2.30 \times RT\tau_p$ may be identified with the difference in extra resonance energy, that is, the additional stabilization due to the conjugation of the substituent group with the π-electronic system, between the transition state and the initial state. The value of 0.90 found for τ_p for the nitro group corresponds to 1.2 kcal./mol. Since the extra resonance energy in nitrobenzene is estimated at 8.5 kcal./mol.[9], that in the transition state will be 9.7 kcal./mol.

Although the exact structure of the transition state is unknown, we may identify it with the structure of the phenylcyclohexadienyl radical[10] (II). The odd electron occupies its non-bonding molecular orbital, and the presence of a substituent group in the radical may be thought to cause the perturbational lowering of the energy of the system. This effect will be greatest for the nitro group, with its comparatively low-lying vacant orbital, resulting in its having the greatest extra resonance energy, in accordance with the observed sequence of the conjugative effect, whereas such an effect becomes much less important for the substituents: chlorine, methoxy and

8) Such division of the electronic effect of a substituent into independent contributions from the inductive and the conjugative effect has first been suggested by Branch and Calvin ("The Theory of Organic Chemistry", Prentice-Hall, Inc., New York (1941), p. 193) for the effect on acid strength and has extensively been applied by Taft ("Steric Effects in Organic Chemistry," Ed. by M. S. Newman, John Wiley & Sons, Inc., New York (1956), p. 577; *J. Am. Chem. Soc.*, **80**, 2436 (1958)) to the consideration of the substituent effect in reaction rates as well.

9) The authors are indebted to Prof. S. Nagakura for this value.

10) Ref. 5, p. 17.

methyl, since these groups are able to contribute only a filled orbital for conjugation. This view is supported by the following consideration based upon the molecular orbital theory. The extra resonance energies in substituted bezenes have been evaluated by Matsen[11] by means of a perturbational treatment with simple molecular orbitals, and those for substituted cyclohexadienyls have now been estimated by the same method as in Matsen's treatment. The results are shown in Table V, which also includes the values similarly calculated for the nitro group, it being assumed that the perturbing vacant molecular orbital of the nitro group has the energy $\alpha+\delta\beta$ ($\delta=-0.5$ or -0.2)[12], and that the coefficient of the atomic orbital of the nitrogen atom constituting the molecular orbital is $1/\sqrt{2}$. The trend seen in the differences in the calculated extra resonance energy between the substrate and the substituted cyclohexadienyl radical shown in the fourth column is in satisfactory agreement with that in the τ_p values, considering the approximate nature of this molecular orbital method.

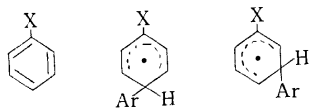

(I) (II) (III)

In this connection, it is to be noted that the extra resonance energies of the substituted cyclohexadienyl radicals (III) simulating the transition state of the arylation at the meta position are calculated to be the same as those in the corresponding substrates (Table V, column 2), except for the case of the nitro group. Even in this case, however, the discrepancy is not serious, being 0.01 and 0.02 for $\delta=-0.5$ and -0.2, respectively. This result is very gratifying, since it means that the conjugative effect is nil for every substituent in accordance with the fact that the Hammett relation has been found to hold for the partial rate factors at the meta position.

Since the polar and the conjugative effect are separately taken into account above, the use of a substituent constant, such as σ_I[13], σ_p^o, or σ_p^n, which measures only the inductive effect, instead of σ_p, might seem more appropriate. The substitution of σ_I in Eq. 1, however, gives too large a value of τ_p for the nitrophenylation of chlorobenzene and anisole, and the use of σ_p^o or σ_p^n gives, although very slightly, too large a value of τ_p again for the nitrophenylation of chlorobenzene and anisole. On the other hand, Brown and Okamoto's σ^+ values[14] give negative values of τ_p for the nitrophenylation of anisole and toluene, indicating that in the *p*-nitrophenylation the electromeric electron-demand at the reaction centre is not so strong as to justify the use of σ^+. The fact that Hammett's σ_p gives the best constancy in τ_p values for each substituted benzene undoubtedly shows that the electromeric electron-demand at the reaction centre, even by an electrophilic radical such as *p*-nitrophenyl, is of so small a magnitude that the use of σ_p is suitable.

Experimental

Melting points are uncorrected.

Solvents.—Nitrobenzene, chlorobenzene, anisole, toluene and benzene were purified as described in Part VI[2].

Substituted Biphenyls Used as Carriers in Isotope Dilution Analysis.—2- and 3-Chlorobiphenyl were prepared according to Elks, Haworth and Hey's method[15] and were purified by chromatography on alumina in petroleum ether followed by recrystallization from methanol, m. p. 35°C and 19°C, respectively.

4-Chlorobiphenyl was prepared and purified as described in Part VI[2].

2- and 3-Methylbiphenyl were prepared by reaction of cyclohexanone with *o*- and *m*-tolylmagnesium bromide followed by dehydration and dehydrogenation, analogously to Hey and Jackson's preparation[16] of 3,4'-bitolyl, but with the use of twice the amount of sulphur in the dehydrogenation; they were then purified by repeated fractional distillations under reduced pressure. The boiling points are: 2-CH_3-, 126°C/13 mmHg (Found: C, 93.02; H, 7.12. Calcd. for $C_{13}H_{12}$: C, 92.81; H, 7.19%); 3-CH_3-, 135~136°C/13 mmHg (Found: C, 92.67; H, 7.21. Calcd. for $C_{13}H_{12}$: C, 92.81; H, 7.19%).

4-Methylbiphenyl was prepared by reaction of *N*-nitroso-*p*-acetotoluidide[17] with benzene and was recrystallized from methanol, m. p. 50.5°C.

4-Methyl-2'-nitrobiphenyl was prepared by reaction of *N*-nitroso-*p*-acetotoluidide[17] with nitrobenzene. After removal of the nitrobenzene, the residue was distilled with superheated steam and the distillate was fractionated by chromatography on alumina in petroleum ether-benzene (4:1) into an oily material and 4-methyl-4'-nitrobiphenyl, m. p. 140°C. The oil was fractionated under reduced pressure, and the distillate (b. p. 190~195°C/17 mmHg) was further purified by chromatography similar to the above to give 4-methyl-2'-nitrobiphenyl, m. p. 37~37.5°C (from methanol).

11) F. A. Matsen, *J. Am. Chem. Soc.*, **72**, 5243 (1950).
12) The energy of the vacant orbital of the nitro group may be estimated to be $\alpha-0.15\beta$ ($\beta=-3$ eV.) from the energy level values quoted by Nagakura and Tanaka (*J. Chem. Phys.*, **22**, 236 (1954)) for the nitro group in nitromethane.
13) R. W. Taft and I. C. Lewis, *J. Am. Chem. Soc.*, **80**, 2436 (1958).
14) H. C. Brown and Y. Okamoto, ibid., **79**, 1913 (1957).
15) J. Elks, J. W. Haworth and D. H. Hey, *J. Chem. Soc.*, **1940**, 1284.
16) D. H. Hey and E. R. B. Jackson, ibid., **1934**, 645.
17) W. S. M. Grieve and D. H. Hey, ibid., **1935**, 689.

Table VI. Decomposition of *N*-nitrosoacet(anilide-^{14}C) at 20.0°C and results of isotope dilution analyses of the products

Exp. No.	Ratio of the portion taken to the total reaction mixture $f\times10^2$	Carrier added $C_6H_5C_6H_4X$ X	*M*, mmol.	Specific activity of biaryl μc./mol.	Amount of biaryl formed μmol.
1	The nitroso compound, 42.1±0.6 mc./mol., 82.5 mg.; the substrate, an equimolar mixture (4.32 g.) of chlorobenzene and benzene; nitrogen evolved 86%				
	7.58	H	4.09	69.8±0.7	89.7
	7.38	2-Cl	3.26	88.0±0.9	92.5
	38.45	3-Cl	7.02	69.2±0.7	30.1
	38.37	4-Cl	3.07	116.3±1.2	22.1
2	The nitroso compound, 42.1±0.6 mc./mol., 82.0 mg; the substrate, an equimolar mixture (3.84 g.) of toluene and benzene				
	8.18	H	2.34	56.2±0.8	38.3
	8.27	2-CH_3	2.47	59.2±0.8	42.1
	23.47	3-CH_3	2.39	57.4±0.8	14.0
	39.97	4-CH_3	1.96	69.2±0.9	8.1

Table VII. Decomposition of *N*-nitroso-(*p*-methyl-^{14}C)-acetanilide at 20.0°C and results of isotope dilution analyses of the products

Exp. No.	Ratio of the portion taken to the total reaction mixture $f\times10^2$	Carrier added 4-$CH_3C_6H_4C_6H_4X$ X	*M*, mmol.	Specific activity of biaryl μc./mol.	Amount of biaryl formed μmol.
3	The nitroso compound, 185.8±1.8 mc./mol., 81.2 mg.; the substrate, an equimolar mixture (4.29 g.) of nitrobenzene, chlorobenzene, and benzene; nitrogen evolved, 55%				
	7.96	H	2.01	226±2	30.7
	3.98	2′-NO_2	4.06	200±2	110
	19.82	3′-NO_2	2.00	202±2	11.0
	3.97	4′-NO_2	2.01	168±2	45.8
	7.93	2′-Cl	4.00	117±2	31.8
	19.88	3′-Cl	2.01	196±3	10.7
	16.92	4′-Cl	2.13	104±1	6.0
4	The nitroso compound, 185.8±1.8 mc./mol., 61.0 mg.; the substrate, an equimolar mixture (3.04 g.) of anisole and benzene; nitrogen evolved, 77%				
	29.81	H	5.98	533±4	57.7
	5.90	2′-OCH_3	2.02	384±3	70.9
	19.87	3′-OCH_3	2.01	384±3	20.9
	23.85	4′-OCH_3	1.46	443±4	14.6
5	The nitroso compound, 185.8±1.8 mc./mol., 63.3 mg.; the substrate, an equimolar mixture (2.75 g.) of toluene and benzene; nitrogen evolved, 82%				
	11.07	H	4.64	151±1	34.1
	11.13	2′-CH_3	12.04	64±1	37.3
	33.30	3′-CH_3	6.04	116±1	11.3
	18.50	4′-CH_3	2.01	129±1	8.7

4-Methyl-3′-nitrobiphenyl was prepared according to Hey, Nechvatal and Robinson's method with some modification. Reduction of 4-methyl-4′-nitrobiphenyl (10 g.) with activated iron and water in benzene[18] followed by acetylation with acetic anhydride gave 4-acetamino-4′-methylbiphenyl (7.5 g.), m. p. 221°C. Into a mixture of this compound (1 g.), acetic acid (15 ml.) and concentrated sulphuric acid (1.6 ml.) maintained at 10°C, fuming nitric acid (d, 1.52; 0.25 g.) was gradually stirred. After 15 min., the mixture was poured into water to yield the 3-nitrated product (m. p. 164°C; 0.7 g.). The procedure for hydrolysis and deamination was the same as that described by Hey, Nechvatal and Robinson[19]. The final product was purified by recrystallization from methanol, m. p. 77.7°C.

The preparation of 4-methyl-4′-nitrobiphenyl was described in Part VII[3].

18) S. E. Hazlet and C. A. Dornfeld, *J. Am. Chem. Soc.*, **66**, 1781 (1944).

19) D. H. Hey, A. Nechvatal and T. S. Robinson, *J. Chem. Soc.*, **1951**, 2892.

2-Chloro-4'-methylbiphenyl was prepared as follows: (a) *N*-Nitroso-*p*-acetotoluidide[17] (157 g.) was allowed to decompose in chlorobenzene (3 l.). The product was isolated from the reaction mixture and fractionated by chromatography on alumina in petroleum ether, giving an oily material and a small amount of 4-chloro-4'-methylbiphenyl, m. p. 124°C. The oil was purified by repeating similar chromatography and distillation under reduced pressure to afford 22 g. of 2-chloro-4'-methylbiphenyl, b. p. 120~123°C/2 mmHg. (b) A mixture of *p*-iodotoluene (110 g.), *o*-iodochlorobenzene (40 g.), copper powder (150 g.), and clean sand (150 g.) was heated 6 hr. at 200~210°C. The reaction mixture was extracted with petroleum ether, and on removal of the solvent from the extract, the residue deposited crystals of 4,4'-bitolyl, which were then filtered off. The filtrate was purified in the same way as described under heading (a), b, p. 112~115°C/1 mmHg (yield, 7 g.). The specimens obtained by both method (a) and method (b) showed the same infrared spectrum (Found: Cl, 17.44. Calcd. for $C_{13}H_{11}Cl$: Cl, 17.48%).

Similarly, 3-chloro-4'-methylbiphenyl was prepared by the Ullmann reaction, m. p. 44~45°C (Found: Cl, 17.36. Calcd. for $C_{13}H_{11}Cl$: Cl, 17.48%).

The preparation of 4-chloro-4'-methylbiphenyl was described in Part VI[2].

2- and 3-Methoxy-4'-methylbiphenyl were prepared by the Ullmann reaction of *o*- and *m*-iodoanisole with *p*-iodotoluene. The experimental procedure was analogous to that mentioned above. Recrystallization of the crude products from methanol yielded the 2-isomer, m. p. 83°C (Found: C, 84.84; H, 7.17. Calcd. for $C_{14}H_{14}O$: C, 84.81; H, 7.12%) and the 3-isomer, m. p. 80°C. (Found: C, 84.72; H, 7.20. Calcd. for $C_{14}H_{14}O$: C, 84.81; H, 7.12%).

The preparation of 4-methoxy-4'-methylbiphenyl was described in part VII[3].

2,4'- and 3,4'-Bitolyl were prepared from 4-methylcyclohexanone and *o*- and *m*-bromotoluene according to Hey and Jackson's method[16] with some modification. The products were purified by repeated distillation under reduced pressure. The boilng points are: 2,4'-$(CH_3)_2$-, 149°C/20 mmHg (Found: C, 92.22; H, 7.87. Calcd. for $C_{14}H_{14}$: C, 92.26; H, 7.74%); 3,4'-$(CH_3)_2$-, 161~162°C/20 mmHg (Found: C, 92.22; H, 7.80. Calcd. for $C_{14}H_{14}$: C, 92.26; H, 7.74%), and the latter melts at 15°C.

4,4'-Bitolyl was prepared by the Ullmann reaction of *p*-iodotoluene and recrystallized from ethanol, m. p. 125°C.

Preparation of Labelled Compounds.—*N*-Nitroso-acet(anilide-^{14}C) (specific activity, 42.1±0.6 mc./mol.) was prepared by a method described elsewhere[20].

(*p*-Methyl-^{14}C)acetanilide was prepared from labelled toluene by acetylation and oximation followed by the Beckmann rearrangement. The detailed experimental procedure is described elsewhere[21].

N-Nitroso-(*p*-methyl-^{14}C)acetanilide was prepared by nitrosating (*p*-methyl-^{14}C)acetanilide (specific activity, 185.8±1.8 mc./mol.; 238 mg.) with nitrosyl chloride (2.6 ml. of a 10% solution in acetic anhydride) in a mixture of acetic acid (2.4 ml.) and acetic anhydride (0.6 ml.) in the presence of fused potassium acetate (0.67 g.) and a trace of phosphorus pentoxide according to the usual method (yield, 180 mg.).

Decomposition of Labelled *N*-Nitroso Compounds and Isotope Dilution Analyses. — The reactions were carried out in an equimolar binary or ternary mixture of aromatic solvents at 20.0°C (see Tables VI and VII); the general procedure for the analysis of the products was analogous to that described in previous papers, but the original reaction mixtures were diluted with acetone instead of benzene. The results of the isotope dilution analyses are summarized in Tables VI and VII.

Labelled biaryls recovered from the reaction mixtures were purified normally by recrystallization from methanol or ethanol until a constant specific activity was reached. The carbon-14 assay is described in Part V[4]. Biphenyl was recrystallized from methanol and finally sublimed. Since the following biaryls were difficult to purify enough for a correct carbon-14 assay, they were converted into suitable derivatives, which can be readily purified to afford specimens pure enough for the radioactivity measurement.

3-Chlorobiphenyl was nitrated by the method described in Part VII[3] to give 3-chloro-4'-nitrobiphenyl, which was purified by repeated recrystallization from methanol.

2- and 3-Methylbiphenyl and 2-chloro- and 2-nitro-4'-methylbiphenyl were converted, by oxidation with potassium permanganate in pyridine by a method similar to Dauben and Tanabe's method[22], into biphenyl-2-carboxylic acid, m. p. 110~111°C, biphenyl-3-carboxylic acid[23], m. p. 160°C, 2-chlorobiphenyl-4'-carboxylic acid, m. p. 247°C (Found: C, 66.95; H, 4.04; Cl, 15.44. Calcd. for $C_{13}H_9ClO_2$: C, 67.11; H, 3.90; Cl, 15.24%), and 2-nitrobiphenyl-4'-carboxylic acid, m. p. 251°C (Found: C, 64.30; H, 3.88; N, 5.92. Calcd. for $C_{13}H_9NO_4$: C, 64.20; H, 3.73; N, 5.76%), respectively. These acids were purified by recrystallizations from ethanol.

In experiments 4 and 5, the 4-methylbiphenyl recovered was nitrated by Grieve and Hey's method[24] to give 4-methyl-4'-nitrobiphenyl, which was then purified by recrystallization from methanol.

Similar nitration of the 2,4'-bitolyl recovered followed by reduction with hydrogen and a Raney nickel catalyst (W-7)[25] in ethanol and acetylation of the resulting amine with acetic anhydride gave monoacetamino-2,4'-bitolyl (Found: N, 6.02. Calcd. for $C_{16}H_{17}NO$: N, 5.85%), m. p. 166°C (from methanol). Similarly, the 3,4'-bitolyl recovered was converted into 4-acetamino-3,4'-bitolyl, m. p. 221°C (from ethanol).

20) H. Kōyama, N. Morikawa and G. Tsuchihashi, *Radioisotopes (Tokyo)*, 11, 107 (1962).
21) N. Morikawa, R. Itô, T. Migita, T. Tanno and O. Simamura, ibid., 8, 246 (1959).
22) W. G. Dauben and M. Tanabe, *J. Am. Chem. Soc.*, 75, 4969 (1953).
23) P. Jacobson, *Ber.*, 28, 2541 (1895).
24) S. M. Grieve and D. H. Hey, *J. Chem. Soc.*, 1932, 1888.
25) "Organic Syntheses", Col. Vol. III (1955), p. 176.

Summary

N-Nitrosoacet(anilide-^{14}C) and *N*-nitroso-(*p*-methyl-^{14}C)acetanilide have been decomposed at 20.0°C in mixtures of benzene and monosubstituted benzenes, and the reaction products have been analyzed for biphenyl and substituted biphenyls by the isotope dilution method. From the results of these competitive experiments, the partial rate factors for the phenylation and *p*-methylphenylation have been calculated (Tables I and II).

The values of the partial rate factor for the meta position give a satisfactory Hammett plot with a slope of +0.05 for the phenylation and one with a slope of +0.03 for the *p*-methylphenylation, suggesting that the *p*-methylphenyl radical has little, if any, measure of polar character.

The correlation of the ρ values for various arylations with the inductive constant for the substituent group on the arylating radical indicates that the effect of the substituent group in the radical is purely inductive in nature.

The partial rate factor for the para position, k_p/k, is found to be related to Hammett's substituent constant by the following equation:

$$\log(k_p/k) = \rho\sigma_p + \tau_p$$

where ρ is the Hammett reaction constant for this arylation as determined from the Hammett plot of the partial rate factors of the meta position. τ_p is found to be tolerably constant for each substituted benzene, irrespective of the nature of the attacking aryl radical, and represents that part of the conjugative effect of the substituent which is independent of the polar nature of the attacking radical.

Molecular orbital calculations have given results which rationalize the trend found in the τ_p values.

Department of Chemistry
Faculty of Science
The University of Tokyo
Hongo, Tokyo

The Photochemical Decomposition of α, α-Diphenyl-β-picrylhydrazyl (DPPH) in Solution. II. Products of the Photolysis and Its Reaction Mechanism

By Atuo SUZUKI*, Makoto TAKAHASI and Kengo SHIOMI

(Received March 27, 1963)

In the preceding paper of this series, the kinetic investigation of the photochemical decomposition of DPPH in solution was reported, and there was proposed a reaction mechanism which is compatible with the results of the kinetic experiments[1]. In order to obtain further detailed information on the decomposition mechanism, the reaction products were also investigated. In paper chromatographical analysis, the R_f values of the reaction products were determined; two of the products were found to be identical with those of α, α-diphenyl-β-picrylhydrazine (I) and α-phenyl-α-(*p*-nitrophenyl)-β-picrylhydrazine (II) respectively[2]. Further, by modifying the method of the photolysis, it became possible to obtain a large amount of the reaction products and to separate the reaction products in a relatively large amount on a cellulose column. Thus, two species of the reaction products were identified unequivocally as α, α-diphenyl-β-picrylhydrazine, and α-phenyl-α-(*p*-nitrophenyl)-β-picrylhydrazine by comparison with authentic specimens prepared by a different method.

The third component in the reaction products (III) (an experimental formula $C_{18}H_{10-11}\cdot N_3O_3$) has not yet been identified with any known compound, although a phenazine-type structure is presumed for it. On the basis of its structure and the previous kinetic results, however, it is presumed that this compound originates from excited DPPH; therefore, a reaction mechanism which involves the nitration of DPPH by the excited DPPH is herein proposed, a mechanism which is compatible with the findings of the previous kinetic experiment.

* Present address: Central Reaserch Institute, Teijin Limited, Hirayama, Hinomachi, Minamitama-gun, Tokyo.

1) Part I, This Bulletin, **36**, 644 (1963).

2) Until recently this compound was believed to be α, α-diphenyl-β-hydroxy-β-picrylhydrazine, but it has recently been demonstrated to be α-phenyl-α-(*p*-nitrophenyl)-β-picrylhydrazine by J. A. Weil, K. V. Sane and J. M. Kinkade, *J. Phys. Chem.*, **65**, 710 (1961).

Results and Discussion

Separation and Identification of the Reaction Products.—*Separation of the Products by Paper Chromatography.*—As a preliminary investigation, the reaction products were chromatographed on a filter paper. Porier[3] has described the separation of various hydrazyl derivatives by paper chromatography using several eluting solvents. In the present case, however, it was found that the most suitable solvent was a mixture of petroleum ether and carbon disulfide (1 : 1 by volume). The R_f values of the reaction products in the presence or absence of air shown in Tables Ia and Ib, which demonstrate that I and II have the same R_f values as those of α,α-diphenyl-β-picrylhydrazine and α-phenyl-α-(p-nitrophenyl)-β-picrylhydrazine respectively.

Table Ia. R_f-Values of reaction products
Decomposition was carried out at 25°C

Solvent	Condition of irradiation	Fraction A	B	C
Benzene	Air present	0.83	0.28	0.04
	Air absent	0.82	0.29	0.04
CCl_4	Air present	0.83	0.29	0.04
	Air absent	0.84	0.27	0.04

Table Ib. R_f-Values of reference substances

	I	II	DPPH
R_f-Value	0.83	0.27	0.84

I: α,α-Diphenyl-β-picrylhydrazine
II: α-Phenyl-α-(p-nitrophenyl)-β-picrylhydrazine

Isolation of the Reaction Products on a Cellulose Column.—Though the separation of the reaction products by paper chromatography is very convenient for the separation of a small amount of the products, it is necessary to obtain a large amount of the products in order to determine the structure of the product III. As a source of light for photolysis, sun-light was substituted for a tungsten lamp in order to complete the photolysis in a short time, and a cellulose column was used to separate a relatively large amount of the reaction products. Benzene was used as a solvent instead of carbon tetrachloride, since the reaction products by sun-light are found to be identical with those obtained under the controlled conditions described in the preceding paper. Three components are isolated on a cellulose column from the reaction products of DPPH, and I and II are confirmed unequivocally to be α,α-diphenyl-β-picrylhydrazine and α-phenyl-α-(p-nitrophenyl)-β-picrylhydrazine respectively by infrared spectra and by mixed melting point determinations with the authentic specimens. The structure of III will be discussed in detail later.

The Determination of the Ratios of the Reaction Products.—The method of the separation of the products on a cellulose column described above was also applied in the quantitative estimation of the reaction products. Known amounts of I, II and III were mixed and fractionated on a cellulose column, and the amount of the eluted products was determined by photometry. The visible and ultraviolet absorption spectra of DPPH, I, II and III are shown in Fig. 1, while the results of the quantitative determination of the reaction products are shown in Table II.

Table II. Fractionation of the three components on a powdered cellulose column

Eluting solvent	Petroleum ether+CS_2 (2 : 1)	Petroleum ether+CS_2 (1 : 1)	Benzene
Product	DPPH+I	II	III
Recovery (%)	99 104	103	98

I: α,α-Diphenyl-β-picrylhydrazine
II: α-Phenyl-α-(p-nitrophenyl)-β-picrylhydrazine
III: $(C_{18}H_{10-11}N_3O_3)_n$

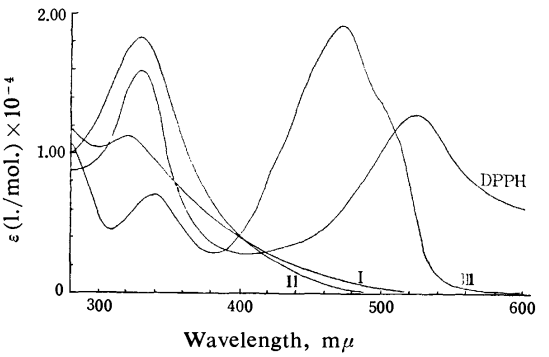

Fig. 1. Visible and ultraviolet absorption spectra of DPPH, α,α-diphenyl-β-picrylhydrazine (I), α-phenyl-α-(p-nitrophenyl)-β-picrylhydrazine (II), and unknown compound (III). ε of III is given by assuming its M.W. = 317.

The table shows that the method is satisfactory for the present purposes. The recovery of more than one hundred per cent of I and II might be due to errors in photometry caused by some impurities coming from the cellulose, which could not be completely removed even by extracting the adsorbent several times with benzene before its use.

Figure 2 gives the ratios of the reaction

3) R. H. Porier, E. J. Kahler and F. Benington, *J. Org. Chem.*, 17, 1437 (1952).

products in a benzene solution after various periods of the reaction time. Since the ratios of I, II and III do not vary markedly in the course of the decomposition, as is shown in Fig. 2, it may be concluded that no one of these three products is a precursor of the other. The total material balance at the final stage of the reaction may be approximated by saying that four moles of DPPH give approximately one mole of I (slightly more than one mole actually), two moles of II, and one mole of III (really slightly less than one mole). In a carbon tetrachloride solution, similar results were obtained, as is shown in Table III.

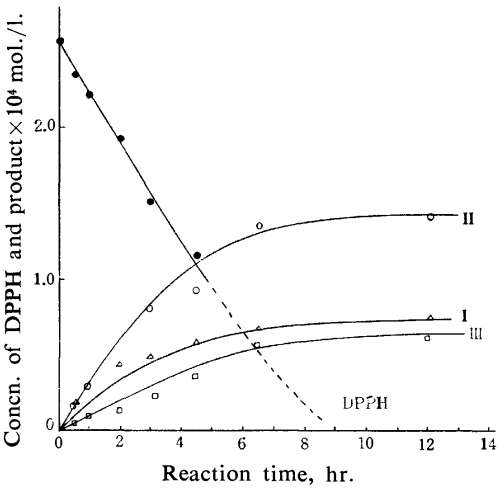

Fig. 2. Concentration-time curves of DPPH products in benzene solution.
I: α,α-Diphenyl-β-picrylhydrazine
II: α-Phenyl-α-(*p*-nitrophenyl)-β-picryl-hydrazine
III: Unknown compound

Investigation of the Structure of III.—*Physical Properties and Molecular Weight.*—The crude substance of III, which was isolated from the decomposition products of DPPH, gives orange-red needles when sublimed at a temperature between 230~250°C. It does not show a clear melting point, but decomposes gradually when heated above 280°C. In ordinary solvents it is sparingly soluble, but it is soluble in concentrated sulfuric acid or hydrochloric acid to give an orange solution without decomposition, indicating that it has basic property. Elemental analysis shows the chemical composition of $(C_{18}H_{10-11}N_3O_3)_n$. The determination of the molecular weight of III was attempted by various methods: the ebullioscopic method in dimethylformamide, the Rast method in camphor or camphor quinone, and the isothermal distillation method, but they produced no appreciable change in either boiling point or melting point within the possible upper limit of concentration, which is unfortunately very small in the available solvents, but the authors could nevertheless conclude that *n* should be more than three.

The Ultraviolet and Infrared Spectra of III.—The ultraviolet spectrum of III indicates a maximum absorption at $\lambda=470$ mμ, and it is

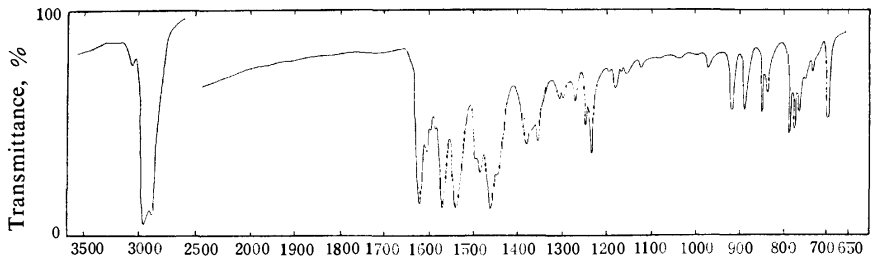

Fig. 3a.

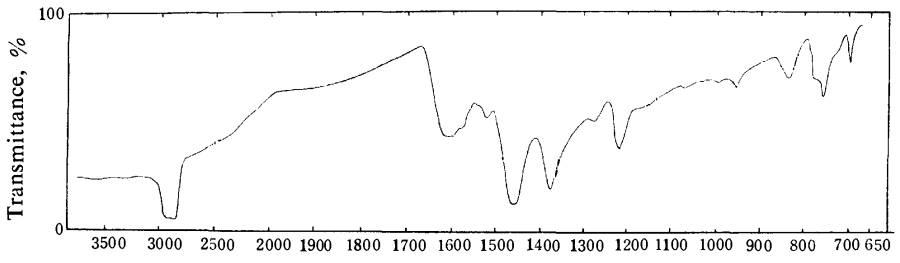

Fig. 3b.

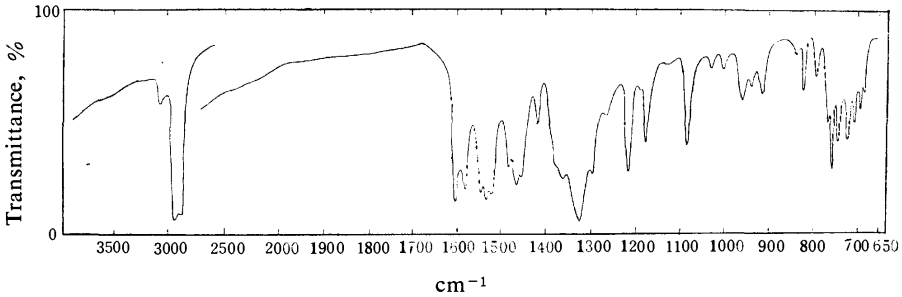

Fig. 3c.

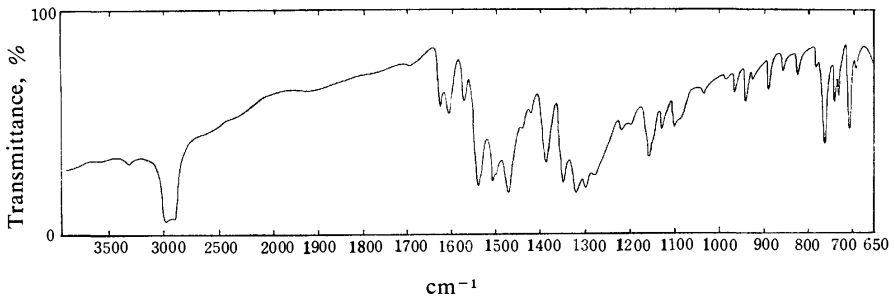

Fig. 3d.

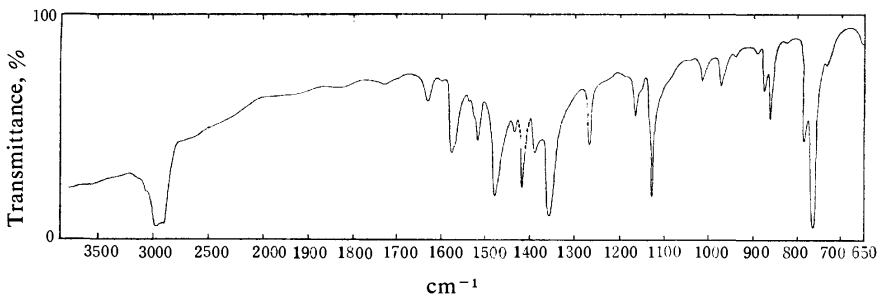

Fig. 3e.

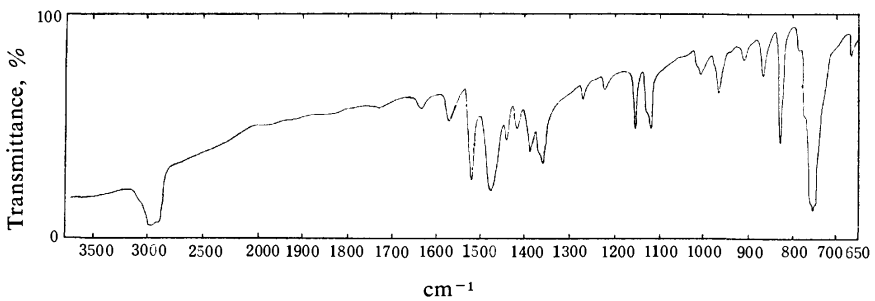

Fig. 3f.

Fig. 3. Infrared absorption spectra of (a) ; III, (b) ; III+HI, (c) : α,α-diphenyl-β-picrylhydrazine, (d) ; 10-phenyl-1,3-dinitro-9,10-dihydrophenazine, (e) ; *N*-oxyphenazine and (f) ; phenazine (in Nujol).

TABLE III. AMOUNT OF THE REACTION PRODUCTS AT THE FINAL STAGE OF THE DECOMPOSITION IN mol./l.$\times 10^5$

Solvent	React. temp. °C	React. time hr.	Initial amount of DPPH*	Amount of products*				Total yield
				I	II	III	I+II+III	$\frac{\text{I+II+III}}{\text{DPPH}}\times 100$
Benzene	25	12	26.0	7.5	14.1	6.2	27.8	107
Benzene	45	12	26.0	7.7	13.2	6.3	27.2	105
CCl_4	25	17	27.7	8.1	14.3	6.0	28.4	103

* Concentration : mol./l.$\times 10^5$

to be noted that the maximum is located at longer wavelengths than those of I and II, suggesting that III has a larger conjugate system than I and II.

The infrared absorption spectrum of III, along with those of II, 10-phenyl-1, 3-diniro-9, 10-dihydrophenazine, phenazine and phenazine oxide as reference substances, are shown in Fig. 3.

No characteristic bands corresponding to the stretching vibration of N–H or O–H are observed in the 3000~3500 cm^{-1} region of the spectrum of III. The absorption bands at 1535 cm^{-1} and 1300 cm^{-1} are assigned to the nitro group. A band at 1235 cm^{-1} is difficult to assign to a unique vibration, but it might originate from the asymmetrical stretching vibration of the ether-type bond R–O–R if the supposed structure of III is accepted. α, α-Diphenyl-β-picrylhydrazine, 10-phenyl-1, 3-dinitro-9, 10-dihydrophenazine, and III have a strong band at 695 cm^{-1} in common, a band which is assigned to an out-of-plane bending vibration of the aromatic C–H of mono-substituted benzene. In mono-substituted benzene, we should expect another absorption band near 750 cm^{-1}; Fig. 3a shows two bands at 755 and 767.5 cm^{-1}, but it is not certain which of the two bands is to be assigned to this bending vibration. Figure 3a also shows bands at 835, 845, 882.5 and 915 cm^{-1}, indicating the presence of poly-substituted benzene nuclei in III.

The Reduction of III with Stannous Chloride.—The chemical formula $(C_{18}H_{10-11}N_3O_3)_n$ indicates the presence of one nitro group in one monomer unit, this combination being compatible with the infrared spectrum of III. In order to confirm the presence of this nitro group and simultaneously to investigate the possibility of the presence of any other reducible group or center, such as *N*-oxide or a free radical electron, the quantitative reduction of III with stannous chloride has been carried out. It has been found that three moles of stannous chloride were consumed per one mole of monomer unit of III, confirming the results of the infrared spectrum and elemental analysis. Further, this result shows that no other easily reducible group or center exists in the compound. The authors also concluded that the original hydrazine bond of DPPH is not left intact in the structure of III, since it is generally known that the usual hydrazine bond is split by stannous chloride to give amino compounds.

The Reaction of III with Hydroiodic Acid.—In order to explain the one extra atom of oxygen, in addition to the nitro group, in the chemical formula $C_{18}H_{10-11}N_3O_3$, the presence of ether-type oxygen was supposed, and the reaction of III with hydroiodic acid was carried out in attempt to open the supposed ether bond. When III was treated with hydroiodic acid, it gave a compound containing one atom of iodine for one unit of III, this compound does not, however, seem to be any simple salt nor molecular complex, because it does not liberate iodide ions when treated with alkali. The infrared spectrum of this compound is very different from that of III, but it does not show any band characteristic of N–H or O–H in the 3000~3500 cm^{-1} region. In spite of this finding, we could not, considering the general high resistivity of the aromatic ether bond to hydroiodic acid, discard the possibility of the presence of ether-type oxygen in III.

The Supposed Structure of III.—The whole of the available data described above is still not sufficient to establish the structure of III, particularly since its molecular weight is not yet known, but the following statements on the structure of III may be accepted at the present stage of knowledge:

(1) Three benzene skeletons are preserved, and one of them is of the mono-substituted type.

(2) One nitro group remains in a benzene nucleus which was originally the picryl group, but it is not known which one of the three nitro group (para or ortho) is thus preserved.

(3) The hydrazine-type $\rangle$N–N$\langle$ bond is split during the reaction to form a phenazine-type ring which is considered to be more stable than the hydrazine derivatives.

It is interesting that Wieland[4] found that the

4) H. Wieland, *Ber.*, **41**, 3478 (1908); **48**, 1078 (1915).

phenazine ring is formed from substituted tetraphenylhydrazines by the action of acid, although the present reaction conditions are different from these in Wieland's experiment.

Summarizing these results, a provisional presentation of the unit structure of III may be shown as follows:

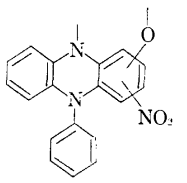

The Material Balance of the Photolysis of DPPH.—According to the experiment determining the ratios of the reaction products, we propose the following stoichiometric relation:

$$4C_{18}H_{12}N_5O_6 \rightarrow C_{18}H_{13}N_5O_6 \text{ (I)} + 2C_{18}H_{12}N_6O_8 + C_{18}H_{10-11}N_3O_3 \text{ (III)}$$

Although there is an excess atom of oxygen on the right hand side, the material balance seems to be fairly statisfactory, considering the accuracy of the quantitative estimation of the reaction products. No definite explanation of the unbalance in the number of oxygen atoms in the above equation is available at present, but it is possible that the oxygen atom is introduced from air or water during the treatment of the reaction products after the irradiation.

In spite of our efforts to find any other reaction product, gas chromatography failed to detect any such volatile substance as nitrobenzene which might be expected to result from the reaction of excited DPPH with the solvent benzene. It was found, however, that some nitrogen oxide existed in the reaction mixture. When the benzene mixture of the reaction products was extracted with water several times, the Gries test showed the presence of nitrous ions in the water extract, but the amount was very small (about one part to 80 parts of DPPH). Further, it was found that III itself produces some nitrogen oxide, most probably nitrogen dioxide, by irradiating its solution. It is presumed that nitrogen oxide comes from the nitro group of III by irradiation, although the detailed mechanism is not known. The nitrogen oxide found in the original reaction mixture of photolysis of III might be produced by the secondary decomposition of III.

The Reaction Mechanism of the Photolysis of DPPH.—In the absence of further data, it is premature to propose a complete scheme for photolysis of DPPH, but our kinetic investigation described in the preceding paper shows that the experimental rate expression fits the following reaction scheme:

$$\begin{aligned} D^* + h\nu &\longrightarrow D^* \\ D^* + (\text{solvent}) &\longrightarrow D \\ D^* + D &\longrightarrow D^*D \\ D^*D &\longrightarrow A + P_1 \\ P_1 + D &\longrightarrow B + P_2 \\ P_2 + D &\longrightarrow C + P_3 \end{aligned}$$

The products described here as A and B, are not directly related to the final products identified in the present work, but the authors assume that excited DPPH transfers its two nitro groups to normal DPPH to give α-phenyl-α-(p-nitrophenyl)-β-picrylhydrazine. The course through which the original excited DPPH is transformed to III is not yet clearly understood, and it might be difficult to describe the process completely in termes of a classical structure formula. The following scheme must be admitted to be rather speculative, but it is given to show some idea of the reaction mechanism:

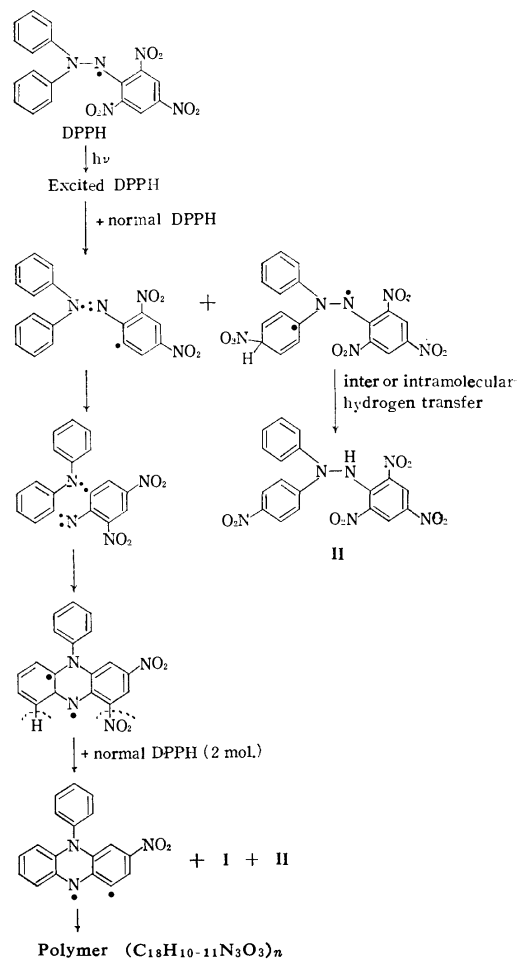

Experimental

The Decomposition of DPPH in a Benzene Solution by Sun-light.—One gram of DPPH was dissolved in 1 l. of purified and dried benzene. In order to increase the surface area of the solution exposed to sun-light, the solution was divided into five glass tubes 2 cm. in diameter by 70 cm. in length, and each tube was sealed without evacuation, leaving air in the space above the surface of the solution. They were exposed to sun-light for about twenty days. By the time the decomposition was completed, the color of the solution had become brown red, giving a brown precipitate. The benzene was removed under reduced pressure, and the residue was fractionated by elution chromatography on a powdered cellulose column measuring 9.0 cm. in diameter by 40 cm. in length and containing 400 g. of adsorbent, using a solvent mixture of petroleum ether and carbon disulfide (2 : 1 by volume) as the eluting solvent. After the first fraction, which was α,α-diphenyl-β-picrylhydrazine (I), came out, the ratio of petroleum ether to carbon disulfide was varied from 2 : 1 to 1 : 1 by volume to elute α-phenyl-α-(*p*-nitrophenyl)-β-picrylhydrazine. The last component was eluted with benzene. Each component was readily distinguishable by the color of the zone. The eluting solvents were distilled off under reduced pressure, and the residue was purified in the following way: I was recrystallized from a mixture of chloroform and alcohol (1 : 1 by volume); 0.12 g. of brick-red crystals (m. p. 171~172°C) were obtained. II was purified by recrystallization from an ethyl acetate-alcohol mixture (1 : 2 by volume); brick-red crystals, (m. p. 152~153°C; weight, 0.21 g.) were obtained. I and II did not depress the melting points of admixture with authentic samples of α,α-diphenyl-β-picrylhydrazine and α-phenyl-α-(*p*-nitrophenyl)-β-picrylhydrazine respectively, and III (0.10 g.) was obtained as a brick-red powder.

The Quantitative Determination of the Reaction Products.—After known amounts of benzene solutions of DPPH, I, II and III were mixed, the solvent was removed by evaporating it under reduced pressure in the dark, and the residue was fractionated on a cellulose column by the method described in the preceding paragraph. The solvents of each fraction were evaporated up to dryness under reduced pressure in the dark, and the residues were dissolved in benzene. From the first fraction the amount of DPPH was determined colorimetrically by absorption at 520 mμ using $\varepsilon=1.28\times10^4$ l./mol., assuming $\varepsilon=0$ for I. The amount of I was obtained from the absorption at 320 mμ minus that of DPPH using $\varepsilon=1.13\times10^4$ l./mol., and $\varepsilon=1.83\times10^4$ l./mol. for I and DPPH respectively. The amounts of II and III were determined by the absorption at 330 mμ ($\varepsilon=1.83\times10^4$ l./mol.) and 470 mμ respectively. The number of moles of III was calculated by assuming its chemical formula to be $C_{18}H_{10}N_3O_3$.

The Determination of the Ratios of the Reaction Products in the Course of the Decomposition.—Fifty milliliters of a benzene solution of DPPH (2.60×10^{-4} mol./l.) was irradiated, and 2 ml. of the solution was pipetted out after various periods of time. Each component in the reaction mixture was determined by the method described in the preceding paragraph.

The Purification of the Product III.—The substance III, which was obtained by column chromatography, has a fairly high purity, but further purification can be achieved by sublimation, giving orange needles. A convenient apparatus for it is shown in Fig. 4.

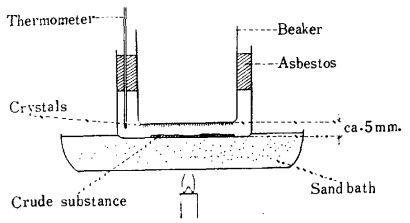

Fig. 4. Apparatus for sublimation of III.

The chemical composition and the visible and ultraviolet absorption spectra after sublimation were consistent with those obtained before sublimation.

Found: C, 68.28; H, 3.47; N, 13.28. Calcd. for $C_{18}H_{10}N_3O_3$: C, 68.35; H, 3.18; N, 13.28. $C_{18}H_{11}N_3O_3$: C, 68.13; H, 3.49; N, 13.24%.

After sublimation; C, 68.10; H, 3.50%.

The Estimation of the Molecular Weight.—The molal elevation constant (K) for dimethylformamide was found to be 18.9°C by using azobenzene. The elevation of the boiling point of the solution of III (0.0171 g.) in dimethylformamide (2.084 g.) was less than 0.10°C, indicating that the number of n is larger than 4.

Because of the low solubility of III in camphor or camphor quinone, as well as because of the coloring of the solutions, the determination of the molecular weight by Rast's method was unsuccessful. The depression of the melting point of a mixture of III (1.3 mg.) with camphor quinone (92.2 mg.) was scarcely observed. If the molecular weight of III is assumed to be about 320, the depression can be expected to be about 2°C in the concentration. When an isothermal distillation method[5] was also applied to III, using benzene as the solvent, the shift of meniscus was hardly noticeable.

The Quantitative Reduction of III with Stannous Chloride in Sulfuric Acid[6].—Nineteen milligrams of III purified by sublimation was suspended in 5 ml. of ethanol which had previously been freed from aldehyde by refluxing it for several hours in a rapid stream of carbon dioxide. When 2 ml. of dilute sulfuric acid (1 : 1 by volume) and 2 ml. of a standard stannous chloride solution (142.1 mg./ml.) were added, the color of III turned reddish violet. During the reduction, a slow stream of carbon dioxide was led into the flask, and the mixture was heated gradually on a water bath. When,

5) R. P. Linstead et al., "A Course in Modern Techniques of Organic Chmistry", Butterworths Scientific Publications, London (1955), p. 150.

6) A. Weissberger et al., "Organic Analysis II", Interscience Publishers, Inc., New York (1954), p. 77.

after half an hour, the reduction had been completed, the contents of the flask were rapidly cooled, diluted with 30 ml. of water, saturated with carbon dioxide, and rapidly titrated against a standard solution of iodine (35.98 mg./ml.), the end point being determined by a pH meter. The difference in the iodine solution between the amount of a blank test and that after the reaction was 1.27 ml., which corresponds to 34.7 mg. of stannous chloride. The theoretical amount of stannous chloride needed to reduce 19.0 mg. of III is 34.2 mg., assuming ing III to have only one nitro group per unit.

The Reaction of III with Hydroiodic Acid.— When a mixture of 10 mg. of III and 0.5 ml. of hydroiodic acid (52%) was heated on a water bath, reaction took place immediately, and the mixture turned black. After heating the mixture of ten minutes, the excess hydroiodic acid was filtered off and the residue was extracted with cold alcohol (95%) several times. The combined alcohol solution was diluted with water to give a dark precipitate which weighed 12.8 mg. when dried at 60°C/2 mmHg for 200 min. The free iodine accompanying the precipitate was completely eliminated in the drying procedure under vacuum.

The Molecular-weight Estimation of the Reaction Product. — When the reaction product (27.8 mg.) of III with hydroiodic acid was dissolved in bromoform (6.322 g.), the depression of the melting point was 0.005°C. As the molal depression constant for bromoform is 14.4°C, the molecular weight was calculated to be 1270, which means that III is a trimer of ($C_{18}H_{10}N_3O_3I$, mol. wt. 443). In such a a case, the depression should be not so large as to enable us to determine the molecular weight precisely, but it may be concluded that the number of n for $(C_{18}H_{10}N_3O_3I)_n$ is larger than 3.

The Determination of Nitrous Ions[7]. — DPPH (10.46 mg. 27 μ mol.) was dissolved in distilled dry benzene (100 ml.) and irradiated for 13 hr., according to the procedure described in the preceding paper, until the decomposition of DPPH had been completed. The reaction mixture was extracted several times with distilled water (in total 100 ml.) until the extract did not show the presence of nitrous ions. The extract was then brought to reaction with Griess' reagent and the amount of nitrous ion was determined colorimetrically, using a calibration curve obtained by an experiment with a known amount of sodium nitrite. The extract was found to contain 10^{-3} mg. of nitrous ions per 100 ml.

The benzene solution of the reaction mixture, which had been completely extracted with water and which was free from nitrous ion, was then divided into two parts; one of these was kept in the dark, and the other was irradiated for another 9 hr.

When the solutions were extracted with distilled water (in total 50 ml.), the one kept in the dark showed a scarcely positive Griess test, but the irradiated one contained 3.3×10^{-3} mg. (0.07 μmol.) of nitrous ions per 50 ml. of solution. The former was fractionated on a cellulose column into three components, and each component was then dissolved in benzene (50 ml.) as before. When these benzene solutions had been further irradiated for 9.5 hr., nitrous ions were detected only in the solution of III. The change in the absorption spectra of III before and after the irradiation was shown in Fig. 5.

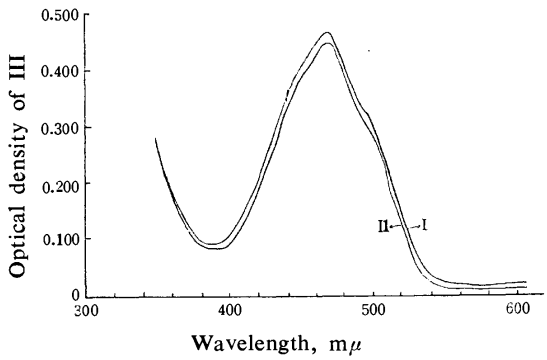

Fig. 5. Change in the absorption spectra of III before and after the irradiation.
I: Immediately after the isolation
II: After irradiation for 9.5 hr.

The other experiment, in which DPPH (10.50 mg.) (27 μ mol.) was dissolved in benzene (100 ml.) and irradiated for 22 hr., showed that the amount of nitrous ions was at most 17.25×10^{-3} mg. (0.37 μ mol.), which corresponds approximately to one part to twenty parts of III, assuming that III is produced in the yield of about 25 per cent from DPPH. Since the photochemical decomposition of III seems to be very slow, the low yield of nitrous ions and the high yield of III in the original reaction mixture of the photolysis of DPPH is understandable.

Summary

1. DPPH in a benzene solution was decomposed by sun-light on a relatively large scale in the presence of air, and the prducts were separated on a cellulose column. The products were identified as α,α-diphenyl-β-picrylhydrazine (I), α-phenyl-α-(p-nitrophenyl)-β-picrylhydrazine (II), and a third component (III) with a chemical composition of $(C_{18}H_{10-11}N_3O_3)_n$ (the n is greater than 3).

2. The method of separation by means of a cellulose column was applied in the quantitative estimation of the reaction products. The ratios of the products in the course of the decomposition were determined. From the ratio at the final stage, the over-all reaction can be written as follows:

$$4\ \mathrm{DPPH} \rightarrow \mathrm{I} + 2\,\mathrm{II} + \mathrm{III}$$

3. The physical and chemical properties of the third component have been described, and a possible structure for III has been proposed.

4. From the material balance and the

7) M. B. Shin, *Ind. Eng. Chem., Anal. Ed.*, 13, 33 (1941).

chemical compositions of the reaction products, it is presumed that the early stage of the decomposition of DPPH induced by light is an intermolecular nitration of DPPH.

Department of Chemistry
College of General Education
The University of Tokyo
Meguro-ku, Tokyo

The Synthesis of 5- and 6-Aminoazulene Derivatives

By Tetsuo NOZOE, Kahei TAKASE and Masao TADA*

(Received February 25, 1963)

In our laboratory, we have made an effort to synthesize azulenes by the action of such active methylenes as malononitrile and ethyl cyanoacetate on troponoids[1-4]. Although this method, using substituted troponoids as the starting material, should provide a suitable method for the synthesis of azulenes with a functional group on the seven-membered ring, very few instances have been reported. We report herein the synthesis of 5- and 6-aminoazulene derivatives from 5-acetamidotropolone (I)[5].

The application of ethyl cyanoacetate, in the presence of one mole of sodium ethoxide, to 5-acetamido-2-methoxytropone (II) afforded two compounds, diethyl 6-acetamido-2-aminoazulene-1, 3-dicarboxylate (IV) and ethyl 6-acetamido-3-cyano-2-hydroxyazulene-1-carboxylate (V), while 5-acetamido-2-(*p*-tolylsulfonyloxy)tropone (III) afforded diethyl 5-acetamido-2-aminoazulene-1, 3-dicarboxylate (VI) and yellow crystals (VII) (m. p. above 270°C). The ultraviolet spectra of these compounds are shown in Figs. 1 and 2.

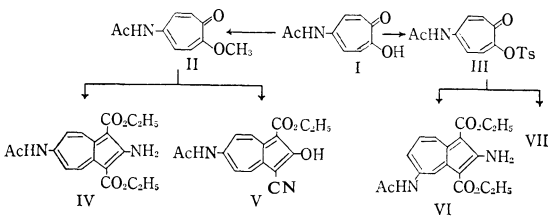

The structural proof of IV, V and VI was based on the analysis and on a comparison of the ultraviolet and infrared spectra with those of known compounds. The validity of the structures proposed was also supported by the well-established general concept that 2-halo- and 2-(*p*-tolylsulfonyloxy)tropones undergo condensation at the 1- and 7-positions of the troponoids, whereas 2-methoxytropones give rise to azulene derivatives derived by condensation at the 1- and 2-positions. The yellow compound (VII), $C_{14}H_{14}O_5N_2$, was shown by ultraviolet spectral evidence not to be an

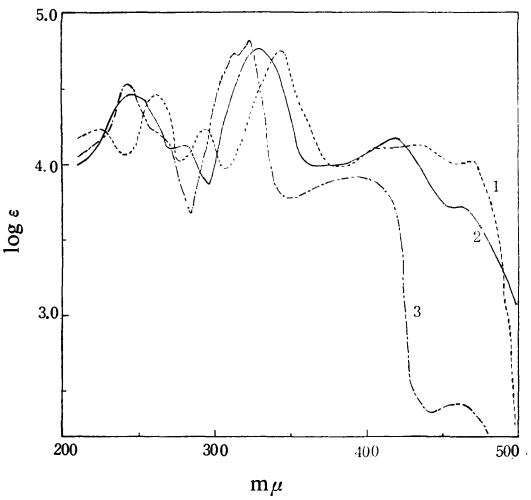

Fig. 1. Ultraviolet absorption spectra in methanol.
1 Diethyl 6-acetamido-2-aminoazulene-1, 3-dicarboxylate (IV)
2 Diethyl 2,6-diaminoazulene-1, 3-dicarboxylate (VIII)
3 Diethyl 2,6-diacetamidoazulene-1, 3-dicarboxylate (IX)

* Present address: The Research Institute for Tuberculosis and Leprosy, Tohoku University, Sendai.

1) T. Nozoe, *Fortschr. Chem. Org. Naturst.*, **13**, 232 (1956); *Croat. chim. Acta*, **29**, 207 (1957); T. Nozoe and S. Ito, *Fortschr. Chem. Org. Naturst.*, **19**, 32 (1961).

2) T. Nozoe, S. Seto and S. Matsumura, *Chem. & Ind.*, **1955**, 1257; T. Nozoe, S. Seto, S. Matsumura and Y. Murase, This Bulletin, **35**, 1179 (1962).

3) T. Nozoe, S. Seto, S. Matsumura and T. Asano, *Proc. Japan Acad.*, **32**, 339 (1956); H. Akino, to be published.

4) T. Nozoe, K. Takase, T. Nakazawa and M. Yasunami, Abstructs of the 13th Symposium on the Reaction Mechanisms of Organic Compounds, Sapporo, Japan (1962), p. 6.

5) T. Nozoe and S. Seto, *Proc. Japan Acad.*, **27**, 188 (1951).

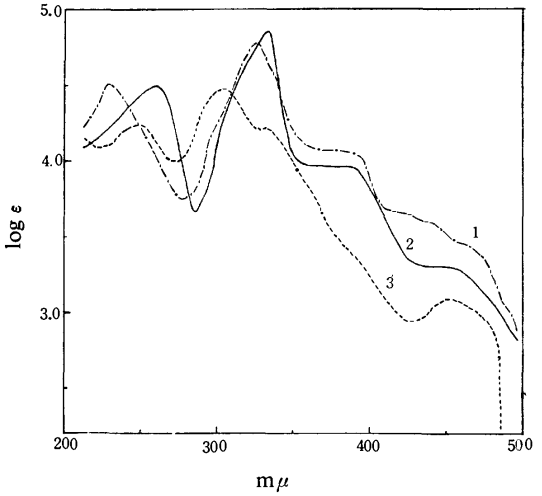

Fig. 2. Ultraviolet absorption spectra in methanol.
1 Ethyl 6-acetamido-3-cyano-2-hydroxyazulene-1-carboxylate (V)
2 Diethyl 5-acetamido-2-aminoazulene-1, 3-dicarboxylate (VI)
3 VII

azulene derivative; its precise structure will be reported on in another paper.

The alkaline hydrolysis of IV afforded a dull brown 2, 6-diamino compound VIII, the acetamido group being predominantly attacked; acetylation of the latter, in turn, gave first IV and then diacetate IX, which was also obtained by the acetylation of IV. Mono Schiff's base was obtained from VIII by the action of benzaldehyde. The diazotization of IV was realized by isoamyl nitrite or sodium nitrite and an excess of sulfuric acid, and decomposition of the diazonium salt formed was carried out by either leaving it standing at room temperature or treating it with active copper and sodium hypophosphite. The reactions carried out in dioxane gave the deaminated product, diethyl 6-acetamidoazulene-1, 3-dicarboxylate (X), while these carried out in aqueous ethanol gave diethyl 6-aminoazulene-1, 3-dicarboxylate (XI), the hydrolysis product of the acetamido group. The acetylation of XI gave X, and the acidic hydrolysis of X afforded XI. XI was obtained also by deamination of the diamino compound VIII, which showing the greater basicity of C_2-amino between the two amino groups. 6-Amino compound XI gave, on alkaline hydrolysis, a dicarboxylic acid XII, the decarboxylation of which in pyridine furnished 6-aminoazulene (XIII) in the form of red prisms (ultraviolet spectrum Fig. 3). XIII is rather unstable and darkens on being left in air for a long time, while its blueish acetate XIV is quite stable (ultraviolet spectrum Fig. 3).

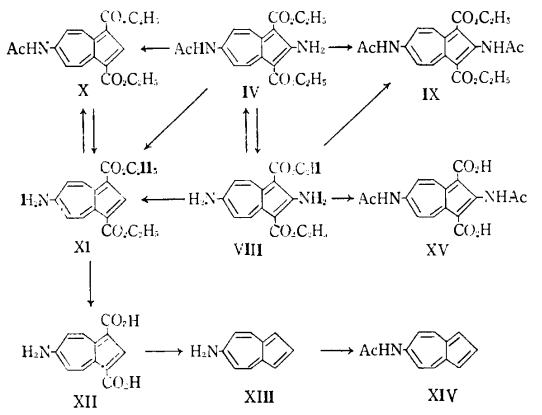

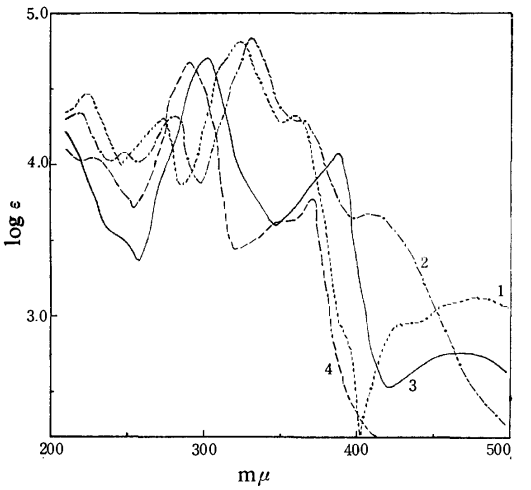

Fig. 3. Ultraviolet absorption spectra in methanol.
1 Diethyl 6-acetamidoazulene-1, 3-dicarboxylate (X)
2 Diethyl 6-aminoazulene-1, 3-dicarboxylate (XI)
3 6-Aminoazulene (XIII)
4 6-Acetamidoazulene (XIV)

In an attempt to derive 2, 6-diaminoazulene, the corresponding dicarboxylic acid XV was obtained from VIII. An attempt to decarboxylate XV on heating, however, resulted in a dark tarry material from which none of the desired product was isolated.

The preferential formation of a 6-acetamido derivative IV on the mild acetylation of 2, 6-diaminoazulene VIII, which contrasts with the preferential diazotization of the 2-amino group, can be explained by the operation of a steric hindrance caused by the presence of the two ethoxycarbonyl groups adjacent to the 2-amino group.

Experimental[6]

The Reaction of 5-Acetamido-2-methoxytropone (II) and Ethyl Cyanoacetate. — To a sodium ethoxide solution prepared from sodium (375 mg.) and absolute ethanol (30 ml.) were added ethyl cyanoacetate (3.6 g.) and then a suspension of II (3.12 g.) in absolute ethanol (50 ml.). The mixture was stirred for 4 hr. and then allowed to stand for 2 days at room temperature. The solvent was removed in vacuo, and water was added. The crystals which separated (2.5 g.) were recrystallized from ethanol to afford IV as yellow needles; m.p. 216~217°C.

Found: C, 62.95; H, 5.42; N, 8.28. Calcd. for $C_{18}H_{20}O_5N_2$: C, 62.78; H, 5.85; N, 8.14%.

λ_{max}^{MeOH} mμ (log ε): 245 (4.49), 280 (4.14), 335 (4.79), 420 (4.14), 462 (3.71). IR (Nujol): 3490, 3335, 1694, 1650, 1637 cm^{-1}.

The Picrate of IV.—M. p. 178~179°C (decomp.); black micro-prisms (from ethanol).

Found: C, 49.90; H, 4.09; N, 12.63. Calcd. for $C_{24}H_{23}O_{12}N_5$: C, 50.26; H, 4.04; N, 12.21%.

The aqueous mother liquor, after the separation of crystals, was extracted with benzene, by which a further crop of IV (0.20 g.) was obtained. The water layer was acidified with 6 N sulfuric acid, and the crystals (m. p. 220~230°C (decomp.)) thereby formed were collected by filtration and recrystallized from ethyl acetate to give V as yellowish brown micro-prisms; m. p. 234~236°C (decomp.); 70 mg.

Found: C, 63.70; H, 4.48; N, 9.02. Calcd. for $C_{16}H_{14}O_4N_2$: C, 64.42; H, 4.73; N, 9.39%.

λ_{max}^{MeOH} mμ (log ε): 232 (4.51), 330 (4.86), 395 (4.01), 420 (3.65) sh, 460 (3.35) sh. IR (Nujol): 3460, 2232, 1781, 1709, 1692 cm^{-1}.

The Reaction of 5-Acetamido-2-(*p*-tolylsulfonyloxy)tropone (III) and Ethyl Cyanoacetate.—The reaction and the working-up of the reaction mixture were carried out in exactly the same way as in the previous section, using sodium (85 mg.), absolute ethanol (12 ml.), ethyl cyanoacetate (0.75 g.) and III (1.00 g.) in absolute ethanol (20 ml.). The crystals which separated (400 mg.) were recrystallized from ethanol to give pale yellow leaflets (VII); m. p. above 270°C.

Found: C, 57.74; H, 5.07; N, 9.54. Calcd. for $C_{14}H_{14}O_5N_2$: C, 57.93; H, 4.86; N, 9.65%.

λ_{max}^{MeOM} mμ (log ε): 247 (4.25), 306 (4.49), 336 (4.23), 454 (3.13).

The mother aqueous liquor give a crystalline substance, 150 mg. of VI, which, after recrystallization from ethanol, gave yellow needles; m. p. 184~185°C.

Found: C, 62.74; H, 5.87; N, 8.06. Calcd. for $C_{18}H_{20}O_5N_2$: C, 62.78; H, 5.85; N, 8.14%.

λ_{max}^{MeOH} mμ (log ε): 263 (4.51), 336 (4.89), 392 (3.98), 450 (3.24) sh. IR (Nujol): 3500, 3370, 3220, 1669 cm^{-1}.

The Picrate of VI.—M. p. 150~151°C (decomp.); pale yellow crystals (from ethanol).

Found: N, 14.28. Calcd. for $C_{30}H_{26}O_{19}N_8$: N, 14.09%.

Diethyl 2, 6-Diaminoazulene-1, 3-dicarboxylate (VIII).—IV (200 mg.) was heated under reflux for 4 hr. with potassium hydroxide (200 mg.) in ethanol (12 ml.); by this procedure 100 mg. of brownish green crystals were precipitated. Recrystallization from benzene afforded VIII as dull brown plates with a metallic luster; m. p. 207~208°C.

Found: C, 63.76; H, 5.56; N, 9.20. Calcd. for $C_{16}H_{18}O_4N_2$: C, 63.56; H, 6.00; N, 9.27%.

λ_{max}^{MeOH} mμ (log ε): 224 (4.25), 262 (4.47), 296 (4.24), 346 (4.74), 430 (4.09), 472 (3.98). IR (Nujol): 3470, 3410, 3320, 3205, 1637 cm^{-1}.

VIII was acetylated to give IV by warming it in acetic anhydride on a water bath for 4 hr.

The Picrate of VIII.—M. p. 180~181°C (decomp.); black needles (from ethanol).

Found: C, 49.89; H, 3.88; N, 13.01. Calcd. for $C_{22}H_{21}O_{11}N_5$: C, 49.71; H, 3.99; N, 13.18%.

The Benzylidene Derivative of VIII.—A solution of VIII (90 mg.), a drop of acetic acid, and benzaldehyde (100 mg.) in ethanol (2 ml.) was warmed on a water bath for 15 min. After the solution had been allowed to stand overnight at room temperature, the crystals (70 mg.) deposited were recrystallized from benzene to recover 20 mg. of VIII. The filtrate was evaporated to dryness, and recrystallization from cyclohexane afforded a benzilidene derivative as orange prisms; m. p. 140~141°C, 15 mg.

Found: C, 70.97; H, 5.58; N, 7.25. Calcd. for $C_{23}H_{22}O_4N_2$: C, 70.75; H, 5.48; N, 7.18%.

IR (Nujol): 3500, 3370, 1686, 1664 cm^{-1}.

Diethyl 2, 6-Diacetamidoazulene-1, 3-dicarboxylate (IX).—A solution of IV in acetic anhydride, in the presence of pyridine, was refluxed on an oil bath for 3 hr. The crystalline residue produced by the evaporation of the solvent was recrystallized from ethanol to give IX as orange needles; m. p. 188~189°C.

Found: C, 62.66; H, 5.74; N, 7.27. Calcd. for $C_{20}H_{22}O_6N_2$: C, 62.16; H, 5.74; N, 7.25%.

λ_{max}^{MeOH} mμ (log ε): 345 (4.56), 316 (4.75), 327 (4.83), 378 (3.90), 398 (3.94), 470 (3.43). IR (Nujol): 3495, 3330, 1714, 1667 cm^{-1}.

The Deamination of IV.—*a) The Formation of Diethyl 6-Acetamidoazulene-1, 3-dicarboxylate (X).*— Into a solution of IV (200 mg.) and concentrated sulfuric acid (0.4 ml.) in dioxane (6 ml.) was added sodium nitrite (50 mg.) in water (2 ml.) with stirring. After the mixture had been stirred for a further 30 min., active copper powder (100 mg.) and sodium hypophosphite (0.8 g.) were added. The mixture was stirred for a further 3 hr. and then allowed to stand overnight at room temperature. The reaction mixture was diluted with water (200 ml.) and extracted with ethyl acetate, and the extract was passed through a column of alumina, yielding X (130 mg.). Recrystallization from ethanol formed orange leaflets; m. p. 221~221.5°C.

Found: C, 65.27; H, 5.57; N, 4.06. Calcd. for $C_{18}H_{19}O_5N$: C, 65.64; H, 5.82; N, 4.25%.

λ_{max}^{MeOH} mμ (log ε): 227 (4.46), 276 (4.30), 329 (4.80), 366 (4.29), 475 (3.04). IR (Nujol): 3320, 1706, 1695, 1667 cm^{-1}.

6) All melting points are uncorrected. Shoulders in the UV spectral data are by sh.

b) The Formation of Diethyl 6-Aminoazulene-1, 3-dicarboxylate (XI).—i) Into a solution of IV (200 mg.) and concentrated sulfuric acid (1.2 ml.) in 60% aqueous ethanol (20 ml.), isoamyl nitrite (180 mg.) was added with stirring while the mixture was being ice-cooled. After the mixture had been stirred for a further 30 min., ethanol (8 ml.) was added and the mixture was allowed to stand overnight at room temperature. The mixture was extracted with ethyl acetate after the addition of water (200 ml.), and the extract was passed through a column of alumina to give XI (10 mg.). The water-layer was adjusted to a slightly alkaline state and extracted with ethyl acetate. By the same purification, XI (90 mg.) was obtained. Recrystallization from ethanol formed orange scales; m. p. 236~237°C, 85 mg.

Found: C, 66.98; H, 6.01; N, 4.87. Calcd. for $C_{16}H_{17}O_4N$: C, 66.88; H, 5.96; N, 4.88%.

λ_{max}^{MeOH} mμ (log ε): 225 (4.34), 252 (4.04), 284 (4.34), 335 (4.82), 365 (4.28), 410 (3.65). IR (Nujol): 3410, 3320, 3205, 1650 cm^{-1}.

The Picrate of XI.—M. p. 209~210°C (decomp.); orangish brown scales (from ethanol).

Found: C, 51.40; H, 4.17; N, 11.20. Calcd. for $C_{22}H_{20}O_{11}N_4$: C, 51.16; H, 3.90; N, 10.85%.

ii) To the diazotized solution of IV (200 mg.) with isoamyl nitrite (180 mg.), active copper powder (100 mg.) and sodium hypophosphite (0.8 g.) were added. The mixture was stirred for 2 hr. and then allowed to stand overnight at room temperature. After removal of the copper powder, the reaction mixture was treated as in i) to obtain XI (145 mg.).

iii) Into a solution of IV (200 mg.) in dioxane (8 ml.) and concentrated sulfuric acid (0.2 ml.), a solution of sodium nitrite (50 mg.) in water (2 ml.) was added with stirring while the mixture was being cooled. After the mixture had been stirred for 15 min., ethanol (5 ml.) and active copper powder (100 mg.) were added, and the mixture was warmed in a water bath for 1 hr. The solution was concentrated to half volume under a reduced pressure and treated as in i) to obtain XI (105 mg.).

The acetylation of XI with acetic anhydride by refluxing it for 10 min. gave X. The hydrolysis of X by refluxing it with 6 N sulfuric acid in ethanol gave XI.

The Deamination of VIII.—A solution of VIII (100 mg.) in 60% aqueous ethanol (10 ml.) and concentrated sulfuric acid (0.6 ml.) was diazotized with isoamyl nitrite (90 mg.) and treated as in the case of the deamination of IV, b-i); XI (20 mg.) was obtained.

6-Aminoazulene-1, 3-dicarboxylic Acid (XII).—A solution of XII (120 mg.) and potassium hydroxide (90 mg.) in 60% aqueous ethanol (15 ml.) was refluxed for 4 hr. The solution was concentrated to half volume under a reduced pressure, and this was then diluted with water (15 ml.) and acidified with 6 N sulfuric acid. The precipitate thereby formed was collected by filtration and repeatedly washed with water, by which process dicarboxylic acid (XII) was obtained as black crystalline powder; m. p. above 275°C; 80 mg.

6-Aminoazulene (XIII).—A solution of XII (80 mg.) in pyridine (2 ml.) was heated at 140~150°C to effect decarboxylation. The residue produced by evaporation of the excess of pyridine was dissolved in benzene and passed through a column of alumina, while the crude material obtained by the concentration of the effluent was recrystallized from ethanol to give XIII (m. p. 106~107°C; 10 mg.) as red scales.

Found: C, 84.12; H, 6.80; N, 9.32. Calcd. for $C_{10}H_9N$: C, 83.88; H, 6.34; N, 9.78%.

λ_{max}^{MeOH} mμ (log ε): 306 (4.70), 390 (4.07), 465 (2.70). in EtOH; 470 (2.71). IR (Nujol): 3420, 3330, 3200 cm^{-1}.

6-Acetamidoazulene (XIV).—A solution of XIII (20 mg.) in acetic anhydride was warmed on a water bath for 5 min. The crystalline residue produced by the evaporation of the solvent was recrystallized from ethanol to give XIV (10 mg.) as blue needles.

Found: C, 78.26; H, 6.07; N, 7.46. Calcd. for $C_{12}H_{11}ON$: C, 77.81; H, 5.99; N, 7.56%.

λ_{max}^{MeOH} mμ (log ε): 230 (4.02), 291 (4.65), 355 (3.60), 374 (3.74). in EtOH; 570 (2.57). IR (Nujol): 3270, 1664 cm^{-1}.

2, 6-Diacetamidoazulene-1, 3-dicarboxylic Acid (XV).—A solution of VIII (20 mg.) and potassium hydroxide (100 mg.) in 60% aqueous ethanol (9 ml.) was refluxed for 7 hr. The solution was concentrated to 1/3 volume under a reduced pressure and diluted with water (20 ml.). The mixture was then extracted with ethyl acetate, and the extract was passed through a column of alumina. From the effluent, a reddish, oily substance was obtained. This was warmed with acetic anhydride on a water bath for 3 hr. The product was crystallized from aqueous ethanol to give XV as a violet brown powder (m. p. 212~213°C; 10 mg.).

Found: N, 8.05. Calcd. for $C_{16}H_{14}O_6N_2$: N, 8.48%.

IR (Nujol): 3470, 3290, 1669, 1650 cm^{-1}.

Expenses for the present series of experiments were defrayed by a grant-in-aid for Scientific Research from the Ministry of Education. The infrared spectra in this paper were measured by using a Shimadzu infrared spectrophotometer IR-27 purchased by a grant-in-aid for Scientific Research from the Toyo Rayon Co., Ltd. The authors wish to express their deep gratitude for these contributions.

Department of Chemistry
Faculty of Science
Tohoku University
Katahira-cho, Sendai

The Synthesis of 5- and 6-Acetylazulene Derivatives

By Tetsuo NOZOE, Kahei TAKASE and Masao TADA*

(Received February 25, 1963)

In a previous paper[1], we reported the synthesis of aminoazulenes from troponoid compounds as a part of a general scheme for the synthetic study of azulenes with the functional group on a seven-membered ring. In this paper, the synthesis of acetylazulenes is reported. The ethylene ketal (II)[2] of 4-acetyltropolone (I)[3] was converted to the corresponding methyl ethers (IIIa and IIIb) and *p*-toluenesulfonate (IVa and IVb), to which the general synthetic method[4-7] of the azulenic compound was then applied.

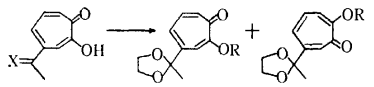

I: X=O IIIa: R=CH_3 IIIb: R=CH_3

II: X= IVa: R=Ts IVb: R=Ts

The reaction of a mixture of methyl ethers (IIIa and IIIb) with ethyl cyanoacetate yielded five azulenic products (ultraviolet spectra: Fig. 1): diethyl 2-amino-5-(1, 1-ethylenedioxyethyl)azulene-1, 3-dicarboxylate (V), ethyl 2-amino-5(or 7)-(1, 1-ethylenedioxyethyl)azulene-1-carboxylate (VI), 1, 3-dicyano-5-(1, 1-ethylenedioxyethyl)-2-hydroxyazulene (VII), ethyl 3-cyano-5(or 7)-(1, 1-ethylenedioxyethyl)-2-hydroxyazulene-1-carboxylate (VIII), and ethyl 3-cyano-7(or 5)-(1, 1-ethylenedioxyethyl)-2-hydroxyazulene-1-carboxylate (IX). The structural assignment of these compounds was based on their analyses, their infrared spectra, and a consideration of the general course of the azulene synthesis[4-7], although the exact locations of the ethoxycarbonyl and cyano groups in VI, VIII and IX with respect of the ethylenedioxyethyl group are not known.

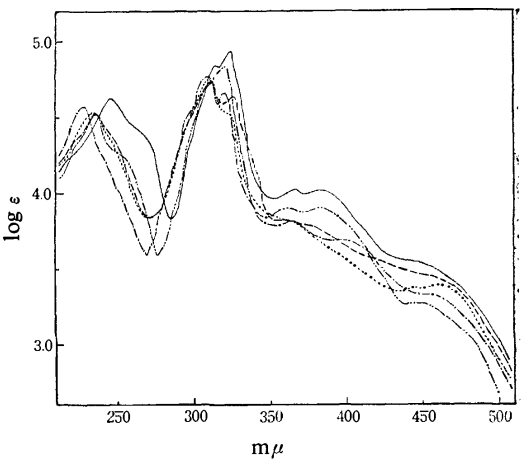

Fig. 1. Ultraviolet absorption spectra of V (——), VI (—·—), VII (—··—), VIII (— — —) and IX (·····) in methanol.

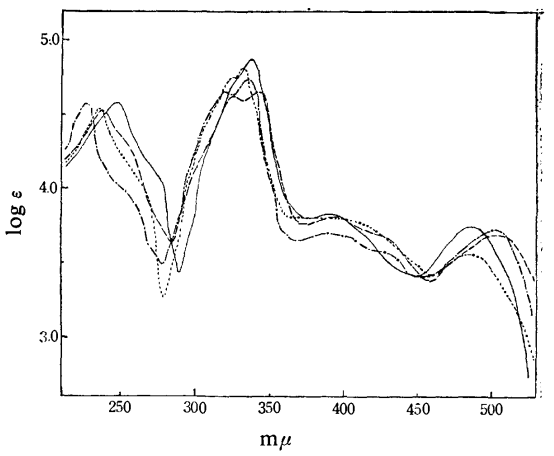

Fig. 2. Ultraviolet absorption spectra of X (——), XI (·····), XII (— — —), and XIII (—·—) in methanol.

When this condensation reaction was carried out in the presence of one molar equivalent of sodium ethoxide, V was obtained as a major product, together with a small amount of VII, VIII and IX, while the reaction with two molar equivalents of sodium ethoxide did not yield V but VII as the major product, accompanied by a small amount of VI. The mild acid hydrolysis of these compounds provoked a cleavage of the ethylene ketal ring to form

* Present address: The Research Institute for Tuberculosis and Leprosy, Tohoku University, Sendai.

1) T. Nozoe, K. Takase and M. Tada, This Bulletin, 36, 1006 (1963).
2) I. Murata, This Bulletin, 34, 577 (1961).
3) T. Nozoe, K. Takase and M. Ogata, *Chem. & Ind.*, 1957, 1070.
4) T. Nozoe, *Fortschr. Chem. Org. Naturst.*, 13, 232 (1956); *Croat. chim. Acta*, 29, 207 (1957); T. Nozoe and S. Ito, *Fortschr. Chem. Org. Naturst.*, 19, 36 (1961).
5) T. Nozoe, S. Seto and S. Matsumura, *Chem. & Ind.*, 1955, 1257; T. Nozoe, S. Seto, S. Matsumura and Y. Murase, This Bulletin, 35, 1179 (1962).
6) T. Nozoe, S. Seto, S. Matsumura and T. Asano, *Proc. Japan Acad.*, 32, 339 (1956); H. Akino, to be published.
7) T. Nozoe, K. Takase, T. Nakazawa and M. Yasunami, Abstracts of the 13th Symposium on the Reaction Mechanisms of Organic Compounds, Sapporo, Japan (1962), p. 6.

the corresponding acetyl compound; diethyl 5-acetyl-2-aminoazulene-1, 3-dicarboxylate (X) from V, ethyl 5(or 7)-acetyl-2-amino-3-cyanoazulene-1-carboxylate (XI) from VI, 5-acetyl-1, 3-dicyano-2-hydroxyazulene (XII) from VII, and ethyl 5(or 7)-acetyl-3-cyano-2-hyroxyazulene-1-carboxylate (XIII) from VIII. The ultraviolet spectra of these substances are shown in Fig. 2.

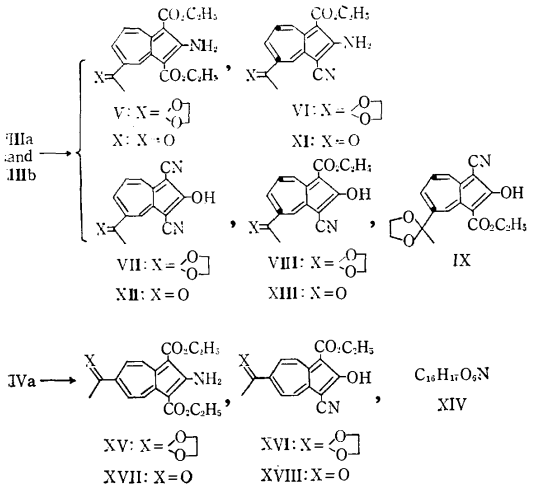

IVb → V

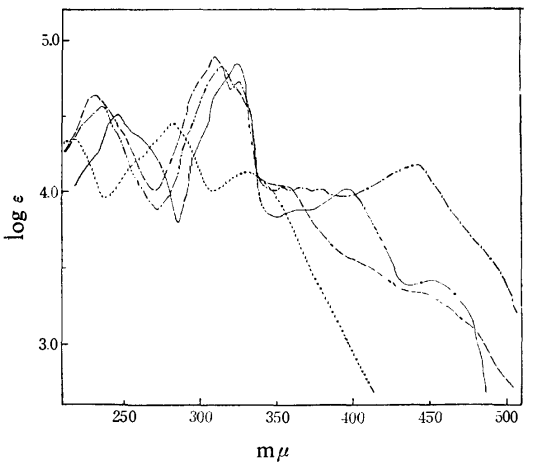

Fig. 3. Ultraviolet absorption spectra of XIV (——), XV (——), XVI (——) and XVIII (——) in methanol.

The reaction of ethyl cyanoacetate on 4-(1, 1-ethylenedioxyethyl)-2-(*p*-tolylsulfonyloxy)tropone (IVa) gave three products, all of which were different from those obtained from IIIa and IIIb. The analyses, the ultraviolet (Fig. 3) and infrared spectra, and the general conception of the nature of the reaction suggested that the first two products were diethyl 2-amino-6-(1, 1-ethylenedioxyethyl)azulene-1, 3-dicarboxylate (XV) and ethyl 3-cyano-6-(1, 1-ethylenedioxyethyl)-2-hydroxyazulene-1-carboxylate (XVI). The third compound XIV, the main product, was assumed not to be azulenic from its ultraviolet spectrum; it has properties similar to those of the substance obtained from 5-acetamido-2-(*p*-tolylsulfonyloxy)tropone[1]. The exact structure, however, can not be drawn. The hydrolysis of ethylene ketal in XV and XVI was effected by diluted acid to give their respective acetylazulenes, XVII and XVIII.

The reaction of ethyl cyanoacetate on the isomeric *p*-toluenesulfonate (IVb), 6-(1, 1-ethylenedioxyethyl)-2-(*p*-tolylsulfonyloxy)tropone, gave the azulene (V) in a low yield, besides the recovery of the starting material. The formation of the azulene (V), the product of the reaction at C_1 and C_2, may be due to the difficulty the reagent has in approaching the 7-position of the tropone because of the presence of the side chain at the 6-position.

The removal of substituents was carried out on ethylenedioxyethylazulenes (V and XV) and acetylazulenes (X and XVII); the diazotization reaction was accomplished by means of large excess of sulfuric acid and isoamyl nitrite or sodium nitrite, the amino group being notably unreactive compared with diethyl 2-aminoazulene-1, 3-dicarboxylate[5]. The decomposition of diazonium salts to yield the corresponding deamination products was achieved by letting the salts stand at room temperature or by warming them in the presence of copper or sodium hypophosphite. In the reactions of V and XV, ethylene ketal was hydrolyzed at the same time; thus, V and X gave diethyl 5-acetylazulene-1, 3-dicarboxylate (XIX), while XV and XVII yielded diethyl 6-acetylazulene-1, 3-dicarboxylate (XX). Dicarboxylic acid XXI obtained by the alkaline hydrolysis of XIX was submitted to thermal decarboxylation to form blue-violet 5-acetylazulene (XXII) ($\nu_{C=O}$ 1664 cm^{-1}), which, though its identify has not yet been established, is probably identical with the product (m. p. 39°C) obtained by Treibs and Quarg[8] by a

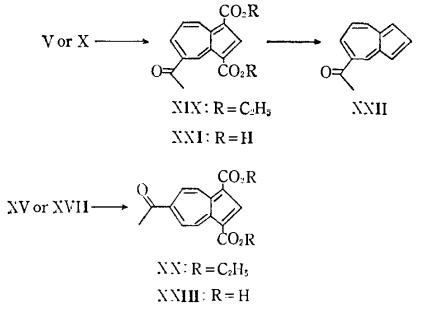

8) W. Treibs and M. Quarg, *Ann.*, **598**, 38 (1956).

ring expansion of indane with diazoketone. The similar hydrolysis of XX to the corresponding dicarboxylic acid XXIII and subsequent thermal decarboxylation yielded a pale green oil, but its small quantity did not allow the product to be characterized.

The alkaline hydrolysis of X and XVII afforded dicarboxylic acid XXIV and XXV respectively, the heating of which in pyridine caused decarboxylation which produced 5-acetyl-2-aminoazulene (XXVI) and 6-acetyl-2-aminoazulene (XXVII) respectively. XXVI was also obtained by the similar decarboxylation of the dicarboxylic acid XXVIII obtained from ethylene ketal V. The ultraviolet spectra of these 5-acetyl- and 6-acetylazulene derivatives are shown in Fig. 4 and Fig. 5. When alkaline hydrolysis of V was carried out in anhydrous ethanol, monocarboxylic acid XXIX was obtained; the decarboxylation of this in pyridine yielded monoester XXX. The acid hydrolysis of XXX gave ethyl 5(or 7)-acetyl-2-aminoazulene-1-carboxylate (XXXI) (ultraviolet spectra in Fig. 6). As the position of ethoxycarbonyl which had under gone alkaline hydrolysis could not be determined, no definite conclusion can be drawn at present concerning the position of the ethoxycarbonyl group in XXX and XXXI.

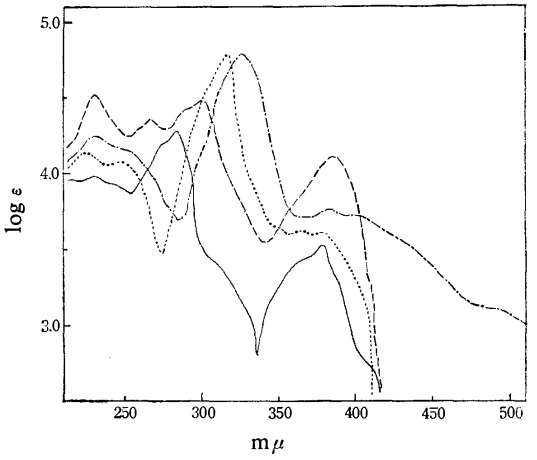

Fig. 4. Ultraviolet absorption spectra of XIX (——), XXII (——), XXVI (– – –) and acetate of XXVI (·····) in methanol.

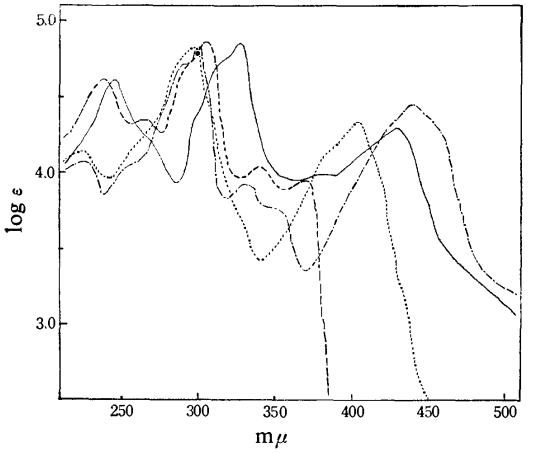

Fig. 5. Ultraviolet absorption spectra of XVII (——), XX (——), XXVII (·····) and acetate of XXVII (– – –) in methanol.

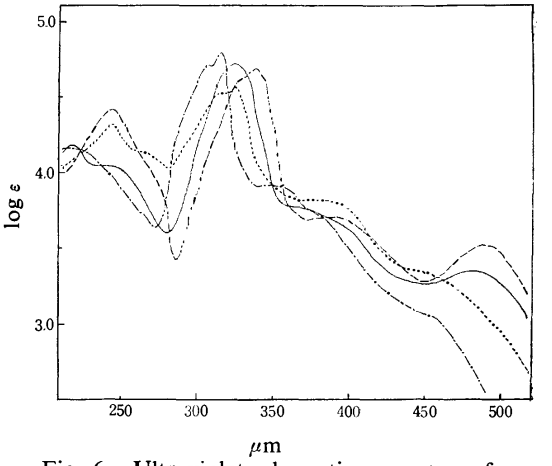

Fig. 6. Ultraviolet absorption spectra of XXIV (——), XXVIII (·····), XXX (——) and XXXI (——) in methanol.

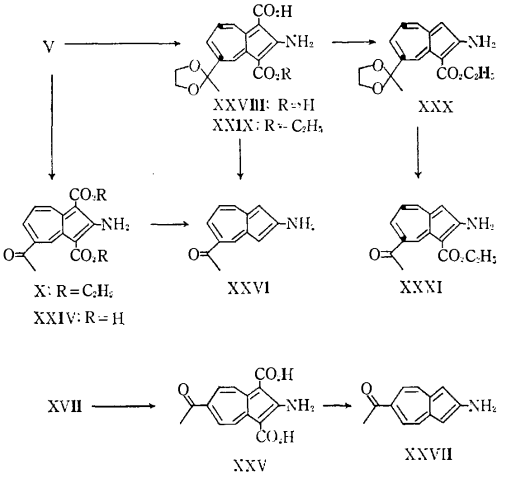

The reactions of these acetylazulene derivatives with ketonic reagents are being investigated and will be reported on in the future.

Experimental[9]

The Reaction of 4-(1, 1-Ethylenedioxyethyl)tropolone Methyl Ether (IIIa and IIIb) and Ethyl Cyanoacetate.—*a) With 1 mol. of Sodium Ethoxide.*—To a sodium ethoxide solution prepared from

9) All melting points are uncorrected. Shoulders in the UV spectral data are designated by "sh".

sodium (1.83 g., 0.036 mol.) and absolute ethanol (80 ml.), ethyl cyanoacetate (6.83 g.) was added. After this mixture had been allowed to stand for 30 min., a solution of methyl ether (a mixture of IIIa and IIIb) (6.9 g., 0.031 mol.) in absolute ethanol (30 ml.) was added, and the new mixture was allowed to stand overnight. The solvent was removed under reduced pressure, water was added, and the separated crystals (m. p. 104~109°C, 7.3 g.) were recrystallized from ethanol to afford V as yellow prisms (m. p. 112~113°C, 6.65 g.).

Found: C, 64.31; H, 6.90; N, 3.82. Calcd. for $C_{20}H_{23}O_6N$: C, 64.33; H, 6.21; N, 3.75%.

λ_{max}^{MeOH} mμ (log ε): 247 (4.88), 317 (5.08), 327 (5.20), 365 (4.25), 387 (4.24), 454 (3.29). IR: (KBr disk) 3445, 3328, 1668; (Nujol) 3460, 3350, 1650 cm^{-1}.

The Picrate of V: M. p. 124.5~126°C; orange needles (from ethanol).

Found: C, 51.70; H, 4.45; N, 9.40. Calcd. for $C_{26}H_{26}O_{13}N_4$: C, 51.82; H, 4.36; N, 9.30%.

The Acetate of V: This was obtained by refluxing V in acetic anhydride for 6 hr.; m. p. 122~123°C; reddish violet needles (from ethanol).

Found: C, 63.55; H, 5.87; N, 3.23. Calcd. for $C_{22}H_{25}O_7N$: C, 63.60; H, 6.07; N, 3.37%.

IR (Nujol): 3490, 3330, 1724, 1701, 1686 cm^{-1}.

From the aqueous mother liquor, crystals (m. p. 225~230°C, 0.20 g.) were obtained after the liquor had been left standing for 3 hr. Recrystallization from benzene formed VIII as yellowish orange silky needles; m. p. 234~237°C (decomp.).

Found: C, 66.56; H, 5.41; N, 4.36. Calcd. for $C_{18}H_{17}O_5N$: C, 66.05; H, 5.24; N, 4.28%.

λ_{max}^{MeOH} mμ (log ε): 237 (4.53), 312 (4.74), 327 (4.63), 365 (3.84). IR: (KBr disk) 3060, 2208, 1647; (Nujol) 2232, 1647 cm^{-1}.

The Acetate of VIII: M. p. 148~149.5°C; pale red scales (from methanol).

Found: C, 65.02; H, 5.19; N, 3.79. Calcd. for $C_{20}H_{19}O_6N$: C, 65.03; H, 5.19; N, 3.79%.

λ_{max}^{MeOH} mμ (log ε): 233 (4.56), 260 (4.29), 303 (4.73), 368 (3.91). IR(KBr disk): 2228, 1772, 1692 cm^{-1}.

The mother liquor was washed with benzene, the water layer was acidified with 6 N sulfuric acid, and the separated crystals (m. p. 225~230°C; 0.45 g.) were recrystallized from ethanol to afford VII as brownish yellow crystals (m. p. 238.5~239°C (decomp.), 0.26 g.).

Found: C, 67.69; H, 4.23; N, 9.70. Calcd. for $C_{20}H_{23}O_6N_2$: C, 68.56; H, 4.32; N, 10.00%.

λ_{max}^{MeOH} mμ (log ε): 230 (4.58), 312 (4.76), 324 (4.65), 367 (3.80), IR (KBr disk): 3020, 2217 cm^{-1}.

The Acetate of VII: M. p. 215~216°C; pale brownish red needles (from ethyl acetate).

Found: C, 67.07; H, 4.38; N, 8.69. Calcd. for $C_{18}H_{14}O_4N_2$: C, 66.93; H, 4.07; N, 8.47%.

λ_{max}^{MeOH} mμ (log ε): 230 (4.54), 303 (4.70), 366.5 (3.79), 480 (2.83). IR (Nujol): 2217, 1783 cm^{-1}.

The filtrate was extracted with benzene, and the crystals thus obtained were recrystallized from a mixture of ethanol and water to form IX, which appeared as pale brownish yellow silky needles (m. p. 214~215°C).

Found: C, 66.23; H, 5.23; N, 4.65. Calcd. for $C_{18}H_{17}O_5N$: C, 66.05; H, 5.24; N, 4.28%.

λ_{max}^{MeOH} mμ (log ε): 236 (4.51), 312 (4.74), 325 (4.52), 453 (3.36). IR (KBr disk): 3060, 2215, 1647 cm^{-1}.

b) With 2 mol. of Sodium Ethoxide.—To a sodium ethoxide solution prepared from sodium (0.18 g., 0.0078 mol.) and absolute ethanol (6 ml.), ethyl cyanoacetate (0.84 g.) was added. After the mixture had been left standing for 30 min., a solution of methyl ether (a mixture of IIIa and IIIb) (0.75 g., 0.0034 mol.) in absolute ethanol (6 ml.) was added, and the mixture was allowed to stand overnight. The solvent was removed under reduced pressure, water was added, and the separated crystals were collected by filtration; m. p. 108~134°C; 0.21 g. Recrystallization from ethanol afforded VI as orangish yellow needles (m. p. 180~182°C, 50 mg.).

Found: C, 65.82; H, 5.51; N, 8.54. Calcd. for $C_{18}H_{18}O_4N$: C, 66.24; H, 5.56; N, 8.56%.

λ_{max}^{MeOH} mμ (log ε): 239 (4.53), 325 (4.80), 368 (3.85), 388 (3.86), 446 (3.25). IR (Nujol): 3490, 3380, 2232, 1675 cm^{-1}.

The mother liquor was washed with benzene, and the aqueous layer was acidified with 6 N sulfuric acid, from which VII (m. p. 218~223°C; 0.52 g.) was obtained.

The Reaction of 4-(1, 1-Ethylenedioxyethyl)-2-(*p*-tolylsulfonyloxy)tropone (IVa) and Ethyl Cyanoacetate.—To a sodium ethoxide solution prepared from sodium (0.39 g.) and absolute ethanol (40 ml.), ethyl cyanoacetate (3.5 g.) was added. After this mixture had been left standing for 30 min., a suspended solution of IVa (5.04 g.) in absolute ethanol (20 ml.) was added, the mixture was stirred for 10 hr., and then it was allowed to stand for 2 days. After removal of the solvent under reduced pressure, water was added to the residue, and the separated crystals were collected (4.25 g.). The crystals were warmed with benzene, and the insoluble part (1.85 g., m. p. 250~256°C) was recrystallized from ethanol to give pale yellow needles of XIV (m. p. 258~259°C).

Found: C, 60.56; H, 5.43; N, 4.41. Calcd. for $C_{16}H_{17}O_6N$: C, 60.18; H, 5.37; N, 4.39%.

λ_{max}^{MeOH} mμ (log ε): 222 (4.34), 288 (4.44), 335 (4.29).

The benzene soluble part was passed through a column of alumina with benzene, and the crystals obtained (m. p. 141~145°C; 1.50 g.) were recrystallized from ethanol to give XV as orangish yellow needles (m. p. 154.5~155°C; 1.15 g.).

Found: C, 64.46; H, 5.62; N, 3.66. Calcd. for $C_{20}H_{23}O_6N$: C, 64.33; H, 6.21; N, 3.75%.

λ_{max}^{MeOH} mμ (log ε): 245 (4.51), 318 (4.71), 327 (4.82), 370 (3.87), 395 (4.00), 450 (3.40). IR (Nujol): 3450, 3345, 1675, 1647 cm^{-1}.

The Picrate of XV: M. p. 137~138°C; orange needles (from ethanol).

The aqueous mother liquor was extracted with benzene to give an oily substance containing a crystalline solid which was then recrystallized from ethanol to give XVI as yellowish orange needles (30 mg.; m. p. 205~206°C).

Found: C, 66.58; H, 5.18; N, 4.40. Calcd. for $C_{18}H_{17}O_5N$: C, 66.02; H, 5.24; N, 4.28%.

λ_{max}^{MeOH} mμ (log ε): 234 (4.61), 313 (4.79), 327 (4.55), 360 (4.12) sh, 450 (3.18) sh. IR (Nujol): 3150, 2222, 1667 cm^{-1}.

The Reaction of 6-(1, 1-Ethylenedioxyethyl)-2-*p*-tolylsulfonyloxy)tropone (IVb) and Ethyl Cyanoacetate.—A sodium ethoxide solution (30 mg. of sodium and 4 ml. of absolute ethanol), ethyl cyanoacetate (250 mg.), and a solution of IVb (360 mg.) in absolute ethanol were treated in the manner described above. After removal of the solvent, water was added and the crystals which had separated were recrystallized from ethanol to give recovered IVb (110 mg.) and the azulene derivative V (10 mg.).

The Hydrolysis of the Ethylene Ketal Group of V, VI, VII, VIII, XV and XVI.—A solution of ethylene ketal in ethanol (40 times) and 6 N sulfuric acid was refluxed for 30 min. and then allowed to cool, by which process a hydrolized compound was obtained, in a nearly quantitative yield.

a) Diethyl 5-Acetyl-2-aminoazulene-1, 3-dicarboxylate (X).—Obtained from V: M. p. 123~124°C; orange micro-prisms (from ethanol).

Found: C, 65.58; H, 5.65; N, 4.43. Calcd. for $C_{18}H_{19}O_5N$: C, 65.64; H, 5.82; N, 4.25%.

λ_{max}^{MeOH} mμ (log ε): 246 (4.55), 328 (4.73), 340 (4.85), 389 (3.78), 490 (3.69). IR (Nujol): 3410, 3320, 1672 cm^{-1}.

The Acetate of X: Obtained by refluxing X in acetic anhydride for 8 hr.; m. p. 161~162°C; reddish violet leaflets (from ethanol).

Found: N, 3.81. Calcd. for $C_{20}H_{21}O_6N$: N, 3.77%.

IR (Nujol): 3380, 1724, 1695, 1686 cm^{-1}.

b) Ethyl 5(or 7)-Acetyl-2-amino-3-cyanoazulene-1-carboxylate (XI).—Obtained from VI; m. p. 199~200°C; orange prisms (from ethanol).

Found: C, 67.81; H, 4.87; N, 9.92. Calcd. for $C_{16}H_{14}O_3N_2$: C, 68.07; H, 5.00; N, 9.92%.

λ_{max}^{MeOH} mμ (log ε): 238 (4.51), 326 (4.63), 336 (4.67), 390 (3.78), 490 (3.51). IR (Nujol): 3470, 3370, 2217, 1686, 1664 cm^{-1}.

c) 5-Acetyl-1, 3-dicyano-2-hydroxyazulene (XII).—Obtained from VII; m. p. 223~225°C; pale brown prisms (from aqueous ethanol).

Found: C, 70.48; H, 3.50; N, 11.61. Calcd. for $C_{14}H_8O_2N_2$: C, 71.18; H, 3.41; N, 11.86%.

λ_{max}^{MeOH} mμ (log ε): 230 (4.57), 324 (4.67), 339 (4.73), 400 (3.67), 504 (3.67). IR (KBr disk): 3010, 2218, 1672 cm^{-1}.

d) Ethyl 5(or 7)-Acetyl-3-cyano-2-hydroxyazulene-1-carboxylate (XIII).—Obtained from VIII; m. p. 204.5~206°C; dull yellowish orange leaflets (from ethanol).

Found: C, 67.25; H, 4.54; N, 5.10. Calcd. for $C_{16}H_{13}O_4N$: C, 67.84; H, 4.63; N, 4.95%.

λ_{max}^{MeOH} mμ (log ε): 235 (4.48), 320 (4.56), 341 (4.63), 380 (3.73), 504 (3.67). IR (KBr disk): 2980, 2220, 1690 cm^{-1}.

The Acetate of XIII: Obtained by refluxing XIII in acetic anhydride; m. p. 169~170°C; brilliant red needles (from ethanol).

Found: C, 66.63; H, 4.61; N, 4.30. Calcd. for $C_{18}H_{15}O_5N$: C, 66.45; H, 4.65; N, 4.31%.

IR (Nujol): 2212, 1779, 1684 cm^{-1}.

e) Diethyl 6-Acetyl-2-aminoazulene-1, 3-dicarboxylate (XVII).—Obtained from XV: m. p. 139~140°C; orange needles (from ethanol).

Found: C, 65.89; H, 5.80; N, 4.38. Calcd. for $C_{18}H_{19}O_5N$: C, 65.64; H, 5.82; N, 4.25%.

λ_{max}^{MeOH} mμ (log ε): 248 (4.60), 330 (4.84), 380 (3.98), 432 (4.30). IR (Nujol): 3510, 3340, 1692, 1669, 1656 cm^{-1}.

f) Ethyl 6-Acetyl-3-cyano-2-hydroxyazulene-1-carboxylate (XVIII).—Obtained from XVI; m. p. 196.5~198°C; pale red granules (from ethanol).

Found: C, 67.84; H, 4.52; N, 4.50. Calcd. for $C_{16}H_{13}O_4N$: C, 67.84; H, 4.63; N, 4.95%.

λ_{max}^{MeOH} mμ (log ε): 240 (4.54), 318 (4.80), 330 (4.66), 357 (3.96), 375 (3.98), 440 (4.12). IR (Nujol): 3200, 2217, 1695, 1667 cm^{-1}.

Diethyl 5-Acetylazulene-1,3-dicarboxylate (XIX).—*a) The Deamination of V in Ethanol.*—To a solution of V (0.50 g.) in 50% aqueous ethanol (25 ml.), concentrated sulfuric acid (4.7 ml.) was added; isoamyl nitrite (2.4 g.) was then added into this mixture with stirring at room temperature. After having been stirred for 4 hr. and having been left standing overnight, the mixture was diluted with water and extracted with benzene. The benzene extract was passed through a column of alumina; from the first effluent, crude crystals of XIX (m. p. 106~109°C; 280 mg.) were obtained. Recrystallization from ethanol formed red needles (m. p. 116.5~117°C).

Found: C, 68.66; H, 5.75. Calcd. for $C_{18}H_{18}O_5$: C, 68.78; H, 5.77%.

λ_{max}^{MeOH} mμ (log ε): 235 (4.54), 272 (4.36), 305 (4.48), 324 (3.94) sh, 395 (4.11), 508 (2.68). IR (Nujol): 1689 cm^{-1}.

From the second effluent, X (20 mg.) was obtained.

When sodium hypophosphite was used on the decomposition of the diazotized solution, XIX (60 mg.) was obtained from V (100 mg.).

b) The Deamination of V in Dioxane.—To a solution of V (100 mg.) in dioxane (3 ml.) and concentrated sulfuric acid (0.4 ml.), a solution of sodium nitrite (50 mg.) in water (0.2 ml.) was dropped in. After this mixture had been stirred for 30 min., active copper powder (100 mg.) was added, and the mixture was warmed on a water bath. The mixture was treated in the above-mentioned method to give XIX (35 mg.).

c) The Deamination of X.—A solution of X (100 mg.) in 50% aqueous ethanol (5 ml.) and concentrated sulfuric acid (4.5 ml.) was diazotized and treated as in a); XIX (30 mg.) was thus obtained.

Diethyl 6-Acetylazulene-1, 3-dicarboxylate (XX).—*a) The Deamination of XV in Ethanol.*—To a solution of XV (100 mg.) in 60% aqueous ethanol (5 ml.), concentrated sulfuric acid (0.6 ml.) was added, and to this mixture, isoamyl nitrite (0.44 g.) was added with stirring at room temperature. After having been stirred for 2 hr. and having been standing overnight, the reaction mixture was diluted with water (20 ml.) and extracted with benzene. The benzene extract was passed through a column of alumina, and from the first effluent, crude crystals

of XX (m. p. 105~106°C; 60 mg.) were obtained. Recrystallization from ethanol formed deep violet blue scales (m. p. 129~130°C).

Found: C, 68.61; H, 5.79. Calcd. for $C_{18}H_{15}O_5$: C, 68.78; H, 5.77%.

λ_{max}^{MeOH} mμ (log ε): 242 (4.62), 270 (4.26), 310 (4.77), 345 (3.93), 375 (2.82), 527 (2.49). IR (Nujol): 1686 cm^{-1}.

b) The Deamination of XV in Dioxane.—Into a solution of XV (200 mg.) in dioxane (6 ml.) and concentrated sulfuric acid (0.4 ml.), a solution of sodium nitrite (50 mg.) in water (2 ml.) was dropped. After this mixture had been stirred for 30 min., active copper powder (100 mg.) and a solution of sodium hypophosphite (0.8 g) in water (93 ml.) were added. After having been stirred an additional for 2 hr., the reaction mixture was treated as in a) From the first effluent, XX (60 mg.) was obtained; from the second effluent, XVII (60 mg.) was obtained.

c) The Deamination of XVII.—XVII (90 mg.) was diazotized and treated as in a); XX (30 mg.) was obtained.

5-Acetylazulene-1, 3-dicarboxylic Acid (XXI).—To a solution of potassium hydroxide (140 mg.) in 70% aqueous ethanol (5 ml.), XX (200 mg.) was added, and the mixture was refluxed for 4 hr. After it had cooled the solution was acidified with 6 N sulfuric acid to give XXI (140 mg.) as dark brown crystals (m. p. above 270°C; sparingly soluble in organic solvents).

5-Acetylazulene (XXII).—The decarboxylation of XXI was carried out under reduced pressure (15 mmHg) at 280~300°C, yielding a violet oil which was then passed through a column of alumina with petroleum ether (b. p. 40~60°C) to give a violet blue oil (XXII). IR (Nujol): 1664 cm^{-1}.

λ_{max}^{MeOH} mμ (log ε): 220 (3.97), 235 (3.98), 392 (4.25), 370 (3.40), 383 (3.50), 564, 584 sh, 612, 670 sh.

6-Acetylazulene-1, 3-dicarboxylic Acid (XXIII).—When XX (150 mg.) was treated as in the above experiment, XXIII (100 mg.) (brown crystals; m. p. above 260°C; sparingly soluble in organic solvents) was obtained. IR (Nujol): 1704 cm^{-1}.

5-Acetyl-2-aminoazulene-1, 3-dicarboxylic Acid (XXIV).—To a solution of potassium hydroxide (100 mg.) in 85% aqueous ethanol (3 ml.), X (100 mg.) was added, and the mixture was refluxed for 5 hr. After the solution had cooled, it was acidified with 6 N sulfuric acid to give XXIV (70 mg.) as a black crystalline powder (m. p. 203~204.5°C (decomp.); sparingly soluble in organic solvents).

Found: C, 60.78; H, 4.04; N, 4.75. Calcd. for $C_{14}H_{11}O_5N$: C, 61.54; H, 4.06; N, 5.13%.

λ_{max}^{MeOH} mμ (log ε): 243 (4.45), 339 (4.75), 385 (3.76), 494 (3.61). IR (KBr disk): 3439, 3325, 1657 cm^{-1}.

6-Acetyl-2-aminoazulene-1, 3-dicarboylic Acid (XXV).—When XVII (180 mg.) was treated as in the above experiment, XXV (130 mg.), (reddish brown crystals; m. p. 265°C (decomp.); sparingly soluble in organic solvents) was obtained.

λ_{max}^{MeOH} mμ (log ε): 246 (4.43), 329 (4.67), 378 (3.86), 434 (4.17). IR (Nujol): 3540, 3340, 1661 cm^{-1}.

2-Amino-5-(1, 1-ethylenedioxyethyl)azulene-1, 3-dicarboxylic Acid (XXVIII).—To a solution of potassium hydroxide (0.80 g.) in ethanol (6 ml.), V (1.00 g.) was added, and the mixture was refluxed for 4 hr. After the mixture had cooled, it was diluted with water and acidified with 6 N sulfuric acid to give XXVIII (0.71 g.) (dull yellowish orange crystals,; m. p. 174~175°C (decomp.); sparingly soluble in organic solvents).

Found: C, 61.71; H, 4.97; N, 4.73. Calcd. for $C_{16}H_{15}O_6N$: C, 60.56; H, 4.77; N, 4.41%.

λ_{max}^{MeOH} mμ (log ε): 345 (4.34), 315 (4.57), 326 (4.62), 380 (3.86) sh. IR (Nujol): 3430, 3340, 1658, 1642 cm^{-1}.

5-Acetyl-2-aminoazulene (XXVI).—*a) From XXIV.*—A solution of XXIV (300 mg.) in pyridine (2 ml.) was heated at 125~130°C to effect decarboxylation. The residue produced by the evaporation of the excess pyridine was dissolved in benzene, and the solution was passed through a column of alumina to give XXVI (m. p. 162~163°C; 130 mg.). Recrystallization from ethanol formed deep violet leaflets (m. p. 167~167.5°C; 110 mg.).

Found: C, 78.05; H, 5.93; N, 7.47. Calcd. for $C_{12}H_{11}ON$: C, 77.81; H, 5.99; N, 7.56%.

λ_{max}^{MeOH} mμ (log ε): 227 (4.25), 322 (4.79), 384 (3.75) 395 (3.72), 490 (3.11) sh. IR: (KBr disk) 3457, 3343, 3238, 1638, 1628; (Nujol) 3460, 3360, 3270, 1645, 1629 cm^{-1}.

Picrate: M. p. 166.5~167.5°C; brownish violet needles (from ethanol).

Found: C, 52.11; H, 5.54; N, 13.21. Calcd. for $C_{18}H_{14}O_8N_4$: C, 52.18; H, 5.77; N, 13.52%.

Acetate: M. p. 176~177°C; deep reddish violet needles (from ethanol).

Found: C, 74.42; H, 5.54; N, 6.16. Calcd. for $C_{14}H_{13}O_2N$: C, 73.99; H, 5.77; N, 6.16%.

λ_{max}^{MeOH} mμ (log ε): 224 (4.11), 250 (4.05), 315 (4.75), 380 (3.59). IR (Nujol): 3380, 1689, 1661 cm^{-1}.

b) From XXVIII.—When XXVIII (400 mg.) was dissolved in pyridine (2 ml.) and treated as in a), XXVI (80 mg.) was obtained.

6-Acetyl-2-aminoazulene (XXVII).—When a solution of XXV (150 mg.) in pyridine (2 ml.) was treated as in the above experiment, XXVII (m. p. 167~168°C; 20 mg.) was obtained. Recrystallization from ethanol formed brilliant brownish yellow scales (m. p. 168.5~169.5°C; 15 mg.).

Found: C, 77.89; H, 6.02; N, 7.50. Calcd. for $C_{12}H_{11}ON$: C, 77.81; H, 5.99; N, 7.56%.

λ_{max}^{MeOH} mμ (log ε): 225 (4.06), 290 (4.69), 301 (4.79), 335 (3.90), 340 (3.74) sh, 440 (4.43). IR (Nujol): 3460, 3340, 3270, 1642 cm^{-1}.

Picrate: M. p. above 270°C; fine black crystals (from ethanol).

Found: N, 12.00. Calcd. for $C_{18}H_{14}O_8N_4$-C_2H_5OH; N, 12.17%.

Acetate; M. p. 198~199°C; blacklish green micro-prisms (from methanol).

Found: C, 73.65; H, 5.97; N, 6.11. Calcd. for $C_{14}H_{13}O_2N$: C, 73.99; H, 5.77; N, 6.16%.

λ_{max}^{MeOH} mμ (log ε): 220 (4.12), 297 (4.83), 404 (4.33). IR (Nujol): 3340, 1704, 1675, 1661 cm^{-1}.

2-Amino-5-(1, 1-ethylenedioxyethyl)azulene-1, 3-dicarboxylic Acid Monoethyl Ester (XXIX).—To a solution of potassium hydroxide (140 mg.) in ethanol (5 ml.), V (400 mg.) was added, and the mixture was refluxed for 4 hr. After it had cooled, the solution was acidified with 6 N sulfuric acid to give XXIX (350 mg.) as brownish yellow crystals (m. p. 161~164°C (decomp.); sparingly soluble in organic solvents).

Found: C, 62.61; H, 5.44; N, 4.22. Calcd. for $C_{18}H_{19}O_6N$: C, 62.60; H, 5.55; N, 4.06%.

λ_{max}^{MeOH} mμ (log ε): 245.5 (4.49), 316 (4.70), 327 (4.80), 370 (3.85), 454 (3.43). IR (KBr disk): 3448, 3327, 1662 cm^{-1}.

p-Bromophenacyl Ester of XXIX.—In a solution of sodium hydroxide (200 mg.) in water (20 ml.), XXIX (100 mg.) was dissolved, and the solution was weakly acidified with 2 N hydrochloric acid. To this solution, a solution of *p*-bromophenacyl bromide (350 mg.) in ethanol (20 ml.) was added, and the mixture was refluxed for 2 hr. The reaction mixture was diluted with water (5 ml.), and the precipitate thereby formed was collected by filtration. Crude crystals of the ester of XXIX (m. p. 186~190°C; 100 mg.) were recrystallized from ethanol to form a pale brown crystalline powder (m. p. 214~215°C, 50 mg.).

Found: C, 58.40; H, 4.17; N, 3.06. Calcd. for $C_{26}H_{24}O_7NBr$: C, 57.57; H, 4.46; N, 2.58%.

Ethyl 2-Amino-5(or 7)-(1, 1-ethylenedioxyethyl)-azulene-1-carboxylate (XXX).—A solution of XXIX (260 mg.) in pyridine (1.5 ml.) was heated at 130~140°C to effect decarboxylation. The residue produced by evaporation of the excess pyridine was dissolved in benzene, and the solution was passed through a column of alumina. A reddish crude substance obtained from the effluent was recrystallized from ethanol to give reddish orange prisms (m. p. 144~145°C; 60 mg.).

Found: C, 67.74; H, 6.31; N, 4.65. Calcd. for $C_{17}H_{19}O_4N$: C, 67.76; H, 6.36; N, 4.65%.

λ_{max}^{MeOH} mμ (log ε): 216 (4.26), 306 (4.77), 316 (4.86), 357 (4.00), 380 (3.80) sh. IR (KBr disk): 3541, 3344, 3287, 1663 cm^{-1}.

Picrate: M. p. 138.5~139.5°C; orange prisms (from ethanol).

Acetate: M. p. 164~165°C; violet red micro-prisms (from ethanol).

Found: C, 66.53; H, 5.99; N, 3.95. Calcd. for $C_{19}H_{21}O_5N$: C, 66.46; H, 6.16; N, 4.08%,

λ_{max}^{MeOH} mμ (log ε): 244 (4.28), 306 (4.84), 316 (4.96), 356 (3.95), 370 (3.97). IR (Nujol): 3500, 1689, 1650 cm^{-1}.

Ethyl 5(or 7)-Acetyl-2-aminoazulene-1-carboxylate (XXXI).—A solution of XXX (50 mg.) in ethanol (2 ml.) and 6 N sulfuric acid (0.02 ml.) was refluxed for 20 min. The reaction mixture was diluted with water (3 ml.) to form XXXI (m. p. 130~132°C; 45 mg.), which was then recrystallized from ethanol to give brownish orange micro-prisms (m. p. 131~132°C; 40 mg.).

Found: C, 69.59; H, 5.49; N, 5.28. Calcd. for $C_{15}H_{15}O_3N$: C, 70.02; H, 5.88; N, 5.44%.

λ_{max}^{MeOH} mμ (log ε): 220 (4.22), 246 (4.10), 331 (4.73), 490 (3.41). IR: (KBr disk) 3313, 3254, 1664, 1612; (Nujol) 3380, 3280, 1656, 1603 cm^{-1}.

Expenses for the present series of experiments were defrayed by a grant-in-aid for Scientific Research from the Ministry of Education. The infrared spectra in this paper were measured with a Shimadzu infrared spectrophotometer IR-27 purchased by a grant-in-aid for Scientific Research from the Toyo Rayon Co., Ltd. The authors wish to express their deep gratitude for these contributions.

Department of Chemistry
Faculty of Science
Tohoku University
Katahira-cho, Sendai

The Reaction of 5- and 6-Acetylazulene Derivatives with Hydrazines. The Formation of Azuleno[4, 3-f]pyrazoles

By Tetsuo NOZOE, Kahei TAKASE and Masao TADA*

(Received February 25, 1963)

In a previous report[1], 5- and 6-acetylazulene derivatives were derived from 4-acetyltropolone. The present paper deals with the reaction of these acetylazulenes with various hydrazines and hydroxylamine. The reaction with unsubstituted hydrazine resulted in the formation of azulenopyrazoles.

The reaction of hydrazine hydrate with diethyl 5-acetylazulene-1, 3-dicarboxylate (I) yielded dull reddish crystals II. When II was heated with potassium hydroxide in ethylene glycol, deep violet crystals III were

* Present address: The Research Institute for Tuberculosis and Leprosy, Tohoku University, Sendai.

1) T. Nozoe, K. Takase and M. Tada, This Bulletin, **36**, 1010 (1963).

formed; III was also obtained by the alkaline hydrolysis of II and the subsequent decarboxylation in quinoline of the resultant dicarboxylic acid IV.

III contains nitrogen and shows a sharp N-H band at 3135 cm^{-1} which disappears upon acetylation to form *N*-acetate (V). The carbonyl frequency (1724 cm^{-1}) of the acetate indicated the attachment of an aromatic system or an electron-attracting group to the imino nitrogen[2]. These spectral observations reveal the structure of III to be that of a methylazulenopyrazole. The infrared spectra of II and its acetate VI exhibited ν_{NH} at 3230 cm^{-1} and ν_{NCOCH_3} at 1733 cm^{-1}, which facts suggest presence of the same ring system in both II and III. The conclusive evidence for the presence of a pyrazole ring was obtained by the alkaline permanganate oxidation of II, upon which 5-methylpyrazole-3, 4-dicarboxylic acid (VII) was obtained. The stability of II to chloranil indicated that II must be a pyrazole and not a pyrazoline derivative. Therefore, II can be formulated as IIa or IIb (see Chart I). Although definite evidence is lacking, we prefer IIa, that is, diethyl 3-methylazuleno [4, 3-f] pyrazole-5, 7-dicarboxylate, to IIb on the basis of the steric hindrance of ethoxycarbonyl at Position 3. Thus, the structures of 3-methylazuleno [4, 3-f] -pyrazole shown in Chart I were assigned to III and IV.

On hydrolysis with a limited amount of alkali, II yielded an ester acid VIII which, on heating in quinoline, gave a monoester IX, althougth the exact position of the ethoxycarbonyl group is not known.

The ultraviolet and visible absorption spectra of these 3-methylazuleno[4, 3-f]pyrazole derivatives are shown in Figs. 1 and 2.

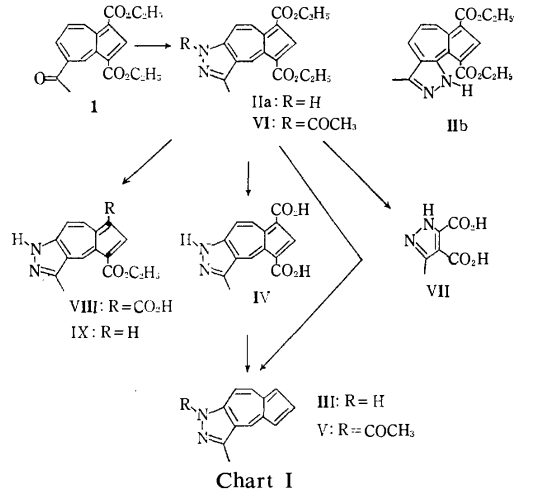

Chart I

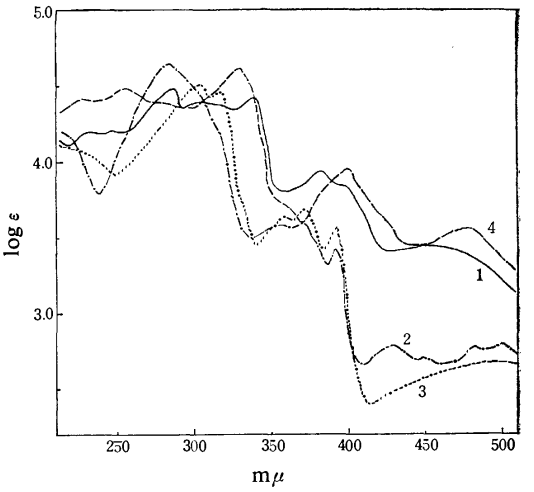

Fig. 1. Ultraviolet absorption spectra in methanol.
1 Diethyl 3-methylazuleno[4,3-f]pyrazole-5,7-dicarboxylate (II)
2 3-Methylazuleno[4,3-f]pyrazole (III)
3 Acetate (V) of III
4 Acetate (VI) of II

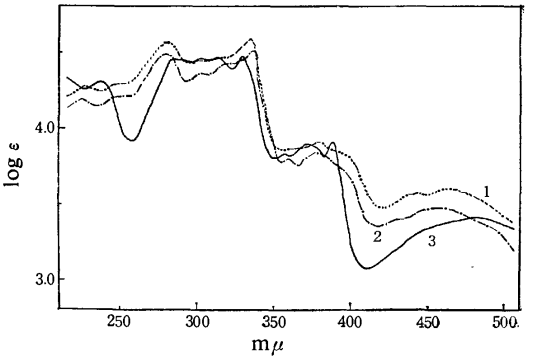

Fig. 2. Ultraviolet absorption spectra in methanol.
1 3-Methylazuleno[4,3-f]pyrazole-5,7-dicarboxylic acid (IV)
2 3-Methylazuleno[4,3-f]pyrazole-5,7-dicarboxylic acid monoethyl ester (VIII)
3 Ethyl 3-methylazuleno[4,3-f]pyrazole-5(or 7)-carboxylate (IX)

This rather unusual ring formation on an azulene nucleus (though such a formation is not without precedent[3], azulenofurane derivative (X)), can be rationalized by the electrophilic nature of the seven-membered ring in

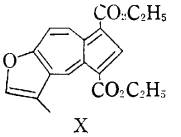

X

2) L. J. Bellamy, "The Infra-red Spectra of Complex Molecules," Methuen, London (1958), p. 213.

3) T. Nozoe, S. Seto and S. Matsumura, *Chem. & Ind.*, 1961, 1715.

azulene enhanced by the presence of the two ethoxycarbonyl groups at Positions 1 and 3, and by the facility of the dehydrogenation of dihydroazulene to azulene. This reaction path is shown in Chart II.

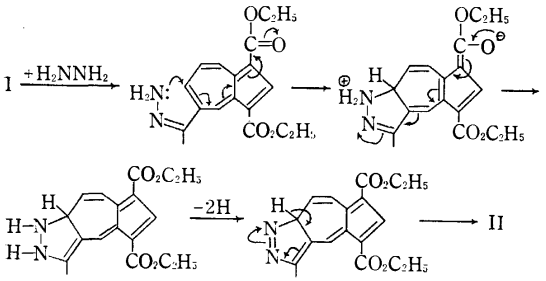

Chart II

This interesting behaviour of I toward hydrazine prompted us to extend our study to other acetylazulenes and other reagents related to hydrazine.

Several experiments revealed that hydrazine is the only reagent to form pyrazole; thus, I gave a normal phenylhydrazone (ν_{NH} 3210 cm^{-1}), a normal *p*-tolylsulfonylhydrazone (ν_{NH} 3210 cm^{-1}) and a normal oxime (ν_{OH} 3350 cm^{-1}). Moreover, 2-amino (XI, XII), 2-acetamido (XIII) or 2-hydroxyl (XIV, XV) groups inhibit the ring formation, giving the normal ketonic derivatives (see the Experimental section). There seems to be no difference if the ethoxycarbonyl or the cyano groups

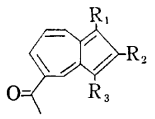

XI: $R_1=R_3=CO_2C_2H_5$; $R_2=NH_2$
XII: $R_1=CN$, $R_3=CO_2C_2H_5$ or $R_1=CO_2C_2H_5$, $R_3=CN$; $R_2=NH_2$
XIII: $R_1=R_3=CO_2C_2H_5$; $R_2=NHCOCH_3$
XIV: $R_1=CN$, $R_3=CO_2C_2H_5$ or $R_1=CO_2C_2H_5$, $R_3=CN$; $R_2=OH$
XV: $R_1=R_3=CN$; $R_2=OH$

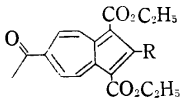

XVI: R=H
XVII: $R=NH_2$

occupy at Positions 1 and 3, inasmuch as electron-releasing amino or the hydroxyl group is situated at Position 2. Furthermore, it is a rather interesting difference that diethyl 6-acetylazulene-1, 3-dicarboxylate (XVI), the position isomer of I, gives only normal hydrazone. According to the SCF electron density calculation for the ground state of azulene[4], the density at Position 6 (0.938) is comparatively lower than that at Position 5 (1.034). The findings described above are consistent with the theoretical calculation.

Experimental[5]

Diethyl 3-Methylazuleno[4, 3-f]pyrazole-5, 7-dicarboxylate (II).—To a solution of diethyl 5-acetylazulene-1, 3-dicarboxylate (I) (130 mg.) in ethanol (2 ml.), 80% hydrazine hydrate (0.1 g.) was added, and the mixture was warmed for 30 min., by which process II (40 mg.) was obtained as dull red micro-prisms (m. p. 252~253°C, after recrystallization from ethanol).

Found: C, 65.99; H, 5.73; N, 8.56. Calcd. for $C_{18}H_{18}O_4N_2$: C, 66.24; H, 5.56; N, 8.58%.

λ_{max}^{MeOH} mμ (log ε): 232 (4.18), 218 (4.44), 307 (4.39), 339 (4.45), 384 (3.94), 460 (3.45). IR (Nujol): 3230, 1692, 1656 cm^{-1}.

Acetate (VI). — Reddish orange micro-prisms (from ethanol); m. p. 121~122°C.

Found: C, 65.46; H, 5.61; N, 8.04. Calcd. for $C_{20}H_{20}O_5N_2$: C, 65.46; H, 5.47; N, 7.61%.

λ_{max}^{MeOH} mμ (log ε): 255 (4.48), 275 (4.38), 328 (4.62), 404 (3.95), 480 (3.53). IR (Nujol): 1733, 1689, 1669 cm^{-1}.

3-Methylazuleno[4, 3-f]pyrazole-5, 7-dicarboxylic Acid (IV).—A solution of II (150 mg.) and potassium hydroxide (200 mg.) in 50% aqueous ethanol (8 ml.) was refluxed for 8 hr. After being cooled, the solution was acidified with 6 N sulfuric acid to give IV (110 mg.) as a brownish red crystalline powder (m. p. above 270°C) which is sparingly soluble in organic solvents.

Found: C, 59.55; H, 4.00; N, 8.90. Calcd. for $C_{14}H_{12}O_4N_2$-$2H_2O$: C, 59.78; H, 4.66; N, 9.96%.

λ_{max}^{MeOH} mμ (log ε): 230 (4.25), 284 (4.54), 304 (4.41), 338 (4.56), 363 (3.82), 460 (3.53). IR (Nujol): 3155, 1661 cm^{-1}.

3-Methylazuleno[4, 3-f]pyrazole (III).—*i) From II.*—To a solution of potassium hydroxide (110 mg.) in ethylene glycol (3 ml.), II (180 mg.) was added, and the mixture was heated at 140~150°C for 6 hr. After being cooled, this solution was diluted with water (40 ml.) and extracted with benzene. Removal of the solvent from the extract gave III (50 mg.) (m. p. 185~186°C), which was recrystallized from aqueous ethanol in the form of purplish red needles (m. p. 186~187°C).

Found: C, 79.20; H, 4.91; N, 15.47. Calcd. for $C_{12}H_{10}N_2$: C, 79.09; H, 5.72; N, 15.38%.

λ_{max}^{MeOH} mμ (log ε): 280 (4.64), 352 (3.59), 370 (3.63), 390 (3.46), 430 (2.79), 500 (2.79). IR (Nujol): 3135, 1613 cm^{-1}.

Acetate (V).—Pale purple scales (from ethanol); m. p. 158~159°C.

Found: C, 75.46; H, 5.56; N, 12.70. Calcd. for $C_{14}H_{12}ON_2$: C, 74.99; H, 5.38; N, 12.49%.

λ_{max}^{MeOH} mμ (log ε): 300 (4.50), 316 (4.44), 359 (3.62),

4) A. Julg, *J. chim. phys.*, **52**, 377 (1955).
5) All melting points are uncorrected.

371 (3.67), 391 (3.55), 495 (2.64). IR (Nujol): 1724, 1684 cm^{-1}.

ii) From IV. — A mixture of IV (120 mg.) and quinoline (1 ml.) was heated at 230~250°C for 2 hr. to effect decarboxylation. The residue produced by the evaporation of the quinoline was dissolved in ethyl acetate and passed through a column of alumina to give III (10 mg.).

The Permanganate Oxidation of II. — Into a solution of II (400 mg.) in a 0.25 N potassium hydroxide solution (100 ml.), finely powdered potassium permanganate (2.32 g.) was added in small portions with stirring at room temperature; the mixture was then stirred a further 6 hr. and allowed to stand overnight. The excess permanganate was decomposed on the addition of methanol, and the precipitated manganese dioxide was filtered off. The filtrate was slightly acidified with 6 N hydrochloric acid and concentrated under a reduced pressure until crystal had begun to separate out. Acetone was added, and the inorganic salts thereby separated were filtered off. After the mother liquor was treated repeatedly in the same way as above, the combined acetone solution was evaporated to dryness; the subsequent addition of a small amount of water gave oxalic acid. From the water-soluble part, 5-methylpyrazole-3,4-dicarboxylic acid (VII) (20 mg.) was obtained (m. p., 233°C (decomp.)); this acid was identified as identical with an authentic specimen[6] by a comparison of the infrared spectra.

3-Methylazuleno[4,3-f]pyrazole-5,7-dicarboxylic Acid Monoethyl Ester (VIII). — To a solution of potassium hydroxide (150 mg.) in 75% aqueous ethanol (8 ml.), II (200 mg.) was added, and the mixture was refluxed for 4 hr. This solution was acidified with 6 N sulfuric acid to give VIII (150 mg.) as brownish red crystals (m. p. 247~250°C (decomp.)).

Found: C, 60.95; H, 4.92; N, 8.58. Calcd. for $C_{16}H_{14}O_4N_2$-H_2O: C, 60.75; H, 5.10; N, 8.86%.

λ_{max}^{MeOH} mμ (log ε): 230 (4.19), 284 (4.55), 304 (4.37), 321 (4.42), 363 (3.79), 380 (3.86), 460 (3.51).

Ethyl 3-Methylazuleno[4,3-f]pyrazole-5 (or 7)-carboxylate (IX). — A mixture of VIII (100 mg.) and quinoline (1.5 ml.) was heated at 230~250°C for 2 hr. to effect decarboxylation. The residue, obtained by the evaporation of the quinoline, was dissolved in benzene and passed through a column of alumina to give red crystals (20 mg.) (m. p. 162~168°C) which were then recrystallized from benzene to form IX (15 mg.) as red prisms (m. p. 202~203°C).

Found: C, 71.03; H, 5.46; N, 10.71. Calcd. for $C_{15}H_{14}O_2N_2$: C, 70.85; H, 5.55; N, 11.02%.

λ_{max}^{MeOH} mμ (log ε): 235 (4.32), 286 (4.47), 302 (4.45), 315 (4.30), 333 (4.29), 373 (3.92), 390 (3.92), 484 (3.41). IR (Nujol): 3145, 1647 cm^{-1}.

Ketonic Derivatives of I.—*a) Phenylhydrazone.*— Violet brown micro-prisms (from ethanol); m. p. 181~182°C.

Found: C, 71.24; H, 5.90; N, 6.54. Calcd. for $C_{24}H_{24}O_4N_2$: C, 71.27; H, 5.98; N, 6.93%.

IR (Nujol) 3310, 1686, 1667 cm^{-1}.

b) p-Tolylsulfonylhydrazone.—Brown micro-prisms (from ethanol); m. p. 206~207°C.

Found: C, 62.16; H, 5.13; N, 5.67. Calcd. for $C_{25}H_{26}O_6N_2S$: C, 62.23; H, 5.43; N, 5.80%.

IR (Nujol): 3210, 1689 cm^{-1}.

c) Oxime. — Brown needles (from ethanol); m. p. 162.5~164°C.

Found: C, 65.38; H, 5.47; N, 4.65. Calcd. for $C_{18}H_{19}O_5N$: C, 65.64; H, 5.82; N, 4.25%.

IR (Nujol): 3350, 1672 cm^{-1}.

Oxime Acetate: Dull red crystals (from ethanol); m. p. 126.5~128°C.

Found: N, 3.77. Calcd. for $C_{20}H_{21}O_6N$: N, 3.33%. IR (Nujol): 1789, 1686 cm^{-1}.

Ketonic Derivatives of XI. — *a) Hydrazone.* — Orange yellow fine crystals (from ethanol); m. p. 128~129°C.

Found: C, 63.01; H, 5.80; N, 11.73. Calcd. for $C_{18}H_{21}O_4N_3$: C, 62.96; H, 6.16; N, 12.24%.

IR (Nujol): 3320, 3250, 3160, 3100, 1667 cm^{-1}.

Hydrazone Monoacetate: Orange yellow fine crystals (from ethanol); m. p. 193~194°C.

Hydrazone Diacetate: Yellow orange needles (from a mixture of ethyl acetate and benzene); m. p. 223~224°C.

Found: C, 62.02; H, 6.04; N, 10.34. Calcd. for $C_{22}H_{25}O_6N_3$: C, 61.81; H, 5.90; N, 9.83%.

IR (Nujol): 3280, 3135, 1730, 1712, 1658 cm^{-1}.

b) Azine. — Orange red micro-prisms (from ethanol); m. p. 224~225°C.

Found: C, 65.12; H, 5.67; N, 8.75. Calcd. for $C_{36}H_{38}O_8N_4$: C, 66.04; H, 5.85; N, 8.56%.

IR (Nujol): 3400, 3250, 1650 cm^{-1}.

Azine Diacetate: Orange red silky needles (from ethyl acetate); m. p. 179.5~181°C.

Found: C, 64.77; H, 5.36; N, 8.12. Calcd. for $C_{40}H_{42}O_{10}N_4$: C, 65.03; H, 5.73; N, 7.58%.

Picrate of Azine Diacetate: Scarlet crystals (from ethanol); m. p. 153~155°C.

Found: N, 9.52. Calcd. for $C_{48}H_{51}O_{18}N_7$: N, 9.67%.

c) p-Tolylsulfonylhydrazone.—Yellow micro-prisms (from ethyl acetate); m. p. 209°C (decomp.).

Found: C, 60.41; H, 5.23; N, 8.63. Calcd. for $C_{25}H_{27}O_6N_3S$: C, 60.35; H, 5.47; N, 8.45%.

IR (Nujol): 3330, 3160, 3100, 1672 cm^{-1}.

p-Tolylsulfonylhydrazone Acetate: Pale red micro-prisms (from ethyl acetate); m. p. 210~210.5°C.

Found: C, 59.39; H, 5.31; N, 7.39. Calcd. for $C_{27}H_{29}O_7N_3S$: C, 60.10; H, 5.42; N, 7.79%.

d) Oxime. — Orange yellow micro-prisms (from ethanol); m. p. 155~156.5°C.

Found: C, 62.50; H, 5.34; N, 7.81. Calcd. for $C_{18}H_{20}O_5N_2$: C, 62.78; H, 5.85; N, 8.14%.

IR (Nujol): 3390, 3260, 1669 cm^{-1}.

Oxime Acetate: Orange needles (from ethanol); m. p. 153~154°C.

Found: C, 62.03; H, 5.46; N, 7.10. Calcd. for $C_{20}H_{22}O_6N_2$: C, 62.16; H, 5.74; N, 7.25%.

IR (Nujol); 3380, 3260, 1756, 1667 cm^{-1}.

e) Phenylhydrazone.—Orange micro-prisms (from ethanol); m. p. 139~139.5°C.

Found: C, 66.79; H, 5.38; N, 8.44. Calcd. for $C_{26}H_{31}O_5N_3$: C, 67.08; H, 6.71; N, 9.03%.

IR (Nujol): 3380, 3240, 1667 cm^{-1}.

6) K. v. Auwers and E. Cauer, *Ann.*, **470**, 304 (1929).

f) Semicarbazone.—Yellowish orange micro-prisms (from aqueous ethanol); m. p. 245~246°C.

Found: C, 59.05; H, 5.35; N, 14.03. Calcd. for $C_{19}H_{22}O_5N_4$: C, 59.00; H, 5.74; N, 14.50%.

IR (Nujol): 3350, 3300, 3160, 3100, 1712, 1664 cm^{-1}.

Ketonic Derivatives of XII.—*a) Hydrazone*.—Yellowish orange micro-prisms (from ethanol); m. p. above 270°C.

Found: N, 16.28. Calcd. for $C_{18}H_{22}O_3N_4$: N, 16.36%.

IR (Nujol): 3300, 3230, 2208, 1667 cm^{-1}.

Hydrazone diacetate: Dull orange micro-prisms (from eshanol); m. p. 192~193°C.

Found: N, 14.49. Calcd. for $C_{20}H_{20}O_4N_4$: N, 14.73%.

IR (Nujol): 3300, 3200, 2193, 1876, 1661 cm^{-1}.

b) Azine.—Orange micro-prisms (from ethyl acetate); m. p. 168°C.

Found: N, 14.53. Calcd. for $C_{32}H_{28}O_4N_6$: N, 14.99%.

IR (Nujol): 3420, 3300, 3200, 2193, 1661 cm^{-1}.

Azine of XIV.—Pale yellowish brown micro-prisms (from ethyl acetate); m. p. 194~195°C (decomp.).

Found: N, 7.47. Calcd. for $C_{40}H_{38}O_{10}N_4$: N, 7.63%.

IR (Nujol): 2222, 1650 cm^{-1}.

Hydrazone of XV.—Orange red powder (from ethanol); m. p. above 265°C.

Found: N, 23.07. Calcd. for $C_{14}H_{10}ON_4$: N, 22.39%.

IR (Nujol): 3380, 3330, 3210, 2193 cm^{-1}.

Hydrazone Acetate.—Pale red micro-prisms (from ethanol); m. p. above 265°C.

Found: C, 63.55; H, 4.37; N, 15.03. Calcd. for $C_{20}H_{20}O_4N_4$: C, 63.15; H, 5.30; N, 14.73%.

IR (Nujol): 3350, 3200, 2208, 1776, 1718, 1684 cm^{-1}.

Hydrazone of XVI.—Dull yellow leaflets (from ethanol); m. p. 232~233°C (decomp.).

Found: C, 65.93; H, 5.93; N, 8.85. Calcd. for $C_{18}H_{20}O_4N_2$: C, 65.84; H, 6.14; N, 8.53%.

IR (Nujol): 3330, 3300, 3250, 1684 cm^{-1}.

Hydrazone Acetate.—Dull yellowish orange micro-needles (from ethanol); m. p. 220°C (blackened).

Found: N, 7.83. Calcd. for $C_{20}H_{22}O_5N_2$: N, 7.56%.

IR (Nujol): 3300, 1706, 1669 cm^{-1}.

Hydrazone of XVII.—Orange micro-prisms (from ethanol); m. p. 125~126°C.

Found: C, 63.39; H, 5.92; N, 12.60. Calcd. for $C_{18}H_{21}O_4N_3$: C, 62.96; H, 6.16; N, 12.24%.

IR (Nujol): 3380, 3250, 3100, 1667 cm^{-1}.

Hydrazone Acetate.—Reddish orange prisms (from ethanol); m. p. 218~219°C.

Found: C, 62.60; H, 5.99; N, 10.80. Calcd. for $C_{20}H_{23}O_5N_3$: C, 62.32; H, 6.02; N, 10.90%.

IR (Nujol): 3350, 3250, 3100, 1724, 1675 cm^{-1}.

Picrate of Hydrazone Acetate: Deep red crystals (from ethanol); m. p. 252.5~253.5°C.

Expenses for the present series of experiments were defrayed by a grant-in-aid for Scientific Research from the Ministry of Education. The infrared spectra in this paper were measured with a Shimadzu infrared spectrophotometer IR-27 purchased by a grant-in-aid for Scientific Research from the Toyo Rayon Co., Ltd. The authors wish to express their deep gratitude for these contributions.

Department of Chemistry
Faculty of Science
Tohoku University
Katahira-cho, Sendai

The Infrared Spectra of Carbonyl Compounds in Alcohols

By Hiroshi MINATO*

(Received December 25, 1962)

The infrared spectra of carbonyl compounds in alcohols have not been studied extensively, but the shift due to the hydrogen bonding is regarded as rather small. Rasmussen et al.[1], for example, report that the carbonyl absorption of diacetone alcohol occurs at 1712 cm^{-1} despite the fact that the hydroxyl frequencies indicate the presence of strong hydrogen bonding. Grove and Willis[2] estimate the influence of hydrogen bonding on some ketones as being not greater than 10 cm^{-1}, and Searles et al.[3] have shown that the carbonyl shift in an equimolar mixture of carbon tetrachloride and methanol is about 8 cm^{-1} with esters, and 7 to 15 cm^{-1} with lactones, depending upon the ring size.

Becker[4] determined the infrared spectra of benzophenone in ethanol and in tetrachloroethylene, and in ethanol observed two bands of about equal intensity at 1666 cm^{-1} and

* Present address: Department of Chemistry, International Christian University, Mitaka, Tokyo.

1) R. S. Rasmusssen, D. D. Tunnicliff and R. R. Brattain, *J. Am. Chem. Soc.*, **71**, 1068 (1949).

2) J. F. Grove and H. A. Willis, *J. Chem. Soc.*, **1951**, 877.

3) S. Searles, M. Tamres and G. M. Barrow, *J. Am. Chem. Soc.*, **75**, 71 (1953).

4) R. S. Becker, *J. Molecular Spectroscopy*, **3**, 1 (1959).

1656 cm^{-1}, and, in tetrachloroethylene, a single band at 1668 cm^{-1}. It appears that this phenomenon has not been mentioned elsewhere, including the excellent reviews on hydrogen bonding recently published[5,6]. In order to obtain general knowledge about carbonyl absorption in alcohols and, particularly, to clarify the nature of the double peak, this investigation was undertaken.

Experimental

Materials.—Methyl *t*-butylperoxy carbonate was prepared by the drop-by-drop addition of a cooled sodium hydroxide solution to an equimolar mixture of *t*-butyl hydroperoxide and methyl chloroformate at −5°C. All the other chemicals were those of the best grade commercially available in the United States and were used without further purification.

Table I. Carbonyl bands in carbon tetrachloride and methanol

	In CCl_4 wave number ν_0	In CH_3OH wave number ν_1	ν_2	$\nu_2-\nu_1$	$\frac{(O.D.)_{\nu_2}}{(O.D.)_{\nu_1}}$
Carbonate					
Di-*t*-butyl carbonate	1739	1739	1712	27	0.53
Di-*m*-cresyl carbonate	1783	1783	1761	22	0.68
Di-*n*-butyl carbonate	1745	1745	1727	18	0.78
Di-*o*-cresyl carbonate	1779	1779	1757	22	0.80
Diethyl carbonate	1748	1748	1730	18	0.81
Ethylene carbonate	1818	1805	1779	26	0.87
Methyl *t*-butylperoxy carbonate[a]	1795 1764	1795	1776	19	1.25[a]
Aldehyde					
Benzaldehyde	1706	(1704)[a]	(1695)[b]	9	
p-Anisaldehyde	1704	(1692)[b]	(1681)[b]	11	
Ketone					
Acetone	1718		1709	9[c]	
2-Heptanone	1718		1706	12[c]	
4-Heptanone	1715		1704	11[c]	
2, 6-Dimethylheptanone-4	1712		1704	8[c]	
Diacetone alcohol	1712		1701	11[c]	
Triacetone alcohol	1698		1698	0	
Benzophenone	1667	1667	1656	11	0.91
Fluorenone	1724		(1712)[b]	12[c]	
Lactone					
γ-Butyrolactone	1779		(1764)[b,d]	15[c]	
γ-Valerolactone	1783		(1764)[b,d]	19[c]	
Ester					
Methyl 3, 5-dinitro benzoate	1742	1739	(1724)[e]	15	(0.27)
Methyl benzoate	1727	1727	1709	18	0.75
Phenyl benzoate	1742	1742	1727	15	0.78
Ethyl benzoate	1724	1721	1704	17	0.84
Ethyl butanoate	1739	1736	1718	18	1.02
Methyl acetate	1745	1745	1730	15	1.09
Isopropyl acetate	1739	1736	1715	21	1.14
Ethyl salicylate	1684	1681[d]		3[c]	

a) This peroxycarbonate is exceptional in that it has two carbonyl bands, 1795 and 1764 cm^{-1} ($O.D._{1764}/O.D._{1795}=0.32$), even in carbon tetrachloride. Recently, Martin reported that di-*t*-butylperoxy carbonate possesses a split carbonyl band, with a high intensity peak at 1825 and a somewhat less intense peak at 1795 cm^{-1} (M. M. Martin, *J. Am. Chem. Soc.*, **83**, 2870 (1961)).
b) The wave numbers in parentheses are inaccurate due to the diffused nature of the bands.
c) These are $\nu_{MeOH}-\nu_{CCl_4}$, not $\nu_2-\nu_1$.
d) The band in methanol is a little broader than that in carbon tetrachloride.
e) These are the shoulders of stronger bands and are not accurate.

5) G. C. Pimentel and A. L. McLellan, "The Hydrogen Bond", W. H. Freeman and Co., London (1960).

6) D. Hadzi (ed.), "Hydrogen Bonding", Pergamon Press, London (1959).

TABLE II. CARBONYL BANDS IN METHANOL AND *t*-AMYL ALCOHOL

	In methanol wave number ν_1	ν_2	$\frac{(O.D.)_{\nu_2}}{(O.D.)_{\nu_1}}$	In *t*-amyl alcohol wave number ν_1	ν_2	$\frac{(O.D.)_{\nu_2}}{(O.D.)_{\nu_1}}$
Phenyl benzoate	1742	1727	0.78	1742	1730	1.00
Benzophenone[a]	1667	1656	0.91	1667	1658	1.21
Isopropyl acetate	1736	1715	1.14	1739	1721	1.74

a) In ethanol, $\nu_1=1667\,cm^{-1}$, $\nu_2=1656\,cm^{-1}$, $(O.D.)_{\nu_2}/(O.D.)_{\nu_1}=1.0$

TABLE III. CARBONYL BANDS OF ISOPROPYL ACETATE IN MIXTURES OF *t*-AMYL ALCOHOL AND CARBON TETRACHLORIDE

Vol. % of *t*-AmOH	$\frac{(t\text{-AmOH})}{(i\text{-PrOAc})}$	Wave number ν_1	ν_2	$\nu_2-\nu_1$	$\frac{(O.D.)_{\nu_2}}{(O.D.)_{\nu_1}}$
4%	1.13	1739			
8	2.25	1736	1724	12	
20	5.6	1739	1724	15	0.78
100	28.2	1739	1721	18	1.74

(The concentration of isopropyl acetate is 0.32 M.)

Infrared Spectra.—The infrared spectra of carbonyl compounds were determined in carbon tetrachloride, methanol or *t*-amyl alcohol by using calcium fluoride cells 0.2 mm. in thickness with a Perkin-Elmer Model 21 infrared spectrophotometer. The concentrations of the carbonyl compounds ranged from ca. 0.1 to 0.3 M, and were chosen so as to show the double peak clearly in alcohols.

Results

The infrared spectra of various carbonates, aldehydes, ketones, lactones and esters were determined in carbon tetrachloride and alcohols. The wave numbers of carbonyl bands in carbon tetrachloride (ν_0) and in alcohols (ν_1 and ν_2), together with the ratios of the optical density of the two bands in alcohols, are shown in Tables I, II, III and IV. The spectrum of the carbonyl absorption of isopropyl acetate in methanol is shown in Fig. 1; this will serve as an example of the doublet bands and also shows the independence of the relative band intensities of the concentration.

The results shown in Tables I—IV may be summarized as follows.

TABLE IV. CARBONYL BAND OF ISOPROPYL ACETATE OF THE VARIOUS CONCENTRATIONS IN METHANOL

Isopropyl acetate mol./l.	$\frac{(O.D.)_{\nu_2}}{(O.D.)_{\nu_1}}$
0.404	1.12
0.305	1.13
0.152	1.21
0.122	1.09
0.061	1.25

($\nu_2=1715$, $\nu_1=1736\,cm^{-1}$)

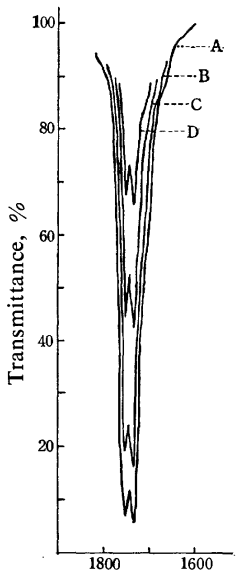

Fig. 1. Carbonyl band of isopropyl acetate in methanol.
Concentration of *i*-PrOAc; A, 0.404; B, 0.305; C, 0.122; D, 0.061 M. Spectral slit-width, 2 cm^{-1}.

1) Except for ethyl salicylate and methyl 3, 5-dinitrobenzoate, all the esters and carbonates appear to give two carbonyl bands in methanol, one at a wave number almost identical with the one in carbon tetrachloride, and the other lower by 15~27 cm^{-1}.

2) Carbonyl bands of aliphatic ketones shift by 9~15 cm^{-1} but do not give two bands in methanol. Benzophenone gives two bands, 11 cm^{-1} apart, while fluorenone seems

to give one broad band which may well in fact consist of two bands.

3) Diacetone alcohol, the carbonyl group of which is already hydrogen-bonded, suffers a further shift as much as 11 cm^{-1} in methanol, whereas the carbonyl absorption of triacetone alcohol is not affected by the change of solvents.

4) Aldehydes seem to give one broad band which may well in fact consist of two bands. The shift of the center of the band is 6~18 cm^{-1}.

5) Lactones gives one broad band in methanol, shifted by 15~19 cm^{-1}.

6) The (Optical density of ν_2)/(Optical density of ν_1) ratio increases as the alcohol is changed from methanol to *t*-amyl alcohol.

7) No significant change in the ratio of the band intensities was observed for various concentrations of isopropyl acetate in methanol.

Discussion

The infrared literature contains numerous examples of monocarbonyl compounds that exhibit two or more prominent bands between 1900 and 1650 cm^{-1}. In the absence of other acceptable explanations, both bands are usually assigned to vibrations involving the carbonyl groups. These doublet carbonyl peaks have been attributed to equilibria between conformational isomers, to Fermi resonance, or to some form of interaction between carbonyl compounds and solvents.

It is not possible to write pairs of stable, conformationally isomeric structures for the carbonyl compounds considered here. In order for the equilibria between conformational isomers to be the cause of the doublet carbonyl bands, it is necessary for the energy difference between two forms to be small enough to allow a significant concentration of the less stable form to exist in equilibrium at room temperature, and the inductive, mesomeric and field effects on the carbonyl group must differ sufficiently in the two forms to induce a significant displacement of the two carbonyl frequencies.

Next, the possibility of attributing these doublet carbonyl bands to Fermi resonance should be examined. Yates and his collaborators[7,8] found that some cyclopent-2-enones exhibited doublet carbonyl bands, the relative intensities of which were dependent on solvents. By a careful examination of the infrared spectra of 5,5-dimethylcyclopent-2-enone, deuterated cyclopent-2-enone and other substituted cyclopent-2-enones, they showed unambiguously that these doublet carbonyl bands arose from Fermi resonance between the carbonyl vibration and the out-of-plane bending vibration of the single ethylenic C–H bond. Angell et al.[9] attributed the double bands of cyclopentanone to the Fermi resonance.

However, the Fermi resonance does not seem to be an acceptable explanation for the doublet carbonyl bands of esters and carbonates in alcohols for the following reason. It is highly unlikely that an accidental degeneracy between the carbonyl stretching mode and an overtone or combination bands would occur through such a wide range of different types of structure. Although Jones et al.[10,11] reluctantly and tentatively attributed the doublet carbonyl bands of unsaturated lactones to Fermi resonance, they were not satisfied with their choice of explanation for the same reason. Yates and Williams[8] found that while 3,4-diphenylcyclopent-2-enone showed a doublet carbonyl absorption at 1718 and 1695 cm^{-1} due to the Fermi resonance with an overtone of the out-of-plane bending vibration of the single ethylenic carbon-hydrogen bond at 860 cm^{-1}, 3,4-diphenyl-5,5-dimethylcyclopent-2-enone showed a singlet carbonyl band since its ethylenic carbon-hydrogen absorption was at 873 cm^{-1}. It is utterly unlikely that the doublet carbonyl bands of all the compounds in Table I arose from an accidental degeneracy between the carbonyl stretching mode and an overtone or combination band, from, i.e., a Fermi resonance.

If these doublet carbonyl bands observed in alcohols cannot be attributed either to equilibria between conformational isomers or to a Fermi resonance, one is forced to believe that these doublet bands are due to some form of interaction between carbonyl compounds and solvents.

If these doublet carbonyl bands in alcohols are due to the hydrogen bonding between the carbonyl oxygen and solvent alcohols, the following three sets of species are conceivably responsible for the doublet bands: 1) non-hydrogen-bonded carbonyl and hydrogen-bonded carbonyl, 2) hydrogen-bonded carbonyl with monomeric alcohol and with polymeric alcohol, and 3) mono-hydrogen-bonded carbonyl and di-hydrogen-bonded carbonyl.

The first set of species does not seem acceptable because of the following two reasons.

7) P. Yates, N. Yoda, W. Brown and B. Mann, *J. Am. Chem. Soc.*, **80**, 202 (1958).
8) P. Yates and L. L. Williams, ibid., **80**, 5896 (1958).
9) C. L. Angell, P. J. Krueger, R. Lauzon, L. C. Leitch, K. Noack, R. J. D. Smith and R. L. Jones, *Spectrochim. Acta*, **11**, 926 (1959).
10) R. N. Jones, C. L. Angell, T. Ito and R. J. D. Smith, *Can. J. Chem.*, **37**, 2007 (1959).
11) R. N. Jones and B. S. Gallagher, *J. Am. Chem. Soc.*, **81**, 5242 (1959).

First, diacetone alcohol, the carbonyl group of which is already hydrogen-bonded, absorbs at 1712 cm^{-1} in carbon tetrachloride, while 2, 6-dimethylheptanone-4 absorbs at 1712 cm^{-1} and heptanone-4 absorbs at 1715 cm^{-1} in the same solvent, the latter two not being hydrogen-bonded. Second, the carbonyl absorption of diacetone alcohol, which is already hydrogen-bonded, is shifted as much as 11 cm^{-1} when its spectrum is taken in methanol.

The second set was chosen by Becker[4] as responsible for the doublet bands of benzophenone in ethanol. He attributed the absorption at 1666 cm^{-1} to the carbonyl group hydrogen-bonded to the monomeric alcohol and the absorption at 1656 cm^{-1} to the carbonyl group hydrogen-bonded to the polymeric alcohol. However, it seems highly unlikely that the ethanol monomer can exist in pure ethanol. The oxygen of the ethanol molecule hydrogen-bonded to a carbonyl group is more basic and should be hydrogen-bonded to other molecules of ethanol.

Therefore, in the absence of other acceptable explanations, the most reasonable explanation for the double bands seems to be that carbonyl compounds in alcohols may exist as both a mono-hydrogen-bonded form and a di-hydrogen-bonded form[12,13]. In Tables I, II and III, ν_1 is attributed to the mono-hydrogen-bonded carbonyl and ν_2 is attributed to the di-hydrogen-bonded carbonyl. These assignments are made on the basis of the following observations: (a) The carbonyl absorption of diacetone alcohol occurs at 1712 cm^{-1} in carbon tetrachloride despite the fact that the hydroxyl frequencies indicate strong hydrogen-bonding (3484cm^{-1}), while 2, 6-dimethylheptanone-4 and heptanone-4 absorb in the same solvent at 1712 and 1715 cm^{-1} respectively, these latter two not being hydrogen-bonded. This fact indicates that the carbonyl absorption of a mono-hydrogen-bonded carbonyl compound occurs at nearly the same wave-number as that of a non-hydrogen-bonded carbonyl compound. (b) Triacetone alcohol, in which two intramolecular hydrogen bondings are possible, absorbs in carbon tetrachloride at 1698 cm^{-1} (compare this value with 1712 cm^{-1} of diacetone alcohol). The carbonyl absorption of triacetone alcohol does not suffer any shift at all when the solvent is changed from carbon tetrachloride to methanol. These facts indicate that a carbonyl absorption is shifted a great deal when the compound is subjected to a condition where di-hydrogen-bonding may take place, and that the carbonyl absorption of a di-hydrogen-bonded carbonyl compound is not affected at all by changing the solvent from carbon tetrachloride to methanol, while that of a mono-hydrogen-bonded carbonyl compound is shifted almost as much as that of a non-hydrogen-bonded carbonyl compound by changing the solvent from carbon tetrachloride to methanol.

It is an interesting question why mono-hydrogen-bonding gives only a small shift while di-hydrogen-bonding gives a rather large shift. A plausible explanation is that, since a carbonyl oxygen probably uses one of its p-orbitals in forming the σ-bond with carbon and another p-orbital in forming the π-bond, two unshared electron pairs are in the 2s and 2p orbitals. Therefore, the first hydrogen-bonding probably takes place by making use of the rich electron density of the unshared p-orbital. This hydrogen bonding probably will not affect the stretching frequency of a carbonyl bond very much. The second hydrogen bonding, however, may strongly affect the stretching frequency of the carbonyl bond, if use must be made of the electrons closer to the carbon-oxygen bond. In other words, extensive hybridization of oxygen orbitals would be required for the formation of two hydrogen bonds, whereas little hybridization would be required to form a single hydrogen bond.

Alkyl ketones are exceptional in that they show only one carbonyl band in methanol, one shifted by 8~12 cm^{-1}. They lack the conjugated π-system which is present in esters, carbonates and aryl ketones. The lack of conjugation and the presence of electron-releasing alkyl groups make alkyl ketones form di-hydrogen-bonds more easily than esters, carbonates or aryl ketones, in which the π-electrons of the carbonyl bond are somewhat spread to the conjugated π-system. In methyl 3, 5-dinitrobenzoate, the π-electrons of the carbonyl bond are strongly pulled to the benzene ring and di-hydrogen-bonded forms are present in a very small quantity, if at all. Methyl trichloroacetate and methyl trifluoroacetate, both of which are esters of strong acids, show only one band in methanol[14], presumably

12) The positions of two molecules of water in the crystalline structure of $Na_2CO_3 \cdot NaHCO_3 \cdot 2H_2O$ are as follows (Ref. 5, p. 264):

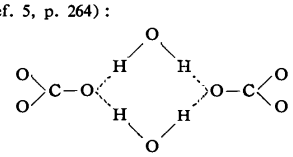

13) The oxygen atoms of water molecules are pictured as hydrogen-bonded to two hydrogens of other water molecules. See, for example, E. S. Gould, "Inorganic Reactions and Structure", Henry Holt and Co., New York (1955), p. 32.

14) T. G. Traylor, private communication.

due to the absence of the di-hydrogen-bonded carbonyl.

In the case of ethyl salicylate, the carbonyl π-electrons are completely spread to the quasi-six membered ring and are not available to form an additional hydrogen-bond. As may be seen in Table I, the carbonyl band of ethyl salicylate is not affected by changing the solvent from carbon tetrachloride to methanol. Its carbonyl band in carbon tetrachloride is at 1684 cm^{-1}, which is 40 cm^{-1} lower than that of ethyl benzoate in carbon tetrachloride and 20 cm^{-1} lower than that of ethyl benzoate in methanol.

Searles et al.[3] found that the shift of the carbonyl band by changing the solvent from carbon tetrachloride to an equimolar mixture of carbon tetrachloride and methanol is 7 cm^{-1} for β-propiolactone, 12cm^{-1} for γ-butyrolactone, and 15 cm^{-1} for δ-valerolactone. These are shifts of the centers of the broad band, and so the bigger shifts may mean a more di-hydrogen-bonded form. The carbonyl band of γ-butyrolactone is further shifted when its infrared spectrum is determined in pure methanol (15 cm^{-1}; see Table I).

The higher (Optical Density of ν_2)/(Optical Density of ν_1) ratio with *t*-amyl alcohol than with methanol may be explained by the fact that self-hydrogen-bonding is much weaker in *t*-amyl alcohol than in methanol[15]. Therefore, the equilibrium, self-bonded alcohol $\rightleftharpoons$ carbonyl-bonded alcohol, is shifted more to the right in the case of *t*-amyl alcohol, even though methanol is a stronger acid. It is presumably only as a hydrogen acceptor that *t*-amyl alcohol is ineffective; accordingly, we have a carbonyl compound able to compete with the oxygen of *t*-amyl alcohol in the hydrogen acceptor role, whereas the carbonyl oxygen cannot compete so well with the oxygen of methyl alcohol.

15) L. J. Bellamy, "The Infrared Spectra of Complex Molecules", John Wiley, New York (1959), p. 101.

Summary

The infrared spectra of some esters, lactones, carbonates, ketones and aldehydes in methanol and *t*-amyl alcohol have been determined. With few exceptions, they showed either two carbonyl peaks separated by 15~27 cm^{-1} or a broad carbonyl peak shifted by 9~19 cm^{-1} from the wave number as determined in carbon tetrachloride. The relative intensities of the two bands are independent of the concentration. Some possible explanations for this phenomenon have been discussed, and as a result these doublet carbonyl bands have been attributed to the mono-hydrogen-bonded carbonyl and the di-hydrogen-bonded carbonyl.

The author would like to thank Professor Paul D. Bartlett of Harvard University for his encouragement to investigation these spectra as a side line to my Ph. D. thesis problem; Professor Teddy G. Traylor of the University of California for his stimulating discussions, and the Bell Telephone Laboratories for a predoctoral research fellowship (1959~1961).

Department of Chemistry
Harvard University
Cambridge 38, Massachusetts
U. S. A.

The Phase Transition of Crystalline Potassium Thiocyanate, KSCN. I. Thermal and Infrared Studies

By Minoru SAKIYAMA, Hiroshi SUGA and Syûzô Seki

(Received January 31, 1963)

From the standpoint of the shape of ions, ionic crystals which consist of spherical cations and spherical anions may be the simplest case; there are found almost no materials of this type which undergo phase transition below their melting temperatures. Two exceptions are, however, silver[1] and cuprous[2] iodides. In those cases, the transitions are known to be due to the positional disorder of the cations in these crystalline lattices.

1) L. W. Strock, *Z. phys. Chem.*, **B25**, 441 (1931); **B31**, 132 (1936): S. Hoshino, *J. Phys. Soc. Japan*, **12**, 315 (1957).

2) J. Krug and L. Sieg, *Z. Naturforsch.*, **7a**, 369 (1952); S. Miyake, S. Hoshino and T. Takenaka, *J. Phys. Soc. Japan*, **7**, 19 (1952).

As the second simplest case, ionic crystals which consist of spherical cations and rod-shaped anions may be cited. They are known to undergo a phase transition which may be related to the change in the direction of the anions. Such ionic crystals include, for example, (1) hydrogen, sodium and potassium cyanides[3], (2) sodium, rubidium and cesium hydroxides[4], and (3) sodium, potassium and rubidium hydrosulfides and hydroselenides[5]. The material studied in this paper, potassium thiocyanate crystal, is known to belong to this category.

Another, simpler case may be the ionic crystals which are composed of spherical anions and radical cations. In this case the phase transition due to the orientational or rotational disorder of the cations is well known. Ammonium halides are the most common instances[6].

Beginning with the view just mentioned, we have studied the phase transition of potassium thiocyanate and ammonium thiocyanate crystals. In the present paper, however, we will confine ourselves to the findings concerning the former.

This crystal is known, by the phase diagram study of Wrzewnewsky[7], to undergo a phase transition at about 142°C. There have also been some crystallographic and structural chemical investigations by some workers.

The room temperature modification of this crystal has been found to belong to the orthorhombic system by Klug[8], while infrared studies of this modification by Jones[9] have shown that the absorption band due to the bending vibration of thiocyanate ions, which should be doubly degenerate, splits into doublets. Plester and Ubbelohde[10] have found in their dilatometric measurements that this substance melts accompanying an anomalously large premelting phenomenon, a phenomenon which they supposed due to the formation of a large number of lattice vacancies. However, our dilatometric study of the extremely purified sample did not show such an anomalous effect[11].

It seemed of interest to elucidate the mechanism of the phase transition of this substance on the basis of our knowledge of crystal structure and of the thermal and other properties. For this purpose, we have carried out differential thermal analysis, specific heat measurements from 0 to 165°C, and measurement of the temperature variation of the infrared absorption bands.

Experimental

Materials.—The potassium thiocyanate used for the present studies (extra pure grade reagent of the Wakō Pure Chemicals Co., Ltd.) was recrystallized twice from water and dried at 150°C under a high vacuum (10^{-5} mmHg).

Apparatus and Procedure.—The differential thermal analysis of this substance was carried out by using an automatically controlled recording apparatus, the details of which have already been reported on[12]. In order to determine the transition temperature accurately and in order to study the thermal behavior in more detail, specific heat measurements were also made in the temperature range from 0 to 165°C by using a conduction calorimeter[13], the heating rate being 0.2~0.3°C/min. A glass-made dilatometer was employed for the measurement of the thermal expansion. The confining liquid used was mercury. It was confirmed that mercury did not react with the sample, even above the melting point[11]. For the infrared measurements, an Hitachi infrared spectrophotometer EPI-2 with sodium chloride, calcium fluoride and potassium bromide prisms was used. Sample spectra were measured in Nujol mull or epitaxially-grown crystal from melt on a potassium bromide plate. The temperature was varied by an electrical heating device of the sample holder, and the temperature was measured by a copper-constantan thermocouple imposed in a hole drilled in a potassium bromide plate.

Results

Dilatometry.—The general trend of the results has been given in a previous paper[11]. The detailed behavior around the transition temperature is reproduced here on a large scale in Fig. 1. The curve does not show any of the discontinuity which is usually found in the first order phase transition. The volume thermal expansion coefficients given in Fig. 2 were calculated at each temperature from dilatometric data.

Differential Thermal Analysis.—The results are shown in Fig. 3. Measurements in the temperature range from −190 to 0°C gave no thermal anomaly, so those results are not reproduced here. The anomaly around 140°C is

3) C. E. Messer and W. T. Ziegler, *J. Am. Chem. Soc.*, **63**, 2703 (1941); J. M. Bijvoet and H. J. Verweel, *Rec. Trav. Chim.*, **54**, 631 (1935).
4) G. von Hevesy, *Z. phys. Chem.*, **73**, 667 (1910); *Z. anorg. Chem.*, **67**, 242 (1910); R. R. Seward, *J. Am. Chem. Soc.*, **64**, 1053 (1942); R. R. Seward and K. E. Martin, ibid., **71**, 3564 (1949).
5) W. Teichert, *Z. anorg. Chem.*, **247**, 113 (1914).
6) A. W. Lawson, *Phys. Rev.*, **57**, 417 (1940).
7) J. B. Wrzewnewsky, *Z. anorg. Chem.*, **74**, 95 (1912).
8) H. P. Klug, *Z. Krist.*, **85**, 214 (1933).
9) L. H. Jones, *J. Chem. Soc.*, **25**, 1069 (1956); **28**, 1234 (1958).
10) D. W. Plester, S. E. Rogers and A. R. Ubbelohde, *Proc. Roy. Soc.*, **A235**, 469 (1956).
11) T. Shinoda, H. Suga and S. Seki, This Bulletin, **33**, 1314 (1960).
12) H. Suga, H. Chihara and S. Seki, *J. Chem. Soc. Japan, Pure Chem. Sec.* (*Nippon Kagaku Zasshi*), **82**, 24 (1961).
13) I. Nitta, S. Seki, M. Momotani, S. Nakagawa and K. Suzuki, *Proc. Japan Acad.*, **26**, 11 (1950).

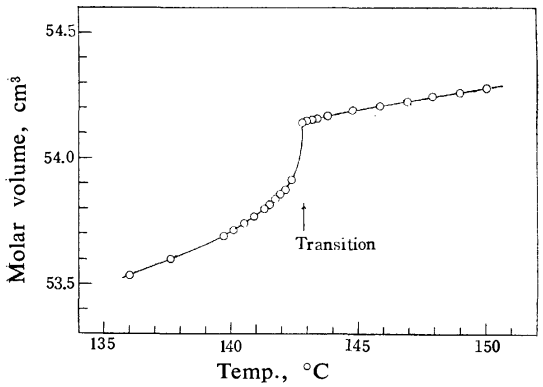

Fig. 1. Temperature variation of molar volume near the transition temperature. (Shinoda, Suga and Seki[11])

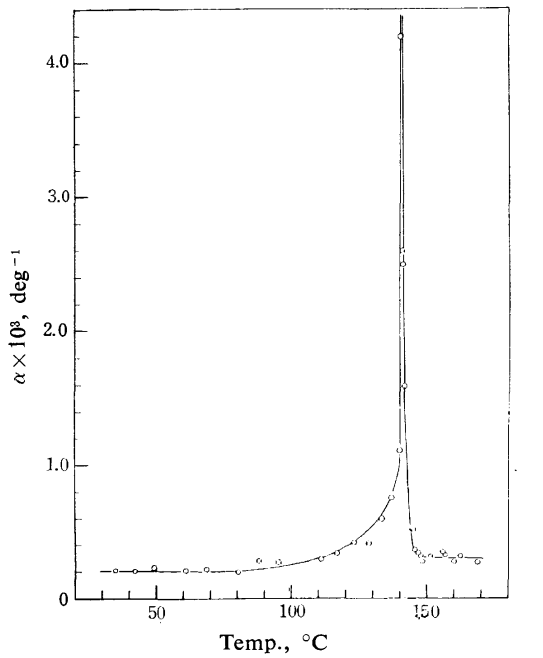

Fig. 2. Volume thermal expansion coefficient vs. temperature curve of potassium thiocyanate crystal.

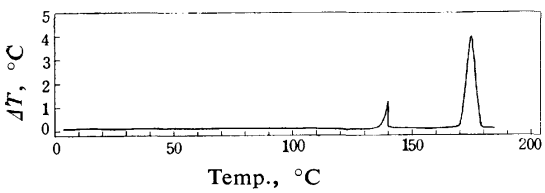

Fig. 3. Differential thermal analysis curve of potassium thiocyanate crystal in the range 0 to 200°C.

due to the phase transition mentioned above, its shape suggesting again that the transition may be of the higher-order type. The higher temperature one at 175°C is ascribed to the melting. As may be seen in the figure, the sharp rise of this curve shows no evidence of the premelting phenomenon suggested by Plester and Ubbelohde[10]. All these results are in good agreement with the results of our dilatometric study[11].

Heat Capacity Measurements.—Heat capacities are tabulated in Table I, while their variation with the temperature is presented in Fig. 4. We can find from this figure that the phase transition is of the so-called "λ-type phase transition", accompanied by a sharp and remarkable rise just below the transition point. No hysteresis phenomenon was observed.

The following thermodynamic quantities were obtained:

Transition temperature: $T_{tr}=139.2°C$

Heat of transition: $\Delta H_{tr}=529.5\pm20$ cal./mol.

Entropy of transition: $\Delta S_{tr}=1.30\pm0.5$ e. u.

TABLE I. HEAT CAPACITY OF POTASSIUM THIOCYANATE

t, °C	C_p cal./deg. mol.	t, °C	C_p cal./deg. mol.
8.58	19.97	99.45	28.17
11.15	20.16	101.67	28.45
13.70	20.35	106.10	29.34
17.48	20.47	108.47	29.74
21.23	20.52	111.77	31.23
24.91	20.62	115.03	31.72
28.36	21.07	118.27	32.74
30.84	21.19	120.01	33.52
34.90	21.45	123.09	34.40
37.26	21.70	127.49	38.27
40.49	22.13	130.03	39.93
43.63	22.52	132.53	44.41
45.03	22.58	135.67	53.53
49.87	22.72	136.93	61.03
51.32	22.81	138.18	78.07
53.13	23.20	139.27	560.70
58.50	23.33	139.52	105.23
63.22	23.81	141.08	33.35
67.92	24.09	142.22	31.96
70.72	24.38	144.26	30.72
75.18	24.71	147.33	29.86
78.57	25.07	152.51	29.83
84.92	25.57	156.67	29.85
87.26	25.75	161.92	29.24
90.75	26.31	167.62	30.20
92.97	26.89	169.67	31.43
95.22	27.18		

Infrared Measurements.—The absorption bands are assigned and the notation used is presented in Table II. Our results almost agreed with those by Jones[9] except in one point. We found a complex structure in the strong bands of the 2000 cm^{-1} region (Fig. 5) which is attributed to the stretching vibration (ν_1) of the C–N bond of SCN^- ions, when

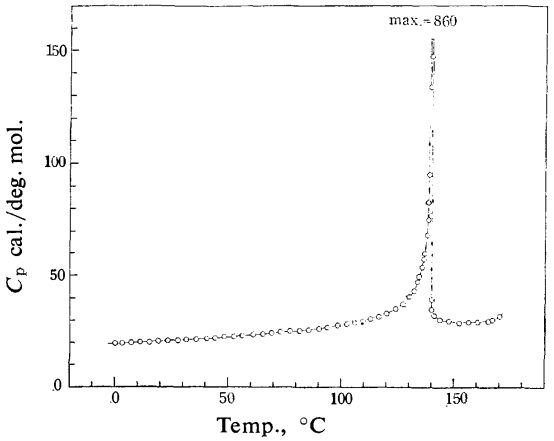

Fig. 4. C_p vs. temperature curve of potassium thiocyanate crystal.

TABLE II. POSITIONS AND ASSIGNMENTS OF INFRARED ABSORPTION BANDS (cm^{-1})

Wave number	Assignment	
469	ν_{2b}	Out of plane bending
483	ν_{2a}	In plane bending
745	ν_3	S-C Stretching
944	$2\nu_{2b}=938$	
966	$2\nu_{2a}=966$	
2018		
2040	ν_1	C-N Stretching
2068		

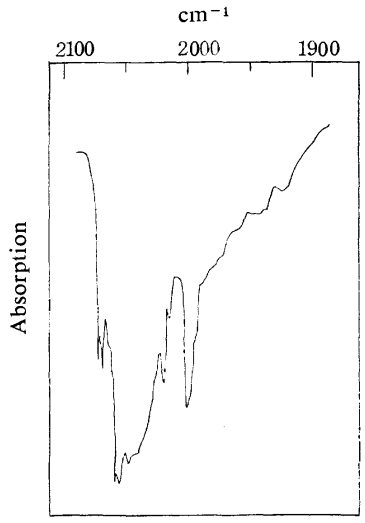

Fig. 5. Infrared spectrum of potassium thiocyanate crystal in the 2000 cm^{-1} region.

we measured with a calcium fluoride prism with an epitaxially-grown sample from the melt.

When the sample was heated, gradual changes in the spectrum were observed. The most characteristic change was the apparent transformation of a doublet in the region of 480 cm^{-1}

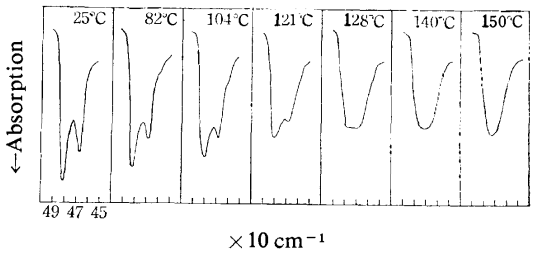

Fig. 6. Temperature variation of ν_{2a} and ν_{2b} bands of SCN^- ion in KSCN crystal.

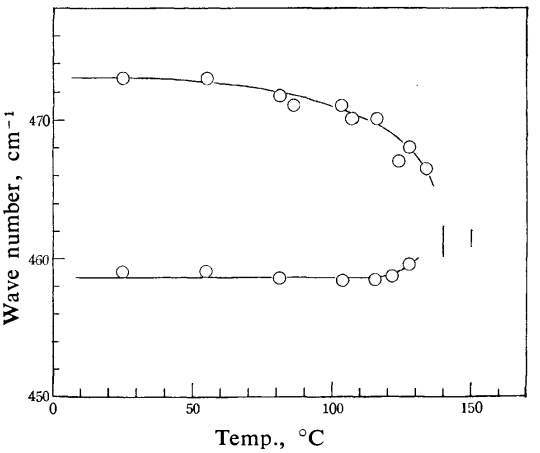

Fig. 7. Temperature dependence of the position of ν_{2a} and ν_{2b} bands of SCN^- ion in potassium thiocyanate crystal.

into a singlet. The behavior of and the variation in the positions of these bands are shown in Figs. 6 and 7. We can find that the 483 cm^{-1} band comes closer to the 469 cm^{-1} band as the temperature increases and the variation in wave number difference of these two bands as a function of the temperature accords with the progress of transition shown in molar volume or heat capacity change. Similar behavior was also observed in the position of the ν_3 band. As to the ν_1 band, little variation was found except for the thermal broadening and smearing of its fine structure.

Discussion

The crystal system of phase II (the room temperature phase) is orthorhombic, with $a=$ 6.66 Å, $b=7.58$ Å, $c=6.635$ Å, $Z=4$, and space group, $D_{2h}^{11}-Pcmb$[8]. The arrangement of ions is schematically given in Fig. 8. The thiocyanate ions lie on a crystallographic b-plane with specified orientations, while potassium ions are sandwiched between the thiocyanate layers.

The molecular symmetry of a "free" thiocyanate ion is $C_{\infty v}$. Three normal modes of vibration, one of which is doubly degenerate,

TABLE III. FACTOR GROUP ANALYSIS OF KSCN CRYSTAL IN PHASE II

$p=16$, $s=8$, $v=4$, $s\text{-}v=4$

D_{2h}^{11}	Screw				Axial glide		Axial glide		N	T	T'	R'	n	IR	Raman
	E	C_2^c	C_2^b	C_2^a	i	σ_c	$\sigma_b=m$	σ_a							
A_{1g}	1	1	1	1	1	1	1	1	7	0	3	1	3	—	$\alpha_{aa}, \alpha_{bb}, \alpha_{cc}$
A_{1u}	1	1	1	1	−1	−1	−1	−1	4	0	2	2	0	—	—
B_{1g}	1	−1	1	−1	1	−1	1	−1	8	0	4	1	3	—	α_{ca}
B_{1u}	1	−1	1	−1	−1	1	−1	1	5	1	2	2	0	M_b	—
B_{2g}	1	1	−1	−1	1	1	−1	−1	5	0	3	2	0	—	α_{ab}
B_{2u}	1	1	−1	−1	−1	−1	1	1	8	1	3	1	3	M_c	—
B_{3g}	1	−1	−1	1	1	−1	−1	1	4	0	2	2	0	—	α_{bc}
B_{3u}	1	−1	−1	1	−1	1	1	−1	7	1	2	1	3	M_a	—
$U_R(p)$	16	0	0	4	0	0	12	0	↑	↑	↑	↑			
$U_R(s)$	8	0	0	4	0	0	4	0							
$U_R(s\text{-}v)$	4	0	0	0	0	0	4	0							
$\pm1+2\cos\phi_R$	3	−1	−1	−1	−3	1	1	1							
$\chi'_R(N)$	48	0	0	−4	0	0	12	0	—						
$\chi'_R(T)$	3	−1	−1	−1	−3	1	1	1	—	—					
$\chi'_R(T')$	21	1	1	−3	3	−1	3	−1	—	—	—				
$1\pm2\cos\phi_R$	3	−1	−1	−1	3	−1	−1	−1							
$\chi'_R(R')$	12	0	0	0	0	0	−4	0	—	—	—	—			

p, s and v: Total number of atoms, ions and polyatomic ions in a Bravais unit lattice, respectively.

ϕ_R: Angle of rotation in the operation R.

$U_R(p)$, $U_R(s)$ and $U_R(s\text{-}v)$: Total number of atoms, ions and polyatomic ions the centers of gravity of which are invariant under the operation R, respectively.

$\chi'_R(N)$, $\chi'_R(T)$, $\chi'_R(T')$ and $\chi'_R(R')$: Characters of representation based on the coordinates of all the degrees of freedom of motion in a Bravais unit lattice, mere translation of the whole of a Bravais unit lattice, translational lattice vibrations of ions, and rotational lattice vibrations, respectively.

N: Total number of degrees of freedom of motion in a Bravais unit lattice.

T, T', R' and n: Numbers of degrees of freedom of translation, translational lattice vibration, rotational lattice vibration and inner vibration of ions in a Bravais unit lattice, respectively.

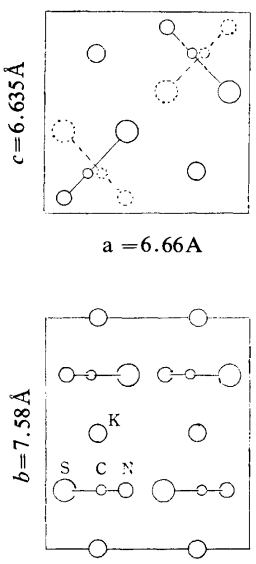

Fig. 8. Schematic representation of the unit cell of potassium thiocyanate crystal.

are those shown in Fig. 9. From the standpoint of site symmetry analysis, Jones[9] explained the splitting of the ν_2 band into a doublet in the crystalline state as the result of the anisotropy of the crystalline field that is brought about by the layer structure of crystal. The absorption bands at 483 and 469 cm^{-1} were assigned on the basis of the polarisation studies to the bending vibrations parallel with (ν_{2a}) and perpendicular to (ν_{2b}) the crystallographic b-plane respectively.

In the present study, a remarkable temperature shift of position was observed to take place in the ν_{2a} and ν_3 bands, both due to a in-plane vibration, while no such tendency was found in the ν_{2b} (out-of-plane) band. These experimental results suggest that phase transition takes place in such a way that the crystalline field parallel with the b-plane around a thiocyanate ion is much influenced in the course of phase transition. As is shown in Fig. 10, the thiocyanate ions in the b-plane are arranged in the closest packing way, so the overlapping of an electron cloud between atoms

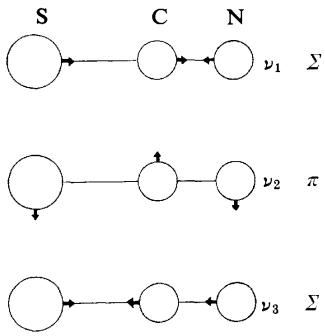

Fig. 9. Schematic representation of normal modes of vibration of SCN^- ion.

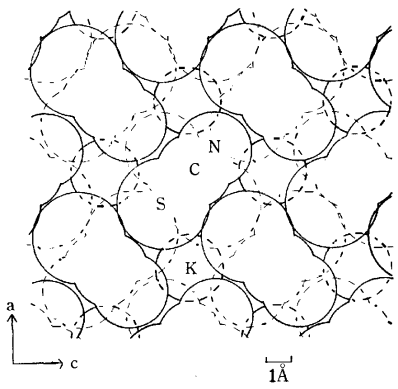

Fig. 10. Schematic representation of the packing of ions projected to b-plane. (phase II).

in the plane is more profound than that between the inter-layer atoms. The above-mentioned remarkable change in the ν_{2a} and ν_3 bands may be understandable by means of this line of explanation.

Now, we should like to proceed to the problem of the thermal properties of the crystal before entering into a discussion of the relationship between the spectroscopic results and the mechanism of phase transition. The molar volume and the thermal expansion coefficient versus the temperature curves reveal that this transition is of a higher order (see Figs. 1 and 2). This means that the crystal structure of the high temperature phase is nearly the same as the low temperature one, with no appreciable change in atomic arrangement. It is also found from the C_p vs. temperature curve that the transition is highly co-operative, as is evident from the sharp rise just below the peak. The amount of transition entropy, 1.30 ± 0.05 e. u., is nearly equal to $R\ln 2 = 1.38$ e. u. Combining these results of transition entropy and of dilatometry, it is strongly suggested that phase I maintains nearly the same arrangement of the centers of gravity of ions and obtains two opposite directions (S–C–N and N–C–S) in one and the same orientation (original to phase II) of anions in equal probability.

Recently, X-ray crystal structure analysis of phase I (the high temperature phase) has been carried out by Yamada and Watanabé[14], who found that the crystal in phase I belongs to the tetragonal system (space group, D_{4h}^{18}–I4/mcm, $Z=4$) and that the electron distribution map of a thiocyanate ion does not differentiate S and C atoms. This means that an averaged structure between two equilibrium directions (S–C–N and N–C–S) in one and the same orientation is obtained. These results are in good agreement with our results.

From these facts, we can conclude that the transition is of the order—disorder type for two directions of thiocyanate ions.

Next, we should like to discuss our spectroscopic results in connection with the mechanism of the phase transition.

As is shown in Figs. 2, 4 and 7, the volume thermal expansion coefficient, the molar heat capacity and the wave number of the infrared ν_{2a} band all start to change at nearly the same temperature, 70°C. These facts show that the temperature shift of the ν_{2a} frequency is intimately related to the progress of the phase transition.

As has been mentioned, the crystal in phase I belongs to the tetragonal system, but the layer structure of the thiocyanate ions is still maintained. Therefore, if the splitting of the ν_2 band observed in phase II is ascribed to the anisotropy of the crystalline field around a

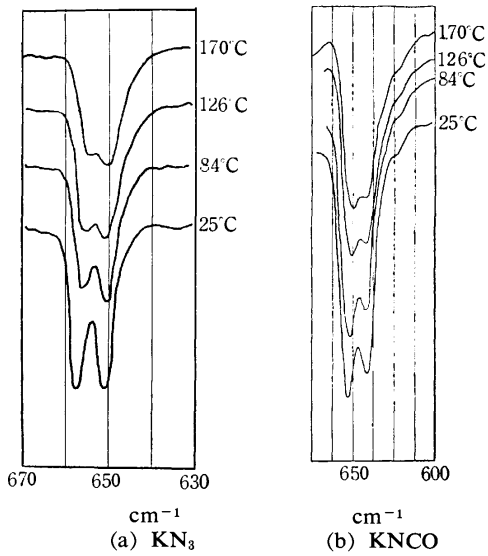

Fig. 11. Temperature variation of infrared ν_2 bands of KN_3 and KNCO crystals.

14) Y. Yamada and T. Watanabé, This Bulletin, 36, 1032 (1963).

thiocyanate ion, a similar ascription should hold also in phase I.

In this respect, we have taken infrared spectra of potassium azide, KN_3 and potassium cyanate, KNCO, crystals for reference. These crystals consist of linear triatomic anions and potassium cations and are quite isomorphous with potassium thiocyanate crystal in phase I (space group, $D_{4h}^{18}-I4/mcm$)[15,16]. In these two crystals the size of anions is the smaller and they are packed more closely, as is reflected in the lattice constants ($a=c=6.096$ Å, $b=7.056$ Å for KN_3 crystal; $a=c=6.07$ Å, $b=7.03$ Å for KNCO crystal), and the thermal motions mainly responsible for the reorientation occur with more difficulty because of their stronger interionic interactions, as is revealed by their higher melting points (355°C for KN_3 and ca. 700°C for KNCO). Spectra of these compounds in the ν_2 region at various temperatures above room temperature are presented in Fig. 11. As is evident from the figure, splitting may be observed at all the temperatures examined, accompanied by a slight shift of higher frequency bands*. From these facts, it is very plausible to assume that we can ascribe the transformation of a doublet into a singlet observed in the ν_2 band of the potassium thiocyanate crystal, not to the fact that this crystal belongs to the tetragonal crystal system in phase I, but rather to an excitation of violent torsional oscillation as well as to a flipping motion which leads to the dynamical directional disordering of the thiocyanate ions.

Inspection of the molecular packing in the potassium thiocyanate crystal of phase II (Fig. 10) shows that out-of-plane motions seem to occur more easily than in-plane motions. Furthermore, from X-ray studies by Yamada and Watanabé[14] it has been established that the expansion of the b axis of a unit cell at the end-point of phase transition is more remarkable than those along the a and c axes ($\Delta b/b\simeq 0.017$, $\Delta a/a\fallingdotseq\Delta c/c\simeq 0.008$). This fact is considered to reflect also the fact that interionic interactions along b-axis are weaker than those along the other two axes, so out-of-plane motions will be more frequently excited than in-plane motions. Although the torsional frequencies of thiocyanate ions are not known, the existence of a lattice frequency of 28 cm^{-1} has been reported by Jones[8]. In any case, it is quite plausible that torsional frequencies are of the order of one-tenth of the bending frequencies. The period of flipping motions from one equilibrium direction to another will be larger than or at least of the same order as those of the torsional oscillation. Therefore, in one period of torsional oscillation some ten cycles or so of bending vibration are possible. Such out-of-plane motions will diminish the repulsive potential, which affects in-plane bending vibration more seriously. Frequent excitation of such kinds of motion all over the crystal will work out to bring about operatively a considerable decrease in the crystalline field around the anions.

Summarizing these results, we may explain the temperature variation of the ν_{2a} band in the following way. When the temperature approaches the transition temperature, the out-of-plane torsional oscillation and the flipping motion of thiocyanate ions are more and more frequently excited; eventually, at the transition point the long-range directional order of thiocyanate ions will disappear completely. Parallel with the progress of the phase transition, the repulsive potential, as well as the anisotropy mentioned above, will be gradually decreased, resulting in the gradual shift of the ν_{2a} band.

Finally, we should like to comment briefly on the results of the factor group analysis of the molecular vibrations of thiocyanate ions in the potassium thiocyanate crystal (phase II). In this case a Bravais unit lattice coincides with a crystallographic unit cell, and there are four potassium cations and four thiocyanate anions in a unit cell. The analysis was performed following the ordinary method; the results are presented in Table III. If a thiocyanate ion is linear, $4\times(3\times3-5)=16$ inner vibrational modes will be present. Nevertheless, only twelve modes are found by this analysis. On the other hand, twelve modes are found for the rotational lattice vibration. If thiocyanate ions are strictly linear, there should be present only $4\times2=8$ rotational vibrational modes in a Bravais unit lattice. Thiocyanate ions are thus found by this analysis to be not strictly linear-shaped but slightly bending, even in the equilibrium configuration, under the influence of the intermolecular interaction. Of the twelve rotational lattice modes, four are out-of-plane modes, distributed among the A_{1u}, B_{1u}, B_{2g} and B_{3g} species. The out-of-plane bending vibration in the nomenclature of the site symmetry analysis corresponds to the rotational lattice modes which fall in B_{1u}.

15) S. B. Hendricks and L. Pauling, *J. Am. Chem. Soc.* 47, 2904 (1925).

16) L. K. Frevel, *Z. Krist.*, 94, 197 (1936); *J. Am. Chem. Soc.*, 58, 779 (1936).

* Infrared spectra of these two crystals have been reported by some authors. For KN_3, see P. Gray and T. C. Waddington, *Trans. Faraday Soc.*, 53, 901 (1957); H. A. Papazian, *J. Chem. Phys.*, 34, 1614 (1961). For KNCO, see T. C. Waddington, *J. Chem. Soc.*, 1959, 2499. These writers have, however, not made any comment regarding on the splitting of the ν_2 band nor have they presented a spectrum chart in which no doublet is observed. We should like to make a more detailed discussion of this point elsewhere in the near future.

As has been mentioned above, in phase I the direction of the thiocyanate ions is disordered. Since the space group of this phase represents the symmetry of the averaged structure, factor group analysis cannot be successfully applied to this phase. However, phase I belongs to the tetragonal system, and at least no positive reasons are available which oblige us to consider that thiocyanate ions bend in this phase. If so, the temperature shift of the ν_{2a} band may be accompanied by the change in molecular shape from slightly bending to strictly linear in the equilibrium configuration, but by no change in the mode of molecular motion. On the other hand, in the bending vibration which falls in the B_{3u} species, a change in the shape of the ions as well as a change in the mode of motion (from a rotational lattice one to a bending one) may be expected to occur, but no appreciable shift in the ν_{2b} frequency is observed.

Summary

The phase transition of the potassium thiocyanate crystal at ca. 140°C has been studied by thermal and infrared methods. The transition is of a higher-order type, accompanied by an entropy change of 1.30 ± 0.05 e. u., which is nearly equal to $R \ln 2$. The infrared band due to the in-plane bending vibration of a thiocyanate ion shifts to lower frequencies in the course of the phase transition. From these results, it has been concluded that the phase transition is connected with the dynamical disordering of the direction of thiocyanate ions in crystal, a disordering which is mainly brought about by the frequent excitation of the out-of-plane torsional oscillation and the flipping motion.

We wish to express our hearty thanks to Professor Isamu Nitta of Kwansei Gakuin University for his valuable advice and continued interest in this study, and also to Drs. Yasusada Yamada and Tatsuo Miyazawa of Osaka University for their kind discussions. This work was partly supported by Scientific Research Funds from the Ministry of Education.

Department of Chemistry
Faculty of Science
Osaka University
Nakanoshima, Osaka

The Phase Transition of Crystalline Potassium Thiocyanate, KSCN. II. X-Ray Study

By Yasusada YAMADA and Tokunosuké WATANABÉ

(Received April 27, 1963)

As has been illustrated in the foregoing paper[1], thermal and infrared absorption data suggest that the mechanism of the phase transition of potassium thiocyanate is described by a model of the order-disorder type transition for the orientation of the rod-shaped thiocyanate ion.

The aim of the present investigation is to confirm the above-mentioned mechanism of transition by the X-ray diffraction method, a proceeding based on the knowledge of the crystal structures below and above the transition temperature.

The crystal structure of the room temperature modification is known. According to Klug[2], potassium thiocyanate is isomorphous with D^{11}_{2h}–Pbcm, and its orthorhombic unit cell, containing four formula units, has the following dimensions:

$$a=6.66\,\text{Å},\ b=6.635\,\text{Å} \text{ and } c=7.58\,\text{Å}$$

Throughout this description, the axes (X, Y, Z) are derived from those of Klug (X', Y', Z') by a transformation: $X=Z'$, $Y=Y'$, $Z=X'$. A structure which gives a fairly good agreement between observed and calculated structure factors is obtained by putting atoms in the following equivalent positions given by D^{11}_{2h}–Pbcm.

4K:

$$u\ \frac{1}{4}\ 0,\ u\ \frac{1}{4}\ \frac{1}{2},\ \bar{u}\ \frac{3}{4}\ 0,\ \bar{u}\ \frac{3}{4}\ \frac{1}{2};$$

4C, 4N, 4S:

1) M. Sakiyama, H. Suga and S. Seki, This Bulletin, **36**, 1025 (1963).
2) H. P. Klug, *Z. Krist.*, **85**, 214 (1933).

$$v\ w\ \frac{1}{4},\ \bar{v}\ \bar{w}\ \frac{3}{4},\ v\ \frac{1}{2}-w\ \frac{3}{4},\ \bar{v}\ \frac{1}{2}+w\ \frac{1}{4};$$

with $u(\mathrm{K})\approx\frac{3}{4}$, $v(\mathrm{S})=0.385$, and $w(\mathrm{S})=0.125$. The suggested parameters for nitrogen are $v(\mathrm{N})=0.080$ and $w(\mathrm{N})=0.400$; for carbon, $v(\mathrm{C})=0.205$ and $w(\mathrm{C})=0.280$. The arrangement of the thiocyanate ions in the unit cell is shown in Fig. 1. All the thiocyanate ions are lying on planes parallel to (0 0 1) and are oriented to the face diagonals, as Fig. 1 shows. The infrared absorption lines referred above correspond to the bending vibrations of the

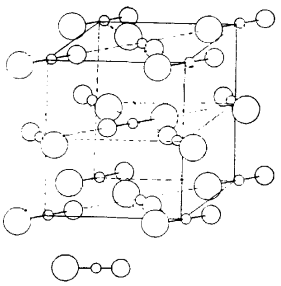

Fig. 1. The arrangement of thiocyanate ions in the low temperature phase.

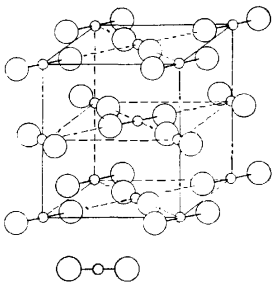

Fig. 2. The arrangement of thiocyanate ions in the high temperature phase.

thiocyanate ions in and out, respectively, of these planes.

The Crystal Structure of the High Temperature Phase

In order to investigate the crystal structure of the high temperature phase, X-ray diffraction experiments were carried out as follows:

The crystals used in the present experiments were obtained by slow evaporation from methanol solutions. In form they are thin rods elongated along [1 0 0]. By a preliminary test, it was found that the transition occurred in a single crystal. The crystals do not shatter on passing the transition temperature, and the process is almost completely reversible.

As the crystal is highly deliquescent, each sample was sealed in a thin, evacuated capillary. Hot air was blown in a constant stream over the capillary mounted on the goniometer in order to maintain the sample at a certain temperature between 160°C and room temperature. A thermocouple was placed at the nozzle of the jet. Before the crystal was set on the goniometer head, another thermocouple was mounted in place of the sample in order to estimate the temperature gradient in the hot air stream. As no appreciable difference was observed between the temperatures read by the two thermocouples, the temperature of the crystal was estimated by the thermocouple placed at the nozzle during the exposure.

Oscillation photographs were prepared by using [1 0 0] and [0 0 1] as the axes of rotation. Precession photographs for the $hk0$ and $hk1$ levels were also prepared.

The general appearance of the oscillation and precession photographs taken at 160°C was very like those taken at room temperature, indicating that the size of the unit cell and the arrangement of the constituent atoms do not change appreciably. However, the symmetry of the reciprocal lattice becomes ditetragonal and many of the weak reflections disappear, though the intensity of reflections from planes with the indices $hk1$ for $h+k+l$ even seems to be affected by the temperature factor alone. The lattice constants are found to be:

$$a=b=6.70\,\text{Å} \text{ and } c=7.73\,\text{Å} \text{ (at 160°C)}$$

To all the extinction rules observed for the room temperature modification, is now added hkl for $h+k+l$ odd. The space groups compatible with these rules are $C^{10}_{4v}-I4\,cm$, $D^{10}_{2d}-I\bar{4}c2$ and $D^{18}_{4h}-I4/mcm$.

Let us now try to derive a structure based upon these space groups, starting first with $C^{10}_{4v}-I4c2$. In this space group, there are two kinds of four-fold and one kind of eight-fold equivalent positions:

$$\left(0\,0\,0,\ \frac{1}{2}\ \frac{1}{2}\ \frac{1}{2}\right)+$$

4a: $0\,0\,z,\ \frac{1}{2}\ \frac{1}{2}\ z;$

4b: $\frac{1}{2}\ 0\ z,\ 0\ \frac{1}{2}\ z;$

8c: $x\ \frac{1}{2}+x\ z,\ \bar{x}\ \frac{1}{2}-x\ z,\ \frac{1}{2}+x\ \bar{x}\ z,$
$\frac{1}{2}-x\ x\ z$

Since there are four formula units in the unit cell, we have to find positions for four potassium, four carbon, four nitrogen and four sulfur atoms. Now, either 4a or 4b will give almost the same arrangement of potassium atoms as in the room temperature modification. However, the carbon, nitrogen and sulfur atoms cannot be placed on either 4a or 4b, because the length of the b-axis is too short to be accommodated with these atoms. Moreover, any one of these structures should give the natural decrease of intensities for $0k0$, e.g., $I_{020}>I_{040}>I_{060}>I_{080}$; this is not, however, the case. The only possibility of placing these atoms is to use 8c, with half a weight on each atom. If we place the potassium atoms on 4a, and the other atoms on 8c with appropriate parameters, we shall arrive at a structure which can easily be derived from the structure of the room temperature modification, the difference being that all the thiocyanate ions are here pointing statistically in two directions, namely, either [1 1 0] and $[\bar{1}\,\bar{1}\,0]$ or $[1\,\bar{1}\,0]$ or $[\bar{1}\,1\,0]$ (See Fig. 2). The same atomic arrangement can also be obtained either from $D^{10}_{2d}-I\bar{4}c2$ or $D^{18}_{4h}-I4/mcm$ by using 4a for potassium and 8h for the other atoms. If the origin of coordinates is shifted to $\frac{1}{4}\,\frac{3}{4}\,\frac{3}{4}$ from that given in International Table I, the positions of atoms can be given by:

$$\left(0\,0\,0,\ \frac{1}{2}\,\frac{1}{2}\,\frac{1}{2}\right)+$$

4K in 4a:

$$\frac{3}{4}\,\frac{1}{4}\,\frac{1}{2},\ \frac{3}{4}\,\frac{1}{4}\,0,\ \frac{1}{4}\,\frac{3}{4}\,0,\ \frac{1}{4}\,\frac{3}{4}\,\frac{1}{2};$$

4C, 4N, 4S in 8c:

$$x\,x\,\frac{1}{4},\ \frac{1}{2}-x\,\frac{1}{2}-x\,\frac{1}{4},\ \frac{1}{2}+x\,\bar{x}\,\frac{1}{4},$$

$$\bar{x}\,\frac{1}{2}+x\,\frac{1}{4},\ \frac{1}{2}+x\,\frac{1}{2}+x\,\frac{3}{4},\ \bar{x}\,\bar{x}\,\frac{3}{4},$$

$$x\,\frac{1}{2}-x\,\frac{3}{4},\ \frac{1}{2}-x\,x\,\frac{1}{4},$$

with half a weight on each.

Comparing these coordinates with those assigned to the atoms in the room temperature modification, it can easily be understood that the structure factor for the high temperature modification has the same expression as those for the room temperature modification with the indices $h+k+1$, even if u(K) is taken to be 3/4 and $w_i=1/2-v_1$. The differences in these three structures given by $C^{10}_{4v}-I4cm$, $D^{10}_{2d}-I\bar{4}c2$ and $D^{18}_{4h}-I4/mcm$ lie in the fact that the site symmetry of the positions of the centers of the mass of the constituent ions corresponds to the following:

	$C^{10}_{4v}-I4\,cm$	$D^{10}_{2d}-I\bar{4}c2$	$D^{18}_{4h}-I4/mcm$
K:	C_4-4	D_2-222	D_4-422
CNS:	$C_{2v}-mm$	D_2-222	$D_{2h}-mmm$

Since the thiocyanate ions are statistically disposed in two directions, or they flip from one direction to the reverse, there is no reason to assume that these thiocyanate ions have a symmetry lower than $D_{2h}-mmm$. The most probable space group is therefore, $D^{18}_{4h}-I4/mcm$. A fairly good agreement between observed and calculated structure factors was found with the following parameters: $x(C)=0.212$, $x(N)=0.110$, $x(S)=0.090$ and $B(\text{overall})=3.1\,\text{Å}^2$. Further refinement was not attempted because of the disordered structure. Though the crystal structure of potassium cyanate[3], KCNO, has not been worked out fully, it seems that it is isomorphous with the high temperature modification of potassium thiocyanate.

The Temperature Dependence of Ordering

It was observed that the intensity of the reflection from those crystal planes whose indices satisfy the relation, $h+k+l=2n+1$, decreases very rapidly as the temperature approaches the transition point. To investigate the temperature dependence of the intensity, the intensity of reflection (0 3 2) was measured at various temperatures by the scintillation-counter method, using monochromatized Mo-K_α radiation. The results are shown in Fig. 3, in which the scale of intensity is chosen arbitrarily. One of the reasons why this reflection was chosen for precise measurement is that there is only a negligible contribution

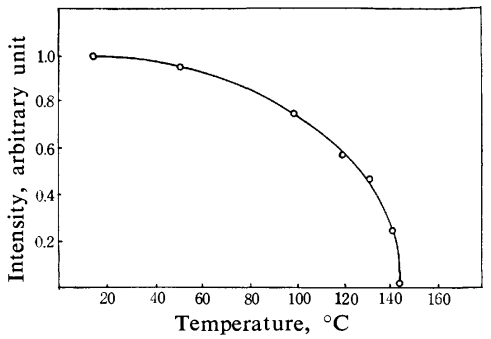

Fig. 3. Temperature dependence of intensity of (0 3 2) reflection.

3) S. B. Hendricks and L. Pauling, *J. Am. Chem. Soc.*, 47, 2904 (1925); L. K. Frevel, *Z. Krist.*, 94, 197 (1936); *J. Am. Chem. Soc.*, 58, 779 (1936).

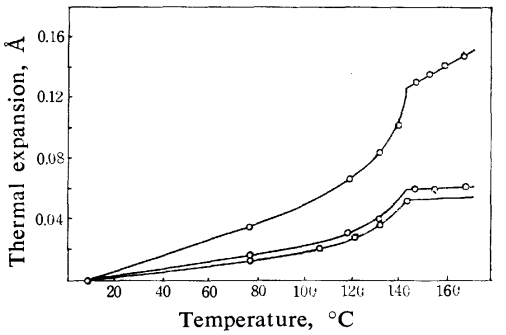

Fig. 4. Thermal expansion of lattice constants.

of the potassium atoms in its structure factor.

It was also observed that the lattice constants show an anomalous expansion near the transition temperature, a finding in accordance with dilatometric data given in the previous investigation. The results are shown in Fig. 4.

The temperature dependence of the reflected intensity directly gives information about the mechanism of the ordering of thiocyanate ions. If we call the arrangement of thiocyanate ions at room temperature " normal ", the high temperature phase can be described as containing an equal number of the normal and of the reverse arrangements of the thiocyanate ions. When the temperature of the crystal is raised, the reverse arrangement sets in and its fraction increases as the temperature rises; finally the crystal contains an equal number of the normal and reverse arrangements above the transition temperature.

Using the long range order parameter, S, which is defined by the relation: $p=1+S/2$, p being the probability that the thiocyanate ion takes in the normal position, we can now write the intensity of the reflection from the crystal planes $(h\,k\,l)$ whose indices satisfy the relation $h+k+l=2n+1$ in the following form:

$$I(hkl)\propto\{f^{r}-f^{w}\}^{2}S^{2}e^{-2M} \qquad (1)$$

where f^{r} represents the scattering amplitude of the thiocyanate ions in the normal position (the equillibrium position at room temperature), f^{w}, that of the same ion in the reverse position, and the factor e^{-2M}, the reduction factor called the Debye-Waller temperature factor. M can be written in the form:

$$M=8\pi^{2}\langle u^{2}\rangle\left(\frac{\sin\theta}{\lambda}\right)^{2}\equiv B(T)\left(\frac{\sin\theta}{\lambda}\right)^{2} \qquad (2)$$

where $\langle u^{2}\rangle$ is the mean-squared displacement of atoms perpendicular to the reflecting crystal plane.

Therefore, the temperature dependence of S relative to the order parameter, $S(T_0)$, at a certain temperature, T_0, can be given by observed intensities as follows:

$$R(T)\equiv\frac{S(T)}{S(T_0)}=\sqrt{\frac{I(T)}{I(T_0)}}\,e^{-M(T)+M(T_0)} \qquad (3)$$

Throughout this study the room temperature, 15°C, was chosen as T_0. To eliminate the $e^{-M(T)+M(T_0)}$ factor, we proceeded as follows. $M(T)$ for $T=160$°C and $T=15$°C were obtained by examining the observed structure factors $F(h\,k\,l)$ with $h+k+l=2n$, because these reflections are independent of the parameter, S, and the temperature dependence of their intensities mainly comes from the excitation of thermal vibrations. The experimental values of $B(T)$ are 3.1 Å^2 for $T=160$°C and 1.9 Å^2 for $T=15$°C. $M(T)$ at any temperature between $T=160$°C and $T=15$°C was obtained by a linear interpolation. The $e^{-M(T)+M(T_0)}$ factor for the (0 3 2) reflection using these values is 0.931 for $T=142$°C (transition temperature). Therefore, the maximum correction due to thermal vibrations is estimated to be about 7%. As $S(T_0)$ can not be obtained experimentally, it must be given more or less arbitrarily, except that the extrapolation of S to $T=0$°K should tend to unity $[S(0°K)=1]$, corresponding to the completely ordered state.

Discussion

Let us look into the mechanism of the ordering. We shall separate the whole lattice into two body-centered tetragonal lattices and assume that the ordering occurs independently in these two lattices. The interaction energy for one sublattice may then be expressed as:

$$U=-\sum_{i}\sum_{j}J_{ij}\mu_i\mu_j \qquad (4)$$

where μ_i is the dipole moment of the i'th ionic radical and can take only two values, $\pm\mu_0$, corresponding to the normal and reversed positions. Using the molecular field approximation, we replace μ_i's by an averaged value, $\langle\mu\rangle$, where

$$\langle\mu\rangle=\mu_0\frac{1+S}{2}-\mu_0\frac{1-S}{2}=\mu_0 S \qquad (5)$$

The interaction energy per ion may then be expressed as

$$U=-\mu_0^{2}\sum_{j}J_{0j}S^{2}\equiv -JS^{2} \qquad (6)$$

Following the usual thermodynamical calculations, we obtain the theoretical values of S versus temperatures which are given by the dotted line in Fig. 5. The open circles in the same figure represent experimental values obtained by Eq. 3, assuming $S(T_0)$ to be equal to the theoretical value. However, extrapolation of the experimental curve (solid line) to $T/T_c=0$ does not give $S=1$, which implies

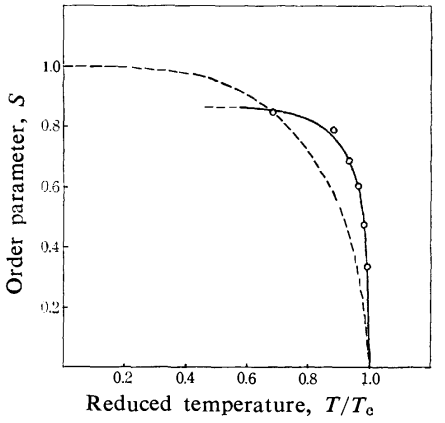

Fig. 5. Temperature dependence of order parameter. Dotted curve is for theoretical value by first approximation. Experimental value is normalized by $S=0.84$.

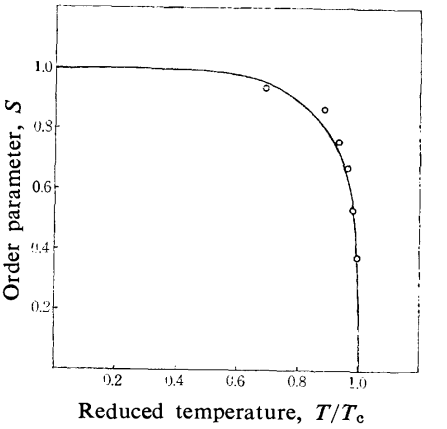

Fig. 6. Temperature dependence of order parameter. Observed values are normalized by $S=0.94$.

that ordering occurs more rapidly in the vicinity of the transition temperature.

As a second approximation, we shall take into account the effect of the volume dependence of the interaction energy, J[4]. If the gain of ordering energy by expansion overcomes the loss of elastic energy, the system will continue to possess the ordering accompanying the anomalous volume expansion near the transition temperature.

A simple calculation along these lines is performed in the Appendix. The results of the calculations give the temperature dependence of S as follows:

$$S=\mathrm{Tanh}\left[\frac{T_c}{T}S+A\frac{T_c}{T}S^3\right]$$
$$A=\frac{2v(\beta_c T_c)^2}{\kappa\alpha^2 k T_c} \qquad (7)$$
$$T_c=2J_0/k$$

where κ is the compressibility; β_c, the anomalous volume expansion coefficient; v, the ionic volume; J_0, the volume-independent part of interaction energy J; k, the Boltzman constant, and α, a parameter given by (A—9), T_c being the Curie temperature. A comparison of the experimental values of the long range order parameter and the values calculated by this equation is given in Fig. 6, where κ is assumed as:

$$\kappa=6.0\times10^{-12}\ \mathrm{cm^2/dyn.}$$

and the following experimental values are used:

$$T_c=142^\circ\mathrm{K}$$
$$\beta_c=4.4\times10^{-4}\ \mathrm{deg^{-1}}$$
$$v=167.5\times10^{-24}\ \mathrm{cm^3}$$

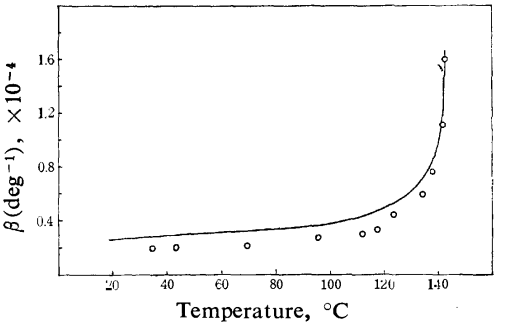

Fig. 7. Temperature dependence of volume expansion coefficient.

For these values,

$$A=0.30$$

As is illustrated in the Appendix, the value of A can not exceed 1/3 for the second order transition, regardless of the value of κ. A comparison of the experimental values of the anomalous volume expansion coefficient β_a and the values calculated by Eq. A—12 is also given in Fig. 7, in which part of the experimental values are given by a dilatation measurement[5].

Substantial accordances in both S and β_a seem to suggest that the transition mechanism is well described by the ordinary molecular field approximation if the volume dependence of the interaction energy is taken into account. The remaining discrepancies may be due to the effect of the excitation of lattice vibrations.

These investigations, however, do not yield any information about the dynamical properties of the flipping motion of the thiocyanate ions.

4) R. Eisenschitz, *Proc. Roy. Soc.*, A **186**, 546 (1938).

5) T. Shinoda, H. Suga and S. Seki, This Bulletin, **33**, 1314 (1960).

Summary

The phase transition of potassium thiocyanate has been investigated by the X-ray diffraction. It was confirmed that it is an order-disorder type transition with regard to the orientation of the thiocyanate ions. The temperature dependence of the ordering and the anomalous volume expansion near the transition temperature seem capable of being interpreted by the molecular field approximation if the volume dependence of the interaction energy is taken into account.

The authors wish to express their thanks to Professor Syūzō Seki for his kind suggestions for conducting this study. They are also indebted to Miss Takako Shinoda, who, kindly offered the dilatation data, and to Mr. Minoru Sakiyama of Osaka University for his helpful discussions in the course of this work.

Department of Physics
Faculty of Science
Osaka University
Nakanoshima, Osaka

Appendix

The free energy per ion concerning order, including elastic energy, is given by

$$F=\frac{1}{2\kappa}\frac{(\delta v_a)^2}{v}-JS^2+\frac{kT}{2}[(1+S)\ln(1+S)+(1-S)\ln(1-S)] \quad \text{(A—1)}$$

where κ is the compressibility, v is the ionic volume and δv_a is the anomalous part of the volume expansion. For small values of δv_a, we have

$$J=J_0+\frac{\partial J}{\partial v}\delta v_a \equiv J_0+J'\delta v_a \quad \text{(A—2)}$$

The equilibrium volume is determined by the energy minimum condition $\delta F/\delta v=0$, which gives:

$$\frac{\delta v_a}{v}=\kappa J' S^2 \quad \text{(A—3)}$$

The substitution of Eq. (A—3) back into (A—1) gives

$$F=-J_0S^2-\frac{\kappa v}{2}J'^2S^4+\frac{kT}{2}[(1+S)\ln(1+S)+(1-S)\ln(1-S)] \quad \text{(A—4)}$$

From the equilibrium condition $\delta F/\delta S=0$, the temperature dependence of S is now given by

$$\frac{4J_0}{kT}+S\frac{4\kappa vJ'^2}{kT}S^3=\mathrm{Tanh}^{-1}S \cong 2(S+\frac{1}{3}S^3+\cdots\cdots) \quad \text{(A—5)}$$

Using the asymptotic form of Tanh S for small S-values, we have an approximate expression for $S(T)$ near the transition temperature as follows:

$$S^2(T)=3\left(\frac{T_c}{T}-1\right)(1-6\kappa vJ'^2)^{-1} \equiv\alpha\frac{\Delta T}{T}\approx\alpha\frac{\Delta T}{T_c} \quad \text{(A—6)}$$

$$T_c=2J_0k$$

$$\alpha=\frac{3}{1-6\kappa vJ'^2}$$

which means that S^2 depends linearly on the temperature near T_c, the Curie temperature. The unknown parameter, J', is calculated by using the experimental value of the anomalous volume expansion coefficient at T_c as follows:

$$\beta_c=\left[\frac{\mathrm{d}\left(\frac{\delta v_a}{v}\right)}{\mathrm{d}T}\right]_{T=T_c}=\kappa J'\left[\frac{\mathrm{d}S^2}{\mathrm{d}T}\right]_{T=T_c} =\kappa J'\frac{\alpha}{T_c} \quad \text{(A—7)}$$

Therefore,

$$S^2=3\left(\frac{T_c}{T}-1\right)\left\{1-6\frac{v(\beta_cT_c)^2}{\kappa\alpha^2}\right\}^{-1} \quad \text{(A—8)}$$

where α is determined by the self-consistency condition:

$$\alpha=\frac{3}{1-\frac{6v(\beta_cT_c)^2}{\kappa\alpha^2}} \quad \text{(A—9)}$$

Finally, we can write the equations to determine S in the form:

$$S=\mathrm{Tanh}\,x \quad \text{(A—10)}$$

$$x=\frac{T_c}{T}S+\frac{T_c}{T}AS^3 \quad \text{(A—11)}$$

$$A=\frac{2v(\beta_cT_c)}{\kappa\alpha^2}$$

S is obtained by plotting S against x as given by (A—10) and (A—11) and looking for the intercept of the two curves. It should be noticed that S^2 as given by (A—8) is infinite for $A\geqq 1/3$, which implies that the asymptotic expansion of $\mathrm{Tanh}^{-1}S$ up to S^3 is invalid for $A\geqq 1/3$. It can be shown that, in this case, S^2 suddenly becomes zero from a finite value at T_c which corresponds to a first order transition.

Further, the anomalous volume expansion coefficient is calculated by the substitution of $S(T)$ in (A—3) as follows:

$$\beta_a=\frac{\mathrm{d}(\mathrm{d}v_a/v)}{\mathrm{d}T}=\kappa J'\frac{\mathrm{d}(S^2)}{\mathrm{d}T} \quad \text{(A—12)}$$

$$=\frac{1}{\alpha}\frac{\mathrm{d}S^2}{\mathrm{d}(T/T_c)}$$

*The Ion-exchange Equilibrium between Cesium and Phenol-sulfonic-acid-type Cation Exchange Resin**

By Hiroyuki TSUBOTA

(Received April 12, 1963)

Many researchers have investigated the specific adsorption of cesium on the phenol-sulfonic-acid-type cation exchange resin as a technique for analyzing cesium in various materials[1-4]. However, studies of the ion-exchange equilibrium with the resin have not yet been carried out, with the exception of one of the Cs^+-Na^+ exchange in a sodium hydroxide solution[5]. In this paper, the distribution coefficients of cesium between several basic solutions and the resin as measured by the batch method are reported. In addition, the phenomenon of the specific adsorption of cesium on the resin from an ammoniacal solution as compared to sodium hydroxide and potassium hydroxide solutions will be discussed.

Experimental

Chemicals.—Diaion BK (phenol-sulfonic-acid-type cation exchange resin) and Duolite C-3 of 60~80 mesh were used**. They were prepared as ammonium, sodium and potassium forms using basic solution of ammonium, sodium and potassium salts respectively. It was confirmed that about 90%, or more, of the phenolic-active groups were in NH_4^+-, Na^+- or K^+-forms. The exchange capacity of the active sulfonic group was 2.0 meq., and that of the phenolic group was 2.2 meq. for 1 g. of air-dried resin. The exchange capacities were determined by measuring the salt-splitting capacities and the exchange capacity in the basic solution.

Solutions of the following composition were used. Various amounts of cesium, with cesium-137 as the tracer, were added to ammoniacal solutions of various concentrations and pH values. The pH value was adjusted by adding ammonium formate. They were prepared in the range of 0.5~7.5 M of total concentration, a pH value of 10~12, and 0~100 mg. of cesium carrier for 50 ml. of solution. Sodium hydroxide plus sodium chloride and potassium hydroxide solutions were prepared in similar ways. All alkaline solutions were kept in CO_2-free air as far as possible.

Instruments.—The pH value of the ammoniacal solution was determined by a glass electrode pH-meter.

The β-activity was measured by a G. M. counter connected with an automatic sample changer. The γ-activity was measured for the photo-peak of 0.66 MeV. by using a well-type NaI(Tl) scintillation counter connected with a single-channel pulse height analyzer.

Measurements.—For each run, 50 ml. of the solution were shaken for 24 hr. with 0.500 g. of the dried ion-exchange resin in a constant temperature bath at 25°C. After an exchange equilibrium had been attained, 5 ml. of the solution were pipetted out, and the radioactivity or cesium concentration of the solution phase (C) was measured. From the C values and the cesium concentration in the initial solution (C_0), the distribution coefficients of cesium (K_d) under various conditions were obtained from the following equation. (Here, the volume decrease of the solution caused by the swelling of the ion exchanger is disregarded).

$$K_d = \{(C_0 - C)/C\}\{50/0.5\}$$
$$= 100 \cdot (C_0 - C)/C \qquad \text{(ml./g.)}$$

In the case of ammoniacal solutions, 2 ml. of the solution were put into a stainless steel counting dish, and the β-activity was measured after drying it under an infrared lamp. In the case of sodium or potassium solutions, 5 ml. of the solution were placed in a capsule and the γ-activity was measured. All measurements were made twice.

Results

$Cs^+-(NH_4^+ + NH_3)$ Exchange System.—The values of the distribution coefficients of cesium when the pH value of the outer solution was varied and the total concentration of the outer solution was kept constant are shown in Fig. 1. Straight lines, the slopes of which were nearly constant for various concentrations, were obtained, although they deviated slightly at both ends. The slopes are expressed as follows:

$$\left(\frac{\partial \log K_d}{\partial \text{pH}}\right)_{[NH_4^+ + NH_3]} = 1.0 \qquad (1)$$

Figure 2 shows the relationship between the distribution coefficients of cesium and the total

* A part of this work was read at the 13th Annual Meeting of the Chemical Society of Japan, Tokyo, April, 1960.

** Similar results for distribution coefficients were obtained. The results for Diaion BK will be reported here.

1) H. S. Miller and G. E. Kline, *J. Am. Chem. Soc.*, 73, 2741 (1951).
2) W. F. Merritt, *Can. J. Chem.*, 36, 425 (1958).
3) J. B. Niday, *Phys. Rev.*, 98, 42 (1955).
4) T. T. Sugihara, H. I. James, E. J. Troianello and V. T. Bowen, *Anal. Chem.*, 31, 44 (1959).
5) H. Kakihana, T. Murase and M. Nakagawa, The 12th Annual Meeting of the Chemical Socity of Japan, Kyoto, April, 1959.

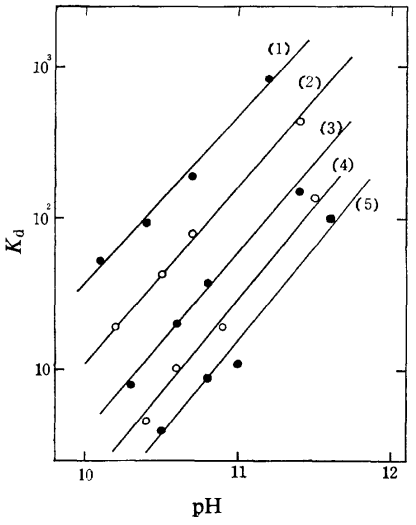

Fig. 1. Distribution coefficients of cesium in $Cs^+-(NH_4^+ + NH_3)$ exchange system.

Total concn. of ammonia, mol./l.
(1) 0.5, (2) 1, (3) 2, (4) 3, (5) 5

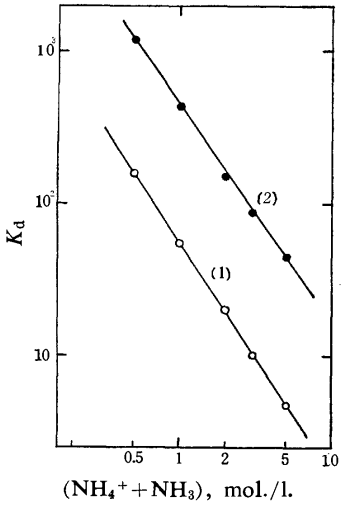

Fig. 2. Distribution coefficients of cesium in $Cs^+-(NH_4^+ + NH_3)$ exchange system.

(1) pH 10.6 (2) pH 11.4

concentration of the outer solution when the pH value of the outer solution was kept constant. They are expressed approximately by the following equation:

$$\left(\frac{\partial \log K_d}{\partial \log [NH_4^+ + NH_3]}\right)_{pH} = -1.6 \qquad (2)$$

where $[NH_4^+ + NH_3]$ denotes the total concentration of the solution.

From Eqs. 1 and 2, the following equation is obtained:

$$\log K_d = pH - 1.6 \log [NH_4^+ + NH_3] + C_1 \qquad (3)$$

where C_1 is the constant for the $Cs^+-(NH_4^+ + NH_3)$ exchange system.

The value when the salt-splitting capacity is 2.0 meq./g.* is as follows:

$$C_1 = -8.8$$

The Cs^+-Na^+ and Cs^+-K^+ Exchange Systems.—The relationship between the distribution coefficients of cesium and the pH value or the concentration of sodium hydroxide when the total sodium concentration in the outer solution was kept constant is shown in Fig. 3. The relation is expressed as follows:

$$\left(\frac{\partial \log K_d}{\partial \log [OH^-]}\right)_{[Na^+]} = 0.25 \qquad (4)$$

or

$$\left(\frac{\partial \log K_d}{\partial pH}\right)_{[Na^+]} = 0.25 \qquad (4')$$

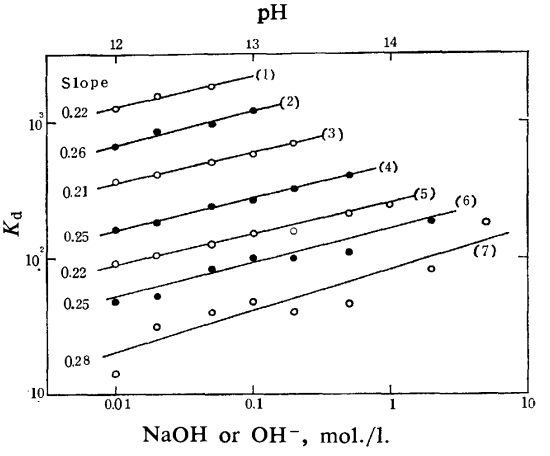

Fig. 3. Distribution coefficients of cesium in Cs^+-Na^+ exchange system.

Total sodium concn., mol./l.
(1) 0.05 (2) 0.1 (3) 0.2 (4) 0.5
(5) 1 (6) 2 (7) 5

Equation 5, which is obtained by rearranging the results shown in Fig. 3, gives the relationship between the distribution coefficients of cesium and the total sodium concentration when the pH value or the concentration of sodium hydroxide in the outer solution is kept constant.

$$\left(\frac{\partial \log K_d}{\partial \log [Na^+]}\right)_{pH} = -0.90 \qquad (5)$$

* Equations 1 and 2 can be formulated even when the quantities of the ion exchnger or the exchange capacities are varied because of the drying state of the resin. However, the value of C_1 in Eq. 3 changes. Therefore, all values of K_d and the constant C_1 are normalized when the salt-splitting capacity, which can be easily determined, is 2.0 meq./g.

From Eqs. 4 and 5, a formula for the Cs^+-Na^+ exchange system may be given with a good approximation as follows:

$$\log K_d = 0.25 \log [OH^-] - 0.90 \log [Na^+] + C_2 \quad (6)$$

where C_2 is the constant for the system, and

$$C_2 = 2.4$$

when the salt-splitting capacity is 2.0 meq./g.

Figure 4 shows the relations between the distribution coefficients of cesium and the

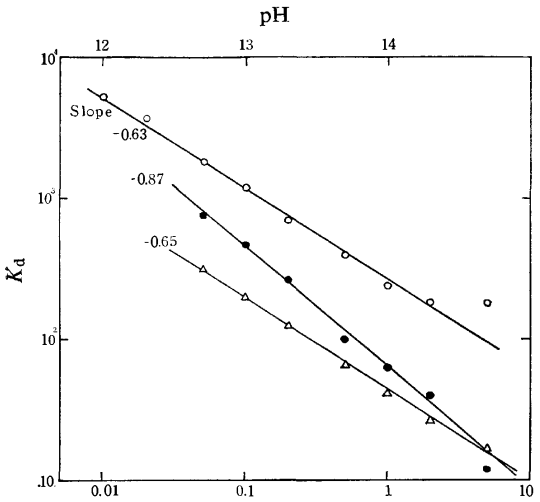

NaOH, KOH or NaCl, mol./l.

Fig. 4. Distribution coefficients of cesium in Cs^+-Na^+ and Cs^+-K^+ exchange system.
The outer solution:
○ Sodium hydroxide solution
● Sodium chloride solution
△ Potassium hydroxide solution

concentration of the outer solution when the outer solution contained only sodium hydroxide or potassium hydroxide, and neither sodium chloride nor potassium chloride. The following equation holds when the outer solution was a sodium hydroxide solution:

$$\log K_d = -0.63 \log [NaOH]_T + C_3 \quad (7)$$

where C_3 is a constant, and

$$C_3 = 2.4 = C_2$$

A similar equation is found when the outer solution was a potassium hydroxide solution:

$$\log K_d = -0.65 \log [KOH]_T + C_4 \quad (8)$$

where C_4 is a constant, and

$$C_4 = 1.7$$

When the outer solution is neutral, i.e., a sodium chloride solution, the distribution coefficients of cesium can be expressed by the following equation:

$$\log K_d = -0.87 \log [NaCl]_T + C_5 \quad (9)$$

where C_5 is a constant, and

$$C_5 = 1.8$$

The $Cs^+-NH_4^+$ Exchange System.—It was very difficult to estimate the ammonium ion concentration in the outer solution exactly, but it was necessary for the rearrangement of the relation expressed by the Eq. 3 for the $Cs^+-(NH_4^+ + NH_3)$ exchange system to provide for the relation of the distribution coefficients of cesium to the ammonium ion concentration. Two ways were tried for the estimation of the ammonium ion concentration in the outer solution, 1) assuming that the ammonium ion concentration is equivalent to the quantities of ammonium formate added to the system, and 2) assuming that the ammonium ion concentration can be calculated by using the dissociation constant of ammonia water $pK = 4.74$ at 25°C[6]. When the ammonium ion concentration was kept constant, the relation between the distribution coefficients of cesium and the pH value of the outer solution can be expressed by the following equation:

$$\left(\frac{\partial \log K_d}{\partial \mathrm{pH}}\right)_{[NH_4^+]} = 0 \quad (10)$$

The relationship between the distribution coefficients and the ammonium ion concentration is shown in Fig. 5. The relationship

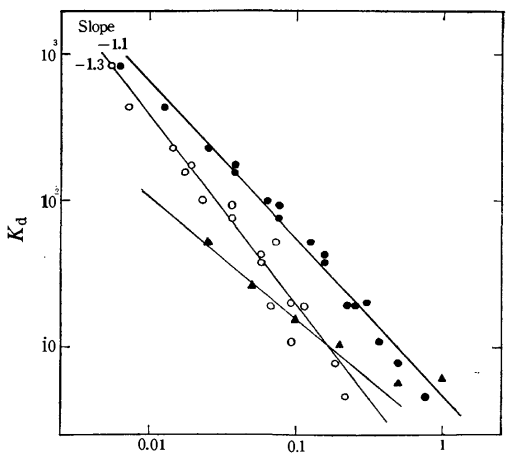

NH_4^+, mol./l.

Fig. 5. Distribution coefficients of cesium in $Cs^+-NH_4^+$ exchange system.
● When NH_4^+ is equivalent to the quantities of ammonium formate added.
○ When NH_4^+ is calculated using the dissociation constant of ammonia water.
▲ When the outer solution is ammonium chloride solution.

6) B. E. Conway, "Electrochemical Data", Elsevier Pub., Amsterdam (1952).

is independent of the pH value and of the total concentration of outer solution, and can be expressed as follows:

$$\log K_d = -1.1 \log [NH_4^+] + C_6 \qquad (11)$$

where C_6 is a constant, and

$$C_6 = 0.62$$

The Variation of the Distribution Coefficients of Cesium with Variation in the Cesium Quantities. — The distribution coefficients of cesium when the cesium quantities in the exchange system were changed are shown in Fig. 6. No simple formula could be found for these variations.

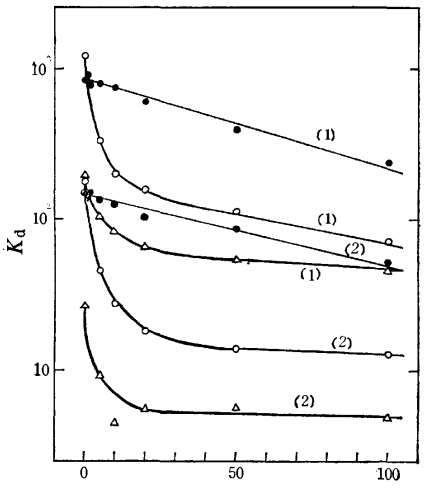

Fg. 6. Relation between distribution coefficients of cesium and amounts of cesium.

● $Cs^+ - (NH_4^+ + NH_3)$ exchange system
(1) Total concn. 0.5 mol./l., pH 11.2 (NH_4^+ 0.006)
(2) Total concn. 2 mol./l., pH 11.4 (NH_4^+ 0.03)
○ $Cs^+ - Na^+$ exchange system
(1) 0.1 mol./l. NaOH
(2) 2 mol./l. NaOH
△ $Cs^+ - K^+$ exchange system
(1) 0.1 mol./l. KOH
(2) 2 mol./l. KOH

Discussion

The observed values of the distribution coefficient of cesium are due to both the sulfonic group and the phenolic group of the resin. Therefore, the adsorption of cesium must be discussed by separating K_d into two functions: K_{dp}, which is due to the phenolic group, and K_{ds}, which is due to the sulfonic group.

$$K_d = K_{dp} + K_{ds} \qquad (12)$$

As the sulfonic acid group is strongly acidic, K_{ds} is probably a function only of the cation concentration in the outer solution $[M^+]$:

$$K_{ds} = B_s [M^+]^{m_s} \qquad (13)$$

where B_s and m_s are constants. Since the phenolic acid group is weakly acidic, however, K_{dp} may be a function of both the cation concentration and the pH value, or $[OH^-]$, of the outer solution:

$$K_{dp} = B_p [M^+]^{m_p} [OH^-]^{n_p} \qquad (14)$$

where B_p, m_p and n_p are constants.

Combining Eqs. 12, 13 and 14,

$$K_d = B_s [M^+]^{m_s} + B_p [M^+]^{m_p} [OH^-]^{n_p} \qquad (15)$$

Differentiating Eq. 15 with respect to $[M^+]$, when $m_s = m_p$,

$$\left(\frac{\partial \log K_d}{\partial \log [M^+]}\right)_{[OH^-]} = \text{const.} \qquad (16)$$

except when $B_s = 0$.

However, differentiating it with respect to $[OH^-]$, for every value of constants, B_s, B_p, B_s, m_p and n_p:

$$\left(\frac{\partial \log K_d}{\partial \log [OH^-]}\right)_{[M^+]} \neq \text{const.} \qquad (17)$$

Moreover, it should be considered that some of the metal ions are associated in the resin phase.

Thus, the results of the experiments cannot be generally expressed by the straight lines shown in Figs. 1—5, but they should be shown according to Eq. 15.

Because Eq. 15 cannot be generally solved, it has to be numerically evaluated. The variation of distribution coefficients, however, may be empirically discussed by assuming that the results are expressed by the straight lines in a limited range, even though it must be discussed more generally using Eq. 15.

The $Cs^+ - Na^+$ Exchange System.—Equation 7, obtained when the outer solution is sodium hydroxide, can be derived from Eq. 6. Sodium hydroxide is almost completely dissociated in an aqueous solution, so that:

$$[Na^+] = [OH^-] \simeq [NaOH]_T \qquad (18)$$

Substituting Eq. 18 in Eq. 6,

$$\log K_d = -0.65 \log [NaOH]_T + C_2 \qquad (6')$$

which is the same as Eq. 7. In the same manner, Eq. 8, obtained for the $Cs^+ - K^+$ exchange system, may be reduced as follows:

$$\log K_d = 0.25 \log [OH^-] - 0.90 \log [K^+] + C_4 \qquad (19)$$

Putting the condition of pH = 7, or $\log [OH^-] = -7$, into Eq. 6,

$$\log K_d = -0.90 \log [Na^+] + 0.65 \qquad (20)$$

The constant term of Eq. 20 is evidently different from that of Eq. 9, obtained when the outer solution is a sodium chloride solution. This fact shows that Eq. 6, which was obtained in the high pH range, cannot be applied in the neutral range*. K_d calculated with Eq. 6 must be larger than K_d calculated by Eq. 9, where the phenolic group plays a part in adsorbing the cesium: therefore,

$$\log K_d \ (6) > \log K_d \ (9)$$

Resolving the equation,

$$[OH^-] > 4.0 \times 10^{-3}$$

or

$$pH > 11.6 \qquad (21)^{**}$$

This shows that the specific adsorption of cesium caused by the phenolic group of the resin may be effective in the range of the pH value over 11.6 for $Cs^+ - Na^+$ exchange system. To increase the specific adsorption of cesium, the concentration of sodium hydroxide must be increased. Consequently, the total adsorption of cesium and K_d will decrease.

The $Cs^+ - (NH_4^+ + NH_3)$ Exchange System.— Equation 11, obtained for the $Cs^+ - NH_4^+$ exchange system, seemed to be inconsistent with the formula obtained for the $Cs^+ - Na^+$ and $Cs^+ - K^+$ exchange systems. This inconsistency can be interpreted as follows. The quantity of cesium A adsorbed on resin is a function of the concentration of the dissociated phenolic groups and of the cation concentration of the solution:

$$A = f\{[OH^-], \ [M^+]\} \qquad (22)$$

From the experimental results mentioned above, function f may be expressed by a power function:

$$A = k_1 [OH^-]^{n_1} [M^+]^{m_1}$$

or

$$K_d = k_2 [OH^-]^n [M^+]^m \qquad (23)$$

Equation 23 can be expressed in a logarithmic form:

$$\log K_d = n \log [OH^-] + m \log [M^+] + k_3 \qquad (24)$$

and for a $Cs^+ - NH_4^+$ exchange system, Eq. 24 is reduced to:

$$\log K_d = n \log [OH^-] + m \log [NH_4^+] + k_3' \qquad (24')$$

On the other hand, in an ammoniacal solution the following relation can be obtained:

$$\frac{[NH_4^+]\,[OH^-]}{[NH_3]} = K_b \qquad (25)$$

where K_b is the dissociation constant of ammonia water. Rearranging Eq. 25,

$$[OH^-] = K_b [NH_3] / [NH_4^+] \qquad (26)$$

As NH_3 may be kept constant before and after the exchange reaction,

$$[OH^-] = K' / [NH_4^+] \qquad (27)$$

Substituting Eq. 27 into Eq. 24',

$$\log K_d = -n \log [NH_4^+] + m \log [NH_4^+] + k_3' + n \log K' = (m-n) \log [NH_4^+] + k_4 \qquad (28)$$

Substituting the values of n and m ($n = 0.25$, $m = -0.90$) which were obtained for the $Cs^+ - Na^+$ and $Cs^+ - K^+$ exchange systems for n and m in Eq. 28 or 24, Eq. 29 can be obtained:

$$\log K_d = (-0.90 - 0.25) \log [NH_4^+] + k_4 = -1.15 \log [NH_4^+] + k_4 \qquad (29)$$

Substituting C_6 for the k_4 of Eq. 29, we can obtain Eq. 11 again. Thus, the tangent of Eq. 29 coincides with that of Eq. 11. This shows that the $Cs^+ - NH_4^+$ exchange is not different from the $Cs^+ - Na^+$ or $Cs^+ - K^+$ exchange.

Because in the $Cs^+ - (NH_4^+ + NH_3)$ exchange system the pH value of the outer solution is less than 11.6, which is the lower limit of pH value for a solution to adsorb cesium specifically with the phenolic group, it is necessary to verify whether or not the specific adsorption of cesium occurs. The distribution coefficients of cesium against NH_4^+ in the ammonium chloride solution shown in Fig. 5 can be attributed to the distribution coefficients caused by the sulfonic group. Because the estimated concentrations of NH_4^+ needed to plot Fig. 5 are uncertain, the results in an ammoniacal solution cannot be quantitatively compared with those in an ammonium chloride solution. The specific adsorption of Cs^+ by the phenolic group may occur in the pH range over 10.5~11, or in the concentration range of $[NH_4^+] < 0.1$ mol./l. In the $Cs^+ - (NH_4^+ + NH_3)$ exchange system, to increase total adsorption of cesium the concentration of NH_4^+ must be kept low and the pH value of the solution must be raised; consequently, the specific adsorption of cesium increases. This characteristic, which is different from that of the $Cs^+ - Na^+$ or $Cs^+ + K^+$ exchange system, is very

---

* This is evident from Eq. 15. Substituting $m_s = m_p = m$ in Eq. 15, the following equation can be obtained:

$$\log K_d = m \log [M^+] + \log\left\{1 + \frac{B_p}{B_s}[OH^-]^{n_p}\right\} + \log B_s$$

When

$$\frac{B_p}{B_s}[OH^-]^{n_p} \gg 1 \quad \text{(in high pH range)}$$

$$\log K_d \simeq m \log [M^+] + n_p \log [OH^-] + \log B_p$$

and when

$$\frac{B_p}{B_s}[OH^-]^{n_p} \ll 1 \quad \text{(in low pH range)}$$

$$\log K_d \simeq m \log [M^+] + \log B_s$$

** It was solved by substituting Eq. 9 as follows:

$$\log K_d = -0.90 \log [NaCl]_T + C_5$$

important in the application of ion exchange to the analysis of cesium.

Because Eq. 15 cannot be generally solved, it has to be numerically evaluated. The results of the numerical calculation of distribution coefficients caused by the adsorption of cesium by phenolic group (K_{d_p}) for the Cs^+-Na^+ exchange system, using the results shown in Figs. 3 and 4, are shown in Fig. 7. The K_{d_p} values for the $Cs^+-(NH_4^+ + NH_3)$ excange system are shown in Fig. 8.

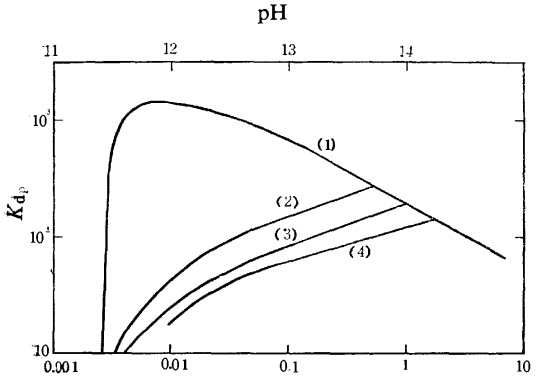

Fig. 7. Distribution coefficients of cesium due to phenolic group of the resin in Cs^+-Na^+ exchange system.

(1) NaOH
(2) $Na^+ = 0.5$ mol./l.
(3) $Na^+ = 1$ mol./l.
(4) $Na^+ = 2$ mol./l.

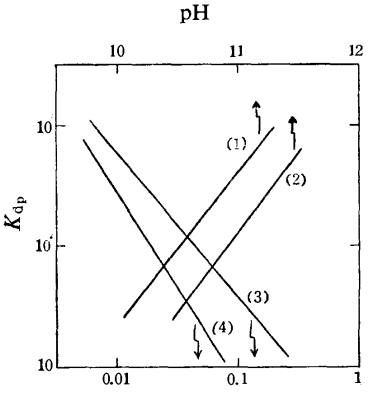

Fig. 8. Distribution coefficients of cesium due to phenolic group of the resin in $Cs^+-(NH_4^+ + NH_3)$ exchange system.

(1) Total concn., 0.5 mol./l.
(2) Total concn., 1 mol./l.
(3) When NH_4^+ is equivalent to the quantities of ammonium formate added.
(4) When NH_4^+ calculated using the dissociation constant of ammonia water.

Summary

1) In the $Cs^+-(NH_4^+ + NH_3)$ exchange system, the distribution coefficients of cesium can be approximately expressed as follows:

$$\log K_d = pH - 1.6 \log [NH_4^+ + NH_3] - 8.8$$

2) In the Cs^+-Na^+ and Cs^+-K^+ exchange systems, the distribution coefficients of cesium can be expressed with a good approximation by:

$$\log K_d = 0.25 \log [OH^-] - 0.90 \log [Na^+] + 2.4$$

and

$$\log K_d = 0.25 \log [OH^-] - 0.90 \log [K^+] + 1.7$$

In the $Cs^+-NH_4^+$ exchange system, the distribution coefficients of cesium can be expressed by:

$$\log K_d = -1.1 \log [NH_4^+] + 0.62$$

3) The specific adsorption of cesium by the active phenolic groups is observed when the pH value of the outer solution is above 12, and high selectivity is obtained above 13 for the Cs^+-Na^+ exchange system. For the $Cs^+-(NH_4^+ + NH_3)$ exchange system, the specific adsorption of cesium is observed above pH 11, and an extremely high selectivity can be obtained when the total concentration of the outer solution is below 1 mol./l.

The author wishes to thank Dr. Hidetake Kakihana and Dr. Terunosuke Nomura of the Tokyo Institute of Technology and Dr. Masami Izawa of the National Institute of Radiological Sciences for their helpful discussions and advice. Thanks are also due to Mr. Kazuo Watari for his assistance in the radioactivity measurements.

National Institute of Radiological Sciences
Kurosuna-cho, Chiba

NOTES

Enamines. IV. The Reaction of 1-Morpholino-1-cyclohexene with Sulfur[1]

By Yujiro NOMURA and Yoshito TAKEUCHI

(Received April 11, 1963)

In a preceding paper of this series[2], the reaction of enamines with hydrogen sulfide was reported; in the present paper, the reaction of an enamine with elementary sulfur will be described. The heating of 1-morpholino-1-cyclohexene (I) with sulfur in the absence of a solvent gave an intractable yellow oil. By refluxing a mixture of I and sulfur in benzene, however, colorless crystals have been obtained and identified as 4a, 9a-dihydroxyperhydrothianthrene (II) by the infrared spectrum, by the elementary analysis and by the melting point test on an admixture with an authentic sample[3]. The assignment of the structure was supported by a successful conversion of II into 1, 2, 3, 4, 6, 7, 8, 9-octahydrothianthrene (III)[4] by the acid treatment.

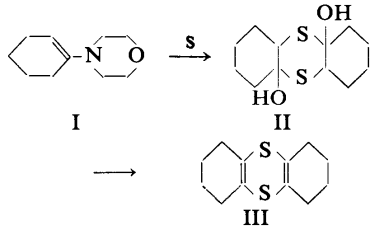

This result may reasonably be explained by assuming the intermediate formation of 2-mercaptocyclohexanone (V), which dimerizes to a 1, 4-dithiane compound (II)[5], since Asinger et al.[3] obtained II by the reaction of 2-chlorocyclohexanone (IV) with sodium hydrogen sulfide.

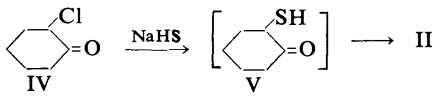

It is postulated that 1-morpholino-1-cyclohexene was attacked by sulfur at the 2-position and that the resulting immonium compound (VI) was hydrolyzed to α-mercaptocyclohexanone as follows:

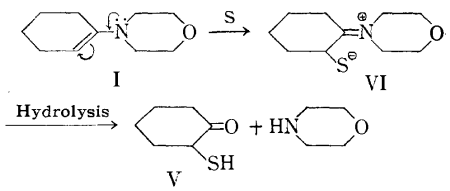

Such is actually the case with the Willgerodt reaction, in which Dauben et al.[6] also assumed an α-mercaptoketone as an intermediate.

II was recovered unchanged, even upon continued heating above its melting point. The OH-stretching frequency of II was observed at 3385 cm^{-1} in both Nujol and the KBr disk. Considering these facts and assuming that the 1, 4-dithiane ring is in the chair form[7], the most probable structure of II may be shown as follows (Fig. 1)*.

We expected that the 3385 cm^{-1} frequency would be shifted to the free OH region on dilution. The OH absorption of II in a carbon

1) Presented in part at the 15th Annual Meeting of The Chemical Society of Japan, Kyoto, April, 1962. Part III of this series: Y. Takeuchi and Y. Nomura, *Sci. Pap. Coll. Gen. Educ. Univ. Tokyo*, **11**, 193 (1961).

2) Y. Nomura and Y. Takeuchi, This Bulletin, **33**, 1743 (1960); cf. C. Djerassi and B. Tursch, *J. Org. Chem.*, **27**, 1041 (1962).

3) F. Asinger, M. Thiel and H. Kaltwasser, *Ann.*, **606**, 67 (1957).

4) B. Milligan and J. M. Swan, *J. Chem. Soc.*, **1961**, 5552.

5) O. Hromatka and E. Engel, *Monatsch. Chem.*, **78**, 38 (1947); O. Hromatka and R. Haberl, ibid., **85**, 830, 1082 (1954).

6) W. G. Dauben, R. P. Ciula and J. B. Rogan, *J. Org. Chem.*, **22**, 363 (1957).

7) Cf. R. E. Marsh, *Acta Cryst.*, **8**, 91 (1955).

* Haberl et al.[8] isolated two isomeric forms of *trans*-2, 5-dihydroxy-2, 5-dimethyl-1, 4-dithiane (VII), the dimer of mercaptoacetone, one of which (VIIa) lost a molecule of water upon heating to give 2, 5-endoxy-2, 5-dimethyl-1, 4-dithiane (VIII), though the other VIIb was recovered unchanged.

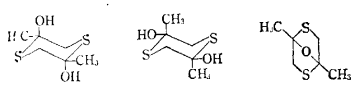

They reported that the OH-strectching frequency of VIIa in Nujol or in the KBr disk was observed at 3300 cm^{-1} due to the intramolecular hydrogen bonding between OH and S, but the frequency of VIIb was observed at 3375 cm^{-1} due to the intermolecular hydrogen bond.

8) R. Haberl, F. Grass, O. Hromatka, K. Brauner and A. Preisinger, *Monatsch. Chem.*, **86**, 551 (1955).

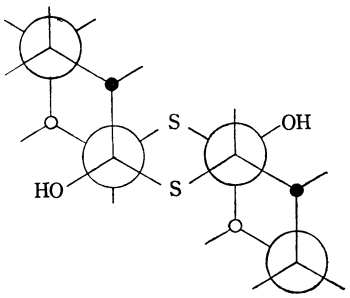

Fig. 1. Newman model of II.

tetrachloride solution, however, gradually disappeared and a strong absorption of $\nu_{C=O}$ appeared at 1710 cm^{-1}, though no absorption due to ν_{S-H} could be observed. II seems to dissociate into monomeric 2-mercaptocyclohexanone in a carbon tetrachloride solution, which has a disagreeable mercaptan-like odor.

Experimental

All melting points were uncorrected. The infrared spectra were determined on a Nihon Bunko Model Koken DS 301 spectrophotometer with a sodium chloride prism.

The Reaction of 1-Morpholino-1-cyclohexene (I) with Sulfur.—To a solution of 33.5 g. (0.2 mol.) of 1-morpholino-1-cyclohexene[9] in 100 ml. of benzene was added 4.8 g. (0.15 g. atom) of powdered stick sulfur. The mixture was heated under reflux for three hours. Refluxing was continued for two more hours after 100 ml. of 6 N hydrochloric acid had been added. The benzene layer was separated, and the aqueous layer was extracted with benzene. The combined benzene solution was washed twice with water, and the solvent was evaporated. The remaining oil was distilled in vacuo under a nitrogen atmosphere. After 1.7 g. of cyclohexanone had been distilled, 4.4 g. of a main fraction (b. p., 115~125°C/17 mmHg) was obtained; this soon solidified upon chilling. After repeated recrystallizations from 2-propanol, colorless crystals melting at 136~136.5°C (lit.[3] m. p. 135~136°C) were obtained. No depression of the melting point was observed on an admixture with authentic 4a, 9a-dihydroxy-perhydrothianthrene. Yield, 4.4 g. (25.1% based on sulfur used). IR ν_{O-H} 3385 cm^{-1} (Nujol, KBr).

Found: C, 54.92; H, 7.74; S, 24.00. Calcd. for $C_{12}H_{20}O_2S_2$: C, 55.34; H, 7.74; S, 24.63%.

A half gram of the material was heated above 160°C for two hours in an oil bath. After cooling, the almost-quantitatively recovered crystals melted at 136°C, and no depression of the melting point was caused by mixing with the initial material.

The Conversion of 4a, 9a-Dihydroxy-perhydrothianthrene (II) to 1, 2, 3, 4, 6, 7, 8, 9-Octahydrothianthrene (III).—To a solution of 0.5 g. of II in 5 ml. of 95% ethanol was added 1 ml. of concentrated hydrochloric acid, and the mixture was refluxed for three hours. After dilution with water, the acid was neutralized by sodium hydrogen carbonate. The resulting crystals were collected and recrystallized twice from 2-propanol. Yield, 0.22 g. (50% theoretical); m. p. 97~98°C (lit.[4] m. p. 97°C). IR $\nu_{C=C}$ 1610 cm^{-1} (Nujol).

Found: S, 28.58. Calcd. for $C_{12}H_{16}S_2$: S, 28.60%.

Department of Chemistry
College of General Education
The University of Tokyo
Meguro-ku, Tokyo

9) S. Hünig, E. Lücke and W. Brenninger, "Organic Syntheses", Vol. 41 (1961), p. 65.

The Calculation of the Energy Levels of Acetaldehyde by a Semi-empirical Molecular Orbital Method Including the Hyperconjugation Effect

By Kōzō Inuzuka

(Received April 12, 1963)

It is well-known that the introduction of a methyl group into unsaturated bond system results in a spectral shift from the spectrum of the unsubstituted parent molecule. A molecular-orbital treatment for a molecule containing a methyl group has been developed by many workers[1]. In this paper, we will calculate the lowest (n, π^*) and (π, π^*) electronic state energies for acetaldehyde by a semi-empirical molecular orbital method[2,3] including a group orbital for the methyl group. The molecular structure of acetaldehyde is shown in Fig. 1[4].

1) For example, C. A. Coulson and V. A. Crawford, *J. Chem. Soc.*, **1952**, 2052; R. S. Mulliken, C. A. Rieke and W. G. Brown, *J. Am. Chem. Soc.*, **63**, 41 (1941); N. Muller, L. W. Pickett and R. S. Mulliken, ibid., **76**, 4770 (1954).

2) R. Pariser and R. G. Parr, *J. Chem. Phys.*, **21**, 466, 767 (1953).

3) T. Anno, I. Matubara and A. Sadō, This Bulletin, **30**, 168 (1957).

4) R. W. Kilb, C. C. Lin and E. B. Wilson, Jr., *J. Chem. Phys.*, **26**, 1695 (1957).

TABLE I. TRANSITION ENERGIES AND OSCILLATOR STRENGTHS OF THE LOWEST n-π^* AND π-π^* TRANSITIONS OF AN ACETALDEHYDE MOLECULE

Orbital jump	Electronic transition	Transition energy, eV.		Oscillator strength	
		Calcd.	Obs.	Calcd.	Obs.
$n\rightarrow\pi_3$	$^3A''\leftarrow{}^1A'$	3.40			
$n\rightarrow\pi_3$	$^1A''\leftarrow{}^1A'$	3.83	3.86[a]	1.57×10^{-4}	3.15×10^{-4}
$\pi_2\rightarrow\pi_3$	$^3A'\leftarrow{}^1A'$	4.83			
$\pi_2\rightarrow\pi_3$	$^1A'\leftarrow{}^1A'$	7.35	7.51[b]	6.83×10^{-2}	

a) V. R. Rao and I. A. Rao, *Indian J. Phys.*, **28**, 491 (1954).
b) A. D. Walsh, *Proc. Roy. Soc.*, **A185**, 176 (1945).

A line combining two hydrogen atoms, H_a and H_b, is perpendicular to the molecular plane, and a third atom, H_c, is contained in its plane as Fig. 1 shows. From the point of view of the

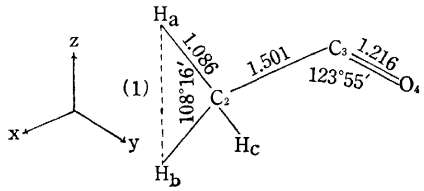

Fig. 1. A model of acetaldehyde molecule; (1) represents a quasi-atom.

molecular orbital method, the methyl group conjugates with the 2pπ orbital of the carbonyl group. For the methyl group, Mulliken[1] used the following group orbitals:

$$\phi_1=(h_a+h_b+h_c)/(3+6S)^{1/2} \qquad [\sigma]$$
$$\phi_2=(2h_c-h_a-h_b)/(6-6S)^{1/2} \qquad [\pi]$$
$$\phi_3=(h_a-h_b)/(2-2S)^{1/2} \qquad [\overline{\pi}]$$

Among these orbitals, the ϕ_3 orbital conjugates with the 2pπ orbitals of the carbonyl group. We assume the ϕ_3 orbital to be a quasi-2pπ orbital; the node is on the midpoint of a line connecting H_a with H_b, and it is separated by 1.086 Å from the neighboring carbon atom. The orbital energy of ϕ_3 is calculated by the following equation:

$$W(\phi_3)=\int \phi_3^* H \phi_3 \, d\tau$$

in which H is a Hartree-Fock type Hamiltonian[5]:

$$H=T+U_{H_3}$$
$$U_{H_3}=-1/r_a-1/r_b-1/r_c+(h_\sigma h_\sigma|+(h_\pi h_\pi|$$
$$-1/2(h_\sigma|h_\sigma-1/2(h_\pi|h_\pi$$

in which $-1/r_i$ is a potential force from a hydrogen nucleus i, and $(h_ih_i|$ and $(h_i|h_i$ are Coulomb and repulsion forces of the h_i electron respectively. For the 1s orbital energy of a hxdrogen atom, we use -13.595 eV., and the three center integrals are calculated by means of Sklar's approximation[6] and Kotani's table[7]. Paoloni proposed a relation between the effective nuclear charge, Z_μ, and one center Coulomb integral, $(\mu\mu|\mu\mu)=3.29_4 Z_\mu^8$. We use the above relation for calculating the effective nuclear charge of the quasi-2pπ orbital.

$$(\phi_3\phi_3|\phi_3\phi_3)=8.430 \text{ eV}.$$

Therefore, we obtain $Z_\mu=2.56$.

The nonbonding orbital for lone pair electrons on the oxygen atom can be approximately represented as follows:

$$\varphi_n=\chi_n$$

χ_n being the 2pπ AO of the oxygen atom, the nodal plane of which is perpendicular to the molecular plane and contains the CO axis. At any rate, we assume that the orbital of the H_3 group participates in hyperconjugation with the residual part of the molecule; the 2pπ group orbital has the effective nuclear charge of 2.56 and the valence state ionization potential of 8.804 eV. The interelectronic Coulomb integrals which appear in this calculation are evaluated according to Roothaan's table[9] for the case of $r>2.80$ Å and according to Pariser-Parr's method[2] for $r\leq2.80$ Å. Particularly, the empirical formula of the interelectronic Coulomb integrals $(H_3H_3|CC)$ is obtained as follows:

$$(H_3H_3|CC)=9.755-2.1680\,r+0.1551\,r^2$$

We use Kon's[10] formula for the calculation of the core integral, β_{CO}, between carbon and oxygen atoms. The core integral, β_{H_3-C}, between H_3 and the neighboring carbon atom, C, is substituted by β_{H_2-C}. β_{H_3-C} can be obtained by assumption of the proportionality relation, $\beta_{H_2-C}/\beta=S_{H_2-C}/S$, where β and S are core and overlap integrals respectively in a benzene molecule. The MO's of acetaldehyde have been obtained by the simple LCAO MO method

5) S. Aono, *Busseiron Kenkyu*, No. 94, 24 (1959).

6) A. L. Sklar, *J. Chem. Phys.*, 7, 984 (1939).
7) M. Kotani, A. Amemiya, E. Ishiguro and T. Kimura, "Table of Molecular Integrals", Maruzen Co., Ltd., Tokyo (1955).
8) L. Paoloni, *Nuovo Cimento*, 4, 410 (1956).
9) C. C. J. Roothaan, *J. Chem. Phys.*, **19**, 1445 (1951).
10) H. Kon, This Bulletin, **28**, 275 (1955).

disregarding overlap integrals. As a methyl group has electron-donating property, it is known that its electronegativity is larger than that of a carbon atom. Accordingly, we adopt the following parameters[1]: $\alpha_{H_3}=\alpha-0.5\beta$, $\alpha_2=\alpha-0.1\beta$, $\alpha_3=\alpha$, $\alpha_4=\alpha+1.5\beta$, $\beta_{12}=2.92\beta$, $\beta_{23}=0.834\beta$, $\beta_{34}=2^{1/2}\beta$, in which α and β are Coulomb and resonance integrals for a benzene molecule. We obtained the following orbitals:

$e_1=-2.8919$

$\varphi_1=0.5547\chi_1+0.6443\chi_2+0.3693\chi_3+0.3753\chi_4$

$e_2=-2.1786$

$\varphi_2=0.3744\chi_1+0.3435\chi_2-0.3726\chi_3-0.7765\chi_4$

$e_3=0.8305$

$\varphi_3=0.2436\chi_1-0.0276\chi_2-0.8288\chi_3+0.5029\chi_4$

$e_4=3.3990$

$\varphi_4=0.7019\chi_1-0.6827\chi_2+0.1496\chi_3-0.0568\chi_4$

in which χ_i represents the $2p\pi$ AO of the ith atom shown in Fig. 1. The results of the calculation are summarized in Table I, together with observed data.

Department of Applied Science
Tokyo Electrical Engineering College
Kanda, Chiyoda-ku, Tokyo

The Proton Magnetic Resonance Spectra of Some Anomeric Glycopyranosides

By Nobuo MORI, Satoshi OMURA, Osamu YAMAMOTO, Teruo SUZUKI and Yojiro TSUZUKI

(Received May 20, 1963)

The α- and β-anomers of glycopyranoses and their derivatives, such as acetates and glycosides, are generally identified on the basis of Hudson's rule of isorotation[1] as well as by infrared absorption spectroscopy[2]. In the latter method, however, there are some difficulties; for example, α-lactose and its acetate can not be distinguished from the corresponding β-anomers[3].

Recently, Lemieux and his co-workers[4] have employed high resolution proton magnetic resonance (NMR) spectroscopy (40 Mc.) for the identification of the anomers of fully-acetylated glycopyranoses and have found that the doublet signals characteristic of the anomeric hydrogens in the equatorial and axial orientaions generally appear around 1.2 and 1.7 p.p.m. (from the chloroform peak) with a splitting of ca. 3 and 8 c. p. s., respectively. However, this method has not yet been used to identify the anomers of other important derivatives, particularly simple alkyl glycosides.

In the present investigation, the NMR spectra in chloroform of some anomeric acetylated glycopyranosides as well as of acetylated lactoses and maltose were measured at room temperature at 60 Mc. and the signals for the anomeric hydrogens were observed. The spectra are shown in Fig. 1, along with those of some acetylglycopyranoses for the sake of comparison.

As far as the spectra of pentaacetyl-β-glycopyranoses (I and II) and the corresponding methyl tetraacetyl-β-glycopyranosides (V and VI) are concerned, it is to be noticed that a doublet signal at 1.65 p. p. m. in the former spectra, that of the anomeric axial hydrogen coupled with the adjacent axial hydrogen, is absent in the latter spectra. In the latter, however, a new doublet signal with a splitting of 6.3 or 7.8 c. p. s. appears at 2.93 p. p. m. This is to be assigned to the anomeric hydrogen in the glycosides. The position of the signal is not surprising, since it is well-known that the signals of the α-protons in etherified alcohols appear at a field higher by ca. 1$\sim$1.5 p. p. m. than those in the corresponding acetates[5] and this shift occurs regardless of the axial and equatorial orientation on a cyclohexane ring[6].

1) C. S. Hudson, *Advances in Carbohydrate Chemistry*, **3**, 15 (1948).
2) S. A. Barker et al., *Chem. & Ind.*, **1952**, 1156; **1953**, 196; *J. Chem. Soc.*, **1954**, 171, 3468, 4211, 4552.
3) Y. Tsuzuki and N. Mori, *J. Chem. Soc. Japan, Pure Chem. Sec.* (*Nippon Kagaku Zassi*), **77**, 992 (1956).
4) R. U. Lemieux, R. K. Kullnig, H. J. Bernstein and W. G. Shneider, *J. Am. Chem. Soc.*, **79**, 1005 (1957); **80**, 6098 (1958)).
5) L. M. Jackman, "Applications of Nuclear Magnetic Resonance Spectroscopy in Organic Chemistry", Pergamon Press, London (1959), p. 55.
6) J. N. Shoolery and M. T. Rogers, *J. Am. Chem. Soc.*, **80**, 5121 (1958).

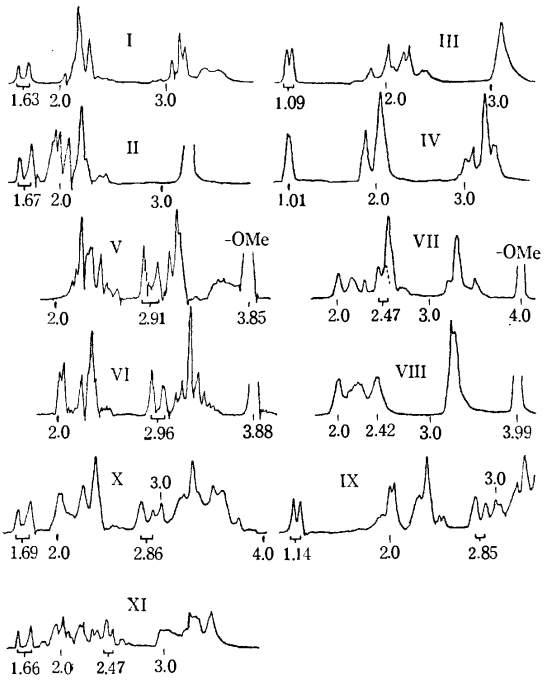

Fig. 1. NMR Spectra of acetylated sugars (in p. p. m. from $CHCl_3$).

Among the spectra of the corresponding α-anomers, a similar difference is observed. The spectrum of pentaacetyl-α-glucose (III) contains a doublet signal at 1.09 p. p. m. which is due to the anomeric equatorial hydrogen coupled with the adjacent axial hydrogen. In the spectrum of methyl tetraacetyl-α-glucoside (VII), the signal is absent, but a similar doublet signal with a splitting of 3 c. p. s. appears at 2.47 p. p. m., seemingly overlapping with a signal at 2.49 p. p. m. Similarly, with pentaacetyl-α-galactose (IV) a signal* which theoretically would be a doublet is present as a singlet at 1.01 p. p. m., while with methyl tetraacetyl-α-galactoside (VIII) a similar one appears at 2.42 p. p. m. Consequently, the signal at 2.45 p. p. m. in the α-glycosides, though not completely separated from other signals, seems to be that of the anomeric hydrogen.

In the spectra of the octaacetates of α- and β-lactose [4-*O*-β-D-galactopyranosyl-α- (IX) and -β-D-glucopyranose (X)], a doublet signal with a splitting of 6.3 or 7.4 c. p. s. appears at 2.86 p. p. m., in addition to the signal of the anomeric hydrogen in the α- or β-glucose unit. The former is of the anomeric axial hydrogen in the β-galactoside unit. In the case of the octaacetate of β-maltose (XI) [4-*O*-α-D-glucopyranosyl-β-D-glucopyranose], two characteristic signals are present, the one at 1.66 p. p. m. with a splitting of 6.7 c. p. s. being due to the anomeric hydrogen in the β-glucose unit and the other at 2.47 p. p. m. with a splitting of 3.5 c. p. s. due to that in the α-glucoside unit.

The above findings may be summarized as follows:

Pentaacetylglycopyranoses
α: 1.05 p. p. m. (J=3 c. p. s.)
β: 1.65 p. p. m. (J=7 c. p. s.)
Methyl tetraacetylglycopyranosides
α: 2.45 p. p. m. (J=3 c. p. s.)
β: 2.93 p. p. m. (J=7 c. p. s.)

Experimental

All compounds were prepared by the methods described in the literature cited; their melting points were as follows:

Pentaacetyl-D-glucopyranose[7], β(I) 131.5~132°C, α(III) 112~112.3°C

Pentaacetyl-D-galactopyranose[8], β(II) 143.5~143.7°C, α(IV) 96.5°C

Methyl tetraacetyl-D-glucopyranoside[7], β(V) 104~105°C, α(VII) 102°C

Methyl tetraacetyl-D-galactopyranoside[9], β(VI) 93~94.5°C, α(VIII) 86~87°C

Octaacetyllactose[10], β(X) 91~91.5°C, α(IX) 151.5°C

Octaacetylmaltose[11], β(XI) 162°C

All the spectra were measured in a 10~20% solution of the compound in chloroform using a Varian Model DP 60 NMR spectrometer equipped with a 60 Mc. r. f. unit. Tetramethylsilane was used in each case as an internal standard. Chemical shifts were obtained by the side-band method and are expressed in p. p. m. from chloroform to make them comparable with the data reported by Lemieux et al.[4]

Tokyo College of Science
Shinjuku-ku, Tokyo
(N. M., S. O. & Y. T.)

Government Chemical Industrial Research Institute, Tokyo
Shibuya-ku, Tokyo
(O. Y. & T. S.)

* Lemieux et al.[4] observed a singlet signal for the anomeric hydrogen in this compound.

7) C. S. Hudson and J. K. Dale, *J. Am. Chem. Soc.*, **37**, 1264 (1915).
8) C. H. Hudson and H. O. Parker, ibid., **37**, 1589 (1915); C. H. Hudson and J. M. Johnson, ibid., **38**, 1223 (1916).
9) J. K. Dale and C. S. Hudson, ibid., **52**, 2534 (1930).
10) C. S. Hudson and J. M. Johnson, ibid., **37**, 1270 (1915).
11) C. S. Hudson and J. M. Johnson, ibid., **37**, 1276 (1915).

SHORT COMMUNICATIONS

The Formation of Lysolecithin by Reductive Cleavage of Egg Yolk Lecithin with Lithium Aluminum Hydride

By Chieko URAKAMI and Kimiko YAMAGUCHI

(Received February 16, 1963)

The preparation of lysolecithins by controlled chemical reactions is of interest since they are utilized as the starting material for resynthesis of "mixed acid" lecithins (two different fatty acids being esterified). Recently, Marinetti[1] has reported that the treatment of lecithin with sodium methoxide at 0°C gives a mixture of α- and β-lysolecithin in a yield of 35%. This process is, however, accompanied by the formation of glycerylphosphorylcholine. Another disadvantage is that in such a polar solvent isomerization of the β-lysolecithin to the α-form and racemization of the β-carbon of the glyceryl moiety occur, though perhaps to only a small extent under the conditions employed. The optical purity of lysolecithin in the resynthesis of lecithins is of prime importance; our method of reductive cleavage of one acyl group of lecithin with lithium aluminum hydride in anhydrous ether is considered to meet this requirement since it has already been demonstrated that the product, glycerylphosphorylcholine formed, on removal of the two acyl groups from L, α-lecithin by the reducing agent retains the configuration of the latter[2]. A further advantage of this reaction is that lysolecithin may be the sole product, provided appropriate reaction conditions are found.

Purified egg yolk lecithin prepared by Hanahan's method[3] was treated with a dilute solution of lithium aluminum hydride in anhydrous ether according to the procedure described previously[2]. The reaction mixture was separated into the ether, aqueous, and inter-phase and the aqueous phase extracted with chloroform. The ether and chloroform solutions were analyzed for inorganic and organic phosphorus and examined by paper-chromatography[4].

Some typical examples of the results obtained are shown in Table I; substantial amounts of organic phosphorus are found in both organic solutions and insignificant amounts in the aqueous phase. Table II shows the R_f values of the products formed. The compound with R_f values higher than 0.2 is considered to be the unchanged lecithin since it was observed in separate experiments that an R_f value of 0.32~0.35 for pure lecithin became smaller, 0.25, when mixed with a large amount of the reduction products (supposedly containing considerable amounts of lysolecithin). The product with an R_f

TABLE I. REACTION CONDITIONS AND RECOVERY OF PHOSPHORUS

Lecithin : $LiAlH_4$ = 1 : 1.5 (mole ratio)

Temp., °C	6	8	8	10
Time, min.	20	20	80	20
Ether phase *P*, %	76.6	67.9	41.5	83.2
Chloroform phase *P*, %	16.7	12.0	30.0	25.8
Aqueous phase *P*, %	1.1	2.7	5.5	7.7

The percentage recoveries are based on the phosphorus content of the lecithin sample employed.

TABLE II. R_f VALUES OF THE PRODUCTS PRESENT IN ETHER AND CHLOROFORM EXTRACT

	Method of detection		
	P	Rhodamine-6G	Compd. assumed
Ether phase	0.10	0.11~0.14	Lysolecithin
	0.25~0.34	0.22~0.24	Lecithin
		0.95	Fatty alcohol
Chloroform phase	0.11~0.14	0.11	Lysolecithin
	0.22~0.29	0.22~0.29	Lecithin
		0.96	Fatty alcohol

Solvent system, diisobutyl ketone : acetic acid : water, 40 : 20 : 3 (v/v/v)

1) G. V. Marinetti, *Biochem.*, **1**, 350 (1962).
2) C. Urakami H. Okura and M. Okada, This Bulletin, **33**, 144 (1960).
3) D. J. Hanahan et al., *J. Biol. Chem.*, **228**, 680 (1957).
4) G. V. Marinetti, *J. Lipid Research*, **3**, 1 (1962).

value 0.10~0.14 is therefore considered to be lysolecithin. The detection of lysolecithin in the ether phase, however, is peculiar as it is generally regarded to be insoluble in ether. This may be explained by the fact that the unchanged lecithin makes lysolecithin soluble in ether, as has been observed by Lea[5]. No detectable amount of glycerylphosphorylcholine was found in the aqueous phase.

Accordingly, these results indicate that the method is promising for the preparation of optically pure lysolecithin, provided optimum reaction conditions are found. Further studies on a maximum extent of the cleavage and identification of the products are in progress.

Osaka City University
Faculty of the Science of Living
Nishi-ku, Osaka (*C. U.*)

Osaka City University
Department of Chemistry
Sumiyoshi-ku, Osaka (*K. Y.*)

5) C. H. Lea et al., *Biochem. J.*, **60**, 353 (1955).

The Synthesis of α-L-Aspartyl-L-serylglycine[1]

By Sidney W. Fox, Tadao Hayakawa and Kaoru Harada

(Received May 22, 1963)

The tripeptide residue, α-L-aspartyl-L-serylglycine, has been found as part of the active site of many esteratic enzymes[2]. The synthesis of this tripeptide is accordingly of interest for studies of catalytic activity *per se*, as a standard intermediate for syntheses of related substances, and as a copolymerized monomer in three-dimensional association with histidine residues in the polymers[3].

The ethyl ester of the tripeptide has been synthesized in this study. Other workers[4] have reported the synthesis of the ethyl ester of glycyl-α-L-aspartyl-L-serylglycine and of the L-aspartyl-*O*-acetyl-L-serylglycylglycine[5]. Attempts in this laboratory to saponify the tripeptide ester led to impure products. The *O*-acetylserine residue may also be subject to racemization when the acetate is removed by the usual treatment. The substituted aspartyl residue is also known to undergo alkaline decomposition easily[6]. The absence of the desired tripeptide from the literature, as well as informal reports of unsuccessful attempts at synthesis, can be explained by the reasons given.

We have devised a route which depends solely upon benzyl or carbobenzyloxy substituents which are entirely removable by hydrogenolysis. This route accordingly avoids any alkaline dederivatization. The sequence is:

$$\text{F-Ser(Bz)-OH (I)} + \text{H-Gly-OBz (II)} \xrightarrow[(90\%)]{\text{DCCD}}$$

$$\text{F-Ser(Bz)-Gly-OBz (III)} \xrightarrow[(71\%)]{} \text{H-Ser(Bz)-Gly-OBz (IV)}$$

$$\text{Z-Asp(OBz}(\beta)\text{)-OH (V)} + \text{IV} \xrightarrow[(47\%)]{\text{DCCD}}$$

$$\text{Z-Asp(OBz)-Ser(Bz)-Gly-OBz (VI)} \xrightarrow[\text{Pd-C}\ (55\%)]{H_2}$$

$$\text{H-Asp-Ser-Gly-OH (VII)}$$

F=Formyl; Z=Carbobenzyloxy; Bz=Benzyl

Except for II and V, none of these compounds were found in the literature. The aspartic acid and serine residues were L throughout.

The *N*-formyl-*O*-benzyl-L-serine was prepared by formylation of *O*-benzyl-L-serine[7], m. p. 133~134°C, $[\alpha]_D^{25} = +54.8°$ (*c* 2.75, ethanol). (Found: N, 6.23. Calcd. for $C_{11}H_{13}O_4N$: N, 6.28%). This substance was reacted with benzyl glycinate and *N*, *N'*-dicyclohexylcarbodiimide (DCCD) in dioxane to yield the formyldipeptide ester (III), m. p. 91~92°C, $[\alpha]_D^{25} = +2.2°$ (*c* 2.43, acetic acid) (Found: C, 65.02; H, 5.92; N, 7.53. Calcd. for $C_{20}H_{22}O_5N_2$: C, 64.85; H, 5.99; N, 7.56%). This compound

1) Aided by Grant No. NsG-173-62 of the National Aeronautics and Space Administration, U. S. A. Contribution No. 9 of the Institute for Space Biosciences.

2) J. A. Cohen, R. A. Osterbaan, H. S. Jansz and F. Berends, *J. Cell. Comp. Physiol.*, **54** Suppl. 1, 231 (1959).

3) S. W. Fox, K. Harada and D. L. Rohlfing, "Polyamino Acids, Polypeptides, and Proteins", Ed. by M. Stahmann, University of Wisconsin Press, Madison (1962), p. 47.

4) A. Van de Linde, H. Kienhuis, A. Verweij and J. P. J. Van der Holst, *Rec. trav. chim.*, **80**, 1305 (1961).

5) L. Benoiton and H. N. Rydon, *J. Chem. Soc.*, **1960**, 3328.

6) S. A. Bernhard, A. Berger, J. H. Carter, E. Katchalski, M. Sela and Y. Shalitin, *J. Am. Chem. Soc.*, **84**, 2421 (1962).

7) K. Okawa, This Bulletin, **29**, 486 (1956).

was deformylated by standing at room temperature in dioxane: benzyl alcohol: hydrochloric acid (5.5 ml.: 5.5 ml.: 1.0 ml. 12 N hydrochloric acid) in an amount equivalent in hydrochloric acid to the formyl ester, for 48 hr. to yield the hydrochloride of IV, which was hygroscopic and not analyzed as such. The hydrochloride had, however, $[\alpha]_D^{25}$ of approximately +8.3° (*c* 6.3, water). The hydrochloride was treated with an equivalent amount of triethylamine in dioxane in an ice bath and filtered from triethylammonium chloride. To the cold filtrate was added β-benzyl *N*-carbobenzyloxy-L-aspartate (V) and DCCD to give the substituted tripeptide (VI), m.p. 129~131°C, $[\alpha]_D^{25} = -4.7°$ (*c* 1.43, dioxane). (Found: C, 67.41; H, 5.99; N, 6.25. Calcd. for $C_{38}H_{39}O_9N_3$: C, 66.95; H, 5.77; N, 6.16%). All four substituents were simultaneously removed by hydrogenolysis with palladium-charcoal in methanol containing an equimolar amount of hydrochloric acid. The hydrochloride of the desired tripeptide (VII) was obtained. The hydrochloride was dissolved in absolute ethanol, the ethanolic solution was filtered from a small amount of insoluble impurity, and the filtrate was treated with an equivalent of pyridine. The free tripeptide (VII) separated immediately. It had d.p. 174~176°C, $[\alpha]_D^{25} = -7.3°$ (*c* 1.54, water). (Found: C, 38.93; H, 5.64; N, 15.20. Calcd. for $C_9H_{15}O_7N_3$: C, 38.99; H, 5.45; N, 15.16%). [Found; on automatic amino acid analyzer (following hydrolysis with 6 N hydrochloric acid at 110°C for 12 hr.): aspartic acid, 0.97; serine, 0.98; glycine, 1.00]. The final tripeptide was found to yield a single spot with ninhydrin when chromatographed on paper in a phenol $-H_2O$ (4:1) solvent, $R_f = 0.17$, with R_f of glycine standard = 0.38.

The tripeptide has little activity for the hydrolysis of *p*-nitrophenyl acetate, and this is additive with that of the free histidine when the two are tested together in solution. Now that the tripeptide is available, it can be included in various kinds of copolymerization with histidine for further tests.

The Chemistry Department and
Institute for Space Biosciences
The Florida State University
Tallahassee, Florida, U. S. A.

The Effect of Water on the Equilibrium Pressure of Ammonium Carbamate

By Eugeniusz BŁASIAK and Andrzej BARAŃSKI

(Received May 30, 1963)

In what follows we are concerned with the effect of the initial amount of water on the equilibrium pressure of ammonium carbamate. We discuss this effect in the temperature range only, where the formation of urea is rather large.

There is some discrepancy between the effects observed by various authors. Kawasumi[1] claims that the pressure of ammonium carbamate does not depend of the amount of water included in the initial sample. On the other hand, Krase and Gaddy[2] and independently Błasiak[3] point out, that the pressure increases with the amount of water. We intend to show that this discrepancy does not exist so as in the reality the "water effect" depends strongly on the loading density.

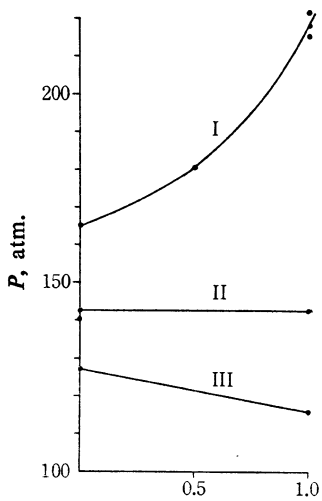

Fig. 1

1) S. Kawasumi, This Bulletin, **26**, 218 (1953).
2) N. W. Krase, V. L. Gaddy, *J. Ind. Eng. Chem.*, **14**, 611 (1922).
3) E. Błasiak, "Technologia związków azotowych (Technology of Nitrogen Compounds)", Vol. II, Collective Publication, Warsaw, P. W. T. (1956), p. 610.

In the figure we show our results obtained for the system $NH_4CO_2NH_2+wH_2O$ at various loading densities at 181°C. The curves I and III refer to the case $D'=0.92$ g./cm^3 and 0.30 g./cm^3 respectively, the curve II to the case $D=0.60$ g./cm^3.

The symbol D means here the initial loading density of ammonium carbamate and D' means the total loading density including the initial content of water. For a given system D, D' and the molar ratio of water to carbamate w, the equation $D'=D(1+0.2308\,w)$ is satisfied.

We see that curve II agrees with the results given by Kawasumi, $t=160$°C, $D=0.60$ g./cm^3, and that curve I agrees with the results obtained by Błasiak, $t=180$°C, $D'\approx 0.9$ g./cm^3. Krase and Gaddy gave no reference to the loading density.

We note that a similar effect was observed for the urea-water system[4].

The detailed discussion of our results will be published in "Chemia Stosowana".

Department of Inorganic Technology
Polytechnic School
Gliwice, Poland (E. B.)

Fertilizer Institute, Tarnów
Department of Inorganic Chemistry
Jagellonian University
Cracow, Poland (A. B.)

4) H. Kinoshita, *Rev. Phys. Chem. Japan*, **21**, 16 (1951).

A New Phenomenon of Storage Light Energy by Solution of Photochromatic 1,1'-Bi(2,4,5-triphenylimidazyl) at Low Temperatures

By Taro HAYASHI and Koko MAEDA

(Received May 30, 1963)

In a study of the mechanism of the chemiluminescence of 2,4,5-triphenylimidazole (lophine), 1,1'-bi(2,4,5-triphenylimidazyl) (I) (m. p. 199~201°C), was obtained as fine, pale yellow prisms. It exhibits both photochromism and thermochromism in a solution and in a solid state[1]. These phenomena were due to the reversible formation of a reddish purple free radical, 2,4,5-triphenylimidazyl-(II), by the dissociation of an N–N bond of compound I with irradiation or heating[2]. This communication deals with a new phenomenon which was found in solutions of this compound and its photochromatic substituted derivatives at low temperatures.

A pale yellow 10^{-3} M benzene solution of 1,1'-bi(2,4,5-triphenylimidazyl) (I) which had been prepared in the dark and sealed in a glass tube after removal of oxygen, was frozen at about −20°C in the dark to a nearly white solid, which soon became a pale yellow solution when kept at room temperature in the dark. The frozen solution did not acquire a reddish-purple color on being irradiated for several minutes with sunlight at −20°C. When this irradiated white solid was, immediately after irradiation, immersed in water at about 15°C in the dark, a reddish-purple color appeared as soon as the solid began to liquefy. In about 15 min. the irradiated frozen solid liquefied to be a deep reddish-purple solution, the color of which was nearly as deep as that acquired by an original pale yellow solution with irradiation at room temperature; it then gradually faded to the original pale yellow when kept in the dark at room temperature. A similar phenomenon was observed when the frozen solution was irradiated at −70°C. The reddish-purple color was attributed to the free radicals (II) produced by the splitting of the N–N bond of compound I, because the solution gave a strong electron spin resonance signal (g=2.003) and the free radical which gave the ESR signal was identified as 2,4,5-triphenylimidazyl (II) by a study of the absorption spectrum. It has, therefore, been concluded that light energy is stored in the frozen solution, to be used later for the splitting of the N–N bond. This phenomenon is a new effect of storage light energy by a frozen solution of the photochromatic compound. It was observed irrespective of the concentration of the solution and of the kind of solvent; it was found, for example, in a 10^{-2} or 10^{-4} M solution in benzene, cyclohexane or carbon tetrachloride.

A pale yellow 10^{-3} M toluene solution of compound I, which, unlike a benzene solution, did not freeze at −20°C, immediately acquired

1) T. Hayashi and K. Maeda, This Bulletin, **33**, 566 (1960); T. Hayashi, K. Maeda, S. Shida and K. Nakada, *J. Chem. Phys.*, **32**, 1568 (1960).

2) T. Hayashi and K. Maeda, This Bulletin, **35**, 2057 (1962).

a deep reddish-purple color when irradiated at about −20°C. From this fact the phenomenon of the storage of light energy seems to be characteristic of a frozen solution. However, the toluene solution did not acquire a reddish-purple color with irradiation at about −70°C. But it did begin to acquire a faint reddish-purple color when kept in a dark room at a temperature near −30°C, the color becoming deeper with a further rise in the temperature. Therefore, the storage of light energy can occur in both a frozen solution and a fluid solution. This phenomenon is primarily to be attributed to the photochromatic molecule in a solution cooled at a low temperature. A similar phenomenon was observed in a solution in *n*-heptane. The freezing of the solution seems to facilitate the storage at a higher temperature to some extent, because a frozen solution in benzene or cyclohexane did not acquire a reddish-purple color upon irradiation at about −20°C but stored light energy to split the N–N bond when the frozen solution liquefied in the dark.

A frozen toluene solution of compound I, which had been cooled at −195°C with liquid nitrogen in the dark, immediately acquired a faint reddish-purple color upon being irradiated at about −195°C. When the temperature rose to about −70°C in the dark or under irradiation, this solid lost its color and became a nearly colorless solution which began to acquire a reddish-purple color near about −30°C in the dark. A similar phenomenon was also observed near −195°C in a frozen solution in benzene, *n*-heptane, cyclohexane or EPA which trapped free radicals formed upon irradiation.

The duration of the storage of light energy by a frozen solution of compound I in benzene, irradiated at −20°C, was measured at −70°C and 0°C. It was found that light energy absorbed could be stored for 100 hr. or more at −70°C, whereas it was completely dissipated in about 6 hr. at 0°C. A fluid toluene solution was also found to be able to store light energy at −70°C for more than 100 hr.

A phenomenon of the storage of light energy, similar to that mentioned above, was also observed in solutions of substituted derivatives of compound I, such as 2-*p*-methylphenyl, 2-*p*-methoxylphenyl, 2-*p*-chlorophenyl, 2,4,5-tri-*p*-methylphenyl and 2,4,5-tri-*p*-chlorophenyl derivatives which were prepared by the method similar to that of compound I.

From the foregoing facts, the following is considered to be the mechanism of the storage of light energy at a low temperature. On irradiation in solution at a low temperature, 1,1'-bi(2,4,5-triphenylimidazyl) must be excited to an unusual metastable state, which is favorably affected by a low, ambient temperature or, especially, by the freezing of the solution. This state may be related to some peculiar state of the N–N bond or to a particular spatial disposition of the two imidazole rings which is related to the temperature. The light energy thus stored in the excited molecule, however, is a little insufficient for the splitting of the N–N bond; therefore, for the effective splitting of the bond, some thermal energy may have to be provided by an elevation of the temperature. The mechanism of the phenomenon observed at −195°C, which, considering from the preliminary investigation of the absorption spectrum, seems to be related to the spatial disposition of the imidazole rings and to that of the phenyl nuclei in the frozen solution, is unknown to us at the present time.

Department of Chemistry
Faculty of Science
Ochanomizu University
Bunkyo-ku, Tokyo

The Enhanced Effect of Anthracene on the Polarographic Maximum of Methyl-p-benzoquinone

By Kiyoko TAKAMURA

(Received June 1, 1963)

The author has been interested in the polarographic behavior of certain quinones in the presence of some polycyclic aromatic hydrocarbons. It is generally known that some polycyclic aromatic hydrocarbons have a suppressing effect on the polarographic maxima of some electroreducible substances[1]. It has been found in the present investigation that, on the other hand, these hydrocarbons are effective in inducing the maxima on the

1) C. E. Searle, *Nature*, **184**, 1716 (1959).

polarograms of some quinones. The results obtained with the methyl-*p*-benzoquinone (MQ)-anthracene (A) system are presented here.

As is shown in Fig. 1, a single wave having a typical maximum was obtained with 1.6×10^{-3} M of MQ in 2-methoxyethanol containing 0.25 M of lithium chloride at 25°C, but this maximum was suppressed by the addition of 0.004% methyl red. Contrary to this, the maximum was enhanced by the addition of A to the original solution. When A was added to the solution containing methyl red as a maximum suppressor, a pronounced maximum was observed to reappear.

The heights of the maxima were measured at varied concentrations of A with or without methyl red, keeping the concentration of MQ constant. In Fig. 2, the results obtained at 25°C are plotted against the concentration of A. Figure 2 shows that the maximum height increases with the increasing A concentration, but it seems gradually to reach to a limiting value. The maximum height obtained at given concentrations of MQ and A was observed to be lowered at higher temperatures and almost to disappear at 45°C.

Although the complete interpretation of the maximum is a very difficult problem, it may

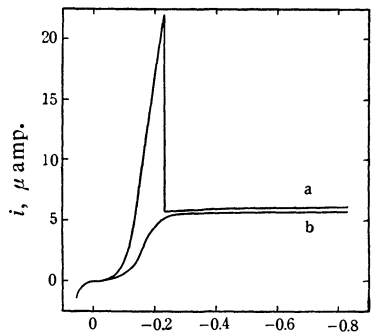

Fig. 1. Polarograms of 1.6×10^{-3} M of MQ obtained in 2-methoxyethanol solutions at 25°C in the absence (curve a) and in the presence of 0.004% methyl red (curve b).

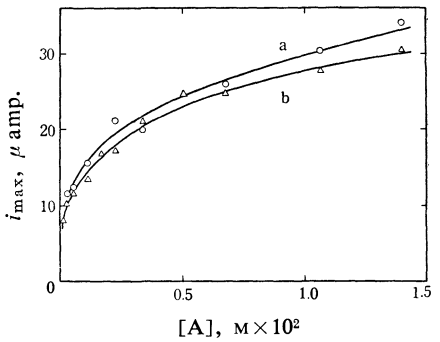

Fig. 2. Relation between maximum current (i_{max}) of MQ and concentration of A in 2-methoxyethanol solutions at 25°C in the absence (curve a) and in the presence of 0.004% methyl red (curve b).
Concentration of MQ is 1.3×10^{-3} M.

be suggested on the basis of the obtained results that the maximum may be attributed to the adsorption of MQ and A on the surface of the dropping mercury electrode. It can be considered that the maximum suppressing action of A is due to the preferential adsorption on the electrode surface. The adsorbed A molecules may prevent the adsorption of electroreducible substances. On the contrary, they should attract MQ and allow it to approach the electrode surface. It is possible that A reacts with MQ to form a charge-transfer complex[2]. Actually, some considerable changes were observed in the infrared spectrum of the mixture of A and MQ (KBr disk). On the assumptions that the complex formed between A and MQ is adsorbed on the electrode surface and that Langmuir's equation is applicable to this system, a consideration of the probable mechanism of the maximum is now in progress. The details will be published later.

The Women's Department
Tokyo College of Pharmacy
Taito-ku, Tokyo

2) M. Chowdhury, *Trans. Faraday Soc.*, **57**, 1482 (1961).

The Infrared Spectra of Tributyl Phosphate Containing Extracted Salts

By Nobufusa SAITO and Akira YAMASAKI

(Received June 25, 1963)

Tri-*n*-butyl phosphate (TBP) is used as an useful extractant for a number of inorganic salts. In the case of extraction using TBP, some chemical evidence has been presented to indicate that the phosphoryl group of TBP plays an important role in the coordination with the extracted salts[1,2]. It has also been recognized that the extraction of inorganic salts brings about the shift of the phosphoryl stretching vibration band towards a lower frequency[3,4].

This study is concerned with the infrared spectra of TBP phases containing extracted chlorides, nitrates and some inorganic complexes. The infrared spectra of the TBP phases (10% benzene solution) were recorded with a Hitachi EPI-2 double-beam infrared spectrometer equipped with sodium chloride optics.

The maxima of the phosphoryl band which appear at 1285 and 1265 cm^{-1} in pure TBP were found to shift towards lower wave numbers upon extraction. It was observed that there were three groups of compounds producing phosphoryl band shifts of different magnitudes. The maximum of the shifted phosphoryl bands appeared at three different ranges of wave numbers: 1155~1175 cm^{-1} for group (I), 1195~1205 cm^{-1} for group (II) and 1260~1265 cm^{-1} for group (III). Some of the results obtained are summarized in Table I.

It has been reported that the compounds of group (I) form disolvates in TBP phase, whereas those of group (II) form trisolvates[1,2,5-8]. It seems likely to us that the magnitude of the phosphoryl band shift has some relationship with the number of TBP molecules coordinated with the extracted salts.

The compounds which are classified as group (III) in Table I exhibited only slight phosphoryl band shifts. These compounds are presumed to be extracted in the form of such complex acids as H_2TeCl_6[9].

The present results seem to indicate that the phosphoryl band shift depends on the degree of solvation of the extracted salts in the TBP phase as well as on the nature and strength of the bond between the phosphoryl group and the salts. Further investigation concerning this phenomenon is in progress.

Department of Chemistry
Faculty of Science
The University of Tokyo
Hongo, Tokyo.

TABLE I

Group	Compound	Nature of aqueous phase	Form of solvate reported	Stretching vibration band of phosphoryl group
(I)	UO_2Cl_2	6 M HCl	$UO_2Cl_2 \cdot 2TBP$[5]	1165
	$UO_2(NO_3)_2$	8 M HNO_3	$UO_2(NO_3)_2 \cdot 2TBP$[1,2,6,7]	1173
	$Zr(NO_3)_4$	8 M HNO_3	$Zr(NO_3)_4 \cdot 2TBP$[6]	1163
	$Th(NO_3)_4$	8 M HNO_3	$Th(NO_3)_4 \cdot 2TBP$[1,2,7]	1175~1180
	$(NH_4)_2[Ce(NO_3)_6]$	(solid)	$Ce(NO_3)_4 \cdot 2TBP$[1,2]	1155
(II)	$La(NO_3)_3$	8 M HNO_3	$La(NO_3)_3 \cdot 3TBP$[1,2,8]	1205
	$Ce(NO_3)_3$	8 M HNO_3	$Ce(NO_3)_3 \cdot 3TBP$[1,2,8]	1205
	$FeCl_3$	6 M HCl	—	1195~1205
	$K_3[TlCl_6]$	6 M HCl	—	1195
(III)	$(NH_4)_2[TeCl_6]$	6 M HCl	$H_2TeCl_6 \cdot 2$~4 TBP[9]	1265
	$(NH_4)_2[SnCl_6]$	6 M HCl	—	1265
	$NH_4[Cr(NCS)_4(NH_3)_2]$	6 M HCl	—	1265
	$HAuCl_4$	6 M HCl	—	1265

1) T. V. Healy and H. A. C. McKay, *Trans. Faraday Soc.*, 52, 633 (1956).
2) T. V. Healy and H. A. C. McKay, *Rec. trav. chim.*, 75, 730 (1956).
3) J. R. Ferraro, *J. Inorg. Nucl. Chem.*, 10, 319 (1959).
4) L. I. Katzin, ibid., 20, 300 (1961).
5) V. B. Shevchenko, I. G. Slepchenko, V. S. Shmidt and E. A. Nenarokomov, *Zhur. Neorg. Khim.*, 5, 1095 (1960).
6) K. Alcock, F. C. Bedford, W. H. Hardwick and H. A. C. McKay, *J. Inorg. Nucl. Chem.*, 4, 100 (1957).
7) K. Alcock, G. F. Best, E. Hesford and H. A. C. McKay, ibid., 6, 328 (1958).
8) D. Scargill, K. Alcock, J. M. Fletcher, E. Hesford and H. A. C. McKay, ibid., 4, 304 (1957).
9) N. Saito, H. Mabuchi and A. Yamasaki, unpublished.

Pure Quadrupole Resonance of Halogens in Potassium Hexahalorhenates(IV)

By Ryuichi IKEDA, Daiyu NAKAMURA and Masaji KUBO

(Received July 1, 1963)

Studies on the pure quadrupole resonance of chlorine in paramagnetic potassium hexachloroiridate(IV) and hexachloroosmate(IV)[1] have shown that metal-ligand bonds in these complexes involve π bond character, because the $d\varepsilon$ orbitals of iridium and osmium ions have one and two holes, respectively. This paper presents some preliminary results obtained for potassium hexachlororhenate(IV), hexabromorhenate(IV) and hexaiodorhenate(IV), rhenium ions in which have three electrons in their degenerate $d\varepsilon$ orbitals leaving three vacancies.

Resonance lines were observed by means of super-regenerative spectrometers described elsewhere[2]. At room temperature, potassium hexachlororhenate(IV) and hexabromorhenate(IV) show a single resonance line for each isotope of halogens. This is in conformity with the cubic structure of these crystals as determined by X-ray analysis[3,4]. On the other hand, the ν_1 as well as ν_2 signal of iodine in potassium hexaiodorhenate(IV) consists of three lines of equal intensity. This indicates the presence of at least three kinds of crystallographically nonequivalent iodine atoms in crystals. Orthorhombic symmetry has already been verified for the crystal structure[5], although detailed structural analysis has not been performed as yet. The observed resonance frequencies are shown in Table I.

Frequency measurements carried out between room and dry ice temperatures have revealed the existence of three transition points at about -4, -16 and -27°C for potassium hexabromorhenate(IV), whereas two transition points are reported to exist at -28 and -48°C from heat capacity[6].

TABLE I. PURE QUADRUPOLE RESONANCE FREQUENCIES OF ^{35}Cl, ^{79}Br AND ^{127}I IN POTASSIUM HEXAHALORHENATES(IV)

Compound		Temp., °C	Frequency, Mc./sec.
K_2ReCl_6		23.0	13.887±0.001
K_2ReBr_6		18.0	112.70±0.03
K_2ReI_6	ν_1	21.0	121.91±0.03 122.99±0.03 123.13±0.03
	ν_2	20.6	243.68±0.07 245.16±0.07 245.34±0.07

It is quite remarkable that the temperature coefficient of resonance frequencies of potassium hexachlororhenate(IV) and hexabromorhenate(IV) is positive (+0.13 and +2.8 kc. sec^{-1} deg^{-1} for K_2ReCl_6 and K_2ReBr_6, respectively, near room temperature), whereas in the majority of cases, the temperature coefficient of pure quadrupole resonance frequencies is negative. Only a few exceptions have ever been reported to this rule (WCl_6[7], $TiBr_4$[8] and $ThCl_4$[9]). No metal complexes have been known to show a negative temperature coefficient of the resonance frequencies. However, the rather abnormal value is not surprising, because the temperature coefficient (-1.0, -0.54, -0.22 and $+0.13$ kc. sec^{-1} deg^{-1} for K_2PtCl_6[2], K_2IrCl_6, K_2OsCl_6[1] and K_2ReCl_6, respectively) increases progressively with increasing electron defficiency in the $d\varepsilon$ orbitals of the central metal ions. It appears that some close parallelism exists between the temperature coefficient of the quadrupole resonance frequencies and the extent of π bond character of metal-ligand bonds. The detailed analysis of experimental results is now in progress and will be published shortly.

Chemistry Department
Faculty of Science
Nagoya University
Chikusa, Nagoya

1) K. Ito, D. Nakamura, K. Ito and M. Kubo, *Inorg. Chem.*, 3, (1963), in press.
2) D. Nakamura, Y. Kurita, K. Ito and M. Kubo, *J. Am. Chem. Soc.*, 82, 5783 (1960).
3) B. Aminoff, *Z. Krist.*, A94, 246 (1936).
4) D. H. Templeton and C. H. Dauben, *J. Am. Chem. Soc.*, 73, 4492 (1951).
5) J. C. Morrow, *J. Phys. Chem.*, 60, 19 (1956); J. Dalziel, N. S. Gill, R. S. Nyholm and R. D. Peacock, *J. Chem. Soc.*, 1958, 4012. Morrow reports that the structure is orthorhombic with four formula weights in a unit cell. However, Dalziel et al. state that the structure can be represented by a body-centered orthorhombic unit cell containing two molecules.
6) R. H. Busey and E. Sonder, *J. Chem. Phys.*, 36, 93 (1962).
7) R. P. Hamlen and W. S. Koski, ibid., 25, 360 (1956).
8) R. G. Barnes and R. D. Engardt, ibid., 29, 248 (1958).
9) A. H. Reddoch, ibid., 35, 1085 (1961).

Studies of Photochemical Reaction. VI. The Synthesis of Methylethyl-α-tetrahydrofurylcarbinol and Ethyl-α-tetrahydrofurylcarbinol

By Kensuke SHIMA and Shigeru TSUTSUMI

(Received February 27, 1963)

In preceding papers[1,2] we have reported the synthesis of *t*-alcohols by means of the photochemical reaction of acetone in tetralin, dioxane and tetrahydrofuran. By these photoreactions, dimethyl-α-tetralylcarbinol, dimethyldioxanylcarbinol and dimethyl-α-tetrahydrofurylcarbinol were easily synthesized. In this paper, we wish to report the synthesis of methylethyl-α-tetrahydrofurylcarbinol (I) and ethyl-α-tetrahydrofurylcarbinol (II) by means of the photochemical reaction of ethyl methyl ketone and propionaldehyde in tetrahydrofuran.

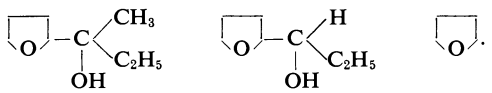

(I) (II) (III)

In the photochemical reaction of ethyl methyl ketone in tetrahdrofuran, *s*-butyl alcohol, methylethyl-α-tetrahydrofurylcarbinol (I) and di-α-tetrahydrofuryl were obtained, as in the photoreaction of acetone in tetrahydrofuran. The new substance, methylethyl-α-tetrahydrofurylcarbinol (I), which can be prepared by other methods only with difficulty, was easily produced.

The photochemical reactions of aldehydes in a liquid phase have been widely studied. Leuschner and Pfordte[3] stated that α-diketones were formed when aldehydes were irradiated. Mayo et al.[4] reported that ethyl cyclohexyl ketone and ethyl-3-cyclohexenylcarbinol were obtained by the reaction of photoactivated propionaldehyde in cyclohexene. It may be predicted that the reactions of photoactivated aldehydes in hydrogen-donor solvents are more complex than those of photo-activated ketones because of the presence of active hydrogen in the aldehyde group. When propionaldehyde was irradiated in tetrahydrofuran, *n*-propyl alcohol and ethyl-α-tetrahydrofurylcarbinol were obtained, and di-α-tetrahydrofuryl was not produced. It was also confirmed that dioxanyldioxane was not produced in the photochemical reaction of propionaldehyde in dioxane. It is assumed that the α-tetrahydrofuryl radical (III), formed by the dehydrogenation of tetrahydrofuran by the photoactivated propionaldehyde, would abstract the hydrogen atom from propionaldehyde without dimerization. Ethyl-α-tetrahydrofurylcarbinol was identified by comparing it with an authentic sample which had been prepared by the following procedure:

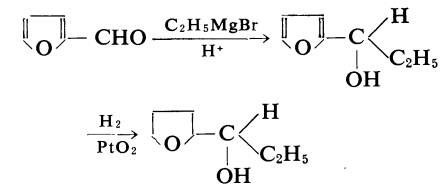

TABLE I. THE REACTION CONDITIONS AND THE YIELDS OF PRODUCTS

Light absorbing reagent (A)	Ethyl methyl ketone	Propionaldehyde
Reaction time, hr.	10	10
A used, g.	48.7	41.7
Tetrahydrofuran used, g.	194.8	203.6
Tetrahydrofuran/(A), mol. ratio	4	4
A consumed, g.	41.7	31.2
Tetrahydrofuran consumed, g.	25.3	22.3
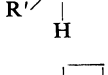 , g.	16.1	4.3
(B) 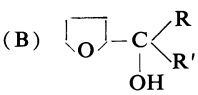 , g.	14.8	10.6
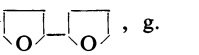 , g.	10.0	—
High boiling residue, g.	18.9	18.3
Unidentified product, g.	6.0	12.3
Wt. % of B in the products	22.3	23.3
Ultimated yield of B based on A consumed, mol. %	18.3	15.4
Ultimated yield of B based on tetrahydrofuran consumed, mol. %	30.2	26.4

R=C_2H_5, R'=CH_3 or H

1) K. Shima, Y. Shigemitsu and S. Tsutsumi, This Bulletin, **35**, 1728 (1962).
2) K. Shima and S. Tsutsumi, ibid, **36**, 121 (1963).
3) G. Leuschner and K. Pfordte, *Ann.*, **622**, 6 (1959).
4) P. de Mayo, J. B. Stothers and W. Templeton, *Proc. Chem. Soc.* (*London*), **1960**, 72; *Can. J. Chem.*, **39**, 488 (1961).

The reaction conditions and yields of the products are summarized in Table I.

Experimental

Materials.—Ethyl methyl ketone and propionaldehyde were purified by fractional distillation: ethyl methyl ketone, b. p., 79~80°C, n_D^{20} 1.3772; propionaldehyde, b. p., 49~50°C, n_D^{20}, 1.3733. Tetrahydrofuran was also purified by distillation over sodium: b. p., 66~67°C, n_D^{20}, 1.4052.

The Photochemical Reaction of Ethyl Methyl Ketone in Tetrahydrofuran.—A mixture of ethyl methyl ketone(48.7g., 0.676mol.)and tetrahydrofuran (194.8 g., 2.706 mol.) was placed in a 300 cc. reaction vessel and irradiated at 11°C in a nitrogen atmosphere for 10 hr. After this irradiation, the reaction product was fractionated to give the following fractions:

	B. p., °C	Weight, g.	n_D^{20}
(1)	64~68	144.5	1.4041
(2)	68~70	19.6	1.4029
(3)	70~81	11.2	1.3862
(4)	~35/13 mmHg	15.8	1.3943
(5)	35~59/13 mmHg	1.8	1.4223
(6)	60~84/13 mmHg	23.6	1.4512
(7)	85~87/13 mmHg	3.4	1.4530
(8)	87~97/13 mmHg	1.9	1.4504
(9)	Residue	18.9	

Fraction 4 was suspected to be *s*-butyl alcohol on the basis of gas chromatography, and it was identified as such by comparing its infrared spectrum with that of an authentic sample. The amounts of ethyl methyl ketone, tetrahydrofuran and *s*-butyl alcohol were estimated by gas chromatography: column, D. N. P. and Si DC 550; carrier gas, H_2, 0.32 kg./cm^2; bridge current, 160 mamp.; column temp., 47°C; retention time: ethyl methyl ketone, 8.5 min. (Si DC 550), 9.5 min. (D.N.P.); tetrahydrofuran, 10 min. (Si DC 550), *s*-butanol: 14 min. (D.N.P.).

It was established that fractions 6 and 7 were mainly composed of two components; they were separated by preparative gas chromatography. Fraction 1, n_D^{20}, 1.4518.

Found: C, 66.54; H, 11.12. Calcd. for $C_8H_{14}O_2$: C, 66.63; H, 11.18%.

The infrared spectrum is shown in Fig. 1. This fraction was confirmed to be methylethyl-α-tetrahydrofurylcarbinol by elemental analysis, study of its infrared spectrum, and comparison of it with the findings of a previous report[2].

The other fraction was di-α-tetrahydrofuryl.

The amounts of methylethyl-α-tetrahydrofurylcarbinol and di-α-tetrahydrofuryl were estimated by gas chromatography: column, Si DC 550, 3 m.; carrier gas, H_2, 0.3 kg./cm^2; bridge current, 160 mamp; column temp., 155°C; retention time: methylethyl-α-tetrahydrofurylcarbinol, 8.2 min.; di-α-tetrahydrofuryl, 11.4 min.

The Photochemical Reaction of Propionaldehyde In Tetrahydrofuran.—A mixture of propionaldehyde (41.0 g., 0.706 mol.) and tetrahydrofuran (203.6 g., 2.83 mol.) was irradiated at 12°C for 10 hr, and the reaction product was fractionally distilled under atmospheric and reduced pressure to give the following fractions:

	B. p., °C	Weight, g.	n_D^{20}
(1)	49~ 52	7.0	1.3710
(2)	52~ 64	5.4	1.3840
(3)	64~ 66	171.5	1.4063
(4)	~ 40/18 mmHg	11.2	1.3852
(5)	40~ 76/18 mmHg	0.7	1.4431
(6)	76~ 92/18 mmHg	20.0	1.4473
(7)	92~100/18 mmHg	2.2	1.4492
(8)	Residue	18.3	

Fraction 4 was assumed to be *n*-propyl alcohol on the basis of gas chromatography, and it was identified as such by means of a mixed melting point test of its 3, 5-dinitrobenzoate with an authentic sample.

Fraction 6 was purified by preparative gas chromatography: b. p., 71~72°C/11 mmHg, n_D^{20}, 1.4483.

The presence of the hydroxyl group was proved by the infrared spectrum. Its 3, 5-dinitrobenzoate was synthesized and recrystallized from ethanol; m. p., 81.2~82.2°C.

Found: C, 51.68; H, 5.10. Calcd. for $C_{14}H_{16}O_8N_2$: C, 51.85; H, 4.97%.

From the above results, this fraction was confirmed to be ethyl-α-tetrahydrofurylcarbinol.

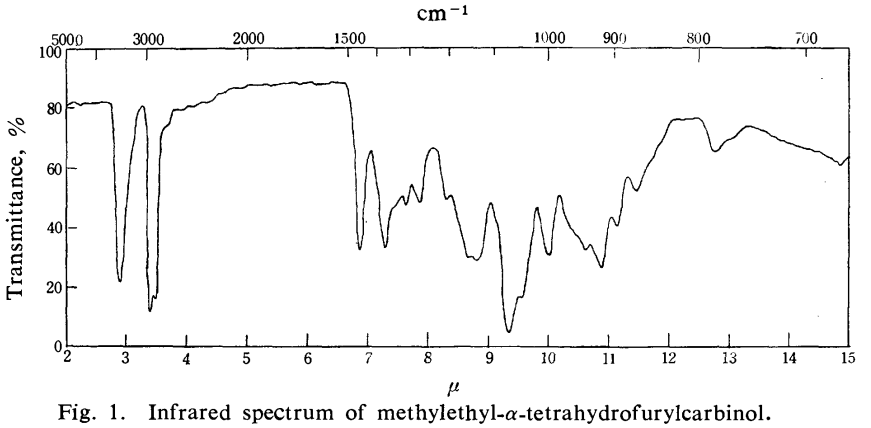

Fig. 1. Infrared spectrum of methylethyl-α-tetrahydrofurylcarbinol.

The Synthesis of Ethyl-α-tetrahydrofurylcarbinol.—Ethyl-α-furylcarbinol was prepared by the reaction of ethylmagnesiumbromide with furfural: b. p., 85~86°C/22 mmHg, n_D^{20}, 1.4763 (lit.,[5] 87~90°C/25mmHg). Ethyl-α-tetrahydrofurylcarbinol[6] was prepared by the hydrogenation of ethyl-α-furylcarbinol in the presence of an Adams catalyst: b.p., 85~95°C/19 mmHg, (lit.,[6] 182~186°C/745 mmHg, n_D^{20}, 1.4485).

Summary

The photochemical reaction of ethyl methyl ketone and propionaldehyde in tetrahydrofuran has been studied. Methylethyl-α-tetrahydrofurylcarbinol and ethyl-α-tetrahydrofurylcarbinol were easily obtained. In the photochemical reaction of propionaldehyde in tetrahydrofuran, di-α-tetrahydrofuryl was not produced, but it was observed to be produced in the photochemical reaction of acetone and ethyl methyl ketone in tetrahydrofuran.

Department of Chemical Technology
Faculty of Engineering
Osaka University
Miyakojima-ku, Osaka

5) R. Douris, *Compt. rend.*, **157**, 723 (1913).
6) J. S. Pierce and R. Adams, *J. Am. Chem. Soc.*, **47**, 1098 (1925).

The Reduction of Aquopentamminechromium(III) Ions at the Dropping Mercury Electrode

By Nobuyuki TANAKA, Yuichi SATO, Reita TAMAMUSHI and Gen SATÔ*

(Received March 14, 1963)

The polarographic behavior of hexamminechromium(III) ions has been reported by several authors.[1-5] In the recent papers by Tanaka and his coworkers,[4,5] the characteristics of the electrode processes of hexamminechromium(III) ions in neutral and acid aqueous solutions have been extensively discussed. In contrast, the polarographic behavior of aquopentamminechromium(III) ions has not been investigated in detail, though the half-wave potential in an acetate buffer has been reported by Friend and Smith.[2]

The present paper is concerned with the reduction of aquopentamminechromium(III) ions at the dropping mercury electrode in aqueous solutions. The study was undertaken in order to find the effect of the substitution of a water molecule for ammonia in the hexamminechromium(III) ion on the reduction at the electrode. The observations in the direct current and the alternating current polarography, including the measurements of Kalousek polarograms and current-time curves, will be presented, and the mechanism of the electrode processes will be discussed.

Experimental

Aquopentamminechromium(III) nitrate was prepared according to the method proposed by Mori[6] and was converted then into chloride.[7] Aquopentamminechromium(III) perchlorate, $[Cr(H_2O)(NH_3)_5](ClO_4)_3$, was precipitated from the solution of the chloride. After recrystallization from water, the complex was identified by measuring its absorption spectra and by determining the chromium and nitrogen contents. Absorption bands were observed at 480 mμ and 365 mμ by the use of a Hitachi *Model EPU-2 spectrophotometer*. The complex was oxidized to chromate with hydrogen peroxide in an alkaline solution, and the chromate content was determined by the spectrophotometric method. Nitrogen was determined by the conventional method.[8]

Found: Cr, 11.38; N, 14.83. Calcd. for $[Cr(H_2O)(NH_3)_5](ClO_4)_3$: Cr, 11.47; N, 15.44%.

This complex is stable for a few months when it is preserved in a silica-gel desiccator in darkness, but for only two or three hours in an acid solution. Gelatin or polyoxyethylene lauryl ether (LEO) was used as a maximum suppressor. All other chemicals used were of a guaranteed reagent grade and were used without further purification.

Direct current (d. c.) polarograms were recorded by a Yanagimoto PB-4 pen-recording polarograph. A Yanagimoto Galvarecorder Y-GR 2 was used to record alternating current (a. c.) polarograms. Kalousek polarograms were recorded with the same

* Present address: Department of Chemistry, Faculty of Science and Technology, Sophia University, Chiyoda-ku, Tokyo.

1) N. Maki, Y. Shimura and R. Tsuchida, This Bulletin, **31**, 413 (1958).

2) J. A. Friend and P. W. Smith, *J. Phys. Chem.*, **63**, 314 (1959).

3) T. C. Ichniowski and A. F. Clifford, *J. Inorg. Nucl. Chem.*, **22**, 133 (1961).

4) N. Tanaka and G. Satô, *Nature*, **197**, 176 (1963).

5) N. Tanaka, K. Ebata and G. Satô, This Bulletin, **36**, 912 (1963).

6) M. Mori, *J. Chem. Soc. Japan, Pure Chem. Sec.* (*Nippon Kagaku Zassi*), **74**, 253 (1953).

7) J. H. S. King, *J. Chem. Soc.*, **127**, 2104 (1925).

8) T. Takagi and E. Hayashi, *J. Chem. Soc. Japan, Pure Chem. Sec.* (*Nippon Kagaku Zassi*), **78**, 445 (1957).

circuit as previously described.[9] Current-time (i-t) curves were recorded by using a Rikadenki ER-J 1 recorder with an RLDC-201 preamplifier. A brown-colored cell of a simple beaker type was used in all measurements. The dropping mercury electrode (DME) used had an m value of 1.76$_6$ mg./sec. and a drop time, t_d, of 4.90 sec./drop, when measured in an air-free 1.0 M potassium nitrate solution at 25°C and −0.5 V. vs. SCE at 50 cm. of the height of mercury reservoir. The potential of the DME was measured against a saturated calomel electrode (SCE), which was connected to the electrolytic solution through a Hume and Harris-type salt bridge. When a. c. polarograms were measured, a platinum wire electrode of a large surface area was inserted in the electrolytic solution as the third electrode; this electrode was terminated at the SCE through a 100 μF capacitor in order to minimize the impedance of the cell. A Hitachi model EHP-1 pH meter was used for the measurement of pH of the solution.

All the measurements were carried out in a thermostat of 25±0.1°C, unless otherwise stated, and the dissolved oxygen in the electrolytic solution was removed by bubbling pure nitrogen gas through the solution. The d. c. and Kalousek polarograms given in this paper were corrected for the residual current and the iR drop across the cell. The half-wave potentials were determined from the plots of log $\bar{i}(\bar{i}_d-\bar{i})$ versus potential.

Results

In the preliminary experiments, aquopentamminechromium(III) was found not to give a well-defined polarographic wave in neutral unbuffered solutions, but to give a well-defined wave in acetate buffers or acid solutions. Typical examples are shown in Fig. 1. In this paper, therefore, only the results obtained in acid solutions are presented.

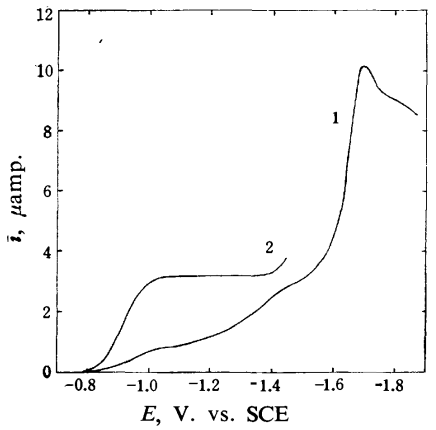

Fig. 1. Polarograms of 1.0 mM $[Cr(H_2O)(NH_3)_5](ClO_4)_3$: (1) in 1.0 M NaCl+0.005% gelatin; (2) in 0.1 M acetate buffer+0.9 M NaCl+0.005% gelatin (pH 4.46).

9) N. Tanaka, R. Tamamushi and M. Kodama, This Bulletin, 33, 14 (1960).

TABLE I. LIMITING CURRENTS OF 1.0 mM $[Cr(H_2O)(NH_3)_5](ClO_4)_3$ AT VARIED HEIGHTS OF THE MERCURY RESERVOIR IN SOLUTIONS CONTAINING 0.9 M NaCl, 0.1 M ACETATE BUFFER AND 0.005% GELATIN

$h_{corr.}$, cm.*	$\bar{i}_l$, μ amp.	$\bar{i}_l/\sqrt{h_{corr.}}$
48.4	3.14	0.452
58.4	3.47	0.454
68.4	3.78	0.457

* Height of mercury reservoir corrected for the back pressure.

The current-potential curves were obtained at various concentrations of aquopentamminechromium(III) ions in 0.1 M acetic acid-sodium acetate buffers containing 0.9 M ammonium chloride and 0.005% gelatin. The limiting current, $\bar{i}_l$, was proportional to the concentration and the value of $\bar{i}_l/C$ was found to be 3.18 μ amp./mM in the concentration range from 0.2 to 2.0 mM. The half-wave potentials were found to be independent of the concentration of the complex. Table I gives the limiting currents measured at different heights of the mercury reservoir. These results clearly indicate that the limiting current is diffusion-controlled. A comparison of the diffusion coefficient of aquopentamminechromium(III) as calculated by the Ilkovič equation and those of hexamminechromium(III)[5] and hexacyanochromate(III)[10] suggests that the wave is of a one-electron reduction. The limiting currents were also measured at various temperatures, and the activation energy for the process controlling the limiting current was calculated according to the method proposed by Vlček[11] to be 5.0 kcal./mol.

Table II presents the diffusion currents, half-wave potentials and slopes of the log-plots which were obtained at 1.0 mM of the complex.

TABLE II. EFFECTS OF pH AND SUPPORTING ELECTROLYTE ON THE POLAROGRAM OF 1 mM $[Cr(H_2O)(NH_3)_5](ClO_4)_3$ IN SOLUTIONS CONTAINING 0.1 M ACETATE BUFFER AND 0.005% GELATIN

Supporting electrolyte added	pH	$\bar{i}_d$ μ amp.	$E_{1/2}$ V. vs. SCE	Slope of log-plot. mV.
0.9 M NaCl	3.46	2.99	−0.924	71
	3.78	3.06	−0.922	72
	4.46	3.17	−0.916	72
	5.58	3.14	−0.929	72
0.5 M NaCl + 0.4 M NH_4Cl	3.77	3.07	−0.925	71
0.9 M NH_4Cl	3.81	3.16	−0.934	72

10) D. N. Hume and I. M. Kolthoff, *J. Am Chem. Soc.*, 65, 1897 (1943).

11) A. A. Vlček, *Collection Czech. Chem. Commun.*, 24, 3538 (1959).

in 0.1 M acetate buffer solutions of various pH's containing either ammonium chloride or sodium chloride or both in a 0.9 M concentration. No appreciable change was observed in the half-wave potentials with the change of pH of the solution. On the other hand, the half-wave potentials were found to shift to more negative potentials with the increasing concentration of supporting electrolytes. Two examples are given in Table III.

TABLE III. EFFECT OF IONIC STRENGTH ON THE POLAROGRAM OF 1.0 mM $[Cr(H_2O)(NH_3)_5](ClO_4)_3$ IN SOLUTIONS CONTAINING 0.1 M ACETATE BUFFEE AND 0.005% GELATIN

Ionic strength	i_d μ amp.	$E_{1/2}$ V. vs. SCE	Slope of log-plot mV.
(A) Adjusted with NaCl.			
0.5	3.17	−0.906	67
1.0	3.12	−0.929	72
1.5	3.04	−0.939	72
2.0	2.85	−0.942	75
(B) Adjusted with NH_4Cl.			
0.5	3.14	−0.898	65
1.0	3.16	−0.934	72
1.5	3.12	−0.944	75
2.0	3.11	−0.950	72

Polarograms of 1.0 mM aquopentamminechromium(III) were recorded at various concentrations of gelatin and LEO in 0.1 M acetate buffers containing 0.9 M ammonium chloride; examples are given in Table IV. The increase in the concentration of gealtin shifts the half-wave potential to more negative potentials. Current-time curves during the life of a mercury drop, which were recorded at −0.94 V. vs. SCE under the same conditions as in Table IV, are reproduced in Fig. 2. In this measurement, the first mercury drop after the initiation of electrolysis was used.[12] The *i-t* curve obtained in the presence of 2×10^{-6} M LEO is nearly the same as that obtained without a maximum suppressor, whereas the presence of gelatin decreases the current to a great extent. Current-time curves were also recorded at various potentials and at various concentrations of gelatin and LEO. The results showed that the addition of 2×10^{-6} M LEO gives satisfactory *i-t* curves. In the absence of a maximum suppressor, however, no satisfactory *i-t* curves were obtained at −1.2 V. vs. SCE.

TABLE IV. EFFECT OF SURFACE ACTIVE SUBSTANCE ON THE POLAROGRAM OF 1.0 M $[Cr(H_2O)(NH_3)_5](ClO_4)_3$ IN SOLUTIONS CONTAINING 0.1 M ACETATE BUFFER AND 0.9 M NH_4Cl

Surface active substance	i_d μ amp.	$E_{1/2}$ V. vs. SCE	Slope of log-plot mV.
None	3.21	−0.911	72
Gelatin, 0.005%	3.21	−0.934	72
Gelatin, 0.01%	3.10	−0.979	75
LEO, 2×10^{-6} M	3.18	−0.918	71

12) J. Kůta and I. Smoler, *Collection Czech. Chem. Commun.*, **24**, 2208 (1959).

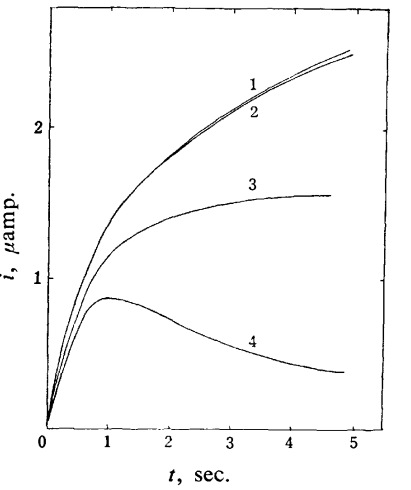

Fig. 2. Current-time curves of 1.0 mM $[Cr(H_2O)(NH_3)_5](ClO_4)_3$ measured at −0.94 V. vs. SCE in solutions containing 0.1 M acetate buffer and 0.9 M NH_4Cl in the absence (curve 1) and in the presence of 2×10^{-6} M LEO (curve 2), 0.005% gelatin (curve 3) and 0.01 % gelatin (curve 4).

Kalousek and a. c. polarograms were recorded to examine the polarographic reversibility of the reduction of the complex. A typical example of the Kalousek polarograms, which was obtained in a solution containing 0.1 M

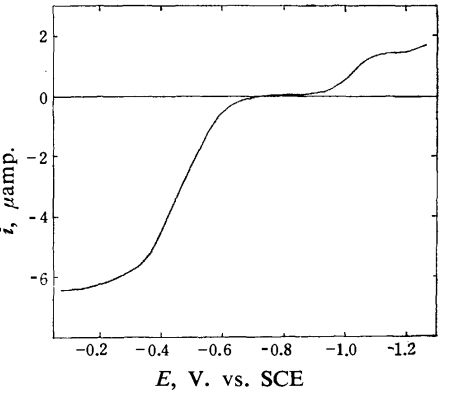

Fig. 3. Kalousek polarogram of 1.0 mM $[Cr(H_2O)(NH_3)_5](ClO_4)_3$ obtained at exchange frequency of 5 cycles/sec. in a solution containing 0.1 M acetate buffer, 0.9 M NH_4Cl and 0.005% gelatin. The potential is set up at −1.2 V. vs. SCE.

acetate auffer, 0.9 M ammonium chloride and 0.005% gelatin, is reproduced in Fig. 3.

Discussion

Aquopentamminechromium(III) gives no well-defined wave in neutral unbuffered solutions because it contains basic ligands and, when reduced, it forms an insoluble film on the surface of the electrode, as has already been reported in the case of the polarographic reduction of hexamminechromium(III).[4,5] In an acid solution, the ammonia molecules that the reduced chromium(II) species liberates are neutralized by hydrogen ions diffusing from the bulk of the solution; consequently, the formation of such an insoluble film is prevented.[4,5] The limiting current of the wave in acid media is diffusion-controlled in every respect; the value of 5.0 kcal./mol. obtained seems appropriate for the activation energy of the diffusion.

The fact that the half-wave potential was almost independent of the hydrogen ion concentration of the solution suggests that the hydrogen ions are not involved in the chemical reaction, if any, preceding the electron transfer (see Table II). Table III shows that the shift of the half-wave potential is due not to an increase in ammonium ion concentration but to an increase in total ionic concentration. It is suggested that no chemical reaction involving ammonium ions takes place prior to the electron transfer.

The reduction of aquopentamminechromium-(III) to chromium(II) species in an acid solution appears to be irreversible in the polarographic sense. A straight log-plot with a reciprocal slope of approximately 70 mV., which is somewhat greater than that expected for a reversible one-electron reduction wave, suggests the irreversible nature of the wave (see Tables II, III and IV). The value of $i_p/(n\bar{i}_d\sqrt{t_d})$, where i_p means the peak current of the a. c. polarogram, $\bar{i}_d$, the average diffusion current of the corresponding d. c. polarogram, and n, the number of electrons involved in the electrode process, represents the degree of polarographic reversibility of the electrode reaction.[13] In Table V, $i_p/(n\bar{i}_d\sqrt{t_d})$ values for the aquopentamminechromium(III) ion and other simple and complex ions are presented. The aquopentamminechromium (III) gives smaller values than that for nickel(II) in a potassium chloride solution, suggesting the complete irreversibility of the reduction of the complex. The irreversibility is supported also by the shape of the Kalousek polarogram (Fig. 3). The increase in exchange frequencies of the on-and-off switch from 5 cycl./sec. to 30 cycl./sec. showed no feature of reversibility.

The instantaneous current at constatnt potential during the life of a mercury drop is given as a function of time,

$$i = k\,t^{x} \qquad (1)$$

where k is a constant. The plot of log i against log t, therefore, should give a straight line with a slope of the value of x. In the case of the reduction of aquopentamminechromium(III), a straight line was obtained only when LEO was added as a maximum suppressor in a concentration of 2×10^{-6} M. The addition of gelatin was found to cause the

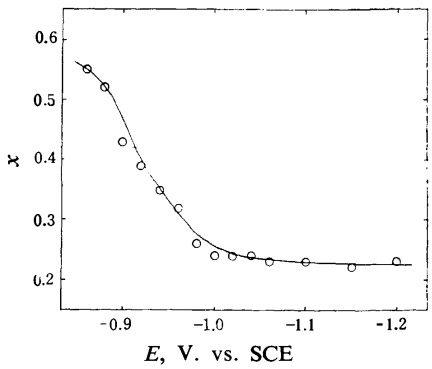

Fig. 4. The values of x in Eq. 1 at varied potentials, measured with 1.0 mM $[Cr(H_2O)(NH_3)_5](ClO_4)_3$ in a solution containing 0.1 M acetate buffer, 0.9 M NH_4Cl and 2×10^{-6} M LEO.

TABLE V. VALUES OF $i_p/n\bar{i}_d\sqrt{t_d}$

Oxidant	Supporting electrolyte*	$i_p/(n\bar{i}_d\sqrt{t_d})$ in amp^{-1}sec$^{-1/2}$
1.0 mM $[Cr(H_2O)(NH_3)_5](ClO_4)_3$	0.9 M NaCl+0.1 M acetate buffer	3.9
1.0 mM $[Cr(H_2O)(NH_3)_5](ClO_4)_3$	0.9 M NH_4Cl+0.1 M acetate buffer	2.8
1.0 mM $[Cr(NH_3)_6]Cl_3$	0.9 M NH_4Cl+0.1 M acetate buffer	9.2
0.5 mM $Cd(NO_3)_2$	1.0 M KNO_3	202
0.5 mM $Zn(NO_3)_2$	1.0 M $NaClO_4$	57.6
0.5 mM $Ni(NO_3)_2$	0.1 M KCl	7.2

* All solutions contain 0.005% gelatin.

13) M. Senda, M. Senda and I. Tachi, *J. Electrochem. Soc. Japan (Denki Kagaku)*, 27, 83 (1959).

shape of the current-time curve to deteriorate and to give no linear plot of log i vs. log t. The values of x at various potentials, therefore, were determined in the presence of 2×10^{-6} M LEO. The plot of x vs. potential, as shown in Fig 4, varies from 0.55 to 0.23 with increasing negative potentials, suggesting that the electrode process is kinetic in nature at the foot of the wave, but diffusion-controlled at the limiting current plateau.

The results obtained from the d. c., the a. c. and the Kalousek polarograms and the current-time curves indicate that the reduction of aquopentamminechromium(III) to chromium-(II) proceeds irreversibly at the dropping mercury electrode and that its overall electrode process in an acid solution may be written as follows:

$$Cr(H_2O)(NH_3)_5^{3+} + e \rightarrow Cr(H_2O)(NH_3)_5^{2+} \quad (2)$$

$$Cr(H_2O)(NH_3)_5^{2+} + n\,H_2O + n\,H^+ \rightarrow Cr(H_2O)_{n+1}(NH_3)_{5-n}^{2+} + n\,NH_4^+ \quad (3)$$

When the electrode reaction is totally irreversible, the following equation holds:[14]

$$\ln\frac{\bar{i}_d-\bar{i}}{\bar{i}} = \ln\{1.13(\Lambda\sqrt{t_d})^{-1}\}+\frac{\alpha nF}{RT}(E-E_{1/2}^r)$$

$$\Lambda=\frac{k_s f_O^{\beta} f_R^{\alpha}}{(D_O^{\beta}D_R^{\alpha})^{1/2}} \qquad (\alpha+\beta=1) \quad (4)$$

where $E_{1/2}^r$ indicates the reversible half-wave potential, k_s, the standard rate constant, α, the transfer coefficient, and f_O and f_R, the activity coefficients of oxidized and reduced forms respectively. If f_O and f_R are assumed to be unity and D_O and D_R, equal to D, Eq. 4 can be simplified. When $\bar{i}$ equals $\bar{i}_d/2$, the equation,

$$\log k_f^\circ = \log 1.13 - \frac{1}{2}\log t_d + \frac{1}{2}\log D + \frac{2.303RT}{\alpha nF}E_{1/2} \quad (5)$$

is obtained, where k_f° indicates the forward rate constant at 0 V. In this paper, a saturated calomel electrode at the observed temperature was used for the reference.

The diffusion coefficients were obtained from the limiting currents with the aid of the Ilkovič equation. The values of log k_f° were determined at various temperatures, as Table VI shows. With these values, the heat of activation of the electrode process, $\Delta H^*_{E=0}$, was calculated to be 40.2 kcal./mol., being referred to the SCE.[15]

Table VI. Log k_f°'s of the reduction of $[Cr(H_2O)(NH_3)_5]^{3+}$ at various temperatures in solutions containing 0.1 M acetate buffer, 0.9 M NH_4Cl and 2×10^{-6} M LEO

Temp. °C	$E_{1/2}$ V. vs. SCE	α	$D^{1/2}\times10^3$ cm. $sec^{-1/2}$	t_d sec.	log k_f°
0.4	−0.972	0.89	1.89	4.40	−18.9
10.0	−0.951	0.88	2.19	4.34	−17.8
17.0	−0.935	0.85	2.46	4.23	−16.6
25.0	−0.918	0.83	2.83	4.12	−15.7
35.0	−0.893	0.83	3.25	4.02	−14.8

Although all experimental results support the irreversible electrode process of reaction 2 and although this irreversibilty seems to be attributed to the electronic rearrangement of aquopentamminechromium(III) from t_{2g}^3 to $e_g t_{2g}^2$,[16] there seems to be another possible mechanism. As has been reported in the case of hexamminechromium(III) ions,[5] reaction 2 may proceed reversibly in the polarographic sense, followed by the rapid aquation of the reduced species, aquopentamminechromium(II) ions. This mechanism would also explain the observations in the a. c. and the Kalousek polarograms. At the present moment, however, it seems not to be possible to decide by which mechanism the electrode reaction proceeds at the dropping mercury electrode.

Summary

The reduction of aquopentamminechromium-(III) ions at the dropping mercury electrode has been studied in acid solutions by means of the measurement of the direct current, the alternating current and the Kalousek polarograms and the current-time curves. The d. c. polarogram gives a well-defined wave corresponding to the one-electron reduction of chromium(III) to chromium(II). All polarograms, including the Kalousek ones, indicate the irreversibility of the reduction of aquopentamminechromium(III) ions. The heterogeneous rate constants at 0 V. vs. SCE at various temperatures have been presented, and the possible mechanisms for the electrode process have been discussed.

The authors wish to thank the Ministry of Education for the financial support granted for this research.

Department of Chemistry
Faculty of Science
Tohoku University
Katahira-cho, Sendai

14) H. Matsuda, *Z. Elektrochem.*, **61**, 489 (1957); **62**, 977 (1958).
15) R. Tamamushi, *Review of Polarography*, **10**, 1 (1962).
16) A. A. Vlček, *Discussions Faraday Soc.*, **26**, 164 (1958).

Dielectric Relaxation and Molecular Structure. I. Relaxation Time and Viscosity

By Kazuo CHITOKU and Keniti HIGASI

(Received March 22, 1963)

Stokes' simple formula for a rigid sphere rotating in a viscous liquid was assumed by Debye[1] to be applicable to a sphere of molecular dimensions surrounded by other molecules of a similar size:

$$\tau=\frac{4\pi\eta a^3}{kT} \tag{1}$$

in which η is the ordinary viscosity[2] of the liquid, a is the radius of the sphere, k is the Boltzmann constant, and T is the absolute temperature.

Equation 1 has been employed widely for thirty years;[3] it has been applied even in the analysis of the relaxation times of nuclear magnetic resonance absorption.[4] It was soon discovered, however, that the molecular radius a obtained from measurements of dielectric relaxation times, τ, in either a liquid or a solution by the use of Eq. 1 is usually only a fraction of the actual radius.[3] In addition, the relaxation time does not follow the increase in viscosity for highly viscous liquids. The concept of internal or microscopic viscosity has been developed[5] to account for this anomaly; however, one can not place much reliance on the estimation of this viscosity of an unmeasurable nature.[6,7]

The object of the present paper is to postulate an empirical relation between the viscosity and the relaxation time and to compare it with Eq. 1. The ordinary viscosity alone will be considered here, since it seems desirable to deal only with measurable quantities. The dielectric measurements in the present report have been limited to dilute solutions, because the relaxation time measured in the liquid state is accompanied with ambiguity because of the choice of an arbitrary conversion ratio from the macroscopic relaxation time to the microscopic relaxation time.[3,8]

Experimental

All the dielectric measurements reported below were made between 1×10^7 and 8×10^7 cycl./sec. (10 ~80 Mc./sec.) with a Hartshorn-Ward apparatus;[9] this measures the loss tangent ($\tan\delta=\varepsilon''/\varepsilon'$) in terms of the capacitance increment (ΔC) corresponding to the half-width of the voltage-resonance curve of the cell-containing circuit.[10] The loss tangents were measured up to 2×10^{-4}. The whole apparatus was kept in an air-thermostat maintained at 25°C.

Our general procedure was checked by measuring a standard substance, benzophenone, in various solvents: *n*-hexane, benzene, carbon tetrachloride and Nujol.

In dilute solutions, both Debye and Onsager equations become:[3]

$$\tan\delta=\frac{(\varepsilon'+2)^2}{\varepsilon'}\,\frac{4\pi n\mu^2}{27kT}\,\frac{\omega\tau}{1+\omega^2\tau^2} \tag{2}$$

where ε' is the dielectric constant of the solvent, n is the number of polar molecules per cubic centimeter, ω is the angular frequency, and τ is the relaxation time. When $\omega\tau\ll1$, this equation reduces to:

$$\tau=\frac{\tan\delta}{\omega c}\,\frac{6750\,kT}{\pi N\mu^2}\,\frac{\varepsilon'}{(\varepsilon'+2)^2} \tag{3}$$

where N is the Avogadro number and c is the molar concentration. The constancy of $\tan\delta/\omega$ over a wide frequency range provides a simple test of Eq. 3. Table I contains results for benzophenone in two solvents, those with the lowest and the highest viscosities. The $\tan\delta/\omega$ values were found constant in all the solvents employed. Using a mean value, $\tan\delta/\omega=6.9\times10^{-12}$, and $\mu=2.94$ D, one finds $\tau=14.7\times10^{-12}$ sec. (14.7 p. sec.) at 25°C in hexane. This is in good agreement with Fairweather's value, 14.3 p. sec.[11] The results are further compared in Table II.

As shown by the above example, the value of the dipole moment in the particular medium is necessary for calculation. Consequently, measurements of dipole moments were carried out by

1) P. Debye, "Polar Molecules," Chemical Catalog, New York (1929).
2) P. Debye, *Trans. Faraday Soc.*, 30, 679 (1934).
3) C. P. Smyth, "Dielectric Behavior and Structure," McGraw-Hill, New York (1955).
4) N. Bloembergen, E. M. Purcell and R. V. Pound, *Phys. Rev.*, 73, 679 (1948).
5) E. Fischer, *Z. Elektrochem.*, 53, 16 (1949).
6) W. Kauzmann, *Rev. Mod. Phys.*, 14, 12 (1942).
7) K. Higasi, "Dielectric Relaxation and Molecular Structure," *Monogr. Res. Inst. Appl. Elec., Hokkaido University*, No. 9 (1961).
8) Cf., for example, J. G. Powles, *J. Chem. Phys.*, 21, 633 (1953); R. C. Miller and C. P. Smyth, *J. Am. Chem. Soc.*, 79, 3310 (1957).
9) K. Chitoku, *Bull. Res. Inst. Appl. Elec.*, 13, 261 (1961).
10) L. Hartshorn and W. H. Ward, *J. Inst. Elec. Engrs.*, 79, 597 (1936); A. Aihara and M. Davies, *J. Colloid Sci.*, 11, 671 (1956).
11) A. Fairweather, *Proc. Phys. Soc.*, B68, 1038 (1955).

TABLE I. RELAXATION TIMES, tan δ AND tan $\delta/\omega c$ OF BENZOPHENONE

1. Solvent, *n*-hexane : 0.2942 mol./l.				
Freq. (Mc./sec.)	16.65	33.43	55.3	75.0
ε'	2.215	2.215	2.222	2.222
$10^3 \times \tan\delta$	0.22	0.42_8	0.70_9	0.96_3
$10^{12} \times \tan\delta/\omega c$	6.8_2	6.9_6	6.9_5	6.9_3
$10^{12} \times \tau$(sec.)	$14._4$	$14._7$	$14._7$	$14._7$
2. Solvent, Nujol : 0.2795 mol./l.				
ε'	2.498_7	2.500	2.506	2.499_3
$10^3 \times \tan\delta$	3.37_8	6.76_5	10.96_1	13.86_1
$10^{12} \times \tan\delta/\omega c$	115.5	115.2	112.9	105.2
$10^{12} \times \tau$(sec.)	$238._9$	$238._3$	$233._2$	$217._6$

TABLE II. RELAXATION TIMES OF BENZOPHENONE

Solvent	Present wrok		Literature		Ref.
	η, c. p. s.	τ, p. sec.	η, c. p. s.	τ, p. sec.	
n-Hexane	0.315/25°C	14.7/25°C	0.32/18°C	14.3/18°C	11
Isooctane	0.480/25°C	18.4/25°C	—	—	
Benzene	0.603/25°C	20.4/25°C		20.4/23°C	12*
				22/19°C	13
p-Xylene	—	—		20.0~21.7/18°C	14
Carbon tetrachloride	0.920/25°C	25.0/25°C	0.70/44°C	26.5/44°C	11
Dioxane	1.160/25°C	24.0/25°C	—	—	
Nujol	137.8/25°C	238.0/25°C	197/19°C	295/19°C	15

* Low frequency measurements based on Eq. 3.

the heterodyne-beat method and with the use of Halverstadt-Kumler's approximation.[16]

Materials.—All chemicals were of the best grade available and were purified before use; their m. p.'s or b. p.'s were checked against the values given in the literature.

Results

Table III summarizes the results of the present measurements. Mixed solvents were employed for substances which were not soluble in pure solvents. Viscosity values are recorded of the solvent itself and also of the dilute solution with which the measurement was carried out; the symbols η_{solv} and η_{solu} are used to mark the distinction between them.

Discussion

Plots of the observed relaxation times against the viscosities do not result in any satisfactory curve. On the other hand, when the logarithms of the relaxation times are plotted against the logarithms of the viscosities, an approximate linear relationship between $\log\tau$ and $\log\eta$ becomes noticeable, as may be seen in Figs. 1 and 2, in which plots are made in the logarithmic scale. For this reason, one can propose the following empirical equation:

$$\log\tau = A + x\log\eta \qquad (4)$$

where A and x are constants relating to the substance alone under a given temperature. In Table IV the A and x values determined by the present series of experiments are recorded.

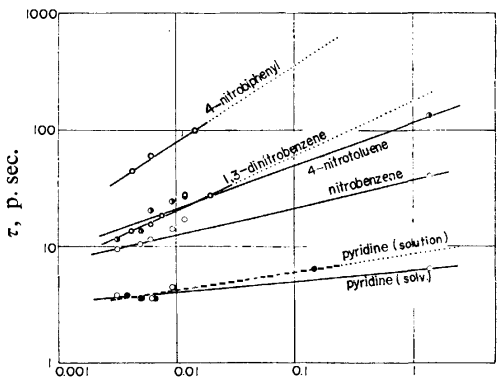

Fig. 1. Dependence of the logarithm of relaxation time of rigid molecules upon the logarithm of the viscosity. Full lines: η_{solv} employed; broken lines: η_{solu} employed.

12) E. Fischer, *Z. Naturforsch.*, **4a**, 707 (1949).
13) D. H. Whiffen and H. W. Thompson, *Trans. Faraday Soc.*, **42A**, 114 (1946).
14) G. Williams, *J. Phys. Chem.*, **63**, 534 (1959).
15) W. Jackson and J. G. Powles, *Trans. Faraday Soc.*, **42A**, 101 (1946).
16) I. F. Halverstadt and W. D. Kumler, *J. Am. Chem. Soc.*, **64**, 2988 (1942).

TABLE III. RELAXATION TIMES OBTAINED IN VARIOUS SOLVENTS (25°C)

1. Solute, Pyridine

Solvent	$\frac{\mu}{D}$	η_{solv} c. p. s.	η_{solu} c. p. s.	τ, p. sec. 34.8 Mc.	56.7 Mc.	77.7 Mc.
n-Hexane	2.25	0.315	0.379	3.75	3.78	3.92
Isooctane	2.27	0.480	0.498	3.67	3.54	3.64
Benzene	2.27	0.603	0.650	3.60	3.50	3.64
Carbon tetrachloride	2.35	0.920	0.942	4.51	4.42	4.60
Nujol	2.23	137.78	15.733	6.43	6.50	6.53

2. Solute, Diphenyl ether

Solvent	$\frac{\mu}{D}$	η_{solv} c. p. s.	η_{solu} c. p. s.	τ, p. sec. 33.4 Mc.	55.3 Mc.	75.0 Mc.
n-Hexane	1.09	0.315	0.728	4.95	5.17	5.38
Isooctane	1.11	0.480	0.818	5.48	5.56	5.47
Benzene	1.16	0.603	1.102	4.62	4.74	4.59
Carbon tetrachloride	1.13	0.920	1.418	7.67	7.69	8.11
Nujol	1.15	137.78	10.998	5.47	5.43	5.90

3. Solute, *m*-Dinitrobenzene

Solvent	$\frac{\mu}{D}$	η_{solv} c. p. s.	τ, p. sec. 16~17 Mc.	33 Mc.	55 Mc.	75 Mc.
n-Hexane-Bz.	3.92	0.415	13.1	13.1	13.7	14.3
Isooctane-Bz.	3.88	0.493	12.7	13.3	14.1	13.5
Benzene	3.84	0.603	14.7	15.7	15.6	15.8
Carbon tetrachloride-Bz.	3.84	0.746	18.3	18.6	18.1	18.9
Dioxane	4.00	1.160	27.4	27.3	27.3	28.3
Nujol-Bz.	3.73	1.921	27.2	27.6	26.6	27.8
4. Solute, Nitrobenzene						
n-Hexane	—	0.135	9.71	9.34	9.57	9.63
Isooctane	—	0.480	10.4	10.4	10.3	10.4
Benzene	4.03	0.603	11.3	11.0	11.1	12.0
Carbon tetrachloride	—	0.920	14.2	14.1	13.9	14.4
Dioxane	—	1.160	17.4	16.9	17.3	17.6
Nujol	—	137.78	40.8	41.2	39.2	40.1
5. Solute, *p*-Nitrotoluene						
n-Hexane	4.47	0.315	10.5	11.7	12.1	11.9
Isooctane	4.49	0.480	13.2	14.5	13.9	14.4
Benzene	4.43	0.603	21.6	20.2	20.1	20.6
Carbon tetrachloride	4.45	0.920	24.3	24.7	23.6	24.9
Dioxane	4.63	1.160	27.3	26.9	26.7	27.0
Nujol	4.54	137.78	139.9	131.2	127.7	134.5
6. Solute, *p*-Nitrobiphenyl						
n-Hexane-Bz.	4.55	0.420	44.7	43.4	43.3	44.8
Benzene	4.48	0.603	61.0	57.9	56.8	58.0
Nujol-Bz.	4.35	1.427	103.9	98.5	97.5	98.2
7. Solute, Benzophenone						
n-Hexane	2.94	0.315	14.4	14.7	14.7	14.7
Isooctane	3.04	0.480	18.3	18.4	20.1	18.9
Benzene	3.05	0.603	21.5	20.4	20.4	20.8
Carbon tetrachloride	3.06	0.920	26.2	24.6	25.5	25.4
Dioxane	3.24	1.160	24.5	23.6	24.4	24.7
Nujol	2.96	137.78	238.9	238.3	233.2	217.6
8. Solute, Benzil						
n-Hexane-Bz.	3.68	0.389	20.3	20.4	20.1	20.3
Benzene	3.71	0.603	24.0	24.8	25.2	25.7
Carbon tetrachloride	3.64	0.920	40.3	37.8	38.5	39.3
Nujol-Bz.	3.60	2.816	55.4	55.5	53.0	54.3

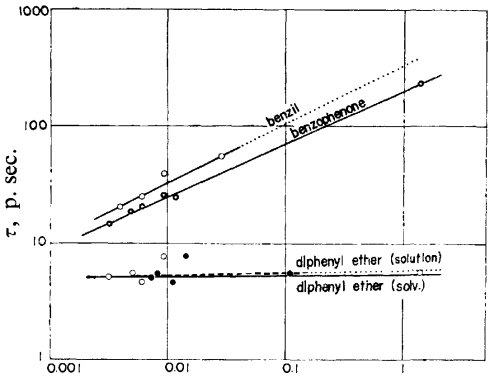

Fig. 2. Dependence of the logarithm of relaxation time of non-rigid molecules upon the logarithm of the viscosity.

TABLE IV. PARAMETER VALUES A AND x OBTAINED FROM THE PRESENT WORK

Substance	A	x
Pyridine	$\bar{1}2.796$	0.09
	$\bar{1}2.940$*	0.16*
Nitrobenzene	$\bar{1}1.575$	0.24
4-Nitrotoluene	$\bar{1}0.071$	0.37
1,3-Dinitrobenzene	$\bar{1}0.246$	0.48
4-Nitrobiphenyl	$\bar{9}.204$	0.66
Diphenyl ether	$\bar{1}2.748$	0.01
	$\bar{1}2.778$*	0.03*
Benzophenone	$\bar{1}0.301$	0.46
Benzil	$\bar{1}0.532$	0.51

* η_{solu} is employed instead of η_{solv}.

Alternatively, we may use η_{solu} instead of η_{solv} in examining the approximate linearity between $\log\tau$ and $\log\eta$. Pyridine in Fig. 1 and diphenyl ether in Fig. 2 show that Eq. 4 is equally valid for any case using either η_{solv} or η_{solu}. The values of A and x marked by an asterisk in Table IV and the broken lines in Figs. 1 and 2 refer to the examination by the use of η_{solu}.

The use of Eq. 2 requires that the dielectric absorption should be of the Debye type, which is not usually possible. In order to examine more fully the validity of Eq. 4, we have to refer to the results of the microwave measurements which account for the deviations from Debye's dispersion. In fact, this has been done by Higasi[7] and was repeated for the present work with equally satisfactory results. Table V records the values of A and x thus obtained.

Now we shall turn to the correlation between Stokes' formula and the new empirical equation. Equation 4 will become identical with Eq. 1 only when the following conditions are satisfied:

TABLE V. PARAMETER VALUES FROM THE LITERATURE

Substance	A	x	y	Ref.
2,2'-Dichloropropane	$\bar{1}2.529$	0.07	0.23	17
2,2'-Dinitropropane	$\bar{1}2.851$	0.16	0.28	17
t-Butyl chloride	$\bar{1}2.423$	0.09	0.21	18
Camphor	$\bar{1}1.190$	0.16	0.29	19,20
1,3-Dichlorobenzene	$\bar{1}1.373$	0.13	—	21
Isoquinoline	$\bar{1}1.591$	0.23	0.47	19,22
1-Chloronaphthalene	$\bar{1}1.712$	0.25	0.38	23
1-Bromonaphthalene	$\bar{1}1.839$	0.27	0.41	23
Acridine	$\bar{1}0.845$	0.69	1.1	19
4-Bromobiphenyl	$\bar{9}.193$	0.66	0.92	19,24

$$A = \log\frac{4\pi a^3}{kT}; \quad x = 1 \tag{5}$$

Tables IV and V both demonstrate that the x parameter is not unity but, rather, is distributed within a wide range: $0<x<1$. This suggests that Stokes' formula is not applicable to a sphere of molecular dimensions.

It is interesting to examine the values of parameter x in the light of molecular structure. For such rigid spherical molecules as 2,2'-dichloropropane and *t*-butyl chloride, one will notice that the x parameter is nearly zero; certainly, the Stokes spherical model is invalid. With an increase in distortion from sphericity, the parameter gradually increases: $x=0.24$ for nitrobenzene and $x=0.66$ for 4-nitrobiphenyl.

For molecules having freedom of internal rotation, the x parameter becomes smaller. This tendency is demonstrated in Fig. 2 in the comparison of diphenyl ether with benzophenone; in the latter kind of molecules, the rotation of the benzene rings does not affect the dipole moment of the molecule, while in the former the molecular moment changes its direction by means of internal rotation.[25] In connection with the internal motion of benzil,[26] it is interesting to find that the x parameter has the fairly large value of 0.46. This leads to a suggestion that benzil is practically a rigid molecule, which is in good agreement with the conclusions of the dipole work.[26]

17) R. S. Holland, G. N. Roberts and C. P. Smyth, *J. Am. Chem. Soc.*, 78, 20 (1956).
18) A. J. Curtis, D. L. McGeer, G. B. Rathmann and C. P. Smyth, ibid., 74, 644 (1952).
19) O. F. Kalman and C. P. Smyth, ibid., 82, 783 (1960).
20) D. W. Whiffen and H. W. Thompson, *Trans. Faraday Soc.*, 42A, 122 (1946).
21) R. J. Meakins, ibid., 54, 1160 (1958).
22) J. Y. H. Chau, R. J. W. Le Fèvre and J. Tardif, *J. Chem. Soc.*, 1957, 2293.
23) E. L. Grubb and C. P. Smyth, *J. Am. Chem. Soc.*, 83, 4122 (1961).
24) H. Kramer, *Z. Naturforsch.*, 15A, 66 (1960).
25) K. Higasi and C. P. Smyth, *J. Am. Chem. Soc.*, 82, 4759 (1960); K. Higasi, This Bulletin, 35, 692 (1962); *Chem. and Chem. Ind. (Kagaku to Kogyo)*, 15, 118 (1962).
26) K. Higasi, This Bulletin, 13, 158 (1938).

The trend of the x parameter is a quantitative description of what has been said qualitatively by Smyth and his co-workers.[27] That is, if the shape of the molecule undergoing dipole rotation departs slightly from that of a sphere, the relaxation time has little dependence upon the viscosity since it can rotate without any considerable displacement of the surrounding molecules. Further, if the molecule is asymmetrical in shape, its rotation must involve the displacement of neighboring molecules and so the relaxation time should depend markedly upon the viscosity of the medium. The concept of the displacement of solvent molecules belongs to a mechanism entirely different from the Newtonian flow on which the Stokes model is theoretically based.

The relation between viscosity and temperature can be expressed by:

$$\eta = B\exp(E_\eta/RT) \tag{6}$$

in which E_η can be called the molar activation energy of viscosity. Similarly, we can write for the time of relaxation,

$$\tau = C\exp(E_\tau/RT) \tag{7}$$

in which C is considered to be independent of the temperature and E_τ, the activation energy for relaxation.

If we take the ratio of E_τ to E_η and denote it by y:

$$y = \frac{E_\tau}{E_\eta} \tag{8}$$

then Eq. 6 will be transformed into:

$$\tau = C\exp(yE_\eta/RT) = (C/B^y)\cdot\eta^y$$

Or, we may write:

$$\log\tau = \log(C/B^y) + y\log\eta \tag{9}$$

Eq. 9 will become identical to Eq. 4, if

$$x = y \quad \text{and} \quad A = \log(C/B^y) \tag{10}$$

27) C. P. Smyth, Ref. 3, pp. 122–123.

The values of x obtained from various solvents using Eq. 4 are compared with the y values obtained for Nujol by Kalman and Smyth[19] from Eq. 8. It is impressive to find in Table V that these two parameters are roughly parallel to each other; $x \simeq y$ and $0 < y \leqslant 1$. The E_τ/E_η ratio is not independent of solvents, and the second condition of Eq. 10 is satisfied only very approximately. These points seem to be reflected in the observed differences between y and x values.

Lastly, we may refer to the frequency dependence of the viscosity. One might point out that the viscosity of Nujol at the frequency of 10~80 Mc./sec. might be different from its static viscosity and that, consequently, the observed relationship might need to be reconsidered. However, this suggestion is untenable. If that be the case, one can not explain why the molecular shape can produce such a considerable variation in x values.

Conclusions

(1) Stokes' formula for a rotating sphere in a viscous medium cannot be applied to a sphere of molecular dimensions.

(2) There exists an empirical relation between the relaxation time, τ, and the viscosity, η:

$$\log\tau = A + x\log\eta$$

in which the x parameter has a value $0 < x \leqslant 1$.

(3) Through the x parameter one can obtain some insight into the mechanism of rotation (internal rotation vs. overall rotation) or one can discuss the shape of the rotating unit.

Acknowledgement is made to the Ministry of Education for a grant-in-aid.

Research Institute of Applied Electricity
Hokkaido University
Sapporo

*The Properties and Infrared Absorption Spectra of Nitrilotriacetate Chelates**

By Yuko TOMITA and Keihei UENO

(Received April 8, 1963)

The metal chelate-forming behavior of nitrilotriacetic acid (hereafter referred to as NTA) has been studied in terms of their properties in a solution,[1] but very few investigations have been undertaken into the NTA chelates in a solid state.[2] Extensive investigation into ethylenedinitrilotetraacetic acid (hereafter referred to as EDTA) chelates, both in a solution and in solid states have proved that the bonding between the EDTA and divalent metals is primarily ionic.[3] In those investigations, infrared absorption spectroscopy provided much information on the nature of the bonding between metal and ligand. For instance, the absorption band for the carbonyl bond of the carboxylate groups was found to shift to higher frequencies with the increasingly covalent character of the metal-carboxylate bond. This observation made it possible to determine whether the bonding in EDTA chelates is essentially ionic or covalent. At the same time, the infrared technique was utilized in differentiating coordinated and uncoordinated carboxyl groups.[4,5] However, this differentiating technique is not always successful; in those complexes whose bonding is primarily ionic, the absorptions of the COOM group and those of the uncoordinated COO^- group occur in the same region, so it is not possible to distinguish between these two cases.

This study, concerned with some of the properties and the infrared spectra of NTA and metal-NTA chelates, attempts to investigate the chelating behavior of NTA in a solid state as well as in a solution and to find a relationship between the carbonyl band and the nature of the metal-carboxylate bond.

Experimental

Infrared Spectra. — The infrared spectra of crystalline complexes were studied in mineral oil mulls and in potassium bromide disks. The solid complexes were pressed into disks, using 0.3~0.5 mg. of chelate mixed with 100 mg. of potassium bromide for each disk. The infrared spectra in aqueous solutions were also taken for those complexes which are soluble enough in water. The aqueous solutions were made with 99.5% D_2O at concentrations of approximately 3~15% by weight, and the spectra were observed using a cell with calcium fluoride windows. The measurements were made with a Nippon Koken model DS 301 double-beam spectrophotometer equipped with sodium chloride optics.

Reagents.—The inorganic salts used in preparing the complexes were reagent grade in all cases. The free acid of NTA (donated by Dojindo & Co.) was analytical grade and was used without further purification.

Preparation of NTA Chelates. Sodium Salt of NTA Chelates ($NaM^{II}Y$[6]).—The following metal carbonates were used in preparing solid chelates: $(MgCO_3)_4 \cdot Mg(OH)_2 \cdot 5H_2O$, $CaCO_3$, $SrCO_3$, $BaCO_3$, $CoCO_3 \cdot 3Co(OH)_2$, $NiCO_3 \cdot 2Ni(OH)_2 \cdot 4H_2O$, $CuCO_3 \cdot Cu(OH)_2 \cdot H_2O$, $(PbCO_3)_2 \cdot Pb(OH)_2$, $ZnCO_3$ and $CdCO_3$. The theoretical amount of inorganic salt was added to a warm suspension of 0.02 mol. of NTA in 50 ml. of water. After complete dissolution, the pH value of the solution was adjusted to 6~7 by adding a 0.01 M solution of sodium carbonate. The solution was heated almost to boiling. To this solution, 200~300 ml. of absolute ethanol was added until the precipitates began to appear, and the resulting solution was cooled in an ice-bath. After filtering the crystals, they were recrystallized from a small amount of water. The finished chelates were immediately placed in a vacuum desiccator for 24 hr.

Hydrogen NTA Chelates ($HM^{II}Y$).—These were prepared in a similar manner, but sodium carbonate was not added to the solution. The separated hydrogen NTA chelates were recrystallized from water and placed in a vacuum desiccator for 24 hr.

Analyses.—The chelates were analyzed for alkaline earths and divalent metals by the EDTA titration technique after the samples had been decomposed with concentrated nitric acid and hydrogen peroxide.[7] For the sodium salt of chelates, sodium was determined by precipitating it as sodium-zinc-uranyl-acetate from the decomposed solution,

* Contribution No. 41 from the Department of Organic Syntheses.

1) G. Schwarzenbach, E. Kampisch and R. Steiner, *Helv. Chim. Acta*, **28**, 828 (1945).

2) M. Mori, M. Shibata, E. Kyuno and Y. Okubo, This Bulletin, **31**, 940 (1958).

3) D. T. Sawyer and P. J. Paulsen, *J. Am. Chem. Soc.*, **81**, 816 (1959).

4) D. H. Busch and J. C. Bailar, ibid., **75**, 4574 (1953).

5) M. L. Morris and D. H. Busch, ibid., **78**, 5178 (1956).

6) Y designate the NTA anion dissociated to trivalent state.

7) Y. Tsuchitani, Y. Tomita and K. Ueno, *Talanta*, **9**, 1023 (1962).

TABLE I. COMPOSITION OF NTA CHELATES INVESTIGATED

Chelate	Metal, %		Sodium, %	
	Calcd.	Found	Calcd.	Found
$NaMgY \cdot 3.5H_2O$	8.16	8.10	7.72	7.68
$NaCaY \cdot 3H_2O$	14.0	14.0	8.05	7.88
$NaSrY \cdot 4H_2O$	23.5	24.0	6.22	6.12
$NaBaY \cdot 3.5H_2O$	33.4	34.0	5.59	5.50
$NaCoY \cdot 2.5H_2O$	18.7	19.0	7.27	7.05
$NaNiY \cdot 3.5H_2O$	17.6	17.0	6.91	6.68
$NaCuY \cdot 2.5H_2O$	19.9	20.6	7.22	7.06
$NaZnY \cdot 3.5H_2O$	19.3	19.4	6.67	6.60
$NaCdY \cdot 3H_2O$	30.3	31.0	6.15	6.08
$NaPbY \cdot 3H_2O$	43.9	44.2	4.87	4.80
$MgHY \cdot 3H_2O$	9.33	9.30		
$CaHY \cdot 2H_2O$	15.1	14.9		
$SrHY \cdot 4H_2O$	25.5	25.4		
$BaHY \cdot 3H_2O$	36.2	36.5		

$Y = N(CH_2COO)_3^{3-}$

followed by EDTA titration.[8,9] The results of the analyses are shown in Table I, along with the proposed formulae.

Results and Discussion

Spectra of Ligand.—In Table II, assignments and wave numbers are given for the important peaks of the NTA chelates of the alkaline earth metals (Mg, Ca, Sr, Ba), divalent metals (Cu, Ni, Zn, Co, Pb) and sodium salts of NTA. There is no significant absorption band between 4000 and 1800 cm^{-1} except for the bands in the 3000~2800 cm^{-1} region, which are assigned to the C-H streching vibration of the CH_2 groups.

The carboxyl group is known to give a strong band in the range between 1735 and 1550 cm^{-1} which is due to the C=O stretching vibration.[10] As it is believed, from the acid dissociation constant data, that NTA ligand acid has a zwitter ion structure, as in the case of EDTA, one may expect a band for carboxylate ion in the 1610~1550 cm^{-1} region for the acid form of NTA. However, no significant absorption band could be found in this region for the free ligand acid. Therefore, it is doubtful that NTA has a zwitter ion structure in the solid state. This situation will be made clearer if one could compare the spectra of the solid state with that of the solution state. However, the spectra of the aqueous solution could not be measured because of the poor solubility of the ligand acid. In this connection, it is noteworthy that a similar situation has been reported for EDTA ligand acid, where no clear band of carboxylate ions, could be found in the expected region. Therefore, the existence of a zwitter ion structure was thought to be doubtful[11] in the solid state, although a very weak shoulder at

TABLE II. INFRARED ABSORPTION PEAKS FOR NTA CHELATES OF ALKALINE EARTH METALS AND DIVALENT METALS

	Stability constant	Ionic radius	-COOH	-COOM	Hydrated $-COO^-$	Crystal $-COO^-$	-CN	D_2O solution -COOM
H_3Y			1728					
Na_2HY			1673		1638	1399		1625
Na_3Y	2.1				1580	1411	1138	1588
$NaMgY \cdot 3.5H_2O$	5.41	0.98		1623	1588	1410	1135	
$MgHY \cdot 3H_2O$			1660	1625				
$NaCaY \cdot 3H_2O$	6.41	1.01		1640	1600	1428	1131	
$CaHY \cdot 2H_2O$			1705	1645				
$NaSrY \cdot 4H_2O$	4.98	1.18		1612	1588	1416	1131	
$SrHY \cdot 4H_2O$			1680	1616				
$NaBaY \cdot 3.5H_2O$	4.82	1.34		1608	1588	1416	1131	
$BaHY \cdot 3H_2O$			1680	1613				
$NaCoY \cdot 2.5H_2O$	10.38	0.78		1622		1411	1127	1596
$NaNiY \cdot 3.5H_2O$	11.53	0.67		1621		1415	1123	1594
$NaCuY \cdot 2.5H_2O$	12.96	0.69		1635*		1418	1115	1612
				1667 1604				
$NaZnY \cdot 3.5H_2O$	10.67	0.70		1624		1412	1127	1599
$NaCdY \cdot 3H_2O$	9.83	0.92		1619		1416	1129	
$NaPbY \cdot 3H_2O$	11.39	1.17		1625		1414	1123	1599

* Anhydrated solid

8) H. Flaschka, *Mikrochemie ver. Mikrochim. Acta*, **39**, 315 (1952).
9) B. Sen, *Z. anal. Chem.*, **157**, 2 (1957).
10) L. J. Bellamy, "The Infrared Spectra of Complex Molecules," John Wiley and Sons, Inc., New York, N. Y. (1958), p. 162.
11) D. Chapman, *J. Chem. Soc.*, **1955**, 1766.

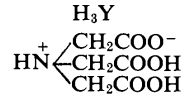

H_3Y

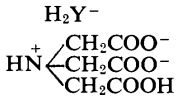

H_2Y^-

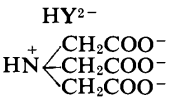

HY^{2-}

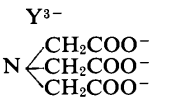

Y^{3-}

In solution			
	1720 cm^{-1} 1623 cm^{-1}	1625 cm^{-1}	1584 cm^{-1}
Solid			
1728 cm^{-1}		1678 cm^{-1} 1638 cm^{-1}	1580 cm^{-1}

1635 cm^{-1} has been assigned to carboxylate ions by one investigator.[12]

In contrast to the NTA free acid, its disodium and trisodium salts were easily soluble in water, so that their spectra were observed both in solid and in solution states. The two bands at 1678 cm^{-1} and 1638 cm^{-1} of disodium NTA in a solid state have been assigned to the $-COOH$ and $-COO^-$ groups respectively. However, in an aqueous solution, only one band, at 1625 cm^{-1}, is observed, indicating that all three carboxyl groups exist as $-COO^-$ and that the proton is attached to the nitrogen atom. This situation has been pointed out by Nakamoto, Morimoto and Martell.[13] Why this singlet carboxyl band splits into a doublet when one goes from a solution to a solid state can be explained in two ways. In one explanation, one of the carboxylate ions of NTA is bonded to the proton of neighboring NTA molecules in the solid state, as is schematically shown below (I). This intermolecular hydrogen bonding will not occur in a solution. The hydrogen-bonded carboxylate group gives rise to an absorption at 1678 cm^{-1}, whereas the free carboxylate group absorps at 1638 cm^{-1}. In

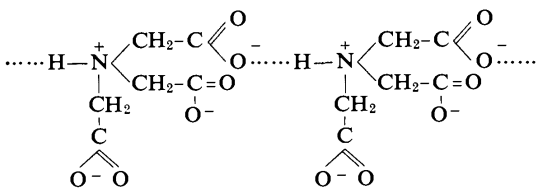

I

another explanation, the stretching vibration of the carboxylate carbonyl bonding will be influenced by the crystal field in the solid state, which will result in the splitting of the singlet band.

Trisodium NTA gives only one band, near 1580 cm^{-1}, both in a solid and in a solution, so it is clear that the three carboxyl groups exist as $-COO^-$, regardless of the state.

The shift of the band for the free carboxylate group from 1625 cm^{-1} in disodium salt to 1584 cm^{-1} in trisodium salt may be caused by the loss of a formal positive charge on the nitrogen atom, as has been discussed by Nakamoto.[13]

The Spectra of Metal Chelates.—It one assumes that NTA behaves as a tetradentate ligand, with all the carboxylate groups coordinated to the central metal ion, only one carboxyl band may be expected in this region for all metal-NTA chelates. However, the infrared spectra of NTA chelates of alkaline earth metals in a solid state show two carboxyl bands, as Table II indicates.

The first group of bands appears in the range between 1640 and 1600 cm^{-1} and can be found in the alkaline earth chelates but in neither free ligand acid nor sodium salts. Therefore, this band can be assigned to the coordinated carboxylate groups. The second group of bands appears in the range between 1600 and 1580 cm^{-1} and can be found in the trisodium salt of NTA as well as in the alkaline earth chelates. However, in the case of the hydrogen complexes and the free acid of NTA, this band has completely disappeared and a new band has appeared around 1700 cm^{-1}, where the absorption band of free carboxylic acid is expected. Therefore, it is quite probable that the band at 1600~1580 cm^{-1} is associated with the uncoordinated carboxylate ions. Similar spectral characteristics have been observed in EDTA chelates, where the coordinated carboxylate group, the uncoordinated carboxyl group and free carboxylic acid were assigned to the bands near 1650, 1750 and 1600 cm^{-1} respectively. From these observations, it is probable that, in the alkaline earth chelates, one of the three carboxyl groups does not coordinate with the central metal ion, but remains free carboxylic acid or carboxylate ions. This conclusion may not be extended to the chelating behavior of NTA in a solution, however, since the spectra were taken on solid samples only and no information on the spectra of the solution state could be obtained because of their poor solubility.

In the case of divalent metal ions other than alkaline earth metals, their chelates

12) D. T. Sawyer and P. J. Paslsen, *J. Am. Chem. Soc.*, **80**, 1597 (1958).
13) K. Nakamoto, Y. Morimoto and A. E. Martell, ibid., **84**, 2081 (1962).

showed a single band, with a shoulder in the carbonyl region. This suggests that NTA behaves as a tetradentate ligand, with all carboxylate groups coordinated with the central metal ion. This is also supported by the information obtained from the spectra of an aqueous solution, in which the shoulder of the carboxyl band disappears and the carboxyl band does not change when the hydrogen complex (HMY) is converted into a sodium complex (NaMY).

Regarding EDTA metal chelates, many papers have been published on the relationship between the carbonyl frequency of a coordinated carboxylate group and the covalent character of the metal-carboxylate bond. Sawyer and Paulsen[3] have summarized the previous data on the EDTA chelates and have concluded as follows: When the coordinated carboxylate band ($\nu_{C=O}$) appears in the 1610~1550 cm^{-1} region, the bonding is primarily ionic. When this band is in the 1650~1625 cm^{-1} region, the bonding is primarily covalent. When the band occurs between these two region, the bonding is probably partially ionic and partially covalent.

In the case of the NTA chelates investigated, the carbonyl bands are always found to occur in the same region, 1640~1600 cm^{-1}, where the carbonyl band of a so-called primarily or partially covalent character is expected to appear. The carbonyl frequencies, therefore, may not be related to the covalent character of the metal-carboxylate bond, and the general rule for judging the nature of the bonding in EDTA chelates cannot be applied to NTA chelates. However, in the case of alkaline earth chelates, the frequency of the carbonyl band in a solid state decreases in the order of calcium > magnesium > strontium > barium. Interestingly, this order is identical with the decreasing order of the chelate stability constant. The plots of the logarithms of stability constants against the wave numbers of the carbonyl bands show a straight line, as Fig. 1 shows. This parallel relationship in alkaline earth chelates can qualitatively be explained as follows. The increase in the stability of the NTA chelates is related to the increase in the covalent nature of the metal-ligand bond. Although the nature of this bonding is primarily ionic, the degree of the contribution of the covalent form II will be greater than that of the ionic form III; this effect results in an increase in the double-bond character of the carbonyl bond.

II III

As to the other divalent metal chelates, it is found that the frequency of the absorption band increases with the increasing stability constant, with the exception of nickel chelates. This relationship was observed in both the solid state and in an aqueous solution.

As has been stated previously, the frequency of the carboxylate band of NTA shifted from 1585 cm^{-1} to 1625 cm^{-1} when the nitrogen atom coordinated with a proton. This is understood to be due to the influence of the formal positive charge on the nitrogen atom. For the NTA chelates, in which the coordination of nitrogen atom with the central metal ion is strong, a similar influence on the carboxylate frequency may be expected. For the alkaline earth chelates, the *N*-metal bonding

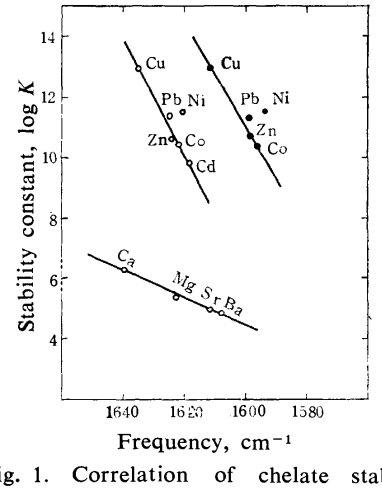

Fig. 1. Correlation of chelate stability constants with C=O absorption frequencies of the chelates.
-○- Hydrated crystal
-●- D_2O solution

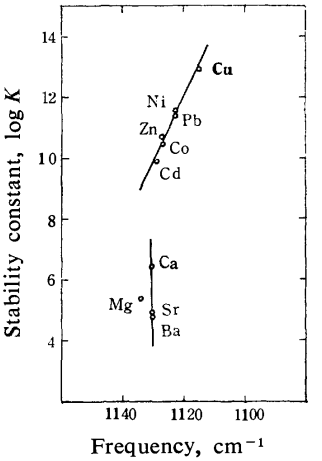

Fig. 2. Correlation of chelate stability constants with C-N absorption frequencies of the chelates.

may not be strong enough to influence the carboxylate frequency. In such a case, the carbonyl frequency must be discussed in relation with the chelate stability.

However, for the NTA chelates of other divalent metals which form more or less strong *N*-metal bonding, their carboxylate frequency will be influenced not only by the carbonyl-metal bonding, but also by the *N*-metal bonding. The coordination of nitrogen atoms to such metal ions is also supported by the shift of the C–N bond, as will be discussed later. Therefore, in this case, one must be careful not to correlate the carboxylate frequency with simply the chelate stability or the nature of the carbonyl-metal bonding.

Carboxylate ions are known to give rise to another peak in the 1420~1390 cm^{-1} region. Accordingly, the band at 1420~1390 cm^{-1} has been assigned to this group, as in Table II. The peak at 1420~1390 cm^{-1} shows some splitting, but no significant relationship between the frequencies of the peaks and the kind of metal ions can be found.

The absorption band in the 1410~1110 cm^{-1} region has been assigned to the C–N bond in NTA chelates.[10] The relationship between the chelate stability and the frequency of the C–N bond for NTA chelates is shown in Fig. 2. The alkaline earth chelates give rise to the peak in the same region, at 1130 cm^{-1}, with the exception of magnesium. On the other hand, the C–N bond of the other divalent metal chelates appears in the 1130~1110 cm^{-1} region, and their frequencies decrease with an increasing stability constant. The corresponding band of the trisodium salt of NTA is found at 1138 cm^{-1}. If one assumes that the coordination of nitrogen to the metal ion results in the lowering of the stretching frequency of the C–N bond, these observations indicate that the *N*-metal bond of alkaline earth chelates is relatively weak and is not sensitive to the metal ions, whereas the bond of other divalent metal chelates is relatively strong and is sensitive to the metal ions. This conclusion may be supported by the fact that these divalent metals form a relatively stable ammine complex, while alkaline earth metals do not form a stable ammine complex.

Summary

Infrared absorption spectra have been observed in NTA and its metal chelates, in solid states as well as in solution. The results indicate that NTA does not exist as zwitter ions in the solid state, that it behaves as a quadridentate ligand for such divalent metals as copper, nickel, cobalt, zinc, cadmium and lead, but that it behaves as a terdentate ligand for the alkaline earth metals. It is also found that the wave number of the $\nu_{C=O}$ band of the coordinated carboxylate group in the NTA chelates tends to shift to a higher value with an increasing chelate stability constant.

A part of the expense of the work reported in this paper was supported by a research grant provided by the Ministry of Education, to whom the authors' thanks are due.

Department of Organic Synthesis
Faculty of Engineering
Kyushu University
Hakozaki, Fukuoka

A Kinetic Study of the Isotopic Exchange of Indium in Indium N-2-Hydroxyethylethylenediamine-N, N', N'-triacetate Complex in Water

By Kazuo SAITO and Michiko TSUCHIMOTO

(Received April 13, 1963)

As an extension of the kinetic study of the isotopic exchange of co-ordination compounds of the d^{10} structure, the present authors have studied the kinetics of indium *N*-2-hydroxyethylethylenediamine-*N*,*N'*,*N'*-triacetate (henceforth written as EDTA–OH with a formula H_3Z) using indium 114 m as tracer. It was previously reported that the exchange rate is measurably slow in an acid solution of pH 2 to 4 but very fast in more acid solutions.[1] The exchange kinetics is quite different from that of the corresponding gallium complex,[2]

1) K. Saito and M. Tsuchimoto, This Bulletin, **35**, 368 (1962).

2) K. Saito and M. Tsuchimoto, *J. Inorg. Nucl. Chem.* **23**, 71 (1961).

and also from that of indium ethylenediamine-*N*,*N*,*N*',*N*'-tetraacetate (henceforth written as EDTA with a formula H_4Y).[3]

This paper gives the results of a kinetic study of the indium EDTA-OH complex $[InZ\cdot OH_2]\cdot H_2O$ with indium in neutral and basic media, and they are compared with the findings regarding the related complexes mentioned above.

Experimental

Preparation of the Complex. — Radioactive EDTA-OH complex of indium was prepared from indium 114 m. (Ammersham; specific activity: 10 μc. per mg.) and extra pure EDTA-OH (Dotite EDTA-OH).[1] The specific activity was 0.41 μc. per mg.

Procedure for Kinetic Runs and Measurement of Radioactivity. — The method was principally the same as that used in the previous work. Uncomplexed indium hydrolyses in aqueous solutions with a pH value of more than 4, and the kinetics was always studied in the presence of tartrate. In neutral solutions up to pH 8.0, 0.0035 M tartrate sufficed to keep 10^{-3} M indium in the aqueous phase, whereas as much as 0.05 M tartrate was required at pH 11. Since tartrate is present in a doubly de-protonated form in the pH region higher than 5, the given figures indicate the concentration of $C_4H_4O_6^{2-}$.

The reaction was very slow in neutral solutions at 25°C, and the kinetics was studied at 40°C. The separation with 8-quinolinol was effected with more ease at this temperature, the separation-induced zero-time exchange being negligible.

Results

The exchange constant, R, is expressed by McKay's formula:

$$R=-2.303\cdot\frac{ab}{a+b}\cdot\frac{\log(1-F)}{t}$$

where a and b are the molar concentrations of the uncomplexed indium and of the indium EDTA-OH complex respectively, t is the lapse of time, and F the fraction of reaction. The kinetics was entirely different in basic and in neutral media. The R values, however, are independent of a and are proportional to b, regardless of the pH value. Such relationships are graphically shown in Figs. 1 and 2. Hence, the reaction constant, k, is expressed by R/b and has a dimension of T^{-1} in the given concentration range.

Exchange in Basic Media.—The pH dependence of k in basic media buffered with various agents, including barbiturate, *p*-hydroxybenzoate and glycine, is shown in Fig. 3. The k values are proportional to the hydroxide ion concentration regardless of the kind of buffering agent, and the rate constant is expressed by $R=k'\cdot b[OH^-]$. The dependence of the k' value upon the concentration of tartrate and the buffering agents is shown in Table I for barbiturate and *p*-hydroxybenzoate solution and in Fig. 4 for glycine solution. The rate

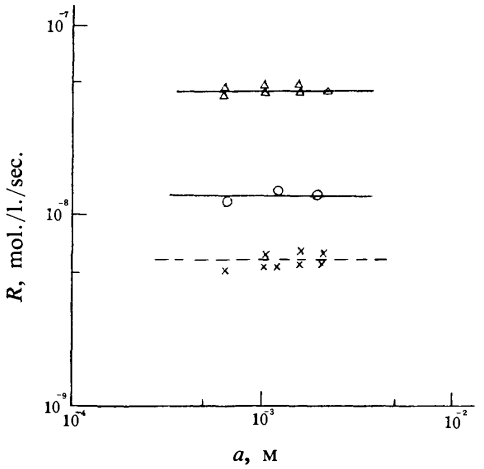

Fig. 1. Relationship between the exchange rate R and the concentration of uncomplexed indium a.
μ=0.30 (KNO_3); b, 1.20×10^{-3} M; Tartrate concn., 0.060 M.
—○— pH, 10.08; 25°C; Barbiturate, 0.0375 M
—△— pH, 8.54; 25°C; Glycine, 0.0625 M
--×-- pH, 7.33; 40°C; Barbiturate, 0.0375 M

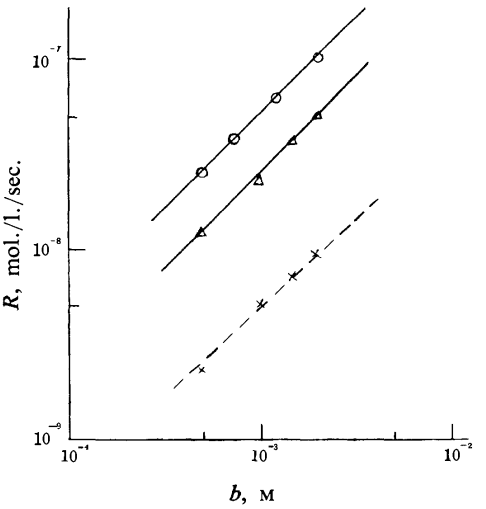

Fig. 2. Relationship between the exchange rate R and the concentration of the indium EDTA-OH complex b.
μ=0.30 (KNO_3); a, 1.20×10^{-3} M; Tartrate concn. 0.060 M
—○— pH, 10.70; 25°C; Barbiturate, 0.0375 M
—△— pH, 8.40; 25°C; Glycine, 0.0625 M
--×-- pH, 7.33; 40°C; Barbiturate, 0.0375 M

3) K. Saito and M. Tsuchimoto, ibid., in press.

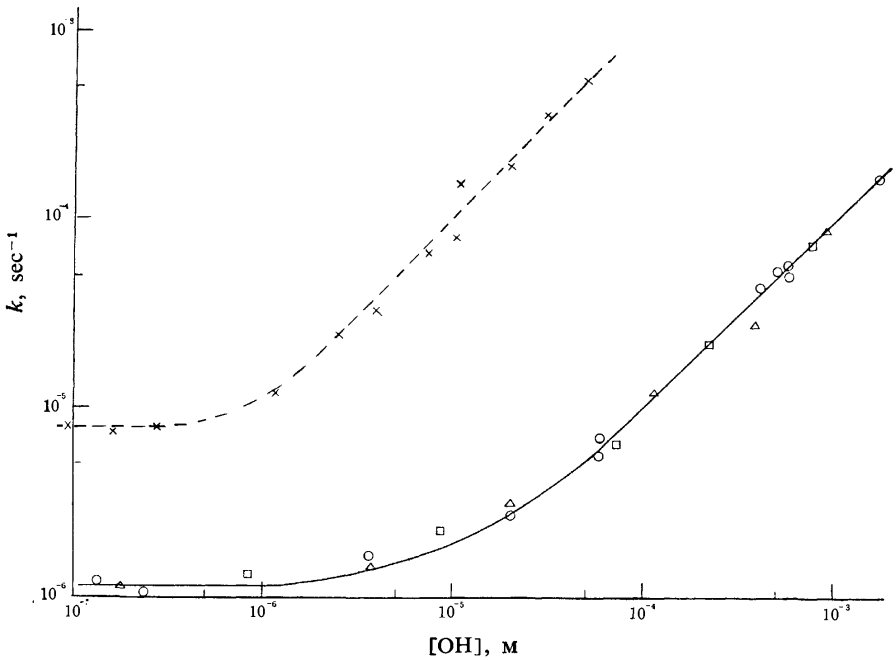

Fig. 3. Relationship between the exchange rate constant k and the hydroxide ion concentration in basic media.
25°C; μ=0.30 (KNO_3); Tartrate concn., 0.060 M
—○— In 0.0375 M barbiturate
—△— In 0.0125 M *p*-hydroxybenzoate
—□— In 0.2 M NH_3 containing 0.032 M NH_4NO_3
--×-- In 0.0625 M glycine

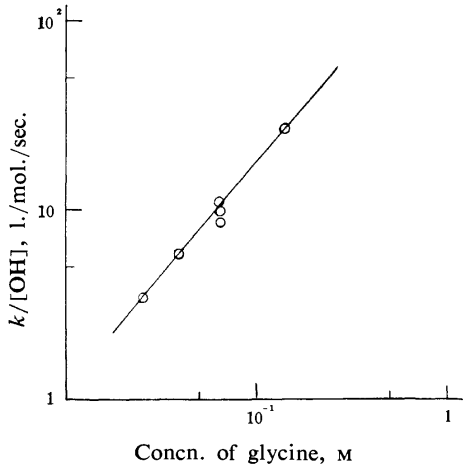

Fig. 4. Influence of the concentration of glycine upon the exchange rate constant k.
25°C; pH, 8.33; μ=0.30 (KNO_3); tartrate, 0.060 M

is affected by the concentration of tartrate and of the former two agents to a small extent. On the other hand, it increases linearly with increase in the concentration of glycinate. The influence of the ionic

Table I. Influence of buffering agents upon the exchange rate constant in basic solutions*

Buffer	Concn. of buffer, M	μ (KNO_3)	k/[OH^-] l./mol./sec.
Na barbiturate	0.025	0.30	0.102
	0.0375	0.30	0.0985
	0.100	0.30	0.175
p-Hydroxybenzoate	0.0075	0.30	0.132
	0.0125	0.30	0.103
	0.0200	0.30	0.187
Ammonia	0.2 (0.032 M NH_4NO_3)	0.30	0.108
Glycine**	0.0625	0.10	9.55
	0.0625	0.30	9.61
	0.0625	0.55	9.21
	0.0625	0.10 (KCl)	10.6
	0.0625	0.55 (KCl)	11.5

* 25°C; Tartrate concn., 0.060 M; Its concentration has little influence upon the rate. (data omitted).
** The influence of the concentration. of glycine is shown in Fig. 4. Change in ionic strength affects the rate to a very small extent in other buffers, too (data omitted).

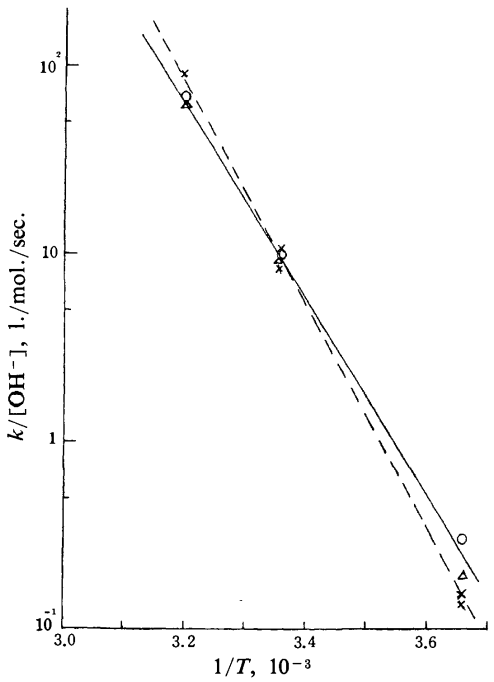

Fig. 5. Temperature dependence of the exchange rate constant in basic media.
μ=0.30 (KNO_3); Tartrate concn., 0.060 M
—○— In 0.0375 M barbiturate
—△— In 0.0125 M *p*-hydroxybenzoate
--×-- In 0.0625 M glycine

strength is small, regardless of the kind of buffering agent used. The temperature dependence in various solutions is shown in Fig. 5; the E_A values are 25 and 27 kcal./mol. in barbiturate (or *p*-hydroxybenzoate) and in glycine solution respectively.

Exchange in Neutral Solutions. — In the pH region from 4 to 8, the exchange reaction proceeds much more slowly than in basic or more acid media; the time taken for one kinetic run was sometimes more than one week, even at 40°C. Hence, the experimental

TABLE II. INFLUENCE OF BUFFER AND IONIC STRENGTH UPON THE EXCHANGE RATE CONSTANT IN THE NEUTRAL REGION*

Buffer	Concn. of buffer, M	μ (KNO_3)	k 10^{-5} sec^{-1}
None	—	0.25	1.38
NaN_3	0.025	0.25	1.52
p-Hydroxybenzoate	0.0125	0.25	1.55
Barbiturate	0.0375	0.25	1.30**
	0.0375	0.10	1.22
	0.0375	0.10 (KCl)	1.25
	0.0375	0.55	1.28
	0.0375	0.55 (KCl)	1.73

* 40°C; Tartrate concn., 0.060 M; pH, 6.13
** Mean value of 12 observations; max. 1.47×10^{-5}, min. 1.09×10^{-5} sec^{-1}

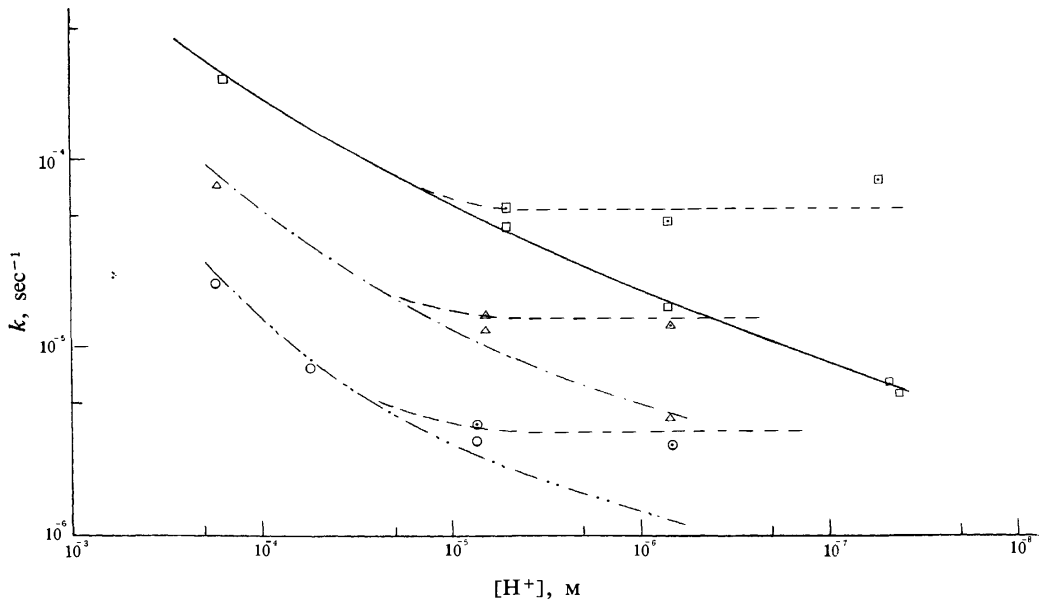

Fig. 6. Dependence of the exchange rate constant upon the hydrogen ion concentration in the neutral region.
40°C; μ=0.25 (KNO_3); no buffer other than tartrate
—·—○—·— In 0.0035 M tartrate ——⊙——
—·—△—·— In 0.0175 M tartrate ——△——
——□—— In 0.060 M tartrate ——▣——

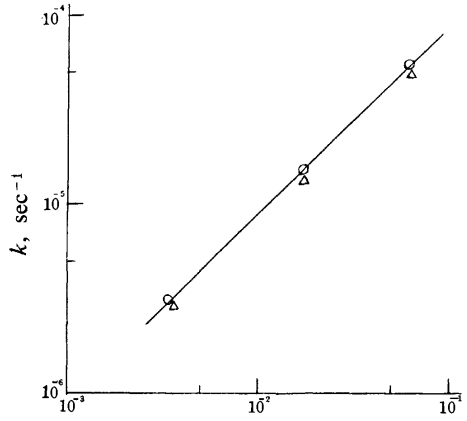

Fig. 7. Relationship between the exchange rate constant k and the concentration of tartrate in the neutral region.
40°C; μ=0.25 (KNO_3)
—○— pH 5.15 —△— pH 6.15

error may be greater. In Fig. 6, the k values are plotted against the hydrogen ion concentration. At a given concentration of tartrate, the rate constant decreases with rise of pH value. The influence of tartrate ions is shown in Fig. 7. (see Discussion). The influence of the buffer and that of the ionic strength are tabulated in Table II. The k values do not appear to be affected significantly by these factors. On the other hand, the rate increases linearly with an increase in the concentration of glycine, as Fig. 8 shows. The temperature dependence of k, which is illustrated in Fig. 9, indicates that the Arrehenius activation energy is 19.2 kcal. per mol. in a tartrate solution, with or without barbiturate, and 24.7 kcal. per mol. in the presence of glycine.

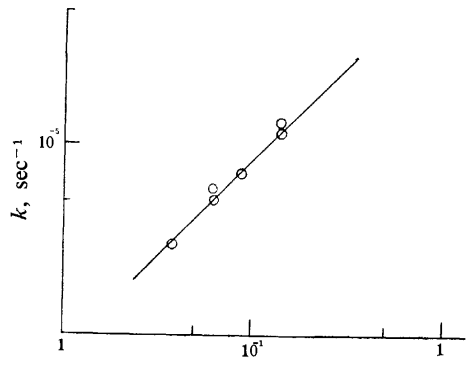

Fig. 8. Influence of the concentration of glycine upon the exchange rate constant in the neutral region.
25°C; μ=0.25 (KNO_3); pH, 7.04; Tartrate concn., 0.060 M

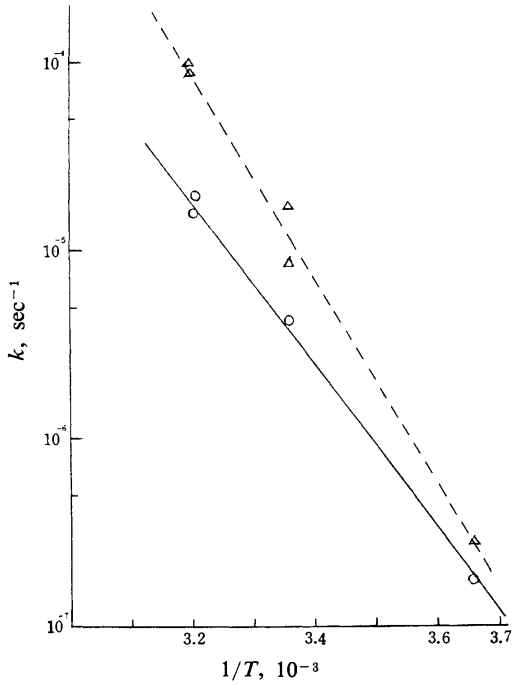

Fig. 9. Temperature dependence of the exchange rate constant in the neutral region.
μ=0.25 (KNO_3); 0.060 M tartrate
—○— Without glycine
--△-- In 0.0625 M glycine

Discussion

The kinetics of the exchange of the indium EDTA-OH complex is quite different from that of the indium EDTA, gallium EDTA or gallium EDTA-OH complex. In neutral solutions, the last three undergo isotopic exchange at an immeasurably slow rate, while the rate for the first-mentioned complex is measurable, although very small as compared with that in an acid or a basic solution. In basic solutions, k is proportional to the hydroxide ion concentration regardless of the kind of buffering agent used (see Table III).

The uncomplexed indium (initially non-radioactive) is present in solutions of a pH more than 4 in the form of a tartrate complex. However, the state of this indium species does not appear to be important in discussing the reaction mechanism because the exchange rate, R, is independent of the concentration of uncomplexed indium.

Exchange in Basic Media. — The indium EDTA-OH has a co-ordinated water, and the dissociation constant to give a proton is 3.6×10^{-6} at 25°C and 5.0×10^{-6} at 40°C. Hence, in basic solutions of pH higher than 8, most of the complex is present in the form of

TABLE III. COMPARISON OF KINETIC DATA FOR INDIUM EDTA AND EDTA-OH COMPLEX AT 25°C

Media		In-EDTA	In-EDTA-OH
	R	$k' \cdot b \cdot [H^+]^3$	$k' \cdot b \cdot [H^+]^1$
Acid	k'	4.3×10 l³/mol³/sec.	1.0×10^{-2} l./mol./sec.
	E_A	18 kcal./mol.	11 kcal./mol.
	R	$< 10^{-10}$ mol./l./sec.	$k \cdot b \cdot [H^+]^0$
Neutral	k	immeasurably slow	1.3×10^{-5} sec^{-1}
	E_A	——	19 kcal./mol.
	R	$k' \cdot b \cdot [OH^-]^2$	$k' \cdot b \cdot [OH^-]^1$
Basic	k'	5.2×10^1 l²/mol²/sec.	1.1×10^{-1} l./mol./sec.
	E_A	25 kcal./mol.	25 kcal./mol.

For simplicity values under representative conditions are given. Details of the experimental conditions are seen in other tables and figures.

hydroxo complex $[InZ \cdot OH]^-$. Since the exchange rate constant, k, is little affected by buffering agents with different structures, such as barbiturate, *p*-hydroxybenzoate and ammonia, the exchange in solutions containing these buffers appears to involve the exchange of the hydroxo complex. Thus, the exchange seems to proceed as follows:

$$[*InZ \cdot OH]^- + OH^- \rightleftarrows [*InZ \cdot O]^{2-} + H_2O$$

(equilibrium to form a conjugate base)

$$[*InZ \cdot O]^{2-} \underset{\text{fast}}{\overset{\text{slow}}{\rightleftharpoons}} [*InO \cdot aq.]^+ + Z^{3-}$$

$$\uparrow\downarrow$$

$$[In \cdot tart_x]^n$$

(rapid exchange of In)

These equations can be simplified as follows:

$$[*InZ \cdot O]^{2-} + [In \cdot tart_x]^n \underset{\text{fast}}{\overset{\text{slow}}{\rightleftharpoons}} [InZ \cdot O]^{2-} + [*In \cdot tart_x]^n$$

Such processes can be alternatively expressed in a somewhat different way as follows:

$$[*InZ \cdot OH]^- + OH^- \rightarrow [*InZ \cdot (OH)_2]^{2-}$$

(attack with hydroxide ions as the rate-determining step)

$$[*InZ \cdot (OH)_2]^{2-} + [In \cdot tart_x]^n \rightleftarrows [InZ \cdot (OH)_2]^{2-} + [*In \cdot tart_x]^n$$

(fast exchange)

Recently, Hoard, Smith and Lind[4] suggested that EDTA complexes of such tervalent metal ions as aluminum, chromium and iron have co-ordination number 7 in the crystalline state. Generally, EDTA–OH forms very similar complexes to EDTA with tervalent metal ions, so that it would not be unreasonable to assume a process involving the attack with hydroxide ions to form an intermediate with co-ordination number 7.

The formation of such an intermediate can also be postulated when it is assumed that the indium EDTA–OH complex has one other mole of co-ordinated water in an aqueous solution. The dissociation constant to give second proton would be so small as compared with that for the first proton that a labile dihydroxo complex is present only as an intermediate state in strongly basic solutions.

$$[*InZ \cdot (OH_2)_2] \rightleftarrows [*InZ \cdot OH_2 \cdot OH]^- + H^+$$

(dissociation of the first proton)

$$[*InZ \cdot OH_2 \cdot OH]^- + OH^- \rightleftarrows [InZ \cdot (OH)_2]^{2-} + H_2O$$

(equilibrium to form a labile dihydroxo complex (conjugate base) as a reaction intermediate)

Nevertheless, nothing decisive can be stated as to the validity of one of the alternative expressions.

Amidst other buffering agents, glycine increases the rate to a marked extent and k' is proportional to the glycine concentration. Such an observation suggests that the reaction mechanism is different from that mentioned above. Acceleration of the exchange reaction by glycine is also seen in the case of the indium EDTA complex, which gives quite different kinetics in the presence and in the absence of glycine.[3] The co-ordinated water in the $[InY \cdot OH_2]^-$ complex is rather easily replaced by other ligands, including halogens and ammonia. In a very similar complex, $[InZ \cdot OH_2]$, the water could also be replaced (although with more difficulty) and the following equilibrium is very likely established in aqueous solutions:

$$[*InZ \cdot OH_2] + NH_2CH_2CO_2H \rightleftarrows [*InZ \cdot NH_2CH_2CO_2H] + H_2O$$

4) J. L. Hoard, G. S. Smith and M. Lind, "Advances in the Chemistry of the Co-ordination Compounds," Ed. by S. Kirschner, McMillan Co., New York (1961), p. 296.

With rise of the pH value, the co-ordinated glycine will liberate a proton to give a complex anion, $[^*InZ\cdot NH_2CH_2CO_2]^-$, which predominates in the given pH region. This anionic complex would interact with hydroxide ions to give a conjugate base, and the exchange reaction would involve a dissociation of the conjugate base.

$$[^*InZ\cdot NH_2CH_2CO_2]^- + OH^- \rightleftarrows [^*InZ\cdot NHCH_2CO_2]^{2-} + H_2O$$

(equilibrium to form a conjugate base)

$$[^*InZ\cdot NHCH_2CO_2]^{2-} + [In\cdot tart_x]^n \overset{\text{slow}}{\underset{\text{fast}}{\rightleftarrows}} [InZ\cdot NHCH_2CO_2]^{2-} + [^*In\cdot tart_x]^n$$

The alternative expression, involving an intermediate with co-ordination number 7 can be similarly written.

Exchange in Neutral Solution. — In the pH region from 4 to 7, the rate constant is much less affected by the pH. In more acid solutions, k values are proportional to the hydrogen ion concentration;[1] this effect is observed at pH below 5. In the acid region, the rate increases in the presence of such acidic radicals as citrate and acetate, and a mechanism involving the replacement of the co-ordinated water by an acid radical was postulated.[1] In the pH region from 5 to 8, the dissociation of co-ordinated water is appreciable, and the effective concentration of the aquo indium EDTA-OH complex $[InZ\cdot OH_2]$ would be decreased to decrease the b value. If the observed k values were corrected on the basis of the effective b values calculated from the dissociation constant, the curves would be as those indicated by broken lines in Fig. 6; i. e., k is independent of the pH at a given concentration of tartrate.

The k vs. tartrate ($C_4H_4O_6^{2-}$, written as "tart" henceforth) concentration curve in Fig. 7 indicates that the corrected k value is proportional to the concentration of tartrate, regardless of the pH. Since the presence of such buffering agents as barbiturate, *p*-hydroxybenzoate and azide (except glycine) does not affect the k value, the replacement of co-ordinated water by tartrate could play an important role in exchange the mechanisms.

$$[^*InZ\cdot OH_2] + tart^{2-} \rightleftarrows [^*InZ\cdot tart]^{2-} + H_2O$$

(equilibrium to form a mixed complex)

If such species underwent isotopic exchange with uncomplexed indium at a measurable rate, the kinetics would be satisfactorily accounted for.

$$[^*InZ\cdot tart]^{2-} + [In\cdot tart_x]^n \overset{\text{slow}}{\underset{\text{fast}}{\rightleftarrows}} [InZ\cdot tart]^{2-} + [^*In\cdot tart_x]^n$$

Generally co-ordinated hydroxide ions are replaced by other ligands with much more difficulty than co-ordinated water, so that the formation of the tartrate complex $[^*InZ\cdot tart]^{2-}$ from the hydroxo complex would not be significant. Hence, the correction of the observed k values on the basis of the effective b values at pH 5 to 8 (broken lines in Fig. 6) would be legitimate. With rise of the pH value, such a species is overwhelmed by the hydroxo complex $[InZ\cdot OH]^-$, which undergoes isotopic exchange at a greater rate through the mechanism mentioned before. Throughout the whole pH range, barbiturate and *p*-hydroxybenzoate do not seem to participate in the exchange reaction.

Acceleration of the exchange reaction by glycine is also observed in the neutral region from pH 5 to 8. Since the rate is independent of the pH in this region, even in the presence of glycine and most glycine is present in an un-ionized form, the formula $[^*InZ\cdot NH_2CH_2\cdot CO_2H]$ would be feasible as an intermediate.

$$[^*InZ\cdot NH_2CH_2CO_2H] + [In\ tart_x]^n \overset{\text{slow}}{\underset{\text{fast}}{\rightleftarrows}} [InZ\cdot NH_2CH_2CO_2H] + [^*In\cdot tart_x]^n$$

With rise of the pH value, the co-ordinated glycine would lose a proton to give an anionic complex, $[InZ\cdot NH_2CH_2CO_2]^-$, which undergoes isotopic exchange through the formation of the conjugate base at a greater rate, as mentioned before.

As has been discussed in this and the preceding paper, the indium EDTA-OH complex is more labile than the indium EDTA complex, as Table III shows. No such difference was observed between the corresponding gallium complexes,[2] which give kinetics similar to that of the indium EDTA complex. Hence, the lability of the indium EDTA-OH complex is rather exceptional amidst similar complexes.

Summary

1) The kinetics of the isotopic exchange of the indium EDTA-OH complex with uncomplexed indium has been studied in neutral and basic solutions, with ^{114m}In as tracer.

2) The exchange rate is independent of the concentration of uncomplexed indium and proportional to that of the EDTA-OH complex, giving the relationship $R=k\cdot b$.

3) In a basic solution buffered by barbiturate, *p*-hydroxybenzoate, or ammonia, the k

value is proportional to the concentration of hydroxide ions and is little affected by the buffer. The Arrhenius activation energy is 25 kcal. per mol., and a mechanism involving the dissociation of hydroxo complex $[InZ \cdot OH]^-$ as the rate-determining step was postulated. The exchange is accelerated by glycine.

4) In a neutral solution with a pH value below 8, the rate is small but measurable. It is independent of the pH value and is little affected by barbiturate or *p*-hydroxybenzoate, and the activation energy is 19 kcal. per mol. The dissociation of a mixed complex containing tartrate as one of the ligands, $[InZ \cdot C_4H_4O_6]^{2-}$, appears to be the rate-determining step. Glycine accelerates the exchange reaction.

5) The feature of the isotopic exchange of the indium EDTA–OH complex is quite different from that of the EDTA complex; the former seems to be much more labile than the latter and similar gallium complexes.

The authors wish to thank the Ministry of Education for its grant-in-aid.

Institute for Nuclear Study
The University of Tokyo
Tanashi, Tokyo

Magnetic Study of Nitro Group

By S. SRIRAMAN, R. SABESAN and S. SRINIVASAN

(Received April 20, 1963)

Introduction of a substituent group for hydrogen in a benzene ring generally resulted a small but detectable change in various physical constants. But the nature of the effect depended much on the position of the group in the ring, and also on the substituting group itself. When a large group like that of the nitro group is substituted in the benzene ring, such changes are found to be large and detectable. Certain anomalous effects were also noticed by different workers, in the case of nitro group. Abe[1] found that *m*-dinitrobenzene showed the maximum absorption band at shorter wavelengths than nitrobenzene. Such a result was also confirmed by Semba.[2] He also measured the equilibrium constants of isomeric nitroanilines and found that the meta compound had a very high value compared with other two isomers. These differences were attributed to the meta-directing property of the nitro group. The resonance structures of the nitro group was also found to contribute largely to the observed changes in the ultraviolet spectrum. Jatkar and Phansalker[3] from their measurements of dipole moments of the nitro-substituted compounds confirmed that the meta directing inductive effect of the nitro group had a considerable influence on the dipole moment.

Bhatnagar and his collaborators[4] detected a variation in the diamagnetic susceptibility depending on the position of the substituting group in the benzene ring, ortho showing a maximum value. Later Cabrera and Fahlenbrach[5] found that in nitrotoluenes the meta compound had a higher value of χ_M than the other two isomers. French,[6] after studying a large number of compounds, noticed an anomalous effect in the case of nitro-substituted compounds. This anomaly was explained by Baddar and Mikhail[7] and later by Mikhail[8], as arising from the contribution of the quinonoid structures of the nitro group to the normal structure. The contribution of the nitro group to the diamagnetic susceptibility was found to vary from 1.45 to 11.74 by Shah et al.[9] But Sriraman and Sabesan[10] found that the behavior of the nitro group, when substituted in the benzene ring, fell generally in line with the observations made by Mikhail,[8] and no serious irregularities were noticed by them. The large changes reported by Shah et al.[9] could not be explained

1) T. Abe, This Bulletin, **33**, 220 (1960).
2) K. Semba, ibid., **33**, 1640 (1960).
3) S. K. K. Jatkar and V. K. Phansalker, *J. Univ. Poona*, 1962, 22 part II 57.
4) S. S. Bhatnagar et al., *Phil. Mag.*, **10**, 101 (1930); **11**, 914 (1931).
5) B. Cabrena and H. Fahlenbrach, *Z. Physik*, **89**, 682 (1934).
6) C. M. Fench, *Trans. Faraday Soc.*, **41**, 676 (1945).
7) F. G. Baddar and H. Mikhail, *J. Chem. Soc.*, **1949**, 2927.
8) H. Mikhail, *J. Chem. Phys.*, **21**, 1004 (1953).
9) S. M. Shah et al., *Curr. Sci.*, **30**, 455 (1961).
10) S. Sriraman and R. Sabesan, *Trans. Faraday Soc.*, **58**, 1080 (1962).
11) S. R. Rao, *Proc. Ind. Acad. Sci.*, **A1**, 123 (1934).

TABLE I

No.	Substance	Mol. wt.	χ_s	χ_M, Exptl.	χ_M, Calcd.	$\Delta\chi_M$	χ_M	Other values	
1	*o*-Dinitrobenzene	168.11	0.398±0.002	66.91	66.70	+0.21	65.98_6	74.3_{13}	
2	*m*-Dinitrobenzene	168.11	0.424±0.002	71.29	66.70	+4.59	70.53_6	72.8_{13}	
3	*p*-Dinitrobenzene	168.11	0.399±0.002	67.08	66.70	+0.38	68.30_6	70.6_{13}	
4	*o*-Chloronitrobenzene	157.56	0.479±0.001	75.50	75.10	+0.40	80.65_9		
5	*m*-Chloronitrobenzene	157.56	0.490±0.001	77.23	75.10	+2.13	76.07_9	74.70_{14}	
6	*p*-Chloronitrobenzene	157.56	0.474±0.001	74.71	75.10	−0.39	79.54_9		
7	*o*-Nitroanisole	153.13	0.518±0.001	79.30	77.20	+2.10	75.28_9		
8	*p*-Nitroanisole	153.13	0.511±0.002	78.23	77.20	+1.03	79.25_9		
9	*o*-Nitrotoluene	137.13	0.523±0.002	71.69	70.60	+1.09	71.85_5	72.19_9	72.28_7
10	*m*-Nitrotoluene	137.13	0.541±0.002	74.16	70.60	+3.56	72.42_5	72.61_9	72.71_7
11	*p*-Nitrotoluene	137.13	0.527±0.002	72.24	70.60	+1.64	70.89_5	69.87_9	72.06_7
12	*o*-Nitroaniline	138.12	0.482±0.002	66.56	67.30	−0.74	68.42_7	66.475_8	66.37_8
13	*m*-Nitroaniline	138.12	0.506±0.001	69.88	67.30	+2.58	68.96_7	70.19_8	67.76_9
14	*p*-Nitroaniline	138.12	0.479±0.002	66.15	67.30	−1.15	66.82_7	60.425_8	66.24_9
15	*o*-Nitrophenol	139.11	0.491±0.002	68.29	65.40	+2.89	70.20_9		
16	*m*-Nitrophenol	139.11	0.498±0.002	69.26	65.40	+3.86	65.60_9		
17	*p*-Nitrophenol	139.11	0.486±0.002	67.59	65.40	+2.19	63.39_9	67.00_{14}	

TABLE II

No.	Substance	Formula	Neutralization of ions*	χ_M Exptl.	$(\chi_M - NO_2)$ Calcd.	Contribution $(NO_2)^{1+}$
1	*o*-Dinitrobenzene	$C_6H_4\cdot NO_2\cdot NO_2$	$B^{2-}1,2+2(NO_2)^{1+}$	66.91	54.80	6.06
2	*m*-Dinitrobenzene	$C_6H_4\cdot NO_2\cdot NO_2$	$B^{2-}1,3+2(NO_2)^{1+}$	71.29	54.80	8.25
3	*p*-Dinitrobenzene	$C_6H_4\cdot NO_2\cdot NO_2$	$B^{2-}1,4+2(NO_2)^{1+}$	67.08	54.80	6.14
4	*o*-Chloronitrobenzene	$C_6H_4\cdot Cl\cdot NO_2$	$B^{2-}1,2+Cl^{1+}+(NO_2)^{1+}$	75.50	68.99	6.51
5	*m*-Chloronitrobenzene	$C_6H_4\cdot Cl\cdot NO_2$	$B^{2-}1,3+Cl^{1+}+(NO_2)^{1+}$	77.23	68.99	8.24
6	*p*-Chloronitrobenzene	$C_6H_4\cdot Cl\cdot NO_2$	$B^{2-}1,4+Cl^{1+}+(NO_2)^{1+}$	74.71	68.99	5.72
7	*o*-Nitroanisole	$C_6H_4\cdot OCH_3\cdot NO_2$	$B^{2+}1,2+(O^{2-}M_1^{1+})^{1-}+(\theta NO_2)^{1-}$	79.30	71.95	7.35
8	*p*-Nitroanisole	$C_6H_4\cdot OCH_3\cdot NO_2$	$B^{2+}1,4+(O^{2-}M_1^{1+})^{1-}+(\theta NO_2)^{1-}$	78.23	71.95	6.28
9	*o*-Nitrotoluene	$C_6H_4\cdot CH_3\cdot NO_2$	$B^{2-}1,2+M^{1+}+(NO_2)^{1+}$	71.69	66.66	5.03
10	*m*-Nitrotoluene	$C_6H_4\cdot CH_3\cdot NO_2$	$B^{2-}1,3+M^{1+}+(NO_2)^{1+}$	74.16	66.66	7.50
11	*p*-Nitrotoluene	$C_6H_4\cdot CH_3\cdot NO_2$	$B^{2-}1,4+M^{1+}+(NO_2)^{1+}$	72.24	66.66	5.58
12	*o*-Nitrophenol	$C_6H_4\cdot OH\cdot NO_2$	$B^{2+}1,2+(\theta NO_2)^{1-}+OH^{1-}$	68.29	61.17	7.12
13	*m*-Nitrophenol	$C_6H_4\cdot OH\cdot NO_2$	$B^{2+}1,3+(\theta NO_2)^{1-}+OH^{1-}$	69.26	61.17	8.09
14	*p*-Nitrophenol	$C_6H_4\cdot OH\cdot NO_2$	$B^{2+}1,4+(\theta NO_2)^{1-}+OH^{1-}$	67.59	61.17	6.42

* The symbols used in column 4 are based on Yang's[16] paper.

satisfactorily, and therefore it was believed that a careful examination of the diamagnetic contribution of the nitro group, taking some more compounds also, might be of interest.

Experimental

The investigations were carried out with a Curie balance.[11] A. R. benzene dried over sodium and distilled over phosphorus pentoxide was used as standard. Its specific susceptibility was taken as -0.702×10^{-6} units. Liquids and solids were purified by standard methods and the purification was continued till specimens of constant susceptibility were obtained. The purified substance was filled in thin-walled glass bulbs, the remaining portion of the bulb being completely evacuated. The solids are powdered and then filled up in the bulb to eliminate orientation effects.

Results

Magnetic susceptibilities of seventeen substances are given in Table I. The observed values are the mean of eight very closely agreeing values, the maximum deviation being shown in the same table. The last column refers to the χ_M values recorded by other workers and is given for the sake of comparison. The theoretical values were calculated by taking atomic and bond values as given by Ingold.[12]

Discussion

In all the nitro compounds studied it is seen that in all cases the meta compound has a higher χ_M value than the other two isomers. Such a result is normally expected as already explained by Sriraman and Sabesan[10]. Also the difference between the experimental values of χ_M and theoretically calculated values are less than two units in most cases and for only a few compounds $\Delta\chi_M$ exceeds three units. This definitely shows that there is no large irregularity in the behavior of the nitrosubstituted compounds and these small differences are explicable by taking into account the inductive and resonance effects[10].

The Contribution of the Group $(NO_2)^{1+}$.— Sriraman and Shanmugasundaram[15] calculated the contribution of the $(NH_2)^{1+}$ value to the diamagnetic susceptibility by treating the shared electrons of the covalent bond as ionic as suggested by Yang[16]. A similar attempt is made to calculate the contribution of $(NO_2)^{1+}$ by taking Angus' modified ionic value[17].

It has been found that the contribution of $(NO_2)^{1+}$ group to the diamagnetic susceptibility, when substituted in the meta position is about eight units and the average contribution is 6.7 units. The atomic contribution of nitro group in organic nitrates was found to be 5.6 by Voiget[18] but in organic nitro compounds he obtained a value of 8.7 units. But the present value of 6.7 units (on the average) for $(NO_2)^{1+}$ is in accordance with the value given by Yang[16] (6.57 units).

The χ_M value of CH_2 when it combined with O^{2-} was taken by Yang as 10.78 units. It is worthy to note that in our present investigation, (χ_M nitroanisole $-\chi_M$ nitrophenol) in ortho and para isomeric compounds are 11.01 and 10.64 respectively, making an average of 10.83, a value very similar to the one obtained by Yang. This arguement cannot be substantiated at this stage until more work is done in this direction.

Summary

The magnetic susceptibilities of several disubstituted aromatic nitro compounds were determined by Curie retorsion method. The contribution of the $(NO_2)^{1+}$ to the diamagnetic susceptibility was evaluated by the method suggested by Yang, taking Angus' modified ionic values.

Department of Physics
Annamalai University
Annamalainager, South India

12) C. K. Ingold, "Structure and Mechanism in Organic Chemistry," Cornell University Press, New York (1953), p. 193.
13) K. Kido, *Sci. Rep. Tohoku. Imp. Univ.*, 24, 701 (1936).
14) A. Bose, *Phil. Mag.*, 21, 1119 (1936).
15) S. Sriraman and D. Shanmugasundaram, This Bulletin, 36, 547 (1963).
16) Tai-Yuan Yang, *J. Chem. Phys.*, **16**, 865 (1948).
17) W. R. Angus, *Proc. Roy. Soc.*, **A136**, 569 (1932).
18) D. Voiget, *Ann. Chim.*, **12**, 393 (1949).

The Crystal Structure of trans-Dichloro-bisethylenediamine-cobalt(III) Nitrate, $[Co\,en_2\,Cl_2]NO_3$

By Shun'ichiro Ooi and Hisao Kuroya

(Received April 1, 1963)

In the last decade, we have carried out the X-ray crystallographic determination of the structures of various *trans*-dihalogeno-bisethylenediaminemetal(III) complexes ("ethylenediamine-praseo salts") having the general formula $[M\,en_2\,X_2]\,Y$, where M is Co or Cr, and X is Cl or Br.[1-3] It has thus been proved that the complex ion is of the centrosymmetrical configuration; namely, i) the two halogen atoms are coordinated to the central metal ion, M, definitely in the trans positions; ii) the ethylenediamine molecule is of the puckered or "gauche-type" structure, which possesses only a two-fold axis of rotation in symmetry, giving a molecular disymmetry to the ligand molecule fixed to M, while, however, iii) the two ethylenediamine molecules are constantly present in the form of an enantiomorphric pair. With the purpose of seeing if any structual changes may be brought to the complex ion in the case of the replacement of Y by the nitrate ion, an attempt has now been made to determine the crystal structure of ethylenediamine-praseo nitrate, $[Co\,en_2\,Cl_2]\,NO_3$. It is well-known that this compound is one of the few slightly soluble nitrates. We have been interested also in this peculiarity.

Experimental

The crystals of $[Co\,en_2\,Cl_2]\,NO_3$ were obtained by slowly adding a dilute solution of nitric acid to an aqueous solution of $[Co\,en_2\,Cl_2]\,Cl\cdot HCl\cdot 2H_2O$. These crystals are green scale-like tablets and are slightly soluble in water. They belong to the monoclinic system, and the unit cell dimensions were found to be:

$a=6.33$ Å, $b=9.25$ Å, $c=10.62$ Å, $\beta=114.5$

The space group was determined to be $P2_1/c$ from the systematic extinctions. The unit cell contains two formula units ($\rho_{obs}=1.75$ and $\rho_{calcd}=1.72$ g. cm^{-3}). Ni$K\alpha$ radiation (1.659 Å) was used, and a multiple film technique was employed in taking Weissenberg photographs about the principal axes. All intensities were measured visually by comparison with a standard scale. The usual correction factors were applied to the observed intensities, and a set of relative $|F_o|$ values was obtained.

Determination of the Structure

In the determination of the structure, $(h\,0\,l)$ and $(0\,k\,l)$ reflections on the Weissenberg photographs were used. As the unit cell contains two formula units, the cobalt atoms and the nitrogen atoms of the nitrate ions must occupy two among the four sets of two-fold special positions, all having point symmetry $\bar{1}$; the cobalt atoms may therefore be placed arbitrarily at the sets of (0 0 0) and (0 1/2 1/2). On the other hand, the nitrate ions are to be located centrosymmetrically on one of the other three sets; in short, a nitrate ion should be in some disordered arrangement, the central nitrogen atom lying on or around the special position referred to above, since the ion has no center of symmetry in its well-known, normal form. Similar disordered structures of the nitrate ion were found in the crystals of bis(glutaronitrilo) and bis(adiponitrilo)copper(I) nitrates and in bis(dimethylglyoximato)-diamminecobalt(III) nitrate.[4-6]

The Patterson projections, $P(UW)$ and $P(VW)$, gave fairly simple patterns, and the approximate position of the chlorine atom could be derived without any trouble. Then, on the basis of the coordinates of cobalt and chlorine atoms only, the structure amplitudes were calculated; in turn, these were found rather consistent with the observed values. Consequently, the signs of all but weak reflections were assumed to be available. From the first Fourier projections, $\rho(XZ)$ and $\rho(YZ)$, we could obtain the approximate position of the ethylenediamine molecule, but not that of the nitrate ion. At this stage, our attempt to pack together the complex cations and nitrate anions, with a view of the $\rho(YZ)$, led us to

1) A. Nakahara, Y. Saito and H. Kuroya, This Bulletin, 25, 331 (1952).
2) S. Ooi, Y. Komiyama, Y. Saito and H. Kuroya, ibid., 32, 263 (1959).
3) S. Ooi, Y. Komiyama and H. Kuroya, ibid., 33, 354 (1960).
4) Y. Kinoshita, I. Matsubara and Y. Saito, ibid., 32, 1216 (1959).
5) Y. Kinoshita, I. Matsubara, T. Higuchi and Y. Saito, ibid., 32, 1221 (1959).
6) K. S. Viswanathan and N. R. Kunchur, *Acta Cryst.*, 14, 675 (1961).

the deduction that the center of the nitrate ion lies close to (0 1/2 0).

Fourier refinements were made as usual. In the case of the a-axis projection, residual electron density due to other components than the complex ion gave a diffuse peak around (X 1/2 0). On the other hand, in the case of the b-axis projection, the residual electron density showed up as a peak around (0 Y 0); however, because of the overlapping of the nitrate ion with the complex ion, the exact coordinates of the nitrate ion could not be elucidated from the Fourier peak.

Taking account of the shape of peak around (X 1/2 0) in the a-axis projection, a model of the disordered structure of the nitrate ion was presented; in this model the ion occupies two different positions in the neighborhood of (0 1/2 0), each of them having a weight of one-half, as shown in Figs. 1, 2 and 3; in these figures, the positions of the two nitrate ions of different orientations are indicated by the

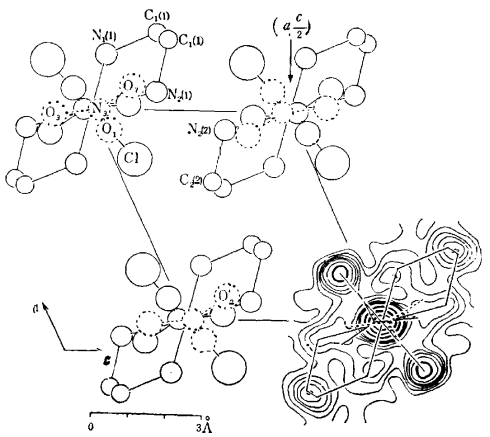

Fig. 1. Structure and electron density projected along b-axis. Contours are drawn at intervals of 2 and 10 e. Å^{-2}, starting at two and twenty electron levels for thin and thick lines, respectively.

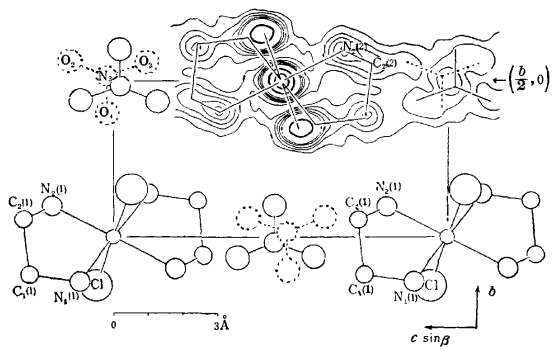

Fig. 2. Structure and electron density projected along a-axis. Contours are drawn in the same manner as Fig. 1.

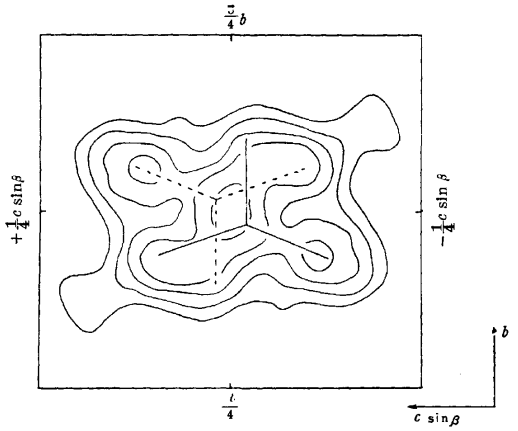

Fig. 3. Residual electron density due to a disordered structure of the nitrate ion projected along a-axis. Contours are drawn at intervals of 1 e. Å^{-2}, starting at two electron level.

dotted and full lines, being related by $\bar{1}$ to one another. Thus, the nitrate ion may take up one of these positions in an asymmetric unit, while the equivalent or the opposite position in any other asymmetric unit may be assumed with quite equal probability; the probability of finding one orientation of the nitrate ion in an asymmetric unit is equal to that of finding another. No unreasonable interatomic distances have been detected in this structure. Possibly, there might be another plausible model which could account for the peak mentioned above. However, no further study was attempted, since the object of the present work was mainly to study the stereochemical configuration of the complex ion.

Table I. Atomic coordinates

Atom	x/a	y/b	z/c
Co	0	0	0
Cl	−0.235	−0.149	0.052
N_1	0.260	−0.133	0.100
N_2	0.083	0.096	0.183
C_1	0.358	−0.112	0.250
C_2	0.322	0.055	0.270
N_3	0.000	0.508	0.017
O_1	−0.100	0.399	0.021
O_2	0.110	0.563	0.129
O_3	−0.023	0.562	−0.096

The atomic coordinates are given in Table I; they gave reliability indices of 0.157 and 0.148 for (0 k l) and (h 0 l) respectively, with the exception of the (1 0 0) reflection, which would be influenced critically by, for instance, extinction effect. Isotropic temperature factors, 4.0 Å^2 for (0 k l) and 3.5 Å^2 for (h 0 l), were used in usual manner.

TABLE II. OBSERVED AND CALCULATED STRUCTURE FACTORS

h	k	l	F_o	F_c	h	k	l	F_o	F_c	h	k	l	F_o	F_c	h	k	l	F_o	F_c
0	0	2	70.8	78.0	2	0	$\bar{12}$	11.6	13.2	0	9	1	6.4	5.2	0	8	5	4.4	− 4.8
0	0	4	54.0	54.0	3	0	$\bar{2}$	26.4	40.0	0	10	1	4.4	− 4.0	0	9	5	5.6	4.8
0	0	6	< 1.8	6.4	3	0	$\bar{4}$	55.6	52.8	0	1	2	30.8	−33.6	0	1	6	10.0	−10.4
0	0	8	6.0	10.8	3	0	$\bar{6}$	43.6	37.2	0	2	2	20.0	27.2	0	2	6	18.8	24.4
0	0	10	< 2.1	2.0	3	0	$\bar{8}$	47.6	42.0	0	3	2	10.8	− 6.0	0	3	6	< 1.9	2.0
1	0	0	70.8	103.2	3	0	$\bar{10}$	9.2	10.8	0	4	2	21.2	19.6	0	4	6	25.6	28.8
1	0	2	70.4	72.8	3	0	$\bar{12}$	5.2	6.4	0	5	2	25.6	23.2	0	5	6	10.0	11.6
1	0	4	41.6	50.0	4	0	$\bar{2}$	71.2	74.0	0	6	2	53.2	44.0	0	6	6	8.4	8.8
1	0	6	57.6	62.8	4	0	$\bar{4}$	25.2	23.6	0	7	2	5.2	− 6.0	0	7	6	8.4	− 7.6
1	0	8	14.0	20.0	4	0	$\bar{6}$	9.2	10.4	0	8	2	24.4	20.0	0	8	6	4.4	7.2
1	0	10	12.4	13.2	4	0	$\bar{8}$	4.8	2.8	0	9	2	13.2	−10.4	0	9	6	7.2	− 6.4
2	0	0	16.4	− 0.4	4	0	$\bar{10}$	< 2.4	1.2	0	10	2	> 1.8	1.2	0	1	7	3.2	5.2
2	0	2	8.0	3.6	4	0	$\bar{12}$	< 1.5	4.0	0	1	3	30.4	30.0	0	2	7	< 2.1	− 2.8
2	0	4	30.8	36.0	5	0	$\bar{2}$	30.4	27.6	0	2	3	49.6	−55.2	0	3	7	23.6	27.2
2	0	6	29.2	36.0	5	0	$\bar{4}$	4.0	4.4	0	3	3	17.2	18.8	0	4	7	7.2	6.8
2	0	8	19.6	21.0	5	0	$\bar{6}$	4.4	− 3.6	0	4	3	8.8	6.0	0	5	7	10.4	13.2
3	0	0	38.4	47.6	5	0	$\bar{8}$	2.0	− 4.8	0	5	3	34.4	28.0	0	6	7	< 1.9	1.6
3	0	2	13.2	− 7.6	5	0	$\bar{10}$	1.2	5.6	0	6	3	14.0	8.8	0	7	7	< 2.1	0.1
3	0	4	16.0	17.6	6	0	$\bar{2}$	8.8	− 4.8	0	7	3	27.2	18.8	0	8	7	9.2	− 6.8
3	0	6	5.2	− 5.2	6	0	$\bar{4}$	8.0	10.8	0	8	3	16.0	−12.4	0	1	8	2.8	− 1.2
3	0	8	7.2	8.4	6	0	$\bar{6}$	5.6	7.6	0	9	3	1.6	− 1.2	0	2	8	20.0	22.8
4	0	0	42.4	39.2	6	0	$\bar{8}$	20.4	20.4	0	10	3	< 1.6	0.1	0	3	8	4.4	2.4
4	0	2	32.0	30.0	6	0	$\bar{10}$	14.0	12.4	0	1	4	40.0	−38.0	0	4	8	18.8	20.0
4	0	4	4.8	6.8	7	0	$\bar{2}$	7.2	9.2	0	2	4	31.2	36.4	0	5	8	3.2	3.2
4	0	6	< 1.8	2.4	7	0	$\bar{4}$	14.0	13.6	0	3	4	18.8	−14.4	0	6	8	4.0	1.2
5	0	0	15.6	13.6	7	0	$\bar{6}$	20.4	18.4	0	4	4	20.8	22.4	0	7	8	4.0	3.2
5	0	2	26.8	21.2	7	0	$\bar{8}$	23.2	19.6	0	5	4	33.2	29.6	0	1	9	4.0	− 2.8
5	0	4	22.0	18.0	0	2	0	91.2	90.4	0	6	4	22.4	20.8	0	2	9	2.4	− 4.4
6	0	0	< 2.1	0.4	0	4	0	45.2	−30.8	0	7	4	6.8	0.8	0	3	9	12.4	15.2
6	0	2	4.4	3.2	0	6	0	24.8	23.6	0	8	4	10.8	15.2	0	4	9	< 2.2	1.2
1	0	$\bar{2}$	88.8	86.8	0	8	0	25.2	20.0	0	9	4	9.6	− 8.0	0	5	9	6.8	8.4
1	0	$\bar{4}$	13.6	−14.4	0	10	0	< 1.9	0.2	0	10	4	6.4	7.2	0	6	9	2.0	5.2
1	0	$\bar{6}$	< 1.6	2.0	0	1	1	54.4	58.0	0	1	5	18.4	23.6	0	1	10	< 2.1	− 0.8
1	0	$\bar{8}$	< 2.1	0.0	0	2	1	20.4	−18.4	0	2	5	40.8	−42.8	0	2	10	10.4	11.2
1	0	$\bar{10}$	9.6	14.4	0	3	1	42.8	−30.8	0	3	5	23.6	28.8	0	3	10	2.4	− 3.2
2	0	$\bar{2}$	28.4	39.2	0	4	1	31.6	24.4	0	4	5	9.6	8.8	0	4	10	11.6	12.4
2	0	$\bar{4}$	4.8	− 1.2	0	5	1	22.0	21.2	0	5	5	12.0	13.2	0	5	10	2.8	− 3.6
2	0	$\bar{6}$	50.0	48.8	0	6	1	23.2	18.8	0	6	5	22.0	20.0	0	1	11	4.8	6.0
2	0	$\bar{8}$	26.8	24.8	0	7	1	50.0	40.4	0	7	5	1.6	2.0	0	2	11	2.0	2.8
2	0	$\bar{10}$	25.2	27.2	0	8	1	6.4	− 5.2										

Results

The geometry of the complex ion herein determined is not significantly different from those reported before. The cobalt atom is surrounded by the four nitrogen atoms of the two ethylenediamine molecules and the two chlorine atoms at the trans-position, forming an octahedral configuration elongated in the Cl–Co–Cl direction. The two ethylenediamine molecules are of the gauche type and are enantiomorphous with one another. The ion has the approximate symmetry of C_{2h}, the two-fold axis of which passes through the central metal atom and bisects the C–C bonds of the ethylenediamine molecules coordinated.

The interatomic distances and bond angles are listed in Table III. The bond length of Co–Cl, 2.26 Å, is a little shorter than the value, 2.33 Å, found in $[Co\,en_2\,Cl_2]\,Cl\cdot HCl\cdot 2H_2O$[1] and $[Co(NH_3)_3H_2O\,Cl_2]\,Cl$,[7] but it ts comparable to that of 2.27 Å in $[Co(NH_3)_5Cl]\,Cl_2$[8] and that of 2.29 Å in $[Co\,pn_2\,Cl_2]\,Cl\cdot HCl\cdot 2H_2O$.[9] The nitrate ion appears to deviate

7) Y. Tanito, Y. Saito and H. Kuroya, This Bulletin, 25, 328 (1952).
8) Y. Komiyama, Y. Shigeta and H. Kuroya, Presented at the 14th Annual Meeting of the Chemical Society of Japan, Tokyo, April, 1961.
9) Y. Saito and H. Iwasaki, This Bulletin, 35, 1131 (1962).

Table III. Interatomic distances and bond angles

Co–Cl	2.26 Å
Co–N_1	1.99 Å
Co–N_2	2.00 Å
N_1–C_1	1.46 Å
N_2–C_2	1.46 Å
C_1–C_2	1.59 Å
N_3–O_1	1.20 Å
N_3–O_2	1.21 Å
N_3–O_3	1.25 Å
$O_1 \cdots N_1$ (1)	2.77 Å
$O_2 \cdots N_1$ (1)	3.02 Å
$O_2 \cdots N_2$ (2)	2.76 Å
$O_3 \cdots N_2$ (2)	3.07 Å
$O_2 \cdots C_2$ (2)	3.33 Å
$O_2' \cdots C_2$ (2)	3.30 Å
Co–N_1–C_1	112.0°
Co–N_2–C_2	106.7°
N_1–C_1–C_2	104.8°
N_2–C_2–C_1	109.7°
N_1–Co–N_2	85.6°
O_1–N_3–O_2	114.6°
O_2–N_3–O_3	124.3°
O_1–N_3–O_3	121.0°

from D_{3h} symmetry, but our measurements are not accurate enough for the shape of the ion to be discussed in detail. The short distances, 2.77, 2.76, 3.02 and 3.07 Å, between the oxygen atoms of the nitrate ion and the nitrogen atoms of the ethylenediamine molecules may be indicative of the presence of hydrogen bonds of the N–H···O type between them.

Recently, a new type of coordination of the ethylenediamine molecule was reported on the crystal of [Hg en Cl_2],[10] where the ethylenediamine molecule is coordinatively bound to two different Hg atoms with its $-NH_2$ radicals in the trans form, thereby forming a $(-Hg-en-)_\infty$ chain, to which the insolubility of this compound in water and alcohol could more or less be attributed. However, as is evident from the findings presented above, no remarkable structual peculiarity to which the slight solubility of the ethylenediamine-praseo nitrate would be even partially due, was found in the present work.

Summary

The crystal structure of *trans*-[Co en_2 Cl_2] · NO_3 has been determined by means of X-ray analysis. The space group is $P2_1/c$ with two formula units in a cell of the dimensions of $a=6.33$ Å, $b=9.25$ Å, $c=10.62$ Å, and $\beta=114.5°$. The crystal is composed of [Co en_2 Cl_2]$^+$ and NO_3^-. The geometry of the complex ion herein determined is not significantly different from those reported before. It has been proposed that the nitrate ion is in a disordered arrangement.

Part of the cost of this investigation was defrayed from the Fund for Scientific Research Expenditure of the Ministry of Education, to which the authors' thanks are due.

Faculty of Science
Osaka City University
Sumiyoshi-ku, Osaka

10) K. Brodersen, *Z. anorg. u. allgem. Chem.*, **298**, 142 (1959).

*The Crystal Structure of Tetramethylenediammonium Chloride**

By Tamaichi ASHIDA and Sakutaro HIROKAWA

(Received May 11, 1963)

There have been fewer published structural investigations of tetramethylenediamine (TDA) in the crystals than of the homologous compounds, ethylenediamine (EDA)[1-5] and hexamethylenediamine,[6-8] both of which are the nearest to TDA in the even-membered series of polymethylenediamines. Recently, the present authors reported a gauche-form of the TDA ion in the crystal of its adipate,[9,10]

* Presented at the 16th Annual Meeting of the Chemical Society of Japan, Tokyo, March, 1963.

1) T. Ashida and S. Hirokawa, This Bulletin, **36**, 704 (1963).
2) A. Nakahara, Y. Saito and H. Kuroya, ibid., **25**, 331 (1952).
3) S. Ooi, Y. Komiyama and H. Kuroya, ibid., **33**, 354 (1960).
4) Y. Okaya and I. Nitta, *Acta Cryst.*, **5**, 564 (1952).
5) K. Sakurai, *J. Phys. Soc. Japan*, **16**, 1205 (1961).
6) W. P. Binnie and J. M. Robertson, *Acta Cryst.*, **2**, 180 (1949).
7) W. P. Binnie and J. M. Robertson, ibid., **3**, 424 (1950).
8) S. Hirokawa, T. Ohashi and I. Nitta, ibid., **7**, 87 (1954).
9) S. Hirokawa and T. Ashida, ibid., **14**, 1004 (1961).
10) S. Hirokawa and T. Ashida, *Memoirs of the Defense Academy*, Vol. II, No. 3, 95 (1962).

though they had expected a planar (trans-) configuration of the ion. Although no investigations so far published have shown the planar configuration of TDA in the crystals, a planar configuration as the cases of EDA[1] and hexamethylenediamine[6-8] may be expected for TDA. Thus, a trans-gauche stereoisomerism like that of EDA is possible for TDA. Tetramethylenediammonium chloride (TDA · Cl) was chosen to be studied in order to elucidate this aspect of the problem. The structural analysis of TDA·Cl may be interesting because the crystal structures of both ethylenediammonium chloride (EDA·Cl)[1] and hexamethylenediammonium chloride[6] have been reported. The present study will show a crystal structure analogous to that of EDA·Cl, and some comparisons between the present crystal and that of EDA·Cl will be made.

Experimental

Tetramethylenediammonium chloride, $H_3N(CH_2)_4NH_3 \cdot 2Cl$, was obtained as white precipitates from ethanol solutions of the components in a stoichiometric molar ratio. The crystals were grown from ethanol-water solutions. The three principal axes of the crystals were designated by referring to those of EDA·Cl.[1] Some of these crystals were obtained as needles elongated along the b-axis, and others, as plates, the main face being (1 0 0). A perfect cleavage perpendicular to the c-axis was found. The crystal belongs to the monoclinic system, and the unit cell dimensions were obtained from the Weissenberg photographs of $(h\,0\,l)$ and $(h\,k\,0)$ by overlapping the powder patterns of aluminum as a standard; they are:

$a=10.73\pm0.01$ Å $\quad b=8.35\pm0.01$ Å

$c=4.60\pm0.01$ Å $\quad \beta=92.5\pm0.3°$

The space group was found to be $P2_1/a$ from the systematic absences of the following spectra: $(0\,k\,0)$ for $k=2n+1$, and $(h\,0\,l)$ for $h=2n+1$. The density, 1.30 g.cm^{-3}, observed by the flotation method corresponds to two formula units in a unit cell; the calculated density is 1.30 g.cm^{-3}.

Weissenberg photographs were taken around the b- and c-axes using CuK_α radiation. The multiple-film technique was used, and the intensities of $(h\,0\,l)$, $(h\,k\,0)$ and a part of the $(h\,k\,1)$ reflections were estimated visually, comparing them with a standard scale. Corrections for polarization and Lorentz factors were made. The linear absorption coefficient of the crystal for CuK_α is rather large ($\mu=64.0$ cm^{-1}). However, the shapes of the crystals used in the experiments were irregular, and no absorption corrections were made.

Structure Determination

Since the crystal belongs to the $P2_1/a$ space group and since the number of formula units in the unit cell is two, the TDA ion has to occupy a center of symmetry of the unit cell. The position of the chloride ion was determined from the projections of the Patterson function along the b- and c-axes. The projections of the electron-density functions along the two principal axes were synthesized by using the structure factors whose phases were assigned by the coordinates of the chloride ion. The maps thus obtained showed the positions of the carbon and nitrogen atoms. The coordinates of the atoms were then refined by successive (F_o-F_c) syntheses. In the course of these refinements, it was found that the contributions of the hydrogen atoms to the structure factors were not negligible; the number of electrons which belong to the hydrogen atoms amount to 16% of the total number of electrons in the crystal. Then, the coordinates of all the hydrogen atoms were calculated geometrically, using the coordinates of the heavier atoms, and these calculations were confirmed on the $(\rho_o-\rho_c)$ maps. These hydrogen atoms were used in the further refinements of the structures, and the *R* factors of the two zones decreased by about 0.02. In these procedures, it was found that if the hydrogen atoms lying near the heavier atoms were disregarded, the coordinates of the heavier atoms cannot be improved by (F_o-F_c) syntheses. In fact, significant shifts in the positions of the atoms, especially carbon and nitrogen, were observed when the hydrogen atoms were included in the calculations. The

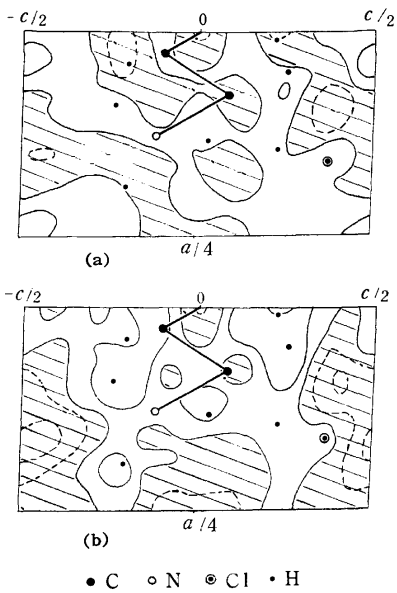

Fig. 1. Final $(\rho_o-\rho_c)$ projected on (0 1 0). (a): ρ_c includes all the atoms; (b): ρ_c does not include any hydrogen atoms. Contours at intervals of 0.4 e. Å^{-2}, broken lines represent negative contours, and negative areas are shaded.

final $(\rho_o-\rho_c)$ maps of $(h\,0\,l)$ are shown in Fig. 1, where significant changes due to the inclusion or exclusion of the hydrogen atoms are observed, not only at the positions of the hydrogen atoms but almost everywhere.

The final atomic coordinates and the temperature factors of the heavier atoms are listed in Table I. Each absolute value of the temperature factors listed in Table I may not have a rigid meaning, however, because no absorption corrections for the intensities were made. The comparisons between the observed and calculated structure factors are shown in Table II. The final R factors are 0.058 and 0.075 respectively for $(h\,0\,l)$ and $(h\,k\,0)$, excluding a few reflections which showed marked

TABLE I. FINAL ATOMIC COORDINATES AND TEMPERATURE FACTORS (Å²)

	x	y	z	B*	B**
C(1)	0.076	0.204	0.079	1.60	1.70
C(2)	0.025	0.063	0.903	2.45	1.70
N	0.126	0.331	0.885	2.35	1.70
Cl^-	0.158	0.600	0.375	1.85	1.70

* Temperature factors obtained for $(h\,0\,l)$.
** Temperature factors obtained for $(h\,k\,0)$.

TABLE II. OBSERVED AND CALCULATED STRUCTURE FACTORS

In each column, the left hand column is the h index, the middle column the observed structure factor, and the right hand column, the calculated structure factor. All structure factors have been multiplied by ten.

$(h\,0\,l)$			0	135	133	8	0	24	5	0	21	0	178	−175	3	62	70
$h\,0\,0$			2	257	−254	10	179	−190	6	130	−116	1	96	102	4	108	103
2	116	124	4	11	1	12	124	109	7	176	180	2	42	52	5	88	−96
4	402	−434	6	166	157	$h\,1\,0$			8	175	158	3	56	−62	6	0	34
6	293	307	8	112	−110	1	107	−100	9	0	−4	4	0	24	7	78	−87
8	0	11	10	57	54	2	125	−126	10	148	−162	5	223	−210	$h,10,0$		
10	184	−186	−2	46	56	3*	410	643	11	50	−59	6	213	−196	0	141	135
12	107	114	−4	224	−214	4	313	−331	12	133	−130	7	37	45	1	0	−22
$h\,0\,1$			−6	121	118	5	0	8	13	0	−13	8	51	51	2	62	−62
0	138	147	−8	19	22	6	0	−16	$h\,4\,0$			9	60	54	3	27	−20
2	144	140	−10	257	−259	7	238	−219	0	305	−324	10	101	104	4	104	−104
4	278	315	−12	8	−1	8	165	163	1	248	−238	11	79	−71			
6	204	−199	$h\,0\,4$			9	163	154	2	150	146	$h\,7\,0$			$(h\,k\,1)$**		
8	107	−97	0	318	−327	10	80	−82	3	62	−60	1	83	−72	$h\,1\,1$		
10	275	269	2	21	22	11	0	27	4	227	223	2	293	−292	0	322	330
12	17	−1	4	129	135	12	55	−48	5	204	214	3	119	−107	3	105	−103
−2*	370	642	6	186	−169	13	126	−100	6	249	−232	4	119	118	4	161	−168
−4	107	−82	8	28	24	$h\,2\,0$			7	126	−112	5	37	33	5	0	−18
−6	276	−277	−2	59	69	0	20	7	8	0	−25	6	82	81	6	261	253
−8	191	184	−4	191	196	1	302	−367	9	171	−182	7	48	49	7	267	282
−10	26	−31	−6	190	−173	2	37	−29	10	150	130	8	163	−164	$h\,2\,1$		
−12	196	−191	−8	61	−52	3	75	−57	11	0	1	9	42	−42	0	217	−217
$h\,0\,2$			−10	65	61	4	72	73	12	79	−65	10	31	29	$h\,3\,1$		
0	57	54	$h\,0\,5$			5	210	189	$h\,5\,0$			$h\,8\,0$			0	372	404
2*	376	488	0	0	14	6	174	174	1	186	184	0	52	−52	$h\,4\,1$		
4	286	−281	2	36	−25	7	259	−246	2	59	48	1	190	207	0	236	196
6	153	−152	4	160	−151	8	0	9	3	291	−276	2	69	−86	−1	0	25
8	290	281	6	68	72	9	79	−66	4	62	−45	3	89	88	−2	229	−188
10	16	23	−2	173	−167	10	52	−56	5	0	30	4	0	−34	−3	136	−137
12	39	−33	−4	44	47	11	182	191	6	103	−106	5	165	−172	−4	50	55
−2	378	−412	−6	118	124	12	31	26	7	92	94	6	31	50	$h\,5\,1$		
−4	289	264				13	84	−87	8	37	−38	7	67	60	0	0	−14
−6	115	104	$(h\,k\,0)$			$h\,3\,0$			9	193	−206	8	0	−19			
−8	318	−319	$h\,0\,0$			1	196	190	10	0	4	9	42	51			
−10	25	−26	2	110	124	2	377	414	11	0	26	$h\,9\,0$					
−12	54	53	4	371	−420	3	224	−187	12	0	−28	1	52	−65			
$h\,0\,3$			6	313	315	4	257	−249	$h\,6\,0$			2	46	−54			

* These reflections were not used for the refinements because of their marked extinction effects.
** These reflections were not used for the refinements, and do not include contributions of the hydrogen atoms.

extinction effects (these are shown with asterisks in Table II).

Discussion of the Results

Some of the important interatomic distances and bond angles in this crystal are shown in Table III and in Fig. 2. Because the TDA ion

TABLE III. IMPORTANT INTERATOMIC DISTANCES (Å) AND ANGLES (deg.)

C(2)-C(2')	1.50	C(2')C(2)C(1)	110.0
C(2)-C(1)	1.52	C(2)C(1)N	110.0
C(1)-N	1.50		
		C(1)NCl(1)	96.2
N-Cl(1)	3.19	C(1)NCl(2)	89.3
N-Cl(2)	3.28	C(1)NCl(3)	94.7
N-Cl(3)	3.28	Cl(1)NCl(2)	101.7
		Cl(1)NCl(3)	127.0
N-Cl(4)	3.28	Cl(2)NCl(3)	129.1
		C(1)NCl(4)	164.4

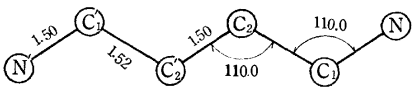

Fig. 2. Dimensions of TDA ion.

occupies a center of symmetry, the four carbon atoms are completely coplanar. The terminal N atoms are also in the plane and join with the carbon atoms to make a coplanar zigzag chain; the displacement of the N atom from the plane of the four carbon atoms is found to be less than 0.001 Å. Thus, in the crystals, the TDA ion was found to have either a trans- or gauche-configuration, depending on the structures of the crystals.

The crystal structure projected on the (001) and the (0 1 0) planes is shown in Figs. 3 and 4. The nitrogen atom has four nearest neighbors among the chloride ions (Cl(1), Cl(2), Cl(3) and Cl(4) in Figs. 3 and 4), the N-Cl distances being 3.19, 3.28, 3.28 and 3.28Å respectively. Such N-Cl lengths are comparable to the values of 3.10~3.30Å found in EDA·Cl,[10] hexamethylenediammonium chloride[6] and several other crystals.[11,12] These four short contacts correspond to the N-H···Cl hydrogen bond distance. However, three of these four contacts, excluding the 'bifurcated' type, may be hydrogen bonds. The C(1)-N-Cl(4) angle (164.4°) is so large that N-Cl(4) may be excluded. The $(\rho_o-\rho_c)$ maps seem to support this view. In the $(\rho_o-\rho_c)$ projected on the

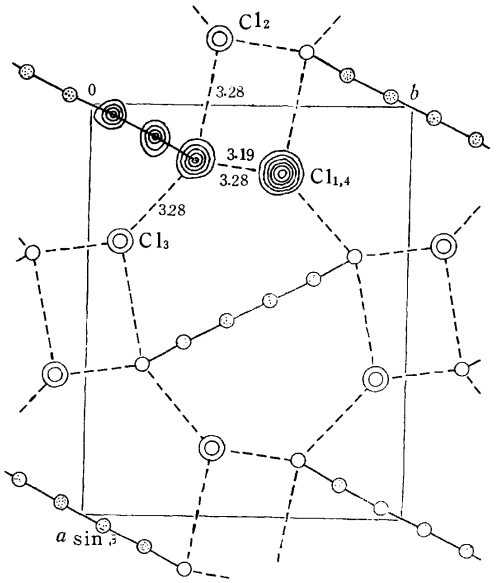

Fig. 3. The structure of TDA·Cl projected on (0 0 1). Broken lines represent hydrogen bonds. In a part of the electron-density function, contours are drawn at an arbitrary equal interval, except at Cl^-, where an interval is three times of that for lighter atoms.

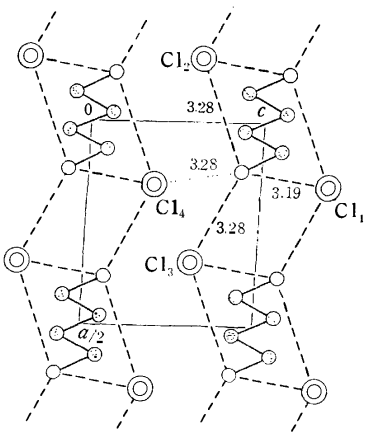

Fig. 4. The structure of TDA·Cl projected on (0 1 0). Broken lines represent hydrogen bonds. A dotted line shows another short contact between N and Cl^-.

(0 0 1) plane, Cl(1) and Cl(4) occupy the same position, and hydrogen atoms were found around the nitrogen atom pointing to Cl(1) or Cl(4), Cl(2) and Cl(3) respectively. On

11) G. C. Pimentel and A. L. McClellan, "The Hydrogen Bond," W. H. Freeman and Co., San Francisco (1960), p. 290.
12) W. Fuller, *J. Phys. Chem.*, **63**, 1705 (1959).

the other hand, in the $(\rho_o - \rho_c)$ maps shown in Fig. 1, no hydrogen atom can be found between N and Cl(4), although in the three other short contacts hydrogen atoms are found to be present. Thus, Cl(1), Cl(2) and Cl(3) are considered as being hydrogen-bonded from the nitrogen atom. Another short contact between N and Cl(4) may be ionic in character; similar short contacts which are not hydrogen bonds have been reported in triazolo-pyrimidine hydrochloride, 3.29 and 3.31 Å.[13] Thus, in this crystal, the three N-H···Cl hydrogen bonds link the organic ions and the chloride ions and make two-dimensional, infinite networks parallel to the (0 0 1) plane. The forces which combine these layers along the c-axis may be van der Waals forces, together with electrostatic forces, if any. These facts explain the perfect cleavage parallel to the (0 0 1) plane.

A Comparison between TDA·Cl and EDA·Cl. —It may be worthwhile to make some comparisons between the structure of this crystal and that of EDA·Cl.[1] The similarity between these two crystals may be interesting if we consider the differences in the dimensions of the organic ions in the two crystals. There are considerable differences between the crystal structure of TDA·Cl and that of hexamethylenediammonium chloide, though the dimensions of the two organic ions differ from each other in just the same way as has been described above.

TABLE IV. CRYSTALLOGRAPHIC DATA OF EDA · Cl AND TDA · Cl

	EDA·Cl	TDA·Cl
a	9.95 Å	10.73 Å
b	6.89 Å	8.35 Å
c	4.42 Å	4.60 Å
β	90.7°	92.5°
Space group	$P2_1/a$	
Z	2	
Symmetry*	Center	
Cleavage**	(0 0 1)	
Needle axis	c	b
Predominant face	(0 0 1)	(1 0 0)

* Symmetry of the organic ion
** Cleavage parallel to

The crystallographic data of both EDA·Cl and TDA·Cl crystals are listed in Table IV. The a- and b-axes of TDA·Cl are a little longer than those of EDA·Cl because of the necessity to accommodate a larger organic ion. Only the crystal habits are different from each other.

The modes of packing of the ions in the crystals or of the hydrogen bonds are said to be, in effect, the same. This was one of the reasons why the possibility of a hydrogen bond between the nitrogen atom and Cl(4) was rejected in the present crystal. These situations may be understood if we compare Figs. 3 and 4 of this paper with Figs. 2 and 3 of the paper on EDA·Cl.[1] In Fig. 3 of this paper, if N is taken out and C(1) is changed to N, the figure thus obtained corresponds roughly to the structure of EDA·Cl projected on the (0 0 1) plane shown in Fig. 2 of Ref. 1. The coordinates of the atoms in both crystals (by Å unit) are listed in Table V for the sake of comparison. The inversions of the signs of the *z*-coordinates of the organic ions are inevitable in order to obtain the same packing. By considering these coordinates of the atoms, the differences in the unit cell dimensions of the two crystals may be elucidated. The equations of the planes of the zigzag chains of the organic ions are:

$$0.901X - 0.434Y + 0.030Z = 0$$

and

$$0.895X - 0.448Y - 0.020Z = 0$$

for TDA·Cl and EDA·Cl respectively, where $X = ax \sin\beta$, $Y = by$, and $Z = cz + ax\cos\beta$. Thus, the orientations of the organic ions to the principal axes are also not very far from each other.

TABLE V. ATOMIC COORDINATES (Å) OF EDA·Cl AND TDA·Cl

		X	*Y*	*Z*
C	EDA	0.259	0.496	0.518
C(2)	TDA	0.270	0.529	−0.458
N	EDA	0.826	1.661	−0.217
C(1)	TDA	0.815	1.705	0.327
N	TDA	1.351	2.762	−0.588
Cl	EDA	1.711	3.996	1.774
Cl	TDA	1.694	5.010	1.651

Summary

The crystal structure of tetramethylenediammonium chloride has been determined by the two-dimensional Fourier method. The crystal belongs to the monoclinic system, with $a=10.73$ Å, $b=8.35$ Å, $c=4.60$ Å and $\beta=92.5°$, and the space group is $P2_1/a$. The tetramethylenediammonium ion has been found to possess a center of symmetry of the unit cell, and the carbon and the nitrogen atoms in the ion, make a coplanar (trans-) zigzag chain. Thus, the tetramethylenediammonium ion has been found to have either a trans- or a gauche-configuration, depending on the structures of the crystals. There are four short approaches

13) P. G. Owston and J. M. Rowe, *Acta Cryst.*, **15**, 231 (1962).

between nitrogen and chloride ions with lengths of 3.19～3.28Å ; three of them have been concluded to be hydrogen bonds. These hydrogen bonds make two-dimensional networks of the ions perpendicular to the c-axis. The structure of this crystal is similar to that of ethylenediammonium chloride, and some comparisons between them have been given.

Department of Chemistry
Defense Academy
Yokosuka

The Effect of Tri-, Tetra-, Penta- and Hexaphosphate on the Crystallization of Strontium Sulfate

By Masaji MIURA, Sadaichi OTANI, Yasuhiro ABE and Chikako FUKUMURA

(Received June 7, 1963)

It is a well-known fact that a very small amount of various condensed phosphates exhibits a striking effect on the stabilization of supersaturated solutions of various inorganic salts, especially those of sparingly soluble calcium salts.[1] In many papers emphasis has been laid on the superior of effect of "hexametaphosphate," a mixture many homologues of polyphosphates, but no work seems to have been done with its individual constituents.

In our previous works,[2,3] the effect of ortho-, pyro-, tri- and trimetaphosphate on the crystallization of strontium sulfate has been investigated in relation to the adsorption of these phosphates on the crystals of strontium sulfate. The purpose of the present work is to study the effect of the higher homologues of polyphosphates, which are the main constituents of the "hexametaphosphate."

Experimental

Radioactive tri-, tetra-, penta- and hexaphosphate were separated by anion-exchange chromatography from a "hexametaphosphate glass" prepared by pyrolysis from a mixture of sodium dihydrogen phosphate and disodium hydrogen phosphate containing ^{32}P.[4] Since these phosphates are gradually hydrolyzed in a solution,[4] all measurements were made with solutions newly prepared and stocked in a cold place. The other reagents used were the same as those used in the previous works.[2,3] The strontium sulfate crystals used as the adsorbent were prepared in a way similar to that used in a previous work,[3] but the crystal size of the product was somewhat larger than that used before.

The effect of the phosphates on the crystallization rate of strontium sulfate was examined by measuring the conductivity decrease in equivalent mixtures of strontium chloride and potassium sulfate solutions containing various amounts of the phosphates. The techniques employed in measuring the conductivity and the adsorption of the phosphates on strontium sulfate have been described in the previous papers.[2,3]

Results and Consideration

The effect of the four kinds of phosphates on the crystallization rate of strontium sulfate is represented by the conductometric data shown in Fig. 1—4. The ordinate of these graphs represents the percentage decrease in the specific conductivity with reference to the total decrease when no phosphate is added.

Figure 5 shows the adsorption isotherms obtained at 25°C and pH 7. This figure shows that the number of moles adsorbed per gram of strontium sulfate decreases with the increase in the chain length of polyphosphate.

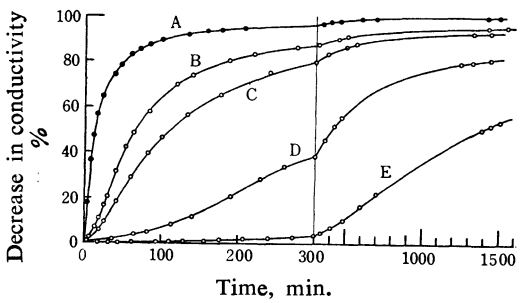

Fig. 1. Decrease in conductivity of 0.01 M $SrSO_4$ solutions containing (A) none, (B) 7×10^{-7}, (C) 1×10^{-6}, (D) 2×10^{-6} and (E) 3×10^{-6} M of triphosphate.

1) L. Rosenstein, U. S. Pat. 2038316 (1936); G. B. Hatch and O. Rice, *Ind. Eng. Chem.*, **31**, 51 (1939); R. F. Reitemeier and T. F. Buehrer, *J. Phys. Chem.*, **44**, 535, 552 (1940); E. J. Burcik, *Producers Monthly*, **19**, 42 (1954).

2) S. Otani, This Bulletin, **33**, 1543 (1960).

3) M. Miura, S. Otani, M. Kodama and K. Shinagawa, *J. Phys. Chem.*, **66**, 252 (1962).

4) W. Wieker, *Z. Elektrochem.*, **64**, 1047 (1960); S. Otani, M. Miura and T. Doi, *J. Chem. Soc. Japan, Ind. Chem. Sec. (Kogyo Kagaku Zasshi)*, **66**, 593 (1963).

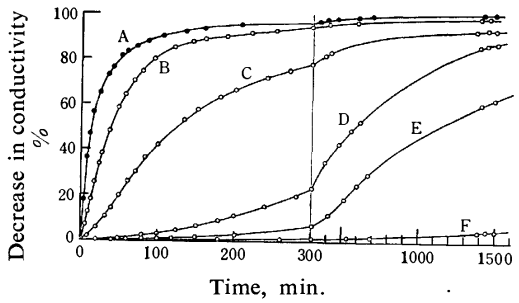

Fig. 2. Decrease in conductivity of 0.01M $SrSO_4$ solutions containing (A) none, (B) 5×10^{-7}, (C) 1×10^{-6}, (D) 1.5×10^{-6}, (E) 2×10^{-6} and (F) 2.5×10^{-6} M of tetraphosphate.

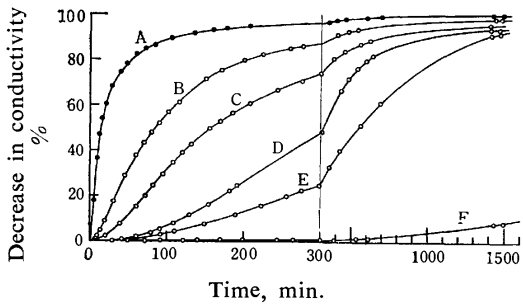

Fig. 3. Decrease in conductivity of 0.01 M $SrSO_4$ solutions containing (A) none, (B) 5×10^{-7}, (C) 7×10^{-7}, (D) 1×10^{-6}, (E) 1.5×10^{-6} and (F) 2×10^{-6} M of pentaphosphate.

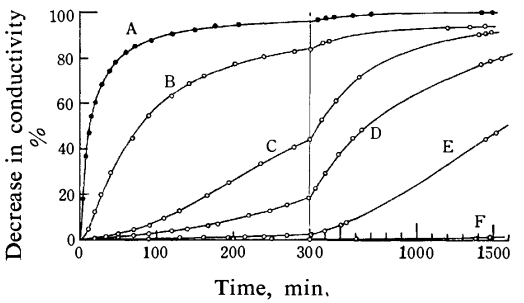

Fig. 4. Decrease in conductivity of 0.01M $SrSO_4$ solutions containing (A) none, (B) 5×10^{-7}, (C) 1×10^{-6}, (D) 1.25×10^{-6}, (E) 1.5×10^{-6} and (F) 2×10^{-6} M of hexaphosphate.

If, however, we represent the same data in terms of the monomer unit, as in Fig. 6, the adsorbed amounts of these phosphates can be illustrated by a common curve almost within the range of experimental error. This fact shows that a tetrahedral PO_4 unit of the polyphosphates adsorbed always occupies, on the average, about the same area of the crystal faces, independent of the chain length of the phosphates examined.

As has been mentioned previously,[3] the average area occupied per triphosphate ion

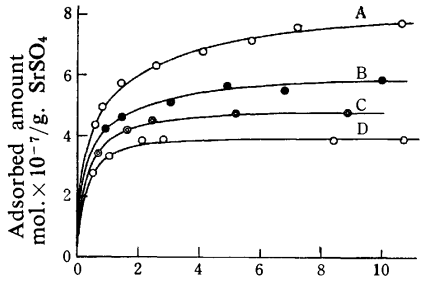

Fig. 5. Adsorption isotherms of tri- (A), tetra- (B), penta- (C) and hexaphosphate (D) at 25°C, pH 7.

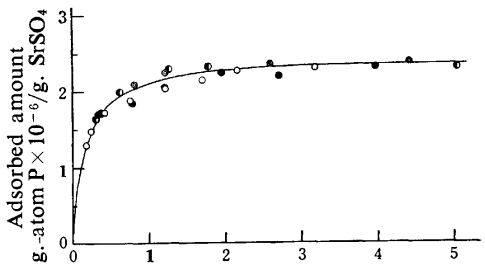

Fig. 6. Adsorption isotherms expressed in terms of the monomer unit.
○ Tri ● Tetra ◎ Penta ◐ Hexa

adsorbed on strontium sulfate is 37Å^2 ; hence, we can estimate the area occupied per PO_4 tetrahedral unit of the phosphates as roughly 12Å^2, independent of their chain length. On the other hand, the areas occupied per ion pair of strontium sulfate on the (1 0 0), (0 1 0) and (0 0 1) faces of its crystal (celestine) were found to be 18.4, 28.7 and 22.4Å^2 respectively.[5] Since the adsorption of phosphates is considered to be caused by some bonding between phosphate anions and Sr^{2+}cations on the crystal face, the above-mentioned data suggest that more than one PO_4 tetrahedral unit may be bound to an Sr^{2+} ion on the crystal faces.

As has been discussed in previous papers,[2,3] the inhibition of the crystallization of strontium sulfate due to the phosphates added may be caused by their adsorption on the crystal nuclei or growing crystals of strontium sulfate. From the similar behavior of the four phosphates in their adsorption on strontium sulfate, their effect on the crystallization rate may be expected to be nearly equivalent in all cases. That this is true may readily be realized if the phosphate concentrations are expressed in monomer units and Figs. 3—6 are then compared with one another. Independent of the

5) S. Otani and M. Miura, *J. Sci. Hiroshima Univ., Ser. A-II*, 27, 11 (1963).

chain length of the phosphates, each monomer exhibits almost the same effect on the crystallization rate. The effects of these phosphates on the habit of the crystals deposited are also similar to one another; spherulites having a nearly spherical shape were obtained from 0.01 M strontium sulfate solutions containing $(5\sim9)\times10^{-6}$ g.-atom P/1. of each phosphate.

In so far as the present work is concerned, "hexametaphosphate" can not be expected to exhibit a far greater effect on the crystallization of strontium sulfate if there is no cooperative effect among the individual constituents.

Department of Chemistry
Faculty of Science
Hiroshima University
Hiroshima

*The Electronic State and Dipole Moment of Diazine Mono-N-oxide**

By Tanekazu KUBOTA** and Haruyuki WATANABE

(Received June 7, 1963)

In previous studies undertaken as part of a programme of physicochemical investigations of various heterocyclic *N*-oxides, one (T. K.) of the present authors has calculated simple molecular orbitals (SMO) and anti-symmetrized molecular orbitals taking into account configuration interactions (ASMO-CI) to elucidate their electronic structures and electronic spectra.[1,2] These results have been compared with these of some physicochemical experiments, such as electronic spectra, dipole moments, infrared spectra, reactivities, etc. As a result, the following set of parameters have been found to be most reasonable for SMO calculation:[3]

$$\alpha_{N^{\delta+}} = \alpha + 1.6\beta,\ \alpha_{O^{\delta-}} = \alpha + 0.8\beta,\ \rho_{NO} = 1$$

where $\alpha_{N^{\delta+}}$, $\alpha_{O^{\delta-}}$ and α are the Coulomb integrals of nitrogen, oxygen and carbon atoms respectively; β is the usual exchange integral between two carbon atoms in benzene; and ρ_{NO} represents the exchange integral of the N–O bond in the β unit. The exponential decrease of inductive effect due to the $N^{\delta+}$ atom, which is the same form as in Jaffé's procedure,[4] was taken into account:

$$\text{Inductive effect} = (1/3)^n \times 1.6\beta$$

where n is the number of bonds between the nitrogen atom and the carbon atom in question.

Further, it was shown that the SMO's and ASMO-CI's calculated under these conditions can reasonably explain the above physicochemical and chemical properties of basic such heterocyclic *N*-oxides[1,2,5] as pyridine *N*-oxide, and quinoline *N*-oxide. Now, as a further extension of these studies, the present authors have investigated the electronic state and the dipole moments of three diazine mono-*N*-oxides, which are convenient in confirming the adequacy of these parameters, from experimental and theoretical (SMO calculation under the conditions described above) points of view.

Experimental

The measurements of dipole moments were carried out at 25°C on dilute solutions in benzene. The dielectric constants were measured by means of a heterodyne beat apparatus provided with a platinum cell.[6] For each solute, determinations were made on solutions of four different concentrations, appropriately chosen below 3 weight per cent. The graphical plot of the dielectric constant, as well as the density of solutions against the concentration in weight per cent, gave a linear dependence within the range of experimental error. The slopes of these straight lines were evaluated by the least-squares method. The molar polarization of the solute was calculated by a method similar to that introduced by Halverstadt and Kumler[7]; it differed, however, in that densities were used rather than the specific volumes. The deformation polarization of each compound was assumed to be 1.05 times the molar refraction approximated with the sum of

* Presented at the 15th Annual Meeting of the Chemical Society of Japan, Kyoto, April, 1962.

** Present address: Department of Physics, The University of Chicago, Chicago 37, Illinois, U. S. A.

1) T. Kubota, *J. Chem. Soc. Japan, Pure Chem. Sec.* (*Nippon Kagaku Zasshi*), **80**, 578 (1959).

2) T. Kubota, This Bulletin, **35**, 946 (1962).

3) The details on the derivation of these paramters have been discussed in Refs. 1 and 2.

4) H. H. Jaffé, *J. Chem. Phys.*, **20**, 279, 778, 1554 (1952): *J. Am. Chem. Soc.*, **76** 3527 (1954).

5) Cf. T. Kubota, *J. Spectroscopical Soc. Japan*, **10**, 83 (1962).

6) Y. Kurita and M. Kubo, *J. Am. Chem. Soc.*, **79**, 5460 (1957).

7) I. F. Halverstadt and W. D. Kumler, ibid., **64**, 2988 (1942).

TABLE I. DIPOLE MOMENTS OF SOME DIAZINE MONO-*N*-OXIDES IN BENZENE SOLUTIONS AT 25°C

Compound	α	β g./cc.	P_2 cc.	MR_D cc.	μ D
Pyrazine 1-oxide	3.38	0.31	82.3	24.6	1.66
4-Methyl-pyrimidine 1-oxide	13.26	0.22	314.0	29.2	3.72
Pyridazine 1-oxide	31.02	0.35	581.3	24.8	5.21

atomic refractions for the D line. Since the values of moments are great, no serious errors are introduced by this assumption, the probable errors being estimated at less than 0.05 D.

The results are shown in Table I, in which α and β denote the changes in the dielectric constant and in the density of the solutions with the weight fraction of the solute; the other notations have their usual meanings. The samples of pyrazine mono-*N*-oxide,[2] 4-methylpyrimidine mono-*N*-oxide[2] and pyridazine mono-*N*-oxide (hygroscopic colorless crystal of m. p. 38~39°C)[8,9] used in this investigation were the same as those reported in detail in previous papers.[2,9] Here, we have employed 4-methylpyrimidine mono-*N*-oxide instead of pyrimidine mono-*N*-oxide because of the difficulty of preparing the latter. Moreover, although the position of the N–O group in 4-methylpyrimidine *N*-oxide has not yet been established, Position 1 in Fig. 2 was inferred to be the most plausible.[10]

MO Calculations and Discussion

The electronic structures of pyrazine mono-*N*-oxide, pyrimidine mono-*N*-oxide and pyridazine mono-*N*-oxide have been calculated by using a simple LCAO-MO (SMO) method, disregarding overlap integrals and electronic interactions.

The various parameters necessary to carry out the calculation are the same as those described at the beginning of this paper, except for the Coulomb integral of pyridine-type nitrogen, which was taken to be the $\alpha+0.4\beta$ derived by Hameka et al.[11] on the basis of the theoretical treatment of the dipole moment of the compounds like pyridine and which was added to the Coulomb potential due to the inductive effect of the $\rangle N^{\delta+}$-group.

In this calculation, pyrazine mono-*N*-oxide was reasonably assumed to belong to the point group C_{2v}. The SMO's of the other two molecules, however, were directly obtained from the original secular equations.

The molecular diagrams thus obtained are shown in Figs. 1, 2 and 3, along with the numbering of atoms. Providing that the benzene heterocyclic ring of these molecules consists of a regular hexagon, with a bond length of 1.38 Å,[12] and that the N–O distance is 1.28 Å,[1,2,13] we have calculated the π-moments on the basis of the π-electron densities given in Figs. 1, 2 and 3. The results are demonstrated in each of the above figures. As in the case of basic heterocyclic *N*-oxides, it is clear from Figs. 1, 2 and 3 that the direction of the π-moment in each diazine mono-*N*-oxide indicates the π-electron transfer from the oxygen atom to the ring, the magnitude of which is greater than that (0.76 D) of pyridine *N*-oxide[2] to be discussed below. This fact is in good agreement with the accepted general tendency; that is, the replacement of one ring carbon atom by a nitrogen atom, which is a more electronegative element than carbon, brings about a greater charge transfer from the N→O group to the ring.

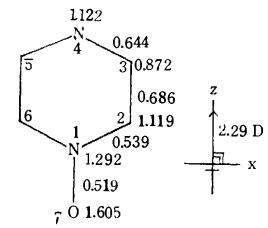

Fig. 1. Molecular diagram and π-moment of pyrazine mono-*N*-oxide.

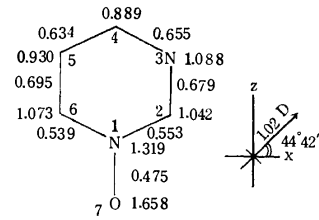

Fig. 2. Molecular diagram and π-moment of pyrimidine mono-*N*-oxide.

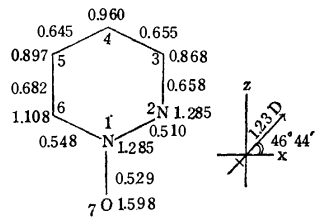

Fig. 3. Molecular diagram and π-moment of pyridazine mono-*N*-oxide.

8) C. F. Koelsch and W. H. Gumprecht, *J. Org. Chem.*, 23, 1603 (1958).
9) H. Watanabe, M. Ogata and H. Kano, *Chem. & Pharm. Bull.*, 11, 29 (1963).
10) E. Ochiai and H. Yamanaka, *Pharm. Bull.*, 3, 175 (1955).
11) H. F. Hameka and A. M. Liquori, *Mol. Phys.*, 1, 9 (1958).
12) This length corresponds to the averaged value of each bond length determined experimentally on pyridine.
13) Y. Namba, T. Oda and T. Watanabe, This Bulletin, 36, 79 (1963).

TABLE II. THE VALUES OF EMPLOYED σ-MOMENTS (D)
(See text)

Bond	Condition 1	Condition 2
$\overset{(+)\ (-)}{N\rightarrow O}$	4.55	4.30**
N—O	0.40	0.40
$\rangle N^*$:	1.0	—
C—N	O[C(sp^2)—N(sp^2)]	0.45

* The moment due to the unshared electron pair. See text.

** This value was cited from Smyth's table. C. P. Smyth: "Dielectric Behaviour and Structure," McGraw-Hill Book Co., New York (1955), p. 244.

It is especially noteworthy to point out that in pyrazine mono-*N*-oxide, a considerable amount of π-electron density is accumulated on the nitrogen atom at position 4, which is furthest apart from the N→O group. On the other hand, the fact that in the case of pyrimidine mono-*N*-oxide the contribution of the meta nitrogen atom to the increase of the π-moment is relatively small shows that the electron migration ability to the meta (3-) N-atom is weak, as is expected from the usual electronic theory. Assuming the mutual interaction between π- and σ- (the moments due to each of the localized bonds) moments to be negligible, we calculated the total dipole moments by means of the vector summation of π- and σ-moments, the latter values of which are listed in Table II. Here the necessary estimation of σ-moments is important. Our estimations were made under two conditions:

Condition 1: In this case we explicitly took into account the moment due to the unshared electron pair (the lone pair moment) on the nitrogen atom in the ring. Recently, Sheibe et al.[14] have reported the NMR chemical shift of pyrimidine in detail, showing that the lone pair moment of the nitrogen atom is, semi-experimentally, 1.2 D by connecting of above chemical shift data with the MO calculation results concerning pyrimidine under the following reasonale conditions: the SMO parameters of the N-atom are 0.5 or 0.4, the C(sp^2)–N(sp^2) σ-moment is nearly zero, as was suggeted by Hameka and Liquori,[11] and the usual C–H σ-moment was adopted. However, since the C–H moment, 0.6 D, adopted by them was somewhat larger than the normal value, we applied 0.4 D[15] to their data to obtain the N-lone pair moment of 1.0 D.

The σ-moment of the N→O bond was assigned as 4.55 D so as to reproduce the observed moment of pyridine *N*-oxide by using the π-moment (0.76 D) estimated experimentally and theoretically by us[1,2] and by other workers[16] and by using the C–N and C–H σ-moments as stated above and as listed in Conditon 1 in Table II.

Condition 2: We have applied the same σ-moments as those employed by Orgel et al.[15] to analyze the dipole moments of many heterocyclic compounds theoretically.[17]

As may be seen from Table III, the agreement between the observed total moments and the calculated ones is relatively good. However, Condition 1 seems to be more reasonable in view of the reproducibility of the observed value and from the theoretical point of view.

Now, the SMO-parameter for aromatic-*N*-oxides, derived previously by us, seems to be suitable to explain the electronic dipole moments for these compounds, including diazine mono-*N*-oxides.

Table IV gives the frontier electron densities of the compounds studied here as defined by Fukui et al.,[19] densities which were successfully applied hitherto to explain the chemical reactivities of the various *N*-oxides.

The chemical reactivity of pyridazine mono-*N*-oxide, which was recently studied in detail by Ogata and Kano,[20] showed that position 4 in the molecule (the para position to the N→O bond) is very active; for example, substituent reaction by a nitrating agent leads to a 4-nitro derivative. These facts agree well with the theoretical prediction inferred

14) W. Seiffert, H. Zimmermann and G. Sheibe, *Angew. Chem.*, 74, 249 (1962).

15) L. E. Orgel, T. L. Cottrell, W. Dick and L. E. Sutton, *Trans. Faraday Soc.*, 47, 113 (1951).

16) A. R. Katritzky, E. W. Randall and L. E. Sutton, *J. Chem. Soc.*, 1957, 1769.

17) The values of many σ-moments have recently been given by R. Daudel et al.[18] on the basis of the theoretical treatment of a σ-bond like C-H, the $\overset{(+)\ (-)}{C\rightarrow H}$ and $\overset{(+)\ (-)}{C\rightarrow N}$ moments being assigned as 0.40 and 1.15 D respectively. It should be noted that the C→N bond moment is very large and that it partly contains the contribution from the lone pair moment of the N-atom, which was prorated to each of the σ-bonds bonded with the N-atom. It seems that the above C→N σ-moment, etc., can not be applied to the C→N bond in the *N*-oxides, because the N-atom in the $\rangle N\rightarrow O$ bond has no lone pair electron. Formally, however, we could explain the observed values with a better accuracy than that of "Condition 2" in Table II by using the σ-moments given by the above authors.

Moreover, although the direction of the C–H bond moment under conditions 1 and 2 is in the direction opposite to that expected theoretically,[18a,b] it should be pointed out that, in the case of Condition 1, the sum of "the lone pair moment of the N-atom" and "the C–H bond moment located at the para-position to the N-atom" is 1.40 D, the value and the direction of which are nearly of the same order as the 1.33 D obtained theoretically by Hameka and Liquori.[11]

18) a) R. Daudel, R. Lefebvre, and C. Moser, "Quantum Chemistry," Interscience. Publ. Inc., New York (1959), p. 206; b) C. A. Coulson and M. T. Rogers, *J. Chem. Phys.*, 35, 593 (1961).

19) K. Fukui, T. Yonezawa and H. Shingu, *J. Chem. Phys.*, 20, 722 (1952); K. Fukui, T. Yonezawa, C. Nagata and H. Shingu, ibid., 22, 1433 (1954).

20) M. Ogata and H. Kano, *Chem. & Pharm. Bull.*, 11, 29, 35 (1963).

TABLE III. THE CALCULATED VALUES OF TOTAL DIPOLE MOMENTS OF SOME *N*-OXIDE COMPOUNDS

Compound	Calculated moment and direction		Observed value*
	Condition 1	Condition 2	
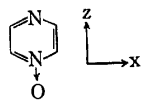	1.27 D	2.01 D	1.66 D
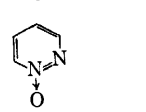	5.18 D	4.94 D	5.21 D
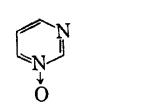	4.02 D	4.26 D	3.72 D**
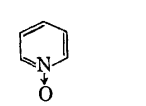	4.19 D	4.39 D	4.19 D[a,5,16]
$(CH_2)_3N\rightarrow O$	4.95 D	5.15 D	5.02 D[b,5,16]

* See Table I.

** This value was obtained on 4-methylpyrimidine *N*-oxide (see "Experimental"). The small effect owing to the methyl group was disregarded on comparison of calculated and observed values. This situation may be allowable for the purpose of the present discussion.

a) A. N. Sharpe and S. Walker, *J. Chem. Soc.*, **1961**, 4522.

b) E. P. Linton, *J. Am. Chem. Soc.*, **62**, 1945 (1940).

TABLE IV. FRONTIER ORBITAL ELECTRON DENSITIES*

	7	1	2	3	4	5	6	ϕ_i**
Pyridazine	0.5780	0.0104	0.0906	0.0334	0.1522	0.0029	0.1324	$(\phi_4 j)^2$
mono-*N*-oxide	0.1694	0.2661	0.2368	0.0253	0.1492	0.1274	0.0259	$(\phi_5 j)^2$
Pyrimidine	0.6189	0.0178	0.1222	0.0099	0.1258	0.0107	0.0948	$(\phi_4 j)^2$
mono-*N*-oxide	0.0980	0.1667	0.0004	0.1846	0.1973	0.0322	0.3209	$(\phi_5 j)^2$
Pyrazine	0.6100	0.0086	0.1211	0.0017	0.1359	—	—	$(\phi_4 j)^2$
mono-*N*-oxide	0.1856	0.2876	0.1112	0.0443	0.2159	—	—	$(\phi_5 j)^2$

* The numbering of each atom is the same as that shown in Figs. 1, 2 and 3.

** ϕ_4 and ϕ_5 denote the highest occupied orbital and the lowest empty orbital, respectively.

from Table IV, in which the frontier electron density on the carbon atom located at position 4 is largest.

Summary

The dipole moments of pyrazine 1-oxide, 4-methylpyrimidine 1-oxide and pyridazine 1-oxide have been measured in benzene solutions and found to be 1.66, 3.72, and 5.21 D respectively. A comparison of these values with those obtained by the SMO calculation, in which the necessary parameters have been theoretically evaluated in detail by us in previous papers,[1,2] shows that the agreement between the observed and calculated values is good.

The authors are grateful to Professor Saburo Nagakura, of the Institute for Solid State Physics, The University of Tokyo, for his kind discussions; and to Mr. Masato Yoshikawa and Dr. Choichiro Asano for their advice on employing an electronic computer in our calculations.

Shionogi Research Laboratory
Shionogi & Co., Ltd.
Fukushima-ku, Osaka

The Photosensitized Oxidation of Leuco-uranine. III. The Kinetics of an Acridine-sensitized Photoöxidation in an Aerated Solution

By Kengo UCHIDA

(Received March 20, 1963)

In previous papers[1-3] the author and his co-workers have studied some properties of leuco-uranine and the kinetics of the acridine-sensitized photoöxidation of leuco-uranine in a deaerated solution. Leuco-uranine prepared by reducing uranine with sodium amalgam was photoöxidized to the colored form by adding some suitable sensitizer to the solution and then by irradiating it with the light appropriate to the sensitizer. In the case of the deaerated solution, leuco-uranine attacked by the triplet state of a sensitizer, i. e., acridine, was transformed into the oxidized form via semiquinone and perhaps with the evolution of molecular hydrogen. The evolved hydrogen, however, could not be successfully detected because of its small quantity.

Now in an aerated solution the rate of the photosensitized oxidation of leuco-uranine is more than ten times slower and the recovery of uranine is less quantitative than in a deaerated solution under suitable conditions. The purpose of the present report is to clarify kinetically the mechanism of this sensitized oxidation in the aerated solution by investigating quantitatively the concentration effect of the dissolved oxygen. The conclusions may be summarized as follows: oxygen rapidly reacts with the triplet state of acridine and produces between them perhaps a molecular complex, which may be similar to that proposed by Schenck.[4] It decomposes mostly into oxygen and acridine, only a little portion participating in the oxidation of leuco-uranine. Therfore, when the concentration of dissolved oxygen is low, oxygen prohibits the formation of uranine, while in the high concentration, the oxidation of leuco-uranine takes place via a different mechanism from that of the deaerated solution which has been elucidated before.[3]

Experimental

Material. — *Leuco-uranine.* — The method of preparation has already been reported in detail.[1] Uranine was reduced with sodium amalgam in an aqueous alkaline solution and recrystallized from ethanol a few times. The crystal was desiccated in a high vacuum.

Acridine.—Tokyo Kasei's acridine was recrystallized twice from a water-ethanol mixture.

Sodium Hydroxide. — The saturated solution was prepared from a G. R. reagent of the Wako Junyaku Co., and the supernatant solution was diluted to the desired concentration.

Disodium Hydrogen Phosphate and Potassium Dihydrogen Phosphate.—G. R. Reagents of the Wako Junyaku Co. were recrystallized three times from an aqueous solution.

Oxygen. — Air was used, and it was purified by removing moisture and carbon dioxide by the use of soda lime, calcium chloride and a trap cooled with dry ice.

Procedure.—Usually the stock solution of leuco-uranine 9.5×10^{-5} M was diluted ten times. In most experiments, the concentration of the acridine used as a sensitizer was about 1.5×10^{-4} M. For the control of the pH value of the solution, a phosphate buffer (about M/30) and sodium hydroxide (for the region of the higher pH values) were used. The pH value was measured with a Hitachi pH meter (model EHP-1).

The concentration of oxygen was controlled in the following way: the sample solution was sufficiently evacuated, repeatedly melted and refrozen in vacuo, and then saturated with oxygen of a definite pressure at 30°C. The oxygen concentration in the solution was calculated with a Bunsen-coefficient, 0.026 at 30°C.[5]

The reaction apparatus was described in detail in the previous paper.[3] The light source was a high-pressure mercury lamp (Matsuda SHL-100 UV), and a specially-designed interference filter transmitting near 490 and 375 mμ was used. This mercury lamp was used as the exciting light (at 365 mμ) and also as the monitoring light (at 490 mμ) with which the absorbance of the solution was measured. From the change of absorbance, the rate of the formation of uranine may easily be evaluated. The reaction cell made of Terex glass is $1\times1\times4$ cm. and has a side arm for evacuation along the long axis. To change the light intensity, the distance between the lamp and the reaction cell was changed, and each time the intensity was measured with a potassium ferrioxalate actinometer.[6] All experiments were performed at 30°C.

1) K. Uchida, S. Kato and M. Koizumi, This Bulletin, 35, 16 (1962).
2) K. Uchida and M. Koizumi, ibid., 35, 1871 (1962).
3) K. Uchida and M. Koizumi, ibid., 35, 1875 (1962).
4) E. g., G. O. Schenck, *Naturwissenschaften*, **40**, 205, 212 (1953).
5) An interporated value in a 0.1N sodium hydroxide aqueous solution; Chemical Society of Japan (ed.), "Handbook of Chemistry (Kagaku Benran)", Maruzen, Tokyo (1958), p. 571.
6) C. A. Parker, *Proc. Roy. Soc.(London)*, **A220**, 104 (1953); C. G. Hatchard and C. A. Parker, ibid., **A235**, 518 (1956).

Results

Determination of the Order of the Reaction with Respect to Leuco-uranine. — The initial rate of the formation of uranine as a function of the initial concentration of leuco-uranine, $[L]_0$, was investigated. A slight variation in the concention of acridine, [A], and in the light intensity, I_0, was standardized by dividing the initial rate by the quantity of absorbed light, since, as will be described later, the rate is proportional to the absorbed light. The

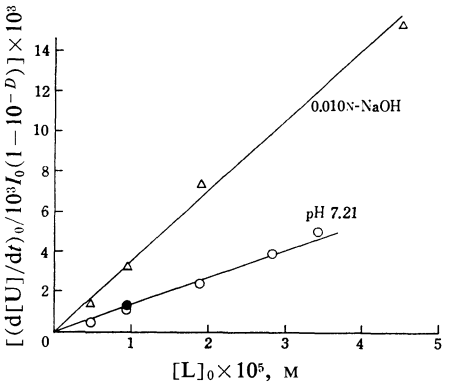

Fig. 1. Dependence of the initial rate on $[L]_0$.
$I_0\sim8\times10^{-8}$ mol. cm^{-2} min^{-1}
$[A]\sim1.3\times10^{-4}$ M
●: Uranine is beforehand added to 5×10^{-6} M (pH 7.21).

results are shown in Fig. 1. It is apparent that the rate is proportional to $[L]_0$. Thus, the rate may be represented as follows:

$$\left(\frac{d[U]}{dt}\right)_0 = k_0'[L]_0 \qquad (1)$$

$$\frac{(d[U]/dt)_0}{10^3 I_{abs}} = \frac{(d[U]/dt)_0}{10^3 I_0(1-10^{-D})} = k_0[L]_0 \qquad (2)$$

where $(d[U]/dt)_0$, [U] and k_0 are the initial rate of the formation of uranine, the concentration of uranine, and the rate constant respectively. I_{abs} is the number of photons (in mol.) absorbed (cm^{-2} min^{-1}) and is represented as $I_0(1-10^{-D})$, where I_0 is the incident light intensity and D, the absorbance of acridine at 365 mμ.

As the initial rates are obtained from the tangent of the plot [U] vs. time t, some error may be inevitable and k_0 may not be entirely accurate. The values of k_0 obtained are 353 l. mol^{-1} for a 0.010 N aqueous alkaline solution and 136 l. mol^{-1} at pH 7.21.

The Effect of the Concentration of Oxygen. —The oxidation of leuco-uranine in a deaerated solution proceeds about ten times faster than in an air-saturated solution. In order to investigate how oxygen behaves in the reaction,

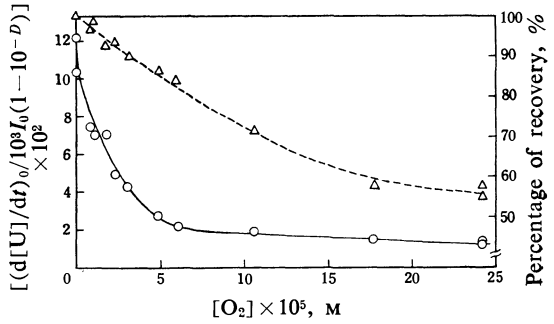

Fig. 2. Effects of $[O_2]$.
0.11 N-NaOH
$I_0=(4.9\sim5.5)\times10^{-8}$ mol. cm^{-2} min^{-1}
$[A]=(1.8\sim2.0)\times10^{-4}$ M
○: $\dfrac{(d[U]/dt)_0}{10^3I_0(1-10^{-D})}$
△: Percentage of the recovery of uranine

the concentration effect of oxygen on the reaction rate was examined. The results are shown in Fig. 2, in which the initial rate is plotted against the concentration of oxygen, $[O_2]$. In the lower concentration region, the rate decreases rapidly with the concentration of oxygen, but the slope of the curve lessens near $[O_2]\sim5\times10^{-5}$ M, and from this concentration up to $[O_2]\sim24\times10^{-5}$ M (air-saturated solution) the rate declines very slowly. From the above results, it is obvious that oxygen suppresses the oxidation, which takes place in vacuo. Judging from a very large retarding effect at the low concentration of oxygen, the rate ought to be negligible in a concentration as high as that in the air saturated solution. However, the fact is that the reaction actually proceeds at an appreciable rate, even in the air-saturated solution. This leads to the conclusion that oxidation of a different mechanism, involving oxygen, is taking place. The percentage of the recovery of uranine after the reaction also decreases with the concentration of oxygen. The results are shown in Fig. 2 with a dashed line.

The Rate Formula. — Let us now discuss a rate formula for each run in the air-saturated solution. Although the total reaction consists of the formation of uranine and the decomposition of the dye, the rate formula for only the former will be considered. It was found that the next equation holds satisfactorily. The interpretation of this equation will be given in the discussion.

$$\frac{d[U]}{dt} = k'([U]_\infty - [U]) \qquad (3)$$

From this,

$$\ln[U]_\infty - \ln([U]_\infty - [U]) = k't \qquad (4)$$

where $[U]_\infty$ is the concentration of uranine at

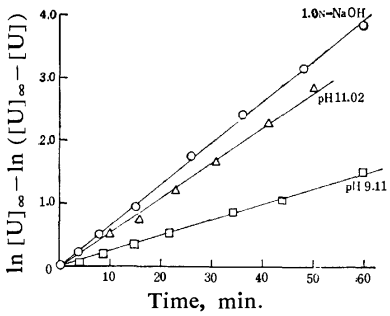

Fig. 3. Plots of $\{\ln [U]_\infty - \ln ([U]_\infty - [U])\}$ against time for typical examples.
$[L]_0 = 9.5\times10^{-6}$ M, $[A] \sim 1.4\times10^{-4}$ M
$I_0 \sim 5.5\times10^{-8}$ mol. cm^{-2} min^{-1}

the end of the reaction and k' is a rate constant. Some examples are shown in Fig. 3.

In the range of lower pH values, however, this equation fails, and when the pH value is lower than 8, the reaction at the initial stage appears to be rather of approximately the zeroth order with respect to the concentration of leuco-uranine. Examples in the range of lower pH values are shown in Fig. 4. Thus the order of the reaction obtained from each run is quite different from that which is obtained from the dependence of the initial rate on the concentration of leuco-uranine, which maintains the first order, as has been mentioned already. This discrepancy suggests that the reaction might be promoted by some reaction products. The problems will be considered in the discussion.

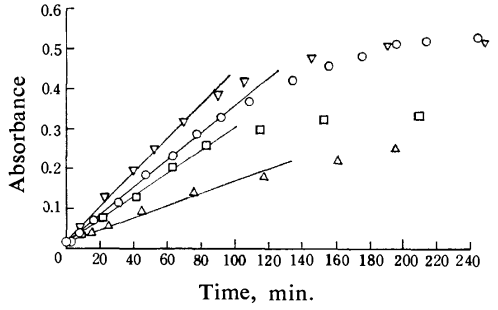

Fig. 4. Dependence of absorbance on the irradiation time.
$[L]_0 = 9.5\times10^{-6}$ M, $[A] = 1.4\times10^{-4}$ M
○: pH 7.2, ▽: pH 6.9, □: pH 6.2,
△: pH 7.2 ($[L]_0 = 4.75\times10^{-6}$ M)

Next, the effects of various factors upon the k' values of the air-saturated solution were examined.

The Effect of Light Intensity. — The results are shown in Fig. 5. As the concentration of acridine differs slightly from sample to sample, the quantity of the absorbed light is used as an abscissa instead of the incident light intensity, I_0. It is calculated from $10^3 I_0(1-10^{-D})$. Figure 5 shows the plot of k' against this quantity. It is apparent that k' increases in proportion to the light intensity.

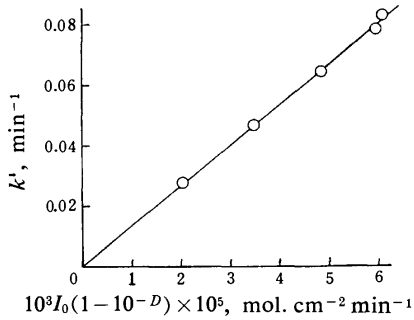

Fig. 5. Plot of k' against I_0.
$[L]_0 = 9.5\times10^{-6}$ M, $[A] = (1.27\sim1.42)\times10^{-4}$ M
$[NaOH] = 0.010$ N

The Effect of the Concentration of Acridine. —The results obtained in region [A] from 0 to 2.06×10^{-4} M are listed in Table I. Since the quantity of the absorbed light is given by $I_0(1-10^{-D})$ and since the k' values are proportional to I_0, as has been mentioned above, it is convenient to plot the value of k'/I_0 against $(1-10^{-D})$ as in Fig. 6. From Fig. 6 it is certain that the values of k' are proportional to the absorbed light under these conditions. Thus, Eq. 3 can be written as follows:

$$\frac{d[U]}{dt} = 10^3 k I_0 (1-10^{-D})([U]_\infty - [U]) \qquad (5)$$

where k is a new rate constant. The value of

Table I. The effect of the concentration of acridine
$[L]_0 = 9.5\times10^{-6}$ M, $[NaOH] = 0.122$ N

$[A]\times10^4$ M	k' min^{-1}	$I_0\times10^8$ mol. cm^{-2} min^{-1}	$k'/I_0\times10^{-5}$ cm^2 mol^{-1}	$1-10^{-D}$	$k\times10^{-3}$ l. mol^{-1}
0	0.00067	7.48	0.0896	0	—
0.160	0.0145	7.48	1.94	0.155	1.25
0.308	0.0265	7.48	3.54	0.276	1.28
0.903	0.0552	7.48	7.38	0.612	1.21
1.42	0.0667	6.73	9.91	0.775	1.28
2.04	0.0845	7.48	11.3	0.881	1.28
2.06	0.0612	5.48	11.2	0.885	1.26

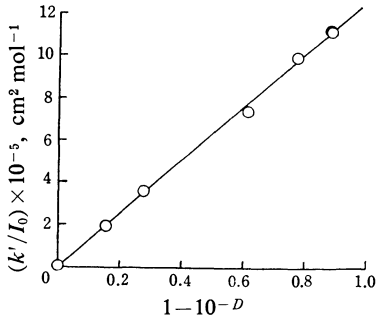

Fig. 6. Plot of k'/I_0 against $(1-10^{-D})$.

$k([U]_\infty-[U])$ gives the quantum yield for the formation of uranine. This is not affected by the concentration of acridine, as Table I shows.

The Effect of the pH Value. — The rate of the formation of uranine varies with the pH value of the solution. The results are listed in Table II. Mention will be made later of the column under $\varphi k_8/k_7$ and $\varphi k_9/k_7$ in Table II. Above a 2 N sodium hydroxide solution, the solubility of acridine is less than 1.5×10^{-4} M, at which value the usual experiments were performed. In the region between pH values of 14 and 11, the k values are almost constant. Below pH 11, they begin to decrease, and at pH~8, Eq. 4 fails; thus the reaction proceeds approximately in the zeroth order respect to the concentration of leuco-uranine at the initial stage. The further decrease of pH seems to increase the rate. The relation between pH values and k values is shown in Fig. 7 by a solid line. It is to be added that the k values in a lower pH region are tentative, since they were obtained from the tangent

TABLE II. THE EFFECT OF THE pH VALUE
$[L]_0=9.5\times10^{-6}$ M, $[A]=(1.4\sim1.5)\times10^{-4}$M
$I_0\sim5.5\times10^{-8}$ mol. cm^{-2} min^{-1}

pH	k', min^{-1}	$k\times10^{-3}$ l. mol^{-1}	Percentage of the recovery %	$\varphi k_8/k_7$	$\varphi k_9/k_7$
14.0	0.0552	1.28	60.2	770	509
13.09	0.0524	1.22	54.7	667	553
12.46	0.0558	1.29	55.3	713	577
12.42	0.0417	0.948	56.2	533	415
11.02	0.0540	1.25	59.5	744	506
10.88	0.0527	1.22	59.8	730	490
10.14	0.0408	1.03	62.5	644	386
9.53	0.0300	0.664	68.2	453	211
9.11	0.0254	0.588	70.7	416	172
8.6	0.0120	0.278	79.7	221	56
8.5	0.00980	0.227	81.0	184	43
7.86	0.00646	0.148	88.1	130	18
6.90	0.0115	0.268	96	257	11
6.28	0.0152	0.358	100	358	0

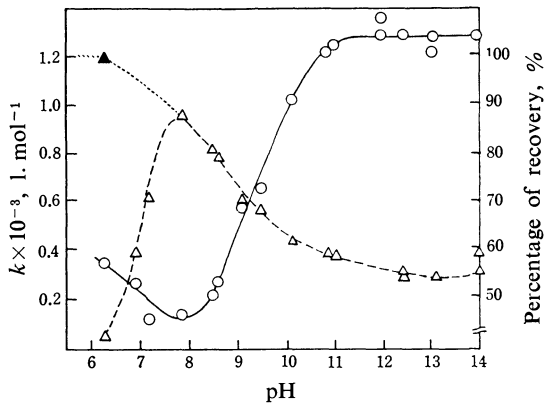

Fig. 7. Effects of the pH value.
○ : k
△ : Percentage of the recovery of uranine
(▲ : after addition of alkali)

at time zero on the plot of the left side of Eq. 4, $\{\ln[U]_\infty-\ln([U]_\infty-[U])\}$, against time. Although the quantity of the produced uranine at the end of the reaction seems to be affected by a very small difference in the experimental conditions and although the reproducibility is not very good, the recovery of uranine at the end of the reaction is about 40~55% at the higher pH values. The percentage begins to increase near pH~11 and approaches 100% at pH~6. The results are shown in Fig. 7 with a dashed line.

In order to make clear why the recovery of the dye is incomplete in high alkalinity, the solution after the reaction was evacuated and again irradiated, but no recovery of uranine was observed. Since the recovery of uranine should take place perfectly in a deaerated solution, the above results show that uranine is partially decomposed irreversibly. The absence of leuco-uranine in the thoroughly irradiated solution was further substantiated by means of paper chromatography.[1] From these results, it is obvious that photolysis of the dye takes place, accompanied by the formation of uranine. This decomposition reaction decreases in magnitude below pH 11.

Since uranine has a pK value of about 7 for the dissociation of univalent into divalent anions,[7] the concentration of univalent anions becomes appreciable below pH 8. As the univalent anions of uranine have absorption maxima at 455 and 475 mμ and as the molar extinction coefficient at 490 mμ is smaller than that of dianions, it is naturally expected that the rise of absorbance at 490 mμ is far less than that in high alkalinity, even when the recovery of the dye really occurs to the same

7) V. Zanker and W. Peter, *Chem. Ber.*, **91**, 572 (1958); L. Lindqvist, *Arkiv. Kemi.*, **16**, 79 (1960).

extent. The recovery of the dye in this pH region was definitely confirmed, however, by adding one drop of an alkaline solution to the thoroughly irradiated solution. Below pH 6, moreover, the neutral molecule of uranine exists in the solution, which has an absorption maximum at 437 mμ, but its extinction coefficient (particularly at 490 mμ) is so much smaller that the absorption can not be recognized at the concentration of 10^{-5} M. Therefore, the experiment below pH 6 cannot be performed for the usual concentration used in the present experiment. However, it was qualitatively confirmed, by a test analogous to that mentioned above, that even with such low pH values uranine is photochemically recovered.

Discussion

In the case of the deaerated solution, leuco-uranine reacts with the triplet state of acridine and becomes an oxidized form via a semi-quinone form. The details of this mechanism have been reported on in a previous papers.[2,3] In the case of the aerated solution, it is clear from the effect of dissolved oxygen that oxygen retards the oxidation reaction. However, if oxygen were to behave only as a retarder, it would be expected that the reaction should be completely suppressed at such a high oxygen concentration as in an air-saturated solution. The experimental results are contrary to the above expectation. Thus, although the rate decreases rapidly with the concentration of oxygen in the lowest region, the decrease becomes less and less near $[O_2] \sim 5 \times 10^{-5}$ M, and even in the air-saturated solution the reaction proceeds at an appreciable rate. These results would imply that the oxidation of leuco-uranine of another type, one involving oxygen, also occurs in addition to the oxidation which involves no oxygen.

From spectroscopic and paper-chromatographic analyses, there is no doubt that the photoöxidized product in the air-saturated solution is uranine[1] and that the acridine acting as a sensitizer does not change at all.

Next, the retardation of the reaction by oxygen will be considered. It is plausible that oxygen attacks and chiefly deactivates the triplet state of acridine. This was confirmed by the following supplementary experiments.

When acridine in an aqueous solution (10^{-4} M in a phosphate buffer of pH 7.3) was irradiated by the light of 365 mμ from a mercury lamp, acridine was photolysed; the quantum yield of the photolysis is 2×10^{-4} in the aerated solution. From the fact that the quantum yield is very small, it is certain that most of the excited state of acridine is deactivated, only a small portion of it being decomposed by the oxygen. When the concentration of oxygen is decreased, the rate of decomposition begins to fall at about $[O_2] \sim 3 \times 10^{-5}$ M. If one assumes that the reaction between an excited molecule and oxygen takes place so fast that the diffusion is the rate-determining process, the above finding implies that oxygen attacks a fairly long-lived excited species, since the dependence of the rate on the concentration of oxygen becomes apparent at such a low concentration. Thus, it is probable that oxygen attacks the triplet state of acridine rather than the singlet excited state. The existence of leuco-uranine in the system would not alter the situation essentially. Now, however, the triplet state of acridine reacts with not only oxygen but also with leuco-uranine at similar rates in this case. Hence it is expected that the concentration effect of oxygen will appear in a somewhat higher concentration. This expectation conforms well to the experimental results, confirming again that oxygen reacts with the triplet state of acridine and not with the excited singlet state. Besides, this is supported by the fact that no quenching of the fluorescence of acridine by oxygen is observed. As for the reaction between oxygen and the triplet state, Schenck[4] has studied many examples of photosensitized oxidation and has proposed that a loosely-bound molecular complex between oxygen and a triplet state of a sensitizer is formed in the course of the photosensitized oxidation. On the basis of Schenck's scheme, it can be considered that the intermediate between oxygen and the triplet state of acridine, $(A^t \cdots O_2)$, is formed during the photosensitized oxidation when acridine is used as a sensitizer, and that most of it may decompose into the original acridine and oxygen and only a little part participate in the recovery of uranine or the irreversible decomposition of the dye.

We will now consider how the decomposition reaction interferes with the recovery of the dye. From the fact that the formation of uranine can be treated satisfactorily with Eqs. 3 and 4, it seems likely that not only is the rate of the formation of uranine (noted below as process [8]) proportional to the concentration of leuco-uranine, as has been shown above, but also the decomposition (noted below as process [9]) is proportional to the concentration of leuco-uranine. Therefore, the relation between the concentration of leuco-uranine and that of uranine may be represented as follows:

$$\{[L]_0 - [L]\}\frac{k_8}{k_8 + k_9} = [U]$$

$$[L] = [L]_0 - \frac{k_8+k_9}{k_8}[U]$$

$$= \frac{k_8+k_9}{k_8}\{[U]_\infty - [U]\} \quad (6)$$

where k_8 and k_9 are the rate constants of processes [8] and [9] respectively. Thus, the fact that the experimental results are satisfactorily analysed by Eq. 3 implies that the decomposition of the dyes occurs simultaneously with the formation of uranine and at a rate proportional to the concentration of leuco-uranine. The ratio of the quantity of uranine formed to that of the dye decomposed at any time is given by the ratio of k_8 to k_9.

Such relations, however, seemingly do not hold at a low pH value, perhaps due to the promotion of the oxidation of leuco-uranine by a certain reaction product. To examine if uranine acts as such a product, the effect of the addition of uranine was examined. As Fig. 1 (a solid circle) shows, the result is that the addition of as much as about 5×10^{-6} M of uranine has no effect on the rate beyond the range of experimental error. Another possibility is that hydrogen peroxide which may be formed during the oxidation of leuco-uranine maintains its existence at a lower pH value and oxidizes leuco-uranine to uranine. It is natural to consider that the formation of hydrogen peroxide is accompanied by the oxidation of leuco-uranine, since this has already been confirmed in the case of the oxidation of the leuco form of thiazine dyes.

Summing up all the processes described above, the next scheme can be proposed:

$$A \xrightarrow{h\nu} A^* \quad [0]$$

$$A^* \rightarrow A \quad [1]$$

$$A^* + OH^- \rightarrow A + OH^- \quad [2]$$

$$A^* \rightarrow A^t \quad [3]$$

$$A^t + OH^- \rightarrow A + OH^- \quad [2']$$

$$A^t \rightarrow A \quad [4]$$

$$A^t + L \rightarrow U + A + H_2 \quad [5]$$

$$A^t + O_2 \rightarrow A^t\cdots O_2 \quad [6]$$

$$A^t\cdots O_2 \rightarrow A + O_2 \quad [7]$$

$$A^t\cdots O_2 + L \rightarrow U + A + (H_2O_2) \quad [8]$$

$$A^t\cdots O_2 + L \rightarrow \text{Decomposition of the dye} \quad [9]$$

where A* is the excited singlet state of acridine and A^t, the triplet state of acridine. Processes [2] and [2'] are observed only in very high concentration of hydroxyl ions.

The application of the steady state method leads to the following equation:

$$\frac{d[U]}{dt} = 10^3 I_0(1-10^{-D})\varphi\left\{\frac{k_5[L]}{k_4+k_5[L]+k_6[O_2]} + \frac{k_6[O_2]}{k_4+k_5[L]+k_6[O_2]}\times\frac{k_8[L]}{k_7+(k_8+k_9)[L]}\right\} \quad (7)$$

where

$$\varphi = \frac{k_3}{k_1+k_3(+k_2[OH^-])}$$

when $[O_2]$ is small, the second term of the right side of this equation can be disregarded. Therefore,

$$\frac{d[U]}{dt} = 10^3 I_0(1-10^{-D})\varphi\frac{k_5}{k_4+k_5[L]+k_6[O_2]}[L] \quad (8)$$

whence

$$\frac{10^3 I_0(1-10^{-D})}{d[U]/dt} = \frac{1}{\varphi}\times\frac{k_4+k_5[L]}{k_5[L]} + \frac{1}{\varphi}\times\frac{k_6}{k_5[L]}[O_2] \quad (9)$$

In agreement with Eq. 9, the plot of the left side of this equation against $[O_2]$ gives a straight line in the region of small $[O_2]$ values, as Fig. 8 shows. From the inclination and the intercept, the values of k_6/k_5 and k_6/k_4 can be evaluated as 1.3 and $(2.2\pm0.5)\times10^5$ l. mol^{-1} respectively. As the value of φ which gives the fraction of the excited singlet state of acridine that goes to the triplet state, the value, 0.24, evaluated in a previous paper[3] was used.

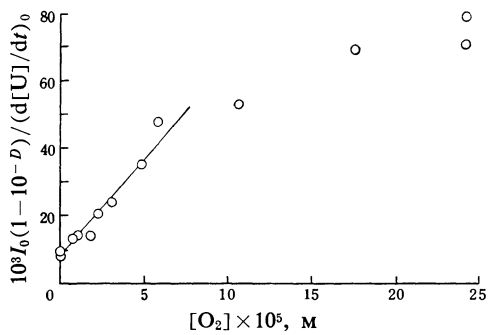

Fig. 8. Plot of $\frac{10^3 I^0(1-10^{-D})}{(d[U]/dt)_0}$ against $[O_2]$.

When the $[O_2]$ value is high, the $k_6[O_2]$ term is so much greater than the $k_5[L]$ term that the first term of Eq. 7 can be disregarded in favor of the second term. From the fact that the overall rate is proportional to [L] up to 4.5×10^{-5} M, one may assume

$$k_7 \gg (k_8+k_9)[L] \quad (10)$$

Thus, the rate of the formation of uranine

may be approximately represented as follows:

$$\frac{d[U]}{dt}=10^3 I_0(1-10^{-D})\varphi\frac{k_6[O_2]}{k_4+k_5[L]+k_6[O_2]}\times\frac{k_8}{k_7}[L] \quad (11)$$

When $[O_2]$ is great, one may put

$$k_6[O_2]\gg k_4+k_5[L] \quad (12)$$

and Eq. 11 is reduced to

$$\frac{d[U]}{dt}=10^3 I_0(1-10^{-D})\varphi\frac{k_8}{k_7}[L] \quad (13)$$

Applying the relation of Eq. 6 to Eq. 13, one gets

$$\frac{d[U]}{dt}=10^3 I_0(1-10^{-D})\varphi\frac{k_8+k_9}{k_7}([U]_\infty-[U]) \quad (14)$$

A comparison of Eq. 14 with Eq. 5 leads to

$$k=\varphi\frac{k_8+k_9}{k_7} \quad (15)$$

The values of $\varphi k_8/k_7$ and $\varphi k_9/k_7$ can easily be obtained from $[U]_\infty$, $[L]_0$, as can the ratio of the quantity of the produced uranine to that of the decomposed dye, i. e., k_8/k_9. The values listed in Table II were obtained in this way. Figure 9 gives the plot of $\varphi k_n/k_7$ ($n=8$ or 9) against pH. Alternatively, the values of $\varphi k_8/k_7$ can also be evaluated from the relation between the initial rate and the initial concentration of leuco-uranine. The agreement between them is rather satisfactory in view of some errors in both values due to the poor reproducibility of the fraction of the produced uranine for the former and the rather inexact procedure of drawing the tangent to the absorbance—time curve at the initial time for the latter.

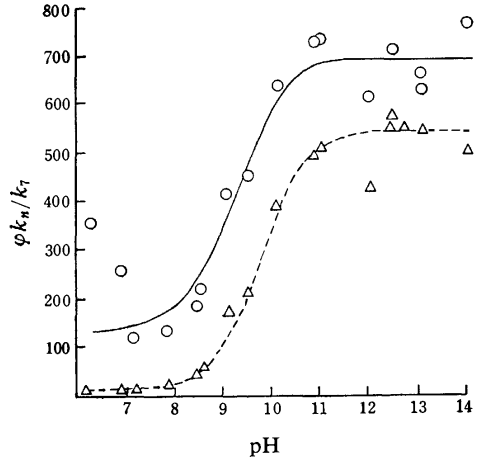

Fig. 9. Plots of $\varphi k_n/k_7$ against the pH value.
○: $\varphi k_8/k_7$ △: $\varphi k_9/k_7$

The pH dependence of the rate in the air-saturated solution is curious at first sight. However, the results can satisfactorily be interpreted in the same way as in the deaerated solution, i. e., on the basis that the various ionic forms of leuco-uranine have different reactivities and, accordingly, have different rate constants. Thus, the next scheme can be written on this basis:

$A^t\cdots O_2 + L^{3-} \rightarrow U$ [i]

$A^t\cdots O_2 + L^{2-} \rightarrow U$ [ii]

$A^t\cdots O_2 + L^{-} \rightarrow U$ [iii]

$A^t\cdots O_2 + L \rightarrow U$ [iv]

$A^t\cdots O_2 + L^{3-} \rightarrow$ Decomposition of the dye [i']

$A^t\cdots O_2 + L^{2-} \rightarrow$ Decomposition of the dye [ii']

$A^t\cdots O_2 + L^{-} \rightarrow$ Decomposition of the dye [iii']

$A^t\cdots O_2 + L \rightarrow$ Decomposition of the dye [iv']

where k_I, k_{II},$\cdots$, k_{Iv}' are the rate constants for each process.

The rate can be approximately given as follows by the use of Eq. 13:

$$\frac{d[U]}{dt}=10^3 I_0(1-10^{-D})\frac{\varphi}{k_7}\times(k_I[L^{3-}]+k_{II}[L^{2-}]+k_{III}[L^{-}]+k_{Iv}[L]) \quad (16)$$

This equation can be rewritten as follows by using the successive dissociation constants of leuco-uranine (K_1, K_2 and K_3):

$$\frac{d[U]}{dt}=10^3 I_0(1-10^{-D})\frac{\varphi}{k_7}\times\frac{(k_{Iv}[H^+]^3+k_{III}K_1[H^+]^2+k_{II}K_1K_2[H^+]+k_IK_1K_2K_3)}{[H^+]^3+K_1[H^+]^2+K_1K_2[H^+]+K_1K_2K_3}[L]_s \quad (17)$$

where $[L]_s$ is the analytical concentration of leuco-uranine. Equation 17 can be changed further as follows by using Eq. 13 again:

$$\frac{\varphi k_8}{k_7}\{[H^+]^3+K_1[H^+]^2+K_1K_2[H^+]+K_1K_2K_3\} \quad (=S)$$

$$=\frac{\varphi}{k_7}\{k_{Iv}[H^+]^3+k_{III}K_1[H^+]^2+k_{II}K_1K_2[H^+]+k_IK_1K_2K_3\} \quad (18)$$

The left side of this equation can now be evaluated, since K_1, K_2 and K_3 have already been determined.[1,3]

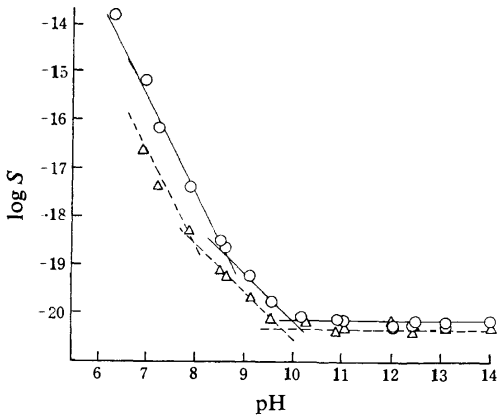

Fig. 10. Plots of $\log S$ against the pH value.
○ : Formation of uranine
△ : Decomposition of the dye

Plotting $\log S$ against pH, it is expected that in the region where the pH value is so small that the first term of the right side overwhelms the other terms, the curve will be a straight line with a slope of -3. As the pH value increases, the straight line gradually curves and joins another straight part having a slope of -2 and then one of 0. Extrapolating each straight line to a pH value of zero, $\varphi k_{\rm I}/k_7$, $\varphi k_{\rm II}/k_7$ and $\varphi k_{\rm III}/k_7$ can be evaluated. The relations are shown in Fig. 10; the following results were obtained:

$$\varphi k_{\rm I}/k_7 = 700 \text{ l. mol}^{-1}$$
$$\varphi k_{\rm II}/k_7 = 400 \text{ l. mol}^{-1}$$
$$\varphi k_{\rm III}/k_7 = 130 \text{ l. mol}^{-1}$$

The value of $\varphi k_{\rm IV}/k_7$ can not be given in the pH region tested in the present experiment. It is to be noted that below pH 8, a slight deviation from the straight line becomes apparent. The values of $\varphi k_8/k_7$ calculated by the use of these values are plotted in Fig. 9 as a solid line. At pH values lower than 8, a deviation from this line is again observed, the experimental values being appreciably larger than the calculated ones. This deviation may be attributed to a somewhat different scheme in the lower pH region, such as the promoting effect of a product which is marked in this pH region.

The values of $\varphi k_9/k_7$ which are related to the decomposition of the dye have been examined in the same manner as was the value of $\varphi k_8/k_7$. The results obtained are as follows:

$$\varphi k_{\rm I}'/k_7 = 550 \text{ l. mol}^{-1}$$
$$\varphi k_{\rm II}'/k_7 = 100 \text{ l. mol}^{-1}$$
$$\varphi k_{\rm III}'/k_7 = 10 \text{ l. mol}^{-1}$$

The values of $\varphi k_9/k_7$ at each pH values were calculated reversely from the above results; the broken curve in Fig. 9 gives the resultant plot. It is seen that this curve fits the experimental values fairly well.

From the above results, it is concluded that the value of $\varphi k_{\rm III}'/k_7$ is much smaller than the values of $\varphi k_{\rm I}'/k_7$ and $\varphi k_{\rm II}'/k_7$, in contrast to the case in the deaerated solution, in which the values of $\varphi k_n/k_{\rm t}$ are not very different from each other.[3] In other words, the univalent anions of leuco-uranine are more stable to the oxidation than the di- and trivalent anions. It is remarkable that the values of $\varphi k_n/k_7$ are very much smaller than those corresponding to the deaerated solution. It will be interesting to investigate whether this difference is due to the difference in the rate constants pertaining to the oxidation of leuco-uranine or to that between the rate constants of the deactivation of the triplet state of acridine and that of the molecular complex, $A^{\rm t}\cdots O_2$; however, this point can not be discussed in the present state of research.

Summary

The mechanism of an acridine-sensitized photoöxidation of leuco-uranine in an aerated solution has been elucidated. The oxidation takes place in a different manner from that in a deaerated solution. That is, oxygen attacks the triplet state of acridine very rapidly and presumably forms a kind of loosely-bound molecular complex. Most of this decomposes into the original acridine and oxygen, so that oxygen suppresses the oxidation of leuco-uranine occurring in the deaerated solution. Denoting the rate constants of the reactions between the triplet state of acridine and leuco-uranine and oxygen, respectively, as k_5 and k_6, the value of k_6/k_5 is given as 1.3. On the other hand, the oxidation of leuco-uranine by oxygen becomes apparent in a high oxygen concentration, such as an air-saturated solution. Namely, the molecular complex consisting of the triplet state of acridine and oxygen reacts with leuco-uranine, and the oxidation of the latter takes place. If one writes the rate constant of this reaction as k_8 and that of the reaction in which the molecular complex decomposes into acridine and oxygen as k_7, one can evaluate the ratio of $\varphi k_8/k_7$ from the experimental results, where the value of φ is the transition probability in which acridine goes to the triplet state from the excited singlet state. An irreversible decomposition of the dye also competes with the above reactions. Putting its rate constant as k_9, the value of $\varphi k_9/k_7$ has been evaluated. The variation of the ratios of $\varphi k_8/k_7$ and $\varphi k_9/k_7$ with the variation in pH values has been interpreted on the basis

that the reactivities of leuco-uranine are different in each ionic species. With the higher values of pH, the quantum yield becomes greater. The quantum yields of the formation of uranine and the irreversible decomposition of the dye have been evaluated as 0.0070 and 0.0055 respectively, yields which are about one thirtieth that in the deaerated solution. In the region of pH values lower than 8, a promoting action of a certain reaction seems to take part in the reaction and the reaction approaches the zeroth order.

The author wishes to express his deep thanks to Professor Masao Koizumi for his cordial encouragement and many helpful discussions throughout this work. He also desires to thank heartily Dr. Shunji Kato for his much valuable advice and Mr. Shigeya Niitsuma for his assistance.

Department of Chemistry
Faculty of Science
Tohoku University
Katahira-cho, Sendai

Appendix

The Confirmation of the Hydrogen Evolution.— In Part I of this series, it was tentatively concluded, on the basis of the results of various kinds of scrutinizing experiments, that the evolution of hydrogen would occur, along with the photosensitized oxidation of leuco-uranine, in the deaerated condition. However, in spite of great effort, we could not succeed at that time in gathering and identifiying the evolved gas, and so the most direct evidence for the hydrogen evolution was lacking. Now, by increasing the quantity of the sample to be irradiated to several times the amount used in the previous paper, the author has succeeded in confirming that hydrogen is evolved. Thus, sample solutions which were about twice as concentrated and the volumes of which were two or four times as great as previous ones were prepared, and the gas evolved during the irradiation was gathered and analysed. As a sensitizer, uranine was used because there is no possibility for the sensitizer itself to be reduced by the evolved hydrogen. It is to be noted, however, that the reproducibility in the feature of the reaction seemed to be rather poor, perhaps because of the use of uranine as a sensitizer. 175~200 ml. of the sample solution ($[L]=9\times10^{-5}$ M, $[U]=(4\sim13)\times10^{-6}$ M and $[NaOH]=2\times10^{-3}$ N) was divided into several portions, each 25~50 ml. in volume, and they were evacuated carefully. After irradiation, all the evolved gas non-condensable at the liquid air temperature was gathered by the use of a small mercury diffusion pump and a Toepler pump. Two similar experiments were then performed; the results obtained are shown in Table III.

Table III. Quantity of gas evolved after irradiation

Exp. no.	Quantity of oxidized leuco-uranine mol.	Volume of gas obtained (reduced to STP*), ml.	Quantity of gas, mol.
I	5.2×10^{-6}	0.149	6.7×10^{-6}
II	5.1×10^{-6}	0.049	2.2×10^{-6}

* Standard temperature (0°C) and pressure (1 atm.)

The gas thus obtained was passed through a tube containing copper(II) oxide at 297°C, and the oxidation product was condensed in a trap cooled by liquid air. The volumes of the non-condensable gases at −183°C, −75°C and at room temperature were determined separately. The results are shown in Table IV.

It is concluded that gas C is water vapor, because water-like mist condensed on the wall when the gas was compressed into a small measuring vessel by the use of a Toepler pump; moreover, its vapor pressure was nearly the same as that of water. The quantity of gas A in Exp. no. I is unexpectedly large; this is perhaps due to the leakage of air during the procedure.

Furthermore, 95% of gases B and C in Exp. no. II disappeared when they were passed through a tube containing sodium hydroxide pellets and were condensed in a trap cooled at about −75°C; so gas B must be carbon dioxide. No organic substance which is not captured by liquid air but which is oxidized into water and carbon dioxide over copper oxide at about 300°C is likely to be produced from leuco-uranine in the reaction.

From the above results, most of the gas evolved in the reaction can be concluded to be hydrogen, but there seems to be some possibility that carbon monoxide might also be produced. The production of the latter might be due to the photochemical reduction of carbonate ions by the hydrogen evolved in the oxidation of leuco-uranine. If one assumes that the equimolar hydrogen is consumed in the reduction of carbonate ions, the quantity of hydrogen initially produced corresponds to 95 and 40% of the oxidized leuco-uranine in the above two experiments. Although the quantitative agreement

Table IV. Quantity of gas after passing through a heated CuO-tube

(Volumes of gases are reduced to STP)

Exp. no.	Gas A Non-condensable at −183°C Volume, ml. (mol.)	Gas B Non-condensable at −75°C Volume, ml. (mol.)	Gas C Non-condensable at room temperature Volume, ml.
I	36×10^{-3} (16×10^{-7})	1.9×10^{-3} (0.9×10^{-7})	($\sim110\times10^{-3}$)
II	1.9×10^{-3} (0.9×10^{-7})	22×10^{-3} (9.6×10^{-7})	($\sim25\times10^{-3}$)

is rather poor in the two experiments, it can be concluded from the above results that the evolution of the hydrogen gas is the main process in the photoöxidation of leuco-uranine in the deaerated solution. It is interesting that carbon monoxide seems to be produced under some conditions; this is perhaps due to the photochemical reduction of carbonate ions.

An NMR Study of Acetaldehyde Methanol Solutions

By Yuzuru FUJIWARA and Shizuo FUJIWARA

(Received April 26, 1963)

Aqueous solutions of acetaldehyde have been investigated utilizing the technique of nuclear magnetic resonance (NMR). The heat of hydration, the equiliblium constants, the chemical shifts, the spin-spin coupling constants, the relative relaxation times and the activation energies for Brownian motions of the molecules have been determined. The probable electronic structures and proton exchange between water and hydrated acetaldehyde have been discussed.[1)]

NMR posseses a considerable advantage for the investigation of the states of such chemically unstable substances as hemiacetal, which forms when acetaldehyde and methanol are mixed. Hemiacetal is difficult to detect by means of other than NMR.

In the present investigation solutions of methanol and acetaldehyde were compared with solutions of water and acetaldehyde. Where no catalyst is used, the rates of the formation of hemiacetal and acetal are so low that measurement of the equilibrium constants for the systems of aldehyde-hemiacetal and aldehyde-acetal are precluded, while the rates of formation are measurable.

Experimental

NMR spectra were obtained at 60 Mc./sec., using a Varian Associates spectrometer. Chemical shifts were measured by the side-band method from the methyl proton signal of free acetaldehyde. Concentrations of various species of hydrogen were determined by measuring the area under the curves with consideration of the power saturation. Acetaldehyde was prepared by the decomposition of commercial para-aldehyde, using sulfuric acid as a catalyst, and by redistillation.

Results and Discussion

It is well known that acetaldehyde and methanol react as follows:

$$CH_3CHO + CH_3OH \rightarrow CH_3CH(OH)(OCH_3)$$

$$CH_3CH(OH)(OCH_3) + CH_3OH \rightarrow CH_3CH(OCH_3)_2 + H_2O$$

The NMR spectra of these solutions are shown in Fig. 1, where the signals for all species of hydrogen appear at separate positions and are unambiguously assigned to their respective curves through such NMR features as fine structure, chemical shift, line width, the concentration dependence of the line intensity, and a comparison of these spectra with the spectra of pure and aqueous solution of dimethylacetal. Three kinds of methoxy methyl hydrogen appear separately in acetal, hemiacetal, and methanol, and three kinds of methyl hydrogen also appear separately in acetal, hemiacetal and acetaldehyde. These phenomena can be explained in terms of the electron density and the long-range magnetic shielding of the C–C and C–O bonds. The anisotropic magnetic effect of C=O on the shift of the methine proton is estimated to be 5.0 p.p.m. on the basis of the difference between the shift of free and that of solvated acetaldehyde; this is not so different from the value of 4.6 p.p.m. obtained from an aqueous solution of acetaldehyde.[1)]

Three kinds of OH hydrogen in water, methanol and hemiacetal form a single broad line in a 60 mol. % solution; its position depends on the concentration (cf. Fig. 2). This suggests a rapid hydrogen exchange, the shift corresponding to the variation of the concentration of each component. In a 10 mol. % solution, these OH hydrogens are separated and have different line widths, i. e., 5.8 c. p. s. for water, 5.3 c. p. s. for hemiacetal, and 6.8 c. p. s. for methanol. If we assume that exchanges are slow[2)] and that the ratios

1) Y. Fujiwara and S. Fujiwara, This Bulletin, **36**, 574 (1963).

2) J. A. Pople, W. G. Schneider and H. J. Bernstein, "High Resolution Nuclear Magnetic Resonance," McGraw-Hill, N. Y. (1958). p, 225.

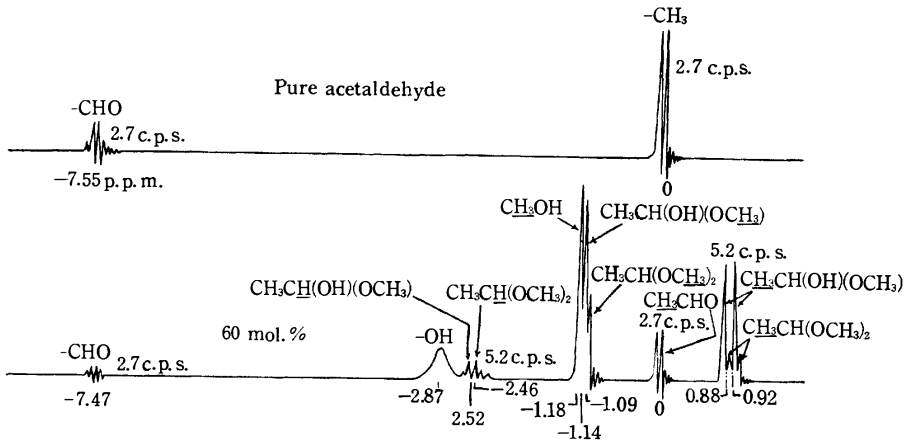

Fig. 1—a

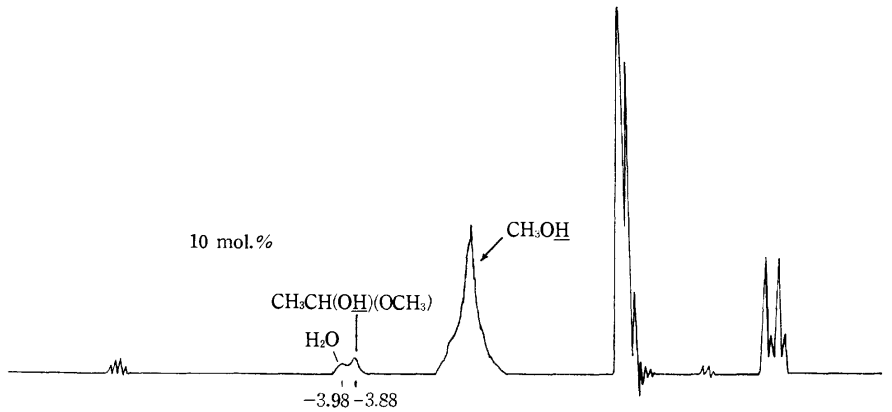

Fig. 1—b NMR spectra of acetaldehyde methanol solution

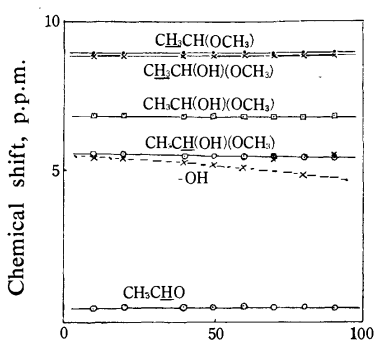

Concentration of Acetaldehyde, mol. %

Fig. 2. Chemical shift of AcH relative to CH_3CHO

of the rates of exchange are constant for common species, one may estimate the exchange rates as in Table I. The order of the values in Table I corresponds to the order of the size of molecules and appears reasonable. Moreover, a comparison of these data with the exchange rate for pure water obtained by

Table I. Rate of hydrogen exchange

		l./mol./sec.
H_2O	— H_2O	$k_{11}=1.6$
MeOH	— MeOH	$k_{22}=0.58$
MeCH(OH) OMe	— MeCH(OH) OMe	$k_{33}=0.35$
H_2O	— MeOH	$k_{12}=0.97$
H_2O	— MeCH(OH) OMe	$k_{13}=0.76$
MeOH	— MeCH(OH) OMe	$k_{23}=0.45$

Meiboom[3] shows that the corresponding value obtained in this laboratory is 0.63 times that of Meiboom. Since his data refer to solutions catalyzed by acid or base, a correction was made to adjust the concentration for this comparison. This can be regarded as a good agreement; the slight discrepancy may be attributed to the role of diffusion due to the different concentration of water. In the present

3) S. Meiboom, *J. Chem. Phys.*, **34**, 375 (1961).

case, the diffusion is somewhat a rate determinant. Arnold[4] has also reported a hydrogen exchange rate for pure ethanol which was about one-third of the value obtained in the present investigation for the exchange between methanol and methanol. This difference undoubtedly results from differences in molecular size.

Molecular motion can be investigated by the measurement of relaxation time, since it depends on the correlation time of the Brownian motion of the molecule. In this case the relative relaxation times were measured by the power saturation method (Fig. 3), assuming an extremely narrow case.[5] The results are shown in Table II, where the temperature dependence of relaxation times is also given. From these data, estimation of the activation energies for the molecular motions was made. Hemiacetal has the largest activation energy; this may be attributed to the restricted motion resulting from the hydrogen bonding with other OH's and is consistent with the case of hydrated acetaldehyde. Hydrated acetaldehyde has a larger value than hemiacetal; this may be explained by the greater tendency of hydrated acetaldehyde to undergo hydrogen bonding than hemiacetal. The activation energy for free acetaldehyde in a methanol solution is estimated to be 1.3 kcal./mol., which agrees quite well with that in an aqueous solution (1.27 kcal./mol.). The small temperature dependence of dimethylacetal may be ascribed to its spherical molecular shape, which hinders rotation very little, to the molecular structure, which has no group which can interact strongly with the surrounding molecules, and to the intermolecular motion, which may considerably contribute to the relaxation.

TABLE II. RELATIVE RELAXATION TIMES

Temp.	Relative relaxation time			E_{ac} kcal./mol.
	+86°C	+30°C	−16°C	
CH_3CHO	1.3	1.0	0.74	1.3
$CH_3CH\langle^{OH}_{OCH_3}$	1.3	0.91	0.51	2.2
$CH_2CH(OCH_3)_2$	1.1	0.91	1.0	~0

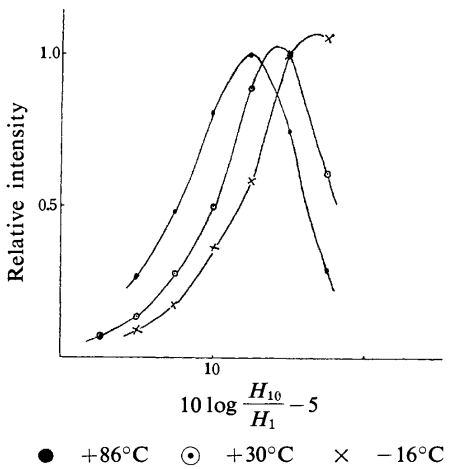

Fig. 3. Power saturation of $CH_3CH(OH)(OCH_3)$

The formation of hemiacetal and acetal from the mixture of acetaldehyde and methanol is very slow when the system is free from a catalyst such as acid or salt. Nevertheless, measurements of their formation rates were made in the case where no catalyst was added. This was necessary in order to avoid the possible disturbance to the system which might be caused by the catalyst and to ascertain the direct interaction of aldehyde with alcohol. The values in Table III were calculated on the assumption that the reverse reactions are negligible and that the methanol content does not vary appreciably during the reaction. The validity of the first assumption was confirmed by observing that the reaction proceeds more rapidly and more extensively in the presence of a catalyst. That of the second was confirmed by measuring the methanol concentration before and after the reaction, which proceeded for 70 days. The agreement of the values obtained at various concentrations is satisfactory and suggests that the calculation based on the above assumption is correct.

TABLE III. REACTION RATE OF AcH-MeOH

Concn., mol./l. AcH	MeOH	$k_1 \times 10^5$* l./mol./hr.	$k_2 \times 10^5$* l./mol./hr.
14.4	6.2	9.0	1.9
12.8	8.5	8.1	2.4
9.2	13.7	8.1	1.9
4.7	18.1	8.7	0.30
Average		8.5 ± 1	2.1 ± 0.5

* $CH_3CHO + CH_3OH \xrightarrow{k_1} CH_3-CH(OCH_3)-OH$

$CH_3-CH(OCH_3)-OH + CH_3OH \xrightarrow{k_2} CH_3-CH-(OCH_3)_2$

Summary

By the NMR method, the methanol solution of acetaldehyde was studied; in this solution all the species of hydrogen of each molecule are measurable, and a kinetic study of the system was readily performed. This could be

4) J. T. Arnold, *Phys., Rev.*, **102**, 136 (1956).
5) N. Bloembergen, E. M. Purcell and R. V. Pound, ibid., **73**, 672 (1948).

compared with any other conventional methods, by which some of the species usually present in the system are directly measured. The formation rates of hemiacetal and acetal were measured as $(8.5 \pm 1) \times 10^{-5}$ and $(2.1 \pm 0.5) \times 10^{-5}$ l./mol./hr., respectively, in the absence of a catalyzer. The hydrogen exchange rates for three kinds of OH's were also obtained. When compared with the related values in the literature, agreement is satisfactory. The relaxation times show a difference in the molecular motion corresponding to molecular structure and in the interaction with surrounding molecules.

The authors wish to thank Mr. Osamu Yamamoto of the Government Chemical Industrial Research Institute and Mr, Naohiro Hayakawa of the Japan Atomic Energy Institute for their aid in obtaining NMR spectra which have been presented in this paper.

Department of Chemistry,
Faculty of Science
The University of Tokyo
Hongo, Tokyo

The Electronic Spectra and Structures of s-Triaminobenzenium and Some Related Ions

By Noboru MATAGA

(Received February 27, 1963)

It has been shown by Köhler and Scheibe[1] that *s*-triaminobenzene (TAB), *s*-triaminoanisol, *s*-triaminoxylene, *s*-triaminomesitylene and phloroglucine trianion (TOB) seem to be easily protonated on the ring carbon in an aqueous solution. When *m*-phenylenediamine is singly protonated, the absorption spectrum of the protonation product is almost the same as that of aniline, and the spectrum of singly protonated aniline is very close to that of benzene. However, the spectrum of singly protonated TAB is quite different from that of *m*-phenylenediamine, and intense band appears at a much longer wavelength. This remarkable change in the spectrum has been ascribed[1] to the formathin of $TABH^+$ protonated on the ring carbon.

In the case of the methyl derivatives of TAB, the wavelength of this intense band is a littler larger than in the case of TAB.

These facts are quite interesting from the viewpoint of the conjugation power of the amino group. The study of the electronic structure and spectrum of $TABH^+$ may be somewhat interesting also in view of the recently developed chemistry[2] of the aromatic hydrocarbons protonated in strongly acidic media.

On the other hand, we have been making some theoretical studies of the electronic spectra and electronic structures of such amino-substituted benzenes as aniline, phenylenediamines and TAB and such amino-substituted nitrogen heterocycles as amino pyridines.[3]

Using the results of these studies, we have attempted to interpret theoretically the electronic spectra and structure of $TABH^+$ and also to give a theoretical basis to the observed stability of the protonated TAB and TOB.

In the following, we shall report the results of these theoretical calculations, together with some discussion.

Theoretical Method

The semiempirical ASMO CI method[4] was used for the calculation of the electronic spectra. The necessary Hückel MO's were calculated by assuming appropiate parameters; that is, all resonance integrals were taken to be the same and equal to β, the Coulomb

1) H. Köhler and G. Scheibe, *Z. anorg. u. allgem. Chem.*, **285**, 221 (1956).

2) a) G. Dallinga, A. A. V. Stuart, P. J. Smit and E. L. Mackor, *Z. Elektrochem.*, **61**, 1019 (1957); E. L. Mackor, A. Hofstra and J. H. van der Waals, *Trans. Faraday Soc.*, **54**, 66, 186 (1958). b) N. Muller, L. W. Pickett and R. S. Mulliken, *J. Chem. Phys.*, **21**, 1400 (1953); *J. Am. Chem. Soc.*, **76**, 4770 (1954). c) T. Morita, *J. Chem. Phys.*, **25**, 1290 (1956); This Bulletin, **31**, 3220 (1958); **32**, 893 (1959); **33**, 1486 (1960).

3) a) N. Mataga, to be published. b) N. Mataga and S. Mataga, This Bulletin, **32**, 600 (1959).

4) a) R. Pariser and R. G. Parr, *J. Chem. Phys.*, **21**, 466, 767 (1953); ibid., **23**, 711 (1955). b) R. Pariser, ibid., **24**, 250 (1956). c) N. Mataga, This Bulletin, **31**, 459, 463 (1958); *Z. physik. Chem. N. F.*, **18**, 285 (1958).

parameter for amino nitrogen, to be 1.2,[5] and that for O^- of TOB, 0.8.*

For the protonation products, the localization model was assumed. That is, if there are $2m$ π-electrons in the framework of n cores of the neutral molecule, then there are $2(m-1)$ π-electrons moving in the framework $n-1$ cores in the protonation product.

Thus, the effect of hyperconjugation[2b,c] with the CH_2 group is not explicitly taken into account in the present treatment. However, its effect on the stabilty of the protonation product will be examined, in an approximate way, in the latter part of this paper.

The procedures for the calculation of the electronic spectra of TAB and $TABH^+$ and the stabilities of the protonated aminobenzenes and TOB were as follows.

A) The Stabilities of the Protonation Products.—As a measure of the stabilities of the protonated species, the so-called localization energies[5-9] were calculated.

In the present case, if the π-energy of the neutral molecule is $2m\alpha+M\beta$, that of the localized system is $2(m-1)\alpha+M_r{}^+\beta$ where the proton is attached at position "r."

The localization energy is given by the difference between the π-energies of the neutral molecule and of the localized system, or by $(M-M_r{}^+)$. If all changes in the σ-bond caused by protonation are treated as being effectively constant throughout a series of aminobenzenes, we can anticipate a correlation[2a,c,8,9] between the calculated localization energies and the experimental basicities.

B) The Electronic Spectra.—The orbital energy of the i-th MO, ε_i, may be written formally:

$$\varepsilon_i=\langle\phi_i|F|\phi_i\rangle=\sum_{\mu,\nu}C_{i\mu}C_{i\nu}\langle\phi_\mu|F|\phi_\nu\rangle$$
$$=\sum_{\mu,\nu}C_{i\mu}C_{i\nu}F_{\mu\nu} \quad (1)$$

where F is the Fock Hamiltonian and ϕ_i is the LCAO MO, for which the Hückel MO's are used in the present calculation:

$$\phi_i=\sum_{\mu}^{n}C_{i\mu}\phi_\mu. \quad (2)$$

The matrix elements of the Fock Hamiltonian in terms of $2p\pi$ AO's may be written as follows:

$$F_\mu=\langle\phi_\mu|F|\phi_\mu\rangle=-I_\mu+(1/2)\cdot P_{\mu\mu}\gamma_\mu+\sum_{\kappa\neq\mu}(P_{\kappa\kappa}-Z_\kappa)\gamma_{\kappa\mu} \quad (3)$$

$$F_{\mu\nu}=\langle\phi_\mu|F|\phi_\nu\rangle=\beta_{\mu\nu}-(1/2)\cdot P_{\mu\nu}\gamma_{\mu\nu} \quad (4)$$

$$\gamma_{\mu\nu}=\langle\phi_\mu(1)\phi_\nu(2)|G_{12}|\phi_\mu(1)\phi_\nu(2)\rangle \quad (5)$$
$$G_{12}=e^2/r_{12}$$

$$P_{\mu\nu}=2\sum_{i}^{\text{occ.}}C_{i\mu}C_{i\nu} \quad (6)$$

In Eqs. 3—5, I_μ is the ionization potential of the μ atom in the appropriate valence state, Z_κ is the core charge of the κ core, $\beta_{\mu\nu}$ is the core resonance integral, and r_{12} in the two electron-operator G_{12} is the inter-electronic distance.

The excitation energy of the $i\rightarrow k$ transition, $E(\chi_{ik})=\langle\chi_{ik}|\mathscr{H}|\chi_{ik}\rangle-\langle\chi_0|\mathscr{H}|\chi_0\rangle$, and the interconfigurational matrix element, $\langle\chi_{ik}|\mathscr{H}|\chi_{jl}\rangle$, may be calculated by the following equations:

$$E({}^1\chi_{ik})=(\varepsilon_k-\varepsilon_i)-\langle\phi_i(1)\phi_k(2)|G_{12}|\phi_i(1)\phi_k(2)\rangle+2\langle\phi_i(1)\phi_k(2)|G_{12}|\phi_k(1)\phi_i(2)\rangle \quad (7)$$

$$\langle{}^1\chi_{ik}|\mathscr{H}|{}^1\chi_0\rangle=\sqrt{2}\langle\phi_k|F|\phi_i\rangle \quad (8)$$

$$\langle{}^1\chi_{ik}|\mathscr{H}|{}^1\chi_{il}\rangle=\langle\chi_k|F|\chi_l\rangle-\langle\phi_i(1)\phi_k(2)|G_{12}|\phi_i(1)\phi_l(2)\rangle+2\langle\phi_i(1)\phi_k(2)|\underset{k\neq l}{G_{12}}|\phi_l(1)\phi_i(2)\rangle \quad (9)$$

$$\langle{}^1\chi_{ik}|\mathscr{H}|{}^1\chi_{jk}\rangle=-\langle\phi_j|F|\phi_i\rangle-\langle\phi_k(1)\phi_j(2)|G_{12}|\phi_k(1)\phi_i(2)\rangle+2\langle\phi_k(1)\phi_j(2)|\underset{i\neq j}{G_{12}}|\phi_i(1)\phi_k(2)\rangle \quad (10)$$

$$\langle{}^1\chi_{ik}|\mathscr{H}|{}^1\chi_{jl}\rangle=-\langle\phi_j(1)\phi_k(2)|G_{12}|\phi_i(1)\phi_l(2)\rangle+2\langle\phi_j(1)\phi_k(2)|\underset{i\neq j,\ k\neq l}{G_{12}}|\phi_l(1)\phi_i(2)\rangle \quad (11)$$

For ${}^3\chi$'s, the third terms in Eqs. 7, 9 and 10 and the second term in Eq. 11 vanish.

In the ASMO CI method used here, the wave function Ψ for an electronic state is approximated by a linear combination of χ_0 and χ_{ik}'s.

5) H. Baba, This Bulletin, 34, 76 (1961).

* In order to determine the Coulomb parameter for O^-, proportionality between α and the valence state ionization potential was assumed, taking the sp^2 hybridized carbon as a reference; i. e., $\delta_O-/\delta_N=(\alpha_O--\alpha)/(\alpha_{N^+}-\alpha)=(I^\pi{}_O\ (\mathrm{tr}^2\mathrm{tr}^c\mathrm{tr}\pi)-I^\pi{}_C)/(I^\pi{}_{N^+}\ (\mathrm{tr}\ \mathrm{tr}\ \mathrm{tr}\pi)-I^\pi{}_C)$, where tr indicates the trigonal hybrid orbital (sp^2).
Using $I^\pi{}_C=11.16$ eV., $I^\pi{}_O=17.7$ eV., $I^\pi{}_{N^+}=28.72$ eV. (J. Hinze and H. H. Jaffé, *J. Am. Chem. Soc.*, **84**, 540 (1962)) and $\delta_N=1.2$, δ_O- was calculated to be 0.45. If we use for $I^\pi{}_{N^+}$ the VESCF value (25.772 eV.) obtained by Brown and Heffernan for pyrrole (Ref. 13), δ_O- can be calculated to be 0.54. Thus, δ_O- seems to be close to 0.5. This value was used at first. However, the electronic spectrum of $TOBH^+$ calculated with this Hückel MO was in poor agreement with the observed data. (S. Mataga and N. Mataga, unpublished.)
Therefore, other values of δ_O- were examined, and it was found that $\delta_O-=0.8$ gave what appeared to be a reasonable result for the spectrum of $TOBH^+$.

6) G. W. Wheland, *J. Am. Chem. Soc.*, 64, 900 (1942).

7) K. Higashi and H. Baba, "Quantum Organic Chemistry," Asakura, Tokyo (1956), p. 273.

8) R. Daudel, R. Lefebvre and C. Moser, "Quantum Chemistry," Interscience, New York (1959), p. 235.

9) A. Streitwieser, Jr., "Molecular Orbital Theory for Organic Chemist," John Wiley & Sons, New York (1961), p. 335.

The oscillator strength, f, is calculated by the method described by Mulliken and Rieke:[10]

$$f=1.085\times10^{11}\omega_{0\alpha}\sum_{r=x,y,z}[M^{r}_{0\alpha}]^{2} \qquad (12)$$

where $\omega_{0\alpha}$ is the frequency in cm^{-1} of the transition from the ground state, Ψ_0, to an excited state, Ψ_α. The necessary fromulas for the calculation of $M^{r}_{0\alpha}$ are given elsewhere.[4b]

C) The Semiempirical Evaluation of Integrals in the ASMO CI Calculation.—The molecular integrals which arise have been evaluated by a semiempirical procedure.

$Z_\mu=1$ for the carbon core and $Z_\kappa=2$ for the core of amino nitrogen which contributes two electrons to the π-system. The I_μ value for carbon was taken to be 11.42 eV., and that for the amino nitrogen, 28.85 eV.[11]

$\gamma_{\mu\nu}$'s were evaluated by the same procedure as before,[12,4c,11] using the valence state ionization potential, I_μ, and the electron affinity, A_μ:

$$\gamma_{\mu\nu}=14.3949/(a+R_{\mu\nu}) \text{ (eV.)} \qquad (13)$$

where $R_{\mu\nu}$ is the distance between the μ and ν atom (in Å). In a homonuclear case,

$$\gamma_\mu=14.3949/a=I_\mu-A_\mu \qquad (14)$$

Thus, $a_C=1.328$Å and $a_N=0.868$Å. For the case of heteronuclear two centers, i. e. carbon and nitrogen, the value of a is the harmonic mean of a_C and a_N. Therefore, $a_{CN}=1.049$Å.

The empirical parameter, $\beta_{\mu\nu}$, was taken into account only for the nearest neighbors and neglected for more distant neighbors: $\beta_{CC}=-2.388$ eV.[12,4c] and $\beta_{CN}=-3.6$ eV.[3a] All C–C bond distances were assumed to be 1.39 Å, and C–N distances, 1.36 Å. D_{3h} and C_{2v} symmetries were assumed for TAB and $TABH^+$ respectively.

The values of F_μ's for the amino nitrogens calculated by Eq. 3 using 28.85 eV. for I_μ, which is the ionization potential of the $2p\pi$ electron of N^+ in the trigonal hybrid state, seem to be too large. For a more refined calculation, the VESCF method[13] proposed by Brown and Heffernan may be useful. Actually, we have calculated the electronic spectra and electronic structure of *p*-phenylenediamine[3a] by the VESCF method and have obtained an improved result compared with that obtained by the ASMO CI calculation similar to the one described above.

However, in the present study, we have not attempted such a refined calculation but have used only a simple procedure which gives appropriate values for the F_μ's of amino nitrogen. That is,

$$\langle F_\mu\rangle_N=\langle F_C\rangle_{AV}+\delta_N\cdot\langle F_{CC}\rangle_{AV} \qquad (15)$$

where $\langle F_C\rangle_{AV}$ is the simple arithmetic mean of F_μ's for carbons, $\langle F_{CC}\rangle_{AV}$ is the same quantity of $F_{\mu\nu}$'s for the nearest neighbor carbon-carbon bonds, and δ_N is the Hückel MO parameter for the Coulomb integral of nitrogen, 1.2.

When $\langle F\rangle_N$ instead of F_N was used, the most suitable value of the core resonance integral, β_{CN}, was -2.399 eV.[3a] the value of β_{CC} being the same as before. Using $\langle F\rangle_N$ and $\beta_{CN}=-2.399$ eV., we have calculated the electronic spectra of some amino-substituted benzenes such as aniline and phenylenediamines and obtained a very good agreement with the observed.[3a]

Results and Discussion

The Hückel MO's and MO energies of TAB, $TABH^+$ (protonated on carbon), TOB and $TOBH^+$ (protonated on carbon) are given in the appendix. The numbering of the atoms in these compounds is given in Fig. 1.

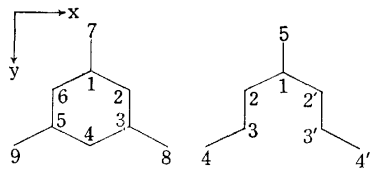

Fig. 1. The numbering of atoms in the base molecule and the corresponding carbonium ion.

A) Comparison of the Calculated Spectra with the Observed.—Using these MO's, the electronic spectra of TAB and $TABH^+$ were calculated by the method described in "Theoretical Method." The calculated spectra are given in Table I together with the observed, and the state functions and energies, taking the energy of the ground configuration, $E(\chi_0)$, as zero, are collected in Table II. The calculated values of such matrix elements as the formal orbital energies, $\langle\psi_i|F|\psi_i\rangle$'s, excitation energies and interconfigurational elements are given in the appendix.

Owing to the D_{3h} symmetry, the transitions to the lowest and the second excited singlet states of TAB respectively are electronically forbidden. These calculated spectra correspond quite well to the very weak absorption bands

10) R. S. Mulliken and C. A. Rieke, *Rep. Progr. Phys.*, 8, 231 (1941).
11) S. Mataga and N. Mataga, *Z. physik. Chem., N. F.*, **19**, 231 (1959).
12) N. Mataga and K. Nishimoto, ibid., **13**, 140 (1957); N. Mataga, This Bulletin, **31**, 453 (1958); N. Mataga, K. Nishimoto and S. Mataga, ibid., **32**, 395 (1959).
13) R. D. Brown and M. L. Heffernan, *Trans. Faraday Soc.*, **54**, 757 (1958); *Australian J. Chem.*, **12**, 319 (1959).

TABLE I. CALCULATED AND OBSERVED SPECTRA OF TAB AND TABH$^+$

TAB	Calcd.		Obs.		TABH$^+$	Calcd.		Obs.	
	$h\nu$, eV.	f	$h\nu$, eV.	f		$h\nu$, eV.	f	$h\nu$, eV.	$\log\varepsilon_{max}$
$^1A'_2$	4.672(4.270)	0	4.4	0	$^1B_1$	3.153(3.121)	0.39	3.4	~3.5
$^1A'_1$	6.016(5.213)	0	5.0	0	$^1A_1$	4.460(4.427)	0.65	4.5	~3.9
$^1E'$	6.191(5.789)	2.2	5.6	$\log\varepsilon_{max}$	$^1A_1$	5.635(5.373)	1.52	?	?
$^3A'_1$	3.341(2.939)	0	?	~4.3	$^1B_1$	6.102(6.070)	0.00	?	?
$^3E'$	4.007(3.605)	0	?	?	$^3B_1$	1.468(1.437)	0	?	?
$^3A'_2$	4.672(4.270)	0	?	?	$^3A_1$	2.096(2.065)	0	?	?
					$^3A_1$	3.774(3.742)	0	?	?
					$^3B_1$	5.237(5.205)	0	?	?

The calculated $h\nu$ values in parentheses are those excluding the ground configuration χ_0 from the configuration interaction. Whether χ_0 was included or not, the calculated f value was almost the same.

TABLE II. THE STATE FUNCTIONS AND ENERGIES FOR TAB AND TABH$^+$

TAB			TABH$^+$		
E, eV.			E, eV.		
−0.4019	$^1A'_1$	$0.9660\chi_0+0.2584(^1\chi_{68}+{}^1\chi_{57})/\sqrt{2}$	−0.0317	$^1A_1$	$0.9972\,\chi_0+0.0338{}^1\chi_{46}-0.0673{}^1\chi_{57}$
4.2705	$^1A'_2$	$(^1\chi_{67}-{}^1\chi_{58})/\sqrt{2}$	3.1215	$^1B_1$	$0.9974{}^1\chi_{56}-0.0714{}^1\chi_{47}$
5.6146	$^1A'_1$	$0.2584\chi_0-0.9660(^1\chi_{68}+{}^1\chi_{57})/\sqrt{2}$	4.4283	$^1A_1$	$0.0145\,\chi_0-0.9633{}^1\chi_{46}-0.2679{}^1\chi_{57}$
5.7891	$^1E'$	$(^1\chi_{67}+{}^1\chi_{58})/\sqrt{2}$	5.6034	$^1A_1$	$0.0739\,\chi_0-0.2662{}^1\chi_{46}+0.9611{}^1\chi_{57}$
		$(^1\chi_{68}-{}^1\chi_{57})/\sqrt{2}$	6.0703	$^1B_1$	$0.0714{}^1\chi_{56}+0.9974{}^1\chi_{47}$
3.3407	$^3A'_1$	$(^3\chi_{68}+{}^3\chi_{57})/\sqrt{2}$	1.4368	$^3B_1$	$0.9787{}^3\chi_{56}-0.2052{}^3\chi_{47}$
4.0072	$^3E'$	$(^3\chi_{67}+{}^3\chi_{58})/\sqrt{2}$	2.0647	$^3A_1$	$0.8457{}^3\chi_{46}-0.5335{}^3\chi_{57}$
		$(^3\chi_{68}-{}^3\chi_{57})/\sqrt{2}$	3.7419	$^3A_1$	$0.5335{}^3\chi_{46}+0.8457{}^3\chi_{57}$
4.6724	$^3A'_2$	$(^3\chi_{67}-{}^3\chi_{58})/\sqrt{2}$	5.2051	$^3B_1$	$0.2052{}^3\chi_{56}+0.9787{}^3\chi_{47}$

in the observed spectra of TAB. Such weak transitions do not exist in the observed spectra of TABH$^+$, and the calculated transition energies are in satisfactory agreement with the observed values. These facts seem to support the assumed structure for TABH$^+$.

B) Calculation of Electronic Spectra with Other Models for TABH$^+$.—Although the results of the calculation described in A agree quite well with the observed spectra of TABH$^+$, we shall examine other models for TABH$^+$.

One of the possible structures of TABH$^+$ is a kind of π-complex,[14] in which the proton is situated on the molecular plane of TAB.

Because of the existence of the proton on the molecular plane, the electronic states of TAB might be considerably changed. The cause of the perturbation in this case will be the electrostatic potential of the proton or the charge-transfer interaction between the π-MO's of TAB and the proton.

We have tried some perturbation calculations using a model in which the proton is situated at the center of and 1.7 Å (half of the interplane distance in graphite) above the molecular plane.

In this model, the perturbing electrostatic potential due to the proton may be written[11] as:

$$\mathscr{H}^p{}_j=-\frac{Z_{H^+}e^2}{r_{pj}} \tag{16}$$

where r_{pj} is the distance between the proton and the j-th electron and $Z_{H^+}e$ is the effective charge of the proton. The formal orbital energy, ε_i, may be modified to ε_i' due to this perturbation.

$$\begin{aligned}\varepsilon_i' &= \varepsilon_i+\langle\phi_i(j)|\mathscr{H}^p{}_j|\phi_i(j)\rangle \\ &\quad+\sum_n\frac{(\langle_i\underline{\phi(j)}|\mathscr{H}^p{}_j|\phi_n(j)\rangle)^2}{\varepsilon_i-\varepsilon_n} \\ &=\varepsilon_i+\sum_\mu C^2{}_{i\mu}\langle\phi_\mu(j)|\mathscr{H}^p{}_i|\phi_\mu(j)\rangle \\ &\quad+\sum_n\frac{(\sum_\mu C_{i\mu}C_{n\mu}\langle\phi_\mu(j)|\mathscr{H}^p{}_j|\phi_\mu(j)\rangle)^2}{\varepsilon_i-\varepsilon_n}\end{aligned} \tag{17}$$

The integral, $V_\mu=\langle\phi_\mu(j)|\mathscr{H}^p{}_j|\phi_\mu(j)\rangle$, was calculated by a formula[15] using Slater AO's with the values of the orbital exponents, $\zeta_C=1.018$, $\zeta_N=1.212$.[11] The second order terms in Eq. 17 were very small compared with those of the first order and were accordingly disregarded as a first approximation.

Therefore, the values of ε_i' necessary for

14) a) M. J. S. Dewar, "Electronic Theory of Organic Chemistry," Oxford University Press (1949); Ref. 7, p. 326; Ref. 9, p. 314. b) S. Nagakura, *Technical Report of ISSP, Ser. A.*, No. 35, Jan., 1962.

TABLE III. STATE FUNCTIONS AND ENERGIES CALCULATED WITH THE ELECTROSTATIC POTENTIAL DUE TO PROTON

E, eV.		
−0.0985	$^1A_1$	$0.9899\chi_0+0.1418(^1\chi_{68}+{}^1\chi_{57})/\sqrt{2}$
3.7596	$^1A_2$	$(^1\chi_{67}-{}^1\chi_{58})/\sqrt{2}$
4.7018	$^1A_1$	$0.1418\chi_0-0.9899(^1\chi_{68}+{}^1\chi_{57})/\sqrt{2}$
5.2782	^1E	$\begin{cases}(^1\chi_{67}+{}^1\chi_{58})/\sqrt{2}\\(^1\chi_{68}-{}^1\chi_{57})/\sqrt{2}\end{cases}$

the calculation of the electronic spetra were calculated as follows:

$$\left.\begin{aligned}\varepsilon_6'=\varepsilon_5'=\varepsilon_5+(0.6972)V_C+(0.3026)V_N\\ \varepsilon_8'=\varepsilon_7'=\varepsilon_7+(0.9074)V_C+(0.0926)V_N\end{aligned}\right\} \quad (18)$$

With the V_μ values, $V_C=-6.8649$ eV., $V_N=-4.4321$ eV. and the interconfigurational matrix elements, $\langle\chi_0|\mathscr{H}^{p_j}|^1\chi_{68}\rangle=\langle\chi_0|\mathscr{H}^{p_j}|^1\chi_{57}\rangle=\sqrt{2}(0.4072)$ eV. The state functions and energies were calculated as shown in Table III.

We can obtain a little red shift of the spectrum in this model of $TABH^+$ also. However, the molecular symmetry of this $TABH^+$ is C_{3v}, and in this symmetry the transition to $^1A_2$ is electronically forbidden and that to $^1A_1$ is polarized perpendicular to the molecular plane. Therefore, we cannot interpret the observed strong band at 3.4 eV. by means of this model. Even if we take into account the charge-transfer interaction between the π-MO's of TAB and the proton, the calculated results will be similar to those of the electrostatic model as long as the proton is situated on the principal axis of the C_3 symmetry.

If the proton is moved to the periphery of TAB, the perturbation will become larger and all π-MO's of TAB will be mixed with each other. Thus, the electronic structure is considerably changed, and the electronic spectra will approach the observed data. However, such interactions may finally lead to the localization or to the hyperconjugation model as the most stable equilibrium form.

Accordingly, the theoretical calculation supports the structure of $TABH^+$ protonated on the ring carbon. The structures of $TABH^+$ similar to the π-complex discussed above may probably be realized in the course of the protonation reaction as an intermediate (outer complex), and the system will shifts to the localized one (inner complex).[14b]

Of course, the reaction involving the movement of the proton in an aqueous solution is very rapid, and the equilibrium between TAB and $TABH^+$ will be realized instantaneously.

C) Effect of Methyl Substitution on the Electronic Spectrum of $TABH^+$.—Although we have calculated here only the electronic spectra of TAB and $TABH^+$ from among the compounds examined by Köhler and Scheibe,[1] a similar interpretation will hold also for other compounds.

The transition energies to the lowest excited singlet states of *s*-triaminoxylenium ($TAXH^+$) and *s*-triaminomesitylenium ($TAMH^+$) ions are smaller by ca. 0.34 eV.[1] than that of $TABH^+$.

The effects of methyl substitutions on the electronic spectra of protonated benzene[16,17] have been discussed by means of both the localization model and the hyperconjugation model.[2c,16]

Calculations and an interpretation similar to those by Morita[2c] may be possible in the present case also. However, we shall make a more simplified explanation as follows.

The lowest excited singlet state of $TABH^+$ is almost completely contributed by $^1\chi_{56}$, as is shown in Table II; that is, the excitation energy to this state is essentially determined by the transition from the highest occupied to the lowest vacant orbitals.

If we assume an inductive model of methyl substitution by taking the Coulomb integral of the substituted carbon to be $\alpha+\delta\cdot\beta$, the orbital energy differences, $\Delta\varepsilon=\varepsilon_6-\varepsilon_5$, for TAB^+ and $TAXH^+$ may be calculate as follows using the MO's given in appendix.

$$\left.\begin{aligned}TABH^+\quad \Delta\varepsilon=-1.0764\,\beta\\ TAXH^+\quad \Delta\varepsilon=-1.0764\,\beta+(0.5531)\delta\cdot\beta\end{aligned}\right\} \quad (19)$$

The value of δ averaged for various methyl substituted aromatics seems to be ~-0.5.[9] If we put $0.34=-(0.5531)\delta\cdot\beta$, assuming $\beta\sim-3$ eV., δ is estimated to be ~-0.2. This value is a little different from the ordinary value, -0.5; nevertheless, the observed bathochromic shift by methyl substitution is, at least qualitatively, well understood by means of this simplified calculation.

D) Similarity of the Electronic Spectrum of $TABH^+$ to Those of Benzenium Ion and Methyl-substituted Benzenium Ions. — As has been discussed in the previous section, the methyl substitution affects the spectrum of $TABH^+$ rather remarkably.

15) C. C. J. Roothaan, *J. Chem. Phys.*, **19**, 1445 (1951).

16) G. Dallinga, E. L. Mackor and A. A. V. Stuart, *Mol. Physics*, **1**, 123 (1958); M. Kilpatrick and H. H. Hyman, *J. Am. Chem. Soc.*, **80**, 77 (1958).

17) J. R. Platt, *J. Chem. Phys.*, **18**, 1168 (1950).

TABLE IV. THE CALCULATED ELECTRONIC SPECTRUM OF BENZENIUM ION

E, eV.	State function	f
−0.0107	$^1A_1$ $0.9992\,\chi_0+0.0243{}^1\chi_{13}-0.0310{}^1\chi_{24}$	
3.4941	$^1B_1$ $0.9991{}^1\chi_{23}-0.0419{}^1\chi_{14}$	0.26
5.2930	$^1A_1$ $0.1028\,\chi_0-0.9106{}^1\chi_{13}-0.4002{}^1\chi_{24}$	0.12
7.0331	$^1A_1$ $0.0380\,\chi_0-0.3896{}^1\chi_{13}+0.9202{}^1\chi^{24}$	1.02
8.1188	$^1B_1$ $0.0419{}^1\chi_{23}+0.9991{}^1\chi_{14}$	1.35

In the case of the substitution for the neutral aromatic hydrocarbon molecules, the amino group affects the spectra to a far greater extent than does the methyl group. Therefore, one might expect that the spectrum of $TABH^+$ is very different from that of benzenium ions or methyl-substituted benzenium ions. However, this is not the case for either the observed spectra or for the calculated spectra. The observed excitation energies to the lowest excited singlet states of benzenium, methyl-substituted benzenium, *s*-triaminobenzenium, methyl-substituted *s*-triaminobenzenium ions, and $TOBH^+$ are not very different from one another and lie approximately between 3.0~3.6 eV. In order to interpret this fact, it will be necessary to compare the MO's and state functions of $TABH^+$ with those of benzenium ion.

The electronic spectrum of benzenium ion has been studied in detail by Morita[2c] using the semiempirical SCF MO CI method. However, for purposes of comparison, the results of theoretical calculations with similar approximations for both compounds may be more reasonable. Accordingly, we have calculated the electronic spectrum of benzenim ion with the same approximations as for $TABH^+$. The calculated energies, state functions and oscillator strengths of transitions from the ground state to the excited states are given in Table IV.

Although the method of calculation used here is less elaborate than that used by Morita, the present results are rather close to Morita's. As is shown in Table IV, the lowest excited singlet state of benzenium ion is almost completely contributed by $^1\chi_{23}$, just as the lowest excited singlet state of $TABH^+$ is almost exclusively contributed by $^1\chi_{56}$. Furthermore, an analogous circumstance holds for other states of both compounds. That is, each excitation energy is essentially determined by the transition from one of the occupied orbitals to one of the vacant orbitals. This may be a remarkable example of the change from the "*round field*" spectra[17] in benzene and TAB (where the configuration interaction is quite strong) to the "*long field*" spectra[17] caused by protonation.

Thus, we have seen the similarity of the state functions of $TABH^+$ to those of benzenium ions, a similarity which corresponds to the resemblance of the observed spectra of these compounds.

Next, we shall show the similarity of the MO's of $TABH^+$ to those of benzenium ions. We can transform the MO's of $TABH^+$ into the following equivalent forms:

$$\left.\begin{aligned}
\phi_4&=0.4084(\phi_2+\phi_{2'})+0.3332(g_3{}^4+g_{3'}{}^4)+0.6665\,g_1{}^4\\
\phi_5&=0.5259(\phi_2-\phi_{2'})+0.4725(g_3{}^5-g_{3'}{}^5)\\
\phi_6&=\qquad\qquad 0.5773(g_3{}^6-g_{3'}{}^6)-0.5773\,g_1{}^6\\
\phi_7&=0.4255(\phi_2-\phi_2')-0.5646(g_3{}^7-g_{3'}{}^7)
\end{aligned}\right\} \tag{20}$$

In these MO's, g is the normalized group orbital for C–NH_2, which can be written as:

$$\left.\begin{aligned}
g^4&=0.3418\phi_C-0.9398\phi_N,\quad g^5=0.5678\phi_C-0.8233\phi_N\\
g^6&=0.8702\phi_C-0.4926\phi_N,\quad g^7=0.9247\phi_C-0.3810\phi_N
\end{aligned}\right\} \tag{21}$$

where, in the same ϕ, $g_3=g_{3'}=g_1$.

The corresponding MO's of benzenium ion are given by:

$$\left.\begin{aligned}
\phi_1&=0.5000(\phi_2+\phi_{2'})+0.2887(\phi_3+\phi_{3'})+0.5773\phi_1\\
\phi_2&=0.5000(\phi_2-\phi_{2'})+0.5000(\phi_3+\phi_{3'})\\
\phi_3&=\qquad\qquad 0.5773(\phi_3+\phi_{3'})-0.5773\phi_1\\
\phi_4&=0.5000(\phi_2-\phi_{2'})-0.5000(\phi_3-\phi_{3'})
\end{aligned}\right\} \tag{22}$$

Thus we can see that the transformed MO's of $TABH^+$ are apparently similar to those of benzenium ion. Of course, the two sets of MO's are not exacty the same but are different from each other to some extent. However, we have described the above transformation of the MO's in order to demonstrate the *geometrial* or *topological* nature of the MO's.

If we transform the base set for the Hückel MO's of $TABH^+$ from $(\phi_1\cdots\phi_8)$ to

$$\left\{\begin{aligned}
&g_1{}^a,\ (g_3{}^a+g_3{}^a)/\sqrt{2},\ g_1{}^b,\ (g_3{}^b+g_{3'}{}^b)/\sqrt{2},\\
&(\phi_2+\phi_{2'})/\sqrt{2},\ (g_3{}^a-g_{3'}{}^a)/\sqrt{2},\\
&(g_3{}^b-g_{3'}{}^b)/\sqrt{2},\ (\phi_2-\phi_{2'}/\sqrt{2}
\end{aligned}\right\}$$

where the group orbitals for C–NH_2 are given by:

$$\begin{aligned}
g^a&=0.870\phi_C-0.493\phi_N\\
g^b&=0.493\phi_C+0.870\phi_N
\end{aligned} \tag{23}$$

then the energy matrix for the Hückel MO's can be written in the following form;

for b_2 species

$$\begin{pmatrix} g_1^a & (g_3^a+g_{3'}^a)/\sqrt{2} & g_1^b & (g_1^b+g_3^b)/\sqrt{2} & (\phi_2+\phi_2)/\sqrt{2} \\ (\alpha-0.5667\beta) & 0 & 0 & 0 & 2(0.87)\beta \\ & (\alpha-0.5667\beta) & 0 & 0 & 2(0.87)\beta \\ & & (\alpha+1.7662\beta) & 0 & 2(0.493)\beta \\ & & & (\alpha+1.7662\beta) & 2(0.493)\beta \\ & & & & \alpha \end{pmatrix}$$

for a_2 species

$$\begin{pmatrix} (g_3^a-g_3^a)/\sqrt{2} & (g_3^b-g_{3'}^b)/\sqrt{2} & (\phi_2-\phi_2)/\sqrt{2} \\ (\alpha-0.5667\beta) & 0 & 2(0.87)\beta \\ & (\alpha+1.7662\beta) & 2(0.493)\beta \\ & & \alpha \end{pmatrix}$$

TABLE V. LOCALIZATION ENERGIES OF SOME AMINOBENZENES AND TOB (in units of β)

Mode of protonation	A. Carbon	B. Amino group
Aniline	2.2498 a)	2.8054
m-Phenylenediamine	1.9562 b)	2.8058
TAB	1.8294	2.8060
TOB	1.6861	—

a) Protonation on para-carbon.
b) Protonation of the carbon atom at ortho-position to both amino groups.

Accordingly, g_a and g_b of each C–NH_2 group are mixed to some extent; that is, the g^i's in (21) can be written as $g^i=c_a{}^i g_a+c_b{}^i g_b$, but $g_1{}^i=g_3{}^i=g^i$ because,

$$\langle g_1^a|\mathscr{H}|(\phi_2+\phi_{2'})/\sqrt{2}\rangle= \langle(g_3^a+g_{3'}^a)/\sqrt{2}|\mathscr{H}|(\phi_2+\phi_{2'})/\sqrt{2}\rangle$$

and

$$\langle g_1^b|\mathscr{H}|(\phi_2+\phi_{2'})/\sqrt{2}\rangle= \langle(g_3^b+g_{3'}^b)/\sqrt{2}|\mathscr{H}|(\phi_2+\phi_{2'})/\sqrt{2}\rangle$$

The calculated spectra of $TABH^+$ and benzenium ion in Tables I and IV respectively indicate that the excitation energy to the lowest excited singlet state of $TABH^+$ is a little smaller than that of benzenium ion. However, this is not the case indeed, the order is just reversed in the observed spectra. This indicates that the present semiempirical ASMO CI method cannot reproduce such a small difference between the observed spectra,** although the calculated excitation energies themselves are close to the observed values.

On the other hand, the difference between the Hückel MO energies of the lowst vacant orbital and the highest occupied orbital can reproduce the observed excitation energy to the lowest excited singlet state quite well, as is described below.

If we assume the inductive parameter for methyl substitution to be ~-0.2, as has already been established, the orbital energy differences may be evaluated as: $-\beta$, -1.0764β, and -1.1β for benzenium ion, $TABH^+$ and mesitylenium ions respectively. The observed excitation energies are 3.1 eV., 3.4 eV. and 3.5 eV. for these ions respectively. Thus, the calculated results agree, at least qualitatively, very well with the observed spectra.

E) The Basicities of TAB and TOB in Comparison with Other Aminobenzenes and Aromatic Hydrocarbons.—As has been described in the "Theoretical Method" section, localization energies due to protonation were calculated as a measure of the stabilities of the protonated species. Calculated results for the protonation of some aminobenzenes and TOB are collected in Table V, where the localization energy is given by $(M-M_r{}^+)$.

As is shown in Table V, the destabilization energy of the π system becomes considerably smaller from aniline to TAB and TOB ($pK\sim9.7$) in mode A, whereas it is almost constant or even slightly increases in mode B. This result is in accordance with the observed data.

Although the effect of hyperconjugation with CH_2 group was not taken into account

** In the present calculation, we have used the same value of the nearest-neighbor core resonance integral for the carbon-carbon bond (β_{CC}) in both $TABH^+$ and benzenium ion. However, there are twice as many π-electrons of $TABH^+$ as those of benzenium ion, whereas the dimension of the core framework of the former is not so large compared with that of the latter. Accordingly, the effective core charge for π-electrons seems to be smaller in $TABH^+$ than in benzenium ion, resulting in the larger overlapping between AO's and, thus, the larger core resonance integrals in the former than in the latter. Moreover, the value of β_{CC} was the same as that used for the neutral aromatic hydrocarbons. Because the effective core charge is larger in benzenium ion than in benzene, a little smaller value of β_{CC} may be more reasonable for benzenium ion.
In general, the calculated spectrum shifts to blue when the values of the core resonance integrals are increased, while a red shift occurs when they are decreased. Therefore, the calculated spectra of $TABH^+$ and benzenium ion will approach the observed values if one adjusts the β_{CC} value in the way described above.

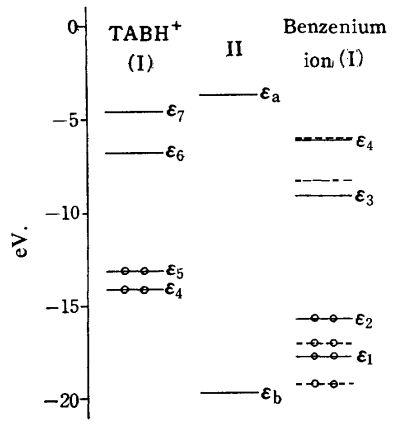

Fig. 2. MO energies for the local systems of $TABH^+$ and benzenium ion, respectively.
In the local system I of benzenium ion, - - - represents the SCF MO energies calculated by Morita.[2c]

either in the calculation of the electronic spectra or in the calculation of the stabilities of the protonated species, it may be examined in some qualitative or semi-quantitative manner.

In the case of $TABH^+$, owing to the presence of the three amino groups, the higher occupied orbitals of the local system I which is indicated in Fig 1b (II is the CH_2 group) may be much more elevated than the highest-occupied orbital of the corresponding local system of benzenium ion.

Actually, this is the case, as is shown in Fig. 2, where the approximate orbital energies for $TABH^+$ and the corresponding quantities for benzenium ion calculated by the present method are indicated, together with the energies of the bonding and antibonding π-orbitals of the CH_2 group as calculated by Morita.[2c] In Fig. 2, the SCF MO energies[2c] for the local system I of benzenium ions are also given for purposes of comparison.

Therefore, the excitation energies from the higher-occupied orbitals of I to the antibonding π-orbital of II(ϕ_a) may not be very large in the case of $TABH^+$. Employing the Pariser-Parr approximation[4a] for the evaluation of the electron repulsion integrals (γ's) between AO's of I and II, the approximate charge transfer (CT) excitation energies in $TABH^+$ were estimated as follows: $E(^1\chi_{5a})\sim4.5$ eV. and $E(^1\chi_{4a})\sim6.4$ eV., where $^1\chi_{5a}\subset B_1$, $^1\chi_{4a}\subset A_1$. Thus, it may be possible that the interactions between these CT configurations and the ground configuration χ_0 stabilize the protonated species.

Mackor et al.[2a] demonstrated an approximate linear relation between the localization energy and log K, where K is the relative basicity constant, in the case of the protonation of many aromatic hydrocarbons.

Although there are only two points for TAB and TOB, the relation between the pK values and the localization eneregies in the present calculation seems to be parallel with that between the values of log K and the localization energies for some aromatic hydrocarbons, as is shown in Fig. 3.

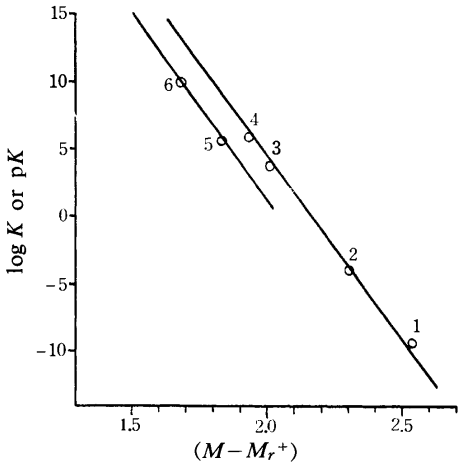

Fig. 3. Relation between the observed basicities and localization enegies.
1. Benzene, 2. Naphthalene, 3. Anthracene, 4. Naphthacene, 5. TAB, 6. TOB.
Localization energies for the polyacene series were taken from Ref. 2a.

Concluding Remarks

The results of the theoretical calculations herein described have revealed that the extraordinarily large proton affinities of TAB and TOB are consistent with the ordinary MO concept of the π-electron system and with the great conjugation power of amino group, and that $TABH^+$ and $TOBH^+$ are carbonium ions similar to the protonation products of benzene and methyl-substituted benzenes. Nevertheless, it is necessary to make a more direct experimental confirmation of the structure of $TABH^+$ by, for example, NMR spectral measurement.

Summary

The electronic spectra and electronic structure of TAB and $TABH^+$ have been studied by the MO method. The calculated spectra agree satisfactorily with the observed values. The stabilities of the protonation products of various aminobenzenes have been studied by Hückel MO calculations. The results of these calculations give an interpretation of the observed facts[1] that TAB in an aqueous solution is easily protonated on the ring

carbon (pK ~5.5), although no such protonation occurs in the case of aniline or *m*-phenylenediamine, where the amino group is protonated. The stability of the protonation product of TOB has also been studied.

It has been pointed out that the spectum of $TABH^+$ is rather similar to that of benzenium ion, although the basicity of the former is much larger than that of the latter. This fact has been explained theoretically.

Further, it has been observed that a relation between the calculated localization energy and the observed basicity constant for the protonation similar to those of many aromatic hydrocarbons approximately holds for TAB and TOB.

The author wishes to express his gratitude to Professor Saburo Nagakura of The University of Tokyo and Dr. Toshifumi Morita of Tokyo Metropolitan University for their thought-provoking discussions. He is also thankful to Dr. Shizuyo Mataga for her assistance in the numerical computations.

Faculty of Science
Osaka City University
Sumiyoshi-ku, Osaka

Appendix I.

Hückel MO's and MO energies of TAB, $TABH^+$, TOB and $TOBH^+$.
(MO energies are in units of β)

MO energy	Symmetry	MO
TAB		
2.4425	a_2''	$\psi_1=0.3792(\phi_1+\phi_3+\phi_5)+0.3105(\phi_2+\phi_4+\phi_6)+0.3052(\phi_7+\phi_8+\phi_9)$
1.9168	e''	$\psi_2=0.3941(\phi_1-\phi_3)-0.2057(\phi_4-\phi_6)+0.5498(\phi_7-\phi_8)$ $\psi_3=0.2275(\phi_1+\phi_3-2\phi_5)-0.1187(\phi_4+\phi_6-2\phi_2)+0.3175(\phi_7+\phi_8-2\phi_9)$
0.9121	a_2''	$\psi_4=0.1366(\phi_1+\phi_3+\phi_5)+0.2994(\phi_2+\phi_4+\phi_6)-0.4744(\phi_7+\phi_8+\phi_9)$
0.5102	e''	$\psi_5=0.2683(\phi_1-\phi_3)-0.5259(\phi_4-\phi_6)-0.3890(\phi_7-\phi_8)$ $\psi_6=0.1549(\phi_1+\phi_3-2\phi_5)-0.3037(\phi_4+\phi_6-2\phi_2)-0.2246(\phi_7+\phi_8-2\phi_9)$
−1.2271	e''	$\psi_7=0.5221(\phi_1-\phi_3)+0.4255(\phi_4-\phi_6)-0.2152(\phi_7-\phi_8)$ $\psi_8=0.3015(\phi_1+\phi_3-2\phi_5)+0.2457(\phi_4+\phi_6-2\phi_2)-0.1242(\phi_7+\phi_8-2\phi_9)$
−2.1546	a_2''	$\psi_9=0.4134(\phi_1+\phi_3+\phi_5)-0.3838(\phi_2+\phi_4+\phi_6)-0.1233(\phi_7+\phi_8+\phi_9)$
		$P_{11}=0.9308,\quad P_{22}=1.2210,\quad P_{77}=1.8461$
$TABH^+$		
2.2644	b_2	$\psi_1=0.3443(\phi_2+\phi_{2'})+0.2599(\phi_3+\phi_{3'})+0.2441(\phi_4+\phi_{4'})+0.5197\phi_1+0.4883\phi_5$
1.9168	a_2	$\psi_2=0.2056(\phi_2-\phi_{2'})+0.3941(\phi_3-\phi_{3'})+0.5499(\phi_4-\phi_{4'})$
1.7662	b_2	$\psi_3=0.2844(\phi_3+\phi_{3'})+0.5024(\phi_4+\phi_{4'})-0.2844\phi_1-0.5024\phi_5$
0.8363	b_2	$\psi_4=0.4084(\phi_2+\phi_{2'})+0.1139(\phi_3+\phi_{3'})-0.3132(\phi_4+\phi_{4'})+0.2277\phi_1-0.6264\phi_5$
0.5102	a_2	$\psi_5=0.5259(\phi_2-\phi_{2'})+0.2683(\phi_3-\phi_{3'})-0.3890(\phi_4-\phi_{4'})$
−0.5662	b_2	$\psi_6=0.5024(\phi_3+\phi_{3'})-0.2844(\phi_4+\phi_{4'})-0.5024\phi_1+0.2844\phi_5$
−1.2270	a_2	$\psi_7=0.4255(\phi_2-\phi_{2'})-0.5221(\phi_3-\phi_{3'})+0.2151(\phi_4-\phi_{4'})$
−1.9008	b_2	$\psi_8=0.4633(\phi_2+\phi_{2'})-0.2935(\phi_3+\phi_{3'})+0.0946(\phi_4+\phi_{4'})-0.5870\phi_1+0.1893\phi_5$
		$P_{11}=0.8056,\quad P_{22}=1.2083,\quad P_{33}=0.7774,\quad P_{44}=1.7276,\quad P_{55}=1.7664$
TOB		
2.3487	a_2''	$\psi_1=0.3945(\phi_1+\phi_2+\phi_3)+0.3359(\phi_2+\phi_4+\phi_6)+0.2547(\phi_7+\phi_8+\phi_9)$
1.6997	e''	$\psi_2=0.4401(\phi_1-\phi_3)-0.2589(\phi_4-\phi_6)+0.4891(\phi_7-\phi_8)$ $\psi_3=0.2541(\phi_1+\phi_3-2\phi_5)-0.1495(\phi_4+\phi_6-2\phi_2)+0.2824(\phi_7+\phi_8-2\phi_9)$
0.6264	a_2''	$\psi_4=0.0867(\phi_1+\phi_3+\phi_5)+0.2767(\phi_2+\phi_4+\phi_6)-0.4992(\phi_7+\phi_8+\phi_9)$
0.3705	e''	$\psi_5=0.1910(\phi_1-\phi_3)-0.5155(\phi_4-\phi_6)-0.4447(\phi_7-\phi_8)$ $\psi_6=0.1103(\phi_1+\phi_3-2\phi_5)-0.2976(\phi_4+\phi_6-2\phi_2)-0.2567(\phi_7+\phi_8-2\phi_9)$
−1.2703	e''	$\psi_7=0.5194(\phi_1-\phi_3)+0.4089(\phi_4-\phi_6)-0.2509(\phi_7-\phi_8)$ $\psi_8=0.2999(\phi_1+\phi_3-2\phi_5)+0.2361(\phi_4+\phi_6-2\phi_2)-0.1448(\phi_7+\phi_8-2\phi_9)$
−2.1751	a_2''	$\psi_9=0.4125(\phi_1+\phi_3+\phi_5)-0.3793(\phi_2+\phi_4+\phi_6)-0.1387(\phi_7+\phi_8+\phi_9)$
		$P_{11}=0.9400,\quad P_{22}=1.2663,\quad P_{77}=1.7936$
$TOBH^+$		
2.1437	b_2	$\psi_1=0.3846(\phi_2+\phi_{2'})+0.2748(\phi_3+\phi_{3'})+0.2045(\phi_4+\phi_{4'})+0.5496\phi_1+0.4090\phi_5$
1.6997	a_2	$\psi_2=0.2589(\phi_2-\phi_{2'})+0.4401(\phi_3-\phi_{3'})+0.4891(\phi_4-\phi_{4'})$
1.4770	b_2	$\psi_3=0.3237(\phi_3+\phi_{3'})+0.4781(\phi_4+\phi_{4'})-0.3237\phi_1-0.4781\phi_5$
0.5815	b_2	$\psi_4=0.3793(\phi_2+\phi_{2'})+0.0735(\phi_3+\phi_{3'})-0.3366(\phi_4+\phi_{4'})+0.1471\phi_1-0.6732\phi_5$
0.3705	a_2	$\psi_5=0.5155(\phi_2-\phi_{2'})+0.1910(\phi_3-\phi_{3'})-0.4447(\phi_4-\phi_{4'})$
−0.6770	b_2	$\psi_6=0.4781(\phi_3+\phi_{3'})-0.3237(\phi_4+\phi_{4'})-0.4781\phi_1+0.3237\phi_5$
−1.2702	a_2	$\psi_7=0.4089(\phi_2-\phi_{2'})-0.5194(\phi_3-\phi_{3'})+0.2509(\phi_4-\phi_{4'})$
−1.9252	b_2	$\psi_8=0.4672(\phi_2+\phi_{2'})-0.2998(\phi_3+\phi_{3'})+0.1100(\phi_4+\phi_{4'})-0.5996\phi_1+0.2200\phi_5$
		$P_{11}=0.8569,\quad P_{22}=1.2491,\quad P_{33}=0.8317,\quad P_{44}=1.6413,\quad P_{55}=1.6981$

Appendix II.

The calculated values of ε_i's, $E(\chi_{ik})$'s and $\langle \chi_{ik}|\mathscr{H}|\chi_{jl}\rangle$'s for TAB and $TABH^+$(in units of eV.).

TAB

$\varepsilon_5=\varepsilon_6=-8.7919$, $E(^1\chi_{67})=E(^1\chi_{58})=5.0298$, $E(^1\chi_{68})=E(^1\chi_{57})=5.5001$

$\varepsilon_7=\varepsilon_8=-0.2811$, $E(^3\chi_{67})=E(^3\chi_{58})=3.9379$, $E(^3\chi_{68})=E(^3\chi_{57})=3.2714$

$\langle ^1\chi_{67}|\mathscr{H}|^1\chi_{58}\rangle=0.7593$, $\langle ^1\chi_{68}|\mathscr{H}|^1\chi_{57}\rangle=-0.2874$, $\langle \chi_0|\mathscr{H}|^1\chi_{68}\rangle=-\sqrt{2}\,(1.3529)$

$\langle ^3\chi_{67}|\mathscr{H}|^3\chi_{58}\rangle=-0.3326$, $\langle ^3\chi_{68}|\mathscr{H}|^3\chi_{57}\rangle=-0.3326$, $\langle \chi_0|\mathscr{H}|^1\chi_{57}\rangle=-\sqrt{2}\,(0.1493)$

$TABH^+$

$\varepsilon_4=-14.0832$, $E(^1\chi_{46})=4.5065$, $E(^1\chi_{56})=3.1365$, $\langle ^1\chi_{46}|\mathscr{H}|^1\chi_{57}\rangle=-0.2905$

$\varepsilon_5=-13.1165$, $E(^3\chi_{46})=2.5422$, $E(^3\chi_{56})=1.5955$, $\langle ^3\chi_{46}|\mathscr{H}|^3\chi_{57}\rangle=0.7569$

$\varepsilon_6=-6.7829$, $E(^1\chi_{57})=5.4935$, $E(^1\chi_{47})=6.0553$, $\langle \chi_0|\mathscr{H}|^1\chi_{57}\rangle=0.3826$

$\varepsilon_7=-4.6151$, $E(^3\chi_{57})=3.2645$, $E(^3\chi_{47})=5.0464$, $\langle \chi_0|\mathscr{H}|^1\chi_{46}\rangle=-0.1734$

$\langle ^1\chi_{56}|\mathscr{H}|^1\chi_{47}\rangle=0.2099$

$\langle ^3\chi_{56}|\mathscr{H}|^3\chi_{47}\rangle=0.7569$

The Infrared Spectra of Troponoid Compounds. VI. The Infrared and Raman Spectra of Tropolone, 3- and 4-Isopropyltropolones

By Yusaku IKEGAMI

(Received March 30, 1963)

In Part IV[1] of this series, the infrared and Raman spectra of tropone (I) and their vibrational assignments were described. Analyses of the infrared spectra of many troponoids can be made on the basis of these findings. Yet, however, for the analyses of the infrared spectra of many tropolones, it is desirable to know the characters and the assignments of the infrared and Raman spectra of some typical tropolones. In the present paper, the Raman spectra of tropolone (II), 4-isopropyltropolone (hinokitiol) (III) and 3-isopropyltropolone (α-thujaplicin) (IV) will be measured in carbon tetrachloride, and the vibrational assignments of these spectra will be discussed, together with their infrared spectra. All these tropolones are colorless crystals and are soluble in organic solvents suitable for the measurement of Raman spectra. Although the Raman spectra of II and III in benzene have been reported on already by Imanishi and Ito,[2,3] more detailed results were obtained in the present measurements.

Measurements

Raman spectra were measured with a Shimadzu automatic-grating Raman spectrometer, type GRS-750, using the Hg-e line (4358 Å) from the Toronto-type mercury lamp as the exciting line. A solution containing ethyl violet and *p*-nitrotoluene in denatured alcohol was used as the filter for the light source.[1] Each sample was measured in carbon tetrachloride (25~35% conc.) by the use of a Raman tube 8 mm. in inner diameter. As the three tropolones are easily colored on exposure to light, the purified samples were preserved in a dark place and caution was taken to shorten the time required for the measurement. Relative intensities in each spectrum (Tables I—III) are given, taking the peak intensity of the most intense line, around 1500 cm^{-1}, as the standard.

Infrared spectra were measured with a Perkin-Elmer model 21 infrared spectrophotometer, using calcium fluoride, sodium chloride and potassium bromide prisms.

Tropolone (m. p. 51°C), 4-isopropyltropolone (m. p. 52°C) and 3-isopropyltropolone (m. p. 34°C) were purified several times by recrystallization and vacuum distillation.

Results and Discussion

Characteristic Features Appearing in the Raman Spectra of Four Troponoids.—The Raman lines observed on three tropolones are shown in Fig. 1, together with those of tropone measured earlier.[1] All these spectra exhibit the most intense line around 1500 cm^{-1}. Further, some strong lines were found which correspond well in their wave numbers and relative intensities to the intense lines of the

1) Y. Ikegami, This Bulletin, **35**, 967 (1962).
2) S. Imanishi and M. Ito, ibid., **28**, 75 (1955).
3) S. Imanishi and M. Ito, ibid., **29**, 632 (1956).

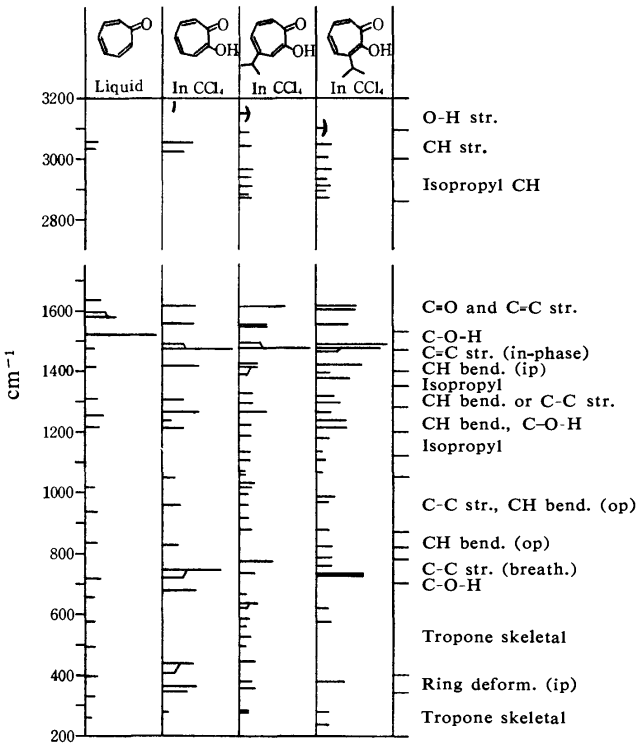

Fig. 1. Raman spectra of four troponoids.

tropone spectrum. Since these characteristic lines in the four troponoids are related to the vibrations of the tropone skeletal part, tentative assignments can be made with reference to the assignments for the spectra of tropone[1] and tropolone[4], as Fig. 1 shows.

The following features in the spectra are illustrated in Fig. 1.

(1) The Raman lines of the three tropolones corresponding to the vibrations belonging to

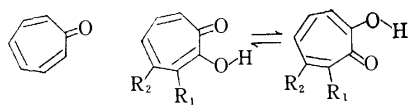

I a b

II: $R_1=R_2=H$
III: $R_1=H$, $R_2=$isopropyl
IV: $R_1=$isopropyl, $R_2=H$

A_1 species of tropone are strong in general. The Raman line due to the C=C in-phase stretching vibration in each spectrum is most intense, but not so strong as that of tropone in the relative intensity.

(2) In a spectrum of 3-isopropyltropolone, it is noticeable that the line due to the C=C in-phase stretching vibration is separated into two lines, at 1489 and 1476 cm^{-1}, with a similar intensity. This fact suggests two possible tautomeric forms, IVa and IVb, for the structure of 3-isopropyltropolone. In the other region, also, some of the Raman lines are found to form pairs, such as 1618 and 1604, 1318 and 1295, 1263 and 1239, 985 and 965, 785 and 758, 728 and 724, and 275 and 234 cm^{-1}.

The existence of similar tautomeric forms must be considered also for 4-isopropyltropolone, and some paired lines, such as 1554 and 1549, 1426 and 1412, 1328 and 1293, 772 and 731, and 280 and 272 cm^{-1}, are pointed out. On the intramolecular hydrogen bonding of tropolone, it has been suggested that a highly mobile tautomeric hydrogen is located by the two equivalent potential minima.[5] Accordingly, it is natural to interpret the vibrational spectra of tropolones on the basis of a consideration of the tautomerism, except for those cases, such as the 5-monosubstituted tropolones, in which two tautomeric forms have the same structural model.

(3) The vibrations due to the C–O–H group are generally strong in the infrared spectra,[4,6,7] but weaker or indistinct in the Raman spectra.

4) Y. Ikegami, ibid., **34**, 94 (1961).

5) H. P. Koch, *J. Chem. Soc.*, **1951**, 512.
6) Y. Ikegami, This Bulletin, **34**, 91 (1961).
7) Y. Ikegami, *J. Japanese Chem.* (*Kagaku-no-Ryoiki*), **38**, 33 (1959).

TABLE I. OBSERVED FREQUENCIES (cm^{-1}) AND THEIR POSSIBLE ASSIGNMENTS FOR TROPOLONE

Infrared Solution[a]	Raman In CCl_4	Assignment
3450 vwb 3151 mb 3120 mb	3229 0.5 b	O-H stretch.[b]
3051 sh 3020 sh	3053 3.0 3023 1.8	CH stretch.
2001 w		2×1000
1970 w		1000+953
1903 vw		2×953
1832 vw		2×917 or 1000+828
1817 sh		953+854
1774 w		917+854
1747 w		
1687 sh		919+767 or 854+828
1618 vs	1618 3.8	C=O and C=C stretch.[c]
1555 s	1559 3.2	C=C and C=O stretch.[c]
1490 vs	1490 sh	C-O-H group[b]
1476 vs	1473 10	C=C stretch. (in-phase)
1444 s		C-C stretch. ? or CH bend. (ip)
1425 sh	1418 4.2	CH bend. (ip)
1355 vw		2×675
1317 sh		767+551
1304 m	1304 1.9	CH bend. (ip) or C-C stretch. ?
1267 vs	1265 4.2	CH bend. (ip)
1251 vs	1239 w	C-O-H group[b]
1213 m	1211 1.9	CH bend. (ip)
1048 vw	1049 0.5	C-C stretch.
1000 vw		CH bend. (op)
953 m	957 1.3	C-C stretch.
917 m		CH bend. (op)
873 w		2×434
854 w		CH bend. (op)
	828 1.1	CH bend. (op)
767 m		CH bend. (op)[b]
	744 8.0	C-C stretch. (ring breath.)
726 sb	719 sh	C-O-H group (op)[b]
713 s		
675 w	678 3.9	Skeletal deform.
654 vw		
551 vw		
434 m	439 2.4	Skeletal deform.
404 m	403 sh	
	360 4.0	Skeletal deform. (ip)
	342 2.4 275 vw	Skeletal deform.

(vs : very strong, s : strong, m : medium, w : weak, vw : very weak, sh : shoulder, b : broad, ip : in-plane, op : out-of-plane)

a) The region of 3600~2000 cm^{-1} was measured by using a calcium fluoride prism. The spectrum was measured in carbon tetrachloride (4000~900 cm^{-1} range) and in carbon disulfide (900~400 cm^{-1}).

b) Refs. 4 and 6. c) Ref. 9.

Therefore, it is fairly difficult to distinguish the vibrations of the tropone skeletal part in the infrared spectra, especially in the finger-print region, because of the overlap with the strong and broad absorptions due to the C-O-H group. On the contrary, almost all of the skeletal vibrations are observed distinctly in the Raman spectra.

(4) In the spectra of 4- and 3-isopropyltropolones, the Raman lines due to the isopropyl group[8] are found in the 2968~2872, 1393~1375 and 1188~1132 cm^{-1} regions.

On the basis of these features, the following

8) R. N. Jones and C. Sandorfy, "Chemical Application of Spectroscopy", Ed. by W. West, Interscience Publishers, New York (1956), pp. 336, 356.

TABLE II. OBSERVED FREQUENCIES (cm^{-1}) AND THEIR POSSIBLE ASSIGNMENTS FOR 4-ISOPROPYLTROPOLONE

Infrared				Raman In CCl_4	Assignment
Solid[a,b]	Liquid[b]	Solution[b,c]	Vapor[d]		
3533 vwb	3450 sh	3450 sh			
3215 sb	3195 sb	3150 m	3140 w	3231 3181 wb 3146	O-H stretch.
		3115 mb			
		3027 w		3088 w 3043 0.4	Ring CH stretch.
2995 sh					
2971 sh					
2957 m	2960 m	2968 s	2980 s	2968 0.7	Asym. CH_3 stretch.
2920 w	2927 w	2931 w	2940 sh	2940 0.5	CH_3 stretch. or 2×1475
				2911 0.5	$1616+1293$?
				2883 w	Tert. CH stretch.
2864 w	2868 w	2872 w	2890 w	2872 0.4	Sym. CH_3 stretch.
		1997 vw			2×998
		1972 vw			
		1900 vw			2×951
1818 w	1804 w	1804 w	1800 w		$911+890$
		1775 vw			2×890
		1700 vw			
1609 vs	1615 vs	1617 vs	1625 vs	1616 5.9	C=O and C=C stretch.
1547 vs	1551 s	1560 s 1546 s	1563 s	1554 1549 3.1	C=C and C=O stretch.
1487 vs	1499 sh	1496 vsb	1498 vs	1495 sh	C-O-H group
1479 vsb 1462 vs	1474 vsb	1472 vsb	1475 vsb	1475 10	C=C stretch. (in-phase)
1449 sh		1442 s	1460 sh		CH_3 degen. deform.
1425 sh 1417 s	1427 s		1422 m	1426 1.3	Ring CH bend. (ip)
1412 sh	1412 s	1410 s		1412 1.3	
1385 sh		1385 vw	1370 sh	1389 sh	CH_3 sym. deform.
1360 w	1369 w	1367 w			
1328 w	1325 w	1330 m		1328 0.7	Ring CH bend. (ip) or C-C stretch. ?
		1320 m	1320 sh		
		1299 sh			
1301 m		1291 sh	1290 sh	1293 0.7	
		1281 m			
1269 vs	1264 vs	1266 vs	1267 vsb	1266 3.0	Ring CH bend. (ip)
	1250 shb	1256 vsb			C-O-H group
1220 sh	1225 sh	1230 sh	1229 sh	1222 0.5	Ring CH bend. (ip)
1188 vsb					C-O-H group
	1185 sh	1182 w	1176 vw	1188 0.4	Isopropyl group
		1142 vw			
		1130 vw		1132 0.2	
1113 w					
1105 m		1100 vw		1106 0.2	
1070 m	1057 w	1066 w	1060 w	1068 vw	
		1058 w		1058 vw	
1013 w	1011 vw	1024 vw 1009 w	1003 w	1030 0.7 1014 0.5	Ring C-C stretch.
998 vw				991 w	Ring CH bend. (op)
960 sh	954 sh	951 sh		957 w	Ring CH bend. (op)
950 s	947 s	946 s	943 m		Ring CH bend. (op)
933 m	913 m	911 m	905 m	914 w	
877 w	891 m	890 m		878 0.3	Ring C-C stretch.
820 s	824 s 790 sh	821 s 790 m	820 m		Ring CH bend. (op)

TABLE II. (Continued)

Infrared				Raman in CCl_4	Assignment
Solid[a,b]	Liquid[b]	Solution[b,c]	Vapor[d]		
767 m	769 m	769 m		772 3.9	Ring C-C stretch. (ring breath.)
756 mb				756 ?	
	735 mb	735 sb	742 mb	731 0.9	C-O-H group (op)
726 m	707 m	722 sh			
655 m	658 s	660 m	658 m	662 vw	Tropone skeletal
	633 sh			635 1.4	
598 m	612 m	610 w		620 sh	
580 sh	582 sh			582 w	
	556 sh			560 vw	
530 sh	522 sh			524 0.3	
503 w	491 w			494 vw	
448 m	444 m			(444 (1)[e])	Ring deform.
				378 0.5	Ring deform.
				353 0.9	
				280 0.2	Ring deform.
				272 0.2	

a) The region of 4000～2000 cm^{-1} was measured as a crystalline film (Ref. 6) and the region lower than 2000 cm^{-1} was measured in a potassium bromide disk.
b) The region higher than 2000 cm^{-1} was measured by using a calcium fluoride prism.
c) In carbon tetrachloride (4000～900 cm^{-1} range) and in carbon disulfide (900～600 cm^{-1}), ca. 5% conc.
d) Ref. 10. e) Ref. 3.

remarks can be made concerning the assignments for the observed frequencies of tropolone, 4- and 3-isopropyltropolones.

Tropolone.—The observed frequencies of tropolone and their assignments are summarized in Table I. The infrared spectra of tropolone in the solid, liquid and vapor states and the assignments regarding the C–O–H group, the CH-stretching and some of the CH-bending vibrations have already been described in Parts II[6] and III[4].

In the 1650～1450 cm^{-1} region, the most intense Raman line, at 1473 cm^{-1}, may easily be assigned to the totally symmetric stretching vibration of three C=C bonds. The two bands at 1618 and around 1555 cm^{-1} may be explained as resulting from the participation of both C=O and C=C stretching vibrations, as has been described in the preceding paper.[9] These frequencies are considerably lower than those of the corresponding bands in tropone as a result of the conjugated chelation in a tropolone structure.

When the Raman spectrum in the 1450～1000 cm^{-1} region is compared with that of tropone, the following lines corresponding to each other in frequency and relative intensity are found:

Tropone; 1412 (0.3), 1309 (0.4), 1254 (1.3), 1217 (0.6), 1017 cm^{-1} (0.2).
Tropolone; 1418 (4.2), 1304 (1.9), 1265 (4.2), 1211 (1.9), 1049 cm^{-1} (0.5).

The vibrational frequencies due to the tropone skeletal part in tropolone are not greatly different from those of tropone. Therefore, the above frequencies can be assigned to the same vibrational modes as those of tropone, as is indicated in Table I. The band at 1265 cm^{-1} is assumed to be related to the vibration of the C–O–H group,[4] and thus this band may be considered the overlap of two bands. The band at 1444 cm^{-1} is assumed to correspond to the band at 1473 cm^{-1} of tropone.

The infrared absorptions at 767 and 726 cm^{-1} are assigned to the CH and OH out-of-plane bending vibrations respectively.[4] Of the remaining frequencies in the 1000～700 cm^{-1} region, the two bands at 957 and 744 cm^{-1} can be assigned to the C–C stretching vibrations, since these bands are strong in the Raman spectrum and correspond well to the vibrations belonging to A_1 species of tropone. The latter was also assigned similarly by Imanishi and Ito.[2,3] The other frequencies observed in this region are assumed mainly to be due to the CH bending vibrations, as indicated in Table I.

The bands in the region lower than 700 cm^{-1} are assigned to the deformation vibrations of the tropone skeleton. Of these, the distinct Raman lines at 678, 360 and 342 cm^{-1} are probably due to vibrations similar to the bands at 653, 396 and 329 cm^{-1} of the tropone spectrum.[1]

4-Isopropyltropolone.—The observed frequencies, obtained from the infrared spectra in the

9) Y. Ikegami, This Bulletin, 35, 972 (1962).

TABLE III. OBSERVED FREQUENCIES (cm^{-1}) AND THEIR POSSIBLE ASSIGNMENTS FOR 3-ISOPROPYLTROPOLONE

Infrared[a]		Raman In CCl_4	Assignment
Liquid	Solution		
3450 wb			
		3102 w	O-H stretch.
3170 mb	3095 wb	3083 w	
	3040 vw	3049 1.0	Ring CH stretch.
	3008 vw	3007 0.5	
2960 s	2962 s	2967 1.0	Asym. CH_3 stretch.
2925 sh	2925 sh	2934 0.3	CH_3 stretch. or 2×1463 ?
		2913 0.7	
2890 sh	2888 sh	2896 w	Tert. CH stretch.
2865 m	2866 m	2872 0.5	Sym. CH_3 stretch.
1618 s	1621 s	1618 5.2	C=O and C=C stretch.
1603 s	1603 s	1604 5.0	
1551 vs	1554 vs	1553 3.7	C=C and C=O stretch.
1493 vs	1495 vs		C-O-H group
		1489 10	C=C stretch. (in-phase)
		1476 9.0	
1465 vs	1465 vs	1463 sh	CH_3 degen. deform.
1425 s	1427 s	1420 6.0	Ring CH bend. (ip)
1394 vs	1395 vs	1393 0.8	CH_3 sym. deform., Ring CH bend. (ip)
1377 s	1378 s	1375 3.8	
	1365 sh		
1350 sh	1345 sh		Tert. CH deform.
1319 vw	1319 vw	1318 1.4	Ring CH bend. (ip) or C-C stretch. ?
1292 s	1295 vs	1295 2.3	
1265 sh	1265 sh	1263 1.0	C-O-H group, Ring CH bend. (ip)
1253 vs	1254 vs		
1233 vs	1237 vs	1239 3.5	
1210 sh	1210 sh	1214 3.4	Ring CH bend. (ip)
1183 w	1182 w	1179 0.6	Isopropyl group
1132 w	1130 w	1132 vw	
1105 w	1105 w	1106 w	
1060 m	1061 m	1065 w	
984 sh	984 m	985 1.4	Ring C-C stretch.
967 m	968 m	965 0.4	
958 sh	953 m		Ring CH bend. (op)
894 sh	888 vw		
875 m	873 m	877 0.6	Ring C-C stretch.
		822 1.2	Ring CH bend. (op)
809 s	809 s		Ring CH bend. (op)
801 sh	799 m		
		785 1.1	Isopropyl group
	764 sh	758 1.0	
742 sb	739 vs		C-O-H group (op)
		728	
720 m	713 m	724 6.2	Ring C-C stretch. (ring breath.)
689 m	690 w		
659 m			
622 m		618 0.6	Tropone skeletal
569 m	572 0.7		
547 vw			
529 vw			
502 vw			
462 m			
426 m			
		376 3.0	Ring deform. (ip)
		275 0.6	Ring deform.
		234 0.6	

a) The region higher than 2000 cm^{-1} was measured by using a calcium fluoride prism.

solid, liquid, solution and vapor states[10] and from the Raman spectrum, are shown in Table II, together with their possible assignments. The OH and CH-stretching absorptions have already been discussed in Part II.[6] Frequencies in the 1650~1470 cm^{-1} region are due to the tropone skeletal stretching and C–O–H group vibrations, as in the case of tropolone.

The bands in the 1460~1442, 1389~1360 and 1188~1130 cm^{-1} regions are assigned, respectively, to the CH_3 degenerate deformation, the symmetric deformation and the skeletal vibrations of the isopropyl group.[8,11] These bands are very weak in both infrared and Raman spectra. The assignments of the remaining bands in the 1470~1000 cm^{-1} region were given with reference to those of tropolone and after consideration of the variation of absorptions according to the changes of state.[4] The Raman lines at 1030 and 1014 cm^{-1}, as well as those at 1426 and 1412 cm^{-1}, are considered to be doublets due to the existence of two tautomeric forms, IIIa and IIIb.

It is possible to assign the intense Raman lines at 878 and 772 cm^{-1} to the ring C–C stretching, and the absorption bands at 950, 820 and 790 cm^{-1},[12] to the CH out-of-plane bending vibrations, which are expected to have a strong intensity. The broad absorption band at 735 cm^{-1} is the OH out-of-plane vibration. The weak bands at 998 and 951 cm^{-1} are probably assigned to the CH out-of-plane vibrations, which are to be expected in this region. The weak absorptions at 1997 and 1900 cm^{-1} can be explained as the overtones of these vibrations.

3-Isopropyltropolone.—The observed frequencies and their possible assignments are summarized in Table III. The bands observed in the 2967~2865 and 3049~3007 cm^{-1} regions belong to the CH stretching vibrations, and their frequencies differ little from those of 4-isopropyltropolone. The broad infrared absorption in 3450~3095 cm^{-1} is assigned to the OH stretching vibration, and the corresponding Raman lines are very weak. This OH absorption, which is strongest at 3170 cm^{-1} in liquid, shifts to 3095 cm^{-1} and its intensity decreases in carbon tetrachloride. The direction of the shift of absorption caused by the change of state agrees with that in the case of tropolone, but the frequencies in each state are lower by about 50 cm^{-1} than those of many tropolones. Such lower frequencies are also observed in the spectra of 3,7-dibromotropolones[13] and 3-quinonyltropolone (3090 cm^{-1}),[14] all of which have a bulky substituent at the 3-position of the tropolone ring.

Frequencies in the 1650~1470 cm^{-1} region are assigned in the same manner as in the case of 4-isopropyltropolone. The Raman line at 1463 cm^{-1} is assigned to the CH_3 degenerate deformation vibration, and the corresponding infrared band shows a strong intensity because of the overlap with the strong and broad absorption due to the C–O–H group. Two bands in 1395~1375 cm^{-1}, one shoulder at 1345 cm^{-1} and two band in 1183~1130 cm^{-1} are all assigned to the vibration due to the isopropyl group. Of these, the strong intensity of the infrared absorption band at 1394 cm^{-1} indicates the overlapping with the ring CH bending absorption, as its to be expected from the fact that 3-bromotropolone shows the absorption band at 1375 and 1353 cm^{-1} (in carbon tetrachloride).

The broad absorption band at 1233 cm^{-1} in the liquid spectrum appears to be related to the C–O–H group. In carbon tetrachloride, this band shifts to the higher wave number side, merging around 1254 cm^{-1}, as in cases of tropolone and 4-isopropyltropolone.[6] The remaining bands in the 1470~1000 cm^{-1} region have been assigned with reference to the assignments for the spectra of tropolone and 4-isopropyltropolone.

As may be seen in Fig. 1, a line at 877 cm^{-1} and two paired Raman lines at 985 and 965 cm^{-1} and at 728 and 724 cm^{-1} are assigned to the ring C–C stretching vibrations. The broad absorption band, strongest at 742 cm^{-1} in the liquid spectrum, shifts to 739 cm^{-1} in carbon tetrachloride; this is assigned to the OH out-of-plane vibration. Among the remaining bands in the 1000~700 cm^{-1} region, those which are strong in the infrared spectrum and weak in the Raman spectrum are probably to be assigned to the CH out-of-plane bending vibrations, as Table III indicates. The two Raman lines at 785 and 758 cm^{-1} are assumed to be due to the isopropyl group.[8] The Raman lines at 618 and 376 cm^{-1} and the paired ones at 275 and 234 cm^{-1}, which are all distinct in the Raman spectrum, are probably to be assigned to the same vibrations as those of tropone at 653, 396 and 259 cm^{-1} respectively.

The author wishes to express his deep gratitude to Professor Susumu Kinumaki, Professor

10) S. Kinumaki, K. Aida and Y. Ikegami, *Sci. Repts. Research Inst., Tohoku Univ., Ser. A*, **8**, 263 (1956).

11) L. J. Bellamy, "The Infrared Spectra of Complex Molecules", Methuen, London (1958), pp. 13, 26.

12) From the results of spectral measurement made on various 2,4- and 2,6-disubstituted tropones, Takase et al. concluded that the absorption bands at 820 and 790 cm^{-1} correspond to the structures of IIIa and IIIb respectively. (K. Takase, M. Yasunami and T. Nozoe; Presented at the 14th Annual Meeting of the Chemical Society of Japan, Tokyo, April, 1961.)

13) K. Ogura and Y. Ikegami, *Bull. Chem. Research Inst. Non-Aqueous Solutions, Tohoku Univ.*, **9**, 23 (1959).

14) S. Seto, Y. Ikegami and H. Sato, ibid., **11**, 85 (1962); S. Seto and H. Sato, This Bulletin, **35**, 349 (1962).

Shuichi Seto and Professor Koyo Aida for their unfailing guidance during the course of this work. He is also indebted to Miss Hisako Minegishi for her technical cooperation in the spectral measurements.

The Chemical Research Institute of Non-Aqueous Solutions
Tohoku University
Katahira-cho, Sendai

Molecular Vibrations and Structures of High Polymers. V.[*1] *The Infrared Active Normal Vibrations of Isotactic Polypropylene, Poly(propylene-2-d), Poly(propylene-1, 1-d_2) and Poly(propylene-3, 3, 3-d_3) in the 1500 ~ 650 cm^{-1} Region*

By Tatsuo MIYAZAWA and Yoshiko IDEGUCHI

(Received May 25, 1963)

Isotactic polypropylene $[-CH_2-CH(CH_3)-]_n$ is structurally typical of a large number of isotactic polymers. Detailed infrared studies of isotactic polypropylene would provide the basic knowledge necessary for vibrational analyses and structure studies of other isotactic polymers. The infrared spectra of isotactic polypropylene and its deuterated derivatives have been measured, and empirical vibrational assignments have been made.[1-6] The effect of isotopic substitutions of the CH, CH_2, and CH_3 groups upon the infrared spectra have been found to be quite complicated. Except for the bands arising from the CH_3 symmetric or asymmetric deformation vibrations or for the bands due to the CH_2 bending vibrations, all the infrared bands in the 1500~650 cm^{-1} region have been found to shift more or less upon the deuterium substitution of any of the CH, CH_2, and CH_3 groups. Therefore, from empirical analyses of the observed isotope effects, all these bands have been considered to be due to hybridized modes of the CH, CH_2, and CH_3 groups.[4] Accordingly, the normal coordinate analyses are indispensable in elucidating the nature of the infrared bands observed for polypropylene and deuterated derivatives.

In our previous studies, general methods were worked out for treating normal vibrations of infinite helical polymers belonging to dihedral groups[7] (for example, polyethylene glycol) or those belonging to cyclic group[8] (for example, isotactic polypropylene). The infrared active normal vibrations of isotactic polypropylene were calculated[8] by the use of the modified Urey-Bradley potential function,[9,10] where the potential constants were transferred from aliphatic hydrocarbons.[11]

The polarized far-infrared spectra of isotactic polypropylene were measured in the 600~280 cm^{-1} region[8] and also in the 400~80 cm^{-1} region, and all the low-frequency infrared active normal vibrations were observed.[12] The normal vibrations of isotactic polypropylene were calculated by the use of the modified Urey-Bradley force field as supplemented by the internal rotation potential about the axial and equatorial C–C bonds and the C-methyl bonds,[13] and the nature of the low-frequency infrared bands were elucidated.[12]

*1 Presented at the Annual Meeting of the Chemical Society of Japan, Tokyo, March, 1963.

1) M. Peraldo and M. Farina, *Chim. e l'Inds.* (*Milano*), **42**, 1349 (1960).
2) C. Y. Liang and F. G. Pearson, *J. Mol. Spectr.*, **5**, 290 (1960).
3) C. Y. Liang, M. R. Lytton and C. J. Boone, *J. Polymer Sci.*, **47**, 139 (1960).
4) C. Y. Liang, M. R. Lytton and C. J. Boone, ibid., **54**, 523 (1961).
5) H. Tadokoro, T. Kitazawa, S. Nozakura and S. Murahashi, This Bulletin, **34**, 1209 (1961).
6) M. P. McDonald and I. M. Ward, *Polymer, Lond.*, **2**, 341 (1961).
7) T. Miyazawa, *J. Chem. Phys.*, **35**, 693 (1961).
8) T. Miyazawa, Y. Ideguchi and K. Fukushima, ibid., **38**, 2709 (1963); International Symposium on Molecular Structure and Spectroscopy, A120, Tokyo, September, 1962.
9) T. Shimanouchi, International Symposium on Molecular Structure and Spectroscopy, C216, Tokyo, September, 1962.
10) M. Tasumi, T. Shimanouchi and T. Miyazawa, *J. Mol. Spectr.*, **9**, 261 (1962).
11) H. Takahashi, *J. Chem. Soc. Japan, Pure Chem. Sec.* (*Nippon Kagaku Zasshi*), **83**, 976 978, 980 (1962).
12) T. Miyazawa, K. Fukushima and Y. Ideguchi, *Polymer Letters*, **1**, 385 (1963), 16th Annual Meeting of the Chemical Society of Japan, Tokyo, March, 1963.
13) T. Miyazawa and K. Fukushima, 16th Annual Meeting of the Chemical Society of Japan, Tokyo, April, 1963.

Unfortunately, however, the far-infrared spectra of the deuterated derivatives of isotactic polypropylene have not yet been published. In the present study, therefore, vibrational analyses were made of the infrared bands of isotactic polypropylene and deuterated derivatives observed in the 1500~650 cm^{-1} region.

Normal Coordinate Treatment

The normal vibrations of isotactic polypropylene, $[-CH_2-CH(CH_3)-]_n$; poly(propylene-2-d), $[-CH_2-CD(CH_3)-]_n$; poly(propylene-1,1-d_2), $[-CD_2-CH(CH_3)-]_n$; and poly(propylene-3,3,3-d_3), $[-CH_2-CH(CD_3)-]_n$ were treated in the present research. The high-frequency C–H stretching modes of the CH, CH_2, and CH_3 groups were separated in a manner described previously.[8] The internal rotation modes about the C–C bonds were not taken into account since the contributions of the internal rotation potential are not appreciable for the vibrations of polypropylene lying above 650 cm^{-1}. An NEAC model 2101 digital computer (Nippon Electric Company, Ltd., Tokyo) was used for the numerical computations involved in the normal coordinate treatment. The $\boldsymbol{G}$ and $\boldsymbol{F}$ matrices[14] for the degenerate normal vibrations of isotactic polypropylene were constructed and diagonalized according to a method described previously.[8]

The internal coordinate (or local symmetry coordinate) vectors, R_n, of the n-th repeating unit are,

where Δr's are the stretching coordinates for which the numbering of carbon and hydrogen atoms are shown in Fig. 1. The elements of the vector $\phi(CH)_n$ in Eq. 1, are; $\Delta\phi(2,n-1;1,n;3,n)$, $\Delta\phi(2,n-1;1,n;5,n)$, $\Delta\phi(2,n-1;1,n;2,n)$, $\Delta\phi(3,n;1,n;5,n)$, $\Delta\phi(3,n;1,n;2,n)$, and $\Delta\phi(5,n;1,n;2,n)$. The elements of the vector $\phi(CH_3)_n$ in Eq. 3 are; $\Delta\phi(1,n;3,n;7,n)$, $\Delta\phi(1,n;3,n;8,n)$, $\Delta\phi(1,n;3,n;9,n)$, $\Delta\phi(8,n;3,n;9,n)$, $\Delta\phi(9,n;3,n;7,n)$, and $\Delta\phi(7,n;3,n;8,n)$. The elements of the vector $\phi(CH_2)_n$ in Eq. 5 are; $\Delta\phi(1,n;2,n;4,n)$, $\Delta\phi(1,n;2,n;6,n)$ $\Delta\phi(1,n;2,n;1,n+1)$, $\Delta\phi(4,n;2,n;6,n)$, $\Delta\phi(4,n;2,n;1,n+1)$, and $\Delta\phi(6,n;2,n;1,n+1)$, where $\Delta\phi$'s are the angle-bending coordinates for which the numbering of the atoms are shown in Fig. 1.

For the CH group of polypropylene, there are two CH bending modes. The CH bending

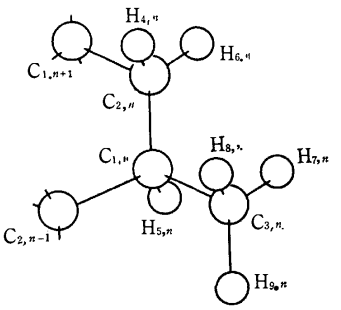

Fig. 1. Numbering of the carbon and hydrogen atoms of isotactic polypropylene chain (right-handed helix).

$$\begin{bmatrix} R_{1,n}\ (\text{CH bend.}^{ax}) \\ R_{2,n}\ (\text{CH bend.}^{eq}) \\ R_{3,n}\ (\delta^s) \\ R_{4,n}\ (\delta^a\ \text{ax.}) \\ R_{5,n}\ (\delta^a\ \text{eq.}) \end{bmatrix} = \begin{bmatrix} 0 & 1/6^{1/2} & 0 & 1/6^{1/2} & 0 & -2/6^{1/2} \\ 0 & -1/2^{1/2} & 0 & 1/2^{1/2} & 0 & 0 \\ 1/6^{1/2} & -1/6^{1/2} & 1/6^{1/2} & -1/6^{1/2} & 1/6^{1/2} & -1/6^{1/2} \\ -2/6^{1/2} & 0 & 1/6^{1/2} & 0 & 1/6^{1/2} & 0 \\ 0 & 0 & -1/2^{1/2} & 0 & 1/2^{1/2} & 0 \end{bmatrix} \phi(CH)_n \tag{1}$$

$$R_{6,n}\ (r_{CM}) = \Delta r(1,n;3,n) \tag{2}$$

$$\begin{bmatrix} R_{7,n}\ (CH_3\ \delta_a^{ax}) \\ R_{8,n}\ (CH_3\ \delta_a^{eq}) \\ R_{9,n}\ (CH_3\ \delta_s) \\ R_{10,n}\ (CH_3\ \text{rock.}^{ax}) \\ R_{11,n}\ (CH_3\ \text{rock.}^{eq}) \end{bmatrix} = \begin{bmatrix} 0 & 0 & 0 & 1/6^{1/2} & 1/6^{1/2} & -2/6^{1/2} \\ 0 & 0 & 0 & 1/2^{1/2} & -1/2^{1/2} & 0 \\ -1/6^{1/2} & -1/6^{1/2} & -1/6^{1/2} & 1/6^{1/2} & 1/6^{1/2} & 1/6^{1/2} \\ -1/6^{1/2} & -1/6^{1/2} & 2/6^{1/2} & 0 & 0 & 0 \\ -1/2^{1/2} & 1/2^{1/2} & 0 & 0 & 0 & 0 \end{bmatrix} \phi(CH_3)_n \tag{3}$$

$$R_{12,n}\ (r_{CC}^{ax}) = \Delta r(1,n;2,n) \tag{4}$$

$$\begin{bmatrix} R_{13,n}\ (\delta) \\ R_{14,n}\ (CH_2\ \text{bend.}) \\ R_{15,n}\ (CH_2\ \text{wag.}) \\ R_{16,n}\ (CH_2\ \text{twist.}) \\ R_{17,n}\ (CH_2\ \text{rock.}) \end{bmatrix} = \begin{bmatrix} 1/30^{1/2} & 1/30^{1/2} & -5/30^{1/2} & 1/30^{1/2} & 1/30^{1/2} & 1/30^{1/2} \\ 1/20^{1/2} & 1/20^{1/2} & 0 & -4/20^{1/2} & 1/20^{1/2} & 1/20^{1/2} \\ 1/2 & 1/2 & 0 & 0 & -1/2 & -1/2 \\ -1/2 & 1/2 & 0 & 0 & 1/2 & -1/2 \\ 1/2 & -1/2 & 0 & 0 & 1/2 & -1/2 \end{bmatrix} \phi(CH_2)_n \tag{5}$$

$$R_{18,n}\ (r_{CC}^{eq}) = \Delta r(2,n;1,n+1) \tag{6}$$

14) E. B. Wilson, Jr., *J. Chem. Phys.*, 7, 1047 (1939); 9, 76 (1941).

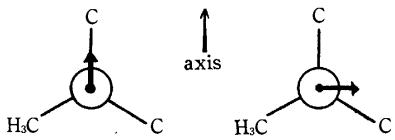

Fig. 2. The axial and equatorial CH bending modes.

mode in the axial direction (CH bend.^{ax}) and the bending mode in the equatorial direction (CH bend.^{eq}) (perpendicular to the helix axis) are given in Eq. 1 and are shown in Fig. 2. For the CH_3 group, there are two asymmetric deformation modes and two rocking modes. The asymmetric deformation mode in the axial direction (CH_3 δ_a^{ax}) and that in the equatorial direction (CH_3 δ_a^{eq}) and the rocking modes in the axial direction (CH_3 rock.^{ax}) and in the equatorial direction (CH_3 rock.^{eq}) are given in Eq. 3 and are shown in Fig. 3.

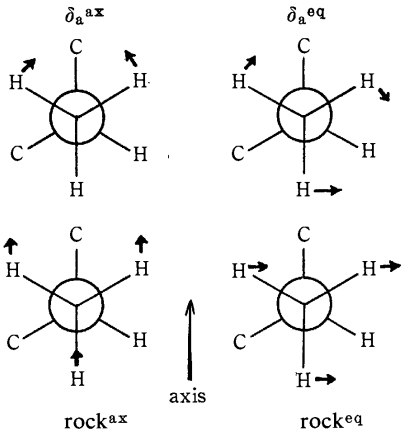

Fig. 3. The axial and equatorial CH_3 asymmetric deformation modes and rocking modes.

In deriving the potential energy matrix, $\boldsymbol{F}$, the modified Urey-Bradley force field[9] was used; the trans-coupling potential[10,11,15] for pairs of C–C–H bond angles in the trans arrangement, the gauche-coupling potential[11] for pairs of C–C–H angles in the gauche arrangement, and the l(C–C–H) angle interaction potential[10,11,16] for the CH_2 group were added as correction terms to the Urey-Bradley force field.[17]

The Urey-Bradley potential constants (in mdyn./Å) of K(C–H) = 3.90 (CH group), K(C–H) = 4.05 (CH_2 group), K(C–H) = 4.05 (CH_3 group), F(H–C–H) = 0.080 and F(H–C–C) = 0.540 were used in correcting for the potential-energy interactions with high-frequency C–H stretching modes.[8]

The C–C stretching constants for the C-methyl bond and the main chain C–C bonds, the H–C–H bending constants for the CH_2 and CH_3 groups, the C–C–H bending constants for the CH, CH_2, and CH_3 groups, the C–C–C bending constant, the C···(C)···C repulsive constants, the intramolecular tension for the CH, CH_2, and CH_3 groups, the trans- and gauche-coupling constants and the angle-interaction constant (l) were adjusted by the

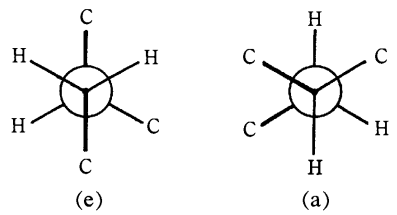

Fig. 4. Spatial arrangement of the carbon and hydrogen atoms of isotactic polypropylene chain (the right-handed helix); (e): as viewed along the equatorial C-C bond; (a): as viewed along the axial C-C bond. Main chain C-C bonds are drawn with heavy lines.

TABLE I. MODIFIED UREY-BRADLEY POTENTIAL CONSTANTS[*1] OF ISOTACTIC POLYPROPYLENE AS ADJUSTED BY THE METHOD OF LEAST SQUARES

K(C-C)	2.11	Axial or equatorial C-C bond
	2.10	C-methyl bond
H(H-C-H)	0.414	CH_3 group
	0.393	CH_2 group
H(H-C-C)	0.222	CH_3 group
	0.205	CH_2 group
	0.225	CH group
H(C-C-C)	0.343	C-CH-C angle
	0.311	C-CH_2-C angle
F(H-C-H)	0.080[*2]	
F(H-C-C)	0.540[*2]	
F(C-C-C)	0.390	
κ	−0.027	CH_3 group
	0.028	CH_2 group
	−0.014	CH group
T	0.104	
G	−0.044	
l(C-C-H)	0.014	CH_2 group

[*1] K, Stretching constant (in mdyn./Å); H, Bending constant (in mdyn./Å); F, Repulsive constant (in mdyn./Å); $F' = -F/10$; κ, Intramolecular tension (in mdyn·Å); T, Trans-coupling constant (in mdyn·Å); G, Gauche-coupling constant (in mdyn·Å); and l(C-C-H), Angle interaction constant (in mdyn·Å)

[*2] Transferred from aliphatic hydrocarbons (Ref. 11).

15) J. Overend and J. R. Scherer, ibid., 35, 1681 (1960).
16) T. Shimanouchi and I. Suzuki, *J. Mol. Spectr.*, 6, 277 (1961).
17) T. Shimanouchi, *J. Chem. Phys.*, 17, 243, 734, 848 (1949).

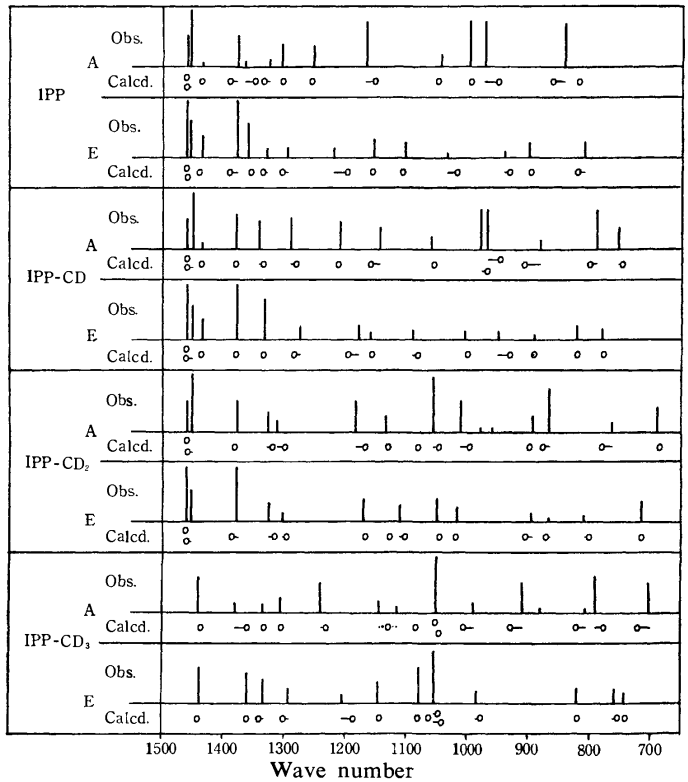

Fig. 5. Observed frequencies (cm^{-1}) and relative intensities (Ref. 1) and calculated frequencies of isotactic polypropylene [IPP], poly(propylene-2-d) [IPP-CD], poly(propylene-1, 1-d_2) [IPP-CD_2], and poly(propylene-3, 3, 3-d_3) [IPP-CD_3].

TABLE II. THE OBSERVED FREQUENCIES*1 (INTENSITY*2) AND THE CALCULATED FREQUENCIES (IN cm^{-1}) AND POTENTIAL ENERGY DISTRIBUTIONS*3 (IN %) OF THE A VIBRATIONS OF ISOTACTIC POLYPROPYLENE IN THE 1500~650 cm^{-1} REGION

ν_0	ν_c	Potential energy distributions
1460 (w)	1462 (ν_7)	CH_3 δ_a^{eq} (65), CH_3 δ_a^{ax} (15)
1454 (s)	1461 (ν_8)	CH_3 δ_a^{ax} (65), CH_3 δ_a^{eq} (20)
1435 (w)	1436 (ν_9)	CH_2 bend. (100)
1378*(m)	1390 (ν_{10})	CH_3 δ_s (65), CH bend. (15)
1365*(vw)	1348 (ν_{11})	CH_2 wag. (40), CH_3 δ_s (35), CH bend. (15)
1326 (w)	1334 (ν_{12})	CH bend.^{ax} (50), CH bend.^{eq} (25)
1304 (m)	1303 (ν_{13})	CH_2 wag. (45), CH_2 twist. (35), CH bend. (15)
1254 (m)	1256 (ν_{14})	CH_2 twist. (35), CH bend.^{ax} (15), CH bend.^{eq} (15)
1168 (s)	1152 (ν_{15})	r_{CC}^{ax} (40), CH_3 rock.^{ax} (20)
1045 (m)	1048 (ν_{16})	r_{CM} (45), r_{CC}^{eq} (30)
998 (s)	995 (ν_{17})	CH_3 rock.^{eq} (40), r_{CM} (25), CH bend. (20), CH_2 twist. (15)
973 (s)	951 (ν_{18})	CH_3 rock.^{ax} (50), r_{CC}^{ax} (25), r_{CC}^{eq} (20)
842 (s)	864 (ν_{19})	CH_3 rock. (30), r_{CC}^{eq} (20), r_{CM} (15)
	819 (ν_{20})	CH_2 rock. (70), CH bend. (20)

*1 The frequencies marked with * were observed by Tasumi and Shimanouchi (Ref. 20) and all the other frequencies were observed by Peraldo and Farina (Ref. 1).

*2 s: strong; m: medium; w: weak; and vw: very weak

*3 CH_3 δ_a, Methyl asymmetric deformation; CH_3 δ_s, Methyl symmetric deformation (see also Fig. 4), r_{CC}^{ax}, Axial C-C stretching; r_{CC}^{eq}; Equatorial C-C stretching; r_{CM}, C-methyl stretching mode.

TABLE III. THE OBSERVED FREQUENCIES*1 (INTENSITY*2) AND THE CALCULATED FREQUENCIES (IN cm^{-1}) POTENTIAL ENERGY DISTRIBUTIONS*3 (IN %) OF THE $E(2\pi/3)$ VIBRATIONS OF ISOTACTIC AND POLYPROPYLENE IN THE 1500～650 cm^{-1} REGION

ν_0	ν_c	Potential energy distributions
1460 (s)	1462 (ν_7)	CH_3 δ_a^{eq} (40), CH_3 δ_a^{ax} (40)
1454 (w)	1461 (ν_8)	CH_3 δ_a^{ax} (45), CH_3 δ_a^{eq} (40)
1435 (m)	1439 (ν_9)	CH_2 bend. (100)
1377 (s)	1390 (ν_{10})	CH_3 δ_s (70), CH bend.^{eq} (15)
1360 (m)	1356 (ν_{11})	CH bend.^{ax} (20), CH bend.^{eq} (15), CH_2 twist. (20), CH_2 wag. (15)
1330 (w)	1336 (ν_{12})	CH_2 wag. (45), CH bend.^{ax} (20), CH_3 δ_s (15)
1296 (w)	1304 (ν_{13})	CH_2 wag. (35), CH bend.^{eq} (25) CH bend.^{ax} (20)
1220 (w)	1197 (ν_{14})	CH_2 twist. (35), CH bend.^{ax} (15), r_{CC}^{eq} (15)
1155 (m)	1156 (ν_{15})	r_{CM} (20), CH bend. (15)
1103 (m)	1107 (ν_{16})	CH_3 rock. (ax : 20, eq : 10), r_{CC}^{ax} (25)
1034 (vw)	1017 (ν_{17})	r_{CM} (30), CH_2 twist. (20), CH bend. (15), CH_3 rock. (15)
941 (w)	931 (ν_{18})	CH_3 rock. (ax : 35, eq : 10), r_{CC}^{ax} (30), r_{CC}^{eq} (15)
899 (m)	896 (ν_{19})	CH_3 rock.^{eq} (40), CH_2 rock. (15), CH bend.^{eq} (15)
809 (m)	821 (ν_{20})	CH_2 rock. (35), r_{CM} (25), r_{CC}^{eq} (20)

*1 *2 *3 See *1 *2 *3 of Table II.

TABLE IV. THE OBSERVED FREQUENCIES*1 (INTENSITY*2) AND THE CALCULATED FREQUENCIES (IN cm^{-1}) AND POTENTIAL ENERGY DISTRIBUTIONS*3 (IN %) OF THE A VIBRATIONS OF ISOTACTIC POLY(PROPYLENE-2-D) IN THE 1500～650 cm^{-1} REGION

ν_0	ν_c	Potential energy distributions
1459 (w)	1459 (ν_7)	CH_3 δ_a^{eq} (85)
1451 (s)	1460 (ν_8)	CH_3 δ_a^{ax} (85)
1435 (w)	1436 (ν_9)	CH_2 bend. (100)
1379 (m)	1380 (ν_{10})	CH_3 δ_s (95)
1342 (m)	1336 (ν_{11})	CH_2 wag. (85)
1291 (m)	1279 (ν_{12})	CH_2 twist. (80)
1210 (m)	1212 (ν_{13})	r_{CC}^{ax} (30), r_{CC}^{eq} (25), CH_3 rock.^{ax} (15), CD bend. (ax : 15, eq : 10)
1145 (m)	1160 (ν_{14})	CH_3 rock. (25), CD bend. (25), r_{CM} (15)
1060 (w)	1054 (ν_{15})	CH_3 rock.^{eq} (30), CH_2 rock. (20)
981 (s)	968 (ν_{16})	r_{CM} (40), CH_3 rock.^{ax} (25), CD bend.^{ax} (20)
969 (s)	947 (ν_{17})	CH_3 rock. (ax : 25, eq : 10), r_{CC}^{ax} (20)
881 (w)	909 (ν_{18})	r_{CC}^{eq} (45), CD bend.^{eq} (20)
790 (s)	800 (ν_{19})	CD bend.^{eq} (30), CD bend.^{ax} (25), CH_3 rock. (eq : 20, ax : 10)
754 (m)	745 (ν_{20})	CH_2 rock. (55), CD bend.^{ax} (25), CD bend.^{eq} (25)

*1 *2 *3 See *1 *2 *3 of Table II.

TABLE V. THE OBSERVED FREQUENCIES*1 (INTENSITY*2) AND THE CALCULATED FREQUENCIES (IN cm^{-1}) AND POTENTIAL ENERGY DISTRIBUTIONS*3 (IN %) OF THE $E(2\pi/3)$ VIBRATIONS OF ISOTACTIC POLY(PROPYLENE-2-D) IN THE 1500～650 cm^{-1} REGION

ν_0	ν_c	Potential energy distributions
1459 (s)	1459 (ν_7)	CH_3 δ_a^{eq} (50), CH_3 δ_a^{ax} (35)
1451 (m)	1460 (ν_8)	CH_3 δ_a^{ax} (50), CH_3 δ_a^{eq} (35)
1435 (m)	1438 (ν_9)	CH_2 bend. (100)
1378 (s)	1380 (ν_{10})	CH_3 δ_s (95)
1334 (m)	1335 (ν_{11})	CH_2 wag. (85)
1273 (w)	1284 (ν_{12})	CH_2 twist. (55)
1179 (w)	1196 (ν_{13})	r_{CM} (20), r_{CC}^{eq} (15), CD bend. (15) CH_3 rock. (15)
1160 (vw)	1158 (ν_{14})	r_{CC}^{ax} (25), CH_3 rock.^{ax} (20), CH_2 twist. (15), CD bend. (15)
1091 (w)	1082 (ν_{15})	CH_3 rock.^{eq} (30), r_{CM} (15)
1005 (w)	1001 (r_{16})	CH_3 rock. (20), CH_2 rock. (20), CD bend. (15)
949 (w)	930 (ν_{17})	r_{CC}^{ax} (40), CH_3 rock. (ax : 30, eq : 10), r_{CC}^{eq} (15)
890 (vw)	891 (ν_{18})	CD bend. (ax : 35, eq : 10), r_{CM} (20), r_{CC}^{eq} (15)
821 (m)	820 (ν_{19})	CD bend. (eq : 35, ax : 10), r_{CM} (20), CH_3 rock.^{eq} (15)
781 (w)	775 (ν_{20})	CD bend.^{ax} (25), CD bend.^{eq} (25), CH_2 rock. (35)

*1 *2 *3 See *1 *2 *3 of Table II.

TABLE VI. THE OBSERVED FREQUENCIES*1 (INTENSITY*2) AND THE CALCULATED FREQUENCIES (IN cm^{-1}) AND POTENTIAL ENERGY DISTRIBUTION*3 (IN %) OF THE A VIBRATIONS OF ISOTACTIC POLY(PROPYLENE-1, 1-D_2) IN THE 1500~650 cm^{-1} REGION

ν_0	ν_c	Potential energy distributions
1461 (w)	1461 (ν_7)	CH_3 δ_a^{eq} (65), CH_3 δ_a^{ax} (20)
1452 (s)	1460 (ν_8)	CH_3 δ_a^{ax} (65), CH_3 δ_a^{eq} (20)
1377 (m)	1382 (ν_9)	CH_3 δ_s (90)
1327 (m)	1318 (ν_{10})	CH bend.^{eq} (55), CH bend.^{ax} (20)
1313 (w)	1301 (ν_{11})	CH bend.^{ax} (60), CH bend.^{eq} (15)
1184 (s)	1167 (ν_{12})	r_{CC}^{ax} (45), CD_2 wag. (20)
1134 (m)	1130 (ν_{13})	CH_3 rock.^{eq} (20), CD_2 twist. (15)
	1082 (ν_{14})	r_{CM} (25), r_{CC}^{eq} (20), CH_3 rock.^{ax} (20)
1058 (s)	1048 (ν_{15})	CD_2 bend. (60), CH_3 rock.^{eq} (15)
1013 (s)	997 (ν_{16})	r_{CM} (30), CD_2 wag. (25), r_{CC}^{eq} (20), CH_3 rock.^{ax} (20)
894 (m)	900 (ν_{17})	CH_3 rock. (eq: 20, ax: 10), CD_2 wag. (20), CD_2 twist. (20)
868 (s)	878 (ν_{18})	CH_3 rock.^{ax} (25), CH_3 rock.^{eq} (20), CD_2 twist. (15), CH bend. (15)
764 (w)	782 (ν_{19})	CD_2 twist. (40), r_{CC}^{eq} (20), r_{CM} (15)
691 (m)	688 (ν_{20})	CD_2 rock. (80)

*1 *2 *3 See *1 *2 *3 of Table II.

TABLE VII. THE OBSERVED FREQUENCIES*1 (INTENSITY*2) AND THE CALCULATED FREQUENCIES (IN cm^{-1}) AND POTENTIAL ENERGY DISTRIBUTIONS*3 (IN %) OF THE E($2\pi/3$) VIBRATIONS OF ISOTACTIC POLY(PROPYLENE-1, 1-D_2) IN THE 1500~650 cm^{-1} REGION

ν_0	ν_c	Potential energy distributions
1461 (s)	1462 (ν_7)	CH_3 δ_a^{eq} (75)
1452 (m)	1460 (ν_8)	CH_3 δ_a^{ax} (80)
1377 (s)	1386 (ν_9)	CH_3 δ_s (85)
1325 (m)	1314 (ν_{10})	CH bend.^{eq} (50), CH bend.^{ax} (15), CH_3 δ_s (20)
1303 (w)	1296 (ν_{11})	CH bend.^{ax} (65), CH bend.^{eq} (20)
1170 (m)	1168 (ν_{12})	r_{CC}^{eq} (35), CD_2 bend. (15)
	1128 (ν_{13})	r_{CC}^{ax} (30), CD_2 wag. (15), r_{CM} (15), CH_3 rock. (15)
1110 (m)	1103 (ν_{14})	CD_2 wag. (20), CH_3 rock.^{eq} (20)
1051 (m)	1043 (ν_{15})	CD_2 bend. (70)
1018 (m)	1020 (ν_{16})	CD_2 wag. (35), CH_3 rock.^{ax} (25), r_{CM} (20)
896 (w)	904 (ν_{17})	CH_3 rock.^{eq} (25), CH_3 rock.^{ax} (15), r_{CC}^{ax} (20)
868 (w)	868 (ν_{18})	CH_3 rock.^{ax} (20), CH_3 rock.^{eq} (20), r_{CC}^{ax} (15), CD_2 twist. (15)
811 (w)	801 (ν_{19})	CD_2 twist. (65)
715 (m)	715 (ν_{20})	CD_2 rock. (45), r_{CM} (15), r_{CC}^{eq} (15)

*1 *2 *3 See *1 *2 *3 of Table II.

TABLE VIII. THE OBSERVED FREQUENCIES*1 (INTENSITY*2) AND THE CALCULATED FREQUENCIES (IN cm^{-1}) AND POTENTIAL ENERGY DISTRIBUTIONS*3 (IN %) OF THE A VIBRATIONS OF ISOTACTIC POLY(PROPYLENE-3, 3, 3-D_3) IN THE 1500~650 cm^{-1} REGION

ν_0	ν_c	Potential energy distributions
1440 (m)	1436 (ν_7)	CH_2 bend. (100)
1379 (w)	1359 (ν_8)	CH_2 wag. (50), CH bend.^{eq} (30)
1334 (w)	1333 (ν_9)	CH bend.^{ax} (55), CH bend.^{eq} (25)
1305 (m)	1304 (ν_{10})	CH_2 wag. (40), CH_2 twist. (35), CH bend. (15)
1239 (m)	1230 (ν_{11})	CH_2 twist. (35), CH bend.^{ax} (25), CH bend.^{eq} (25)
1145 (w)	1128 (ν_{12})	r_{CC}^{ax} (55)
1115 (w)	1083 (ν_{13})	CD_3 δ_s (65), r_{CM} (50)
1051 (s)	1049 (ν_{14})	CD_3 δ_a^{ax} (45), CD_3 δ_a^{eq} (40)
	1045 (ν_{15})	CD_3 δ_a^{ax} (50), CD_3 δ_a^{eq} (40)
989 (w)	1006 (ν_{16})	r_{CC}^{eq} (35), CD_3 δ_s (25)
909 (m)	928 (ν_{17})	r_{CM} (20), r_{CC}^{eq} (15), CD_3 rock.^{eq} (15), CH_2 twist. (15)
807 (vw)	820 (ν_{18})	CH_2 rock. (70), r_{CM} (15)
791 (s)	775 (ν_{19})	CD_3 rock.^{ax} (40), CD_3 rock.^{eq} (25)
703 (m)	720 (ν_{20})	CD_3 rock.^{eq} (40), CD_3 rock.^{ax} (30)

*1 *2 *3 See *1 *2 *3 of Table II.

TABLE IX. THE OBSERVED FREQUENCIES*1 (INTENSITY*2) AND THE CALCULATED FREQUENCIES (IN cm^{-1}) AND POTENTIAL ENERGY DISTRIBUTIONS*3 (IN %) OF THE $E(2\pi/3)$ VIBRATIONS OF ISOTACTIC POLY(PROPYLENE-3, 3, 3-D_3) IN THE 1500~650 cm^{-1} REGION

ν_0	ν_c	Potential energy distributions
1438 (s)	1439 (ν_7)	CH_2 bend. (100)
1361 (m)	1361 (ν_8)	CH bend. (eq: 30, ax: 10), CH_2 wag. (20), CH_2 twist. (25)
1333 (m)	1339 (ν_9)	CH_2 wag. (45), CH bend.^{ax} (35)
1293 (m)	1299 (ν_{10})	CH_2 wag. (35), CH bend.^{eq} (30), CH bend.^{ax} (25)
1206 (w)	1184 (ν_{11})	CH_2 twist. (35), CH bend.^{ax} (15), r_{CC}^{eq} (15)
1145 (m)	1143 (ν_{12})	r_{CM} (30), CH bend. (15)
1081 (m)	1079 (ν_{13})	r_{CC}^{ax} (35), CD_3 δ_s (15), r_{CC}^{eq} (15)
	1061 (ν_{14})	CD_3 δ_s (55), CD_3 δ_a (20)
1054 (s)	1044 (ν_{15})	CD_3 δ_a^{eq} (70), CD_3 δ_a^{ax} (15)
	1040 (ν_{16})	CD_3 δ_a^{ax} (55), CD_3 δ_a^{eq} (20)
984 (w)	976 (ν_{17})	CH_2 rock. (15), r_{CM} (15)
821 (m)	818 (ν_{18})	CH_2 rock. (30), r_{CM} (20), r_{CC}^{eq} (15)
759 (m)	753 (ν_{19})	CD_3 rock.^{ax} (35), CD_3 rock.^{eq} (30)
743 (w)	739 (ν_{20})	CD_3 rock.^{eq} (40), CD_3 rock.^{ax} (25)

*1 *2 *3 See *1 *2 *3 of Table II.

TABLE X. THE OBSERVED*1 AND CALCULATED FREQUENCIES BELOW 650 cm^{-1} AND THE CALCULATED POTENTIAL ENERGY DISTRIBUTIONS (IN %)*2 OF ISOTACTIC POLYPROPYLENE [IPP], POLY(PROPYLENE-2-D) [IPP-CD], POLY(PROPYLENE-1, 1-D_2) [IPP-CD_2] AND POLY(PROPYLENE-3, 3, 3-D_3) [IPP-CD_3]

	IPP		ν_c		
ν_0	ν_c	Potential energy distributions	IPP-CD	-CD_2	-CD_3
528	514 (ν_{21}^E)	δ^a (35), δ (25)	498	488	490
460	435 (ν_{22}^E)	δ^s (70)	428	391	407
456	479 (ν_{21}^A)	δ^a (75)	470	453	445
398	391 (ν_{22}^A)	δ^s (45), δ^a (30)	387	371	360
321	309 (ν_{23}^E)	δ^a (65)	307	293	285
251	260 (ν_{23}^A)	δ^a (45), δ^s (30)	257	238	248
	138 (ν_{24}^E)	δ^a (55), δ (45)	137	131	127
	118 (ν_{24}^A)	δ (50), δ^a (20)	114	110	110

*1 Observed in previous studies (Refs. 8 and 12). Only the frequencies above 250 cm^{-1} are listed for comparisons.

*2 δ^s and δ^a, the symmetric and asymmetric deformations, respectively, of the CH_2-$CH(CH_3)$-CH_2 group; δ, the C-CH_2-C deformation.

method of least squares.[18] The initial set of these constants as transferred from ethane, propane, and isobutane[11] have been described previously[8]. All the fundamental frequencies of $[-CH_2-CH(CH_3)-]_n$, $[-CH_2-CD(CH_3)-]_n$, $[-CD_2-CH(CH_3)-]_n$, and $[-CH_2-CH(CD_3)-]_n$ observed by Peraldo and Farina[1] in the 1500~650 cm^{-1} region and the skeletal frequencies of $[-CH_2-CH(CH_3)-]_n$[8,12] (A species: 456, 398 and 251 cm^{-1}; $E(2\pi/3)$ species: 528, 460 and 321 cm^{-1}) were used for the adjustment of potential constants. The potential constants thus obtained are shown in Table I. A common stretching constant K(C-C) was used for the axial C-C bond and for the equatorial C-C bond since the arrangements of the carbon and hydrogen atoms adjacent to these C-C bonds are the same, as Fig. 4 shows. In the adjustments of the potential constants, the elements of Jacobian matrices (derivatives of frequencies with respect to potential constants) were calculated by means of an equation reported previously.[19]

The trans-coupling ($T=0.104$) and gauche-coupling ($G=-0.044$) constants of polypropylene agree closely with the corresponding constants for polyethylene ($T=0.100$ and $G=-0.033$) and for ethane ($T=0.107$ and $G=-0.025$).[9] It is interesting to note that the gauche constant is nearly equal to $-T/2$.

The frequencies calculated with the final set of potential constants may be compared

18) D. E. Mann, T. Shimanouchi, J. H. Meal and L. Fano, *J. Chem. Phys.*, 27, 43 (1957).

19) T. Miyazawa, *J. Chem. Soc. Japan, Pure Chem. Sec. (Nippon Kagaku Zasshi)*, 76, 1132 (1955).

TABLE XI. THE L MATRIX ELEMENTS FOR THE A VIBRATIONS OF ISOTACTIC POLYPROPYLENE IN THE 1500~650 cm^{-1} REGION

S_i*	ν_7 1462	ν_8 1461	ν_9 1436	ν_{10} 1390	ν_{11} 1348	ν_{12} 1334	ν_{13} 1303	ν_{14} 1256	ν_{15} 1152	ν_{16} 1048	ν_{17} 995	ν_{18} 951	ν_{19} 864	ν_{20} 819
CH bend.^{ax}	−1	1	1	2	−3	9	3	−5	2	−1	−3	1	2	2
CH bend.^{eq}	−2	−1	1	5	−4	−7	4	−4	0	3	−3	0	1	−3
δ^s	0	0	0	0	0	0	1	2	1	1	−2	0	−2	1
δ^a (ax)	0	0	0	−1	1	−1	0	0	3	1	1	0	−1	0
δ^a (eq)	0	0	0	1	−1	−1	−1	0	0	−1	−1	1	0	0
r_{CM}	0	0	0	0	2	0	0	0	0	3	2	0	1	1
CH_3 δ_a^{ax}	−6	13	−2	−1	1	−2	0	2	2	0	0	2	1	0
CH_3 δ_a^{eq}	12	7	1	2	−1	−2	0	−3	1	−1	2	1	−1	0
CH_3 δ_s	−1	0	0	11	8	1	−1	1	0	1	1	0	0	0
CH_3 rock.^{ax}	2	−4	0	0	0	−1	−1	2	5	−1	−1	6	3	−1
CH_3 rock.^{eq}	−4	−2	0	0	−1	−1	0	−4	2	−2	6	2	−3	2
r_{CC}^{ax}	0	0	0	1	−1	1	−1	−1	−3	0	0	2	1	0
δ	0	0	−1	0	0	1	−1	−1	−2	−1	1	0	2	−1
CH_2 bend.	−1	1	15	−1	1	0	0	0	0	0	0	0	0	0
CH_2 wag.	1	0	−1	−4	8	−2	8	−2	0	−2	−1	0	0	0
CH_2 twist.	0	0	0	2	−3	1	7	7	−1	−1	4	−1	1	0
CH_2 rock.	0	0	0	1	−1	−3	0	0	−1	−2	−1	0	2	6
r_{CC}^{eq}	0	0	0	0	0	−1	0	−1	1	−2	0	−2	1	−1

* For the notation of the symmetry coordinates, see *3 of Table II.

with the observed frequencies in Tables II—X and in Fig. 5. Except for the unobserved fundamentals, the r. m. s. frequency deviations for the vibrations lying in the 1500~650 cm^{-1} region are: $[-CH_2-CH(CH_3)-]_n$: 1.0%, $[-CH_2-CD(CH_3)-]_n$: 1.1%, $[-CD_2-CH(CH_3)-]_n$: 1.0%, and $[-CH_2-CH(CD_3)-]_n$: 1.2%, and the overall deviation is 1.1%. In view of the small number (a total of 16) of potential constants as compared with the large number (a total of 108) of observed frequencies, a frequency deviation as small as this indicates that these potential constants may now be used for the elucidation of the nature of observed fundamental vibrations. Therefore, the potential energy distributions ($F_{ii}L_{ip}^2/4\pi^2c^2\nu^2$) were also calculated as shown in Tables II–X for the A and E($2\pi/3$) vibrations of polypropylene and the deuterated derivatives. Only the terms greater than 15% are listed in Tables II–X.

For nondegenerate vibrations, the normal modes may be expressed by the elements of the L matrix. When the p-th normal vibration is excited, the i-th internal coordinate (or local symmetry coordinate) of the n-th repeating unit is given by

$$R_{i,n} = (1/N)^{1/2} L_{ip} Q_p \qquad (7)$$

where Q_p is the normal coordinate for the p-th vibration and $(1/N)^{1/2}$ is the normalization factor. On the other hand, for degenerate vibrations of a helical molecule associated with the phase difference of δ, the normal modes may be expressed by the amplitude factor $L_{ip}(\delta)$ and the phase angle $\varepsilon_{ip}(\delta)$. When the p-th degenerate vibration is excited, the i-th internal coordinate of the n-th unit is given by:

$$R_{i,n} = (2/N)^{1/2} L_{ip}(\delta)\{Q_{pa}(\delta)\cos[n\delta + \varepsilon_{ip}(\delta)] + Q_{pb}(\delta)\sin[n\delta + \varepsilon_{ip}(\delta)]\} \qquad (8)$$

where $Q_{pa}(\delta)$ and $Q_{pb}(\delta)$ are the p-th pair of normal coordinates with the phase difference of δ.[8] The L matrix elements [in units of 1/10·Å·(atomic weight)$^{1/2}$] for the A vibrations of isotactic polypropylene are listed in Table XI. The amplitude factor [in units of 1/10·Å·(atomic weight)$^{1/2}$] and the phase angle (in degrees) for the E($2\pi/3$) vibrations are listed in Table XII, where the phase angles were taken in the range of $+90°\sim-90°$ with the result that the values of a number of L_{ip}'s were taken to be negative.

CH_2 Bending Vibrations

The band of polypropylene at 1435 cm^{-1} is also observed for $[-CH_2-CD(CH_3)-]_n$ and $[-CH_2-CH(CD_3)-]_n$, but not for $[-CD_2-CH(CH_3)-]_n$. This band is assigned to the CH_2 bending vibration.[1,4] As is shown in Tables II—V, VIII and IX, the potential energy of this vibration is almost exclusively associated with the CH_2 bending mode.

For $[-CH_2-CH(CD_3)-]_n$, the bands due to the A and E components have been resolved at 1440 (parallel: ∥) and 1438 cm^{-1} (perpendicular: ⊥), respectively.[1] The infrared

20) M. Tasumi and T. Shimanouchi (private communication).

TABLE XII. THE AMPLITUDE FACTORS AND PHASE ANGLES*1 FOR THE $E(2\pi/3)$ VIBRATIONS OF ISOTACTIC POLYPROPYLENE IN THE 1500～650 cm^{-1} REGION

S_i*2	ν_7 1462	ν_8 1461	ν_9 1439	ν_{10} 1390	ν_{11} 1356	ν_{12} 1336	ν_{13} 1304	ν_{14} 1197	ν_{15} 1156	ν_{16} 1107	ν_{17} 1017	ν_{18} 931	ν_{19} 896	ν_{20} 821
CH bend.^{ax}	−1 (0)	1 (−5)	1 (−25)	1 (−5)	6 (0)	5 (0)	−6 (−75)	−4 (5)	−3 (60)	2 (80)	1 (45)	1 (−20)	−1 (25)	2 (25)
CH bend.^{eq}	−1 (0)	−1 (0)	−1 (−50)	5 (0)	−5 (−5)	3 (35)	6 (45)	3 (−15)	3 (0)	2 (−75)	−2 (−45)	−1 (−80)	−3 (−15)	1 (−55)
δ^s	0	0	0	0	0	1 (−80)	−1 (−35)	2 (60)	−2 (60)	−1 (85)	−2 (−60)	0	1 (15)	0
δ^a (ax)	0	0	0	0	−1 (0)	−1 (25)	−1 (35)	1 (−80)	1 (−40)	2 (15)	0	−1 (65)	0	0
δ^a (eq)	0	0	1 (−20)	1 (5)	−1 (5)	1 (20)	0	1 (−85)	−2 (5)	1 (45)	−1 (30)	−1 (−40)	−1 (25)	−1 (60)
r_{CM}	0	0	0	0	1 (−10)	−1 (20)	−1 (55)	0	2 (0)	1 (−15)	2 (0)	0	−1 (25)	−2 (−35)
CH_3 δ_a^{ax}	−10 (0)	10 (0)	−1 (5)	−1 (−5)	−2 (−5)	−2 (20)	−2 (55)	1 (−10)	−1 (40)	2 (−5)	−1 (−75)	2 (0)	−1 (15)	0
CH_3 δ_a^{eq}	10 (0)	10 (0)	0	2 (5)	−2 (10)	2 (40)	2 (35)	−2 (70)	1 (60)	1 (25)	1 (−85)	1 (−30)	2 (−10)	0
CH_3 δ_s	−1 (5)	0	0	12 (0)	5 (−5)	−6 (10)	−3 (65)	0	1 (0)	0	1 (−5)	0	0	0
CH_3 rock.^{ax}	3 (0)	−3 (0)	0	0	−1 (0)	−1 (25)	−2 (50)	1 (−25)	−3 (40)	5 (0)	−2 (−65)	5 (0)	−2 (10)	1 (35)
CH_3 rock.^{eq}	−3 (0)	−3 (0)	0	1 (5)	−1 (10)	1 (45)	2 (30)	−4 (75)	2 (45)	3 (25)	3 (−80)	3 (−30)	5 (0)	0
r_{CC}^{ax}	0	0	0	0	1 (−35)	1 (−20)	0	−1 (−25)	1 (75)	−2 (10)	−1 (50)	2 (−20)	−1 (−5)	−1 (−80)
δ	0	0	−1 (5)	−1 (20)	0	−1 (55)	−1 (85)	−1 (−70)	3 (25)	0	1 (40)	1 (−25)	0	1 (65)
CH_2 bend.	−1 (−35)	1 (0)	15 (0)	0	−2 (30)	−1 (0)	0	0	1 (35)	0	0	0	0	0
CH_2 wag.	−1 (90)	0	0	−5 (−20)	5 (25)	−8 (−55)	7 (0)	−2 (−85)	−1 (10)	2 (20)	−1 (−50)	0	0	0
CH_2 twist.	0	1 (20)	1 (0)	−2 (60)	6 (30)	3 (−50)	−1 (−45)	6 (0)	2 (60)	3 (−25)	−4 (50)	−1 (−15)	−1 (−45)	0
CH_2 rock.	0	0	0	−1 (65)	−1 (−50)	−1 (5)	2 (−60)	−4 (80)	−3 (−85)	−2 (−75)	2 (−25)	−1 (−15)	−3 (40)	4 (0)
r_{CC}^{eq}	0	0	0	−1 (45)	1 (55)	0	0	−1 (50)	1 (45)	1 (−75)	1 (85)	1 (65)	1 (15)	1 (25)

*1 Phase angles are listed in parentheses. *2 For the notation of the symmetry coordinates, see *3 of Table II.

intensity ratio for these CH_2 bending vibrations has been calculated to be A : E = 1.8 : 1,[21] where the C-C-C bond angle has been assumed to be 114.5°.*2 In fact, the parallel peak at 1440 cm^{-1} has been found to be slightly stronger than the perpendicular peak at 1438 cm^{-1} (Fig. 4f of Ref. 1).

For neither $[-CH_2-CH(CH_3)-]_n$ nor $[-CH_2-CD(CH_3)-]_n$ has the band at 1435 cm^{-1} been resolved into two components. Furthermore, the calculated frequencies of the A and E CH_2 bending vibrations are essentially the same. Accordingly, the strong $\perp$ dichroism of the band at 1435 cm^{-1} indicates that the E vibration is appreciably stronger than the A vibration; the observed ratio (A : E) is very different from the ratio estimated from the spatial structure or from the ratio observed for $[-CH_2-CH(CD_3)-]_n$. Since the spatial structure of isotactic polypropylene will not change much upon isotopic substitution, the appreciably weak relative intensity of the A component is possibly associated with the normal mode (or hybridization). It may be seen in Tables XI and XII that the hybridization of the methyl asymmetric deformation mode is greater for the CH_2 bending vibration (ν_9) of the A species than the corresponding ν_9 vibration of the E species. For $[-CH_2-CH(CH_3)-]_n$ and $[-CH_2-CD(CH_3)-]_n$, the asymmetric deformation frequencies of the methyl group lie within 30 cm^{-1} of the CH_2 bending frequency and so slight hybridization may well be expected, even though the methyl group is separated from the CH_2 group by the CH group. The slight coupling of the CH_2 bending mode and the CH_3 asymmetric deformation modes is also suggested from the higher frequency shift of the CH_2 bending band upon the deuteration of the CH_3 group.

CH_3 Deformation Vibrations

Asymmetric Deformation Modes. — The $\parallel$ band at 1454 cm^{-1} and the $\perp$ band at 1460 cm^{-1} of polypropylene are also observed for $[-CH_2-CD(CH_3)-]_n$ and $[-CD_2-CH(CH_3)-]_n$, but not for $[-CH_2-CH(CD_3)-]_n$. These bands are assigned to the asymmetric deformation vibrations of the CH_3 group.[1,4,6] The calculated A and E frequencies (ν_7 and ν_8) are nearly the same. Neither the band at 1460 nor that at 1454 cm^{-1} has been resolved into two components, and the dichroism is not strong. Apparently, the 1460 cm^{-1} ($\perp$) band due to the E vibration is overlapped by the corresponding $\parallel$ band due to the A vibration, and the 1454 cm^{-1} ($\parallel$) band due to the A vibration is overlapped by the corresponding $\perp$ band due to the E vibration.

Symmetric Deformation Modes. — The $\perp$ band of $[-CH_2-CH(CH_3)-]_n$ at 1377 cm^{-1} is also observed for $[-CH_2-CD(CH_3)-]_n$ and $[-CD_2-CH(CH_3)-]_n$ but not for $[-CH_2-CH\cdot(CD_3)-]_n$.*3 This band is assigned to the CH_3 symmetric deformation vibration. The frequencies calculated for the corresponding A and E vibrations are essentially the same. Accordingly, the perpendicular dichroism of the band at 1377 cm^{-1} indicates that the perpendicular band due to the E vibration is stronger than the parallel band due to the A vibration. The intensity ratio of the A and E bands has been estimated by Krimm[21] to be 0.4 : 1.0, a figure in good agreement with the observed intensity ratio.

The Normal Vibrations of Polypropylene $[-CH_2-CH(CH_3)-]_n$

In our previous study, the normal vibrations of isotactic polypropylene were treated by the use of potential constants as transferred from other hydrocarbons[8]. In the present study, the gauche-coupling potential and the l(C-C-H) potential were introduced, and the potential constants were refined by the method of least squares. Therefore, the potential energy distributions calculated in the present study differ somewhat from the previous ones. In the following discussions, the nature of the normal vibrations will be discussed, referring to the potential energy distributions as listed in Tables II—IX and to the normal modes as listed in Tables XI and XII.

CH_2 Wagging and Twisting Modes and CH Bending Mode.—In the region between 1370 and 1200 cm^{-1}, four parallel bands (1365, 1326, 1304, and 1254 cm^{-1}) and four perpendicular bands (1360, 1330, 1296, and 1220 cm^{-1}) have been observed for $[-CH_2-CH(CH_3)-]_n$. Similar spectra have also been observed for $[-CH_2-CH(CD_3)-]_n$, but not for either $[-CH_2-CD(CH_3)-]_n$ or $[-CD_2-CH(CH_3)-]_n$. As is shown in Tables II, III, XI, and XII, these bands of $[-CH_2-CH(CH_3)-]_n$ arise from the hybridized vibrations of the CH_2 wagging and twisting modes and from those of the axial and equatorial CH bending modes.

Upon the deuteration of the CH group, two parallel bands (at 1342 and 1291 cm^{-1}) and two perpendicular bands (1334 and 1273 cm^{-1}) have been observed for $[-CH_2-CD(CH_3)-]_n$.

21) S. Krimm, *Fortschr. Hochpolymer.-Forsch.*, 2, 51 (1960).

*2 If the C-C-C bond angle is assumed to have the tetrahedral value, the intensity ratio is derived as A : E = 1 : 1.

*3 As will be discussed later, the parallel band of $[-CH_2-CH(CD_3)-]_n$ at 1379 cm^{-1} is assigned to the ν_8^A vibration (see Table VIII).

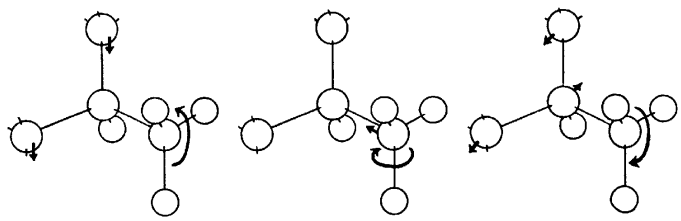

Fig. 6. Schematic representations of the normal modes of the ν_{15}, ν_{17} and ν_{18} vibrations (A species) of isotactic polypropylene.

These bands are due to the CH_2 wagging and twisting modes, which are not hybridized with the CH bending modes (Tables IV and V). On the other hand, for $[-CD_2-CH(CH_3)-]_n$, two parallel bands (1327 and 1313 cm^{-1}) and two perpendicular bands 1325 and 1303 cm^{-1}) have been observed[1] (Tables VI and VII). These bands arise from the CH bending modes (axial and equatorial), which are not hybridized with either the CH_2 wagging or twisting modes. It is interesting to note that the 'intrinsic' CH_2 wagging and twisting frequencies observed for $[-CH_2-CD(CH_3)-]_n$, as well as the 'intrinsic' CH bending frequencies observed for $[-CD_2-CH(CH_3)-]_n$, all lie in the narrow region of 1350~1270 cm^{-1}. Naturally the CH_2 wagging and twisting modes and the CH bending modes are extensively hybridized for the molecule of $[-CH_2-CH(CH_3)-]_n$.

In our previous study, the weak ∥ band at 1254 cm^{-1} and the weak ⊥ band at 1220 cm^{-1} were considered to arise primarily from the CH_2 twisting modes. Actually, however, these frequencies are much lower than the 'intrinsic' CH_2 twisting frequencies as observed for $[-CH_2-CD(CH_3)-]_n$. The A vibration at 1254 cm^{-1} is due to the CH_2 twisting mode as coupled with the CH bending mode in the H–C–methyl plane, whereas the E vibration at 1220 cm^{-1} is due to the CH_2 twisting mode as coupled with the CH bending mode perpendicular to the H–C–methyl plane.

CH_3 and CH_2 Rocking Modes and C–C Stretching Modes.—In the region between 1200 and 900 cm^{-1}, five strong parallel bands due to the A vibrations and five perpendicular bands due to the E vibrations are observed. As Tables II, III, XI, and XII show, these bands of polypropylene arise from the hybridized vibrations of the axial and equatorial CH_3 rocking, the axial and equatorial C–C stretching, the C–methyl stretching, and the CH_2 rocking modes.*5

The parallel bands at 1168, 998, 973 and 842 cm^{-1} are the strongest peaks of polypropylene. As Table II shows, all these bands are associated with the methyl rocking modes. However, the hybridization of the C–C stretching modes is appreciable for these vibrations. Thus, the band at 1168 cm^{-1} is primarily associated with the axial C–C stretching mode as coupled with the axial methyl rocking mode. The band at 1045 cm^{-1} is due to the asymmetric stretching mode of the C-methyl bond and the equatorial C–C bond. The band at 998 cm^{-1} is due to the equatorial rocking mode coupled with the C-methyl bond, whereas the band at 973 cm^{-1} is due to the axial rocking mode as coupled with the antisymmetric stretching mode of the axial and equatorial C–C bonds. The band at 842 cm^{-1} is associated with the methyl rocking mode in the H–C-methyl plane coupled with the symmetric stretching mode of the C-methyl and the equatorial C–C bonds. The hybridizations of the C–C stretching modes and the methyl rocking modes are schematically shown in Fig. 6 for the A vibrations at 1168, 998 and 973 cm^{-1}.

It might be anticipated that the intensities of the parallel bands at 1168 and 973 cm^{-1} are due to the methyl rocking modes in the axial direction. However, the intensity of the band at 998 cm^{-1} is as strong as those of the bands at 1168 or 973 cm^{-1}, although the vibration at 998 cm^{-1} is largely associated with the equatorial methyl rocking mode. Apparently more extensive studies are necessary for a detailed discussion of the intensities of bands arising from much hybridized modes.

*4 The assignments by Liang et al.[4] were: 1360 (⊥), 1330 (⊥), CH_2 wag.+CH bend.; 1304 (∥) and 1296 (⊥), CH_2 twist.+CH and CH_3 bend.; 1255 (∥) and 1220 cm^{-1} (⊥), CH bend.+CH_2 rock.+CH_3 rock. The assignments by McDonald and Ward[6] were: 1360 (⊥), 1304 (∥), 1254 (∥), and 1220 (⊥), CH bend.; 1330 (⊥), CH_2 wag.; and 1296 cm^{-1} (⊥), CH_2 twist.

*5 The assignments by Liang et al.[4] were: 1168 (∥) and 1155 (⊥), CH_3 rock.+CH_2 and CH bend.; 1103 (⊥), 1045 (∥), 998 (∥), 941 (∥) and 899 (⊥), r_{CC}; 973 (∥), CH_3 rock.+CH_2 and CH rock.; 840 (∥) and 809 (⊥), CH_2 rock.+CH and CH_3 rock. The assignments by McDonald and Ward[6] were: 1168 (∥), CH_3 rock.+r_{CC}; 1103 (⊥), 941 (⊥), 899 (⊥) and 809 (⊥), CH bend.+r_{CC}; 1045 (∥), r_{CC}+CH_3 rock.; 998 (∥), r_{CC}+CH_3 rock.+CH_2 rock.; 973 (∥), CH_3 rock.+CH_2 rock.+r_{CC}; 842 (∥), CH_2 rock.+CH_3 rock.+r_{CC}.

The perpendicular band of polypropylene at 1155 cm^{-1} has also been observed in the Raman effect[22]. This band corresponds to the calculated ν_{15}^{E} frequency of 1156 cm^{-1}. Although the ν_{15}^{E} perpendicular band and the ν_{15}^{A} parallel band lie close to each other, these vibrations are quite different from each other. Thus the ν_{15}^{E} vibration is primarily associated with the C-methyl stretching mode as coupled with the CH bending modes modes in the axial and equatorial directions, but it is not much associated with the methyl rocking modes. On the other hand, the three perpendicular bands at 1103, 941 and 899 cm^{-1} are due to the methyl rocking modes, where the contributions of the axial or equatorial C–C stretching modes are also appreciable.

The band at 1103 cm^{-1} is due to the methyl rocking mode in the axial direction ($\varepsilon=0°$), the rocking mode in the equatorial direction ($\varepsilon=25°$), and the axial C–C stretching mode ($\varepsilon=10°$), with small phase angle differences among them. The band at 941 cm^{-1} is due to the axial methyl rocking mode ($\varepsilon=0°$), the equatorial rocking mode ($\varepsilon=-30°$), the axial C–C stretching mode ($\varepsilon=-20°$), and the equatorial C–C stretching mode ($\varepsilon=65°$). The axial and equatorial C–C stretching modes for this vibration are almost 90° out-of-phase. The band at 899 cm^{-1} is due to the equatorial methyl rocking mode ($\varepsilon=0°$), the equatorial CH bending mode ($\varepsilon=-15°$), and the CH_2 rocking mode ($\varepsilon=40°$), all of which take place in the equatorial direction. The methyl rocking mode and the CH bending mode are almost in phase for this vibration.

The perpendicular band at 809 cm^{-1} is due to the CH_2 rocking mode ($\varepsilon=0°$), coupled with the C-methyl stretching mode ($\varepsilon=-35°$) and the equatorial C–C stretching mode ($\varepsilon=25°$). On the other hand, the ν_{20}^{A} vibration calculated at 819 cm^{-1} is primarily due to the the CH_2 rocking mode. The displacements of the hydrogen atoms associated with this rocking mode are nearly perpendicular to the helix axis; this vibration has not, however, yet been located in the infrared absorption.

The Normal Vibrations of Poly(propylene-2-d) $[-CH_2-CD(CH)_3-]_n$

CH_2 Wagging and Twisting Modes.—As has been discussed before, the CH_2 wagging and twisting modes of $[-CH_2-CH(CH_3)-]_n$ are coupled with the CH bending modes. However, the CH_2 wagging and twisting modes of $[-CH_2-CD(CH_3)-]_n$ are almost free from the coupling with the CD bending modes, since the "intrinsic" CD bending frequencies are much lower than the 'intrinsic' CH_2 wagging and twisting frequencies. As Tables IV and V show, the parallel band of $[-CH_2-CD(CH_3)-]_n$ at 1342 cm^{-1} and the perpendicular band at 1334 cm^{-1} are associated almost exclusively with the CH_2 wagging mode. The parallel band at 1291 cm^{-1} and the perpendicular band at 1273 cm^{-1} are associated with the CH_2 twisting modes in accordance with the assignment made by Liang et al.[4]*6

The CH_2 wagging and twisting frequencies of propane are 1336 and 1278 cm^{-1} respectively.[11] These vibrations of propane are also free from much coupling with other modes. Therefore, the 'intrinsic' CH_2 wagging and twisting frequencies may be taken to be about 1335 cm^{-1} and 1280 cm^{-1} respectively.

CD Bending, CH_3 and CH_2 Rocking, and C–C Stretching Modes.—For $[-CH_2-CD(CH_3)-]_n$, eight parallel bands and seven perpendicular bands are observed[1] in the 1250~650 cm^{-1} region; all these bands arise from the hybridized vibrations of the CD bending, CH_3 rocking, CH_2 rocking, and C–C stretching modes. (No single band is due to a 'pure' mode.) All these modes have their intrinsic frequencies in the 1100~800 cm^{-1} region. For highly symmetric molecules, symmetry elements (such as twofold axes or planes of symmetry) impose restrictions upon the couplings among those vibrational modes, even though their 'intrinsic' frequencies lie in the same frequency region. However, the molecular chain of isotactic polypropylene does not have such symmetry elements, and all those vibrational modes of $[-CH_2-CD(CH_3)-]_n$ are subject to extensive hybridization.

The bands at 1060 (∥) and 1091 cm^{-1} (⊥) have been assigned to the C–D bending mode.[6] However, to judge from the normal coordinate analysis, these bands are not very much associated with the CD bending modes. Rather, the A vibration at 1060 cm^{-1} is due to the equatorial methyl rocking mode coupled with the CH_2 rocking mode, while, on the other hand, the E vibration at 1091 cm^{-1} is due to the equatorial methyl rocking mode coupled with the C-methyl stretching mode.*7

The parallel bands at 981, 969 and 790 cm^{-1} are the strongest peaks in the 1250~650 cm^{-1} region. The ν_{16}^{A} vibration is associated with the C-methyl stretching mode, the axial methyl rocking mode, and the axial CD bending

22) M. C. Tobin, *J. Opt. Soc. Am.*, 49, 850 (1959).

*6 McDonald and Ward[6] also have assigned the bands at 1334 (⊥) and 1291 cm^{-1} (∥) to the CH_2 wagging and twisting modes respectively.

*7 Weak bands were observed at 1049 (∥) and 1016 cm^{-1} (⊥) and were assigned to CD bending modes.[6] These bands, however, are not identified in the spectra reported by Peraldo and Farina (Fig. 2b of Ref. 1).

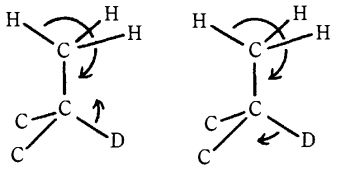

(a) (b)

Fig. 7. Schematic representations of the A vibrations of isotactic poly(propylene-2-d) at 790 cm^{-1} (a) and 1145 cm^{-1} (b).

mode. The ν_{17}^{A} vibration is associated with the methyl rocking mode perpendicular to the D-C-methyl plane as coupled with the axial C-C stretching mode.

The medium intensity band at 1210 cm^{-1} (‖) has been considered to be due to the coupling of the methyl rocking mode and the C-C stretching mode.[8] However, as Table IV shows, this band is due to the antisymmetric stretching mode of the axial and equatorial C-C bonds as coupled with the CD bending mode perpendicular to the D-C-methyl plane.

The strong parallel band at 790 cm^{-1} is due to the coupling of the CD bending mode and the CH_3 rocking mode (both in the D-C-methyl plane), as is schematically shown in Fig. 7a. On the other hand, the medium intensity band at 1145 cm^{-1} is primarily due to the other hybridization of the CD bending and methyl rocking modes, as shown in Fig. 7b. This vibration is, therefore, the counterpart of the A vibration at 790 cm^{-1}.

The CH_2 rocking mode (A species) of $(-CH_2-CD(CH_3)-]_n$ is strongly coupled with the CD bending mode (nearly perpendicular to the D-C-methyl plane). This band appears to be much stronger than the corresponding A vibration of $[-CH_2-CH(CH_3)-]_n$ calculated at 819 cm^{-1}. This is possibly due to the greater coupling of the CH_2 bending mode with the CD bending mode.

It is noteworthy that the perpendicular bands of $[-CH_2-CD(CH_3)-]_n$ are much weaker than the parallel bands observed in the 1250 ~650 cm^{-1} region although these E vibrations are also due to the hybridizations of the CD bending, CH_3 and CH_2 rocking, and C-C stretching modes, as are the A vibrations (Tables IV and V).

The Normal Vibrations of Poly(propylene-1, 1-d_2), $[-CD_2-CH(CH_3)-]_n$

CH Bending Modes.—As has been discussed before, the CH bending modes of $[-CH_2-CH(CH_3)-]_n$ are coupled with the CH_2 wagging and twisting modes. However, the CH bending modes of $[-CD_2-CH(CH_3)-]_n$ are almost free from couplings with the CD_2 wagging or twisting modes. As Tables VI and VII show, the parallel bands at 1327 and 1313 cm^{-1} and the perpendicular bands at 1325 and 1303 cm^{-1} are almost exclusively due to the CH bending modes. The CH bending displacements of the ν_{10}^{A} and ν_{11}^{E} vibrations are perpendicular to the H-C-methyl plane, whereas the CH bending displacements of the ν_{11}^{A} and ν_{10}^{E} vibrations are in the H-C-methyl plane.

The CH bending vibration of isobutane, which is observed at 1330 cm^{-1}, is not much coupled with other vibrational modes. Taking into account the CH bending frequencies of isobutane as well as of $[-CD_2-CH(CH_3)-]_n$, the 'intrinsic' CH bending frequency may be taken as ca. 1320 cm^{-1}.

CD_2 Rocking Modes.—The parallel band of $[-CD_2-CH(CH_3)-]_n$ at 691 cm^{-1} is primarily due to the CD_2 rocking mode, as Table VI shows. The intensity of this band is much stronger than the corresponding band (ν_{20}^{A}) of $[-CH_2-CH(CH_3)-]_n$. The perpendicular band at 716 cm^{-1} is due to the CD_2 rocking mode, coupled with the C-methyl stretching mode and the equatorial C-C stretching mode.

CD_2 Bending.—The perpendicular band at 1051 cm^{-1} corresponds to the calculated ν_{15}^{E} frequency of 1042 cm^{-1}, and this band is considered to be due to the CD_2 bending mode (Table VII). On the other hand, the strong parallel band at 1058 cm^{-1} appears to correspond to the ν_{15}^{A} vibration calculated at 1048 cm^{-1} or to the ν_{14}^{A} vibration calculated at 1082 cm^{-1}. The ν_{15}^{A} vibration is associated with the CD_2 bending mode, coupled with the equatorial methyl rocking mode. The ν_{14}^{A} vibration is associated with the hybridization of the axial methyl rocking mode and of the antisymmetric stretching mode of the C-methyl and C-C bonds.

CD_2 Wagging and Twisting Modes, CH_3 Rocking Modes, and C-C Stretching Modes.—The parallel band at 1134 cm^{-1} is due to the methyl rocking mode (in the H-C-methyl plane) coupled with the CD_2 twisting mode. The perpendicular band at 1110 cm^{-1} corresponds either to the ν_{14}^{E} vibration calculated at 1103 cm^{-1} or to the ν_{13}^{E} vibration calculated at 1128 cm^{-1}. The ν_{14}^{E} vibration is associated with the CD_2 wagging mode and the methyl rocking mode in the H-C-methyl plane.

The parallel band at 1184 cm^{-1} is due to the axial C-C stretching mode, coupled with the CD_2 wagging mode, whereas the perpendicular band at 1170 cm^{-1} is due to the equatorial C-C bond, coupled with the CD_2 bending mode. The nature of the infrared bands of poly(propylene-1, 1-d_2) in this region of the spectrum are too complicated for empirical analyses based on the isotope shifts.

The parallel bands at 894 and 868 cm^{-1} are due to the methyl rocking modes, coupled with the CD_2 wagging or twisting modes, as Table VI shows. The methyl rocking motion of the ν_{17}^A vibration (calculated at 900 cm^{-1}) is nearly perpendicular to the H-C-methyl plane, whereas the rocking motion of the ν_{18}^A vibration (calculated at 878 cm^{-1}) is nearly in the H-C-methyl plane. The parallel band at 1013 cm^{-1} arises from the antisymmetric stretching mode of the C-methyl and equatorial C–C bonds, coupled with the CD_2 wagging and methyl rocking mode.

The perpendicular band at 896 cm^{-1} is due to the methyl rocking mode (perpendicular to the H-C-methyl plane), coupled with the axial C–C stretching mode. The band due to the ν_{18}^E vibration is possibly overlapped by the strong parallel band at 868 cm^{-1}. The methyl rocking mode of the ν_{18}^E vibration is nearly in the H-C-methyl plane.

The weak parallel band at 764 cm^{-1} and the perpendicular band at 811 cm^{-1} are primarily due to the CD_2 twisting modes, as Table VI and VII show.

The Normal Vibrations of Poly(propylene-3, 3, 3-d_3), $[-CH_2-CH(CD_3)-]_n$

CH_2 Wagging and Twisting Modes and CH Bending Modes. — For isotactic $[-CH_2-CH\cdot(CD_3)-]_n$, four parallel bands and four perpendicular bands are observed in the 1400～1200 cm^{-1} region.[1] The absorption spectra in this region are very similar to the spectra of $[-CH_2-CH(CH_3)-]_n$. These bands arise from the coupling of the CH_2 wagging, CH bending, and CH_2 twisting modes, as Tables VIII and IX show*8. It may be seen that the A vibrations of $[-CH_2-CH(CD_3)-]_n$ at 1379, 1334, 1305 and 1239 cm^{-1} closely correspond to the A vibrations of $[-CH_2-CH(CH_3)-]_n$, except for a slight hybridization of the methyl symmetric deformation mode. Also the E vibrations of $[-CH_2-CH(CD_3)-]_n$ at 1361, 1333, 1293, and 1206 cm^{-1} correspond to the E vibrations of $[-CH_2-CH(CH_3)-]_n$ at 1360, 1330, 1296, and 1220 cm^{-1} respectively.

CD_3 Asymmetric Deformation Modes. — The strong parallel band at 1051 cm^{-1} corresponds to the ν_{14}^A and ν_{15}^A vibrations (calculated at 1049 and 1045 cm^{-1} respectively), and the strong perpendicular band at 1054 cm^{-1} corresponds to the ν_{15}^E and ν_{16}^E vibrations (calculated at 1044 and 1040 cm^{-1}, respectively). As Tables VIII and IX show, these bands are associated almost exclusively with the asymmetric deformation modes of the CD_3 group.

Liang et al. have assigned the bands at 1051 and 1054 cm^{-1} to the overlapped A and E components of all the asymmetric and symmetric deformation modes of the CD_3 group.[4] On the other hand, McDonald and Ward have assigned the strong bands at 1051 (∥) and 1145 cm^{-1} (⊥) to the symmetric and asymmetric deformation modes, respectively, of the CD_3 group.[6] As for the bands due to the symmetric modes, the present normal coordinate analysis favors the assignment made by Liang et al.

CD_3 Symmetric Deformation Mode.—The CD_3 symmetric deformation modes are strongly coupled with the C–C stretching modes. The weak parallel band at 1115 cm^{-1} appears to correspond to the ν_{13}^A vibration calculated at 1083 cm^{-1}. This vibration arises from a strong coupling between the CD_3 symmetric deformation mode and the C-methyl stretching mode. The perpendicular band at 1081 cm^{-1} corresponds either to the ν_{13}^E vibration calculated at 1079 cm^{-1} or to the ν_{14}^E vibration calculated at 1061 cm^{-1}. The ν_{13}^E vibration is associated with the axial and equatorial C–C stretching modes, coupled with the CD_3 symmetric deformation mode, whereas the ν_{14}^E vibration is primarily due to the CD_3 symmetric deformation mode, coupled with the asymmetric deformation mode. The parallel band at 989 cm^{-1} corresponds to the ν_{16}^A vibration and is due to the equatorial C–C stretching mode and the CD_3 symmetric deformation mode.

CD_3 Rocking Mode.—The parallel bands of $[-CH_2-CH(CD_3)-]_n$ at 791 and 703 cm^{-1} and the perpendicular bands at 759 and 743 cm^{-1} are associated almost exclusively with the CD_3 rocking modes, as Tables VIII and IX show.*9 The 'intrinsic' CD_3 rocking frequency appears to be much lower than the intrinsic frequencies of the CH_2 wagging and twisting modes or the C–C stretching mode. For the A vibration at 791 cm^{-1} and the E vibration at 759 cm^{-1}, the CD_3 rocking mode is nearly perpendicular to the H-C-methyl plane, whereas for the A vibration at 703 cm^{-1} and the E vibration at 743 cm^{-1} the CD_3 rocking mode is nearly parallel to the H-C-methyl plane.

CH_2 Rocking Mode and C–C Stretching Modes. —The parallel band at 807 cm^{-1} and the perpendicular band at 821 cm^{-1} are primarily due to the CH_2 rocking modes, coupled with the

*8 The bands at 1305 (∥) and 1293 (⊥) were assigned by Liang et al.[4] to the CH_2 twisting modes. The assignments by McDonald and Ward[6] were: 1379 (∥) and 1333 (⊥), CH_2 wag; 1293 (⊥), CH_2 twist; 1361 (⊥), 1305 (∥), 1239 (∥), and 1206 cm^{-1} (⊥), CH bend.

*9 The bands at 1081 (⊥), 909 (∥), and 791 cm^{-1} (∥) have been considered to be due in part to the CD_3 rocking modes.[6]

C-methyl or equatorial C–C stretching modes.*[10] The parallel band at 909 cm^{-1} is due to the symmetric stretching mode of the C-methyl and equatorial C–C bonds (coupled with the equatorial CD_3 rocking mode and the CH_2 twisting mode). On the other hand, the strong perpendicular band at 1145 cm^{-1} is due to the C–methyl stretching mode and the CH bending mode.

The Liquid Spectra of Isotactic Polypropylene and Its Deuterated Derivatives

On the basis of the potential energy distributions as well as on that of the normal modes calculated for the crystalline spectra, one may also assign the bands observed in the liquid spectra of isotactic polypropylene and its deuterated derivatives.

Localized Modes.—The effect of melting upon the infrared spectra of isotactic polypropylene[23,24] and its deuterated derivatives[1] have been studied, and several absorption bands have been found to persist upon melting. For example, strong bands are observed at 1380 cm^{-1} and 1460 cm^{-1} for $[-CH_2-CH\cdot(CH_3)-]_n$, $[-CH_2-CD(CH_3)-]_n$, and $[-CD_2-CH(CH_3)-]_n$, but not for $[-CH_2-CH(CD_3)-]_n$. These peaks are assigned to the symmetric and asymmetric deformation modes, respectively, of the methyl group. Similarly, for $[-CH_2-CH(CD_3)-]_n$ in the liquid state, a strong band is observed at 1052 cm^{-1}. This band corresponds to the strong bands at 1054 ($\parallel$) and 1051 cm^{-1} ($\perp$) in the crystalline state and is assigned to the asymmetric deformation modes of the CD_3 group in the liquid state.

The strong band at 1446 cm^{-1} is observed for $[-CH_2-CH(CD_3)-]_n$ and is assigned to the CH_2 bending mode. For $[-CH_2-CH(CH_3)-]_n$ and $[-CH_2-CD(CH_3)-]_n$ in the liquid state, the band due to the CH_2 bending mode is overlapped by the strong band arising from the asymmetric methyl deformation modes. For $[-CD_2-CH(CH_3)-]_n$, a medium intensity band is observed at 1057 cm^{-1}. This band appears to correspond to the ν_{15}^{A} (1058 cm^{-1}) and ν_{15}^{E} vibration (1051 cm^{-1}) and is assigned to the CD_2 bending mode.

The frequencies of the symmetric and asymmetric deformation vibrations of the CH_3 group or the bending vibrations of the CH_2 group do not shift essentially upon melting. As Tables II–IX show, the potential energy of these vibrations is concentrated in one vibrational mode, while the atomic displacements are localized in the methyl or the methylene groups. Therefore, even though the main chain of isotactic polypropylene carries out internal-rotation rearrangements above the melting point, these localized vibrations of the methyl or the methylene groups are not very much influenced by the thermal motions of the backbone chain. The bands arising from localized vibrations in the liquid state may be as strong and sharp as the corresponding bands in the crystalline state.

CH_2 Wagging and Twisting Modes.—On the basis of these considerations, it would be anticipated that the bands due to 'localized' vibrations in the liquid state will be stronger and more well-defined as the localization becomes higher. In fact, for $[-CH_2-CD(CH_3)-]_n$, a strong band is observed at 1333 cm^{-1}; this band is assigned to the CH_2 wagging mode in the liquid state. As has been discussed before, the CH_2 wagging vibration of this molecule is free from coupling with other modes, and its vibrational displacements are much localized in the $C-CH_2-C$ group. The frequency of this band agrees closely with the 'intrinsic' CH_2 wagging frequency taken at 1335 cm^{-1}. In the crystalline state, the CH_2 wagging frequencies ($\nu_{11}^{A}=1342$ cm^{-1} and $\nu_{11}^{E}=1334$ cm^{-1}) are split by 8 cm^{-1}.

The liquid band of $[-CH_2-CD(CH_3)-]_n$ at 1282 cm^{-1} corresponds to the 'intrinsic' CH_2 twisting frequency of 1280 cm^{-1} and is assigned to the CH_2 twisting mode in the liquid state. As has been discussed before, the twisting mode of this molecule is also free from much coupling with other vibrational modes, and the vibrational displacements are greatly localized in the $C-CH_2-C$ group. In the crystalline state, the twisting frequencies are split into the A component at 1291 cm^{-1} and the E component at 1273 cm^{-1}.

CH Bending Modes.—For $[-CD_2-CH(CH_3)-]_n$, a strong band is observed at 1318 cm^{-1} in the liquid state. This band corresponds to the 'intrinsic' CH bending frequency of 1320 cm^{-1}. The CH bending vibrations of this molecule are not much coupled with other vibrational modes.

For $[-CH_2-CH(CD_3)-]_n$ in the liquid state, four bands are observed[1] at 1358, 1326 (shoulder), 1293, and 1235 cm^{-1}. These peaks arise from the CH_2 wagging and twisting modes and the CH bending modes in the liquid state. These frequencies, however, are shifted slightly but distinctly from the 'intrinsic' frequencies of the CH_2 wagging, twisting and CH bending modes, indicating vibrational couplings among these modes, even in the liquid state. Vibrational couplings among these

*[10] The parallel band at 710 cm^{-1} was assigned to the CH_2 rocking mode by McDonald and Ward.[6]

23) G. Natta, *J. Polymer Sci.*, 16, 143 (1955).

24) K. Abe and K. Yanagisawa, ibid., 36, 536 (1959).

modes should depend upon the internal-rotation conformations about the axial and equatorial C–C bonds. Therefore, theoretical analyses of these couplings will be useful for conformation studies of isotactic polypropylene chains in the liquid state.

CD_3 Rocking Modes. — For $[-CH_2-CH\cdot(CD_3)-]_n$ in the liquid state, two medium-intensity bands are observed at 790 and 709 cm^{-1}. The band at 790 cm^{-1} corresponds to the $\nu_{19}{}^A$ (791 cm^{-1}) and $\nu_{19}{}^E$ vibrations (759 cm^{-1}) of the crystalline state, vibrations which are associated with the CD_3 rocking mode perpendicular to the H–C-methyl plane. On the other hand, the liquid band at 709 cm^{-1} corresponds to the $\nu_{20}{}^A$ (703 cm^{-1}) and $\nu_{20}{}^E$ vibrations (743 cm^{-1}), which are associated with the CD_3 rocking mode in the H–C-methyl plane. As Tables VIII and IX show, these vibrations of the crystalline state are associated exclusively with the CD_3 rocking modes, and the vibrational displacements are localized, at least in the CD_3–$CH\langle^{C}_{C}$ group. These CD_3 rocking modes involve the vibrational displacement of the main-chain carbon atoms and, in fact, the A and E frequencies of the ν_{19} or ν_{20} vibrations are split by 30~40 cm^{-1}. These splittings are reduced upon melting when the main chain conformations are not rigid. On the other hand, the internal rotation conformation of the CD_3–$CH\langle^{C}_{C}$ group does not change upon the rearrangement of the CD_3 group from one staggered form to another. Therefore, the CD_3 rocking modes are not influenced by the internal rotation of the CD_3 group, and well-defined bands due to the CD_3 rocking modes may well be expected, even in the liquid state. Accordingly, the liquid band at 790 cm^{-1} is assigned to the CD_3 rocking mode perpendicular to the H–C-methyl plane, whereas the band at 709 cm^{-1} is assigned to the CD_3 rocking mode in the H–C-methyl plane.

The CD_3 rocking frequencies of perdeuterated ethane, C_2D_6, are observed at 970 cm^{-1} (E_g) and 594 cm^{-1} (E_u). Since the splitting of these rocking frequencies arises from the trans- and gauche-coupling potential term,[9,11] the 'intrinsic' CD_3 rocking frequency may be taken to have an average value of about 780 cm^{-1} [~(970+594)/2]. The CD_3 rocking vibration of $[-CH_2-CH(CD_3)-]_n$ at 790 cm^{-1} corresponds to the intrinsic frequency derived from deuteroethane.

CH_3 Rocking and C–C Stretching Modes.— For $[-CH_2-CH(CH_3)-]_n$ two strong bands are observed at 1151 cm^{-1} and 971 cm^{-1} in the liquid state. These liquid bands are possibly associated with 'localized' vibrational modes of the CH_3–$CH\langle^{C}_{C}$ group modes, which are not influenced by the internal rotation rearrangements, at least of the CH_3 group.

The intrinsic CH_3 rocking frequency may be estimated at about 1000 cm^{-1} [~(1190+821)/2] from the CH_3 rocking frequencies (E_g: 1190 cm^{-1} and E_u: 821 cm^{-1}). The liquid band of $[-CH_2-CH(CH_3)-]_n$ at 971 cm^{-1} corresponds to this intrinsic frequency and is considered to be associated primarily with the CH_3 rocking modes in the liquid state. On the other hand, the contributions of the C–C stretching modes are possibly greater for the liquid band at 1151 cm^{-1} than that of the methyl rocking mode. Since the degenerate C–C stretching vibration of isobutane,[11] CH_3–$CH\langle^{CH_3}_{CH_3}$, is observed at 1166 cm^{-1}, the liquid band of polypropylene at 1151 cm^{-1} is possibly associated with the asymmetric stretching mode, coupled with the methyl rocking mode of the CH_3–$CH\langle^{C}_{C}$ group. Naturally, these tentative assignments should be examined further by means of theoretical treatment of the liquid spectra. Nevertheless, these considerations are supported by the observation of a corresponding strong band at 1140 cm^{-1} in the liquid spectra of $[-CH_2-CH(CD_3)-]_n$, a band which may not be ascribed to the methyl rocking mode. More extensive analyses of the liquid spectra of isotactic polypropylene and deuterated derivatives will be important for conformation studies of the isotactic polymeric chain, and, accordingly, theoretical developments in the treatment of the liquid spectra of flexible polymeric chains are highly desirable.

Summary

The infrared active normal vibrations of isotactic polypropylene and its deuterated derivatives in the crystalline state have been treated by the general method derived previously.[8] The modified Urey-Bradley force field has been used; the trans- and gauche-coupling potential terms for the H–C–C angles and the angle-interaction terms for the methylene group have been added to the Urey-Bradley force field. A total of 16 potential constants have been adjusted by the method of least squares, and a total of about 100 infrared-active frequencies have been calculated with the r. m. s. frequency deviation as small as 1.1%. The potential energy distributions have been calculated, together with the normal modes, and the nature of the inferred bands observed in the 1500~650 cm^{-1} region

have been elucidated. Vibrational assignments for the well-defined liquid bands of isotactic polypropylene and its deuterated derivatives have also been made.

The authors wish to thank Professor Takehiko Shimanouchi of the University of Tokyo for his encouragement and his stimulating discussions and Dr. Kunio Fukushima of Osaka University and Dr. Takaharu Ohnishi and Dr. Hiroaki Takahashi of the University of Tokyo for their helpful discussions.

Institute for Protein Research
Osaka University
Kita-ku, Osaka

The Electron Spin Resonance of o-Substituted Benzophenone Ketyls

By Kazuhiro MARUYAMA,*1 Rikuhei TANIKAGA and Ryozo GOTO

(Received April 20, 1963)

Previous papers[1,2] in this series have shown that ketyls of those benzophenone derivatives which consist of non-substituted phenyl groups and ortho-substituted phenyl groups (i. e., 2-methylbenzophenone, 2, 6-dimethylbenzophenone, 2, 6-dimethyl-4-*t*-butylbenzophenone, 2, 4, 6-trimethylbenzophenone and 2-methylcyclohexyl phenyl ketone—group I) give extremely different ESR spectra from those of the ketyls of benzophenone and para-substituted benzophenone derivatives (i. e., 4-methylbenzophenone, 4, 4'-dimethylbenzophenone, 4-*t*-butylbenzophenone, 4, 4'-di-*t*-butylbenzophenone, 4-methoxybenzophenone, 4, 4'-dimethoxybenzophenone and 4-ethylbenzophenone—group II). That is, although the ketyls of group II give well-resolved spectra, the ketyls of group I give less well-resolved spectra consisting of four broad lines. We have speculated that these four broad lines might be caused by a larger accumulation of free electron spin on a non-substituted phenyl group — especially an accumulation at two ortho- and para-positions. In order to confirm this hypothesis, the ESR spectrum of the ketyl of d_5-phenyl 2-methylphenyl ketone was studied. Two other pieces of experimental evidence were also obtained in support of the authors' view.

Results and Discussion

The Ketyl of the d_5-Phenyl 2-Methylphenyl Ketone.[*2] — The ESR spectra of the ketyls of the d_5-phenyl 2-methylphenyl ketone (I) and of the phenyl 2-methylphenyl ketone (II) are shown in Fig. 1. ESR measurement was done in a dilute solution of the ketyl in tetrahydrofuran (THF). When these two spectra are compared, the difference is quite clear. II gives four broad lines with a total width of 21.7 gauss, while I gives a single line with a smaller total width of 18.5 gauss. Since the

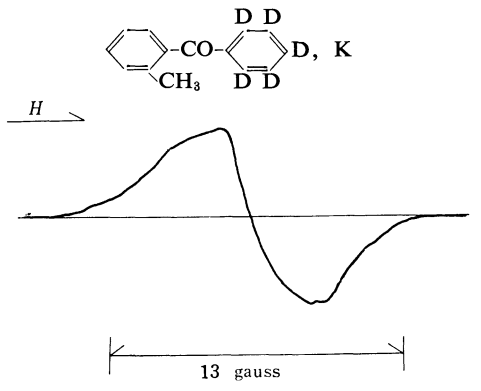

Fig. 1 (a)

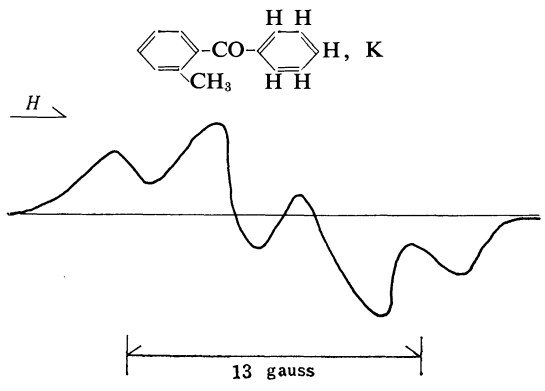

Fig. 1 (b)

1) R. Goto, K. Maruyama, R. Tanikaga and Y. Deguchi, This Bulletin, **35**, 1746 (1962).
2) K. Maruyama, R. Tanikaga and R. Goto, *J. Chem. Soc. Japan, Pure Chem. Sec.* (*Nippon Kagaku Zasshi*), **84**, 75 (1963).

*1 This author is now in Washington University as a research associate.

*2 This part of the work was done under the support of the United States Air Force and the National Science Foundation of the U. S. A.

nuclear spin of deuterium is one, seven lines should be observed if the free electron spin is accumulated exclusively into two ortho- and para-positions of the non-substituted phenyl group. However, line broadening is caused by the thermal motion of the ortho methyl on the other phenyl group (time-dependent local field change), as is evident from the previous paper and from the following experimental results. The nuclear magnetic moment of deuterium is one-seventh that of protium. The results obtained above are, therefore, reasonable.

The Ketyl of the 2-Methylphenyl 4'-*t*-Butylphenyl Ketone. — The ESR spectrum of the ketyl of the 2-methylphenyl 4'-*t*-butylphenyl ketone was obtained in a dilute solution of THF (Fig. 2). The spectrum consists of three broad lines. The intensity ratio of the lines is 1 : 2 : 1. This fact also shows that the free electron spin is exclusively accumulated at two ortho-positions of the 4'-*t*-butyl-substituted phenyl group.

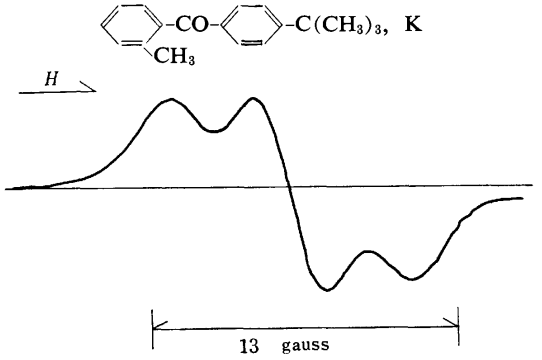

Fig. 2

The Ketyl of the 2-Methylphenyl 3'-Chlorophenyl Ketone. — The ESR spectrum of the ketyl of the 2-methylphenyl 3'-chlorophenyl ketone was observed in a dilute solution of THF (Fig. 3). The spectrum consists of four broad lines. The intensity ratio of the spectrum lines is nearly 1 : 3 : 3 : 1. This result shows that the free electron spin density of the meta positions of the non-ortho-substituted phenyl group is nearly zero or, at least, very small.

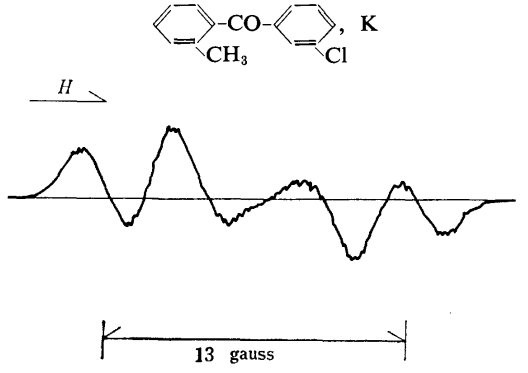

Fig. 3

Discussion

All the results so far obtained show that the free electron spin of the ketyl of the benzophenone derivative which is constructed form the non-ortho-substituted phenyl and the ortho-substituted phenyl is delocalized mainly on a non-ortho-substituted phenyl of the two phenyl groups. If we could assume that the splitting parameter for aromatic hydrocarbons (23 gauss) is also applicable to these ketyls, we could say that about fifty per cent of the free electron spin is located on the non-substituted phenyl group, since the splitting between the four broad lines is about five gauss in almost all cases. The rest of the free electron spin will reside on the $\cdot\dot{C}-OK$ group. The structure of the ketyl has been the subject of extensive investigations.[3-8] Recently Hirota[9] showed the possibility of the existence of paramagnetic dimers due to the dimerization of monomer ion pairs. The simplest representation of ketyl structure, however, is III.

$$C_6H_5-\dot{C}(O^{\ominus}K^{\oplus})-C_6H_4X$$

III

X=*o*-, *m*-, *p*-, CH_3, CH_3O, $C(CH_3)_3$, Cl, etc.

From the said results, the spatial arrangement of the ketyl which consists of the non-ortho-substituted phenyl group and the ortho-substituted phenyl group is to be represented by IV.

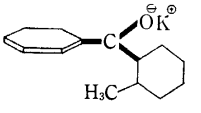

IV

That is to say, the ortho-substituted phenyl group is bent out of the plane of the three central bonds because of the steric hindrance

3) E. Beckmann and T. Paul, *Ann.*, **266**, 1 (1891).
4) W. Schlenk and T. Weickel, *Ber.*, **44**, 1182 (1911).
5) W. Schlenk and A. Thal, ibid., **46**, 2840 (1913).
6) W. E. Bachmann, *J. Am. Chem. Soc.*, **55**, 1179 (1933).
7) R. N. Doesher and G. W. Wheland, ibid., **56**, 2011 (1934).
8) C. B. Wooster, ibid., **56**, 2436 (1934).
9) N. Hirota, Thesis work in Washington University (1962).

of the ortho methyl group. Deguchi[10] reported recently that the diphenyl nitric oxide derivative, which has an ortho substituent, gave an extraordinarily broad ESR spectra although the other derivatives gave a well-resolved hyperfine structure. He was inclined to consider that most of the electron spin densities must be delocalized on nitrogen and on the ortho methyl group. However, this may be far from the truth. The same explanation as has been presented for ketyls may apply.

Experimental

The Preparation of the Ketyl and Measurement. — Ketyls were produced by the reduction of the corresponding ketones with a potassium metal. The measuring apparatus of the ESR was a usual vacuum vessel. THF was dried over K-Na alloy.

Synthesis of Material. — d_5-Phenyl 2-methylphenyl ketone was synthesized from d_6-benzene (99.5 atom%) and *o*-toluyl chloride using the usual Friedel-Crafts reaction (b. p. 131°C/2 mmHg). d_6-Benzene was synthesized by the exchange reaction between benzene and D_2SO_4 (concn. 50 mol. %). D_2SO_4 was made by mixing D_2O and anhydrous SO_3 (γ-form).

The physical constants of the other ketones are as follows:

	Boiling point
2-Methylphenyl 4'-*t*-butylphenyl ketone	160°C/2.0 mmHg
2-Methylphenyl 3'-chlorophenyl ketone	144~148°C/ 3.5 mmHg

10) Y. Deguchi, This Bulletin, **35**, 260 (1962).

Summary

The ESR spectra of the potassium ketyls of d_5-phenyl 2-methylphenyl ketone (I), phenyl 2-methylphenyl ketone (II), 2-methylphenyl 4'-*t*-butylphenyl ketone and 2-methylphenyl 3'-chlorophenyl ketone have been measured in a tetrahydrofuran solution.

II gave four broad lines, and I, a single line with a smaller total width. It is considered that the ortho-substituted phenyl group is bent out of the plane of the three central bonds because of the steric hindrance of the ortho methyl group, and that then the free electron spin is accumulated at a non-substituted phenyl group — especially at the ortho- and para-positions.

The findings on the other ketyls support the above hypothesis.

A part of this work was done at the laboratory Professer S. I. Weissman at Washington University. The authors would like to express their sincere gratitude for his valuable discussion and for the use of his apparatus. The remainder of the work was done with the help of a scientific research grant of the Japanese Ministry of Education.

Department of Chemistry
Faculty of Science
Kyoto University
Sakyo-ku, Kyoto

Synthetic Studies of the Derivatives of Nitroacetic Acid. I. The Preparation of Nitroacetic Ester and the Synthesis of α, β-Unsaturated α-Nitrocarboxylic Esters

By Sumio UMEZAWA and Shonosuke ZEN

(Received April 30, 1963)

The Steinkopf method[1] for the preparation of nitroacetic ester has been modified, and it has been found that, when dipotassium nitroacetate is esterified with ethanol and hydrogen chloride in the presence of a dehydrating agent such as magnesium sulfate, the yield of ethyl nitroacetate is greatly raised, to 78%, probably because the decomposition of nitroacetic acid by the Nef reaction[2] is prevented by the dehydrating agent.

α, β-Unsaturated α-nitroesters have been prepared by the reactions shown in Chart 1.

This is a general synthesis of α, β-unsaturated α-nitroesters. Although the literature contains some examples[3] of the preparation of α, β-unsaturated α-nitroesters, esters of the sort form a relatively unknown class of compounds and are expected to be extraordinary reactive.

1) W. Steinkopf, *Ann.*, **434**, 21 (1923).
2) J. U. Nef, ibid., **280**, 263 (1894); W. E. Noland, *Chem. Revs.*, **55**, 137 (1955).
3) H. B. Hill and O. E. Black, *Am. Chem. J.*, **32**, 232 (1904); L. Bouveault and A. Wahl, *Compt. rend.*, **131**, 687 (1900); P. Friedländer, J. Mähly and M. Lazarus, *Ann.*, **229**, 203 (1885); A. Dornow and H. Menzel, ibid., **580**, 43 (1952).

TABLE I. β-ACETOXY-α-NITROESTERS AND α,β-UNSATURATED α-NITROESTERS

Compound	B. p., °C/mmHg	n_D^{20}	Formula	Analysis Found C, %	Found H, %	Found N, %	Calcd. C, %	Calcd. H, %	Calcd. N, %	Yield %
IV	84~92/0.2	1.4360	$C_8H_{13}O_6N$	44.26	5.68	6.86	43.83	5.98	6.39	52.9
V	98.5~107/0.04~0.05	1.440	$C_{10}H_{17}O_6N$	48.22	6.63	6.19	48.58	6.93	5.67	88.5
VI	118~120/0.04	1.4498	$C_{11}H_{17}O_8N$	45.39	5.91	4.78	45.36	5.85	4.80	65
VII	72~75/3	1.4535	$C_6H_9O_4N$	45.72	5.38	8.21	45.28	5.66	8.80	62.5
VIII	72.5~79.5/0.7	1.4548	$C_8H_{13}O_4N$	50.44	6.82	7.74	51.33	7.00	7.48	80
IX	125~130/0.2	1.4788	$C_9H_{13}O_6N$	—	—	6.12	—	—	6.06	29.8

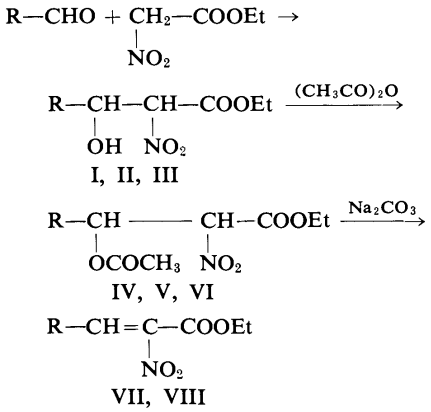

(I, IV, VII: R=CH_3; II, V, VIII: R=n-C_3H_7; III, VI: R=EtOOC—CH_2)

Chart 1

Ethyl β-hydroxy-α-nitrocarboxylates (I and II) were prepared by the general method used by Rodionov and Belikov.[4]

The condensation of sodium ethyl formylacetate with ethyl nitroacetate in aqueous sodium carbonate gave diethyl β-hydroxy-α-nitroglutarate (III), which is a potential intermediate to β-hydroxyglutamic acid.

The acetylation of ethyl β-hydroxy-α-nitrobutyrate (I) with acetic anhydride in the presence of a small quantity of sulfuric acid gave ethyl β-acetoxy-α-nitrobutyrate (IV). Ethyl β-acetoxy-α-nitrocaproate (V) and diethyl β-acetoxy-α-nitroglutarate (VI) were prepared from ethyl β-hydroxy-α-nitrocaproate (II) and diethyl β-hydroxy-α-nitroglutarate (III) by an analogous procedure.

The treatment of the ethyl β-acetoxy-α-nitrocarboxyrates with anhydrous sodium carbonate in benzene at room temperature resulted in deacetylation and dehydration, giving ethyl α,β-unsaturated α-nitrocarboxylates; ethyl α-nitrocrotonate (VII) and ethyl 2-nitro-2-hexenoate (VIII) have been obtained by this procedure from IV and V respectively (Table I).

4) K. M. Rodionov and V. M. Belikov, *Chem. Abstr.*, **49**, 1550 (1955). The preparation of ethyl β-hydroxy-α-nitrobutyrate (I) and of ethyl β-hydroxy-α-nitrovalerate is described.

TABLE II. INFRARED SPECTRA OF α,β-UNSATURATED α-NITROESTERS (liquid, cm^{-1})

Compound	Ester CO	C=C	C—NO_2
VII	1742	1667	1542, 1346
VIII	1742	1660	1544, 1347
IX*	1750	1659	1588, 1310

* Carbon tetrachloride

The treatment of diethyl β-acetoxy-α-nitroglutarate (VI) with sodium carbonate by the procedure described above failed to produce the corresponding α,β-unsaturated α-nitroester. The condensation of sodium ethyl formylacetate[5] (1.0 mol.) with ethyl nitroacetate (2.0 mol.) in the presence of an amine such as n-butylamine or diethylamine (1.0 mol.) gave diethyl α-nitroglutaconate (IX) by the reactions shown in Chart 2.

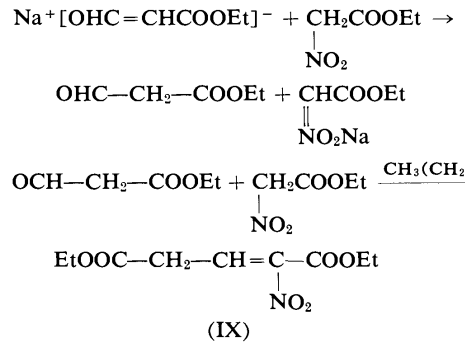

Chart 2

Experimental

Ethyl Nitroacetate.—A mixture of powdered dipotassium nitroacetate (50 g., 0.27 mol.) and anhydrous magnesium sulfate (10 g.) in absolute ethanol (300 g.) was stirred and cooled −8~−10°C, and dry hydrogen chloride was passed into the mixture. After the mixture absorbed 42 g. (1.15 mol.) of hydrogen chloride, the mixture was stirred

5) M. Cogan, *Bull. soc. chim. France*, [5] **8**, 125 (1941); S. M. McElvain and R. L. Clake, *J. Am. Chem. Soc.*, **69**, 2657 (1947); W. Deuschell, *Helv. Chim. Acta*, **35**, 1587 (1952).

for an additional hour and allowed to stand overnight at room temperature. The inorganic salt which separated was removed by filtration, and the ethanol was evaporated under reduced pressure at about 30°C. The residue was dissolved in benzene (100 ml.), and the solution was washed with a small quantity of a 5% sodium carbonate solution to neutralize the reaction product. After drying with anhydrous magnesium sulfate, followed by the evaporation of the solvent, the product was distilled under reduced pressure to give ethyl nitroacetate, b. p. 102~105°C/23 mmHg, yield 30.2 g. (78.2%).

Ethyl β-Hydroxy-α-nitrocaproate (II).—A solution of anhydrous sodium acetate (0.107 g.) in water (1.1 ml.) was added to a solution of *n*-butyraldehyde (8.48 g., 0.118 mol.) in ethanol (11.3 ml.) at below 10°C. To this solution ethyl nitroacetate was added drop by drop (14.1 g., 0.118 mol.), while the temperature was maintained at 8~14°C. Stirring was continued for 3.5 hr. to give a clear, pale-yellow solution. After the removal of the solvent under reduced pressure, the residue was dissolved in ether (200 ml.) and the solution was acidified with 10% hydrochloric acid and washed with a small quantity of water. The ethereal solution was dried with anhydrous magnesium sulfate and evaporated. The resulting residue was distilled under reduced pressure to ethyl β-hydroxy-α-nitrocaproate, b. p. 102~114°C/3 mmHg, n_D^{20} 1.4479, yield 14 g. (64.2%).

Found: C, 46.76; H, 7.45; N, 7.26. Calcd. for $C_8H_{15}O_5N$: C, 46.80; H, 7.37; N, 6.83%.

Diethyl β-Hydroxy-α-nitroglutarate (III).—Ethyl nitroacetate (7.5 g. 0.054 mol.) was added to a solution of concentrated hydrochloric acid (4.5 ml.) in water (7 ml.) below −10°C. Into this mixture was added sodium ethyl formylacetate (7.2 g., 0.05 mol.) rapidly under vigorous stirring. The solution was strongly acidic. Then a 5% aqueous sodium carbonate (about 45 ml.) which had been cooled to about 5°C was added to the reaction mixture to make pH 7.2~7.6, and the mixture was stirred at about 0°C for 1 hr. After the mixture had been made acidic (pH 1~2) by the addition of concentrated hydrochloric acid (about 4.5 ml.) under cooling in an ice-bath, the mixture was extracted with benzene. The benzene extract was dried over anhydrous sodium sulfate, and then the solvent was removed by evaporation, giving a yellow sirup. This product was subjected to fractional distillation under reduced pressure in the usual way. After small fore-runs of unchanged ethyl nitroacetate and triethyl trimesate, diethyl β-hydroxy-α-nitroglutarate distilled at 120~123°C/0.08 mmHg, n_D^{20} 1.4616; yield 3.5 g. (26%); infrared spectrum (liquid): 3480 (OH), 1750 (ester CO), 1565 and 1375 cm^{-1} (C-NO_2).

Found: C, 44.87; H, 5.63; N, 5.71. Calcd. for $C_9H_{15}O_7N$: C, 43.37; H, 6.07; N, 5.62%.

The agreement between the found and calculated values of analysis was not very good, probably because the sample was accompanied with a trace of triethyl trimesate, the removal of which by distillation was difficult. However, acetylation gave an analytically pure sample of the acetate of III, as will be described below.

Ethyl β-Acetoxy-α-nitrobutyrate (IV).—A mixture of ethyl β-hydroxy-α-nitrobutyrate (I) (9.0 g., 0.05 mol.), acetic anhydride (5.7 g., 0.056 mol.) and concentrated sulfuric acid (0.04 ml.) was stirred at 60°C for 30 min. After the removal of acetic acid and acetic anhydride by distillation under reduced pressure, the residue was subjected to fractional distillation to give the title compound; yield, 5.9 g.

Ethyl α-Nitrocrotonate (VII).—To a solution of ethyl-β-acetoxy-α-nitrobutyrate (IV) (5.0 g. 0.023 mol.) in dry benzene (2.5 ml.) anhydrous sodium carbonate (1.21 g., 0.0114 mol.) was added; the mixture was stirred at about 60°C for about 5 min. until the evolution of carbon dioxide ceased. When the temperature of the mixture had fallen to room temperature, additional dry benzene was added and the mixture was stirred. The benzene-layer was dried with anhydrous sodium sulfate, and the solvent was removed by distillation. The residue was fractionated under reduced pressure to give a colorless oil, b. p. 72~76°C/3 mmHg, yield 2.27 g. Repeated distillation gave an analytically pure sample of ethyl α-nitrocrotonate.

Diethyl α-Nitroglutaconate (IX).—To a mixture of sodium ethyl formylacetate (6.0 g., 0.04 mol.) and ethyl nitroacetate (11.6 g., 0.086 mol.) in absolute ethanol, *n*-butylamine (3.2 g., 0.04 mol.) was added, and the mixture was refluxed on a water bath for 8 hr. After the mixture had stood overnight at room temperature, the precipitate of sodium ethyl nitroacetate was removed by filtration and the reddish brown filtrate was concentrated by evaporation. To the concentrate dry benzene (90 ml.) was added to precipitate additional sodium ethyl nitroacetate, this was removed again by filtration. After cooling to about 10°C, the benzene solution was washed with a small quantity of 20% acetic acid and with water. The benzene solution was dried over anhydrous sodium sulfate overnight, and filtered, and the solvent was removed, going an oily residue. This residue was fractionated under reduced pressure to give a crude product of diethyl α-nitroglutaconate; b. p. 144~158°C/0.1~0.5 mmHg, yield 3.0 g. (29.8%). When the product was allowed to stand, a small quantity of crystalline triethyl trimesate separated. After removal of this trimesate, the oily product was repeatedly fractionated.

The authors are indebted to Mr. Saburo Nakada of this Laboratory for his microanalysis.

Department of Applied Chemistry
Faculty of Engineering
Keio University
Koganei-shi, Tokyo

Synthetic Studies of the Derivatives of Nitroacetic Acid. II. The Synthesis of Isoxazolecarboxylic Acids from α, β-Unsaturated α-Nitroesters[1,2]

By Shonosuke ZEN and Sumio UMEZAWA

(Received April 30, 1963)

In a preliminary communication[3] we have shown that the treatment of α, β-unsaturated α-nitroesters with *n*-butylamine in ligroin or absolute ethanol gives derivatives of isoxazole-3, 5-dicarboxylic acid. In the present paper, we report a more detailed study of the new synthesis of isoxazole compounds.

When an excess of *n*-butylamine was added to a solution of diethyl α-nitroglutaconate,[4] it was found that considerable heat was evolved and, after the solution was allowed to stand at room temperature, crystals of 3, 5-bis(*n*-butylcarbamoyl)-4-(*n*-butylcarbamoylmethyl)-isoxazole (I) were deposited in almost a quantitative yield.

Moreover, we have found that the cyclization reaction is generally applicable to the synthesis of 4-substituted isoxazole-3, 5-dicarboxylic acids. The treatment of ethyl α-nitrocrotonate[4] with an excess of *n*-butylamine in absolute ethanol, followed by refluxing for several hours, gave 4-methyl-3, 5-bis(*n*-butylcarbamoyl)-isoxazole (II); 4-*n*-propyl-3, 5-bis(*n*-butylcarbamoyl)isoxazole (III), 4-phenyl-3, 5-bis(*n*-butylcarbamoyl)isoxazole (IV), 4-(*p*-chlorophenyl)-3, 5-bis(*n*-butylcarbamoyl)isoxazole (V) and 4-(*p*-nitrophenyl)-3, 5-bis(*n*-butylcarbamoyl)isoxazole (VI) have been obtained from ethyl 2-nitro-2-hexenoate,[4] ethyl α-nitrocinnamate,[5] ethyl *p*-chloro-α-nitrocinnamate[5] and ethyl 4, α-dinitrocinnamate[5] respectively by the same general procedure (Table I).

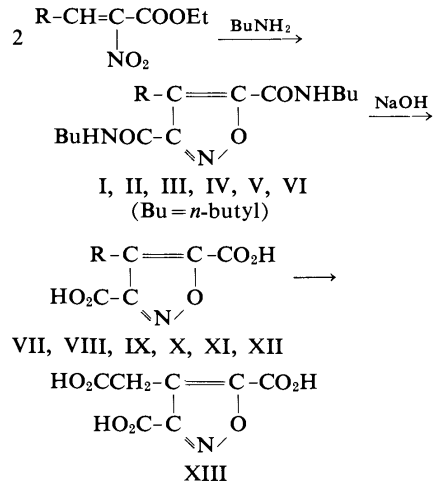

I, VII: R=BuHNOCCH$_2$; II, VIII: R=CH$_3$; III, IX: R=*n*-C$_3$H$_7$; IV, X: R=C$_6$H$_5$; V, XI: R=(*p*)Cl-C$_6$H$_4$; VI, XII: R=(*p*)NO$_2$-C$_6$H$_4$

Chart 1

By mild alkaline hydrolysis with 10% sodium hydroxide in 50% aqueous ethanol, the above-mentioned butylamides of isoxazolecarboxylic acids have been converted into the corresponding free acids of 4-substituted isoxazoles. Thus, 4-methylisoxazole-3, 5-dicarboxylic acid (VIII), 4-(*n*-propyl)isoxazole-3, 5-dicarboxylic acid (IX), 4-phenylisoxazole-3, 5-dicarboxylic acid (X), 4-(*p*-chlorophenyl)isoxazole-3, 5-dicarboxylic acid (XI) and 4-(*p*-nitrophenyl)isoxazole-3, 5-dicarboxylic acid (XII) have been obtained in high yields. The hydrolysis of 3, 5-bis(*n*-butylcarbamoyl)-4-(*n*-butylcarbamoylmethyl)isoxazole (I) at about 60°C gave 4-(*n*-butylcarbamoylmethyl)isoxazole-3, 5-dicarboxylic acid (VII), while more drastic hydrolysis achieved by refluxing for about seven hours with 10% sodium hydroxide in 50% aqueous ethanol afforded 3, 5-dicarboxyisoxazole-4-acetic acid (XIII) (Table II).

Evidence for the structures of the above-mentioned isoxazole derivatives could be deduced from the hydrolysis products. It has been known that isoxazoles are cleaved at the N–O and C=C bonds or C–C bond by drastic hydrolysis with alkali.[6] The drastic alkaline hydrolysis of 4-phenyl-3, 5-bis(*n*-butylcarbamoyl)isoxazole (IV) resulted in the formation of phenylacetic acid (IV') and oxalic acid. Moreover, the hydrolysis of 4-(*p*-dimethylaminophenyl)-3, 5-bis(*n*-butylcarbamoyl)isoxazole (XIV)[7] by an analogous treatment afforded *p*-dimethylaminophenylacetic acid (XIV') and oxalic acid. The above hydrolysis of IV and

1) Presented in part before the Division of Organic Chemistry of the Annual Meeting of the Chemical Society of Japan, Kyoto, April, 1959.
2) Abstracted in part from the Ph. D. thesis presented to Keio University by Shonosuke Zen.
3) S. Umezawa and S. Zen, This Bulletin, 33, 1016 (1960).
4) S. Umezawa and S. Zen, ibid., 36, 1143 (1963).
5) A. Dornow and H. Menzel, *Ann.*, 580, 43 (1952).
6) L. Claisen, *Ber.*, 42, 65 (1909); C. Munsante, *Gazz. chim. ital.*, 72, 537 (1942); S. Takagi and H. Yasuda, *J. Pharm. Soc. Japan* (*Yakugaku Zassi*), 79, 467 (1959).
7) The synthesis of this isoxazole derivative will be described in the next paper.

Table I. 4-Substituted 3,5-bis(*n*-butylcarbamoyl)isoxazoles

Compound	Procedure	M. p. °C	Solvent for recrystallization	Formula	Analysis Found C, %	Found H, %	Found N, %	Calcd. C, %	Calcd. H, %	Calcd. N, %	Yield %
I	—	179~179.5	a	$C_{19}H_{32}O_4N_4$	60.41	8.22	15.15	59.97	8.48	14.73	100 (nearly)
II	A B	84~86	b	$C_{14}H_{23}O_3N_3$	60.32	7.95	15.18	59.76	8.24	14.94	A: 5.5 B: 14.2
III	B	111.5~113	b	$C_{16}H_{27}O_3N_3$	61.63	8.61	13.60	62.11	8.80	13.58	34.1
IV	B	160~162	a	$C_{19}H_{25}O_3N_3$	66.86	6.90	12.55	66.43	7.34	12.24	64.6
V	B	125~127.5	c	$C_{19}H_{24}O_3N_3Cl$	60.60	6.27	11.23	60.39	6.41	11.12	50
VI	B	135	d	$C_{19}H_{24}O_5N_4$	58.52	6.34	14.66	58.75	6.23	14.43	40.3

a ethanol; b ligroin; c 70% ethanol; d *n*-propanol-petroleum ether

Table II. 4-Substituted isoxazole-3,5-dicarboxylic acids

Compound	Procedure	M. p., °C (decomp.)	Solvent for recrystallization	Formula	Analysis Found C, %	Found H, %	Found N, %	Calcd. C, %	Calcd. H, %	Calcd. N, %	Yield %	Neutralization equivalent Found	Neutralization equivalent Calcd.
VII	C	156.5~157	e	$C_{11}H_{14}O_6N_2$	48.95	5.11	10.38	48.89	5.22	10.37	94	—	—
VIII	D	212~212.5	e	$C_6H_5O_5N$	42.25	3.11	7.97	42.11	2.95	8.19	94.8	85.3	85.6
IX	D	176~177	f	$C_8H_9O_5N$	47.98	4.81	6.96	48.24	4.57	7.03	99	100.9	99.5
X	C	183~183.5	g	$C_{11}H_7O_5N$	56.87	2.97	6.08	56.66	3.03	6.01	87.6	115.7	116.6
XI	C	187~187.5	g	$C_{11}H_6O_5NCl$	49.68	2.65	5.45	49.35	2.25	5.25	94	138.8	133.8
XII	C	172~174	g	$C_{11}H_6O_7N_2$	47.80	2.60	9.89	47.49	2.17	10.07	80	142.0	139.1
XIII	—	104~108 (m. p.)	e	$C_7H_5O_7N$	39.02	2.42	6.57	39.08	2.34	6.51	98	72.3	71.7

e dioxane-chloroform; f ethylene chloride; g dioxane-ethylene chloride-ligroin

Tabl III. Infrared spectra of 4-substituted isoxazole-3,5-dicarboxylic acids (Nujol, cm^{-1})

Compound	Crystalline water	Carboxyl OH	Carboxyl CO	Isoxazole[8] Ring stretching	Isoxazole[8] Ring breathing	Isoxazole[8] Ring deformation
VIII	3545~3478	2620~2530	1723	1622, 1492	1039	862
IX	3533, 3438	2640~2530	1717	1601, 1490	1072	904
X	3500~3334	2610~2520	1717	1610, 1505	1046	865
XI*	3511~3356	2586~2356	1720	1610, 1502	1042	862
XII*	—	2600~2300	1725	1608, 1508	1020	849
XIII	3480, 3342	2620~2540	1715	1623, 1488	1044	867

* KBr

XIV can be easily explained by the reaction sequence shown in Chart 2.

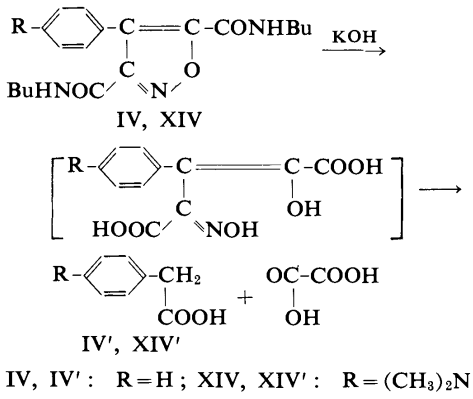

Chart 2

Reaction Mechanism.—The formation of isoxazole derivatives described above suggests that a key intermediate in the reaction sequence may be an addition compound (XIX) formed by the addition of nitroacetate to an α,β-unsaturated α-nitroester. Therefore, it seems reasonable to suggest that the initial step involves the base-catalyzed cleavage of α,β-unsaturated α-nitroester to liberate the nitroacetic ester moiety, which may be in equilibrium with the original unsaturated nitroester, followed by the addition of the former to the latter to give the above-mentioned key intermediate. It then cyclize to form an isoxazole derivative (XX) by the elimination of its water and nitrous acid.

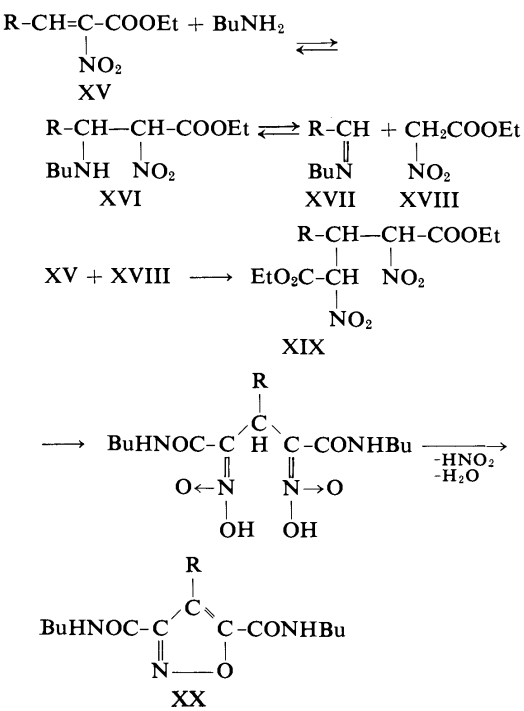

Chart 3

Fortunately, we could isolate a Schiff base (XVII), benzylidene-*n*-butylamine, from the mother liquor of the 4-phenyl-3, 5-bis(*n*-butylcarbamoyl)isoxazole (IV) which is obtained from ethyl α-nitrocinnamate by refluxing it with *n*-butylamine in absolute ethanol. Evidently, the initial reaction involves the addition of butylamine to an α,β-unsaturated α-nitroester (XV), while the adduct (XVI) generates nitroacetic ester (XVIII), which adds to the α,β-unsaturated α-nitroester in the presence of a basic catalyst (*n*-butylamine) in a way similar to that of the Michael reaction to give the key intermediate (XIX), as is outlined in Chart 3.

As was expected, the addition of ethyl nitroacetate to the above reaction-systems resulted in a significant increase in the yields of isoxazole derivatives.

Experimental

3, 5-Bis(*n*-butylcarbamoyl)-4-(*n*-butylcarbamoylmethyl)isoxazole (I). — Into a mixture of diethyl α-nitroglutaconate[4] (0.50 g., 0.0022 mol.) in ligroin (2 ml.) was added *n*-butylamine (1.0 g., 0.013 mol.) under stirring. During this period considerable heat was evolved, and the color of the solution changed to a yellowish brown. When the solution was left standing at room temperature, there were deposited crude crystals of I, which were then collected and washed with a small quantity of ethanol; m. p. 176~178°C, yield 0.41 g. (nearly quantitative). Recrystallization from ethanol gave an analytically pure sample.

4-Methyl-3, 5-bis(*n*-butylcarbamoyl)isoxazole (II). —(An example of procedure A) A mixture of ethyl α-nitrocrotonate[4] (1.0 g., 0.0063 mol.), absolute ethanol (2 ml.) and *n*-butylamine (2.75 g., 0.038 mol.) was refluxed for 3 hr. After standing at room temperature overnight, the solvent was removed by distillation to give a reddish brown sirup, which was then taken in hot ligroin, filtered, and cooled to give colorless needles of the title compound; m. p. 82~85°C; yield 0.035 g. (5.5%). Recrystallization from ligroin gave an analytically pure sample.

(An example of procedure B) By the addition of ethyl nitroacetate.—A mixture of ethyl α-nitrocrotonate (1.06 g., 0.0066 mol.), ethyl nitroacetate (0.88 g., 0.0066 mol.) and *n*-butylamine in absolute ethanol was refluxed for 10.5 hr. After the solution had been left standing at room temperature overnight, the solvent was removed by distillation to give a deep yellow residue, which was then recrystallized from ligroin (yield, 0.19 g.). The product was found to be identical with the product prepared by procedure (A) above by undepressed m. p. and infrared spectra.

8) A. R. Katritzky and A. J. Boulton, *Spectrochimica Acta*, 17, 238 (1961).

4-(*n*-Butylcarbamoylmethyl)isoxazole-3, 5-dicarboxylic Acid (VII).—(An example of procedure C) A mixture of 3,5-bis(*n*-butylcarbamoyl)-4-(*n*-butylcarbamoylmethyl)isoxazole (1.14 g.) and 10% sodium hydroxide in 50% aqueous ethanol (110 ml.) was warmed at 50~55°C for 2 hr. while being stirring. After the removal of the ethanol by distillation under reduced pressure, the aqueous solution was acidified with hydrochloric acid and then extracted with ether. The extract was dried over anhydrous sodium sulfate, filtered, and evaporated to give a powdery residue (yield 0.74 g.). Recrystallization gave colorless needles of the title compound.

3, 5-Dicarboxylsoxazole-4-acetic Acid (XIII).—A mixture of 3,5-bis(*n*-butylcarbamoyl)-4-(*n*-butylcarbamoylmethyl)isoxazole (I) (0.80 g.) and 10% sodium hydroxide in 50% aqueous ethanol (25 ml.) was refluxed for 7 hr. After the removal of the ethanol by distillation, aqueous solution was acidified with hydrochloric acid and extracted with ether. The ethereal extract was dried over anhydrous sodium sulfate, filtered and evaporated to give a pale-yellow powder (yield 0.44 g.). Recrystallization gave colorles needles of the titlec ompound.

4-Methylisoxazole-3, 5-dicarboxylic Acid (VIII).—(An example of procedure D) A mixture of 4-methyl-3,5-bis(*n*-butylcarbamoyl)isoxazole (II) (0.82 g.) and 10% sodium hydroxide in 50% aqueous ethanol (33 ml.) was refluxed for 2 hr. and worked up as has been described in the preparation of XIII (yield, 0.47 g.).

The Ring Opening of 4-Phenyl-3, 5-bis(*n*-butylcarbamoyl)isoxazole.—A mixture of 4-pheny-3,5-bis(*n*-butylcarbamoyl)isoxazole (1.0 g.) and 28.5% potassium hydroxide in 50% aqueous ethanol (55 ml.) was refluxed for about 4 hr. After the ethanol had been removed by distillation, the aqueous solution was cooled to about 5°C, acidified with hydrochloric acid, and extracted with ether. The ethereal extract was dried over anhydrous sodium sulfate, filtered, and evaporated to give a crystalline residue (yield 0.55 g.). The product was then extracted with benzene.

The soluble part obtained by the evaporation of the benzene extract was washed with petroleum ether to give crystals of phenylacetic acid, m. p. 74~77°C; yield 0.25 g. (64%). Mixed m. p. with an authentic specimen of phenylacetic acid was undepressed.

The insoluble part in benzene was recrystallized from dioxane-chloroform to give colorless crystals of oxalic acid dihydrate, m. p. 97.5~99°C; yield 16 mg. Mixed m. p. with an authentic sample of oxalic acid dihydrate was undepressed.

The Ring Opening of 4-(*p*-dimethylaminophenyl)-3, 5-bis(*n*-butylcarbamoyl)isoxazole.—A mixture of 4-(*p*-dimethylaminophenyl)-3,5-bis(*n*-butylcarbamoyl)isoxazole[7] (0.5 g.) and 10% sodium hydroxide in 50% aqueous ethanol (10 ml.) was refluxed for 2 hr. After the ethanol had been removed by distillation, the aqueous solution was acidified to pH 5.4~5.6 with hydrochloric acid and extracted with ether. The ethereal extract was dried over anhydrous sodium sulfate, filtered and evaporated to give a crystalline residue, yield 0.12 g. (51.6%). Recrystallization from ligroin gave colorless plates of *p*-(dimethylamino)phenylacetic acid, m. p. 109.5~110.5°C.[9]

Found: C, 67.46; H, 7.21; N, 7.50. Calcd. for $C_{10}H_{13}O_2N$: C, 67.02; H, 7.31; N, 7.82%.

Paperchromatography of the mother-liquor which remained after extraction with ether showed the presence of oxalic acid.

The Isolation of Benzylidene-*n*-butylamine from the Reaction Mixture Obtained from Ethyl α-Nitrocinnamate and *n*-Butylamine.—A mixture of ethyl α-nitrocinnamate (1.0 g., 0.0048 mol.), *n*-butylamine 1.32 g., 0.019 mol.) and absolute ethanol (4 ml.) was refluxed for 8 hr. After the solution had been left standing at room temperature, the resulting crystals of 4-phenyl-3,5-bis(*n*-butylcarbamoyl)-isoxazole (IV) was collected by filtration. Concentration of the filtrate gave the second crop; the total yield of IV was 0.187 g. (23.5%). The mother liquor which separated from the second crop was distilled under reduced pressure to give a colorless liquid boiling at 95~112°C/12 mmHg.

The product was extracted with benzene. The removal of benzene by evaporation, followed by vacuum distillation, gave benzylidene-*n*-butylamine, b, p. 110~111°C/13 mmHg., yield 92 mg., which was found by infrared spectra to be identical with an authentic specimen.

Summary

1) α,β-Unsaturated α-nitroesters react with *n*-butylamine to give 4-substituted isoxazole-3, 5-carboxylic butylamides. This is a new synthesis of isoxazole derivatives.

2) The mechanistic features of the above reaction have been explained.

3) The mild alkaline hydrolysis of the above butylamides gave 4-substituted isoxazole-3, 5-dicarboxylic acids.

This work has been supported in part by a grant from the Kawakami Memorial Foundation, to which the authors' thanks are due. The authors are also indebted to Mr. Saburo Nakada of this Laboratory for the microanalytical data.

Department of Applied Chemistry
Faculty of Engineering
Keio University
Koganei-shi, Tokyo

9) Reported m. p. 112~113°C. M. Okubo and R. Goto, *J. Chem. Soc. Japan, Pure Chem. Sec.* (*Nippon Kagaku Zasshi*), 82, 261 (1961).

Synthetic Studies of the Derivatives of Nitroacetic Acid. III. The Synthesis of Isoxazole-3, 5-dicarboxylic Acids from Schiff Bases and Nitroacetic Ester[1]

By Sumio UMEZAWA and Shonosuke ZEN

(Received April 30, 1963)

The authors have previously reported[2] that dibutylamides of 4-substituted isoxazole-3, 5-dicarboxylic acids were obtained when α, β-unsaturated α-nitrocarboxylates were treated with an excess of *n*-butylamine in an anhydrous solvent; they also presented the reaction mechanism of the new synthesis.

If the mechanism presented by the authors is valid, one should be able to obtain the derivatives of isoxazole-3, 5-dicarboxylic acids by the reaction of Schiff bases (1) with nitroacetic ester (2) in the presence of basic catalysts by means of the scheme outlined in Chart 1.

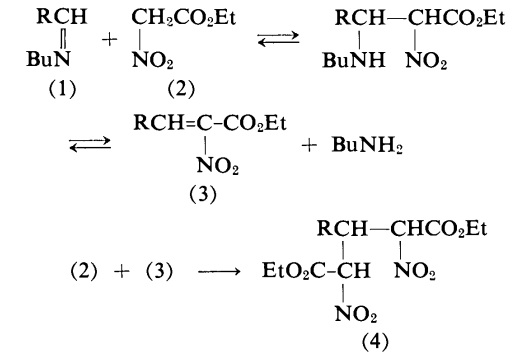

Chart 1

The authors have already mentioned, in a previous paper,[2] the sequel of the path from (4) to the isoxazole derivatives.

This expectation has now been realized. When an excess of *n*-butylamine (about five moles) was added to a mixture of Schiff base (one mole) and ethyl nitroacetate (two moles) in absolute ethanol, an exothermic reaction occurred. After refluxing for several hours, the mixture was concentrated to give a crystalline solid of 3, 5-bis(*n*-butylcarbamoyl) derivatives of isoxazole.

By this general procedure the following compounds, I—XVII, have been prepared from the corresponding Schiff bases and ethyl nitroacetate:

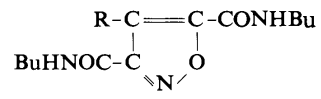

I—XVII

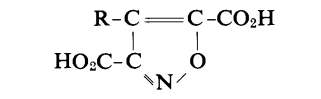

VI', IX'*, XI', XIII'*, XIV', XVII'

Aliphatic series:

R

I: CH_3
II: n-C_3H_7
III: $(CH_3)_2C{=}CH(CH_2)_2{-}CHCH_2$ (with CH_3 on the last CH)

Aromatic series:

IV: C_6H_5
V: $(p)Cl{-}C_6H_4$
VI, VI': $(2,4)Cl_2C_6H_3$
VII: $(p)NO_2{-}C_6H_4$
VIII: $(m)NO_2{-}C_6H_4$
IX: $(p)CH_3CONH{-}C_6H_4$
IX'*: $H_2N{-}C_6H_4$
X: $(p)(CH_3)_2NC_6H_4$
XI, XI': 1-Naphthyl
XII: 9-Anthryl

Heterocyclic series:

XIII, XIII'*: 2-Furyl
XIV, XIV': 2-Thienyl
XV: 2-Pyrrolyl
XVI: 2-Pyridyl
XVII, XVII': 3-Indolyl

Citronellylidene-*n*-butylamine failed to give isoxazole compounds, whereas citronellylidenebenzylamine gave 4-(2, 6-dimethyl-2-octenyl)-3, 5-bis(benzylcarbamoyl)isoxazole (III) by means of a reaction with ethyl nitroacetate in the presence of an excess of benzylamine. Indole-3-aldehyde and *n*-butylamine failed to give a Schiff base; however, 3-indolylidenaniline could be used to give 4-(3-indolyl)-3, 5-bis-(*n*-butylcarbamoyl)isoxazole (XVII) by means of the general procedure.

1) Presented in part before the Division of Organic Chemistry of the 14th and 15th Annual Meetings of the Chemical Society of Japan, Tokyo, April, 1961, and Kyoto, April, 1962. Preliminary communication: S. Zen and S. Umezawa, This Bulletin, 34, 890 (1961).
2) S. Zen and S. Umezawa, This Bulletin, 36, 1146 (1963).

* Dimethyl ester were caused to crystallize.

As an example using a primary amine other than *n*-butylamine the treatment of benzylidenebenzylamine with ethyl nitroacetate in the presence of an excess of benzylamine by analogous reaction conditions gave 4-phenyl-3,5-bis(benzylcarbamoyl)isoxazole (XVIII) in 84% yield.

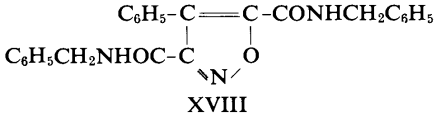

XVIII

XIX

The di-*n*-butylamine Schiff base of terephthalaldehyde, namely, *p*-xylylidene-di(*n*-butylamine), also gave a diisoxazolyl derivative of benzene (XIX) upon the treatment of one mole of the Schiff base with four moles of ethyl nitroacetate and an excess of *n*-butylamine.

An alternative method, in which aldehydes and an primary amine are used instead of a Schiff base, also gave a 4-substituted isoxazole-3,5-dicarboxylic acid. However, the yield by this alternative method have been found to be generally lower than corresponding yields by the first-mentioned method.

4-(*p*-Sulfamoylphenyl)-3(or 5)-(*n*-butylcarbamoyl)-5(or 3)-(ethoxycarbonyl)isoxazole (XX) was obtained by the alternative procedure in good yield.

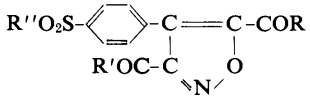

XX: R, R'=BuHN, C_2H_5O or vice versa; R''=NH_2

XX': R, R', R''=OH

The above amide derivatives of isoxazole-3,5-dicarboxylic acid have been hydrolyzed mildly with sodium hydroxide in aqueous ethanol by the procedure described in a proceding paper[2] to give the corresponding 4-substituted isoxazole-3,5-dicarboxylic acids. In general, the derivatives substituted for aliphatic groups at the 4-position gave better yields when the reaction mixture was refluxed, while the derivatives substituted by aromatic or heterocyclic groups at the same position gave better yields when the reaction mixture was warmed at 50~60°C for several hours.

The hydrolysis of 4-(*p*-acetamidophenyl)-3,5-bis(*n*-butylcarbamoyl)isoxazole (IX) and 4-(2-furyl)-3,5-bis(*n*-butylcarbamoyl)isoxazole (XIII) failed to give crystalline products of free acids; their methyl ester have, however, been crystallized.

Experimental

4-Methyl-3,5-bis(*n*-butylcarbamoyl)isoxazole (I). —(A typical example of the general method).— Into a solution of ethylidene-*n*-butylamine[3] (1.50 g., 0.015 mol.) in absolute ethanol (5 ml.) was added ethyl nitroacetate (4.03 g., 0.03 mol.) under stirring. During this period considerable heat was evolved; the temperature of the reaction mixture rose to 60°C from 18°C. *n*-Butylamine (5.53 g., 0.076 mol.) was then added to the mixture. When the exothermic reaction had subsided, the reaction mixture was gently refluxed for 5 hr. After the solution had been left standing at room temperature, the solvent was removed by distillation to give a reddish brown sirup, which was allowed to stand in a refrigerator to give crystals of the title compound, yield 0.46 g. (10.9%) which were then recrystallized from ligroin to give feathery crystals, m. p. 84~86°C. The product was found by undepressed mixed melting point and infrared spectra to be identical with the authentic specimen[2] prepared from ethyl α-nitrocrotonate.

II-XI, XIV, XVI and XIX were prepared by the general procedure (Tables I and II).

4-(9-Anthryl)-3,5-bis(*n*-butylcarbamoyl)isoxazole (XII).—The reaction mixture obtained from 9-anthrylidene-*n*-butylamine (2.09 g.), ethyl nitroacetate (2.31 g.) and *n*-butylamine (2.92 g.) was refluxed for 9 hr. After the mixture had cooled to room temperature, water (about 10 ml.) was added to give a crude crystalline solid. The product was dissolved in ethanol (11 ml.), and the solution was diluted with water (6 ml.) to give a crystalline solid. This was again dissolved in benzene (7.3 ml.) and diluted with ligroin, whereupon there separated analytically pure crystals of the title compound (yield 0.34 g.); UV (methanol): 255 mμ (ε, 235000).

4-(2-Furyl)-3,5-bis(*n*-butylcarbamoyl)isoxazole (XIII). — The reaction mixture obtained by the general method from 2-furylidene-*n*-butylamine[5] (7.55 g.), ethyl nitroacetate (13.3 g.) and *n*-butylamine (18.5 g.) was refluxed for 9 hr. and allowed to stand, whereupon it gave a crude solid (yield 5.60 g.) The mother liquor was concentrated, and the residue was extracted with hot cyclohexane. When the cyclohexane extract was cooled, the second crop was obtained; (yield 3.64 g.; total 55.5%). Recrystallization from cyclohexane gave colorless feathery crystals (UV (methanol): a shoulder at 246 mμ (ε, 16000), 308 mμ (ε, 10700)).

4-(2-Pyrrolyl)-3,5-bis(*n*-butylcarbamoyl)isoxazole (XV).—The reaction mixture obtained by the general procedure from 2-pyrrolylidene-*n*-butylamine (1.0 g.), ethyl nitroacetate (1.8 g.) and *n*-butylamine

3) L. Kahorec, *Acta Phys. Austrica*, **1**, 307 (1948).
4) A. R. Katritzky and A. J. Boulton, *Spectrochim. Acta*, **17**, 238 (1961).
5) J. E. Beatty and J. R. Stevens, *J. Am. Chem. Soc.*, 71, 703 (1949).

TABLE I. 4-SUBSTITUTED 3,5-BIS(*n*-BUTYLCARBAMOYL)ISOXAZOLES

Compound	M. p. °C	Solvent for recrystallization	Formula	Analysis Found C, %	Found H, %	Found N, %	Calcd. C, %	Calcd. H, %	Calcd. N, %	Yield %
III	126~128	a	$C_{28}H_{33}O_3N_3$	72.44	7.03	9.52	73.17	7.27	9.14	19.8
VI	139~140.5	b	$C_{19}H_{23}O_3N_3Cl_2$	55.41	5.77	10.44	55.34	5.63	10.19	51.5
VIII	168~169	b	$C_{19}H_{24}O_5N_4$	58.80	6.11	14.51	58.75	6.23	14.43	57
IX	159~160	c	$C_{21}H_{28}O_4N_4$	63.13	6.92	13.19	62.98	7.05	13.99	48
X	117.5~118.5	b	$C_{21}H_{30}O_3N_4$	65.74	7.95	14.80	65.26	7.82	14.50	30.8
XI	181.5~183	a	$C_{23}H_{27}O_3N_3$	70.61	6.68	10.64	70.20	6.92	10.68	52.5
XII	159~162	d	$C_{27}H_{29}O_3N_3$	73.43	6.33	9.56	73.11	6.59	9.47	9.6
XIII	127~127.5	e	$C_{17}H_{23}O_4N_3$	61.15	7.02	12.76	61.24	6.95	12.61	55.5
XIV	120~123	a	$C_{17}H_{23}O_3N_3S$	58.55	6.56	12.06	58.44	6.64	12.03	50
XV	180~182	f	$C_{17}H_{24}O_3N_4$	61.56	7.41	17.03	61.42	7.28	16.86	4.8
XVI	128~129	b	$C_{18}H_{24}O_3N_4$	62.90	6.83	16.46	62.77	7.02	16.27	21.4
XVII	184.5~185.5	b	$C_{21}H_{26}O_3N_4$	66.00	7.01	14.38	65.95	6.85	14.65	44
XIX	255~257	a	$C_{32}H_{44}O_6N_6$	63.28	7.02	13.89	63.14	7.29	13.81	45.4

a ethanol; b ethanol-water; c *n*-propanol-ligroin; d benzene-ligroin; e cyclohexane f *n*-hexane

(2.45 g.) was refluxed for 14 hr., and the solvent was removed by distillation to give a tarry residue, which was then extracted with benzene. The benzene solution was evaporated to give again a tarry residue. This residue was again extracted with hot *n*-hexane (30 ml.), and the hexane extract was cooled to give crystals of the title compound; yield 0.072 g.; recrystallized from *n*-hexane to give slightly violet needles; UV (methanol): 247~255 mμ (ε, 7900).

4-(3-Indolyl)-3, 5-bis(*n*-butylcarbamoyl)isoxazole (XVII). — The reaction mixture obtained by the general procedure from indolylidenaniline[6] (1.0 g.), ethyl nitroacetate (1.2 g.) and *n*-butylamine (1.7 g.). was refluxed for 6.5 hr. and evaporated to give a dark red tar, which was then caused to crystallize by treatment with aqueous ethanol (yield 0.77 g.) Repeated recrystallization from 50% ethanol gave yellow needles (UV (methanol): a shoulder at 281 mμ (ε, 8510) and 288 mμ (ε, 7400)).

4-Phenyl-3, 5-bis(benzylcarbamoyl) isoxazole (XVIII).—To a mixture of benzylidenebenzylamine (1.95 g.) and ethyl nitroacetate (2.66 g.) benzylamine (5.35 g.) was added, and the mixture was refluxed for 2 hr. After the mixture had stood at room temperature, the resulting solid was collected by filtration; yield 3.46 g. (84%) recrystallized from ethanol to give colorless needles of the title compound, m. p. 199.5~200°C.

Found: C, 72.98; H, 4.99; N, 10.30. Calcd. for $C_{25}H_{21}O_3N_3$: C, 72.98; H, 5.14; N, 10.21%.

The hydrolysis of the product with 10% sodium hydroxide in 50% ethanol at 50~60°C for 2 hr. gave 4-phenylisoxazole-3,5-dicarboxylic acid[2] in 69% yield.

The Alternative Method Using Aldehydes and Primary Amine Instead of Schiff Bases. — To a mixture of an aldehyde (1.0 mol.) and ethyl nitroacetate (2.0 mol.) in absolute ethanol *n*-butylamine (6 mol.) was added; the mixture was refluxed for 5 hr. and worked up in a manner similar to that described in the preparation of the above-described 4-substituted isoxazole-3,5-dicarboxylic dibutylamides. Yields by the alternative method are shown in comparison with those obtained through Schiff bases in Table II.

TABLE II. THE YIELD OF 4-SUBSTITUTED ISOXAZOLE-3,5-DICARBOXYLIC DIBUTYLAMIDES

Compound	Yield, %* Through Schiff bases	By the alternative method
I	10.9	24.0
II	29.5	22.9
IV	66.5	38
V	47.5	42.4
VI	51.5	21.4
VIII	57.0	36
XX	—	68.2

* Crude products

4-(*p*-Sulfamoylphenyl)-3(or 5)-(*n*-butylcarbamoyl)-5(or 3)-(ethoxycarbonyl) isoxazole (XX).—Prepared by the alternative method from *p*-sulfamoylbenzaldehyde[7] (1.0 g.), ethyl nitroacetate (1.45 g.), *n*-butylamine (2.37 g.) and absolute ethanol (1.6 ml.); yield 1.47 g. (68.2%); recrystallized from *n*-butanol as colorless feathery crystals, m. p. 120~123°C; UV: 243 mμ (ε, 16400); IR (Nujol): 3340, 3260, 1750, 1674, 1549, 1329, 1195 (-SO_2N=), 1618, 1500, 1014 and 851 cm^{-2}.

Found: C, 51.52; H, 5.48; N, 10.28. Calcd. for $C_{17}H_{21}O_6N_3S$: C, 51.63; H, 5.35; N, 10.63%.

4-(2, 4-Dichlorophenyl) isoxazole-3, 5-dicarboxylic Acid (VI').—Prepared from 4-(2,4-dichlorophenyl)-3,5-bis(*n*-butylcarbamoyl)isoxazole (VI) (1.2 g.) by

6) M. p. 133~135°C. Reported m. p. 126~127°C by R. Majima and M. Kotake, *Ber.*, 58B, 2039 (1925).

7) T. P. Sycheva and M. N. Shchukina, *Chem. Abstr.*, 49, 932 (1955).

TABLE III. 4-SUBSTITUTED ISOXAZOLE-3,5-DICARBOXYLIC ACIDS

Compound	M. p., °C (decomp.)	Solvent for recrystallization	Formula	Analysis Found C, %	Found H, %	Found N, %	Calcd. C, %	Calcd. H, %	Calcd. N, %	Yield %	Neutrarization equivalent Found	Neutrarization equivalent Calcd.
VI′	183～186	a	$C_{11}H_5O_5NCl_2$	44.10	1.97	4.85	43.75	1.65	4.64	59.5	155.4	151.0
XI′	198.5～199.5	b	$C_{15}H_9O_5N$	63.42	3.30	5.06	63.61	3.20	4.96	35.3	140.4	141.6
XIV′	158～159	c	$C_9H_5O_5NS$	46.00	2.25	5.41	45.20	2.11	5.86	67.9	114.5	119.6
XVII′	211～213	d	$C_{13}H_8O_5N_2$	56.90	3.53	9.98	57.36	2.96	10.29	56.5	138.3	136.1
XX′	143～145	d	$C_{11}H_7O_8NS$	42.20	2.96	4.79	42.17	2.26	4.48	87	104.5	104.4

a ether-ligroin ; b water ; c dioxane-ligroin ; d dioxane-chloroform

TABLE IV. INFRARED SPECTRA OF 4-SUBSTITUTED ISOXAZOLE-3,5-DICARBOXYLIC ACIDS (Nujol, cm^{-1})

Compound	Crystalline water	Carboxyl OH	Carboxyl CO	Isoxazole[4] Ring stretching	Isoxazole[4] Ring breathing	Isoxazole[4] Ring deformation
VI′	3350	2650～2550	1733	1610, 1495	1040	866
XIV′	3517～3350	2595～2350	1751, 1724	1612, 1465	1044	862
XVII′	3425	2666～2380	1717	1605, 1420	1015	844
XX′	3345～3230	2660～2520	1722	1600, 1496	1017	901

TABLE V. SCHIFF BASES OF *n*-BUTYLAMINE

No.	Compound	Formula	B. p., °C/mmHg	M. p., °C	Analysis Found N, %	Analysis Calcd. N, %	Yield %
1	2,4-Dichlorobenzylidene-*n*-butylamine	$C_{11}H_{13}NCl_2$	127～130/2.5	—	—	—	70.1
2	*p*-Acetamidobenzylidene-*n*-butylamine	$C_{13}H_{18}ON_2$	—	108～110*	12.79	12.83	94.5
3	*p*-(Dimethylamino)benzylidene-*n*-butylamine	$C_{13}H_{20}N_2$	131～135/3	—	—	—	77
4	1-Naphthylidene-*n*-butylamine	$C_{15}H_{17}N$	167～169/7	—	6.43	6.63	81.5
5	9-Anthrylidene-*n*-butylamine	$C_{19}H_{19}N$	—	64～ 65**	5.24	5.36	91.6
6	2-Pyrrolylidene-*n*-butylamine	$C_9H_{14}N_2$	91～92.5/3	—	18.69	18.65	79.5
7	2-Pyridylidene-*n*-butylamine	$C_{10}H_{14}N_2$	81～82.5/3	—	—	—	76
8	*p*-Xylylidene-di(*n*-butylamine)	$C_{16}H_{24}N_2$	159～160/3	—	—	—	84
9	Citronellylidene-*n*-butylamine	$C_{14}H_{27}N$	93～95.5/3	—	6.64	6.69	65.5

* Recrystallized from benzene ; colorless plates

** Recrystallized from aqueous ethanol ; yellow needles

a procedure similar to that described in the preceding paper.[2] Hydrolysis was carried out at 50~60°C for 2 hr.; yield 0.52 g.; recrystallized from ether-ligroin to give colorless plates.

A sample free from crystalline water was analyzed.

XI' XIV' and XVII' were prepared by a similar procedure (Tables III and IV).

Dimethyl 4-(*p*-Aminophenyl)isoxazole-3, 5-dicarboxylate (IX').—A mixture of 4-(*p*-acetamidophenyl)-3, 5-bis(*n*-butylcarbamoyl)isoxazole (IX) (10.6 g.) and 10% sodium hydroxyde in 50% aqueous ethanol (430 ml.) was refluxed for 2 hr. After the mixture had stood at room temperature, a small quantity of an insoluble matter was removed by filtration, and then ethanol (1.0 l.) was added to the filtrate to give disodium salt of the title compound; yield 5.27 g. (68.1%); m. p.>300°C. A sample of the salt (0.36 g.) was suspended in absolute methanol (11 ml.), and the mixture was saturated with hydrogen chloride gas while being cooled. After standing at room temperature overnight, the solution was evaporated to dryness. The residue was dissolved in water, and the solution was made alkaline with a 5% sodium carbonate solution to pH 8.7~9.0, followed by extraction with methylene chloride.

The extract was dried over anhydrous sodium carbonate and evaporated to give an yellow solid yield 0.10 g. (28%); recrystallization from ethyl acetate-ligroin gave yellow needles of the title compound, m. p. 163~166°C.

Found: C, 57.01; H, 4.10; N, 10.27. Calcd. for $C_{15}H_{12}O_5N_2$: C, 56.52; H, 4.38; N, 10.14%.

Dimethyl 4-(2-Furyl)isoxazole-3, 5-dicarboxylate (XIII').—A mixture of 4-(2-furyl)-3, 5-bis(*n*-butylcarbamoyl)isoxazole (1.67 g.) and 10% sodium hydroxide in 50% ethanol (20 ml.) was warmed at 55~60°C for 1 hr. The dark brown mixture thereby obtained was evaporated under reduced pressure to remove the ethanol, acidified with hydrochloric acid, and extracted with ether. Evaporation of the ethereal extract gave a dark brown sirup (1.22 g.) which failed to crystallize. A part of the residue (0.9 g.) was dissolved in absolute methanol (40 ml.); the solution was then saturated with dry hydrogen chloride gas and left to stand at room temperature. After the removal of the methanol by distillation, the resulting sirup with dissolved in chloroform (30 ml.) and washed with a 5% sodium carbonate solution and water. The chloroform solution was dried over anhydrous sodium sulfate and evaporated to give a dark brown sirup, which was caused to crystallize, giving needles yield, 0.1 g. (10%); recrystallized from *n*-hexane; colorless needles, m. p. 63~64.5°C.

Found: C, 52.44; H, 3.62; N, 5.80. Calcd. for $C_{11}H_9O_6N$: C, 52.59; H, 3.61; N, 5.58%.

4-(*p*-Sulfophenyl)isoxazole-3, 5-dicarboxylic Acid (XX'). — A mixture of 4-(*p*-sulfamoylphenyl)-3(or 5)-(*n*-butylcarbamoyl)-5(or 3)-(ethoxycarbonyl)isoxazole (XX) (0.30 g.) and 10% sodium hydroxide in 50% aqueous ethanol (20 ml.) was warmed at about 60°C for 2 hr. while being stirred. After removal of the ethanol, the aqueous solution was acidified with hydrochloric acid to pH 2.0 and extracted with ether. The extract was dried over anhydrous sodium sulfate, filtered, and evaporated to give a yellow powder (0.22 g.), which was a partially hydrolized product. A part (0.1 g.) of the product was dissolved in 10% aqueous sodium hydroxide (2.0 ml.), and the solution was refluxed for 1 hr. After acidified with hydrochloric acid to pH 4.0, the solution was extracted with ether. The ethereal extract was dried over anhydrous sodium sulfate, filtered, and evaporated to give a yellow powder (0.1 g.). Recrystallization from dioxane-chloroform gave colorless needles.

Schiff Base (Table V). — Prepared by a general procedure illustrated by the following examples.

n-Butylidene-n-butylamine.—A mixture of *n*-butylaldehyde (5.04 g., 0.07 mol.) and *n*-butylamine (5.11 g., 0.07 mol.) in benzene (15 ml.) was refluxed for 30 min. After the mixture had been dried over anhydrous sodium sulfate, the benzene was removed and the residue was distilled under reduced pressure to give the Schiff base, b. p. 113.5~114°C/20 mmHg, yield 4.10 g. (46.1%).

Citronellylidene-n-benzylamine. — A mixture of citronellal (5.0 g.) and benzylamine (3.8 g.) in benzene (30 ml.) was stirred and allowed to stand for 1 hr. The benzene layer was then separated and dried over anhydrous sodium sulfate. After the removal of the benzene, the residue was distilled under reduced pressure to give the Schiff base, b. p. 150~151.5°C/5.5 mmHg, yield 4.76 g. (60.3%).

Found: N, 5.86. Calcd. for $C_{17}H_{25}N$: 5.76%.

Summary

1) Schiff bases react with ethyl nitroacetate in the presence of *n*-butylamine or benzylamine to give 4-substituted isoxazole-3, 5-dicarboxylic amides. This is a new synthesis of isoxazole derivatives.

2) Twenty kinds of 4-substituted isoxazole-3, 5-dicarboxylic amides, including aliphatic, aromatic and heterocyclic derivatives, have been prepared.

3) Seven of the above-mentioned amides have been hydrolyzed to give the corresponding 4-substituted isoxazole-3, 5-dicarboxylic acids.

4) Some Schiff bases have been described.

This work has been supported in part by a grant from the Kawakami Memorial Foundation, to which the authors' thanks are due. The authors are also indebted to Mr. Saburo Nakada of this Laboratory for the microanalytical data.

Department of Applied Chemistry
Faculty of Engineering
Keio University
Koganei-shi, Tokyo

*Corundum α-Al_2O_3 Formation from the Dehydration of Boehmite γ-AlOOH under Hydrothermal Conditions. I. Factors Determining the Grain Size of Corundum and a Proposal for the Formation Mechanism**

By Goro YAMAGUCHI and Hiroaki YANAGIDA

(Received May 22, 1963)

The fact that aluminum hydroxides are transformed into corundum through dehydration in a relativery low temperature range near 400°C under hydrothermal conditions has been noted by Laubengayer and Weisz,[2] Ervin and Osborn[3] and Kennedy,[4] while the temperature of transformation by calcination in air is usually above 1000°C. Using this reaction, the present authors obtained grains consisting of separated single crystals of corundum of a uniform size and habit of hexagonal plate or column ;[5] the grains showed excellent qualities as abrasive material.[6] It is worth clarifying the mechanism of this reaction as an approach to the investigation of the processes of solid phase formation. The solubilities of corundum and boehmite under the condition of corundum formation from boehmite have been discussed in a previous paper.[7] In the present paper, the grain size of corundum crystals obtained under various hydrothermal conditions with such varying factors as reaction temperature, hydrothermal pressure and quantity of the seed crystals of corundum, has been measured to provide other information for a discussion of the formation mechanism.

Experimental

Procedure.—Aluminum hydroxide, boehmite or gibbsite is weighed and laid in a Bridgeman-sealed Morey-type reactor with an aqueous solution of alkali. The reactor is then heated to an appointed temperature within 15 min. in an electric furnace and kept at the temperature for enough hours to convert the boehmite completely into corundum. The hydrothermal pressure is calculated from the relation among the pressure, volume and temperature of the water after the table of Kennedy.[8] The reactor is quenched to room temperature, also within 15min. and the corundum residue is washed out with pure water into a glass beaker.

Grain Size Determination. — The grain size of corundum is measured by the sedimentation method using Shimadzu's sedimentograph. Glycerol diluted with pure water is used as a sedimentation medium. The viscosity of the medium is calculated from the relation among the viscosity, density and temperature of glycerin diluted with water.[9]

Results

1) The Effect of Reaction Temperature.— The grain size of corundum crystals obtained when the pressure was 1000 atm., the solvent was a 0.1 N sodium hydroxide solution, and the temperature was 460 to 550°C was measured. The results are shown in Fig. 1, while the appearance of the corundum crystal is shown in Fig. 2. The shape of the corundum crystal is scarecely at all similar to that of boehmite,

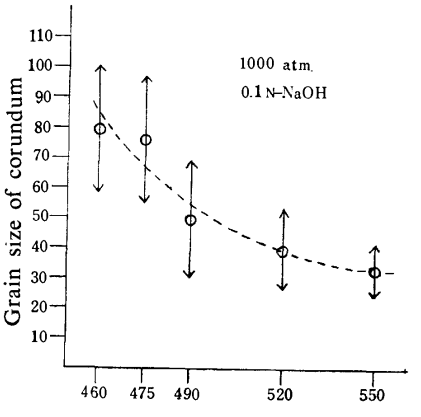

Fig. 1. Relation between grain size of corundum and hydrothermal temperature.

* This paper is subtitled "Investigations into the Processes of Solid Phase Formation" No. 2. The first paper was "On the Reaction Mechanism of Boehmite Formation from the Dehydration of Gibbsite"[1].

1) G. Yamaguchi and H. Yanagida, *J. Chem. Soc. Japan, Ind. Chem. Sec.* (*Kogyo Kagaku Zasshi*) **66**, 770 (1963).

2) A. W. Laubengayer and R. S. Weisz, *J. Am. Chem. Soc.*, **65**, 247 (1943).

3) G. Ervin, Jr. and E. F. Osborn, *J. Geol.*, **59**, 391 (1951).

4) G. C. Kennedy, *Am. J. Sci.*, **257**, 563 (1959).

5) G. Yamaguchi and H. Yanagida, Abstracts of the 13th Annual Meeting of the Chemical Society of Japan, No. 5A27 (Tokyo, April, 1960).

6) G. Yamaguchi, H. Yanagida, Y. Suwa and S. Soejima, Symposium on Artificial Minerals, No. 2-2 (Osaka, November, 1961)

7) G. Yamaguchi, H. Yanagida and S. Soejima, This Bulletin, **35**, 1789 (1962).

8) G. C. Kennedy, *Am. J. Sci.*, **248**, 540 (1950).

9) "Kagaku-Benran" Ed. by the Chemical Society of Japan, Maruzen Co., Ltd., Tokyo 1958.

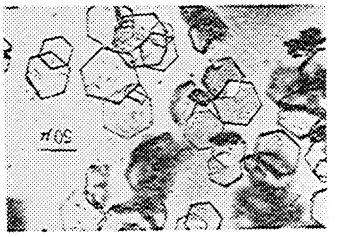

Fig. 2. Corundum obtained at 490°C under 1000 atm.

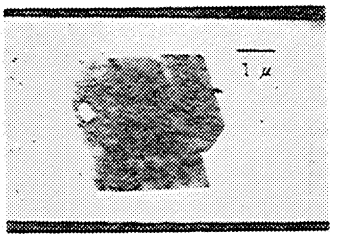

Fig. 3. Boehmite as starting material.

the starting material, as Fig. 3 shows. This suggests that the reaction of corundum formation under the conditions of the present section is due to a dissolution-precipitation process. The activation energy of the nucleation process of corundum should be larger than that of crystal growth judging from the fact that the grain size of corundum is decreased with the rise of temperature.

2) The Effect of Hydrothermal Pressure.—The grain size of corundum obtained when the temperature was 500°C, the solvent was a 0.1 N sodium carbonate solution, and the hydrothermal pressure was 250 to 1500 atm. was also measured. The results are shown in Fig. 4. The appearance of the crystals of corundum are shown in Figs. 5 and 6. The figures show that corundum obtained under lower hydrothermal pressure has a less perfect shape than that obtained under higher pressure. The former seems to be composed of aggregates of small crystals. This phenomenon is closely related to that of boehmite formation from gibbsite under various hydrothermal pressure.[1] In that case, boehmite was formed in its own rhombic tabular shape, as is shown in Fig. 3, when the nucleus of boehmite was formed and grew practically in a free hydrothermal solvent, while boehmite was formed as an aggregate of fine crystals with the original shape of gibbsite when the processes took place within the original grain. In the present case of corundum formation from boehmite, the nucleus formation and the crystal growth of corundum seem to occur practically in a free hydrothermal solvent not enclosed within boehmite grain when the hydrothermal pressure is higher, and so when the solvent is rich and dence, whreas the processes seems to occur within the grain when the pressure is lower, and so when the solvent is poor in outer free space.

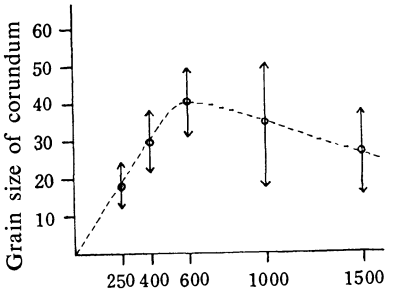

Fig. 4. Relation between grain size of corundum and hydrothermal pressure.

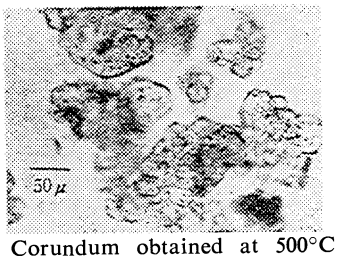

Fig. 5. Corundum obtained at 500°C under 250 atm.

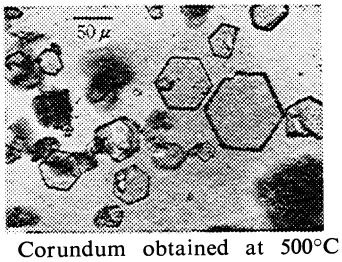

Fig. 6. Corundum obtained at 500°C under 1000 atm.

3) The Effect of the Addition of Seed Crystals of Corundum.—Corundum was formed from boehmite hydrothermally above 440°C when no seed crystal of corundum was added.[2,5,7] The equilibrium point between boehmite and corundum, however, should be 370°C under 1000 atm.[10-12] An equilibrium relation between two species must be discussed for the condition when the two co-exist, if the reaction of the formation of the more stable phase is of great activation energy of nucleation.[11] By the addition of seed crystals of corundum, the induction period before the initiation of corundum formation can be considerably

10) H. Yanagida "Research on the Synthesis of Minerals," Master Degree Thesis, The University of Tokyo (1960).
11) H. Yanagida, "Hydrothermal Reactions of Aluminas," Ph. D. Thesis, The University of Tokyo (1963).
12) G. Yamaguchi and H. Yanagida, to be published later in This Bulletin.

TABLE I. EFFECT OF ADDITION OF SEED CRYSTAL OF CORUNDUM UPON THE GRAIN SIZE OF NEWLY FORMED CORUNDUM IN 0.01 N NaOH SOLUTION UNDER 1000 ATM. AT 450°C

Addition of seed crystals of corundum			Newly formed corundum
		Surface area	
μ	g.	cm^2	μ
—	—	—	55.0±16.0
2.1	0.5	2.5×10^3	2.8± 1.1
2.1	1.0	5.0×10^3	1.8± 1.2
47.0	0.5	100	29.2± 7.5
500	0.1	2.0	34.2±10.4

shortened,[11,12] as Table I shows, the grain size of the newly-formed corundum is decreased. The results was obtained when the temperature was 450°C, the solvent was a 0.01 N sodium hydroxide solution, and the pressure was 1000 atm. with the addition of various quantities, of seed crystals of corundum. The larger the surface area of the seed crystals of corundum, the finer the size of the newly-formed corundum. It is supposed, therefore, that the crystal as seed promotes the nucleus formation. Since the effect was also observed when the seed crystal was far separated from boehmite grain in the reactor, the nucleation process must also take place in outer free space, not enclosed within the original boehmite grain, when some seed crystals are present. The seed crystal grew a little and the boehmite grain was converted into corundum even when boehmite existed metastably without any addition of corundum seed crystals. Moreover, the corundum crystal newly obtained from boehmite behaves as new seed. Just after the initiation of corundum formation when no seed crystals of corundum were added, as has been in preseding sections, therefore, the corundum behaved as seed and the nucleation process and the growth took place in the free space instead.

Summary of the Results and Some Suggestions.—The results may be summarized as follows; (1) The corundum crystal in most cases is in the shape of hexagonal plate (the habit modification is discussed in another paper)[13] except when the hydrothermal pressure is lower and the solvent is poor. (2) The grain size of corundum decreases with the rise of the reaction temperature. (3) By the addition of seed crystals of corundum, the grain size of newly-formed corundum can be decreased. These findings suggest that; (a) the reaction of corundum formation is closely related to that of boehmite formation from gibbsite; (b) according to the first finding, the reaction is carried out through a hydrothermal dissolution-precipitation process; (c) the nucleation process is of a higher activation energy than the growth; (d) the nucleus is formed both within the original boehmite grain and in the free space of a solution (the latter contribution becomes larger if the solvent is rich enough or if some corundum seed crystals have formerly been added); (e) after the initiation of corundum formation, the newly-formed corundum acts as new seed, and (f) the process of crystal growth takes place practically always in the free space of a solution, not within the original boehmite grain; the growth within it is noticeable when the outer solvent is poor, as when hydrothermal pressure is low.

13) G. Yamaguchi, H. Yanagida and S. Ono, *J. Ceram. Assoc. Japan*, 71, 182 (1963).

Conclusion

A Proposal for the Mechanism of Corundum Formation under Hydrothermal Conditions. — Considering these results, the present authors propose the reaction schema shown in Fig. 7 for the formation mechanism of corundum under hydrothermal conditions. This schema

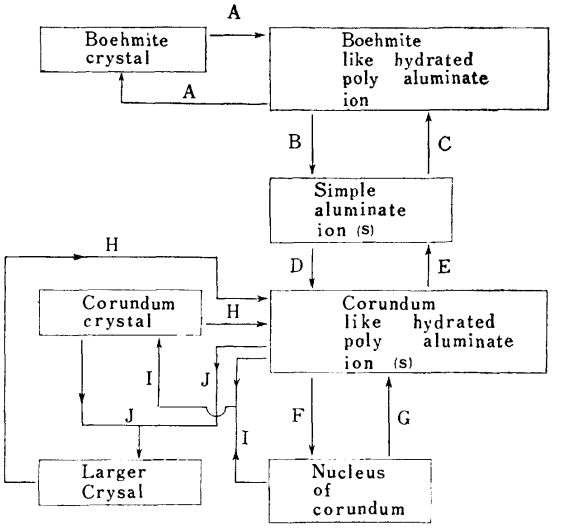

Fig. 7. Reaction schema for corundum formation.

is closely related to that of boehmite formation from the dehydration of gibbsite.[1] In that schema, gibbsite and boehmite were in the positions of boehmite and corundum respectively in the present schema. The most important hypothesis of these proposals is the existence of certain hydrated polyions whose structure is like the corresponding crystal lattice. Process A in Fig. 7 involves the dissolution of boehmite to boehmite-like hydrated polyions and process A', the precipitation of boehmite.

Process A′ is more complex in fact and is carried out through a cycle similar to that of the F, G, H and I processes; it is, however, written here in a simplified way. Process B indicates the dissociation of boehmite-like hydrated polyions into such simpler ones as $Al(OH)_4^-$ or $Al(H_2O)_2(OH)_4^-$, and C, the process of their association. The dissolution equation of aluminas in the previous paper[7] shows that an equilibrium among A, B, C and D has already been attained when the reaction temperature reaches above 400°C. Process D indicates the association of the simpler aluminate ions into corundum-like hydrated poly-aluminate ions, and E, the process of the dissociation. Process D, the present authors propose, is of high activation energy and it becomes the rate-determining one when the poly ions are not present at all. The seed crystals of corundum, whether added formerly or newly formed, supply the polyions according to Process H. The corundum-like hydrated poly aluminate ions are characterized by the structure of the two nearest aluminum ions being jointed through three oxygen atoms as in corundum lattice, while that of the boehmite-like one is of the nearest two aluminum ions being jointed through one or two oxygen atoms as in boehmite lattice. Process F indicates the nucleus formation of corundum crystal through the polymerization of the corundum-like polyions and G, the process of its depolymerization. Further polymerization results in the precipitation of corundum crystals according to Process I. The corundum crystals grows through Process J and at the same time supplies the polyions through the Process H.

Explanation of the Results According to the Reaction Schema.—The results in the present work can be explained with this reaction schema as follows. Finding (1) in the summary of the results in the preceding section is due to the reaction schema of a dissolution-precipitation process; Finding (2) is interpreted as meaning that the activation energy of the nucleation of corundum, Processes D and F, especially D at the early stage of the reaction, when any corundum seed crystals are not added, is larger than that of crystal growth J, and Finding (3) is due to the fact that the addition of corundum seed crystals makes it possible to initiate Process F and to promote Process D through Process H, and (e), therefore, is due to the fact that newly-formed corundum supplies the polyions through the Process H.

A reaction mechanism of corundum formation under hydrothermal condition has been discussed on the basis of the findings that the grain size of corundum varies with the hydrothermal conditions of temperature, pressure, and the addition of corundum seed crystals. The present authors have proposed a reaction schema by adapting the conception of hydrated poly aluminate ions with crystal lattice structure as proposed in the previous paper.[1] The reaction schema will be discussed also in a later paper[12] in connection with the results concerned with the reaction velocity of corundum formation under various hydrothermal conditions.

We wish to thank Mr. Toru Hashimoto for his co-operation in this work.

Department of Industrial Chemistry
Faculty of Engineering
The University of Tokyo
Hongo, Tokyo

The Crystal Structure of Purpureo Salt, $[Co(NH_3)_5Cl]Cl_2$

By Yoshihiko SHIGETA, Yoshimichi KOMIYAMA and Hisao KUROYA

(Received May 25, 1963)

A series of monoacido-pentaammine-cobalt-(III) complexes of the $[Co(NH_3)_5L]X_2$* type have been extensively investigated with respect to their light absorptions, their substitution reactions, and so on. However, there have been few reports on their crystal structures. In 1935, West determined the crystal structure of the chloro-pentaamine-rhodium(III) chloride, $[Rh(NH_3)_5Cl]Cl_2$[1] and, furthermore, found, by means of the powder photographic method, that the corresponding cobaltic salt is isotype to this rhodium(III) compound; he did not, however, give any details of the structure of the former.

Therefore, in order to determine exactly the way of packing in the crystalline state, the chloro-pentaammine-cobalt(III) chloride or "purpureo salt," $[Co(NH_3)_5Cl]Cl_2$, was taken up, and an X-ray analysis of its crystal structure was attempted. It should be noted that this compound is one of the most fundamental of the Werner complexes.

Experimental

Purpureo-cobaltic salt was prepared by Jörgensen's method.[2] The crystals for our X-ray work were grown slowly at room temperature from an aqueous solution as concentrated as possible. They are orthorhombic-bipyramidal, showing a pseudo-regular octahedral shape.

Ni$K\alpha$ radiation (1.659 Å) was used, and a multiple-film technique was employed in taking Weissenberg photographs about the three principal axes. The dimensions of the unit cell, the space group, and other crystallographic data were found to be as follows:

$a=13.34\pm0.03$, $b=10.33\pm0.03$, $c=6.73\pm0.02$ Å;

Puma-D_{2h}^{16}, $Z=4$,

$\rho_{obs}=1.77$ g. cm^{-3} (25°C), $\rho_{calcd}=1.79$ g. cm^{-3}

The relative intensities were estimated visually by comparison with a standard scale. The usual correction factors were applied by means of the chart given by Cochran,[3] while no correction for absorption was made.

* L denotes any univalent acid-radical working as a ligand.

1) C. D. West, *Z. Krist.*, **91**, 181 (1935).
2) S. M. Jörgensen, *Z. anorg. Chem.*, **17**, 461 (1898).
3) W. Cochran, *J. Sci. Inst.*, **25**, 253 (1949).

Determination of the Structure

Possibly, this compound is isostructural with the corresponding rhodium(III) compound, as has already been suggested by West. Therefore, the first trial model, based on the structure of the corresponding rhodium(III) compound, was immediately set up, the bond lengths and bond angles being properly adjusted. The agreement was fairly good between the observed structure amplitudes and those calculated for this model.

Then, all the parameter values were refined by the usual procedure of successive approximations. The final parameters are listed in Table I, while the final electron density projection along the b-axis is shown in Fig. 1. The observed structure factors are compared with the calculated ones in Table II. The atomic scattering factors used for calculating the structure factors were those listed in the International Tables. An overall temperature factor was used in the form of $\exp(-B\sin^2\theta/\lambda^2)$, where B has the value of 2.0 Å^2.

TABLE I. ATOMIC COORDINATES

Atom	x/a	y/b	z/c
Co	0.395	0.250	0.176
Cl(1)	0.528	0.250	−0.033
N_1	0.283	0.250	0.353
N_2	0.303	0.250	−0.055
N_3	0.487	0.250	0.407
N_4	0.395	0.059	0.176
N_5	0.395	0.441	0.176
Cl(2)	0.148	0.000	0.158

The $R=\sum||F_o|-|F_c||/\sum|F_o|$ reliability factors are 0.104, 0.073 and 0.121 for ($hk0$), ($0kl$) and ($h0l$) respectively. The weighted mean value of R is 0.109 for the observed reflections up to $\sin\theta/\lambda=0.590$.

Description of the Structure

The structure projected upon a plane normal to the b-axis is shown in Fig. 2, which corresponds to Fig. 1. Evidently, the crystal is composed of complex cations, $[Co(NH_3)_5Cl]^{2+}$, and chloride anions in an arrangement of the CaF_2-type; thus, the compound is essentially ionic.

TABLE II. OBSERVED AND CALCULATED STRUCTURE FACTORS

h k l	F_o	F_c	h k l	F_o	F_c	h k l	F_o	F_c	h k l	F_o	F_c	h k l	F_o	F_c
2 0 0	10.2	10.1	6 0 3	10.0	8.4	7 0 7	4.6	3.7	10 6 0	24.8	−20.6			
4 0 0	28.5	−30.3	7 0 3	16.5	−13.3	2 1 0	26.8	30.1	10 7 0	0	0.7			
6 0 0	9.7	6.9	8 0 3	6.1	5.1	2 2 0	22.4	−21.8	10 8 0	2.5	− 2.0			
8 0 0	19.3	18.1	9 0 3	16.0	16.4	2 3 0	12.7	−13.2	10 9 0	0	− 0.6			
10 0 0	4.8	5.0	10 0 3	4.9	4.0	2 4 0	6.7	5.3	12 1 0	6.4	6.9			
12 0 0	2.3	− 3.4	11 0 3	18.9	14.9	2 5 0	24.8	22.8	12 2 0	6.2	6.2			
14 0 0	1.9	− 3.5	12 0 3	3.0	2.0	2 6 0	17.6	−14.7	12 3 0	0	− 3.1			
0 2 0	19.1	−18.7	13 0 3	11.0	−10.4	2 7 0	9.3	−10.3	12 4 0	3.1	− 2.3			
0 4 0	68.0	66.4	14 0 3	2.5	2.1	2 8 0	2.6	2.5	12 5 0	6.1	6.7			
0 6 0	18.8	−19.0	1 0 4	23.0	21.2	2 9 0	7.3	8.2	12 6 0	3.9	5.0			
0 8 0	30.5	31.2	2 0 4	5.7	6.4	2 10 0	9.3	− 8.7	12 7 0	0	− 3.0			
0 10 0	9.0	− 9.2	3 0 4	17.7	17.7	2 11 0	7.7	− 7.7	14 1 0	2.2	− 0.8			
0 12 0	18.3	18.1	4 0 4	13.1	13.9	2 12 0	0	1.8	14 2 0	15.5	14.4			
0 0 2	14.1	−13.8	5 0 4	16.2	−16.5	4 1 0	4.8	− 2.7	14 3 0	2.3	1.3			
0 0 4	15.2	−15.3	6 0 4	3.2	− 1.9	4 2 0	32.4	−26.0	14 4 0	1.2	− 1.2			
0 0 6	20.6	22.0	7 0 4	13.9	−14.1	4 3 0	10.1	7.3	14 5 0	1.4	− 0.5			
1 0 1	13.5	−13.4	8 0 4	6.1	− 6.0	4 4 0	17.8	−17.1	0 1 1	31.8	−30.0			
2 0 1	9.1	10.5	9 0 4	1.9	− 1.4	4 5 0	1.2	0.4	0 3 1	9.3	13.5			
3 0 1	13.9	−12.2	10 0 4	3.4	1.7	4 6 0	11.0	− 7.6	0 5 1	23.2	−22.4			
4 0 1	25.3	25.2	11 0 4	0	1.6	4 7 0	2.9	2.1	0 7 1	7.9	− 8.0			
5 0 1	5.9	5.4	12 0 4	2.1	− 1.9	4 8 0	8.4	− 8.1	0 9 1	8.8	− 8.3			
6 0 1	0	− 1.2	13 0 4	0	1.7	4 9 0	0	− 1.2	0 11 1	7.7	7.8			
7 0 1	10.8	9.7	1 0 5	11.6	−11.8	4 10 0	6.5	− 4.7	0 2 2	21.4	−17.0			
8 0 1	28.3	−25.4	2 0 5	4.5	1.8	4 11 0	1.2	0.0	0 4 2	5.1	− 6.6			
9 0 1	10.6	− 8.2	3 0 5	2.7	− 2.7	6 1 0	14.9	−15.0	0 6 2	6.2	− 5.3			
10 0 1	6.8	6.2	4 0 5	4.6	− 4.5	6 2 0	14.7	14.4	0 8 2	1.6	− 2.4			
11 0 1	8.3	− 6.2	5 0 5	5.7	6.5	6 3 0	6.9	7.6	0 10 2	3.8	− 3.5			
12 0 1	25.4	19.1	6 0 5	0	1.3	6 4 0	11.7	8.5	0 1 3	8.5	7.8			
13 0 1	15.9	11.7	7 0 5	3.4	1.2	6 5 0	13.9	−13.4	0 3 3	5.7	− 5.5			
14 0 1	0.9	0.1	8 0 5	21.7	21.8	6 6 0	15.5	14.4	0 5 3	6.7	6.3			
15 0 1	7.6	6.4	9 0 5	11.0	− 9.2	6 7 0	6.9	7.6	0 7 3	5.1	− 4.3			
1 0 2	28.3	−28.0	10 0 5	3.8	2.1	6 8 0	9.1	8.2	0 9 3	4.3	3.5			
2 0 2	8.2	8.8	11 0 5	4.9	− 4.6	6 9 0	5.9	− 6.6	0 11 3	3.7	− 3.1			
3 0 2	34.8	−34.8	12 0 5	7.6	− 9.8	6 10 0	9.1	9.0	0 2 4	10.2	− 9.0			
4 0 2	30.4	30.2	1 0 6	0	− 0.5	6 11 0	5.6	6.2	0 4 4	10.7	−11.1			
5 0 2	22.8	20.8	2 0 6	0	− 0.4	8 1 0	22.8	−23.4	0 6 4	7.3	− 5.8			
6 0 2	10.1	9.1	3 0 6	5.7	− 4.5	8 2 0	1.4	− 0.1	0 8 4	7.3	− 6.6			
7 0 2	10.1	12.2	4 0 6	17.9	−16.5	8 3 0	17.2	16.1	0 10 4	4.5	− 4.0			
8 0 2	7.6	− 8.3	5 0 6	7.6	− 6.5	8 4 0	14.5	13.3	0 1 5	18.9	17.7			
9 0 2	12.7	− 9.5	6 0 6	2.1	− 0.7	8 5 0	21.8	−19.9	0 3 5	12.7	−13.1			
10 0 2	0	− 2.5	7 0 6	0	0.1	8 6 0	2.8	− 2.4	0 5 5	15.8	15.2			
11 0 2	0	− 0.5	8 0 6	5.3	7.4	8 7 0	12.7	12.2	0 7 5	10.4	−10.3			
12 0 2	3.8	− 2.5	9 0 6	0	− 1.6	8 8 0	8.2	7.5	0 9 5	9.0	8.7			
13 0 2	5.1	− 3.6	10 0 6	2.1	− 0.7	8 9 0	11.0	−10.1	0 2 6	5.3	2.5			
14 0 2	0	− 1.0	1 0 7	4.6	2.4	8 10 0	2.3	− 1.5	0 4 6	16.6	17.0			
15 0 2	4.2	− 2.6	2 0 7	2.7	5.0	10 1 0	2.2	0.4	0 6 6	1.2	− 0.4			
1 0 3	3.6	− 1.6	3 0 7	6.1	− 6.9	10 2 0	23.7	−23.0	0 8 6	9.6	10.6			
2 0 3	6.3	− 6.4	4 0 7	10.1	9.4	10 3 0	1.1	0.9	0 1 7	0	− 2.3			
3 0 3	6.1	2.6	5 0 7	0	1.3	10 4 0	0	0.8	0 3 7	1.4	− 0.4			
4 0 3	3.8	5.6	6 0 7	0	− 0.6	10 5 0	0	0.5	0 5 7	0	− 2.9			
5 0 3	26.8	−26.8												

The interatomic distances and bond angles, calculated on the basis of the atomic parameters in Table I, are listed in Table III.

The cobalt atom is surrounded by four nitrogen atoms at the corners of a square (Co–$N_{2\sim5}$, 1.97 Å), with one more nitrogen atom (Co–N_1, 1.91 Å) and one chlorine atom (Co–Cl (1), 2.27 Å) just below or above,

completing a slightly distorted octahedral coordination. One remarkably shorter distance between Co and $NH_3(1)$, which is in trans-position to Cl, has been found also in the case of $[Co(NH_3)_3(NO_2)_2Cl]$.[4] The other Co-N bonds are normal in length, as in $[Co(NH_3)_6]^{3+}$, where the nitrogen atoms are all equidistant from the cobalt atom (Co–N, 2.02 Å or so).

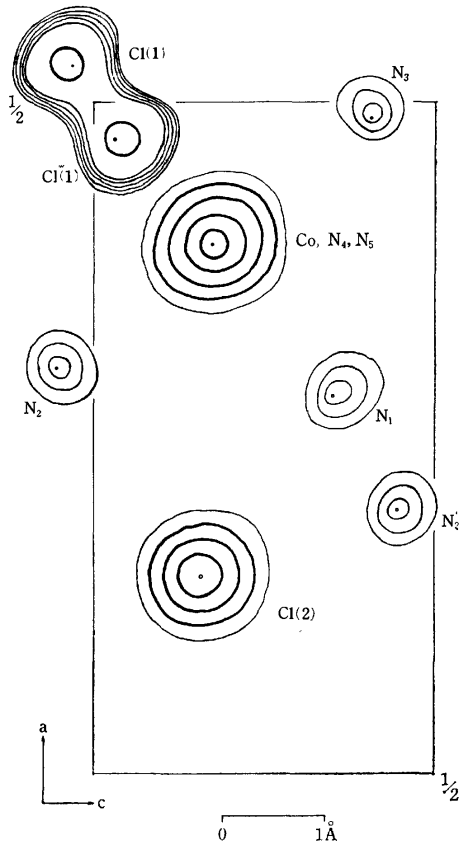

Fig. 1. Contours are drawn at intervals of 2e. $Å^{-2}$, starting at two electron level. Contours above 10e. $Å^{-2}$ are drawn at 10e. $Å^{-2}$ with thick lines.

The occurrence of one significantly shorter Co–NH_3 bond is to be noted. This may be because, working as a strongly electronegative ligand, the chlorine atom exerts its influence, if any, most effectively upon a ligand lying in the trans position to it, since to a first approximation the chlorine atom and the ligand can be regarded as bound to one another through the d_{z^2}, p_z and s orbitals of the central cobalt atom.

According to West, there is no distinction between the five Rh–NH_3 bonds involved in $[Rh(NH_3)_5Cl]^{2+}$. This might be shown not to be the case, however, if the structure of this rhodium(III) compound* were more refined.

4) Y. Tanito, Y. Saito and H. Kuroya, This Bulletin, 26, 420 (1953).

Table III. Interatomic distances and bond angles

Co—Cl(1)	2.27 Å
Co—N_1	1.91
Co—N_2	1.97
Co—N_3	1.98
Co—N_4	1.97
Co—N_5	1.97
Cl(1)···Cl(2)	3.95
N_3···Cl(2)	3.39
N_4···Cl(2)	3.60
N_5···Cl(2)	3.60
N_3'···Cl(2)	3.57
N_4'···Cl(2)	3.35
N_5'···Cl(2)	3.35
N_1'···Cl(2)	3.43
N_2''···Cl(2)	3.61
N_4''···Cl(2)	3.36
N_5''···Cl(2)	3.36
N_1''···Cl(2)	3.41
Cl'''(1)···Cl(2)	4.06
N_2'''···Cl(2)	3.29
N_4'''···Cl(2)	3.59
N_5'''···Cl(2)	3.59
Cl(1)···N_1''	3.61
Cl(1)···N_3'	3.81
Cl(2)···Cl'(2)	4.34
∠N-Co-N	90.0°
Cl(1)-Co-N	90.0
Co—N_4···Cl(2)	101.0
Co—N_5···Cl(2)	101.0
Co—N_3···Cl(2)	107.0
Co—N_3'···Cl(2)	93.8
Co'—N_4'···Cl(2)	100.0
Co'—N_5'···Cl(2)	100.0
Co'—N_1'···Cl(2)	99.1
Co''—N_2''···Cl(2)	93.4
Co''—N_4''···Cl(2)	101.5
Co''—N_5''···Cl(2)	101.5
Co''—N_1''···Cl(2)	93.7
Co'''—N_2'''···Cl(2)	111.5
Co'''—N_4'''···Cl(2)	91.2
Co'''—N_5'''···Cl(2)	91.2

* However, our recalculation based on the atomic coordinates reported by West revealed that the four NH_3-groups are not exactly in a plane normal to the N-Rh-Cl axis (see Fig. 3).

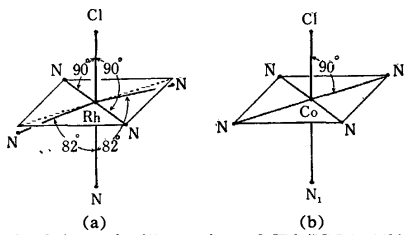

Fig. 3. Schematic illustration of $[Rh(NH_3)_5Cl]^{2+}$ (a) and $[Co(NH_3)_5Cl]^{2+}$ (b) ion.

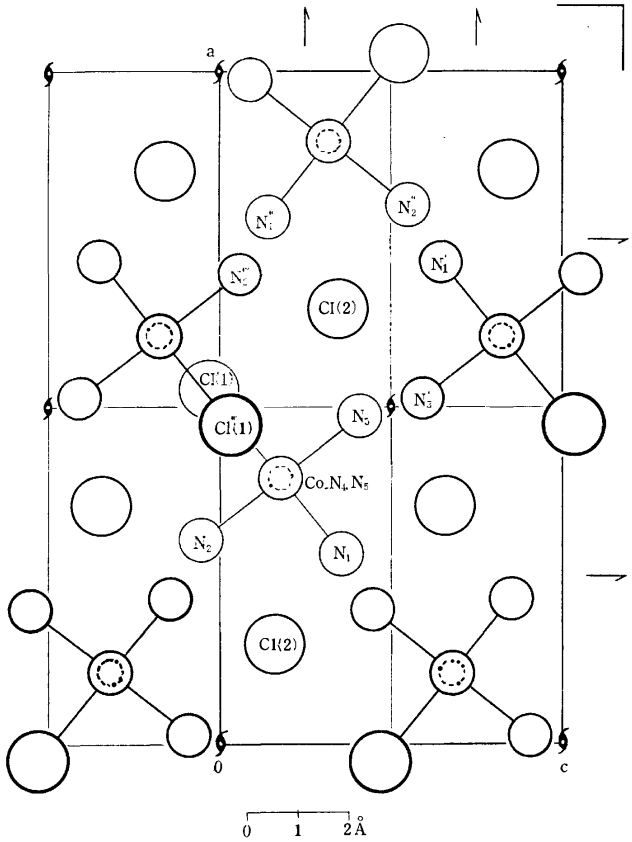

Fig. 2. Projection of the structure along the b-axis.

A chloride anion Cl(2) in the outer atmosphere is surrounded by fourteen NH_3 groups at distances ranging from 3.29 Å to 3.61 Å, as well as by two coordinated chlorine atoms at distances of 3.95 Å and 4.06 Å. Considerations of the distances of $NH_3\cdots Cl(2)$, the angles of Co–N···Cl(2) and the way of packing lead us to the view that the hydrogen bonding is not unfavorable for the following four links of N–H···Cl(2):

	N···Cl(2)	∠Co–N···Cl(2)
N_3—H···Cl(2)	3.39 Å	107.0°
N_5'—H···Cl(2)	3.35	100.0
N_4''—H···Cl (2)	3.36	101.5
N_2'''—H···Cl (2)	3.29	111.5

Summary

The crystal structure of $[Co(NH_3)_5Cl]Cl_2$ has been determined by the two-dimensional Fourier method. The orthorhombic unit cell has dimensions of $a=13.34$, $b=10.33$ and $c=6.73$ Å, and it contains four formula units. The space group is Pnma–D_{2h}^{16}.

The shape and the size of a complex ion were found to be approximately similar to those of the crystal of the corresponding rhodium(III) compound.

One NH_3 group is co-ordinated to the central cobalt atom in the trans position to the chlorine atom; the Co–N(1) distance is 1.91 Å, rather shorter than the four other Co–N distances, 1.97 Å.

Part of the cost of this study has been defrayed by a grant from the Ministry of Education, to which the authors' thanks are due.

Faculty of Science
Osaka City University
Sumiyoshi-ku, Osaka

X-Ray Diffraction Studies of the Molecular Complexes of Tetracycline Salts

By Shigeharu INOUYE and Yoichi IITAKA

(Received April 22, 1963)

In addition to the usual 1 : 1 type of molecular compounds formed by an antibiotic tetracycline with such other substancs as γ-butyrolactone,[1] urea,[2] or methanol,[3] tetracycline sulfate forms a series of complexes with the general formula: [2 tetracycline] sulfate·complexing agent·10 water, where "complexing agent" denotes a second molecule, such as an aliphatic carboxylic acid or a derivative of urea, having a rather smaller molecular volume. In a dry atmosphere, however, the decahydrate readily loses 4 molec. of water to form a relatively stable hexahydrate, while the crystal lattices are simultaneously rearranged. The latter dehydrated sulfate-complexes have been the subject of previous investigations,[4,5] and from the close resemblance of their X-ray diffraction powder patterns, a clathrate-like structure has been suggested for them. The formation of similar sulfate-complexes has been observed with oxytetracycline, but not with chlorotetracycline.[6]

This communication is concerned with a crystallographic investigation of the decahydrated sulfate-complexes, together with a classification of the powder patterns of various salt-complexes, including fluosilicate-, hydrochloride-, and nitrate-complexes, as well as of sulfate-complexes.

Experimental

Preparation.—Neutral hydrated tetracycline or oxytetracycline (1 mmol.) is dissolved in water (3~5 ml.) by the addition of strong acid (1~1.5 mequiv.). The complexing agent (2.5 mmol.) is dissolved in the solution under gentle heating. Removing unsoluble compounds by filtration, the solution is cooled to obtain the salt-complexes as crystallites. When guanidine sulfate, dimethylglyoxime or glyoxal, for example, is added to the solution as a complexing agent, crystals are obtained in which water molecules are enclosed in place of guanidine sulfate, etc.

Most of the salt-complexes were obtained as fine crystalline powders. However, when the supersaturated solution was kept in a refrigerator without shock for several days, some of the sulfate-complexes grew in a form of needles elongated along the b-axis, showing {001} as the principal face and often twinned on {001}. The single crystals are yellow in color and show a marked pleochroism.

When the salt anion is sulfate or fluosilicate, the salt-complexes usually crystallize as decahydrates. Hexahydrates of these salt-complexes are prepared by storing the original decahydrates over silica gel at room temperature overnight. Most of the hydrochloride- and nitrate-complexes, as well as a few of the sulfate- and fluosilicate-complexes, crystallize from an aqueous solution directly as hexahydrates. In Table I, the hexahydrates that crystallize directly are distinguished by an asterisk.

Analysis.—The chemical analyses of the composition of the salt-complexes have been reported in previous papers.[4-7] The specific gravity of a single crystal was determined by flotation in a mixture of carbon tetrachloride and chloroform at 20°C. The values given in Table II, however, are not expected to be more accurate than $\pm$ 0.02, since the crystals were subjected to dehydration.

X-Ray Measurement.—X-Ray diffraction powder patterns were taken by means of CuK_α radiation using a Norelco diffractometer. The powder patterns of the decahydrates were measured using undried specimens, for they are readily converted into partially dehydrated forms when exposed to dried air.

Single crystal X-ray photographs of oscillation, rotation, and Weissenberg were taken by means of CuK_α radiation. The unit cell parameters recorded in Table II were calculated mainly from the oscillation and (*h*0*l*) Weissenberg photographs about the b-axis. The mean errors for the monoclinic cell dimensions are *a*, $\pm$ 0.04; *b*, $\pm$ 0.02; *c*, $\pm$ 0.04 Å, and β, $\pm$ 0.2°, whilst for orthorhombic cells, they are $\pm$ 0.04, $\pm$ 0.03, and $\pm$ 0.05 Å for the a, b, and c-axes respectively. In the case of the dehydrated sulfate-complexes, the errors may exceed the above values, since the reflections consist of diffuse spots. A comparison among the intensities of corresponding X-ray reflections was made mainly on the (*h*0*l*) and (*h*1*l*) Weissenberg photographs for the 11 different salt-complexes of the *d*α form shown in Table II.

1) E. Gans and T. Higuchi, *J. Am. Pharm. Assoc.*, **46**, 587 (1957).
2) L. L. Smith, S. A. Muller, M. Marx, R. Winterbottom and A. P. Doerschuk, *J. Org. Chem.*, **23**, 721 (1958).
3) A. Soder and W. Siedel, Japanese Pat. 34-8746 (1959).
4) H. Ogawa and S. Inouye, *Bull. Agr. Chem. Soc. Japan*, **24**, 657 (1960).
5) S. Inouye, *Chem. Pharm. Bull.*, **9**, 417 (1961).
6) S. Inouye and H. Ogawa, *Agr. Biol. Chem.*, **25**, 333 (1961).
7) S. Inouye, Thesis, The University of Tokyo (1962).

TABLE I. CLASSIFICATION OF SALT-COMPLEXES OF TETRACYCLINE (TC) AND OXYTETRACYCLINE (OTC) ACCORDING TO X-RAY DIFFRACTION POWDER PATTERNS

Decahydrate

Salt-complex of the *dα* Form

TC Sulfate-complex
Acetic acid
Acrylic acid
Aspartic acid
Cyanamide
Dicyanodiamide
Formic acid
Fumaric acid
Glycolic acid
Hydantoin
Malonic acid
Methyl hydrogenoxalate
Monobromoacetic acid
Monochloroacetic acid
Oxalic acid
Propionic acid
Pyrazine
Succinimide
Thioacetic acid
Water

TC Fluosilicate-complex
Acetic acid
Dicyanodiamide
Formamide
Formic acid
Hydantoin
Monochloroacetic acid
Succinimide

OTC Sulfate-complex
Acetic acid
Monochloroacetic acid
Propionic acid

Salt-complex of the *dβ* Form

TC Sulfate-complex
Ascorbic acid
Glutaric acid
Malonic acid
Parabanic acid

Other Salt-complex

TC Sulfate-complex
Dimethyl carbonate
Pyruvic acid

TC Hydrochloride-complex
Oxalic acid

TC Fluosilicate-complex
Oxalic acid

OTC Sulfate-complex
Fumaric acid
Oxalic acid
Succinic acid

Hexahydrate

Salt-complex of the *hγ* Form

TC Sulfate-complex
Acetic acid
Aspartic acid
Cyanamide
Dicyanodiamide
Formic acid
Fumaric acid
Glycolic acid
Hydantoin
Malonic acid
Monochloroacetic acid
Oxalic acid
Pyrazine
Water

OTC Sulfate-complex
Acetic acid
Monochloroacetic acid
Oxalic acid

Salt-complex of the *hδ* Form

TC Sulfate-complex
Acetic acid
Acrylic acid
Ascorbic acid
Biuret*
Dimethyl carbonate
Formamide*
Glutaric acid
Malonic acid
Methyl hydrogenoxalate
Monobromoacetic acid
Monochloroacetic acid
Propionic acid
Pyruvic acid
Thioacetic acid
Thioglycolic acid

Urethan*

TC Hydrochloride-complex
Oxalic acid
Pyrazine*
Succinimide*

TC Nitrate-complex
Biuret*
Oxalic acid*

TC Fluosilicate-complex
Acetic acid

TC Hydrobromide-complex
Oxalic acid*

OTC Hydrochloride-complex
Pyrazine

Other Salt-complex

TC Sulfate-complex
Parabanic acid

TC Hydrochloride-complex
Hydantoin*
Parabanic acid*

TC Nitrate-complex
Hydantoin*
Parabanic acid*
Succinimide*

TC Fluosilicate-complex
Biuret*
Dicyanodiamide
Formamide
Formic acid
Hydantoin
Urethan*

* The salt-complex that crystallizes directly as a hexahydrate.

Results and Discussion

Table I shows a classification of the salt-complexes according to their powder patterns. Many of the salt-complexes belong to one of four distinct groups, that is, the *dα*, *dβ*, *hγ*, *hδ* forms, in which *dα* and *dβ* are the crystal forms found in decahydrates, and *hγ* and *hδ* are those found in hexahydrates. Figure 1 illustrates their typical powder patterns. Besides these, several other variations of the above forms are also recognized; these are shown in Table I as "other salt-complex," but they are not mentioned further in this paper.

The general characters of each of these four forms are set out below.

The *dα* Form.—*Sulfate-complexes.*—To this group belong most of the sulfate-complexes of decahydrate, namely, 19 members so far examined. Since all of them show striking

TABLE II. UNIT CELLS AND SPECIFIC GRAVITIES OF SALT-COMPLEXES

Tetracycline salt-complex	Form	System	a, Å	b, Å	c, Å	β	Specific gravity	
							Calcd.	Found
Sulfate-acetic acid	$d\alpha$	Monoclinic	15.87	10.50	17.36	109°00′	1.49	1.49
Sulfate-aspartic acid	$d\alpha$	Mcnoclinic	15.82	10.50	17.32	109°12′	1.49[d]	1.49
Sulfate-fumaric acid	$d\alpha$	Monoclinic	15.81	10.50	17.34	108°36′	1.56[e]	1.52
Sulfate-malonic acid	$d\alpha$	Monoclinic	15.93	10.50	17.50	109°12′		
Sulfate-monobromoacetic acid	$d\alpha$	Monoclinic	15.79	10.49	17.46	108°40′	1.58	1.55
Sulfate-monochloroacetic acid	$d\alpha$	Monoclinic	15.90	10.50	17.38	108°48′	1.525	1.52
Sulfate-oxalic acid	$d\alpha$	Monoclinic	15.72	10.50	17.44	109°06′	1.555	1.53
Sulfate-propionic acid	$d\alpha$	Monoclinic	15.72	10.49	17.40	108°24′	1.51	1.49
Sulfate-water[a]	$d\alpha$	Monoclinic	15.90	10.50	17.35	109°12′	1.46	1.47
Sulfate-water[b]	$d\alpha$	Monoclinic	15.82	10.49	17.31	109°00′	1.46	1.47
Fluosilicate-monochloroacetic acid	$d\alpha$	Monoclinic	15.91	10.49	17.50	109°00′		
Oxytetracycline sulfate-acetic acid	$d\alpha$	Monoclinic	15.79	10.50	17.40	108°12′	1.52	1.515
Sulfate-glutaric acid	$d\beta$	Orthorhombic	16.05	10.50	32.40	90°00′		
Sulfate-malonic acid	$d\beta$	Orthorhombic	15.97	10.53	32.13	90°00′	1.55	1.52
Sulfate-oxalic acid[c]	$h\gamma$	Monoclinic	16.02	10.50	14.69	102°		
Sulfate-water[c]	$h\gamma$	Monoclinic	16.00	10.50	14.83	102°		

a) The dodecahydrate crystallized in the presence of guanidine sulfate.
b) The dodecahydrate crystallized in the presence of dimethylglyoxime.
c) The hexahydrate prepared by the partial dehydration of the decahydrate.
d) Calculated for $2C_{22}H_{24}O_8N_2$-H_2SO_4-2/5$C_4H_7O_4N$-10H_2O.
e) Calculated for $2C_{22}H_{24}O_8N_2$-H_2SO_4-4/5$C_4H_4O_4$-10H_2O.

similarities in their powder patterns, it was assumed that they possess essentially the same unit cell dimensions and symmetry. In order to confirm this point, X-ray single crystal patterns of 9 different kinds of sulfate-complexes were examined; it was, indeed, found that the unit cell dimensions are nearly

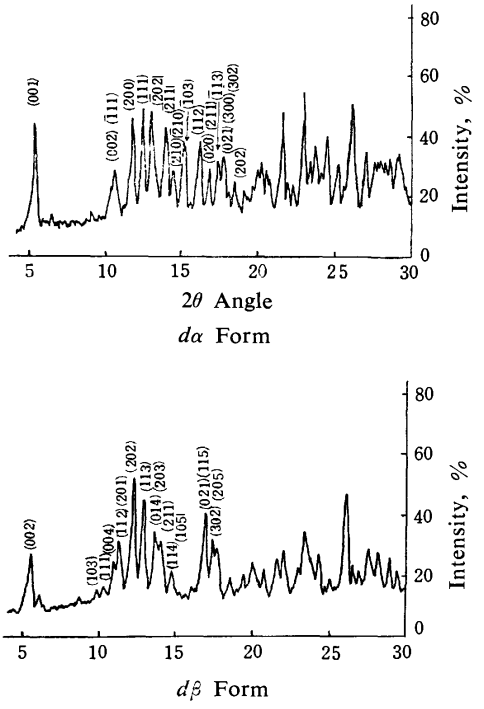

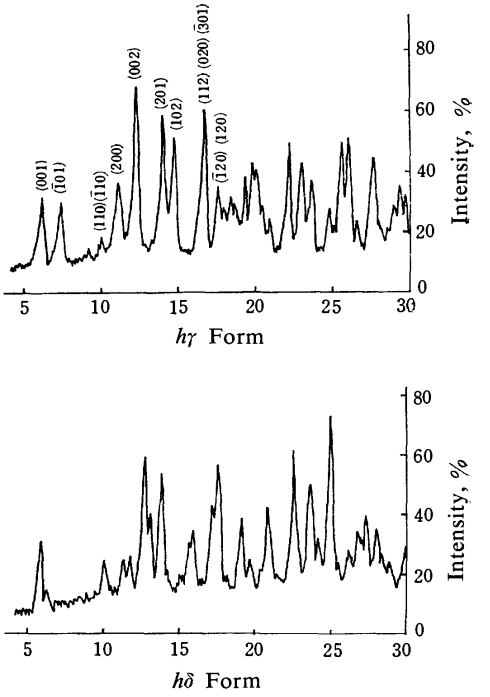

Fig. 1. X-Ray diffraction powder patterns of the four crystal forms.

the same in all of them, as Table II shows. Generally, the cell dimensions are in the range a=15.7~15.9, b=10.5, c=17.3~17.5 Å, and β=108~109°. Taking into consideration the optically-active character of the tetracycline

melecule coupled with the systematic absence, $(0\,k\,0)$ when k is odd, the space group of the $d\alpha$ form was determined as $P2_1$. In nearly every case, there are [2 molec. of tetracycline], one sulfate, one molecule of a complexing agent, and 10 molec. of water in each asymmetric unit, as calculated from the cell volume and the density given in Table II.

Fluosilicate-complexes. — Seven of the fluosilicate-complexes so far examined gave powder patterns very similar to those of the corresponding sulfate-complexes. The isomorphous series of sulfate-complexes, therefore, seems to be extended to include the fluosilicate-complexes. In fact, the monoclinic cell parameters of the fluosilicate-monochloroacetic acid complex were found to be $a=15.91$, $b=10.49$, $c=17.50$ Å and $\beta=109°00'$, figures are indistinguishable from those of its sulfate-complex.

Oxytetracycline Sulfate-complexes.—In addition to the oxytetracycline sulfate-acetic acid complex, whose cell parameters were $a=15.79$, $b=10.50$, $c=17.40$ Å, and $\beta=108°12'$, two more members (sulfate-propionic acid and -monochloroacetic acid complexes) are found to belong to the $d\alpha$ form.

The above results, together with the similar compositions of the salt-complexes, indicate that the molecular packings within the isomorphous salt-complexes of the $d\alpha$ form are very similar. No influence of the complexing agent was observed in determining the crystal structure. Molecules so chemically diverse as water, formic acid, oxalic acid, hydantoin, and dicyanodiamide are considered to be interchangeable in the $d\alpha$-type unit cell without any considerable enlargement or contraction of the cell dimensions.

In the isomorphous molecular compounds, which contained such a variety of chemical compounds, it does not seem likely that the binding force arises primarily from ion-dipole interactions as in the case of the tetraethylammonium bromide succinimide complex.[8] The formation of such a co-ordination compound is subjected to restriction not only by a charge distribution of the complexing agents but also by dimensional factors, so that even chemically-analogous substances may not form similar co-ordination compounds.[9] Therefore, it seems reasonable that the crystal strcutures of the $d\alpha$ form consist of an almost identical framework of the tetracycline (or oxytetracycline) molecules enclosing spaces capable of containing a complexing agent, just as those observed in inclusion compounds.

Further sppport for this point comes from a consideration of the restricted size (50~120 Å^3) and shape (co-planarity) of the complexing agent, as has been discussed previously,[7] and particularly from a detailed comparison of the X-ray diffraction intensities as a whole. Among the $d\alpha$-type sulfate-complexes given in Table II, there is a notable intensity resemblance when due allowance is made for the differences in absorption effect. For example, the difference in intensity between the sulfate-monobromoacetic acid and -propinic acid complexes of tetracycline is less than the difference between two sulfate-acetic acid complexes of tetracycline and oxytetracycline. Since the crystal structures of these complexes are isomorphous, it is to be expected that the differences in intensity of the corresponding reflections are due largely to the different scattering contributions of the complexing agents. However, the above finding suggests that they make only a small contribution. This may be explained, as in the case of the β-quinol clathrate,[10] by the freedom of motion or the statistical disorderness of the complexing agents in the cavities.

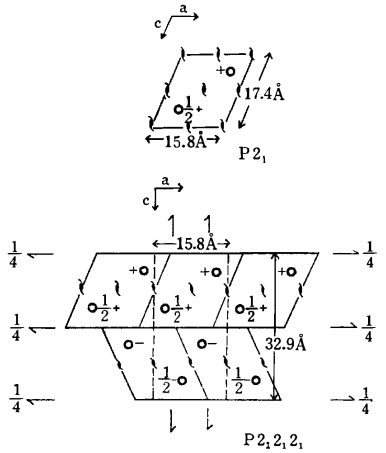

Fig. 2. Relationship between the $d\alpha$ type monoclinic cell ($P2_1$) and the $d\beta$ type orthorhombic cell ($P2_12_12_1$) (projection along [010]).

The $d\beta$ Form.—The $d\beta$ from is found in a few decahydrated sulfate-complexes, that is, sulfate-malonic acid, -glutaric acid, -parabanic acid and ascorbic acid complexes. Since sulfate-malonic acid complex also crystallizes in the $d\alpha$ form, the $d\beta$ form is evidently a polymorphic modification of the $d\alpha$ form. The crystals of the $d\beta$ form are orthorhombic, with the space group $P\,2_12_12_1$ and with cell dimensions of $a=16.0$, $b=10.5$, $c=32.1$~32.4 Å ; there are 4 units in a cell, each unit consisting of [2

8) H. M. Powell and E. Wait, *J. Chem. Soc.*, **1958**, 1866.
9) H. M. Powell, *J. Inorg. & Nuclear Chem.*, **8**, 546 (1958).
10) D. E. Palin and H. M. Powell, *J. Chem. Soc.*, **1947**, 208.

tetracycline] sulfate, one complexing agent and 10 water molecules. A comparison of these parameters with those of the $d\alpha$ form reveals that a and b are almost identical with those of the $d\alpha$ form, whilst c corresponds to $2c_{d\alpha}\sin\beta$. If two monoclinic cells of the $d\alpha$ form are twinned, as in Fig. 2, where the twinning axis is the twofold screw axis lying at $y=1/4$ or 3/4 in the (001), the newly-formed orthorhombic cell has cell dimensions and a space group which are nearly identical with those of the $d\beta$ form. It is, therefore, possible that the $d\beta$ form is really a monoclinic substance submicroscopically twinned, thus exhibiting orthorhombic symmetry.* If so, the molecular packing must be essentially the same in both the $d\alpha$ and $d\beta$ forms, in spite of the apparent differences in unit cell dimensions and symmetry.

In this connection, it is interesting to note that the monoclinic crystals of the $d\alpha$ form are often twinned on a plane parallel to (001), giving apparent orthorhombic symmetry on the $h0l$ reflections. However, a careful examination of the Weissenberg photographs shows that they are, in fact, made up of the superposition of the sets of reflections from each of the untwinned crystals. In this case, therefore, each component part of the twinned crystal is large enough compared with a coherent region of X-rays.

The $h\gamma$ Form.—The $h\gamma$ form is found in the hexahydrates produced by the partial dehydration of the decahydrated sulfate-complexes: about one-half of the $d\alpha$-type sulfate-complexes fall into the $h\gamma$ form on dehydration. When a single crystal of the $d\alpha$-type sulfate-oxalic acid or -water complex was kept in dried air for a few minutes, diffuse spots due to the partial dehydrates appeared on the X-ray photograph, superposed on the normal diffraction spots. From the oscillation and ($h0l$) Weissenberg photographs about the b-axis of the dehydrated crystals, the approximate monoclinic cell dimensions of the $h\gamma$ form were found to be $a=16.0$, $b=10.5$, $c=14.7$ Å and $\beta=102°$ (Table II). The reliability of the proposed parameters may be judged further from the indexing of the powder pattern shown in Table III, in which there is no significant discrepancy between the observed and calculated diffraction angles.

Since all the powder patterns belonging to the $h\gamma$ form are very similar, it is reasonable, as in the case of the $d\alpha$ form, to assume the existence of the same essential framework among the $h\gamma$-type sulfate-complexes. It is to be noted, however, that, unlike the $d\alpha$ and $h\delta$ forms, where other salt-complexes besides sulfate-complexes are isomorphous members, the formation of the $h\gamma$ form is limited to the sulfate-complexes, insofar as we have been able to determine. This suggests that a sulfate anion plays an important part in determining the common framework of the $h\gamma$ form.

Table III. Indexing and Comparison of the Observed and Calculated Diffraction 2θ Angles for the Powder Patterns of the $d\alpha$ and $h\gamma$ Forms

$d\alpha$ Form			$h\gamma$ Form		
hkl	Calcd.	Found	hkl	Calcd.	Found
001	5.35°	5.35°	001	6.1 °	6.1 °
002, $\bar{1}11$	10.7	10.7	$\bar{1}01$	7.4	7.3
			$\bar{1}10$	10.15	10.05
200	11.9	11.9	200	11.3	11.3
111	12.5	12.5	002	12.3	12.3
$\bar{2}02$	13.25	13.2	201	14.0	14.0
$\bar{2}11$	14.2	14.1	102	14.6	14.6
210	14.6	14.6	112, 020, $\bar{3}01$	16.9	16.8
$\bar{1}03$	15.3	15.3			
112	16.2	16.2	120	17.8	17.7
020	16.9	16.9			
$\bar{1}13$	17.5	17.5			

As may be seen from a comparison of the cell parameters of the $d\alpha$ and $h\gamma$ forms, it is apparent that the escape of 8 mol. of water from the the $d\alpha$-type unit cell causes a decrease in the c-axis length (2.7 Å) and in the β angle (7°). According to an infrared analysis,[11] the lattice deformation probably corresponds to the approach of a complexing agent to a sulfate anion. In contrast to the $d\alpha$ form, where the sulfate anion holds tetrahedral symmetry as a whole, in the $h\gamma$ form a splitting of the sulfate bands is observed, this can be reasonably interpreted as a lowering of the T_d symmetry caused by interaction between a complexing agent and a sulfate anion.

The $h\delta$ Form.—The $h\delta$ form is a polymorphic modification of the $h\gamma$ form, for some of the hexahydrates, for example, sulfate-acetic acid or -monochloroacetic acid complex, crystallize in both of these forms. Though its unit cell dimensions were not determined, many hexahydrates of the sulfate-, nitrate-, hydrochloride-, and hydrobromide-complexes belong to this group (Table I).

A particularly interesting phenomenon observed in this group is that the powder patterns of 4 different kinds of salt-complexes, namely, the hydrochloride-oxalic acid, hydrobromide-oxalic acid, nitrate-oxalic acid and

* Such submicroscopic twinning is often found in minerals (T. Ito, "X-Ray Studies on Polymorphism," Maruzen, Tokyo (1950)).

11) S. Inouye, *Chem. Pharm. Bull.*, in press (1963).

sulfate-methyl hydrogenoxalate complexes, are quite similar to one another, suggesting the isomorphous replacement of Cl^-, Br^-, NO_3^- and SO^{2-} anions among these crystals.

Summary

An examination of the salt-complexes of tetracycline and oxytetracycline by the X-ray powder method has shown the presence of at least four different kinds of crystal structures, i. e., the *dα*, *dβ*, *hγ*, and *hδ* forms. Among them, the *dα* form has been studied in detail by the use of single crystals. The monoclinic unit cell dimensions of the *dα* crystals do not vary much either with a salt anion or with a complexing agent, and the intensities of the various reflections so far examined are very similar. On the basis of these findings, it is suggested that the crystal structures of the *dα*-type salt-complexes consist of an almost identical framework of tetracycline or oxytetracycline molecules which encloses spaces capable of containing complexing agents of various types. The orthorhombic *dβ* form is a polymorphic modification of the *dα* form, probably arising from submicroscopically polysynthetic twinning of the latter.

The authors wish to express their gratitude to Professor Toshihiko Okamoto and Professor Masamichi Tsuboi of the University of Tokyo, and to Dr. Hiroshi Ogawa of this laboratory, for their interest and encouragement. Thanks are also due to Dr. Kazuhiko Ohta and Messrs. Katsumi Hamano and Tomoya Ogawa for the use of their X-ray facilities.

Central Research Laboratories of
Meiji Seika Kaisha, Ltd.
Morooka, Yokohama (S. I.)

Faculty of Pharmaceutical Sciences
The University of Tokyo
Hongo, Tokyo (Y. I.)

A Consideration of the Q-e Scheme. IV. A Theoretical Approach to Price-Alfrey's Polarity Term

By Nariyoshi KAWABATA, Takayuki FUENO, Teiji TSURUTA and Junji FURUKAWA

(Received April 24, 1963)

Part I of this series[1] described a revised pattern of Price-Alfrey's *Q-e* scheme[2] which assumed the *e*-value of styrene to be equal to zero. In Part II,[3] we tried to give some theoretical background for this scheme. We divided the conjugation-stabilization energy between the monomer and the attacking radical, E_{RM}, into four terms by means of the following equation:

$$E_{RM} = E_{RoMo} + E_R + E_M + E'_{RM} \quad (1)$$

Here, E_{RoMo} is the stabilization energy between the polyethylene radical and the ethylene monomer, and E_R and E_M are the increments in the stabilization energy over E_{RoMo} as the standard introduced by the substituents in the polymer radical and in the monomer molecule respectively. E'_{RM} is the surplus increment in the stabilization energy introduced by the substituents of the radical and the monomer. We proposed relations 2 to 4 for the *P*-, *Q*- and *e*-terms:

$$P \propto \exp(E_R/\boldsymbol{RT}) \quad (2)$$

$$\ln Q_1 - \ln Q_2 = (E_{M_1} - E_{M_2})/\boldsymbol{RT} \quad (3)$$

$$e_R e_M = -E'_{RM}/\boldsymbol{RT} \quad (4)$$

The classical interpretation of the *P*-, *Q*- and *e*-terms is obviously different from ours, especially in the explanation of the polarity term. According to the classical interpretation,[2b] *e* is proportional to the charge on the end group of the radical or the monomer. Both of the two interpretations correlate with experimental facts; therefore, some theoretical interrelation may exist between them. The electronic charge on the end group of the radical or the monomer seems to be introduced mainly by heteroatoms. Therefore, we tried to investigate the effect of heteroatoms on the *Q-e* terms.

1) N. Kawabata, T. Tsuruta and J. Furukawa, *Makromol. Chem.*, **51**, 70 (1962).
2) a) T. Alfrey, Jr., and C. C. Price, *J. Polymer Sci.*, **2**, 101 (1947). b) T. Alfrey, Jr., J. J. Bohrer and H. Mark, "Copolymerization," Interscience Publisher, New York (1952).
3) N. Kawabata, T. Tsuruta and J. Furukawa, *Makromol. Chem.*, **51**, 80 (1962).

The Effect of Heteroatoms on the Conjugation-stabilization Energy. — In Part II of this series,[3] we proposed relations 2—4 for the *P*-, *Q*- and *e*-terms. Therefore, we would like now to investigate the effect of heteroatoms on the stabilization energy in order to examine their effect on the *Q-e* terms.

The conjugation-stabilization energy, E_{RM}, was calculated by the following equation.[3-5]

$$E_{RM}=2\left(\sum_{i}^{occ}\sum_{j}^{unocc}-\sum_{j}^{occ}\sum_{i}^{unocc}\right)\frac{(C_r^j)^2(C_m^i)^2}{E_j-E_i}(\Delta\beta)^2+\left(\sum_{i}^{occ}-\sum_{i}^{unocc}\right)\frac{(C_r^h)^2(C_m^i)^2}{E_h-E_i}(\Delta\beta)^2 \quad (5)$$

where C_r^j and C_m^i are the coefficients of the rth and the mth atomic π-orbitals in the jth and the ith molecular orbitals belonging to the eigenvalues E_j and E_i in the radical and the monomer respectively. E_h and C_r^h are the energy of the half-occupied orbital of the radical and the coefficient of the rth π-orbital in this MO respectively. $\sum^{occ}$ and $\sum^{unocc}$ imply summation over all the occupied (except the half-occupied) and all the unoccupied molecular orbitals. When the r'th atom of the radical and the m'th atom of the monomer are replaced with the heteroatoms Y and X respectively, E_j, E_i, $(C_r^j)^2$ and $(C_m^i)^2$ will become,[6] respectively:

$$E_i+\delta E_i=E_i+(C_m^i)^2\delta X \quad (6)$$

$$E_j+\delta E_j=E_j+(C_{r'}^j)^2\delta Y \quad (7)$$

$$(C_m^i)^2+\delta(C_m^i)^2=(C_m^i)^2+2C_m^iC_{m'}^i\sum_{p\neq i}\frac{C_m^pC_{m'}^p}{E_i-E_p}\delta X+\lambda_m(\delta X)^2 \quad (8)^*$$

$$(C_r^j)^2+\delta(C_r^j)^2=(C_r^j)^2+2C_r^jC_{r'}^j\sum_{q\neq j}\frac{C_r^qC_{r'}^q}{E_j-E_q}\delta Y+\lambda_r(\delta Y)^2 \quad (9)^*$$

where δX and δY are the respective increments of the Coulomb integrals for the heteroatoms X and Y. E_{RM} then becomes

$$E_{RM}=2\left(\sum_{i}^{occ}\sum_{j}^{unocc}-\sum_{j}^{occ}\sum_{i}^{unocc}\right)\times\frac{\{(C_m^i)^2+\delta(C_m^i)^2\}\{(C_r^j)^2+\delta(C_r^j)^2\}}{(E_j+\delta E_j)-(E_i+\delta E_i)}(\Delta\beta)^2+\left(\sum_{i}^{occ}-\sum_{i}^{unocc}\right)\times\frac{\{(C_m^i)^2+\delta(C_m^i)^2\}\{(C_r^h)^2+\delta(C_r^h)^2\}}{(E_h+\delta E_h)-(E_i+\delta E_i)}(\Delta\beta)^2 \quad (10)$$

Therefore, when, by the use of Eq. 11, we separate the stabilization energy into four terms in order to investigate the effect of the heteroatoms, the E_r, E_m and E'_{rm} terms can be given by Eqs. 12—14.[7] Here, E_r and E_m are the increments in the stabilization energy introduced by the heteroatom of radical Y and by that of monomer X respectively. E'_{rm} is the surplus increment in the stabilization energy introduced by the heteroatoms of the radical and the monomer.

$$E_{RM}=E_{r_0m_0}+E_r+E_m+E'_{rm} \quad (11)$$

$$E_r=C_r(\delta Y)^2 \quad (12)^*$$

$$E_m=C_m(\delta X)^2 \quad (13)^*$$

$$E'_{rm}=-C'_{rm}(\delta X)(\delta Y) \quad (14)$$

C_m, C_r and C'_{rm} are positive constants characteristic of a series of monomers having a same skeletal structure, in which only the r'th atom of the radical and the m'th atom of the monomer are replaced by various heteroatoms.

A Theoretical Approach to Price-Alfrey's Polarity Term. — In Part II of this series,[3] we proposed relations 2—4. According to Price and Alfrey,[2] the rate constant of the propagation step, k_p, is expressed by:

$$k_p=PQ\exp(-e_Re_M) \quad (15)$$

Here, the polarity term is the product of e_R and e_M. Further, $e_{R_1}=e_{M_1}$ is assumed for the radical and the monomer of type 1. In these two points, Eq. 4 does not conform to the concept of Price and Alfrey. However, for each series of isoelectronic monomers having a same skeletal structure, in which a fixed

* $\lambda_m=(C_{m'}^i)^2\left(\sum_{p\neq i}\frac{C_m^pC_{m'}^p}{E_i-E_p}\right)^2+2C_m^iC_{m'}^i\sum_{l\neq i}\sum_{p\neq i}\frac{C_m^lC_{m'}^l(C_{m'}^p)^2}{(E_i-E_l)(E_i-E_p)}-2C_m^i(C_{m'}^i)^3\sum_{l\neq i}\frac{C_m^lC_{m'}^l}{(E_i-E_l)^2}$

$\lambda_r=(C_{r'}^j)^2\left(\sum_{q\neq j}\frac{C_r^qC_{r'}^q}{E_j-E_q}\right)^2+2C_r^jC_{r'}^j\sum_{n\neq j}\sum_{q\neq j}\frac{C_r^nC_{r'}^n(C_{r'}^q)^2}{(E_j-E_n)(E_j-E_q)}-2C_r^j(C_{r'}^j)^3\sum_{n\neq j}\frac{C_r^nC_{r'}^n}{(E_j-E_n)^2}$

* When the reference monomer and the reference radical are alternant hydrocarbons, the 1st order terms cancel after summation. Therefore, Eqs. 12 and 13 are free from 1st order terms. When the reference monomer or the reference radical is a non-alternant hydrocarbon, Eqs. 12 and 13 may not be correct, although such a case is of rare occurrence.

4) M. J. S. Dewar, *J. Am. Chem. Soc.*, 74, 3341 (1952).
5) T. Yonezawa, K. Hayashi, C. Nagata, S. Okamura and K. Fukui, *J. Polymer Sci.*, 14, 312 (1954); K. Hayashi, T. Yonezawa, C. Nagata. S. Okamura and K. Fukui, ibid., 20, 537 (1956).
6) C. A. Coulson and H. C. Longuet-Higgins, *Proc. Roy. Soc.*, A191, 39 (1947).
7) N. Kawabata, T. Fueno, T. Tsuruta and J. Furukawa, *J. Chem. Soc. Japan, Ind. Chem. Sec.* (*Kogyo Kagaku Zasshi*), 66, 836 (1963).

TABLE I. REVISED *Q*-*e* VALUES

Vinyl compound	*e*	*Q*
Vinylidene cyanide	3.5	200
Methyl α-phenylacrylate[9]	2.8	21
N-Vinylpyridinium-fluoroborate[10]	2.4	3.6
Di-β-chloroethyl itaconate	2.3	3.0
Methyl α-chloroacrylate	2.0	9
1,1-Dihydroperfluorobutyl acrylate	2.0	3.0
Chloroprene	2.0	2.0
p-Potassium styrenesulfonate	1.9	5.5
Acrylamide	1.9	3.0
Acrylonitrile	1.9	2.7
α-Acetoxyacrylonitrile	1.8	5
N-Benzylidene-4-methacryloxy-aniline	1.8	4
α,β,β-Trifluorostyrene	1.8	1.5
Methacrylonitrile	1.7	3.3
Dibutyl itaconate	1.6	3.8
Itaconic acid	1.6	3.3
Dimethy itaconate	1.6	2.1
n-Butyl vinyl sulfonate	1.6	0.4
Acrylic acid	1.6	0.4
N,*N*,*N*-Triethyl-*N*-(2-methacryloxy-ethyl)-ammonium iodide	1.5	4
Methyl vinyl ketone	1.5	3.5
Methacrylic acid	1.5	3.0
Acrolein	1.5	1.6
n-Octyl acrylate	1.5	1.5
Butyl acrylate	1.5	1.3
Abietyl acrylate	1.5	1.3
Methyl vinyl sulfone	1.5	0.5
Phenyl vinyl sulfone	1.5	0.3
Methyl thiolacrylate	1.4	3.0
Methyl acrylate	1.4	1.3
Pentachlorostyrene	1.4	0.8
Chlorotrifluoroethylene	1.4	0.14
Vinyl perfluorobutyrate	1.4	0.1
Tetrafluoroethylene	1.4	0.07
2,3-Dichloro-1,3-butadiene	1.3	25
4-Vinylpyrimidine	1.3	6
Stearyl methacrylate	1.3	1.9
β-Chloroethyl acrylate	1.3	1.8
Hydronopyl acrylate	1.3	1.5
Vinyl trifluoroacetate	1.3	0.03
p-Nitrostyrene	1.2	5.3
p-Sulfonamidostyrene	1.2	4.3
Methyl isopropenyl ketone	1.2	3.0
Ethyleneglycol dimethacrylate	1.2	2.9
Methacrolein	1.2	2.3
Decyl methacrylate	1.2	2.0
Methyl methacrylate	1.2	1.9
Ethyl methacrylylaminoacetate	1.2	1.8
Nonyl methacrylate	1.2	1.7
Ethyl methacrylate	1.2	1.5
Vinyl fluoride	1.2	0.09
p-Cyanostyrene	1.1	3.6
2-Vinylpyridine	1.1	1.8
Vinylidene chloride	1.1	0.5
2-Chloroallyl alcohol	1.1	0.08
m-Nitrostyrene	1.0	2.2
4-Vinylpyridine	1.0	1.7
n-Butyl methacrylate	1.0	1.5
Vinyl isothiocyanate	1.0	1.3
Ethyl acrylate	1.0	1.3
Allyl alcohol	1.0	0.15
2-(*N*,*N*-Dimethylamino)-4-vinylpyrimidine	0.9	2.9
Methacryloxymethylpentamethyl-disiloxane	0.9	1.3
Isobutyl methacrylate	0.9	1.2
2-Chloroallyl chloride	0.9	0.2
Allyl chloride	0.9	0.03
n-Octyl methacrylate	0.8	2.9
2,5-Bis(trifluoromethyl)styrene	0.8	2.2
Glycidyl methacrylate	0.8	1.5
n-Hexyl methacrylate	0.8	1.0
Methacrylamide	0.8	0.7
4-Methacryloxybenzylideneaniline	0.7	4.0
2-Fluoro-1,3-butadiene	0.7	2.0
m-Bromostyrene	0.7	1.8
Isopropenyl methacrylate	0.7	1.5
Allyl laurate	0.7	0.03
6-Chloro-2-vinylnaphthalene	0.6	2.5
m-Chlorostyrene	0.6	1.6
p-Iodostyrene	0.6	1.6
p-Chlorostyrene	0.6	1.4
p-Bromostyrene	0.6	1.4
N-(1,1-Dihydroperfluorobutyl)-*N*-ethyl acrylamide	0.6	1.2
4-Chloro-1-vinylnaphthalene	0.6	1.2
n-Amyl methacrylate	0.6	0.9
N-Vinylsuccinimide	0.6	0.14
Dimethallyl oxalate	0.6	0.06
Diallyl phthalate	0.6	0.03
4-Methacryloxybenzilidene-4'-chloroaniline	0.5	6
n-Propyl methacrylate	0.5	1.5
3-Trifluoromethylstylene	0.5	1.4
t-Butyl methacrylate	0.5	1.3
Isopropenylacetylene	0.5	0.6
4,6-Diamino-2-vinyl-*s*-triazine	0.4	2.6
Vinyl chloride	0.4	0.06
Sodium styrenesulfonate	0.3	2.6
o-Chlorostyrene	0.3	1.8
2-Methyl-5-vinylpyridine	0.3	1.3
Vinyl bromide	0.3	0.05
5-Ethyl-2-vinylpyridine	0.2	1.3
N-Methyl methacrylamide	0.2	0.4
Pentachlorophenyl vinyl sulfide	0.2	0.25
Vinyl isocyanate	0.2	0.13
Vinyl palmitate	0.2	0.02
Vinyl caprate	0.2	0.01
Vinyl dichloroacetate	0.1	0.05
2-Vinylphenanthrene	0.0	4

TABLE I. continued.

Vinyl compound	*e*	*Q*
3-Vinylphenanthrene	0.0	4
2-Vinylthiophene	0.0	2.9
2-Vinylquinoline	0.0	2.0
2-Vinylnaphthalene	0.0	2.0
Vinylacetylene	0.0	1.6
1-Vinylnaphthalene	0.0	1.5
p-Trimethoxysilylstyrene	0.0	1.4
N-(*p*-Tolyl) methacrylamide	0.0	1.3
1,3-Butadiene	0.0	1.3
α-Acetoxystyrene	0.0	1.1
m-Vinylphenol	0.0	1.1
m-Methylstyrene	0.0	1.0
Styrene	(0.0)	(1.00)
p-Trimethylsilylstyrene	0.0	1.0
o-Methylstyrene	0.0	0.9
N-Phenyl methacrylamide	0.0	0.9
Phenylacetylene	0.0	0.7
N-Ethyl methacrylamide	0.0	0.3
Isopropenyl isocyanate	0.0	0.14
Vinyl ethyl oxalate[11]	0.0	0.12
Vinyl formate	0.0	0.10
Vinyl chloroacetate	0.0	0.05
Vinyl butyrate	0.0	0.03
Vinyl propionate	0.0	0.03
Vinyl benzoate	0.0	0.03
Vinyl undecylenate	0.0	0.03
Vinyl pelargonate	0.0	0.03
N-Vinyl-2-oxazolidinone	0.0	0.03
Vinyl acetate	0.0	0.02
Tris(trimethylsiloxyl) vinylsilane	0.0	0.02
Vinyl laurate	0.0	0.01
Ethylene	0.0	0.01
Allyl acetate	0.0	0.01
2-Vinylmercaptobenzothiazole	−0.1	1.5
2,5-Dimethylstyrene	−0.1	1.0
p-Methylstyrene	−0.1	0.9
N-(*p*-Chlorophenyl) methacrylamide	−0.1	0.7
Ethyl vinyl sulfide	−0.1	0.2
Vinyl levulinate	−0.1	0.02
Bis(trimethylsiloxyl) vinylmethylsilane	−0.1	0.02
p-Acetylaminostyrene	−0.2	1.3
β-Isopropenylnaphthalene	−0.2	0.9
p-Methoxystyrene	−0.2	0.9
Divinyl sulfide	−0.2	0.5
N-Methyl-*N*-vinyl-*p*-toluenesulfonamide	−0.2	0.08
N-Vinylpyrrolidone	−0.2	0.08
Isopropenyl acetate	−0.2	0.03
Vinyl isocaproate	−0.2	0.03
Vinyl caprylate	−0.2	0.02
Vinyl pinonate	−0.2	0.02
Vinyl stearate	−0.2	0.02
Vinyl caproate	−0.2	0.02
Isoprene	−0.3	2.0
α-Methylstyrene	−0.3	1.1
N-(*p*-Anisyl) methacrylamide	−0.3	0.25
p-Dimethylaminostyrene	−0.4	1.0
Phenyl vinyl sulfide	−0.6	0.2
Isobutylene	−0.6	0.02
Methyl vinyl sulfide	−0.7	0.2
9-Vinyl carbazole	−0.9	0.2
N-Ethyl-*N'*-vinylurea	−1.1	0.05
N-Vinylurethane	−1.4	0.06
Isobutyl vinyl ether	−1.4	0.02

carbon atom of a reference monomer (ethylene, butadiene, styrene or another neutral monomer) is replaced by such a heteroatom as oxygen, nitrogen, etc., the surplus energy term, E'_{RM}, seems to satisfy the concept. For these series of monomers, Eqs. 2−4 can, respectively, be reduced to

$$P \propto \exp(E_r/\boldsymbol{RT}) \tag{16}$$

$$\ln Q - \ln Q_0 = E_m/\boldsymbol{RT} \tag{17}$$

$$e_R e_M = -E'_{rm}/\boldsymbol{RT} \tag{18}$$

Here, Q_0 is the *Q*-value of the reference monomer of a monomer series. From Eqs. 12, 13 and 14, Eqs. 16, 17 and 18 can, respectively, be reduced to:

$$P \propto \exp\{(C_r/\boldsymbol{RT})(\delta Y)^2\} \tag{19}$$

$$\ln Q - \ln Q_0 = (C_m/\boldsymbol{RT})(\delta X)^2 \tag{20}$$

$$e_R e_M = (C'_{rm}/\boldsymbol{RT})(\delta X)(\delta Y) \tag{21}$$

Here, C_r, C_m and C'_{rm} are constants characteristic of a series of monomers having a same skeletal structure. As can be seen in Eq. 21, the polarity term may reasonably be separated into two terms, e_R and e_M, for such a monomer series.

$$e_R = -\sqrt{C'_{rm}/\boldsymbol{RT}}(\delta Y) \tag{22}$$

$$e_M = -\sqrt{C'_{rm}/\boldsymbol{RT}}(\delta X) \tag{23}$$

The assumption by Price and Alfrey that $e_{R_1} = e_{M_1}$ for the radical and the monomer of type 1 also seems to be reasonable for a monomer series of the same skeletal type.

Revised *Q-e* Values. — On the basis of the copolymerization data collected by Young,[8] we calculated the revised *Q-e* values by assuming the *e*-value of styrene to be equal to zero. These values are given in Table I.

We also calculated the $e_R e_M$ values as the

8) L. J. Young, *J. Polymer Sci.*, 54, 411 (1961).
9) K. Chikanishi, unpublished finding.
10) Irl. N. Duling and C. C. Price, *J. Am. Chem. Soc.*, 84, 578 (1962).
11) N. Kawabata, T. Tsuruta and J. Furukawa, *Makromol. Chem.*, 48, 106 (1961).

products of the relevant e-values given in Table I. These $e_R e_M$ values were compared with the e_{RM} values.[1] For each series of isoelectronic monomers having a same skeletal structure, the average deviation of $e_R e_M$ from e_{RM} was about 7%. However, for other pairs of radical and monomer, the average error was nearly 35%. This finding shows the validity of our conclusion that the expression by Price and Alfrey is reasonable for a series of monomers having a same skeletal structure.

An Electrostatic Interpretation of the Polarity Term.—According to the classical interpretation,[2b] e is proportional to the charge on the end group of the radical or the monomer. In fact, a linear relation was observed between $q_R q_M$ and $e_R e_M$.[3] That is,

$$e_R e_M \propto q_R q_M \tag{24}$$

Here, q_R and q_M are π-electronic charges on the end groups of the radical and the monomer respectively. According to Price,[12] it would be a reasonable speculation to write

$$e_R e_M = \varepsilon_R \varepsilon_M / rDkT \tag{25}$$

Here, ε_R and ε_M are actual charges on the end groups of the radical and the monomer respectively. D is the effective dielectric constant, and r is the distance of separation in the activated complex. However, there has often been proposed a different opinion that the electron transfer from a donor radical to an acceptor monomer, or vice versa, in the activated complex may account for the alternation tendency.[3,13-18] For a series of monomers having a same skeletal structure, q_R and q_M can be expressed as follows on the basis of Eqs. 8 and 9:

$$q_R = -2\sum_{j}^{occ} \delta(C_r^j)^2 e - \delta(C_r^h)^2 e = C_R(\delta Y) \tag{26}$$

$$q_M = -2\sum_{i}^{occ} \delta(C_m^i)^2 e = C_M(\delta X) \tag{27}$$

Here, C_R and C_M are negative constants characteristic of the series of monomers. From Eqs. 22 and 26,

$$e_R = -(\sqrt{C'_{rm}/\boldsymbol{RT}}/C_R)q_R \tag{28}$$

From Eqs. 23 and 27,

$$e_M = -(\sqrt{C'_{rm}}/\boldsymbol{RT}/C_M)q_M \tag{29}$$

The correlation of the polarity term with the product of π-electronic charges (Eq. 24) seems to be ascribable to the relations 28 and 29.

Summary

Previously, we pointed out the correlations of the P-, Q- and e-terms with the components of the conjugation-stabilization energy between monomers and attacking radicals. In the present paper, the effect of heteroatoms on the components of the stabilization energy was investigated. For each series of isoelectronic monomers, in which a fixed carbon atom of a reference monomer (ethylene, styrene, butadiene or another neutral monomer) is replaced by a heteroatom (oxygen, nitrogen, etc.), we obtained the relations: $\ln Q - \ln Q_0 = (C_m/\boldsymbol{RT})(\delta X)^2$, $P \propto \exp(C_r/\boldsymbol{RT})(\delta Y)^2$, $e_R = -\sqrt{C'_{rm}/\boldsymbol{RT}}(\delta Y)$ and $e_M = -\sqrt{C'_{rm}/\boldsymbol{RT}}(\delta X)$. Here, C_m, C_r and C'_{rm} are positive constants characteristic of the monomer series, while δX and δY are the Coulomb integral increments of the heteroatoms (relative to a carbon atom) in the monomer X and the radical Y respectively. Q_0 is the Q-value of the reference monomer of the series. The e-values of the reference monomers were all assumed to be zero. The opinions of Price and Alfrey that the polarity term is the product of e_R and e_M and that $e_{R_1} = e_{M_1}$ for the radical and the monomer of type 1 seem to be not only convenient but also reasonable for a series of monomers having a same skeletal structure. The π-electronic charges, q_R and q_M, on the end groups of the radical and the monomer seem to be correlated with e_R and e_M in such a manner that $e_R = -(\sqrt{C'_{rm}/\boldsymbol{RT}}/C_R)q_R$ and $e_M = -(\sqrt{C'_{rm}/\boldsymbol{RT}}/C_M)q_M$. Here, C_R and C_M are negative constants characteristic of the series of monomers. The correlation of the polarity term with the electrostatic interaction between the charges of the radical and the monomer seems to be ascribable to these relations.

Department of Synthetic Chemistry
Kyoto University
Sakyo-ku, Kyoto

12) T. C. Schwan and C. C. Price, *J. Polymer Sci.*, **40**, 457 (1959).
13) F. M. Lewis, C. Walling, C. Cummings, E. R. Briggs and F. R. Mayo, *J. Am. Chem. Soc.*, **70**, 1519 (1948).
14) P. D. Bartlett and K. Nozaki, ibid., **68**, 1495 (1946).
15) F. R. Mayo and C. Walling, *Chem. Revs.*, **46**, 191 (1950).
16) F. R. Mayo, F. M. Lewis and C. Walling, *J. Am. Chem. Soc.*, **70** 1529 (1948).
17) G. S. Levinson, *J. Polymer Sci.*, **60**, 43 (1962).
18) P. J. Flory, "Principles of Polymer Chemistry," Cornell University Press, Ithaca (1953), Chap. 5.

The C-H Stretching Spectra and Intensities of Dihalogenomethanes and Intermolecular Interaction

By Utako KANBAYASHI

(Received April 17, 1963)

Many experiments and theoretical considerations concerning the vibrational spectra of dihalogenomethanes have been carried out.[1-7] Regarding the C–H stretching bands of each compound in the condensed phase, a band existing between 2970 and 3000 cm^{-1} was assigned to ν_1 (a symmetric stretching vibration) and another between 3040 and 3070 cm^{-1}, to ν_6 (an antisymmetric stretching vibration).

In the C–H stretching region of the infrared spectrum of dichloromethane vapor, there is found only a doublet centered at 2995 cm^{-1}. In the dilute solution state, a band of weak intensity appears on the high frequency side (3048 cm^{-1} in the case of the carbon tetrachloride solution), whereas none is observed in the vapor state. As the concentration of the solute increases, the absorptivity* of this band also increases, while that of the band of low frequencies (2983 cm^{-1} in the carbon tetrachloride solution) decreases. In the pure liquid, the former is much stronger than the latter, as Josien et al.[8] have indicated.

In ordinary cases, where the existence of intermolecular interaction, rotational isomerism, etc. can be ignored, neither the frequency nor the absorptivity of an infrared band changes appreciably as a function of the concentration in a non-polar solvent. Considering this well-known fact, it is very interesting to find such experimental results as have been presented above.

Experimental

The commercial products of dichloromethane, chlorobromomethane, dibromomethane, and diiodomethane were purified by distillation. Dimethoxymethane-d_6 was prepared at the author's laboratory.[9] The purity of these compounds was checked by means of gas chromatography.

The infrared spectra in the C–H stretching region were obtained by means of a Perkin-Elmer model 12 C spectrophotometer equipped with a lithium fluoride prism. The recording of spectra in the vapor state was made in cells with path lengths of 10 cm. and 100 cm. on dichloromethane and chlorobromomethane, 100 cm. on dibromomethane, and 10 cm. on dimethoxymethane-d_6, all at a total pressure of 1 atm. The recording of spectra in solution was made with carbon tetrachloride and carbon disulfide as the solvents, and at the following volume percentage concentrations: dichloromethane—50% (cell thickness, 0.10 mm.), 10% (0.2 and 0.5 mm.) and 1.0% (0.5 and 1.0 mm.); chlorobromomethane—50% (0.05 and 0.1 mm.), 10% (0.2 and 0.5 mm.) and 2% (0.5 and 1.0 mm.); dibromomethane—50% (0.01, 0.03 and 0.05 mm.), 10% (0.2 mm.) and 2% (1.0 mm.); diiodomethane—50% (0.03 and 0.05 mm.), 10% (0.2, 0.5 and 1.0 mm.), 5% (1.0 mm.) and 2% (1.0 and 5.0 mm.); and dimethoxymethane-d_6 (in carbon tetrachloride solution only)—25% (0.15 mm.). In the pure liquids spectral, measurements were made in cells 0.05 and 0.03 mm. thick for dichloromethane and chlorobromomethane, 0.03 and 0.014 mm. thick for dibromomethane and diiodomethane, and 0.014 mm. thick for dimethoxymethane-d_6.

Spectra were also obtained with a Perkin-Elmer model 21 spectrophotometer equipped with a sodium chloride prism on the compounds in the vapor state, in solution (solvent: carbon tetrachloride and carbon disulfide) and as pure liquids. Especially on dichloromethane, the variation in intensity and frequency with concentration was observed minutely with varied concentrations—the CH_2 bending vibration* (1425 cm^{-1}) and the CH_2 rocking vibration (895 cm^{-1}) in carbon tetrachloride solution, and the CH_2 wagging vibration (1154 cm^{-1}) and the C–Cl stretching vibrations (740 and 707 cm^{-1}) in carbon disulfide solution.

As for the Raman spectra, observation was made by means of a Cary model 81 spectrophotometer on dichloromethane, chlorobromomethane and dibromomethane in pure liquid and in carbon tetrachloride solution (50, 20 and 10% by volume). On the compounds in pure liquid, the qualitative degrees of depolarization were measured by alternately wrapping the Raman tube with two types of polarizing cylinders.

1) J. W. Straley, *J. Chem. Phys.*, 23, 2183 (1955).
2) J. Wagner, *Z. physik. Chem.*, 45, 69 (1940).
3) Ta-You Wu, *J. Chem. Phys.*, 10, 116 (1942).
4) J. C. Decius, ibid., 16, 214 (1948).
5) T. Shimanouchi, ibid., 17, 848 (1949).
6) E. K. Plyler and W. S. Benedict, *J. Research Natl. Bur. Standards*, 47, 202 (1951).
7) I. Suzuki and T. Shimanouchi, *J. Mol. Spectroscopy*, 6, 277 (1961).
8) M.-L. Josien, N. Fuson and A. Lafaix, *Compt. rend.*, 249, 256 (1959).
* $\frac{1}{cl}\log_{10}\frac{I_0}{I}$
9) K. Nukada, *Spectrochimica Acta*, 18, 745 (1962). *Reports Gov. Chem. Ind. Research Inst. Tokyo* (to be published).

* In pure liquid, dichloromethane has a band at 1425 cm^{-1} and a very weak shoulder at 1445 cm^{-1}. When it is diluted with carbon tetrachloride, the intensity at 1445 cm^{-1} becomes larger, but that at 1425 cm^{-1} becomes a bit smaller.

Results

Variation of the Relative Intensities.—*Infrared Spectra.*—The ratio of the absorbance of ν_6 to that of ν_1 (D_6/D_1) was computed from the observed spectra of the dihalogenomethanes and dimethoxymethane-d_6 by means of the base-line method.* In the cases of carbon tetrachloride and carbon disulfide solutions, plots of the observed values of D_6/D_1 against the concentration yield straight lines (see Figs. 2 and 3). If these straight lines are extended to zero concentration, the values of D_6/D_1 at

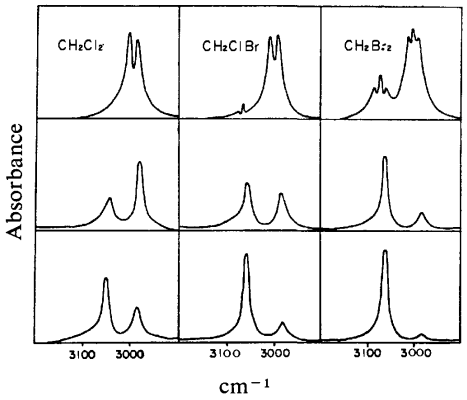

Fig. 1. C-H stretching spectra of CH_2Cl_2, CH_2ClBr, and CH_2Br_2 in vapor, carbon tetrachloride solution and in pure liquid.**
Upper row: Vapor
Middle row: Solution in carbon tetrachloride 10% by volume
Bottom row: Pure liquid

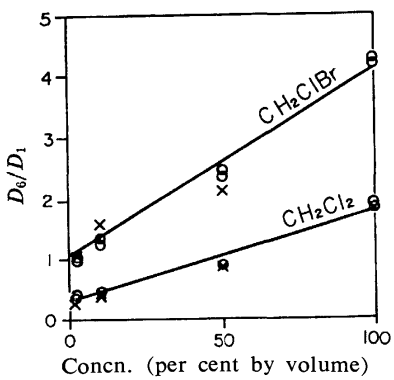

Fig. 2. Plot of D_6/D_1 vs. concentration in CCl_4 and CS_2 solutions for CH_2Cl_2 and CH_2ClBr.
○ CCl_4 solution and pure liquid
× CS_2 solution

* Since spectra were obtained with a single-beam spectrophotometer, the reproducibility of the observed values of absorbances was not very good. For this reason, ratios of absorbances were calculated.

** The absorptivities of C-H stretching bands vary with the kind of compound as well as with phase. So the absorbance is plotted on the ordinate axis.

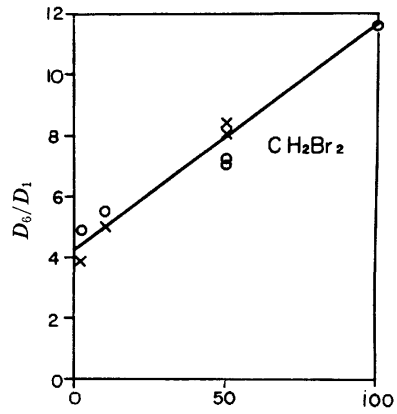

Fig. 3. Plot of D_6/D_1 vs. concentration in CCl_4 and CS_2 solutions for CH_2Br_2.
○ CCl_4 solution and pure liquid
× CS_2 solution

TABLE I. C-H STRETCHING FREQUENCIES OF DICHLOROMETHANE, CHLOROBROMOMETHANE, DIBROMOMETHANE AND DIIODOMETHANE IN cm^{-1}

	Infrared		Raman	
	ν_1	ν_6	ν_1	ν_6
Dichloromethane				
Vapor	3002, 2988	—	(3002)[a]	
Solution (CCl_4)[b]	2983	3048	2984	3044
Solution (CS_2)[b]	2974	3039		
Liquid	2987	3054	2986	3051
Solid	2983	3054		
Chlorobromomethane				
Vapor	3008, 2993	3078, 3065, —		
Solution (CCl_4)[b]	2987	3058	2986	3055
Solution (CS_2)[b]	2980	3049		
Liquid	2985	3059	2986	3055
Dibromomethane				
Vapor	3017, 3005, 2996	3087, 3077, 3065		
Solution (CCl_4)[b]	2986	3066	2993	3065
Solution (CS_2)[b]	2979	3059		
Liquid	2988	3064	2986	3060
Diiodomethane				
Vapor				
Solution (CCl_4)[b]	2981	3061		
Solution (CS_2)[b]	2975	3053		
Liquid	2968	3046		

a) J. Rud Nielsen and N. E. Ward, *J. Chem. Phys.*, **10**, 81 (1942).
b) Frequencies obtained by extrapolating to zero concentration are shown.

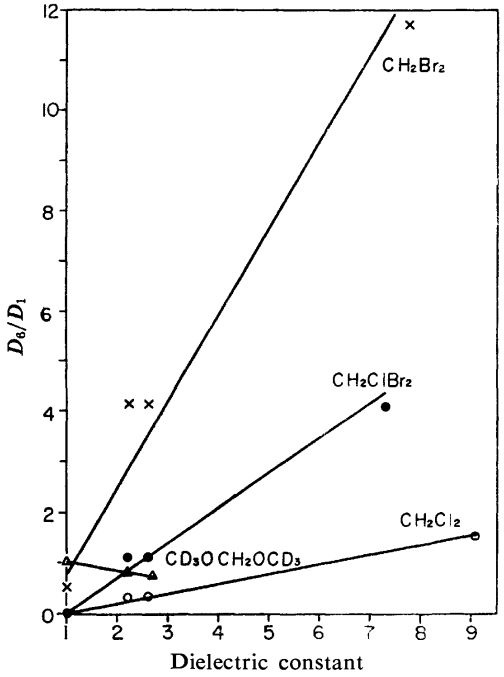

Fig. 4. Plot of D_6/D_1 vs. the dielectric constant of the medium for CH_2Cl_2 (○), CH_2ClBr (●), CH_2Br_2 (×) and CD_3OCH_2O-CD_3 (△).

infinite dilution in carbon tetrachloride and carbon disulfide solutions are obtained. Then, in the cases of chlorobromomethane, dibromomethane and dimethoxymethane-d_6, if the values of D_6/D_1 are plotted against the dielectric constants of the media (vapor, carbon tetrachloride, carbon disulfide and pure liquid), they fall on a straight line. (Fig. 4) Moreover, in the case of dichloromethane, if the values of D_6/D_1 in pure liquid and in carbon tetrachloride and carbon disulfide solutions are plotted against the dielectric constants of the media, the value of D_6/D_1 obtained by setting the dielectric constants at one (vapor) by extrapolation is nearly zero. This agrees well with the author's interpretation that, in vapor, the intensity of ν_6 is extremely weak. Details of this interpretation are given below.

As Fig. 4 shows, the value of D_6/D_1 increases with the dielectric constant in the cases of dichloromethane, chlorobromomethane and dibromomethane, but decreases in the case of dimethoxymethane-d_6.

In the case of dichloromethane, the variations in the band intensities with the concentration in the sodium chloride prism region, were observed to be smaller than those in the C-H stretching region.

Raman Spectra.—The relative intensity of ν_1 and ν_6 were estimated in the cases of dichloromethane, chlorobromomethane and dibromomethane in the pure liquid and in carbon tetrachloride solutions of various concentrations. The ratio of the peak intensity of ν_6 to that of ν_1 (h_6/h_1) shows no variation beyond the range of experimental errors. The values of h_6/h_1 are 0.16～0.18 for dichloromethane, 0.17～0.18 for chlorobromomethane, and 0.28～0.29 for dibromomethane.

Frequency Shifts.—When the compound is in a solution, the frequency shifts of ν_1 and ν_6 are linear functions of the concentration in both the infrared and Raman spectra. The slope varies with the kind of compound as well as with the kind of band and solvent. The frequencies shown in Table I for carbon tetrachloride and carbon disulfide solutions were obtained by extrapolation to zero concentration. When the compound is in a vapor, carbon tetrachloride solution or carbon disulfide solution, the relation between $(\nu_{vapor}-\nu_{solution})/\nu_{vapor}$ and $(\varepsilon-1)/(2\varepsilon+1)$ is approximately linear. However, the value in the case of a pure liquid is not on the same line.

Discussion

Assignment of C-H Stretching Vibrations of the Dichloromethane Molecule in Vapor. — In the infrared spectra of dichloromethane in the condensed phases, single bands are observed at about 2980 and 3050 cm^{-1}. However, in the vapor, only a doublet centered at 2995 cm^{-1} is found, and no band is observed in the vicinity of 3050 cm^{-1}. Straley[1] has reported the doublet as being due to a partial overlapping of ν_1 and ν_6. However, the present author has concluded, on the basis of the following considerations, that the doublet at 2995 cm^{-1} corresponds to ν_1, showing P and R branches, and that ν_6, which may exist in a higher frequency region, is not observed because of its very weak intensity (see Fig. 1). This result is in good agreement with Kagarise's.[10]

(1) In the infrared spectrum of chlorobromomethane vapor, a band of weak intensity is observed at 3065 cm^{-1} in addition to the doublet centered at 3000 cm^{-1}. These two bands, which are also observed in the condensed phase, can reasonably be assigned to ν_6* and ν_1 respectively. In the case of dibromomethane, the bands at 3005 and 3077 cm^{-1} in the vapor are also observed in the condensed phase and can be reasonably assigned to ν_1 and ν_6 respectively. In both cases, the difference in frequency between ν_1 and ν_6 is 60～80 cm^{-1} irrespective of the phase. Assuming that

10) R. E. Kagarise, *Spectrochim. Acta* (in press).

* The asymmetric C-H stretching vibration in the cases of chlorobromomethane and dimethoxymethane-d_6 molecules is also represented by ν_6.

Straley's assignment is correct in the case of dichloromethane, the difference in frequency in the vapor is 14 cm^{-1}, while that in the condensed phase is 60~70 cm^{-1}. This frequency difference of 14 cm^{-1} in the vapor is abnormally small when compared with the other dihalogenomethanes.

When the compounds are in vapor, the intensity of ν_6 is much weaker than that of ν_1 in the case of chlorobromomethane but not very different in the case of dibromomethane. When the compounds are in the condensed phase, the intensity of ν_6 compared with that of ν_1 increases in the order of: dichloromethane → chlorobromomethane → dibromomethane. If the same tendency exists in vapor, it must be expected that the intensity ratio of ν_6 to ν_1 is smaller in the case of dichloromethane than in the case of chlorobromomethane.

(2) The dichloromethane molecule is a nearly prolate symmetric top* and ν_1 is a type-B band, while ν_6 is a type-C band. It is inferred from the band contours of the other fundamental bands, overtones and combination bands[11] of dichloromethane that the type-B bands lack a Q branch, while the type-C bands have a relatively strong Q branch. The doublet of dichloromethane centered at 2995 cm^{-1} does not exhibit a prominent Q branch; therefore, it is reasonably regarded as a type-B band.

In the case of a nearly prolate symmetric top, the approximate value of the separation of the maxima of P and R branches is given as follows;

$$\Delta\nu = \sqrt{\frac{8kT}{hc}} \cdot \frac{B+C}{2}$$

As estimated by this formula, $\Delta\nu$ is 13 cm^{-1} in the case of dichloromethane, a value which is in good accordance with the observed separation of 14 cm^{-1}, between the maxima of the doublet at 2995 cm^{-1}.

Variation of the Infrared Intensities of the C–H Stretching Bands and Intermolecular Interaction.—The intensities of the C–H stretching bands of dihalogenomethanes vary extraordinarily with the dielectric constant of the medium, as is shown in Fig. 4, but the frequency shifts are comparatively small, as Table I shows. According to Josien et al.,[8] in the case of dichloromethane the ratios between the integrated intensities in a dilute carbon tetrachloride solution (0.15 mol./l.) and in pure liquid are 1 : 0.6 for ν_1 and 1 : 2.4 for ν_6.

According to Polo et al.,[12] the ratio of the infrared intensity in the condensed phase to that in vapor hinges solely on the refractive indices of the media as estimated by the Debye model. In other words, the ratio between the intensities in vapor is identical with the ratio in the condensed phase.

If Polo's theory were valid, the intensity of any band in the carbon tetrachloride solution would be nearly equal to that in pure liquid, since the refractive index of dichloromethane (1.42) is nearly equal to that of carbon tetrachloride (1.46). Nevertheless, it is observed that the absorptivities of ν_1 and ν_6 vary markedly with the concentration of both in carbon tetrachloride and carbon disulfide solutions. Such variation cannot be explained by the simple model mentioned above, rather, it suggests the existence of some intermolecular interaction, as Polo indicated. Caldow et al.[13,14] have made an experimental study of the effect of solvents on the absorption bands of hydrogen cyanide. They have concluded that the observed solvent effects in the case of hydrogen cyanide result from the superposed contributions of both bulk dielectric effects and intermolecular interaction between a solute molecule and a solvent molecule. It is considered reasonable, therefore, that the remarkable concentration effect on the infrared intensities of ν_1 and ν_6 in the case of dichloromethane result from intermolecular interaction. In this case the interaction between solute molecules (dichloromethane) is more predominant than the interaction between a solute molecule and a solvent molecule (carbon tetrachloride or carbon disulfide); it is observed that the intensity ratio between ν_1 and ν_6 in solution approaches the ratio in vapor as the solution is diluted (see Fig. 4). Kagarise concluded also that dichloromethane forms a complex with aceton.[10]

Hydrogen bonding generally causes not only a large variation in the intensity of the stretching band, but also a remarkable lowering of its frequency. In such cases, the effect of intermolecular interaction has more influence on the intensity than on the frequency. Therefore, to presuppose the existence of intermolecular interaction in the case of dichloromethane seems not to contradict the experimental finding that the frequency shift is comparatively small. In chlorobromomethane and dibromomethane, a similar variation is also observed; therefore, a similar interaction

* $I_A = 2.6\times10^{-39}$, $I_B = 25.6\times10^{-39}$ and $I_C = 27.7\times10^{-39}$ g.cm²

11) E. K. Plyler and W. S. Benedict, *J. Res. Nat. Bur. Stand.*, 49, 1 (1952).

12) S. R. Polo and M. K. Wilson, *J. Chem. Phys.*, 23, 2376 (1955).

13) G. L. Caldow and H. W. Thompson, *Proc. Roy. Soc. (London)*, A254, 1 (1960).

14) G. L. Caldow and H. W. Thompson, ibid., A254, 17 (1960).

is presupposed. Again, in the case of dimethoxymethane-d_6, where such an interaction seems negligible, the variation in the ratio of intensities (D_6/D_1) is smaller than in the cases of dihalogenomethanes, and its slope against the dielectric constants of media is opposite to the slope in dihalogenomethanes (see Fig. 4).

The author wishes to express her thanks to Dr. Kenkichi Nukada for the opportunity given to perform this research and for his helpful advice and critical remarks, and to Dr. Shinnosuke Saeki, for their valuable suggestions.

The author is also grateful to Dr. Kazuo Amaya and Mrs. Kazuko Sasaki for their measuring of the dielectric constant of chlorobromomethane.

For aid in completing this English manuscript, acknowledgement is due to Professor R. E. Kagarise and Mr. Norizo Maeda.

Government Chemical Industrial Research Institute, Tokyo
Shibuya-ku, Tokyo

Synthese von 3,6-Disubstituierten 2-Hydroxypyrazinen

Von Mitsuo MASAKI und Masaki OHTA

(Eingegangen am 27. April, 1963)

Die Untersuchungen über Aspergillsäure, ein von dem Moder, *Aspergillus flavus*,[1] produziertes Antibiotikum, zogen den Schluss,[2] dass die Substanz 3-Isobutyl-6-*sek*.-butyl-2-hydroxypyrazin-1-oxyd oder tautomere Hydroxamsäure (I) darstellt.

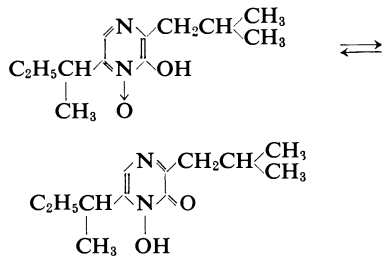

(I)

Zwei Methoden zur Synthese von 2-Hydroxypyrazinen, welche an 3 und 6 Stellungen zwei ungleiche Substituenten aufweisen, sind bereits von Spring et al. berichtet worden. Die erste Synthese geht von dem aus α-Oximino-aldehyd mit α-Amino-nitril erhaltenen 3,6-disubstituierten 2-Aminopyrazin-1-oxyd aus, das bei der Reduktion mit Natriumdithionit den Deoxykörper ergibt, der durch Behandlung mit salpetriger Säure zu 3-Isobutyl-6-*sek*.-butyl-2-hydroxypyrazin umgewandelt wurde.[2] Die zweite Synthese beruht auf der Dehydratisierung von DL-Leucyl-DL-isoleucinanhydrid mit Phosphorylchlorid zu 3-*sek*.-Butyl-6-isobutyl-2-hydroxypyrazin.[3]

In der vorliegenden Arbeit beschreiben wir, dass man durch die direkte Cyclisierungsreaktion zu 3,6-disubstituierten 2-Hydroxypyrazinen gelangen kann, indem man einen *N*-(2-Keto-alkyl)-aminosäureester (IV) mit Ammoniak in Methanol kondensiert.

Kürzlich berichteten wir,[4] dass durch die Umsetzung von α-Halo-oxim mit Aminosäureester in ätherischer Lösung *N*-(2-Oximinoalkyl)-aminosäureester (II) leicht zugänglich ist, der bei Hydrolyse mit Alkali die entsprechende Carbonsäure liefert. Verbindungen vom Typus IV liessen sich durch Verseifung

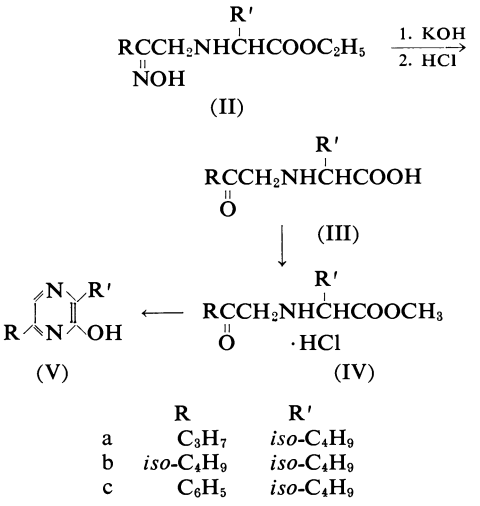

	R	R′
a	C_3H_7	*iso*-C_4H_9
b	*iso*-C_4H_9	*iso*-C_4H_9
c	C_6H_5	*iso*-C_4H_9

1) E. C. White und J. H. Hill, *J. Bact.*, **45**, 433 (1943).
2) G. T. Newbold, W. Sharp und F. S. Spring, *J. Chem. Soc.*, **1951**, 2679. vgl. J. D. Dutcher, *J. Biol. Chem.*, **171**, 321 (1947).
3) J. J. Gallagher, G. T. Newbold, W. Sharp und F. S. Spring, *J. Chem. Soc.*, **1952**, 4870.
4) M. Masaki und M. Ohta, Dieses Bulletin, **36**, 922 (1963).

der Oximinogruppe der *N*-(2-Oximino-alkyl)-aminosäuren, und durch die anschliessende Veresterung der entstandenen *N*-(2-Keto-alkyl)-aminosäure (III), erhalten.

In der Gegenwart von Benzaldehyd[5] wurde *N*-(2-Oximinopentyl)-leucin mit Salzsäure in 60 proz. Ausbeute zur *N*-(2-Keto-pentyl)-leucin (III-a) verseift, welche mit Methanol und Chlorwasserstoff *N*-(2-Keto-pentyl)-leucin-methylester-hydrochlorid (IV-a) lieferte. Dieses Ester-hydrochlorid gab durch Behandlung mit Ammoniak in Methanol bei Zimmertemperatur 3-Isobutyl-6-propyl-2-hydroxypyrazin (V-a), dessen Konstitutionsbeweis durch Elementar-Analyse und Ultraviolet-spektrum erreicht wurde. Die letzte Stufe der Synthese ist die Oxydation, die in den meisten Pyrazin-synthesen allgemein ist.

Durch dieses Verfahren konnten wir weiter 3, 6-Diisobutyl-2-hydroxypyrazin ("Flavacol") (V-b)[6] und 3-Isobutyl-6-phenyl-2-hydroxypyrazin (V-c), ausgehend von den entsprechenden *N*-(2-Oximino-alkyl)-leucinen, synthetisieren.

Zur Synthese von 2-Hydroxypyrazin-1-oxyd oder tautomerer Hydroxamsäure dürfte der durch die oben erwähnte Methode zugänglich gewordene *N*-(2-Keto-alkyl)-aminosäureester (IV) als Zwischenprodukt erwartet werden.[7]

Beschreibung der Versuche

***N*-(2-Keto-pentyl)-leucin (III-a).** — Eine Lösung von 2 g *N*-(2-Oximinopentyl)-leucin[4] in 20 ccm 3N Salzsäure wurde mit 2 g Benzaldehyd und 20 ccm Methanol versetzt und die klare Lösung wurde bei Zimmertemperatur stehengelassen. Nach 3 Tagen wurde die Lösung unter vermindertem Druck auf ca. 10 ccm eingeengt, dann 2 mal mit Äther gewaschen und mit Natriumcarbonat neutralisiert, wobei sich die Keto-aminosäure ausschied, die 2 mal mit Wasser nachgewaschen wurde. Rohausb. 1.2 g. Farblose Nädelchen vom Schmp. 184~186°C (aus Methanol).

Gef.: C, 61.27; H, 9.64; N, 6.59. Ber. für $C_{11}H_{21}O_3N$: C, 61.36; H, 9.83; N, 6.51%.

Bei der Einwirkung von Hydroxylamin auf dieses Keton wurde das Oxim quantitativ erhalten.

***N*-(2-Keto-pentyl)-leucin-methylester-hydrochlorid (IV-a).**—Eine Suspension von 0.6 g III-a in 15 ccm Methanol wurde unter Durchleitung von trockenem Chlorwasserstoff 2 Stdn am Rückfluss gekocht und die erhaltene Lösung wurde über Nacht stehengelassen. Der beim Eindampfen des Lösungsmittels hinterbliebene Rückstand wurde unter vermindertem Druck über Kaliumhydroxyd getrocknet und aus Essigester umkristallisiert. Ausb. 0.6 g. Farblose Nadeln vom Schmp. 90~91.5°C (Sintern bei 70~74°C).

Gef.: N, 5.08. Ber. für $C_{12}H_{23}O_3N \cdot HCl$: N, 5.29%.

3-Isobutyl-6-propyl-2-hydroxypyrazin (V-a).— Eine Lösung von 0.5 g IV-a in 12 ccm Methanol sättigte man mit Ammoniak und liess die Lösung bei Zimmertemperatur stehen. Nach 2 Tagen wurde die Lösung unter vermindertem Druck eingeengt und der Rückstand wurde in Essigester mit Aktivkohle behandelt, und wieder wurde die Lösung unter vermindertem Druck abgedampft. Der ölige Rückstand wurde mit 3 N Salzsäure extrahiert, dann der Extrakt mit Aktivkohle behandelt und unter vermindertem Druck zur Trockene eingedampft. Der kristallinische Rückstand wurde mit Natriumbicarbonatlösung und dann mit Wasser gewaschen. Rohausb. 0.3 g. Farblose Nadeln vom Schmp. 136.5~137°C (aus Äthanol). UV-Spektrum in Äthanol: λ_{max} 2280 A(ε=7400) und 3260 A(ε=7400).

Gef.: C, 67.91; H, 9.00; N, 14.64. Ber. für $C_{11}H_{18}ON_2$: C, 68.00; H, 9.34; N, 14.42%.

***N*-(2-Keto-isohexyl)-leucin (III-b).**—Eine Lösung von 3 g *N*-(2-Oximino-isohexyl)-leucin[4] in 20 ccm 3 N Salzsäure versetzte man mit 2 g Benzaldehyd und 18 ccm Methanol, liess die erhaltene Lösung 3 Tagen bei Zimmertemperatur stehen und arbeitete dann weiter auf wie beim III-a. Rohausb. 1.9 g. Farblose Nädelchen vom Schmp. 178~179°C (aus Methanol).

Gef.: C, 62.59; H, 10.19; N, 6.05. Ber. für $C_{12}H_{23}O_3N$: C, 62.85; H, 10.11; N, 6.11%.

3, 6-Diisobutyl-2-hydroxypyrazin (V-b). — Wie beim IV-a wurde 0.6 g III-b mit Methanol und Chlorwasserstoff verestert, wobei 0.7 g rohes *N*-(2-Keto-isohexyl)-leucinmethylester-hydrochlorid (IV-b) erhalten wurde. Eine Lösung von 0.55 g IV-b vom Schmp. 114~116°C (aus Benzol-Äther) in 20 ccm Methanol wurde mit Ammoniak gesättigt und nach 2 tägigem Stehenlassen bei Zimmertemperatur wurde das Reaktionsgemisch wie beim V-a aufgearbeitet, dabei wurde 0.25 g rohes V-b erhalten. Umkristallisierung aus Äthanol ergab farblose Kristalle vom Schmp. 149~151°C (Gef.: N, 13.33%. Lit.[6] Schmp. 144.5~147°C). UV-Spektrum in Äthanol: λ_{max} 2290 A(ε=6700) und 3250 A(ε=7400).

Salzsäuresalz von *N*-Phenacyl-leucin (III-c).— Man löste 5 g *N*-(2-Phenyl-2-oximinoäthyl)-leucin[4] in 40 ccm 3 N Salzsäure auf und liess bei Zimmertemperatur stehen. Bald fing ein farblose Niederschlag (Salzsäuresalz von III-c) sich auszuscheiden an. Nach 24 stdg. Stehen wurde der Niederschlag abgesaugt. Rohausb. 5 g. Farblose Nadeln vom Schmp. 194°C (aus 3N Salzsäure).

Gef.: C, 58.79; H, 6.91; N, 4.89. Ber. für $C_{14}H_{19}O_3N \cdot HCl$: C, 58.84; H, 7.01; N, 4.90%.

***N*-Phenacyl-leucin-methylester-hydrochlorid (IV-c).**—Eine Suspension von 0.9 g Salzsäuresalz von III-c in 20 ccm Methanol wurde wie beim IV-a aufgearbeitet. Farblose Prismen vom Schmp. 133~135°C (aus Essigester). Ausb. 0.6 g.

Gef.: N, 4.61. Ber. für $C_{15}H_{21}O_3N \cdot HCl$: N, 4.67%.

Freie Base: Leicht zersetzliche, farblose Nadeln vom Schmp. 53°C (aus Petroläther).

5) R. Fischer und T. Wieland, *Chem. Ber.*, **93**, 1387 (1960).

6) G. Dunn, G. T. Newbold und F. S. Spring, *J. Chem. Soc.*, **1949**, 2586.

7) Tatsächlich erhielten wir schon durch Behandlung des Keto-amino-ester mit Hydroxylamin eine Spur Substanz, die mit Eisenchlorid eine deutliche Farbreaktion zeigt. Wir untersuchen dies jetzt und werden bald davon Mitteilung machen.

3-Isobutyl-6-phenyl-2-hydroxypyrazin (V-c).— Man löste 0.5 g IV-c in 20 ccm Methanol auf, leitete Ammoniak bis zur Sättigung und liess dann die Lösung bei Zimmertemperatur stehen. Nach 2 Tagen wurde die Lösung unter vermindertem Druck eingedampft, der ölige Rückstand wurde in Essigester aufgelöst und nach der Entfernung des unlöslichen Ammoniumchlorides wurde die Lösung wieder eingedampft, inzwischen wurde ein Luftstrom durch die Lösung eingeleitet, um die Luftoxydation zu vervollständigen. Der ölige Rückstand wurde mit 6 N Salzsäure extrahiert und nach Behandlung mit Aktivkohle der Extrakt mit 2 N Natronlauge neutralisiert, wobei sich ein brauner Niederschlag (0.16 g) ausfiel, der aus Äthanol umkristallisiert wurde. Gelbe Nadeln vom Schmp. 167~168.5°C. UV-Spektrum in Äthanol: λ_{max} 2390 A(Schulter $\varepsilon=6800$), 2500 A($\varepsilon=8000$) und 3280 A($\varepsilon=13000$).

Gef.: C, 73.21; H, 6.97; N, 12.21. Ber. für $C_{14}H_{16}ON_2$: C, 73.65; H, 7.06; N, 12.27%.

Laboratorium für Organische Chemie
Tokyo Institut für Technologie
Meguro-ku, Tokyo

The Luminescence Spectra of Triply-ionized Dysprosium and Terbium in Alkaline Earth Fluorides

By Eiichi IWASE and Seijiro NISHIYAMA

(Received May 14, 1963)

The three principal luminescence bands of the samarium(III) ion, which is embedded in alkaline earth fluorides, show, according to Tomaschek,[1] a blue shift as the matrix is changed in the sequence of calcium fluoride, strontium fluoride and barium fluoride. Here the blue shift refers to the displacement of bands towards the larger frequency side of the spectrum. Yoshimura[2] verified this regularity of the blue shift with a much greater number of bands of samarium(III) luminescence appearing in the sequence of matrices just mentioned. Furthermore, Evert[3] studied the luminescence of another rare earth ion, namely, the praseodymium(III) ion, embedded in sulfides as well as in oxides of alkaline earth elements, and put forward two suggestions, though they did not explicitly concern the luminescence in the matrices of alkaline earth fluorides. One of his suggestions was that a blue shift may also occur in the luminescence spectrum of the praseodymium(III) ion embedded in the sequence of alkaline earth fluorides with ascending lattice-constants; the other suggestion is that, with this sequence of matrices, there may be seen the "contraction of the luminescence spectrum," i.e., the decrease occurs in the frequency-intervals of the luminescence bands of the praseodymium(III) ion. This paper presents the results of investigations of the luminescence spectra of dysprosium(III) and terbium(III) ions embedded in the matrices of calcium fluoride, strontium fluoride and barium fluoride; this investigation was undertaken for the purpose of ascertaining what the effects of the crystal-field strength of these matrices on the f-f transitions of the said triply-ionized rare earths are really like.

1) R. Tomaschek, *Z. Elektrochem.*, **36**, 737 (1930); *Physik. Z.*, **33**, 878 (1932); *Acta Phys. Polon.*, **5**, 403 (1936).
2) J. Yoshimura, *Sci. Papers, Inst. Phys. Chem. Research* (Tokyo), **23**, 224 (1933).
3) H. Evert, *Ann. Physik*, [5] **12**, 107, 137 (1932).

Experimental

By means of the reactions between alkaline earth nitrates and hydrofluoric acid in aqueous solutions, precipitates of calcium fluoride, strontium fluoride and barium fluoride were prepared; they were then soaked with a nitrate solution of either dysprosium(III) or terbium(III) and calcined at about 900°C for 30 min. These rare earths were made by the Lindsay Chemical Division, the American Potash & Chemical Corporation, and were of 99.9% purity. The concentration of the rare earth ions in the matrix is always made to be about 0.1%.

The excitation to the luminescence is done in a small Urbain tube by cathode-ray bombardment at room temperature, and the luminescence thus provoked is spectrographically investigated by employing a glass-prism spectrograph of Feuss.

In the matrix-sequence of calcium fluoride, strontium fluoride and barium fluoride, the intensity of the luminescence generally decreases so markedly that, in order to make sure of a proper and detailed comparison among the luminescence spectra, the duration of the exposure to the photographic plate had to be varied, for instance,

several minutes for the luminescence in the calcium fluoride matrix and several hours for that in the barium fluoride matrix.

Results and Discussion

Figures 1—3 are, respectively, the schematic representations of the luminescence spectra of dysprosium(III) and terbium(III) ions which are embedded in the calcium fluoride, strontium fluoride and barium fluoride matrices.

In a comparatively recent work by Chatterjee[4] on the luminescence spectra of dysprosium(III) and terbium(III) ions, calcium fluoride was selected as their matrix. From our experiments on the luminescence spectra, it is now confirmed that a fairly great number of the bands observed by him should be ascribed to the presence of praseodymium, samarium and either terbium or dysprosium as impurities in the dysprosium and terbium preparates.

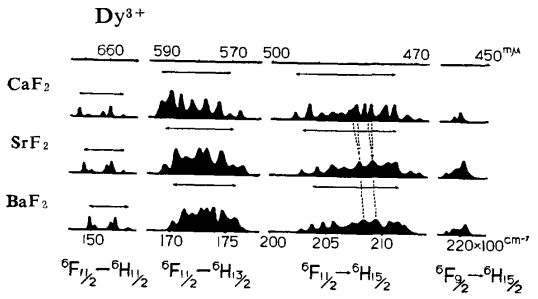

Fig. 1

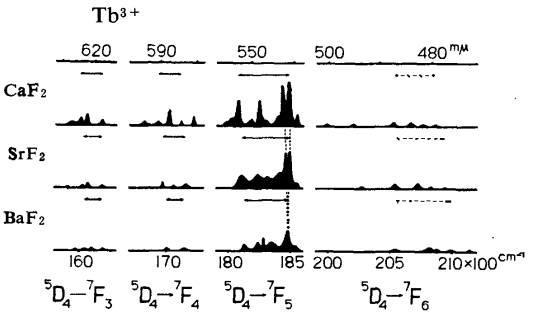

Fig. 2

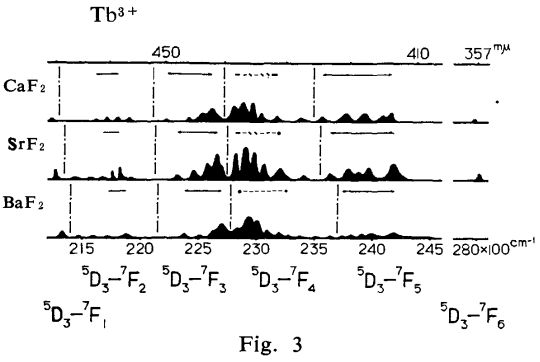

Fig. 3

Our measurements cover the frequency regions 14800~21200 cm^{-1} and 15900~26300 cm^{-1} for the luminescence of dysprosium(III) and terbium(III) ions respectively. As is shown in Table I, the total number of observed bands of the dysprosium(III) ion is 28, 26 and 27 for the luminescence found in the calcium fluoride, strontium fluoride and barium fluoride matrices respectively. Similarly, that of the terbium(III) ion is 46, 42 and 40 for the luminescence found in the calcium fluoride, strontium fluoride and barium fluoride matrices respectively.

TABLE I

	Total number of observed bands			Number of bands showing blue shift	
	CaF_2	SrF_2	BaF_2	$CaF_2 \rightarrow SrF_2$	$SrF_2 \rightarrow BaF_2$
Dy^{3+}	28	26	27	25	22
Tb^{3+}	46	42	40	35	33

The four systems of the bands of dysprosium(III) ions around 15100, 17300, 20800 and 22000 cm^{-1} are assigned, respectively, to the 6F11/2→6H11/2, 13/2, 15/2 and 6F9/2→6H15/2 transitions. To make these assignments of bands, the data given by Dieke and others,[5] are referred to.

Ten band-groups of the terbium(III) luminescence around 16100, 17100, 18300, 20700, 21300, 21800, 22500, 23200, 23900 and 26200 cm^{-1} are, respectively, assigned to the 5D4→7F3, 4, 5, 6 and 5D3→7F1, 2, 3, 4, 5, 6 transitions. To make these assignments of bands, the data given by Gobrecht[6] and Dieke and others[5] are taken into consideration.

The outermost electron-shell of all the triply-ionized rare earths is, as is well known, of a configuration having two 5s and six 5p electrons. Because of the shielding of this electronic structure of the closed-shell type, the f-f transitions of these ions would not be very much affected by an external force, and when these ions are embedded in various matrices, all the observed luminescence bands due to the f-f transitions are sharp and the proper correspondences between them may be ascertained comparatively easily.

When the matrix is restricted to alkaline earth fluorides with a comparatively simple structure of cubic fields (O_h^5), the lattice-constant is increased in the successive order of

4) N. Chatterjee, *Z. Physik*, **113**, 96 (1939).

5) G. H. Dieke and S. Singh, *J. Opt. Soc. Am.*, **46**, 495 (1956).

6) H. Gobrecht, *Ann. Physik*, [5] **28**, 673 (1937).

calcium fluoride, strontium fluoride and barium fluoride. Accordingly, the effects of crystal-field strength on a foreign cation embedded in the site of alkaline earth ions may be decreased in this order.

The detailed and comparative studies of the luminescence spectra of triply-ionized rare earths embedded in these alkaline earth fluorides imply the elucidation of the effects on the f—f transitions under the application of different crystal-field strengths. From the measurements described above, three items of interest may generally be settled. The first is the displacement of bands caused by changing the matrix. The second is the relative values of overall crystal-field splittings observed in the transitions with the definite total angular momentums of J an J'. The third is the determination of the splitting of certain individual bands under the influence of more intense crystal fields.

Concerning the first item, the following facts should be mentioned. If the matrix is changed in a sequence of increasing lattice-constants, namely, calcium fluoride → strontium fluoride, then 25 bands of the dysprosium(III) ion are found to follow the regularity of the blue shift as is shown in Table I. Similarly, this is the case with the 22 bands of the dysprosium(III) ion for the matrix-sequence strontium fluoride→barium fluoride. As to the luminescence of the terbium(III) ion, the blue shift is observed with 35 bands on changing the matrix calcium fluoride→strontium fluoride, and with 33 bands for the change of matrix strontium fluoride→barium fluoride.

Concerning the second item, Table II indicates that, with the decrease in the lattice-constant of the matrix in the successive order

Table II. Magnitudes of relative crystal-field splittings $\Delta\nu$ observed in $^6F_{11/2}\rightarrow{}^6H_{J'}$ transitions

Dy^{3+}		CaF_2		SrF_2		BaF_2
$J'=11/2$	ν	15270 cm^{-1}		15290		15320
	ν'	14880		14930		14980
	$\Delta\nu$	390	>	360	>	340
13/2		17520		17560		17590
		16900		16940		17020
		620	≒	620	>	570
15/2		21090		21110		21150
		20210		20280		20370
		880	>	830	>	780

of barium fluoride, strontium fluoride and calcium fluoride, each of the overall crystal-field splittings of the 6H11/2, 13/2, and 15/2 levels of the dysprosium(III) ion is increased. Here ν and ν' are the wave number of the bands. This effect may be assumed to occur almost directly proportionately to the crystalfield strength of the matrices. In other words, if the matrices are arranged in the order of descending crystalfield strength, namely, in the sequence of calcium fluoride, strontium fluoride and barium fluoride, it can then be called a "contraction of spectrum" using Evert's term. Tables III—IV demonstrate how the relation of the socalled contraction of spectrum also holds generally for the band-systems of terbium(III) luminescence. However, there are exceptions for the two band-systems belonging to the 5D4→7F6 and 5D3→7F4 transitions, in which is seen, on the contrary, an "expansion of spectrum."

Finally, it is note worthy that the splitting of some individual bands under the influence of a more intense crystalfield is found in the luminescence spectra of dysprosium(III) and terbium(III) ions. The two intense bands at 20830 and 20940 cm^{-1} observed in the barium

Table III. Magnitudes of relative crystal-field splittings $\Delta\nu$ observed in $^5D_4\rightarrow{}^7F_{J'}$ transitions

Tb^{3+}		CaF_2		SrF_2		BaF_2
$J'=3$	ν	16190 cm^{-1}		16190		16200
	ν'	16010		16030		16050
	$\Delta\nu$	180	>	160	>	150
4		17120		17160		17150
		16930		16980		17000
		190	>	180	>	150
5		18480		18490		18480
		18080		18100		18120
		400	>	390	>	360
6		20850		20950		21000
		20520		20540		20550
		330	<	410	<	450

Table IV. Magnitudes of relative crystal-field splittings $\Delta\nu$ observed in $^5D_3\rightarrow{}^7F_{J'}$ tansitions

Tb^{3+}		CaF_2		SrF_2		BaF_2
$J'=2$	ν	21800 cm^{-1}		21830		21890
	ν'	21620		21660		21720
	$\Delta\nu$	180	>	170	≒	170
3		22620		22660		22700
		22230		22320		22380
		390	>	340	>	320
4		23170		23210		23280
		22810		22820		22840
		360	<	390	<	440
5		24160		24180		24190
		23560		23630		23740
		600	>	550	>	450

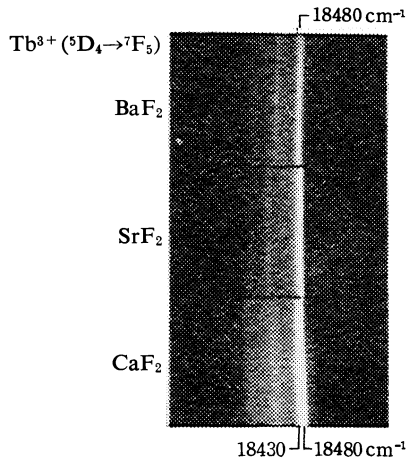

Fig. 4. Splitting of individual band in the crystalfield.

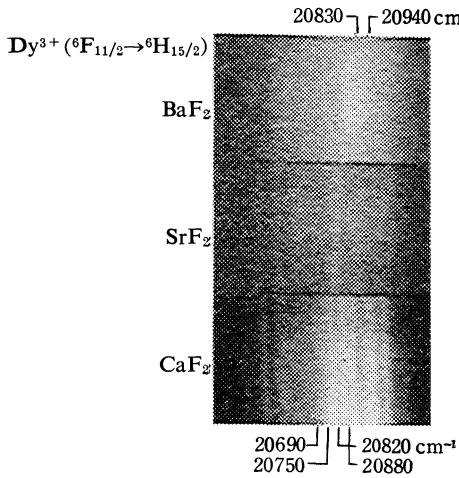

Fig. 5. Splitting of individual bands in the crystalfield.

TABLE V. SPLITTING OF INDIVIDUAL BANDS IN THE CRYSTAL FIELD

	BaF_2 cm^{-1}	SrF_2 cm^{-1}	CaF_2 cm^{-1}	$\Delta\nu$ cm^{-1}
Dy^{3+} $^6F_{11/2}\rightarrow{}^6H_{15/2}$	20830	20780	20690 20750	60
	20940	20900	20820 20880	60
Tb^{3+} $^5D_4\rightarrow{}^7F_5$	18480	18460 18490		30
			18430 18480	50

fluoride matrix are ascribed to the 6F11/2→6H15/2 transition, and these bands correspond to the two bands in the strontium fluoride matrix appearing at 20780 and 20900 cm^{-1}. On changing the matrix strontium fluoride→calcium fluoride, the band at 20780 cm^{-1} observed in strontium fluoride is found to split into two components of 20690 and 20750 cm^{-1} ($\Delta\nu=60\,cm^{-1}$) in the more intense crystalfield of calcium fluoride, while the other band of 20900 cm^{-1} in strontium fluoride similarly splits into two, of 20820 and 20880 cm^{-1} ($\Delta\nu=60\,cm^{-1}$), in calcium fluoride. It should be mentioned that the magnitude of each of these $\Delta\nu$ splittings is 60 cm^{-1}. The most intense band of terbium(III) luminescence is ascribed to a 5D4→7F5 transition and is observed at 18480 cm^{-1} in the barium fluoride matrix. In the more intense crystalfield of the strontium fluoride matrix, it splits into two components of 18460 and 18490 cm^{-1} ($\Delta\nu=30\,cm^{-1}$), while in the most intense crystalfield of the calcium fluoride matrix, it splits into components of 18430 and 18480 cm^{-1} ($\Delta\nu=50\,cm^{1}$). It should be emphasized that the magnitude of these splittings, namely 30 and 50 cm^{-1}, may be taken as the approximate measure of the relative strength of the crystalfield for the matrices of barium fluoride, strontium fluoride and calcium fluoride.

Summary

(i) The luminescence spectra of dysprosium(III) and terbium(III) ions have been measured in the cubic field (O_h^5) of calcium fluoride, strontium fluoride and barium fluoride under excitation by cathode-ray-bombardment.

(ii) The displacement of the luminescence bands of dysprosium(III) ion has been studied with relation to the matrices mentioned above, a blue shift being observed, with 25 and 22 bands as the matrix was changed in successive sequences of calcium fluoride to strontium fluoride and strontium fluoride to barium fluoride respectively. Similarly, this was the case with 35 bands of the terbium(III) luminescence when, the matrix was changed from calcium fluoride to strontium fluoride, and with 33 bands for that from strontium fluoride to barium fluoride.

(iii) The magnitude of the relative crystalfield splittings $\Delta\nu$ of the luminescence bands of dysprosium(III) and terbium(III) ions was reported in relation to the increasing strength of the crystal field, i. e., in the sequence of matrices barium fluoride, strontium fluoride and calcium fluoride. For the dysprosium(III) luminescence, the crystalfield splittings observed in the 6F11/2→6H11/2, 6F11/2→6H13/2 and 6F11/2→6H15/2 transitions had a tendency to increase in the matrix-sequence barium fluoride, strontium fluoride and calcium fluoride. In the case of the terbium(III) luminescence, variations similar to that found in the dysprosium(III) luminescence took place in the crystalfield splittings of the 5D4→7F3, 5D4→7F4,

5D4→7F5, 5D3→7F2, 5D3→7F3 and 5D3→7F5, transitions, while the reverse was the case with the 5D4→7F6 and 5D3→7F4 transitions.

(iv) It was found that the band appearing at 18480 cm^{-1} in the luminescence spectrum of the terbium(III) ion embedded in barium fluoride splits into its respective two components when the terbium ion was embedded in matrices of strontium fluoride and calcium fluoride with a more intense crystalfield strength. The magnitudes of these splittings, 30 and 50 cm^{-1} as observed in strontium fluoride and calcium fluoride respectively, are presumably proportional to the differences between the crystalfield strength for barium fluoride, strontium fluoride and calcium fluoride.

The authors wish to thank Professor S. Nagakura, Professor S. Sugano and Professor S. Shionoya of the Institute for Solid State Physics, the University of Tokyo, for their interest and helpful discussions.

The Institute of Physical and Chemical Research
Bunkyo-ku, Tokyo

The Luminescence Spectra of Triply-ionized Rare Earths in the Calcination Products of Some Magnesium Compounds

By Eiichi IWASE and Seijiro NISHIYAMA

(Received May 14, 1963)

According to Tomaschek,[1] the luminescence spectra of samarium(III) ions embedded in the matrices of magnesium oxide, which are derived from the thermal treatment of magnesia usta, magnesium sulfate and magnesium chloride, are different from one another, although these matrices have the same X-ray diffraction diagram.

From the chemical point of view, the thermal decomposition of magnesium compounds does not always give rise to a simple and high-quality magnesium oxide, and the few fragments of the starting magnesium compounds remaining in the calcination products may be expected, in some cases, to have a remarkable effect on the luminescence spectra of the triply-ionized rare earths embedded therein. These effects would be detectable in variations of relative intensity, spectral position and sharpness of the luminescence bands. Therefore, measurements have been made of the luminescence spectra of the europium(III), terbium(III), and dysprosium(III) as well as of the samarium(III) ions embedded in calcination products derived from three kinds of magnesium compounds. This paper will present the experimental results obtained and some interpretations relating to them.

1) R. Tomaschek and O. Deutschbein, *Ann. Physik*, [5] **16**, 943 (1933); R. Tomaschek, *Acta Phys. Polon.*, **5**, 405 (1936).

Experimental

High-quality crystals of $Mg(NO_3)_2 \cdot 6H_2O$, $MgSO_4 \cdot 7H_2O$ and $MgCl_2 \cdot 6H_2O$ are soaked with a nitrate solution of one of the rare earths just mentioned, and then subjected to a calcination at about 900°C for 30 min. Some portions of these calcination products are then further heated in a flame of town gas mixed with oxygen at about 1800°C for 5 min. The concentration of the rare earth added is made to be 0.1 % of the matrix. The excitation to the luminescence is done in a small Urbain tube by cathode-ray bombardment at room temperature, and the luminescence thus yielded is spectrographically investigated by employing the glass-prism spectrograph of Feuss.

Results and Discussion

Figures. 1—4 are the schematic representations of luminescence spectra of, respectively, the samarium(III), europium(III), terbium(III) and dysprosium(III) ions which are embedded in the calcination products derived from $Mg(NO_3)_2 \cdot 6H_2O$, $MgSO_4 \cdot 7H_2O$ and $MgCl_2 \cdot 6H_2O$ at 900 and 1800°C. The most intense bands in each of the luminescence spectra are shown in Table I. Comparing the results obtained on the matrix calcined at 900°C with those calcined at 1800°C, there will be found either a simple displacement of the band of maximum intensity or a simple interchange of intensity with another band. The former situation is

TABLE I. THE MOST INTENSE LUMINESCENCE BANDS OF TRIPLY-IONIZED RARE EARTHS EMBEDDED IN CALCINED MAGNESIUM COMPOUNDS

Starting matrix	Calcination temp., °C	Sm^{3+} cm^{-1}	Eu^{3+} cm^{-1}	Tb^{3+} cm^{-1}	Dy^{3+} cm^{-1}
$Mg(NO_3)_2 \cdot 6H_2O$	900	16370	16750	17830 18310 18360	16830
	1800	16300	16750	18360	16840 17100
$MgSO_4 \cdot 7H_2O$	900	16360	16750	18460	17310
	1800	16320	16260	18020 22750 23580 23710	16850
$MgCl_2 \cdot 6H_2O$	900	17540	16750	18390	17360
	1800	16140	16180 16760	18260	16830

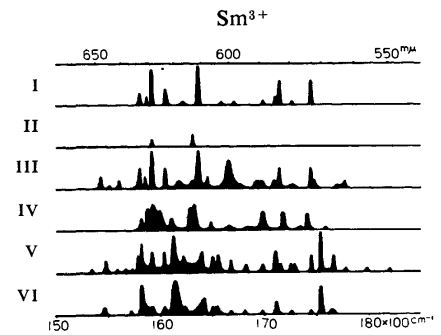

			Number of bands observed
I	$Mg(NO_3)_2 \cdot 6H_2O$	900°C	13
II	$Mg(NO_3)_2 \cdot 6H_2O$	1800°C	2
III	$MgSO_4 \cdot 7H_2O$	900°C	22
IV	$MgSO_4 \cdot 7H_2O$	1800°C	15
V	$MgCl_2 \cdot 6H_2O$	900°C	27
VI	$MgCl_2 \cdot 6H_2O$	1800°C	18

Fig. 1

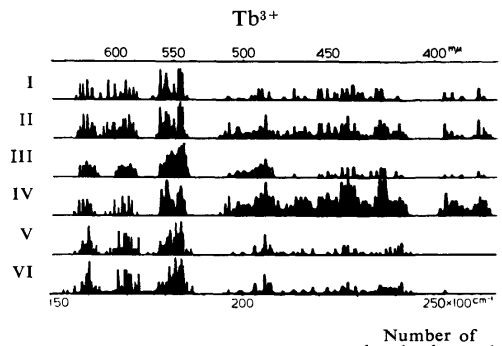

			Number of bands observed
I	$Mg(NO_3)_2 \cdot 6H_2O$	900°C	56
II	$Mg(NO_3)_2 \cdot 6H_2O$	1800°C	83
III	$MgSO_4 \cdot 7H_2O$	900°C	53
IV	$MgSO_4 \cdot 7H_2O$	1800°C	75
V	$MgCl_2 \cdot 6H_2O$	900°C	68
IV	$MgCl_2 \cdot 6H_2O$	1800°C	68

Fig. 3

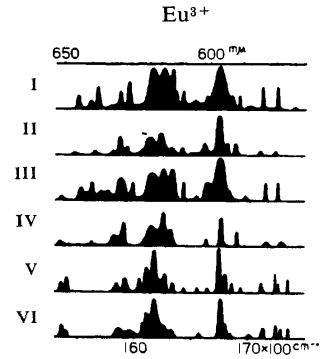

			Number of bands observed
I	$Mg(NO_3)_2 \cdot 6H_2O$	900°C	17
II	$Mg(NO_3)_2 \cdot 6H_2O$	1800°C	14
III	$MgSO_4 \cdot 7H_2O$	900°C	18
IV	$MgSO_4 \cdot 7H_2O$	1800°C	12
V	$MgCl_2 \cdot 6H_2O$	900°C	20
VI	$MgCl_2 \cdot 6H_2O$	1800°C	18

Fig. 2

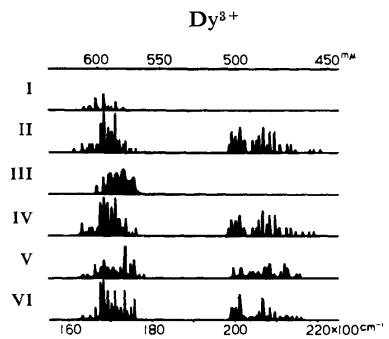

			Number of bands observed
I	$Mg(NO_3)_2 \cdot 6H_2O$	900°C	8
II	$Mg(NO_3)_2 \cdot 6H_2O$	1800°C	40
III	$MgSO_4 \cdot 7H_2O$	900°C	6
IV	$MgSO_4 \cdot 7H_2O$	1800°C	36
V	$MgCl_2 \cdot 6H_2O$	900°C	28
VI	$MgCl_2 \cdot 6H_2O$	1800°C	32

Fig. 4

seen in the case of the samarium(III) luminescence in the $Mg(NO_3)_2 \cdot 6H_2O$-derived and $MgSO_4 \cdot 7H_2O$-derived matrices, while the latter situation is seen in the cases of the samarium(III) luminescence in the $MgCl_2 \cdot 6H_2O$-derived matrix, the europium(III) luminescence in the $MgSO_4 \cdot 7H_2O$-derived matrix, the terbium(III) luminescence in the $MgCl_2 \cdot 6H_2O$-derived matrix and the dysprosium(III) luminescence in the $MgSO_4 \cdot 7H_2O$-derived as well as the $MgCl_2 \cdot 6H_2O$-derived matrices. In some cases, circumstances are more complicated and a variation in the number of bands with the maximum intensity is seen. For instance, in the case of the terbium(III) luminescence given by the $Mg(NO_3)_2 \cdot 6H_2O$-derived matrix, one of three bands having equal maximum intensity remains unchanged in its intensity, while the other two are weakened. Thus, the bands with maximum intensity decrease in number. On the other hand, an increase in the number of bands with maximum intensity is seen, for instance, in the cases of the europium(III) luminescence given by the $MgCl_2 \cdot 6H_2O$-derived matrix and of the dysprosium(III) luminescence given by the $Mg(NO_3)_2 \cdot 6H_2O$-derived matrix, where the original band of maximum intensity is displaced and another band is intensified up to an intensity equal to that of the original one, while in the terbium(III) luminescence given by the $MgSO_4 \cdot 7H_2O$-derived matrix, the original band of maximum intensity is weakened and the other four bands tend to have an intensity equal to that of the original band. Thus, the bands of maximum intensity increase in number.

On the right of Figs. 1—4 are indicated the total number of observed bands of samarium(III), europium(III), terbium(III) and dysprosium(III) ions. When the calcination-temperature is elevated, the total number of bands of samarium(III) and europium(III) ions decreases on the contrary, that of terbium(III) ions increases with the exception of the case of the $Mg(NO_3)_2 \cdot 6H_2O$-derived matrix. Here the total number of bands remains almost unchanged. In the case of the luminescence of dysprosium(III) ions, the total number of bands increases when the calcination temperature is raised.

Generally speaking, calcination at a different temperature causes a comparatively small change in the total number of luminescence bands given by the $MgCl_2 \cdot 6H_2O$-derived matrix.

So far as the matrix calcined at 900°C is concerned, the total number of observed luminescence bands of the triply-ionized rare earths embedded in the $MgCl_2 \cdot 9H_2O$-derived matrix is much larger than in the $Mg(NO_3)_2 \cdot 6H_2O$-derived and $MgSO_4 \cdot 7H_2O$-derived matrices.

When the samarium(III), europium(III), terbium(III) and dysprosium(III) ions embedded in the matrices of magnesium compounds calcined at 900°C are subjected to further heat treatment at 1800°C, the total intensity of luminescence is changed. It is interesting to note that the magnitude of the intensity-variation of luminescence can be arranged in the sequence of increasing atomic number of these rare earths; the most marked decrease in the total intensity of luminescence is effected for samarium(III) ions, whereas the most marked increase is for dysprosium(III) ions. For europium(III) and terbium(III) ions a moderate decrease and a moderate increase in the total intensity of luminescence are observed respectively.

As the result of the elevation of the calcination temperature, the relative intensity of luminescence bands appearing side by side in the spectrum is sometimes reversed in order. For the europium(III) luminescence, this is the case with the band-couple of 15880 and 15950 cm^{-1} in the matrix derived from $Mg(NO_3)_2 \cdot 6H_2O$ and with those of 15360 and 15400 cm^{-1}, as well as with 15840 and 15920 cm^{-1} in the matrix derived from $MgCl_2 \cdot 6H_2O$. For the terbium(III) luminescence a similar reversal of intensity is observed in the bands of 15920, 16000 and 16060 cm^{-1} in the matrix derived from $Mg(NO_3)_2 \cdot 6H_2O$.

In the case of $Mg(NO_3)_2 \cdot 6H_2O$, thermal conversion to magnesium oxide goes forward so smoothly that the luminescence spectrum of each of the triply-ionized rare earths embedded in magnesium oxide is obtained in its pure form. As was expected, the thermal decomposition to magnesium oxide does not proceed easily for $MgSO_4 \cdot 7H_2O$. Turbidimetric analyses of SO_4^{2-} as barium sulfate sol (Table II, upper line) show that about 2/3 of the starting material is decomposed to magnesium oxide by calcining at 900°C for 30 min. in an electric furnace and that about 1/4 of the sulfate component still remains in a product subjected to further heating in a flame of town gas mixed with oxygen at 1800°C for 5 min. Due to the sulfate component remaining in the matrix calcined at 900°C, a number of characteristic diffuse bands and their conglomeration are

Table II. Examples of chemical analyses of remaining components in calcined products

Starting substances	900°C 30 min.	1800°C 5 min.
$MgSO_4 \cdot 7H_2O$	25.66%	19.52%
$MgCl_2 \cdot 6H_2O$	0.000147	0.000038

seen. When further decomposition occurs following heat treatment at 1800°C, the feature of the luminescence spectrum approaches that in pure magnesium oxide. Although the thermal decomposition to magnesium oxide is readily obtainable with $MgCl_2 \cdot 6H_2O$, the luminescence spectrum of each of the triply-ionized rare earths embedded therein has an appearance considerably different from the luminescence spectrum obtained in the $Mg(NO_3)_2 \cdot 6H_2O$-derived matrix; these rare earth ions give intense and sharp luminescence bands peculiar to the respective chloride-derived matrix. Examples of turbidimetric analyses as silver chloride sol (Table II, lower line) show 147 p.p.m. of chlorine content for a product calcined at 900°C for 30 min. and 38 p.p.m. of chlorine content for that calcined at 1800°C for 5 min. The quantity of chlorine ions existing in the matrix corresponds to about 64 and 17 mol. % of that of the rare earth ions respectively. It should be mentioned that even such a minute quantity of chlorine ions found in the matrix would have quite remarkable effects over the whole luminescence spectrum of the rare earth ions existing therein.

If it can be assumed that the luminescence spectrum of each of the triply-ionized rare earths embedded in either the $MgSO_4 \cdot 7H_2O$-derived or $MgCl_2 \cdot 6H_2O$-derived matrix is composed of two kinds of bands (one, the kind of bands observed in pure magnesium oxide and the other, the kind of bands characteristic of the matrix with either a sulfate or chloride component remaining therein), the composition of the luminescence spectrum, as well as the mixing ratio of these two kinds of luminescence bands, would be such as shown in Table III.

Table III. Mixing ratio of bands characteristic of magnesium sulfate- or chloride-derived matrix and those due to pure magnesia in luminescence spectrum of triply-ionized rare earth

Starting matrix	Sm^{3+}	Eu^{3+}	Tb^{3+}	Dy^{3+}
$MgSO_4 \cdot 7H_2O$	11/11	9/9	16/37	4/2
$MgCl_2 \cdot 6H_2O$	17/10	12/8	29/39	14/14

Table IV gives the frequency of some principal luminescence bands of samarium(III), europium(III), terbium(III) and dysprosium(III) ions, which is considered to be inherent in the matrices derived from $MgSO_4 \cdot 7H_2O$ and $MgCl_2 \cdot 6H_2O$ by the calcination at 900°C.

Table IV. Principal luminescence bands of triply-ionized rare earth characteristic of the sulfate-derived and chloride-derived matrices
(Calcination temp. 900°C)

Starting matrix	Sm^{3+} cm^{-1}	Eu^{3+} cm^{-1}	Tb^{3+} cm^{-1}	Dy^{3+} cm^{-1}
$MgSO_4 \cdot 7H_2O$				16990
	16460	15520	18150	17150
	16640	15700	18460	17310
		15980		17560
$MgCl_2 \cdot 6H_2O$	16130	16050	16010	17360
	17540	16100	18090	
		16180	18260	

Summary

(i) The luminescence spectra of samarium(III), europium(III), terbium(III) and dysprosium(III) ions embedded in the calcination products of $Mg(NO_3)_2 \cdot 6H_2O$, $MgSO_4 \cdot 7H_2O$ and $MgCl_2 \cdot 6H_2O$ have been studied under excitation by cathode-ray bombardment at room temperature. The calcination of these ions was carried out either at about 900°C for 30 min. or by further heating at about 1800°C for 5 min.

(ii) The luminescence spectrum of each of the rare earth ions in magnesium oxide matrix was obtained in its pure form in the case of the calcination products derived from $Mg(NO_3)_2 \cdot 6H_2O$. A number of distinguishing diffuse luminescence bands were observed arising from the sulfate component remaining in the calcination products derived from $MgSO_4 \cdot 7H_2O$. Calcination products derived from $MgCl_2 \cdot 6H_2O$ had a composition very near that of magnesium oxide and contained only a small amount of chlorine. When the triply-ionized rare earths here investigated were embedded in these calcination products, several intense and sharp luminescence bands were found which cannot be ascribed to those observed in pure magnesium oxide, but presumably result from their chlorine content.

(iii) The luminescence spectra of these triply-ionized rare earths embedded in the matrices derived from the calcination of $MgSO_4 \cdot 7H_2O$ and $MgCl_2 \cdot 6H_2O$ were considered to be constituted of the bands observed in the matrix of pure magnesium oxide and those characteristic of a matrix containing either a sulfate- or chloride-component. The frequencies of some of the principal bands characteristic of the presence of sulfate- and chloride-components have been given for each of the triply-ionized rare earths investigated here.

(iv) As to the intensity of the luminescence of samarium(III), europium(III), terbium(III) and dysprosium(III) ions embedded in the matrices of calcined magnesium compounds, the magnitude of variation arising from heat treatment at elevated temperatures may be arranged

in the order of rare earth ions with increasing atomic numbers 62~66, the most marked decrease being seen in the luminescence of samarium(III) ions with the smallest atomic number (62), and the most marked increase, in that of dysprosium(III) ions with the largest atomic number (66).

The Institute of Physical and Chemical Research
Bunkyo-ku, Tokyo

The Structure of Bromoemimycin

By Chihiro TAMURA

(Received June 10, 1963)

The purpose of this investigation was to elucidate the molecular structure of emimycin by means of X-ray crystal analysis. Emimycin is an antibiotic which is obtained from Streptomyces griseochromogenes.[1] It has a partial inhibition against various species of bacteria and some yeasts. The chemical formula $C_8H_8N_4O_4$ was assigned to emimycin on the basis of the chemical analysis and molecular weight determination. When we started our crystal structure analysis of emimycin, nothing was known of its structure except that it had one hydroxyl group. By the direct bromination of emimycin with aqueous bromine, a bromine derivative was obtained in a form of crystals suitable for X-ray analysis. To this compound as used in this investigation, a compound which we call bromoemimycin, the formula $C_8H_6N_4Br_2O_4$ was assigned.

Experimental

Crystals of bromoemimycin were obtained by letting an aqueous solution stand for a week in a refrigerator. They are colorless long needles elongated along the c-axis. The crystal was found to be orthorhombic. The dimensions of the unit cell were obtained using higher order reflections on oscillation photographs:

$$a = 8.68 \pm 0.03\,\text{Å}$$
$$b = 11.84 \pm 0.05\,\text{Å}$$
$$c = 5.35 \pm 0.02\,\text{Å}$$
$$\text{Volume} = 549\,\text{Å}^3$$

The systematic absences were found to be $(0\,k\,l)$ for $k+l$ odd, and $(h\,0\,l)$ for h odd. Therefore, the space group was determined to be $Pna2_1$ or Pnam. These space groups require four or eight molecules in the unit cell. The density, as measured by the floatation method using a mixture of carbon tetrachloride and tetrabromoethane, was 2.25 g.cm^{-3}. From the volume of the unit cell and the density of the crystal thus obtained, the molecular weights are calculated to be 186 or 93, which are approximately one-half or one-quarter of the expected value. However, the latter value is unlikely, because the total atomic weights of the chemical formula requires 191 as the least value. This suggests that the true moleular formula should be $C_4H_3N_2BrO_2$, which gives a calculated density of 2.31 g.cm^{-3}, compatible with the observed value.

Intensities were obtained by the multiple-film technique, using an integrated Weissenberg camera. Filtered CuK_α radiation was used throughout. Three-dimensional intensity data were collected for $(h\,k\,l)$ l up to 3, for $(h\,k\,l)$ h up to 3, and for $(h\,0\,l)$ and $(h\,1\,l)$. The intensities were visually estimated using a standard calibrated strip.

Correction for the Lorentz and polarization factors were made in the usual way. Absorption correction was not made, since the cross-sections of the specimens used are 0.03×0.05 mm. for the c-axis and 0.02×0.05 mm. for the b-axis.

The structure factors were put on an approximately absolute scale by Wilson's method.[2] The temperature factor for all those atoms were taken as 2.2 Å^2, except for the bromine atom. McWeeny's f-curves[3] were employed for the light atoms, while that of Thomas[4] was used for the bromine atom.

Determination of the Structure

Since the c-axis is the shortest, it was expected that the projection of the structure on the (0 0 1) plane would show the maximum resolution of the molecular structure. This projection belongs to the same plane group pgg, no matter whether the space group is $Pna2_1$ or Pnam. Patterson syntheses were carried out using intensities of both the ordinary and modified types, the latter having been described by Takaki et al.[5]

1) M. Terao, K. Karasawa, N. Tanaka, H. Yonehara and H. Umezawa, *J. Antibiotics, Ser. A*, **13**, 401 (1960).

2) A. J. C. Wilson, *Acta Cryst.*, **2**, 318 (1949).

3) R. McWeeny, ibid., **4**, 513 (1951).

4) L. H. Thomas and K. Umeda, *J. Chem. Soc.*, **1957**, 293.

5) Y. Takaki, T. Oda and M. Sakata, Japan Applied Physics 9th Conference, 1962.

Fig. 1. Patterson projection on the (0 0 1) plane, ordiary type, $P(UV)$.

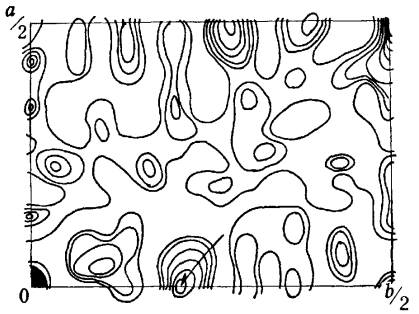

Fig. 2. Patterson projection on the (0 0 1) plane, modified type, $P'(UV)$, as $b=3$.

$$P'(UV)=\sum\sum F^2(1-e^{-b(\sin\theta/\lambda)^2})^2 \times\cos 2\pi hx\cdot\cos 2\pi ky$$

These projections showed that the bromine-bromine vector lay very close to the b-axis. The approximate coordinates of the bromine atom was found to be:

$$x=0.0$$
$$y=0.1$$

Modified Fourier projections of the structure on the (0 0 1) plane were calculated, using the signs derived from the position of the heavy atom alone.

$$\rho'(xy)=\sum\sum F(1-e^{-b(\sin\theta/\lambda)^2}) \times\cos 2\pi hx\cdot\sin 2\pi ky$$

It was prepared with 56 terms (47% of the total reflection), using cosine terms only, as the assumed position of the bromine atom was on the b-axis.

Several models of the molecular structure fit the Fourier projection. However, it contains false peaks because all the sine terms were disregarded. Closer examination showed that the bromine atom was situated slightly out of the b-axis. By the trial and error method, the coordinates of the bromine atom were assigned to the following positions:

$$x=0.010$$
$$y=0.105$$

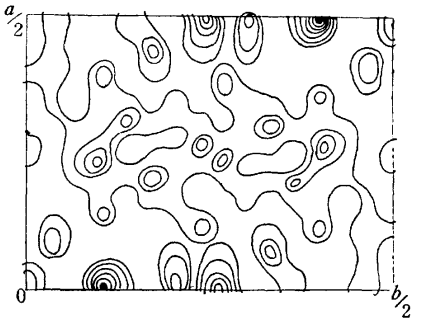

Fig. 3. Modified Fourier projection on the (0 0 1) plane.

A modified Fourier map was synthesized based on the new coordinates of the bromine atom, terms of doubtful sign being omitted. The number of terms used in this calculation was 107 out of a total of 121 observed reflections.

This Fourier projection indicates that the molecule has a six-membered ring system, with the replacements at the 1, 2 and 3 position and with position 2 taking the bromine atom, although it was not possible to distinguish carbon, nitrogen and oxygen atoms. The contribution of the light atoms were then included to determine the phases of the sturcture factors. In this calculation, all the atoms except bromine were treated as nitrogen atoms. The temperature factors for all those light atoms were taken as 2.2 Å^2, and that of bromine, as 1.5 Å^2.

In the second Fourier map, the locations of the oxygen atoms were easily recognized from the peak heights in the electron density distribution. This was also supported by the R-factor, when oxygen atoms were placed at positions 1 and 3. The six compounds listed below were considered (Fig. 4.), which are the six-membered ring systems of the meta substituents for the oxygen atoms. Compound III is already known,[6] and compound IV is difficult to fit because of its chemical properties.

$D(x, y)$ differential syntheses were calculated for the refinements of the atomic coordinates and for the distinction between carbon and nitrogen atoms. The mean value of the scattering factors of carbon and nitrogen was used for all the atoms in the pyrazine ring. These projections clearly showned the presence of anisotropy in the thermal vibrations of the bromine atom in the direction of the maximum amplitude lying almost parallel to the a-axis. The reliability factor became 18% when a correction of anisotropic temperature factors

6) G. W. Kenner, B. Lythgoe, A. R. Todd and A. Topham, *J. Chem. Soc.*, 1943, 388.

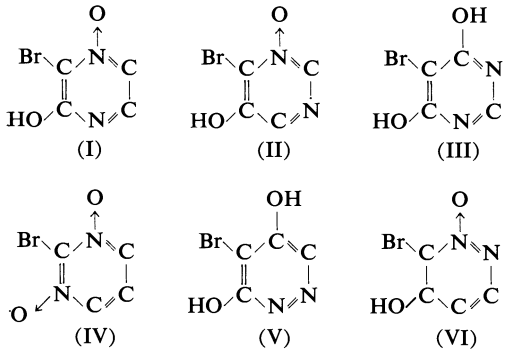

Fig. 4. Six possible structure formulae, as expected.

to bromine was made. To distinguish nitrogen from carbon atoms, $D(x, y)$ syntheses were carried out four times (Fig. 5). One can see that positions 1 and 4 have higher electron densities than those at positions 2, 3, 5 and 6. This suggests that positions 1 and 4 are occupied by nitrogen atoms. Furthermore, we have made structure factor calculations based on the following models:

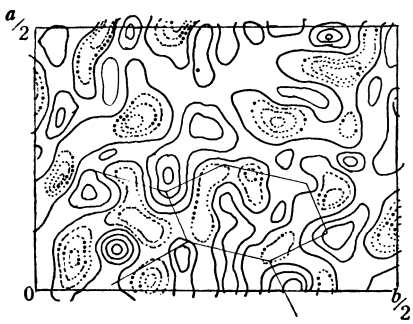

Fig. 5. Differential synthesis, on the (0 0 1) plane.

TABLE I. *R*-FACTOR CALCULATIONS FOR FOUR ESTIMATED MODELS

Model No.	Br	O	N	C	*R*-Factor %
1	9	7,8	1,2	3,4,5,6	17.5
2	9	7,8	1,3	2,4,5,6	17.7
3	9	7,8	1,4	2,3,5,6	15.9
4	9	7,8	2,4	1,3,5,6	16.9

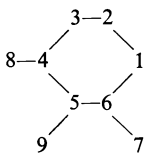

From these calculations also, the best model is found to be the one in which nitrogen atoms occupy positions 1 and 4.

The peak heights of electron density in the final Fourier synthesis is shown to be seven electrons per Å^2 for positions 1 and 4, and six electrons per Å^2 for positions 2, 3, 5 and 6. Thus, from these three results, we concluded that nitrogen atoms occupy positions 1 and 4. The final reliability factor reached 12.3% for $(h\,k\,0)$.

The systematic absences required as a possible space group $Pna2_1$ or Pnam. However, the fact that four molecules in the unit cell combined with the following face, suggested that the space group in $Pna2_1$. If it is Pnam, molecules are required to lie on the mirror planes, which are 2.67Å appart. Judging from the (0 0 1) projection, it seems very unlikely for the molecules to have such an arrangement. Furthermore, Wilson's test revealed that the space group has no center of symmetry. The space group was confirmed later by structrure factor calculations.

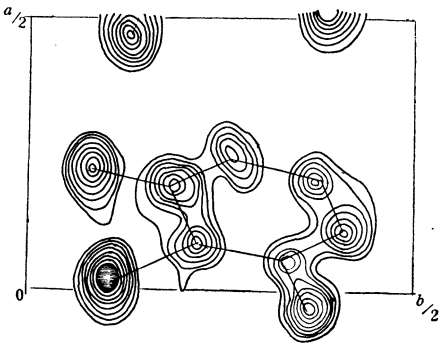

Fig. 6. Final Fourier map of bromoemimycin contours are drawn at intervals of 1 eÅ^2 except for bromine.

Now that the y-coordinate of the bromine atom was obtained by the (0 0 1) projection, and since the space group of the crystal $Pna2_1$ allowed the z-coordinate of this atom to be given at 0, we carried out Fourier analysis $\rho(x, y)$ based on the phases given by bromine. Although this projection contained overlappings of the molecule, it was possible to assign the z-coordinates of the light atoms by referring to the y-coordinates already obtained by the (0 0 1) projection. Two cycles of $D(y, z)$ syntheses were carried out for the refinements. The reliability factor for $(0\,k\,l)$ became 14.3%.

The observed and calculated structure factors are shown in Table II for $(h\,k\,0)$, and in Table III for $(0\,k\,l)$.

The final coordinates of the carbon, nitrogen, oxygen and bromine atoms are shown in Table IV.

TABLE II. COMPARISON OF CALCULATED AND OBSERVED STRUCTURE FACTORS (0 0 1).
Values are multiplied by 1/4

h k l	F_o	F_c	*h k l*	F_o	F_c	*h k l*	F_o	F_c	*h k l*	F_o	F_c
0 0 0	—	89	2 11 2	3.0	2.4	5 1 0	13.0	15.5	7 9 0	5.3	5.4
2	4.8	− 3.3	12	3.1	− 4.0	2	8.1	10.6	10	2.1	1.1
4	32.9	−35.9	13	2.9	2.9	3	4.8	− 5.5	11	1.8	1.6
6	21.6	−20.7	14	7.8	− 8.3	4	6.3	7.0			
8	11.6	11.3	15	0.0	− 0.8	5	14.0	−14.0	8 0 0	5.6	4.2
10	14.7	15.8				6	6.4	− 7.2	1	0.0	− 1.0
12	0.0	− 0.2	3 1 0	14.7	16.8	7	3.4	− 3.4	2	2.7	2.6
14	10.0	− 9.6	2	1.8	2.7	8	5.0	− 5.2	3	2.2	2.3
			3	3.2	− 3.4	9	6.5	6.3	4	3.7	− 2.9
1 1 0	16.3	16.0	4	4.3	− 3.1	10	1.4	2.0	5	0.0	− 1.0
2	4.4	3.4	5	22.2	−23.5	11	8.3	− 8.1	6	6.3	− 6.9
3	5.5	− 5.4	6	4.0	− 5.0	12	3.5	2.9	7	1.7	− 2.4
4	1.0	− 0.7	7	2.8	− 1.8	13	3.5	− 4.8	8	3.4	3.4
5	15.6	−17.8	8	2.9	− 2.1				9	0.0	− 0.6
6	3.5	2.3	9	13.5	−15.8	6 0 0	6.7	6.2	10	3.6	3.5
7	7.4	− 6.5	10	8.5	8.0	1	5.7	5.7			
8	2.4	− 1.6	11	5.1	5.5	2	4.4	4.3	9 1 0	3.0	4.0
9	16.7	15.8	12	0.0	0.0	3	5.1	5.4	2	3.5	4.4
10	3.7	− 2.6	13	7.8	− 8.0	4	10.0	−10.5	3	2.7	− 2.6
11	7.8	8.0	14	2.3	− 1.3	5	2.6	− 0.8	4	3.5	3.0
12	2.1	1.1				6	3.4	− 2.7	5	2.7	− 3.1
13	8.1	− 7.8	4 0 0	26.2	24.2	7	2.3	− 3.5	6	5.1	− 5.2
14	0.0	0.2	1	1.0	− 1.0	8	4.1	4.5	7	0.0	0.1
15	5.2	− 7.2	2	3.6	3.7	9	2.4	− 3.1	8	1.3	− 1.5
			3	1.3	0.1	10	6.2	6.7	9	0.0	1.9
2 0 0	21.8	21.8	4	16.0	−16.4	11	2.5	3.0			
1	17.5	17.0	5	2.3	1.9	12	1.8	− 1.7	10 0 0	2.3	3.2
2	7.7	5.7	6	9.5	−10.7				1	1.0	1.5
3	7.1	6.4	7	4.4	− 3.8	7 1 0	6.5	5.9	2	0.7	1.4
4	24.0	−24.3	8	9.5	9.4	2	6.6	8.2	3	3.0	4.5
5	0.6	2.1	9	0.0	− 0.7	3	3.8	− 4.0	4	2.0	− 1.9
6	6.7	− 6.0	10	7.4	8.3	4	2.0	2.0	5	0.0	0.8
7	3.2	− 3.3	11	1.2	2.9	5	7.1	− 7.1	6	1.4	− 1.4
8	11.7	11.1	12	0.0	− 1.0	6	3.7	− 4.6			
9	5.7	− 5.3	13	2.9	2.6	7	2.3	2.7	11 1 0	0.0	1.3
10	10.9	11.5	14	5.3	− 7.2	8	3.4	− 3.3	2	0.0	0.5

TABLE III. COMPARISON OF CALCULATED AND OBSERVED STRUCTORS (1 0 0)
Values are multiplied by 1/4

h k l	F_o	F_c	*h k l*	F_o	F_c	*h k l*	F_o	F_c	*h k l*	F_o	F_c
0 1 1	16.6	22.2	0 6 2	13.9	15.7	0 11 3	11.2	9.1	0 1 5	11.8	8.1
3	17.6	22.3	8	16.3	15.1	13	8.1	7.3	3	9.7	9.8
5	12.5	11.7	10	15.5	11.5				5	2.6	2.2
7	18.9	16.5	12	6.1	4.5	0 0 4	14.0	13.0	7	4.5	6.4
9	8.5	4.0	14	4.4	4.0	2	4.1	2.2	9	3.4	3.0
11	15.8	12.4				4	14.4	11.8			
13	5.4	5.8	0 1 3	11.2	11.4	6	9.2	8.9	0 0 6	8.8	10.7
			3	22.2	24.0	8	9.2	11.2	2	2.2	1.8
0 0 2	28.5	30.6	5	6.3	9.4	10	9.8	7.9	4	5.7	7.4
2	9.6	8.2	7	16.3	14.9	12	4.6	5.3	6	2.8	5.3
4	22.5	23.4	9	8.8	6.7						

TABLE IV. FRACTIONAL ATOMIC COORDINATES

Atom	x	y	z
Br	0.014	0.106	0.000
O_1	−0.043	0.363	0.055
O_2	0.223	0.081	0.395
N_1	0.114	0.409	0.330
N_2	0.190	0.182	0.362
C_1	0.062	0.329	0.186
C_2	0.090	0.218	0.195
C_3	0.245	0.265	0.500
C_4	0.203	0.381	0.516

Discussion of the Results

From the coordinates of the atoms obtained, the molecular structure of bromoemimycin was determined to be 2-bromo-3-hydroxy-pyrazine-*N*-oxide-1. Therefore, the emimycin should have the structure 3-hydroxyl-pyrazine-*N*-oxide-1.

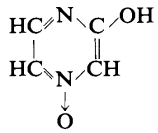

It is interesting to see that the structure of emimycin resembled that of the antibiotic aspergillic acid.[7] The molecular formula of aspergillic acid is:

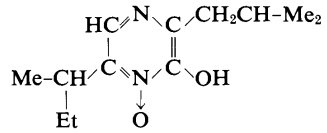

The pyrazine ring of the bromoemimycin is planar, and the equation of the best plane as determined by the methods of least squares is:

$$0.222x+y-0.820z-0.524=0$$

The displacements of the atoms within the ring and O_1, O_2 and Br from this plane are shown in Table V.

The molecule can be described as a planar

TABLE V. DISPLACEMENTS OF ALL ATOMS FROM THE PYRAZINE RING PLANE

Atom	Displacements, Å
C_1	0.04
C_2	−0.02
N_1	0.02
C_3	−0.03
C_4	0.06
N_2	−0.05
O_1	−0.17
O_2	−0.38
Br	0.11

7) G. T. Newbold, W. Sharp and F. S. Spring, ibid., 1951, 2679.

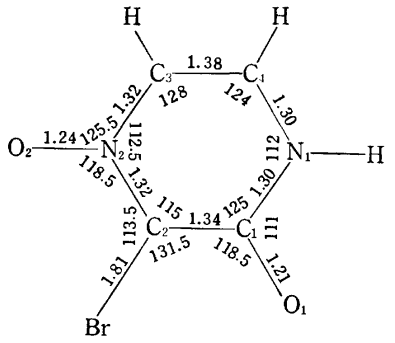

Fig. 7. The bond lengths and angles of the bromoemimycin.

pyrazine ring, but the oxygen of *N*-oxide is about 0.4Å apart from the pyrazine ring plane. The other oxygen and the bromine atom departed slightly from its plane.

The bond lengths and bond angles are given in Fig. 8.

The C_1–O_1 bond length 1.21Å, appears to be significantly shorter than the reported value, 1.39Å, for the ⩾C–OH bond in β-naphthol.[8] This might mean that the ⩾C=O bond here has a strong double bond character, so that the hydrogen atom may be attached to N_1. It may form a hydrogen bond with the carbonyl oxygen atom. It is expected that a keto-enol tautomerism similar to that found in the case of α-pyridone occurs.[9] The N_2–O_2 bond length is found to be 1.24Å, which is the same as that reported[10] for the N–O bond in phenazine-5, 10-*N*-oxide. The C–Br bond length is 1.81Å, which is considerably shorter than the reported value, 1.88Å,[11] for *o*-bromo-benzoic acid. This suggests that the C–Br bond is associated with a double bond character. The C–N bonds within the pyrazine ring are considerably shorter than those reported for those in pyrazine, 1.334Å,[12] and in pyrazinamide, 1.348Å.[13] The C–C bonds are also shorter than the mean value for benzene, 1.39Å.

The molecular arrangements are shown in Fig. 8 and Fig. 9.

The closest intermolecular interatomic distances occur between O_1 of molecule A and O_2' and N_2' of molecule B. The distances

8) H. C. Watson and A. Hargreaves, *Acta Cryst.*, 11, 556 (1958).
9) B. R. Penfold, ibid., 6, 591 (1953).
10) Y. Namba, T. Oda and T. Watanabé, This Bulletin, 36, 79 (1963).
11) G. Fergson and G. A. Sim, *Acta Cryst.*, 15, 346 (1962).
12) P. J. Wheatley, ibid., 10, 182 (1957).
13) Y. Takaki, Y. Sasada and T. Watanabé, ibid., 13, 693 (1960).

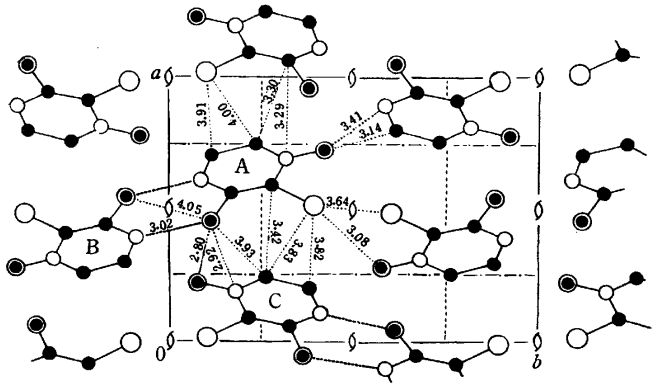

Fig. 8. Projection of the structure on (0 0 1). The hydrogen bonds are indicated by bold dotted lines. Other intermolecular atomic distances are shown by thin dotted lines.

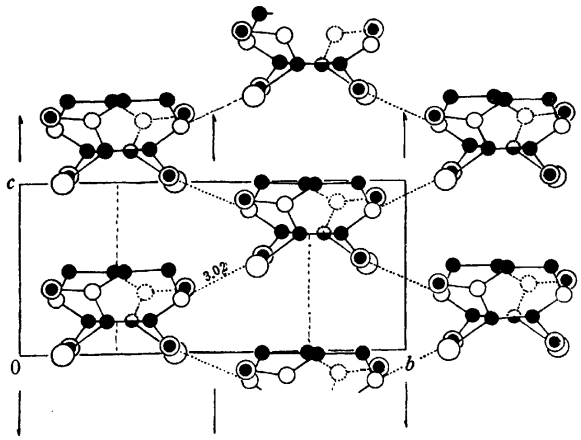

Fig. 9. The projection on (0 1 0), the hydrogen bonds are indicated by dotted lines.

are 2.81Å for $O_1 \cdots O_2'$ and 2.92Å for $O_1 \cdots N_2'$, and one might expect hydrogen bonds between those atom. However, there are no hydrogen atoms associated with these atoms, and the interatomic distances mentioned above may well be explained by the van der Waals contacts.

Another short interatomic distance, 3.02Å, is found between N_1 of molecule A and O_1'' of molecule C. It appears that a hydrogen bond would exist between these atoms. If the tautomerism occurs, as has been suggested earlier, the molecular chain along the screw axis may be stabilized by the synchronized oscillation of the hydrogen atoms.[14]

The distance between O_2 and Br', 3.08Å, is considerably shorter than the accepted value of the van der Waals radii sum, 3.48Å. It may not be possible to discuss this contact because of the inaccurate z-coordinates. Though we do not know the electronic state of the oxygen atom of the *N*-oxide group, nor the van der Waals radius of the atom in question, however, one might also suggest that this shortening is due to the charge-transfer effect.[15]

Another shorter intermolecular contact, 3.14Å, occurs between the O_2 atom of the *N*-oxide group and the ring C_4 atom; this distance does not differ significantly from the reported value in *N*-oxyphenazine, 3.11Å.[16]

I wish to thank Professor Tokunosuké Watanabé of Osaka University and Professors Toshizo Titani, Kazuo Hata, and Einosuke Fukushima of the Tokyo Metropolitan University for their useful discussions of this work. I am also grateful to Director Munetoshi

14) M. L. Huggins, *Nature*, 139, 550 (1937).

15) T. L. Charlton and J. Trotter, *Acta Cryst.*, 16, 313 (1963).

16) R. Curti, V. Riganti and S. Loechi, ibid., 14, 133 (1961).

Matsui and Dr. Akira Ito of this Laboratory for their encouragement, and to Mr. Michiya Terao for suppling the crystals. I am also indebted to Dr. Yoshio Sasada, Institute for Protein Research, Osaka University, and Dr. Yoshito Takaki, Osaka University of Liberal Arts and Education for their detailed discussions.

Physical Chemistry Section
Takamine Laboratory
Sankyo Co., Ltd.
Shinagawa-ku, Tokyo

Electronic Properties of Quaterrylene, $C_{40}H_{20}$

By Yusei MARUYAMA, Hiroo INOKUCHI and Yoshiya HARADA

(Received June 25, 1963)

Experimental studies of the electrical and optical behaviour of organic semiconductors have been carrried out for a number of materials.[1] In the polycyclic aromatic hydrocarbon series quaterrylene, $C_{40}H_{20}$ (Fig. 1), with eleven benzene rings, is one of the largest molecules ever studied as an organic semiconductor.

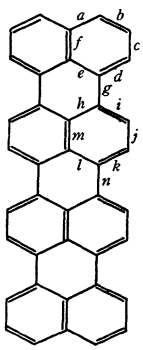

Average lengths

$a=1.392\pm0.009$ Å
$b=1.374\pm0.007$
$c=1.425\pm0.004$
$d=1.405\pm0.008$
$e=1.396\pm0.012$
$f=1.432\pm0.015$
$g=1.526\pm0.007$
$h=1.405\pm0.015$
$i=1.366\pm0.012$
$j=1.425\pm0.018$
$k=1.379\pm0.008$
$l=1.408\pm0.005$
$m=1.430\pm0.009$
$n=1.529\pm0.006$

Fig. 1. Quaterrylene ($C_{40}H_{20}$).

Quaterrylene was synthesized by Clar et al.[2] and also by Zinke and his coworkers.[3] Though there is some confusion between them it generally seems to be true that it is synthesized by a condensation of perylene. The crude material applied in the work was provided by Rütgerswerke-Aktiengeselschaft A. G., Germany, and was regarded as "Clar's quaterrylene" on the basis of its optical absorption spectra.

The crystal and molecular structure of quaterrylene (Clar's quaterrylene) was studied by Shrivastava and Speakman[4] in connection with X-ray analysis. They found that quaterrylene is isotypic with perylene; it crystallizes in the monoclinic system with $a=11.25$ Å, $b=10.66$ Å, $c=19.31$ Å, $\beta=100.6°$ and with four molecules per unit cell, while the space group is $P2_1/a$. The molecule lies with its greatest length almost exactly perpendicular to the ab plane. The bond lengths are shown in Fig. 1; the mean length of the peri-bonds connecting the naphthalenic residues is assessed at 1.53 ± 0.01 Å.

An aromatic compound with a larger molecular size would have a higher electrical conductivity. Therefore, it is expected that reliable results concerning semiconductive behaviour would be found when this hydrocarbon is applied for the observations of Shrivastava and Speakman. In this article, we are presenting a more quantitative figure of organic semiconductors obtained through a study of the electronic properties of quaterrylene.

Further, the simple molecular orbital calculation for this molecule will in due course enable the present authors to explain its spectroscopical data.

Experimental Procedures

Purifications.—The microcrystals of quaterrylene were dark green, but its thin films were violet. The hydrocarbon was extraordinarily stable, as it could be heated to about 500°C without decomposition and without melting. Since they were virtually insoluble in all solvents at room temperature, ordinary methods for the purification of organic compounds, for recrystallization and for chromatography could not be applied. Therefore, sublimation was the most useful technique for purification and also for making single crystals in this case.

1) H. Inokuchi and H. Akamatu, "Solid State Physics," Vol. 12, Academic Press, New York (1961), p. 93.
2) E. Clar, W. Kelly and R. M. Laird, *Mh. Chem.*, **87**, 391 (1956).
3) A. Zinke, H. Nussmuller and R. Ott, ibid., **86**, 853 (1955); A. Zinke, E. Zeschko and R. Ott, ibid., **91**, 445 (1960).
4) H. N. Shrivastava and J. C. Speakman, *Proc. Roy. Soc.*, **257**, 477 (1960).

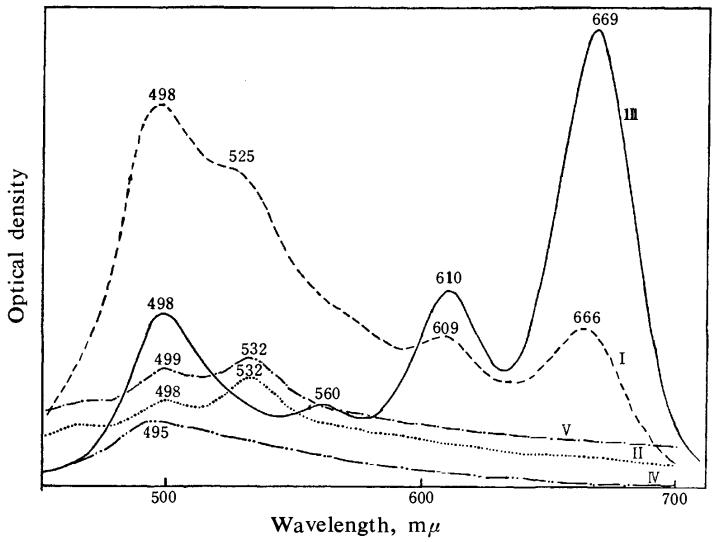

Fig. 2. The optical absorption spectra in the course of purification.

Impurities included in the matrix were soluble in trichlorbenzene. Therefore, the filtration technique was also employed for purification. Before filtration, the hydrocarbon was sublimed three times in vacuum of 10^{-5} mmHg at about 450°C. The compound was also dark green-coloured microcrystals. A suspension of quaterrylene in trichlorobenzene possessed no absorption peaks in a visible region because of its insolubility at room temperature. It was rather soluble in that solvent at about 100°C; the solution was blue at that temperature. The absorption spectrum for this step is shown as curve I in Fig. 2. When the hot solution was cooled, its colour changed to a light reddish violet from blue and dark green powders were precipitated. This spectrum is shown as II in Fig. 2. The powders which were filtered off from the solution were suspended again in cold trichlorobenzene. No absorption peaks could be found in the spectrum at room temperature, but at about 100°C several peaks appeared on the spectral response curve. The spectrum is shown as III in the figure.

A remarkable difference between curves I and III is the disappearance of the peak of 525 mμ in the latter spectrum. When the solution was cooled, only the peak of 495 mμ survived (curve IV). On the other hand, the filtered solution possessed 499 mμ and 532 mμ absorption peaks (curve V), and no considerable change in spectra was obtained by means of heating and cooling.

In order to examine the solvent effect on the absorption spectra, α-methylnaphthalene was employed in place of trichlorobenzene. This spectrum is illustrated as curve VI, which corresponds to curve I. Since no noticeable difference could be found between them, it can be concluded that the solvent effect is to be neglected.

When III and V are compared, it seems that the 530 mμ peak originates in impurities which are soluble in cold trichlorobenzene. On the basis of these results, the typical absorption spectrum of quaterrylene is possibly curve III: this agrees with the finding of Clar.[2]

The absorption spectrum of the evaporated thin film is shown in Fig. 3, along with that of the solution.

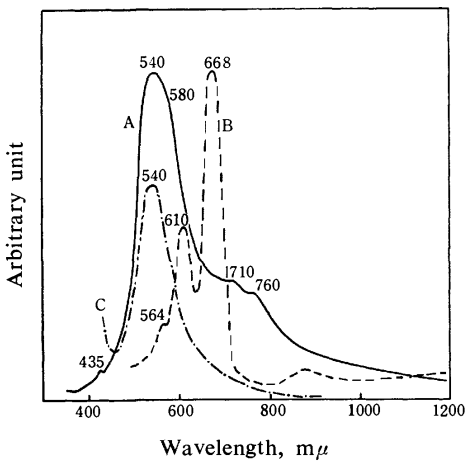

Fig. 3. The optical absorption spectra of thin film (A) and of solution (B) of quaterrylene. Curve C shows the spectral response of photo-emf.

In ordinary aromatic hydrocarbons, the positions of their absorption peaks for the solid state only shift to the long wave length side compared with those for the solution state. For quaterrylene, however, this was not the case, and, further, no correspondence between their absorption peaks and the intensity ratios of both their spectra was found.

Preparation of Single Crystals.—Because of the insolubility of quaterrylene for any solvent, it was difficult to obtain a single crystal sufficient in size to measure the resistivity by deposition from a

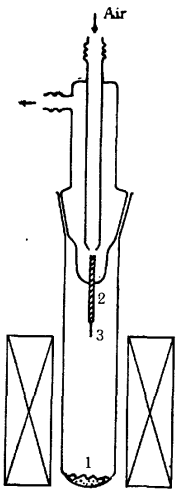

Fig. 4. The sublimation vessel used to make single crystals.

solution or by cooling the molten material. Thereby, a slow sublimation of quaterrylene in a vacuum vessel, as is shown in Fig. 4, was applied to make a single crystal. The bottom (1) of a glass tube which had been evacuated to a pressure of 10^{-5} mmHg was heated by a surrounding electric furnace. Before starting the sublimation, a tiny needle-like single crystal (3) to be used as a nucleus was stuck on the top of the tungsten rod (2), which is cooled with circulated air. Upon being heated at 350°C for a long period, the single crystal grew to a fairly large one, 0.2 mm.×0.2 mm.× 5.0 mm. The direction of the long axis of the crystal was b.

Preparation of Conductivity Cells.—The cells of the thin film of quaterrylene were prepared by the method of vacuum evaporation. When the evaporation speed was controlled to be slow, the prepared films were lustrously violet and very stable. They seemed to be better-oriented films than those of other aromatics. Thin aluminium or silver films which had also been evaporated in vacuo were employed for the electrodes of cells, as is shown in Fig. 5.

The powdered specimens compressed in an insulating cylinder were also applied measured for resistivity.

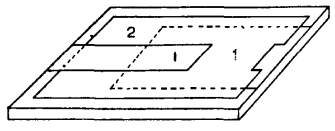

(1) Sandwich-type

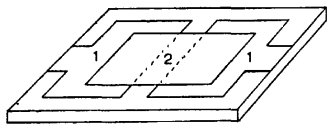

(2) Surface-type

Fig. 5. The electrode arrangement of cells. Electrodes (1) and quaterrylene (2).

Preparation of the Single Crystals for a Polarized Light Absorption.—In the course of the vacuum evaporation of quaterrylene, when a substrate, a glass plate, was heated to the proper temperature from the back by an electrical heater, fairly large single crystals grew on the film. In fact, the evaporation had to proceed very slowly in this case; it took several hours to accomplish it under a pressure of 10^{-5} mmHg.

For that duration, the substrate was kept at about 250°C, and the evaporation gun, at about 450°C. Following this method, one or two flat single crystals 50 $\mu\times100\,\mu\times100$ Å (thickness) could be found on the film under a polarization microscope, and, as they showed oblique extinction, the crystal faces were possibly ac plane. It is expected that the polarized light absorption spectra of these crystals will probably show dichroism and "Davydov Splitting."

Experimental Results

The measurements of the electrical resistivity were made with a Cary vibrating-reed electrometer, model 31, for four types of specimens; compressed powders, single crystals, sandwich-type films, and surface-type films. For the last two types of cells, the photoconductivity measurements were also made using a Hitachi photo-electric spectrometer, model EPU-2, or a projector lamp as the light sources. Their dark resistivities are listed in Table I.

Table I. The electrical resistivity, ρ_{15} of quaterrylene $\rho=\rho_0\exp(\Delta\varepsilon/2kT)$

Type of specimen	ρ_{15}, Ωcm.	$\Delta\varepsilon$, eV.
Powder	10^{10}	0.6
Single crystal	10^{6}	—
Sandwich-type	10^{13}	0.6
Surface-type	10^{5}	0.6

From the results of the two types of film cells, a substantial anisotropy of the resistivity was found by a factor of $10^{7}\sim10^{8}$; 10^{5} Ωcm. for the surface-type cell and 10^{13} Ωcm. for the sandwich-type cell.[5] The $\Delta\varepsilon$ values listed in the same table were calculated from the temperature dependence of the resistivity in the range of 15~150°C in air.

Quaterrylene was very stable against an applied electric field; the hydrocarbon could be subjected to a very high voltage, $10^{6}\sim10^{7}$ V./cm. The relation between the dark current and their applied potential is given in Fig. 6.

In the sandwich-type cell, a photovoltage appeared when it was illuminated by a visible light. As the photoelectromotive force (abbreviated as photo-emf.) originates in the

5) H. Inokuchi, H. Kuroda and H. Akamatu, This Bulletin, 34, 749 (1961).

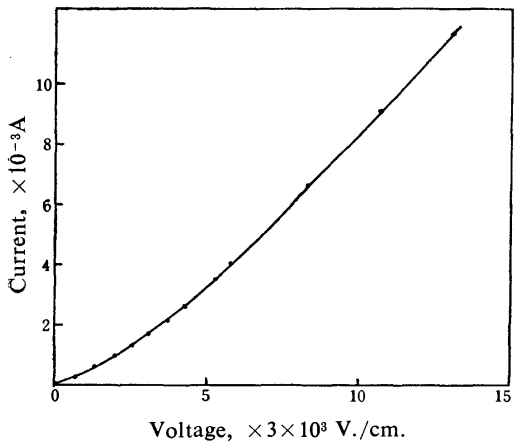

Fig. 6. The dark current versus the applied potential for the sandwich-type cell.

contact layer between the metal and the aromatics, the surface conditions of both are essential to this effect. Therefore, during the preparation of the cell and also during the measurement of the voltage, it must be kept in vacuo.* The apparatus which is convenient for such treatments is in preparation; therefore, the following data concerning photo-emf. are tentative.

In the present experiment the photovoltaic cell was made of a quaterrylene thin film sandwiched between two aluminium films on a glass plate. However, it was exposed to air for only a few minutes needed to place it in the other vessel for measurement. The photovoltage attained the maximum value of 135~270 mV. when the light intensity was 40 μW/cm^2. The cells were sensitive to a very weak light;* the dependence on the light intensity is shown in Fig. 7. The spectral response of photo-emf. is in Fig. 3 compared with the optical absorption spectrum for the film.

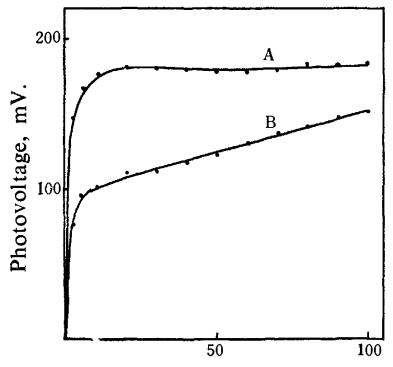

Fig. 7. The photovoltage versus the light intensity. Curve (A) is illuminated from the front of the cell and (B), from the back.

Photoconductivity measurements were also made for the surface-type and the sandwich-type cells; the former was less sensitive than the latter. The rectifying effect of the photoconduction was scarcely recognized; therefore, it could not be determined by this method whether the sign of the predominant charge carrier is plus or minus.

Pulsed photoconductivity measurement was applied to the evaporated films because of the impossibility of gaining single crystals sufficiently large to find the sign of the charge carrier and the charge mobility. The evaporation of quaterrylene was made onto a "Mylar" sheet, and then the film was covered with another Mylar sheet. The film thickness was several microns. A short light pulse, approximately a few μsec. long, was applied to the film through the conducting glass electrode, which was held against the back face of one Mylar sheet.** The applied electric field varied from about 1×10^6 V./cm. to 2×10^6 V./cm. The photocurrent was fairly small in comparison with that for anthracene;[6] therefore, a large electric field was necessary in order to obtain photocurrent enough for the detector, a Tektronix oscilloscope, type 545 A. The mobility of the charge carriers was calculated from the $\mu = d^2/Vt$ relation, where μ is the mobility; d, the film thickness; V, the voltage applied and t, the time between the light pulse and the saturation point in the charge pulse. The transit time, t, was very small and comparable to the light pulse duration; therefore, its estimation was rather difficult. The mobility was in the order of 10^{-3} cm^2/V. sec. and was very low in comparison with that of anthracene.[6] The scattering of the charge carriers at the crystalline boundaries in the film specimen may be partly responsible for this low value.

The ionization potential of solid quaterrylene was found from the photoemission

* When the surfaces of the specimens were in direct contact with air during the preparation of the cell, the photovoltaic behaviour was rather irregular. For example, the glass plate, which was exposed to air after the evaporation of the aluminum electrode (the front-side electrode) on the substrate in a vacuum vessel, was placed in another vessel to make a thin film of the aromatics. After the aromatics had been evaporated, the cell was removed to the former vessel and the electrode(the back-side electrode) was evaporated on the aromatic film. The photovoltaic cell showed a photo-emf. of the same sign when it was illuminated from either side of the electrode. In this case, it was supposed that the contact layer between the aromatics and the back-side electrode was responsible for the induced photo-emf. because the surface of the front electrode was poisoned with air.

* The measurement had to be made in a dark room because it was affected by stray room light.

** The details of the apparatus will be appear elsewhere.

6) R. G. Kepler, *Phys. Rev.*, 119, 1226 (1960).

spectrum of the evaporated film. The evaporated film on a glass plate was placed on a centre of a glass vessel, the inner-surface of which had been coated entirely with colloidal graphite as an electron collector, excepting a quartz window for introducing a light. When a monochromatic light was introduced into the vacuum photoemission cell of quaterrylene, a fairly strong photoelectric current was found. The threshold value of its spectral response, as is illustrated in Fig. 8, was around 250 mμ, 4.9 eV.

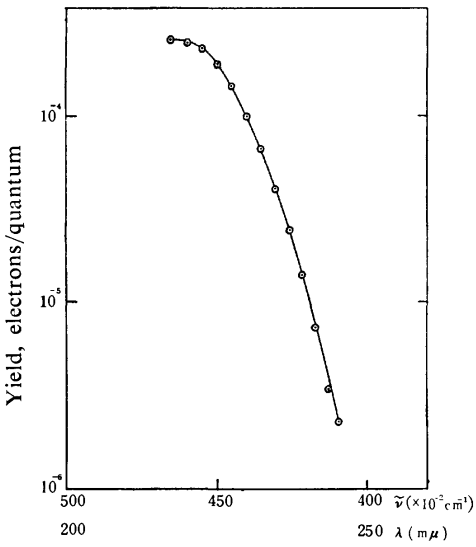

Fig. 8. The quantum yield of the photoemission of quaterrylene.

Discussion

Because the semiconductivity of quaterrylene is fairly high, its numerical values may be employed in further quantitative considerations. This is also true for the photovoltaic effect.

When contact is made between semiconductive material and metal, it is believed that the potential barrier corresponding to the contact potential difference is established. In the case of quaterrylene, such a model was employed to interpret its photovoltaic effect. Supposing the band-type model for the organic semiconductors, the following schematic diagram may be introduced for the system of quaterrylene and aluminium. In the diagram, the band gap, 0.6 eV., is based on the results of the temperature dependence of semiconduction, and the ionization potential, 4.9 eV., is based on the photoemission data. The potential barrier height which is essential for this case is $\Delta\varepsilon/2$ (half of the band gap). When the contact layer is illuminated by a light which has enough energy to excite electrons from the filled band to the conduction band excited electrons are driven to the metal by the electric field which has been built in that layer. (Holes may flow in the opposite direction.) This flow of charge carriers can be detected as photocurrents by the electrometer when the circuit is closed. In the case of an open circuit condition (in the experiment, the insulating resistance of the apparatus was greater than 10^{15} Ω), the driven carriers accumulate to build a field which prevents the further flow of the carriers. At last, equilibrium is achieved when the Fermi level of quaterrylene is lowered by the amount of the barrier height in dark. Therefore, the photovoltage, which is measured by the electrometer, is the difference between the Fermi level of aluminium and that of quaterrylene, that is, $\Delta\varepsilon/2$.[7] On this basis, the experimental data for photovoltage, 100$\sim$300 mV., seemed rather reasonable, since the $\Delta\varepsilon/2$ is about 0.3 eV.

The optical absorption spectra of quaterrylene have several interesting points, and the observation of the polarized light absorption of the single crystals made by the method previously described has been made preliminarily. The work of quantitative assignment is in progress.

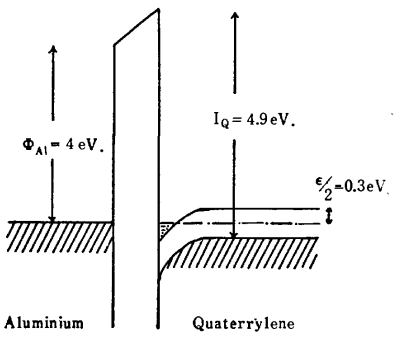

Fig. 9. A schematic energy diagram for the system of quaterrylene in contact with aluminium.

Summary

Quaterrylene ($C_{40}H_{20}$) is a dark green-coloured aromatic hydrocarbon and is extraordinarily stable, as it can be heated to over 500°C without decomposition. The semiconduction of the aromatic hydrocarbon possesses a substantial anisotropy by a factor of $10^7\sim10^8$; the resistivity in the direction parallel to the b axis is 10^6 Ωcm. (for a single crystal) or 10^5 Ωcm. (for a surface-type cell) and that perpendicular to the b axis is 10^{13} Ωcm.

7) H. Inokuchi, Y. Maruyama and H. Akamatu, This Bulletin, **34**, 1093 (1961).

However, their energy gaps are around 0.6 eV.

From its pulsed photoconduction of the thin film, a drift mobility has been estimated in the order 10^{-3} cm^2/V. sec. However, the rectifying effect of the photoconduction can scarcely be recognized; that is to say, it seems that the mobilities of the holes and electrons in crystal are almost the same.

Further, its photovoltage between aluminium and quaterrylene has a value of 0.1~0.3 V., while the ionization potential of the hydrocarbon is 4.9 eV. judging from the threshold value of the spectral response of the photoelectric emission.

From these results, a energy level diagram has been introduced for the system of the aromatic hydrocarbon-aluminium contact when a band-type model is employed as the organic semiconductor.

The Institute for Solid State Physics
The University of Tokyo
Azabu, Tokyo

*The Structure of Todomatuic Acid. The Synthesis of (±)-Dihydro-desoxo-todomatuic Acid**

By Masao NAKAZAKI and Sachihiko ISOE

(Received February 25, 1963)

The chemical investigation of todomatuic acid (I) was initiated by Tuchihashi and Hanzawa,[1] who isolated an acid on the hydrolysis of the high boiling fraction (b. p. 207~210°C/12 mmHg) of an oil which had been obtained as a by-product when *Abies sachalinensis* MAST. (todo matu) was digested with sulfite in the pulp industry. They described the sesquiterpene acid, todomatuic acid (m. p. 58.5°C; b. p. 200~215°C/3 mmHg; n_D^{50} 1.4891, d_4^{50} 1.0233, $[\alpha]_D^{32.5}$ +85.84°) and suggested the formula of $C_{15}H_{24}O_3$. They also established the presence of a carbonyl group by preparing various carbonyl derivatives: semicarbazone (m. p. 193°C), thiosemicarbazone (m. p. 149~150°C), and *p*-nitrophenylhydrazone (m. p. 154~155°C). That this compound was a ketone rather than an aldehyde was assumed as a results of its negative Schiff and Legal tests. Furthermore, the natural compound absorbed one mole of hydrogen over a palladium-on-carbon catalyst to give dihydrotodomatuic acid (b. p. 182~183°C/3 mmHg).

These facts, together with other evidence (the molecular formula, the molecular refraction index, etc.) led them to conclude correctly that this natural product is an unsaturated monocyclic sesquiterpene carboxylic acid with one keto group. Some further observations on the structure of todomatuic acid, observations which eventually led to its correct structure assignment, are due to Momose.[2] He found that, on oxidative degradation with potassium permanganate, I gave oxalic acid and an acyclic saturated ketodicarboxylic acid, $C_{13}H_{22}O_5$ (semicarbazone, decomp. p. 185~186°C). The further oxidation of $C_{13}H_{22}O_5$ with nitric acid gave isovaleric acid (IV) and racemic β-(α-carboxyethyl)glutaric acid (V), which was found to be identical with a synthetic specimen.[3]

These findings indicate that the acyclic saturated ketodicarboxylic acid $C_{13}H_{22}O_5$ could be either IIIa or IIIb, corresponding to structure I or II respectively for todomatuic acid. The structure formula I was Momose's choice, because I is compatible with the isoprene rule and several sesquiterpenes[4] (see Fig. 4) can be found posssesing the same carbon skeleton (bisabolene type) as I; of these, atlantone[5] (VI) is especially noteworthy, for in it the keto group and the endocyclic double bond are located in the same place as in I.

It seems desirable, however, to provide more convincing evidence to prove unambiguously[6]

* For a preliminary account of this work, see M. Nakazaki and S. Isoe, This Bulletin, **34**, 741 (1961).

1) R. Tuchihashi and T. Hanzawa, *J. Chem. Soc. Japan (Nippon Kwagaku Kwaishi)*, **61**, 1041 (1940).

2) T. Momose, *J. Pharm. Soc. Japan (Yakugaku Zasshi)*, **61**, 288 (1941).

3) Z. H. Skraup, *Monatsh.*, **21**, 907 (1900).

4) J. L. Simonsen and D. H. R. Barton, "The Terpenes," Vol. III, Cambridge Univ. Press, Cambridge (1952), pp. 9–25.

5) A. S. Pfau and P. A. Plattner, *Helv. Chim. Acta*, **17**, 129 (1934).

6) Momose's explanation for the formation of $C_{13}H_{22}O_5$ instead of a homologous ketodicarboxylic acid seems awkward.

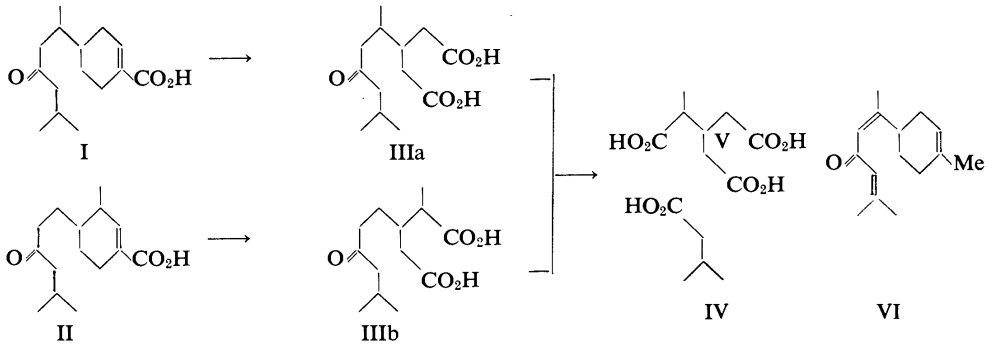

Fig. 1

the structure of this unusual monocyclic sesquiterpene carboxylic acid, preferably by a synthetic approach. In this paper, the synthesis of (±)-dihydro-desoxo-todomatuic acid and the establishment of the absolute configuration of todomatuic acid will be reported.

First we wanted to ascertain the exact location of the carboxyl group on the cyclohexene ring by means of Barbier-Wieland degradation, hoping that a cyclohexanone derivative, our prime objective, would prove to be a useful key substance for structure determination as well as for a synthetic approach.

The Wolff-Kishner reduction of todomatuic acid yielded desoxy-todomatuic acid (VIIa) (Fig. 2) (m. p. 59~60°C), which was esterified with diazomethane to afford the methyl desoxo-todomatuate (VIIc) (b. p. 130~131°C/1 mmHg). The catalytic hydrogenation of VIIc over an Adams catalyst gave methyl dihydro-desoxo-todomatuate (VIIIa) (b. p. 117~119°C/1 mmHg), which gave the carbinol VIIIc with phenylmagnesium bromide. The unsaturated compound VIIId, obtained from VIIIc on dehydration by boiling with acetic anhydride and pyridine, was ozonolyzed. After the ozonide had been decomposed with zinc powder, the neutral fraction boiling at 100~110°C/1 mmHg was purified by chromatography on alumina. An oil which showed infrared absorption at 1704 cm^{-1} (six-membered cyclic ketone) was converted directly into semicarbazone (m. p. 151~152°C). If the structure of todomatuic acid is represented correctly by I, this ketone should be 2-(4-oxocyclohexyl)-6-methylheptane (IX). Our next project was, therefore, the synthsis of this compound.

p-Anisyl-isohexylketone (Xa) (Fig. 3), obtained by the Friedel-Crafts reaction of anisol

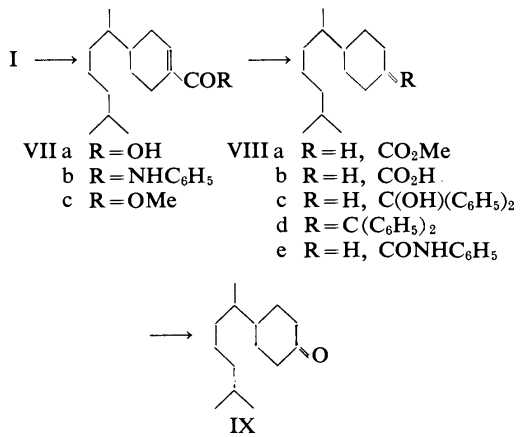

Fig. 2

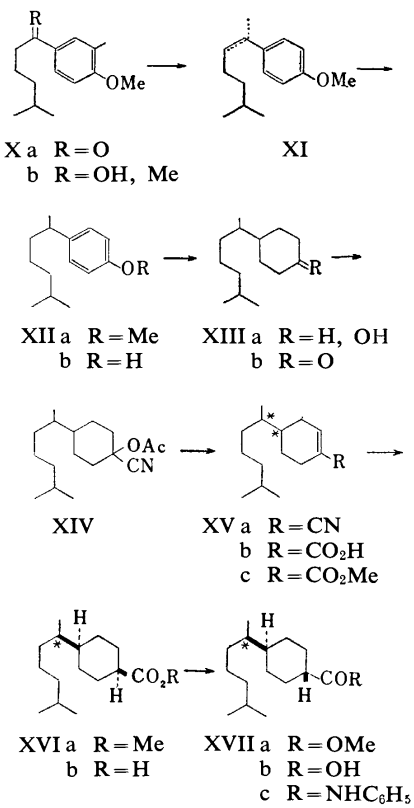

Fig. 3

and 5-methylhexanoyl chloride, was converted into the carbinol Xb with methylmagnesium bromide, and then Xb was dehydrated by boiling it with acetic anhydride to afford the unsaturated phenol ether XI. The catalytic hydrogenation of XI gave XIIa, which was hydrolyzed by boiling it with hydroiodic acid in an acetic acid solution to afford the phenol XIIb. The high pressure catalytic hydrogenation of XIIb (Raney nickel 130 atms., 140~150°C) yielded the alcohol XIIIa, which was oxidized with potassium dichromate in sulfuric acid to (±)-2-(4-oxocyclohexyl)-6-methylheptane (XIIIb) (b. p. 113~114°C/1 mmHg, semicarbazone, m. p. 149~150°C), whose infrared absorption spectrum was found superimposable on that of the ketone IX from the natural product. These findings firmly established the structure of todomatuic acid (I). Our attention was next directed to introduce a carboxyl group to the C_1 position of the ketone XIIIb in order to synthesize (±)-dihydro-desoxo-todomatuic acid (VIIIb).

The ketone XIIIb was heated with potassium cyanide in acetic anhydride to give the cyanohydrin acetate XIV, which was pyrolyzed at 1 mmHg by passing it through a heated Pyrex tube (600°C) packed with ceramic Rashig rings to afford the unsaturated cyanide XVa, which was then hydrolyzed to the unsaturated acid XVb (b. p. 163~165°C/1 mmHg). Although two racemic forms[7] were expected for the structure XVb because of the presence of two asymmetric carbon atoms, the infrared absorption spectrum of the synthetic XVb was found identical with that of (+)-desoxotodomatuic acid (VIIa).

In order to provide more unambiguous evidence, it seemed desirable to compare compounds with only one asymmetric center. The synthetic XVb was esterified with diazomethane, and the methyl ester thus obtained was catalytically hydrogenated on an Adams catalyst, affording the saturated methyl ester XVIa, probably the cis form predominantly. Equilibration of the methyl ester XVIa by boiling it with sodium ethoxide yielded the more stable trans methyl ester XVIIa, which was then saponified to (±)-*trans*-2-(4-carboxycyclohexyl)-6-methylheptane (XVIIb) (b. p. 152~155°C/1 mmHg; n_D^{18} 1.4723); its anilide XVIIc melted at 105~106°C. In order to compare the above mentioned synthetic XVIIb with the saturated acid VIIIb obtained from the natural product, it is necessary to convert VIIIb to the trans form; this was accomplished by the equilibration of the methyl ester VIIIa by boiling it with sodium ethoxide. Saponification of the optically active trans methyl ester thus prepared gave (+)-*trans*-dihydro-desoxo-todomatuic acid (XVIIb), b. p. 150~153°C/1 mmHg; $[\alpha]_D^{27}$ +14.1°; n_D^{18} 1.4723 (the anilide, m. p. 115~116°C), whose infrared spectrum was found to be superimposable on that of the synthetic XVIIb in every detail.

Having thus accomplished the synthesis of (±)-dihydro-desoxo-todomatuic acid, let us now proceed to discuss the absolute configuration of todomatuic acid. As can be seen from the structure formula of todomatuic acid (I) (Fig. 4; the molecular rotations are shown below the structure formula of the relevant compounds), it has two asymmetric centers (C_4 and C_7). The absolute configuration around C_4 will be discussed first. Since todomatuic acid (I) and desoxo-todomatuic acid (VIIa) show almost equal rotation values ($[M]_D$ +233° and $[M]_D$ +224° respectively), the keto groups on the side chains seem to have little effect on the optical rotations. The same is true for the asymmetric center at C_7; dihydro-desoxo-todomatuic acid XIXa, lacking the asymmetric center at C_4, exhibits very little rotation, showing a predominant contribution of the asymmetric center at C_4 to the optical rotation of the unsaturated compounds I and VIIa.

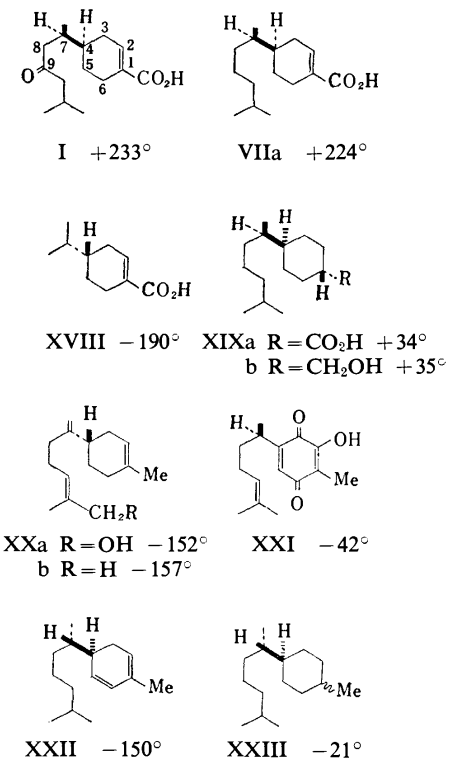

Fig. 4

7) Pyrolysis at 600°C can hardly be stereo-specific, and the products, XVa, XVb and XVc, may be a mixture of two racemic forms.

Therefore, it is safe to compare todomatuic acid (I) and desoxo-todomatuic acid (VIIa) with (−)-phellandric acid (XVIII) ($[M]_D$ −190°),[8] despite the fact that I and VIIa have extra asymmetric centers in the side chains. One of Mills' empirical rules[9] tells us that I and VIIa have the (R)-configuration opposite natural (−)-phellandric acid (XVIII) at the C_4 center. Among the four bisabolene type sesquiterpenes whose absolute configurations have been established (lancerol (XXa),[10] bisabolene (XXb),[11] perezone (XXI)[12] and zingiberene (XXII)[13]), is particularly suitable to compare zingiberene's asymmetric center in the side chain with that of todomatuic acid (I). Hexahydrozingiberene (XXIII) ($[M]_D$ −21°),[14] which has only one asymmetric center in the side chain, can be compared with (+)-dihydro-desoxo-todomatuic acid (XIXa), since the substitutions at C_1 are too remote from the asymmetric centers on C_7 to affect the signs of rotation in both compounds. A more relevant comparison is that of XXIII with the alcohol XIXb, $[M]_D$ +35°, prepared from XIXa by lithium aluminum hydride reduction. Since the hydroxymethyl group has almost the same polarizability as the methyl group,[15] the fact that XIXb and XXIII show opposite rotations of about the same order indicates that these compounds have opposite configurations in the side chains. This deduction assigns the (R)-configuration to the asymmetric center, C_7, of todomatuic acid. Although the specific rotation[5] reported for atlantone (VI) is very small (+1∼+6°),[16] it is very interesting to note that todomatuic acid and atlantone are the only two sesquiterpene ketones of the bisabolene type with a positive optical rotation so far isolated from conifers.

These facts are of interest in connection with the taxonomy of conifers,[17] suggesting the same absolute configuration at the C_4 asymmetric centers in both compounds.

Experimental*

Todomatuic Acid (I). — Crude todomatuic acid (80 g.), obtained from the hydrolysis of the high boiling fraction of sulfite oil, was recrystallized from petroleum ether (b. p. 35∼60°C) to give 41 g. of a pure compound, m. p. 57∼59°C, $[\alpha]_D^{13}$ +92.50° (*c* 1.2 in ethanol) (lit.:[1] m. p. 58.5°C, $[\alpha]_D$ +85.84° (in ethanol)).

Found: C, 71.56; H, 9.57. Calcd. for $C_{15}H_{24}O_3$: C, 71.38; H, 9.57%.

The semicarbazone prepared from I was recrystallized from diluted ethanol decomp. p. 190°C (lit.:[1] decomp. p. 193.2∼193.7°C).

Found: C, 61.92; H, 8.83; N, 13.42. Calcd. for $C_{16}H_{27}O_3N_3$: C, 62.09; H, 8.80; N, 13.59%.

(+)-Desoxo-todomatuic Acid (VIIa).—In a copper flask, 12 g. of sodium was dissolved in 230 cc. of diethylene glycol, and a mixture of 21 g. of todomatuic acid and 20 cc. of hydrazine (prepared from commercially available 80% hydrazine hydrate by azeotropic dehydration with toluene) was then added. The reaction mixture was heated at 180∼190°C, and the generated water was co-distilled with excess hydrazine. Heating was continues for 24 hr., and then 15 cc. of hydrazine was added. The reaction mixture was heated for another 24 hr. and then poured into ice water. After the aqueous solution was made acidic with concentrated hydrochloric acid, this was extracted with benzene. The benzene extract was dried over anhydrous magnesium sulfate. Removal of the solvent gave a viscous residue which distilled at 164∼166°C/1 mmHg to give 13.8 g. of a viscous oil. After this oil had stood at room temperature, the product crystallized. Recrystallization from diluted methanol gave crystals which melted at 50∼60°C, $[\alpha]_D^{27}$ +94.3° (*c* 1.18 in ethanol).

Found: C, 75.90; H, 11.18. Calcd. for $C_{15}H_{26}O_2$: C, 75.58; H, 11.00%.

The anilide VIIIb was prepared by the usual procedure and recrystallized from petroleum ether and then from diluted methanol; m. p. 78∼79°C.

Found: C, 80.36; H, 10.15; N, 4.77. Calcd. for $C_{21}H_{31}ON$: C, 80.46; H, 9.97; N, 4.47%

(+)-*trans*-Dihydro-desoxo-todomatuic Acid (XVIIb).—To 40 cc. of an ether solution of diazomethane prepared from 4 g. of *N*-nitrosomethylurea, a solution of 2 g. of desoxo-todomatuic acid in 50 cc. of ether was added. After being kept at room temperature for 2 hr., the excess diazomethane was decomposed with acetic acid. After the mixture had been washed with water and dried over anhydrous magnesium sulfate, the solvent was removed

8) R. G. Cook, A. K. Macbeth and T. B. Swanson, *J. Chem. Soc.*, **1940**, 808.

9) J. A. Mills, ibid., **1952**, 4976.

10) A. Birch and A. R. Murray, ibid., **1951**, 1888. The absolute configuration was established by Mills[9] by comparing its rotation with that of limonene.

11) A. Eschenmoser, J. Schreiber and W. Keller, *Helv. Chim. Acta*, **34**, 1667 (1951). The absolute configuration was established by Mills[9] by a comparison of its rotation with that of limonene.

12) F. Kögl and A. G. Boer, *Rec. trav. chim.*, **54**, 779 (1935); cf. also Ref. 13.

13) A. Eschenmoser and H. Schinz, *Helv. Chim. Acta*, **33**, 171 (1950); D. Arigoni and O. Jeger, ibid., **47**, 881 (1954). See also Ref. 11.

14) F. W. Semmler and A. Becker, *Ber.*, **46**, 1816 (1913); L. Ruzicka and A. G. van Veen, *Ann.*, **468**, 143 (1929).

15) J. Brewster. *J. Am. Chem. Soc.*, **81**, 5475 (1959).

16) The fact that the proton at C_4 is labile might be responsible for the racemization through enolization. According to Mills,[9] an optically pure compound with the VI structure should show at least $[M]_D$+150°. Compare this with the molecular rotations of XXa and XXb (Fig. 4).

17) H. Erdtman, "Chemistry of Some Heartwood Constitutions of Conifers and their Physiological and Taxonomic Significance," in A. Todd, Ed., "Progress in Organic Chemistry," Vol. I, Academic Press Inc., Pub., New York (1952), p. 22.

* The analyses were performed in the microanalytical laboratory of the Institute of Polytechnics, Osaka City University.

to afford a liquid which was distilled to give 1.9 g. of methyl desoxo-todomatuate (VIIc) (b. p. 130~131°C/1 mmHg). The catalytic hydrogenation of 1.9 g. of VIIc in 30 cc. of ethanol with 0.5 g. of an Adams catalyst gave 1.7 g. of methyl dihydro-desoxo-todomatuate, (VIII) (b. p. 117~119°/1 mmHg). To a sodium ethoxide solution prepared from 0.2 g. of sodium and 11 cc. of absolute ethanol, 1.7 g. of methyl dihydro-desoxo-todomatuate (VIIIa) was added. After the solution had been refluxed for 1 hr., the methyl ester was saponified by boiling it with 1 g. of potassium hydroxide and 5 cc. of water. After the ethanol had been distilled off, the reaction mixture was refluxed for 4 hr. and then diluted with 20 cc. of water. The alkaline solution was washed with ether and was made acidic with concentrated hydrochloric acid. After this solution had been extracted with ether and dried over anhydrous magnesium sulfate, the solvent was removed to give a viscous oil which distilled at 150~153°C/1 mmHg, affording 1.6 g. of an oil. $[\alpha]_D^{27}$ +14.1° (*c* 1.77 in ethanol), n_D^{18} 1.4723. The anilide prepared from XVIIb was recrystallized from ethanol, m. p. 115~116°C.

Found: C, 80.14; H, 10.62; N, 4.49. Calcd. for $C_{21}H_{33}ON$: C, 79.94; H, 10.54; N, 4.44%.

The Wieland-Barbier Degradation of Methyl (+)-Dihydro-desoxo-todomatuate (VIIIa).—To a Grignard solution prepared from 4 g. of magnesium, 30 g. of bromobenzene and 100 cc. of ether, a solution of 4 g. of the methyl ester VIIIa in 30 cc. of ether was added. After the solution had been refluxed for 15 min., the ether was removed and replaced by 50 cc. of benzene; then the reaction mixture was heated in an oil bath (110°C) for 12 hr. The Grignard complex was decomposed with cold diluted hydrochloric acid and extracted with ether. After being dried over anhydrous magnesium sulfate, the ether extract was concentrated to give an oil which was distilled to yield 4.5 g. of the tertiary alcohol VIIIc (b. p. 200~205°C/1 mmHg). The tertiary alcohol VIIIc (8.8 g.) was dehydrated by heating it with 200 cc. of acetic anhydride and 40 cc. of pyridine for 4 hr. The reaction mixture was poured into ice water and extracted with ether. The ether extract was washed with diluted hydrochloric acid and a 5% sodium carbonate solution successively and then dried over anhydrous magnesium sulfate. Removal of the solvent gave an oil which was then distilled to afford 7.2 g. of the unsaturated compound VIIId (b. p. 205~210°C/1 mmHg). To a solution of 7.2 g. of the unsaturated compound VIIId in 75 cc. of chloroform, a stream of ozone (2%) was passed for 1 hr. The ozonide was decomposed with 8 cc. of acetic acid and 6 g. of zinc powder. After being freed from the zinc powder, the chloroform solution was washed with a diluted sodium carbonate solution and then concentrated. The residue was distilled at 1 mmHg to give two fractions: 1. b. p. 100~110°C. 1 g; 2. b. p. 190~210°C. 5.4 g. The higher boiling fraction was shown to be recovered unsaturated compound VIIId by examination of its infrared spectrum; it was then ozonolyzed again to afford 0.7 g. of the low boiling fraction (b. p. 110~120°C/1 mmHg). The combined low boiling fractions were dissolved in 20 cc. of petroleum ether and passed through a column containing 35 g. of alumina. Elution with petroleum ether-ether (10 : 1) gave 0.2 g. of an oil which exhibited an absorption at 1704 cm^{-1} infrared spectrum; this was directly converted into semicarbazone. The semicarbazone was recrystallized from diluted ethanol, m. p. 151~152°C.

Found: C, 67.38; H, 11.02; N, 15.97. Calcd. for $C_{15}H_{29}ON_3$: C, 67.37; H, 10.93; N, 15.72%.

***p*-Anisyl-isohexylketone (Xa).**—A mixture of 44.3 g. of 5-methylhexanoic acid and 35 cc. of thionyl chloride was heated on a water bath for 30 min. After the excess thionyl chloride had been removed, the residue was distilled to yield 45 g. of 5-methylhexanoyl chloride (b. p. 70~71°C/1 mmHg). To a stirred mixture of 53.4 g. of aluminum chloride and 150 cc. of carbon disulfide, 45 g. of the acid chloride was added over a 10 min. period under cooling. After 36.7 g. of anisole had been added over a 30 min. period, stirring was continued for another 30 min.; then the temperature of the reaction mixture was gradually brought to room temperature. The reaction mixture was decomposed with ice and extracted with ether. The ether extract was washed with water, a 10% sodium hydroxide solution and water successively, and then dried over anhydrous magnesium sulfate. Removal of the solvent gave a residue which distilled to yield 56.6 g. of Xa, b. p. 131~133°C/1 mmHg.

Found: C, 76.27; H, 9.34. Calcd. for $C_{14}H_{20}O_2$: C, 76.32; H, 9.15%.

The semicarbazone prepared from Xa was recrystallized from ethanol to give prisms, m. p. 124~125°C.

Found: C, 65.11; H, 8.54; N, 15.10. Calcd. for $C_{15}H_{23}O_2N_3$: C, 64.95; H, 8.36; N, 15.5%.

2-*p*-Anisyl-6-methylheptane (XIIa).—To a suspension of 18 g. of magnesium in 250 cc. of ether, a stream of methyl bromide was passed until the magnesium was consumed. A solution of 56 g. of the ketone Xa in 100 cc. of ether was added to the Grignard solution for over 1 hr., and the reaction mixture was refluxed for 2 hr. After diluted hydrochloric acid had been added to decompose the Grignard complex, the reaction mixture was extracted with ether. Removal of the solvent gave the crude alcohol Xb, which was refluxed with 150 cc. of acetic anhydride for 3 hr. The solution was concentrated at reduced pressure and the residual oil was distilled, giving 47.8 g. of the unsaturated compound XI (b. p. 107~113°C/1 mmHg). Two grams of Raney nickel were added to a solution of 47.8 g. of the unsaturated compound XI in 30 cc. of ethanol and hydrogenated in a steel bomb at 25 atm. of hydrogen at 30~40°C. The product boiled at 107~113°C/1 mmHg and weighed 47.5 g.

Found: C, 81.95; H, 11.13. Calcd. for $C_{15}H_{24}O$: C, 81.76; H, 10.98%.

2-(4-Hydroxyphenyl)-6-methylheptane (XIIb).—A mixture of 42 g. of XIIa, 115 cc. of hydroiodic acid (b. p. 127°C), 40 cc. of acetic anhydride and 1 g. of red phosphorus was refluxed for 2 hr. After 60 cc. of acetic anhydride had been added, heating

was resumed for another 2 hr. The reaction mixture was then poured into ice water and extracted with benzene. The benzene extract was washed with water and dried over anhydrous magnesium sulfate. Removal of the solvent and distillation gave 38 g. of XIIb, b. p. 127~128°C/1 mmHg.

Found: C, 80.42; H, 10.80. Calcd. for $C_{14}H_{22}O$: C, 81.50; H, 10.75%.

2-(4-Hydroxycyclohexyl)-6-methylheptane(XIIIa).—The phenol (38 g.) XIIb was catalytically hydrogenated in 70 cc. of ethanol with 2 g. of Raney nickel in a steel bomb (140~150°C, 130 atm. of hydrogen) for 3 hr. After being freed from the catalyst, the product was distilled to give 37.5 g. of the cyclohexanol derivative XIIIa, b. p. 120~121°C/1 mmHg.

Found: C, 79.75; H, 12.19. Calcd. for $C_{14}H_{28}O$: C, 79.18; H, 13.29%.

2-(4-Oxocyclohexyl)-6-methylheptane (XIIIb).—To a solution of 18.5 g. of potassium dichromate in 142 cc. of water, 16.3 cc. of concentrated sulfuric acid was added. To the stirred dichromate solution, 37.0 g. of the alcohol XIIIa was added at 57~58°C. The mixture was then stirred for 20 min., cooled to room temperature and extracted with ether. The ether extract was washed with water and with a 5% sodium hydroxide solution successively, and then dried over anhydrous magnesium sulfate. Removal of the solvent and distillation gave 27.5 g. of XIIIb (b. p. 113~114°C/1 mmHg).

Found: C, 79.96; H, 12.91. Calcd: for $C_{14}H_{16}O$: C, 79.93; H, 12.46%.

The semicarbazone prepared from XIIIb was recrystallized from diluted ethanol, m. p. 149~150°C. The mixed melting point with the semicarbazone (m. p. 151~152°C) of IX from todomatuic acid was 149.5~150°C, and their infrared spectra in a Nujol mull or carbon disulfide were superimposable in every detail.

Found: C, 67.53; H, 10.78; N, 15.73. Calcd. for $C_{15}H_{29}ON_3$: C, 67.37; H, 10.93; N, 15.72%.

2-(4-Cyano-4-acetoxycyclohexyl)-6-methylheptane (XIV).—A mixture of 20 g. of the ketone XIIIb and 22.8 g. of acetic anhydride was added slowly to a chilled solution of 14.6 g. of potassium cyanide in 145 cc. of water and then stirred for 13 hr. at room temperature. The reaction mixture was neutralized with a sodium carbonate solution and extracted with ether. The ether extract was washed with water and dried over anhydrous magnesium sulfate. When the solvent was removed at reduced pressure, the cyanohydrin began to decompose. The crude cyanohydrin was directly acetylated by heating it with 10 cc. of acetic anhydride and 1.3 g. of acetyl chloride for 1 hr. After concentration at reduced pressure, the residue was distilled to give 3.5 g. of XIV, b. p. 145~147°C/1 mmHg. The ketone XIIIb was recovered from a low boiling fraction.

2-(4-Carboxycyclohex-3-enyl)-6-methylheptane (XVb).—Five grams of the acetate XIV were passed through a heated Pyrex tube (600°C) packed with ceramic Rashing rings at reduced pressure (1 mmHg) over 1.5 hr. The decomposition products were collected in a trap chilled in a dry ice-acetone bath. After being diluted with ether, the product was washed with water and dried over anhydrous magnesium sulfate. The solvent was removed, and the residue was distilled to give 2.11 g. of the unsaturated cyanide XVa (b.p. 130~132°C/1 mmHg). The cyanide XVa (2.0 g.) was hydrolyzed by heating it with a solution of 1.5 g. of potassium hydroxide in 13 cc. of water with 15 cc. of diethylene glycol for 30 hr. After being made acidic with concentrated hydrochloric acid, the mixture was extracted with benzene. Removal of the solvent gave a residue which was hydrolyzed further by refluxing it with an ethanolic sodium ethoxide solution (prepared from 0.5 g. of sodium and 20 cc. of ethanol). The reaction mixture was diluted with water and washed with benzene. The unsaturated acid XVb precipitated by adding diluted hydrochloric acid was extracted with ether. Removal of the solvent gave an oil which distilled to afford 1.5 g. of XVb, b. p. 163~165°C/1 mmHg. The infrared spectrum was found superimposable on that of (+)-desoxo-todomatuic acid (VIIa).

Found: C, 75.34; H, 10.99. Calcd. for $C_{15}H_{26}O_2$: C, 75.58; H, 11.00%.

***trans*-2-(4-Carboxycyclohexyl)-6-methylheptane (XVIIb).**—The unsaturated acid XVb (1.2 g.) was dissolved in 50 cc. of ether and esterified with a diazomethane ether solution prepared from 2.4 g. of nitrosomethylurea. After the reaction mixture had been allowed to stand at room temperature for 3 hr., the excess diazomethane was decomposed with a small amount of acetic acid. The mixture was washed with a diluted sodium cabonate solution and then water. After being dried over anhydrous sodium sulfate, the solvent was removed to give an oil which distilled at 128~130°C/1 mmHg. The yield was 1.2 g. The methyl ester XVc was dissolved in 20 cc. of ethanol and catalytically hydrogenated with 80 mg. of an Adams catalyst for 12 hr. Removal of the catalyst and the solvent gave 1.1 g. of an oil which was distilled, b. p. 117~120°C/1 mmHg. The saturated ester (XVIa) (1.1 g.) was added to an ethanolic sodium ethoxide solution prepared from 0.1 g. of sodium and 5 cc. of ethanol, and the solution was refluxed for 1 hr. After a solution of 0.7 g. of sodium hydroxide in 8 cc. of water had been added, the mixture was refluxed for 8 hr. The solution was acidified with diluted hydrochloric acid and extracted with ether. Removal of the solvent and distillation of the residue gave an oil (1.0 g.) (b. p. 152~155°C/1 mmHg; n_D^{18} 1.4723) whose infrared absorption spectrum was found superimposable in every detail on that of natural (+)-*trans*-dihyro-desoxo-todomatuic acid. The anilide prepared from XVIIb was recrystallized from diluted methanol to give needles, m. p. 105~106°C. The mixed melting point with the anilide from natural (+)-*trans*-dihydro-desoxo-todomatuic acid (m. p. 115~116°C) was 103~104°C.

Found: C, 80.42; H, 10.76; N, 4.64. Calcd. for $C_{21}H_{33}ON$: C, 79.94; H, 10.54; N, 4.44%.

The Lithium Aluminum Hydride Reduction of Methyl (+)-*trans*-Dihydro-desoxo-todomatuate (XVIIa).—To a slurry of 0.57 g. of lithium aluminium hydride and 10 cc. of ether, a solution of 2.0 g. of the optically active methyl ester XVIIa in 10 cc. of ether was added over a 45 min. period.

After the reaction mixture had been refluxed for 1.5 hr. and then cooled in an ice bath, the excess lithium aluminum hydride was decomposed with ethyl acetate. Twenty cubric centimeters of 2 N hydrochloric acid were added, and the reaction mixture was extracted with ether. The ether extract was washed with water and dried with anhydrous sodium sulfate. Removal of the solvent gave a viscous oil which was then distilled to afford 1.5 g. of a liquid, b. p. 152~155°C/4 mmHg; n_D^{31} 1.4663, $[\alpha]_D^{31}$ +15.5° (*c* 30.4 in chloroform).

This work was partially supported by a grant-in-aid for fundamental scientific research from the Ministry of Education, to which the author's thanks are due. They also are very grateful to Mr. Yoshio Ohta for his technical assistance and to Mr. Sohei Sato, Dai Shyowa Pulp Ind. Co., for generously supplying them with crude todomatuic acid.

Department of Chemistry
Institute of Polytechnics
Osaka City University
Kita-ku, Osaka

On the Absolute Configuration of threo-1, 2-Diphenyl-2-hydroxyethylamine

By Masao NAKAZAKI

(Received February 25, 1963)

The (R)-configuration of (−)-1, 2-diphenylethylamine (Ia) has been established[1] by the degradation of its (+)-*N*-acetyl derivative Ib to D-aspartic acid (II), and the analgesic property of (−)-*N*, *N*-dimethyl-1, 2-diphenylethylamine (Ic), derived from Ia, has been attributed to its configuration similar to that of (−)-morphine (Fig. 1).

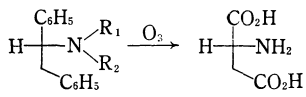

Ia $R_1=R_2=H$ II
b $R_1=Ac$, $R_2=H$
c $R_1=R_2=Me$

Fig. 1

However, this assignment of the absolute configuration to Ia has been found to be inconsistent with the findings of La Manna and his collaborators,[2] who obtained (+)-Ia (the enantiomer of Ia) from (+)-*threo*-1, 2-diphenyl-2-hydroxyethylamine (VIIa) by replacing the hydroxyl group with a chlorine atom with phosphorus pentachloride and by the subsequent hydrogenolysis of the chloro derivative (Fig. 2). The L-configuration* had been assigned to the (+)-*threo* isomer VIIa by Weijlard et al.,[3] who reported that they had converted the *N*-formyl derivative IVb of the D(−)-*erythro* isomer IVa, whose absolute configuration had been proved unambiguously,[4] into the (+)-*threo* isomer VIIa by treating it with thionyl chloride, which is believed to allow only the hydroxyl group to epimerize.[5]

Once this assignment of the L-configuration of the (+)-*threo* isomer VIIa is accepted as correct, it is more than natural that La Manna et al. were led to give the (R)-configuration to (+)-1, 2-diphenylethylamine instead of to the (−)- isomer Ia. However, a very curious situation arose when they found that the D(−)-*erythro* isomer IVa afforded (−)-Ia by the same treatment applied to the (+)-*threo* isomer VIIa.

1) M. Nakazaki, *Chem. & Ind.*, **1962**, 1577; This Bulletin, **36**, 161 (1963).

2) P. Pratesi, A. La Manna and L. Fontanella, *Il Farmaco (Pavia), Ed. Sci.*, **10**, 673 (1955); *Chem. Abstr.*, **50**, 10057 (1956).

* The configurations of the formulations in this paper are in accord with Fischer's convention referring to the asymmetric center at C_2 (Figs. 2 and 3).

3) J. Weijlard, K. Pfister. 3rd, E. F. Swanezy, C. A. Robinson and M. Tishler, *J. Am. Chem. Soc.*, **73**, 1217 (1951).

4) A. McKenzie and D. J. C. Pirie (*Ber.*, **69**, 876 (1936)) correlated the configuration at C_2 of IVa with D(−)-mandelic acid (IIIa) via D(−)-benzoin (IIIb) and D(−)-benzoin oxime (IIIc) (Fig. 2). (Cf. also A. McKenzie and H. Wren, *J. Chem. Soc.*, **93**, 309 (1908).) The erythro configuration of IVa was established by J. Reed and I. G. M. Campbell (ibid., **1930**, 2377) and by A. Weissberger and H. Bach (*Ber.*, **64**, 1094 (1934); **65**, 63 (1935)). On the predominant formation of the erythro derivative IVa by the reduction of benzoin oxime (IIIc), see D. J. Cram and F. A. Abd Elhafez, *J. Am. Chem. Soc.*, **74**, 5824 (1952).

5) A mechanism involving the intermediate stages V and VI had been suggested. There is ample evidence to support the idea of the epimerization at the center carrying the hydroxyl group (Cf. D. F. Elliot, *J. Chem. Soc.*, **1950**, 62; G. Fodor, V. Bruckner, J. Kiss and G. Óheggi, *J. Org. Chem.*, **14**, 337 (1949),). Weijlard et al.[3] cites much relevant literature.

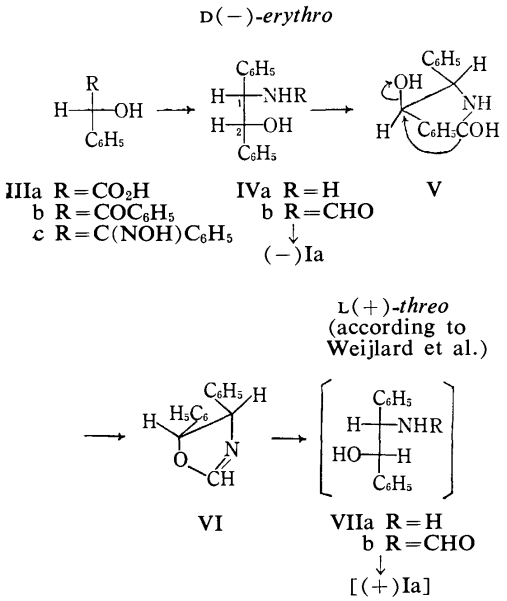

Fig. 2

Since, according to Weijlard et al.,[3] the D(−)-*erythro* isomer IVa and the (+)-*threo* isomer VIIa both have the same configuration at C_1 (the carbon atom carrying amino group) (Fig. 2), both compounds may be expected to give the same optically-active 1, 2-diphenylethylamine. To circumvent this difficulty, La Manna and his collaborators suggested that "the replacement of the hydroxyl group (of D(−)-*erythro* isomer IVa) by a chlorine atom by means of phosphorus pentachloride may involve inversion of the configuration at the C_1 center (the carbon atom bearing amino group) which is not directly concerned in the replacement."[2]

Since the absolute configuration of (−)-1, 2-diphenylethylamine (Ia) was unambiguously determined[1] by correlating it directly to D-aspartic acid (II), one is forced to assume, contrary to the suggestion of La Manna et al.,[2] that it must not be the D(−)-*erythro* isomer IVa but the (+)-*threo* isomer VIIa which epimerizes at the center of C_1 while the hydroxyl group is replaced at C_2 with phosphorus pentachloride.

However, the awkwardness has still remained, demanding some reasonable mechanism to explain this curious epimerization at C_1; no relevant parallel to which could be found in the literature. This contribution is primarily concerned with the revision of the absolute configuration of *threo*-1, 2-diphenyl-2-hydroxyethylamine (VIIa) originally proposed by Weijlard et al.,[3] so as to avoid the awkward circumstance mentioned above.

A survey of the literature reveals that

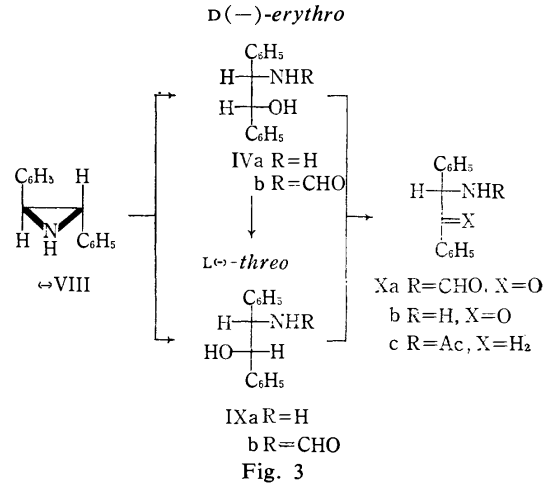

Fig. 3

Weissberger and Bach[6] performed an experiment (Fig. 3) which indicated clearly that (−)-*erythro* isomer IVa and (−)-*threo* isomer IXa have the same configuration at C_1; in this experiment they obtained these two optically-active diastereoisomers from (−)-*trans*-1, 2-diphenylethyleneimine (VIII)[7] on hydrolysing it with diluted sulfuric acid. Because the (−)-*erythro* isomer IVa resulted from the *trans*-opening of the (−)-*trans* ethyleneimine, VIII has been shown to have the D-configuration by correlating it with D(−)-mandelic acid IIIa[4] (Fig. 2); the (−)-*threo* isomer which is formed by the cis-opening of the VIII, differing from IVa only at the configuration of C_2 must have the L-configuration, contrary to the conclusion of Weijlard et al., as Fig. 3 shows. This deduction[8] was further supported by the conversion of the *N*-formyl derivatives of both D(−)-*erythro*- (IVb) and L(−)-*threo*- 1, 2-diphenyl-2-hydroxyethylamine (IXb) to the same (R)(+)-desylamine hydrochloride (Xb)[9] by sodium

6) A. Weissberger and H. Bach, *Ber.*, 65, 631 (1932).

7) Since the absolute configuration of D(−)-*erythro*-1, 2-diphenyl-2-hydroxyethylamine (IVa) has been established, (−)-*trans*-1, 2-diphenylethyleneimine is shown to be 1(S), 2(S)-diphenylethyleneimine (VIII).

8) P. Pratesi, A. La Manna and G. Vitali (*Il Farmaco (Pavia) Ed. Sci.*, 15, 387 (1960); *Chem. Abstr.*, 54, 24472 (1960)) reached the same conclusion by obtaining the same optically-active (+)-*N*-acetyl-1, 2-diphenylethylamine (Ib) m. p. 164~165°C, $[\alpha]_D$ +14° by hydrogenolysis of the *N*, *O*-diacetyl derivatives of IVa and IXa.

9) This finding also confirms the absolute configuration of (S)(−)-desylamine (the enantiomer of Xb) and the retention of the configuration in the conversion of (S)(−)-desylamine to D(−)-benzoin (IIIb) reported by A. McKenzie and D. J. Cruickshank (*Ber.*, 69, 876 (1936)), although their deduction of these facts was not complete until the compounds, m. p. 141~142°C ($[\alpha]_D$−10° from (D)-benzoin oxime, $[\alpha]_D$+10.4° from (+)-desylamine)) were shown to be of the erythro form of 1, 2-diphenyl-2-hydroxyethylamine.[4] This has been pointed out by C. K. Ingold (1951) in his personal communication to the editor of Beilstein, "Handbuch der Organischen Chemie." (IV Auflage, Bd. 14, zweites Ergänzungswerk, Springer, Berlin (1951), p. 62).

dichromate oxidation, followed by hydrolysis of the resulting *N*-formyldesylamine (Xa).[10]

These results are in harmony with La Manna's finding mentioned above that the (+)-*threo* isomer (now known to be of the D-configuration, the enantiomer of IXa) and the D(−)-*erythro* isomer IVa gave optically-active 1,2-diphenylethylamines with opposite rotations; hence it is not necessary to assume a rather incredible epimerization at C_1 in the replacement reaction of the hydroxyl group at C_2 of the erythro isomer IVa with phosphorus pentachloride.

Let us turn now to the conversion of the *N*-formyl derivative IVb of the D(−)-*erythro* isomer IVa into the (+)-*threo* isomer (now known to have the D-configuration; the enantiomer of IXa) with thionyl chloride reported by Weijlard et al. In order to accommodate their finding to the established absolute configurations (vide supra) of *erythro*- and *threo*-1,2-diphenyl-2-hydroxyethylamine, it seems inevitable, although improbable, to assume the epimerization at C_1 against overwhelming evidence which support the epimerization at the carbon atom C_2 carrying the hydroxyl group under these reaction conditions. On duplicating their isomerization experiment of the *N*-formyl derivative IVb of the D(−)-*erythro* isomer with thionyl chloride, it was found that the *threo* isomer showed, rather surprisingly, $[\alpha]_D -122°$, which has been shown to have the L-configuration IXa (vide supra); this is contrary to the finding of Weijlard et al.

This finding also indicates that the isomerization follows the usual, well-established path, affording an isomer which differs in the configuration of the carbon atoms carrying the hydroxyl groups (V→VI, in Fig. 2).

This error in the measurement of the optical rotation has been responsible for creating a chaos of puzzling phenomena, confusing La Manna and his collaborators in their determination of the absolute configuration of 1,2-diphenylethylamine (Ia).

It may be worthwhile to mention here another attempt to determine the absolute configuration of 1,2-diphenylethylamine (Ia), an attempt which eventually led to a conclusion opposite to ours.[1] Lyle[11] suggested the (R)-configuration for (+)-1,2-diphenylethylamine (the antipode of Ia) because its positive plain rotatory dispersion curve is very close the summation curve of (R)(+)-α-methylbenzylamine and (S)(+)-amphetamine which she considered to be the components of (+)-1,2-diphenylethylamine molecule. The reason why she was led to the wrong conclusion must be sought in her failure to take account of the phenyl-phenyl interaction and of the hydrogen bond between the phenyl groups and the amino groups, as well as the conformational asymmetry emphasized by Brewster.[12]

Experimental

(±)-*erythro*-1,2-Diphenyl-2-hydroxyethylamine ((±)-IVa).—To a solution of 5.7 g. of benzoin-α-oxime in 60 cc. of 90% ethanol was added 0.5 g. of 10% palladium-charcoal catalyst, together with 6 cc. of 5.5 N ethanolic hydrochloric acid; this mixture was then shaken at 40°C in an atmosphere of hydrogen for 6 hr. After the catalyst had been filtered out, the filtrate was concentrated to about 1/3 of the original volume. The crystals (1.1 g.) which were deposited upon the addition of water were recrystallized from benzene to afford hydrobenzoin, m. p. 135~136°C. The aqueous solution was made basic with concentrated aqueous ammonia to yield 3.97 g. of racemic IVa, m. p. 152~158°C. Recrystallization from methanol raised the m. p. to 157~160°C (lit.:[3] m. p. 163°C).

The Hydrochloride.—To a solution of 1 g. of racemic IVa in 10 cc. of ethanol was added 1.2 cc. of 5.5 N ethanolic hydrochloric acid, followed the addition of 10 cc. of ether to precipitate the hydrochloride of IVa (1.1 g.), m. p. 228°C (lit.:[3] m. p. 219~220°C).

***N*-Formyl-(±)-*erythro*-1,2-diphenyl-2-hydroxyethylamine** ((±)-IVb).—One gram of the hydrochloride of racemic IVa was dissolved in 3 cc. of formamide, and the mixture was heated at 150°C for 15~20 min. After being cooled to room temperature, the reaction mixture was diluted with 20 cc. of water to precipitate crystals which were then collected and washed with water to yield 0.61 g. of racemic IVb. Recrystallization from ethanol gave needles which weighed 0.61 g. and which melted at 180~182°C (lit.:[3] m. p. 179~181°C).

(±)-*N*-Formyldesylamine ((±)-Xa) from (±)-IVb.—A solution of 0.21 g. of racemic IVb in 3 cc. of acetic acid was added to a stirred solution of 0.27 g. of sodium dichromate dihydrate in 4 cc. of acetic acid at 10°C over 1/2 hr. The solution was then brought slowly to room temperature (10°C) and allowed to stand overnight. After being heated at 50°C for 20 min., the reaction mixture was diluted with 70 cc. of water and kept in a refrigerator overnight; 76 mg. of prismatic crystals (m. p. 199~120°C) precipitated. Recrystallization from benzene-petroleum ether did not raise the melting point. An infrared spectrum in Nujol indicated major peaks at 3360 (NH), 1685, and 1660 cm^{-1} (CO).

Found: C, 75.2; H, 5.6; N, 6.0. Calcd. for $C_{15}H_{13}O_2N$: C, 75.30; H, 5.48; N, 5.85%.

(±)-Desylamine ((±)-Xb) Hydrochloride from (±)-Xa.—After a mixture of 86 mg. of racemic

10) Optically-active *N*-formyldesylamine could not be obtained in a crystalline state, but the racemic variety was in prism form, m. p. 119~120°C.

11) G. G. Lyle, *J. Org. Chem.*, 25, 1779 (1960).

12) J. Brewster, *J. Am. Chem. Soc.*, 81, 5475 (1959).

Xa and 4 cc. of 2 N hydrochloric acid had been refluxed for 2 hr., the solution was evaporated to dryness in a vacuum. The crystalline residure was dissolved in 5 cc. of water and treated with Norit. The filtrate was then concentrated to about 0.5 cc., and 1 cc. of concentrated hydrochloric acid was added. The mixture was allowed to stand in a refrigerator to precipitate fine needles, which were then collected and washed with concentrated hydrochloric acid. The (±)-desylamine hydrochloride, after being dried in a desiccator over sodium hydroxide pellets, decomposed at 220~225°C and weighed 40 mg. (lit.:[3]) the optically active hydrochloride, m. p. 230°C).

(±)-*threo*-1,2-Diphenyl-2-hydroxyethylamine ((±)-IXa).—A mixture of racemic IVb and 3.0 cc. of thionyl chloride was stirred at 0~5°C for 20 min., and the reaction mixture was brought slowly to room temperature over a 1 hr. period. After the excess thionyl chloride had been decomposed with 20 g. of ice, the reaction mixture was refluxed for 2 hr. After being cleared with Norit, the solution was made basic with a 3 N sodium hydroxide solution to precipitate the racemic IXa, which was then washed with water and dried to yield 1.1 g. of crystals, m. p. 128°C. Recrystallization from ethanol gave 0.9 g. of prisms, m. p. 129~130°C (lit.:[3]) m. p. 126~128°C).

The hydrochloride (decomp. p. 205~210°C) was prepared following the procedure described for the erythro isomer IVa. The yield was quantitative (lit.:[3]) decomp. p. 200~201°C).

***N*-Formyl-(±)-*threo*-1, 2-diphenyl-2-hydroxyethylamine ((±)-IXb).**—Following the procedure described for the erythro isomer IVb, a mixture of 0.83 g. of the hydrochloride of racemic IXa and 3 cc. of formamide was heated to give 0.65 g. of racemic IXb, m. p. 146~149°C after recrystallization from diluted ethanol (lit.:[3]) m. p. 145~146°C).

(±)-Desylamine ((±)-Xb) Hydrochloride from (±)-IXb.—A solution of 0.60 g. of the racemic IXb in 7 cc. of acetic acid was added gradually to a stirred solution of 0.81 g. of sodium dichromate dihydrate in 12 cc. of acetic acid at 10°C over a 1/2 hr. period. After being allowed to stand over-night at room temperature, the mixture was heated at 50°C for 1/2 hr. This mixture was diluted with 200 cc. of water, saturated with sodium chloride, and then extracted with ether. The ether extract was washed with a dilute sodium hydrogen carbonate solution and then with a saturated sodium chloride solution. The ether extract was dried over anhydrous magnesium sulfate and was concentrated to give 0.42 g. of a viscous residue (the odor of benzaldehyde was noticed) which was then hydrolyzed by boiling it with 10 cc. of 2 N hydrochloric acid for 2 hr. The solution was concentrated under reduced pressure to give a crystalline mass, which was washed with benzene. The residue was dissolved in a small amount of water and concentrated again after treatment with Norit. To the clear solution (about 1 cc.) 3 cc. of concentrated hydrochloric acid was added to precipitate (±)-desylamine hydrochloride, which decomposed at 225~230°C and which weighed 0.12 g.

Found: N, 5.5. Calcd. for $C_{14}H_{14}ONCl$: N, 5.66%.

D(−)-*erythro*-1,2-Diphenyl-2-hydroxyethylamine (IVa).—A mixture of 11.1 g. of racemic IVa and 7.9 g. of L-glutamic acid was dissolved in 330 cc. of 50% ethanol and was kept in a refrigerator to precipitate the L-glutamate of the (−)-amine IVa as fine needles, which were then recrystallized from 50% ethanol. The L-glutamate melted at 213°C with decomposition. $[\alpha]_D^{20}$ −50.0° (*c* 0.42 in water) (lit.:[3]) decomp. p. 215°C, $[\alpha]_D^{25}$ −50.3° (*c* 0.65 in water)). The L-glutamate (6.63 g.) was dissolved in 100 cc. of water, and the D(−)-*erythro* base IVa was precipitated by adding concentrated aqueous ammonia. The base was collected and washed with water to give 3.5 g. of crystals, which melted at 141~144°C after recrystallization from ethanol. $[\alpha]_D^{24}$ −6.4° (*c* 1.25 in ethanol) (lit.:[3]) m. p. 143°C, $[\alpha]_D^{25}$ −10.1° (*c* 0.59 in ethanol)).

The hydrochloride which was prepared following the procedure for the racemic compound decomposed at 215°C, $[\alpha]_D^{21}$ −59.0° (*c* 1.0 in water) (lit.:[3]) decomp. p. 213.5~214.5°C, $[\alpha]_D^{25}$ −69.5° (*c* 0.65 in water)).

Found: N, 5.2. Calcd. for $C_{14}H_{16}ONCl$: N, 5.61%.

***N*-Formyl-D(−)-*erythro*-1,2-diphenyl-2-hydroxyethylamine (IVb).**—The *N*-formyl derivative IVb, which was prepared following the procedure for the racemic erythro amine, melted at 201~202°C after recrystallization from ethanol, $[\alpha]_D^{22}$ +2.6° (*c* 0.45 in ethanol).

Found: C, 74.4; H, 6.3; N, 5.8. Calcd. for $C_{15}H_{15}O_2N$: C, 74.66; H, 6.27; N, 5.81%.

(+)-Desylamine (Xb) Hydrochloride obtained by the Oxidation of IVb.—A solution of 0.411 g. of IVb in 8 cc. of acetic acid was added to a stirred solution of 0.56 g. of sodium dichromate dihydrate in 6 cc. of acetic acid over a 15 min. period at 0°C. After being stirred for 1 hr. at 0°C, the solution was allowed to stand overnight at room temperature. The reaction mixture was then poured into 200 cc. of water and extracted with ether. The ether extract was washed with a dilute sodium hydrogen carbonate solution and then with a saturated sodium chloride solution. After drying over anhydrous magnesium sulfate, the solvent was removed to give crude *N*-formyl-(+)-desylamine (an oil, $[\alpha]_D^{22}$ +227° (*c* 1.4 in ethanol)), which was hydrolyzed directly by boiling it with 10 cc. of 2N hydrochloric acid for 2 hr. The solution was concentrated under reduced pressure to give a crystalline residue which was dissolved in a small amount of water and treated with Norit. The filtrate freed from Norit was concentrated again to 3 cc., and then 6 cc. of concentrated hydrochloric acid was added to precipitate (+)-desylamine hydrochloride, which decomposed at 225°C and which weighed 60 mg., after drying in a vacuum desiccator over sodium hydroxide pellets., $[\alpha]_D^{21}$ +189° (*c* 1.0 in water) (lit.:[13]) $[\alpha]_D^{16}$ +223.2° (*c* 2.54 in water)).

Found: C, 68.0; H, 5.7. Calcd. for $C_{14}H_{14}ONCl$: C, 67.87; H, 5.69%.

13) A. McKenzie and N. Walker, *J. Chem. Soc.*, **1928**, 646.

The Isomerization of *N*-Formyl-D(−)-*erythro*-1,2-diphenyl-2-hydroxyethylamine (IVb) to L-(−)-*threo* Isomer IXa.—A mixture of 1.5 g. of *N*-formyl-D(−)-*erythro* amine IVb and 3 cc. of thionyl chloride was stirred at 0°C for 5 min., and then the temperature of the mixture was gradually raised to room temperature (15°C) over a 45 min. period. The solution was poured onto 100 g. of ice to decompose the excess thionyl chloride, and the reaction mixture was refluxed for 2 hr. The solution was cleared with Norit and was made basic with a 4 N sodium hydroxide solution to precipitate 1.4 g. of L(−)-*threo* amine IXa, which was collected and washed with water. The amine was recrystallized from ethanol to give needles which melted at 114~116°C, $[\alpha]_D^{22}$ −122° (*c* 1.0 in ethanol) (lit.:[3] m. p. 115.2~115.8°C $[\alpha]_D^{24}$ −123.7° (*c* 1.2 in ethanol) for the "D(−)-*threo*" isomer).

Found: C, 78.8; H, 7.1; N, 6.4. Calcd. for $C_{14}H_{15}ON$: C, 78.84; H, 7.09; N, 6.57%.

The hydrochloride which was prepared following the procedure for the racemic threo compound decomposed at 230°C, $[\alpha]_D^{18}$ −122° (*c* 1.2 in ethanol). (lit.:[3] decomp. p. 220~221°C, $[\alpha]_D^{23}$ +84.7° (*c* 0.01 in water) for the hydrochloride of the "L(+)-*threo*" isomer).

***N*-Formyl-L(−)-*threo*-1,2-diphenyl-2-hydroxyethylamine (IXb).**—The *N*-formyl-L(−)-*threo* isomer IXb which was prepared following the procedure used for the racemic compound melted at 116~119°C after recrystallization from 50% ethanol, $[\alpha]_D^{18}$ +11.3° (*c* 1.2 in ethanol).

Found: C, 74.2; H, 6.2; N, 5.9. Calcd. for $C_{15}H_{15}O_2N$: C, 74.66; H, 6.27; N, 5.81%.

(+)-Desylamine (Xb) Hydrochloride from IXb. Following the procedure used for the oxidation of IVa, 0.469 g. of IXb was oxidized with 0.58 g. of sodium dichromate dihydrate in acetic acid to give 70 mg. of (+)-desylamine hydrochloride, which decomposed at 225°C, $[\alpha]_D^{23}$ +130° (*c* 0.51 in water). Its infrared spectrum was found superimposable on that of (+)-desylamine hydrochloride derived from IVa (in a Nujol mull).

The author is very grateful to the Nitto-kasei Co. for its financial support. He is also indebted to Drs. Tetsuo Shiba (Osaka University) and Setsuji Sakurai (Ajinomoto Co.) for their generous gifts of L-glutamic acid. A part of the expense of this research was defrayed by the grant-in-aid for fundamental scientific research from the Ministry of Education, to which the author's thanks are due.

Department of Chemistry
Faculty of Engineering Science
Osaka University
Shibahara, Toyonaka

*Studies on the Absorptiometric Determination of Microamounts of Boron. V. The Necessity of Methyl or Ethyl Oxalate in the Color Reaction of Boric Acid with Curcumin**

By Masatoshi MIYAMOTO

(Received May 4, 1963)

The color reaction of boric acid with curcumin, whereon the most sensitive method for absorptiometric determination of boron is based, is well-kown, but it has not yet been clearly revealed although when Schulemberger[1] first studied the reaction in 1866. Spicer and Strickland[2] have, however, contributed valuable information on the reaction product. The present paper deals with facts concerning the color reaction overlooked for a long time. The study has been initiated with the purpose of extracting an effective product from a curcumin-oxalic acid reagent solution sufficiently aged by refluxing;[3] thus, it is hoped, a stable and reliable reagent for instant use can be obtained.

Results and Discussion

The Effects of Various Acids on Color Reaction.—It has been reported that the presence of oxalic,[4] tartaric[5] and salicylic[6] acids intensify the color resulting from the reaction between

* Presented at the Symposium on Analytical Chemistry held by the Japan Society for Analytical Chemistry, Tokushima, October, 1962.

1) M. E. Schulemberger, *Bull. Soc. Chim.*, [2], **5**, 194 (1866).

2) G. S. Spicer and J. D. H. Strickland, *J. Chem. Soc.*, **1952**, 4644, 4650.

3) M. Miyamoto, *Japan Analyst* (*Bunseki Kagaku*), **11**, 635 (1962).

4) C. E. Cassal and H. Gerrans, *British Food Journal*, 210 (1902).

5) F. Michel, *Mikrochemie ver. Mikrochim. Acta*, **29**, 63 (1941); *Chem. Abstr.*, **35**, 5412 (1941).

6) C. H. Cribb and F. W. F. Arnaud, *Analyst*, **31**, 147 (1906).

Table I. Effect of various acids on color development

Exp., No.	Curcumin solution*1		Net absorbancy at 550 mμ for 1 μg. boron in the presence of		
	Solvent	Acid added	None	Oxalic acid	Hydrochloric acid
1	Ethanol	—	—	0.126	0.021
2	Ethanol	Hydrochloric	0.098*2	0.311*3	—
3	Ethanol	Oxalic	0.404	—	0.400
4	Ethanol	Malonic	0.190	0.326	—
5	Ethanol	Tartaric	0.000	0.152	—
6	Ethanol	*o*-Phthalic	0.016	0.011	0.000
7	Ethanol	Salicylic	0.000	—	—
8	Acetone	—	—	—	0.000
9	Acetone	Oxalic	0.068	—	0.362
10	Diethyl ketone	Oxalic	0.124	—	0.120

*1 Refluxed for 4 hr.
*2 Analogous absorbancies were obtained for 0.5, 1.5 and 2.0 μg. of boron.
*3 Proportional to the amounts of boron.

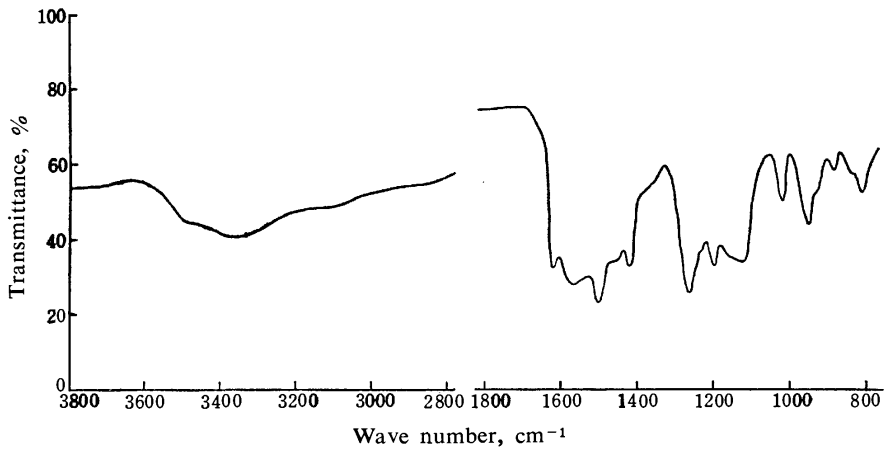

Fig. 1. Infrared absorption spectrum of curcumin.
Curcumin, 0.5 mg., and KBr, 200 mg.

curcumin and boric acid. The author's results in the 4th column of Table I show that the presence of oxalic acid is effective for the color reaction under the conditions stated in the experimental section below, whereas those of hydrochloric, malonic, tartaric, *o*-phthalic and salicylic acids are ineffective (cf. Nos. 2 to 7). The slight effect of malonic acid may possibly be attributed to small amounts of oxalic acid contaminating the malonic acid used (cf. "Effect of various esters" below). No correlation is observed between the effects and the first dissociation constants of the acids added to a curcumin solution. The effect of oxalic acid on the reaction is unique.

A comparison of the results shown in the 5th column, Nos. 1 and 2, shows that the presence of hydrochloric acid promotes the color reaction in the presence of oxalic acid. This may be attributed to the effect of hydrochloric acid (hydrogen ions) on the aging reaction of a reagent solution, whereby aging reaction proceeds during evaporation for the color reaction. However, the aging reaction does not proceed enough during the evaporation, as is revealed by a lower result of No. 2, 5th column, than that of No. 3, 4th column. In either cases, both oxalic and hydrochloric acids were present at the evaporation stage; a curcumin-oxalic acid solution aged fairly enough by 4 hours' refluxing[3] was used in the latter case. Tartaric and *o*-phthalic acids are not only ineffective but also interfere with the color reaction in the presence of oxalic acid, as is shown in the 5th column. This may be attributed to the formation of borate

TABLE II. INFRARED ABSORPTION BANDS OF CURCUMIN

Wave number, cm^{-1}		Assigned to
Author	Reported[9]	
3360	3400	-OH (Hydrogen bonded)
1625	1625	>C=O (Conjugated hydrogen bonded ring of β-diketone)
1570	1600 ?	-C=C- (Conjugated)
1510	1500	-C=C- (Ring)
1430	—	-OH (β-Diketone[10])
1265	—	-OH (Phenolic[11]) >C=O (Conjugated hydrogen bonded ring of β-diketone[10])
1200	—	-OH (Phenolic[11]), -C-O-C- (Aryl)
1125	—	?
1025	—	-C-O-C- (Aryl)
960	962	-C=C- (Trans), -OH (β-Diketone[10])

complexes* with the acids.

When acetone is used as the solvent in preparing a reagent solution, the reagent solution gives an intense color only in the presence of hydrochloric acid (cf. Nos. 8 and 9). A reagent solution prepared with diethyl ketone as the solvent gave a little coloration (cf. No. 10). However, because of insufficient data, no conclusion was possible except that the solution might not have a strong color-developing power, if, indeed, it has any.

The foregoing results indicate that the presence of oxalic acid is necessary in the color reaction between boric acid and curcumin when ethanol is used as the solvent in preparing a reagent solution and that the presence of both of hydrochloric and oxalic acids is required when acetone is used as the solvent. These facts suggest a close relation between the color reaction and the solvent of the reagent solution used.

The Aging Reaction of the Curcumin-Oxalic Acid Reagent.—*Absorption Spectrum.*—The aging phenomenon of a curcumin-oxalic acid reagent solution is pronounced in an ethanol medium. However, no interpretation of this phenomena has been made thus far. The structure[8,9] of curcumin reveals no possibility of a reaction whereby curcumin reacts with either oxalic acid or ethanol in the solution or is converted to a compound effective in the coloration of boric acid. The structure was confirmed by absorption spectroscopic studies. The infrared and near-ultraviolet absorption curves obtained by the author are shown in Figs. 1 and 2, respectively. The infrared absorption bands of a purified curcumin in the solid

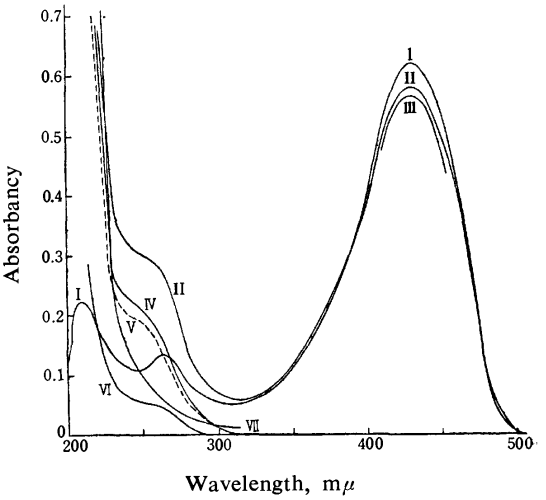

Fig. 2. Absorption spectra of ethanolic solutions of curcumin-oxalic acid reagent and related compounds.
I: Curcumin, 1.09×10^{-5} M
II: Curcumin-oxalic acid (refluxed for 6 hr.), 1.09×10^{-5} and 3.97×10^{-3} M, respectively
III: Curcumin-oxalic acid (left to stand for 29 days), the same concentrations as curve II
IV: Oxalic acid (refluxed for 6 hr.) or diethyl oxalate, 3.97×10^{-3} M
V: Difference between curves I and II
VI: Oxalic acid (fresh solution), 1.5×10^{-3} M
VII: Oxalic acid (aqueous solution), 1.5×10^{-3} M

state may be assigned as shown in Table II. The absorption band, max 265 mμ and ε 12500, observed in an ethanol medium indicates the possible existence of the keto-enol ring structure[12] of curcumin in the medium (cf. curve

* The complex formation of boric acid with tartaric acid in an acid medium is suggested by the increasing solubilities[7] of boric acid in water with the increasing amounts of tartaric acid added.

7) W. F. Linke, "Solubilities of Inorganic and Metal-organic Compounds," Vol. I, D. Van Nostrand, New York (1958), p. 267.

8) V. Lampe, *Ber.*, 51, 1347 (1918).

9) L. J. Bellamy, G. S. Spicer and J. D. H. Strickland, *J. Chem. Soc.*, 1952, 4653.

10) S. Bratož, D. Hadži, and G. Rossmy, *Trans. Faraday Soc.*, 52, 464 (1956).

11) K. Kuratani, *J. Chem. Soc. Japan, Pure Chem. Sec. (Nippon Kagaku Zassi)*, 73, 928 (1952).

12) D. S. Rasmussen, D. D. Tunnicliff and R. R. Brattain, *J. Am. Chem. Soc.*, 71, 1068 (1949).

I, Fig. 2). Only a little decrease in the absorbancy of a curcumin-oxalic acid reagent solution at 430 mμ was observed after it had been refluxed for 6 hr., indicating a good stability[3] of the reagent solution (cf. curves I and II). A decrease of about 10% was also observed after allowing reagent solution to stand at room temperature for 29 days. However, no appreciable change in the shape of the absorption curve was observed in either case.

A comparison of curve I, obtained for a curcumin solution, with curve II obtained for an aged reagent solution leads to curve V, analogous to the absorption curve of the ethyl oxalate (curve IV) but different from that of oxalic acid (curve VII). Seemingly this implies that the aging reaction may simply be the esterification reaction of oxalic acid with the ethanol used as a solvent rather than a reaction with which curcumin is concerned. This expectation was substantiated by the facts that a fresh curcumin solution to which ethyl oxalate has been added develops the color with boric acid as much as a sufficiently aged reagent solution does and that this is also the case when a refluxed ethanolic solution of oxalic acid has been added instead of the ester. On the contrary, a very weak coloration takes place with a refluxed ethanolic curcumin solution to which a fresh ethanolic solution of oxalic acid has been added. The results obtained are shown in Tables III and IV.

Table III. Color development with a curcumin solution mixed with an oxalic acid solution

Curcumin soln.	Oxalic acid soln.	Net absorbancy at 550 mμ for 1 μg. boron
Fresh	Fresh	0.090
Refluxed	Fresh	0.087
Refluxed	Refluxed	0.395
Fresh	Refluxed	0.399

Table IV. Effect of various esters on the color development

Oxalate ester	Solvent	Net absorbancy at 550 mμ for 1 μg boron
Dimethyl	Methanol	0.355
Diethyl	Methanol	0.392
Diethyl	Ethanol	0.405
Diethyl	Acetone	0.404
Di-*n*-butyl	Ethanol	0.003
Di-*n*-butyl	*n*-Butanol	0.002

The Effects of Various Esters.—As Table IV shows, a curcumin solution to which diethyl oxalate has been added develops the color with boric acid independently of the solvent used in preparing the reagent solution. Dimethyl oxalate acts as does diethyl oxalate. Dibutyl oxalate (presumably any higher ester of oxalic acid than propyl oxalate) and esters other than that of oxalic acid do not contribute to the color reaction at all. These facts indicate the unique and important role of dimethyl oxalates in the color reaction.

Acetone has been frequently used as a solvent in place of ethanol in preparing a curcumin-oxalic acid reagent solution. It is dimethyl or diethyl oxalate but not oxalic acid which enables the reagent solution to develop the color with boric acid. The ester should be formed from alcoholic impurities in any acetone used. This will be seen from the fact that the purer the acetone, the lower the intensity of the resulting color, as Table V shows. No difference in the shape of the absorption curve was observed between the colored product obtained from an acetonic curcumin-oxalic acid solution and that obtained from an ethanolic curcumin-diethyl oxalate solution (cf. curves II and III, Fig. 3). It has been

Table V. Color development with curcumin and oxalic acid dissolved in various purity grades of acetone

Acetone	Net absorbancy at 550 mμ for 1 μg. boron	
	Fresh soln.	Refluxed soln.
JIS 1st grade	0.200	—
JIS special grade	—	0.362
Absorption spectroscopic grade	0.138	0.203
Purified	0.017	0.104

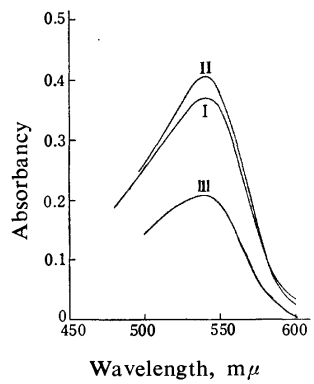

Fig. 3. Absorption spectra of ethanolic solutions of colored products.
Reagent solutions used are:
I: Curcumin-dimethyl oxalate as a methanolic solution
II: Curcumin-diethyl oxalate as an ethanolic solution
III: Curcumin-oxalic acid as an acetonic solution refluxed for 8 hr.

said[13] that commercial acetone some times contains methanol as an impurity. The author observed strong absorption bands at 206.5 and 214 mμ and around 1.9 μ which may be attributed to such impurities as water and alcohols present in commercial acetones.

With this view, the role of hydrochloric acid in the color reaction, whereby an acetonic reagent solution is able to develop a strong color with boric acid with the aid of hydrochloric acid (cf. Table I), may be understood as that of an acid catalyst in the esterification which occurs during evaporation for the color reaction. The presence of insufficient amounts of either of the esters in the reaction mixture may cause low and scattered results. For this reason,* the amounts of aqueous sample solutions assigned to the color reaction should be regulated[3] in order to retain ethyl oxalate against hydrolysis. The fact that an insufficiently aged reagent solution or a reagent solution containing relatively small amounts of oxalic acid results in low and scattered results[14] may also be attributed to insufficient amounts of ethyl oxalate formed in the reagent solutions. Seemingly, for the same reason, highly precise results may hardly be expected by using an acetonic reagent solution prepared with a commercially available acetone containing even relatively small amounts of alcoholic impurities, even if a working curve is renewed for a particular reagent solution prepared with a particular lot of acetone as the solvent.

The Composition of the Colored Product. — The composition of the colored product has been studied by Schulemberger[1] and by Clarke and Jackson.[15] Spicer and Strickland[2] have presented a structure for a red complex, rosocyanin,** formed in the presence of hydrochloric acid; they have found the boron curcumin ratio to be 1 to 2. They have also stated that another red complex, rubrocurcumin, having a 1 to 1 to 1 composition of boron, curcumin, and oxalic acid is formed when the reaction takes place in the presence of oxalic acid, and they have presented a structure for this complex. However, the foregoing discussion reveals that further studies of the colored products, especially of rubrocurcumin, are necessary.

No distinct difference in absorption maximum and shape was observed between absorption curves of ethanolic solutions of the colored product obtained in the presence of methyl and ethyl oxalate respectively (cf. curves I and II, Fig. 3). This might imply that the same product is obtained in the presence of either of the esters. The author leaves uncovered such problems as the role of the esters in the reaction mechanism and the composition of colored product, merely indicating that methyl or ethyl oxalate is necessary for the color reaction between curcumin and boric acid.

Experimental

The chemicals, such as curcumin, oxalic acid, ethanol and hydrochloric acid, the apparatus, the procedure of color development, and the method of measuring color intensity are the same as in the previous reports.[8,14,16] The other chemicals used were of JIS special or guaranteed grade. The methanol, acetone, and diethyl ketone used as solvents for preparing curcumin-oxalic acid solutions had been purified by distillation with a quartz apparatus after having been dried with anhydrous sodium carbonate. Variations will be indicated for particular cases.

The Effect of Various Acids on Color Development. — A boric acid solution containing 1.00 μg. of boron associated with either one of the other substances, 2.00 mg. (3.2 meq.) of oxalic acid, or 1 meq. of hydrochloric acid was subjected to the color reaction with a curcumin solution containing one of the various acids to be tested. The curcumin solution was prepared by dissolving 40.0 mg. of curcumin and 80.0 meq. of hydrochloric, oxalic, malonic, tartaric, *o*-phthalic or salicylic acid in 100 ml. of ethanol, acetone, or diethyl ketone. This mixture was refluxed for 4 hr. in order to promote an aging reaction such as might take place in the case of an ethanolic curcumin-oxalic acid solution. The refluxing was continued for 8 hr. in the case of an acetonic solution because of the low boiling point of acetone. The reaction product was extracted by ethanol, and the absorbancy was measured at 550 mμ. Blank tests gave absorbancies less than 0.033. The results are shown in Table I.

Absorption Spectra. — The infrared absorption spectrum of curcumin was obtained with a recording spectrophotometer, Hitachi Model EPI-2, a pellet consisting of 0.5 mg. of curcumin and 200 mg. of potassium bromide being used. The curcumin was purified by recrystallization[14] from ethanol until a constant melting point, 173°C, was obtained. The results are shown in Fig. 1. For obtaining the absorption spectra of the various solutions shown in Fig. 2, a manual spectrophotometer, Hitachi Model EPU-2, equipped with 1 cm. cells was used, the reference liquids being the same

13) T. Kuwata, "Yozai," Maruzen Co., Tokyo (1940), p. 258.

* The hydrolysis of the resultant colored product during evaporation for the reaction may not be a principal reason for regulating the volume of the aqueous sample solution to be taken. The coloration is observed at the end of the evaporation, and it proceeds further by baking.[3]

** Rosocyanin, so called by these workers, should be distinguished from the "rosocyanine" of the previous workers.[1,15]

14) M. Miyamoto, *Japan Analyst (Bunseki Kagaku)*, **12**, 115 (1963).

15) L. Clarke and C. L. Jackson, *Am. Chem. J.*, **39**, 696 (1908).

16) M. Miyamoto, *Japan Analyst (Bunseki Kagaku)*, **12**, 120 (1963).

as the solvents of the sample solutions. Ethanolic solutions of curcumin-oxalic acid, curcumin, oxalic acid, and diethyl oxalate were diluted with ethanol to an appropriate concentration just before the measurements so as to give appropriate absorbancies, although their concentration was originally 40.0 mg./100 ml. and 0.400 M as to the curcumin and oxalic acid equivalent respectively. For obtaining the absorption spectra of reaction products extracted by ethanol, a recording spectrophotometer, Hitachi Model EPS-2, and 1 cm. celles were used, the reference liquid being ethanol. The results are shown in Fig. 3.

Color Development with a Curcumin and an Oxalic Acid Solutions Prepared Independently.—An ethanolic solution of curcumin, 80.0 mg./100 ml., and one of 0.800 M oxalic acid were prepared. Two milliliter portions of the solutions were mixed together just before use, and the color-developing power of the mixed solutions was tested by using 1.00 μg. of boron. The test was also carried out after the solutions had been independently subjected to refluxing for 2 hr. The results are shown in Table III.

The Effects of Various Esters.—A reagent solution containing 40.0 mg. of curcumin and 40.0 mmol. of the various esters to be tested was prepared by dissolving the respective substances in methanol, ethanol, acetone, or *n*-butanol. The color-developing power of the solution was tested by using 1.00 μg. of boron. The esters tested were dimethyl, diethyl, and di-*n*-butyl oxalates. The results are shown in Table IV. When *n*-butanol was the solvent, two layers were formed by adding the reagent solution to a boric acid solution, and the system was not dried by the evaporation at 55°C leaving the solvent because of its high boiling point. In this case, it was assumed that drying completed when the aqueous layer had disappeared. None of the color-developing power was observed when the oxalate esters were replaced by any of the following esters: the dimethyl and diethyl esters of acetic, malonic, and *o*-phthalic acids, and methyl and ethyl salicylates.

Color Development with Curcumin and Oxalic Acid Dissolved in Various Purity Grades of Acetone.—Curcumin-oxalic acid solutions were prepared by using various purity grades of acetone as a solvent. Immediately after the preparation, the color-developing power of the solutions was tested by using 1.00 μg. of boron, to which 1.00 meq. of hydrochloric acid had previously been added. The test was also carried out after the solutions had been refluxed for 8 hr. The results are shown in Table V. Of the various grades of acetone, a spectroscopic-grade aceton was that of Eastman Kodak, and a purified acetone was obtained by the following procedure: acetone, JIS first grade, was stirred in the presence of powdered potassium permanganate for 3 days, then double distilled after dehydration with anhydrous sodium carbonate.

Summary

The coloration of microamounts of boric acid with an ethanolic solution takes place in the presence of oxalic, but not in that of other acids. Near-ultraviolet, visible, and infrared absorption spectroscopic studies have revealed that the aging reaction of an ethanolic curcumin-oxalic acid reagent solution is simply the esterification of the oxalic acid with the solvent used. The resulting diethyl oxalate is necessary to the color reaction. The role of the ester has not been interpreted yet; however, it is so unique that it can be performed only by dimethyl oxalate, not by the other esters. The esterification of oxalic acid in an acetonic reagent solution may be attributed to the presence of alcoholic impurities present in aceton used. The composition of the colored reaction product, rubrocurcumin, presented by Spicer and Strickland[2] has not been substantiated yet in relation to the necessity of the esters to the color reaction.

The author is indebted to Mr. Yasuo Suzuki for his experimental work. Acknowledgement is also made to Drs. Kenji Ono and Yoshinaga Oka, Professors of Tohoku University, for their encouragement, to Dr. Akira Tomita for his installation of the study equipment, and to the Tokai Electrode Mfg. Co., Ltd., for the permission to publish the results.

Research Laboratory
Tokai Electrode Mfg. Co., Ltd.
Fujisawa, Kanagawa-ken

Studies of the Pyrimidine Derivatives. XXV. The Reaction of Alkoxycarbonylthiocyanates and Related Compounds with the Sodium Salt of Thiamine*

By Akira TAKAMIZAWA, Kentaro HIRAI and Keiko MATSUI

(Received May 22, 1963)

In previous papers of this series,[1,2] the syntheses of many *S*-alkoxycarbonylthiamine (I) and *O*,*S*-bis(alkoxycarbonyl)thiamine (II) derivatives have been reported. It has also been shown that *O*,*S*-bis(ethoxycarbonyl)thiamine (DCET) (IIa) has a thiamine activity approximately equivalent to that of thiamine hydrochloride (III) that it is highly absorbed when administered orally, and that the high thiamine level is maintained for a longer time than that of III.[3] In an attempt to obtain a reagent which can introduce the alkoxycarbonyl group into thiamine under mild conditions, the present authors first took up alkoxycarbonylthiocyanate (IV).

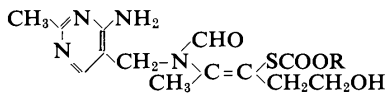

(I)

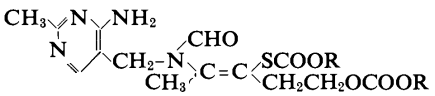

(II) a) R=C_2H_5
b) R=C_4H_9

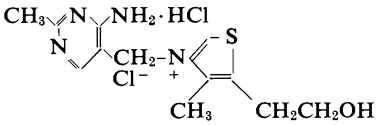

(III)

KSCN+ClCOOR ⟶ N≡C-S-COOR + S=C=N-COOR
(IV) a) R=C_2H_5 (V) a) R=C_2H_5
b) R=C_4H_9 b) R=C_4H_9

KSCN+$ClCOSC_2H_5$ ⟶ S=C=N-$COSC_2H_5$
(VI) (VII)

KSCN+ClCOR ⟶ S=C=N-COR
(VIII) a) R=C_6H_5
b) R=CH_3

KSCN+$ClCOOCH_2CH=CH_2$ ⟶ S=C=N-$CH_2CH=CH_2$ +
(IX) (X)

S=C=N-$COOCH_2CH=CH_2$
(XI)

KSCN+$BrCH_2CH=CH_2$

Chart 1

Dixon and Taylor[4] reported that potassium thiocyanate reacted with ethyl chloroformate and with acylchloride in acetone solutions to give ethoxycarbonylisothiocyanate (Va) and acylisothiocyanate (VIII) respectively. We reinvestigated the reaction of ethyl chloroformate with potassium thiocyanate and obtained two oily substances with b. p. 25.5~26.7°C/1.8 mmHg and b. p. 41.2~41.9°C/2.0 mmHg. The elementary analyses of both substances agreed with the formula $C_4H_5O_2SN$, and it was suggested that they were the isomeric each other. The infrared spectrum of the former showed absorptions at 1960~1990 cm^{-1} for the -N=C=S group and at 1750 cm^{-1} (C=O)

* Part XXIV of this series: A. Takamizawa, K. Hirai, Y. Hamashima and H. Sato, submitted to *Chem. Pharm. Bull.*

1) A. Takamizawa and K. Hirai, ibid., 10, 1102 (1962).
2) A. Takamizawa, K. Hirai and Y. Hamashima, ibid., 10, 1107 (1962).
3) a) T. Minesita, M. Morita and T. Iwata, *Ann. Rep., Shionogi Research Lab.*, 12, 6 (1962); b) Vitamin B_1, New Deriv. Research Sub-Comm., Japan, *Vitamins*, 25, 516 (1962).
4) A. E. Dixon and J. Taylor, *J. Chem. Soc.*, 93, 684 (1908).

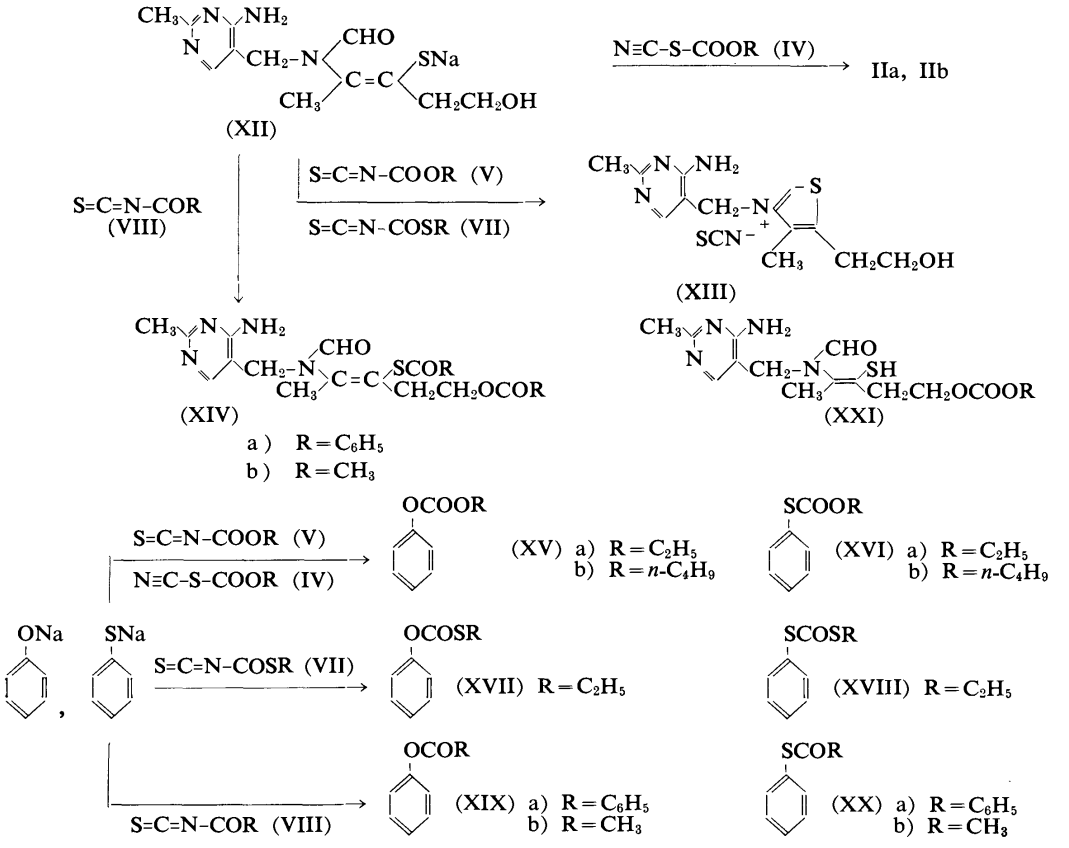

Chart 2

and at 1220~1260 cm^{-1} (C–O) respectively for the –N–C–O– group (Fig. 1). The spectrum of the latter showed the –C≡N band at 2190 cm^{-1}, and C=O and C–O bands at 1770 cm^{-1} and 1140~1190 cm^{-1} respectively for the –S–C–O– group (Fig. 4). From these results, the former should be ethoxycarbonyl isothiocyanate (Va), and the latter, ethoxycarbonylthiocyanate (IVa). These structures were also confirmed by their ultraviolet spectra. Hosoya, Tanaka and Nagakura[5] have shown that the ultraviolet spectrum of thioacetamide has the absorption maximum characteristic of the C=S group at 318 mμ (ε, 60). The ultraviolet spectrum of the former substance (isothiocyanate) showed the absorption maximum at 325 mμ (ε, 61.9). On the other hand, no absorption was found in the latter substance (thiocyanate) (Fig. 5).

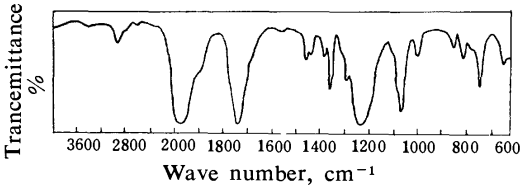

Fig. 1. Infrared spectrum of ethoxycarbonylisothiocyanate (Va). (film)

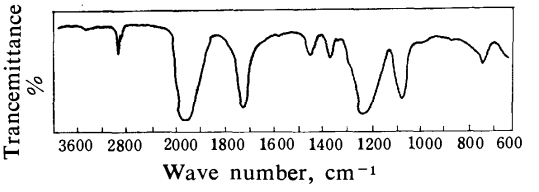

Fig. 2. Infrared spectrum of butoxycarbonylisothiocyanate (Vb). (film)

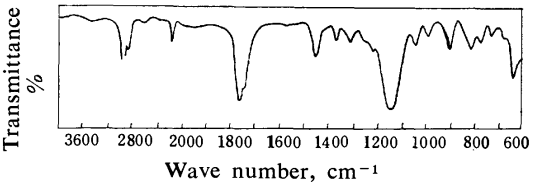

Fig. 3. Infrared spectrum of butoxycarbonylthiocyanate (IVb). (film)

5) H. Hosoya, J. Tanaka and S. Nagakura, This Bulletin, 33, 850 (1960).

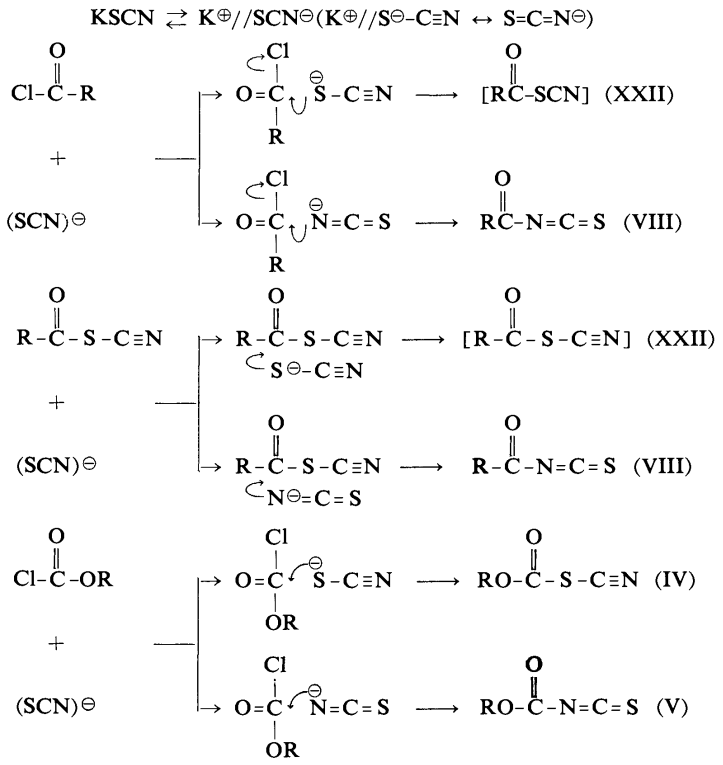

Chart 3

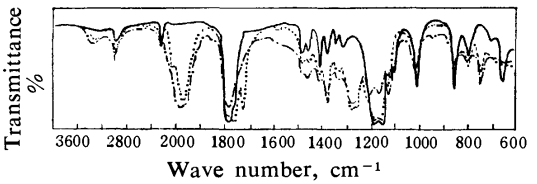

Fig. 4. Infrared spectrum of IVa and its spectral change with the left time in acetone solution in the presence of KSCN.
1. Original IVa (——)
2. After 20 min. at room temperature (------)
3. After 45 min. at room temperature (—·—·)

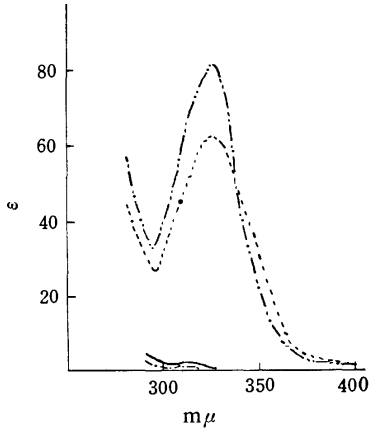

Fig. 5. Ultraviolet spectra of IVa (——), IVb (------), Va (—·—·—) and Vb (··—··—).

As it was interesting that two isomers were obtained in this reaction, investigations on analogous compounds were carried out. The reaction of butyl chloroformate with potassium thiocyanate gave two isomers, buthoxycarbonylthiocyanate (IVb) and butoxycarbonyl isothiocyanate (Vb), whose structures were confirmed by their infrared and ultraviolet spectra. The infrared spectrum of Vb showed the -N=C=S band at 1970~1990 cm^{-1}, the C=O band at 1750 cm^{-1} and the C–O band at 1240~1250 cm^{-1} for the $-\overset{}{N}-\overset{O}{\overset{\|}{C}}-O-$ group (Fig. 2), while that of IVb showed the -C≡N band at 2190 cm^{-1}, the C=O band at 1765 cm^{-1} and the C–O band at 1155~1165 cm^{-1} for the $-S-\overset{O}{\overset{\|}{C}}-O-$ group (Fig. 3). Moreover, although the ultraviolet spectrum of Vb exhibited the absorption maximum at 323 mμ (ε, 81) no maximum was observed with IVb (Fig. 5).

Further, the reaction of potassium thiocyanate with thioethoxycarbonylchloride (VI) gave only one product, the isothiocyanate (VII). Similarly, benzoylchloride and acetylchloride did not give the thiocyanates, but only the respective isothiocyanates, VIIIa[4,6] and VIIIb[4]. Their structures were confirmed by infrared

6) J. C. Ambelang and T. B. Johnson, *J. Am. Chem. Soc.*, **61**, 632 (1939).

TABLE I. PRODUCTS OBTAINED FROM THE REACTION OF RCl WITH KSCN

RCl	Product	Yield, %	B. p., °C/mmHg	UV λ_{max}^{EtOH} mμ (ε)
$ClCOOC_2H_5$	$S{=}C{=}N{-}COOC_2H_5$	30	25.5~26.7/1.8	325 (61.9)
	$N{\equiv}C{-}S{-}COOC_2H_5$	30	41.2~41.9/2.0	
$ClCOOC_4H_9$	$S{=}C{=}N{-}COOC_4H_9$	34	59.0~61.0/6.0	323 (81.8)
	$N{\equiv}C{-}S{-}COOC_4H_9$	21	54.0~55.5/2.0	
$ClCOSC_2H_5$	$S{=}C{=}N{-}COSC_2H_5$	61	50.0~50.5/3.0	328 (94.7)
	$N{\equiv}C{-}S{-}COSC_2H_5$	0		
$ClCOC_6H_5$	$S{=}C{=}N{-}COC_6H_5$	76	102~103 /4.8	340 (133)
	$N{\equiv}C{-}S{-}COC_6H_5$	0		
$ClCOCH_3$	$S{=}C{=}N{-}COCH_3$	20	39.5~40.5/21	333 (53.2)
	$N{\equiv}C{-}S{-}COCH_3$	0		
$ClCOOCH_2{-}CH{=}CH_2$	$S{=}C{=}N{-}CH_2CH{=}CH_2$	30.9	38.0~40.8/8.0	
	$S{=}C{=}N{-}COOCH_2{-}CH{=}CH_2$	3.5	40.8~50.5/7.0	325 (69.6)

TABLE II. REACTION PRODUCTS AND YIELDS

Reagent	Thiamine sodium salt		C_6H_5ONa		C_6H_5SNa	
	Product	Yield, %	Product	Yield, %	Product	Yield, %
$N{\equiv}C{-}S{-}COOC_2H_5$	DCET	26	$C_6H_5OCOOC_2H_5$	42	$C_6H_5SCOOC_2H_5$	52
$S{=}C{=}N{-}COOC_2H_5$	B_1-SCN	trace	$C_6H_5OCOOC_2H_5$	24	$C_6H_5SCOOC_2H_5$	33
$N{\equiv}C{-}S{-}COOC_4H_9$	IIb	21	$C_6H_5OCOOC_4H_9$	51	$C_6H_5SCOOC_4H_9$	64
$S{=}C{=}N{-}COOC_4H_9$	B_1-SCN	trace	$C_6H_5OCOOC_4H_9$	31	$C_6H_5SCOOC_4H_9$	47
$S{=}C{=}N{-}COSC_2H_5$	B_1-SCN	trace	$C_6H_5OCOSC_2H_5$	39	$C_6H_5SCOSC_2H_5$	38
$S{=}C{=}N{-}COCH_3$	DAT	34	$C_6H_5OCOCH_3$	42	$C_6H_5SCOCH_3$	50
$S{=}C{=}N{-}COC_6H_5$	DBT	26	$C_6H_5OCOC_6H_5$	56	$C_6H_5SCOC_6H_5$	60

TABLE III. BOILING POINTS AND ELEMENTAL ANALYSES OF THE PRODUCTS

	B. p., °C/mmHg (m. p., °C)	Formula	Analysis % Calcd. C	Calcd. H	Found C	Found H
$C_6H_5OCOOC_2H_5$	56~57/2	$C_9H_{10}O_3$	65.05	6.07	65.18	6.12
$C_6H_5OCOOC_4H_9$	95~96/2	$C_{11}H_{14}O_3$	68.02	7.63	68.57	7.34
$C_6H_5OCOSC_2H_5$	80~85/3	$C_9H_{10}O_2S$	59.86	5.53	59.21	5.56
$C_6H_5OCOCH_3$	83~84/14	$C_8H_8O_2$	70.57	5.92	71.04	6.29
$C_6H_5OCOC_6H_5$	(68.5~70.5)	$C_{13}H_{10}O_2$	78.77	5.09	78.66	5.05
$C_6H_5SCOOC_2H_5$	93~95/5	$C_9H_{10}O_2S$	59.31	5.53	58.96	5.69
$C_6H_5SCOOC_4H_9$	109~109.5/4	$C_{11}H_{14}O_2S$	62.82	6.71	63.60	7.06
$C_6H_5SCOSC_2H_5$	100~101/2	$C_9H_{10}OS_2$	54.51	5.08	54.47	5.25
$C_6H_5SCOCH_3$	76~77/3	C_8H_8OS	63.12	5.23	62.98	5.41
$C_6H_5SCOC_6H_5$	(54)	$C_{13}H_{10}OS$	72.86	4.70	72.38	4.72

and ultraviolet spectra. When allyl chloroformate (IX) was used, however, besides a small amount of allyloxycarbonyl isothiocyanate (XI), allylisothiocyanate (X) was afforded, along with decarboxylation. X was identified by the infrared spectra of the product obtained by the reaction of allyl bromide with potassium thiocyanate in dimethylformamide.[7] These results are listed in Table I.

Next, the behaviors of these thiocyanate and isothiocyanate derivatives in relation to the sodium salt of thiamine (XII) were investigated. The reaction of alkoxycarbonylthiocyanate (IV) with thiamine sodium salt (XII) produced *O*,*S*-bis(alkoxycarbonyl)thiamine (II). However, when alkoxycarbonyl isothiocyanate (V) was used, a small amount of thiamine thiocyanate (XIII) was obtained as the only product. On the other hand, benzoylisothiocyanate (VIIIa) and acetylisothiocyanate (VIIIb) gave *O*, *S*-dibenzoylthiamine (XIVa)[8,9] and *O*, *S*-diacetylthiamine (XIVb)[8] respectively.

Analogously, IV or V reacted with simple phenol and thiophenol to give alkoxycarbonyl phenol (XV) and alkoxycarbonylthiophenol (XVI) respectively. Similarly, thioalkoxy carbonyl isothiocyanate (VII) gave thioalkoxycarbonyl phenol (XVII) or thioalkoxycarbonyl

7) S. Yoneda, H, Kitano and K. Fukui, *J. Chem. Soc. Japan, Ind. Chem. Soc.* (*Kogyo Kagaku Zasshi*), **65**, 1816 (1962).

8) T. Matsukawa and H. Kawasaki, *J. Pharm. Soc.* (*Yakugaku Zasshi*), **73**, 705, 709 (1953).

9) S. Yoshida, ibid., **74**, 993 (1954).

thiophenol (XVIII), and acylisothiocyanate (VIII) gave acylphenol (XIX) or acylthiophenol (XX). From these facts, it became clear that these thiocyanate or isothiocyanate derivatives can be used for alkoxycarbonylation or acylation reactions. These results are summarized in Table II.

Acyl- or alkoxycarbonylphenol and thiophenol are obtained in better yields than diacyl- and bis(alkoxycarbonyl)-thiamine respectively, possibly because phenol and thiophenol are much more reactive than the thiol-type thiamine. Thiocyanates gave a better yield than isothiocyanates. From Table II, the power of acylation and alkoxycarbonylation may tentatively ranked as follows:

$$RCOCl \geq (RCOSCN) > ROCOCl \geq RCONCS \geq ROCOSCN > ROCONCS$$

In the reaction with thiamine, it was noticed that IV, having reactive carbonyl, could react with thiamine, which has a relatively weak activity, and that at the first step, *S*-alkoxycarbonylthiamine (I) was formed and then a S→O rearrangement of the alkoxycarbonyl group occurred to give *O*-alkoxycarbonylthiamine (XXI) in the presence of alkali. The SH group of (XXI) was further alkoxycarbonylated to yield *O*,*S*-bis(alkoxycarbonyl)thiamine (II).[2]

While V seemed to have no carbonyl reactive enough to interact with the SH group of thiamine, VIII was much more active and reacted with XII to give *O*,*S*-diacylthiamine (XIV).

When a 2.5 molar equivalent of alkyl chloroformate was used in the reaction with potassium thiocyanate, IV and V were given in ratio of 1 : 1; this ratio was not changed by the increase of the mole of alkyl chloroformate. When an equimolar equivalent of alkyl chloroformate was used, however, V was given predominantly. Ethoxycarbonylthiocyanate (IVa) was thermally stable and did not change upon being boiled in ethanol in the presence of acetic acid. When a small amount of potassium thiocyanate or potassium acetate was added, however, IVa was readily converted into Va, even at room temperature. This conversion was traced by the infrared spectrum of this reaction mixture. As is shown in Fig. 4, the N=C=S and N–C–O bands increased with the decrease in the C≡N and S–C–O bands. It was considered that IV would convert into V by the reaction with potassium thiocyanate.

The mechanism of these reactions may be explained as follows: In an acetone solution the thiocyanato ion takes the form of an ion pair, and the S site or N site of this ion attacks the carbonyl carbon of acylchloride to give acylthiocyanate (XXII) and acyl isothiocyanate (VIII) as the respective transient products. Since XXII was considered to be the powerful acylation agent, however, it reacted with the thiocyanato ion to yield the stable acylisothiocyanate (VIII).

In the same manner, the reaction between the thiocyanato ion and alkyl chloroformate gives alkoxycarbonylthiocyanate (IV) and isothiocyanate (V). However, as the activity of IV is considerably weaker, the excess of alkyl chloroformate consumes the thiocyanato ion and IV is not able to participate in the reaction with the thiocyanato ion. As a result, IV and V are isolated in the reaction mixture.

Experimental

Ethoxycarbonylthiocyanate (IVa) and Ethoxycarbonylisothiocyanate (Va).—Into a solution of 244 g. (2.5 mol.) of potassium thiocyanate in 2.5 l. of acetone was added 633 g. (5.75 mol.) of ethyl chloroformate dropwise with stirring at room temperature. After the solution had been stirred for 4 hr. at room temperature, the separating potassium chloride was filterd off and the filtrate was concentrated. Distillation of the residue yielded 200.5 g. of the liquid with a b. p. of 43~58°/6.0 mmHg. The fractional distillation of this liquid (119.1 g.) gave 32.1 g. of IVa and 26.5 g. of Va.

IVa; b. p. 25.5~26.7°C/1.8 mmHg. $n_D^{25.3}$ 1.4930.
Found: C, 36.79; H, 4.06; N, 10.40; S, 24.07. Calcd. for $C_4H_5O_2NS$: C, 36.63; H, 3.84; N, 10.68; S, 25.21%.

Va: b. p. 41.2~41.9°C/2.0 mmHg.*1 $n_D^{25.3}$ 1.4570.
Found: C, 36.86; H, 4.33; N, 10.13. Calcd. for $C_4H_5O_2NS$: C, 36.63; H, 3.84; N, 10.68%. λ_{max}^{EtOH} 325 mμ (ε, 61.9).

Butoxycarbonylthiocyanate (IVb) and Butoxycarbonylisothiocyanate (Vb).—To a solution of 9.8 g. (0.1 mol.) of potassium thiocyanate in 100 cc. of acetone 27.2 g. (0.2 mol.) of butyl chloroformate was added dropwise. Treating it as above gave 8.7 g. of the liquid with a b. p. of 38~74°C/4~5 mmHg. The fractional distillation of this liquid (35 g.) gave 10 g. of VIb and 6.0 g. of Vb.

IVb: b. p. 54.0~55.5°C/2.0 mmHg. $n_D^{24.5}$ 1.4545.
Found: C, 44.87; H, 5.96; N, 8.66. Calcd. for $C_5H_9O_2SN$: C, 45.25; H, 5.69; N, 8.79%.

Vb: b. p. 59.0~61.0°C/6.0 mmHg. $n_D^{24.5}$ 1.4820.
Found: C, 46.18; H, 6.22; N, 8.82. Calcd. for $C_5H_9O_2SN$: C, 45.25: H, 5.69; N, 8.79%. λ_{max}^{EtOH} 323 mμ (ε, 81).

Thioethoxycarbonyl Isothiocyanate (VII).—To a solution of 14.6 g. (0.15 mol.) of potassium thiocyanate in 150 cc. of acetone 37.4 g. (0.3 mol.) of thioethoxycarbonyl chloride was added dropwise. Treatment as above gave 9.0 g. (61.2%) of (VII); b. p. 50.0~50.5°C/3.0 mmHg. $n_D^{23.5}$ 1.5788. IR ν_{max}^{film}

*1 Ref. 4: b. p. 83°C/30 mmHg.

1930～1970 (-N=C=S), 1685 (C=O) cm^{-1}. UV: 328 mμ (ε, 94.7).

Found: C, 33.17; H, 3.60; N, 9.59; S, 43.27. Calcd. for $C_4H_5OS_2N$: C, 32.63; H, 3.42; N, 9.52; S, 43.56%.

Benzoylisothiocyanate (VIIIa).—This was obtained from 9.7 g. (0.1 mol.) of potassium thiocyanate in 100 cc. of acetone and 28.0 g. (0.2 mol.) of benzoyl chloride after treating them as described above. Yield, 12.4 g. (75.6%). B. p., 102～103°C/4.8 mmHg.*2 IR ν_{max}^{film} 1930～1970 (-N=C=S), 1690 (C=O) cm^{-1}. UV: λ_{max}^{EtOH} 340 mμ (ε, 133).

Found: C, 59.04; H, 3.21; N, 8.43; S, 19.23. Calcd. for C_8H_5ONS: C, 58.81; H, 3.09; N, 8.58; S, 19.65%.

Acetylisothiocyanate (VIIIb).—This was obtained from 9.7 g. (0.1 mol.) of potassium thiocyanate in 100 cc. of acetone and 15.7 g. (0.2 mol.) of acetyl chloride after treating them as described above. Yield, 2.0 g. (19.8%). B. p. 39.5～40.5°C/21 mmHg.*3 $n_D^{23.5}$ 1.5190. IR ν_{max}^{film}: 1950～1980 (-N=C=S), 1725 (C=O) cm^{-1}. UV: λ_{max}^{EtOH} 333 mμ (ε, 53.2).

Found: C, 36.92; H, 3.43; N, 12.66; S, 29.91. Calcd. for C_3H_3ONS: C, 35.63; H, 2.99; N, 13.85; S, 31.71%.

Allylisothiocyanate (X) and Allyloxyisothiocyanate (XI).—To a solution of 14.7 g. (0.15 mol.) of potassium thiocyanate in 150 cc. of acetone 36.2 g. (0.3 mol.) of allyl chloroformate was added dropwise and the mixture was treated as above. Fractional distillation of the yielded product gave 4.6 g. (30.9%) of X and 0.77 g. (3.5%) of XI.

X: b. p. 38～40.8°C/8 mmHg.*4

Found: C, 48.52; H, 5.28; N, 13.48. Calcd. for C_4H_5NS: C, 48.44; H, 5.08; N, 14.12%.

It was identified with the product obtained by the method of Yoneda et al.[7] by infrared spectra.

XI: b. p. 48.5～50.5°C/7 mmHg. IR ν_{max}^{film}; 1960～1990 (-N=C=S), 1750 (C=O), 1220～1250 (C-O-C) cm^{-1}. UV: λ_{max}^{EtOH} 325 mμ (ε, 69.6).

Found: C, 42.87; H, 3.81; N, 9.57. Calcd. for $C_5H_5O_2NS$: C, 41.95; H, 3.52; N, 9.78%.

***O*, *S*-Bis(ethoxycarbonyl)thiamine (IIa) Hydrochloride.**—Into the suspension of 3.6 g. (0.01 mol.) of the sodium salt of thiamine[10] (XII) in *n*-propyl alcohol was added 3.3 g. (0.025 mol.) of IVa dropwise with stirring. During this reaction, the reaction mixture was maintained at pH 8.8～9.0 by the addition of alcoholic sodium ethoxide. After stirring for 2 hr. at room temperature, *n*-propyl alcohol was removed by vacuum distillation. Residue was dissolved in 20% hydrochloric acid and after being washed with ether, extracted with chloroform thoroughly. This chloroform extract was dried over anhydrous magnesium sulfate, and the chloroform was removed. The sirup obtained was induced to crystallize by treating it with ether and then recrystallized from the mixture of ethyl acetate and ethanol to give 1.26 g. (26.2%) of IIa hydrochloride in the form of colorless prisms m.p. 121～123°C. This product was identified with an authentic sample of IIa hydrochloride[1] by infrared spectra.

***O*, *S*-Bis(butoxycarbonyl)thiamine (IIb) Hydrochloride.**—This was prepared from 3.6 g. (0.01 mol.) of the sodium salt of thiamine (XII) in EtOH and 3.2 g. (0.02 mol.) of IVb as described above. The yield of IIb hydrochloride was 1.1 g. (21.2%); m. p. 86～88°C. The infrared spectrum of this product was identical with that of an authentic sample of IIb hydrochloride.[2]

Thiamine Thiocyanate (XIII).—This compound was obtained in a trace amount from XII by the reaction of either Va, Vb, or VII after treating it as above. It was then recrystallized from water to give colorless prisms, m. p. 180～181°C (decomp.). The infrared spectrum of this product was identical with that of an authentic sample of XIII.

***O*, *S*-Dibenzoylthiamine (DBT) (XIVa).**—To a suspension of 2.8 g. (0.06 mol.) of XII in ethanol 2.5 g. (0.15 mol.) of VIIIa was added dropwise as described above for the preparation of II. After the removal of ethanol, the residue was dissolved in ethyl acetate and washed with water and a diluted sodium hydroxide aqueous solution. After being dried over anhydrous magnesium sulfate, ethyl acetate was removed to give colorless crystals. Recrystallization from diluted ethanol gave 0.98 g. (25.5%) of colorless prisms; m. p. 172°C. The infrared spectrum was identical with that of the sample obtained by the other method.[8,9]

Found: C, 63.58; H, 5.43; N, 11.24; S, 6.62. Calcd. for $C_{26}H_{26}O_4N_4S$: C, 63.65; H, 5.34; N, 11.42%.

***O*, *S*-Diacetylthiamine (DAT) (XIVb).**—To a suspension of 3.9 g. (0.11 mol.) of XII in ethanol 2.2 g. (0.22 mol.) of VIIIb was added dropwise as described above for the preparation of II. After the removal of ethanol, the residue was dissolved in water and extracted with benzene. This benzene extract was shaken with 3% acetic acid, and the acetic acid layer was thoroughly extracted with chloroform. The chloroform extract was dried over anhydrous magnesium sulfate, and the chloroform was removed. The residual sirup was treated with ether to give colorless crystals; yield 1.35 g. (34.0%). Recrystallization from benzene-petroleum benzine gave colorless prisms (m. p. 118～119.5°C), whose infrared spectrum was identical with that of the sample obtained by the other method[8].

Found: C, 52.44; H, 6.12; N, 15.00. Calcd. for $C_{16}H_{22}O_4N_4S$: C, 52.44; H, 6.05; N, 15.29%.

The Acylation and Alkoxycarbonylation of Phenol and Thiophenol.—To a suspension of 0.03 mol. of dry sodium salt of phenol or thiophenol in ethanol 0.03 mol. of various alkoxycarbonylthiocyanates, isothiocyanates or acylisothiocyanates were added. After the mixture had been stirred for 2 hr. at room temperature, the ethanol was removed ether was added to the residue, and the separated sodium thiocyanate was filtered off. The esher solution fractionally distilled.

The Infrared Spectral Change of Ethoxycarbonyl Thiocyanate (IVa) in the Presence of

*2 Ref. 4: b. p. 119°C/10 mmHg.
*3 Ref. 4: b. p. 30～32°C/9～10 mmHg.
*4 Ref. 7: b. p. 151～152°C.
10) O. Zima and R. R. Williams, *Ber.*, **73**, 941 (1940).

Potassium Thiocyanate.—To a solution of 2.3 g. (0.0175 mol.) of IVa in acetone 0.34 g. (0.0035 mol.) of potassium thiocyanate was added and the mixture was stirred at room temperature. After 20 min. and 45 min., a part of the reaction mixture was taken up, the acetone was removed, and the infrared spectrum of the residual oil was taken. The results are shown in Fig. 4.

The authors express their deep gratitude to Professor Masao Tomita, Professor Shojiro Uyeo of the Kyoto University, and Dr. Ken'ichi Takeda, the Director of this laboratory, for their kind encouragement, and to Professor Saburo Nagakura of The University of Tokyo for his reading of this manuscript and for his invaluable suggestions. Thanks are also due to Assistant Professor Hideki Sakurai of the Kyoto University for his helpful discussion and to the members of the Analysis Room of this laboratory for their elementary analyses.

Shionogi Research Laboratory
Shionogi & Co., Ltd.
Fukushima, Osaka

NOTES

Selective Reduction of Phosphatides with Lithium Aluminum Hydride. II. Reductive Cleavage of Phosphatidic Acid

By Chieko URAKAMI and Mitsuko OKADA

(Received February 20, 1963)

In a previous paper[1] we had reported that the reductive cleavage of lecithin with lithium aluminum hydride in anhydrous ether gave rise to L, α-glycerylphosphorylcholine, a finding which was later confirmed by De Haas and Van Deenen[2] by the resynthesis of L, α-lecithins and L, α-lysolecithins from L, α-glycerylphosphorylcholine prepared by our method. A similar cleavage of the two acyl groups of the phosphatidic acid molecule may be attained by controlling reaction conditions so as to give L, α-glycerylphosphoric acid if no further reduction of the phosphate moiety occurs.

The method described by Kates[3] was followed for the preparation of the sodium salt of phosphatidic acid by subjecting purified (by column chromatography) egg yolk lecithin to the action of the lecithinase C of carrot roots and for the liberation of the free acid. The analytical results, the examination by paper chromatography,[4] and analyses for phosphorus and ester bond[5] indicate that the product so obtained consisted of approximately 70% phosphatidic acid and of some such as impurities fatty acids and their esters.

Difficulty was experienced in purifying the sample because phosphatidic acid is known to be highly labile; it is hydrolyzed even on exposure to moist air* or its ethanol solution is allowed to stand at room temperature.[6]

Since phosphatidic acid is a monoester of orthophosphoric acid, an extra mole of the hydride reagent would be required to compensate its acidity in addition to the one mole needed for the cleavage of the two fatty acid residues. Therefore, mole ratios higher than 1 : 2 (phosphatidic acid : lithium aluminum hydride) were considered in the present study; the reaction time was varied from 10 to 30 min. within a temperature range of 8~15°C. The procedure employed for reduction of the free acid in anhydrous ether with lithium aluminum hydride was essentially the same as that described earlier.[1] The aqueous phase separated from the reaction mixture was passed through a small column of Amberlite IR-112 and

1) C. Urakami, H. Okura and M. Okada, This Bulletin, **33**, 144 (1960).
2) G. H. De Haas and L. L. M. Van Deene, *Tetrahedron Letters*, No. 22, 7 (1960).
3) M. Kates, *Can. J. Biochem. Physiol.*, **33**, 575 (1955).
4) F. M. Heunnekens et al., *J. Biol. Chem.*, **206**, 443 (1954).
5) F. C. Bauer, Jr., and E. F. Hirsch, *Arch. Biochem.*, **20**, 242 (1949).
6) J. Olley, *Chem. & Ind.*, **1954**, 1069.
* Private commuication from Baer.

the eluate and the ethereal phase initially separated from the reaction mixture were analyzed for phosphorus, α-glycerylphosphoric acid-phosphorus[7,8] and ester bond.[5] The best conditons found from these studies appeared to be a mole ratio of phosphatidic acid to the hydride reagent of 1 : 2, at 10°C, and for 20 min; a typical example of the results obtained is shown in Table I.

TABLE I. RECOVERY OF PHOSPHORUS IN THE AQUEOUS AND ETHEREAL PHASES

Reaction conditions:		
Rhosphatidic acid : $LiAlH_4$ = 1 : 2, 10°C, 20 min.		
Sample wt., 18.2 mg. (equivalent to 492 μg. of α-GP-P)		
Reaction products:		
Aqueous phase	P_i, μg.	0.0
	α-GP-P, μg.[a]	456 ± 6
	%	92.6 (97.9)
	α-GP-P, μg.[b]	473 ± 2
Ethereal phase	Ester[c]	trace
	Total P	—

P_i stands for inorganic phosphorus, α-GP-P α-glycerylphosphoric acid-phosphorus.

a) Burmaster's method.[7]

b) Voris' method.[8]

c) The quantitative method[5] was employed; a trace amount detected may be due to the presence of fatty acid esters. The figures in parentheses are corrected for a loss of phosphorus during the course of elution through a column of Amberlite IR-112, the average recovery of the lithium salt of glycerylphosphoric acid being 94.5%.

An attempt to isolate the reaction product in the aqueous phase according to the method of Long and Maguire[9] was made with 200 mg. of the phosphatidic acid, but an amount of the barium salt of glycerylphosphoric acid obtained was so small that its rigorous purification could not be attained. Consequently, examination of its optical rotation was not possible (its specific rotation is known to be small, $[\alpha]_D = -1.2$[10]). However, the analytical results revealed that the sample isolated contained 77% α-glycerylphosphoric acid, the chief impurity being barium carbcnate; the amount of periodate consumed was equivalent to the content of α-glycerylphosphoric acid-phosphorus determined by Burmaster's method,[7] and no β-glycerylphosphoric acid-phosphorus was detected.

The fact that L, α-lecithin when treated similarly with the hydride reagent, gives rise to L, α-glyceylphosphoric acid[1] provides the reasonable assumption that the α-glycerylphosphoric acid obtained here retains the L-configuration of the natural acid. Further work is indicated, of course, but this method, involving a single-step reaction appears, to be preferable for the structural determination of naturally-occurring phosphatidic acids to the diazomethanolysis recommended by Baer,[11] which requires hydrogenation previous to interaction with diazomethane.

Osaka City University
Faculty of the Science of Living
Nishi-ku, Osaka (C. U.)

Tokushima Univesity
Kosokagaku Kenkyusho (M. O.)

7) C. F. Burmaster., *J. Biol. Chem.*, **164**, 233 (1946).
8) L. Voris et al., ibid., **133**, 491 (1940).
9) C. Long and M. F. Maguire, *Biochem. J.*, **54**, 612 (1953).
10) E. Baer, *J. Biol. Chem.*, **185**, 615 (1950).
11) E. Baer and J. Maurukas, ibid., **212**, 39 (1955).

A Study of the Structure of Pyridine Extracts from Coals by High Resolution Nuclear Magnetic Resonance Spectroscopy

By Gen TAKEYA, Mitsuomi ITOH, Akira SUZUKI and Susumu YOKOYAMA

(Received April 30, 1963)

Hitherto, various studies of hydrogen distribution in coals have been made by such methods as infrared[1] and broad-line NMR spectroscopy.[2] Of these analytical methods, although it would seem that the high resolution NMR method has some important advantages, only a few papers[3] have been published reporting on studies of the constitution of coal or coal-like materials made using it.

The present report deals with the constitution of the pyridine extracts of some Japanese coals, a study based upon their hydrogen distribution. The pyridine extracts of Yubari, Taiheiyo, Sumiyoshi and Sohya coal were separated from the solvent, dried and redissolved into deutero-pyridine, C_5D_5N. The C_5D_5N solutions (18~20%) of the coal extracts thus prepared were examined by NMR spectroscopy at 60 Mc. with a JNM-3H-60 NMR spectrometer.

The distribution of hydrogen was estimated from the intensities of the three different NMR bands. H_a represents the aromatic hydrogen atom which was situated ca. 7.5 p.p.m. from the tetramethyl silane peak in the NMR spectra; H_α, the hydrogen atom at α-positions to the aromatic rings (ca. 2.6 p.p.m.), and H_o, the hydrogen on the other saturated carbon atoms (ca. 1.5 p.p.m.). It has been confirmed by Ikenoue that the resonance peak for phenolic hydrogens in a pyridine solution appeared at a far lower position of the applied magnetic field than 8.5 p.p.m.[4]

From the contents of the different types of hydrogen atoms and the elementary analysis, the structural parameters: f_a (carbon aromaticity), σ (the measure of the substitution of the aromatc systems) and H_{au}/C_a (the aromatic hydrogen-to-carbon ratio of the hypothetical unsubstituted aromatic material) which were introduced by Brown et al.[3a] have been calculated for the pyridine extracts of coals. A new parameter of the length of the aliphatic carbon chain is proposed by the present authors

TABLE I. ANALYTICAL AND STRUCTURAL DATA OF THE PYRIDINE EXTRACTS

Coal sample		Yubari	Taiheiyo	Sumiyoshi	Sohya
Yield of extract (d. a. f.)		18.5	16.7	15.8	16.6
Pyridine extract analysis (d. a. f.)*	C	83.73	80.28	78.05	76.78
	H	6.39	7.13	6.51	6.42
	O	9.88	12.59	15.44	16.80
C/12 ($\propto$ C)		6.98	6.69	6.50	9.40
H/1 ($\propto$ H)		6.39	7.13	6.51	6.42
O/16 ($\propto$ O)		0.62	0.79	0.95	1.05
Hydrogen distribution (fraction)	H_a/H	0.151	0.053	0.064	0.105
	H_α/H	0.224	0.183	0.195	0.191
	H_o/H	0.625	0.764	0.741	0.704
Structural parameters	f_a	0.61	0.50	0.53	0.55
	σ	0.58	0.79	0.79	0.71
	H_{au}/C_a	0.54	0.55	0.58	0.66
	H_o/H_α	2.9	4.2	3.8	3.7
Numbers of aromatic condensed ring		6	6	5~6	4
Length of aliphatic C-chain		4	5	5	5

* These data are revised by substraction of phenolic hydrogen.

1) For example, D. W. van Krevelen, "Coal", Elsevier, Amsterdam (1961), pp. 363-372.
2) Ibid., pp. 382—391.
3) a) J. K. Brown, W. R. Ladner and N. Sheppard, *Fuel*, 39, 79 87 (1960). b) J. F. M. Oth and H. Tschamler, *Brennstoff-Chem.*, 42, 378 (1961); 43, 177 (1962).
4) Private communication from Dr. T. Ikenoue (Tohoku University, Sendai).

on the basis of the following relation: $\mathbf{H}_o/\mathbf{H}_\alpha=(\mathbf{H}_o/\mathbf{H})/(\mathbf{H}_\alpha/\mathbf{H})$. In the derivation of the above four parameters, nitrogen and sulfur (less than 2% d. a. f.-basis) in coal constituents have been disregarded. Furthermore, two assumptions were made regarding the constitution of coal: (1) all oxygen elements are attached directly to the aromatic systems; i. e., practically all oxygen occurs as phenolic OH and quinone groups, and (2) the aromatic rings are not directly linked by a C–C bond.[3a]

Assumption 1 may be accepted on the basis of our experimental results,[5] which show that more than 60% of the oxygen involved in the four parent sample coals appears as phenolic OH and quinone groups; assumption 2 is reasonable since a high degree of C–C crosslinking between aromatic systems is unlikely because of the large steric interactions of the aromatic systems involved. A realistic value for x and y in Brown's relations appears to be close to 2, as Brown et al. have set forth.[3a]

The structural parameters, f_a, σ, $\mathbf{H}_{au}/\mathbf{C}_a$ and above $\mathbf{H}_o/\mathbf{H}_\alpha$, calculated on the above assumptions, together with the features for the mean structure which are inferred from these parameters, are given in Table I.

Faculty of Engineering
Hokkaido University
Sapporo

5) G. Takeya et al., the 14th Annual Meeting of the Chemical Society of Japan, Tokyo, April 4, 1961.

The NMR Spectrum of Acrylonitrile

By Kazunaga MURAYAMA and Kenkichi NUKADA

(Received June 25, 1963)

The NMR spectrum of acrylonitrile at the resonance frequency under 60 Mc. shows a very complicated ABC pattern, and the interpretation of the spectrum cannot be carried out without utilizing a high speed computer.

On the other hand, at the resonance frequency of 100 MC,* the spectrum showed a nearly AMX-type pattern (Fig. 1), and it was very easy to obtain the relative chemical shifts and spin coupling constants by using a simple rule of line splitting (case A).

A slightly more accurate treatment, in which the spin system was assumed to be ABX, was also carried out according to the method of Pople et al.[1] (caseB). In the latter case, the absolute values of each parameter were not

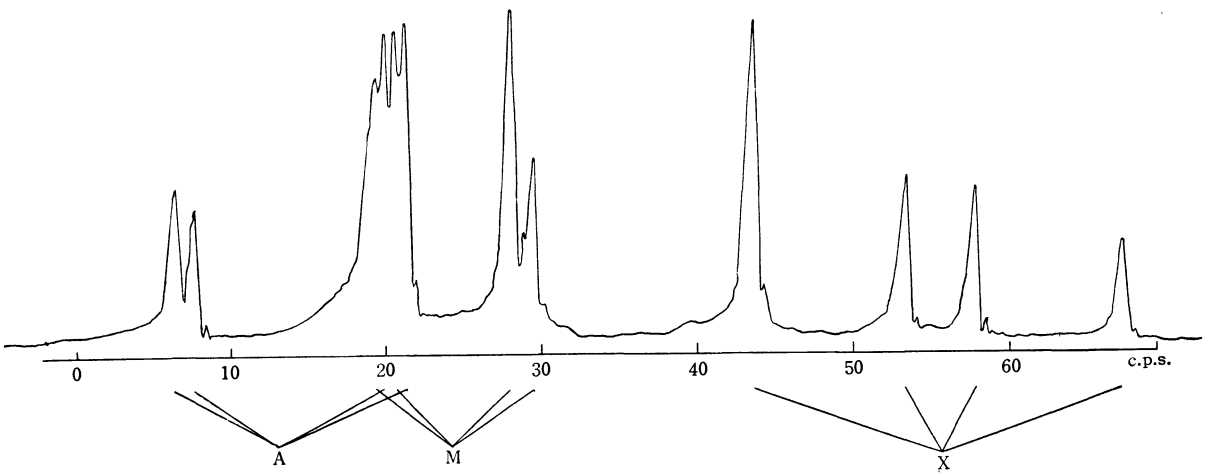

Fig. 1. NMR spectrum of acrylonitrile at 100 Mc.

* The NMR spectrum was recorded with a Varian HR-100 spectrometer.

1) J. A. Pople, W. G. Schneider and H. J. Bernstein, "High Resolution Nuclear Magnetic Resonance," McGraw-Hill, New York (1959), Chap. 6.

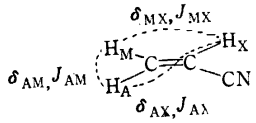

Fig. 2. Parameters for acrylonitrile.

TABLE I. CHEMICAL SHIFTS δ AND COUPLING CONSTANTS J OF ACRYLONITRILE (c. p. s.)

	δ_{AM}	δ_{AX}	δ_{MX}	J_{AM}	J_{AX}	J_{MX}
Case A	11.7	45.0	33.3	1.4	14.7	10.0
Case B	11.6	45.0	33.4	1.4	14.4	9.5
Castellano's Data[2]	10.0	47.9	37.9	1.7	18.0	11.0

essentially different from those of the former case. The relative sign between J_{AX} and J_{MX} (see Fig. 2), could, however, be determined to be positive in case B.

The results are illustrated in Table I, which compares them with the data obtained at 40 Mc. by Castellano et al.,[2] which data are reduced to the values at 100 Mc. The coincidence among these data is satisfactory.

Basic Research Laboratories
Toyo Rayon Company, Ltd.
Kamakura-shi, Kanagawa

2) S. Castellano and J. S. Waugh, *J. Chem. Phys.*, 43, 295 (1961).

The Production of High Specific Activities of Tin

By Shouzow FUKUSHIMA, Satori HAYASHI,[*1] Sanshiro KUME, Hideo OKAMURA, Kiyoteru OTOZAI, Koh SAKAMOTO,[*2] Ryuzo TSUJINO[*3] and Yasukazu YOSHIZAWA

(Received January 5, 1963)

Radioactive substances of a high specific activity are very useful in nuclear spectroscopy and in the tracer technique. In this work the production of the two long-lived radioactivities of tin, ^{113}Sn and ^{117m}Sn, was studied by means of cyclotron bombardment. These nuclides can be obtained separately from targets of a natural isotopic abundance by means of a cyclotron with a fixed frequency, provided the two reactions, ^{113}In(d, 2n)^{113}Sn and ^{115}In(α, pn)^{117m}Sn, are aimed at respectively. The purposes of the present investigation are to determine the thick target yield for these reactions and to establish the procedure for preparing the high specific activities of tin from the irradiated target.

Maxwell et al.[1] have reported procedures for the preparation of high specific activities of tin by means of alpha particle-induced reaction on cadmium of a natural abundance. In this case ^{113}Sn and ^{117m}Sn are produced concomitantly from the reactions ^{110}Cd(α, n)^{113}Sn, ^{111}Cd(α, 2n)^{113}Sn and ^{114}Cd(α, n)^{117m}Sn. In the present work, the thick target yields for these nuclides have also been determined.

Experimental

Thick Target Yield.—*Bombardment.*—Indium and cadmium plates of about 150 mg./cm^2 were bombarded with 11.2 MeV. deuterons or 22.1 MeV. alpha particles from the 110 cm. cyclotron of Osaka University. The target materials were 99.9% chemically pure. They were soldered on a water-cooled block of copper and irradiated at the "external target" position. The incident particle energies were degraded with aluminum absorbers and estimated from the range-energy relation.[2] The beam current was kept as low as about 2 μ amp. to prevent the target materials from melting. Total activations of about 2 μ amp.$\times$0.5 hr.=3600 microcoulombs were performed.

The total numbers of incident projectiles were determined by the use of monitor foils, by, that is, chromium and silver foils for deuterons and alpha particles respectively. The excitation function for the ^{52}Cr(d, 2n)^{52}Mn reaction[3] and the ^{107}Ag+$\alpha\rightarrow$ ^{109}Cd reaction[4] were used for the calibration.*

Source Preparation.—The procedures of chemical separations before the measurement of the tin activities were as follows. The irradiated cadmium target was dissolved in aqua regia. About 20 mg. of a iron(III) carrier was added, and the tin activity was coprecipitated with ferric hydroxide from a 2 N ammonia solution. The precipitate was then redissolved in 2 ml. of diluted hydrochloric acid.

The irradiated indium target was treated with hydrochloric acid, and a 20 mg. carrier of tin was added. The tin activity was separated from a 0.5 N hydrochloric acid solution as a sulfide. The sulfide was dissolved in 2 ml. of concentrated hydrochloric acid.

Activity Measurement.—The tin activities produced were measured with a gamma ray scintillation spectrometer. After the interfering activities had decayed off after several days, the activities of the 2 ml. liquid sample mentioned above were measured spectrometrically in a 1(3/4)$''\times$2$''$ well-type NaI scintillator. The photopeaks of the 390 keV. gamma ray from ^{113}Sn$-^{113m}$In and the 160 keV. gamma ray from ^{117m}Sn were measured. When both activities were contained, the contribution of the Compton part of the 390 keV. gamma ray to the 160 keV. photopeak was subtracted.

The counting efficiencies of the photopeaks (counting rates per disintegration rate) for both activities were calculated from several data as shown in Table I.

The Obtained Thick Target Yield.—The Thick target yields of the In+d, In+α and Cd+α reactions at some incident particle energies are summarized in Table II.

The Excitation Function for the ^{115}In(α, pn)^{117m}Sn Reaction.—The low values of thick target yields for the ^{115}In(α, pn)^{117m}Sn reaction suggest that the studied region of alpha particle energies is too low for the high-yield production of the activity. In order to study further the energy dependency of the yields in the higher region, the excitation function up to 40 MeV. for this reaction was obtained

*1 Present address: Public Health Research Institute of Osaka Prefecture, Osaka

*2 Present address: Radiation Center of Osaka Prefecture, Sakai, Osaka

*3 Present address: Yanagimoto Mfg. Co., Ltd., Kyoto

1) R. D. Maxwell, H. R. Haymond, D. R. Bomberger, W. M. Garrison and J. G. Hamilton, *J. Chem. Phys.*, 17, 1005 (1949).

2) H. Bichsel, R. F. Mozley and W. A. Aron, *Phys. Rev.*, 105, 1788 (1957).

3) P. Kafalas and J. W. Irvine, Jr., ibid., 104, 703 (1956).

4) S. Fukushima, S. Hayashi, S. Kume, H. Okamura, K. Otozai, K. Sakamoto and Y. Yoshizawa, *Nuclear Physics*, 41, 275 (1963).

* In the latter case two processes, ^{107}Ag(α, pn)^{109}Cd and ^{107}Ag(α, 2n)^{109}In$\rightarrow^{109}$Cd, are involved.

TABLE I. COUNTING EFFICIENCIES FOR ^{113}Sn AND ^{117m}Sn

Nuclide	Measured gamma ray MeV.	Photopeak efficiency	Total internal conversion coefficient	Intensity of the gamma ray per one disintegration	Counting efficiency
^{113}Sn	0.393	0.28	0.54	0.65	0.19
^{117m}Sn	0.159	0.95	41.0	0.79	0.74
	0.161	0.95	0.31		

TABLE II. THICK TARGET YIELDS* IN $\mu c./\mu amp.\ hr.$ FOR ^{113}Sn AND ^{117m}Sn FROM THE REACTIONS In+d, In+α AND Cd+α

In+d reaction		In+α reaction		Cd+α reaction		
E_d (MeV., LAB)	^{113}Sn	E_α (MeV., LAB)	^{117m}Sn	E_α (MeV., LAB)	^{113}Sn	^{117m}Sn
7.1	$1.1(0.7)\times10^{-2}$	16.6	$3(4)\times10^{-4}$	11.5	—	$1.7\ (0.2)\times10^{-3}$
9.1	$9.1(0.6)\times10^{-2}$	19.1	$7(1)\times10^{-3}$	14.8	$2.3(0.2)\times10^{-2}$	$2.0(0.3)\times10^{-1}$
10.9	$2.6(0.2)\times10^{-1}$	20.8	$4.7(0.5)\times10^{-2}$	20.8	$3.2(0.2)\times10^{-1}$	$1.1(0.1)\times10^{0}$

* The values in the brackets are the estimated standard deviations.

by the use of the stacked foil method.

Indium was electrolytically deposited in a 10 mg./cm² thickness on a silver plate of 25 mg./cm², and the indium foil was stacked together with the backing. The excitation function was measured in the energy region of 40~22 MeV. with alpha particles of 40 MeV. from the 160 cm. cyclotron of the Institute for Nuclear Study, the University of Tokyo, and in the 22~12 MeV. region with alpha particles of 22 MeV. from the 110 cm. cyclotron of Osaka University. The incident energy for each foil was estimated from the range-energy relationship in silver.[2] After the appropriate chemical isolation of tin, the radioactivity of ^{117m}Sn was measured by the same method. The observed cross section was corrected for the straggling effect, the foil thickness and the initial beam energy spread.[4] The correction amounts, for example, to about 13% at 17 MeV.

The cross sections thus obtained for the $^{115}In(\alpha, pn)^{117m}Sn$ reaction are given in Table III and are expressed as the excitation function in Fig. 1. The thick target yield curve for this reaction calculated from the excitation function and the range-energy relation is shown in Fig. 2, together with the values of the thick target yields already given in Table II. Figure 2 shows that the yield at 40 MeV. is about twentyfold that at 20 MeV.

TABLE III. MEASURED CROSS SECTIONS FOR THE REACTION $^{115}In(\alpha, pn)^{117m}Sn$

E_α (MeV., LAB)	Cross section (mb.) with standard deviation
11.9	0.01 ± 0.02
14.9	0.04 ± 0.01
17.7	0.64 ± 0.06
22.1	$5.9\ \pm0.8$
27.1	$14\ \pm2$
31.5	$16\ \pm2$
35.4	$16\ \pm2$
39.1	$13\ \pm2$

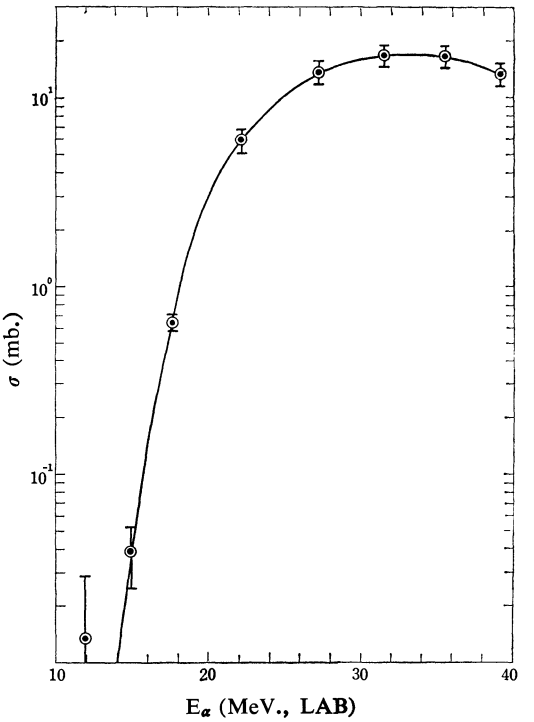

Fig. 1. Excitation function of the reaction $^{115}In(\alpha, pn)^{117m}Sn$.
Points: observed cross sections
Flags: standard deviations accompanied with the observed points
Solid curve: excitation fuction

The Preparation of High Specific Activities of Tin.—*Carrier-free Isolation.*—The irradiated indium target was dissolved in concentrated hydrochloric acid. After the addition of 20 mg. each of copper and of cadmium carriers, the tin activity was coprecipitated with copper sulfide by hydrogen sulfide

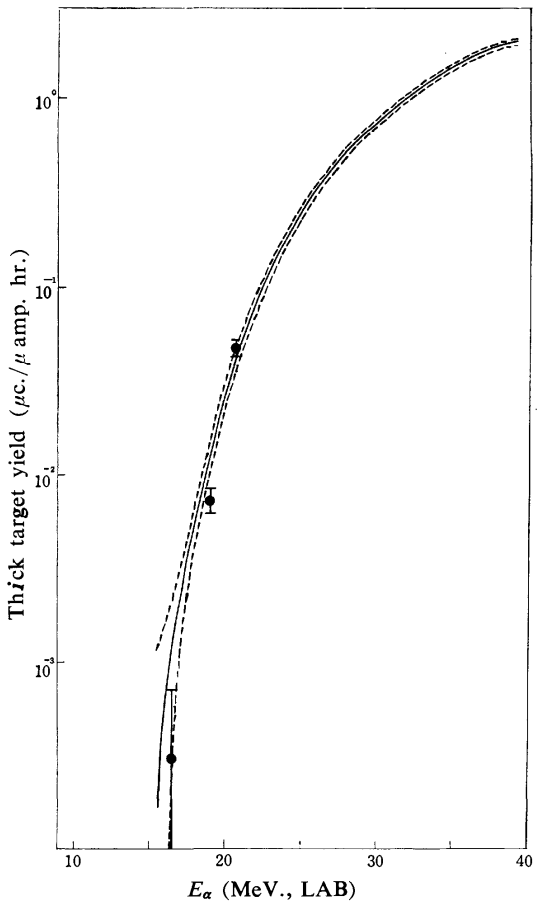

Fig. 2. Thick target yield curve for the reaction $^{115}In(\alpha, pn)^{117m}Sn$.
Solid curve: thick target yield curve calculated from the excitation function
Broken curves: upper and lower limits of the standard deviations
Closed circles: experimental values as shown in Table I
Flags: standard deviations in experimental values

from a 0.5 N hydrochloric acid solution. The sulfide was dissolved in a small amount of aqua regia, and the solution was evaporated almost to dryness. The residue was dissolved in 0.5 N hydrochloric acid. The tin activity was then again coprecipitated with copper sulfide from the solution containing 10 mg. each of indium and of cadmium carriers, After three coprecipitations, the copper sulfide with the tin activity was dissolved in a small amount of aqua regia, and then with water and hydrochloric acid; 10 ml. of a 2 N hydrochloric acid solution was obtained. The solution was passed through a column, 8 mm. in diameter, containing 3 ml. of Amberlite CG-400. After a complete elution of the copper by 30 ml. of 2 N hydrochloric acid, the carrier-free tin activity was eluted out with 25 ml. of 2 N nitric acid.

The irradiated cadmium target was dissolved in aqua regia. The solution was diluted with water, and 20 mg. of a iron(III) carrier was added. The tin activity was coprecipitated with ferric hydroxide from a 2 N ammonia solution. The reprecipitated ferric hydroxide was dissolved in hydrochloric acid, and 20 mg. each of indium and of copper carriers were added. Hydrogen sulfide was passed into the 0.5 N hydrochloric acid solution, and the tin activity was coprecipitated with copper sulfide. From this precipitate the carrier-free activity in a nitric acid solution was obtained by the same procedures as in the case of the indium target mentioned above.

Efficiencies of the carrier-free isolations of the tin activity are shown in Table IV. The nitric acid solution thus obtained has about 1 mg. of residue.

Table IV. Efficiencies of carrier-free isolations of the tin activity

Target	Chemical yield of Sn activity, %	Decontamination factor of In	Cd
In	87	>10^6	>10^3
Cd	94		

Electrolytic Deposition.—In order to obtain a sample for beta ray spectrometry, the activity was collected by means of an internal electrolysis from a 0.3 N hydrochloric acid solution. The apparatus for the internal electrolysis shown in Fig. 3. The anode is a zinc plate, while the cathode is a thin layer (10 μg./cm²) of gold deposited in vacuo on a thin "Mylar" tape (500 μg./cm², 2 mm.×15 mm.). About 80% of the activity was deposited in 20 hr. It must be noted that the tin activity is dissolved back into the hydrochloric acid solution in a moment if the external circuit is cut off.

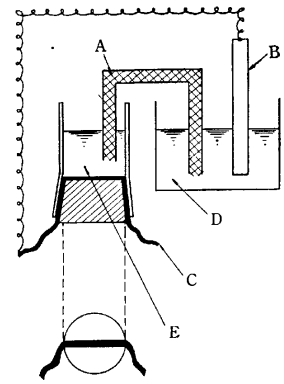

Fig. 3. Apparatus for the internal electrolysis.
A: Salt bridge (3% agar-agar, KCl satd.)
B: Zn-anode
C: Au-cathode (deposited in vacuo on "Mylar")
D: Anodic electrolyte (0.1 N $ZnCl_2$)
E: Cathodic electrolyte (0.3 N HCl, carrier-free tin activity, 0.2 ml.)

Discussion

If either ^{113}Sn or ^{117m}Sn is required separately, the In+d or In+α reactions respectively

may be used. However, if these nuclides can co-exist, the Cd+α reaction is preferable because of high thick target yield in the studied energy range and because of the higher melting point of cadmium than of indium.

The values of the thick target yield observed directly for the $^{115}In(\alpha, pn)^{117m}Sn$ reaction are in good agreement with the values from the excitation function at the energies lower than 21 MeV. If the values for the higher energies are necessary, the calculated values are available.

The separation procedure for the carrier-free activity by coprecipitation and ion exchange herein presented is efficient despite its simplicity in comparison with the distillation method.[1]

The tin activity was deposited internal-electrolytically on a gold film on "Mylar" foil (2 mm. × 15 mm.) and was used as a sample source for the beta ray spectrometer of Osaka University.[5] The L and M conversion electrons of the 159 keV. gamma ray were resolved separately.[6] Thus, the specific activity of the sample was sufficiently high so as to let the spectrometer exhibit its resolving power (0.2%) fully, even at the low energy region.

Summary

The production of high specific activities of tin, ^{113}Sn and ^{117m}Sn, with a cyclotron had been studied. Thick target yields for the reactions (A) $^{113}In(d, 2n)^{113}Sn$, (B) $^{115}In(\alpha, pn)^{117m}Sn$ and (C) $^{110}Cd(\alpha, n)^{113}Sn + ^{111}Cd(\alpha, 2n)^{113}Sn + ^{114}Cd(\alpha, n)^{117m}Sn$ were determined for several incident particle energies. The reactions A and B are available for the production of the single tin activity. Reaction C is preferable to the others in the total yields of tin activities for the energy range studied, i.e., up to the energy of about 5 MeV. per nucleon of the incident particle. A thick target yield for reaction B has also been obtained from the excitation function up to the alpha particle energy of 40 MeV. The procedures for the carrier-free isolation of the tin activity from indium and cadmium targets by coprecipitation and ion exchange have also been described.

The authors are indebted to Dr. Y. Koh of Osaka City University for his help throughout the work. They are also grateful to the members of the cyclotron group of Osaka University, and to both the cyclotron and radiochemical groups of the Institute for Nuclear Study, the University of Tokyo.

Department of Radiochemistry
Faculty of Science
Osaka University
Nakanoshima, Osaka

5) T. Katoh, M. Nozawa, Y. Yoshizawa and Y. Koh, *J. Phys. Soc. Japan*, **15**, 2140 (1960).
6) Y. Koh, private communication.

A Theoretical Assignment of the ESR Spectra of Cyclohexadienyl and Phenyl Radicals

By Keiji MOROKUMA, Shun-ichi OHNISHI, Takao MASUDA and Kenichi FUKUI

(Received January 23, 1963)

The assignment of observed unknown ESR spectra to a certain radical is often liable to involve some ambiguities; for example, the radicals from benzene and substituted benzenes cause trouble.

Fischer[1] irradiated benzene, toluene, ethylbenzene, cumene, fluorobenzene and chlorobenzene with an electron beam at 77°K and in all of the compounds studied observed the same spectrum, which consisted of a main triplet of the splitting of 50±2 gauss, each component of which separated into four triplets with the splittings 10.6±0.5 gauss (quartet) and 2.6± 0.2 gauss (triplet). He ascribed the spectrum to the cyclohexadienyl radical, $C_6H_7\cdot$, with the largest splitting (50 gauss) said to be that of the two methylene protons, with the splitting (10.6 gauss), that of the two ortho and the one para protons, and with the smallest splitting (2.6 gauss), that of the two meta protons.

Ohnishi et al.[2] studied ESR spectra of

1) H. Fischer, *Kolloid Z.*, **180**, 64 (1962).

2) S. Ohnishi, T. Tanei and I. Nitta, *J. Chem. Phys.*, **37**, 2402 (1962).

radicals produced by the electron beam irradiation at 77°K of benzene, toluene, chlorobenzene, phenylcyclohexane, benzoic acid and xylenes. For benzene at observation temperatures lower than −50°C, they obtained a triplet spectrum with a quartet structure, each component having a finer triplet structure with splittings of 47.5 gauss (triplet), 10.4 gauss (quartet) and 2.5 gauss (triplet). At the higher temperature this spectrum disappeared, while there remained another singlet spectrum with the width of 25 gauss. They attributed the former complex spectrum, which is very close to that observed by Fischer, to the cyclohexadienyl radical, as did Fischer, while the latter singlet spectrum was ascribed to the phenyl radical, $C_6H_5\cdot$. Kuwata[3] observed a broad spectrum from UV-irradiated halogenobenzenes which was considered to originate from the phenyl radical.

On the other hand, Chkheidze et al.[4] irradiated benzene with an electron beam and observed a triplet spectrum with the intensity ratio of 1 : 2 : 1 and with the splitting of 45.0±1.5 gauss; each component of this spectrum separated into a quartet with the splitting of 10.2±0.5 gauss. Though the spectrum seems to resemble very closely those found by Fischer and by Ohnishi et al., Chkheidze et al. assigned the spectrum to the phenyl radical, where the largest triplet was assigned to the two ortho protons and the quartet, to the two meta and one para protons.

As we have explained here, the assignment of the two kinds of observed spectra, the triplet with quartet structures and the broad singlet, is a matter still to be settled. Judging from the historical evidence that theoretical calculations and discussions have offered a great foundation for the interpretation of ESR spectra, it seems to be worthwhile to make a calculation on cyclohexadienyl and phenyl radicals and to compute the spin densities or the coupling constants of protons. Recently Fischer[5] presented a molecular orbital calculation on the spin density of the cyclohexadienyl radical to support his assignment. In the present paper the authors will make a valence bond calculation on both radicals, will compare the results with the two observed spectra, and will give the theoretical choice between the two assignments of the spectra.

The Valence Bond Calculation of Proton-coupling Constants in the Cyclohexadienyl Radical

The Model of the $C_6H_7\cdot$ Radical. — The cyclohexadienyl radical is treated as a system

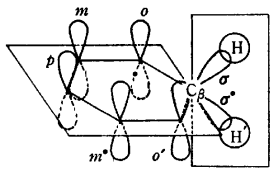

Fig. 1. Model of C_6H_7 radical.

consisting of 9 electrons on the following 9 atomic orbitals (Fig. 1):

- o: 2pπ orbital on one of the ortho carbons
- o': 2pπ orbital on the other ortho carbon
- m: 2pπ orbital on one of the meta carbons
- m': 2pπ orbital on the other meta carbon
- p: 2pπ orbital on the para carbon
- σ: Hybridized orbital on the carbon β directed to the AO H
- σ': Hybridized orbital on the carbon β directed to the AO H'
- H: Hydrogen 1s orbital on the hydrogen bonding with σ
- H': Hydrogen 1s orbital on the other hydrogen bonding with σ'

The plane on which the σ H and the σ' H' bonds are located is always assumed to be perpendicular to the molecular plane. As the hybridization of the methylene carbon, C_β in Fig. 1, and the bond length of the C_β–C_{ortho} bond do not seem to have been determined experimentally, we employed the following four different sets of configurational parameters in order to see the variation of the calculated results arising from these configurational differences.

a) The hybridization of the carbon β in the C_β–C_{ortho} bonds is assumed to be sp^2, which implies that the C–C bonds in benzene are not affected by a hydrogen addition; therefore, the hybridization of the σ and σ' orbitals is sp^5 (s nature 1/6 and p nature 5/6). The C_β–C_{ortho} bond length (r) is assumed to be 1.39Å, the C–C bond length in benzene.

b) The same hybridization as in a). The C_β–C_{ortho} bond length is 1.54Å, the bond length of a normal C–C single bond.

c) The carbon β is assumed to have the tetrahedral configuration: that is, all the valence orbitals of the carbon β are sp^3 hybridized. The C_β–C_{ortho} bond length is 1.39Å.

d) The same hybridization as in c). The bond length is 1.54Å.

In all of the four sets, the C_o–C_β–$C_{o'}$ angle is assumed to be 120°; this choice of angle affects the calculated value of the spin density scarcely at all.

3) K. Kuwata, private communication.
4) I. I. Chkheidze, Yu. N. Molin and N. Ya. Buben, *Dokl. Akad. Nauk. SSSR*, **130**, 1291 (1960).
5) H. Fischer, *J. Chem. Phys.*, **37**, 1094 (1962).

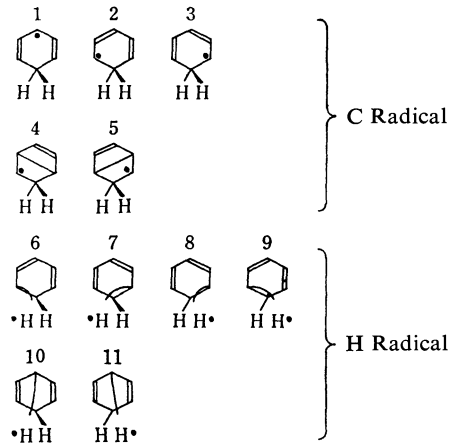

Fig. 2. Canonical structures taken into calculation of C_6H_7.

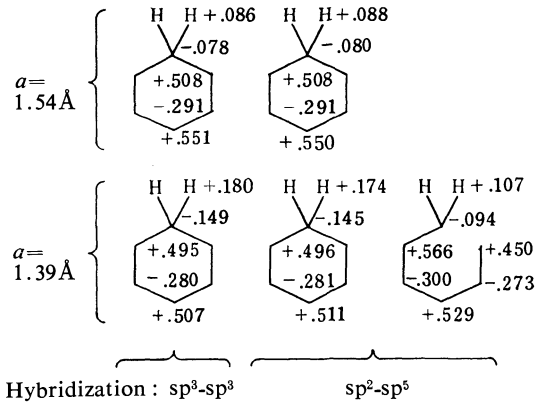

Fig. 3. Calculated spin density of C_6H_7 radical.

Canonical Structures. — Of all the possible canonical structures that have maximum bondings, 11 structures of lower energies corresponding to Kekulé and Dewar structures are taken into account on calculation. They are illustrated in Fig. 2.

Atomic Integrals.—The method of the evaluation of the necessary atomic integrals is the same as in the previous paper,[6] mainly the method of van Vleck[7] and of Karplus et al.[8], except for Altman's[9] exchange integrals between $p\pi$ orbitals. The values of the $p\pi$-$p\pi$ exchange integrals employed are $N_{\pi\pi\pi\pi}$ (1.39Å) $=-2.27$ eV. and $N_{\pi\pi\pi\pi}$ (1.54Å) $=-1.24$ eV. Exchange integrals between non-neighboring atomic orbitals are completely neglected.

Calculation Results.—The calculated coefficients of all the canonical structures in the ground state wave function are collected in Table I, from which the spin densities are derived in Fig. 3.

Figure 3 also gives the result of a comparative calculation on an imaginary compound in which the interaction of one of the ortho carbons with the methylene group is omitted. One can clearly see that the ring formation very markedly increases the spin density on the methylene proton; the calculated spin density on the methylene protons in a ring compound is almost twice as large as in an open-chain compound.

In Fig. 3 it is also obvious that the change of the hybridization of the carbon β have little effect on the spin distribution. Thus, the observed coupling constants seem to offer no information on the hybridization.

On the other hand, the change in the C_β-C_{ortho} distance, that is, the change in the exchange integral between C_β and C_{ortho}, exerts a great influence on the spin density in the methylene group. Elongation of the C_β-C_{ortho} bond length from 1.39Å to 1.54Å reduces the methylene proton spin density by half.

From these calculated values of spin density are derived the proton coupling constants in Table II, constants which are independent of the hybridization of C_β. The coupling constants of "σ" protons, that is, of ortho, meta and para protons, are calculated by the following popular relationship between the spin density on the adjacent carbon $p\pi$ orbital, ρ_C, and the proton isotropic constants, a_H:

$$a_H = Q_{HC}\rho_C \qquad (1)$$

where Q_{HC} is taken to be, as usual, -22.5

TABLE I. COEFFICIENTS OF CANONICAL STRUCTURES IN THE GROUND STATE WAVE FUNCTION OF C_6H_7

Hybridization of carbon C_1	C_1-C_{ortho} distance, Å	Coefficient				
		C_1	C_2, C_3	C_4, C_5	C_6, C_7, C_8, C_9	C_{10}, C_{11}
sp^3-sp^3	1.54	+0.3955	−0.3118	+0.0986	+0.0572	+0.0055
sp^2-sp^5	1.54	+0.3951	−0.3100	+0.0993	+0.0584	+0.0053
sp^3-sp^3	1.39	+0.3737	−0.2499	+0.1058	+0.1152	+0.0093
sp^2-sp^5	1.39	+0.3752	−0.2537	+0.1051	+0.1118	+0.0086

6) K. Morokuma and K. Fukui, This Bulletin, **36**, 534 (1963).
7) J. H. van Vleck, *J. Chem. Phys.*, **1**, 219 (1933); **2**, 20 (1934).
8) M. Karplus and D. H. Anderson, ibid., **30**, 6 (1959); M. Karplus, ibid., **30**, 11 (1959).
9) S. L. Altman, *Proc. Roy. Soc.*, **A210**, 327, 343 (1951-2).

TABLE II. CALCULATED AND OBSERVED PROTON-COUPLING CONSTANTS OF C_6H_7 RADICAL

Proton	Isotropic coupling constant (in gauss)			
	Calculated[b]		Observed	
	$r=1.54$Å	$r=1.39$Å	Ohnishi[2] and Fischer[1]	Chkheidze[4]
Ortho	−11.4	−11.1∼11.2	10.4∼10.6	10.2 (meta)[a]
Para	−12.4	−11.4∼11.5	10.4∼10.6	10.2 (para)[a]
Meta	+ 6.5	+ 6.3	2.5∼ 2.6	—
Methylene	+36∼37	+73∼76	47.5∼50.0	45.2 (ortho)[a]
Spectrum (lines)	3×4×3	3×4×3	3×4×3	3×4 (Assigned to $C_6H_5\cdot$)

a) Assignment by Chkheidze.[4] Assigned to $C_6H_5\cdot$ radical.
b) No matter what the hybridization of C_β is.

gauss.[10] The isotropic coupling constants of methylene protons are related to spin densities on them by the equation:

$$a_H = Q_H \rho_H \qquad (2)$$

Though a_H is theoretically given as +507 gauss, a smaller value, +420 gauss, which has been previously used by the authors in a similar valence bond calculation on a deformed methylene group,[6] would be more appropriate. This is mainly due to our disregard of any contribution of ionic structures. The coupling constants in Table II are calculated with the latter Q_H value.

The Valence Bond Calculation of Proton-coupling Constants in the Phenyl Radical

The Model of the $C_6H_5\cdot$ Radical. — In the phenyl radical, the migration of the odd electron may be achieved in several ways. One example is such a mechanism as the σ-π interaction between the non-bonding σ orbital and the pπ orbital, both on the carbon, C_1 (see Fig. 4), followed by the π-π migration to the pπ orbital on the ortho carbon and then by σ-π interaction between the ortho pπ orbital and the ortho C–H bond. However, this mechanism seems less significant because of the double σ-π interaction, which would bring about a spin density on the ortho proton of the order of 1/500.

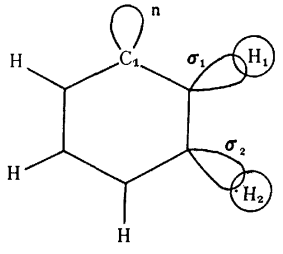

Fig. 4. Model of C_6H_5 radical.

A more probable mechanism would be direct interaction between the non-bonding σ orbital and the ortho C–H bond in the molecular plane. Therefore, in the present section we adopted the model in Fig. 4, consisting of 5 electrons on the following 5 atomic orbitals:

n: sp^2 hybridized non-bonding orbital on the carbon C_1
σ_1: sp^2 hybridized orbital on the ortho carbon, making a C–H bond with H_1
H_1: hydrogen 1s orbital on the hydrogen H_1
σ_2: sp^2 hybridized orbital on the meta carbon, making a C–H bond with H_2
H_2: hydrogen 1s orbital on the hydrogen H_2

For the sake of simplicity, the C–H bonds on only one side of the n orbital are considered. The inclusion of the other side would not affect the result seriously. Moreover, the para C–H bond is not taken into account, for the spin density of the para proton derived by the direct and in-plane interaction is relatively small and its order of magnitude can be estimated by the above calculation.

The change of the hybridization of the carbon, C_1, is not taken into consideration, for the change of the hybridization does not seem to affect the results. The C_1–C_{ortho} bond length is fixed as 1.39Å and the C_o–C_1–$C_{o'}$ angle, 120°. As the elongation of the C_1–C_{ortho} bond would reduce the coupling, as we saw in the previous section, the results of this calculation give the maximum value of the coupling constant.

Canonical Structures and Integrals. — All of the independent canonical structures that have the maximum bonding number, five structures in all, are taken as bases of the calculations, they are shown in Fig. 5. Ionic structures are not included in the present calculation at all. Integrals are evaluated by the same methods as in the preceding section.

Calculation Result.—The normalized ground state wave function is obtained as follows:

10) H. M. McConnell and D. B. Chesnut, *J. Chem. Phys.*, **28**, 107 (1958).

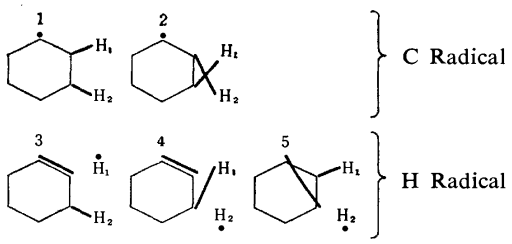

Fig. 5. Canonical structures taken into calculation of C_6H_5.

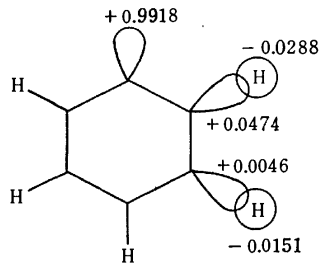

Fig. 6. Calculated spin density of C_6H_5 radical.

$$\Psi = 1.1338\phi_1 + 0.0968\phi_2 + 0.1144\phi_3 + 0.0673\phi_4 + 0.1779\phi_5 \quad (3)$$

where ϕ_i is the i-th canonical structure (for the numbering of them, see Fig. 5). From this function is derived the spin density shown in Fig. 6. The spin density is almost completely localized on the non-bonding hybridized orbital, n, on the carbon C_1; the phenyl radical may be said to be essentially a localized radical. From the spin densities in Fig. 6 the coupling constants of the ortho and meta protons are calculated by means of Eq. 2. The results are shown in Table III.

TABLE III. CALCULATED AND OBSERVED PROTON-COUPLING CONSTANTS OF $C_6H_5\cdot$ RADICAL

Proton	Coupling constants (in gauss)		
	Calculated	Observed	
		Ohnishi[2]	Chkheidze[4]
Ortho	−12.1	—	45.0
Meta	− 6.3	—	10.2
Para	—	—	10.2
Spectrum (lines)	3×3×2	1 ($\Delta H_{msl} \simeq 25$ gauss)	3×4

The Assignment of Observed Spectra and Discussion

After inspection of the calculated proton-coupling constants of the cyclohexadienyl radical $C_6H_7\cdot$, the complex spectrum, the triplet with finer structures of four triplets, observed by Ohnishi et al. and by Fischer, may safely be assigned to the cyclohexadienyl radical (see Table II). Agreement with the observed and the calculated spectra seems to be very good.* Though the coupling constant of methylene protons depends on the C_β–C_{ortho} bond length, the coincidence with the experimental value of 47.5∼50.0 gauss is accomplished at the bond length between 1.54 Å (C–C single bond) and 1.39 Å (C–C bond in benzene). This would be rational in the cyclohexadienyl radical, for it is produced from the regular hexagonal benzene molecule by hydrogen addition.

On the other hand, according to the theoretical results in Table III, the phenyl radical is considered to give a triplet with finer triplet structures. The singlet spectrum observed by Ohnishi has the width of 25 gauss between the maximum slopes and, depending on conditions, has slight nicks, showing that it might be a triplet. The large width just corresponds to the unresolved hyperfine structures of the theoretically-predicted splittings of 12 gauss. Thus, this broad singlet spectrum may safely be assigned to the phenyl radical. Chkheidze's assignment, in which the largest coupling constants, of 45 gauss, are attributed to ortho positions of the phenyl radical, does not correspond to the theoretical result at all. His spectrum, which is like those of Ohnishi and Fischer, would have to be ascribed to the cyclohexadienyl radical.

By the aid of this valence bond calculation, it seems that a theoretical basis can be given for the assignment of the two kinds of observed ESR spectra from irradiated benzene.

Summary

Two kinds of spectra—a triplet with a finer structure of four triplets, and a singlet--are known to be observed in ESR of irradiated benzene, and two different assignments of these spectra have been proposed—one assigning the triplet to the cyclohexadienyl radical and the singlet to the phenyl radical, and the other assigning the triplet to the phenyl radical. In the present paper, in order to give ground for a theoretical choice between the assignments, a valence bond calculation on the spin distribution of cyclohexadienyl and phenyl radicals has been carried out. On the cyclohexadienyl radical, though the numerical value of the spin density for methylenic protons is dependent on the C–$C_{methylene}$ bond length, the calculated spectrum is in good agreement with the observed triplet with four

* The coupling constant calculated for meta protons is a little too large. This seems to be either a general trend or a defect of the simple valence bond calculation of the conjugated system.

triplets. On the other hand, the phenyl radical has been shown theoretically to be an essentially localized radical and to give a singlet spectrum, which also agrees with that of the observed singlet.

Numerical calculations were carried out on the KDC-I digital computer of Kyoto University.

Faculty of Engineering
Kyoto University
Sakyo-ku, Kyoto
(K. M., T. M. & K. F.)

Osaka Laboratories
Japanese Association for
Radiadion Research on Polymers
Mii, Neyagawa, Osaka
(S. O.)

Chemical Reaction in a Shock Wave. I. The Ignition Delay of a Hydrogen-Oxygen Mixture in a Shock Tube

By Shiro FUJIMOTO

(Received February 22, 1963)

Many studies have been published about the reaction of hydrogen-oxygen mixtures.[1-4] In order to clarify the mechanism of this reaction, measurements of the induction period, during which the extent of reaction cannot be detected by the measuring instrument, are very useful.*,[5] Measurements of this induction period at low temperatures and low pressures have been already published[5] and those at high temperatures and low pressures have been conducted by Schott and Kinsey[3] and by Strehlow.[4]

In order to ignite the combustible mixture, there are various methods, such as ignition by electric spark,[6,7] by compression waves,[8] and by hot surfaces and by hot wires.[9] Howewer, the shock-tube technique is most useful for the measurement of the induction period or ignition delay, because the shock wave heats the mixture to a desired temperature almost instantaneously and homogeneously.

In the present experiment, the author tried to measure the induction period of a hydrogen-oxygen mixture in a shock tube at a moderate temperature and a rather high pressure ($825 \leq T_r \leq 1360°K$, $670 \leq P_r \leq 2670$ mmHg and $7.6\times10^{-4} \leq [O_2] \leq 3.0\times10^{-3}$ mol./l.); he tried also to examine the mechanisms proposed by other authors, whose measurements have been conducted under different conditions.

Experimental

The shock tube,[10] made from mild steel, has a square cross section with an inside lateral of 5 cm. and is divided into two sections, the reservoir chamber, A, 60 cm. in length and the test chamber, C, 180 cm. in length. Chambers A and C are separated by several sheets of cellophane film which can be punctured by the needle, N.

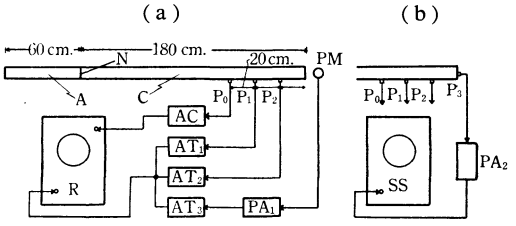

Fig. 1. Schematic diagram of the measuring system.
(a) Photo-multipler circuit with shock tube
(b) Piezo-gauge circuit, otherwise similer to (a)

1) M. Steinberg and W. E. Kaskan, "5th Symposium on Combustion," Baltimore, The Williams and Wilkins Co., (1955), p. 664.

* For example, Schott et al.[3] defined this period as the time during which the OH concentration reaches the threshold of detectability.

2) J. A. Fay and E. Lekawa, *J. Appl. Phys.*, **27**, 261 (1956).

3) G. L. Schott and J. L. Kinsey, *J. Chem. Phys.*, **29**, 1177 (1958).

4) R. A. Strehlow, presented before the Division of Fuel Chemistry, American Chemical Society, St. Louis, Missouri, March, 1961.

5) N. N. Semenov, "Some Problems in Chemical Kinetics and Reactivity," Vol. II., Princeton Univ. Press, Princeton, New Jersey (1959), p. 163.

6) M. V. Blane, P. G. Guest, G. von Elbe and B. Lewis, *J. Chem. Phys.*, **15**, 798 (1947).

7) W. Roth, P. G. Guest, G. von Elbe and B. Lewis, ibid., **19**, 1530 (1951).

8) B. P. Mullins, "Spontaneous Ignition of Liquid Fuels," Butterworths, London (1955), p. 13.

9) W. Jost, "Explosions und Verbrenunggsvorgänge in Gasen," Springer, Berlin (1939). p. 36.

10) M. Suzuki, H. Miyama and S. Fujimoto, This Bulletin, **31**, 819 (1958).

A brief scheme of the measuring system is shown in Fig. 1. As the shock wave passes down the tube, a signal on the piezo gauge, P_0, is thereby actuated; this signal is amplified through the amplifier circuit (AC) and triggers a raster-oscilloscope, Type SS 5101, made by the Iwasaki Communication Apparatus Co., which can respond to a time up to 1 μsec. The subsequent piezo gauges, P_1 and P_2, are actuated by the downward travelling shock wave, and the signals are fed through amplifier thyratron circuits (AT_1) and (AT_2), again on the raster-oscilloscope, thus providing a measurement of the incident shock speed. The measurement of the ignition was made in two ways. One method depends upon a raster-oscilloscope pattern actuated by a photo-multiplier (Fig. 1-(a)). A light signal initiated by the light emission of the gas mixture passes through a transparent plastic window, hits a photo-multiplier tube, and, appears in the sweep on the raster-oscilloscope, thus making possible an estimation of the exact time of ignition. A sample raster-oscilloscope pattern is shown in Fig. 2.

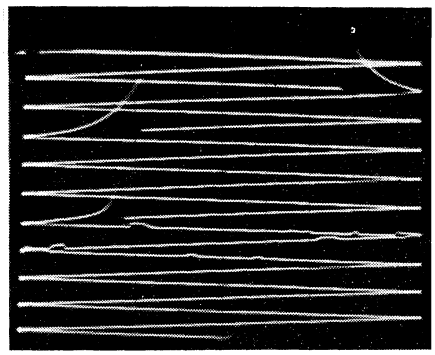

Fig. 2. Raster-oscilloscope diagram (an example).
N_2; 80%Ar+20%($2H_2+O_2$)
ω=740 m./sec., τ=298 μsec.
The 1st and 2nd signals are those from velocity gauges and 3rd signal is from photomultiplier gauge.

In the second method, measurements are carried out by using a piezo-gauge placed at the bottom of the shock tube. A pressure disturbance, accompanied by gas detonation, through a preamplification circuit (PA_2) (Fig. 1-(b)), gives a relevant pressure pattern on a synchroscope (Type 5302 of the Iwasaki Communication Apparatus Co.); this enables one to determine the exact time of the ignition. A sample pattern is given in Fig. 3. Both methods were applied for each run of measurements; the results obtained from the two ways were satisfactorily concordant. Piezogauges have been used by several investigators in shock studies.[11,12] A gauge of this type, made in this laboratory, has proven eminently successful as a detector of weak shock waves.

11) W. W. Willmarth, *Rev. Sci. Inst.*, **29**, 218 (1958).
12) B. Greene and G. B. Kistiakowsky, *J. Am. Chem. Soc.*, **72**, 1080 (1950).

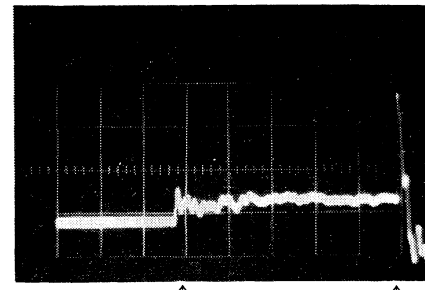

Reflected shock wave Start of ignition

Fig. 3. Synchroscope pattern of a signal from the piezogauge on the bottom of the shock tube.
N_2; 70%Ar+30% ($2H_2+O_2$)
ω=733 m./sec., τ=530 μsec.

As a driver gas in the reservoir, A, nitrogen was used. In the test chamber, C, $0.067H_2+0.033O_2+0.900Ar$, $0.133H_2+0.067O_2+0.800Ar$ and $0.2H_2+0.1O_2+0.7Ar$ were used. In the present report, only ignitions caused by reflected shock waves will be described.

Results and Discussion

From Fig. 2, where a sample of a raster-oscilloscope diagram is shown, the incident shock velocity, ω, and ignition delay, τ, at various shock conditions can be obtained; they are tabulated in Tables I and II. For the evaluation of the τ values, it is assumed that the ignition occurs at the wall of the end plate of the shock tube; a Schlieren picture taken by Strehlow[4] seems to justify this assumption. Applying the usual process

TABLE I. VALUES OF ω, τ, T_r, P_r, and O_2 FOR 70%Ar+30%($2H_2+O_2$) PHOTO-MULTIPLIER METHOD

P_1 mmHg	ω m./sec.	τ μsec.	T_r °K	P_r mmHg	O_2 mol./l. $\times 10^3$
100	666	2227	825	1208	2.348
50	683	2019	870	673	1.241
50	692	1525	891	702	1.264
50	703	1302	909	734	1.295
50	707	1059	918	750	1.310
50	719	1014	945	789	1.340
50	736	888	987	847	1.376
50	764	543	1053	955	1.455
50	797	177	1131	1074	1.525
50	830	156	1215	1223	1.616
50	840	130	1242	1266	1.635
50	844	143	1254	1286	1.647
50	851	115	1269	1317	1.665
50	862	109	1308	1373	1.685
50	870	117	1323	1408	1.708
50	885	84	1362	1478	1.740

TABLE II. VALUES OF ω, τ, T_r, P_r AND O_2 FOR 70%Ar+30%($2H_2+O_2$) PIEZOGAUGE METHOD

P_1 mmHg	ω m./sec.	τ μsec.	T_r °K	P_r mmHg	O_2 mol./l. $\times 10^3$
100	694	1220	894	1416	2.540
100	709	1142	924	1511	2.622
100	717	1164	942	1565	2.655
100	722	1120	948	1577	2.670
100	725	1020	960	1618	2.701
100	733	958	978	1672	2.741
100	735	630	984	1686	2.749
100	740	624	996	1730	2.785
100	744	160	1008	1765	2.810
100	746	158	1010	1775	2.814
100	749	190	1017	1800	2.840
100	752	179	1026	1818	2.841
100	754	160	1029	1835	2.860
100	763	120	1050	1905	2.910
100	769	154	1065	1949	2.935
100	772	126	1071	1975	2.960
100	773	120	1074	1982	2.962
100	778	138	1086	2020	2.988

of calculation,[13] the temperature, T_r, and the pressure, P_r, of the reflected shock wave and the concentration of oxygen behind the reflected shock wave are also tabulated in Tables I and II. In this procedure, a constant value of γ is assumed.*1

Steinberg and Kaskan[1] found a linear relationship between $\log_{10}\tau$ and $1/T_r$ for a $2H_2+O_2$ mixture without dilution. Schott and Kinsey[3] measured the formation of OH in the shock wave-induced combustion of H_2 and O_2 by using the ultraviolet absorption of OH and found a linear relationship between $\log_{10}\tau[O_2]$ and $1/T$ as follows:

$$\log_{10}\tau[O_2]\ (\text{mol.}\,l^{-1}\,\text{sec.}) = -10.647+(3966\pm625)/T \qquad (1)$$

Strehlow[4] obtained a similar result by using a conventional shock tube and the Schlieren system. In comparison with their results, our results are shown in Fig. 4. Although the position of our least square line is different from that of the other authors, the slope of the line is about the same. The least square line is expressed as follows;

$$\log_{10}\tau[O_2]\ (\text{mol.}\,l^{-1}\,\text{sec.}) = -9.581+3559/T_r \qquad (2)$$

The difference in the position of lines can not be explained as arising from experimental error, because the uncertainty of the τ value is less than 1 μsec. and that of T_r, less than 1%.*2

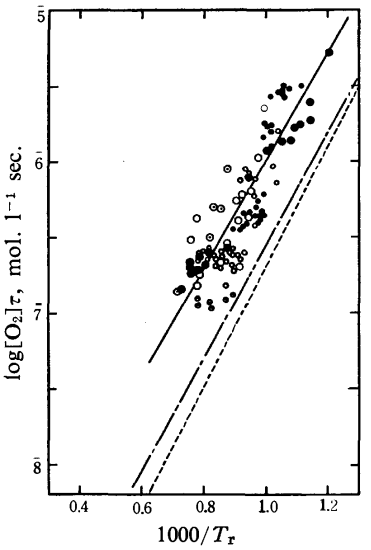

Fig. 4. Relation between $\log_{10}[O_2]\tau$ and $1/T_r$ for $2H_2+O_2$ with argon.

	Photo-multiplier method	Piezo gauge method
70%Ar+30%($2H_2+O_2$)	●	●
80%Ar+20%($2H_2+O_2$)	○	○
90%Ar+10%($2H_2+O_2$)	⊙	⊙
Strehlow's line	—·—·—	
Schott's line	----------	

In order to explain the induction time, τ, Semenov assumed the following reactions:

$$OH + H_2 \rightarrow H_2O + H \qquad (I)$$

$$O_2 + H \rightarrow OH + O \qquad (II)$$

$$O + H_2 \rightarrow OH + H \qquad (III)$$

Schott and Kinsey[3] also adopted Semenov's mechanism and derived the similar equation:

$$\tau[O_2] \propto \frac{1}{k_2} = \exp(E_2/RT)$$

In the derivations described above, Reaction IV is disregarded because of its low reactoin velocity compared with that of reaction II.

$$H + O_2 + M \rightarrow HO_2 + M \qquad (IV)$$

If reaction IV is taken into account, the following relation is derived:

$$\tau[O_2] \propto \frac{1}{k_2\{1-k_4[M]/2k_2\}}$$

13) I. I. Glass, W. Martin and G. N. Patterson, "A Theoretical and Experimental Study of the Shock Tube," UTIA Report No. 2, November, 1953.

*1 In the present experiment, the hydrogen-oxygen mixture is diluted with argon and the temperature is not very high. Therefore, the variation of γ with the temperature is not so large as to decrease the value of T_r beyond the range of experimental error.

*2 This uncertainty is guessed from the accuracy of the measuring instrument. However, according to the experimental results, the fluctuation of τ at a definite temperature is ±8% and the fluctuation of T_r at a definite τ value is ±5%.

Under the experimental conditions of Schott and Kinsey[3] $k_4[M]/2k_2$ is far less than 1 and the $\tau[O_2] \propto (1/k_2)$ relation may be applied. However, under the present experimental conditions, where pressure is comparatively high and temperature is low, $k_4[M]/2k_2$ can not be ignored in comparison with 1. According to Lewis and von Elbe,[14] $2k_2/k_4[M]$ is expressed as follows;

$$2k_2/k_4[M] = \frac{0.0556}{f_{H_2}+0.35f_{O_2}+0.20f_{Ar}} \times \frac{T}{P} \times \exp -\left[\frac{17000}{803R}\left(\frac{803}{T}-1\right)\right]$$

where is the mole fraction of the components of the mixture, P is the pressure in mmHg, and T is the absolute temperature. By using this equation, $k_4[M]/2k_2$ under the present experimental conditions can be calculated as follows.

T, °K	$k_4[M]/2k_2$
900	1.64
1000	0.69
1100	0.35
1200	0.20
1300	0.14

Obviously, $k_4[M]/2k_2$ is not ignored, and, therefore, reaction IV must be taken into consideration. However no quantitatively satisfactory explanation for the difference between our data and that of the others shown in Fig. 4 has yet been obtained. Also, it is difficult to explain why the value, 16.3 kcal., of the activation energy obtained by using the slope of the line in Fig. 4 is very close to those of Schott (18.1 kcal.) and Strehlow (16.5 kcal.). It is supposed that the simple scheme described above does not express the situation correctly.*3 In order to obtain a fully satisfactory explanation, it is necessary to conduct a more detailed study.

14) B. Lewis and G. von Elbe, "Combustion Flams and Explosions of Gasee," Academic Press Inc., New York (1961), p. 45.

Summary

The values of the ignition delay of a hydrogen-oxygen mixture with a diluent in the reflected shock waves were measured by using a shock tube equipped with a piezo gauge for shock velocity measurements and a photomultiplier or another piezo gauge for the measurement of the time of ignition.

There was the following relationship between the ignition delay, τ, and the temperature, T_r, behind the reflected shock wave:

$$\log_{10}\tau\,[O_2]\ (\text{mol. } l^{-1}\ \text{sec.}) = -9.581 + 3559/T_r$$

where $825 \leq T_r \leq 1360$°K and $7.6\times10^{-4} \leq [O_2] \leq 3.0\times10^{-3}$ mol./l. The difference between this relationship and that set forth by other authors has been discussed.

The author wishes to express his gratitude to Professor Momotaro Suzuki of Defense Academy and Dr. Hajime Miyama of the Basic Resarch Laboratories of Toyo Rayon Co., Ltd., for their many helpful discussions during the course of this study, and to Mr. Tsuneo Kase for his help in performing the experiments.

Department of Chemistry
Defense Academy
Yokosuka

*3 According to Dr. W. C. Gardiner's private communication to Dr. H. Miyama, it appears that there are three reactions in the induction time that have almost the same rate constants.

The Electronic Spectra of Aromatic Molecular Crystals. II. The Crystal Structure and Spectra of Perylene

By Jiro TANAKA

(Received March 27, 1963)

The electronic absorption spectra of aromatic molecular crystals have been investigated from several viewpoints in order to confirm the polarizations and the symmetry properties of excited states, and in order to discover the mechanism of electronic interactions in molecular crystals.[1] In spite of the many experiments which have been reported hitherto, few have been concerned with the same molecule in different crystalline forms. Perylene has two crystalline forms; the first was shown by Donaldson, Robertson and White[2] to have a dimeric structure, while a new form, herein reported, is monomeric and analogous to the structures of naphthalene and anthracene. The electronic spectra of the two crystalline forms has been studied, and it has been shown that the charge-transfer resonance interaction is very important, particularly in the dimeric crystal. The anomalous fluorescence of dimers of pyrene and naphthalene in a solution[3] and of pyrene and other substances in the crystalline state[4,5] have attracted attention; the present study provides an explanation of the mechanism of anomalous fluorescence.

Crystal Structure.—It is proposed to designate the previously-known form of perylene by α and the new one by β. Crystals of both the α and β forms have been obtained together from petroleum ether or benzene solutions, but they are easily distinguished from each other by their general appearance. The α form is usually obtained as a rectangular, tabular, yellow crystal (monoclinic), while the β form is obtained as hexagonal, greenish-yellow prisms (monoclinic). The β form is transformed into α at about 140°C. At and below room temperature, both forms are stable, and no transformation was found at lower temperatures.

X-Ray rotation and Weissenberg photographs show that the β form belongs to the $P2_1/a$ space group and give the following crystal data: $a=11.27\pm0.03$, $b=5.88\pm0.02$, $c=9.65\pm0.03$ Å, $\beta=92.1\pm0.3°$; absent spectra; ($h0l$) when h is odd and ($0k0$) when k is odd; space group, $P2_1/a$ (C^5_{2h}); two molecules per unit cell; the center of the molecule is at the origin; volume of the unit cell, 394.3 Å^3. It should be noted that the lattice constants are similar to those of the α form except for b, which is about half of the α form (α has $a=11.35$, $b=10.87$, $c=10.31$ Å and $\beta=100.8°$; space group $P2_1/a$ with four molecules in the unit cell.[2]

The crystal structure analysis has been carried out with the aid of a and b axes projection. The $h0l$ and $0kl$ reflections were recorded with a Weissenberg camera using Cu$K\alpha$ radiation. The multiple-film technique was used, and the intensity data were obtained by

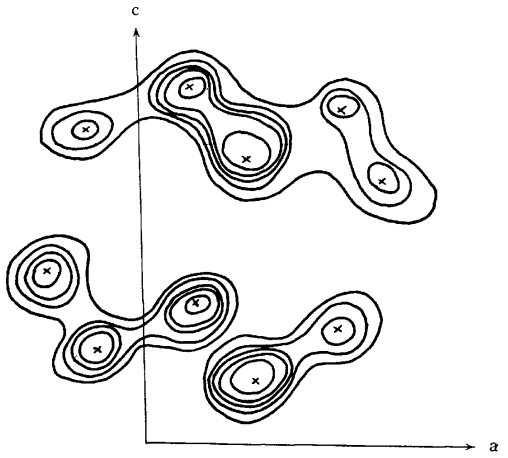

Fig. 1. Fourier map for the b-axis projection.

TABLE I

	x	y	z
C_1	0.092	0.170	0.044
C_2	0.169	0.323	0.117
C_3	0.214	0.331	0.270
C_4	0.177	0.190	0.344
C_5	0.091	0.020	0.292
C_6	0.044	−0.132	0.365
C_7	−0.050	−0.285	0.322
C_8	−0.083	−0.310	0.175
C_9	−0.037	−0.150	0.097
C_{10}	0.044	0.010	0.143

1) J. Tanaka, *Prog. Theoret. Physics*, Suppl. **12**, 183 (1959).
2) D. M. Donaldson, J. M. Robertson and J. G. White, *Proc. Roy. Soc.*, **A220**, 311 (1953).
3) Th. Förster, Paper presented at the International Symposium on Molecular Structure and Molecular Spectroscopy, Tokyo, 1962.
4) J. Ferguson, *J. Chem. Phys.*, **28**, 765 (1958).
5) B. Stevens, *Spectrochim. Acta*, **18**, 439 (1956).

TABLE II. OBSERVED AND CALCULATED STRUCTURE FACTORS

	Obs.	Calcd.		Obs.	Calcd.		Obs.	Calcd.		Obs.	Calcd.
001	80	86	404	5	5	$60\bar{1}\bar{1}$	5	− 5	020	60	− 86
002	120	−129	405	17	− 18	800	64	− 62	022	14	5
003	57	56	406	21	− 21	803	12	− 20	023	22	− 25
004	110	−105	408	10	3	804	54	61	024	17	18
005	88	82	4010	8	6	805	50	48	027	31	24
006	9	18	$40\bar{1}$	85	− 80	806	15	− 23	029	8	− 7
009	10	− 5	$40\bar{2}$	28	− 20	$80\bar{1}$	12	10	0211	5	− 5
200	114	136	$40\bar{3}$	14	14	$80\bar{2}$	8	4	032	5	− 2
201	63	− 61	$40\bar{4}$	23	− 32	$80\bar{3}$	7	4	033	5	21
202	40	27	$40\bar{5}$	14	17	$80\bar{4}$	11	− 11	036	8	13
203	34	− 40	$40\bar{8}$	41	32	$80\bar{5}$	26	− 18	038	9	− 9
204	131	−123	$40\bar{9}$	16	13	$80\bar{9}$	7	7	040	14	− 6
205	11	− 11	$40\bar{1}\bar{0}$	9	− 9	1002	3	− 1	041	6	− 5
206	30	29	600	34	− 34	1003	15	23	042	8	− 17
208	17	− 13	601	34	− 32	1004	37	42	043	8	− 6
209	29	− 16	602	14	32	$120\bar{4}$	6	7	044	7	7
$20\bar{1}$	116	149	605	12	12	011	7	− 8	047	18	18
$20\bar{2}$	12	− 12	$60\bar{1}$	8	10	012	23	− 23	049	2	− 2
$20\bar{3}$	39	48	$60\bar{2}$	7	4	013	6	− 1	054	6	6
$20\bar{6}$	6	6	$60\bar{4}$	65	− 48	014	41	− 42	055	7	10
$20\bar{7}$	22	− 36	$60\bar{5}$	26	− 20	015	43	− 34	060	42	39
$20\bar{8}$	10	− 10	$60\bar{6}$	12	4	016	12	15	061	11	12
$20\bar{9}$	7	11	$60\bar{7}$	22	− 22	017	14	16	062	9	− 7
400	6	− 4	$60\bar{8}$	33	33	019	14	− 11	064	12	− 11
401	32	41	$60\bar{9}$	46	44	0110	6	− 2	065	13	− 13
403	5	− 7	$60\bar{1}\bar{0}$	5	− 9	0111	6	3			

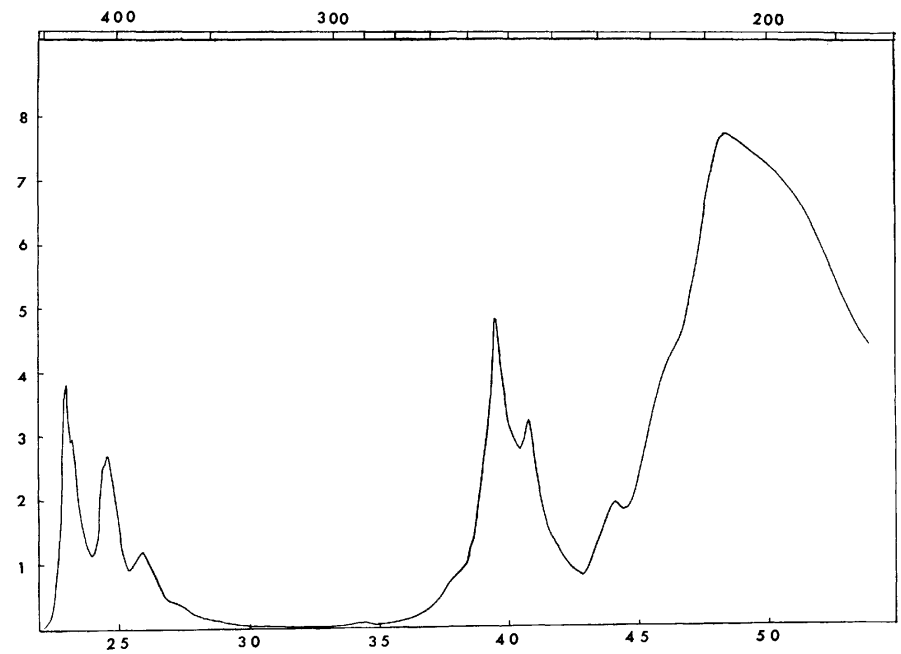

Fig. 2. Absorption spectrum of perylene in *n*-heptane.
Ordinate; molecular extinction coefficient (in units of 10^4)
Abscissa; lower, frequency (in $10^3\,cm^{-1}$), upper, wavelength (in mμ)

visual comparison with crystal-reflected calibration spots of known relative exposures. In the *h0l* zone, 69 intensities out of 140 were measured, and 41 out of 78 for 0*kl*. The appropriate molecular orientation was deduced from the spectra of single crystals. A comparison with the spectrum showed that the directions of the long (L) and the short (M) axes of the molecules must be nearly the same in the two forms. Assuming that the tilts of the molecules on the axes are same in the two forms, the signs of the structure factors were determined; the first Fourier *h0l* projection showed the positions of all the carbon atoms. After a few cycles of refinement, the x and z parameters shown in Table I were obtained. The structure factors were calculated using the same temperature factor for all atoms, $B=4.2$, and at this stage of refinement, R (for the observed F_{h0l} reflection only) is 0.17. The calculated structure factors are compared in Table II with the observed values. The Fourier map for the b axis projection is shown in Fig. 1. The 0*kl* Fourier projection did not show resolved atoms because of serious overlapping in this projection. Assuming that the molecule is planar and has nearly the same structure as in the α form, the y parameters shown in Table I may be derived and the structure factors F_{0kl} shown in Table II may be calculated. For the observed 0*kl* reflections, the R factor is 0.27. Although, at this stage of refinement, the agreement between observed and calculated values is not sufficiently good to discuss the shape of the molecule, it seems reasonable to regard the β form as having a different structure from the α form and as resembling the structures of naphthalene and anthracene. For convenience in the following discussion, we will regard the α form as a

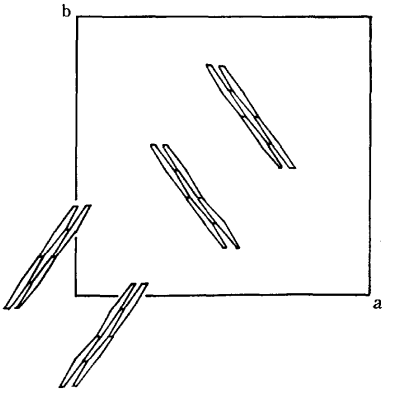

(a)

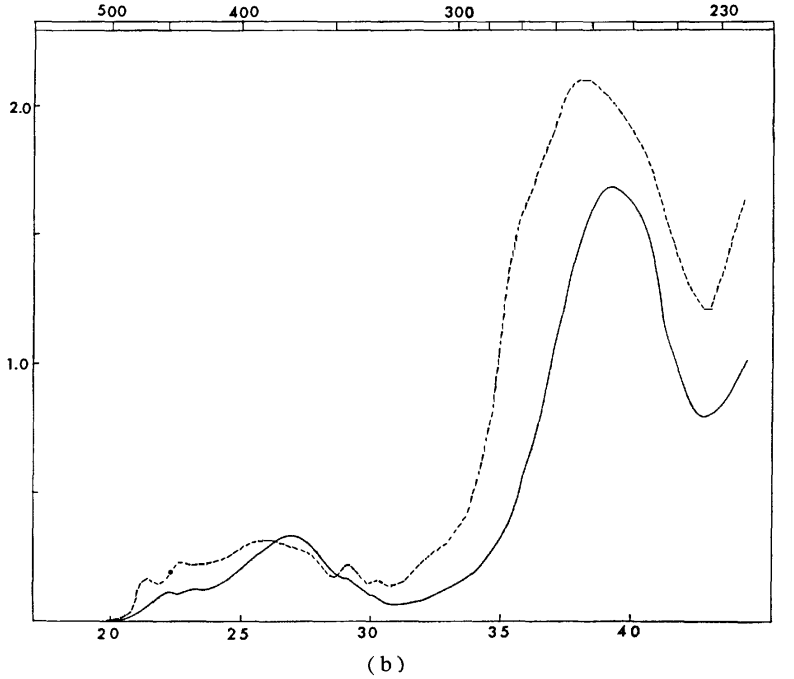

(b)

Fig. 3. (a) Projection of molecules in α crystal form onto (001) plane. (b) Absorption spectrum of α form through (001) plane.
—— Light polarized parallel to a-axis
------ Light polarized parallel to b-axis
Ordinate; optical density
Abscissa; lower, frequency (in $10^3\,cm^{-1}$), upper, wavelength (in mμ)

dimer structure and the β form as a monomer structure of perylene.

The Absorption Spectrum of the Perylene Crystals.—The electronic absorption spectrum of perylene in the *n*-heptane solution shown in Fig. 2 has been measured by using a Cary Model 14 spectrophotometer. Three strong absorption bands are clearly seen at 23050 cm^{-1} (f=0.33), at 39600 cm^{-1} (f=0.44) and at 48500 cm^{-1} (f=2.2), and another weaker bands, at 44200 cm^{-1}. Following the Hückel MO theory, the transition between the highest occupied and the lowest vacant orbital produces an excited state of symmetry $^1B_{2u}$, where the molecular symmetry is taken as D_{2h} and the two-fold axis is along the L-axis. This transition is allowed along the L-axis. The difference in orbital energy is 0.647β, and the second one, of the same symmetry, is at 1.347β, so that we can estimate roughly the energy of the first transition by the Pariser-Parr method[6] by taking only the interaction between the highest occupied MO i and the lowest vacant MO j and by disregarding the other orbitals. The excitation energy, ΔE, is then given by;

$$\Delta E = 0.674\beta + K_{ij} \quad (1)$$

where K_{ij} represents the exchange electron integral between MO i and j;

$$K_{ij} = \int \varphi_i^*(1)\varphi_j^*(2)\,1/r_{12}\varphi_i(2)\varphi_j(1)\mathrm{d}\tau_1\mathrm{d}\tau_2$$

The numerical calculation of ΔE, carried out with β taken as -2.371 eV.,[7] gives 2.84 eV., the observed value being 2.85 eV. Of course, this agreement occurs because of the cancellation of terms due to exchange integrals which

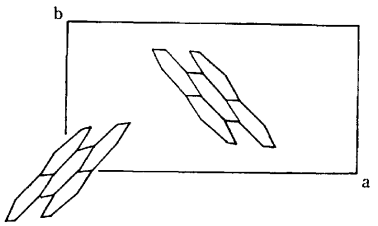

(a)

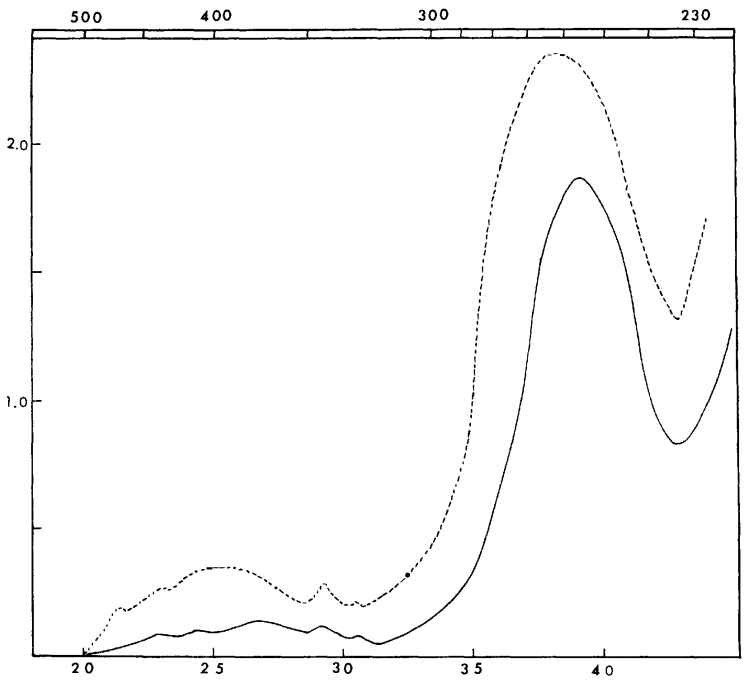

(b)

Fig. 4. (a) Projection of molecules in β crystal form onto (001) plane. (b) Absorption spectrum of β form through (001) plane.
—— Light polarized parallel to a-axis
------ Light polarized parallel to b-axis
Ordinate; optical density
Abscissa; lower, frequency (in 10^3 cm^{-1}), upper, wavelength (in mμ)

6) R. Pariser and R. G. Parr, *J. Chem. Phys.*, **21**, 466, 767 (1953).

7) R. Pariser, ibid., **24**, 250 (1956).

TABLE III

Band (cm^{-1})	Polarization (direction of the transition moment)	Direction cosine to crystal axes		Calculated oscillator strength*		Calculated and observed dichroic ratio	
α Form		$\cos\theta_a$	$\cos\theta_b$	a	b	a : b(calcd.)	a : b(obs.)
23050	L-axis	0.117	0.014	0.0143	0.0002	71.5 : 1.0	0.82 : 1.0
39600	M-axis	0.618	0.783	0.535	0.856	1.0 : 1.60	1.0 : 1.46
β Form							
23050	L-axis	0.343	0.044	0.122	0.002	61.0 : 1.0	0.35 : 1.0
39600	M-axis	0.615	0.771	0.526	0.829	1.0 : 1.57	1.0 : 1.25

* The value of $3f\cos^2\theta_{a,b}$ is presented, where f is the oscillator strength of the solution's absorption band. For 23050 cm^{-1} band the values of $\cos\theta_{a,b}$ of the L-axis polarization are used, and for the 39600 cm^{-1} band, the M-axis values are used.

TABLE IV

Band of solution cm^{-1}	f	Assignment	α Form: Band in crystal		α Form: Splitting		β Form: Band in crystal		β Form: Splitting	
			a	b	(obs.)	(calcd.)	a	b	(obs.)	(calcd.)
23050	0.15	$^1B_{2u}$ (L-axis)	22200	21400	800	1020	22930	21370	1560	2360
24610	0.10		23150	22730	420	635	24390	23040	1350	1470
26000	0.07		25380	24750	630	450	26670	25000	1670	1180
—		charge transfer	27000	26450	550					
34500			29180	29180	0		29240	29240	0	
			30300	30300	0		30300	30300	0	
39600 40860	0.44	$^1B_{3u}$ (M-axis)	39100	38600	500	−214	39100	38200	900	−2460
44200	0.15									
48500	2.17									

have been neglected and of the effect of configurational interaction with other higher excited states. However, it seems certain that the 23050 cm^{-1} band corresponds to the $^1B_{2u}$ excited state and is polarized along the L-axis. The 39600 cm^{-1} band is presumably polarized along the short axis (M-axis), since the next higher level is often orthogonal to the first level.

The crystalline absorption spectra of both the α and β forms presented in Figs. 3 and 4 have been obtained through the (001) plane by the method described in a previous paper.[8] The projection of molecules onto the (001) plane is also shown in Figs. 3 and 4. Hochstrasser[9] has discussed the spectrum of the α form in the 20000~30000 cm^{-1} region, but his labeling of the crystal axes seems to be misprinted; his a-axis should be read as b and his b-axis as a. In the present study, all crystalline axes were determined by X-ray rotation photograph. Based on the oriented gas model, the intensities of the crystalline absorption bands can be predicted as in Table III. Referring to the values of the direction cosine in Table III, it can be seen that the intensity of the absorption band polarized along the L-axis should be far less than the M-axis polarized band in the (001) spectrum if the oscillator strengths are the same. The f values of the 23050 cm^{-1} and 39600 cm^{-1} bands are of the same order of magnitude, so it can be shown from the spectra (Figs. 3 and 4) that the 23050 cm^{-1} band corresponds to the excited level of $^1B_{2u}$ symmetry, while the 39600 cm^{-1} band belongs to $^1B_{3u}$ symmetry. The observed dichroic ratios for the 39600 cm^{-1} band are in good agreement with the calculated values; hence the oriented gas model holds well for the 39600 cm^{-1} band in both the α and β forms.

Table IV lists all the observed band positions and assignments. The splitting of bands has been observed for 39600 cm^{-1} band; values of 500 cm^{-1} and 900 cm^{-1} are recorded for the $E_a - E_b$ splitting in the α and β forms.

The calculation of the Davydov splitting has been carried out by the standard method, taking into consideration the dipole-dipole interaction of molecules within a 20Å sphere.

8) J. Tanaka, This Bulletin, 36, 833 (1963).
9) R. Hochstrasser, *Can. J. Chem.*, 39, 451 (1961).

For the β form, the two excited state wave functions Ψ^{γ} and Ψ^{δ}, which are active along the a and b axes respectively, are written as:

$$\Psi^{\gamma}=\frac{1}{\sqrt{2N}}\left(\sum_{j=1}^{N}\varphi'_{1j}-\sum_{i=1}^{N}\varphi'_{2i}\right)$$
$$\Psi^{\delta}=\frac{1}{\sqrt{2N}}\left(\sum_{j=1}^{N}\varphi'_{1j}+\sum_{i=1}^{N}\varphi'_{2i}\right) \quad (2)$$

where φ'_{1j} represents a crystal wave function in which a molecule on the $1j$th site is excited and where φ'_{2i} denotes a crystal wave function in which the $2i$th site molecule is excited. The summation over N means that the excitation moves through the $2N$ molecules; $i=1, 2, \cdots, N$, $j=1, 2, \cdots, N$. The splitting between b and a axes (E_b-E_a) may then be given by

$$E_b-E_a=2V_{12}$$
$$=2\sum_{i=1}^{N}\int\varphi_1(1)\varphi'_1(1)H\varphi_2(2)\varphi'_{2i}(2)d\tau_1d\tau_2 \quad (3)$$

where $\varphi'_1(1)$ and $\varphi'_{2i}(2)$ are the excited state wave functions of the 1st and $2i$th molecules, and H is Hamiltonian of the system. The coordinates of transition dipoles chosen for the 1st and 2nd molecules are 1 (xyz) 2 $(1/2-x, 1/2+y, \bar{z})$; they are related to each other by the screw axis rotation about the b-axis.

For the α form, the excited states which belong to the B_u and A_u representation of the C^5_{2h} space group and which are active along the a- and b-axes respectively are written by:

$$\Psi^{\zeta}=\frac{1}{\sqrt{4N}}\left(\sum_{i=1}^{N}\varphi'_{1i}-\sum_{j=1}^{N}\varphi'_{2j}-\sum_{k=1}^{N}\varphi'_{3k}+\sum_{l=1}^{N}\varphi'_{4l}\right)$$
$$\Psi^{\varepsilon}=\frac{1}{\sqrt{4N}}\left(\sum_{i=1}^{N}\varphi'_{1i}-\sum_{j=1}^{N}\varphi'_{2j}+\sum_{k=1}^{N}\varphi'_{3k}-\sum_{l=1}^{N}\varphi'_{4l}\right) \quad (4)$$

where φ'_{1i}, φ'_{2j}, φ'_{3k}, and φ'_{4l} represent the crystal wave functions in which the $1i$, $2j$, $3k$, and $4l$ molecules are excited. They are related to each other by the symmetry operation of the crystal. The coordinates of transition dipoles chosen are 1 (x, y, z), 2 $(\bar{x}, \bar{y}, \bar{z})$, 3 $(1/2-x, 1/2+y, \bar{z})$ and 4 $(1/2+x, 1/2-y, z)$. The excitation transfer matrix elements for Ψ^{ζ} and Ψ^{ε} are given by:

$$V^{\zeta}=\frac{1}{4}\ (-V_{11}-V_{13}+V_{14}+V_{23}-V_{24}-V_{34})$$
$$V^{\varepsilon}=\frac{1}{4}\ (-V_{11}+V_{13}-V_{14}-V_{23}+V_{24}-V_{34}) \quad (5)$$

the notation for V_{12} is given in Eq. 3. The splitting between a and b axes is given by:

$$E_a-E_b=V_{14}-V_{13} \quad (6)$$

The calculated energies V_{12}, V_{13} and V_{14}, using the Hamiltonian for the dipole-dipole interaction only, are given in Table V.

The splittings calculated for the 39600 cm^{-1} band are -214 cm^{-1} and -2460 cm^{-1} for the α and β forms respectively, but the observed values are 500 cm^{-1} and 900 cm^{-1}. The calculated values do not agree even in sign for the two forms. Presumably the interaction with higher excited levels will be strong enough to change the energy level in the crystal.

In the region of the first absorption band near 20000~32000 cm^{-1}, we have found more important deviations from the oriented gas model based on the solution spectrum. First of all, we have noticed a broad band appearing in both the α and the β forms instead of the sharp vibrational band in solution, although, even at room temperature, some vibrational structure can be seen. The Davydov splitting has been calculated assuming both the L-axis polarization and the weak interaction model of Simpson and Peterson,[10] although the general pattern of the spectrum seems to be intermediate coupling. The results are listed in Table IV. It shows a general agreement between the observed and the calculated values, but the former is smaller than the latter. This discrepancy is attributed to the interaction with other excited states, particularly the charge transfer state, to the inadequacy of the dipole-dipole approximation, and to the overestimation of the transition moment in crystal because a large hypochromism was observed for this band.

TABLE V

α Form

V_{13}		V_{14}	
$^1B_{2u}$(L)	$^1B_{3u}$(M)	$^1B_{2u}$(L)	$^1B_{3u}$(M)
-802	-562	882	-768

β Form

V_{12}	
$^1B_{2u}$(L)	$^1B_{3u}$(M)
-1840	1184

All energies in $cm^{-1}/Å^2$. The explicit form for V_{12} is, for example, given by:

$$V_{12}=\frac{-e^2}{R^3}\mu^2\{2\cos\theta_z\cos\theta_{z'}-\cos\theta_x\cos\theta_{x'}-\cos\theta_y\cos\theta_{y'}\}$$

where R is the distance between the centers of two transition moments, μ is its magnitude (Å), and $\cos\theta_z$, $\cos\theta_{z'}$, $\cos\theta_x$, $\cos\theta_{x'}$, $\cos\theta_y$ and $\cos\theta_{y'}$ are the direction consines of the transition moments on each molecule referred to the axis drawn between the two centers as the Z axis, with the X and Y axes orthogonal to the Z axis.

10) W. T. Simpson and D. L. Peterson, *J. Chem. Phys.*, **26**, 588 (1957).

In the α form spectrum near 25000~28000 cm^{-1}, we have found another absorption band, one which we have assigned to the charge transfer between molecules for the following reasons. First of all, this band is particularly apparent in the dimer form, in which the charge transfer interaction should be larger than in the monomer form. However, the intensity of this type of band cannot be expected to be large since in the ground-state crystal configuration, the molecules are separated by about 3.5Å and since the electron overlap is relatively small. Therefore, this band will appear by borrowing intensity from the $^1B_{2u}$-allowed excited state by configurational mixing. Still, however, it has a different dichroic ratio ($D_b : D_a$) to the first two absorption bands near 21000~23000 cm^{-1}. The band is rather stronger along the a-axis than along the b-axis, which is another reason for assigning it to a different origin. The theoretical study of the electronic structure of the aromatic-excited dimer of perylene has recently been made by Murrell and Tanaka,[11] who show that the perylene dimer has four excited singlet states in this region and that the allowed charge transfer band should appear at about 26600 cm^{-1} (cf. Fig. 5 and the $^1G \rightarrow {}^1R_u$ transition at 3.5Å). The observed band is at 26500~27000 cm^{-1}; hence, its assignment to the charge transfer is supported by the theoretical treatment.

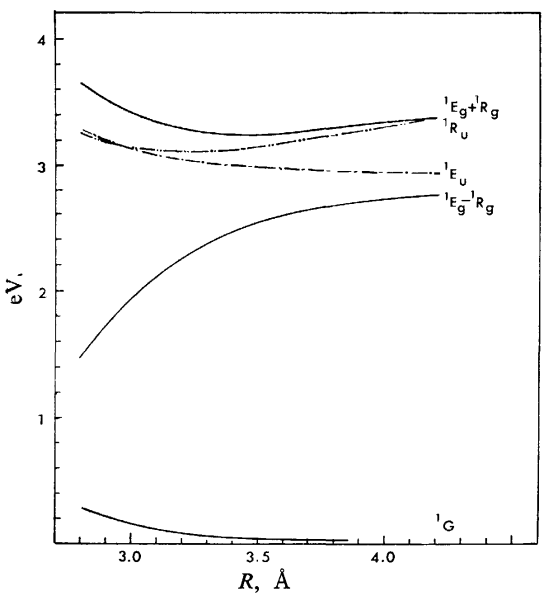

Fig. 5. Energy level diagram for the perylene dimer (only lower excited singlet levels having $^1B_{2u}$ symmetry are shown).
Ordinate; energy in eV.
Abscissa, distance between two molecules

The direction of the transition moment of this charge transfer band is of interest when compared with that in other molecular complexes, where the direction is vertical to the aromatic ring.[12] In the case of the aromatic dimer, the intensity is probably mainly due to the interaction with the allowed transition of the molecule, and the direction is along the molecular axis in the plane rather than vertical to it. The spectrum of the α form shows that the band is stronger along the a-axis, where the molecular L-axis lies.

The splitting of the charge transfer band along the a and b axes is, though less definite, nearly 550 cm^{-1}. This magnitude is so large that we must also consider the migration of the charge transfer state (the locally-ionized state) in the crystal. Although the charge transfer state will polarize the crystal and distort the lattice to some extent, its migration in the crystal introduces a new mechanism of photoconduction in aromatic crystals. By means of this mechanism, the locally-ionized state is considered to move rather easily, and its dissociation into electron and hole at an electrode surface will result in a transport of the electric charge. The band width of this state, or the excitation transfer matrix element between molecules, will be large than the usual band width of molecular orbitals in crystals; hence, the charge mobilities in molecular crystals will be increased.

The energy level of the charge transfer state for the monomer crystal (β form) can be estimated by the same method. Following the previous treatment,[11] it is given by $I-A-C$, where I is the ionization potential of the molecule, A, its electron affinity, and C the electrostatic coulomb force between electron and hole. Introducing the numerical values of $(I-A)=5.89$ eV. and $C=2.07$ eV. for $R=6.35$Å separation leads to a charge transfer state at 3.82 eV. (30800 cm^{-1}), a state which could not be observed in the longer wavelength region and one which is hidden under the strong transition to the $^1B_{3u}$ state.

Next we will discuss the hypochromism of the transition to the $^1B_{2u}$-excited state. It is seen from the projection in Figs. 3—4 that the L-axis is almost along the a-axis of the crystal. In this structure it is expected that absorption should appear only along the a-axis, not along the b-axis for the L-axis polarization band. However, the experimental results shows that the reverse is the case; it is rather stronger along the b-axis than along the a-axis. In

11) J. N. Murrell and J. Tanaka, *Mol. Phys.* (to be published); G. J. Hoijtink and E. Konijnenberg, *Z. phys. Chem.* (to be published).

12) K. Nakamoto, *J. Am. Chem. Soc.*, 74, 1739 (1952).

TABLE VI. INTENSITY RATIOS OF THE $^1B_{2u}$ BAND TO THE $^1B_{3u}$ BAND

	Calculated		Observed	
	a-Axis $^1B_{2u} : {}^1B_{3u}$	b-Axis $^1B_{2u} : {}^1B_{3u}$	a-Axis $^1B_{2u} : {}^1B_{3u}$	b-Axis $^1B_{2u} : {}^1B_{3u}$
α Form	0.027 : 1.00	0.0002 : 1.00	0.20 : 1.00	0.17 : 1.00
β Form	0.230 : 1.00	0.0025 : 1.00	0.11 : 1.00	0.21 : 1.00

Table VI the calculated and observed values of the intensity ratio of the $^1B_{2u}$ band to the $^1B_{3u}$ band are compared. It is seen that in the β form the observed a-axis absorption is greatly reduced while it is increased along the b-axis; in the α form it increases in both directions, but to a greater extent along the b-axis. The increase along the b-axis may be explained by mixing with the next higher excited levels, but the decrease in the intensity, particularly along the a-axis, cannot be explained simply by the interaction with the allowed transition at higher energies. As has been mentioned previously, the transition to the charge transfer state has very little transition moment, so the interaction with this state may result in the hypochromism of the $^1B_{2u}$ transition. This mechanism for hypochromism is reasonable if we consider the symmetry properties of these excited states. Both the $^1B_{2u}$ and the charge transfer states involve the excitation of an electron from the highest occupied to the lowest vacant orbital of the same molecule or of the nearest neighbor molecule. Therefore, the symmetries of the molecular orbitals concerned are the same and the mixing of these states is allowed. For the $^1B_{3u}$ excited state, however, no interaction with the lowest charge transfer state can be expected since the symmetry of the molecular orbital is different. Therefore, hypochromism, and other types of deviation from the oriented gas model, will be found only in the $^1B_{2u}$ excited state and is, in fact, observed in the crystalline spectrum.

In the α form the intensification of the charge transfer band and the decrease in the intensity of the $^1B_{2u}$ transition caused by this interaction is observed along the a-axis. For the β form, however, because the charge transfer absorption is at a higher energy region and cannot be discerned, we found only a decrease in the intensity of the $^1B_{2u}$ transition.* In the crystal the interaction will take place not only between a pair of molecules in the dimer but through neighboring molecules, and the energy level of the charge transfer state will form a band, the excitation transfer will occur more efficiently, and stronger hypochromism may be expected. The L-axis of the molecule, along which direction the interaction of molecular orbitals takes place, exactly coincides with the a-axis of both crystal forms, so that strong hypochromism is seen only along the a-axis. If the L-axis is not along the a-axis, but somewhere between the a- and b-axes, then hypochromism will be observed in both crystal directions.

Finally, it must be mentioned that at 29200 and 30500 cm^{-1} there are new absorption bands which are not observed in solution. These bands will be of a different origin rather than vibrational progressions of the $^1B_{2u}$ state because no splitting is observed in either the α or β forms. A very weak absorption band in the solution spectrum at about 34500 cm^{-1} is difficult to correlate without further information.

The Fluorescence Spectrum of Perylene Crystals.—The fluorescence spectra of both the α and the β forms have been measured by the recording spectrofluorometer of Professor Makishima's labotatory.* The machine consists of a mercury excitation lamp, a Kipp and Zonen double monochromator, and a

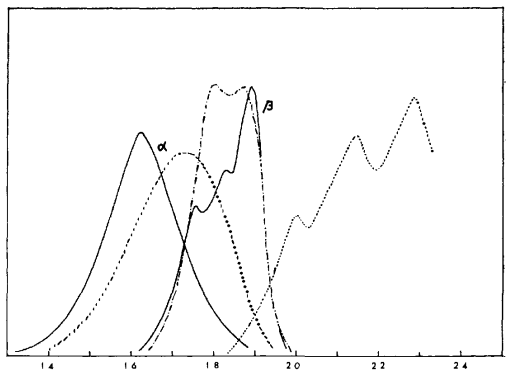

Fig. 6. Fluorescence spectrum of perylene.
------ solution in *n*-heptane
α form: —— at 77°K
---- at room temperature
β form: —— at 77°K
·—· at room temperature
Abscissa; frequency (in 10^3 cm^{-1})
Ordinate; intensity (in arbitrary units)

* The intensification of the charge transfer band along the a-axis, which will occur under the strong absorption band of the $^1B_{3u}$ transition, will influence the dichroic ratio of the $^1B_{3u}$ bands of the β form. In fact, the smaller observed value as compared with the calculated value or with the α form can be explained on this basis.

* The author wishes to express his thanks to Professors S. Makishima and S. Shionoya for the use of their spectrofluorometer.

photoelectric recording system. The spectra at room temperature and at the temperature of liquid nitrogen are shown in Fig. 6, together with the solution spectrum. It is most remarkable that the β form emits a green fluorescence at about 18950 cm^{-1}, while the α form glows yellow to red in the region of 16000 to 17000 cm^{-1} and shifts markedly with the temperature. The green emission of the β form is regarded as a monomer emission of the crystal, while the red emission of the α form is considered to be a dimer emission.

We will now discuss the origin of the dimer emission band from the theoretical point of view. First, a qualitative description of the charge transfer interaction, following Nagakura and Tanaka's one-electron approximation,[13] will be given. Let us consider the interaction between the two ground state molecules. The wave function and the resonance energy for the charge transfer are given by:

$$\Psi = a\varphi_1 + b\theta_2$$
$$\Delta E = \frac{2\beta^2}{I_P - E_A}, \quad \beta = \int \varphi_1 H \theta_2 d\tau \qquad (4)$$

where φ_1 is the highest occupied orbital of the donor molecule and θ_2 is the lowest vacant orbital of the acceptor molecule. Because of the symmetry of φ_1 and θ_2 (which are orthogonal if we take only the directly opposite interaction in the most symmetrical dimer), the resonance integral β will be very small; hence, no self-molecular complex can be formed between unexcited molecules, even if the relevant alternant hydrocarbon behaves as a good electron donor or acceptor in a mixed system. However, if one molecule is in the excited state, interaction takes place between φ_2 and θ_2, and the symmetry of the orbitals obviously favors a large interaction. Therefore, the molecule in the excited state (the $^1B_{2u}$ excited state in the case of perylene) will be stabilized to a greater extent by a charge transfer complex formation with another unexcited molecule of the same species. It is well established that the absorption and fluorescence spectra of a molecular complex appear in completely different positions from those of the individual molecules and are mainly determined by the values of I_p, E_A and β in Eq. 7. Hence, it is quite reasonable that the fluorescence of the excited dimer appears at longer wavelengths where there is no corresponding molecular transition. This is the qualitative explanation of the larger red shift of the excited dimer emission band.

Recently a more sophisticated quantitative treatment of this problem has been evolved by Murrell and Tanaka, and by Hoijtink and Konijnenberg.[11]

The calculation based on a non-overlap approximation which takes into account the exciton type interaction between the ^1E_u and ^1E_g states* shows that the splitting of this type is not enough to explain the observed shift and gives the wrong order when compared to the observed shifts for naphthalene, pyrene and perylene. When electron overlap and delocalization are considered, and when the Hamiltonian matrix elements are evaluated, it is shown that the interaction between ^1E_g and ^1R_g produces a large splitting, with only a very slight splitting for the $^1E_1$ and ^1R_u states. Figure 5 shows the results of the calculation for this configurational interaction. It is seen that the $^1E_g - {}^1R_g$ state is most stabilized by electron delocalization between the molecules. Although the transition between the ground state and the $^1E_g - {}^1R_g$ state is forbidden by symmetry, long wave emission band of the dimer certainly corresponds to this transition because this is the only state which is greatly stabilized by charge resonance interaction. If the dimer is not completely symmetric, as in the crystal, the selection rule will not strictly forbid emission from the lowest singlet level. The stabilization of this level is greater, the shorter the molecular separation, so it is conceivable that the molecules will approach each other following the excitation of one of them. This means that a self-molecular complex has been formed between two molecules, of which one is in the excited state. Figure 5 shows that the red shift is mainly due to the stabilization of the $^1E_g - {}^1R_g$ state, but it is also due, to some extent, to the repulsion of the ground state at the closer molecular approach. The estimation of this distance is very difficult and necessarily involves guesswork, but a comparison of the observed and calculated values suggests a separation of 3.1~3.2 Å. At this distance the stabilization of the $^1E_g - {}^1R_g$ state is about 0.6 eV., and the repulsion in the ground state is about 0.1 eV.

13) S. Nagakura and J. Tanaka, *J. Chem. Phys.*, **22**, 236 (1954).

* The notations for the electronic configuration of the dimer, in which only the $^1B_{2u}$ local excited state and the charge transfer state are considered, are as follows:

Configuration		
Ground	$^1A^1A$	G
Excited Resonance	$^1A^*{}^1A - {}^1A^1A^*$	^1E_u
	$^1A^*{}^1A + {}^1A^1A^*$	^1E_g
Charge Resonance	$^1(^2A^+{}^2A^- - {}^2A^-{}^2A^+)$	^1R_u
	$^1(^2A^+{}^2A^- + {}^2A^-{}^2A^+)$	^1R_g

$$^1A^1A = |\varphi_1\bar{\varphi}_1\theta_1\bar{\theta}_1|$$

$$^1A^*{}^1A = \sqrt{1/2}\{|\varphi_1\bar{\varphi}_2\theta_1\bar{\theta}_1| - |\bar{\varphi}_1\varphi_2\theta_1\bar{\theta}_1|\}$$

$$^1(^2A^+{}^2A^-) = \sqrt{1/2}\{|\varphi_1\bar{\theta}_2\theta_1\bar{\theta}_1| - |\bar{\varphi}_1\theta_2\theta_1\bar{\theta}_1|\}$$

where φ_1, θ_1 and φ_2, θ_2 are wave functions of the highest occupied and lowest vacant orbitals of each molecule and $^1A^*$ is the lowest singlet excited state of $^1B_{2u}$ symmetry.

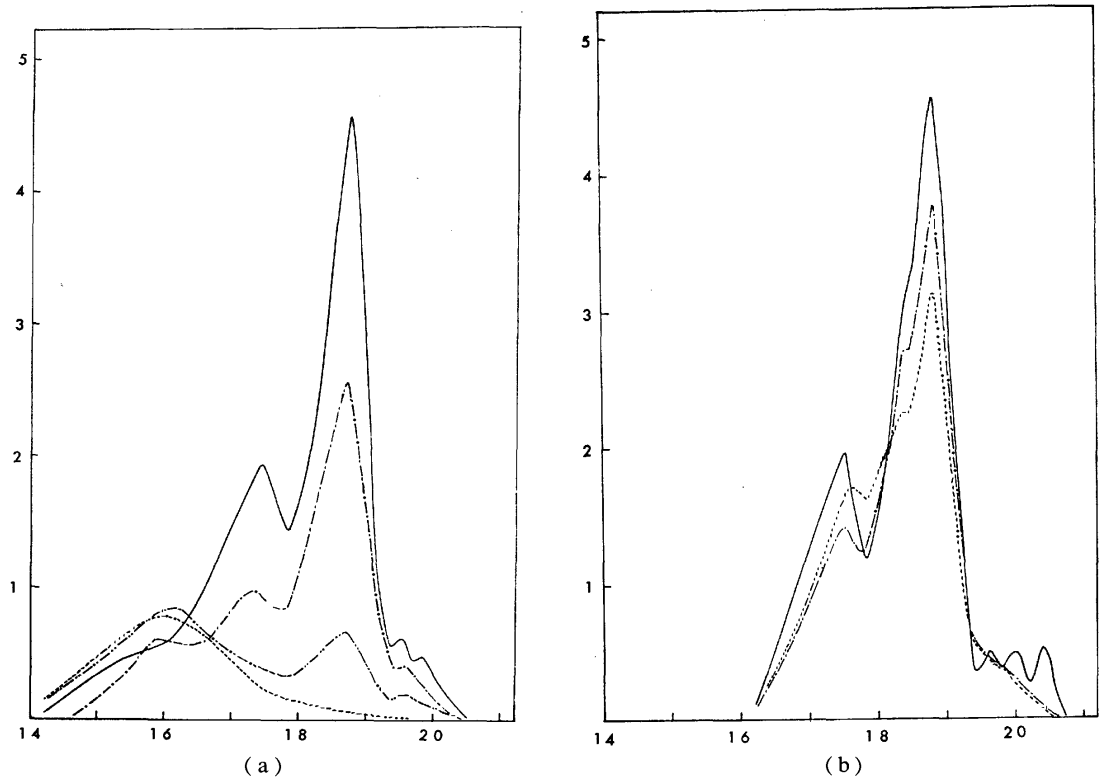

Fig. 7. Fluorescence spectrum of perylene crystals.

(a) α Form
—— at 4.2°K -·-·- at 33°K -···- at 50°K ----- at 70°K
(b) β Form
—— at 4.2°K -·-·- at 28°K ---- at 80°K
Abscissa; frequency (in $10^3\,cm^{-1}$)
Ordinate; intensity of fluorescence (in arbitrary units, but with the same scale for different temperatures)

The dimer emission band shifts remarkably from 17300 cm^{-1} at room temperature to 16250 cm^{-1} at 77°K. This proves that the potential function of the excited state is rather shallow and that the population of the state is easily affected by the temperature.

The β form fluorescence shows a vibrational structure, but the α form is structureless. This is explained by the potential curves of Fig. 5. The emission of the dimer form takes place between the excited state stabilized by charge transfer interaction and the ground state destabilized by repulsive interaction. Since the potential in the ground state is repulsive, discrete vibrational levels do not exist for this state and its population is continuous. Therefore, the dimer emission band has no vibrational structure.

Further experimental support for the idea of the movement of the molecule in the excited state in the α-form crystal is given by the fluorescence measurement at the temperature of liquid helium. The fluorescence spectra of α and β forms between 4.2 to 77°K are shown in Figs. 7(a) and 7(b). The β form emission does not change in shape or position, but it does decrease in intensity with an increase in temperature; this is presumably due to the enhancement of the radiationless relaxation process at higher temperatures. In contrast to the small change of the β form emission, the yellow-red emission of the α form changes to green at 4.2°K with no accompanying crystalline phase transition.* By increasing the temperature to 77°K, the red emission appears again, and at intermediate temperatures both red and green emissions are observed.

* The phase transformation from β to α occurs at about 140°C. The β form is the metastable form at room temperature, and it is inconceivable that the $\alpha \rightarrow \beta$ transformation occurs at a lower temperature. In fact, we can recover the α crystal after its immersion in liquid helium without any of the damage to the original shape which would be expected if a phase transition had occurred.

Therefore, it is most probable that the dimer emission is prohibited at the temperature of liquid helium because the molecules are frozen out and cannot approach each other after excitation. In Fig. 5 we have considered only the energy of some molecular orbitals; however, the interaction between the other orbitals will give additional repulsion at a shorter molecular separation. The resultant potential function for the total system is as drawn in Fig. 8, in which the potential barrier appears at intermediate separation. Following the excitation of one molecule in the dimer with the nuclear separation fixed (the Franck-Condon principle) (process 1), it will relax into the lower of the singlet excited levels by radiationless process 2, cross the barrier (process 3) to the lowest of the singlet excited levels by changing the nuclear separation, and then emit at smaller energies (process 4). However, if the system is frozen out, the molecule has insufficient energy to surmount this potential barrier and hence remains at the larger molecular separation, with less stabilization of the excited energy level. In fact, the fluorescence spectrum of the α form between 4~25°K shows only a green emission which is nearly the same as that of the β form, indicating that no stabilization of the excited state occurs because of the prohibition of the molecular movement. In the range between 25~40°K, the green emission is slowly quenched and the red emission appears instead, while above 40°K the quenching of the green and the appearance of the red occur more rapidly.

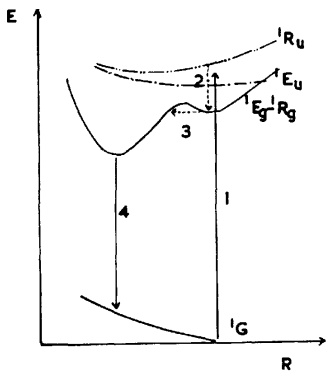

Fig. 8. Potential energy curve for the excited dimer including total repulsive energy.

The rate process of the movement of the molecule to the closest position has been analyzed by the measurement of the intensity of the emission bands. We assume that the number of molecules frozen at the lattice sites is proportional to the intensity of the green emission; the decrease in the green emission intensity is considered to be proportional to the number of molecules which cross the barrier. The temperature dependence of the ratio at the red emission to the green emission is shown in Fig. 9, where the abscissa is $1/T$ and the ordinate is the logarithm of the intensity ratio of the red to the green emission in an arbitrary unit. The kinetic scheme for the movement of the molecule after the excitation is given as follows:

$M + h\nu \rightarrow M^*$

(1) Molecules excited in the crystalline site

$M^* \rightarrow M + h\nu_G$

(2) Green emission, rate constant k_2

$M^* + M \rightarrow M_2^*$

(3) Excited dimer formation, rate constant k_3

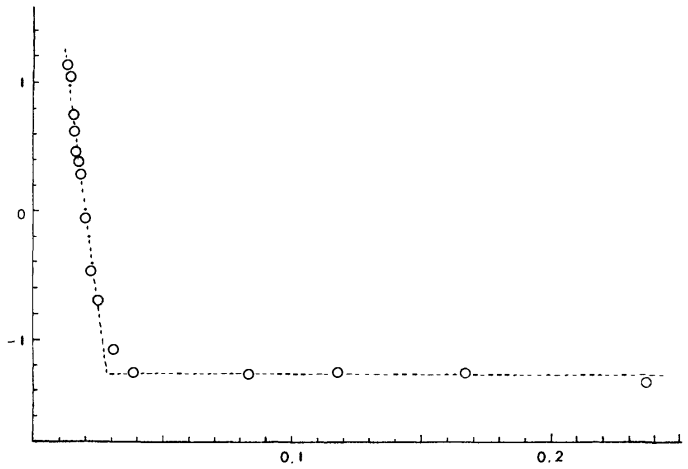

Fig. 9. Change in intensity ratio of red to green emission of the α form crystal with temperature.

TABLE VII

	Solution			β Form			α Form at 4.2°K		
	Abs.	Emis.	Shift	Abs.	Emis.	Shift	Abs.	Emis.	Shift
1st	23050	22800	250	21370	18880	2490	21400	18700	2700
2nd	24700	21500		22990	18400		22800		
3rd	26000	20000		25830	17550		25060	17420	

The band positions are expressed in wave numbers. The crystalline absorption is the mean value for the a- and b-axes.

$M_2^* \rightarrow 2M + h\nu_R$

(4) Red emission from an excited dimer, k_4

$M_2^* \rightarrow 2M$

(5) Radiationless deactivation of an excited dimer, k_5

$M^* \rightarrow M$

(6) Radiationless deactivation of an excited monomer, k_6

The molecule in the crystal is constantly illuminated; hence, the concentration of M* in 1 is assumed to be constant. At the lower temperature, between 4.2 to 25°K, no appreciable decrease in the green emission is observed, so process 2 predominates with the natural emission coefficient of k_2. The numerical value of k_2 is estimated from the absorption oscillator strength, f, by the use of the following relation:[14]

$$k_2 = \frac{1}{1.5}\frac{g_l}{g_u} f\nu^2 = 1.2\times10^8/\text{sec.} \qquad (10)$$

where g_l and g_u are the spin multiplicity of the lower and upper states and ν is the absorption frequency in wave numbers.

The intensities of the green and the red emission bands are given by

$$I_G = \frac{k_2[M^*]}{k_2+k_6}, \quad I_R = k_4[M_2^*] = \frac{k_4}{k_4+k_5}\cdot k_3[M^*] \qquad (11)$$

where [M*] and [M_2*] denote the concentration of the monomer and dimer molecules excited. The intensity ratio of the red to the green emission is given by

$$\frac{I_R}{I_G} = \frac{k_4[M_2^*]}{\frac{k_2[M^*]}{k_2+k_6}} = \frac{k_4 k_3(k_2+k_6)}{k_2(k_4+k_5)} = \frac{k_4(k_2+k_6)}{k_2(k_4+k_5)} A_3 e^{-h\nu/kT} \qquad (12)$$

where $k_3 = A_3 e^{-h\nu/kT}$.

It follows that if we take the logarithm of I_R/I_G in the ordinate and $1/T$ in the abscissa, we are able to estimate the activation energy of process 3. Figure 9 shows this relationship, the activation energy obtained from the slope between 40~80°K is $\nu = 285\ \text{cm}^{-1}$. This energy corresponds to the potential barrier in Fig. 8. At higher temperatures, most excited molecules go to the lowest state and emit a red fluorescence. The natural emission coefficient, k_4, estimated from comparison of the intensities of the red and green emission bands, gives $f = 0.089$. This fairly large value suggests a dipole-allowed transition, which is posible if the structure of the dimer is not completely symmetric and if the emission is not symmetry-forbidden.

The polarization of the dimer emission has been measured and the intensity was nearly the same in the a- and b-axes directions. However, the direction of the transition moment of the dimer emission band will not be discussed further, for we do not know the orientation of the excited molecule in the crystal.

Summarizing the above discussion, the mechanism of the red (dimer) emission is as follows:

After the excitation of one molecule of the dimer pair, the charge transfer resonance interaction taking place is larger at the shorter molecular separation, so the molecules approach each other and the excited dimer is formed. The emisson from this stabilized state to the repulsive ground state appears at longer wavelengths. At very low temperatures, the motion of the molecule is inhibited and no stabilization by the excited-dimer formation can occur.

The present phenomenon somewhat resembles the quenching of the impurity fluorescence at very low temperatures.[15] However, the mechanism of the emission is quite different, since the impurity fluorescence occurs by exciton migration to an impurity site, coupled with lattice vibrations, whereas the present phenomenon takes place by the movement of the molecule itself at each site in the crystal where a molecule is excited.

The emission of the β form appears at about

14) G. N. Lewis and M. Kasha, *J. Am. Chem. Soc.*, **66**, 2100 (1944).

15) Y. Kanda and H. Sponer, *J. Chem. Phys.*, **29**, 798 (1958); L. E. Lyons and J. W. White, ibid., **29**, 447 (1958); K. Gschwendtner and H. C. Wolf, *Naturwiss.*, **48**, 42 (1961).

18880 cm^{-1}; its vibrational progressions are tabulated in Table VII, together with those for the solution and α-form emissions. The β-form emission does not change position when the temperature is changed from 77 to 4.2°K. When the shifts of the first peak of the fluorescence from the first peak in the absorption is compared for the β form and for the solution, it is seen that a larger shift occurs in the β-form emission. The explanation for this stabilization of the excited state must be sought in such interaction as the charge transfer, but it is rather strange that the β-form and the α-form emissions at the temperature of liquid helium do not differ greatly. In fact, the first peak position differs by only about 180 cm^{-1}; the shift from the absorption peak is 2700 cm^{-1} for the α form and 2490 cm^{-1} for the β form, and the structure of the vibrational progression is certainly different. In view of the greater dependence of the charge-transfer resonance interaction on the nuclear separation, it is rather difficult to explain the almost identical emission bands from the different crystalline forms at low temperatures, but experiments show that the difference is rather small. The small peaks of the β-form emission near 20000 cm^{-1} are due to surface states.

As a result of the observation of a green emission from the β and α forms at the temperature of liquid helium, an alternative explanation for the observation by Hochstrasser[16] of perylene-pyrene charge transfer fluorescence can be given. Of couse, the possibility of charge-tranfer resonance interaction between perylene-pyrene cannot be ruled out, but it should certainly be smaller than in the cases of perylene-perylene or pyrene-pyrene because the molecular orbitals concerned are of different types. The emission at 5250 Å of perylene in pyrene is almost identical with the β-form emission; therefore, it should be interpreted as a monomer emission of perylene in pyrene crystal.

16) R. Hochstrasser, *J. Chem. Phys.*, 36, 1099 (1962).

Summary

A new crystalline form of perylene has been found and its crystal structure has been determined by the two-dimensional X-ray diffraction method. The new form is monomeric, while the previously known form has a dimeric structure. The electronic absorption and fluorescence spectra of both forms have been measured; on the basis of these data, an assignment is proposed for the observed transitions. Although the fluorescence spectrum of the monomer form shows a small shift, that of the dimer form shows a larger shift than would be expected from the absorption spectrum. This is explained as a stabilization of the lowest excited singlet state by a charge-transfer resonance interaction between the molecules in a pair. Because this stabilization increases as the distance between two molecules decreases, it is suggested that the molecules in a pair approach each other after excitation. At the liquid helium temperature the motion of molecules in the crystal will be frozen out, the larger stabilization of the excited level cannot occur, and the green emission which is characteristic of the monomer form is observed from the dimer form. The rate process of the molecular motion at lower temperatures has been analyzed.

The author would like to express his thanks to Professor Saburo Nagakura for his continued encouragement of this work and to Professor Yoshihiko Saito and Mr. Hazime Iwasaki for their kind advice on crystal structure analysis. The author would also like to thank to Dr. John N. Murrell for discussions and hospitality during his stay in Sheffield. He also wishes to thank Dr. Brian Stevens of Sheffield University and Dr. Stephen C. Wallwork of Nottingham University for their criticism of the manuscript.

The Institute for Solid State Physics
The University of Tokyo
Azabu, Tokyo

The Application of the Archibald Ultracentrifugal Method to the Determination of the Micellar Molecular Weight of the Anionic Surface Active Agents

By Kinji KAKIUCHI, Ken'ichi HATTORI and Toshizo ISEMURA

(Received April 18, 1963)

Although the sedimentation equilibrium method of ultracentrifugation gives a reliable molecular weight, it requires a very long time to attain the equilibrium state. Archibald[1] has suggested procedures by which molecular weight can be determined without waiting for the equilibrium state. As he has shown, the sedimentation equilibrium equation always holds at the meniscus and at the bottom of a liquid column within the cell. The equations are given by:

$$M_m = \frac{RT}{(1-\bar{v}\rho_0)\omega^2}\left(\frac{dc/dr}{rc}\right)_m \qquad (1)$$

for the meniscus, and

$$M_b = \frac{RT}{(1-\bar{v}\rho_0)\omega^2}\left(\frac{dc/dr}{rc}\right)_b \qquad (2)$$

for the bottom, where M is the molecular weight; R, the gas constant; T, the absolute temperature; $\bar{v}$, the partial specific volume of the solute; ρ_0 the density of the solvent; ω, the angular velocity; c, the solute concentration; r, the distance measured from the axis of the rotor to the meniscus or bottom of the liquid column within the cell, and the suffixes m and b, the meniscus and bottom of the liquid column respectively.

The Archibald ultracentrifugal method has been increasingly applied to the determination of the micellar weights of nonionic surface active agents[2,3] in an aqueous solution. It is worthwhile to investigate whether or not this method can also be applied to the determination of the miceller weight of anionic surface active agents. The purpose of the present investigation, therefore, is to confirm the applicability of the Archibald method to anionic surface active agents. The systems studied in the present investigation are the aqueous solution of sodium dodecyl sulfate (SDS) and the formalin condensates of sodium β-naphthalene sulfonate (β-NF). The latter compounds have the formula:[4]

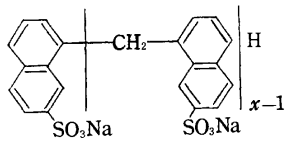

where x is the number of naphthalene nuclei, 1, 2, 3, ·····, 8, 9.5 (average) and 13.5 (average).

Experimental

Apparatus.—The experiments were performed in a Hitachi Analytical Ultracentrifuger, UCA-1 type (maximum speed 60000 r.p.m.), equipped with a Schlieren cylindrical lens system. The temperature was measured with a radiation thermocouple provided a continuous indication of the temperature of the base of the rotor, with an accuracy of ± 0.1°C. To make the photographs more clear a piece of human hair was used for the inclined slit.

For each test a given sample of a definite concentration in water or in a sodium chloride solution was placed in a conventional cell. At a fixed speed of rotation, six photographs of the sedimentation pattern were taken at intervals of ten minutes. At the same time, the corresponding temperatures of the rotor were measured, and their average value was used for the calculations. The temperature was 20 ± 3°C.

The patterns are shown in Fig. 1. dc/dr corresponds to the vertical axis, since in our present experimental concentration we assume that dc/dr is proportional to dn/dr (n: refractive index). r corresponds to the horizontal axis. By measuring the area under the curve of the meniscus or bottom, it is possible to obtain a numerical value proportional to the decreased or increased concentration. Similarly, three patterns obtained from the boundary-forming cell give the average value proportional to the initial concentration by measuring the area under the curve. Thus, the apparent concentration at the meniscus and bottom at every interval of time is determined. The molecular weights at any one time are given by Eqs. 1 and 2, which represent the molecular weights at both the meniscus and bottom of the cell.[5,6] We denote these as

1) W. J. Archibald, *J. Phys. and Colloid Chem.*, **51**, 1504 (1949).
2) C. W. Dwiggins, Jr., R. J. Bolen and H. N. Dunning, *J. Phys. Chem.*, **64**, 1175 (1960).
3) F. Tokiwa and T. Isemura, This Bulletin **35**, 1737 (1962).
4) K. Hattori and Y. Tanino *J. Chem. Soc. Japan, Ind. Chem. Sec.* (*Kogyo Kagaku Zasshi*), **66**, 55 (1963).
5) G. Kegeles, S. M. Klainer and W. J. Salem, *J. Phys. Chem.*, **61**, 1286 (1957).
6) H. K. Schachman, "Ultracentrifugation in Biochemistry," Academic Press, New York and London (1959).

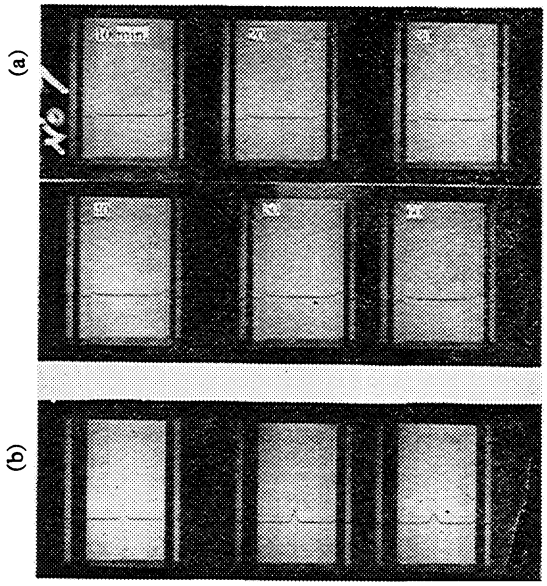

Fig. 1. Photographs for Archibald method.
(a) Pictures correspond to 10, 20, 30, 40, 50 and 60 min. after attaining 15200 r.p.m.
(b) Pictures from boundary-forming cell. By measuring the area it is possible to obtain the concn. of the initial solution, c_0.

$M_m(t)$ and $M_b(t)$ respectively. $M_m(t)$ or $M_b(t)$ tends to decrease or increase with time according as the solution is non-ideal or polydisperse. To obtain the appearent weight-average molecular weights of the solutes, M_0, $M_m(t)$ or $M_b(t)$ should be extrapolated to time zero.

$M_m(t)$ was exclusively used to obtain reliable data from the meniscus rather than the bottom. There is a possibility of an increase in micellar weight upon the addition of silicone oil[7] for the formation of the bottom surface.

The partial specific volume was calculated by the equation:

$$\bar{v}=\frac{1}{\rho_0}\left[1-\frac{\rho-\rho_0}{W}\right] \qquad (3)$$

Here ρ is the density of a solution containing W g. solute in 1 ml., and ρ_0 is the density of the solvent. The densities were determined by the picnometer of Lipkin et al.[8]

Materials. — *Sodium Dodecyl Sulfate (SDS).* — The dodecyl alcohol used for preparing sodium dodecyl sulfate was purified by fractional distillation under reduced pressure several times. It contained no homologues detectable by gas chromatographical analysis, and its hydroxyl value was found to be 301.0 (calcd. 301.1). Sodium dodecyl sulfate was prepared by the method of Dreger et al.,[9] followed by repeated recrystallization from ethanol and by extraction with petroleum ether. The aqueous solution of the purified propuct showed no minimum point in its surface tension-concentration curve.

The partial specific volume of SDS was found to be 0.825 in water and 0.855 in a 0.01～0.1 M sodium chloride solution.

The Condensates of Sodium β-Naphthalene Sulfonate (β-NF).—These compounds with x=1～8 were purified by a method previously reported.[4] The purity was confirmed by "one spot" on the paper chromatogram analysis. β-NF's with x=9.5 and 13.5 were synthesized by the usual methods and were not purified further except by dialysis to remove lower polymers. Their molecular weights were determined by infrared spectra.[10] Table I summarizes the partial specific volumes of β-NF in water and in a 0.1 M sodium chloride solution.

Table I. Partial specific volume of β-NF (at 25°C, concn. 1%)

x	Distilled water	0.1 M Sodium chloride
1	0.637	0.612
2		0.591
3		0.576
4		0.621
5		0.595
6		0.635
7		0.627
8		0.600
9.5		0.597
13.5	0.632	0.635
Average value	0.634	0.610

Results and Discussion

The determination of the micellar molecular weights of the ionic-surface active agent by the Archibald method has not previously been reported. The reason seems to have been that the micelle of ionizable molecules is disintegrated by the increasing repulsion between ionic groups because the micelles sediment faster, leaving the counter ions behind.

The Archibald method may be applicable to the determination of the micellar molecular weight if the disintegration of the micelle is prevented by adding a neutral electrolyte to the solution, although the micellar weight might be dependent on the concentration of the added electrolyte.

The Micellar Molecular Weight of Sodium Dodecyl Sulfate. — Table II summarizes the micellar molecular weights, M_0, of SDS at different concentrations in water or in a sodium chloride solution. In the absence of sodium chloride, SDS has a very low number of association, indicating the disintegration of the micelle mentioned above in the ultracentrifugal field.

7) S. M. Klainer and G. Kegeles, *Arch. Biochem. Biophys.*, **63**, 247 (1956).
8) M. R. Lipkin, J. A. Davison, W. T. Harvey and S. S. Kurty, *Ind. Eng. Chem. Anal. Ed.*, **16**, 55 (1944).
9) E. E. Dreger, G. I. Keim, G. D. Miles, L. Shedlovsky and J. Ross, *Ind. Eng. Chem.*, **36**, 610 (1944).
10) K. Hattori and K. Konishi, *J. Chem. Soc. Japan, Ind. Chem. Sec. (Kogyo Kagaku Zasshi)*, **66**, 59 (1963).

TABLE II. MICELLAR MOLECULAR WEIGHTS OF SDS (M_0)

Exp. No.	Concn. of SDS, %	Concn. of NaCl, M	Temp. °C	Micellar M. W.	No. of Association
.1	1.00	0.00	21.1	2.06×10^3	7.1
12	0.65	0.00	19.2	3.80×10^3	13
2	0.50	0.00	20.8	7.05×10^3	24
3	0.25	0.00	21.2	8.00×10^3	28
13	0.20	0.00	22.7	3.90×10^3	15
7	1.00	0.01	23.0	6.64×10^3	23
14	2.00	0.10	21.3	1.41×10^4	49
4	1.00	0.10	19.6	1.32×10^4	46
5	0.50	0.10	18.0	2.37×10^4	82
6	0.25	0.10	19.4	3.37×10^4	117
11	0.10	0.10	20.9	1.41×10^4	49
7	1.00	0.20	23.4	2.50×10^4	87

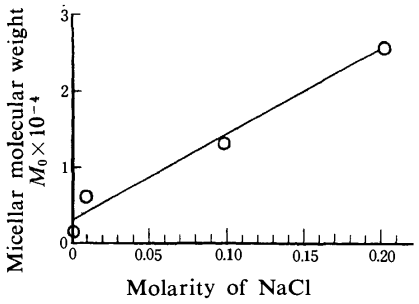

Fig. 2. Plots of micellar molecular weight of SDS as a function of molarity of sodium chloride. Concn. of SDS, 1.00%.

McBain and Hutchinson[11] are of the opinion that the micellar molecular weight of SDS is not changed by the addition of excess sodium chloride, that the effective volume of the micelle is enlarged, and that solubilizing power increases as the charge decreases. It is expected that the micellar molecular weight of SDS is obtainable in the presence of a neutral electrolyte. As Fig. 2 shows, however, the M_0 of a 1.00% SDS solution is proportional to the concentration of sodium chloride and, within the range of concentration of sodium chloride studied, the micellar molecular weight has no tendency to attain any limiting value.

The published values of the micellar molecular weight of SDS are very diverse, and the number of association, n, ranges over 40 to 80, as follows: 1.15×10^4 ($n=40$),[12] 1.14×10^4 ($n=40$),[13] 2.05×10^4 ($n=71$),[14] 2.3×10^4 ($n=79$)[15] and 1.80×10^4 ($n=62$)[16] are obtained by light scattering; $1.12\sim2.02\times10^4$ ($n=39\sim70$),[17] by diffussion and 1.70×10^4 ($n=57$),[18] by small angle X-ray scattering.

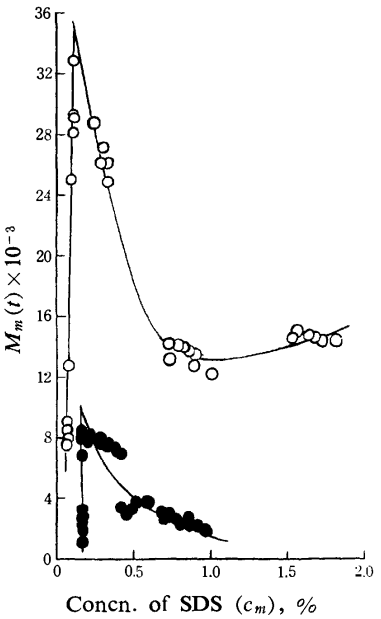

Fig. 3. Micellar molecular weight $M_m(t)$ as a function of the concn. of SDS. The concns. of SDS denote c_m at any time in the centrifugal run.

○: in 0.1 M sodium chloride solution
●: in water

Figure 3 shows the changes of $M_m(t)$ with the concentration of SDS at the meniscus, which varies with the time of the centrifugal run. It is clear that the numbers of association are varied from 40 to 80 at concentrations of more than 0.5% SDS in a sodium chloride solution. In the absence of sodium chloride, the numbers of association are much

11) M. E. L. McBain and E. Hutchinson, "Solubilization and Related Phenomena," Academic Press Inc., Publishers New York (1955), p. 176.
12) H. V. Tarter, *J. Colloid Sci.*, **14**, 115 (1959).
13) L. M. Kushner and W. D. Huffard, *J. Colloid Sci.*, **10**, 429 (1955).
14) H. V. Tarter and A. C. M. Lelong, *J. Phys.C hem.*, **59**, 1185 (1955).
15) J. M. Rhillips and J. K. Mysels, ibid., **59**, 325 (1955).
16) L. H. Princen and J. K. Mysels, *11th Technical Report Project (NR) 356-254, Office of Naval Research* (1958).
17) E. Hutchinson and J. C. Melrose, *Z. Phys. Chem.*, [NF] **2**, 117 (1954).
18) W. Philippoff, *Discussions Faraday Soc.*, **11**, 96 (1951).

smaller. Below the concentration of 0.5% SDS, the curves of the numbers of association vs. concentration abruptly show a sharp maximum point. The concentrations of SDS at a sharp maximum point are 0.16% and 0.13% in water and in 0.1 M sodium chloride respectively. These values agree with the reported values for critical micelle concentration (CMC).[19,20] Clearly the addition of sodium chloride lowers the CMC of SDS. Tartar[12] and Kolthoff[19] reported that the CMC of SDS decreased from 0.25% to 0.174~0.177% upon the addition of 0.1 M sodium chloride. Moreover, it is noted that above the CMC the slope of the linear relationship between $M_m(t)$ and time is positive, while below the CMC its slope is negative. Figure 4 illustrates that $M_m(t)$ increases with time above the CMC but decreases below the CMC.*

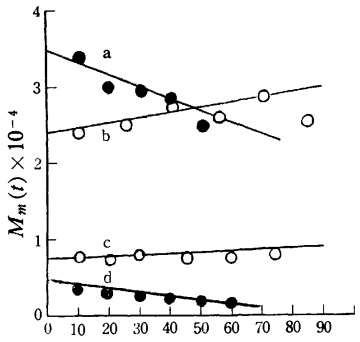

Fig. 4. Plots for $M_m(t)$ vs. time of centrifugation.

a : SDS 0.25%, NaCl 0.1 M
b : SDS 0.50%, NaCl 0.1 M
c : SDS 0.50%, NaCl (not contained)
d : SDS 0.20%, NaCl (not contained)

As Fujita et al.[21] have pointed out, $M_m(t)$ or $M_b(t)$ is a function of time. They also pointed out that the $M_m(t)$ of polystyrene in methyl ethyl ketone increased with time and that $M_b(t)$ decreased in an approximately linear fashion, but that they could be extrapolated to give the same intercept at $t=0$ in agreement with the theoretical requirement. Whether the slope of the $M_m(t)$-time curve is positive or negative depends on either the non-ideality or the polydispersity of the solution. It is supposed that non-ideality is predominant in the SDS solution above the CMC but the polydispersity is predominant below the CMC.

In the concentration of the critical micelle region, as Fig. 3 shows, it is necessary for us to handle with care a detailed treatment of the behavior by means of thermodynamic and hydrodynamic argument. However, it is very difficult to ascribe these deviations from the ideality to any non-ideality of the solute accompanied not only by the change of equilibrium between the micelle and the free ion but also by the disintegration of the micelle at the ultracentrifugal field. Goldberg[22] and Fujita et al.[21] have pointed out that in the application of the Archibald method the chemical potential is expressed in terms of both the concentration and the activity coefficient, γ, of the solute. For simplicity of theoretical development, they considered only two component systems, a homogeneous solute and a solvent. For such a solution the equation reduces to:

$$1/M_0 = 1/M_W + \boldsymbol{B}c + \text{higher terms in } c \quad (4)$$

where the coefficient $\boldsymbol{B}$ refers to the initial slope of $\ln\gamma$ at $c=0$ and, hence, is independent of the concentration, and M_W is the weight-average melecular weight. This equation indicates that a plot for $1/M_0$ vs. c allows an evaluation of M_W from its intercept at $c=0$ $\boldsymbol{B}$ from its initial slope. $\boldsymbol{B}$ corresponds to the second virial coefficient of light scattering. Fujita et al. have pointed out that for polystyrene in methyl ethyl ketone the plots for $1/M_0$ vs. concentration deviate from a straight line at relatively low concentrations and increase sharply with a further increase in c. This steep upward curvature suggests that the third and higher terms in the above equation would be quite different from those in the equation derived from the theory of light scattering.

In non-ideal solutions, the extended form of the Svedberg equation[23] reduces to:

$$M = \frac{\boldsymbol{R}T\mathrm{s}}{D(1-\bar{v}\rho)}\left[1-\frac{\mathrm{d}\ln\gamma}{\mathrm{d}\ln c}\right] \quad (5)$$

At an infinite dilution, the term in brackets becomes unity. Creeth[24] has shown that in a thallous sulfate-water system, $\mathrm{d}\ln\gamma/\mathrm{d}\ln c$ is positive within the range of his experimental concentration. This discrepancy between Eq.

19) I. M. Kolthoff and W. J. Stricks, *J. Phys. and Colloid Chem.*, **52**, 915 (1948).
20) J. Powney and C. C. Addison, *Trans. Faraday Soc.*, **33**, 1243, 1253 (1937).
* The concentrations described in Fig. 4 are those for the prepared samples. In the coures of the centrifugal run the solute sediments partially form the meniscus. Accordingly, the concentration of SDS at the meniscus, c_m, decreases gradually. Although the concentration of sample (a), 0.25%, is actually above the CMC, c_m decreases below the CMC soon after the beginning of ultracentrifugation with this solution.
21) H. Fujita, H. Inagaki, T. Kotake and H. Utiyama, *J. Phys. Chem.*, **66**, 4 (1962).
22) R. J. Goldberg, *J. Phys. Chem.*, **57**, 194 (1953).
23) J. W. Williams, K. E. Van Holde, R. L. Baldwin and H. Fujita, *Chem. Revs.*, **58**, 715 (1958).
24) J. M. Creeth, *J. Phys. Chem.*, **66**, 1228 (1962).

TABLE III. MICELLAR MOLECULAR WEIGHTS OF β-NF (M_0)

Exp. No.	Nuclear No.	Concn. of β-NF, %	Concn. of NaCl, M	Temp. °C	Micellar M. W.	No. of Association
4	1	1.00	0.00	18.0	1.46×10^2	0.50
3	1	1.00	0.10	20.0	1.80×10^2	0.81
12	2	1.00	0.10	20.7	3.42×10^2	0.72
13	3	1.00	0.10	21.3	1.43×10^2	2.00
14	4	1.00	0.10	17.9	1.33×10^3	1.86
21	5	1.00	0.10	19.6	2.90×10^3	2.42
16	6	1.00	0.10	20.1	2.91×10^3	2.02
17	7	1.00	0.10	19.4	4.67×10^3	2.73
18	8	1.00	0.10	21.2	5.40×10^3	2.80
5	9.5	1.00	0.10	16.6	7.00×10^3	3.06
2	13.5	1.00	0.00	22.5	4.30×10^3	1.32
20	13.5	0.25	0.10	19.3	3.18×10^4	9.76
19	13.5	0.50	0.10	22.4	2.48×10^4	7.31
1	13.5	1.00	0.10	23.4	2.25×10^4	7.13

5 and the experimental results is due to the incomplete dissociation of the electrolyte.

As has been described in the experimental part, it has been assumed that the difference between the refractive indices and the partial specific volumes does not depend on SDS concentration within the range of the experimental conditions. However, these values of free ions differ slightly from those of the micelle formed above the CMC.[25,26] Though it is difficult to explain the abnormally high association observed, it might be due to the incomplete dissociation of counter ions, accompanied by the change of the equilibrium between the micelle and the free ion of SDS at a given instant of centrifugation.

The Micellar Molecular Weight of Condensates of Sodium β-Naphthalene Sulfonate.—The association of purified β-NF in water has never been studied quantitatively. It is expected that the association would occur since their molecular structure is similar to that of direct dyes.[27] In fact, at concentrations above ca. 0.015%, the association of these compounds is shown in the light of their ultraviolet spectra[28]. The Archibald method in a cylindrical lens-Schlieren optical system is not easily applicable to such low concentration regions, and its use introduces appreciable errors. Table III summerizes the molecular weights, M_0, obtained for 0.25~1.0% β-NF solutions in 0.1 M sodium chloride.

In the absence of an elctrolyte the number of association of β-NF with $x=1$ and 13.5 nearly agrees with the value for non-association. The dependency of M_0 on the concentration of β-NF is not significant at concentrations below 1.00% when 0.10 M sodium chloride is present.

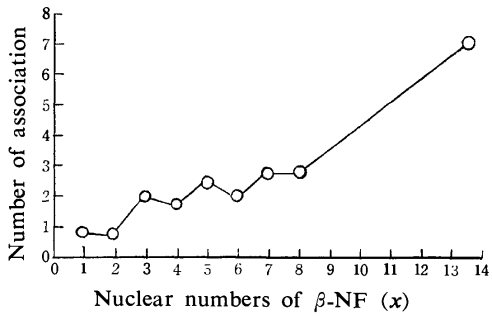

Fig. 5. Relation of number of association to x of 1.00% β-NF in 0.1 M NaCl.

Figure 5 shows that the number of association of β-NF in its 1.0% solution dissolved in 0.1 M sodium chloride increases with the number of nuclei, x, suggesting that the intermolecular van der Waals attraction[29,30] becomes stronger as x increases. The slopes of the curves of $M_m(t)$ against time for β-NF were found always to be negative. This indicates that polydispersity is more predominant than non-ideality in this case. This is reversed in the case of a SDS solution more concentrated than the CMC

Summary

(1) The values of the micellar molecular weight of SDS in water and in a sodium chloride solution could not be obtained by

25) H. B. Klevens, *J. Phys. and Colloid Chem.*, **52**, 130 (1948).
26) W. D. Harkins, R. W. Mattoon and M. L. Corrin, *J. Colloid Sci.*, **1**, 105 (1946).
27) I. Vickerstaff, "The Physical Chemistry of Dyeing," London and Edinburgh, Oliver and Boyd, 2. ed., (1954).
28) K. Hattori and Y. Tanino. *J. Chem. Soc. Japan, Ind. Chem. Sec.* (*Kogyo Kagaku Zasshi*), **66**, 65 (1963).
29) R. H. Peters and H. H. Sumner, *J. Soc. Dye. Colourists*, **71**, 130 (1955).
30) C. H. Giles and A. S. A. Hassen, ibid., **74**, 846 (1958).

the Archibald method, whereas the observed M_0 may represent the relative values, each corresponding to a given instant of centrifugation. However, a CMC could be definitely determined which agreed with the values reported by other workers. As may be noted from the slope of the dependency of M_0 on time, the SDS solution is non-ideal above the CMC while it is polydisperse below the CMC. The abnormally high association in the critical micelle region might be caused by the incomplete dissociation of counter ions, accompanied by a change in the equilibrium between the micelle and the free ion of SDS at a given instant of centrifugation.

(2) When the electrolyte is absent, β-NF's presumably exist in a monomeric state, but in a 0.1 M sodium chloride solution they associate, the degree of association being proportional to the x. In the region of 0.25~1.0% concentration, micelles of β-NF were observed to be polydisperse.

One of the authors (K. H.) gratefully acknowledges the support given by Mr. Zen'ichi Miyagawa, Director of the Central Research Laboratory, Kao Soap Co., Ltd. They both wish to thank Mr. Fumikatsu Tokiwa, Kao Soap Co., Ltd., for his supply of purified SDS.

Institute for Protein Research
Osaka University
Kita-ku Osaka (K. K. & T. I.)

Central Research Laboratory
Kao Sorp Co., Ltd.
Wakayama (K. H.)

Thermal and Radiation Oxidations of Benzene to Phenol in Aqueous Solutions Containing Metal Ions at Elevated Temperatures. III.[1,2] *The Effect of Copper Ions*

By Hiroshi HOTTA, Nobutake SUZUKI and Akira TERAKAWA[3]

(Received April 18, 1963)

In this paper the results of the oxidation of benzene to phenol in cupric aqueous solutions will be discussed and will be compared with the results for iron salt solutions reported in Part II.[2] The most distinctive point is that cuprous ions are unstable because of the fast rate of oxidation by the oxygen dissolved in contrast to ferrous ions which are stable.

Experimental

Aqueous Solutions.—Cupric sulfate was dissolved initially by 0.01 M in 0, 0.01 and 0.1 N sulfuric acid; cupric chloride was similarly dissolved in hydrochloric acid. All reagents were of guaranteed grade.

Apparatus and Procedure. — The experimental procedure, described in detail previously,[1,2] may be outlined as follows: 1 cc. of benzene was put on 15 cc. of an aqueous solution in a hard-glass tube set in a 50 cc. stainless-steel reactor under an oxygen pressure of 30 atm., and then this system was heated by the programming heater and kept for 30 min. at a given temperature. When irradiated by cobalt-60 gamma rays, the dose was about 14000 r. for 25 min.

Analytical.—The yield of phenol was determined from the optical density of the ether extract at 273.5 mμ, as in Part II.[2]

The concentration of cupric species dissolved in the solution after reaction was determined from the optical density of the cupric-oxine complex in chloroform.[4] The concentration of ferrous species was measured in the form of the α, α'-dipyridyl complex.

Results and Discussion

The Irradiated Solutions of Cupric Sulfate.—The total amount of phenol produced in the irradiated 0.01 M cupric sulfate solutions of 0, 0.01 and 0.1 N sulfuric acid is plotted as the function of the reaction temperature by the solid marks and the solid lines in Fig. 1. A small amount of precipitates was found only at temperatures higher than 180°C, in contrast to the case of iron salts.[1]

1) Part I: H. Hotta and N. Suzuki, This Bulletin, **36**, 717 (1963).
2) Part II: H. Hotta, A. Terakawa, K. Shimada and N. Suzuki, ibid., **36**, 721 (1963).
3) Present address: Showa Denko Co., Minato-ku, Tokyo.
4) K. Motojima and H. Hashitani, *Japan Analyst (Bunseki Kagaku)*, **9**, 151 (1960).

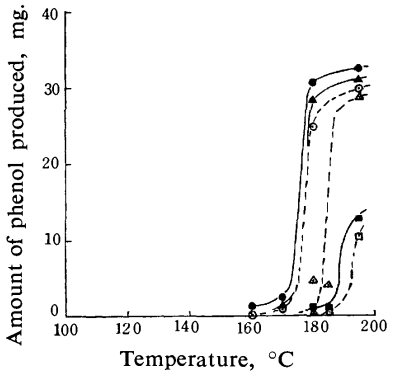

Fig. 1. Yields of phenol in 0.01 M cupric sulfate solutions with radiation (solid marks) and without radiation (open marks) in neutral (● and ⊙), in 0.01 N (▲ and △) and in 0.1 N (■ and ⊡) sulfuric acid.

According to Part II,[2] the reaction scheme of the radiation oxidation of benzene in an aerated aqueous solution of copper salt at elevated temperatures is assumed to be as follows:

$$H_2O \xrightarrow{\sim\!\!\sim} H,\ OH,\ H_2,\ H_2O_2 \qquad (1)$$

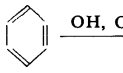

(2)

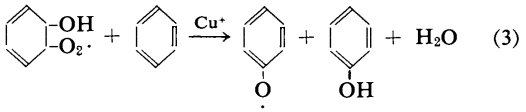

(3)

$$PhO + PhH = PhOH + Ph \qquad (4)$$

$$Ph + O_2 = PhO_2 \qquad (5)$$

$$PhO_2 + PhH = PhO_2H + Ph \qquad (6)$$

$$PhO_2H + Cu^{2+} = PhO_2 + H^+ + Cu^+ \qquad (7)$$

$$PhO_2H + Cu^+ = PhO + OH^- + Cu^{2+} \qquad (8)$$

(Ph: phenyl radical)

In ferric sulfate solutions, it was assumed in Part II that the initiation of the chain oxidation of benzene (reaction 3) is to be attributed to a trace amount of ferrous ion present initially, as ferric ions are reduced successively through the propagation process (cf. reaction 7) once initiated. However, in cupric sulfate solutions, such a cuprous ion propagating the chain process (reactions 3 and 8) cannot be present, for cuprous ions, unlike ferrous ions, are readily oxidized by oxygen. Therefore, scarcely any phenol is produced up to 160°C, as Fig. 1 shows, unlike the case of ferric sulfate solutions.[2]

Phenol production is considerably suppressed in the 0.1 N sulfuric acid. This is mainly due to the acceleration of cuprous oxidation;

$$Cu^+ + O_2 + H^+ = Cu^{2+} + HO_2 \qquad (9)$$

On the other hand, as the open marks and dotted lines in Fig. 1 show, phenol is produced in the non-irradiated solutions at somewhat higher tempetatures than in the irradiated ones.

The Effect of Copper Metal in the Sulfate Solutions.—The amounts of phenol produced in the solutions with the composition given in Table I and containing 2 g. of copper metal pieces (99.99% purity), are shown in Fig. 2 by solid marks for the irradiated cases and by open marks for the non-irradiated cases. As Fig. 2 shows, when copper metal is present in the aqueous phase, the yield of phenol is large, even at lower temperatures, regardless of irradiation or non-irradiation, as in the ferrous solution.[2] This is especially clear in solution a.

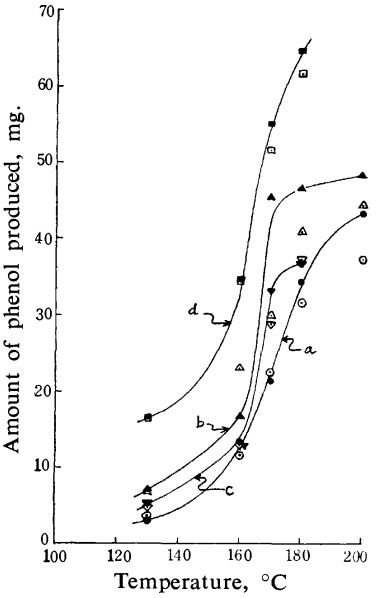

Fig. 2. Yields of phenol in (a) neutral 0.01 M cupric sulfate solution (● and ⊙), (b) 0.01 M cupric sulfate solution of 0.01 N sulfuric acid (▲ and △), (c) 0.01 N sulfuric acid (▼ and ▽) and (d) 0.1 N sulfuric acid (■ and ⊡) with radiation (solid marks) and without radiation (open marks). These systems contained 2 g. of copper metal pieces, respectively.

This fact supports the above assumption that scarcely any production of phenol in the cupric solution below 160°C is due to the lack of cuprous ions. Since cuprous ions are supplied continuously by the corrosion of the copper metal, the yield of phenol increases with an increase in the acidity. The concentration of cupric species in the solution after the reaction, given in Table I, is almost the same over the entire temperature range,

TABLE I. EFFICIENCIES OF COPPER METAL DISSOLVED FOR PHENOL PRODUCTION

System	Composition			Temp.	γ-Rays	Phenol produced to metal dissolved,	(Cu^{2+}) after reaction
	H_2SO_4 N	$CuSO_4$ M	Cu-metal g.	°C		mole ratio	M
a	0	0.01	2	160	Yes	>300	0.0101
					No	130	0.0107
				170	Yes	110	0.0114
					No	260	0.0106
b	0.01	0.01	2	160	Yes	27	0.0143
					No	20	0.0182
				170	Yes	83	0.0139
					No	24	0.0188
c	0.01	0	2	160	Yes	12	0.0078
					No	12	0.0079
				170	Yes	23	0.0089
					No	27	0.0087
d	0.1	0	2	160	Yes	5.5	0.0447
					No	5.4	0.0448
				170	Yes	8.4	0.0465
					No	8.5	0.0434

independent of the increase in phenol yield. As the acidity increases, the number of metal ions dissolved increases, as does the yield of phenol. Therefore, the efficiency of the copper metal dissolved for phenol production, i. e., the mole ratio of the phenol produced to the copper metal dissolved, is the greatest for the neutral solution a, as Table I shows. This means that the majority of the cuprous ions produced from metal are oxidized by oxygen independent of the phenol production.

It should be noticed that phenol production is accelerated even for the case of solution a in Fig. 2, in which the concentration of cupric species increases only a little. This means that a trace amount of cuprous ions is sufficient to initiate the chain process. When a solution containing cupric ions is in contact with copper metal, the equilibrium constant of the disproportionation,

$$Cu^{2+} + Cu \rightleftharpoons 2Cu^{+} \qquad (10)$$

is

$$K_{10} = \frac{\sqrt{(Cu^{2+})}}{(Cu^{+})} = 10^{3}$$

at room temperature.[5] The production of cuprous ions in the neutral solution may be due to a slight corrosion of copper metal by the decomposed product of sulfate ions as well as to reaction 10.

It may be concluded from the mole ratios in Table I that the chain length of the oxidation reaction is at least 100 for 10 mg. of phenol produced. On the other hand, the *G*-value of phenol is 320 for 10 mg. of phenol produced at 160°C in the irradiated neutral ferric sulfate solution (from Figs. 2 and 4 in Part II.[2]) For this case, it is supposed that the apparent *G*-value of OH radical as the initiator of phenol production (reaction 2) is less than 3 in spite of the various paths for the OH radical production (cf. Part II), if one assumes that the efficiencies of ferrous and cuprous ions are equivalent for the whole chain process.

Cupric-Ferric Solutions. — In the aerated cupric-ferric solution at room temperature, ferrous ions are produced due to the reactions[6-8]

$$Cu^{2+} + HO_2 = Cu^{+} + H^{+} + O_2 \qquad (11)$$

and

$$Cu^{+} + Fe^{3+} = Cu^{2+} + Fe^{2+} \qquad (12)$$

However, in the cupric solution without ferric ions under high oxygen pressure at elevated temperatures, since cuprous ions are not scavenged by ferric ions if reduced, the equilibrium between reactions 9 and 11 depends on the oxygen pressure. Therefore, cupric ions are considered not to be reduced by reaction 11 in the solutions in Fig. 1.

Moreover, even in the irradiated and non-irradiated neutral and 0.1 N sulfuric acid solutions of 0.01 M cupric-0.01 M ferric[9] sulfate,

5) I. Grenthe, *J. Am. Chem. Soc.*, 83, 360 (1961).

6) E. J. Hart, *Radiation Research*, 2, 33 (1955).

7) W. G. Barb, J. H. Baxendale, P. George and K. R. Hargrave, *Trans. Faraday Soc.*, 47, 462 (1951).

8) M. Cher and N. Davidson, *J. Am. Chem. Soc.*, 77, 793 (1955).

9) The concentration of 0.01M is not of ferric sulfate but of ferric ions.

in fact, ferrous ions were not produced, indicating that cupric ions are seemingly not reduced after all.

Next, benzene was oxidized in this neutral cupric-ferric solution. The amount of phenol produced (triangle marks) and the ferrous concentration (circle marks) are shown in Fig. 3 by solid marks for the irradiated case and by opon marks for the non-irradiated case. The ferrous concentration less than 1×10^{-5} M is unreliable.

In Fig. 3, the yield of phenol is much smaller than in the respective 0.01 M cupric and 0.01 M[9] ferric sulfate solutions, and scarcely any phenol is produced, even at 190°C, in the non-irradiated cupric-ferric solution. This means that, even if ferrous ions are produced by the oxidation process of benzene, they are reoxidized by the back path of reaction 12, and then the cuprous ions produced are consumed at once by the excess oxygen. Therefore, the oxidation process of benzene cannot be propagated successively. The mole ratios of the phenol produced to the ferrous concentration for the irradiated case are 22 and 54 at 170°C and 190°C respectively (cf. Fig. 3), suggesting such a consumption of ferrous ions.

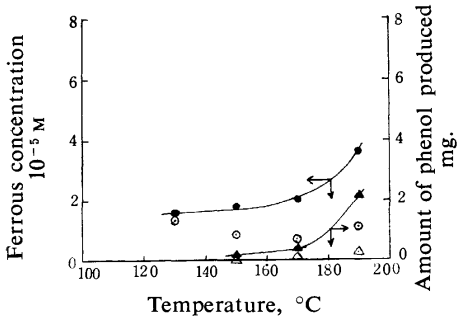

Fig. 3. Yields of phenol in the irradiated (▲) and non-irradiated (△) 0.01 M cupric-0.01 M ferric sulfate solution, and the corresponding ferrous concentrations (● and ⊙) after reaction.

These ratios are much larger than in the iron salt solutions discussed in Part II.[2] That is, the fast rate of cuprous oxidation kills not only the activity of cuprous ions but also that of ferrous ions.

Cupric Chloride Solutions.—The results of cupric chloride solutions in 0, 0.01 and 0.1 N hydrochloric acid are shown in Fig. 4 by marks similar to those in Fig. 1. Phenol production is suppressed in the presence of chloride ions, as has been seen in the iron chloride solution.[2]

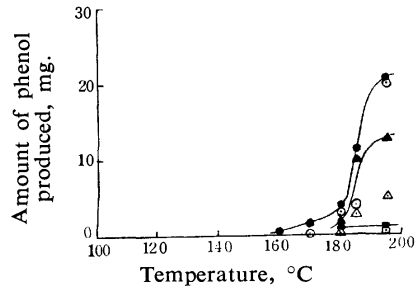

Fig. 4. Yields of phenol in 0.01 M cupric chloride solutions with radiation (solid marks) and without radiation (open marks) in neutral (● and ⊙), in 0.01 N (▲ and △) and in 0.1 N (■ and ⊡) hydrochloric acid.

Summary

The yield of phenol increases abruptly above 170°C in the cupric sulfate solutions. When the solutions contain copper metal pieces, phenol is produced, even below 160°C, regardless of irradiation or non-irradiation. On the other hand, scarcely any phenol is produced in the cupric-ferric sulfate solution, even at 180°C. These facts are to be attributed to the fast rate of cuprous oxidation by oxygen.

Japan Atomic Energy Research Institute
Tokai, Ibaraki-ken

Experimental Sensitivity Data for Radioactivation Analysis with 14 MeV. Neutrons

By Yuzuru KUSAKA, Haruo TSUJI and Takayoshi ADACHI

(Received April 25, 1963)

The recent improvements, in such accelerators as the Cockcroft-Walton or Van de Graaff type in the shape, the operating methods, the available neutron fluxes and the cost of neutron generators, make them particularly useful as the neutron source in radioactivation analysis.[1-3]

In such machines 14 MeV. neutrons are produced by the $^{3}H(d, n)^{4}He$ nuclear reaction, using deuterons accelerated at 100 to 150 kV. The neutrons so produced can participate in (n, p), (n, α), (n, n) and (n, 2n) reactions for various nuclides. As the radioactivities produced by the reaction are generally of short half-lives, fast radioactivation is made possible for many elements.

Several concise summaries of theoretical sensitivity values for various elements activated by 14 MeV. neutrons have been published.[4,5] Although these data are very useful for a rough estimation of the sensitivities of each element, they are only approximate, mainly because of the inaccuracy of the present cross section value in the 14 MeV. neutron reaction.

This paper will describe experimental results concerned with the sensitivity, results which have been obtained by an experimental method with practical applications as an industrial routine analysis; it will also discuss radioactivity which has not been described in the sensitivity data so far published.

Experimental

Neutron Source.—A thick tritiated zirconium target (3 curies; The Radiochemical Centre, Amersham, Buckinghamshire, England) was bombarded with a deuteron beam of 100 to 170 KeV. and of 5 to 10 μamp. by the Cockcroft-Walton type accelerator of Konan University. The neutron strength during the irradiation was continuously measured by a proportional counter with a cesium iodide scintillator which had been set in the accelerator tube to count the associated alpha particles from the T-D reaction. The absolute neutron flux at the sample position was determined by the activation method of standard copper foil, the beta radioactivity of which was measured by a 4π gas-flow counter using Q gas.

Sample Transfer System and Neutron Irradiation.—A polyethylene "bunny" capsule (1.3 cm. i. d., 4.6 cm. long, 0.1 cm. thick) containing the sample was transferred, by means of a vacuum cleaner (500 watt), between the irradiation position, which was set to come to the sample center 3.5 cm. below the target, and the radioactivity detector through a flexible vinyl tubing (1.8 cm. i. d., 10 m. long). Irradiation was started by turning on the accelerator beam switch, and it was timed with a stop watch. At the end of 10.0 min. irradiation, the transfer system was turned on to bring the "bunny" capsule back to the well of the scintillation detector. The average travel time of the capsule from the irradiation position to the detector was 3.5 sec.

Radioactivity Measurement.—The radioactivity induced in the sample was measured by a shielded well-type sodium iodide-scintillation detector (Harshow, 4.45 cm. dia., 5.08 cm. height, well: 1.91 cm. dia., 3.81 cm. deep) optically contacted with a photomultiplier tube (RCA 6342-A). Pulses from the phototube were fed to a linear-amplifier and then to a single-channel pulse height analyzer, the output from which was fed to a scaler.

The gross gamma ray counting was done for 10.0 min. in the sensitivity determination. In another run using the same sample, the decay curve was traced for an appropriate length of time and, consequently, the produced radioactive nuclide was analyzed. In the runs the countings were started after only 5.0 sec. of irradiation. However, the oxide, carbonate, acetate and nitrate samples were started after 40 sec., it being necessary first to eliminate the influence of the ^{16}N produced by the (n, p) reaction on oxygen.

Using the mean value of neutron flux observed during the irradiation, all the net counts, which were obtained by subtracting the counts in the empty capsule from the counts with the sample, were normalized to the data in a standard neutron flux (1.0×10^{5} neutrons per cm^{2} per sec.) and were also corrected for the variations in the weight of each sample.

Irradiation Sample.—A definite amount of the sample was pressed into a pellet (1.2 cm. dia., less than 3.4 cm. long) and put in the bottom of the "bunny" capsule.

The chemical forms of the samples were as

1) E. A. Burrill and M. H. MacGregor. *Nucleonics*, **18**, No. 12, 64 (1960).
2) Y. Kusaka, *Isotopes and Radiation (Doitai to Hoshasen)*, **4**, 79 (1961).
3) W. W. Meinke and R. W. Shideler, *Nucleonics*, **20**, No, 3, 60 (1962).
4) R. F. Coleman, *Analyst*, **86**, 39 (1961).
5) A. S. Gillespie, Jr., and W. W. Hill, *Nucleonics*, **19**, No. 11, 170 (1961).

follows: the elements of silver, aluminum, arsenic, bismuth, calcium, cerium, cobalt, chromium, copper, iron, indium, iridium, lithium, magnesium, manganese, molybdenum, nickel, phosphorus, platinum, rhodium, ruthenium, sulfur, antimony, selenium, silicon, tin, tantalum, tellurium, thallium, tungsten, zinc and zirconium; the oxides of dysprosium, gallium, germanium, mercury, lanthanum, niobium, lead, praseodymium, samarium, titanium, vanadium and yttrium; the carbonates of cesium, potassium, sodium and rubidium; the acetates of barium and strontium; fluorine as polytetrafluoroethylene; bromine as dibromobenzene; iodine as methyl iodide; nitrogen as ammonium nitrate and oxygen as oxalic acid.

Results

Radioactive Nuclide Produced by Fast Neutron Reaction. — The nuclides so produced were analyzed by the decay curves obtained in the radioactivity measurements. The quantity expressed with the counting rate of the nuclide at the end of irradiation has been plotted against the half-life of the radioactivity; it is shown in Fig. 1. In Fig. 1 the nuclide is marked with the parent isotope in the nuclear reaction, while the waved line shown under the reaction mark indicates the activation to the metastable state of an isomeric pair. The nuclear reactions shown with the black point, that is, in cerium, germanium, gold, rubidium and selenium, have not been described in previously-published sensitivity data[4,5] but, nevertheless, produce considerable amounts of radioactivity.

In Fig. 1 the ambiguous weak radioactivities of less than 100 counts per min. are not plotted.

In the other experiments, the sensitivity for the activation analysis has been estimated. In these cases the sensitivity was assumed to be the quantity of the element needed to give 500 counts in a 10-min. measurement. However, in oxygen and gold only 100 counts was adopted in the 1 min. measurement; this was because of their short-lived radioactivities. The results are shown in Table I.

TABLE I. SENSITIVITY FOR RADIOACTIVATION ANALYSIS

Element	Sensitivity mg.	Element	Sensitivity mg.
Br	18.5	Zn	260
Cu	21.2	Mn	290
Pr	24.6	O	352
Si	28.9	Zr	390
Rb	59.5	N	435
Ga	63.9	Na	490
P	65.1	Mo	497
Sb	67.4	Cd	503
Ba	76.1	Cl	505
Ag	81.6	Mg	537
Al	86.1	Ge	540
Cr	170	Sr	625
F	181	Au	685
Ce	196	Hg	690
Se	200	K	890
V	250		

More than 1 g.: As, Bi, Ca, Co, Cs, Fe, Hf, I, Ir, La, Li, Nb, Ni, Pb, Pt, Ru, S, Sm, Sn, Ta, Te, Ti, Tl, W, Y

A Consideration of Experimental Error.—The experimental error in the results described above was caused mainly by the fluctuations of the neutron flux on the sample during irradiation. A typical example of the fluctuation curve is shown in Fig. 2. In the adopted

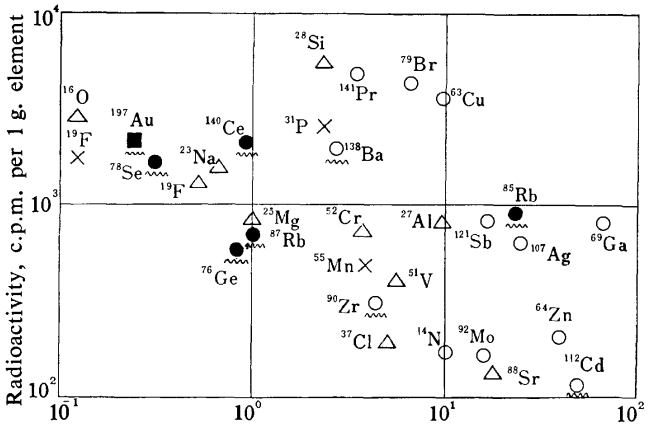

Fig. 1. Radioactive nuclide produced by 14 MeV. neutron reaction.
○: (n, 2n) reaction △: (n, p) reaction
×: (n, α) reaction □: (n, n′) reaction

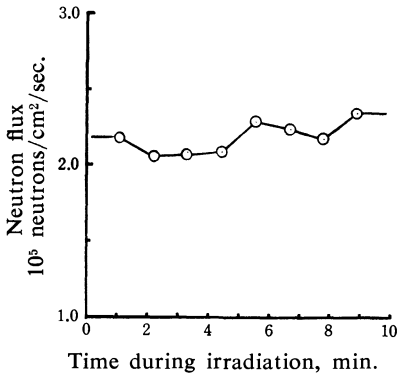

Fig. 2. Fluctuation of neutron flux during irradiation.

neutron flux itself, which was the mean value of the plots in Fig. 2, an uncertainty of 2.9% is estimated. In all the runs, an approximate 3.5% error could be assumed.

However, when relatively short-lived nuclides were to be measured, the neutron flux fluctuations near the end of irradiation become important and, therefore, the results tend to be less reliable. Although the theoretical error estimations in such nuclides are very difficult, roughly a 10% error was inferred from the experiments.

The neutron flux variation in the sample set at the irradiation position gave about a 5% error as a maximum. However, after the flux distribution had been determined by the activation method of copper monitor foils set at various positions in a polyethylene " bunny " capsule during irradiation, the corrections for sample position (sample thickness) were made in all the experimental results and, therefore, the error based on sample position became negligibly small.

Discussion

The short-lived radioactivities produced in germanium, selenium, rubidium and cerium are probably produced by (n, 2n) reactions; that is, they are due to Ge-75 m (48 sec.), Se-77 m (19 sec.), Rb-84 m (23 min.), Rb-86 m (1.02 m) and Ce-139 m (55 sec.). The radioactivity produced in gold might be due to the Au-197 m (7.2 sec.) produced by the (n, n') reaction.

It is possible improve the sensitivity by using a more sensitive gamma ray detector or higher neutron fluxes. Even in these cases, however, the relative sensitivity values are not expected to differ greatly from the data reported in the present paper. It is, therefore, believed that the present data will be useful in a general consideration of radioactivation analysis by 14 MeV. neutrons.

The authors wish to thank Dr. Kazunori Yuasa, Mr. Bunzaburo Saeki and Mr. Yoshinao Fujiwara of the Department of Physics of Konan University for their helpful discussions of the problem and their kind assistance in the use of the accelerator. The cost of this research was partly defrayed by a grant from the Scientific Research Expenditure Fund of the Ministry of Education, to which the authors' thanks are due.

Department of Chemistry
Faculty of Science
Konan University
Higashinada-ku, Kobe

The Composition of the Volatile Oil Obtained from the Leaves of Torreya nucifera and the Structure of Torreyol

By Tsutomu SAKAI, Kiichi NISHIMURA, Hiroaki CHIKAMATSU* and Yoshio HIROSE

(Received May 1, 1963)

The volatile oil obtained from *Torreya nucifera Sieb. et Zucc.* was first examined by Shinozaki;[1] α-pinene, camphene, limonene (ca. 60%), cadinene, and a crystallin sesquiterpenic alcohol (m. p. 137~138°C), which was named torreyol, were found to be its components. The structure of torreyol was shown by Nishida and Uota[2] to be represented by formula I on the basis of the fact that torreyol gave cadinene dihydrochloride upon reaction with hydrogen chloride and yielded acetone

* Present address: Department of Chemistry, Faculty of Engineering Science, Osaka University, Toyonaka, Osaka.

1) E. Shinozaki, *J. Soc. Chem. Ind.* (*Kōgyō-Kwagaku Zasshi*), **25**, 768 (1922).

2) K. Nishida and H. Uota, ibid., **43**, 150 (1940); **44**, 225 (1941).

by ozonolysis. The structure of cadinene dihydrochloride, at that time, was said by Ruzicka and Stoll[3] to be represented by structure II, and this formula was used in the study by Nishida and Uota. Later, this structure for cadinene dihydrochloride was found to be incorrect, and the revised structure, III, for it was suggested by Campbell and Soffer.[4] Therefore, the structure of torreyol also needed to be revised. Herout and his co-workers[5,6] reported that the physical properties of torreyol strikingly resemble those of δ-cadinol.

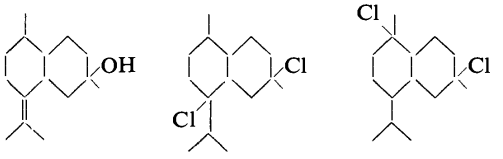

I II III

The purpose of this study is to elucidate the structure of torreyol and to obtain more precise data on the composition of the volatile oil.

Experimental

Two hundred and twenty-four grams of the volatile oil were obtained from 30.5 kg. of the leaves of *Torreya nucifera* by extraction with methanol, followed by steam distillation of the methanol extract. For the effectual recovery of torreyol and other sesquiterpene alcohols, the oil was treated by the following procedure. The oil was first separated by distillation under reduced pressure into a low-boiling fraction and a residual fraction containing mainly sesquiterpene alcohols. The latter was cooled, and the deposited crystals were collected. The same procedure was repeated on the filtrate until no crystalline material was deposited. The combined crystals were recrystallized from dilute ethanol. The oil recovered from the mother liquors of the recrystallization and the final filtrate were further separated by adsorption chromatogaphy on neutral alumina into three fractions, namely, a hydrocarbon fraction, a liquid sesquiterpene alcohol fraction, and a crystalline sesquiterpene alcohol fraction. By the above procedures, the original oil was separated into the following three fractions:

Fraction A: A low-boiling fraction separated by distillation, and a hydrocarbon fraction separated by adsorption chromatography on alumina. (209 g.)

Fraction B: A liquid sesquiterpene alcohol fraction separated by adsorption chromatography on alumina. (8.1 g.)

Fraction C: Crystalline sesquiterpene alcohol. (6.9 g.)

Fraction A.—Fraction A was further fractionated by distillation with Podbielniak's 13 mm.×2ft. Heli-Grid column under reduced pressure, followed by adsorption chromatography on silica gel. Each fraction was analyzed by gas chromatography, spectroscopy, and chemical methods. The course of the fractional distillation is presented in Fig. 1.

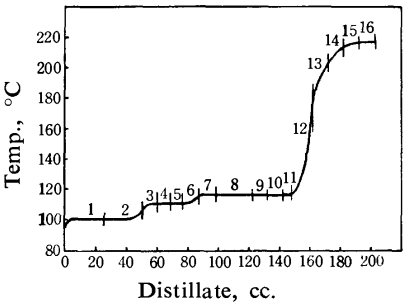

Fig. 1. The fractional distillation curve (50 mmHg).

The last fraction (fraction 17, 6 cc.) was recovered from the final residue by steam distillation.

Fractions 1 and 2 consisted only of α-pinene.

Fraction 3 was a mixture of hydrocarbons, which the infrared spectrum showed to contain myrcene. The myrcene was removed from the mixture as a maleic acid adduct. By adsorption chromatography of the unreacted portion, α-pinene, 3-carene, limonene, and γ-terpinene were isolated.

Fractions 4 to 6 contained limonene and myrcene.

Fractions 7 to 11 consisted only of limonene.

Fraction 12, the wide boiling range fraction, was a mixture of hydrocarbons and oxygen-containing compounds. The major constituents of this fraction were limonene and terpinolene. Minute amounts of linalool, terpinen-4-ol, citronellol, phenylethyl acetate and methyl salicylate were also found to be present by chromatographic separation.

Fractions 13 and 14 were complicated mixtures of hydrocarbons judged by gas chromatographic analysis to consist of at least nine hydrocarbons. However, it was so difficult to separate them by adsorption chromatography that only δ-cadinene, γ-cadinene, β-elemene, and two unknown sesquiterpene hydrocarbons could be isolated. Besides, fraction 13 contained small amounts of citronellol, geraniol and an unidentified carbonyl compound.

Fractions 15 to 17 consisted of relatively pure δ-cadinene.

Fraction B.—Fraction B, the liquid sesquiterpene alcohol fraction separated by adsorption chromatography on neutral alumina, was percolated again through a silica gel column. It contained nerolidol, two sesquiterpene alcohols, and an unidentified aromatic carbonyl compound.

One of the sesquiterpenic alcohols seemed to be identical with the so-called "cadinenol" isolated by Herout and his co-workers[5,7] from Juniper berry oil. The structure of cadinenol has not yet been

3) L. Ruzicka and M. Sotll, *Helv. Chim. Acta*, 7, 94 (1924).
4) W. P. Campbell and M. D. Soffer, *J. Am. Chem. Soc.*, 64, 417 (1942).
5) V. Herout and V. Sykora, *Tetrahedron*, 4, 246 (1958).
6) V. A. Pentegova, O. Motl and V. Herout, *Doklady Acad. Nauk SSSR*, 138, 850 (1961).
7) J. Pliva, M. Horak, V. Herout and F. Sorm, "Die Terpene. Der Spektrum und phys. Konstanten. Teil I. Sesquiterpene," Akademie-Verlag, Berilin (1960).

established. The infrared spectrum and the retention time on the gas chromatography of the alcohol isolated here were both identical with those of cadinenol, although the crystallization of the isolated alcohol was not effected by the seeding of an authentic sample of cadinenol. By referring to the values of the optical rotation of cadinenol ($[\alpha]_D$ −89°) and the isolated alcohol ($[\alpha]_D$ +69°), it was concluded that the isolated alcohol was an optical antipode of (−)-cadinenol obtained from Juniper berry oil.

The other sesquiterpene alcohol was difficult to separate from cadinenol, and its ultimated purity did not exceed 60%. The infrared spectrum of this compound was not identical with that of any known sesquiterpene alcohol, and further study was abandoned because there was an insufficient quantity of it.

Fraction C.—Fraction C was almost pure torreyol; m. p. 138~139°C. Sublimation and recrystallization from 50% ethanol afforded pure torreyol; m. p. 139.5~140.5°C, $[\alpha]_D^{18}$ 118.6° (*c* 2.075, ethanol).

The physical constants of the torreyols reported previously were m. p. 137~138°C[1] and 141~142°C[2], and $[\alpha]_D$ +99°19′[1] and +107°13′[2].

The findings on the composition of the volatile oil are summarized in Table I.

Table I. The composition of the volatile oil.

Compound	%
Iimonene	41.4
α-Pinene	23.0
Myrcene	6.8
Terpinolene	0.7
3-Carene	0.3
γ-Terpinene	0.1
Citronellol	0.7
Terpinen-4-ol	0.4
α-Terpineol	0.3
Linalool	+
Geraniol	+
Methyl salicylate	0.2
Phenylethyl acetate	0.1
Unidentified carbonyl compound	0.1
δ-Cadinene	13.6
γ-Cadinene	2.0
β-Clemene	0.8
Sesquiterpene hydrocarbon I	1.0
Sesquiterpene hydrocarbon II	0.8
Torreyol (now δ-cadinol)	3.1
Cadinenol	1.2
Nerolidol	0.6
Sesquiterpene alcohol	1.0
Sesquiterpene hydrocarbon mixture	2.5
Unidentified carbonyl compound I	0.3
Unidentified carbonyl compouod II	0.2

The Structure of Torreyol

Upon treatment with hydrogen chloride in dioxane-water, torreyol gave cadinene dihydrochloride; m. p. 119°C, $[\alpha]_D^{14}$ +40.8° (*c* 0.735, ethyl acetate). On the basis of the value of the optical rotation, the identity of the infrared spectrum, and the depression of the mixed melting point with (−)-cadinene dihydrochloride (m. p. 117~118°C, $[\alpha]_D^{14}$ −40.7°), it can be said that the dihydrochloride of torreyol is undoubtedly (+)-cadinene dihydrochloride.

The oxidation of torreyol with potassium permanganate yielded a dihydroxy-ketone (m. p. 143~144°C).[8] No acetone was detected by the ozonization of torreyol. These findings prove the previously suggested. Formula I for torreyol to be untenable; on the other hand, by a direct comparison of the mixed melting point and the infrared spectrum with an authentic sample,[9] torreyol was proved to be identical with (+)-δ-cadinol. It was an optical antipode of pilgerol[10] isolated from the oil of *Pilgerodendron uniferum* by Erdtman.[11]

Table II. The physical constants of δ-cadinol

Name	M. p., °C	α_D	Source	Ref.
δ-Cadinol	139 ~140	−109	*Juniperus communis*	5
Albicaulol	138 ~139	−102.3*1	*Pinus albicaulis*	8
Pilgerol	140 ~141	−107	*Pilgerodendron uniferum*	10
Cedrelanol	139 ~140	−106	*Cedrela odorata Brasilensis*	12
δ-Cadinol	141	+118.4*2	*Pinus sibirica*	6, 13
Sesquigoyol	135.5	+ 99.5*2	*Pinus pentaphylla*	14
Torreyol	139.5~140.5	+118.6*3	*Torreya nucifera*	

*1 at 23°C *2 at 20°C *3 at 18°C

8) W. G. Dauben, B. Weinstein, P. Lim and A. B. Anderson, *Tetrahedron*, 15, 217 (1961).
9) V. Herout, private communication.
10) H. Erdtman, Z. Telechowicz and and F. G. Toploss, *Acta Chem. Scand.*, **1956**, 1563.
11) H. Erdtman, private communication.
12) G. Chiurdoglu, R. R. Smolders and A. Soquet, *Bull. soc. chim. Belg.*, 70, 468 (1961).
13) V. A. Pentegova, O. Motl and V. Herout, *Collect. Czechoslov. Chem. Commun.*, 26, 1362 (1961).
14) Y. Sebe, *J. Chem. Soc. Japan (Nippon Kwagaku Kwaishi)*, 61, 1269 (1940).

The structure of (−)-δ-cadinol has to be represented by formula IV, proposed by Dauben and his co-workers;[8] therefore the structure of (+)-δ-cadinol has to be shown by formula V.

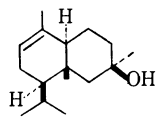

IV

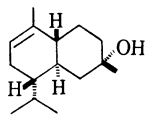

V

The physical constants of δ-cadinol obtained from various sources are shown in Table II.

Summary

It was found that the volatile oil from the leaves of *Torreya nucifera* contains limonene, 41.4%; α-pinene, 23.0%; myrcene, 6.8; terpinolene, 0.7%; 3-carene, 0.3%; γ-terpinene, 0.1%; citronellol, 0.7%; terpinen-4-ol, 0.4%; α-terpineol, 0.3%; methyl salicylate, 0.2%; phenylethyl acetate, 0.1%; δ-cadinene, 13.6%; γ-cadinene, 2.0%; β-elemene, 0.8%; torreyol (δ-cadinol), 3.1%; (+)-cadinenol, 1.2%; nerolidol, 0.6%; small amounts of linalool and geraniol; two unknown sesquiterpenic hydrocarbons, 1.8%; an unknown sesquiterpene alcohol, 1.0%, and three unidentified carbonyl compounds.

The authors wish to express their deep thanks to Professor V. Herout, Institute of Chemistry, Czechoslovak Academy of Science, for his valuable suggestions and kind supply of authentic samples of cadinenol and δ-cadinol. They are also indebted to Professor H. Erdtman, Organisk-kemiska Institutionen, Kungl. Tekniska Högskolan, for his kind help in identifying torreyol with pilgerol.

The Institute of Food Chemistry
Kita-ku, Osaka

Synthesis of DL-Glutamic Acid from 1, 1, 1, 5-Tetrachloropentane

By Kazuo SAOTOME and Toshiaki YAMAZAKI

(Received May 22, 1963)

Various amino acids have been synthesized by Russian authors using ethylene-carbon tetrachloride telomers as the starting raw materials. In the previous papers,[1,2] the present authors have reported on the synthesis of DL-lysine from 1, 1, 1, 5-tetrachloropentane which had been prepared by the telomerization of ethylene and carbon tetrachloride. This paper presents a novel way for the synthesis of DL-glutamic acid from 1, 1, 1, 5-tetrachloropentane. The process involves the five steps shown below:

$$\underset{\text{(I)}}{Cl(CH_2)_4CCl_3} \rightarrow \underset{\text{(II)}}{HO(CH_2)_4CCl_3} \rightarrow \underset{\text{(III)}}{HOOC(CH_2)_3CCl_3} \rightarrow \underset{\text{(IV)}}{HOOC(CH_2)_2CH{=}CCl_2} \rightarrow \underset{\text{(V)}}{HOOC(CH_2)_2CHClCOOH} \rightarrow \underset{\text{(VI)}}{HOOC(CH_2)_2CHNH_2COOH}$$

Since the trichloromethyl group in I is inert towards a nucleophilic reagent, the chlorine atom at the other end can be substituted selectively by the hydroxy group in an aqueous alkaline solution. In a laboratory, however, the saponification of the acetoxy derivative of I prepared by treating I with potassium acetate in glacial acetic acid is a more convenient method.

According to Nesmeyanov et al.,[3] the oxidation of II by chromic anhydride in glacial acetic acid gave III, but in a poor yield. In our study, II was oxidized with potassium permanganate in an aqueous solution to afford III in a yield over 90%. The trichloroethyl group in aliphatic compounds is converted to dichlorovinyl group by heating in the presence of such a Lewis acid as ferric chloride.[4] The dehydrochlorination of III using such stronger Lewis acids as aluminum chloride and ferric chloride resulted only in a poor yield. However, when III was heated in the presence of a relatively weaker Lewis acid such

1) K. Saotome and Y. Kodaira, This Bulletin, **35**, 2010 (1962).
2) K. Saotome, *J. Chem. Soc. Japan, Ind. Chem. Sec.* (*Kogyo Kagaku Zasshi*), **65**, 1061 (1962).
3) A. N. Nesmeyanov, L. I. Zakharkin and R. Kh. Freidlina, *Izv. Akad. Nauk, Otd. Khim. Nauk*, **1955**, 40.
4) A. N. Nesmeyanov, R. Kh. Freidlina and L. I. Zakharkin, *Quart. Rev.*, **10**, 330 (1956).

as zinc chloride or bismuth chloride, IV was found to be affoded in a good yield. Nesmeyanov et al.[3] synthesized IV through another process, in which dichloropropenylmalonic acid prepared from 3,3,3-trichloropropene-1 by malonic synthesis was decarboxylated.

The synthesis of α-chlorocarboxylic acid by the chlorination of compounds containing a dichlorovinyl group in an acid medium has been reported recently.[5] The conjugated addition of chlorine to the dichlorovinyl group is considered to proceed according to the following scheme:

$$RCH{=}CCl_2 \xrightarrow[HA]{Cl_2} [RCHCl\text{-}CCl_2A] \xrightarrow{H_2O}$$
$$RCHClCOOH + 2HCl + HA$$

A chlorine atom and an acid residue (A) are added to the double bond of the dichlorovinyl group, and the resulting adduct is decomposed with water to give α-chlorocarboxylic acid.

Freidlina et al.[6] synthesized several amino acids by the ammonolysis of α-chlorocarboxylic acids which had been prepared by the above method. In their reports, DL-glutamic acid was also prepared from 5,5-dichloro-4-pentenoic acid (IV). Since the separation of α-chloroglutaric acid as crystals is somewhat difficult, they obtained the diethyl ester of α-chloroglutaric acid by treating the crude product with ethanol. The ammonolysis of diethyl α-chloroglutarate was carried out with ethanol-ammonia. They obtained DL-glutamic acid in a 70% yield after the hydrolysis of the amination product with hydrochloric acid. Another reason why Freidlina et al. converted the chlorination product to diethyl α-chloroglutarate may be the complicated behavior of α-chloroglutaric acid in ammonolysis.

According to Kawai,[7] the ammonolysis of α-chloroglutaric acid in aqueous ammonia at a temperature above 200°C proceeds according to the following scheme:

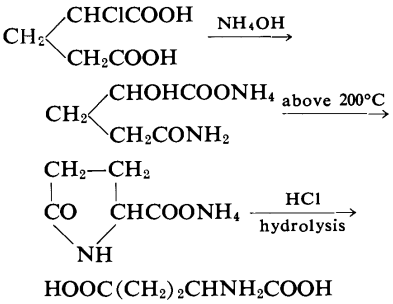

$HOOC(CH_2)_2CHNH_2COOH$

DL-glutamic acid

In our process, α-chloroglutaric acid was separated as crystals from the chlorination product. The ammonolysis of α-chloroglutaric acid was carried out in aqueous ammonia at 260°C, and the resulting product was hydrolyzed with hydrochloric acid to afford DL-glutamic acid in a 87% yield.

Experimental

1,1,1-Trichloro-5-hydroxypentane (II).—A mixture of 786 g. of I, 660 g. of potassium acetate and 900 ml. of glacial acetic acid was refluxed for 16 hr. in the presence of the catalyst iodine (1.5 g.). The reaction mixture was diluted with water after the acetic acid had been evaporated under reduced pressure. The oily layer and the benzene extract from the aqueous layer were then combined and washed with water. Distillation of the extract under reduced pressure afforded 1,1,1-trichloro-5-acetoxypentane; b. p. 79~80°C/1 mmHg, n_D^{20} 1.4683. Yield, 805 g. (92.0%).

The acetate prepared above was saponified with sodium hydroxide in aqueous methanol (1 : 1) at room temperature. The reaction mixture, after being allowed to stand overnight, was neutralized with hydrochloric acid and extracted with benzene. The distillation of the benzene extract under reduced pressure afforded a quantitative amount of II; b. p. 78~80°C/1 mmHg, n_D^{20} 1.4878 (lit.[3] b. p. 112~113°C/10 mmHg, n_D^{20} 1.4897).

5,5,5-Trichlorovaleric Acid (III).—Into an aqueous solution of potassium permanganate heated in a water bath, II was stirred in drop by drop. The reaction was continued for a few hours after the

TABLE I. THE OXIDATION OF 1,1,1-TRICHLORO-5-HYDROXYPENTANE

$HO(CH_2)_4CCl_3$ g.	$KMnO_4$ g.	H_2O ml.	Temp. °C	Time hr.	$HOOC(CH_2)_3CCl_3$ g.	Yield, %
19.1	23.5	140	45~50	(1.0)*+2.0	15.5	75.8
95.5	143	650	50~55	(1.0) +2.0	89.5	87.5
95.5	190	650	55~60	(2.0) +2.0	88.5	85.0
95.5	160	600	55~60	(1.0) +3.0	96.0	93.8
95.5	160	650	55~60	(1.5) +3.0	94.0	92.0

* The value in ( ) represents the time used for the addition of $HO(CH_2)_4CCl_3$.

5) A. N. Nesmeyanov, R. Kh. Freidlina, V. N. Kost and T. T. Vassilyeva, *Tetrahedron*, **17**, 69 (1962).
6) R. Kh. Freidlina, V. N. Kost and T. T. Vassilyeva, *Izv. Akad. Nauk, Otd. Khim. Nauk*, **1959**, 826.
7) Y. Kawai, *J. Chem. Soc. Japan, Pure Chem. Sec.* (*Nippon Kagaku Zasshi*), **80**, 1321 (1959).

TABLE II. THE DEHYDROCHLORINATION OF 5,5,5-TRICHLOROVALERIC ACID

$HOOC(CH_2)_3CCl_3$ g.	Lewis acid g.	Solvent AcOH, g.	Temp. °C	Time hr.	$HOOC(CH_2)_2CH=CCl_2$ g.	Yield, %
50.0	$FeCl_3$ 0.5	—	90～100	4.0	21.0	51.0
50.0	$AlCl_3$ 1.0	—	100～110	4.0	26.5	64.5
41.0	$BiCl_3$ 1.5	—	140～150	3.0	28.0	83.2
41.0	$BiCl_3$ 2.0	—	140～150	4.0	28.5	84.6
41.0	$ZnCl_2$ 1.5	—	120～130	4.0	27.0	80.3
41.0	$BiCl_3$ 1.5	12	140～150	4.0	27.5	81.2
41.0	$BiCl_3$ 1.0+0.5*	12	140～150	2.0+2.0	28.5	84.6
41.0	$ZnCl_2$ 1.0+0.5	12	120～130	2.0+2.0	26.5	78.7

* The catalyst was added in two portions 1.0 g. at the beginning of the reaction, and then 0.5 g. after 2 hr.

TABLE III. THE CHLORINATION OF 5,5-DICHLORO-4-PENTENOIC ACID

$HOOC(CH_2)_2CH=CCl_2$ g.	Acid g.	Temp. °C	Time hr.	$HOOC(CH_2)_2CHClCOOH$ g.	Yield, %
25.0	H_2SO_4 (96%) 31	5～10	3	17.0	69.5
20.0	H_2SO_4 (96%) 32	5～10	5	13.0	68.5
26.0	H_2SO_4 (90%) 65	5～10	5	20.0	78.0
31.0	H_2SO_4 (90%) 90	3～ 8	5	25.0	82.0
32.0	H_2SO_4 (92%) 80	3～ 8	5	22.0	70.0
20.0	HCOOH 60	3～ 8	5	16.0	81.5
26.0	CH_3COOH 80	3～ 8	5	18.0	70.5

addition of the reactant. The excess permanganate was decomposed by adding a small amount of methanol. The manganese dioxide which was precipitated was filtered from the reaction mixture and washed several times with hot water. The filtrate was then cooled and acidified with hydrochloric acid. The white crystals which precipitated were collected and dried over calcium chloride under reduced pressure. Recrystallization from petroleum ether afforded III; m. p. 64°C (lit. m. p. 65°C).

Found: C, 29.19; H, 3.41; Cl, 51.82. Calcd. for $C_5H_7O_2Cl_3$: C, 29.23; H, 3.43; Cl, 51.77%.

Details of the reaction are shown in Table I.

5,5-Dichloro-4-pentenoic Acid (IV). — The dehydrochlorination of III was investigated using several Lewis acids as catalysts. The reaction was carried out by heating and simultaneously stirring III in the presence of the catalyst. After the evolution of hydrogen chloride had ceased, the reaction mixture was washed with water, then distilled under reduced pressure to afford IV; b. p. 95～97°C/1 mmHg, n_D^{20} 1.4888 (lit.[3] b. p. 93～94°C/1 mmHg, n_D^{20} 1.4898).

Found: C, 35.32; H, 3.68; Cl, 41.83. Calcd. for $C_5H_6O_2Cl_2$: C, 35.53; H, 3.58; Cl, 41.96%.

The reaction conditions and the yields are shown in Table II.

As Table II shows, when a stronger Lewis acid ($AlCl_3$ or $FeCl_3$) was used as the catalyst, the resinous by-product increased and the yield of IV decreased. The best result was obtained when bismuth chloride was used as the catalyst. The effect of acetic acid as a solvent was not prominent.

α-Chloroglutaric Acid (V). — Into sulfuric acid cooled in ice-water, IV was dissolved slowly to make a clear solution. Chlorine gas was passed through this solution while it gas being stirred at a temperature below 10°C. The reaction was continued for a few hours until the evolution of hydrogen chloride had ceased. The reaction mixture was then poured into ice-water, and the product was extracted with ether. The ether extract was washed several times with water and dried with anhydrous sodium sulfate. After the evaporation of the ether, the residue was further dried under reduced pressure to obtain the crystals of V. Recrystallization from chloroform afforded white crystals; m. p. 95～97°C, (lit. m. p. 98°C).

Found: C, 36.19; H, 4.24; Cl, 21.43. Calcd. for $C_5H_7O_4Cl$: C, 36.05; H, 4.24; Cl, 21.29%.

In this reaction, formic and acetic acids were also applied in place of sulfuric acid. The reaction product was then treated as in the case of sulfuric acid. Details of the reaction are shown in Table III.

DL-Glutamic Acid (VI).—In an autoclave equipped with a magnetic stirrer, V (5.0 g.) and aqueous ammonia were placed. The reaction was carried out at the temperature of 260±5°C for 4 hr. The reaction mixture was concentrated almost to dryness on a water bath to remove any free ammonia. The residue was then dissolved in 40 ml. of hot water and filtered.

To this filtrate 40 ml. of concentrated hydrochloric acid was added, and the mixture was refluxed for 4 hr. to hydrolyze the reaction product. The solution was again concentrated to dryness under reduced pressure to remove hydrochloric acid. The solid product was dissolved in 100 ml. of water, and the solution was decolorized by boiling it with

active charcoal. The decolorized solution was then concentrated to about 30 ml. An aliquot of this solution was directed to the sample for the quantitative analysis of VI. The pH of the rest of the solution was adjusted at 3.2 (the isoelectric point of glutamic acid) and stored in a refrigerator. White crystals precipitated. Recrystallization from water gave VI; m. p. 185°C (lit. m. p. 185°C). This was identified by paper chromatography with an authentic sample and was shown to be one-spot.

Found: C, 40.67; H, 6.38; N, 9.39. Calcd. for $C_5H_9O_4N$; C, 40.82; H, 6.17; N, 9.52.

The Quantitative Analysis of DL-Glutamic Acid. —Five milliliters of the decolorized solution was diluted to 100 ml., of which 0.01 ml. was taken on a filter paper; the components other than DL-glutamic acid were removed by electrophoresis. The DL-glutamic acid was then extracted with ethanol from the paper, and the resulting solution was analyzed by electrophotometry. The DL-glutamic acid content was determined by comparison with the standard extinction curve. The relation between the concentration of aqueous ammonia and the yield is show in Table IV.

In Tabl IV, the yield may be seen to decrease as the concentration of ammonia increases.

TABLE IV. THE AMMONOLYSIS OF α-CHLOROGLUTARIC ACID

α-Chloroglutaric acid	Aqueous NH_3		DL-Glutamic acid	
g.	ml.	concn., %	g.	Yield, %
5.0	50	13.5	3.84	87
5.0	50	20.0	3.31	75
5.0	50	28.0	3.09	70

Summary

DL-Glutamic acid has been synthesized from 1, 1, 1, 5-tetrachloropentane. The process involves five steps through 1, 1, 1-trichloro-5-hydroxypentane (92%), 5, 5, 5-trichlorovaleric acid (94%), 5, 5-dichloro-4-pentenoic acid (85%), α-chloroglutaric acid (82%), and DL-glutamic acid (87%). The over-all field from 1, 1, 1, 5-tetrachloropentane to DL-glutamic acid was 52%.

In the dehydrochlorination of 5, 5, 5-trichlorovaleric acid to 5, 5-dichloro-4-pentenoic acid, rather weak Lewis acid catalysts, such as bismuth chloride and zinc chloride were found to give the best results.

The authors wish to expess their deep thans to Dr. Gentaro Noyori of the Noguchi Institute for his kind advice on the ammonolysis of α-chloroglutaric acid.

Technical Research Laboratory
Asahi Chemical Industry Co., Ltd.
Itabashi-ku, Tokyo

Oligomers and Polymers Containing Triple Bonds. II. Derivatives of Ethynylazobenzene

By Hisaya TANI, Sigeru TANAKA and Fumio TODA

(Received May 11, 1963)

Previous studies[1,2] have shown that various diethynyl compounds react with cupric or cuprous salts to produce linear and stable polymers containing triple bonds. In the present paper, the preparation of 4-ethynyl- and 4,4'-diethynylazobenzene and the polymerization of the latter will be described.

The treatment of 4-acetylazobenzene[3] (II), prepared from *p*-aminoacetophenone (I) and nitrosobenzene, with phosphorus pentachloride and then with a large excess of sodium amide in liquid ammonia, resulted in the formation of *trans*-4-ethynylazobenzene (IIIa), together with a small amount of cis-isomer (IIIb). When a nearly theoretical amount of sodium amide was employed, however, 4-(chloroethynyl)-*trans*-azobenzene (IVa) and IIIa were obtained in almost equal yields.

Confirmatory evidence for the configurations of IIIa and IIIb was found in the following experimental results: the relationship between the electronic absorption properties of IIIa and IIIb resembled that between those of *cis*- and *trans*-azobenzene (Fig. 1), and IIIa (m. p. 81~82°C) was eluted with carbon tetrachloride faster than was IIIb (m. p. 183.5°C) during the course of chromatography on alumina. It has previously been well known that cis-derivatives of azobenzene are more strongly adsorbed on

1) H. Tani, F. Toda and K. Matsumiya, This Bulletin, **36**, 391 (1963).
2) H. Tani, K. Murayama and F. Toda, *Chem. & Ind.*, **1962**, 1980.
3) F. Kunckell, *Ber.*, **33**, 2641 (1900).

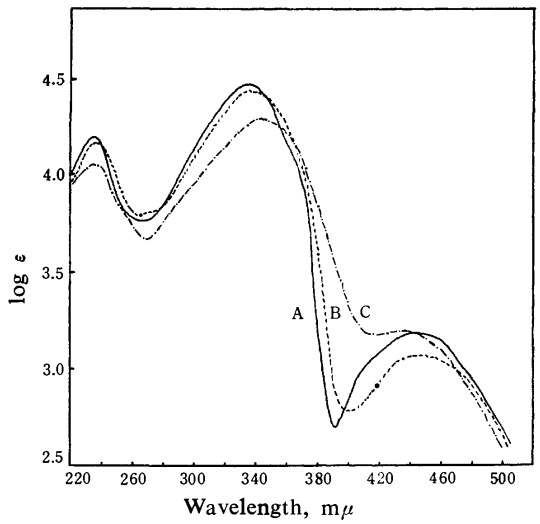

Fig. 1. Electronic absorption spectra.
A 4-Ethynyl-*trans*-azobenzene (III_a)
B 4-(Chloroethynyl)-*trans*-azobenzene (IV_a)
C 4-Ethynyl-*cis*-azobenzene (III_b)
all in dioxane.

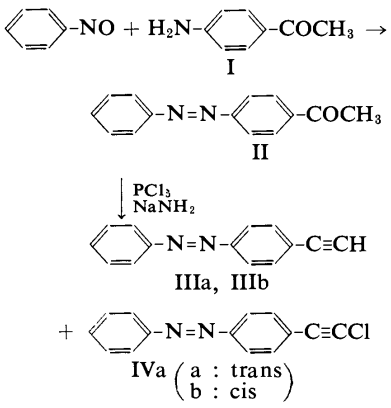

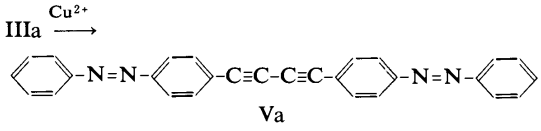

alumina and have higher melting points than do trans-derivatives. The configurations assigned to all the remaining compounds obtained in the present work were similarly confirmed.

IIIa gave, on oxidative coupling with cupric acetate in pyridine, the normal product Va in a good yield.

The formation of IVa in the course of the conversion of II to III may offer valuable evidence for the initial formation of 4-(1,2,2-trichloroethyl)azobenzene, from which IVa and further IIIa were produced by the action of sodium amide.

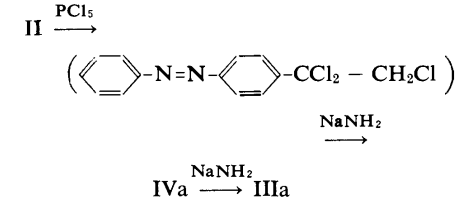

4,4'-Diethynyl-*trans*-azobenzene (VIIa) was prepared from 4,4'-diacetylazoxybenzene (VI), which had been obtained by the oxidation of I with neutralized Caro's acid[4] or with perboric acid,[5] by the reduction of azoxy group with phosphorus trichloride, followed by treatment with the same method as was employed for II. When phosphorus oxychloride and chloroform were used as solvents in the reduction process, 4,4'-diethynylazoxybenzene (VIII) and 4-ethynyl-4'-acetyl-*trans*-azobenzene (IXa) were formed as the respective by-products. The electronic spectra of VIIa, VIII and IXa, indicating valuable evidence for their configuration, are shown in Fig. 2.

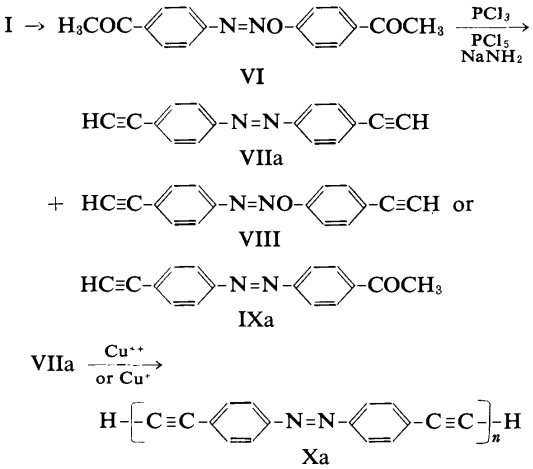

The polymerizations of VIIa with copper salt catalysts in pyridine or in dimethylformamide, as summarized in Table I, resulted in the formation of insoluble and infusible reddish brown or dark brown solids. The infrared and electronic absorption spectra indicated that these products were conjugated linear polymers. When polymerizations were carried out in pyridine, the linear dimer of VIIa (Xa, $n=2$) was obtained. This is because of the low solubility of the initially-formed dimer in the solvent used for the polymerization. When the polymerization was carried out in dimethylformamide, linear hexamer (Xa, $n=6$) was obtained. It is not clear whether the

4) J. C. E. Simpson, *J. Chem. Soc.*, **1952**, 2606.
5) S. Mehta and M. V. Vakilwala, *J. Am. Chem. Soc.*, **74**, 563 (1952).

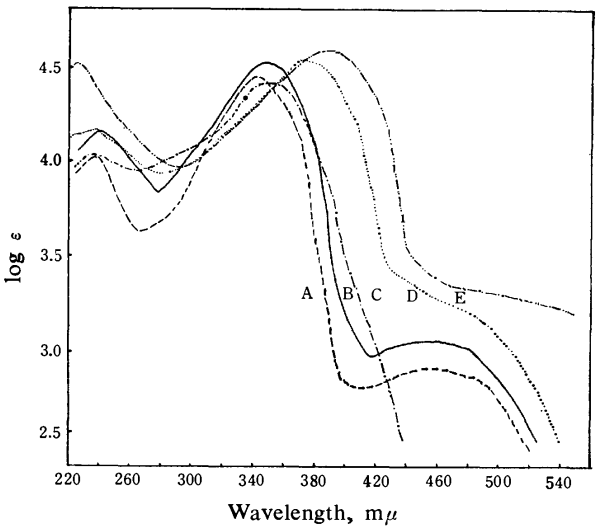

Fig. 2. Electronic absorption spectra.
A 4-Ethynyl-4'-acetyl-*trans*-azobenzene (IXa)
B 4, 4'-Diethynyl-*trans*-azobenzene (VIIa)
C 4, 4'-Diethynylazoxybenzene (VIII)
D 4, 4'-Bis(phenyl-*trans*-azo)diphenyldiacetylene (Va)
E 4, 4'-Bis(*p*-ethynylphenyl-*trans*-azo)diphenyldiacetylene (Xa, $n=2$); all in dioxane.

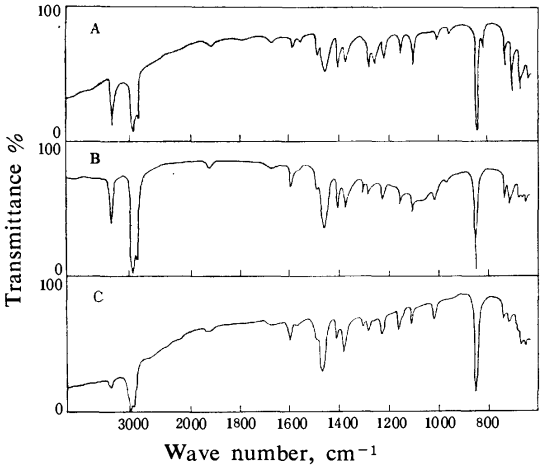

Fig. 3. Infrared absorption spectra.
A 4, 4'-Diethynyl-*trans*-azobenzene (VIIIa)
B 4, 4'-Bis(*p*-ethynylphenyl-*trans*-azo)diphenyldiacetylene (Xa, $n=2$)
C Polymer (Xa, $n=6$)
all in Nujol mull.

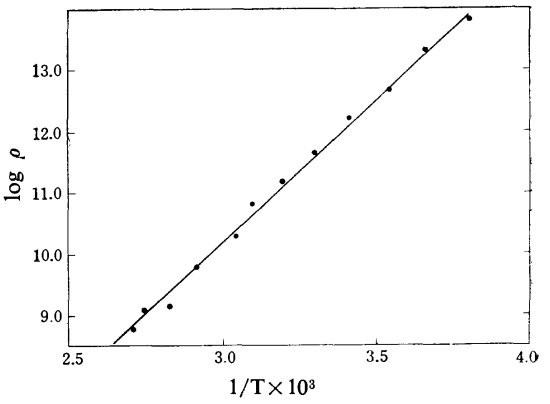

Fig. 4. Resistance-temperature characteristic for Xa, $n=6$.

difference in the degree of polymerization is due to the basicity of the solvent or to the solubility of the oligomer in the solvent.

The degree of polymerization of all the polymers thus obtained was estimated by comparing the intensity at the ethynyl maximum (3300 cm^{-1}) in the infrared spectra of these polymers with that of VIIa, used as a reference standard (Fig. 3). This estimation was based on the assumption that the absorbancy of the ethynyl band is not affected by the length of the conjugation system. This assumption was justified by comparing the electronic spectra of Xa, $n=2$ with that of Va, as shown in Fig. 2; these spectra show that Xa, $n=2$ absorbs at wave lengths longer by ca. 11 mμ than does Va. It is most reasonable to consider that this bathochromic shift is attributable to the two additional ethynyl substituents. On the other hand, the shift exhibited when one more ethynyl group was introduced in to IIIa is 14 mμ (Figs. 1 and 2), which is comparable to the value (11 mμ) of the shift due to the conversion of Va to Xa, $n=2$.

TABLE I. POLYMERIZATION OF 4, 4'-DIETHYNYL-*trans*-AZOBENZENE (VIIa)

VIIa mg.	Catalyst mg.		Solvent* ml.	Reaction temp., °C	Reaction time, min.	Atmosphere	Color	Product mg.	Degree of polymerization
65.75	CuCl	50.0	P 30	40～ 45	30	O_2	Brown	61.0	2
16.25	CuCl	14.2	P 10	95～100	90	O_2	Reddish Brown	14.63	2
10.75	CuCl	19.2	D 7	61～ 62	60	O_2	Dark Brown	2.90	6
13.02	CuCl	11.7	D 7.5	95～ 98	30	O_2	Dark Brown	2.96	3
20.30	$Cu(OAc)_2$	35.3	P 10	60	90	air	Brown	16.8	2
11.74	$Cu(OAc)_2$	20.86	D 8	62	35	air	Reddish Brown	5.84	2

* P, Pyridine D, Dimethylformamide

The resistivities of Xa, $_{n=6}$ at 25° and at 0°C were found to be 3.8×10^{12} and 3.9×10^{-4} ohm. cm. respectively. The temperature dependence of the resistivity obeyed the following relation:

$\rho=\rho_0\exp. \Delta\varepsilon/2kT$ where $\Delta\varepsilon=1.85$eV. (Fig. 4)

From the above data, it is apparent that this polymer has the typical characteristics of an organo-semiconductor.

Experimental*

4-Ethynyl-*trans*-azobenzene (IIIa) and 4-Ethynyl-*cis*-azobenzene (IIIb).—A mixture of 4-acetylazobenzene (2.2 g., 0.01 mol.), phosphorus pentachloride (2.4 g., 0.011 mol.), and phosphorus oxychloride (20 ml.) was heated at 60°C for 1 hr. The crude chloride obtained by the evaporation of phosphorus oxychloride under reduced pressure was dissolved in dry ether, and the solution was then added to sodium amide in liquid ammonia (sodium 1.0 g., 0.044 g. atom, liquid ammonia 100 ml.). After the evaporation of the ammonia, the crude product was extracted with ether. The ethereal layer was washed with water and dried over sodium sulfate. The residue obtained by the evaporation of the ether was chromatographed on alumina.

The orange crystals obtained from the fraction eluted with carbon tetrachloride were recrystallized from *n*-hexane to give 4-ethynyl-*trans*-azobenzene (IIIa); 160 mg. as orange leaflets; m. p. 81～82°C. IR: KBr disk, 3270 (ethynyl), 1414 (azobenzene), 843 (*p*-disubstituted benzene) and 769, 675 cm^{-1} (monosubstituted benzene). UV: $\lambda_{max}^{Dioxane}$: 234 mμ (ε, 15500), 334 (28200), 442 (1400).

Found: C, 81.36; H, 4.88; N, 13.38. Calcd. for $C_{14}H_{10}N_2$: C, 81.53; H, 4.89; N, 13.58%.

Elution with benzene, followed by recrystallization from *n*-hexane, yielded a small amount of 4-ethynyl-*cis*-azobenzene (IIIb) as orange needles; m. p. 183.5°C. IR: KBr disk, 1400 (azobenzene), 845 (*p*-disubstituted benzene), and 773, 685 cm^{-1} (monosubstituted benzene). UV: $\lambda_{max}^{Dioxane}$: 234 mμ (ε, 11800), 344 (20000), 415 (1500), 432 (1500).

Found: N, 13.37. Calcd. for $C_{14}H_{10}N_2$: N, 13.58%.

* All melting points are uncorrected.

The mercury salt of IIIb (orange) did not melt, but turned black at ca. 245°C. IR: KBr disk, 2130 (acetylene), 1410 (azobenzene), 850 (*p*-disubstituted benzene) and 770, 685 cm^{-1} (monosubstituted benzene).

4-(Chloroethynyl)-*trans*-azobenzene (IVa).—4-Acetylazobenzene (5.1 g., 0.023 mol.) was treated with phosphorus pentachloride (5.0 g., 0.024 mol.) in phosphorus oxychloride (30 ml.) and then with sodium amide in liquid ammonia (sodium 1.5 g., 0.065 g. atom, liquid ammonia 150 ml.) in the manner described above. The ammonia was removed, and the residue was extracted with ether. The ether layer was washed with water and dried over magnesium sulfate. After evaporation of the solvent, the crude material remaining was chromatographed on alumina from carbon tetrachloride.

Recrystallization of the crystals obtained from the first fraction (eluted with carbon tetrachloride 700 ml.) from *n*-hexane afforded IVa (200 mg.), in the form of orange leaflets; m. p. 107.5°C. IR: KBr disk, 2210 (acetylene), 1410 (azobenzene), 838 (*p*-disubstituted benzene) and 763, 675 cm^{-1} (monosubstituted benzene). UV: $\lambda_{max}^{Dioxane}$: 221 mμ (ε, 10900) 236 (14600) 338 (26800), 445 (1100).

Found: C, 69.27; H, 3.67; N, 11.56; Cl, 14.70. Calcd. for $C_{14}H_9N_2Cl$: C, 69.86; H, 3.77; N, 11.64; Cl, 14.73%.

From the second fraction (eluted with carbon tetrachloride 800 ml.), there was obtained the crude solids, the recrystallization of which from *n*-hexane gave orange leaflets (200 mg.; m. p. 78～79°C), identified as 4-ethynyl-*trans*-azobenzene (IIIa) by comparing their infrared spectrum and melting point with those of an authentic sample.

4, 4'-Bis(phenyl-*trans*-azo)diphenyldiacetylene (Va).—To a solution of IIIa (100 mg.) in pyridine (20 ml)., cupric acetate monohydrate (2.0 g.) was added; the mixture was then stirred at 60°C for 30 min. The solid precipitates which formed were collected by filtration and washed with a small amount of pyridine. The solid was dried and then recrystallized from chloroform to yield Va (95 mg.) (quantitative yield) as orange leaflets; m. p. 243～234.5°C (decomp.). UV: $\lambda_{max}^{Dioxane}$: 238 mμ (ε, 13800), 374 (33100), 448 (2200).

Found: C, 80.73; H, 4.42; N, 13.70. Calcd. for $C_{28}H_{18}N_4$: C, 81.93; H, 4.42; N, 13.65%.

4, 4'-Diacetylazoxybenzene (VI).—*Procedure (A).*—A mixture of *p*-aminoacetophenone (1, 2.7 g., 0.02 mol.), acetic acid (80 ml.), and sodium perborate (3.3 g., corresponding to 0.02 g. atom of oxygen) was heated at 60°C for 2hr. The precipitates which had separated after the addition of water were collected, washed with water, dried, and then recrystallized from alcohol to give VI, 700 mg. (25%) as yellow leaflets; m. p. 187~190°C. IR: KBr disk, 1685 (ketone), 1462, 1360 (methyl), 1410 (azobenzene), 1260 (aromatic ketone) and 844 cm^{-1} (*p*-disubstituted benzene). UV: $\lambda_{max}^{Dioxane}$: 274 mμ (ε, 10900), 338 (21900).

When the reaction was carried out at 52°C and 30°C, VI was obtained in a yield of 15 and 11% respectively.

Found: C, 67.96; H, 5.05; H, 9.63. Calcd. for $C_{16}H_{14}N_2O_3$: C, 68,07; H, 5.00; N, 9.92%.

Procedure (B).—A solution of *p*-aminoacetophenone (1, 9.7 g., 0.072 mol.) in dioxane (10 ml.) was added to neutral Caro's acid (0.18 N, 900 ml.). After the solution had been shaken for 10 min. at room temperature, the precipitates which had formed were collected by filtration, washed with water, and dried. Recrystallization of the product from acetone afforded VI 3.2 g. (32%) as yellow needles (m. p. 195.5°C), which showed no depression of melting point upon being mixed with the sample prepared in procedure (A). When 0.07 N Caro's acid was used, the yield of VI was lowered to 14%.

4, 4'-Diethynyl-*trans*-azobenzene (VIIa) and 4, 4'-Diethynylazoxybenzene (VIII).—A mixture of 4, 4'-diacetylazoxybenzene (2.8 g., 0.01 mol.), phosphorus oxychloride (40 ml.), and phosphorus trichloride (1.5 g., 0.01 mol.) was treated at 50°C for 30 min. To this warm mixture, phosphorus pentachloride (4.5 g., 0.02 mol.) was added, and the mixture was heated at 50°C for 1 hr. After removal of the phosphorus oxychloride and phosphorus trichloride by distillation in vacuo, the crude chloride which remained was suspended in dry ether (200 ml.), and the resulting suspension was added drop by drop to sodium amide in liquid ammonia (sodium 2.3 g., 0.1 g. atom, liquid ammonia 100 ml.), Stirring was continued for a further 30 min. The residue which remained after the evaporation of the ammonia was decomposed with water and extracted with ether. The ether layer was washed with water and dried over sodium sulfate. After evaporation of the solvent, the crude material was chromatographed on alumina. The crude crystals which were obtained from the first fraction, eluted with carbon tetrachloride, were recrystallized from *n*-hexane, giving VIIa (10 mg.) as orangered needles. Although VIIa did not show a melting point and turned black in the usual m. p. measurement, it melted at 201~202°C with decomposition when immersed at 198°C. IR: Nujol mull, 3270 (ethynyl), 1925 (acetylene), 1419 (azobenzene) and 848 cm^{-1} (*p*-disubstituted benzene). UV $\lambda_{max}^{Dioxane}$: 239 mμ (ε, 14100), 264 (shoulder) (7600), 348 (30200), 450 (1100).

Found: C, 83.52; H. 4.41; N, 12.46. Calcd. for $C_{16}H_{10}N_2$: C, 83.45; N, 4.38; N, 12.17%.

On the other hand, from the second fraction, eluted with benzene, orange yellow crystals were obtained. The crystals were recrystallized from *n*-hexane to yield VIII (10 mg.) as orange yellow leaflets; m. p. 141.5~142.5°C. UV $\lambda_{max}^{Dioxane}$: 230 mμ (ε, 11700), 349 (21400), 480 (shoulder) (100).

Found: C, 77.40; H, 4.29; N, 11.53. Calcd. for $C_{16}H_{10}N_2O$: C, 78.03; H, 4.09; N, 11.38%.

4, 4'-Diethynyl-*trans*-azobenzene (VIIa) and 4-Acetyl-4'-ethynyl-*trans*-azobenzene (IXa).—A solution of 4, 4'-diacetylazoxybenzene (5.5 g., 0.02 mol.) in chloroform (80 ml.) with was treated phosphorus trichloride (2.7 g.) at 50°C for 1 hr. The resultant mixture was then heated with phosphors pentachloride (8.4 g., 0.04 mol.) at 50~60°C for 1 hr. The crude chloride which remained after the evaporation of the chloroform and phosphorus trichloride was treated with sodium amide in liquid ammonia (sodium 3.5 g., 0.15 g. atom; liquid ammonia 150 ml.). After removal of the ammonia, the residue was decomposed with water and extracted with ether. The ether layer was washed with water and then evaporated to leave the crude product, which was chromatographed on alumina from benzene. The first fraction gave the desired compound (VIIa) as orange-red leaflets (96 mg.; m. p. 201~202°C (decomp., immersed at 198°C) after recrystallization from *n*-hexane.

When the crystals which were obtained from the second fraction were recrystallized from aqueous ethanol, IXa (14 mg.) was obtained as orange leaflets; m. p. 163°C. IR: KBr disk, 3240 (ethynyl), 2090 (acetylene), 1660, 1264 (acetyl), 1414 (azo) and 850 cm^{-1} (*p*-disubstituted benzene). UV $\lambda_{max}^{Dioxane}$: 236 mμ (ε, 10000), 344 (22400), 455 (600).

Found: C, 76.27; H, 4.99; N, 10.76. Calcd. for $C_{16}H_{12}N_2O$: C, 77.40; H, 4.87; N, 11.28%.

Electric Constants.—Electric constants were measured for the tablet of Xa, $n=6$, on which indium had been sublimed in vacuo. The tablet was made by applying a pressure of 6000 kg./cm^2 on the powder of the polymer in a tube 13 mm. in diameter for a 30-min. period.

The authors wish to express their thanks to Mr. Yoshinobu Murakami of the Matsushita Electric Industrial Co., Ltd., for his measurements of the electric constants and also to Mr. Masakazu Okumiya of this faculty for his microanalyses.

Department of Polymer Science
Faculty of Science
Osaka University
Nakanoshima, Osaka

Studies of Pyridotropolones. VII.[1,2] *Several Condensation Reactions of Isopropylpyrido[3, 2-d]tropolones*

By Kameji YAMANE, Tadashi MATSUMOTO and Akira YOKOO

(Received May 14, 1963)

Regarding the condensation reaction of pyridotropolones, one of the present authors, Yamane,[3] has previously reported that nitroso compound I of 8-isopropyl-2-methylpyrido-[3, 2-d] tropolone afforded a quinoxalo compound II by the condensation with *o*-phenylenediamine, and that 5-amino compound III, which was obtained by the catalytic reduction of I, gave an oxazolopyridotropone derivative IV upon being treated with acetic anhydride. Kikuchi and Muroi[4] reported that pyrido-[3, 2-d] tropolone and its 2-methyl derivative gave quinoxaline derivatives by condensation with *o*-phenylenediamine, and that 2-methylpyrido [3, 2-d] tropolone afforded a 2-styryl compound by condensation with benzaldehyde. The present authors carried out similar condensation reactions of isopropylpyrido [3, 2-d]-tropolones. Furthermore, some derivatives of pyridoindolotropones were obtained by reaction with phenylhydrazine.

As was reported by Kikuchi and Muroi,[4]

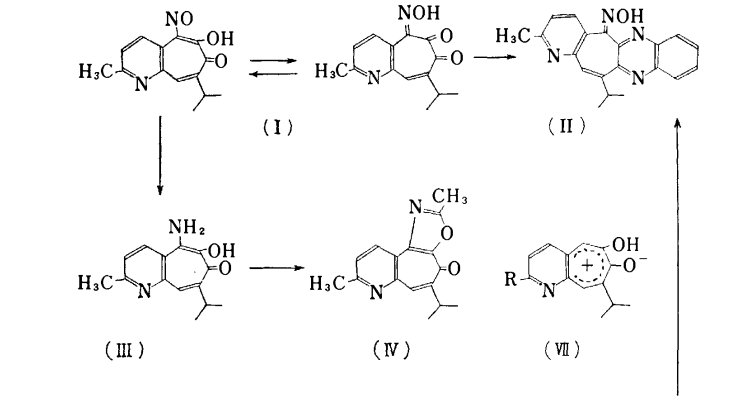

(I) (II) (III) (IV) (VII) (VI) (V) (VIII)

a : R_2=-CH(CH$_3$)$_2$, R_3=H

b : R_2=H, R_3=-CH(CH$_3$)$_2$

a : R_1=H, R_2=-CH(CH$_3$)$_2$, R_3=H

b : R_1=CH_3, R_2=-CH(CH$_3$)$_2$, R_3=H

c : R_1=R_2=H, R_3=-CH(CH$_3$)$_2$

d : R_1=CH_3, R_2=H, R_3=-CH(CH$_3$)$_2$

e : R_1=R_2=R_3=H

Scheme I

1) This work was presented at the Meeting of the Kyushu District of the Chemical Society of Japan, Fukuoka, October, 1961.

2) Part VI: K. Yamane, This Bulletin, **34**, 42 (1961).

3) K. Yamane, *J. Chem. Soc. Japan, Pure Chem. Sec.* (*Nippon Kagaku Zasshi*), **80**, 1175 (1959).

4) K. Kikuchi and T. Muroi, presented at the Tohoku Local Meeting of the Chemical Society of Japan, Sendai, June, 1960.

(IX) (X)

Scheme II

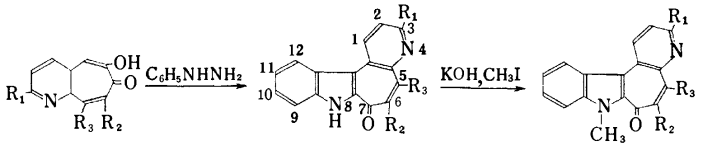

(XI) (XII) (XIII)

a : $R_1=H$, $R_2=-CH(CH_3)_2$, $R_3=H$

b : $R_1=CH_3$, $R_2=-CH(CH_3)_2$, $R_3=H$

c : $R_1=R_2=H$, $R_3=-CH(CH_3)_2$

Scheme III

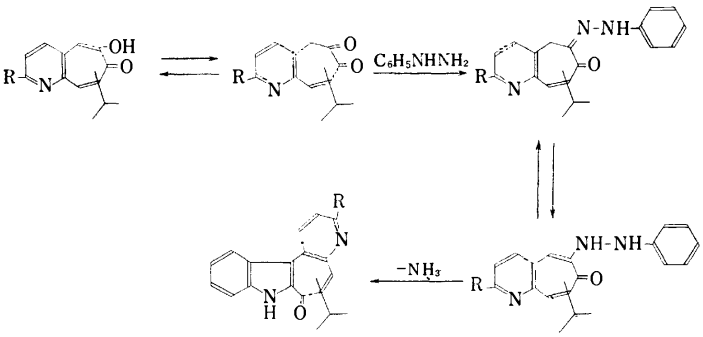

Scheme IV

8-isopropyl-2-styrylpyrido[3, 2-d]tropolone (VIa) and 9-isopropyl-2-styrilpyrido [3, 2-d] tropolone (VIb) were obtained from the reaction of benzaldehyde with 8-isopropyl-2-methylpyrido-[3, 2-d] tropolone (Vb) and with 9-isopropyl-2-methylpyrido[3, 2-d]tropolone (Vd) respectively.

Attempts to prepare quaternary salts of 8-isopropylpyrido [3, 2-d] tropolones by reaction with methyl iodide, ethyl iodide and ethyl *p*-toluenesulfonate were unsuccessful. This was probably due to the decrease in the electron density at the nitrogen atom through the contribution of the structure VII.

The heating of 8- and 9-isopropyl derivatives (Va, Vb and Vc) with *o*-phenylenediamine in acetic acid afforded quinoxaline derivatives in a good yield, as in the case[4] of pyrido [3, 2-d] - tropolone. Kikuchi and Muroi[4] proposed a structure (IX or X) for the condensation product. Treating VIIIb with amyl nitrite in an acidic medium gave II.[3] VIIIe was not acylated by acetyl chloride or benzoyl chloride in pyridine. The infrared spectrum of VIIIe has no absorption bands at the NH region and exhibits an absorption band at 1453 cm^{-1} due to the CH_2 deformation vibration. From these facts, it may be concluded that the condensation product VIII exists not as formula IX but as quinoxalo structure X (Schemes I and II).

The heating of 8-isopropyl-2-methylpyrido-[3, 2-d] tropolone (XIb) with phenylhydrazine in acetic acid unexpectedly gave yellow crystals (XIIb) of formula $C_{20}H_{18}ON_2$ in place of a phenylhydrazone. This suggests that one molecule of ammonia was lost during the reaction. The crystals did not react either with carbonyl reagents or with acylating agents, but *N*-methyl compound XIII was obtained by a method similar to that used in the case of

carbazole. The infrared spectrum of XIIb shows peaks at 1620 cm^{-1} and 3300 cm^{-1}. 8- and 9-isopropyl analogs (XIa and XIc) also gave similar compounds (XIIa and XIIc respectively). The ultraviolet absorption spectra of these compounds are shown in Fig. 2. From these facts it may be assumed that the condensation products have the pyrido[3, 2-d]-indolo[2, 3-b]tropone structure (Scheme III). It is interesting that the mother substance, pyrido[3, 2-d]tropolone and its 2-methyl derivative, gave no pyridoindolotropones. Further studies are now in progress. The mechanism of this condensation reaction seems to be analogous to Fischer's indole syntheses, as Scheme IV shows.

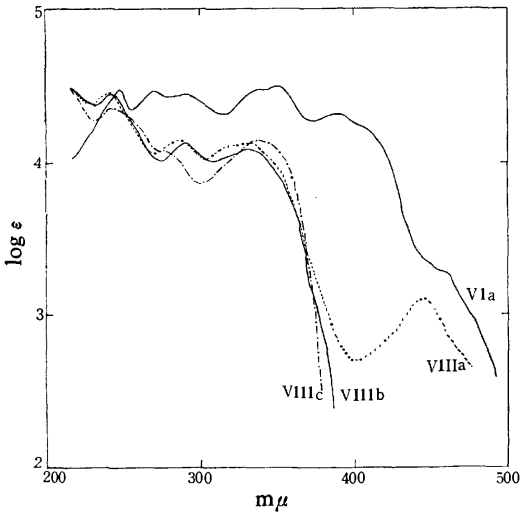

Fig. 1. Ultraviolet absorption spectra of VIa, VIIIa, VIIIb and VIIIc in methanol.

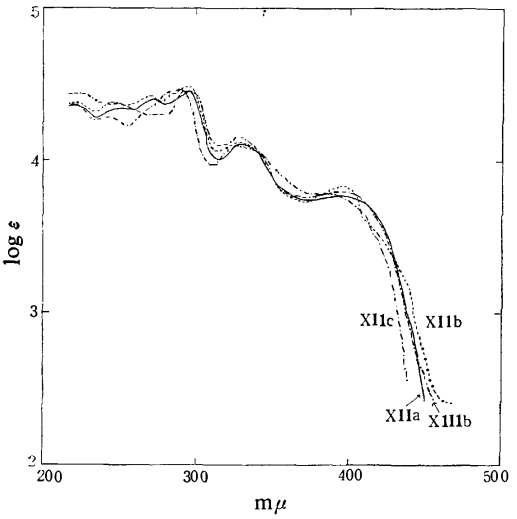

Fig. 2. Ultraviolet absorption spectra of XIIa, XIIb, XIIc and XIIIb in methanol.

Experimental[5]

8-Isopropyl-2-styrylpyrido[3,2-d]tropolone (VIa).—A mixture of Vb (0.4 g.), benzaldehyde (0.2 cc.) and a small amount of zinc chloride in a sealed tube was heated for 3 hr. at 150~160°C. The reaction mixture was diluted with water, and a reddish brown precipitate was then filtered out and sublimed under reduced pressure. The yellow sublimate was recrystallized from methanol to give yellow needles; m. p. 142~142.5°C.

Found: C, 79.45; H, 6.10; N, 4.21. Calcd. for $C_{21}H_{19}O_2N$: C, 79.47; H, 6.03; N, 4.11%.

9-Isopropyl-2-styrylpyrido[3, 2-d]tropolone (VIb).—This was prepared from Vd by a method similar to that described above. Yellow needles; m. p. 182~183°C.

Found: C, 79.36; H, 6.21; N, 4.23. Calcd. for $C_{21}H_{19}O_2N$: C, 79.47; H, 6.03; N, 4.11%.

The Quinoxalo Derivative of 8-Isopropylpyrido-[3,2-d]tropolone (VIIIa).—A mixture of Va (0.4 g.) and *o*-phenylenediamine (0.22 g.) in acetic acid (1.5 cc.) was refluxed for 4 hr. After being cooled, the reaction mixture was diluted with water and made alkaline with aqueous ammonia. The syrupy matter which separated was washed with water and dried in a vacuum dessicator. Recrystallization from ethanol gave pale brownish yellow needles; m. p. 133~134°C (0.43 g., yield 81%).

Found: C, 79.04; H, 5.99; N, 14.54. Calcd. for $C_{19}H_{17}N_3$: C, 79.41; H, 5.96; N, 14.62%.

The Quinoxalo Derivative of 8-Isopropyl-2-methylpyrido[3, 2-d]tropolone (VIIIb).—A mixture of Vb (0.4 g.) and *o*-phenylenediamine (0.2 g.) was treated by a method similar to that described above. Colorless cubic crystals; m. p. 149.5~150.5°C (0.45 g., yield 86%).

Found: C, 79.59; H, 6.18; N, 13.70. Calcd. for $C_{20}H_{19}N_3$: C, 79.70; H, 6.35; N, 13.94%.

The Reaction of VIIIb with Amyl Nitrite.—To a solution of VIIIb (0.5 g.) in concentrated hydrochloric acid (2 cc.), amyl nitrite (3 cc.) was added at room temperature; the mixture was then warmed at 50°C in a water bath to deposit the hydrochloride of II. After the mixture had been allowed to stand overnight, the hydrochloride was filtered and washed with ethanol. Yield, 0.56 g. Recrystallization from ethanol gave colorless plates melting at 259~260°C (decomp.). The hydrochloride (0.12 g.) was dissolved in a large amount of 1 N sodium hydroxide solution by heating on a water bath. After insoluble matter had been removed by hot filtration, the filtrate was acidified with acetic acid and allowed to stand at room temperature to cause crystallization. Recrystallization from alcohol gave a free base, II, as pale yellow plates melting at 238~238.5°C (0.1 g.); the plates were found to be identical with the authentic sample[3] by the mixed melting point and the infrared spectrum.

The Quinoxalo Derivative of 9-Isopropylpyrido-[3,2-d]-tropolone (VIIIc).—A mixture of Vc (0.1 g.) and *o*-phenylenediamine (0.05 g.) was

5) The microanalyses were carried out by Mrs. K. Kodaira and Miss A. Iwanaga (Nozoe Laboratory), to whom deep gratitude is here expressed.

treated as in VIIIa. Colorless plates, m. p. 158.5～159°C (0.11 g., yield, 81%).

Found: C, 79.56; H, 5.61; N, 14.77. Calcd. for $C_{19}H_{17}N_3$: C, 79.41; H, 5.96; N, 14.62%.

6-Isopropylpyrido[3, 2-d]indolo[2, 3-b]tropone (XIIa).—A mixture of XIa (0.3 g.) and phenylhydrazine (0.19 g.) in acetic acid (1.5 cc.) was refluxed for 10 hr. After it had cooled, the crystals were collected by filtration and washed with water. Recrystallization from ethanol gave yellow needles; m. p. 185.5～186.5°C (0.17 g., yield 42%).

Found: C, 79.34; H, 6.22; N, 9.38. Calcd. for $C_{19}H_{16}ON_2$: C, 79.14; H, 5.59; N, 9.72%.

6-Isopropyl-3-methylpyrido[3, 2-d]indolo[2, 3-b]-tropone (XIIb).—A mixture of XIb (0.3 g.) and phenylhydrazine (0.15 g.) was treated as in XIIa. Yellow needles; m. p. 220～221°C (0.21 g., yield 53%).

Found: C, 79.50; H, 5.85; N, 9.45. Calcd. for $C_{20}H_{18}ON_2$: C, 79.44; H, 6.00; N, 9.27%.

Picrate.—Orange yellow prisms; m. p. 223～224°C (from ethanol).

Found: N, 12.94. Calcd. for $C_{26}H_{21}O_8N_5$: N, 13.18%.

N-Methyl Compound (XIIIb).—A mixture of XIIb (0.1 g.) and potassium hydroxide (0.05 g.) was heated in a test tube at 230～240°C. After the mixture had cooled, red potassium salt was refluxed with methyl iodide (1 g.) for 3 hr. The excess methyl iodide was then evaporated, and the residue was extracted with benzene. The benzene extracts were treated with charcoal, and the solvent was distilled out. The residue was recrystallized from ethanol to give yellow needles; m. p. 147～148°C, (0.08 g., yield 76%).

Found: C, 80.09; H, 6.13; N, 8.34. Calcd. for $C_{21}H_{20}ON_2$: C, 79.71; H, 6.37; N, 8.85%.

5-Isopropylpyrido[3, 2-d]indolo[2, 3-b]tropone (XIIc).—A mixture of XIc (0.13 g.) and phenylhydrazine (0.13 g.) in acetic acid (1.5 cc.) was refluxed for 8 hr. After the reaction mixture had cooled, water was added, and the product was recrystallized from ethanol to give yellow needles melting at 255°C (by Kofler block). (A very poor yield).

Found: C, 79.24; H, 5.79; N, 9.14. Calcd. for $C_{19}H_{16}ON_2$: C, 79.14; H, 5.59; N, 9.72%.

The present research was financed by a grant-in-aid for Scientific Research granted by the Ministry of Education. The authors wish to express their hearty thanks to Professor Tetsuo Nozoe, and Assistant Professor Toshio Mukai of Tohoku University and Assistant Professor Katsuo Kikuchi of Yamagata University for their helpful advice.

Chemical Institute
Faculty of Science
Okayama University
Tsushima, Okayama

*Studies on Amino-hexoses. VI. The Synthesis of Phenyl 2-Acetamido-3-O-(D-1'-carboxyethyl)-2-deoxy-α- and β-D-Glucopyranoside and Their Methyl Esters**

By Kazuhiko YAMAMOTO, Mamoru FUJINAGA and Yoshio MATSUSHIMA

(Received June 5, 1963)

A new aminosugar named muramic acid has been discovered in uridine pyrophosphate peptide complexes in *Staphylococcus aureus*[1] and was determined to be 2-amino-3-*O*-(D-1'-carboxyethyl)-2-deoxy-D-glucose.[2] It has been found to be distributed among the cell walls of a number of bacteria. Lysozyme, the enzyme which exerts a bacteriolytic action, has been found to split the cell-wall polysaccharide-peptide complex called muco-peptide at the site of the glycosidic bond of the *N*-acetyl-muramic acid component.[3] However, the substrate specificity of lysozyme is not very clear because of the complexity of the chemical structure of the mucopeptide.

One of the present authors has reported on a convenient method for synthesizing *N*-acetyl-muramic acid glycosides.[4] The present paper will describe the synthesis of phenyl *N*-acetyl-α- and β-muramide and their methyl esters by this method and will also describe the action of lysozyme on these model substrates.

* Presented in part at the 16th Annual Meeting of the Chemical Society of Japan, Tokyo, April, 1963.

1) J. T. Park. *J. Biol. Chem.*, **194**, 885 (1952).

2) R. E. Strange and L. H. Kent, *Biochem. J.*, **71**, 333 (1959).

3) L. R. Berger and R. S. Weiser, *Biochim. Biophys. Acta*, **26**, 517 (1957); W. Brumfitt, A. C. Wardlan and J. T. Park, *Nature*, **181**, 1783 (1958); M. R. Salton and J. M. Ghuysen, *Biochim. Biophys. Acta*, **36**, 552 (1959); H. Pelzer, ibid., **63**, 229 (1962).

4) Y. Matsushima and J. T. Park, *J. Org. Chem.*, **27**, 3581 (1962).

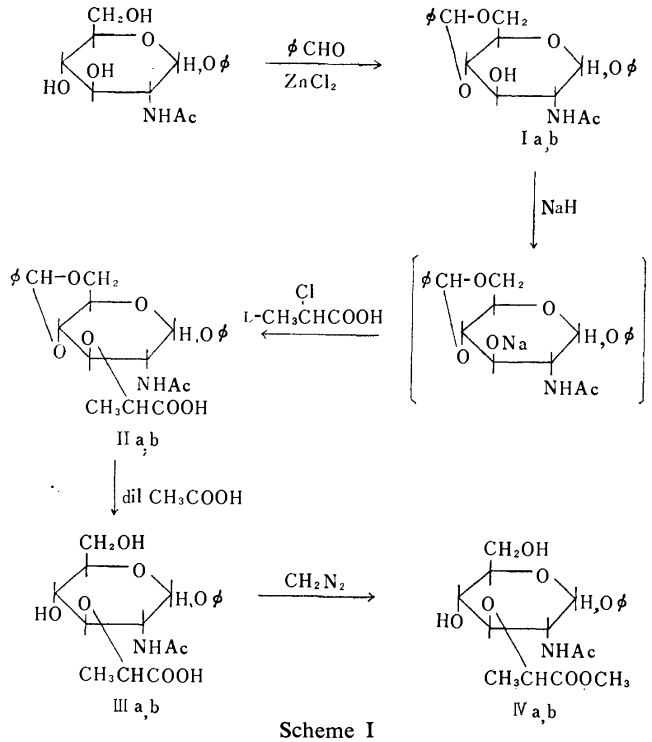

Scheme I

Phenyl α- and β-D-glucosaminide were prepared according to the methods cited.[5,6] These phenyl glycosides were converted by the usual method into 4,6-*O*-benzylidene derivatives, and the latter were condensed with L-α-chloropropionic acid, as has been reported.[4] The debenzylation with dilute acetic acid of these condensation products yielded phenyl *N*-acetyl-α- and β-muramide repectively. Methylation with diazomethane gave the respective methyl esters. The procedure of the synthesis is shown in Scheme I.

Lysozyme action[7] was tested on these acids as well as on methyl esters over a range of pH values. It was found that no appreciable cleavage of the phenyl group occurred in either α- or β-anomer.

Experimental

Phenyl 2-Acetamido-4,6-*O*-benzylidene-2-deoxy-α-D-glucopyranoside (Ia).—Four grams of phenyl 2-acetamido-2-deoxy-α-D-glucopyranoside,[5] 40 g. of freshly distilled benzaldehyde, and 4.0 g. of anhydrous zinc chloride were kept in a tightly closed polyethylene bottle while being mechanically shaken at room temperature for 24 hr. The reaction mixture was then poured into 1000 ml. of cold water, and the water layer was separated by decantation from the oily product. This product was washed three times with petroleum ether, at which the product turned into a fine powder which was recrystallized from methanol. The crystals melted at 282~284°C. $[\alpha]_D^{18}$ +182.7 (*c* 0.684, pyridine). The yield was 4.3 g. (82.9%).

Found: C, 62.39; H, 6.24; N, 3.61. Calcd. for $C_{21}H_{23}O_6N \cdot H_2O$: C, 62.52; H, 6.25; N, 3.47%.

Phenyl 2-Acetamido-4,6-*O*-benzylidene-2-deoxy-β-D-glucopyranoside (Ib). — Two grams of phenyl 2-acetamido-2-deoxy-β-D-glucopyranoside[6] were treated as in the case of the α-anomer (Ia). After recrystallization from methanol, the product melted at 254°C with decomposition. $[\alpha]_D^{24}$ −27.1 (*c* 5.10, pyridine). The yield was 2.3 g. (90%).

Found: C, 62.27; H, 6.31; N, 3.47. Calcd. for $C_{21}H_{23}O_6N \cdot H_2O$: C, 62.52; H, 6.25; N, 3.47%.

Phenyl 2-Acetamido-4,6-*O*-benzylidene-3-*O*-(D-1'carboxyethyl)-2-deoxy-α-D-glucopyranoside (IIa). —Five grams of Ia were dissolved in dry hot dioxane (450 ml.) under mechanical stirring; after the addition of 2.5 g. of sodium hydride (a fine powder dispersed in mineral oil at a ca. 50% concentration), the mixture was kept at 90°C for 150 min. Eight grams of L-α-chloropropionic acid[8] were added when the temperature had gone down to 60°C. The mixture became a heavy paste and was vigorously stirred for 50 min. 5.5 g. of sodium hydride were again added, where-upon the mixture became thin. The temperature was again raised

5) S. Roseman and A. Dorfman, *J. Biol. Chem.*, **191**, 607 (1951).

6) B. H. Leaback and P. G. Walker, *J. Chem. Soc.*, **1957**, 4754.

7) Crystalline egg-white lysozyme was used. Cf. J. M. Ghuysen and M. R. J. Salton, *Biochim. Biophys. Acta*, **40**, 462 (1960).

8) Shou-Cheng J. Fu, S. M. Birnbaum and J. P. Greenstein, *J. Am. Chem. Soc.*, **76**, 6054 (1954).

to 90°C for a short time, and then the mixture was allowed to stand overnight at room temperature. After the cautious addition of 100 ml. of water to decompose the excess sodium hydride, concentration in vacuo gave a thick yellow brown syrup, which was then washed with petroleum ether and dried in vacuo. The aqueous solution (1000 ml.) of the product, after it had once been filtered from a trace of insoluble matter, was made acidic (pH=2.0~2.2) by adding, drop by drop, 6 N hydrochloric acid while the solution was cooled by ice water. The slightly yellow crystals which precipitated were filtered, washed with water, and recrystallized from ethanol. The colorless crystals melted at 243~244°C. $[\alpha]_D^{20}$ +185.6 (*c* 0.388, pyridine). The yield was 4.5 g. (75.9%).

Found: C, 62.48; H, 5.91; N, 3.27. Calcd. for $C_{24}H_{27}O_8N$: C, 63.01; H, 5.95; N, 3.06%.

Phenyl 2-Acetamido-4, 6-*O*-benzylidene-3-*O*-(D-1'-carboxyethyl)-2-deoxy-β-D-glucopyranoside (IIb).—2.4 g. of Ib were treated as in the case of IIa. The crystals from ethanol melted at 248~249°C with decomposition. $[\alpha]_D^{28}$ −15.0 (*c* 2.93, pyridine). The yield was 2.3 g. (81%).

Found: C, 60.72; H, 6.15; N, 2.97. Calcd. for $C_{24}H_{27}O_8N \cdot H_2O$: C, 60.62; H, 6.15; N, 2.95%.

Phenyl-2-Acetamido-3-*O*-(D-1'-carboxyethyl)-2-deoxy-α-D-glucopyranoside (IIIa).—Four grams of IIa were boiled for exactly 10 min. in 820 ml. of 67% acetic acid. After evaporation of the mixture in vacuo, the repeated addition of a small amount of water, and evaporation in vacuo until no odor of acetic acid remained, there remained an amorphous residue which failed to crystallize. $[\alpha]_D^{20}$ +164.5 (*c* 0.106, pyridine).

Phenyl 2-Acetamido-3-*O*-(D-1'-carboxyethyl)-2-deoxy-β-D-glucopyranoside (IIIb).—One gram of IIb was treated as in the case of IIIa. The product was recrystallized from water. The crystals melted at 192~193°C with decomposition. $[\alpha]_D^{19}$ −4.1 (*c* 3.83, pyridine).

Found: C, 55.77; H, 6.02; N, 3.84. Calcd. for $C_{17}H_{23}O_8N$: C, 55.28; H, 6.28; N, 3.79%.

Phenyl 2-Acetamido-3-*O*-(methyl D-1'-ethylcarboxylate)-2-deoxy-α-D-glucopyranoside (IVa).—An ethereal solution of diazomethane was dropped into a solution of IIIa in 50 ml. of methanol which had been cooled with ice water. The reagent was added until a consistent yellow color remained. The residue which was obtained by evaporating the solution in vacuo was recrystallized from a mixture of ethyl acetate and petroleum ether. The colorless crystals melted at 170~175°C with decomposition. $[\alpha]_D^{20}$ +169.6 (*c* 1.256, ethyl acetate). The yield was 2.2 g. (65.7%).

Found: C, 56.73; H, 6.76; N, 3.75. Calcd. for $C_{18}H_{25}O_8N$: C, 56.39; H, 6.57; N, 3.65%.

Phenyl 2-Acetamido-3-*O*-(methyl D-1'-ethylcarboxylate)-2-deoxy-β-D-glucopyranoside (IVb).—One gram of a crude specimen of IIIb was treated with diazomethane as in the case of IVa. The crystalline product obtained melted at 216~217°C with decomposition. $[\alpha]_D^{14}$ +5.3 (*c* 3.90, pyridine). The yield was 0.7 g. (83%).

Found: C, 56.47; H, 6.57; N, 3.65. Calcd. for $C_{18}H_{25}O_8N$: C, 56.39; H, 6.56; N, 3.65%.

The Hydrolysis of IIa and IIb to 2-Amino-3-*O*-(D-1'-carboxyethyl)-2-deoxy-D-glucose (Muramic Acid).—IIa and IIb both gave a single spot of muramic acid on a papergram after hydrolysis with 2 N hydrochloric acid at 100°C for 4~5 hr. Runs were made along with an authentic muramic acid specimen in a solvent system of phenol-water (75 : 25); the R_f value of the spot developed with ninhydrin was about 0.51. These findings confirm the previously-assigned structures II—V.

Summary

A convenient method for the synthesis of anomeric phenyl glycosides of *N*-acetyl muramic acid and their methyl esters has been described. The test of lysozyme action on these model substrates was negative.

The expenses of this research were covered by U. S. Public Health Service Grant No. AI-04586-02.

The authors are indebted to Dr. James T. Park of the Department of Microbiology, Tufts University School of Medicine, for his gift of *N*-acetyl-glucosamine.

Department of Chemistry
Osaka University
College of Science
Kita-ku, Osaka

The Determination of Water Contents in Low Polymers of Formaldehyde by the Karl Fischer Method. II. The Determination of the Total Amounts of Adsorbed Water and Bound Water by the Methanol Absorption Method

By Kaname MUROI and Kunihiko OGAWA

(Received June 7, 1963)

In the previous paper,[1] the present authors reported a method for the determination of adsorbed water and bound water separately in low polymers of formaldehyde by using the Karl Fischer method. Recently, on the basis of the already-established method of determining the trace content of water in gases by Karl Fischer titration,[2] the same authors have developed a simple methanol absorption method for determining the sum of the amounts of adsorbed water and bound water in low polymers of formaldehyde. In the present method, the sample was pyrolyzed in a steam of dry nitrogen; the water vapor thus formed was absorbed in methanol, which was then titrated with a Karl Fischer reagent.

Experimental

Materials.—Both commercial-grade and special-class reagents of paraformaldehyde were used without further purification. The α-polyoxymethylene was supplied by our laboratory. The methanol was dried by magnesium metal. The propylene glycol was dried by boiling. The Karl Fischer reagent SS "Mitsubishi," free of methanol and supplied by the Mitsubishi Chemical Industries, was used (titer: 3.0 mg. H_2O/ml.).

Apparatus and Procedure. — The apparatus is illustrated in Fig. 1. Titration flask, F, was kept at about 10°C by running water through the jacket, G. One hundred milliliters of dry methanol was added to F through a side arm, H. Dry nitrogen, adjusted to a constant velocity of about 0.2 l./min., was passed to A, D and F. The methanol in F was titrated to the dead stop-end point with the Karl Fischer reagent. One to three grams of the sample were added to A through the side arm B. The tubing, D, was heated to about 100°C with a tape heater, E, and then A was heated at 200~250°C with a mantle heater, C. The water formed by pyrolyzing the sample was absorbed in cool methanol in F, and the water content in methanol was titrated every 5~10 min. with the Karl Fischer reagent. The dead stop-end point was attained after 30 min.; then the heating of A was stopped. The percentage of water was calculated from the titration value of the Karl Fischer reagent.

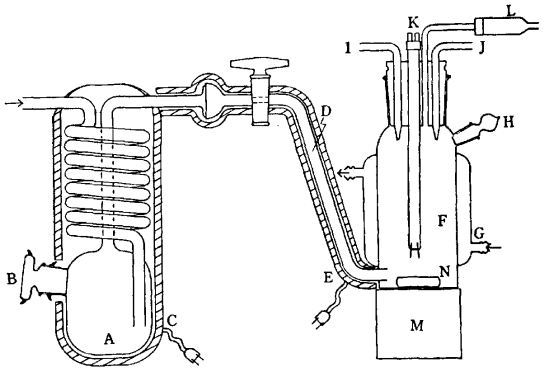

Fig. 1. Apparatus for the methanol absorption method.

A: Pyrolysis flask, 75 ml.
B: Side arm for sampling
C: Mantle heater, 200 W.
D: Conduit tube for gaseous formaldehyde
E: Tape heater, 100 W.
F: Titration flask, 200 ml.
G: Condenser
H: Side arm for methanol
I: Buret for standard water-in-methanol solution
J: Buret for Karl Fischer reagent
K: Platinum electrode
L: Outlet (with drying tube)
M: Magnetic stirrer
N: Stirrer bar

After A had been cooled to room temperature, the sample was added to A again through the side arm B, and the water contents was determined continuously by the same procedures. The bound water content was given by the difference in values between this method and the previously-reported methanol extraction method.[1]

Results and Discussion

In this method, the authors mainly attempted to find an adequate solvent to absorb the gas formed by the pyrolysis of the polymer. Since formaldehyde is known to be readily soluble in alcohols with evolution of heat and is known not to yield formaldehyde gas, the glycol reported in previous paper,[1] which

1) K. Muroi and K. Ogawa, This Bulletin, **36**, 965 (1963).
2) K. Muroi, *Japan Analyst (Bunseki Kagaku)*, **10**, 847 (1961).

Table I. Effects of interferences on the determination of water in formaldehyde at various temperature

Titration temp. °C	Nature of end point (visual titration)		Amount of water formed at 10 min's by interfering reaction in end point mg.
	Color change	Stability	
10	Good	Fairly stable	0
20	Good	Fairly stable	0
30	Good	Stable	0
40	Poor	Fades stowly	0.12
50	Very poor	Fades	0.35

do not react with formaldehyde below about 100°C, were first used as absorbing solvents of the gas; it was found, however, that the glycols did not absorb the gas completely. Then methanol, which has the strongest affinity for formaldehyde among primally alcohols, was used. The interference of formaldehyde with the Karl Fischer titration was studied. Mitchell et al.[3] have reported that formaldehyde does not interfere with the direct titration of an ordinary Karl Fischer reagent. On the contary, Iliceto et al.[4] have reported that formaldehyde interfered with the results of the Karl Fischer titration. To study the interference of the formaldehyde which was adsorbed in methanol, 3 g. of paraformaldehyde was pyrolyzed and absorbed in 50 ml. of methanol. Then the methanol solution was titrated with a Karl Fischer reagent at various temperatures. The water content thus measured and the nature of the titration end point visually observed are listed in Table I. It was found that the formaldehyde reacted with methanol very slowly above 30°C, and that it did not react at all below 30°C. From these results, as well as from the fact that the rate of the vaporization of methanol on the bubbling of a dry nitrogen carrier decrease with a decrease in the temperature, the methanol solution in flask F was kept at 10°C. Though the time necessary for analysis procedure not depended on the flow rate of the dry nitrogen carrier gas but, rather, mainly on the heating temperature of flask A, the optimum flow rate for reducing the vaporization loss of methanol was found to be 0.2 l./min. Table II lists the water content values in the various types of low polymers of formaldehyde determined by this method. An excellent reproducibility was obtained. Table III lists the water content values in the same samples as determined by this method and by the propylene glycol dissolution method reported in the previous paper.[1] The agreement between the two methods was remarkably good. When this method was compared with the propylene glycol dissolution method, it was found that this method had these advantages:

1) The operation of this method is simple, it is not affected by the moisture in the air, and the reproducibility is good.

2) The propylene glycol dissolution method can not be applied to samples pyrolized above about 170°C, but this method is applicable to such samples.

3) It has been found that the propylene glycol dissolution method is interfered with the small amount of an alkali component contained in commercially-available paraformaldehyde, but in this method, this small

Table II. Results of determination of water contents by methanol absorption method for various type of low polymer formaldehyde

Sample	Water content %
Commercial grade paraformaldehyde	13.64
	13.56
	13.73
Special grade reagent paraformaldehyde	2.30
	2.31
	2.31
α-Polyoxymethylene	0.61
	0.61
	0.61

Table III. Comparison of water contents in various type of low polymer of formaldehyde determined by methanol absorption method and propylene glycol dissolution method

Sample	Water content, %	
	Methanol absorption method	Propylene glycol dissolution method
85% Paraformaldehyde	13.64	13.68
95% Paraformaldehyde	3.45	3.46
Special grade reagent paraformaldehyde	2.31	2.31
α-Polyoxymethylene	0.61	0.61

3) W. M. D. Bryant, J. Mitchell, Jr. and D. M. Smith, *J. Am. Chem. Soc.*, 62, 3504 (1940).

4) A. Iliceto and S. Bezzi., *La Chemica e I. Industria*, 42, 728 (1960).

TABLE IV. RESULTS OF CALCULATIONS OF THE DEGREES OF POLYMERIZATION FROM THE CONTENT OF BOUND WATER

Sample	Water content, %		Bound water %	Degree of polymerization
	Methanol absorption method	Methanol extraction method		
85% Paraformaldehyde	13.58	7.86	5.72	10
95% Paraformaldehyde	3.45	0.53	2.72	21
Special grade reagent paraformaldehyde	2.31	0.30	2.01	30
α-Polyoxymethylene	0.61	0.24	0.37	162

TABLE V. RESULTS ON THE VARIATION OF WATER CONTENTS IN PARAFORMALDEHYDE IN AIR

	Days on shelf					
	0	1	3	5	7	10
Adsorbed water, %	8.1	7.8	7.6	6.6	4.2	2.7
Bound water, %	6.1	7.7	4.3	3.1	3.0	2.9

amount of an alkali component remains in the pyrolysis flask A and does not enter into the titration flask F; therefore, titration is not interfered with alkali. Table IV lists the adsorbed water content value and the summed content of adsorbed water and bound water in various types of low polymers of formaldehyde as determined by the methanol extraction method and by this method. The difference in the values corresponds to the content of bound water in the polymers from which the average degree of polymerization was calculated. Table V lists the results of the variation of adsorbed water and bound water in paraformaldehyde in air with time. At first, both adsorbed and bound water decreased rapidly. After 5 days, while bound water was stabilized at the value of about 3% (n=about 20), adsorbed water was still decreasing slowly. The authors are now studying the processes of the depolymerization of paraformaldehyde from the variation of adsorbed and bound water.

Summary

The summed content of adsorbed water and bound water in low polymers of formaldehyde has been determined by the following method: (1) The sample is pyrolized in a steam of dry nitrogen. (2) The water thus formed is absorbed in methanol. (3) The water content of the methanol solution is determined by titrating with a Karl Fischer reagent. A comparison between the present method and the propylene glycol dissolution method reported in the previous paper has made it evident that the present method is easy in its operations and is applicable to polymers having a wide range of polymerization. It has also been found that formaldehyde does not react with methanol below 30°C.

Central Research Laboratory
Mitsubishi Chemical Industries Ltd.
Kawasaki, Kanagawa

The Absorption Spectra of Cobalt(III) Complexes. III.[1] *The Spin-forbidden Bands*

By Junnosuke FUJITA and Yoichi SHIMURA

(Received May 11, 1963)

In marked contrast to the extensive work on the first and the second absorption bands of cobalt(III) complexes, relatively few investigations have been made of the weak absorption bands observed on the longer wavelength side adjacent to the first band. According to the ligand field theory,[2] the former two can be assigned to the spin-allowed transitions and the weak latter to the spin-forbidden transitions, although all these bands between the d levels of the cobalt(III) ion split because of the field perturbations of ligands.

Previously, Yoneda et al.[3] have reported on the existence of some weak absorption bands in the near infrared spectra (0.8~1.3 μ) of $[Co(CO_3)(NH_3)_4]NO_3$ and $K_3[Co\ ox_3]$. Inamura and Kondo[4] have also found weak bands in this region for some polynuclear cobalt(III) complexes. Later, Jørgensen[5] studied the nature of these weak bands and assigned them to the spin-forbidden transitions. More recently, Linhard and Weigel[6] have carefully measured the near infrared spectra of $[Co\ en_3]^{3+}$, $[Co(NH_3)_6]^{3+}$ and $[Co(X)(NH_3)_5]^{2+}$ ($X=F^-$, Cl^-, Br^-, I^-) and shown that each complex has two absorption bands due to the spin-forbidden transitions which correspond well with the theoretical assignment.[2] These two bands were named the A and the B bands, beginning from the longer wavelength side.

In order to investigate the nature of these A and B bands in more detail, as has been done for the first and the second bands,[1] we have measured the absorption spectra of about fifty complexes of cobalt(III). By combining these findings with those on the first and the second bands, it will be possible to discuss the experimental relationships among them in this paper.

Experimental

A Beckman DU spectrophotometer was used to obtain the absorption spectra in the range between 25 and 120 ($\times 10^{13}$/sec.). Aqueous solutions almost saturated were used to measure the near infrared spectra. All measurements were made at room temperature.

The complexes used in this work were prepared according to the methods described in the available literature, except for several new compounds which will be described below. All the compounds were recrystallized carefully before measuring the weak absorption bands.

***trans*-Chloro-nitro-bis(ethylenediamine)-cobalt(III) Perchlorate, *trans*-$[Co(Cl)NO_2\ en_2]ClO_4$.**—A finely powdered *trans*-$[Co(NO_2)_2\ en_2]NO_3$ was dissolved in hydrochloric acid (1 : 1). The crude product was precipitated from this clear solution by the addition of solid sodium perchlorate. The red precipitate which was filtered off was dissolved again in hydrochloric acid (1 : 1). The addition of perchloric acid (60%) to this solution resulted in the formation of orange red crystals, which were then filtered, washed with alcohol and dried in air. This complex was anhydrous.

Found: ClO_4^-, 27.1. Calcd. for $[Co(Cl)NO_2\text{-}en_2]ClO_4$: 27.6%.*

***trans*-Bromo-nitro-bis(ethylenediamine)-cobalt(III) Perchlolate, *trans*-$[Co(Br)NO_2\ en_2]ClO_4$.**—The mixture of 4 g. *trans*-$[Co(NO_2)_2\ en_2]Br\cdot 2H_2O$ and 6 ml. concentrated hydrobromic acid ($d=1.48$) was warmed on a water bath while being stirred. After the evolution of gas ceased, the resulting materials were kept in a cool place for a while. Then the precipitate was separated; it was the crude product of *trans*-$[Co(Br)NO_2\ en_2]Br$ and could be recrystallized from concentrated hydrobromic acid by the addition of acetone. The pure perchlorate was prepared by the addition of perchloric acid (60%) to the solution of this precipitate in concentrated hydrobromic acid. The complex was separated as anhydrous, brownish red crystals.

Found: ClO_4^-, 23.8. Calcd. for $[Co(Br)NO_2\text{-}en_2]ClO_4$: 24.6%

Tetrammine-mono(ethylenediamine)-cobalt(III) Bromide Monohydrate, $[Co(NH_3)_4\ en]Br_3\cdot H_2O$.—This complex was prepared by the method described previously.[8]

Potassium Pentacyano-nitro-cobaltate(III), $K_3[Co(CN)_5NO_2]$.—The mixture containing 8 g. of $[Co(NO_2)(NH_3)_5]Cl_2$ and 10 g. of potassium cyanide

1) Parts I and II of this series: Y. Shimura and R. Tsuchida, This Bulletin, **28**, 572 (1955); **29**, 311 (1956).
2) Y. Tanabe and S. Sugano, *J. Phys. Soc. Japan*, **9**, 766 (1954).
3) H. Yoneda, S. Kida and M. Kobayashi, *J. Chem. Soc. Japan, Pure Chem. Sec.* (*Nippon Kagaku Zassi*), **73**, 518 (1952).
4) Y. Inamura and Y. Kondo, ibid., **74**, 627 (1953).
5) C. K. Jørgensen, *Acta Chem. Scand.*, **8**, 152 (1953).
6) M. Linhard and M. Weigel, *Z. physik. Chem. N. F.*, **11**, 308 (1957).
* For the analysis of the perchlorate ion, the method of Linhard and Stirn[7] was employed.
7) M. Linhard and G. Stirn, *Z. anorg. Chem.*, **265**, 105 (1952).
8) Y. Shimura, This Bulletin, **31**, 311 (1958).

TABLE I. SUMMARY OF THE MEASUREMENT

The frequencies are given in 10^{13}/sec., and the intensities by log ε in parentheses

Complex	A Band	B Band	I Band	II Band	B–A	II–I	I–A	Ref.
$[Co(NH_3)_6]Cl_3$	40.1(1.42)	ca. 51(1.8)	62.9(1.76)	88.3(1.68)	10.9	25.4	22.8	
$[Co\ en_3]Cl_3 \cdot 3H_2O$	41.5(1.52)	ca. 52(1.8)	63.9(1.94)	88.4(1.90)	10.5	24.5	22.4	
$[Co(NH_3)_4\ en]Br_3 \cdot H_2O$	40.8(1.47)	ca. 51(1.9)	63.6(1.83)	88.4(1.76)	10.2	24.8	22.8	
$[Co\ dip_3](ClO_4)_3 \cdot 3H_2O$	43.5(0.04)	—	66.6(1.84)	—	—	—	23.1	9
$[Co\ en_2\ phen]SO_4Cl \cdot 2H_2O$	42.2(1.88)	—	64.6(2.01)	—	—	—	22.4	9
$[Co(l\text{-}leu)\ en_2]Cl_2$	38.0(1.72)	ca. 49(0.1)	61.5(2.02)	86.1(2.06)	11.0	24.6	23.5	
$[Co\ ox(NH_3)_4]Cl$	35.8(1.81)	ca. 46(0.0)	58.7(1.91)	84.0(2.11)	10.2	25.3	22.9	
$[Co\ CO_3en_2]Cl \cdot H_2O$	34.7(0.05)	ca. 45(0.3)	58.4(2.13)	83.0(2.09)	10.3	24.6	23.7	
$[Co(phthal)en_2]Br \cdot 3H_2O$	ca. 33 (1.91)	ca. 43(0.1)	55.6(1.92)	ca. 85 (2.07)	10.0	19.4	22.6	9
$[Co(salic)(NH_3)_4]Cl \cdot H_2O$	35.0(0.18)	—	56.6(2.20)	ca. 78 (2.5)	—	21.4	21.0	9
$[Co(salic)en_2]Cl \cdot 2H_2O$	37.0(0.08)	—	58.2(2.36)	ca. 79 (2.6)	—	20.8	21.2	9
fac-$[Co(gly)_3] \cdot H_2O$	33.0(0.02)	ca. 46(0.3)	57.7(2.20)	80.2(2.15)	13.0	22.5	24.7	
mer-$[Co(gly)_3] \cdot 2H_2O$	29.8(1.82)	ca. 42(1.9)	55.7(2.00)	80.6(2.18)	12.2	24.9	25.9	
fac-$[Co(dl\text{-}ala)_3]$	33.2(0.12)	ca. 45(0.3)	57.9(2.27)	80.3(2.21)	11.8	22.4	24.7	
mer-$[Co(dl\text{-}ala)_3]$	30.3(1.96)	ca. 43(0.1)	55.6(2.00)	80.9(2.18)	12.7	25.3	25.3	
fac-$[Co(picol)_3]$	34.6(0.22)	ca. 46(0.3)	58.3(2.17)	79.6(2.24)	11.4	21.3	23.7	9
mer-$[Co(picol)_3]$	ca. 34 (0.08)	—	57.8(2.02)	80.0(2.34)	—	22.2	23.8	9
cis-$NH_4[Co\ ox_2(NH_3)_2] \cdot H_2O$	31.2(0.02)	ca. 42(0.3)	54.0(2.04)	78.2(2.30)	10.8	24.2	22.8	
cis-$K[Co(CO_3)_2(NH_3)_2] \cdot 3H_2O$	27.3(0.64)	ca. 40(0.9)	52.2(2.24)	76.0(2.41)	12.7	23.8	24.9	10
$Na[Co\ ox_2en] \cdot H_2O$	33.3(1.91)	ca. 44(0.2)	55.6(1.93)	77.9(2.12)	10.7	22.3	22.3	10
$K[Co\ malo_2en] \cdot H_2O$	33.3(0.02)	ca. 43(0.2)	55.6(1.96)	77.9(2.08)	9.7	22.3	22.3	10
$Na[Co\ edta] \cdot 4H_2O$	30.8(1.96)	ca. 43(0.4)	55.9(2.51)	78.1(2.36)	12.2	22.2	25.1	
cis-(N)-$K[Co(ada)_2] \cdot 3/2H_2O$	28.4(0.00)	ca. 41(0.2)	53.4(2.18)	79.0(2.13)	12.6	25.6	25.0	10
cis-(N)-$K[Co(ata)gly] \cdot 2H_2O$	27.3(0.07)	ca. 40(0.3)	53.0(2.35)	78.2(2.23)	12.7	25.2	25.7	10
$K_3[Co\ ox_3] \cdot 3H_2O$	25.0(0.25)	ca. 38(0.5)	49.7(2.17)	70.9(2.30)	13.0	21.2	24.7	
cis-$[Co(Cl)NH_3en_2]Cl_2 \cdot 2H_2O$	35.8(1.64)	ca. 47(0.1)	56.9(1.86) 65.6(1.36)	82.2(1.87)	11.2	25.3	21.1	14
cis-$[Co(NO_2)_2en_2]Cl$	ca. 45 (1.8)	—	68.8(2.27)	—	—	—	23.8	
trans-$[Co(NO_2)_2en_2]Cl$	ca. 48 (1.5)	—	70.0(2.30)	—	—	—	22.0	
trans-$[Co(Cl)NO_2en_2]ClO_4$	ca. 41 (1.6)	—	62.5(1.97)	—	—	—	21.5	
trans-$[Co(Br)NO_2en_2]ClO_4$	ca. 42 (0.7)	—	60.0(2.12)	—	—	—	18.0	
cis-$[Co(N_3)_2(NH_3)_4]ClO_4$	33.0(0.12)	—	55.8(2.42)	—	—	—	22.8	
trans-$[Co(N_3)_2(NH_3)_4]N_3$	31.8(1.86)	—	53.0(2.49)	—	—	—	21.2	
$Na_2[Co(NO_2)edta] \cdot 3H_2O$	26.4(1.81)	ca. 38(1.9)	51.4(1.97) 60.4(2.32)	—	11.6	—	25.0	
$K_2[Co(Cl)edta] \cdot 3H_2O$	27.2(1.89)	ca. 39(0.3)	51.6(2.38)	74.5(2.43)	11.8	22.9	24.4	
$Na[Co(Br)edtaH] \cdot 3H_2O$	30.0(0.25)	ca. 39(0.6)	51.0(2.34)	—	9.0	—	21.0	
$K_3[Co(CN)_6]$	ca. 75 (1.9)	—	96.8(2.29)	116.8(2.12)	—	20.0	21.8	
$K_4[Co(CN)_5SO_3] \cdot 3H_2O$	ca. 70 (0.7)	—	89.6(2.59)	—	—	—	19.6	
$K_3[Co(CN)_5NO_2]$	ca. 66 (0.9)	—	ca. 86 (2.5)	—	—	—	20	
$K_3[Co(CN)_5N_3] \cdot 2H_2O$	ca. 57 (1.9)	—	78.9(2.86)	—	—	—	21.9	
$K_3[Co(CN)_5Cl]$	59.6(0.04)	—	76.9(2.31)	ca. 99 (2.1)	—	22.1	17.3	11
$K_3[Co(CN)_5Br]$	58.4(0.95)	—	75.6(2.21)	—	—	—	17.2	11
$K_3[Co(CN)_5I]$	60.7(1.98)	—	ca. 73 (2.3)	—	—	—	13.7	11
$[Co(CN)_2en_2](SO_4)_{1/2} \cdot 3/2H_2O$	49.6(1.71)	—	74.4(1.95)	97.3(1.94)	—	22.9	24.8	

dissolved in 100 ml. of water was warmed on a water-bath while being stirred. After the evolution of gaseous ammonia, the orange yellow solution obtained was filtered and kept at room temperature for a while. The addition of methanol to the solution gave a pale yellow precipitate, which was then filtered off, washed with alcohol and ether, and dried in air. Recrystallization from the aqueous solution to obtain well-formed pale yellow crystals was effected by the slow addition of methanol and by leaving it to stand in a refrigerator.

Found: Co, 16.5; C, 16.40; N, 23.51. Calcd. for $K_3[Co(CN)_5NO_2]$: Co, 16.73; C, 17.05; N, 23.85%.

Potassium Pentacyano-azido-cobaltate(III) Dihydrate, $K_3[Co(CN)_5N_3]\cdot 2H_2O$.—The recrystallized yellow crystals of this complex were obtained by almost the same method as the nitro-complex, described above, using 8.4 g. of $[Co(N_3)(NH_3)_5]Cl_2$ and 10 g. of potassium cyanide. The only difference was that the reaction took place at room temperature, without the complex being warmed on a water-bath.

Found: Co, 15.8; C, 15.77; N, 30.15; H_2O, 9.53. Calcd. for $K_3[Co(CN)_5N_3]\cdot 2H_2O$: Co, 15.33; C, 15.75; N, 29.15; H_2O, 9.37%.

Potassium Pentacyano-sulfono-cobaltate(III) Trihydrate, $K_4[Co(CN)_5SO_3]\cdot 3H_2O$.—To 50 ml. of an aqueous solution containing 10 g. of $K_3[Co(CN)_5Br]$, 5 g. of $K_2SO_3\cdot 2H_2O$ dissolved in 50 ml. of water was added. The resulting solution was heated on a water-bath until the initial reddish color turned pale yellow. After the solution had cooled, the addition of methanol to the filtered solution gave pale-yellow crystals, which were then filtered off, washed with alcohol and ether, and dried in air. These were recrystallized from the aqueous solution by the addition of methanol.

Found: Co, 12.5; C, 12.26; N, 15.08; H_2O, 11.52. Calcd. for $K_4[Co(CN)_5SO_3]\cdot 3H_2O$: Co, 12.29; C, 12.52; N, 14.60; H_2O, 11.27%.

Results and Discussion

In Table I are listed the numerical data for the A, the B, the first, and the second absorption bands. Some typical absorption curves of all the spectra measured are shown in Figs. 1—6.

From these data, the following conclusions may be obtained.

1) The spectrochemical series[1,12] determined experimentally for the first and the second bands is also valid for the A and the B bands. This indicates that the lower the frequencies of the first and the second bands, the lower the corresponding A and B bands. In Fig. 1, the spectra of the cobalt(III) complexes of the ammine-oxalato series are shown to illustrate how the successive substitutions of ammonia by oxalate ions cause shifts in all these bands and how the magnitude of the shifts is proportional to the degree of substitution.[1]

2) As may be seen in Fig. 7, there is a linear relationship between the frequencies of the A band and those of the first band. A similar relation is seen between the first and the second bands[13] (Fig. 8), and also between the A and the B bands (Fig. 9). This indicates that these bands are closely related to

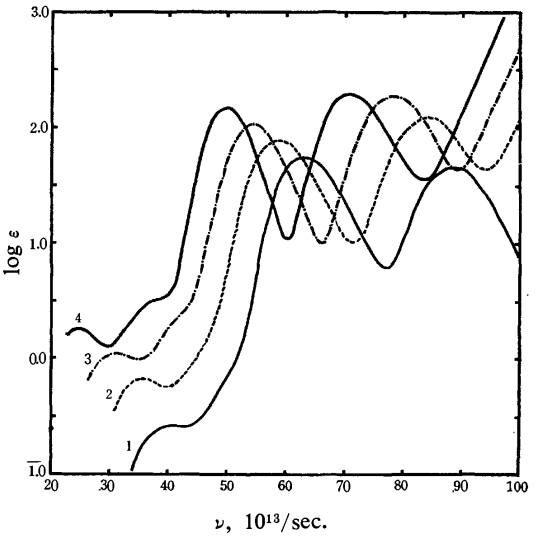

Fig. 1. Absorption spectra of: 1, $[Co(NH_3)_6]^{3+}$; 2, $[Co\,ox(NH_3)_4]^{+}$; 3, $[Co\,ox_2(NH_3)_2]^{-}$; 4, $[Co\,ox_3]^{3-}$.

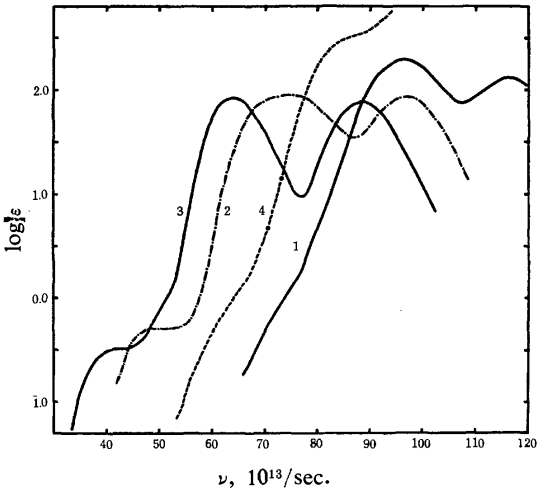

Fig. 2. Absorption spectra of: 1, $[Co(CN)_6]^{3-}$; 2, $[Co(CN)_2en_2]^{+}$; 3, $[Coen_3]^{3+}$; 4, $[Co(CN)_5SO_3]^{4-}$.

9) N. Matsuoka, Y. Shimura and R. Tsuchida, *J. Chem. Soc. Japan, Pure Chem. Sec.* (*Nippon Kagaku Zasshi*), **82**, 1637 (1961).
10) J. Hidaka, Y. Shimura and R. Tsuchida, This Bulletin, 35, 567 (1962).
11) J. Fujita, will be reported in detail later.
12) R. Tsuchida, This Bulletin, **13**, 388, 436 (1938).
13) K. Sone, *J. Chem. Soc. Japan, Pure Chem. Sec.* (*Nippon Kagaku Zassi*), **71**, 270, 316 (1950).

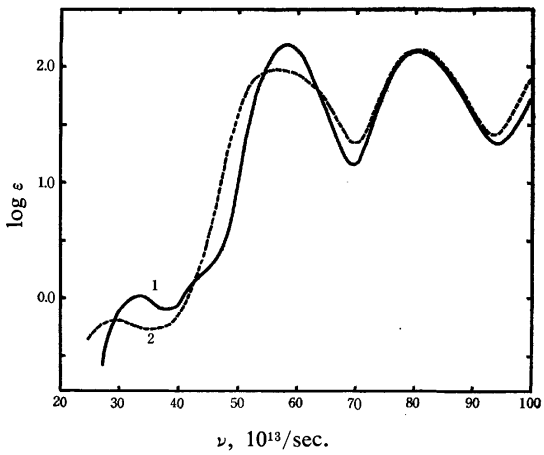

Fig. 3. Absorption spectra of: 1, fac-[Co(gly)$_3$]; 2, mer-[Co(gly)$_3$].

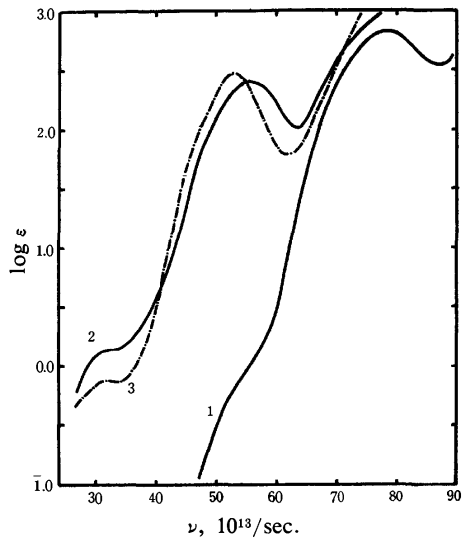

Fig. 4. Absorption spectra of: 1, $[Co(CN)_5N_3]^{3-}$; 2, *cis*-$[Co(N_3)_2(NH_3)_4]^+$; 3, *trans*-$[Co(N_3)_2(NH_3)_4]^+$.

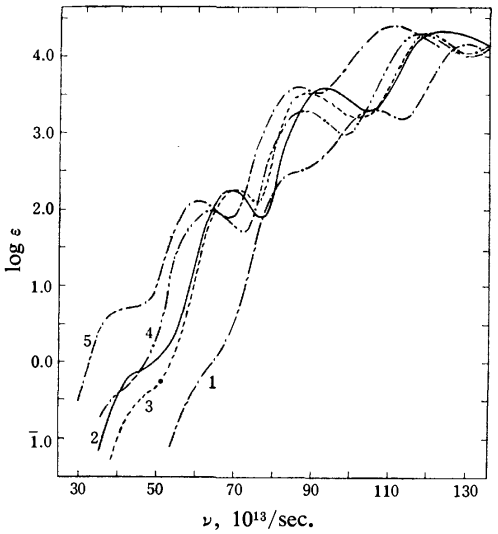

Fig. 5. Absorption spectra of: 1, $[Co(CN)_5NO_2]^{3-}$; 2, *cis*-$[Co(NO_2)_2\,en_2]^+$; 3, *trans*-$[Co(NO_2)_2\,en_2]^+$; 4, *trans*-$[Co(Cl)NO_2\,en_2]^+$; 5, *trans*-$[Co(Br)NO_2\,en_2]^+$.

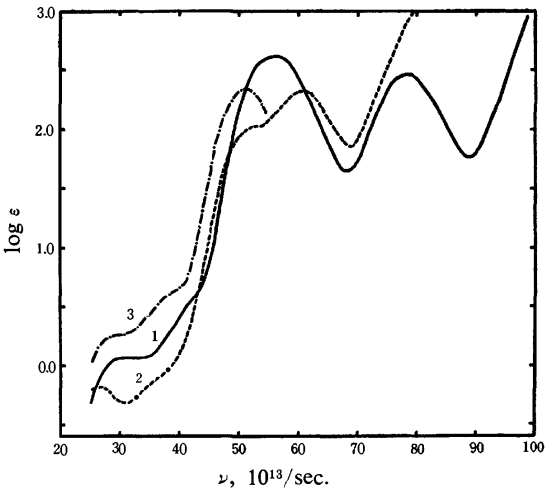

Fig. 6. Absorption spectra of: 1, [Co edta]$^-$; 2, [Co(NO$_2$) edta]$^{2-}$; 3, [Co(Br) edtaH]$^-$.

each other in origin, in agreement with the theoretical assignment.

3) The slope of the straight line for the relation between the A band and the first band (Fig. 7) indicates that the frequency separation between these bands becomes smaller as the first band shifts to a shorter wavelength. For this reason, the spin-forbidden bands, especially the B band, of a complex, the first band of which appears in the shorter wavelength region, are often hidden by the strong first band. For the ion $[Co(CN)_6]^{3-}$, for example, only the band is observed as a shoulder on the foot of the first band, as may be seen in Fig. 2.

4) The absorption intensities of the A and the B bands are usually about 1/100 as weak as those of the first and the second bands. For most complexes, as the intensity of the first band increases, the intensity of the A band increases also. A parallel relationship exists, therefore, between the first and the A bands in both the frequencies of absorption maxima and the intensities. Figures 1 and 3 show such relationships clearly.

5) The absorption curves shown in Figs. 4 and 5 indicate that the absorption intensity of the A band in a cis-complex is higher than that in the corresponding trans-complex. This may be due to the lower molecular symmetry in a cis-complex as compared with that in a trans-complex.

6) The absorption intensities of the A bands

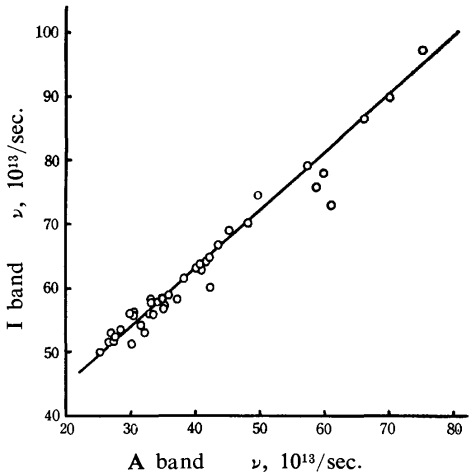

Fig. 7. The linear relation between the A and the I bands.

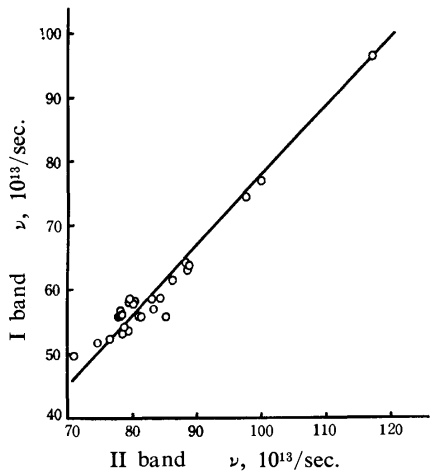

Fig. 8. The linear relation between the I and the II bands.

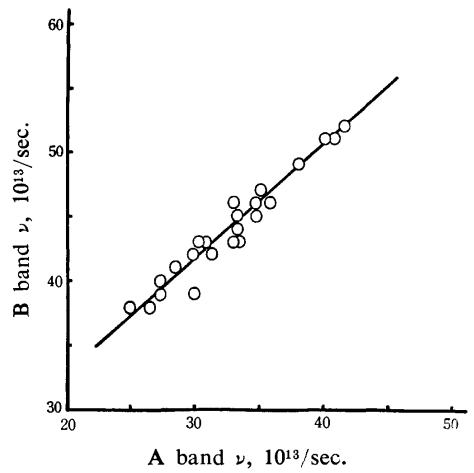

Fig. 9. The linear relation between the A and the B bands.

in bromo-complexes are quite high compared with those of the other complexes (Figs. 5 and 6). The same observation has been made on the spectrum of $[Co(Br)(NH_3)_5]^{2+}$ by Linhard and Weigel.[6] Furthermore, the linear relationship mentioned above between the maximum positions of the first band and those of the A band does not hold for these bromo-complexes. If the data for the bromo-complexes are plotted, as in Fig. 7, these points deviate considerably from a straight line. In other halogeno-complexes such as $[Co(I)(NH_3)_5]^{2+}$,[6] *cis*- and *trans*-$[Co(X)NH_3\,en_2]^{2+}$ ($X=Br^-$, I^-)[14] or a series of halogeno-pentacyanocobalt(III) complexes, $[Co(CN)_5X]^{3-}$ ($X=Cl^-$, Br^-, I^-),[11] the same anomalies have been observed.

7) As may be seen in Figs. 3 and 6, in a complex the first band of which splits, the A band is broad. This indicates that the band splittings may also occur in the A bands. In the case of $[Co(NO_2)edta]^{2-}$, a linear relationship for the A and the first bands shown in Fig. 7 exists, if the observed A band is plotted against the low frequency component (Ia) of the first band. If the mean frequency of the two components of the first band is taken, however, the linear relationship breaks down. This suggests that the other component of the A band which corresponds to the high frequency component of the first band (Ib) may be hidden under or may be overlapped by the B band.

All the conclusions 1)—7) mentioned above coincide well with the theoretical assignments of the weak bands A and B to the spin-forbidden transitions, $^1A_{1g}\rightarrow{}^3T_{1g}$ and $^1A_{1g}\rightarrow{}^3T_{2g}$ respectively, in the expression of an O_h-symmetry approximation. The numerical data listed in Table I may be useful in determining the "nephelauxetic series"[15] of these low-spin d^6 complexes.

Summary

The near infrared, visible and near ultraviolet absorption spectra of about fifty complexes of cobalt(III) have been measured and the data discussed mainly in order to find the relationships existing among the two weak spin-forbidden bands and the two well-known spin-allowed bands.

Department of Chemistry
Faculty of Science
Osaka University
Nakanoshima, Osaka

14) T. Yasui and Y. Shimura, This Bulletin, 36, 1286 (1963).
15) C. E. Schäffer and C. K. Jørgensen, *J. Inorg. Nuclear Chem.*, 8, 143 (1958); C. K. Jørgensen, *Progr. Inorg. Chem.*, 4, 73 (1962).

The Absorption Spectra of Cobalt(III) Complexes. IV.[1] *The Preparation and the Absorption Spectra of Monohalogenomonoamine-bis(ethylenediamine)-cobalt(III) Complexes*

By Takaji YASUI and Yoichi SHIMURA

(Received May 11, 1963)

It is well known that $[Co\,Cl(amine)en_2]^{2+}$ and $[Co\,Br(amine)en_2]^{2+}$ ions are formed in the reactions of chloro- and bromo-praseo salts, respectively, with aliphatic or aromatic primary amines,[2-4] but not with secondary and tertiary amines. In the cases of $[Co\,Cl(NH_3)en_2]^{2+}$ and $[Co\,Br(NH_3)en_2]^{2+}$ ions, both the cis and the trans isomers have been prepared by Werner,[5] and the cis salts have been resolved into the optically active isomers. The geometrical structures of the complexes containing organic amines, however, have not been precisely determined. A few studies[2,4] have been made trying to resolve the complexes by the use of α-bromo-*d*-camphorsulfonate, but none of these efforts have succeeded. Bailar and Clapp[4] investigated the reactions of an optically-active violeo salt with the organic amines, but they could not isolate the reaction products with optical activities, except for an optically-active complex of *p*-toluidine, *cis*-$[Co\,Cl(p\text{-toluidine})en_2]\,Cl_2$.

In the present paper, a few complexes which belong to the corresponding iodo series, i. e., *trans*- and *cis*-$[Co\,I(NH_3)en_2]\,I_2$ and *cis*-$[Co\,I(amine)en_2]\,I_2$ (amine = methylamine and pyridine), have been newly synthesized. Furthermore, some missing members of the chloro and the bromo series have also been prepared. The absorption spectra of the complexes have been measured in the region of 210~1200 mμ, with especially great care in the near-infrared region, and the results will be discussed mainly in relation to the geometrical structures of the complex ions.

Experimental

Measurements.—A Beckman DU quartz spectrophotometer was used for the measurements of the absorption spectra in the 210~1200 mμ region. All the aqueous solutions of the complexes obeyed Beer's law at concentrations of $1\sim10^{-5}$ mol./l. The measurements for the dilute solutions were made rapidly in the cold to avoid the aquotization of the complex ions.

The absorption spectrum of *cis*-$[Co\,I(NH_3)en_2]I_2$ coincided well with that of the corresponding chloride, *cis*-$[Co\,I(NH_3)en_2]Cl_2$. Therefore, the effects of the outer-sphere anions have not been considered as long as no extra hydrogen halide or halide salt was added to the sample solutions.

Materials.—*trans-[Co Cl(NH$_3$)en$_2$]Cl$_2$·H$_2$O.*— This compound was prepared from *trans*-$[Co\,Cl(NCS)\text{-}en_2]NCS$ by the procedure of Werner.[6] The color of the crystals isolated was ruby red.

cis-[Co Cl(amine)en$_2$]Cl$_2$.—The complex containing NH_3 instead of amine was prepared by the method of Werner[7] and was recrystallized from concentrated hydrochloric acid. The crystals were reddish in color and needle-shaped. The compounds containing methyl-, ethyl- or *n*-propyl-amine, or pyridine, instead of ammonia, were prepared by similar procedures. The *n*-propylamine complex is a new compound.

Found: C, 23.18; H, 7.50; N, 19.31; H_2O, 4.82. Calcd. for $C_7H_{25}N_5Cl_3Co\cdot H_2O = [Co\,Cl(C_3H_9N)(C_2H_8N_2)_2]Cl_2\cdot H_2O$: C, 23.43; H, 7.50; N, 19.16; H_2O, 4.96%.

cis-[Co Cl(aniline)en$_2$]Cl$_2$.— This complex was prepared by the method of Bailar and Clapp.[4] The toluidine complex, *cis*-$[Co\,Cl(p\text{-toluidine})en_2]Cl_2\cdot H_2O$, was obtained by a similar method. These complexes of aromatic amines are less soluble in water than those of aliphatic amines.

trans-[Co Br(NH$_3$)en$_2$]Br$_2$·H$_2$O. — The compound was obtained by the method of Werner,[8] but this was somewhat modified as follows. A pure complex, *trans*-$[Co(OH_2)(NH_3)en_2]Br_3$, was suspended in an appropriate amount of concentrated hydrobromic acid and was gently heated to 70°C. After being kept for a few minutes at this temperature, the color of the solution changed from orange to violet. This solution was then cooled to room temperature and alcohol was added. By letting the solution stand in an ice-bath, the compound was obtained as reddish violet crystals.

cis-[Co Br(NH$_3$)en$_2$]Br$_2$·H$_2$O. — This salt was obtained by the reactions of the bromo-praseo salt, *trans*-$[Co\,Br_2en_2]Br$, with aqueous ammonia upon

1) Part III of this series: J. Fujita and Y. Shimura, This Bulletin, **36**, 1281 (1963).
2) J. Meisenheimer and E. Kiderlen, *Ann.*, **438**, 238 (1924).
3) A. Ablov, *Bull. soc. chim. France*, 3, 2270 (1936); 4, 1783 (1937).
4) J. C. Bailar, Jr., and L. B. Clapp, *J. Am. Chem. Soc.*, **67**, 171 (1945).
5) A. Werner, *Ann.*, **386**, 55 (1912); *Ber.*, 44, 1887 (1911).
6) A. Werner, *Ann.*, **386**, 176 (1912).
7) A. Werner, ibid., **386**, 55 (1912).
8) A. Werner, ibid., **386**, 182 (1912).

cooling in a freezing mixture.[9] The same compound was also obtained by dehydrating *cis*-[Co(OH$_2$)(NH$_3$)en$_2$]Br$_3$ in a drying apparatus.

cis-[Co Br(methylamine)en$_2$]Br$_2$. — This compound was prepared by the same procedure as was the ammine complex, *cis*-[Co Br(NH$_3$)en$_2$]Br$_2$.

cis-[Co Br(amine)en$_2$]Br$_2$.—The ethylamine, *n*-propylamine and pyridine complexes were easily synthesized from bromo-praseo salt and the respective amines. The latter two complexes are new.

Found: C, 17.86; H, 5.23; N, 14.70. Calcd. for $C_7H_{25}N_5Br_3Co$=[Co Br(C_3H_9N)($C_2H_8N_2$)$_2$]Br$_2$: C, 17.59; H, 5.27; N, 14.65%.

Found: C, 21.70; H, 4.28; N, 14.25. Calcd. for $C_9H_{21}N_5Br_3Co$=[Co Br(C_5H_5N)($C_2H_8N_2$)$_2$]Br$_2$: C, 21.71; H, 4.25; N, 14.06%.

trans-[Co I(NH$_3$)en$_2$]I$_2$. — A finely powdered, pure complex, *trans*-[Co(OH$_2$)(NH$_3$)en$_2$]I$_3$,[10] was spread on a watch-glass and was dehydrated in vacuo at room temperature for two or three days. The color of the powder changed from brown to brownish-black. The crude product obtained was purified as follows. A more soluble by-product was extracted by a small amount of water; the greenish residue remaining was then dissolved in a large quantity of water, and the solution was filtered. In an ice-bath, the greenish crystals were deposited from the filtrate. The crystals collected by filtration were recrystallized repeatedly from water by the addition of potassium iodide. The greenish-brown crystals obtained were washed with cold water, with alcohol, and then with acetone. The trans-salt was less soluble in water than the corresponding cis salt.

Found: C, 8.31; H, 3.57; N, 12.00. Calcd. for $C_4H_{19}N_5I_3Co$=[Co I(NH$_3$)($C_2H_8N_2$)$_2$]I$_2$: C, 8.33; H, 3.32; N, 12.14%.

cis-[Co I(NH$_3$)en$_2$]I$_2$.—Purified *cis*-[Co(OH$_2$)(NH$_3$)en$_2$]I$_3$ was spread on a watch-glass and dehydrated in a drying apparatus at 70~75°C for about three hours. The color of the compound gradually changed from brown to brownish-black. The crude product was dissolved in a little amount of water, and then the solution was filtered. To the filtrate, powdered potassium iodide was added. After this solution had cooled in an ice-bath, a large number of dark brown, hexagonal crystals were deposited. The product separated by filtration was recrystallized from water by the addition of potassium iodide, and it was washed with cold water, with alcohol and then with acetone.

Found: C, 8.15; H, 3.50; N, 12.15. Calcd. for $C_4H_{19}N_5I_3Co$=[Co I(NH$_3$)($C_2H_8N_2$)$_2$]I$_2$: C, 8.33; H, 3.32; N, 12.14%.

cis-[Co I(methylamine)en$_2$]I$_2$. — Twenty grams of *cis*-[Co Cl(methylamine)en$_2$]Cl$_2$·H$_2$O was dissolved in 30 ml. of an aqueous solution of potassium hydroxide (1:5). After it had stood for a while, the solution was filtered with a glass filter. When an excess of concentrated hydrobromic acid was added to the filtrate drop by drop and cooled in an ice-bath, crystals began to deposit. After the solution had cooled in an ice-bath for a few hours, a large amount of the mono-aquo bromide, [Co(OH$_2$)(methylamine)en$_2$]Br$_3$ was obtained. This complex was transformed to the iodide by double decomposition with potassium iodide.

By the dehydration of the mono-aquo iodide, [Co(OH$_2$)(methylamine)en$_2$]I$_3$, at 80~85°C for two to three hours, a crude, brownish-black product was obtained. The recrystallization was made by a procedure to that used with *trans*-[Co I(NH$_3$)en$_2$]I$_2$. After repeated recrystallizations, the crystal was a dark greenish-brown, hexagonal plate. This is sparingly soluble in water.

Found: C, 10.40; H, 3.69; N, 11.68. Calcd. for $C_5H_{21}N_5I_3Co$=[Co I(CH_5N)($C_2H_8N_2$)$_2$]I$_2$: C, 10.16; H, 3.58; N, 11.85%.

cis-[Co I(pyridine)en$_2$]I$_2$. — The aquo complex, [Co(OH$_2$)(pyridine)en$_2$]I$_3$, was obtained by a method similar to that used for the methylamine complex, and this was dehydrated at 70~80°C for a day. From the crude product, a more soluble substance was extracted with a little water. A large amount of water was saturated with the greenish residue, and the solution was filtered. A few drops of saturated potassium iodide solution were then added to the filtrate. The solution was cooled in an ice-bath until dark green, octahedral crystals were deposited. A pure sample was sparingly soluble in water.

Found: C, 17.22; H, 3.35; N, 10.54. Calcd. for $C_9H_{21}N_5I_3Co$=[Co I(C_5H_5N)($C_2H_8N_2$)$_2$]I$_2$: C, 16.92: H, 3.31; N, 10.96%.

The aquo complexes, [Co(OH$_2$)(aniline)en$_2$]I$_3$ and [Co(OH$_2$)(*p*-toluidine)en$_2$]I$_3$, which were obtained by procedures similar to those used for the pyridine complex, were unstable. Therefore, the corresponding iodo-amine complexes could not be isolated.

Results and Discussion

The Near-infrared Absorption Spectra. — It has been known that the cobalt(III) complexes generally have two weak absorption bands in the near-infrared region,[1,11-13] of which the band appearing at the longer wavelength is named the A band and the band at the shorter wavelength, the B band. In most cases the B band is overlapped by the so-called first band, which is located just adjacent to the B band in a shorter wavelength and which has a moderate intensity.

The absorption maxima of the complexes of the [Co X(NH$_2$-R)en$_2$]X$_2$ type, which were measured in aqueous solutions, are summarized in Table I. In Figs. 1 and 3—5, the representative absorption curves are shown. As may be understood from the table and the figures, the molar extinction coefficients of the A bands increase by a factor of about ten in each substitution of the ligand X in the

9) A. Werner, ibid., **386**, 111 (1912).
10) A. Werner, ibid., **386**, 185 (1912).
11) C. K. Jørgensen, *Acta Chem. Scand.*, **8**, 1502 (1954).
12) M. Linhard and M. Weigel, *Z. physik. Chem. N. F.*, 11, 308 (1957).
13) Y. Tanabe and S. Sugano, *J. Phys. Soc. Japan*, **9**, 766 (1954).

TABLE I. ABSORPTION MAXIMA OF THE $[Co\,X(NH_2\text{-}R)en_2]X_2$-TYPE COMPLEXES

ν_{max} 10^{13} sec^{-1} (log ε)

Structure	R-NH_2*	X	A Band	I Band		II Band	Charge transfer band	
				Ia	Ib**			
trans	NH_3	Cl	34.1(ī.52)	56.7(1.62)	66.2(1.28)	83.3(1.66)	109.7(2.98)	133 (4.28)
		Br	33.3(0.67)	55.1(1.71)	66.4(1.30)		93.8(2.81)	120 (4.24)
		I	32.7(1.47)	52.2(1.85)			78.5(3.41)	105.5(4.23)
cis	NH_3	Cl	35.8(ī.64)	56.9(1.86)	65.6(1.36)	82.2(1.87)	110.3(2.98)	131 (4.28)
		Br	33.9(0.69)	55.6(1.92)	65.0(1.43)		94.7(2.85)	117 (4.24)
		I	33.3(1.50)	52.5(2.06)			80.0(3.48)	105 (4.25)
cis	Me-NH_2	Cl	35.3(ī.69)	56.9(1.89)	65.0(1.40)	81.8(1.92)	108.8(3.02)	131 (4.29)
		Br	33.3(0.64)	55.1(1.90)			94.7(2.88)	119 (4.27)
		I	33.0(1.47)	52.2(2.04)			79.0(3.45)	105 (4.22)
cis	Et-NH_2	Cl	35.1(ī.66)	56.9(1.87)	64.8(1.41)	81.8(1.92)	108.7(3.00)	131.5(4.30)
		Br	33.0(0.66)	55.1(1.91)			94.5(2.89)	119 (4.27)
cis	Pr-NH_2	Cl	35.0(ī.69)	56.9(1.89)	64.6(1.43)	81.7(1.94)	109.0(3.00)	131 (4.35)
		Br	33.3(0.64)	55.0(1.92)			94.5(2.90)	119 (4.30)
cis	Py	Cl	35.6(ī.73)	57.1(1.88)	64.6(1.49)	81.5(1.91)	106.6(2.94)	129 (4.38)
		Br	33.3(0.71)	55.1(1.93)			91.1(2.88)	116 (4.24)
		I	33.2(1.57)	51.7(2.05)			75.0(3.41)	100.5(4.18)
cis	Anil	Cl	ca. 34.5(ī.96)	56.5(2.01)				
		Br	32.7(0.63)	55.0(1.93)				
cis	Tol	Cl	ca. 34.3(ī.94)	56.4(1.98)				

* Me-NH_2 = Methylamine; Et-NH_2 = Ethylamine; Pr-NH_2 = *n*-Propylamine; Py = Pyridine; Anil = Aniline; Tol = *p*-Toluidine

** Values calculated from the observed curves by the separation of the Ia component.

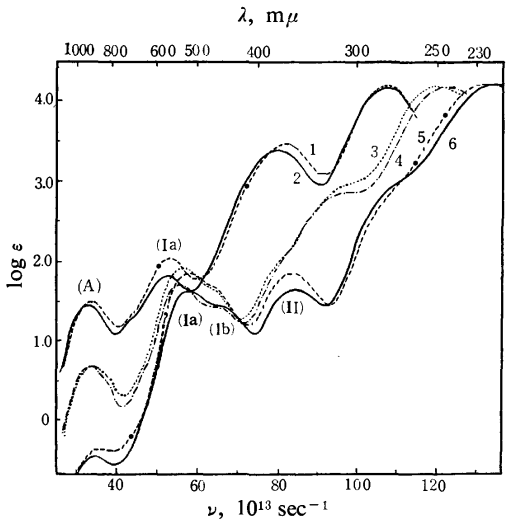

Fig. 1. Absorption curves of:
1. *cis*-$[Co\,I(NH_3)en_2]I_2$
2. *trans*-$[Co\,I(NH_3)en_2]I_2$
3. *cis*-$[Co\,Br(NH_3)en_2]Br_2\cdot 2H_2O$
4. *trans*-$[Co\,Br(NH_3)en_2]Br_2\cdot H_2O$
5. *cis*-$[Co\,Cl(NH_3)en_2]Cl_2$
6. *trans*-$[Co\,Cl(NH_3)en_2]Cl_2\cdot H_2O$

order of $Cl^- \rightarrow Br^- \rightarrow I^-$. This factor is larger than that of the first band. This finding agrees well with Linhard's finding for the halogenopentammine cobalt(III) complexes.[12] The first and the second bands of the cobalt(III) complexes arise from the forbidden transitions between the splitted d-energy levels which have the same spin-multiplicity, while the A and B bands arise from those between the levels of the different spin-multiplicity values (from singlet to triplet). More particulary, the A and B bands are spin-forbidden and their intensities are very weak, in accordance with the theoretical considerations.[13]

If the A band arises from the splitted d-levels, it is expected that the bands will split because of the lower symmetries of the halogeno-amine complexes, just as the first bands split to Ia and Ib. As may be seen in Fig. 4, a weak splitting of the A bands was observed in some of the bromo complexes. In Fig. 1, the absorption spectra of the trans- and the cis-forms of $[Co\,X(NH_3)en_2]X_2$ are shown. The A band of the trans-form is at a longer wavelength and has a weaker intensity than that of the corresponding cis-form.

For the measurements of the A bands, rather concentrated solutions were necessary in most cases because of the lower absorption intensities of the complexes in this region. For some cases, two or three irregular fine structures were observed on the longer wavelength side of the A bands. It could be ascertained that such a phenomenon arose from the difference in the concentrations of the solvent water between the sample and the reference cells. For example, the near-infrared absorption spectra of water and of *trans*-$[Co\,Cl(NH_3)en_2]Cl_2\cdot H_2O$ are shown in Fig. 2. The A

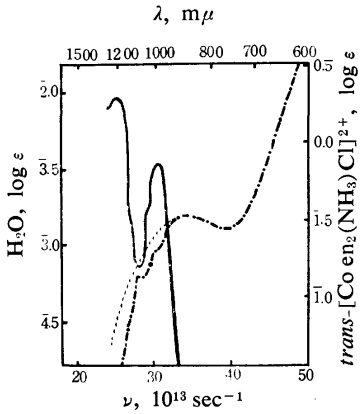

Fig. 2. Absorption curves of solvent water and the complex ion in the near-infrared region.

——: Water ·—·— Complex ion
----: Absorption curve corrected for the absorption by the solvent water which is present in excess in the reference cell.

band of the complex shows minima in a region corresponding to that of the absorption maxima of the solvent water (30.7 and 29.1×10^{13} sec^{-1}).

The Visible and Ultraviolet Spectra. — The so-called first and second absorption bands which appear in the visible and ultraviolet region also belong to the d-d transitions. The first bands of the complexes concerned split into two components, Ia and Ib, because of the lower symmetries of the complex ions (Figs. 1 and 3). In the iodo complexes, only the Ia components are observed, while the Ib components are hidden under the strong charge-transfer bands, as Fig. 5 shows. The molar extinction coefficient of the first band increases with an increase in the atomic weight of the coordinated halogen, but this is not so remarkable as that of the A band.

The absorption spectra of the trans- and the cis-forms of $[Co\,X(NH_3)en_2]X_2$, ($X=Cl^-$, Br^-) showed some differences in the Ia bands. The difference in the intensities was about 0.2 by log ε. The iodo-ammine complexes also showed the same trend. It was concluded, therefore, that the complex which showed a higher intensity in the Ia band was the cis-form, while that which showed a lower intensity was the trans-form (Fig. 1). If this conclusion is applicable to the complexes containing organic amines, it may be possible to determine the geometrical structures of theses complexes. As is shown in Table I and Figs. 3—5, the intensities of the Ia bands of the complexes which have aliphatic amines are almost identical with those of the cis-forms of $[Co\,X(NH_3)en_2]X_2$. Therefore, all these complexes, except for those containing aromatic amines, probably have the cis configuration. This conclusion agrees with the inference by Meisenheimer and Kiderlen[2] and that by Bailar et al.[4] The first absorption bands of the complexes of aromatic amines do not necessarily coincide with those of *cis*-$[Co\,X(NH_3)\,en_2]X_2$, because of the overlapped specific absorption bands of the aromatic amines (Fig. 3). The spectrum of the bromo-aniline complex, however, coincides very well with that of *cis*-$[Co\,Br(NH_3)en_2]Br_2$, as Fig. 4 shows.

In their spectral features the pyridine complexes resemble the aliphatic amine complexes.

As for the ultraviolet spectra of the chloro- and bromo-amine complexes, some studies

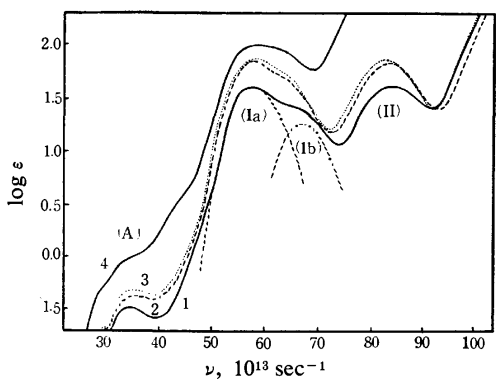

Fig. 3. Absorption curves of:

1. *trans*-$[Co\,Cl(NH_3)en_2]Cl_2\cdot H_2O$
2. *cis*-$[Co\,Cl(NH_3)en_2]Cl_2$
3. *cis*-$[Co\,Cl(NH_2\cdot Me)en_2]Cl_2\cdot H_2O$
4. *cis*-$[Co\,Cl(Anil)en_2]Cl_2$

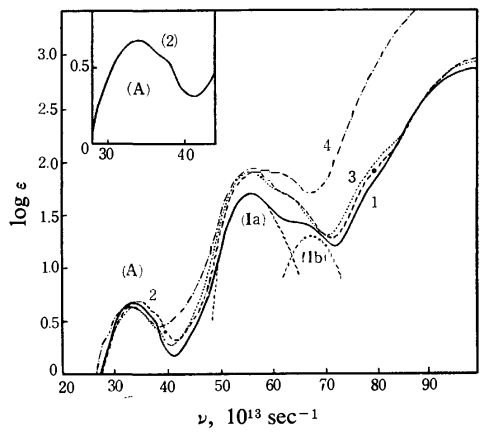

Fig. 4. Absorption curves of the bromo complexes:

1. *trans*-$[Co\,Br(NH_3)en_2]Br_2\cdot H_2O$
2. *cis*-$[Co\,Br(NH_3)en_2]Br_2\cdot 2H_2O$
3. *cis*-$[Co\,Br(NH_2\text{-}Me)en_2]Br_2$
4. *cis*-$[Co\,Br(Anil)en_2]Br_2\cdot 1/2H_2O$

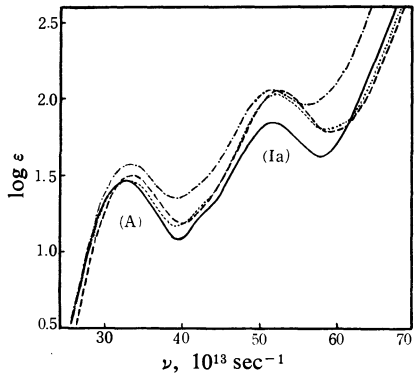

Fig. 5. Absorption curves of the iodo-complexes:
——— *trans*-[Co I(NH_3)en_2]I_2
------ *cis*-[Co I(NH_3)en_2]I_2
····· *cis*-[Co I(NH_2-Me)en_2]I_2
—·—· *cis*-[Co I(Py)en_2]I_2

have been reported by Ablov and Filippov.[14,15] We investigated all the chloro-, bromo-, and iodo-amine complexes in this region. As Table I and Fig. 1 show, the charge transfer bands shift to longer wavelength in the following order of ligand halogens: $Cl^- \rightarrow Br^- \rightarrow I^-$. Some differences between the spectra of the trans- and the cis-forms were also noted in this region.

14) A. Ablov and M. P. Filippov, *Zhur. Neorg. Khim.*, **2**, 42 (1957); *Chem. Abstr.*, **51**, 17441i (1957).
15) A. Ablov and M. P. Filippov, *Zhur. Neorg. Khim.*, **2**, 2390 (1957); *Chem. Abstr.*, **53**, 2774i (1959).

Summary

The four iodo-amine complexes and some chloro- and bromo-amine complexes belonging to [Co X(NH_2-R)en_2]X_2 type have been newly synthesized to complete the series.

From the measurements of the near-infrared, visible and ultraviolet absorption spectra, the geometrical structures of the complexes have been determined. The ammine complexes, [Co X(NH_3)en_2]X_2, exist in both the cis- and the trans-forms, but the organic amine complexes, [Co X(NH_2-R)en_2]X_2, exist only in the cis-form.

The weak splitting of the A band has been observed for the first time in the bromo-amine complexes.

Department of Chemistry
Faculty of Science
Osaka University
Nakanoshima, Osaka

High-kinetic Energy Fragment Ions from Aliphatic Hydrocarbons under Electron Impact. III. Nine Hydrocarbons Ranging from C_2 to C_4

By Toshikazu TSUCHIYA

(Received May 30, 1963)

In previous papers, we have described a method for measuring the kinetic energy of the fragement ions observed in the mass spectra of hydrocarbons[1] and have reported some findings.[2] In the present work, we will measure the kinetic energies of the fragment ions of nine hydrocarbons by the method and will discuss the findings in an attempt to clarify the mechanism of the decomposition of molecules into various high-kinetic energy fragment ions.

The samples were standard one obtained from the Takachiho Chemicals Co.; their nominal purities were 99% or higher and we found them to be pure by a mass spectrometer. The procedure of measurement has been described previously.[1] The approximate values of the appearance potential of a few high-kinetic energy fragment ions were measured by the vanishing current method, using neon as the calibrating gas.

Results

The results of these measurements are given in Tables I—III. The previously-reported data, for ethylene, propane and methyl high-kinetic energy ions from 1, 3-butadiene,[1] are also included for the purpose of comparison. Table I summarizes the measurements of the kinetic energies of fragment ions. The measured peak height values are given in Table

1) T. Tsuchiya, *J. Chem. Soc. Japan, Pure Chem. Sec.* (*Nippon Kagaku Zasshi*), **35**, 1221 (1962).
2) T. Tsuchiya, *J. Chem. Phys.*, **36**, 568 (1962).

TABLE I. EXCESS KINETIC ENERGY OF FRAGMENT IONS (in eV.)

Compound	m/e									
	12	13	14	15	16	25	26	27	28	29
Ethylene		2.1	2.2							
Ethane		2.2	2.1	2.5	2.6					
Propylene		2.5	2.6	2.6			1.2	1.3		
Propane		2.5	2.4	2.4	2.6		1.3	1.2	1.1	
n-Butane		2.3	2.3	2.3	2.4		1.8	1.8	1.8	1.9
Isobutane		2.4	2.6	2.5	2.7			1.4	1.7	
1-Butene	2.3	2.3	2.4	2.4	2.4	1.8	1.8	1.9	1.9	
cis-2-Butene	2.2	2.3	2.4	2.5	2.6	1.7	1.8	1.9	1.9	
trans-2-Butene	2.3	2.3	2.4	2.4	2.5	1.7	1.8	1.9	1.9	
Isobutene	2.3	2.4	2.6	2.7	2.9		1.8	1.9	1.9	
1, 3-Butadiene	2.3	2.3	2.5	2.4		1.7	1.8	2.0		

TABLE II. INTENSITY OF IONS

The upper row for each compound is the intensity of the ions with excess kinetic energy, the lower one, that of the ions with thermal energy only (in arbitrary units)

Compound	m/e																
	12	13	14	15	16	25	26	27	28	29	36	37	38	39	40	41	42
Ethylene		1.7 11.2	4.7 16.7														
Ethane		0.9 6.3	3.5 11.5	8.9 16.5	0.4 0.4												
Propylene		1.0 3.3	4.7 10.6	5.9 11.2			4.6 26.1	6.9 68.8									
Propane		0.6 3.0	3.8 9.0	17.5 19.6	0.5 0.6		4.9 43.0	13.8 177	7.5 130								
n-Butane		0.6 1.2	2.5 4.0	24.0 17.0	0.4 0.5		4.7 37.6	12.4 203	3.3 119	2.1 175			+	+		+	
Isobutane	0.3 0.7	0.9 1.6	4.0 6.2	31.8 27.4	1.0 0.8		1.8 19.1	2.6 164					+	+	+	+	+
1-Butene	0.5 1.4	1.0 2.5	4.4 6.6	17.6 15.8	0.3 0.4	1.3 4.9	6.6 50.1	8.8 145	1.8 101				+	+ + +	+ +	+	
cis-2-Butene	0.5 1.2	0.7 1.7	2.8 3.5	17.3 11.3	0.1 0.1	1.3 6.1	8.8 51.8	10.5 140	2.6 96			+	+	+ +	+		
trans-2-Butene	0.2 1.1	0.6 1.3	2.7 3.3	16.5 9.4	0.2 0.4	0.9 5.9	8.5 49.2	10.2 130.5	3.4 91.2			+	+	+ +	+		
Isobutene	0.6 1.7	1.4 2.5	6.0 6.4	21.7 14.2	0.4 0.4		3 24	3 93	0.4 63	0.4 32	+ +	+	+	+ + +	+	+	
1, 3-Butadiene	1.1 3.6	2.0 3.7	4.9 5.4	7.4 1.8		1.2 10.5	9.3 63.5	10.9 176				+	+	+ +	+		

TABLE III. APPEARANCE POTENTIAL OF HIGH KINETIC ENERGY IONS (in eV.)

Compound	m/e			
	14	15	26	27
Ethylene	35±4			
Ethane		30±3		
Propylene	30±3	29±3	38±3	30±3

II, where the upper row for each substance shows the values for the high-kinetic energy peaks,* or satellite peaks, and the lower one, the values for the thermal energy peaks. Table III gives the rough values of the estimated appearance potentials of some satellite peaks.

Discussion

Hustrulid[3] and Mohler[4] have discussed the mechanism of the formation of KE ions and have proposed that KE ions result from the dissociation of doubly-charged ions formed by electron impact. For convenience, this mecha-

* For convenience, ions having excess kinetic energies will hereafter be called KE ions, while those having thermal energies corresponding to the temperature of the ion-source will be called TE ions.

3) A. Hustrulid, P. Kusch and J. T. Tate, *Phys. Rev.*, 54, 1037 (1938).

4) F. L. Mohler, V. H. Dibeler and R. M. Reese, *J. Chem. Phys.*, 22, 394 (1954).

TABLE IV. BOND ENERGY D, IONIZATION ENERGY I, AND APPEARANCE POTENTIAL A (eV.)

D		I		A			
CH_3-C_2H_3	3.9[a]	C_2H_3	10.3[c]	C_2H_4	$\rightarrow$ $C_2H_3^+$+H	14.0[b]
CH_3-CH_3	3.7[a]	CH_3	10.0[b]	C_2H_4	$\rightarrow$ CH_2^++CH_2	19.3[b]
CH_2-H	3.5[b]	CH_2	11.9[b]	CH_2	$\rightarrow$ C^++2H	18.0[b]
$C_2H_2^+$-H	3.8[b]	CH	11.1[b]			
CH_2^+-H	5.3[b]	C	11.3[b]			
CH^+-H	3.5[b]					

a J. S. Roberts and H. A. Skinner, *Trans. Faraday Soc.*, **45**, 339 (1949).
b F. H. Field and J. L. Franklin, "Electron Impact Phenomena," Academic Press, New York (1957).
c M. B. Wallenstein, Thesis, Univ. Utah, 1951.

nism will hereafter, as in the previous report, be referred to as the H-M mechanism.

***m/e* 16.**—In some cases weak doublets are observed at *m/e* 16, as Table II shows. One or more of the following ions can contribute to the peak at *m/e* 16: (a) rearrangement ions of the sample material, (b) isotope ions of the *m/e* 15 ion, (c) ions from impurities contained in samples such as the parent ion of methane and oxygen ions from oxygen or from water, and (d) the background peaks of oxygen ions from oxygen or from water. The contributions from (c) and (d) could be eliminated by scrutinizing the kinetic energy value of the satellites[5] and the sensitivity of the instrument and by referring to the *m/e* 32 and to the *m/e* 18 peaks. After the isotope contribution was subtracted, it was found that some of the *m/e* 16 satellites of ethane, propane, *n*-butane, isobutane, and isobutene are due to inherent high-kinetic energy ions. Presumably, these ions are methane ions, produced by rearrangement. Though the intensities of the satellites are small, the following trends, concerning the intensity of *m/e* 16 KE ions, can be seen from Table I. The longer the carbon chain of a molecule, the smaller the intensity of the KE ion. Whereas the isostructure has a favorable effect on KE ion production, double bond has a negative influence.

Ethane.—In the following discussions, the numbers shown after each reaction equation indicate the energy of the formation of the KE ions, as computed from the values in Table IV and the measured KE values of the concerned ions in eV. These computed energies represent the lower limits of the true energies of formation, since the produced fragments may possibly be in the excited state.

The following reactions were investigated as reactions giving CH_3^+ KE ions according to the H-M mechanism:

$$C_2H_6 \rightarrow C_2H_6^{2+} \rightarrow \begin{cases} 2CH_3^+ & 28.7 \quad (1) \\ CH_3^+ + CH_2^+ + H & 33.6 \quad (2) \\ CH_3^+ + CH^+ + 2H & 37.2 \quad (3) \end{cases}$$

For example, the energy of the formation of CH_3^+ KE ions, $F(CH_3^+)$, in reaction 2 was computed by the following cycle:

$$F(CH_3^+) = D(CH_3\text{–}CH_3) + 2I(CH_3) + D(CH_2^+\text{–}H) + E(CH_3^+) + E(CH_2^+) + E(H)$$

Where

D(X–Y): the dissociation energy of the X–Y bond,
I(X): the ionization potential of the radical X,
E(Y); the kinetic energy of the radical or ion Y.

From the experimental values in Table I and from the data in Table IV, $F(CH_3^+)$ is found to be:

$$F(CH_3^+) = 33.6 + E(H)$$

Other F values were computed in a similar way.

The appearance potential of the CH_3^+ ion, $A(CH_3^+)$, is 30±3 eV. (Table III). The F value for reaction 1 is compatible with the experimental value, $A(CH_3^+)$. The experimental value for the total kinetic energy, which is the summation of the kinetic energies of the ions, 5.0 eV., differs from the value, 5.6 eV., calculated by Mohler et al.[4] Taking into consideration, however, the fact that the computation of Mohler et al. contains an assumption about the distance between charges, reaction 1 may also be valid.

Reactions 2 and 3 are both accompanied with neutral fragments. Comparing the F values with $A(CH_3^+)$, these reactions are considered to be improbable. If hydrogen is produced as a molecule instead of atoms, however, reaction 3 is not impossible.

Apart from the H-M mechanism, the following reactions were investigated:

5) J. D. Morrison and H. E. Stanton, *J. Chem. Phys.*, **28**, 9 (1958).

$$C_2H_6 \rightarrow C_2H_6^+ \rightarrow \begin{cases} CH_3^+ + CH_3 & 18.7 \quad (4) \\ CH_3^+ + CH_2 + H & 22.2 \quad (5) \\ CH_3^+ + CH + 2H & 26.5 \quad (6) \\ CH_3^+ + C + 3H & 28.9 \quad (7) \end{cases}$$

In computing the F values, the kinetic energies of the neutral fragments as a whole were assumed to be equal to that of the CH_3^+ ion, i. e., 2.5 eV. The energy of formation for reaction n, F_n, was computed as before. D(CH-H) = 4.3 eV., necessary to determine F_6, was calculated from the equation:

$$D(\text{CH-H}) = I(CH_2) + D(CH^+\text{-H}) - I(CH)$$

From a similar cycle, D(H-C-H) was found to be 6.7 eV. and was used to obtain F_7.

Comparing the $A(CH_3^+)$ values with the F values, reactions 4 and 5 can be eliminated, provided the products are not in the excited state. Since we know very little about the energies of the neutral fragements in reactions 4 and 5, nothing can be inferred from their F values about these reactions. The summation of the intensities of ions other than the m/e 15 ion is about one-half of the intensity of the m/e 15 ion (Table II). Accordingly, only some m/e 15 ions are produced in pairs with other KE ions, since equal numbers of the two species of an ion pair are necessarily produced by a particular reaction and the sensitivities of those ion pairs in Eqs. 1—7 are reasonably assumed to be approximately equal.[2] Thus, the CH_3^+ KE ion seems to be produced from ethane by reaction 1 according to the M-H mechanism and by some of the reactions 4—7 with neutral fragments, if the produced fragments are excited appropriately.

C_3H_6.—When a doubly-charged molecular ion dissociates, the two resulting fragments have equal momentum. As has been discussed previously,[2] pairs of ions were selected in this respect and the following reactions were investigated:

$$C_3H_6 \rightarrow C_3H_6^{2+} \rightarrow \begin{cases} CH_3^+ + C_2H_3^+ & 28.1 \quad (8) \\ C_2H_3^+ + CH_2^+ + H & 33.4 \quad (9) \\ C_2H_3^+ + CH^+ + 2H & 36.8 \quad (10) \\ C_2H_2^+ + CH^+ + 3H & 40.5 \quad (11) \end{cases}$$

Mohler et al.[4] gave 3.7 eV. as their "Coulomb energy" for propane. Using an appropriate value[6] for the distance between end carbon atoms in propylene, instead of that in propane,[7] computation similar to Mohler gives 3.9 eV. as the "Coulomb energy" of propylene. The summation of the kinetic energies of the ion pair in reaction 8 is 3.9 eV. (Table I), which agrees with the computed value. $A(C_2H_3^+)$ in Table III is also compatible with the energy of the formation of 8.

6) D. R. Lide, Jr., and E. E. Mann, *J. Chem. Phys.*, **27**, 868 (1957).

7) L. Pauling and L. O. Brockway, *J. Am. Chem. Soc.*, **59**, 1223 (1937).

While the energies of the formation of reactions 9 and 10 are incompatible with the appearance potentials (Table III), that of reaction 11 is compatible with $A(C_2H_2^+)$ in Table III, provided we assume that the hydrogen atoms produced have no kinetic energy. Thus 8 and 11 seem to be important reactions from the standpoint of the H-M mechanism.

Apart from the H-M assumption, the following reactions were investigated because their energies of formation are reasonable when compared with the measured appearance potentials of the corresponding ions. In deriving the energy of formation, the momentum of the KE ions and of the neutral fragments as a whole were assumed to be conserved.

Among the reactions producing the CH_3^+ KE ion only, reaction 12 requires an energy of formation less than $A(CH_3^+)$:

$$C_3H_6 \rightarrow C_3H_6^+ \rightarrow CH_3^+ + CH_2 + CH \qquad 25.9 \quad (12)$$

Similarly, for CH_2^+, we have reaction 13:

$$C_3H_6 \rightarrow C_3H_6^+ \rightarrow CH_2^+ + CH_2 + CH + H \qquad 31.2 \quad (13)$$

For $C_2H_3^+$ and $C_2H_2^+$, we have:

$$C_3H_6 \rightarrow C_3H_6^+ \rightarrow \begin{cases} C_2H_3^+ + C + 3H & 28.0 \quad (14) \\ C_2H_2^+ + C + 4H & 31.4 \quad (15) \end{cases}$$

As the neutral fragments produced may be excited, 12—15 are feasible reactions from the standpoint of the energy of formation.

The sum of the peak heights of high-energy ions in the C_1 group is about 11.6, while that of those in the C_2 group is 11.5 (Table II). As has already been reported for propane,[2] this suggests that the two groups of ions are produced simultaneously in pairs and that the contributions of 12—15 may be of little importance.

C_4 Compounds.—The KE values and the intensities of KE ions of a mass number higher than m/e 30 could not be measured because the resolving power of the present instrument was insufficient, although the presence of KE ions could be recognized clearly because of partly-overlapped satellites. The KE values in this m/e range were roughly estimated to be about 0.8 eV. The number of + marks in Table II indicates the approximate intensity of the KE ions.

Although the results of the present experiment on C_4 compounds are insufficient to describe the phenomena accurately, the following points are conceivable. The KE of each m/e 12~15 ion is larger than that of each m/e 25~29 ion, but the magnitude of momentum is in the reverse order. By the H-M mechanism, when a doubly-charged molecular ion dissociates, the two resulting fragments have equal momentum. Since the kinetic energies of the m/e 40 group ions are, roughly,

0.8 eV., their momentum is in the same range as that of *m/e* 12~15 group ions. The summation of the KE of the two groups is about 3 eV., a value which is nearly the same as the total KE value computed by Mohler et al.[4]* Thus, the reaction giving the two groups of ions *m/e* 12~15 and *m/e* 40 simultaneously is possible from this point of view.

The intensities of the *m/e* 15 KE ions of isobutane and isobutene are very large, and they might be produced in pairs with neutral fragments. As in the case of the H–M mechanism, the process can be considered as follows: From Table I, it is seen that the KE of isobutene is 2.7 eV. and that that of isobutane is 2.5 eV. Although the precision of the present experiment is ±0.2 eV., the order of magnitude of the KE values is reliable, i. e., the *m/e* 15 KE value of isobutene is larger than that of isobutane. The C–C distance of isobutane is 1.54±0.02 Å,[8] while that of isobutene between the tertiary carbon atom and the CH_3 radical is 1.50 Å.[9] We assume that, in a section along the C–C bond of the potential energy diagram of the two substances, the potential energy curve for the ground states and for the upper repulsive state, along which a molecule dissociates into a CH_3^+ ion and another fragment, are nearly the same. Since the C–C distance of isobutene is smaller than that of isobutane, the Franck-Condon region corresponding to isobutene crosses the potential energy curve for the upper state at a region higher than in isobutane; consequently, the KE of *m/e* 15 ion from isobutene is larger than that from isobutane.

* *n*-Butane, 2.9; Isobutene, 3.7; 1-Butene, 3.0 eV.

8) J. Y. Beach and J. Walter, *J. Chem. Phys.*, **8**, 303 (1940).

9) G. R. Somayajulu, ibid., **31**, 919 (1959).

Summary

Fragment ions produced by electron impact with excess kinetic energies from into nine hydrocarbons ranging from C_2 to C_4 have been investigated. Fragment ions of a higher mass number could not be measured. The decomposition mechanism of propylene has been explained by the mechanisms proposed by Hustrulid and by Mohler et al. To explain the decomposition of other molecules, reactions producing ions with excess kinetic energy as well as neutral fragments must also be taken into consideration.

The author would like to express his thanks to Dr. Akira Kuboyama for his advice and to Mr. Ryuzo Shiota for his valuable discussions and survey of the manuscript.

Government Chemical Industrial Research Institute, Tokyo
Shibuya-ku, Tokyo

The Viscometric Properties of Polyesters. I. A Comparison between Crystalline and Amorphous Polyesters

By Ryuzo NAKATSUKA

(Received May 23, 1963)

The need for knowledge of the factors influencing the viscometric property of linear polyesters and for an interpretation based on the molecular theories of these relationships has increased with the technological advances of recent years. In order to gain a satisfactory understanding of flow, detailed data are required on well-defined polymers, linear polyesters for example, over a wide range of temperature.

Fox et al.[1] have reviewed recent research on the viscosity of polymers and their concentrated solutions. In their review the experimental problems, the data actually measured and the empirical laws of flow are discussed, and besides, the results are interpreted in terms of qualitative quantitative molecular theories of flow.

The purposes of this experiment are, (1) to deduce the relationship between the chemical structure and the viscometric property of long chain polyesters, (2) to gain detailed information about viscosity over a wide range of temperature, and (3) to point out several interesting problems incident to these results.

1) T. G. Fox, S. Gratch and S. Loshaek, "Rheology," Vol. I, Academic Press, New York (1956), Chap. 12.

For polyester, Flory[2] has already measured their viscosity extensively and has quantitatively examined the influence of molecular weight and temperature on viscosity.

Takayanagi et al.[3] have also studied the temperature dependence of viscosity over a wide range of temperature and applied Bueche's[4] theory to their results. The present author has suggested in a previous report[5] that, for the study of the viscometric property of polyeters, it might be necessary to compare the crystalline with the amorphous polyesters in connection with the viscometric property in the super-cooled liquid state of low molecular substance.[7] Moreover, for the purpose of confirming this opinion, the viscosity of aliphatic polyesters with similar simple chemical structures has been studied in detail. However, discussions of the viscosity of polyesters should be based on exact and detailed experimental results for many kinds of polyesters over a wide range of viscometric conditions; therefore, the present experiment may be considered only an attempt in this direction.

Experimental

The Measurement of Viscosity.—Generally it is important to select a suitable instrument for rheological studies. The rotational viscometer is more useful than the capillary one to obtain the temperature dependence of a steady flow viscosity over a wide range of temperature. The former can easily measure viscosity in several seconds at any desired temperature; therefore, there is little need of a fine temperature regulator if the temperature of the apparatus is observed closely.

Under normal conditions of measurement, for the purposes of this experiment, we may regard the linear long chain polyesters with relatively low molecular weights (about 2000) as almost Newtonian fluids.[5]

The viscometer used in this experiment was as follows:

Rotational viscometer (Brookfield type)
Measuring range: $10^{-1}\sim10^{3}$ poises
Shear rate: 6~60 r.p.m. (4-stage change)

The Preparation of the Polyesters.—Aliphatic long chain polyesters with a low viscosity were prepared by the ordinary method. The combinations of acid and glycol are shown in Table I.

The polyesters were prepared in a 2-liter, 4-necked flask equipped with a thermometer, an inlet tube for inert gas, a device for the azeotropic removal of water, and a mechanically-sealed agitator. In most cases 3 mol. of acid and 3.3 mol. of glycol were reacted under a xylene reflux until the acid number was reduced to approximately 50; this was accomplished by the continuous agitation arising from the introduction of a stream of inert gas. Next, such residual volatile matters as water, glycol and acid were removed by vacuum distillation until the acid number was reduced to approximately 30.

Measurement of the Melting Point of the Crystalline Polyester.—In the polyesters used in this experiment, we can easily distinguish the crystalline from the amorphous one. A certain group of polyesters changes abruptly from the transparent liquid state to the opaque solid state at a certain temperature if they are cooled slowly in the melted state. As a result of the solidification, no viscosity under this temperature can be obtained. On the contrary, there is an other group of polyesters which cannot solidify or for whom it is extremely difficult to solidify from the melted state, even when kept at a low temperature near the glass transition point for several days.

In this report the former and the latter groups of polyesters are termed the crystalline and the amorphous respectively. If the temperature dependence of the infrared spectrum of polyester is studied, the crystalline band is observed for the crystalline, but not for the amorphous.[8]

The melting point of the crystalline was measured with a polarizing microscope. Usually the value of the melting point of any crystalline polymer is somewhat different from its solidifying point which can be pointed out in measuring its viscosity.

Results and Discussion

As the full curve of viscosity can be obtained easily over a wide range of viscosity (about $10^{-1}\sim10^{6}$ poises) in the case of amorphous long chain polyesters of a low viscosity, it seems that these kinds of polyesters may serve as typical models for rheological studies.

The aliphatic saturated polyesters used in this experiment are listed in Table I.

The temperature dependence of the steady flow viscosity in the range of $10^{-1}\sim10^{3}$ poises is shown in Figs. 1—2 for amorphous polyesters and in Fig. 3 for crystalline polyesters.

Within the limits of these aliphatic long chain polyesters, the viscosity-versus-temperature curves are very similar to one another; the very small difference in viscosity may depend on the change in chemical structure.

Since all samples were prepared to have similar molecular weights (1600~2000), the results of this experiment are not considered to have been remarkably affected by the differences in molecular weights of the samples.

2) P. J. Flory, *J. Am. Chem. Soc.*, **62**, 1057 (1940).
3) M. Takayanagi and S. Kuriyama, *J. Chem. Soc. Japan, Ind. Chem. Sec.* (*Kōgyō Kagaku Zassi*), **59**, 49 (1956).
4) F. Bueche, *J. Chem. Phys.*, **21**, 1850 (1953).
5) R. Nakatsuka, Y. Yoshida, *Kagaku to Kogyo* (*Osaka*), **30**, 82 (1956).
6) P. J. Flory, "Principles of Polymer Chemistry," Cornell University Press (1953), p. 49.
7) C. Dodd and Hu Pak Mi, *Proc. Phys. Soc.*, **B 62**, 454 (1949); N. N. Greenwood and R. L. Martin, ibid., **A 215**, 46 (1952).
8) Presented at the 12th Annual Meeting of Thermosetting Resins, Osaka, October, 1962.

TABLE I. MELTING POINT OF SOLID-STATE POLYESTER (°C)

Type	Glycol		Acid			
			Su (2)	Ad (4)	Az (7)	Se (8)
Ordinary type	Et	(4)	—	—	—	69
	Pr	(5)	—	—	36	49
	i-Bu	(5′)	—	a	a	a
	n-Bu	(6)	34	45	39	53
	Pe	(7)	—	—	41	51
Ether type	DE	(7)	a	a	0	33
	DP	(7′)	a	a	a	a
	TE	(10)	a	a	a	29

Note

	Conventional	IUPAC
Su:	Succinic Acid	Butanedioic acid
Ad:	Adipic acid	Hexanedioic acid
Az:	Azelaic acid	Nonanedioic acid
Se:	Sebacic acid	Decanedioic acid
Et:	Ethylene glycol	1,2 Ethanediol
Pr:	—	1,3 Propanediol
i-Bu:	—	1,3 Butanediol
n-Bu:	—	1,4 Butanediol
Pe:	—	1,5 Pentanediol
DE:	Diethylene glycol	2,2′-Dihydroxydiethyl ether
DP:	Dipropylene glycol	2,2′-Dihydroxydipropyl ether
TE:	Triethylene glycol	1,2-Ethanediol bis(2-hydroxy-ethyl ether)

(2) a: Amorphous c: Crystalline

(3) Figures listed in brackets indicate the numbers of members in the main chain belonging to an acid or glycol component of the linear polyester, and a figure with a prime corresponds to a linear polyester with side chains.
For example:

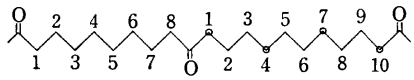

Se (8) TE (10)
Triethylene sebacate (8—10 polyester)

TABLE II. CENTER OF THE "TRANSITION AREA" FOR VISCOUS FLOW (°C)

Type	Glycol		Acid			
			Su (2)	Ad (4)	Az (7)	Se (8)
Ordinary type	Et	(4)	—	—	—	c
	Pr	(5)	—	—	c	c
	i-Bu	(5′)	79	72	45	32
	n-Bu	(6)	c	c	60	c
	Pe	(7)	—	—	c	c
Ether type	DE	(7)	80	51	53	c
	DP	(7′)	75	46	27	34
	TE	(10)	71	52	34	c

A Comparison between the Crystalline and the Amorphous Polyesters.—Aliphatic linear polyesters without side chains are generally crystalline, with the exception of diethylene adipate and several polymers similar to it.[6] As Table I shows, what are called "ether-type polyesters" with ether bonds in the main chain, prepared from such polyglycols as diethylene or triethylene glycol, show a peculiar behavior in their crystallizing tendency.

Though such "ether-type polyesters" without side chains[6] as diethylene adipate are generally recognized to be amorphous, several crystalline "ether-type polyesters" were found among the samples prepared and used in this experiment. Accordingly, we can easily select several sets of polymers very similar in chemical structure, while differing in crystallinity, and compare their viscosities. For example, triethylene azelate is amorphous and triethylene sebacate is crystalline, while both are very similar in chemical structure and viscometric

property over the range of temperature higher than their melting points.

In other words, as is apparent from Figs. 1 and 2, the difference in viscosities between sebacate and azelate in combination with various glycols is so little as to be almost negligible, independently of whether they are crystalline or amorphous.

The relation between chemical structure and crystallizing tendency is shown in Table I.

It seems well established by Table I (1) that every polyester with side chains which was prepared from 1,3-butanediol or dipropyleneglycol is amorphous; (2) that all the ordinary aliphatic-saturated polyesters without side chains or ether bonds in the main chains are crystalline, and (3) that "ether-type polyesters" without side chains are not always crystalline. For example, triethylene azelate and triethylene sebacate are similar in chemical structure, but the former is amorphous and the latter crystalline. Yet both show a very similar viscosity vs. temperature behavior within a comparatively wide temperature range, including the melting point of the latter.

The difference in the crystallizing tendencies of polyesters is probably caused by the intramolecular rotation of the ether bond being easier than that of the methylene bond. From Table I, it may be found that the crystallizing tendencies are relative to the ratio, (m/n), of the number of methylene members of the acid

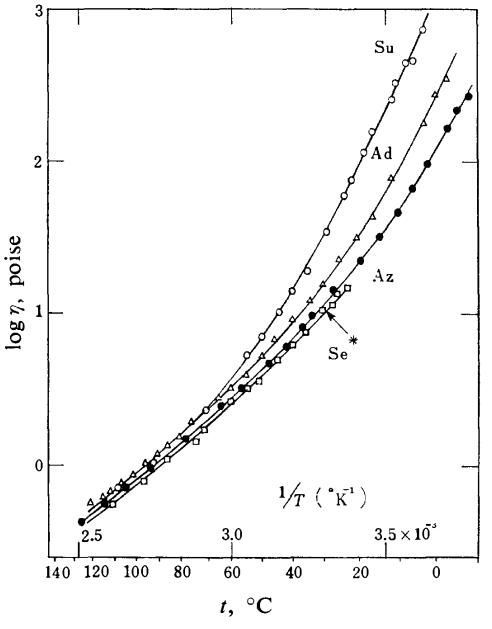

Fig. 1. Relationship between viscosity and temperature (triethylene glycol series).

* Crystalline polyester
↓ Melting point

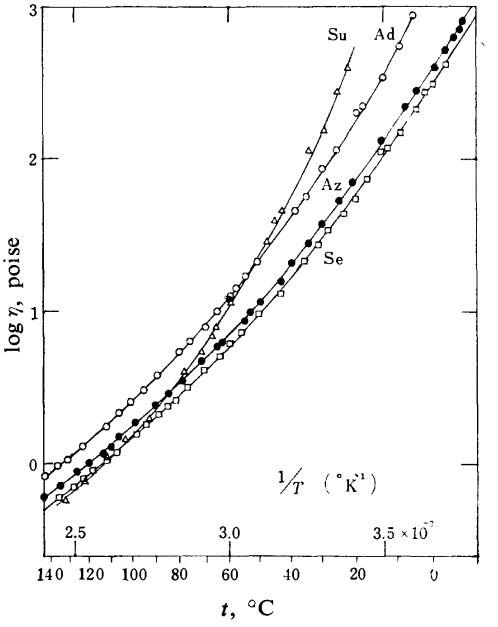

Fig. 2. Relationship between viscosity and temperature (1,3 butanediol series).

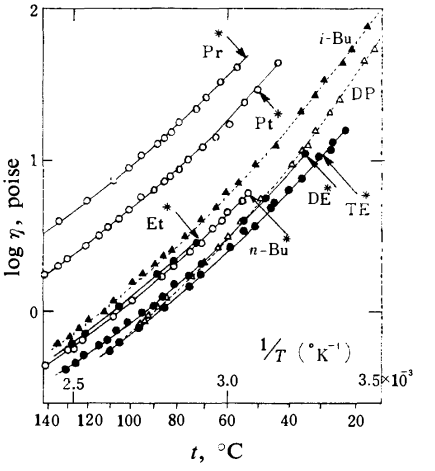

Fig. 3. Relationship between viscosity and temperature (sebacic acid series).

* Crystalline polyester
↑ Melting point

component, (m), to the number of oxygen plus methylene members of the glycol component, (n), in the "ether-type polyesters." That is, "ether-type polyesters" may be shown as follows:

$$-\overset{\overset{O}{\|}}{C}-(CH_2)_m-\overset{\overset{O}{\|}}{C}-O-(-CH_2-CH_2-O-)_{(n-1)/3}-\overset{\overset{O}{\|}}{C}-$$

Acid component — Glycol component

The corresponding numbers for various acid or glycol components are shown in Table I.

For example, in crystalline diethylene sebacate, the numbers of chain members of the acid and the glycol components are 8 and 7 respectively. On the contrary, in amorphous diethylene adipate, the numbers are 4 and 7 respectively. It can be said that "ether-type polyesters" in which m/n is approximately equal to 1 are crystalline.

In order to study their crystallizing tendency further, some polyesters were prepared from such a higher aliphatic dibasic acid as brassylic acid. Both diethylene brassylate (11—7 polyester) and triethylene brassylate (11—10 polyester) were crystalline, as was to be expected.

However, the author believes that further investigation into this matter is required in order to conclude that the ratio of the numbers of members between the methylene of the acid and the ether chain of the glycol is very significant in the crystallizing tendency of "ether-type polyesters."

The $\log \eta$ vs. $1/T$ curves are shown in Figs. 1 and 2 for the amorphous and in Fig. 3 for the crystalline. The slopes of these curves are proportional to the apparent activation energy (E^*) for viscous flow in the Andrade equation:

$$\ln \eta = \ln A + E^*/RT$$

where A and E^* are constants, and R is the gas constant.

Generally, over a wide range of temperature, no apparent activation energy (E^*) of any polyester is constant, no can the curve of $\log \eta$ against $1/T$ be regarded as a straight line.

The findings on the connection between the viscometric property and the crystallizing tendency are as follows:

As Figs. 1—3 show, in the range of temperature higher than the point corresponding to their melting points, all $\log \eta - 1/T$ curves of polyesters used in this experiment are nearly parallel to one other, in spite of their differences in crystallinity and their differences in chemical structure.

Therefore, in a perfectly molten state, or in a state wherein molecules can flow practically free of molecular interaction, the E^* values of the polyesters practically coincide and tend to approach a fixed value when the temperature is raised.

Moreover, when polyesters with similar chemical structures, such as several pairs of sebacate and azelate combined with the same glycol, are compared, it may be seen that almost all the $\log \eta - 1/T$ curves overlap over a wide range of temperature when they are shifted along the η-axis.

On the contrary, in the range of temperature lower than the point corresponding to the melting point of the crystalline counterpart, the discrepancy in the temperature dependence of the viscosity of amorphous polyesters may be ascribed to the differences in their chemical structures.

By comparing the temperature dependence of the viscosity of the crystalline polyesters with that of the amorphous ones, it may be seen that the mechanism of the viscous flow of the latter changes discontinuously in a certain temperature region near the melting point of the corresponding crystalline polyesters. In other words, it seems that in the range of temperature lower than the melting point of crystalline polyesters, a certain sort of force acting on molecules of the crystalline polyesters also exists in the case of the corresponding amorphous polyesters and that this is a cause of the change in their viscous flow state.

"Transition Area" near the Melting Point.— As has been stated above, it has been inferred that there exists a "transition area" for viscous flow in amorphous polyesters in the region of temperature near the melting point of crystalline polyesters with similar chemical structures.

When the temperature is raised beyond the "transition area," the viscous flow of every polyester aproaches an "Andrade liquid state." Though the absolute values of the viscosity of all polyesters are not always equal, their apparent activation energies at a fixed temperature become almost equal. That is, if the difference in molecular weight between polyesters is negligible, the A constant in the Andrade equation depends upon the chemical structure, but the E^* constant does not. With temperature change within the "transition area," the viscous flow state of each polyester begins to change remarkably according to its chemical structure. When the temperature is lowered near the glass transition temperature of each polyester, the $\log \eta - T$ curves, independently of the chemical structure of each, become parallel with one another.

It is clear that the effect of chemical structure on viscosity becomes most remarkable near the "transition area." For example, as Fig. 1 shows, in the case of the triethylene glycol series, the longer the chain of the acid component, the smaller the value of the apparent activation energy.

This relation can be more directly represented by plotting the curves of $\log \eta - 1/T^2$ in Figs. 4 and 5. The curve for each polyester is virtually represented by two intersecting straight lines.

This point of intersection may be regarded as a center of the "transition area" of each amorphous polyester; in the case of crystalline polyesters, with the exception of diethylene

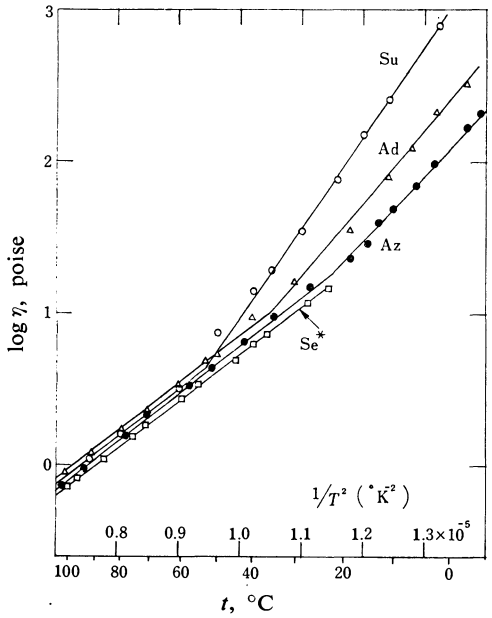

Fig. 4. Relationship between viscosity and temperature (triethylene glycol series).

* Crystalline polyester
↓ Melting point

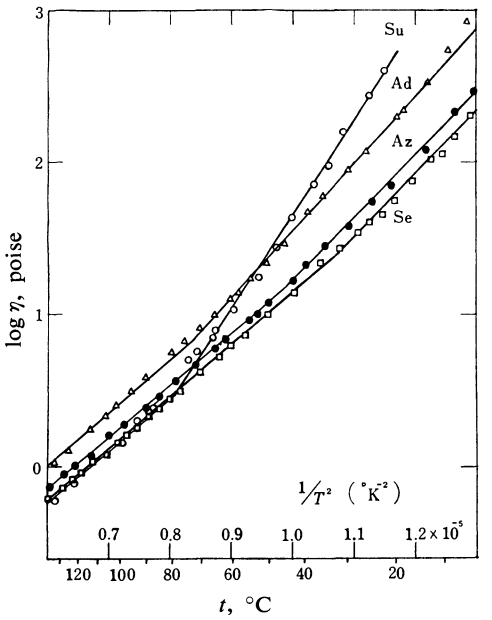

Fig. 5. Relationship between viscosity and temperature (1,3 butandicl series).

azelate whose rate of crystallization is very slow, this point is near the melting point. Therefore, it can be considered that practically no viscosity curve exists beyond this point. As to the relation between $\log\eta$ and $1/T$, all straight lines under this point are almost parallel with one another, irrespective of chemical structure. The values of the "center of transition area" determined by this method are shown in Table II.

By comparing Table I with Table II, it may clearly be seen that the center of the "transition area" of an amorphous polyester almost corresponds to the melting point of a crystalline polyester. This experimental fact shows the close connection between the "transition area" and the melting point.

The Temperature Dependence of the Activation Energy for the Viscous Flow near the "Transition Area".—The relationship between E^* and $1/T$ over the range of viscosity 10^{-1} $\sim 10^3$ poises is shown in Figs. 6 and 7. For example, as Fig. 6 shows, these relations are represented as nearly S-type curves, and the center of the "transition area" is regarded as being practically the point at which the slope of the E^*-1/T curve is steepest. The values of the viscosity and apparent activation energy at this point reach about 10 poises and about 11 kcal./mol. respectively.

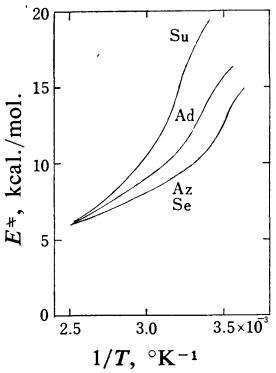

Fig. 6. Apparent activation energy for viscous flow (triethylene glycol series).

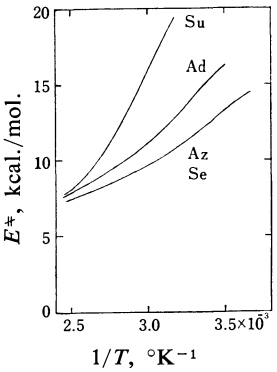

Fig. 7. Apparent activation energy for viscous flow (1,3 butanediol series).

The E^*-1/T curve in the range of high viscosity (10^3~10^6 poises) will be shown in a the next report of the present series.

As has been stated above, by studying the relations between $\log\eta$ and $1/T$, $\log\eta$ and $1/T^2$, and E^* and $1/T$, it may be easily deduced that there is a "transition area" for the viscous flow in the case of aliphatic long-chain polyesters. However, this concept is quite different from that regarding the glass transition point discussed previously, because the abrupt changes of temperature dependence in the infrared absorption[8] and in the refractive index are not observed in the transition area." In the "transition area" for the viscous flow, the viscous flow mechanism changes suddenly and, accordingly, it should be possible to distinguish viscometric properties between the higher and the lower temperature.

However, at present, it can be said with certainty only that no abrupt change in the arrangement of long chain molecules as shown at the crystallizing point has yet occurred at this stage.

In this manner, the existence of the "transition area" is more clearly shown in the relationship between E^* and $1/T$ than in the $\log\eta - 1/T$ curves.

Every apparent activation energy (E^*) at a certain temperature within the "transition area" differs from the others according to the chemical structure of each polyester, and the abrupt rise of E^* in the same area shows the change of interaction among linear polyester molecules with many dipoles.

The effects of chemical structure on E^* may be compared approximately as follows:

Glycol series

dipropylene glycol $>$ diethylene glycol $>$ triethylene glycol $\fallingdotseq$ 1,3-butanediol

Acid series

succinic acid $\gg$ adipic acid $>$ azelaic acid $\gg$ sebacic acid

It seems usual that the larger the chain between two adjacent carbonyl groups in a homologous series of polyesters, the lower the apparent activation energy near the "transition area." This phenomenon may be caused by the diluting effect of larger chains for dipole interaction.

However, it seems unusual that both triethylene glycol and 1,3-butanediol have the effect of reducing E^*, in spite of the fact that the side chains of 1,3-butanediol generally increase the E^* value because of their effect of reducing the fluxibility of long-chain molecules.

From these experimental results, it may be presumed that the methylene chain is more flexible than the ether chain in the "transition area" for viscous flow, and that the ether bond has a smaller dependence of intramolecular rotation on the temperature than does the methylene bond.

Summary

From the study of the viscosity of aliphatic long-chain polyesters over a wide range of temperatures, the following results have been obtained:

(1) Among aliphatic long-chain polyesters with ether bonds in the main chains, several crystalline polyesters have been obtained.

(2) Accordingly, it has been possible to compare the temperature dependence of the viscosity of the amorphous and the crystalline polyesters with similar chemical structures.

(3) When the temperature is raised, every apparent activation energy for viscous flow (E^*) approaches a fixed value, independently of the chemical structure of the polyester.

(4) However, the viscous flow state of the amorphous polyester changes discontinuously in connection with the chemical structure near the melting point of the corresponding crystalline polyester.

(5) In the "transition area" for viscous flow, the viscosity and the apparent activation energy (E^*) are, respectively, about 10 poises and 11 kcal./mol.

The author is indebted to Professor Hiromu Murata of the Faculty of Science, Hiroshima University for his helpful discussions and encouragement throughout the work, and to Dr. Keiji Oshima, Director of the Osaka Municipal Technical Institute for his advice and encouragement. He also wishes to express his gratitude to Mr. Tadao Nakao, Senior Managing Director of the Sumitomo Bakelite Co., Ltd., and Director of the Central Research Laboratory of the same company, for permission to publish this paper, and to Mr. Kyosuke Miki and Mr. Shozo Yoshizumi of this Laboratory for their valuable assitstance.

Central Research Laboratory
Sumitomo Bakelite Co., Ltd.
Totsuka, Yokohama

The Normal Vibrations of Polyglycine I

By Kunio FUKUSHIMA, Yoshiko IDEGUCHI and Tatsuo MIYAZAWA

(Received June 12, 1963)

The molecular structure and vibrational spectra of polyglycine I, $(-CH_2CONH-)_n$, are closely related to those of polypeptides and proteins. According to X-ray analyses,[1] it has been concluded that the chain conformation of polyglycine I is in the β-conformation. On the basis of this conformation, measurements and partial assignments of the infrared absorption bands of polyglycine I in the spectral region between 2 and 30 μ have been made by Shimanouchi et al. using a sample prepared by them.[2]

We are interested in the relationship between the chain conformation of polypeptides and their normal frequencies, especially the characteristic amide frequencies and skeletal frequencies. We have calculated the normal vibrations of polyglycine I and its *N*-deuterated species in order to elucidate the nature of the normal vibrations characteristic of β-chain polypeptides, in which the molecular chain is in the all-trans zig-zag conformation.

Internal Co-ordinates

According to X-ray investigations,[1] the molecule of polyglycine I belongs to the factor group C_{2v}. Therefore, the twenty-six normal vibrations (characteristic amide vibrations and skeletal vibrations) of the polyglycine I molecule are grouped into nine A_1, nine B_1, four A_2 and four B_2 vibrations. Of these, only the infrared active in-plane vibrations, A_1 and B_1 will be treated in the present study.

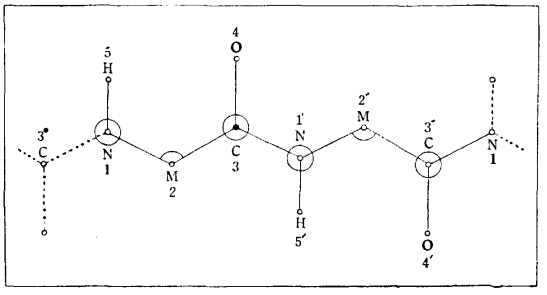

Fig. 1. Numbering of the atoms of the polyglycine I molecule.

The calculations were carried out according to Wilson's ***GF*** matrix method[3]; the methylene groups were treated as mass points, as the aim of these calculations was the analysis of only skeletal vibrations and characteristic amide vibrations. The molecular model is presented in Fig. 1; the internal co-ordinate vectors belonging to the m-th unit of the infinite molecular chain of the polyglycine I molecule will be denoted as $R^{(m)}$ and $R'^{(m)}$. The internal co-ordinates used are;

$$R_1^{(m)} \quad \Delta r_{NH} = \Delta r_{15}$$
$$R_2^{(m)} \quad \Delta\gamma_{NH} = (1/\sqrt{2})\Delta(\alpha_{513'} - \alpha_{215})$$
$$R_3^{(m)} \quad \Delta\beta_{NH} = (1/\sqrt{6})\Delta(2\alpha_{3'12} - \alpha_{513'} - \alpha_{215})$$
$$R_4^{(m)} \quad \Delta r_{NM} = \Delta r_{12}$$
$$R_5^{(m)} \quad \Delta\alpha_{NMC} = \Delta\alpha_{321}$$
$$R_6^{(m)} \quad \Delta r_{MC} = \Delta r_{23}$$
$$R_7^{(m)} \quad \Delta r_{CO} = \Delta r_{34}$$
$$R_8^{(m)} \quad \Delta\gamma_{CO} = (1/\sqrt{2})\Delta(\alpha_{432} - \alpha_{1'34})$$
$$R_9^{(m)} \quad \Delta\beta_{CO} = (1/\sqrt{6})\Delta(2\alpha_{231'} - \alpha_{1'34} - \alpha_{432})$$
$$R_{10}^{(m)} \quad \Delta r_{CN} = \Delta r_{31'}$$
$$R'^{(m)}_1 \quad \Delta r'_{NH} = \Delta r_{1'5'}$$
$$R'^{(m)}_2 \quad \Delta\gamma'_{NH} = (1/\sqrt{2})\Delta(\alpha_{31'5'} - \alpha_{5'1'2'})$$
$$R'^{(m)}_3 \quad \Delta\beta'_{NH} = (1/\sqrt{6})\Delta(2\alpha_{2'1'3} - \alpha_{31'5'} - \alpha_{5'1'2'})$$
$$R'^{(m)}_4 \quad \Delta r'_{NM} = \Delta r_{1'2'}$$
$$R'^{(m)}_5 \quad \Delta\alpha'_{NMC} = \Delta\alpha_{1'2'3'}$$
$$R'^{(m)}_6 \quad \Delta r'_{MC} = \Delta r_{2'3'}$$
$$R'^{(m)}_7 \quad \Delta r'_{CO} = \Delta r_{3'4'}$$
$$R'^{(m)}_8 \quad \Delta\gamma'_{CO} = (1/\sqrt{2})\Delta(\alpha_{2'3'4'} - \alpha_{4'3'1})$$
$$R'^{(m)}_9 \quad \Delta\beta'_{CO} = (1/\sqrt{6})\Delta(2\alpha_{13'2'} - \alpha_{2'3'4'} - \alpha_{4'3'1})$$
$$R'^{(m)}_{10} \quad \Delta r'_{CN} = \Delta r_{3'1}$$

where r_{ij} and α_{ijk} represent the bond length between atoms, i and j, and the bond angle formed by atoms, i, j and k respectively.

1) C. W. Bunn and E. V. Garner, *Proc. Roy. Soc.*, **A189**, 39 (1947); W. T. Astbury, *Nature*, **163**, 722 (1949); C. H. Bamford, L. Brown, E. M. Cant, A. Elliot, E. W. Hanby and B. R. Malcolm, ibid., **176**, 396 (1955).

2) S. Suzuki, Y. Iwashita, T. Shimanouchi and M. Tsuboi, Abstracts of the International Symposium on Molecular Structure and Spectroscopy, Tokyo (1962), A110.

3) E. B. Wilson, *J. Chem. Phys.*, **7**, 1047 (1939); **9**, 76 (1941).

	...	$R'^{(m-1)}$	$R^{(m-1)}$	$R'^{(m)}$	$R^{(m)}$	$R'^{(m+1)}$	$R^{(m+1)}$	...
⋮								
$R'^{(m-1)}$	$\tilde{B}$	A	B					
$R^{(m-1)}$		$\tilde{B}$	A	B				
$R'^{(m)}$			$\tilde{B}$	A	B			
$R^{(m)}$				$\tilde{B}$	A	B		
$R'^{(m+1)}$					$\tilde{B}$	A	B	
$R^{(m+1)}$						$\tilde{B}$	A	B
⋮								

Fig. 2. Form of $\boldsymbol{G}$, $\boldsymbol{F}$ matrix of polyglycine I.

TABLE I. FORCE CONSTANTS (mdyn./Å) AND MOLECULAR PARAMETERS

K(N-H)	5.6	H(H-N-C)	0.35	F(H. N. C)	0.50
K(N-C)	5.5	H(C-N-M)	0.30	F(C. N. M)	0.30
K(N-M)	3.4	H(H-N-M)	0.15	F(H. N. M)	0.50
K(M-C)	3.1	H(N-M-C)	0.20	F(N. M. C)	0.30
K(C=O)	8.5	H(O=C-M)	0.30	F(O. C. M)	0.50
		H(M-C-N)	0.30	F(M. C. N)	0.50
		H(O=C-N)	0.35	F(O. C. N)	1.50
		r_{NH}	1.00Å	α_{HNC}, α_{CNM}, α_{MNH},	
		r_{NM}	1.47Å	α_{NMC}, α_{OCM}, α_{MCN},	
		r_{MC}	1.54Å	α_{NCO}.....120°	
		r_{CO}	1.21Å		
		r_{CN}	1.32Å		

By the use of these internal co-ordinate vectors, the $\boldsymbol{G}$ matrix of the polyglycine I molecule was constructed; it is expressed in the form shown in Fig. 2.

Potential Energy

The Urey-Bradley potential energy[4] of the polyglycine I molecule is expressed as:

$$V=\sum_{m,i,j}K'_{ij}r_{ij}^{(m)}[\Delta r_{ij}^{(m)}]+(1/2)K_{ij}[\Delta r_{ij}^{(m)}]^2+\sum_{m,i,j,k}H'_{ijk}r_{ij}^{(m)}r_{jk}^{(m)}[\Delta\alpha_{ijk}^{(m)}]+(1/2)H_{ijk}r_{ij}^{(m)}r_{jk}^{(m)}[\Delta\alpha_{ijk}^{(m)}]^2+\sum_{m,i,j,k}F'_{ik}q_{ik}^{(m)}[\Delta q_{ik}^{(m)}]+(1/2)F_{ik}[\Delta q_{ik}^{(m)}]^2$$

For the term containing F'_{ik} and F_{ik}, the summation is taken for all i and k combinations which correspond to the index i and k in α_{ijk}. In the above formula, m is the index for chain units, while $r_{ij}^{(m)}$, $r_{jk}^{(m)}$ and $q_{ik}^{(m)}$ represent the equilibrium value of the interatomic distance.

The Reduction of the Secular Equation

For a long chain molecule such as polyglycine I, only the vibrations in which all units in the molecular chain vibrate in phase are optically active.[5] Since the polyglycine I molecule has a plane of symmetry as well as a two-fold screw axis (fiber axis), the optically-active vibrations are classified into four species, A_1, B_1, A_2 and B_2. The A_1 and B_1 vibrations are symmetric with respect to the molecular plane, whereas the A_2 and B_2 vibrations are antisymmetric with respect to this plane. From the $\boldsymbol{G}$ and $\boldsymbol{F}$ matrices of infinite order shown in Fig. 2, the $\boldsymbol{G}$ and $\boldsymbol{F}$ matrices for the optically-active A_1 and B_1 vibrations were constructed by the symmetry co-ordinates shown below:

$$S_i=(1/\sqrt{N})\sum_m(R_i^{(m)}+R'^{(m)}_i) \quad \text{for } A_1 \text{ species} \tag{2}$$

$$S'_i=(1/\sqrt{N})\sum_m(R_i^{(m)}-R'^{(m)}_i) \quad \text{for } B_1 \text{ species} \tag{3}$$

In these equations, N is the total number of chain units in the polyglycine I molecular chain.

The secular equations (10th order) for the A_1 and B_1 vibrations

$$|\boldsymbol{G}_A\boldsymbol{F}_{A_1}-\lambda E|=0 \tag{4}$$

$$|\boldsymbol{G}_{B_1}\boldsymbol{F}_{B_1}-\lambda E|=0 \tag{5}$$

were solved by an NEAC model 2101 electronic computer. The force constants and the molecular parameters used in this calculation are listed in Table I. The calculated normal frequencies and the diagonal terms of potential

4) T. Shimanouchi, *J. Chem. Phys.*, **17**, 243, 734, 848 (1949).
5) S. E. Whitcomb, H. H. Nielsen and L. H. Thomas, *J. Chem. Phys.*, **8**, 143 (1940).

TABLE II. OBSERVED AND CALCULATED FREQUENCIES OF POLYGLYCINE I AND *N*-DEUTERATED POLYGLYCINE I AND CALCULATED ^{15}N ISOTOPE SHIFTS OF FREQUENCIES*

	Polyglycine I			*N*-Deuterated polyglycine I		
	ν_o	ν_c	^{15}N Shift	ν_o	ν_c	^{15}N Shift
A_1		176	− 1		173	− 2
		223	− 2		221	− 1
	628(IV)	589	− 2		587	− 2
	987	991	−13	935(III′)	963	− 3
	1112	1101	−11		984	− 9
	1235(III)	1305	− 3		1153	−10
	1524(II)	1518	−17	1475(II′)	1425	−19
	1685(I)	1652	− 2		1642	− 2
B_1		278	− 1		278	− 1
		541	− 6		518	− 5
	773(IV)	741	− 3		737	− 3
		874	− 9		863	− 7
	1015	1001	−16		984	−13
	1215(III)	1295	− 3		1037	− 4
	1524(II)	1512	−17	1475(II′)	1425	−19
	1630(I)	1647	− 1		1632	− 1
A_1, B_1	3300(νNH)	3340	− 7	2500(νND)	2438	−11

* ν_o Observed frequency, cited from Ref. 2 ν_c Calculated frequency

energy distributions are shown in Tables II and III respectively. The L^x matrix, which is used for the transformation from the normal co-ordinate vector, Q, into the cartesian co-ordinate vector fixed to the molecule, X, was calculated by the following formulae;[6]

$$X = L^x Q \tag{6}$$

$$L^x = M^{-1}\tilde{B}FL\Lambda^{-1} \tag{7}$$

The schematic representations of the atomic displacements thus calculated are shown in Figs. 3 and 4. The ^{15}N isotope shifts of the normal frequencies of the polyglycine I molecule were calculated by the following equation:[7]

$$\lambda_a = (1/m'_n - 1/m_n)(m_n)^2 \times [(L^x_{na})^2 + (L^y_{na})^2 + (L^z_{na})^2] \tag{8}$$

λ_a : The isotope shift of the a-th frequency parameter
m_n : The mass of the n-th atom
m'_n : The mass of the isotope atom
$(L^x)_{na}$: The vector associated with the n-th atom in the a-th normal vibration

$$(L^x)_{na} = \begin{pmatrix} L^x_{na} \\ L^y_{na} \\ L^z_{na} \end{pmatrix}$$

The calculated isotope shifts of the normal frequencies are shown in Table II.

Discussion

Polyglycine I is in the antiparallel chain-pleated sheet structure in the crystalline state.[1] Therefore, the assignment of the infrared absorption bands has to be made according to this structure, which contains interchain hydrogen bonds. Each of the internal vibrations of the polyglycine I molecule splits into two normal vibrations in the case of the polyglycine I crystal as follows:[8]

Molecule	Crystal	Selection rule
A_1	(0, 0)	IR inactive
	(0, π)	IR active
B_1	(π, 0)	IR active
	(π, π)	IR active
A_2	(0, 0)	IR inactive
	(0, π)	IR inactive
B_1	(π, 0)	IR active
	(π, π)	IR active

In principle, all the infrared active vibrations of the polyglycine I crystal are expected to appear in the infrared absorption. However, except for the amide I, II and III vibrations the frequency difference of each pair of splitted

6) B. L. Crawford, Jr., and W. H. Fletcher, ibid., **19**, 141 (1951).
7) T. Miyazawa, Abstracts of the 15th Annual Meeting of the Chemical Society of Japan, Kyoto (1962), p. 20211.
8) T. Miyazawa, *J. Chem. Phys.*, **32**, 1647 (1960).

TABLE III. THE DIAGONAL TERMS OF POTENTIAL ENERGY DISTRIBUTIONS OF POLYGLYCINE I MOLECULE AND *N*-DEUTERATED SPECIES

Polyglycine I molecule, A_1 vibration

ν_c	S_1	S_2	S_3	S_4	S_5	S_6	S_7	S_8	S_9	S_{10}
	S_i									
3340	1.0	0.0	0.0	0.0	0.0	0.0	0.0	0.0	0.0	0.0
1652	0.0	0.0	0.1	0.0	0.0	0.0	0.8	0.1	0.0	0.1
1518	0.0	0.0	0.7	0.1	0.0	0.0	0.0	0.0	0.1	0.4
1304	0.0	0.0	0.3	0.0	0.0	0.3	0.1	0.0	0.1	0.3
1101	0.0	0.0	0.0	0.7	0.0	0.2	0.0	0.1	0.0	0.0
991	0.0	0.2	0.0	0.0	0.1	0.2	0.2	0.1	0.1	0.1
589	0.0	0.0	0.0	0.0	0.1	0.1	0.0	0.0	0.7	0.0
223	0.0	0.3	0.0	0.0	0.1	0.0	0.0	0.6	0.0	0.0
176	0.0	0.4	0.0	0.0	0.5	0.0	0.0	0.0	0.1	0.0

Polyglycine I molecule, B_1 vibration

ν_c	S'_1	S'_2	S'_3	S'_4	S'_5	S'_6	S'_7	S'_8	S'_9	S'_{10}
	S'_i									
3340	1.0	0.0	0.0	0.0	0.0	0.0	0.0	0.0	0.0	0.0
1647	0.0	0.0	0.1	0.0	0.0	0.0	0.8	0.1	0.0	0.1
1512	0.0	0.0	0.6	0.1	0.0	0.1	0.0	0.0	0.1	0.4
1294	0.0	0.0	0.3	0.1	0.0	0.2	0.1	0.0	0.1	0.3
1001	0.0	0.1	0.0	0.5	0.0	0.1	0.1	0.0	0.1	0.2
874	0.0	0.0	0.0	0.3	0.0	0.5	0.0	0.0	0.1	0.0
741	0.0	0.3	0.0	0.1	0.1	0.2	0.0	0.0	0.3	0.0
541	0.0	0.0	0.0	0.0	0.2	0.0	0.0	0.7	0.1	0.0
278	0.0	0.3	0.0	0.0	0.2	0.0	0.0	0.0	0.4	0.0

N-Deuterated polyglycine I molecule, A_1 vibration

ν_c	S_1	S_2	S_3	S_4	S_5	S_6	S_7	S_8	S_9	S_{10}
	S_i									
2438	1.0	0.0	0.0	0.0	0.0	0.0	0.0	0.0	0.0	0.0
1642	0.0	0.0	0.0	0.0	0.0	0.0	0.8	0.1	0.0	0.2
1425	0.0	0.0	0.2	0.1	0.0	0.2	0.0	0.0	0.1	0.7
1153	0.0	0.0	0.4	0.1	0.0	0.1	0.1	0.0	0.0	0.1
984	0.0	0.2	0.2	0.2	0.1	0.1	0.1	0.1	0.0	0.0
963	0.0	0.0	0.2	0.5	0.0	0.4	0.0	0.0	0.1	0.0
587	0.0	0.0	0.0	0.0	0.1	0.1	0.0	0.0	0.7	0.0
221	0.0	0.3	0.0	0.0	0.1	0.0	0.0	0.6	0.0	0.0
173	0.0	0.4	0.0	0.0	0.5	0.0	0.0	0.0	0.1	0.0

N-Deuterated polyglycine I molecule, B_1 vibration

ν_c	S'_1	S'_2	S'_3	S'_4	S'_5	S'_6	S'_7	S'_8	S'_9	S'_{10}
	S'_i									
2438	1.0	0.0	0.0	0.0	0.0	0.0	0.0	0.0	0.0	0.0
1632	0.0	0.0	0.0	0.0	0.0	0.0	0.9	0.1	0.0	0.2
1425	0.0	0.0	0.2	0.1	0.0	0.2	0.0	0.0	0.1	0.6
1037	0.0	0.0	0.7	0.0	0.0	0.1	0.0	0.0	0.1	0.0
984	0.0	0.1	0.0	0.4	0.0	0.1	0.1	0.0	0.1	0.2
863	0.0	0.0	0.0	0.3	0.0	0.4	0.1	0.0	0.0	0.0
737	0.0	0.3	0.0	0.1	0.1	0.2	0.0	0.0	0.3	0.0
518	0.0	0.0	0.1	0.0	0.2	0.0	0.0	0.6	0.1	0.0
278	0.0	0.3	0.0	0.0	0.2	0.0	0.0	0.0	0.4	0.0

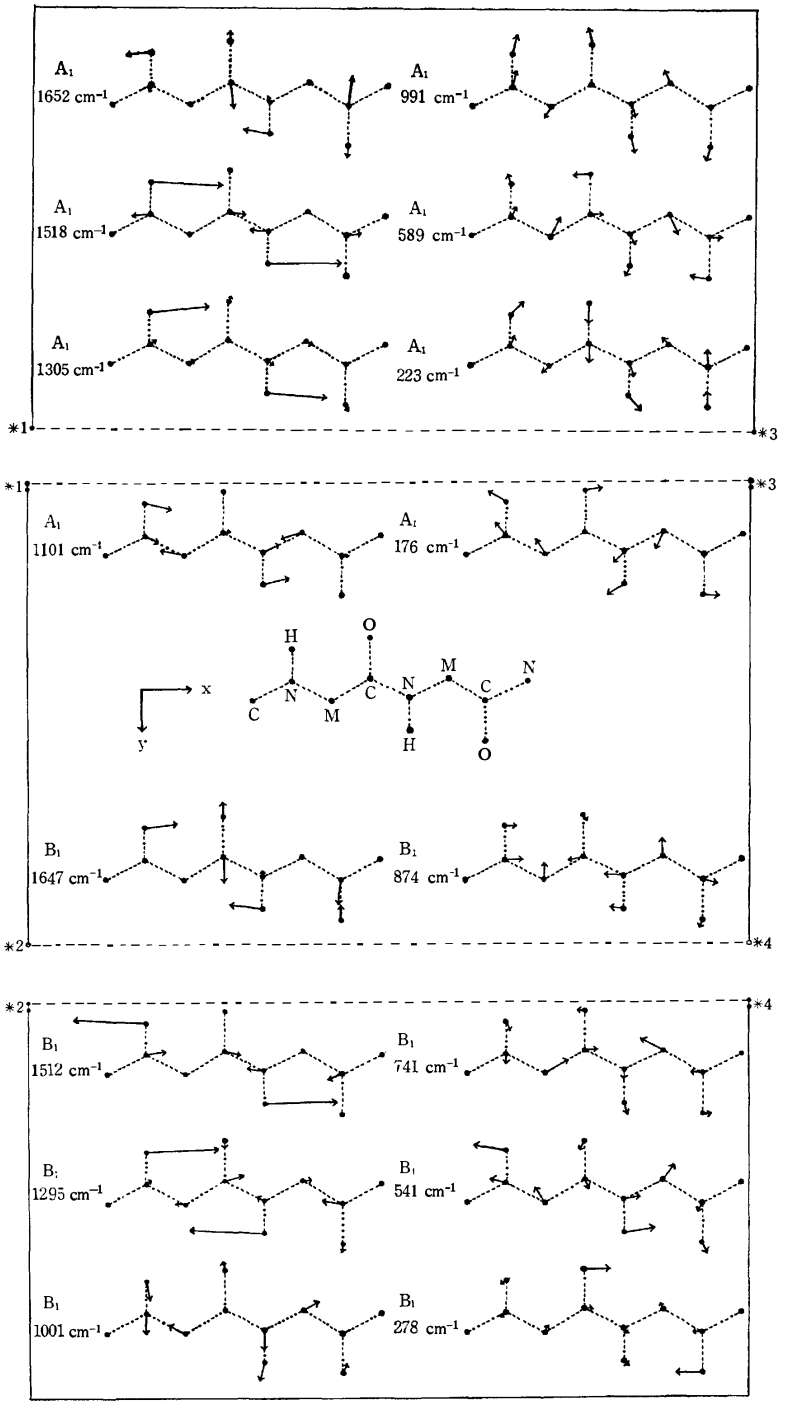

Fig. 3. Calculated normal modes of the A_1 and B_1 vibrations of polyglycine I.

bands may be very small in the case of in-plane vibrations. Therefore, detailed assignments on the basis of the selection rule for the crystal were made only for the amide I, II and III vibrations; the assignments of the other vibrations were made according to the selection rule based on the molecular symmetry. Accordingly, the bands assigned to the B_1 vibrations are considered to be due to the $\nu(\pi, 0)$ and $\nu(\pi, \pi)$ vibrations.

Characteristic Amide Vibrations.—Among the vibrations characteristic of polypeptides, six

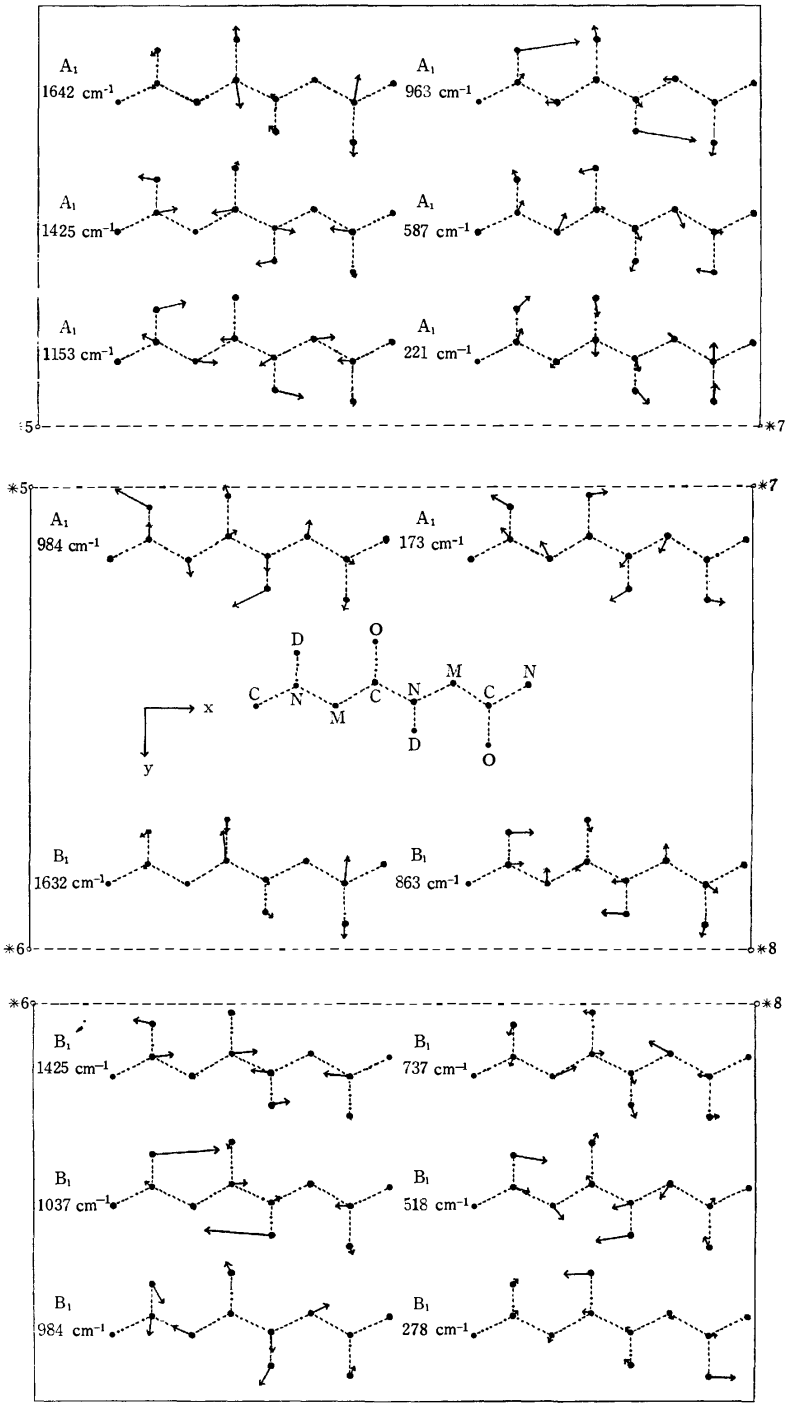

Fig. 4. Calculated normal modes of the A_1 and B_1 vibrations of *N*-deuterated polyglycine I.

vibrations (amide I, amide II, amide III, amide IV, amide II′ and amide III′) are treated as the in-plane vibrations of polyglycine I and its *N*-deuterated compound. The nature of these vibrations will now be discussed.

Amide I Vibration.—As Table III shows, this vibration is the antisymmetric stretching vibration of the O=C–N skeleton, in which the ratios of the energy associated to the C=O and C–N bonds are 0.78 : 0.14 for the A_1 vibration and 0.78 : 0.10 for the B_1 vibration. There are three types of amide I vibrations, $\nu(0, \pi)$,

$\nu(\pi, 0)$ and $\nu(\pi, \pi)$. The frequency of the $\nu(0, \pi)$ vibration is higher than those of $\nu(\pi, 0)$ and $\nu(\pi, \pi)$. These vibrations have been observed at 1688 cm^{-1} ($\nu(0, \pi)$) and 1630 cm^{-1} ($\nu(\pi,0)$). The direction of the transition moment associated with the $\nu(0, \pi)$ vibration is parallel to the fiber axis. Since the C=O bonds are nearly perpendicular to the chain axis, the C=O bond transition moments are largely canceled in the $\nu(0, \pi)$ vibration. Therefore, this vibration is expected to be weak in intensity. For the $\nu(\pi, 0)$ vibration, in which the direction of the transition moment is perpendicular to the fiber axis, the contribution of the C=O bond moment change is great. Therefore, the intensity of this vibration is expected to be strong. The assignments of the 1685 cm^{-1} band to $\nu(0, \pi)$ and the 1630 cm^{-1} band to $\nu(\pi, 0)$ reasonably follow from a consideration of their intensities.

Amide II Vibration. — This is the coupled vibration of the N-H in-plane bending and the amide C-N stretching vibrations. The degree of the coupling of these two vibrations is nearly the same for the A_1 and B_1 vibrations. These vibrations are observed at 1524 cm^{-1}.

Amide II' Vibration. — This is the coupled vibration of the C-N stretching, the N-D in-plane bending and the C-M stretching vibrations.

Amide III Vibration.—To this vibration, the contributions of the N-H in-plane bending, the C-M stretching and the N-C stretching modes are important. The couplings of these modes are different for the A_1 and B_1 vibrations, as Table IV shows. The frequency of the A_1 vibration is higher than that of the B_1 vibration. The $\nu(0, \pi)$ (A_1) vibration appears at 1236 cm^{-1} and the $\nu(\pi, 0)$ and $\nu(\pi, \pi)$ (B_1) vibrations at 1214 cm^{-1}.

Amide III' Vibration.—To this vibration, the N-D in-plane bending mode contributes mainly; however, the contributions of skeletal stretching modes are also important.

Amide IV Vibration. — In this vibration, the frequency difference between the A_1 and B_1 vibrations is large. The calculated A_1 frequency is 589 cm^{-1} while the calculated B_1 frequency is 741 cm^{-1}. The A_1 vibration is an almost pure C=O in-plane bending vibration with a small contribution by the C-M stretching mode, whereas the B_1 vibration is a coupled vibration of the C=O in-plane bending, C-N-M skeletal deformation and C-M stretching modes. In the A_1 vibration, all the C=O bonds displace in phase, with a resultant strong transition moment along the molecular chain, so the intensity of this vibration may be expected to be very strong. Therefore, the strong band at 628 cm^{-1} is assigned to this vibration. In the B_1 vibration the bond moment change associated with the C=O in-plane bending mode will not contribute much to the total dipole moment change, and the transition moment of this B_1 vibration is possibly due to the dipole moment change of the C-N-M skeletal mode. Since the intensity of this B_1 vibration is considered to be weak, the weak band at 773 cm^{-1} is assigned to this vibration.

Nature of the Skeletal Vibrations. — The skeletal vibrations of polyglycine I are important in studying the changes in the polypeptide chain conformation. From the results of the calculations, the nature of the skeletal vibrations of the β-type polypeptide chain with no side chains has been made clear.

Skeletal Stretching Vibrations.—There are four skeletal stretching vibrations in the polyglycine I molecule, two belonging to the A_1 species and the other two belonging to the B_1 species. As Table II shows, the A_1 vibration calculated at 1101 cm^{-1} is the antisymmetric stretching vibration of the N-M-C skeleton. The band at 1112 cm^{-1} is assigned to this vibration. The other A_1 vibration, calculated at 991 cm^{-1}, is the C-M stretching vibration coupled with the M-C-N and C-N-M skeletal deformation modes. The band at 987 cm^{-1} is assigned to the A_1 vibration. For the B_1 species, the vibration calculated at 1001 cm^{-1} is the antisymmetric stretching vibration of the C-N-M skeleton coupled with the C-N-M skeletal deformation mode. The band at 1015 cm^{-1} is assigned to this vibration. The other B_1 vibration calculated at 874 cm^{-1} is the symmetric stretching vibration of the N-M-C skeleton. The band due to this vibration has not yet been identified.

Skeletal Deformation Vibrations. — There are four skeletal deformation vibrations, two belonging to the A_1 species and two belonging to the B_1 species. The A_1 vibrations include the antisymmetric skeletal deformation vibration of the M-C-N-M skeleton calculated at 223 cm^{-1} and the antisymmetric skeletal deformation vibration of the C-N-M-C skeleton calculated at 176 cm^{-1}. The two skeletal deformation frequencies of the B_1 species are very different from those of the A_1 species. The B_1 vibrations include the symmetric deformation vibration of the C-N-M-C skeleton, coupled with the amide IV vibration calculated at 278 cm^{-1}, and the symmetric deformation vibration of the N-M-C-N skeleton (calculated frequency at 541 cm^{-1}).

Institute for Protein Research
Osaka University
Kita-ku, Osaka

An Unsaturated Cyclic Alcohol in the Nonsaponifiable Matter of the Liver Oil of the Crab, Paralithodes Camtschatica

(Received June 21, 1963)

By Suketaka ITO[*1] and Yoshiyuki TOYAMA[*2]

The presence of an unsaturated alcohol with the formula $C_{10}H_{18}O_2$ in the nonsaponifiable matter of the liver oil of the crab, *Palalithodes Camtschatica*, was reported forty years ago by Tsujimoto.[1] This alcohol, named kanyl alcohol by him, was shown to be an unsaturated monohydric alcohol, whereas the nature of the other oxygen atom was not decided. It was postulated as having a branched chain of carbon atoms or a cyclic structure from the fact that both this alcohol and its hydrogenation product had low freezing points. The hydroxyl group of this alcohol was inferred to be located in a position which is unfavorable for urethan formation, since neither phenyl urethan nor α-naphthyl urethan of a crystalline form could be obtained from this alcohol. Later, Nakamiya[2] reinvestigated a fraction corresponding to the kanyl alcohol of Tsujimoto and concluded that kanyl alcohol was not a uniform substance but a mixture of different components.

In this study, the liquid fraction was separated from the nonsaponifiable matter of the liver oil of the crab, *Paralithodes Camtschatica*. The acetate of this fraction was fractionally distilled to give an acetate fraction which accords with Tsujimoto's kanyl alcohol in its refractive index, saponification value and iodine value. However, when this fraction was subjected to chromatography on silica gel, a main fraction and a by-fraction were collected in the ratio of approximately 2 : 1. The gas-liquid chromatography of these two fractions indicated that while the by-fraction contained at least several components, the main fraction consisted almost exclusively of a uniform substance. When the main fraction was studied further, the conclusion was reached that the free alcohol, $C_{12}H_{20}O_2$, corresponding to this acetate fraction is α-octa-2, 5-dienyl-β-hydroxytetrahydrofuran.

*1 Present address: Department of Industrial Chemistry, Faculty of Engineering, Shinshu University, Nagano-shi.

*2 Present address: Department of Applied Chemistry, Faculty of Engineering, Toyo University, Kawagoe, Saitama-ken.

1) M. Tsujimoto, *Repts. Govern. Chem. Ind. Res. Inst., Tokyo*, 23 [3], 25 (1928); 24 [4], 9 (1929).

2) Z. Nakamiya, *Bull. Inst. Phys. Chem. Res.*, 19, 790 (1940).

Experimental

The Properties of Liver Oil.—A 37.35 kg. batch of livers separated from crabs, *Paralithodes Camtschatica*, caught in northern waters was supplied by the Nihon Suisan K. K. It was heated on a water bath to remove the bulk of the water; the concentrated material, 11 kg., was extracted with ether, yielding 2.033 g. of oil. The oil was completely soluble in acetone. It was a dark brown liquid with a peculiar odor and had the following characteristics: d_4^{20} 0.9280, n_D^{20} 1.4796, A. V. 89.4, S. V. 160.4, I. V. (Wijs) 174.1[*3] and nonsaponifiable matter 11.0 %.

The Separation of the Liquid Fraction of Nonsaponifiable Matter and the Fractional Distillation of Its Acetate.—A crude nonsaponifiable matter was separated from the oil by saponification with potassium hydroxide in ethanol, followed by the extraction of the soap solution with ether in the usual way. A 202 g. portion of the crude nonsaponifiable matter was dissolved in 600 ml. of hot methanol, and the solution was cooled with ice to separate 53 g. of a crystalline solid which consisted chiefly of cholesterol. The solid was filtered, and the material recovered from the filtrate was dissolved in 440 ml. of hot acetone. When the acetone solution was cooled, 14.5 g. of a crystalline solid was separated and filtered. This solid consisted chiefly of batyl alcohol, together

TABLE I. THE FRACTIONAL DISTILLATION OF THE ACETATE OF LIQUID NONSAPONIFIABLE MATTER

Fraction	B. p. °C/3.5 mmHg	Yield g.	n_D^{23}	S. V.	I. V.
1	~130	6.0	1.4599	259.8	124.6
2	130~140	12.3	1.4642	266.5	142.1
3	140~150	2.2	1.4645	277.9	129.5
4	150~160	1.3	1.4644	274.4	116.7
5	160~170	1.9	1.4634	275.2	96.1
6	170~180	1.8	1.4627	268.4	92.1
7	180~190	3.3	1.4609	259.5	78.9
8	190~200	2.5	1.4594	245.8	67.3
9	200~210	6.0	1.4586	228.2	57.1
10	210~219	16.0	1.4582	225.6	50.3
11	219~220	6.4	1.4590	224.4	49.8
12	220~223	15.1	1.4605	218.1	56.1
13	223	6.7	1.4663	211.5	71.7
14	Residue	13.0	—	—	—

*3 The abbreviations A. V., S. V. and I. V. are used for acid value, saponification value and iodine value respectively.

with a small amount of cholesterol. From the acetone filtrate a liquid fraction of nonsaponifiable matter was recovered (n_D^{22} 1.4898, A. V. 8.4 and I. V. 142.8). It was acetylated by refluxing it with acetic anhydride to give an acetate of S. V. 206.9 and I. V. 100.7. A 145 g. portion of this acetate was distilled to give a distillate of b. p. 110~223°C/2 mmHg, S. V. 231.2 and I. V. 84.3. The fractional distillation of this distillate (94.5 g.) gave the results shown in Table I.

Fraction 1 and fractions 3—6 in Table I were refractionated. A fraction approximating fraction 2 was separately collected and united to fraction 2. This united fraction was fractionated further to give, eventually, 8.7 g. of a fraction with b. p. 130~135°C/2 mmHg, n_D^{22} 1.4624, S. V. 265.0 and I. V. 143.9. These values approximate those for kanyl acetate reported by Tsujimoto:[1] n_D^{20} 1.4623, S. V. 251 and I. V. 145.

The Chromatography of the Acetate Fraction (B. p. 130~135°C/2 mmHg).—This fraction (8.5 g.) was chromatographed on silica gel and eluted with hexane and then with hexane-ether (100 : 0.5, 100 : 1 and 100 : 2). Each 100 ml. of the eluate was separately collected, giving a total of 60 fractions. The chromatogram is shown in Fig. 1. The eluate

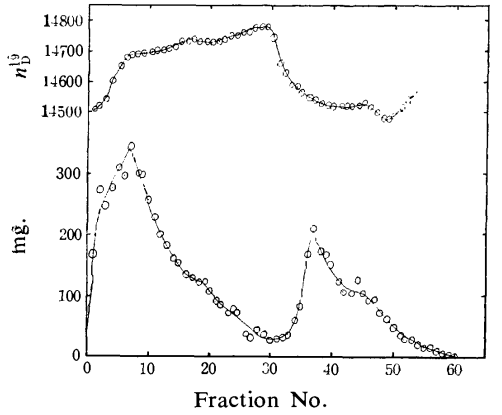

Fig. 1. Elution chromatogram of the acetate fraction, b. p. 130~135°C/2 mmHg.

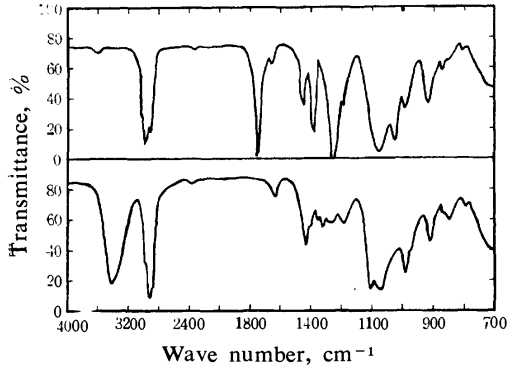

Fig. 2. Infrared spectra of the fraction A (upper) and the free alcohol (lower). Film on NaCl flats.

fractions 5—14 were united, and 2.6 g. of united material were rechromatographed on silica gel. After the earlier and later eluate fractions had been removed, the intermediate fractions, 2.05 g. in total (n_D^{20} 1.4703~1.4712) were combined into a fraction A of S. V. 235.5 and I. V. 196.5 (calculated for $C_{12}H_{19}O \cdot OCOCH_3$: S. V. 235.4 and I. V. 213.0). Fraction A was analyzed by gas-liquid chromatography at 210°C, using a 225 cm×6 mm. column of diethylene glycol succinate polyester on Celite 545. The chromatogram indicated that this fraction contained a uniform substance almost exclusively. The infrared spectra of this fraction and the free alcohol obtained by saponification are shown in Fig. 2.

The eluate fractions 36—46 in Fig. 1 were united, and the united material, 1.55 g., was chromatographed on silica gel to give 0.96 g. of a fraction B having S. V. 322.7 and I. V. 107.6, but this fraction was found by gas-liquid chromatography to be a complicated mixture of different components.

Alkali-Isomerization and Ozonolysis of Fraction A. — Fraction A, after isomerization with a 6.6% solution of potassium hydroxide in ethylene glycol at 180°C for 25 min., exhibited the characteristic absorption of conjugated dienes, $k_{233}=37.6$.

A 100 mg. portion of fraction A in 10 ml. of chloroform was ozonized at −15°C. Then 10 ml. of water was added to the solution, and the mixture was gradually heated from 20°C to 90°C while a current of hydrogen was being passed through the mixture. The volatile substances formed were carried off by the hydrogen current and passed successively through a trap containing a solution of 2,4-dinitrophenylhydrazine in 2 N hydrochloric acid and a trap containing a solution of barium hydroxide. A considerable amount of precipitates of barium carbonate was formed in the second trap. The precipitates of 2,4-dinitrophenylhydrazone (DNPH) formed in the first trap were filtered. The DNPHs in the filtrate were recovered by extraction with benzene, followed by washing of the benzene solution with 2 N hydrochloric acid and water, and finally by the distilling off of the benzene. The total yield of crude DNPHs was 294 mg. Crude DNPHs were chromatographed on silica gel. Two eluate fractions were collected using hexane and hexane-ether as the eluants. The first eluate fraction gave 90 mg. of a DNPH which was then purified by rechromatography on silica gel, followed by recrystallization from hexane. The purified substance was in the form of orange yellow needles of m. p. 155.5~156.5°C (lit.[3] 155°C for propionaldehyde DNPH).

Found: N, 23.40. Calcd. for $C_9H_{10}N_4O_4$: N, 23.50%.

The second eluate fraction gave 78 mg. of a DNPH which was purified by rechromatography on silica gel and recrystallization from hexane to give, eventually, yellow needles of m. p. 165~165.5°C (lit.[4] 168.5°C for acetaldehyde DNPH). No depression of the melting point was observed on admixture with an authentic specimen of acetaldehyde DNPH.

3) C. F. H. Allen, *J. Am. Chem. Soc.*, **52**, 2955 (1930).
4) W. M. D. Bryant, ibid., **60**, 2814 (1938).

A Saturated Alcohol from the Hydrogenation Product of Fraction A.—Fraction A was hydrogenated in ethanol using platinum black as the catalyst. The hydrogenation product was saponified to give a crude saturated alcohol which had n_D^{17} 1.4581 and I. V. 6.2. It was a pale yellow liquid with a solidifying point below −15°C, which was negative to the iodoform reaction. This material was used as a saturated alcohol in the experiments described below.

Phenyl Urethan. — A solution of 50 mg. of the saturated alcohol in 3 ml. of benzene, which had been dried over metallic sodium, was refluxed with 50 mg. of phenyl isocyanate for 30 min. When the solvent and the excess of the reagent were distilled off, the reaction product, phenyl urethan, was obtained in a yield of 80 mg. It did not solidify on standing at room temperature. Only after repeated heating and cooling did it begin to solidify. After repeated recrystallizations from hexane, fibrous crystals of m. p. 57.5~58.5°C were obtained.

Found: C, 71.22; H, 9.08; N, 4.84. Calcd. for $C_{19}H_{29}O_3N$: C, 71.44; H, 9.15; N, 4.39%.

The Oxidation of the Saturated Alcohol with Chromic Acid. — A solution of 100 mg. of chromic anhydride in 5 ml. of 90% acetic acid was gradually added to a solution of 180 mg. of the saturated alcohol in 10 ml. of glacial acetic acid; the resulting solution was allowed to stand overnight at room temperature. Then the solution was heated at 60°C for 15 min., and the reaction product was extracted with ether. The ether solution was washed succesively with a solution of sodium bisulfite, water, a solution of sodium carbonate and water. When the ether was distilled off, 162 mg. of the reaction product remained. To a solution of this material in 5 ml. of ethanol was added the reagent prepared from 0.2 g. of 2,4-dinitrophenylhydrazine, 1 ml. of sulfuric acid, 1.5 ml. of water and 5 ml. of ethanol. The mixture was heated at 60°C for 10 min. and then allowed to stand for 24 hr. The precipitates of crude DNPH formed were filtered. Yield, 152 mg. These were purified by chromatography on silica gel and elution with hexane and hexane-ether. The material obtained from the main eluate fraction was purified further by repeated recrystallizations from hexane to give, eventually, 35 mg. of yellow needles of m. p. 84.5~85.5°C.

Found: C, 57.13; H, 6.91; N, 14.83. Calcd. for $C_{18}H_{26}N_4O_5$: C, 57.13; H, 6.93; N, 14.81%.

The Oxidative Cleavage of the Saturated Alcohol with Potassium Permanganate. — To a solution of 90 mg. of the saturated alcohol in 30 ml. of acetone an excess of potassium permanganate in small portions was added, and the mixture was refluxed for 7 hr. The reaction product was treated in the usual way, and 46 mg. of an acidic substance was separated. This was converted to the methyl ester, and the latter was analyzed by gas-liquid chromatography (temperature: 160°C). Methyl pelargonate, together with a small amount of methyl caprylate and oenanthate, was identified.

The Preparation of *n*-Dodecane by the Reduction of the Reaction Product of the Saturated Alcohol and Hydrogen Iodide. — Six grams of hydrogen iodide (d=1.7) were added to a solution of 205 mg. of the saturated alcohol in 2 ml. of glacial acetic acid, and the mixture was refluxed for 1 hr. The reaction product was extracted with ether, and the ether solution was washed successively with a solution of sulfurous acid, a solution of sodium bicarbonate, and water. When the ether was distilled off, there remained 380 mg. of the reaction product, which was regarded as alkyl iodide by its infrared spectrum.*4 To a solution of 160 mg. of this iodide in 35 ml. of ether, which had been dried over metallic sodium, 200 mg. of lithium aluminum hydride were added and the solution was refluxed for 2 hr. The reaction product was separated in the usual way. Yield, 63 mg. *n*-Dodecane was identified by gas-liquid chromatography (temperature: 100°C).

The Ozonolysis of the Debromination Product of the Alkyl Bromide Derived from the Saturated Alcohol.—To a solution of 190 mg. of the saturated alcohol in 2 ml. of glacial acetic acid 10 g. of hydrogen bromide (d=1.49) were added, and the mixture was refluxed for 5 hr. The reaction product was separated in the usual way. Yield, 267 mg. This was considered to be alkyl bromide from its infrared spectrum.*4 The bromide was dissolved in 15 ml. of glacial acetic acid, and 750 mg. of zinc powder were added to the solution. After this solution had been refluxed for 2 hr., the debromination product was obtained by extraction with ether. The debromination product (130 mg.) in 10 ml. of methylene chloride was ozonized at −15°C. The ozonide was decomposed by adding 5 ml. of a 10% solution of potassium hydroxide and 1 ml. of 30% hydrogen peroxide, after which the mixture was gradually heated to 85°C while passing a current of nitrogen through it. The alkaline solution was then acidified with diluted sulfuric acid and distilled. The distillate, after neutralization with a N/10 solution of potassium hydroxide, was evaporated, and the residue was taken up with ethanol. The ethanol solution was concentrated to a volume of 2~3 ml. Benzyl bromide in an amount equivalent to the alkali required for the neutralization of the distillate was added to the concentrated ethanol solution, and the mixture was refluxed for 25 min. The benzyl esters thus obtained were extracted with ether. Yield, 63 mg. These were analyzed by gas-liquid chromatography (temperature: 200°C); benzyl propionate and pelargonate were identified as the main components.

Discussion

Since cholesterol and batyl alcohol are the main components of the crystalline solid which was obtained by recrystallizations of the total nonsaponifiable matter from methanol and acetone, and since batyl and selachyl acetates are found as main components of the higher-boiling acetate fractions (Table I) of the liquid nonsaponifiable matter, cholesterol, batyl

*4 The absorption bands associated with the hydroxyl and ether groups in the original unsaturated alcohol were absent in the spectrum of this substance.

alcohol and selachyl alcohol are considered to be major components of the total nonsaponifiable matter.

An acetate fraction (b. p. 130~135°C/2 mmHg) obtained by the fractional distillation of the acetate of liquid nonsaponifiable matter accorded with Tsujimoto's kanyl acetate in its properties, but this fraction was found to be a heterogeneous mixture by gas-liquid chromatography. Of the two eluate fractions (A and B) obtained by column chromatography of this fraction on silica gel, fraction A consisted of a uniform substance, while fraction B was found to be a mixture of different components. Hence, kanyl alcohol is not a uniform substance but a mixture which contains a peculiar alcohol as a main component, namely, the alcohol of fraction A. Since fraction A was readily separated by column chromatography, it appears to be of a series quite different from the other component acetates.

It may be seen from Fig. 2 that the infrared spectra of fraction A and the free alcohol obtained therefrom show an absorption band at 1075 cm^{-1} which may be assigned to the C–O stretching vibration of aliphatic ethers or five- or six-membered cyclic ethers,[5] while the infrared spectrum of the free alcohol shows an absorption band at 1105 cm^{-1} which may be assigned to the C–O stretching vibration of secondary alcohols. Since the formula of the saturated alcohol obtained by the hydrogenation of fraction A is demonstrated as $C_{12}H_{24}O_2$ by analyses of its phenyl urethan and of the DNPH obtained from its oxidation product (ketone), the formula of the unsaturated alcohol should be $C_{12}H_{20}O_2$, since it has two double bonds, as is seen from its iodine value of 241.4. The proportion of carbon and hydrogen atoms indicated that there should be a cyclic group in its molecule.

Fraction A has an alkali-conjugatable diene $=CHCH_2CH=$, and the ozonolysis of fraction A gives propionaldehyde as a cleavage product. Accordingly, fraction A should have the group $CH_3CH_2CH=CHCH_2CH=CH-$. Further, the oxidative scission of the saturated alcohol with potassium permanganate yields pelargonic acid as a main cleavage product. Hence, the saturated alcohol should have a straight chain of 9 carbon atoms; $CH_3(CH_2)_7CH<$. This fact, together with the fact that the reduction of the alkyl iodide derived from the saturated alcohol with lithium aluminum hydride yields *n*-dodecane, leads to the conclusion that the unsaturated alcohol is α-octa-2, 5-dienyl-β-hydroxytetrahydrofuran:

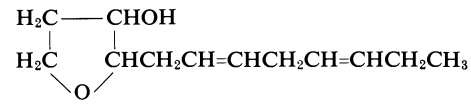

This structure is also consistent with the fact that the ozonolysis of the debromination product of the alkyl bromide derived from the saturated alcohol yields pelargonic and propionic acids.

Department of Applied Chemistry
Faculty of Engineering
Nagoya University
Chikusa-ku, Nagoya

5) L. J. Bellamy, "The Infrared spectra of Complex Molecules," Methuen & Co., Ltd., London (1958), pp. 116, 119.

The Rearrangement Reaction of Levulinic Acid in a Selenium Dioxide-catalyzed Hydrogen Peroxide Oxidation

By Noboru SONODA and Shigeru TSUTSUMI

(Received May 10, 1963)

In previous reports[1-4] we described the synthesis of carboxylic acids from dialkyl ketones and aryl alkyl ketones by oxidation with hydrogen peroxide using a selenium dioxide catalyst. Our findings have shown that the process of the formation of carboxylic acids from an unsymmetrical dialkyl ketone involved the migration of one of the alkyl groups to the α-carbon atom of the other

1) N. Sonoda and S. Tsutsumi, This Bulletin, **32**, 505 (1959).
2) N. Sonoda, T. Yamaguchi and S. Tsutsumi, *J. Chem. Soc. Japan, Ind. Chem. Sec.* (*Kogyo Kagaku Zasshi*), **63**, 737 (1960).
3) N. Sonoda and S. Tsutsumi, This Bulletin, **33**, 1440 (1960).
4) N. Sonoda and S. Tsutsumi, ibid., **34**, 1007 (1961).

alkyl group and the oxidation of the carbonyl group to a carboxyl group. This observation led us to guess that keto-acid might be oxidized to dibasic acid with the same number of carbon atoms as the original keto-acid; therefore, levulinic acid was used as the starting material.

The oxidation of levulinic acid with hydrogen peroxide was carried out in a tertiary butyl alcohol solution in the presence of a catalytic amount of selenium dioxide at 82°C. Distillation of the reaction mixture under reduced pressure afforded glutaric acid as the main acid product; a small amount of methylsuccinic acid was also isolated as the isomer of glutaric acid.

Several studies[5-11] have been made of the syntheses of glutaric acid derivatives from levulinic acid. Hara and Fujise[5] have reported the one-step synthesis of glutaramide from levulinic acid by a Willgerodt reaction, and recently Motoki and Odaka[9-11] have studied a method for the syntheses of various derivatives of glutaric acid. In these cases, however, no rearrangement of the carbon skelton was observed, because these reactions proceeded via a process involving the reduction of the carbonyl group and the oxidation of the active methyl group. In the present case, glutaric acid may be formed by the intramolecular migration of the β-carboxyethyl group to the methyl carbon atom and by the oxidation of the original carbonyl group to the carboxyl group; these possibilities are based on the rearrangement behavior[1,12] of unsymmetrical dialkyl ketones. Furthermore, the evidence of the rearrangement was supported by the fact that the methylsuccinic acid isolated was produced by the migration of the methyl group to the methylene carbon atom adjacent to the carbonyl group:

$$CH_3-\overset{\overset{O}{\|}}{C}-CH_2-CH_2-COOH \xrightarrow{H_2O_2\text{-}SeO_2}$$

$$HOOC-CH_2-CH_2-CH_2-COOH$$
$$+\ HOOC-\underset{\underset{CH_3}{|}}{CH}-CH_2-COOH$$

It has been shown that the active species of this rearrangement reaction may be peroxyselenous acid $\left(HOO-Se\begin{matrix}\nearrow O\\ \searrow OH\end{matrix}\right)$ generated by the oxidation of selenium dioxide with hydrogen peroxide in the reaction system,[12] so that the rearrangement may be caused by the attack of peroxyselenous acid on levulinic acid in a process similar to that described in the previous reports.[4,12]

The reactivity of levulinic acid was considerably lower than that of dialkyl ketone with a low molecular weight, so that the yield of C_5-dibasic acids amounted to about 10% of the levulinic acid used, and a fairly good recovery of the starting levulinic acid was observed in spite of an excess amount of hydrogen peroxide having been used.

Small amounts of β-acetylacrylic acid and of fumaric acid were also isolated as by-products. Raymond[13] has reported that the oxidation of various esters of levulinic acid yielded the corresponding esters of β-acetylacrylic acid by dehydrogenation. Accordingly, it was assumed that β-acetylacrylic acid might be produced by the action of the selenium dioxide used as the catalyst in the present case:

$$CH_3-\overset{\overset{O}{\|}}{C}-CH_2-CH_2-COOH \xrightarrow{SeO_2}$$

$$CH_3-\overset{\overset{O}{\|}}{C}-CH=CH-COOH$$

Fumaric acid may be generated by the oxidative cleavage of β-acetylacrylic acid or by the dehydrogenation of succinic acid[14] with selenium dioxide. Succinic acid can be formed by the oxidative cleavage of levulinic acid, but the formation of succinic acid was not detected in the present experiment.

Experimental

Material.—Levulinic acid used in this experiment was purified by the distillation of the commercial product; b. p. 152°C/21 mmHg (reported[15] b. p. 138~140°C/10 mmHg).

Oxidation of Levulinic Acid. — To 150 ml. of a tertiary butyl alcohol solution[16] containing 1.0 g. of selenium dioxide and 0.3 mol. of hydrogen peroxide, 17.4 g. (0.15 mol.) of levulinic acid was added. The hydrogen peroxide was completely consumed by the refluxing of the solution for

5) Y. Hara and S. Fujise, *J. Chem. Soc. Japan, Pure Chem. Sec.* (*Nippon Kagaku Zassi*), **74**, 698 (1953).
6) M. Matsui, H. Kubo and M. Kibi, *J. Agr. Chem. Soc. Japan*, **29**, 893 (1955).
7) T. Takenishi and O. Simamura, This Bulletin, **27**, 207 (1954).
8) S. Fujise, Y. Nakamura and Y. Nishizawa, *J. Chem. Soc. Japan, Pure Chem. Sec.* (*Nippon Kagaku Zassi*), **75**, 348 (1954).
9) S. Motoki and A. Odaka, ibid., **77**, 401 (1956).
10) S. Motoki, ibid., **82**, 256 (1961).
11) S. Motoki, ibid., **82**, 740 (1961).
12) N. Sonoda and S. Tsutsumi, *Technol. Repts. Osaka Univ.*, **13**, 223 (1963).
13) S. Raymond, *J. Am. Chem. Soc.*, **72**, 3296 (1950).
14) S. Astin, A. C. C. Newman and H. L. Riley, *J. Chem. Soc.*, **1933**, 391.
16) Y. Hachihama and I. Hayashi, *J. Chem. Soc. Japan, Ind. Chem. Sec.* (*Kōgyō Kagaku Zassi*), **54**, 695 (1951).
16) For the preparation of the oxidative reagent, see Ref. 1.

12 hr., and at this stage a small amount of metallic selenium was deposited. After the removal of the solvent by distillation from the reaction mixture, the residual high-boiling liquid was distilled under reduced pressure and was divided into two fractions: fraction A, 11.5 g., b. p. <150°C/3.5 mmHg; fraction B, 2.8 g., b. p. 150~160°C/3.5 mmHg; residue, ca. 2.5 g., resinous substance containing metallic selenium.

Fraction A was kept for two days at room temperature, and the deposited crystalline material was then fitered (0.5 g.) and recrystallized from benzene to yield 0.3 g. of β-acetylacrylic acid; m. p. 125°C (reported[17] m. p. 125~126°C). Upon admixture with an authentic sample of β-acetylacrylic acid, the melting point was not depressed, and the infrared spectrum of the product was identical with that of an authentic sample.

Found: C, 52.61; H, 5.48. Calcd. for $C_5H_6O_3$: C, 52.63; H, 5.30%.

After the removal of β-acetylacrylic acid by filtration, the residual liquid was redistilled under reduced pressure, giving a trace amount of β-acetylacrylic acid and 8.7 g. of unchanged levulinic acid; the infrared spectra of these samples closely resembled those of authentic materials.

Fraction B, which partly contained crystalline materials, was cooled at 0°C overnight, and the solid which was then deposited was filtered and dissolved into hot benzene. After the removal of a small amount of insoluble substance, the hot benzene solution was cooled and the crystalline material deposited was filtered and recrystallized from benzene to yield 1.2 g. of glutaric acid; m. p. 96~97°C (lit.[18] m. p. 97°C)). Upon admixture with an authentic sample of glutaric acid, the melting point was not depressed, and the infrared spectrum of the product was identical with that of an authentic sample.

Found: C, 45.67; H, 6.22. Calcd. for $C_5H_8O_4$: C, 45.45; H, 6.10%.

The substance insoluble in hot benzene was purified three times by sublimation at 200°C/25 mmHg, yielding 0.03 g. of fumaric acid, which melted at 286~288 °C (sealed tube) (lit.[19] m. p. 286~287°C); the mixed melting point with an authentic sample showed no depression, and the infrared spectrum of the product was identical with that of an authentic sample.

Found: C, 41.67; H, 3.62. Calcd. for $C_4H_4O_4$: C, 41.39; H, 3.47%.

The residual liquid obtained from fraction B by the filtration of the solid materials was cooled at 0°C for a few days, and 0.6 g. of the solid deposited was filtered. After recrystallization was repeated from benzene containing a small amount of ether, there was obtained 0.2 g. of methylsuccinic acid, which melted at 108~109°C (reported[20] m. p. 110°C); the mixed melting point with an authentic sample (m. p. 109~109.5°C), synthesized by the hydrolysis of ethyl β-cyanobutyrate showed no depression, and the infrared spectrum of the product was identical with that of an authentic sample; neutral equivalent, 65.9 (theoretical value, 66.1).

Found: C, 45.13; H, 5.90. Calcd. for $C_5H_8O_4$: C, 45.45; H, 6.10%.

Summary

The selenium dioxide-catalyzed oxidation of levulinic acid with hydrogen peroxide in *t*-butyl alcohol gave glutaric acid and methylsuccinic acid as the rearrangement products. The glutaric acid may be formed by the migration of the β-carboxyethyl group to the methyl carbon atom and by the oxidation of the carbonyl group to the carboxyl group, and the formation of methylsuccinic acid may be due to the migration of the methyl group to the methylene carbon atom adjacent to the carbonyl group.

Department of Chemical Technology
Faculty of Engineering
Osaka University
Miyakojima, Osaka

17) F. R. Goss and C. K. Ingold, *J. Chem. Soc.*, 1928, 1976.
18) R. L. Shriner, R. C. Fuson and D. Y. Curtin, "The Systematic Identification of Organic Compounds," 4th Ed., John Wiley & Sons, Inc., New York, N. Y. (1956).
19) H. U. v. Vogel, "Chemiker Kalender," Springer Verlag, Berlin (1956).
20) E. P. Kohler and F. R. Butler, *J. Am. Chem. Soc.*, 48, 1045 (1926).

Studies of Isocyanides. I. The Formation of Urethanes and Ureas from Isocyanides

By Masaya OKANO, Yoshihiko ITŌ, Tatsuya SHŌNO and Ryohei ODA

(Received May 13, 1963)

In recent years new addition reactions of isocyanides have been widely developed by Ugi and his co-workers. Their studies mainly covered the reactions with several carbonyl and similar compounds, such as ketenes, carboxylic acids, acyl chlorides and Schiff bases.[1] It seems that these new reactions, as well as the well-known Passerini reaction,[2] essentially involve an electrophilic attack by the positive carbon of these reagents on the negatively-charged carbon of isocyanides. Since the electrophilic nature of *t*-butyl hypochlorite[3] and *N*-bromosuccinimide (NBS)[4] in aromatic halogenations and that of hydroxylamine[5] (with a Lewis acid catalyst) in aromatic amination have previously been established, we have now examined the reactions of these electrophiles with isocyanides, which may be expected to yield urethanes and ureas, after successive hydrolysis if necessary.

When cyclohexyl isocyanide was treated with *t*-butyl hypochlorite in the presence of zinc chloride catalyst, an instantaneous reaction took place, and a 20% yield of *t*-butyl *N*-cyclohexylcarbamate, in addition to cyclohexyl isocyanate (16%), was obtained by successive treatment with water. In the absence of the catalyst, however, the isocyanate (40%) was the sole product. Similarly, the addition of phenyl isocyanide to *t*-butyl hypochlorite, followed by hydrolysis, afforded *t*-butyl *N*-phenylcarbamate in a 69% yield. The use of other Lewis acid catalysts (e.g., aluminum trichloride, boron trifluoride and ferric chloride) is not suitable, since isocyanide itself rapidly converts to a tarry matter when the catalysts are added. A reasonable path for this reaction would involve the formation of an imidoyl-chloride intermediate,[6] as in the case of the reaction between isocyanide and acyl chloride:[7]

$$R\text{-}N\rightleftarrows C + t\text{-}BuOCl \xrightarrow{ZnCl_2\ cat.} \left[R\text{-}N{=}C\begin{matrix}Cl\\OBu\text{-}t\end{matrix}\right] \xrightarrow{H_2O} RNHCOOBu\text{-}t$$

$$R = C_6H_{11},\ C_6H_5$$

The reaction of cyclohexyl isocyanide with wet NBS (containing ca. 5~10% of water) proceeded smoothly at room temperature and gave a 21% yield of *N*-(cyclohexylcarbamoyl) succinamic acid after hydrolysis. When the reaction was conducted under completely anhydrous conditions, the formation of a tarry matter was observed after a short induction period and the above acid could not be isolated by successive treatment with water. A preliminary test indicated that the addition of zinc bromide caused the decomposition of NBS; therefore, no effort was made to examine the zinc salt-catalyzed reaction. An analogous reaction of phenyl isocyanide with *N*-bromoacetamide (NBA) yielded the expected adduct, *N*-acetyl-*N'*-phenylurea, in a 38% yield. Since this type of reaction proceeds smoothly even in the dark, an ionic process appears to be favorable; on this point, however, more conclusive evidence would be desirable.

$$C_6H_{11}\text{-}N\rightleftarrows C + \begin{matrix}CH_2\text{-}CO\\|\\CH_2\text{-}CO\end{matrix}NBr \rightarrow \left[C_6H_{11}\text{-}N{=}C\begin{matrix}Br\\N\end{matrix}\begin{matrix}CO\text{-}CH_2\\|\\CO\text{-}CH_2\end{matrix}\right] \xrightarrow{H_2O} C_6H_{11}NHCONHCOCH_2CH_2COOH$$

$$C_6H_5\text{-}N\rightleftarrows C + CH_3CONHBr \rightarrow \left[C_6H_5\text{-}N{=}C\begin{matrix}Br\\NHCOCH_3\end{matrix}\right] \xrightarrow{H_2O} C_6H_4NHCONHCOCH_3$$

Lastly, the treatment of a mixture of cyclohexyl isocyanide and hydroxylamine hydrochloride with zinc chloride afforded a 42% yield of *N*-cyclohexylurea, as shown in the following equation:

1) I. Ugi et al., *Chem. Ber.*, **94**, 734, 1116, 2233, 2797, 2802 (1961); *Angew, Chem.*, **74**, 10 (1962).
2) M. Passerini, *Gazz. chim. ital.*, **51**, 181 (1921) [*Chem. Abst.*, **16**, 556 (1922)].
3) D. Ginsberg, *J. Am. Chem. Soc.*, **73**, 2723 (1951).
4) S. D. Ross, M. Finkelstein and R. C. Petersen, ibid., **80**, 4327 (1958). NBS is generally considered to be a homolytic brominating agent, especially for an allylic system; however, Ross et al. recently cited the possibility of the heterolytic bromination of reactive aromatics with NBS.
5) C. Graebe, *Ber.*, **34**, 1778 (1901); G. F. Jaubert, *Compt. rend.*, **132**, 841 (1901).
6) Unfortunately, an attempt to isolate the intermediate oil was not successful because of its thermal instability.
7) I. Ugi and U. Fetzer, *Chem. Ber.*, **94**, 1116 (1961).

$$C_6H_{11}\text{-}N\rightleftharpoons C + \underset{(HCl\ salt)}{NH_2OH} \xrightarrow{ZnCl_2\ cat.}$$

$$\left[C_6H_{11}\text{-}N{=}C\begin{matrix}NH_2\\OH\end{matrix}\right] \rightarrow C_6H_{11}NHCONH_2$$

Unfortunately, in a similar reaction with phenyl isocyanide, no adduct could be isolated from the tarry reaction product. Phenylhydroxylamine also did not give the expected *N*-cyclohexyl-*N'*-phenylurea under similar conditions; rather, somewhat unexpectedly, *N*,*N'*-dicyclohexylurea (53%) was obtained. Controlled experiments in which the isocyanide was treated with phenylhydroxylamine alone or with zinc chloride alone did not afford any product. Thus, it is highly probable that phenylhydroxylamine acts as an oxygen donor, though the reaction mechanism is not quite clear.

Experimental[8]

The Reaction of Cyclohexyl Isocyanide with *t*-Butyl Hypochlorite.—Into a mixture of 5.4 g. (0.05 mol.) of *t*-butyl hypochlorite (prepared by the procedure of Teeter and Bell[9]) and 1.3 g. (0.01 mol.) of zinc chloride in 20 ml. of dry ethylene dichloride, 5.5 g. (0.05 mol.) of cyclohexyl isocyanide was added dropwise with stirring, at such a rate that the reaction temperature was kept below 10°C. The stirring was continued at that temperature for an additional hour, and then the reaction mixture was allowed to stand overnight at room temperature. After removal of the unchanged hypochlorite and the solvent, the residue was poured into water. After this mixture had stood for 2 hr., the organic layer that separated was extracted with ether. The ethereal solution was washed twice with water, dried, and evaporated. The resulting oil was distilled in vacuo to yield 1.0 g. (16%) of cyclohexyl isocyanate (b. p. 60~65°C/18 mmHg), identified as dicyclohexylurea (m. p. 228°C), and a dark residue. Recrystallization of the residue from methanol afforded 2.0 g. (20%) of *t*-butyl *N*-cyclohexylcarbamate (m. p. 68~69°C). The melting point was undepressed on admixture with a sample prepared from cyclohexyl isocyanate and *t*-butyl alcohol.

Found: C, 66.13; H, 10.64; N, 7.42. Calcd. for $C_{11}H_{21}NO_2$: C, 66.29; H, 10.62; N, 7.03%.

When this reaction was carried out in the absence of the catalyst, only cyclohexyl isocyanate (40%) was isolated.

The Reaction of Phenyl Isocyanide with *t*-Butyl Hypochlorite.—The procedure employed was similar to that used for the above reaction except that dry dioxane was used as the solvent. The working up of the reaction mixture, as described above, gave *t*-butyl *N*-phenylcarbamate (69%), which after recrystallization from ethanol melted at m. p. 134~135°C. No mixed melting point depression was observed with an authentic material prepared by the usual method. In the non-catalyzed reaction, phenyl isocyanate (13%) was the sole isolable product.

The Reaction of Cyclohexyl Isocyanide with NBS.—After 8.9 g. (0.05 mol.) of NBS had been moistened with 0.9 g. of water, the mixture was gradually stirred into a solution of 5.5 g. (0.05 mol.) of cyclohexyl isocyanide and 50 ml. of dry carbon tetrachloride. The reaction temperature was maintained at ca. 10~15°C by means of a water bath. At the end of the addition, a color change from dark red to yellow was observed. Then the reaction mixture was allowed to stand overnight at room temperature. The solid that separated was collected and treated with water. There were obtained 1.3 g. (11%) of *N*-(cyclohexylcarbamoyl), succinamic acid, which after recrystallization from acetone had an m. p. of 162~164°C. Some additional product was also obtained from the solvent layer; it weighed 1.2 g. (10%). The acid showed no depression in melting point when mixed with an authentic material which had been prepared from *N*-cyclohexylurea and succinic anhydride in acetic acid.

Found: C, 54.68; H, 7.52; N, 11.44. Calcd. for $C_{11}H_{18}N_2O_4$: C, 54.53; H, 7.48; N, 11.56%.

The Reaction of Phenyl Isocyanide with NBA. In a smimilar way, 7.2 g. (0.07 mol.) of phenyl isocyanide was added dropwise to a mixture of 9.5 g. (0.07 mol.) of wet NBA (prepared by the procedure of Oliveto and Gerold[10]) and 50 ml. of dry chloroform. The reaction mixture was worked up as in the preceeding experiment to give 4.7 g. (38%) of *N*-acetyl-*N'*-phenylurea. Recrystallization from ethanol gave the pure product (m. p. 183°C). No depression in melting point was observed upon admixture with an authentic material which had been prepared by the addition reaction of acetamide to phenyl isocyanate.[11]

The Reaction of Cyclohexyl Isocyanide with Hydroxylamine Hydrochloride.—A mixture of 3.5 g. (0.05 mol.) of hydroxylamine hydrochloride, 5.5 g. (0.05 mol.) of cyclohexyl isocyanide, 1.3 g. (0.01 mol.) of zinc chloride and 30 ml. of dioxane was heated at 50°C for 3 hr. with stirring. The reaction mixture was evaporated in vacuo to remove dioxane, and the residue was poured into 30 ml. of water; then the solution was made slightly basic with aqueous sodium hydroxide. The crude product which separated from the solution was redissolved in ethanol to remove zinc hydroxide, and the alcohol was evaporated to dryness. Recrystallization of the resulting solid from water afforded 3.0 g. (42%) of *N*-cyclohexylurea (m. p. 189°C). A mixed melting point with an authentic sample, prepared from cyclohexyl isocyanate and aqueous ammonium hydroxide, showed no depression.

The Reaction of Cyclohexyl Isocyanide with Phenylhydroxylamine.—A mixture of 6.5 g. (0.06 mol.) of phenylhydroxylamine, 5.5 g. (0.05 mol.) of cyclohexyl isocyanide, 1.3 g. (0.01 mol.) of zinc chloride and 30 ml. of dioxane was stirred at 50°C for 25 hr. After removal of the solvent in vacuo,

8) All boiling and melting points are uncorrected.
9) H. M. Teeter and E. W. Bell, "Organic Syntheses," 32, 20 (1952).
10) E. P. Oliveto and C. Gerold, ibid., 31, 171 (1951).
11) P. F. Wiley, *J. Am. Chem. Soc.*, 71, 1310 (1949).

the reaction mixture was poured into water, and the organic layer was extracted with ether. The evaporation of the ether and the unreacted isocyanide in vacuo afforded 3.0 g. (53%) of *N,N'*-dicyclohexylurea. Two recrystallizations from acetone or ethanol gave a pure sample (m. p. 228°C), which was identified with an authentic sample by a mixed melting point determination.

Summary

The reactions of isocyanides with alkyl hypochlorite, *N*-bromoamides, and hydroxylamine have been investigated. Cyclohexyl and phenyl isocyanides give *t*-butyl carbamates (urethanes) by the zinc chloride-catalyzed reaction with *t*-butyl hypochlorite, followed by treatment with water. An analogous reaction with *N*-bromosuccinimide or *N*-bromoacetamide in the presence of a small amount of water gives the corresponding acylureas. On treatment with hydroxylamine hydrochloride and zinc chloride, cyclohexyl isocyanide affords *N*-cyclohexylurea.

Institute for Chemical Research
Kyoto University
Takatsuki, Osaka (M. O.)

Department of Synthetic Chemistry
Faculty of Engineering
Kyoto University
Sakyo-ku, Kyoto
(Y. I., T. S. & R. O.)

Studies of the Synthetic Inorganic Ion Exchanger. II.[1] *The Properties of Stannic Phosphate*

By Yasushi INOUE

(Received May 25, 1963)

The stannic phosphates, a group of synthetic inorganic ion exchangers which would be expected to have radiation and thermal stability, have been prepared by various methods and their compositions, ion exchange capacities and chemical stabilities have been investigated, as the preceding report describes.[1]

The exchanger, precipitated from a slightly acidic solution by mixing phosphate with stannic in the ratio of over two to one, has the stoichiometric composition of $PO_4^{3-}/Sn^{4+}=5/4$. It is in the form of white, hard and semitransparant granules and can be used for column operation. The neutral salt decomposition capacity is about 1.3~1.4 meq./g., considerably higher than that of natural inorganic ion exchangers. As to chemical stability, stannic phosphate is comparatively stable in mineral acid, except in concentrated hydrochloric acid, but in alkaline solutions it is unstable, even in a 0.1 N sodium hydroxide solution.

For the purpose of evaluating the availability for a typical ion exchanger like an ion exchange resin, the mutual separation of the alkali metal has been conducted. By using various concentrations of ammonium chloride as eluants, the complete separation of sodium, potassium and cesium from one other has been achieved with a relatively small column. The object of this report is to contribute to the knowledge concerning such fundamental properties of this exchanger as its ion exchange characteristics, its thermal stability and its radiation stability. Moreover, the recommended preparation method and the structure of the exchanger are suggested.

Experimental

Preparation. — The synthetic method has been outlined in the previous report, but the procedure was not detailed.[1] From the evidence which is to be presented later, the following procedure is most recommended. This method corresponds to that used for No. 7 in the first report of this series.

Two hundred and ten grams of stannic chloride pentahydrate were dissolved in 600 ml. of distilled water while it was being heated, and it was then filtered to remove the suspended materials. Into this solution 1.2 l. of a 1.2 N sodium hydroxide solution containing 187 g. of sodium dihydrogen phosphate dihydrate was added rapidly, stirring vigorously at room temperature. At first, the flocculent precipitate was formed, then the gel structure grew from one minute to the next, and finally the solution completely coagulated as a gelatinous mass. After the solution had thus stood for several hours, distilled water was added, and it was stirred to obtain a homogeneous suspension. After the gelatinous suspension had settled down, the supernatant liquid was decanted. This procedure was repeated

1) Y. Inoue, *J. Inorg. Nucl. Chem.*, in press.

several times till the pH of the washings (nearly 3) remained constant. At the last stage of washing, the precipitate was filtered through fine filter paper under suction, washed twice or three times by distilled water, removed from the funnel, and dried at room temperature till it shrank. The gel thus obtained broke down easily to small particles with cracking and with slight evolution of heat when it was immersed in water. If the gel did not break down to the desired particle size, it was ground in a porcelain mortar and sized by sieving. To convert it thoroughly to the hydrogen form, it was then immersed in 1 N nitric acid or 1 N hydrochloric acid for two or three days (the solution was sometimes renewed in the course of immersion), washed several times by distilled water, filtered, and dried in air. In the present work, an exchanger of a 100~200 mesh size was used unless otherwise stated, except in the K_d determination, in which a 200~350 mesh was used.

Titration Curves.—These were determined by the standard technique.[2] A half gram of stannic phosphate was equilibrated with 75 ml. of a solution containing sodium chloride and sodium hydroxide, the total sodium concentration being 0.1 M. After the mixture had stood for three days with intermittent shaking, the pH of the supernatant liquid was measured on a Toa Dempa pH meter. As will be described later, the titration curves were different from batch to batch, therefore, the samples of the same batch were used throughout one set of experiments.

Distribution Coefficients. — Batch distribution coefficients were determined by equilibrating weighed amounts (usually 500 mg.) of the ion exchanger with 50 ml. of suitable solutions for two or three days in a thermostat at 25°C. The acidities of solutions containing 10^{-3} M of the cation in question were adjusted by dilute nitric acid. This was followed by filtration of the mixture, and analysis and pH measurement of the filtrate were then made. The metallic ion content of the exchanger after equilibrium was estimated from the difference between the total initial and final concentrations of metal present in the solutions.

Distribution coefficients were calculated by means of the usual relationship.

$$K_d = \frac{\text{meq. of cation in exchanger/g. of exchanger}}{\text{meq. of cation in solution/ml. of solution}}$$

The analyses of sodium, potassium, rubidium, cesium, copper, gallium, zinc, strontium, calcium, iron and cobalt were carried out radiometrically using ^{24}Na, ^{42}K, ^{86}Rb, ^{137}Cs, ^{64}Cu, ^{72}Ga, ^{65}Zn, ^{89}Sr, ^{45}Ca, ^{59}Fe and ^{60}Co respectively as tracers. The analysis of lithium was made by flame photometry; manganese, by the persulfate oxidation-permanganate photometric method; chromium, by the diphenyl carbazide photometric method; and ammonium, by the extraction-photometric method.

Rate of Exchange.—This was measured by almost the same method as K_d determination. The temperature employed was 25°C or 80°C, and exchangers of a 100~200 mesh or a 200~350 mesh were used. From the analytical results of an aliquot of the supernatant liquid taken every suitable time interval, the rate of exchange was determined. In this case, 500 mg. of the exchanger was used with 100 ml. of the solution.

Gamma-ray Irradiation.—The samples, sealed in a hard glass tube, were irradiated by a 10000 curies cobalt-60 gamma-ray irradiation facility of The Japan Atomic Energy Research Institute at the dose rate of 1.11×10^6 r./hr. for a definite period. After this irradiation, the samples were conditioned as described before; then the titration curves, exchange capacities, selectivity and so on were measured. When irradiation was done in an aqueous solution, 8 g. of the exchangers were immersed in 8 ml. of the solutions.

Treatment of the Exchanger with High Temperature Water. — Ten grams of exchanger were immersed in 50 ml. of distilled water; this was treated for eight days in static autoclaves up to 300°C. The samples were then taken out of the autoclaves and conditioned as described above; then the titration curves, exchange capacities, selectivities and so on were measured.

Another Experimental Method. — The densities of the exchangers were measured by the usual manner, using a 5 ml. pycnometer. The column operation and the measurement of the exchange capacity were carried out as described in the first report. The exchange capacity is the "hydrogen liberation capacity" as defined in the previous report.

Thermogravimetry was performed with Shimadzu Model T-1A thermal analysis equipment, employing an TB-1 thermal balance as additional equipment. Measurement was carried out in air at a heating rate of 10°C/min. over the temperature range from 20°C to 800°C.

In the X-ray diffraction experiments, copper K_α radiation was employed.

Results

The Recommended Method for the Synthesis of Stannic Phosphate.—The yields and densities of the stannic phosphates obtained by six typical preparation methods are presented in Table I. Densities are about 2.0~2.4 g./cm^3, and no differences among the methods of preparation were observed. From the exchange capacities and physical properties described in the first report, the mixing ratio of stannic to phosphate of 2 to 1 is the most appropriate. As to yield, from the economical point of view, that for stannic chloride would be most important. The No. 7 sample shows the highest yield per unit amount of stannic chloride. Putting the above results together, the synthetic method of No. 7 is most recommended.

Titration Curves.—The titration curves of stannic phosphates prepared by various methods are represented in Fig. 1. The curves show that the stannic phosphates are weakly acidic

2) N. E. Topp and K. W. Pepper, *J. Chem. Soc.*, **1949**, 3299.

TABLE I. VARIOUS PROPERTIES OF STANNIC PHOSPHATE

Sample No.	Synthetic method			Yield g.	PO_4^{3-}/Sn^{4+}*	Hydrogen* liberation capacity meq./g.	Density g./cm³
	$NaH_2PO_4 \cdot 2H_2O$, g.	NaOH g.	$SnCl_4 \cdot 5H_2O$ g.				
3	94	72	210	159	0.912	1.21	2.06
6	94	76	210	161	0.565	0.98	2.40
7	187	48	210	200	1.28	1.35	2.17
9	187	96	210	90	1.04	1.26	2.22
13	187	36	105	76	1.25	1.41	2.26
20	108	48	210	140	0.56	0.78	2.29

* From the data of the first report.

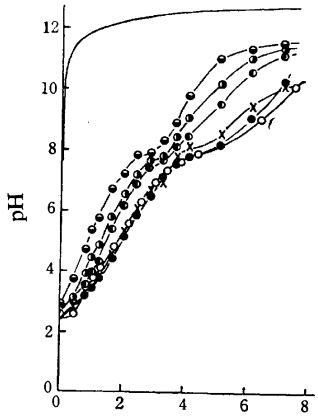

Fig. 1. Titration curves of stannic phosphate. Legend: -◑- No. 3; -◐- No. 6; -○- No. 7; -●- No. 9; -×- No. 13; -◒- No. 20; — In the absence of exchanger

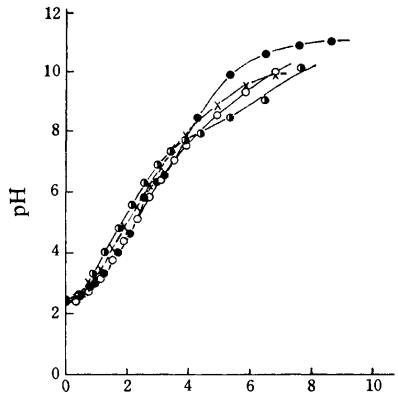

Fig. 2. Titration curves of stannic phosphate prepared by the recommended procedure.
Legend: -○- Batch No. 1; 200~350 mesh exchanger; conditioning solution HCl
-×- Batch No. 1; 200~350 mesh exchanger; conditioning solution HNO_3
-●- Batch No. 2; 100~200 mesh exchanger; conditioning solution HCl
-◑- Batch No. 3; 100~200 mesh exchanger; conditioning solution HNO_3

cation exchangers and possess several dissociable hydrogen atoms over a range of pK_a values. The lack of sharpness of the inflection points suggests that there may be somewhat overlapping values of pK_a. However, it seems that the most acidic exchange group has a pK_a value of approximately three. This value probably corresponds to the pK_a value of the second hydrogen ion of the activated phosphoric acid group. In an acidic solution this dissociable hydrogen is most important, and it is considered that the neutral salt decomposition capacities result from one hydrogen ion of the $H_2PO_4^-$. From the practical point of view, it is sufficient to pay special attention to this exchanging group.

The reproducibility of the preparation was fairly good from the point of view of exchange capacity, as has been discussed in the preceding report, but variations in the titration curves have been observed between different batches; these variations are usually most marked in the high pH region (above 8) of the curve. This is perhaps attributable to the unstability in the face of an alkaline medium. The general pattern is, however, fairly constant in the pH range of less than 8, as Fig. 2 shows. The influence on the shape of the titration curves

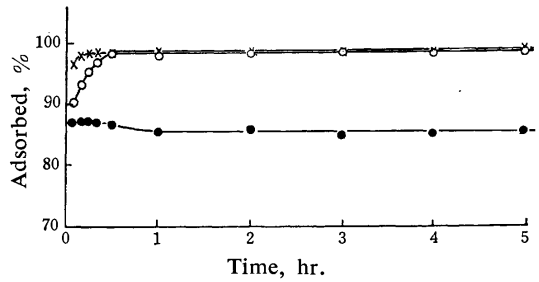

Fig. 3 a). Rate of exchange of cesium (temperature 25°C).
Legend: -○- Conc. of Cs C. F.; 100~200 mesh of exchanger
-×- Conc. of Cs C. F.; 200~350 mesh of exchanger
-●- Conc. of Cs 10^{-3} M; 200~350 mesh of exchanger

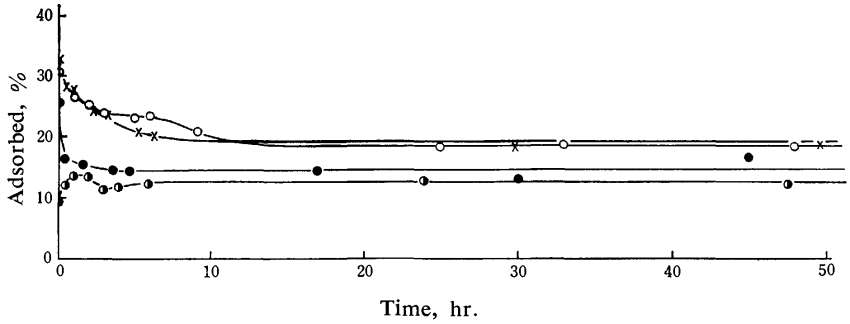

Fig. 3 b). Rate of exchange of sodium.
Legend: -×- Conc. of Na 10^{-3} M; 100~200 mesh of exchanger; 25°C
-○- Conc. of Na 10^{-3} M; 200~350 mesh of exchanger; 25°C
-◑- Conc. of Na 10^{-2} M; 200~350 mesh of exchanger; 25°C
-●- Conc. of Na 10^{-3} M; 200~350 mesh of exchanger; 80°C

of the different acids by which the exchangers are converted to the hydrogen form, has been investigated, hydrochloric acid gives titration curves more acidic than nitric acid, but this effect is not very great. No effect of particle size on the titration curves was recognized.

Rate of Exchange.—To evaluate the time of standing indispensable for batch experiments, the rate of exchange was investigated using a 100~200 mesh or a 200~350 mesh exchanger at 25°C and 80°C (cf. Fig. 3). Carrier-free ^{137}Cs, 10^{-3} M cesium, 10^{-2} M sodium and 10^{-3} M sodium ion were used as the exchanging cations.

When the concentration of the exchanging cation was 10^{-3} M, the maximum adsorption was attained immediately after the exchangers were immersed in a solution; thereafter the amount of exchange gradually decreased with the lapse of time. After ten or twenty four hours, equilibrium was reached. On the contrary, when the concentration was 10^{-2} M or a tracer concentration, the amount of adsorbed cation gradually increased and then reached constant. In the case of 80°C, equilibrium was attained within two hours, and it was apparent that the exchange rate was accerelated by a high temperature. As a result of the above investigation, to be on the safe side, a standing period for two or three days is recommended for batch equilibrium experiments.

Distribution Coefficients. — The distribution coefficients of various cations are tabulated in Table II. They were measured using nearly neutral solutions of the cations in question. The pH of the solution in equilibrium with the exchanger was also measured, as the table shows.

The affinity series for alkali metal follows the pattern shown by many organic exchangers, viz.

$$Li < Na < NH_4 < K < Rb < Cs$$

Table II. Distribution coefficients of cations
500 mg. of exchanger/50 ml. of solution, at 25°C, 10^{-3} M/l.

Cation	Compound used	pH	K_d, ml./g.
Li^+	Chloride	2.70	11.4±0.6
Na^+	Chloride	2.53	28.9±0.3
NH_4^+	Chloride	2.70	147±4
K^+	Chloride	2.49	356±13
Rb^+	Chloride	2.57	735±6
Cs^+	Chloride	2.57	1343±12
Ca^{2+}	Chloride	2.48	2247±121
Sr^{2+}	Nitrate	2.40	602.8±11.2
Zn^{2+}	Nitrate	2.03	315.0±6.6
Cu^{2+}	Nitrate	2.59	$(5.87\pm0.38)\times10^3$
Mn^{2+}	Sulfate	2.60	2090±122
Fe^{2+}	Sulfate	1.00	7.6
Co^{2+}	Chloride	1.97	96.70±2.00
Fe^{3+}	Sulfate	0.91	4207±172
Ga^{3+}	Nitrate	2.20	$(1.35\pm0.07)\times10^4$
Cr^{3+}	Sulfate	2.48	3595±318

There are, however, differences between the behavior of ion exchange resins and stannic phosphates. For example, it is interesting to note that calcium is adsorbed more selectively than strontium and that ferric ions show an exceptionally high distribution coefficient. The reason for this is not clear, although it might be due to a specific chemical interaction other than a simple ionic reaction.

Thermal Stability.—*Heat Treatment in Air.*— In order to obtain a rough idea of the thermal stability of the stannic phosphate, a thermogravimetric analysis was conducted on material which had been dried at room temperature (cf. Fig. 4). Also, the weight losses and exchange capacities of the exchangers dried to a constant weight at temperatures ranging from 110 to 410°C are shown in Table III.

Figure 4 shows a step-by-step decomposition

curve. It is assumed that the weight loss observed from room temperature to 200°C mainly corresponds to the desorption of water retained in the gel structure and that structural water is lost at the inflection point near 350°C. The weight loss obtained from the thermal analysis curve is generally identical with that obtained by heating to a constant weight, but at 110°C these values differ from one other. This difference is perhaps due to the non-equilibrium condition of the thermal analysis. This is clear from the fact that the thermal analysis curve shows a steep slope near 110°C.

The exchange capacity does not change upon heat treatment at 110°C, provided the correction due to the weight loss is performed. However, it is reduced to half when it is heated to 210°C. If stannic phosphate is treated at 410°C to a constant weight, the cation exchange capacity completely diminishes. The

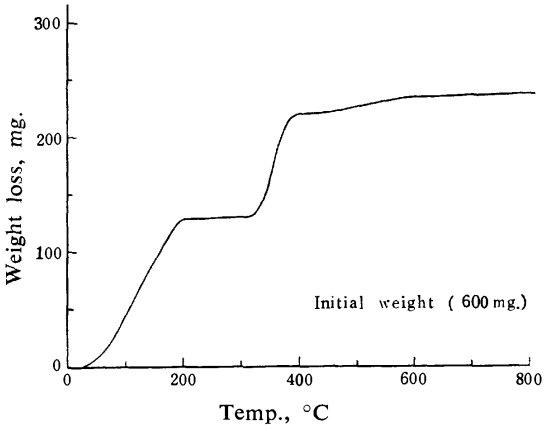

Fig. 4. Thermogram for stannic phosphate.

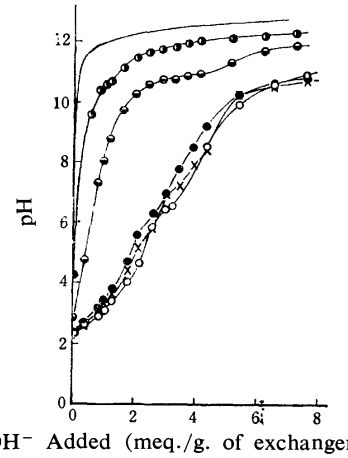

Fig. 5. Titration curves of stannic phosphate as a function of drying temperature.
Legend : -○- Room temperature ; -×- 110°C; -●- 210°C ; -◒- 320°C ; -◑- 410°C ;— In the absence of exchanger

TABLE III. EFFECT OF HEAT TREATMENT IN AIR

Temp.	Exchange capacity, meq./g.		Weight, mg.	
°C	Calculated value	Experimental value	Calculated value	Experimental value
Room temp.	1.28	1.35	600	600
110	1.62	1.62	475	475
210	0.81	0.82	468	469
320	—	0.23	461	460
410	—	0.02	392	392

titration curves obtained by the samples dried at various temperatures give support to this observation ; that is to say, the titration curve of stannic phosphate dried at 320°C shows a considerable decrease in the most acidic exchange group. At 410°C, the inflection point originating from the most acidic hydrogen ions completely disappears (Fig. 5).

To evaluate the separation abilities of the stannic phosphates dried at temperatures higher than room temperature, the separation of sodium and cesium was conducted by the same method as in the preceding paper. Even in the sample dried at 110°C one can not separate these ions, presumably because of the tailing of the elution curve. Thus, the stannic phosphates dried at temperatures 110°C or higher cannot be used as cation exchangers.

Heat Treatment in an Aqueous Solution.—As has been mentioned above, the stannic phosphate is not stable against heat treatment in air. To know whether or not this is also true in an aqueous solution, an examination was conducted of the ion exchange properties of a stannic phosphate refluxed with distilled water or 7 N nitric acid for five hours and then treated with distilled water in a static autoclave up to 300°C for eight days. The results are summarized in Table IV and Fig. 6. When stannic phosphate is treated both in water and 7 N nitric acid at their boiling points, its external appearance does not change, but at 200°C it slightly loses its transparency. At 250°C the particles break down to some extent. If the temperature of water rises to 300°C, the particles completely break down and disperse into

TABLE IV. EFFECT OF HEAT TREATMENT IN AQUEOUS SOLUTIONS

Solution	Temp. °C	Time	Exchange capacity meq./g.
—	—	—	1.23
7 N HNO_3	100	5 hr.	1.17
H_2O	100	5 hr.	1.22
H_2O	100	8 days	1.22
H_2O	200	8 days	1.27
H_2O	250	8 days	1.10

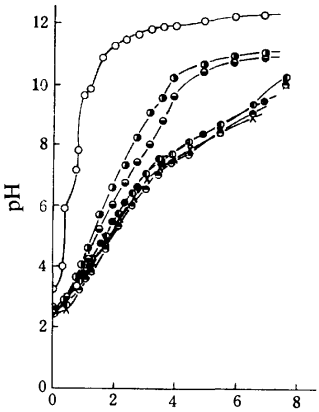

Fig. 6. Effect of heat treatment in aqueous solution on the titration curves of stannic phosphate.
Legend: -◐- In 7 N HNO_3, at boiling point, 5 hr.; -◓- In H_2O, at boiling point, 5 hr.; -●- In H_2O, 100°C, 8 days; -◒- In H_2O, 200°C 8 days; -◑- In H_2O, 250°C, 8 days; -○- In H_2O, 300°C, 8 days

the water as a suspension and, therefore, the exchanger cannot be used.

The exchange capacity does not change up to 200°C, but it slightly decreases upon treatment at 250°C; the titration curves show a similar trend. Samples treated at 300°C do not only break down physically, but they also completely lose their cation exchange capacity, as Fig. 6 shows. Moreover, in the same way as in the preceding section, the separation of sodium and cesium was carried out. These separations go well using stannic phosphate treated in water at temperatures up to 250°C.

It is apparent from the above results that stannic phosphate can be used in pressurized, high-temperature water or in boiling concentrated nitric acid.

Radiation Stability.—The exchange capacities and titration curves of the irradiated samples are shown in Table V and Fig. 7 respectively. These coincide with those of reference runs within the range of experimental error. The separation of sodium and cesium gose as well as before, and it is concluded that stannic phosphate is stable against irradiation of about 10^9 r.

X-Ray Diffraction.—The results are shown in Fig. 8. Stannic phosphate dried at room temperature shows a weak line at d=4.14 Å, and one more line appears at d=3.73 Å when the sample dried at 110°C is used. When the drying temperature is 410°C, it shows 7 lines; however, the spacings of these lines do not coincide at all with that of the lines which appear in the diffraction patterns of exchangers

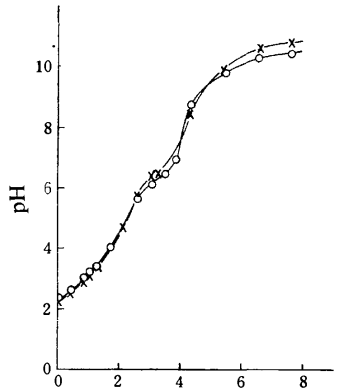

Fig. 7. Effect of irradiation on the titration curve of stannic phosphate.
Legend: -×- Reference; -○- 10^9 r

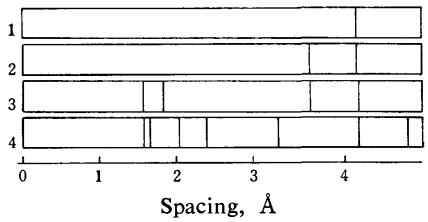

Fig. 8. X-Ray diffraction.
1: Dried at room temperature
2: Dried at 110°C
3: Dried at 210°C
4: Dried at 410°C

TABLE V. EFFECT OF RADIATION

Environment	Dose, r	Exchange capacity meq./g.
Reference	—	1.44
Air	1.10×10^8	1.40
Air	1.13×10^9	1.40
H_2O	1.02×10^9	1.45
7 N HNO_3	1.02×10^9	1.45

dried at 210°C or a lower temperature. This suggests that some remarkable changes in structure may occur between 210°C and 410°C. There are only a small number of diffraction lines, and the intensities of these lines are so weak that the relative intensity can not be determined. Consequently, the stannic phosphate has a nearly amorphous structure, and, therefore, a detailed analysis of the results is impossible.

Discussion

Structure.—On the basis of the results concerning the properties of the exchanger hitherto obtained, one can put forward the following assumptions.

a) When the air-dried exchanger is heated at 110°C to a constant weight, the weight loss measured is due to water retained in the gel structure; this water completely volatilizes off at this temperature. (About 20.8% of this water is contained in an air-dried exchanger.)

b) The neutral salt decomposition capacity results from one hydrogen ion of the H_2PO_4– group. The strongly dissociable hydrogen ions due to one-half of the H_2PO_4–groups disappear at 210°C, and the other half, at 320°C with the condensation of the H_2PO_4– groups. The titration curves support this assumption.

c) The weight loss near 350°C is due to the loss of structual water. This assumption is supported by the evidence of X-ray diffraction study and by the marked change in appearance.

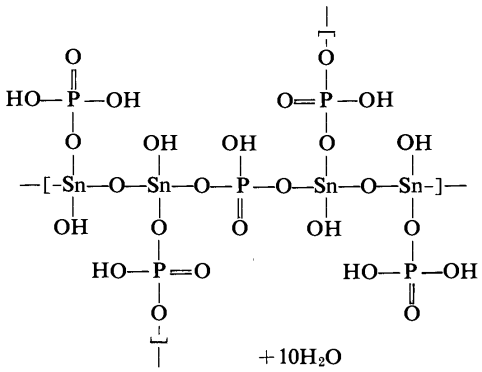

Fig. 9. Structure of stannic phosphate.

Taking the composition of stannic phosphate (P/Sn=5/4) and the above assumptions into consideration, the structure represented in Fig. 9 may be inferred.

The neutral salt decomposition capacities and weight losses calculated on the basis of the above assumptions are presented in Table III. These values and experimental results agree fairly well.

It seems that the arrangement of such a unit structure is not very regular because the X-ray diffraction patterns display a nearly amorphous structure.

Rate of Exchange.—The separation of sodium and cesium did not go well when stannic phosphate dried at 110°C was used, even though the exchange capacity was unchanged. This is mainly due to prolonged tailing, and it is perhaps also attributable to the slow rate of exchange. On the other hand, this phenomenon does not occur when stannic phosphate treated in water even at so high a temperature as 250°C is used. If one thinks of the rate-determining step as particle diffusion, as has been made clear in the case of zirconium phosphate,[3] and if one considers that ions migrate through adsorbed water, the above phenomenon may be explained well.

The findings of Fig. 3 can be illustrated as follows. When the concentration of exchanging cations is 10^{-3} M, which corresponds to about one-seventh of the exchange capacity, the cations are adsorbed in a high distribution coefficient immediately after the exchanger comes in contact with the solution. Part of the cations, once adsorbed on the exchanger, are liberated into the solution at a finite rate in consequence of the decrease in the distribution coefficient, which is accompanied by the drop of the pH of the solution; then equilibrium is attained. The adsorption curve when a 10^{-2} M solution is used, differs from that obtained when the concentration is 10^{-3} M. In this case the exchanging cations added are not adsorbed rapidly in so high a distribution coefficient as when the pH of the solution is high. As a result of this fact and of the pH change of the solution during the exchange step, such a curve as represented in Fig. 3 is obtained. On the other hand, in the case of infinite dilution, no pH change of the solution occurs during the adsorption process and the exchange occurs in a simple adsorption process.

Ion Exchange Equilibria.—Assuming that the exchanging ion is a simple cation, which does not undergo complexing, polymerization or hydrolytic reaction in the media of interest, and assuming that only one type of exchanging group contributes to the ion exchange reaction, the ion exchange equilibria may be written in the form:

$$M^{n+} + nHR = MR_n + nH^+ \quad (1)$$

with the equilibrium constant:

$$K = \frac{(MR_n)\,[H^+]^n \gamma_{MR_n} \gamma_{H^+}^n}{[M^{n+}]\,(HR)^n \gamma_{M^{n+}} \gamma_{HR}^n} \quad (2)$$

where brackets is the concentration of the ion in the aqueous phase, parentheses is the concentration in the exchanger phase, and γ is the activity coefficient. K is the equilibrium constant. Equation 2 is useful as an ion exchange equation, at least under some limiting conditions, if the activity coefficients in the exchanger phase do not vary rapidly.

With organic exchangers, the activity coefficient ratio, $\gamma_{MR_n}/\gamma_{HR}^n$, for the exchanger phase is essentially constant if exchange reactions are carried out in moderately dilute electrolyte solutions, if one of the adsorbed ions occurs at dilute concentrations, and if no complexing or hydrolytic reactions occur. The composition of the exchanger is, therefore,

3) G. H. Nancollas and R. Paterson, *J. Inorg. Nucl. Chem.*, 22, 259 (1961).

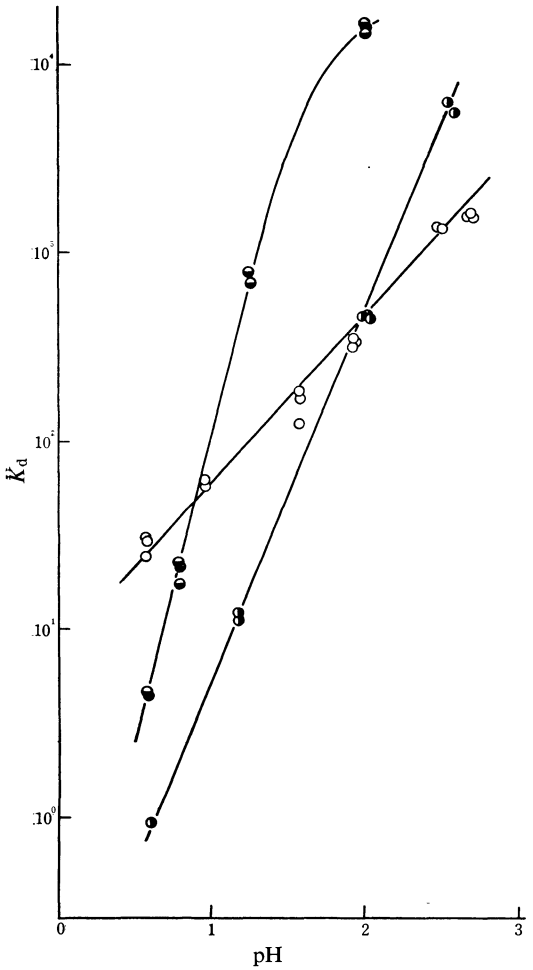

Fig. 10. Distribution coefficients for Cs(I), Cu(II) and Ga(III) on stannic phosphate at different pH.
Legend: -○- Cs(I); -◑- Cu(II); -◒- Ga(III)

essentially independent of the concentration of the adsorbed ions and Eq. 2 simplifies to:

$$K_d [H^+]^n \frac{\gamma_{H^+}^n}{\gamma_{M^{n+}}} = \text{const.} \quad (3)$$

where the distribution coefficient, K_d, is defined by:

$$K_d = \frac{(MR_n)}{[M^{n+}]} \quad (4)$$

If the ionic strength of the solution is low, the activity coefficient, $\gamma_{M^{n+}}$, will be unity. Equation 3 can, therefore, be rewritten to:

$$\log K_d = \text{const.} + n \times \text{pH} \quad (5)$$

According to Eq. 5, a plot of log K_d vs. pH should be a straight line with a slope of n.

This relationship has been verified for cesium(I), copper(II) and gallium(III) ions, as illustrated in Fig. 10. This relationship shows that only one type of exchange reaction contributes to the reaction in such a low pH as less than 3.

Summary

A recommended procedure for the preparation of stannic phosphate and a discussion of its ion exchange properties have been presented.

Some of the results obtained are as follows.

1) The density of the stannic phosphate is 2.17 g./cm^3.

2) Stannic phosphate is a weakly acidic cation exchanger and possesses several dissociable hydrogen atoms in the range of pK_a values. In a weakly acidic solution, in which the exchanger is useful, the exchange group having the pK_a value of approximately three is most important.

3) The ion exchange equilibrium can be elucidated by the mass action law.

4) The affinity series for alkali metal coincides with the usual relationship observed in the ion exchange resin.

5) The rate-determining step is assumed to be the migration of ions through the water retained in the gel structure.

6) Stannic phosphate is unstable against heat treatment in air; that is, the separation of alkali metal does not go well with the exchanger dried at 110°C due to the slow rate of exchange.

7) It is fairly stable against heat treatment in water; that is, it undergoes only a slight decrease in ion exchange capacity even when it is treated in water at 250°C for 8 days.

8) It is stable against irradiation of about 10^9 r.

9) The structure of stannic phosphate has been suggested on the basis of its thermal decomposition curve, its exchange capacity, its titration curves, and its X-ray diffraction patterns.

The author wishes to thank Dr. Hidehiro Goto and Dr. Shin Suzuki of Tohoku University for their guidance, discussion and continuous encouragement.

This project was partly financed by a grant-in-aid for Fundamental Scientific Research provided by the Ministry of Education, to which the authors' gratitude is due.

The Research Institute for Iron Steel and Other Metals
Tohoku University
Katahira-cho, Sendai

Studies of the Synthetic Inorganic Ion Exchanger. III. The Separation of the Fission Product by Means of a Stannic Phosphate Cation Exchanger

By Yasushi INOUE

(Received June 8, 1963)

Previously, stannic phosphate, one of the synthetic inorganic ion exchangers which would be expected to have radiation and thermal stability, has been prepared and its fundamental properties investigated, as has been described in preceding reports.[1,2]

Stannic phosphate is one of the polybasic acids which have several dissociable hydrogen atoms. However, the functional group, with the pK_a value of approximately three, is most important in a weakly acidic solution, and in such a solution this exchanger is useful; therefore, it may be assumed that, from the practical point of view, stannic phosphate is a weakly acidic cation exchanger with only one functional group. The ion exchange equilibrium can be elucidated from the mass action law; the ion exchange properties of stannic phosphate are also affected by heat treatment in air. For instance, the separation of alkali metals does not proceed well when the exchanger is dried at 110°C because of the slow rate of exchange. On the other hand, stannic phosphate is fairly stable against heat treatment in water; that is, it changes for the worse only in a slight decrease in exchange capacity even when it is treated in water at 250°C. It is so stable against radiation that is not affected at all by gamma ray irradiation up to 10^9 r. Thus, the stannic phosphate has been shown to be, for the most part, a good cation exchanger except for a few shortcomings such as unstability against alkaline solutions and against heat treatment in air; as an example of practical applications, the mutual separation of various nuclides in a fission product cooled for one or two years has been carried out using ammonium chloride and nitric acid as eluants. The results will be described below.

Experimental

Reagents and Apparatus. — *Reagents.* — *Ion Exchanger:* Stannic phosphate prepared by the method described previously was used.[2]

Radioactive Isotopes: The kinds of radioactive isotopes, their suppliers, commercial forms and the methods of pretreatment are shown in Table I. Their radiochemical purity was certified by gamma ray spectrometry or by analyses of their beta ray absorption curves before use.

Other chemicals, such as nitric acid and ammonium chloride, were of the highest purity grade.

Apparatus.—All pH measurements were performed with a Toa Dempa pH meter, model HM-5, calibrated with the appropriate buffer solutions prior to the experiments. Measurements of beta rays and gamma rays were made by a Hitachi Model RT-1 G. M. counter and a Hitachi well-type scintillation counter respectively. A Hitachi Model RDA-2 single-channel gamma-ray spectrometer or TMC-400 channel pulse-height-analyzer Model 406-6 were used for the measurement of the gamma-ray spectra.

Procedures.—The column was prepared as follows. To 2 g. of a dried exchanger in hydrogen form (100~200 mesh) sufficient distilled water was added to allow thorough enough mixing to expell any adhering air bubbles. After mixing, the slurry was poured into a glass column, 7 mm. in internal diameter, using glass wool as a column support. The column thus prepared had the height of 40 mm.. When the ammonium form exchanger was used, the column was conditioned by the passage of 50 ml. of a 3 M ammonium chloride solution, followed by that of 50 ml. of distilled water, at the flow rate of 0.5~0.6 ml./min.

The flow rate of the influent was kept nearly constant, 10~12 drops per min. corresponding to 0.5~0.6 ml./min., throughout this experiment.

For making elution curves, effluents were received in polyethylene test tubes every 2 g. by means of a Toyo Kagaku Sangyo Model SF-200A fraction collector unless otherwise noted; their radioactivity was measured with the well-type scintillation counter. When beta rays were used for the measurement of radioactivity, one drop of effluent was received on aluminum dishes every 2 g. and their radioactivity was measured with the G. M. counter in the usual manner. The identification of the nuclides present in the effluent and the determination of their radiochemicl purity were made by gamma ray spectrometry and by analyses of beta-ray absorption curves at several important points on the elution curves.

The content of rare earth in the cesium fraction was determined in the following way: To the sample solution, 5 mg. of cesium and 20 mg. of lanthanum

1) Y. Inoue, *J. Inorg. Nucl. Chem.*, in press.
2) Y. Inoue, This Bulletin, **36**, 1316 (1963).

TABLE I. RADIOACTIVE ISOTOPES USED IN THIS WORK

Nuclide	Supplier	Commercial form	Pre-treatment
F. P.	Oak Ridge National Laboratory, U. S. A.	Nitrate	Treated with HNO_3: Cooled for about 1.5 years
^{89}Sr	Oak Ridge National Laboratory, U. S. A.	Chloride	^{90}Y removal by ion exchange: Converted into HNO_3 form
^{106}Ru-^{106}Rh	Radiochemical Center, England	Trichloride	Converted to HNO_3 form
^{95}Zr-^{95}Nb	Oak Ridge National Laboratory, U, S. A.	Oxalate	Each nuclide is separated by means of TTA extraction: Converted to HNO_3 form
^{137}Cs	Oak Ridge National Laboratory, U. S. A.	Chloride	Converted to HNO_3 form
^{144}Ce(III)	Radiochemical Center, England	Trichloride	H_2O_2 reduction
^{144}Ce(IV)	Radiochemical Center, England	Trichloride	$KBrO_3$ oxidation-ether extraction-back extracted into dil. HNO_3
^{90}Sr-^{90}Y	N. V. Philips-Roxane Pharmaceutish-Chemishe Industrie "Duphar", Holland	Chloride	Converted to HNO_3 form

were added as carriers, and a slight excess of ammonium hydroxide solution was also added to precipitate lanthanum hydroxide. The precipitate thus formed was filtered, washed, and dissolved into a possibly small amount of hydrochloric acid. Precipitation was repeated until the activity of the lanthanum hydroxide became free from that of the cesium. Then the precipitate was put into a polyethylene sample tube and its activity was measured by the well type scintillation counter.

Results

Distribution Coefficients.—To contribute to the establishment of the method of separation, the distribution coefficients of various nuclides contained in the fission product were determined in a nitric acid medium, as shown in Table II.

^{95}Zr and ^{95}Nb show high distribution coefficients of about 3×10^3 ml./g. extending over a wide range of acidity. This is perhaps attributable to the formation of insoluble phosphates. On the contrary, although there is a slight tendency for ruthenium to adsorb from concentrated nitric acid on the exchanger bed, the distribution coefficients for ruthenium are nearly zero throughout the wide range of acidity. For ^{137}Cs, ^{89}Sr, ^{90}Y, ^{144}Ce(III) and ^{144}Ce(IV), the distribution coefficients decrease with increasing acidity in accordance with the usual relationship observed in ion exchange resins. It is noticeable that cesium has exceedingly high distribution coefficients. It is assumed that a zirconium-niobium equilibrium mixture and ruthenium may be easily separated from the remaining nuclides because of their peculiar behavior toward the exchanger. Therefore, at first the conditions for the mutual separation of ^{137}Cs, ^{89}Sr and ^{144}Ce, and of ^{90}Sr and ^{90}Y were determined; then the behavior of zirconium-niobium and ruthenium towards the column operation was investigated.

The Separation of ^{137}Cs and ^{89}Sr.—As Table II indicates, the separation of ^{137}Cs and ^{89}Sr by the hydrogen-form exchanger was intended using nitric acid as the eluant. In this case, strontium shows a gently sloping elution curve when acidity is low; the peak of the elution curve cannot become sharp until the acidity of the eluant is increased to more than 5 N. Cesium is in part eluted with nitric acid of a high concentration such as 5 N, but the major part of it remains on the top of the column.

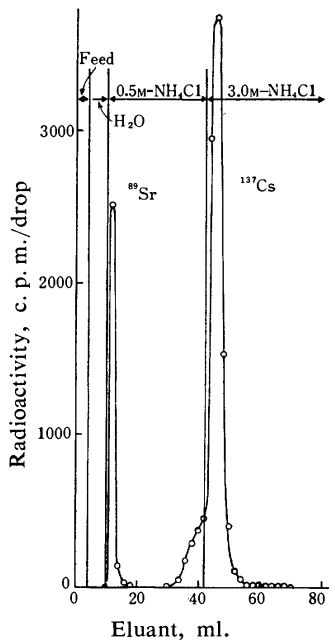

Fig. 1. Separation of ^{137}Cs and ^{89}Sr by hydrogen-form exchanger.

TABLE II. DISTRIBUTION COEFFICIENTS IN NITRIC ACID SOLUTION (ml./g.)

Acidity (N)	Nuclide							
	^{95}Zr	^{95}Nb	^{137}Cs	^{89}Sr	^{90}Y	^{144}Ce(III)	^{144}Ce(IV)	^{106}Ru*
0.1	2.7×10^3	2.2×10^3	3.8×10^3	6.7×10	1.4×10^3	9.3×10^2	6.5×10^2	~0
0.5	3.5×10^3	2.6×10^3	1.3×10^3	~7	1.6×10	1.2×10	1.1×10	~0
1.0	3.5×10^3	2.7×10^3	1.8×10^2	~2	~3.6	~4	~1	~0
3.0	3.6×10^3	2.5×10^3	1.0×10^2	~2	~2	~2	~1	~3
10.0	3.7×10^3	4.0×10^3	~3.7	~0	~0	~0	~0	~8

* The species of ^{106}Ru is not identified.

Therefore, cesium and strontium cannot be separated with the hydrogen-form exchanger using nitric acid as the eluant. When ammonium chloride is used, the sharp peaks of ^{89}Sr and ^{137}Cs appeared in the 0.5 M and 3.0 M fractions respectively, as Fig. 1 shows. The amount of cesium remaining on the column after the elution is only 0.1% or less of the total cesium present; therefore, it is concluded that the separation is complete. When the ammonium-form exchanger is used instead of the hydrogen-form, the elution of strontium by 0.5 M ammonium chloride solution is not sharp, as Fig. 4 shows. To get a sharp elution curve, it is necessary to add a little hydrogen ion to the eluant, as shown in Fig. 5. According to this principle, strontium and cesium can be separated on the ammonium-form exchanger by a step elution technique using 0.1 N nitric acid-0.2 M ammonium chloride and 3 M ammonium chloride as the eluants respectively.

The Separation of ^{89}Sr and ^{144}Ce and of ^{90}Sr and ^{90}Y.—The separation of ^{89}Sr and ^{144}Ce was carried out using a hydrogen-form exchanger,

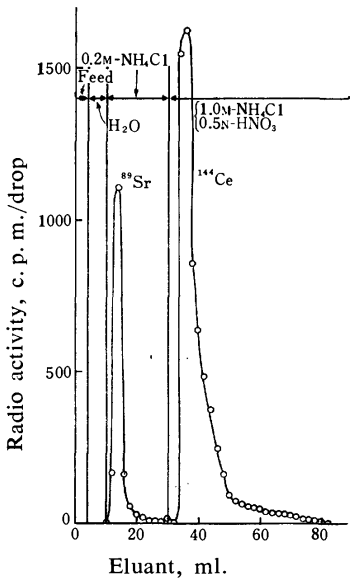

Fig. 2. Separation of ^{89}Sr and ^{144}Ce by hydrogen-form exchanger.

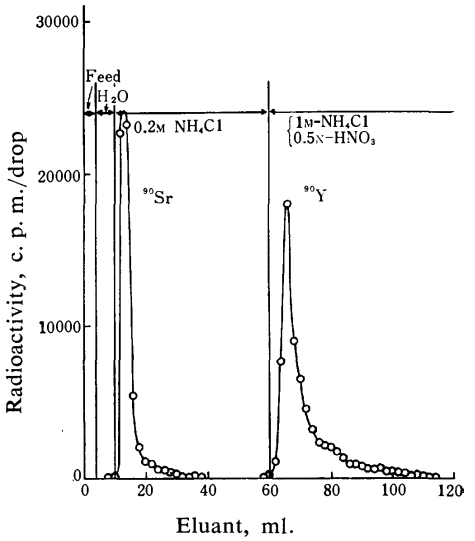

Fig. 3. Separation of ^{90}Sr and ^{90}Y by hydrogen-form exchanger.

as Fig. 2 shows. As to strontium, the elution was performed in a manner similar to that in Fig. 1. Because cerium is eluted only in a small part when ammonium chloride is used alone, whatever concentrated solution may be used, it is necessary to add hydrogen ions to some extent for the complete elution of cerium. In this case, however, the addition of ammonium chloride is not always necessary and cerium can be completely eluted by nitric acid above 1 N alone, as Fig. 10 shows.

In the case of the ammonium-form exchanger, in contrast to the hydrogen-form, strontium is completely eluted with dilute ammonium chloride as 0.5 M only with the aid of nitric acid, as shown in Figs. 4 and 5. Figure 6 shows that cerium is not eluted at all with a 0.1 N nitric acid-0.2 M ammonium chloride solution. Therefore, these nuclides can be separated according to this principle (Fig. 7). The separation of a ^{90}Sr–^{90}Y equilibrium mixture is possible in an analogous manner, as Figs. 3 and 8 show.

The Separation of ^{137}Cs and ^{144}Ce.—Applying the fact that cerium can not be eluted by

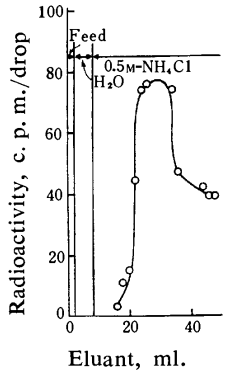

Fig. 4. Elution of strontium by 0.5 M ammonium chloride (ammonium-form exchanger).

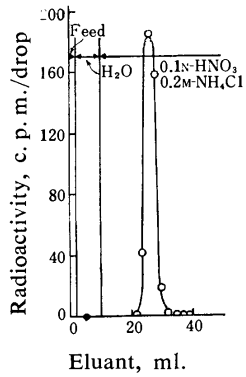

Fig. 5. Elution of strontium by 0.1 N nitric acid−0.2 M ammonium chloride (ammonium-form exchanger).

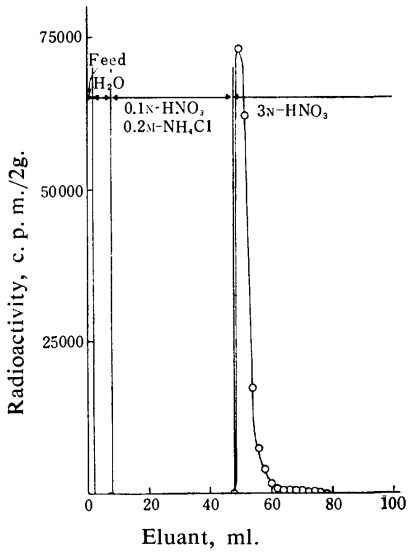

Fig. 6. Elution of cerium by hydrogen-form exchanger.

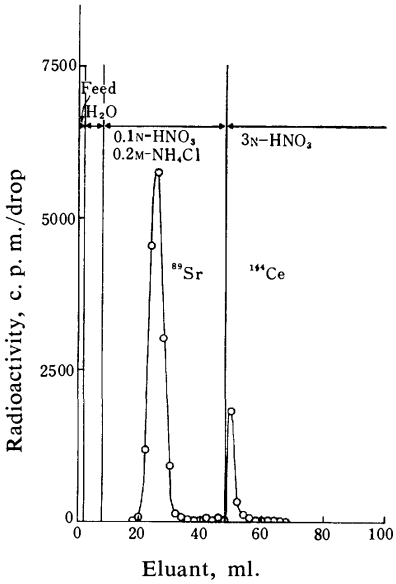

Fig. 7. Separation of ^{89}Sr and ^{144}Ce by ammonium-form exchanger.

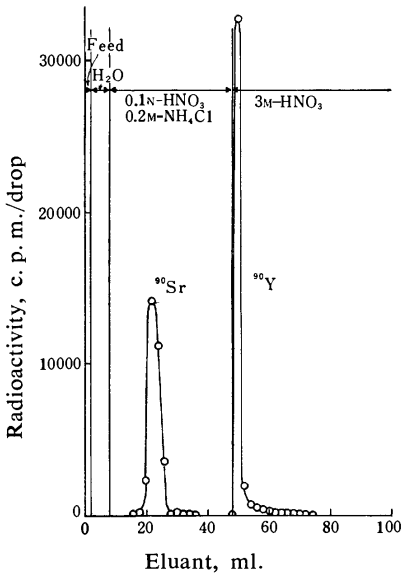

Fig. 8. Separation of ^{90}Sr and ^{90}Y by ammonium-form exchanger.

ammonium chloride alone, the separation of cesium and cerium has been carried out with the hydrogen-form exchanger, as shown in Fig. 9. It is necessary to note that the small peak appears in the beginnig of the 3 M ammonium chloride fraction. The analytical results show that this is mainly due to cerium. This is attributable to the elution of cerium with the hydrogen ions which are liberated from the hydrogen-form exchanger when the concentrated ammonium chloride solution is

passed through it. Therefore, the complete separation of cesium and cerium on the hydrogen-form exchanger is impossible. However, as represented in Fig. 10, cerium is seldom eluted by 3 M ammonium chloride from the ammonium-form exchanger. On the basis of the above results, it is assumed that cesium and cerium can be separated by the step elution technique using 3 M ammonium chloride and 3 N nitric acid as the respective eluants. It is apparent from Fig. 11 that well-defined curves are obtained and that the separation is complete.

The Adsorption of Zirconium and Niobium. —The behavior of the zirconium-niobium equilibrium mixture was investigated in detail with the column operation in order to determine whether or not the results of the batch experiments could be applied to the column separation experiment. Ten milliliters of a 0.1 N nitric acid solution containing a zirconium-niobium equilibrium mixture were applied to the top of the column, and the column was then washed with 50 ml. of 5 N nitric acid. The leakage of ^{95}Zr–^{95}Nb from the column bed amounts to about 4.5 per cent, and the uptake is not complete. However, from the shape of

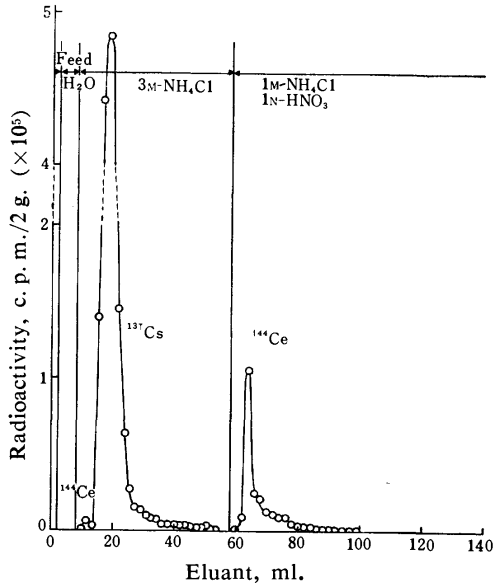

Fig. 9. Separation of ^{137}Cs and ^{144}Ce by hydrogen-form exchanger.

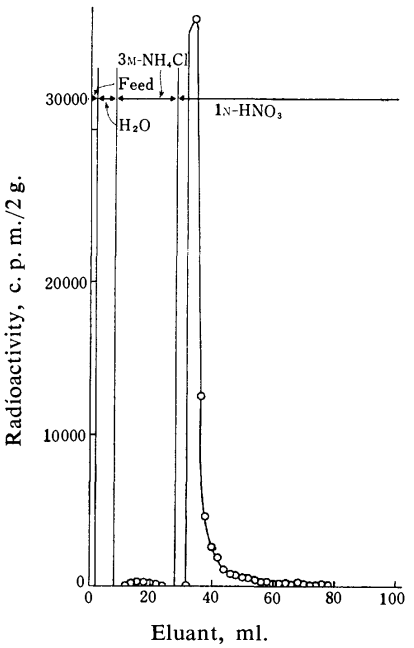

Fig. 10. Elution curve of cerium by ammonium-form exchanger.

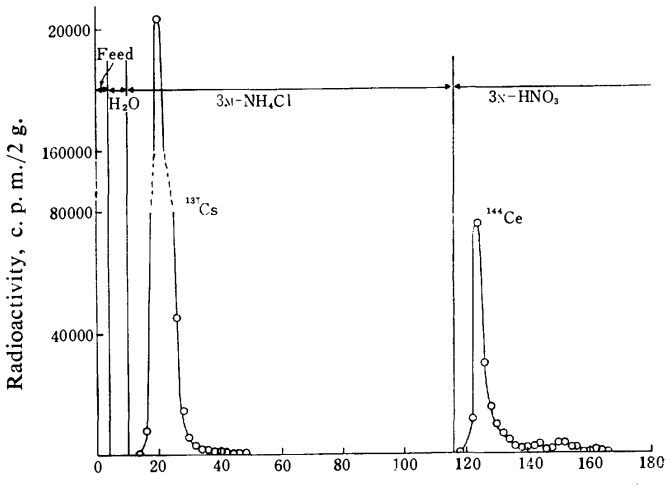

Fig. 11. Separation of ^{137}Cs and ^{144}Ce by ammonium-form exchanger.

the breakthrough curve it seems that the leakage from the exchanger bed does not occur by the elution of ions once retained on exchanger, but takes place during the adsorption step (Fig. 12a). Such peculiar behavior can probably be attributed to the presence of a radiocolloidal form of zirconium. This seems quite possible, since the stock solution was only 0.1 N in free acid. On the basis of the above considerations, a zirconium solution which had been treated with hot concentrated nitric acid for a few hours was used immediately after being diluted to the desired acidity, but no decrease in the leaked activity was observed. When the effluent is passed through the exchanger bed three times, zirconium can be adsorbed almost completely, but this method cannot be used in the practical separation of the fission product because the separation of cesium and strontium is interfered with by this operation. The unadsorbed zirconium is almost completely washed out with 10 ml. of distilled water, as Fig. 12(b) shows. In order

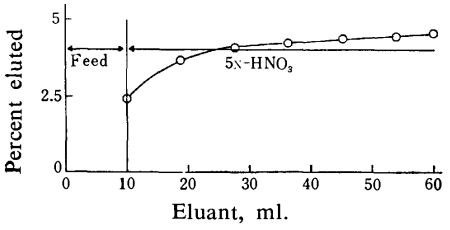

Fig. 12 (a). Breakthrough curve of zirconium by 5 N nitric acid.

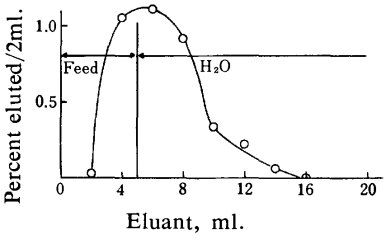

Fig. 12 (b). Breakthrough curve of zirconium by water.

to make sure, the distribution coefficients of zirconium and niobium in a 1 N nitric acid solution were determined as a function of the ammonium nitrate concentration; it was found that these elements can be completely retained on the column, even in the concentrated salt solution. Putting these findings together, it is apparent that the total zirconium and niobium activity can be precisely estimated from the sum of the activity remaining on the column after the elution is finished and the sum of the leaked activity during the adsorption step.

The Adsorption of Ruthenium.—The behavior of ruthenium was investigated in detail with the column operation in order to determine whether or not the results of batch experiments could be applied to the column operation.

Ten milliliters of a 0.1 N or 0.2 N nitric acid solution containing ruthenium activity was passed through the exchanger bed. When the level of the solution reached the top of the exchanger bed, nitric acid of the same concentration was percolated through and the effluent was collected every 10 ml. The results are presented in Fig. 13. The curves represent the accumulated percentage value of the eluted activity as a function of the effluent volume. When the ruthenium solution which has been treated with concentrated nitric acid is used, only about 40% of ruthenium activity is eluted. When the ruthenium treated enough with fuming nitric acid is used, more ruthenium is eluted, but the percentage still does not reach 80%. When the concentration of the eluant is 0.2 N nitric acid, the 90% mark of the ruthenium is broken through. However, strontium is also completely eluted under these conditions, so this concentration is unfavorable for the elution of ruthenium in the separation of the fission product. The reason for the discrepancy between this and the batch experiment is not clear; at any rate, it is impossible to separate ruthenium from the other nuclides with the column operation. Consequently, the complete separation of fission product cannot be effected without the separation of ruthenium in advance by a method other than the ion exchange.

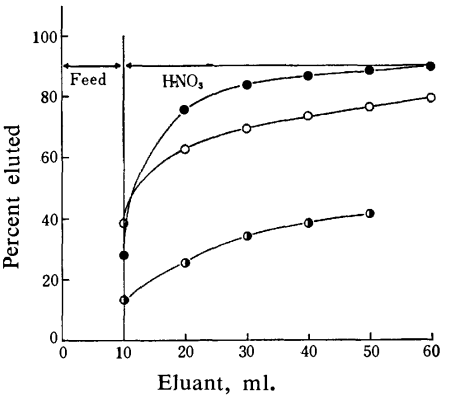

Fig. 13. Elution of ruthenium.
-◑- Eluant: 0.1 N-HNO_3
-○- Eluant: 0.1 N-HNO_3, treated with fuming nitric acid
-●- Eluant: 0.2 N-HNO_3, treated with fuming nitric acid

The Volatilization of Ruthenium.—It is advisable to remove ruthenium without the introduction of foreign salts. It was found in detailed

TABLE III. SEPARATION OF SYNTHETIC SAMPLES

Experimental No.	^{137}Cs Yield, %	^{137}Cs Yield, % corrected	^{144}Ce-^{144}Pr Yield, %	^{144}Ce-^{144}Pr Yield, % corrected	^{95}Zr-^{95}Nb Yield, %	^{89}Sr Yield, %
1	114.2	104.9	73.3	98.7	110.2	98.9
2	111.5	102.2	81.6	107.0	98.9	98.7
3	112.9	103.6	78.4	103.7	90.7	103.6
Mean		103.5		103.1	99.9	100.4

TABLE IV. ANALYSIS OF FISSION PRODUCT
(measured by well type scintillation counter)

	Analytical result						Total
	E. P. used	Sr	Cs*	R. E.*	Zr-Nb	Ru	
c. p. m.	771675	7463	103083	483242	10288	163308	767384
%	100	1.0	13.4	62.6	1.3	21.2	99.5

* Contamination of Cs with R. E. is corrected.

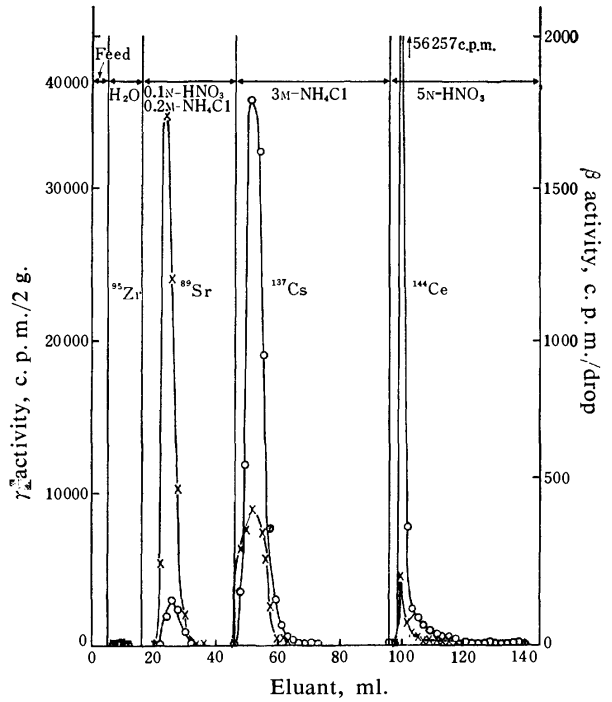

Fig. 14. Separation of synthetic sample.

examinations that the best method for removing ruthenium was the volatilization from boiling concentrated perchloric acid. Not less than 99% of ruthenium is removed by the boiling of concentrated perchloric acid solution, and this procedure does not affect the following ion exchange separation. It is necessary, however, to boil off ruthenium violently instead of fuming it gently.

The Separation of a Fission Product Solution. —Putting the above results together, the mutual separation of various nuclides contained in a fission product is carried out in the following way: To the sample solution, 5 ml. of concentrated perchloric acid is added, and this is boiled until a yellow color has once appeared and then diminished. (It is advisable to lead the distillate into water in order to prevent any health hazard.) Then the residual solution is evaporated almost to dryness on the hot plate. After cooling, 1 ml. of 1 N nitric acid is added, heated to dissolve the residue, and diluted to 10 ml. with water. This is poured into an ammonium-form exchanger bed;

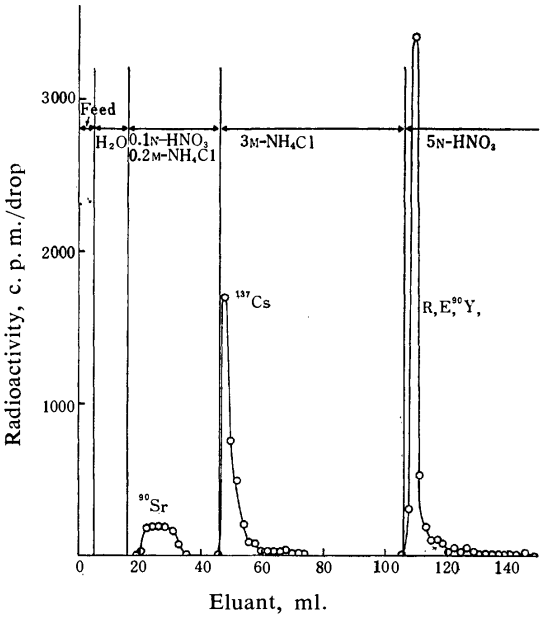

Fig. 15. Separation of fission product.

when the level of the solution reaches the top of the exchanger bed, 10 ml. of water, 30 ml. of 0.1 N nitric acid-0.2 M ammonium chloride, 60 ml. of 3 M ammonium chloride, and 60 ml. of a 5 N nitric acid solution are passed through the column successively.

The separation of a synthetic sample containing nearly equal activities of ^{89}Sr, ^{137}Cs, ^{95}Zr–^{95}Nb, ^{106}Ru and ^{144}Ce is shown in Fig. 14. Although the shape of the elution curve shows that satisfactory separation is achieved, it is observed from the analytical results that there is a contamination by cerium of the cesium fraction. The material balance represented in Table III convinces one of this observation. The corrected values obtained by the analysis of the cesium fraction are also shown in Table III; these values agree quite well within the experimental error.

The results of the separation of the fission product are shown in Fig. 15 and Table IV. The reason for the contamination of the cesium fraction is not clear, although it is assumed that the elution step of strontium may affect the separation.

Summary

The mutual separation of various nuclides contained in fission product has been carried out with a stannic phosphate cation exchanger. Various concentrations of nitric acid and ammonium chloride solutions have been used as eluants, and the separation has been performed on hydrogen- and ammonium-form exchangers.

The separations of ^{89}Sr–^{137}Cs, ^{89}Sr–^{144}Ce, ^{137}Cs–^{144}Ce and ^{90}Sr–^{90}Y were easy and complete except for that of ^{137}Cs–^{144}Ce on a hydrogen-form exchanger. ^{95}Zr and ^{95}Nb were almost completely adsorbed on the exchanger over a wide range of acidity and salt concentration; therefore, they were not eluted at all. As the behavior of ^{106}Ru is complex and its separation from other nuclides is impossible, it is necessary to separate the ruthenium from the fission product in advance by a method other than that of ion exchange.

With reference to the above results, the total analysis of the fission product on an ammonium-form exchanger has been carried out. It is almost complete except for the contamination of rare earth in the cesium fraction.

The author wishes to thank Dr. Hidehiro Goto and Dr. Shin Suzuki of Tohoku University for their guidance, discussion and continuous encouragement.

Part of the expenses for this investigation have been defrayed by a grant-in-aid by the Ministry of Education.

The Research Institute for Iron Steel and Other Metals
Tohoku University
Katahira-cho, Sendai

Syntheses of 23-Ketositosterol and Its Derivatives

By Ken-ichi MORITA,* Takeshi IWAMA and Yoshiaki KAMANO**

(Received March 27, 1963)

In connection with other studies, it was necessay to prepare sitosterol derivatives with oxygen functions at the C_{22} and C_{23} carbon atom, respectively. This article describes a method for the introduction of oxygen functions into the C_{23} carbon atom of sitosterol.

The peroxybenzoic acid oxidation of 3β-acetoxy-5α-chlorostigmast-22-ene (II)[1] proceeded stereospecifically and gave a single isomer of 5α-chloro-3β-acetoxy-22ξ, 23ξ-epoxystigmastane (III). Bladon et al.[2] have reported that the peroxybenzoic acid oxidation of 3β-acetoxy-5α, 8α-epidioxyergosta-6, 9 (11), 22-triene gives two isomers of 3β-acetoxy-22ξ, 23ξ-epoxy-5α-hydroxyergosta-7, 9(11)-diene. The difference is probably due to the alkyl side chains at C_{24}. The side chain at C_{24} is an ethyl group with an α-configuration[3] in the stigmastane series, whereas it is a methyl group with a β-configuration[4] in the ergostane series. The oxide ring of compound III probably has the α-configuration, since an examination of the

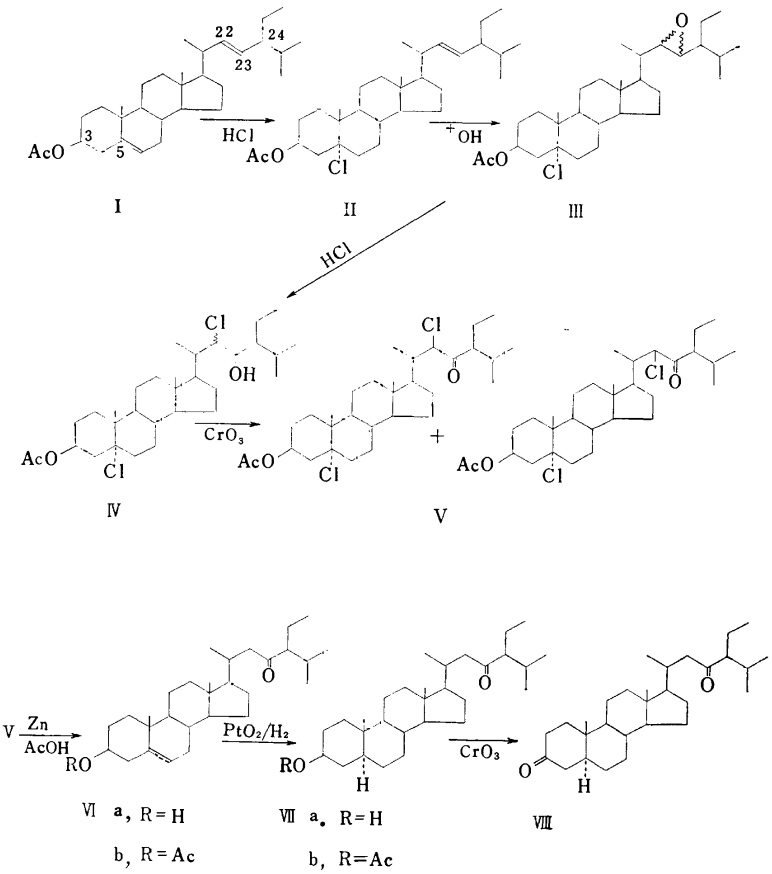

* To whom inquiry about this paper should be addressed. Present address: Basic Research Laboratories, Toyo Rayon Co., Kamakura, Japan.

** Present address: Taisho Pharmaceutical Co., Ltd., Toshima-ku, Tokyo.

1) E. M. Chamberlin, E. Tristram, T. Utne and J. M. Chemerda, *J. Am. Chem. Soc.*, 79, 456 (1957).

2) P. Bladon, P. B. Clayton, C. W. Greenhalgh, H. B. Henbest, E. R. H. Jones, B. J. Lovell, G. Silverstone, G. W. Wood and G. F. Wood, *J. Chem. Soc.*, 1952, 4883.

3) Y. Kishida, *Chem. Pharm. Bull.*, 8, 357 (1960).

4) L. F. Fieser, "Steroids," Reinhold Publishing Co., New York (1959), p. 339.

Dreiding model[5] seems to indicate that the α-side of the Δ^{22}-double bond of compound II is less hindered.

The treatment of compound III with hydrogen chloride in acetic acid gave a chlorohydrin mixture. The chromic acid oxidation of the chlorohydrin gave two isomeric chloroketones: isomer A [(m. p. 161~162°C, $[\alpha]_D$+43°, λ_{max} 305 mμ (ε, 57), and isomer B (m. p. 178~179°C $[\alpha]_D$+17°, λ_{max} 298 mμ (ε, 60)]. It is possible that one, after formed, was in part epimerized to the other. Both the isomers possess the 22-chloro-23-keto structure (V), as the following evidence shows. Both gave the same keto acetate on reduction with zinc dust and acetic acid. The hydrogenation of the keto acetate on an Adam platinum catalyst in an acidic medium, followed by an alkaline hydrolysis, gave a saturated keto alcohol. The chromic acid oxidation of the saturated keto alcohol gave a diketone (m. p. 159~160°C, $[\alpha]_D$+54.4°) which was different from the stigmastane-3, 22-dione (m. p. 176~177°C, $[\alpha]_D$+21.8°) obtained by Fischer and Mägerlein.[6] Therefore, the only possible structure for the diketone is VIII (stigmastane-3, 23-dione). When the crude oxidation product of the chlorohydrin (IV) was treated with zinc dust and acetic acid the only isolable ketone was 3β-acetoxystigmast-5-en-23-one (VIb). The attack of the chloride ion upon the oxide III occurred exclusively at the C_{22} carbon atom.

It is noteworthy that the prolonged hydrogenation of 3β-acetoxystigmast-5-en-23-one (VIb) on a platinum oxide catalyst in an acidic medium furnished saturated ketone VIIb in a good yield. No hydroxy compound was formed.[7] The treatment of 3β-acetoxystigmast-5-en-23-one (VIb) with hydroxylamine hydrochloride in pyridine[8] uner reflux for 30 hr., under the condition which give oximes from hindered ketones, gave the unchanged starting material. The attempted esterification of 3β-acetoxy-5α, 22ξ-dichlorostigmastan-23-one (V) by Baeyer-Villiger reaction (peroxybenzoic acid in chloroform for one month) also failed. These facts indicate that the C_{23}-keto group in a stigmastane series is sterically highly hindered.

The reduction of compound VIb with lithium aluminum hydride gave epimeric diols. Two isomers were separated as benzoates (IX) (major one: m. p. 130~130.5°C, $[\alpha]_D$ −9°; minor one: m. p. 160~162°C, $[\alpha]_D$ −31°). According to Cram's rule[9] for the steric control of asymmetric induction, the major isomer may have the α-configuration.

The treatment with an alkali and the reacetylation of compound III gave 3β-acetoxy-22ξ,

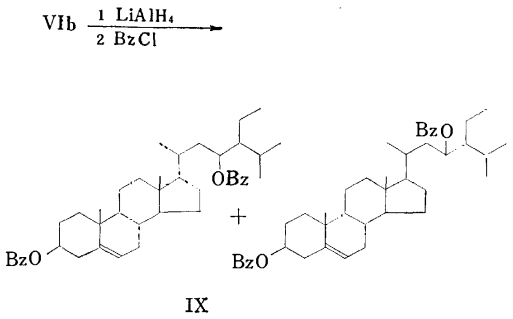

IX

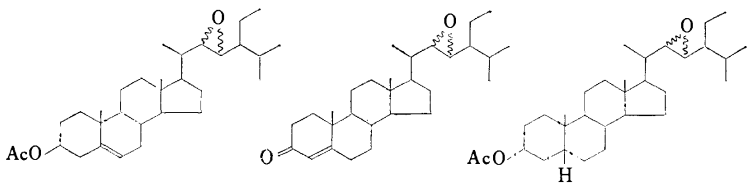

X XI XII

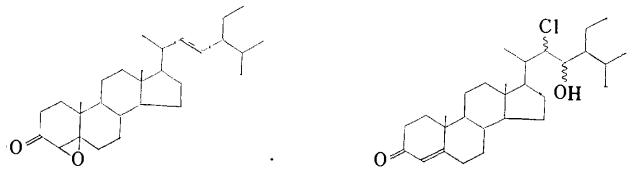

XIII XIV

5) A. S. Dreiding, *Helv. Chim. Acta*, 42, 1339 (1959).
6) F. G. Fischer and H. Mägerlein, *Ann.*, 636, 88 (1960).
7) In this connection, it may be noted that the reduction of sargasteryl acetate (3β-acetoxy-20-isostigmasta-5, 24(28)-diene) with platinum oxide in ethyl acetate gave 5, 6-dihydrosteryl acetate. Cf. K. Tsuda, R. Hayatsu, Y. Kishida and S. Akagi, *J. Am. Chim. Soc.*, **80**, 921 (1958), footnote 8.
8) E. B. Hershberg, E. P. Oliveto and R. Rausser, *Chem. & Ind.*, **1958**, 1477.
9) D. J. Cram and F. A. A. Elhafez, *J. Am. Chem. Soc.*, **74**, 5828 (1952).

23ξ-epoxystigmast-5-ene (X). The peracid oxidation of stigmasta-4, 22-dien-3-one[10] and 3α-acetoxy-5β-stigmast-22-ene[11] gave the corresponding oxides, XI and XII respectively. The oxidation of stigmasta-4, 22-dien-3-one with alkaline hydrogen peroxide gave 4, 5-oxide XIII. The treatment of XI with hydrogen chloride gave a corresponding chlorohydrin XIV. The 22ξ-chloro-23ξ-hydroxy structure was assigned by analogy with a previous reaction.

The dehydrohalogenation of V was attempted as the means of obtaining $\Delta^{20(22)}$-23-ketone by treatment with *s*-collidine or lithium carbonate in dimethylformamide, but no such compound could be isolated, although the crude product showed a slight ultraviolet absorption around 230~240 mμ. The only isolable compound was epimeric 3β-acetoxy-22ξ-chlorostigmast-5-en-23-one (XV.)

The purity of the compounds described in this article was examined by thin-layer chromatography; the R_f values of some of the compounds are recorded in Table I.

TABLE I. THIN-LAYER CHROMATOGRAPHY OF STIGMASTANE DERIVATIVES (BENZENE, SILICA GEL G)

No	Compound	R_f
1	Stigmast-5-ene-3β, 23ξ-diol	0.02
2	3β-Hydroxy-stigmastan-23-one (VIIa)	0.03
3	3β-Hydroxy-stigmast-5-en-23-one (VIa)	0.03
4	Stigmast-4-ene-3, 23-dione	0.03
5	Cholesterol	0.07
6	Stigmasterol	0.07
7	Stigmastane-3, 23-dione (VIII)	0.19
8	3β-Acetoxystigmastan-23-one (VIIb)	0.29
9	3β-Acetoxystigmast-5-en-23-one (VIb)	0.30
10	3β-Acetoxy-5α-chloro-22ξ, 23ξ-epoxystigmastane (III)	0.30
11	3β-Acetoxy-22ξ, 23ξ-epoxystigmast-5-ene (X)	0.34
12	3β-Acetoxy-5α, 22ξ-dichlorostigmastan-23-one (V) (Isomer A, m. p. 161~162°C)	0.33
13	3β-Acetoxy-5α, 22ξ-dichlorostigmastan-23-one (V) (Isomer B, m. p. 178~179°C)	0.30
14	3β-Acetoxy-22ξ-chlorostigmast-5-en-23-one (XV) (Isomer A, m. p. 166.5~168°C)	0.37
15	3β-Acetoxy-22ξ-chlorostigmast-5-en-23-one (XV) (Isomer B, m. p. 177.5~180.5°C)	0.33
16	3β-Acetoxy-5α-chlorostigmast-22-ene (II)	0.48
17	Cholesteryl acetate	0.51
18	Stigmasteryl acetate (I)	0.51
19	3β, 23ξ-Dibenzoxystigmastane (IX) (Isomer A, m. p. 159~162°C)	0.62
20	3β, 23ξ-Dibenzoxystigmastane (IX) (Isomer B, m. p. 130~130.5°C)	0.67

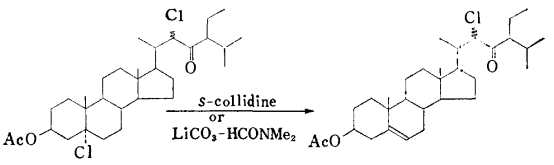

V XVa, b

Experimental[12]

3β-Acetoxy-5α-chlorostigmast-22-ene (II).—This material was prepared essentially by the procedure previously described.[1] The presence of acetic acid (100 ml. for 100 g. of stigmasteryl acetate) increased the yield. The product was obtained as needles; m. p. 183~184°C, $[\alpha]_D^{19}$ −7° (*c* 0.997) (reported m. p. 183~185°C, $[\alpha]_D^{24}$ −8.1°)

3β-Acetoxy-5α-chloro-22ξ, 23ξ-epoxystigmastane (III).—To a cold solution of 18.4 g. of II in 184 ml. of chloroform was added 45 ml. of a chloroform solution of peroxybenzoic acid containing 1.3 molar equivalents of the peracid. The mixture was then allowed to react at 0~3°C for fifteen days. The excessive peracid was decomposed with 10% aqueous potassium iodide, and the liberated iodine was titrated with 0.1N sodium thiosulfate (1.05 mol. of peracid were consumed). The chloroform solution was washed with 10% aqueous potassium carbonate and water and dried over anhydrous sodium sulfate. The chloroform was expelled under reduced pressure (the inner temperature was kept below 50°C). Recrystallization from ethyl acetate gave 12.5 g. of needles; m. p. 137~138°C, $[\alpha]_D^{22}$ −15° (*c* 0.46).

Found: C, 73.49; H, 10.34; Cl, 7.34. Calcd. for $C_{31}H_{51}O_3Cl$: C, 73.41; H, 10.14; Cl, 6.99%.

3β-Acetoxy-22ξ, 23ξ-epoxystigmast-5-ene (X).—To a solution of 3.2 g. of III in 150 ml. of ethyl alcohol was added a solution of sodium carbonate (3.2 g.) in water (18 ml.); the mixture was then heated under reflux for 5 hr. the usual manipulation gave 2.9 g. of an oil which was acetylated by treating it with acetic anhydride (5 ml.) and pyridine (11 ml.) overnight at room temperature; 3 g. of an sticky oil was thus obtained. Chromatography and recrystallization form methanol gave crystals (m. p. 114.5~115°C, $[\alpha]_D^{17}$ −71° (*c* 0.47)).

Found: C, 79.09; H, 10.71. Calcd. for $C_{31}H_{50}O_3$: C, 79.10; H, 10.71%.

22ξ, 23ξ-Epoxystigmast-4-en-3-one (XI).—Stigmasta-4, 22-dien-3-one (500 mg., m. p. 125~126°C) was dissolved in 2 ml. of chloroform containing 170 mg. of perbenzoic acid. The mixture was allowed to react at room temperature for three days in the

10) G. Slomp, Jr., Y. F. Shealy, J. L. Johnson, R. A. Donia, B. A. Johnson, R. P. Holysz, R. L. Pederson, A. O. Jensen and A. C. Ott, ibid., 77, 1216 (1955).
11) D. H. R. Barton and C. J. W. Brooks, ibid., 72, 1633 (1950).

12) All melting points were uncorrected. Rotations were measured in chloroform solution. Infrared spectra were determined with a Perkin-Elmer Model 21. Ultraviolet spectra were determined with a Hitachi Type EPU-2. We are indebted to Miss Sachiko Yoshikawa for measurements of rotations and some technical assistance and to Sankyo Co. for analyses.

dark. The usual manipulation gave 600 mg. of a cake which was chromatographed on 16 g. of alumina. Elution with a mixture of petroleum-ether and benzene (2 : 8) gave 200 mg. of the starting material. Further elution with chloroform gave 250 mg. of crystals (m. p. 117.5~118.5°C) after recrystallization from methanol. The infrared spectrum showed the absence of a Δ^{22}-double bond (970 cm^{-1}).

Found: C, 81.73; H, 10.83. Calcd. for $C_{29}H_{46}O_2$: C, 81.63; H, 10. 86%.

4β, 5β-Epoxystigmast-22-en-3-one (XIII).—To a stirred solution of 500 mg. of stigmasta-4, 22-dien-3-one in 20 ml. of methanol, 1.2 ml. of 4 N sodium hydroxide and 3 ml. of 30% hydrogen peroxide were added at 0~3°C. The mixture was then left to stand for 48 hr., poured into water and extracted with ether. The evaporation of ether and the crystallization of the residue from methanol gave 350 mg. of crystals (m. p. 120~122°C). The infrared spectrum showed the presence of a Δ^{22}-double bond (970cm^{-1}). The β-configuration of the oxide was assumed, since cholest-4-en-3-one gave 4β, 5β-epoxycholestan-3-one when similarly treated.[13]

Found: C, 81.25; H, 11.32. Calcd. for $C_{29}H_{46}O_2$: C, 81.63; H, 10.86%.

3α-Acetoxy-22ξ, 23ξ-epoxy-5β-stigmastane (XII). —This material was prepared by a procedure similar to that described for compound III. Recrystallization from methanol gave crystals (m. p. 105~107°C).

Found: C, 78.32; H, 11.34. Calcd. for $C_{31}H_{52}O_3$: C, 78.76; H, 11.08%.

5α-Chlorostigmast-22-en-3-one. — Two hundred milligrams of 5α-chlorostigmast-22-en-3β-ol [m. p. 153.5~155°C (from benzene-methanol)], prepared from stigmasterol and hydrochloric acid by a procedure similar to that employed in the preparation of 3β-acetoxy-5α-chlorostigmast-22-ene (II), was dissolved in 5 ml. of chloroform and treated with 100 mg. of chromic acid in a mixture of 0.5 ml. of water and 10 ml. of acetic acid at room temperature overnight. Crystallization of the product from benzene-methanol gave 100 mg. of crystals (m. p. 136~136.5°C, $[\alpha]_D^{18}$ −5° (*c* 0.41)).

Found: C, 77.78; H, 10.62; Cl, 7.75. Calcd. for $C_{29}H_{47}OCl$: C, 77.90; H, 10.60; Cl, 7.93%.

Semicarbazone; m. p. 216~218°C.

Found: C, 71.73; H, 9.54; Cl, 7.02; N, 8.35. Calcd. for $C_{30}H_{50}OClN_3$: C, 71.46; H, 9.99; Cl, 7.03; N, 8.33%.

3β-Acetoxy-5α, 22ξ-dichlorostigmastan-23ξ-ol (IV).—To a solution of 21.3 g. of 3β-acetoxy-5α-chloro-22ξ, 23ξ-epoxystigmastane (III) in 200 ml. of chloroform, 270 ml. of a 4% solution of hydrogen chloride in glacial acetic acid was added, and the mixture was allowed to stand for 24 hr. at room temperature. The reaction mixture was then poured into water and extracted with chloroform three times. The combined chloroform extract was washed with 5% aqueous potassium carbonate and water, dried over anhydrous magnesium sulfate, and concentrated under reduced pressure to give 23 g. of a yellow foam.

Crystallization from a 1 : 1 mixture of ethyl acetate and ethyl alcohol gave 10.0 g. of the first crop (m. p. 157~160°C) and 6.5 g. of the second crop (m. p. 152~156°C). The analytical sample was recrystallized from acetone; m. p. 162~164°C, $[\alpha]_D^{20}$ 0° (*c* 0.69).

Found: C, 68.71; H, 9.70; Cl, 12.73. Calcd. for $C_{31}H_{52}O_3Cl_2$: C, 68.48; H, 9.64; Cl, 13.04%.

22ξ-Chloro-23ξ-hydroxystigmast-4-en-3-one (XIV).—One gram of 22ξ, 23ξ-epoxystigmast-4-en-3-one (XI) was dissolved in 15 ml. of a 5% solution of hydrogen chloride in glacial acetic acid, and the mixture was allowed to react for 24 hr. at 0~5°C. The product was crystallized from methanol to 0.65 g. of crystals (m. p. 216~218°C).

Found: C, 75.51; H, 10.27; Cl, 7.86. Calcd. for $C_{29}H_{47}O_2Cl$: C, 75.20; H, 10.23; Cl, 7.65%.

3β-Acetoxy-22ξ-chlorostigmastan-23-one (V). — To a stirred solution of 11.5 g. of 3β-acetoxy-22ξ-chlorostigmastan-23ξ-ol (IV) in a mixture of 80 ml. of chloroform and 80 ml. of glacial acetic acid, a solution containing 6 g. of chromic acid in a mixture of 6 ml. of water and 90 ml. of acetic acid was added at 20~30°C over a 3-hr. period. The mixture was continuously stirred for a further twenty hours at room temperature. Excessive chromic acid was decomposed with 30 ml. of ethanol (stirred for 1 hr.), and the mixture was poured into water. The chloroform extracts were combined, washed with 5% aqueous sulfuric acid (three times) and water (three times), dried over anhydrous sodium sulfate, and concentrated. The residue was crystallized from acetone to 8.5 g. of crystals (m. p. 145~150°C). The crude material was used for the next reaction.

The fractional recrystallization of the crude crystals gave two compounds that were found to be epimeric isomers.

Isomer A: m. p. 161~162°C; $[\alpha]_D^{14}$ +43° (*c* 1.0).

Found: C, 69.13; H, 9.52; Cl, 12.85. Calcd. for $C_{31}H_{50}O_3Cl_2$: C, 68.74; H, 9.36; Cl, 13.09%.

UV $\lambda_{max}^{CHCl_3}$ 305 mμ (ε, 57); IR (KBr) 1732, 1714, 1247 cm^{-1}.

Isomer B: m. p. 178~179°C; $[\alpha]_D^{13}$ +17° (*c* 1.0).

Found: C, 68.77; H, 9.24; Cl, 13.16. Calcd. for $C_{31}H_{50}O_3Cl_2$: C, 68.74; H, 9.36; Cl 13.09%.

UV $\lambda_{max}^{CHCl_3}$ 298 mμ (ε, 60); IR (KBr) 1733, 1707, 1241 cm^{-1}.

3β-Acetoxy-22ξ-chlorostigmast-5-en-23-one (XV). —Five grams of crude V (m. p. 145~150°C) were dissolved in 60 ml. of *s*-collidine, and the mixture was heated under reflux for 24 hr. The precipitated collidine hydrochloride was then removed by filtration and washed with ether. The mother liquor was diluted with more ether and washed with 10% sulfuric acid and water. The evaporation of the ether gave 4.5 g. of a brown oil. Crystallization from ethyl alcohol gave 1.5 g. of needles (m. p. 160~163°C). Further recrystallization from methylenechloride-acetone gave isomer A, 166.5~168°C, $[\alpha]_D^{19}$ −31° (*c* 0.67).

Found: C, 73.33; H, 9.80; Cl, 7.49. Calcd. for $C_{31}H_{49}O_3Cl$: C, 73.70; H, 9.78; Cl, 7.02%.

UV $\lambda_{max}^{CHCl_3}$ 296 mμ (ε, 93), IR (Nujol) 1736, 1256, 802 cm^{-1}.

13) P. A. Plattner, H. Heusser and A. B. Kulkarni, *Helv. Chim. Acta*, 31, 1822 (1948).

The mother liquor of the first crystallization of the above experiment was concentrated to a brown oil, which was then chromatographed on 60 g. of florisil packed in petroleum ether. Elution with 1% acetone in petroleum ether and recrystallization from acetone gave 230 mg. of isomer B; m. p. 177.5~180.5°C; $[\alpha]_D^{19}$ −63° (*c* 0.67).

Found: C, 73.78; H, 9.78; Cl, 7.47. Calcd. for $C_{31}H_{49}O_3Cl$: C, 73.70; H, 9.78; Cl, 7.02%.

UV $\lambda_{max}^{CHCl_3}$ 297 mμ (ε, 65); IR(Nujol) 1729, 1251, 800 cm^{-1}.

Further elution gave no crystalline material.

3β-Acetoxystigmast-5-en-23-one (VIb). — Seven grams of crude V (m. p. 145~150°C) were dissolved in 140 ml. of glacial acetic acid, and 7 g. of zinc dust was added with swirling. The mixture was then heated under reflux for 3 hr. After cooling, excessive zinc dust was removed and washed with benzene. The mother liquor was diluted with water and extracted with benzene. The combined benzene extract was washed with a saturated solution of sodium bicarbonate in water, dried over anhydrous sodium sulfate, and concentrated. The residue (6.9 g.) was dissolved in a small amount of methylene chloride and the solution was put on 200 g. of a florisil column packed in petroleum ether (b. p. 35~70°C). Elution with petroleum ether (fractions Nos. 1 and 2) and recrystallization from benzene-methanol gave 189 mg. of aliphatic saturated hydrocarbon (paraffin), which was present in the stigmasterol extracted from soybean oil[14] as an impurity; m. p. 67~69°C; IR (KBr) 2590, 2870, 1475, 1470, 734, 723 cm^{-1}. (Found: C, 84.78; H, 14.67%.) The Liebermann-Burchard and Beilstein reactions were both negative. Futher elution with 1% ethyl acetate in petroleum ether (Nos. 19—24) and recrystallization from ethyl acetate gave 1.53 g. of an unidentified material; m. p. 136~138.5°C (sintering at 127°C). The infrared spectrum showed the presence of an acetate and the absence of a hydroxyl group and of a Δ^{22}-double bond and no ketone band other than that of an acetate (Found: C, 77.01; H, 10.33). Further elution with 1% and 2% ethyl acetate in petroleum ether (Nos. 44—107) and recrystallization from acetone gave 2.4 g. of 3β-acetoxystigmast-5-en-23-one (VIa); m. p. 153~154°C, $[\alpha]_D^{18}$ −16° (*c* 0.69).

Found: C, 79.22; H, 10.39. Calcd. for $C_{31}H_{50}O_3$: C, 79.10; H, 10.71%.

UV $\lambda_{max}^{CHCl_3}$ 291 mμ (ε, 46); IR (KBr) 1733, 1709, 1249, 1037, 800 cm^{-1}.

3β-Hydroxystigmast-5-en-20-one (VIa). — The alkakine hydrolysis of VIb gave a free corresponding alcohol of VIb. Recrystallization from acetone gave crystals; m. p. 157~157.5°C, $[\alpha]_D^{18}$ −11° (*c* 0.62).

Found: C, 80.85; H, 11.39. Calcd. for $C_{29}H_{48}O_2$: C, 81.25; H, 11.29%.

UV $\lambda_{max}^{CHCl_3}$ 291 mμ, (ε, 67); IR(KBr) 3465, 1716, 1700 (shoulder), 794 cm^{-1}.

Stigmast-4-ene-3, 23-dione.—The Oppenauer oxidation of VIa gave stigmast-4-ene-3, 23-dione; m. p. 122~123°C, $[\alpha]_D^{19}$ +93° (*c* 0.68).

Found: C, 81.08; H, 10.61. Calcd. for $C_{29}H_{46}O_2$: C, 81.63; H, 10.87%.

UV λ_{max}^{MeOH} 241 mμ (ε, 16300); IR(Nujol) 1712, 1678, 1623 cm^{-1}.

3β, 23α(and β)-Dibenzoxystigmast-5-ene (IX).— To a solution of 500 mg. of 3β-acetoxystigmast-5-en-23-one (VIb) in dry tetrahydrofuran, 0.4 g. of lithium aluminum hydride was added; the mixture was then heated under reflux for 5 hr. After the mixture had been allowed to stand overnight, the product was isolated in a conventional way to give 490 mg. of a solid. A portion of the solid was recrystallized from methylene chloride-ethyl alcohol to form crystals; m. p. 178~180°C, $[\alpha]_D^{19}$ −34° (*c* 0.69).

Found: C, 80.52; H, 11.56. Calcd. for $C_{29}H_{50}O_2$: C, 80.87; H. 11.70%.

The remaining solid (445 mg.) was converted into a benzoate by treating it with benzoyl chloride-pyridine at 50°C for 6 hr.; it was then allowed to stand at room temperature overnight after which the benzoate was chromatographed on 100 g. of alumina (Sumitomo Kagaku Co., 100 mesh). Elution with 1% ethyl acetate in petroleum ether and recrystallization from ethyl acetate-methanol gave 282 mg. of needles; m. p. 130~130.5°C, $[\alpha]_D^{18}$ −9° (*c* 0.67).

Found: C, 80.45; H, 9.10. Calcd. for $C_{43}H_{58}O_4$: C, 80.83; H, 9.15%.

Further elution with the same solvent and recrystallization from ethyl acetate-methanol gave 54 mg. of needles; m. p. 159~162°C, $[\alpha]_D^{19}$ −31° (*c* 0.86).

Found: C, 80.21; H, 8.95. Calcd. for $C_{43}H_{58}O_4$: C, 80.83; H, 9.15%.

The two isomers gave similar infrared spectra.

3β-Acetoxystigmastan-23-one (VIIb). — 3β-Acetoxystigmast-5-en-23-one (VIb) (942 mg.) was dissolved in a mixture of 40 ml. of dry ether and 20 ml. of acetic acid (distilled over potassium permanganate), and then 44 mg. of platiunm oxide was added. The mixture was agitated with hydrogen. After 58 ml. of hydrogen had been absorbed during a 30-min. period, the absorption of hydrogen ceased. The product was isolated in the usual way and was recrystallized from ethanol to give 747 mg. of crystals; m. p. 151~152°C, $[\alpha]_D^{17}$ +27° (*c* 0.68).

Found: C, 78.47; H, 10.97. Calcd. for $C_{31}H_{52}O_3$: C, 78.76; H, 11.09%.

UV $\lambda_{max}^{CHCl_3}$ 291 mμ (ε, 54); IR(Nujol) 1733, 1704, 1250 cm^{-1} (no absorption at 800 cm^{-1}). The tetranitromethane test was negative.

3β-Hydroxystigmastan-23-one (VIIa).—To a solution of 540 mg. of 3β-acetoxystigmastan-23-one (VIIb) in a mixture of 10 ml. of methylene chloride and 10 ml. of methanol, a solution of 0.1 g. of potassium hydroxide in 1 ml. of water was added; the mixture was allowed to stand overnight. The usual manipulation gave 525 mg. of crystals; m. p. 175~175.5°C; $[\alpha]_D^{17}$ +40° (*c* 0.65).

Found: C, 80.53; H, 11.49. Calcd. for $C_{29}H_{50}O_2$: C, 80.87; H, 11.70%.

UV $\lambda_{max}^{CHCl_3}$ 290 mμ (ε, 49); IR(Nujol) 3460, 3333, 1714, 1695 cm^{-1}.

Stigmastane-3, 23-dione (VIII).—To a solution of 200 mg. of 3β-hydroxystigmastan-23-one (VIIa)

14) For the isolation of stigmasterol from phytosterol, see, T. Yamada and K. Morita, *J. Japan Oil Chemist's Association*, 11, 290 (1962).

in a mixture of 1 ml. of methylene chloride and 10 ml. of acetic acid, 0.1 g. of chromic acid in 0.5 ml. of water was added; the mixture was allowed to stand overnight. After the decomposition of the excessive chromic acid with ethyl alcohol, the product was extracted with methylene chloride. The extract was washed with aqueous sodium carbonate and water, dried over anhydrous sodium sulfate, and concentrated. The residue was crystallized from ethanol to give 118 mg. of crystals; m. p. 159~160°C; $[\alpha]_D^{17}$ +54° (*c* 0.68).

Found: C, 80.97; H, 11.17. Calcd. for $C_{29}H_{48}O_2$: C, 81.25; H, 11.29%.

UV $\lambda_{max}^{CHCl_3}$ 290 mμ (ε, 71); IR (Nujol) 1724, 1709 cm^{-1}.

3β-Acetoxy-22ξ-chlorostigmast-5-en-23ξ-ol.—*From 3β-Acetoxy-5α, 22ξ-dichlorostigmastan-22ξ-ol.*—A solution of 800 mg. of 3β-acetoxy-5α, 22ξ-dichlorostigmastan-23ξ-ol (IV) in 16 ml. of *s*-collidine was heated under reflulx for 17 hr. The mixture was poured into water and extracted with chloroform. The chloroform extract was washed with diluted sulfuric acid and water, dried with anhydrous sodium sulfate, and concentrated to dryness. The residual crude material (780 mg.) was chromatographed on 24 g. of florisil. Elution with benzene and recrystallization from acetone gave crystals (m. p. 168.5~169.5°C). The Beilstein test was positive.

Found: C, 73.48; H, 9.86; Cl, 7.04. Calcd. for $C_{31}H_{51}O_3Cl$: C, 73.41; H, 10.13; Cl, 6.99%.

From 3β-Acetoxy-22ξ, 23ξ-epoxystigmast-5-ene (X).—To a solution of 300 mg. of oxide X in 20 ml. of glacial acetic acid, 6 ml. of a 5% solution of hydrogen chloride in acetic acid was added; the mixture was then heated at 65~70°C for 2 hr. The reaction mixture was poured into water, and the precipitated solid was collected by filtration. Recrystallization of the dried sample from acetone gave crystals with a m. p. 166~168°C. Mixed melting point determination with the 3β-acetoxy-22ξ-chlorostigmast-5-en-23ξ-ol obtained above showed no depression, and the infrared spectra were identical.

Thin-layer Chromatography.—Silica gel G was used as the adsorbent (0.25 mm. thick) and benzene was used as the eluant. A spray reagent was prepared by dissolving potassium permanganate (0.1%) in 5% aqueous sodium carbonate.[15] Slightly different R_f values were obtained for each run. The values in Table I are averages of several runs. A mixture of stigmasterol, 3β-acetoxystigmast-5-en-23-one and stigmasteryl acetate was chosen as the reference mixture; it was run each time with the other compounds.

The authors are indebted to Professor Susumu Mori, Tokyo Metropolitan University, and to Dr. Mitsuo Nakamura and Mr. Ryoji Mamine, Directors of the institute, for their encouragement.

Sugiyama Chemical Research Institute
Mitaka, Tokyo

15) We are indebted to Professor H. Dannenberg (Max-Plank-Institite für Biochemie) for the information about the reagent.

An Abnormal Reaction of Hypohalous Acids with Hindered Double Bonds

By Ken-ichi MORITA,* Yoshiaki KAMANO** and Takeshi IWAMA

(Received March 27, 1963)

The isolation of stigmast-5-ene-3α, 7α, 22α-triol from the leaves of the horse chestnut[1] and of Tochinoki *(Aesculum turbinata)*[2] prompted us to investigate methods for the introduction of the oxygen atom into the side chains of stigmastane derivatives.[3] During the course of our investigation, we observed that the double bond of stigmast-22-ene derivatives gave dihalides instead of halohydrins upon conventional treatment with positive halogen compounds such as *N*-bromoacetamide, *N*-bromosuccinimide, isocyanuric bromide or isocyanuric chloride in aqueous dioxane in the presence of perchloric acid. This paper deals with the mechanism of this abnormal reaction.

The treatment of 3β-acetoxy-5α-chlorostigmast-22-ene (II) with *N*-bromoacetamide (NBA), *N*-bromosuccinimide (NBS) or isocyanuric bromide (ICB)[4] in aqueous dioxane in

* To whom inquiry about this paper should be addressed. Present address: Basic Research Laboratories, Toyo Rayon Co., Ltd., Kamakura, Japan.

** Present address: Taisho Pharmaceutical Co., Ltd., Toshima-ku, Tokyo.

1) F. G. Fischer and H. Mägerlein, *Ann.*, **636**, 88 (1960). There is some doubt on the configuration of an hydroxyl group at C_3.

2) K. Morita, T. Iwama and S. Yoshikawa, unpublished result.

3) K. Morita, T. Iwama and Y. Kamano, This Bulletin, **36**, 1332 (1963).

4) K. Morita, ibid., **31**, 347 (1958).

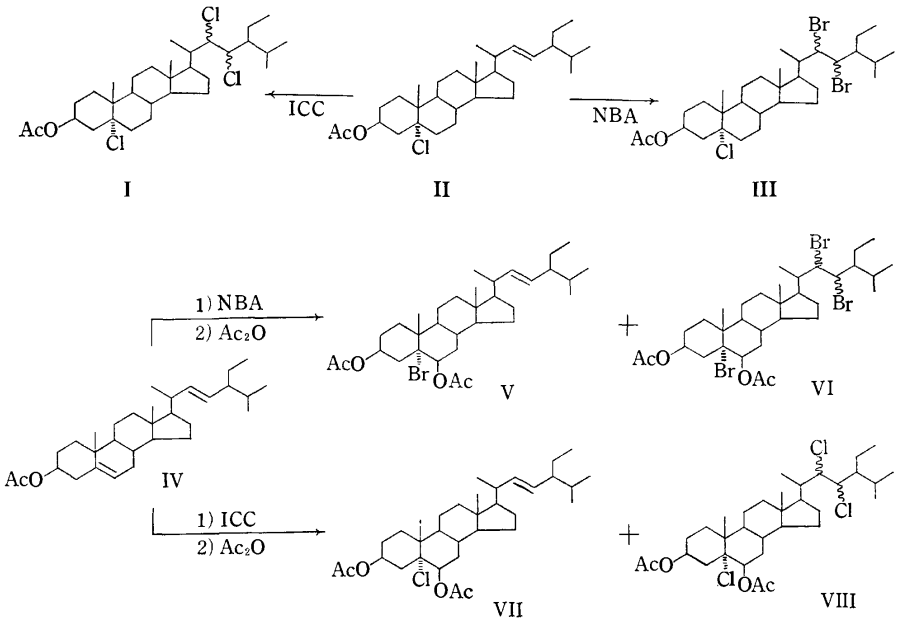

I II III IV V VI VII VIII

the presence of perchloric acid gave 3β-acetoxy-5α-chloro-22ξ, 23ξ-dibromostigmastane (III), while treatment with isocyanuric chloride (ICC) gave 3β-acetoxy-5α, 22ξ, 23ξ-trichlorostigmastane.[5,9]

The treatment of stigmasteryl acetate (IV) with 1.4 molar equivalents of *N*-bromoacetamide in aqueous dioxane in the presence of perchloric acid, followed by acetylation and careful chromatography, gave the starting material (IV), 5α-bromo-3β, 6β-diacetoxystigmast-22-ene (V) and 3β, 6β-diacetoxy-5α, 22ξ, 23ξ-tribromostigmastane (VI). The treatment of stigmasteryl acetate (IV) with 1.4 molar equivalents of isocyanuric chloride, followed by acetylation and chromatography, gave the starting material IV 5α-chloro-3β, 6β-diacetoxystigmast-22-ene (VII) and 3β, 6β-diacetoxy-5α, 22ξ, 23ξ-trichlorostigmastane (VIII). These results clearly show that the Δ^{22}-double bond gives dihalides under reaction conditions where the Δ^{5}-double bond gives halohydrins.

The mechanism[6] of the addition of hypohalous acids to olefins is probably the formation of halogenium ring intermediates, IX, followed by an attack of the water molecule on halogenium ions, IX, to furnish halohydrins, X.

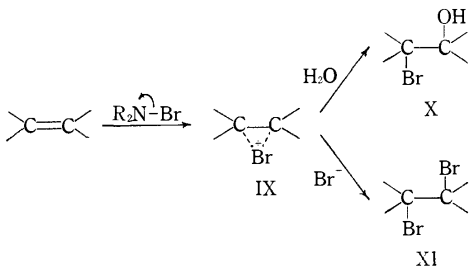

IX X XI

Fieser and Rajagopalan[7] reported that the brief refluxing of 5α, 6α-epoxycholestan-3β-ol (XII) with periodic acid in aqueous acetone afforded pure triol, XIV, in a 94% yield. It may most probably be assumed that the reaction proceeds through an oxonium ion intermediate, XIII, that is then attacked by water

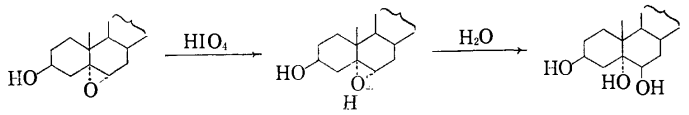

XII XIII XIV

5) When stigmasta-4, 22-dien-3-one was treated with *N*-bromoacetamide or isocyanuric chloride, a small amount of a bromohydrin or a chlorohydrin was obtained, respectively (see experimental part). Therefore, some halohydrins may be present in the mother liquor of the crystallization.

6) Cf. E. S. Gould, "Mechanism and Structure in Organic Chmistry," Henry Holt and Co., New York (1959), pp. 514-527. See also D. J. Cram and G. Hammond, "Organic Chemistry," McGraw-Hill, New York (1959), p. 341.

7) L. F. Fieser and S. Rajagopalan, *J. Am. Chem. Soc.*, 71, 3938 (1949).

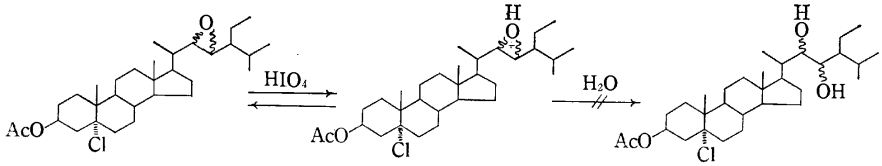

XV XVI

molecule to afford triol, XIV, since the treatment of XII with most acids other than periodic acid either produces esters (CH_3COOH, H_2SO_4) or effects a displacement (HCl).[8]

Similar hydrolytic fission was attempted with 3β - acetoxy - 5α - chloro - 22ξ, 23ξ - epoxystigmastane[13] (XV) under more drastic conditions without observing any fission of the oxide ring. This fact supports the assumption that the rear side of the 22ξ, 23ξ-oxonium ring XVI is so sterically hindered[14] as to prevent the attack of the water molecule.

We now come to the assumption that the 22ξ, 23ξ-halogenium ions are also inert against the attack of the water molecule, since the configuration of the epoxide ring[16] in XV and that of the halogenium ion ring in the intermediate should be the same. Accordingly, the Br^- or Cl^- that may be present in a small concentration determines whether the reaction will give dibromide X, or dichloride. The reactivity of the Br^- or Cl^- against the halogenium ion, IX, should be greater than that of the water molecule because of their greater polarizability, although the bulkiness of the Br^- and Cl^- are comparable to it.

The evidence presented in this article supports the theory that the water molecule and not the OH^- species attack the halogenium ion intermediate to form halohydrins.

Experimental[17]

3β-Acetoxy-5α, 22ξ, 23ξ-trichlorostigmastane (I).—To a solution of 1.0 g. of 3β-acetoxy-5α-chlorostigmast-22-ene (II)[13] (m. p. 183~185°C) in 60 ml. of dioxane containing 0.3 ml. of 60% perchloric acid and 6 ml. of distilled water, 0.7 g. of isocyanuric chloride (purity 82%) was added; the mixture was then allowed to stand for 50 hr. at room temperature. The mixture was poured into water and extracted with ether. The ethereal extract was washed with 10% aqueous sodium bisulfite, 10% aqueous sodium carbonate and water, dried over anhydrous sodium sulfate, and concentrated. The recrystallization of the residue from ethyl acetate gave 0.3 g. of crystals; m. p. 208~209°C, $[\alpha]_D^{15}$ +20° (*c* 0.67).

IR (KBr) 1736, 1241 cm^{-1}; (no hydroxyl and no Δ^{22}-double bond absorption).

Found: Cl, 18.31. Calcd. for $C_{31}H_{50}O_2Cl_3$: Cl, 18.9%.

3β - Acetoxy - 5α - chloro - 22ξ, 23ξ - dibromostigmastane (III).—*With N-Bromoacetamide.*—Into a suspension of 5 g. of 3β-acetoxy-5α-chlorostigmast-22-ene (II) in 200 ml. of dioxane, 15 ml. of water, 1.5 ml. of 60% perchloric acid and 1.3 g. of *N*-bromoacetamide was added. The mixture was then warmed at 50°C for 30 min. and allowed to stand at room temperature overnight. Recrystallization of the product from benzene-methanol gave 0.9 g. of crystals; m. p. 205~206°C, $[\alpha]_D^{17}$ +9° (*c* 1.01).

IR (KBr) 1730, 1239 cm^{-1}; (no hydroxyl and no Δ^{22}-double bond).

Found: BrCl, 29.91. Calcd. for $C_{31}H_{51}O_2ClBr_2$: BrCl, 29.94%.

With N-Bromosuccinimide or Isocyanuric Bromide.[4]—When a similar reaction was carried out using *N*-bromosuccinimide or isocyanuric bromide instead of *N*-bromoacetamide, compound III was obtained in 35 and 60% yields respectively. The identity was established by the mixed melting point and infrared spectra. The better yield observed with isocyanuric bromide is probably due to the ease in liberating bromine.

With Bromine.—To a stirred solution of 1 g. of 3β-acetoxy-5α-chlorostigmast-22-ene (II) in 20 ml. of carbon tetrachloride, a solution of 0.33 g. of

8) L. F. Fieser, "Steroids," Reinhold Publishing Co., New York (1959), p. 196.

9) Mori reported that cholest-5-ene gave 5α, 6α-dichlorocholestane[10] instead of a chlorohydrin when treated with bleaching powder in ether in the presence of acetic acid, whereas cholestery esters,[11] cholesteryl halides[12] and cholest-5-en-3-one[13] gave the corresponding chlorohydrins under the same condition. The reason for this is not clear, but it is conceivable that C_3-substituents may have something to do with it and also the concentration of Cl^- may be greater in the system of bleaching-powder-acetic acid. Dihalides are usually formed as by-products when one uses dilute solutions of halogens in water to generate hypohalous acids, since halogens are present in the system as a result of equilibration. We know no examples of positive halogen compounds to attack olefins with the formation of dihalides.

10) S. Mori, *J. Chem. Soc. Japan, Pure Chem. Sec.* (*Nippon Kagaku Zassi*), 74, 89 (1953).

11) S. Mori, ibid., 64, 981 (1943); 74, 39 (1953).

12) S. Mori, ibid., 74, 42, 89 (1953).

13) S. Mori, K. Morita and F. Mukawa, *Proc. Japan Acad.*, 32, 585 (1956).

14) In this connection, it may be noted that C_{22}-keto[16] and C_{23}-kete group in stigmastane series are sterically highly hindered.[13] Attempted fission of the epoxide ring of XV with $LiAlH_4$ in refluxing ether (24 hr.) failed.

15) Fischer and Mägerlein (Ref. 1) reported that C_{22}-carbonyl group in stigmastane derivatives did not form semicarbazones.

16) The configuration of the ring is probably α, since an examination of the Dreiding model seems to indicate that the α-side of Δ^{22}-double bonds of stigmastene derivatives are less hindered (cf. Ref. 13).

17) All melting points were uncorrected. Rotations were measured in chloroform solution. Infrared spectra were determined with a Perkin-Elmer Model 21. We are indebted to miss Sachiko Yoshikawa for some technical assistance and to Sankyo Pharmaceutical Co. for analyses.

bromine in 50 ml. of the same solvent was added over a period of 30 min. at 0°C; the mixture was then allowed to stand at the same temperature overnight. The product was isolated in the way described above. There was obtained 0.6 g. of needles (m. p. 205~206°C) (Found: BrCl, 29.71%). The identity was established by the mixed melting point and by the infrared spectra.

The Reaction of 3β-Acetoxy-5α-chloro-22ξ, 23ξ-dibromostigmastane (III) with Polling Pyridine. —A solution of 0.7 g. of III in 6 ml. of pyridine was heated under reflux for 11 hr. After it had cooled, the mixture was poured into water and the precipitated solid was collected by filtration. The solid was chromatographed on 30 g. of alumina (300 mesh, Wako Junyaku Co.). Elution with benzene-ether (9:1) and recrystallization from ethanol gave 250 mg. of crystals (m. p. 130~135°C). Although the material showed a weak ultraviolet absorption around 236 mμ, its infrared spectrum was identical with that of stigmasteryl acetate. Three more recrystallizations from ethanol gave pure stigmasteryl acetate (m. p. 138~139°C) (Found: C, 82.35; H, 10.75%).

The Reaction of *N*-Bromoacetamide with Stigmasteryl Acetate (IV). — To a mechanically-stirred solution of 13.6 g. (3 mmol.) of stigmasteryl acetate (IV) in 300 ml. of dioxane containing 3 ml. of 60% perchloric acid and 3 ml. of water, was added 5.8 g. (1.4 mol. eq.) of *N*-bromoacetamide over a period of 5 hr. at room temperature. The reaction mixture was allowed to stand overnight. Then 3% aqueous sodium bisulfite, and a large amount of water were successively added to the stirred solution. The product was extracted with ether four times. The combined ethereal solution was washed with water, dried over anhydrous magnesium sulfate, and evaporated to give 18.6 g. of an oil. The oil was acetylated by treatment with 50 ml. of acetic anhydride and 100 ml. of pyridine overnight at room temperature. The usual manipulation gave 18.6 g. of an oil containing crystals and an oil which was chromatographed on 410 g. of alumina (100 mesh, Sumitomo Kagaku Co.). Elution with 2% ethyl acetate in petroleum ether (b. p. 35~70°C) (fraction, Nos. 7—9) gave 2.58 g. of stigmasteryl acetate (IV). Further elution with the same solvent (Nos. 11—15) gave 4.8 g. of crude 5α-bromo-3β,6β-diacetoxystigmast-22-ene (V) which, on recrystallization from methylene chloride-ethanol, gave 3.5 g. of crystals with a m. p. of 152~155.5°C. The analytical sample was prepared by further recrystallization from ethyl acetate to needles; m. p. 156~158°C; $[\alpha]_D^{18}$ −68° (*c* 0.67, $CHCl_3$).

IR (KBr) 1736, 1244, 1236 (acetate); 973 cm^{-1} (Δ^{22}-double bond).

Found: C, 67.05; H, 9.06; Br, 12.78. Calcd. for $C_{33}H_{53}O_4Br$: C, 66.76; H, 9.00; Br, 13.46%.

Elution with 3 and 4 per cent of ethyl acetate in petroleum ether (Nos. 22—26) gave 462 mg. of crude 5α,22ξ,23ξ-tribromo-3β,6β-diacetoxystigmastane (VI). Recrystallization from methanol gave crystals; m. p. 211.5~212°C, $[\alpha]_D^{18}$ −73° (*c* 0.67, $CHCl_3$).

IR (Nujol) 1745 (shoulder), 1733, 1250, 1230 cm^{-1} (acetate).

Found: C, 52.99; H, 7.09; Br, 32.43. Calcd. for $C_{33}H_{52}O_4Br_3$: C, 52.60; H, 7.09; Br, 31.82%.

Elution with 10% ethyl acetate in petroleum ether (Nos. 32—39) gave 777 mg. of unidentified crystals, IR (Nujol) 3236, 1067, 970, 880, 800 and 765 cm^{-1} (Found: C, 81.80; H, 11.35; Br, 0%), while elution with 20% and 50% ethyl acetate in petroleum ether (Nos. 40—43) (2.276 g.) and recrystallization from ethyl acetate gave other unidentified crystals (m. p. 217.5~218°C). IR (Nujol) 3521, 1712, 1282, 1256, 1038, 970, 878 and 866 cm^{-1}. (Found: C, 74.15; H, 10.67; Br, 3.08%.)

All fractions not described here were uncrystallizable oils.

3β, 6β-Diacetoxy-5α, 22ξ, 23ξ-tribromostigmastane (VI) from V. — To a solution of 2.0 g. of 5α-bromo-3β,6β-diacetoxystigmast-22-ene (V) in 50 ml. of dioxane containing 0.5 ml. of 60% perchloric acid and 0.5 ml. of water, 0.7 g. of *N*-bromoacetamide was added; the mixture allowed to stand overnight at room temperature. The mixture was then poured into water containing some sodium bisulfite, and the product was well extracted with ether. The ethereal solution was washed with aqueous sodium carbonate and with water, dried over anhydrous sodium sulfate, and evaporated. The product was crystallized from methylene chloride-ethanol to give 1.6 g. of VI (m. p. 209~211°C). Its identity was established by the mixed melting point and the infrared spectra.

The Reaction of Isocyanuric Chloride with Stigmasteryl Acetate (IV).—Into a solution of 8 g. (1.7 mmol.) of stigmasteryl acetate (IV) in 150 ml. of dioxane containing 2 ml. of 60% perchloric acid and 2 ml. of water, 2.3 g. of isocyanuric chloride (83% purity) was added with swirling and the mixture was stored in the dark at room temperature (26°C) overnight. When the product was isolated as above, 9.666 g. of the yellow oil were acetylated by treatment with 5 ml. of acetic anhydride and 15 ml. of pyridine overnight at room temperature to give 9.8 g. of an oil, which was chromatographed on 300 g. of alumina (100 mesh, Sumitomo Kagaku Co.). Elution with 2% ethyl acetate in petroleum ether (b. p. 35~70°C) (fraction Nos. 8 and 9) gave 1.586 g. of stigmasteryl acetate (IV) (m. p. 138~138.5°C). Further elution with the same solvent (Nos. 15—21) gave 1.68 g. of 5α-chloro-3β,6β-diacetoxystigmast-22-ene (VII) with a m. p. of 147~151°C. The analytical sample was recrystallized from acetone; m. p. 153~153.5°C, $[\alpha]_D^{18}$ −51° (*c* 0.68).

Found: C, 72.35; H, 9.68; Cl, 6.25. Calcd. for $C_{33}H_{53}O_4Cl$: C, 72.16; H, 9.73; Cl, 6.46%.

Further elution with 2% ethyl acetate in petroleum ether (Nos. 22—24) and recrystallization from methanol gave 361 mg. of 3β,6β-diacetoxy-5α,22ξ,23ξ-trichlorostigmastane (VIII), m. p. 215~217°C, $[\alpha]_D^{18}$ −37° (*c* 0.60).

Found: C, 63.65; H, 8.48; Cl, 17.30. Calcd. for $C_{33}H_{53}O_4Cl_3$: C, 63.91; H, 8.61; Cl, 17.15%.

Bromohydrin of Stigmasta-4,22-dien-3-one.—To a stirred solution of 5 g. of stigmasta-4,22-dien-3-one (m. p. 121~123°C) in a mixture of 100 ml. of ether, 300 ml. of acetone and 30 ml. of water, 1.5 ml. of 60% perchloric acid and 2.0 g. (1.2 mol.) of *N*-bromoacetamide were added; the mixture was

then allowed to stand at room temperature for 24 hr. The product was extracted with ether, washed with 10% aqueous sodium bisulfite and 10% aqueous sodium carbonate and water, dried, and concentrated. The residue was repeatedly recrystallized from acetone to give a small amount of crystals; m. p. 210~212°C $[\alpha]_D^{18}$ +51° (*c* 0.69).

IR (KBr) 3466, 1661 and 1618 cm^{-1} (no Δ^{22}-double bond absorption).

Found: Br, 16.17. Calcd. for $C_{29}H_{47}O_2Br$: Br, 15.85%.

A similar result was obtained when dioxane was used as the solvent instead of a mixture of ether and acetone.

No attempt was made to isolate the dibromide that should be present in the reaction mixture.

The structure of the bromohydrin is pobably 23ξ-bromo-22ξ-hydroxystigmast-4-en-3-one, since the opening of the oxide of the Δ^{22}-double bond of 3β-acetoxy-5α-chlorostigmast-22-ene with hydrogen chloride gave a 22ξ-chloro-23ξ-hydroxy compound.[13] The course of the entering groups to the oxide ring (for Cl^-) and the course to the bromonium ring (for H_2O) are probably the same.

Chlorohydrin of Stigmasta-4, 22-dien-3-one.—To a stirred solution of 0.9 g. of stigmasta-4, 22-dien-3-one in a mixture of 60 ml. of dioxane and 6 ml. of water, 0.3 ml. of 60% perchloric acid and 0.7 g. of isocyanuric chloride (purity 63.3%) were added; the mixture was then allowed to stand for 48 hr. The product was extracted as described above, and the residue was repeatedly recrystallized from benzene-methanol to give a small amount of crystals (m. p. 216~218°C). The mixed melting point with the bromohydrin of stigmasta-4,22-dien-3-one described above showed no depression, and the infrared spectrum showed the presence of hydroxyl and α, β-unsaturated ketone groups.

Found: C, 75.51; H, 10.27; Cl, 7.86. Calcd. for $C_{29}H_{47}O_2Cl$: C, 75.20; H, 10.23; Cl, 7.65%.

A similar result was obtained when we used a mixture of ether and acetone instead of dioxane as the solvent.

The Reaction of 3β-Acetoxy-5α-chloro-22ξ, 23ξ-epoxystigmastane (XV) with Hydroiodic Acid.—To a solution of 200 mg. of 3β-acetoxy-5α-chloro-22ξ, 23ξ-epoxystigmastane (XV) in 8 ml. of glacial acetic acid, 5 ml. of hydroiodic acid in 10 ml. of acetic acid were added; the mixture was then allowed to stand at room temperature for 20 hr. in the dark. The mixture was poured into water and extracted with ether. The usual manipulation gave 145 mg. of 3β-acetoxy-5α-chlorostigmast-22-ene (II) (m. p. 183~184°C).

Its identity was established by the mixed melting point determination and by a comparison of the infrared spectra.

An Attempted Reaction of 3β-Acetoxy-5α-chloro-22ξ, 23ξ-epoxystigmastane (XV) with Periodic Acid.—To a solution of 0.5 g. of XV[13] (m. p. 137~138°C) in 20 ml. of acetone, 0.4 g. of periodic acid in 6.5 ml. of distilled water was added; the mixture was then heated under reflux for 2 hr. and allowed to stand overnight. The reaction mixture was extracted with ether, and the ethereal extract was washed with water, dried and concentrated. Recrystallization of the residue gave 0.4 g. of the starting material; m. p. and mixed m. p. 137~138°C.

The authors are indebted to Professor Susumu Mori, Tokyo Metropolitan University, and to Dr. Mitsuo Nakamura and Mr. Ryoji Mamine, Directors of the Institute, for their encouragement.

Sugiyama Chemical Research Institute
Mitaka, Tokyo

The Spectrophotometric Determination of Titanium with Hydrogen Peroxide and Xylenol Orange[1)]

By Makoto Otomo

(Received June 18, 1963)

The yellow complex of titanium-hydrogen peroxide has been widely used for the spectrophotometric determination of titanium.[2-4)] By treatment of the complex with EDTA, Sweeter and Bricker[5)] found a new complex, the absorption spectrum of which differed from that of titanium-hydrogen peroxide. Recently Musya and Ogawa[6)] applied the above reaction to the spectrophotometric determination of titanium and clarified the composition of the

1) This work was presented at the Tohoku Branch Meeting of the Chemical Society of Japan, Hirosaki, October, 1962.

2) A. Weissler, *Ind. Eng. Chem., Anal. Ed.*, **17**, 695 (1945).

3) F. D. Snell and C. T. Snell, "Colorimetric Methods of Analysis," Vol. II, D. Van Nostrand Co., Inc., New York (1949), p. 423.

4) E. B. Sandell, "Colorimetric Determination of Traces of Metals," Interscience Publishers, Inc., New York (1950), p. 572.

5) P. B. Sweeter and C. E. Bricker, *Anal. Chem.*, **26**, 196 (1954).

6) S. Musya and K. Ogawa, *J. Chem. Soc. Japan, Pure Chem. Sec. (Nippon Kagaku Zassi)*, **78**, 1686 (1957).

new complex. No workers, however, have yet applied such a reaction to the spectrophotometric determination of metals with xylenol orange in the presence of a "third reactant."

The present author has dealt with a number of metal chelates of xylenol orange and has found that, upon the addition of the third reactants, most of these chelates do not produce any new complex which is useful for the spectrophotometric determination of the corresponding metals. When, however, titanium(IV) salt is treated with xylenol orange in the presence of hydrogen peroxide, a new, red complex with an absorption maximum at about 535 mμ is formed. This study was undertaken to determine the conditions under which up to 70 μg. of titanium could be determined spectrophotometrically and to ascertain the composition of the new chelate by means of appropriate spectrophotometric techniques.

Experimental

Reagents and Apparatus.—The solutions of titanium and xylenol orange and the spectrophotometer used were the same as those reported on previously.[7]

A solution of hydrogen peroxide was used after standardizing it as usual against a standard solution of potassium permanganate. Perchloric acid was used for all acidity adjustments because of its low complexing action.

All experiments were carried out at 25±0.5°C.

Standard Procedure for the Determination of Titanium.—To a 25 ml. volumetric flask containing up to 70 μg. of titanium, 0.2 to 5 ml. of a 0.3% solution of hydrogen peroxide, 3.5 to 6 ml. of a 1×10^{-3} M solution of xylenol orange, and 2 to 3 ml. of a 0.5 N solution of perchloric acid were added. The solution was diluted to the mark with water, mixed, and allowed to stand for about 15 min. The absorbance of the solution was then measured at 532 mμ against a solution containing the same amounts of hydrogen peroxide, xylenol orange and perchloric acid.

Results and Discussion

Absorption Spectra.—The absorption spectrum of the titanium-hydrogen peroxide-xylenol orange complex is greatly affected in its shape by the concentration of perchloric acid and also by the amount of hydrogen peroxide and xylenol orange. Under the conditions described above, however, a reproducible spectrum with an absorption maximum at about 532 mμ* was obtained. The spectra thus obtained are shown in Fig. 1.

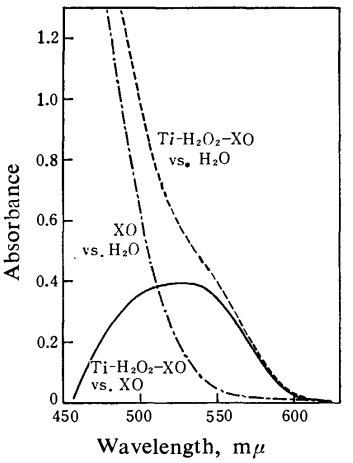

Fig. 1. Absorption spectra.
Ti: 32.4 μg., H_2O_2: 0.3% soln. 1ml., XO: 1.65×10^{-4} M, $HClO_4$: 0.05 M

The Effect of Acidity.—A choice of perchloric acid concentration is quite significant, for the absorption maximum and also the stability of the color are greatly affected by the concentration of perchloric acid. A series of solutions containing 23.2 μg. of titanium, 3.3 ml. of a 1×10^{-3} M solution of xylenol orange, and varying amounts of perchloric acid were prepared. The results obtained will be summarized in the following three sections.

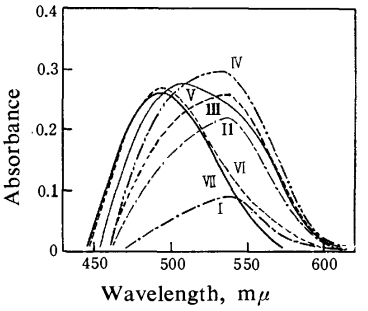

Fig. 2. Effect of acidity on the spectra of the Ti-H_2O_2-XO complex.
Ti: 23.2 μg., H_2O_2: 0.3% soln. 5ml., XO: 1.32×10^{-4} M, $HClO_4$ concn.: I; 0.174 M, II; 0.116 M, III; 0.078 M. IV; 0.06~0.04 M, V; 0.029 M, pH: VI; 4.0, VII; 4.5~5.0

The Relationship between Acid Concentration and Absorption Spectra.—Figure 2 shows the effect on the absortion spectra of the concentration of perchloric acid added to the solution containing titanium, hydrogen peroxide and xylenol orange. From the inspection of the curves, it is found that, depending on the concentration of perchloric acid two different absorbing species can subsequently be formed; one of them, which is formed in the considerably high acidic region, has an absorption

7) M. Otomo, This Bulletin, to be published.

* The absorption maximum shifts subsequently to 535 mμ with the increasing amount of titanium.

maximum at 535 mμ, while the other, which is formed in the slightly acidic region, has an absorption maximum at 495 mμ. In the practical spectrophotometric determination of titanium, the former complex was used; thereby not only could the hydrolysis of titanium be prevented, but also the interference of other cations could be conveniently reduced.

Maximum Color Development.—The reaction is not as rapid as the speed (about 15 min.) required for maximum color development. Figure 3 shows that the maximum absorbance is obtained over the perchloric acid concentration range 0.04 to 0.06 N.

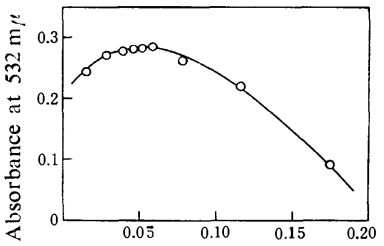

Fig. 3. Effect of acidity.
Ti: 23.2 μg, H_2O_2: 0.3% soln. 5ml.,
XO: 1.32×10^{-4} M

The Relationship between Acid Concentration and Color Stabiliy.—The stability of the color increases with the perchloric acid concentration. In solutions at low concentrations of perchloric acid, the absorbance of the colored solution decreases slowly with time, probably because of the hydrolysis of titanium. In solutions at high acidities, the color is stable for a long period, but the color development is not complete. When, however, the perchloric acid concentration was kept at 0.04 to 0.06 N, the absorbance of the solution remained constant for several ten minutes.

The Effect of the Amount of Hydrogen Peroxide.—It was found that the amount of hydrogen peroxide considerably affects the position of the absorption maximum and the stability of the color. These relations are summarized in Table I. The maximum and constant absorbance is obtained when 0.2 to 5 ml. of a 0.3% solution of hydrogen peroxide is added. Under these conditions, an absorption maximum is found at 532 mμ and the absorbance of the solution remains constant for about 30 min. When a too small amount of hydrogen peroxide is added, the color is indeed stable for a long period, but too low an absorbance is obtained. With a large amount of hydrogen peroxide, on the other hand, a relatively higher absorbance is obtained, but the color becomes somewhat unstable.

Table I. Effect of amount of hydrogen peroxide

Titanium taken, 23.2 μg.
Xylenol orange, 1.65×10^{-4} M
Perchloric acid, 0.05 N

H_2O_2 added		Absorption maximum mμ	Absorbance at absorption maximum	Period of time min.*
	ml.			
0.03%,	0.1	520	0.221	30～ >80
	0.25	525	0.254	20～>100
0.3%,	0.1	525	0.274	20～>100
	0.25	532	0.282	15～ >45
	1	532	0.284	15～50
	5	535	0.282	15～50
3%,	1	535	0.275	20～50
	3	535	0.271	20～50
	5	535	0.263	20～50
	8	535	0.265	10～30

* In which the absorbance of the colored solutions being kept constant.

The Effect of the Addition of Xylenol Orange.—The maximum color development was obtained when 3.5 to 6 ml. of a 1×10^{-3} M solution of xylenol orange was used. Under these conditions, no visual shift in the position of the absorption maximum was observed.

The Order of the Addition of Reagents.—Varying the order in which the reagents were added had no significant effect on the results. In all cases, the color was completely developed within 15 min.

Beer's Law.—As is shown in Fig. 4, the calibration plot obeys Beer's law over the concentration range investigated, 7 to 70 μg. of titanium. The molar extinction coefficient is found to be 15000 at 532 mμ and the sensitivity, 0.003 μg. per cm^2. This sensitivity is comparable with that of the thymol method[8]

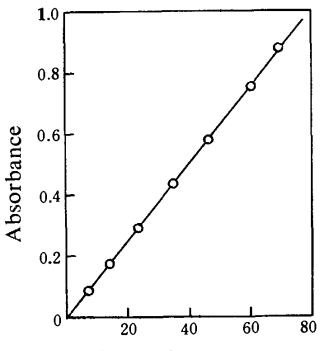

Fig. 4. Calibration curve at 532 mμ.
H_2O_2: 0.3% soln. 0.5 ml., XO: 1.65×10^{-4} M, $HClO_4$: 0.051 M

8) V. Lenher and W. G. Crawford, *J. Am. Chem. Soc.*, 35, 138 (1913).

Table II. Effect of cations on titanium determination

Titanium taken, 32.4 μg. (0.68 μmol.)
Cations added, each 0.5 μmol.

Cation	Titanium found μg.	Deviation μg.
Aluminum(III)	32.4	± 0
Bismuth(III)	55.4	+23.1
Calcium(II)	32.5	+ 0.1
Cadmium(II)	32.8	+ 0.4
Cerium(III)	32.4	± 0
Cobalt(II)	32.4	± 0
Chromium(III)	32.4	± 0
Copper(II)	33.0	+ 0.6
Iron(III)	54.3	+21.9
Gallium(III)	64.0	+31.6
Mercury(II)	33.0	+ 0.6
Lanthanum(III)	32.4	± 0
Magnesium(II)	33.0	+ 0.6
Manganese(II)	32.6	+ 0.2
Molybdenum(VI)	32.5	+ 0.1
Neodymium(III)	32.3	− 0.1
Nickel(II)	32.5	+ 0.1
Lead(II)	32.5	+ 0.1
Palladium(II)	36.0	+ 3.6
Tin(IV)	47.0	+14.6
Thorium(IV)	71.0	+38.6
Thallium(III)	45.4	+13.0
Uranium(VI)	32.3	− 0.1
Vanadium(IV)	34.4	+ 2.0
Tungsten(VI)	32.5	+ 0.1
Zinc(II)	32.4	± 0
Zirconium(IV)	55.4	+23.0

Table III. Effect of anions on titanium determination

Titanium taken, 32.4 μg.
Xylenol orange, 1.63×10^{-4} M
Hydrogen peroxide added, 0.3% soln. 1 ml.
Perchloric acid, 0.05 N

Anion Present	Added μmol.	Titanium found μg.	Deviation μg.
Chloride	500	32.5	+0.1
Fluoride	0.5	32.3	−0.1
	1	30.7	−1.7
	2.5	26.6	−5.8
Nitrate	500	32.3	−0.1
Sulfate	100	32.4	±0
	200	32.2	−0.2
	500	30.7	−1.7
Oxalate	0.1	32.3	−0.1
	0.2	31.3	−1.1
	1	23.5	−8.9
Phosphate	20	32.3	−0.1
	50	31.8	−0.6
	140	29.8	−2.6
Tartrate	10	32.5	+0.1
	50	31.6	−0.8
	100	29.4	−3.0
Citrate	25	32.5	+0.1
	50	31.7	−0.7
	150	29.5	−2.9
NTA	0.1	31.1	−1.3
	0.25	28.1	−4.3
EDTA	0.1	29.1	−3.3
	0.25	23.8	−8.6

or that of the chromotropic acid method,[9] and it is much higher than that of the tiron method[10] or that of the resoflavine method.[11]

The Effect of Diverse Ions.—Separate tests were made to elucidate the interference of various cations as well as that of anions on the determination of titanium. The results are shown in Tables II and III.

Complex Formation.—Some attempts were made to establish the nature of the complex in solution and to determine the composition of the complex.

(1) The Mole Ratio Method.—The mole ratio method was employed to determine the molar ratio of xylenol orange to the titanium-hydrogen peroxide complex. A known aliquot of a titanium solution was treated preliminarily with an excess of hydrogen peroxide to form the yellow titanium-hydrogen peroxide complex. Varying amounts of a xylenol orange solution were then added, and the absorbance of the mixture was measured at 15 wavelengths between 420 and 600 mμ. The concentration of perchloric acid was held constant at 0.048 N. Some typical plots are shown in Fig. 5. It is seen that changes in the slope occur at a mole ratio of 1, indicating the presence of a 1 : 1 complex between xylenol orange and the titanium-hydrogen peroxide complex.

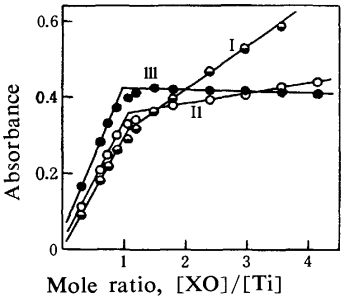

Fig. 5. Mole ratio method applied for Ti-H_2O_2-XO complex.
Ti: 2.713×10^{-5} M, H_2O_2: 8.2×10^{-3} M
$HClO_4$: 0.051 M, I: 510 mμ, II: 530 mμ, III: 550 mμ

9) E. B. Sandell, "Colorimetric Determination of Traces of Metals," Interscience Publishers, Inc., New York (1950), p. 577.
10) J. H. Yoe and A. R. Armstrong, *Anal. Chem.*, **19**, 100 (1947).
11) G. Charlot, *Anal. Chim. Acta*, **1**, 244 (1947).

(2) The Application of the Method of Lewis and Skoog.—In order to determine the combining ratio of titanium, a spectrophotometric method described by Lewis and Skoog[12] was applied in which the perchloric acid concentration was high enough for the complex formation to be quite incomplete. The concentration of perchloric acid was held constant at 0.4 N. Under these conditions, it is possible to assume that the equilibrium concentrations of the reactants are not appreciably different from their initial concentrations. The reaction producing the absorbing species is assumed to be

$$m\,\mathrm{Ti} + n\,\mathrm{H_2O_2} + p\,\mathrm{XO} \rightleftharpoons (\mathrm{Ti})_m(\mathrm{H_2O_2})_n(\mathrm{XO})_p$$

The equilibrium constant for this reaction can be expressed in terms of the apparent molar extinction coefficient, ε_c, of the complex and the absorbance, D, of the color-developing solution, which is measured against the reference solution containing the same amounts of perchloric acid and the reactants.

$$K'_{\mathrm{Ti}} = (D/\varepsilon_c)/[\mathrm{Ti}]^m[\mathrm{H_2O_2}]^n[\mathrm{XO}]^p \quad (1)$$

If the conditions are now chosen so that the reaction does not proceed very far to the right, the initial concentration of the reactants, $[\mathrm{Ti}]_i$, $[\mathrm{H_2O_2}]_i$ and $[\mathrm{XO}]_i$, can be substituted for the equilibrium concentration.

Thus,

$$K'_{\mathrm{Ti}} = (D/\varepsilon_c)/[\mathrm{Ti}]_i^m[\mathrm{H_2O_2}]_i^n[\mathrm{XO}]_i^p \quad (2)$$

which may be written as

$$\log D = m\log[\mathrm{Ti}]_i + n\log[\mathrm{H_2O_2}]_i + p\log[\mathrm{XO}]_i + \log K'_{\mathrm{Ti}}\varepsilon_c \quad (3)$$

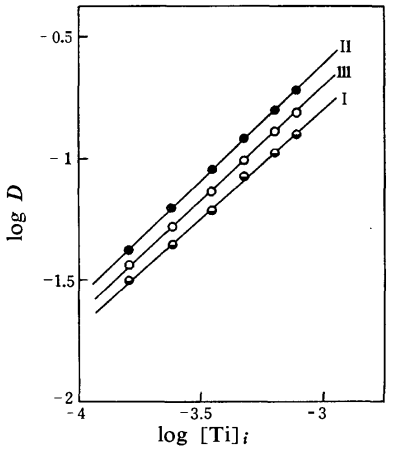

Fig. 6. Plots of log D vs. log$[\mathrm{Ti}]_i$.
$[\mathrm{H_2O_2}]_i$: 1.64×10^{-3} M, $[\mathrm{XO}]_i$: 1.55×10^{-4} M, $HClO_4$: 0.40 M, I: 510 mμ, II: 530 mμ, III: 550 mμ

12) C. Lewis and D. A. Skoog, *J. Am. Chem. Soc.*, **84**, 1101 (1962).

If $[\mathrm{H_2O_2}]_i$ and $[\mathrm{XO}]_i$ are held constant, a plot of log D vs. log $[\mathrm{Ti}]_i$ should yield a straight line with slope m. When the experimental data were treated in this way, a good straight line with a slope of 0.95 (as an average at six wavelengths between 510 and 560 mμ) was obtained. Some of these data are plotted in Fig. 6.

(3) The Combining Ratio of Hydrogen Peroxide.—It now becomes necessary to determine the combining ratio of hydrogen peroxide. An interesting spectrophotometric method, which makes possible the interpretation of the experimental data for systems involving three components, was recently described by Newman and Hume.[13] This method, however, is not directly applicable to the present system, involving titanium, hydrogen peroxide and xylenol orange. Therefore, a modified method was developed. Assuming the following equilibrium:

$$\mathrm{Ti} + \mathrm{XO} + n\,\mathrm{H_2O_2} \rightleftharpoons \mathrm{Ti\cdot XO\cdot(H_2O_2)}_n$$

the equilibrium constant, $K'_{\mathrm{H_2O_2}}$, may be defined as;

$$K'_{\mathrm{H_2O_2}} = [\mathrm{Ti\cdot XO\cdot(H_2O_2)}_n]/[\mathrm{Ti}][\mathrm{XO}][\mathrm{H_2O_2}]^n \quad (4)$$

If two species, xylenol orange and the complex, are absorbing and if the absorbance is measured against the solution containing the same amounts of the reactants except for hydrogen peroxide, the following relationship may hold:

$$D = \varepsilon_c[\mathrm{Ti\cdot XO\cdot(H_2O_2)}_n] \quad (5)$$

where D is the observed absorbance and ε_c is the apparent molar extinction coefficient of the complex. The initial concentrations of titanium, xylenol orange and hydrogen peroxide in any given experiment are, respectively:

$$[\mathrm{Ti}]_i = [\mathrm{Ti}] + [\mathrm{Ti\cdot XO\cdot(H_2O_2)}_n]$$
$$[\mathrm{XO}]_i = [\mathrm{XO}] + [\mathrm{Ti\cdot XO\cdot(H_2O_2)}_n] \quad (6)$$

and

$$[\mathrm{H_2O_2}]_i = [\mathrm{H_2O_2}] + n\,[\mathrm{Ti\cdot XO\cdot(H_2O_2)}_n]$$

If the initial concentration of xylenol orange is considerably higher than that of titanium, the equilibrium concentration of xylenol orange may be assumed to equal its initial concentration. Substituting Eqs. 5 and 6 into Eq. 4, rearranging it, and then taking logarithms,

$$\log\{D/([\mathrm{Ti}]_i\,\varepsilon_c - D)\} = \log K'_{\mathrm{H_2O_2}} + \log[\mathrm{XO}]_i + \log\{([\mathrm{H_2O_2}]_i - nD)/\varepsilon_c\}^n \quad (7)$$

If the proper value of n is assumed, a plot of

13) L. Newman and D. N. Hume. ibid., **79**, 4571 (1957).

$$\log\{D/([\mathrm{Ti}]_i\,\varepsilon_c - D)\} \text{ vs. } \log\{([\mathrm{H_2O_2}]_i - nD)/\varepsilon_c\}^n$$

should yield a straight line with a unit slope. When the experimental data were treated in this way and the value of n was assumed to be one, a good straight line with a slope of 0.9 ± 0.03 was obtained. Values of n equal to one-half and two were tried unsuccessfully. These findings hold for solutions containing a fixed amount of titanium (2.709×10^{-5} M) and xylenol orange (1.653×10^{-4} M) and varying amounts of hydrogen peroxide (0.286 to 4.090 $\times10^{-4}$ M). In all the experiments, the concentration of perchloric acid was held constant at 0.048 N.

(4) Conclusion.—From the foregoing results, it is possible to conclude that a 1 : 1 : 1 complex is formed as a result of the reaction of titanium with hydrogen peroxide and xylenol orange.

The formation constant, K_c, of the complex can be calculated from Eq. 3, using the data obtained in section 2 and the step-by-step acid dissociation constants of xylenol orange[14] (see also Ref. 7). The results, along with the apparent molar extinction coefficients at six wavelengths, are summarized in Table IV. The value of the formation constant agrees approximately with that (1.8×10^{37}) calculated from Eq. 7.

Table IV. Formation constant, K_c, and apparent molar extinction coefficient, ε_c, of the complex

Wavelength, mμ	ε_c	K_c*
510	14000	4.0×10^{37}
520	14500	4.7×10^{37}
530	14800	5.4×10^{37}
540	14200	5.7×10^{37}
550	12600	5.4×10^{37}
560	10300	4.0×10^{37}
	Av.	4.8×10^{37}

* An average value at six different concentrations of titanium.

14) B. Řehák and J. Körbl, *Collection Czechoslov. Chem. Communs.*, 25, 797 (1960).

Summary

Although almost no color reaction occurs when titanium is treated with a solution of xylenol orange at pH below 2, the addition of hydrogen peroxide as a third reactant yields a new, red complex with an absorption maximum at about 535 mμ. On the basis of the above reaction, a new method for the spectrophotometric determination of titanium has been described. The color stability is affected by the amount of hydrogen peroxide and xylenol orange. When, however, 0.2 to 5 ml. of a 0.3% solution of hydrogen peroxide and 3.5 to 6 ml. of a 1×10^{-3} M solution of xylenol orange are used for less than 70 μg. of titanium and a total volume of 25 ml., the color obtained is stable for at least 30 min. Beer's law is obeyed over the 7 to 70 μg. range of titanium. The mole ratio method and the two spectrophotometric methods have been employed to determine the composition of the complex. It has been concluded that a 1 : 1 : 1 complex is formed under the conditions investigated.

The author wishes to acknowledge the kind guidance and the many helpful suggestions of Professor Kôichi Tonosaki.

Department of Chemistry
Faculty of Literature and Science
Hirosaki University
Hirosaki, Aomori

Cadmium Sulfodichlorohydroxydimethylfuchsondicarboxylate Chelate—A Spectrophotometric Study

By Satendra P. SANGAL and Arun K. DEY

(Received May 28, 1963)

Sulfodichlorohydroxydimethylfuchsondicarboxylic acid (trisodium salt; trivial name Chrome Azurol S; Color Index 43825) has extensively been used in these laboratories as a colorimetric reagent[1] and as a chelating agent for metal chelate formation in aqueous solution.[2-6] The use of Chrome Azurol S as a chelatochromic indicator in the complexometric determination of thorium has also been reported.[7] The present communication reports our work on the composition and stability of the cadmium(II)-Chrome Azurol S chelate.

Experimental

Materials.—Solutions of cadmium sulfate and Chrome Azurol S (B. D. H.) were prepared in double distilled carbon dioxide free water.

Instruments.—For the absorbance measurements a Unicam SP 500 spectrophotometer was used.

pH measurements were done with a Leeds and Northrup direct reading pH indicator.

Results and Discussion

Behavior of the Reagent as a Colloidal Electrolyte.—Dey et al. reported earlier[8] that

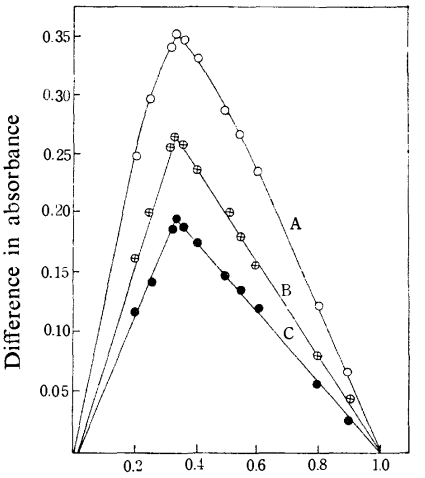

Fig. 1. Composition of the chelate using absorbance measurements by the method of continuous variations at 540 mμ, pH 11.0.
Curve A: Concn. of $CdSO_4$ 5.0×10^{-4} M
Curve B: Concn. of $CdSO_4$ 3.33×10^{-4} M
Curve C: Concn. of $CdSO_4$ 2.50×10^{-4} M

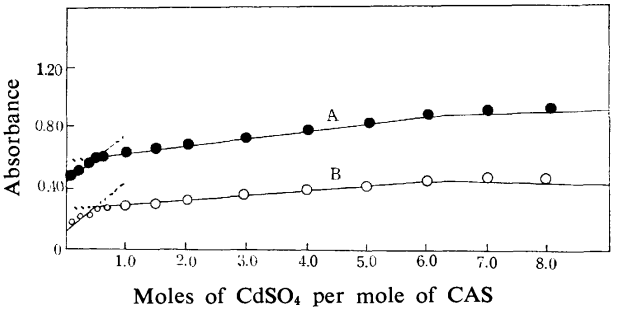

Fig. 2. Composition of the chelate using absorbance measurements by the mole ratio method at 540 mμ, pH 11.0.
Curve A: Concn. of CAS 2.0×10^{-4} M
Curve B: Concn. of CAS 1.0×10^{-4} M

1) A. K. Dey, S. C. Srivastava, R. L. Seth, S. N. Sinha and S. P. Sangal, 7th Int. Coord. Chem. Conf., Stockholm and Uppsala (Sweden), paper No. 7 B (1962).
2) S. C. Srivastava and A. K. Dey, *Inorg. Chem.*, 2, 216 (1963).
3) S. C. Srivastava, S. N. Sinha and A. K. Dey, *J. prakt. Chem.*, (iv) **19**, 229 (1963).
4) S. C. Srivastava and A. K. Dey, *J. Inorg. Nucl. Chem.*, **25**, 217 (1963).
5) R. L. Seth and A. K. Dey, *J. Ind. Chem. Soc.*, **39**, 773 (1962).
6) S. P. Sangal and A. K. Dey, ibid., 40, 464 (1963).
7) S. P. Sangal and A. K. Dey, *Z. anal. Chem.*, **178**, 415 (1961).
8) S. C. Srivastava, R. L. Seth and A. K. Dey, *J. Colloid Sci.*, **17**, 86 (1962).

TABLE I. THE COMPOSITION OF THE CHELATE BY THE CONTINUOUS VARIATIONS METHOD

Total volume 50 ml.

Experiment	Curve	$c^* \times 10^{-4}$ M	p†	λ mμ	Volume of $CdSO_4$ at peak, ml.	Composition of the chelate Cd : CAS
I (Fig. 1)	A	5.00	1.0	540	16.67	1 : 2
	B	3.33	1.0	540	16.67	1 : 2
	C	2.50	1.0	540	16.67	1 : 2
**Ia	A	5.00	1.0	560	16.67	1 : 2
	B	3.33	1.0	560	16.67	1 : 2
	C	2.50	1.0	560	16.67	1 : 2
**Ib	A	2.50	0.5	540	10.00	1 : 2
	B	5.00	2.0	540	25.00	1 : 2
**Ic	A	2.50	0.5	560	10.00	1 : 2
	B	5.00	2.0	560	25.00	1 : 2

** Figs. omitted to economise space.
CAS: Chrome Azurol S
* Concentration of cadmium sulfate
† The ratio c'/c, c' being the concentration of CAS.

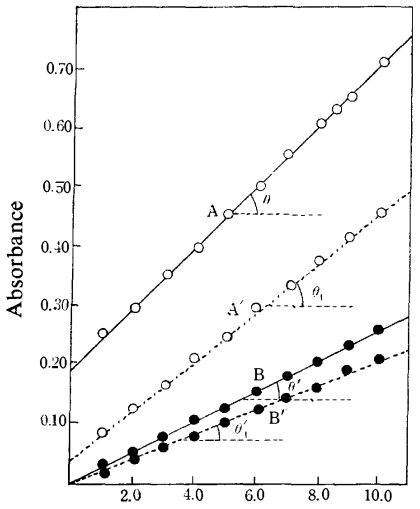

Volume of the variable component, ml.

Fig. 3. Composition of the chelate using absorbance measurements by the slope ratio method at pH 11.0.
20 ml. of (2×10^{-4} M) excess component + x ml. of (2.5×10^{-4} M) variable component + ($30-x$) ml. water.
AA', $CdSO_4$ varying; BB', CAS varying; Solid line 540 mμ and broken line 560 mμ.

$$\frac{\tan\theta}{\tan\theta'} = 1.9 \qquad \frac{\tan\theta_1}{\tan\theta_1'} = 2.0$$

Chrome Azurol S behaves as a colloidal electrolyte in concentrated solutions. Therefore, during these investigations solutions were used of the order of 10^{-4} M so that the solutions may behave as true solution.

Effect of Time on the Chelate.—The chelate formation was found to be immediate and the absorbance values remained constant upto 48 hr. However, the solutions were kept for half an hour to attain equilibrium.

Nature of the Chelate Formed.—The method of Vosburgh and Cooper[9] was employed. Mixtures containing cadmium sulfate and Chrome Azurol S in the ratio of 0 : 1, 1 : 1, 1 : 2, 1 : 4 and 1 : 5 (pH 11.0) were prepared and their absorbances measured at various wavelengths. The results show that the region of maximum absorbance of Chrome Azurol S lies at 430 mμ, whereas, that of the mixtures at 540 mμ. This shows clearly that only one chelate having λ_{max} 540 mμ is formed under the conditions of study.

Stoichiometry of the Components.—The composition was studied using three different methods viz. (i) the method of continuous variations,[10] (ii) mole ratio method[11] and the (iii) slope ratio method.[12] Measurements were made at pH 11.0, adjusted by ammonia added to the mixtures. The results obtained by the continuous variations method are summarized in Table I.

From Table I and Fig. 1 it is clear that the composition of the chelate is $Cd(CAS)_2$. This is further corroborated by the mole ratio method (Fig. 2) and slope ratio method (Fig. 3).

TABLE II. STABILITY CONSTANTS K

Method employed	pH	log K at 25°C	ΔG (kcal.) at 25°C
Method of Dey et al.	11.0	9.1±0.2	−12.7±0.2
Mole ratio method	11.0	9.0±0.2	−12.5±0.2

9) W. C. Vosburgh et al. *J. Am. Chem. Soc.*, **63**, 437 (1941); **64**, 1630 (1942).
10) P. Job, *Compt. rend.*, **180**, 928 (1928); *Ann. Chim.* (10) **9**, 133 (1928).
11) J. H. Yoe and A. L. Jones, *Ind. Eng. Chem. Anal. Ed.*, **16**, 111 (1944).
12) A. E. Harvey and D. L. Manning, *J. Am. Chem. Soc.*, **12**, 4488 (1950).

Effect of pH on the Stability of the Chelate.—Mixtures containing cadmium sulfate and Chrome Azurol S in the ratio of 1:2 were prepared, and their absorbances were measured at various wavelengths after adjusting their pH to different values. It was observed that the λ_{max} of the chelate which is 540 mμ holds good between pH 9.5 to 11.5. This shows that the chelate is stable within this range of pH.

Calculations of the Stability Constant *K*.—The stability constants were calculated using the method of Dey et al.[13,14] and the mole ratio method.[11] The results are given in Table II.

13) A. K. Mukherji and A. K. Dey, *J. Inorg. Nucl. Chem.*, **6**, 314 (1958); *Anal. Chim. Acta*, **18**, 329 (1958).
14) S. K. Banerji and A. K. Dey, *Z. anorg. Chem.*, **309**, 226 (1961); R. L. Seth and A. K. Dey, ibid., **321**, 278 (1963).

Summary

Sulfodichlorohydroxydimethylfuchsondicarboxylate forms a 1:2 violet colored chelate (λ_{max} 540 mμ) with cadmium(II). The chelate is stable between pH 9.5 and 11.5. The values of stability constant as determined by two different methods are 9.1 and 9.0, at 25°C.

The authors are thankful to the Council of Scientific and Industrial Research, India for the award of a fellowship to one of them (S. P. S.).

Chemical Laboratories
University of Allahabad
Allahabad, India

Behavior of Chromotropic Acid as a Colloidal Electrolyte in Aqueous Solution

By Satendra P. SANGAL

(Received June 6, 1963)

A number of organic reagents have been used in these laboratories as complexants, and during the study of composition and stability of their metal chelates spectrophotometrically, it was observed that they deviated from stoichiometry when the solutions employed were not dilute. This was found to be due to the behavior of the reagents as colloidal electrolytes. In concentrated solutions, such reagents display colloidal behavior, but when extremely dilute they show the characteristics of true solutions. The reagents so far investigated from this point of view in these laboratories are ammonium aurintricarboxylate,[1] sodium alizarin-3-sulfonate,[2] *p*-nitrobenzene azochromotropic acid,[3] 7-iodo-8-hydroxy-quinoline-5-sulfonic acid,[4] sulfodichlorohydroxydimethylfuchsondicarboxylic acid,[5] sodium 2-naphthol-3, 6-disulfonic acid,[6] and 1-(*o*-arsonophenylazo)-2-naphthol-3, 6-disulfonic acid.[7]

Chromotropic acid has widely been studied and it is observed that it forms colored chelates with many metals. As a part of a detailed study on the composition and stability of the metal chelates of chromotropic acid, its behavior as a colloidal electrolyte has been investigated and the results are communicated in this paper.

Experimental

Instruments. — Electrical conductance of the reagent in solution was measured with a Leeds and Northrup Kohlrausch Slidewire with an audiofrequency oscillator in the circuit, operated by 220/50 cycles a. c. mains, and using a dip type measuring cell having a cell constant 0.5875.

Materials.—Solutions of the reagent was prepared by dissolving chromotropic salt (B. D. H.) in conductivity water.

1) A. K. Mukherji and A. K. Dey, *J. Colloid Sci.*, **13**, 99 (1958).
2) A. K. Mukherji and A. K. Dery, *Kolloidzschr.*, **158**, 147 (1958).
3) S. C. Srivastava, R. L. Seth and A. K. Dey, *J. Ind. Chem. Soc.*, in course of publication.
4) S. C. Srivastava, R. L. Seth and A. K. Dey, *Kolloidzschr.*, **183**, 73 (1962).
5) S. C. Srivastava, R. L. Seth and A. K. Dey, *J. Colloid Sci.*, **17**, 86 (1962).
6) S. N. Sinha, S. C. Srivastava and A. K. Dey, ibid., **17**, 601 (1962).
7) S. P. Sangal and A. K. Dey, *J. Sci. Ind. Res.*, **21B**, 600 (1962).

Results and Discussion

The electrical conductance of solutions of chromotropic salt was determined at different dilutions at 25°C, and the curve obtained by plotting the square root of the concentration of reagent solution against molar conductance (Fig. 1, Table I) is not linear and resembles that of colloidal electrolytes as recorded by

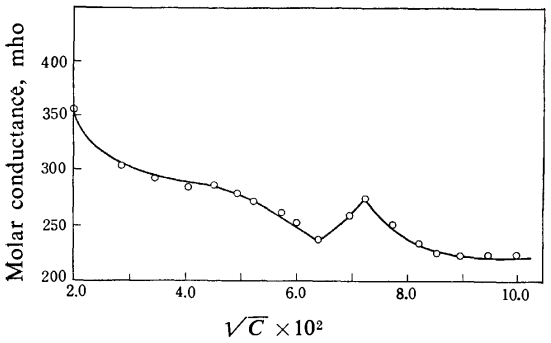

Fig. 1. Variation of molar conductance with concentration.

TABLE I. VARIATION OF MOLAR CONDUCTANCE WITH CONCENTRATION

Concentration of chromotropic acid, M	$\sqrt{C} \times 10^2$	Molar conductance mho
0.0004	2.00	357
0.0008	2.83	304
0.0012	3.46	292
0.0016	4.00	282
0.0020	4.47	287
0.0024	4.89	278
0.0028	5.27	274
0.0032	5.65	265
0.0036	6.00	268
0.0040	6.32	265
0.0044	6.64	239
0.0048	6.99	258
0.0052	7.21	261
0.0056	7.41	271
0.0060	7.74	253
0.0068	8.24	236
0.0072	8.47	250
0.0080	8.94	250
0.0092	9.50	250
0.0100	10.00	250

McBain.[8] It would have been a straight line if the system behaved as a true electrolyte and the Debye-Hückel equation would have been applicable.

The specific conductance of the aqueous solution of chromotropic acid was also determined at different temperatures (Table II).

8) J. W. McBain, "Colloid Science," D. C. Heath and Co., Boston (1950).

TABLE II. VARIATION OF SPECIFIC CONDUCTANCE WITH TEMPERATURE

Concentration of chromotropic acid, M	Specific conductance mho $\times 10^4$						
	0°	10°	20°	30°	40°	50°	60°C
0.003	2.9	3.5	4.7	5.8	7.0	8.2	9.4
0.005	4.7	5.2	6.4	8.8	9.9	11.7	14.1
0.010	8.1	10.5	12.7	17.6	20.5	24.0	26.0

The curve obtained by plotting specific conductance against temperature (Fig. 2) was extrapolated to give the temperature of zero conductance which was found to be −20.0°C. The temperature coefficient per degree centigrade per hundred units of conductance at 35°C calculated from Fig. 2 is shown in Table III.

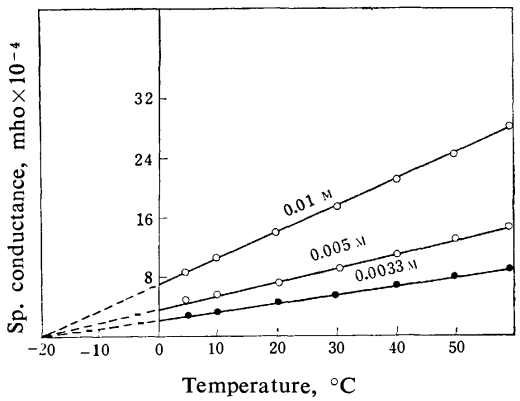

Fig. 2. Variation of specific conductance of chromotropic acid solution with temperature.

TABLE III. TEMPERATURE COEFFICIENT OF CONDUCTANCE

Concn. of chromotropic acid, M	Sp. cond. at 35°C (from graph) mho $\times 10^4$	Temp. coefficient per degree centigrade	Temp. coefficient per hundred of the conductance
0.003	6.5	0.10	1.5
0.005	10.0	0.16	1.6
0.010	19.5	0.33	1.7

The results conclusively establish the colloidal nature of the reagent. Mushran and Prakash[9] as a result of their investigations with a number of colloidal systems found that in general the temperature of zero conductance of true electrolytes lies near about −40°C, whereas, in the case of colloidal electrolytes this temperature ranges between −15 and −35°C. Shivapuri and Prakash[10] also corroborated these results from their study on the

9) S. P. Mushran and S. Prakash, *J. Phys. Chem.*, **50**, (1946).
10) T. N. Shivapuri and S. Prakash, *Curr., Sci.*, 18, 403 (1949).

colloidal behavior of a number of dyes in aqueous solution. Also the temperature coefficient per degree centigrade per hundred units of conductance at 35°C in colloidal systems and colloidal electrolytes is mostly below 2.0.

Hence on the basis of the above results it is concluded that chromotropic acid behaves as a colloidal electrolyte. In the determination of the composition and stability of the chelates the colloidal characteristics of the chelating agent plays a significant part due to what non-stoichiometric ratios are often arrived at. Therefore, for physico-chemical studies it is advisable to work with extremely dilute solutions when the chelating agent behaves as a true solution.[11]

Summary

The nature of chromotropic acid as a colloidal electrolyte has been established from electrical conductance studies. The curve obtained by plotting the square root of concentration and molar conductance of the reagent solution is not linear and resembles that of a colloidal electrolyte. The temperature coefficient per degree centigrade per hundred units of conductance at 35°C is between 1.5 and 1.7. The temperature of zero conductance, determined by extrapolation, is −20.0°C.

The author is thankful to Dr. Arun K. Dey for his valuable guidance throughout the progress of this work. Thanks are also due to the Council and Scientific and Industrial Research, New Delhi for an award of a fellowship.

Chemical Laboratories
University of Allahabad
Allahabad, India

11) A. K. Dey, *J. Colloid Sci.*, 3, 473 (1948).

The Preparation of Dimer Aldehydes and Dimer Alcohols in an Oxo Reactor. I. Modifiers Effective in Producing Dimer Aldehydes and the Hydrogenation of the Aldehydes with Synthesis Gas

By Hiroshi UCHIDA and Akio MATSUDA

(Received July 2, 1963)

The oxo process has here been modified to produce aldehydes with $2n+2$ carbon atoms in an oxo reactor, starting with an olefin of n carbon atoms. The modified oxo process was previously reported to use zinc metal and such zinc compounds as naphthenate and acetylacetonate as the modifiers,[1-3] together with a cobalt carbonyl catalyst. However, previous work[4] in our own laboratory has established that the hydroformylation rate is considerably decreased in the presence of zinc, presumably owing to the formation of an oil-soluble mixed carbonyl of $[Co(CO)_4]_2Zn$. The mixed carbonyl had already been discovered by Hieber and Schulten.[5] The present paper deals first with search for more efficient modifiers and then with another attempt to obtain alcohols from the corresponding aldehydes by hydrogenation with the synthesis gas at the pressure prevalent in the oxo reaction conditions without removal of the cobalt carbonyl. Although the hydrogenation process using synthesis gas has been known for a long time,[6] hydrogenation at a reasonable rate could be achieved only with difficulty under the pressure of the oxo reaction.[7]

Experimental

The synthesis run was conducted in a 300 cc. stainless-steel autoclave. The autoclave was connected by a copper tube and a needle valve to a pressure vessel (0.5 l. in volume) into which an equimolecular mixture of hydrogen and carbon monoxide had been compressed at the pressure of a little above 200 kg./cm^2. It was equipped with a stirrer with a vertical movement. A solution containing dicobalt octacarbonyl crystals, a solvent, and a modifier were placed in the autoclave. After

1) P. A. Lobo, A. T. Ashton, D. C. Clidon and L. N. Vernon, *Chem. Eng.*, **1961**, Dec. 11, p. 70.
2) R. B. Mason, U. S. Pat. 2811567 (1957).
3) C. L. Aldridge et al., U. S. Pat. 2942034 (1960).
4) K. Bando, unpublished.
5) H. Hieber and H. Schulten, *Z. anorg. u. allgem. Chem.*, **243**, 145 (1939).
6) M. Orchin, "Advances in Catalysis," Vol. V, Academic Press Inc., N. Y. (1953), p. 385.
7) J. Berty, E. Olbad and L. Markó, *Chem. Tech.*, **5**, 283 (1957).

flushing the air out with the synthesis gas, the autoclave was loaded with some propylene and pressured with the synthesis gas from the pressure vessel to about 140 kg./cm^2 at room temperature; then the autoclave was heated. It took about 20 min. to heat the autoclave to 150°C. Thereafter, the stirring mechanism was started. During the reaction period, the temperature was controlled at 150±1°C, and the pressure in the autoclave was maintained at 200 kg./cm^2 by the continuous introduction of the synthesis gas from the pressure vessel through the needle valve. Pressure falls in the pressure vessel with time were recorded. The amounts of synthesis gas calculable from the pressure falls stood for the gas consumption in the hydroformylation. After the reaction period of an hour or two hours, the autoclave was cooled in running water and the gas was purged and metered while the liquid product was weighed. In several cases, the gas was analyzed for unreacted propylene. The composition of the liquid product was determined gas chromatographically by means of a 3 m. column of cellite plus P. E. G. 1500, while the unreacted propylene was measured by means of a 2 m. column of alumina plus silicon oil.

The propylene was 93 mol.% pure and contained 6.5 mol.% propane and 0.5 mol.% ethane according to the gas chromatographic analysis. Solvents such as cyclohexane and *n*-butyraldehyde, which were free from any impurities detectable from gas chromatographic analyses, were obtained by the fractional distillation of the commercial products. Dicobalt octacarbonyl was manufactured by the reaction between cobalt carbonate in benzene and the synthesis gas at high pressure. The liquid content after the reaction was cooled to deposit crystals of the carbonyl, which were then stored for use in a pressure vessel under carbon monoxide.

A variety of the modifiers were examined for their effects on both the dimerization of aldehydes and the rate of hydroformylation. Among these, magnesium methylate, isopropylates of aluminum and titanium, and zinc naphthenate were from commercial sources; all of them except the last were supplied by the Kawakami Institute, Inc. The zinc isopropylate was prepared from zinc chloride and sodium isopropylate, while the zinc acetylacetonate was prepared from zinc carbonate and acetylacetone. The acetylacetonates of vanadium ($VO(C_5H_7O_2)_2$), chromium ($Cr(C_5H_7O_2)_3$), molybdenum ($MoO_3(C_5H_7O_2)_2$), and zirconium ($Zr(C_5H_7O_2)_4\cdot 10H_2O$) were prepared, according to the method described in the literature,[8] by reacting acetylacetone with vanadium pentoxide, with chromium trichloride in the presence of urea, with molybdenum trioxide, and with zirconium oxychloride ($ZrOCl_2\cdot 8H_2O$) in the presence of sodium carbonate respectively. The acetylacetonate of magnesium was the product obtained by the reaction between magnesium foil and acetylacetone, while that of titanium was prepared from titanium isopropylate and acetylacetone. Stannous oleate was prepared by the extraction with ether of a mixture of aqueous sodium oleate and aqueous stannous chloride, followed by the evaporation of the ether. In the experimental runs to study the hydrogenation of dimer aldehydes with the synthesis gas, the carbonyl of iron, besides that of cobalt, was used. It was prepared in a way which has been described elsewhere.[9]

8) "Inorganic Syntheses," II, (1946) p. 121; V, (1957) p. 115, 130; VI, (1960) p. 147.

Results and Discussion

The Effects of Modifiers on the Hydroformylation Rate and on the Yield of Dimer Aldehydes. — On the reasonable assumption[10] that the initial rate of hydroformylation is of the first order with respect to propylene concentration, the magnitude of an initial rate constant, k, evaluated by the aid of the formula $k=(1/t)\ln[c_0/(c_0-V/2)]$, where t is the reaction time (min.), c_0 is the initial amount of propylene (mole), and V is the amount of the consumed synthesis gas (mole) as estimated as mentioned afore,[11] gives an appoximate measure of the initial rate. In the present study, k is conventionally calculated by putting the value of t as the point at which $c_0-V/2$ is equal to $0.9\,c_0$.

Tables I and II summarize the results of experimental runs made to examine the effects of modifiers. The reaction conditions differ in some respects between series I of Table I and series II of Table II. The main difference is that in the former series cyclohexane was used as the reaction medium, while *n*-butyraldehyde was used in the latter series. Accordingly, the effects of modifiers can not be compared directly throughout the runs of the two series. However, an approximate and reasonable comparison is possible if the data with no modifiers in each of the series and the data with the modifiers (magnesium methylate and aluminum isopropylate) that are common to both the series are taken into consideration.

The choice of *n*-butyraldehyde as the reaction medium in series II was made after a few preliminary experiments, according to which a larger content of the dimer aldehydes in the product, as well as a higher rate of hydroformylation, was obtained by its use.[12] Moreover, the choice is preferable in view of the fact that in the industrial oxo reactor for aldehyde production from propylene, the

9) H. Uchida, *Rpt. Gn't. Chem. Ind. Research Inst. Tokyo*, **44**, 43 (1949).

10) A. R. Martin, *Chem. & Ind.*, **1954**, 1536.

11) For a more rigorous estimation of V, the change of the partial pressure of propylene in the gas phase of the autoclave should be taken into account, since the partial pressure decreases with the progress of the hydroformylation.

12) The experimental data will be reported elsewhere in detail.

hydroformylation proceeds in the medium of butyraldehydes.

In the tables, the conversion is calculated on the basis of the amount of synthesis gas consumed, or more accurately, of the amount of propylene unconverted. Data of the former calculation are shown in brackets. The product composition in Table I shows the composition of liquid product exclusive of cyclohexane, while that in Table II shows the composition of the total liquid product. The residue stands for matter not yet identified.

Although a comparatively small amount of zinc compound causes an increase in the yield of dimer aldehydes without much reduction of the rate of hydroformylation, a greater amount completely inhibits the progress of the reaction. The inhibition is similarly observed with zirconium acetylacetonate and stannous oleate. The acetylacetonates of titanium and vanadium considerably increased the yield of dimer aldehydes, with some decrease in the rate. Aluminum isopropylate and the acetylacetonates of chromium and molybdenum have scarcely any effect upon either the dimerization or the rate. In contrast to the above modifiers, magnesium compounds such as methylate and acetylacetonate appear to be significant in effectively increasing the yield of dimer aldehydes without any reduction of the hydroformylation rate. The investigation will hereafter be conducted by emphasizing the magnesium compounds.

The Dimerization Rate of *n*-Butyraldehyde in the Presence of Magnesium Methylate. — In order to obtain more comprehensive knowledge on the effect of magnesium methylate, the rates of the dimerization of *n*-butyraldehyde at the pressure and the temperature of the oxo reaction were measured in the presence of either dicobalt octacarbonyl or magnesium methylate, and then in the presence of both of them. The measurement was conducted by means of the determination of the contents of C-4 and C-8 aldehydes in several liquid samples (1 cc.) withdrawn from the initial charge of *n*-butyraldehyde (20 cc.) by means of a dip tube at time intervals over the dimerization period. The results are shown in Fig. 1 as plots of the respective aldehyde contents vs. the reaction time. The figure also includes the plots of the residue. The dimerization takes place in the presence of dicobalt octacarbonyl alone (curve I); the extent of this dimerization is rather high compared with that due to the presence of magnesium methylate alone (curve II). In their simultaneous presence (curve III), the extent is considerably increased, and the C-8 aldehydes are produced in an amount greater

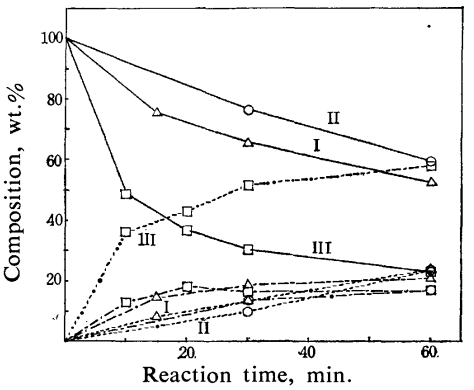

Fig. 1. Dimerization of *n*-butyraldehyde under high pressure of the 1 : 1 synthesis gas. Reaction temperature, 150°C; the synthesis gas pressure, 200 kg./cm². Full line, *n*-butyraldehyde: dotted line, C-8 aldehydes; dotted and dashed line, residue.
-△- In the presence of 0.8 mmol. $Co_2(CO)_8$
-○- In the presence of 0.8 mmol. $Mg(OCH_3)_2$
-□- In the presence of 0.8 mmol. $Co_2(CO)_8$ plus 0.8 mmol. $Mg(OCH_3)_2$

than the sum of the respective amounts of curves I and II.[13]

The Effects of Organic Bases on the Hydroformylation Rate and on the Yield of Dimer Aldehydes. — It had already been established that the rate of hydroformylation is increased by the addition of small amounts of organic bases.[14] With the intention of increasing the rate, the reaction was now carried out in the presence of one of the two organic bases, either pyridine or *N*, *N*-dimethylaniline, in addition to dicobalt octacarbonyl and magnesium methylate. The results are listed in Table III, which also includes the product composition after hydrogenation in the usual way, using a cobalt catalyst. Pyridine unexpectedly caused an increase in the yield of dimer aldehydes with an approximately equal rate, while *N*, *N*-dimethylaniline caused an increase in the rate with an invariable yield. The remarkable effect of pyridine can be seen more readily with the composition of the product after hydrogenation (cf. numerals in brackets).

The Direct Synthesis of C-8 Alcohols from Propylene in the Oxo Reactor. — As is recognizable in the foregoing tables, the products of hydroformylation at 150°C always contain

13) As for the C-8 aldehydes in the products along curve II, only unsaturated ones are present, whereas in the products along curves I and III, the saturated ones are increasingly present with the passage of reaction time. The product of curve III after the reaction period of an hour contains a greater amount of the saturated C-8 aldehydes than of the unsaturated ones. Detailed data on the produt composition will be reported elsewhere.

14) I. Wender, H. W. Sternberg and M. Orchin, "Catalysis," Vol. V, Reinhold Publ. Corp., New York (1957), p. 109.

TABLE I. EFFECTS OF MODIFIERS ON HYDROFORMYLATION RATE AND YIELD OF DIMER ALDEHYDES (Series I)

Exp. No.	$Co_2(CO)_8$ mmol.	Modifier mmol.	Conversion %	k 10^{-2} min^{-1}	Product composition, wt.%						
					n-C_3H_7CHO	i-C_3H_7CHO	n-C_4H_9OH	i-C_4H_9OH	$C_7H_{13}CHO$	$C_7H_{15}CHO$	Residue
1	0.27	None	(80)	1.5	50.9	27.5	0.9	0.4	1.5	1.9	16.9
2	0.27	Zn naphthenate 0.53	(40)	0.4	26.2	28.6	3.5	1.6	13.1	13.5	13.5
3	0.27	Zn isopropylate 0.53	(50)	0.5	32.0	26.0	1.7	1.5	11.4	14.0	13.4
4	0.27	Al isopropylate 1.07	(80)	1.5	49.8	24.9	2.3	1.4	1.2	3.9	16.5
5	0.40	None	(100)	2.5	47.5	23.4	2.6	1.1	3.5	5.6	16.3
6	0.40	Mg methylate 0.85	99.5	2.6	30.8	26.6	2.1	1.1	3.7	21.9	13.8
7	0.50	Mg methylate 1.07	(100)	3.4	28.7	27.1	3.1	2.2	3.5	21.7	13.7
8	0.53	Ti isopropylate 1.07	(70)	1.3	25.7	24.6	4.6	2.3	4.3	22.1	16.4

The reaction conditions were as follows: The pressure was 200 kg./cm^2, the temperature was 150±1°C, and the reaction period was 2 hr. The initial charge included 0.2±0.01 mol. C_3H_6 and 0.056 mol. C_6H_{12}, besides $Co_2(CO)_8$ and modifiers.

TABLE II. EFFECTS OF MODIFIERS ON HYDROFORMYLATION RATE AND YIELD OF DIMER ALDEHYDES (Series II)

Exp. No.	Modifier[a)]	Conversion %	k 10^{-2} min^{-1}	Product composition, wt.%						
				n-C_3H_7CHO	i-C_3H_7CHO	n-C_4H_9OH	i-C_4H_9OH	$C_7H_{13}CHO$	$C_7H_{15}CHO$	Residue
9	None	(98)	5.6	48.0	19.6	3.7	0.9	0.7	9.4	17.7
10	Al isopropylate	97.0	5.5	46.4	19.3	2.9	1.0	1.1	8.7	20.5
11	Mg methylate	(99)	5.8	35.6	19.2	3.1	1.1	3.1	22.6	15.4
12	Mg acetylacetonate	98.5	5.8	38.4	19.7	3.2	1.0	3.8	17.2	16.6
13	Ti acetylacetonate	93.2	3.3	35.8	18.5	3.5	1.4	6.9	13.4	20.5
14	V acetylacetonate	(94)	3.6	34.4	19.5	3.5	1.0	1.1	17.8	22.7
15	Cr acetylacetonate	(94)	4.5	47.3	21.2	3.2	1.7	1.6	9.2	15.8
16	Mo acetylacetonate	95.0	4.4	45.8	18.8	2.1	1.3	1.0	6.3	24.7
17	Zn acetylacetonate	0	0	—	—	—	—	—	—	—
18	Zr acetylacetonate	0	0	—	—	—	—	—	—	—
19	Sn oleate	0	0	—	—	—	—	—	—	—

a) The amount of modifiers was 0.8 mmol. throughout the runs. The reaction was carried out in the same way as in series I except that 0.068 mol. of n-C_3H_7CHO was used in place of cyclohexane and the reaction duration was an hour.

Table III. Effects of additions of organic bases

Exp. No.	Organic base mmol.	Conversion %	k 10^{-2} min^{-1}	Product composion, wt.%[a]								
				n-C_3H_7CHO	*i*-C_3H_7CHO	*n*-C_4H_9OH	*i*-C_4H_9OH	$C_7H_{13}CHO$	$C_7H_{15}CHO$	2-Ethyl-4-methylpentanol	2-Ethyl-hexanol	Residue
20	None	98.2	6.5	28.9(1.2)	20.7(0.4)	4.1(29.5)	3.0(22.4)	0 (0)	29.0(1.7)	0(2.3)	0(26.6)	14.3(15.9)
21	Pyridine (2.0)	(95)	5.1	22.0(1.2)	22.8(2.7)	3.0(16.0)	1.0(23.5)	5.0(0)	33.2(1.0)	0(3.8)	0(39.8)	13.0(12.0)
22	*N*,*N*-Dimethylaniline (2.0)	99.1	10.6	29.2(0.9)	20.2(0.5)	4.9(30.4)	1.4(21.7)	2.1(0)	28.8(3.1)	0(2.8)	0(26.6)	13.4(14.0)

a) The numerals in brackets correspond to the product after the hydrogenation in the usual way.
The reaction conditions were quite the same as in the runs in Table II. The initial charge included 0.2±0.01 mol. C_3H_6, 0.068 mol. *n*-C_3H_7CHO, 0.4 mmol. $Co_2(CO)_8$, and 1.6 mmol. $Mg(OCH_3)_2$, without or with an organic base.

Table IV. Hydrogenation of modified oxo product with 2 : 1 synthesis gas in the presence of iron pentacarbonyl

Exp. No.	Mg methylate mmol.	Pyridine mmol.	$Fe(CO)_5$ mmol.	k 10^{-2} min^{-1}	Product composition, wt.%								
					n-C_3H_7CHO	*i*-C_3H_7CHO	*n*-C_4H_9OH	*i*-C_4H_9OH	$C_7H_{13}CHO$	$C_7H_{15}CHO$	2-Ethyl-4-methylpentanol	2-Ethyl-hexanol	Residue
23	0.8	3.0	None	3.1	7.3	22.4	3.6	0.9	17.6	25.8	0	0	22.4
24	0.8	3.0	0.4	—	3.3	1.6	20.6	24.1	0	3.5	1.9	27.6	17.4
25	0.8	3.0	0.8	2.9	2.3	1.6	17.5	23.3	0	4.5	2.3	29.9	18.6
26	0.8	3.0	1.6	—	1.3	1.0	20.0	25.3	0	3.0	2.3	28.8	18.3
27	0.8	3.0	3.0	3.2	2.2	1.8	16.5	21.1	0	2.2	2.9	29.5	23.8
28	0.8	0	0.8	16.4	2.2	0.4	28.2	23.2	0	0	1.9	21.0	23.1
29	0.8	1.0	0.8	8.3	2.9	1.0	24.9	23.6	0	3.2	2.2	22.3	19.9
30	0.8	2.0	0.8	5.5	2.4	0.6	23.1	23.4	0	2.1	2.7	29.4	16.3
31	0.8	4.0	0.8	3.3	2.0	2.5	14.2	22.7	0	5.9	3.5	28.5	20.7
32	1.2	4.0	0.8	3.0	3.2	3.5	15.6	25.3	0	5.7	3.7	35.3	7.7
33	1.6	4.0	0.8	4.9	2.2	1.1	15.8	27.2	0	2.7	3.5	40.1	7.4

The initial charge contained 0.2±0.01 mol. C_3H_6, 0.068 mol. *n*-C_3H_7CHO, and 0.4 mmol. $Co_2(CO)_8$, besides $Mg(OCH_3)_2$ and pyridine.

Table V. Dicobalt octacarbonyl remaining undecomposed after hydrogenation of oxo product

Exp. No.	Gas composition H_2 : CO	$Fe(CO)_5$ mmol.	Undecomposed metal carbonyl		Product composition, wt.%									
			Co mg. atom/l.	Fe eq.	*n*-C_3H_7CHO	*i*-C_3H_7CHO	*n*-C_4H_9OH	*i*-C_4H_9OH	*n*-$HCO_2C_4H_9$	*i*-$HCO_2C_4H_9$	$C_7H_{15}CHO$	*n*-$C_3H_7CH(OC_4H_9)_2$	*i*-$C_3H_7CH(OC_4H_9)_2$	Residue
34	1 : 1	None	1.2	0	5.0	2.5	57.6	9.5	3.1	2.0	2.8	7.7	2.7	7.1
35	1 : 1	1.6	5.9	11.0	0.6	0.1	72.6	11.7	3.8	2.4	2.2	2.3	0	4.3
36	1.5 : 1	None	1.0	0	10.1	6.4	42.8	7.6	1.9	1.2	2.2	16.7	7.0	4.1
37	1.5 : 1	1.6	3.8	10.6	0.7	0.1	73.7	12.7	4.1	2.1	1.6	1.0	0	4.0
38	2 : 1	None	0.5	0	8.4	4.3	53.5	7.8	2.7	1.3	3.8	9.3	3.2	5.7
39	2 : 1	1.6	1.8	10.3	0.6	0.1	72.0	12.9	3.3	1.7	2.4	1.4	0	5.6

The initial charge consisted of 0.44±0.01 mol. C_3H_6, 0.5 mol. *n*-C_3H_7CHO, and 0.8 mmol. $Co_2(CO)_8$, without or with 1.6 mmol. $Fe(CO)_5$.

minor amounts of butanols. Wender et al.[15] pointed out that the hydrogenation of butyraldehyde to butanol proceeded smoothly at 185°C under 200 atm. of the synthesis gas, but they presented no experimental data on the rate. According to our preliminary experiments, the hydrogenation, even at this high temperature, proceeded at a rate lower than that as did propylene hydroformylation at 150°C, when a considerable amount of aldehydes, particularly of dimer aldehydes, used to remain after hydrogenation of an hour. A higher temperature, for instance, one of 200°C might naturally be expected to increase the hydrogenation rate. Nevertheless, the hydrogenation stopped soon after the temperature rose to 200°C, because of the decomposition of the dicobalt octacarbonyl to cobalt metal (cf. Exp. No. 23 in Table IV). In this connection, Berty et al.[7] had already stated that not only the simple elevation of temperature to 200°C, but also the higher pressure of 300 atm., could barely bring about the hydrogenation of octylaldehyde. The higher pressure, however, was not economical from a practical point of view.

Previous data available for the equilibrium concentration of metal carbonyls under carbon monoxide, of dicobalt octacarbonyl by Berty et al.,[7] and of iron pentacarbonyl by Pichler et al.[16] indicated that the latter metal carbonyl was more stable at a high temperature at a fixed carbon monoxide pressure. Moreover, our previous paper[17] reported that iron pentacarbonyl was a catalyst capable of hydrogenating methylacrylate to methylpropionate with a gas mixture including hydrogen and carbon monoxide. On the basis of these findings, an attempt has been made to carry out the hydroformylation in the presence of iron pentacarbonyl, besides that of dicobalt octacarbonyl and magnesium methylate, and then to effect, without any treatment of the oxo product, the hydrogenation of the resulting aldehydes to the corresponding alcohols by the simple elevation of the temperature to 200°C.

In the experimental runs, $2H_2$: 1CO synthesis gas at 200 kg./cm^2 was used in place of the 1 : 1 synthesis gas used in the preceding runs, since hydrogen and carbon monoxide were to be consumed in the ratio of 2 : 1. The hydroformylation was conducted at 150°C for an hour, followed by a rapid temperature rise to 200°C, which was accompanied by a temporary pressure rise to 210~217 kg./cm^2. Thereafter, the pressure was fixed at 200 kg./cm^2, which level was maintained during the hydrogenation period of an hour by the continuous introduction of the 2 : 1 synthesis gas from the pressure vessel.

The results are listed in Table IV. It has now been proved that in the presence of iron pentacarbonyl almost all C-8 as well as C-4 aldehydes are hydrogenated to the corresponding alcohols, whereas in its absence the aldehydes are left unhydrogenated. Pyridine again effects the dimerization favorably, resulting in a greater yield of C-8 alcohols, but it, in this series of runs, decreases the rate of hydroformylation to some extent (cf. Exp. Nos. 28, 29, 30, and 31). The yield of C-8 alcohols is increased by increasing the amount of magnesium methylate (cf. Exp. Nos. 31, 32, and 33).[18]

It has, however, remained unclarified whether cobalt carbonyl or iron carbonyl is the catalyst for the hydrogenation. It may be plausible that part of the cobalt carbonyl, at least, should be left as such in the product after the hydrogenation if the carbonyl does catalyze the hydrogenation. To confirm this, the carbonyl content in the product was determined. The hydroformylation and hydrogenation procedures were similar to those described just above, but they differed in some details; the runs were made with no modifiers for aldehyde dimerization, and in the hydrogenation stage hydrogen was supplied from another pressure vessel. Moreover, caution was exercised to avoid contamination of the product because of the corrosion of the autoclave material with carbon monoxide; this was avoided by using another shaking 400 cc. autoclave, the whole inner surface of which was lined with titanium. After the hydrogenation, the carbonyls of cobalt and, at the same time, of iron remaining dissolved in the liquid products were determined in the following way; the carbonyls in the filtrate free from finely divided metal precipitates were quantitatively decomposed into sulfates with sulfuric acid, and the resulting metal ions were determined by means of a chelate titration method using EDTA.

15) I. Wender. M. Orchin and H. H. Storch, *J. Am. Chem. Soc.*, 72, 4842 (1950).
16) H. Pichler and H. Wallenda, *Brennstoff-chem.*, 21, 133 (1956).
17) H. Uchida and K. Bando, This Bulletin, 29, 953 (1956).
18) Most of the residue in Table IV is probably a mixture of compounds whose individual boiling points are higher than that of octylalcohol. The porducts from runs Nos. 24-26 and 29-33 were collected and removed from octylalcohol, together with the lower boiling constituents, by distillation. The composition of the material at the bottom, amounting to 14% of the total product, was then determined by means of a gas chromatographic procedure (for details of the procedure, cf. our previous paper[19]): it proved to include 4.5 2-ethylhexyl-isobutyrate, 12.3 2-ethylhexyl-*n*-butyrate, and 19.0 2-ethyl-1, 3-hexanediol in wt. %.
19) A. Matsuda and H. Uchida, *Rpt. Gn't. Chem. Ind. Research Inst. Tokyo*, 57, 50 (1962).

The product obtained from a raw material consisting of 0.5 mol. *n*-butyraldehyde, 0.44± 0.01 mol. propylene, 0.8 mmol. dicobalt octacarbonyl, and 1.6 mmol. iron pentacarbonyl should contain respective carbonyls equivalent to about 20 mg. atom cobalt and 20 mg. atom iron per liter.

The results, as summarized in Table V, indicate that only minute amounts of dibutyracetals and of butyraldehydes remain unhydrogenated in the product from the raw material including iron pentacarbonyl, while a greater amount remains in the product from the raw material including no iron pentacarbonyl, and that under relatively high pressures of carbon monoxide, the oil-soluble cobalt in the former product is about three times the amount of that in the latter product. The hydrogen absorption, in the absence of iron pentacarbonyl, stopped in a short time after the temperature was raised to 200°C, but in the presence of iron pentacarbonyl, it took place continuously until the hydrogenation was nearly completed. An additional fact sheds light on the role played by iron pentacarbonyl; a hydrogenation run of *n*-butyraldehyde (3 mol.) carried out in the presence of iron pentacarbonyl (3 mmol.) alone at 200 kg./cm^2 of the 1 : 1 synthesis gas showed scarcely any absorption of hydrogen, even after a prolonged reaction of 10 hr.[20] These facts lead to the conclusion that iron pentacarbonyl is not the real catalyst for the hydrogenation of the aldehyde but that it contributes to the hydrogenation by suppressing, at high temperatures, the decomposition of the dicobalt octacarbonyl that does catalyze the hydrogenation.

20) The product consisted of 12.1 *n*-butyraldehyde, 2.3 *n*-butanol, 1.1 C-8 saturated aldehydes, 3.4 *n*-butyr-*n*-butyrate, 67.5 C-8 unsaturated aldehydes, and 13.5 residue in wt. %.

Summary

Among the modifiers which have been tested, magnesium compounds are the most effective in producing a great amount of dimer aldehydes in the course of the propylene hydroformylation. The addition does not result in any reduction of the hydroformylation rate at 150°C. A certain amount of C-4 aldehydes had already been dimerized in the presence of dicobalt octacarbonyl alone, but the amount of dimerized aldehydes is greatly increased by the further addition of magnesium compounds, the total amount exceeding the sum of the amounts obtainable in the presence of either one of them. Moreover, the addition of an organic base further increases the yield of dimer aldehydes to some extent.

When starting with the raw material also containing iron pentacarbonyl, the hydrogenation of the aldehydes with the synthesis gas can be accomplished by the simple elevation of the temperature to 200°C. In the hydrogenation stage, iron pentacarbonyl does not behave as the catalyst for itself, but it contributes to the hydrogenation by suppressing, at that high temperature, the decomposition of the dicobalt octacarbonyl that is the real catalyst.

Government Chemical Industrial Research Institute, Tokyo
Shibuya-ku, Tokyo

The Electronic Spectra and Electronic Structures of the Nitrobenzene and Nitrotoluene Anions

By Akira ISHITANI, Keiji KUWATA, Hiroshi TSUBOMURA* and Saburo NAGAKURA

(Received June 28, 1963)

Recently the study of the electronic and ESR spectra of anion radicals of organic compounds has made remarkable progress. The ESR spectra of the nitrobenzene and nitrotoluene anions have been observed by several research workers, and the hyperfine structures of these spectra have been analyzed.[1-7] The electronic spectra of these anions, however,

* Present address: Faculty of Engineering Science, Osaka University, Toyonaka, Osaka.

1) T. L. Chu, G. E. Pake, D. E. Paul, J. Townsend and S. I. Weissmann, *J. Phys. Chem.*, **57**, 504 (1953).

2) G. E. Pake, S. I. Weissmann and J. Townsend, *Trans. Faraday Soc.*, **19**, 147 (1955).

3) R. L. Ward and M. P. Klein, *J. Chem. Phys.*, **28**, 518 (1958).

4) R. L. Ward, ibid., **30**, 852 (1959).

5) D. H. Geske and A. H. Maki, *J. Am. Chem. Soc.*, **82**, 2671 (1960).

6) R. L. Ward, ibid., **83**, 1296 (1961).

7) A. H. Maki and D. H. Geske, ibid., **83**, 1852 (1961).

have never been observed. In view of this, we undertook to measure their electronic absorption spectra in parallel with their ESR spectra for the purpose of deepening our knowledge about the electronic structures of substituted benzene ion radicals. Furthermore, in order to clarify the nature of the observed electronic absorption bands, a theoretical study of the π-electron system of the nitrobenzene anion has been carried out by considering the configurational interaction among several electron configurations, such as ground, locally excited and charge-transfer configurations.

Experimental

Commercial nitrobenzene of E. P. grade was purified by vacuum distillation. Commercial *p*-nitrotoluene of E. P. grade was purified by repeating recrystallization from ethanol. Tetrahydrofuran (abbreviated hereafter to THF) and dimethoxyethane (abbreviated hereafter to DME) used as solvents were dried over calcium chloride, refluxed with sodium metal for two days, and fractionally distilled. Since the anion radicals are very sensitive to oxygen and moisture, their preparations and the measurements of their ESR and electronic spectra must be done in vacuo (10^{-4}~10^{-5} mmHg). Therefore, a vacuum line system with a tube attached for the ESR measurement and a quartz cell of 1 cm. path length for the electronic absorption measurement was used for the preparation of the anion radicals (see Fig. 1). They were prepared by keeping the 10^{-2}~10^{-3} M solutions of nitrobenzene or nitrotoluene in contact with a pure alkali metal film made by distillation in vacuo.

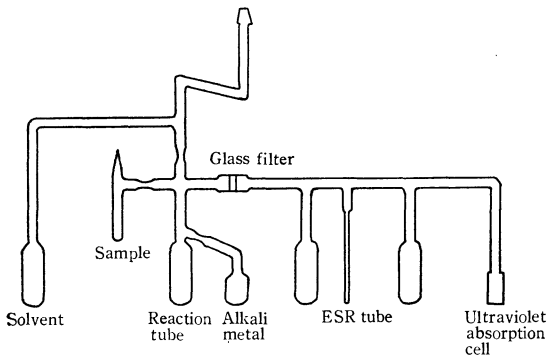

Fig. 1. The vacuum line system.

A Cary recording spectrophotometer model 14 M was used for the measurements of the near infrared, visible and ultraviolet absorption spectra. The ESR spectra were measured with a Hitachi ESR spectrometer model MPU-2B (X band, 100 kc. modulation).

Experimental Results

The Electronic Absorption of the Nitrobenzene Anion. — The DME solution of nitrobenzene turned a shallow brown when in contact with a potassium metal film and showed the ESR spectrum. With the progress of the reaction, the ESR absorption became stronger, the 260 mμ band of neutral nitrobenzene gradually decreased its intensity, and at the same time new absorption bands appeared. The color of the solution changed from brown to reddish orange and then to deep reddish purple. The electronic absorption spectrum and ESR spectrum of this solution were measured in parallel. The observed electronic absorption spectrum is shown in Fig. 2. The observed hyperfine structure of the ESR spectrum was explained well on the basis of the coupling constants determined by Ward et al.[6] The spin concentration of the solution was determined, with the result that 5~10% of nitrobenzene was converted into the radical in the solution.

The observed electronic spectrum of the solution consists of five absorption bands. However, great caution must be used in the identification of the electronic spectrum, since the solution might contain not only the nitrobenzene anion radical but also other by-products. When the solution was exposed to air, it immediately changed color from reddish purple to yellow and no longer showed the ESR signal. The electronic spectrum of the solution of the decomposed products was measured and compared with that of the anion radical solution. From this comparison, it was concluded that, among the five bands shown in Fig. 2, the two bands at 292 and 560 mμ which disappeared when the anion radical solution was in contact with air may safely be ascribed to the nitrobenzene anion.

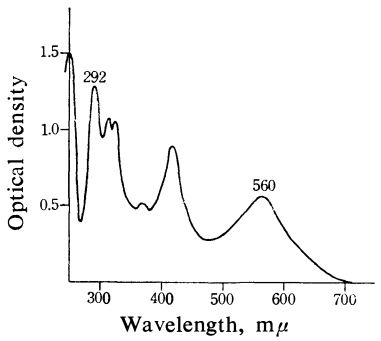

Fig. 2. The electronic spectrum of the DME solution of the nitrobenzene anion.

The Electronic Spectrum of the *p*-Nitrotoluene Anion.—A similar experimental study was also carried out with *p*-nitrotoluene. When in contact with a potassium metal film, the THF solution of *p*-nitrotoluene turned blue and gave the electronic spectrum

shown in Fig. 3. This spectrum is composed of three bands at 302, 607 and 875 mμ. The ESR spectrum was also measured; the result was completely coincident with that obtained by Maki et al.[7] The three electronic absorption bands shown in Fig. 3 and the ESR spectrum disappeared in parallel when the solution was exposed to air. Therefore, the 302, 607 and 875 mμ bands may safely be assigned to the *p*-nitrotoluene anion.

Theoretical

Molecular orbital calculations of the π-electron system of the nitrobenzene anion were carried out in order to clarify the nature of the observed transition bands and obtain some knowledge about the electronic structure of the anion radical. In the actual calculations, the nitrobenzene anion was separated into two components; the benzene anion and the nitro group. The interaction between the components was calculated by taking into account the interaction among such

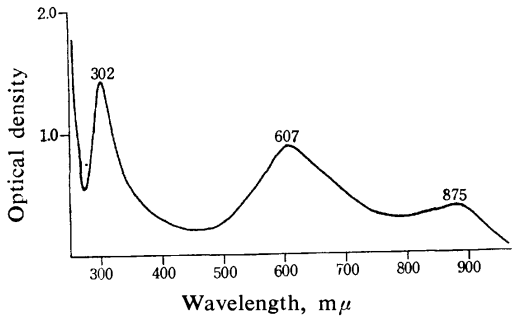

Fig. 3. The electronic spectrum of the THF solution of the *p*-nitrotoluene anion.

π-electron configurations as ground, locally excited and charge-transfer configurations. In order to perform this kind of calculation, we need knowledge about the energy values and wave functions for the respective components. Therefore, first of all, the calculation of the benzene anion was carried out.

The calculation of the energy levels of the benzene anion was carried out by considering the configurational interaction among the two ground and nine excited π-electron configurations which are obtained by putting seven π-electrons into the molecular orbitals of the neutral benzene. The detailed description of our calculations may be omitted, since similar calculations have been made by Hoijtink.[8] In the actual calculation, the approximation of zero differential overlap was adopted.[9] The repulsion integrals of the (AA/AA) and (AA/BB) types necessary for the evaluation of the configuration energies and the interaction energies between the configurations were obtained by the method of Pariser and Parr.[9] The finally-evaluated energy levels and wave functions are given in Table I. These results are in good agreement with those obtained by Hoijtink.[8]

Using the above results about the π-electron structure of the benzene anion, the energy levels and wave functions of the nitrobenzene anion were calculated by a method similar to that used for the theoretical consideration of the π-electron structures of the nitromethyl anion,[10] nitrobenzene,[11] nitroamide, and ethyl nitrate.[12] That is to say, the effect of the nitro group on the energy levels of the benzene anion was considered in terms of the configuration interaction among the ground, locally excited and charge-transfer configurations. The geometrical configuration of the nitrobenzene anion necessary for the actual calculation was assumed to be equal to that of nitrobenzene itself as determined by Trotter.[13]

In the evaluation of the ground configuration energy, electrostatic interaction energy was taken into account. This is because there is a large heterogeneity in the π-electron distribution of the nitro group and the nitrogen atom is positively charged to a great extent. The thirteen locally excited configurations were considered. The energy values of the twelve configurations caused by the local excitation within the benzene anion were calculated by adding electrostatic interaction energy to the calculated excitation energy of the benzene anion given in Table I. The energy of the configuration locally excited within the nitro group was determined from the experimental value of the $\pi \rightarrow \pi^*$ transition energy of the nitromethane[9] and the electrostatic energy.

In addition to these, a charge-transfer configuration which is caused by moving an electron in the highest occupied orbital of the benzene anion to the lowest vacant orbital of the nitro group was taken into consideration. The energy of this configuration was obtained as follows: (Ionization potential of the benzene anion) − (electron affinity of the nitro group) = (electron affinity of benzene) − (electron affinity of the nitro group) = −0.54 −0.4 = −0.94 (eV.) The electron affinity of benzene was taken from the paper by Hush

8) G. J. Hoijtink, *Mol. Phys.*, **2**, 85 (1959).
9) R. Pariser and R. G. Parr, *J. Chem. Phys.*, **21**, 466, 767 (1953).
10) S. Nagakura, *Mol. Phys.*, **3**, 152 (1960).
11) *J. Mol. Spectroscopy*, to be published.
12) This Bulletin, to be submitted.
13) J. Trotter, *Acta Cryst.*, **12**, 884 (1959).

TABLE I. ENERGY LEVELS AND WAVE FUNCTIONS OF THE BENZENE ANION

Energy, eV.	Wave function*
0	$\Psi_1=\phi_1$
0	$\Psi_2=\phi_2$
2.390	$\Psi_3=-0.2318\phi_4+0.2318\phi_6-0.1640\phi_{7a}-0.2839\phi_{7b}+0.8860\phi_9$
4.895	$\Psi_4=-0.2667\phi_4+0.6842\phi_6+0.2559\phi_{7a}+0.6287\phi_{7b}+0.0001\phi_9$
4.895	$\Psi_5=-0.2666\phi_3+0.6842\phi_5+0.2559\phi_{8a}+0.6288\phi_{8b}$
5.534	$\Psi_6=\ 0.6454\phi_4+0.4606\phi_6+0.4501\phi_{7a}-0.4107\phi_{7b}+0.0001\phi_9$
5.534	$\Psi_7=\ 0.6455\phi_3+0.4605\phi_5+0.4502\phi_{8a}-0.4106\phi_{8b}$
7.081	$\Psi_8=\ 0.4427\phi_4-0.4432\phi_6+0.3136\phi_{7a}+0.5425\phi_{7b}+0.4636\phi_9$
6.072	$\Psi_9=\ 0.4998\phi_3-0.5003\phi_5+0.3535\phi_{8a}+0.6124\phi_{8b}$
7.536	$\Psi_{10}=-0.5124\phi_4-0.2637\phi_6+0.7789\phi_{7a}-0.2473\phi_{7b}-0.0002\phi_9$
7.536	$\Psi_{11}=-0.5123\phi_3-0.2638\phi_5+0.7790_{8a}-0.2472\phi_{8b}$

* ϕ_i's are the wave functions of the π-electron configurations used for the calculation of the benzene anion. They are represented by the following equations:

$\phi_1=|\varphi_1\bar{\varphi}_1\varphi_2\bar{\varphi}_2\varphi_3\bar{\varphi}_3\varphi_5|$

$\phi_2=|\varphi_1\bar{\varphi}_1\varphi_2\bar{\varphi}_2\varphi_3\bar{\varphi}_3\varphi_4|$

$\phi_3=|\varphi_1\bar{\varphi}_1\varphi_2\bar{\varphi}_2\varphi_3\varphi_5\bar{\varphi}_5|$

$\phi_4=|\varphi_1\bar{\varphi}_1\varphi_2\varphi_3\bar{\varphi}_3\varphi_4\bar{\varphi}_4|$

$\phi_5=|\varphi_1\bar{\varphi}_1\varphi_2\bar{\varphi}_2\varphi_3\varphi_4\bar{\varphi}_4|$

$\phi_6=|\varphi_1\bar{\varphi}_1\varphi_2\varphi_3\bar{\varphi}_3\varphi_5\bar{\varphi}_5|$

$\phi_{7a}=1/\sqrt{2}\,(|\varphi_1\bar{\varphi}_1\varphi_2\bar{\varphi}_2\varphi_3\bar{\varphi}_4\varphi_5|-|\varphi_1\bar{\varphi}_1\varphi_2\bar{\varphi}_2\bar{\varphi}_3\varphi_4\varphi_5|)$

$\phi_{7b}=1/\sqrt{6}\,(|\varphi_1\bar{\varphi}_1\varphi_2\bar{\varphi}_2\varphi_3\bar{\varphi}_4\varphi_5|+|\varphi_1\bar{\varphi}_1\varphi_2\bar{\varphi}_2\bar{\varphi}_3\varphi_4\varphi_5|-2|\varphi_1\bar{\varphi}_1\varphi_2\bar{\varphi}_2\varphi_3\varphi_4\bar{\varphi}_5|)$

$\phi_{8a}=1/\sqrt{2}\,(|\varphi_1\bar{\varphi}_1\varphi_2\varphi_3\bar{\varphi}_3\varphi_4\bar{\varphi}_5|-|\varphi_1\bar{\varphi}_1\bar{\varphi}_2\varphi_3\bar{\varphi}_3\varphi_4\varphi_5|)$

$\phi_{8b}=1/\sqrt{6}\,(|\varphi_1\bar{\varphi}_1\varphi_2\varphi_3\bar{\varphi}_3\varphi_4\bar{\varphi}_5|+|\varphi_1\bar{\varphi}_1\bar{\varphi}_2\varphi_3\bar{\varphi}_3\varphi_4\varphi_5|-2|\varphi_1\bar{\varphi}_1\varphi_2\varphi_3\bar{\varphi}_3\bar{\varphi}_4\varphi_5|)$

$\phi_9=|\varphi_1\bar{\varphi}_1\varphi_2\bar{\varphi}_2\varphi_3\bar{\varphi}_3\varphi_6|$

where φ_i's are the molecular orbitals of benzene.

TABLE II. ENERGIES AND WAVE FUNCTIONS OF THE π-ELECTRON CONFIGURATIONS USED FOR THE CALCULATIONS OF THE NITROBENZENE ANION

Wave function*	Energy, eV.	Symmetry**	Character
$\phi'_1=\Psi_1\,\lvert\,\varphi_a\bar{\varphi}_a\varphi_b\bar{\varphi}_b\,\rvert$	−0.857	S	Ground configurations
$\phi'_2=\Psi_2\,\lvert\,\varphi_a\bar{\varphi}_a\varphi_b\bar{\varphi}_b\,\rvert$	−0.733	A	
$\phi'_3=\Psi_3\,\lvert\,\varphi_a\bar{\varphi}_a\varphi_b\bar{\varphi}_b\,\rvert$	1.599	S	Locally (in the benzene ring) excited configurations
$\phi'_4=\Psi_4\,\lvert\,\varphi_a\bar{\varphi}_a\varphi_b\bar{\varphi}_b\,\rvert$	4.057	S	
$\phi'_5=\Psi_5\,\lvert\,\varphi_a\bar{\varphi}_a\varphi_b\bar{\varphi}_b\,\rvert$	4.150	A	
$\phi'_6=\Psi_6\,\lvert\,\varphi_a\bar{\varphi}_a\varphi_b\bar{\varphi}_b\,\rvert$	4.785	S	
$\phi'_7=\Psi_7\,\lvert\,\varphi_a\bar{\varphi}_a\varphi_b\bar{\varphi}_b\,\rvert$	4.699	A	
$\phi'_8=\Psi_8\,\lvert\,\varphi_a\bar{\varphi}_a\varphi_b\bar{\varphi}_b\,\rvert$	6.290	S	
$\phi'_9=\Psi_9\,\lvert\,\varphi_a\bar{\varphi}_a\varphi_b\bar{\varphi}_b\,\rvert$	5.281	A	
$\phi'_{10}=\Psi_{10}\,\lvert\,\varphi_a\bar{\varphi}_a\varphi_b\bar{\varphi}_b\,\rvert$	6.747	S	
$\phi'_{11}=\Psi_{11}\,\lvert\,\varphi_a\bar{\varphi}_a\varphi_b\bar{\varphi}_b\,\rvert$	6.741	A	
$\phi'_{12a}=1/\sqrt{2}\,(\lvert\,\varphi_1\bar{\varphi}_1\varphi_2\bar{\varphi}_2\varphi_3\bar{\varphi}_3\varphi_4\varphi_a\bar{\varphi}_a\varphi_b\bar{\varphi}_c\,\rvert-\lvert\,\varphi_1\bar{\varphi}_1\varphi_2\bar{\varphi}_2\varphi_3\bar{\varphi}_3\varphi_4\varphi_a\bar{\varphi}_a\bar{\varphi}_b\varphi_c\,\rvert)$	5.894	S	Locally (in the nitro group) excited configurations
$\phi'_{12b}=1/\sqrt{6}\,(\lvert\,\varphi_1\bar{\varphi}_1\varphi_2\bar{\varphi}_2\varphi_3\bar{\varphi}_3\varphi_4\varphi_a\bar{\varphi}_a\varphi_b\bar{\varphi}_c\,\rvert+\lvert\,\varphi_1\bar{\varphi}_1\varphi_2\bar{\varphi}_2\varphi_3\bar{\varphi}_3\varphi_4\varphi_a\bar{\varphi}_a\bar{\varphi}_b\varphi_c\,\rvert-2\lvert\,\varphi_1\bar{\varphi}_1\varphi_2\bar{\varphi}_2\varphi_3\bar{\varphi}_3\bar{\varphi}_4\varphi_a\bar{\varphi}_a\varphi_b\varphi_c\,\rvert)$	5.894	S	
$\phi'_{13a}=1/\sqrt{2}\,(\lvert\,\varphi_1\bar{\varphi}_1\varphi_2\bar{\varphi}_2\varphi_3\bar{\varphi}_3\varphi_5\varphi_a\bar{\varphi}_a\varphi_b\bar{\varphi}_c\,\rvert-\lvert\,\varphi_1\bar{\varphi}_1\varphi_2\bar{\varphi}_2\varphi_3\bar{\varphi}_3\varphi_5\varphi_a\bar{\varphi}_b\varphi_c\,\rvert)$	5.832	A	
$\phi'_{13b}=1/\sqrt{6}\,(\lvert\,\varphi_1\bar{\varphi}_1\varphi_2\bar{\varphi}_2\varphi_3\bar{\varphi}_3\varphi_5\varphi_a\bar{\varphi}_a\varphi_b\bar{\varphi}_c\,\rvert+\lvert\,\varphi_1\bar{\varphi}_1\varphi_2\bar{\varphi}_2\varphi_3\bar{\varphi}_3\varphi_5\varphi_a\bar{\varphi}_b\varphi_c\,\rvert-2\lvert\,\varphi_1\bar{\varphi}_1\varphi_2\bar{\varphi}_2\varphi_3\bar{\varphi}_3\bar{\varphi}_5\varphi_a\bar{\varphi}_a\varphi_b\varphi_c\,\rvert)$	5.832	A	
$\phi'_{14}=\lvert\,\varphi_1\bar{\varphi}_1\varphi_2\bar{\varphi}_2\varphi_3\bar{\varphi}_3\varphi_a\bar{\varphi}_a\varphi_b\bar{\varphi}_b\varphi_c\,\rvert$	−0.94	S	Charge-transfer configuration

* φ_a, φ_b, φ_c, are the molecular orbitals of the nitro group evaluated by Tanaka (J. Tanaka, *J. Chem. Soc. Japan, Pure Chem. Soc. (Nippon Kagaku Zasshi)*, **78**, 1636 (1957)).

** S and A mean symmetric and antisymmetric, respectively, with respect to the symmetry plane perpendicular to the plane of the nitrobenzene anion.

and Pople.[14] The electron affinity of the nitro group was taken to be 0.4 eV., the value used for the calculation of a series of nitro compounds.[10-12] The energies and wave functions of the configurations taken up in the present calculations are shown in Table II.

The off-diagonal matrix elements (H_{ij}'s) of the total electronic Hamiltonian which represent the interaction between two appropriate configurations were evaluated by the aid of the method presented by Pople[15] and by Murrell and Longuet-Higgins.[16] The results are shown in Table III. The repulsion integrals necessary for the evaluation of the interaction energies between configurations locally excited in different parts of the molecule were obtained in the same way as in the case of the benzene anion. The interaction energies between the charge-transfer configuration and the others are expressed using the core resonance integral, β_{CN}, between the adjacent nitrogen and carbon atoms. The best value of β_{CN} was estimated to be -2.30 eV. for neutral nitrobenzene.[10] It may be expected that the $|\beta_{CN}|$ of the nitrobenzene anion is larger than that of neutral nitrobenzene. In the present calculations, β_{CN} was estimated to be -3.0 eV. By solving the secular equation composed of the elements given in Tables II and III by the aid of an electronic computer (IBM 7090), the energy levels and wave functions of the nitrobenzene anion were evaluated. (see Fig. 4). Of these, the lowest four energy levels and their wave functions are shown in Table IV.

TABLE III. OFF-DIAGONAL MATRIX ELEMENTS USED FOR THE CALCULATIONS OF THE NITROBENZENE ANION

$H_{1.14}$	$=-1.214$ eV.	$(0.408\ \beta_{CN})$
$H_{3.12a}$	$=0.162$	
$H_{3.14}$	$=-0.761$	$(0.254\ \beta_{CN})$
$H_{4.12a}$	$=0.066$	
$H_{5.13a}$	$=0.176$	
$H_{6.12a}$	$=-0.036$	
$H_{7.13a}$	$=-0.302$	
$H_{8.12a}$	$=0.317$	
$H_{8.14}$	$=-0.398$	$(0.133\ \beta_{CN})$
$H_{10.12a}$	$=-0.281$	
$H_{11.13a}$	$=-0.070$	

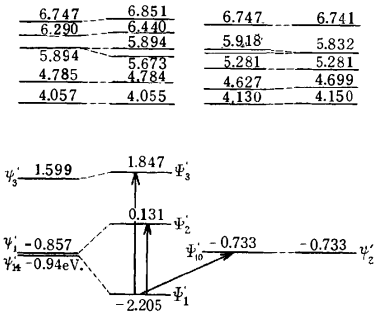

Fig. 4. The energy diagram of the nitrobenzene anion.

Furthermore, the oscillator strength (f) values of the three longer wavelength transitions were calculated by means of the usual equation, $f=1.085\times10^{-5}\nu Q^2$, where Q and ν are the transition moment (in units of Å) and the evaluated transition energies (in units of cm^{-1}) respectively. The evaluated oscillator strength values are shown in Table V, together with observed and calculated transition energies.

TABLE V. OBSERVED AND CALCULATED DATA FOR THE ABSORPTION SPECTRUM OF THE NITROBENZENE ANION

Transition	Transition energy, eV. Obs.	Calcd.	Calculated oscillator strength
$\Psi'_1 \rightarrow \Psi'_{10}$	—	1.471	1.64×10^{-3}
$\Psi'_1 \rightarrow \Psi'_2$	2.214	2.336	4.13×10^{-1}
$\Psi'_1 \rightarrow \Psi'_3$	4.245	4.052	5.51×10^{-2}

TABLE IV. THE LOWEST FOUR ENERGY LEVELS OF THE NITROBENZENE ANION AND THEIR WAVE FUNCTIONS

Energy, eV.	Wave function	Symmetry
$W_1=-2.205$	$\Psi'_1=0.6616\phi'_1+0.1470\phi'_3+0.0000\phi'_4-0.0000\phi'_6+0.0346\phi'_8-0.0001\phi'_{10}-0.0043\phi'_{12a}+0.7345\phi'_{14}$	S
$W_2=0.131$	$\Psi'_2=0.7365\phi'_1-0.3115\phi'_3-0.0002\phi'_4+0.0001\phi'_6-0.0393\phi'_8+0.0005\phi'_{10}+0.0110\phi'_{12a}-0.5991\phi'_{14}$	S
$W_3=1.847$	$\Psi'_3=0.1408\phi'_1+0.9380\phi'_3+0.0011\phi'_4-0.0004\phi'_6-0.0255\phi'_8-0.0021\phi'_{10}-0.0358\phi'_{12a}-0.3136\phi'_{14}$	S
$W_{10}=-0.733$	$\Psi'_{10}=\Psi'_2$	A

14) N. S. Hush and J. A. Pople, *Trans. Faraday Soc.*, 51, 600 (1955).
15) J. A. Pople, *Proc. Phys. Soc.*, **A68**, 81 (1955).
16) H. C. Longuet-Higgins and J. N. Murrel, ibid., **A68**, 601 (1955).

Discussion

On the basis of the comparison of the calculated transition energies and oscillator strengths with the observed results, the 560 mμ and 292 mμ bands can safely be ascribed to the $W_1 \rightarrow W_2$ and $W_1 \rightarrow W_3$ transitions respectively. As may easily be seen from the wave functions given in Table IV, the W_1 and W_2 states may be said to be mainly caused by the resonance interaction between the ground and charge-transfer configurations, although there are also small contributions from locally excited configurations. Therefore, the strongest 560 mμ band may be regarded as the intramolecular charge-transfer band. In the upper state of the 292 mμ band, the contribution of the local excitation within the benzene anion is large, amounting to 88%. Therefore, this band can be interpreted as the shifted band of the 600 mμ band of the benzene anion. It is noteworthy that the band of the benzene anion shows a large blue shift when the nitro group is introduced. This blue shift phenomenon exhibits a striking contrast to the red shift phenomena usually observed with the 260 mμ band of the neutral benzene molecule.[17] In the case of the nitrobenzene anion, the resonance between the ground and charge-transfer configurations is strong; consequently, the stabilization energy of the ground configuration due to the resonance is larger than that of the locally excited configuration. This is the reason why the 600 mμ band of the benzene anion shows the blue shift when the nitro group is introduced.

In addition to the above-mentioned two bands, the theoretical results show that another weak band, one corresponding to the $W_1 \rightarrow W_{10}$ transition, may appear in the near infrared region, say, the 800 mμ region. Although a weak and broad absorption was found in that region, no clear absorption peak could be observed in the case of the nitrobenzene anion.

This may be due to the fact that the band should be very weak, as is revealed by the small value of the calculated oscillator strength; moreover, the solvent absorption in the expected wavelength region prevents any accurate absorption measurement. In the case of the *p*-nitrotoluene anion, we observed the absorption peak at 875 mμ. This may correspond to the same transition.

17) S. Nagakura and H. Baba, *J. Am. Chem. Soc.*, 74, 5693 (1952).

TABLE VI. ODD ELECTRON DENSITIES AND COUPLING CONSTANTS OF THE NITROBENZENE ANION

Atom	Odd electron density		Coupling constant, gauss obs.
	Calcd.	Obs.	
N	0.2651	0.212	10.33
C^o	0.0401	0.124	3.46
C^m	0.0401	0.040	1.13
C^p	0.1495	0.138	3.86

The observed coupling constants[6] and the odd electron densities derived from them are shown in Table VI, together with the theoretical values of odd electron densities evaluated by the use of the wave function Ψ_1' in Table IV. The odd electron densities on the ring carbon atoms, ρ_i^C's, were obtained using the usual equation, $\rho_i^C = a_i^H / Q_H$.[18] Here a_i^H is the observed coupling constant of the ring proton adjacent to the carbon atom under consideration and Q_H was taken to be 28 gauss.[19] The odd electron density on the nitrogen atom, ρ^N, was obtained by using a similar equation, $\rho^N = a^N / Q_N$, where a^N the observed coupling constant and Q_N was assumed to be 49 gauss, the mean value of the coupling constants of nitrogen in the anion radicals of several aliphatic nitro compounds.[20] The odd electron densities estimated from the coupling constants are in good agreement with the theoretical ones except in the case of the ortho carbon atom.

The Institute for Solid State Physics
The University of Tokyo
Azabu, Tokyo (K. I., H. T. & S. N.)

Department of Chemistry, Faculty of Science
Osaka University
Nakanoshima, Osaka (K. K.)

18) H. M. McConnell, *J. Chem. Phys.*, 25, 890 (1956).
19) H. S. Jarrett, ibid., 25, 1289 (1956).
20) D. H. Geske and J. L. Ragle, *J. Am. Chem. Soc.*, 83, 3532 (1961).

NOTES

The Oxidation of (+)-p-Menth-3-ene with Selenium Dioxide

By Takayuki SUGA, Masako SUGIMOTO and Tamon MATSUURA

(Received March 8, 1963)

The oxidation of (+)-*p*-menth-3-ene with *t*-butyl chromate has been recorded to afford (+)-*p*-menth-3-en-2-one (major product) and (±)-*p*-menth-3-en-5-one (minor product),[1] but only the latter ketone was produced by oxidation with selenium dioxide in an alcoholic solution.[2,3] The action of selenium dioxide in acetic acid appears not to have been described as yet. We have now investigated this reaction in an 8 : 11 mixture* of glacial acetic acid and acetic anhydride in order to check the position of the oxidative attack.

The oxidation was carried out at 50°C for 40 hr. with an equimolar amount of selenium dioxide. *p*-Menth-3-en-5-yl acetate (I; 35% based on the sample taken), *p*-menth-3-en-5-ol (II; 18%) and *p*-menth-3-en-5-one (III; 8%) were obtained, all of them optically inactive. No oxidation product resulting from the attack on the other allylic methylene (2-position) could be isolated in spite of a careful examination. This finding was further supported by the fact that such successive treatments as saponification of the whole reaction products, oxidation with chromic trioxide-pyridine complex and final dehydrogenation gave thymol as the resultant. Not even a trace of carvacrol, which should be derived from C_2-oxidation products, could be detected.

The hydroxyl group of II and the acetoxy group of I apparently possessed trans-configuration with respect to the methyl group attached to C_1, as II and I were converted into the 3, 5-dinitrobenzoate which coincided with that of the (±)-*trans-p*-menth-3-en-5-ol characterized by Macbeth et al.[4]

In order to explain both the formation of the optically inactive oxidation products and the attack on only C_5-active methylene, we suppose the formation of a carbonium ion intermediate IV in the resonance state, when

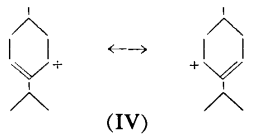

(IV)

selenium dioxide attacks *p*-menth-3-ene. The I (major product) is explained as resulting from the reaction between IV and the solvent (i. e., the acetoxy anion). II may be formed when water, which is considered to be produced by the attack of the oxidant, reacts on IV, and then II is party oxidized to yield III.

Experimental

Sample.—(+)-*p*-Menth-3-ene[5] (b. p. 168~169°C, n_D^{25} 1.4490, d_4^{25} 0.8080, $[\alpha]_D^{25}$ +114.9°) was prepared from (−)-menthol by the pyrolysis of methyl (−)-menthylxanthate (m. p. 39.5~40.5°C). The racemization procedure with *p*-toluenesulfonic acid[6] showed the hydrocarbon to consist of (+)-*p*-menth-3-ene (72%) and (+)-*p*-menth-2-ene (28%). However, the isolation of pure *p*-menth-3-ene was so difficult that the hydrocarbon mixture was used without further purification.

Oxidation.—To the sample hydrocarbon (41.5 g.) dissolved in a mixture of glacial acetic acid (41 g.) and acetic anhydride (56 g.), selenium dioxide (33.3 g.) was added in seven portions over a 15-hr. period at 50°C under agitation in an atmosphere of nitrogen. After the mixture had been stirred at the same temperature for a further 25 hr., it was subjected to steam-distillation. The residue seemed to be metallic selenium and a selenium-containing polymerized substance. The distillate, after being treated as usual, gave a neutral oil (26.0 g., $[\alpha]_D^{13}$ +3.7° (l, 1), E. V. 160.3), the chromato-strip chromatogram[7] of which exhibited three spots corresponding to those of I, II and III respectively.

1) K. Fujita, This Bulletin, **34**, 968 (1961).
2) E. Borgwardt and E. Schwenk, *J. Am. Chem. Soc.*, **56**, 1185 (1934).
3) R. Kitaoka, *Repts. Osaka Ind. Research Inst.* (*Ôsaka Kôgyo Gijutsu Shikenjo Hôkoku*), No. 316, 1 (1960).
* The *t*-butyl chromate oxidation of *p*-menth-3-ene[1] has been carried out in benzene containing glacial acetic acid and acetic anhydride in the same ratio as above.
4) A. K. Macbeth, B. Milligan and J. S. Shannon, *J. Chem. Soc.*, **1953**, 2574.
5) L. Tschugaeff, *Ber.*, **32**, 3332 (1899); W. Hückel, W. Tappe and G. Legutke, *Ann.*, **543**, 197 (1940).
6) J. P. Wibaut, H. C. Beyerman and H. B. Van Leeuwen, *Rec. trav. chim.*, **71**, 1032 (1952).
7) J. G. Kirchner, J. M. Miller and G. J. Keller, *Anal. Chem.*, **23**, 420 (1951); J. M. Miller and J. G. Kirchner, ibid., **25**, 1107 (1953).

The Identification of Reaction Products.—(1) On treating the neutral oil (8.00 g.) with an excess of 2, 4-dinitrophenylhydrazine in ethanolic hydrochloric acid, only 2, 4-dinitrophenylhydrazone (2.03 g., m. p. and mixed m. p. 145~146°C) of (±)-III was obtained.

(2) The neutral oil (5.00 g.) was treated with a 2 N hydrochloric acid solution of 2, 4-dinitrophenylhydrazine and subjected to steam-distillation in a neutral medium, and an oil (3.98 g.) containing no ketone (by the IR spectrum) was obtained. The oil was chromatographed on a silica gel column with a 17 : 3 (in vol.) mixture of isopropyl ether and *n*-hexane as the eluant, and was separated into three fractions. The first fraction (0.07 g.) was the unchanged hydrocarbon, which was found to consist of *p*-menth-3-ene and *p*-menth-2-ene by infrared spectrum comparison. The second fraction (1.92 g., b. p. 93~94°C/9 mmHg, n_D^{25} 1.4555, d_4^{25} 0.9344, $[\alpha]_D^{20}+0.12°$*, $\nu_{C=O}$ 1736 cm^{-1}, ν_{C-O-} 1239 cm^{-1}) was (±)-I, which was identified by converting it into (±)-II. The third fraction (1.76 g., b. p. 92°C/10.5 mmHg, n_D^{25} 1.4770, d_4^{25} 0.9134, $[\alpha]_D^{20}$ ±0°, ν_{OH} 3344 cm^{-1}, ν_{C-OH} 1028 cm^{-1}) was (±)-II, which was identified by converting it into the 3, 5-dinitrobenzoate (m. p. 141.5~142°C; lit.[4], m. p. 142°C as (±)-*trans*-*p*-menth-3-en-5-yl 3, 5-dinitrobenzoate) and also into (±)-III on chromic trioxide-pyridine complex oxidation.

(3) The neutral oil (3.7 g.) was successively subjected to saponification with 0.5 N alcoholic potassium hydroxide, oxidation with chromic trioxide-pyridine complex, and dehydrogenation with palladium charcoal (palladium content: 30%) at 230°C for 15 hr. A phenolic substance (1.4 g., m. p. 49~51°C) was thus obtained, which was identified as thymol by the mixed melting point determination. The gas chromatogram of the substance did not show the peak corresponding to carvacrol, but a single peak was observed.

* Judging from the gas chromatogram, which exhibited a small peak of the sample hydrocarbon in addition to a main peak of the acetate, the ester was contaminated with a small amount of the unchanged hydrocarbon. Accordingly, this small optical rotation value is due to the hydrocarbon.

Summary

The oxidation of (+)-*p*-menth-3-ene by selenium dioxide in a mixture of glacial acetic acid and acetic anhydride was examined with special attention paid to the position of the oxidative attack, i. e., the C_2- or C_5-position of the hydrocarbon. Careful examination of the reaction product showed that this oxidation yielded only (±)-*p*-menth-3-en-5-yl acetate (major product), (±)-*p*-menth-3-en-5-ol and (±)-*p*-menth-3-en-5-one. Thus, this oxidant selectively attacks an active methylene group at the C_5-position of *p*-menth-3-ene.

Department of Chemistry
Faculty of Science
Hiroshima University
Hiroshima

The Redetermination of the Lattice Constants of Phenazine 5, 10-Dioxide

By Yoshiyuki NAMBA, Tsutomu ODA and Tokunosuké WATANABÉ

(Received June 6, 1963)

In a previous paper,[1] we have reported on the crystal structure of phenazine 5, 10-dioxide. Quite independently, another paper on the same subject has been published by Curti et al.[2]

The atomic coordinates and the crystal structure derived therefrom agree in both papers in the main. However, there are small differences in the unit cell dimensions between the two investigations. Therefore, we have carried out a careful determination of the unit cell dimensions on two specimens, one prepared by us and another kindly sent to us by Professor Curti. It was not possible to get more accurate values for the spacings on the basis of powder diffractometry because of overlapping. A Weissenberg camera was used, and the Debye-Sherrer reflections from pure sodium chloride were superimposed on reflections from a single crystal of phenazine 5, 10-dioxide. There were no significant differences between the unit cell dimentions obtained from the two specimens. They are:

$$a = 7.75 \pm 0.02\,\text{Å}, \qquad b = 4.09 \pm 0.02\,\text{Å},$$

$$c = 15.36 \pm 0.05\,\text{Å}, \text{ and } \beta = 104°48' \pm 10'.$$

The new data are closer to those of Curti et al. Fortunately, there are no serious changes necessary between the intramolecular atomic distances reported in the previous paper, except

1) Y. Namba, T. Oda and T. Watanabé, This Bulletin, **36**, 79 (1963).
2) R. Curti and V. Riganti, *Instituto Lombardo (Rend. Sc.)*, **A94**, 117 (1960).

that the value of 1.39 Å for the C_6–N bond should be revised to 1.36 Å. There are slightly larger changes in the intermolecular atomic distances between molecules related by the unit translation along the b-axis, namely, +0.09 Å on the average, the largest being between C_5 and O′ (Fig. 5), for which the reported value, 3.45 Å, should be read as 3.59 Å.

Laboratory of Physical Chemistry
Osaka University of
Liberal Arts and Education
Tennoji, Osaka (Y. N. & T. O.)
Department of Physics
Osaka University, Osaka (T. W.)

The Spectral Dependence of the Photoconduction and the Mobility of the Charge Carrier in a Single Crystal of the Pyrene-Tetracyanoethylene Complex

By Haruo KURODA, Keitaro YOSHIHARA and Hideo AKAMATU

(Received June 13, 1963)

Photoconduction has been observed with solid molecular complexes involving polycyclic aromatic hydrocarbons as an electron donor and 1, 3, 5-trinitrobenzene (TNB), bromanil, or tetracyanoethylene (TCNE) as an electron acceptor.[1] In the electronic spectra of these solid complexes, the absorption bands associated with the intermolecular charge-transfer excitation have been found in the visible region.[2,3] We have shown in a previous paper[1] that a weak photoconductive sensitivity in the wavelength region of the first charge-transfer band is appreciably dependent on the process of the crystal preparation, while the sensitivity in the shorter wavelength region is not. It seemed, therefore, that it would be interesting to examine the photoconduction with a well-grown single crystal of these complexes.

We obtained a single crystal of the pyrene-TCNE complex by slowly evaporating the solvent from a chloroform solution containing equivalent amounts of pyrene and TCNE. The crystal thus prepared showed a marked photoconductive sensitivity, a sensitivity much higher than that of various other charge-transfer complexes. We have examined the spectral dependence of photoconduction with a single crystal a few millimeters square and about one millimeter thick. The results obtained with a surface-type cell are shown in Fig. 1, together with the spectral dependence curve for a polycrystalline specimen which was grown from the melt of the complex. The spectral dependence curve of a single crystal rises steeply in the wave number region from 15000 to 20000 cm^{-1}. No photoconduction could be detected practically in the region corresponding to the first charge-transfer band, in contrast to the spectral dependence for a polycrystalline specimen. The threshold of photoconduction can be located at 13500 cm^{-1} (1.67 eV.), a value which coincides with the energy gap, 1.5~1.6 eV., determined from the temperature dependence of the dark conductivity. It is evident, therefore, that the photoconduction observed in the lower wave number region with a polycrystalline specimen is not an intrinsic one.

The determination of the crystal structure of this complex is now in progress. The preliminary results show, that it is monoclinic, with the cell dimensions $a=14.58$ Å, $b=7.34$ Å $c=8.09$ Å and $\beta=92.4°$, and that it belongs to the $P2_1/a$ space group. Two molecules of pyrene and two molecules of TCNE are contained in a unit cell. The face of a plate-like single crystal is the bc plane, in which the transition moment of the charge-transfer excitation is nearly parallel to the c-axis. However no appreciable anisotropy was found in the dark conductivity or in the photoconductivity.

The drift mobility of the charge carriers in this complex was determined from the observation of the photocurrent pulse[4] produced by an irradiation of a light pulse 1 μ sec. in duration from an air-gap spark. At room temperature, the drift mobility in the direction perpendicular to the bc plane was 0.15~0.2 cm^2/V. sec. for the electron and 0.05~0.08 cm^2/V. sec. for the positive hole. These values are smaller than the drift mobility of charge carriers in an anthracene crystal.[4,5] We could

1) H. Akamatu and H. Kuroda, *J. Chem. Phys.*, to be published.
2) H. Kuroda, M. Kobayashi, M. Kinoshita and S. Takemoto, ibid., **36**, 457 (1962).
3) H. Kuroda, K. Yoshihara and H. Akamatu, This Bulletin, **35**, 1604 (1962).
4) O. H. LeBlanc, Jr., *J. Chem. Phys.*, **33**, 626 (1960).
5) R. G. Kepler, *Phys. Rev.*, **119**, 1226 (1960).

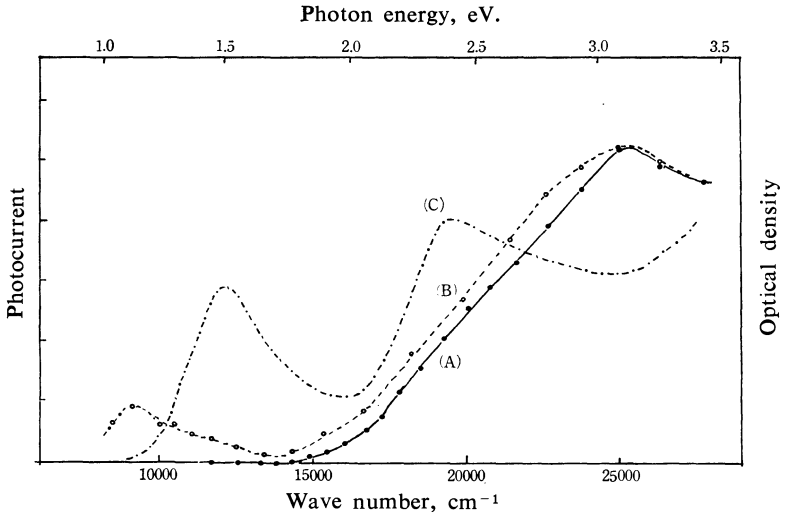

Fig. 1. Spectral dependence of photoconduction of pyrene-TCNE complexes.
(A) Single crystal, (B) Polycrystalline specimen, (C) Absorption spectrum

not detect any appreciable change in the mobility from 5°C to 40°C. These results seem to indicate that the carriers in the pyrene-TCNE complex are of a more localized nature than those in anthracene or in other simple organic solids. This is quite reasonable if we suppose, as we have postulated in the previous papers,[2,3] that in the lowest conduction state of a solid molecular complex such as pyrene-TCNE, an conduction electron moves in the crystal lattice primarily by jumping from one acceptor molecule to another acceptor molecule, while a positive hole moves from one donor molecule to another donor molecule. The height of the photocurrent pulse was almost three times as much for the electron as for the positive hole. The stationary photocurrent was also higher when the light was irradiated through the negative electrode than in the reverse case. These results indicate that electrons make a larger contribution to the photoconduction than positive holes. This is probably the result of the difference in mobility.

Department of Chemistry
Faculty of Science
The University of Tokyo
Hongo, Tokyo

SHORT COMMUNICATIONS

*The Solid Complex of Silver Nitrate and Ethylene**

By Kimio TARAMA, Mitsuhiko SANO and Kengo TATSUOKA

(Received August 9, 1963)

The syntheses of a number of solid complexes of silver nitrate with several olefins have been reported in the literatures,[1,2] but there seems to have been no mention of the solid complex with ethylene. In this laboratory, the solid complex of silver nitrate with ethylene has been prepared from an aqueous solution under

* Reported at the 16th Annual Meeting of the Chemical Society of Japan, Tokyo, April, 1963.

1) M. A. Bennet, *Chem. Revs.*, **63**, 611 (1962).
2) J. W. Kraus and E. A. Stern, *J. Am. Chem. Soc.*, **84**, 2893 (1962).

Table I. Composition of the complex

Sample*	1	2	3
Silver, mol.	2.97×10^{-3}	4.10×10^{-3}	5.70×10^{-3}
Ethylene, mol.	1.48×10^{-3}	2.01×10^{-3}	2.83×10^{-3}
Nitrate ion, mol.	2.91×10^{-3}	3.91×10^{-3}	5.48×10^{-3}
C_2H_4/Ag, mol. ratio	0.498	0.490	0.497
NO_3/Ag, mol. ratio	0.981	0.954	0.962

* Samples 1, 2 and 3 were dried for 6 hr., 4 hr. and 5 min. respectively.

suitable temperature and silver-nitrate concentration conditions. In this paper the method of preparation and some properties will be reported.

Experimental.—The silver nitrate used was reagent grade. The purity of the ethylene was 99.6%; no other olefins were detected by gas chromatographic analysis. In the preparation of the solid complex, when ethylene gas was bubbled through the saturated aqueous solution of the silver nitrate (6 N) at 0°C, a white precipitate appeared. This precipitate in solution disappeared when nitrogen gas instead of ethylene was bubbled through this solution, and it was repeatedly regenerated by the repetition of the above-mentioned procedure. The resulting solid precipitate was isolated from the solution and dried on a glass filter cooled at 0°C by passing ethylene over it under a pressure of about 800 mmHg.

The dried samples were stored at the temperature of dry ice in glass containers in an ethylene atmosphere. The equilibrium pressure data were obtained with a manometric apparatus. The ethylene content of the complex was calculated from the amount of gas resulting from the complete decomposition of the samples, and then the amount of silver in the residue was measured gravimetrically in the analytical form of silver chloride and that of nitrate ions, by ultraviolet method.

Results and Discussion.—The solid silver nitrate-ethylene complex is in the form of white needle-like crystals and is stable only at temperature below about −30°C or under higher partial pressures of ethylene, like other silver salt-olefin complexes.[1] This complex dissociates quantitatively to ethylene and crystal silver nitrate without forming polymerized or oxidized products of ethylene at 30°C. The analytical data of this complex are presented in Table I. The quantities of ethylene released from the complex correspond closely to 0.5 mol. of ethylene par mole of silver nitrate for three samples. These samples also indicate no change in the composition of the complex with the contamination of the water. The ratio of nitrate ions to silver is about unity. These analytical data lead to the conclusion that the composition of the complex

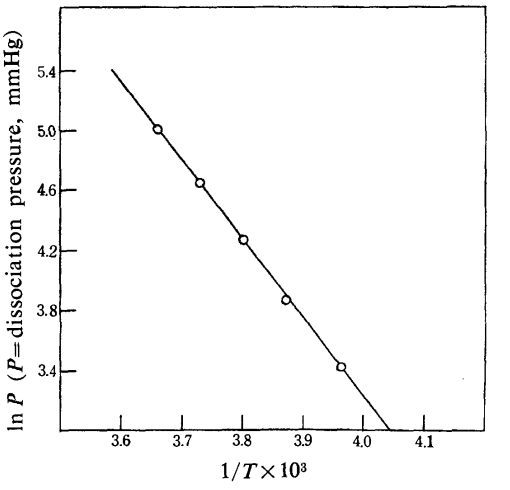

Fig. 1. Dissociation pressure of $(AgNO_3)_2\cdot C_2H_4$.

is $(AgNO_3)_2\cdot C_2H_4$. Equilibrium pressures (P) in the temperature range from 253°K to 273°K are illustrated in Fig. 1. From these data the heat of dissociation is calculated to be 10.6± 0.2 kcal. for $(AgNO_3)_2\cdot C_2H_4$. This is about twice as large as the value (5.8 kcal.)* for $AgNO_3\cdot C_2H_4$ in an aqueous solution.

The complex formation between silver ions and ethylene may be described by the following equations in an aqueous solution.[3]

$$Ag^+ + C_2H_4 \overset{K_1}{\rightleftarrows} Ag^+\cdot C_2H_4 \quad (1)$$

$$Ag^+\cdot C_2H_4 + Ag^+ \overset{K_2}{\rightleftarrows} (Ag^+)_2\cdot C_2H_4 \quad (2)$$

$$Ag^+\cdot C_2H_4 + C_2H_4 \overset{K_3}{\rightleftarrows} Ag^+\cdot (C_2H_4)_2 \quad (3)$$

Trueblood and Lucas found K_1 to be 85.3 and K_2 0.15 at 25°C by distribution methods.[4] These equilibrium constants indicate that the fraction of $(Ag^+)_2C_2H_4$ in silver and ethylene complexes in an aqueous solution is very small, but that in higher concentrations of silver nitrate, the concentration of the species having this composition will rise in accordance with the reaction of Eq. 2; then the species will be

3) S. Winstein and H. Lucas, ibid., 60, 836 (1938).
4) K. N. Trueblood and H. J. Lucas, ibid., 74, 1338 (1952).

able to precipitate if its solubility is sufficiently low at 0°C.

The structure of this complex will be reported later.

Department of Fuel Chemistry
Faculty of Engineering
Kyoto University
Sakyo-ku, Kyoto

A New Catalyst System for the Polymerization of Tetrahydrofuran

By Iwao YAMASHITA, Minoru SERIZAWA and Takaharu MIYAKAWA

(Received August 21, 1963)

The ring-opening polymerization of tetrahydrofuran (THF) by the use of metal halides or triethyl aluminum as a catalyst has recently been reported by several authors.[1] In such cases, a cocatalyst or comonomer, such as alkyl halides, ortho acid esters, hydrogen halides, alkylene oxides, oxethanes, diketene, β-propiolactone, and phenyl isocyanate, have been used together with the catalyst.

We have now examined the polymerization of THF by the use of organometallic compounds (Et_3Al, Et_2AlCl, Et_2Zn) or metal halides ($BF_3 \cdot Et_2O$, $AlCl_3$, $FeCl_3$) in the presence of phosphorus pentaoxide (P_2O_5) and have found that Et_3Al was the most effective of the substances examined.

Bulk polymerization was carried out in a nitrogen atmosphere in a sealed test tube. The polymeric product was isolated by pouring the reaction mixture into a large quantity of water containing hydrochloric acid. The crude polymer was washed with methanol and then dissolved in THF at room temperature by leaving it standing for 24 hr. The THF-soluble fraction was recovered by again pouring the solution into a large excess of water and then drying it in vacuo. The THF-insoluble fraction was washed with THF and dried in vacuo.

Several results of the polymerization of THF by the use of the P_2O_5-Et_3Al system are shown in Table I and Figs. 1 and 2. The effect of P_2O_5 is obvious. Both the THF-soluble and the THF-insoluble fraction contain a small amount phosphorus.*

When the THF-soluble fraction was compared with polytetrahydrofuran prepared by the method of Muetterlies[3] (catalyst: PF_5), considerable differences in the thermal properties were noticed, whereas the X-ray diffraction patterns and infrared spectra of the two polymers were similar. On the other hand, an apparent difference was found between those of the THF-soluble fraction and those of the

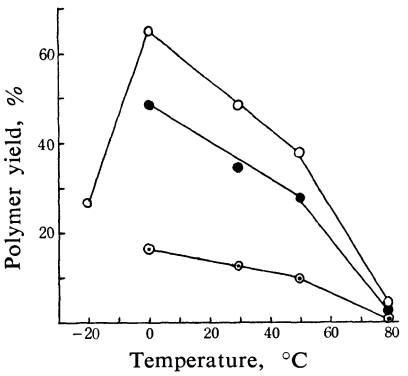

Fig. 1. The yield of polymer vs. polymerization temperature.
Catalyst, $1/2P_2O_5$ (2 mol. %)-Et_3Al (2 mol. %)
Polymerization time, 24 hr.
○: Total yield
●: Yield of THF-insoluble fraction
⊙: Yield of THF-soluble fraction

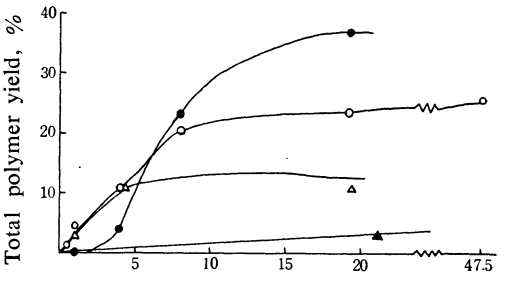

Fig. 2. The total polymer yield vs. polymerization time.
Catalyst, $1/2P_2O_5$ (2 mol. %)-Et_3Al (1 mol. %)
●: 0°C, ○: 30°C, △: 50°C, ▲: 80°C

1) See, for example, H. Meerwein, *Angew. Chem.*, **72**, 927 (1960); T. Saegusa et al., presented at the Meeting of the Society of Polymer Science, Osaka, November, 1962.

* The quantitative analysis of the phosphorus in the polymer was carried out by the Nakamura's method.[2]

2) M. Nakamura, *J. Agr. Chem. Soc. Japan (Nogei Kagaku Zasshi)*, **24**, 1 (1950).

3) E. L. Muetterties, U. S. Pat. 2856370 (1958).

TABLE I. POLYMERIZATION OF THF BY Et_3Al-P_2O_5 SYSTEM
EFFECT OF AMOUNT OF P_2O_5
THF: 0.05 mol., Et_3Al: 0.001 mol. (2 mol. %), Polymerization at 30°C for 24 hr.

$1/2P_2O_5$ / Et_3Al	Total yield %	THF-sol. fraction			THF-insol. fraction	
		Yield %	η_{sp}/c*	P Content %	Yield %	P Content %
0	0	—	—	—	—	—
0.2	5.7	5.6	—	—	0.1	0.92
0.6	22.6	6.1	2.28	—	16.5	0.83
1.0	48.5	13.5	1.75	0.17	35.0	0.90
1.6	34.2	9.2	2.58	—	25.0	1.92
2.0	43.0	12.7	2.79	—	30.3	1.19

* Measured on a solution of 0.2 g. polymer in 100 ml. benzene at 30°C.

THF-insoluble fraction. These differences seem to have some relation to their phosphorus contents.

Further details of the reaction mechanism of such a catalyst system and such properties of polymers will be published elsewere.

Government Industrial Research Institute, Osaka
Oyodo-ku, Osaka

The Electrokinetic Potential and Surface Acidity of Titanium Dioxide

By Tetsuo MORIMOTO and Masashi SAKAMOTO

(Received August 24, 1963)

When an insoluble metal oxide is in equilibrium with water, the solid will be covered with surface hydroxyl groups as a result of surface hydration. The present communication deals with the dependence of the electrokinetic potential and the surface acidity of titanium dioxide on its heat treatment in order to clarify the dissociation of surface hydroxyl groups on titanium dioxide.

Titanium dioxide obtained by the hydrolysis of titanium sulfate was treated with ammonium hydroxide to remove contaminating sulfate groups. After having been sufficiently washed with water, the sample was dried and calcined at given temperatures. The electrokinetic potentials obtained in water by the streaming-potential method are shown in Fig. 1. The charge of titanium dioxide is positive on the samples treated at 100 to 700°C, but it changes to a negative value after treatment at higher temperatures. An isoelectric point appears on a sample treated at about 800°C, which agrees with the transition temperature of anatase to rutile.

In the next place, the surface acidity of these samples was examined by the dye-adsorption method. To prepare the dye solution, 10 mg. of methylred was dissolved in 100 ml. of isooctane.[1] 0.2 g. of titanium dioxide was then shaken with 4 ml. of the dye solution. After the adsorption of dye molecules, the

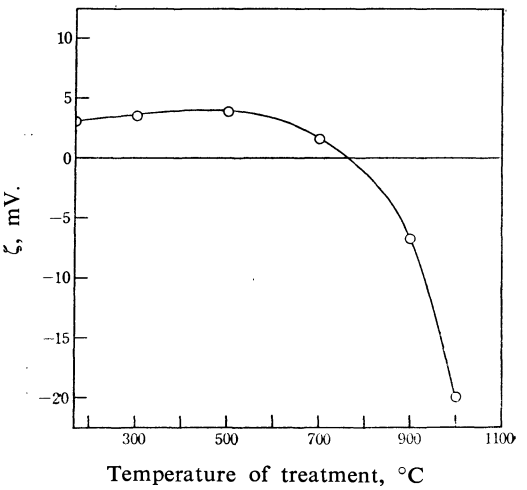

Fig. 1. Electrokinetic potential (ζ) of titanium dioxide.

1) K. Tanabe and M. Katayama, *J. Res. Inst. Catalysis, Hokkaido Univ.*, 7, 106 (1959); C. Walling, *J. Am. Chem. Soc.*, 72, 1164 (1950).

reflectance of the powder was measured by a spectrophotometer. The color of the adsorbed dyestuff was a basic one, yellow, in the samples treated at lower temperatures, but in the samples treated at 1000°C it was an acidic color, red, as is recorded in Fig. 2. Thus the change in the surface acidity of titanium dioxide appears to correspond to the transition temperature of the crystal, as in the case of the electrokinetic potential.

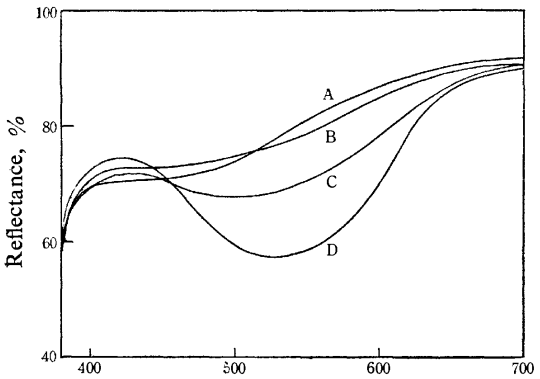

Fig. 2. Reflection spectra of methylred adsorbed on titanium dioxide, treated at A, 100°C; B, 500°C; C, 700°C; D, 1000°C.

It is possibly considered that the surface hydroxyl groups situated on titanium dioxide dissociate as follows:

$$\equiv TiOH \rightarrow \equiv Ti^{+} + OH^{-} \quad (1)$$

$$\equiv TiOH \rightarrow \equiv TiO^{-} + H^{+} \quad (2)$$

Dissociation resulting from Eq. 1 will give a positive charge on the surface and a basic color for the indicator, while that from Eq. 2 a negative charge and an acidic color. Judging from the present investigation, it is plausible that, on treatment at temperatures lower than 800°C, the dissociation of surface hydroxyl groups on titanium dioxide follows Eq. 1, while on treatment at higher temperatures it follows Eq. 2.

It is known that the distances between neighboring oxygens are longer than about 3.00Å in basic metal hydroxide crystals, while in acidic ones they are less than 2.70Å.[2] The crystallographic data on titanium dioxide, described by Cromer and Herrington,[3] are represented in Table I. If we assume that

Table I. Oxygen-oxygen distances in anatase and rutile, Å

Anatase	Rutile
2.802	2.779
2.446	2.526
3.040	

the surface of titanium dioxide is hydrated to form surface hydroxyl groups without varying the O–O distances greatly from those given in Table I, it may be expected that rutile has an acidic surface and anatase, a basic one. Rather we may propose from the present results that the exposed surfaces of anatase are rich in longer O–O bonds. In conclusion, the fact that titanium dioxide may have either a positive or a negative charge according to its modifications should play an important role in the interfacial phenomena of titanium dioxide.

Department of Chemistry
Faculty of Science
Okayama University
Tsushima, Okayama

2) R. Kiriyama, "Kōzō Muki-Kagaku," Kyōritsu, Tokyo (1955).
3) D. T. Cromer and K. Herrington, *J. Am. Chem. Soc.*, 77, 4708 (1954).

The Separation and Determination of Polycyclic Aromatic Hydrocarbons by Thin Layer Chromatography

By Hidetsuru MATSUSHITA, Yasutomo SUZUKI and Hiroyuki SAKABE

(Received August 28, 1963)

This study presents a method for the separation and the quantitative determination of polycyclic aromatic hydrocarbons by thin-layer adsorption chromatography.

Anthracene, pyrene, 1, 2-benzanthracene, 3, 4-benzpyrene, perylene and 1, 12-benzperylene were used as samples. They were all proved to be chromatographically pure. As the adsorbent layer, silica gel Woelm for thin layer chromatography (M. Woelm · Eschege, Germany) was used in a thickness of about 300 μ. The chromatoplate was activated by heating at 100°C for 15 min. in an electric furnace and then by heating it at 60°C and 0.1 mmHg for 30 min. in a vacuum desiccator. The activated plate was transferred quickly onto a hot metal plate of about 60°C, and 3 μl. of a benzene solution of the test sample were spotted on it. The ascending development was carried out in a chromatographic chamber using as the developing solvent *n*-hexane, *o*-dichlorobenzene and pyridine (10 : 1 : 0.5). The humidity in the chromatographic chamber was about 25%. The developing time was about 60 min., and the height of development was about 12 cm. Spots of the separated hydrocarbons on the plate were detected by fluorescence under a 365 mμ ultraviolet light.

The minimum values of aromatic hydrocarbons detectable by this method were within the range of 0.13 μg. to 0.0017 μg., as Table I shows. As these values obtained by acetylated paper chromatography have been reported to be 2 μg. to 5 μg.,[1] this method is very sensitive in detecting these compounds.

TABLE I. R_f VALUES AND MINIMUM DETECTABLE VALUES OF POLYCYCLIC AROMATIC HYDROCARBONS BY THIN LAYER CHROMATOGRAPHY

Substance	R_f value[1]	Minimum detectable value, μg.
Anthracene	0.51	0.03
Pyrene	0.41	0.13
1,2-Benzanthracene	0.32	0.010
3,4-Benzpyrene	0.23	0.007
Perylene	0.19	0.0017
1,12-Benzperylene	0.15	0.002

1) To obtain these R_f values, samples were spotted in 5 min. on a hot metal plate (ca. 60°C) in a room of 49% relative humidity at 29°C and developed in a chromatographic chamber of 27% relative humidity at 29°C for 60 min.

It must be noticed that the R_f values were highly affected by the humidity in the chromatographic chamber as well as by that in the environmental air in which samples were spotted. An increase in the humidity gave larger R_f values, resulting in an unsatisfactory separation of the aromatic hydrocarbons.

In this study, a linear relationship was found between the area of spot and the logarithm of the amount of aromatic hydrocarbon (Fig. 1). On the basis of this relationship, aromatic hydrocarbons were determined with an accuracy of ±5% if such experimental conditions as activation and humidity were fixed. In this connection, it is recommended that the amount of an unknown sample is calculated using a calibration curve which is drawn from three or more spots of known amounts of pure hydrocarbon on the plate on which the unknown sample is spotted.

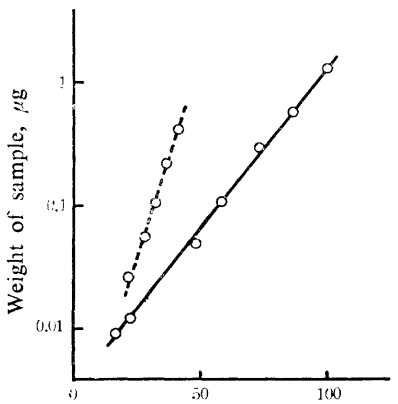

Fig. 1. Relationship between area of spot and logarithm of weight for 3,4-benzpyrene (——) and for 1,2-benzanthracene (----) on the thin layer chromatoplate.

This method might offer a useful tool for the microdetermination of carcinogenic hydrocarbons such as 3,4-benzpyrene in air pollutants, exhaust gases or the smoke of cigarettes.

National Institute of Industrial Health
Kizuki-sumiyoshi, Kawasaki

1) Th. Wieland and W. Kracht, *Angew. Chem.*, **69**, 172 (1957).

The Self-diffusion Coefficients of Carbon Dioxide, Hydrogen Carbonate Ions and Carbonate Ions in Aqueous Solutions

By Kunihiko KIGOSHI and Takusei HASHITANI

(Received September 17, 1963)

The distribution of natural radiocarbon and man-made radiocarbon in the atmosphere and the ocean depends on the exchange rate of carbon between the atmosphere and the ocean.[1] In recent publication Bolin[2] has pointed out that this carbon exchange between the atmosphere and the ocean depends on the diffusion of carbonates ions in the sea water.

This short communication will present the results of studies of the self-diffusion of carbon dioxide, hydrogen carbonate ions and carbonate ions in aqueous solutions. The measurements of the self-diffusion coefficients were made using a modified Northrop-McBain type diaphragm cell. Both the upper and the lower compartments of the cell were filled with solutions of the same chemical composition. The solutions contain carbon dioxide, hydrogen carbonate ions, carbonate ions and sodium ions, and they were adjusted to pH 4.0, 8.0 and 12.5. More than 99% of the carbon atoms in the solution were contained as carbon dioxide molecules in the solution of pH 4.0, as hydrogen carbonate ions in the solution of pH 8.0, and as carbonate ions in the solution of pH 12.5. Therefore, each solution could be regarded as a pure solution of these molecules or ions. The concentration of carbon-containing ions in these solutions was held ca. 0.1 F while that of carbon dioxide was ca. 0.06 F. The carbon tracer C-14 was present in the lower compartment of the cell.

After the diffusion had continued for one or two days, barium carbonate was precipitated from the solution in each compartment. By β-rays assays of these precipitates, the diffusion coefficients of carbon dioxide, hydrogen carbonate ions and carbonate ions in aqueous solutions shown in Table I were obtained. The cell constant was determined by the diffusion of a 0.1 F potassium chloride solution into pure water, assuming a standard value of 1.87×10^{-5} cm^2/sec. for the diffusion coefficient of this solution.[3]

TABLE I. SELF-DIFFUSION COEFFICIENTS OF CO_2, HCO_3^- AND CO_3^{2-} (10^{-5} cm^2/sec.)

Temp., °C	CO_2	HCO_3^-	CO_3^{2-}
0.0	0.953±0.013	0.521±0.011	0.414±0.011
25.0	1.94 ±0.023	1.09 ±0.015	0.804±0.008
30.0	2.18 ±0.019	1.28 ±0.015	0.974±0.005

The details of the experimental procedure and a discussion of the hydration of carbon dioxide, hydrogen carbonate ions and carbonate ions in aqueous solutions based on the measured self-diffusion coefficients will be published in the near future in this Bulletin.

Department of Physics and Chemistry Gakushuin University Mejiro, Tokyo

1) K. Kigoshi, *J. Radiation Research*, 1-2, 111 (1960).
2) B. Bolin, *Tellus*, 12, 274 (1960).
3) R. H. Stokes, *J. Am. Chem. Soc.*, 72, 763 (1950).

*The Separation of Amino Acids with an Ion-exchange Membrane**

By Yujiro HARA

(Received February 8, 1962)

The group separation of a mixture of amino acids obtained from the hydrolysis of gluten has been carried out by electrodialysis, using the homogeneous ion-exchange membrane of the styrene-butadiene copolymer. It has been found that the five-compartment use of a cation-exchange membrane (C-2, with a water content of 50% and a specific resistance of 100 Ω-cm.) and an anion-exchange membrane (A-3, with a water content of 55% and a specific resistance of 120 Ω-cm.) effects a successful separation of amino acids into neutral, basic, and acidic groups. However, 10~20% of the neutral amino acids migrated to the basic and acidic amino acid groups.

The separation of amino acids by electrodialysis using such ordinary semi-permeable membranes as biological and collodion membranes has previously been attempted.[1] However, this method has not yet been carried out on an industrial scale because of the difficulty of manufacturing large-sized membranes with good electric properties and stability for long use. Moreover, ordinary semi-permeable membranes have a very low permselectivity; therefore, they cannot prevent the leakage of the hydrogen and hydroxyl ions formed in the electrode chambers. This makes it difficult to adjust the hydrogen ion concentration of amino acid solutions in the intermediate compartments. The author adopted ion-exchange membranes as diaphragms in the electrodialysis, and the experiments were carried out using homogeneous ion-exchange membranes of the styrene-butadiene copolymer produced by Kuwata and Yoshikawa.[2]

Experimental

The separation of amino acids by electrodialysis using ion-exchange membranes was limited to the separation of such groups as the acidic (AA), neutral (NA), and basic (BA) groups, all with similar isoelectric points. Various ion-exchange membranes have been made by polymerization or condensation.[3] The ion exchange membranes used in the present experiments were derived from the styrene-butadiene copolymer (commercial SBR) which has a styrene content of 50%.

The styrene-butadiene copolymer membrane has an advantage that the pore-size of the membrane can be changed by adjusting the butadiene content of the copolymer and/or by controlling the cross-linking reaction. Consequently, this kind of membrane is preferable over other ion exchange membranes for the separation of amino acids. The properties of these membranes are shown in Table I. The porosity of the membranes is compared in terms of the value of the water content (W), the water permeation ratio[4] (K), and the specific resistance (Ω-cm.) of the membranes.

An electrodialysis apparatus,* separated by two sets of anion- and cation-membranes (7.5×7.5 cm.), as illustrated in Fig. 1 (each intermediate compartment was 7.5×7.5×1.0 cm.), was used, with a nickel plate (7.0×7.0 cm.×0.3 mm.) as a cathode and a carbon electrode 7.5×7.5×0.8 cm.) as an anode. The experiment was carried out by changing the cation-exchange membrane, C_1, and the anion-exchange membrane, A_2, in various ways. The A_1 and C_2 membranes in Fig. 1 were fixed throughout the experiment by A-1 and C-1 respectively. A sodium chloride solution (0.1~0.2%) was placed in the intermediate compartments A and C, and 70 cc. of a solution (pH 5.6) containing 10% of mixed amino acids (Table II) obtained from the hydrolysis of gluten and by adjusting the pH in the vicinity of the isoelectric point of neutral

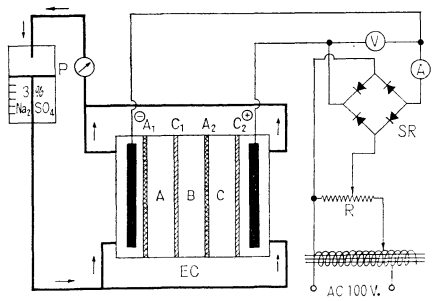

Fig. 1. Apparatus.

* This article reports on part of a long-range research program on ion-exchange membranes being led by Professor T. Kuwata and Assistant Professor S. Yoshikawa of The University of Tokyo.

1) G. L. Foster and C. L. Schmidt, *Biochem. J.*, **40**, 1709 (1926); K. Ikeda and S. Suzuki, U. S. Pat. 1015890 (1912).

2) T. Kuwata and S. Yoshikawa, Japanese Pat. 239596, 239724, 248669.

3) S. Yoshikawa, *J. Soc. Org. Chem. Japan*, **15**, 603 (1957).

4) "Kogyo Butsurikagaku," Ed. by Kogyo Butsurikagaku Kenkyu-kai, 2nd Ed., Korona-sha, Tokyo, p. 111.

* Electrodialysis cells made by assembling the various compartments in the form illustrated in Fig. 2 (for intermediate compartments) and in Fig. 4 (for electrode compartments) as indicated in a previous paper[5] were used.

5) Y. Hara, *J. Chem. Soc. Japan, Ind. Chem. Sec.* (*Kogyo Kagaku Zasshi*), **65**, 885 (1962).

Table I. Properties of the ion-exchange membranes used

Type	Notation	Ion-exchange capacity of membrane meq./g.	Fixed ion concentration in membrane meq./g.	Water content of membrane*1 W, %	Water permeation ratio*2 K, $\times 10^{-16}$ cm^3	Specific resistance Ω-cm.	Ion selective permeability n, 0.1 N NaCl	Thickness mm.
Cation-exchange membrane	C-1	1.05	2.57	33.4	0.24	272	0.90	0.24
	C-2	1.32	2.13	50.1	0.32	100	0.92	0.28
Anion-exchange membrane	A-1	1.68	3.91	31.2	0.18	300	0.90	0.23
	A-2	1.69	3.16	47.2	0.23	250	0.91	0.26
	A-3	1.78	1.84	54.8	0.45	120	0.85	0.45

*1 This value was calculated on the basis of the total weight of the resin comprising the membrane, excluding any supporting material.

*2 The degree of the penetration of a diaphragm is a value indicating the size and distribution of pores derived from Poiseville's law on the assumption that the cross-section of pores of a diaphragm is round. This is ordinarily indicated by the quantity (cc.) which transfers 1 cm^2 of diaphragm 1 cm. thick in one hour under a static pressure of 1 cm. of a water column when a 0.5 N sucrose solution and water are placed on opposite sides of the diaphragm.

Table III. Group separation of amino acids mixture

Runs No.	Electrodialysis cell: Ion-exchange membranes C_1	A_2	Catholyte	Anolyte	Initial current density amp./dm^2	Period of operation hr.	Experimental results: pH variation of the solution in each compartment A	B	C	Behavior of separating amino acids in each fraction A	B	C
1	C-1	A-1	3% Na_2SO_4	3% Na_2SO_4	0.3	5.0	10<	3.8	9.0	BA Gly Leu Ser Val Pro Ala Thr	NA His AA	AA Gly
2	C-1	A-1	3% Na_2SO_4	3% Na_2SO_4	0.1	24.0	8.8	5.6	8.6	Arg Lys Gly Pro Ser Thr Val Leu	NA His Arg AA	AA
3	C-1	A-1	N NaOH	N NaOH	0.1	24.0	10<	8.6	10<	Arg Lys Gly Leu Val Pro	BA NA AA	AA
4	C-1	A-1	N HCl	N NaOH	0.1	—	1	3.0	10<	—	— AA	AA Gly Ser
5	C-2	A-2	3% Na_2SO_4	3% Na_2SO_4	0.2	5.0	9.0	5.0	10.0	Arg Lys Gly Ser Ala Val	NA His Glu	AA
6	C-2	A-2	3% Na_2SO_4	3% Na_2SO_4	0.13	24.0	8.2	4.8	10	Arg Lys Gly Ser	NA His Glu	AA Gly Ser
7	C-2	A-3	3% Na_2SO_4	3% Na_2SO_4	0.15	22.0	8.0	5.6	8.2	Arg Lys Gly Ser Ala	NA His	AA Gly Ser Val Ala Leu
8	C-2	A-3	3% Na_2SO_4	3% Na_2SO_4	0.2	20.0	5.6	5.8	6.8	Arg Lys Gly Ser Ala Val Lew	NA His	AA Gly Ser Val Ala Leu
9	C-2	A-3	3% Na_2SO_4	3% Na_2SO_4	0.46	5.0	5.6	5.4	4.4	BA Gly Ser Ala Val Leu	NA	AA Gly Ser Val Ala Leu
10	C-2	A-3	6% Na_2SO_4	6% Na_2SO_4	0.5	3.5	10<	5.2	7.4	BA Gly Ser Ala Val Leu	NA	AA Gly Ser Val Ala Leu
11	C-2	A-3	6% Na_2SO_4	6% Na_2SO_4	0.8	2.0	10<	5.2	7.0	BA Gly Ser Ala Val Leu	NA	AA Gly Ser Val Ala Leu
12	C-1	A-3	6% Na_2SO_4	6% Na_2SO_4	0.5	2.5	—	5.2	—	BA Gly Ser Ala Val Leu	NA Arg His	AA
13	C-1	A-3	6% Na_2SO_4	6% Na_2SO_4	0.36	5.0	—	5.2	—	BA Gly Ser Ala Val Leu	BA NA AA	AA

TABLE II. COMPOSITION OF AMINO ACIDS MIXTURE USED

Kind of amino acids	Notation	Content %
Glutamic acid	Glu	12.7
Aspartic acid	Asp	
Acidic amino acids	AA	12.7
Glycine	Gly	5.3
Alanine	Ala	4.4
Leucine	Leu	18.5
Isoleucine	Ileu	
Valine	Val	7.2
Methionine	Met	
Proline	Pro	10.4
Serine	Ser	3.3
Threonine	Thr	2.0
Phenylalanine	Phe	8.5
Neutral amino acids	NA	71.5
Arginine	Arg	6.9
Histidine	His	5.4
Lysine	Lys	3.5
Basic amino acids	BA	15.7
		Sum 99.9

amino acids, were placed in the intermediate compartment B. Colloidal deposits on the C_1 cation-exchange membrane cause electric resistance when peptide and fumin are present in the feed amino acids, perticularly in the case of imperfect hydrolysis. Therefore, the muddy matter in the feed solution of amino acids was filtered off and purified through an ion-exchange resin bed. A 3~6% sodium sulfate solution was used as an electrolyte solution in the cathodic and anodic chamber and was circulated in the direction of the arrow at the rate of 1.0 l./hr. in order to cancel out the H ions and OH ions produced in the electrode solution at all times and thus to prevent any effect of pH fluctuation on the intermediate solution.

If the electrodialysis is carried out in such a way, sulfate ions will be furnished from the cathode to the A compartment and sodium ions from the anode to the C compartment, and, consequently, the pH of the solution of the B compartment will not be much changed during the electrodialysis.

The experiment was carried out using various kinds of anion- and cation-exchange membranes and under various operating conditions, such as current density, operating time, kind of electrolyte and pH of the solution of each compartment during electrodialysis. The degree of amino-acid separation was measured by two-dimensional paper partition chromatography and was determined quantitatively by the dinitrophenyl-paper chromatography method.[6]

Results and Discussion

To carry out a group separation of amino acids smoothly, it is necessary to keep the feed solution, viz., the solution in the intermediate compartment B at a constant pH during the electrodialysis. The pH fluctuation of the compartment B solution is due to the electrolysis of water within the membrane in addition to the effect of the H ions or OH ions formed on the electrodes. The effect of the H or OH ions can be minimized by mixing electrode solutions during circulation. When the sizes of the amino acid molecules are about as large as or larger than the pore-size of the ion-exchange membrane, the electrolysis of water occurs by forced electric current. Because of this phenomenon, the pH in each intermediate compartment varies markedly during electrodialysis.

The results are summarized in Table III. As No. 1 shows, when membranes having the smallest pore-size, C-1 and A-1, were adopted as membranes C_1 and A_2, respectively electrolysis of water took place apparently at an initial current density of 0.3 amp./dm^2 and the solution in compartment B gradually became acidic. In No. 2, if the initial current density was decreased at 0.1 amp./dm^2 and if the period of dialysis was extended, no electrolysis of water took place, but the results of paper partition chromatography showed that the separation of amino acids was imperfect. In Nos. 3 and 4, when sodium hydroxide or hydrochloric acid and sodium hydroxide were used as the electrolytes, the pH of the solution in the B compartment became unstable and the separation of amino acids was imperfect. In Nos. 5 and 6, when membranes wit ha little larger pore-sizes, C-2 and A-2, were adopted as membranes C_1 and A_2 respectively, the fluctuation of the pH of the solution in the intermediate compartment B was noticeable, even at a low current density, and it was found from the results of paper partition chromatography that a considerable amount of histidine and glutamic acid still remained in the B compartment. When the A-3 membrane, with the largest pore-size, was adopted as membrane A_2 almost no electrolysis of water took place, even at the high initial current density of 0.8 amp./dm^2, as Nos. 7—11 show, and the separation of amino acids took place within a short time. Further, the results of paper partition chromatography showed that no acidic and basic amino acids remained in the solution of the B compartment, although a small amount of remaining histidine was noticed in the feed solution at a current density below 0.2 amp./dm^2.

On the other hand, when the C-1 membrane, which has a smaller pore-size, was adopted as the C_1 membrane insteat of the C-2 membrane, both the basic and acidic groups remained in the solution of the B compartment,

6) S. Blackburm and A. G. Lowther, *Biochem. J.*, 48, 126 (1951).

as shown in Nos. 12 and 13. Therefore, the separation of amino acids was unfavorably achieved. Further, it was found that when a set of C-2 and A-3 membranes, both of which have a larger pore-size, was applied and when electrodialysis was performed by applying a high initial current density (0.5~0.8 amp./dm^2), no electrodialysis of water took place and a favorable result was obtained.

TABLE IV. QUANTITATIVE ANALYSIS OF AMINO ACIDS SEPARATED BY DNP-PPC METHOD (Run No. 11)

Kind of amino acids	Each fraction of separated amino acids in the intermediate compartments, %		
	A	B	C
Glutamic acid	0	0	100
Aspartic acid	0	0	100
Glycine	10.0	81.7	8.2
Alanine	6.9	85.6	7.4
Leucine, Isoleucine	4.3	89.9	6.0
Valine, Methionine	6.7	86.3	7.0
Proline	5.7	89.0	5.1
Serine	7.0	81.5	12.1
Threonine	8.9	75.4	15.7
Phenylalanine	3.3	83.6	13.3
Neutral amino acids	7.2	84.3	9.4
Arginine	100	0	0
Histidine	100	0	0
Lysine	100	0	0

The results of the quantitative analysis on each fraction by means of the dinitrophenyl-paper partition chromatography method as an example (No. 11), are shown in Table IV, where the separation was almost ideal. These results show the complete absence of basic and acidic amino acids in the neutral amino acids remaining in the B compartment and a few per cent of neutral amino-acid transfer to both the basic and the acidic amino acid groups. This tendency is especially noted in neutral amino acids, which have a smaller molecular weight, and is probably due to the electro-osmosis accompanying the electrodialysis. In addition, it is interesting to note that some of the neutral amino acids, such as serine and threonine, which have an hydroxyl group, and phenylalanine, which has a phenyl ring, show a marked tendency to transfer to the acidic amino acid group. This seems to be because these amino acids have a particular affinity for the anion-exchange membrane.

The author is deeply indebted to Dr. Tadashi Yawataya and his co-workers of the Asahi Glass Co., Ltd., for the generous supply of the ion-exchange membranes used in this work, and to Mr. Toshisaburo Yamana of the Daigo Nutritive Chemicals Co., Ltd., for leading some of the experiments reported on in this paper.

Research Laboratories
Takeda Chemical Industries, Ltd.
Osaka

The Complex Formation of Boron Fluoride with Lower Olefin at Low Temperatures. I. The Isotope Effects and Absorption Spectra of Boron Fluoride-Propylene and -Ethylene Systems

By Ryohei NAKANE, Tsunao WATANABE, Osamu KURIHARA and Toshiyuki ŌYAMA

(Received December 12, 1962)

The complexes of π donors with vacant-orbital acceptors, e.g., unsaturated hydrocarbons with Friedel-Crafts catalysts, have been considered not likely to be very stable,[1] although mono-olefin can form complexes with such transition metals as platinum(II) and silver(I). Evans et al.[2] denied the possibility of any stable complex of isobutylene with boron fluoride. In a preceding paper,[3] however, we proposed that propylene may form a stable liquid complex with boron fluoride at low temperatures. This proposal has its basis in the fact that the equilibrium constant of the isotopic exchange between boron fluoride gas and boron fluoride in a propylene solution is much larger than the vapor pressure ratio of

1) R. Mulliken, *J. Phys. Chem.*, **56**, 818 (1952).
2) A. Evans and M. Polanyi, *J. Chem. Soc.*, **1947**, 252.
3) R. Nakane, T. Watanabe and O. Kurihara, This Bulletin, **35**, 1747 (1962).

isotopic boron fluorides. In other words, the unusual concentration of boron-10 in the liquid phase of boron fluoride with propylene can be explained only by assuming the formation of the liquid complex. In this report more accurate values of the isotopic exchange, as obtained by further measurements, are given, together with the absorption spectra of the complex. Similar measurements of the boron fluoride-ethylene system have also been made.

Experimental

Material. — Tank boron fluoride, propylene, ethylene and propane were purified by repeated bulb-to-bulb distillation in vacuo at temperatures from −112°C (the melting point of carbon disulfide) to that of liquid nitrogen. The inside of the distillation bulb was coated with evaporated sodium to remove any trace of residual oxygen and water. In all cases, good care was taken to assure the purity of the gas, for the purity attained by the boron fluoride and propylene used in the previous work might be somewhat insufficient.

The Measurement of the Isotope Effect. — The equilibrium constant of the isotopic exchange was measured by the shaking method.[4] The apparatus used is shown in Fig. 1. The flask with a break-off seal (a), a stopcock (1) and a universal joint (b) was connected to an appropriate vacuum line. The volume was approximately 300 ml. First the

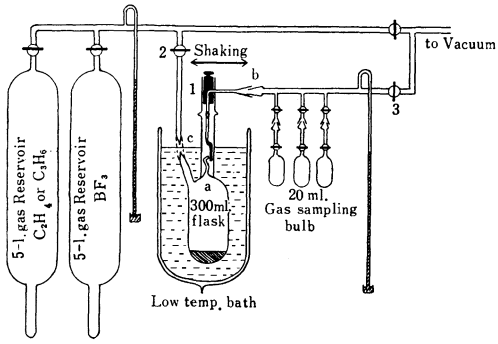

Fig. 1. The shaking type of gas-liquid contactor for the determination of equilibrium constant for low temperature exchange.

entire appartus was evacuated. Known amounts of purified propylene or ethylene and boron fluoride were then introduced through a stopcock (2) into the flask and frozen with liquid nitrogen. The glass tube (c) connecting the flask with the stopcock (2) was sealed off, then the flask was closed and isolated from the vacuum line. The flask was immersed in a low temperature bath at the melting point of carbon disulfide (−112°C). From the known volume of the flask, the total amounts of introduced propylene or ethylene, and of boron fluoride, and the amounts of boron fluoride in the gas phase (m mol.) and in the liquid phase (M mol.) were calculated. Since a large excess of boron fluoride in the liquid phase was used (at least in the ratio of 20 to 1), the value of m/M was small enough to assume that the isotopic composition in the liquid phase remains almost unchanged throughout the experiments. The equilibrium constant was, accordingly, so determined by only measureing the $^{10}B/^{11}B$ ratio in the gas phase before and after the equilibration, that sampling in the liquid phase was not necessary.

The flask was vigorously shaken by a shaker for approximately 2 hr., after which the joint (b) was connected to a set of 20 ml. sampling tubes. After the connecting line to stopcock (1) and the sampling tubes had been evacuated, stopcock (3) was closed. Then the seal (a) was broken by a smart turning of stopcock (1) and the gas in the flask was allowed to flow into the sampling tubes one by one. This way of sampling was suitable for checking whether or not the normal gas boiling from the liquid phase as a result of the sudden drop of pressure affected the isotopic composition of the sampled gas in the flask. The result of the analysis was that only when the pressure of gaseous boron fluoride in the flask was low was the gas sampled last in the three tubes not to be relied upon because of the dilution.

For the boron fluoride-propylene system, the sampled gas was directly analyzed by means of a mass spectrometer, for there was only a very little trace of propylene in it. On the other hand, for the boron fluoride-ethylene system it was necessary to introduce ammonia gas to produce a solid ammonia-boron fluoride complex because about a half of the sampled gas was ethylene. After the unreacted ethylene gas had been evacuated, the ammonia-boron fluoride complex was heated with sulfuric acid to regenerate the boron fluoride, which was then analyzed by means of the mass spectrometer.

The equilibrium constant was obtained from the analyzed values corrected by the m/M effect.

Our 15 cm., 60°-sector-type mass spectrometer, which was made by Mr. Hoshino in our laboratory several years ago, has recently had its electric source improved; thereby more accurate values than in the preceding investigations could be obtained.

The Measurement of the Ultraviolet Absorption Spectrum. — The ultraviolet absorption spectrum was measured on a Cary recording spectrophotometer of the 14 M type. A vessel made of quartz as shown in Fig. 2 was devised for the measurement at low temperatures. The double-wall container, A, was evacuated after the fashion of a Dewar vessel in order to obtain thermal insulation and was filled with a cooling agent, liquid nitrogen or melting carbon disulfide (−112°C). After the center tube, B, had been evacuated, the specimen was let into it through stopcock C from a gas reservoir provided and then condensed. When a large quantity of the specimen had condensed, its temperature at the bottom, B′, of the tube became slightly higher than the temperature of the cooling agent, but it remained constant. A beam of ultraviolet light was passed through B′ in a path length

4) R. Nakane and O. Kurihara, *Sci. Papers Inst. Phys. Chem. Research (Tokyo)*, **56**, 161 (1962).

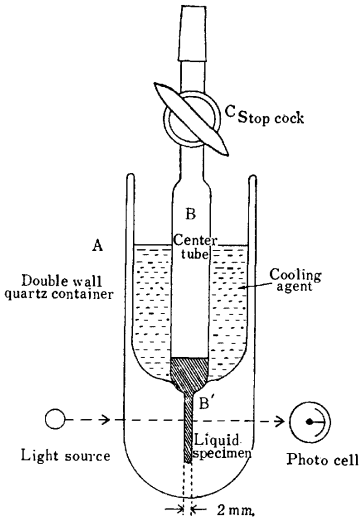

Fig. 2. Apparatus used for obtaining ultraviolet low temperature absorption spectrum.

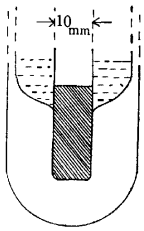

Fig. 2'

of approximately 2 mm. This transmission-type cell has the advantages that it can be used with any spectrometer and that its construction is far simpler than the cells used by Potts[5] and Reid[6]; it is also suitable for a low-temperature liquid measurement, as in the present work.

Results and Discussion

The Isotope Effect.—Results concerning the isotope effect are shown in Table I. The value of the equilibrium constant when propylene is contained in the liquid phase of a system is always larger than when the system has no propylene, but when ethylene is contained in the liquid phase, the value is the same as that of the isotopic exchange between gaseous and liquid boron fluoride, that is, the vapor pressure ratio of isotopic molecules $^{11}BF_3$ to $^{10}BF_3$. These results seem to suggest that boron fluoride forms a stable liquid complex with propylene at $-112°C$, but not with ethylene, which only dissolves into liquid boron fluoride. This is because the equilibrium constant for the isotopic exchange is

Table I. Equilibrium constant of boron isotope exchange in boron fluoride-mono-olefin system at $-112°C$

System	Mole ratio of olefin to BF_3 in the liquid phase	Vapor press. mmHg	Equilibrium constant $\left[\frac{^{10}B}{^{11}B}\right]_{liq}/\left[\frac{^{10}B}{^{11}B}\right]_{gas}$
BF_3	0	300	1.011 ± 0.002
BF_3-Ethylene	1	440	1.011 ± 0.002
BF_3-Propylene	1	170	1.018 ± 0.002
	3	120	1.018 ± 0.002
	4	75	1.018 ± 0.002

well correlated with the energy states of the molecules, especially with their vibration energies. Therefore, the fact that the equilibrium constant of the boron fluoride-ethylene system and the vapor pressure ratio of isotopic molecules have the same value shows that the dissolution of liquid ethylene into liquid boron fluoride has no appreciable effect on the vibrational energy of the molecule; in other words, the structure of boron fluoride in a liquid ethylene solution is not different from that of liquid boron fluoride itself. On the other hand, the fact that the value of the equilibrium constant of the boron fluoride-propylene system is larger than the vapor pressure ratio of isotopic molecules shows that a new molecule, the vibrational energy of which is different from that of boron fluoride, is formed, as in the case of the boron fluoride-ether complex.[7] This can be explained as follows: propylene polarizes as the result of the inductive transfer of the charge from the methyl radical to the double bond. Electron-deficient boron atoms in the boron fluoride act as very strong electron-acceptors. Hence, when boron fluoride is dissolved in liquid propylene, the charge is transferred from β-carbon atoms of propylene to boron atoms, causing the β-carbon atoms to become partially bonded covalently to boron atoms and the structure of boron fluoride molecule to become deformed to some extent from the original planar to tetrahedral. As a result, the interatomic distances between the boron atom and the three fluorine atoms of the molecules are changed, causing a change in the vibrational energy of the molecule. Thus, the results of the experiment made on the isotope effect in the present work prove that, with propylene, at low temperatures, boron fluoride can form stable complexes which are not π-complexes but σ-complexes.

Thus, in the boron fluoride-propylene system, isotopic exchange occurs between gaseous

5) W. Potts, Jr., *J. Chem. Phys.*, 23, 65 (1955).
6) C. Reid, *J. Am. Chem. Soc.*, 76, 3264 (1954).
7) A. Palko, G. Begun and L. Landau, *J. Chem. Phys.*, 37, 552 (1962).

boron fluoride and the liquid boron fluoride-propylene complex as follows:

$$^{10}BF_3(gas) + {}^{11}BF_3 \cdot C_3H_6(liq.) \overset{K}{\rightleftharpoons} {}^{11}BF_3(gas) + {}^{10}BF_3 \cdot C_3H_6(liq.)$$

where $K = 1.018 \pm 0.002$ $(-112°C)$

while in the boron fluoride-ethylene system the isotopic exchange is according to the following equation:

$$^{10}BF_3(gas) + {}^{11}BF_3(\text{in ethylene soln.}) \overset{K}{\rightleftharpoons} {}^{11}BF_3(gas) + {}^{10}BF_3(\text{in ethylene soln.})$$

where $K = 1.011 \pm 0.002$ $(-112°C)$

In a table given in the preceding paper, mention was made of the precipitation of a white solid matter when the mole ratio of boron fluoride in the liquid phase to propylene in a solution was 1:1. This precipitated material was a polymer; its amount increased with the increase of boron fluoride in the liquid phase. When, however, the materials used were sufficiently pure, the amount of the precipitate, the polymer, was not much, which facilitated the measurement of the isotope effect and of the absorption spectrum of a mole ratio 1:1 solution of the propylene-boron fluoride system.

The Absorption Spectrum. — The forming of a complex of propylene with boron fluoride can be established by the measurement of the ultraviolet absorption spectrum.

Figure 3 shows the absorption spectra of liquid propylene from 28000 cm^{-1} to 50000 cm^{-1} at the melting point temperatures of itself and of carbon disulfides.

Potts[5] examined the absorption spectra of methylated ethylenes in a rigid glass form at low temperatures and observed a weak absorption in the 40000~48000 cm^{-1} region, an absorption which he assigned to the $T \leftarrow N$ absorption ($^3B_{1u}$—$^1A_{1g}$). On the contrary, Mulliken[8] asserted that this absorption was not $T \leftarrow N$ band, but $T_R \leftarrow N$ band (state T_R is of $^3B_{3u}$ with the same electron configuration as of the R state of $^1B_{3u}$), because the above bands showed a vibrational frequency interval of about 1400 cm^{-1}, an interval which agrees well with the 1375 cm^{-1} spacing found in the $R \leftarrow N$ transition ($^1B_{3u}$—$^1A_{1g}$), whereas if it is the $T \leftarrow N$ absorption, the vibrational frequency interval should be comparable to that (about 850 cm^{-1}) of the V state.

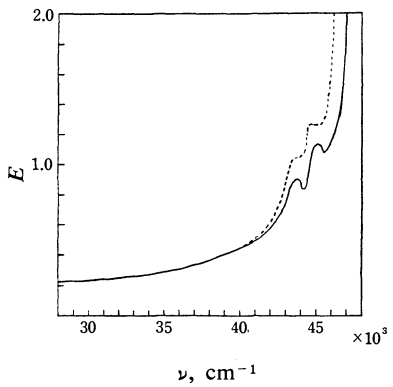

Fig. 3. Absorption spectrum of liquid propylene [solid curve, at the melting point temperature of itself; dashed curve, nearly $-112°C$].

As Fig. 3 shows, two weak absorptions of liquid propylene were found at 45000±100 cm^{-1} and 43650±100 cm^{-1} at low temperatures. The close similarity between the two positions and the vibrational frequency intervals of both the absorption bands of liquid propylene observed by the authors and those of methylated observed by the authors and those of methylethylene shown by Potts indicates that the former bands are none other than those caused by the singlet-triplet transition $T_R \leftarrow N$ ($^3B_{3u}$—$^1A_{1g}$).

When mixtures of boron fluoride with propylene (1:1) are cooled to a low temperature of about $-100°C$, a colorless liquid appears which freezes at a temperature a little higher than $-160°C$. The absorption spectra at the melting point temperatures of itself and of carbon disulfide are shown in Fig. 4. In both cases the main features are the same, and the $T_R \leftarrow N$ absorption in propylene disappeared in the 43650~45000 cm^{-1} region and did not reappear even at longer wavelengths. No blue-shift could be detected, either, for the absorption of a stronger intensity was still observed.

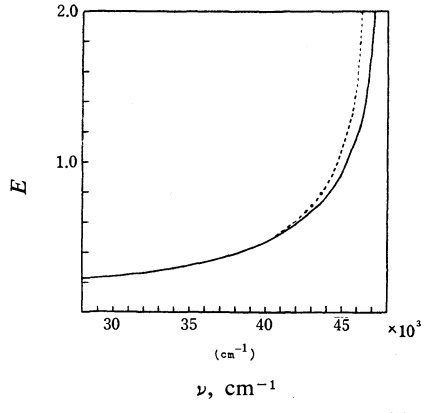

Fig. 4. Absorption spectrum of liquid boron fluorid-propylene system (1:1) [solid curve, at the melting point temperature of itself (nearly $-160°C$); dashed curve, nearly $-112°C$].

8) R. Mulliken, ibid., 33, 1596 (1960).

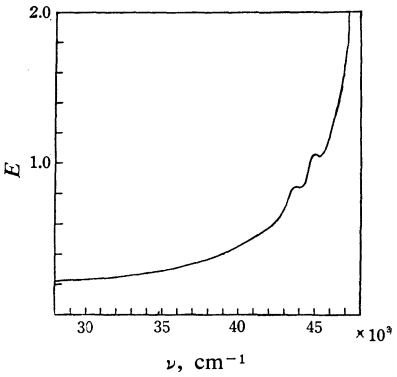

Fig. 5. Absorption spectrum of liquid propylene-propane system (1 : 1) nearly [−185°C].

For the sake of comparison, the absorption spectrum of propylene in a propane solution (1 : 1) was measured at low temperatures, but in this case the $T_R \leftarrow N$ bands of propylene were observed in their original positions, as Fig. 5 shows.

In ordinary circumstances, the Rydberg bands may be expected to become observable in the gas phase but not in liquids or in the liquid phase at low temperatures, for their large-sized orbitals will probably be strongly perturbed by closely-situated solvent molecules.[5] However, the fact that the two absorption bands in 43650 and 45000 cm^{-1} caused by the $T_R \leftarrow N$ transition are observed in liquid propylene or in its propane solution at low temperatures shows that, when the molecules are merely linked by van der Waals' force, Rydberg orbitals are not perturbed by the neighboring molecules, even in the liquid phase, and that electrons can be excited from the π-bonding orbital of the $\rangle C{=}C\langle$ bond to the Rydberg orbital. However, the disappearance of the absorption bands upon the addition of boron fluoride shows that the boron fluoride molecule, being different from the propylene and propane molecules, can closely approach the propylene molecule and strongly perturb the large-sized Rydberg orbitals of propylene molecules.

That the boron fluoride molecules can closely approach propylenes is a sure indication of the smallness of the distance between the boron atom and the β-carbon atom of propylene molecules in a liquid compared with the van der Waals' distance, which causes the formation of a molecular complex. Thus, the disappearance of the $T_R \leftarrow N$ bands of propylene upon the addition of boron fluoride can be attributed to the complex formation.

However, it is considered that the σ-complex formed is not $CH_3{-}\overset{+}{C}H{-}CH_2{-}\overset{-}{B}F_3$, which was formerly assumed to be the intermediate product in polymerization,[9] but $\overset{\delta+}{CH_3{-}CH}{=}CH_2 \rightarrow \overset{\delta-}{B}F_3$ for the $V \leftarrow N$ bands indicating the presence of a double bond were still observed.

On the other hand, in ethylene the $T_R \leftarrow N$ absorption, being obscured by the long-wavelength tail of strong $V \leftarrow N$ bands, is hardly traceable; therefore, the effect of boron fluoride upon ethylene could not be examined.

The Relation between Complex Formation and Polymerization.—Before Evans et al.[2] showed that a co-catalyst such as water is necessary for the polymerization of isobutylene by a boron fluoride catalyst, many investigators assumed hypothetically that unstable complexes are formed as intermediate products in polymerization, condensation and other reactions in which boron fluoride is used as a catalyst. Moreover, they all, including Evans, denied the existence of a stable complex of boron fluoride with mono-olefin, and this conclusion has been generally accepted since. In the present investigation, however, it was found for the first time that boron fluoride, which is a Friedel-Crafts catalyst, can form a stable liquid σ-complex with a polar mono-olefin such as propylene at low temperatures, whereas no σ-complex formation with a non-polar mono-olefin such as ethylene could be detected.

The polymerization of well-purified propylene does not proceed either at a low or at room temperature, but in the presence of a co-catalyst such as water a solid polymer at low temperatures and a liquid polymer at room temperature are produced at atmospheric pressure. Therefore, it is obvious that the formation of the σ-complex has no direct connection with the mechanism of polymerization; at low temperatures, the reaction of σ-complex formation proceeds parallel with the reaction of polymerization. On the other hand, ethylene, which is a non-polar mono-olefin, cannot form a σ-complex with boron fluoride at low temperatures and does not polymerize at atmospheric pressure, even in the presence of a co-catalyst such as water, although an oily polymer is obtained at higher pressure.[10]

Summary

The equilibrium constant of the isotopic exchange between boron fluoride gas and boron fluoride in a propylene solution at −112°C

9) C. Price and J. Ciskowski, *J. Am. Chem. Soc.*, **60**, 2499 (1938).

10) A. Topchiev, S. Zavgorodnii and Ya. Paushkin, "Boron Fluoride and its Compounds as Catalysts in Organic Chemistry," Pergamon Press, London (1959), p. 174.

has been determined by means of a shaking-type gas-liquid contactor. When the mole ratio of propylene to boron fluoride in the liquid phase was larger than 1, the value of the constant obtained was 1.018. In the boron fluoride-ethylene system, the value of the constant is equal to the vapor pressure ratio of the isotopic boron fluorides, i. e., 1.011.

In the measurement of the absorption spectrum of liquid propylene at low temperatures, two weak absorptions were observed at 43650 and 45000 cm^{-1}. They were assigned to the $T_R \leftarrow N$ transition. When boron fluoride was added to liquid propylene at low temperatures, these absorption bands disappeared, although the $V \leftarrow N$ bands were still observed.

The above findings lead to the following conclusion: boron fluoride can form stable liquid σ-complexes with polar mono-olefins such as propylene at low temperatures; these complexes are not the intermediate products in polymerization by a boron fluoride catalyst. On the other hand, ethylene, which is a non-polar mono-olefin and which does not polymerized at atmospheric pressure, cannot form a stable σ-complex with boron fluoride, even at low temperatures.

The authors wish to express their deep thanks to Dr. Shizu Tonomura for her kind advice on measuring the absorption spectra.

The Institute of Physical and Chemical Research
Bunkyo-ku, Tokyo

*Some Theoretical Considerations of Quasi-reversible and Irreversible Electrode Reactions in Oscillographic Square-wave Polarography**

By Koichi OKAMOTO

(Received March 20, 1963)

The new oscillographic polarograph reported on in a previous paper[1] is a combination of Barker's square-wave polarograph and Randles' single-sweep oscillographic polarograph in which the anodic sweep process was newly equipped in order to observe the anodic wave. By this polarograph, the a.c. polarographic wave (square-wave polarographic wave) in the cathodic process and also in the anodic process under the rapid sweeping of the applied d.c. voltage can be obtained.

The charging current, which appears in a rapid voltage sweep system, as in this oscillographic polarograph, is eliminated by the positive feed-back of the cell current to the d.c. amplifier, as has been described in the previous paper,[1] and also by the gating method proposed by Barker.[2] The a.c. polarographic wave in this polarograph, therefore, can be considered to give the faradaic current independent of the charging current.

The theoretical treatment of the reversible electrode reaction in the oscillographic square-wave polarograph has been reported on in a previous paper.[3] In this paper, some theoretical considerations of the quasi-reversible and the irreversible reactions will be presented.

I. Fundamental Equation.—The generalized equation, which represents the polarographic current, $j(t)$, in this polarograph, is expressed as Eq. 1 :[4,5]

$$\Psi(t) = (k_G f/\sqrt{D}\,)\left\{e^{-\alpha\zeta(t)} - [e^{-\alpha\zeta(t)} + e^{\beta\zeta(t)}] \times (1/\sqrt{\pi}) \int_o^t \Psi(s)\,(t-s)^{-1/2}\mathrm{d}s\right\} \quad (1)$$

where

$$\Psi(t) = j(t)/n\boldsymbol{F}q\sqrt{D_{\mathrm{ox}}}{}^{*}\boldsymbol{C}_{\mathrm{ox}} \quad (2)$$

$$\zeta(t) = (n\boldsymbol{F}/\boldsymbol{RT})\,[E(t) - \boldsymbol{E}^{r}{}_{1/2}] \quad (3)$$

$$k_G = (k_f^0)^{\beta}(k_b^0)^{\alpha}, \quad f = ({}_{\mathrm{ox}}f)^{\beta}(f_{\mathrm{red}})^{\alpha},$$

$$\sqrt{D} = (\sqrt{D_{\mathrm{ox}}})^{\beta}(\sqrt{D_{\mathrm{red}}})^{\alpha}$$

f_{ox} and f_{red}=activity coefficients of the oxidized and the reduced forms of a depolarizer;

k_f^0 and k_b^0=reaction rate of the potential

* Oscillographic Square-Wave Polarography. Part V.

1) Y. Saitō and K. Okamoto, *Rev. Polarography*, **10**, 227 (1962).

2) G. C. Barker, *Anal. Chim. Acta*, **18**, 118 (1958).

3) K. Okamoto, *Rev. Polarography*, in press.

4) H. Matsuda, *Z. Elektrochem.*, **59**, 494 (1955).

5) H. Matsuda, ibid., **62**, 977 (1958).

determinig process of the oxidation and the reduction of a depolarizer under the normal hydrogen potential;

α and β=transfer coefficients ($\alpha+\beta=1$);

E=electrode potential vs. hydrogen electrode;

$E(t)$=applied potential expressed as a function of time and

$E^{r}_{1/2}$=reversible half-wave potential.

The $\Psi(t)$ function can be expanded into the power series of $(nF/RT)\Delta E$.[4] The first term in the series gives the d.c. component of the electrode current and is expressed as Eq. 4 for the cathodic wave and as Eq. 6 for the anodic wave. The second term gives the a.c. component and is expressed as Eq. 5 for the cathodic and as Eq. 7 for the anodic.

The cathodic waves, in which the electrode potential is given by $E(t)=E_o-vt-\Delta E\,V(t/\Theta)$, are expressed as Eqs. 4 and 5:[4,5]

D.c. component:

$$j^{c}_{0}(t)/nFq\sqrt{D_{ox}}{}^{*}C_{ox}=\Psi^{c}_{0}(t)=\lambda\left\{(1+e^{\xi})^{-1}-(1/\sqrt{\pi})\int_{0}^{t}\Psi^{c}_{0}(s)(t-s)^{-1/2}ds\right\} \quad (4)$$

A.c. component:

$$j^{c}_{1}(t)/nFq\sqrt{D_{ox}}{}^{*}C_{ox}=\Psi^{c}_{1}(t)=\lambda\left\{F^{c}(\xi;\lambda)V(t/\Theta)-(1/\sqrt{\pi})\int_{0}^{t}\Psi^{c}_{1}(s)(t-s)^{-1/2}ds\right\} \quad (5)$$

The anodic waves, where $E(t)=E_1+vt-\Delta E\times V(t/\Theta)$, are expressed as Eqs. 6 and 7:[3-5]

D.c. component:

$$j^{a}_{0}(t)/nFq\sqrt{D_{red}}{}^{*}C_{red}=\Psi^{a}_{0}(t)=\lambda\left\{(1+e^{\xi})^{-1}-\left[(1/\sqrt{\pi})\int_{0}^{\theta}\Psi^{c}_{0}(s)(t-s)^{-1/2}ds+(1/\sqrt{\pi})\int_{\theta}^{t}\Psi^{a}_{0}(s)(t-s)^{-1/2}ds\right]\right\} \quad (6)$$

A.c. component:

$$j^{a}_{1}(t)/nFq\sqrt{D_{red}}{}^{*}C_{red}=\Psi^{a}_{1}(t)=\lambda\left\{F^{a}(\xi;\lambda)V(t/\Theta)-\left[(1/\sqrt{\pi})\int_{0}^{\theta}\Psi^{c}_{1}(s)(t-s)^{-1/2}ds+(1/\sqrt{\pi})\int_{\theta}^{t}\Psi^{a}_{1}(s)(t-s)^{-1/2}ds\right]\right\} \quad (7)$$

where

$$\zeta(t)=(nF/RT)[E(t)-E^{r}_{1/2}] \quad (8)$$

$$\lambda=(k_G f/\sqrt{D})(e^{-\alpha\xi}+e^{\beta\xi}) \quad (9)$$

$$F^{c}(\xi;\lambda)=[4\cosh^{2}(\xi/2)]^{-1}+(\alpha-\beta e^{-\xi})[\lambda(1+e^{-\xi})]^{-1}\Psi^{c}_{0}(t) \quad (10)$$

$$F^{a}(\xi;\lambda)=[4\cosh^{2}(-\xi/2)]^{-1}+(\beta-\alpha e^{\xi})[\lambda(1+e^{\xi})]^{-1}\Psi^{c}_{0}(t) \quad (11)$$

$\xi=(nF/RT)vt-\zeta_o$ for Eqs. 4, 5, 9 and 10

$\xi=(nF/RT)v(t-\theta)+\zeta_1$, for Eqs. 6, 7, 9 and 11 (11')

Other variables and constants are used with the same meaning as in the previous paper.[3]

II. Quasi-Reversible Case.—In quasi-reversible reactions, no simplification of Eqs. 10 and 11 can be made. The calculation of the a.c. component, therefore, must be started from the calculation of the d.c. component.

The mathematical procedures for calculating the d.c. component in the cathodic process, $\Psi^{c}_{0}(t)$, under the projected conditions, such as $\alpha=0.3$, 0.5 and 0.7 and $\Lambda=10$, 1, 10^{-1} and 10^{-2} (see Eq. 12), have already been shown by Matsuda.[4] For this paper, the numerical calculations of $\Psi^{c}_{0}(t)$ were carried out by means of the electronic computer, and then the following calculation of the a.c. component $\Psi^{c}_{1}(t)$ in a cathodic process was made using the d.c. component obtained.

1. Cathodic Process.—i) D.C. Component.— The quasi-reversible case[4] can be defined as $15\geqq\Lambda\geqq 10^{-2(1+\alpha)}$. In this case, Eq. 4 can be numerically dissolved by the same mathematical procedures as were used by Matsuda.[4] The results are shown in Figs. 1-a, b and c. The $\Psi^{c}_{0}(-\xi)$ and ξ-values at the summit point of each curve are summarized in Table I.

ii) A.C. Component.—In order to calculate the a.c. component using the d.c. components shown in Fig. 1, Eqs. 9 and 10 are transformed into Eqs. 12 and 13;

$$\Lambda=(k_G f/\sqrt{D})(nFv/RT)^{-1/2} \quad (12)$$

$$\Psi(t)=(nFv/RT)^{1/2}\Psi(\xi) \quad (13)$$

They can be rewritten to Eqs. 14 and 15:

$$\lambda=\Lambda(nFv/RT)^{1/2}(e^{-\alpha\xi}+e^{\beta\xi}) \quad (14)$$

$$F^{c}(\xi;\lambda)=[4\cosh^{2}(\xi/2)]^{-1}+(\alpha-\beta e^{-\xi})\times(1+e^{-\xi})^{-1}(e^{-\alpha\xi}+e^{\beta\xi})^{-1}\Lambda^{-1}\Psi^{c}_{0}(\xi) \quad (15)$$

On the other hand, as has already been shown by Matsuda,[4] by applying Fourier's expansion method, Eq. 5 may be expressed as Eq. 16:

$$j^{c}(\xi)=nFqD_{ox}{}^{1/2}{}^{*}C_{ox}(nF\Delta E/RT)\times\Theta^{-1/2}F^{c}(\xi;\lambda)\,\psi_{sq}(t/\Theta;\lambda\sqrt{\Theta/2\pi}) \quad (16)$$

where ψ_{sq} is the same function as in a previous work;[3] it is graphically shown in Fig. 2.

The theoretical equation of a.c. polarograms, $j^{c}(-\xi)$, are shown in Figs. 3-a, b and

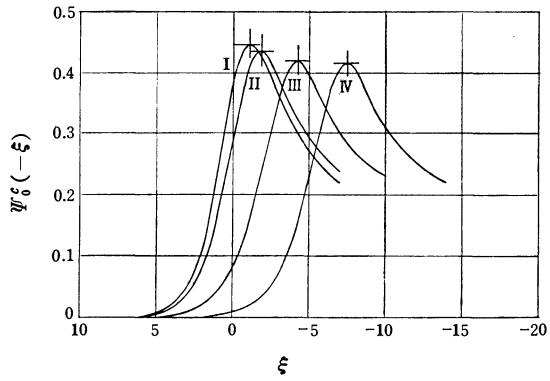

Fig. 1-a. $\alpha=0.7$.

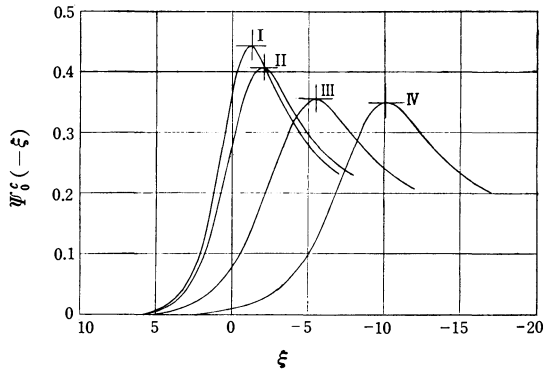

Fig. 1-b. $\alpha=0.5$.

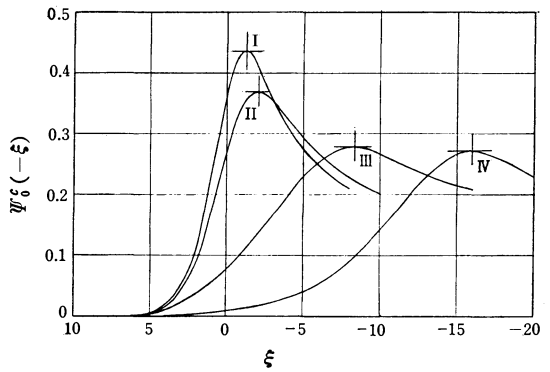

Fig. 1-c. $\Psi_0^c(-\xi)\sim\xi$ Relation (quasi-reversible) $\alpha=0.3$. I: $\Lambda=10^1$, II: $\Lambda=10^0$, III: $\Lambda=10^{-1}$, IV: $\Lambda=10^{-2}$.

c, where the following numerical values are adopted: $n=2$, $q=2\times10^{-2}$cm^2, $D_{ox}=10^{-5}$cm$^2\cdot$sec^{-1}, $\Delta E=5$ mV., $^*C_{ox}=5\times10^{-4}$mol./l., $\Theta=1.667\times10^{-4}$sec., $T=25°$C, $\alpha=0.3$, 0.5 and 0.7, and $\Lambda=10^1$, 10^0, 10^{-1} and 10^{-2}. The summit current values, $(j_s)_{quasi}$, the summit potential values, $(\xi_s)_{quasi}$, and the half-width values, $(\xi_{s/2})_{quasi}$, are summarized in Table II. These values can be expressed as Eqs. 17, 17', 18 and 19:

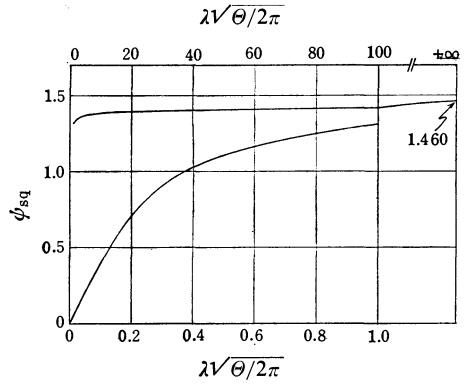

Fig. 2. The relation between ψ_{sq} ($t/\Theta=0.9$ and 1.9; $\lambda\sqrt{\Theta/2\pi}$) and $\lambda\sqrt{\Theta/2\pi}$.

$$(j_s)_{quasi}=K(\Lambda,\alpha)(j_s)_{rev} \tag{17}$$

$$K(\Lambda,\alpha)=[F(\xi;\lambda)\times\psi_{sq}(t/\Theta;\lambda\sqrt{\Theta/2\pi})]_{quasi}/0.365 \tag{17'}$$

$$(\xi_s)_{quasi}=(\xi_s)_{rev}-\Xi(\Lambda,\alpha) \tag{18}$$

$$(\xi_{s/2})_{quasi}=\Delta(\Lambda,\alpha)(\xi_{s/2})_{rev} \tag{19}$$

where

$(j_s)_{rev}=67.15\ \mu$amp

$(\xi_s)_{rev}=0$

$(\xi_{s/2})_{rev}=3.6_0$

The $K(\Lambda,\alpha)$, $\Xi(\Lambda,\alpha)$ and $\Delta(\Lambda,\alpha)$ functions are shown in Figs. 4, 5 and 6. The relation of $(j_s)_{quasi}$ and $(\xi_s)_{quasi}$ of the a.c. waves to $(i_s)_{quasi}$ and $(\xi_s)^{DC}_{quasi}$ of the d.c. waves are also listed in Table II in the form of $(j_s)_{quasi}/(i_s)_{quasi}$ and $(\xi_s)^{DC}_{quasi}-(\xi_s)_{quasi}$.

2. Anodic Process. — The d.c. component $\Psi_0^a(-\xi)$, and the a.c. component, $\Psi_1^a(-\xi)$, can be obtained by Eqs. 6 and 7, but the

Table I. The summit potential and current of the d.c. wave (quasi-reversible)

α	Λ	$(\xi_s)^{DC}_{quasi}$	$\Psi_0^c(\xi)$	$(i_s)_{quasi}$*
0.7	10^1	− 1.1	0.445	47.9μamp.
	10^0	− 1.9	0.435	46.9
	10^{-1}	− 4.3	0.418	45.0
	10^{-2}	− 7.5	0.415	44.7
0.5	10^1	− 1.3	0.441	47.5
	10^0	− 2.1	0.407	43.8
	10^{-1}	− 5.5	0.356	38.3
	10^{-2}	−10.1	0.350	37.7
0.3	10^1	− 1.3	0.436	46.9
	10^0	− 2.1	0.369	39.7
	10^{-1}	− 8.3	0.278	29.9
	10^{-2}	−15.9	0.271	29.2

* $(i_s)_{quasi}$ was calculated by the equation: $(i_s)_{quasi}=n\boldsymbol{F}q\ D_{ox}^{1/2*}\ C_{ox}(n\boldsymbol{F}v/\boldsymbol{R}T)^{1/2}\Psi_0^c(\xi)$ where, $v=4$ V./sec. and other constants were shown in the section II-1-ii.

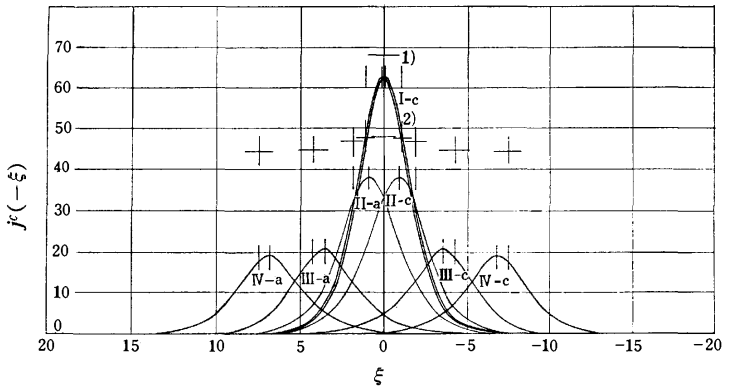

Fig. 3-a. $\alpha=0.7$.

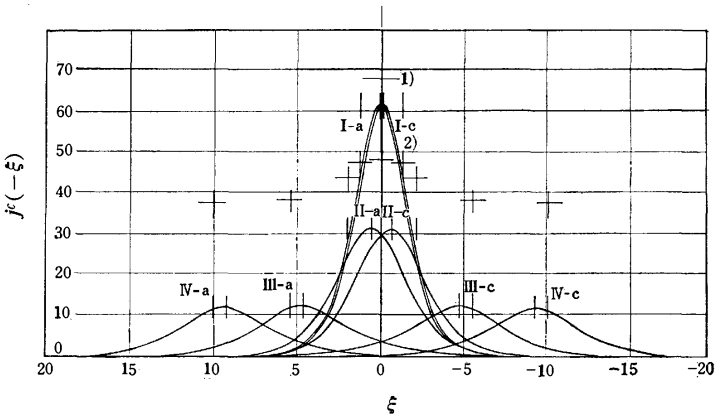

Fig. 3-b. $\alpha=0.5$.

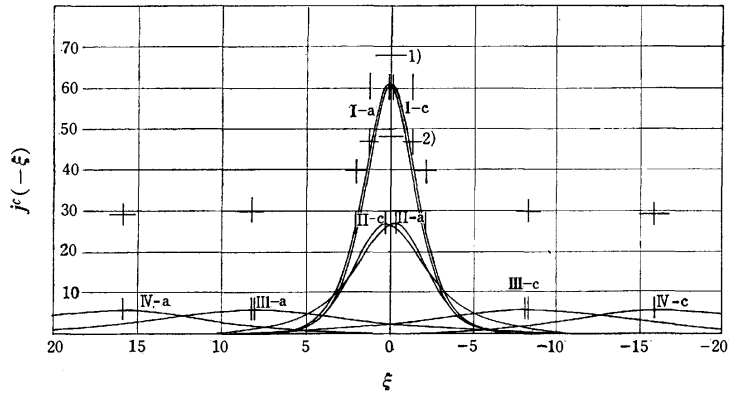

Fig. 3-c. $\alpha=0.3$.

$j^c(-\xi)\sim\xi$ Relation (quasi-reversible).
I: $\Lambda=10^1$, II: $\Lambda=10^0$, III: $\Lambda=10^{-1}$, IV: $\Lambda=10^{-2}$. −c: cathodic, −a: anodic.

1) The summit current of reversible a.c. wave.
2) The summit point of quasi-reversible d.c. wave.

integrations in these equations can not be carried out, because the $\Psi_0^c(-\xi)$ values can not be virtually calculated up to the ξ-value of $-\infty$.

In the reversible case, an approximation technique was employed[3] in order to obtain the effect of the change of the turning point of the sweeping d.c. voltage. Namely, when the d.c. voltage is swept to the ξ-value of $-\infty$, the influence from a prior cathodic

TABLE II. THE SUMMIT POTENTIAL AND CURRENT, AND THE HALF-WIDTH OF THE A. C. WAVE (QUASI-REVERSIBLE)

α	Λ	$(j_s)_{quasi}$	$(\xi_s)_{quasi}$	$(\xi_{s/2})_{quasi}$	$\frac{(j_r)_{quasi}^*}{(i_s)_{quasi}}$	$(\xi_s)_{quasi}^{DC}-(\xi_s)_{quasi}$
0.7	10^1	62.6_4	− 0.1	3.6_0	1.30_7	1.0
	10^0	38.0_6	− 0.9	4.1_0	0.81_1	1.0
	10^{-1}	20.8_8	− 3.5	4.2_0	0.46_4	0.8
	10^{-2}	19.1_6	− 6.7	4.2_5	0.42_9	0.8
0.5	10^1	61.6_7	− 0.1	3.6_0	1.29_5	1.2
	10^0	31.1_5	− 0.5	4.9_0	0.71_1	1.6
	10^{-1}	12.4_3	− 4.7	6.2_0	0.32_4	0.8
	10^{-2}	11.8_3	− 9.3	6.2_5	0.31_3	0.8
0.3	10^1	60.7_4	− 0.1	3.6_5	1.29_3	1.2
	10^0	26.8_0	+ 0.3	5.1_0	0.67_4	2.4
	10^{-1}	5.8_2	− 8.1	13.6_0	0.19_4	0.2
	10^{-2}	5.6_6	−15.9	13.8_0	0.19_3	0.0

* Refer to the Table I.

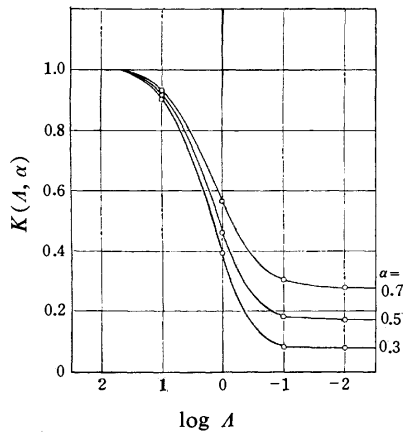

Fig. 4. $K(\Lambda, \alpha)\sim\log \Lambda, \alpha$ relation.

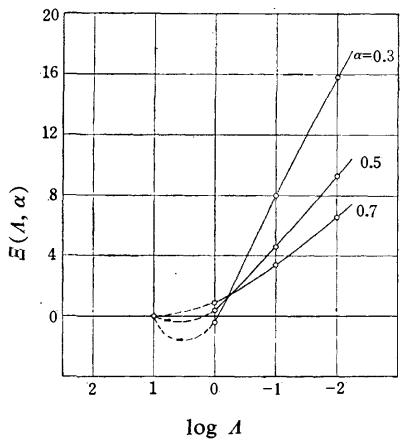

Fig. 5. $\Xi(\Lambda, \alpha)\sim\log \Lambda, \alpha$ relation.

sweep upon the following anodic sweep is negligible. For this reason, the anodic waves having a form symmetrical to the corresponding cathodic waves were employed for calculating both the d. c. and a. c. anodic components. The d. c. anodic waves, therefore, have the forms symmetrical to the cathodic waves with respect to the zero point (see Figs. 1-a, b and c).

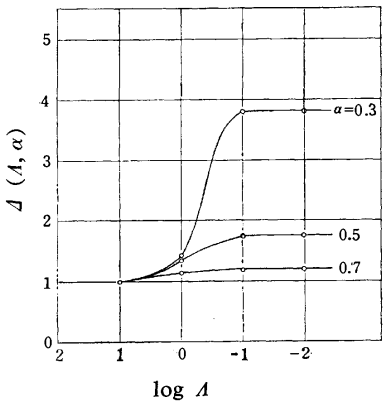

Fig. 6. $\Delta(\Lambda, \alpha)\sim\log \Lambda, \alpha$ relation.

TABLE III. THE SUMMIT POTENTIALS AND THE SUMMIT CURRENTS OF THE D. C. WAVES (irreversible)

Sweep process	$\xi_0^*-\xi_1^*$	$\frac{-\xi_1^*}{\xi_0^*-\xi_1^*}$	$(\xi_s^*)_{irr}^{DC}$	$\Psi_0(\xi^*)_{irr}$
Cathodic	—	—	−0.78	+0.496
Anodic	20	1/4	+0.9	−0.324
	20	1/2	+0.9	−0.372
	40	1/2	+0.7	−0.407
	80	1/2	+0.7	−0.433

The a. c. anodic waves are expressed as Eq. 20 and are shown in Figs. 3-a, b and c:

$$j^a(\xi)=nFqD_{red}^{1/2}\ {}^*C_{red}(nF\Delta E/RT)\times\Theta^{-1/2}F^a(\xi\,;\lambda)\phi_{sq}(t/\Theta\,;\lambda\sqrt{\Theta/2\pi}) \quad (20)$$

where λ and $F^a(\xi\,;\lambda)$ are given by Eqs. 9 and 11 respectively. The relations between the summit potentials, the summit currents, the half-width and $\ln\Lambda$ and α, and between the

summit potentials of a. c. and of d. c. waves are also the same to those of the cathodic waves (see Table II).

III. Irreversible Case.—*1. Cathodic Process.*—*i) D. C. Component.* — The irreversible case is defined by the condition: $\xi \geqq 4.6$ or $e^{-\xi} \leqq 10^{-2}$, as has already been indicated by Matsuda.[5] Eqnations. 10 and 9 are, therefore, simplified to Eqs. 21 and 22 respectively:

$$F^c(\xi\,;\lambda) = (k_G f/\sqrt{D})\,\alpha\lambda\Psi_0^c(t) \tag{21}$$

and

$$\lambda = (k_G f/\sqrt{D})\,e^{-\alpha\xi} \tag{22}$$

Eq. 4 is also changed to Eq. 23:

$$\Psi_0^c(\xi) = (k_G f/\sqrt{D})\,(nFv/RT)^{-1/2} e^{\alpha\xi} \times \left\{1-(1/\sqrt{\pi})\int_{-\zeta}^{\xi}\Psi_0^c(\eta)\,(\xi-\eta)^{-1/2}\mathrm{d}\eta\right\} \tag{23}$$

In order to eliminate the $(k_G f/\sqrt{D})\,(nFv/RT)^{-1/2}$ term, the transformation as Eqs. 24-a, b and c, Eq. 12 and Eq. 25 are introduced into Eq. 23:

$$\alpha\xi = \xi^* - \ln \Lambda^* \tag{24-a}$$

$$\alpha\eta = \eta^* - \ln \Lambda^* \tag{24-b}$$

$$\Lambda/\sqrt{\alpha} = \Lambda^* \tag{24-c}$$

$$\Psi(\xi)/\sqrt{\alpha} = \Psi_{\mathrm{irr}}(\xi^*) \tag{25}$$

Eq. 26 is then derived:

$$e^{-\xi^*}\Psi_{\mathrm{irr}}(\xi^*) = 1-(1/\sqrt{\pi}) \times \int_{-\alpha\zeta+\ln\Lambda^*}^{\xi^*}\Psi_{\mathrm{irr}}(\eta^*)\,(\xi^*-\eta^*)^{-1/2}\mathrm{d}\eta^* \tag{26}$$

This equation can be dissolved by the numerical integration, as has been shown by Matsuda;[4] the $\Psi_{\mathrm{irr}}(-\xi^*)\sim\xi^*$ curve calculated (again by the author) is shown in Fig. 7-a, while the values at their summit points are listed in Table III.

ii) A. C. Component.—By the use of Fourier's expansion technique in the same manner as Matsuda,[5] Eq. 5 is changed to Eq. 27:

$$j_1^c(\xi) = nFq\ D_{\mathrm{ox}}^{1/2}\,{}^*C_{\mathrm{ox}}(\alpha nF\Delta E/RT) \times \Theta^{-1/2}(nFv/RT)^{1/2}\psi_0^c(\xi)\,(k_G f/\sqrt{D})^{-1}e^{-\alpha\xi} \times \psi_{\mathrm{sq}}(t/\Theta\,;\ (k_G f/\sqrt{D})\,e^{\alpha\xi}\sqrt{\Theta/2\pi}) \tag{27}$$

The final equation, 28, is obtained by introducing Eqs. 24—25 and 12 into Eq. 27; i. e.,

$$j_{\mathrm{irr}}^c(\xi^*) = nFq\ D_{\mathrm{ox}}^{1/2}\,{}^*C_{\mathrm{ox}}(\alpha nF\Delta E/RT) \times \Theta^{-1/2}e^{-\xi}\Psi_0^c(-\xi^*)\psi_{\mathrm{sq}}(t/\Theta\,;\ (\alpha nFv/RT)^{1/2} \times (\Theta/2\pi)^{1/2}e^{\xi^*}) \tag{28}$$

where $\Psi_0^c(-\xi^*)$ is the d. c. component already described in Section III-1-i, while the values of $\psi_{\mathrm{sq}}(t/\Theta\,;\ (\alpha nFv/RT)^{1/2}(\Theta/2\pi)^{1/2}e^{\xi^*})$ can be

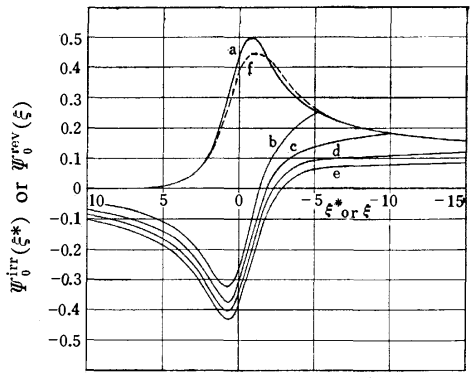

Fig. 7. The relation between $\Psi_0^{\mathrm{irr}}(\xi^*)$ and ξ^* (irreversible).

a : cathodic
b : anodic. $\xi_0^*-\xi_1^*=20$, $-\xi_1^*/(\xi_0^*-\xi_1^*)=1/4$
c : anodic. $\xi_0^*-\xi_1^*=20$, $-\xi_1^*/(\xi_0^*-\xi_1^*)=1/2$
d : anodic. $\xi_0^*-\xi_1^*=40$, $-\xi_1^*/(\xi_0^*-\xi_1^*)=1/2$
e : anodic. $\xi_0^*-\xi_1^*=80$, $-\xi_1^*/(\xi_0^*-\xi_1^*)=1/2$
f : $\Psi_0^{\mathrm{rev}}(\xi)\sim\xi$ (reversible)

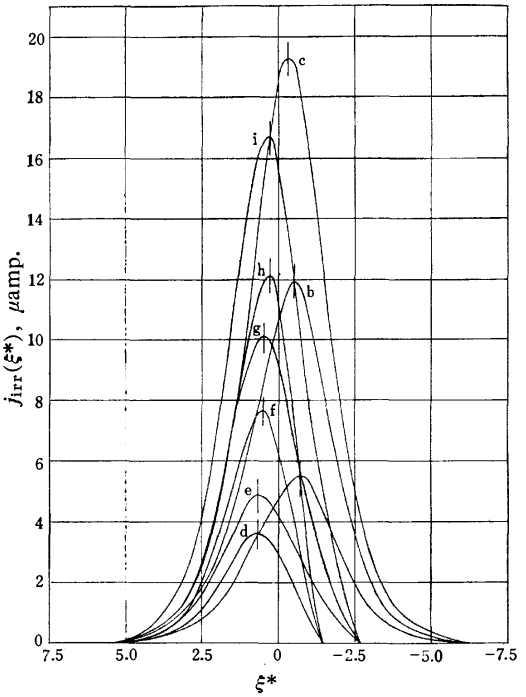

Fig. 8. The relation between $j_{\mathrm{irr}}(\xi^*)$ and ξ^* (irreversible)

a cathodic : $\alpha=0.3$.
b cathodic : $\alpha=0.5$.
c cathodic : $\alpha=0.7$.
d anodic : $\beta=0.3$, $\xi_0^*-\xi_1^*=20$, $-\xi_1^*/(\xi_0^*-\xi_1^*)=1/4$
e anodic : $\beta=0.3$, $\xi_0^*-\xi_1^*=80$, $-\xi_1^*/(\xi_0^*-\xi_1^*)=1/2$
f anodic : $\beta=0.5$, $\xi_0^*-\xi_1^*=20$, $-\xi_1^*/(\xi_0^*-\xi_1^*)=1/4$
g anodic : $\beta=0.5$, $\xi_0^*-\xi_1^*=80$, $-\xi_1^*/(\xi_0^*-\xi_1^*)=1/2$
h anodic : $\beta=0.7$, $\xi_0^*-\xi_1^*=20$, $-\xi_1^*/(\xi_0^*-\xi_1^*)=1/4$
i anodic : $\beta=0.7$, $\xi_0^*-\xi_1^*=80$, $-\xi_1^*/(\xi_0^*-\xi_1^*)=1/2$

TABLE IV. THE SUMMIT POTENTIALS AND CURRENTS, AND THE HALF-WIDTH VALUES OF THE A. C. WAVES (IRREVERSIBLE)

Sweep process	Transfer coefficient	$\xi_0^*-\xi_1^*$	$\frac{-\xi_1^*}{\xi_0^*-\xi_1^*}$	$(\xi_s^*)_{irr}$	$(\xi_{s/2}^*)_{irr}$	$(j_s)_{irr}$ (μ amp.)	$\frac{(j_s)_{irr}^*}{(i_s)_{irr}}$
Cathodic	$\alpha=0.7$	–	–	-0.3	2.9_5	19.3	0.43
	$\alpha=0.5$	–	–	-0.5	3.0_5	12.0	0.31
	$\alpha=0.3$	–	–	-0.7	3.2_0	5.6	0.19
Anodic	$\beta=0.7$	20	1/4	$+0.3$	2.4_5	12.1	0.42
		80	1/2	$+0.3$	2.8_0	16.7	0.42
	$\beta=0.5$	20	1/4	$+0.5$	2.5_0	7.7	0.31
		80	1/2	$+0.5$	2.8_5	10.5	0.31
	$\beta=0.3$	20	1/4	$+0.7$	2.5_5	3.7	0.19
		80	1/2	$+0.7$	2.9_5	4.9	0.19

* $(i_s)_{irr}$ Values were calculated by the equations:
$(i_s)^c_{irr}=n\boldsymbol{F}qD_{ox}^{1/2}*C_{ox}\ (\alpha n\boldsymbol{F}v/\boldsymbol{RT})^{1/2}\ \Psi_0^c(\xi^*)_{irr}$ for the cathodic wave.
$(i_s)^a_{irr}=-n\boldsymbol{F}qD_{red}^{1/2}*C_{red}(\beta n\boldsymbol{F}v/\boldsymbol{RT})^{1/2}\ \Psi_0^a(\xi^*)_{irr}$ for the anodic wave.
where, n, $\boldsymbol{F}$, q, $D^{1/2}{}_{ox(or\ red)}$, $*C_{ox(or\ red)}$ and T are the same to these in the section II-1-ii, and $v=4$ V. sec^{-1}.

obtained from the $\Psi_{sq}\sim\lambda\sqrt{\Theta/2\pi}$ curve shown in Fig. 2.

Theoretical a. c. polarograms, $j^c_{irr}(\xi^*)$, taken under the same conditions as in Section II-1-ii, except the values of Λ, are shown in Fig. 8. The irreversible polarogram is very much affected by the magnitude of the transfer coefficient, and the wave height becomes very much lower than the reversible case. The variations of the summit potentials, $(\xi_s^*)_{irr}$, the half- widths, $(\xi_{s/2}^*)_{irr}$, the summit currents, $(j_s)_{irr}$, and the ratios to the d. c. summit currents, $(j_s)_{irr}/(i_s)_{irr}$, obtained from Fig. 8 are summarized in Table IV.

2. Anodic Process.—i) D. C. Component.—The second term in Eq. 6 is equivalent to Eq. 4. The first term, designated by $\Psi_0^1(\xi)$, can, on the other hand, be calculated in the following manner: when the variables, t and s, are transformed as Eqs. 11′ and 29,

$$\eta=\zeta_1-n\boldsymbol{F}v(s-\theta)/\boldsymbol{RT} \tag{29}$$

where

$$\zeta_1=(n\boldsymbol{F}/\boldsymbol{RT})(E_1-E^r{}_{1/2})$$

$\Psi_0^1(\xi)$ is expressed as Eq. 30:

$$\Psi_1^0(\xi)=(k_Gf/\sqrt{D})(n\boldsymbol{F}v/\boldsymbol{RT})^{-1/2}e^{\beta\xi}(1/\sqrt{\pi})\times\int_{\zeta_1}^{\zeta_0}\Psi^c(\eta)(\xi+\eta-2\zeta_1)^{-1/2}\mathrm{d}\eta \tag{30}$$

Further transformation of this equation by the use of Eqs. 31-a, b, c, and d, and Eq. 12 leads to a simpler equation, 32:

$$\beta\xi=\xi^*-\ln\Lambda^* \tag{31-a}$$
$$\beta\eta=\eta^*-\ln\Lambda^* \tag{31-b}$$
$$\Lambda/\sqrt{\beta}=\Lambda^* \tag{31-c}$$
$$\Psi(\xi)/\sqrt{\beta}=\Psi_{irr}(\xi^*) \tag{31-d}$$

$$\Psi^1_{irr}(\xi^*)=(1/\sqrt{\pi})\int_{\beta\zeta_1+\ln\Lambda^*}^{\beta\zeta_0+\ln\Lambda^*}\Psi^c_{irr}(\eta^*)\times[\xi^*+\eta^*-2(\beta\zeta_1+\ln\Lambda^*)]^{-1/2}\mathrm{d}\eta^* \tag{32}$$

When the sweeping range of the d. c. voltage is as wide as $\zeta_0\gg10$ and $\zeta_1\ll-10$, Eq. 32 may be approximately expressed by Eq. 33:

$$\Psi^1_{irr}(\xi^*)=(1/\sqrt{\pi})\times\int_{-\infty}^{\infty}\Psi^c_{irr}(\eta^*)(\xi^*+\eta^*-2\xi_1^*)^{-1/2}\mathrm{d}\eta^* \tag{33}$$

where

$$\xi_1^*=\beta\zeta_1+\ln\Lambda^*$$

The $\Psi^c_{irr}(\eta^*)$ function has a maximum value of $\eta^*=0.78$ as Fig. 7-a shows. Therefore, the approximation method used in a previous paper[3] is applied to Eq. 33 under the assumption that the $\Psi^c_{irr}(\eta^*)$ reaches a maximum at $\eta^*=0$; therefore, Eq. 34 can be obtained:

$$\Psi^1_{irr}(\xi^*)\fallingdotseq(1/\sqrt{\pi})(\xi^*-2\xi_1^*)^{-1/2}\times\int_{-\infty}^{\infty}\Psi^c_{irr}(\eta^*)\mathrm{d}\eta^* \tag{34}$$

Since the integral term in Eq. 34 cannot be virtually calculated, the following approximation method is employed. When the $\Psi^c_{rev}(\xi)$ function for the revesible case and $\Psi^c_{irr}(\xi^*)$ for the irreversible case are compared with each other, as in Fig. 7, the arease within ξ or $\xi^-=7\sim-10$ are found to be almost equivalent. Moreover, since the more negative the ξ or ξ^* values, the more reversible the electrode reactions, the integral value of $\Psi^c_{irr}(\xi^*)$ more and more approaches that of $\Psi^c_{rev}(\xi)$ with increasing negative shift of ξ or ξ^*-values. For these reasons, the integral value

of $\Psi^c_{irr}(\xi^*)$ can be considered to be the equivalent to that of $\Psi^c_{rev}(\xi)$ for all ξ or ξ^* values. The integral value in Eq. 33, may, therefore, be approximated by Eq. 35 in a manner similar to the reversible case:[3]

$$\int_{-\infty}^{\infty}\Psi^c_{irr}(\eta^*)d\eta^* \fallingdotseq \int_{-\infty}^{\infty}[\cosh^2(\eta/2)]^{-1}d\eta=4 \quad (35)$$

The d.c. component in an irreversible anodic electrode reaction can be finally expressed as Eq. 36:

$$\Psi^a_{irr}(\xi^*)=(1/\sqrt{\pi})(\xi^*_0-\xi^*_1)^{-1/2}[\xi^*/(\xi_0^*-\xi_1^*)-2\xi_1^*/(\xi_0^*-\xi_1^*)]^{-1/2}-\Psi^c_{irr}(\xi^*) \quad (36)$$

where

$$\xi_0^*=\beta\zeta_0+\ln \Lambda^*$$

The relations between $\Psi^a_{irr}(\xi^*)$ and ξ^* for some ξ_0^* and ξ_1^* values are shown in Figs. 7-b, c, d and e. The values at their summit points are listed in Table III.

ii) A. C. Component.—The first integral term in Eq. 7, which represents the influence of a cathodic sweep upon an anodic process, can be neglected for the same reason as that adapted in the reversible case.[3] The generalized equation can, therefore, be shown as Eq. 37:

$$\Psi^a_1(t)=\lambda\left\{F(\xi;\lambda)V(t/\Theta)-(1/\sqrt{\pi})\times\int_{\Theta}^{t}\Psi^a_1(s)(t-s)^{-1/2}ds\right\} \quad (37)$$

The final equation, 38, which expresses the theoretical a.c. polarographic wave in the anodic process, can be obtained by means of the same mathematical technique as that in Section III-1-ii:

$$j^a_1(\xi^*)=nFqD_{red}^{1/2}{}^*C_{red}(\beta nF\Delta E/RT)\times\Theta^{-1/2}e^{-\xi^*}\Psi^a_0(\xi^*)\psi_{sq}(t/\Theta;\beta nFv/RT)^{1/2}\times(\Theta/2\pi)^{1/2}e^{\xi^*} \quad (38)$$

where $\Psi^a_0(\xi^*)$ is the d.c. component in the range of $\Psi^a_0(\xi^*)\leqq 0$, which was already obtained in Section III-2-i and which is also shown in Figs. 7-b. c. d. and e.

Some of the theoretical polarograms calculated by Eq. 38 under the same conditions as in Section II-1-ii, but in this case using β, D_{red} and C_{red} instead of α, D_{ox} and C_{ox} respectively, are shown in Figs. 8-d—i.

The variations of the summit potentials, $(\xi_s^*)_{irr}$, the half-widths, $(\xi_{s/2}^*)_{irr}$, the summit currents, $(j_s)_{irr}$ and the ratios to the d.c. summit currennts, $(j_s)_{irr}/(i_s)_{irr}$ with the vallues of β and the turning potentials are summarized in Table IV.

As is shown in Fig. 8, the summit potential of the irreversible anodic wave is more positive than that of the cathodic waves. Their wave heights are lower than the cathodic waves because of the influence of the turning point of applied d.c. voltage, and they are affected by the values of the transfer coefficient β.

The asymmetric forms of the anodic a.c. waves such as Figs. 8-d-i, are due to the insufficiently negative value of the turning point of the d.c. applied voltage. If the turning point is selected at the infinite negative value, a symmetric wave may be otained.

IV. Discussion.—The polarographic wave of the quasi-reversible reaction in the author's polarograph is very much influenced by the magnitude of the reaction rate constant and by the transfer coefficient in a manner almost identical with that of the conventional a.c. polarograph.

The summit current, $(j_s)_{quasi}$, decreases with the decrease in the Λ-values and also with that in the α-values, as is shown in Fig. 4. The transition range in the said figure corresponds to the quasi-reversible region, and the decrement of $K(\Lambda, a)$ in this region is comparatively larger than that of the same function for Randles' single sweep polarograph reported by Matsuda.[4] The summit potential, $(\xi_s)_{quasi}$, changes with the changes in the α- and Λ-values in rather a complicated way, as Fig. 5 shows. This relation is not equivalent to that of Randles' polarograph. When the reaction rate, $\Lambda(=(k_af/\sqrt{D})(nFv/RT)^{-1/2})$, is in the range of $10^1\sim10^0$, and also when the transfer coefficient, α, is as small as 0.3, the the summit potential tends to shift to the potentials more positive than that of the reversible wave, $[(\xi_s)_{rev}=0]$. This interesting result is also observed in the conventional a.c. polarographic wave.[5] The value of the half-width, $(\xi_{s/2})_{quasi}$, also changes with the α- and Λ-values, as Fig. 6 shows. The smaller the values of the transfer coefficient and of the reaction rate, the broader the wave. This relation is most predominant in the case of a transfer coefficient with a small value, e.g., $\alpha=0.3$. The summit currents of a.c. waves at $\Lambda=10^1$ are larger than those of d.c. waves independently of the values of α, as is shown in Table II, and they decrease rather remarkably in a manner similar to that of $K(\Lambda, \alpha)$ in Fig. 4.

The $(\xi_s)_{quasi}$ summit potential is always at a potential more positive than the $(\xi_s)^{quasi}_{DC}$ summit potential as is seen in Table II. The difference between them, however, decreases with a decrease in the value of the transfer coefficient; finally it becomes negligibly small at $\alpha=0.3$ and $\Lambda=10^{-2}$, as Table II shows.

The theoretical findings on the quasi-reversible electrode reaction in the author's polarograph may be useful for the estimation of the

reversibility and of the reaction rate constant.

The polarographic wave of an irreversible electrode reaction can not be observed clearly by the conventional a. c. method because of its very low height and its obscure form. This is true also in the oscillographic square-wave polarograph, in which the d. c. applied voltage sweeps very rapidly. However, the measurement of such an irreversible wave can be effectively carried out by the observation of a higher anodic wave instead of that of a lower cathodic wave. This is one of the merits of this equipment.

As is shown in Table IV, the summit potential, $(\xi_s^*)_{\mathrm{Irr}}$, is affected by the magnitude of the transfer coefficient in the manner: $(\xi_s^*)^c_{\mathrm{Irr}} = -0.7$, -0.5 and -0.3 for $\alpha=0.3$, 0.5 and 0.7 in the cathodic process, and $(\xi_s^*)^a_{\mathrm{Irr}}=0.7$, 0.5 and 0.3 for $\beta=0.3$, 0.5 and 0.7 in the anodic process respectively. No effect of the change of the turnnig point of the d. c. applied voltage upon the summit potential is predicted, as the table shows. The summit currents in both cathodic and anodic processes are also affected by the transfer coefficient; and their relations are almost linear, as Fig. 9 shows. The influence of the change of the turning point of the d. c. voltage upon the summit currents of the anodic waves is rather remarkable, as is shown in Table IV. When the voltage is turned back at such insufficiently negative potentials as $\xi^*=-5$ or -10, an asymmetric anodic wave lower in height than the corresponding cathodic wave is obtained, as Fig. 8 shows.

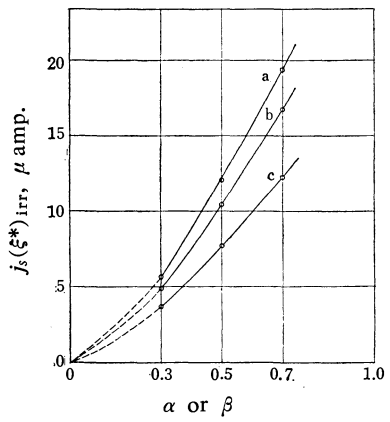

Fig. 9. The dependence of the summit current $j_s(\xi^*)_{\mathrm{Irr}}$ to the transfer coefficient.
a cathodic
b anodic, $\xi_0^*-\xi_1^*=80$, $-(\xi_1^*/\xi_0^*-\xi_1^*)=1/2$
c anodic. $\xi_0^*-\xi_1^*=20$, $-(\xi_1^*/\xi_0^*-\xi_1^*)=1/4$

The discussion or the evaluation of the theoretical results of the a. c. wave could be carried out in more detail if the a. c. wave were expressed in the form of some known and simple function. Such a trial, however, is not easy, so in this paper the discussions were made on the basis of the discontinuous values obtained by the numerical calculations of the integral equations.

Conclusion

Some theoretical considerations of the quasi-reversible and the irreversible electrode reactions in oscillographic square-wave polarograph have been carried out according to a mathematical procedure similar to that used in the reversible reaction.

The equations which represent the quasi-reversible polarographic wave in the cathodic and also in the anodic sweep processes have been derived. The polarographic wave of the quasi-reversible reaction is very much influenced by the magnitude of the transfer coefficient and by that of the reaction rate. Generally speaking, the smaller the above values, the lower the wave height; the summit potential tends to shift to more positive values when $10^0>\Lambda>10^{-1}$ and to more negative values when the Λ-value is less than 10^{-1}.

The theoretical equation of irreversible waves in the cathodic and the anodic sweep processes have also been derived. The wave height of the irreversible electrode reaction is much lower than that of the reversible reaction and is dependent on the transfer coefficient. The summit potentials in two sweep processes do not coincide with each other.

The author is very much indebted to Professor Taichirō Fujinaga, Kyōto University, for his guidance, to Dr. Hiroaki Matsuda, Government Chemical Industrial Research Institute, Tokyo, for his advice, and to Dr. Munetoshi Matsui and to Dr. Akira Itō, both of this laboratory, for affording facilities for this investigation.

Physical Chemistry Section
Takamine Laboratory, Sankyo Co., Ltd.,
Shinagawa-ku, Tokyo

Synthesis of Long-chain Aliphatic Compounds from Cyclododecatriene

By Hirosi TAKAHASI and Muneaki YAMAGUCHI

(Received March 21, 1963)

Dialkyl 1, 16-hexadecandioate, a starting material of 16-membered ring compounds, has been synthesized by the following methods: (1) treating α, ω-dibromoalkane with dialkyl sodiomalonate[1] or potassium cyanide[2]; (2) treating the monochloride of α, ω-dicarboxylic acids with organo cadmium compounds;[3] (3) alkylating 1, 3-cyclohexandione with 1, 4-dibromobutene[4] followed by ring opening, and (4) the electrolytic coupling of α, ω-dicarboxylic acids.[5] The present paper reports a synthesis of diethyl 1, 16-hexadecandioate from 1, 5, 9-cyclodecatriene, as well as syntheses of certain long-chain aliphatic compounds as intermediates of the hexadecandioate.

cis, trans, trans-1, 5, 9-Cyclododecatriene was treated with hydrogen peroxide in formic acid to give 2-formoxy-*cis, trans*-5, 9-cyclododecadienol in a 76% yield; its hydrolysis yielded *cis, trans*-5, 9-cyclodecadiene-*cis*-1, 2-diol[6] (I) melting at 160~161°C with small amounts of an isomer melting at 164~165°C.

The 1, 2-diol I gave *cis*-1, 2-cyclododecanediol[7] upon hydrogenation over palladium-charcoal. The configurations of the two olefinic bonds are considered to be cis and trans on the basis of the infrared absorptions of 2-formoxy-*cis, trans*-5, 9-cyclododecadienol and *cis, trans*-5, 9-cyclododecadiene-1, 2-diol isopropylidene ketal (II) near 970 and 700 cm^{-1}.[8] The structure of the isomer melting at 164~165°C is currently under investigation.[9]

The treatment of *cis, trans*-5, 9-cyclododecadiene-*cis*-1, 2-diol with lead tetraacetate yielded *cis, trans*-5, 9-dodecadiene-1, 12-dial (III) in a 63% yield. The compound gave succinic acid in a 91% yield upon ozonolysis followed by oxidative decomposition, thus excluding the possibility of double-bond migration. The configurations of the two olefinic bonds are considered to be cis and trans on the basis of the infrared absorbance of the dialdehyde at 970 cm^{-1} relative to that of *cis, trans, trans*-1, 5, 9-cyclododecatriene.

The dialdehyde was treated with lithium aluminum hydride to give *cis, trans*-5, 9-dodecadiene-1, 12-diol (IV) in a 79% yield.

cis, trans-5, 9-Dodecadiene-1, 12-dial was heated with ethyl hydrogen malonate and catalytic amounts of piperidine in pyridine to give 2, 6, 10, 14-hexadecatetraene-1, 16-dioate (V) in a 71% yield. This compound gave a mixture of oxalic and succinic acid upon ozonolysis followed by hydrolysis. Upon catalytic hydrogenation over palladium-charcoal, the compound absorbed four moles of hydrogen to give diethyl 1, 16-hexadecanedioate (VI). Attempts to prepare diethyl 6, 10-hexadecadiene-1, 16-dioate by partial hydrogenation over palladium-charcoal or Raney-nickel were unsuccessful.

Experimental[10]

2-Formoxy-*cis, trans*-5, 9-cyclododecadienol. — To 1150 g. of formic acid (80%), 1050 g. of acetic anhydride and 3 ml. of concentrated sulfuric acid were added. The solution was then mixed with 440 g. of *cis, trans, trans*-1, 5, 9-cyclododecatriene[11] and hydrogen peroxide (30%) was added dropwise under stirring. The reaction temperature rose to near 100°C after 350 g. of hydrogen peroxide had been added, and the mixture became homogeneous. The solution was stirred until the peroxide disappeared, and then the solvent was removed in a vacuum. From the distillate, 58 g. of cyclododecatriene were recovered unchanged. The residue was distilled to give 398 g. of a fraction boiling at 150~160°C/10 mmHg (76% based on the reacted cyclododecatriene). By redistillation, a fraction boiling at 155°C/10 mmHg was collected.

1) N. L. Prake, H. W. Carhart and R. Mozingo, *J. Am. Chem. Soc.*, **63**, 617 (1949).
2) P. Chuit and T. Hausser, *Helv. Chim. Acta*, **12**, 850 (1929).
3) A. Kreuchunas, *J. Am. Chem. Soc.*, **75**, 3339 (1953).
4) H. Stetter and W. Dierichs, *Ber.*, **85**, 1061 (1952).
5) L. Ruzicka, M. Stoll and H. Schinz, *Helv. Chim. Acta*, **11**, 1174 (1928).
6) The same diol has been obtained by treating 1, 5, 9-cyclododecatriene with perbenzoic acid; see L. I. Zakharkin and V. V. Korneva, *Doklady Akad. Nauk. S. S. S. R.*, **132**, 1078 (1960).
7) V. Prelog and M. Speck (*Helv. Chim. Acta*, **38**, 1786 (1955)) have reported on the infrared spectra of *cis*- and *trans*-1, 2-cyclododecanediol. Both diols can be easily differentiated by the spectra.
8) Both of these compounds are liquid and gave infrared absorptions at the C-H bending region much more clearly than the original diol.
9) The isomer gave analytical data in accord with cyclododecadienediol. On catalytic hydrogenation over palladium-charcoal, two moles of hydrogen were absorbed, and the hydrogenated product gave oxalic acid upon oxidation with pottasium permanganate.
10) All temperatures are uncorrected.
11) G. Wilke, *Angew. Chem.*, **75**, 10 (1963); H. Takahasi and M. Yamaguchi, *J. Org. Chem.*, **28**, 1409 (1963).

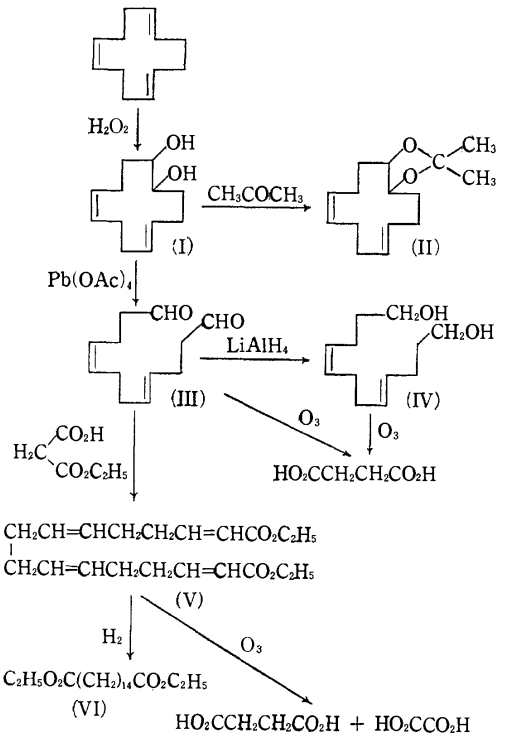

Found: C, 69.40; H, 8.85. Calcd. for $C_{13}H_{20}O_3$: C, 69.61; H, 8.99%.

The infrared spectrum of the compound showed the absorptions of the trans and cis double bonds near 970 and 700 cm^{-1}.

***cis, trans*-5, 9-Cyclododecadiene-*cis*-1, 2-diol.**—To a mixture of 500 g. of *cis, trans, trans*-1, 5, 9-cyclododecatriene, 1300 g. of formic acid (80%), 1200 g. of acetic anhydride and 3 ml. concentrated sulfuric acid, 390 g. of hydrogen peroxide (31%) were added. The mixture was stirred until the peroxide disappeared, and then the solvent was removed in a vacuum. From the distillate, 62 g. of the starting cyclododecatriene were obtained. The residue was vigorously refluxed with 1.2 l. of a 20% sodium hydroxide solution for 2 hr. After the mixture had cooled the crystals were filtered, washed with water, and recrystallized from 400 ml. of alcohol to give 320 g. of crude *cis, trans*-5, 9-cyclododecadiene-*cis*-1, 2-diol melting at 150~153°C. The filtrate was concentrated to give 30 g. of the crude 1, 2-diol. The total yield was 66%. A pure specimen was obtained by recrystallization from alcohol; m. p. 160~161°C. The compound showed the infrared absorptions of the trans and cis double bonds at 970 and 700 cm^{-1}.

The mother liquor was distilled in a vacuum to give a fraction boiling at 170~190°C/5 mmHg. This fraction partially crystallized after standing overnight at room temperature, and the solids were filtered to give 2 g. of crystals melting at 156~160°C. By recrystallization from acetone, a pure specimen was obtained; m. p. 164~165°C. Mixed melting point with *cis, trans*-5, 9-cyclododecadiene-*cis*-1, 2-diol showed a depression; m. p. 145~157°C.

Found: C, 73.51; H, 10.26. Calcd. for $C_{12}H_{20}O_2$: C, 73.43; H, 10.27%.

***cis, trans*-5, 9-Cyclododecadiene-*cis*-1, 2-diol Isopropylidene Ketal.**—A mixture of 5 g. of *cis, trans*-5, 9-cyclododecadiene-*cis*-1, 2-diol, 50 ml. of acetone and 10 g. of anhydrous copper sulfate was stirred at room temperature for 3 days. After the copper sulfate had been filtered, the acetone was removed and the residue was distilled in a vacuum to give 4.5 g. (69%) of *cis, trans*-5, 9-cyclododecadiene-*cis*-1, 2-diol isopropylidene ketal; b. p. 128~131°C/3 mmHg, m. p. 41~42°C.

Found: C. 76.24; H, 10.27. Calcd. for $C_{15}H_{24}O_2$: C, 76.23; H, 10.24%.

The compound gave the infrared absorptions of the double bonds at 970 and 730 cm^{-1} (liquid).

***cis, trans*-5, 9-Dodecadiene-1, 12-dial.**—Lead tetraacetate was prepared from 450 g. of trilead tetraoxide and 1.4 l. of acetic acid. Into a mixture of 100 g. of *cis, trans*-5, 9-cyclododecadiene-*cis*-1, 2-diol and 150 g. of potassium carbonate in 1 kg. of xylene, lead tetraacetate was stirred in small portions under a nitrogen atmosphere over a 3 hr. period, the mixture was then allowed to stand overnigh after having been stirred for an additional hour. The mixture was filtered, and the solid was washed with xylene. The xylene solutions were washed with water and dried over anhydrous sodium sulfate. After the solvent had been removed, 63 g. of *cis, trans*-5, 9-dodecadiene-1, 12-dial boiling at 140~160°C/4 mmHg were obtained in a 63% yield. A pure specimen was obtained by redistillation; b. p. 147~148°C/4mmHg, n_D^{20} 1.4799, d_4^{20} 0.9625.

Found: C, 73.94; H, 9.42. Calcd. for $C_{12}H_{18}O_2$: C, 74.19; H, 9.34%.

The compound (in a carbon disulfide solution) gave infrared absorptions of the trans and cis double bonds at 970 and 710 cm^{-1} respectively, and the infrared absorbance of this compound in a 6.0 mmol. % carbon disulfide solution at 970 cm^{-1} was of the same degree as that of *cis, trans, trans*-1, 5, 9-cyclododecatriene in a 3.0 mmol. % carbon disulfide solution.

2, 4-Dinitrophenylhydrazone: m. p. 110~111°C.

Found: C, 52.08; H, 4.81; N, 20.09. Calcd. for $C_{24}H_{26}N_8O_8$: C, 51.98; H, 4.72; N, 20.21%.

The Ozonolysis of *cis, trans*-5, 9-Dodecadiene-1, 12-dial.—Ozone was introduced into a solution of 3 g. of the sample and 30 ml. of acetic acid, and the ozonized solution was treated with hydrogen peroxide. When the solution was concentrated, 5 g. of succinic acid melting at 180~182°C was obtained in a 91% yield. Its paper chromatography gave a single spot of succinic acid.

***cis, trans*-5, 9-Dodecadiene-1, 12-diol.**—To a solution of 39 g. of *cis, trans*-5, 9-dodecadiene-1, 12-dial in 100 ml. of ether, 4 g. of lithium aluminum hydride were added over a 2 hr. period; the mixture was then refluxed for 3 hr. while being stirred. After it had stood overnight, the mixture was poured into 100 g. of ice-water and extracted with ether after having been treated with hydrochloric acid. The extracts were washed with water and dried over anhydrous sodium sulfate. After the ether had been removed, the residue was distilled to give 31 g. (79.4%) of a fraction boiling at 165~

170°C/4 mmHg. Redistillation gave *cis, trans*-5, 9-dodecadiene-1, 12-diol; b. p. 167~168°C/4 mmHg, n_D^{20} 1.4889, d_4^{20} 0.9558.

Found: C, 72.81; H, 11.13. Calcd. for $C_{12}H_{22}O_2$: C, 72.68; H, 11.18%.

Bis(phenylurethane): m. p. 72.0~72.5°C.

Found: C, 71.35; H, 7.36; N, 6.35. Calcd. for $C_{26}H_{32}N_2O_4$: C, 71.53; H, 7.39; N, 6.42%.

Diethyl 2, 6, 10, 14-Hexadecatetraene-1, 16-dioate.—A solution of 19 g. of *cis, trans*-5, 9-dodecadiene-1, 12-dial, 50 g. of ethyl hydrogen malonate, and 1 ml. of piperidine in 70 ml. of pyridine was refluxed under a nitrogen atmosphere for 4 hr. The solution was then concentrated, and the residue was distilled in a vacuum to give 23 g. (71%) of a fraction boiling at 220~230°C/6 mmHg. and 4 g. of residue. A pure specimen was obtained by redistillation; b. p. 196~197°C/2 mmHg, n_D^{20} 1.4899, d_4^{20} 0.9919.

Found: C, 71.36; H, 8.98. Calcd. for $C_{20}H_{30}O_4$: C, 71.23; H, 9.04%.

The ozonolysis followed by the hydrolysis of the compound gave a mixture of oxalic and succinic acid.

Attempts to Synthesize Diethyl 6, 10-Hexadecadiene-1, 16-dioate.—An alcohol solution of 6.7 g. (0.02 mol.) of diethyl 2, 6, 10, 14-hexadecatetraene-1, 16-dioate was hydrogenated over palladium-charcoal (or Raney-nickel). After 1 l. (0.045 mol.) of hydrogen had been absorbed, the catalyst was filtered off and the filtrate was distilled to give 5.5 g. of a fraction boiling at 220~240°C/6 mmHg. The fraction gave a mixture of oxalic, succinic and adipic acid by ozonolysis followed by hydrolysis.

Diethyl 1, 16-Hexadecandioate.—An alcohol solution of 6.7 g. (0.02 mol.) of diethyl 2, 6, 10, 14-hexadecatetraene-1, 16-dioate was hydrogenated over palladium-charcoal (or Raney-nickel) for 7 hr. After 1.7 l. (0.08 mol.) of hydrogen had been absorbed, the catalyst was filtered and the filtrate was distilled to give 5.5 g. of diethyl 1, 16-hexadecandioate boiling at 220~240°C/6 mmHg.

By hydrolysis, this compound gave 1, 16-hexadecandioate; m. p. 119~120°C.

The authors wish to express their thanks to Professor Hitosi Nozaki of Kyoto University for his extremely helpful suggestions and his readings of the manuscript.

Government Industrial Research Institute, Osaka
Oyodo-ku, Osaka

Sorboses. I. Syntheses of 2, 3-O-Isopropylidene-6-amino-6-deoxy-α-L-sorbofuranoses[1]

By Kanji TOKUYAMA, Masumi KIYOKAWA and Nobuyuki HŌKI

(Received April 9, 1963)

Although 1- and 2-amino derivatives of L-sorbose (I) are known,[2] the 6-amino derivative has not yet been described. In this paper we will report on the synthesis of 6-amino-6-deoxy- and 1, 6-diamino-1, 6-dideoxy-2, 3-*O*-isopropylidene-α-L-sorbofuranoses.

The synthesis was achieved by the schemes outlined in Chart I. For the introduction of an amino group into the C-6 position of a sugar, the tosylation of the hydroxyl group at only this position was desired. At the outset, 1-*O*-acetyl-2, 3-di-*O*-isopropylidene-α-L-sorbofuranose (IV) was prepared to protect all the other hydroxyl groups, and is stable under alkaline conditions and hydrolysable with acid.

The acetylation of 2, 3 : 4, 6-di-*O*-isopropylidene-α-L-sorbofuranose (II)[3] with acetic anhydride in pyridine gave 1-*O*-acetyl-2, 3 : 4, 6-di-*O*-isopropylidene-α-L-sorbofuranose (III), which was hydrolyzed with 60% acetic acid to give IV. The tosylation of IV with one mole of tosyl chloride in pyridine gave a sirup mixture of the expected 6-tosylate, 1-*O*-acetyl-2, 3-*O*-isopropylidene-6-*o*-tosyl-α-L-sorbofuranose (V) and ditosylate, 1-*O*-acetyl-2, 3-*O*-isopropylidene-4, 6-di-*O*-tosyl-α-L-sorbofuranose (VI). The latter was obtained from IV by treating it with more than 2 mol. of tosyl chloride. The separation of those two tosylates was achieved by alumina chromatography, but with poor yields. The purification of 2, 3-*O*-isopropylidene-6-anilino-6-deoxy-α-L-sorbofuranose (X), which was obtained by the treatment of V with aniline, was also difficult. The deacetylation of V by ethanolic sodium hydroxide gave 2, 3-*O*-isopropylidene-6-*O*-tosyl-α-L-sorbofuranose (VII) as silky crystals. The deacetylation of VI gave a

1) Presented at the Division of Organic Chemistry of the 16th Annual Meeting of the Chemical Society of Japan, Tokyo, April, 1963.

2) K. Heynes, H. Paulsen, R. Eichstedt and M. Rolle, *Chem. Ber.*, **90**, 2039 (1957).

3) T. Reichstein, *Helv. Chim. Acta*, **17**, 311 (1934).

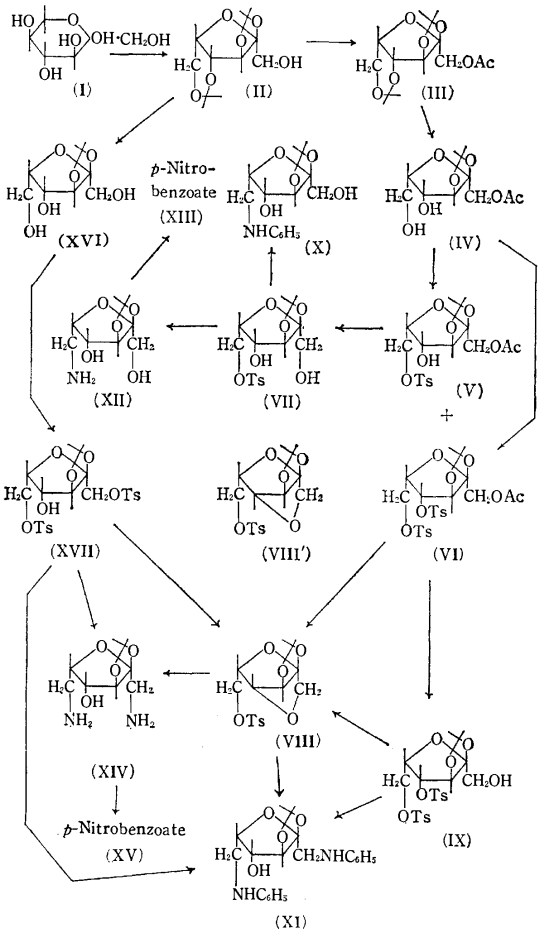

Ac=CH_3CO-
Ts=*p*-toluenesulfonyl-

Chart I

crystalline compound, the infrared spectrum of which exhibited no hydroxyl groups, suggesting that the compound is either 2,3-*O*-isopropylidene-6-*O*-tosyl-1,4-anhydro-α-L-sorbofuranose (VIII) or 1,4-anhydro-α-L-psicose (VIII'). Therefore, the deacetylation of the mixture of V and VI, followed by either fractional crystallization or alumina chromatography, was carried out successfully to give two tosylates, VII and VIII (or VIII').

The heating of VII with aniline gave X, while that with liquid ammonia gave 2,3-*O*-isopropylidene-6-amino-6-deoxy-α-L-sorbofuranose (XII) as a sirup, which was converted into a crystalline *p*-nitrobenzoate (XIII).

The structure of anhydrosugar (VIII or VIII') was also investigated. The deacetylation of VI with alcoholic sodium hydroxide gave an anhydrosugar (VIII or VIII'), while that with liquid ammonia at room temperature gave 2,3-*O*-isopropylidene-4,6-di-*O*-tosyl-α-L-sorbofuranose (IX), which was then easily converted into the same anhydrosugar when treated with alcoholic sodium hydroxide. On the other hand, the partial hydrolysis of II to 2,3-*O*-isopropylidene-α-L-sorbofuranose (XVI), followed by tosylation, gave 2,3-*O*-isopropylidene-1,6-di-*O*-tosyl-α-L-sorbofuranose (XVII).[4,5] Reacting with alcoholic sodium hydroxide, XVII was converted into an anhydrosugar which showed an infrared absorption band identical with the above-described anhydrosugar. The latter course has no opportunities for Walden inversion. Therefore, the structure of anhydrosugar was established as VIII. It is noteworthy that no Walden inversion was observed in the reaction of VI to VIII.

The treatment of VIII with aniline gave dianilinosorbose. Under the same conditions, XVII gave the same product. From these results the dianilinosorbose was confirmed to be 2,3-*O*-isopropylidene-1,6-dianilino-1,6-dideoxy-α-L-sorbofuranose (XI). Similarly, the treatment of VIII as well as of XVII with liquid ammonia gave 2,3-*O*-isopropylidene-1,6-diamino-1,6-dideoxy-α-L-sorbofuranose (XIV) as a sirup, which was then converted into a crystalline *p*-nitrobenzoate (XV). The two 1,6-diamino-sorboses, XI and XIV, were also prepared from IX, with the amines via VIII as a probable intermediate.

The infrared absorption spectra of the above-described sorbofuranoses are summarized in Table I. Previously, Barker and Stephens reported that the compounds containing a furanose or hydrofuranol ring exhibit infrared absosption of the A, B, C and D types at 924±

Table I. Infrared absorption bands of sorbofuranoses

Compound	Frequencies (cm^{-1}) of absolute bands				
	Type A	Type B	Type C	Type D	Other peaks
II	945	890	855	830	765
III	980	901	858	835	770
IV	985	888	860	828	770
VII	946	898	870	828	792
VIII	935	895	858	818	780
IX	977	900	865	827	770
X	938	892	866	823	760
XI	934	892	860	812	742
XIII	982	895	863	824	778
XV	944	880	855	830	720
XVI	980	891	864	830	750
XVII	958	890	856	818	765
Mean and standard derivation	958±24	895±7	864±6	823±7	

4) T. I. Temnikova and V. V. Sklyarava, *Zh. Prikl. Khim.*, 27, 1131 (1954); *Chem. Abstr.*, 49, 2952 (1955).
5) H. Ohle, *Ber.*, 71, 562 (1938).

13, 879±7, 858±7 and 799±17 cm^{-1}, respectively.[6] These four types of infrared absorption bands are also characteristic of sorbofuranoses, but their positions then shift to higher frequencies to some extent, appearing at 958±24, 895±7, 864±6 and 823±7 cm^{-1} respectively. 1,2-*O*-Isopropylidene-α-L-sorbopyranose[5] and methyl α-L-sorbopyranoside[7] showed no absorption bands of these four types. Instead, they exhibited absorptions at 910 and 902, 890 and 880, and 772 and 792 cm^{-1}, positions which were identical with those of D-glucopyranose as suggested by Barker et al.[8] These facts are very useful in determining whether or not sorboses are of the furanose type.

Experimental[9]

1-*O*-Acetyl-2,3:4,6-di-*O*-isoproylidene-α-L-sorbofuranose (III).—Into a cooled solution of 200 g. of 2,3:4,6-di-*O*-isopropylidene-α-L-sorbofuranose (II) in 300 ml. of dry pyridine, 200 g. of acetic anhydride in portions were stirred. After having been stirred at 0~5°C for 4 hr. and after standing overnight at room temperature, the reaction mixture was poured onto 800 g. of ice. The product was then extracted with benzene, washed with a sodium bicarbonate solution, dried, and evaporated in vacuo. The residue was distilled to give a colorless sirup, which crystallized immediately. Yield: 204 g. (88%); b. p. 168°C/6 mmHg; m. p. 52°C $[\alpha]_D^{19}$ −16.4 (*c* 1.038, acetone).

Found: C, 55.95; H, 7.51; CH_3CO, 13.96. Calcd. for $C_{14}H_{22}O_7$ (302): C, 55.63; H, 7.29; CH_3CO, 14.23%.

1-*O*-Acetyl-2,3-*O*-isopropylidene-α-L-sorbofuranose (IV).—A solution of 170 g. of 1-*O*-acetyl-2,3:4,6-di-*O*-isopropylidene-α-L-sorbofuranose (III) in 200 ml. of 60% acetic acid was warmed at 80°C for 40 min. The reaction mixture was cooled, made alkaline with sodium carbonate, and then extracted with chloroform. After the removal of the solvent, the residue was distilled to give a colorless sirup. Yield: 88 g. (67.2%); b. p. 205°C/11 mmHg; $[\alpha]_D^{23}$ +7.3 (*c* 0.987, acetone).

Found: C, 50.41; H, 7.07; CH_3CO, 16.26. Calcd. for $C_{11}H_{18}O_7$ (262): C, 50.38; H, 6.87; CH_3CO, 16.41%.

The Tosylation of 1-*O*-Acetyl-2,3-*O*-isopropylidene-α-L-sorbofuranose (IV).—Into a solution of 100 g. of 1-*O*-acetyl-2,3-*O*-isopropylidene-α-L-sorbofuranose (IV) in 300 ml. of dry pyridine, 73 g. of tosyl chloride in small portions were stirred while the mixture was being cooled in ice water. After having been stirred at room temperature for 4 hr., the reaction mixture was poured into 600 ml. of a saturated sodium carbonate solution and then extracted with chloroform, which had been washed with water, dried and evaporated to dryness in vacuo to a sirup (A). Yield: 118 g. i) Ten grams of the A sirup was fractionated by alumina chromatography with chloroform. The first fraction was 0.15 g. of 1-*O*-acetyl-2,3-*O*-isopropylidene-4,6-di-*o*-tosyl-α-L-sorbofuranose (VI), $[\alpha]_D^{23}$ −3.8 (*c* 1.03, acetone).

Found: C, 52.40; H, 5.64; S, 10.80. Calcd. for $C_{25}H_{30}O_{11}S_2$ (570): C, 52.63; H, 5.26; S, 11.22%.

The other compound purely isolated was 0.18 g. of 1-*O*-acetyl-2,3-*O*-isopropylidene-6-*O*-tosyl-α-L-sorbofuranose (V), $[\alpha]_D^{23}$ +4.2 (*c* 0.790, acetone).

Found: C, 52.35; H, 5.88; S, 7.90. Calcd. for $C_{18}H_{24}O_9S$ (416): C, 51.99; H, 5.77; S, 7.69%.

ii) The 4,6-ditosylate VI was also obtained from IV, along with more than 2 mol. of tosyl chloride, by using the same procedure.

iii) A solution of 50 g. of the A sirup in a solution of 8 g. of sodium hydroxide, 60 ml. of water and 280 ml. of ethanol was warmed at 50°C for 40 min. After the solvent had been removed, the residue was extracted with chloroform, which had been washed with water, dried and evaporated to dryness in vacuo to a sirup. a) Recrystallization from ethanol gave 12 g. of 2,3-*O*-isopropylidene-6-*O*-tosyl-1,4-anhydro-α-L-sorbofuranose (VIII). The mother liquor was evaporated to dryness in vacuo. Recrystallization from petroleum ether and ethyl acetate gave 16 g. of 2,3-*O*-isopropylidene-6-*O*-tosyl-α-L-sorbofuranose (VII). b) The sirup dissolved in chloroform was passed through an alumina column and evaporated to dryness. Recrystallization from ethanol gave 12 g. of 2,3-*O*-isopropylidene-6-*O*-tosyl-1,4-anhydro-α-L-sorbofuranose (VIII). The column was eluted out with alcohol. The alcohol solution was evaporated in vacuo. Recrystallization of the residue from petroleum ether and ethyl acetate gave 10 g. of 2,3-*O*-isopropylidene-6-*O*-tosyl-α-L-sorbofuranose (VII).

2,3-*O*-Isopropylidene-6-*O*-tosyl-α-L-sorbofuranose (VII).—A solution of 2 g. of 1-*O*-acetyl-2,3-*O*-isopropylidene-6-*O*-tosyl-α-L-sorbofuranose (V) in 20 ml. of 0.5 N ethanolic potassium hydroxide was warmed at 50°C for 1 hr. To the reaction mixture 100 ml. of chloroform were then added. The chloroform layer was washed with water, dried, and evaporated to dryness. Recrystallization from petroleum ether and ethyl acetate gave 1.1 g. (61.2%) of colorless needles; m. p. 105°C, $[\alpha]_D^{22}$ +15.1 (*c* 1.075, acetone).

Found: C, 51.70; H, 6.05; S, 8.55. Calcd. for $C_{16}H_{22}O_8S$ (374): C, 51.34; H, 5.88; S, 8.56%.

2,3-*O*-Isopropylidene-6-*O*-tosyl-1,4-anhydro-α-L-sorbofuranose (VIII).—This was prepared from 2g. of 1-*O*-acetyl-2,3-*O*-isopropylidene-4,6-di-*O*-tosyl-α-L-sorbofuranose (VI) and 20 ml. of ethanolic potassium hydroxide in a 62% yield by the above-described procedure. M. p. 115°C (recrystallized from ethanol), $[\alpha]_D^{24}$ −11.6 (*c* 1.035, acetone).

Found: C, 53.74; H, 5.62; S, 9.01. Calcd. for $C_{16}H_{20}O_7S$ (356): C, 53.96; H, 5.62; S, 8.99%.

The anhydrosorbose VIII was also obtained from 2,3-*O*-isopropylidene-4,6-di-*O*-tosyl-α-L-sorbofuranose (IX) or 2,3-*O*-isopropylidene-1,6-*O*-tosyl-α-L-sorbofuranose (XVII) in a similar yield by the above-described procedure.

6) S. A. Barker and R. Stephens, *J. Chem. Soc.*, **1954**, 4550.
7) R. L. Whistler and R. M. Hixon, *J. Am. Chem. Soc.*, **59**, 2047 (1937).
8) S. A. Barker, E. G. Bourne, M. Stacy and D. H. Wiffen, *J. Chem. Soc.*, **1954**, 171.
9) All melting points are uncorrected.

2,3-*O*-Isopropylidene-4,6-di-*O*-tosyl-α-L-sorbofuranose (IX).—A solution of 10 g. of 1-*O*-acetyl-2,3-*O*-isopropylidene-4,6-di-*O*-tosyl-α-L-sorbofuranose (VI) in 10 ml. of liquid ammonia was allowed to stand overnight at room temperature. After the liquid ammonia had been removed, a brown sirup was obtained, the solution of which in 50 ml. of chloroform had been washed with water, dried, and evaporated to dryness in vacuo to a sirup. Alumina chromatography with chloroform gave 0.5 g. of colorless needles as a second fraction; m. p. 125°C (recrystallized from ethanol), $[\alpha]_D^{23}$ +8.4 (*c* 1.003, acetone).

Found: C, 52.33; H, 5.48; S, 11.55. Calcd. for $C_{23}H_{28}O_{10}S_2$ (528): C, 52.23; H, 5.34; S, 12.14%.

2,3-*O*-Isopropylidene-6-anilino-6-deoxy-α-L-sorbofuranose (X).—A solution of 2 g. of 2,3-*O*-isopropylidene-6-*o*-tosyl-α-L-sorbofuranose (VII) and 2 g. of potassium carbonate in 20 ml. of aniline was heated while being stirred at 160~170°C for 20 hr. The reaction mixture was then cooled and extracted with three 60 ml. portions of chloroform, which had been washed with water, dried and evaporated in vacuo to get a dark brown sirup. Recrystallization from ethanol gave 0.7 g. of colorless needles; m. p. 140°C, $[\alpha]_D^{24}$ +32.6 (*c* 0.859, acetone).

Found: C, 61.46; H, 7.35; N, 4.59. Calcd. for $C_{15}H_{21}NO_5$ (295): C, 61.02; H, 7.12; N, 4.75%.

2,3-*O*-Isopropylidene-1,6-dianilino-1,6-dideoxy-α-L-sorbofuranose (XI).—This was obtained from 2g. of 2,3-*O*-isopropylidene-6-*O*-tosyl-1,4-anhydro-α-L-sorbofuranose (VIII) and 2 g. of potassium carbonate in 20 ml. of aniline by the above-described procedure for 2,3-*O*-isopropylidene-6-anilino-6-deoxy-α-L-sorbofuranose (X). Recrystallization from ethanol gave 0.8 g. of the sample for analysis; m. p. 151°C, $[\alpha]_D^{25}$ +10.3 (*c* 1.020, acetone).

Found: C, 68.36; H, 7.20; N, 7.78. Calcd. for $C_{21}H_{26}N_2O_4$ (370): C, 68.11; H, 7.04; N, 7.57%.

The dianilino compound XI was also prepared in a similar yield from either 2,3-*O*-isopropylidene-1,6-di-*O*-tosyl-α-L-sorbofuranose (XVII) or 2,3-*O*-isopropylidene-4,6-di-*O*-tosyl-α-L-sorbofuranose (IX) by the same procedure.

2,3-*O*-Isopropylidene-6-amino-6-deoxy-α-L-sorbofuranose (XII).—A solution of 5 g. of 2,3-*O*-isopropylidene-6-*o*-tosyl-α-L-sorbofuranose (VII) in 10 ml. of liquid ammonia was heated on a boiling water-bath for ten days. After the liquid ammonia had been removed, the residue, dissolved in 100 ml. of chloroform, was passed through an alumina column (50 g. of alumina was used) and evaporated to dryness in vacuo. A solution of 1 g. of the residue and 2 g. of *p*-nitrobenzoyl chloride in 15 ml. of dry pyridine was stirred at room temperature for 10 hr. The reaction mixture was poured into a saturated aqueous solution of sodium carbonate while being cooled and was extracted with chloroform which had been washed with water and evaporated to dryness in vacuo. Three recrystallizations from petroleum ether and ethyl acetate gave 1.4 g. of colorless needles (XIII); m. p. 235°C (decomp.), $[\alpha]_D^{30}$ +25.3 (*c* 0.364, acetone).

Found: C, 54.22; H, 3.91; N, 8.32. Calcd. for $C_{30}H_{26}N_4O_{14}$ (666): C, 54.05; H, 3.91; N, 8.41%.

A solution of 1 g. of XIII in 50 ml. of 10% methanolic sodium hydroxide was refluxed for 1.5 hr. After the methanol had been removed, the residue was extracted with chloroform, and the extracts were washed with water saturated with sodium chloride, dried, treated with charcoal, and evaporated to dryness in vacuo to a sirup. Yield: 0.2 g., $[\alpha]_D^{23}$ +28.1 (*c* 1.030, acetone).

Found: C, 49.63; H, 7.69; N, 6.07. Calcd. for $C_9H_{17}NO_5$ (219): C, 49.32; H, 7.76; N, 6.39%.

2,3-*O*-Isopropylidene-1,6-diamino-1,6-dideoxy-α-L-sorbofuranose (XIV).—This was prepared from 5 g. of 2,3-*O*-isopropylidene-6-*O*-tosyl-1,4-anhydro-α-L-sorbofuranose (VIII) and 10 ml. of liquid ammonia by the above-described procedure. *p*-Nitrobenzoate (XV): m. p. 110~115°C (decomp.) (by five recrystallizations from petroleum ether and benzene), $[\alpha]_D^{23.5}$ −69.5 (*c* 0.243, acetone).

Found: C, 53.88; H, 4.24; N, 10.79. Calcd. for $C_{30}H_{27}N_5O_{13}$ (665): C, 54.14; H, 4.06; N, 10.53%.

The 1,6-diaminosorbose (XIV) was obtained as colorless plates. M. p. 52°C, $[\alpha]_D^{30}$ −8.36 (*c* 1.078, acetone).

Found: C, 49.80; H, 7.95; N, 13.01. Calcd. for $C_9H_{18}N_2O_4$ (218): C, 49.54; H, 8.26; N, 12.84%.

The authors wish to express their deep gratitude to Dr. Ken'ichi Takeda, Director of this laboratory, and to Dr. Kaname Hamamoto, Assistant Director of this laboratory, for their encouragement. The authors are also indebted to the other members of this laboratory who measured the optical rotation and made the elementary analysis.

Shionogi Research Laboratory
Shionogi & Co., Ltd.
Fukushima-ku, Osaka

Darstellung und Acetolyse von isomeren Decalylcarbinyltosylaten

Von Nobuo Mori

(Eingegangen am 22. April, 1963)

In der Cyclohexanreihe im allgemeinen solvolysieren sich axiale Tosylate etwa 3~4-mal rascher als die entsprechenden äquatorialen Isomere; die Reaktionsbeschleunigung wird hauptsächlich durch die sogenannte 1, 3-diaxiale Wechselwirkung zwischen der axialen Tosylatgruppe und dem axialen Wasserstoffatom an C_3 order C_5 in den axialen Formen verursacht,[1] und sie steigt ja mit der Zahl der Wechselwirkung.[2] Auch bei der Solvolyse von gewissen äquatorialen Cyclohexyltosylaten, die eine grosse Gruppe wie Methyl in der 1- oder 3-axialen Lage besitzen, wird ähnlich eine ziemlich grosse Beschleunigung trotz der äquatorialen Form erfahren; das kommt daher, dass ihre Ionisierung auch durch Beteiligung der 1- oder 3-axialen grossen Gruppe unterstützt wird. Von einigen Beispielen der Beschleunigung wird zunächst die Solvolyse von *cis*- und *trans*-1, 3-Dimethylcyclohexylbromid[3] angeführt, worin die cis Form mit äquatorialem Bromatom auch mit einer praktisch gleichen Geschwindigkeit wie die der trans Form mit axialem Bromatom acetolysiert wird. Ähnlich acetolysieren sich äquatoriale *cis*-3, 3, 5-Trimethylcyclohexyl-[4] und 2α-Cholestanyl-tosylat[5] rascher als äquatoriale *cis*-3-Methylcyclohexyl- und als 3β-Cholestanyl-tosylat; die Tatsache wurde in ähnlicher Weise auf die grössere Wechselwirkung zwischen der axialen Methylgruppe an C_3 und dem axialen Wasserstoffatom an C_1 in den ersten Verbindungen zurückgeführt.

Im Anschluss an das Problem über solche 1, 3-diaxiale Wechselwirkung, und zwar besonders zur Klärung des Konstellationseinflusses auf die Reaktionsfähigkeit von den axialen und äquatorialen Toluolsulfoxymethylgruppen in der Cyclohexanreihe wurde früher die Acetolyse von *cis*- und *trans*-4-*t*-Butylcyclohexylcarbinyltosylat, die beide das Butyl in Äquatorialstellung enthalten dürfen, aufgeführt, wobei die cis Form ja 4.2-mal rascher als der trans Isomer reagierte.[6] In bezug auf die Untersuchungen erschien es mir interessant und zweckmässig, auch konstellativ einheitliche, isomere Decalylcarbinyltosylate zu studieren.

In der vorliegenden Mitteilung werden somit eine Methode zur Darstellung von bisher unbekannten *cis-cis*-1-, *cis-cis*-2-, *trans-trans*-1- und *trans-cis*-2-Decalylcarbinyltosylaten* und ihre Acetolyse berichtet.

Darstellung von Isomeren Decalylcarbinyltosylaten.—Die vier Tosylate sind in üblicher Weise,[7] mit der praktisch vollständigen Beibehaltung von Konfiguration, aus den entsprechenden Decahydronaphthoesäuren dargestellt worden. Von den acht theoretisch möglichen *cis*- und *tran*-Decahydro-1- und -2-naphthoesäuren sind bisher fünf in reiner Form bekannt.[8] Von denen dürfen vier Verbindungen, nämlich die *cis-cis*-1-, *cis-cis*-2, *trans-trans*-1- und *trans-cis*-2-Säuren, in der rein (die *trans*-Reihe) oder praktisch rein (die *cis*-Reihe) äquatorialen Konstellation vorliegen, somit sind sie zur vorliegenden Untersuchung zweckmässig, während die einzige übrige, nämlich die *cis-trans*-2-Säure, unzweckmässig ist, weil sie etwa in Konstellation uneinheitlich angesehen wird.

In diesem Versuch wurden darum die ersteren vier Säuren als Ausgangsmateriale zur Darstellung der Decalylcarbinyltosylate benützt. Von den Säuren wurden also die *trans-trans*-1- und *trans-cis*-2-Säuren zwar aus den entsprechenden Chlordecalinen in üblicher Weise[8-11] durch Carbonierung ihrer Grignard-Reagenzien hergestellt, während die *cis-cis*-1- und *cis-cis*-2-Isomere durch Hydrierung von 1- und 2-Naphthoesäuren mit Hilfe von Raney-Nickel an Stelle des Platinoxyds[8,12] in ziemlich guter Ausbeute erhalten wurden. Die gereinigten Säuren wurden dann durch Veresterung und

1) S. Winstein und H. J. Holness, *J. Am. Chem. Soc.*, 77, 5562 (1955).
2) I. Moritani, S. Nishida und M. Murakami, ebenda, 81, 3420 (1959).
3) T. D. Nevitt und G. S. Hamond, ebenda, 76, 4124 (1954).
4) Hp. Fischer, C. A. Grob und W. Schwarz, *Tetrahedron Letters*, No. 1, 25 (1962).
5) S. Nishida, *J. Am. Chem. Soc.*, 82, 4290 (1960).

* Alle Konfigurationen werden von den relativen Stellen der Wasserstoffatome an C_9, C_{10} und C_9, C_1 oder C_9, C_2 gezeigt.

6) N. Mori, Dieses Bulletin, 35, 1755 (1962).
7) Zum Beispiel, N. Mori, ebenda, 34, 1567 (1961).
8) W. G. Dauben, R. C. Tweit und C. Mannerskantz, *J. Am. Chem. Soc.*, 76, 4422 (1954).
9) G. Tsatsas, *Ann. Chim. (Paris)*, [11] 19, 217 (1944).
10) W. G. Dauben und R. C. Tweit, *J. Am. Chem. Soc.*, 76, 3196 (1954).
11) W. Borsche und E. Lange, *Ann.*, 434, 219 (1923).
12) W. G. Dauben und E. Hoerger, *J. Am. Chem. Soc.*, 73, 1504 (1951).

TABELLE I. KONFIGURATIONEN* UND KONSTANTEN DER DARGESTELLTEN DECALINDERIVATE

Substituent X	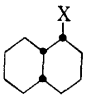	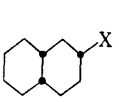	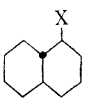	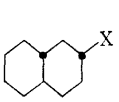
	cis-cis-1	cis-cis-2	trans-trans-1	trans-cis-2
-COOH (Schmp. °C)	125	81	102	106
$-COOC_2H_5$ (n_D^{25})	1.4767	1.4755	1.4700	1.4685
(d_4^{25})	1.0014	0.9988	0.9826	0.9784
$-CH_2OH$ (Schmp. °C)	55	68.8	Flüssig	31.5
$-CH_2OTs$ (Schmp. °C)	67.5	56.2	74.5	62

nachfolgende Reduktion mit Lithiumaluminiumhydrid zu den entsprechenden Decalylcarbinolen umgesetzt, die dann zum Schluss tosyliert wurden.

In der folgenden Tabelle werden nun die dargestellten Decahydronaphthoesäuren, als auch ihre Ester, Carbinole und Tosylate zusammen mit ihren Konstanten angegeben.

Wie man in der Tabelle sieht, sind immer die Brechungsindizes als auch die spezifische Gewichte der Äthylester von der cis-Reihe, deutlich höher als diejenigen der entsprechenden Ester von der trans-Reihe, was wohl von Auwers-Skita Regel[13] erwartet wird.

Acetolyse von Decalylcarbinyltosylaten.—Die Acetolyse der vier Decalylcarbinyltosylate wurde jederzeit bei 110.1°C in Gegenwart von etwas überschüssigem Natriumacetat ausgeführt. Zum Vergleich wurden weiter auch *cis*- und *trans*-4-*t*-Butylcyclohexylcarbinyltosylate, die früher nur in Abwesenheit von der Base solvolysiert wurden, unter den gleichen Bedingungen acetolysiert; die Geschwindigkeiten in beiden Fällen sind beinah dieselben. Die folgende Tabelle zeigt die Verhältnisse von den Acetolysegeschwindigkeitskonstanten zusammen mit ihren als energetisch günstig angesehenen, gestaffelten Konstellationen von I bis zu VI.

Es ist von Interesse, dass die Geschwindigkeitskonstanten der vier Decalylcarbinyltosylate, die hauptsächlich in den entsprechenden äquatorialen Konstellationen von II zu V bzw. in etwas deformierten Formen vorliegen dürfen, zwischen den der *cis*- und *trans*-4-*t*-Butylcyclohexylcarbinyltosylate liegen, trotzdem die Zahl der sogenannten 1, 3-diaxialen Wechselwirkung auf die Tosylatgruppe jedenfalls eins ist, wie später erwähnt werden wird. Wie die gaschromatographische Analyse des Reaktionsprodukts ergibt, treten bei der Acetolyse bei 145~150°C ausschliesslich das Methylenderivat und Carbinylacetat auf. Das Verhältnis von der Eliminierung zu der Substitution zeigt eine regelmässige Zunahme mit der bei 110°C gemessenen Geschwindigkeitskonstante.

Dann könnte man erwarten, dass der Unterschied in den Reaktivitäten vorwiegend von der sterischen Spannung abhängig ist, welche nicht nur auf die Tosylatgruppe, sondern auf die ganze Toluolsulfoxymethylgruppe wirkt und welche bei Ionisierung zu einem Carboniumion nachlässt.

Früher wurde gezeigt,[6] dass sich das axiale *cis*-4-*t*-Butylcyclohexylcarbinyltosylat 4.2-mal rascher als der entsprechende äquatoriale trans-Isomer acetolysiert, und dass die Reaktionsbeschleunigung unter anderm auf die sterische Spannung zurückzuführen ist, welche durch die relative grosse Wechselwirkung zwischen dem Wasserstoffatom in der Methylengruppe und den axialen Wasserstoffatomen an C_3 und C_5 in der Konstellation von I verursacht wird und welche bei Ionisierung zu einem Carboniumion nachlässt. Durch solch eine auf das Methylen-Wasserstoffatom wirkende sterische Spannung kann sich der oben angegebene Unterschied in der Acetolysegeschwindigkeit von den Tosylaten folgendermassen, zahlenmässig, erklären.

Wie man in der Tabelle sieht, bedeutet die Wechselwirkung vom Typus A immer die 1, 3-diaxiale Wechselwirkung zwischen der Tosylatgruppe und dem Wasserstoffatom, während diejenige vom Typus B die 1, 3-diaxiale Wechselwirkung zwischen den Wasserstoffatomen in der Methylengruppe und in 3-Stellung, und auch weiter diejenige vom Typus C die Wechselwirkung zwischen den zwei Wasserstoffatomen in der Methylengruppe und in 4-Stellung. Von diesen drei Wechselwirkungen, könnte die vom Typus C den höchsten Einfluss auf die Ionisierung des Tosylatmoleküls ausüben, weil die an der Wechselwirkung vom Typus C sich beteiligenden zwei Wasserstoffatome zueinander näher als in 1, 3-diaxialer Stellung stehen, somit das Molekül in einem höheren gespannten Zustand sein sollte.

13) K. von Auwers, *Ann.*, **420**, 84 (1920); A. Skita, *Ber.*, **53**, 1792 (1920); A. Skita und W. Faust, ebenda, **64**, 2878 (1931).

* Die Stellen der Wasserstoffatome werden in den Formeln mit schwarzen Tupfen gezeigt, diese Tupfen zeigen, dass ein Wasserstoffatom auf der Fläche des Moleküls liegt.

Tabelle II. Konstellationen, relative Reaktionsgeschwindigkeiten und Verhaltnis vom Olefin zum Acetat

Konstellation vom Tosylat	Wechselwirkung vom Typus A(TsO:H)	B(H:H)	C(H:Ⓗ)	Relative Reaktionsgeschwindigkeiten	Verhaltnis vom Olefin zum Acetat
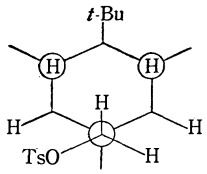 (I) *cis*-4-*t*-Butylcyclohexylcarbinyl	1	1	2	4.07	1.0
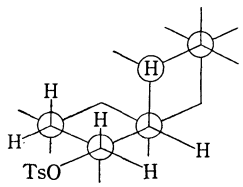 (II) *cis-cis*-1-Decalylcarbinyl	1	2	1	3.00	0.92
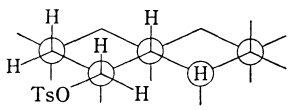 (III) *trans-trans*-1-Decalylcarbinyl	1	2	1	2.51	0.80
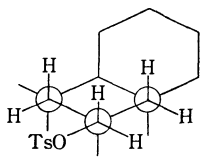 (IV) *cis-cis*-2-Decalylcarbinyl	1	3	0	1.60	0.65
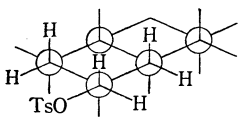 (V) *trans-cis*-2-Decalylcarbinyl	1	3	0	1.14	0.53
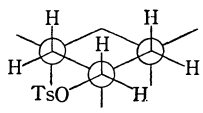 (VI) *trans*-4-*t*-Butylcyclohexylcarbinyl	1	3	0	1.00	0.47

Vorausgesetzt, dass die Abnahme der Wechselwirkung, u. a. vom Typus C, beim Übergang des Grundzustandes in den Carboniumion, hauptsächlich den Nachlass der Spannung im Tosylatmolekül verursacht, so lässt sich die Grösse ihrer Acetolysegeschwindigkeit überhaupt nur auf Grund von der Wechselwirkungszahl vom Typus C leicht erklären.

Wie die Tabelle lehrt, ist die Zahl vom Typus A in allen Konstellationen eins, während die vom Typus C eine regelmässige Zunahme mit der Geschwindigkeitskonstante und die vom Typus B eine Abnahme zeigen. Daraus folgt, dass hauptsächlich die Wechselwirkung vom Typus C die Acetolysegeschwindigkeit kontrolliert.

Vergleicht man noch die drei Tosylate von IV, V und VI miteinander, welche die gleiche Wechselwirkung (A+3B) enthalten, so sieht man, dass die rein äquatoriale *trans-cis*-2-Tosylat-(V) und als rein äquatorial angesehene *trans*-4-*t*-Butyl-verbindungen (VI) fast gleich

schnell reagieren, und zwar verläuft die Reaktion von V rascher nur um den Faktor 1.14 als die von VI, aber das als fast rein äquatorial angesehene *cis-cis*-2-Tosylat (IV) acetolysiert sich 1.6-mal so rasch wie VI. Für diese erhöhte Reaktivität von IV scheint die uneinheitliche Konstellation vorantwortlich zu sein, weil der axiale Konstellationsisomer ziemlich rascher als der äquatoriale Isomer (IV) reagieren will.

Nach einer ähnlichen Ursache acetolysiert sich auch das als fast rein angesehene *cis-cis*-1-Tosylat (II) etwas racher als der rein äquatoriale *trans-trans*-1-Isomer (III), trotz der gleichen Wechselwirkungszahl (A+2B+C).

Beschreibung der Versuche

Alle Schmelzpunkte sind korrigiert.

***cis-cis*-1-Decahydronaphthoesäure.**—Eine schwach alkalische wässrige Lösung von 1-Naphthoesäure (10 g) in einer 5-proz. Natriumhydroxydlösung wurde in Gegenwart von Raney-Nickel (5 g) unter einem anfänglichen Druck von 75 Atom. bei 190～200°C hydriert. Nachdem die Aufnahme des Wasserstoffs beendet war, wurde das Reaktionsgemisch abgesaugt und dann unter Eiskühlung und Umrühren mit konzentrierter Salzsäure angesäuert, um eine sauere Substanz auszufällen. Die Substanz wurde abgesaugt und mit Wasser gewaschen. Das Rohprodukt (9 g) wurde mehrmals aus Ameisensäure umkristallisiert, bis der Schmelzpunkt konstant wurde, dabei wurden Schuppchen (3 g) vom Schmp. 123.5～125.5°C erhalten.

***cis-cis*-2-Decahydronaphthoesäure.**—2-Naphthoesäure (10 g) wurde wie bei der *cis-cis*-1-Säure hydriert. Das Reaktionsgemisch wurde abgesaugt und dann unter Eiskühlung und Umrühren mit Salzsäure angesäuert. Das ausgefallene Öl wurde in Äther aufgenommen, die ätherische Lösung über Natriumsulfat getrocknet und dann verdampft. Der ölige Rückstand erstarrte nach Stehenlassen einige Tage im Kühlschrank zu einer farblosen Kristallmasse, und er wurde aus etwas Hexan zweimal umkristallisiert, wobei Nädelchen (3 g) vom Schmp. 76～79°C erhalten wurden. Ein Teil vom Produkt ergab nach noch einer Umkristallisierung aus etwas Hexan Nadeln vom Schmp. 80.5～81.5°C.

***trans-trans*-2-Decahydronaphthoesäure.**—Reines *trans*-Decalin (300 g) wurde nach der bekannten Methode von Dauben und Tweit,[10] indessen bei einer höheren Temperatur von 10～15°C und im Laufe von einigen Stunden chloriert, wobei ein Gemisch von *trans*-1- und *trans*-2-Chlordecalin (120 g) vom Siedp. 100～117°C/12 Torr. erhalten wurde. Die Grignard-Lösung aus dem Chlordecalingemisch (52 g), Magnesium (12 g) und Jod (0.05 g) in wasserfreiem Äther (300 ccm) wurde unter starkem Umrühren und Kühlen mit Eis-Kochsalz bei −10～−5°C mit getrocknetem Kohlendioxyd so lange behandelt bis die Reaktionstemperatur nicht mehr anstieg, danach unter Kohlendioxyd noch 30 Min gerührt. Das Reaktionsgemisch wurde in der Kälte mit eiskalter verd. Schwefelsäure umgesetzt, und dann wurde die ätherische Schicht einmal mit Salzlösung gewaschen und zweimal mit 10-proz. Natriumhydroxydlösung extrahiert. Die alkalische Lösung wurde unter Eiskühlung mit konz. Salzsäure angesäuert, um ein saueres Öl auszufällen, das in der Kälte sich kristallisierte. Nach einigemaligem Umkristallisieren aus Hexan ergaben sich Blättchen (6 g) vom Schmp. 105.5～106.5°C. Diese Säure gab ein Amid als Blättchen vom Schmp. 205～206°C.

***trans-trans*-1-Decahydronaphthoesäure.**—Aus der Mutterlauge der Umkristallisierung der *trans-cis*-2-Säure wurde wenige reine *trans-trans*-1-Decahydronaphthoesäure (1 g) vom Schmp. 102°C (aus wässrigem Äthanol) nach der chromatographischen Methode von Dauben und Tweit[10] getrennt.

Auch nach der anderen Methode[8] wurde diese Säure durch Carbonierung von einer Grignardlösung des bei Chlorierung vom *trans-trans*-1-Decalol gewonnen reinen *trans-trans*-1-Chlordecalins dargestellet. Nach zweimaligen Umkristallisierungen aus wässrigem Äthanol ergaben sich Nadeln vom Schmp. und Misch-Schmp. 100～101°C. Der Misch-Schmp. mit der bei 106°C schmelzenden *trans-cis*-2-Säure war 85～88°C.

***cis-cis*-1-Decahydronaphthoesäureäthylester.**—Die reine *cis-cis*-1-Säure (4.3 g) wurde in eine Lösung von konz. Schwefelsäure (1 ccm) in absolutem Äthanol (50 ccm) zugesetzt und 1.5 Stdn. unter Rückfluss erhitzt, und dann wurde das Lösungsmittel unter vermindertem Druck abgedampft. Der Rückstand wurde in Äther aufgenommen, mit Wasser und 10-proz. Natriumcarbonatlösung gewaschen und über Natriumsulfat getrocknet. Nach Abdampfen von Äther wurde der ölige Rückstand in Vakuum destilliert. Ausb. 3.8 g, Siedp. 145～151°C/19.5 Torr. Die Hauptfraktion (2.9 g) vom Siedp. 148～150°C/19.5 Torr. hatte n_D^{25} 1.4767, d_4^{25} 1.0014 und MR_D 59.31 (Ber. 59.80).

***cis-cis*-2-Decahydronaphthoesäureäthylester.**—Dieser Ester wurde in ähnlicher Weise wie bei der 1-Ester aus der *cis-cis*-2-Säure (2.5 g) vom Schmp. 76～79°C hergestellt. Ausb. 2.4 g, Siedp. 145～152°C/19.5 Torr. Die Hauptfraktion (1.8 g.) von Siedp. 148～150°C/19.5 Torr. zeigte n_D^{25} 1.4755, d_4^{25} 0.9988 und MR_D 59.32 auf.

***trans-trans*-1-Decahydronaphthoesäureäthylester.**—Die reine *trans-trans*-1-Säure (3.0 g) lieferte den Ester (3.0 g) vom Siedp. 143～146°C/19.5 Torr. Die Hauptfraktion (2.5 g) vom 144～145°C/19.5 Torr. hatte n_D^{25} 1.4700, d_4^{25} 0.9826 und MR_D 59.71.

***trans-cis*-2-Decahydronaphthoesäureäthylester.**—Die reine *trans-cis*-2-Säure (4.5 g) ergab den Ester (4.2 g) vom Siedp. 145～150°C/20 Torr. Die Hauptfraktion (2.2 g) vom Siedp. 145～148.5°C/20 Torr. hatte n_D^{25} 1.4685, d_4^{25} 0.9784 und MR_D 59.37.

***cis-cis*-Decalyl-1-carbinol und dessen Tosylat.**—Zu einer Suspension von Lithiumaluminiumhydrid (1.4 g) in getrocknetem Äther (50 ccm) wurde eine Lösung des *cis-cis*-1-Säureesters (3.7 g) in getrocknetem Äther (30 ccm) unter Eiskühlung bei 0～5°C tropfenweise zugegeben, und nach der Entfernung des Eisbades noch 30 Min bei Raumtemperatur gerührt. Das Reaktionsgemisch wurde unter Eiskühlung mit verd. Schwefelsäure umgesetzt, und die organische Schicht wurde, nach dem Waschen mit Salzlösung, über Kaliumcarbonat getrocknet und

abgedampft. Der ölige Rückstand wurde in Vakuum destilliert, wobei ein zähes farbloses Öl (2.5 g) vom Siedp. 136～139°C/12 Torr. erschien, das im Kühlschrank zu einer Kristallmasse bald erstarrte. Die Ausbeute der Hauptfraktion war 2.5 g, Siedp. 138～138.5°C/12 Torr. Nach Umkristallisieren aus wässrigem Äthanol ergab sie Nadeln von Schmp. 55°C.

Fef. C, 78.66; H, 11.77. Ber. für $C_{11}H_{20}O$: C, 78.51; H, 11.98%.

Das Carbinol (1.5 g) in wasserfreiem Pyridin (5 cc) wurde bei 0～5°C mit pulverisiertem *p*-Toluolsulfochlorid (2.0 g) behandelt und nach Stehenlassen über Nacht im Kühlschrank zu einem Gemisch von Eis und konz. Salzsäure eingegossen. Das ausgefallene Öl erstarrte bald. Nach Absaugen wurde es zweimal aus Äthanol umkristallisiert. Das gereinigte Tosylat (2.0 g) war Blättchen vom Schmp. 67～67.5°C.

Gef. C, 67.15; H, 8.22. Ber. für $C_{18}H_{26}O_3S$: C, 67.06 H, 8.13%.

***cis-cis*-Decalyl-2-carbinol und dessen Tosylat.**—Bei ähnlicher Behandlung des *cis-cis*-2-Säureesters (2.2 g) mit Lithiumaluminiumhydrid (1.0 g) wie bei der *cis-cis*-1-Verbindung ergab sich ein Carbinol (1.4 g) als ein zäher Sirup vom Siedp. 145～148°C/20 Torr. Die Hauptfraktion (1.0 g) vom Siedp. 147～147.5°C/20 Torr. hatte n_D^{25} 1.4983, d_4^{25} 0.9891 und MR_D 49.87 (Ber. 50.56). Nach Stehenlassen einige Tage im Eisschrank erstarrte die Fraktion zu einem Kristallbrei. Nach dem Abpressen auf Ton und Umkristallisieren aus wässrigem Äthanol formten sich Nadeln vom Schmp. 68.6～68.8°C.

Gef. C, 78.61; H, 12.24%.

Das Carbinol (1.1 g) ergab ein Tosylat (1.0 g) als Nadeln, Schmp. 56.0～56.2°C aus wässrigem Äthanol. Der Misch-Schmp. mit dem bei 62°C schmelzenden *trans-cis*-2-Carbinyltosylat deprimiert zu 43.5～45.5°C.

Gef. C, 67.33; H, 8.30%.

***trans-trans*-Decalyl-1-carbinol und dessen Tosylat.**—Aus dem *trans-trans*-1-Säureester (2.8 g) und Lithiumaluminiumhydrid (1.2 g) ergab sich ein Carbinol (1.6 g), ein zäher Sirup vom Siedp. 133～136°C/12 Torr. Die Hauptfraktion (1.6 g) vom Siedp. 132～132.5°C/11.5 Torr. zeigte n_D^{25} 1.4952, d_4^{25} 0.9808 und MR_D 50.05 auf. Das Carbinol (1.0 g) ergab ein Tosylat (1.1 g) als Blättchen vom Schmp. 74.5°C aus wässrigem Äthanol.

Gef. C, 66.80; H, 8.41%.

***trans-cis*-Decalyl-2-carbinol und dessen Tosylat.**—Aus dem *trans-cis*-2-Säureester (4.0 g) und Lithiumaluminiumhydrid (1.5 g) ergab sich ein Carbinol (3.0 g) als ein zäher Sirup vom Siedp. 142～145°C/20 Torr, das im Kühlschrank zu einer Kristallmasse erstarrte. Die Ausbeute der Hauptfraktion war 2.5 g, Siedp. 144～144.5°C/20 Torr., und die Kristallmasse schmolz bei 29～30°C. Nach Umkristallisieren aus wässrigem Äthanol ergaben sich Nadeln vom Schmp. 31～31.5°C.

Gef. C, 78.28; H, 12.22%.

Das Carbinol (2.0 g) lieferte ein Tosylat (2.7 g) als Nadeln vom Schmp. 62°C nach Umkristallisieren aus Äthanol.

Gef. C, 67.12; H, 8.16%.

Messungen

Essigsäure.—Eisessig wurde zweimal durch Gefrieren gereinigt, mit 3% Essigsäureanhydrid und 1% Natriumacetat unter Rückfluss 2 Stdn. erhitzt, und dann fraktioniert.

Messungen von Acetolysegeschwindigkeit.—Das Tosylat und ein wenig Überschüss vom Natriumacetat wurden in 50 ccm Essigsäure gelöst, und auf 7～8 Ampullen verteilt, die sofort zugeschmolzen und in einem auf 110.1 ±0.1°C eingestellten Thermostat gebracht wurden. Nach einer bestimmten Zeit wurde eine Ampulle rasch auf 10°C abgekühlt, 5 ccm der Lösung sofort mit 0.05 N-Essigsäure Perchlorsäure mit Bromphenolblau als Indikator titriert, um das unreagierte Natriumacetat zu bestimmen. Die Geschwindigkeitskonstante (k) wurde nach der Formel erhalten:

$$k = (2.303/t)\log\{a/(a-x)\}$$

hier a: Anfangskonzentration des Tosylats, x: Konzentration der nach der Zeit t verbrauchten Base.

Die berechneten Intervallkonstanten befanden sich jedenfalls innerhalb der Fehlergrenzen

Tabelle III. Acetolyse von *trans-cis*-2-Decalylcarbinyltosylat in Anwesenheit von Natriumacetat bei 110.1°C

Zeit Sek.	AcONa ×10² Mol./l	Tosylat ×10² Mol./l	Intervallkonstante, k ×10⁵, Sek^{-1}
0.0	3.215	3.110	—
6600	3.021	2.916	0.977
12600	2.853	2.748	0.977
18000	2.703	2.598	0.997
21600	2.622	2.517	0.977
25200	2.534	2.429	0.981
28200	2.472	2.367	0.966
		Mittelwert	0.978

Tabelle IV. Acetolysegeschwindigkeitskonstanten bei 110.1±0.1°C

Tosylat vom	Tosylat ×10² Mol./l	AcONa ×10² Mol./l.	Konstante k, ×10⁵ Sek^{-1}
cis-4-*t*-Butylcyclohexylcarbinol	1.93	2.06	3.47
	1.55	—	3.35*
cis-cis-1-Decalylcarbinol	3.11	3.21	2.56
trans-trans-1-Decalylcarbinol	2.04	2.66	2.14
cis-cis-2-Decalylcarbinol	3.11	3.21	1.36
trans-cis-2-Decalylcarbinol	3.11	3.22	0.978
trans-4-*t*-Butylcyclohexylcarbinol	3.09	3.21	0.851
	1.85	2.10	0.871
	1.40	—	0.768*

* Wert bei 110.0°C[6])

von 3% aus dem Mittelwert. Beispielsweise wird ein typischer Verlauf der Acetolyse von *trans-cis*-2-Decalylcarbinyltosylat in Tabelle III gezeigt. Tabelle V zeigt die mittelen Acetolysegeschwindigkeitskonstanten erster Ordnung von den Tosylaten.

Acetolyse.—Acetolyse von den Tosylaten und Analyse der Acetolyseprodukte wurden auf jeden Fall in folgender Weise ausgeführt. 1 g Tosylat und 0.3 g Natriumacetat wurden in 35 ccm Essigsäure unter Rückfluss 35 Stdn. bei 145~150°C erhitzt. Die schwach gelbliche oder farblose Lösung wurde mit Wasser und Äther verdünnt, und dann ein grosser Teil der Essigsäure bei 0°C mit einer verdünnten Natriumhydroxydlösung neutralisiert. Die getrennte ätherische Schicht wurde mit Wasser, mit einer Natriumcarbonatlösung und wieder mit Wasser gewaschen. Aus der über Natriumsulfat getrockneten ätherischen Lösung wurde der Äther in Vakuum abgedampft. Ein schwach gelblicher öliger Rückstand wurde jedenfalls in fast quantitative Ausbeute (0.5~0.6 g) erhalten, welcher nach dem Ergebnis der gaschromatographischen Analyse nur aus einem Methylenderivat und Carbinylacetat bestand.

Der gaschromatographische Versuch wurde bei 180°C mit einem Gaschromatograph GCG-2 von Yanagimoto ausgeführt, in welchem eine Thermosol-2-Säule (2 m), Helium als Trägergas und eine aufgegebene Menge 6 μl benützt wurden. Die Gaschromatographiken der Reaktionsprodukte hatten jedenfalls nur zwei Piks mit Retentionszeiten ca. 6 und 60 Min. Der erste Pik war vom Methylenderivat und der letzte Pik vom Carbinylacetat, nach dem Befunde der unter den gleichen Bedingungen erhaltenen Retentionszeiten vom authentischen 2-Methylen-*trans*-decalin und *trans-cis*-2-Decalylcarbinylacetat. Das Flächenverhältnis vom Methylenderivat zum Acetat wurde berechnet, welches in Tabelle II gezeigt wird.

Ich danke herzlich Herrn Prof. Dr. Yojiro Tsuzuki für seinen Rat und Herrn Sadatoshi Akahori im Laboratorium für Organische Chemie der Universität Tokio, für die Elementaranalysen.

Die wissenschaftliche Hochschule zu Tokyo
(Tokyo Rika Daigaku)
Shinjuku-ku, Tokyo

Intramolecular Hydrogen Bonding in Some Aliphatic α- and β-Hydroxy-carboxylates

By Nobuo MORI, Satoshi OMURA, Osamu YAMAMOTO, Teruo SUZUKI and Yojiro TSUZUKI

(Received July 19, 1963)

High resolution proton magnetic resonance (NMR) spectroscopy has recently been employed as a powerful means for investigating various types of hydrogen bonds. It is useful when the changes in the chemical shift of a proton involved in the formation of a hydrogen bond are sufficiently large,[1] and it is useful as an indicator of hydrogen-bond formation similar to the changes in X–H stretching frequency due to the formation of a hydrogen bond.[2]

The formation of intramolecular hydrogen bonds in dilute solutions in non-polar solvents is a simple case, since in general only one species is involved. For various *o*-substituted phenols in carbon tetrachloride, the change in the chemical shift of the hydroxyl-proton due to the formation of an intramolecular hydrogen bond has been correlated with the corresponding change in the O–H stretching frequency.[3,4] In addition, the dilution-shift curves of *o*-halophenols[4,5] in carbon tetrachloride, quite different from that of phenol itself, are generally of an s-shape, with a reversal of the curvature at a relatively high concentration.

1) J. A. Pople, W. G. Schneider and H. J. Bernstein, "High Resolution Nuclear Magnetic Resonance," McGraw-Hill Book Co., New York, N. Y. (1959), p. 400.

2) G. C. Pimental and A. L. McClellan, "The Hydrogen Bond," W. H. Freeman and Co., San Francisco (1960), p. 142.

3) A. L. Porte, H. S. Gutowsky and I. M. Hunsbenger, *J. Am. Chem. Soc.*, **82**, 5057 (1960); J. R. Merrill, *J. Phys. Chem.*, **65**, 2023 (1961).

4) L. W. Reeves, *Can. J. Chem.*, **38**, 736 (1960); L. W. Reeves, E. A. Allan and K. O. Strømme. ibid., **38**, 1249 (1960); E. A. Allan and L. W. Reeves, *J. Phys. Chem.*, **66**, 613 (1962).

5) C. M. Huggins, G. C. Pimental and J. N. Shoolery, ibid., **60**, 1311 (1956).

The intramolecular hydrogen bonding in some aliphatic α- and β-hydroxy-carboxylates, particularly *d*-tartrates, has previously been studied by means of optical rotation[6] and by infrared spectroscopy.[7] The present paper will report on further investigation of the esters carried out by NMR and infrared spectroscopy.

Experimental

All ethyl esters were prepared by Fischer's method from hydroxy-carboxylic acids and ethyl alcohol in the presence of dry hydrogen chloride and were repeatedly fractionated. These esters are of the racemic form, unless otherwise stated, and are listed in Table I.

All the NMR spectra of the esters were measured in pure liquid or in solutions in varions concentrations up to 0.002 mol./l. in carbon tetrachloride at 20°C with a Varian Model DP 60 NMR spectrometer; chemical shifts were read by the sideband method, using tetramethylsilane (TMS) as an internal standard. Each shift in the table is the average of at least two independent measurements. Full analysis of the signals in the spectra could readily be made on the basis of the chemical shift and the relative intensity.

Many data of the infrared measurement were taken from the previous works,[7] while others were obtained in a similar manner at 20°C; the pure liquid measurement, however, was carried out with a Hitachi EPI-002 infrared spectrometer equipped with a sodium chloride prism and the solution measurement, with a Perkin-Elmer 21 spectrometer equipped with a lithium fluoride prism. The infrared and the NMR data obtained for the hydroxyl groups in the esters are shown in Table I.

Results and Discussion

Infrared Measurements of the Hydroxyl Groups. — The infrared spectra of the pure liquid esters display in each case one broad absorption band at a frequency of from 3420 to 3500 cm^{-1}, higher than the 3350 cm^{-1} of the hydroxyl in pure ethanol, as seen in Table I.

Table I. Chemical shifts and frequencies of hydroxyl groups

	Ethyl ester	B. p. °C/mmHg	Chemical shift $-\delta_{OH}$, c.p.s. from TMS			Frequency (ν_{OH}, cm^{-1})		
			δ_1[a]	δ_0[b]	$\Delta\delta$	ν_1[a]	ν_0[c]	$\Delta\nu$
I	Glycolate	75.0/35	267	103	164	3427	3545 (st) 3611 (w)	118
II	Lactate	72.5/37	259	126	133	3436	3543 (st) 3613 (w)	107
III	α-Hydroxyisobutyrate	65.5/31	238	145	93	3478	3544 (st) 3606 (w)	66
IV	β-Hydroxypropionate	79/12	250	85	166	3426	3582 (st) 3625 (sh)	156
V	β-Hydroxybutyrate	78/12	247	116	131	3430	3560 (st) 3625 (sh)	130
VI	Malate	144/24.3	246	137	109	3441	3535 (st) 3590 (sh)	94
VII	*d*-Tartrate	156.5/12	248	143	107	3454	3532 (st) 3588 (w)	78
VIII	*meso*-Tartrate	156/13.5 M. p. 58°C	—	145	—	—	3534 (st) 3584 (sh)	—
IX	*cis*-Hexahydrosalicylate	91.5/5	214	138	76	3494	3540 (st)	43
X	*trans*-Hexahydrosalicylate	92/3.5	237	124	113	3474	3560 (st) 3593 (st)	86
	α-Methoxypropionate	90/138						
	Methanol[d]		295	29	266			
	Ethanol[d]		320	42	278	3350	3631	281
	Isopropanol[d]		306	50	256			
	t-Butanol[d]		283	48	235			

a) Value for pure liquid.
b) Value extrapolated to infinite dilution in CCl_4.
c) Value at a concentration of ca. 0.02~0.04 mol./l. in CCl_4. "st" means a strong band, "w" a weak band and "sh" a shoulder.
d) The reported values in J. C. Davis, K. S. Pitzer and C. N. Rao, *J. Phys. Chem.*, **64**, 1744 (1960) were converted from Me-peak to TMS as standard.

6) T. M. Lowry and J. O. Cutter, *J. Chem. Soc.*, **121**, 532 (1925); W. Kauzmann and H. Eyring, *J. Chem. Phys.*, **9**, 41 (1941); Y. Tsuzuki, *J. Chem. Soc. Japan, Pure Chem. Sec.* (*Nippon Kagaku Kwaisi*), **64**, 282, 290 (1943).

7) a) Y. Tsuzuki et al., ibid., **75**, 1030, 1033 (1954); b) N. Mori, Y. Tsuzuki and Tsubomura, ibid., **77**, 459 (1956).

Of particular interest is the steric effect of the methyl group on the O–H frequency. The OH frequency of the α-hydroxy-esters increases in the order of the glycolate (3427 cm^{-1}), the lactate (3436 cm^{-1}) and the α-hydroxy-isobutyrate (3478 cm^{-1}) ; in the β-hydroxy- esters a similar trend is found for the β-hydroxypropionate (3426 cm^{-1}) and the β-hydroxybutyrate (3430 cm^{-1}). This is undoubtedly to be attributed to a weaker intermolecular hydrogen bond resulting from steric hindrance by the methyl group.

Preliminary measurements of the lactate and the tartrate carried out in concentrations of up to ca. 0.002 mol./l. have shown that the position of the O–H band is displaced with a decreasing concentration towards a higher frequency and that, simultaneously, a shoulder or an additional weak band appears, overlapped with the first strong band. At different concentrations below ca. 0.05 mol./l., the positions and relative intensities of the bands were substantially independent of the concentration. Accordingly, the spectra of the other esters were measured in a concentration near 0.03 mol./l. in carbon tetrachloride. The results of the measurement in solution are shown in Figs. 1—5.

In the α-hydroxy-esters, the strong and the weak bands appear at ca. 3545 and 3610 cm^{-1} respectively. The former should be assigned to the hydroxyl group intramolecularly associated with the carbonyl in the carboxylate

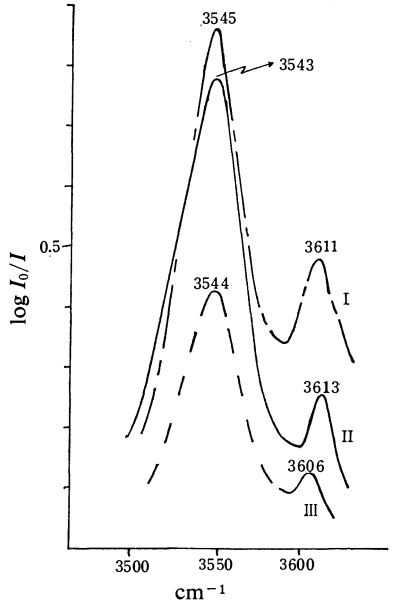

Fig. 1. IR spectra of hydroxyl groups in CCl_4.
I Ethyl glycolate, 0.002 mol./l., 30 mm. cell
II Ethyl lactate, 0.004 mol./l., 31 mm. cell
III Ethyl α-hydroxyisobutyrate, 0.002 mol./l., 30 mm. cell

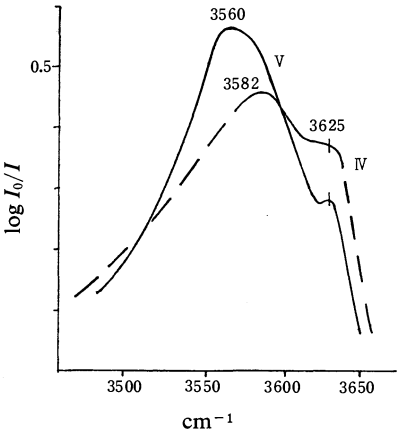

Fig. 2. IR spectra of hydroxyl groups in CCl_4.
IV Ethyl β-hydroxypropionate, 0.04 mol./l., 3 mm. cell
V Ethyl β-hydroxybutyrate, 0.046 mol./l., 3 mm. cell.

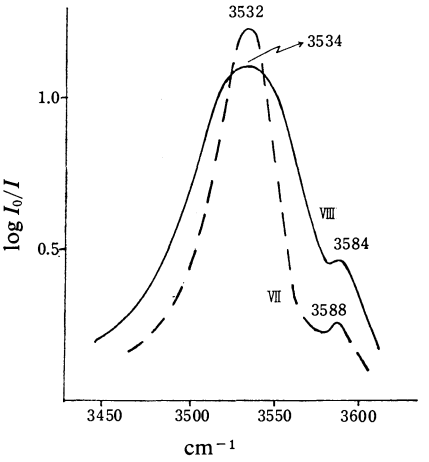

Fig. 3. IR spectra of hydroxyl groups in CCl_4.
VII Ethyl *d*-tartrate, 0.030 mol./l., 3 mm. cell
VIII Ethyl *meso*-tartrate, 0.010 mol./l., 30 mm. cell

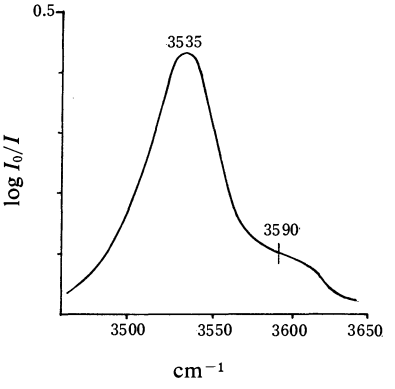

Fig. 4. IR spectrum of the hydroxyl group in ethyl malate in 0.026 mol./l. in CCl_4. (3 mm. cell).

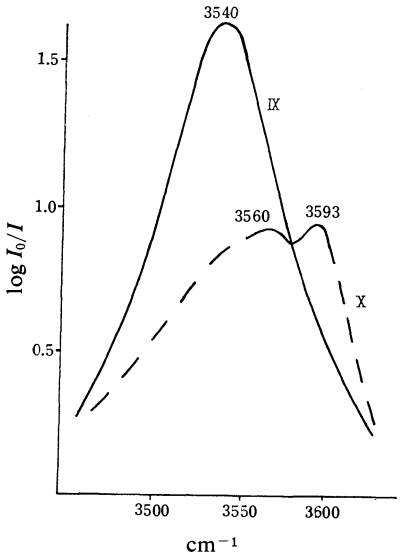

Fig. 5. IR spectra of hydroxyl groups in CCl_4.
IX Ethyl *cis*-hexahydrosalicylate, 0.03 mol./l., 30 mm. cell
X Ethyl *trans*-hexahydrosalicylate, 0.03 mol./l., 30 mm. cell.

group, as has been suggested in a previous paper.[7b] On the other hand, the latter is considerably lower than the 3631 cm^{-1} of the free hydroxyl of ethanol, although near that (3580~3610 cm^{-1}) of the intramolecularly hydrogen-bonded hydroxyl in many aliphatic diols.[8] Nevertheless, it is not evident whether the weak band is due to the hydroxyl associated with the ether-oxygen in the carboxylate group or to the free hydroxyl, because the electron-attracting nature of the carboxylate group would cause the absorption band of the α-hydroxyl to shift towards a lower frequency.

In all the β-hydroxy-esters except the isomeric hexahydrosalicylates, the strong band appears at 3560 or 3582 cm^{-1}; this is due to the hydroxyl intramolecularly associated with the carbonyl in the carboxylate group. The weak band at 3625 cm^{-1} may be due to the hydroxyl, either free or associated in a manner similar to that in the corresponding case of the α-hydroxy-esters. This may be compared with the 3630 cm^{-1} of the free hydroxyl in methyl 3-hydroxyurs-12-en-24-oate:[9]

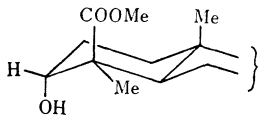

8) L. P. Kuhn, *J. Am. Chem. Soc.*, **74**, 2492 (1952).
9) A. R. H. Cole and G. T. A. Müller, *J. Chem. Soc.*, **1959**, 1224.

Further, when the frequencies of the hydroxyls in the α- and β-hydroxy-esters in a liquid (ν_1) and in a dilute solution (ν_0) are compared, the values of ν_0 for the strong band due to the α-hydroxyl are seen to be lower by 15~30 cm^{-1} than those for the β-hydroxyl; an even more remarkable difference is found in the values of $\nu_0-\nu_1$ or $\Delta\nu$. Consequently, this seems to be directly related to the strength of the intramolecular hydrogen bond in the α- and β-hydroxy-esters, which form a five- and a six-membered ring respectively. It is also of interest that, as the number of methyl groups on the carbon atom with the hydroxyl group increases, the frequencies of both the weak and the strong bands decrease and there is a simultaneous decrease in the intensity of the former band relative to that of the latter, as can be seen in Figs. 1 and 2. However, this is not surprising, since the methyl group would bring about a geometry faborable to form a stronger intramolecular hydrogen bond. Similarly, in isomeric ethyl hexahydrosalicylates, the intramolecular hydrogen bond of the hydroxyl formed with the carbonyl in the cis form is considered to be stronger than that of the trans form.

Chemical Shifts of Hydroxyl-protons and Other Protons.—As may be seen in Table I, the signal position (δ_1) of the hydroxyl-proton in each of the α- and β-hydroxy-esters in the pure liquid state moves towards a higher field with the increasing number of methyl groups on the carbon atom with the hydroxyl group. Such a trend is also seen in the series of alcohols except methanol, as may be seen in the table. This is undoubtedly due to a weaker intermolecular hydrogen bond resulting from steric hindrance by the methyl group, as has been pointed out in connection with the infrared measurement. Figure 6 shows the dilution-shift curves for some of the esters investigated. The insert in the figure, plotted on a larger scale, shows the detailed low-concentration measurements extrapolated to infinite dilution. The chemical shifts (δ_0) of the hydroxyl-protons in the table are those extrapolated to infinite dilution. It is of interest that the value of δ_0 in each of the α- and β-hydroxy-esters increases with the increased number of methyl groups on the carbon atom having the hydroxyl group, although no such trend is seen in the series of alcohols except methanol. Consequently, this must be related to the intramolecular hydrogen-bonding strength in the esters.

It is known that a stronger intramolecular hydrogen bond results in a lower value of the dilution shift, as may be seen, for example, in *o*-chlorophenol[5] in a carbon tetrachloride

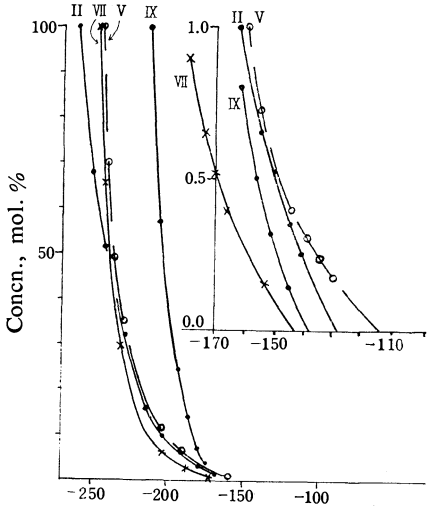

Chemical shift from TMS (60 Mc.), c.p.s.

Fig. 6. Changes in chemical shifts of hydroxyl protons in CCl_4. The numbers on the figure refer to the numbered compounds in Table I.

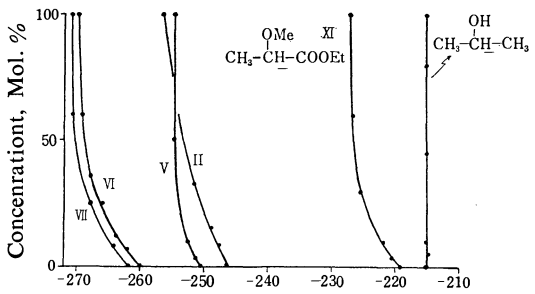

Chemical shift from TMS (60 Mc.), c.p.s.

Fig. 7. Dilution shifts for the proton on a carbon atom having a hydroxyl group in CCl_4. The numbers on the figure refer to the numbered compounds in Table I.

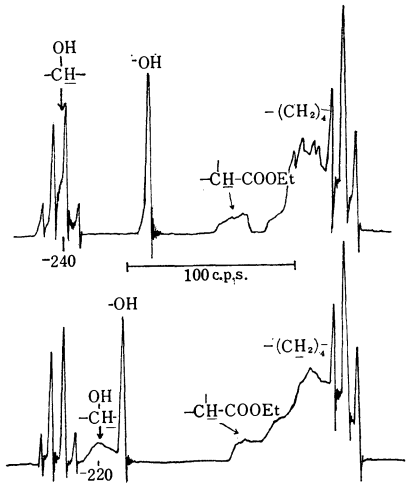

c.p.s. from TMS

Fig. 8. NMR spectra of isomeric hexahydrosalicylates in CCl_4 (20 mol. %) at 60 Mc.
IX *cis*-Isomer
X *trans*-Isomer

solution, where the dilution shift of the hydroxyl-proton is only 0.8 p.p.m. as compared with 2.8 p.p.m. of the phenols containing no intramolecular hydrogen bond; also, in β-chloroethanols[10] the value is 3.5 p.p.m., which is lower than the 4.5 p.p.m. of ethanol itself. Accordingly, the relatively low dilution shifts of 1.3~2.8 p.p.m. of the hydroxyl-protons in the esters are substantially caused by the intramolecular hydrogen bond formed in them. However, the curves of the dilution shifts for the esters, as shown in Fig. 6, are generally of an L-shape, differnt from that of *o*-chlorophenol, which features the reversal of the curvature at ca. 20 mol. % in carbon tetrachloride.[5] A similar reversal of curvature was observed even with ethanol itself at a low concentration of 1.5 mol. %[11] and also with some alcohols.[10] This might seem to lead to the conclusion that, even in a concentration as low as 1 mol. % (or ca. 0.01 mol./l.) or below, each of the esters consists of a system of monomers and intermolecularly associated species, with a decreasing proportion of the latter to the former on further dilution. This is strikingly different from the findings based on the infrared measurement of the hydroxyl group in a dilute solution, where substantially all molecules are present as monomer even in a concentration as high as 0.1 mol./l. This contradiction may be settled by a possible assumption that the changes in the chemical shift of the hydroxyl-proton on dilution are caused not only by the dissociation of the polymer, but also partially by some other factors such as those which would bring about the dilution shifts of protons other than the hydroxyl-proton, as will be mentioned later. Consequently, a dilution-shift curve of the hydroxyl-proton resulting from such factors would be superimposed on a real hydrogen-bond-shift curve of the proton to produce the dilution-shift curve of an apparent L-shape without the reversal of curvature.

In all the esters investigated, a similar dilution shift has also been observed for protons other than the hydroxyl-proton, most especially for the proton on the carbon atom with the hydroxyl group. The changes in the chemical shift of such protons in some of the esters are shown in Fig. 7. In general, the dilution shift of the proton on the carbon atom with

10) T. M. Conner and C. Reid, *J. Mol. Spectroscopy*, **7**, 32 (1961).
11) E. D. Becker, U. Liddle and J. N. Shoolery, ibid., **2**, 1 (1958).

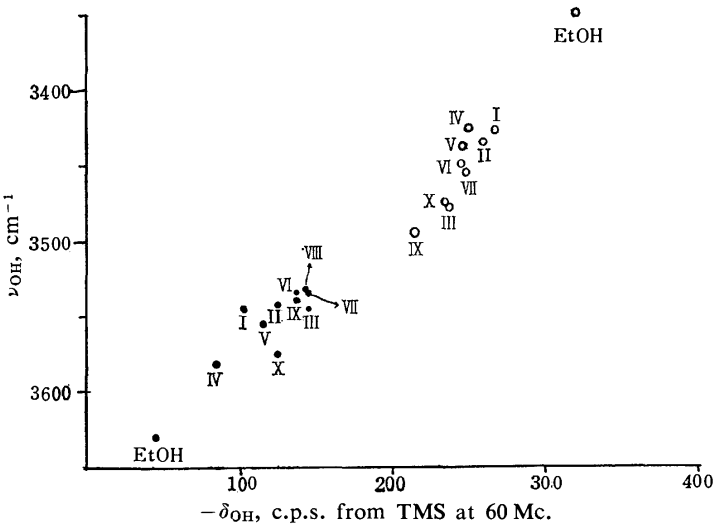

Fig. 9. Correlation of the chemical shift (δ_{OH}) with the frequency (ν_{OH}). The numbered points on the figure refer to the numbered compounds in Table I.
○ Pure liguid ● Infinitely diluted solution in CCl_4

either the hydroxyl or carboxylate group, A or B, is ca. 5 c. p. s. towards a higher field, while that of the proton on the carbon atom with both groups C is ca. 10 c.p.s. in the same direction. Further, the signals due to the methyl- and methylene-protons in the ethyl-carboxylate group shift by 3 c.p.s. towards a lower field. These shifts seem to have no direct relation to the hydrogen bonding, since there is a shift of 8 c.p.s. for the α-proton in ethyl α-methoxypropionate, but no shift for the α-proton in isopropanol.

$$\underset{\text{OH}}{\overset{|}{\text{-CH-}}} \qquad \text{-CH}_2\text{-COOC}_2\text{H}_5 \qquad \underset{\text{OH}}{\overset{|}{\text{-CH-}}}\text{COOC}_2\text{H}_5$$

(A) (B) (C)

Intramolecular Hydrogen Bonding in Ethyl Tartrates, Malate and Isomeric Hexahydrosalicylates.—*Ethyl meso-Tartrate.*—The infrared spectrum of ethyl *meso*-tartrate in Fig. 3 displays on strong absorption band at 3534 cm^{-1}, with a shoulder at 3584 cm^{-1}; the relative intensity of the former to the latter is ca. 10. As for the form of the intramolecular hydrogen bonding of this ester in a dilute solution in carbon tetrachloride, conformation I seems to be the most preferable of the three I—III given below. This suggestion is based on the facts that the frequency of the strong band is very close to that of the α-hydroxyl group, especially in ethyl lactate and α-hydroxyisobutyrate, but it is almost completely different from those of the β-hydroxyl group and some diols. Furthermore, the chemical shift of the hydroxyl-proton in infinite dilution is substantially equal to those of the α-hydroxy-esters, but quite different from those of the β-hydroxy-esters. On the other hand, the shoulder seems to be due to the hydroxyl associated with the carbonyl in the β-carboxylate group in the same molecule. Conformation III, containing a hydrogen bond between the two hydroxyls, is unlikely, at least in a carbon tetrachloride solution, because of the relatively high steric repulsion between the groups in the conformation.

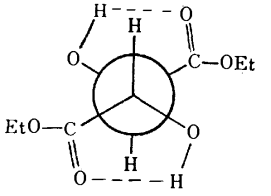

I

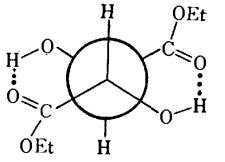

II

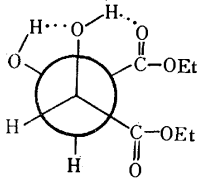

III

Ethyl d-Tartrate.—The infrared spectrum of this ester in Fig. 3 contains two bands, at 3532 and 3588 cm^{-1}, the relative intensity of the former to the latter being ca. 10. The frequencies of the bands and also the chemical shift in infinite dilution are the same as those of

ethyl *meso*-tartrate; therefore, the strong band should be assigned to the hydroxyl associated with the α-carboxylate-carbonyl in conformation IV, as has been suggested in a previous paper.[7b] It is not evident whether or not the weak band is due to the hydroxyl in conformation V or VI.

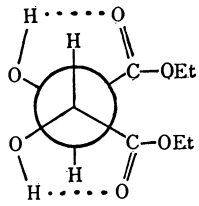

IV

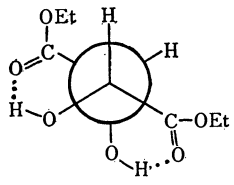

V

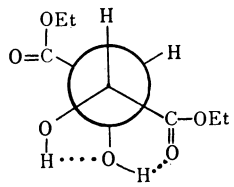

VI

Ethyl Malate.—The strong band at 3535 cm^{-1} in Fig. 4 may be assigned to the hydroxyl forming the same type of intramolecular hydrogen bond as in the α-hydroxy-esters. This assignment is borne out by almost the same chemical shift of the hydroxyl-proton as that of the tartrates. The shoulder near 3590 cm^{-1} may be due to the hydroxyl associated with the β-carboxylate-carbonyl.

Ethyl cis- and trans-Hexahydrosalicylates.—According to the NMR spectra (60 Mc.) of isomeric 4-*t*-butylcyclohexanols[12] and decalols[13], the axial hydrogen on the carbon atom with the hydroxyl group appears in a field higher by ca. 30 c.p.s. than the signal position of the epimeric equatorial hydrogen (−235 c.p.s. from TMS), the two signals being broadened unresolved spin-spin multiplets. This fact is useful in the conformational analysis of the isomeric ethyl hexahydrosalicylates.

The NMR spectrum of the cis form in carbon tetrachloride in Fig. 8-IX displays a signal at ca. −240 c.p.s. overlapped with that of the methylene protons in the ethylcarboxylate group. On the other hand, the spectrum of the trans form in Fig. 8-X has a broadened signal at ca. −220 c.p.s. The infrared spectrum of the cis ester in Fig. 5 has only one strong absorption band, at 3450 cm^{-1}; consequently, conformation VII, containing an intramolecular hydrogen bond of the axial hydroxyl with the carbonyl in the equatorial carboxylate group, shold be assigned for this isomer. On the other hand, the infrared spectrum of the trans form in Fig. 5 contains two bands at 3560 and 3593 cm^{-1} with the intensity ratio of ca. 3 : 1. The former may be due to the hydroxyl associated with the carbonyl in conformation VIII, and the latter, to one associated with the ether-oxygen in conformation IX.

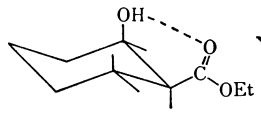

VII

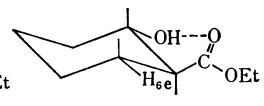

VIII

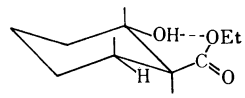

IX

The Correlation between Chemical Shifts and Frequencies.—For various *o*-substituted phenols in a dilute solution in carbon tetrachloride, the change in the chemical shift of the hydroxyl-proton on the formation of an intramolecular hydrogen bond has been correlated with the corresponding change in the O–H stretching frequency.[3,4] Gränacher reported a similar correlation for intermolecular hydrogen bonds.[14] In the present work, the chemical shifts of the hydroxyl-proton of the hydroxy-ester in the pure liquid state and in infinite dilution in carbon tetrachloride have been correlated with the stretching frequencies of the O–H band in the respective states. Figure 9 shows graphically the correlation between the above two parameters for all the esters studied as well as for ethanol for the purpose of comparison. All plots of the chemical shifts against the frequencies lie roughly on a straight line between the plots for ethanol in the liquid state and in infinite dilution.

Department of Chemistry
Tokyo College of Science
Shinjuku-ku, Tokyo
(N. M., S. O. & Y. T.)

Government Chemical Industrial
Research Institute, Tokyo
Shibuya-ku, Tokyo
(O. Y. & T. S.)

12) A. H. Lewin and S. Winstein, *J. Am. Chem. Soc.*, **84**, 2464 (1952).
13) J. I. Musher, ibid., **83**, 1146 (1961).
14) I. Gränacher, *Helv. Phys. Acta*, **34**, 272 (1961).

*The Chelating Behavior of Catechol-4-sulfonate with Iron(III) Ion**

By Yukito MURAKAMI and Katsuyuki NAKAMURA

(Received May 11, 1963)

Disodium 1,2-dihydroxybenzene-3, 5-disulfonate (Tiron) was found to form blue, violet and red complexes with iron(III)[1,2] in aqueous media, and these were referred to the 1 : 1, 2 : 1 and 3 : 1 (ligand to metal) complexes respectively.[2] Later, the interaction of Tiron with iron(III) in aqueous media at the ionic strength of 0.1 M was investigated quantitatively by means of both potentiometric and spectrophotometric methods, and the stability constants of the chelates were evaluated.[3] These investigations established the information that two sulfonate groups favor the strong coördinate bond formation and, thus, that Tiron may form various stable chelates with iron(III) in aqueous media.

For the present work, a catechol derivative with only one sulfonate group at the 4-position, monopotassium salt of catechol-4-sulfonic acid, was selected and the effect of a sulfonate group on the chelating behavior of the catechol with iron(III) was investigated.

Experimental

Reagent-grade $Fe(NO_3)_3 \cdot 9H_2O$ produced by the Wako Pure Chemical Industries, Ltd. was used to prepare an aqueous stock solution of iron(III) ions which was standardized by chelatometric titration. The method for the preparation of potassium catechol-4-sulfonate was described in a previous paper.[4]

The procedure for potentiometric titration was largely the same as has been mentioned elsewhere.[5] However, this procedure was modified in some occasions, since equilibrium was reached only slowly in the major pH region of potentiometric titrations when a sufficient amount of the ligand was not present. In the modified procedure (*the batch method*), a series of bottles containing measured amounts of the metal ion, ligand species, and a supporting electrolyte were used; varying amounts of a standard base were added in these bottles. These solutions were allowed to equilibrate at 30±0.1°C for 12~24 hr. in a nitrogen atmosphere, and then the pH of each sample was recorded. The pH readings thus obtained were verified by subsequent pH measurements from time to time.

The visible absorption spectra of the iron(III)-catechol-4-sulfonate system were measured with a Hitachi EPS-2-type recording spectrophotometer at various hydrogen ion concentrations. The hydrogen ion concentrations of the solutions were adjusted by adding proper amounts of a standard base (sodium hydroxide) or a standard acid (nitric acid). The concentrations of iron(III) ion, of catechol-4-sulfonate, and of the supporting electrolyte (potassium nitrate) in stock solutions were adjusted at 2.50×10^{-1} M, 7.50×10^{-4} M, and 0.10 M respectively.

Results and Discussion

Systems with Enough Ligand Present.—The potentiometric titration curve of the iron(III)-catechol-4-sulfonate system at a 10 : 1 molar ratio of ligand to metal ion is illustated in Fig. 1. Alkalimetric titration (from the lower pH region) and acidimetric titration (from the

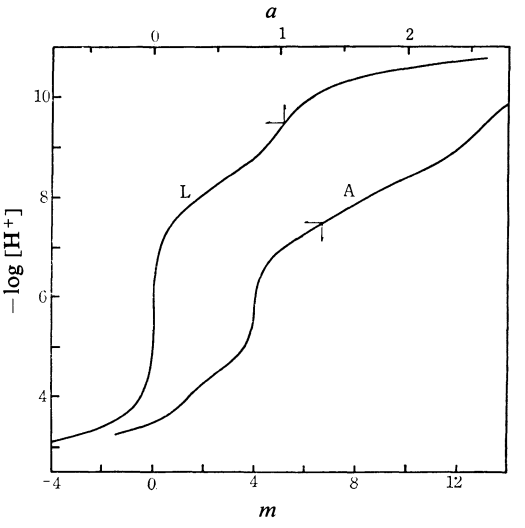

Fig. 1. Potentiometric titration of Fe(III)-catechol-4-sulfonate chelate system at 10 : 1 molar ratio (A) and potassium catechol-4-sulfonate alone (L). Total ligand concentrations: A, 2.00×10^{-3} M; L, 1.00×10^{-3} M; m=moles of base added per gram-ion of metal; a=moles of base added per mole of ligand; t=30°C; μ=0.10 M (KNO_3).

* Contribution No. 46 from the Department of Organic Synthesis, Faculty of Engineering, Kyushu University.

1) J. H. Yoe and A. L. Jones, *Ind. Eng. Chem., Anal. Ed.*, **16**, 111 (1944).
2) A. E. Harvey, Jr., and D. L. Manning, *J. Am. Chem. Soc.*, **72**, 4488 (1950).
3) G. Schwarzenbach and A. Willi, *Helv. Chim. Acta*, **34**, 528 (1951).
4) Y. Murakami, K. Nakamura and M. Tokunaga, This Bulletin, **36**, 669 (1963).
5) Y. Murakami, This Bulletin, **35**, 52 (1962); *J. Inorg. Nucl. Chem.*, **24**, 679 (1962).

higher pH region) of the system brought about titration curves which coincide with each other satisfactorily. The equilibrium of the solution at each addition of base or acid was established in a sufficiently short period of time, even though both titrations required some time (approximately 30 min.) for the attainment of the equilibrium in the region of $m=4$. Three inflection regions were observed in titration curve A in Fig. 1; the most significant of these was the one found at the m-value of 4. The first small inflection was observed in the region between 1.5 and 2.0 in m-value, while another one was found around $m=13$. The former corresponds to the formation of the 1 : 1 chelate, while the latter corresponds to the formation of the 3 : 1 chelate and to the liberation of the first proton of the free ligand existing in the solution. The steep jump of the titration curve at $m=4.0$ is undoubtedly ascribed to the completion of the 2 : 1 chelate formation.

Figure 2 shows titration curves for solutions containing a 3 : 1 ratio of ligand to metal ion. No precipitates were observed throughout titrations as in the case of the 10 : 1 system. In the alkalimetric titration of the 3 : 1 system, equilibrium of the titrating solutions was reached quickly in an acidic buffer region lying below $m=1.5$, where the 1 : 1 chelate formation is predominant, while it was established rather gradually in the second buffer region ($2.0<m<4.0$). A very slow establishment of equilibrium was observed in the second inflection region ($m=4.0$); the pH reading did not becomes stationary in a few hours of elapse. Then, the pH equilibration was completed in approximately half an hour for each addition of a base in the third buffer region, lying between 4.0 and 6.0 in m-value. Meanwhile, the 3 : 1 system was also titrated with an acid from the higher pH range. A good agreement of the titration curve with that obtained by alkalimetric titration was observed, except in the second buffer region and in the second inflection range. In order to clarify the extremely noticeable disagreement of both curves in the second inflection range and the minor one in the second buffer region, the third titration curve in Fig. 2 was obtained by the batch method, the procedure for which has been mentioned in the preceding section. It was ascertained that the equilibrium of the system was gained after 12 hr., even in the second inflection region. The pH reading drifted downward in alkalimetric titration in the range of slow equilibration, while it tended upward in acidimetric titration in the same range, so that the truly equilibrated curve may be expected to lie between these two titration curves. During the titration of the iron(III)-catechol-4-sulfonate system, the color of the solution varied remarkably, as in the case of the iron(III)-Tiron system, from a greenish blue in the first buffer region ($m<1.7$; $-\log[H^+]<4.0$) through a violet in the second buffer region ($m=4$; $-\log[H^+]=5.5\sim6.7$) to a deep red in the higher pH range ($m>6$; $-\log[H^+]>9.0$).

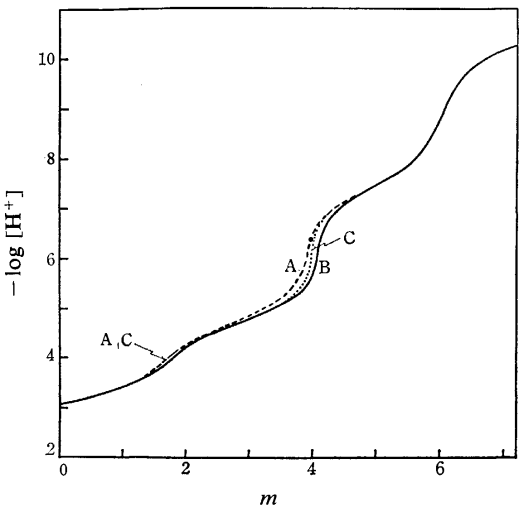

Fig. 2. Potentiometric titration of Fe(III)-catechol-4-sulfonate chelate system at total ligand concentration of 1.00×10^{-3} M with 3 : 1 molar ratio of ligand to metal ion : A, alkalimetric titration; B, acidimetric titration; C, batch method (equilibrated for 12~24 hr.); m=moles of base added per gram-ion of metal; $t=30°C$; $\mu=0.10$ M (KNO_3).

Such a slow establishment of equilibrium reading in the 3 : 1 titration curves may not be due to the hydrolysis of any iron(III) chelates, but to the slow rates of chelate-forming reactions. The following experimental results may support this statement. Firstly, the equilibration rate was accelerated in the presence of enough ligand i. e., in the 10 : 1 system, and no precipitates were observed in solutions of the 3 : 1 system which contained different amounts of base and which were left for a long enough period of time. Secondly, in the 3 : 1 system were observed two distinct inflection regions at $m=4.0$ and 6.0, which may be ascribed to the formation of the 2 : 1 and the 3 : 1 chelate respectively.

1 : 1 and 2 : 1 Systems.—It was rather difficult to examine the behavior of the chelate systems when the amount of ligand species present in the system was not enough to occupy all the coördination sites of the nuclear metal ion. The titration curves for 1 : 1 and 2 : 1 molar ratios of ligand to metal ion are shown in Fig. 3. The pH drifting was observed to start above $m=1.0$ ($-\log[H^+]=3.1$) in the

1 : 1 titration, while such a tendency of pH drifting was extreme above $m \approx 4.0$ in the 2 : 1 titration. The slow rates of both the chelate formation and the hydrolysis reaction of the chelates seem to make the system complex. The extensive hydrolysis of the partially-chelated metal ion conceivably occurs in this case in a manner similar to that in the iron-(III)-kojate chelate system.[5]

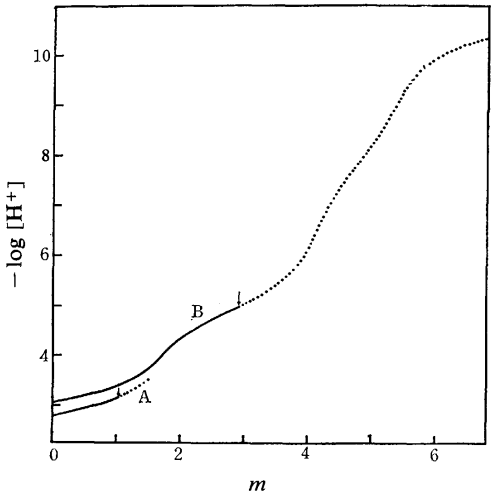

Fig. 3. Potentiometric titration of Fe(III)-catechol-4-sulfonate chelate system at total ligand concentration of 1.00×10^{-3} M, with these molar ratios of ligand to metal ion: A, 1 : 1; B, 2 : 1; t=30°C; μ=0.10 M (KNO_3). Dotted curves represent non-equilibrated titration; arrows indicate points where pH drifting became noticeable.

Stability Constants.—The stability constants calculated by the aid of Bjerrum's method[6] are shown in Table I, along with the data on the corresponding Tiron chelates reported by Schwarzenbach and Willi.[3] Because of the slow establishment of the equilibrium state, the stability constants for the 2 : 1 and the 3 : 1 chelate were evaluated with a lower precision. Moreover, the stability constant for the 1 : 1 chelate was not evaluated with enough accuracy due to some complexity of the system.

TABLE I. STABILITY CONSTANTS OF Fe(III) CHELATES
30.0±0.1°C; μ=0.10 M (KNO_3)

Ligand	$\log K_1$	$\log K_2$	$\log K_3$
Catechol-4-sulfonate	>17	14.0	9.1
Tiron[3]*	20.7	15.2	11.0

* t=20~22°C; μ=0.1 M (KCl)
For the definition of the stability constants, see Ref. 4.

Visible Absorption Spectra.—The visible absorption spectra of the 3 : 1 chelate system were measured at various pH's. The main absorption maximum of the chelate solution, which may be ascribed to the d-d transition of the metal-electron, is plotted as a function of the pH value of the chelate solution in Fig. 4. The color changes of the iron(III)-catechol-4-sulfonate system in aqueous media may be attributed to the stepwise formation of various chelates; the 1 : 1 chelate in the lower, the 2 : 1 in the middle, and the 3 : 1 in the higher pH region. The absorption maxima of these chelates in aqueous media are indicated in Table II, together with those of the Tiron chelates. It seems that the difference in stability constants between the iron(III)-Tiron and the iron(III)-catechol-4-sulfonate chelates does not cause any appreciable spectral shifts among

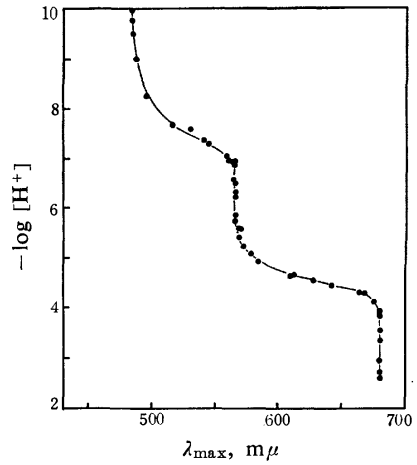

Fig. 4. Variation in absorption maximum of Fe(III)-catechol-4-sulfonate chelate system with hydrogen ion concentration, at total ligand concentration of 7.50×10^{-4} M with 3 : 1 molar ratio of ligand to metal ion; μ=0.010 M (KNO_3).

TABLE II. VISIBLE ABSORPTION SPECTRA OF THE Fe(III) CHELATES

Ligand	Absorption maximum, mμ			Intensity, log ε	
	1 : 1 Chelate	2 : 1 Chetate	3 : 1 Chelate	2 : 1 (565 mμ)	3 : 1 (483 mμ)
Catechol-4-sulfonate	680	565	483	3.62	3.74
Tiron[1,2]	—	560	480	—	—

6) J. Bjerrum, "Metal Ammine Formation in Aqueous Solution," P. Haase & Son, Copenhagen (1942).

the corresponding chelates in these systems. It seems, therefore, that Tiron and catechol-4-sulfonate produce similar ligand fields for the iron(III) ion.

Summary

Both potentionmetric and spectrophotometric measurements have been carried out in order to study the chelating tendencies of catechol-4-sulfonate with iron(III) ions in aqueous media at the ionic strength of 0.10 M. Even in the 3 : 1 (ligand to metal ion) system, the equilibrium of the titrating solution was established gradually, except in the lower pH range. When the amount of the ligand was not sufficient to satisfy the coördination number of the iron(III) ion, the titration system became complicated because of both the slow attainment of equilibrium in the chelate formation and the hydrolysis of the chelates.

The stability of the iron(III)-catechol-4-sulfonate was found to be slightly less than that of the corresponding iron(III)-Tiron chelates. The visible absorption spectral data indicated that Tiron and catechol-4-sulfonate produce similar ligand fields for the iron(III) ion.

Department of Organic Synthesis
Faculty of Engineering
Kyushu University
Hakozaki, Fukuoka

The Re-activation Analysis of Aluminum—The Activation Analysis of Aluminum with Special Reference to Yield Determination

By Yuichiro KAMEMOTO and Shigeru YAMAGISHI

(Received May 13, 1963)

In an activation analysis using short-lived nuclides with radiochemical separation, the chemical yield has been determined by, for instance, the gravimetry, volumetry, photometry, polarography and tracer method. The yield determination by these methods requires a long period of time, however; therefore, these methods cannot be used in rapid determination. A method in which the chemical yield is determined by re-irradiating the counted sample and which can be completed in a short time is suitable for rapid determination.

On the other hand, it is not desirable, from the standpoint of the precise determination of the chemical yield, that other methods, such as the gravimetry, volumetry, photometry and polarography, be applied to the yield determination of elements being analyzed after their activity has been counted.

When the correction factor of chemical yield is previously determined by a radioisotope tracer under the same conditions as the practical and is used for the correction of chemical yield in each separation, there is the disadvantage that an error is produced by the difference between the chemical yields obtained in the individual separations.

The present authors have devised an activation analysis in which the chemical yield is easily corrected by the re-activation of the counted sample; they have designated this method "re-activation analysis".[1)]

After the addition of a carrier to the irradiated sample solution, the element to be determined is isolated in a radiochemically pure form by solvent extraction, transferred into a polyethylene tube, and its γ-ray spectrum measured. It is then allowed to decay to a negligible activity level and sealed again in a polyethylene tube. This sample is re-activated with neutrons and counted. The element is determined by the induced activity from the first irradiation, which is corrected for the chemical yield calculated from the induced activity from the second irradiation. In other words, the technique of non-destructive activation analysis is applied to determine the yield of radiochemical separation in normal destructive activation analysis. This method has the advantage of determining the chemical yield without loss of the counted sample.

This method has been satisfactorily applied to the determination of aluminum.

1) Y. Kamemoto and S. Yamagishi, *J. Chem. Soc. Japan, Pure Chem. Sec.* (*Nippon Kagaku Zasshi*), **84**, 291 (1963).

Theoretical

This re-activation technique consists of these steps: the first irradiation of a sample, the addition of a carrier, radiochemical separation, the counting of the induced activity from the first irradiation, the sealing of the counted sample in a polyethylene tube, cooling, a second irradiation, and the counting of the induced activity from the second irradiation. For rapid radiochemical separation, a solvent extraction method was adopted. In this method the carrier to be added is sometimes limited to a rather small amount. Therefore, the amount of the element to be determined cannot be disregarded in the calculation of the chemical yield. From these considerations, an equation for determining the element in the sample from the induced activities from the first and the second irradiation was derived as follows:

$$\text{Chemical yield} = \frac{W_c'}{W_c + W} \tag{1}$$

where

W: weight of the aluminum in the sample (g.),

W_c: weight of the aluminum carrier added to the first irradiated sample (g.),

W_c': weight of the aluminum isolated from the sample after the addition of the carrier (g.).

When the chemical yield is 100%, the induced activity, A, from the first irradiation is:

$$A = A_{sam} \times \frac{W_c + W}{W_c'} \tag{2}$$

where A_{sam} is activity of the ^{28}Al isolated from the first irradiated sample.

The specific activity in the first irradiation is the same in unknown and the standard samples.

Therefore,

$$A/W = A_{st}/W_{st} \tag{3}$$

where

A_{st}: the induced activity of the standard aluminum from the first irradiation,

W_{st}: the amount of the standard aluminum for the first irradiation.

From Eqs. 2 and 3,

$$W = \frac{A_{sam} \times W_c \times W_{st}}{A_{st} \times W_c' - A_{sam} \times W_{st}} \tag{4}$$

The specific activity in the second irradiation is also the same in the unknown and the standard samples.

Therfore,

$$A_{sam}'/W_c' = A_{st}'/W_{st}' \tag{5}$$

where

A_{sam}': the induced activity of the ^{28}Al isolated from the second irradiation,

A_{st}': the induced activity of the ^{28}Al of the standard aluminum from the second irradiation,

W_{st}': the amount of standard aluminum for the second irradiation.

From Eqs. 4 and 5,

$$W = \frac{A_{sam} \times W_c \times W_{st}}{(A_{st} \times A_{sam}' \times W_{st}'/A_{st}') - A_{sam} \times W_{st}} \tag{6}$$

Experimental

Standard Sample.—4.7 mg. of a spectrographically pure aluminum rod made by Johnson Matthey Co., Ltd., was dissolved in 1 ml. of sulfuric acid. After evaporation, the residue was dissolved in water and diluted to 50 ml. This solution was further diluted to give several solutions of different aluminum concentration. Each 1 ml. of the standard solution was sealed in a polyethylene tube and placed in the center of a capsule packed with soft paper.

Sample. — Samples containing different amounts of aluminum, manganese, sodium and magnesium were prepared in the same way as the aluminum standard.

Apparatus. — The JRR-1 reactor was used as a neutron source, while the RCL-256 channel pulse-height analyzer with a 1.75×2 inch NaI (Tl) crystal (well type) attached was used as a counter.

Neutron Irradiation.—All irradiations were made in the No. 16 experimental hole (pneumatic tube) at a neutron flux of about 3×10^{11} n/cm^2/sec. The first irradiation was continued for 3 min., and the second irradiation, for 10 sec.

Procedure. — This method consists of the first irradiation, the addition of the carrier, solvent extraction, counting, the second irradiation, cooling, and counting. The above procedure was repeated for each sample with the reactor always in the same stationary state.

The sample solution irradiated in the reactor for 3 min. was transferred into a separating funnel. An aluminum carrier solution (94.0 μg. Al) was added to this solution. After the further addition of 50 ml. of an oxine solution containing 30 mg. of oxine, 1.5 ml. of an acetic acid solution and 2.5 g. of sodium acetate, aluminum was extracted with 5 ml. of benzene.[2-4] The organic phase was transferred into a polyethylene tube, which was then mounted in the NaI (Tl) crystal 5 min. after the end of the irradiation; it was counted for 2 min., and the resultant γ-ray spectrum was measured. The polyethylene tube containing the benzene phase was sealed again and was kept sufficiently long to allow the aluminum-28 activity decay. It was then irradiated again for 10 sec. and cooled for 2 min., and the γ-ray spectrum was measured for one minute.

2) E. Sudo, ibid., 72, 718 (1951).
3) H. Nishida, *Japan Analyst* (*Bunseki Kagaku*), 4, 39 (1955).
4) S. Yokosuka, ibid., 5, 71 (1956).

In the first irradiation, the standard sample was irradiated for 3 min. and measured for the γ-ray spectra 5 min. after irradiation in the same manner as for the unknown sample. In the second irradiation, the standard sample was irradiated for 10 sec., cooled for 2 min., and counted for one minute.

In each of the resultant gamma spectra, the height of the photopeak due to the 1.78 MeV. γ-ray from the ^{28}Al was measured.

Results and Discussion

γ-Ray Spectrum.—An example of the γ-ray spectrum of ^{28}Al, which was measured after irradiation and extraction, is shown in Fig. 1.

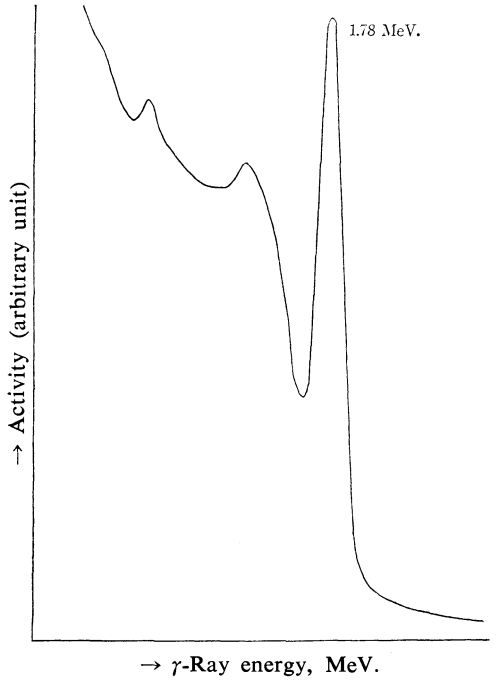

Fig. 1. γ-Ray spectrum of ^{28}Al of sample No. 10.

Calibration Curve. — The calibration curves of aluminum for the first and the second irradiation are shown in Figs. 2 and 3 respectively.

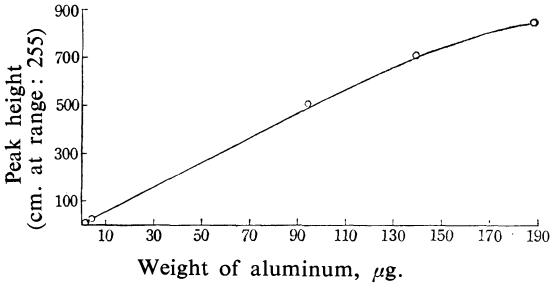

Fig. 2. Calibration curve of aluminum for the first irradiation.

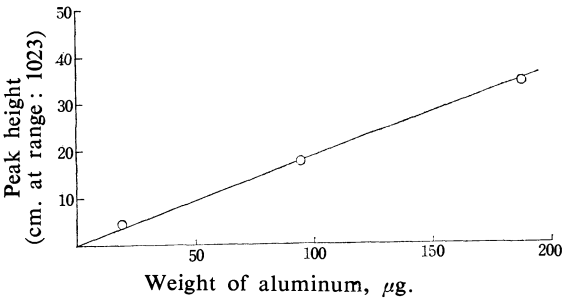

Fig. 3. Calibration curve of aluminum for the second irradiation.

In the concentration ranges of aluminum of 0~100 and 0~190 μg. for the first and the second irradiation respectively, the relation between activity and concentration was linear. Therefore, in these concentration ranges aluminum could be determined with each standard sample in the first and the second irradiation.

Result.—The determination results of aluminum by this method are shown in Table I.

Table I. Analytical results by this method

Sample No.	Sample: Al added μg.	Sample: Other element added, mg.	Al found μg.
1	3.76	0	3.34
2	3.76	0	3.97
3	3.76	0	3.73
4	3.76	0	3.81
5	3.76	0	3.72
6	1.88	0	1.92
7	0.94	0	0.99
8	3.76	Mn, 1	4.64
9	3.76	Mn, 0.1	4.45
10	3.76	Mg, 1	3.69
11	3.76	Mg, 0.1	3.80
12	3.76	Na, 1	3.78

The coefficient of the variation was 1.22% for the determination of 3.76 μg. of aluminum. This value is the total error produced in this method, including the error due to the neutron flux variation in the reactor.

Interference.—The γ-rays which may be confounded with the γ-ray of aluminum at 1.78 MeV. are that at 1.734 MeV. of ^{90}Y, at 1.81 MeV. of ^{56}Mn, and at 1.853 MeV. of ^{88}Rb. The interefence by ^{56}Mn, ^{24}Na and ^{166}Ho must also be taken into account because of their high activation cross sections and saturation factors.[5]

The present authors also examined the interference by sodium and manganese which

5) T. Nakai, S. Yajima, M. Okada, K. Shiba and T. Moki, *J. Chem. Soc. Japan, Pure Chem. Sec.* (*Nippon Kagaku Zasshi*), **81**, 104 (1960).

was sometimes observed in the non-destructive determination of aluminum.

Since sodium and rubidium were not extracted with an oxine-benzene solution, these elements did not affect the determination of aluminum in the present method. It could be considered that manganese did not affect it either because of its non-extractability with an oxine-benzene solution. However, some interference by manganese was found. This interference may be due to some precipitation of manganese hydroxide at the pH value of the extraction step.

The induced activities of sodium and manganese obstruct the photopeak of aluminum or cause a pile-up phenomena in the γ-ray spectrum when the amount of these elements in the sample material is 25$\sim$250 times as much as that of the aluminum. In such cases, the non-destructive determination of aluminum is not practicable. In the proposed method, sodium does not affect the determination of aluminum. Manganese causes an error of about 18% in the determination of aluminum, but a semi-quantitative determination is possible. These results show the advantages of the present method over other non-destructive methods.

Division of Chemistry
Japan Atomic Energy Research Institute
Tokai-mura, Ibaraki

*The Nuclear Magnetic Resonance Spectra of Olefinic Protons and the Substituent Effects. III. Trans-forms of Methyl β-Substituted Acrylates, β-Substituted Vinyl Methyl Ketones and β-Substituted Acryloyl Chlorides**

By Jun NIWA and Hazime KASIWAGI

(Received June 4, 1963)

It was reported in Part I that a Hammett-type relationship was applicable to the chemical shifts of olefinic protons situated at the cis-position to terminal substituents in the trans-forms of ω-substituted styrenes and in those of 1-substituted propenes ($RCH_A=CH_BX$, invariable substituent; R=C_6H_5, CH_3).[1] In these systems, the invariable substituent was an electron-repulsive methyl group or an aromatic ring which might constitute a conjugated system with the olefinic part. The present authors are concerned with such systems in which the invariable substituent of a series of compounds is strongly electron-attractive and conjugates with the olefinic part.

As examples of such systems, a series of trans-forms of methyl β-substituted acrylates, β-substituted vinyl methyl ketones and β-substituted acryloyl chlorides were chosen. The authors have investigated the results of the NMR absorption of these compounds from the viewpoint of a Hammett-type relationship. Moreover, the trends of the proton shifts in these compounds have been compared with those of ω-substituted styrenes and 1-substituted propenes.

Experimental

Two Varian 4300-B type spectrometers operating at 56.4 Mc. and 60 Mc. were used in obtaining the spectra. The conditions of measurement were the same as described in Part I.[1]

All the compounds examined have a trans-configuration. The acrylate derivatives are as follows: Methyl β-methylcrotonate, methyl crotonate, methyl acrylate, methyl cinnamate, methyl β-bromoacrylate, methyl β-chloroacrylate, dimethyl fumarate, methyl β-acetylacrylate and β-methoxycarbonylacryloyl chloride. The spectra of the corresponding free acids were also measured in glacial acetic acid. The methyl vinyl ketone derivatives are as follows: Methyl vinyl ketone, methyl styryl ketone and methyl acetylacrylate. As for the acryloyl chloride derivatives, crotonyl chloride, cinnamoyl chloride and β-methoxycarbonylacryloyl chloride were used. The synthesized compounds had the following properties: β-Methyl crotonic acid, m. p. 66~67°C; its ester, b. p. 132°C; β-chloroacrylic acid, m. p. 83.5~84°C; its ester, b. p. 22°C under 12 mmHg; β-bromoacrylic acid, m. p. 115~116°C; its ester, b. p. 20°C under 5 mmHg; β-methoxycarbonylacryloyl chloride, b. p. 65°C under 15 mmHg. Methyl

* Presented at the 15th Annual Meeting of the Chemical Society of Japan, Kyoto, April, 1962.

1) H. Kasiwagi and J. Niwa, This Bulletin, 36, 405 (1963).

acrylate (b. p. 80.5°C), methyl crotonate (b. p. 118~119°C), crotonic acid (m. p. 71~72°C), fumaric acid (m. p. 286~287°C), methyl β-acetyl acrylate (b. p. 196.8~197.3°C) and methyl vinyl ketone (b. p. 33~34°C under 130 mmHg) were commercially obtained and purified.* The physical properties of the other compounds were described in Part I.

Results and Discussion

The spectra of olefinic protons of methyl β-substituted acrylates, β-substituted vinyl methyl ketones and β-substituted acryloyl chlorides are of the simple AB-type, with the exception of those of methyl crotonates, methyl acrylate and methyl vinyl ketone. Methyl crotonate gives the spectra corresponding to the ABX_3-type, while the spectra of methyl acrylate and methyl vinyl ketone are attributed to the ABC-type. In the spectra of β-methoxycarbonylacryloyl chloride, a single signal was observed for the olefinic protons. The analyses of the spectra of methyl acrylate and methyl vinyl ketone have been compared with the results obtained by Castellano and Waugh[2] and by Brügel et al.[3] respectively. The chemical shifts obtained by the analysis of the spectra are summarized in Table I.

In series of compounds here examined ($RCH_A{=}CH_BX$, $R{=}CO_2CH_3$, $COCH_3$, COCl), since the invariable substituent (R) conjugates with the olefinic part, it may be expected that the olefinic proton shifts would be governed by Hammett's substituent effect, at least qualitatively. Meanwhile, the authors have observed that a qualitative relationship exists between the shifts of protons (H_A) situated at the cis-position to substituents in mono-substituted ethylenes[4] ($RCH_A{=}CH_BX$, R=H) and Hammett's σ. The τ-values of the proton shifts are shown in the table. The authors examined Hammett's substituent effects for the proton shifts in these four systems, comparing the former systems with the latter. In this case, it must be taken into account that the magnetic anisotropy of the substituents and other magnetic effects act as disturbing factors in the investigation of polar substituent effects. As has been considered in Part I, however, such disturbing factors do not seem to be much for the shifts of H_A, with the exception of a few cases. This would imply that the chemical shifts of H_A in these compounds are governed mainly by the polar substituent effects.

Similarly, as in Part I, Fig. 1 shows the relationship between the τ-values of H_A in these compounds and Hammett's σ_p. Figure 2 also shows the relationship between the τ-values of H_A and Taft's parameter, $0.40\,\sigma_I + 0.70\,\sigma_R$.[5] In the figures, the plot for the H_A of styrene is corrected to 4.79 p. p. m.[1,4,6] and that of acrylonitrile, to 3.80 p. p. m.[7] In the series of β-substituted acrylates, the H_A of methyl cinnamate may also be lowered by the

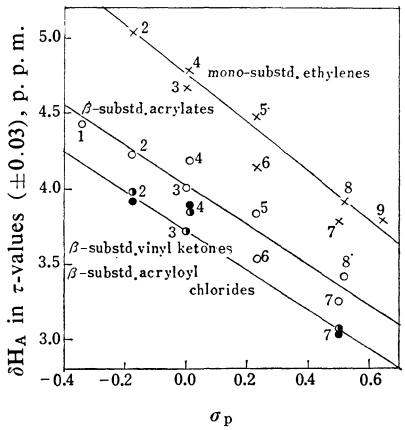

Fig. 1. The cis-proton chemical shifts of $RCH_A{=}CH_BX$, plotted vs. Hammett's σ_p. The substituents X are: 1, $(CH_3)_2$; 2, CH_3; 3, H; 4, C_6H_5; 5, Cl; 6, Br; 7, CO_2CH_3; 8, $COCH_3$; 9, CN.

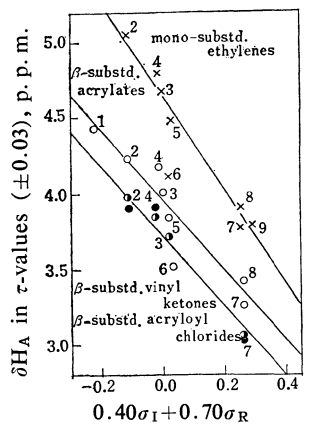

Fig. 2. The cis-proton chemical shifts of $RCH_A{=}CH_BX$, plotted vs. Taft's parameter, $0.40\,\sigma_I + 0.70\,\sigma_R$. The substituents X are: 1, $(CH_3)_2$; 2, CH_3; 3, H; 4, C_6H_5; 5, Cl; 6, Br; 7, CO_2CH_3, 8, $COCH_3$; 9, CN.

* Products of the Tokyo Kasei Kogyo Co., Ltd., and of the Wako Pure Chemical Industries, Ltd.

2) S. Castellano and J. S. Waugh, *J. Chem. Phys.*, **34**, 295 (1961).

3) W. Brügel, Th. Ankel and F. Krückberg, *Z. Elektrochem.*, **64**, 1121 (1961).

4) C. N. Banwell and N. Sheppard, *J. Mol. Phys.*, **3**, 351 (1960); A. A. Bothner-By and C. Naar-Colin, *J. Am. Chem. Soc.*, **83**, 231 (1961).

5) R. W. Taft, Jr., ibid., **79**, 1045 (1957); R. W. Taft, Jr., and I. C. Lewis, ibid., **80**, 2436 (1958).

6) C. E. Johnson, Jr., and E. A. Bovey, *J. Chem. Phys.*, **29**, 1012 (1958).

7) G. S. Reddy, J. H. Goldstein and L. Mandell, *J. Am. Chem. Soc.*, **83**, 1300 (1961).

TABLE I. PROTON CHEMICAL SHIFTS OF ACRYLIC ACID, METHYL ACRYLATE, METHYL VINYL KETONE, ACRYLOYL CHLORIDE, ETHYLENE AND THEIR DERIVATIVES,
$RCH_A=CH_BX$ (R : CO_2CH_3, $COCH_3$, COCl, H)

Chemical shifts in τ-values in p. p. m., ± 0.03 p. p. m.

a) Trans-forms of β-substituted acrylic acid and their methyl esters

Substituent	R : CO_2H[a]			R : CO_2CH_3		
	δH_A	δH_B	δH_C	δH_A	δH_B	δCO_2CH_2-H
$(CH_3)_2$	4.31			4.44		6.40
CH_3	4.20	2.93		4.24	3.13	6.36
H	4.05	3.71	4.31	4.01	3.78	6.32
C_6H_5	3.54	2.21		3.69	2.43	6.31
Br	3.47	2.23		3.52	2.43	6.27
Cl	3.72	2.48		3.84	2.69	6.29
CO_2H	3.12	3.12				
CO_2CH_3				3.26[b]	3.26[b]	6.25[b]
$COCH_3$				3.43	3.06	6.22
COCl				3.04	3.04	6.15

b) Trans-forms of β-substituted vinyl methyl ketone and β-substituted acryloyl chloride

Substituent	R : $COCH_3$		R : COCl	
	δH_A	δH_B	δH_A	δH_B
CH_3	3.99	3.24	3.91	2.81
H	3.72	3.91		
C_6H_5	3.35	2.55	3.41	2.20
CO_2CH_3	3.06	3.43	3.04	3.04

c) Mono-substituted ethylenes

Substituent	R : H	
	δH_A	δH_B
CH_3[e]	5.04	4.27
H[d]	4.67	4.67
C_6H_5[d]	4.29	3.31
	4.36[e]	3.35[e]
Br[d]	4.12	3.51
Cl[d]	4.48	3.70
CO_2CH_3[e]	3.78	4.01
$COCH_3$[e]	3.91	3.72
CN[d]	4.09	4.47

a) The values were obtained from measurement with the glacial acetic solution owing to the low solubility of the compounds in carbon tetrachloride.
b) Measurement was performed with the saturated solution in carbon tetrachloride.
c) Adopted from tha data measured in the same concentration by Bothner-By et al. A. A. Bothner-By and C. Naar-Colin, *J. Am. Chem. Soc.*, **83**, 231 (1961).
d) Cited from the data measured in the same concentration by Banwell et al. C. N. Banwell and N. Sheppard, *J. Mol. Phys.*, **3**, 351 (1960).
e) Measured by the authors.

long-range shielding effect of the benzene ring, which is situated at the cis-position to H_A. If the magnitude of the lowering effect is estimated as in styrene, the τ-value of H_A may be corrected to 4.19 p. p. m. This correction may, however, be overestimated, because the methoxycarbonyl group in this compound is strongly electron-attractive, which would diminish the effect of the benzene ring current. As for the Cl, Br, CO_2CH_3 and $COCH_3$ groups, the consideration made in Part I would hold in the present systems. In Figs. 1 and 2 a rough correlation may be observed, but it seems to be somewhat disintegrated compared with ω-substituted styrenes and 1-substituted propenes. Moreover, it is also observed that the plots for the corresponding substituents in the ethylene derivatives and in the β-substituted acrylates deviate similarly from the correlation line. Therefore, the same kind of correlation may be expected among the H_A-shifts themselves in both systems. In Fig. 3 a fairly clear

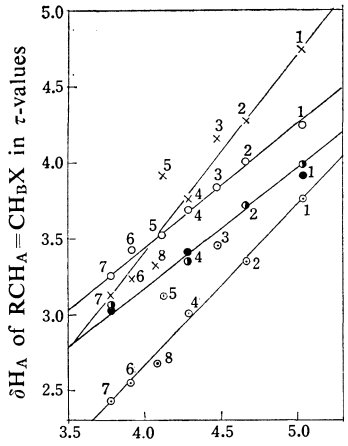

Fig. 3. The correlation among δH_A of methyl β-substd. acrylates (○), β-substd. vinyl methyl ketones (◑), β-substd. acryloyl chlorides (●), ω-substd. styrenes (⊙) and 1-substd. propenes (×). The substituents X are; 1, CH_3; 2, H; 3, Cl; 4, C_6H_5; 5, Br, 6, $COCH_3$, 7, CO_2CH_3, 8, CN.

correlation among them may be observed. This suggests that, in these systems, the modes of the transmission of substituent effects are essentially similar. Figure 3 also shows the relation between the H_A-shifts of ω-substituted styrenes (and 1-substituted propenes) and those of the ethylene derivatives. In this case, however, the correlation is considerably disintegrated. Especially, the plots for halogen substituents deviate largely from the correlation line. (With regard to the origin of the anomalous behavior of the H_A-shifts caused by halogen atoms, further invetigation is necessary.) On the other hand, it was reported in Part I that a fairly clear correlation existed between the H_A-shifts of ω-substituted styrenes (and 1-substituted propenes) and the ortho-proton shifts of mono-substituted benzenes. From what has been stated above with regard to the modes of the transmission of substituent effects, these six olefinic systems may be classified into two types — one is the system rather resembling the benzene derivatives, and the other, the ethylene derivatives. This may correspond to the difference between the natures of the conjugated systems, of which the former has the electron-repulsive invariable substituents and the latter, the electron-attractive. Also, the slope of each correlation line decreases, on the whole, in the order of the σ-value of the invariable substituent, namely, $CH_3 > H \simeq C_6H_5 > CO_2CH_3 \simeq COCH_3 \simeq COCl$. This probably illustrates how the overall trends of the H_A-shifts in each system are uniformly governed by the polar nature of the invariable substituent.

As for the shielding of the H_B protons at the β-position, their behavior can not be discussed concurrently with those of the H_A-shifts from the viewpoint of Hammett's substituent effect. Moreover, there is no clear correlation between the H_B-shifts of β-substituted acrylates and those of the ethylene derivatives. Similarly to what has been reported in Part I, however, the order of the H_B-shifts of these compounds may be qualitatively determined by both the electronegativity of the first atom and the magnetic anisotropy of the substituent group.

As is shown in Fig. 4, in trans-forms of methyl β-substituted acrylates the chemical shifts of the methyl proton of the methoxycarbonyl group are determined by Hammett's σ_p, although their spread does not exceed about 0.2 p. p. m. in any of the derivatives. This relation corresponds with the fact that the pK_a-values of the trans-forms of β-substituted acrylic acids are represented by the usual Hammett equation.[8]

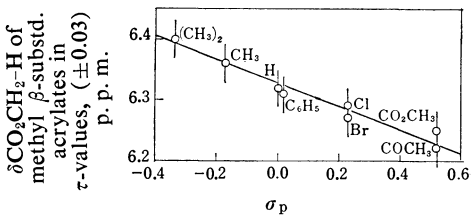

Fig. 5. The methyl proton shifts of methoxycarbonyl groups of methyl β-substituted acrylates, plotted vs. Hammett's substituent constants, σ_p.

Summary

In the NMR absorption of the trans-forms of β-substituted acrylates, β-substituted vinyl methyl ketones and β-substituted acryloyl chlorides, the chemical shifts of protons situated at the cis-position to the substituents have been roughly determined by Hammett's σ_p and Taft's parameter, $0.40\,\sigma_I + 0.70\,\sigma_R$. From a comparison of the H_A-shifts of the six olefinic systems ($RCH_A{=}CH_BX$, R = CH_3, C_6H_5, H, CO_2CH_3, $COCH_3$, COCl), these systems have been classified into two types—one, systems resembling the benzene derivatives, and the other, resembling the ethylene derivatives. Nevertheless, it has also been observed that the slope of each correlation line, on the whole, decreased in the order of the σ-value of the invariable substituent. The methyl proton shifts of β-substituted *trans*-acrylates, too,

8) M. Charton and H. Meislich, ibid., **80**, 5941 (1958).

depend upon Hammett's σ_p. The shifts of the proton (H_B) at the β-positon can not be discussed from the viewpoint of Hammett's substituent effect. However, they relate qualitatively with the electronegativity of the first atom of the substituent group.

The authors wish to take this opportunity to thank Dr. Naoya Nakagawa of the University of Electro-Communications for his helpful discussions. Thanks are also due Dr. Yo-ichiro Mashiko of the Government Chemical Research Institute and Dr. Ichiro Yamaguchi and Dr. Naohiro Hayakawa of the Japan Atomic Research Institute for kindly giving permission to use the spectrometers of those institutions.

Chemical Laboratory
Department of General Education
Nagoya University
Chikusa-ku, Nagoya

The Rheological Properties of Concentrated Suspensions. I. Some Theoretical Considerations Based on a Network Model

By Masaharu TAKANO*

(Received June 6, 1962)

At very small deformations, certain concentrated disperse systems show viscoelastic properties resembling these of polymer solutions. The elasticity of disperse systems is not that of an entropic nature as that of polymer systems. It is generally accepted that the elastic properties of such disperse systems are due to a three-dimentional network formed by the flocculation or aggregation of the dispersed solid particles. Tobolsky and Eyring[1] have derived a theory of the viscoelastic deformation of a polymer network. This theory is based essentially on a generalized Maxwell model as modified by Eyring's non-linear viscous elements. Recently van den Tempel[2] has extended this theory to the creep behavior of plastic disperse systems at very small deformations.

It is the purpose of this paper to extend this theory in order to explain the stationary flow properties of concentrated suspensions at very low rates of shear and their dynamic properties at low frequencies on the basis of a network model.

A. The Flocculation of Spherical Particles

The typical mechanical properties of fluocculated systems are originated from the network structure formed by their dispersed particles. They are evidently influenced by the concentration, surface characteristics, shape, and size distribution of the dispersed particles. The mechanical and thermal conditions during the preparation and the storage of the system are also of great influence. For the sake of simplicity, let us consider the particles to be uniform spheres.

The kinetics of the flocculation of spherical particles has been discussed theoretically by von Smoluchowski,[3] Overbeek,[4] Goodeve and Whitfield[5] and others. The rate of flocculation and the stationary size-distribution of the flocculate in the flowing suspension are generally determined by three factors: the Brownian motion of the particles, the effect of the shearing force, and the interaction energy between neighboring particles.

Flocculates increase in size by linking upon collision with each other and decompose by the breaking of the internal links. The rate of increase of the number of the k-fold flocculates† by collision per unit volume is given by the following equation, at finite concentrations:[4]

---

* Present address: Pulp and Paper Research Institute of Canada, Montreal, Quebec, Canada.

1) A. Tobolsky and H. Eyring, *J. Chem. Phys.*, **11**, 125 (1943).

2) M. van den Tempel, *J. Colloid Sci.*, **16**, 284 (1961).

3) M. Von Smoluchowski, *Physik. Z.*, **17**, 557, 585 (1916); *Z. physik. Chem.*, **92**, 129 (1917).

4) J. Th. G. Overbeek, "Colloid Science," Vol. I, Ed. by H. R. Kruyt, Elsevier Publ. Co., Amsterdam (1952), p. 278.

5) C. F. Goodeve and G. W. Whitfield, *Trans. Faraday Soc.*, **34**, 511 (1938).

† The k-fold flocculate means a flocculate constituted of k particles.

$$\mathrm{d}\nu_k/\mathrm{d}t=(1/2)\sum_{\substack{i=1\\j=k-i}}^{i=k-1}4\pi D_{ij}R_{ij}\nu_i\nu_j-\nu_k\sum_{i=1}^{\infty}4\pi D_{ki}R_{ki}\nu_i+(2\dot{\gamma}/3)\times\{\sum_{\substack{i=1\\j=k-i}}^{i=k-1}R^3_{ij}\nu_i\nu_j-2\nu_k\sum_{i=1}^{\infty}R^3_{ki}\nu_i\} \quad (1)$$

where ν_i is the number of the i-fold flocculates per unit volume, D_{ij} and R_{ij} are the mutual diffusion constant and the radius of interaction between the i-fold flocculates and the j-fold flocculates respectively, and $\dot{\gamma}$ is the rate of shear. The first and the second term represent the increase and the decrease of the k-fold flocculates by thermal collision respectively. The third and the fourth term correspond to the rates of change of the number of flocculates by shearing force. For unlinked particles, the first and the third term vanish. Therefore,

$$\mathrm{d}\nu_1/\mathrm{d}t=-\nu_1\sum_{i=1}^{\infty}4\pi D_{1i}R_{1i}\nu_i-(4\dot{\gamma}/3)\nu_1\sum_{i=1}^{\infty}R^3_{1i}\nu_i \quad (2)$$

Some of the flocculates decompose to smaller flocculates as the result of thermal and mechanical actions. The rate of loss of the k-fold flocculates per unit volume is

$$-\mathrm{d}\nu_k/\mathrm{d}t=\nu_k(\boldsymbol{kT}/\boldsymbol{h}\sigma)\exp\{-(\Delta F-f\lambda)/\boldsymbol{kT}\}-\sum_{j=k+1}^{\infty}\{2\nu_j/(j-1)\}(\boldsymbol{kT}/\boldsymbol{h}\sigma)\times\exp\{-(\Delta F-f\lambda)/\boldsymbol{kT}\} \quad (3)$$

where $\boldsymbol{k}$ and $\boldsymbol{h}$ are the constants of Boltzmann and Planck respectively, T is the absolute temperature, ΔF, the mean free energy of activation for breaking a link between particles in a flocculate, λ, the critical distance for breaking a link, and f, the mean shearing force on a link. σ is the mean number of links to be broken for generating two smaller fragments from a flocculate. It is effectively larger than one when some circular structures are involved in the flocculates. In Eq. 3 the first term represents the decomposition of the k-fold flocculates, while the second term represents the generation of the k-fold flocculates by the decomposition of larger flocculates. For unlinked particles, the first term vanishes; therefore,

$$-\mathrm{d}\nu_1/\mathrm{d}t=-\sum_{j=2}^{\infty}\{2\nu_j/(j-1)\}\times(\boldsymbol{kT}/\boldsymbol{h}\sigma)\exp\{-(\Delta F-f\lambda)/\boldsymbol{kT}\} \quad (4)$$

For $k\geqq 2$, the net rate of the increase of the k-fold flocculates per unit volume is given by the summation of Eqs. 1 and 3:

$$\mathrm{d}\nu_k/\mathrm{d}t=(1/2)\sum_{\substack{i=1\\j=k-i}}^{i=k-1}4\pi D_{ij}R_{ij}\nu_i\nu_j-\nu_k\sum_{i=1}^{\infty}4\pi D_{ki}R_{ki}\nu_i+(2\dot{\gamma}/3)\{\sum_{\substack{i=1\\j=k-1}}^{i=k-1}R^3_{ij}\nu_i\nu_j-2\nu_k\sum_{i=1}^{\infty}R^3_{ki}\nu_i\}-\{\nu_k-\sum_{j=k+1}^{\infty}2\nu_j/(j-1)\}(\boldsymbol{kT}/\boldsymbol{h}\sigma)\times\exp\{-(\Delta F-f\lambda)/\boldsymbol{kT}\} \quad (5)$$

For unlinked particles, it is given by the summation of Eqs. 2 and 4:

$$\mathrm{d}\nu_1/\mathrm{d}t=-\nu_1\sum_{i=1}^{\infty}4\pi D_{1i}R_{1i}\nu_i-(4\dot{\gamma}/3)\nu_1\sum_{i=1}^{\infty}R^3_{1i}\nu_i+\sum_{j=2}^{\infty}\{2\nu_j/(j-1)\}(\boldsymbol{kT}/\boldsymbol{h}\sigma)\times\exp\{-(\Delta F-f\lambda)/\boldsymbol{kT}\} \quad (6)$$

The summations in Eqs. 5 and 6 are very complicated and can not be carried out without any assumptions or approximations. When the radii of the i-fold flocculates and of the j-fold flocculates are not too widely different, we obtain the following approximation:[4]

$$D_{ij}R_{ij}\fallingdotseq 2D_1R_1$$

where D_1 is the diffusion constant of an unlinked particle and R_1 the distance of interaction between unlinked particles. Under the same conditions, we have another approximation:

$$R^3_{ij}\fallingdotseq R^3_1(i+j)/2\phi_c$$

where ϕ_c is the mean fraction of volume occupied by particles in a multiple flocculate.

Substituting these approximations into Eqs. 5 and 6, we have, for $k\geqq 2$:

$$\nu_k/\mathrm{d}t=4\pi D_1R_1\{\sum_{\substack{i=1\\j=k-i}}^{i=k-1}\nu_i\nu_j-2\nu_k\sum_{i=1}^{\infty}\nu_i\}+(\dot{\gamma}R^3_1/3\phi_c)\{\sum_{\substack{i=1\\j=k-i}}^{i=k-1}(i+j)\nu_i\nu_j-2\nu_k\sum_{i-1}^{\infty}(k+i)\nu_i\}-\{\nu_k-\sum_{j=k+1}^{\infty}2\nu_j/(j-1)\}\times(\boldsymbol{kT}/\boldsymbol{h}\sigma)\exp\{-(\Delta F-f\lambda)/\boldsymbol{kT}\} \quad (7)$$

and for $k=1$:

$$\mathrm{d}\nu_1/\mathrm{d}t=-8\pi D_1R_1\sum_{i=1}^{\infty}\nu_i\nu_1-(2\dot{\gamma}R^3_1/3\phi_c)\nu_1\sum_{i=1}^{\infty}(1+i)\nu_i+\{\sum_{j=2}^{\infty}2\nu_j/(j-1)\}(\boldsymbol{kT}/\boldsymbol{h}\sigma)\times\exp\{-(\Delta F-f\lambda)/\boldsymbol{kT}\} \quad (8)$$

The total rate of the increase of flocculates per unit volume is obtained by summing up Eq. 7 with respect to k and by then adding Eq. 8:

$$\mathrm{d}\sum_{k=1}^{\infty}\nu_k/\mathrm{d}t = -4\pi D_1 R_1\Big(\sum_{k=1}^{\infty}\nu_k\Big)^2 - (2\dot{\gamma}R_1^3/3\phi_c)\nu_0\Big(\sum_{k=1}^{\infty}\nu_k\Big) + \Big(\sum_{k=1}^{\infty}\nu_k-\nu_1\Big)(\boldsymbol{kT}/\boldsymbol{h}\sigma) \times \exp\{-(\Delta F-f\lambda)/\boldsymbol{kT}\} \quad (9)$$

where $\nu_0=\sum_{k=1}^{\infty}k\nu_k$ is the total number of primary particles per unit volume.

As $\mathrm{d}\sum_{k=1}^{\infty}\nu_k/\mathrm{d}t=0$ at a stationary state, the number of flocculates per unit volume is

$$\sum_{k=1}^{\infty}\nu_k = \frac{\left(\begin{array}{c}(\boldsymbol{kT}/\boldsymbol{h}\sigma)(1-\nu_1/\sum_{k=1}^{\infty}\nu_k)\\ \times\exp\{-(\Delta F-f\lambda)/\boldsymbol{kT}\}-(2\dot{\gamma}R_1^3/3\phi_c)\nu_0\end{array}\right)}{4\pi D_1 R_1} \quad (10)$$

In concentrated disperse systems, the number of unlinked particles may be negligible compared with the total number of flocculates. Therefore,

$$\sum_{k=1}^{\infty}\nu_k = \frac{\left(\begin{array}{c}(\boldsymbol{kT}/\boldsymbol{h}\sigma)\exp\{-(\Delta F-f\lambda)/\boldsymbol{kT}\}\\ -(2\dot{\gamma}R_1^3/3\phi_c)\nu_0\end{array}\right)}{4\pi D_1 R_1} \quad (11)$$

The diffusion constant of the unlinked particles, D_1, and the total number of primary particles, ν_0, are expressed by the following equations respectively:

$$D_1=\boldsymbol{kT}/3\pi\eta R_1$$

and

$$\nu_0=6\phi/\pi R_1^3$$

where R_1 is the diameter of the primary particles, η, the viscosity of the medium, and ϕ, the volume fraction of solid dispersed particles.

Therefore, Eq. 11 can be rewritten as follows:

$$\sum_{k=1}^{\infty}\nu_k=(3\eta/4\boldsymbol{h}\sigma)\exp\{-(\Delta F-f\lambda)/\boldsymbol{kT}\} -3\eta\dot{\gamma}\phi/\boldsymbol{kT}\pi\phi_c \quad (12)$$

If no flocculates have any circular structures, the total number of the links between particles per unit volume is

$$L_o=\sum_{k=1}^{\infty}(k-1)\nu_k=\nu_0-\sum_{k=1}^{\infty}\nu_k \quad (13)$$

This equation holds in the case of linear or branched structures. However, actually, certain circular structures may be formed in flocculates. Let n_k equal the average number of links involving a given particle in an k-fold flocculate;

$$\mathrm{d}n_k/\mathrm{d}t=K(k-1)/V_k-\beta n_k$$

where K is the rate constant of link formation and β is the rate constant of the link rupture without any generation of smaller fragments. V_k is the volume occupied by a k-fold flocculate and is given approximately by $k\pi R_1^3/6\phi_c$. At a stationary state,

$$n_k=K(k-1)/\beta V_k=6K\phi_c(k-1)/k\pi\beta R_1^3$$

Considering the fact that each link is shared by two particles, the number of links in a k-fold flocculate is

$$b_k=3K\phi_c(k-1)/\pi\beta R_1^3$$

The total number of the links between particles per unit volume is, therefore:

$$L'=\sum_{k=1}^{\infty}b_k\nu_k=(3K\phi_c/\pi\beta R_1^3)\Big(\nu_0-\sum_{k=1}^{\infty}\nu_k\Big) \quad (14)$$

The rate constants, K and β, are given approximately by the following equations:[4]

$$K=4\pi D_1' R_1+(4\dot{\gamma}/3)R_1^3$$

and

$$\beta=(1-1/\sigma)(\boldsymbol{kT}/\boldsymbol{h})\exp\{-(\Delta F-f\lambda)/\boldsymbol{kT}\}$$

where D_1' is the mutual diffusion constant of the particles involved in a multiple flocculate.

As σ is the mean number of links between two fragments of a flocculate, the total number of links between particles per unit volume is

$$L'=\sum_{k=1}^{\infty}\sigma(k-1)\nu_k=\sigma\Big(\nu_0-\sum_{k=1}^{\infty}\nu_k\Big) \quad (14')$$

When we compare Eq. 14' with Eq. 14,

$$\sigma=3K\phi_c/\pi\beta R_1^3 \quad (15)$$

and when we substitute the β given above into Eq. 15,

$$\sigma=1+3K\phi_c/\pi R_1^3(\boldsymbol{kT}/\boldsymbol{h})\exp\{-(\Delta F-f\lambda)/\boldsymbol{kT}\} \quad (15')$$

Combining Eq. 15 with Eq. 12, we obtain

$$L'=\{(6/\pi R_1^3)+(3\eta\dot{\gamma}/\boldsymbol{kT}\pi\phi_c)\}\sigma\phi - (3\eta/4\boldsymbol{h})\exp\{-(\Delta F-f\lambda)/\boldsymbol{kT}\} \quad (16)$$

In this equation the second term is independent of the concentration. Therefore, a critical concentration, ϕ_{crit}, above which links between particles would appear, is

$$\phi_{crit}=\frac{(3\eta/4\boldsymbol{h})\exp\{-(\Delta F-f\lambda)/\boldsymbol{kT}\}}{\{(6/\pi R_1^3)+(3\eta\dot{\gamma}/\boldsymbol{kT}\pi\phi_c\}\sigma} \quad (17)$$

This critical concentration may be lowered with the increase in the ΔF value.

B. The Mechanical Properties of Concentrated Suspensions

In order to explain the viscoelastic properties of suspensions, van den Tempel[2] assumed that at very small deformations the interparticle links could be distinguished into two kinds: the primary links, which remain intact during measurement, and the secondary links, which may break and reform during an experiment. However, van den Tempel did not give the precise nature of the primary links and neglected the shearing force acting on the medium; this force can not be ignored in suspensions of a highly viscous medium.

In the model considered here, the primary links may be explained by considering the circular structures in the flocculate. The flocculates are distributed homogeneously in the system. In a stationary state, the total number of the links, L', between dispersed particles is held constant, but the sizes of the flocculates are changed incessantly by interactions between the flocculates.

For the sake of simplicity, let us assume, as van den Tempel did, that the flocculate is an assembly of chains, each chain consisting of a linear array of dispersed perticles placed very close together and oriented in three mutually-perpendicular directions in the cube. In such an equivalent model, linkages between neighboring perticles in a chain may be considered to be composed of σ links on the average when we accept the presence of circular structures in the flocculates, as stated in the definition of σ in Section A. Moreover, if the mutual distance between neighboring particles in a chain is negligible compared to the diameter of the particles, the number of links in one direction is $L'R_1/3$ per unit area; in other words, a cross section of the cube perpendicular to the chains cuts through $L'R_1/3$ links per unit area. In the present equivalent model, the σ links between two neighboring perticles must be broken simultaneously in order to separate them. Two kinds of behavior of the bonds between particles may be considered upon deformations of the system: the one is the breaking of bonds following the re-formation of another bond between another pair of particles, and the other is the elongation of bonds without the separation of particles, in the stationary state. The probability of the simultaneous breaking of σ links, which is necessary for breaking the bonds, may be $1/\sigma$; therefore, that of the other type of deformation may be $(1-1/\sigma)$. The former corresponds to the secondary bonds and the latter to the primary bonds proposed by van den Tempel. However, he considered a special case in which σ equals one and in which all particles in the system are involved in a flocculate.

When the shearing force acting on the medium can not be ignored, the total shear stress, S, tangential to the cross section considered is expressed as follows:

$$S=\eta\dot{\gamma}+f_1N_1+f_2N_2 \tag{18}$$

where η is the effective viscosity of the medium involving the hydrodynamic effect of particles, and f_1 and f_2 are the mean forces acting on the primary links and on the secondary links respectively. N_1 and N_2 are the numbers of links cut by a cross section of unit area. In the present model,

$$N_1=(1-1/\sigma)L'R_1/3 \tag{19}$$

$$N_2=(1/\sigma)L'R_1/3 \tag{20}$$

The rate of shear of the primary links is governed by the rate of the stretching of unbroken links, while that of the secondary links in expressed as a sum of the rate of link-stretching and the rate of the breaking of the links:[1,2]

$$\dot{\gamma}_1=(n_1/g_1)(\mathrm{d}f_1/\mathrm{d}t) \tag{21}$$

$$\dot{\gamma}_2=(n_2/g_2)(\mathrm{d}f_2/\mathrm{d}t)+(2n_2\lambda_2\boldsymbol{kT}/\boldsymbol{h}) \times\exp(-\Delta F_2/\boldsymbol{kT})\sinh(f_2\lambda_2/\boldsymbol{kT}) \tag{22}$$

where it has been assumed that the strain is increased by λ_2 whenever two particles separate. The number of links per unit chain length in the direction normal to the shear plane and the the mean stiffness of the links are called n and g respectively.

According to the definitions,

$$n_1=(1-1/\sigma)(1/R_1) \tag{23}$$

$$n_2=(1/\sigma)(1/R_1) \tag{24}$$

So long as coherence in the sample is maintained, the shear stress is distributed over the medium, the primary links and the secondary links in such a way that the rate of shear is the same throughout:

$$\dot{\gamma}=\dot{\gamma}_1=\dot{\gamma}_2 \tag{25}$$

Stationary Flow Properties. — In stationary flow experiments, the total shear stress and the rate of shear are constant during measurement:

$$\mathrm{d}S/\mathrm{d}t=0 \tag{26}$$

and

$$\mathrm{d}\dot{\gamma}^2/\mathrm{d}t^2=0 \tag{27}$$

As L' and σ may be assumed not to be changed in the stationary flow, n_1, n_2 N_1 and N_2 are considered, from Eqs. 19, 20, 23 and 24, to be constant during measurement.

Consequently, from Eqs. 26, 27, 18 and 21,

$$N_1\mathrm{d}f_1/\mathrm{d}t=-N_2\mathrm{d}f_2/\mathrm{d}t=N_1g_1\dot{\gamma}/n_1 \tag{28}$$

Therefore, integrating Eq. 21, we have the mean force acting on primary links at an instant as follows:

$$f_1=\int_0^{t_1}(g_1\dot{\gamma}/n_1)\mathrm{d}t=\int_0^{\gamma_1}(g_1/n_1)\mathrm{d}\gamma=(g_1/n_1)\gamma_1 \tag{29}$$

where it has been assumed that n and g are independent of the strain and where γ_1 means the mean strain of primary links at the instant, t_1.

Substituting Eqs. 28 and 29 into Eq. 22, and combining the result with Eq. 18, we obtain

$$S=\eta\dot{\gamma}+(N_2\boldsymbol{k}T/\lambda_2)\sinh^{-1}\{\dot{\gamma}\tau_2\lambda_2(N_1g_1/n_1+N_2g_2/n_2)/N_2\boldsymbol{k}T\}+(N_1g_1\gamma_1/n_1) \tag{30}$$

where the relaxation time, τ_2, is defined by Eq. 31.

$$\tau_2=(\boldsymbol{h}/2g_2\lambda_2^2)\exp(\Delta F_2/\boldsymbol{k}T) \tag{31}$$

At very low rates of shear, approximately,

$$S=\eta\dot{\gamma}+(N_1g_1/n_1+N_2g_2/n_2)\tau_2\dot{\gamma}+(N_1g_1/n_1)\gamma_1 \tag{32}$$

The (N_1/n_1) and (N_2/n_2) parameters are generally given by functions of the concentration and the rate of shear. According to Eqs. 19, 20, 23 and 24, the parameters are

$$(N_1/n_1)=(N_2/n_2)=L'R_1^2/3 \tag{33}$$

When Eq. 33 is combined with Eqs. 16 and 17,

$$(N_1/n_1)=(N_2/n_2)=(R_1^2/3)(6/\pi R_1^3+3\eta\dot{\gamma}/\boldsymbol{k}T\pi\phi_c)\sigma(\phi-\phi_{crit}) \tag{34}$$

where σ is the same as that given by Eq. 15'.

Substituting Eq. 34 into Eq. 32, we obtain

$$S=\eta_{pl}\dot{\gamma}+S_o \tag{35}$$

where η_{pl} and S_o are the plastic viscosity and the yield value, respectively, given by

$$\eta_{pl}=\eta+(R_1^2/3)(g_1+g_2)\tau_2(6/\pi R_1^3+3\eta\dot{\gamma}/\boldsymbol{k}T\pi\phi_c)\sigma(\phi-\phi_{crit}) \tag{36}$$

and

$$S_o=(R_1^2/3)g_1\gamma_1(6\pi R_1^3+3\eta\dot{\gamma}/\boldsymbol{k}T\pi\phi_c)\sigma(\phi-\phi_{crit}) \tag{37}$$

The plastic viscosity and the yield value will increase linearly above the critical concentration, ϕ_{crit}, given by Eq. 17. However, after all particles are involved in a flocculate in all the space available in the system, the ϕ_c included in σ must be equal to ϕ; therefore, σ increases linearly with the concentration ϕ. In such a region, the plastic viscosity and the yield value must be quadratic functions of the concentration.

If the terms concerning the shearing force in Eqs. 15', 16 and 17 are negligibly small at very low rates of shear, the (N_1/n_1) and (N_2/n_2) parameters may be considered to be independent of the rates of shear. In such a case, we have

$$(N_1/n_1)=(N_2/n_2)=(2/\pi R_1)\sigma'(\phi-\phi'_{crit}) \tag{34'}$$

where

$$\sigma'=1+(12D'\boldsymbol{h}\phi_c/R_1^2\boldsymbol{k}T)\exp(\Delta F/\boldsymbol{k}T) \tag{15''}$$

and

$$\phi'_{crit}=(\eta\pi R_1^3/8\boldsymbol{h})\exp(-\Delta F/\boldsymbol{k}T)/\sigma' \tag{17'}$$

When we substitute Eq. 34' into Eq. 32, and combine the result with Eq. 35,

$$\eta_{pl}=\eta+(g_1+g_2)\tau_2(2/\pi R_1)\sigma'(\phi-\phi'_{crit}) \tag{36'}$$

and

$$S_o=(2/\pi R_1)g_1\gamma_1\sigma'(\phi-\phi'_{crit}) \tag{37'}$$

In this case, the plastic viscosity and the yield value, η_{pl} and S_o, are independent of the rates of shear; therefore, Eq. 35 represents the typical behavior of a Bingham body.

Dynamic Properties at Very Small Deformations.—We consider dynamic properties when the network structure formed by particles is not broken irreversibly by the shearing force.

When the network is subjected to a sinusoidal shear strain,

$$\gamma=\gamma_0\exp(\boldsymbol{j}\omega t) \tag{38}$$

the mean shear force acting on the primary links is given, by integrating Eq. 21 with Eqs. 25 and 38, as follows:

$$f_1=(g_1/n_1)\gamma_0\exp(\boldsymbol{j}\omega t) \tag{39}$$

Similarly, the force on the secondary links is given by integrating Eq. 22 with the first order approximation that $\sinh(f_2\lambda_2/\boldsymbol{k}T)$ equals $(f_2\lambda_2/\boldsymbol{k}T)$ at very small shear stresses:

$$f_2=(g_2/n_2)\gamma_0\exp(\boldsymbol{j}\omega t)(\boldsymbol{j}\omega\tau_2+\tau_2^2\omega^2)/(1+\tau_2^2\omega^2) \tag{40}$$

where τ_2 is the same as that given by Eq. 31 and where it has been assumed that the values of n_2 and g_2 are independent of the shear strain.

If the medium shows its own viscoelasticity, Eq. 18 alters:

$$S=\eta'_m(\omega)\dot{\gamma}+G'_m(\omega)\gamma+f_1N_1+f_2N_2 \tag{41}$$

where $G'_m(\omega)$ and $\eta'_m(\omega)$ are the dynamic modulus and the dynamic viscosity of the medium involving the hydrodynamic effect of particles.

Substituting Eqs. 39 and 40 into Eq. 41, we have

$$S=\{\eta'_m(\omega)+(N_2g_2/n_2)\tau_2/(1+\tau_2^2\omega^2)\}\boldsymbol{j}\omega\gamma_0\times\exp(\boldsymbol{j}\omega t)+\{G'_m(\omega)+(N_1g_1/n_1)+(N_2g_2/n_2)\tau_2^2\omega^2/(1+\tau_2^2\omega^2)\}\times\gamma_0\exp(\boldsymbol{j}\omega t) \tag{42}$$

If we denote the dynamic modulus and the dynamic viscosity of the whole system at very small deformations as $G'_s(\omega)$ and $\eta'_s(\omega)$ respectively, the shear force is expressed by

$$S=\eta'_s(\omega)\boldsymbol{j}\omega\gamma_0\exp(\boldsymbol{j}\omega t)+G'_s(\omega)\gamma_0\exp(\boldsymbol{j}\omega t) \tag{43}$$

Comparing Eq. 42 with Eq. 43, we have

$$G'_s(\omega)=G'_m(\omega)+(N_1g_1/n_1)+(N_2g_2/n_2)\tau_2^2\omega^2/(1+\tau_2^2\omega^2) \tag{44}$$

$$\eta'_s(\omega)=\eta'_m(\omega)+(N_2g_2/n_2)\tau_2/(1+\tau_2^2\omega^2) \tag{45}$$

In the case of a simply viscous medium, the first term in Eq. 44 vanishes and the first term in Eq. 45 is independent of the frequency.

At very small deformations, the network may be considered not to be changed by the shearing force. In Eqs. 44 and 45, the (N_1/n_1) and (N_2/n_2) parameters may, therefore, be given by Eq. 34' as functions of the concentration. Consequently, at very small deformations, we have

$$G'_s(\omega)=G'_m(\omega)+(2/\pi R_1)\times\{g_1+g_2\tau_2^2\omega^2/(1+\tau_2^2\omega^2)\}\sigma'(\phi-\phi'_{crit}) \tag{46}$$

$$\eta'_s(\omega)=\eta'_m(\omega)+(2/\pi R_1)g_2\times\{\tau_2/(1+\tau_2^2\omega^2)\}\sigma'(\phi-\phi'_{crit}) \tag{47}$$

where σ' and ϕ'_{crit} are the same as those given by Eqs. 15'' and 17'.

When we compare Eqs. 46 and 47 with Eqs. 36' and 37', we recognize similarities between the concentration dependence of dynamic properties and that of the plastic viscosity at very low rates of shear. The dynamic properties will increase linearly above a critical concentration, ϕ'_{crit}, given by Eq. 17' and after all the particles are involved in a flocculate in all the space available in the system, the dynamic properties must be be quadratic functions of the concentration.

The Correlation between the Dynamic Properties and the Stationary Flow Properties.—The correlation of the dynamic properties and the stationary flow properties can be deduced by comparing the derived equations with one other. The dynamic viscosity and the dynamic modulus at very small deformations are given by Eqs. 46 and 47. On the other hand, the plastic viscosity and the yield value in stationary flow experiments are generally given by Eqs. 36 and 37, while they are given by Eqs. 36' and 37' at infinitesimal rates of shear.

By comparing Eq. 47 with Eqs. 36 and 36', we can deduce the following relations between the viscosities: (i) when the primary links are absent in the system, the dynamic viscosity at lower frequencies coinsides with the plastic viscosity at very low rates of shear, and (ii) when the primary links exist, the plastic viscosity at infinitesimal rates of shear may be larger than the dynamic viscosity at lower frequencies. However, in the latter case, the plastic viscosity at finite rates of shear may be practically larger or smaller than the dynamic viscosity at lower frequencies, depending on the sensitivity of links to the shear force, since σ and ϕ_{crit} depend on the shearing force exponentially, as Eqs. 15' and 17 show.

When we compare Eq. 46 with Eqs. 37 and 37', we can see that the dynamic modulus at lower frequencies also relates to the yield value in simple shear experiments. At infinitesmal rates of shear, the yield value may be given by a product of γ_1 and the dynamic modulus at lower frequencies.

The Dependence of the Dynamic Properties on Amplitude.—The mean stiffness of links in Eqs. 39 and 40 may be decreased with an increase in the amplitude of shear strain, since the links between solid particles generally have a non-linear dependence of the stiffness on the particle separation. Besides, the network formed by particles may be changed by the shearing force and the rate of shear at larger deformations, as predicted by Eq. 9 in Section A. At larger stresses, therefore, the (N_1/n_1) and (N_2/n_2) parameters in Eqs. 44 and 45 are not given by Eq. 34'. In such a case, the parameters may be approximated to those mean values through sinusoidal motions and may be given by functions of the amplitudes of the shear rate and of the shearing force acting on the links.

If we denote the parameters at the amplitudes of the shear rate $\dot{\gamma}_0$ and of the shearing force f_0 as $(N_1/n_1)_{\dot{\gamma}_0,f_0}$ and $(N_2/n_2)_{\dot{\gamma}_0,f_0}$, so long as a first order approximation that $\sinh(f_2\lambda_2/\boldsymbol{kT})$ equals $(f_2\lambda_2/\boldsymbol{kT})$ is acceptable, the dependence of the dynamic properties on the amplitude of the shearing force is given by the following equations:

$$\{G'_s(\omega)-G'_m(\omega)\}_{\dot{\gamma}_0,f_0}/\{G'_s(\omega)-G'_m(\omega)\}_{\dot{\gamma}_0\fallingdotseq 0,f_0\fallingdotseq 0}=\psi(\dot{\gamma}_0,f_0)\{g_1+g_2\tau_2^2\omega^2/(1+\tau_2^2\omega^2)\}_{\dot{\gamma}_0,f_0}/\{g_1+g_2\tau_2^2\omega^2/(1+\tau_2^2\omega^2)\}_{\dot{\gamma}_0\fallingdotseq 0,f_0\fallingdotseq 0} \tag{48}$$

and

$$\{\eta'_s(\omega)-\eta'_m(\omega)\}_{\dot{\gamma}_0,f_0}/\{\eta'_s(\omega)-\eta'_m(\omega)\}_{\dot{\gamma}_0\fallingdotseq 0,f_0\fallingdotseq 0}=\psi(_0,\dot{\gamma}f_0)\{g_2\tau_2/(1+\tau_2^2\omega^2)\}_{\dot{\gamma}_0,f_0}/\{g_2\tau_2/(1+\tau_2^2\omega^2)\}_{\dot{\gamma}_0\fallingdotseq 0,f_0\fallingdotseq 0} \tag{49}$$

where

$$\psi(\dot{\gamma}_0,f_0)=(N_1/n_1)_{\dot{\gamma}_0,f_0}/(N_1/n_1)_{\dot{\gamma}_0\fallingdotseq 0,f_0\fallingdotseq 0}=(N_2/n_2)_{\dot{\gamma}_0,f_0}/(N_2/n_2)_{\dot{\gamma}_0\fallingdotseq 0,f_0\fallingdotseq 0} \tag{50}$$

As $\tau_2g_2=(\boldsymbol{h}/2\lambda_2^2)\exp(\Delta F_2/\boldsymbol{kT})$ in Eq. 49 may be independent of the amplitude of the shearing force, Eqs. 48 and 49 can be rewritten as

follows at lower frequencies:

$$\{G'_s(\omega)-G'_m(\omega)\}_{\dot{\gamma}_0,\ f_0}/\{G'_s(\omega)-G'_m(\omega)\}_{\dot{\gamma}_0\fallingdotseq 0,\ f_0\fallingdotseq 0}=\psi(\dot{\gamma}_0,\ f_0)(g_1)_{\dot{\gamma}_0,\ f_0}/(g_1)_{\dot{\gamma}_0\fallingdotseq 0,\ f_0\fallingdotseq 0} \tag{48'}$$

and

$$\{\eta'_s(\omega)-\eta'_m(\omega)\}_{\dot{\gamma}_0,\ f_0}/\{\eta'_s(\omega)-\eta'_m(\omega)\}_{\dot{\gamma}_0\fallingdotseq 0,\ f_0\fallingdotseq 0}=\psi(\dot{\gamma}_0,\ f_0) \tag{49'}$$

In conclucion, it is thought that the dynamic modulus is influenced by the amplitude more remarkably than is the dynamic viscosity at lower frequencies.

Summary

The rheological properties of concentrated suspensions have been considered theoretically by the use of a network model in which the particles are linked at random by thermal and mechanical actions.

The effects of particle size, the viscosity of the medium and the mean free energy of the activation for breaking links between particles have been taken into account in the calculation of the number of interparticle links.

The links between particles have been conveniently distinguished into two kinds in stationary states: the primary links, which are elongated without the separation of neighboring particles in an instant, and the secondary links, which are broken and reformed reversibly in an instant. The primary links originate from circular structures in the flocculates.

The dynamic properties at very small deformations and the stationary flow properties have been derived theoretically as functions of the concentration and of the frequency or the rate of shear by assuming a generalized Maxwell model modified by Eyring's non-linear viscous elements.

The correlation of the dynamic properties and the stationary flow properties and the dependence of the dynamic properties on amplitude have been considered theoretically by the use of the present network model.

The author is much indebted to Professor Hirotaro Kambe of the Aeronautical Research Institute, The University of Tokyo, for his many stimulating discussions and suggestions.

Aeronautical Research Institute
The University of Tokyo
Meguro-ku, Tokyo

The Rheological Properties of Concentrated Suspensions. II. Stationary Flow Properties and the Influence of Additives and of Particle Size

By Masaharu TAKANO and Hirotaro KAMBE

(Received July 2, 1963)

It is generally accepted that the rheological properties of concentrated suspensions are connected with the state of flocculation and that the contribution of larger flocculates to the properties is predominant at low shearing stresses.[1,2] The rheological behavior of such flocculated systems is appreciably influenced by a trace of an adsorbate as well as by the size distribution of particles, which changes the energy of the interaction between particles. There is yet, however, no definite interpretation of the relations between the rheological properties and structures of the flocculates formed by particles in the ststem. In such concentratrated suspensions, it would be reasonable to assume that dispersed particles are partially linked with each other by weak attractive forces and that the links between particles are broken by a shearing force depending on the rate of shear.[2-5] A network model composed of links with various relaxation times would be an appropriate base for an explanation of the plastic behavior of such concentrated suspensions at low rates of shear where links between particles are not appreciably broken by the shearing force.[6,7]

1) M. Senô, *J. Chem. Soc. Japan, Pure Chem. Sec.*, (*Nippon Kagaku Zassi*), **78**, 66 (1957); *Month. J. Inst. Ind. Sci., Univ. Tokyo*, (*Seisan Kenkyû*), **11**, 36 (1959).

2) I. M. Krieger and T. J. Dougherty, *Trans. Soc. Rheol.*, **3**, 137 (1959).

3) C. F. Goodeve and G. W. Whitfield, *Trans. Faraday Soc.*, **34**, 51 (1938).

4) S. Peter and I. Stolle, *Z. physik. Chem. N.F.*, **11**, 251 (1957).

5) T. Gillespie, *J. Colloid Sci.*, **15**, 219, 313 (1960).

6) A. Tobolsky and H. Eyring, *J. Chem. Phys.*, **11**, 125 (1954).

7) M. van den Tempel, *J. Colloid Sci.*, **16**, 284 (1961).

In a previous paper,[8] several equations were proposed for the stationary flow properties of concentrated suspensions at low rates of shear, assuming that there are certain circular structures in flocculates and that the links between particles can be conveniently distinguished into two parts at any instant in the stationary flow: the primary links, which are elongated without the separation of neighboring particles, and the secondary links, which are broken and reformed with the separation of particles.

It is the purpose of this paper to measure the stationary flow properties of various concentrated suspensions at very low rates of shear and to compare the findings with the theoretical predictions.

Experimental

Materials.—The characteristics of the pigments and media used in this work are listed in Table I. Barium sulfate-III was the same as barium sulfate-I except that the former was covered by sodium stearate. Linseed oil contains free fatty acids in itself and is more polar than polyisobutylene, which consists essentially of linear hydrocarbons with short methyl side chains, as shown in Table I.

The Preparation of Suspensions.—First a paste containing 70% pigments by weight was made. This paste was then passed through a paint mill three times and diluted by a medium to give a suspension of the required concentration. The diluted suspension was passed once more through the mill. Additives were added to the pigment before the pigment was mixed with the medium. An exact concentration of pigment was determined by igniting the suspension. Pigments had not been dried before being mixed with the medium except when the effect of water was examined experimentally.

Apparatus.—The stationary flow properties were measured with capillary viscometers and a rotational viscometer.

(a) Capillary Viscometers.—The capillary viscometers used in this work are improved Bingham viscometers, as illustrated in Fig. 1. The radii of the capillaries are 0.1493 and 0.1079 cm. and their lengths are 5.0 and 4.5 cm. respectively. The flow volume of measurement was selected so small as 0.10 cm^3 in order that the effects of head difference might be ignored during measurement. Measurements were made, alternately under pressure and by suction, in a water bath controlled at 30±0.02°C after the sample had been kept in it for 30 min.

The shear stress, S_a, and the shear-rate, $f(S_a)$,

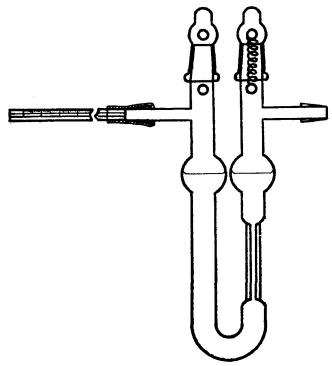

Fig. 1. Improved Bingham viscometer.

Table I-a. Characteristics of materials

Material	Density at 30°C g./cm^3	Viscosity at 30°C poises	Dielectric constant at 24.7°C, 50 kc./sec. e.s.u.
Linseed oil-I	0.9595	21.1	3.40
Linseed oil-II	0.9615	40.2	3.40
Linseed oil-III	0.9605	59.3	3.40
Polyisobutylene-I	0.883	137.3	1.90
Polyisobutylene-II	0.8825	129.6	1.90
Barium sulfate	4.50	—	10.25[a]
Water	0.996	0.008	76.5
Sodium stearate	1.07	—	3.125[b]

Table I-b. Particle sizes and purity of pigments

Pigment	Particle sizes			Weight loss		
	$(\overline{R})$ μ	$(\overline{R^2})^{1/2}$ μ	$(\overline{R^3})^{1/3}$ μ	at 105°C wt. %	by ignition wt. %	Total wt. %
Barium sulfate-I	0.075	0.079	0.082	0.32	1.34	1.66
Barium sulfate-II	0.265	0.283	0.311	0.20	1.51	1.71
Barium sulfate-III (covered by sodium stearate)	0.075	0.079	0.082	0.20	2.30	2.50

a) F. Wachholtz and A. Franceson, *Kolloid Z.*, **92**, 75 (1940).
b) K. D. Pathak and B. V. Bhide., *J. Indian Chem. Soc.*, **30**, 47 (1953).

8) M. Takano, This Bulletin, **36**, 1418 (1963).

at the wall of the capillary are given by the following equations:

$$S_a = a\Delta P/2L$$

$$f(S_a) = (1/\pi a^3)\{3Q + S_a(dQ/dS_a)\}$$

where a and L are the radius and the length of capillary respectively, ΔP is the pressure, and Q, the flow volume per unit time. The apparent shear rate is given as follows:

$$\dot{\gamma}_a = 4Q/\pi a^3$$

For the Bingham flow, the yield value, S_0, and the plastic viscosity, η_{pl}, are:

$$S_0 = a\Delta P_0/2L$$

$$\eta_{pl} = (\pi a^4/8QL)\{\Delta P - 4\Delta P_0/3 + (\Delta P_0/3)(\Delta P_0/\Delta P)^3\}$$

$$\fallingdotseq (\pi a^4/8QL)(\Delta P - \Delta P_0)$$

where ΔP_0 is the pressure below which the sample does not flow.

(B) Brookfield Rotational Viscometer.—The Brookfiedl viscometer used in this work is a commercial instrument which has a cylinder driven at the four constant speeds of 2, 4, 10 and 20 rev./min. However, three cylinders are exchangeable. The diameters of the cylinders are 3.039, 5.027 and 7.059 mm., and the lengths are 4.995, 5.053 and 5.009 cm. respectively. A container which had a radius of about 5 cm. and a depth of about 8 cm. was used directly as a vessel for the measurements.

Measurements were made after the sample had been kept for three hours in a water bath controlled at 30±0.02°C.

The stationary flow curves were obtained by using Engelhardt's extrapolation method.[9] The yield value and the plastic viscosity for Bingham flow have been calculated by means of the following equations:

$$S_0 = M_0/2\pi a^2 L$$

$$\eta_{pl} = (M/4\pi\omega L)(1/a^2 - 1/b^2) + (S_0/\omega)\ln(a/b)$$

where M is the torque acting on the inner cylinder, M_0, the critical torque below which the sample does not flow, L, the immersed length of the inner cylinder, ω, the angular velocity of the inner cylinder, and a and b, the radii of the inner and outer cylinder respectively. The apparent rate of shear, $\dot{\gamma}_a$, is given as follows:

$$\dot{\gamma}_a = 2\omega/\{1 - (a/b)^2\}$$

Experimental Results

Typical Newtonian and Bingham behavior was observed at lower rates of shear, as illustrated in Figs. 2 and 3.

The plastic viscosity and the yield value of various suspensions are listed in Tables II and III. The values listed in the tables were mainly obtained with capillary viscometers. However, some data were obtained by the Brookfield viscometer at 2 and 4 rev./min., as it was very difficult to obtain reproducible data at a stationary flow for thixotropic suspensions when capillary viscometers were used. The dependences of the relative plastic viscosity and the yield value are shown in Figs. 4 and 5.

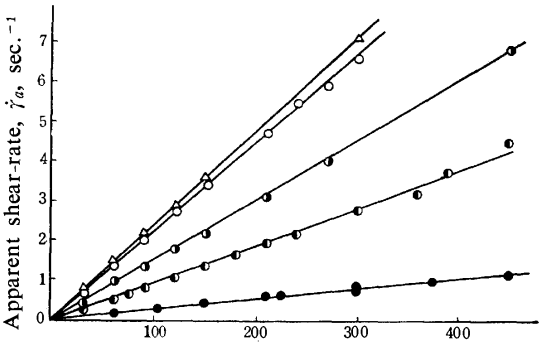

Fig. 2. Newtonian flow of suspensions of barium sulfate-I in linseed oil-II at various concentrations: (△) 0 vol.%, (○) 2.26vol. %, (◑) 8.18 vol.%, (◐) 17.14 vol.% and (●) 30.86 vol.%.

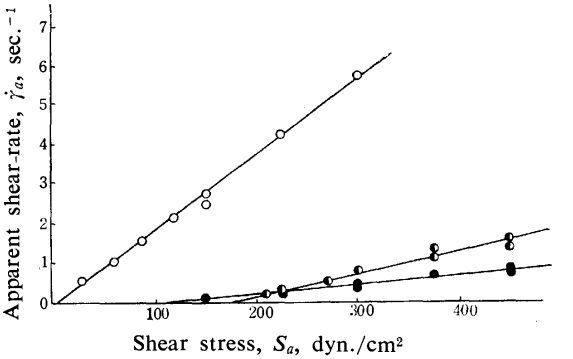

Fig. 3. Bingham flows of various suspensions: (○) 2.40 vol.% barium sulfate-III in linseed oil-II, (◐) 7.14 vol. % barium sulfate-III in linseed oil-II and (●) 2.09 vol.% barium sulfate-I in polyisobutylene-II.

When linseed oil was used as the medium, the yield value was not observed and the dependence of the relative plastic viscosity on the concentration was relatively simple, except when the particles were covered by sodium stearate. The adsorption of sodium stearate on the surfaces of particles increases the plastic viscosity and generates the yield value at lower concentrations.

When polyisobutylene is used as the medium, the yield value appears above the critical concentration determined by the particle size, and the plastic viscosity also increases remarkably above the critical concentration. The coating of the particles by sodium stearate

9) W. von Engelhardt and H. Lübben, *Kolloid Z.*, 147. 1 (1956).

TABLE II. RHEOLOGICAL PROPERTIES OF SUSPENSIONS OF BARIUM SULFATE IN LINSEED OIL (30°C)

Suspension	Concn. vol. %	Plastic viscosity poises	Relative plastic viscosity	Yield value dyn./cm²
Barium sulfate-I in linseed oil-II	0	40.2	1.00	0
	2.26	43.7	1.09	0
	8.18	67.1	1.67	0
	17.14	111.8	2.78	0
	30.86	420.8	10.45	0
Barium sulfate-II in linseed oil-I	0	21.1	1.00	0
	1.82	22.5	1.07	0
	7.16	30.2	1.43	8.2
	17.28	51.2	2.43	0
Barium sulfate-II in linseed oil-II	0	40.2	1.00	0
	2.04	45.1	1.12	0
	7.90	55.8	1.39	0
	16.67	89.0	2.21	0
	31.50	268.1	6.67	0
Barium sulfate-III in linseed oil-II	0	40.2	1.00	0
	2.40	51.2	1.27	7.34
	7.14	164.1	4.08	174.
	14.81*	595.	14.8	1060.

* Obtained by use of a Brookfield viscometer.

TABLE III. RHEOLOGICAL PROPERTIES OF SUSPENSIONS OF BARIUM SULFATE IN POLYISOBUTYLENE (30°C)

Suspension	Concn. vol. %	Plastic viscosity poises	Relative plastic viscosity	Yield value dyn./cm²
Barium sulfate-I in polyisobutylene-II	0	129.6	1.00	0
	2.09	421.3	3.25	105.6
	4.57*	871.	6.72	364.
	7.50*	—	—	—
Barium sulfate-II in polyisobutylene-I	0	137.3	1.00	0
	1.81	145.0	1.06	0
	4.47	159.7	1.17	0
	7.50	412.0	3.00	119.9
	16.11*	1577.	11.5	683.3
Barium sulfate-III in polyisobutylene-II	0	129.6	1.00	0
	2.10	195.7	1.51	36.7
	4.54	218.6	1.69	49.2
	8.21*	280.	2.16	222.5

* Obtained by use of a Brookfield viscometer.

lessens the appreciable dependence of the stationary flow properties on the concentration.

In both cases, suspensions of barium sulfate-I exhibit a higher dependence of the stationary properties on the concentration than

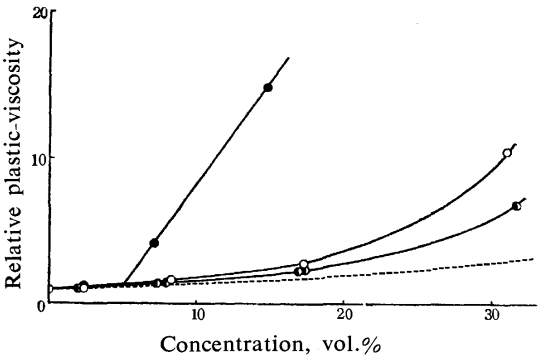

(a) Suspensions of barium sulfate in linseed oil.

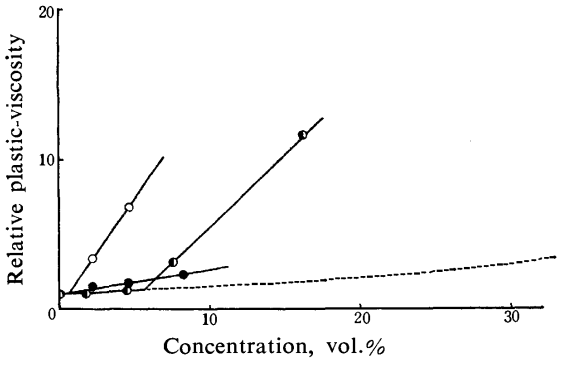

(b) Suspensions of barium sulfate in polyisobutylene.

Fig. 4. Concentration dependence of the relative plastic-viscosity.
Symbols: (○) barium sulfate-I, (◐) barium sulfate-II and (●) barium sulfate-III. A dotted line represents Vand's equation.

do those of barium sulfate-II. In these cases, it seems not to be important that the particles had not been dried before being mixed with the medium. The effect of the adsorption of water on the stationary flow properties of suspensions of barium sulfate-I in linseed oil was examined experimentally; the findings are listed in Table IV. A minor quantity of water below 2 wt.% based on pigment does not appreciably change the flow properties of the system.

According to electron-microscopic observations, the shapes of these particles are approximately hexahedral, but the size distribution of particles differs from particle to particle, as shown in Table I-b. The weight losses of these particles by their being dried and by ignition are listed in Table I-b.

Sedimentation volumes of the particles in various media are listed in Table V. Barium sulfate-I shows a larger volume than barium sulfate-II in polar and non-polar media.

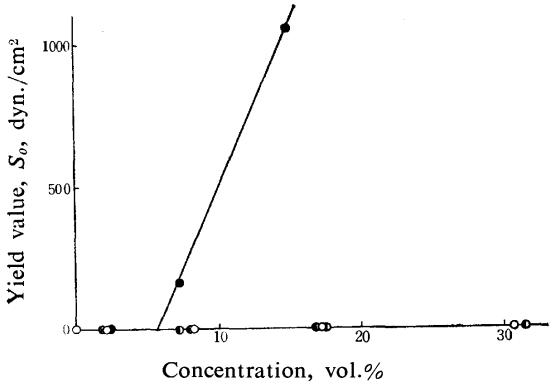

(a) Suspensions of barium sulfate in linseed oil.

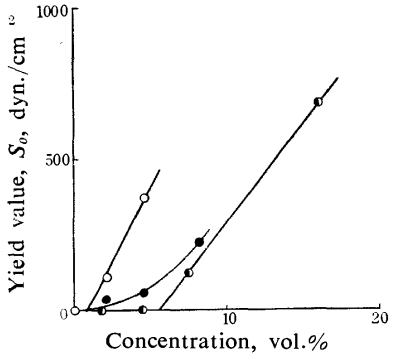

(b) Suspensions of barium sulfate in polyisobutylene.

Fig. 5. Concentration dependence of the yield value.
Symbols: (○) barium sulfate-I, (◐) barium sulfate-II and (●) barium sulfate-III.

TABLE IV. INFLUENCE OF ADDITION OF WATER UPON THE RHEOLOGICAL PROPERTIES IN SUSPENSION OF BARIUM SULFATE IN LINSEED OIL (12.54 VOL. %, AT 30°C)

Suspension	Concn. wt. % based on pigment	Plastic viscosity poises	Relative plastic viscosity	Yield value dyn./cm^2
Barium sulfate-I in linseed oil-III	0	116.7	1.97	0
	0.5	105.1	1.77	0
	1.0	113.6	1.92	0
	2.0	110.9	1.87	0
	3.0	207.9	3.50	0

TABLE V. SEDIMENTATION VOLUME OF PIGMENTS (cm^3/g.) AT ROOM TEMPERATURE

Pigment	in H_2O	in CCl_4	in C_6H_6
Barium sulfate-I	2.34	3.64	2.12
Barium sulfate-II	1.06	1.04	1.20

The time dependence and shear-rate dependence of the flow properties were examined qualitatively by the Brookfield viscometer.

When linseed oil was used as medium, thixotropic behavior was observed slightly in suspensions of barium sulfate-I and -II, and remarkably in suspensions of barium sulfate-III.

When polyisobutylene was used as the medium on the other hand, anti-thixotropic behaviors[10] were observed, as illustrated in Figs. 6 and 7. Suspensions of barium sulfate-I have a greater tendency toward anti-thixotropic behavior than do those of barium sulfate-II. The anti-thixotropic behavior, however, disappears and normal thixotropic behavior is

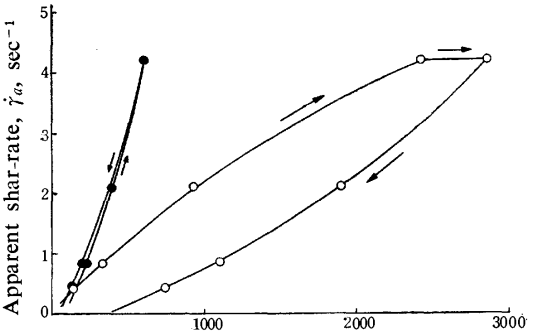

Fig. 6. Time dependence of flow property: (○) 4.54 vol.% suspension of barium sulfate-I in polyisobutylene-II and (●) 4.57 vol.% suspension of barium sulfate-III in polyisobutylene-II. Each point was obtained after rotating of the inner cylinder at a given speed for 5 min.

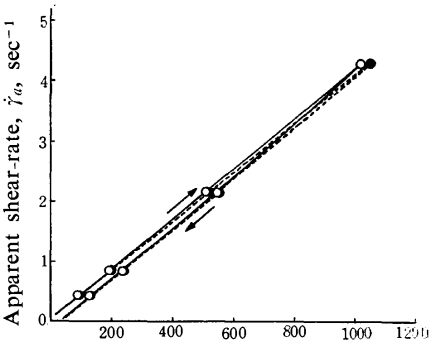

Fig. 7. Time dependence of flow property for a 4.47 vol.% suspension of barium sulfate-II in polyisobutylene-I: (○) after the sample was kept still for 30 min., and (●) after the sample was kept still for three weeks. Each point as obtained after rotating of the inner cylinder at a given speed for 5 min.

10) J. Crane and D. Schiffer, *J. Polymer Sci.*, 23, 93 (1957).

observed when the particles are covered by sodium stearate.

Discussion

According to the experimental results described above, it is evident that the particle sizes and the polarities of the medium and of the additive appreciably influence the state of flocculation and the flow properties of the system.

In the previous paper,[8] it was proposed that the plastic viscosity and the yield value of flocculated systems at very low rates of shear may be given by the following equations:

$$\eta_{pl}=\eta+(g_1+g_2)\tau_2(2/\pi R_1)\sigma'(\phi-\phi'_{crit}) \quad (1)$$

and

$$S_o=(2/\pi R_1)g_1\gamma_1\sigma'(\phi-\phi'_{crit}) \quad (2)$$

where η is the effective viscosity of a medium involving the particles, g_1 and g_2 are the mean stiffnesses of the primary links and of the secondary links between particles respectively, τ_2 is the relaxation time of the secondary links, R_1, the diameter of the particles, ϕ, the volume fraction of the particles, σ', the mean number of links to be broken in order to separate two particles, γ_1, the mean strain of primary links in a stationary flow, and ϕ'_{crit}, the critical concentration above which stationary links between particles appear appreciably.

In Eqs. 1 and 2, the parameters, τ_2, σ' and ϕ'_{crit}, are given as follows at very low rates of shear:

$$\tau_2=(\boldsymbol{h}/2g_2\lambda_2^2)\exp(\Delta F/\boldsymbol{kT}) \quad (3)$$

$$\sigma'=1+(12D_1'\boldsymbol{h}\phi_c/R_1^2\boldsymbol{kT})\exp(\Delta F/\boldsymbol{kT}) \quad (4)$$

and

$$\phi'_{crit}=(\eta\pi R_1^3/8\boldsymbol{h})\exp(-\Delta F/\boldsymbol{kT})/\sigma' \quad (5)$$

where $\boldsymbol{h}$ and $\boldsymbol{k}$ are the constants of Planck and Boltzmann respectively, ΔF is the mean free energy of activation for breaking the links between particles (which equals those of secondary links effectively), λ_2 is the distance increased whenever the secondary links are broken, T, the absolute temperature, D_1', the mutual diffusion constant of particles involved in a flocculate, and ϕ_c, the volume fraction occupied by particles in flocculates.

According to theoretical considerations, the plastic viscosity and the yield value must increase linearly above the critical concentration, ϕ'_{crit}, given by Eq. 5. After all particles are involved in one flocculate occupying the entire space available in the system, these flow properties must be quadratic functions of the concentration, since the ϕ_c included in σ' must be equal to the ϕ in such a region. These theoretical predictions seem to agree with the experimental findings, at least qualitatively, in flocculated systems.

The critical concentration, ϕ'_{crit}, can be obtained experimentally, and the mean free energy of activation for breaking the links between particles ΔF can be evaluated by using Eq. 5 with an assumption of the value of σ'. The critical concentration and the energy, ΔF, evaluated in this way are listed in Table VI. In these flocculated systems, the mean free energy of activation for breaking the links between particles seems to have the order of $30\sim36\boldsymbol{kT}$, slightly depending on the assumed value of σ'. The order of energy, ΔF, agrees with the values, $38\sim46\boldsymbol{kT}$, obtained by van den Tempel for suspensions of glyceryltristearate in either groundnut oil or paraffin oil.[7]

Table VI. Critical concentration and the mean free energy of activation for breaking the links between particles

Flocculated system	Critical concn. ϕ'_{crit}, vol. %	ΔF, $\boldsymbol{kT}$ $\sigma'=1$	$\sigma'=2$	$\sigma'=3$
Barium sulfate -III in linseed oil-II	5.0	31.0	30.3	29.8
Barium sulfate -I in polyisobutylene-II	0.8	34.0	33.3	32.8
Barium sulfate -II in polyisobutylene-I	5.6	36.0	35.3	34.9
Barium sulfate -III in polyisobutylene-II	0.5	34.4	33.7	33.3

In non-polar mediums, the most generally occurring type of interaction between particles may be considered to be the van der Waals-London attraction. For solvated spherical particles, the mean free energy of activation for breaking the links between two neighboring particles, ΔF, is given approximately by the following equation:[11-13]

$$\Delta F=(A_m^{1/2}-A_p^{1/2})^2R_1/24(\delta+2\Delta) \quad (6)$$

where A_m and A_p are the Hamaker parameters of medium and particles, δ is the distance between the surfaces of solvated particles, and Δ is the thickness of the layer of the bound medium.

For particles adsorbed by an additive, the interaction energy is[13]

11) H. C. Hamaker, *Physica*, 4, 1058 (1937).
12) M. J. Vold, *J. Colloid Sci.*, 9, 451 (1954).
13) M. J. Vold, ibid., 16, 1 (1961).

$$\Delta F=(A_s^{1/2}-A_m^{1/2})^2(R_1+2\Delta)/24\delta + (A_s^{1/2}-A_p^{1/2})^2R_1/24(\delta+2\Delta) + (A_s^{1/2}-A_p^{1/2})(A_m^{1/2}-A_s^{1/2}) \times R_1(R_1+2\Delta)/12(\delta+\Delta)(R_1+\Delta) \quad (7)$$

where A_s is the Hamaker parameter of the additive and Δ, the thickness of the layer of the additive.

The parameter, A, of a given homogeneous material with q_i, q_j atoms per cubic centimeter is defined as

$$A=\pi^2\sum_i\sum_j q_iq_j\lambda_{ij} \quad (8)$$

where λ_{ij} is the van der Waals parameter between two kinds, i and j, of atoms depending mainly on the polarizabilities of the atoms concerned. However, there is no simple method evaluate the value of A.

For the sake of simplicity, we will consider the van der Waals-London attraction between molecules. In this way, we have the approximate parameter for a given homogeneous material:

$$A=\pi^2q^2\lambda \quad (8')$$

and the parameter, λ, between two molecules:[14]

$$\lambda=(3/4)\alpha^2eI \quad (9)$$

where q is the number of molecules per cubic centimeter, α, the polarizability of the molecule, e, the charge of an electron, and I, the first ionization potential of the molecule. The polarizabilities of non-polar molecules can be evaluated by measurement of the dielectric constant:

$$\alpha=(3M/4\pi dN)(\varepsilon-1)/(\varepsilon+2) \quad (10)$$

where M is the molecular weight, N, Avogadro's constant, d, the density, and, ε, the dielectric constant at sufficiently higher frequencies.

By substituting Eqs. 9 and 10 into Eq. 8', and by combining the result with the following relation:

$$q=(dN/M)$$

we obtain

$$A=(3/4)^3eI(\varepsilon-1)^2/(\varepsilon+2)^2 \quad (11)$$

For non-polar materials, Eq. 11 will give an approximate value of the A parameter. For polar materials, however, Eq. 11 may only give an approximate order of the parameter.

Assuming $I=13.5$ eV., which is the first ionization potential of hydrogen atom for linseed oil, polyisobutylene and water, and using the dielectric constants listed in Table I-a, we estimated the magnitudes of A for each material. Similarly, for barium sulfate and sodium stearate, we assumed $I=5.21$ eV. for $Ba \rightarrow Ba^+$ and $I=5.09$ eV. for $Na \rightarrow Na^+$. The resultant evaluated values are listed in Table VII. Although these values were roughly estimated as described above, their orders of magnitudes of A agreed with those estimated in another way.[13]

TABLE VII. ORDERS OF THE MAGNITUDES OF PARAMETERS A

Material	A, erg.
Linseed oil	1.81×10^{-12}
Polyisobutylene	4.88×10^{-13}
Barium sulfate	2.00×10^{-12}
Sodium stearate	5.91×10^{-13}
Water	8.55×10^{-12}

By substituting these values of A into Eqs. 6 and 7 and by comparing the results with the experimental results stated above, we can estimate the distance between particles as shown in Table VIII. The thickness of the layer of sodium stearate was calculated from the concentration, ca. 1 wt.% based on pigment. In suspensions of barium sulfate-I and -II in linseed oil, the energy of the interaction between particles owing to the van der Waals-London attraction is very small when the distance between the surfaces of solid particles is larger than 10Å. The critical concentration, ϕ'_{crit}, given by Eq. 5 does not appaer up to the closest packing. This evaluation agrees with the experimental finding that no critical concentration can be observed up to the highest concentration.

The inefficiency of the addition of water to the suspensions in linseed oil can also be explained by assuming the van der Waals-London attraction between particles.

TABLE VIII. INTERACTION PARAMETERS BETWEEN PARTICLES

	$BaSO_4$-III in linseed oil-II	$BaSO_4$-I in P.I.B. -II	$BaSO_4$-II in P.I.B. -I	$BaSO_4$-III in P.I.B. -II
$\delta+2\Delta$, Å	11.8	12.1	43.3	55.3
2Δ, Å	10.3	—	—	10.3
δ, Å	1.5	—	—	45.0
$\Delta F/kT$	30.5	33.6	35.4	33.1
σ'	1.5	1.5	1.8	1.3
g_1, g_2 dyn./cm.	2250.	64.7	5.35	33.5
λ_2, Å	108.	276.	471.	622.
$\gamma_1\times10^5$	4.51	134.	3460.	92.1
$\tau_2\times10^5$, sec.	3.52	254.	6980.	614.

14) F. London, *Z. Phys.*, 63, 245 (1930)

The mean stiffness of links between particles may be given by the following equation:

$$g=(1/3)(\mathrm{d}^2\Delta F/\mathrm{d}\delta^2) \qquad (12)$$

If we assume the D_1' in Eq. 4 can be approximated by the diffusion constant of unlinked particles $D_1=kT/3\pi\eta R_1$, and that ϕ_c may be approximated by ϕ'_{crit}, the other parameters, σ', γ_1 and λ_2, may be evaluated from the concentration dependences of the plastic viscosity and the yield value by using Eqs. 1, 2, 3 and 4. The results are listed in Table VIII. However, it has been assumed that g_1 equals g_2 and that the interaction between particles is merely the van der Waals-London attraction.

Summary

The stationary flow properties of concentrated suspensions of barium sulfate in linseed oil and of those in polyisobutylenes have been measured at very low rates of shear with capillary viscometers and a Brookfield viscometer.

The dependence of the plastic viscosity and the yield value on the concentration, the particle sizes, and the polarizabilities of the medium and of the additive have been measured and explained by using a network model and by assuming van der Waals-London attraction between particles.

In suspensions of barium sulfate in linseed oil, the plastic viscosity and the yield value do not change on the addition of water below 2 wt. % based on pigments, and their dependence on the concentration of particles is monotonous. However, these values increase when the particles are covered with sodium stearate above a critical concentration.

In suspensions of barium sulfate in polyisobutylene, the plastic viscosity and the yield value appreciably increase above the critical concentration determined by the particle sizes, and these values decrease when the particles are covered with sodium stearate.

In both cases, a higher plastic viscosity and yield value are observed for suspensions of smaller particles in the same medium.

In suspensions of barium sulfate in polyisobutylene, antithixotropic behavior is observed at very low rates of shear. When the particles were covered by sodium stearate, the abnormal behavior disappears and normally thixotropic behavior is observed.

For plastic systems, the mean free energy of activation for breaking links between particles has been evaluated at $30\sim36kT$. If we assume van der Waals-London attraction between particles, the distance between the surfaces of solid particles is within the range of 10～55 Å, depending on the particle sizes and the presence of an additive.

Other parameters, the mean number of links to be broken for separating particles, the mean stiffness of links and other data have been approximately evaluated by assuming van der Waals-London attraction between particles.

The authors would like to express their gratitude to Professor Emeritus Bunnosuke Yamaguchi for his kind advice and also to Mr. Sentaro Yoshimoto for assisting in the experimental work described in this paper.

Aeronautical Research Institute
The University of Tokyo
Meguro-ku, Tokyo

The Gas Chromatographic Separation and Characterization of δ-Cyclogeraniolene and α-Cyclogeraniolene Formed from Isophorone by Wolff-Kishner Reduction[1]

By Atsuaki ARAI, Ching-Chung YAO and Iwao ICHIKIZAKI

(Received June 6, 1963)

Some isomers of cyclogeraniolene are known to serve as starting substances applicable[2-4] in the synthesis of ionone analogs. These isomers have been prepared by the cyclization of geraniolene[5,6] or by the dehydrative cyclization of 2, 6-dimethyl-5-hepten-2-ol[7,8] in the presence of various acidic catalysts; they have not, however, hitherto been separated in a pure state except in a single case in which δ- and ε-isomers,[8] i. e., 3, 5, 5- and 3, 3, 5-trimethylcyclohexene, were isolated in a reliable purity[9] from the dehydration products of dihydroisophorol.

A recent publication[10] describing how the modified Wolff-Kishner reduction of isophorone gave only the α-isomer, 2, 4, 4-trimethylcyclohexene, has prompted us to report on the isolation and characterization of δ- and α-isomers from the reaction products obtained during our independent studies.

We have found that the above reduction carried out at 160~170°C produces, in a 55% yield, an inhomogeneous hydrocarbon along with a small amount of isophorone hydrazone and isophorone azine. The hydrocarbon mixture thus obtained gave, on gas chromatography, two large peaks which accounted for ca. 30 and 70% of the total. A very small peak at a much lower retention time was also detected thereby, but it has not yet been identified. The relative amounts of the two main components scarcely changed under the reaction conditions programmed from 140 to 200°C, while that of the minor component varied over a range of 0~3%. The separation of these isomers was not sufficiently achieved even by careful distillation techniques, whereas the two principal components were completely isolated from the above mixture by preparative scale-gas chromatographic trapping.

The faster-eluted cyclogeraniolene gave, on ozonolysis, 2, 4, 4-trimethylhexanedioic acid, and the other major isomer yielded isogeronic acid in a high yield. Therefore, the former was considered to be δ-cyclogeraniolene and the latter to be α-cyclogeraniolene. The structural assignment was further confirmed by the NMR spectra, as will be described in the Experimental section.

The formation of the δ-isomer in the above reaction is not unexpected, as it has previously been recognized[11,12] that the Wolff-Kishner reduction of α, β-unsaturated carbonyl compounds in an alicyclic series gives essentially two olefinic isomers, of which one possesses the olefinic bond at the same position as before, while the other has a bond which has migrated to the site of the original carbonyl group.

We have found a linear relationship between the refractive indices and mole ratios for several mixtures of α- and δ-cyclogeraniolenes. The observed refractive values of both pure isomers (α, n_D^{25} 1.4433; δ, n_D^{25} 1.4383) were in good agreement with those estimated by graphical extrapolation. Alkonyi's "α-cyclogeraniolene," [10] n_D^{25} 1.4408, is possibly inhomogeneous and is contaminated by an appreciable amount of δ-isomers and/or other substances.

Finally, isophorone azine,[10] which was obtained on the Wolff-Kishner reduction, as has been mentioned, was also formed when isophorone hydrazone was allowed to stand for a long period at room temperature.

1) Presented at the 6th Symposium on Perfumery, Terpene and Essential Oil Chemistry, Ina, August, 1962.
2) A. Brenner and H. Schinz, *Helv. Chim. Acta*, 35, 1615 (1952).
3) Cf. R. Vonderwahl and H. Schinz, ibid., 35, 1997, 2005 (1952).
4) Cf. A. Arai and I. Ichikizaki, This Bulletin, 35, 818 (1962).
5) C. Harris and E. Weil, *Ber.*, 37, 845 (1904).
6) L. Bateman, J. I. Cunneen and E. S. Waight, *J. Chem. Soc.*, 1952, 1714.
7) A. Brenner, U. Steiner and H. Schinz, *Helv. Chim. Acta*, 35, 1336 (1952).
8) Cf. G. C. Oppenlander and A. R. Day, *J. Org. Chem.*, 21, 961 (1956).
9) G. Slomp, M. Inatome, C. E. Bowers, J. M. Derfer and K. W. Greenlee, ibid., 25, 514 (1960).
10) I. Alkonyi, *Chem. Ber.*, 94, 2486 (1961).
11) G. Lardelli and O. Jeger, *Helv. Chim. Acta*, 32, 1817 (1949).
12) S. Nagahama, H. Kobayashi and S. Akiyoshi, This Bulletin, 35, 1140 (1962).

Experimental[13]

The Wolff-Kishner Reduction of Isophorone. — A mixture of isophorone (69 g.), triethylene glycol (300 g.), 80% hydrazine hydrate (140 g.) and potassium hydroxide (93 g.) was heated at a bath temperature of 160~170°C for 2 hr. The reaction mixture was distilled at the same temperature to separate the product, which was obtained as an azeotropic mixture with a b. p. range of 123~135°C. The residue was again refluxed for 2 hr. and distilled. There was also obtained a pale yellow product boiling at 125~165°C. The combined distillates were then separated, and the water layer was extracted with ether. The extract and the organic layer were combined, washed with a saturated sodium chloride solution, dried over sodium sulfate and concentrated in vacuo. Distillation through a 20 cm. Vigreux column gave (1) a colorless liquid (39 g.) (b. p. 65~67°C/80 mmHg), (2) a pale yellow oil (8.5 g.) (b. p. 120~127°C/20 mmHg) and (3) a viscous yellow oil (8.3 g.) (b. p. 143~145°C/3 mmHg), which solidified immediately to give yellow prisms.

The low boiling fraction 1 was redistilled over sodium (1 g.) using a small Vigreux column to give a mobile liquid (38.2 g.) (b. p. 67.5~68°C/80 mmHg, n_D^{25} 1.4420), which on gas chromatography employing a 9 m., 30% PEG-6000-on-Celite DM-14A column at 128°C with a hydrogen flow rate of 35 ml./min. gave three peaks with the retention times of 18 min. 18 sec., 21 min. 18 sec. and 24 min. 42 sec. respectively. The second and third peak, accounting for 29 and 69% of the above fraction, are due to δ- and α-cyclogeraniolene respectively. The first peak, accounting for 2%, is due to the hydrocarbon, which has not yet been characterized. The relative amounts of this compound changed over a range of only 0~3% under several W.-K. reduction conditions (4~13 hr. at 140~200°C).

The distillation of fraction 2 gave a pale yellow oil (7.8 g.) which boiled at 125~127°C/21 mmHg and which solidified gradually when left standing. Crystallization from ether-petroleum ether (5 : 1) yielded isophorone hydrazone as colorless needles (m. p. 72~73°C), which was treated with the Brady reagent to give isophorone 2,4-dinitrophenylhydrazone as dark-red needles (m. p. 146~147°C) (Lit. m. p. 147~148°C[14]).

Isophorone hydrazone was unstable and, on exposure to air, yielded an orange-yellow tarry product with an isophorone-like odor from which isophorone azine, identified by the mixture melting point determination and by infrared comparison with an authentic sample, was obtained.

The yellow solid obtained from the high boiling fraction 3 was recrystallized from methanol to give isophorone azine in the form of yellow leaflets; m. p. 148.5~149°C (Lit. m. p. 147~148°C[10]). ν_{max}^{KBr} 3034, 1641 (C=N), 1580 (conju. C=C), 1381, 1362 (*gem*-dimethyl), 1121, 898 and 835 cm^{-1}.

Found: C, 79.54; H, 10.07; N, 9.91. Calcd. for $C_{18}H_{28}N_2$: C, 79.36; H, 10.36; N, 10.28%.

The treatment of this compound with the Brady reagent gave, in a quantitative yield, isophorone 2,4-dinitrophenylhydrazone; m. p. 146~147.5°C.

The Gas Chromatographic Separation of δ-Cyclogeraniolene and α-Cyclogeraniolene from the Hydrocarbon Mixture.—The hydrocarbon mixture (59 g., n_D^{25} 1.4419) consisting of 0.5% an unknown component, 28.5% δ-isomers and 71.0% α-isomers was injected in 6 ml. portions into a Beckmann "Megachrom" equipped with a 12 ft.×5/8 in.φ, Apiezon "J" on a firebrick column at 123°C with a 135°C pre-heated inlet and a nitrogen flow (inlet/outlet=15/1 (p. s. i.)). After the usual procedure, there were finally obtained three fractions: (1) 11.4 g. (retention time, 27 min. 48 sec.), (2) 34.0 g. (32 min. 32 sec.), and (3) 6.3 g. (the mixed hydrocarbon recovered). The distillation of fraction 1 through a 40 cm. Vigreux column over sodium (1 g.) gave δ-cyclogeraniolene (9.9 g.) as a colorless mobile liquid (b. p. 132.4~132.6°C/760 mmHg, n_D^{25} 1.4384, n_D^{15} 1.4428), which was gas chromatographed on a 2.5 m. column of 25% PEG-6000 substrate to show a single peak. (Lit. b. p. 133.58°C, n_D^{20} 1.4406[9]). ν_{max}^{film} 3014, 1653, 714, 672 (cis -CH=CH-), 1461 ($-CH_2-$), 1398, 1387 and 1367 cm^{-1} (CH_3). NMR absorptions:[13] a multiplet in the 8.40~8.88 τ region (2H, CH_2 in the 4-position); an apparent triplet at 8.26 τ (2H, allylic CH_2 in the 6-position); a multiplet at 7.94 τ (1H, allylic CH in the 3-position); two peaks at 9.12 and 9.09 τ (6H, *gem*-dimethyl); a doublet at 9.04 τ (3H, CH_3 in the 3-position, J=5.01 c.p.s.), and an apparently unresolved doublet at 4.59 τ (2H, vinyl CH=CH, J=0.9 c.p.s., half-width=3.5 c.p.s.).

Found: C, 86.98; H, 12.92. Calcd. for C_9H_{16}: C, 87.02; H, 12.98%.

Fraction 2 was distilled through the same column to afford α-cyclogeraniolene (32.1 g.) as a colorless mobile liquid (b. p. 137~138°C/760 mmHg, n_D^{25} 1.4433), which was proven to be completely homogeneous by gas chromatographic analysis. (Lit. b. p. 103~105°C/200 mmHg;[7] b. p. 135°C, n_D^{25} 1.4408;[10] b. p. 54°C/40 mmHg[15]). ν_{max}^{film} 3042, 1679, 805 (>C=CH-), 1458 ($-CH_2-$), 1381 and 1363 cm^{-1} ($-CH_3$). NMR absorptions:[13] a triplet at 8.64 τ (2H, CH_2 in the 5-position); a multiplet at 7.91 τ (4H, two allylic CH_2 in the 3- and 6-positions); two peaks at 9.03 and 8.97 τ (6H, *gem*-dimethyl); a singlet at 8.27 τ (3H, CH_3 in the 2-position), and a multiplet at 4.33 τ (1H, olefinic C-H).

Found: C, 87.05; H, 13.03. Calcd. for C_9H_{16}: C, 87.02; H, 12.98%.

The retention time ratios to cyclohexene as the standard of the two isomeric cyclogeraniolenes and related substances, when measured at 136°C by a 3 m., 30% PEG-6000-on-Celite DM-14B column with

13) All melting points were measured on a Kofler block and are uncorrected. The infrared spectra were recorded on a Nippon Bunkô, model IRS, recording spectrometer using sodium chloride optics, while the gas chromatographic analyses were performed with a Kotaki Super Fractioner, model GU-21. The NMR spectra were determined at 56.4 Mc./s. with a Varian V-4300C high resolution NMR spectrometer using a 20 vol. % solution in carbon tetrachloride and tetramethylsilane as the internal standard.

14) A. W. Fort, *J. Org. Chem.*, **26**, 332 (1961).

15) B. Willhalm, U. Steiner and H. Schinz, *Helv. Chim. Acta*, **41**, 1359 (1958).

a 25 ml./min. rate of hydrogen flow, are: the unknown hydrocarbon, 1.26; ε-cyclogeraniolene, 1.37; δ-cyclogeraniolene, 1.45, and α-cyclogeraniolene, 1.67.

2,4,4-Trimethylhexanedioic Acid.—Ozonized oxygen (*c* 17 g./m³) was passed through a solution of δ-cyclogeraniolene (1.5 g.) in carbon tetrachloride (10 ml.) at a flow rate of 30 l./hr. over a period of 2.5 hr. The temperature was maintained at −10°C by cooling. Acetic acid (5 ml.) and 30% hydrogen peroxide (1.5 ml.) were added, and the resulting solution was allowed to stand overnight at room temperature. After the bulk of solvent had been removed in vacuo, the residue was treated as usual to give a colorless, viscous oil (0.65 g.) (b. p. 160～180°C/6 mmHg (bath temp.)), which solidified when stored for a week in a refrigerator. Crystallization afforded colorless prisms; m. p. 71°C (Lit. m. p. 69.7～70.0°C,[9] 72～73.5°C[16]). The dianilide crystallized from benzene in the form of colorless prisms; m.p. 165°C (Lit. m.p. 164～165°C,[16] 162.8～163.3°C[17]).

Isogeronic Acid.—α-Cyclogeraniolene (1.5 g.) in carbon tetrachloride (15 ml.) was ozonized, and the reaction mixture was treated in the manner described for δ-isomer. A colorless viscous oil (1.0 g., 67.0%) (b. p. 162～165°C/5 mmHg) was obtained.

Found: C, 62.32; H, 9.42. Calcd. for $C_9H_{16}O_3$: C, 62.76; H, 9.36%.

The semicarbazone crystallized from methanol in the form of colorless prisms; m. p. 200～201°C (Lit. m. p. 197～198°C,[10] 198°C[18]).

The authors wish to express their deep appreciation to Dr. Yo-ichiro Mashiko and Dr. Hiroshi Tomita of the Government Chemical Industrial Research Institute of Tokyo for their help in the use of the Beckmann "Megachrom" and to Dr. Naohiro Hayakawa of the Japan Atomic Energy Research Institute for his measurement of the NMR spectra. They are also indebted to Dr. Toshiaki Nishida of this laboratory for his valuable discussions of the NMR spectra and for his kind supply of a pure sample of ε-cyclogeraniolene.

Laboratory of Organic Chemistry
Kobayasi Institute of Physical Research
Kokubunji, Tokyo

16) R. H. Mazur, *J. Org. Chem.*, **26**, 1289 (1961).
17) O. Wallach, *Ann.*, **343**, 40 (1905).
18) F. Tieman and R. Schmidt, *Ber.*, **31**, 883 (1898).

The Mechanism of Ethylenimine Formation by the Action of Grignard Reagents on Ketoximes

By Shoji EGUCHI and Yoshio ISHII

(Received June 7, 1963)

It has been known that certain substituted ethylenimines are obtained by the action of aliphatic or aromatic Grignard reagents on aryl alkyl ketoximes, followed by the non-acidic decomposition of Grignard complexes.[1]

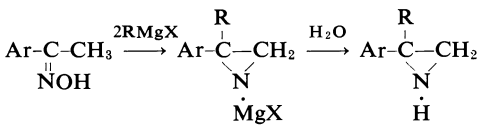

In this paper this cyclization reaction will be examined using acetophenone oxime I as a ketoxime and ethylmagnesium bromide as a Grignard reagent; as will be seen, an azirine derivative VIII has been found to be an intermediate in these reactions.

Campbell et al.[1] proposed the following reaction process involving the Grignard complex III as an intermediate:

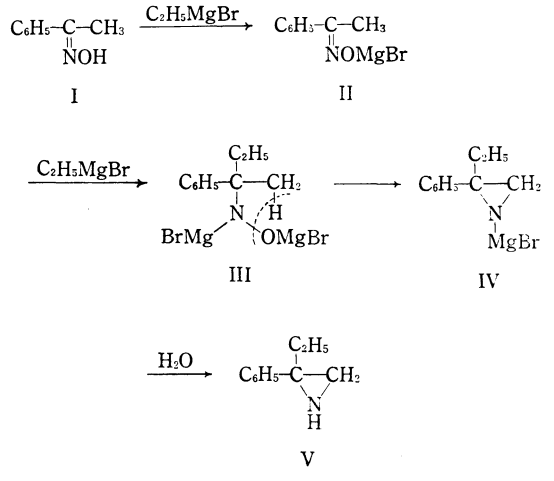

1) K. N. Campbell and J. F. Mckenna, *J. Org. Chem.*, **4**, 198 (1939); K. N. Campbell, B. K. Campbell and E. P. Chaput, ibid., **8**, 99 (1943); K. N. Campbell, B. K. Campbell, J. F. Mckenna and E. P. Chaput, ibid., **8**, 103 (1943); K. N. Campbell, B. K. Campbell, L. G. Hess and I. J. Schaffner, ibid., **9**, 184 (1944).

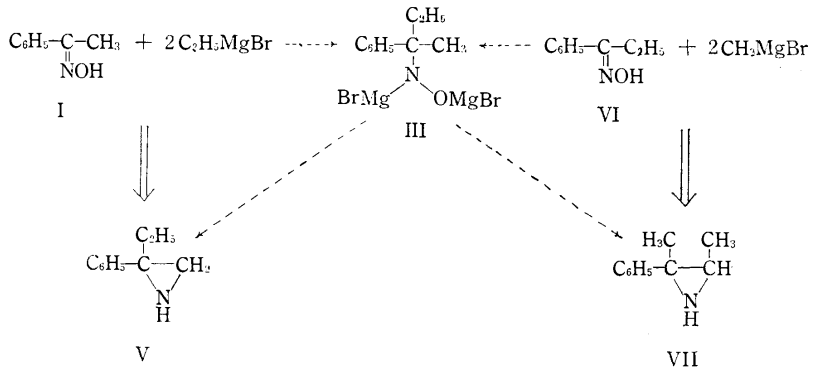

If this were actually the case, the same product would be expected from the reaction of acetophenone oxime (I) and ethylmagnesium bromide as from that of propiophenone oxime (VI) and methylmagnesium bromide, since the same intermediate complex III should be formed from these two reaction systems.

However, Henze and Compton[2] reported that the former reaction system afforded 2-phenyl-2-ethylethylenimine (V), while the latter yielded 2-phenyl-2, 3-dimethylethylenimine (VII). By gas chromatographic analysis we have confirmed their findings.

From these results, it may be concluded that an α-carbon atom of the alkyl group in the oxime becomes a member of the ethylenimine ring.

An explanation of this fact has been suggested based on the configuration of the starting oxime and the proximity of the OMgBr group to the hydrogen of the alkyl group.[2] In the intermediate complex III, however, the carbon-nitrogen single bond can not be fixed and no allylic hydrogen exists any longer; accordingly it is difficult to explain the selective cyclization in these reactions since the hydrogen atoms of the two alkyl groups become more or less equivalent.

An alternative and more plausible formulation is that the acidic hydrogen of the alkyl group is abstracted by an excess of the Grignard reagent, followed by cyclization to an azirine ring VIII, and that the reaction of the Grignard reagent on this azirine intermediate finally affords the substituted ethylenimine compounds as follows:

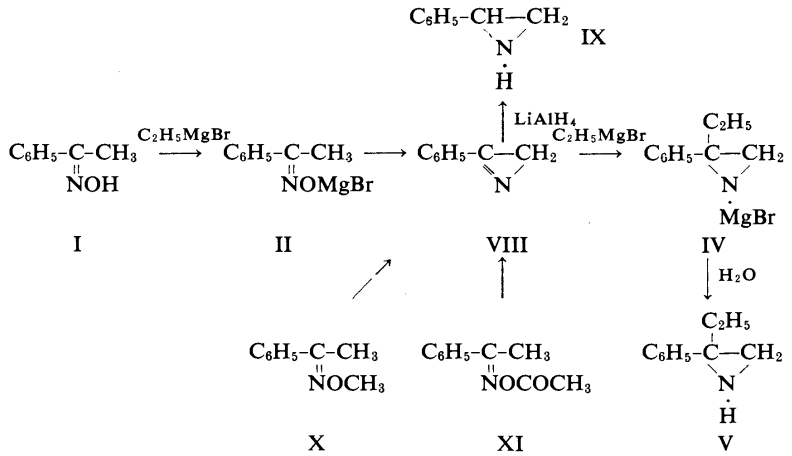

The Neber rearrangement[3] of an oxime tosylate by a base is an example similar to this cyclization process. The mechanism of the Neber rearrangement has been reported by Cram and his co-workers,[4] who proved the intermediate to be an azirine derivative.

When the phenylazirine (VIII) was treated with ethylmagnesium bromide and the resultant complex was decomposed by ice-ammonium chloride, 2-phenyl-2-ethylethylenimine (V) was obtained as expected. Lithium aluminum hydride reduction of the C=N double bond of the azirine gave styrenimine (IX).

The reaction of acetophenone oxime with

2) H. R. Henze and W. D. Compton, ibid., **22**, 1036 (1957).

3) P. W. Neber and A. Friedolsheim, *Ann.*, **449**, 109 (1926); P. W. Neber and G. Huh, ibid., **515**, 283 (1935); P. W. Neber, A. Burgard and W. Thier, ibid., **526**, 277 (1936).

4) D. J. Cram and M. J. Hatch, *J. Am. Chem. Soc.*, **75**, 33, 38 (1953).

ethylmagnesium bromide containing lithium aluminum hydride was examined, and the reaction products were analyzed by gas chromatography. It was found that 2-phenyl-2-ethylethylenimine (V) was produced in this reaction, together with a small amount of styrenimine (IX). On the other hand, from the reaction of lithium aluminum hydride with acetophenone oxime, no trace of styrenimine could be detected.

The intermediate complex II was obtained by the addition of one mole of ethylmagnesium bromide to the oxime I in ether. The complex II was stable upon being heated at 150°C without a solvent, but it yielded the ethylenimine V when treated with an excess of ethylmagnesium bromide (about 2 mol.) at about 95°C in a toluene-ether (1 : 1) mixture. The second mole of the Grignard reagent presumably reacts with the complex II as a base to produce a carbanion:

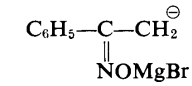

Acetophenone oxime methyl ether (X) and its acetate XI also reacted with an excess of the Grignard reagent under the same conditions to afford the ethylenimine V in a relatively high yield.

These findings clearly support the proposed mechanism for the ethylenimine formation from the action of the Grignard reagent on oximes.

Experimental

The infrared absorption spectra were measured with a Nippon Bunko IRS infrared spectrometer, using rock salt prisms. The gas chromatographic analyses were carried out on a Shimazu gas chromatograph, Model GC-1B.

2-Phenyl-2-ethylethylenimine (V).—Almost the same procedure as that of Campbell[1] was employed in the reactions of oximes and Grignard reagents. One mole of ethylmagnesium bromide in 250 ml. of ether and 250 ml. of toluene was prepared. With the solution kept at ca. 100°C, 34 g. (0.25 mol.) of acetophenone oxime was added dropwise with stirring. After the addition of the oxime, the mixture was kept at 105°C for 1 hr. The reaction mixture was then poured onto a cracked ice-ammonium chloride mixture, and the organic layer was extracted with ether several times. The combined ether extracts were dried over anhydrous magnesium sulfate. After the mixture had stood overnight, the solvent was removed under reduced pressure (water aspirator) below 80°C. The vacuum distillation of the oily residue gave about 15~20 g. of 2-phenyl-2-ethylethylenimine (V); yield 40~54%; b. p. 85~87°C/7 mmHg, n_D^{20} 1.5319 [lit.,[1] b. p. 85~86°C/7 mmHg, n_D^{20} 1.5318]. The infrared spectrum of V exhibited prominent bands at 3200, 3000, 2900, 1600, 1495, 1450, 1370, 1230, 1145, 870, 770, and 710 cm^{-1}. Phenyl thiourea, m. p. 98~99°C [lit.,[1] m. p. 99~100°C], $\nu_{C=S}^{KBr}$ 1590 cm^{-1}. The gas chromatographic analyses of V through a 1.5 m. column packed with 30% Cerite-545 and PEG-6000 revealed a single peak.

Acetophenone oxime methyl ether (b. p. 80~81°C/10 mmHg) and acetophenone oxime acetate (m. p. 53~55°C, $\nu_{C=S}^{KBr}$ 1770 cm^{-1}) were also treated with the Grignard reagent under the same conditions, to give 2-phenyl-2-ethylethylenimine (V) in yields of 63% and 64%, respectively.

2-Phenyl-2, 3-dimethylethylenimine (VII).—Propiophenone oxime (VI) (0.25 mol.) was treated with 1 mol. of methylmagnesium bromide under conditions similar to those when I was treated with ethylmagnesium bromide. A 50% yield of VII resulted; b. p. 89~91°C/7 mmHg; n_D^{20} 1.5242 [lit.,[2] b. p. 85~95°C/10 mmHg, n_D^{20} 1.5288]; phenyl thiourea, m. p. 120~122°C [lit.,[2] m. p. 122~123°C], $\nu_{C=S}^{KBr}$ 1590 cm^{-1}. Gas chromatography showed two peaks which may correspond to a 98 : 2 mixture of the cis and trans isomers. No peak corresponding to 2-phenyl-2-ethylethylenimine (V) was observed.

The Reaction of Acetophenone Oxime with Lithium Aluminum Hydride-Grignard Reagent Mixture.*—Acetophenone oxime, 13.5 g. (0.1 mol.) in 50 ml. of toluene, was added drop by drop at 85°C to a Grignard reagent-lithium aluminum hydride mixture which had been prepared from 9.6 g. of magnesium (0.4 mol.), 50 g. of ethyl bromide and 1.0 g. (0.026 mol.) of lithium aluminum hydride in 300 ml. of an ether-toluene (1 : 1) mixture. After the addition, the mixture was refluxed for about 1 hr. The reaction mixture was poured onto a cracked ice-ammonium chloride mixture, and the organic layer was extracted with ether 5 times. The extracts were dried over anhydrous magnesium sulfate, and then the solvent was removed under reduced pressure (water aspirator). Distillation of the remaining oily material gave 6 g. of an amine-imine mixture, b. p. 94~95°C/10 mmHg, n_D^{20} 1.5352. Gas chromatographic analysis showed that this was a mixture of 64% 2-phenyl-2-ethylethylenimine, 1% styrenimine and 35% α-phenylethylamine.

The same reaction of acetophenone oxime with the Grignard reagent-lithium aluminum hydride mixture in ether at a lower temperature was also carried out, but gas chromatography showed the basic products were then 72% ethylaniline and 28% α-phenylethylamine. The lithium aluminum hydride reduction of acetophenone oxime in ether produced 60% α-phenylethylamine and 40% ethylaniline.[5]

The Reaction of Phenylazirine (VIII) **with Lithium Aluminum Hydride and the Grignard Reagent.**—2-Phenylazirine (VIII), which had been obtained from the pyrolysis of α-azidostyrene,[6] was treated with lithium aluminum hydride in the

* It has been reported that the reducing properties of an ether solution of $Mg(AlH_4)_2$, formed from $LiAlH_4$ and the Grignard reagent, are similar to those of the ether solution of $LiAlH_4$; E. Wiberg and R. Bauer, *N. Naturforsch.*, **5b**, 397 (1950); *Chem. Abstr.*, **45**, 4593 (1951).

5) D. R. Smith, M. Maienthal and J. Tipton, *J. Org. Chem.*, **17**, 294 (1952).

6) G. Smolinsky, ibid., **27**, 3557 (1962).

usual manner. Styrenimine (IX) was obtained in a 30% yield; b. p. 88~90°C/9 mmHg, n_D^{20} 1.5610 [lit.,[7] b. p. 94~95°C/10 mmHg, n_D^{20} 1.5588]. Gas chromatography showed a single peak. The reaction of phenylazirine with ethylmagnesium bromide in ether gave 2-phenyl-2-ethylethylenimine (V) in a 55% yield. The relatively low yield of styrenimine and V from these reactions may be due to the dimerization of phenylazirine, since an unidentified, yellow, high-boiling material (b. p. 140~145°C/2 mmHg) was also obtained.

The Isolation of Complex II. — When one mole of ethylmagnesium bromide in ether was introduced into an ethereal solution of acetophenone oxime at room temperature, a white solid was obtained in a high yield (ca. 95%). This solid showed $\nu_{C=N}^{KBr}$ 1613 cm^{-1} (very strong[8]), and by hydrolysis acetophenone oxime was reproduced. When the complex II was treated with an excess of ethylmagnesium bromide in a manner described before, 2-phenyl-2-ethylethylenimine (V) was obtained (65%). However, complex II neither reacts with one mole of the Grignard reagent nor changes upon being heated at 150°C for 1 hr. without a solvent.

7) S. J. Brois, ibid., **27**, 3532 (1962).
8) Y. Kuroda and M. Kimura, This Bulletin, **36**, 464 (1963).

Summary

The reactions of aryl alkyl ketoximes with aliphatic Grignard reagents have been carried out under various conditions.

Gas chromatographic analyses of the reaction products showed the formation of an ethylenimine ring in which an α-carbon of the alkyl group in oximes constitutes a member of the ethylenimine ring. The reaction of acetophenon oxime with ethylmagnesium bromide containging lithium aluminum hydride produced 2-phenyl-2-ethylethylenimine, together with styrenimine.

A reaction process similar to that of the Neber rearrangement has then been proposed on the basis of the above findings.

Department of Applied Chemistry
Faculty of Engineering
Nagoya University
Chikusa-ku, Nagoya

The Synthesis of New Meso-ionic Compounds from Cyanomethyl Dithiobenzoate[1]

By Masaki OHTA and Masatoshi SUGIYAMA

(Received June 8, 1963)

In our previous paper on meso-ionic compounds,[2] it was reported that 3-phenylsydnoneimine hydrochloride (II) was prepared by the action of hydrogen chloride upon *N*-nitrosoanilinoacetonitrile (I). Recently, the synthesis of sydnoneimine hydrochlorides and sydnoneimines substituted with an acyl-, carbamoyl- or thiocarbamoyl- group at the exocyclic nitrogen atom has been reported by Daeniker and Druey.[3]

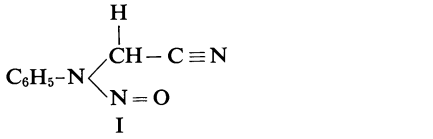

I

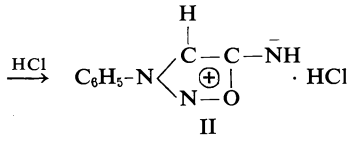

II

The formation of a sydnoneimine ring involves both a bond formation by the intramolecular addition between polar groups, i. e., a nitroso and a cyano group, and a proton transfer to a nitrogen of the cyano group. As the thioketo group is a strong polar group like the nitroso group, it is reasonable to expect that ring formation would occur with cyanomethyl dithioesters by means of a similar mechanism. The present paper reports the synthesis of a new type of meso-ionic compound, "dithioloneimine,"* containing two sulfur atoms in a ring.

The reaction of potassium dithiobenzoate

1) This paper is the part XVII of studies on meso-ionic compounds.

2) H. Kato, M. Hashimoto and M. Ohta, *J. Chem. Soc. Japan, Pure Chem. Sec.* (*Nippon Kagaku Zassi*), **78**, 707 (1957).

3) H. U. Daeniker and J. Druey, *Helv. Chim. Acta*, **45**, 2426 (1962).

* The free base of IV is referred to as "dithioloneimine" and was derived from an unknown "dithiolone" with the structure written below. The synthesis of dithiolone is now under way in our laboratory.

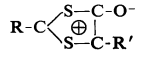

with chloroacetonitrile in ethanol or in methanol gave a red, oily product, identified as cyanomethyl ester III, which could be purified neither by crystallization nor by distillation even in a nitrogen atmosphere because of decomposition; therefore, the oily intermediate was used for further experiments. When dry hydrogen chloride was passed into an ethereal solution of III, dithioloneimine hydrochloride was separated out; it was very hygroscopic in air and was identified as the picrate.

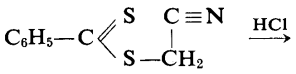

III

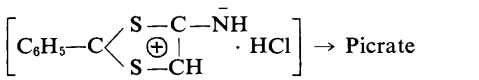

IV V

In contrast to sydnoneimine hydrochloride, which is easily acylated with acyl chlorides in the presence of alkali, IV seemed to be very unstable towards alkali and could not be acylated in the presence of weak alkali. By the action of benzoyl chloride on III in an ethereal solution, the hydrochloride of the *N*-benzoyl derivative VIa was obtained. When acetyl chloride was used in place of benzoyl chloride, the hydrochloride of the *N*-acetyl derivative VIb was obtained.

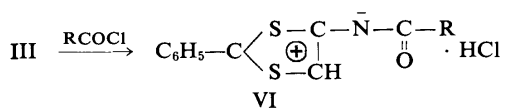

VI

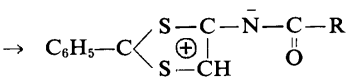

VII

VIa $R=C_6H_5$ VIb $R=CH_3$

These hydrochlorides of *N*-acyldithioloneimines are yellow, but their free bases are brilliant red. It is known that some dithioesters show thermochromism in a solution. For example, a solution of methyl α-dithionaphthoate in ethyl benzoate is yellow-orange, but it becomes red-orange when heated.[4] Yellow crystals of VIa or of its solution in benzene or in xylene turn red when heated and then become yellow again when cooled.

When α-chlorophenylacetonitrile was treated with potassium dithiobenzoate, an oily intermediate VIII was obtained which gave 2, 5-diphenyldithioloneimine hydrochloride when treated with hydrogen chloride. Unexpectedly, when VIII was treated with benzoyl chloride, the same dithioloneimine hydrochloride was obtained. The reason for the formation of this hydrochloride instead of the *N*-benzoyl derivative is not clear.

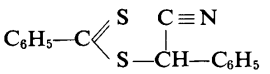

VIII

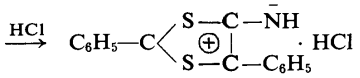

IX

The structural evidence for dithioloneimines based on elementary analysis and its infrared spectrum. The disappearance of the C≡N stretching band at 2260 cm^{-1} and the appearance of a CH stretching band at 3020~3050 cm^{-1} suggest the formation of a meso-ionic ring. A CO stretching band of *N*-acylsydnoneimine hydrochlorides was observed at 1720 cm^{-1},[3] but in case of *N*-acyldithioloneimine hydrochlorides, this band shifts to 1650~1670 cm^{-1}.

Experimental

2-Phenyldithioloneimine Picrate (V). — Thirty-eight grams of chloroacetonitrile were added drop by drop below 40°C to an ethanol solution (500 ml.) of potassium dithiobenzoate prepared from 98 g. of benzotrichloride by Crawholl's procedure;[5] the mixture was then stirred for an hour at room temperature under a slow stream of nitrogen. The filtration of the reaction mixture and the removal of the ethanol from the filtrate gave 47 g. of a red oil which was identified as III by its infrared spectrum but which could not be purified by distillation because it decomposed when heated above 80°C.

The red oil was dissolved in 100 ml. of ether and dried with sodium sulfate. Dry hydrogen chloride was passed through 10 ml. of an ethereal solution of III, the hygroscopic precipitate obtained was quickly dissolved in 10 ml. of ethanol, and 1 ml. of a saturated alcoholic solution of picric acid was added to the resulting solution. Then the alcoholic solution was heated to a boil; when it had cooled, there separated out red needles, which were recrystallized from ethanol (m. p. 157.5~158.5°C).

Found: C, 42.50; H, 2.30; N, 13.09. Calcd. for $C_{15}H_{10}N_4O_7S_2$: C, 42.66; H, 2.39; N, 13.26%.

2-Phenyl-1-*N*-benzoyldithioloneimine Hydrochloride (VIa).—To 20 ml. of the ethereal solution of III prepared above, 7.2 g. of benzoyl chloride were added while the mixture was shaken well, the mixture was then kept standing for a day at room temperature. The precipitate was filtered off and crystallized three times from ethanol to give 4.3 g. of yellow needles (m. p. 214~215°C (decomp.)), which showed λ_{max}^{EtOH} 398 mμ (ε 15100).

4) A. Schoenberg, S. Nickel and D. Cernik, *Ber.*, 65, 289 (1932).

5) J. C. Crawholl and D. F. Elliott, *J. Chem. Soc.*, **1951**, 2071.

Found: C, 57.42; H, 3.62; N, 4.28. Calcd. for $C_{16}H_{12}NOS_2Cl$: C, 57.57; H, 3.62; N, 4.19%.

2-Phenyl-*N*-acetyldithioloneimine Hydrochloride (VIb).—To 20 ml. of the ethereal solution of III, 4 g. of acetyl chloride were added while the solution was being cooled and shaken; the mixture was then kept standing for a day. The precipitate was filtered off, crystallized from ethanol, and recrystallized from isopropyl alcohol to give 4.5 g. of yellow crystals (m. p. 207°C (decomp.)), which showed λ_{max}^{EtOH} 398 mμ (ε 13800).

Found: C, 48.43; H, 3.45; N, 5.38. Calcd. for $C_{11}H_{10}NOS_2Cl$: C, 48.60; H, 3.71; N, 5.15%.

2-Phenyl-*N*-benzoyldithioloneimine (VIIa).—To 100 ml. of an aqueous solution of VIa (1 g.) 10 ml. of a saturated aqueous solution of sodium hydrogen carbonate was added, and the mixture was shaken with benzene. The benzene layer was then dried with sodium sulfate. The removal of the benzene gave 0.6 g. of red needles (m. p. 176~177°C (decomp.)), which showed λ_{max}^{EtOH} 472 mμ (ε 9090).

Found: C, 64.30; H, 3.48; N, 4.73. Calcd. for $C_{16}H_{11}NOS_2$: C, 64.63; H, 3.73; N, 4.71%.

2-Phenyl-*N*-acetyldithioloneimine (VIIb). — To 100 ml. of an aqueous solution of VIb (1 g.), 10 ml. of a saturated aqueous solution of sodium hydrogen carbonate was added, and the mixture was shaken with benzene. The benzene layer was then dried with sodium sulfate. The removal of the benzene gave 0.55 g. of red crystals, which was recrystallized twice from benzene-petrolium ether; m. p. 184~185°C (decomp).

Found: C, 55.63; H, 3.16; N, 5.56. Calcd. for $C_{11}H_9NOS_2$: C, 56.10; H, 3.86; N, 5.95%.

2, 5-Diphenyldithioloneimine Hydrochloride (IX).—7.6 g. of α-chlorophenylacetonitrile[6] which had been prepared from mandelonitrile[7] and thionyl chloride were added under a slow stream of a nitrogen current below 40°C to 100 ml. of potassium dithiobenzoate in ethanol prepared from 9.8 g. of benzotrichloride; the mixture was then stirred for an hour at room temparature. The filtration of the reaction mixture and the removal of ethanol of the filtrate gave a red oil, to which 20 ml. of water was added and extracted with two portions of ether of 50 ml. each. The ethereal layer was dried with sodium sulfate, and dry hydrogen chloride was passed through one-half of the ethereal layer. When the solution was kept standing for two days at room temparature, gave dark red crystals which were recrystallized from acetone (m. p. 166~167° (decomp.)), the crystals showed λ_{max}^{EtOH} 487 mμ (ε 21800).

Found: C, 58.42; H, 3.74; N, 4.52. Calcd. for $C_{15}H_{12}NS_2Cl$: C, 58.92; H, 3.92; N, 4.58%.

To the other half of the ethereal solution, benzoyl chloride was added; after the mixture had been kept standing over night, red crystals were filtered off. Recrystallization from acetone gave dark red needles which were identified as IX by their infrared spectrum and by elementary analysis.

The authors are indebted to Miss Toshiko Aoyagi for her elementary analysis and to Mr. Yutaka Hachimori for his ultraviolet spectral data.

Laboratory of Organic Chemistry
Tokyo Institute of Technology
Meguro-ku, Tokyo

6) F. Barrow and F. J. Thorneycroft, ibid., **1934**, 722.
7) H. Gilman and A. H. Blatt, "Organic Syntheses," Coll. Vol. I, 336 (1961).

The Separation and Structure Determination of an Eicosatrienoic and an Eicosadienoic Acid in Nagi Seed Oil[*1]

By Suketaka ITO,[*2] Yoshito KOYAMA[*3] and Yoshiyuki TOYAMA[*4]

(Received June 8, 1963)

The presence of an eicosatrienoic acid in the seed oil of Nagi, *Podocarpus Nagi*, has been reported in a previous study by Koyama and Toyama.[1] However, the structure of this acid has not yet been determined; it is only known that this acid, after isomerization with alkali, shows the characteristic absorption of conjugated dienes without showing that of conjugated trienes.

In this study, the presence of an eicosadienoic

*1 A Synopsis of this paper has already been published in Japanese; *J. Chem. Soc. Japan, Pure Chem. Sec.* (*Nippon Kagaku Zasshi*), **84**, 92 (1963).

*2 Present address: Department of Industrial Chemistry, Faculty of Engineering, Shinshu University, Nagano-shi.

*3 Present address: Aichi Prefectural Research Institute for Food Industry, Nishi-ku, Nagoya.

*4 Present address: Department of Applied Chemistry, Faculty of Engineering, Toyo University, Kawagoe, Saitama-ken.

1) Y. Koyama and Y. Toyama, *J. Chem. Soc. Japan, Pure Chem. Sec.* (*Nippon Kagaku Zassi*), **78**, 1223 (1957). The eicosatrienoic acid of Nagi seed oil was carelessly named "podocarpic acid" by these authors, but this nomenclature should be withdrawn since the same name had already been given to a different resin acid (cf. A. C. Oudemans, *Ber.*, **6**, 1122, 1125 (1873)).

acid besides the eicosatrienoic acid in Nagi seed oil has been indicated by gas-liquid chromatography (GLC). For the separation of these two acids, the methyl ester of the fatty acids of Nagi seed oil was subjected to repeated urea-adduct segregation; a crude eicosatrienoate fraction and a fraction rich in eicosadienoate were thus separated. The crude eicosatrienoate fraction was purified further by column chromatography to give the eicosatrienoate fraction. The fraction rich in eicosadienoate was fractionally distilled to give the eicosadienoate fraction. The positions of the double bonds in the eicosatrienoate and in the eicosadienoate were determined by the oxidative ozonolysis of the respective methyl ester fractions and also, in the case of the eicosatrienoate, by the oxidative ozonolysis of the nonadecatrienyldimethylcarbinol and the hydroxyeicosadienoate derived from it.

Experimental

Properties of the Oil.—The Nagi seed oil used in this study was extracted with acetone from Nagi seeds collected in Nara in late November, 1960. The yield of the oil from 3 kg. of seeds was 270 g. It is a pale yellow liquid with a faint aroma. The characteristics of the oil and of its fatty acids are as follows:

Oil: n_D^{20} 1.4802, acid value 1.2, saponification value 188.0, iodine value 151.4, and nonsaponifiable matter 0.64%.

Fatty acids: n_D^{20} 1.4704, neutralization value 193.5, and iodine value 162.4.

Fatty Acid Composition.—The methyl ester of fatty acids, freed from nonsaponifiable matter, was prepared from the oil in the usual way. It had a refractive index (n_D^{20}) of 1.4634, a saponification value of 186.5 and an iodine value of 153.9, and it was analyzed by GLC. All GLC analyses were performed using a conventional GLC apparatus with a thermoconductivity detector. Column: 225 cm. in length and 6 mm. in diameter, packed with 60~80 mesh Celite 545 coated with 20% diethylene glycol succinate polyester. Temperatures: 230°C for the methyl ester fractions of fatty acids, 200°C for the methyl esters of the dibasic cleavage products of ozonolysis, and 170°C for the benzyl esters of monobasic cleavage products of ozonolysis. Helium flow rate: 80 ml./min. The peaks on the chromatogram were identified by the addition of reference samples or by a comparison of the retention times. With diethylene glycol succinate polyester as the fixed liquid phase, the retention time of the methyl eicosenoate is almost equal to that of the linolenate, whereas with propylene glycol succinate polyester as the fixed liquid phase, the retention times for these two methyl esters are significantly different.[2] The chromatogram of the fatty acid methyl esters of Nagi seed oil using propylene glycol succinate polyester as the fixed liquid phase showed the peak corresponding to the eicosenoate but no peak corresponding to the linolenate. The composition of the fatty acid methyl esters was calculated by the half-band width method. The results are shown in Table I.

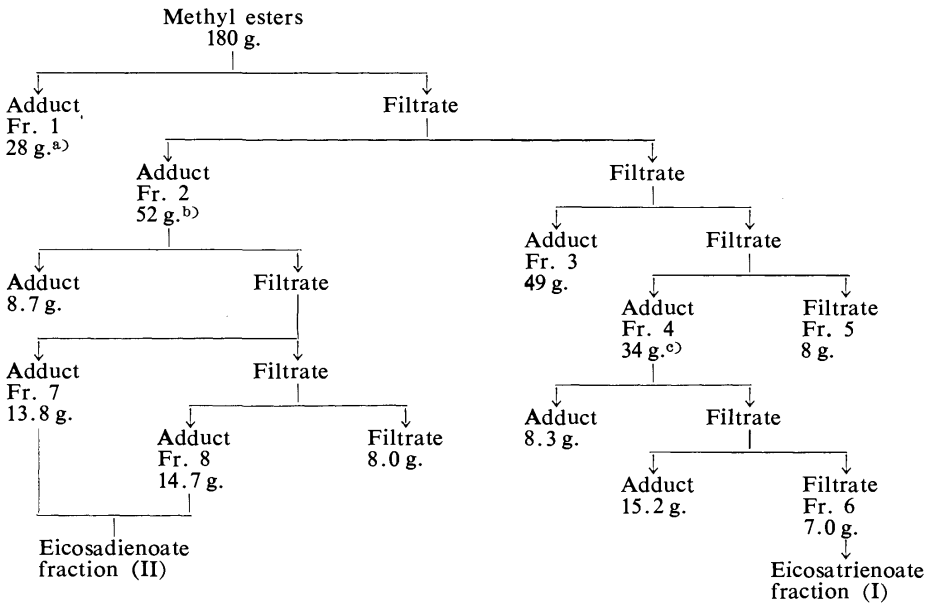

Fig. 1. Scheme of the urea-adduct segregation of methyl esters.

a) The yields for adducts and filtrates are those for methyl ester regenerated therefrom.
b) The succeeding segregation was performed with 46.5 g. of this fraction.
c) The succeeding segregation was performed with 32.0 g. of this fraction.

2) S. Ito and K. Fukuzumi, *J. Chem. Soc. Japan, Ind. Chem. Sec.* (*Kogyo Kagaku Zasshi*), **65**, 1963 (1962).

TABLE I. THE COMPOSITION OF THE FATTY ACID METHYL ESTERS OF NAGI SEED OIL

Methyl ester	Wt. %[a)]
Palmitate	3.8
Stearate	1.9
Oleate	21.4
Linoleate	37.8
Eicosenoate	1.8
Eicosadienoate	9.6
Eicosatrienoate	23.7

a) Corrected. Cf. Ref. 2.

The Urea-adduct Segregation of Methyl Esters. —Methyl esters were prepared by refluxing 200 g. of oil with 600 ml. of methanol and 0.6 g. of metallic sodium for 30 min., and then by extracting them with hexane after the solution had been cooled to room temperature. A 180 g. portion of the methyl esters thus obtained was treated with 180 g. of urea and 1350 ml. of methanol; the crystalline urea-adduct (Fr. 1) was then filtered off at room temperature and washed with hexane. The material recovered from the hexane washing was added to the methanol filtrate and then treated with another 150 g. of urea. The urea-adduct (Fr. 2) was filtered and washed as before. The filtrate was treated further with urea in a similar manner to give urea-adduct fractions (Fr. 3 and Fr. 4) and the final filtrate fraction (Fr. 5) as shown schematically in Fig. 1. The methyl ester fractions regenerated from Frs. 1—5 were analyzed by GLC to ascertain the relative distribution of the eicosatrienoate and of the eicosadienoate in these fractions. It was found that, although Fr. 2 contained more oleate and linoleate than eicosadienoate and eicosatrienoate, the proportion of the amount of eicosadienoate to eicosatrienoate in this fraction was relatively large. Fraction 4 contained eicosatrienoate and linoleate but no eicosadienoate. Fraction 5 appeared to contain almost exclusively the eicosatrienoate as a regular methyl ester, but oxidized and polymerized methyl esters and some other impurities were also concentrated in this fraction. Fractions 2 and 4 were subjected to further fractionation using urea, as Fig. 1 shows.

Methyl Eicosatrienoate and Eicosadienoate. — The methyl ester fraction regenerated from Fr. 6 in Fig. 1 was found by GLC to contain no methyl ester other than the eicosatrienoate. It was purified further by elution chromatography using hexane and hexane-ether (100 : 0.5) as the eluants and an adsorption column, 20.6 cm. in height and 3.0 cm. in diameter, packed with 70 g. of activated silica.

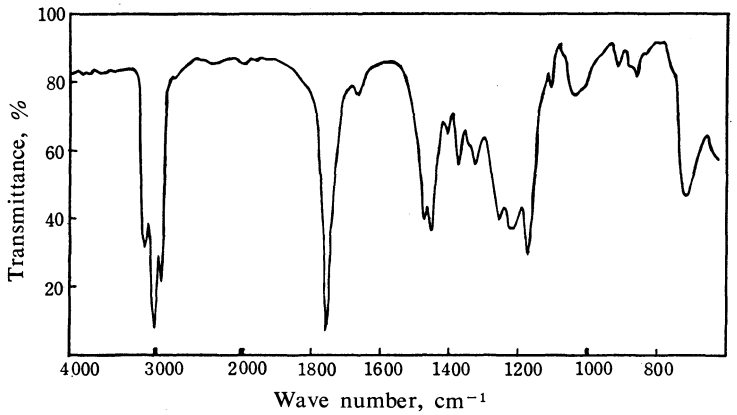

Fig. 2. Infrared spectrum of the fraction I (film on NaCl flats).

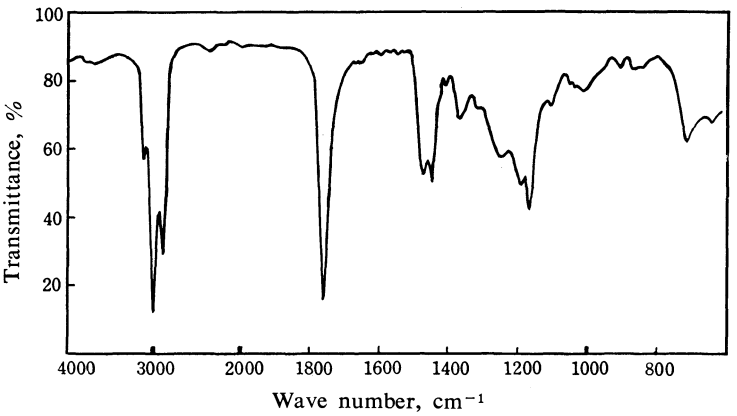

Fig. 3. Infrared spectrum of the fraction II (film on NaCl flats).

When the first and last eluates were removed, 6.1 g. of the methyl eicosatrienoate fraction (I) was obtained.

The methyl ester fractions regenerated from Fr. 7 and Fr. 8 in Fig. 1 were united, and the united fraction was fractionally distilled under 2 mmHg using a fractionating column, 90 cm. in height and 1.8 cm. in diameter, packed with stainless steel rings, 4 mm. in diameter. Thirteen fractions were separately collected. The lower boiling fractions consisted predominantly of the methyl ester of C_{18}-acids. The 12th fraction, 1.2 g., was used as the methyl eicosadienoate fraction (II) in this study. The chromatograms of GLC indicated that, while fraction I consists almost exclusively of methyl eicosatrienoate, fraction II is not a pure methyl eicosadienoate fraction but is contaminated more or less with other unsaturated methyl esters. The characteristics of fractions I and II are shown in Table II.

Table II. The characteristics of methyl eicosatrienoate (I) and eicosadienoate (II)

	I[a]	II[b]
n_D^{32}	1.4660	1.4572
Saponification value	174.9 (175.1)	175.6 (174.0)
Iodine value	235.5 (237.6)	154.7 (157.4)
Hydrogen absorption ml./mmol.	67.2 (67.5)	—

a) The figures in parentheses are the values calculated for $C_{21}H_{36}O_2$.
b) The figures in parentheses are the values calculated for $C_{21}H_{38}O_2$.

The hydrogenation of fractions I and II with palladium black in ether gave methyl arachidate. The infrared spectra of I and II exhibited no absorption at 965 cm^{-1} (Figs. 2 and 3). The ultraviolet absorptions of fractions I and II after isomerization with 21% potassium hydroxide in ethylene glycol at 180°C for 15 min. were measured. After the isomerization both fractions exhibited the characteristic absorptions of conjugated dienes, $k_{233}=85.0$ for fraction I and $k_{233}=71.5$ for fraction II. In the region of conjugated trienes, 268 mμ, fraction II after the isomerization exhibited no absorption, while fraction I after the isomerization exhibited only a minor absorption, one which is possibly to be ascribed to the presence of a small amount of preformed conjugated trienes in fraction I.

The Ozonolysis of Fractions I and II.—A 100 mg. portion of I was ozonized in 3 ml. of methylene chloride at −15°C by passing ozonized oxygen (4.5%) through the solution for 2 hr. at a flow rate of 80 ml. per min. Then, 2 ml. of 30% hydrogen peroxide and 5 ml. of a 5% aqueous solution of potassium hydroxide were added to the ozonide solution, and the mixture was gradually heated to 80°C in the course of 2 hr., during which period nitrogen bubbles were allowed to pass through the mixture. The reaction mixture was then distilled, and the distillate was neutralized with a 0.1 N solution of potassium hydroxide and evaporated to dryness. The residue was taken up with 20 ml. of ethanol, and the ethanol solution was concentrated to a volume of 2~3 ml. Finally, benzyl bromide in an amount equivalent to the amount of potassium hydroxide required to neutralize the distillate was added to the concentrated ethanol solution, and the mixture was refluxed for 20 min. After the mixture had cooled, the extraction of the reaction mixture with ether gave 94 mg. of benzyl esters. Benzyl formate, acetate and caproate were identified by GLC. Another 100 mg. portion of I was ozonized in the same way, and the ozonide was decomposed by gradually heating the ozonide solution with 2 ml. of 30% hydrogen peroxide and 5 ml. of water up to 90°C in the course of 3 hr., during which period nitrogen bubbles were allowed to pass through the mixture. The reaction product was then evaporated in vacuo for the removal of the bulk of the water, and the residue was taken up with ether. The ether solution was dried over anhydrous sodium sulfate. After distilling off the ether, the residue was esterified with sulfuric acid and methanol to give methyl esters of dibasic acids (68 mg.), in which methyl glutarate and adipate were identified as the main components by GLC.

A 100 mg. portion of II was ozonized, and the ozonide was treated in the same way as has been described for I. From the distillate, benzyl esters were obtained in a yield of 92 mg. Benzyl formate, acetate and caproate were identified by GLC. The distillation residue was extracted with ether, and the ether extract was converted to methyl esters with sulfuric acid and methanol. Yield: 63 mg. Methyl undecanedioate was identified as the main component by GLC.

The Preparation and Ozonolysis of Nonadecatrienyldimethylcarbinol. — A solution of 400 mg. of fraction I in 10 ml. of ether was added to a Grignard reagent prepared from 400 mg. of methyl iodide, 70 mg. of magnesium turnings, and 5 ml. of ether in the usual way. The mixture was then refluxed for 1 hr., and the reaction product was hydrolyzed by the successive addition of water and of dilute hydrochloric acid. The product was obtained by extraction with ether in a yield of 402 mg. It could be recognized as nonadecatrienyldimethylcarbinol by the pattern of the preparation and by the infrared spectrum shown in Fig. 4. This tertiary, unsaturated alcohol was subjected to ozonolysis, and the ozonide was treated in the same way as has been described for fraction I. From 200 mg. of alcohol 97 mg. of methyl esters of dibasic acids were obtained; in these esters methyl adipate and succinate, together with glutarate, were identified by GLC.

Methyl Hydroxyeicosadienoate.—A 4.0 g. portion of the fatty acid obtained from fraction I by saponification was dissolved in 30 ml. of ether and brominated at −15°C, yielding 1.35 g. of an ether-insoluble bromide which had a m. p. of 152~152.5°C (reported,[1] 152~152.5°C) after recrystallization from carbon tetrachloride and which was regarded as hexabromoarachidic acid. A solution of 1.10 g. of recrystallized hexabromide in 80 ml. of ethanol-ether (1 : 1) was neutralized with a solution of potassium hydroxide and refluxed for 4 hr. After 1.5 to 2 hr. from the beginning of this refluxing, potassium bromide was formed and precipitated

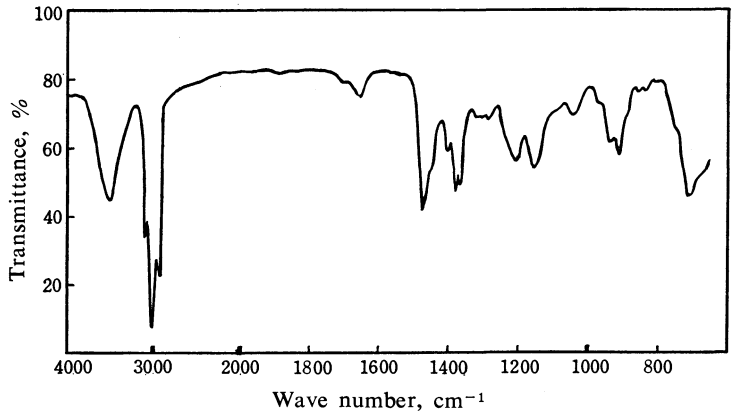

Fig. 4. Infrared spectrum of nonadecatrienyldimethylcarbinol derived from the fraction I (film on NaCl flats).

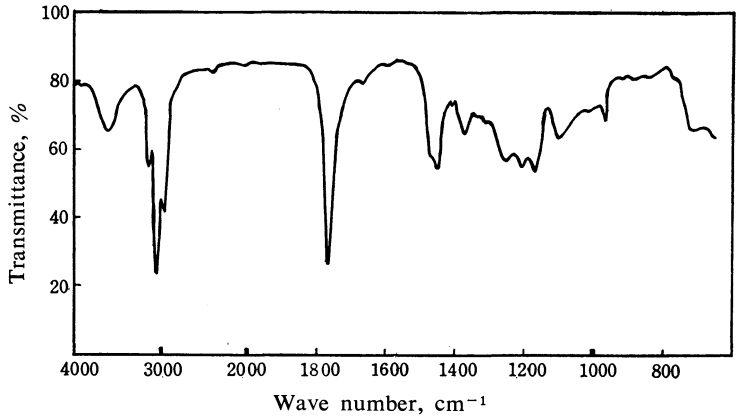

Fig. 5. Infrared spectrum of methyl hydroxyeicosadienoate derived from the fraction I (film on NaCl flats).

from the solution. The reaction product was extracted with ether, and the ether solution was washed with alkali to remove the unchanged hexabromoarachidic acid. After distilling off the ether from the ethereal solution, 634 mg. of a neutral substance (bromolactone) was obtained. Yield: 64% of theory. To 625 mg. of this substance were added 500 mg. of zinc powder and 13 ml. of methanol, and the mixture was refluxed for 1 hr. Then, 250 mg. of zinc powder, 7 ml. of methanol and 1 ml. of concentrated sulfuric acid were added, and the mixture was refluxed further for 1 hr. The reaction product obtained by extraction with ether was found to be free from bromine. Yield: 334 mg. The debromination product could be recognized as methyl hydroxyeicosadienoate by the pattern of the preparation and by the infrared spectrum (Fig. 5). It had a refractive index (n_D^{31}) of 1.4772 and an iodine value of 155.6 (calcd. for $C_{21}H_{38}O_3$: 149.9). The isomerization product obtained under the same conditions as have been described for fractions I and II exhibited the characteristic absorption of conjugated dienes, $k_{233}=70.8$.

A solution of 100 mg. of the debromination product in 3 ml. of methylene chloride was ozonized at −15°C for 1.5 hr. Then, 10 ml. of a 5% solution of potassium hydroxide and 500 mg. of silver oxide were added to the ozonide solution, and the mixture was heated at 70°C for 3 hr. during which period nitrogen bubbles were allowed to pass through the mixture. The alkaline solution was filtered. The filtrate was acidified with diluted sulfuric acid and then distilled. The distillate was subjected to a procedure similar to that described for fractions I and II to give 103 mg. of benzyl esters. Benzyl formate, acetate and caproate were identified by GLC.

Discussion

Both methyl eicosatrienoate (I) and eicosadienoate (II), upon hydrogenation, give methyl arachidate. Accordingly, I and II have no branched chain. The ethylenic linkages in I and II are of the all-cis form, since the infrared spectra of I and II (Figs. 2 and 3) show no absorption at 965 cm^{-1}. After isomerization with alkali, I and II show the characteristic absorption of conjugated dienes at 233 mμ.,

indicating that both I and II have the $=CHCH_2CH=$ group of the divinylmethane type.

The ozonolysis of II gives formic, acetic and caproic acids as the monobasic acids and *n*-undecanedioic acid as the dibasic acid. Among these cleavage products, formic and acetic acids may be regarded as secondary decomposition products of malonic acid or of its precursor resulting from the $=CHCH_2CH=$ group. Accordingly, $CH_3(CH_2)_4CH=$ and $=CH(CH_2)_9COOCH_3$ are the terminal groups of II.

From these results, the free fatty acid corresponding to II may be concluded to be all-*cis*-11, 14-eicosadienoic acid.

The ozonolysis of I gives formic, acetic and caproic acids as the monobasic acids, and adipic and glutaric acids as the dibasic acids. Formic and acetic acids are considered to be secondary decomposition products originating from the $=CHCH_2CH=$ group. Hence, the free fatty acid of I is found to have the terminal group $CH_3(CH_2)_4CH=$ on the methyl side and either $=CH(CH_2)_4COOH$ or $=CH(CH_2)_3COOH$ as the terminal group on the carboxyl side. However, the oxidative ozonolysis of the nonadecatrienyldimethylcarbinol derived from I gives succinic acid in a large proportion, together with glutaric and adipic acids as the dibasic cleavage products. Hence, the terminal group on the carboxyl side should be $=CH(CH_2)_3COOH$. As for the arrangement of the two intermediate groups, $=CHCH_2CH=$ and $=CH(CH_2)_4CH=$, the results of the ozonolysis of hydroxydienoate (I') derived from I indicate that the $=CHCH_2-CH=$ group is adjacent to the terminal group, $CH_3(CH_2)_4CH=$, since the hydroxydienoate contains an alkali conjugatable diene, $=CHCH_2-CH=$, and since on ozonolysis it gives formic, acetic and caproic acids as the monobasic cleavage products. On the basis of these findings, the free fatty acid corresponding to I may be concluded to be all-*cis*-5, 11, 14-eicosatrienoic acid. The hydroxydienoate I' is methyl 5-hydroxy-11, 14-eicosadienoate.

Department of Applied Chemistry
Faculty of Engineering
Nagoya University
Chikusa-ku, Nagoya

Univalent-Bivalent Ion-exchange Equilibria on Some Permselective Membranes

By W. G. B. MANDERSLOOT

(Received June 3, 1963)

This study was undertaken in connection with preferential ion transport in electrodialytic ion transfer through permselective membranes and therefore the ion pairs studied were selected from those encountered in natural waters: Cl/SO_4 in the case of anion exchange resins and Na/Ca in the case of cation exchange resins.

In the equilibrium state the electrochemical potential of each mobile particle is equal inside and outside the resin. If a constant partial molar volume is assumed for each particle it may be shown[1] that for the ion i:

$$E_i=\bar{\varphi}_i-\varphi_i=\frac{1}{z_i\boldsymbol{F}}\left[\boldsymbol{RT}\ln\frac{a_i}{\bar{a}_i}-\pi V_i\right] \quad (1)$$

in which E is the Donnan potential, φ the electrical potential, z the electrovalency of the ion, $\boldsymbol{F}$ Faraday's constant, $\boldsymbol{R}$ the gas constant, T the absolute temperature, a the single ion activity, π the swelling pressure and V the partial molar volume; barred symbols refer to the resin phase. Helfferich[1] applies Eq. 1 to both the competing counterion species i and j, assuming $\bar{\varphi}_i=\bar{\varphi}_j$ and therefore $E_i=E_j$, and assuming a constant π. Tye[2] has pointed out that counterions and co-ions are on different electrical potentials and the same, although possibly less so, should hold for two different counterions i and j. Therefore we will equate φ_i and φ_j rather than E_i and E_j:

$$\varphi_i=\varphi_j \quad (2)$$

Combining Eqs. 1 and 2:

$$\ln\left[\frac{a_j}{\bar{a}_j}\right]^{z_i}\left[\frac{\bar{a}_i}{a_i}\right]^{z_j}=-\frac{\pi}{\boldsymbol{RT}}[z_jV_i-z_iV_j]-\frac{z_iz_j\boldsymbol{F}}{\boldsymbol{RT}}[\bar{\varphi}_i-\bar{\varphi}_j] \quad (3)$$

1) F. Helfferich, *Ionenaustauscher*, Vol. 1, *Verlag Chemie*, Weinheim/B (1959), pp. 133, 154.

2) F. L. Tye, *J. Chem. Soc.*, **1961**, 4784.

In the exchange of i and j not only the two counterions are involved but also a certain amount of water and therefore we replace in Eq. 3 the difference in partial molar volumes by the total volume change (in the resin) involved in the exchange of i and j, $(z_j\overline{V}_i - z_i\overline{V}_j)$. Furthermore, it will be assumed that π is proportional to the equivalent fraction $\overline{X}_j$ of j in the resin:

$$\pi = \pi_i + \overline{X}_j(\pi_j - \pi_i) \tag{4}$$

in which π_i and π_j denote the swelling pressures in the single ionic forms of the resin. When the single ion activities in Eq. 3 are replaced by molalities according to

$$a_i = f_i m_i, \text{ etc.} \tag{5}$$

and the molalities are in turn replaced according to

$$X_i = \frac{z_i m_i}{z_i m_i + z_j m_j}, \text{ etc.} \tag{6}$$

and defining the relative affinity coefficient K_j^i by:

$$K_j^i \equiv \left[\frac{X_j}{\overline{X}_j}\right]^{z_i}\left[\frac{\overline{X}_i}{X_i}\right]^{z_j} \tag{7}$$

then, combination of 3–7 and conversion to logarithms gives:

$$\ln k_j^i = (z_j - z_i)\ln\frac{z_i m_i + z_j m_j}{z_i\overline{m}_i + z_j\overline{m}_j} + \ln\frac{f_i^{z_j}}{f_j^{z_i}} + \ln\frac{\overline{f}_j^{z_i}}{\overline{f}_i^{z_i}} - [z_j\overline{V}_i - z_i\overline{V}_j] \times \frac{\pi_i + \overline{X}_j[\pi_j - \pi_i]}{RT} - \frac{z_i z_j F}{RT}(\overline{\varphi}_i - \overline{\varphi}_j) \tag{8}$$

The first term on the right hand side is the external/internal concentration ratio term which disappears when $z_i = z_j$. This term is mainly responsible for the increase in affinity for multivalent ions (compared with univalent ions) when the external total electrolyte concentration is decreased. The term varies slightly with $\overline{X}_j$ because of the amount of water involved in the exchange, which causes m_i and m_j to change with $\overline{X}_j$.

The second term is the external activity coefficient ratio term which is somewhat dependent on X_j and therefore also on $\overline{X}_j$ and, depending on the ionic species involved, the term can change considerably with external concentration.

The thired term is the internal activity coefficient ratio term which is difficult to estimate; one should be very cautious when considering an analogy with concentrated electrolyte solutions.

The fourth term is the pressure-volume term which is dependent on $\overline{V}$ and therefore on total external concentration (increased swelling of the resin at lower external concentration) and, as shown, it is also dependent on $\overline{X}_j$.

The last term is the electrical term which can be expected to be quite independent of external concentration and $\overline{X}_j$.

Experimental

Ion exchange resin membranes used were:

	Cation exchanger	Anion exchanger
Permaplex[3]	C-20	A-20
T. N. O.[4]	C-60	A-60
A. M. F.[5]	3129 B-56	3129 B-96
A. C. I.[6]	Yes	Yes
C. S. I. R.[7]	—	TA

From each membrane four circular pieces with a diameter of 1.5 in. were cut and brought to the sodium or chloride form with several amounts of 2 N sodium chloride after which the samples were rinsed with distilled water. The pieces were then equilibrated for two days with renewed amounts of mixed solutions of sodium chloride and calcium chloride (0.15N) or sodium chloride and sodium sulfate (0.5N, 0.15N or 0.01N). In a number of cases ohmic resistance measurements were carried out on the membranes in the equilibrating solution. On each piece of membrane measurements were made on two different small areas (2.3 cm^2) and for each material the reported values are the average of eight measurements.

Equilibration and Resistance Measurements at 25°C. —The four pieces of each material were weighed together after thorough blotting with filter paper. Calcium was then displaced from the cation exchange resins by leaching with 25 ml. amounts of 1N sodium chloride and calcium was determined by complexometric titration with EDTA. Chloride and SO_4 were displaced from the anion exchange resins by leaching with 25 ml. amounts of 2 N sodium nitrate. Chloride in the leach was determined by Mohr titration and SO_4 by complexometric titration using photometric endpoint detection. The NO_3 form of the membranes was weighed. The membranes were in the complete sodium or chloride form before each new equilibration with a mixed solution. All equilibrations were carried out with the same four pieces of material. Finally, the membranes were rinsed free of absorbed electrolyte and dried to constant weight sodium or chloride form in a vacuum desiccator over phosphorus(V) oxide.

Results and Discussion

Change in Water Content.—The weight of the samples varied linearly with internal

3) The Permutit Co., Ltd., England.
4) Central Technical Institute T. N. O., Netherlands.
5) American Machine & Foundry Comp., U. S. A.
6) Asahi Chemical Industry, Japan.
7) J. R. Parrish and R. Stevenson, S. A. Council for Scientific and Industrial Research, S. A. Pat. 2793/60; Brit. Pat. 907079.

TABLE I. CHANGE IN WATER CONTENT IN ION EXCHANGE

Increase in water content in the replacement of:	Total external electrolyte concn., N	Permaplex	T. N. O.	A. M. F.	A. C. I.	C. S. I. R.
Ca by Na, g. mol./g. eq.	0.15	0.4	4.7	1.1	1.1	—
Internal molality of Na-form, g.-eq./1000 g. H_2O	0.15	3.4	2.0	9.3	7.5	—
Cl by SO_4, g. mol./g. eq.	0.01	2.4	1.3	2.7	2.0	1.8
	0.15	2.5	1.3	2.7	1.9	—
	0.50	2.2	1.5	2.6	3.4?	1.1
NO_3 by SO_4, g. mol./g. eq.	0.01	5.7	4.3	4.9	4.0	3.9
	0.15	5.4	3.9	4.9	3.6	—
	0.50	4.9	3.5	4.3	3.9	2.9
Internal molality of Cl-form, g.-eq./1000 g. H_2O	0.01	5.5	7.0	6.2	4.3	5.3

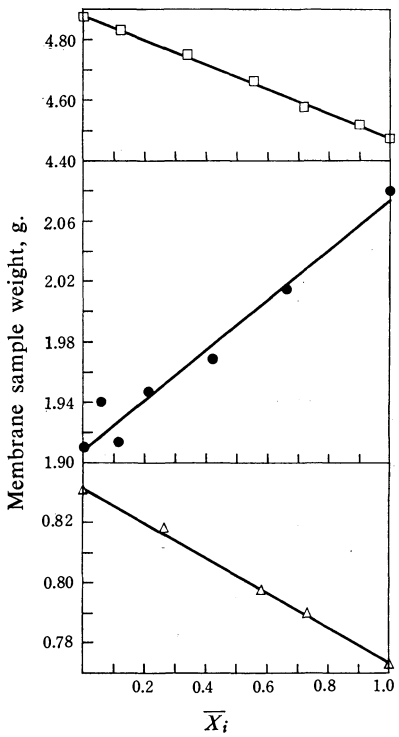

Fig. 1. Weight change of membrane samples.
i=Monovalent ion
△ A. M. F. 3129 B-96, Cl/SO_4,
● T. N. O. C-60, Na/Ca,
□ Permaplex A-20, Cl/SO_4

counterion composition, examples being shown in Fig. 1. After correcting for the change due to the counterions themselves it was possible to arrive at the constant amount of water involved in the exchange of i and j. The constancy is the basis for Eq. 4. As indicated by Boyd et al.[8] the amount of water involved is not necessarily constant in resins with low degrees of crosslinking; the resin membranes are usually highly crosslinked.

The observed water content changes have been summarized in Table I. In the cation exchange resins the amount of water involved in the Ca/Na exchange tends to be low in the resins of high internal molality. The hydration of the ions in the resin decreases with increasing internal molality (degree of crosslinking).[9]

The result for Permaplex C-20 seems to deviate, but it should be remembered that these heterogeneous membranes contain liquid interstices between the ion exchange resin grains embedded in the inert matrix. This leads to a higher water content for the membrane than for the resin itself[10] and consequently to a low calculated internal molality. It may also lead to low values for the change in water content, if the volume changes of the resin particles are partly compensated by changes in the size of the interstices.

In the anion exchange resins the amount of water involved in the Cl/SO_4 or NO_3/SO_4 exchange decreases, in general, with increasing external electrolyte concentration, i. e., with decreasing swelling of the resin and consequently an increasing internal molality. The correlation of water content change with the internal molalities of the different membranes is less clear and it should be remembered that, although in general the high concentration of fixed ions is due to crosslinking, the degree of crosslinking itself should still be taken into account. The C. S. I. R.-T. A. resin, for instance, is very highly crosslinked but does not have the highest concentration of fixed ions.

In general, we may conclude that the amount of water involved in ion exchange is dependent

8) G. E. Boyd, S. Lindenbaum and G. E. Myers, *J. Phys. Chem.*, **65**, 577 (1961).

9) H. Ohtaki, K. Gonda and H. Kakihana, This Bulletin, **33**, 293 (1961); *Z. Electrochem*, **67**, 87 (1963).

10) D. K. Hale and D. J. McCauley, *Trans. Faraday Soc.*, **57**, 135 (1961).

on the amount of water present in the resin and on the rigidity (crosslinking) of the polymer network.

Conductivity.—Conductances were measured only in 0.15 N solutions. The results are given in Figs. 2 and 3. In the cation exchange resins interaction is noticeable only at high calcium loading. The calcium form of the resin is less swollen and the observed effect could be explained by an uneven distribution of counterions through the resin, caused by heterogeneity in the crosslinking of the resin.

The form of the curve obtained for the heterogeneous Permaplex C-20 membranes can be explained as follows. At low $\overline{X}_{Ca}$ the calcium ions in the membrane will be located mainly inside the resin particles and then they cannot hinder the movement of Na^+ on the particle surface. If surface transport makes up a large portion of total transport, the conductivity of the membrane decreases little when only a small amount of calcium is present. Evidence that surface transport is indeed important in heterogeneous membranes comes from selective ion transport in a d.c. field, in which the transport ratios are more in favor of the common monovalent ions than would be expected from the ratios of internal concentrations and mobilities. At high $\overline{X}_{Ca}$ the calcium ions are present on the particle surface as well (area of little crosslinking) and the interaction is then similar to, though possibly less than, that in homogeneous membranes.

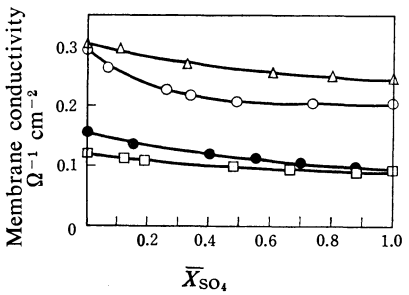

Fig. 2. Membrane conductivity at 25°C in 0.15N $NaCl/Na_2SO_4$ solution.

△ A. M. F. 3129 B-96
○ A. C. I.
● T. N. O. A-60
□ Permaplex A-20

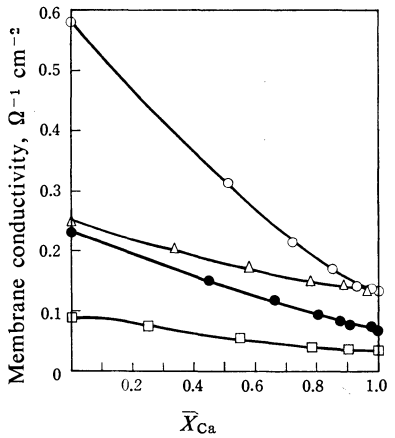

Fig. 3. Membrane conductivity at 25°C in 0.15 N $NaCl/CaCl_2$ solution.

△ A. M. F. 3129 B-56
○ A. C. I.
● T. N. O. C-60
□ Permaplex C-20

In the anion exchange resins the interaction is strong at any $\overline{X}_{SO_4}$, particularly in the A. C. I. membrane. The chloride form of the resin is less swollen and the observed effect could again be explained by an uneven distribution of counterions through the resin. In this case the ions causing the highest swelling of the resin are the less mobile (bivalent) ions, and the differences in the conductivities of the two single ionic forms of the resin are considerably smaller than in the case of Ca/Na in the cation exchange resins in which the less mobile (bivalent) ions cause the lowest swelling. Conductivities appear to give some indication of the electrostatic forces between fixed ions and counterions.

Ion Exchange Equilibrium. — The relative affinity coefficient K_{Ca}^{Na} is given in Fig. 4 and $K_{SO_4}^{Cl}$ is given in Fig. 5. In both types of resin K varies with $\overline{X}$ and in the discussion of Eq. 8 several reasons have already been indicated. This equation does not incorporate the influence of heterogeneity in the resin. This heterogeneity can have several causes. If the fixed ions are of a different chemical nature (e.g., $-COO^-$ and $-SO_3^-$), then the resin is bifunctional[11] and K_j^i changes sharply at $\overline{X}$ corresponding to the fraction of fixed ions of one kind; or, fixed ions of identical chemical nature are attached to the polymer network in different positions.[12-14] Reichenberg and McCauley[15] attributed the strong dependence of K on $\overline{X}$ in highly crosslinked resins to heterogeneity in the degree of crosslinking through the resin (sometimes interpreted as a range of pore sizes[16,17]); the result

11) J. P. Cornaz and H. Deuel, *Helv. Chim. Acta*, **39**, 1227 (1956).
12) I. H. Spinner, J. Ciric and W. F. Graydon, *Can. J. Chem.*, **32**, 143 (1954).
13) G. E. Myers and G. E. Boyd, *J. Phys. Chem.*, **60**, 521 (1956).
14) O. D. Bonner, V. F. Holland and L. L. Smith, ibid., **60**, 1102 (1956).
15) D. Reichenberg and D. J. McCauley, *J. Chem. Soc.*, **1955**, 2741.
16) K. Uberreiter and G. Kanig, *J. Chem. Phys.*, **18**, 399 (1950).
17) Ref. 1, p. 13.

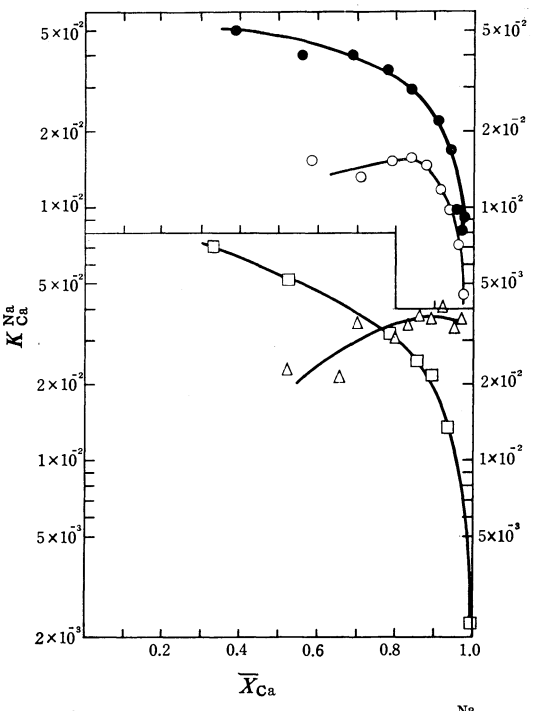

Fig. 4. Relative affinity coefficient K^{Na}_{Ca}.

● T. N. O. C-60 ○ A. C. I.
□ Permaplex C-20 △ A. M. F. 3129 B-56

is a multifunctional resin. Högfeldt[18] has shown that both a bifunctional and a multifunctional treatment can be used to explain the same set of experimental data. Glueckauf and Watts[19,20] indicated that heterogeneous crosslinking is an important factor with respect to some other resin (or membrane) properties as well, i. e., electrolyte uptake and salt diffusion. It was also shown[21] that their approach does not lead to a quantitative theory of ion exchange equilibra.

The most remarkable feature in Fig. 4 is the strong decrease in K^{Na}_{Ca} at high $\overline{X}_{Ca}$; the more calcium is present in the resin the higher the affinity for calcium. The deviating result for the A. M. F. membrane remains unexplained.

Between $X_{Ca}=0$ and $X_{Ca}=1$ the concentration ratio term in Eq. 8 varies only by 5～10%. Changes in the external activity coefficient term can be estimated at 0.3%. There is no *a priori* reason why the internal activity coefficient term should decrease greatly at high $\overline{X}_{Ca}$. The electrical term in Eq. 8 can be assumed to remain approximately constant and the pressure-volume term should bring about a gradual decrease in K^{Na}_{Ca} with increasing $\overline{X}_{Ca}$.

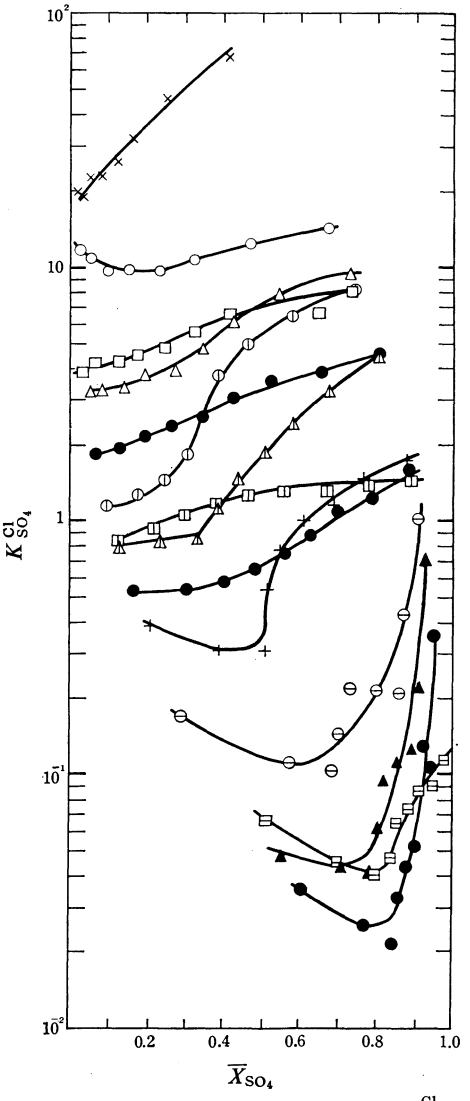

Fig. 5. Relative affinity coefficient $K^{Cl}_{SO_4}$.

Total external concn.	0.01N	0.15N	0.50N
T. N. O. A-60	●	●	●
Permaplex A-20	⊟	⊞	□
A. M. F. 3129 B-96	▲	△	△
A. C. I.	⊖	⊕	○
C. S. I. R.-TA	+		×

If the resin is heterogeneous with respect to crosslinking, then at high $\overline{X}_{Ca}$ the few sodium ions will be situated preferentially in the areas of least crosslinking, forming islands of high swelling, which are squeezed by the elastic forces in the surrounding more crosslinked area. A serious deviation from proportionality between π and $\overline{X}_{Ca}$ may then occur. In should be noted that the strong decrease in K^{Na}_{Ca} occurs in the same range of $\overline{X}_{Ca}$ in

18) E. Högfeldt, *Ark. f. Kemi*, **13**, 491 (1959).
19) E. Glueckauf and R. E. Watts, *Nature*, **191**, 904 (1961).
20) E. Glueckauf and R. E. Watts, *Proc. Roy. Soc.*, **268A**, 339 (1962).
21) E. Glueckauf, ibid., **268A**, 350 (1962).

which interaction with respect to conductivity was observed.

With respect to the Cl/SO_4 equilibria on the anion exchange resins (Fig. 5) attention is drawn to the sharp increase in affinity for chloride at high $\overline{X}_{SO_4}$ and low external concentration. This affinity is generally higher in the highly crosslinked resins (A. C. I. and C. S. I. R.-T. A.) where the sharp increase starts at $\overline{X}_{SO_4}=0.6$ and $\overline{X}_{SO_4}=0.4$ respectively, while in the other resins it starts only at approximately $\overline{X}_{SO_4}=0.75$. In the shape of the curves for higher external concentrations there is some indication that the increase is then less sharp but starts at a much lower $\overline{X}_{SO_4}$. In all casses less swelling is connected with a higher affinity for chloride.

The contribution of the concentration ratio term to $K^{Cl}_{SO_4}$ changes by 15~30% with $\overline{X}_{SO_4}$ across the ranges of $\overline{X}_{SO_4}$ investigated at each exteral concentration. The external activity coefficient term can be estimated from

$$\frac{f^2_{Cl}}{f_{SO_4}}=\frac{f^2_{Cl}\cdot f^2_{Na}}{f_{SO_4}\cdot f^2_{Na}}=\frac{\gamma^4_{NaCl^*}}{\gamma^3_{Na_2SO_4^*}} \qquad (9)$$

in which γ is the mean ion activity coefficient. [At the same ionic strength $I=(1+1/2X_{SO_4})\times(m_{Cl}+2m_{SO_4})$]. Values derived from listed data[22] are given in Table II. The increase

Table II. Estimated values for $\frac{f^2_{Cl}}{f_{SO_4}}$

External concn., N	$X_{SO_4}=0$	$X_{SO_4}=1$
0.01	1.8	2.0
0.15	5.1	6.5
0.50	10.7	16.8

in affinity for chloride with external concentration is due not only to the concentration ratio term but also to a considerable change in the external activity coefficient ratio.

In a resin with hetrogeneous crosslinking the chloride ions are preferentially situated in regions with relatively high crosslinking and, when at high $\overline{X}_{SO_4}$ the SO_4 ions invade these regions, pressure-volume effects increase the affinity for chloride. The influence of heterogeneity can be expected to be strongest when the resin is in its most swollen state (low external concentration or high $\overline{X}_{SO_4}$); in regions of low crosslinking the swelling changes more with external concentration than in regions of high crosslinking.[23]

The high affinity for chloride does not occur in the resins with the highest internal molality (see Table I) but in the resins with the highest degree of crosslinking. This is a strong indication that the pressure-volume term is of relative importance.

Summary

The relative affinity coefficient K^i_j is shown to be dependent on the ratio of external and internal total concentrations, the ratio of the external activity coefficients and of the internal activity coefficients, a pressure-volume term and an electrical term. K^i_j is therefore dependent on the "loading" of the resin $\overline{X}_j$.

Several cation exchange resins exhibit a very strong affinity for calcium at high calcium loading and this affinity increases sharply with $\overline{X}_{Ca}$; this effect is attributed to heterogeneity in the crosslinking of the resin and it is a strong indication that here the pressure-volume term plays a decisive rôle.

The pressure-volume term appears to be of relative importance also in the Cl/SO_4 equilibrium on anion exchange resins, particularly when these are highly crosslinked. Heterogeneity in the crosslinking probably causes the sharp increase in affinity for Cl at high SO_4 loading and low (0.01N) external concentration.

Conductivity measurements on the resins in single and mixed forms is useful to get an indication of the binding forces between counterions and fixed ions and these measurements can also reveal interactions which may have a bearing on ion exchange equilibrium.

The author wishes to express his sincere thanks to Mr. J. Venlet who carried out the experimental work and who assisted in the data evaluation.

Chemical Engineering Group
Council for Scientific and Industrial Research
Pretoria, South Africa

22) R. Parsons, "Handbook of Electrochemical Constants," Butterworths, London (1959).

23) R. J. Stewart and W. F. Graydon, *J. Phys. Chem.*, **61**, 164 (1957).

A Molecular Orbital Treatment of Phosphate Bonds of Biochemical Interest. II. Metal Chelates of Adenosine Triphosphate

By Kenichi FUKUI, Akira IMAMURA and Chikayoshi NAGATA

(Received June 20, 1963)

In our previous paper[1] attempts were made by way of the simple LCAO MO method to correlate the energy-donor ability of adenosine triphosphate (ATP) with the π electronic energy of this compound. However, it was found that, so far as only the phosphate part is considered, the π electronic energy change of ATP in the course of hydrolysis, the reactivity index, and the π electron density at the phosphorus atom are not significantly different from those of such other high energy phosphate compounds as adenosine diphosphate (ADP), phosphoenol pyruvate (PEP) and acetyl phosphate (ACP), nor from those of such low energy phosphate compounds as adenosine monophosphate (AMP) and glycerol 1-phosphate (GLP).

These findings could not explain the efficiency of ATP as a biological specific. That is, among many so-called high energy phosphate compounds, ATP holds a unique position in the sense that ATP alone is, in general, used as an energy source in *in vivo* energy transfer reactions. Therefore, some other factors must be taken into consideration in order to explain the biochemical characteristic of ATP. This was pointed out by the present authors in the previous paper, where the possible importance of the metal chelate formation of ATP in the *in vivo* reaction was suggested. In fact, the participation of metal ions in the biological functions of ATP has been established in many experiments. In line with these experiments, various models of ATP-metal complex have been proposed. However, no detailed discussion and calculation have yet been carried out.

In the present paper, a comparison will be made of such theoretical indices as the stabilization energy due to the formation of metal chelate, the reactivity index and the π electron density for various models with the experimental facts, especially with the enzymatic hydrolysis of ATP. On the basis of this comparison, the most probable structure of the ATP-metal complex will be sought.

1) K. Fukui, K. Morokuma and C. Nagata, This Bulletin, 33, 1214 (1960).

The Method of Calculation and the Models Adopted

As in the previous paper, the calculations were carried out by means of the simple LCAO MO method. For the sake of comparison, the same values for the parameters of the Coulomb and the resonance integrals of phosphorus and oxygen atoms have been adopted as in the previous paper. However, in these calculations it was necessary to determine the parameters for the chelate-forming part of the ATP-metal complex. The resonance integrals between the metal and the oxygen atom or the nitrogen atom, $l_{M-O}\beta$, or $l_{M-N}\beta$, are both taken to be $0.4\,\beta$, where β is the resonance integral of two adjacent carbon atoms in benzene. This value was determined by considering the distance of the chelate bond and also the nature of the orbitals participating in the π conjugation.*

The value of Coulomb integral for the metal, α_M, is difficult to determine. Therefore, calculations have been carried out for model 2 for various values, for $\alpha+3\beta$, $\alpha+\beta$, $\alpha-\beta$ and $\alpha-3\beta$. The theoretical indices obtaiaed by utilizing these varying parameters are not very different from one another, and the qualitative conclusion is not changed with these varying parameters. Therefore, the calculations for some models have been carried out for two parameters, $\alpha+\beta$, and $\alpha-\beta$. For model 1, rather tedious calculations are required, therefore, the calculations have been carried out for the $\alpha+\beta$ parameter value.

By utilizing these parameters, such theoretical indices as the stabilization energy due to the chelate formation, the superdelocalizability and the total π electron density at the phosphorus atoms have been calculated for the following models (Fig. 1).

* The resonance integrals between oxygen and metal have been tentatively determined to be 0.4β, which may be an intermediate value between that of oxygen-phosphorus bond in ATP, 0.6β, and that of the usual hydrogen bond. For many kinds of metals, the values of resonance integral are probably different. But so far as the relative comparison on the stability of chelate compounds is concerned, the change in the resonance integral can be included in the change in the Coulomb integral, so that the approximate estimation of the resonance integral may not cause any serious errors in these calculations.

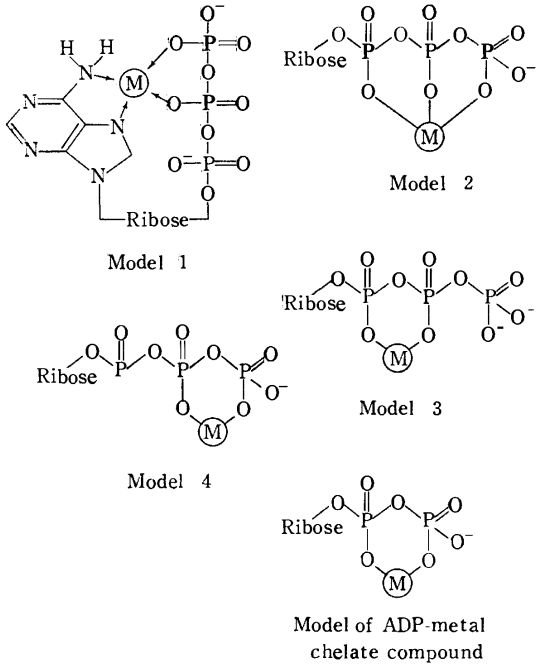

Fig. 1. The models of metal chelate compounds adopted in the calculation.

Model 1 represents the ATP-metal complex making a chelate between the adenine and the phosphate parts. Taking the metal as the magnesium cation, Szent-Györgyi[2] postulated a quadridentate chelate. Epp[3] et al. suggested, on the basis of their infrared data of ATP in the presence of and in the absence of Mg^{2+}, that such a complex formation could be recognized, although no direct evidence was obtained as to whether the complex formation was intramolecular or intermolecular.

In addition, James,[4] on the basis of the data on the rotatory dispersion of ATP, ADP and AMP, suggested the existence of some interaction between adenine and phosphate parts. Model 2 was proposed by Melchior[5] in view of the higher stability of the ATP-metal complex than those of ADP and AMP.

Theoretically there exist two other possible chelate complex structures between the polyphosphate chain and the metal. They are designated as models 3 and 4; the theoretical indices have been calculated with respect to these structures, and also for the ADP-chelate complex for the sake of comparison.

2) A. Szent-Györgyi, "Biogenetics," Academic Press, New York (1957).
3) A. Epp, T. Ramasarma and I. R. Wetter, *J. Am. Chem. Soc.*, **80**, 724 (1958).
4) B. H. Levendahl and T. W. James, *Biochim. Biophys. Acta*, **21**, 298 (1956).
5) N. Melchior, *J. Biol. Chem.*, **206**, 615 (1954).

In ATP there are two sites at which chelation can take place, that is, the amino group of the purine ring or the polyphosphate chain. In order to decide the site where the metal ion combines with the ATP molecule, Khan and Martell[6] measured the equilibrium constant of the ATP complex with various metal ions and concluded that the amino group of the purine ring is probably not involved in the chelate formation of ATP, because little or no interaction was observed between metal ions and adenosine. In view of these experiments, there is no need to consider the ATP-metal chelation on the purine ring only. Needless to say, however, model 1 can not be eliminated by this experiment, because in that model the participation of both the purine ring and the polyphosphate parts are considered.

Results and Discussion

Stabilization Energy Due to the Metal Chelate Formation.—In Table I, the stabilization energies calculated with regard to various models for ATP-metal complexes are indicated. For the sake of comparison, the calculated results for the ADP-metal complex are also included. As may clearly be seen in this table, the stabilization energies for models 3 and 4 are considerably smaller than those for models 1 and 2. Therefore, the latter two models are more plausible than the former two. The propriety of models 3 and 4 is, moreover, threatened conclusively by the fact that the stabilization energies for models 3 and 4 are smaller than that of the ADP-metal complex; this finding contradicts the fact that the ATP

Table. I. Stabilization energy due to metal chelate formation

Chelate compound	The value of the Coulomb integral of the metal, α_M	Stabilization energy (in units of β)
ADP-metal chelate compound	$\alpha+\beta$	3.609
	$\alpha-\beta$	3.800
ATP-metal chelate compound model 1	$\alpha+\beta$	7.890
ATP-metal chelate compound model 2	$\alpha+3\beta$	9.326
	$\alpha+\beta$	9.330
	$\alpha-\beta$	9.614
	$\alpha-3\beta$	9.503
ATP-metal chelate compound model 3	$\alpha+\beta$	2.442
	$\alpha-\beta$	2.634
ATP-metal chelate compound model 4	$\alpha+\beta$	1.109
	$\alpha-\beta$	1.301

6) M. M. T. Khan and A. E. Martell, *J. Phys. Chem.*, **66**, 10 (1962).

complex has a higher stability than those of ADP or AMP. Hence, from the standpoint of the stabilization energy, model 1 or 2 remains the most favorable.

Reactivity Indices and Enzymatic Hydrolysis. —As reactivity indices such as the superdelocalizability for nucleophilic attack, $S_r^{(N)}$, and the π electron density at the phosphorus atoms of ATP- and ADP-metal complexes have been calculated; they are indicated in Tables II and III. Superdelocalizability, S_r, is

TABLE II. SUPERDELOCALIZABILITY, S_r, OF THE PHOSPHORUS ATOM FOR NUCLEOPHILIC ATTACK

Compound	The value of the Coulomb integral of the metal α_M	$S_{P_1}^{(N)}$	$S_{P_2}^{(N)}$	$S_{P_3}^{(N)}$
ADP(phosphate part only)		1.182	1.099	
ADP-metal chelate compound	$\alpha+\beta$	1.094	1.180	
	$\alpha-\beta$	1.100	1.188	
ATP(phosphate part only)		1.183	1.191	1.099
ATP-metal chelate compound model 1	$\alpha+\beta$	1.182	1.101	1.180
ATP-metal chelate compound model 2	$\alpha+3\beta$	1.094	1.102	1.181
	$\alpha+\beta$	1.093	1.101	1.180
	$\alpha-\beta$	1.100	1.106	1.188
	$\alpha-3\beta$	1.097	1.104	1.184
ATP-metal chelate compound model 3	$\alpha+\beta$	1.093	1.100	1.098
	$\alpha-\beta$	1.100	1.107	1.099
ATP-metal chelate compound model 4	$\alpha+\beta$	1.182	1.101	1.180
	$\alpha-\beta$	1.182	1.108	1.188

a good index representing the reactivity of atom r in conjugated molecules, the greater the value of a position, the more reactive that position. Accordingly, from Table II, a prediction for the most susceptible position in ATP for the nucleophilic attack is possible. That is, for models 1 and 4, the innermost and the terminal phosphorus atoms (they are referred to as P_1 and P_3, respectively) are expected to be most susceptible to nucleophilic attack, whereas model 2 predicts the following order of reactivity: $P_3 > P_2 > P_1$, where the middle phosphorus atom is designated as P_2. For model 3 and also for free ATP, P_2 is predicted as the most reactive.

In comparing these theoretical predictions with the experimental positions of enzymatic hydrolysis, we can choose the model 1 as the most probable chelate complex of ATP, because the theoretical indices for this model explain well the experimental position of enzymatic hydrolysis. That is, the most commonly encountered type of reaction of ATP is the cleavage of the terminal phosphate group, P_3; moreover, not a few reactions involving the cleavage of the innermost group, P_1, have also been recognized. On the other hand, the middle phosphate group is very resistant to such enzymatic attacks. These situations are schematically shown in Fig. 2, in which the position of cleavage is shown by an arrow. The theoretical values for model 4 explain well the experimental position of enzymatic hydrolysis, but this model is not suitable in view of the stabilization energy, as has been stated in the previous section.

TABLE III. TOTAL π ELECTRON DENSITY, q_r, OF THE PHOSPHORUS ATOM

Compound	The value of the Coulomb integral of the metal α_M	q_{P_1}	q_{P_2}	q_{P_3}
ADP (phosphate part only)		0.270	0.329	
ADP-metal chelate compound	$\alpha+\beta$	0.279	0.272	
	$\alpha-\beta$	0.276	0.268	
ATP (phosphate part only)		0.269	0.268	0.329
ATP-metal chelate compound model 1	$\alpha+\beta$	0.270	0.277	0.272
ATP-metal chelate compound model 2	$\alpha+3\beta$	0.278	0.276	0.270
	$\alpha+\beta$	0.279	0.277	0.272
	$\alpha-\beta$	0.276	0.275	0.268
	$\alpha-3\beta$	0.277	0.275	0.269
ATP-metal chelate compound model 3	$\alpha+\beta$	0.279	0.278	0.329
	$\alpha-\beta$	0.276	0.275	0.329
ATP-metal chelate compound model 4	$\alpha+\beta$	0.269	0.277	0.272
	$\alpha-\beta$	0.269	0.274	0.268

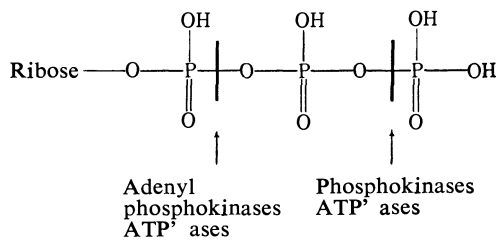

Fig. 2. Positions of the enzymatic cleavage of ATP (After Ref. 7).

In Table III the total π electron densities for various models are indicated. The smaller the value in the table, the more reactive the position for the nucleophilic attack. Also, in this case an identical conclusion is obtained as in the case of the superdelocalizability. That is, model 1 remains the most probable structure in *in vivo* reactions.

A Comparison of the Theoretical Indices with the Nuclear Magnetic Resonance Spectra of ATP.—Recently an ever-increasing number of data have been accumulated regarding the nuclear magnetic resonance (NMR) spectra of ATP, but no quantitative data for the theoretical analysis is available. Therefore, in this paper some qualitative discussions will be undertaken in comparison with the results of Cohn's experiment.[7] Cohn measured the shift in resonance frequency of the three phosphorus atoms in ATP relative to that of H_3PO_4. The shift for P_2 was largest and appeared at higher magnetic fieldes, while the spectra of P_1 and P_3 were superimposed upon each other and appeared at lower magnetic fields than those of P_2. If the chemical shift is exclusively influenced by the electron density, we can expect, on the basis of the above experiment, the following order of electron density at the phosphorus atoms in ATP: $P_2 > P_1 \sim P_3$. However, as may be seen in Table III, the degree of the electron densities in free ATP is $P_3 > P_2 \sim P_1$. This discrepancy means that the chemical shift of phosphorus atoms is influenced not only by the electron density around them, but also by other factors. That is, the contribution from the terms of the diamagnetism as well as the paramagnetism should be taken into consideration in order to explain correctly the shift of the phosphorus atom in ATP.

The authors wish to acknowledge that some of the calculations were carried out on the automatic computer, KDC-1, of Kyoto University.

Faculty of Engineering
Kyoto University
Sakyo-ku, Kyoto (*K. F.*)

Electrical Communication Laboratory
Nippon Telegraph and Telephone
Musashino, Tokyo (*A. I.*)

National Cancer Center Research Institute
Chuo-ku, Tokyo (*C. N.*)

7) M. Cohn, "Mechanisms of Enzymic Cleavage of of Some Organic Phosphates" presented at the Symposium on Enzymatic Reaction Mechanisms, held at Gatlinburg, Tennessee, April, 1959.

Kinetics of the Catalytic Hydrogen Peroxide Oxidation of Thiodiglycol in Aqueous Solutions

By Yoshiro OGATA and Yasuhiko SAWAKI

(Received June 27, 1963)

In order to compare the catalytic activities of various inorganic compounds and to discover new catalysts in the aqueous hydrogen peroxide oxidation, the catalytic oxidation of thiodiglycol (TDG) was investigated.

$$(HOCH_2CH_2)_2S + H_2O_2 \rightarrow (HOCH_2CH_2)_2SO + H_2O \quad (1)$$

The rate of the uncatalyzed hydrogen peroxide oxidation of TDG has been reported by Ross[1] to follow the second-order kinetics. We found that molybdate exhibited a stronger catalytic activity than well-known tungstates and selenous acid. The kinetics of sodium molybdate (SM)-catalyzed oxidation has also been investigated, since the mechanism of the catalysis of molybdates had not previously been clarified in detail.[2]

The present paper describes the rate data and a probable mechanism of the SM-catalyzed hydrogen peroxide oxidation of TDG in aqueous solution. In the course of this study, the rate of the oxidation of TDG by yellow sodium peroxymolybdate (YPM), together with the absorption spectra of the SM-hydrogen peroxide system, were measured.

1) S. D. Ross, *J. Am. Chem. Soc.*, **68**, 1484 (1946).

2) Molybdates have been used in the hydrogen peroxide oxidation of organic compounds in the following experiments: a) I. D. Raacke-Fels, C. H. Wang, R. K. Robins and B. E. Christensen, *J. Org. Chem.*, **15**, 627 (1950); b) A. R. Bader, *J. Am. Chem. Soc.*, **73**, 3731 (1951); c) K. Kahr and C. Berther, *Chem. Ber.*, **93**, 132 (1960); d) G. Toennies and J. T. Kolb, *J. Biol. Chem.*, **140**, 131 (1941); e) J. C. Ghosh and B. C. Kar, *J. Indian Chem. Soc.*, **11**, 485 (1934).

Experimental

Materials.—TDG was purified by vacuum distillations; b. p. 131~134°C/3 mmHg. YPM was synthesized according to the Kobosev-Sokolov procedure.[3] All the catalysts used were commercial reagents of G. R. grade.

Typical Procedure for Kinetic Measurements.—A buffered aqueous solution containing TDG, a catalyst, sodium acetate and acetic acid was thermostated at the reaction temperature; the reaction was started by adding a known amount of aqueous hydrogen peroxide. Aliquots were taken out at appropriate intervals of time, and their peroxide contents were determined iodometrically.

The SM-catalyzed oxidation was carried out in aqueous media at pH 0.5~6.2 and in aqueous sulfuric acid. No appreciable change in the rates was observed when the oxidation was started by mixing TDG with a prepared mixture of SM and hydrogen peroxide, or when the reaction was carried out in a brown flask.

The kinetics of oxidation by YPM was studied by means of the iodometry of active oxygen in a buffered reaction mixture of YPM and TDG.

Ultraviolet Absorption Spectra.—Absorption spectra (210~500 mμ) were measured with a SM-H_2O_2 system in order to obtain some information on active species in the SM-catalyzed hydrogen peroxide oxidation. An absorption maximum was observed at the wavelength of 310 mμ with a solution at pH 4.7 or at 326 mμ with one at pH 0.8. No absorption maximum appeared in 210~500 mμ with an aqueous solution of hydrogen peroxide-TDG and with an aqueous solution of TDG-SM.

Reaction Products Criterion.—To examine the reaction products, a mixture of SM (0.002 mol.), hydrogen peroxide (0.12 mol.) and TDG (0.1 mol.) in 100 ml. of water was kept standing at 25° for two hours. After the evaporation of the water under reduced pressure, the residue was dissolved in alcohol, the SM being filtered off. On recrystallization from alcohol crystals (11.3 g.) of thiodiglycol sulfoxide (82%) were obtained; m. p. 110.5~111.5°C (lit.[4] m. p. 111°C).

Upon the treatment of thiodiglycol sulfoxide (15×10^{-3} M), the reaction product, with a mixture of SM (1×10^{-4} M) and H_2O_2 (8×10^{-3} M) at 25°C and pH 4.7 or 0.8 for 4 hr., no appreciable oxidation occurred.

Results and Discussion

The Examination of the Catalyst Activity.—Sulfides, in general, can be oxidized to sulfoxides by hydrogen peroxide at room temperature.[5] Ross[1] has reported that the second-order rate constant for the uncatalyzed hydrogen peroxide oxidation of thiodiglycol (TDG) in aqueous solutions of pH 4~6 was 2.17×10^{-3} l. mol^{-1} sec.$^{-1}$ at 25°C.

Our examinations of the catalytic activities of various inorganic compounds at 25°C and pH 4.7 gave the following data:

Compounds with some activity:

$Na_2MoO_4 > Na_2WO_4 \gg H_2SeO_3 \gg NH_4VO_3$, Na_2TeO_4, $UO_2(OAc)_2$, and $Cu(OAc)_2$

Compounds with no activity:

$AgNO_3$, $MgCl_2$, $BaCl_2$, $CaCl_2$, $Zn(OAc)_2$, $ZnSO_4$, $CdCl_2$, $HgCl_2$, $Hg(OAc)_2$, $Al_2(SO_4)_3$, $Na_2B_4O_7$, $NaBO_3$, $NaBO_2$, Tl_2SO_4, $Zr(OAc)_4$, $NaHCO_3$, Na_2CO_3, $Pb(OAc)_2$, $NaNO_3$, NaH_2PO_4, $Na_2P_2O_7$, Na_2HPO_3, $(NaPO_3)_n$, $Cr_2(SO_4)_3$, Cr_2O_3, K_2SO_4, $Na_2S_2O_3$, $KHSO_4$, $Mn(OAc)_2$, $KClO_3$, $KClO_4$, $NaClO_2$, $NaBrO_3$, KIO_3, KIO_4, $CoSO_4$, $Co(OAc)_2$, $Ni(OAc)_2$, and V_2O_5

TABLE I. CATALYZED HYDROGEN PEROXIDE OXIDATION OF TDG IN AQUEOUS SOLUTIONS AT 25°C AND pH 4.7

Initial concn.: H_2O_2, 0.02570 M; TDG, 0.03960 M

Catalyst	Concn. of catalyst M$\times10^{-4}$	Rate constant[a]		Catalyst coeff.[a]	
		$k_2\times10^3$ l. mol^{-1} sec^{-1}	$k_1\times10^3$ sec^{-1}	k_2^c l^2 mol^{-2} sec^{-1}	k_1^c l. mol^{-1} sec^{-1}
Na_2MoO_4	1	—	6.56	—	6.54
Na_2WO_4	1	69.2	—	670	—
H_2SeO_3	10	4.12	—	1.93	—
NH_4VO_3	10	2.54	—	0.35	—
Na_2TeO_4	10	2.42	—	0.23	—
$UO_2(OAc)_2$	10	2.39	—	0.20	—
$Cu(OAc)_2$	10	2.37	—	0.18	—
None	0	2.17	—	—	—

a) $v=k_2[H_2O_2][TDG]=(k_0+k_2^c[Catalyst])[H_2O_2][TDG]$ or $v=k_1[TDG]=k_1^c[Catalyst]-[TDG]$.

3) N. J. Kobosev and N. N. Sokolov, *Z. anorg. u. allgem. Chem.*, **214**, 321 (1933).
4) J. Bougault and P. Robin, *Compt. rend.*, **171**, 355 (1920).
5) M. Gazdar and S. Smiles, *J. Chem. Soc.*, **93**, 1833 (1908).

Compounds with side reactions:

$CuCl_2$, $CuSO_4$, $Ce_2(SO_4)_3$, $ZrOCl_2$, $NaNO_2$, $NaHSO_3$, KSCN, $K_2Cr_2(SO_4)_4$, $Fe_2(SO_4)_3$, $K_3Fe(CN)_6$, $K_4Fe(CN)_6$, $NaBiO_3$, and Na_2TeO_3

It is evident in Table I that molybdate and tungstate are both active catalysts, while selenous acid is less active. However, the other four, NH_4VO_3, Na_2TeO_4, $UO_2(OAc)_2$ and $Cu(OAc)_2$, show only a small activity. It is of interest to note that the rate of SM-catalyzed oxidation is independent of the concentration of hydrogen peroxide, following the first-order kinetics with TDG, while the oxidations with other catalysts satisfy the second-order kinetics. The comparison of the catalytic activities of sodium molybdate (SM) and tungstate seems less significant, since their kinetics are different. It is obvious, however, that the completion of oxidation with molybdate is faster than that with tungstate. The SM-catalyzed oxidation will be discussed in detail later.

Table II. Rate data on the oxidation of TDG with SM-H_2O_2 in the range of $[H_2O_2]>2[SM]$

Initial concn., $M\times10^3$ [SM]	[H_2O_2]	[TDG]	pH (Added compound)	Temp., °C	$k_1\times10^4$ sec^{-1}
A) Effect of initial concentrations of hydrogen peroxide and TDG					
0.050	5.070	2.670	4.7 (AcOH-AcONa)	25	2.57
0.050	5.098	5.340	4.7 (AcOH-AcONa)	25	2.76
0.050	5.012	8.010	4.7 (AcOH-AcONa)	25	2.75
0.050	12.50	8.010	4.7 (AcOH-AcONa)	25	2.67
0.050	25.02	10.68	4.7 (AcOH-AcONa)	25	2.82
2.0	5.63	9.03	4.7 (AcOH-AcONa)	0	18.3
2.0	8.53	9.03	4.7 (AcOH-AcONa)	0	18.8
2.0	8.47	4.51	4.7 (AcOH-AcONa)	0	18.2
0.025	9.705	9.027	0.8 (H_2SO_4)	25	12.2
0.025	9.705	13.54	0.8 (H_2SO_4)	25	12.2
0.025	6.470	13.54	0.8 (H_2SO_4)	25	12.2
B) Effect of the acidity of the solutions					
0.025	11.12	12.17	−0.60[a] (H_2SO_4)	25	11.9
0.025	11.12	12.17	−0.31[a] (H_2SO_4)	25	11.8
0.025	11.12	12.17	+0.02[a] (H_2SO_4)	25	12.2
0.025	11.12	12.17	+0.15[a] (H_2SO_4)	25	12.5
None	52.99	42.43	−0.60[a] (H_2SO_4)	25	75.8[b]
None	52.99	42.43	−0.31[a] (H_2SO_4)	25	133[b]
None	52.99	42.43	−0.04[a] (H_2SO_4)	25	236[b]
None	52.99	42.43	+0.15[a] (H_2SO_4)	25	355[b]
C) Effect of temperature					
0.025	8.52	9.03	4.7 (AcOH-AcONa)	0	0.275
0.025	8.46	9.03	4.7 (AcOH-AcONa)	5	0.401
0.025	9.85	9.03	4.7 (AcOH-AcONa)	10	0.599
0.025	10.80	12.17	4.7 (AcOH-AcONa)	20	1.15
0.025	13.53	16.22	4.7 (AcOH-AcONa)	25	1.62
0.025	10.80	12.17	4.7 (AcOH-AcONa)	30	2.09
0.025	8.52	9.03	0.8 (H_2SO_4)	0	2.97
0.025	8.46	9.03	0.8 (H_2SO_4)	5	4.01
0.025	9.85	9.03	0.8 (H_2SO_4)	10	5.66
0.025	10.80	12.17	0.8 (H_2SO_4)	20	9.54
0.025	13.53	16.22	0.8 (H_2SO_4)	25	11.9
0.025	10.80	12.17	0.8 (H_2SO_4)	30	15.9
None	52.99	42.43	4.7 (AcOH-AcONa)	20	14.0[b]
None	52.99	42.43	4.7 (AcOH-AcONa)	25	21.1[b]
None	52.99	42.43	4.7 (AcOH-AcONa)	30	31.5[b]
None	52.99	42.43	4.7 (AcOH-AcONa)	35	45.9[b]

a) Acidity function, $-H_0$.
b) Second-order rate constant ($l.\,mol^{-1}\,sec^{-1}$); $v=k_2\,[H_2O_2]\,[TDG]$.

Peroxytungstates have been suggested as active oxidation species in the tungstate-catalyzed epoxidation of olefins,[6] and peroxyselenious acid, in the selenium dioxide-catalyzed oxidation of dimethyl aniline[7] and ketones.[8]

No catalytic action of vanadic acid, a well-known catalyst,[9] was observed under these conditions, although a faint activity was appreciable with ammonium vanadate. Faint catalytic activities were also observed with sodium tellurate, cuprous acetate and uranyl acetate. The uranyl acetate is known to catalyze the hydrogen peroxide oxidation of primary amines.[10] Ferric and ferrous salts showed no appreciable activity.

The Mechanism of SM-catalyzed Oxidation. —*Rate Equations.*—The rate of SM-catalyzed oxidation is independent of the concentration of hydrogen peroxide and is first-order with respect to TDG if the concentration ratio of hydrogen peroxide vs. SM exceeds 2, as Table II-A and Fig. 1 show. These pseudo-first order rates are proportional to the concentration of SM (Fig. 2). Thus, if $[H_2O_2] > 2$ [SM], the rate equation is expressed as:

$$v = k_1 [TDG] = k_1^c [SM] [TDG] \quad (2)$$

([SM] is the initial concentration of Na_2MoO_4.) However, if $[H_2O_2]/[SM]$ is less than 2, the rate is second-order (Table III and Fig. 1):

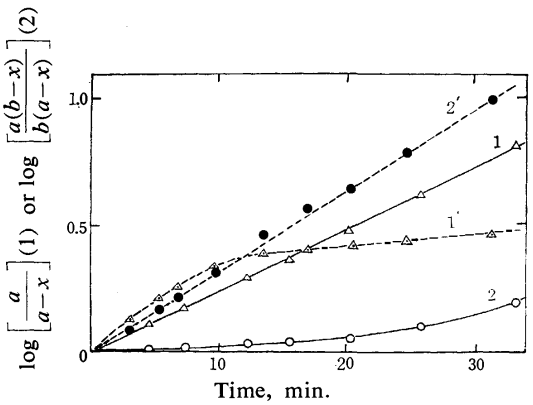

Fig. 1. Comparison of first-order (1) and second-order (2) rate equations at 0°C and pH 4.7.

	$[TDG]_{Init}$ (a), M×10³	$[H_2O_2]_{Init}$ (b), M×10³	[SM] M×10³
1 (△), 2 (○) ——	9.03	8.53	1
1'(▲), 2'(●) ------	5.42	3.70	2

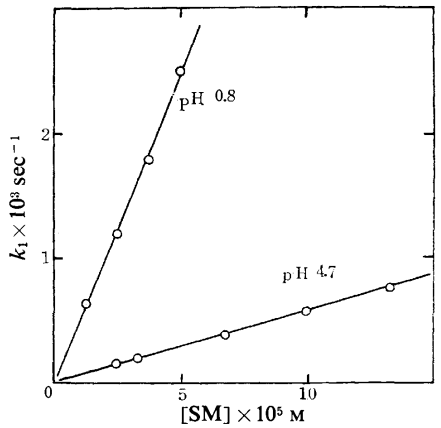

Fig. 2. Effect of concentration of SM on the rate in the range of $[H_2O_2] > 2[SM]$ at 25°C.

TABLE III. RATE DATA ON THE OXIDATION OF TDG WITH SM-H_2O_2 IN THE RANGE OF $[H_2O_2] < 2[SM]$; pH=4.7 (AcOH-AcONa) at 0°C

Initial concn. M×10³			k_2' a) 1. mol^{-1}. sec^{-1}
[SM]	$[H_2O_2]$	[TDG]	
2.0	0.924	1.806	0.856
2.0	1.924	1.806	0.862
2.0	2.879	1.806	0.749
2.0	2.879	2.709	0.706
2.0	2.879	4.514	0.786
2.0	3.611	1.924	0.860
2.0	3.695	5.417	0.711
4.0	2.879	4.514	0.856
6.0	2.879	4.514	0.783

a) $v = k_2'$ [Active oxygen] [TDG]

$$v = k_2' [\text{Active oxygen}] [TDG] \quad (3)$$

Here, [Active oxygen] expresses the concentration of active oxygen determined iodometrically. The value of k_2' holds constant while [SM] is vavied, in so far as $[H_2O_2] < 2[SM]$.

The pseudo-second order rate constant of the uncatalyzed oxidation is calculated from Table II-C and Table VI to be acout 2.0×10^{-3} l. mol^{-1} sec^{-1}, which is about 1/400 of the value of k_2', 0.797 l. mol.$^{-1}$ sec^{-1}. Hence, k_2' is not the rate for hydrogen peroxide itself, but that for other active oxidizing species.

It is quite probable that one mole of SM is transformed quantitatively to a reactive intermediate by two moles of hydrogen peroxide:

$$SM + 2H_2O_2 \overset{\text{fast}}{\rightleftarrows} \text{intermediate}$$

$$\frac{1}{2}\text{(intermediate)} + (HOCH_2CH_2)_2S \xrightarrow{\text{slow}} (HOCH_2CH_2)_2SO$$

6) a) M. Mugdan and D. P. Young, ibid., 1949, 2988; b) K. A. Saegebarth, *J. Org. Chem.*, 24, 1212 (1959); c) Z. Raciszewski, *J. Am. Chem. Soc.*, 82, 1267 (1960).
7) Y. Ogata and I. Tabushi, This Bulletin, 32, 215 (1959).
8) N. Sonoda and S. Tsutsumi, ibid., 32, 505 (1959); 33, 1440 (1960); 34, 1006 (1961).
9) W. Treibs, *Chem. Ber.*, 72, 1194 (1934).
10) K. Kar and C. Berther, ibid., 93, 132 (1960).

TABLE IV. RELATION OF ABSORBANCE WITH THE RATIO $[H_2O_2]/(2[SM])$
$[SM]=0.5\times10^{-3}$ M, pH=4.7

$[H_2O_2]\times10^3$ M	$\frac{[H_2O_2]}{2[SM]}$ (A)	$E_{1cm.}$ (310 mμ)	$\frac{E_{1cm.}\ (310\ m\mu)}{0.492}$ (B)	B/A
0.1635	0.164	0.072	0.147	0.900
0.3270	0.327	0.152	0.310	0.950
0.4905	0.491	0.226	0.460	0.938
0.6792	0.679	0.327	0.665	0.983
1.358	1.36	0.496	—	—
2.038	2.04	0.486	—	—
3.232	3.23	0.490	—	—
40	40	0.495	—	—

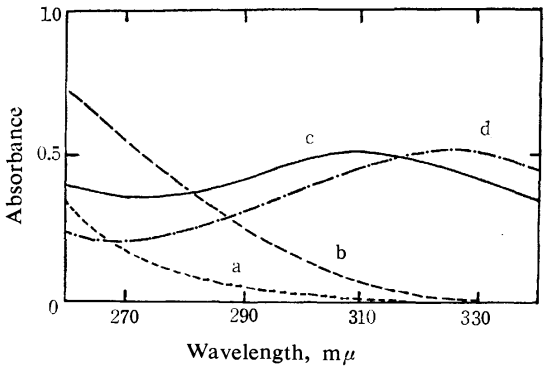

Fig. 3. Absorption spectra of SM-H_2O_2 in aqueous solutions (a) SM at pH 4.7 (AcOH-AcONa) (b) SM at pH 0.8 (H_2SO_4) (c) SM-H_2O_2 at pH 4.7 (AcOH-AcONa) (d) SM-H_2O_2 at pH 0.8 (H_2SO_4).

Assuming that the formation of the intermediate is rapid and complete and that excess hydrogen peroxide has no effect on the rate, the rate sould be independent of the concentration of hydrogen peroxide when $[H_2O_2]>2[SM]$.

Reactive Species in Solutions.—The formation of the complex, YPM, was expected from the previous equations; this expectation was confirmed by the identification of YPM by means of ultraviolet spectrophotometry, together with the comparison of the data on oxidation by SM-H_2O_2 with those on oxidation by YPM.

As shown in Fig. 3, an absoption maximum appeared at 310 mμ (pH 4.7) or at 326 mμ (pH 0.8) in the aqueous hydrogen peroxide-SM system, each maximum being identical with that of synthetic YPM at the corresponding pH. The absorbance of the aqueous hydrogen peroxide-SM system was determined at pH 4.7 with various concentrations of hydrogen peroxide while [SM] was kept constant (Table IV). The absorbance at 310 mμ did not increase with an increasing amount of hydrogen peroxide in the range of $[H_2O_2]>2[SM]$. Therefore, two moles of hydrogen peroxide and one mole of SM react almost quantitatively to yield YPM. The shift of the absorption maximum up to 326 mμ (pH 0.8) suggests that YPM may exist in another form in the realm of higher acidity.

TABLE V. OXIDATION OF TDG WITH YPM AT 0°C AND pH 4.7 (AcOH-AcONa)

Initial concn., M×10³		k''_2[a]
[Active oxygen]	[TDG]	l. mol^{-1} sec^{-1}
0.831	1.806	0.824
1.661	1.806	0.694
1.661	3.612	0.792

a) $v=k''_2$ [Active oxygen] [TDG]

Table V shows the rate data on the oxidation of TDG by YPM, data which satisfy the second-order kinetics:

$$v=k_2''\ [\text{Active oxygen}]\ [\text{TDG}] \quad (4)$$

Here, [Active oxygen] means the concentration of the active oxygen determined iodometrically. This pseudo-second order rate constant, k_2'', is identical with k_2' in Eq. 3 within the range of experimental error. These facts suggest the following mechanism at pH 3~6:

$$Na_2MoO_4 \overset{\text{fast}}{\rightleftarrows} 2Na^+ + MoO_4^{2-} \quad (5)$$

$$MoO_4^{2-} + 2H_2O_2 \overset{\text{fast}}{\rightleftarrows} HMoO_6^- + H_2O + OH^- \quad (6)$$

$$HMoO_6^- + (HOCH_2CH_2)_2S \overset{\text{slow}}{\longrightarrow} HMoO_5^- + (HOCH_2CH_2)_2SO \quad (7)$$

$$HMoO_5^- + (HOCH_2CH_2)_2S \overset{\text{fast}}{\longrightarrow} H^+ + MoO_4^{2-} + (HOCH_2CH_2)_2SO \quad (8)$$

Assuming that all the SM is converted to $HMoO_6^-$ in this pH range and that a and b are the initial concentrations of $HMoO_6^-$ and TDG respectively, and x, the decrease of TDG at time t, the rate is expressed as:

$$v=k_2''\ [HMoO_6^-]\ [\text{TDG}]$$
$$=k_2''\left(a-\frac{x}{2}\right)(b-x)$$

or

$$k_2''t=\frac{2}{b-2a}\ln\frac{2a(b-x)}{b(2a-x)} \quad (9)$$

Equation 9 is equal to Eqs. 3 and 4, and satisfies Eq. 2, if $[HMoO_6^-]$ is constant and equal to the initial concentration of SM.

SM reacts with two moles of hydrogen peroxide to form Na_2MoO_6 (YPM) and with four moles of hydrogen peroxide to form red sodium peroxymolybdate Na_2MoO_8, an unstable peroxide decomposing to YPM at room temperature.[3,11] It has been found that YPM exists in a neutral aqueous solution in the form of monoanion II.[12]

$$\underset{\text{(I)}}{MoO_2(OOH)(OOH)} \rightleftarrows \underset{\text{(II)}}{MoO_2(OO^-)(OH)}+H^+$$

Here the first ionization constant of I, K_1, is 3×10^{-3} and the second ionization constant, K_2, is 7×10^{-10}; hence the dissociation of II is almost negligible in a neutral solution.[12] When [SM] exceeds 2×10^{-3} M, SM exists in the form of polymolybdate,[13] which reacts also with hydrogen peroxide to give II.[14] These facts strongly suggest that the active species at pH 3~6 is $HMoO_6^-$.

The Effect of Acidity.—The effect of the acidity of the solution on the SM-catalyzed oxidation rate is shown in Table II-B and Fig. 4. The rate increases with the increasing acidity of the solution; the plot of log k vs. pH in the pH range of 2~3 fits a line of the unit slope (Fig. 4).

The rate constant at pH below 2 becomes independent of the acidity, as is obvious from the data obtained in dilute aqueous sulfuric acid (Table II-B). However, the uncatalyzed oxidation is accelerated by acid at pH below 2, and this is probably the well-known acid catalysis in the hydrogen peroxide oxidation. The plot of log k_2 vs. $-H_0$ gave a straight line with a slope of 0.90. The activation energies were calculated to be 11.2 kcal. mol^{-1} at a pH above 3 and 9.21 kcal. mol^{-1} at a pH below 2 (Table VI).

These facts imply two distinct active species, those at pH values below 2 and those above 3. Furthermore, the ultraviolet absorption spectrophotometry described above also endorses the presence of two active species at different pH's. It is most probable that YPM at pH above 3 exist as $HMoO_6^-$ (II), while at pH below 2 they exist as H_2MoO_6 (I), which should be more active than $HMoO_6^-$. The ratio of $[H_2MoO_6]$ to $[HMoO_6^-]$ was calculated to be 100 : 3 at pH 1 and 1 : 30 at pH 4 by means of the first ionization constant of H_2MoO_6 as determined by Csányi.[12] The shift of the absorption maximum from 310 to 326 mμ with a decreasing pH value is explicable by the transformation of $HMoO_6^-$ to H_2MoO_6. Considering the ionization constants of H_2MoO_6, H_2MoO_6 should be about nine times as active as $HMoO_6^-$ at 25°C.

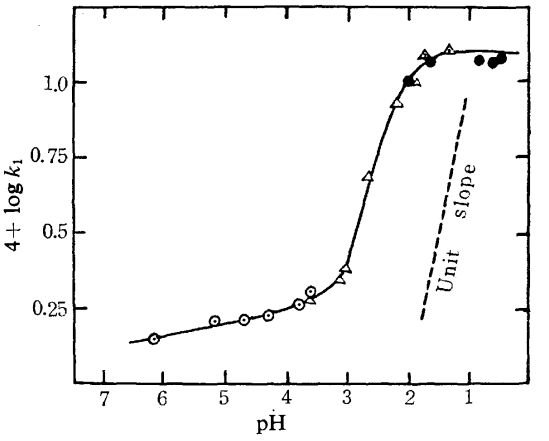

Fig. 4. Effect of pH of reaction mixture on the first-order rate constant k_1 at 25°C.
⊙ AcOH-AcONa
△ HCl-KCl
◬ HCl
● H_2SO_4

TABLE VI. ENERGY OF ACTIVATION AND ENTROPY OF ACTIVATION (calcd. from Table II-C)

[SM] $M\times10^{-5}$	pH	ΔE kcal. mol^{-1}	ΔS (25°C) cal. $deg^{-1}\cdot mol^{-1}$
None	4.7	14.25	−32.3
2.5	4.7	11.17	−38.4
2.5	0.8	9.21	−41.0

Summary

The catalytic activities of some inorganic compounds for the hydrogen peroxide oxidation of thiodiglycol (TDG) have been examined in aqueous media at 25°C and at pH 4.7. It has been found that the order of catalytic activities was: Na_2MoO_4, $Na_2WO_4 \gg H_2SeO_3 > NH_4VO_3$, Na_2TeO_4, $UO_2(OAc)_2$, $Cu(OAc)_2$. The rates of oxidation using all these catalysts, except sodium molybdate, may be expressed as $v=k_2[H_2O_2][TDG]$.

The kinetics of this reaction has been

11) L. J. Csányi, *Acta. Chim. Acad. Sci. Hung.*, **14**, 269 (1958); *Chem. Abstr.*, **52**, 19647 (1958).
12) J. J. Csányi, *Maggar Kém. Folyóirat*, **61**, 1 (1955); *Chem. Abstr.*, **49**, 15412 (1955).
13) G. Carpéni, *Bull. soc. chim. France*, **1947**, 484.
14) L. H. Csányi, *Acta Chim. Acad. Sci. Hung.*, **14**, 79 (1958); *Chem. Abstr.*, **52**, 19647 (1958).

studied in detail, especially with the sodium molybdate (SM) catalyst, by means of iodometry. The oxidation in the range $[H_2O_2] > 2[SM]$ follows the pseudo-first-order kinetics: $v = k_1^c[SM][TDG]$. The rate at pH below 2 is several times faster than that at pH 3~6, the energies of the activation at pH's below 2 and at 3~6 being 9.21 and 11.2 kcal. mol^{-1} respectively. The oxidation in the range of $[H_2O_2] < 2[SM]$ follows the second-order kinetics: $v = k_2'$[Active oxygen][TDG]. The values of k_2' were identical with the second-order rate constants obtained in the oxidation of thiodiglycol by yellow sodium peroxymolybdate. It is probable that dihydroperoxymolybdate, $HMoO_6^-$, produced rapidly from Na_2MoO_4 and hydrogen peroxide, oxidizes thiodiglycol. The increase in the rate with a decreasing pH may be due to the transformation of $HMoO_6^-$ to more active H_2MoO_6, since the Na_2MO_4-hydrogen peroxide system gave two different ultraviolet absorption maxima corresponding to $HMoO_6^-$ and H_2MoO_6 at pH 4.7 and 0.8 respectively.

Department of Applied Chemistry
Faculty of Engineering
Nagoya University
Chikusa-ku, Nagoya

Polymerization and Polymers of Itaconic Acid Derivatives. V. The Copolymerization Reactivity of Itaconic Acid in an Aqueous Solution[1,2]

By Susumu NAGAI

(Received July 12, 1963)

Studies of the copolymerization of itaconic acid have been reported by several workers.[3-7] Concerning the effect of pH value on the copolymerization reactivity of itaconic acid, however, no information has been produced in the literature available to the author.

In the preceding report[1] on the homopolymerization of itaconic acid in an aqueous solution, it was shown that an increase in the pH values of the solution caused a great decrease in the rate of polymerization. For the interpretation of this phenomenon, it was suggested that itaconic acid in the dianionic form polymerizes poorly.

Therefore it became of interest to determine whether or not itaconic acid in the dissociated state is able to copolymerize with other monomers. In the present paper, the effect of pH value on the copolymerization reactivity of the acid with acrylonitrile is described.

Experimental

Materials.—Acrylonitrile was purified by Thomas' method.[8] Itaconic acid was recrystallized two times from water. Potassium persulfate was also recrystallized from water and was used as a polymerization initiator. Deionized water, prepared by treating water with ion-exchange resin, was used as the solvent of the copolymerization.

The Copolymerization Procedure and the Treatment of the Copolymer.—Three pH values, 1.5, 4.6 and 9.5, were selected for the copolymerization systems of itaconic acid and acrylonitrile in an aqueous solution. In order to adjust the pH, hydrochloric acid or potassium hydroxide was added to the solution of itaconic acid.

Potassium persulfate, the itaconic acid solution with its pH adjusted, and acrylonitrile were charged for the polymerization into a clean glass tube. The total volume of the solution in each batch was 50 ~60 cc. After they had been flushed with nitrogen, the tubes were sealed and immersed in a water-bath regulated to the polymerization temperature of 50°C. and then kept still for several hours.

The copolymer formed was soluble or insoluble to the solution depending on both the composition of the copolymer and the pH value of the system. For the system in which the copolymer precipitated, it was easy to separate the copolymer from the unreacted monomers by filtration. When, however, the

1) Part IV of this series: S. Nagai and K. Yoshida, *Chem. High Polymers, Japan*, **17**, 746 (1960).
2) Presented at the 11th Annual Meeting of the Society of Polymer Science, Japan, Nagoya, May, 1962.
3) R. G. Fordyce and C. G. Ham, *J. Am. Chem. Soc.*, **69**, 695 (1947).
4) J. Exner and M. Bohdanecky, *Chem. Abstr.*, **48**, 8583 (1954).
5) M. Uchida and H. Nagao, *J. Chem. Soc. Japan, Ind. Chem. Sec. (Kogyo Kagaku Zasst)*, **60**, 494 (1957).
6) T. Higuchi and M. Imoto, ibid., **61**, 1053 (1958).
7) C. S. Marvel and T. Shepherd, *J. Org. Chem.*, **24**, 599 (1959).
8) W. M. Thomas and J. J. Pellon, *J. Polymer Sci.*, **13**. 329 (1954).

copolymer did not precipitate in the copolymerization medium at the acid pH, the solution was first neutralized by the addition of potassium hydroxide to pH 7, and then an excess amount of calcium chloride solution was rapidly stirred in at about 50°C to form the calcium salts of the itaconic monomer and the copolymer.[9] The calcium salt of the copolymer obtained was a fine powder and was insoluble to the solution, while that of the monomer was soluble. The copolymer salt was so finely suspended in the solution that it was difficult to isolate the salt by suction filtration through a glass filter. Accordingly, the suspension was centrifuged to recover the precipitates, and the upper solution was then decanted. The precipitates were washed with hot water and centrifuged again. This procedure was repeated several times until no chlorine ions were found in the washings. Then the copolymer was dried.

After copolymerization at a slightly alkaline pH, the solution of this system changed its color to yellow; the addition of a calcium chloride solution caused no recovery of the copolymer. In this case, however, the addition of hydrochloric acid precipitated the copolymer, with a yellow color, at about pH 3~4. Before being dried, the precipitate was dissolved again in water and reprecipitated by the addition of hydrochloric acid.

The Analysis of the Copolymer.—The acrylonitrile content of the copolymer was determined by nitrogen analysis using Kieldahl's method. The ash obtained from the copolymer was analyzed for calcium by the titration of EDTA and for potassium by the gravimetric method or by flame photometry.* Then the itaconic acid content was calculated from that of acrylonitrile, considering the calcium and potassium content of the copolymer.

Results and Discussion

The results of the copolymerization of three systems I, II and III, at different pH values are presented in Table I. In these cases, itaconic acid is designated as monomer 2, while acrylonitrile is monomer 1.

The Relationship between the pH of the System and the Dissociation of Itaconic Acid.—The copolymerization was carried out in the pH ranges of 1.0~2.2 (I), 4.7~5.3 (II) and 9.8~7.1 (III). It can be considered on the basis of Fig. 1,[10] which shows the relationship between the pH value and the degree of dissociation of itaconic acid, that the compositions of the acid in these systems are as follows:

(I) $IA > 97\%$

(II) $IA^- \simeq 80\%$, $IA \simeq IA^{2-} \simeq 10\%$

(III) $IA^{2-} > 97\%$

where IA means the undissociated form, IA^- means the first step dissociated monoanion, and IA^{2-} means the second-step dissociated dianion.

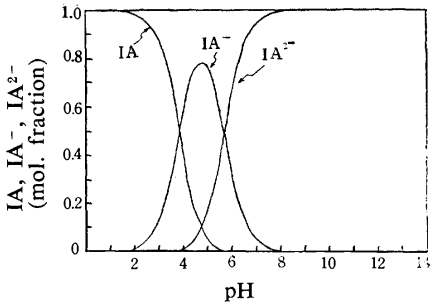

Fig. 1. Dissociation curves of itaconic acid against pH. IA, IA^- and IA^{2-} mean undissociated, first step dissociated and second step dissociated forms of itaconic acid, respectively.

The Precipitation of the Copolymer in the Copolymerization System.—In the cases of both I and II, the copolymer rich in acrylonitrile precipitated during the polymerization, while the copolymer rich in itaconic acid did not precipitate. The copolymer of an intermediate composition was partly precipitated and partly dissolved in the solution. (Cf., e.g., Table I, I-3.) However, in the case of III, no precipitates were found, presumably because of the great solubility of the copolymer composed, even though only in part, of itaconic dianion, whose water solubility is very large.

The Rate of Copolymerization.—In the acid pH copolymerization, a great decrease in the rate of copolymerization was observed as the composition of itaconic acid increased. This phenomenon had already been reported and explained by Uchida;[5] itaconic acid acts as a retarder in the emulsion copolymerization with acrylonitrile. Thus, itaconic acid monomers (M_2) add predominantly to the polymer radicals in competition with acrylonitrile monomers, i.e., $r_1 < 1 < r_2$. This results in a yield of polymer radicals with the itaconic units whose homopropagation ability is comparatively poor added at the growing ends.

However, in the neutrallized solution of the present work, rates of copolymerization which were rather large in comparison with those in acid pH copolymerization were observed in the range of 0.2~0.4 mol. fractions of M_2. The most probable interpretation of this phenomenon is that the relationship between r_1 and r_2 is now changed, as will be mentioned below; i.e., $r_1 > r_2 \simeq 0$, with a larger r_1

9) This method has previously been described by H. Ito and S. Suzuki in the case of the copolymerization of acrylonitrile with acrylic acid; *J. Chem. Soc. Japan, Ind. Chem. Sec.* (*Kogyo Kagaku Zassi*), **58**, 627 (1955).

* The author wishes to thank Miss Muyo Higashiura et al. of the Inorganic Analysis Laboratory of the Institute for their kind directions for the analysis.

10) This figure has already been presented in the preceding report.[1]

TABLE I. RESULTS OF COPOLYMERIZATION OF ITACONIC ACID (M_2) WITH ACRYLONITRILE (M_1) AT VARIOUS pH *1

Exp. No.	Monomer composition $M_2/(M_1+M_2)$ mol. fraction	Time hr. : min	pH	Conversion*2	Rate of copolymerization %/hr.	Copolymer composition $m_2/(m_1+m_2)$ mol. fraction
I-1	0.0574	1 : 0	1.20～1.40	6.2	6.2	0.0476*3
I-1′	0.0627	2 : 0	1.33～1.70	13.0	6.5	0.070*3
I-2	0.127	2 : 0	1.31～2.20	2.8	1.4	0.180*3
I-3	0.176	4 : 40	1.37～2.00	4.4	0.94	0.32～0.35*4
I-4	0.252	6 : 15	1.35～2.10	5.2	0.84	0.452
I-5	0.308	12 : 40	1.20～1.40	8.8	—	0.488
I-6	0.342	16 : 50	1.33～2.00	9.1	—	0.551
I-7	0.543	16 : 50	1.31～2.00	4.5	—	0.692
I-8	0.705	4 : 20	1.00～1.15	3.1	0.72	0.785
I-9	0.844	5 : 30	1.00～1.20	1.8	0.33	0.890
II-1	0.0661	1 : 37	4.80～5.25	14.0	8.75	0.037*3
II-2	0.115	1 : 37	4.70～5.10	12.0	7.5	0.042*3
II-3	0.187	2 : 35	4.70～5.12	4.0	1.6	0.221*3
II-4	0.290	6 : 00	4.70～4.80	—	—	0.390
II-5	0.426	4 : 20	4.70～4.89	3.3	0.76	0.532
II-6	0.565	5 : 30	4.70～4.66	4.5	0.82	0.594
II-7	0.713	6 : 00	4.70～5.00	—	—	0.672
II-8	0.789	3 : 55	4.70～4.80	1.3	0.33	0.775
III-1	0.0671	1 : 25	9.20～7.40	7.6	5.35	0.0137
III-2	0.184	2 : 30	9.20～7.33	13.0	5.2	0.26
III-2′	0.194	5 : 05	9.00～7.20	25.5	5.0	—
III-3	0.227	7 : 30	8.30～7.98	28.0	—	0.330
III-4	0.328	2 : 30	9.77～7.64	11.8	4.75	0.327
III-4′	0.307	12 : 40	8.68～7.40	25.1	—	0.332
III-5	0.394	2 : 30	9.57～7.50	7.5	3.0	0.405
III-5′	0.379	15 : 35	8.00～7.10	20.5	—	—
III-6	0.456	2 : 35	9.35～8.40	2.3	0.9	0.421
III-7	0.736	7 : 45	9.20～8.40	very low		0.522
III-8	0.803	4 : 20	9.43～8.51	very low		0.652

* The initiator, potassium persulfate, was used in concentrations of 1/200 mol. per monomers.

*2 The conversion data represent the copolymers of AN and IA recalculated from those for the experimentally-obtained copolymers containing Ca and K.

*3 The copolymer is insoluble to the aqueous solution.

*4 Some of the copolymers are insoluble.

TABLE II. COPOLYMERIZATION PARAMETERS OBTAINED*

Series	pH	M_2	r_1	r_2	Q_2	e_2
I	1.0～2.2	IA >97%	0.25	1.57	0.55	0.22
II	4.7～5.3	IA^- ≃max.	0.30	0.60	—	—
III	9.8～7.1	IA^{2-} >97%	0.43	0.1	0.12	−0.58

* The Q and e values of acrylonitrile used for this calculation are 0.41 and 1.2 respectively.

and a smaller r_2 than those for the acid pH copolymerization, thus accelerating the consumption of M_1 and increasing the rate of copolymerization.

When more than a 0.4 mol. fraction of itaconic acid was used, the rate of conversion became very small.

The Composition of the Copolymer and the Copolymerization Parameters.—The calculation of the monomer reactivity ratios was carried out according to Lewis and Mayo's method, as shown in Fig. 2, except for runs which yielded precipitated copolymers, because the unexpected absorption of the unreacted monomers to the precipitated polymers might have occurred.

Figures 3—5 show the relationship between the monomer and the copolymer compositions. The curve represents the calculated values for

r_1 and r_2, while the points represent the experimentally-determined compositions. Each curve rides sufficiently on the respective experimental points, except for those systems excluded from the calculation.

Figure 3 shows that when itaconic acid is undissociated, copolymers with acrylonitrile always contain an excess fraction of itaconic acid compared with the fraction of the acid in the monomer mixtures. On the other hand, when itaconic acid is ionized to the second step dissociated form, the "azeotropic" points are observed on a composition of about 0.4 mol. fraction of M_2, as shown in Fig. 5. Figure 4 shows an example of the results obtained by the copolymerization at intermediate pH values when IA, IA^- and IA^{2-} are all involved in the reaction.

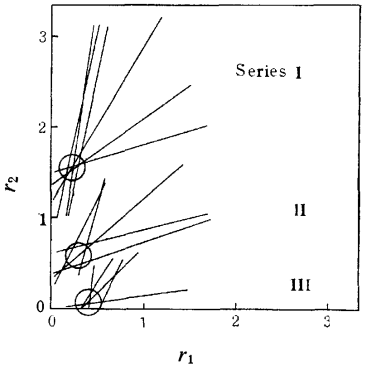

Fig. 2. Calculation diagram of reactivity ratios.

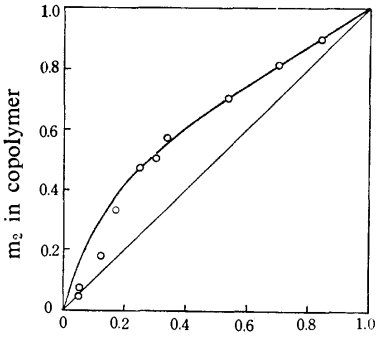

Fig. 3. Relationship between monomer composition and the initial copolymer composition. (Series I)

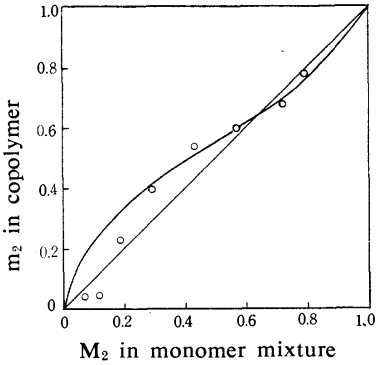

Fig. 4. Relationship between monomer composition and the initial copolymer composition. (Series II)

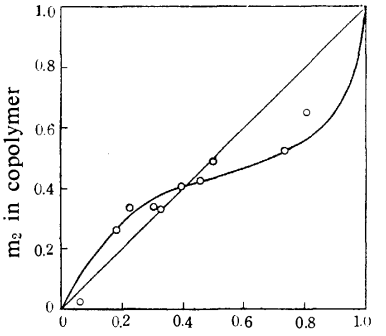

Fig. 5. Relationship between monomer composition and the initial copolymer composition. (Series III)

The monomer reactivity ratios and the Q-e values calculated according to the method of Alfrey and Price are summarized in Table II.

As for the monomer reactivity ratios, it is observed that r_2 decreases from 1.57 to 0.1 according as itaconic acid changes from the undissociated form to the second-step dissociated anion. This fact suggests that, in accordance with the finding reported in the previous paper,[1] for all practical purposes the second-step dissociated itaconic dianion does not homopolymerize.

During the considerable change in r_2 above mentioned, however, a comparatively small change is observed in r_1, one ranging from 0.25 to 0.43. This finding demonstrates that the itaconic dianion has yet a considerable reactivity to copolymerization.

Concerning the corresponding changes in Q and e values, Q_2 varies from 0.55 to 0.12, while e_2 varies from 0.22 to -0.58, according as itaconic acid changes from IA to IA^{2-}. If this finding is compared with that of acrylic acid, some interesting facts are observed. In the case of acrylic acid, Ito and Suzuki reported[9] that Q varies from 0.40 to 0.11, while e varies from 0.25 to -0.15, according as the acid changes from the undissociated form to the anion. It may be due to the similar structures of acrylic and itaconic acid from the point of view of resonance stabilization that the two monomers have similar Q values,

showing similar changes in response to the changes in the dissociation degree. Further, probably responsible for the second step dissociation of itaconic acid against the only one step dissociation of acrylic acid is the fact that the change in the *e* value of itaconic acid is much larger than the change of that of acrylic acid.

Summary

The copolymerization of itaconic acid with acrylonitrile has been carried out in aqueous solutions of three different pH values. From the composition data obtained, the monomer reactivity ratios and the *Q-e* values have been calculated. The results indicate that itaconic acid, when ionized to the second-step dissociated form, is able to copolymerize with other monomers, while it is almost completely unable to homopolymerize.

The author wishes to express his gratitude to Dr. Keinosuke Yoshida and Dr. Taizo Uno for their encouragement and to Mr. Yasushi Yoshinaga for his cooperation in the experiments.

The Osaka Municipal
Technical Research Institute
Kita-ku, Osaka

The Nuclear Magnetic Resonance Spectra of Triethylaluminum and Diethylaluminum Monohalides

By Osamu YAMAMOTO

(Received July 5, 1963)

The high resolution proton magnetic resonance spectra of a considerable number of metal alkyls have been studied in recent years; special attentions has been directed to ethyl compounds[1-4] in an attempt to correlate the electronegativity of the metal with the internal chemical shift of the ethyl group. An empirical linear relation between them was first proposed by Dailey and Shoolery[5] and later modified by Shoolery[6] for substituents of lower electronegativity through altering the empirical constants of the equation. The modified form of the equation is:

$$x = 0.62\delta + 2.07 \qquad (1)$$

where x is the electronegativity of the metal atom and δ is the internal chemical shift in p. p. m., i. e., the difference between the methyl and the methylene proton shifts.

It can easily be predicted from the equation that if x is equal to the constant term, the δ value is zero, and that if x is less than the constant term, δ is negative; that is, the methyl protons will be less shielded than the methylene protons. The spectrum shows the "inverted ethyl signals." These have clearly been demonstrated by Baker for tetraethyllead and diethylaluminum chloride respectively.[1]

Aluminum alkyls occupy an interesting position in structural chemistry because of their dimeric forms;[7,8] consequently, they have been studied extensively by means of X-ray[9] and electron diffraction[10] as well as by Raman[11-15] and infrared[12,14,16-18] spectroscopy. Some studies of the proton magnetic

1) E. B. Baker, *J. Chem. Phys.*, **26**, 960 (1957).
2) P. T. Narasimhan and M. T. Rogers, *J. Am. Chem. Soc.*, **82**, 34 (1960).
3) P. T. Narasimhan and M. T. Rogers, ibid., **82**, 5983 (1960).
4) P. T. Narasimhan and M. T. Rogers, *J. Chem. Phys.*, **34**, 1049 (1961).
5) B. P. Dailey and J. N. Shoolery, *J. Am. Chem. Soc.*, **77**, 3977 (1955).
6) J. N. Shoolery, Lecture Notes, *Varian Associates Conference* (1957); see also Ref. 3.
7) A. W. Laubengayer and W. F. Gilliam, *J. Am. Chem. Soc.*, **63**, 477 (1941).
8) K. S. Pitzer and H. S. Gutowsky, ibid., **68**, 2204 (1946).
9) P. H. Lewis and R. E. Rundle, *J. Chem. Phys.*, **21**, 986 (1953).
10) L. O. Brockway and N. R. Davison, *J. Am. Chem. Soc.*, **63**, 3287 (1941).
11) K. W. F. Kohlrausch and J. Z. Wagner, *Z. phys. Chem.*, **B52**, 185 (1942).
12) E. G. Hoffmann, *Z. Elektrochem.*, **64**, 616 (1960).
13) C. P. Van der Kelen and M. A. Herman, *Bull. soc. chim. Belges*, **65**, 362 (1956).
14) M. P. Growenewege, *Z. phys. Chem.*, (*N. F.*), **18**, 147 (1958).
15) O. Yamamoto, This Bulletin, **35**, 619 (1962).
16) K. S. Pitzer and R. K. Sheline, *J. Chem. Phys.*, **16**, 552 (1948).
17) E. G. Hoffmann and G. Schomburg, *Z. Elektrochem.*, **61**, 1101 (1957).
18) G. Schomburg and E. G. Hoffmann, ibid., **61**, 1110 (1957).

resonance spectra of these compounds have also been reported.[1,19,20] These compounds, however, except for methyl derivatives, give moderately complicated spectra, and the reported values of the chemical shifts, δ, and the coupling constant, J, are based on the firstorder approximation of the analysis.

In the present paper, the δ and the J values for triethylaluminum and diethylaluminum monohalides will be revised by a rigorous A_3B_2 analysis of the spectra; moreover, some consideration will be given for the internal chemial shifts and the coupling constants of the compounds. At the same time, the dilution effect on the δ values will be considered.

Experimental

The proton magnetic resonace spectra were obtained by means of a Varian Associate DP-60 spectrometer equipped with V-4311 R-F units of 40 and 60 Mc./sec., the usual sideband technique being employed. The spectra were obtained with pure liquid samples as well as solutions in benzene.

The solvent was dehydrated and purified by the conventional methods. All the materials used were prepared by Grosse and Mavity's methods.[21] Since aluminum alkyls are in general very reactive with air and moisture, the purified samples were transferred into cylindrical sample tubes (5 mm. o. d.) in a high vacuum apparatus; appropriate amounts of solvent, if employed, were directly distilled therein, and then the tubes were sealed off.

Results

The spectra obtained at 40 Mc./sec. using the pure liquid samples are reproduced in Figs. 1—4. The triplet-like signals on the lower field side are due to the methyl protons, and the higher field side signals, to the

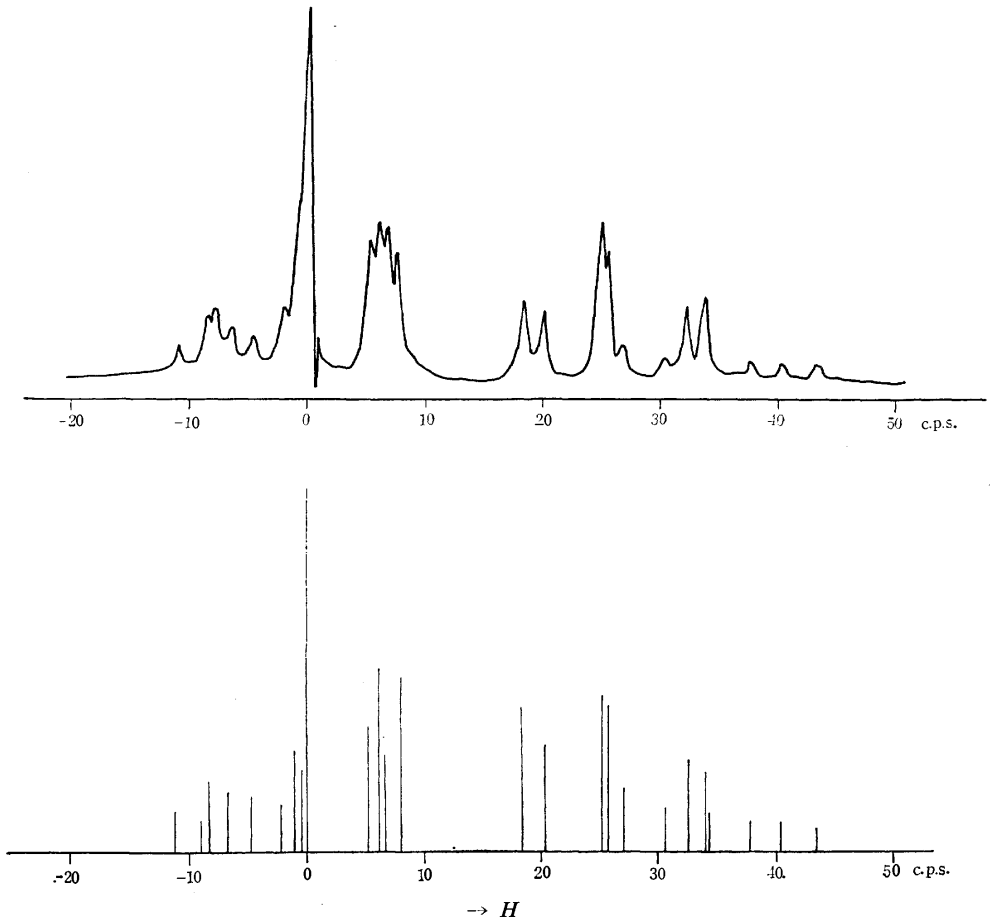

Fig. 1. Observed and calculated spectra of triethylaluminum in pure liquid state at 40 Mc./sec.

19) E. G. Hoffmann, ibid., 64, 144 (1960).
20) M. P. Growenewege, J. Smidt and H. de Vries, *J. Am. Chem. Soc.*, **82**, 4425 (1960).
21) A. von Grosse and J. M. Mavity, *J. Org. Chem.*, **5**, 106 (1940).

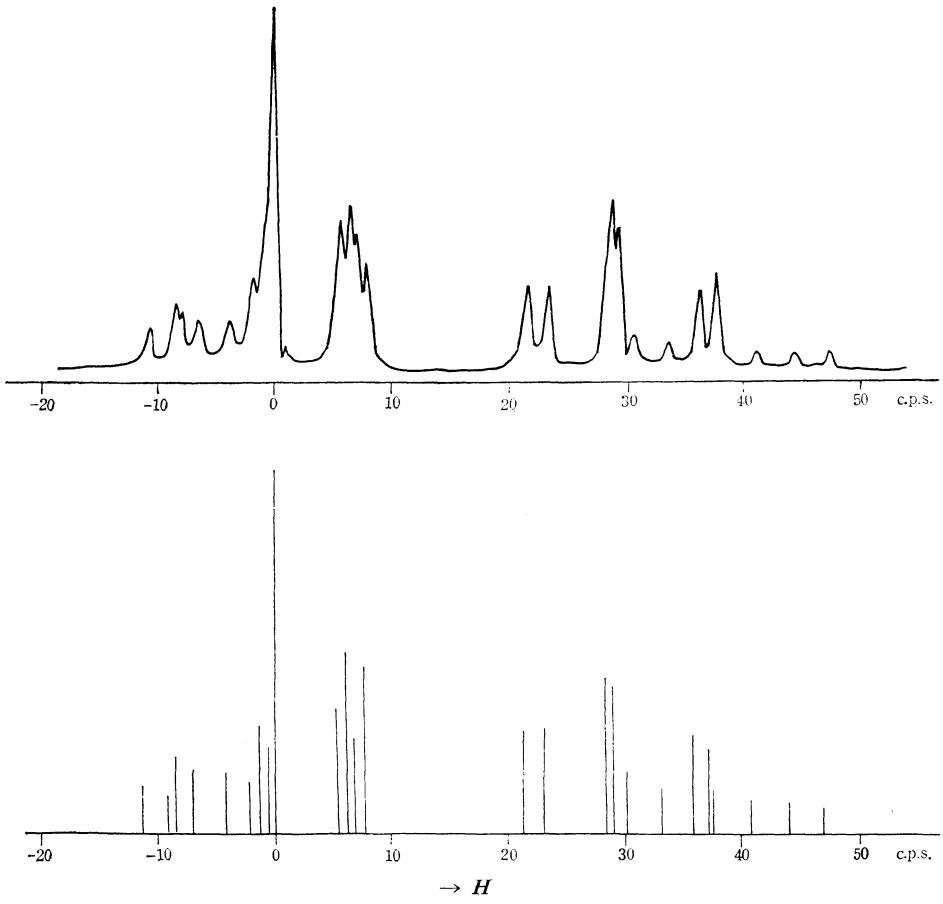

Fig. 2. Observed and calculated spectra of diethylaluminum chloride in pure liquid state at 40 Mc./sec.

TABLE I. OBSERVED AND CALCULATED SPECTRA OF TRIETHYLALUMINUM AT 40 Mc./sec. The designation for the transitions is according to Narasimhan and Rogers.[2]

Transition at the limit $J \to 0$	Frequency c.p.s.		Relative intensity		Transition at the limit $J \to 0$	Frequency c.p.s.		Relative intensity	
	Calcd.	Obs.	Calcd.	Obs.		Calcd.	Obs.	Calcd.	Obs.
CH_3-transition					CH_2-transition				
$Q_3T_1 \to Q_1T_1$	−11.3	−11.4	1.4	1.7	$Q_3T_0 \to Q_3T_{-1}$	18.5	18.5	4.8	4.6
$D_1T_1 \to D_{-1}T_1$	−8.9	−8.7	1.1	3.9	$Q_3T_1 \to Q_3T_0$	20.3	20.3	3.6	3.4
$Q_1T_1 \to Q_{-1}T_1$	−8.2	−8.1	2.4		$D_1T_0 \to D_1T_{-1}$	25.2	25.3	5.2	11.8
$Q_{-1}T_1 \to Q_{-3}T_1$	−6.6	−6.6	2.0	2.3	$D_1T_1 \to D_1T_0$	25.8	25.8	4.9	
$Q_3T_0 \to Q_1T_0$	−4.6	−4.7	1.8	2.5	$Q_1T_1 \to Q_1T_0$	27.0	26.9	2.0	
$D_1T_0 \to D_{-1}T_0$	−2.1	−2.2	1.6	20.0	$Q_1T_0 \to Q_1T_{-1}$	30.6	30.6	1.4	1.4
$Q_1T_0 \to Q_{-1}T_0$	−1.0	−1.2	3.5		$D_{-1}T_1 \to D_{-1}T_0$	32.6	32.5	3.1	3.2
$Q_{-1}T_0 \to Q_{-3}T_0$	−0.5	−0.7	2.8		$D_{-1}T_0 \to D_{-1}T_{-1}$	34.1	34.1	2.8	3.9
QS and DS transition	0.0	0.0	12.0		$Q_{-1}T_0 \to Q_{-1}T_{-1}$	34.3		1.3	
$Q_{-1}T_{-1} \to Q_{-3}T_{-1}$	5.3	5.4	4.2	18.3	$Q_{-1}T_1 \to Q_{-1}T_0$	37.7	37.6	1.0	1.2
$Q_1T_{-1} \to Q_{-1}T_{-1}$	6.1	6.1	6.2		$Q_{-3}T_1 \to Q_{-3}T_0$	40.0	40.4	1.0	1.0
$D_1T_{-1} \to D_{-1}T_{-1}$	6.7	6.7	3.2		$Q_{-3}T_0 \to Q_{-3}T_{-1}$	43.4	43.4	0.8	0.7
$Q_3T_{-1} \to Q_1T_{-1}$	7.6	7.5	5.8						

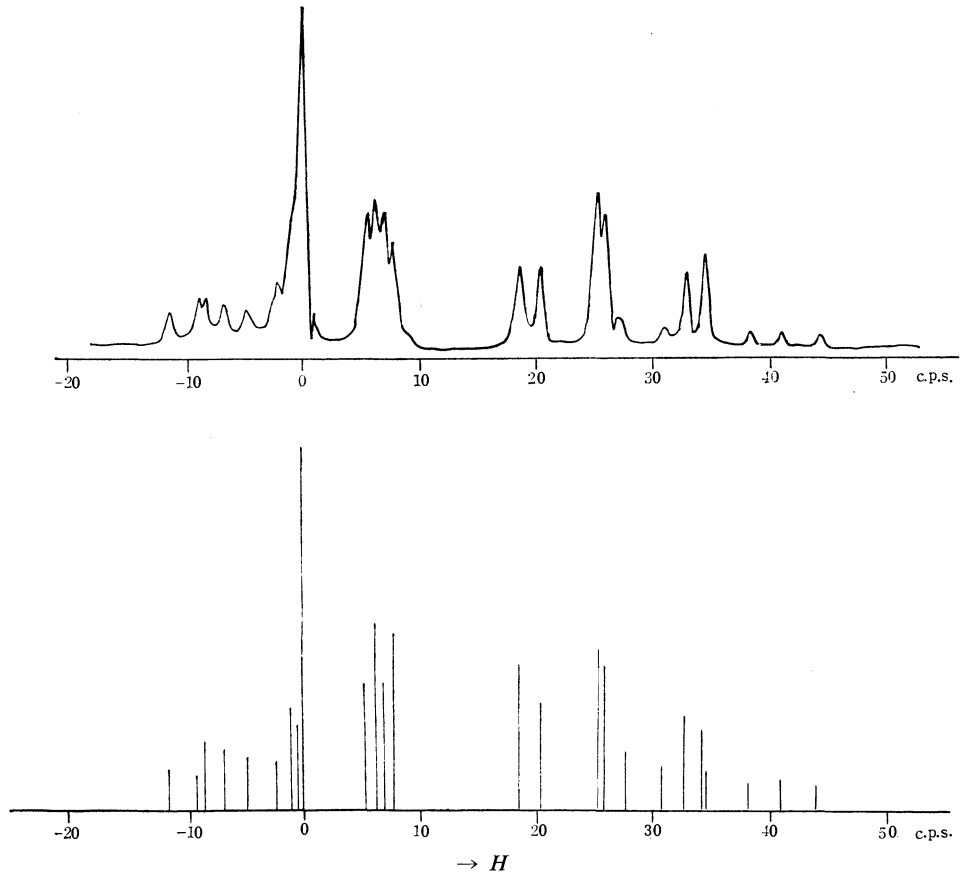

Fig. 3. Observed and calculated spectra of diethylaluminum bromide in pure liquid state at 40 Mc./sec.

methylene protons, so the spectra show "inverted ethyl signals." The individual spectral lines are somewhat broadened, probably because of the nuclear spin of aluminum ($I=5/2$).

The analysis of the spectra as an A_3B_2 system was accomplished using a NEAC-2101 digital computor. Three equivalent protons of the methyl group and two of the methylene group were treated as composite spin particles which have total spin angular momenta of 3/2 and 1 respectively. The initial assignment of the signals was determined by comparison with the theoretical spectra calculated for various J/δ values in advance. Since the observed spectra were not very muth deformed from the first-order triplet-quartet spectra (when J/δ is quite small), the assignments were rather easy. All the data from the observed lines according to the tentative assignment were fed into the input of the computor, and calculations were made to obtain the stationary state energies and the transition intensities. The program further proceeded to iteration, using the least-squares method for the difference between the observed and the calculated frequencies.

TABLE II. δ AND J_{CH_3, CH_2} VALUES OBTAINED FROM A_3B_2 ANALYSIS OF THE SPECTRA EOR TRIETHYLALUMINUM AND DIETHYLALUMINUM MONOHALOGENIDES IN THE PURE LIQUID STATE

Compound	δ, p.p.m.		J_{CH_2, CH_3} c.p.s.	
	40 Mc.	60 Mc.	40 Mc.	60 Mc.
$Al(C_2H_5)_3$	−0.72	−0.72	7.9_3	8.0_1
$Al(C_2H_5)_2Cl$	−0.81	−0.82	8.1_1	8.1_2
$Al(C_2H_5)_2Br$	−0.73	−0.73	8.0_8	8.0_7
$Al(C_2H_5)_2I$	−0.60	−0.60	8.0_5	8.1_1

The numerical details of the calculation are shown in Table I for only the 40 Mc. spectrum of triethylaluminum, while schematic illustrations of the theoretical spectra for each compound are given at the bottom in Figs. 1—4. The δ and the J values obtained both at 60 and 40 Mc./sec. for the pure liquid samples are summarized in Table II.

The spectra of benzene solutions were obtained only with 60 Mc./sec.; similar calculations were made to obtain the δ values,

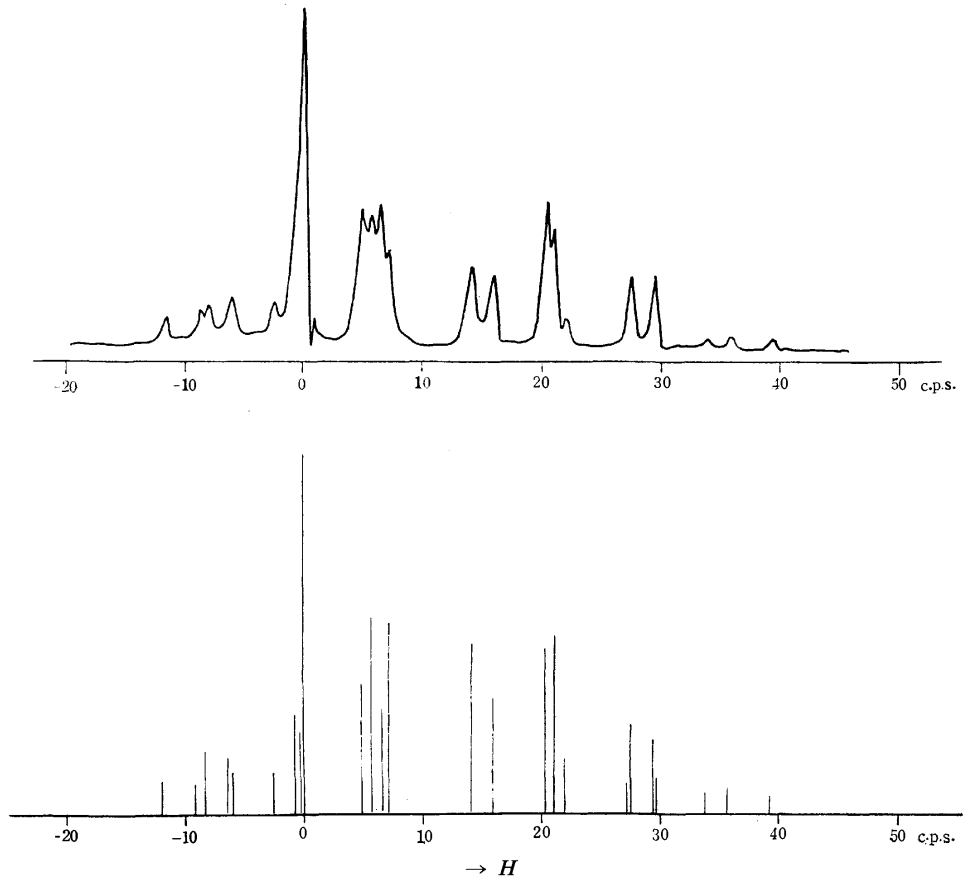

Fig. 4. Observed and calculated spectra of diethylaluminum iodide in pure liquid state at 40 Mc./sec.

which are shown in Fig. 5 plotted against the concentration.

Discussion

Coupling Constants. — The agreement in the J values at 40 Mc./sec. and at 60 Mc./sec. assures the accuracy of the obtained spin-spin coupling constants between the methyl and the methylene protons, J_{CH_3, CH_2}. All of the values are found to be near 8.0 c. p. s. and to be approximately the same as those obtained with other metal compounds (See Table III). Hence, it seems that the coupling constants, J_{CH_3, CH_2}, in the ethyl groups of such metal compounds are independent of the nature of the metal atoms attached to the ethyl groups.

The Dilution Effect of Benzene on δ Values.— Narasimhan and Rogers[3] have suggested that it would be preferable to obtain the δ values at infinite dilution in an inert solvent. Originally Dailey and Shoolery[5] employed 50 volume % benzene solutions in correlating the δ values with the electronegativity of metals. Although benzene is not necessarily an adequate solvent because of its considerable solvent effect, other solvents commonly used in NMR measurements cannot be employed in the case of metal alkyls because of the overlap of the signals and/or the reaction between the solvent and the solutes.

Thus, it is necessary to obtain the δ values at infinite dilution using benzene as the solvent and to observe their differences from those obtained with pure liquid samples for each

TABLE III. J_{CH_2, CH_3} OF SOME METAL ETHYL COMPOUNDS

Compound	J_{CH_3, CH_2}, c. p. s.	Ref.
$P(C_2H_5)_3$	7.6	4
$Sn(C_2H_5)_4$	8.2	4
$Hg(C_2H_5)_3$	7.0	2
$Pb(C_2H_5)_4$	8.2	4
$Zn(C_2H_5)_2$	8.6	3
$Ge(C_2H_5)_4$	7.8	3
$Ga(C_2H_5)_3$	9.1	3
$Si(C_2H_5)Cl_3$	8.0	3
$Si(C_2H_5)_2Cl_2$	8.0	3

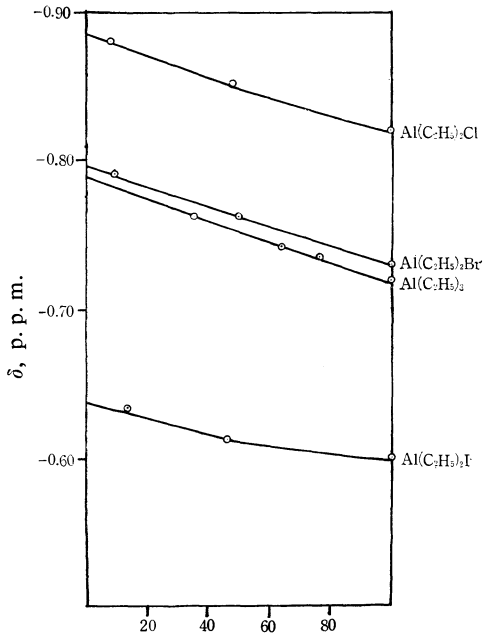

Fig. 5. Solvent effect benzene on δ values of $Al(C_2H_5)_3$ and $Al(C_2H_5)_2X$.

particular metal compound. Figure 5 shows the dilution effect on the δ values obtained in the present work. It may be seen from this figure that the maximum difference is about 0.1 p. p. m., the extent being quite large.

As far as the electronegativity of the metal itself is concerned, it is not so much affected by such a change in δ values as indicated by Narasimhan and Rogers.[3] However, when the effect of substituents attached to the metal atom on the δ values, as will be described below, is involved, the dilution effect plays more or less a significant role; in these instances, one must discuss the problem using δ values obtained under substantially the same conditions.

The Effects of Substituents Attached to the Metal Atom on the δ Values. — As is shown in Fig. 5 and Table II, the δ values of the diethylaluminum monohalides increase as the substituents change from chlorine through bromine to iodine. (Throughout the discussion below, the sign of δ is taken into account when the δ values are compared.) Figure 6 shows that the methyl protons, which are at the γ-position to the halogens, do not change in the resonance position throughout the compounds under the same conditions of dilution. Thus, the difference in δ values for these compounds is due to the methylene proton shifts. The methylene protons are at the β-position to the halogens and are, hence, influenced by the substituents.

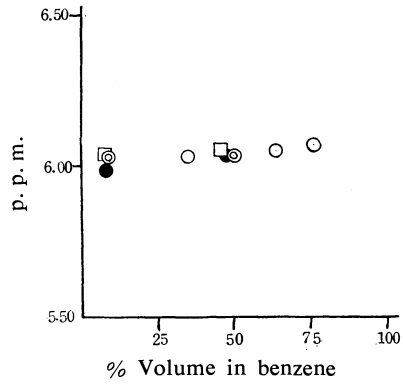

Fig. 6. Chemical shifts of the methyl signals in $Al(C_2H_5)_3$ and $Al(C_2H_5)_2X$ in benzene (referred to solvent benzene).

○ $Al(C_2H_5)_3$ ◎ $Al(C_2H_5)_2Br$
● $Al(C_2H_5)_2Cl$ □ $Al(C_2H_5)_2I$

In the CH_3-CH_2-X type compounds it has already been found that, for a simple atomic substituent, the shift to a lower field of the protons at the β-position, i. e., the methyl proton shift, increases in the order of the substituent from upper to lower down the periodic table.[22] The shielding by a β group to the methyl protons is largely controlled by the diamagnetic anisotropy of the substituent, with a smaller contribution from its inductive effect. Thus, the extents of the low field shifts increase in the descending order of chlorine, bromine and iodine. This order is contrary to that of the electronegativity but is consistent with that of the diamagnetic polarizability of the atom.

The same is true for the methylene protons of diethylaluminum monohalides. Thus, since the methylene protons in these compounds are shifted to lower fields in the order of chloride, bromine, and iodine by the diamagnetic anisotropy of the halogen atoms and since the methyl signals are substantially invariant, diethylaluminum monohalides have δ values increasing in the order of chlorine, bromine and iodine.

Triethylaluminum, which has a larger δ value than diethylaluminum monochloride, provides another problem. As was mentioned above, the substitution of the halogen atom at the β-position to a certain group of protons causes the proton signal or signals to shift to a lower field. This can be interpreted in terms of the electron-withdrawing power of the halogen atoms. For example, diethylsilane dichloride has a larger δ value (+0.01 p.p.m.)

22) L. M. Jackman, "Applications of Nuclear Magnetic Resonance Spectroscopy in Organic Chemistry," Pergamon Press, New York (1959), p. 53.

than tetraethylsilane (−0.42 p. p. m.).[3,23] A similar consideration will lead to a larger expected value for δ in diethylaluminum monochloride than in triethylaluminum, but actually the reverse is true.

Growenewege, Smidt, and de Vries[20] reported that trimethylaluminum, which gives a sharp singlet signal at room temperature, shows two separate signals at −78°C, one of which appears at higher and the other at lower fields than that of the original one. They assigned the higher signal to the terminal methyl protons and the lower one to the bridged methyl protons of trimethylaluminum dimer. The fact that trimethylaluminum gives only one singlet signal at room temperature was attributed to the rapid exchange between the terminal and the bridged methyl groups.

Since triethylaluminum has also been reported to have a dimeric form in liquid or in solutions,[7,8] the fact that the obtained spectra can be interpreted by a simple A_3B_2 system rather than by the superposition of two different A_3B_2 spectra must be responsible for the rapid exchange between the terminal and the bridged ethyl groups, as in the trimethylaluminum. In these circumstances the observed signals will be a weighted mean of the two A_3B_2 signals. If it is assumed that in this case also both the methyl signals are at approximately the same position and that the ethyl bridge is formed through the methylene group, i. e.,

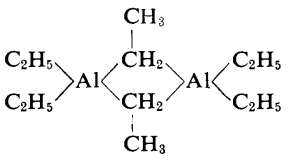

then the terminal methylene signals which are observed when the rapid exchange does not occur may be expected to appear at higher fields than the methylene signals observed at room temperature; therefore, the δ value of the terminal ethyl groups would be smaller than the δ value of diethyl aluminum monochloride. Then the apparent abnormality of the δ values of triethylaluminum may be eliminated. The confirmation of this assumption requires the low temperature spectra of triethylaluminum, work on which is now proceeding in this laboratory.

Baker in his early paper[1] suggested that the aluminum atom in triethylaluminum has a greater tendency to donate an electron to the methylene group than in diethylaluminum chloride, so that the former has a larger δ value. However, this conception seems to be improbable to judge the discussion of tetraethylsilane and diethylsilane dichloride mentioned above.[3]

The Electronegativity of Aluminum. — The electronegativity of the aluminum atom evaluated from Eq. 1 with the δ value of triethylaluminum at infinite dilution turns out to be 1.58. The electronegativity of metals can be obtained by various methods, including the method using the vibrational frequency of the methyl derivatives of the metals.[24-28] Several relationships between the electronegativity and the symmetric deformation frequency of the methyl group have been proposed. The following experimental formula, for instance, has been presented by Takenaka:[26]

$$\delta_{CH_3} = 375 \log(x/r^2_{cx}) + 1366 \qquad (2)$$

where δ_{CH_3} is the symmetric deformation frequency of the methyl group in cm^{-1}, x is the electronegativity of the metal atom, and r_{cx} is the distance between carbon and the metal atom in Å.

If the obtained values, 1.58 for the electronegativity of aluminum and 2.00Å for the terminal Al–C distance,[9] are used, one obtains 1215 cm^{-1} for δ_{CH_3}, which agrees approximately with the observed value, 1200 cm^{-1}, for the symmetric deformation of the methyl group in trimethylaluminum.[12] When the electronegativity which would be obtained for the terminal ethyl signal of triethylaluminum is substituted into formula 2 above, one can expect a smaller δ_{CH_3} value and the agreement between the observed and the expected values will be much improved.

The author wishes to express his hearty thanks to Dr. Shinnosuke Saëki of the Government Chemical Industrial Research Institute, Tokyo, for his kind advice and discussions regarding computor calculation, and to Mr. Joseph Yamada of the same Institute for his experimental work.

Government Chemical Industrial Research Institute, Tokyo
Shibuya-ku, Tokyo

23) Assuming the bridge structure in the aluminum compounds and comparing the substituents attached to the metal atom, diethylsilane dichloride rather than triethylsilane monochloride is appropriate, the δ value of the latter having not yet been reported but predicted to be −0.215 p. p. m. by Narasimhan and Rogers.[3]

24) N. Sheppard, *Trans. Faraday Soc.*, 51, 1465 (1955).
25) J. K. Wilmshurst, *J. Chem. Phys.*, 26, 426 (1957).
26) T. Takenaka, *J. Chem. Soc. Japan, Pure Chem. Sec.* (*Nippon Kagaku Zasshi*), 82, 1309 (1961).
27) T. Takenaka, ibid., 83, 267 (1962).
28) T. Takenaka and R. Gotoh, ibid., 83, 997 (1962).

Reaction of Tropylium Ion with Tropolone[1]

By Tetsuo NOZOE, Takahiro TEZUKA and Toshio MUKAI

(Received July 12, 1963)

In a previous paper[2] the authors reported on the reaction of tropylium ion with β-naphthol. Since tropolone is regarded as a compound analogous to phenols in its chemical behavior, especially toward electrophilic reagents,[3] it is to be expected that a reaction would take place between tropylium ion and tropolone. The present paper will describe this reaction and the structure and reactions of the products obtained.

The reaction of equimolecular amounts of tropylium bromide and sodium salt of tropolone affords three kinds of acidic substances with recovery of tropolone. They are yellowish needles, (I) $C_{14}H_{12}O_2$ (m. p. 89°C), (II) $C_{14}H_{12}O_2$ (m. p. 127°C) and (III), $C_{21}H_{18}O_2$ (m. p. 137°C), which were obtained in 20, 18 and 36% yields respectively. From their analytical values, the red coloration with ferric chloride, which is characteristic of tropolone derivatives, and a consideration of the preferential attack of the electrophilic reagent at the 3- and 5-positions of the tropolone ring, I and II have been assumed to be 3- or 5-(7-tropyl)tropolone. The coupling of I with *p*-toluenediazonium chloride results in the formation of a crystalline azo dye (IV) $C_{21}H_{18}O_2N_2$ (m. p. 159°C), which indicates that I is 3-(7-tropyl)tropolone with no substituent at the 5-position.[4] II also affords an azo dye (V) $C_{14}H_{12}O_2N_2$ (m. p. 200°C) by coupling with *p*-toluenediazonium chloride. However, its analytical value reveals that the tropyl group of the 5-position of II would be replaced by the *p*-tolylazo group. In fact, V is found to be identical with the known 5-(*p*-tolylazo)tropolone[5] by a comparison of their infrared absorption spectra; there is no depression of their mixed melting point. Since the reaction is considered to proceed as depicted below, II is certainly 5-(7-tropyl)tropolone. There are some examples of the same type of replacement reaction in tropolone derivatives; that is, the 5-hydroxymethyl[6] and 5-morphorinomethyl groups[6] at the 5-position are replaced with the *p*-tolylazo group.

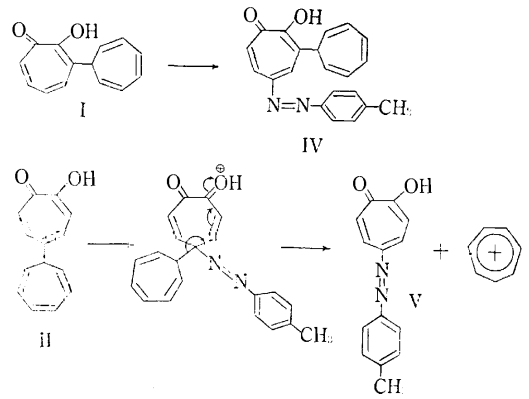

As Figs. 1, 2 and 3 show, the ultraviolet spectra and nuclear magnetic resonance spectra[7] of I and II support the correctness of the structure of I and II. In their nuclear magnetic spectra, I and II exhibit five groups of signals, a, b, c, d and e, which have intensity ratios corresponding to 1, 2, 4, 4 and 1 protons respectively. The triplet signal, a, the quartet, b and the multiplet, c, are ascribed to the C_7, $C_{1,6}$ and $C_{2,3,4,5}$ protons of the tropyl group, and d and e are attributed to the tropolone-ring proton and that of the hydroxyl group respectively. The symmetrical signal d of II is especially characteristic of the A_2B_2 system,[8] indicating II to be 5-(7-tropyl)tropolone. The e signal shifts to a lower field when one drop of acetic acid is added.

The acidic compound III couples with *p*-toluenediazonium salt in pyridine, affording an azo dye (VI) $C_{28}H_{24}O_2N_2$ (m. p. 188°C). III also gives a crystalline sodium salt and a hydrazine salt which readily regenerates III on acidifying. From these facts and from the

1) Presented at the 14th Annual Meeting of the Chemical Society of Japan, Kyoto, April, 1961.

2) T. Nozoe, S. Ito and T. Tezuka, *Chem. & Ind.*, 1960, 1088; T. Nozoe, T. Mukai, S. Ito and T. Tezuka, to be published.

3) T. Nozoe et al., "Comprehensive Organic Chemistry" (Daiyuki-Kagaku), Vol. 13, Asakura Publishing Co., Tokyo (1960), p. 124.

4) In general, it is known that tropolone derivatives with a substituent at the 5-position do not give an azo dye in the crystalline state. This method is often used for the diagnosis of the existence of a 5-substituent.

5) T. Nozoe, S. Seto, Y. Kitahara, M. Kunori and Y. Nakayama, *Proc. Japan Acad.*, 26, (7) 38 (1950).

6) S. Seto and K. Ogura, This Bulletin, 32, 493 (1959).

7) All NMR spectra were measured in the Laboratory of Professor Hazato of the Chemical Research Institute of Non-aqueous Solutions, Tohoku University.

8) L. M. Jackman, "Application of Nuclear Magnetic Resonance Spectroscopy in Organic Chemistry," Pergamon Press, London (1959), p. 92.

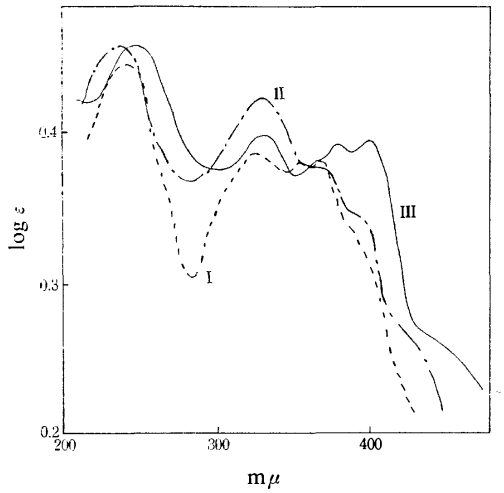

Fig. 1. UV spectra of I, II and III in methanol.

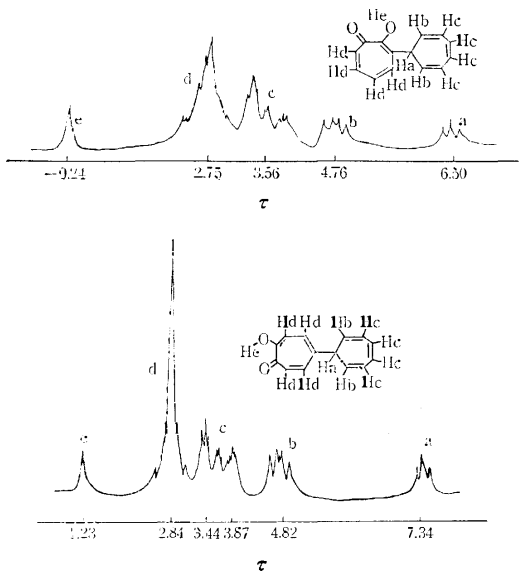

Figs. 2 and 3. NMR spectra of I and II in carbon tetrachloride (40 Mc.), with cyclohexane as an internal reference.

analytical value, III is assumed to be 3, 7-di-(7-tropyl)tropolone. The ultraviolet spectrum shown in Fig. 1 supports the assignment of III as a tropolone derivative. In the infrared spectrum, however, there is no absorption band due to the hydroxyl group and III does not show any coloration with ferric chloride in an organic solvent, such as benzene and chloroform; it does, however, show a red coloration in *n*-butanol. Since III is 3, 7-di(7-tropyl)tropolone, not a 3, 5-derivative, these abnormalities concerning the infrared spectrum and coloration can be understood from the steric hindrance of the tropyl groups situated in the 3- and 7-positions. Actually, III gives only one methyl ether (VII) (m. p. 86°C), upon being treated with diazomethane. Nine moles of hydrogen are absorbed when III is hydrogenated over platinum oxide, yielding a compound (VIII) $C_{21}H_{36}O_2$ (m. p. 60°C) which shows a band at 3500 cm^{-1} for a hydroxyl and at 1700 cm^{-1} for a carbonyl group.

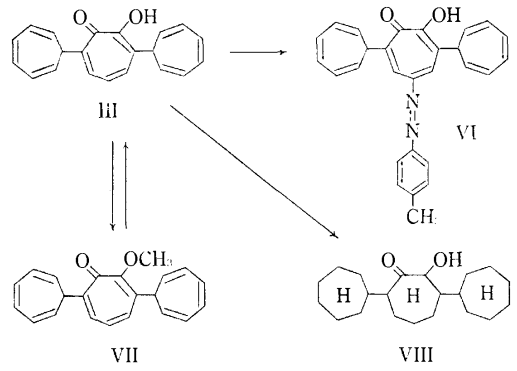

The NMR spectrum of III, shown in Fig. 4, furnishes additional evidence concerning its structure. There are also five groups of absorption signals, a, b, c, d and e. The symmetrical shape of the a triplet which appears at 6.48τ, at almost the same field as a of I, supports the theory that the two tropyl groups are situated in equivalent positions, that is, the 3- and 7-positions. If they were not at equivalent positions, they would give rise to the double triplet in this region of field. The signal d at 2.69τ, ascribed to the tropolone-ring proton, shows AB_2 type coupling.[8] This fact also supports the idea that III is 3, 7-di-(7-tropyl)tropolone.

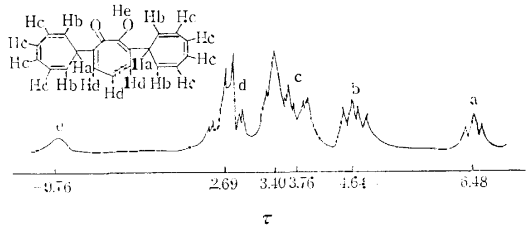

Fig. 4. NMR spectrum of III in carbon tetrachloride (40 Mc.), with cyclohexane as an internal reference.

The distillation of the mixture obtained from the reaction of tropylium ions and tropolone at the bath temperature of 180°C, before separating I, II and III, affords two additional acidic compounds; (IX) $C_{14}H_{12}O_2$ (m. p. 98°C) and (X) $C_{14}H_{12}O_2$ (m. p. 60°C). They are assumed to be isomeric monotropyltropolones resulting from a shift of the hydrogen during heating, because of their

analytical values and the red coloration with ferric chloride characteristic of tropolones. On coupling with *p*-toluenediazonium chloride, IX does not afford any crystalline azo compound, but X does afford an azo dye, (XI) $C_{21}H_{18}O_2N_2$ (m. p. 148°C).[4]

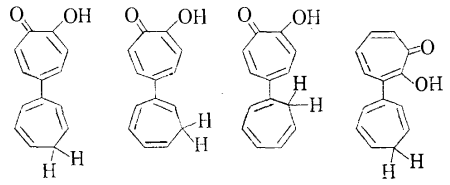

IXa IXb IXc X

This fact indicates that IX is 5- and that X is 3-tropyltropolone isomeric to II and I. In the case of IX, there are three possible formulas in which double bonds of the tropyl group are conjugated to the tropolone ring; IXa, IXb and IXc. In fact, the ultraviolet spectra of IX and X are shifted to a longer wavelength region than those of I and II, as Fig. 5 shows. However, IXc can be ruled out, because its NMR spectrum shows a triplet with the area of two protons at 7.71τ which is attributed to the C_7 proton of the tropyl group. Recently, ter Borg, Kloosterziel and Van Meurs[9] reported that 7-deuterocycloheptatriene, when heated at 100~140°C, rearranged to 3-deuterocycloheptatriene as a result of the 1, 5-transannular shift of hydrogen. Nozoe and his co-workers also reported that 7-tropylbenzene[10] and 4-(7-tropyl)phenol[11] rearranged to the corresponding 2 or 3-tropyl derivatives upon being heated with or without a base. According to ter Borg et al., IXa would be a more favorable formula than IXb, while X would have the similar isomeric formulas. It is necessary to do more detailed study in order to elucidate the structure of IX and X and to clarify the thermorearrangement of I, II and III. The results of this series of studies will be published in this Bulletin.

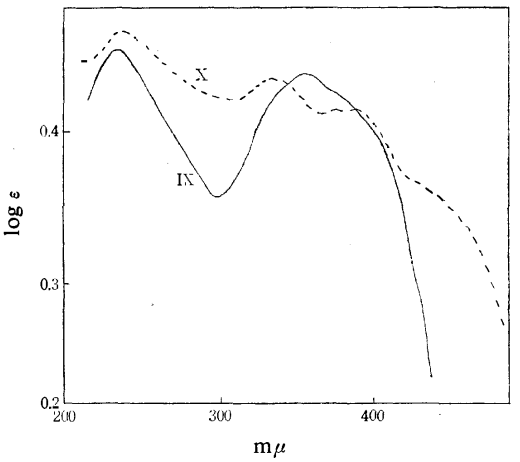

Fig. 5. UV spectra of IX and X in methanol.

Experimental[12,13]

The Reaction of Tropylium Bromide and Tropolone Sodium Salt: The Formation of 3-(7-Tropyl)- (I), 5-(Tropyl)- (II) and 3, 7-Di(7-tropyl)tropolone (III).—To a suspension of the sodium salt prepared from 10 g. of tropolone (0.0821 mol.) in 80 ml. of absolute ethanol, 13.6 g. (0.0795 mol.) of tropylium bromind were added. The reaction mixture was refluxed for 5.5 hr. After the sodium bromide had been filtered off, the evaporation of the solvent afforded 17 g. of an oil, which was found by paper chromatography to be a mixture of four kinds of tropolone derivatives. The fractional recrystallization of the sodium salt obtained from the oil from a water-ethanol mixture gave five fractions as follows. (1) The acidification of 2.8 g. of the most sparing soluble portion by 2 N hydrochloric acid afforded 2.2 g. of yellow crystals (m. p. 125~131°C), which on recrystallization from a benzene-ethanol mixture gave yellow needles (III) (m. p. 137°C). IR (KBr): no OH group, 1600, 1550 (C=O and C=C), 748, 695 cm^{-1} (7-tropyl group).[14]

Found: C, 83.44; H, 5.86. Calcd. for $C_{21}H_{18}O_2$: C, 83.42; H, 6.00%.

Treating III with hydrazine hydrate gave hydrazine salt (m. p. 160°C (decomp.)) as pale yellow needles.

Found: N, 8.80. Calcd. for $C_{21}H_{22}O_2N_2$: N, 8.38%.

(2) The acidification of 2.0 g. of the second sparing soluble portion afforded 1.2 g. of crystals (m. p. 60~65°C), the recrystallization of which from ethanol gave yellow needles (I) (m. p. 88~89°C). IR (Nujol): 3120 (OH), 1615, 1600, 1550 (C=O, C=C) 755, 704 cm^{-1} (7-tropyl group).[14]

Found: C, 79.25; H, 5.70. Calcd. for $C_{14}H_{12}O_2$: C, 79.22; H, 5.70%.

(3) The acidification of 2.3 g. of sodium salt afforded 1.1 g. of crystals (m. p. 100°C), the recrystallization of which from benzene gave yellow needles (II) (m. p. 126~127°C). IR (Nujol): 3200 (OH) 1615, 1550 (C=O and C=C) 755 and 704 cm^{-1} (7-tropyl group).[14]

Found: C, 79.69; H, 5.71. Calcd. for $C_{14}H_{12}O_2$: C, 79.22; H, 5.70%.

(4) The acidification of 1.6 g. of sodium salt afforded crystals (m. p. 40~45°C), which were identified as tropolone by a comparison of the infrared spectra.

9) A. P. ter Borg, H. Kloosterziel and N. Van Meurs, *Chem. & Ind.*, 1962, 359.
10) T. Nozoe, T. Mukai, T. Tezuka and K. Osaka, *J. Chem. Soc. Japan. Pure Chem. Sec.* (*Nippon Kagaku Zasshi*), 83, 662 (1963).
11) T. Nozoe and K. Kitahara, *Chem. & Ind.*, 1962, 1192.
12) All melting points are uncorrected.
13) The microanalyses were carried out by Miss Ayako Iwanage and Mutsuko Suzuki in this Laboratory.
14) K. Conrow, *J. Am. Chem. Soc.*, 81, 5461 (1959).

(5) The acidification of 1 g. of the most easily soluble portion afforded 0.85 g. of oil, which was not studied in more detail.

The Coupling of 3-(7-Tropyl)tropolone (I) with *p*-Toluenediazonium Chloride. The Formation of Azo Dye (IV).—To a solution of 60 mg. of I dissolved in 0.3 ml. of pyridine, an aqueous solution of *p*-toluenediazonium chloride prepared from 30 mg. of *p*-toluidine in the usual way was added drop by drop while the solution was cooled by ice. The reaction mixture was then stirred for 1 hr., diluted with water, and extracted with chloroform. After the mixture had been dried on sodium sulfate, the evaporation of the solvent afforded 90 mg. of red crystals (IV) with a melting point of 157 ~158°C after recrystallization from the benzene-ethanol mixture.

λ_{max}^{MeOH} mμ (log ε): 233 (4.13), 297 (3.88), 390 (4.37) and 440 (sh).

Found: C, 76.31; H, 4.25; N, 8.33. Calcd. for $C_{21}H_{18}O_2N_2$: C, 76.34; H, 5.49; N, 8.48%.

The Reaction of 5-(7-Tropyl)tropolone (II) with *p*-Toluenediazonium Chloride. The Formation of Azo Dye (V).—To a solution of 38 mg. of II dissolved in 0.2 ml. of pyridine, an aqueous solution of *p*-toluenediazonium chloride prepared from 15 mg. of *p*-toluidine was added drop by drop while the solution was being cooled by ice, and stirring was continued for 1.5 hr. The crystals precipitated were collected by filtration to give 25 mg. of red crystals (m. p. 145~150°C). Recrystallization from a benzene-ethanol mixture afforded orange needles (V) (m. p. 199~200°C), which were identified with authentic 5-(*p*-tolylazo)tropolone[5] by a comparison of their infrared spectra and by a mixed melting point determination.

The Coupling of 3, 7-Di(7-tropyl)tropolone (III) with *p*-Toluenediazonium Chloride. The Formation of Azo Dye (VI). — To a solution of 100 mg. of sodium salt of III dissolved in 2 ml. of pyridine, an aqueous solution of *p*-toluenediazonium chloride prepared from 60 mg. of *p*-toluidine was added drop by drop while the solution was being cooled by ice. After the mixture had been stirred for 1.5 hr. at 0~5°C, the filtration of the reaction mixture afforded 135 mg. of red crystals (m. p. 155~160°C), the recrystallization of which from benzene gave orange needles (VI) (m. p. 187~188°C).

λ_{max}^{MeOH} mμ (log ε): 265 (4.35), 295 (4.27), 402 (4.49) and 436 (4.45).

Found: C, 80.34; H, 5.41; N, 5.79. Calcd. for $C_{28}H_{24}O_2N_2$: C, 79.97; H, 5.75; N, 6.66%.

The Formation and Hydrolysis of Methyl Ether (VII) of 3, 7-Di(7-tropyl)tropolone (III). — To 5 ml. of a 2.8% ether solution of diazomethane containing a few drops of methanol, 100 mg. of III were added and the mixture was allowed to stand overnight at room temperature. The removal of the ether afforded 70 mg. of crystals (m. p. 80~82°C), which on recrystallization from methanol gave yellowish crystals (VII) (m. p. 85~86°C). IR (Nujol): no OH group, 1590, 1560 (C=O and C=C), 745, 704 cm^{-1} (tropyl group).

λ_{max}^{MeOH} mμ (log ε): 322 (3.80).

Found: C, 83.51; H, 5.79. Calcd. for $C_{22}H_{20}O_2$: C, 83.51; H, 6.37%.

The solution of 7 mg. of VII dissolved in 1 ml. of ethanol containing five drops of 6 N hydrochloric acid was refluxed for 30 min. After the removal of the ethanol and dilution with water, the reaction mixture was extracted with benzene. Evaporation of benzene extract, after it had been dried on sodium sulfate, afforded 5 mg. of crystals (m. p. 130°C), which were found to be identical with III by a comparison of their infrared spectra.

The Catalytic Hydrogenation of 3, 7-Di(7-tropyl)-tropolone (III). — A solution of 38 mg. of III dissolved in 2 ml. of ethanol was catalytically reduced in the presence of 10 mg. of platinum oxide at an ordinary temperature and pressure. 26 ml. of hydrogen (9 molar equivalent) were absorbed over a 70 min. period. After the removal of the catalyst by filtration, evaporation of the ethanol afforded 32 mg. of colorless crystals (m. p. 52~55°C), the recrystallization of which from ethanol gave colorless needles (VIII) (m. p. 59~60°C). IR (oily state): 3500 (OH), 2900, 2850 (CH) 1700 cm^{-1} (C=O).

Found: C, 78.77; H, 10.87. Calcd. for $C_{21}H_{36}O_2$: C, 78.69; H, 11.32%.

The Separation of Isomeric Compounds (IX and X) from the Reaction of Tropylium Bromide and Tropolone. — The reaction of 13.6 g. of tropylium bromide and 10.0 g. of tropolone was carried out in as the way described above. The oily product thus obtained was distillated under reduced pressure to give three fractions as follows. (1) 3.94 g. of an oil (b. p. 90°C/3 mmHg) which crystallized to colorless crystals (m. p. 40°C). Recrystallization from benzene gave crystals, melting at 47°C, which were identified as recovered tropolone by a comparison of their infrared spectra. (2) 1.21 g. of an oil (b. p. ~190°C/3 mmHg). (3) 2.41 g. of an oil (b. p. 190~192°C/3 mmHg). Fractions 2 and 3 were found to be almost the same by a comparison of their infrared spectra and by paper chromatography which showed the existence of two major components. The sodium salt obtained from 2 g. of fraction 3 was fractionally recrystallized from a water-ethanol mixture to give the following fractions. From the most sparing fraction, 635 mg. of the salt was obtained, which on acidification with 2 N hydrochloric acid it gave 350 mg. of crystals (m. p. 65~67°C). Recrystallization from petroleum ether afforded yellow needles (IX) (m. p. 97~98°C). IR (KBr): 3180 (OH), 1602, 1550 (C=O, C=C), 750, 732 cm^{-1}.

Found: C, 79.03; H, 5.64. Calcd. for $C_{14}H_{12}O_2$: C, 79.22; H, 5.70%.

The acidification of 1.02 g. of the second fraction of the salt afforded 750 mg. of crystals (m. p. 40~50°C), which on recrystallization from ethanol gave yellow needles (X) (m. p. 59~60°C). IR (KBr): 3235 (OH), 1600, 1594, 1545 (C=O, C=C) 725, 704 cm^{-1}.

Found: C, 78.04; H, 5.36. Calcd. for $C_{14}H_{12}O_2$: C, 79.22; H, 5.70%.

The oil, obtained from 300 mg. of the most easily soluble salt by acidifying it with acid, could not be identified because of its lability.

The Coupling of 3-Tropyltropolone (X) with *p*-Toluenediazonium Chloride.—To a solution of 160

mg. of X dissolved in 1 ml. of pyridine, *p*-toluenediazonium chloride prepared from 97 mg. of *p*-toluidine was added drop by drop while the solution was being cooled by ice. After it has been stirred and ice-cooled for 2 hr. and had been diluted with water, the reaction mixture was extracted with chloroform. The extract was washed with water, dried on sodium sulfate and evaporated to give 120 mg. of red crystals (m. p. 120~125°C), the recrystallization of which from a benzene-ethanol mixture afforded yellow needles (XI) (m. p. 148~149°C).

λ_{max}^{MeOH} mμ (log ε): 233 (4.22), 307 (4.13), 400 (4.53) and 440 (sh).

Found: C, 76.91; H, 5.43; N, 7.82. Calcd. for $C_{21}H_{18}O_2N_2$: C, 76.34; H, 5.49; N, 8.43%.

The authors wish to express their gratitude to Professor Genjiro Hazato and his colleagues of the Chemical Institute of Non-aqueous Solutions, Tohoku University, for their measurement of the NMR spectrum and to the Sankyo Co. for its donation of a research fund which covered a part of the expenses for this work. The infrared and ultraviolet spectrophotometers used in this study were purchased with a grant-in-aid for Fundamental and Technical Research from the Toyo Rayon Co., Ltd., to whom the authors are grateful.

Department of Chemistry
Faculty of Science
Tohoku University
Katahira-cho, Sendai

*Absolute Configuration of Nupharamine**

By Ichiro KAWASAKI, Shigeru MATSUTANI and Takeo KANEKO

(Received July 12, 1963)

Nupharamine is a minor alkaloid isolated from the root of *Nuphar japonicum* DC. Although structure I was assigned to nupharamine by Arata and Ohashi,[1,2] the configurations of the three asymmetric carbons involved in this alkaloid have not yet been ascertained.

A number of natural products containing a piperidine ring have been isolated, and their chemical structures, together with their stereochemistry, have been elucidated. Leonard and Ryder[3] synthesized 2-butyl-3-methyl piperidine, which had been obtained from lupinane by cyanogenbromide degradation,[4] and found that the infrared spectra of its trans and of its cis isomer differ from one other. This finding led us to guess that the conformation of nupharamine could be determined through its spectral behavior. Recent studies of methyl quinolizidine have indicated that an axial and an equatorial group showed peaks at different positions in the NMR spectra.[5,6] This finding played a important role in the determination of the configuration of deoxynupharidine, the main alkaloid of this plant.[6] As will be described in the following scheme, we wish here to elucidate the conformation of nupharamine by the chemical correlation of it with deoxynupharidine and its diastereoisomer.

Anhydronupharamine was obtained from nupharamine by heating it with hydrochloric acid and then neutralizing it with sodium hydrogen carbonate according to Ohashi's procedure. As this product seemed to be a mixture of two isomers which have double bonds at different positions, it was separated into IIIA and IIIB isomers by chromatography on an alumina column. While the infrared spectrum of the IIIB isomer showed bands at 1360 cm^{-1} and 1380 cm^{-1}, both assigned to the *gem*-dimethyl group, that of the other isomer, IIIA, showed no such bands, but, rather, two distinctive bands at 875 cm^{-1} and 880 cm^{-1}. On the other hand, only the latter band was recognized in the infrared spectrum of anhydrotetrahydronupharamine (VIIIA), which had been derived from tetrahydronupharamine by a similar procedure and no longer contained a furan ring. Therefore, this band (880 cm^{-1}) should be assigned to a double bond of the $CH_2=C<$ type, while the former band (875 cm^{-1}) should be assigned to the furan ring.

* Short Communication, This Bulletin, **36**, 623 (1963).

1) Y. Arata and T. Ohashi, *J. Pharm. Soc. Japan* (*Yakugaku Zasshi*), **77**, 792 (1957).

2) T. Ohashi, ibid., **79**, 729, 734 (1959).

3) N. J. Leonard and B. L. Ryder, *J. Org. Chem.*, **18**, 598 (1953).

4) K. Winterfeld and F. W. Holschneider, *Ber.*, **64**, 137 (1931).

5) T. M. Moynehan, K. Schofield, R. A. Y. Jones and A. R. Katritzky, *J. Chem. Soc.*, **1962**, 2637.

6) M. Kotake, I. Kawasaki, T. Okamoto, S. Matsutani, S. Kusumoto and T. Kaneko, This Bulletin, **35**, 1335 (1962).

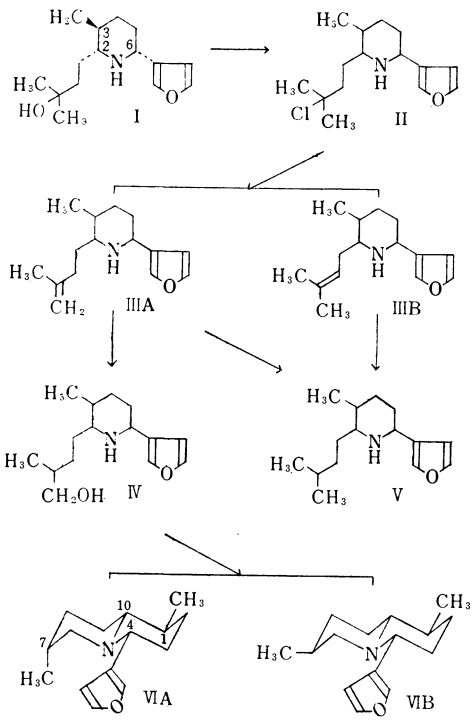

Fig. 1

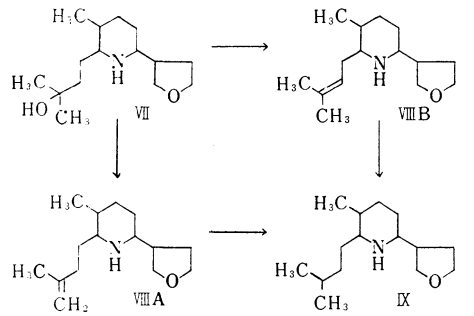

Fig. 2

When the isomer VIIIA or VIIIB was hydrogenated, the same compound, tetrahydrodeoxynupharamine (IX), was obtained in both cases. Similarly, the isomers IIIA and IIIB gave the same hydrogenation product, deoxynupharamine.

These facts indicate that IIIA contains a terminal double bond and that IIIB, an internal double bond in their molecules. With diborane in tetrahydrofuran, IIIA was converted to an organoborane compound, which was then oxidized to isonupharamine (IV) by alkaline hydrogen peroxide. IV was chlorinated with thionyl chloride and then cyclized with methanolic potassium hydroxide to afford a quinolizidine derivative. It was a mixture of diastereoisomers at C-7. The separation of both isomers was carried out by chromatography on an alumina column. From the observation of the infrared spectrum and of the levo rotatory power, one isomer, VIA, was found to be identical with natural deoxynupharidine. The other isomer, VIB, gave an infrared spectrum identical with that of 1(e), 7(e)-dimethyl-4(e)-[furyl-(3)]-quinolizidine[7] and a showed 1-equatorial methyl doublet at 0.86 p.p.m. and a 7-equatorial one at 0.68 p.p.m. in the NMR spectrum. The NMR spectra of isomer of deoxynupharidine are shown in the following table:**

Deoxynupharidine		Axial p.p.m.	Equatorial p.p.m.
1-epi	1-Me	1.19	
	7-Me	1.09	
Natural	1-Me		0.89
	7-Me	1.10	
7-epi	1-Me		0.86
	7-Me		0.68

The difference between the chemical shifts of the axial and equatorial methyl groups may be due to the long-range shielding effect of a magnetically-anisotropic carbon-carbon single bond or to the diamagnetic anisotropy which arises from furan ring currents. The C-methyl proton resonance signal for the equatorial methyl group (0.89~0.68 p. p. m.) was found to be at a higher field than the signal for the axial methyl group (1.19~1.09 p. p. m.). This observation indicates that the compound VIB must carry both methyl groups on equatorial conformation.

From the results obtained, it was concluded that the configurations of the asymmetric carbons, C_2, C_3, and C_6, of nupharamine are identical with those of the C_{10}, C_1 and C_4 of *l*-deoxynupharidine respectively and that, therefore, their absolute configurations may be deduced to be C_2(R), C_3(S) and C_6(R).

Experimental

Chloronupharamine (II).—a) A solution of 2 g. of nupharamine in 20 ml. of 10% hydrochloric acid was heated on a steam bath for 40 min. and then evaporated in vacuo. The residue was dissolved in small amounts of acetone and kept in a refrigerator. The deposited hydrochloride was recrystallized from acetone or ethanol-ether (1 : 5); 0.3 g.; m. p. 194°C (decomp.).

b) To a solution of 1 g. of nupharamine in 15 ml. of anhydrous ether, 0.7 g. of ice-cooled thionyl

7) F. Bohlmann, E. Winterfeld, P. Studt, H. Lautrent, G. Boroshewoki and K-M. Kleine, *Chem. Ber.*, **94**, 3151 (1961).

** These values were determined at 60 Mc. with a Varian A-60 spectrometer in a benzene solution (using TMS as the internal standard).

chloride were added and then kept at 50°C for 15 min. The solvent was evaporated. The residue was dissolved in 5 ml. of ethanol-ether (1 : 5) and kept in a refrigerator. The obtained hydrochloride (0.7 g.) melted at 196°C (decomp.).

Found : C, 58.59 ; H, 8.17. Calcd. for $C_{15}H_{25}O_2$-NCl_2 : C, 58.82 ; H, 8.27%.

Anhydronupharamine, IIIA and IIIB.—A solution of 1 g. of chloronupharamine-hydrochloride in water was carefully made basic with sodium carbonate and extracted with ether. The ether solution was dried and the ether was removed by distillation. The product was obtained as an oil (b. p. 113～120°C/3 mmHg, 0.75 g ; 91.4%) which was negative in a Beilstein test. The oil (1.55 g.) obtained was dissolved in petroleum ether and chromatographed on an alumina (55 g.) column.

Fraction	Elute	Volume ml.	Weight g.
1	Petr. ether	280	0
2	Petr. ether : ether (5%)	155	0.33
3	Petr. ether : ether (5%)	150	0.28
4	Petr. ether : ether (5%)	250	0.28
5	Petr. ether : ether (1 : 1)	200	0.29
6	Ether	250	0.31
7	Ethanol	100	0.43

The infrared spectrum of fraction 2 showed bands at 1505 and 875 cm^{-1} (the furan nucleus) and at 1380 and 1360 cm^{-1} (*gem*-dimethyl), and that of fraction 5 at 1505 and 875 cm^{-1} (the furan nucleus) 880 cm^{-1} (CH_2=C<) and 1380 cm^{-1}.

Deoxynupharamine (V).—A solution of 0.95 g. of anhydronupharamine (IIIA) in 20 ml. of alcohol was hydrogenated over 10% of palladium-on-charcoal at room temperature and in an ordinary atmosphere. After 98 ml. of hydrogen (one equivalent 90 ml.) had been absorbed over a 14 hr. period, the reduction product was taken up in the usual manner and crystallized as hydrochloride ; m. p. 232～233°C.

Found : C, 66.14 ; H, 9.60. Calcd. for $C_{15}H_{25}ON$-HCl : C, 66.27 ; H, 9.64%.

The hydrogenation of IIIB gave hydrochloride (m. p. 232～233°C) ; these crystals were shown to be identical with those obtained from IIIA (mixed m. p. 232～233°C). The infrared spectra of both hydrochloride were also identical.

Anhydrotetrahydronupharamine, VIIIA and VIIIB.—Tetrahydronupharamine VII (1.7 g. ; its perchloride, m. p. 212°C (decomp.)) was dissolved in 40 ml. of ether ; then a solution of 0.8 g. of thionyl chloride in 20 ml. of ether was slowly added while being ice-cooled. The mixture was warmed at 40～50°C for 3 hr. and then evaporated. The residue was made basic with an aqueous sodium bicarbonate solution and extracted with ether. The ether solution was dried, and the solvent was removed by evaporation. The residual oil (1.3 g.) was chromatographed on an alumina column (80 g.).

The infrared spectrum of fraction 5 showed a band at 880 cm^{-1}, indicating the presence of a CH_2=C< group.

Fraction	Elute	Volume ml.	Weight g.
1	Petr. ether : ether (5%)	200	0
2	Petr. ether : ether (10%)	200	0.14
3	Petr. ether : ether (20%)	250	0.48
4	Ether	100	0.26
5	Ether	400	0.30
6	Ethanol	200	0.04

Tetrahydrodeoxynupharamine (IX).—The anhydrotetrahydronupharamines, VIIIA and VIIIB, gave identical tetrahydrodeoxynupharamine (IX) when reduced over a platinum catalyst. Its hydrochloride was recrystallized from acetone to give colorless needles (m. p. 195°C).

Isonupharamine (IV).—To a mixture of 1.66 g. of anhydronupharamine (IIIA) and 0.61 g. of sodium borohydride in 80 ml. of tetrahydrofuran, a solution of 3.07 g. of boron trifluoride etherate in 10 ml. of tetrahydrofuran was added slowly under an nitrogen atmosphere. After being kept at room temperature for 4 hr., the reaction mixture was decomposed with 2 ml. of water, and then 2 ml. of 6 N sodium hydroxide and 2 ml. of 30% hydrogen peroxide were stirred in. After the mixture had been kept at 45～50°C for 30 min., the solvent layer was separated from a precipitate, which was extracted several times with boiling ether. The solvent layer and the combined ether extracts were mixed up, and the solvent was evaporated. The residue was dissolved in ether, washed with water and dried. On distillation, 1.0 g. of IV (b. p. 145～152°C (bath temp.)/0.001 mmHg.) was obtained. The perchlorate was recrystallized from ethyl acetate to give colorless needles (m. p. 164～166°C).

Found : C, 51.35 ; H, 7.47 ; Cl, 10.07. Calcd. for $C_{15}H_{23}ON$-$HClO_4$: C, 51.20 ; H, 7.44 ; Cl, 10.07%.

Deoxynupharidine, VIA and VIB.—To a solution of 1 g. of isonupharamine (IV) in 10 ml. of ether, 0.5 g. of thionyl chloride in 5 ml. of ether was added slowly. After being kept at 40～50°C for 30 min., the reaction mixture was mixed with 10 ml. of water and 40 ml. of methanol ; it was then made basic potassium hydroxide. The mixture was refluxed for 2 hr. The precipitated inorganic salt was filtered off. The filtrate was made acidic with hydrochloric acid and evaporated in vacuo. Then the residue was neutralized and extracted with ether. The ether extract was dried and evaporated to give an oil (0.6 g.), which was dissolved in petroleum ether ; an insoluble substance (0.07 g.) was then filtered off. The chromatography of this petroleum ether solution on an alumina column (80 g.) resulted in the separation of the following fractions :

Fraction	Elute	Volume ml.	Weight g.
1	Petr. ether	100	0.02
2	Petr. ether	100	0.02
3	Petr. ether	100	0.01
4	Petr. ether : ether	100	0.39
5	Ether	100	0.07

Fraction 4 was rechromatographed on an alumina column (65 g.).

Fraction	Elute	Volume ml.	Weight g.
4-1	Petr. ether : ether (5%)	120	0
4-2	Petr. ether : ether (10%)	65	0.05
4-3	Petr. ether : ether (15%)	105	0.12
4-4	Petr. ether : ether (20%)	105	0.07
4-5	Petr. ether : ether (30%)	65	0.05
4-6	Ether	130	0.10

The infrared spectrum of fraction 4-2 was identical with that of natural deoxynupharidine. The optical rotation of this fraction showed $[\alpha]_D$ $-76.8°$ (*c* 5.6 in ethanol). The corresponding fraction of another run showed $[\alpha]_D$ $-97.11°$ (*c* 1.7 in ethanol), and the hydrochloride melted at 256~258°C (cf. natural deoxynupharidine: $[\alpha]_D$ $-109.86°$).

Found: C, 66.98; H, 8.91; N, 5.00. Calcd. for $C_{15}H_{23}ON$-HCl: C, 66.77; H, 8.97; N, 5.19%.

The infrared spectrum of fraction 4-3 was identical with that of *dl*-7(epi)-deoxynupharidine: $[\alpha]_D$ $-110°$ (*c* 1.06 in ethanol); the hydrochloride, m. p. 246~248°C.

Found: C, 66.50; H, 8.86; N, 5.22.

The authors wish to express their thanks to Dr. Kenichi Takeda and Dr. Kazuo Tori of the Shionogi Research Laboratory for his measurement of the NMR spectra. Part of the expenses for this study were defrayed by a grant from the Ministry of Education, to which the authors' thanks are due.

Department of Chemistry
Faculty of Science
Osaka University
Nakanoshima, Osaka

Compounds Related to Acridine. I. Condensation of Acridine Derivatives Having Active Methyl Group and Aromatic Nitroso Compounds*

By Otohiko TSUGE, Minoru NISHINOHARA and Masashi TASHIRO

(Received July 13, 1963)

The basic condensation of the active methylene or the methyl group and the aromatic nitroso compound in general has been known as the Ehrlich-Sachs reaction[1] and has been considered a useful synthetic route to the corresponding ketone or aldehyde. It has been established in recent years that this reaction is accompanied by an oxidative reaction to form the nitrone, besides the anil, as a by-product. It is also known that these two products are difficult to separate.

Recently,[2] we found that the reaction of 7-methyl-4, 5-dihydroindeno [1, 7-bc] acridine (I) with *p*-nitrosodimethylaniline did not take place in the presence of an alkaline catalyst (sodium carbonate, potassium carbonate or piperidine) ; on the other hand, the presence of a catalytic amount of a mineral acid, especially hydrochloric acid, afforded the nitrone compound in a fairly good yield, while only a small amount of the anil compound was formed.

The present investigation was undertaken in order to elucidate the role of hydrochloric acid (HA) as a condensation agent in the reaction of 9-methyl- (II), 2, 9-dimethyl- (III), 4, 9-dimethyl- (IV), 2-chloro-9-methyl- (V), 7-methylbenz [c] - (VI) or 12-methylbenz [a] acridine (VII), which are similar to I in their chemical structures, with several nitroso compounds : nitrosobenzene (VIII), *p*-nitrosodimethyl- (IX), *p*-nitrosodiethylaniline (X) and *p*-nitrosophenol (XI).

These compounds and their reaction products are depicted in Chart 1.

Although the reaction of II with nitroso compounds, especially IX, in the presence of an alkaline catalyst has been investigated by a number of workers, Chardonnens and Heinrich[3] first successfully separated and identified acridine-9-carboxaldehyde anils and *N*-(*p*-substituted phenyl)-α-(9-acridyl) nitrones ; the major product was found to be the anil in most cases.

On the other hand, only a little information has been available regarding the condensation of substituted 9-methylacridines or methylbenzacridines and the nitroso compound. Porai-Koshits and others[4] reported that a

* Presented in part at the 16th Annual Meeting of the Chemical Society of Japan, Tokyo, April, 1963.

1) P. Ehrlich and F. Sachs, *Ber.*, **32**, 2341 (1899).

2) H. Saikachi, O. Tsuge and M. Tashiro, *J. Pharm. Soc. Japan* (*Yakugaku Zasshi*), **80**, 584 (1960).

3) L. Chardonnens and P. Heinrich, *Helv. Chim. Acta*, **32**, 656 (1949).

4) A. E. Porai-Koshits and G. S. Ter-Sarkisyan, *Izvest. Akad. Nauk S. S. S. R., Otdel. Khim. Sci.*, **1951**. 601.

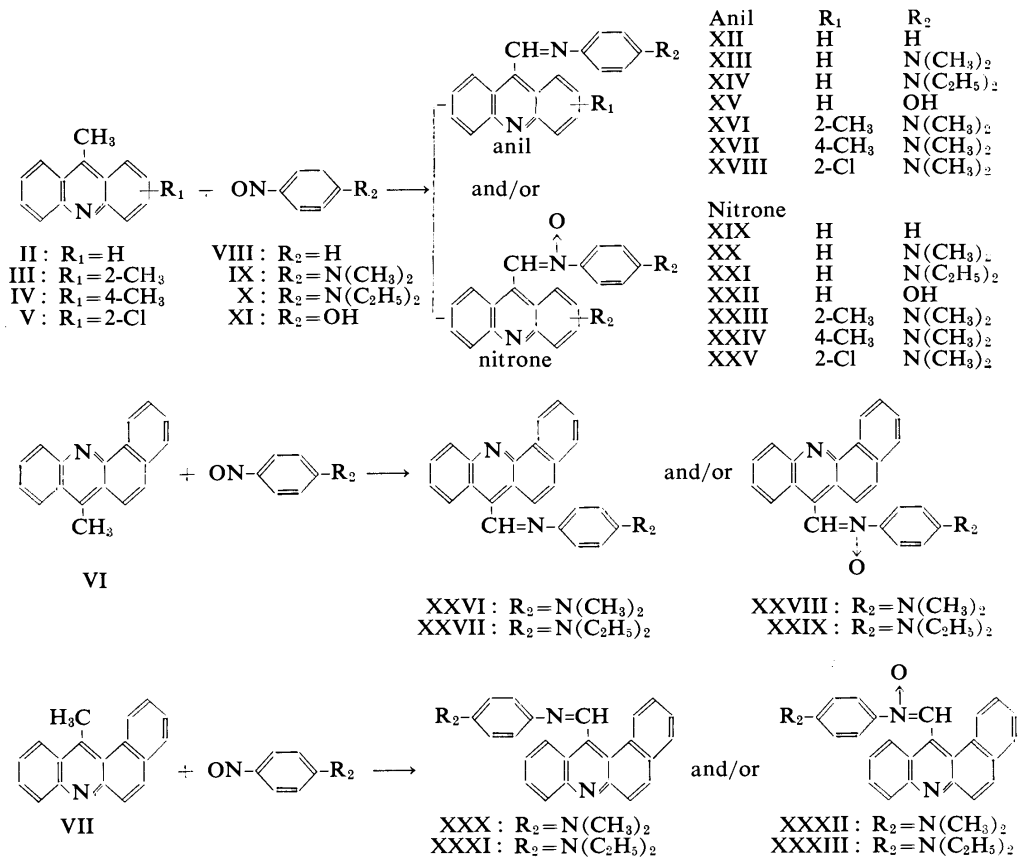

Chart 1

nitrone compound was formed by the reaction of the dimethylsulfate of VI with IX. It was reported by Mikhailov and Ter-Sarkisyan[5] that the condensation of III and IX with sodium carbonate or the ultraviolet illumination of a mixture of VII and the hydrochloride of IX in methanol gave the corresponding nitrone compounds in a poor yield.

Now, the addition of a small amount of HA in place of an alkaline catalyst to the reaction mixture of the acridine derivatives and nitroso compounds mentioned above in ethanol, revealed interesting results, as had been expected. In addition, this paper will also deal with the infrared spectra of the anil and nitrone compounds.

Results and Discussion

As the optimum conditions for obtaining a nitrone compound by the reaction of I with IX in the presesnce of HA had not been determined, in the reaction of II with IX the effect of reaction conditions on the yield of

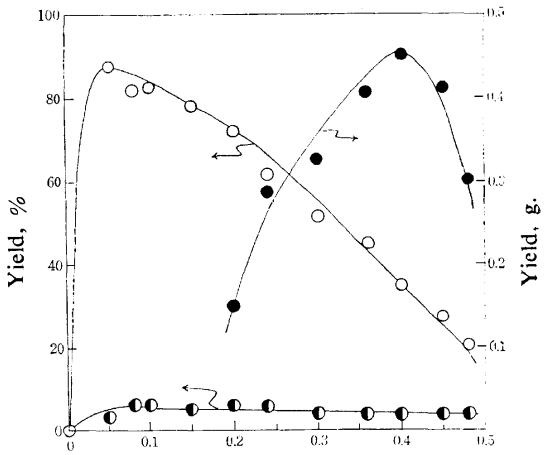

Fig. 1. Effect of hydrochloric acid.

Mixtures of II (1.0 g.) and IX (1.6 g.) in the presence of the specified amounts of HA (d^{27} 1.1748) in ethanol (50 ml.) were refluxed for 2 hr.

-○-○- Nitrone (XX)
-◐-◐- Anil (XIII)
-●-●- Higher melting compound (XXXIV)

5) B. M. Mikhailov and G. S. Ter-Sarkisyan, ibid., 1954, 656.

acridine-9-carboxaldehyde *N*-(*p*-dimethylaminophenyl)anil (XIII) or of *N*-(*p*-dimethylaminophenyl)-α-(9-acridyl)nitrone (XX) was first examined.

Effect of the Amount of Hydrochloric Acid.—The results are given in Fig. 1. In contrast with the condensation in the presence of sodium carbonate, the main product was the nitrone XX, whose yield was greatly affected by the amount of HA. The maximum yield of XX was obtained when the molar ratio of HA to II was about 0.08 (0.03 ml. in Fig. 1); its yield rapidly decreased with the increase in the amount of the HA. While the yield of the anil XIII was little affected by the HA, it was very poor.

On the other hand, if the molar ratio of HA to II was over about 0.5 (0.2 ml. in Fig. 1), the higher melting substance (XXXIV)[6] (m. p. over 300°C) began to be formed. When equimolecular amounts of II and of HA were used, the maximum yield of XXXIV was obtained. On the other hand, a large amount of a resinous material came to be formed as the amount of the HA increased.

Effect of the Reaction Time.—The effects of the reaction time on the yields of XIII and XX in the presence of HA or sodium carbonate are shown in Fig. 2. It is clear that HA greatly accelerated the rate of the condensation of II and IX in comparison with sodium carbonate, and that the nitrone XX was formed in a good yield in a short while. In the case of sodium carbonate, more of the anil XIII was obtained than of the nitrone XX, but both yields were very poor, as had been reported by Chardonnens and Heinrich.[3]

Effect of the Amount of *p*-Nitrosodimethylaniline (IX).—The results are given in Table I. The treatment of II with two or three molecular amounts of IX afforded the nitrone XX in an excellent yield. In particular, it is to be emphasized that even when an equimolecular amount of IX was used, XX was formed in a fairly good yield.

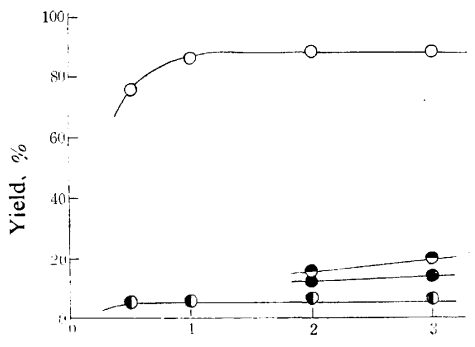

Fig. 2. Effect of the reaction time.
-●-●- Anil (XIII) } In the presence of HA
-○-○- Nitrone (XX) }
-●-●- Anil (XIII) } In the presence of Na_2CO_3
-●-●- Nitrone (XX) }

6) The structure of XXXIV will be published elsewhere in the near future.

Table I. Effect of the amount of IX*

IX**	Product, %	
	Anil (XIII)	Nitrone (XX)
1	4.1	74.8
2	5.0	85.3
3	4.5	90.0

* Mixtures of II (1.0 g.) and the specified amounts of IX in the presence of HA (0.05 ml., d^{27} 1.1748) in ethanol (50 ml.) were refluxed for 3 hr.
** Moles per mole II

Kröhnke and his co-workers[7,8] have suggested the mechanism for the formation of the anil and nitrone in the presence of an alkaline catalyst depicted in Chart 2:

$$R\text{-}CH_3 + ON\text{-}R' \longrightarrow$$

$$R\text{-}CH_2\text{-}\underset{\displaystyle OH}{\underset{|}{N}}\text{-}R' \text{-(A)-} \begin{cases} \xrightarrow{-H_2O} R\text{-}CH{=}N\text{-}R' \\ \xrightarrow{-H_2} R\text{-}CH{=}\overset{\displaystyle O}{\hat{N}}\text{-}R' \end{cases}$$

Chart 2

That is, the aldol-type intermediate (A) is formed by the condensation of active methyl and the nitroso compound, and the dehydration of the intermediate (A) chiefly proceeds to give the anil. Simultaneously, the nitrone compound is formed as a by-product by the dehydrogenation. The dehydrogenation is mainly ascribed to the oxidative property of the nitroso compound according to the following scheme:

$$R\text{-}CH_2\text{-}\underset{\displaystyle OH}{\underset{|}{N}}\text{-}R' + 2\ ON\text{-}R' \longrightarrow R\text{-}CH{=}\overset{\displaystyle O}{\hat{N}}\text{-}R' + R'\text{-}N{=}\overset{\displaystyle O}{\hat{N}}\text{-}R'$$

Furthermore, they proposed that the intermediate (A) may be dehydrogenated in a certain degree by air, and that the corresponding phenylhydroxylamine, which is yielded by the reduction of the nitroso compound, is disproportionate to the original nitroso compound and aniline derivative: $2R'\text{-}NO + H_2 \rightarrow 2R'\text{-}NHOH \rightarrow R'\text{-}NO + R'\text{-}NH_2$.

According to this mechanism, at least two moles of the nitroso compound are needed to form one mole of the nitrone compound.

7) F. Kröhnke, *Ber.*, 71, 2583 (1938).
8) F. Kröhnke, H. Leister and I. Vogt, *Chem. Ber.*, 90, 2792 (1959).

TABLE II. EFFECT OF THE SUBSTITUENT IN NITROSOBENZENES

Nitrosobenzene		Catalyst**	Reaction	Product***			
Kind	Amounts*		time, hr.	Anil	Yield, %	Nitrone	Yield, %
VIII	4	Na_2CO_3	3	XII	—	XIX	53.7
VIII	3	HCl	2	XII	42.9	XIX	+
IX	2	Na_2CO_3	3	XIII	16.9	XX	8.5
IX	2	HCl	2	XIII	4.3	XX	87.2
X	1	Na_2CO_3	6	XIV	53.1	XXI	9.1
X	2	HCl	2	XIV	40.0	XXI	27.3
XI	2	K_2CO_3	3	XV	—	XXII	47.1
XI	2	HCl	3	XV	82.3	XXII	—

* Moles per mole II

** Data with sodium carbonate as a catalyst were quoted from Ref. 3.

*** Yields based on II and a plus-sign, +, means a small amount.

However, the fact that the nitrone XX was obtained in a good yield, even if an equimolecular amount of IX was used, as Table I shows, does not appear to be explained by Kröhnke's mechanism. The mechanism will be considered elsewhere in the near future.

Effect of the Substituent in Aromatic Nitroso Compounds.—Chardonnens and Heinrich[3] also reported that the kind of aromatic nitroso compound affected the relative amounts of the products, the anil and the nitrone. As has been described above, contrary to the case of sodium carbonate, the nitrone XX was chiefly afforded when the mixture of II and IX with a catalytic amount of HA in ethanol was refluxed. Accordingly, it seemed of interest to clarify the variation in the relative amounts of the anil and of the nitrone when the condensations of II and several nitrosobenzenes VIII—XI were carried out in the presence of a catalytic amount of HA in a boiling ethanol solution. The results are summarized in Table II.

Table II shows interesting features regarding the relative amounts of the anil and of the nitrone compound. In the treatment of II and nitrosobenzene (VIII) with sodium carbonate, *N*-phenyl-α-(9-acridyl)nitrone (XIX) was obtained as a major product in place of acridine-9-carboxaldehyde *N*-phenylanil (XII). On the other hand, when HA was used the product ratio of these two compounds was reversed, and the anil XII was formed as the main product.

As has been mentioned above, IX reacted with II in the presence of HA to give the nitrone compound in an excellent yield. The condensation of II and *p*-nitrosodiethylaniline (X) with HA or sodium carbonate afforded acridine-9-carboxaldehyde *N*-(*p*-diethylaminophenyl)anil (XIV) as the major product. In the case of the former, however, *N*-(*p*-diethylaminophenyl)-α-(9-acridyl)nitrone (XXI) was also formed in a fairly large amount.

Drozdov and Yavorskaya[9] have reported that the condensation of II and *p*-nitrosophenol (XI) with sodium carbonate leads to the formation of *N*-(*p*-hydroxyphenyl)-α-(9-acridyl)-nitrone (XXII) (m. p. 230~231°C) in a 60% yield. We carried out the reaction of II with XI in the presence of HA or potassium carbonate as a condensation agent; acridine-9-carboxaldehyde *N*-(*p*-hydroxyphenyl)anil (XV) (m. p. 275°C) or the nitrone compound (XXII) (m. p. 235°C (decomp.)) was obtained in a 82.3 or a 47.1% yield respectively. The melting point of the anil XV reported by Drozdov and Yavorskaya[9] was 225°C (decomp.), but XV prepared by the condensation of acridine-9-carboxaldehyde and *p*-aminophenol melted at 275°C.

Reaction of Other Acridines with Nitroso Compounds. — We have attempted to clarify the relation between the effect of HA and sodium carbonate on the condensation of other acridines and nitroso compounds. It has been reported that the treatment of 2, 9-dimethylacridine (III) with IX in the presence of sodium carbonate in boiling methanol for 5 hr. afforded *N*-(*p*-dimethylaminophenyl)-α-(2-methyl-9-acridyl)nitrone (XXIII) in about a 26% yield.[5] We carried out the reaction of III with IX in the presence of HA or sodium carbonate in boiling ethanol. In the case of HA, 2-methylacridine-9-carboxaldehyde *N*-(*p*-dimethylaminophenyl)anil (XVI) was obtained in a good yield, but XXIII, in only a trace amount. As reported by Mikhailov and Ter-Sarkisyan,[5] in the presence of sodium carbonate only the nitrone XXIII was obtained in a poor yield.

4, 9-Dimethyl- (IV) or 2-chloro-9-methylacridine (V), treated with IX in the presence of HA, condensed to afford 4-methylacridine- (XVII) or 2-chloroacridine-9-carboxaldehyde *N*-(*p*-dimethylaminophenyl)anil (XVIII) in a fairly

9) N. S. Drozdov and E. V. Yavorskaya, *Zhur. Obshchei Khim.*, **30**, 3421 (1960).

TABLE III. CONDENSATION OF OTHER ACRIDINES AND NITROSO COMPOUNDS

Acridine	Nitroso* compound	Catalyst	Reaction time, hr.	Anil	Product** Yield, %	Nitrone	Yield, %
III	IX	HCl	3	XVI	77.4	XXIII	+
III	IX	Na_2CO_3	3	XVI	—	XXIII	22.2
IV	IX	HCl	3	XVII	36.6	XXIV	44.9
IV	IX	Na_2CO_3	3	XVII	—	XXIV	15.2
V	IX	HCl	3	XVIII	54.8	XXV	37.7
V	IX	Na_2CO_3	3	XVIII	43.6	XXV	+
VI	IX	HCl	3	XXVI	15.5	XXVIII	14.6
VI	X	HCl	3	XXVII	37.4	XXIX	—
VII	IX	HCl	1	XXX	+	XXXII	82.6
VII	X	HCl	1	XXXI	—	XXXIII	61.5

* Two moles per mole acridine compounds were used.

** Yields based on acridines and a plus-sign, +, means a trace amount.

good yield; the corresponding nitrone, *N*-(*p*-dimethylaminophenyl)-α-(4-methyl-9-acridyl)-(XXIV) or *N*-(*p*-dimethylaminophenyl)-α-(2-chloro-9-acridyl)nitrone (XXV), was also produced. However, the basic condensation of IV or V with IX afforded only the nitrone XXIV or anil XVIII respectively in a low yield.

The methylbenzacridines VI—VII, as well as I, did not react with IX or X in the presence of an alkaline catalyst, but they did react to give the anil and/or nitrone with HA. In the condensation of VI and IX, benz[c]acridine-7-carboxaldehyde *N*-(*p*-dimethylaminophenyl)anil (XXVI) and *N*-(*p*-dimethylaminophenyl)-α-(7-benz[c]acridyl) nitrone (XXVIII) were obtained in almost the same yield, but both yields were poor. However, VI with X reacted to give only the corresponding anil, benz[c]acridine-7-carboxaldehyde *N*-(*p*-diethylaminophenyl)anil (XXVII).

On the other hand, VII with IX or X smoothly reacted to afford the nitrone, *N*-(*p*-dimethylaminophenyl)- (XXXII) or *N*-(*p*-diethylaminophenyl)-α-(12-benz[a]acridyl)nitrone (XXXIII) respectively, in a fairly good yield, although the corresponding anil was not formed. These results are summarized in Table III.

Mikhailov and Ter-Sarkisyan[10] have reported that the order of the reactivity of the methyl component in the reaction with *m*-nitrobenzaldehyde was as follows: II>VI>VII; 4-picoline>4-quinaldine>1-methylbenzo[f]quinoline>4-methylbenzo[h]quinoline.

When the reactivity of the methyl group in VI and VII in the reaction with IX or X is compered, the latter is greater than the former. This seems to be the same as with the relationship of benzoquinoline derivatives mentioned above; it shows that the steric factor alone is not always predominate.

10) B. M. Mikhailov and G. S. Ter-Sarkisyan, *Izvest. Akad. Nauk S. S. S. R., Otdel. Khim. Nauk*, **1954**, 846.

TABLE IV. STRETCHING VIBRATIONS OF C=N AND N-O

Compound (XII—XXV) R_1	R_2	$\nu_{C=N}$, cm^{-1} Anil	Nitrone	ν_{N-O}, cm^{-1} (Nitrone)
H	H	1613	1612	1054
H	$N(CH_3)_2$	1621	1606	1048
H	$N(C_2H_5)_2$	1620	1607	1049
H	OH	1616	1613	1047
2-CH_3	$N(CH_3)_2$	1610	1597	1048
4-CH_3	$N(CH_3)_2$	1621	1612	1020
2-Cl	$N(CH_3)_2$	1615	1601	1047
Compound (XXVI—XXIX)				
	R_2			
	$N(CH_3)_2$	1623	1610	1061
	$N(C_2H_5)_2$	1618	—	—
Compound (XXX—XXXIII)				
	$N(CH_3)_2$	1625	1613	1036
	$N(C_2H_5)_2$	—	1608	1042

The structure assignments of all anils and nitrones described above were made on the basis of the infrared spectra as well as of elemental analyses.

Furthermore, all the anils or nitrones were almost quantitatively hydrolyzed to afford the corresponding formyl derivatives, which formed the anils by condensation with anilines.

Infrared Spectra of the Anils and Nitrones.— The infrared spectra of the above-mentioned anils and nitrones were measured in Nujol mull; the characteristic absorption bands for the C=N bond of the Schiff base type and for the *N*-oxide group were thus established. The observed frequencies are summarized in Table IV. The spectra of the anil XIII and nitrone XX as one example are shown in Fig. 3. In general, the C=N stretching frequency in the nitrone compounds was observed at a lower frequency region than that in the anil compounds; this shows that the double-bond

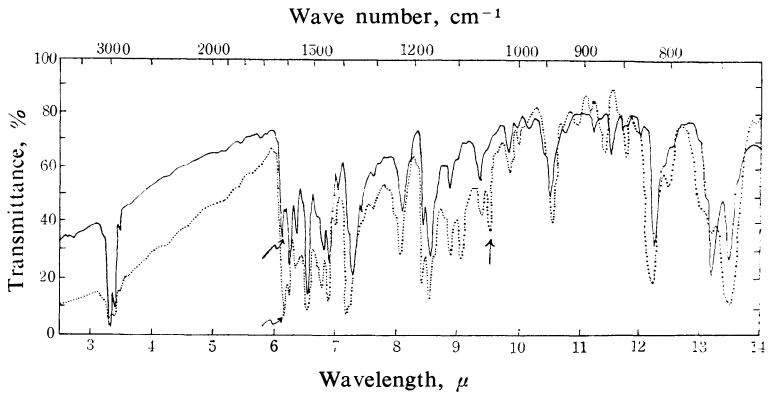

Fig. 3. Infrared spectra of the anil (XIII) and nitrone (XX) in Nujol mull.
—— (XIII), ···· (XX)

character of C=N in the former is smaller than that in the latter, as was expected.

In all nitrone compounds, the moderate absorption band always appeared around 1050 cm^{-1}. The N–O stretching frequency in aliphatic tertiary amine *N*-oxides,[11] aromatic nitroso compounds[12] or pyridine *N*-oxides[13] is assigned to the region of 950, 1380~1340 or 1200~1300 cm^{-1} respectively.

Since the N–O bond in the above-mentioned nitrone compounds is considered by mesomerism to have a greater double-bond character than that in aliphatic tertiary amine *N*-oxides and a smaller one than that in aromatic nitroso compounds or pyridine *N*-oxides, it is expected that the N–O band of the present nitrones will appear at a higher frequency region than that of aliphatic *N*-oxides and at a lower region than the aromatics.

Consequently, it seems to be appropriate for the observed band at around 1050 cm^{-1} to be assigned to the N–O streching frequency in the nitrone compounds.

Experimental[14]

Preparation of Methylacridines II—VII.—The reaction conditions in the preparation of 9-methylacridine (II) by the Bernthsen method were examined.[15] It was found that the yield of II became better as the amount of zinc chloride increased and that the following procedure afforded II in a fairly good yield in spite of the relatively short reaction time.

A mixture of diphenylamine (10.0 g.) and glacial acetic acid (10 ml.) in the presence of anhydrous zinc chloride (40.0 g.) was heated to 220°C, while being stirred; the excess acetic acid was thus evaporated, and the mixture was then held at 220~230°C for 6 hr. The reaction mixture was digested with hot 10% aqueous sulfuric acid and then strongly alkalified with concentrated aqueous ammonia to dissolve zinc chloride. The insoluble residue was extracted with benzene and, after separation, the benzene layer was extracted again with 10% aqueous sulfuric acid. The extract with dilute sulfuric acid was alkalified by the addition of aqueous ammonia, upon which yellow crystals separated out. Filtration gave 10.0 g. (87.5%) of crude II (m. p. 103~110°C), which on chromatography on alumina and then recrystallization from petroleum benzine afforded pale yellow needles (m.p. 118~118.5°C) (reported, 117~118°C[16]). (Found: C, 87.02; H, 5.71; N, 7.60%).

According to this procedure, the following acridines were prepared from the corresponding diarylamine, 2-methyl-, 4-methyl-, 2-chlorodiphenylamine, 1-phenyl- or 2-phenylnaphthylamine; 2, 9-dimethylacridine (III): pale yellow needles (from petroleum benzine), m. p. 89.5~90°C (reported, 90°C[16]). Yield, 45.5%. (Found: C, 86.62; H, 6.44; N, 6.86 %). 4, 9-Dimethylacridine (IV): pale yellow needles (from petroleum benzine), m. p. 53.5~54°C. Yield, 51.2%.

Found: C, 86.51; H, 6.03; N, 6.72. Calcd. for $C_{15}H_{13}N$: C, 86.92; H, 6.33; N, 6.76%.

2-Chloro-9-methylacridine (V): pale yellow needles (from petroleum benzine), m. p. 124~125°C (reported, 124°C[17]). Yield, 71.5%. (Found: C, 73.92; H, 4.50; N, 6.18%). 7-Methylbenz[c]acridine (VI): pale yellow scales (from benzene), m. p. 124~125°C (reported, 125.5°C[4]). Yield, 68.4%. (Found: C, 88.76; H, 5.09; N, 5.98%). 12-Methylbenz[a]acridine (VII): pale yellow scales (from benzene), m. p. 144~145°C (reported, 144~145°C[18]). Yield,

11) A. Palm and H. Werbin, *Can. J. Chem.*, 32, 858 (1954).
12) K. Nakamoto and R. E. Rundle, *J. Am. Chem. Soc.*, 78, 1113 (1956).
13) H. Shindo, *Chem. Pharm. Bull. Japan*, 7, 791 (1959).
14) All melting points are uncorrected.
15) A. Bernthsen, *Ann.*, **224**, 1 (1884). This synthesis of 9-substituted acridines consists of heating a mixture of an aromatic or aliphatic carboxylic acid with diphenylamine and zinc chloride at 200~270°C for about 20 hr.
16) H. Jensen and F. Rethwisch, *J. Am. Chem. Soc.*, 50, 1144 (1928).
17) A. Campbell et al. have reported that they obtained V by the reaction of 2, 9-dichloroacridine with ethyl sodiomalonate (*J. Chem. Soc.*, **1958**, 1145).
18) A. E. Porai-Koshits and G. S. Ter-Sarkisyan, *Izvest. Akad. Nauk S. S. S. R., Otdel. Khim. Sci.*, **1951**, 771. VI or VII was prepared by the reaction of the corresponding diarylamine with acetic anhydride in a 48.8 or a 26.8% yield respectively.

83.7%. (Found: C, 88.95; H, 5.21; N, 5.80%).

Reaction of 9-Methylacridine (II) with Nitrosobenzene (VIII).—To a solution of II (1.0 g.) and VIII (1.1 g.) dissolved in ethanol (50 ml.), HA (0.03 ml.) was added.[19] The resultant solution was refluxed on a water bath and, after one hour, additional VIII (0.5 g.) was placed into the reaction mixture: it was then refluxed for another hour. A large part of the ethanol was evaporated in vacuo, and the residue was allowed to stand overnight. Filtration gave the anil (XII) (0.52 g.) as yellowish brown crystals; m. p. 158~160°C. The filtrate was evaporated to dryness, and the residue obtained was dissolved in benzene. The benzene solution was chromatographed on alumina to separate XII (0.18 g.) (m. p. 159~160°C) and the nitrone (XIX) (m. p. 200°C (decomp.)) in a small amount. The combined anil (XII) was recrystallized from ethanol to give yellow scales; m. p. 161.5°C (reported, 163°C[3]). This compound was identical with the authentic substance which had been prepared by the condensation of acridine-9-carboxaldehyde (XXXV) and aniline. (Found: C, 85.15; H, 5.06; N, 9.88%). The recrystallization of the crude nitrone from ethanol afforded yellow prisms; m. p. 227°C (decomp.) (reported, 220°C (decomp.)). (Found: C, 80.04; H, 4.88; N, 9.45%).

Reaction of II with *p*-Nitrosodimethylaniline (IX).—To a solution of II (1.0 g.) and IX (1.6 g.) in ethanol (50 ml.), HA (0.2 ml.) was added. The refluxing of the reaction mixture resulted in the precipitation of reddish brown crystals in several minutes. After having been refluxed for 2 hr., the mixture was allowed to stand overnight. Filtration gave reddish brown crystals (1.39 g.) which, on washing with hot benzene (5ml.×2), left the nitrone (XX) (1.26 g.) (m. p. 240°C (decomp.)). Recrystallization from a large amount of benzene afforded reddish brown prisms; m. p. 243°C (decomp.) (reported, 243°C (decomp.)[3]). (Found: C, 77.90; H, 5.83; N, 12.31%). The benzene washings were evaporated to give a small amount of the anil (XIII) as red crystals which, on recrystallization from ethanol, afforded red prisms; m. p. 248°C (reported, 248°C[3]). (Found: C, 80.98; H, 5.86; N, 13.01%). The ethanol filtrate after reaction was concentrated in vacuo and then cooled to give 0.15 g. of a higher melting compound (XXXIV); m. p. over 300°C. (Found: C, 79.39, 79.29; H, 4.78, 4.71; N, 7.31, 7.71%).

The results of other reactions under varying conditions are shown in Figs. 1 and 2 and Table I.

Reaction of II with *p*-Nitrosodiethylaniline (X).—A solution of II (1.0 g.), X (1.7 g.) and HA (0.03 ml.) in ethanol (50 ml.) was refluxed for 2 hr. After a large part of the ethanol had been evaporated in vacuo, filtration afforded brown crystals (1.2 g.). The crystals were washed with 15 ml. and then with 5 ml. of hot benzene to leave 0.5 g. of the nitrone XXI, which, on recrystallization from ethanol, gave orange prisms (m. p. 207~208°C (decomp.)) (reported, 208°C (decomp.)[3]). (Found: 77.94; H, 6.30; N, 11.37%). The benzene washings were evaporated to give the anil XIV (0.4 g.), which, on recrystallization from ethanol, afforded dark violet prisms (m. p. 168~169°C (reported, 165°C[3])). (Found: C, 81.38; H, 6.66; N, 11.90%).

Reaction of II with *p*-Nitrosophenol (XI).—*With HA.*—A solution of II (1.0 g.), XI (1.3 g.) and HA (0.03 ml.) in ethanol (50 ml.) was refluxed for 3 hr. After the mixture had stood overnight, filtration afforded dark brown crystals (1.21 g.); m. p. 265~269°C. Recrystallization from chlorobenzene gave brown plates; m. p. 274~275°C. This compound was proved, by the admixed m. p. and by the infrared spectrum, to be identical with the anil (XV) (m. p. 275°C (reported, 225°C (decomp.)[9])) which was obtained from the condensation of the aldehyde XXXV and *p*-aminophenol.

Found: C, 80.20; H, 4.93; N, 9.24. Calcd. for $C_{20}H_{14}ON_2$: C, 80.52; H, 4.73; N, 9.39%.

With Potassium Carbonate.—The similar reaction of II (0.55 g.) with XI (0.7 g.) in the presence of potassium carbonate (40 mg.) in ethanol (30 ml.) gave 0.42 g. of the nitrone (XXII), which, on recrystallization from chlorobenzene, afforded dark yellowish green scales (m. p. 235°C (decomp.)) (reported, 230~231°C[9]).

Found: C, 75.99; H, 4.65; N, 9.09. Calcd. for $C_{20}H_{14}O_2N_2$: C, 76.42; H, 4.49; N, 8.91%.

Reaction of 2,9-Dimethylacridine (III) with IX.—A mixture of III (0.5 g.), IX (0.7 g.) and HA (0.02 ml.) in ethanol (50 ml.) was refluxed for 3 hr. and then allowed to stand overnight. Filtration gave crystals which, on being washed with hot benzene (5 ml.×8), left 30 mg. of red crystals; m. p. 217~219°C (decomp.). Recrystallization from chlorobenzene afforded red prisms of the nitrone (XXIII) (m. p. 220°C (decomp.)) (reported, 224~225°C[5]).

Found: C, 77.47; H, 5.70; N, 12.04. Calcd. for $C_{23}H_{21}ON_3$: C, 77.72; H, 5.96; N, 11.82%.

The benzene washings were evaporated in vacuo to give red crystals (0.65 g.), which, on recrystallization from benzene, afforded dark red prisms (m. p. 223°C). This compound was identical with the anil XVI obtained by the condensation of aldehyde XXXVI and *p*-dimethylaminoaniline, as will be mentioned below.

Found: C, 81.48; H, 6.53; N, 12.07. Calcd. for $C_{23}H_{21}N_3$: C, 81.39; H, 6.24; N, 12.38%.

In the presence of concentrated aqueous sodium carbonate (4 drops) in place of HA, the same reaction afforded the nitrone (0.19 g.).

2-Methylacridine-9-carboxaldehyde (XXXVI).—A mixture of XXIII (0.5 g.) in 12% aqueous hydrochloric acid (10 ml.) was heated on a water bath for 30 min. After the mixture had cooled, the precipitated crystals were filtrated and washed with aqueous ammonia. Yield, 0.295 g. (94.8%); m. p. 137~139°C. Recrystallization from the benzene-petroleum benzine mixture gave the aldehyde (XXXVI) as orange needles; m. p. 145°C (reported, 136~138°C[5]).

Found: C, 81.50; H, 5.23; N, 6.48. Calcd. for $C_{15}H_{11}ON$: C, 81.43; H, 5.01; N, 6.33%.

A mixture of XXXVI (0.1 g.), *p*-dimethylaminoaniline (0.1 g.) and acetic acid (1 drop) in ethanol

19) HA used in this experiment: d^{17} 1.1748.

(10 ml.) was refluxed for 2 hr. After the mixture had cooled, filtration afforded 0.14 g. (90.0%) of the anil XVI as dark red prisms (m. p. 223°C).

Reaction of 4, 9-Dimethylacridine (IV) with IX.—The similar treatment of IV (1.0 g.), IX (1.5 g.) and HA (0.03 ml.) in ethanol (50 ml.) gave benzene-soluble dark red crystals (0.61 g.) (m. p. 188~189°C) and benzene-insoluble orange crystals (0.75 g.) (m. p. 204~205°C (decomp.)). The recrystallization of the former from benzene afforded dark red prisms; m. p. 188~189°C. This compound was proved, by the admixed m. p. and infrared spectrum, to be identical with the anil XVII prepared by the condensation of the corresponding aldehyde XXXVIII and *p*-dimethylaminoaniline, as will be described below.

Found: C, 81.48; H, 6.53; N, 12.07. Calcd. for $C_{23}H_{21}N_3$: C, 81.39; H, 6.24; N, 12.38%.

The latter was recrystallized from chlorobenzene to afford orange plates (m. p. 207~208°C (decomp.)), whose infrared spectrum and elemental analyses showed the nitrone XXIV.

Found: C, 77.73; H, 5.99; N, 11.81. Calcd. for $C_{23}H_{21}ON_3$: C, 77.72; H, 5.96; N, 11.82%.

The reaction of IV (0.5 g.) with IX (0.75 g.) in the presence of concentrated aqueous sodium carbonate (4 drops) in ethanol (25 ml.) afforded 0.13 g. of the nitrone XXIV (m. p. 207~208°C (decomp.)).

4-Methylacridine-9-carboxaldehyde (XXXVIII).—The hydrolysis of 0.5 g. of the mixture of the anil XVII and nitrone XXIV obtained above with 12% aqueous hydrochloric acid (10 ml.) afforded the aldehyde XXXVIII (0.27 g.) (m. p. 112~113°C), which, on recrystallization from petroleum benzine, gave yellow needles (m. p. 114°C).

Found: C, 81.51; H, 5.34; N, 6.55. Calcd. for $C_{15}H_{11}ON$: C, 81.43; H, 5.01; N, 6.33%.

The anil XVII (m. p. 189°C) was quantitatively obtained by a condensation of the aldehyde XXXVIII and *p*-dimethylaminoaniline similar to that in the case of XXXVII.

Reaction of 2-Chloro-9-methylacridine (V) with IX.—A mixture of V (1.0 g.), IX (1.32 g.) and HA (0.03 ml.) in ethanol (50 ml.) was refluxed for 3 hr. After the mixture had stood overnight, the obtained crystals were dissolved in hot chlorobenzene (100 ml.). After they had cooled, filtration gave orange scales (0.62 g.) (m. p. 230°C (decomp.)), which, on recrystallization from chlorobenzene, showed a m. p. of 235°C (decomp.). This compound was confirmed as the nitrone XXV from the infrared spectrum and elemental analyses.

Found: C, 70.25; H, 5.14; N, 11.25. Calcd. for $C_{22}H_{18}ON_3Cl$: C, 70.30; H, 4.83; N, 11.18%.

The filtrate was evaporated in vacuo to give dark red crystals (0.86 g.), which, on recrystallization from chlorobenzene, showed a m. p. of 207~208°C. This compound was identical with the anil XVIII prepared from the corresponding aldehyde XXXIX and *p*-dimethylaminoaniline.

Found: C, 73.35; H, 5.23; N, 11.49. Calcd. for $C_{22}H_{15}N_3Cl$: C, 73.43; H, 5.04; N, 11.68.

The similar reaction of V (0.5 g.) with IX (0.66 g.) in the presence of concentrated aqueous sodium carbonate (4 drops) afforded the anil (0.34 g.) (m. p. 202~204°C), and a small amount of the nitrone.

2-Chloroacridine-9-carboxaldehyde (XXXIX).—The hydrolysis of 0.5 g. of the above mixture of the anil and nitrone with 12% aqueous hydrochloric acid gave 0.31 g. of the aldehyde XXXIX (m. p. 162~163°C), which, on recrystallization from petroleum benzine, afforded yellow needles (m. p. 169°C).

Found: C, 69.72; H, 3.35; N, 5.88. Calcd. for $C_{14}H_9ONCl$: C, 69.58; H, 3.34; N, 5.80%.

The condensation of XXXIX and *p*-dimethylaminoaniline similar to that in the case of XXXVII afforded the anil XVIII (m. p. 209°C) quantitatively.

Reaction of 7-Methylbenz[c]acridine (VI) with Nitroso Compound.—*With IX.*—To a solution of VI (2.0 g.) and IX (2.5 g.) in ethanol (70 ml.), HA (2 drops) was added, and the mixture was refluxed for 3 hr. After the mixture had stood overnight, filtration gave yellowish brown crystals (0.47 g.) (m. p. 220~228°C (decomp.)), which, on recrystallization from benzene, afforded the nitrone XXVIII as orange prisms (m. p. 240°C (decomp.)) (reported, 236~237°C (decomp.)[4]). (Found: C, 79.68; H, 5.40; N, 10.56%). The filtrate was evaporated to give a resinous material, which was then dissolved in benzene. The benzene solution was chromatogaphed on alumina to separate unreacted VI (0.79 g.) and red crystals (0.48 g.) (m. p. 188~197°C). The latter was recrystallized from benzene to give the anil XXVI as red prisms (m. p. 214~215°C).

Found: C, 83.24; H, 5.88; N, 11.24. Calcd. for $C_{26}H_{21}N_3$: C, 83.17; H, 5.64; N, 11.19%.

With X.—The similar treatment of VI (1.0 g.) with X (1.25 g.) in the presence of HA (1 drop) in ethanol (50 ml.) afforded unchanged VI and red crystals (0.61 g.) (m. p. 156~160°C), which, on recrystallization from ethanol, showed a m. p. of 167~168°C and appeared as red prisms. This red compound was proved to be the anil XXVII by its elemental analyses and infrared spectrum.

Found: C, 83.11; H, 6.23; N, 10.36. Calcd. for $C_{28}H_{25}N_3$: C, 83.34; H, 6.22; N, 10.41%.

Reaction of 12-Methylbenz[a]acridine (VII) with a Nitroso Compound.—*With IX.*—A solution of VII (1.0 g.) and IX (1.24 g.) in a mixture of ethanol (50 ml.) and HA (1 drop) was refluxed for 1 hr. After the mixture had cooled, filtration gave yellow needles (1.33 g.) (m. p. 234°C (decomp.)), which, on recrystallization from *o*-dichlorobenzene, showed a m. p. of 235°C (decomp.). This compound was proved to be the nitrone XXXII by its elemental analytical values and infrared spectrum.

Found: C, 79.62; H, 5.70; N, 10.75. Calcd. for $C_{26}H_{21}ON_3$: C, 79.77; H, 5.41; N, 10.73%.

The filtrate was then evaporated, and the residue was dissolved in benzene. The benzene solution was chromatographed on alumina to afford red prisms (m. p. 168~169°C) in a small amount. This compound was proved to be the anil XXX by its elemental analyses and infrared spectrum.

Found: C, 83.09; H, 5.60; N, 11.23. Calcd. for $C_{26}H_{21}N_3$: C, 83.17; H, 5.67; N, 11.19%.

With X.—A mixture of VII (1.0 g.), X (1.25 g.) and HA (1 drop) in ethanol (50 ml.) was heated

under reflux for 1 hr. After the reaction mixture had been concentrated in vacuo, filtration afforded yellow crystals (1.12 g.) (m. p. 204~205°C (decomp.)), which, on recrystallization from ethanol, gave yellow needles (m. p. 208~209°C (decomp.)). This compound was the nitrone XXXIII.

Found: C, 79.93; H, 5.89; N, 10.26. Calcd. for $C_{28}H_{25}ON_3$: C, 80.14; H, 6.00; N, 10.02%.

The authors are deeply grateful to Messrs. H. Matsui and K. Hikida of the Institute of Pharmaceutical Sciences of this university for their measurement of the infrared spectra, and to the staff of the Analytical Service Centre of this university for their elemental analyses.

The Research Institute of Science and Industry
Kyushu University
Hakozaki, Fukuoka

The Ultraviolet Absorption Spectra and the Hydrolysis of $\overset{4}{P}\text{-}\overset{3}{P}\text{-}\overset{4}{P}$-Acid[1]

By Norimasa YOZA and Shigeru OHASHI

(Received July 15, 1963)

It is well known that the popular and fundamental oxo acids of phosphorus, i. e., hypophosphorous, phosphorous, hypophosphoric, orthophosphoric, and condensed phosphoric acid, do not show any remarkable absorption in the ultraviolet wavelength region of 220~400 mμ. However, in the course of a systematic spectrophotometric study of the oxo acids of phosphorus, the authors found that some of the compounds which contain P–P linkages exhibit absorption spectra in that ultraviolet region. One of them is the oxo acid of phosphorus with lower oxidation numbers, which has the following structural formula and which is represented by the abbreviated formula indicated below (A chemical name has not yet been given to this acid):

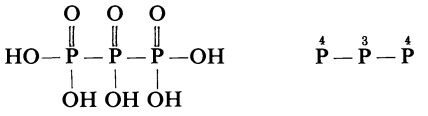

Acid form Abbreviated formula

The present investigation revealed that the absorption spectra of the $\overset{4}{P}\text{-}\overset{3}{P}\text{-}\overset{4}{P}$-acid vary remarkably with the pH of the solution and that this variation of the spectra can be explained in connection with a pH titration curve of this acid reported by Blaser and Worms.[2]

Blaser and Worms performed the hydrolysis of the $\overset{4}{P}\text{-}\overset{3}{P}\text{-}\overset{4}{P}$-acid in nitric acid solutions; its rates were measured by means of iodometric and bromometric titrations. In the present investigation, the hydrolysis of this acid was carried out in perchloric acid solutions in order to minimize the hindrance arising from the complex formation between an acid as a medium and metal ions, a formation of which will be encountered in a future study concerning the effect of the metal ions on the hydrolysis of the $\overset{4}{P}\text{-}\overset{3}{P}\text{-}\overset{4}{P}$-acid. The rates of its hydrolysis were readily determined by the ultraviolet spectrophotometric method. By the present investigation it was found that the rate constant of the hydrolysis of the $\overset{4}{P}\text{-}\overset{3}{P}\text{-}\overset{4}{P}$-acid increases linearly with the activity of perchloric acid.

Experimental

Materials.—The salts* of $\overset{1}{P}$-, $\overset{3}{P}$-, $\overset{5}{P}$-, and $\overset{5}{P}\text{-O-}\overset{5}{P}$-acid were commercial reagents, while the salts* of $\overset{3}{P}\text{-O-}\overset{3}{P}$, $\overset{2}{P}\text{-}\overset{4}{P}$-, $(\text{-}\overset{3}{P}\text{-})_6$-ring, $\overset{3}{P}\text{-O-}\overset{4}{P}\text{-}\overset{4}{P}$-, $\overset{4}{P}\text{-}\overset{3}{P}\text{-}\overset{4}{P}$-, $\overset{3}{P}\text{-O-}\overset{5}{P}$-, $\overset{4}{P}\text{-}\overset{4}{P}$-, $(\text{-}\overset{4}{P}\text{-}\overset{4}{P}\text{-O-})_2$-ring, $\overset{4}{P}\text{-}\overset{4}{P}\text{-O-}\overset{4}{P}\text{-}\overset{4}{P}$-, and $\overset{5}{P}\text{-O-}\overset{4}{P}\text{-}\overset{4}{P}$-acid were supplied by Blaser and Worms.

Buffer Solutions. — The pH of the solutions was adjusted with perchloric acid, citric acid, sodium acetate, sodium monohydrogen orthophosphate, sodium dihydrogen orthophosphate, sodium tetraborate decahydrate, sodium carbonate, and sodium hydroxide.[3]

1) Abbreviated formulas of this kind have been proposed by Blaser and Worms. The Arabic numerals attached to the phosphorus atoms represent their oxidation numbers. See B. Blaser and K.-H. Worms, *Z. anorg. u. allgem. Chem.*, **300**, 225 (1959).

2) B. Blaser and K.-H. Worms, ibid., **300**, 250 (1959).

* The chemical formulas of these salts were shown in a previous paper; cf. Ref. 4.

3) R. A. Robinson, "The Structure of Electrolytic Solutions," John Wiley & Sons Inc., New York (1959), p. 253.

The Measurement of Absorbances. — The measurement of absorbances was carried out with a Shimadzu photoelectric spectrophotometer QB-50 with 1.00 cm. silica cells. In order to keep the cell temperature constant, water of a constant temperature was circulated into a cell mount.

The Determination of the Rate Constants. — Hydrolytic reactions were started by mixing perchloric acid solutions and sample solutions, both of which had been preequilibrated thermally in a constant-temperature bath. The rate constants were calculated from the data obtained by measuring the decrease of the absorbances at 215 mμ with time.

Paper Chromatography and Colorimetry.—The ascending technique was employed for paper chromatographic identification[4] of reaction products. ^{3}P- and ^{4}P-^{4}P-acid were determined colorimetrically with a molybdenum(V)-molybdenum(VI) reagent.[5]

Results and Discussion

There have been no studies of the ultraviolet absorption spectra of oxo acids of phosphorus, especially of the lower oxo acids of phosphorus, which have been recently discovered. Therefore, it was first tested whether any of the oxo acids of phosphorus in aqueous solutions give absorption spectra in the ultraviolet region of 220~400 mμ. It was verified that, of ^{1}P-, ^{3}P-, ^{3}P-O-^{3}P-, ^{2}P-^{4}P-, ^{3}P-O-^{4}P-^{4}P-, ^{3}P-O-^{5}P-, ^{4}P-^{4}P-, ^{4}P-^{4}P-O-)$_2$-ring, ^{4}P-^{4}P-O-^{4}P-^{4}P-, ^{5}P-O-^{4}P-^{4}P-, ^{5}P-, and ^{5}P-O-^{5}P-acid in aqueous solutions none afford any ultraviolet absorption spectra. However, it was found that ^{4}P-^{3}P-^{4}P- and (-^{3}P-)$_6$- ring acid in aqueous solutions show characteristic absorption spectra in the ultraviolet region. It may be possible to analyze the ^{4}P-^{3}P-^{4}P- or (-^{3}P-)$_6$- ring acid quantitatively or qualitatively in the presence of other oxo acids of phosphorus by means of the ultraviolet absorption spectra. It is interesting to note that both of these acids have more than two P-P linkages in their structures.

In this paper only the absorption spectra of the ^{4}P-^{3}P-^{4}P-acid will be discussed. As for the (-^{3}P-)$_6$-ring acid, there are two maxima at 206 and 221 mμ in its absorption spectrum when the pH of the solution is 6.7. For the complete explanation of the absorption spectra of this acid, however, further investigation is required.

The Absorption Spectra of ^{4}P-^{3}P-^{4}P-Acid.—The absorption spectra of the ^{4}P-^{3}P-^{4}P-acid were measured at various pH values. As Figs. 1 and 2 show, the shapes of the absorption spectra vary remarkably with the pH change of the solutions.

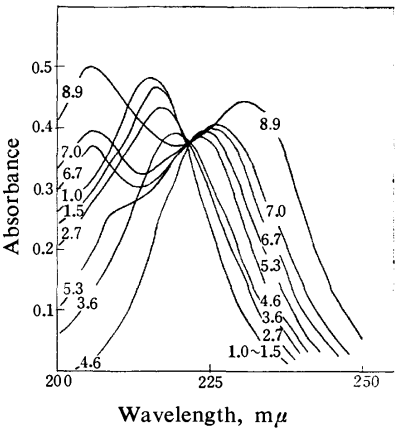

Fig. 1. pH dependence of the absorption spectra of ^{4}P-^{3}P-^{4}P-acid (1.54×10^{-4} M) in aqueous solutions (pH 1.0~8.9).

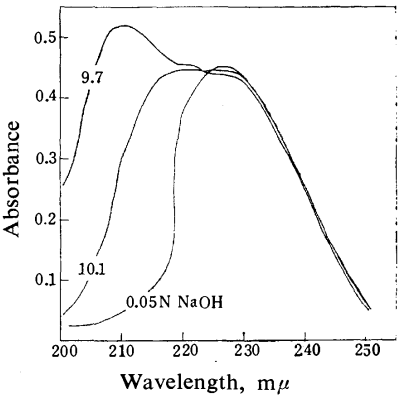

Fig. 2. pH dependence of the absorption spectra of ^{4}P-^{3}P-^{4}P-acid (1.54×10^{-4} M) in aqueous solutions (pH 9.7—0.05 N NaOH).

In an alkaline solution with a pH higher than 11, the spectrum exhibit the maximum absorption at the wavelength of 226 mμ. With the decreasing pH of the solution, the absorbance in the range of the shorter wavelengths increases. Thus, for instance, the absorption spectrum taken at pH 8.9 has two maxima at 205 and 230 mμ. With a further decrease of pH, the peak at 205 mμ diminishes, the maximum at 230 mμ shifts towards the shorter wavelength, and at last the absorption spectrum with only one peak appears. For example, at pH 4.6 one can observe a spectrum with its maximum at 224 mμ only.

When the pH of the solution decreases further, the maximum shifts more and more towards the shorter wavelength side while, at

4) S. Ohashi and N. Yoza. This Bulletin, 36, 707 (1963).
5) N. Yoza and S. Ohashi, report presented at the 16th Annual Meeting of the Chemical Society of Japan, Tokyo, April, 1963.

the same time, its absorbance increases. At pH 1 the spectrum indicates a maximum at 215 mμ. In the range of pH lower than 1, the absorption maximum at 215 mμ is always observed. However, in this range, the $\overset{4}{P}\text{-}\overset{3}{P}\text{-}\overset{4}{P}$-acid is unstable, and the intensity of the absorbance decreases with time.

There have been reports on the pH dependence of the absorption spectra of some dibasic acids, such as sulfurous acid.[3] In these cases the variations of the absorption spectra with the pH value have been attributed to the transformation between ionized and unionized species of the molecule in question.

As for $\overset{4}{P}\text{-}\overset{3}{P}\text{-}\overset{4}{P}$-acid, an analogous discussion is possible in comparison with the pH titration data for this acid. The pH titration curve[2] of $\overset{4}{P}\text{-}\overset{3}{P}\text{-}\overset{4}{P}$ acid exhibits three inflection points at pH values, ca. 11, 9 and 5, corresponding to $P_3O_8^{5-}$, $HP_3O_8^{4-}$ and $H_2P_3O_8^{3-}$ respectively.

It is reasonable to assign the characteristic ultraviolet absorption spectra of $\overset{4}{P}\text{-}\overset{3}{P}\text{-}\overset{4}{P}$-acid to three successively ionized species, $P_3O_8^{5-}$, $HP_3O_8^{4-}$, and $H_2P_3O_8^{3-}$, and to one unionized species, $H_5P_3O_8$, as indicated in Table I. The peak at 226 mμ is attributed to the negatively-charged anion formed by the removal of five protons from the unionized molecule, while the spectrum with the maxima at 205 and 230 mμ is assigned to the unsymmetrical species with four negative charges. Similarly, the spectrum with the maximum at 224 mμ is ascribed to the species with three negative charges, and the spectrum with the maximum at 215 mμ, to the unionized species of $\overset{4}{P}\text{-}\overset{3}{P}\text{-}\overset{4}{P}$-acid.

Table I. Relation between the ultraviolet absorption spectra of the $\overset{4}{P}\text{-}\overset{3}{P}\text{-}\overset{4}{P}$-acid and pH of the solutions

Species	Stability	Maximum of the spectrum mμ	pH of the solution
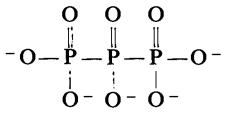	Stable	226	11
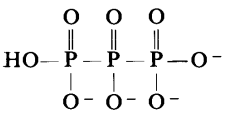	Stable	205 230	9
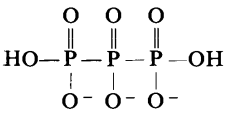	Stable	224	5
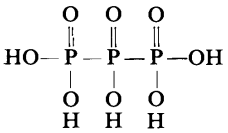	Unstable (hydrolysis)	215	1

The Hydrolytic Decomposition of $\overset{4}{P}\text{-}\overset{3}{P}\text{-}\overset{4}{P}$-Acid.—The rate of the hydrolysis of $\overset{4}{P}\text{-}\overset{3}{P}\text{-}\overset{4}{P}$-acid is quite slow in a solution of low acidity, but it is catalytically accelerated by the addition of acid. It was confirmed by Blaser and Worms[2] that the hydrolysis of $\overset{4}{P}\text{-}\overset{3}{P}\text{-}\overset{4}{P}$-acid in 1.5 N nitric acid proceeds by the following two paths;

$$\overset{4}{P}\text{-}\overset{3}{P}\text{-}\overset{4}{P}\text{-Acid} \rightarrow \overset{3}{P}\text{-Acid} + \overset{4}{P}\text{-}\overset{4}{P}\text{-Acid} \quad \text{(A)}$$

$$\overset{4}{P}\text{-}\overset{3}{P}\text{-}\overset{4}{P}\text{-Acid} \rightarrow \overset{5}{P}\text{-Acid} + \overset{2}{P}\text{-}\overset{4}{P}\text{-Acid} \rightarrow \overset{5}{P}\text{-Acid} + 2\overset{3}{P}\text{-Acid} \quad \text{(B)}$$

Table II. Rate constants of the hydrolysis of the $\overset{4}{P}\text{-}\overset{3}{P}\text{-}\overset{4}{P}$-acid in perchloric acid solutions of various concentrations (measured at 215 mμ and 30.4°C)

No.	Concentrations of perchloric acid, N	Rate constants, min^{-1}
1	0.240	6.98×10^{-4}
2	0.480	1.73×10^{-3}
3	0.720	2.50×10^{-3}
4	0.960	3.30×10^{-3}
5	1.20	4.07×10^{-3}
6	1.44	4.90×10^{-3}
7	1.68	7.16×10^{-3}
8	1.92	8.92×10^{-3}
9	2.16	1.04×10^{-2}
10	2.40	1.34×10^{-2}
11	2.64	1.61×10^{-2}
12	2.88	1.88×10^{-2}

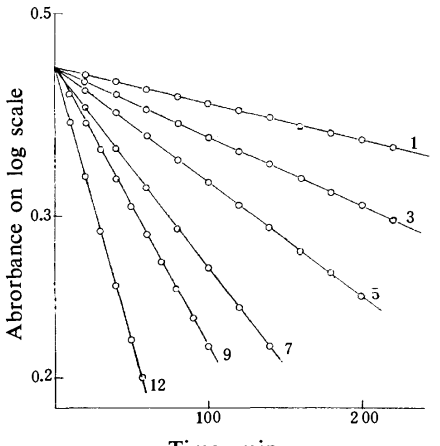

Fig. 3. The hydrolysis of $\overset{4}{P}\text{-}\overset{3}{P}\text{-}\overset{4}{P}$-acid ($1.64\times10^{-4}$ M) in perchloric acid.
The numbers in this figure correspond to the numbers in Table II.

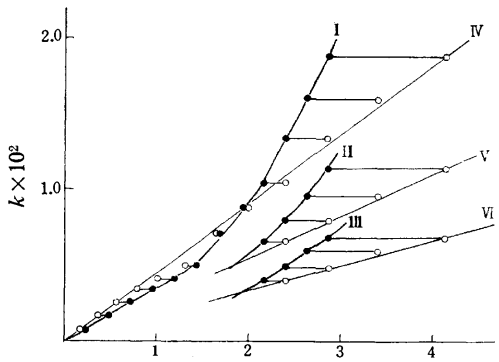

Fig. 4. Relationship between the rate constant, k, of the hydrolysis of $^{4}_{}\text{P}\text{-}^{3}_{}\text{P}\text{-}^{4}_{}\text{P}$-acid and the concentration of perchloric acid.
I, II and III; k vs. normality at 30.4, 25.0 and 20.0°C
IV, V and VI; k vs. activity at 30.4, 25.0 and 20.0°C

and that 82% of the $^{4}_{}\text{P}\text{-}^{3}_{}\text{P}\text{-}^{4}_{}\text{P}$-acid is decomposed by Path A and 18% of it by Path B.

However, it was found by the present investigation, paper chromatographically and colorimetrically, that equimolar amounts of $^{3}_{}\text{P}$ and $^{4}_{}\text{P}\text{-}^{4}_{}\text{P}$-acid are produced by the hydrolysis of the $^{4}_{}\text{P}\text{-}^{3}_{}\text{P}\text{-}^{4}_{}\text{P}$-acid in perchloric acid solutions. Therefore, it was concluded that the hydrolysis of the $^{4}_{}\text{P}\text{-}^{3}_{}\text{P}\text{-}^{4}_{}\text{P}$-acid in perchloric acid solutions proceeds only by Path A. The difference between the reaction mechanisms for the hydrolysis of the $^{4}_{}\text{P}\text{-}^{3}_{}\text{P}\text{-}^{4}_{}\text{P}$-acid in nitric acid and in perchloric acid solutions can not be explained at the present state of knowledge.

The decrease in the concentration of $^{4}_{}\text{P}\text{-}^{3}_{}\text{P}\text{-}^{4}_{}\text{P}$-acid by hydrolysis can be readily pursued by measuring the absorbances at 215 mμ due to the unionized species of this acid, because the hydrolysis products, $^{3}_{}\text{P}$- and $^{4}_{}\text{P}\text{-}^{4}_{}\text{P}$- acid, do not show any absorption. As shown in Fig. 3, the hydrolysis of $^{4}_{}\text{P}\text{-}^{3}_{}\text{P}\text{-}^{4}_{}\text{P}$-acid follows the first order rate law. Thus, the rate constant, k, is calculated from the equation:

$$k=\{2.303/(t_2-t_1)\}\log(E_1/E_2)$$

where E_1 and E_2 represent the absorbances at 215 mμ measured at the times t_1 and t_2 respectively. The rate constants obtained for the disappearance of the $^{4}_{}\text{P}\text{-}^{3}_{}\text{P}\text{-}^{4}_{}\text{P}$-acid in the perchloric acid solutions of various concentrations at 30.4°C are presented in Table II, from which it can be seen that the rate constant increases considerably with the increase in the acidity.

In Fig. 4, the rate constants measured at 30.4, 25.0 and 20.0°C are plotted against the normalities and activities of perchloric acid. Since there are not sufficient data on the activity coefficients of perchloric acid, some of them have been obtained graphically by interpolation from the known data[6] for 0.1, 0.2, 0.3, 0.4, 0.5, 0.6, 0.7, 0.8, 0.9, 1.0, 1.2, 1.4, 1.6, 1.8, 2.0, 2.5, and 3.0 N perchloric acid. It can be concluded that there is a linear relationship between the rate constant of the hydrolysis of the $^{4}_{}\text{P}\text{-}^{3}_{}\text{P}\text{-}^{4}_{}\text{P}$-acid and the activity of perchloric acid.

Activation Energy.—From the rate constants measured at three different temperatures, one can estimate the activation energy for the hydrolysis of $^{4}_{}\text{P}\text{-}^{3}_{}\text{P}\text{-}^{4}_{}\text{P}$-acid to be 16.6 kcal. per mol. This value is considerably smaller than that for the hydrolysis at the P–P linkage of hypophosphoric acid, 20~25 kcal. per mol.[7]

Summary

It has been found that $^{4}_{}\text{P}\text{-}^{3}_{}\text{P}\text{-}^{4}_{}\text{P}$-acid in aqueous solutions shows characteristic ultraviolet absorption spectra, which vary remarkably with the pH change of the solutions. The spectra having absorption maxima at 226, both 205 and 230, 224, and 215 mμ can be assigned to $P_3O_8^{5-}$, $HP_3O_8^{4-}$, $H_2P_3O_8^{3-}$, and $H_5P_3O_8$ respectively.

The rates of the hydrolysis of the $^{4}_{}\text{P}\text{-}^{3}_{}\text{P}\text{-}^{4}_{}\text{P}$-acid in the perchloric acid solutions have been determined by measuring the absorbance at 215 mμ. The hydrolysis follows the first order rate law. The hydrolysis products are $^{3}_{}\text{P}$- and $^{4}_{}\text{P}\text{-}^{4}_{}\text{P}$-acid. The rate constant is in the linear function with the activity of perchloric acid. The activation energy has been estimated to be 16.6 kcal. per mol.

The authors wish to express their hearty thanks to Professor Jun Yoshimura for his kind suggestions made in the course of this work. The authors also wish to thank Dr. Bruno Blaser and Dr. Karl-Heinz Worms for supplying the samples used in this study.

Department of Chemistry
Faculty of Science
Kyushu University
Hakozaki, Fukuoka

6) "Handbook of Analytical Chemistry," McGraw-Hill Book Company Inc., New York (1963), p. 10.
7) J. R. Van Wazer, "Phosphorus and its Compounds," Interscience Publishers, New York (1958), p. 411.

The Chemical Compositions of Crystals and Glasses of the $NaPO_3$-Na_2SiO_3 and $NaPO_3$-SiO_2 Systems

By Shigeru OHASHI and Fumio OSHIMA*

(Received July 20, 1963)

Several attempts to prepare condensed phosphates containing other oxoacid anions have been made. Thilo and his coworkers[1-7] have, for instance, succeeded in making condensed arsenate-phosphates,** which are composed of P-O-P, As-O-P, and As-O-As linkages. Some investigations have been carried out of the chemical compositions of condensed sulfate-phosphates[8] and condensed vanadate-phosphates,[9] which contain S-O-P and V-O-P linkages respectively.

Silicic acid has a tendency toward polymerization, which in turn leads to the formation of various condensed silicates. From the structural analogy between condensed phosphates and condensed silicates, it is to be expected that condensed phosphate-silicates containing P-O-Si linkages will be formed. Investigations[10-12] of the reaction of silicic acid with orthophosphoric acid have revealed the existence of silicon diphosphate, SiP_2O_7. An investigation of the CaO-P_2O_5-SiO_2 system by du Plessis[13] has disclosed that when a glass of calcium phosphate-silicate is dissolved in water, it gives a mixture of polyphosphates the average chain length of which decreases with the increase in the silicon dioxide content of the glass. Some physical and chemical properties of glasses of the Na_2O-P_2O_5-SiO_2, Na_2O-P_2O_5-B_2O_3, and Na_2O-P_2O_5-Al_2O_3 systems have recently been reported by Takahashi.[14] Although the $NaPO_3$-SiO_2 and KPO_3-SiO_2 systems have also been studied by du Plessis,[13] there have not been sufficient data available on the chemical compositions of the substances belonging to these systems.

The present investigation was undertaken to determine the chemical compositions of crystals and glasses of $NaPO_3$-Na_2SiO_3 and $NaPO_3$-SiO_2 systems. It was found by this work that glassy substances of these systems contain P-O-Si linkages, but not crystalline substances.

Experimental

Glassy Substances. — In a platinum crucible a certain amount (4~12 g.) of monosodium dihydrogen orthophosphate dihydrate was dehydrated and melted by heating and then converted into a glass of sodium metaphosphate (Graham's salt) by cooling the melt in the platinum crucible. In the case of the $NaPO_3$-Na_2SiO_3 system, after the weight of the glass had been measured, calculated amounts of silicon dioxide and of sodium carbonate were placed on the glass in the crucible. As for the $NaPO_3$-SiO_2 system, a mixture of only sodium metaphosphate and silicon dioxide was used. Then, the mixture of these two or three materials was melted at 1400°C for 1.5 hr. The melt was quenched by pouring it onto a copper plate and by pressing it with another copper plate. By this procedure, glasses of the $NaPO_3$-Na_2SiO_3 system with P/Si ratios of 6, 10, 15, 20, 30, 50, 75, 100 and 200, and glasses of the $NaPO_3$-SiO_2 system with P/Si ratios of 10, 20 and 50 were prepared. All the glasses thus obtained were colorless.

Crystalline Substances. — A mixture of sodium metaphosphate, silicon dioxide, and sodium carbonate or a mixture of sodium metaphosphate and silicon dioxide was heated at 1500°C for 1.5 hr. The melt was crystallized by cooling it slowly down to 200°C at the rate of 100°C/hr. By this treatment, crystals of the $NaPO_3$-Na_2SiO_3 system with P/Si ratios of 0.5, 0.7, 0.85, 1, 1.15, 1.3, 1.5, 2, 3 and 4, and crystals of the $NaPO_3$-SiO_2 system with P/Si ratios of 0.5, 1, 2, 3 and 4

* Present address: Laboratory of Chemistry, Fukuoka Gakugei University, Shiobaru, Fukuoka.

** These compounds are tentatively named by the present authors according to Rule 6.3 for double salts, triple salts, etc. in "Nomenclature of Inorganic Chemistry" reported by the commission of International Union of Pure and Applied Chemistry in 1957.

1) E. Thilo and I. Plaetschke, *Z. anorg. u. allgem. Chem.*, **260**, 297 (1949).
2) E. Thilo and G. Schulz, ibid., **266**, 34 (1951).
3) E. Thilo, G. Schulz and E.-M. Wichmann, ibid., **272**, 182 (1953).
4) E. Thilo and L. Kolditz, ibid., **278**, 122 (1955).
5) E. Thilo and K. Dostál, ibid., **298**, 100 (1959).
6) I. Grunze, K. Dostál and E. Thilo, ibid., **302**, 221 (1959).
7) F. Wodtcke and E. Thilo, *Monatsberichte der Deutschen Akademie der Wissenschaften zu Berlin*, **1**, 508 (1959).
8) K. J. Shaver and J. G. Stites, Jr., "The Heteropolymeric System Na_2O-P_2O_5-SO_3," a report presented at the 131st National Meeting of the American Chemical Society, Miami, Florida, April, 1957.
9) S. Ohashi and T. Matsumura, This Bulletin, **35**, 501 (1962).
10) A. Boulle and R. Jary, *Compt. rend.*, **237**, 161, 328 (1953).
11) R. Jary, *Ann. Chim. (Paris)*, [13], **2**, 58 (1957).
12) V. N. Sveshnikova and E. P. Danilva, *Zhur. Neorg. Khim.*, **2**, 928 (1957).
13) D. J. du Plessis, *Angew. Chem.*, **71**, 697 (1959).
14) K. Takahashi, "Binary Phosphate, Silicophosphate, Borophosphate and Aluminophosphate Glasses, their Properties and Structure," a report presented at the 6th International Congress on Glass, Washington, July, 1962.

were prepared. All the crystals thus obtained were white.

X-Ray Diffractometry. — The samples were ground with an agate mortar until they could pass through a 150 mesh screen. Their diffraction patterns were taken with a Rigaku Denki Geigerflex diffractometer with nickel-filtered CuK_α radiation.

Paper Chromatography. — Solvents A and B as reported by Bernhart and Chess[15] were used. Solvent A was made by mixing 25 ml. of a 20% trichloroacetic acid solution, 10 ml. of water, and 65 ml. of acetone. Solvent B was made by mixing 25 ml. of a 20% trichloroacetic acid solution, 17 ml. of water, and 58 ml. of acetone.

Solvent A was used for the separation of ortho-, di-, tri-, trimeta-, and long-chain- phosphates. A sample solution was placed at the center of a circular paper, 18 cm. in diameter, of Toyo No. 51A and developed for 2 hr. at 10~12°C.

Solvent B was used for the separation of individual chain phosphates from ortho- through tridecaphosphate and long-chain phosphates. Filter paper of Toyo No. 51A was cut into a sheet of 60 by 8 cm., with one end tapered to leave a central 5 by 0.8 cm. strip. The sample solution was placed at the upper end of the central strip of the paper sheet and developed for 5 days at 5°C.

After it had dried, the paper was sprayed with a perchloric acid-molybdate solution so as to convert the phosphates into molybdophosphate. After it had again dried, the paper was exposed to ultraviolet radiation in order to reduce the molybdophosphate a blue complex. Each phosphate species on the paper chromatogram was identified by the similar treatment of a reference solution of a known mixture of phosphates.

The demarcation between the bands was made close to the rear edge of each band in order to minimize the effects of hydrolysis, and the elution of each band was carried out by Smith's[16] method. The paper was cut at the demarcation line, and each band was placed in a 25 ml. Erlenmeyer flask, to which 10 ml. of 0.1 N ammonia was added. The resulting solution was transferred into a 25 ml. volumetric flask, and 10 ml. of water and 2 ml. of Lucena-Conde and Prat's reagent[17] were added. All the bands from each paper must be treated in the same way. Therefore, all the flasks containing solutions from one paper were placed in a boiling water bath at one time, removed at the same time after they had been heated for 1 hr., cooled, and diluted to the mark with water. The absorbance of the solution was measured with a Hirama electrophotometer at 800 mμ.

Lucena-Conde and Prat's Reagent.[17] — Ammonium molybdate tetrahydrate (8.15 g.) was dissolved in 60 ml. of water. To 30 ml. of this solution, 50 ml. of 12 N hydrochloric acid and 56 ml. of 36 N sulfuric acid were slowly added. After the mixture had cooled, 12 N hydrochloric acid was added to bring the volume back to 136 ml. To 25 ml. of the initial molybdate solution, 12.5 ml. of 12 N hydrochloric acid, 12.5 ml. of water, and finally, 10 ml. of mercury were added in turn. The mixture was shaken for 5 min. and filtered to obtain 40 ml. of a ruby-red solution of molybdenum (V). This ruby-red solution was stirred into the acid solution of molybdenum(VI) mentioned above and diluted to 200 ml. to give an emerald green solution.

The Measurement of the Average Chain Length of Polyphosphates. — In a 250 ml. Erlenmeyer flask, 0.1~1 g. of a glass was dissolved in about 150 ml. of water. After most of the silicate ions in the sample solution had been deposited, the deposit was filtered off. According to the pH titration method proposed by Van Wazer, Griffith, and McCullough,[18,19] the average chain length (polymerization degree) of the polyphosphates produced by the hydrolysis of a given sample was measured as follows.

An appropriate amount of the filtrate was acidified with dilute hydrochloric acid and then titrated with 0.1 N sodium hydroxide. The volume of the 0.1 N sodium hydroxide consumed between two inflection points located at approximately pH 4.5 and 9.5 was measured. Another suitable amount of the filtrate was mixed with 0.2 g. of potassium chloride and boiled with hydrochloric acid in order to hydrolyze completely all the condensed phosphates. The residue was treated with water and then titrated with the 0.1 N sodium hydroxide. If the titer for the first titration per unit weight of the sample is A and if the titer for the second one is A_h, the average chain length, $\bar{n}$, is given by the equation, $\bar{n}=2A_h/A$, on the assumption that ortho- and ring phosphates are not present.

Results and Discussion

The samples of both $NaPO_3$–Na_2SiO_3 and $NaPO_3$-SiO_2 systems with P/Si ratios smaller than 4 were obtained as crystalline substances containing amorphous substances. The chemical compositions of these crystalline substances can be estimated from the data obtained by the X-ray diffractometry and the paper chromatography. When the samples are treated with water, all the phosphates are dissolved in it. As for silicon, crystalline silicon dioxide is not dissolved in water, while a greater part of the soluble silicates deposits, only a smaller part of it remaining in the solution. Although the paper chromatographic behavior of silicate ions in the sample solution has not been confirmed, silicate ions do not interfere at all with the separation of condensed phosphates.

The data for the $NaPO_3$–Na_2SiO_3 system with P/Si ratios of 0.5~4.0 are given in Table I. In the X-ray diffraction patterns of the samples with P/Si ratios of 0.85~1.50,

15) D. N. Bernhart and W. B. Chess, *Anal. Chem.*, 31, 1026 (1959).
16) M. J. Smith, ibid., 31, 1023 (1959).
17) F. Lucena-Conde and L. Prat, *Anal. Chim. Acta*, 16, 473 (1957).
18) J. R. Van Wazer, E. J. Griffith and J. F. McCullough, *Anal. Chem.*, 26, 1755 (1954).
19) E. J. Griffith, ibid., 28, 525 (1956).

TABLE I. CHEMICAL COMPOSITIONS OF SUBSTANCES OF THE $NaPO_3$-Na_2SiO_3 SYSTEM WITH P/Si RATIOS OF 0.500~4.00

P/Si	X-Ray diffractometry					Paper chromatography			
	Phosphate				α-Cristobalite	Phosphate, P%			
	Ortho	Unknown (ortho)	Di	Tri*		Ortho	Di	Tri	Higher
0.500	###	±	±	−	±	100	0	0	0
0.700	###	±	±	−	±	100	0	0	0
0.850	−	###	±	−	±	100	0	0	0
1.00	−	###	±	−	###	100	0	0	0
1.15	−	###	+	−	###	85.8	14.2	0	0
1.30	−	###	##	−	###	65.1	34.9	0	0
1.50	−	###	###	−	###	51.7	48.3	0	0
2.00	−	+	###	−	###	16.4	83.6	0	0
3.00	−	−	###	###	##	0	43.7	53.1	3.2
4.00	−	−	##	###	+	0	26.7	64.5	8.8

* High temperature form

there are unknown peaks of a strong intensity at spacings of 2.63 and 4.29 Å and of a medium intensity at spacings of 2.79 Å. According to an unpublished paper by Ohashi and Ikeda, these unknown peaks, which have been observed for certain samples of the $NaPO_3$-Na_2SO_4 system, are assumed to be due to one of the modifications of trisodium orthophosphate. The discussions below are based on this assumption.

The crystalline substance of the sample with the P/Si ratio of 1.00 is composed of trisodium orthophosphate and α-cristobalite. Therefore, it is quite evident that when a mixture of sodium metaphosphate and sodium metasilicate with a mole ratio of 1 : 1 is melted, the following reaction occurs:

$$NaPO_3 + Na_2SiO_3 \rightarrow Na_3PO_4 + SiO_2 \quad (1)$$

The crystalline substances of the samples with P/Si ratios smaller than 1.00 contain trisodium orthophosphate but not α-cristobalite. For these samples, the silicon dioxide produced by Eq. 1 reacts further with an excess of sodium metasilicate to form a glassy sodium silicate. The crystalline substances of the samples with P/Si ratios larger than 1.00 contain α-cristobalite and two of the following three phosphate species; trisodium orthophosphate, tetrasodium diphosphate, and pentasodium triphosphate (high-temperature form). The α-cristobalite content in these samples, of course, decreases with the increase in the P/Si ratio. The orthophosphate content decreases and that of diphosphate increases when the P/Si ratio increases from 1.00 to 2.00. With the further increase in the P/Si ratio, the diphosphate content decreases and that of triphosphate increases. These facts indicate that the trisodium orthophosphate produced by Eq. 1 reacts further with an excess of sodium metaphosphate to form di- and triphosphate.

Small amounts of chain phosphates longer than triphosphate were found in the aqueous solutions of the samples with P/Si ratios of 3.00 and 4.00. Since anhydrous crystals of such chain phosphates as hexasodium tetraphosphate and heptasodium pentaphosphate have not been obtained as yet, it is reasonable to consider that the chain phosphates longer than triphosphate in the samples mentioned above compose an amorphous phase, in which di- and triphosphate are probably incorporated to some extent.

The data for the $NaPO_3$-SiO_2 system with P/Si ratios of 0.5~4.0 are given in Table II. The crystalline phases of all the samples are composed of α-cristobalite and trisodium trimetaphosphate. Some of them also contain small amounts of α-tridymite. Ortho-, di-, and triphosphates were found by paper chromatography in the aqueous solutions of the samples. These ortho- and chain phosphates may be derived from amorphous substances, because the X-ray diffraction patterns of these samples do not exhibit any peaks due to phosphates other than trisodium trimetaphosphate. However, the structure of these amorphous substances can not be determined from only the data presented here. It was disclosed that the crystalline substances of neither system contains P–O–Si linkages.

When the samples of the glassy substances with P/Si ratios larger than 6 are treated with water, almost all of the silicate ions deposit as silicic acid. All phosphate species and a trace amount of silicate ions come into the solution. The compositions of the phosphate species in the sample solutions were determined

TABLE II. CHEMICAL COMPOSITIONS OF SUBSTANCES OF THE $NaPO_3$-SiO_2 SYSTEM WITH P/Si RATIOS OF 0.500~4.00

P/Si	X-Ray diffractometry			Paper chromatography phosphate, P%		
	Trimeta-phosphate	α-Cristo-balite	α-Tridy-mite	Ortho	Di+Tri	Trimeta
0.500	+	##	−	4.8	20.5	74.7
1.00	##	##	+	0.9	20.7	78.4
2.00	##	##	+	1.0	21.3	77.4
3.00	##	##	+	1.6	21.9	76.5
4.00	##	##	±	1.8	21.8	76.4

TABLE III. CHEMICAL COMPOSITIONS OF POLYPHOSPHATES PRODUCED BY THE HYDROLYSIS OF GLASSY SUBSTANCES OF THE $NaPO_3$-Na_2SiO_3 AND $NaPO_3$-SiO_2 SYSTEMS

P/Si	Phosphate, P%													
	Ortho	Di	Tri	Tetra	Penta	Hexa	Hepta	Octa	Ennea	Deca	Hen-deca	Do-deca	Tri-deca	High poly
The $NaPO_3$-Na_2SiO_3 system														
6.00	3.1	12.8	14.4	16.8	14.7	10.8	7.6	5.2	4.3	3.2	2.4	4.7		0
10.0	2.7	11.1	11.3	11.5	12.3	9.8	8.4	7.2	5.7	4.6	3.3	3.0	2.8	6.3
15.0	2.3	8.8	9.3	9.4	10.7	8.7	8.3	7.6	5.3	4.8	3.7	3.3	2.9	14.9
20.0	1.9	5.6	6.1	7.8	9.1	7.6	7.8	7.1	6.3	5.3	3.8	3.7	3.4	24.5
30.0	1.3	3.5	4.5	4.7	7.4	5.3	6.2	5.9	4.9	4.9	3.5	3.3	3.1	41.5
50.0	0.6	2.2	3.6	3.0	5.0	4.5	5.2	4.0	4.5	4.0	3.0	2.8	2.6	55.0
75.0	0.4	1.3	2.0	2.2	4.3	3.2	4.3	3.5	3.5	3.6	2.3	1.9	1.8	65.7
100	0.3	1.2	1.3	1.9	2.8	2.1	3.2	3.3	2.8	2.4	2.1	1.8	1.7	73.1
200	0.3	0.6	0.7	1.1	2.9	1.4	2.2	1.8	2.1	1.8	1.7	1.4	1.3	80.7
The $NaPO_3$-SiO_2 system														
10.0	2.3	7.1	7.2	7.4	8.0	7.4	6.8	5.8	5.6	4.6	4.3	3.9	2.9	26.7
20.0	1.5	4.5	4.8	5.7	7.5	5.7	5.9	5.8	5.0	4.6	3.8	3.1	3.1	39.0
50.0	0.7	2.1	3.1	3.5	5.8	3.7	5.2	3.4	4.1	3.7	3.3	2.8	2.5	56.1
R_f	0.72	0.58	0.52	0.47	0.42	0.37	0.32	0.27	0.23	0.19	0.16	0.13	0.11	

by paper chromatography. The results for the samples of the $NaPO_3$-Na_2SiO_3 and $NaPO_3$-SiO_2 systems are given in Table III. By the technique employed in the present investigation, it was possible to separate each member of the chain phosphates from orthophosphate through tridecaphosphate. The contents of the chain phosphats longer than tridecaphosphate were determined as a whole and are given as high polyphosphates in Table III.

Paper chromatograms developed with Solvent B for the reference solutions of trimeta- and tetrametaphosphate reveal that trimeta- and tetrametaphosphate have the same R_f values as penta- and heptaphosphate respectively. The paper chromatographic analysis by the use of Solvent A disclosed that the sample solutions contain small quantities of trimeta-, tetrametaphosphate, and, probably, ring phosphates larger than tetrametaphosphate. For instance, in the solutions of the samples of the $NaPO_3$-Na_2SiO_3 system with P/Si ratios of 10 and 20, 2.1 and 2.0 percent of the phosphorus are present as trimetaphosphate, and 1.1 and 1.5 per cent of the phosphorus, as tetrametaphosphate respectively. Therefore, the true penta- and heptaphosphate contents are considered to be a little smaller than the values given in Table III. Although it is not sure where the ring phosphates larger than tetrametaphosphate are located on the paper chromatograms developed with Solvent B, their quantities are probably small enough to be disregarded. When the P/Si ratio increases, the contents of the chain phosphates from ortho- to hexaphosphate decrease, while those of the high polyphosphates increase. With the increase in the P/Si ratio, the contents of the chain phosphates from hepta- to tridecaphosphate first increase and then decrease. If all the distributions of the phosphate species are considered, it is evident that the average chain length of the polyphosphates increases with the increase in the P/Si ratio. Conversely speaking, when the quantity of sodium metasilicate added to a sodium metaphosphate

glass increases, the contents of the shorter chain phosphates in the sample solutions increase.

The average chain lengths of the polyphosphates in the sample solutions were determined by the pH titration method. Since the quantities of orthophosphate and ring phosphates in the sample solutions are less than several per cent, the effect of their presence on the calculation of the average chain length of the polyphosphates is disregarded in the following discussion. The fact that the average chain length, $\bar{n}$, increases in the P/Si ratio is indicated by curves A and B in Fig. 1. It is well known that the average chain length, $\bar{n}$, of polyphosphates in a sodium phosphate glass is given by the equation, $Na/P=(\bar{n}+2)/\bar{n}$, where Na/P is the atomic ratio of both the elements. Assuming that there is no interaction between a sodium phosphate glass and silicon dioxide in a melted state, one can calculate the average chain length of polyphosphates in the sample solution. If the P/Si ratio of the $NaPO_3$-Na_2SiO_3 system is x, the Na/P ratio is equal to $(x+2)/x$ and, therefore, $\bar{n}$ is equal to x. Curve C in Fig. 1 indicates this relation, $\bar{n}=x$. The great discrepancy between curves A and C means that the above assumption is not correct. As for the $NaPO_3$-SiO_2 system, the average chain length of polyphosphates based on the same assumption should be the same as that of a sodium metaphosphate glass, approximately 80~200. Curve B again indiate that the above assumption can not be employed.

Therefore, a sodium phosphate glass seems to react with silicon dioxide at a high temperature to form P–O–Si linkages. There are four types of possible structures containing one or more P–O–Si linkages.

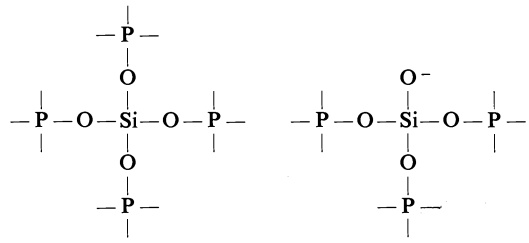

Structure A Structure B

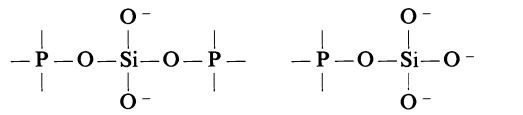

Structure C Structure D

The average chain length, $\bar{n}$, of polyphosphates produced by the hydrolytic scission of P–O–Si linkages in condensed phosphate-silicate of the $NaPO_3$-Na_2SiO_3 system is given by Eq. 2:

$$(\bar{n}+2)/\bar{n}=(x+y+2-z)/x \qquad (2)$$

where x, y, or z is the number of phosphorus atoms, P–O–Si linkages, or $Si-O^-$ linkages per atom of silicon respecctively. Similarly, $\bar{n}$ for the $NaPO_3$-SiO_2 system is given by Eq. 3:

$$(\bar{n}+2)/\bar{n}=(x+y-z)/x \qquad (3)$$

For structure A, B, C, or D, y is 4, 3, 2, or 1 and z is 0, 1, 2, or 3 respectively. The average chain lengths of polyphosphates derived from the condensed phosphate-silicates with various P/Si ratios, x, were calculated by Eq. 2 or 3. As is shown in column I of Table IV, even the calculated values of the average chain length based on structure A are considerably larger than the experimental values when x is greater than 50.

Other factors that shorten the average chain length of the polyphosphates produced from the condensed phosphate-silicates are the existence of branching points in phosphate chains and the presence of composition water and of other impurities. If all these factors are represented by the factor b, Eqs. 2 and 3 are modified into Eqs. 4 and 5 respectively:

$$(\bar{n}+2)/\bar{n}=(x+y+2-z+bx)/x \qquad (4)$$

$$(\bar{n}+2)/\bar{n}=(x+y-z+bx)/x \qquad (5)$$

where b is given with respect to an atom of phosphorus. If b is arbitrarily set at 0.04, the average chain lengths shown in column II of Table IV are obtained by means of Eqs. 4 and 5. When b is zero, Eqs. 4 and 5 are reduced to Eqs. 2 and 3 respectively. Therefore, if $0<b<0.04$, the average chain length

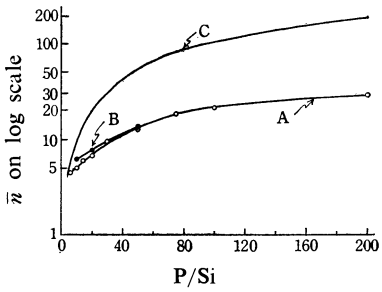

Fig. 1. Variation of average chain lengths of polyphosphates derived from the glasses with P/Si ratios.
A: Experimental values for the $NaPO_3$-Na_2SiO_3 system
B: Experimental values for the $NaPO_3$-SiO_2 system
C: Calculated values for the $NaPO_3$-Na_2SiO_3 system on the assumption that there is no interaction between a sodium metaphosphate glass and silicon dioxide in a melted state

TABLE IV. AVERAGE CHAIN LENGTHS OF POLYPHOSPHATES DERIVED FROM CONDENSED PHOSPHATE-SILICATES

	x P/Si	$\bar{n}$ Found	Column I $\bar{n}$ calcd. by Eq. 2 or 3 Structure				Column II $\bar{n}$ calcd. by Eq. 4 or 5 (b=0.04) Structure			
			A	B	C	D	A	B	C	D
$NaPO_3$–Na_2SiO_3 system	6	4.5	2.0	**3.0**	**6.0**	∞	1.9	**2.8**	**5.3**	50
	10	5.1	3.3	**5.0**	10	∞	3.1	**4.5**	8.3	50
	15	6.0	5.0	**7.5**	15	∞	**4.5**	**6.5**	12	50
	20	6.7	**6.7**	10	20	∞	**5.9**	**8.3**	14	50
	30	9.6	**10**	15	30	∞	**8.3**	**12**	19	50
	50	12.7	17	25	50	∞	**13**	17	25	50
	75	17.7	25	38	75	∞	**17**	21	30	50
	100	21.2	33	50	100	∞	**20**	25	33	50
	200	28.9	67	100	200	∞	**29**	33	40	50
$NaPO_3$–SiO_2 system	10	6.2	**5.0**	10	∞		**4.5**	**8.4**	50	
	20	7.7	10	20	∞		**8.3**	14	50	
	50	14.2	25	50	∞		**17**	25	50	

calculated by Eq. 4 or 5 for a sample with a certain P/Si ratio lies between the corresponding values of $\bar{n}$ given in columns I and II of Table IV. The average chain length of a pure sodium metaphosphate (Graham's salt) is usually in the range from 80 to 200, depending on the conditions of the preparation. Hence, the b factor for Graham's salt is calculated by the equation, $(\bar{n}+2)/\bar{n}=(1+b)/1$, to be 0.025~0.01. Therefore, the assumption that b is less than 0.04 in the present discussion is not unreasonable. As can be seen in Table IV, the calculated values for the average chain lengths printed in boldface type are close to the experimental values. Structure D appears unlikely to occur. In view of the above discussion, it seems reasonable to conclude that, with the increase in the P/Si ratio, the structural framework of the glasses of the condensed phosphate-silicates is transformed successively from structure C to structure B and then to structure A.

Summary

Crystals and glasses of the $NaPO_3$–Na_2SiO_3 and $NaPO_3$–SiO_2 systems with various P/Si ratios have been prepared from sodium metaphosphate, silicon dioxide, and sodium carbonate. The samples with P/Si ratios in the range from 0.05 to 4.00 have been obtained as crystalline substances containing amorphous substances, while those with P/Si ratios in the range from 6.00 to 200 have been obtained as glassy substances. By the X-ray diffractometry and the paper chromatography, it has been revealed that the crystals of neither system contains any P–O–Si linkages. By the paper chromatography and the pH-titration method, it has been disclosed that the glassy substances of either system with P/Si ratios higher than 6 are hydrolyzed to give mixtures of polyphosphates when dissolved in water. The lower the P/Si ratio, the more shorter chain polyphosphates are formed. The variation in the average chain length of the polyphosphates with the P/Si ratio indicates that these glassy substances are condensed phosphate-silicates containing P–O–Si linkages. Three structural types of P–O–Si linkages have been proposed for the condensed phosphate-silicates.

Department of Chemistry
Faculty of Science
Kyushu University
Hakozaki, Fukuoka

The Thermal Condensation of Formaldehyde with Aliphatic Olefins

By Shoji WATANABE and Kyoichi SUGA

(Received July 18, 1963)

The addition of formaldehyde to olefins is known as the Prins reaction.[1] In a previous paper,[2] the preparation of a limonenylcarbinol, 1,8(9)-*p*-menthadien-10-yl-carbinol, and its various derivatives was reported. The present paper describes the thermal condensation of paraformaldehyde with aliphatic olefins in the presence of acetic anhydride.

Various workers have shown that the principal products of thermal olefin-formaldehyde condensations are unsaturated primary alcohols in which the double bond is located at a position adjacent to its original site in the starting olefins.[3] In this study all condensations were carried out in acetic anhydride, at temperatures varying from 180 to 210°C, the products obtained being mainly acetates.

$$R\text{-}\overset{3}{C}H_2\text{-}\underset{R'}{\overset{2}{C}}\text{=}\overset{1}{C}H_2 + CH_2O \rightarrow R\text{-}\overset{3}{C}H\text{=}\underset{R'}{\overset{2}{C}}\text{-}\overset{1}{C}H_2\text{-}CH_2OH$$

The isoprene process is in two stages. The first stage involves the use of the Prins reaction, in which isobutylene is reacted with formaldehyde under mild conditions to give 4,4-dimethylmethadioxane as the principal product. The 4,4-dimethyl-methadioxane is then decomposed to isoprene in the second stage, with a recycle of the by-product formaldehyde. This method is used as the industrial process for making isoprene.[4,5] In the presence of acetic acid and acetic anhydride, the reaction of isobutylene with formaldehyde was studied.[6] The authors also studied the thermal condensation of isobutylene (I) with paraformaldehyde under various reaction conditions in an attempt to prepare an unsaturated primary alcohol, 3-methyl-3-buten-1-ol (III).

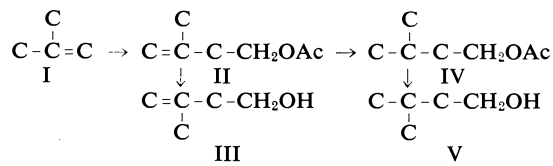

From the condensation of isobutylene (I) with paraformaldehyde in the presence of acetic anhydride (at 180°C), 3-methyl-3-butenyl-acetate (II) was obtained in ca. a 30% yield. The hydrolysis of this II gave 3-methyl-3-buten-1-ol (III). The structure of III was established as (1) by reduction and hydrolysis or by hydrolysis and reduction, giving 3-methyl-butan-1-ol (V). II and III showed strong absorption in their infrared spectra at 890 cm^{-1}, indicating that they possessed the end methylene group.

In this condensation reaction, some etheric compounds, the structure of which was not determined, were obtained in ca. 13% yield.

As catalysts, aluminum chloride, zinc chloride, boron trifluoride etherate, iron carbonyl, titanium tetrachloride and anhydrous stannic chloride were used, and the products were analyzed with gas-liquid chromatography. The results are shown in Table I. From this results, it is established that the condensation gave the acetate of the unsaturated primary alcohol 3-methyl-3-buten-1-ol (III) and etheric compounds.

The condensation of 2-ethyl-1-hexene (VI) with paraformaldehyde at 220°C in the presence of acetic anhydride gave an acetate VII in ca. a 66% yield. By the saponification of this acetate VII, the corresponding alcohol VIII was obtained. Analysis, the hydroxy value and the bromine value indicated that the product was an adduct of one mole of formaldehyde to VI ($C_9H_{18}O$ VIII). The infrared absorption spectrum showed the absorption band characteristic of a primary alcohol type at 1050 cm^{-1}, and those characteristic of a trisubstituted ethylene type at 1660 cm^{-1} and 830 cm^{-1}. The gas liquid chromatogram of VIII showed two peaks, the areas of which were nearly equal. From these facts, it is thought that VIII is a mixture of $VIII_A$ and $VIII_B$. The reduction of VIII gave a saturated primary alcohol (IX), the gas-liquid chromatogram of which showed only one peak. The

1) H. J. Prins, *Proc. Acad. Sci. Amsterdam*, **22**, 51 (1919); *J. Chem. Soc.*, **118**, 42 (1920).
2) K. Suga and S. Watanabe, This Bulletin, **32**, 1100, 711 (1959).
3) a) O. Kriebitz, *Ber.*, **32**, 57 (1899); b) A. T. Blomquist, M. Passer, C. S. Schollenberger and J. Wolinsky, *J. Am. Chem. Soc.*, **79**, 4972 (1957); c) G. Ohloff, *Arch. Pharm.*, **287**, 258 (1954); d) K. Suga and S. Watanabe, *J. Chem. Soc. Japan, Pure Chem. Sec.* (*Nippon Kagaku Zasshi*), **83**, 749, 1142 (1962).
4) A. Y. Giraud, *Chem. Eng. Progress*, **57**, (9), 66 (1961).
5) K. Fukui, Y. Ōe, H. Kitano, *J. Chem. Soc. Japan., Ind. Chem. Sec.* (*Kogyo Kagaku Zasshi*), **62**, 1667 (1959).
6) A. T. Blomquist and J. A. Verdol, *J. Am. Chem. Soc.*, **77**, 78 (1955).

TABLE I

Additive component	Main products (yield, %)		
	Lower boiling point fraction	C C=C-C-CH_2OAc	Higher boiling point fraction
Acetic anhydride		25	10
Acetic anhydride*		30	10
$SnCl_4$			8
$SnCl_4$, Acetic anhydride			21
$AlCl_3$	3		
BF_3, Acetic anhydride			21
$Fe(CO)_4$, Acetic anhydride		35	10
$Fe(CO)_4$	30		15
$TiCl_4$, Acetic anhydride		15	5
$TiCl_4$	10		

* The initial pressure with H_2 was 100 kg./cm^2.

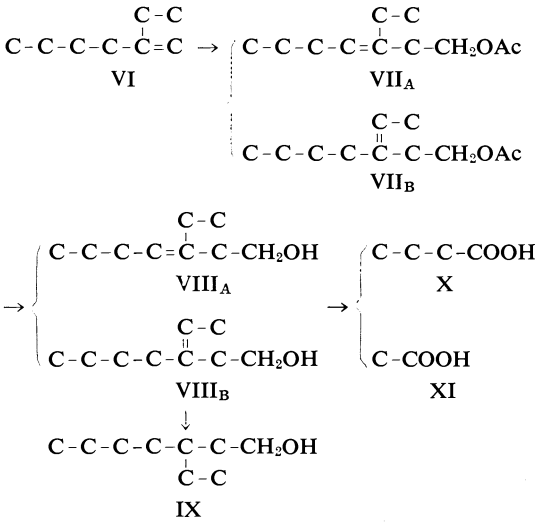

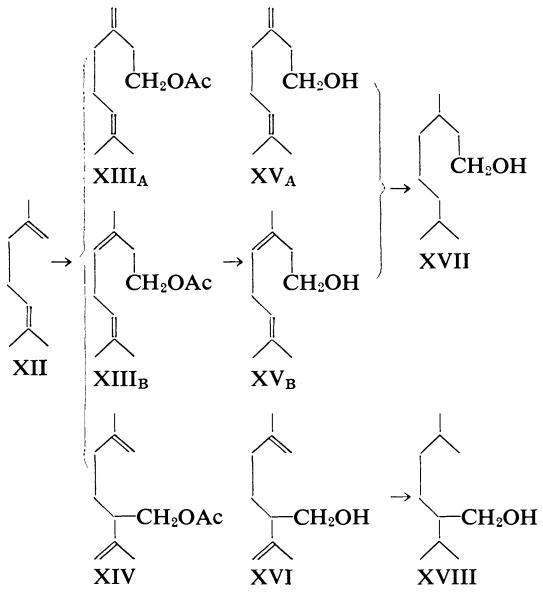

oxidation of VIII with potassium permanganate gave lactic acid (X) and acetic acid (XI). From the above results, it has been concluded that the alcohol VIII was an equivalent mixture of 3-ethyl-3-heptenol ($VIII_A$) and 3-ethylidene-heptanol ($VIII_B$).

The condensation of formaldehyde with 2, 6-dimethyl-1, 5-heptadiene (XII) under conditions similar to those used for 2-ethyl-1-hexene gave a mixture of three unsaturated alcohols, XV_A, XV_B and XVI, in ca. a 40% yield. This product, which showed a narrow boiling point range, gave no solid derivatives, and its direct separation into the three isomeric components with fractional distillation was unsuccessful. The reduction of the mixture of the alcohols, XIII and XIV, gave a product composed of 65% tetrahydrogeraniol (XVII) and 35% tetrahydrolavanduol (XVIII). This composition was established by comparing the gas-liquid chromatogram of the reduction product with those of known mixtures of pure XVII and XVIII. The mixture of XVII and XVIII was separated by means of column chromatography, using activated alumina gel. XVII and XVIII were identical in infrared spectra with authentic XVII and XVIII. Similarly, the mixture of XV and XVI was separated by means of liquid chromatography, using activated alumina gel.

The infrared absorption spectrum of XV indicates the presence of a primary alcohol group (absorption peak at 1050 cm^{-1}), an end methylene group (at 890 cm^{-1}) and a trisubstituted ethylene group (at 825 cm^{-1}). These results suggest a mixture of 3-methylene-7-methyl-6-octen-1-ol (XV_A) and 3, 7-dimethyl-3, 6-octadien-1-ol (XV_B) for the XV. Similarly, the infrared absorption spectrum of XVI indicates the presence of a primary alcohol group (absorption peak at 1050 cm^{-1}) and an end methylene group (890 cm^{-1}). These results

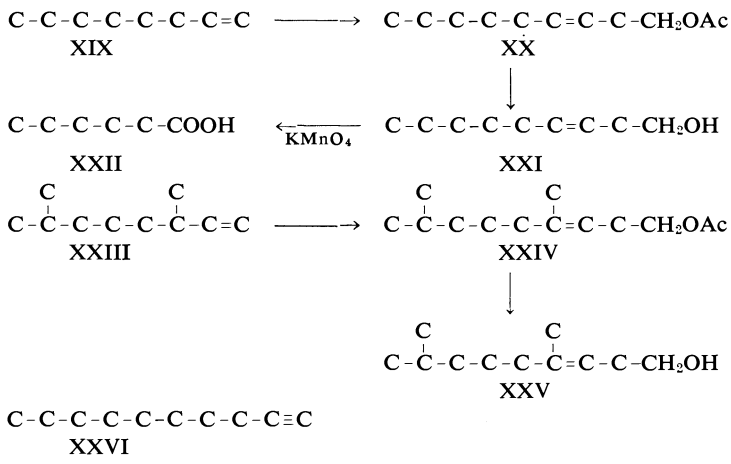

suggest the structure of 2-isopropenyl-5-methyl-5-hexenol for the XVI. As has been mentioned above, the procedure for synthesizing C_{10}-terpene alcohols from C_9-unsaturated olefins and formaldehyde with thermal condensation is a new method. The preparation of various terpene alcohols using this method is now in progress at our laboratory.

From the condensation of octene-1 (XIX), 3-nonen-1-ol acetate (XX) was obtained in ca. a 30% yields. The hydrolysis of this product gave 3-nonen-1-ol (XXI). The oxidation of this alcohol with potassium permanganate gave the known hexanoic acid, indicating that the structure was 3-nonen-1-ol. The infrared absorption spectrum of XXI indicates the presence of a trans configuration (at 965 cm^{-1}).

Similarly, from the condensation of 3, 7-dimethyl-1-octene (XXIII), 4, 8-dimethyl-3-nonen-1-ol (XXV) was obtained in ca. a 30% yield through the acetate XXIV. Analysis, quantitative acetylation, the bromine value and the infrared absorption spectrum (825 cm^{-1}, 1050 cm^{-1}) indicated that the structure was 4, 8-dimethyl-3-nonen-1-ol (XXV).

The condensation of paraformaldehyde with decyn-1 (XXVI) under conditions similar to those above mentioned did not give any alcoholic compounds.

From the condensation of octene-2 (XXVII), an unsaturated acetate (XXVIII) was obtained in ca. an 11% yield. The saponification of XXVIII gave an unsaturated primary alcohol XXIX. The gas liquid chromatography of XXIX showed that it consisted of two components, and the saturated alcohol XXX consisted of two components, too. This product, which showed a narrow boiling point range, gave no solid derivatives, however, and its direct separation into the two isomeric components by means of fractional distillation and liquid chromatography was unsuccessful. The

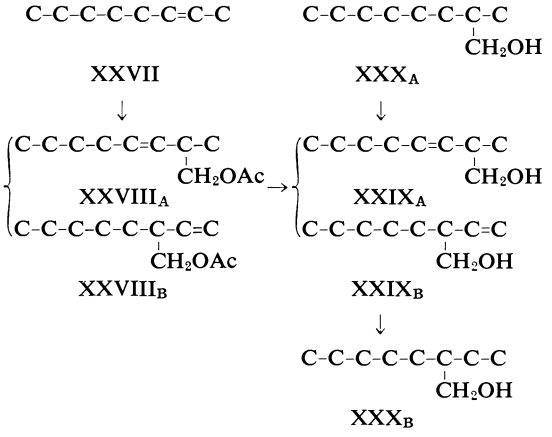

infrared absorption spectrum indicates the presence of a primary alcohol group (absorption peak at 1040 cm^{-1}), an end vinyl group (absorption peaks at 910 cm^{-1} and 990 cm^{-1}) and a trans configuration of –CH=CH– (absorption peak at 967 cm^{-1}) The product III prepared by the catalytic hydrogenation of XXIX had no double bonds as an end vinyl group and a trans configuration visible in the infrared absorption spectrum. These results suggest the mixture of 2-methyl-3-octen-1-ol ($XXIX_A$) and 3-oxymethyl-1-octene ($XXIX_B$) for the original unsaturated alcohol.

Under conditions similar to those used for XXVII, the condensations of oleic acid, methyl oleate, oleylalcohol and oleylacetate, which has a disubstituted double bond (–CH=CH–), yielded no good results.

From the condensation of 2, 6-dimethyl-2-octene (XXXI), an acetate (XXXII) was obtained. The saponification of this acetate gave an unsaturated primary alcohol XXXIII. Analysis ($C_{11}H_{22}O$), the hydroxyl value and the bromine value indicated that the product was an adduct of one mole of formaldehyde

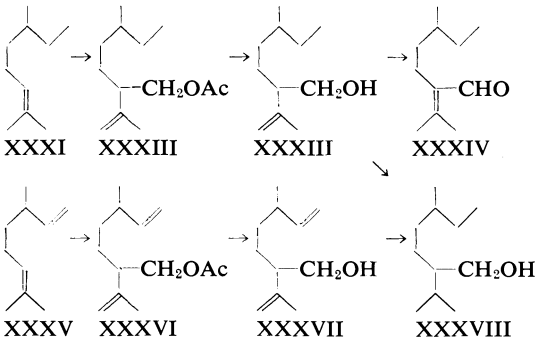

to XXXI. The infrared absorption spectrum showed the absorption bands characteristic of a primary group (absorption peak at 1040 cm^{-1}) and of an end methylene group (strong band at 855 cm^{-1}). Formula XXXIII was established on the basis of a comparison with the infrared spectrum of the product XXXVIII prepared by the catalytic hydrogenation of the end methylene group of the carbinol XXXIII. The hydrogenated carbinol XXXVIII showed remarkable doublet absorption peaks at 1380 cm^{-1} arising from an isopropyl radical. From the above results, it was concluded that the structure of the alcohol XXXIII is 3-methyl-2-(3'-methyl-1'-pentyl)-3-buten-1-ol. By the action of chromic anhydride in glatial acetic acid, an α,β-unsaturated aldehyde, 3-methyl-2-(3'-methyl-1'-pentyl)-2-buten-1-al (XXXIV), was obtained. It gives positive reactions with Schiff's reagent and with Tollen's reagent. The major absorption peaks at 243 mμ in the ultraviolet absorption spectrum suggested the presence of a conjugated enal grouping.

When the proportions of XXXI, paraformaldehyde and acetic anhydride were changed, the yields of XXXII were examined by means of gas-liquid chromatography (Table II). The use of 0.5 mol. of acetic anhydride and 1.25 mol. of paraformaldehyde per mole of XXXI gave the best results.

Similarly, from the condensation of 2, 6-dimethyl-2, 7-octadiene (XXXV), 2, 6-dimethyl-3-oxymethyl-1,7-octadiene (XXXVII) was obtained. The infrared absorption spectrum showed the absorption bands characteristic of a primary alcohol at 1040 cm^{-1}, of an end methylene group at 890 cm^{-1}, and of an end vinyl group at 910 and 990 cm^{-1}. The product prepared by the catalytic hydrogenation of XXXVII was identical in infrared absorption spectrum, gas-liquid chromatogram and other physical constants with the XXXVIII which had been prepared from the known XXXIII. These results suggest the structure of 2, 6-dimethyl-3-oxymethyl-1, 7-octadiene (XXXVII) for the original alcohol.

From the condensation of 2, 3-dimethyl-2-pentene (XXXIX), which has a tetrasubstituted double bond, an unsaturated alcohol was obtained in a poor yield, but the structure was not determined.

Finally, from the condensation of myrcene (XXXX), which has a conjugated diene, no alcoholic compound was obtained, only an unsaturated hydrocarbon as the main product

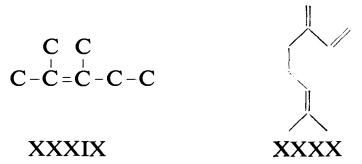

XXXIX XXXX

TABLE II. REACTION OF 2,6-DIMETHYL-2-OCTENE (XXXI) WITH PARAFORMALDEHYDE

Experimental No.	XXXI mol.	Paraformaldehyde mol.	Acetic-anhydride mol.	Recovered XXXI %	XXXII %	High boiling point fraction %	Residue %
1	1.0	1.0	1.0	90	0	0	10
2	1.0	1.25	1.0	87	3	0	10
3	1.0	1.5	1.0	90	0	0	10
4	1.0	1.25	0.25	48	22	0	30
5	1.0	1.25	0.5	2	51	17	30
6	1.0	1.25	0.75	52	21	2	25
7	1.0	1.25	1.0	77	3	0	20
8	1.0	1.0	0.26	39	28	8	25
9	1.0	1.0	0.49	15	48	7	30
10	1.0	1.0	0.55	38	32	5	25
11	1.0	1.0	0.65	82	8	8	10
12	1.0	1.0	1.0	100	0	0	10
13							

Reaction temperature 220°C, reaction time 5 hr.
Gas chromatography; Column; Reoplex 400 (20%) on celite 545, 2.25 m.
Carrier gas; He 47.5 ml./min. Column Temp.; 170°C
Apparatus; Shimadzu GC-1A Type

in ca. a 35% yield. The molecular weight (280), the boiling point (140~150°C/3 mmHg), and the bromine value indicated that the product was a dimer of XXXX. The infrared absorption spectrum did not show the existence of an oxygenated compound.

The foregoing observations indicate that the thermal condensation of paraformaldehyde with aliphatic olefins in the presence of acetic anhydride occurs most readily with end methylene-type olefins, $CH_2=CR_1R_2$, and that trisubstituted olefins ($R_1CH=CR_2R_3$), disubstituted olefins and vinyl olefins ($CH_2=CHR_1$ and $R_1CH=CHR_2$) and tetrasubstituted olefins ($R_1R_2C=CR_3R_4$) are less reactive in these orders.

Experimental

Materials.—The properties of the materials used are summarized in Table III.

The Condensation with Paraformaldehyde (General Method).—A mixture of 1 mol. of an olefin, 1 mol. of paraformaldehyde, and 0.5 mol. of acetic anhydride was heated at 180~220°C in an stainless autoclave for several hours. The reaction mixture was extracted with ether. The ethereal solution was then washed with water and drid over anhydrous sodium sulfate. Fractional distillation gave a crude acetate. By saponification with the alcoholic potassium hydroxide of the acetate, the corresponding alcohol was obtained.

The Condensation of Isobutylene (I) with Formaldehyde.—From a mixture of 19 g. of isobutylene (I), 11 g. of paraformaldehyde, and 15 g. of acetic anhydride (reaction temperature, 200~210°C; reaction time, 4 hr.), 15 g. of a crude product was obtained. The crude product (150 g.) fractionally distilled to give the following fractions: (a) 24 g. of the forerun (b. p. 70~140°C); (b) 60 g. of II (b. p. 144°C; d_4^{30} 0.8910; n_D^{29} 1.4150; molecular refraction, 36.00 (calcd. for $C_7H_{12}O_2$, F_1, 35.713); bromine value, 115.01 ($C_7H_{12}O_2$, F_1, 124.7); (c) 33 g. of higher condensation products (b. p. 144~160°C); (d) 30 g. of residue.

The infrared spectrum of the II compound showed strong absorption at 890 cm^{-1} (an end methylene group) and at 1740 cm^{-1} and 1240 cm^{-1} (acetate).

The quantitative hydrogenation of II in methanol using a Raney nickel catalyst required 98% of one molar equivalent of hydrogen. The product was identical with an authentic isoamyl acetate (IV) in infrared absorption spectrum, gas chromatogram and other physical constants.

The saponification of II in the usual way gave 3-methyl-3-butene-1-ol (III); b. p. 132°C, n_D^{20} 1.4340; d_4^{20} 0.8533. The infrared spectrum of III showed strong absorption at 890 cm^{-1} (an end methylene group) and at 1050 cm^{-1} (a primary alcohol group). The quantitative hydrogenation of II in ethyl alcohol using a palladium-carbon catalyst required one molar equivalent of hydrogen. The product was identical with an authentic isoamyl alcohol (V) in infrared absorption spectrum, gas chromatograph and other physical constants.

The Condensation of 2-Ethyl-1-hexene (VI) with Formaldehyde. — From a mixture of 112 g. of VI, 36 g. of paraformaldehyde and 51 g. of acetic anhydride (reaction temperature, 220°C; reaction time, 6 hr.), 122 g. of the crude VII was obtained. The saponification of VII gave a mixture of $VIII_A$ and $VIII_B$. B. p. 81°C/6 mmHg; d_4^{15} 0.8345; n_D^{22} 1.4541; molecular refraction, 45.84 (Calcd. for $C_9H_{17}OH$, F_1, 44.95); hydroxy group, 11.97% (Calcd. for monohydric alcohol, 11.96%); bromine value, 128.4 (Calcd. for $C_9H_{17}OH$, 112.4); infrared absorption spectrum, 1045 cm^{-1}, 1660 cm^{-1} and 830 cm^{-1}.

Found: C, 76.01; H, 12.32. Calcd. for $C_9H_{18}O$: C, 76.02; H, 12.76%.

2-Ethyl-heptanol (IX).—Upon the hydrogenation of VIII in methanol at 130°C under high pressure (40 kg./cm^2) using a Raney nickel catalyst, one molecular equivalent of hydrogen was absorbed. The reduced product IX was carefully distilled. B. p. 79~80°C/6 mmHg.

The Oxidation of VIII with Potassium Permanganate.—A mixture of 29 g. of potassium permanganate, 35 g. of concentrated sulfuric acid and 300 cc. of water was added to a mixture of 10 g. of VIII and 30 cc. of acetone over an hour's time. After the mixture had been left alone overnight,

TABLE III

Olefins	Boiling point °C/mmHg	d_4^t	n_D^t	Note
Isobutylene (I)				From Mitsubishi Oil Co., Ltd.
2-Ethyl-1-hexene (VI)	66~70/120	d_4^{13} 0.7314	n_D^{22} 1.4149	
2,6-Dimethyl-1,5-heptadiene (XII)	69~70/ 80	d_4^{13} 0.7593	n_D^{18} 1.4461	
Octene-1 (XIX)	70.5/140	d_4^{15} 0.7213	n_D^{25} 1.4071	
3,7-Dimethyl-1-octene (XXIII)	58/ 19	d_4^{29} 0.7476	n_D^{31} 1.4190	
Decyne-1 (XXVI)	98~102/ 40			
Octene-2 (XXVII)	121~123	d_4^{24} 0.7178	n_D^{24} 1.4123	
2,6-Dimethyl-2-octene (XXXI)	82~84/ 57		n_D^{20} 1.4300	
Dihydromyrcene (XXXV)	60/ 18	d_4^{17} 0.7540	n_D^{18} 1.4448	
2,3-Dimethyl-2-pentene (XXXIX)	88	d_4^{20} 0.7383	n_D^{25} 1.4094	
Myrcene (XXX)				From Takasago Perfumery Co., Ltd.

TABLE IV

Fraction No.	Boiling point °C/mmHg	Yield g.	Gas-liquid chromatograph		
			$XV_A(B)$*	$XV_B(C)$*	XVI(A)**
1	79/7～94/5	2			
2	94/5～87/2	4	25	17	58
3	87/2	4	31	26	43
4	87/2	4	37	22	31
5	87/2～87.5/2	4.2	42	42	16
6	87.5/2～90/2	5	41	57	2
7	90/2～135/2	5			
The crude alcohol			39	26	35

* Geraniol type ** Lavanduol type

the precipitated part was filtered off. After the reaction-mixture had been alkalined with sodium carbonate, it was evaporated. The concentrated solution was then acidified with sulfuric acid and extracted with ether. After the ether had been evaporated, the residue was an analyzed by gas liquid chromatography; lactic acid (X) and acetic acid (XI) were recognized by comparing then with authentic samples.

The Condensation of 2, 6-Dimethyl-1, 5-heptadien (XII) with Formaldehyde. — From a mixture of 41 g. of XII, 10 g. of paraformaldehyde and 17 g. of acetic anhydride (reaction temperature, 220°C; reaction time, 4 hr.), 25 g. of crude acetate (b. p. 89～90°C/2 mmHg) was gained. The saponification of this product gave 20 g. of a mixture of XXV and XXVI. This was distilled to give the fractions in Table IV.

The Hydrogenation of XV and XVI.—Upon the hydrogenation of 4 g. of Fr. 2 (Table IV) in methanol at 120°C using a Raney nickel catalyst, two molecular equivalents of hydrogen were absorbed. The reduced product was shown to be a mixture of tetrahydrogeraniol (XVII) (40%) and tetrahydrolavanduol (XVIII) (60%) by gas-liquid chromatography.

The Separation of Mixture of XVI and XVII. —The chromatography of 2 g. of the above-mentioned saturated alcohol (XVII, XVIII) with an activated alumina using benzene (150 cc.) and acetone (150 cc.) gave 100 mg. of tetrahydrogeraniol (purity, 90%) and 100 mg. of tetrahydrolavanduol (XVIII) (purity, 90%) from the elution of acetone. XVII and XVIII were identified by a comparison of the infrared absorption spectra and the gas-liquid chromatography results with those of authentic samples.

Found: C, 75.57; H, 13.53. Calcd. for $C_{10}H_{22}O$ (XVII): C, 75.88; H, 14.01%.

Found: C, 75.62; H, 13.92. Calcd. for $C_{10}H_{22}O$ (XVIII): C, 75.88; H, 14.01%.

Separation of a Mixture of XV and XVI.— The chromatography of 2 g. of the mixture of XV and XVI with an activated alumina using benzene (150 cc.) and acetone (150 cc.) gave 200 mg. of a mixture of XV_A and XV_B (purity, 80%) and 70 mg. of XVI (purity, 80%) from the elution of acetone.

Condensation of Octene-1 (XIX) with Formaldehyde.—From a mixture of 45 g. of XIX, 20.5 g. of acetic anhydride and 14.5 g. of paraformaldehyde (reaction temperature, 220°C; reaction time, 5.5 hr.), 22 g. of a crude acetate (XX) (b. p. 110～120°C/20 mmHg) was gained. The saponification of the product gave 14 g. of XXI. B. p. 114～116°C/25 mmHg; d_4^{12} 0.8630; n_D^{12} 1.4550; molecular refraction, 44.90 (Calcd. for $C_9H_{18}O$, F_1, 44.82); hydroxy group, 11.50% (Calcd. for monohydric alcohol, 11.95%); bromine value, 103.2 (Calcd. for $C_9H_{18}O$, F_1, 112.3); the gas chromatogram shows one peak.

α-Naphthylurethan. — This was prepared as usual and was recrystallized from petroleum benzine. M. p. 75.5°C.

Found: N, 4.42. Calcd. for $C_{20}H_{25}NO_2$: N, 4.498%.

Oxidation of XXV with Potassium Permanganate.—A mixture of 25 g. of potassium permanganate, 21 g. of sulfuric acid and 300 cc. of water was added to 10 g. of XXV over an hour's time while the mixture was agitated. After the mixture had then been left alone overnight, the precipitated material was filtered off. The filtrate was alkalined with potassium hydroxide and then evaporated. After the concentrated solution had been acidified with sulfuric acid, it was extracted with ether. The ether solution was distilled to give 2 g. of caproic acid (XXII), which was identical with the IR and GC of the authentic sample of XXII.

p-Bromphenatylester.—This was prepared as usual and was recrystallized from methanol. It has a m. p. of 72°C, which does not depress the m. p. of an authentic XXII *p*-bromphenatylester with an m. p. of 72°C.

The Condensation of 3, 6-Dimethyl-1-octene (XXIII) with Formaldehyde.—From a mixture of 31 g. of XXIII, 6,7 g. of paraformaldehyde and 11 g. of acetic anhydride (reaction temperature, 220°C; reaction time, 10 hr.), 7 g. of a crude acetate XXIV was obtained. The saponification of XXIV gave 4 g. of XXV. B. p. 120～124°C/20 mmHg; d_4^{29} 0.8363; n_D^{30} 1.4462; molecular refraction, 54.21 (Calcd. for $C_{11}H_{22}O$, F_1, 54.26); bromine value, 75.2 (Calcd. for $C_{11}H_{22}O$, F_1, 93.9); hydroxy group, 9.91% (Calcd. for monohydric alcohol, 9.98%).

Found: C, 76.88; H, 12.85. Calcd. for $C_{11}H_{22}O$ (XXV): C, 77.58; H, 13.02%.

The Condensation of Decyn-1 (XXVI) with Formaldehyde.—From a mixture of 30 g. of XXVI, 6.7 g. of paraformaldehyde and 13.5 g. of acetic anhydride (reaction temperature, 220°C; reaction

time, 10 hr.), no acetate was obtained.

The Condensation of Octene-2 (XXVII) with Formaldehyde.—From a mixture of 40 g. of XXVII, 12.5 g. of paraformaldehyde and 18.17 g. of acetic anhydride (reaction temperature, 200~210°C; reaction time, 11 hr.), 7 g. of a crude acetate (XXVIII) (b. p. 80~88°C/9 mmHg) were obtained. The saponification of 20 g. of XXVIII in the usual way gave 14 g. of XXIX (b. p. 92~95°C/7 mmHg; $n_D^{29.5}$ 1.4430; $d_4^{29.5}$ 1.1864; bromine value, 103 (Calcd. for $C_{19}H_{18}O$, F_1, 112); hydroxy group, 13.5% (Calcd. for monohydric alcohol 11.98%); the gas chromatogram shows one peak). The infrared spectrum of the compound XXIX showed a strong absorption at 1040 cm^{-1} (a primary alcohol group) and at 967 cm^{-1}, 910 cm^{-1} and 990 cm^{-1} (a terminal vinyl group and a disubstituted trans-type double bond).

Found: C, 76.01; H, 12.71. Calcd. for $C_9H_{18}O$ (XXIX): C, 76.02; H, 12.75%.

The hydrogenation of XXIX in a methanol solution using a Pd-C catalyst absored one molar equivalent of hydrogen. This infrared absorption spectrum showed no absorption peaks of any double bonds.

Condensation of 2, 6-Dimethyl-2-octene (XXXI) with Formaldehyde. — From a mixture of 32 g. of XXXI, 16 g. of acetic anhydride and 6 g. of paraformaldehyde (reaction temperature 220°C; reaction time, 5 hr.), 10 g. of a crude acetate XXXII were obtained (b. p. 90~97°C/7 mmHg). This (137 g.) was distilled to give the following fractions: (a) 59 g. of XXXII (b. p. 81~81.5°C/3 mmHg; n_D^{10} 1.4504; d_4^{10} 0.8913; molecular refraction, 64.06 (Calcd. for $C_{13}H_{24}O_2$, 63.42); saponification value, 240 (Calcd. for $C_{13}H_{24}O_2$, 264); bromine value, 65.3 (Calcd. for $C_{13}H_{24}O_2$: F_2, 75.3); the gas chromatogram shows one peak); (b) 12 g. of higher condensation products (b. p. 120~130°C/2 mmHg.; d_4^{21} 0.9313; n_D^{21} 1.4745; bromine value, 85.8; hydroxyl group, 13.5%).

The saponification of XXXII (20 g.) gave an alcoholic compound, XXXIII (12 g.). B. p. 92~93°C/5 mmHg; n_D^{10} 1.4615; d_4^{10} 0.8598; molecular refraction, 54.43 (Calcd. for $C_{11}H_{22}O$: F_1, 54.06%); hydroxyl group, 9.15% (Calcd. for $C_{11}H_{22}O$, 9.99%); bromine value, 80.5 (Calcd. for $C_{11}H_{22}O$, 93.9); the gas chromatogram shows one peak.

Found: C, 76.60; H, 13.11. Calcd. for $C_{11}H_{22}O$ (XXXIII): C, 77.46; H, 13.00%.

2, 6-Dimethyl-3-oxymethyl-octane (XXXVII). — The quantitative hydrogenation of XXXIII in methanol using a Raney nickel catalyst in an autoclave (initial H_2 pressure, 35 kg./cm^2) required 99% of one molar equivalent of hydrogen. From 3 g. of XXXIII there were obtained 2 g. of XXXVII (b. p. 89~91°C/5 mmHg; n_D^8 1.4520; the gas chromatogram shows one peak).

3-Methyl-2-(3'-methyl-1'-pentyl)-2-buten-1-al (XXXIV).—To a mixture of 6 g. of XXXIII, 10 g. of acetone and 10 g. of glacial acetic acid, a mixture of 12 g. of chromic anhydride, 30 g. of acetic acid, 5 g. of water and 2 g. of concentrated sulfuric acid was added over a 30 minute period at 0°C while the mixture was being vigorously agitated. After the mixture had then been stirred for 4.5 hr., it was poured into a large amount of water and extracted with ether. The extracts were washed with water and dried over anhydrous sodium sulfate. By fractional distillation, 2 g. of XXXIV were obtained (b. p. 68~72°C/1~2 mmHg; λ_{max} 243 mμ, ε 1310). This substance gave a positive reaction with Schiff's reagent and reduced an ammoniacal silver nitrate solution.

2,4-Dinitrophenylhydrazone.—This was prepared as usual and was recrystallized from a mixture of pyridine and methanol. M. p. 209°C: λ_{max} 390 mμ ε 4080.

Found: N, 17.69. Calcd. for $C_{17}H_{24}O_4N_4$: N, 16.56%.

The Condensation of 3, 7-Dimethyl-1, 6-octadiene (XXXV) with Formaldehyde.—From a mixture of 79 g. of XXXV, 17 g. of paraformaldehyde and 28.5 g. of acetic anhydride (reaction temperature, 200°C; reaction time, 4 hr.), 25 g. of crude XXXVI (b. p. 100~130°C/4 mmHg) were obtained. The saponification of this product (92 g.) gave 71 g. of a crude alcohol. This was distilled to give the following fractions: (a) 28 g. of XXXVII (b. p. 81.5°C/3 mmHg; n_D^{26} 1.4645; d_4^{26} 0.8590; molecular refraction, 54.36 (Calcd. for $C_{11}H_{20}O$: F_2, 53.59); hydroxyl group, 9.06% (Calcd. for monohydric alcohol, 10.1%); bromine value, 201 (Calcd. for $C_{11}H_{20}O$: F_2, 189.9); the gas chromatography shows one peak).

Found: C, 77.49; H, 12.19. Calcd. for $C_{11}H_{20}O$ (XXXVII): C, 78.49; H, 11.98%.

(b) 5 g. of higher condensation products (b. p. 100~110°C/3 mmHg).

Hydrogenation of 2, 6-Dimethyl-3-oxymethyl-1, 7-octadiene (XXXVII).—The quantitative hydrogenation of XXXVII in isopropylalcohol using Raney nickel in an autoclave (initial H_2 pressure, 38 kg./cm^2) required 98% of two molar equivalents. B. p. 93°C/3 mmHg; n_D^5 1.4523. The infrared spectrum and the gas-liquid chromatogram of this product agreed with XXXVIII, which had been similarly prepared from XXXIII.

The Condensation of 2, 3-Dimethyl-2-pentene (XXXIX) with Formaldehyde.—From a mixture of 26 g. of XXXIX, 9 g. of paraformaldehyde and 13 g. of acetic anhydride (reaction temperature, 220°C; reaction time, 8 hr.), 3 g. of a crude acetate (b. p. 120~125°C/3 mmHg) were obtained. The saponification of this product gave 0.5 g. of an alcoholic compound, the structure of which was not determined.

Condensation of Myrcene (XXXX) with Formaldehyde.—From a mixture of 45 g. of XXXX, 10 g. of paraformaldehyde and 17 g. of acetic anhydride (reaction temperature, 210~220°C; reaction time, 5 hr.), the following main fraction was obtained: (a) 13.7 g. of an unsaturated hydrocarbon (b. p. 140~150°C/3 mmHg: d_4^{25} 0.8793; n_D^{25} 1.5001; bromine value, 205; molecular weight, 280).

Absorption Spectra. — The infrared absorption spectra were measured by using a Koken IRS spectrophotometer, while the ultraviolet absorption spectrum were measured with a "Shimadzu" photometric spectrophotometer Type QB-50 using isopropyl alcohol as the solvent.

Gas-Liquid Chromatography. — Gas-liquid chromatography was measured under the following

conditions: II, III, IV, V, VI, XII, XIX, XXI, XXIII, XXVI, XXVII, XXXI, XXXV, XXXIX and XXXX: column; LAC-2R-446 (20%) on Celite 545, 2 m.; temperature, 120°C; carrier gas He 45 ml./min.

VII, VIII, IX, XIII, XIV, XV, XVI, XVII, XVIII, XX, XXI, XXIV, XXV, XXVIII, XXIX, XXX, XXXII, XXXIII, XXXIV, XXXVI, XXXVII and XXXVIII: Temperature, 180°C; the other conditions were the same as above.

X, XI and XXII: column; Silicone D C 200 on Celite 545, 2 m.; temperature, 150°C; carrier gas, He 45 ml./min.

The authors are indebted to the Takasago Perfumery Co., Ltd., for providing materials.

Department of Applied Chemistry
Faculty of Technology
Chiba University
Matsudo-shi, Chiba

Remark on the Solvent Effects upon the Electronic Spectra of Naphthalene Derivatives

By Noboru MATAGA

(Received July 20, 1963)

In one of our previous papers[1] we reported on the absorption and fluorescence spectra of naphthylamines and isomeric aminobenzoic acids in various organic solvents. This sort of study, in which the effects of solvents on both the absorption and fluorescence spectra are investigated, is important in order to obtain detailed information on the electronic structures of complex aromatic molecules as well as on the nature of the molecular interaction in solutions.

It has been observed that the hydrogen bonding between the solute and the solvent molecules, especially that between the alcohol and amino nitrogen of naphthylamines or aminobenzoic acids, affects the electronic spectra of the latter two quite remarkably. This fact has been ascribed to the rearrangement of the hydrogen bond between the solute and solvent molecules during the lifetime of the excited solute molecule.

In the present report, we shall describe additional experimental findings concerning the electronic spectra of some aromatic hydrocarbon derivatives, such as naphthylamines, naphtholate ions and aniline in aqueous and alcohol solutions; we shall also discuss the rearrangement of the solute-solvent interaction in the excited state and the role of the Franck-Condon principle in the spectral shifts.

Experimental

The details of the apparatus for the measurement of the absorption and fluorescence spectra have been described elsewhere.[1-3] The samples of the solutes were the same as were used before.[1,3]

Experimental Results and Discussion

The Importance of the Franck-Condon Principle in the Solvent Shifts of π-π^* Spectra.— As has been demonstrated in our previous report,[1] the solute-solvent interactions in alcohol solutions affect the absorption spectra of naphthylamines only slightly, whereas they cause a very large red shift of the fluorescence spectra compared to the case of *n*-hexane or cyclohexane solutions.

The hydrogen-bonding interaction in alcohol solutions of naphthylamines probably involves the following types of hydrogen bonds:

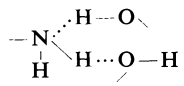

The hydrogen bond of the $-H-H\cdots O<$ type (type D) causes a red shift of the absorption spectrum, whereas the $-N\cdots H-O<$ type (type A) hydrogen bond causes a blue shift of the absorption spectrum; this is because the former is favorable while the latter is unfavorable to the charge migration from the substituent to the aromatic ring.

The hydrogen-bonding interaction of the A type is certainly much weaker in the excited

1) N. Mataga, This Bulletin, 36, 654 (1963).

2) N. Mataga, Y. Torihashi and Y. Kaifu, *Z. physik. Chem. N. F.*, 34, 379 (1962).

3) N. Mataga and Y. Kaifu, *Mol. Phys.*, in press.

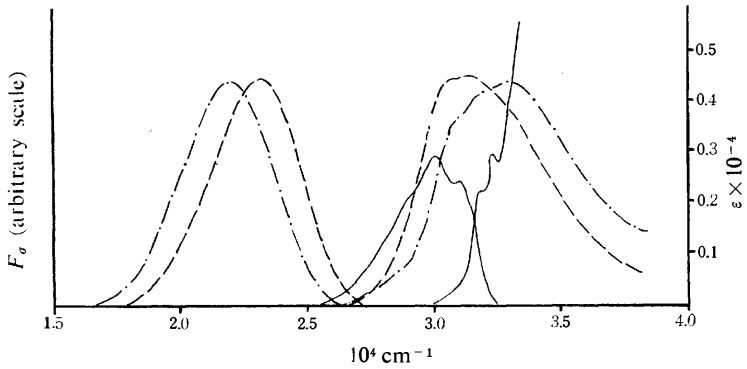

Fig. 1. Absorption and fluorescence spectra of α-naphthylamine in various solvents.
Solvents : ---- 60% (weight) H_2SO_4, – – – Ethanol, —·— H_2O (neutral).
Concentrations of solute : 2×10^{-3} mol./l. in 60% H_2SO_4 and ca. 0.8×10^{-4} mol./l. in the other solvents.

TABLE I. THE WAVE NUMBERS OF THE BAND MAXIMA OF ANILINE, α- AND β-NAPHTHYLAMINES IN ETHANOL AND IN AQUEOUS SOLUTIONS (IN UNITS OF $10^4\,cm^{-1}$)

Solvent	Aniline		α-Naphthylamine		β-Naphthylamine	
	σ_a^m	σ_f^m	σ_a^m	σ_f^m	σ_a^m	σ_f^m
EtOH	3.52	2.95	3.13	2.31	2.96	2.46
H_2O	3.58	2.91	3.30	2.19	3.02	2.43

state,*1 while that of the D type is a little stronger in the excited state than in the ground state. The former circumstance is related to the fact that the basicity of the amino nitrogen is much weaker in the excited state than in the ground state, as has been demonstrated by Förster[4] in the case of naphthylamines in an aqueous solution. Moreover, the type D hydrogen bond may be strengthened by the cooperative interaction between alcohol molecules in the hydrogen-bonded chain.

These hydrogen-bonding interactions, as well as the dipole-dipole and dipole-polarization interactions with the surrounding solvent molecules, which are much stronger in the excited state than in the ground state, may cause the very large $\Delta\sigma$ value (the wave number difference between the maxima of the absorption, (σ_a^m), and of the fluorescence spectra, (σ_f^m), respectively) of the alcohol solution.

The effects of the solute-solvent interactions on the spectral shifts described above may be far greater in the aqueous solution than in the alcohol solution because of the more extensive hydrogen bonding interactions and dipolar interactions in the former solution.

As an example of very large spectral shifts in the hydroxylic solvent, the absorption and fluorescence spectra of α-naphthylamine in ethanol and water (neutral), together with those in 60% (weight) sulfuric acid solution, are shown in Fig. 1. In the last solvent, the amino nitrogen is protonated in both the ground state and the fluorescence state.

The wave numbers of the band maxima of α- and β-naphthylamines in ethanol and in an aqueous solution are collected in Table I. The wave numbers of the band maxima of naphthylamines in some of the other organic solvents have been given elsewhere.[1]

As can be seen from Fig. 1 and Table I, the σ_a^m values of naphthylamines in aqueous (neutral) solutions are greater than those in alcohol solutions, whereas the σ_f^m values in the aqueous solutions are much smaller than those in alcohol solutions. Therefore, the $\Delta\sigma$ value is quite large in the aqueous solution. For example, $\Delta\sigma\sim11100\,cm^{-1}$ in the aqueous

*1 In the potential energy curve for the type A hydrogen bonding which was given in our previous report (Fig. 7 of Ref. 1), the equilibrium distance between the proton donor and the acceptor in the case of the type A hydrogen bond was assumed to be larger in the excited state than in the ground state. However, this assumption is rather doubtful. Because the extent of the charge migration from the nitrogen lone pair orbital to the ring is much greater in the excited state than in the ground state, the lone pair orbital may be more contracted in the excited state than in the ground state. Accordingly, the equilibrium distance between the donor and the acceptor may be a little smaller in the excited state than in the ground state. This circumstance is analogous to the case of the blue shift of the absorption and the red shift of the emission in the n-π spectra shown by Krishna and Goodman (V. G. Krishna and L. Goodman, *J. Chem. Phys.*, 33, 381 (1960)), although the extent of the orbital contraction may be smaller in the present case than in the case of the n-π^* transition.

4) Th. Föster, *Z. Elektrochem.*, 54, 531 (1950).

neutral solution compared to $\sim 8200\,cm^{-1}$ in ethanol and $\sim 4800\,cm^{-1}$ in *n*-hexane in the case of α-naphthylamine.*2 This wave number difference is greater, the larger the sum of the Franck-Condon destabilization energies in the excited and ground states. The present experimental results, which demonstrate the blue shift of the absorption spectrum and the large red shift of the fluorescence spectrum in a more polar solvent, indicate that the Franck-Condon principle, including the various solute-solvent interactions, plays a very important role in the solvent shifts of the electronic spectra.

Table I also contains the σ_a^m and σ_f^m values of aniline in ethanol and in the aqueous neutral solution. We can observe from Table I that the solvent shifts of the spectra in this case are quite analogous to those in the case of naphthylamines.

If we take the spectrum in such non-polar aliphatic hydrocarbons as *n*-hexane and cyclohexane as a reference, then the sum of the Franck-Condon destabilization energies resulting from the solute-solvent interactions in the excited and ground states may be expressed as the difference between the $\Delta\sigma$ value in a polar solvent and that in the hydrocarbon solvent. The Franck-Condon destabilization energy of aniline in an aqueous solution amounts to $3400\,cm^{-1}$. This value is much smaller than the corresponding quantity for α-naphthylamine ($6300\,cm^{-1}$), although it is larger than that for β-naphthylamine ($2900\,cm^{-1}$).

The Similarity of the Electronic Spectra of Naphtholate Ions to Those of Naphthylamines. —Before ending the present article, we would like to note the similarity between the electronic spectra of naphtholate ions in the aqueous solution and those of naphthylamines in the aqueous solution. The conjugation power of $-O^-$ seems to be only a little larger than that of the amino group, as one can see from the electronic absorption spectra of many aromatic hydrocarbon derivatives which have $-O^-$ and $-NH_2$ substituents. Actually, the most appropriate values of the Coulomb parameter for the calculation of Hückel MO's seem to be 0.8[5] for $-O^-$ and 1.2[6] for the amino nitrogen.

The σ_a^m values of α- and β-naphtholate ions are $30300\,cm^{-1}$ and $29000\,cm^{-1}$ respectively*3. These σ_a^m values are smaller than the corresponding values of naphthylamines, in accordance with the stronger conjugation power of $-O^-$ than the amino group. However, the $\Delta\sigma$ values for the naphtholate ions ($9300\,cm^{-1}$ for the α-isomer and $5200\,cm^{-1}$ for the β-isomer) are rather close to those of naphthylamines. The value for the β-naphthol molecule in an aqueous solution is $2200\,cm^{-1}$, which is much smaller than that of the ion (α-naphthol molecule is not fluorescent in an aqueous solution).

Thus, although the wave numbers of the maxima of both the absorption and the fluorescence spectra of naphtholate ions are a little smaller than those of naphthylamines, the spectra of each isomer of naphtholate ions and naphthylamines are similar to each other and the characteristics[1] of the spectrum of each isomer are well maintained in naphtholate ions as well.

Summary

The importance of the Franck-Condon principle in the solvent shifts of π–π^* spectra has been discussed with reference to aniline and naphthylamines in alcohol and aqueous solutions. The blue shift of the absorption spectra and the red shift of the fluorescence spectra in these polar solvents have been interpreted in terms of the Franck-Condon destabilization energies, including the solute-solvent hydrogen bonding interactions and the dipolar interactions. In addition to this, the similarity of the electronic spectra of naphtholate ions to those of naphthylamines has been pointed out with reference not only to the absorption spectra but also to the fluorescence spectra.

Faculty of Science
Osaka City University
Sumiyoshi-ku, Osaka

*2 As has been discussed in the previous report,[1] the fluorescent state of α-naphthylamine is plausibly ^1L_a, although the lowest absorbing singlet state seems to be ^1L_b. In the case of β-naphthylamine, ^1L_b is the relevant excited state for both light absorption and fluorescence. Therefore, the σ_a^m value indicated in the text for α-naphthylamine is that of ^1L_a.

5) N. Mataga, This Bulletin, **36**, 1109 (1963).
6) H. Baba, ibid., **34**, 76 (1961); H. Baba and S. Suzuki, ibid., **34**, 82 (1961).

*3 As has been discussed in Ref. 1, the ^1L_a band shifts strongly to the red in constrast to the ^1L_b band, which shifts to the red only slightly upon the substitution of an electron-donating group at the α position.

The ^1L_b band of α-naphtholate ion is overlapped by the ^1L_a band more extensively than that of α-naphthylamine because the red shift of the ^1L_a band relative to that of the ^1L_b band is greater for the $-O^-$ substitution than for the amino substitution. In view of this, the σ_a^m value for α-naphtholate ion indicated in the text can quite plausibly be assigned to ^1L_a.

Formaldehyde Resins. LXVI.[1] *The Base-catalyzed Reaction of Benzamides with Formaldehyde*

By Minoru Imoto and Mitsue Kobayashi

(Received July 21, 1963)

Three years ago, the present authors stated[2] that the rate of the reaction of amide with formaldehyde in the presence of hydrochloric acid was represented by the following equation:

$$R = k[\mathrm{HCl}][\mathrm{R\text{-}CONH_2}][\mathrm{CH_2O}]$$

For the reaction, an S_E2 mechanism was proposed, illustrated by the following two steps:

i) $\mathrm{CH_2O + HCl \rightarrow {}^{+}CH_2OH + Cl^-}$

ii) $\mathrm{R\text{-}CONH_2 + {}^{+}CH_2OH \rightarrow R\text{-}CO^{-}\overset{\overset{+}{\mathrm{CH_2OH}}}{\underset{\underset{\mathrm{H^+}}{}}{\mathrm{NH}}}}$

$$\rightarrow \mathrm{R\text{-}CONHCH_2OH + H^+}$$

In the present paper, the base-catalyzed reaction of monosubstituted benzamides with formaldehyde will be studied kinetically. The following results have been obtained: (i) The rate of the reaction increased linearly with the concentration of formaldehyde, until the concentration reached a certain value. Above this value, the rate remained constant; i.e., the rate was independent of the concentration of formaldehyde. (ii) The reaction rate constants fit Hammett's equation. (iii) An S_E1 mechanism is proposed for the base-catalyzed reaction of benzamide with formaldehyde.

Experimental

Materials.—The preparation of six kinds of *m*- or *p*-substituted benzamides and the purification of dioxane have been described in the previous paper.[2] As a catalyst, a 0.0428 N aqueous solution of sodium hydroxide was used.

Kinetic Procedures.—All reactions were carried out at 30°C (±0.05°C). A required amount of amide was weighed into a 50 ml. volumetric flask. The amide was dissolved in 25 ml. of dioxane. The flask was placed in a thermostat kept at 30°C for at least 30 min. The formaldehyde solution and distilled water were also kept at the same temperature. A 0.6 ml. volume of the catalyst and then a required amount of the formaldehyde solution were added to the flask. In order to avoid the effect of carbon dioxide in the atmosphere, the catalyst solution was added through a microburette in an atmosphere of air freed from carbon dioxide. The solution was then immediately diluted to 50ml. with distilled water. After a thorough mixing, the solution was brought into a reaction vessel which had been placed in the thermostat. The rate of the consumption of formaldehyde was determined by the KCN-method, as has been described in the case of an acid-catalyzed reaction.[2]

Experimental Errors Anticipated. — (1) The *N*-methylol amide produced may decompose to formaldehyde and amide in the presence of the base. However, Ugelstadt has concluded that the back reaction could be neglected until the reaction reached the consumption of ca. 10% of formaldehyde.[3]

(2) The benzamide may be hydrolyzed with the base catalyst into benzoic acid and ammonia. Ugelstadt has also concluded that this hydrolysis was negligible.

(3) As is known, formaldehyde is changed into formic acid and methanol by the Cannizzaro reaction. However, under the conditions described above, this reaction was so small as to be negligible, as Table I shows.

Table I. The consumption of formaldehyde at 30°C

($[\mathrm{CH_2O}]_0 = 0.05$ mol./l., catalyst 0.6 ml./50 ml.)

Reaction time min.	Decrease in $[\mathrm{CH_2O}]_0$ content $\times 10^{-3}$ mol./l.	Decrease in $[\mathrm{CH_2O}]_{\mathrm{OCH_3}}$ content $\times 10^{-3}$ mol./l.
2	0	0.5
5	0.1	1.8
25	0.1	2.6
45	0.28	6.0
60	0.28	—

In Table I, the decrease in $[\mathrm{CH_2O}]_0$ content indicates the concentration of formaldehyde consumed by the Cannizzaro reaction in the absence of amide. The decrease in $[\mathrm{CH_2O}]_{\mathrm{OCH_3}}$ content was the result of the consumption of formaldehyde by the reaction of formaldehyde with *p*-methoxybenzamide. In the present reaction, the *p*-methoxybenzamide was the most inactive amide. Even in this case, however, the $[\mathrm{CH_2O}]_0$ decrease was only a twentieth of that of $[\mathrm{CH_2O}]_{\mathrm{OCH_3}}$.

An Estimation of the Initial Rate of Reaction. —Figure 1 shows a typical example of the reaction course. The ordinate, -[F], showed the concentration of consumed formaldehyde. Extrapolating the

1) LXV: M. Imoto, N. Kotani and T. Toda, *J. Chem. Soc. Japan, Ind Chem. Soc.* (*Kogyo Kagaku Zasshi*), in press.

2) Part LIII of this series: M. Imoto and M. Kobayashi, This Bulletin, 33, 1651 (1960).

3) J. Ugelstadt, Dissertation, Leiden University (1955).

remaining concentration of formaldehyde, [F], to time zero, the initial concentration of formaldehyde, $[F]_0$, was estimated. The inclination of the curve of -[F] vs. time at time zero gave the rate of the reaction, $-d[F]/dt$.

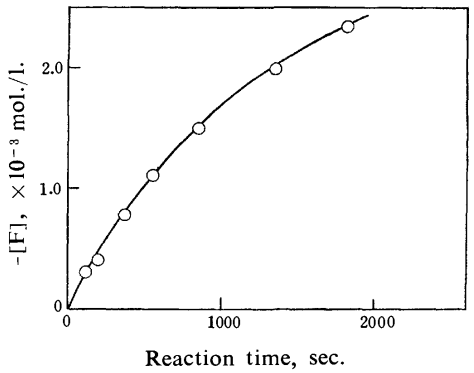

Fig. 1. The consumption of formaldehyde vs. the reaction time.
($[F]_0=0.0955$ mol./l., $[C_6H_5CONH_2]_0=0.05$ mol./l., at 30°C)

Results and Discussion

Reaction-orders of the Reactants.—Ugelstadt[3] has previously given the following rate equation for the base-catalyzed reaction of benzamide with formaldehyde:

$$R=-d[F]/dt$$
$$=k[C_6H_5CONH_2][CH_2O][OH^-] \quad (1)$$

To confirm Ugelstadt's formula, the rate of the consumption of formaldehyde, R, was investigated at various concentrations of benzamide and formaldehyde.

The Reaction-order of Benzamide.—While the concentrations of formaldehyde and of the catalyst were kept at 0.05 mol./l. and 0.60 ml./50 ml. respectively, the rate was measured in various concentrations of benzamide over the range from 0.0125 to 0.05 mol./l. As Fig. 2 shows, a linear relationship was obtained.

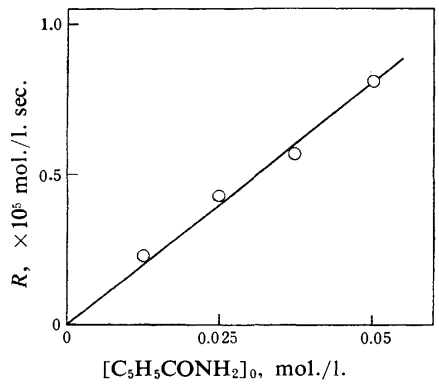

Fig. 2. The relationship between R and $[C_6H_5CONH_2]_0$.

The reaction, therefore, was of the first order with benzamide.

The Reaction-order of Formaldehyde.—While the concentration of benzamide was kept at 0.05 mol./l., the concentration of formaldehyde was changed from 0.013 to 0.200 mol./l. The result obtained was peculiar, as is shown in Fig. 3. Such a relationship between $[F]_0$ and R was found for the first time.

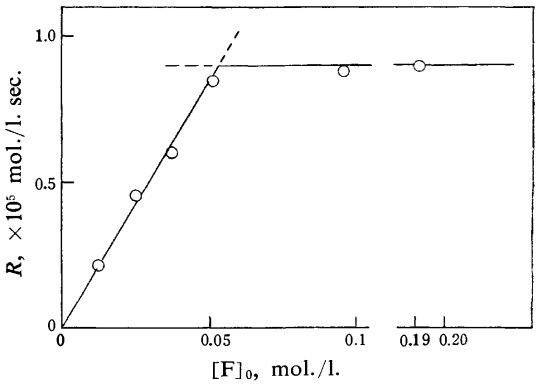

Fig. 3. The relationship between R and $[F]_0$.
0.6 ml. of the catalyst was added.

When the concentration of formaldehyde was less than ca. 0.05 mol./l., the reaction was of the first order with formaldehyde. However, in a higher concentration of formaldehyde than this characteristic concentration, the reaction order of formaldehyde became zero. A similar bending point in the curve of R vs. $[F]_0$ was also observed in the reaction of every substituted benzamide, as Fig. 4 shows.

The Reaction-order of Sodium Hydroxide.—According to the paper by Ugelstadt, it may be assumed that the reaction-order of $[OH^-]$ was first under the conditions described above. This will also be confirmed by us in a later paper.[4]

From the results obtained, the experimental rate equation can be represented as follows: In the case of a lower concentration of formaldehyde than usual:

$$R_2=\frac{-d[F]}{dt}$$
$$=k_2[C_6H_5CONH_2][CH_2O][OH^-] \quad (2)$$

By a higher concentration of formaldehyde than usual;

$$R_1=\frac{-d[F]}{dt}=k_1[C_6H_5CONH_2][OH^-] \quad (3)$$

The Effect of the Polar Character on the Reaction Rate. — The electron-releasing or attracting group substituted in the benzene

4) Part LXVII of this series: M. Imoto and A. Ninagawa, This Bulletin, 36, 1508 (1963).

nucleus of benzamide was expected to have a strong effect on the rate of the reaction. While the concentration of the substituted benzamide was kept constant (0.05 mol./l.), the relationship between R and $[F]_0$ was measured. The results obtained are illustrated by Fig. 4.

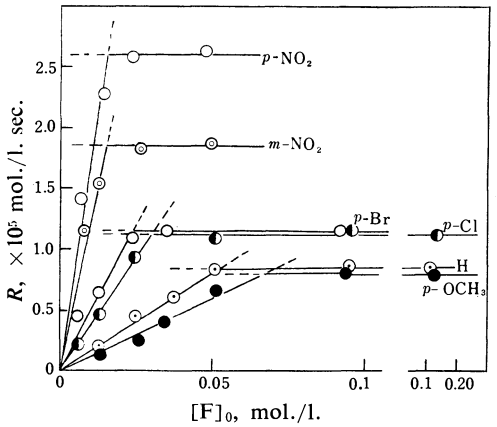

Fig. 4. The relationship between the initial concentration of formaldehyde and R. $[X\text{-}C_6H_4CONH_2]=0.05$ mol./l. Catalyst=0.6 mi./50 ml.

From the results of the experiments illustrated in Fig. 4, the reaction constants, $k_1[OH^-]$ and $k_2[OH^-]$, were calculated. (Table II).

These values of $k[OH^-]$ were correlated with Hammett's equation. The linear relationship shown in Fig. 5 was obtained.

TABLE II. RATE CONSTANTS FOR SUBSTITUTED BENZAMIDE

Benzamide	$k_1[OH^-]$	$k_2[OH^-]$	σ
p-OCH_3	1.60	1.92	−0.268
H	1.80	3.51	0.0
p-Cl	2.32	6.91	+0.227
p-Br	2.40	9.61	+0.232
m-NO_2	3.72	38.5	+0.710
p-NO_2	5.28	41.8	+0.778

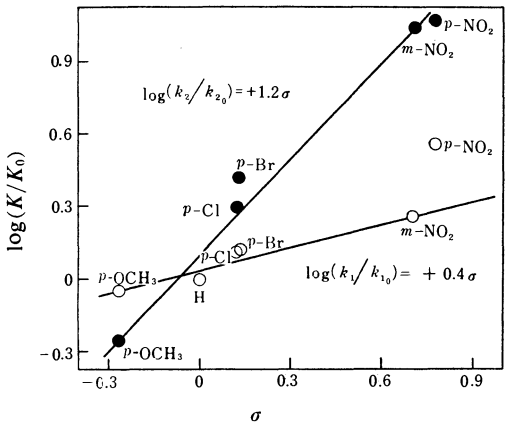

Fig. 5. Plots for Hammett's equation.

The Reaction Mechanism of Benzamide with Formaldehyde in the Presence of a Base Catalyst.—Ugelstadt has concluded that the reaction of benzamide proceeded via three steps:

i) $R\text{-}CONH_2 + B \rightarrow R\text{-}CONH^- + BH^+$

ii) $R\text{-}CONH^- + CH_2O \rightarrow RCONH\text{-}CH_2O^-$

iii) $RCONHCH_2O^- + BH^+ \rightarrow RCONHCH_2OH + B$

Of these three steps, it is clear that iii is not the rate-determining step. Ugelstadt considered step ii to be rate-determining and kinetically derived Eq. 1. However, this conception can not completely interpret the present results.

Step i may be concluded to be the slowest step from the consideration that, when an electron-attracting group is introduced into the phenyl nucleus, the release of protons from the NH_2 group of benzamide by the attack of hydroxyl ions becomes easier. This conception may be experimentally demonstrated, as in Fig. 5. In the range of the lower, and also of the higher, concentrations of formaldehyde, the signs of ρ were positive. The values of ρ were estimated to be +1.2 and +0.4 respectively.

The mechanism presented above may be classified as S_E1, namely, a unimolecular electrophilic substitution. The existence of Eq. 2 in the range of the lower concentration of formaldehyde was, apparently, consistent with the theory of S_E2. However, a new conception was applicable as follows: By step ii $X\text{-}C_6H_4CONH^-$ reacts immediately with formaldehyde, which exists in the solvated cage. Accordingly, until formaldehyde reaches the saturating concentration in the solvated cage, the rate of the consumption of formaldehyde is dependent on the added amounts of formaldehyde. In case the concentration of formaldehyde is higher than the saturated concentration in the solvated cage, the rate of the consumption of formaldehyde is independent of the amounts of formaldehyde.

It can be accepted that the bending points in the curves in Fig. 5 may be indicative of the saturated concentration of formaldehyde in the solvated cage. These points were obtained by extending the upward and lying lines to the crossing points. The concentrations of formaldehyde at this point were denoted as $[F]_c$.

In the ion of $X\text{-}C_6H_4CONH^-$, if X is an electron-attracting group, the electron-density about the nitrogen atom becomes smaller than when an electron-releasing group such as X is present. It is to be anticipated that the smaller

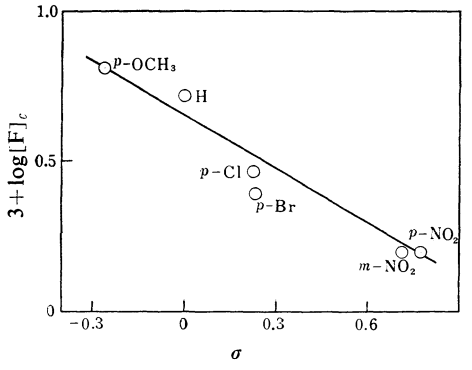

Fig. 6. The relation of the saturating concentration of formaldehyde in solvated cage with Hammett's constants.

the electron-density about the nitrogen atom, the smaller the solvating ability of the ion of $X\text{-}C_6H_4CONH^-$. The values of $[F]_c$ were estimated as follows: *p*-OCH_3 0.065 mol./l., H 0.052, *p*-Cl 0.0305, *p*-Br 0.024, *m*-NO_2 0.015, and *p*-NO_2 0.015. The results obtained here were applied to Hammett's equation, as Fig. 6 shows. These results strongly supported the conception of S_E1.

Summary

The mechanism of the reaction of the substituted benzamides with formaldehye in dioxane-water (1 : 1) in the presence of sodium hydroxide has been studied kinetically. Equations 2 and 3 have been obtained. An electron-attracting group increased the rate of the reaction, while an electron-releasing group decreased it. The reaction rates fit Hammett's equation. It was concluded that the S_E1-mechanism is suitable for interpreting the results obtained.

Faculty of Engineering
Osaka City University
Kita-ku, Osaka

Formaldehyde Resins. LXVII.[1] *On the Reaction Order of Sodium Hydroxide and on the Salt-effect of Sodium Bromide in the Base-catalyzed Reaction of Benzamide with Formaldehyde*

By Minoru IMOTO and Akira NINAGAWA

(Received July 26, 1963)

In the preceding paper,[1] the base-catalyzed reaction of benzamide and its para-substituted derivatives was investigated, and the following results were obtained. The rate equation was found to be:

$$R_2 = \frac{-d[CH_2O]}{dt} = k_2[C_6H_5CONH_2][CH_2O][OH^-] \quad (1)$$

at a lower concentration of formaldehyde than usual and

$$R_1 = \frac{-d[CH_2O]}{dt} = k_1[C_6H_5CONH_2][OH^-] \quad (2)$$

at a higher concentration of formaldehyde than usual, moreover, the reaction mechanism was assumed to be as follows:

i) $R\text{-}CONH_2 + B \rightleftarrows R\text{-}CONH^- + BH^+$

ii) $R\text{-}CONH^- + CH_2O \rightarrow R\text{-}CONHCH_2O^-$

iii) $R\text{-}CONHCH_2O^- + BH^+ \rightleftarrows R\text{-}CONHCH_2OH + B$

For k_2 and k_1 of Eqs. 1 and 2, Hammett's rule was applied, and a linear relationship was established. The reaction constants, ρ, were +1.2 and 0.4 respectively. The positive ρ values indicated an easiness of the loss of the proton from an amide group when the substituent was of the electron-withdrawing type. Granted that step i was the slowest step, the reaction was interpreted as S_E1. The change in the reaction order of formaldehyde from one to zero was explained by the idea of the "solvated cage."

The present paper concerns the determination of the reaction order of sodium hydroxide and the relationship between the concentration of sodium hydroxide and the bending concentration of formaldehyde, $[F]_c$, which corresponds to the critical point of the reaction order of formaldehyde. Also, studies of the salt-effect of sodium bromide and of the constancy of the pH value through the reaction will be reported on.

1) LXVI: M. Imoto and M. Kobayashi, This Bulletin, **36**, 1505 (1963).

Experimental

Reagents.—The methods used in the preparation and purification of benzamide and dioxane have already been described in a previous paper.[2] An aqueous solution of sodium hydroxide was used as the catalyst. In order to avoid a change in its concentration due to carbon dioxide absorption from air, the storing bottle was directly connected to a microburette and the solution was pushed into the burette by air pressure through a potassium hydroxide absorber tube. Sodium bromide was of a commercially special grade.

Experimental Procedures. — The reaction was carried out at 15±0.05°C, and the rate was determined by the following procedure. Benzamide (0.657 g.) was weighed into a 50 ml. graduated flask so as to produce a 0.1 mol./l. solution; this was dissolved in 35 ml. of dioxane, and then a repuired amount of the catalyst was added. While the mixture was kept in a constant-temperature bath at 15°C for twenty minutes, a formaldehyde solution and purified water were also kept at the same temperature in the same bath. The formaldehyde solution was then pipetted into the benzamide solution, and the whole mixture was then diluted to a total volume of 50 ml. immediately and mixed well by shaking it in the bath. The reaction mixture was then transferred to a reaction vessel that had also been kept in the constant-temperature bath. The addition of formaldehyde was taken as the start of the reaction; after that time aliquot samples were taken at a constant time intervals. The aliquot was then mixed with the quenching solution, which had been cooled in ice water for twenty minutes, and then the amount of residual formaldehyde was determined by the KCN-method, which has been described in a previous paper.[1]

When a salt was present in the reaction system, a water solution of sodium bromide was added just before the addition of the catalyst.

The values of pH were measured by means of a Hitachi-Horiba potentiometer Type P.

Quenching of the Reaction.—Among the number of tests made to quench the reaction, the best results were obtained with a mixture of a buffer solution (0.1 N KH_2PO_4 and 0.1 N Na_2HPO_4) and potassium cyanide with a pH value of 10.0 cooled in ice water for twenty minutes before use. The results obtained are shown in Fig. 1.

After the quenching, the titration of formaldehyde had to be done immediately, for the reaction was stopped for a short period only, after which the reverse reaction took place.

The Start of the Reaction. — The following two methods had been considered to be the start of the reaction:

(a) The time of the addition of formaldehyde, following the addition of the sodium hydroxide solution to the benzamide.

(b) The time of the addition of the sodium hydroxide solution, following the addition of formaldehyde.

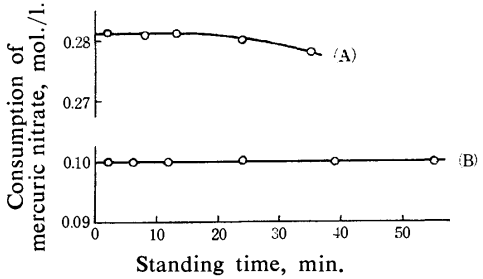

Fig. 1. The standing time in the quenching solution vs. the amount of mercuric nitrate consumed.
(A) The titration of the reacting solution; $[Benzamide]_0=0.100$ mol./l., $[CH_2O]_0=0.100$ mol./l., $[NaOH]=4.0\times10^{-4}$ mol./l., reaction time=29 min.
(B) The titration of the formaldehyde solution, as a blank test; $[CH_2O]_0=0.100$ mol./l.

Both were found to be the same; method a was chosen.

Calculation of the Reaction Rate.—The amount of formaldehyde consumed was given by the difference between the amounts of mercuric nitrate needed for an aliquot sample and for a blank test in which no benzamide was present. The rate of the disappearance of formaldehyde was computed in the manner described in the foregoing paper. Figure 2 shows some typical examples of the consumption of formaldehyde.

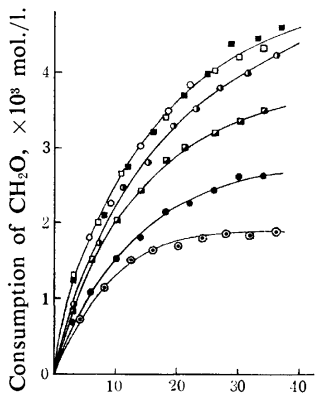

Fig. 2. The consumption of formaldehyde vs. reaction time at 15±0.05°C.
$[Benzamide]_0=0.100$ mol./l., $[NaOH]=4.47\times10^{-4}$ mol./l.
$[CH_2O]_0=0.129$ mol./l. (□) 0.064 mol./l. (◪)
0.107 (■) 0.043 (●)
0.099 (○) 0.021 (⊙)
0.085 (◑)

Results

The Order of the Reaction with Respect to Each Reactant.—The reaction was carried out with various concentrations of formaldehyde

2) Part LIII of this series: M. Imoto and M. Kobayashi, This Bulletin, 33, 1651 (1961).

between 0.011 and 0.155 mol./l. for each concentration of sodium hydroxide of 6.12×10^{-4}, 4.48×10^{-4}, 3.28×10^{-4}, and 2.18×10^{-4} mol./l., and their relation with the initial rate of the consumption of formaldehyde (R) was obtained as in Fig. 3, from which the order of the reaction with respect to formaldehyde and sodium hydroxide, and the relationship of the sodium hydroxide concentration to the bending concentration of formaldehyde $[F]_c$ were studied. Of these the reaction had already been reported in a previous paper to be of the first order with respects to formaldehyde; the present study was undertaken in order to reconfirm it.

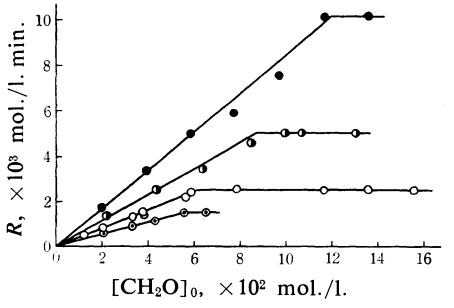

Fig. 3. Consumption rate (R) vs. the concentration of formaldehyde in the presence of various amounts of sodium hydroxide.
$[Benzamide]_0=0.100$ mol./l.
$[NaOH]=6.12\times10^{-4}$ mol./l. (●), 4.47×10^{-4} mol./l. (◑), 3.28×10^{-4} mol./l. (○), and 2.18×10^{-4} mol./l. (⊙)
The same symbols used in Figs. 4, 5 and 6 to represent these same [NaOH] value.

Order of the Reaction with Respect to Formaldehyde. — At each concentration of sodium hydroxide, a linear relationship between the lower concentrations of formaldehyde and R was obtained; at the higher concentrations of formaldehyde, it had no effect on the rate, showing the order of the reaction to be zero. The logarithmic plots of low formaldehyde concentrations and R are shown in Fig. 4. The values of tan α were found to be 1.00, 0.82, 0.97 and 0.93 at the respective concentrations of sodium hydroxide. The reaction, therefore, was found to be of the first order with respect to formaldehyde in the range of lower concentrations.

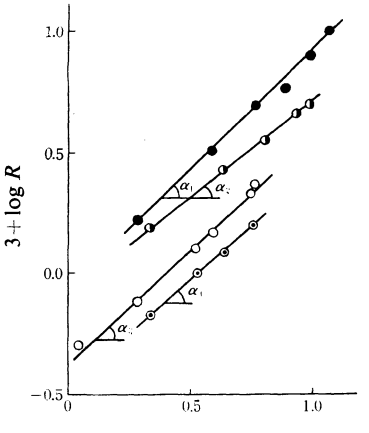

Fig. 4. The relationship between R and the concentration of formaldehyde before the bending point.
tan $\alpha_1=1.00$ tan $\alpha_3=0.97$
tan $\alpha_2=0.82$ tan $\alpha_4=0.93$

The Order of the Reaction with Respect to Sodium Hydroxide.—The logarithmic plots of sodium hydroxide concentration and R at the formaldehyde concentration of 0.40 mol./l., shown already in Fig. 3, gave the straight line in Fig. 5, and tan α was found to be 1.00. Thus the order of the reaction with respect to sodium hydroxide was found to be of the first order.

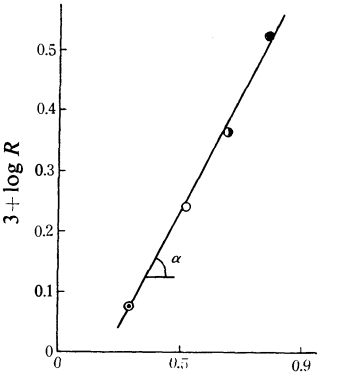

Fig. 5. The relationship between sodium hydroxide concentration and R at $[CH_2O]_0=0.40$ mol./l.
tan $\alpha=1.00$

The Relationship between the Bending Concentration of Formaldehyde and Sodium Hydroxide Concentration.—Figure 6 shows the relationship between the logarithmic plots of the bending concentration of formaldehyde, where the order of the reaction turned from first to zero, and the sodium hydroxide concentration. It was made clear that the slope was 0.93 and that the relationship between the bending concentration of formaldehyde, $[F]_c$, and the sodium hydroxide concentration was of the first order.

Measurement of pH.—As Figs. 7 and 8 show, the pH values of the reaction systems were found to be constant throughout the reaction. Therefore, it was not necessary to consider the various sub-reactions which could cause a change in pH value.

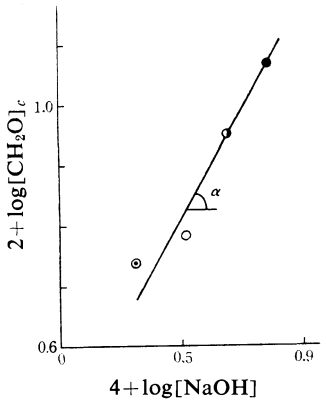

Fig. 6. The relationship between the formaldehyde concentration at the bending point and the sodium hydroxide concentration.
$\tan\alpha=0.93$

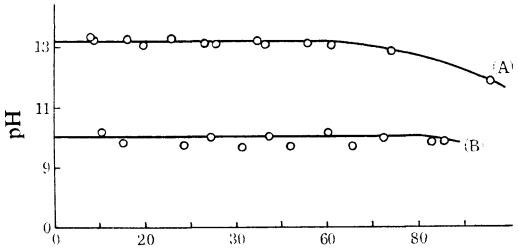

Fig. 7. The pH of the reaction mixture vs. time.
$[Benzamide]_0=0.100$ mol./l., $[CH_2O]_0=0.100$ mol./l.
$[NaOH]=4.47\times10^{-4}$ mol./l. (A), 2.18×10^{-4} mol./l. (B)

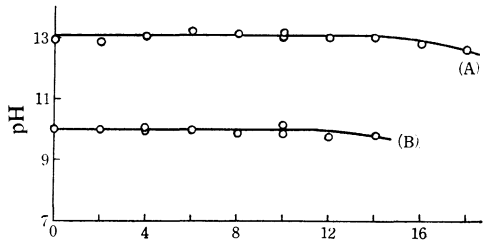

Fig. 8. The pH of the reaction mixture at time zero vs. the formaldehyde concentration.
$[Benzamide]_0=0.100$ mol./l.
$[NaOH]=4.47\times10^{-4}$ mol./l. (A), 2.18×10^{-4} mol./l. (B)

The Salt Effect of Sodium Bromide. — The results obtained are illustrated in Fig. 9. The pH value was constant through the reaction in the presence of sodium bromide.

Activation Energy. — The activation energy of the reaction of benzamide with formaldehyde in the presence of sodium hydroxide was computed as 8.25 kcal./mol. on the basis of the experiments at 15, 20, 25, and 30°C (Fig. 10).

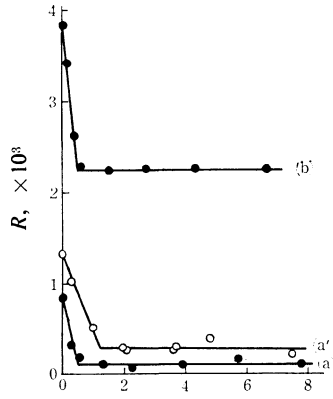

Fig. 9. The salt effect of sodium bromide on the reaction rate of benzamide with formaldehyde.
$[Benzamide]_0=0.100$ mol./l.
$[CH_2O]_0=0.100$ mol./l. (○), 0.040 mol./l. (●)
Upper line (b): $[NaOH]\ 7.37\times10^{-4}$ mol./l.
Lower two line (a') (a): $[NaOH]\ 3.28\times10^{-4}$ mol./l.

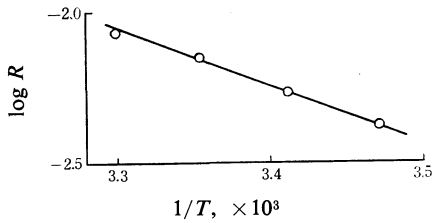

Fig. 10. The determination of activation energy.
$[Benzamide]_0=0.100$ mol./l.
$[CH_2O]_0=0.105$ mol./l.
$[NaOH]=3.5\times10^{-4}$ mol./l.

Discussions

The rate equation derived from the present experimental results has shown a good agreement with Eqs. 1 and 2 obtained by Imoto and Kobayashi in the foregoing paper.[1] On the basis of the formation of $RCON^-H$ anions by the reaction of OH^- with the amide, Imoto and Kobayashi have concluded that the mechanism of this reaction was like S_E1, and that thus the anion formed was caged by the solvent and by other molecules to form a so-called "solvated cage," in which formaldehyde reacted with the anion to introduce methylol groups. If this were the reaction, the rate of the disappearance of formaldehyde in a solvated cage had to be proportional to the formaldehyde concentration, unless it reached the saturation

concentration in the cage. When added formaldehyde gave a higher concentration than the saturation concentration in a solvated cage, it existed at the outer side of the cage, missing the reaction with the anion, and the rate of the consumption of formaldehyde was not affected by the formaldehyde concentration. If the reaction proceeds in that fashion, the concentration of $RCON^-H$ increases with an increase in the sodium hydroxide concentration. In other words, the number of solvated cages increases with an increase in the sodium hydroxide concentration, and when the formaldehyde concentration increases, the amount of formaldehyde coming into the solvated cages also increases, therefore, it can be expected that the saturation concentration of formaldehyde will be increased linearly with an increase in the sodium hydroxide concentration. There should be a linear relationship between the critical bending concentration of formaldehyde in Fig. 3 and the sodium hydroxide concentration. As is shown in Fig. 6, the experimental results agreed well with what had been expected. The peculiar effect of sodium bromide shown in Fig. 9 can also be explained by the solvated cage theory. With the concentration of sodium bromide, the concentration of sodium ions in the cage increases, resulting in a decreas in the formaldehyde concentration in the cage. Inevitably the consumption rate of formaldehyde decreases rapidly, until sodium ions reach an equilibrium concentration in the cage. After the equilibrium is achieved, the rate may be kept constant. As the lower two curves in Fig. 9 show, the bending point of a' with respect of sodium bromide is situated at a higher concentration than that of a. This phenomenon can be understood by the cage theory, considering that the concentration of formaldehyde in a' is 0.1 mol./l. and that in a is 0.04 mol./l. The equilibrium concentration of sodium cations should be lower in the case of a' than in that of a.

Those results strongly support the S_E1 mechanism of the reaction of benzamide with formaldehyde in the presence of a base catalyst.

Summary

A kinetic study of the reaction of benzamide with formaldehyde in the presence of sodium hydroxide has been made. The following results have been obtained: (1) A linear relationship is obtained between the concentration of sodium hydroxide and the critical bending concentration of formaldehyde where the reaction-order changes from one to zero. (2) The pH value is constant throughout the reaction. (3) The rate of the reaction decreases upon the addition of sodium bromide. However, the decrease reaches a miuimum at a definite concentration of sodium bromide. After this point, the salt has no effect on the rate. (4) The activation energy has been computed as 8.25 kcal./mol. The findings (1) and (3) have been explained by the solvated cage theory.

Faculty of Engineering
Osaka City University
Kita-ku, Osaka

Charge Mobility in Pyrene Crystals

By Kenji OHKI, Hiroo INOKUCHI and Yusei MARUYAMA

(Received August 6, 1963)

Recently, Murrell has calculated the overlap integrals between the molecular orbitals of different anthracene molecules in the crystal lattice.[1] Further, LeBlanc has reported on the band structure of anthracene.[2] In this report, we will extend Murrell's study to the pyrene crystal in order to find a correlation between the calculated and experimental values of charge mobility in a direction perpendicular to its ab plane.*

1) J. N. Murrell, *Mol. Phys.*, **4**, 205 (1961).
2) O. H. LeBlanc, *J. Chem. Phys.*, **35**, 1275 (1961).

Theoretical

The Coordinates.—The crystal structure of pyrene is monoclinic prismatic with a space group $C_{2h}^5-P2_1/a$ and with $a=13.60\pm0.05$ Å, $b=9.24\pm0.03$ Å, $c=8.37\pm0.10$ Å and $\beta=100.2\pm0.2°$; its detailed analysis has been obtained by the X-ray method by Robertson and White.[3]

* The calculation of overlap integrals in a direction parallel to the ab plane will be reported on elsewhere.
3) J. M. Robertson and J. G. White, *J. Chem. Soc.*, **1947**, 358.

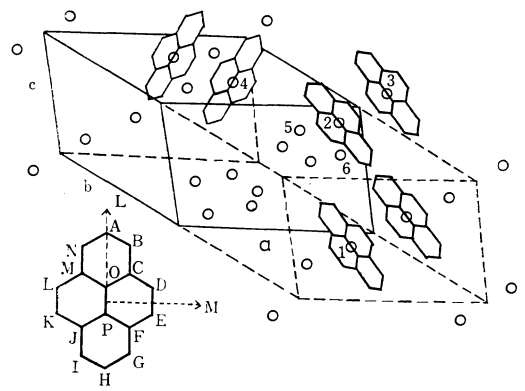

Fig. 1. Arrangement of pyrene molecules in the crystal lattice.

Employing their findings, the relation between neighbouring molecules in the crystal is drawn in Fig. 1; the numbers 1, 2,···, 6 denote pyrene molecules in the crystal. Further, the terms of A, B, C, ···, O and P are carbon atoms in the pyrene molecule, as the same figure shows. From the orthogonal coordinates (X, Y, Z) of the sixteen atoms of the pyrene molecule in the crystal lattice, the distances between two atomic centres in a perpendicular direction to the ab plane are estimates as follows:

(a) Distances between molecule 1 and molecule 2.

N_1G_2**$=3.541$ Å $M_1E_2=4.945$ Å $N_1F_2=4.032$ Å

$M_1F_2=4.703$ Å $N_1E_2=3.827$ Å $L_1G_2=3.827$ Å

$N_1D_2=4.921$ Å $L_1F_2=4.945$ Å $M_1G_2=4.032$ Å

$K_1G_2=4.921$ Å

(b) Distances between molecule 1 and molecule 3. All distances are more than 5 Å.

(c) Distances between molecule 1 and molecule 4.

$N_1N_4=4.899$ Å $B_1M_4=4.672$ Å

$B_1N_4=4.042$ Å $B_1L_4=4.366$ Å

(d) The distance between molecule 1 and molecule 5.

$N_1I_5=4.356$ Å

(e) Distances between molecule 1 and molecule 6.

$N_1B_6=4.042$ Å $B_1M_6=4.612$ Å

$N_1N_6=4.899$ Å $L_1B_6=4.366$ Å

When the overlap integrals between two atomic orbitals are calculated, any integrals between two orbitals which are more than 5.0Å are disregarded, for the integrals decrease exponentially with the distances of the two atomic centres. Therefore, none of intermolecular distances greater than 5 Å are indicated in the above chart. Furthermore, as is described in the following section, the density of the unpaired electrons at the A, H, O or P atom positions is null. Thereby, all terms including A, H, O and P are also disregarded.

The Calculation of Overlap Integrals. — The overlap integral (S) between two molecules, a and b, are

$$S=\int \phi_k^a \phi_k^b \, d\tau = \sum_{ij} C_{ki}C_{kj} \int \chi_i^a * X_j^b d\tau \qquad (1)$$

because ϕ_k^a, the molecular orbital, is derived from a linear combination of atomic orbitals, χ_i^a.

To obtain C_{ki} and $k(C_{kj})$, the simple Hückel theory has been applied. The Hückel functions for the hole and the electron are given in Fig. 2.[4]

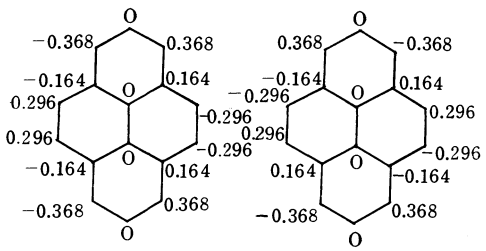

For hole For electron

Fig. 2. The Hückel functions for hole and electron.

Further, the terms of $\int \chi_j^a * \chi_j^b \, d\tau$ are calculated in association with Mulliken's method.[5] On the basis of this work on a master formula for the Slater-AO overlap integral, two of the terms are considered to find the overlap integral between two molecules:

$$S(2p\pi, 2p\pi) = (120)^{-1} p^5 [5A_4 - 6A_2 + A_0] \quad (t=0) \qquad (2)$$

$$S(2p\sigma, 2p\sigma) = (120)^{-1} p^5 [5A_4 - 18A_2 + 5A_0] \quad (t=0) \qquad (3)$$

where $A_k(p) \equiv \int_1^\infty \xi^k e^{-p\xi} d\xi$

$$= e^{-p} \sum_{\mu=1}^{k+1} \left[k!/p^\mu (k-\mu+1)! \right];$$

in the above equation $\mu (=Z_n/(n-\delta))$ is 1.45 for C^-, 1.625 for C, and 1.80 for C^+. Further, $p \equiv 1/2(\mu_a+\mu_b)R/a_H$, $t \equiv (\mu_a-\mu_b)/(\mu_a+\mu_b)$, R is the distance between atoms, and a_H is the

** N_1G_2 denotes the distance between the N atom of molecule 1 and the G atom of molecule 2.

4) C. A. Coulson and R. Daudel, "Dictionary of Values of Molecular Constants," Vol. II, Centre de la Recherche Scientifique and ICI (1955).

5) R. S. Mulliken, C. A. Rieke, D. Orloff and H. Orloff, *J. Chem. Phys.*, **17**, 1248 (1949).

Bohr radius.

From these relations, $S(2p\pi, 2p\pi)$ and $S(2p\sigma, 2p\sigma)$ have been calculated as in Table I.

As Table I shows, the overlap integral, S, monotonously decreases with an increase in the parameter, p. In association with the curve of relation, p-S, the values of S for the atomic pair have been evaluated.

These atomic orbitals are defined by the vectors $\boldsymbol{n}_a$ and $\boldsymbol{n}_b$, and the separation of the orbitals, by $\boldsymbol{R}$. Thereby, the overlap integral, S_{ab}, is described as:

$$-S_{ab}=\frac{(\boldsymbol{n}_a\boldsymbol{R})(\boldsymbol{n}_b\boldsymbol{R})}{\boldsymbol{n}_a\boldsymbol{n}_b{}^2\boldsymbol{R}}\,S(2p\sigma, 2p\sigma)-\left[\frac{\boldsymbol{n}_a\boldsymbol{n}_b}{n_an_b}\cdot\frac{(\boldsymbol{n}_a\boldsymbol{R})(\boldsymbol{n}_b\boldsymbol{R})}{n_an_bR}\right]S(2p\pi, 2p\pi) \tag{4}$$

In this consideration, we must calculate the directions of the π-orbital vectors in the pyrene crystal lattice. In accordance with the crystallographical study by Robertson and White, the orientations of molecules in the lattice are:

$$\chi_L=61.1^\circ:\ \chi_M=52.2^\circ:\ \chi_N=128.7^\circ$$
$$\cos\chi_N=-0.6248$$
$$\psi_L=77.7^\circ:\ \psi_M=52.4^\circ:\ \psi_N=40.2^\circ$$
$$\cos\psi_N=0.7630$$
$$\omega_L=31.9^\circ:\ \omega_M=120.1^\circ:\ \omega_N=80.5^\circ$$
$$\cos\omega_N=0.1648$$

where χ, ψ and ω are the angles at which the molecular axes L and M (Fig. 1) and their perpendicular, N, make the a, b and c′ crystallographic axes (c′ is perpendicular to a and b). Thereby, the directions of the π-orbital vectors for molecules 1, 2 and 3 are (−0.6248, 0.7630, 0.1648) or (0.6248, −0.7630, −0.1648), and for molecules 4, 5 and 6, (−0.6248, −0.7630, 0.1648) or (0.6248, 0.7630, −0.1648).

On the basis of the above calculations, the overlap integrals for the hole and the electron in the pyrene crystal are summarized in Table II. These integrals may be proportional to the mobility of the charge carriers.

TABLE I. THE OVERLAP MASTER TABLE

p	$S(2p\sigma, 2p\sigma)$	$S(2p\pi, 2p\pi)$
10.00	3.491×10^{-2}	5.342×10^{-3}
10.50	2.564×10^{-2}	3.656×10^{-3}
11.00	1.866×10^{-2}	2.491×10^{-3}
11.50	1.347×10^{-2}	1.691×10^{-3}
12.00	0.9652×10^{-2}	1.136×10^{-3}
12.50	0.6869×10^{-2}	0.7686×10^{-3}
13.00	0.4853×10^{-2}	0.5155×10^{-3}
13.50	0.3416×10^{-2}	0.3447×10^{-3}
14.00	0.2389×10^{-2}	0.2298×10^{-3}
14.50	0.1662×10^{-2}	0.1527×10^{-3}
15.00	0.1151×10^{-2}	0.1013×10^{-3}
15.50	0.0794×10^{-2}	0.06695×10^{-3}

TABLE II. THE OVERLAP INTEGRAL BETWEEN TWO PYRENE MOLECULES

Overlap integral between two molecules (a-b)		Hole	Electron
a	b		
1	2	4.13×10^{-4}	0.71×10^{-4}
1	4	-2.62×10^{-4}	-1.90×10^{-4}
1	5	-1.92×10^{-4}	-1.92×10^{-4}
1	6	-2.39×10^{-4}	-1.87×10^{-4}

Experimental and Discussion

Fairly large single crystals of purified pyrene, the method of preparation of which has already been described in a previous report,[6] were studied to find their carrier mobilities. The apparatus to find them was designed following suggestion by Kanzaki.[7] A pyrene crystal (4) approximately 1 to 2 mm. thick (d) was mounted between a pair of Mylar insulating sheets (3) serving as blocking layers. Between two metal electrodes, one of them a copper electrode (1) and the other a conducting glass one (5), an electrical potential (V) was applied, and a short light pulse with μ sec. along was illuminated on the surface of the crystal, as is shown in Fig. 3 schematically. Under the influence of a polarity of the electric field, one of the charge carriers drifted through the crystal. Therefore, the mobilities (μ) of both carriers, the electron (μ_e) and the hole (μ_h),

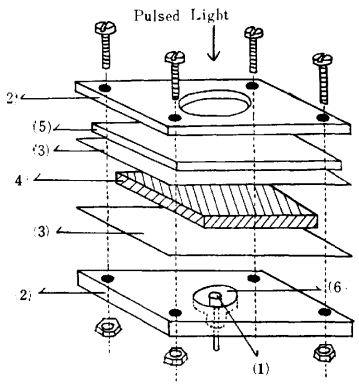

Fig. 3. The apparatus to observe the charge mobility in organic crystals. (1) Copper electrode, (2) copper holder, (3) Mylar sheet as blocking layer, (4) pyrene crystal, (5) conducting glass electrode and (6) teflon insulating bush.

6) H. Inokuchi and K. Ohki, This Bulletin, 36, 105 (1963).

7) H. Kanzaki, T. Ninomiya and K. Kido, *J. Phys. Chem. Solids*, 22, 309 (1961).

were calculated from the relation $\mu=d^2/Vt$, where t is the time of drift in crystal.* In accordance with the above equation, the mobilities were observed to be $\mu_e\sim3.0\,cm^2/V.sec.$ and $\mu_h=1.2\pm0.1\,cm^2/V.sec.$ at room temperature respectively.

LeBlanc has found from the transient photocurrent with cathode illumination that the hole mobility in the polycrystalline pyrene is $\mu_h=0.35\pm0.03\,cm^2/V.sec.$ at 100°C and $\mu_h=0.28\pm0.03\,cm^2/V.sec.$ at 149°C.[8] The same author has also reported that the photocurrent with an illuminated cathode, which was fifty times smaller than that with an illuminated anode, is too weak to use to estimate the electron mobility. In contrast with his work, in this experiment, the electron mobility (μ_e) could be estimated from the weak photocurrent using cathode illumination, although with difficulty.

To judge from the theoretical calculations in Table II, the hole mobility was larger than that of the electron. This discrepancy between experimental and theoretical works may result from a rough approximation of the above calculation applying the overlap integral; in the future we hope to have a more reliable theoretical treatment for organic semiconductors.

* To avoid the effect of the time constant of the apparatus on the preceding relation, the value of the resistor as an input impedance was $10^5\,\Omega$, the applied potential was 10^3 V., and the thickness of the crystal was 1.4 mm.

8) O. H. LeBlanc, *J. Chem. Phys.*, **37**, 916 (1962).

Summary

To estimate the charge mobility in a direction perpendicular to the ab plane in the sixteen atoms of the aromatic hydrocarbon crystal, pyrene, the overlap integrals between two molecules have been calculated. On the basis of these results, the hole mobility (μ_h) has been found to be twice that of the electron mobility (μ_e). However, judging from the transient photocurrent of the pyrene crystal, μ_e ($\sim3\,cm^2/V.sec.$) was considerably larger than μ_h ($1.2\,cm^2/V.sec.$). This discrepancy may be eliminated by the introduction of a more accurate theoretical treatment.

The Institute for Solid State Physics
The University of Tokyo
Azabu, Tokyo

The Application of Intermittent Illumination to the Bleaching of Dye. I. A General Consideration of the Method

By Masao KOIZUMI and Yoshiharu USUI

(Received June 17, 1963)

It is well-known that intermittent illumination (the sector method) has been successfully applied to kinetic studies of polymerization, but it has not yet been introduced in the photobleaching reaction of dye solutions. It is certain, however, that this method would also afford valuable information about the behavior of the intermediate produced by the irradiation of the dye solution. For example, if a certain intermediate with a lifetime of τ absorbs light, there is a possibility that the reaction is accelerated by an intermittent illumination with a frequency comparable with $1/\tau$, as compared with the case in which it is illuminated by a light with a lower frequency. There will be many other cases in which such specific effects may be anticipated. We undertook such experiments by employing the stroboscope light as a light source. This consists of successive flashes, the duration of which is several microseconds and the frequency of which can be changed within a certain region. Furthermore, one flash can emit a considerable amount of light. It is expected that such a light source has, in some cases, certain advantages over an intermittent light source by means of a sector.

The object of the present paper is to discuss the basic points necessary for such a quantitative application. For example, two factors, the intensity and the frequency of the flash, when varied over a wide range, may have some specific effects on the reaction which may be attributed to the method itself; therefore, it is necessary to consider them beforehand. For example, when the intensity of the flash is increased beyond a certain limit,

the quantity of the reaction will become independent of the intensity. The present paper will first discuss four subjects which are closely connected with the experimental results to be presented later.

The Establishment of the Steady State.—When a certain intermediate with a rather long life, τ, is generated by an illumination, its concentration will rise with a successive flash. It is desirable to know the number of flashes which are necessary to get the maximum concentration of the intermediate (X) and the value of the latter when the net reaction does not take place. These findings will be helpful in considering the situation in which the eventual reaction proceeds.

The Effect of ν on the Quantity of Reaction at Various Flash Intensities when $\nu \ll 1/\tau$.—Even when the frequency of the (successive) flashing ν is substantially smaller than $1/\tau$, the quantity of the reaction is still affected by ν in a specific manner depending on the flash intensity. This effect may be said to be due to the method itself. The general features may perhaps be summarized as follows:

A) At a constant light quantity per second, the larger ν may increase the quantity of the reaction per second more or less according to the intensity.

B) At a constant light intensity of one pulse, the quantity of reaction per each successive flash is independent of ν. However, the average quantity of reaction per flash decreases with ν.

The Effect of ν when $\tau \approx 1/\nu$.—A complicated effect due to the method itself may be anticipated.

Some Relations between I and ν Effects when a Genuine Frequency Effect exists.—For example, the case in which X absorbs light and induces an additional reaction will be considered.

I. The Establishment of the Steady State

Let us consider the case in which no net reaction takes place and yet an intermediate, X, with a suitable lifetime, τ, is produced. Upon successive flashes, the concentration of X increases until X^o_n and X^f_n practically reach the constant value (see Fig. 1).

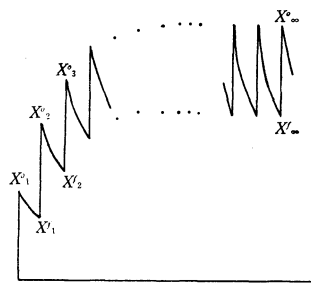

Fig. 1. Change in the concentration of X when no net reaction occurs.

The number of flashes necessary to realize this situation can be derived as follows:
Put the initial concentration of dye as C_o and the concentrations of dye immediately after each flash and just before the next flash, respectively, as C^o_n and C^f_n.

$$\left.\begin{array}{l} C_o \rightarrow C^o_1 \rightarrow C^o_2 \rightarrow \cdots\cdots \\ \qquad X^o_1 \rightarrow X^o_2 \rightarrow \cdots\cdots \end{array}\right\}$$

$$\left.\begin{array}{l} C^f_1 \rightarrow C^f_2 \rightarrow \cdots\cdots \\ X^f_1 \rightarrow X^f_2 \rightarrow \cdots\cdots \end{array}\right\}$$

If $(1-f)$ fraction of dye is changed to X by each flash and if the ratio of X^f_n to X^o_n is g, the following relations hold:

1st pulse

$$C^o_1 = C_o f \qquad X^o_1 = C_o(1-f)$$
$$C^f_1 = C_o - X^f_1 \qquad X^f_1 = C_o(1-f)g$$
$$= C_o(1-g+fg)$$

2nd pulse

$$C^o_2 = C_o\{1-(1-f)g\}f$$
$$X^o_2 = C_o\{1-(1-g+fg)f\}$$
$$C^f_2 = C_o\{1-g+fg(1-g)+f^2g^2\}$$
$$X^f_2 = gX^o_2$$

3rd pulse

$$C^o_3 = C^f_2 f$$
$$X^o_3 = C_o[1-\{1-g+fg(1-g)+f^2g^2\}f]$$
$$C^f_3 = C_o[(1-g)+fg(1-g)$$
$$+f^2g^2(1-g)+f^3g^3]$$
$$X^f_3 = gX^o_3$$

n-th pulse

$$C^f_n = C_o\{(1-g)+fg(1-g)+\cdots$$
$$\cdots+(fg)^{n-1}(1-g)+f^ng^n\}$$
$$= \frac{C_o}{1-fg}\{(1-f)f^ng^{n+1}+(1-g)\}$$

Changing $(1-f)$ to f for convenience:

$$C^f_n = \frac{C_o\{(1-f)^ng^{n+1}f+(1-g)\}}{1-(1-f)g} \tag{1a}$$

$$X^f_n = \frac{C_ofg\{1-(1-f)^ng^n\}}{1-(1-f)g} \tag{1b}$$

$$C^o_n = \frac{C_o\{(1-f)(1-g)+(1-f)^ng^n\}}{1-(1-f)g} \tag{1c}$$

$$X^o_n = \frac{C_of\{1-(1-f)^ng^n\}}{1-(1-f)g} \tag{1d}$$

For $n \rightarrow \infty$:

$$C^f{}_\infty = \frac{1-g}{1-(1-f)g} C_o \qquad (1'a)$$

$$C^o{}_\infty = \frac{(1-f)(1-g)}{1-(1-f)g} C_o \qquad (1'c)$$

$$X^f{}_\infty = \frac{C_o f g}{1-(1-f)g} \qquad (1'b)$$

$$X^o{}_\infty = \frac{C_o f}{1-(1-f)g} \qquad (1'd)$$

If X returns to the ground state dye according to the first order reaction, then $g = \exp(-k/\nu)$, where k is a rate constant and ν, the frequency of the flash.

If the light absorption is proportional to $C\varepsilon$ (assuming the cell length to be 1 cm.), f can be written as $\Phi\varepsilon\alpha$, where α is a fraction of the excited dye which reaches X, and Φ is the light quantity per pulse (see II).

As an example, let us consider the case when $f=0.1$ and $k \approx 10\ \mathrm{sec}^{-1}$. For 100 pulses per sec. (100 pps),

$$g = e^{-k/\nu} \approx 0.9 \qquad X^f{}_\infty \approx 0.47 C_0$$

It can be estimated that the second term in Eqs. 1a, b, c and d becomes less than 1% of the first term when $n=20$. For 10 pps, g is ca. 0.4, $X^f{}_\infty$ is ca. 6% of C_o, and two or three flashes would be enough for X^f to get within 10% of this $X^f{}_\infty$ value.

If $f=0.01$, $k \approx 10\ \mathrm{sec}^{-1}$, and $\nu=100$, $X^f{}_\infty$ would be about 8% of the concentration of the ground state dye, and the second term in Eq. 1b becomes one per cent of the first term when n equals 40.

II. Intensity Effect ($\nu \ll 1/\tau$)

The high intensity of the flash is favorable to a large reaction rate. However, if it is too large, the absorption of light is so close to the saturation point that a quantitative treatment is rather troublesome. What kind of effect may be expected when the intensity approaches the saturation value? How is it influenced by the frequency of the flash? What is the largest possible intensity which is not accompanied with complicating effects? These questions must be answered before we can deal with our problem quantitatively.

Let us take the case when the reaction proceeds through X with a rather long τ. At first, however, only the $\nu \ll 1/\tau$ region, where no genuine kinetic effect is expected, will be considered. The scheme is written as follows:

$$\mathrm{D} \rightarrow \mathrm{D}^* \rightarrow \mathrm{X} \overset{k_d}{\rightarrow} \mathrm{D}, \qquad k_s = k_r + k_d$$
$$\downarrow k_r$$
$$\text{Product}$$

a) The 1 pulse per sec., total light quantity; Φ_o (photons per cm^2).

In case the absorption is more or less close to the saturation ($1000\,\Phi_o\varepsilon\alpha \lessapprox 1$; see below), the fractions of light absorbed are a little different in the earlier and in the later stages of one flash, although its duration is as short as several microseconds. Differentiating Φ_o into small parts, one can put

$$\mathrm{d}\Phi_{ab} = \varepsilon C \mathrm{d}\Phi_o$$

assuming C to be small enough. If α part of the molecules excited is transferred to X,

$$\alpha \mathrm{d}\Phi_{ab} = -\mathrm{d}C/1000$$

Hence:

$$-\mathrm{d}C = 1000\,\alpha C \varepsilon \mathrm{d}\Phi_o$$

Integration gives

$$\ln \frac{C_o}{C} = 1000\,\alpha\varepsilon\Phi_o$$

Putting the decrease of C during the flash as ΔC,

$$\Delta C = \alpha\Phi_{ab} = C_o(1 - e^{-1000\Phi_o\alpha\varepsilon})$$

The quantity of reaction by one flash (R_o) is

$$R_o = \Phi_{ab}\ \alpha\frac{k_r}{k_s} = C_o\frac{k_r}{k_s}(1 - e^{-1000\Phi_o\alpha\varepsilon}) \qquad (2)$$

Now let us treat the case in which the following approximation holds, i.e., the case in which f in I, where f is approximated by $\Phi_o\alpha\varepsilon$, must be replaced by $f - f^2/2$. Besides, $1000\Phi_o$ will be replaced by Φ from now on.

$$R_o = \Phi_{ab}\alpha\frac{k_r}{k_s} \approx C_o\frac{k_r}{k_s}\left\{\Phi\alpha\varepsilon - \frac{(\Phi\alpha\varepsilon)^2}{2}\right\}$$
$$= C_o\frac{k_r}{k_s}\left(f - \frac{f^2}{2}\right) \qquad (3)$$

b) The ν times illumination for one second with the flash of Φ.

For the first flash:

$$\Delta C = C_o\frac{k_r}{k_s}\left(f - \frac{f^2}{2}\right) = C_o f'$$

For each successive flash, the initial concentration, C_n, and the quantity of reaction, R_n, may be given as follows:

Flash No.	Initial concn.	R_n*	$\sum R_n$**
1	C_o	$C_o f'$	$C_o f'$
2	$C_o(1-f')$	$C_o(1-f')f'$	$\{C_o f'(1-f')+1\}$
3	$C_o(1-f')^2$	$C_o(1-f')^2 f'$	$\{C_o f(1-f')^2 + (1-f')+1\}$
4	$C_o(1-f')^3$	⋮	⋮
⋮	⋮	⋮	⋮
ν	$C_o(1-f')^{\nu-1}$	$C_o(1-f')^{\nu-1}f'$	$C_o(1-(1-f')^\nu)$

* R_n: Quantity of reaction to each flash
** $\sum R_n$: Total quantity of the reaction

The total quantity of the reaction for one second when $\nu f' < 1$:

$$\sum_{n=1}^{\nu} R_n = C_0\{1-(1-f')^{\nu}\}$$
$$= C_0\left\{\nu f' - \frac{\nu(\nu-1)}{2!}f'^2 + \frac{\nu(\nu-1)(\nu-2)}{3!}f'^3 + \cdots\right\}$$

and

$$\nu f' = \nu\frac{k_r}{k_s}\left(f - \frac{f^2}{2}\right)$$
$$= \nu\frac{k_r}{k_s}\left\{\Phi\alpha\varepsilon - \frac{(\Phi\alpha\varepsilon)^2}{2}\right\}$$
$$\frac{\nu(\nu-1)}{2!}f'^2 = \frac{\nu(\nu-1)}{2}\left(\Phi^2\alpha^2\varepsilon^2\frac{k_r^2}{k_s^2} + \cdots\right)$$

Hence,

$$\sum_{n=1}^{\nu} R_n \doteqdot \nu\frac{k_r}{k_s}C_0\left[\Phi\alpha\varepsilon - \frac{(\Phi\alpha\varepsilon)^2}{2}\left\{1+(\nu-1)\frac{k_r}{k_s}\right\}\right] \quad (4)$$

In order for $\sum_{n=1}^{\nu} R_n$ to be proportional to the light intensity (within 10 %), the second term must be less than 10 % of the first term.

So,

$$\Phi\alpha\varepsilon < \frac{0.2}{1+(\nu-1)\frac{k_r}{k_s}} \quad (5)$$

This shows that the limit for the linearity largely depends on k_r/k_s. For small values of k_r/k_s, the critical value of Φ does not depend on ν, and for the value of k_r/k_s close to 1, it approaches to $1/\nu$ of that for 1 pps. For instance, in the case of 100 pps, $\Phi_0\varepsilon\alpha$ must be less than 0.004 when $k_r/k_s \approx 0.5$. It is desirable to perform the experiment in the Φ region where the linearity holds approximately irrespective of ν. In the region of Φ treated here, $(1/\nu)\sum_{n=1}^{\nu} R_n$ decreases with the larger ν, and so a correction is needed to get a genuine effect if it is observed.

For example, in the case of 100 pps,

$$\sum_{n=1}^{\nu} R_n = 100\frac{k_r}{k_s}\Phi\alpha\varepsilon C_0\left[1-\frac{1}{2}\left\{1+99\frac{k_r}{k_s}\right\}\Phi\alpha\varepsilon\right] \quad (6)$$

and in case of 10 pps,

$$\sum_{n=1}^{\nu} R_n = 10\frac{k_r}{k_s}\Phi\alpha\varepsilon C_0\left[1-\frac{1}{2}\left\{1+9\frac{k_r}{k_s}\right\}\Phi\alpha\varepsilon\right] \quad (6')$$

c) The light quantity per second $I_0=\nu\Phi$ is kept constant.

The critical intensity (light quantity per second) below which the linearity holds, increases remarkably with the value of ν. Putting the light quantity per second as $I_0=\nu\Phi$, the quantity of reaction per second, $\sum_{n=1}^{\nu} R_n$, is given by:

$$\sum_{n=1}^{\nu} R_n = C_0\frac{k_r}{k_s}I_0\alpha\varepsilon\left[1-\frac{I_0\alpha\varepsilon}{2\nu}\left\{1+(\nu-1)\frac{k_r}{k_s}\right\}\right] \quad (7)$$

Thus, for 1 pps,

$$\sum_{n=1}^{\nu} R_n = C_0\frac{k_r}{k_s}I_0\alpha\varepsilon\left\{1-\frac{1}{2}I_0\alpha\varepsilon\right\}$$

for 10 pps,

$$\sum_{n=1}^{\nu} R_n = C_0\frac{k_r}{k_s}I_0\alpha\varepsilon\left\{1-\frac{I_0\alpha\varepsilon}{10}\left(\frac{1}{2}+\frac{9}{2}\frac{k_r}{k_s}\right)\right\}$$

for 100 pps,

$$\sum_{n=1}^{\nu} R_n = C_0\frac{k_r}{k_s}I_0\alpha\varepsilon\left\{1-\frac{I_0\alpha\varepsilon}{100}\left(\frac{1}{2}+\frac{99}{2}\frac{k_r}{k_s}\right)\right\}$$

III. Specific Effect When the Lifetime of X is Comparable with $1/\nu$

Even when no genuine kinetic effect is present, a certain frequency effect may be expected when the lifetime of X is comparable with $1/\nu$. Therefore, it is necessary to examine such an effect before the quantitative investigation can be made. It is, however, perhaps impossible to get an exact expression generally applicable to all cases. Here one has to be satisfied with treating two problems approximately.

a) An approximate expression for the quantity of reaction by n pulses when $nf<1$.

b) An appoximate expression for the quantity of reaction in unit time as a function of ν when $f_0=\nu f=$const. (<1).

a) X produced by each flash goes to the product by the fraction $q=k_r/k_s$. The remaining portion returns to the original dye step by step according to the flashing condition and contributes further to the total quantity of reaction. Thus, if X_n represents the quantity of X produced by the nth flash, then $(1-q)(1-g)X_n$ goes back to the original dye before the commencement of the $(n+1)$th flash. gX_n represents the portion of X_n at the commencement of the $(n+1)$th flash. In the same way, $gX_n(1-g)(1-q)$ returns to the original dye during the period between $(n+1)$-th and the $(n+2)$th flash. These processes continue until the end of all flashings; the situations are similar for all X_n.

On the basis of the above reasoning, one gets a general expression for X_n produced*

* The meaning of X_n is different from X^0_n or X^f_n.

by the nth flash. For the sake of simplicity, $(1-g)(1-q)$ is set as r.

For the 1st flash,

$$X_1=C_of$$

for the 2nd flash

$$X_2=\{C_of(1-f)+X_1fr\}$$

for the 3rd flash,

$$X_3=\{C_of(1-f)^2+X_1f(1-f)r+X_1fgr\}+X_2fr$$

for the 4th flash,

$$X_4=C_of(1-f)^3+X_1fr\{(1-f)^2+g(1-f)+g^2\}+X_2fr\{(1-f)+g\}+X_3fr$$

for the 5th flash,

$$X_5=C_of(1-f)^4+X_1fr\{(1-f)^3+g(1-f)^2+g^2(1-f)+g^3\}+X_2fr\{(1-f)^2+g(1-f)+g^2\}+X_3fr\{(1-f)+g\}+X_4fr$$

Hence, for the nth flash,

$$X_n=C_of(1-f)^{n-1}+X_1fr\{(1-f)^{n-2}+g(1-f)^{n-3}+g^2(1-f)^{n-4}+\cdots+g^{n-2}\}+X_2fr\{(1-f)^{n-3}+g(1-f)^{n-4}+g^2(1-f)^{n-5}+\cdots+g^{n-3}\}$$
$$\vdots$$
$$+X_{n-2}fr\{(1-f)+g\}+X_{n-1}fr$$

This is simplified as follows:

$$X_n=C_of(1-f)^{n-1}+rf\left[X_1\frac{\{(1-f)^{n-1}-g^{n-1}\}}{1-f-g}+X_2\frac{\{(1-f)^{n-2}-g^{n-2}\}}{1-f-g}\cdots+X_{n-2}\frac{\{(1-f)^2-g^2\}}{1-f-g}+X_{n-1}\frac{\{(1-f)-g\}}{1-f-g}\right] \quad (8)$$

Similarly,

$$X_{n-1}=C_of(1-f)^{n-2}+rf\left[X_1\frac{\{(1-f)^{n-2}-g^{n-2}\}}{1-f-g}+X_2\frac{\{(1-f)^{n-3}-g^{n-3}\}}{1-f-g}\cdots+X_{n-3}\frac{\{(1-f)^2-g^2\}}{1-f-g}+X_{n-2}\frac{(1-f-g)}{1-f-g}\right]$$

$$\cdots\cdots\cdots\cdots\cdots\cdots$$

$$X_3=C_of(1-f)^2+rf\left[X_1\frac{\{(1-f)^2-g^2\}}{1-f-g}+X_2\frac{1-f-g}{1-f-g}\right]$$

$$X_2=C_of(1-f)+rfX_1\frac{(1-f-g)}{1-f-g}$$

$$X_1=C_of$$

To get a simple expression, one has to draw attention to the condition $nf<1$ and has to cut down all the terms higher than f^3.

Then, $X_n=C_of(1-f)^{n-1}+C_orf^2\left[\frac{(1-f)^{n-1}-g^{n-1}}{1-f-g}+\frac{(1-f)\{(1-f)^{n-2}-g^{n-2}\}}{1-f-g}+\frac{(1-f)^2\{(1-f)^{n-3}-g^{n-3}\}}{1-f-g}+\cdots+(1-f)^{n-2}\frac{(1-f-g)}{(1-f-g)}\right]$

This is reduced to the following equation:

$$X_n=C_of(1-f)^{n-1}+\frac{C_orf^2}{1-f-g}\left\{(n-1)(1-f)^{n-1}+\frac{g^n-g(1-f)^{n-1}}{1-f-g}\right\}$$

In the same way,

$$X_{n-1}=C_of(1-f)^{n-2}+\frac{C_orf^2}{1-f-g}\left\{(n-2)(1-f)^{n-2}+\frac{g^{n-1}-g(1-f)^{n-2}}{1-f-g}\right\}$$

$$\cdots\cdots\cdots\cdots\cdots\cdots$$

$$X_3=C_of(1-f)^2+\frac{C_orf^2}{1-f-g}\left\{2(1-f)^2+\frac{g^3-g(1-f)^2}{1-f-g}\right\}$$

$$X_2=C_of(1-f)+\frac{C_orf^2}{1-f-g}\left\{(1-f)+\frac{g^2-g(1-f)}{1-f-g}\right\}$$

$$X_1=C_of$$

By means of the formula of the geometric progression, one gets

$$\sum X_n = C_o\{1-(1-f)^n\} + \frac{C_o r f^2}{1-f-g}\left[\frac{(1-f)-(n-1)(1-f)^n}{f} + \frac{(1-f)^2-(1-f)^n}{f^2} + \frac{g^2-g^{n+1}}{(1-f-g)(1-g)} - \frac{g(1-f)\{1-(1-f)^{n-1}\}}{(1-f-g)f}\right] \quad (9a)$$

and the quantity of the reaction, R, is given by:

$$R \equiv q\sum X_n \quad (9b)$$

It is to be added that when $g=0$, the above equation leads to

$$q\sum X_n = C_o\left\{nfq - \frac{n(n-1)}{2}f^2q^2\right\} \quad (10)$$

This is just the expression obtained from $C_o\{1-(1-f)^n\}$, which is the quantity of reaction when the interval of flash is long enough. From Eq. 9a one can easily calculate the quantity of reaction by n flashes for arbitrary values of f, g and q. These calculations must be performed for a set of successive flashes irrespective of the time spent by n flashes. For example, if one sets $f=0.001$, $n=101$, $g=0.5$, and $q\approx 0$, then the quantity of reaction is about 5 % smaller than when $g=0$. Thus, it is expected generally that the shorter the period of flash, the less the quantity of the reaction. It is worth mentioning here that the above formulas (9) hold only when $nf \ll 1$; a much larger effect would be expected if f is larger.*

b) The quantity of reaction per second when $f_o=\nu f=$const. (<1), where ν is the frequency of flash, is easily obtained by an extension of the treatment given in a). The case in which ν is very small need not be considered, since the situations are just the same as with a). When ν is large, g is approximately equal to 1 and is written as follows:

$$g = e^{-k_s/\nu} \approx 1-\frac{k_s}{\nu}, \quad 1-g=\frac{k_s}{\nu}$$

Further, one can replace $(1-f)^\nu$ by e^{-f_o}. Starting from Eq. 8, one can derive following expression by substituting the above relations. (It should be added that all terms higher than f^3 are disregarded.)

$$q\sum_{n=1}^{\nu} X_n = C_0\{1-e^{-f_o}\}q + \frac{C_o q(1-q)k_s f_o^2(\nu-1)}{2(k_s-f_o)\nu} - \frac{C_o q(1-q)k_s f_o^2(\nu-1)}{2\nu(k_s-f_o)}\left\{1+\frac{k_s f_o}{\nu(k_s-f_o)}\right\} \quad (11)$$

If ν is large enough, Eq. 11 is simplified as follows (in the approximation to f_o^2):

$$q\sum_{n=1}^{\nu} X_n = C_o\{1-e^{-f_o}\}q \doteqdot C_o\left\{f_o q - \frac{f_o^2}{2}q\right\} \quad (12)$$

This is to be compared with the quantity of reaction per second obtained under the assumption of a steady state illumination, when X and the product, P, are respectively, produced according to the following relations:

$$\frac{dX}{dt} = \alpha\varepsilon I_o C = k_s X \quad (13)$$

$$\frac{dP}{dt} = -\frac{dC}{dt} = k_r X \quad (14)$$

Equation 13 is restricted to the case where $\alpha\varepsilon C$ is small enough. When I_o is moderately large, the quantity of the reaction per second, R, may be approximately given as follows:

$$R = C_o\left\{\frac{k_r}{k_s}I_o\alpha\varepsilon - \frac{1}{2}\frac{k_r^2}{k_s^2}I_o^2\alpha^2\varepsilon^2\right\} = C_o\left\{f_o q - \frac{1}{2}f_o^2 q^2\right\} \quad (15)$$

Thus, when ν is large enough, the quantity of reaction per second is $(1/2)f_o^2 q(1-q)$ less than that of the steady illumination. It is to be noted that Eq. 15 is different from Eq. 12 in the f_o^2 term and that it is equal to Eq. 10 if one replaces n with ν and takes it large enough. Comparing Eq. 15 with Eq. 7, one can say that when $\tau < 1/\nu$, the quantity of reaction per second (when $I_o=\nu\Phi=$const.) for the frequency ν is $(1/2\nu)(1-k_r/k_s)I_o^2\alpha^2\varepsilon^2(k_r/k_s)$ less than that of the steady illumination at I_o.

Summing up the results obtained in III and II, one can say as follows. As the frequency of flashing is made larger under the condition $\nu f = f_o =$const., then the quantity of reaction per second increases and tends to the value of the steady illumination in the $\tau < 1/\nu$ region, but it decreases when τ becomes larger than $1/\nu$. Further, one can say that when $f_o \approx 0.1$, the ordinary kinetic treatment may be used as in the steady illumination. Thus, it would be better to deal with the rate constant evaluated by the usual method rather than with the quantity of reaction per pulse or per second. The condition for linearity is more stringent for the latter (see IV).

IV. A Model Case

One model case will be considered as an example in which a genuine kinetic frequency effect is to be expected. It is the case in which X absorbs light and then reacts. For this case, an argument similar to that given in III can be made.

* f represents $\Phi\alpha\varepsilon$, but this is an approximation. An exact expression for $(1-f)$ is e^{-f}.

The first flash produces the intermediate X in the amount $X_1=C_of$. During the dark period, the fraction of X_1 which goes to the product is $(1-g)q$ and $r=(1-g)(1-q)$ returns to the ground state. The second flash then produces X in the amount $C_of(1-f)+X_1rf$. The situations up to this point are just the same as in III. The difference appears during the second flash, in which the remaining fraction of X_1, i.e., gX absorbs light and some portion of it contributes to the reaction. Thus the g included explicitly in Eq. 8 is reduced to some extent and should be replaced by such a quantity as $g'=g(1-\varepsilon'\alpha'\Phi)$ (when $\varepsilon'\alpha'\Phi$ is small enough). This implies that the fraction $g\varepsilon'\alpha'\Phi$ goes to the product by the absorption of light. Analogous processes go on to the end of all the flashings and the situations are similar for all X_n.

However, the above situations are too complicated to be considered exactly; one must here be content with the treatment of the extreme case in which all the gX reacts upon the absorption of light. In this case one has only to put $g=0$ in Eq. 9. The contribution of X_n to the quantity of reaction is in general given by $X_n\{(1-g)q+g\}$. Another point to be noted, however, is that the summation must be done to the $(n-1)$th flash, because X_n produced by the last flash goes to the product by the amount of X_nq.

Thus, the quantity of the product is given by;

$$R'=\sum_1^{n-1}X_{n-1}\{(1-g)q+g\}+X_nq$$

By applying Eq. 9 (putting $g=0$) and Eq. 8, one gets:

$$\begin{aligned}R'=&C_o\{1-(1-f)^n\}q+C_o\{1-(1-f)^{n-1}\}\\&\times g(1-q)+C_orf^2q\left\{\frac{1-(n-2)(1-f)^{n-2}}{f}\right.\\&\left.+\frac{(1-f)-(1-f)^{n-2}}{f^2}+(n-1)(1-f)^{n-2}\right\}\\&+C_orf^2g(1-q)\left\{\frac{1-(n-2)(1-f)^{n-2}}{f}\right.\\&\left.+\frac{(1-f)-(1-f)^{n-2}}{f^2}\right\}\end{aligned}\tag{16}$$

Apart from f^2 terms, one gets from Eqs. 16, 9 and 10:

$$\begin{aligned}R'-R&=C_o\{1-(1-f)^{n-1}\}g(1-q)\\&\fallingdotseq(n-1)C_ofg(1-q)\end{aligned}\tag{17}$$

and

$$\frac{R'-R}{R}=\frac{n-1}{n}\frac{g(1-q)}{q}\tag{18}$$

The above two formulas are, of course, the maximum values possible for given g and q values, but they make some general features clear. Thus, according to them, the effect is zero when $q=k_r/k_s=1$ and increases with the value of g. Since $g=\exp(-k_s/\nu)$, the effect becomes apparent in the frequency region where $\nu\gtrsim k_s$. Equation 17 does not, however, indicate the intensity effect correctly. This is natural since the above treatment concerns only the extreme case when the light absorption by X is large enough. If one treats the general case, a complicated function involving $g\varepsilon'\alpha'\Phi$ in both denominator and numerator would result.

The situations will be clarified, at least approximately, by the steady state treatment. Thus, if one assumes that $\alpha'\varepsilon'I_oX(=k'\varepsilon'I_oX)$ of X undergoes the photo-reaction, then

$$I_o\alpha\varepsilon(C-X)=k_sX+\alpha'\varepsilon'I_oX$$

and if one assumes X is very small compared with C,

$$\frac{-dC}{dt}=\frac{I_o\alpha\varepsilon C_o(k_r+k''I_o)}{k_s+k''I_o}\tag{19}$$

In the absence of any extra reaction,

$$\frac{-dC}{dt}=I_o\alpha\varepsilon C_o\frac{k_r}{k_s}\tag{20}$$

Hence, the ratio R'/R in this case is given approximately by

$$\frac{R'}{R}=\frac{1+(k''/k_r)I_o}{1+(k''/k_s)I_o}\tag{21}$$

and

$$\frac{R-R'}{R}=\frac{k''I_o(1/k_r-1/k_s)}{1+(k''/k_s)I_o}\tag{22}$$

These values are, in general, not independent of I_o. To sum up, the genuine effect begins to appear at such a frequency when $\nu\gtrsim k_s$ and, in addition, $k''I_0(=\alpha'\varepsilon'I_0)$ should be at least comparable with k_r. The intensity exponent for $R'-R$ lies between the first and the second order.

Summary

The method of intermittent illumination by means of flashes of very short duration has been criticized, particularly with regard to the frequency and intensity of the flash. It has been concluded that when f_o (the fractional decrease of the starting substance per second due to the absorption of light) is less than 0.1, the kinetics for the steady illumination will hold within a few per cent. A model case in which a certain intermediate absorbs light and causes an addition reaction has been discussed.

The authors wish to thank Professor Shunji Kato for his helpful discussions.

Department of Chemistry
Faculty of Science
Tohoku University
Katahira-cho, Sendai

The Application of Intermittent Illumination to the Bleaching of Dye. II. The Methylene Blue-Amine System

By Shunji KATO, Yoshiharu USUI and Masao KOIZUMI

(Received June 17, 1963)

The method of intermittent illumination has been successfully applied to the kinetic studies of photopolymerization in which the termination consists of the mutual interaction of two growing radicals. However, the method has not yet been introduced into the field of the photobleaching of dye. Although the situation in dye chemistry is quite different from that of photopolymerization, there seems to be, among the published results, some cases which suggest certain intermittent light effects. For example Ainsworth[1] observed a saturation effect in the photobleaching of thiazine dyes by ferrous ion and attributed it to the formation of a certain complex which is susceptible to photobleaching but which requires a rather long time to form. According to him, the scheme can be shown as follows:

$$\begin{array}{ccccc} (D-A)^* & \longrightarrow & \cdots\cdots & \longrightarrow & Y \longrightarrow \text{Product} \\ h\nu\uparrow & & & & \downarrow \\ (D-A) & \longleftarrow & A & \longleftarrow & D+A \end{array}$$

where (D—A) is a labile complex of the dye D and the electron donor A.

If the frequency of flash is great enough, then the $D+A \rightarrow (D—A)$ process cannot respond and the quantum yield should decrease with the increase in frequency.

Another case is the photobleaching of methylene blue by means of trimethylamine.[2] In this case the existence of a certain intermediate with the lifetime of the order of minutes and with absorption spectra in the region neighboring that of the dye has been suspected. The scheme can be written as follows:

$$D \xrightarrow{h\nu} D' \longrightarrow X \longrightarrow \text{Product}$$
$$\downarrow \qquad \downarrow$$
$$D \qquad D$$

X is the intermediate in question. In this case, the quantity of the reaction should increase when the interval of flash, $1/\nu$, becomes smaller than the lifetime of X. In both these cases, some kind of intensity effect is also to be expected if the intensity is varied over a wide range. However, the intermittent light method is more direct and affords more detailed information.

In this paper some findings on the methylene blue-trimethylamine system will be reported, along with the details of the apparatus and the procedures for checking the method. As a light source a flash of short duration (several micro-seconds) was used. Its merit was that it gave a considerable amount of light in a very short time and so made the interval of successive flashes easily controllable. Such a light source, we believe, has in these cases some advantages over the intermittent light obtained by means of a sector.

Experimental

Materials. — *Methylene Blue.* — Merck's dye was recrystallized twice from *n*-butyl alcohol and then from redistilled water, and then dried in a vacuum for ten hours. The molar extinction coefficient at 665 mμ is 7.12×10^4.

Trimethylamine.—The trimethylamine (TMA) free base was prepared by the reaction of ammonium chloride with paraformaldehyde by the ordinary method. It was purified by removing the moisture and a trace of ammonia by high vacuum distillation from the dry ice-methanol to liquid air bath four times. The purity of TMA was checked by a Shimadzu gas chromatograph; and the sample could be stored without any change as long as it was degassed and kept in a refrigerator.

Sodium Borate. — A commercial G. R. reagent was recrystallized from redistilled water two or three times.

Intermittent Irradiation Apparatus.—A stroboscope by Nihon Denshi Sokki (Japan Electronic Instrument, Co.), with a xenon flash unit attached was used. It made possible the intermittent illumination of any frequency from 1 to 500 p.p.s (pulse per second). For lower frequency illumination (1 p.p.s.~1 p.p.m.), triggering was done with a microswitch driven by a synchronous motor (p.p.m. denotes pulse per minute). The xenon flash lamp was a U-shaped glass tube, 70 mm. long and 8 mm. in diameter. The separation of its legs was 15 mm. It was connected to a 1 μF capaciter charged up to about 1500 V. The voltage was almost constant for frequencies lower than 1 p.p.s., but it dropped appreciably for higher frequencies. The light intensity was varied by means of neutral filters.

The Cell Compartment.—A sample cell and an actinometer cell were placed side by side, separated

1) S. Ainsworth, *Z. Electrochem.*, **64**, 93 (1960).
2) H. Obata and M. Koizumi, This Bulletin, **30**, 136, 142 (1957); **32**, 125 (1959).

by a dark sheet, in a water-circulating thermostat. The cell was rectangular, $1\times1\times4$ cm., and was connected to a glass tube, which was sealed at the top. Figure 1 shows the top view. The cells, filters and lamp were placed as close together as possible. As is shown in the figure, the sample was illuminated with red light, while the actinometer was illuminated with full light.

Actinometry.—A ferrioxalate actinometer was used to measure the relative light quantity. However, there were two questions to solve beforehand. One was that the antinometer itself may have a frequency effect. If the reaction under pulse irradiation proceeded in a way different from the ordinary way, its quantum yield would depend on the pulse frequency. Another is that the wavelength region sensitive to the actinometer is different from that absorbed by methylene blue. Thus, if the wavelength distribution of the flash light varies with the frequency, the ratio of the intensity of red light to the shorter one, which is effective on the actinometer, will not be constant. This can result in a false frequency effect. These two problems were solved in the following ways.

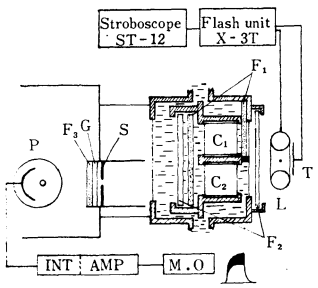

Fig. 1. Schematic diagram of the irradiation apparatus.

L : Xe-flash lamp
C_1 : Sample cell
C_2 : Actinometer cell
F_1 : WR-2 Cut-off filter
F_2 : Neutral filter
F_3 : Interference filter
S : Slit
G : Frosted glass
P : Photocell (PT-25-VI)
T : Trigger
INT-AMP : Integrating and amplifier circuit unit
M.O : Electromagnetic oscillograph

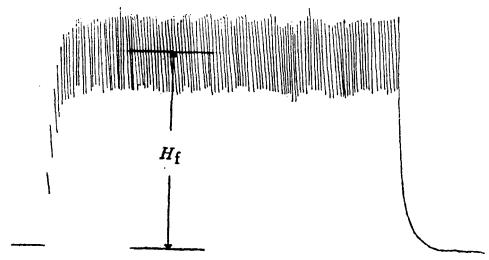

Fig. 2. Oscillogram for 1 p.p.s. The height (H_f) is proportional to the light quantity.

The actinometer was irradiated by the strobo-flash and, at the same time, the current of a photo-tube receiving the same light through a red filter was recorded with an electromagnetic oscillograph. A cathode follower with an integrating circuit was used to smooth out the pulse signal. It was found that the conversion in the actinometer, irrespective of the frequency, was just proportional to the light quantity measured from the oscillogram, as Fig. 2 shows. The area under the trace gives a measure of the light quantity received by a photo-tube during the period. Thus, it was established that the light quantity from the ferrioxalate actinometer can be safely used as a measure of the light quantity absorbed by methylene blue. The factor to convert the former to the latter was measured at 3~4.

Procedure.—An aqueous borate buffer solution (3×10^{-2} M, pH=9.18), containing 1×10^{-5} M methylene blue and 5.0×10^{-3} M TMA, was sealed into a reaction cell after having been degassed by means of repeated pumping in a liquid air bath.

The sample cell and an actinometer cell were illuminated in the cell compartment at 30°C, and the spectral change was followed with a Hitachi EPU-2A spectrophotometer. Since it was confirmed that in the present case there was no shift in the absorption peak in the course of photobleaching, the reaction was followed by the decrease in absorbancy at the peak.

Results

Some Reaction Features. — First, some features of the reaction under pulse illumination were compared with those under steady illumination. In the case of the photobleaching of methylene blue (MB) in the evacuated buffer solution or in alcohol under steady illumination, the shift in the absorption peak of the remaining dye was, to some extent, accompanied by bleaching. This point was, therefore, examined. However, there proved to be no such phenomenon in the present system. Thus, the spectrum of the remaining dye after appreciable bleaching had its maximum peak in exactly the same position as that in the original dye. It was further established that almost all the bleaching reaction consists of the formation of leuco dye; this was established by the absorption spectra of the product and by the fact that the introduction of air to an almost completely bleached solution recovers all of the dye. Another point which was examined concerns the fact that, in steady illumination, a slight increase in the absorption peak of the dye was observed after the interruption. After the 10 p.p.s. irradiation of a sample containing 1.0×10^{-5} M MB, 5×10^{-3} M $(CH_3)_3N$ and 3×10^{-2} M borate by an Xe-lamp by the use of a WR-2 red filter, the absorption spectrum of the sample in the 500~800 mμ region was examined, within 100 sec. and after a long lapse of time in the dark. The examination showed no

change within the range of experimental error, unlike the results obtained under steady illumination. Similar experiments were also conducted using the solution bleached to about one-half by flashes of 10 and 100 p.p.s.; the absorption spectra did not show any change after the sample had been stored 100 hr. in the dark. The cause of such a different behavior under the present conditions is unknown.

However, except for such trivial differences, there is no doubt that quite a similar photoreduction takes place under intermittent illumination and under steady illumination.

Kinetic Results.— It has been shown in the previous paper that the kinetic law for steady illumination can be applied approximately, with a range of error of only a few percent, for pulse illumination in the case of a first order reaction if $f_0 \leq 0.1$. This situation does not alter in other cases.

Now, the kinetics of the reaction of the present system under steady illumination can be better described as of the second order than as of the first order*. Hence, the experimental results in this paper were dealt with in the same way.

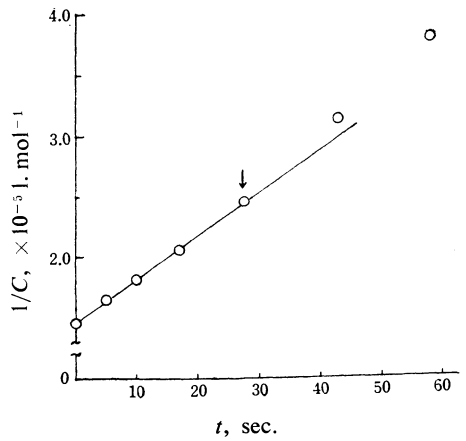

Fig. 3. Applicability of the second order rate formula.

[TMA] $=5.0\times10^{-3}$ M [MB] $=6.7\times10^{-6}$ M
Intermittent frequency; 100 p.p.s.
↓ Marks forty percent bleaching point

As Fig. 3 shows, the reciprocals of the concentration (C) give a good straight line against the time (t) in the initial stage up to about forty percent bleaching, although a slight deviation becomes apparent when the bleaching proceeds further.

From the above results it is clear that the rate formula for the steady illumination really holds for the pulse illumination. Therefore, one can discuss the frequency effect in terms of the second order rate constant, k. To do so, however, a comparison of k must be made at the same light quantity per second.

Hence, the intensity of the flash was controlled by means of neutral filters, and several experiments were performed at various intensities for each frequency. Figure 4 and Table I show the results for 1, 10 and 100 p.p.s. To make the comparison easier, a multiple scale was employed. It is evident from the figure that k in all cases gives a linear plot. This implies that k is proportional to I_0; i.e.,

TABLE I. SECOND ORDER RATE CONSTANT (k) AT VARIOUS LIGHT INTENSITIES

[MB] $=8.8\times10^{-6}$ M [TMA] $=5.0\times10^{-3}$ M
[Borate] $=3.0\times10^{-2}$ M pH $\simeq$ 9.2 (30°C)

Frequency p.p.s.	I_0* (photons·l^{-1} sec^{-1})	k (l. mol^{-1}· sec^{-1})	$k_0\times10^{15}$ (photons^{-1}· mol^{-1} l^2)
100	0.98×10^{18}	1.36×10^3	
100	1.36×10^{18}	2.12×10^3	1.45
100	1.99×10^{18}	2.86×10^3	
100	2.20×10^{18}	3.48×10^3	
10	0.88×10^{17}	1.50×10^2	
10	2.20×10^{17}	3.40×10^2	1.42
10	2.84×10^{17}	3.61×10^2	
10	4.09×10^{17}	4.92×10^2	
1	2.06×10^{16}	2.18×10	
1	4.93×10^{16}	4.92×10	1.04
1	6.22×10^{16}	6.51×10	
1	7.40×10^{16}	8.00×10	

* The light quantity is obtained by ferrioxalate actinometer.

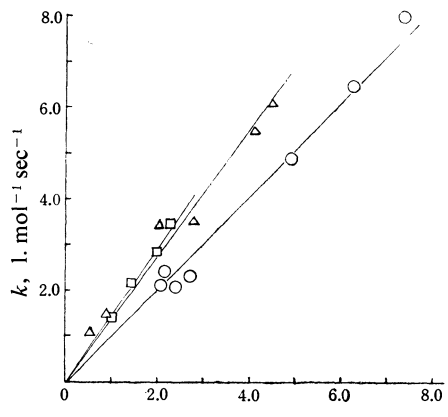

Fig. 4. Intensity effect on k in MB-TMA-borate buffer solution.

○ 1 p.p.s.: k in unit of 10, $I_0^{(1)}$ in unit of 10^{16}
△ 10 p.p.s.: k in unit of 10^2, $I_0^{(10)}$ in unit of 10^{17}
□ 100 p.p.s.: k in unit of 10^3, $I_0^{(100)}$ in unit of 10^{18}

* To be published shortly. Quite a different rate formula had previously been proposed,[2] but later works including the present one, have disproved it.

$$k = k_0 I_0 \quad (1)$$

where k_0 depends only on ν. To show this it will better to denote k_0 by $k_0^{(\nu)}$.

Equation 1 is exactly the relation that holds for steady illumination. This again supports the similarity in kinetics in the two case. Figure 4 further shows that the inclinations in the case of 10 and 100 p.p.s. are appreciably larger than that for 1 p.p.s. In other words, $k_0^{(100)}$ and $k_0^{(10)}$ are larger than $k_0^{(1)}$. Although there seems to be some inconsistency between relation 1 and the dependence of k_0 on ν in view of formula 21 given in the previous paper (see Discussion), there is no doubt that the frequency effect can be discussed in terms of k_0.

When relation 1 had been established, it was utilized to obtain the values of k_0 in the region of 1 p.p.m. to 1 p.p.s. in a few experiments. The $k_0^{(\nu)}$ values thus obtained are given in Table II. It is evident that in the range from 1 p.p.s. to 1 p.p.m. there is no intermittent light effect beyond the range of experimental error, which is somewhat larger than that in the higher frequency region.

Figure 5 shows the plot of $k_0^{(\nu)}/k_0^{(1)}$ against $\log \nu$. It is apparent that $k_0^{(\nu)}$ is nearly

TABLE II. FREQUENCY EFFECT ON $k_0^{(\nu)}$

Frequency	$\log \nu$	$k_0^{(\nu)}/k_0^{(1)}$
100 p.p.s.	2.0	1.42
10 p.p.s.	1.0	1.40
1 p.p.s.	0	1.10
12 p.p.m.	−0.7	0.75
6 p.p.m.	−1.0	0.97
1 p.p.m.	−1.8	0.96

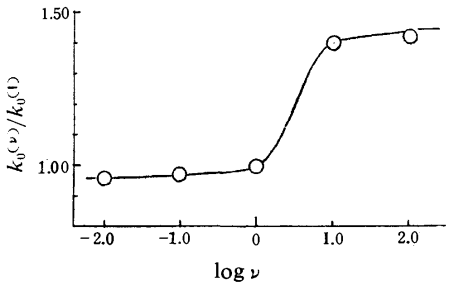

Fig. 5. Frequency effect on $k_0^{(\nu)}$.
[MB] = 8.8×10^{-6} M [TMA] = 5.0×10^{-3} M
[Borate] = 3.0×10^{-2} M

TABLE III. SECOND ORDER RATE CONSTANT (k) AT VARIOUS LIGHT INTENSITIES

[MB] = 8.8×10^{-6} M [TMA] = 5.0×10^{-3} M
pH = 10.3 (30°C)

Frequency p.p.s.	I_0* (photons·sec^{-1})	k (l. mol^{-1} sec^{-1})	$k_0\times10^{14}$ (photons^{-1} mol^{-1} l^2)
100	0.47×10^{18}	0.78×10^4	
100	0.57×10^{18}	0.90×10^4	1.50
100	0.86×10^{18}	1.30×10^4	
100	1.49×10^{18}	2.20×10^4	
10	0.38×10^{17}	0.38×10^3	
10	0.70×10^{17}	0.82×10^3	1.16
10	1.10×10^{17}	1.28×10^3	
10	1.75×10^{17}	2.09×10^3	
1	0.57×10^{16}	0.73×10^2	
1	1.53×10^{16}	1.55×10^2	1.02
1	1.83×10^{16}	1.83×10^2	
1	2.71×10^{16}	2.70×10^2	

* The light quantity is obtained by ferrioxalate actinometer.

TABLE IV. FREQUENCY EFFECT ON $k_0^{(\nu)}$

Frequency	$\log \nu$	$k_0^{(\nu)}/k_0^{(1)}$
100 p.p.s.	2.0	1.48
10 p.p.s.	1.0	1.14
1 p.p.s.	0	1.00
6 p.p.m.	−1.0	0.89
1 p.p.m.	−1.8	0.87

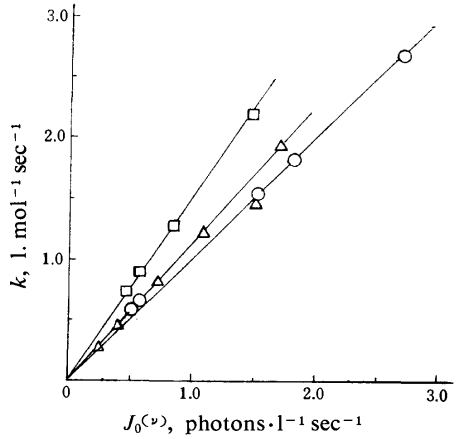

Fig. 6. Intersity effect on k in MB-TMA aq. solution.
○ 1 p.p.s.: k in unit of 10^2, $I_0^{(1)}$ in unit of 10^{16}
△ 10 p.p.s.: k in unit of 10^3, $I_0^{(10)}$ in unit of 10^{17}
□ 100 p.p.s.: k in unit of 10^4, $I_0^{(100)}$ in unit of 10^{18}

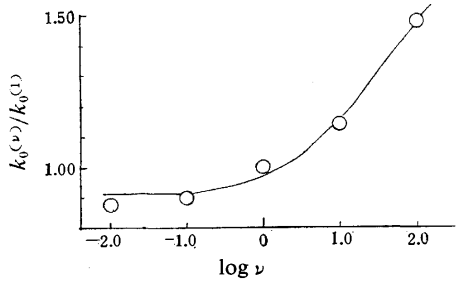

Fig. 7. Frequency effect on $k_0^{(\nu)}$.
[MB] = 8.8×10^{-6} M [TMA] = 5.0×10^{-3} M

constant below 1 p.p.s., while it increases by about fifty percent between 1 and 10 p.p.s.

Similar experiments were conducted using a solution of methylene blue (1×10^{-5} M) and trimethylamine (5.0×10^{-3} M). The analysis was made in the same way. The results are shown in Tables III and IV, and in Figs. 6 and 7. $k_0^{(\nu)}$ in this case increases considerably between 10 p.p.s. and 100 p.p.s.

Discussion

It is evident from the above results that there is a certain frequency effect, although the frequency interval, in which the effect becomes apparent, differs slightly at pH=9.2 (a borate buffer solution) and at pH=10.3 (without borate ions).

The following discussion mainly concerns the former case, which was studied in more detail, but the discussion will also be applicable to the latter, at least in its essential points. In the first place, there is no doubt that a genuine frequency effects, since, as was discussed in the previous paper, a silght decrease in $k_0^{(\nu)}$ should be expected in the $\nu\approx1/\tau$ region when I_0=const. and in the absence of a genuine effect (see II and III of the previous paper). The positive effect is to be expected in the following two cases.

a) The case in which certain intermediate X absorbs light and induces a reaction according to the following scheme.—If the lifetime (τ_X) of X is longer than the period of pulse $1/\nu$, additional photoreaction occurs; if the lifetime is shorter, it does not.

$$\mathrm{D} \xrightarrow{h\nu} \mathrm{D}^{\prime} \longrightarrow \mathrm{X} \xrightarrow[k_r]{(h\nu')} \text{Prod.}$$
$$\mathrm{D}^{\prime} \xrightarrow{k_d} \mathrm{D}$$

b) The case where a bimolecular reaction of X occurs.—In this case the effect is due rather to the increase in intensity accompanied by the rise in frequency. However, the present results can not be interpreted by this scheme for the following reason. The experimental results show that $k_0^{(10)}$ is about ten percent larger than $k_0^{(1)}$. Hence, it should be possible to observe a somewhat larger effect by making the intensity of the 1 p.p.s. flash about ten times. However, this is not the case, as is evident from Fig. 5. On the other hand, all the experimental results can be comprehended by scheme a) on the basis of the arguments given in the previous paper. The details will be described below, along with the important conclusions derived from them. First of all, the lifetime of X is estimated to be about one second on the basis of the finding that $k_0^{(\nu)}$ is nearly constant at frequencies below 1 p.p.s. but sharply rises between 1 to 10 p.p.s. In other words, k_s ($=k_d+k_r$) is estimated to be about 1. There is no other intermediate with a longer lifetime. The authors would like to deny the existence of an intermediate with a lifetime as long as a minute, as has been claimed.[2] This is due perhaps to a subsidiary process such as the photoadsorption of dye on the wall.

Another important conclusion is that the intermediate has quite a large absorbance. Thus for the effect to be observed, $\alpha'\varepsilon' I_0$ (ε'; the absorbance of X, α; the probability of the photoreaction of X) should be comparable with k_r (see IV of the preceeding paper). If k_r is 0.1~0.01, then from I_0 for 10 p.p.s., ε' ought to be $10^4\sim10^5$, assuming that $\alpha'\approx1$.

Two other comments must be made. One is about the finding that $k_0^{(\nu)}$ is approximately proportional to I_0 for the 100, 10, and 1 frequencies respectively (see Fig. 4); the other is about the unexpectedly small difference in the effect for 10 p.p.s. and for 100 p.p.s.

From the argument given in III of the previous paper, when the genuine effect does not exist, $k_0^{(\nu)}$ should decrease to some extent in the $\tau\approx1/\nu$ region (if $f_0\approx1$) and the decrease should be larger with the increase in f_0. In the present work, the maximum f_0 for 10 p.p.s. and for 100 p.p.s. is 0.1α and 0.6α respectively, and if α is not too small, a moderate deviation from linearity, especially in the latter case, is to be expected. When the genuine effect exists, however, relation 22 in the previous paper must hold approximately. From the values of k_s, k_r and $\alpha'\varepsilon' I_0$ estimated above, however, the deviation from linearity (opposite to that mentioned above) would not be very large.

Taking into consideration the two opposite effects, one may understand the approximate linearity observed. At any rate, the accuracy of the experiment is not good enough to detect this deviation.

As for the equal magnitude of the effects for 10 p.p.s. and for 100 p.p.s., it is due partially to the fact that f_0 in the latter case is quite close to 1. Alternatively, it is possible that the value of g lies quite close to 1, even at $\nu=10$.

In summary, the above scheme seems to be consistent with all the experimental results.

A slight difference between the effect of the system containing borate ion (pH=9.2) and that of the one without it suggests the dependence of the character of X on some anion. There is, however, one curious point: X has quite a large absorption in the visible region. It is possible that X is not an intermediate essentially connected with the reaction but rather the ground state dye observed immediately after having been recovered from some excited

species or some intermediate.* In connection with this, it is worth mentioning that no transient absorption spectrum with a life near one second has ever been observed in our laboratory** in the 300～500 mμ region.

In order to clarify the nature of X, further studies of the systems containing anions other than the borate ion are desirable.

Summary

A new apparatus for intermittent illumination has been designed and applied to the system of methylene blue and trimethylamine. A frequency effect has been discovered and established to be genuine. Thus, when the frequency is raised, the rate constant for the buffered and for the non-buffered solution shows an increase of about forty percent, but in the former case, between 1 p.p.s. and 10 p.p.s., and in the latter one between 10 p.p.s. and 100 p.p.s.

If it is assumed that a certain intermediate X absorbs light and induces the additional reaction, the extinction coefficient of X ought to be 10^4～10^5 in order to interpret the observed effect. Hence, it is likely that the intermediate in question is not an intermediate in true sense of the word, but the ground state dye in a slightly modified state.

Department of Chemistry
Faculty of Science
Tohoku University
Katahira-cho, Sendai

* Such a modified form of dye was assumed by Ainsworth and Havemann. Thus, Ainsworth proposed the formation of a complex by the dye and the ferrous ion; he thought that the dye, just when recovered from the triplet, is in a somewhat different state. Havemann assumes a similar complex formation. However, the effect in such cases would be opposite to the one in the present case. (R. Havemann and H. Pietsch., *Z. physik. Chem.*, **211**, 26, 61 (1959).

** To be reported in the near future.

NOTES

The Synthesis of Ethyl β-Ionylideneacetate by the Wittig Reaction

By Yozo Ishikawa

(Received June 14, 1963)

β-Ionylideneacetate is an important key intermediate for preparing Vitamin A and related compounds. The chief difficulty encountered in the synthesis of this ester lies in maintaining the conjugated polyene system in the molecule. The Wittig reaction using triphenylphosphine has been reported by Pommer and his coworkers[1] to be a favorable method for preparing this ester and its vinylogs, in which the formation of *retro*-compounds has scarcely ever been observed.

This paper will describe the synthesis of ethyl β-ionylideneacetate by means of a Wittig reaction using diethyl carbethoxymethylphosphonate prepared from triethyl phosphite and ethyl bromoacetate.

Ethyl *trans*-β-ionylideneacetate (I) was obtained by the reaction of β-ionone with diethyl carbethoxymethylphosphonate carbanion prepared from the phosphonate and sodium amide in tetrahydrofuran.[2] I was reduced with lithium aluminum hydride to *trans*-β-ionylideneethanol, which was then oxidized with manganese dioxide to *trans*-β-ionylideneacetaldehyde for purposes of identification. The properties of these derivatives were in good agreement with those reported in the literature.

An attempt to synthesize β-ionylideneacetaldehyde diethylacetal by the reaction of β-ionone with diethyl β,β-diethoxyethylphosphonate carbanion derived from monochloroacetaldehyde diethylacetal and diethyl phosphite was unsuccessful.

1) E. g., H. Pommer, *Angew. Chem.*, **72**, 811 (1960).

2) H. Takahashi, K. Fujiwara and M. Ohta, This Bulletin, **35**, 1498 (1962). An analogous reaction of diethyl carbethoxymethylphosphonate with ketones has been reported by B. C. Kovalev, L. A. Yanovskaya and V. F. Kucherov, *Izv. Akad. Nauk SSSR, Otd. Khim. Nauk*, 1876 (1962); *Chem. Abstr.*, **58**, 9148 (1963). These authors showed that β-ionone failed to react and was recovered unchanged.

Experimental[3]

Ethyl *trans*-β-Ionylideneacetate (I).—In a dry nitrogen atmosphere, a solution of 11.2 g. of diethyl carbethoxymethylphosphonate in 10 cc. of tetrahydrofuran was stirred into a suspension of 2 g. of sodium amide in 30 cc. of tetrahydrofuran while the suspension was being cooled in a water bath. After the stirring had continued for 6 hr., during which period scarcely any evolution of ammonia could be observed, a solution of 10 g. of β-ionone in 20 cc. of tetrahydrofuran was added drop by drop. The resulting mixture was stirred for an additional 2 hr. and then allowed to stand overnight at room temperature. After the solvent had been distilled off, the residual resinous product was decomposed with water and extracted with ether. The ethereal layer was washed with water and dried over anhydrous sodium sulfate. The solvent was evaporated, and the residue was distilled in vacuo to give ethyl *trans*-β-ionylideneacetate (I). Yield: 11 g. (80.4%); b. p. 148~154°C/2 mmHg; d_4^{17} 0.9700; λ_{max} 257, 300 mμ (lit.,[4] 257, 302 mμ); IR-spectrum (liq.): 965 cm^{-1} (*trans* -CH : CH-), 1715, 1240 cm^{-1} (ester).

Found: C, 77.98; H, 10.14; Calcd. for $C_{17}H_{26}O_2$: C, 77.82; H, 9.99%.

3) The UV absorption spectra were measured in isopropyl alcohol. Elementary analyses were performed at the Institute of Physical and Chemical Research, Tokyo.

trans-β-Ionylideneethanol (II).—I was reduced with lithium aluminum hydride to II;[4] b. p. 120~130°C/0.1 mmHg; λ_{max} 240, 267 mμ (lit.,[5] λ_{max} 240, 265 mμ); IR-spectrum (liq.): 3340, 995 cm^{-1} (prim. alcohol), 965 cm^{-1} (*trans* -CH : CH-).

trans-β-Ionylideneacetaldehyde (III).—II was oxidized with manganese dioxide to III;[4] b. p. 105~110°C/0.01 mmHg; λ_{max} 275, 327 mμ (lit.,[5] 273, 327 mμ); 2, 4-dinitrophenylhydrazone: m. p. 198°C (lit.,[4] 198°C); λ_{max} 413 mμ.

Found: N, 14.10; Calcd. for $C_{21}H_{26}N_4O_4$: N, 14.07%; semicarbazone: m. p. 194~195°C (lit.,[4] 194~195°C); λ_{max} 324 mμ.

Found: N, 15.20; Calcd. for $C_{16}H_{25}N_3O$: N, 15.26%.

The author is indebted to Professor Kyoichi Suga and Mr. Shoji Watanabe of Chiba University for their cordial guidance throughout this work.

Miyoshi Oil & Fat Co., Ltd.
Katsushika-ku, Tokyo

4) C. D. Robeson, J. D. Cawley, L. Weisler, M. H. Stern, C. C. Eddinger and A. J. Chechak, *J. Am. Chem. Soc.*, **77**, 4111 (1955).

5) H. O. Huisman, A. Smit, P. H. van Leeuwen and J. H. van Rij, *Rec. trav. chim.*, **75**, 977 (1956).

The Reaction Products from Resorcinol Dimethyl Ether and Cinnamoyl Chloride by the Friedel-Crafts Reaction

By Sumu MATSUEDA, Kazuo SANNOHE and Yoshinori SAITO

(Received June 19, 1963)

In 1926 Simonis and Danischewski[1] synthesized 2, 6-dimethoxychalcone (I) (m. p. 80°C) by the Friedel-Crafts reaction between resorcinol dimethyl ether and cinnamoyl chloride over aluminum chloride in carbon disulfide; I was then converted into 6-methoxy-2-hydroxychalcone (II) (m. p. 108°C). In 1947 Seshadri and Venkoteswarln[2] obtained 6-methoxy-2-hydroxychalcone (III) (m. p. 127~129°C) by the Kostanecki's method, treating 6-methoxy-2-hydroxyacetophenone with benzaldehyde in an alkaline medium. In 1950 Oliverio and Schiavello[3] reported that 6-methoxy-2-hydroxychalcone (IV) (m. p. 64°C) could be obtained by letting 6-methoxy-2-hydroxyacetophenone react with benzaldehyde in an ethanolic sodium hydroxide solution. They noticed the different melting points of II, III and IV, but they suggested that these differences might be attributed to the polymorphism, which is often observed in chalcones. The present paper will discuss the structure of II, III and IV. We have found that I and II are not 2, 6-derivatives but 2, 4-derivatives.

In the Friedel-Crafts reaction of resorcinol dimethyl ether, the substitution reaction at the 4-position (*o*, *p*-orientation) is perhaps more suitable than that at the 2-position (*o*,*o*-orientation) from the standpoint of the steric effect of these methoxy groups. A normal substitution reaction can take place at

1) H. Simonis and S. Danischewski, *Ber.*, **59**, 2914 (1926).
2) T. R. Seshadri and V. Venkoteswarln, *Proc. Indian Acad. Sci.*, **26A**, 189 (1947).
3) Aleardo Oliveris and Aldo Schiavello, *Gazz. Chim. Ital.*, **80**, 788 (1950).

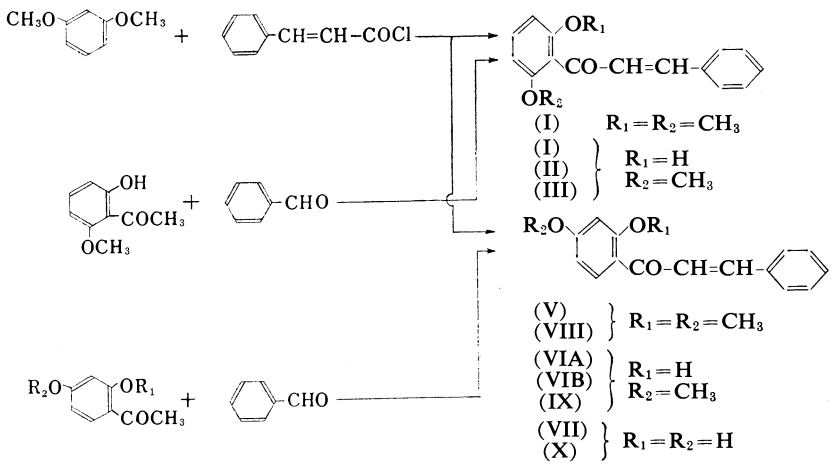

the 4-position, as in the case of Simonis and Danischewski, giving 2, 4-dimethoxychalcone and 4-methoxy-2-hydroxychalcone.

A product (V) in the form of yellow needles (m. p. 79~80°C) is obtained by means of the same procedure as Simonis and Danischewski. This product is comfirmed to be equal to I by converting V into monomethoxymonohydroxychalcone (VIB) (m. p. 107~108°C), which is identified as the II obtained by Simonis and Danischewski. On the other hand, by means of comparison of their mixed melting point and ultraviolet and infrared absorption spectra, the compound V is identified as 2, 4-dimethoxychalcone (VIII) (m. p. 79~80°C), an authentic sample of which is synthesized by means of Geismann's method.[4] 4-Methoxy-2-hydroxychalcone (IX) (m. p. 107~108°C), which is identical with an authentic sample,[5] is obtained from VIII under the same conditions as with Simonis and Danischewski. The identity of IX and VIB (=II) is established by the mixed melting point and absorption spectra of ultraviolet and infrared. It is concluded that cinnamoyl chloride does not attack the 2-position of the benzene nucleus of resorcinol dimethyl ether but rather attacks the 4-position, producing not 2, 6-dimethoxychalcone but 2, 4-dimethoxychalcone.

We also obtained, from the reaction of Simonis and Danischewski, 4-methoxy-2-hydroxychalcone (VIA) (m. p. 107~108°C) and 2, 4-dihydroxychalcone (VII) (m. p. 150~151°C) by means of elution chromatography on alumina. These compuonds show the typical ultraviolet absorption spectra of the chalcone structure and the absence of any flavanones, which isomerize easily from these chalcones. The average ratio of the yield of V, VIA and VII is about 70 : 10 : 5. Resorcinol dimethyl ether is carefully purified, confirming that it does not contain any trace of either monomethyl ether or raw resorcinol by means of gas chromatography. Therefore, the formation of VIA and VII may be attributed to a catalytic demethylation of aluminum chloride.

4) T. A. Geissman and R. O. Clinton, *J. Am. Chem. Soc.*, **68**, 697 (1945).
5) J. Shinoda, *J. Pharm. Soc. Jap.* (*Nippon Yakugaku Zasshi*), **48**, 214 (1928).

Experimental

The authentic compounds, 2, 4-dimethoxychalcone (VIII), 4-methoxy-2-hydroxychalcone (IX) and 2, 4-dihydroxychalcone (X), are prepared from the corresponding acetophenone derivatives and benzaldehyde by means of the usual chalcone syntheses.

Resorcinol Dimethyl Ether.—A sample of the dimethyl ether of resorcinol purified by repeated fractional distillations, was shown by gas chromatography (Silicone D. C. 550) to contain no such impurities such as the monomethyl ether of resorcinol and raw resorcinol.

Friedel-Crafts Reaction.—Forty grams of resorcinal dimethyl ether and 50 g. of cinnamoyl chloride were dissolved in 270 ml. of carbon disulfide. Into this solution 38 g. of fine pulverized aluminum chloride were then added while all were cooled with ice. After having been stirred for 1 hr. at room temperature, the reacted mixture was refluxed for 3 hr. at 50°C. Then the aluminum complex was filtered off, washed with carbon disulfide and ether. The complex was decomposed with ice water containing hydrochloric acid. The product dissolved in benzene and was purified by chromatography on alumina. The first eluted compound Vl was recrystallized from alcohol, yielding 56 g. of yellow needles (m. p. 79~80°C).

Found : C, 76.07 ; H, 5.86. Calcd. for $C_{17}H_{16}O_3$: C, 76.10 ; H, 6.01%.

λ_{max} (in alcohol) 230, 280 and 300~320 (plain curve) mμ. The major bands in the infrared absorption spectrum (KBr-disk) are : 3100 m, 3066 m, 2996 m, 2950 m, 2846 m, 1665 s, 1620 s, 1590 s, 1500 s, 1460 m, 1455 m, 1442 m, 1337 s, 1320 m, 1292 s, 1257 s, 1223 s, 1205 m, 1186 m, 1165 m, 1152 m,

1135 s, 1072 w, 1050 w, 1029 m, 1020 m, 1000 m, 987 m, 925 w, 865 w, 830 s, 806 m, 773 w, 768 s, 733 w and 698 w cm^{-1}

V showed no melting point depression when combined with authentic 2, 4-dimethoxychalcone (VIII), and it showed the same infrared absorption spectra as VIII. The second elute VI was recrystallized from petroleum benzine, to give 7.2 g. of yellowish orange needles (m. p. 107~108°C).

Found : C, 75.50 ; H, 5.62. Calcd. for $C_{16}H_{14}O_3$: C, 75.57 ; H, 5.55%.

λ_{max} (in alcohol) 220, 255 and 310~340 (plain curve) mμ. The major bands in the infrared absorption spectrum (KBr-disk) are : 3510 m, 3100 w, 3020 w, 3000 w, 2960 w, 2935 m, 2840 m, 1630 s, 1580 s, 1570 s, 1505 m, 1490 m, 1475 w, 1455 m, 1413 m, 1365 s, 1320 m, 1298 m, 1278 m, 1225 s, 1130 s, 1070 w, 1015 m, 998 m, 982 w, 975 m, 955 m, 850 m, 838 w, 807 m, 789 w, 765 s, 735 w and 674 w cm^{-1}.

VI showed no melting point depression when mixed with authentic 4-methoxy-2-hydroxychalcone (IX). The infrared absorption spectra of these compounds were quite similar. On the other hand, by means of methylation with dimethyl sulfate and sodium hydroxide, VI was converted into dimethoxy derivatives in the form of yellow needles (m. p. 80°C), which agreed with VIII. The last elute VIII was recrystallized from benzene, yielding 4.5 g. of yellowish orange needles (m. p. 150~151°C).

Founb : C, 74.85 ; H, 5.11. Calcd. for $C_{15}H_{12}O_3$: C, 74.99 ; H, 5.03%.

λ_{max} (in alcohol) 240, 255 and 310~350 (plain curve) mμ. The major bands in the infrared absorption spectrum (KBr-disk) are : 3360 s, 3080 m, 3000 w, 2930 m, 2850 w, 1640 s, 1630 s, 1590 s, 1520 s, 1498 m, 1442 s, 1420 m, 1382 s, 1333 m, 1283 m, 1200 broad, 1143 s, 1065 m, 1022 w, 985 m, 950 m, 838 m, 825 w, 785 m, 752 s, 728 w and 710 w cm^{-1}.

VII showed the same infrared absorption spectra as and no melting point depression when combined with authentic 2, 4-dihydroxychalcone (X). VII was then converted into VIII by means of methylation with dimethyl sulfate and sodium hydroxide.

The authors are grateful to Dr. Shin-ichiro Fujise and Dr. Sekio Mitsui for their kind guidance in this work.

Department of Chemistry
Faculty of Literature and Science
Hirosaki University
Hirosaki, Aomori

The Reaction of Sodium Metaphosphate with Disodium Sulfate at a High Temperature

By Shigeru OHASHI and Kozo IKEDA*

(Received June 20, 1963)

Poni and Cernătescu[1] have reported that a new compound with the formula Na_3SPO_7 which has an S–O–P linkage, can be prepared by the fusion of an equimolar mixture of sodium hydrogen sulfate and disodium hydrogen orthophosphate. The investigation of the same reaction by Audrieth, Mills, and Netherton[2] has revealed that the reaction proceeds according to Eqs. 1 and 2:

$$n\mathrm{NaHSO_4} + n\mathrm{Na_2HPO_4} \xrightarrow{200^\circ\mathrm{C}} n\mathrm{Na_2SO_4} + n\mathrm{NaH_2PO_4} \quad (1)$$

$$n\mathrm{NaH_2PO_4} \xrightarrow{600\sim800^\circ\mathrm{C}} (\mathrm{NaPO_3})_n\text{-glass} + n\mathrm{H_2O} \quad (2)$$

where n is the average chain length of the polyphosphates in the glass. It has been concluded that the final products are disodium sulfate and a glass of sodium metaphosphate and that a sulfate-phosphate copolymer such as Na_3SPO_7 can not be formed by this reaction, at least in the temperature range of 200~800°C.

The present authors have investigated the reaction of equimolar mixtures (S/P=1) of glassy sodium metaphosphate and disodium sulfate at temperatures higher than 800°C. The mixtures were melted in platinum crucibles at 1300 and 1400°C for 1 hr. and then rapidly cooled. The products were white crystalline substances.

It was found that when the mixture is heated at such high temperatures, a considerable amount of sulfur trioxide is expelled from the melt, while phosphorus pentaoxide is not expelled. Chemical analyses of the reaction

* Present address: Institute for Thermal Spring Research, Okayama University, Misasa, Tottori-ken.

1) M. Poni and R. Cernătescu, *Ann. Sci. Univ. Jassy*, **28**, Sect. I, 3 (1942); *Chem. Abstr.*, **42**, 4480 (1948).

2) L. F. Audrieth, J. R. Mills and L. E. Netherton, *J. Phys. Chem.*, **58**, 482 (1954).

TABLE I. DATA OBTAINED BY THE X-RAY DIFFRACTOMETRY AND THE PAPER CHROMATOGRAPHY FOR THE SAMPLES OF THE $NaPO_3$-Na_2SO_4 AND $NaPO_3$-Na_2SiO_3 SYSTEMS

	X-Ray diffractometry				Paper chromatography P%	
	Unknown	Diphosphate	Na_2SO_4	α-Cristobalite	Orthophosphate	Diphosphate
The $NaPO_3$-Na_2SO_4 system, prepared at						
1300°C	+++	++	+	−	39.5	60.5
1400°C	+++	++	+	−	50.8	49.2
The $NaPO_3$-Na_2SiO_3 system P/Si						
1.00	+++	±	−	+++	100	0
1.15	+++	+	−	+++	85.8	14.2
1.30	+++	++	−	+++	65.1	34.9
1.50	+++	+++	−	+++	51.7	48.3
2.00	+	++	−	+++	16.4	83.6

products revealed that 63.5 or 80.75% of the total sulfur was expelled as sulfur trioxide when the mixture was prepared at 1300 or 1400°C respectively. If one assumes that no compounds with S–O–P linkages are produced in the sample, the reaction can be represented by Eq. 3:

$$(NaPO_3)_n + nNa_2SO_4 \rightarrow Na_{n+2nx}P_nO_{3n+nx} + n(1-x)Na_2SO_4 + nxSO_3 \quad (3)$$

where x is a fraction of the sulfur expelled as the sulfur trioxide with respect to the total sulfur, while $Na_{n+2nx}P_nO_{3n+nx}$ represents a mixture of sodium phosphates.

The X-ray diffraction pattern of the sample exhibits peaks due to considerable amounts of tetrasodium diphosphate and an unknown species with a small amount of disodium sulfate. The following three peaks are characteristic of the unknown species; two peaks of strong intensity at spacings of 2.63 and 4.29 Å, and a peak of medium intensity at a spacing of 2.79 Å. On the other hand, it was found in the laboratory of the present authors that there were three peaks, with spacings quite identical to those described above, in the X-ray diffraction patterns of certain samples of a sodium metaphosphate-sodium metasilicate system, which will be described in a separate paper.

The data obtained by the X-ray diffractometry and the paper chromatography of the samples of both the systems are shown in Table I. The latter data indicate that considerable amounts of orthophosphate are present in the sample solutions of both the systems. It may be possible to assume that crystalline substances with structural frameworks such as I, II, III, or IV are hydrolyzed to give orthophosphate when dissolved in water. However,

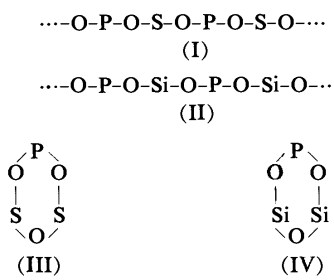

it is difficult in general to assume that a substance containing S–O–P linkages and one containing P–O–Si linkages both give a group of peaks located at quite identical spacings. Therefore, it seems reasonable to assume that the unknown peaks in question may be due to a kind of trisodium orthophosphate.

Therefore, it may be concluded that the main reaction of an equimolar mixture of sodium metaphosphate and disodium sulfate at a high temperature proceeds according to Eq. 3 and that no compound with S–O–P linkages, at least as a major component in the crystalline substances, is formed by this reaction. A pattern of normal trisodium orthophosphate exhibits three characteristic peaks at spacings of 2.55, 2.70, and 4.25 Å. The discrepancy between the spacings of the peaks due to normal trisodium orthophosphate and those due to the unknown species discussed in this paper remains an unsolved problem.

Department of Chemistry
Faculty of Science
Kyushu University
Hakozaki, Fukuoka

The Catalytic Activity of Metal Oxides of the Fourth Period in the Hydrogen-Oxygen Reaction. A Commentary on a Paper by Popovskii and Boreskov

By Isamu KOMURO,* Haruhiko YAMAMOTO and Takao KWAN

(Received July 1, 1963)

In spite of many efforts[1] to correlate the catalytic activity of metal oxides with such electronic properties of the corresponding oxides as the semiconductivity and the electronic configuration of the metal ion, there still remain some cases where the classical oxidation-reduction concept[2] sounds better than modern electronic interpretations. Undoubtedly, the catalyst activity of metal oxide is so sensitive to the mode of preparation or to the surrounding atmosphere that difficulty is often encountered in interpreting the observed activity data, the temperature threshold for a reaction in a majority of cases being a conventional measure of the catalyst activity.

Recently Popovskii and Boreskov[3] investigated the hydrogen-oxygen reaction on the metal oxides of the fourth period in a systematic and careful manner. Excess oxygen was used so that the catalyst activity might be compared at a certain oxidation level. The rate data were given in terms of the volume of hydrogen consumed per unit hour and per unit area of the metal oxides at temperatures of 150 and of 300°C respectively.

Their data are reproduced in Fig. 1 in relation to the atomic number of the constituent metal ion in the way they adopted.

The order of the catalyst activity was found to be:

$$Co_3O_4 > CuO > MnO_2 > NiO > Fe_2O_3 > Cr_2O_3 > V_2O_5 > ZnO > TiO_2$$

at 150°C. The activity at 300°C was nearly parallel with this. While such an activity series was consistent with the familiar relationship in respect to the type of semiconductor, i. e., *p*-type>*n*-type, Popovskii and Boreskov favored the parallel relationship with a work function series of these oxides proposed as:

$$CuO > NiO > V_2O_5 > ZnO > TiO_2$$

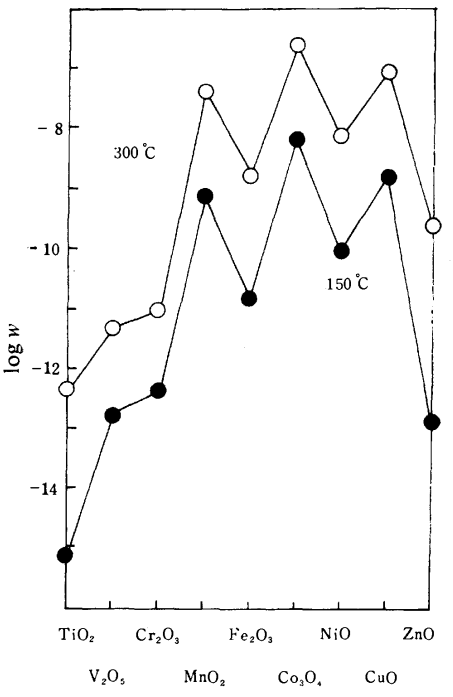

Fig. 1. The catalytic activity of metal oxides of the fourth period for the hydrogen-oxygen reaction after Popovskii and Boreskov.[3]

suggesting that the electron transfer from the substrate to the oxide is rate-controlling.

It should be noted, however, that the work function of metal oxide is in general sensitively dependent on the pretreatment of the oxide as well as on the atmosphere. At present the value of the work function, as far as metal oxide is concerned, does not seem to be well-established. It has been reported[4] that the work function of zinc oxide is, at an oxidation level, greater by 1.0 eV. or even more than that of nickel oxide, contrary to the above order proposed by Popovskii and Boreskov.

On the other hand, it would be interesting to see if the relative catalytic activity of the

* Present address: Research Laboratory, Mitsubishi Petrochemical Co., Ltd., Mizonokuchi, Kawasaki.

1) See, for example, F. S. Stone, "Advances in Catalysts," Vol. 13, Academic Press, New York (1962), p. 1.

2) Sol Weller and S. E. Voltz, *Z. physik. Chem. N. F.*, 5, 100 (1955); S. Makishima, Y. Yoneda and Y. Saito, International Congress on Catalysis, Paris, 1960.

3) V. V. Popovskii and G. K. Boreskov, *Prob. Kin. Cata. Nauk. S. S. S. R.*, 10, 67 (1960).

4) H. H. Jacobs, *J. Appl. Phys.*, 17, 596 (1946); F. Wilessov and A. Terenin, *Naturwiss.*, 46, 167 (1959).

oxides quoted above accords with the relative reducibility of the corresponding oxide by hydrogen. Let us, therefore, investigate how the bond strength of oxygen with the surface may be correlated with the catalyst activity.

The chemisorption of hydrogen would be instantaneous under the experimental conditions; the H_2–D_2 exchange reaction is known to occur on the metal oxides at much lower temperatures.[5] The same may perhaps be true with the oxygen chemisorption. It is assumed that the act of depriving the chemisorbed oxygen atom to yield water is rate-controlling. Let us assume, moreover, that the heat of the formation of metal oxide per g. atom oxygen is a measure of the strength of the oxygen-surface bond. The heat of formation of metal oxide per g. atom oxygen does not depend appreciably on the valency state of the constituent metal ion, at least for the metal oxides under investigation. Current investigations[6] fortunately indicate that there is a close correspondence between the chemisorption and the formation of the bulk compounds. Thus, one may expect some kind of regular relation between the catalyst activity of the metal oxides of the fourth period and the heat of the formation of the corresponding metal oxide. Table I shows the heats of formation of metal oxides per g. atom oxygen,

TABLE I. THE HEAT OF FORMATION OF METAL OXIDE PER G. ATOM OXYGEN AND THE KINETIC DATA FOR THE HYDROGEN-OXYGEN REACTION AT 150°C

Catalyst	Heat of formation $\Delta H°$, cal.	$\Delta H°$/g. atom oxygen cal.	Rate, w cc./hr. cm^2	Activation energy kcal.
TiO_2	228350	114180	6.3×10^{-16}	21
V_2O_5	381960	76390	1.8×10^{-13}	18
Cr_2O_3	274670	91560	4.1×10^{-13}	18
Fe_2O_3	202960	67650	1.4×10^{-11}	15
MnO_2	126400	63200	$\sim10^{-9}$*	14
Co_3O_4	—	63000**	6.5×10^{-9}	11
NiO	57640	57640	2.6×10^{-10}	8
CuO	37740	37740	4.9×10^{-9}	13
ZnO	84670	84670	1.3×10^{-13}	24

* Estimated from the plot of Fig. 1.
** Mean of CoO (56910) and Co_2O_3 (207300).
The thermochemical values were taken from "Handbook of Chemistry and Physics," 42nd Ed., Chemical Rubber Publishing Co. (1960).

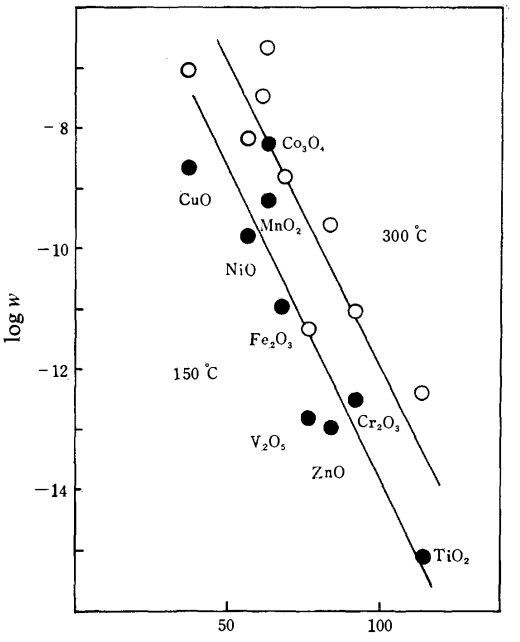

Fig. 2. The relation between the catalytic activity of metal oxides and the heat of formation of metal oxides per g. atom oxygen.

together with the kinetic data for the hydrogen-oxygen reaction obtained by Popovskii and Boreskov.

An attempt was made to plot the rate data ($\log w$) against the heat of formation of metal oxide as given by the third column of Table I. This plot is shown in Fig. 2.

It may be seen from Fig. 2 that an approximately linear relationship exists between the catalyst activity of the metal oxides and the heat of formation of these oxides at 150 and 300°C respectively. It is shown, in other words, that the weaker the oxygen-surface bond, the faster the rate of hydrogen-oxygen reaction.

Sachtler et al.[7] described the relative catalytic activity of metals in the decomposition of formic acid by the use of the heat of formation of metal formate, arriving at a so-called volcano-shaped curve. The present approach is quite similar to this. The use of the heat of formation in any way instead of the strength of the surface bond must, of course, be only approximate. However, it does seem useful as one can readily correlate the kinetic data in terms of the thermodynamic quantities available in the "Handbook."

5) D. A. Dowden, N. Mackenzie and B. M. W. Trapnell, *Proc. Roy. Soc.*, **A237**, 245 (1956).
6) M. W. Roberts, *Nature*, **188**, 1020 (1960); D. Brennan, D. O. Hayward and B. M. W. Trapnell, *Proc. Roy. Soc.*, **A256**, 81 (1960); W. M. H. Sachtler and L. L. van Reijen, *Shokubai*, **4**, 147 (1962); K. Tanaka and K. Tamaru, ibid., **4**, 328 (1962).
7) J. Fahrenfort, L. L. van Reijen and W. M. H. Sachtler, *Z. Elektochem.*, **64**, 716 (1960); W. M. H. Sachtler, Lecture read before the Catalysis Club of Japan, July 26, 1961, Sapporo.

Indeed, there is a rough parallelism between the activation energy of the hydrogen-oxygen reaction given in the fifth column and the heat of formation of metal oxide per g. atom oxygen given by the third column of Table I. It is hoped that modern electronic theory will be successfully applied on the basis of knowledge gained from the classical viewpoint.

One of the authors (I. K.) especially wishes to thank Dr. Yoshio Murata, the General Manager of The Research Laboratory, Mitsubishi Petrochemical Co., Ltd., for his support of this survey.

Division of Physicochemical Technology
Faculty of Pharmaceutical Sciences
The University of Tokyo
Hongo, Tokyo

Note added in proof.—An explanation compatible with this commentary was put forward very recently by Boreskov, Dzisyak and Kasatkina (*Kin. Kata.*, **4**, 388 (1963)) in the homomolecular exchange of oxygen isotope on metal oxides; these authors noted that the calalytic activity of metal oxides of the fourth period in the above-mentioned reaction or in the hydrogen-oxygen reaction may be determined by the bond energy of oxygen with the surface and not by the electronic work function of the oxides.

The Chelating Behavior of β-Aminoethylmercaptan with Alkaline Earth Metals[*1]

By Yuichi TSUCHITANI,[*2] Takeshi ANDO and Keihei UENO

(Received July 22, 1963)

During the course of our investigation into the syntheses of new chelating agents, an intermediate product, β-aminoethylmercaptan (hereafter referred to as AEM), drew our attention as a masking agent in the chelatometric titration.[1] This investigation also made it necessary that we get basic information on the chelating behavior of this bidentate ligand with various metal ions.

Many papers have been published on the chelate-forming properties of AEM in solid[2,3], as well as in solution states;[4-7] the reported data on the chelate stability constant include data on such metal ions as cadmium(II), cobalt(II), nickel(II), lead(II) and zinc(II).[8] However, no information is available on its chelating behavior with alkaline earth metals. This paper will report the results of the chelate stability measurement of AEM with alkaline earth metals.

Experimental

Reagents. — AEM which had been obtained as hydrochloride from the Evans Chemitics, Inc., New York, was recrystallized repeatedly from ethanol in a nitrogen atmosphere. The material was very hygroscopic and had to be stored in nitrogen over phosphorus pentaoxide. It melted at 70~70.5°C in a sealed tube (reported m. p. 70.2 ~70.7°C[9]).

Found: C, 20.81; H, 6.90%. Calcd. for $C_2H_7NS \cdot HCl$: C, 21.13; H, 7.10%.

The purity of the material was also checked by the iodometry of the -SH group; it was found to be 99.37±0.40%. The strength of the aqueous solution of the reagent decreased by 0.5~1.0% over a 3-day period even when it was kept in nitrogen in a refrigerator; therefore, the exact strength of the solution was estimated by taking the mean value of the strengths before and after measurement.

All the metal ions used in this study were in nitrate form; the concentration of their solutions was determined by the EDTA titration.

The Measurement of the Dissociation and the Chelate Stability Constants. — The experimental method consisted of the potentiometric titration of the ligand in the absence and in the presence of

*1 Contribution No. 44 from the Department of Organic Synthesis, Faculty of Engineering, Kyushu University.

*2 Present address: Central Research Laboratory, Ajinomoto Co., Kawasaki.

1) K. Yamaguchi and K. Ueno, *Talanta*, **10**, 1041 (1963).

2) R. V. G. Ewens and C. S. Gibson, *J. Chem. Soc.*, **1949**, 431.

3) D. C. Jicha and D. H. Busch, *Inorg. Chem.*, **1**, 872, 878 (1962).

4) K. A. Jensen, *Z. anorg. u. allgem. Chem.*, **229**, 265 (1936).

5) R. G. Neville and G. Gorin, *J. Am. Chem. Soc.*, **78**, 4891, 4893 (1956); **79**, 518 (1957).

6) E. Felder, A. Rosigno and R. Radica, *Gazz. chim. ital.*, **85**, 453 (1955).

7) N. C. Li and R. A. Mannig, *J. Am. Chem. Soc.*, **77**, 5225 (1955).

8) J. Bjerrum et al., "Stability Constants, Part I: Organic Ligands," Chem. Soc., London (1957).

9) Product data on AEM hydrochloride, Evans Chemitics, Inc., New York.

the metal ions, using a 0.10 N sodium hydroxide solution as the titrant. The ionic strength was kept constant at $\mu=0.10$ with potassium nitrate, while the concentrations of the ligand and the metal ions were kept at $1\sim2\times10^{-3}$ M. Titrations were carried out with solutions with 1 : 1 and 1 : 2 metal ligand ratios at 25 ± 0.1°C in a current of nitrogen in the absence of atmospheric and dissolved oxygen.

The hydrogen ion concentration was measured by means of a Hitachi Horiba Model P pH-meter with a glass and a calomel electrode. A fluctuation in the pH value was seen when a fresh glass electrode was used; only reproducible readings were taken as the titration data.

Results and Discussion

The acid dissociation constant of the ligand was calculated, according to Bjerrum's method, from the titration curve of the ligand in the absence of metal ions (Fig. 1). The equilibria and the dissociation constants to be determined are expressed as:

$$H_2A^+ \rightleftharpoons H^+ + HA\,;\ k_1=(H^+)(HA)/(H_2A^+)$$

$$HA \rightleftharpoons H^+ + A^-\,;\ k_2=(H^+)(A^-)/(HA)$$

where H_2A^+ represents the protonated ligand ($HSCH_2CH_2N^+H_3$). The values of pk_1 and pk_2 were obtained from Bjerrum's formation curve, and their accuracies were checked by the successive approximation method of Carlson, McReynolds and Verhoek.[10] As Table I shows, these values agree fairly well with the reported values when the differences in experimental conditions are taken into account.

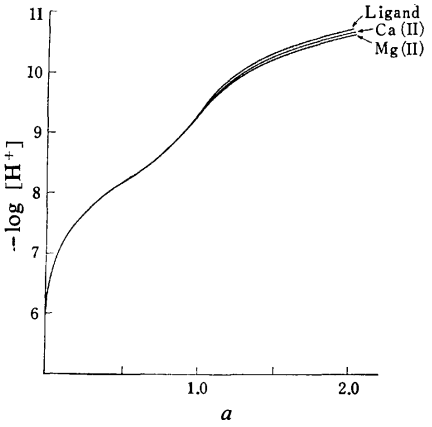

Fig. 1. Titration curves of AEM with and without the metal ions.
$t=25$°C; $\mu=0.10$ (KNO_3); Concentration of ligand, about 1×10^{-3}

The titration curves of the solutions with a 1 : 1 metal to ligand ratio for calcium(II) and magnesium(II) are shown in Fig. 1. Although the titration of solutions with a 1 : 2 ratio was also carried out, no indication of the formation of a 1 : 2 chelate was found. The chelate stability constant for the 1 : 1 may be defined as follows:

$$M^{2+} + A^- \rightleftharpoons MA^+\,;$$

$$K_{MA}=(MA^+)/(M^{2+})(A^-)$$

where M^{2+} and A^- represent alkaline earth metal ions and the deprotonated ligand $H_2NCH_2CH_2S^-$ respectively. The chelate stability constants for alkaline earth metals were calculated from these titration curves according to the method developed by Chaberek and Martell.[11] When the data obtained from the titration curves in a range of $a=1.4\sim1.7$ were employed, the agreement of the calculated values on each metal ion were not satisfactory. Therefore, fairly consistent values from the narrower range of $a=1.48\sim1.57$ were taken as the chelate stability constants. The main reasons for such a deviation may be an error

TALE I. ACID DISSOCIATION CONSTANTS AND CHELATE STABILITY CONSTANTS OF AEM AND SOME RELATED COMPOUNDS

Ligand	pk_1	pk_2	log K_{MA} for			
			Ba	Ca	Mg	Sr
β-Aminoethylmercaptan						
25°C, $\mu=0.10$	8.19	10.73	1.37	2.21	2.30	1.55
25°C, $\mu=0.15$	8.35	10.81				
Iminodiacetic acid						
20°C, $\mu=0.10$	2.98	9.89	1.67	2.59	2.94	—
Glycine						
20°C, $\mu=0.2$	2.35	—	0.77	1.38	3.44	—
Glycolic acid						
20°C, $\mu=0.2$	3.71	—	0.66	1.11	0.92	0.80

All data except those of the first line are taken form Ref. 8.

10) G. A. Carlson, J. P. McReynolds and F. H. Verhoek, *J. Am. Chem. Soc.*, **67**, 1334 (1945).

11) S. Chaberek, Jr. and A. E. Martell, ibid., **74**, 5052 (1952).

in pH measurement, an error which would increase with decreasing chelate stability, and the decomposition of ligands in the alkaline region. As is shown in Table I, the chelate stability constants for alkaline earth metals are not very high, but they are still appreciable. These values are comparable to those of iminodiacetic acid and are somewhat higher than those of glycolic acid and glycine. The same order of increasing stability, barium< calcium<magnesium, is observed for AEM, glycine and iminodiacetic acid, all of which have nitrogen as one of the donor atoms. These findings suggest that the coordination of nitrogen in AEM is effective, even in the case of alkaline earth metals. In the chelate stability investigation into the marcaptoethyl derivative of iminodiacetic acid,[12] it has been found that the coordination of the $-S^-$ group contributes very little to the chelate stability in the case of alkaline earth metals. Therefore, it is very likely that the chelate formation of AEM with alkaline earth metals takes place mainly through the coordination of the amino nitrogen of the ligand.

Part of the expense of this investigation have been defrayed by a grant from the Ministry of Education, to which the authors' thanks are due.

Department of Organic Synthesis
Faculty of Engineering
Kyushu University
Hakozaki, Fukuoka

12) G. Scharzenbach, G. Anderegg, W. Schneider and H. Senn, *Helv. Chim. Acta*, **38**, 1147 (1955).

*The Polymerization of 3,3-Bis(chloromethyl)oxetane with Boron Trifluoride-Diethyl Etherate in the Presence of Glycidyl Methacrylate**

By Takayuki Otsu, Shuzo Aoki and Minoru Imoto

(Received July 27, 1963)

Recently Saegusa and his colaborators[1] reported that three-membered cyclic ethers, such as propylene oxide and epichlorohydrin, showed a cocatalytic effect on the polymerization of tetrahydrofuran and 3,3-bis(chloromethyl)oxetane with Lewis acid catalysts. We also found that glycidyl methacrylate and glycidyl acetate could serve as both cocatalyst and comonomer in the polymerization of tetrahydrofuran catalyzed by boron trifluoride-diethyl etherate.[2] Several copolymers of tetrahydrofuran and 3,3-bis(chloromethyl)oxetane with some other three-membered cyclic ethers have been prepared.[3] This paper is concerned with the polymerization of 3,3-bis(chloromethyl)oxetane with boron trifluoride-diethyl etherate in the presence of glycidyl methacrylate.

Experimental

3,3-Bis(chloromethyl)oxetane, glycidyl methacrylate and boron trifluoride-diethyl etherate were carefully distilled in nitrogen atmosphere under reduced pressure. The middle fraction was collected and used. Methylene chloride was washed with aqueous sodium carbonate and then with distilled water, dried over calcium chloride, and distilled. The polymerization and copolymerization were carried out in a glass-stoppered tube. After a specified time, the polymerization mixture was poured into methanol. The polymer precipitated was filtered off on a glass filter, washed with methanol, and dried under vacuum. The composition of the copolymer was calculated from the results of the chlorine analysis.

Results and Discussion

The effects of the catalyst concentration and of the polymerization temperature on the polymerization rate of 3,3-bis(chloromethyl)-oxetane in the presence of glycidyl methacrylate and boron trifluoride-diethyl etherate were investigated. The results are shown in Table I. The yield of the polymer increased with the increases in the concentration of

* Vinyl Polymerization. LXXXII.

1) T. Saegusa, H. Imai and J. Furukawa, *Makromol. Chem.*, **54**, 218 (1962); T. Saegusa, H. Imai, S. Hirai and J. Furukawa, *J. Chem. Soc., Japan, Ind. Chem. Sec.* (*Kogyo Kagaku Zasshi*), **66**, 474 (1963).

2) T. Otsu, K. Goto, S. Aoki and M. Imoto, *Makromol. Chem.*, in press.

3) H. Meerwein, D. Delfs and H. Morschel, *Angew. Chem.*, **72**, 927 (1960); W. J. Murbach and A. Adicoff, *Ind. Eng. Chem.*, **52**, 772 (1960); L. A. Dickinson, *J. Polymer Sci.*, **58**, 857 (1962).

TABLE I. THE EFFECTS OF BORON TRIFLUORIDE-DIETHYL ETHERATE-GLYCIDYL METHACRYLATE CONCENTRATION AND POLYMERIZATION TEMPERATURE ON THE POLYMERIZATION OF 3,3-BIS(CHLOROMETHYL)OXETANE

Run No.	Boron trifluoride-diethyl etherate g.	Glycidyl methacrylate g.	3,3-Bis(chloromethyl)oxetane g.	CH_2Cl_2 ml.	Temp. °C	Time hr.	Yield g.
B-1	0.4	0	4.0	10	−78	3	0.3
15	0.05	0.05	4.0	10	−78	48	0.4
3	0.1	0.1	4.0	10	−78	48	0.6
16	0.4	0.4	4.0	10	−78	1.5	0.8
17	1.0	1.0	4.0	10	−78	1.5	1.3
3	0.1	0.1	4.0	10	−78	48	0.6
11	0.1	0.1	4.0	10	30	5	0.7
4	0.1	0.5	4.0	10	−78	48	0.1
9	0.1	0.5	4.0	10	0	48	0.3
12	0.1	0.5	4.0	10	30	2	1.8
5	0.1	2.0	4.0	10	−78	48	trace
10	0.1	2.0	4.0	10	0	48	0.1

TABLE II. THE RESULTS OF COPOLYMERIZATION OF 3,3-BIS(CHLOROMETHYL)OXETANE WITH GLYCIDYL METHACRYLATE*

Run No.	Boron trifluoride-diethyl etherate g.	Glycidyl methacrylate g.	3,3-Bis(chloromethyl)oxetane g.	Temp. °C	Time hr.	Yield g.	Cl (%) in copolymer
3	0.1	0.1	4.0	−78	48	0.6	
4	0.1	0.5	4.0	−78	48	0.1	
5	0.1	2.0	4.0	−78	48	trace	
6	0.1	4.0	4.0	−78	48	trace	
B-2	0.4	0	4.0	0	0.5	2.0	45.67**
18	0.4	0.2	4.0	0	0.37	1.0	45.60
21	0.4	0.5	4.0	0	0.25	0.2	43.37
19	0.4	1.0	4.0	0	3	0.5	39.31
22	0.4	2.0	4.0	0	0.5	0.1	40.75
20	0.4	4.0	4.0	0	4	0.2	33.15

* 10 ml. of CH_2Cl_2 was used as a diluent.
** Calcd. for $C_5H_8OCl_2$: Cl, 45.73%.

boron trifluoride-diethyl etherate-glycidyl methacrylate and in the polymerization temperature; therefore, it was clear that glycidyl methacrylate serves as a cocatalyst for the polymerization of 3,3-bis(chloromethyl)oxetane as well as for that of tetrahydrofuran.[2)]

Table II shows the results of the copolymerization of 3,3-bis(chloromethyl)oxetane with glycidyl methacrylate at −78 and 0°C. As can be seen from Tables I and II, the yield of the polymer decreased as the concentration of glycidyl methacrylate increased relative to the concentration of boron trifluoride-diethyl etherate. These results may be interpreted in terms of the decreased reactivity of the oxonium cation derived from glycidyl methacrylate, since the carbon-carbon double bond in glycidyl methacrylate was quite inert for

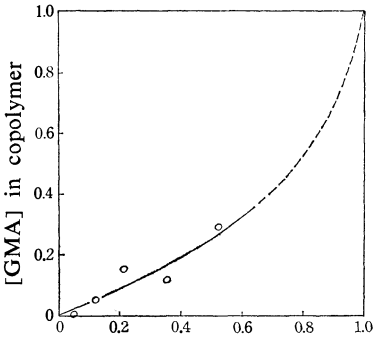

Fig. 1. Monomer-copolymer composition curve for copolymerization of 3,3-bis(chloromethyl)oxetane with glycidyl methacrylate at 0°C.

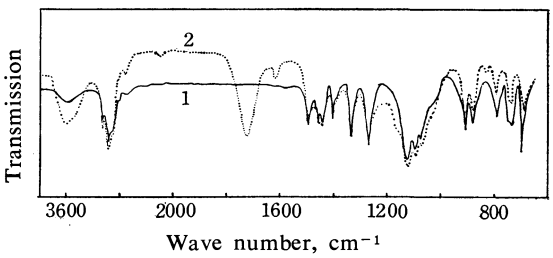

Fig. 2. Infrared spectra of poly-3,3-bis(chloromethyl)oxetane (1) and 3,3-bis(chloromethyl)-oxetane-glycidyl methacrylate copolymer (2) in KBr disk.

the cationic polymerization of tetrahydrofuran, as has been reported in a previous paper.[2)]

From the chlorine contents in the copolymer (Table II), a monomer-copolymer composition curve for this copolymerization at 0°C was drawn (cf. Fig. 1). The apparent monomer reactivity ratios were calculated to be:

r(3, 3-bis(chloromethyl)oxetane) = 2.6

r(glycidyl methacrylate) = 0.2

These values are the same as those obtained for the tetrahydrofuran-glycidyl methacrylate copolymerization.[2)]

The infrared spectrum of the copolymer (Fig. 2) shows absorption bands at 1730 and 1640 cm^{-1} due to a carbonyl group and a carbon-carbon double bond respectively, evidently arising from the glycidyl methacrylate unit of the polymer chain. Accordingly, it has been concluded that only the three-membered cyclic ether (epoxy) group in glycidyl methacrylate participated in the copolymerization with the 3,3-bis(chloromethyl)oxetane catalyzed by boron trifluoride-diethyl etherate.

Department of Applied Chemistry
Faculty of Engineering
Osaka City University
Kita-ku, Osaka

SHORT COMMUNICATIONS

The Free Radical of Quinone Formed on Active Alumina

By Tsutomu TAKAMURA and Jiro KASHIWAKURA

(Received August 21, 1963)

It has been observed that violet or pink coloration is produced by the absorption of *p*-benzoquinone, Q, or chloranil on active alumina. This has led to the assumption that quinones changed to semiquinone, because a similar coloration has been observed in the course of semiquinone formation in a homogeneous alkaline solution.[1)]

Pure active alumina (99.99% purity after complete drying) obtained by the amalgam method was heated at about 400°C to expel adsorbed water and was then cooled in air. The white alumina thus treated turned pink or violet when it was suspended in a carbon tetrachloride solution of chloranil. The color tone was found to depend upon the water content of the alumina. A low water content gave an orange or pink color, and a high water content, violet or brown. When Q was used instead of chloranil, a brownish violet coloration developed.

When the near-ultraviolet spectrum of Q absorbed on the alumina was measured by the KBr disk method, two adsorption bands were observed, at 415 and 430 mμ. This indicates the formation of semiquinone, whose characteristic bands are known to appear at 407 and 430 mμ in an aqueous solution.[2)] The ESR spectrum was recorded for the alumina degassed at 400°C for 3 hr. under the pressure of 10^{-5} mmHg, followed by the adsorption of Q in vacuo. The spectrum of alumina showed a single absorption band whose peak-to-peak separation of the derivative form was approximately 10 gauss and the *g* value of which was

1) B. Venkataraman and G. Frankel, *J. Am. Chem. Soc.*, **77**, 2707 (1955); W. Llaig and J. C. Saleld, *Naturwiss.*, **47**, 516 (1960).

2) M. Eigen and P. Matthies, *Chem. Ber.*, **94**, 3309 (1961).

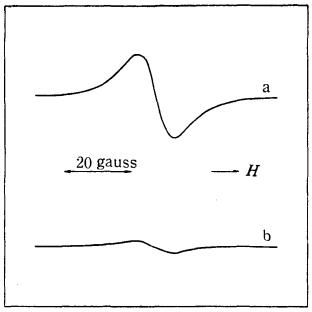

Fig. 1. ESR spectra of *p*-benzoquinone adsorbed on the alumina treated with (curve b) and without (curve a) antimony trichloride.

2.00 (Fig. 1, curve a), while only a very weak signal could be obtained when the alumina had previously been treated with Lewis acid composed of antimony trichloride or maleic anhydride (Fig. 1, curve b).

Although no detailed ESR spectrum of semiquinone could be obtained, the findings regarding the near-ultraviolet and ESR spectra seem to indicate the formation of a semiquinone. Two mechanisms can generally be considered in the formation of a semiquinone from Q. One is the charge-transfer mechanism, where some Lewis base transfers one electron to the delocalized π orbital of Q; the other is that one proposed by Eigen and Matthies,[2] where the hydroxide ion attaches to the 2-position of Q, after which a porton is released and an equimole is formed of hydroxy-*p*-benzosemiquinone and *p*-benzosemiquinone.

If the formation of a semiquinone on active alumina occurs through the above-mentioned mechanisms, some basic sites must be present on the alumina surface. The ESR results of Lewis acid-treatment support the assumption that the basic sites which cause semiquinone formation are present on the alumina. It has been reported that water or oxygen plays an important role in the formation of a semiquinone in a homogeneous solution.[1,2] Since the present findings regarding the ESR signal obtained for the sample prepared in vacuo indicate little influence by oxygen, a further study of the influence of water in connection with the basicity of active alumina has since been conducted.

Central Research Laboratory
Tokyo Shibaura Electric Co., Ltd.
Komukai, Kawasaki

Electron Spin Resonance Spectra of Nitrophenol Anion Radicals

By Kisaburo UMEMOTO, Yasuo DEGUCHI and Taitiro FUJINAGA

(Received September 3, 1963)

Though the electron spin resonance of the nitrophenol anion radical could not be studied by the reduction method using alkali metals, we have observed the ESR spectra of *p*-, *m*- and *o*-nitrophenol anion radicals generated by electrochemical reduction by following a method similar to that of Maki et al.[1] Electrolysis was carried out in a 10^{-3} molar acetonitrile solution containing 0.1 N tetra-*n*-propylammonium perchlorate as the

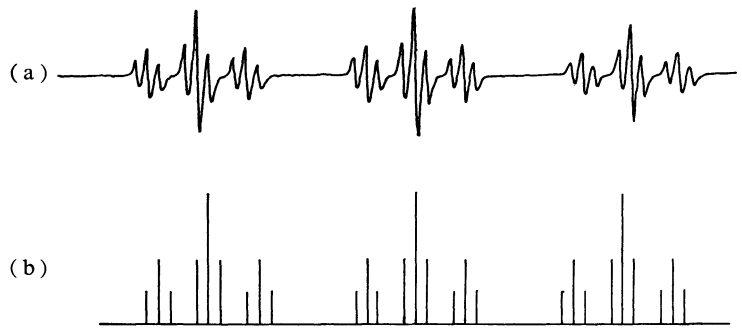

Fig. 1. (a) ESR spectrum of *p*-nitrophenol.
(b) Spectrum constructed from the coupling constants shown in Table I.

1) C. H. Geske and A. G. Maki, *J. Am. Chem. Soc.*, **82**, 2671 (1960).

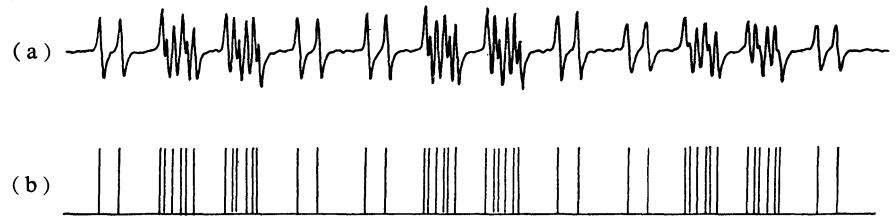

Fig. 2. (a) ESR spectrum of *m*-nitrophenol.
(b) Spectrum constructed from the coupling constants shown in Table I.

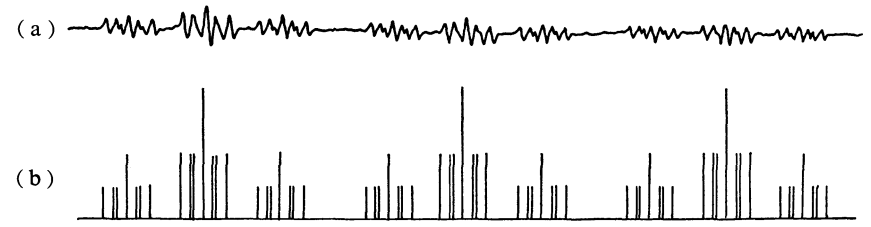

Fig. 3. (a) ESR spectrum of *o*-nitrophenol.
(b) Spectrum constructed from the coupling constants shown in Table I.

TABLE I. COUPLING CONSTANTS OF NITROPHENOL ANION RADICALS

Substance	Coupling constants* (in gauss)
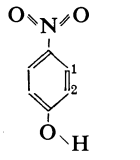 *p*-Nitrophenol	$a_N = 13.8$ $a_{H_1} = 3.14$ $a_{H_2} = 0.72$
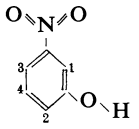 *m*-Nitrophenol	$a_N = 12.3$ $a_{H_1} = 3.33$ $a_{H_2} = 2.98$ $a_{H_3} = 2.76$ $a_{H_4} = 0.92$
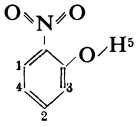 *o*-Nitrophenol	$a_N = 12.5$ $a_{H_1} = 3.59$ $a_{H_2} = 3.59$ $a_{H_3} = 1.01$ $a_{H_4} = 0.61$ $a_{H_5} = 0.46$

* The assignment of these coupling constants was not confirmed by the deuterium substitution but supposed from the results of the Hückel MO calculations.

supporting electrolyte.

The spectrum of *p*-nitrophenol is shown in Fig. 1a. The three major groups are presumably the hyperfine structures due to the nitrogen splitting, each of them consisting of three triplets caused by two pairs of equivalent protons. These protons are considered to be those which are attached to the ortho- and meta-positions of the benzene ring. The proton hyperfine structure of the hydroxyl group was not observed in this case. The hyperfine coupling constants are shown in Table I, where the results of the Hückel MO calculations have been referred to for the assignment of the coupling constant in each position of the molecule.

The ESR spectrum of *m*-nitrophenol is shown in Fig. 2a. It seems that the proton hyperfine siructure of the hydroxyl group does not show up as in the case of *p*-nitrophenol, and that the two protons in the ortho-positions with respect to the nitro group are not equivalent. Thus this spectrum can be explained well on the basis of the obtained coupling constants shown in the table. The results seem particularly interesting when compared with those obtained with *m*-nitrotoluene, *m*-chlorobenzene and *m*-bromonitrobenzene, in which the ortho-protons are equivalent.[2)]

The ESR spectrum of *o*-nitrophenol is shown in Fig. 3a. There is a distinct nitrogen triplet, each element of which consists of from nineteen to twenty-one lines. These absorption lines can not be understood without taking account the hyperfine coupling of the proton in the hydroxyl group. Though proton splitting constants have not yet been definitely assigned to each of the protons, this spectrum can be explained fairly well on the basis of the splitting constants shown in the table. The participation of the hydroxyl-group proton in the hyperfine coupling of *o*-nitrophenol might

2) T. Fujinaga, Y. Deguchi and K. Umemoto., unpublished results.

be caused by the hydrogen bonding of the hydroxyl-group proton to the nitro-group.

The hydrogen bonding effect in *o*-nitrophenol has already been observed from its infrared spectra,[3] but we believe that the present report is the first ESR observation of the hydrogen bonding in *o*-nitrophenol.

Other anion radicals of substituted nitrobenzenes have also been prepared electrolytically, and a good deal of information on the electrode process has been obtained by the use of ESR spectroscopy. These findings will be reported in due course.

Department of Chemistry
Faculty of Science
Kyoto University
Sakyo-ku, Kyoto

3) M. Tsubori, This Bulletin, **25**, 385 (1952).

A Nonenzymatic Approach to the Selective Cleavage of Threonine Peptides

By Takeo KANEKO and Toshishige INUI

(Received September 4, 1963)

It has previously been reported that threonine was easily cyclized with phosgene in an alkaline solution to an oxazolidone carboxylic acid.[1] It has also been found that the cyclization of *N*-benzoyl-DL-threonine methyl ester with phosgene to an *N*-benzoyl oxazolidone derivative through a chlorocarbonyl intermediate proceeded in a similar way when the methods of Bergel[2] and Ben-Ishai[3] were applied. In this case, the *N*-benzoyl oxazolidone derivative produced could be hydrolyzed to the oxazolidone carboxylic acid in one step.* In this hydrolysis, only the benzoyl group could be removed in safety from the oxazolidone ring. In connection with this finding, it seemed that it would be of great interest to investigate whether threonine dipeptide, which involves a piptide linkage between the amino group of threonine and the carboxyl group of another amino acid, can be cyclized to an oxazolidone derivative and then cleft to an oxazolidone carboxylic acid and free amino acid.

From a reaction of *N*-benzyloxycarbonyl-(Z)-DL-ananyl-DL-threonine methyl ester[4] (DL-DL-I; m. p. 103.5~105°C) with phosgene, an *O*-chlorocarbonyl compound (m. p. 103.5~104.5°C; Found: C, 51.12; H, 5.26; N, 6.91. Calcd. for $C_{17}H_{21}N_2O_7Cl$: C, 50.94; H, 5.28; N, 6.99%) was obtained. It was cyclized to DL-*trans*-3-(Z-DL-alanyl-)-4-methoxycarbonyl-5-methyl-2-oxo-oxazolidine (DL-DL-II; m.p. 129.5~130°C; Found: C, 56.16; H, 5.52; N, 7.60. Calcd. for $C_{17}H_{20}N_2O_7$: C, 56.40; H, 5.53; N, 7.69%). To a solution of 2.46 g. of the oxazolidone derivative (DL-DL-II) in 38 ml. of methanol, 15.1 ml. (2 eq.) of 0.90 N potassium hydroxide were added. The reaction mixture was kept at room temperature for 1.5 hr. After evaporating the methanol in vacuo, the aqueous solution which remained was acidified with hydrochloric acid to pH 3 and then extracted with ethyl acetate. From the extract, Z-DL-alanine[5] (DL-DL-III; m. p., 113.5~114.5°C; yield: 1.32 g. (88%)) was isolated. An additional amount of hydrochloric acid was added to the remaining acidic aqueous solution (pH 1), which was then evaporated to dryness in vacuo. From an extract of the

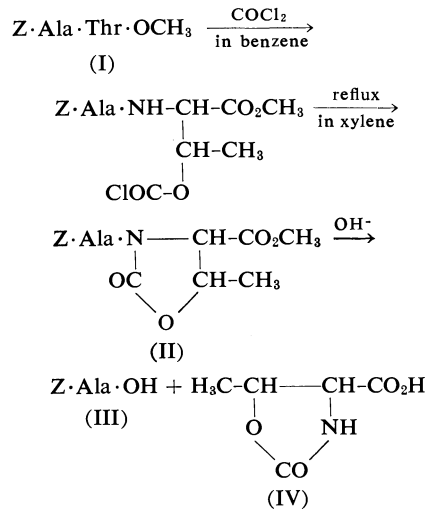

1) T. Kaneko and T. Inui, *J. Chem. Soc. Japan, Pure Chem. Sec.* (*Nippon Kagaku Zasshi*), **82**, 1075 (1961).
2) F. Bergel and R. Wade, *J. Chem. Soc.*, **1959**, 941.
3) D. Ben-Ishai, *J. Am. Chem. Sac.*, **78**, 4962 (1956).
* This study will be reported on elsewhere.
4) Th. Wieland, K. Freter and E. Goss, *Ann.*, **626**, 154 (1959).
5) M. Bergmann and L. Zervas, *Ber.*, **65**, 1192 (1932).

residue with ethyl acetate, DL-*trans*-oxazolidonecarboxylic acid[1] (DL-IV; m. p. 126.5~127.0°C; yield: 0.89 g. (91%)) was obtained. In the case of the reaction of an optically-active peptide (L-L-I; m. p. 131.7~132.2°C; $[\alpha]_D^{16.5}$ −23.6° (MeOH)), the oxazolidone peptide (L-L-II) obtained was hydrolyzed in a way similar to that used for DL-DL-II to L-III[6] (m. p., 86~87°C; $[\alpha]_D^{13}$ −13.8° (AcOH)) and L-IV[7], (m. p. 139.0~139.8°C; $[\alpha]_D^{11}$ +40.7° (H_2O)) in yields of 71% and 60% respectively.

Z-Glycyl-DL-threonine methyl ester (m. p., 110.5~111.8°C) was also cyclized to the corresponding oily oxazolidone peptide by the action of phosgene; this was followed by hydrolysis to give Z-glycine[5] and DL-IV in yields of 71% and 76% respectively.

Similarly, a tripeptide, Z-L-alanyl-L-alanyl-L-threonine methyl ester (m. p. 181.0~181.5°C; $[\alpha]_D^{11}$ −56.5° (MeOH)) was also cyclized to the corresponding oily oxazolidone peptide ester, which afforded Z-L-alanyl-L-alanine[8] (m. p., 149.5~151.0°C; $[\alpha]_D^{13.5}$ −32.5° (MeOH)) and L-IV by a mild alkaline hydrolysis.

These results indicated that this selective cleavage of threonine peptide occurred with no recemization at the peptide linkage in which an amino group of the threonine residue participated.

Department of Chemistry
Faculty of Science
Osaka University
Nakanoshima, Osaka

6) M. Hund and V. duVigneaud, *J. Biol. Chem.*, **124**, 699 (1938).

7) T. Inui and T. Kaneko, *J. Chem. Soc. Japan, Pure Chem. Sec.* (*Nippon Kagaku Zasshi*), **82**, 1078 (1961).

8) W. H. Stein, S. Moore and M. Bergmann, *J. Biol. Chem.*, **154**, 191 (1944).

NMR Studies of Rates of the Inversion of o, o'-Bridged Biphenyls[1]

By Michinori Ōki, Hiizu Iwamura and Naohiro Hayakawa

(Received September 17, 1963)

In the course of infrared spectral study, it became necessary to know the rates of the inversion of 9, 10-dihydrophenanthrene (I), 2, 7-dihydro-3, 4 : 5, 6-dibenzoxepin (II), and their derivatives. Since the half-lives of the inversion of these samples are expected to be too short to allow the conventional optical resolution which is inevitable for the polarimetric method,[2,3] the authors adopted the NMR technique,[4] which has lately been successfully applied to the analyses of the rate processes.[5,6]

If I and II are fixed as non-planar or if the half-lives of their inversion are relatively long, the spectra of the bridging methylene groups will be composed of the A_2B_2- and AB-spin patterns respectively, since the two protons on a methylene group are situated in a different magnetic environment. This is the case in III, IV and VI.[7] III shows a broad signal at τ, 7.38, δ_{AB} being less than 5 c. p. s., while IV shows an exact AB-quartet at τ, 6.00 (center), with $\delta_{AB}=19.6$ c. p. s. and $J_{AB}=11.0$ c. p. s.

On the contrary, I, II and V show a singlet

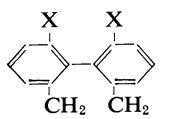

I; X=H
III; X=CH_3
V; X=CH_2-

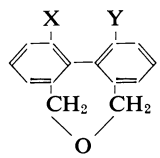

II; X=Y=H
IV; X=Y=CH_3
VI; X+Y=CH_2OCH_2
VII;* X+Y=CH_2CH_2
VIII;* X=H, Y=NO_2

* New compounds prepared by dehydrating the corresponding bis(hydroxymethyl)biphenyls with *p*-toluenesulfonic acid. VII; m. p. 92~93°C, Found: C, 86.51; H, 6.39, Calcd. for $C_{16}H_{14}O$: C, 86.45; H, 6.35%. VIII; m. p., 115°C, Found: C, 69.84; H, 4.68; N, 5.78, Calcd. for $C_{14}H_{11}O_3N$: C, 69.90; H, 4.59; N, 5.80%.

1) Presented in part at the 16th Annual Meeting of the Chemical Society of Japan, Tokyo, April, 1963.

2) R. Kuhn and O. Albrecht, *Ann.*, **455**, 272 (1927).

3) R. Adams and H. C. Yuan, *Chem. Revs.*, **12**, 261 (1932).

4) The NMR spectra were measused on a Varian V-4300 spectrometer operating at 56.4 Mc./sec., and variable with a temperature probe accessory and a Dewar probe insert attached. The samples were dissolved in carbon disulfide containing 1% tetramethyl silane to make a 5% solution.

5) A typical example can be seen in the study of the chair-chair interconversion of cyclohexane (F. R. Jensen, D. S. Noyce, C. H. Sederholm and A. J. Berlin, *J. Am. Chem. Soc.*, **84**, 386 (1962)).

6) Lately, Meyer and Meyer (ibid., **85**, 2170 (1963)) have shown the applicability of the NMR method to the study of the rates of rotation of 2, 2'-bis(hydroxymethyl)biphenyls; their report prompted the present authors to report these preliminary findings.

7) K. Mislow and M. A. W. Glass (ibid., **83**, 2780 (1961)) were the first in observing the non-equivalent methylene-bridge protons in VI.

methylene signal at room temperature and retain the singlet at temperatures as low as $-90°C$. The rates of the inversion are estimated to be not less than $10^2\ sec^{-1}$ at $-90°C$, and by assuming $\log A=12$,[8] the activation energy of the inversion is obtained as less than 9 kcal./mol.

VII, at room temperature, also gives two singlet signals at τ, 7.20 and τ, 5.75; these signals are due to the protons on the $-CH_2CH_2-$ and $-CH_2OCH_2-$ groups respectively. Interestingly, the latter signal begins to lower and broaden gradually as the temperature goes down to $-50°C$, and at $-55°C$, separation into vague multiplet sets in. At $-60°C$, a resonance pattern of a characteristic AB-quartet is clearly recognized. At $-80°C$ or lower, the signal is rigorously determined as $\delta_{AB}=25.9$ c. p. s. and $J_{AB}=11.4$ c. p. s. Even at this temperature, the signal at the higher applied magnetic field will not separate into an apparent multiplet but is only broadened a little. Since the δ_{AB} of the methylene protons on the $-CH_2CH_2-$ group is smaller, the averaging of the resonance signals is still occurring in the rate process through which the signal due to $-CH_2OCH_2-$ with a larger δ_{AB} does not coalesce. Assuming that the relation, $\tau=\sqrt{2}/2\,\pi\delta_{AB}=1/2k$, holds when the quartet signal coalesces to a broad singlet, k is found to be $58\ sec^{-1}$ at $-55°C$. The exchange broadening of two interacting nuclear spin resonance signals has been treated theoretically by Alexander.[9] For the fast exchange limit, the height of the coalesced singlet relative to that at $\tau\rightarrow 0$, can be related to the mean life-time. From the limiting slope, $\tau\rightarrow 0$, together with the velocity obtained above at the very temperature of coalescence, the energy of activation and the Arrhenius factor of inversion are determined:

$E=11.2\pm 2$ kcal./mol., and $\log A=12.9\pm 1.5$.

Since the two methylene groups in VIII are no longer equivalent, VIII exhibits double AB-quartets at room temperature; CH_2 substituting the benzene ring without a nitro group, τ, 5.77 (center), $\delta_{AB}=27.0$, and $J_{AB}=11.80$ c. p. s.; and CH_2 substituting the benzene nucleus with a nitro group τ, 5.61 (center), $\delta_{AB}=15.1$, and $J_{AB}=11.4$ c. p. s. Thus the rate of inversion may be estimated to be less than $50\ sec^{-1}$ at room temperature. As the temperature rises, the quartet singnal at a lower applied magnetic field begins to broaden and coalesce (at 48°C) earlier than that at a higher magnetic field (at 56°C). From the two coalescence temperatures of the resonance signals with a different chemical shift, the kinetic parameters of the rate process are determined as follows: $E=15.5\pm 2$ kal./mol. and $\log A=12.0\pm 1.5$.

Department of Chemistry
Faculty of Science
The University of Tokyo
Hongo, Tokyo (M. Ōki & H. Iwamura)

Japan Atomic Energy Research Institute
Tokai-mura, Ibaragi (N. Hirota)

8) On an average, $\log A$ of the inversion in *o, o'*-bridged biphenyls is 12 (D. M. Hall and M. M. Harris, *J. Chem. Soc.*, **1960**, 490).

9) S. Alexander, *J. Chem. Phys.*, **37**, 967 (1962).

The Absolute Configuration of the Tris-l-propylenediamine Cobalt(III) Ion, L-[Co l-pn$_3$]$^{3+}$

By Yoshihiko SAITO, Hitoshi IWASAKI and Hiroko OTA

(Received September 19, 1963)

The absolute configuration of the optically-active tris-*l*-propylenediamine cobalt(III) ion has been determined. Crystals of L-[Co *l*-pn$_3$]-Br_3 (pn: propylenediamine, $NH_2CHCH_3CH_2$-NH_2) were prepared, and their crystal structure was completely determined.[1] Commercial *d, l*-propylenediamine was resolved with *d*-tartaric acid according to the method described by O'Brien and Toole.[2] The *l*-pn was heated with purpureo-chloride, $[CoCl(NH_3)_5]Cl_2$. The reaction mixture was then dissolved in a small amount of water. When concentrated hydrobromic acid was added to the solution, crystals of the bromide were precipitated. By recrystallization from water, well-formed prismatic crystals deep orange-red in color were obtained. They are hexagonal, with the space

1) H. Iwasaki, H. Ota and Y. Saito, to be published.

2) T. D. O'Brien and R. C. Toole, *J. Am., Chem. Soc.*, **76**, 6009 (1954).

group $P6_3$; $a=11.03\pm0.03$, $c=8.59\pm0.03$ Å and $Z=2$ (Cu$K\alpha$, $\lambda=1.542$ Å).

The structure is essentially ionic, consisting of positively-charged complex ions and bromide anions. The arrangement of these ions in the crystals is closely related to that found in 2D $[Co\,en_3]Cl_3\cdot NaCl\cdot 6H_2O$.[3] A perspective drawing of the complex ion, $[Co\,l\text{-}pn_3]^{3+}$ is presented in Fig. 1.

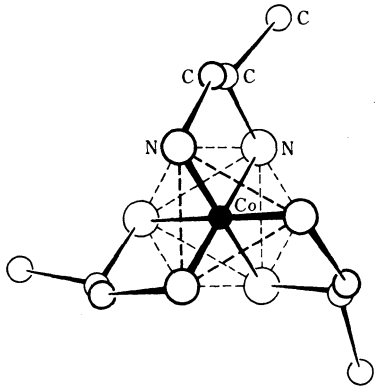

Fig. 1. A perspective drawing of the complex ion, $[Co\,l\text{-}pn_3]^{3+}$.

The complex ion has a three-fold axis of symmetry through the central cobalt atom. All the three ligands, therefore, should have identical configurations. The general features of the complex ion are very similar to those of $[Co\,en_3]^{3+}$ (en: ethylenediamine).[3,4] The five-membered Co-pn rings are puckered, and the C–C bonds in these rings are nearly parallel to the three-fold axis, taking "lel" forms in Bailar's notation.[5] The presence of the substituted methyl groups does not seem to disturb the five-membered ring. The methyl carbon bonds are equatorial with respect to the plane of the ring. The absolute configuration of the complex ion was determined by using absorption-edge technique.[6] Anomalous dispersion effects were taken into account for both the cobalt and bromine atoms, the correction factors for the f-values being:

$$\Delta f'(\mathrm{Co}) = -2.2 \qquad \Delta f''(\mathrm{Co}) = 3.9$$
$$\Delta f'(\mathrm{Br}) = -0.9 \qquad \Delta f''(\mathrm{Br}) = 1.5$$

for Cu$K\alpha$ radiation.[7] The atomic parameters and Bijvoet inequalities were refined on the differential Fourier program at the same time. Some of the observed and calculated relations between $I(h\,k\,l)$ and $I(h\,k\,\bar{l})$, the latter being equivalent to $I(\bar{h}\,\bar{k}\,\bar{l})$ because of the symmetry of the space group, are compared in Table I.

Table I. Determination of the absolute configuration

$h\,k\,l$	Calcd.		Obs.	
	I_{hkl}	$I_{hk\bar{l}}$	I_{hkl}	$I_{hk\bar{l}}$
1 3 1	378	124	>	
1 5 1	85	48	>	
1 6 1	42	101	<	
1 8 1	27	2	>	
3 1 1	934	721	>	
3 5 1	19	75	<	
4 6 1	5	34	<	
5 1 1	0	38	<	

From these accordances in the table, it may be found that the complex ion $[Co\,l\text{-}pn_3]^{3+}$ shown in Fig. 1 corresponds to the laevorotatory form with respect to the Na D lines. If the three methyl groups of $[Co\,l\text{-}pn_3]^{3+}$ are replaced by hydrogen atoms, the absolute configuration of the complex ion, L-$[Co\,en_3]^{3+}$,[8] is obtained. In fact, the optical rotatory dispersion curves of L-$[Co\,en_3]^{3+}$ and L-$[Co\,l\text{-}pn_3]^{3+}$ correspond to one another.[9] The absolute configuration of the propylenediamine, which has an asymmetric carbon atom in the molecule, could be determined at the same time. The results confirm the previous conclusion of our X-ray investigation[10] and agree with the chemical convention.[11,12]

The calculation of the structure factors was carried out on the PC-2 computer of this Institute.

Institute for Solid State Physics
The University of Tokyo
Azabu, Tokyo

3) K. Nakatsu, M. Shiro, Y. Saito and H. Kuroya, This Bulletin **30**, 158 (1957).
4) K. Nakatsu, Y. Saito and H. Kuroya, ibid., **29**, 428 (1956).
5) E. J. Corey and J. C. Bailar, Jr., *J. Am. Chem. Soc.*, **81**, 2620 (1959).
6) J. M. Bijvoet, A. F. Peerdeman and A. J. van Bommel, *Nature*, **168**, 271 (1951).
7) C. H. Dauben and C. F. Templeton, *Acta Cryst.*, **8**, 841 (1955).
8) Y. Saito, K. Nakatsu, M. Shiro and H. Kuroya, This Bulletin, **30**, 795 (1957).
9) A. P. Smirnoff, *Helv. Chim. Acta*, **3**, 177 (1920).
10) Y. Saito and H. Iwasaki, This Bulletin, **35**, 1131 (1962).
11) H. Reihlen, E. Weinbrenner and G. v. Hessling, *Ann.*, **494**, 143 (1932).
12) S. Schnell and P. Karrer, *Helv. Chim. Acta*, **38**, 2036 (1955).

*An Ion Exchange Method for the Determination of Cesium-137 and Strontium-90 in Fallout**

By Hiroyuki TSUBOTA

(Received March 20, 1963)

Several methods for the determination of cesium-137 and strontium-90 in fallout deposits have been reported,[1-6] some of them including ion-exchange techniques. The main aim of the radiochemical analysis of fallout has been the determination of cesium-137 and strontium-90, the most important radionuclides among the fission products because of their long half-lives. It is, therefore, necessary to develop a more rapid and less tedious method for these important radionuclides than the conventional ones.

The methed reported here for the determination of cesium-137 and strontium-90 from the same sample is based on three previous studies by the the present author and his coworker. The first work dealt with the phenomena of the hydrolysis of metal ions adsorbed on cation exchange resin.[7] The second described the ion-exchange separation of a small quantity of strontium from a large quantity of calcium.[8] The third presented fundamental data for the specific adsorption of cesium by a phenol-sulfonic acid type cation-exchange resin.[9]

Experimental

Chemicals. — *Cation Exchange Column A.* — H^+-form of Amberlite CG-120 (sulfonic-acid type cation exchange resin), 100~200 mesh, 2.0×15 cm. column.

Cation Exchange Column B.—Diaion BK (phenol-sulfonic-acid type cation exchange resin), 100~120 mesh, equilibrated with "solution II," 1.0×4 cm. column.

Elutriant I. — 1 : 1 mixture of a 2 M ammonium acetate solution and methanol.

Elutriant II.—2 M ammonium acetate solution.

Solution I.—A mixture of a 5 M ammonium formate solution and 5 M aqueous ammonia in the ratio of 1 : 40 (pH 11.3).

Solution II.—A tenfold diluted solution of solution I (pH 11.0).

All chemicals used were of reagent grade.

Radioactivity Measurement. — Gamma-activity was measured by a scintillation counter with a single-channel pulse height analyzer, and the β-activity by an anti-coincidence low-background Geiger-Muller counter.

Procedure.—As a result of extensive studies of the analytical procedure, the following method was established for the analysis of monthly fallout deposits collected on a 50×50 cm. tray.

An extract of the fallout deposit with 6 N hydrochloric acid was subjected to analysis after organic matter had been decomposed with nitric acid and after silica had been removed by a conventional procedure. The extract was evaporated to dryness, and then the residue was dissolved in 5~10 ml. of 3 N hydrochloric acid and diluted with water to 30~50 ml. The solution was passed through column A and the column was washed with 50 ml. of water. Then, 300 ml. of elutriant I was passed through the column at the flow rate of 2~3 ml./min. Sodium, potassium, magnesium and calcium were eluted in this portion. In the next step, cesium and strontium were eluted with 225 ml. of elutriant II. The effluent was evaporated to dryness on a water bath, and the residue was heated under an infrared lamp; thus the ammonium formate in the residue could be sublimed.

Two milliliters of solution I and 10 ml. of water were added to the vessel to dissolve the residue. The total strontium content of the solution was determined by titration with a 0.01 M EDTA standard solution adding 1 ml. of a 0.01 M magnesium-EDTA solution, and Eriochrome Black T as an indicator. After the titration, a volume of EDTA nearly equal to the titre was further added, and the solution was diluted to 20 ml. with water. The solution was poured into column B. The column was washed with 20 ml. of a mixture of 2 ml. of solution I, a volume of EDTA equal to the titre, and water.

Strontium-90 activity in the effluent was determined with a low-background Geiger-Muller counter by the usual yttrium-milking method after the EDTA had been decomposed with nitric acid and hydrogen peroxide. The γ-activity of the cesium-137 remaining in the column was measured with

---

* The manual form of the procedure reported here was included in an article in *Japan Analyst* (*Bunseki Kagaku*), **9**, 787 (1960).

1) F. J. Bryant, A. C. Chamberlain, A. Morgan and G. S. Spicer, AERE. HP: R-2353 (1957).

2) Radiation Council, Japan Atomic Energy Commission, "Methods of Analysis for Strontium-90" (1960), "Methods of Analysis for Cesium-137" (1962), Science and Technology Agency, Japanese Government (In Japanese).

3) Health and Safety Laboratory, HASL manual standard procedures, with revision and modifications in August 1959. NYO-4700 (1960).

4) T. T. Sugihara, H. I. James, E. J. Troianello and V. T. Bowen, *Anal. Chem.*, **31**, 44 (1959).

5) T. Sotobayashi and S. Koyama, *J. Faculty of Sciences, Niigata Univ., Ser. I*, **3**, No. 2, 103 (1962).

6) H. Tsubota, *Japan Analyst* (*Bunseki Kagaku*), **9**, 783 (1960).

7) H. Tsubota and H. Kakihana, *J. Chem. Soc. Japan, Pure Chem. Sec.* (*Nippon Kagaku Zasshi*), **82**, 1650 (1961).

8) H. Tsubota, This Bulletin, to be published.

9) H. Tsubota, ibid, **36**, 1038 (1963).

a scintillation counter, by taking the resin out from the column into a suitable vessel with water and by drying under an infrared lamp. Alternatively, cesium-137 was eluted from the column with 30 ml. of a 1 : 1 mixture of 1 M formic acid and a 1 M ammonium formate solution. The effluent was evaporated to dryness, and the residue was sublimed under an infrared lamp. The vessel was rinsed thoroughly with 5 ml. of a 1 : 1 mixture of 1 M formic acid and 1 M ammonium formate to dissolve the cesium. The solution was transferred to a stainless steel counting dish and again evaporated to dryness under an infrared lamp to expel the ammonium formate completely. The β-activity of cesium-137 in the dish was measured with a low-background Geiger-Muller counter.

Examination of the Procedure

To check the efficiency of separation, an artificial solution with a composition similar to the extract of fallout was used. Its composition is shown in Table I.

TABLE I. CHEMICAL COMPOSITION OF ARTIFICIAL FALLOUT SAMPLE

Metal ion	Content, mg.
Na^+	200
K^+	50
Mg^{2+}	50
Ca^{2+}	120
Fe^{3+}	80
Al^{3+}	40

Total: About 1.5 g. as chlorides (ca. 30 meq.)

The Behavior of Metal Ions which Tend to be Hydrolyzed.—The artificial fallout solution containing cerium and zirconium labeled with cerium-144 and zirconium-95 was passed through column A. The column was treated with elutriants I and II by the procedure mentioned above, and the effluent was divided into 10 ml. fractions. The radioactivity measurement of cerium and zirconium and the colorimetrical determination of ferric and aluminum ions were carried out in each fraction. Very small amounts of these metal ions were sometimes detected in the fraction collected before the calcium fractions but not in other fractions. It was thus verified that metal ions which tend to be hydrolyzed are not eluted from the cation exchange column with elutriant I (containg methanol), a finding which is in accordance with the former findings with aqueous elutriants.[7]

The Elution of Strontium and Cesium from Column A.—Figures 1 and 2 show the elution curves from column A for artificial fallout solutions containing varying amounts of cesium labeled with cesium-137 and for those containing various amounts of calcium. The elutriants

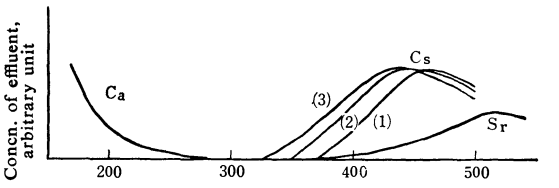

Fig. 1. Separation of cesium from calcium.
Column: Amberlite CG-120, 2.0 ϕ × 15 cm.
Sample: Artificial fallout solution containing cesium and 10 mg. of strontium
Elutriant: 1 : 1 mixture of 2 M ammonium acetate aqueous solution and methanol
Curve (1): Amount of cesium is 0 mg. (carrier-free Cs-137).
Curve (2): Amount of cesium is 5 mg.
Curve (3): Amount of cesium is 10 mg.

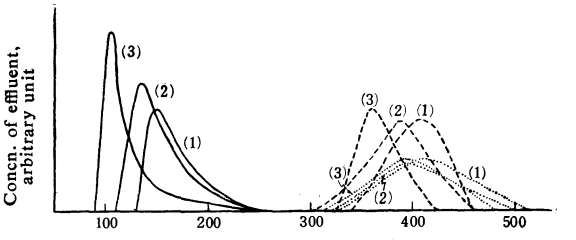

Fig. 2. Elution curves of calcium, strontium and cesium.
Column: Amberlite CG-120, 2.0 ϕ × 15 cm.
Sample: Artificial fallout solution containing 10 mg. of cesium and 20 mg. strontium. Amounts of calcium were varied; curve 1, 120 mg.; curve 2, 180 mg.; and curve 3, 240 mg.
Elutriant: 300 ml. of elutriant I and 230 ml. of elutriant II.
——: Elution curves of calcium
·····: Elution curves of strontium
- - -: Elution curves of cesium

used are specified along each curve in the figures. From the figures, it is evident that strontium is eluted together with cesium and that both ions are eluted later than and are well separated from calcium. The effect of the change in calcium concentration, as actually encountered in the fallout, can also be shown. The increasing calcium concentration makes the separation more complete. These findings are in agreement with the former findings.[8]

The Capacity of Column A.—The column dimensions were decided upon by assuming that the maximum dimensions would be required if all the cations in the artificial solution were to be replaced by calcium. By using a column 15 cm. long and 2 cm. in diameter, fallout extract, the cation content of which is equivalent to at least 30 meq., would be treated. A sample of greater cation content than that

TABLE II. ADSORPTION OF STRONTIUM ON A COLUMN OF PHENOL-SULFONIC ACID TYPE CATION EXCHANGE RESIN*1

Sample solution*2	Radioactive tracers added	Radioactivity found*4			
		In the effluent of			In the column %
		Sample solution %	Washing solution*3		
			0~25 ml., %	25~50 ml., %	
A	Sr-89	27.0	2.1	0.0	68.5
A	Sr-90+Y-90	24.6	2.1	0.0	70.8
B	Sr-89	97.6	3.3	0.1	0.7
C	Sr-89	95.5	4.5	0.0	0.04
C	Sr-90+Y-90	82.0	20.8	0.0	0.02
C	Cs-137	0.0	0.0	0.0	99.1

*1 1.0 ϕ×4 cm. column.
*2 50 ml. of solution II, containing 10 mg. (0.11 mmol.) of Sr carrier, and EDTA (A) 0, (B) 0.11 mmol. and (C) 0.22 mmol. respectively.
*3 Solution II containing EDTA (A) 0, (B) 0.11 mmol. and (C) 0.11 mmol. respectively.
*4 Added radioactivity was taken as 100%.

of the artificial solution can be treated by a larger column. The length of the column (L cm.) necessary to treat W g. (as chlorides) of a sample is given by:[8]

$$L=10+5\frac{W}{1.5}$$

and the volume of elutriant (V ml.) by:

$$V=V_0\frac{L}{15}$$

where V_0 is the volume of elutriant required when the value of W is 1.5. Actually, 2 g. of chlorides can be treated with a column 15 cm. long, as will be shown later in Table III. Hence, L calculated in this manner has reasonable allowance.

The Separation of Cesium and Strontium with Column B.—Cesium is adsorbed on a phenol-sulfonic-acid type cation exchange resin from an ammoniacal solution.[9] When solution II containing strontium labeled with radioactive strontium was passed through column B and the column was washed with solution II, a considerable amount of strontium remained in the column, as is shown in Table II. When EDTA was added to the sample solution and washing solution, however, no strontium (nor yttrium) remained. Even when twice as much EDTA as strontium was added to solution II, cesium was not eluted until 150 ml. of the washing solution had passed.

The cesium adsorbed on the resin could not be eluted with water, and was eluted very slowly with a neutral solution of sodium or ammonium salt, but it was eluted easily and completely with acidic solutions. Elution curves for cesium from column B with different elutriants are shown in Fig. 3. The elution

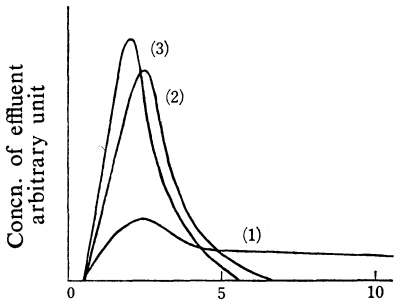

Volume of effluent, in the unit of column volume

Fig. 3. Elution curves of cesium from a column of phenol-sulfonic acid type cation exchange resin.
Column: Diaion BK, 1.0 ϕ×4 cm.
Elutriant: (1) 0.5 N HCl
Elutriant: (2) 3 N HCl
Elutriant: (3) 1 : 1 mixture of 2 M formic acid and 2 M ammonium formate.

curve with 0.5 N hydrochloric acid consists of two parts, a high peak probably due to elution from the phenolic group, the tailing part probably due to elution from the sulfonic group. Elution curves with concentrated acids, such as 3 N hydrochloric acid or a 2 M formate buffer solution, had a typical form of favorable elution.

Results

The analysis was carried out by using an artificial fallout solution containing labeled strontium and cesium. The results are shown in Table III. The recovery was 98±4% for strontium and 99±3% for cesium.

The results of analyses of monthly fallout deposits are shown Table IV. In this case, samples were collected on the roof of the

TABLE III. RECOVERY OF STRONTIUM AND CESIUM*1

Radioactive and non-active cations added to the artificial solution				Radioactive and non-active cations found		
Ca*2 mg.	Sr*3 mg.	Cs mg.	Radioactive nuclide*4	Sr mg.	Sr-90 %	Cs-137 %
80	10.2	10.0	Sr-90	10.1_5	93.7	—
80	10.2	10.0	Cs-137	10.0_3	—	99.0
80	0.30	10.0	Sr-90, Cs-137	0.32	99.3	102.9
80	1.20	1.00	Sr-90, Cs-137	1.15	102.1	95.6
0	1.12	1.00	F. P. (less Sr-90, Cs-137)*5	—	(20.1 c.p.m.)	
0	10.2	1.00	Sr-90, Cs-137	8.40	79.7	56.3
0	10.2	1.00	Sr-90, Cs-137	9.90	98.2	97.1

*1 Column length is 15 cm. for each run except for the last run (20 cm.). Amount of the artificial solution corresponds to 1.5 g. of chlorides for first 5 runs and 3.0 g. for last 2 runs.
*2 Amount of calcium added to the artificial solution, which contains 120 mg. of calcium.
*3 Including the strontium in the calcium salt as an impurity.
*4 Radioactivity added were:
Sr-90: 43.4×10^3 c.p.m.
Cs-137: 6.7×10^3 c.p.m.
*5 Mixture of fission products (cooled for 3 months) from which Sr-90 and Cs-137 were removed. Total radioactivity added was about 5×10^5 c.p.m.

TABLE IV. RESULTS OF RADIOCHEMICAL ANALYSES OF CESIUM-137 AND STRONTIUM-90 IN MONTHLY FALLOUT DEPOSITS

Collected in	Present method		Precipitation method	
	Cs-137 mc./km²	Sr-90 mc./km²	Cs-137 mc./km²	Sr-90 mc./km²
May 1959	3.93	1.91	4.10	1.86
June	2.32	0.78	2.60	0.78
July	0.98	0.17	0.84	0.17
Aug.	0.44	0.13	0.29	0.14
Sept.	0.54	0.09	0.29	0.09
Oct.	0.47	0.04	0.21	0.03
Nov.	0.28	0.03	0.32	0.04
Dec.	0.17	0.08	0.18	0.09
Jan. 1960	0.19	0.08	0.18	0.07

National Institute of Health in Tokyo, Japan, and the hydrochloric acid extracts of the sample were divided into two portions, one being analyzed by the present method and the other by the usual fuming acid-tungsto-silicate-perchlorate method.[2] The agreement between the results of these two methods was satisfactory as a whole.

The author wishes to thank Professor Yasuo Miyake of Tokyo Kyoiku University, Professor Hidetake Kakihana of the Tokyo Institute of Technology, Professor Yasushi Kitano of Nagoya University, and Dr. Masami Izawa, the Chief of the Chemistry Division, the National Institute of Radiological Sciences, for their helpful discussions of this work. Special thanks are given to Mr. Takashi Nagai of the National Institute of Health, who made many data available for the analysis of radiocesium.

National Institute of Radiological Sciences
Kurosuna-cho, Chiba-shi

Oxidation of Alicyclic Compounds with Pernitrous Acid

By Tadao INOUE, Noboru SONODA and Shigeru TSUTSUMI

(Received May 4, 1963)

It has been reported by many workers[1-5] that the reaction of hydrogen peroxide with nitrous acid, nitrate, nitrite, etc. produces unstable peroxy compounds of nitrogen. Baeyer and Villiger[1] inferred the formation of an unstable pernitrous acid as an intermediate during the reaction between hydrogen peroxide and nitrous acid, and Rasig[2] showed the presence of pernitric acid (formulated as HNO_4) from the fact that a mixture of hydrogen peroxide and nitrous acid was a stronger oxidizing agent than either of its components. Kortum and Finckh[3] observed that the transient yellow color solution, prepared by mixing acidified hydrogen peroxide with sodium nitrite, had an ultraviolet absorption band with a maximum close to that of nitrate ions, but about fifteen times more intense and much broader. Halfpenny and Robinson[4] suggested the formation of pernitrous acid and further proposed the homolytic fission of pernitrous acid to give a hydroxy radical and nitrogen dioxide on the grounds of the polymerization of methylacrylate or reaction with simple aromatic compounds.

Laville et al.[5] supported the above considerations and postulated the nitration process of quinoline by the free radical mechnism. Recently, Johnson and Lockett[6] reported the mechnism of pernitrous acid formation from their observation of the effect of oxygen and hydrogen peroxide on the oxidzing action of nitrous acid. This investigation was carried out in order to obtain some information about the oxidation behavior of aliphatic compounds with the pernitrous acid produced as an active oxidizing species in the reaction system. Cyclohexane and cyclohexene were chosen as the starting materials.

Results and Discussion

When cyclohexane and cyclohexene were oxidized by hydrogen peroxide containing nitrous acid in a slightly acidic solution, several compounds were obtained as the reaction products. When cyclohexane was treated with pernitrous acid at 0~2°C, cyclohexanol was obtained as the main product, and cyclohexanone, cyclohexyl nitrate and nitrocyclohexane were also confirmed by gas chromatography, infrared spectra and/or the identification of derivatives. It was assumed that these products would be produced by the following course, in which the hydroxy radical resulting from the homolytic fission of pernitrous acid initially attacks cyclohexane and in which, after the abstraction of the hydrogen atom, the cyclohexyl radical formed reacts with the ·OH, ·ONO and ·NO_2 radicals.

$$H_2O_2 + HNO_2 \rightarrow HOONO + H_2O$$

$$HOONO \rightarrow \cdot OH + \cdot ONO \leftrightarrow \cdot NO_2$$

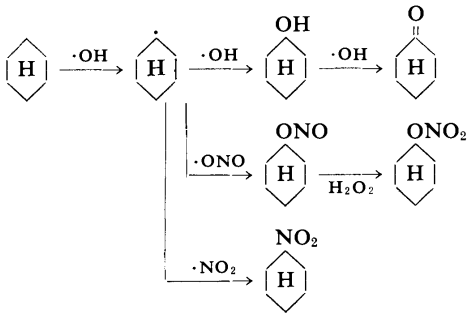

It seems to us that the reaction proceeds step by step and that cyclohexyl nitrate and cyclohexanone would be formed by the oxidation with the ·OH radical and H_2O_2 respectively. Halfpenny and Robinson[4] suggested that the reaction of pernitrous acid with aromatic compounds might proceed by homolytic processes involving the successive addition of the ·OH and ·NO_2 radicals to the aromatic nucleus and that the abstraction of nuclear hydrogen by the hydroxy radical would not occur. However, the reaction of saturated hydrocarbons with these agents may proceed via the immediate hydrogen abstraction, followed by recombination with other radicals.

1) A. Baeyer and V. Villiger, *Ber.*, **34**, 755 (1901).
2) F. Rasig, *Z. angew. Chem.*, **17**, 1419 (1904); *Ber.*, **40**, 4585 (1907).
3) G. Kortum and B. Finckh, *Z. physik. Chem.*, **B48**, 32 (1941).
4) E. Halfpenny and P. L. Robinson, *J. Chem. Soc.*, **1952**, 928, 939.
5) J. R. Laville and W. A. Waters, *J. Chem. Soc.*, **1954**, 400.
6) A. Johnson and A. P. Lockett, *Proc. Chem. Soc.*, **1961**, 218.

Cyclohexene was treated with pernitrous acid prepared from nitrous acid and an excess amount of hydrogen peroxide. From the water-insoluble part of the reaction products, cyclohexanol, cyclohexanone, cyclohexene-3-ol and cyclohexen-3-one were detected as oxygen-containing components; they were considered to be formed by the attack of the hydroxy radical on the double bond or the α-hydrogen atom of cyclohexene. The presence of nitrocyclohexane, 3-nitrocyclohexene and cyclohexyl nitrate as nitrogen-containing components may be assumed on the basis of the analysis of the infrared spectrum and the physical properties. *trans*-2-Nitrocyclohexyl nitrate was also isolated as a higher boiling product which might be formed by the hydrogen peroxide oxidation of the *trans*-2-nitrocyclohexyl nitrite produced by the reaction of the nitro radical with cyclohexene.[7] *trans*-2-Nitrocyclohexanol was obtained as a main product from the water-soluble part. The reduction of this part with lithium aluminum hydride gave *trans*-2-aminocyclohexanol and *trans*-cyclohexan-1, 2-diol, which was considered to be derived from *trans*-hydroxycyclohexyl nitrate. The presence of the nitrite was also detected by the infrared spectrum of the water-soluble part. In this experiment, no cis-isomers of these products were detected. The formation of *trans*-2-nitrocyclohexanol indicated that the simultaneous hydroxylation and nitration of the olefinic double bond with pernitrous acid might be possible. The yield of α-nitroalcohol was fairly low for the synthetic purpose because of the less selectivity of the reaction. The whole reaction might be interpreted by the free radical mechanism shown below. The hydroxy radical formed by the homolytic fission of pernitrous acid may attack an olefinic double bond or an α-hydrogen, and then the α-hydroxycyclohexyl radical or the cyclohexyl radical will be formed as the respective first intermediates, whereas the nitro radical may add to a double bond or may recombine with free radicals formed in this reaction system. These intermediate radicals may react with other radicals or may disproportionate to produce various products.

When an excessive amount of sodium nitrite was used to prepare the pernitrous acid, 1-nitrocyclohexene and cyclohexane-φ-nitrosite were isolated in addition to the products described above. There products may be derived from the reaction of free nitrous

$$HOONO \rightarrow \cdot OH + \cdot ONO \leftrightarrow \cdot NO_2$$

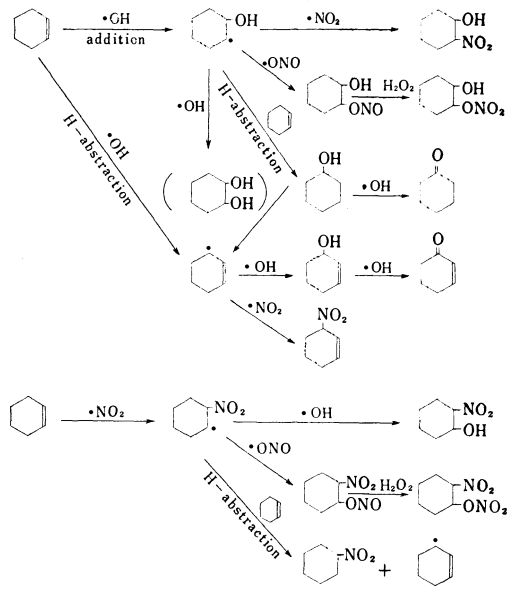

acid.[8]

Cyclohexane-φ-nitrosite is produced in addition to the reaction product of pernitrous acid, so the excess amount of hydrogen peroxide must be used to avoid these side reactions.

Experimental

Materials.—The cyclohexane used was purified by treating it with fuming sulfuric acid and then by fractional distillation: b. p. 80.7°C, $n_D^{20}=1.4263$ (lit.[9] b. p. 80.7°C). Cyclohexene was prepared by the dehydration of cyclohexanol, and it was purified by fractional distillation before used: b. p. 82.5°C, $n_D^{20}=1.4449$ (lit.[10] b. p. 82.6°C).

These materials were confirmed to be pure by gas chromatography.

The Reaction of Cyclohexane with Pernitrous Acid.—Cyclohexane (1 mol.) was emulsified with a solution containing 100 ml. of 6% hydrogen peroxide, 5 ml. of 3 N hydrochloric acid and 80 ml. of water in 1 l. four-necked flask in a nitrogen atmosphere. A 5% sodium nitrite solution (150 ml.) and a 6% hydrogen peroxide solution (288 ml.) were simultaneously vigorously stirred drop by drop into the emulsion for about 1 hr. at 0~2°C. The stirring was continued a further 4 hr. The organic layer from four runs experiments was separated and dried over anhydrous sodium sulfate. After the removal of the unreacted cyclohexane, the residual liquid was distilled under reduced pressure and 1 g. of an oily liquid (b. p. 39~60°C/10 mmHg) was obtained; this was assumed to be

7) H. Baldock, N. Levy and C. W. Scaife, *J. Chem. Soc.*, **1949**, 2627.
8) A. V. Topchiev and E. L. Fantalova, *Doklady Akad. Nauk S.S.S.R.* **88**, 83 (1953).
9) A. Weiberger, "Technique of Organic Chemistry," Vol. VII, Interscience Publisher, Inc., New York (1955), p. 52.
10) H. Gilman, "Organic Syntheses." Coll. Vol. I, 183 (1956).

a mixture of mono-functional cyclohexane derivatives. Four peaks were detected in this fraction by gas chromatography; two of them were identical with the those of cyclohexanol and cyclohexanone respectively; (column, silicon-550; 130°C). The fraction showed infrared absorption bands at 3320 cm^{-1} (OH); 1690 cm^{-1} (C=O); 1620, 1280, and 868 cm^{-1} (ONO_2) and 1545 and 1375 cm^{-1} (NO_2).[11] The reduction of this fraction with lithium aluminum hydride gave cyclohexylamine, which was identified as the hydrochloric acid salt (m. p. 203~204°C (lit.[12] m. p. 203~204°C)). This showed the presence of nitrocyclohexane in the above fraction. Cyclohexyl nitrate was assumed to be present on the basis of the infrared spectrum.

The Reaction of Cyclohexene with Pernitrous Acid.—A 5% sodium nitrite solution (150 ml.) and a 6% hydrogen peroxide solution (288 ml.) were added to an emulsion containing a 6% hydrogen peroxide solution (100 ml.), water (80 ml.) 3 N-hydrochloric acid (5 ml.) and cyclohexene (82 g.) in the manner described in the reaction of cyclohexane. The organic layer separated from ten runs was extracted with an aqueous sodium bicarbonate solution and was washed with water. After being dried over sodium sulfate, the organic layer was distilled to remove unreacted cyclohexene, and the residual oil was distilled under reduced pressure. From the fraction (1.2 g.) with a b. p. of 45~57°C/3 mmHg, cyclohexanol, cyclohexanone, cyclohexyl nitrate and nitrocyclohexane were identified by gas chromatography, and 3-nitrocyclohexene was assumed to be present on the ground of its characteristic bands in the infrared spectrum: 1545 and 1368 cm^{-1} (NO_2) and 1665 cm^{-1} (C=C). The infrared analysis of this nitro-compound agreed with that of Brown.[13] The fraction (1.3 g.) (b. p. 58~120°C/3 mmHg) was purified by chromatography using a silica gel column according to the procedure of Stevens;[14] it was judged to be *trans*-2-nitrocylohexyl nitrate from a comparison of its infrared spectrum with that of an authentic sample.[13] A mixture of the sodium carbonate solution and the washed water was acidified with N hydrochloric acid and mixed with the aqueous layer from ten runs. The resultant aqueous solution was extracted with chloroform, and the extract was dried over anhydrous sodium sulfate. The chloroform was evaporated, and 18.5 g. of the oily residue was distillated under reduced pressure; the following fractions were obtained:

Fraction 1: 7.8 g., b. p. 39~64°/3 mmHg
Fraction 2: 7.7 g., b. p. 65~104°C/3 mmHg
Residue: 2.9 g.

Fraction 1 was divided into three portions by preparative gas chromatography using a silicon-550 packed column. Each portion was distilled under reduced pressure. Cyclohexanol (3.4 g.) was isolated and identified as its α-naphthylurethane: (m. p. 128~128.5°C (lit.[15] m. p. 128°C)); a mixed melting point with an authentic sample was not depressed.

Found: C, 57.79; H, 6.88. Calcd. for $C_{17}H_{19}NO_2$: C, 57.81; H, 7.11%.

The second portion (0.6 g. of liquid; b. p. 42~43°C/3 mmHg) was identified as cyclohexen-3-ol by the infrared spectrum and its α-naphthylurethane derivative (m. p. 154~155°C (lit.[16] m. p. 155°C)); a mixed melting point with an authentic sample showed no depression.

Found: C, 76.19; H, 6.15. Calcd. for $C_{17}H_{17}NO_2$: C, 76.38; H, 6.41%.

The third portion (1.4 g. of liquid; b. p. 54~56°C/3 mmHg) was assumed to be cyclohexen-3-one on the basis of the bromine test and its infrared spectrum, which showed the strong characteristic band at 1680 cm^{-1} (conjugated carbonyl). Fraction 2 showed characteristic bands at 3320 cm^{-1} (OH); 1548 and 1375 cm^{-1} (NO_2); and 1625, 1275, 865, 760, and 690 cm^{-1} (ONO_2). Fraction 2 was reduced with lithium aluminum hydride. Fraction 2 (7.7 g.) was added drop by drop to a well-stirred solution of lithium aluminum hydride (9.0 g.) in ether (200 ml.). After the reaction mixture had been kept at 33°C for 5 hr., water (50 ml.) and a 20% aqueous solution of sodium potassium tartrate (150 ml.) were stirred in. The aqueous layer which separated was saturated with sodium chloride and then extracted with ether and ethanol. After these extracts had been mixed with the organic layer, the resultant mixture was dried over magnesium sulfate and the solvent was evaporated. The residual liquid was distilled under reduced pressure and 3 g. of a liquid (b. p. 70~94°C/3 mmHg) was obtained. This fraction was cooled at 0°C, and the deposited crystalline solid was filtered. Recrystallization from a *n*-hexane-ligroin mixture gave *trans*-cyclohexan-1, 2-diol (0.7 g.), which was considered to be derived by the reduction of *trans*-hydroxycyclohexyl nitrite or *trans*-2-hydroxycyclohexyl nitrate (m. p. 103~104°C (lit.[17] m. p. 103~103.5°C)); a mixed melting point with an authentic sample showed no depression.

Found: C, 62.09; H, 10.40. Calcd. for $C_6H_{12}O_2$: C, 62.04; H, 10.41%.

The filtrate was dissolved in 50 ml. of benzene, and dry hydrogen chloride was passed through the solution. Recrystallization of the deposited solid gave 2 g. of *trans*-2-aminocyclohexanol hydrochloride (m. p. 175~176°C (lit.[18] m. p. 176~177°C)).

Found: C, 47.56; H, 9.29. Calcd. for $C_6H_{14}NOCl$: C, 47.52; H, 9.31%.

The Reaction of Cyclohexene with Hydrogen Peroxide and a Concentrated Sodium Nitrite Solution. — Cyclohexene (82.1 g.) was emulsified with a mixture of sulfuric acid (10 ml.) and water (80 ml.), and a sodium nitrite solution (69 g. in 250 ml. of water) and a 6% hydrogen peroxide solution (450 ml.) containing 17 ml. of water and 3 ml. of concentrated sulfuric acid were simultaneously added drop by drop to the emulsion at equal rate

11) J. F. Brown, *J. Am. Chem. Soc.*, **77**, 6341 (1955).
12) O. Wallack, *Ann.*, **343**, 46 (1905).
13) J. F. Brown, *J. Am. Chem. Soc.*, **77**, 6341 (1955).
14) T. Stevens and W. D. Emmons, ibid., **79**, 6008 (1957).
15) R. R. L. Shriner, R. C. Fason and D. Y. Curtin, "The Systematic Identification of Organic Compounds," 4th Ed., John Wiley & Sons, Inc., New York (1956).
16) F. Clarke and L. N. Owen, *J. Chem. Soc.*, **1950**, 2103.
17) A. Roebuck and H. Adkins, "Organic Syntheses," Coll. Vol. III, 217 (1948).
18) G. E. McCasland, R. N. Clark and H. E. Caster, *J. Am. Chem. Soc.*, **71**, 637 (1949).

over a 2 hr. period while dry nitrogen was passed at −5∼−10°C. The products, obtained from the two runs described above, were separated into three parts: a crystalline solid (1.6 g.) water-soluble products (10.0 g.) and water-insoluble products (5.5 g.). This solid was identified as cyclohexane-φ-nitrosite from its infrared spectrum which was in full accordance with that of Brown[19] (m. p. 153°C (decomp.)); it recrystallized from ethyl acetate; and a mixed melting point with an authentic sample showed no depression.

Found: C, 45.69; H, 6.52. Calcd. for $C_{12}H_{20}N_4O_6$: C, 45.56; H, 6.37%.

Distillation of the water-insoluble products gave 3-nitrocyclohexene (b. p. 54∼56°C/1 mmHg Found: C, 56.82; H, 7.28. Calcd. for $C_6H_{10}NO_2$: C, 56.68; H, 7.14% and 1-nitrocyclohexene (b. p. 64∼65°C/1 mmHg.

Found: C, 56.61; H, 7.29. Calcd. for $C_6H_{10}NO_2$: C, 56.68; H, 7.14%.

The infrared spectra of these nitro-compounds agreed with those of Brown.[11] Treatment of 1-nitrocyclohexene with semicarbazide acetate in methanol gave 2-nitrocyclohexylsemicarbazide after several days (m. p. 163∼163.5°C (decomp.), from ethanol (lit.[20] m. p. 163°C)).

Found: C, 41.77; H, 6.97. Calcd. for $C_7H_{14}N_4O_3$: C, 41.62; H, 6.98%.

A small amount of *trans*-2-nitrocyclohexanol was obtained from the water-soluble products (b. p. 94∼95°C/1 mmHg).

Found: C, 49.62; H, 7.91. Calcd. for $C_6H_{11}NO_3$: C, 49.64; H, 7.64%.

Department of Chemical Technology
Faculty of Engineering
Osaka University
Miyakojima-ku, Osaka

19) J. F. Brown, ibid., **77**, 6341 (1955).

20) A. V. Topchiev and E. L. Fantalova, *Doklady Akad. Nauk S.S.S.R.*, **88**, 83 (1953).

The Electronic Spectra of Nitrones and the Solvent Effect on Them[*1]

By Tanekazu KUBOTA,[*2] Masumi YAMAKAWA[*2] and Yutaka MORI[*3]

(Received May 7, 1963)

The spectroscopic behavior and the electronic states of such heterocyclic *N*-oxides as pyridine and quinoline *N*-oxides have been reported by the present authors[1-3] and by other workers.[4] Nitrone, the general formula of which can be expressed as I, may also be considered to be a kind of conjugated tertiary amine *N*-oxide. If the oxygen atom in I shows considerable resonance interaction with the rest of the molecule, a spectroscopic behavior similar to that of heterocyclic *N*-oxides may be expected for nitrones. For example, in

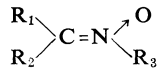

(I)

aldonitrones, where R_1 and R_2 in I are an aryl group and a hydrogen atom respectively, the above-mentioned resonance structure may be written as II–IV.

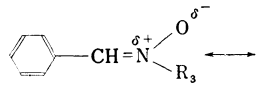

(II)

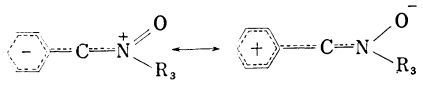

(III) (IV)

Although a few reports on the electronic spectra of nitrones have been published by several workers,[5-7] a detailed spectroscopic investigation from the above view-point has not been made. For this paper, the electronic spectra of a total of fifteen nitrones, all of which contain a benzene ring as at least one

*1 Presented at the International Symposium on Molecular Structure and Spectroscopy, Tokyo, September, 1962.

*2 Shionogi Research Laboratory, Shionogi & Co., Ltd., Fukushima-ku, Osaka. T. Kubota's present address: Department of Physics, The Univesity of Chicago, Chicago 37, Ill., U. S. A.

*3 Osaka Gakugei University, Tennoji-ku, Osaka.

1) See T. Kubota, *J. Spectroscopical Soc. Japan*, **10**, 83 (1962).

2) Y. Matsui and T. Kubota, *J. Chem. Soc. Japan, Pure Chem. Sec.* (*Nippon Kagaku Zasshi*), **83**, 985 (1962).

3) T. Kubota and M. Yamakawa, This Bulletin, **35**, 555 (1962).

4) N. Hata and I. Tanaka, *J. Chem. Phys.*, **36**, 2072 (1962).

5) O. H. Wheeler and P. H. Gore, *J. Am. Chem. Soc.*, **78**, 3363 (1956).

6) B. W. Langley, B. Lythgoe and N. V. Riggs, *J. Chem. Soc.*, **1951**, 2309; **1952**, 4191.

7) P. Brocklehurst, *Tetrahedron*, **18**, 299 (1962).

substituent of R_1, R_2 and R_3 in I, and such related compounds as anils and oximes, have been extensively examined in various solvents. The results thus obtained will be compared with the findings on spectroscopic behavior obtained previously on heterocyclic *N*-oxides. In addition, the configurations of the typical nitrones were also assumed from the measurement of the dipole moments and from their reactivities.[8]

Experimental

Measurement.—The ultraviolet absorption spectra were measured with a Hitachi recording spectrophotometer, model EPS-2 at 23°C and at a slow scanning speed, using matched quartz cells with a 1 cm. light path. The infrared spectra were measured with a Perkin-Elmer 12-C recording spectrometer provided with LiF optics and with a Nippon-Bunko DS-201-B recording spectrometer with NaCl optics. Special care was taken in the region of the OH-stretching frequency. The dipole moments were measured at 25°C in benzene or dioxane. The dielectric constants of dilute solutions were measured by the heterodyne beat method, using a platinum cell.[9] The experiments were made for concentrations lower than 1%, a good linear relationship between the dielectric constants and the weight fractions of a sample being obtained within the range of experimental error. From

TABLE I. THE ELEMENTARY ANALYSIS, MELTING POINTS, SYNTHETIC METHODS, AND THE NUMBERING OF NITRONES

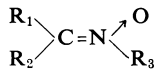

No.	Formula R_1	R_2	R_3	m. p. °C	C, % Calcd.	C, % Obs.	H, % Calcd.	H, % Obs.	N, % Calcd.	N, % Obs.	Synthetic method
1	Ph	H	CH_3	83.5~84.0	71.09	71.24	6.71	6.93	10.36	10.20	A
2**	Ph	H	CH_2-Ph	82 ~83	79.59	79.59	6.20	6.36	6.63	6.93	B
3	*p*-CH_3-Ph	H	CH_3	120.5	72.45	72.39	7.43	7.46	9.39	9.32	A
4*	*p*-Cl-Ph	H	CH_3	135	56.65	56.60	4.75	4.76	8.26	8.09	A
5	*p*-NO_2-Ph	H	CH_3	207~208	53.33	53.27	4.48	4.71	15.44	15.40	A
6	Ph	H	Ph	113~113.5	79.16	79.34	5.62	5.78	7.10	6.83	A
7	*p*-CH_3O-Ph	H	Ph	117~118	73.99	74.22	5.77	5.99	6.16	6.20	A
8	*p*-NO_2-Ph	H	Ph	182~183	64.46	64.46	4.16	4.27	11.57	11.63	A
9*	Ph	H	*p*-Cl-Ph	174	67.39	67.36	4.35	4.46	6.05	6.07	A
10	Ph	H	*o*-CH_3-Ph	118~119.5	79.59	79.72	6.20	6.25	6.63	6.65	A
11	Ph	H	*m*-CH_3-Ph	93~94	79.59	79.62	6.20	6.42	6.63	6.54	A
12	Ph	H	*p*-CH_3-Ph	123~124	79.59	79.71	6.20	6.20	6.63	6.56	A
13**	CH_3	Ph	CH_3	118~119	72.45	72.17	7.43	7.47	9.39	9.56	A'
14	Ph	Ph	CH_3	106.5~108.0	79.59	79.61	6.20	6.14	6.63	6.93	C
15	Ph	Ph	Ph	221~222	83.45	83.82	5.53	5.79	5.13	5.08	D

A: Ph-CHO+R-NH-OH → Ph-CH=N(→O)-R [a,b]

a) O. H. Wheeler and P. H. Gore, *J. Am. Chem. Soc.*, **78**, 3363 (1956).
b) O. L. Brady and F. P. Dunn, *J. Chem. Soc.*, **1926**, 2411.

A': 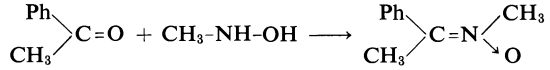 This method will be reported by Y. Mori.

B: A. C. Cope and A. C. Haven, Jr., *J. Am. Chem. Soc.*, **72**, 4896 (1950).

C: 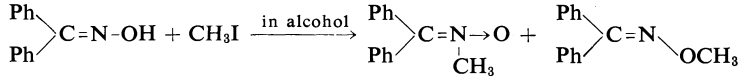

(This nitrone was synthesized by methylating the benzophenonoxime with methyl iodide): c.f. L. Alessandri, *Atti della Reale Accademia dei Lincei* 5, **23**, II. 134 (1914).

D: 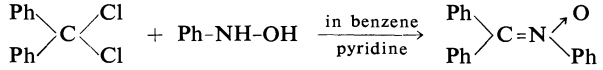

This new method will be reported by Y. Mori.

*: The elementary analysis for chlorine

	Calcd.	Obs.
4)	20.90	20.87
9)	15.30	15.36

**: This configuration is not certain but is most probable.

8) The report on the chemical reactivities will be published shortly in the *Jounral of the Chemical Society of Japan, Pure Chem. Sec.* (*Nippon Kagaku Zasshi*), by Mori et al.

9) Y. Kurita and M. Kubo, *J. Am. Chem. Soc.*, **79**, 5460 (1957).

TABLE II. THE ELEMENTARY ANALYSIS, MELTING POINTS, SYNTHETIC METHODS, AND THE NUMBERING OF THE RELATED COMPOUNDS OF NITRONE

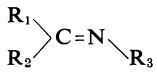

No.	Formula			m. p., °C	C, %		H, %		N, %		Synthetic method
	R_1	R_2	R_3		Calcd.	Obs.	Calcd.	Obs.	Calcd.	Obs.	
16	C_6H_{11}	CH_3	OH	60	68.04	68.51	10.71	10.79	9.92	9.93	E
17	Ph	H	OH	35.5							E
18	Ph	CH_3	OH	58	71.09	70.69	6.71	6.70	10.36	10.46	E
19	Ph	Ph	OH	144	79.16	79.21	5.62	5.76	7.10	7.12	E
20*	*p*-Cl-Ph	H	OH	110	54.04	54.01	3.89	4.05	9.00	8.82	E
21*	H	*p*-Cl-Ph	OH	142	54.04	53.52	3.89	3.97	9.00	9.10	E
22	Ph	H	OCH_3	101～102/ 38 mmHg							C
23	Ph	H	OCH_3	60～61	79.59	79.41	6.20	6.39	6.63	6.69	C
24	Ph	H	CH_3	76～76.5/ 18 mmHg							F
25	Ph	Ph	Ph	52	86.15	86.44	6.12	5.92	7.73	7.74	F
26	Ph	Ph	Ph	113～113.5	88.68	88.69	5.87	5.90	5.44	5.82	F

E: 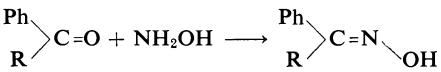 (by the usual method)

F: 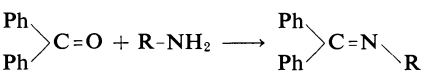 (by the usual method. c. f. G. Reddelien, *Ber.*, **42**, 4759 (1909))

* : The elementary analysis for chlorine

	Calcd.	Obs.
20)	22.79	22.74
21)	22.79	23.20

the slope of this straight line, the molar polarization of the solute was calculated by a method similar to that of Halverstadt-Kumlar.[10] The deformation polarization of nitrones was assumed to be 1.05 times the molar refraction estimated as the sum of the bond refractions.

Materials.—The solvents were purified by the method recommended by Weissberger and Proskauer;[11] special care was taken to remove contaminating water from the organic solvents. The synthetic method, microanalytical data, estimated configurations and physical properties of the nitrones and the related compounds are shown in Tables I and II, together with the numbering of the samples.

Results and Discussion

On the Electronic Spectra of Nitrones.—Figures 1 and 2 give the absorption spectra of nitrones and the related compounds in nonpolar solvents, while Table III lists the absorption maxima and the intensities of the compounds measured in various solvents. As may clearly be seen in Fig. 1, nitrones apparently show a characteristic strong π-π^* band in the region of 280～370 mμ as well as one or two additional bands with a relatively low intensity in the region of 200～260 mμ, the positions of which bands are dependent upon the kind of substituent. The molecular extinction coefficient (ε) of the former is about 20000. With regard to the examination of the character of the spectra of nitrones, a comparison of the spectra of the corresponding anils, oximes, etc., with those of nitrones would seem to be very important and interesting. Detailed investigations of the electronic spectra of anil-type compounds were carried out by Ebara,[12] by Brocklehurst,[7] and by other workers,[13-15] with results consistent with ours (see Fig. 2).

The spectra of compounds 17–24, which are oxime or anil-type compounds with no benzene ring on the *N*-atom, apparently consist of a rather weak band with vibronic structures at the longest wavelength region, a strong band continuing from the above weak band, and a strong band in the 200～230 mμ region. Each of these spectra is essentially similar to

10) I. F. Halverstadt and W. D. Kumler, ibid., **64**, 2988 (1942).
11) A. Weissberger and E. P. Proskauer, "Organic Solvents," 2nd Edition, Interscience Pub., Inc., New York (1955).
12) N. Ebara, This Bulletin, **33**, 534 (1960); **34**, 1151 (1961).
13) C. Wiegand and E. Merkel, *Ann.*, **550**, 175 (1942).
14) H. Zollinger, "Azo and Diazo Chemistry," Interscience Pub., Inc., New York & London (1961), p. 316.
15) M. B. Robin and W. T. Simpson, *J. Chem. Phys.*, **36**, 580 (1962).

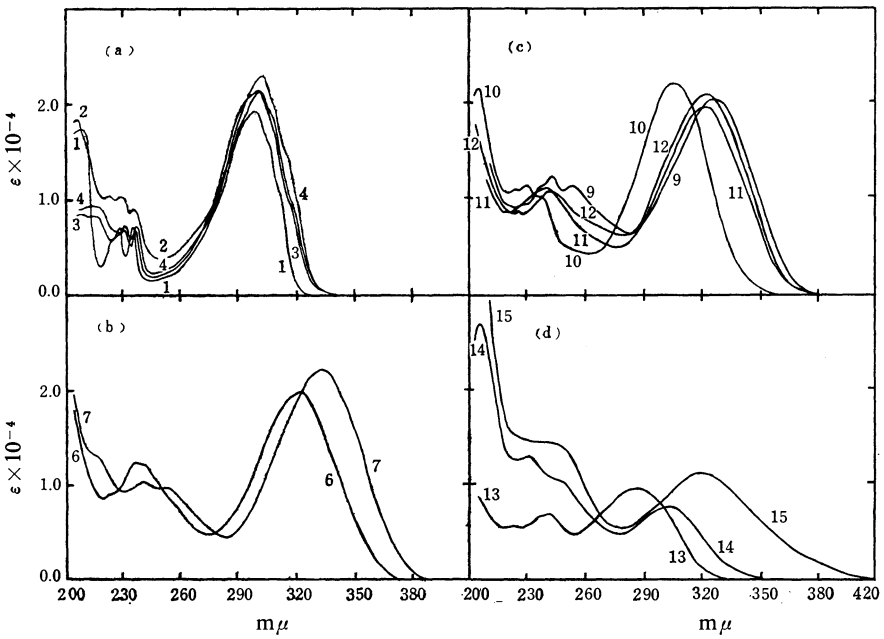

Fig. 1. The spectra of nitrones in *n*-heptane.
(The numbering of each curve is the same as that in Tables I and II.)

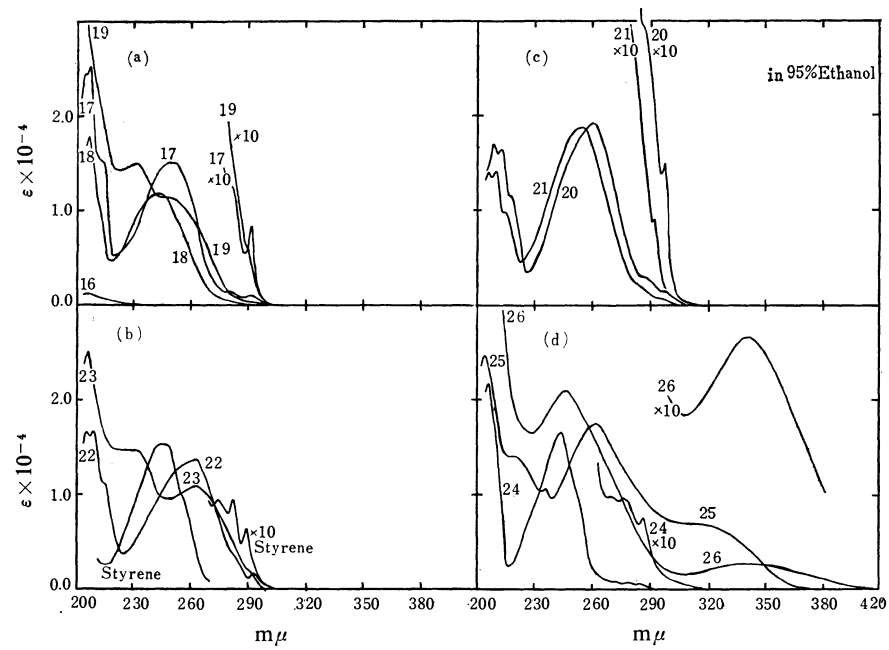

Fig. 2. Spectra of the related compounds of nitrone in *n*-heptane.
(The numbering of each curve is the same as that in Tables I and II.)

that of styrene. which is shown in Fig. 2 and the electronic state of which has been analyzed theoretically and experimentally by workers.[16-19] On the basis of these investigations, these absorption bands may reasonably be assigned to the ^1L_b, ^1L_a, and ^1B_b bands, according to

16) J. F. Music and F. A. Matsen, *J. Am. Chem. Soc.*, **72**, 5256 (1950).
17) W. W. Robertson, J. F. Music and F. A. Matsen, ibid., **72**, 5260 (1950).
18) H. C. Longuet-Higgins and J. N. Murrell, *Proc. Phys. Soc.*, **68**, 601 (1955).
19) R. H. Dyck and D. S. McClure, *J. Chem. Phys.*, **36**, 2326 (1962).

TABLE III. THE ε_{max}*1 AND THE λ_{max}*1 OF NITRONES AND THEIR RELATED COMPOUNDS IN VARIOUS SOLVENTS

Nitrones

No.	Compound	CCl_4		*n*-Heptane		EtOH		MeOH		H_2O	
		λ_{max}	ε_{max}	λ_{max}	ε_{max}	λ_{max}	ε_{max}	λ_{max}	ε_{max}	λ_{max}	ε_{max}
1	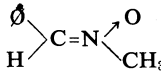			207.5	17490	206.8	9510	207.0	8310	203.9	10370
				229.2	7390	223.2	8700	222.3	7780	218.3	9180
				235.8	7380						
		300.9	19890	298.3	19330	291.6	21150	290.0	19250	286.0	18570
2*2	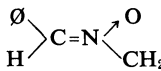			205.5	18170	206.8	17800	207.2	16750	202.8	20330
				222.6	10470						
				229.4	10470	223.2	10400	221.7	9970		
				236.7	8910						
		304.0	20110	300.7	21710	295.5	21560	295.0	20950	291.4	21420
3	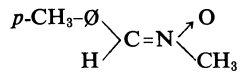			215.8	8210	208.0	9270	207.6	8150		
				224.0	6020	225.8	8980	218.3	6840	217.8	8230
				230.9	7470	231.7	7820	224.7	8340	222.3	9360
				238.0	7070			230.3	7070	227.7	7580
		304.0	22080	300.5	21830	295.8	24650	295.2	22880	292.3	22800
4	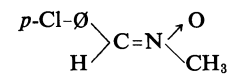			216.7	9510	208.2	9270	207.5	9480		
				223.8	7310	226.6	7610	225.7	7910	222.3	9520
				231.0	7520	233.6	7040	232.3	7260	229.0	7890
				237.9	7430						
		305.1	23280	302.9	23140	298.0	22650	296.8	22980	294.0	22980
5	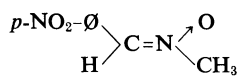			247.2	—	247.0	10400	247.2	10170	247.8	9500
		348.6	—	345.2	—	339.9	15810	336.6	15570	328.3	15230
6	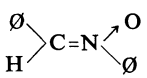			238.0	12320	231.8	10680	230.2	9930	202.2	19980
										225.8	10340
				243.0	12120						
		324.9	19630	322.6	19900	315.5	20180	313.0	19210	308.0	21420
7	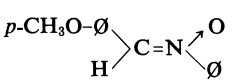			241.4	10410	238.3	11630	237.6	11710	231.6	10200
				254.0	9770						
		339.0	22900	336.0	22050	332.0	26700	330.5	28200	325.0	25000
8	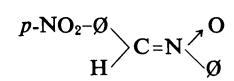			246.4	—						
				253.6	—	245.0	9140	244.4	9290		
				266.0	—	265.4	9660	263.2	10000	268.6	—
		365.0	20830	361.0	—	356.0	19550	353.5	20420	341.0	—

TABLE III (continued)

Nitrones (continued)

No.	Compound	CCl_4		*n*-Heptane		EtOH		MeOH		H_2O	
		λ_{max}	ε_{max}	λ_{max}	ε_{max}	λ_{max}	ε_{max}	λ_{max}	ε_{max}	λ_{max}	ε_{max}
9	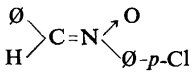	328.0	21400	243.9 253.8 327.5	12210 11250 20120	234.4 320.5	10750 22350				
10	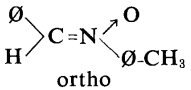 ortho	311.0	20750	205.6 226.0 231.2 238.0 307.4	21200 11080 11490 10380 22000	207.2 225.7 300.5	17560 10290 21770	207.2 224.5 299.0	17250 10070 21590	202.3 295.6	20350 20800
11	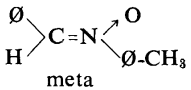 meta	324.9	19850	212.3 241.7 323.3	10740 11670 19650	207.5 233.0 315.4	18100 10250 20600			203.8 222.6 308.7	21730 9560 20800
12	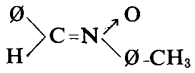 para	326.0	21450	205.0 226.4 242.6 324.0	17100 9060 11240 20930	206.0 233.7 317.2	13960 9800 22010	206.6 232.0 315.3	14600 10230 23600		
13*2	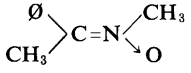	286.2	11040	221.0 237.1 240.7 286.6	5640 6700 6840 9470	210.8 260.5	8220 11690	208.7 258.0	8430 11030	207.7 253.8	10350 12000
14	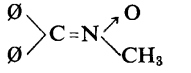	307.8	7780	206.8 231.8 303.9	26870 13060 7570	208.0 233.7 293.1	23580 14130 6950			205.5 230.6 282.0	— — —
15	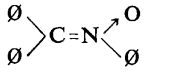	324.0	11270	206.1 234.6 320.0	33060 14530 11240	210.5 233.7 312.2	20680 15810 10800	207.6 232.9 310.5	28770 15400 10780	203.3 231.7 310.0	— — —

*1 : ε_{max} and λ_{max} in the region less than 215 mμ are a little ambiguous because of the limitation in the apparatus.

*2 : This configuration is not certain but is most probable.

TABLE III (continued)
The related compounds of nitrones

No.	Compound	CCl_4		*n*-Heptane		EtOH		MeOH		H_2O	
		λ_{max}	ε_{max}	λ_{max}	ε_{max}	λ_{max}	ε_{max}	λ_{max}	ε_{max}	λ_{max}	ε_{max}
16	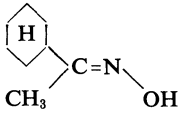			205.2	1380					206.4	2140
17	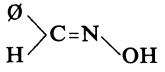			205.5 208.3 213.7 250.2 280.8 291.2	25170 25200 15370 15160 1269 821					204.7 252.0 291.2	24370 15290 1043
18	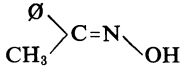			207.7 244.0	18060 11990					205.0 241.4	18050 11210
19	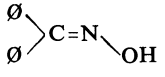			205.0 231.3 248.0	33230 15130 11460						
20	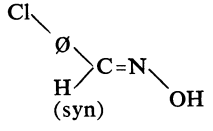					207.8 212.6 218.4 260.0 297.4	17160*3 16520 11490 19240 1530				
21	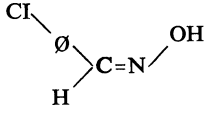					206.6 210.5 253.3 292.0	14130*3 14100 18860 914				
22	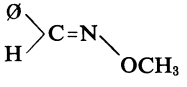			207.3 211.3 216.8 262.1 293.0	16620 16880 11340 13890 1609	208.6 210.6 261.0 293.0	17170 17520 14000 1743				
23	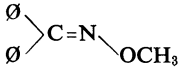			206.9 232.0 263.0	25190 14700 11060	210.2 232.0 263.0	19300 13990 10810				

TABLE III (continued)
The related compounds of nitrones (continued)

No.	Compound	CCl_4		*n*-Heptane		EtOH		MeOH		H_2O	
		λ_{max}	ε_{max}	λ_{max}	ε_{max}	λ_{max}	ε_{max}	λ_{max}	ε_{max}	λ_{max}	ε_{max}
24	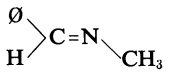	278.0 288.0	1240 893	205.5 244.0 269.1 277.0 286.9	21740 16660 999 973 751	208.5 245.3 278.0 286.8	15430 15930 1330 884			204.6 250.0 280.7	16030 14110 1632
25	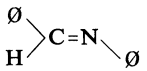			204.2 218.5 235.3 261.6 310.0	25430 14080 10770 17480 7285	206.7 218.0 235.0 263.0 306.0	20640 14390 9071				
26	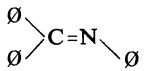	344.0	2965	206.5 246.0 340.9	38710 21120 2639	210.3 246.0 333.0	31140 19780 2744	208.4 245.7 330.6	32660 19840 2779		

*3: In 95% ethanol.

The absorption band of compound 21 shifts to more blue region than that of compound 20, because there is a little steric hindrance for which the benzene ring and the side chain are not in the same plane.*4

*4: B. Jersler, *Nature*, **180**, 1410 (1958); **166**, 741 (1950).

TABLE IV. THE RELATIONSHIP BETWEEN C_{CH_3OH} AND $(E-E_{NO})/C_{CH_3OH}$

C_{CH_3OH} mol./l.	E_{280}	$E-E_{NO}$	$(E-E_{NO})/C_{CH_3OH}$	E_{270}	$E-E_{NO}$	$(E-E_{NO})/C_{CH_3OH}$	E_{304}	$E_{NO}-E$	$(E_{NO}-E)/C_{CH_3OH}$
0.0000	0.506	—	—	0.279	—	—	0.720	—	—
0.05165	0.565	0.059	1.142	0.316	0.037	0.716	0.703	0.017	0.329
0.1033	0.593	0.087	0.842	0.340	0.061	0.591	0.670	0.050	0.484
0.1550	0.613	0.107	0.690	0.358	0.079	0.510	0.656	0.064	0.413
0.2066	0.636	0.130	0.629	0.380	0.101	0.489	0.647	0.073	0.353
0.2583	0.640	0.134	0.519	0.385	0.106	0.410	0.635	0.085	0.329
0.3099	0.652	0.146	0.471	0.396	0.117	0.378	0.631	0.089	0.287
0.4358	0.661	0.155	0.356	0.402	0.123	0.282	0.620	0.100	0.229
0.5448	0.674	0.168	0.308	0.420	0.141	0.259	0.615	0.105	0.193

Platt's notation and in the order given above, as Figs. 2a–2d show. In the case of the absorption spectra of nitrones, we could not explicitly find the band corresponding to ^1L_b, but it may be hidden below the strongest π-π^* band.[20] Moreover, in the case of oximes or anils, we could not obviously find the absorption band corresponding to those of nitrones appearing in the 200~250 mμ region with relatively low intensity and fine structures. These facts clearly suggest that the difference in electronic structures between nitrones and anil-type compounds is fairly large, and that the resonance structures, for example as shown in II–IV, must be taken into consideration.

Recently, the abnormal electronic spectra of such anils as benzylidene aniline have been found by several authors[7,12] and have been discussed from the standpoint of steric hindrance by comparison with the spectra of stilbene or azobenzene. These authors concluded that benzylidene aniline has no planar structure and that two benzene rings are considerably twisted with regard to each other. Spectral curves similar to those obtained by previous authors were also recorded by us for the benzylidene aniline. As may be understood from Figs. 1a, 1b, 1c and 1d, however, in the case of *N*-phenyl benzaldoxime and its analogous nitrones distinctly different spectra from those of, for instance, the benzylidene aniline were observed. These spectra are analogous to those of nitrones with no benzene ring on the *N*-atom in molecules and show, at the longest wavelength region, the strongest π-π^* band, which depends on the nature of the substituent introduced in the benzene ring, as may be seen in Figs. 1a, 1b, and 1c and Table I. This character is similar to that of the spectra shown by normal nitrones, as has been mentioned before, where the steric hindrance may be inferred to be small. This fact indicates that the electronic structure of these nitrones differs considerably from that of, for instance, the benzylidene aniline and that these nitrones may be closely represented by a planar structure, although some steric hindrance may be inferred from the the molecular model shown in Fig. 3.[21]

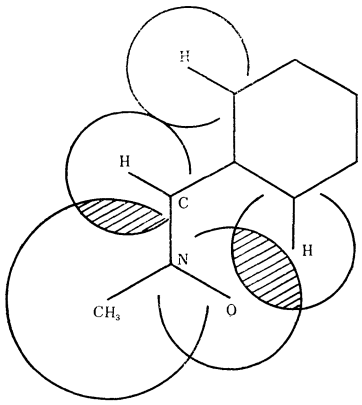

Fig. 3. Molecular model of *N*-methyl benzaldoxime.

Steric Effect on the Electronic Spectra of Nitrones.—It should be clearly noted in Fig. 1d that the intensity of the π-π^* band of *N*-methyl or *N*-phenyl benzophenonoxime is much lower than that of *N*-phenyl benzaldoxime. The same tendency can also be found in the spectra of *N*-methyl acetophenonoxime, the intensity of the π–π^* band of which is much lower than that of *N*-methyl benzaldoxime.

As an example, Fig. 4 shows the molecular model of *N*-methyl benzophenonoxime drawn by the aid of Pauling's van der Waals radii.[21] From this figure it is evident that these nitrones have a considerable steric hindrance for planar structure and that, as is often the case,

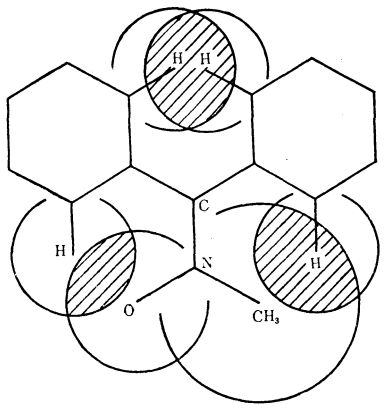

Fig. 4. Molecular model of *N*-methyl benzophenonoxime.

such a steric hindrance is the main reason for the decrease in the intensity of the characteristic strong π-π^* band of nitrones because the resonance among such canonical structures as II–IV may be hindered by the steric hindrance. The spectroscopic behavior of *N*-methyl acetophenonoxime is of especial interest. This compound can be obtained only by the replacement of the side chain C–H group of *N*-methyl benzaldoxime by a C–CH_3 group.

It is well known that the effect of methyl substitution on the electronic spectra of conjugated systems is rather small. Nevertheless, a serious difference was observed between the

20) Detailed theoretical calculation results on this point will be published in the next paper.

21) L. Pauling, "The Nature of the Chemical Bond," 3rd Edition, Cornell University Press, New York (1956), p. 260. C–H, 1.08Å; C–C (aromatic), 1.40; C–C (–Ph), 1.43; C–CH_3, 1.52; C–N, 1.48; N→O, 1.33; C=N 1.32.

spectra of *N*-methyl benzaldoxime and those of *N*-methyl acetophenonoxime. Namely as may be seen in Figs. 1a and 1d, the intensity of the latter is very weak. It seems probable that the steric effect is the main reason for this, as may, for example, be seen in Fig. 5. In this molecule the configuration of the benzene part and the side chain part may depart more from the coplanar structure than from the structure of *N*-methyl benzaldoxime.[22]

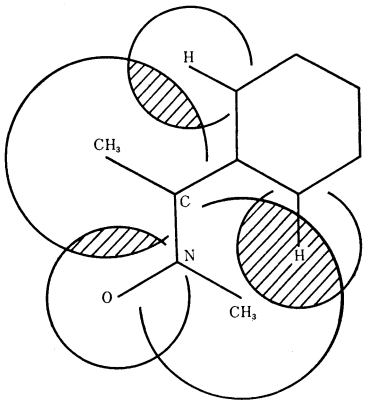

Fig. 5. Molecular model of *N*-methyl acetophenonoxime on the assumption of the "anti" form of phenyl group against N→O bond.

The fact that compound 10 absorbs light at a shorter wavelength than the π-π^* bands of compounds 11 and 12 may also be explained by considering the structure.

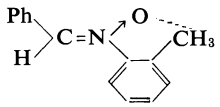

Solvent Effect on the Electronic Spectra of Nitrones and Their Related Compounds.—As may clearly be seen in Table I, the blue shift of the absorption bands of all nitrones is caused by the increasing polarity of those solvents which contain active hydrogen atoms which can form hydrogen bonds. This phenomenon is analogous to that discovered generally in heterocyclic *N*-oxides and may be considered to be due to the reason discussed in detail in our previous papers.[1,3] It is conceivable that hydrogen bonding, such as $\gg$N→O···H (solvent), plays an important role in the blue shift phenomenon. In order to make a more detailed study concerning the contribution of the hydrogen-bonding effect, we made an experiment on three component systems (*N*-methyl benzaldoxime, methanol and *n*-heptane). The change in the spectra of *N*-methyl benzaldoxime upon the addition of methanol is shown in Fig. 6. The behavior

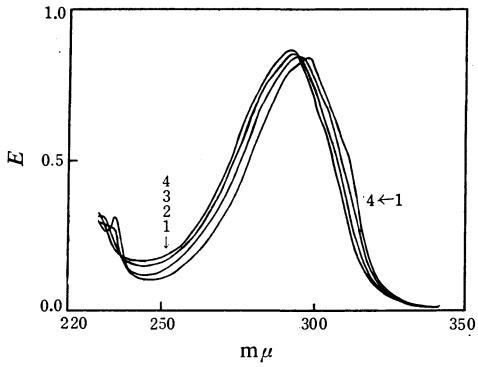

Fig. 6. The UV spectra of *N*-methyl benzaldoxime in *n*-heptane containing methanol.
Concentrations of methanol (mol./l.)
1 : 0.0000 2 : 0.1033 3 : 0.3099 4 : 0.5448
Concentration of *N*-methyl benzaldoxime : 4.217×10^{-5} mol./l.
Temp. : 26.8°C Light path : 1.0 cm.

of the spectra suggests that the equilibrium shown in Eq. 1 may exist.[27]

$$N\rightarrow O + HO\text{–}CH_3 \rightleftarrows N\rightarrow O\cdots HO\text{–}CH_3 \qquad (1)$$

This fact is also supported by the behavior of the OH-stretching band of methanol when nitrone is added, as is shown in Fig. 7. From Eq. 1, the following equation is obtained:

$$K=\frac{[C_{NO\cdots H}]}{[C_{NO}-C_{NO\cdots H}]\ [C_{CH_3OH}-C_{NO\cdots H}]} \qquad (2)$$

where C_{NO}, C_{CH_3OH} and $C_{NO\cdots H}$ are the concentrations of nitrone, methanol and the associated compound respectively. Under the experimental conditions shown in Fig. 6, $C_{CH_3OH}\gg C_{NO\cdots H}$. Then, Eq. 3 is easily obtained by appling the Lambert-Beeer law.

22) The configuration shown in Fig. 5 is also supported by the fact that mutual interaction like $\gg$N-O···H_3C- can be expected. The interaction of this type has often been reported in the heterocyclic *N*-oxides, such as α-picoline *N*-oxide.[4,23-25] Furthermore, this structure is more reasonable from the stand-point of chemical reactivities.[26]

23) N. Ikekawa and Y. Sato, *Pharm. Bull. Japan*, **2**, 400 (1954).

24) T. Kubota, *J. Pharm. Soc. Japan*, **77**, 785 (1957).

25) N. Hata, This Bulletin, **34**, 1440 (1961).

26) Y. Mori, to be published.

27) In this case, it was found that the fine structure at about 293.4 mμ disappeared rapidly upon the addition of a small amount of methanol, and no fine isosbestic point could be obtained. This shows some contribution from effects other than the hydrogen bonding. However, it is clear that the shift due to the hydrogen-bonding effect is the largest. This fact is also supported by the behavior of the infrared spectra shown in Fig. 7.[27a]

27a) See also footnote 3, and the following paper concerning the investigation of infrared spectra: H. Shindo and B. Umezawa, *Chem. Pharm. Bull.*, **10**, 492 (1962).

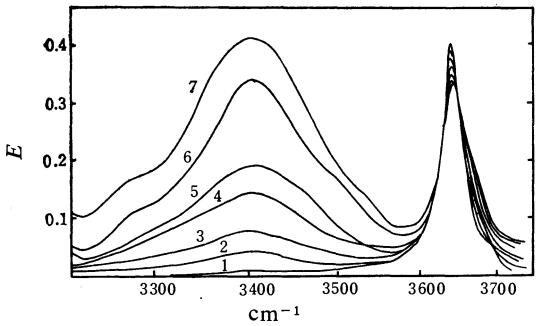

Fig. 7. The O-H stretching bands of methanol in carbon tetrachloride containing *N*-methyl benzaldoxime.
Concentration of *N*-methyl benzaldoxime ($\times 10^{-3}$ mol./l.)
1: 0.0000 2: 4.380 3: 9.510 4: 19.9
5: 27.6 6: 52.9 7: 79.4
Concentration of methanol: 0.0102 mol./l.
Temp.: 24.0°C Light path: 1.0 cm.

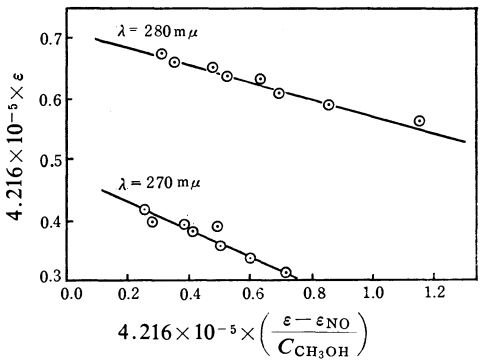

Fig. 8. The relationship between ε and $(\varepsilon-\varepsilon_{NO})/C_{CH_3OH}$ for *N*-methyl benzaldoxime.

$$\varepsilon=\frac{1}{K}\left(\frac{\varepsilon_{NO}-\varepsilon}{C_{CH_3OH}}\right)+\varepsilon_{NO\cdots H} \qquad (3)$$

where ε is an apparent molecular extinction coefficient, and ε_{NO} and $\varepsilon_{NO\cdots H}$ are the molecular extinction coefficients of nitrone and the hydrogen-bonding compound respectively. The relations of Eq. 3 at various wavelengths are shown in Fig. 8 and Table IV. The averaged value of K is 5.6 l./mol., while the degree of blue shift caused by hydrogen bonding (1:1) is about 642 cm^{-1}. In addition, the degree of the red shift of the OH-stretching band resulting from this hydrogen bonding effect is about 238 cm^{-1}. In the case of *N*-methyl acetophenonoxime, its absorption bands shift largely to blue upon the addition of a small quantity of methanol, as is shown in Fig. 9, where no good isosbestic point could be obtained. The absorption bands of oximes and anils did not show such a large blue shift with the increasing polarity of solvents as was found for

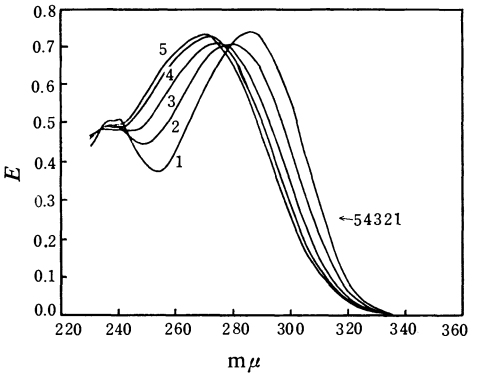

Fig. 9. The UV spectra of *N*-methyl acetophenonoxime in *n*-heptane containing methanol.
Concentrations of methanol (mol./l.)
1: 0.0000 2: 0.02596 3: 0.05192
4: 0.07788 5: 0.10384
Concentration of *N*-methyl acetophenonoxime: 1.184 mg./100 ml.
Temp.: 30°C Light path: 1.0 cm.

nitrones or heterocyclic *N*-oxides.[1] Generally, the solvent effect on the spectra of these compounds is very small. These results suggest that the blue shift is characteristic of conjugated *N*-oxides; this phenomenon was always observed in both heterocyclic *N*-oxides and nitrones. It seems that hydrogen bonding, such as N→O···H–O– (solvents), plays an important role in this phenomenon.[28]

On the Configuration of Nitrones.—Whether the conjugated system of nitrones is a syn or an anti form is very important for the analysis of these spectra, which has been described before and which will be discussed in the next paper more fully, and for the problem of the steric hindrance, which was discussed in the previous section. The configurations of nitrones are inferred from the methods of synthesis,[29] their reactivities,[29] and the measurement of the dipole moments which are

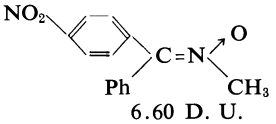

6.60 D. U.

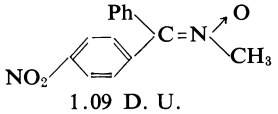

1.09 D. U.

28) After we finished work on this paper, we learned of the paper by Kinko Shinzawa, of the Tokyo Institute of Technology, read at "The Symposium on Photochemistry" held by the Chemical Society of Japan, in Nagoya, October 17, 1962, in which she found that free nitrone (benzylidene aniline *N*-oxide) and hydrogen-bonded nitrone clearly show a different behavior in the quantum yield of the photochemical reaction.
29) Y. Mori, to be published.

TABLE V. THE DIPOLE MOMENTS OF COMPOUNDS 1, 5, AND 8*

Compound	α	β	$P_{2\infty}$, cc.	MR_D, cc.	μ, D.	Solvent
1	10.02	0.21	290.24	39.89	3.49	Benzene
5	26.88	0.30	835.5	45.56	6.20	Dioxane
8	20.98	0.31	886.58	65.31	6.32	Dioxane

*: In this Table, α and β denote the changes in the dielectric constant and in the density of the solutions with the weight fraction of the solute respectively, and other notations have their usual meaning.

shown in Table V. The dipole moments of the following compounds were measured by Taylar and Sutton.[30]

The dipole moment of the compound in which the nitrophenyl group is cis against the *N*-oxide group is 6.60 D. U., but that for the trans form is 1.09 D. U. The measured dipole moments of 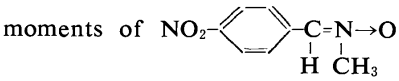 and 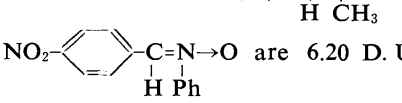 are 6.20 D. U. and 6.32 D. U. respectively. Therefore, it may reasonably be considered that these configurations are the anti form, that is, that the nitrophenyl group is cis to the *N*-oxide group. The nitrone configurations shown in Table I have been decided on the basis of the reasonable assumption that the nitrones synthesized with the same method have the same configuration. This rule may be safely applied for compounds of this type.

It seems that these configurations give a reasonable explanation of the steric effect on the spectra of nitrones and for the reactivity of these compounds.[29]

Summary

The ultraviolet spectra of nitrones, the configurations of which were assumed from their dipole moments and chemical reactivities, and their related compounds have been measured in various solvents. The following results have been obtained:

(1) Nitrones show a characteristic strong π–π^* band in the 280~370 mμ region as well as one or two additional bands with a relatively low intensity in the 200~260 mμ region. The molecular extinction coefficient (ε) of the former is about 20000. The decrease in intensity of the π-π^* band is observed in the spectra of the sterically-hindered compounds.

(2) These bands always show a blue shifs with the increasing polarity of the solvent. The general rule of solvent effect on heterocyclic *N*-oxides applies also to nitrones, the conjugated *N*-oxide band of which has the same property as that of heterocyclic *N*-oxides.

(3) It has been confirmed by ultraviolet and infrared spectra that the formation of a hydrogen bond such as N→O···H (solvent) plays an important role in this blue shift phenomenon.

The authors wish to express their deep gratitude to Professor Emeritus Eiji Ochiai of The University of Tokyo for his kind guidance throughout the course of this work; to Professor Saburo Nagakura of the Institute for Solid State Physics, The University of Tokyo, for his valuable discussions and for reading the manuscript; to Dr. Ken'ichi Takeda, Director of this Research Laboratory, and Dr. Noboru Mataga of Osaka Municipal University for their valuable advice; to Dr. Haruyuki Watanabe of this Research Laboratory for the measurement of the dipole moments and for valuable advice, and to Mr. Mamoru Takasuka for the measurement of the infrared spectra.

Shionogi Research Laboratory
Shionogi & Co., Ltd.
Fukushima-ku, Osaka (T. K. & M. Y.)

Laboratory of Organic Chemistry
Osaka Gakugei University
Tennoji-ku, Osaka (Y. M.)

30) T. W. J. Taylar and L. E. Sutton, *J. Chem. Soc.*, 1933, 63; 1931, 2190.

The Electronic Structures and Electronic Spectra of Benzylidene Methyl Amine N-Oxide[*2] and Its Related Compounds*[*1]

By Tanekazu KUBOTA[*3] and Masumi YAMAKAWA

(Received May 9, 1963)

In a previous paper,[1] the electronic spectra of many nitrones and their related compounds were recorded, and the configurations of some nitrones were determined by measuring their dipole moments. As a result, we found that the behavior of the electronic spectra of nitrones, especially with regard to solvent effects, is very similar to that of heterocyclic *N*-oxides. That is, in hydrogen-bonding solvents, a remarkable blue shift of the electronic spectra is always observed with an increase in solvent polarity. In addition, it was established that the electronic spectra of nitrones without a large steric hindrance exhibit a behavior which can be expressed as resonance hybridization, such as I, II and III.

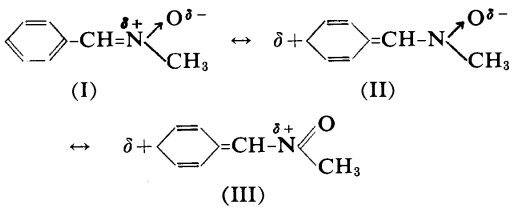

(I) (II) (III)

It seems important to make more detailed studies of the above points from the theoretical and experimental points of view. This paper will report the theoretical results obtained on the basis of the molecular orbital theory (MO). These results will be compared with those of experiments on benzylidene methyl amine *N*-oxide, which is a basic nitrone, and its related compounds.

Experimental

The ultraviolet absorption spectra were measured with a Hitachi recording spectrophotometer, Model EPS-2. Measurements were usually carried out at room temperature and at a slow scanning speed, using a 1 cm. light path quartz cell. The organic solvents used were purified according to the methods recommended by Weissberger and Proskauer;[2] special care was taken to remove any contaminating water. The anhydrous ethanol containing hydrogen chloride was prepared by introducing hydrogen chloride gas, which has been carefully dried with concentrated sulfuric acid, into anhydrous ethanol. The concentration of hydrochloric acid was decided by titration with a sodium hydroxide solution. The samples used were benzylidene methyl amine, its *N*-oxide, and benzaldoxime *O*-methyl ether.[3] The synthetic and purification methods and the physical properties of these compounds were reported in a previous paper.[1]

Experimental Results

The electronic structure and the spectrum of benzylidene methyl amine *N*-oxide were analyzed according to the following system, where styrene was selected as the basic compound, because the electronic structure and the electronic spectra of styrene have been investigated in detail by several authors, as will be mentioned later. Figure 1 shows the spectra of styrene[4] and benzylidene methyl amine and its *N*-oxide, these spectra being measured by a method previouly reported.

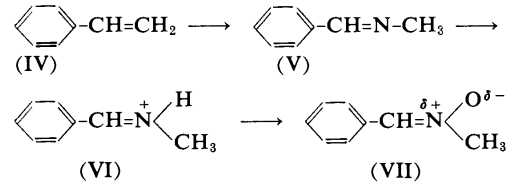

(IV) (V) (VI) (VII)

The Absorption Spectra of Proton-Addition Compounds of Benzylidene Methyl Amine (V) and Its Related Compound.—Compound V is relatively unstable in an acid solution and decomposes easily to each component, benzaldehyde, etc. This is easily detected by the fact that the absorption spectrum of V varies considerably with time, the final one being the same as that of benzaldehyde.

However, the spectrum corresponding to VI

*1 Presented at the International Symposium on Molecular Structure and Spectroscopy, Tokyo, September, 1962.

*2 The tertiary amine N-oxides of this type are frequently called "nitrone."

*3 Present address: Department of Physics, The University of Chicago, Chicago 37, Ill., U. S. A.

1) T. Kubota, M. Yamakawa and Y. Mori, This Bulletin, **36**, 1549 (1963).

2) A. Weissberger and E. Proskauer, "Organic Solvents," 2nd Ed. Interscience Pub., Inc., New York (1955).

3) This is a syn-type compound; that is,

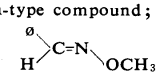

4) The spectrum of styrene has been cited in these papers: a) E. M. Layton, Jr., *J. Mol. Spectroscopy*, **5**, 181 (1960); b) E. Merkel, *Z. Elektrochem.*, **63**, 373 (1959); c) Landolt-Börnstein, "Zahlenwerte und Funktionen," I. Band 3 Teil, Springer-Verlag, Berlin (1951), p. 266.

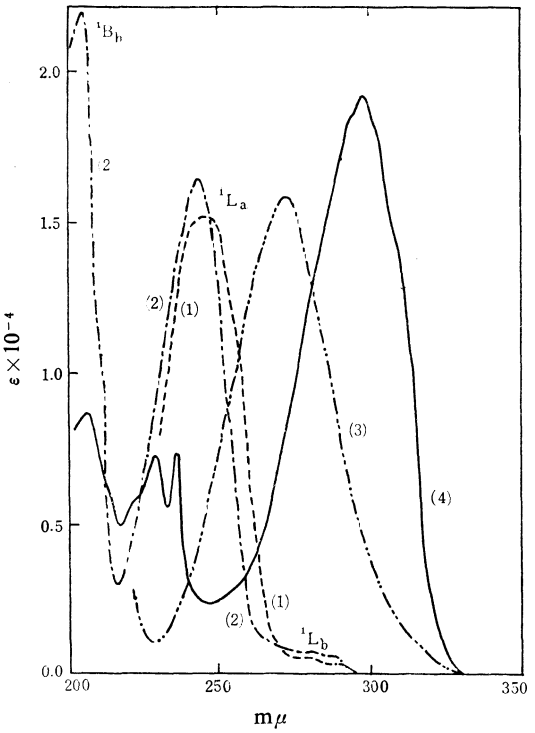

Fig. 1. The absorption spectra of the compounds.
(1) ---- Styrene in cyclohexane
(2) —·—· Ph-CH=N-CH_3 in *n*-heptane
(3) ----- Ph-CH=$\overset{+}{N}$H-CH_3 in 3.57 N H_2SO_4
(4) —— Ph-CH=N→O in *n*-heptane
CH_3

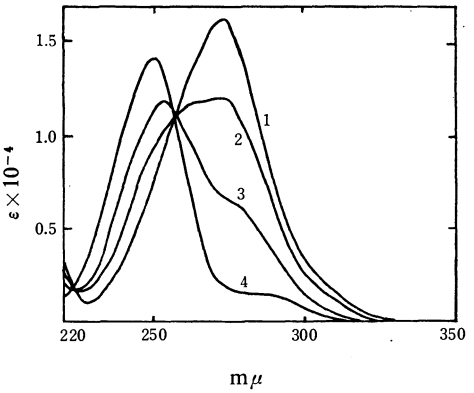

Fig. 2. Time dependence of the absorption spectra of Ph-CH=N-CH_3 in 3.57 N H_2SO_4.
1. After about 10 min. 2. After about 1 hr.
3. After about 4 hr. 4. Benzaldehyde

can be obtained by recording the spectra as soon as possible after dissolving V in sulfuric acid solutions of various concentrations. The recorded spectra are shown in Figs. 1 and 2. The absorption spectra of V dissolved in anhydrous ethanol containing hydrochloric acid also show a time dependence, but the mechanism of decomposition may be considered to be different from that in the acidic aqueous solution mentioned above,[5] because the spectrum obtained after 2 hr. is completely different from that of benzaldehyde. As has been stated above, however, the spectrum of VI was also obtained by recording it quickly after the sample had been dissolved. The spectra in various acid concentrations are shown in Fig. 3.

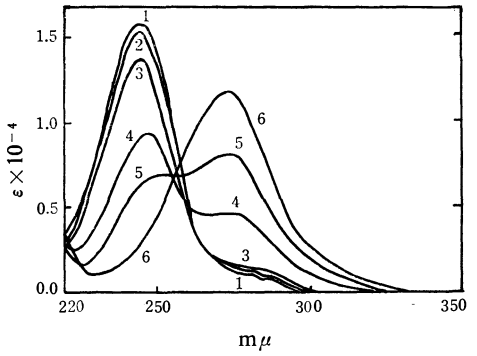

Fig. 3. The spectra of Ph-CH=N-CH_3 in anhydrous ethanol containing hydrogen chloride of various concentrations.
Concentrations of HCl
1. 0.000 mol./l.
2. 1.996×10^{-5}
3. 3.992×10^{-5}
4. 9.98×10^{-5}
5. 1.996×10^{-4}
6. 9.98×10^{-4}
The spectra were recorded as soon as possible after dissolving the sample in solvents.

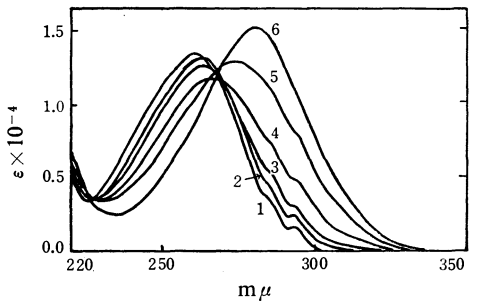

Fig. 4. The spectra of Ph-CH=N-OCH_3 in anhydrous ethanol containing hydrogen chloride of various concentrations.
Concentrations of HCl
1. in abs-EtOH
2. 4.83 mol./l.
3. 5.80
4. 6.76
5. 7.73
6. 8.69

5) Considering that weter may play an important role in the decomposition of V to benzaldehyde, etc., in an acidic aqueous medium, we carried the experiment out under the anhydrous condition.

On the other hand, benzaldoxime *O*-methyl ether is stable in an acidic medium, and the spectra of the proton-addition compound could be recorded easily, as may be seen in Fig. 4. In this case it may reasonably be thought that the proton addition will occur at the nitrogen atom in the molecule.

A comparison of the spectrum of benzaldoxime *O*-methyl ether with that of V shows that the former absorbs light at a longer wavelength than the latter. The resonance effect of the OCH_3 group may be the main reason for this.

Theoretical

In order to analyze the electronic structure and the spectrum of benzylidene methyl amine *N*-oxide (VII), MO methods were applied to the IV, V, VI and VII compounds. As VII is quite a complex molecule, in practice it is difficult to treat it under higher order conditions. In this paper, the theoretical calculations were based on the π-electron approximation, partly taking electron repulsion terms into account and including the zero differential overlap approximation, proposed by Goodman and Shull[6] and by Baba and Suzuki,[7] to interpret the spectra of benzene derivatives.

Electronic State and Spectroscopic Exchange Integrals, β_s's, of Styrene.—The electronic spectrum and the electronic structure of styrene have been reported by many workers, and the spectrum has reasonably been assigned.[4a,8-11] As is shown in Fig. 1, the absorption bands of styrene have been assigned to ^1L_b, ^1L_a and ^1B_b (Platt's notation) in the order of decreasing wavelength. It may reasonably be considered that these bands are related to the four orbitals ϕ_3, ϕ_4, ϕ_5 and ϕ_6 in the Hückel MO's of styrene shown in Fig. 5.[12,13] Here, the configuration $^1\chi_{4\to5}$ arising from the one electron transition from ϕ_4 to ϕ_5 has the symmetry of $^1A_1$ and the lowest transition energy. The other transitions belonging to the $^1A_1$ symmetry have far larger transition energies than that of $^1\chi_{4\to5}$ (cf. Fig. 5). The interaction between $^1\chi_{4\to5}$ and other $^1A_1$ configurations seems to be relatively small. Assuming that the transition energy, $1.3243\,\beta$, of the $^1\chi_{4\to5}$ configuration, obtained from the simple molecular orbital (SMO) calculations, is equal to the observed value, 5.009 eV., for the ^1L_a band, we can obtain 3.78 eV. for the spectroscopic exchange integral β_s belonging to $^1A_1$. This value was applied to the calculations for V, VI and VII. The configurations, $^1\chi_{4\to6}$ and $^1\chi_{3\to5}$, belonging to $^1B_1$ have the same energy, since styrene is an alternant hydrocarbon. Therefore, the two excited states corresponding to Eqs. 1 and 2 may be written:

$$\Psi_1=\frac{1}{\sqrt{7}}(^1\chi_{3\to5}-{}^1\chi_{4\to6}) : {}^1B_1^- \tag{1}$$

$$\Psi_2=\frac{1}{\sqrt{2}}(^1\chi_{3\to5}+{}^1\chi_{4\to6}) : {}^1B_1^+ \tag{2}$$

These correspond to the ^1L_b and the ^1B_b bands respectively. The interaction between $^1\chi_{3\to5}$ and $^1\chi_{4\to6}$ was calculated by means of Eq. 3:

$$(^1\chi_{4\to6}|H|{}^1\chi_{3\to5})=2(36|G|54)^{MO}-(36|G|45)^{MO} \tag{3}$$

The values of (pp/pp) and (pp/qq), which are one-center and two-center π-coulomb repulsion integrals respectively, were calculated on the basis of Pariser-Parr's Ball approximation.[14] The quantity (pp/pp) is obtained from the relation: $(pp/pp)=I_p-E_A$.

In the case of the $2p\pi$-electron in the carbon atom, as was seen in a previous paper,[15] the ionization potential (I_p) and the electron affinity (E_A) on the valence state of sp^3 (V_i) were taken from the data of Pritchard and Skinner.[16] These data lead to $(pp/pp)_c=11.42-0.58=10.84$ eV.

When the distance (γ) between nuclei $\geqq 2.80$ Å, the quantity (pp/qq) is given by Eq. 4 on the basis of the Ball approximation:[14]

$$(pp/qq)_{eV}=\frac{7.1975}{\gamma}\left[\left\{1+\left(\frac{1}{2\gamma}\right)^2(R_p-R_q)^2\right\}^{-1/2}+\left\{1+\left(\frac{1}{2\gamma}\right)^2(R_p+R_q)^2\right\}^{-1/2}\right] \tag{4}$$

Since Slater's effective nuclear charge of the $2p\pi$-electron in the carbon-atom is 3.25, $R_p=R_q=1.4145$ Å is obtained by the aid of the Pariser-Parr method. However, for the case of $\gamma<2.80$ Å, the quantity (pp/qq) is obtained by

6) L. Goodman and H. Shull, *J. Chem. Phys.*, **27**, 1388 (1957).
7) H. Baba and S. Suzuki, ibid., **32**, 1706 (1960).
8) J. F. Music and F. A. Matsen *J. Am. Chem. Soc.*, **72**, 5256 (1950).
9) H. C. Longuet-Higgins and J. N. Murrell, *Proc. Phys. Soc.*, **68**, 7-A, 601 (1955).
10) W. W. Robertson, J. F. Music and F. A. Matsen. *J. Am. Chem. Soc.*, **72**, 5260 (1950).
11) J. R. Platt, *J. Chem. Phys.*, **18**, 1168 (1950).
12) We have assumed here that IV, V, VI and VII have the symmetry of C_{2v} from the view-point of π-electron systems, and that all exchange integrals are equal to β.
13) C. A. Coulson and R. Daudel, "Dictionary of Values of Molecular Constants," Vol. III, Centre National de la Récherche Scientifique, I. C. I. Ltd., Paris, p. 50.
14) R. Pariser and R. G. Parr, *J. Chem. Phys.*, **21**, 466, 767 (1953).
15) T. Kubota, This Bulletin, **35**, 946 (1962); *J. Chem. Soc. Japan, Pure Chem. Sec.* (*Nippon Kagaku Zasshi*), **80**, 578 (1959).
16) H. O. Pritchard and H. O. Skinner, *Chem. Revs.*, 55, 745 (1955).

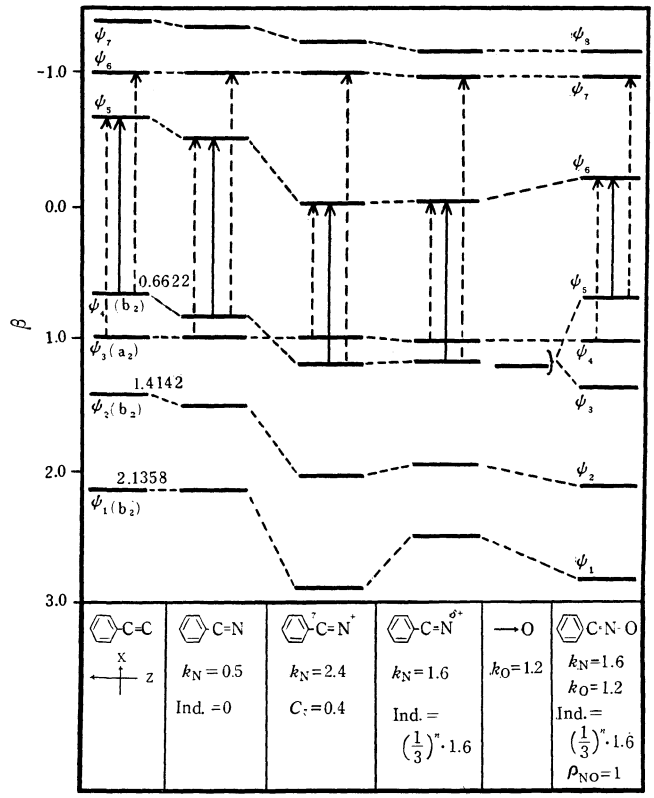

Fig. 5. The orbital energies of styrene, benzylidene methyl amine and its related compounds, and benzylidene methyl amine *N*-oxide.

extrapolating the values evaluated at longer distances to $\gamma=0$, using Eq. 5 as determined by the method of quadratic equation:

$$(pp/qq)=0.2463\gamma^2-2.8237\gamma+10.84 \qquad (5)$$

The values of $(pp/qq)_c$ and of Eq. 3 thus obtained are shown in Table I.

On the basis of the SMO approximation, $E(^1\chi_{4\to6})$ and $E(^1\chi_{3\to5})$ are equal to 1.66215 β, as can be understood from Fig. 5. The interaction between them leads to the two states shown in Fig. 6, in which the observed values of ^1L_b and ^1B_b are also given.[4a]

Table I. The values of various integrals
(Unit is in eV.)

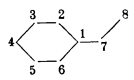

(11/11) = 10.84
(11/22) = 7.370
(11/33) = 5.441
(11/44) = 4.865

Configuration interaction matrix elements between two $^1B_1$ states.

$(^1\chi_{4\to6}\|H\|^1\chi_{3\to5})$	Compounds
0.6032	Ph−C=C
0.6281	Ph−C=N
0.5814	Ph−C=N$^{\delta+}$
$(^1\chi_{4\to6}\|H\|^1\chi_{5\to7})$	
0.3677	Ph−C=N→O

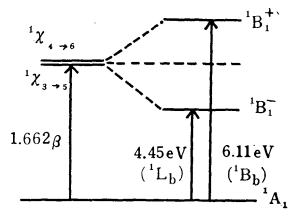

Fig. 6. The configuration interaction between $^1\chi_{4\to6}$ and $^1\chi_{3\to5}$ states in styrene.

Now, the spectroscopic exchange integral, β_s, is evaluated to satisfy the observed values in Fig. 6.[17] $\beta_s=3.04$ eV. is obtained to reproduce the observed value of ^1L_b, whereas $\beta_s=3.31$ eV. is obtained from that of the ^1B_b band. The difference between these two β_s values apparently results from the fact that

17) The dimensions of styrene were estimated on the basis of the bond order-bond length relation derived by Coulson.[18,24] We assumed that the benzene ring is a regular hexagon, the bond distance of which is 1.40 Å. It should be noted that the terms (pp/qq) necessary to calculate Eq. 3 are reduced to those consisting of the carbon atoms appearing in the benzene ring in the molecule because of the assumed C_{2v} symmetry.

18) C. A. Coulson, *Proc. Roy. Soc.*, **A207**, 91 (1951).

TABLE II. SIMPLE MOLECULAR ORBITALS

("Eigenvalue" shows the δ in the equation: $E=\alpha+\delta\beta$)

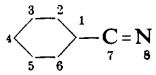

	Eigenvalue	Symmetry	C_{i4}	C_{i3}	C_{i2}	C_{i1}	C_{i7}	C_{i8}
ϕ_1	2.15033	b_2	+0.29424	+0.31636	+0.38603	+0.51374	+0.33265	+0.20157
ϕ_2	1.50352	b_2	+0.45320	+0.34070	+0.05905	−0.25192	−0.49686	−0.49512
ϕ_3	1.00000	a_2	0	+0.50000	+0.50000	0	0	0
ϕ_4	0.84491	b_2	+0.43872	+0.18534	−0.28212	−0.42371	+0.20625	+0.59797
ϕ_5	−0.50310	b_2	+0.37706	−0.09485	−0.32934	+0.26054	+0.52761	−0.52598
ϕ_6	−1.00000	a_2	0	+0.50000	−0.50000	0	0	0

$C_{i2}=\pm C_{i6}$: $C_{i3}=\pm C_{i5}$ (+ and − represent b_2 and a_2 orbitals respectively). $\varepsilon_7=-1.36792$: $\varepsilon_8=-2.12775$

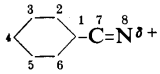

	Eigenvalue	Symmetry	C_{i4}	C_{i3}	C_{i2}	C_{i1}	C_{i7}	C_{i8}
ϕ_1	2.48625	b_2	+0.11593	+0.14411	+0.23953	+0.43721	+0.53024	+0.59830
ϕ_2	1.95552	b_2	+0.36826	+0.36007	+0.32875	+0.26333	−0.18937	−0.53265
ϕ_3	1.03970	a_2	0	+0.49504	+0.50491	0	0	0
ϕ_4	1.17915	b_2	+0.53955	+0.31811	−0.17074	−0.50932	−0.16854	+0.40047
ϕ_5	−0.02882	b_2	+0.34519	−0.00497	−0.34495	+0.03535	+0.68260	−0.41908
ϕ_6	−0.96069	a_2	0	+0.50491	−0.49504	0	0	0

$C_{i2}=\pm C_{i6}$: $C_{i3}=\pm C_{i5}$ (+ and − represent b_2 and a_2 orbitals respectively). $\varepsilon_7=-1.17856$: $\varepsilon_8=-2.02342$

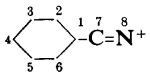

	Eigenvalue	Symmetry	C_{i4}	C_{i3}	C_{i2}	C_{i1}	C_{i7}	C_{i8}
ϕ_1	2.89629	b_2	+0.02657	+0.03848	+0.08487	+0.20734	+0.43076	+0.86797
ϕ_2	2.04204	b_2	+0.36504	+0.37271	+0.39605	+0.43604	+0.09830	−0.27462
ϕ_3	1.00000	a_2	0	+0.50000	+0.50000	0	0	0
ϕ_4	1.20279	b_2	+0.55039	+0.33100	−0.15226	−0.51414	−0.31387	+0.26217
ϕ_5	−0.00867	b_2	+0.36064	−0.00156	−0.36063	+0.00469	+0.72121	−0.29942
ϕ_6	−1.00000	a_2	0	+0.50000	−0.50000	0	0	0

$C_{i2}=\pm C_{i6}$: $C_{i3}=\pm C_{i5}$ (+ and − represent b_2 and a_2 orbitals respectively). $\varepsilon_7=-1.24063$: $\varepsilon_8=-2.09181$

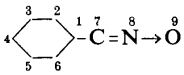

	Eigenvalue	Symmetry	C_{i1}	C_{i2}	C_{i3}	C_{i4}	C_{i7}	C_{i8}	C_{i9}
ϕ_1	2.80865	b_2	+0.24348	+0.10736	+0.05169	+0.03681	+0.42584	+0.72544	+0.45096
ϕ_2	2.12615	b_2	+0.47043	+0.38909	+0.33378	+0.31397	+0.13840	−0.25000	−0.26993
ϕ_3	1.36987	b_2	−0.40396	−0.03880	+0.35310	+0.51553	−0.40395	+0.06604	+0.38876
ϕ_4	1.03970	a_2	0	+0.50491	+0.49504	0	0	0	0
ϕ_5	0.69624	b_2	−0.27258	−0.24954	+0.11363	+0.32640	+0.35775	+0.33086	−0.65677
ϕ_6	−0.19804	b_2	+0.10732	−0.29936	−0.03030	+0.30595	+0.55838	−0.51570	+0.36888
ϕ_7	−0.96069	a_2	0	−0.49504	+0.50491	0	0	0	0

$C_{i2}=\pm C_{i6}$: $C_{i3}=\pm C_{i5}$ (+ and − represent b_2 and a_2 orbitals respectively). $\varepsilon_8=-1.18828$: $\varepsilon_9=-2.02446$

the calculated values of Eq. 3 are not suitable. If one calculates the value of Eq. 3 so as to reproduce the observed ^1L_b and ^1L_a bands, one obtains 0.8307 eV., which is a little greater than that listed in Table I. The main reasons for this discrepancy are as follows: (a) The MO's used here are not the SCF-MO, which are believed to be most desirable. (b) We assumed that the symmetry of styrene is C_{2v}. (c) In these calculations, only the configuration interaction (C. I.) between $^1\chi_{3\to5}$ and $^1\chi_{4\to6}$ was evaluated. If we are rigorous we must consider the C. I. among the other configurations. Therefore, 3.17 eV., that is, the mean value between 3.04 eV. and 3.31 eV., was adopted here as the approximate value for the β_s corresponding to the $^1B_1$ bands. This value was applied to the calculations of V, VI and VII.

The SMO Calculations for Benzylidene Methyl Amine (V) and Its Proton-Addition Compound (VI).—The SMO's on V and VI were calculated by a method analogous to that used for styrene. In this case, the selection of the Coulomb integral is important for the N-hetero atom in Eq. 6:

$$\alpha_{hetero} = \alpha + k_{hetero}\beta \qquad (6)$$

So far, much information about the Coulomb integral for the heterocyclic nitrogen atoms has been obtained by many authors. It has been reported that the value 0.4~0.5 is the best for the parameter, k_N, of the sp^2 type, just as for the nitrogen atom in pyridine.[19] Assuming that the parameter of the nitrogen atom in V is nearly equal to that in pyridine, we used $k_N = 0.5$.[19a] For the $k_N{}^+$ of the $\rangle\overset{+}{N}$–H type, we made use of 2.4 (0.4 β is adopted on the carbon atom adjacent to the N^+-atom), which was decided by the SCF-MO calculations for the pyridine cation.[20] The results are listed in Table II.

The SMO Calculation of Benzyliden Methyl Amine *N*-Oxide (VII).—This compound is the simplest and most typical nitrone. Previously, we studied the electronic structure of such heterocyclic *N*-oxides as pyridine *N*-oxide and determined reasonable parameters to describe the hetero atoms of these molecules. Here, in order to compare the results of nitrones with those of heterocyclic *N*-oxides, the parameters,[21] except for that of the oxygen atom of VII, were taken to be equal to those of the heterocyclic *N*-oxides derived previously by us: $k_N = 1.6$, and inductive effects $= (1/3)^n \cdot k_N$.

Furthermore, under the conditions mentioned above, we also calculated the SMO of the hypothetical molecule 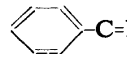 , which is obtained by dividing the VII into the composite systems consisting of the oxygen atom and its residual part.[22] The MO's thus obtained are listed in Table II. Next, the parameter of the oxygen atom in VII was determined so as to reproduce the observed dipole moment (3.49 D. U.) of VII.[1] As was described in a previous paper,[1] although VII is probably distorted somewhat from a planar structure, for the sake of simplicity the planar structure was assumed for the calculation of the dipole moment. The molecular dimensions of VII were obtained by a method analogous to that used in the calculation of styrene. The bond-order bond-length relation was used, where the order-length relationships of the N–O and C–N bonds are the same as those of our previous papers,[15] and as those used in Kobayashi's and in Cox and Jeffrey's papers respectively.[23] Moreover, we assumed that each of the C–C–N and C–N–O angles is 120°, the configuration of the molecule being the same as that discussed in a previous paper,[1,24] and that the benzene ring is a regular hexagon.

The values of the σ-moments were determined with reference to those obtained by the analysis of the dipole moments of, for instance, pyridine *N*-oxide, and diazine mono *N*-oxide[15,26] and by the analysis of the NMR

19) a) N. Mataga and K. Nishimoto, *Z. Phys. Chem. N. F.*, **13**, 140 (1957); b) See also T. Kubota, *Progress Reports on Electronic Processes in Chemistry*, **2**, 39 (1960), published by the Japanese Reseach Group on Electronic States.

20) S. Mataga and N. Mataga, *Z. physik. Chem. N. F.*, **19**, 231 (1959).

21) The effect based on the methyl group was neglected.

22) It seems to be very useful to compare the energy level of the oxygen atom with those of the residual part stated above.

23) a) E. G. Cox and G. A. Jeffrey, *Proc. Roy. Soc.*, **A207** 110 (1951); b) H. Kobayashi, *J. Chem. Soc. Japan, Pure Chem. Sec.* (*Nippon Kagaku Zasshi*), **82**, 272 (1961).

24) The dimensions and configurations for V, VI and VII are as follows:

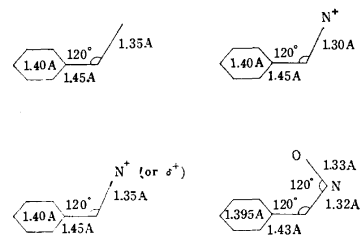

The dimensions of VII were estimated by averaging the molecular diagrams obtained by using the following two sets of parameters: $k_N = 1.6$, inductive effects $= (1/3)^n k_N$, $\rho_{NO} = 1$ and $k_O = 0.8$; $k_N = 1.6$, $k_O = 0.8$, $\rho_{NO} = 0.7$, and inductive effects $= 0$.[15,25] These averaged values are almost the same as those in the molecular diagram shown in Fig. 10.

25) The latter set of parameters is nearly equal to that adopted by W. Maier, A. Saupe and A. Englert, *Z. physik. Chem. N. F.*, **10**, 273 (1957).

26) T. Kubota and H. Watanabe, This Bulletin, **36**, 1093 (1963), where the symbol "N–O" in Table II must be read as H–C because of misprint.

spectra of pyridimine:[27] $\overset{(+)}{N}\rightarrow\overset{(-)}{O}$ (dative bond) $=4.55$ D., $\overset{(+)}{H}-\overset{(-)}{C}=0.40$ D., $C(sp^2)-N(sp^2)=0.0$ D., and the lone pair moment of the $N(sp^2)$ atom is 1.0 D. Under these conditions, the MO's were calculated by using the various parameters of the oxygen atom. It was found that $k_O=1.2$ is a suitable value. The results thus obtained are shown in Table II. It is important to point out that 1.2 is larger than the value decided previously for pyridine *N*-oxide (0.8β). This fact shows that the electron migration from the oxygen atom to the conjugated system in VII is smaller than that in heterocyclic *N*-oxides, as will be mentioned in a later section.

The Calculation of the Transition Energy and the Oscillator Strength of Benzylidene Methyl Amine (V), Its Proton-Addition Compound VI, and Benzylidene Methyl Amine *N*-Oxide (VII).—These values are calculated by using the MO's and the eigen values shown in Table II and the spectroscopic exchange integrals, β_s, mentioned in the preceding section. The one electron transition from the highest occupied orbital to the lowest vacant orbital belongs to the $^1A_1$ symmetry (shown with a solid arrow line in Fig. 5); this state may be expressed by a single configuration as in the case of styrene. Both transitions shown with a dotted arrow line in Fig. 5 belong to the $^1B_1$ symmetry, and these will interact with each other, as may be seen in Table I. The observed and calculated values of electronic spectra are shown in Fig. 7, in which the observed values are indicated by a circle. The transition moment corresponding to each excited state was also computed. The numbers shown in Fig. 7 indicate the square value of $\vec{Q}$:

$$\vec{Q}=\int \Psi_g(^1\Gamma)\,\vec{\gamma}\,\Psi_{exc.}\ (^1\Gamma)d\tau \qquad (7)$$

where $\Psi_{exc.}$ ($^1B_1^{\pm}$) is as shown in Table III. Under our approximation, $\vec{Q}$ is reduced to each term expressed as $q_{i-j}=\sqrt{2}\sum_\nu C_{i\nu}\cdot C_{j\nu}\cdot\vec{\gamma}_\nu$.[28] Assuming that side chain group in the molecules has the bent structure (120°), the calculation of the transition moments for the $^1A_1$ species was carried out.[24] The $^1A_1$ level has a transition moment along the long axis of molecules, while the $^1B_1$ levels have their transition moments parallel with the X-axis, as Fig. 5 shows. The character of the $^1B_1$ bands may be considered to be localized in the benzene ring.

Discussion and Results

On the Electronic Spectra of Benzylidene Methyl Amine *N*-Oxide (VII) and Its Related Compounds.—As is shown in Fig. 7, the calculated values of V agreed well with the observed values. It should be noted that the level arising from $^1B_1^-$ increases to an intensity slightly more than that of styrene[29] because the MO is disordered when the nitrogen atom is introduced.

The calculated transition energy and intensity of the $^1A_1$ level of VI are also in good agreement with the experimental results, as may be seen in Fig. 7. Furthermore, on the basis of this calculation, it is thought that a band having the $^1B_1$ symmetry will exist in the longest wavelength region. An inspection of the experimental curve of VI in Figs. 1, 2 and 3 will show that the curve in the above wavelength region has a considerably prolonged tail, where an absorption band may be hidden. In the light of the calculated results, this hidden band may conceivably be ascribed to the $^1B_1^-$ band, although the calculated value does not thoroughly agree with the observed value. The main reason for this disagreement on the $^1B_1^-$ level may be attributed to the selection of Coulomb parameters (i.e., the $k_{N^+}=2.4$ used here for N^+ is relatively large). Therefore, the MO values, ψ_4 and ψ_5, of styrene shown in Fig. 5 are largely stabilized in spite of the small change of the ψ_3 and ψ_6 MO's. As a result, the $^1B_1^-$ level undergoes a large red shift. When a large net charge such as N^+ is introduced into the molecule, it is believed that the same treatment of the VI as of the pyridine cation is not totally valid. The calculated results of VII shown in Fig. 7 differ from those of other compounds in the following points: a band having the $^1B_1$ symmetry and a lower intensity than that of the strong $^1A_1$ band existing at about 4 eV. must appear in the region of 5.35 eV. In fact, we can find a new band having vibrational structures at about 5.35 eV., as may be seen in Figs. 1, 7 and Table III.[30] On the basis of the above findings, we may reasonably conclude

27) W. Seiffert, H. Zimmermann and G. Sheibe, *Angew. Chem.*, 74, 249 (1962).

28) R. S. Mulliken and C. A. Rieke, *Report Progress Physics*, 8, 231 (1941); R. Daudel, R. Lefebrre and C. Moser, "Quantum Chemistry," Interscience Publishers, New York (1959).

29) On this approximation, if the vibronic interaction is not considered, the $^1B^-_1$ of styrene is forbidden by accident.

30) We could not obviously conclude from this calculation whether or not the absorption band arising mainly from the $^1\chi_{3\rightarrow6}$ configuration ($^1A_1$) is overlapped in this band. A problem analogous to this was discussed by Inuzuka in the case of the compound:

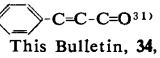

[31]

31) K. Inuzuka, This Bulletin, 34, 1557 (1961).

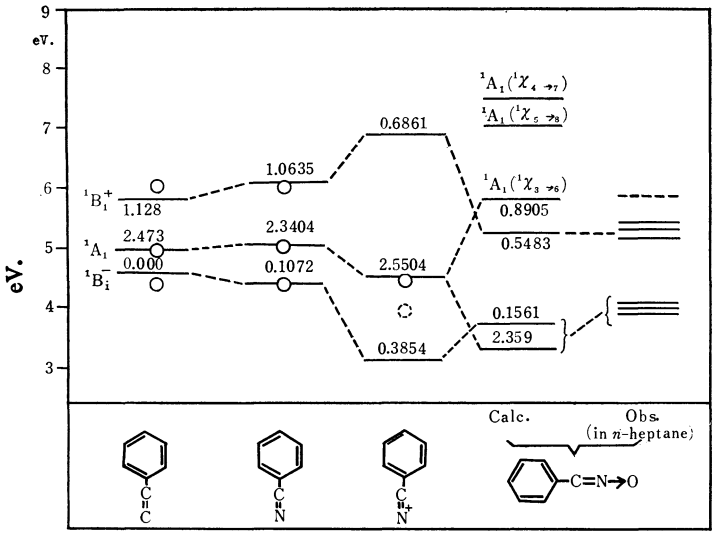

Fig. 7. The calculated energy levels, the observed values, and Q^2 values (refer to equation 7 in text.)
○: Observed value (Number is the value of Q^2)

TABLE III. THE CALCULATED AND OBSERVED VALUES OF $^1A_1$ AND $^1B_1$ BAND

Compound	$^1A_1$ Obs.	$^1A_1$ Calcd.	$^1B_1^-$ and $^1B_1^+$ Obs.	$^1B_1^-$ and $^1B_1^+$ Calcd.	Wave functions of $^1B_1^-$ and $^1B_1^+$ states	
Ph-C=C	5.009	5.009	4.451	4.666	$1/\sqrt{2}$ $(^1\chi_{3\to5}-{}^1\chi_{4\to6})$	$^1B_1^-$
			6.112	5.872	$1/\sqrt{2}$ $(^1\chi_{3\to5}+{}^1\chi_{4\to6})$	$^1B_1^+$
Ph-C=N	5.081	5.095	4.475	4.477	0.9092 $(^1\chi_{3\to5})$ −0.4164 $(^1\chi_{4\to6})$	$^1B_1^-$
			6.033	6.136	0.4164 $(^1\chi_{3\to5})$ +0.9092 $(^1\chi_{4\to6})$	$^1B_1^+$
Ph-C=N$^+$	4.531	4.579	~4.0[a]	3.197	Only single configuration: $^1\chi_{3\to5}$	$^1B_1^-$
Ph-C=N→O	b)	3.382	b)	3.829	0.9682 $(^1\chi_{4\to6})$ −0.2501 $(^1\chi_{5\to7})$	$^1B_1^-$
	5.976[c]	5.930[c]	5.259	5.347	0.2501 $(^1\chi_{4\to6})$ +0.9682 $(^1\chi_{5\to7})$	$^1B_1^+$
			5.410[c]			
			5.551			

a) Estimated value from the recorded curve.
b) $^1B_1^-$ band will be hidden below the strong $^1A_1$ band appearing at 3.974 eV., 4.066 eV., 4.157 eV. (maximum), and 4.226 eV. in *n*-heptane solution.
c) See footnote 30 in the text.

that the characteristic strong π-π^* band of VII can be assigned to a $^1A_1$ band superposed on a weak $^1B_1$ band, although the calculated energy levels do not perfectly agree with the observed levels because of various approximations and assumptions made in carrying out the calculations. From the standpoint of what has been mentioned above, it should be emphasized that the change in the electronic state in becoming the *N*-oxide compound is very large. It can be stated that the excited wave function of the strong π-π^* band ($^1A_1$) consists mainly of the $^1\chi_{5\to6}$ configuration. The comparison between the ψ_5 and ψ_6 MO's of the VII compound shown in Table II suggests that the charge transfer from the oxygen atom to the conjugated system can be expected when the π-π^* transition from ψ_5 to ψ_6 takes place; this finding is similar to that of heterocyclic *N*-oxides.[15,32] The observed blue shift phenomenon of the π-π^* band always caused by the solvent effect on nitrone compounds[1] may be considered to be due to the decrease in the π-electron density at the oxygen atom of the N→O bond in the excited state, because the hydrogen bonding power at the excited state may decrease in this case.

The Molecular Diagrams of V, VI and VII. —Figures 8a, b, c, show the molecular diagrams calculated on the basis of the results described in the "Theoretical" section. A comparison of the molecular diagram in Fig. 8c with those of heterocyclic *N*-oxide compounds[15] is of much interest from the following standpoints:

32) T. Kubota and M. Yamakawa, ibid., 35, 555 (1962).

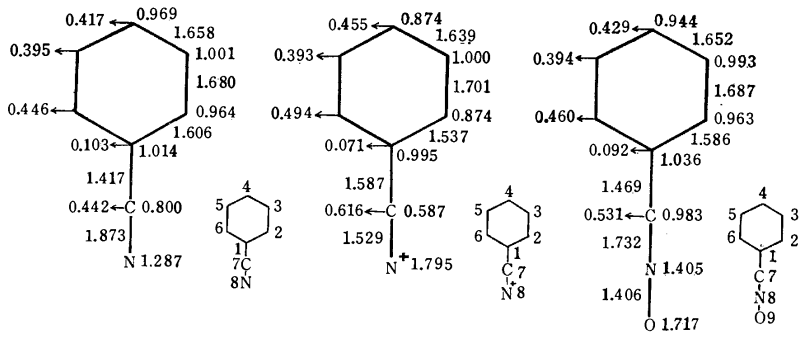

(a) (b) (c)

Fig. 8. The molecular diagrams of the compounds shown in Fig. 7.

(i) The double bond character of the N→O bond is decreased;

(ii) The net-charge at the carbon atom 7, which is adjacent to the N→O bond, becomes positive, and

(iii) The electron migration to a benzene ring from the N→O group is comparatively small.

The investigation of the infrared spectra of many nitrones published recently by Shindo[33] shows that the N→O stretching frequency of VII, which was assigned to the very strong band appearing at 1171 cm^{-1}, exists at a longer wavelength than the frequency (1265 cm^{-1}) of pyridine *N*-oxide.[15] This fact is believed to be in agreement with the conclusion obtained from the molecular diagram. The application of Fukui's frontier orbital method,[34] giving a good predictition for the reactivities of heterocyclic *N*-oxides,[15] to the prediction of the reactivities of nitrones is also of interest.

As may easily be understood from the MO's in Table II, the frontier electron density at C_7 (except for the nitrogen and oxygen atoms) is largest in both frontier orbitals, ψ_5 and ψ_6. This fact suggests that the carbon atom, C_7, is very active in both electrophilic and nucleophilic reactions, and that this position may be easily attacked by reagents. In the course of our experiments, as has been stated in the "Experimental" section, we have also established that VII, etc., (i. e., nitrones) are relatively unstable in an acidic medium and show behavior indicating that the carbon atom, C_7, is the reaction center. Thus the spectrum of VII changes into that of benzaldehyde in an acidic aqueous medium and into a composite spectrum of compounds considered to be HCl-addition substances to the C=N bond in the molecule in mixed solvents consisting of absolute alcohol and absolute hydrogen chloride. In the later case, the altered spectra are analogous to those of simple benzene derivatives. These facts support our theoretical predictions.

33) H. Shindo and B. Umezawa, *Chem. Pharm. Bull.*, **10**, 492 (1962).

34) K. Fukui, T. Yonezawa and H. Shingu, *J. Chem. Phys.*, **20**, 722 (1952); K. Fukui, T. Yonezawa, C. Nagata and H. Shingu, ibid., **22**, 1433 (1954).

Summary

The ultraviolet absorption spectra of benzylidene methyl amine, its proton-addition compound and benzylidene methyl amine *N*-oxide have been examined under various conditions. SMO calculations on those compounds have been carried out, and various physicochemical properties have been discussed.

On the basis of these calculations, the spectra of the above compounds have reasonably been assigned by using the spectroscopic exchange integrals $\beta_s(^1A_1)$ and $\beta_s(^1B_1)$, which were evaluated from the spectra and the MO, including C. I., of styrene.

The authors wish to express their deep gratitude to Professor Saburo Nagakura of the Institute for Solid State Physics, The University of Tokyo, for his valuable discussions and for reading the manuscript; to Dr. Ken'ichi Takeda, Director of this Research Laboratory, Dr. Noboru Mataga of Osaka Municipal University, and Professor Yuzuru Ooshika of Kwansei Gakuin University for their valuable discussions; and to Dr. Yutaka Mori of Osaka Gakugei Univerity for supplying samples.

Shionogi Research Laboratory
Shionogi & Co., Ltd.
Fukushima-ku, Osaka

The Hypersensitization of Photoconduction in Microcrystalline Zinc Oxide

By Eiichi INOUE and Takashi YAMAGUCHI

(Received May 9, 1963)

As is well known, microcrystalline zinc oxide exhibits remarkable photoconduction as long as its surface is covered with chemisorbed oxygen, but it becomes a surprisingly poor photoconductor as the oxygen is removed from the surface.[1] In a previous paper,[2] we have reported that the photoconduction characteristics can be further improved if the chemisorbed oxygen is replaced with appropriate electron-affinitive molecules. In the present paper, an enhancement of the photoconductivity of microcrystalline zinc oxide by the adsorption of some electron-affinitive molecules, such as iodine, phthalic anhydride and *p*-chloranil, will be described. The spectral response of the photocurrent and the temperature dependence of dark- and photo-currents have been studied. Rose Bengal, an organic dye which is widely used for the optical sensitization of zinc oxide photoconduction, was added to the above-mentioned systems, to be adsorved together with the electron-affinitive molecules, and the spectral response of the photoconduction has been measured.

It has been found that the electron-affinitive molecules are chemically adsorbed on zinc oxide not only to change the surface barrier height of zinc oxide, but also to co-operate with the dye molecule on the surface and to increase the photoconductive sensitivity of zinc oxide in its proper (ultraviolet) and also in its dye-sensitized (visible) wavelength regions. We shall call such a co-operative optical sensitization in the visible region "the hyper-sensitization of photoconduction."

Experimental

The microcrystalline zinc oxide used was Merck's reagent, 0.3 μ in particle size. It had a purity of 99.95%, containing calcium (0.015 %), lead (0.01 %) and sulfates (0.01%) as impurities. The adsorption of the electron-affinitive molecule onto the zinc oxide was made in the dark from an alcoholic solution. In order to study the hypersensitization, a small amount of Rose Bengal was further adsorbed by the same method onto thus-prepared zinc oxide, which had already adsorbed the electron-affinitive molecule. During these processes, no attempt was made to remove chemisorbed oxygen from the zinc oxide; therefore, the oxygen is considered to remain on the surface, forming a co-adsorbed layer with the electron-affinitive molecule or with the dye and the electron-affinitive molecule. The prepared samples of zinc oxide were coated in the dark on glass plates to a thickness of 40 to 50 μ. Two aluminum strips used as electrodes were placed 0.5 cm. apart on each of the specimens to accomplish a surface-type arrangement. In order to eliminate any pre-irradiation history of the zinc oxide employed, every specimen was kept in the dark for 50 hr. or more before its electric current was measured with a vibrating-reed electrometer. The contact between the electrode and the specimen was known to be ohmic from the linear relationship observed between the applied voltage (ranging from 5 to 100 V./cm.) and the current. A photographic tungsten lamp was used as the light source for measurement, while white light and a xenon arc were combined with a double monochromator for spectral study.

Results

The Sensitization of the Photoconduction.— When zinc oxide which had chemisorbed oxygen further adsorbed 0.03 mol.% of iodine,

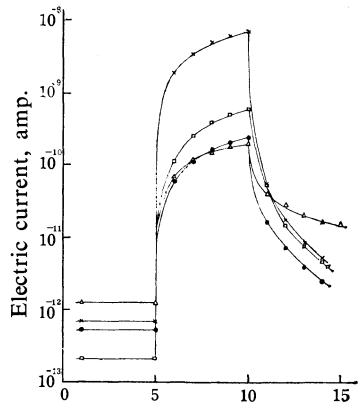

Fig. 1. Rise and decay of photocurrent in zinc oxide-oxygen-electron affinitive molecule systems.

- ● ZnO-O_2
- △ ZnO-O_2-*p*-chloranil (0.03 mol.%)
- □ ZnO-O_2-iodine (0.03 mol.%)
- × ZnO-O_2-phthalic anhydride (0.03 mol.%)

1) W. Ruppel, H. J. Gerritsen and A. Rose, *Helv. Phys. Acta*, **30**, 495 (1957).

2) E. Inoue, I. Maki and T. Yamaguchi, *J. Chem. Soc. Japan, Ind. Chem. Sec.* (*Kogyo Kagaku Zasshi*), **66**, 428 (1963).

phthalic anhydride or *p*-chloranil, the photocurrent was found to increase markedly, while the dark current scarcely changed at all or even decreased. Figure 1 shows the photocurrents of zinc oxide-oxygen-electron affinitive molecule systems measured with a white light with an intensity 1.3×10^{-2} W/cm^2.

When the above specimens were dyed with Rose Bengal of 0.0052 mol.%, the photocurrents, upon irradiation with the same light, increased further, as Fig. 2 shows. All the

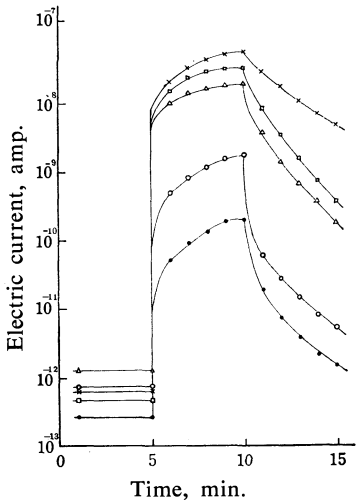

Fig. 2. Rise and decay of photocurrent in zinc oxide-oxygen-electron affinitive molecule-dye systems.

- ● ZnO-O$_2$
- ○ ZnO-O$_2$-Rose Bengal (0.0052 mol.%) (1)
- △ (1)+0.01 mol. % *p*-chloranil
- □ (1)+0.01 mol. % iodine
- × (1)+0.01 mol. % phthalic anhydride

specimens hereto used were prepared by coating the zinc oxide samples with silicone resin (7% by volume) as a binder for convenience. It was assumed that the influence of the resin on the photoconduction in each specimen is similar and that it, therefore, can be disregarded. From these measurements, it has been made clear that the electron-affinitive molecule adsorbed on the zinc oxide surface has a distinct effect on the photoconduction of zinc oxide.

Figure 3 illustrates the spectral response of photoconduction in the zinc oxide-oxygen-electron-affinitive molecule systems. The sensitization of the photoconductivity occurs only in the ultraviolet region, not in the visible region, except in the case of *p*-chloranil. In the case of phthalic anhydride, which was found to be the most effective, a double peak was found in the action spectrum. The cause of the double peak has not yet been determined. The system with *p*-chloranil showed a slight

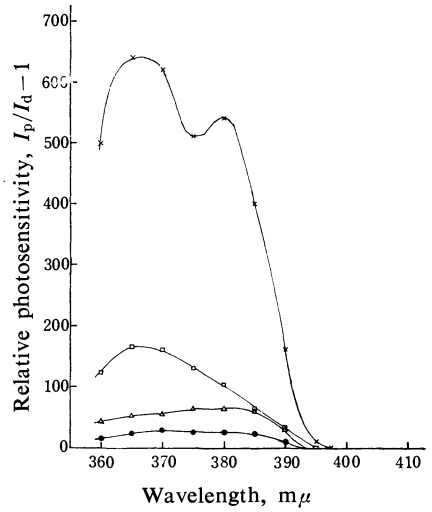

Fig. 3. Spectral response of photoconduction in zinc oxide-oxygen-electron affinitive molecule systems.

- ● ZnO-O$_2$
- △ ZnO-O$_2$-*p*-chloranil (0.03 mol. %)
- □ ZnO-O$_2$-iodine (0.03 mol. %)
- × ZnO-O$_2$-phthalic anhydride (0.03 mol. %)

response in the visible region which was too small to be shown in Fig. 3. The wavelength where the small response appears coincides with that of light absorption by *p*-chloranil. The results in Fig. 3 indicate a process whereby the electron-affinitive molecule is chemisorbed on the zinc oxide surface and there draws an electron from the crystal, making a depletion layer which decreases the dark conductivity of zinc oxide. When the system is irradiated with the light which zinc oxide absorbs, the chemisorbed molecule may get physisorbed or desorbed into the atmosphere. This process will lead to an increase in the photocurrent, as is the case in the zinc oxide-oxygen system mentioned at the beginning of this paper.[1] Therefore, the sensitization of the photoconduction under investigation should be considered to be caused by the chemisorption of the electron-affinitive molecule and, therefore, not by the optical sensitization effect. Here, the optical sensitization refers to a type of sensitization caused by light absorption by the sensitizer itself, as has been found in dye-sensitized silver halide in the photographic process.

The spectral response of photoconduction in the zinc oxide-oxygen-electron affinitive molecule-Rose Bengal systems is shown in Fig. 4. A remarkable optical sensitization is found in the visible region, where the light is strongly absorbed by Rose Bengal (420~600 mμ); *p*-chloranil, is an exceptional case, for it shows

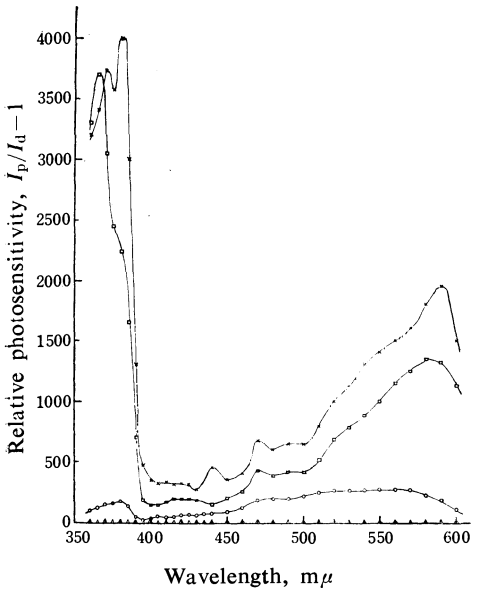

Fig. 4. Spectral response of photoconduction in zinc oxide-oxygen-electron affinitive molecule-dye systems.

○ ZnO-O_2-Rose Bengal (1)
× (1)+Phthalic anhydride
□ (1)+Iodine
△ (1)+*p*-Chloranil

very little effect. The efficiency of sensitization, however, varies from one electron-affinitive molecuce to another. It should be noticed here that the photoconductivity in the ultraviolet region is also much increased by the presence of Rose Bengal. Since Rose Bengal does not absorb light of this wavelength region, the increase can not be caused by optical sensitization. It is most likely that the sensitizing effect by the electron-affinitive molecule is intensified by the co-adsorption of Rose Bengal.

With the zinc oxide co-adsorbed *p*-chloranil and Rose Bengal, this effect has not been observed (see Fig. 4), though quite a large effect of sensitization was observed upon irradiation with the intense white light (see Fig. 2). The discrepancy between the two results can probably be explained by the difference between the incident light—white light and monochromatic light. A superposing effect of the photocurrent, which seems to be responsible for this discrepancy, will be described in the next paragraph.

The photocurrents in the zinc oxide-oxygen-Rose Bengal system and in the zinc oxide-oxygen-*p*-chloranil-Rose Bengal system were measured with ultraviolet (365 mμ), visible (577 mμ) and combined (365 mμ+577 mμ) lights. Here the intensities of the ultraviolet light and the visible light were held constant at 3.24×10^{-6} W/cm². As may be seen in Fig. 5, the photocurrents under co-irradiation were considerably larger than the sum of the photocurrents under separate irradiation. Evidently, there is a co-operative process for the sensitization of the photoconduction in the system,

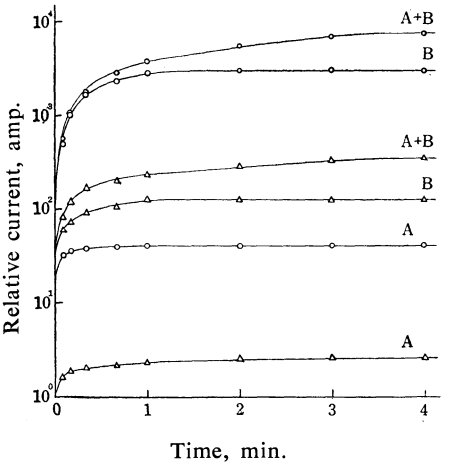

Fig. 5. Rise of photocurrent in dyed zinc oxide irradiated with light of 365 mμ (A), 577 mμ (B) or 365 mμ+577 mμ (A+B).

○ ZnO-O_2-Rose Bengal
△ ZnO-O_2-*p*-chloranil-Rose Bengal

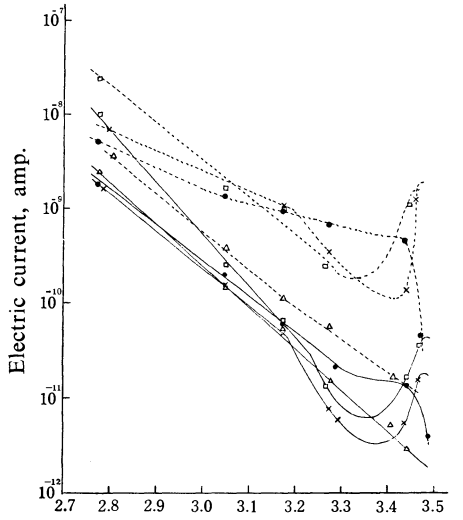

Fig. 6. Temperature dependence of dark- (solid line) and photo-current (broken line). (Light intensity 1.0×10^{-6} W/cm², applied voltage 40 V./cm.)

	Activation energy, eV.	
	dark-	photo-
● ZnO-O_2 (1)	0.89	0.66
△ (1)+*p*-Chloranil	0.76	0.47
□ (1)+Iodine	0.90	0.76
× (1)+Phthalic anhydride	0.79	0.30

which takes place when the system is irradiated simultaneously with ultraviolet and visible lights. We shall call such an effect "the superposing effect of the photocurrent."

The Temperature Dependence of the Electric Current. — The change in photoconductivity upon the adsorption of an electron-affinitive molecule can be caused by the change in the electron density of the zinc oxide crystal and also by the change in surface barrier height. The latter can be roughly estimated from a measurement of the thermal activation energy of the dark-current, which is determined from the temperature dependence of the dark-current.

Figure 6 illustrates the temperature dependence of dark- and photo-currents from 20°C to 90°C in each system without Rose Bengal. The thermal activation energy of the zinc oxide-oxygen system in the dark (~0.9 eV.) is maintained in the zinc oxide-oxygen-iodine system too, but those of other systems are smaller. The photoconduction requires less activation energy than the dark conduction in each of the systems investigated. It is certain that the adsorption of the electron-affinitive molecule causes a change in the activation energy of conduction which corresponds to a change in the barrier height or surface level.

Discussion

The sensitization of the photoconduction in the ultraviolet region in microcrystalline zinc oxide is considered to be due to the chemisorption and not to the optical effect. This is evident from Fig. 3, where the enhancement of the photoconductivity is not found in the visible region in spite of the fact that the adsorbed molecules more or less absorb light of this region. The chemisorption of the electron-affinitive molecule would increase the dark resistivity of the system by decreasing the electron density in the zinc oxide crystal as well as by changing the surface barrier height, while the chemisorbed molecule may get desorbed or physisorbed when the system is irradiated with the light which is absorbed by zinc oxide, leading to the marked decrease in resistivity. This change in resistivity upon irradiation may depend upon the electron affinity of the chemisorbed molecule and also on the concentration of chemisorbed molecules on the surface. When the electron-affinitive molecule is adsorbed on zinc oxide, the surface level may become more shallow than when only oxygen is present, and at the same time the surface level density may increase.

When both the electron-affinitive molecule and Rose Bengal are adsorbed on zinc oxide, the hypersensitization of the photoconduction takes place (cf. the visible region of Fig. 4). Here, supposedly the electron-affinitive molecule co-operates with Rose Bengal in the optical sensitization process. In other words, the optical sensitization of the photoconduction is intensified by the chemisorbed molecule. Such a process may be understood by adopting Weigl's postulate[4] on the dye-sensitization mechanism. When the system is irradiated with visible light, the Rose Bengal molecule absorbs the light and injects an electron into the conduction band of zinc oxide. The positively-charged dye ion thus formed captures an electron from a chemisorbed negative molecular ion, e. g., iodine ion or phthalic anhydride ion, returns to the original neutral molecule, and absorbs light again. By repeating this, the chemisorbed molecular ion density on the surface gradually decreases and the surface barrier of zinc oxide is finally eliminated. Therefore, the photosensitivity depends upon the nature and on the surface density of both the dye and the electron-affinitive molecule. However, another possible process, in which an exciton produced by light in dye aggregates elevates an electron from the chemisorbed negative ion directly up to the conduction band of zinc oxide, can not be excluded. One of the present authors (E. I.) and Maki have reported that the photodesorption of oxygen from dye-sensitized zinc oxide occurs upon irradiation with light absorbed by the dye.[5] This fact supports the processes hypothesized above.

The co-operative effect of the electron-affinitive molecule and dye in the ultraviolet region (Fig. 4) may differ from the above-discussed effect in the visible region. In this case, the fact that Rose Bengal does not absorb ultraviolet light of 350~400 mμ eliminates the possibility of the optical sensitization. This co-operative effect is probably to be attributed to the change in the surface level of zinc oxide upon the chemisorption of the electron-affinitive molecule.

The superposing effect of the photocurrent in the zinc oxide-oxygen-dye system upon irradiation with the mixed light of the ultraviolet and visible regions (Fig. 5) can be explained as follows. When the dye-sensitized zinc oxide is irradiated with ultraviolet[6] or visible[5] light separately, the photodesorption of the oxygen occurs and photocurrent increases,

3) S. R. Morrison, *Advances in Catalysis*, 7, 259 (1955).
4) J.W. Weigl, Preprint in "Internationales Kolloquiume über Wissenshaftliche Photographie," Zürich, September, 1961.
5) E. Inoue and I. Maki, The 16th Annual Meeting of Chemical Society of Japan, Tokyo, April. 1963.
6) D. J. W. Bevan and J. S. Anderson, *General Discussion Faraday Soc.*, 8, 238 (1950).

in different processes. The rate of photocurrent increase should depend on the rate of photodesorption. Under ultraviolet light irradiation, the chemisorbed atomic oxygen ion combines with a hole photo-produced in the valence band of zinc oxide and becomes an neutral atom. Then two oxygen atoms recombine on the surface to form a molecule which gets desorbed into the ambient. On the other hand, under visible light irradiation, oxygen atoms produced by the process mentioned in the discussion of the hypersensitization recombine to form molecules which leave the surface. In both processes, the rate-determining step would be the recombination of the oxygen atoms, a step which is proportional to the square of the oxygen atom concentration on the surface. The rate of the photo-desorption oxygen by co-irradiation with ultraviolet and visible lights will thus become larger than the sum of the rates by separate irradiation. This is considered to be the best possible explanation for the superposing effect of the photo-conduction.

The above findings on the sensitization of the photoconduction in microcrystalline zinc oxide can well be employed in order to raise the photosensitivity of the electrophotographic layer in which zinc oxide powder is dispersed in dielectric resin.

The authors wish to thank Mr. Isamu Maki, Mr. Fumio Kawamura and Mr. Yoshimitsu Tsuchiya for their earnest assistance during this investigation.

Graphic Engineering Laboratory
Tokyo Institute of Technology
Meguro-ku, Tokyo

The Spectrophotometric Determination of Titanium with Xylenol Orange[1]

By Makoto Otomo

(Received May 31, 1963)

Titanium(IV), in a slightly acidic solution buffered with acetic acid and sodium acetate, reacts with xylenol orange to give red or reddish-violet complexes, each consisting of one molecule of the reagent to one atom of titanium. The red complex formed by adding an excess of xylenol orange to a titanium solution is applicable to the spectrophotometric determination of titanium. The present paper will describe the conditions which permit the spectrophotometric determination of titanium at microgram levels and the results of a study of complex formation.

Experimental

Stock Solution of Titanium.—Titanium dioxide, prepared by igniting the precipitates which result from the hydrolysis of titanium tetrachloride (E. Merck Co., Ltd.), was fused with about five times as large a mixture of ammonium sulfate and sulfuric acid. The fused mass, after cooling, was dissolved in 6 N sulfuric acid and then diluted with distilled water to make the solution about 0.1 M in titanium sulfate. The resultant solution was standardized by the volumetric method described by Ishimaru.[2] A working standard solution was prepared by diluting the above solution with distilled water.

Perchloric Acid and Sodium Perchlorate.—In a study of complex formation, perchloric acid and sodium perchlorate solutions were used to maintain constant the hydrogen ion concentration and the ionic strength. The latter was prepared from reagent grade perchloric acid and sodium carbonate.

The other reagents and apparatus used were the same as those reported previously.[3] All experiments were carried out at 25±0.5°C.

Standard Procedure.—To a solution in a 25 ml. volumetric flask, which contained up to 40 μg. of titanium, were added 10 ml. of an acetate buffer (pH 3 to 4.5) and 4 ml. of a 1×10^{-3} M solution of xylenol organge. The solution was diluted to the mark with water and then mixed. After about 30 min., the absorbance of the solution was measured at the desired wave length (502 or 532 mμ), using a reagent blank as the reference.

Results and Discussion

Preliminary experiments showed that the variation in pH value had no significant effect on the absorption spectra of the solution,

1) This work was first presented at the Tôhoku-Hokkaido Branch Meeting of the Chemical Society of Japan, Hakodate, July, 1962.

2) S. Ishimaru, *J. Chem. Soc. Japan, Pure Chem. Sec.* (*Nippon Kwagaku Kwaishi*), **59**, 667 (1938).

3) M. Otomo, This Bulletin, **36**, 137 (1963).

provided the pH of the solution was maintained below 5 and a sufficient excess of xylenol orange was used.

Absorption Spectra.—Figure 1 gives the absorption spectra of solutions containing 35 μg. of titanium and xylenol orange added in various amounts, 3.5×10^{-5} to 1.44×10^{-4} M. There are two absorption bands; the intense absorption band with its maximum at about 440 mμ is due to the xylenol orange, which increases in intensity with the addition of the reagent, while the absorption found at the longer wavelengths seems to be due to the overlap of the titanium-xylenol orange complex band with that of the xylenol orange. It is found that the latter band at about 555 mμ slightly shifts toward shorter wavelengths with the increasing amounts of xylenol orange and that, at the same time, the intensity of the absorbance at this wavelength decreases gradually; for example, when the concentrations of xylenol orange are kept at 3.2×10^{-5}, 4.0×10^{-5}, and 4.8×10^{-5} M, the absorption maxima are found at 555, 552 and 550 mμ respectively. The further addition of xylenol orange causes disappearance of the absorption maximum, giving small shoulders. Further, an isosbestic point can be observed at 532 mμ, where the absorption curves for different solutions with a fixed amount of titanium cross each other, suggesting that titanium reacts with xylenol orange to form at least two absorbing entities which are in equilibrium with each other and also with the free xylenol orange. Similar phenomena have also been observed in the xylenol orange complexes of aluminum,[4] gallium[5] and thallium.[5]

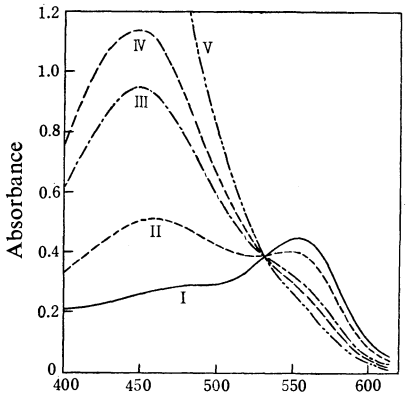

Fig. 1. Absorption spectra of Ti-XO complex at pH 3.0.
Ti: 35 μg., XO: I, 3.2×10^{-5} M; II, 4.8×10^{-5} M; III, 7.2×10^{-5} M; IV, 9.6×10^{-5} M; V, 1.44×10^{-4} M.

4) M. Otomo, This Bulletin, **36**, 809 (1963).
5) M. Otomo, unpublished work.

When, however, more than 3.5 ml. of a 1×10^{-3} M solution of xylenol orange is added and the same amount of this solution is used as the reference, the maximum absorption was always found at about 502 mμ (see Fig. 2), strongly suggesting the existence of only one form of the complex under the conditions so far studied.

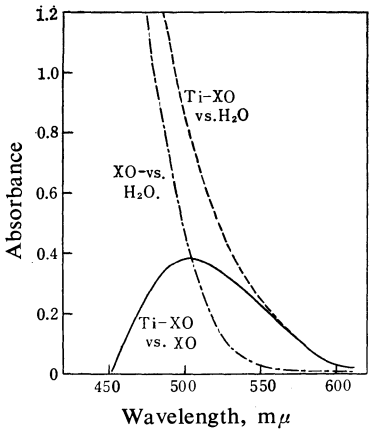

Fig. 1. Absorption spectra of XO and its Ti complex at pH 3.0.
Ti: 35 μg., XO: 1.6×10^{-4} M

The Effect of pH Value.—The effect of pH value on the color development was examined by measuring, at 502 mμ, the absorbance of a colored solution containing 25 μg. of titanium and 4 ml. of a 1×10^{-3} M solution of xylenol orange, the pH being adjusted to the desired value by means of an acetate buffer solution. From the curve shown in Fig. 3, it is found that the maximum and constant absorbance is obtained over the pH range 3 to 4.5. At a pH of less than 1.5, the complex does not

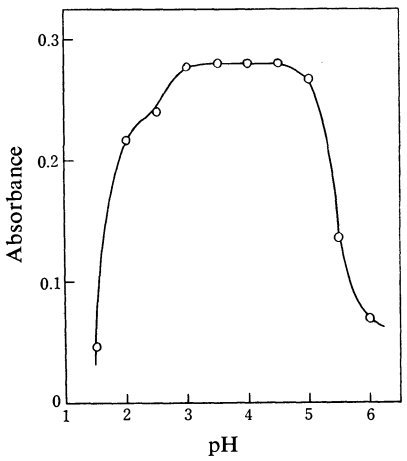

Fig. 3. Effect of pH on color development.
Ti: 25 μg., XO: 1.65×10^{-4} M

give any red coloration. At a pH above 4.5, the absorbance at 502 mμ decreases sharply with the increasing pH value, probably because of hydrolysis of the titanium. A constant absorbance was also obtained at 532 mμ (isosbestic point) provided the pH of the solution was kept between 3 and 4.5.

The Effect of the Addition of the Reagent.—The effect of reagent concentration on the color development was studied with solutions containing 25 μg. of titanium and varying amounts of a 1×10^{-3} M solution of xylenol orange. The absorbance measurement was made at three wavelengths, 502, 532 and 552 mμ. The results are shown in Fig. 4. When more than 3.5 ml. of the reagent solution is added, the absorbance at neither 502 mμ nor 532 mμ is affected by the further addition of the reagent. On the other hand, the absorbance at 552 mμ decreases sharply with the additional reagent unless a large amount of the reagent is used.

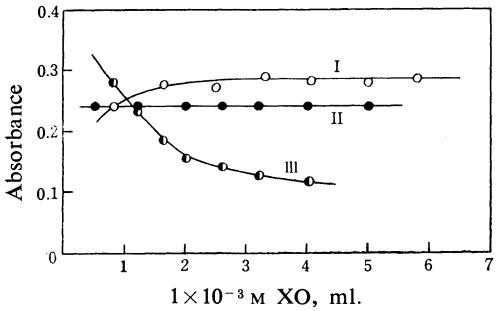

Fig. 4. Effect of addition of reagent (at pH 4.0).
Ti: 25 μg., I: 502 mμ, II: 532 mμ, III: 552 mμ

The Effect of the Standing Time.—The red color of the titanium-xylenol orange complex is stable for at least several hours.

Calibration.—Figure 5 shows that the plots of the absorbance-titanium concentration obey Beer's law over the ranges up to 25 μg. of titanium at 502 mμ and up to 40 μg. of titanium at 532 mμ. The absorbance measurements were made with solutions in which the pH value was adjusted (1) to 4.0 for the measurements at 502 mμ, and (2) to 3.0 for the measurements at 532 mμ. The latter pH value was chosen to minimize the interferences from other cations, which formed complexes with xylenol orange at the higher pH values to give positive errors. The apparent molar extinction coefficients were calculated as 18000 at 502 mμ and 11700 at 532 mμ, respectively.

The Effect of Diverse Ions. — Such anions as chloride, nitrate and sulfate do not interfere, even when present in large amounts. Large amounts of oxalate and tartrate give erroneous results, because they reduced the absorbance of the solution, probably by forming complexes with titanium. Since fluoride, phosphate and EDTA ions can form some stable complexes with titanium, they give large negative errors, even when added in small amounts.

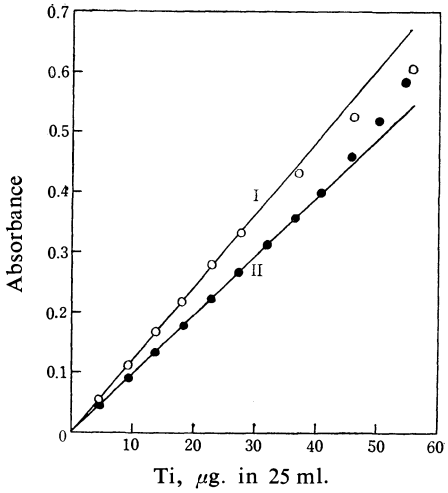

Fig. 5. Calibration curves.
XO: 1.6×10^{-4} M, I: 502 mμ, II: 532 mμ

Of the 26 cations tested, aluminum, iron(III), tin(II), thorium, yttrium vanadium(IV) interfere with the titanium determination by forming colored solutions.

Complex Formation.—The appearance of an isosbestic point, which has already been shown in Fig. 1, suggests that two complexes, one a red complex with its absorption maximum at 502 mμ and the other a reddish-violet one with its absorption maximum at about 555 mμ, are in equilibrium with each other. On the basis of the above suggestion, a study was made to determine the composition of the two complexes and to calculate the formation constants. In order to calculate the formation constants, however, it must be considered that xylenol orange is a polybasic acid* and that, therefore, the stability of the complexes is greatly dependent on the pH value under investigation. In all the solutions used in this study, therefore, the perchloric acid concentration was maintained constant at 0.020 M and the ionic strength was kept constant at 0.50.

* The stepwise acid dissociation constants of xylenol orange have been determined by Řehák and Körbl[6] as $pk_1=2.58$, $pk_2=3.23$, $pk_3=6.37$, $Pk_4=10.46$, and $pk_5=12.28$.

6) B. Řehák and J. Körbl, *Collection Czechoslov. Chem. Communs.*, **25**, 797 (1960).

The Red Complex with its Absorption Maximum at 502 mμ. — This complex is formed when xylenol orange is added in excess to a titanium solution. Although numerous methods have been developed for interpreting spectrophotometric data as they are presented in various cases, none is directly applicable to this particular system. Consequently, a method has been developed which is a modification of that of McConnell and Davidson.[7]

Assuming that the formation of the red complex is in accordance with the following equation:

$$TiO^{2+} + nXO \rightleftharpoons TiO(XO)_n + npH^+$$

the equilibrium constant, K, may be given by:

$$K = [TiO(XO)_n][H^+]^{np}/[TiO^{2+}][XO]^n \quad (1)$$

where XO is the total unbound xylenol orange, $TiO(XO)_n$ is the total titanium-xylenol orange complex, and p is the number of hydrogen ions liberated from one molecule of xylenol orange by the chelation. Unknown charges are omitted. The species of titanium(IV) present at the acidity and concentration level used is TiO^{2+} according to the notations of Musha and Ogawa[8] and of Sone and Tanaka.[9] The apparant formation constant, K', may be expressed as:

$$K' = K/[H^+]^{np} = x/(a-x)(b-nx)^n \quad (2)$$

where x is the molar concentration of the complex, and a and b are the initial molar concentrations of titanium and xylenol orange respectively. If a large excess of xylenol orange is present, the value of $b-nx$ will essentially equal the initial concentration of xylenol orange, b. The formation constant may then be written:

$$K' = x/(a-x)b^n \quad (3)$$

If the molar extinction coefficient of xylenol orange is represented as ε_{XO} and that of the complex, as ε_C, the absorbance of the solution, D, at any wavelength may be written:

$$D = (\varepsilon_C - n\varepsilon_{XO})x + \varepsilon_{XO}b \quad (4)$$

If the absorbance is measured against the solution containing the same amount of xylenol orange as b, D may be reduced to:

$$D = (\varepsilon_C - n_{XO})x \quad (5)$$

Solving for x and substituting it into Eq. 3 yields:

$$D = (\varepsilon_C - n\varepsilon_{XO})a - D/K'b^n \quad (6)$$

The values of D obtained at various concentrations of xylenol orange are plotted against D/b^n. With the correct choice of n, this should give a straight line, the slope of which is $-1/K'$, and the intercept, $(\varepsilon_C - n\varepsilon_{XO})a$. Values of n equal to one-half and two were tried unsuccessfully. Only a choice of n equal to one made the data interpretable. Thus, the only complex present is a 1 to 1 complex. Some of the results are shown in Fig. 6.

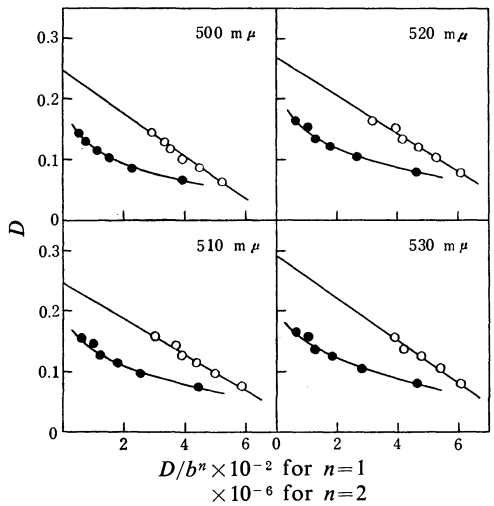

Fig. 6. Plots of D vs. D/b^n.
$HClO_4$: 0.020 M, μ: 0.50 M $NaClO_4$, a: 1.935 $\times 10^{-5}$ M
-○-: $n=1$, -●-: $n=2$

This graphical technique for evaluating the formation constant, K', was applied to data obtained at eight wavelengths, at 10 mμ intervals from 500 to 570 mμ. These eight values of K' were averaged to give a mean value of $K' = 2.9 \times 10^3$, with a standard deviation of 0.3×10^3.

Further, two other methods, one of which has been described by Andrews and Keefer[10] and the other of which has been reported previously by the present author,[11] were applied for the calculation of the formation constant. Both methods showed that a 1 to 1 complex is also formed in the presence of excess xylenol orange. As the mean values for K', 3.1×10^3 and 2.9×10^3 were obtained respectively; these are in good agreement with the value obtained above.

The Reddish-Violet Complex with Its Absorption Maximum at 555 mμ.—This complex is formed by adding titanium in excess to a solution of xylenol orange. The method of

7) H. McConnell and N. Davidson, *J. Am. Chem. Soc.*, **72**, 3164 (1950).
8) S. Musha and K. Ogawa, *J. Chem. Soc. Japan*, (*Nippon Kagaku Zassi*), **78**, 1686 (1957).
9) K. Sone and M. Tanaka, "Teisei Bunsekikagaku," A Translation of Charlot, "L'Analyse Qualitative et les Réaction en Solution" (In Japanese), Kyoritsu Shuppan, Tokyo (1958), p. 263.
10) R. M. Keefer and L. J. Andrews, *J. Am. Chem. Soc.* **74**, 1891 (1952).
11) M. Otomo, This Bulletin, **36**, 889 (1963).

Frank and Oswalt[12] was applied here: if a 1 to 1 complex is formed, the following equilibrium may exist:

$$TiO^{2+} + XO \rightleftarrows TiO(XO) + qH^+$$

$$K' = [TiO(XO)]\,[H^+]^q / [TiO^{2+}]\,[XO] \qquad (7)$$

where q is the number of hydrogen ions liberated from one molecule of xylenol orange by the chelation. At a constant acidity, the following relation may finally be derived:

$$ab/(D-\varepsilon_{XO}b) = (a+b)/(\varepsilon_C-\varepsilon_{XO}) + 1/K'(\varepsilon_C-\varepsilon_{XO}) \qquad (8)$$

where a and b are the initial molar concentrations of titanium and xylenol orange respectively. D is the absorbance of the solution, ε_{XO} and ε_C are the molar extinction coefficients of xylenol orange and the complex respectively, and K' is the apparant formation constant. If the first assumption is correct, on plotting the values of $ab/(D-\varepsilon_{XO}b)$ at various concentrations of titanium against the values of $a+b$, a straight line with slope $1/(\varepsilon_C-\varepsilon_{XO})$ and intercept $1/K'(\varepsilon_C-\varepsilon_{XO})$ should be obtained. Some of the results obtained are summarized in Fig. 7. From this figure, it is clear that a straight-line relationship is completely satisfied between $ab/(D-\varepsilon_{XO}b)$ and $a+b$, showing that a 1 to 1 complex is also formed. The formation constant, as a mean value of the values found at ten wavelengths between 520 and 610 mμ, was found to be 1.9×10^4, with a standard deviation of 0.5×10^4.

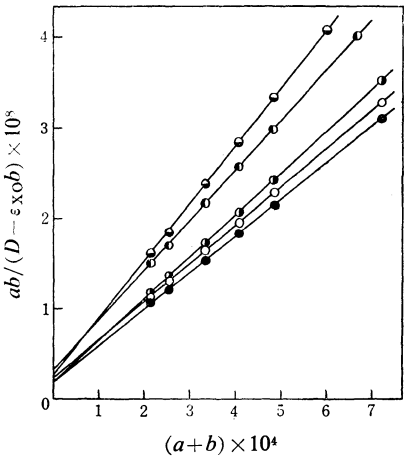

Fig. 7. Plots of $ab/(D-\varepsilon_{XO}b)$ vs. $(a+b)$.
$HClO_4$: 0.020 M, μ: 0.50 M $NaClO_4$
XO: 2×10^{-5} M, -◒-: 520 mμ
-◑-: 530 mμ, -●-: 550 mμ
-○-: 560 mμ, -◐-: 580 mμ

From the foregoing results, it may be concluded that, depending on the amount of the reagent, titanium forms either of two 1 to 1 complexes, a red complex with its absorption maximum at 502 mμ and a reddish-violet one with its absorption maximum at 555 mμ, the latter being more stable than the former. It was also found that the experimental data are satisfied only by assuming the existence of mononuclear 1 to 1 complexes. Although two interesting models of the position of the chelation ring in the xylenol orange complexes of niobium(V) and thallium(III) have been described by Cheng et al.[13] and by Busev et al.[14] respectively*, it is not possible to obtain definite information on the structure of these titanium-xylenol orange complexes on the basis of the experimental results described in the present paper and of the unpublished result. The present author is also, therefore, investigating the structural configuration of these complexes; the results will be presented elsewhere.

Summary

A new method for the spectrophotometric determination of titanium has been described. This method is based on the formation of the colored complex between titanium and xylenol orange in a slightly acidic solution. The effects of pH and the reagent concentration on the color development of the complex have been thoroughly investigated, and experimental conditions which make possible the determination of titanium at microgram levels have been devised. The compositions of the two 1 to 1 complexes have been determined from the data of spectrophotometric measurements. The apparant formation constants of these complexes have also been calculated.

The author wishes to express his hearty thanks to Professor Kôichi Tonosaki for his kind guidance and encouragement throughout this study, and to Dr. Katsumi Yamamoto of the Faculty of Science, Tohoku University, for this valuable advice.

Department of Chemistry
Faculty of Literature and Science
Hirosaki University
Hirosaki, Aomori

12) H. S. Frank and R. L. Oswalt, *J. Am. Chem. Soc.*, **69**, 1321 (1947).
13) K. L. Cheng and B. L. Goydish, *Talanta*, **9**, 987 (1962).
14) A. I. Busev and V. G. Tiptsova, *Zhur. Anal. Khim.*, **15**, 573 (1960).
* They both suggested that the chelation occurs through at least the displacement of the phenolic hydrogen atom.

*Hydroxyl Radicals in the γ-Radiolysis of Aqueous Benzene Solutions**

By Minoru TSUDA

(Received June 1, 1963)

The results of studies of the γ-irradiation of aqueous gelatin solutions[1,2] suggest that hydroxyl radicals play an important role in the radiation induced crosslinking of high polymers in aqueous solutions.[3] With dilute aqueous solutions it is ordinarily true that only water absorbs the incident energy. The dissociation of the water leads to the production of hydroxyl radicals, which then attack the solute. The hydroxyl radical can abstract hydrogen atoms from solutes such as organic polymers to produce polymer radicals. This process can be considered an oxidation of the polymer solute. In an oxygen-free solution, hydrogen atoms may also abstract hydrogen from the polymer solute. The polymer radicals produced may then combine with each other to produce crosslinks. However, experiments in this laboratory suggest that hydrogen atoms*1

$$RH + OH^{\cdot} \rightarrow R^{\cdot} + H_2O$$
$$RH + H^{\cdot} \rightarrow R^{\cdot} + H_2$$
$$R^{\cdot} + R^{\cdot} \rightarrow R - R$$

are quite ineffective, although hydroxyl radicals promote crosslinking considerably.[2,3] Hydrogen atoms apparently preferably combine to produce hydrogen molecules. If hydrogen atoms can be changed to hydroxyl radicals, an increase in the extent of crosslinking is to expected.

Dainton et al. have shown that nitrous oxide is capable of reacting with the 'basic form' of the hydrogen atom produced by the γ-radiolysis of water to produce hydroxyl radicals and nitrogen.[4,5] The occurrence of such a reaction should increase the yield of crosslinking. The present author has, accordingly, studied the effect of nitrous oxide on

$$N_2O + H^{\cdot} \rightarrow OH^{\cdot} + N_2$$

the γ-radiolysis of an aqueous benzene solution. Benzene was used instead of a polymeric substance in order to simplify the analysis of the experimental results.

Previous studies[7-10] of the oxidation of benzene in oxygen-free aqueous solutions by γ-irradiation have been interpreted in terms of the following sequence of reactions:

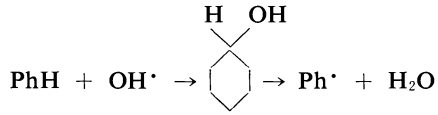

$$PhH + H^{\cdot} \rightarrow PhH_2 \rightarrow \text{Polymer}$$
$$Ph^{\cdot} + Ph^{\cdot} \rightarrow Ph_2$$
$$Ph^{\cdot} + OH^{\cdot} \rightarrow PhOH$$

In aerated solutions the following reaction also occurs:

$$Ph^{\cdot} + O_2 + H_2O \rightarrow PhOH + H_2O_2$$

This schema shows that the oxidation of benzene is effected by hydroxyl radicals, but not by hydrogen atoms. Therefore, the yield of hydroxyl radicals is estimated from the yield of the oxidized products, namely, phenol and biphenyl, from benzene. The production of a small amount of oxygen by the primary action of γ-rays on water and nitrous oxide merely results in an increase in the yield of phenol. The total yields of biphenyl and phenol from benzene in the presence of nitrous oxide should equal the radical yields of water upon radiolysis, provided that nitrous oxide does in fact change all the hydrogen atoms into hydroxyl radicals. According to Allen,[11] the radical yields (G_H and G_{OH} for ^{60}Co-gamma rays) for irradiated water are 2.85± 0.15 and 2.4 respectively in neutral solutions.

Hydrogen peroxide also reacts with hydrogen atoms to give hydroxyl radicals.[9] Therefore, hydrogen peroxide can also be used to study the effect of hydroxyl radicals in the oxidation of

* Presented at the Autumn Meeting of the Chemical Society of Japan, Tokyo, November, 1961.

1) Y. Tomoda and M. Tsuda, *Tokyo Kogyo Shikensho Hokoku*, **55**, 490 (1960).

2) Y. Tomoda and M. Tsuda, *J. Polymer Sci.*, **54**, 321 (1961).

3) Y. Tomoda and M. Tsuda, *Nature*, **190**, 905 (1961).

*1 The hydrogen atoms described here may be better represented by solvated electrons.

4) F. S. Dainton and D. B. Peterson, *Nature*, **186** 878 (1960).

5) F. S. Dainton and S. A. Sills, ibid., **186**, 879 (1960).

6) Chemical Society of Japan, "Kagaku-Benran," Maruzen Co., Ltd.. Tokyo (1958), p. 572.

7) G. Stein and J. Weise, *J. Chem. Soc.*, **1949**, 3245.

8) J. H. Baxendale and D. Smithies, *J. Chem. Phys.*, **23**, 604 (1955).

9) P. V. Phung and M. Burton, *Radiation Research*, **7**, 199 (1957).

10) J. H. Baxendale and D. Smithies, *J. Chem. Soc.*, **1959**, 779.

11) A. O. Allen, "The Radiation Chemistry of Water and Aqueous Solutions," D. Van Nostrand Co. Inc., Princeton (1961), p. 46.

organic compounds. However, in this case it is also necessary to consider the possibility

$$H_2O_2 + H^\cdot \rightarrow OH^\cdot + H_2O$$

of the consumption of hydroxyl radicals by hydrogen peroxide (reaction 1), which will compete with reaction 2. However, it is known

$$OH^\cdot + H_2O_2 \rightarrow H_2O + HO_2 \quad (1)$$

$$PhH + OH^\cdot \rightarrow PH^\cdot + H_2O \quad (2)$$

that, at a high concentration of hydrogen peroxide, the decomposition of the peroxide proceeds through a chain-reaction mechanism,[12] and that hence, the production of oxygen does not result in the consumption of any hydroxyl radicals at all.

Experimental

A 3000 curie ^{60}Co source was used for all irradiations. The dose rate, which was measured with a Fricke Dosimeter, was 1.98×10^5 rads/hr.

Fifty grams of water were weighed into a 100 ml. ampoule, and oxygen was completely removed by passing nitrogen gas through the water for 30 min. After the addition of 2 ml. of benzene, the ampoule was sealed. In the case of the nitrous oxide solutions, flushing with nitrogen for 30 min. was followed by passing nitrous oxide through the water for 30 min. at 3~5°C, prior to the addition of the 2 ml. of benzene. Hydrogen peroxide solutions were prepared by the addition of 10 ml. of an 8.91 mol./l. aqueous hydrogen peroxide solution which had been acidified with sulfuric acid to give the final solution, with a pH of 3, in order to prevent the spontaneous decomposition of the hydrogen peroxide.[13] The ampoules were vigorously agitated for 10 min. immediately before γ-irradiation in order to ensure the saturation of the solution with benzene. All irradiations were carried out at 25°C by a time scale.

Biphenyl was analyzed according to the method of Phung and Burton.[9] Phenol was analyzed by the method of Baxendale et al.[8,14,15] Phenol was extracted from the sample with ether after biphenyl and benzene had first been removed by extraction with *n*-hexane, and it was determined spectrometrically using an absorption at 273.5 mμ. A correction was applied for the distribution of phenol between water and *n*-hexane. With samples containing hydrogen peroxide, correction must be made for the absorption by hydrogen peroxide at 273.5 mμ. The contribution by hydrogen peroxide to the absorption at 273.5 mμ was calculated from the absorption at 247 mμ. (Biphenyl, which also absorbs at 247 mμ, was removed by extraction with *n*-hexane prior to the spectrometric analysis.)

12) Ref. 11, p. 102.
13) Y. Shibata, "Muki-Kagaku Zensho II-1-1," Maruzen Co., Ltd., Tokyo, (1951), p. 238.
14) J. H. Baxendale and J. Magee, *Discussions Faraday Soc.*, **14**, 160 (1953).
15) J. Goodman and J. Steigman, *J. Phys. Chem.*, **62**, 1020 (1958).

Results

G-Values were calculated from the gradient of the lines Fig. 1 and Fig. 2.

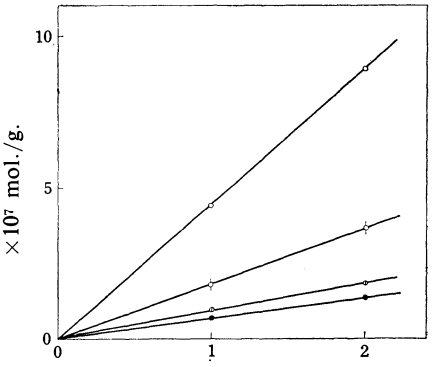

Fig. 1. Ordinate: Amounts of phenol and biphenyl produced in one gram of water (mole).

Phenol { N_2 ●, N_2O ○ } Biphenyl { N_2 ⊕, N_2O ○ }

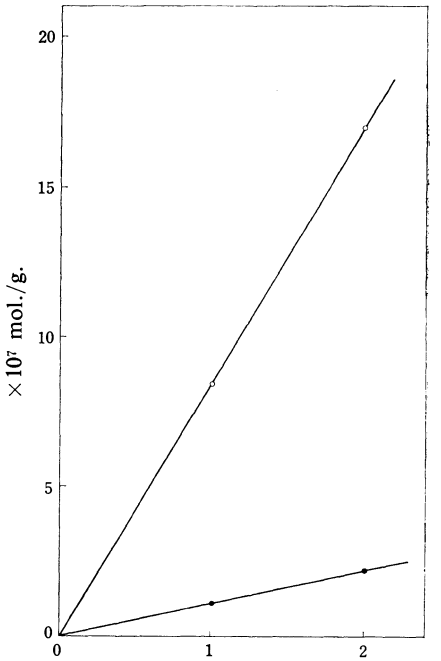

Fig. 2. Ordinate: Amounts of phenol and biphenyl produced in one gram of water containing hydrogen peroxide (mole).
Phenol ○ Biphenyl ●

TABLE I. CONDITIONS AND *G* VALUES

Condition	$G(Ph_2)$	$G(PhOH)$
Nitrogen	0.45	0.35
Nitrous oxide	2.15	0.90
Hydrogen peroxide	0.55	4.11

TABLE II

	$G(Ph_2)$	$G_1(PhOH)$	$G_2(PhOH)$	$G(PhOH)$[a]	$G((OH)PhH\cdot)$[b]
N_2	0.45	0.23	0.12	0.35	1.48
N_2O	2.15	0.78	0.12	0.90	5.98
H_2O_2	0.55	0.28	3.83	4.11	5.49

a) $G(PhOH)=G_1(PhOH)+G_2(PhOH)$
b) $G((OH)PhH\cdot)=2G(Ph_2)+2G_1(PhOH)+G_2(PhOH)$

The yield of biphenyl for oxygen-free (N_2-saturated) benzene solutions agrees with the value obtained by Baxendale and Smithies[8], but it is smaller than that reported by Phung and Burton.[9] The yield of phenol reported for oxygen-free benzene solutions is substantially in accordance with other reports.[8,9]

Discussion

The 'basic form' of the hydrogen atom produced by the dissociation of irradiated water seems to be a solvated electron, e_{aq}^-, and it preferably reacts with nitrous oxide[16] and hydrogen peroxide.[17-21]

$$e_{aq}^- + N_2O \rightarrow N_2 + H_2O_2^- \rightarrow N_2 + OH\cdot + OH^-$$

$$e_{aq}^- + H_2O_2 \rightarrow H_2O_2^- \rightarrow OH\cdot + OH^-$$

Under the present experimental conditions, the concentration ratio $[H_2O_2]/[H^+]$ was about 10^3 (pH ~3), and the ratio of the rate constants for the $H_2O_2+e_{aq}^-$ and $H^++e_{aq}^-$ reactions is about 1/2.[20] Therefore, the production of the acidic form of the hydrogen atom, H, should be negligible in the present case.

In nitrous oxide solutions the yield of hydroxyl radicals should be $2(G(Ph_2)+G(PhOH))=6.10$, which is larger than the expected value of 5.25 ± 0.15 (the sum of G_H and G_{OH}).[11] The discrepancy may be partly due to the oxygen produced by the decomposition of water and nitrous oxide.

In hydrogen peroxide solutions the yield of hydroxyl radicals should be $2G(Ph_2)+G(PhOH)=5.21$ because of the presence of the large amount of oxygen produced by the radiolysis of hydrogen peroxide.

Recently, Dorfman et al. reported the production of hydroxycyclohexadienyl radicals in the process of the radiolysis of an aqueous benzene solution.[22] The discussion of our data in terms of their mechanism may be necessary. They proposed the following sequence of reactions:

$$PhH + OH\cdot \rightarrow (OH) \leftarrow PhH\cdot$$

$$2(OH)PhH\cdot \rightarrow ((OH)PhH)_2 \rightarrow Ph_2$$

$$2(OH)PhH\cdot \rightarrow PhOH + (OH)PhH_2 \quad (3)$$

$$(OH)PhH\cdot + O_2 \rightarrow (OH)PhHO_2\cdot \rightarrow PhOH + HO_2\cdot$$
$$\downarrow$$
$$\text{Peroxide (a small part)} \quad (4)$$

$(OH)PhH_2$ may change to $PhH+H_2O$. In deaerated solutions,[22] $G(Ph_2)$ ~0.5 and $G(PhOH)$ ~0.23. The distribution of hydroxycyclohexadienyl radicals between biphenyl and phenol seems to be about 2:1. This ratio of distribution was applied to our data (Table II). $G_1(PhOH)$ is the yield of phenol produced by reaction 3, $G_2(PhOH)$ is that by reaction 4, and $G(PhOH)$ is the experimental result. $G((OH)PhH\cdot)$ should equal the radical yield of water, (G_H+G_{OH}).

In oxygen-free solutions our result for $G((OH)PhH\cdot)$ agrees with that obtained by Dorfman et al.[22]

According to Allen,[11] G_H in an atmosphere with a high concentration of oxygen is larger by 0.1 in G value than the ordinary value. Therefore, $G((OH)PhH\cdot)$ should be 5.35 ± 0.15 in hydrogen peroxide solutions; the experimental result agrees with this expected value.

In nitrous oxide solutions the same value of $G_2(PhOH)$ as in deaerated solutions was applied. The value of $G((OH)PhH\cdot)$ is 10% larger than the expected value.

Summary

Some experiments have been made in order to prove the hypothesis that the hydroxyl radical plays an important role in the oxidation of organic compounds by γ-radiolysis in aqueous solutions. Nitrous oxide and hydrogen peroxide have been found to be capable of converting radiation-induced hydrogen atoms (or their stoichiometrically-equivalent

16) F. S. Dainton and D. B. Peterson, *Proc. Roy. Soc.*, **A267**, 443 (1962).
17) P. E. Riesz and B. E. Burr, *Radiation Research*, **16**, 663 (1962).
18) N. F. Barr and A. O. Allen, *J. Phys. Chem.*, **63**, 928 (1959).
19) E. Hayon and A. O. Allen, ibid., **65**, 2181 (1961).
20) G. Czapski and A. O. Allen, ibid., **66**, 262 (1962).
21) W. M. Garrison, B. M. Weeks and S. Cole, *Nature*, **193**, 129 (1962).
22) L. M. Dorfman, R. E. Bühler and I. A. Taub, *J. Chem. Phys.*, **36**, 549, 3051 (1962).

species) into hydroxyl radicals. In the γ-radiolysis of aqueous benzene solutions in the presence of nitrous oxide or hydrogen peroxide, the yield of the oxidation products from benzene has been found to equal, as had been expected, the sum of the yields of hydrogen atoms and hydroxyl radicals from water.

Government Chemical Industrial Research Institute, Tokyo
Hiratsuka, Kanagawa

The Absorption Spectra of Oil-soluble Dyes Solubilized by a Polysoap and a Monosoap

By Fumikatsu TOKIWA

(Received June 3, 1963)

Polysoaps constitute a very special class of soap. In a certain sense the micelles are already formed, because each molecule of polysoap may be regarded as the equivalent of a micelle, each molecule acting as a prefabricated soap micelle.[1] The phenomena associated with the critical concentration and the micelle equilibrium should, accordingly, be absent from polysoap solutions. From this point of view the polysoap is entirely different from ordinary soaps. Strauss and his co-workers[1-5] have extensively studied the solubilization effects of cationic polysoap, formed by adding dodecyl bromide to polyvinylpyridine, and have found that polysoap molecules undergo a considerable change in their structure upon solubilization. They have also pointed out that the solubilization mechanism depends on the nature of the solubilizates.[3,5]

However, no systematic study has as yet been reported either of the solubilization of oil-soluble dyes by polysoap or of the differences between polysoap and monosoap in the solubilization mechanisms of the dyes. The results of such a study, dealing with 1-benzeneazo-2-naphthol and three 1-nitrobenzeneazo-2-naphthols, are presented in this paper and in a subsequent paper. These three 1-nitrobenzeneazo-2-naphthols are equivalent in molecular weight, differing only in the position of the nitro group in the benzene ring.

Spectral measurement furnishes a simple means of obtaining information on the states of solubilized dyes in polysoap and monosoap solutions, although such a measurement is qualitative. In this experiment the absorption spectra of the dyes were measured in polysoap and monosoap solutions, and also in some hydrocarbons for purposes of comparison. The polysoap used was an *n*-dodecyl bromide addition compound of poly-2-vinylpyridine, while the monosoap was *n*-dodecyl-α-picolinium bromide, which seems to be closely related in its chemical structure to the polymeric unit of the above polysoap.

The present paper is a study of absorption spectra, leading to an understanding of the states of solubilized dyes in polysoap and monosoap solutions and of the way in which they are solubilized.

Experimental

Polysoap (*n*-Dodecyl Bromide Addition Compound of Poly-2-vinylpyridine).—Poly-2-vinylpyridine was prepared by polymerizing freshly-distilled 2-vinylpyridine (b. p. 57°C at 17 mmHg) in ligroin (purified by sulfuric acid) in the presence of benzoyl peroxide at 40°C for 3 days, followed by the purification procedure described by Strauss et al.[6] The nitrogen content of the purified polymer was 13.29%; calcd. 13.33%. (All the nitrogen analyses reported in this paper were performed by the Elementary Analysis Center, Kyoto University.) The intrinsic viscosity, $[\eta]$, in 92 weight per cent ethanol was 0.636 at 25°C; this value corresponds to a molecular weight of 1.27×10^5 and a degree of polymerization of 1.2×10^3, assuming that the values of K and α in a viscosity equation, $[\eta]=KM^{\alpha}$, are equal to those of poly-4-vinylpyridine.[7]

The polymer was then quaternized with *n*-dodecyl

1) L. H. Layton and U. P. Strauss, *J. Colloid Sci.*, **9**, 149 (1954).
2) M. E. L. McBain and E. Hutchinson, "Solubilization," Academic Press, New York (1955), p. 236.
3) U. P. Strauss and N. L. Gershfeld, *J. Phys. Chem.*, **58**, 747 (1954).
4) U. P. Strauss and S. S. Slowata, ibid., **61**, 411 (1957).
5) U. P. Strauss and L. H. Layton, ibid., **57**, 352 (1953).
6) U. P. Strauss and E. G. Jackson, *J. Polymer Sci.*, **6**, 649 (1951).
7) A. G Boyes and U. P. Strauss, ibid., **22**, 463 (1956).

bromide (b. p. 112°C at 3.0 mmHg, prepared from dodecyl alcohol of a high purity) in nitroethane at 80°C for 13 days. Purification was accomplished as reported by Strauss et al.,[6] using petroleum ether instead of isoöctane and ligroin. The polysoap finally purified contained 6.72% nitrogen and 16.70% bromine. The polysoap gave a slightly acidic pH in water (the 0.10% solution had a pH of 3.48). Titration with sodium hydroxide gave an average value of 4.82×10^{-3} equivalent of hydrogen ions per gram of polysoap. From these analytical data, it follows that 33.5% of the nitrogen is quaternized with *n*-dodecyl bromide, while 10.0% carries hydrogen bromide. Only one-third of the nitrogen reacted with *n*-dodecyl bromide in spite of the high temperature and the long time of reaction.

Monosoap (*n*-Dodecyl-*α*-picolinium Bromide).—Monosoap was prepared by the quaternization of *α*-picoline with *n*-dodecyl bromide according to the ordinary method. The soap was then purified by repeated recrystallization from acetone. The nitrogen was 4.08% (calcd. 4.09%); Br, 23.16% (calcd. 23.35%).

Oil-soluble Dyes.—The four dyes, 1-benzeneazo-2-naphthol (abbreviated to BAN) and 1-(*ortho*-, *meta*- and *para*-)nitrobenzeneazo-2-naphthol (abbreviated to *o*-nitro-BAN, *m*-nitro-BAN and *p*-nitro-BAN respectively), were synthesized by coupling diazotized aniline or nitroaniline with *β*-naphthol in alkaline solutions. The starting materials—aniline, (*ortho*-, *meta*- and *para*-)nitroaniline, and *β*-naphthol—were purchased from the Wako Pure Chemicals Co. The crude dyes were thoroughly washed with water and dried in vacuo. The purification of the dyes was carried out by repeated recrystallization from benzene or a benzene-methanol mixture. The dyes were finally obtained as fine crystalline powders.

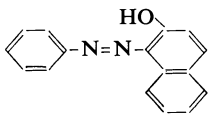

BAN

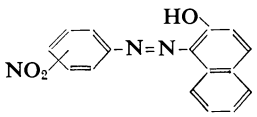

(*o*-, *m*-, *p*-)Nitro-BAN

The wavelengths of the absorption maxima (λ_{max}) of these dyes in ethanol and the molar extinction coefficients (ε_{max}) at the maxima are listed in Table I.

TABLE I. THE λ_{max} AND ε_{max} OF OIL-SOLUBLE DYES

Dyes	λ_{max}, mμ	ε_{max}, $\times10^{-4}$
BAN	485	1.46
o-Nitro-BAN	495	2.11
m-Nitro-BAN	478	1.65
p-Nitro-BAN	491	2.52

The Preparation of Polysoap Solutions.—Polysoap solutions were prepared according to the method of Strauss et al.[4,8] The residual HBr was removed from the polysoap by ion-exchange as follows: an anion-exchange resin, Amberlite IRA-410, in the hydroxide form, contained in a bag made of Visking's dialysis casing, was immersed briefiy in an aqueous solution of the polysoap to raise the pH to around 6.

Solubilization.—The solubilization was run in a water bath at 30±0.1°C for 55 hr. to attain equilibrium. The method used was the same as that used in a previous investigation.[9] In the present experiment, appropriate concentrations of polysoap and monosoap were chosen for the solubilization of dyes on the basis of the results of a preliminary experiment, for the reason described under "Results and Discussion."

Absorption Spectra. — Spectral measurements were performed with a Shimadzu Model RS-27 automatic spectrophotometer at room temperature (about 30°C) immediately after the solubilization.

Results and Discussion

Figures 1 and 2 show the absorption spectra of solubilized dyes in polysoap and in monosoap solutions respectively. Since the solubilizing power of polysoap and monosoap is highly dependent on the structure of the dyes (this will be reported on in more detail in a subsequent paper), it is difficult to compare the spectra of the dyes solubilized by equal concentrations of polysoap and monosoap. It is, therefore, necessary to choose appropriate concentrations of soaps in order to obtain the maximum absorbance of solubilized dyes ranging from 0.6 to 0.8, a convenient range for the comparison of the spectra Unfortunately, the polysoap solution itself exhibits a slight yellow color depending on the

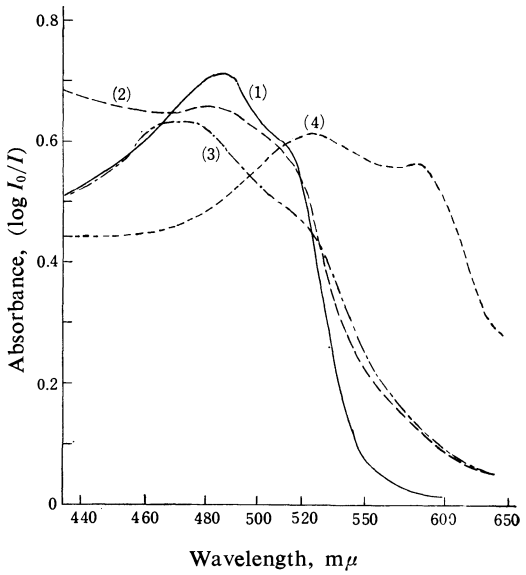

Fig. 1. Absorption spectra of oil-soluble dyes solubilized by polysoap.
(1) BAN (2) *o*-Nitro-BAN
(3) *m*-Nitro-BAN (4) *p*-Nitro-BAN

8) L. H. Layton, E. G. Jackson and U. P. Strauss, ibid., 9, 295 (1952).

9) F. Tokiwa, This Bulletin, 36, 222 (1963).

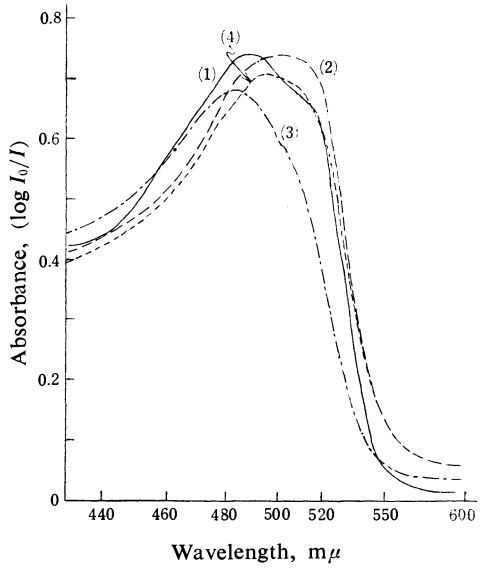

Fig. 2. Absorption spectra of oil-soluble dyes solubilized by monosoap.

(1) BAN (2) *o*-Nitro-BAN
(3) *m*-Nitro-BAN (4) *p*-Nitro-BAN

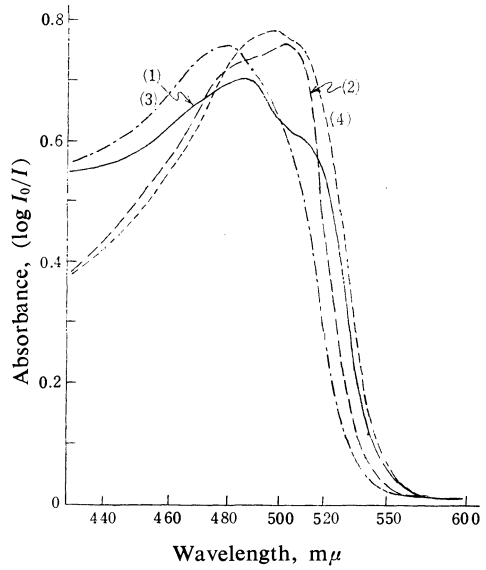

Fig. 3. Absorption spectra of oil-soluble dyes in benzene.

(1) BAN (2) *o*-Nitro-BAN
(3) *m*-Nitro-BAN (4) *p*-Nitro-BAN

concentration, although its spectrum has no absorption maximum, as Fig. 5 shows. This makes the spectrum of the dye somewhat obscure because of the overlap of dye and polysoap spectra. Therefore, to show the spectrum of the dye alone, without the contribution from polysoap, each spectrum shown in Fig. 1 has been obtained by substracting the absorbance of polysoap from the observed absorbance.

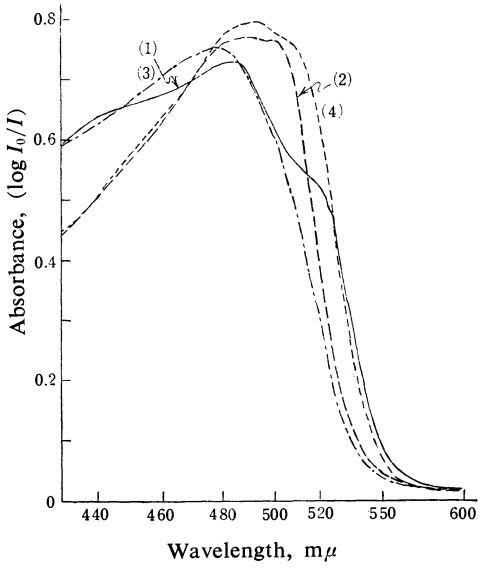

Fig. 4. Absorption spectra of oil-soluble dyes in hexane.

(1) BAN (2) *o*-Nitro-BAN
(3) *m*-Nitro-BAN (4) *p*-Nitro-BAN

Table II. The λ_{max} of the dyes in soap solutions and hydrocarbons

Dyes	λ_{max}, mμ			
	Polysoap	Monosoap	Benzene	Hexane
BAN	487	488	486	485
o-Nitro-BAN	480	502	502	(490)～500
m-Nitro-BAN	465～475	483	481	479
p-Nitro-BAN	523, 582	495	495	493

It is generally accepted that, in most aqueous solutions of ordinary soaps, the solubilization of oil-soluble dyes occurs in the interior of the micelles.[10] Therefore, if the dyes studied are solubilized in the interior of the soap micelle, which consists of a dense hydrocarbon region, then some similarities are to be expected between the spectra of the dyes solubilized in soap solutions and those of the dyes dissolved in hydrocarbons.[11] Figures 3 and 4 illustrate the spectra of four dyes in benzene and in hexane respectively. Aside from the shapes of the spectra, one notes that the wavelength of the absorption maximum of each dye in a monosoap solution corresponds closely to that in hydrocarbons (Table II). The wavelength difference is between 0 and 4 mμ; in benzene the difference is much less.

10) M. E. L. McBain and E. Hutchinson, "Solubilization," Academic Press, New York (1955), pp. 45, 147.
11) L. Michaelis and S. Granick, *J. Am. Chem. Soc.*, **67**, 1212 (1945).

This may indicate that the dyes studied are solubilized in the hydrocarbon region of monosoap micelles. In the case of BAN, furthermore, its spectra in both polysoap and monosoap solutions show a good similarity, as may be seen in Figs. 1 and 2. The similarity suggests that the way of the solubilization of BAN by both soaps is nearly the same. This suggestion is supported by the fact that the amounts of BAN solubilized by the two soaps are nearly equal, as will be shown in a following paper.

When one compares Fig. 1 with Figs. 2, 3 and 4, on the other hand, one notes that the spectra of nitro-BAN in polysoap solutions are not similar either to those in monosoap solutions or to those in hydrocarbons. These differences in spectra may be considered to arise from the fact that the state of nitro-BAN solubilized by the polysoap is not similar to that of nitro-BAN solubilized by the monosoap; they also suggest that nitro-BAN molecules are solubilized in different ways by the two soaps. It has been proposed that benzene and heptanol are solubilized between the polar heads of the side-chains of polysoap, in a manner similar to the micelle penetration which occurs with such polar materials as alcohols in ordinary soap solutions.[3,5] By analogy, whatever the detailed mechanism may be, the difference in spectra could be explained as follows: The loci of the solubilization of dyes in the polysoap molecule are not only the dense hydrocarbon region of the interior but also the polar region near the polymer backbone. In this case, the nitro group of the dye molecule seems to play an important role in the solubilization. Among the three nitro-BAN's, *p*-nitro-BAN exhibits a behavior totally different from that observed for the other dyes; that is, its two absorption maxima appear in the longer wavelength region. In view of the fact that the structures of these nitro-BAN molecules differ only in the position of the nitro group on the benzene ring, the solubilization of nitro-BAN molecules may depend upon their molecular volumes as well as on their polarities.

When the polysoap solution containing solubilized *p*-nitro-BAN was diluted with a large amount of ethanol (about 5 times by volume), the two peaks of its spectrum, at 523 and 582 mμ, disappeared and, simultaneously, a new absorption maximum arose, the wavelength of which is approximately equal to that of the maximum observed in hydrocarbons or in a monosoap solution. Any change in the spectrum of the dye molecule may be attributed to the redistribution of the electrons in the molecule.[11,12] Therefore, this means that dilution by ethanol changes the electron distribution in the *p*-nitro-BAN molecule; it also suggests that the electron distribution in this molecule is strongly affected by the polar region of the polysoap molecule as a result of the solubilization. In the case of the solubilization of *p*-nitro-BAN, especially, the polar region of the polysoap appears to act as a strong solubilizing locus.

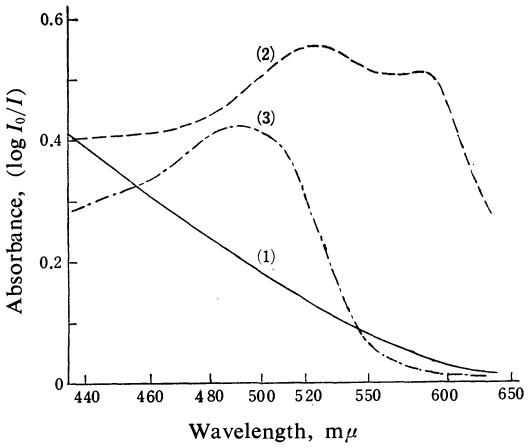

Fig. 5.
(1) Absorption spectrum of polysoap (1.0% aqueous solution): and the effect of dilution with ethanol on the spectrum of *p*-nitro-BAN
(2) Before dilution
(3) After dilution

Summary

The absorption spectra of several oil-soluble dyes, 1-benzeneazo-2-naphthol and three 1-nitrobenzeneazo-2-naphthols, have been measured in aqueous solutions of polysoap and monosoap and in hydrocarbons. The spectra of the above dyes in monosoap solutions are similar to those in hydrocarbons, while the spectra of dyes with a nitro group in polysoap solutions, especially the spectrum of *p*-nitro-BAN, are different. The differences in the solubilization behavior of the dyes in polysoap and in monosoap solutions and the ways in which the dyes are solubilized have been discussed. It has also been proposed that the loci of the solubilization in the polysoap molecule are not only the dense hydrocarbon region in the interior but also the polar region near the polymer backbone. In this case, the nitro group of the dye molecule seems to play an important role in the solubilization.

12) I. Maruta and F. Tokiwa, *J. Chem. Soc. Jacan, Pure Chem. Sec.* (*Nippon Kagaku Zasshi*), **82**, 1657 (1961); I. Maruta, ibid., **83**, 788 (1962).

The author wishes to express his thanks to Professor Toshizo Isemura of Osaka University for his kind advice. He also wishes to express his appreciation to Mr. Zenichi Miyagawa, Director of these Research Laboratories, for the permission to publish this paper, to Dr. Iwao Maruta for his advice, and to Miss Nobuko Kusui for her help in this work.

Research Laboratories
Kao Soap Co., Ltd.
Sumida-ku, Tokyo

The Solubilization of Oil-soluble Dyes by a Polysoap and a Monosoap

By Fumikatsu TOKIWA

(Received June 3, 1963)

In the preceding paper[1] the solubilization of oil-soluble dyes by polysoap was discussed by comparing the dye spectra in polysoap solutions with those in monosoap solutions and in hydrocarbons. In order better to understand the difference in solubilization between polysoap and monosoap, as well as the effect of solubilizate structure on the amounts solubilized, studies have now been made of the solubilizing power, viscosity and electrical conductivity of both polysoap and monosoap solutions.

The results of such studies are presented in this paper. As solubilizates, 1-benzeneazo-2-naphthol and three different 1-nitrobenzeneazo-2-naphthols were used, the same dyes as were employed in the preceding paper. The polysoap was obtained by the quaternization of poly-2-vinylpyridine with *n*-dodecyl bromide; the monosoap was *n*-dodecyl-*α*-picolinium bromide.

Experimental

Materials. — The materials used were polysoap (a *n*-dodecyl bromide addition compound of poly-2-vinylpyridine), monosoap (*n*-dodecyl-*α*-picolinium bromide) and four oil-soluble dyes; 1-benzeneazo-2-naphthol and three forms of 1-nitrobenzeneazo-2-naphthols (*ortho*, *meta* and *para*), which are abbreviated to BAN, *o*-nitro-BAN, *m*-nitro-BAN and *p*-nitro-BAN respectively. These materials were also used in the preceding investigation.[1]

A polyelectrolyte, poly-2-vinyl-*N*-ethylpyridinium bromide, was prepared from ethyl bromide and the poly-2-vinylpyridine described in the preceding paper. The method of Strauss et al.[2,3] was employed for preparing poly-4-vinyl-*N*-ethylpyridinium bromide. Analysis gave nitrogen 7.57%, bromine 32.3%.

Procedures.—Solubilizations were run in a water bath for 55 hr. to attain equilibrium, the method described in a previous paper[4] being employed. The amounts of solubilized dyes were determined by optical density measurements using a spectrophotometer, Hitachi Model EPU-2A.

Electrical conductivities were measured with a conductance bridge, Yanagimoto Model MY-7; the platinium electrodes were slightly platinized, and the cell constant was 0.482. The water used in preparing the solutions had a specific conductance of $1.0 \sim 1.5 \times 10^{-6}$ ohm^{-1} cm^{-1}.

The viscosities were measured with Ostwald-type viscometers, the flow times for pure water at 30°C being 67.7 and 140.5 sec.

Results and Discussion

The relationship between the solubilizing power of polysoap and the structure of oil-soluble dyes is shown in Fig. 1, where the extent of the solubilization of dyes is plotted against the concentration of polysoap. Figure 2 illustrates this relationship for monosoap. BAN, which contains no nitro group, is, in both soap solutions, more solubilized than the other dyes at any given soap concentration. This indicates that the introduction of a nitro group on the BAN molecule causes a lowering of the solubilization, probably because of the increase in its molecular volume[5] and the change in its polarity. The polysoap has greater solubilizing power, especially for dyes with a nitro group, than the monosoap. As for the dyes with a nitro group, it can be seen from Figs. 1 and 2 that in polysoap solutions the order of the amount solubilized is *m*-nitro-BAN>*p*-nitro-BAN>*o*-nitro-BAN, while in

1) F. Tokiwa, This Bulletin, **36**, 1585 (1963).
2) U. P. Strauss, S. J. Assony, E. G. Jackson and L. H. Layton, *J. Polymer Sci.*, **9**, 509 (1952).
3) U. P. Strauss and N. L. Gershfeld, *J. Phys. Chem.*, **58**, 747 (1954).
4) F. Tokiwa, This Bulletin, **36**, 222 (1963).
5) L. H. Layton and U. P. Strauss, *J. Colloid Sci.*, **9**, 149 (1954).

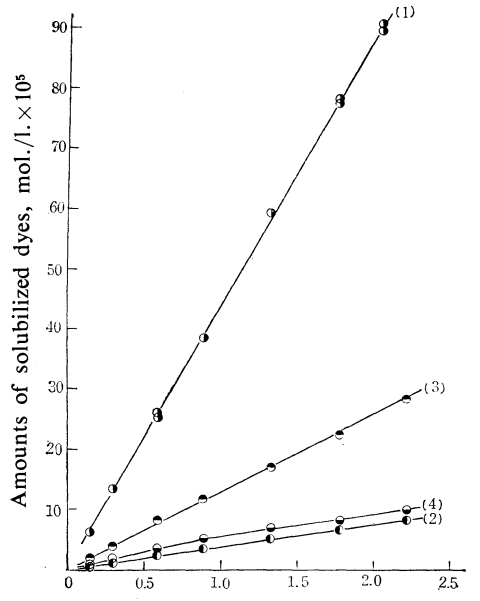

Fig. 1. The extent of solubilization of oil-soluble dyes plotted against the concentration of polysoap at 30°C.

(1) BAN (2) *o*-Nitro-BAN
(3) *m*-Nitro-BAN (4) *p*-Nitro-BAN

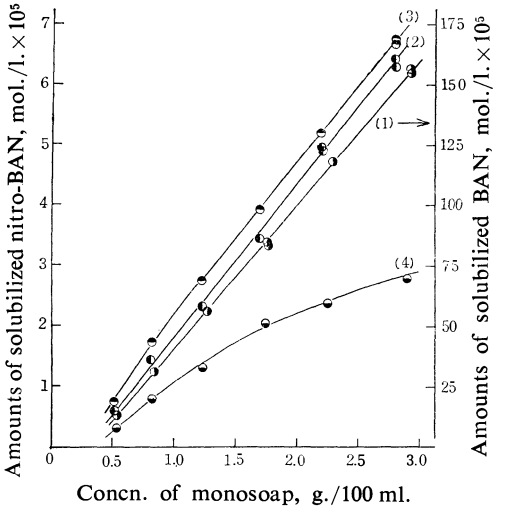

Fig. 2. The extent of solubilization of oil-soluble dyes plotted against the concentration of monosoap at 30°C.

(1) BAN (2) *o*-Nitro-BAN
(3) *m*-Nitro-BAN (4) *p*-Nitro-BAN

monosoap solutions it is *m*-nitro-BAN>*o*-nitro-BAN>*p*-nitro-BAN. These results suggest that the solubilization depends not only on the volumes of the dye molecule, which may not considerably differ from one another in this case, but also on its structure.

The solubilizing powers of polysoap and monosoap at concentrations of 10.0 and 20.0 g./l. for each of the four dyes are compared in Table I, where the symbols C and S denote the concentration of soaps (g./l.) and the amount of solubilized dyes (mol./l.) respectively. The value of S/C represents the number of dye molecules solubilized by a gram of solubilizer. Comparing the values of S/C for polysoap and for monosoap, we find that the polysoap is a better solubilizer of the dyes with a nitro group than the monosoap. It is also of interest to calculate the value of T, the number of dye molecules which are solubilized per dodecyl group, since the presence of the dodecyl groups plays an important role in the solubilization.[3] These values are also given in Table I. From Table I, furthermore, we can calculate the ratio of the S/C-value of polysoap to that of monosoap (A) and the ratio of the T-value of polysoap to that of monosoap (B) at a given soap concentration. These values, which are listed in Table II, show more clearly the characteristics of the solubilization by polysoap and monosoap.

The significant feature of these results is the relatively high solubilization of the dyes with a nitro group in polysoap solutions. These results are most likely due to the greater number of soap molecules contained in a polysoap molecule; probably, also, the soap molecules form larger and hence more efficient micelles when they are attached to a polymer chain than when they are free. The hydrocarbon chain of the polymer, too, may contribute to the solubilization. The fact that the structure of polysoap molecules is less compact and more disordered than that of monosoap micelles[7,8] may also play a role. However, the way in which the solubilizing efficiency depends on the position of the nitro group in the dye molecule is not clear.

In order to learn more about the polysoap and monosoap molecules when they are saturated with the dyes, the viscosities of the solutions were measured. The effects of saturation with dyes on the viscosities of polysoap and monosoap solutions, in which the dyes reached their respective solubilization limits, are shown in Figs. 3 and 4, where the reduced viscosity, η_{sp}/C, is given as a function of the concentration of soaps. For comparison, the viscometric behavior of polyelectrolyte without a dodecyl side-chain is also illustrated in Fig. 3.

The curve of the polyelectrolyte is a familiar pattern: the reduced viscosity, which is very

6) U. P. Strauss and L. H. Layton, *J. Phys. Chem.*, **57**, 352 (1953).
7) H. B. Klevens, *J. chim. phys.*, **49**, 615 (1952).
8) H. B. Klevens, *Kolloid-Z.*, **128**, 61 (1952).

TABLE I. SOLUBILIZATION LIMITS

Soap	C g./l.	BAN S mol./l. $\times 10^5$	BAN S/C mol./g. $\times 10^6$	BAN T mol./mol. C_{12} $\times 10^3$	*o*-Nitro-BAN S mol./g. $\times 10^5$	*o*-Nitro-BAN S/C mol./g. $\times 10^6$	*o*-Nitro-BAN T mol./mol. C_{12} $\times 10^3$
Monosoap	10.0	40.0	40.0	13.7	1.82	1.82	0.622
	20.0	100	50.0	17.1	4.36	2.18	0.746
Polysoap	10.0	43.7	43.7	24.6	3.80	3.80	2.14
	20.0	87.2	43.6	24.5	7.40	3.70	2.08

Soap	C g./l.	*m*-Nitro-BAN S mol./l. $\times 10^5$	*m*-Nitro-BAN S/C mol./g. $\times 10^6$	*m*-Nitro-BAN T mol./mol. C_{12} $\times 10^3$	*p*-Nitro-BAN S mol./g. $\times 10^5$	*p*-Nitro-BAN S/C mol./g. $\times 10^6$	*p*-Nitro-BAN T mol./mol. C_{12} $\times 10^3$
Monosoap	10.0	2.18	2.18	0.746	1.06	1.06	0.363
	20.0	4.72	2.36	0.807	2.21	1.11	0.380
Polysoap	10.0	13.0	13.0	7.32	5.40	5.40	3.04
	20.0	25.8	12.9	7.26	9.20	4.60	2.59

TABLE II. THE COMPARISON OF THE SOLUBILIZING POWER OF POLYSOAP AND THAT OF MONOSOAP

Concn. of soap g./l.	BAN A	BAN B	*o*-Nitro-BAN A	*o*-Nitro-BAN B	*m*-Nitro-BAN A	*m*-Nitro-BAN B	*p*-Nitro-BAN A	*p*-Nitro-BAN B
10.0	1.09	1.80	2.09	3.44	5.96	9.81	5.09	8.37
20.0	0.872	1.43	1.70	2.79	5.47	9.00	4.14	6.82

A: (S/C-value of polysoap)/(S/C-value of monosoap)
B: (T-value of polysoap)/(T-value of monosoap)

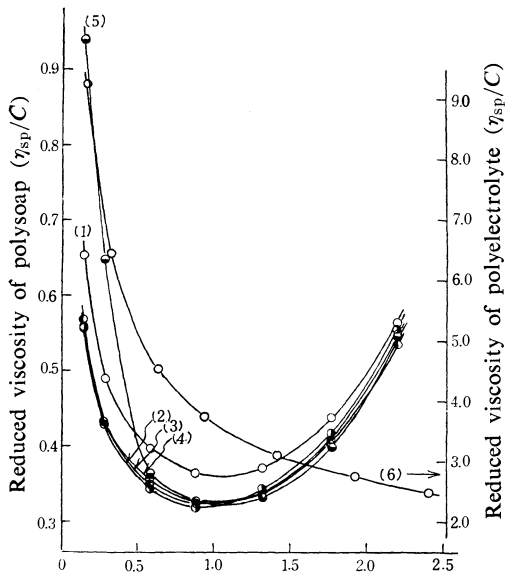

Concn. of polysoap, g./100 ml.

Fig. 3. The effect of saturation with dyes on the viscosity of polysoap at 30°C.

(1) None (2) BAN
(3) *o*-Nitro-BAN (4) *m*-Nitro-BAN
(5) *p*-Nitro-BAN
(6) Viscometric behavior of poly-2-vinyl-*N*-ethylpyridinium bromide at 30°C.

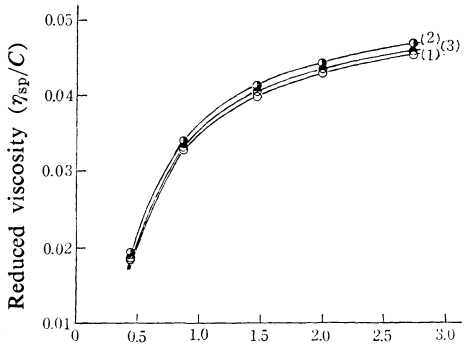

Concn. of monosoap, g./100 ml.

Fig. 4. The effect of saturation with dyes on the viscosity of monosoap at 30°C.

(1) None (2) BAN
(3) *m*-Nitro-BAN: *o*-nitro-BAN and *p*-nitro-BAN are similar to curve 3.

large at a high dilution because of the highly extended configuration of the flexible polyions, decreases with an increasing polymer concentration as the electrostatic repulsion between ionized groups is diminished. Since reduced viscosity can be interpreted as a measure of the effective specific volume of a polymer molecule,[3,9] the structure of the polysoap

9) U. P. Strauss, N. L. Gershfeld and E. H. Crook, *J. Phys. Chem.*, **60**, 577 (1956).

molecule in water is considerably more compact than that of the polyelectrolyte molecule. The effect of attaching dodecyl chains to a flexible polymer chain is to pull the polymer molecule together.

Now, let us consider the state of monosoap micelles and polysoap molecules after the solubilization of the dyes. In the case of the monosoap, the very small change in viscosity may be explained as being due to the swelling of the micelles as a result of the dye solubilization.[10] On the other hand, the addition of the dyes to a polysoap solution decreases the viscosity, except for that of *p*-nitro-BAN at low concentrations of polysoap. The observed decrease in viscosity can be ascribed to the contraction of polysoap molecules as a result of the dye solubilization. However, the difference in the effect of the structure of dyes on the viscometric behavior of polysoap is small, with the one exception described below.

Among the dyes studied, *p*-nitro-BAN produced an extra-ordinary increase in the viscosity of the polysoap solution upon its solubilization. The reason for this experimental finding is not clear. However, the steep rise of curve 5 in Fig. 3 in the low concentration region of polysoap may be an indication of either an anomalous extension of polysoap molecules or of an anomalous interaction among different polysoap molecules. According to Strauss et al.[3] the following mechanism also seems possible. The dye molecules are predominantly solubilized, with their polar nitro groups located in the polar region near the polymer backbone and with their hydrophobic portions extending into the hydrocarbon region of the polysoap molecule. This will contract the polar region, which, therefore, will be less able to shield the hydrocarbon region from the aqueous medium. The hydrocarbon which is thus exposed at the surface of the polysoap molecule will be attracted by the van der Waals force to similarly-exposed hydrocarbon of other polysoap molecules, with the resul that the polysoap molecules will tend to stick to one another. However, the reason why such an anomalous increase in viscosity occurs exclusively in the case of the solubilization of *p*-nitro-BAN and why it appears in the low concentration region of polysoap is not explainable by the above mechanism.

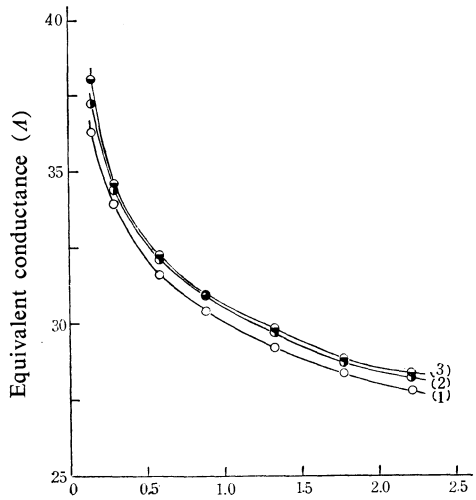

Fig. 5. The effect of saturation with dyes on the equivalent conductance of polysoap at 30°C.
(1) None (2) BAN
(3) *p*-Nitro-BAN: *o*-nitro-BAN and *m*-nitro-BAN are similar to curve 2.

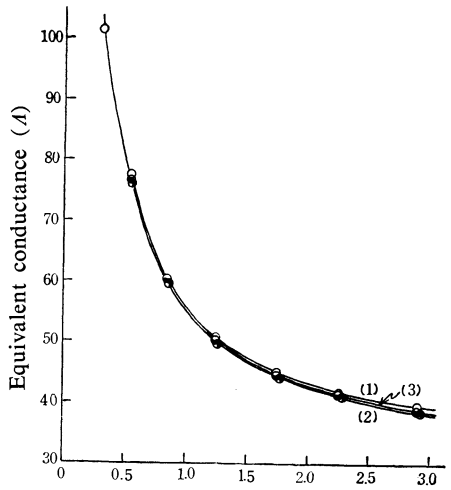

Fig. 6. The effect of saturation with dyes on the equivalent conductance of polysoap at 30°C.
(1) None (2) BAN
(3) *p*-Nitro-BAN: *o*-nitro-BAN and *m*-nitro-BAN are similar to curve 3.

To find out more about the nature of these effects, a study was also made of the electrical conductance of polysoap solutions containing solubilized dyes. Figure 5 illustrates the effect of saturation with dyes on the equivalent conductance, Λ, as a function of the polysoap concentration, where the values of Λ are based on the bromide-ion content of the polysoap. A similar figure for the monosoap is given in Fig. 6.

With the monosoap, the conductance is affected very little by solubilized dyes. With

10) A. F. H. Ward and A. G. Chitale, *Proc. 2nd Int. Cong. Surface Activity*, Vol. 1, 319 (1956).

the polysoap, contrary to expectation, each solubilized dye produces a small increase in conductance, but no significant difference among them could be found. This suggests that the locus of the solubilization of the dyes inside the polysoap molecule does not strongly affect the conductance. The finding also eliminates the possibility that the anomalous increase in viscosity with *p*-nitro-BAN is caused directly by the electrical charge effect.

Summary

The solubilization of several oil-soluble dyes, 1-benzeneazo-2-naphthol (BAN) and three 1-nitrobenzeneazo-2-naphthols (nitro-BAN), by a polysoap and a monosoap has been studied by measuring the solubilizing power, the viscosity and the electrical conductance of the solutions of both soaps.

The polysoap is a better solubilizer than the monosoap. BAN was more solubilized than nitro-BAN at any given concentration of soap. The amount of nitro-BAN solubilized by the polysoap was increased in the order *m*-nitro-BAN > *p*-nitro-BAN > *o*-nitro-BAN, while the solubilization by the monosoap was in the order *m*-nitro-BAN > *o*-nitro-BAN > *p*-nitro-BAN. However, there appears to be no simple interpretation of the effect of the structure of dyes upon the solubilization. The addition of the dyes to the polysoap solutions decreased the viscosity, except for that of *p*-nitro-BAN at low concentrations of polysoap. *p*-Nitro-BAN produced an anomalous increase in the viscosity, the reason for this being not certain. In the case of polysoap, every solubilized dye produced a small increase in electrical conductance, but no significant difference among them could be found.

The author wishes to express his deep thanks to Professor Toshizo Isemura of Osaka University for his kind advice. He also wishes to express his appreciation to Mr. Zenichi Miyagawa, Director of these Research Laboratories, for the permission to publish this paper, to Dr. Iwao Maruta for his advice, and to Miss Nobuko Kusui for her help in this work.

Research Laboratories
Kao Soap Co., Ltd.
Sumida-ku, Tokyo

*The Synthesis of Chelating Agents. II. The Synthesis of Aminoacetone-N,N-diacetic Acid and Its Chelating Behavior with Metal Ions**

By Takeshi ANDO

(Received June 7, 1963)

A great deal of work has been done in the preparation of iminodiacetic acid (IDA) derivatives. However, very little has been reported in the literature on the synthesis of derivatives which have a carbonyl group as an additional coordinating site. The only such compound related to the carbonyl derivative is *N*-acetoamidoiminodiacetic acid (*N*-AIDA), which has been reported on by Schwarzenbach and his co-workers.[1)]

This paper will report on the synthesis as well as on the chelating behavior of a new chelating agent, aminoacetone-*N*, *N*-diacetic acid (AADA), or 1-amino-2-propanone-*N*, *N*-diacetic acid, which is the first iminodiacetic acid derivative to have a keto group as an additional coordinating site. This compound was prepared by the condensation of monobromoacetone with an iminodiacetic acid dimethyl ester, followed by the hydrolysis of the resulting ester.

By comparing the chelating behavior of AADA with that of similar ligands which do not have an additional coordinating group, we have been able to obtain information on whether or not the aliphatic keto carbonyl group can coordinate to the metal ions of the first transition group or the alkaline earth group.

Schwarzenbach and his co-workers investigated the chelation behavior of various iminodiacetic acid derivatives which have different

* Contribution No. 48 from the Department of Organic Synthesis, Faculty of Engineering, Kyushu University.

1) G. Schwarzenbach, G. Anderegg, W. Schneider and H. Senn, *Helv. Chim. Acta*, **38**, 1147 (1955).

additional coordinating groups, they suggested that the coordinating site of the acetoamido group of *N*-AIDA was not the amino group but the carbonyl group.[1] In this connection, it is also of interest to compare the chelating behavior of AADA with that of *N*-AIDA in order to make certain whether or not the coordination of the acetoamido group of *N*-AIDA occurs exclusively of the carbonyl group.

The chelate stability measurements were therefore carried out, by the pH titration method, on solutions with 1 : 1 and 1 : 2 metal ligand ratios in order to determine the first and second stability constants. The metal ions chosen in this study were copper(II). nickel(II) lead(II), zinc(II), cadmium(II), cobalt(II), calcium(II), strontium(II) and magnesium(II).

The results of the stability constant measurements indicate that the chelating behavior of AADA is very similar to that of *N*-AIDA; it is proved that the coordination of the carbonyl group of AADA to metal ions is appreciable, and that the coordination site of the acetoamido group of *N*-AIDA is also the carbonyl group, as has previously been suggested by Schwarzenbach and his co-workers.[1]

Experimental

The Synthesis of AADA.—A solution of 30 g. (1.86 mol.) of an iminodiacetic acid dimethyl ester[2] in 30 ml. of ethylacetate was added dropwise with stirring to a solution of 13.1 g. (0.95 mol.) of monobromoacetone[3] in 90 ml. of ethylacetate, and the mixture was then kept at 60~70°C under reflux for 4hr. After the mixture had cooled, the resulting white crystals of iminodiacetic acid dimethyl ester hydrobromide were filtered off and repeatedly washed with 100 ml. of ethylacetate. About 21 g. of the hydrobromide was recovered.

The mixture of the filtrate and the washing reagent was concentrated to evaporate ethyl acetate under reduced pressure, the temperature of the solution being kept below 50°C. The residue, a pale yellow oil (24 g.), was a crude aminoacetonediacetic acid dimethyl ester containing a small amount of unreacted monobromoacetone. To a solution of this ester in 30 ml. of ethanol, 80 ml. of water and 33 g. of solid $Ba(OH)_2.8H_2O$ were added; the mixture was then refluxed on a boiling water bath for 2 hr. with occasional shaking. After the mixture had cooled, barium sulfate was precipitated by adding a theoretical amount of sulfuric acid. The precipitate was then filtered off with the aid of Celite and repeatedly washed with hot water.

The mixture of the filtrate and the washing reagent was concentrated to 30~40 ml. under reduced pressure, the temperature being kept below 60°C. To the concentrated solution, 200 ml. of ethanol was added, and the mixture was stored in a refrigerator overnight to complete the precipitation of the free acid of AADA; the crude product was then filtered off and recrystallized from 80% methanol five times. Yield, 12.5 g. (70%). Pure AADA consists of white, bulky crystals which decompose at 190~191°C.

Found: C, 44.44; H, 5.86; N, 7.37, 7.29. Calcd. for $C_7H_{11}NO_5$: C, 44.25; H,6.05; N, 7.41%.

AADA is very soluble in water, soluble in boiling methanol and acetone, very slightly soluble in boiling ethanol, and insoluble in benzene and ether. The solid sample is sensitive to acid or alkaline vapor, and it must be stored in a tightly closed container. The aqueous solution gradually decomposes and rapidly turns yellow at a high temperature. The decomposition is also accerelated by an acid or base.

Measurement.—The experimental method and the conditions in this study are similar to those described in a previous paper.[4] A Hitachi-Horiba Model P pH meter equipped with extension glass and calomel electrodes was used to measure the hydrogen ion concentration. The temperature of the titration solutions was kept at 25.0±0.1°C, while the ionic strength was maintained at approximately 0.10 M with potassium nitrate.

The concentration of the ligand for the determination of the acid dissociation constants was about 0.001~0.002 M. For the titration of solutions of 1 : 1 metal ligand ratio, the initial concentrations were about 0.001M of each component. For the 1 : 2 solutions, the concentrations of metal ions and ligand were about 0.001 M and 0.002 M respectively.

Calculations

The equilibrium constants described in this paper may be summarized as follows:

$$pk_1 = -\log\frac{(HA^-)(H^+)}{(H_2A)}$$

$$pk_2 = -\log\frac{(A^{2-})(H^+)}{(HA^-)}$$

$$K_{MA} = \frac{(MA)}{(M^{2+})(A^{2-})}$$

$$K_{MA_2} = \frac{(MA_2{}^{2-})}{(MA)(A^{2-})}$$

The acid dissociation constants were obtained by a direct algebraic method described previously,[4] and the results were checked by a modified Bjerrum method.[5]

The 1 : 1 metal chelate titration curves were used for the calculation of the first stability constants by means of the algebraic method reported on in a previous paper.[4]

2) J. V. Dubsky, *Ber.*, **50**, 1694 (1917).
3) P. A. Levene, "Organic Syntheses," Coll. Vol. II, 88 (1948).
4) T. Ando, This Bulletin, **35**, 1395 (1962).
5) S. Chaberek, Jr., and A. E. Martell, *J. Am. Chem. Soc.*, **74**, 5052 (1952).

The data obtained from the 1 : 2 curves for heavy metals were utilized as a basis for the calculation of their first and second chelate stability constants according to the modified Bjerrum method which has been described in detail by Chaberek and Martell.[5] The final equation which was employed in this paper is:

$$\bar{n}=\frac{1}{C_M}\left[C_A-\left(\frac{(H^+)^2}{k_1\cdot k_2}+\frac{(H^+)}{k_2}+1\right)(A^{2-})\right]$$

where

$$(A^{2-})=\frac{(2-a)C_A-(H^+)+(OH^-)}{2(H^+)^2/k_1\cdot k_2+(H^+)/k_2}$$

where C_A and C_M are the total concentrations of ligand and metal ion species respectively, and where a is the number of moles of sodium hydroxide added per mole of ligand.

However, the exact values of the constants were obtained by the successive approximation procedure developed by Carlson, McReynolds and Verhoek.[6]

Results and Discussion

Titration Curves. — The corrected potentiometric titration curves for AADA with or without an equivalent amount of metal ions are given in Fig. 1. The curve for the free acid is similar in shape to those of IDA and its homologues, but the inflection at one equivalent of the base which corresponds to the formation of the monosodium salt is considerably weaker than those of IDA and its homologues.

During the titration of the solutions with a 1 : 1 metal ligand ratio, a little pH fluctuation was found in the vicinity of $a=1.8$ for cadmium and cobalt, and in the vicinity of $a=2.0$ for copper, nickel and lead, but no fluctuation was observed in the case of zinc and other metal ions. It is interesting to note on these curves that zinc and cadmium form more stable chelates with AADA than does cobalt in the low pH region. This chelating behavior is rather similar to that of 2-hydroxyethyliminodiacetic acid (2-HIDA) and *N*-AIDA, but it is different from that of IDA and *N*-methyliminodiacetic acid (MIDA).

The titration curves for the solutions with a 1 : 2 metal ligand ratio are illustrated in Fig. 2. The curves for alkaline earth metals were not observed, because it is not likely that they form any stable 1 : 2 chelate with this ligand. A similar chelating tendency for zinc and for cadmium was also observed in this case, and a fluctuation of pH was experienced in the case of cadmium and cobalt in the pH region above 7. The curve for zinc apparently shows a considerably strong inflection at three moles of base per mole of metal ion. This indicates that the formation of 1 : 1 and of 1 : 2 chelates occurs in separate pH regions. This two-step reaction may be expressed as follows:

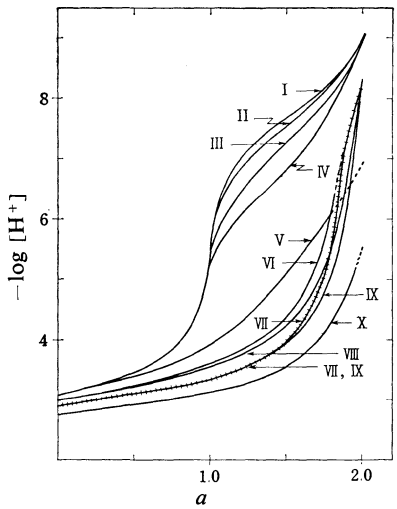

Fig. 1. Titration curves for 1 : 1 solution with 0.1 N NaOH. Concentration of ligand and metal ions……1×10^{-3} M. I, ligand; II, Mg(II); III, Sr(II); IV, Ca(II); V, Co(II); VI, Cd(II); VII, Pb(II); VIII, Zn(II), IX, Ni(II); X, Cu(II). a denotes moles of base added per mole of ligand.

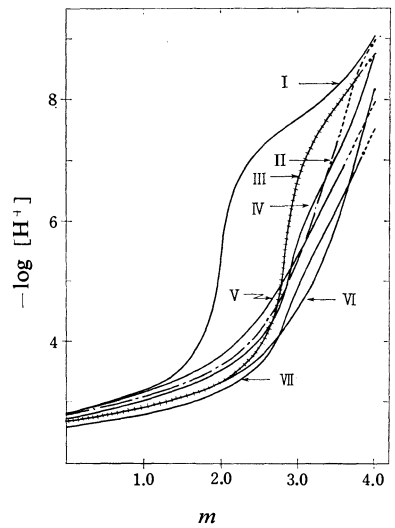

Fig. 2. Titration curves for 1 : 2 solution with 0.1 N NaOH. Concentration of ligand……2×10^{-3} M, metal ion……1×10^{-3} M. I, ligand; II, Cd(II); III, Pb(II); IV, Zn(II); V, Co(II); VI, Ni(II); VII, Cu(II). m denotes moles of base added per mole of metal ion.

6) G. A. Carlson, J. P. McReynolds and F. H. Verhoek, ibid., **67**, 1334 (1945).

the formation of 1:1 chelate in the lower pH region:

$$H_2A + M^{2+} + 2OH^- \rightarrow MA + 2H_2O$$

$$H_2A + OH^- \rightarrow HA^- + H_2O$$

the formation of 1:2 chelate in the higher pH region:

$$MA + HA^- + OH^- \rightarrow MA_2^{2-} + H_2O$$

A similar inflection was also observed on the curves for copper and cobalt, although it is much weaker.

The curve for lead is so unusual that no decisive interpretation can be made. However, the curve indicates that AADA forms a considerably stable 1:1 chelate with lead in the low pH region, and that the chelate changes into a hydroxo-complex or a polynuclear complex in the higher pH region.

Formation Functions.—The Bjerrum formation functions for certain metal chelates of AADA are given in Fig. 3. In the case of

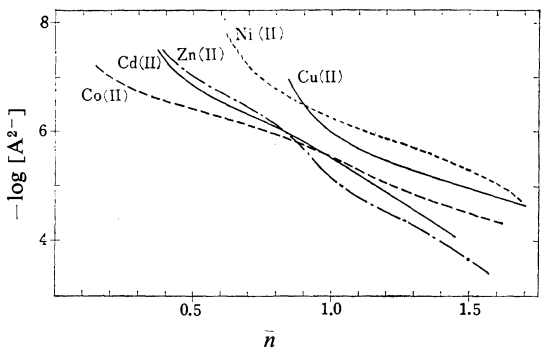

Fig. 3. Formation functions of some divalent metal chelates of AADA. Concentration of ligand……2×10^{-3}, metal ion……1×10^{-3} M; $t=25°C$; $\mu=0.1$ (KNO_3).

copper and nickel, the Bjerrum method could not be employed for the determination of K_{MA} because the values for $-\log(A^{2-})$ were not available at $\bar{n}=0.5$. It was also impossible to determine directly the K_{MA_2} for cadmium from the $-\log(A^{2-})$ value at $\bar{n}=1.5$, for some precipitation occurred in this region. However, K_{MA} at $\bar{n}=0.5$ for nickel was conveniently calculated from the known values of $K_{MA}\cdot K_{MA_2}$ at $\bar{n}=1.0$ and K_{MA_2} at $\bar{n}=1.5$, and the value of K_{MA_2} at $\bar{n}=1.5$ for cadmium, were similarly derived from the values of $K_{MA}\cdot K_{MA_2}$ at $\bar{n}=1.0$ and K_{MA} at $\bar{n}=0.5$.

The formation curve for lead was found to be so unusual that the chelating behavior of AADA for lead was thought to be quite different from that of the other IDA derivatives.

Equilibrium Constants.—The acid dissociation and chelate stability constants of AADA are listed in Table I, along with the corresponding values of some IDA derivatives.

The values of the acid dissociation constants determined by the algebraic method agree reasonably well with those obtained by the modified Bjerrum method. The pk_2 value of AADA indicates that the substitution for a methyl group or hydrogen by a acetyl group apparently results in a marked decrease in the basicity of the imino nitrogen. The same effect was also observed with *N*-AIDA.

The chelate stability constants calculated by these two methods agree well within the range of experimental error for nickel, zinc and cadmium. However, in the case of cobalt, the K_{MA} value obtained by the algebraic method may be erroneous, for the overlapping of 1:1 and 1:2 chelate formation in the 1:1 titration curve is disregarded in the derivation of the stability constant. Therefore, the agreement of the two values for cobalt is not very good.

The K_{MA} values for lead which were calculated from the data of the titration curve in the range of $a=1.1\sim1.7$ did not agree well. Only if the data from the narrower range of $a=0.8\sim1.1$ were chosen were fairly consistent values obtained; their mean values are listed in the table for lead chelate. Therefore, this value may not be accurate enough. The determination of K_{MA_2} for lead by the Bjerrum method was unsuccessful, as has been described before. Above a pH of about 3.5, the reaction of AADA with lead seems to be very complicated; a further investigation will be necessary to analyse the titration curves.

The errors of these stability constants are ±0.1 of log unit. Therefore, the value of two decimal places in the constant means nothing for the below discussion.

The Effect of the Carbonyl Group on the Chelate Stability.—If the carbonyl group is involved in the coordination of AADA to metal ions, it will behave as a quadridentate ligand. Thus, for the metal ions with the coordination number of 4, AADA will form a stable 1:1 chelate; the formation of 1:2 chelate will be more difficult than in the case of such tridentate ligands as IDA or MIDA. This will result in a larger difference between $\log K_{MA}$ and $\log K_{MA_2}$. For the metal ions with the coordination number of 6, the situation will also be the same, although the difference between $\log K_{MA}$ and $\log K_{MA_2}$ is smaller than in the former case. The values of the difference for some metal chelates are also shown in Table I. It may be seen from the table that the tendency of AADA to form a 1:2 chelate from a 1:1 chelate is less marked for zinc and cadmium than for nickel and cobalt. This

TABLE I. ACID DISSOCIATION CONSTANTS OF IDA AND THE DERIVATIVES AND STABILITY CONSTANTS OF THEIR CHELATES (μ=0.10; KNO_3)

Ligand	Acid dissociation constant		Stability constant								
			Cu(II)	Pb(II)	Ni(II)	Zn(II)	Cd(II)	Co(II)	Ca(II)	Sr(II)	Mg(II)
AADA (t=25°C) 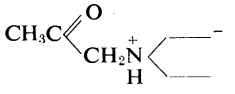	pk_1 2.62	log K_{MA}*1	(9.0_5)	(7.7_0)	7.7_4	6.9_6	6.9_2	6.1_7	4.0_8	3.6_2	2.7_2
		log K_{MA}*2			7.3_2	7.0_1	6.8_4	6.4_0			
	pk_2 7.71	log K_{MA_2}	4.9_4		5.2_9	3.6_4	4.1_2	4.5_2			
		Δ log K_D*3	(4.1_1)		2.0_3	3.3_7	2.7_2	1.8_8			
MIDA (t=20°C) 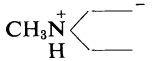 1)	pk_1 2.12	log K_{MA}	10.09		8.37	7.66	6.77	7.62	3.75	2.85	3.44
		log K_{MA_2}	6.83		7.22	6.43	5.75	6.29			
	pk_2 9.65	Δ log K_D*3	3.26		1.15	1.23	1.02	1.33			
IDA (t=30°C) 5),7),8)	pk_1 2.54	log K_{MA}	10.55		8.30	7.02	5.30	7.01	2.59*4		2.94*4
		log K_{MA_2}	5.65		6.35	5.14	4.18	5.34			
	pk_2 9.12	Δ log K_D*3	4.90		1.95	1.88	1.12	1.67			
***N*-AIDA** (t=20°C) 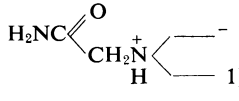 1)	pk_1 2.3	log K_{MA}	9.68	8.40	8.02	7.30	7.08	6.91	3.96	3.03	2.47
		log K_{MA_2}	3.26	2.24	3.88	2.24	3.60	3.30			
	pk_2 6.60	Δ log K_D*3	6.42		4.14	5.06	3.48	3.61			

*1 log K_{MA} obtained by algebraic method. *2 log K_{MA} obtained by Bjerrum method. *3 Δ log K_D=log K_{MA}−log K_{MA_2} *4 Determined at 20°C

7) G. Schwarzenbach, A. Willi and R. O. Bach, *Helv. Chim. Acta*, **30**, 1303 (1945).

8) H. Senn and G. Schwarzenbach, unpublished results (cited from; S. Chaberek and A. E. Martell, "Sequestering Agents," John Wiley & Sons, Inc., New York, (1959) p. 552).

can be understood if one remembers that zinc and cadmium have a coordination number of 4 of tetrahedral configuration, while nickel and cobalt have a coordination number of 6 for a octahedral configuration. A somewhat similar tendency is observed in *N*-AIDA, which is also believed to be a quadridentate ligand for the above-mentioned metal ions, while tridentate ligands such as IDA and MIDA show an ease of 1 : 2 chelate formation.

As has been discussed above, it is quite probable that the carbonyl group is involved in the coordination of AADA to metal ions. If this is the case, this will result in an increase of 1 : 1 chelate stability in comparison with those similar ligands which have no additional coordinating group. In order to examine such an additional stability for the various *N*-substituted IDA derivatives, Schwarzenbach and his co-workers have employed the linear correlation method.[1] According to this method, an increase in the stability which is due to the additional coordinating group is estimated as a difference between the stabilities of the new ligand and of a hypothetical ligand which has no additional coordinating group but which does have the same basicity of imino nitrogen as the new ligand. This comparison can be made by drawing a correlation line of $\log K_{MA}$ versus pk_2 for a series of *N*-alkyl substituted iminodiacetic acids, such correlation lines for selected metal ions are shown in Fig. 4. These lines were drawn using the data from the Schwarzenbach's paper.[1] If the stability of the new ligand increases upon the introduction of an additional coordinating group, the plot of $\log K_{MA}$ versus pK_2 for such a ligand must be above the correlation line; the degree of deviation from the line is a measure of the additional stability due to the additional coordinating group. The increased stabilities of AADA measured by this method, which is expressed as $\Delta \log K_T$, are graphically shown in Fig. 5, along with those of some related IDA derivatives.

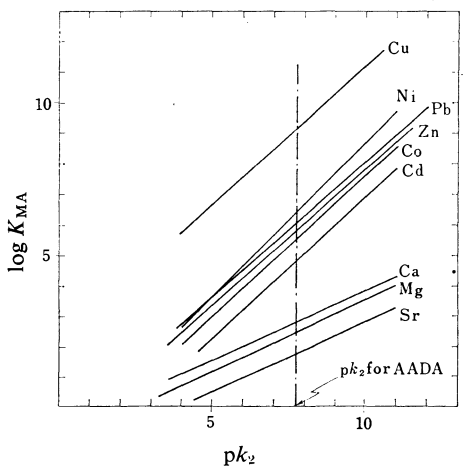

Fig. 4. Correlation lines for the selected metal ions.

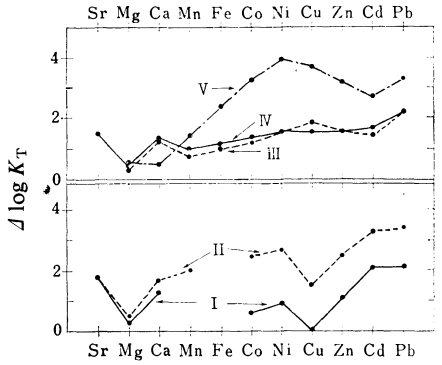

Fig. 5. Increased stability ($\Delta \log K_T$) due to an additional coordinating site.

Ligand : $R-\overset{+}{N}H\begin{cases}CH_2COOH\\CH_2COO^-\end{cases}$

	R
I,	$CH_3-CO-CH_2-$
II,	$H_2N-CO-CH_2-$
III,	$CH_3-O-CH_2CH_2-$
IV,	$HO-CH_2CH_2-$
V,	$H_2N-CH_2CH_2-$

As is clear from curve I of Fig. 5, the contribution of the carbonyl coordination in AADA is appreciable, with the exceptions of magnesium and copper. The chelating tendency of AADA is also found to be very similar to that of *N*-AIDA (curve II); such a resemblance would indicate that the coordination of the acetoamido group of *N*-AIDA occurs exclusively through the carbonyl oxygen, as has previously been suggested by Schwarzenbach. It is interesting to note that, with the exception of copper, the chelating tendencies of AADA and *N*-AIDA are somewhat similar to those of the *N*-hydroxyethyl and *N*-methoxyethyl derivatives of IDA (curves IV and III respectively), both of which have coordinating oxygen. However, they are quite different from that of aminoethyliminodiacetic acid (curve V), which has amino nitrogen as an additional coordinating site.

In the case of copper, no increase in stability is observed at all, probably because the square planar configuration of copper ion is not favorable for the coordination of the carbonyl oxygen of AADA.

It may also be seen from Fig. 4 that the degree of contribution of the carbonyl coordination to the 1 : 1 chelate stability is greater

in *N*-AIDA than in AADA. This indicates that the basicity of the carbonyl oxygen in the acid amide group is stronger than in the aliphatic keto group, this situation being consistent with the result from the electronic theory of organic molecules.

Summary

1) Aminoacetone-*N*, *N*-diacetic acid or 1-amino-2-propanone-*N*, *N*-diacetic acid has been synthesized. This is the first iminodiacetic acid derivative to have a keto group as an additional coordinating site.

2) The acid dissociation constant and the chelate stability constants of this ligand have been determined by the pH titration method, at 25°C and 0.10 M ionic strength, for such metal ions as copper(II), lead(II), nickel(II), zinc(II), cadmium(II), cobalt(II), calcium(II), strontium(II) and magnesium(II).

3) It has been proved that the coordination of the carbonyl oxygen of this ligand to metal ions is appreciable, and the increase in the chelate stability has been explained by the contribution of the carbonyl coordination.

The author is grateful to Professor Keihei Ueno for his guidance during the course of this investigation. He also wishes to thank Mr. M. Shido, Mrs. S. Shido and Miss T. Tahara for performing the elemental analysis. Finally, this work was supported in part by a scientific research grant of the Ministry of Education, to which the author's thanks are due.

Department of Organic Synthesis
Faculty of Engineering
Kyushu University
Hakozaki, Fukuoka

Amperometric Determinations of Metals with Chloramine T

By G. S. DESHMUKH and M. C. ESHWAR*

(Received June 12, 1963)

Erdey and co-workers[1] reported the application of ascorbic acid for direct and indirect determination of vanadium(V) using variamine blue as indicator. An ascorbimetric method[2] was also investigated by Erdey for the determination of cerium(IV) and chromium(VI). Various workers[3-5] found the reduction of pentavalent vanadium by arsenous oxide as too slow, and the reaction was therefore catalysed by iodide :[5] Analytical determination of Ce^{4+} was carried out with arsenous oxide using osmium tetroxide or iodine monochloride as catalyst and ferroin as indicator. Lang[8] studied the reduction of chromic acid with H_3AsO_3. Various workers[9-11] investigated the reduction of vanadium(V) to vanadium(IV) by hydrazine in sulfuric acid. Bray[11] and Cuy discarded the reaction for analytical determination, due to the occurrence of a partial side reaction resulting in the formation of ammonia and hydrazoic acid. Kolthoff[12] inferred that the oxidation of hydrazine proceeds smoothly to nitrogen and water in presence of sufficient concentration of hydrochloric acid. Benrath and Ruland[13] studied the oxidation of hydrazine by ceric sulfate. A review of the literature however, revealed that the reduction of Cr^{6+} with hydrazine has not been attempted.

Earlier results from these laboratories reported the utility of chloramine T in the oxidation of ascorbic acid,[14] arsenious oxide[16] and hydrazine sulfate[15] amperometrically at the rotating platinum wire micro-electrode. Following this, an investigation on the possibility of reducing V^{5+}, Ce^{4+} and Cr^{6+} by the

* Present address: Planning & Development Division, Fertiliser Corporation of India Ltd., Sindri.

1) L. Erdey, E. Bodor and I. Buzas, *Acta. Chim. Acad. Sci. Hung.*, **7**, 227 (1955).
2) L. Erdey, *Magyar. Kém. Folyóirat.*, **56**, 262 (1950).
3) E. Bobtelsky and A. Glasner, *J. Am. Chem. Soc.*, **64**, 1462 (1942).
4) E. Zintl and P. Zaimis, *Z. angew. Chem.*, **40**, 1286 (1927); cf., *Z. anal. Chem.*, **76**, 55 (1929).
5) G. Gaudefroy, *Compt. rend.*, **234**, 1171 (1952).
6) K. Gleu, *Z. anal. Chem.*, **95**, 305 (1933).
7) H. H. Willard and P. Young, *J. Am. Chem. Soc.*, **55**, 3260 (1933).
8) R. Lang, *Z. anorg. u. allgem. Chem.*, **152**, 197 (1926).
9) K. A. Hofmann and F. Küspert, *Ber.*, **31**, 64 (1897).
10) A. W. Browne and F. F. Shetterley, *J. Am. Chem. Soc.*, **29**, 1305 (1907).
11) W. C. Bray and E. J. Cuy, ibid., **46**, 858 (1924).
12) I. M. Kolthoff, ibid., **46**, 2009 (1924).
13) A. Benrath and K. Ruland, *Z. anorg. u. allgem. Chem.*, **114**, 267 (1920).
14) G. S. Deshmukh and M. C. Eshwar, *J. Sci. Ind. Res. (Ind.)*, **19B**, 502 (1960).
15) G. S. Deshmukh and M. C. Eshwar, *Ann. Chim., Rome*, communicated.
16) G. S. Deshmukh, M. C. Eshwar and M. S. V. Rao, *Chemist-Analyst.*, **51**, 70 (1962).

above reductants, and titrating the excess reductant with chloramine T was taken up.

Experimental

Reagents and Apparatus. — Stock solution of vanadium(V) was prepared by dissolving an accurately weighed amount of vanadium pentoxide (E. Merck) in sodium carbonate (AnalaR) and the solution was made slightly acidic with hydrochloric acid. The vanadium content of this solution was checked by the method of Willard and Young.[17] Ceric sulfate solution was obtained by the usual method and the strength of this solution was determined with a standard solution of ferrous ammonium sulfate. A decinormal solution of potassium dichromate was prepared from a pure E. Merck (G. R.) sample. Approximately decinormal solutions of ascorbic acid and hydrazine sulfate were obtained from pure samples, while that of arsenious oxide was prepared as suggested by Pierce and Haenisch[18] and standardised amperometrically with chloramine T.[14-16]

A solution of chloramine T, approximately N/10, was prepared from a pure sample and standardised iodometrically with sodium thiosulfate. Iodine monochloride solution was 0.005 M. A sodium citrate-citric acid buffer (pH ~5.8), prepared by mixing 3 vol. of 0.5 M sodium citrate, 1 vol. of 0.5 M citric acid and 1 vol. of water, was used to control the pH of the reaction mixture. A simple form of amperometric unit, with an impressed potential of +0.3 volt vs. S. C. E., was used.

Determination of Vanadium

The reduction of V^{5+} to V^{4+} with hydrazine sulfate was found to be smooth, resulting in the formation of nitrogen and water. The possibility of the side reaction reported[10,11] was overcome by using hydrochloric acid instead of sulfuric acid, for acidifying the vanadium solution. Ascorbic acid also was found to reduce V^{5+} to V^{4+} quantitatively, with the formation of dehydroascorbic acid and water. In strongly acidic solutions, the reduction of vanadium(V) by arsenous oxide required more than 24 hr. for completion. However, iodine monochloride was found to catalyse the reaction, and it was also observed that the reaction was accelerated with an increase in the concentration of the catalyst. It was seen that the reaction required 10~15 min. for completion, when 1.0 ml. of iodine monochloride (0.005 M) was added. Accordingly, all the experiments with arsenous oxide were carried out using 1.0 ml. iodine monochloride as catalyst. For titration of excess hydrazine sulfate, 0.25 ml. of iodine monochloride was added as catalyst. The amount of iodine monochloride added to catalyse the reduction of vanadate by arsenous oxide, also served for titration of excess arsenous oxide. The reduction is found to be quantitative with each reductant under the above operating conditions according to:

$$2VO_3^- + C_6H_8O_6 + 6H^+ \rightarrow 2VO^{2+} + C_6H_6O_6 + 4H_2O \quad (1)$$

$$4VO_3^- + As_2O_3 + 12H^+ \rightarrow 4VO^{2+} + As_2O_5 + 6H_2O \quad (2)$$

$$4VO_3^- + N_2H_4 + 12H^+ \rightarrow 4VO^{2+} + N_2 + 8H_2O \quad (3)$$

Hence, 1.0 ml. of $NC_6H_8O_6$, or NAs_2O_3, or $NN_2H_4 \cdot H_2SO_4$ $\equiv$ 0.05094 g. of vanadium

Determination of Cerium

Tetravalent cerium was reduced quantitatively to trivalent state by ascorbic acid with the formation of dehydroascorbic acid and water, whereas the reduction with arsenous oxide was rather slow. The latter reaction was found to be accelerated by the addition of 0.25 ml. (5 drops) of iodine monochloride (0.005 M), which also served for titration of excess arsenous oxide with chloramine T. The procedure with hydrazine under similar conditions presented certain difficulties, detrimental to its utility as an analytical tool and could not therefore be pursued at the present stage. Ascorbic acid and arsenious oxide were, however, suitable for the quantitative determination of cerium.

$$2Ce(SO_4)_2 + C_6H_8O_6 \rightarrow Ce_2(SO_4)_3 + C_6H_6O_6 + H_2SO_4 \quad (4)$$

$$4Ce(SO_4)_2 + As_2O_3 + 2H_2O \rightarrow 2Ce_2(SO_4)_3 + As_2O_5 + H_2SO_4 \quad (5)$$

Hence, 1.0 ml. of $NC_6H_8O_6$, or NAs_2O_3 $\equiv$ 0.1401 g. of cerium

Determination of Chromium

Reduction of Cr^{6+} to Cr^{3+} was complete with all the three reductants viz., ascorbic acid, arsenous oxide and hydrazine sulfate. The reaction products presumably are dehydroascorbic acid, arsenic pentoxide and nitrogen respectively. Whereas the titration of excess ascorbic acid was carried out in presence of citrate buffer only, that of excess arsenite and

17) H. H. Willard and P. Young, *Ind. Eng. Chem., Anal. Ed.*, 6, 48 (1934).
18) W. C. Pierce and E. L. Haenisch, "Quantitative Analysis," John Wiley & Sons, Inc., New York (1948), p. 242.

Table I. Determination of vanadium

With $C_6H_8O_6$ Amount of V			With As_2O_3 Amount of V			With $N_2H_4 \cdot H_2SO_4$ Amount of V		
Taken mg.	Found mg.	Error %	Taken mg.	Found mg.	Error %	Taken mg.	Found mg.	Error %
5.266	5.257	−0.17	5.098	5.126	+0.55	2.463	2.477	+0.57
3.949	3.944	−0.13	4.078	4.093	+0.37	2.155	2.138	−0.79
2.633	2.646	+0.49	3.059	3.068	+0.29	1.847	1.842	−0.27
1.975	1.955	−1.01	2.549	2.565	+0.63	1.478	1.489	+0.74
1.317	1.313	−0.30	2.039	2.053	+0.69	1.232	1.217	−1.22
1.054	1.055	+0.095	1.529	1.527	−0.13	1.109	1.119	+0.90

Table II. Determination of cerium

With $C_6H_8O_6$ Amount of Ce			With As_2O_3 Amount of Ce		
Taken mg.	Found mg.	Error %	Taken mg.	Found mg.	Error %
34.34	34.24	−0.29	17.17	17.14	−0.17
25.75	25.80	+0.19	12.88	12.88	Nil
17.17	17.10	−0.41	8.586	8.634	+0.56
12.87	12.83	−0.31	6.869	6.889	+0.29
8.584	8.592	+0.093	6.010	5.984	−0.43
6.868	6.926	+0.84	5.152	5.182	+0.58

Table III. Determination of chromium

With $C_6H_8O_6$ Amount of Cr			With As_2O_3 Amount of Cr			With $N_2H_4 \cdot H_2SO_4$ Amount of Cr		
Taken mg.	Found mg.	Error %	Taken mg.	Found mg.	Error %	Taken mg.	Found mg.	Error %
3.472	3.447	−0.72	3.472	3.485	+0.37	3.472	3.477	+0.14
2.604	2.622	+0.69	2.604	2.575	−1.11	2.604	2.610	+0.23
1.736	1.711	−1.44	1.736	1.738	+0.11	1.736	1.741	+0.29
1.519	1.526	+0.46	1.302	1.296	−0.46	1.302	1.304	+0.15
1.302	1.295	−0.54	1.040	1.037	−0.29	1.128	1.125	−0.27
1.042	1.054	+1.15	0.8680	0.8638	−0.48	0.9548	0.9468	−0.83

hydrazine required iodine monochloride to catalyse the oxidation. The quantitative reduction proceeds as follows:

$$K_2Cr_2O_7 + 3C_6H_8O_6 \rightarrow 2KCrO_2 + 3C_6H_6O_6 + 3H_2O \quad (6)$$

$$2K_2Cr_2O_7 + 3As_2O_3 \rightarrow 4KCrO_2 + 3As_2O_5 \quad (7)$$

$$2K_2Cr_2O_7 + 3N_2H_4 \rightarrow 4KCrO_2 + 3N_2 + 6H_2O \quad (8)$$

Hence, 1.0 ml. of $NC_6H_8O_6$, or NAs_2O_3, or $NN_2H_4 \cdot H_2SO_4$ $\equiv$ 0.01734 g. of chromium

Procedure.—An aliquot of VO_3^-, Ce^{4+} or $Cr_2O_7^{2-}$ solution was taken in a 150 ml. Pyrex beaker, to which an appropriate quantity of the reductant viz., ascorbic acid, arsenous oxide and hydrazine sulfate was added. One milliliter of iodine monochloride (0.005 M) was added for accelerating vanadium(V)-arsenic(III) reaction, and 0.25 ml. for that of cerium(IV)-arsenic(III) reaction. For titration of excess arsenous oxide in $Cr_2O_7^{2-}$ determination and of excess hydrazine sulfate (in VO_3^-, $Cr_2O_7^{2-}$ determinations), 0.25 ml. (5 drops) of iodine monochloride was added as catalyst. In each case, 10~15 ml. of sodium citrate-citric acid buffer (pH ~5.8) was introduced to maintain an overall pH of 4.3~4.9. The contents were diluted approximately to 50 ml. and titrated amperometrically with chloramine T at a potential of +0.3 volt vs. S. C. E.

Observations are returned in 3 short tables.

Summary

An indirect procedure for the determination of V^{5+}, Ce^{4+} and Cr^{6+} is given. Three reductants, viz., ascorbic acid, arsenous oxide and hydrazine have been employed for reduction of each oxidant. Iodine monochloride

has been used as catalyst in the reduction of V^{5+} and Ce^{4+} by arsenous oxide. Reduction of Ce^{4+} with hydrazine presented certain difficulties and is not pursued at the present stage. The excess reductant in each case is determined amperometrically with chloramine T at the rotating platinum wire micro-electrode, and an impressed potential of +0.3 volt vs. S.C.E. The titrations are performed at a pH of 4.3~4.9, using citrate-citric acid buffer. For titration of excess arsenous oxide and $N_2H_4 \cdot H_2SO_4$, 0.25 ml. of iodine monochloride (0.005 M) has been employed as catalyst. The procedure, which is rapid and accurate, has been employed for determination of amounts up to 1.05 mg. vanadium, 5 mg. cerium and 0.86 mg. chromium.

Authors' thanks are due to Professor G. B. Singh for facilities and to the Ministry of Scientific Research & Cultural Affairs, Government of India, for the award of a scholarship to one of us (M.C.E).

Division of Analytical Chemistry
Banaras Hindu University
Banaras, India

*Studies on Mixture Dyeing. II. The Kinetics of a Mixture of Chrysophenine G and Sirius Red 4B**

By Minoru SEKIDO and Zenzo MORITA

(Received June 14, 1963)

In the previous paper,[1] the mixture dyeing whose dyebath contained an equimolar mixture solution of Benzopurpurine 4B and Sky Blue 6B was kinetically investigated. There was a great difference in surface concentration between the two dyes owing to the great difference in affinity between them. Therefore, because of the sharp gradient of the concentration of Benzopurpurine 4B the interaction between the two dyes in the substrate, especially the effect of the blue dye on the diffusion of the red dye, could not be estimated quantitatively.

In this paper, the mixture dyeing of Chrysophenine G (C. I. Direct Yellow 12) and Sirius Red 4B (C. I. Direct Red 81), which are very similar to each other in dyeing property, has been studied; the single dyeings of these dyes have also been carried out in order to discuss quantitatively their behavior in the mixture dyeing.

First, the equilibrium adsorption from the single and mixture dyebath was investigated. Then, on the basis of the obtained results, the dyeing conditions for kinetic study were determined.

In order to estimate the effect of the yellow dye on the diffusion of the red dye, the surface concentration of the former dye was gradually increased at a constant surface concentration of the latter dye, and vice versa; diffusion experiments were then carried out. When both dyes had equal surface concentrations, the kinetics of mixture dyeing has been investigated. The temperature effect of mixture dyeing has also been studied.

Experimental

Materials.—A cellophane sheet made by the Tokyo Cellophane Co., Ltd., was used as the dyeing substrate. It was scoured with distilled water and conditioned in a desiccator with 50% sulfuric acid.

Purified dyes were used throughout. They were prepared from commercial dyes (Kayaku Chrysophenine GX (KYK) and Suprazo Red 4B (MDW)) by the method of Robinson and Mills.[2] The absence of colored impurities was verified by paper chromatography.

Equilibrium Dyeing.—The dyeings were carried out following the method of Horiki et al.[3] Pieces of the sample, weighing from 25 to 35 mg., were dyed in 200 ml. of dyeing liquor at 90, 85 and 80°C. The dyeing duration was one day (90°C) or two days (85 and 80°C). In the case of the single dyeing, the dye concentrations of the equilibrium dyebath were as shown in Figs. 1 and 2. Those of the mixture dyeing shown in Tables III, IV and V, were determined by a large number of preliminary experiments. After dyeing, the pieces of the sample

* Presented at the 15th Annual Meeting of the Chemical Society of Japan, Kyoto, April, 1962.

1) Part I: M. Sekido and Z. Morita, This Bulletin, **35**, 1375 (1962).

2) C. Robinson and H. A. T. Mills, *Proc. Roy. Soc.*, **A131**, 576 (1931).

3) Y. Horiki, Y. Tanizaki and N. Ando, This Bulletin, **33**, 163 (1960).

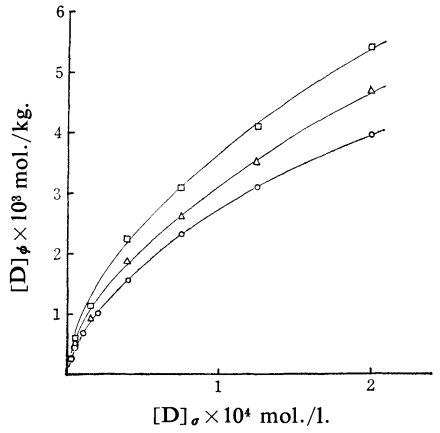

Fig. 1. Adsorption isotherms of Chrysophenine G.

NaCl: 3.0×10^{-2} mol./l.
—○— 90°C, —△— 85°C, —□— 80°C

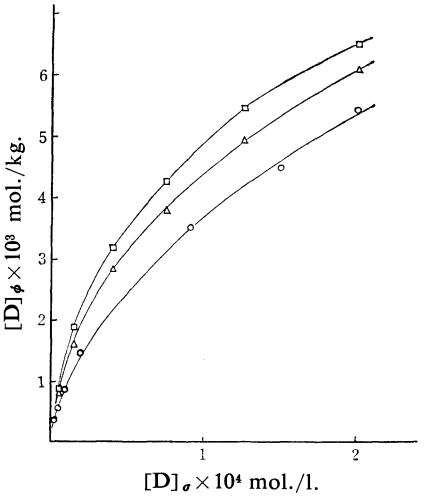

Fig. 2. Adsorption isotherms of Sirius Red 4B.

NaCl: 3.0×10^{-2} mol./l.
—○— 90°C, —△— 85°C, —□— 80°C

were quickly rinsed in a dilute sodium chloride aqueous solution, dried, and stripped in 25% aqueous pyridine. The strippings were analyzed by determining the optical densities at the wavelength of maximum absorption for each component by the use of a Hitachi EPB-V type spectrophotometer (405 and 520 mμ). The absorption spectra of the mixture dye in an aqueous pyridine solution were found to be additive. The concentration of sodium chloride was 0.03 mol./l. for every dyebath.

Diffusion.—The experimental methods were similar to those reported before.[1] The dyeing times were 500 min. (90°C), 750 min. (85°C) or 1000 min. (80°C). The dyeing condition, namely, the concentrations in the mixture dyeing, were determined by the results of the equilibrium adsorption.

Theoretical*

Dyeing Equilibrium.—The adsorption isotherms are obtained from the equilibrium dyeing measurements. According to Vickerstaff,[4] the isotherms are also derived from the theoretical considerations for any particular dyebath and substrate system. The standard affinity of direct dye anions for the substrate, $\Delta\mu^0$ (kcal./mol.), can be calculated by

$$-\Delta\mu^0 = RT\ln\frac{[D]_\phi [Na]_\phi{}^z}{V^{z+1}} - RT\ln[D]_\sigma [Na]_\sigma{}^z \quad (1)$$

$$[Na]_\phi = [D]_\phi\left\{\frac{z}{2}+\left(\frac{z^2}{4}+\frac{V^2[Na]_\sigma[Cl]_\sigma}{[D]_\phi{}^2}\right)^{1/2}\right\} \quad (2)$$

where $[D]_\phi$ (mol./kg.) denotes the concentration of adsorbed dye anions in the substrate at equilibrium; $[Na]_\phi$ (mol./kg.), the concentration of the sodium ions in the substrate at equilibrium; $[Na]_\sigma$ and $[Cl]_\sigma$ (mol./l.), the concentrations of the sodium and the chloride ions in the dyebath at equilibrium; z, the valency of the dye anions; R, the gas constant; T, the absolute temperature, and V (l./kg.), the internal volume of the substrate. In this case, the volume term was taken to be 0.45.

Kinetics.—The theory of diffusion has been reported on before.[1] The distribution of Chrysophenine G and Sirius Red 4B in the substrate in the mixture dyeing, as shown in Results and Discussion, is similar in shape to that in the single dyeing. The diffusion equation of mixture dyeing, therefore, may be given by

$$\frac{\partial C_1}{\partial t} = D_{11}\frac{\partial^2 C_1}{\partial x^2} + D_{12}\frac{\partial^2 C_2}{\partial x^2} \approx D_1'\frac{\partial^2 C_1}{\partial x^2} \quad (3)$$

$$\frac{\partial C_2}{\partial t} = D_{21}\frac{\partial^2 C_2}{\partial x^2} + D_{22}\frac{\partial^2 C_2}{\partial x^2} \approx D_2'\frac{\partial^2 C_2}{\partial x_2} \quad (4)$$

where D_1' and D_2' (cm^2/min.) denote the apparent diffusion coefficient of each dye in the mixture dyeing. The other symbols are as given before.[1] These six diffusion coefficients have been calculated by the same methods as in the previous paper.[1]

Results and Discussion

Single Dyeing.—The adsorption isotherms of the two dyes at 90, 85 and 80°C are shown in Figs. 1 and 2, and the standard affinity, calculated by Eqs. 1 and 2, in Table I. The

* Chrysophenine G denotes dye 1 and Sirius Red 4B, dye 2; they are shown by subscripts such as D_{11} $[D_2]_\phi$.

4) T. Vickerstaff, "The Physical Chemistry of Dyeing," 2nd ed., Oliver and Boyd, London (1954), p. 194.

TABLE I. STANDARD AFFINITY OF DIRECT DYES

Temp., °C	Chrysophenine G	Sirius Red 4B
90	$-(3.40\pm0.06)$	$-(3.73\pm0.06)$
85	$-(3.51\pm0.07)$	$-(3.90\pm0.07)$
80	$-(3.62\pm0.06)$	$-(3.94\pm0.07)$

diffusion coefficients at various surface concentrations are shown in Tables III, IV and V. The surface concentration, C_i^0, in diffusion experiments are assumed to be equal to the equilibrium adsorption, $[D_i]_\phi$, obtained from Figs. 1 and 2 for the same concentration in a dyebath. These results show that the two dyes have similar dyeing properties, although Chrysophenine G has a little larger diffusion coefficient and a little lower affinity than Sirius Red 4B.

The activation energies of diffusion at a constant surface concentration are given in Table II. They decrease with an increase in the surface concentration.

TABLE II. APPARENT ACTIVATION ENERGY OF DIFFUSION

	$C_0\times10^3$	E
Chrysophenine G	2.5	9.89
	3.0	8.35
	3.5	7.86
	4.5	5.79
Sirius Red 4B	2.5	16.9
	3.0	16.3
	3.5	14.7
	4.0	12.9

Mixture Dyeing.—The equilibrium adsorptions in mixture dyeing, which correspond to the expected dyeing condition described before, are as shown in Tables III, IV and V. In the kinetic study, three kinds of dyeing conditions and three dyeing temperatures are employed.

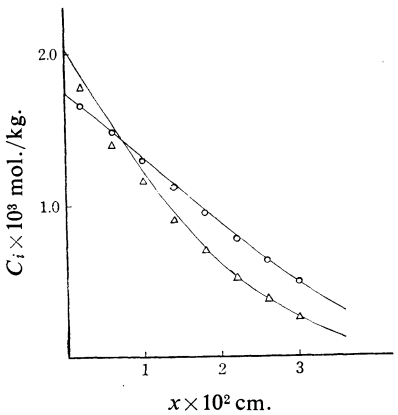

Fig. 3. Dye distribution in mixture dyeing.
○ Chryrophenine G, △ Sirius Red 4B
—— Theoretical curve; $[D_1]_\sigma=9.40\times10^{-5}$, $[D_2]_\sigma=6.35\times10^{-5}$,
NaCl: 3.0×10^{-2} mol./l.; 90°C; 500 min.
(Cf. Table III, Exp. No. 1)

The surface concentration, C_i^0, in diffusion experiments was assumed, as in single dyeing, to be equal to the equilibrium adsorption from the same concentration in the dyebath. As shown in Fig. 3, the surface concentration in diffusion experiments is a little different from the equilibrium adsorption under the same conditions, but this difference does not affect the calculation of the cross-term diffusion coefficients.

When the surface concentration of yellow dye at 90°C is maintained constant and that of red dye is gradually increased, the apparent diffusion coefficient of yellow dye, D_1', increases gradually. In this case, because of the concentration dependence of the diffusion coefficient, D_{22} (the diffusion coefficient of the red dye) increases with an increase in the surface concentration. D_{11} (that of the yellow dye) may not increase for the same reason. However, D_1' increases gradually with an increase in $[D_2]_\phi(=C_2^0)$. This, therefore, may be due to the effect of red dye on the diffusion of yellow dye. The diffusion of red dye may also be affected by yellow dye. As the surface concentration of the yellow dyes, however, is maintained constant, the yellow dyes may be almost identical in their effect on the diffusion of red dye, as Table III shows.

When the surface concentration of red dye is maintained constant, the reverse phenomenon is observed; namely, D_2' increases gradually. The effect of yellow dye on the diffusion of red dye seems to be smaller than in the reverse case. Such a situation is also observed when the surface concentrations of the two dyes are equal; these phenomena may be interpreted by means of the combination effect of the two dyeing conditions mentioned above.

D_{11}, D_{12}, D_{21} and D_{22} should be estimated simultaneously. As has been stated before, D_{11} and D_{22} determined by the single dyeing. Because of the activity of the dye and other factors, D_{11} and D_{22} may vary with the concentration of the two respective dyes. Although the concentration dependence of these diffusion coefficients has been investigated by O'Donnell and Gosting,[5] it can not be estimated from these experimental results with adequate experimental accuracy. As the absolute values of D_{12} are larger than those of D_{21}, and as D_{21} approximates to zero, it is considered, as has been stated before, that the effect of yellow dye on the diffusion of red dye is smaller than in the reverse case.

5) I. J. O'Donnell and L. J. Gosting, "The Structure of Electrolyte Solutions," Ed. by W. J. Hamer, John Wiley & Sons, Inc., New York (1959), Chap. 11.

TABLE III. MIXTURE DYEING AT 90°C

Exp. No.	$[D_1]_\sigma$ $\times 10^4$	$[D_2]_\sigma$ $\times 10^4$	$[D_1]_\phi$ $\times 10^3$	$[D_2]_\phi$ $\times 10^3$	D_{11} $\times 10^7$	D_{12} $\times 10^7$	D_{21} $\times 10^7$	D_{22} $\times 10^7$	D_1' $\times 10^6$	D_2' $\times 10^7$	
1	0.94_0	0.63_5	2.01	2.35	6.5	3.0	-0.012_5	5.2	1.10	5.51	
2	1.02	0.82_0	1.96	2.69	6.5	2.8	−0.049	5.7	1.31	5.96	
3	1.08	1.04	2.00	3.20	6.5	2.5	−0.007	6.1	1.37	6.13	$[D_1]_\phi$=const.
4	1.14	1.27	1.93	3.45	6.5	2.3	−0.002	6.2	1.50	6.35	
5	1.20	1.52	1.94	3.81	6.5	2.1	−0.001	6.3	1.58	7.28	
6	1.17	0.51_0	2.43	2.09	7.2	3.5	−0.44	4.7	1.25	5.59	
7	1.45	0.56_0	2.71	2.08	7.8	3.9	−0.61	4.7	1.26	5.38	
8	1.59	0.57_8	2.90	2.07	8.4	4.5	-0.75_9	4.7	1.32	6.24	$[D_2]_\phi$=const.
9	1.72	0.60_3	3.10	2.10	8.9	5.0	−0.88	4.7	1.38	6.75	
10	1.97	0.62_5	3.51	2.09	9.6	5.6	-1.07_1	4.7	1.40	6.74	
11	0.88_5	0.46_5	2.03	1.96	6.5	3.2	-0.27_5	4.6	1.25	5.76	
12	1.26	0.72_3	2.46	2.50	7.2	3.4	-0.23_0	5.4	1.37	6.13	
13	1.53	0.88_0	2.60	2.60	7.6	3.5	-0.27_7	5.6	1.52	6.58	$[D_1]_\phi=[D_2]_\phi$
14	2.31	1.39	3.20	3.16	8.9	4.2	-0.45_0	6.1	1.65	7.19	
15	2.82	1.75	3.60	3.60	9.8	5.1	-0.55_0	6.4	1.74	8.96	

TABLE IV. MIXTURE DYEING AT 85°C

Exp. No.	$[D_1]_\sigma$ $\times 10^5$	$[D_2]_\sigma$ $\times 10^5$	$[D_1]_\phi$ $\times 10^3$	$[D_2]_\phi$ $\times 10^3$	D_{11} $\times 10^7$	D_{22} $\times 10^7$	D_1' $\times 10^7$	D_2' $\times 10^7$	
1	8.22	5.63	2.25	2.61	6.0	4.0	8.7	4.5	
2	8.71	6.75	2.27	2.89	6.0	4.3	10.0	5.0	
3	9.13	8.15	2.34	3.29	6.0	4.7	9.3	4.2	$[D_1]_\phi$=const.
4	9.50	9.50	2.29	3.47	6.0	4.9	8.8	4.5	
5	9.95	12.5	2.27	4.13	6.0	5.4	13.0	4.9	
6	11.6	16.8	2.27	4.80	6.0	5.9	16.0	5.8	
7	7.46	4.25	2.07	2.12	5.5	3.5	8.7	3.9	
8	9.95	5.67	2.45	2.47	6.4	3.9	8.7	3.8	
9	12.4	7.75	2.64	2.79	6.9	4.2	13.0	4.8	$[D_1]_\phi=[D_2]_\phi$
10	19.8	13.6	3.71	3.80	8.9	5.2	14.0	5.6	
11	25.1	17.5	4.16	4.18	9.6	5.5	16.0	6.6	

TABLE V. MIXTURE DYEING AT 80°C

Exp. No.	$[D_1]_\sigma$ $\times 10^4$	$[D_2]_\sigma$ $\times 10^5$	$[D_1]_\phi$ $\times 10^3$	$[D_2]_\phi$ $\times 10^3$	D_{11} $\times 10^7$	D_{22} $\times 10^7$	D_1' $\times 10^7$	D_2' $\times 10^7$	
1	1.00	5.10	3.22	2.79	6.8	2.8	7.5	3.3	
2	1.24	5.46	3.64	2.76	7.7	2.8	7.8	3.3	
3	1.48	5.77	4.14	2.72	8.4	2.8	8.1	3.7	$[D_2]_\phi$=const.
4	1.75	6.18	4.43	2.72	8.7	2.8	11.0	3.5	
5	2.02	6.55	4.96	2.78	9.0	2.8	10.0	3.6	
6	2.28	6.90	5.23	2.69	9.1	2.8	10.0	3.5	
7	0.79_0	4.75	2.52	2.54	5.2	2.7	6.2	2.9	
8	1.03	6.35	3.02	2.95	6.4	2.9	8.3	3.3	
9	1.32	8.35	3.40	3.43	7.2	3.2	12.0	4.0	$[D_1]_\phi=[D_2]_\phi$
10	1.65	11.1	4.03	4.00	8.3	3.4	8.9	3.4	
11	2.00	14.0	4.11	4.10	8.4	3.5	6.7	3.5	
12	2.49	18.9	4.74	4.75	9.0	3.7	9.0	4.1	

The distributions of these dyes in the substrate are very different from those in the mixture of Benzopurpurine 4B and Sky Blue 6B. This may be explained as follows. Chrysophenine G and Sirius Red 4B are similar to each other in distribution, while Benzopurpurine 4B and Sky Blue 6B are not. It follows that the effect of the two dyes on the diffusion of each dye is smaller in the former case than in the latter and that the dye distributions in

the present experiments, as shown in Fig. 3, may be Fickian. However, as Fig. 3 shows, the distribution of two dyes in the substrate agrees well with the theoretical curves in the previous paper.[1] Therefore, the unusual distribution of Sky Blue 6B may not be a particular one, and the shape of the dye distribution in the mixture dyeing may be determined by the value of the diffusion coefficients of the dye and the ratio of the surface concentrations; i.e., the dye distribution in the mixture dyeing may be Fickian only when the two dyes are similar to each other in dyeing property.

At 85°C, the dyeing condition of the constant surface concentration of yellow dye and the equal surface concentration of the two dyes are employed. The results are shown in Table IV. At 80°C, the dyeing condition of the constant surface concentration of red dye and the equal surface concentration of the two dyes are employed; the results are shown in Table V. Similar phenomena such as those at 90°C, are observed. As the results exhibit a little scatter, the cross-term diffusion coefficients have not been calculated.

Judging from the difference between D_1' and D_{11} or D_2' and D_{22}, the temperature effect on mixture dyeing seems to decrease with a decrease in the temperature. This is inconsistent with the cases of Benzopurpurine 4B and Sky Blue 6B. This temperature effect is considered to be caused by various complicated factors, such as the activity and the affinity of dye, which vary with the temperature. Therefore, it may not be possible to discuss it simply. The absorption spectra of the dye mixture in the substrate were additive, even in the case of a mixture of Chrysophenine G and Sky Blue 6B, in contrast with those in an aqueous solution.[6] Therefore, in the substrate, there may not be such a strong interaction to vary the absorption spectra as in a solution, and so the same complex between two dyes as in a solution may not result. The main factor influencing the diffusion in mixture dyeing may be a competition of available surfaces in the substrate. Then the dye with the smaller diffusion coefficient or with the larger affinity has a more profound effect on the diffusion of the dye with a larger diffusion coefficient or with a smaller affinity than in the reverse case. The results of these experiments confirm these hypotheses.

Summary

1) The single and mixture dyeing of Chrysophenine G (C. I. Direct Yellow 12) and Sirius Red 4B (C. I. Direct Red 81) have been examined kinetically.

2) The affinity and the diffusion coefficient of each dye at 90, 85 and 80°C have been evaluated. The apparent activation energy of diffusion at a constant surface concentration has been calculated.

3) In the mixture dyeing, although the apparent diffusion coefficient of each dye became larger than that in the single dyeing, whose surface concentration was similar to that in the mixture dyeing, the dye with the smaller diffusion coefficient had a more profound effect on the diffusion of the dye with the larger diffusion coefficient than in the reverse case.

Laboratory of Dyeing Chemistry
Tokyo Institute of Technology
Meguro-ku, Tokyo

6) M. Sekido and Z. Morita, unpublished work.

The Electronic Spectra and Electronic Structures of Amino-substituted Benzenes

By Noboru MATAGA

(Received June 1, 1963)

Theoretical studies of the electronic structures and spectra of complex aromatic molecules seem to be of increasing importance from various viewpoints. The electronic spectra and electronic structures of substituted aromatic hydrocarbons for instance, have been the subject of a number of theoretical investigations.[1-12]

Baba and Suzuki[12] have made a comparative study of the electronic spectra of phenol and aniline and also of those of naphthols and naphthylamines. These calculations, as well as those by some of the other investigators,[5,9] employed molecular orbitals delocalized over all the cores of the molecules, in contrast to the method of the composite system, where a molecule is regarded as being made up of several fragments and where the interactions among the wave functions of these fragments are calculated to give the wave functions for the whole molecule.[7,8] The latter method is quite suitable for determining the correlation between the spectrum of a molecule and the spectra of fragments of which the molecule is composed and also for ascertaining the extent of charge transfer (CT) interaction among these fragments in the molecule.

Of course, these two methods are not essentially independent of each other. Recently, Fischer-Hjalmars[13] has developed an elegant method for transforming the wave functions calculated by the former method into those obtained by the latter method using natural spin orbital of Löwdin;[14] she has applied that method to toluene and aniline. In the case of aniline, the result of this transformation was rather close to the wave functions calculated by Murrell[7] with the method of the composite system.

As has been said above, the electronic spectrum and the electronic structure of aniline, among other amino-substituted benzenes, have been studied in detail. However, the electronic structures and spectra of poly-substituted amino-benzenes have not been studied in detail.

Because of the strong conjugation of the amino group with the π-electron system of the aromatic ring, perturbation methods* seem to be poor approximations for systematically interpreting the electronic spectra of amino-substituted aromatics; therefore, a variational method should be employed for this study.

Because of this strong conjugation power of the amino group, the electronic structure of the aromatic hydrocarbon will be considerably affected by this substitution. Actually, Köhler and Scheibe[15] have demonstrated that *s*-triaminobenzene is easily protonated on the ring carbon in an almost neutral aqueous solution, whereas aniline, as well as *m*-phenylenediamine, is protonated on the amino-nitrogen. This is a remarkable example of substitution effecting a large change in the physico-chemical property of a molecule.

We have studied this very interesting phenomenon by means of molecular orbital calculations and have shown that the calculated electronic spectrum of the protonated *s*-triaminobenzene agrees satisfactorily with the observed spectrum, and also that the quite large proton affinity of this molecule is in accordance with the results of the calculations.[16]

In view of the circumstances described above, it seems to be desirable to study the electronic spectra and electronic structures of amino-substituted aromatics in a more systematic way.

1) A. L. Sklar, *J. Chem. Phys.*, **7**, 984 (1939).
2) K. F. Herzfeld, *Chem. Revs.*, **41**, 233 (1949).
3) F. A. Matsen, *J. Am. Chem. Soc.*, **72**, 5243 (1950).
4) S. Nagakura and H. Baba, ibid., **74**, 5693 (1952).
5) I. Fischer, *Ark. Fys.*, **5**, 377 (1952).
6) L. Goodman, I. G. Ross and H. Shull, *J. Chem. Phys.*, **26**, 474 (1957); L. Goodman and H. Shull, ibid., **27**. 1388 (1957).
7) H. C. Longuet-Higgins and J. N. Murrell, *Proc. Phys. Soc.*, **A68**, 601 (1955); J. N. Murrell, ibid., **A68**, 969 (1955).
8) S. Nagakura and J. Tanaka, *J. Chem. Phys.*, **22**, 236 (1954); S. Nagakura, ibid., **23**, 1441 (1955); J. Tanaka and S. Nagakura, ibid., **24**, 1274 (1956).
9) K. Nishimoto and R. Fujishiro, This Bulletin, **31**, 1036 (1958); K. Nishimoto, to be published.
10) Y. I'Haya, *J. Am. Chem. Soc.*, **81**, 6120, 6127 (1959).
11) N. Mataga and S. Mataga, This Bulletin, **32**, 600 (1959).
12) H. Baba, ibid., **34**, 76 (1961); H. Baba and S. Suzuki, ibid., **34**, 82 (1961).
13) I. Fischer-Hjalmars, *Ark. för Fys.*, **21**, 123 (1962); Preprint for the International Symposium on Molecular Structure and Spectroscopy, Tokyo, Japan, September, 1962.
14) P.-O. Löwdin, *Phys. Rev.*, **97**, 1474 (1955).
* In the sense of the expansion of the secular determinant in a series.
15) H. Köhler and G. Scheibe, *Z. anorg. u. allgem. Chem.*, **285**, 221 (1956).
16) N. Mataga, This Bulletin, **36**, 1109 (1963).

Accordingly, we have taken up several amino-benzenes, such as aniline, isomeric phenylene-diamines (PDA) and *s*-triaminobenzene (TAB), and also several amino-substituted nitrogen heterocycles, such as 4-amino-pyridine, 1, 4-di-aminotetrazine and melamine.

In the present report, mainly the results for amino-substituted benzenes will be described.

Method of Calculation

Although our method of calculation in this report is based on the semiempirical ASMO method[12,17,18] with a zero differential overlap, we have tried various approaches including the VESCF[19,20] calculation on *p*-PDA, because the electronic structures of amino-derivatives appear to be much more complicated than those of parent hydrocarbons and simple *n*-heterocycles, where the -CH= groups of the parent hydrocarbon are replaced by -N=.

One of the difficulties with calculation using the MO's delocalized over all the cores of the molecule is the assessment of the core potential at amino nitrogen, which can contribute two electrons to the π-system, in contrast to the case of aromatic hydrocarbons or *n*-heterocycles, where the core potentials for π-electrons are fairly uniform. A similar difficulty arises in the case of pyrrole, for which Brown and Heffernan used the VESCF method.[20]

The outline of our procedure of calculation is as follows:

i) The calculation of Hückel MO's, assuming appropriate values of Coulomb and resonance parameters ($\alpha_N=\alpha+1.2\beta$, $\beta_{CN}=\beta$[12]).

ii) The antisymmetrization of Hückel MO's.

iii) The calculation of electronic spectra invoking configuration interaction (CI) or SCF calculation using Hückel MO's as the starting wave functions, and then the calculation of the electronic spectra by the CI method.

Although the necessary formulas for the ASMO CI calculation have been given elsewhere,[17,18] they will now be described briefly.

The Hückel MO's (ϕ_i's) are expressed by linear combinations of $2p\pi$ AO's ($\phi_1 \cdots\cdots \phi_{2n}$) of carbon and nitrogen:

$$\psi_1=\sum_{\mu}^{2n} c_{i\mu}\phi_\mu \tag{1}$$

The Hamiltonian for $2m$ π-electrons can be written as:

$$\mathscr{H}=\sum_{i}^{2m}\mathscr{H}_i^{\text{core}}+\sum_{i<j}^{2m} e^2/r_{ij} \tag{2}$$

where $\mathscr{H}_i^{\text{core}}$ is the core Hamiltonian for the ith electron and r_{ij} is the interelectronic distance.

By means of the Fock Hamiltonian, $F=\mathscr{H}^{\text{core}}+G$, the apparent orbital energies are expressed by:

$$\varepsilon_i=\langle\psi_i|F|\psi_i\rangle=\sum_{\mu,\nu} c_{i\mu}c_{i\nu}\cdot\langle\phi_\mu|F|\phi_\nu\rangle=\sum_{\mu,\nu} c_{i\mu}c_{i\nu}F_{\mu\nu} \tag{3}$$

Putting $\langle\phi_\mu(i)|\mathscr{H}_i^{\text{core}}|\phi_\nu(i)\rangle=\beta_{\mu\nu}$, the matrix elements of Fock Hamiltonian in terms of AO's are written as:

$$\left.\begin{aligned} F_{\mu\mu}&=-I_\mu+(1/2)P_{\mu\mu}\gamma_{\mu\mu}+\sum_{\kappa\neq\mu}(P_{\kappa\kappa}-Z_\kappa)\gamma_{\kappa\mu}\\ F_{\mu\nu}&=\beta_{\mu\nu}-(1/2)P_{\mu\nu}\gamma_{\mu\nu}\end{aligned}\right\} \tag{4}$$

The excitation energies for the $i\rightarrow k$ transition, $E(^{1,3}\chi_{ik})=\langle^{1,3}\chi_{ik}|\mathscr{H}|^{1,3}\chi_{ik}\rangle-\langle\psi_0|\mathscr{H}|\chi_0\rangle$, where χ_0 is the ground electronic configuration, and the interconfigurational matrix elements, $\langle^{1,3}\chi_{ik}|\mathscr{H}|\cdot{}^{1,3}\chi_{jl}\rangle$, are calculated by the following equations:

$$E(^{1,3}\chi_{ik})=(\varepsilon_k-\varepsilon_i)-(\langle ik|G|ik\rangle-\langle ik|G|ki\rangle)\pm\langle ik|G|ik\rangle \tag{5}$$

$$\langle^{1,3}\chi_{ik}|\mathscr{H}|^{1,3}\chi_{il}\rangle=\varepsilon_{kl}-(\langle ik|G|il\rangle-\langle ik|G|li\rangle)\pm\langle ik|G|li\rangle,\quad k\neq l \tag{6}$$

$$\langle^{1,3}\chi_{ik}|\mathscr{H}|^{1,3}\chi_{jk}\rangle=-\varepsilon_{ji}-(\langle kj|G|ki\rangle-\langle kj|G|ik\rangle)\pm\langle kj|G|ik\rangle,\quad j\neq i \tag{7}$$

$$\langle^{1,3}\chi_{ik}|\mathscr{H}|^{1,3}\chi_{jl}\rangle=-(\langle jk|G|il\rangle-\langle jk|G|li\rangle)\pm\langle jk|G|li\rangle,\quad i\neq j,\ k\neq l \tag{8}$$

$$\langle^1\chi_{ik}|\mathscr{H}|\chi_0\rangle=\sqrt{2}\,\varepsilon_{ki} \tag{9}$$

In these equations, $\varepsilon_{ki}=\langle\psi_k|F|\psi_i\rangle$, $\langle jk|G|li\rangle=\langle\psi_j(i)\psi_k(j)|e^2/r_{ij}|\psi_l(i)\psi_i(j)\rangle$, the + signs before the last terms in the right hand side are for singlets, and the − signs are for triplets. Thus, only the singly-excited configurations and the ground configuration are taken into account.

In the case of the SCF calculation, the secular equation:[21]

$$\sum_{\nu}F_{\mu\nu}c_{i\nu}=\varepsilon_i c_{i\mu} \tag{10}$$

must be solved by an iterative procedure.

In the VESCF method of Brown and Heffernan,[19,20] the SCF procedure involves the dependence of all the integrals except $\beta_{\mu\nu}$ on the charge distribution, $P_{\mu\mu}$.

The wave function, Ψ, for an electronic state is given by a linear combination of χ's. The oscillator strength, f, is calculated by the following equation:

$$f=0.08754\times\nu_{oa}\sum_{r=x,y,z}[m^r_{oa}]^2 \tag{11}$$

where ν_{oa} is the excitation energy in units of eV. of the transition from the ground state, Ψ_0, to an excited state, Ψ_a. The necessary formulas for the calculation of the transition moment, m^r_{oa}, have been given elsewhere.[17b]

Let us now consider the evaluation of integrals. They have been evaluated by semiempirical procedures. $Z_\kappa=1$ for the carbon core and $Z_\kappa=2$ for the core of amino nitrogen, which contributes two electrons to the π-system. The I_μ values for carbon were taken to be 11.42 eV., and that for the amino nitrogen, 28.85 eV.[22]

17) a) R. Pariser and R. G. Parr, *J. Chem. Phys*, **21**, 466, 767 (1953); ibid., **23**, 711 (1955); b) R. Pariser, ibid., 24, 250 (1956).

18) N. Mataga, This Bulletin, **31**, 453, 459, 463 (1958); *Z. Phys. Chem. N. F.*, **18**, 19 (1958).

19) R. D. Brown and M. L. Heffernan, *Trans. Faraday Soc.*, 54, 757 (1958); *Australian J. Chem.*, **12**, 543, 554 (1959).

20) R. D. Brown and M. L. Heffernan, ibid., **12**, 319, 330 (1959).

21) J. A. Pople, *Trans. Faradaday Soc.*, **49**, 1375 (1953); *Proc. Phys. Soc.*, **A68**, 81 (1955).

$\gamma_{\mu\nu}$'s were evaluated by the same procedure as before.[18,23,24] For the evaluation of m^r and $\gamma_{\mu\nu}$, all nearest neighbor C–C bond distances are assumed to be 1.39Å, and those of C–N bonds, 1.36Å.[5] The core resonance integral, $\beta_{\mu\nu}$, was taken into account only for the nearest neighbors and was neglected for more distant neighbors; the same value as before[18,23,24] was used for β_{CC}, namely, $\beta_{CC}=-2.388$ eV. However, the most suitable value for β_{CN} in the present approximation is not yet known. We have calculated the electronic spectrum of *p*-PDA assuming various values for β_{CN} in order to find out the β_{CN} value which fits the observed excitation energy. In this way, the best value of β_{CN} for reproducing the excitation energies to the first and the second excited singlet states has been found to be -3.6 eV.

We have calculated the electronic spectra of some amino-substituted benzenes and nitrogen heterocycles, such as aniline, *p*-PDA, TAB, 4-aminopyridine, 4,4'-diaminotetrazine and melamine, with this β_{CN} value. However, the agreement between the calculated and observed spectra is not very satisfactory with this β_{CN} value.

One of the main causes for this unsatisfactory agreement seems to be as follows. The value of I_μ for the amino-nitrogen (28.85 eV.) used in the above calculation (Approximation A) is the ionization potential of the $2p\pi$ electron of N^+ in the trigonal hybrid state. This value appears to be too large; the real value is probably smaller than this value and a little larger than that for neutral nitrogen because the actual core for a π-electron at amino-nitrogen is not N^{2+} but is partially shielded because of the existence of another π-electron. Moreover, this value of β_{CN} seems to be too large because the overlap between the $2p\pi$ AO's on the amino-nitrogen and the substituted carbon respectively may not be larger than the corresponding overlap between the nearest neighbor carbons.

In view of these circumstances, we should examine other semiempirical procedures more appropriate to the present case. One of the possible procedures is to regard I_μ or $F_{\mu\mu}$ for amino nitrogen as an adjustable parameter and to select the most suitable value for reproducing the observed spectra satisfactorily. For this purpose, we have used a simplified procedure which gives appropriate values for the $F_{\mu\mu}$'s of amino-nitrogen, That is,

$$\langle F_{NN}\rangle=\langle F_{CC}\rangle_{AV}+\delta_N\cdot\langle F_{12}\rangle_{AV} \qquad (12)$$

where $\langle F_{CC}\rangle_{AV}$ is the simple arithmetic mean of $F_{\mu\mu}$'s for carbon, $\langle F_{12}\rangle_{AV}$ is the same quantity of $F_{\mu\nu}$'s for the nearest neighbor carbon-carbon bonds, and δ_N is the Hückel MO parameter for the Coulomb integral of nitrogen, 1.2.

When $\langle F_{\mu\mu}\rangle$ of Eq. 12 instead of $F_{\mu\mu}$ of Eq. 4 is used for amino-nitrogen, the most suitable value of the core resonance integral β_{CN} appears to be -2.399 eV., the β_{CC} value being the same as before. Therefore, in this approximation, $\beta_{CN}\approx\beta_{CC}$; this result seems to be physically reasonable.

For a more refined calculation, the VESCF method of Brown and Heffernan[19,20] may be used. An analogous idea of "differential ionization" has been proposed by I'Haya.[25]

In the VESCF method, it is assumed that Slater's rule for the effective charges of atoms is applicable to a continuous variation in electron density. Accordingly, the effective charge, Z_μ, of the μ atom is expressed as a function of $P_{\mu\mu}$:

$$Z_\mu=N_\mu-\lambda_\mu-0.35(\sigma_\mu+P_{\mu\mu}) \qquad (13)$$

where N_μ is the atomic number and σ_μ is the number of σ-electrons associated with the μ atom in the molecular framework, e. g., 3 for carbon and the amino-nitrogen. λ_μ is the contribution from the inner shell electrons, and $\lambda_\mu=1.35$ for carbon and nitrogen in the present case.

If the I_μ's are plotted against the Z_μ's for the (sp^3, V_4) valence state of the iso-electronic series, C, N^+ and O^{2+}, and for the (sp^4, V_3) valence state of the iso-electronic series, C^-, N and O^+ respectively, the curves are accurately parabolic. In this way, the form of the relationship between the valence state ionization potential, I_μ, and Z_μ has been established.[26] Therefore, $\gamma_{\mu\nu}$'s can be calculated easily from the relations:

$$\gamma_{\mu\mu}(sp^3, V_4)=I_\mu(sp^3, V_4)-A_\mu(sp^3, V_4)$$
$$=I_\mu(sp^3, V_4)-I_\mu(sp^4, V_3)$$
$$a_{\mu\mu}=14.3949/\gamma_{\mu\mu}$$

and

$$a_{\mu\nu}=2a_{\mu\mu}a_{\nu\nu}/(a_{\mu\mu}+a_{\nu\nu})$$

Thus, in this SCF procedure, the I_μ's and $\gamma_{\mu\nu}$'s become functions of $P_{\mu\mu}$'s from their dependence on Z_μ's. We have applied this method to *p*-PDA.

Results and Discussion

The Hückel MO's and MO energies of aniline and isomeric PDA's are given in Appendix I. The numberings of the atoms in these molecules are given in Fig. 1. The MO's and MO energies of TAB are given elsewhere.[16] C_{2v} symmetry is assumed for aniline, *o*- and *m*-PDA, while D_{2h} symmetry is assumed for *p*-PDA.

Using these Hückel MO's, the electronic spectrum of *p*-PDA was calculated, assuming various β_{CN} values as described in the Method-of-Calculation section. The results are indicated in Fig. 2. The observed excitation energy to the lowest excited singlet state of *p*-PDA is nearly 4 eV. This value can be repoduced by taking either $\beta_{CN}=-1.2$ eV. or $\beta_{CN}=-3.6$ eV. However, with $\beta_{CN}=-1.2$ eV. the disagreement between the calculated and observed values of the excitation energy to the second excited singlet state is considerable (observed value

22) S. Mataga and N. Mataga, *Z. Phys. Chem. N. F.*, **19**, 231 (1959).
23) K. Nishimoto and N. Mataga, ibid., **12**, 335 (1957); N. Mataga and K. Nishimoto, ibid., **13**, 140 (1957).
24) N. Mataga and K. Nishimoto and S. Mataga, This Bulletin, **32**, 395 (1959).
25) Y. I'Haya, *Mol. Phys.*, **3**, 513, 521 (1960).
26) S. Mataga and N. Mataga, This Bulletin, **32**, 521 (1959).

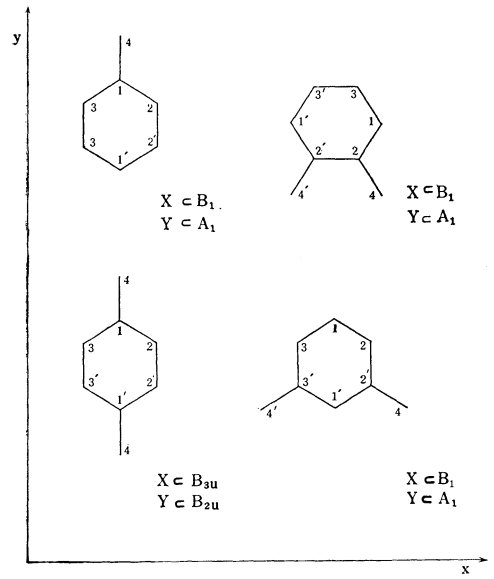

Fig. 1. The numbering of atoms in aminobenzenes.

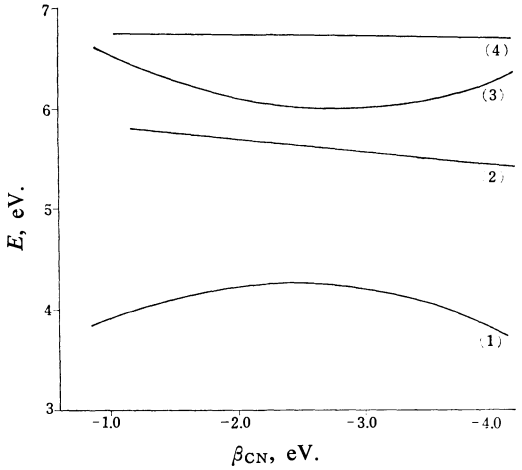

Fig. 2. The change of the excited singlet state energies of *p*-PDA as a function of the β_{CN} values.
(1) $\Psi(^1B_{3u}) = a^1\chi_{56} - b^1\chi_{47}$
(2) $\Psi(^1B_{2u}) = c^1\chi_{57} + d^1\chi_{46}$
(3) $\Psi(^1B_{3u}) = b^1\chi_{56} + a^1\chi_{47}$
(4) $\Psi(^1B_{2u}) = d^1\chi_{57} - c^1\chi_{46}$

TABLE I. CALCULATED ELECTRONIC SPECTRA OF ANILINE AND *p*-PDA (APPROXIMATION A) IN COMPARISON WITH THE OBSERVED VALUES

Aniline

$-E$, eV.		State function	f_{calcd}	$h\nu_{obs}$, eV.	f_{obs}
−0.0038	$(^1A_1)_0$	$0.9997\,\chi_0 + 0.0062^1\chi_{46} + 0.0174^1\chi_{35} + 0.0133^1\chi_{26}$			
4.7315	$(^1B_1)_I$	$0.8906^1\chi_{45} - 0.4457^1\chi_{36} + 0.0898^1\chi_{25}$	0.048	4.33[a]	0.026[a]
5.8192	$(^1A_1)_I$	$0.0140\,\chi_0 - 0.8867^1\chi_{46} - 0.4609^1\chi_{35} - 0.0339^1\chi_{26}$	0.19	5.29[a]	0.17[a]
6.5055	$(^1B_1)_{II}$	$0.3964^1\chi_{45} + 0.8577^1\chi_{36} + 0.3273^1\chi_{25}$	0.53	6.29[a]	—
6.7601	$(^1A_1)_{II}$	$0.0115\,\chi_0 + 0.4564^1\chi_{46} - 0.8849^1\chi_{35} + 0.0924^1\chi_{26}$	1.18	—	—
8.8382	$(^1B_1)_{III}$	$0.2229^1\chi_{45} + 0.2560^1\chi_{36} - 0.9406^1\chi_{25}$	0.60	—	—
9.2173	$(^1A_1)_{III}$	$0.0139\,\chi_0 + 0.0727^1\chi_{46} - 0.0661^1\chi_{35} - 0.9951^1\chi_{26}$	0.039	—	—
3.3026	$^3A_1$	$0.7419^3\chi_{35} + 0.6537^3\chi_{46} - 0.1490^3\chi_{26}$	0	3.32[b]	—
3.7528	$^3B_1$	$0.9639^3\chi_{45} + 0.2435^3\chi_{36} - 0.1073^3\chi_{25}$	0	—	—
3.9669	$^3A_1$	$0.6658^3\chi_{35} - 0.7445^3\chi_{46} + 0.0486^3\chi_{26}$	0	—	—
5.0724	$^3B_1$	$0.2543^3\chi_{45} - 0.9617^3\chi_{36} + 0.1018^3\chi_{25}$	0	—	—
7.4190	$^3A_1$	$0.0791^3\chi_{35} + 0.1352^3\chi_{46} + 0.9876^3\chi_{26}$	0	—	—
7.5601	$^3B_1$	$0.0784^3\chi_{45} + 0.1255^3\chi_{36} + 0.9890^3\chi_{25}$	0	—	—

p-PDA

E, eV.		State function	f_{calcd}	$h\nu_{obs}$, eV.	$\log \varepsilon_{obs}^{max}$
−0.0077	$^1A_g^+$	$0.9995\,\chi_0 + 0.0300^1\chi_{37}$			
3.9958	$^1B_{3u}^-$	$0.8816^1\chi_{56} - 0.4720^1\chi_{47}$	0.07	3.93[c]	3.3[c]
5.4923	$^1B_{2u}^+$	$0.9410^1\chi_{57} + 0.3385^1\chi_{46}$	0.47	5.04[c]	3.9[c]
6.0996	$^1B_{3u}^+$	$0.4720^1\chi_{56} + 0.8816^1\chi_{47}$	0.75	—	—
6.7012	$^1B_{2u}^-$	$0.3385^1\chi_{57} - 0.9410^1\chi_{46}$	1.15	—	—
7.6985	$^1B_{1g}$	$^1\chi_{36}$	0	—	—
8.5038	$^1A_g^-$	$0.0300\,\chi_0 - 0.9995^1\chi_{37}$	0	—	—
2.9611	$^3B_{3u}^+$	$0.9739^3\chi_{56} + 0.2268^3\chi_{47}$	0	—	—
3.1059	$^3B_{2u}^+$	$0.8114^3\chi_{57} + 0.5843^3\chi_{46}$	0	—	—
3.8815	$^3B_{2u}^-$	$0.5843^3\chi_{57} - 0.8114^3\chi_{46}$	0	—	—
4.6262	$^3B_{3u}^-$	$0.2268^3\chi_{56} - 0.9739^3\chi_{47}$	0	—	—
6.7462	$^3B_{1g}$	$^3\chi_{36}$	0	—	—
7.3274	^3A_g	$^3\chi_{37}$	0	—	—

a) See Ref. 12.
b) M. Kasha, *Chem. Revs.*, **41**, 401 (1947).
c) W. F. Forbs and I. R. Leckie, *Can. J. Chem.*, **36**, 1371 (1958).

$\sim$5 eV.). Accordingly, $\beta_{CN}=-3.6$ eV. has been chosen in this approximation.

A Comparison of the Calculated with the Observed Spectra. — Using this β_{CN} value, the electronic spectrum of aniline has been calculated and a more extensive CI calculation of *p*-PDA than that given in Fig. 2 has been carried out. The calculated results are shown in Table I, together with the observed values.

The calculated excitation energies are a little larger than the observed values. The calculated relative spacing among $^1A_g^+$, $^1B_{3u}^-$ and $^1B_{2u}^+$ states of *p*-PDA is especially unsatisfactory. That is, the calculated energy difference, $E(^1B_{2u}^+)-E(^1B_{3u}^-)$, is ca. 0.5 eV. larger than the observed value. Even if we use other values for β_{CN} between -2 eV.$\sim$ -3.6 eV., this unsatisfactory result is not very much improved, and with β_{CN} values other than -3.6 eV., the agreement between the observed and calculated excitation energies to the $^1B_{3u}^-$ state become worse, as can be seen from Fig. 2. Thus, the present approximation seems to give rather unsatisfactory results. The reason for this may be the use of too large a value for I_n or F_{NN}, as has already been discussed in the Method-of-Calculation Section. Accordingly, we have tried the next approximation, i. e., the use of Eq. 18. The electronic spectra of aniline and *p*-PDA as

Table II. Calculated electronic spectra of aniline and isomeric PDA's (approximation B) in comparison with the observed values*

Aniline

E, eV.		State function	f_{calcd}
-0.0100	$(^1A_1)_0$	$0.9992\,\chi_0-0.0379^1\chi_{46}+0.0150^1\chi_{35}$	—
4.5224	$(^1B_1)_I$	$0.8851^1\chi_{45}-0.4653^1\chi_{36}$	0.05
5.4552	$(^1A_1)_I$	$0.0305\,\chi_0+0.9405^1\chi_{46}+0.3384^1\chi_{35}$	0.31
6.5556	$(^1B_1)_{II}$	$0.4653^1\chi_{45}+0.8851^1\chi_{36}$	0.84
6.7148	$(^1A_1)_{II}$	$0.0269\,\chi_0+0.3378^1\chi_{46}-0.9408^1\chi_{35}$	1.04

p-PDA

E, eV.		State function	f_{calcd}
-0.0081	$^1A_g^-$	$0.9998\,\chi_0-0.0159^1\chi_{37}$	—
3.8957	$^1B_{3u}^-$	$0.8342^1\chi_{56}-0.5514^1\chi_{47}$	0.04
5.1268	$^1B_{2u}^+$	$0.9659^1\chi_{57}+0.2589^1\chi_{46}$	0.52
5.7989	$^1B_{3u}^+$	$0.5514^1\chi_{56}+0.8342^1\chi_{47}$	0.77
6.6660	$^1B_{2u}^-$	$0.2589^1\chi_{57}-0.9659^1\chi_{46}$	0.99
6.9036	$^1A_g^+$	$0.0159\,\chi_0+0.9998^1\chi_{37}$	0

o-PDA

E, eV.		State function	f_{calcd}	$h\nu_{obs}$, eV.	$\log\varepsilon_{obs}^{max}$
-0.0784	$^1A_1$	$0.9931\,\chi_0-0.1045^1\chi_{56}+0.0525^1\chi_{47}$	—	—	—
4.3423	$^1A_1$	$0.0661\,\chi_0+0.8719^1\chi_{56}+0.4852^1\chi_{47}$	0.09	4.29	3.5
5.0209	$^1B_1$	$0.9344^1\chi_{57}-0.3561^1\chi_{46}$	0.22	5.26	3.8
6.0700	$^1B_1$	$0.3561^1\chi_{57}+0.9344^1\chi_{46}$	0.62	—	—
6.2653	$^1A_1$	$0.1228\,\chi_0-0.5576^1\chi_{56}+0.8210^1\chi_{47}$	1.34	—	—
3.0737	$^3B_1$	$0.8723^3\chi_{57}-0.4889^3\chi_{46}$	0	—	—
3.0843	$^3A_1$	$0.9808^3\chi_{56}-0.1947^3\chi_{47}$	0	—	—
3.7112	$^3B_1$	$0.4889^3\chi_{57}+0.8723^3\chi_{57}$	0	—	—
4.5082	$^3A_1$	$0.1947^3\chi_{56}+0.9808^3\chi_{47}$	0	—	—

m-PDA

E, eV.		State function	f_{calcd}	$h\nu_{obs}$, eV.	$\log\varepsilon_{obs}^{max}$
-0.0131	$^1A_1$	$0.9988\,\chi_0-0.0489^1\chi_{57}-0.0065^1\chi_{46}$	—	—	—
4.4527	$^1B_1$	$0.8279^1\chi_{56}-0.5608^1\chi_{47}$	0.03	4.23	3.4
5.2759	$^1A_1$	$0.0467\,\chi_0+0.8891^1\chi_{57}+0.4552^1\chi_{46}$	0.19	5.16	3.8
5.9196	$^1A_1$	$0.0231\,\chi_0+0.5911^1\chi_{57}-0.8062^1\chi_{46}$	0.65	—	—
5.9793	$^1B_1$	$0.5608^1\chi_{56}+0.8279^1\chi_{47}$	1.31	—	—
3.0501	$^3A_1$	$0.9205^3\chi_{57}+0.3907^3\chi_{46}$	0	—	—
3.3867	$^3B_1$	$0.9306^3\chi_{56}+0.3659^3\chi_{47}$	0	—	—
4.0046	$^3A_1$	$0.3907^3\chi_{57}-0.9205^3\chi_{46}$	0	—	—
4.3946	$^3B_1$	$0.3659^3\chi_{56}-0.9306^3\chi_{47}$	0	—	—

* The observed values are taken from Ref. c of Table I.

well as those of *o*- and *m*-PDA have been calculated with this approximation.

The calculated results are shown in Table II, where the observed results for *o*- and *m*-PDA are given for purposes of comparison.

One can see from Tables I and II that the agreement between the calculated and the observed excitation energies is more satisfactory in Approximation B than in Approximation A, although less extensive configuration interactions are invoked to obtain the results given in Table II.

The calculation predicts that the excitation energies to the lowest excited singlet states of *o*- and *m*-PDA will be larger than that of *p*-PDA; this is in accordance with the observed results. Furthermore, the values of the excitation energies themselves, as well as the relative spacings among the excited states, are given correctly.* These results appear to support the agreements described in Sec. II against Approximation A. However, the procedure of Approximation B seems to be rather arbitrary. Therefore, we have examined a more "theoretical" procedure, i. e., the VESCF method, in the case of *p*-PDA.

The calculated spectrum and the VESCF MO's are given in Table III and Appendix II respectively. The β_{CN} value used in this calculation was the same as that in Approximation B.

As one can see from Table III, the calculated excitation energies are a little smaller than the observed values, although the energy difference between the $^1B_{2u}{}^+$ and $^1B_{3u}{}^-$ states is correctly given. It seems to be possible that one can fit the observed spectrum if one selects a somewhat different β_{CN} value and repeats the SCF calculation. However, we shall not attempt such a calculation here, for this is quite a laborious procedure.

TABLE III. THE CALCULATED ELECTRONIC SPECTRUM OF *p*-PDA (VESCF METHOD)

	State function	$h\nu$, eV.	f
^1A_g	χ_0		—
$^1B_{3u}{}^-$	$0.9624^1\chi_{56}-0.2715^1\chi_{37}$	3.5693	0.12
$^1B_{2u}{}^+$	$0.9819^1\chi_{57}+0.1892^1\chi_{36}$	4.7091	0.69
$^1B_{3u}{}^+$	$0.2715^1\chi_{56}+0.9624^1\chi_{37}$	6.6306	0.64
$^1B_{2u}{}^-$	$0.1892^1\chi_{57}-0.9819^1\chi_{36}$	6.6332	0.98
$^1B_{1g}$	$^1\chi_{46}$	5.5513	0
^1A_g	$^1\chi_{47}$	6.3188	0
$^3B_{2u}{}^+$	$0.9624^3\chi_{57}+0.2714^3\chi_{36}$	2.4436	0
$^3B_{3u}{}^+$	$0.9930^3\chi_{56}+0.1182^3\chi_{37}$	2.5324	0
$^3B_{2u}{}^-$	$0.2714^3\chi_{57}-0.9624^3\chi_{36}$	3.7282	0
$^3B_{3u}{}^-$	$0.1182^3\chi_{56}-0.9930^3\chi_{37}$	5.3898	0
$^3B_{1g}$	$^3\chi_{46}$	4.8127	0
^3A_g	$^3\chi_{47}$	4.8400	0

* Quite recently, the electronic spectrum of aniline has been examined in detail up to the vacuum ultraviolet region (K. Kimura, H. Tsubomura and S. Nagakura, presented at the 16th Annual Meeting of the Chemical Society of Japan, April, Tokyo, 1963). According to this measurement, the energy difference between $\Psi(^1B_1)_{II}$ and $\Psi(^1A_1)_{II}$ amounts to 0.33 eV. In our present study, it is calculated to be 0.26 eV. in Approximation A and 0.16 eV. in Approximation B.

The Relation between the Simple Hückel MO Calculation and the Present One. — In the present method, the electronic repulsions are explicity taken into consideration in the calculation of the electronic spectra. However, because of the zero differential overlap approximation, the present method appears to be essentially similar to the simple Hückel MO method. Among the matrix elements of the Fock Hamiltonian, the diagonal element, $F_{\mu\mu}$, and the non-diagonal element, $F_{\mu\nu}$, between the nearest neighbor AO's have appreciable values, whereas the $F_{\mu\nu}$ between the more distant neighbors has a very small value. This circumstance corresponds quite well to the fact that, in the simple Hückel MO method, only the Coulomb integral, α, and the resonance integral, β, between the nearest neighbor AO's are taken into account. Furthermore, the $F_{\mu\mu}$ values for the ring carbons are not very different from each other throughout the mono-, di- and tri-substituted aminobenzenes. The $F_{\mu\mu}$ values for the ring carbons of these compounds are in the range -5.5 eV.~ -6 eV.; the average value is ~ -5.8 eV. This value is rather close to that of the alternant hydrocarbon, -6 eV.

$F_{\mu\mu}$ in Eq. 4 can be rewritten as:

$$F_{\mu\mu} = -(I_\mu + A_\mu)/2 + (P_{\mu\mu}-1)\cdot\gamma_{\mu\mu}/2 + \sum_{\kappa\neq\mu}(\delta Q_\kappa)\gamma_{\mu\kappa} \qquad (14)$$

where $\delta Q_\kappa = (P_{\kappa\kappa} - Z_\kappa)$. When the μth atom is one of the ring carbons, this equation can be further rewritten as:

$$F_{\mu\mu}(\mathrm{C}) = -(I_\mu + A_\mu)/2 - (\delta Q_\mu)\cdot\gamma_{\mu\mu}/2 + \sum_{\kappa}^{\mathrm{all}}(\delta Q_\kappa)\cdot\gamma_{\mu\kappa} \qquad (15)$$

If the electron distribution of the parent hydrocarbon is not very much disturbed by the substitution, the $F_{\mu\mu}(\mathrm{C})$ value may be close to $-(I_\mu + A_\mu)/2$, the $F_{\mu\mu}(\mathrm{C})$ value of the parent hydrocarbon, because the δQ values are small in this case.

As has been described above, this circumstance seems to hold approximately, even in the case of amino-substituted benzenes, in spite of the great conjugation power of the amino group. We can expect that $F_{\mu\mu}(\mathrm{C})$ will become smaller when the Hückel MO parameter, δ_N, becomes smaller. Actually, if we assume $\delta_N \sim 0.8$ in the case of TAB, $F_{\mu\mu}(\mathrm{C})$ becomes ca. -5.0 eV.

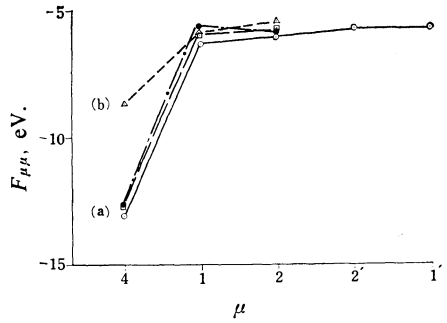

Fig. 3. $F_{\mu\mu}$ values of some aminobenzenes.
(a) Approximation A. —— Aniline
— — *p*-PDA —·— TAB
(b) VESCF approximation for *p*-PDA.
$\mu=7$ is for the amino group of TAB.

Some examples of the $F_{\mu\mu}$ values in aminobenzenes are shown in Fig. 3.

As has been described at the beginning of this article, we have calculated the electronic spectra and electronic structures of some aminobenzenes protonated on the ring carbon, employing the localization model.[16] In this case, for example in the benzenium ion, four electrons move in the field of five positive carbon cores. Therefore, the core field is much stronger in this case than in the case of neutral aminobenzene molecules, although, again in this case, we can observe that the $F_{\mu\mu}$(C) values are fairly uniform. Namely, $F_{\mu\mu}(C) \approx -10\pm0.5$ eV., throughout aniline protonated on para-carbon, *m*-PDA protonated on the carbon atom at the ortho-position to both amino groups and $TABH^+$. This $F_{\mu\mu}$(C) value is rather close to the average $F_{\mu\mu}$(C) value of the benzenium ion, -10.5 eV.

The non-diagonal matrix element, $F_{\mu\nu}$(C), between the nearest neighbor carbon AO's may be rewritten as:

$$F_{12}(C) = \beta_{12} - \frac{1}{2}(P^0_{12} + \Delta P_{12})\gamma_{12}$$

$$= F^0_{12} - \frac{1}{2}(\Delta P_{12})\cdot\gamma_{12} \qquad (16)$$

where F^0_{12} is the matrix element of the parent hydrocarbon because, in the present approximations except for the VESCF method, the β_{12} and γ_{12} are the same as those of the parent hydrocarbon.

We can observe that the F_{12}(C) values are not very different from each other throughout the aminobenzene molecules. The average value for these molecules is -4.063 eV.; this is close to the F_{12}(C) value for benzene, -4.1538 eV. However, as Fig. 4 shows, we can observe a definite linear relation between the F_{12}(C) value averaged over all the nearest neighbor pairs of an aminobenzene and the

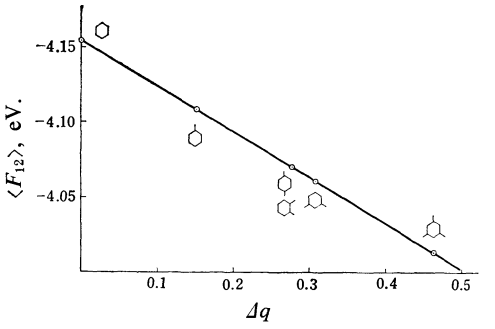

Fig. 4. $\langle F_{12}\rangle_{AV}$ versus Δq relation for aminobenzenes.

Δq value, the total of the charge which has migrated to the ring from the substituents.

Because the F_{12}(C) value in the present approximation is essentially determined by the P_{12} value, this fact indicates the linear relation between Δq and P_{12} averaged over all the nearest neighbor μ-ν pairs ($\langle P_{12}\rangle$), as is shown in Fig. 5.

Remarks on the Relations among the Charge Migrations, Bond Orders and the Extra Delocalization Energies. — As Fig. 5 shows, the linear relation between $\langle P_{12}\rangle$ and Δq seems to

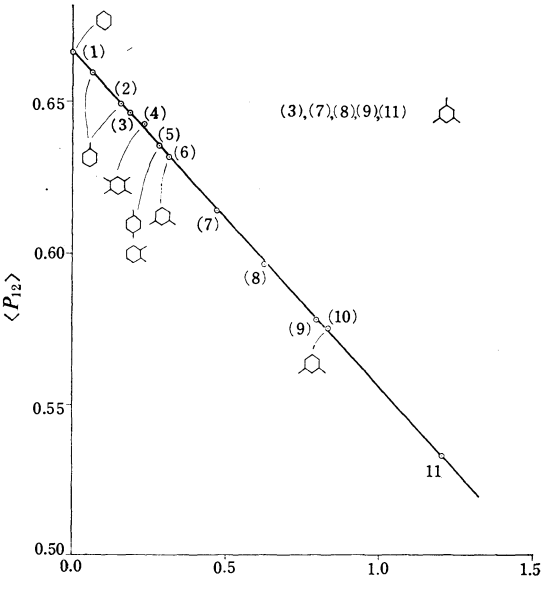

Fig. 5. $\langle P_{12}\rangle$ versus Δq relation for some substituted benzenes.
(1), (3), (4): $\delta_X=1.5$, $\beta_{CX}=0.7\beta$
(2), (5), (6), (7): $\delta_X=1.2$, $\beta_{CX}=\beta$
(8): $\delta_X=0.8$, $\beta_{CX}=\beta$
(9): $\delta_X=0.5$, $\beta_{CX}=\beta$
(10), (11): $\delta_X=0$, $\beta_{CX}=\beta$
The values for the case of $\delta_X=1.5$ and $\beta_{CX}=0.7\beta$ are taken from Ref. 27 and others are calculated by the present author.

hold almost exactly, at least in the case of the benzene derivatives, because the number of the substituents and the Coulomb parameter δ_X are varied from 1 to 4 and from 0 to 1.5 respectively, and the parameters for the resonance integral, β_{CX}, are of two kinds, 0.7 and 1.0.

Thus, the linear relation in this case can be expressed as;

$$\langle P_{12}\rangle = \langle P_{12}\rangle_0 - (0.11)\cdot \Delta q \qquad (17)$$

where $\langle P_{12}\rangle_0 = 2/3$, the bond order of benzene.

Furthermore, we can see an almost complete linear relation between the extra-delocalization energy (vertical), $\Delta\varepsilon$ and Δq, as can be seen from Fig. 6. The $\Delta\varepsilon$ versus Δq relation in Fig. 6 involves various amino-substituted nitrogen heterocycles in addition to the amino-substituted benzenes. The Hückel MO parameters for the amino group of the former compounds are the same as those of aminobenzenes, and the parameters for the ring nitrogen are the same as were used before,[18] i. e., $\delta_N = 0.5$ and $\beta_{CN} = \beta$. The analogous linear relation between $\Delta\varepsilon$ and Δq has already been demonstrated for hydroxy derivatives of benzene and naphthalene, assuming $\delta_O = 1.5$ and $\beta_{CO} = 0.7\beta$.[27]

Qualitatively speaking, we can expect a larger Δq value, the greater the $\Delta\varepsilon$ value, in accordance with the concept of the intra-

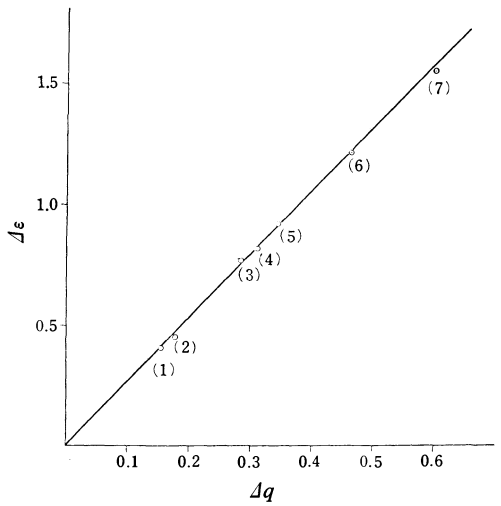

Fig. 6. $\Delta\varepsilon$ versus Δq relation for some amino-substituted benzenes and nitrogen heterocycles.
(1) Aniline (2) 4-Aminopyridine
(3) *p*- and *o*-PDA (4) *m*-PDA
(5) 4,4′-Diaminotetrazine
(6) TAB (7) Melamine
$\Delta\varepsilon$ is in unit of $-\beta$.

molecular charge transfer interaction.[7,8,11,28] Furthermore, we can anticipate a smaller $\langle P_{12}\rangle$ value, the larger the Δq value, because the charge is transferred from the substituents to the antibonding orbitals of benzene or *N*-heterobenzenes.

As we can see from Appendix I and Figs. 5 and 6, the $\Delta\varepsilon$, Δq and $\langle P_{12}\rangle$ values of substituted benzenes are approximately proportional to the number of the substituents when the same parameter value is used for the substituents. This fact suggests that we may be able to derive such a proportionality relation by the perturbation method. However, this proportionality and the linear relations seem to be rather peculiar, especially in view of the strong conjugation power of the amino group, which probably invalidates perturbation calculation. Nevertheless, we will examine here whether such a perturbation calculation is possible or not in the case of amino-substituted alternant hydrocarbons.

Now, the energy matrix for the secular determinant may be written as follows according to the LCMO approximation:

$$\begin{pmatrix}
\varepsilon_1^b & & & & \eta_{11}^b \cdots & \eta_{1\sigma}^b \cdots & \eta_{1n}^b \\
& \ddots & & & \vdots & \vdots & \vdots \\
& & \varepsilon_j^b & & \eta_{j1}^b \cdots & \eta_{j\sigma}^b \cdots & \eta_{jn}^b \\
& & & \ddots & \vdots & \vdots & \vdots \\
& & & \varepsilon_m^b & \eta_{m1}^b \cdots & \eta_{m\sigma}^b \cdots & \eta_{mn}^b \\
& & & & \eta_{11}^a \cdots & \eta_{1\sigma}^a \cdots & \eta_{1n}^a \\
& & & & \vdots & \vdots & \vdots \\
& & & & \eta_{j1}^a \cdots & \eta_{j\sigma}^a \cdots & \eta_{jn}^a \\
& & & & \vdots & \vdots & \vdots \\
& & & & \eta_{m1}^a \cdots & \eta_{m\sigma}^a \cdots & \eta_{mn}^a \\
& & & & \lambda_1 & & 0 \\
& & & & & \ddots & \\
& & & & & \lambda_\sigma & \\
& & & & 0 & & \ddots
\end{pmatrix} \qquad (18)$$

In Eq. 18, the ε^a's and ε^b's are the orbital energies of the antibonding and bonding orbitals of the hydrocarbon respectively, and the λ_σ's are those of the lone pair orbitals of the substituents. $\eta_{j\sigma}$ is the matrix element between the jth MO ψ_j of the hydrocarbon and the lone pair orbital, θ_σ, of the σth substituent; that is,

$$\eta_{j\sigma}^a = \int \psi_j^a \mathscr{H}_{\text{eff}} \theta_\sigma \mathrm{d}\tau$$

$$\eta_j^b = \int \psi_j^b \mathscr{H}_{\text{eff}} \theta_\sigma \mathrm{d}\tau$$

If $(\varepsilon_1^b)'$, $\cdots$, $(\varepsilon_m^b)'$, $(\varepsilon_1^a)'$, $\cdots$, $(\varepsilon_m^a)'$, $\cdots$, and $(\lambda_1)'\cdots(\lambda_n)'$ are the exact solutions of the secular equation, then, because of the invariance of trace,

27) K. Nishimoto, This Bulletin, **32**, 445, 699 (1959).

28) S. Nagakura, *Mol. Phys.*, **3**, 105 (1960).

$$\sum_j^m[(\varepsilon_j^a)'+(\varepsilon_j^b)']+\sum_\sigma^n(\lambda_\sigma)'$$

$$=\sum_j^m[\varepsilon_j^a+\varepsilon_j^b]+\sum_\sigma^n\lambda_\sigma \quad (19)$$

Accordingly,

$$\Delta\varepsilon=2\sum_j^m[\varepsilon_j^b-(\varepsilon_j^b)']+\sum_\sigma^n[\lambda_\sigma-(\lambda_\sigma)']$$

$$=2\sum_j^m[(\varepsilon_j^a)'-\varepsilon_j^a] \quad (20)$$

If we approximate $(\varepsilon_j^a)'$ by the second order perturbed energy, then, from Eq. 18,

$$(\varepsilon_j^a)'\cong\varepsilon_j^a+\sum_\sigma^n(\eta_{j\sigma}^a)^2/(\varepsilon_j^a-\lambda_\sigma) \quad (21)$$

From 20 and 21,

$$\Delta\varepsilon\cong2\sum_j^m\sum_\sigma^n(\eta_{j\sigma}^a)^2/(\varepsilon_j^a-\lambda_\sigma)$$

$$=2\sum_j^m\sum_\sigma^n(c_{js}^a\beta_{s\sigma})^2/(\varepsilon_j^a-\lambda_\sigma) \quad (22)$$

In deriving Eq. 22, we have used the ordinary approximation,

$$\eta_j^a=\int\psi_j^a\mathscr{H}_{\text{eff}}\theta_\sigma d\tau$$

$$=\sum_\mu c_{j\mu}^a\int\phi_\mu\mathscr{H}_{\text{eff}}\theta_\sigma d\tau\cong c_{js}^a\beta_{s\sigma} \quad (23)$$

where σth substituent is attached to the sth carbon.

In the case of aminobenzenes, Eq. 22 can be further simplified as follows:

$$\Delta\varepsilon=2\beta^2[\sum_s(c_{1s}^a)^2/(\varepsilon_1^a-\lambda)$$

$$+\sum_s(c_{2s}^a)^2/(\varepsilon_2^a-\lambda)+\sum_s(c_{3s}^a)^2/(e_3^a-\lambda)]$$

$$=(0.407)\cdot n_s\cdot(-\beta) \quad (24)$$

where n_s is the number of the substituents; this equation holds almost exactly.

The approximate MO corresponding to 21 may be written as:

$$(\psi_j^a)'\cong\psi_j^a+\sum_\sigma^n(\eta_{j\sigma}^a)\theta_\sigma/(\varepsilon_j^a-\lambda_\sigma)$$

and the normalized form of $(\psi_j^a)'$ is:

$$(\psi_j^a)'\cong[\psi_j^a+\sum_\sigma^n(\eta_{j\sigma}^a)\theta_\sigma/(\varepsilon_j^a-\lambda_\sigma)]/$$

$$[1+\sum_\sigma^n\{\eta_{j\sigma}^a/(\varepsilon_j^a-\lambda_\sigma)\}^2]^{1/2} \quad (25)$$

If (ψ_j)''s are the exact solutions of the secular equation, there exists the following relation for the coefficients, $c_{j\sigma}$'s, of θ_σ:

$$\sum_j^{m+n}(c_{j\sigma}^b)^2+\sum_j^m(c_{j\sigma}^a)^2=1$$

Accordingly,

$$\Delta q=2[n_s-\sum_j^{m+n}\sum_\sigma^n(c_{j\sigma}^b)^2]=2\sum_j^m\sum_\sigma^n(c_{j\sigma}^a)^2 \quad (26)$$

From 23, 25 and 26, the expression for Δq may be written as:

$$\Delta q\cong2\sum_j\left[\frac{\sum_s(c_{js}^a)^2}{(\varepsilon_j^a-\lambda)^2}\cdot\left\{1+\frac{\sum_s(c_{js}^a)^2}{(\varepsilon_j^a-\lambda)^2}\right\}^{-1}\right] \quad (27)$$

where $\lambda_\sigma=\lambda=1.2$.

If we neglect the second term in the curled bracket compared to 1, then Eq. 27 can be rewritten in the following form:

$$\Delta q\cong(0.170)\cdot n_s \quad (28)$$

However, because the exact value of Δq for aniline is 0.155, Eq. 34 is not a very good approximation.

If we use Eq. 27, the Δq values are calculated to be 0.160, 0.317 and 0.467 for aniline, *m*-PDA and TAB respectively. These values are fairly close to the exact values and are approximately proportional to the number of substituents.

Thus the linear relation between $\Delta\varepsilon$ and Δq and the proportionality of these quantities to n_s in the case of aminobenzenes can be accounted for approximately by the perturbation method.** However, when smaller δ_X values are used, the perturbation method becomes quite a poor approximation.

The calculation of $\langle P_{12}\rangle$ by the perturbation method gives quite poor results. In any way, we cannot explain the linear relation between $\langle P_{12}\rangle$ and Δq for the wide range of parameter values shown in Fig. 5.

The MO of a substituted benzene can be written in the LCMO form as follows:

$$\psi_i=\sum_{j=1}^6c_{ij}\psi_j^B+\sum c_{i\sigma}\theta_\sigma \quad (29)$$

where $\psi_1^B\cdots\psi_6^B$ are the MO's of benzene from the lowest bonding to the highest anti-bonding orbitals.

From Eq. 29, we can derive the following equation;

$$6\cdot\langle P_{12}\rangle=\sum_i^v(2c_{i6}^2+c_{i4}^2+c_{i5}^2)$$

$$-\sum_i^v(2c_{i1}^2+c_{i2}^2+c_{i3}^2) \quad (30)$$

where $\sum_i^v$ means the summation over the vacant orbitals of the substituted benzene.

** The following points should be noted here. In several parts of this paper, we have insisted that the perturbation method in the sense of the expansion of the secular determinant in a series seems to be a poor approximation for amino-substituted aromatics. The calculation of the orbital energies and MO's themselves for the occupied orbitals of these compounds by the perturbation method is certainly a very poor approximation. Therefore, we cannot use the perturbation method for the calculation of the electronic spectra. However, we can use this method to calculate some ground state quantities, such as $\Delta\varepsilon$ and Δq, expanding only the unoccupied orbitals which are affected only slightly by the substitution.

On the other hand, the expression for Δq can be written as:

$$\Delta q = 2\sum_{i}^{v}\sum_{\sigma} c_{i\sigma}^2 = 2\sum_{i}^{v}(1-\sum_{j=1}^{6} c_{ij}^2)$$
$$= 6 - 2\sum_{i}^{v}(2c_{i1}^2 + c_{i2}^2 + c_{i3}^2)$$
$$- 2\sum_{i}^{v}(2c_{i6}^2 + c_{i4}^2 + c_{i5}^2) + 2\sum_{i}^{v}(c_{i1}^2 + c_{i6}^2) \quad (31)$$

From 30 and 31 we can derive the following relation between $\langle P_{12}\rangle$ and Δq:

$$\langle P_{12}\rangle = 0.5 + \sum_{i}^{v}(c_{i1}^2 + c_{i6}^2)/6$$
$$- \sum_{i}^{v}(2c_{i1}^2 + c_{i2}^2 + c_{i3}^2)/3 - \Delta q/12 \quad (32)$$

When the ionization potential of the lone pair orbital of the substituent becomes infinitely large, Δq, $\sum_{i}^{v} c_{i1}^2$ and $\sum_{i}^{v}(2c_{i1}^2 + c_{i2}^2 + c_{i3}^2)$ approach zero, and $\sum_{i}^{v} c_{i6}^2$ approaches 1. Thus $\langle P_{12}\rangle$ becomes the bond order of benzene, 2/3.

Even in the case of amino-substituted benzene, $\sum_{i}^{v}(c_{i1}^2 + c_{i6}^2)$ may perhaps be close to unity and $\sum_{i}^{v}(2c_{i1}^2 + c_{i2}^2 + c_{i3}^2)$, to zero. For example, in the case of aniline, $\sum_{i}^{v}(c_{i1}^2 + c_{i6}^2) = 0.986$, $\sum_{i}^{v}(2c_{i1}^2 + c_{i2}^2 + c_{i3}^2) = 0.007$, and $\sum_{i}^{v}(c_{i1}^2 + c_{i6}^2) = 0.971$, while $\sum_{i}^{v}(2c_{i1}^2 + c_{i2}^2 + c_{i3}^2) = 0.014$ for *m*-PDA. Thus, the sum of the first two terms in the right-hand side of Eq. 32 is approximately equal to the bond order of benzene, and the sum of the 3rd and the fourth terms may be close to $(0.1)\cdot\Delta q$.

In this way, we can "*understand*" to some extent the linear relation between $\langle P_{12}\rangle$ and Δq, although this is not a "*proof*" of the relation in Eq. 17, which holds for a wide range of Hückel MO parameters.

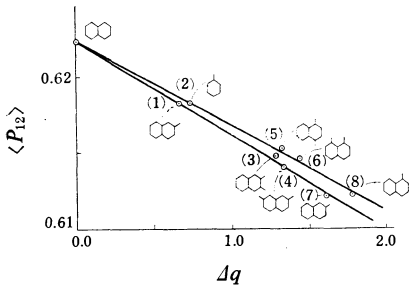

Fig. 7. $\langle P_{12}\rangle$ versus Δq relation for some substituted naphthalenes.
(1)—(6): $\delta_X = 1.5$, $\beta_{CX} = 0.7\beta$ (Taken from K. Nishimoto and R. Fujishiro, This Bulletin, **35**, 390 (1962) and Ref. 27)
(7), (8): $\delta_X = 1.2$, $\beta_{CX} = \beta$ (Taken from Ref. 9)

This sort of approximate linear relation between $\langle P_{12}\rangle$ and Δq holds not only for the benzene derivatives but also for the naphthalene derivatives, as Fig. 7 shows, although there is a slight difference between the α- and β-derivatives in this case.

A Comparison of the Calculated Dipole Moments of Aniline in the Ground State, as Well as in the Excited State, with the Experimental Values. — Using the wave functions given in Tables I and II, we have calculated the π-moment of aniline and compared it with the observed values.

The theoretical expression for the dipole moment in terms of the state function, Ψ, is given by:

$$\vec{\mu} = \langle \Psi | \boldsymbol{M} | \Psi \rangle \quad (33)$$

where $\boldsymbol{M} = \sum_{\tau} e_\tau \boldsymbol{r}_\tau$

e_τ and $\boldsymbol{r}_\tau$ are the charge and the position vector of τth particle respectively. In the π-electron approximation, $\boldsymbol{M}$ can be separated into two parts:

$$\boldsymbol{M} = e\sum \boldsymbol{r}_\lambda + \sum e_\kappa \boldsymbol{r}_\kappa$$

The first summation is over π-electrons, and the second, over the cores.

The necessary formulas for the expansion of 33 have been given elsewhere.[17a,29]

The ground state dipole moment of aniline has been calculated to be:

2.20 D. (Approximation A)

and 1.72 D. (Approximation B)

On the other hand, from the experimental value Smith[30] has estimated the π-moment of aniline to be $\sim$1.67 D., which is very close to the value calculated with Approximation B.

In addition to this study of the ground state dipole moment, we have calculated the π-moment in the lowest-excited singlet state.

On the other hand, we can use the difference between the solvent shifts of the absorption and fluorescence spectra in order to get experimental information on the electronic structure of the excited molecule.[29,31,33]

We have measured the absorption and fluorescence spectra of aniline in several solvents. The light source for the fluorescence measurement was a 300 W. Xenon discharge

29) N. Mataga, This Bulletin, **36**, 654 (1963).
30) J. W. Smith, *J. Chem. Soc.*, **1961**, 81.
31) N. Mataga et al., This Bulletin, **28**, 690 (1955); **29**, 465 (1956).
32) E. Lippert, *Z. Naturforsch.*, **10a**, 541 (1955); *Z. Elektrochem.*, **61**, 962 (1957).
33) E. G. McRae, *J. Phys. Chem.*, **61**, 562 (1957).

tube with a stabilizer. The fluorescence was excited at 285 mμ, the monochromatic exciting light from the Xenon discharge tube being taken out by a quartz prism monochromator. Aniline, which had been purified[34] by the standard method and stored in a vacuum and in a dark place, was distilled in a vacuum before use. The other details of the experimental procedures have been described elsewhere.[29,35]

Using the experimental results given in Table IV and by means of the following equation,[31,32] we can estimate the difference between the dipole moment in the excited state ($\vec{\mu}_e$) and that in the ground state ($\vec{\mu}_g$); i. e., $\vec{\Delta\mu}=(\vec{\mu}_e-\vec{\mu}_g)$, where the excited state is the fluorescence state.

$$hc(\sigma_a^m-\sigma_f^m)\simeq\text{Const.}+2\left[\frac{D-1}{2D+1}-\frac{n^2-1}{2n^2+1}\right]\frac{(\vec{\Delta\mu})^2}{a^3} \quad (34)$$

In Eq. 34, σ_a^m and σ_f^m are the wave numbers of a peak of the fluorescence band and that of the corresponding absorption band respectively. D and n are the dielectric constant and the refractive index of the solvent respectively, and a is the cavity radius in Onsager's theory of the reaction field.

TABLE IV. THE WAVE NUMBERS OF THE BAND MAXIMA OF ANILINE IN SEVERAL SOLVENTS (in unit of $10^4\,cm^{-1}$)

Solvent	σ_a^m	σ_f^m	$\sigma_a^m-\sigma_f^m$
Cyclohexane	3.48	3.14	0.34
Dichloroethane	3.47	3.07	0.40
n-Butylacetate	3.44	3.00	0.44
Acetonitrile	3.46	2.99	0.47

There are some ambiguities concerning the magnitude of a, although perhaps $a\simeq 2\sim 2.5$ Å. For these a values, $\vec{\Delta\mu}$ values are estimated to be 2~2.5 D. because $(\vec{\Delta\mu})^2/a^3\sim 2000\,cm^{-1}$.

It should be noted here that, if the change in the π-electronic structure induced by the electronic excitation is small, the observed $\vec{\Delta\mu}$ value represents approximately the difference between the π-moment in the excited state and that in the ground state. The theoretical $\vec{\Delta\mu}$ values are calculated as follows:

$\vec{\Delta\mu}=4.82$ D. (Approximation A)

and $\vec{\Delta\mu}=4.12$ D. (Approximation B)

Although the theoretical values are a little larger than the experimental values, their order of magnitudes is the same.

In our previous work[29] on the experimental and theoretical estimation of the $\vec{\Delta\mu}$ values of naphthylamines, it has been argued that the MO calculation may overestimate the $\vec{\Delta\mu}$ values.

If the calculated $\vec{\Delta\mu}$ value in the present case is reduced by multiplying by the same factor as before, i. e., 1/4, then the theoretical value becomes smaller than the experimental value, as was the case in the previous work.

In the case of naphthylamines, it has been suggested that the structure of the amino group changes a little during the life time of the excited state and that this is the cause of the observed value of $\vec{\Delta\mu}$ being larger than the theoretical value.

However, it is not quite certain whether or not the same factor to reduce the calculated $\vec{\Delta\mu}$ value as for naphthylamines is appropriate in the present case. Therefore, we cannot discuss in detail the structural change of the amino group during the life time of the excited state.

Summary

The electronic spectra and electronic structures of amino substituted benzenes have been studied by the semiempirical MO method, with the explicit inclusion of the electron repulsion.

According to the calculated results, we can interpret the difference between the spectra of various poly-substituted aminobenzenes; also, the calculated excitation energies and oscillator strengths are in satisfactory agreement with the observed values.

The relation between the present calculation and the simple Hückel MO calculation has been analyzed. Moreover, several interesting relations between the Hückel MO quantities of substituted benzenes and naphthalenes have been demonstrated and discussed.

The calculated π-moment of aniline in the ground state is in satisfactory agreement with the experimental value. Furthermore, the π-moment of aniline in the lowest excited singlet state has been calculated and compared with the experimental value obtained from the measurement of the solvent shifts of the absorption and fluorescence spectra.

The present author wishes to express his hearty thanks to Dr. Kichisuke Nishimoto and Dr. Shizuyo Mataga for their helpful discussions.

Faculty of Science
Osaka City University
Sumiyoshi-ku, Osaka

34) N. Mataga and S. Tsuno, This Bulletin, **30**, 711 (1957).
35) N. Mataga, Y. Torihashi and Y. Kaifu, *Z. Phys. Chem. N. F.*, **34**, 379 (1962).

APPENDIX I. HÜCKEL MO'S AND MO ENERGIES OF ANILINE AND ISOMERIC PDA'S (MO ENERGIES ARE IN UNITS OF β)

MO energy	MO
Aniline	
2.2565	$\psi_1(b_2)=0.3556(\phi_2+\phi_3)+0.2596(\phi_{2'}+\phi_{3'})+0.2301\phi_{1'}+0.5429\phi_1+0.5140\phi_4$
1.5712	$\psi_2(b_2)=0.1203(\phi_2+\phi_3)+0.4037(\phi_{2'}+\phi_{3'})+0.5139\phi_{1'}-0.2145\phi_1-0.5782\phi_4$
1.0000	$\psi_3(a_2)=0.5000(\phi_2-\phi_3)+0.5000(\phi_{2'}-\phi_{3'})$
0.5750	$\psi_4(b_2)=0.3866(\phi_2+\phi_3)-0.1332(\phi_{2'}+\phi_{3'})-0.4634\phi_{1'}+0.3556\phi_1-0.5692\phi_4$
−1.0000	$\psi_5(a_2)=0.5000(\phi_2-\phi_3)-0.5000(\phi_{2'}-\phi_{3'})$
−1.1431	$\psi_6(b_2)=0.2001(\phi_2+\phi_3)+0.3297(\phi_{2'}+\phi_{3'})-0.5771\phi_{1'}-0.5585\phi_1+0.2384\phi_4$
−2.0596	$\psi_7(b_2)=0.4113(\phi_2+\phi_3)-0.3779(\phi_{2'}+\phi_{3'})+0.3669\phi_{1'}-0.4691\phi_1+0.1439\phi_4$
	$P_{11}=0.934,\ P_{22}=1.081,\ P_{2'2'}=0.996,\ P_{1'1'}=1.064,\ P_{44}=1.845$
p-PDA	
2.3503	$\psi_1(b_{1u})=0.3100(\phi_2+\phi_{2'}+\phi_3+\phi_{3'})+0.4186(\phi_1+\phi_{1'})+0.3639(\phi_4+\phi_{4'})$
1.9708	$\psi_2(b_{3g})=0.1395(\phi_2-\phi_{2'}+\phi_3-\phi_{3'})+0.4144(\phi_1-\phi_{1'})+0.5376(\phi_4-\phi_{4'})$
1.1299	$\psi_3(b_{1u})=0.3028(\phi_2+\phi_{2'}+\phi_3+\phi_{3'})+0.0393(\phi_1+\phi_{1'})-0.5612(\phi_4+\phi_{4'})$
1.0000	$\psi_4(b^2_g)=0.5000(\phi_2+\phi_{2'}-\phi_3-\phi_{3'})$
0.3370	$\psi_5(b_{3g})=0.2842(\phi_2-\phi_{2'}+\phi_3-\phi_{3'})+0.3799(\phi_1-\phi_{1'})-0.4403(\phi_4-\phi_{4'})$
−1.0000	$\psi_6(a_u)=0.5000(\phi_2-\phi_{2'}-\phi_3+\phi_{3'})$
−1.2802	$\psi_7(b_{1u})=0.2493(\phi_2+\phi_{2'}+\phi_3+\phi_{3'})-0.5684(\phi_1+\phi_{1'})+0.2292(\phi_4+\phi_{4'})$
−2.1077	$\psi_8(b_{3g})=0.3869(\phi_2-\phi_{2'}+\phi_3-\phi_{3'})-0.4285(\phi_1-\phi_{1'})+0.1295(\phi_4-\phi_{4'})$
	$P_{11}=0.986,\ P_{22}=1.076,\ P_{44}=1.860$
o-PDA	
2.4120	$\psi_1(b_2)=0.2799(\phi_1+\phi_{1'})+0.4769(\phi_2+\phi_{2'})+0.1982(\phi_3+\phi_{3'})+0.3935(\phi_4+\phi_{4'})$
1.7094	$\psi_2(a_2)=0.2252(\phi_1-\phi_{1'})+0.3018(\phi_2-\phi_{2'})+0.0830(\phi_3-\phi_{3'})+0.5926(\phi_4-\phi_{4'})$
1.5231	$\psi_3(b_2)=0.2827(\phi_1+\phi_{1'})-0.1098(\phi_2+\phi_{2'})+0.5406(\phi_3+\phi_{3'})-0.3403(\phi_4+\phi_{4'})$
0.7930	$\psi_4(a_2)=0.5421(\phi_1-\phi_{1'})+0.1275(\phi_2-\phi_{2'})+0.3023(\phi_3-\phi_{3'})-0.3135(\phi_4-\phi_{4'})$
0.3509	$\psi_5(b_2)=0.2049(\phi_1+\phi_{1'})+0.3876(\phi_2+\phi_{2'})-0.3156(\phi_3+\phi_{3'})-0.4564(\phi_4+\phi_{4'})$
−1.0859	$\psi_6(b_2)=0.5475(\phi_1+\phi_{1'})-0.3320(\phi_2+\phi_{2'})-0.2624(\phi_3+\phi_{3'})+0.1452(\phi_4+\phi_{4'})$
−1.1841	$\psi_7(a_2)=0.0983(\phi_1-\phi_{1'})+0.4177(\phi_2-\phi_{2'})-0.5341(\phi_3-\phi_{3'})-0.1752(\phi_4-\phi_{4'})$
−2.1183	$\psi_8(a_2)=0.3815(\phi_1-\phi_{1'})-0.4671(\phi_2-\phi_{2'})-0.3411(\phi_3-\phi_{3'})+0.1408(\phi_4-\phi_{4'})$
	$P_{11}=1.090,\ P_{22}=0.994,\ P_{33}=1.059,\ P_{44}=1.860$
m-PDA	
2.3640	$\psi_1(b_2)=0.2841(\phi_2+\phi_3)+0.4313(\phi_{2'}+\phi_{3'})+0.2404\phi_1+0.3650\phi_{1'}+0.3707(\phi_4+\phi_{4'})$
1.9168	$\psi_2(a_2)=0.2057(\phi_2-\phi_3)+0.3941(\phi_{2'}-\phi_{3'})+0.5498(\phi_4-\phi_{4'})$
1.3450	$\psi_3(b_2)=0.4008(\phi_2+\phi_3)-0.0568(\phi_{2'}+\phi_{3'})+0.5962\phi_1-0.0848\phi_{1'}-0.3931(\phi_4+\phi_{4'})$
0.6696	$\psi_4(b_2)=0.0962(\phi_2+\phi_3)-0.2232(\phi_{2'}+\phi_{3'})+0.2876\phi_1-0.6666\phi_{1'}+0.4210(\phi_4+\phi_{4'})$
0.5102	$\psi_5(a_2)=0.5259(\phi_2-\phi_3)+0.2683(\phi_{2'}-\phi_{3'})-0.3890(\phi_4-\phi_{4'})$
−1.0684	$\psi_6(b_2)=0.3275(\phi_2+\phi_3)+0.2633(\phi_{2'}+\phi_{3'})-0.6134\phi_1-0.4930\phi_{1'}-0.1162(\phi_4+\phi_{4'})$
−1.2271	$\psi_7(a_2)=0.4255(\phi_2-\phi_3)-0.5221(\phi_{2'}-\phi_{3'})+0.2152(\phi_4-\phi_{4'})$
−2.1101	$\psi_8(b_2)=0.3763(\phi_2+\phi_3)-0.4373(\phi_{2'}+\phi_{3'})-0.3567\phi_1+0.4145\phi_{1'}+0.1321(\phi_4+\phi_{4'})$
	$P_{11}=0.992,\ P_{22}=1.139,\ P_{2'2'}=0.933,\ P_{1'1'}=1.170,\ P_{44}=1.846$

APPENDIX II. VESCF MO'S AND MO ENERGIES OF *p*-PDA (MO ENERGIES ARE IN UNITS OF eV.)

MO energy	MO
−13.6929	$\psi_1(b_{1u})=0.3435(\phi_2+\phi_{2'}+\phi_3+\phi_{3'})+0.4406(\phi_1+\phi_{1'})+0.2642(\phi_4+\phi_{4'})$
−12.2245	$\psi_2(b_{3g})=0.1711(\phi_2-\phi_{2'}+\phi_3-\phi_{3'})+0.4903(\phi_1-\phi_{1'})+0.4484(\phi_4-\phi_{4'})$
− 9.9838	$\psi_3(b_{2g})=0.5000(\phi_2+\phi_{2'}-\phi_3-\phi_{3'})$
− 9.5396	$\psi_4(b_{1u})=0.2674(\phi_2+\phi_{2'}+\phi_3+\phi_{3'})-0.0605(\phi_1+\phi_{1'})-0.5943(\phi_4+\phi_{4'})$
− 7.4495	$\psi_5(b_{3g})=0.2645(\phi_2-\phi_{2'}+\phi_3-\phi_{3'})+0.2938(\phi_1-\phi_{1'})-0.5232(\phi_4-\phi_{4'})$
− 0.4914	$\psi_6(a_u)=0.5000(\phi_2-\phi_{2'}-\phi_3+\phi_{3'})$
0.0951	$\psi_7(b_{1u})=0.2457(\phi_2+\phi_{2'}+\phi_3+\phi_{3'})-0.5498(\phi_1+\phi_{1'})+0.2775(\phi_4+\phi_{4'})$
2.6572	$\psi_8(b_{3g})=0.3882(\phi_2-\phi_{2'}+\phi_3-\phi_{3'})-0.4162(\phi_1-\phi_{1'})+0.1589(\phi_4-\phi_{4'})$
	$P_{11}=1.049,\ P_{22}=1.077,\ P_{44}=1.796$

The Quenching Action of Pyridine and Quinoline on the Fluorescence of Naphthalene Derivatives

By Takuji MIWA and Masao KOIZUMI

(Received June 19, 1963)

The influence of the hydrogen bond on the fluorescent properties of aromatic compounds has been studied by seveval authors, including Mataga and Koizumi,[1] Kasha[5] and Weller.[6] Mataga particularly has performed some systematic studies using various combinations of acceptor and donor.[1-4] One of his most interesting findings is that an aromatic fluorescer is strongly quenched when it is hydrogen-bonded directly with another π-electronic system. Thus, for example, the fluorescence of naphthol and acridine is largely quenched by, respectively, pyridine and phenol. He has proposed, as a mechanism for such a quenching process, that the charge transfer from quencher to fluorescer or from fluorescer to quencher via the hydrogen bond occurs, followed by the vibronic energy dissipation. In connection with this hypothesis, it seemed interesting to extend the study to systems in which the possibility of an electronic energy transfer via the hydrogen bond is conceivable. In such cases there is also a possibility that the quenching efficiency depends on the wavelength of the exciting light. Very few examples of such systems have ever been studied, perhaps because the complicated character of such systems is supposed to make the analysis of the results very troublesome.

We have sttempted such an experiment using naphthol and naphthylamine as hydrogen-donating fluorescers and quinoline, as a hydrogen-accepting quencher; for the sake of comparison, we have also studied the effect of quinoline on the fluorescence of 2-naphthylmethylether and *N, N*-dimethyl-2-naphthylamine, both of which are unable to form hydrogen bonds. We have found appreciable quenching, even in the latter cases. In connection with these rather unexpected results, therefore, some experiments have been made with the use of pyridine as a quencher, and, further, the solvent effect has been studied to some extent.

Experimental

Materials.—*2-Naphthylamine.* — A G. R. sample was dissolved in dilute hydrochloric acid, filtered, and neutralized by soduim hydroxide. The precipitate obtained, after being filtered and dried, was submitted to repeated crystallization from a water-ethanol mixture and to sublimation in vacuo.

N, N-Dimethyl-2-naphthylamine. — The mixture of methyl iodide and 2-naphthylamine, with sodium hydroxide added, was heated for ten hours at 120°C in a sealed vessel. The product was extracted by chloroform, and the raw crystal was obtained by evaporating the solvent. For further purification, recrystallization from methanol and sublimation under reduced pressure were repeated several times (m. p. 43.2°C).

2-Naphthol.—A G. R. sample was recrystallized from a water-ethanol mixture and sublimed in vacuo.

2-Naphthylmethylether. — A concentrated sulfuric acid solution of 2-naphthol and methyl alcohol was refluxed for four hours at 125°C. The product was extracted by benzene and washed with an aqueous alkaline solution until no existence of a phenolic hydroxy group was detected by a Millon test. The crystal obtained by evaporating the solvent, after several recrystallizations from ethanol, was dried in a calcium chloride desiccator (m. p. 72.1°C).

Quinoline. — Synthesized quinoline manufactured by Tokyo Kasei was dried over barium oxide for more than a week and was twice distilled in vacuo.

Pyridine.—A G. R. reagent of Wako-Junyaku was dehydrated by making the azeotrope with benzene. Ordinary distillation, fractional distillation with a packed column and vacuum distillation were performed in succession.

n-Hexane.—After being shaken for a long time with fuming sulfuric acid diluted with concentrated sulfuric acid, this was washed with water, neutralized with an aqueous alkaline solution, treated with alkaline potassium permanganate, washed again with water, and then dried over calcium chloride. It was further distilled from over sodium metal or phosphorous pentoxide. The fraction (67.5~68.5°C) was used.

1) N. Mataga, Y. Kaifu and M. Koizumi, *Nature*, **175**, 731 (1955); This Bulletin, **29**, 115 (1956); N. Mataga and S. Tsuno, ibid., **30**, 368, 711 (1957).
2) N. Mataga, ibid., **31**, 481 (1958).
3) N. Mataga, ibid., **31**, 487 (1958).
4) N. Mataga, Y. Torihashi and Y. Kaifu, *Internattonal Symposium on Molecular Structure and Spectroscopy, September* 1962, *Science councll of Japan*, D. 113-1~4; *Z. Phys. Chem., N. F.*, **34**, 379 (1962); N. Mataga and Y. Kaifu, *J. Chem. Phys.*, **36**, 2804 (1962).
5) M. Ashraf El-Bayoumi and M. Kasha, ibid., **34**, 2181 (1961).
6) A. Weller, *Naturwlss.*, **7**, 175 (1955); *Z. Elektrochem.*, **60**, 1144 (1956). A. Weller and K. H. Grellmann, ibid., **64**, 145 (1960).

Benzene.—A G. R. sample of Wako-Junyaku was shaken with concentrated sulfuric acid, treated with an aqueous alkaline solution, washed with water, and then dried over calcium chloride. Three recrystallizations in a ice bath and fractional distillation through a packed column were performed.

Ethanol.—A G. R. sample of Wako-Junyaku was fractionally distilled through a column packed with stainless spirals.

Anthracene.—A sample of a high purity was kindly supplied by Professor Shimpachiro Kato of the University of Tokyo.

The purity of 2-naphthylmethylether and of *N*, *N*-dimethyl-2-naphthylamine was checked by I. R., while that of pyridine and quinoline was checked by gas chromatography.

Apparatus.—A block diagram of fluorometer is shown in Fig. 1.

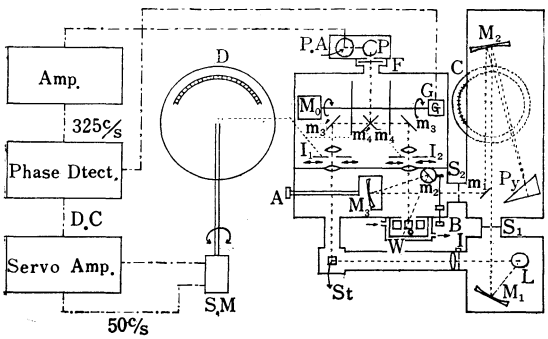

Fig. 1. Fluorometer.
A, B: screw for adusting focus, C: wavelength disk, D: intensity disk, F: filter, G: generator, I, I_1, I_2: iris, L: light source, M_0: synchronous motor, m_1, m_2, m_3, m_4, m_3', m_4': mirror, M_1, M_2, M_3: concave mirror, o: sample, P: photomultiplier, P. A: priamplifier, Py: prism. S_1, S_2: slit, S. M: reversible motor, St: standard material, W: water jacket

This apparatus is constructed in such a way that the solution is illuminated obliquely from the front, the exciting light being focused close to the cell. The fluorescent light coming out from the same front is compared with a standard beam taken through another path from the same light source; by mechanically balancing the intensity of the two beams, the ratio of the two can be read directly on a scale-disk. The apparatus is suitable for systems with a large optical density. The exciting light from a 500W Xenon lamp of Ushio Kogyo was made monochromatic by a prism monochromator. A RCA 1P28 photomultiplier was used. The absorption spectra were measured by means of a Hitachi spectrophotometer, and the fluorescence spectra, by the same apparatus with its fluorescence attachments.

The Procedure, the Calibration of the Apparatus and an Outline of the Analysis.—The measurement was made in the following way. The relative intensity against the standard light beam was measured with a solution containing only a fluorescer and with a solution containg the same concentration of fluorescer and various amounts of quencher at the same time. From these measurements the ratio of the former, F_0, to the latter, F, was calculated. The measurement was made at constant temperatures and at various wavelengths in the region from 260 to 350 mμ. The concentration was 10^{-3} M for 2-naphthylamine and *N*, *N*-dimethyl-2-naphthylamine, and 2.5×10^{-3} M for 2-naphthol and 2-naphthylmethylether. The concentration of quencher was varied over a suitable range according to the situations.

After the scale of the intensity ratios and of the wavelengths had been calibrated in a suitable way, the depth effect or the effect of the optical density of the system on the measured fluorescence intensity was examined. This effect is, of course, mainly due to the quantity of the absorption of light, but it is expected that the effect partially depends on the geometric condition characteristic of the apparatus. Thus, the emitting position varies according to the optical density of the solution, thereby affecting the measured intensity. This effect is expected to be especially large when the optical density is rather small and when the exciting beam penetrates into the inner part of the solution. This is the reason why the experimental calibration is desirable.

To examine this effect quantitatively, the solution of anthracene in *n*-hexane was used as a sample for calibration, since it has been well established by many investigations[7-9,10] that its fluorescence

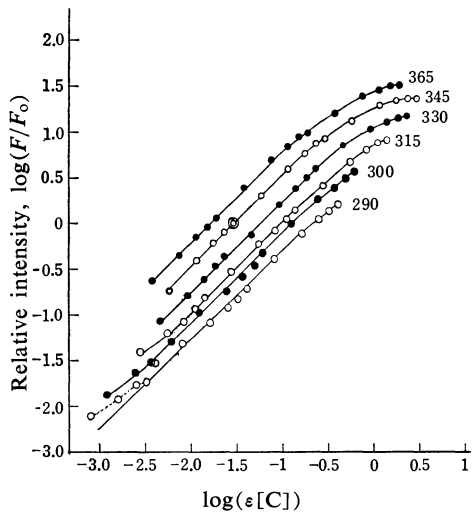

Fig. 2. Relation between fluorescence intensity and optical density for the solution of anthracene in *n*-hexane. All the (F/F_0) values are the relative ones, the value for 10^{-5} M anthracene solution at 345 mμ being taken as a standard (denoted by ◎ in the figure). The number is exciting wavelength (mμ).

7) Cf., for example, W. H. Melhuish, *J. Phys. Chem.*, **65**, 229 (1961); W. R. Ware, ibid., **66**, 455 (1962).
8) G. Weber and F. W. J. Teale, *Trans. Faraday Soc.*, **54**, 640 (1958). J. Ferguson, *J. Mol. Spectroscopy*, **3**, 177 (1959).
9) E. J. Bowen and A. Norton, *Trans. Faraday Soc.*, **35**, 45 (1939).
10) A. Dammers-de Klerk, *Mol. Phys.*, **1**, 141 (1958).

quantum yield is independent of the wavelength[8] and that, further, its concentration quenching is practically of no importance up to about 10^{-3} M.[9] Moreover, the experimental conditions quite similar to those for the systems to be studied can be chosen. Actually the concentration of anthracene in *n*-hexane was varied from 2×10^{-6} M to 10^{-3} M. The relations obtained between the optical density of the solution and the measured fluorescence intensity are shown in Fig. 2.

The dependence of the position of the curves on the frequency is no doubt due to the intensity distribution of the exciting light. In the region of low optical density, all the curves have the same unit slope, while they tend to constant values characteristic for each frequency. The latter phenomena are mainly due to the situations approaching the complete absorption of exciting light. In fact, the plot of $\log(F/F_0)$ against $\log(1-e^{-2.303\varepsilon[C]})$ gives a straight line, with a unit slope for each frequency. From the results in Fig. 2 one can estimate the intensity distribution of the exciting light. In most of the experiments the optical density was so high that the intensity of the fluorescence was believed to be independent of it, but in a few cases where the optical density was lower, the correction factor for the incomplete absorption of light was estimated from Fig. 2.

To interpret the relation between F_0/F and the concentration of the quencher, it is necessary in general to take into account the inner filter effect of the absorption of the quencher, the effect of hydrogen bond formation in the ground state, and lastly, the genuine quenching effect. As has been shown by Mataga[4] and by one of the present authors[11] (M. K.), the quenching effect via the hydrogen bond formation must be treated in just the same way as in the case of dynamical quenching, in contradistinction to the case of the enhancement of fluorescence intensity. The prerequisite for the method of analysis, that is, the complete suppression of fluorescence by hydrogen bonding, is supported by the fact that the fluorescence spectra of naphthylamine and naphthol are not affected by the addition of enough pyridine or quinoline to effect an appreciable change in the absorption spectra of the fluorescer. This fact enables us further to disregard the possibility of the reabsorption of the fluorescence by a quencher due to the slight overlapping of the fluorescence spectra and the absorption spectra of the quencher. In addition, the fluorescence intensity of quinoline is so weak that it can be disregarded in comparison with the fluorescence of 2-naphthylamine and 2-naphthol. Thus, it is most plausible to analyze the experimental results on the basis of the assumption that only free fluorescer molecules can emit fluorescence and that the pyridine or quinoline molecules which attack the excited fluorescer molecules cause the quenching phenomenon. In some cases, however, the influence on the fluorescence due to the inner filter effect of the quencher and the influence of the existence of a hydrogen-bonded complex are so great that it is very difficult to obtain the exact value of the quenching constant. It is desirable that any particular device is, if possible, used case by case.

11) M. Koizumi, Symposium on the Electronic States of Molecules, held by the Chemical Society of Japan, October, 1961.

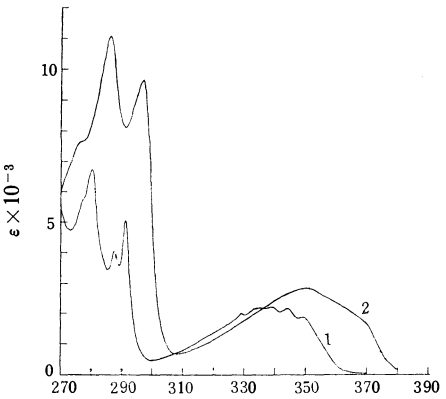

Fig. 3a. Absorption spectra in *n*-hexane.
1; 2-Naphthylamine
2; *N*, *N*-Dimethyl-2-naphthylamine

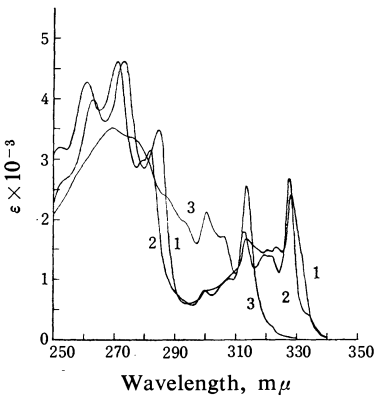

Fig. 3b. Absorption spectra in *n*-hexane.
1; 2-Naphthol, 2; 2-Naphthylmethylether, 3; Quinoline

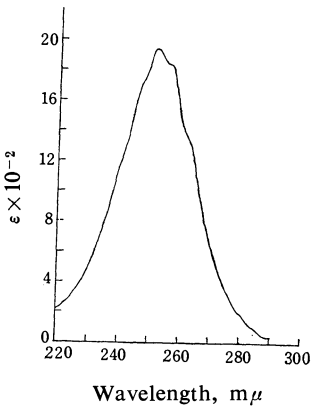

Fig. 3c. Absorption spectrum of pyridine in *n*-hexane.

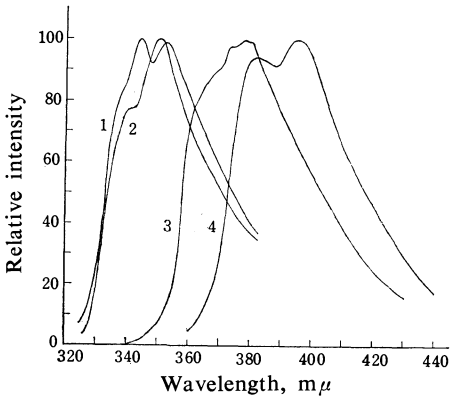

Fig. 3d. Fluorescence spectra (arbitrary unit).
1; 2-Naphthylmethylether 5×10^{-4} M/l. in *n*-hexane
2; 2-Naphthol 2×10^{-4} M/l. in *n*-hexane
3; 2-Naphthylamine 10^{-3} M/l. in *n*-hexane
4; *N*, *N*-Dimethyl-2-naphthylamine 10^{-3} M/l. in *n*-hexane

Results

Absorption Spectra and Fluorescence Spectra.—The absorption spectra of some fluorescers and quenchers and the fluorescence spectra for the former are shown in Fig. 3, a, b, c and d.

The Equilibrium Constant of the Hydrogen Bond Formation in the Ground State.—This was obtained spectroscopically by the usual method. Changes in the absorption spectra in the case of 2-naphthol—pyridine and in the case of 2-naphthol—quinoline, both in *n*-hexane, are shown in Fig. 4, a and b.

The equilibrium constant was evaluated by using the following equation:

$$\frac{d^{\lambda}-d_{o}^{\lambda}}{[A]}=\varepsilon'^{\lambda}K[D_o]-Kd^{\lambda} \qquad (1a)$$

$$K=\frac{[A]\,(d_{o}^{\lambda}-d'^{\lambda})+[A']\,(d^{\lambda}-d_{o}^{\lambda})}{[A]\,[A']\,(d'^{\lambda}-d^{\lambda})} \qquad (1b)$$

where [A] or [A'] and [D_o] denote, respectively, the total concentration of quencher and the total concentration of fluorescer, where d^{λ} or d'^{λ} and d_o^{λ} are the optical densities at the wavelength λ in the presence and in the absence of a quencher respectively, and where ε'^{λ} is the molar extinction coefficient of the hydrogen-bonded complex at λ. As Fig. 5 shows, the 1a relation holds quite satisfactorily.

The values obtained from 1a are given in Table I, together with the pertinent data published in the literature. The values from 1a are in good agreement with the average values obtained numerically from 1b.

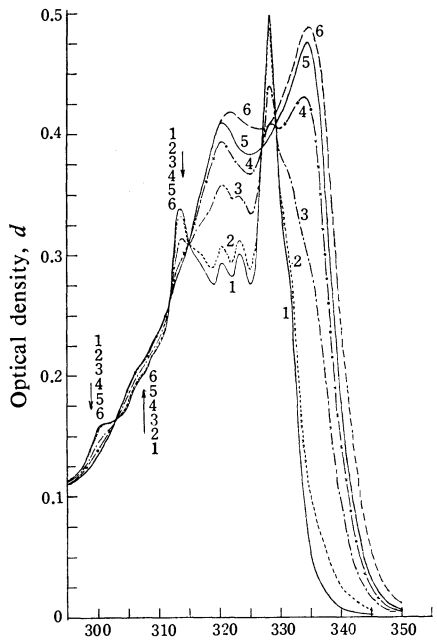

Fig. 4a. Absorption spectra of 2-naphthol (2×10^{-4} M/l.)—pyridine in *n*-hexane at 21°C. The contribution by pyridine is eliminated by substracting the absorption of pyridine solution of corresponding concentration. Concentration of pyridine (M/l.).
1; 0, 2; 9.943×10^{-4}, 3; 9.943×10^{-3}, 4; 4.972×10^{-2}, 5; 2.486×10^{-1}, 6; 2.486

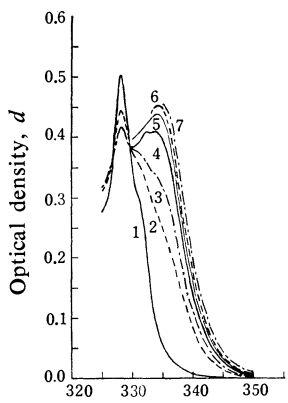

Fig. 4b. Absorption spectra of 2-naphthol (2×10^{-4} M/l.)—quinoline in *n*-hexane at 21°C. The contribution by quinoline is eliminated by substracting the absorption of quinoline solution of corresponding concentration.
Concentration of quinoline (M/l.).
1; 0, 2; 6.767×10^{-3}, 3; 1.353×10^{-2}, 4; 3.384×10^{-2}, 5; 6.767×10^{-2}, 6; 1.353×10^{-1}, 7; 3.384×10^{-1}

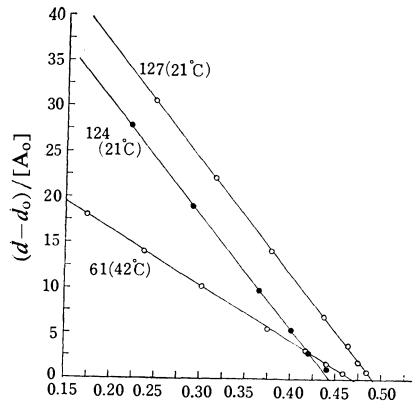

Fig. 5. The procedure for obtaining the hydrogen bonding formation constant K. The numbers represent the value of K at the given temperature.
○ : 2-Naphthol—Pyridine in *n*-hexane at 334 mμ.
● : 2-Naphthol—Quinoline in *n*-hexane at 336 mμ.

TABLE I. THE EQUILIBRIUM CONSTANT K OF THE HYDROGEN BOND FORMATION

System	Solvent	Temp. °C	K
2-Naphthol—Pyridine	*n*-Hexane	21	125
		42	61
	Benzene[2]	14	41
2-Naphthol—Quinoline	*n*-Hexane	21	125
2-Naphthylamine—Pyridine	Cyclohexane[4]	15	12
	Benzene[2]	13	0.2

2-Naphthylamine and *N*, *N*-Dimethy-2-naphthylamine in *n*-Hexane.—In the case of *N*, *N*-dimethyl-2-naphthylamine—quinoline which has no ability to act as a hydrogen donor, there are two factors which must be taken into account: (i) the genuine quenching effect and (ii) the inner filter effect due to the absorption of quinoline. On this basis, F_0/F is expressed as follows:

$$F_0/F=\frac{1-e^{-\alpha_D[D]d}}{1-e^{-(\alpha_D[D]+\alpha_A[A])d'}}\left(\frac{\varepsilon_D[D]+\varepsilon_A[A]}{\varepsilon_D[D]}\right)$$
$$\times(1+k[A])=\frac{1-e^{-\alpha_D[D]d}}{1-e^{-(\alpha_D[D]+\alpha_A[A])d'}}$$
$$\times\left\{1+\left(k+\frac{\varepsilon_A}{\varepsilon_D[D]}\right)[A]+k\frac{\varepsilon_A}{\varepsilon_D[D]}[A]^2\right\} \quad (2)$$

where [D] and [A] are the concentrations of fluorescer and of quencher respectively, where α_D, α_A, ε_D and ε_A are, respectively, the molar absorbancy of fluorescer and quencher and the molar extinction coefficient of fluorescer and quencher, and where k is the quenching constant. The first term on the right side concerns the absorption of light, and its denominator can always be well approximated by 1, while for the numerator this is not always possible in the region where α_D is rather small. The value was estimated from the calibration curves of Fig. 2. F_0/F divided by this value will be denoted as $(F_0/F)_{corr.}$. It is to be added that there is no overlapping of the fluorescence spectra and the absorption spectra of quinoline, even in such a high concentration of the latter as 0.388 M. As required by Eq. 2, the plot of $(F_0/F)_{corr.}-1$ against [A] gives a concave curve upward, while the plot of $((F_0/F)_{corr.}-1)/[A]$ against [A] gives a good straight line, as is shown in Fig. 6.

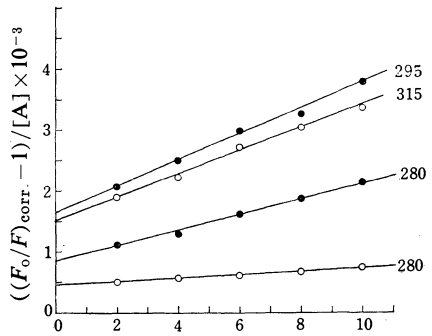

Fig. 6. Plot of $((F_0/F)_{corr.}-1)/[A]$ against the concentration of quinoline [A]. The number is the exciting wavelength (mμ).
● : 2-Naphthylamine (10^{-3} M/l.)—Quinoline in *n*-hexane at 20°C.
○ : *N*, *N*-Dimethyl-2-naphthylamine (10^{-3} M/l.)—Quinoline in *n*-hexane at 20°C.

From the slope and intercept one gets $k\varepsilon_A/\varepsilon_D[D]$ and $k+\varepsilon_A/\varepsilon_D[D]$; k can be evaluated if the values of ε_A and ε_D under the experimental conditions are estimated. In this system, however, the absorption spectra of quinoline do not overlap with those of the fluorescer in the region >335 mμ, and so the correct value of k can be obtained from the linear plot of $(F_0/F)_{corr.}-1$ against [A] at these wavelengths. Thus, in this case,

$$(F_0/F)_{corr.}-1=k[A] \quad (3)$$

The values obtained are $k=90$ (20°C) and $k=100$ (40°C).

This is a result somewhat unexpected, since Mataga[2] found previously that pyridine, the basicity of which is quite similar to quinoline, does not quench the fluorescence of *N*, *N*-dimethyl-2-naphthylamine at all (see Discussion).

In the case of 2-naphthylamine—quinoline, the hydrogen bond is formed with quinoline. However, the equilibrium constant of its formation, as has already been mentioned, is quite small, and under the experimental conditions the change in the absorption spectra due to the hydrogen bond formation is negligible. Therefore, all the effects of hydrogen bond formation such as (i) the increase in the reabsorption of fluorescence, (ii) the decrease in the fluorescence due to the reduced number of free molecules, and (iii) the change in the inner filter effect can be disregarded. Hence Eq. 2 is equally well applicable in this case. In fact, the plot of $(F_0/F)_{corr.}-1$ against [A] gives a concave curve upward, while the plot of $((F_0/F)_{corr.}-1)/[A]\sim[A]$ gives a good straight line (Fig. 6). As in the case of *N*, *N*-dimethyl-2-naphthylamine—quinoline, however, a more exact value of k can be obtained from the results in the $\sim$335 mμ region, where the absorptions of the two substances do not overlap and where Eq. 3 satisfactorily holds. The values obtained are $k=120$ (20°C) and $k=140$ (40°C).

The Frequency Effect on the Quenching Constant in the Cases of 2-Naphthylamine—Quinoline and *N*,*N*-Dimethyl-2-naphthylamine—Quinoline.—Since there is some difficulty in obtaining the correct value of k at various frequencies on the basis of Eq. 2, the dependence of k on the frequency was examined in the following way. From Eq. 2 one can calculate $\varepsilon_D/\varepsilon_A$ if k is assumed to be constant, irrespective of the frequency, and to have the same value as that at 335 mμ, where there is no overlapping of absorptions. If the values of $(\varepsilon_A/\varepsilon_D)$ at various frequencies obtained from the calculation coincide with those from the observed ε_A and ε_D values, one may conclude that there is no frequency effect on k. In the opposite case, one will have to recognize the dependence of k on the frequency. The result is, as Figs. 7 and 8 show, that there is a very good correspondence between the two.

Thus there is no doubt that k is constant, independent of the frequency.

2-Naphthylmethylether and 2-Naphthol in *n*-Hexane.—In the case of 2-naphthylmethylether—quinoline, the absorption spectra of the two substances overlap over the whole wavelength region. Therefore, $\varepsilon_A/\varepsilon_D$ values were estimated from the molar extinction coefficient and k was calculated for various frequencies on the basis of Eq. 2. The value is $k=53$ (21°C), irrespective of the wavelength.

In the case or 2-naphthol—quinoline, there are three kinds of effects which reduce the fluorescence intensity: (i) the genuine quenching action, (ii) the inner filter effect, and

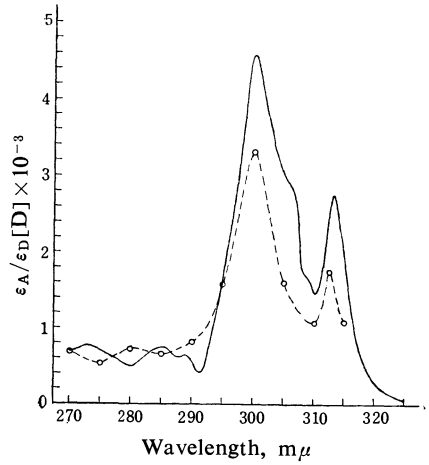

Fig. 7. Inner filter effect for 2-naphthylamine—quinoline in *n*-hexane. Full line and dotted line represent respectively the calculated value $\varepsilon_A/\varepsilon_D[D]$ and the observed value.

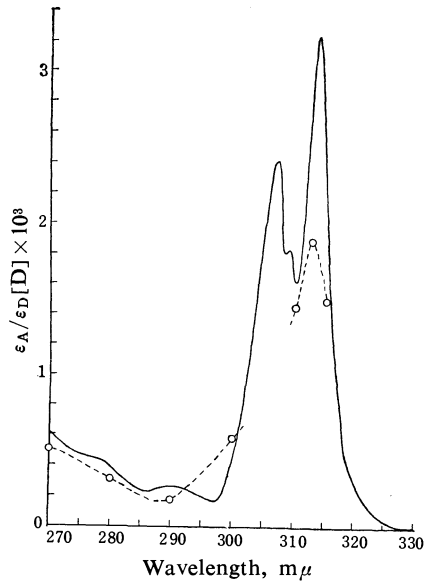

Fig. 8. Inner filter effect for *N*, *N*-dimethyl-2-naphthylamine—quinoline in *n*-hexane. Full line and dotted line represent respectively the calculated value $\varepsilon_A/\varepsilon_D[D]$ and the observed value.

(iii) the formation of the nonfluorescent hydrogen-bond complex in the ground state. Taking these three effects into account, one can derive the following equation:

$$(F_0/F)_{corr.}=(1+k[A])\times\left(1+\frac{\varepsilon_A[A]}{\varepsilon_D[D]}+\frac{\varepsilon_{DA}K}{\varepsilon_D}[A]\right)$$

where K is the equilibrium constant of the

hydrogen bond formation. The above equation is further changed as follows by putting $[D] = [D_o]/(1+K[A])$:

$$(F_o/F)_{corr.}-1=\left(k+\frac{\varepsilon_A+K[D_o]\,\varepsilon_{DA}}{\varepsilon_D[D_o]}\right)[A]+\left(k\frac{\varepsilon_A+K[D_o]\,\varepsilon_{DA}}{\varepsilon_D[D_o]}+\frac{K\varepsilon_A}{\varepsilon_D[D_o]}\right)[A]^2+k\frac{K\varepsilon_A}{\varepsilon_D[D_o]}[A]^3 \quad (4)$$

As Fig. 9 shows,

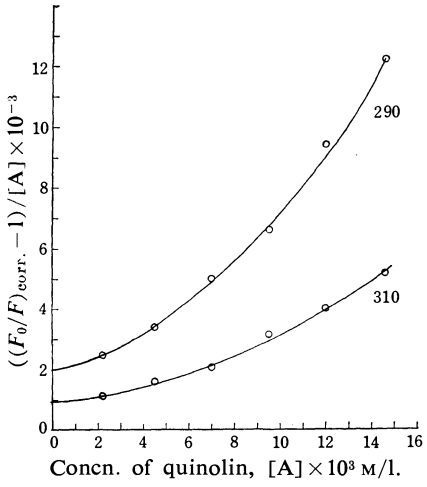

Fig. 9. Plot of $((F_o/F)_{corr.}-1)/[A]$ against the concentration of quinoline [A] for 2-naphthol (10^{-3} M/l.)—quinoline in *n*-hexane at 21°C. The number is exciting wavelength (mμ).

the plot of $((F_o/F)_{corr.}-1)/[A]$ against [A] gives a concave curve upward and so Eq. 4 is considered to fit the experimental results. However, the exact value of k could not be obtained because the other two effects are considerably larger than the genuine quenching action and made the treatment erroneous. It was roughly estimated that $k\approx100$ irrespective of the wavelength.

It is to be added here that in these two cases, quinoline has absorption spectra the long wavelength part of which overlaps slightly with the fluorescence spectra and that, moreover, there is some possibility that the nonfluorescent hydrogen-bonded complex reabsorbs the fluorescence to some extent. Of course, the above treatment does not take any account of these possibilities.

Pyridine as a Quencher. — All the above results, which concern cases where quinoline acts as a quencher, are rather unexpected in view of the results and the proposed mechanism by Mataga,[2] because 2-naphthylmethylether and *N*, *N*-dimethyl-2-naphthylamine, which are both incapable of forming a hydrogen bond, are appreciably quenched by quinoline. Therefore, the quenching action of pyridine was reexamined.

N, N-Dimethyl-2-naphthylamine and 2-Naphthylmethylether.—In the case of these two substances, the effect, if it exists, must be due to the genuine quenching action. The result reconfirmed Mataga's observation[2] that there was not any slight quenching action of pyridine.

2-Naphthylamine and 2-Naphthol. — Taking into account the genuine quenching action and the effect due to the formation of a nonfluorescent hydrogen-bonded complex in the ground state, the following equation can be derived:

$$(F_o/F)_{corr.}-1=\left(k+\frac{\varepsilon'}{\varepsilon}K\right)[A]+k\frac{\varepsilon'}{\varepsilon}K[A]^2 \quad (5)$$

where ε' and ε are, respectively, the molar extinction coefficient of the hydrogen-bonded complex and the free fluorescer, k and K are, respectively, the quenching constant and the equilibrium constant of the hydrogen-bond formation.

In the case of 2-naphthylamine, the plot of $(F_o/F)_{corr.}-1$ against [A] gives a good straight line. This is because the quilibrium constant of the hydrogen-bond formation in the gound state is so small in this case that it can safely be disregarded. From the slope one gets $k=116$ (23°C) and $k=133$ (40°C).

In the case of 2-naphthol, $(F_o/F)_{corr.}-1\sim[A]$ gives a concave curve upward, while $((F_o/F)_{corr.}-1)/[A]\sim[A]$ gives a good straight line and from its slope one gets $kK\varepsilon'/\varepsilon$. At the wavelength where $\varepsilon'\approx\varepsilon$, one gets $k=117$ (21°C) by using the value $K=125$ (21°C).

The Quenching Phenomena in Ethanol and Benzene.—To get a better insight into the mechanism of quenching, analogous experiments for several systems were made in ethanol and benzene. The results for benzene were qualitatively similar to those in *n*-hexane except that the quenching constants in all cases are somewhat less than those in *n*-hexane. In the case of ethanol, however, some extraordinary results were obtained. Thus, pyridine was found slightly to quench the fluorescence of *N,N*-dimethyl-2-naphthylamine.[3] The quenching constant evaluated by applying the Stern-Volmer equation (Eq. 3) is $k=15$ (25°C). However, the fluorescence of 2-naphthylmethylether was not affected at all by the addition of pyridine.* In the case of 2-naphthylamine

* This result contradicts Mataga's remark that this compound shows considerable quenching (see Ref. 3).

—pyridine, the plot of $(F_0/F)_{corr.}-1$ against [A] gives a good straight line and from the slope one gets $k=16$ (25°C). These findings can be comprehended if one considers that both fluorescer and quencher are hydrogen-bonded with ethanol almost completely (see Discussion). When quinoline was used as a quencher, treatment similar to that used in the case of *n*-hexane can be applied, and for 2-naphthylamine and *N*,*N*-dimethyl-2-naphthylamine, quite reliable *k*-values were obtained. No reliable value for 2-naphthylmethylether could be obtained.

The quenching constants so far obtained are tabulated in Table II.

Discussion

In such non-polar solvents as *n*-hexane and benzene, pyridine can be a quencher only when hydrogen bond formation is possible; thus 2-naphthylamine and 2-naphthol are quenched remarkably, while *N*, *N*-dimethyl-2-naphthylamine and 2-naphthylmethylether are not quenched at all. In such cases, therefore, there is no doubt that the hydrogen bond plays an important role in the quenching process. However, the fact that *N*, *N*-dimethyl-2-naphthylamine and 2-naphthylmethylether are quenched to some extent by quinoline indicates that hydrogen bonding is not always necessary for quenching. Particularly, the result that *N*, *N*-dimethyl-2-naphthylamine is quenched by quinoline to almost the same extent as 2-naphthylamine strongly suggests that quite a different molecular process than hydrogen bonding is participating in these quenching phenomena, although it seems natural to consider that hydrogen bond formation plays a role of another type or makes it easy for the afore-mentioned molecular process to occur.

As to the nature of the molecular process which causes quenching in our cases, it seems that all the results are consistent with the mechanism involving a charge transfer from fluorescer to quencher. Thus, firstly, the finding that *N*, *N*-dimethyl-2-naphthylamine is quenched more than 2-naphthylmethylether by quinoline (in *n*-hexane) may be attributed to the larger electron-releasing power of the dimethylamino group than that of the methoxy group and, secondly, the difference between the quenching action of pyridine and quinoline may be due to the difference in their electron-accepting power, though this is not conclusive because of the lack of data on electron affinity. The results obtained in ethanol also favor this view. Thus, in this solvent both pyridine and quinoline, as well as fluorescers, form the hydrogen bond, mainly with ethanol, and the hydrogen bonding between quencher and fluorescer is almost completely suppressed. Now, if one makes the plausible assumption that the effect of the hydrogen bonding between fluorescer and ethanol is of less significance than that of the hydrogen bonding between quencher and ethanol, then, for example, 2-naphthylamine and *N*, *N*-dimethyl-2-naphthylamine may be expected to be affected equally by pyridine and by quinoline. The results are quite consistent with this expectation, since the quenching constants of pyridine and quinoline are about the same for both substances. Further, the fact that *N*, *N*-dimethyl-2-naphthylamine is quenched by pyridine, but not in non-polar solvents, may be interpreted by supposing that pyridine in ethanol gets a larger electron-accepting power because of the hydrogen bond formation with ethanol. Lastly, the finding that 2-naphthylmethylether, unlike *N*, *N*-dimethyl-2-naphthylamine, is not quenched by pyridine in ethanol may again be attributed to the lower electron-releasing power of the methoxy group compared with the dimethylamino group. Thus, it is very tempting to attribute the present quenching phenomena to the charge transfer from fluorescer to quencher. However, it seems somewhat peculiar that quinoline and pyridine act as electron-accepting agents; further studies will be necessary to confirm the above view.

Next, let us discuss the rate-determining step of the quenching process. As Table II shows, the temperature coefficient of the quenching constant is positive in all cases, irrespective of whether hydrogen bonding occurs or not. Besides, in similar systems, such as 2-naphthylamine—pyridine and 2-naphthol—pyridine, or in 2-naphthylamine—quinoline and 2-naphthol—quinoline in non-polar solvents, the quenching constant is of the same order, although the equilibrium constant of the hydrogen bonding in the ground state is quite different.[2,4] From these facts it is very plausible that the rate-determining step in quenching is the process of diffusion. To confirm this view, the quenching constant, k, was calculated by the well-known formula $k_q=4\pi N(D_A+D_B)(r_A+r_B)/1000$; it was then compared with the experimental values. In this equation D_A and D_B are the diffusion coefficients of fluorescer and quencher which were calculated from the experimental formula of Thakar;[12] r_A+r_B was assumed to be 7.5Å,[13] and τ was set as equal to 10^{-8} sec. The results are given in Table III, while the

12) P. E. Othmar and M. S. Thakar, *Ind. Eng. Chem.*, **45**, 589 (1939).
13) A. Weller, *Z. Elektrochem.*, **64**, 55 (1960).

TABLE II. QUENCHING CONSTANTS

Quencher / Solvent / Fluorescer	Quinoline			Pyridine		
	n-Hexane	Benzene	Ethanol	*n*-Hexane	Benzene*	Ethanol
2-Naphthylamine	120(20°C)[1] 140(40°C)[2]	70(30°C)[7]	75(28°C)[10] 85(50°C)[11]	116(25°C)[15] 133(40°C)[16]	60(23°C)[21]	16(25°C)[23]
N, *N*-Dimethyl-2-naphthylamine	90(20°C)[3] 100(40°C)[4]	73(30°C)[8] 78(50°C)[9]	87(25°C)[12] 100(50°C)[13]	0(25°C)]17] 0(40°C)[18]	0(23°C)[22]	15(25°C)[24]
2-Naphthol	100(21°C)[5]			117(21°C)[19]		2(21°C)[25]
2-Naphthylmethyl-ether	53(25°C)[6]		60(21°C)[14]	0(21°C)[20]		0(21°C)[26]

The number [*i*] corresponds to that in Fig. 10.
* N. Mataga, This Bulletin, **31**, 484 (1958).

TABLE III. THE VALUES OF k CALCULATED FROM $k_q=4\pi N(D_A+D_B)(r_A+r_B)/1000$

Quencher / Solvent / Fluorescer	Quinoline			Pyridine		
	n-Hexane	Benzene	Ethanol	*n*-Hexane	Benzene	Ethanol
2-Naphthylamine	234(20°C)[1] 334(40°C)[2]	140(30°C)[7] 191(50°C)	80(30°C)[10] 119(50°C)[11]	266(20°C)]15] 378(40°C)[16]	158(30°C)[21] 216(50°C)	91(30°C) 135(50°C)
N, *N*-Dimethyl-2-naphthylamine	218(20°C)[3] 305(40°C)[4]	131(30°C)[8] 178(50°C)[9]	75(30°C)[12] 111(50°C)[13]	250(20°C)[17] 348(40°C)[18]	149(30°C)[22] 204(50°C)	85(30°C)[24] 127(50°C)
2-Naphthol	238(20°C)[5]	142(30°C)	81(30°C)	268(20°C)[19]	160(30°C)	92(30°C)[25]
2-Naphthyl-methylether	227(20°C)[6]	136(30°C)	78(30°C)[14]	258(20°C)[20]	154(30°C)	89(30°C)[26]

The number [*i*] corresponds to that in Fig. 10.

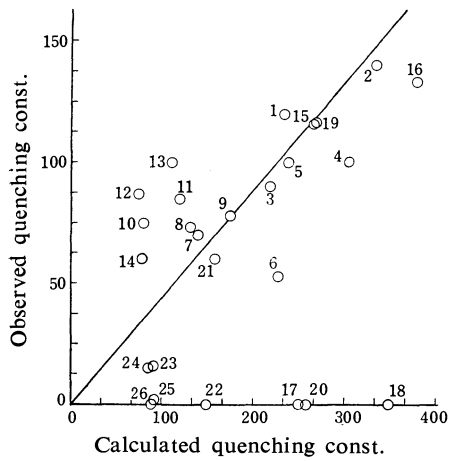

Fig. 10. Plot of the calculated quenching constants against the observed ones. The numbers in the figure correspond to the systems listed in Tables II and III.

comparison between the experimental and calculated values is shown in Fig. 10.

Broadly speaking, the correlation between the experimental and calculated values is rather good.

Thus, 2-naphthylamine—pyridine, 2-naphthol—pyridine, 2-naphthylamine—quinoline and *N*, *N*-dimethyl-2-naphthylamine—quinoline, all in nonpolar solvents, are close to the drawn line. It is clear that the difference between benzene and *n*-hexane is mainly due to the difference in viscosity, which affects the *D*-value. For all cases where the quenching constants are conspicuously small, such as *N*, *N*-dimethyl-2-naphthylamine—pyridine ($k=0$), 2-naphthylmethylether—pyridine ($k=0$) and 2-naphthylmethylether—quinoline, all in nonpolar solvents, there is no question that the genuine quenching process is rate-determining, completely or, at least, partially.

The feature in ethanol is somewhat anomalous. Thus, in the cases of 2-naphthylamine—quinoline and *N*, *N*-dimethyl-2-naphthylamine—quinoline, the observed values are appreciably larger than those which would be expected from the calculated values. Perhaps the calculated values are incorrect because of the improper estimation of τ, D_A, D_B, r_A and r_B. For *N*, *N*-dimethyl-2-naphthylamine—pyridine and 2-naphthylamine—pyridine, the observed k-values are less than the calculated values; this is certainly because the genuine quenching process is rate-determining.

At any rate, it is clear that in nonpolar solvents the quenching process is in many cases so rapid that it is determined by the process of diffusion, irrespective of the molecular mechanism of quenching. Thus, in the case of 2-naphthylamine—pyridine or 2-naphthol—pyridine in nonpolar solvents, k is considered to depend on the rate with which two molecules encounter one another with a mutual

orientation suitable for forming the intermolecular hydrogen bond. It is remarkable that the quenching in *N,N*-dimethyl-2-naphthylamine—quinoline seems to be diffusion rate-determining.

To summarize the above discussion, it is certain that the molecular process essential for quenching in the present systems is something other than hydrogen bonding, although it is clear that the latter plays an impotant role. According to Mataga,[4] charge transfer via the hydrogen bond makes the vibronic energy transfer feasible.

According to the view of the present authors, however, the main cause of the quenching is the charge transfer from fluorescer to quencher; the hydrogen bonding is considered, at least partly, to make it easy for this process to occur by increasing the electron density on the amino or hydroxy groups. The following fact might also have to be taken into account. If charge migration occurs from the electron-releasing group, such as a methoxy or amino group, to a ring in the excited state of the fluorescer, then a lone-pair on the hetero-atom in a quencher molecule will be able to act as a donor to these groups in a somewhat electron-deficient state. This will then make it easier for the charge transfer from fluorescer to quencher through π-π interaction to occur.

To sum up, our model of quenching process may be written schematically as follows:

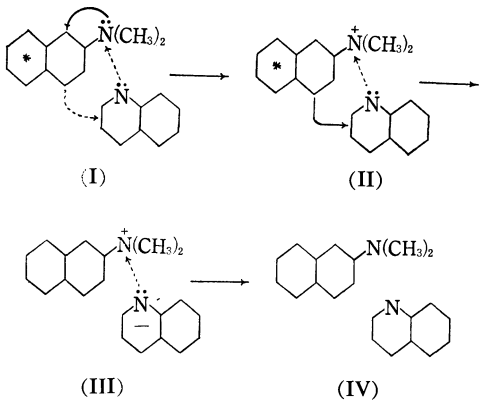

The essential point for quenching is I→II→III; the mechanism for III→IV is rather indifferent.

To verify the above speculation, the role of the quencher as an electron acceptor and the role of the hetero-atom in the quencher, which possibly acts as a donor, are the key-points which further studies should attack.

In concluding the discussion, brief comment should be made on the frequency effect of the quenching constant and on the experiment for the depth effect using anthracene.

The finding that quenching is independent of the frequency in 2-naphthylamine—quinoline and in *N,N*-dimethyl-2-naphthylamine—quinoline is quite natural and self-evident if one considers the conclusion obtained in the present paper, i.e., the fact that the rate-determining step of quenching is diffusion, since in such a situation the excited fluorescer molecule is sure to attain the equilibrium condition with regard to vibration and rotation and from the standpoint of interaction with the solvent molecules before the quenching process commences.

As to the effect of concentration on the fluorescence of anthracene, some anomalous results have recently been reported by Dammers-de Klerk.[10] According to him, the concentration quenching in *n*-hexane begins in a rather low concentration region, the fluorescence quantum yield at 10^{-3} M being about 1/5 that of the extreme dilute solution. Our present results do not show any such decrease in this concentration but conform quite well with the data of other authors.[9] Although our experiment was made in the presence of oxygen, Damers-de Klerk's results seem to be very doubtful. Förster[14] has also expressed this same opinion recently.

Summary

The quenching constants (k) of quinoline for the fluorescence of several substances in *n*-hexane have been determined. The values obtained are as follows; they are independent of the frequency of the exciting light.

2-Naphthylamine	120 (20°C)	140 (40°C)
N,N-Dimethyl-2-naphthylamine	90 (20°C)	100 (40°C)
2-Naphthol	100 (21°C)	
2-Naphthylmethyl-ether	53 (21°C)	

The results clearly show that the hydrogen bond is not necessary for the quenching to occur, in contradiction to the mechanism proposed by Mataga[4] for the case in which pyridine is used as a quencher.

To elucidate the mechanism, the quenching phenomena in the fluorescence of the above substances have been further studied in benzene and ethanol, using pyridine and quinoline as quenchers. The most notable finding has been that, in ethanol, pyridine can quench the fluorescence of 2-naphthylamine and *N,N*-

14) E. Döller and Th. Förster, *Z. Phys. Chem., N. F.*, **31**, 274 (1962).

dimethyl-2-naphthylamine equally well, the k value for 25°C being, respectively, 16 and 15.

A mechanism has been proposed which involves the charge transfer from fluorescer to quencher. When the quenching is considerable, the rate-determining step is the diffusion process, irrespective of the molecular mechanism for the quenching.

Department of Chemistry
Faculty of Science
Tohoku University
Katahira-cho, Sendai

The Photoreduction of Acridine in Deaerated and Aerated Alcohol Solutions.[1] *II.*

By Shigeya NIIZUMA and Masao KOIZUMI

(Received July 24, 1963)

In the preceding paper,[1] Kato, Minagawa and one of the present authors (M. K.) studied the photoreduction of acridine in ethanol and observed the following facts:

i) A solution of aridine, 1×10^{-4} M, in ethanol free from oxygen, when illuminated by 365 mμ, produces acridan, the quantum yield being about 0.13, independent of the temperature.

ii) In an air-saturated solution, the photoreduction goes on at the rate of about one-third of the evacuated solution.

iii) For both cases, the rate is simply proportional to the absorption of light.

iv) When the concentration of oxygen is varied, the reaction proceeds at the same rate as that of the air-saturated solution so long as the oxygen concentration is much larger than that of acridine. However, when the oxygen concentration becomes of the order of the acridine concentration, then the earlier part of the reaction proceeds at a rate approximately equal to that of the air-saturated solution, although at a certain point the rate increases rather suddenly to that of the oxygen-free solution.

The forth finding above was interpreted by assuming that, in the presence of oxygen, the acridan-producing reaction (with no consumption of oxygen) and the oxygen-consuming reaction (with no production of acridan) proceed simultaneously and that, when the existent oxygen is exhausted, only the former reaction survives. On this basis, the rate of oxygen consumption was calculated to be about twice as large as that of the reduction of acridine. A tentative scheme was proposed which can interpret the above results.

Now, in the present paper we will extend the study to the reaction in methanol and isopropanol and discuss all the results so far obtained, including those for ethanol, on the basis of the same scheme.

Experimental

Sample.—Acridine was purified by the method described in the previous paper. The concentration of acridine is always 1×10^{-4} M, while ε at 365 mμ is 1.12×10^{4}, 1.14×10^{4}, 1.19×10^{4} for methanol, ethanol and isopropanol solutions respectively.

Methanol.—Iwai Kasei's methanol (G. R.) was used without further purification.

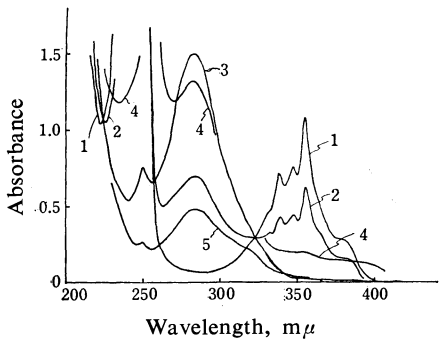

Fig. 1. The absorption spectra of acridine and the photoproducts in methanol solution. [A] $=1\times10^{-4}$ M

1 Before illumination (initial)
2 Short time illumination
3 30 min. illumination (photoproduct)
4 Long time illumination
} air-saturated solution
5 Long time illumination; degassed solution

A large decrease in the optical density of curve 5 is due to the precipitation of the photoproduct (see text).

1) S. Kato, S. Minagawa and M. Koizumi, This Bulletin, **34**, 1026 (1961). This paper shoud be numbered I.

Isopropanol. — Wako Junyaku's isopropanol was twice distilled. (B. p. 81.9~82.1°C) An impurity causing a slight absorption near 240 mμ was eliminated by the purification.

Procedure.—The procedures for degassing and the apparatus are almost the same as in the previous paper. The exciting light was 365 mμ from a high-pressure mercury lamp, and the reaction was followed by the change in the optical density of the sample at 365 mμ in a reaction cell (1×1×4 cm.). The intensity of the exciting light was measured by a potassium ferri-oxalate actinometer and found to be ca. 0.21×10^{-7} and 0.65×10^{-8} M sec^{-1} cm^{-2} for methanol and isopropanol respectively.

Results

The Absorption Spectra of Products. — The absorption spectra of the products in each solvent are shown in Figs. 1, 2 and 3. As can be seen in Figs. 1, 2 and 3 the main product in the case of methanol and ethanol is acridan, irrespective of the presence or absence of oxygen. The differences in the absorbance in the 230~300 mμ region for the aerated and deaerated solutions might be partially due to different by-products or to the small contribution of accompanied side reactions. The latter is plausible in view of the fact that prolonged illumination, after the depression of the optical density down to practically zero in the 350 mμ region, causes a gradual rise in the same region (cf. curve 4 in Fig. 1). When the ethanol solution of the product is kept for a long time, a white precipitate[2] is produced which may be attributed to acridan. In the case of isopropanol, the products in the degassed solution and in the air-saturated solution are different. In the former case, the product is judged to be acridan, while in the latter case the spectra with the peaks at 250, 345, 355 mμ resemble those of diacridan.[3] It is to be added that there is a clear isosbestic point in the change of acridine into acridan.

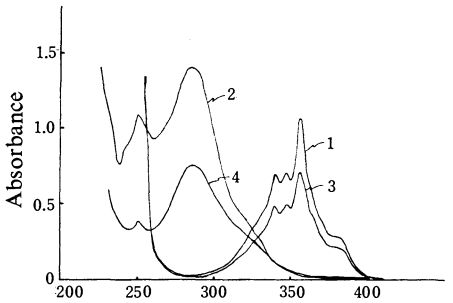

Fig. 2. The absorption spectra of acridine and the photoproducts in ethanol solution.
$[A]_{air\text{-}sat}=1\times10^{-4}$ M
$[A]_{degassed}=0.7\times10^{-4}$ M
1 Before illumination } air-saturated
2 After illumination } solution
3 Before illumination } degassed solu-
4 After illumination } tion

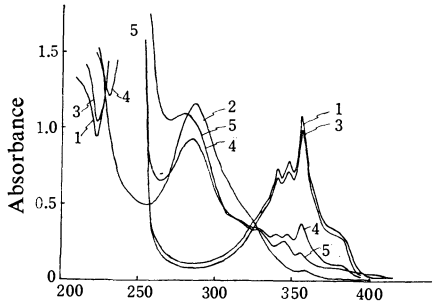

Fig. 3. The absorption spectra of acridine and the photoproducts in isopropanol solution.
$[A]\approx1\times10^{-4}$ M
1 Before illumination } degassed solu-
2 After illumination } tion
3 Before illumination (initial)
4 Short time illumination } air-saturated solution
5 After illumination (photoproduct)

A Comparison of Aerated and Deaerated Solutions.—When the reaction is proportional to the absorption of light, the relation

$$-\frac{dc}{dt}=\frac{kI_0}{d}(1-e^{-\alpha cd})\times10^3 \qquad (1)$$

must hold, where c, t, I_0, d and α are respectively the concentration of acridine (M), the time of reaction, the quantum yield, the light intensity (M/sec. cm^2), the thickness of the cell (1 cm.), and the absorption coefficient at 365 mμ. The integration of Eq. 1 leads to

$$\ln(e^{\alpha cd}-1)=\ln(e^{\alpha c_0 d}-1)-1000k\alpha I_0 t \qquad (2)$$

Equation 2 can represent very well the results in methanol and isopropanol and for both the air-saturated and oxygen-free solutions. From the linear plot of $\ln(e^{\alpha cd}-1)\sim t$ one gets $1000k\alpha I_0$, and so the value of k (quantum yield) can be calcurated using the values of α and I_0. A few examples of the plots are shown in Fig. 4. The values of k are summarized in Table I.

From Table I we can say that k-values are generally independent of the temperature, and that the ratio of k_d (for an oxygen-free solution) and k_a (for an air-saturated solution) is ca. 4, ca. 3 and ca. 2.8 for methanol, ethanol and isopropanol. It is worth mentioning that, for the degassed solutions, k is practically the same for methanol and for ethanol, while it is much smaller for isopropanol.

2) V. Zanker and H. Schnith, *Chem., Ber.*, **92**, 2210 (1959).
3) V. Zanker and P. Schmid, *Z. physik. Chem.*, **17**, 11 (1958).

TABLE I. *k*-VALUES OBTAINED

Condition	Solvent			
	Ethanol	Methanol	Methanol	Isopropanol
Air-saturated solution	0.040_3(25°C)	0.028_4(25°C)	0.038_1(15°C)	0.031_8(25°C)
	0.045_6(25°C)	0.034_4(25°C)	0.028_3(15°C)	0.030_5(25°C)
	0.044_9(25°C)	0.032_7(25°C)	0.031_2(15°C)	0.034_5(25°C)
Average	0.043±0.002	0.032±0.003	0.033±0.003	0.032±0.002
Oxygen free solution	0.12_8(13.3°C)*	0.12_6(25°C)	0.12_3(15°C)	0.087(25°C)
	0.12_1(25°C)*	0.13_6(25°C)	0.13_6(15°C)	0.086(25°C)
	0.13_4(25°C)*	0.12_5(25°C)	0.12_5(15°C)	0.093(25°C)
				0.093(25°C)
Average	0.129±0.003*	0.129±0.004	0.128±0.006	0.090±0.003

* S. Minagawa's data

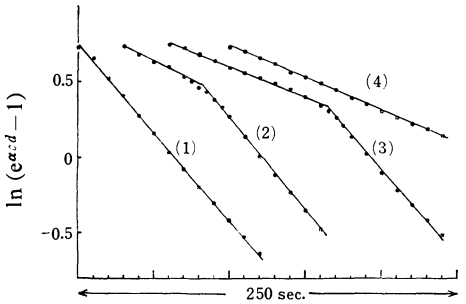

Fig. 4. Plots of ln ($e^{acd}-1$) vs. time for acridine in isopropanol solution.
[A] = 1×10^{-4} M
(1) Degassed soln. (2) [O_2] = 0.6×10^{-4} M
(3) [O_2] = 1.5×10^{-4} M (4) Air-saturated soln.

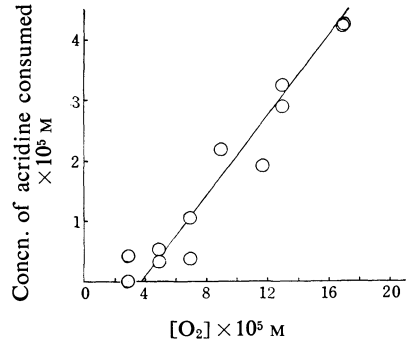

Fig. 5. Plots of the decrease of acridine concentration before the breaking point of the decay curve vs. the initial concentration of dissolved oxygen in methanol solution.

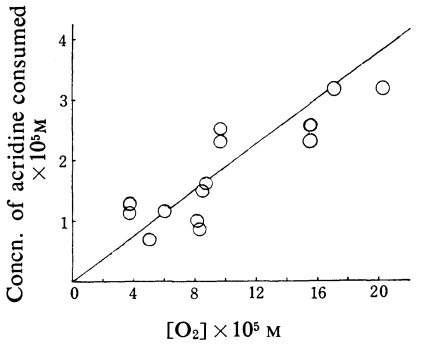

Fig. 6. Plots of the decrease of acridine concentration before the breaking point of the decay curve vs. the initial concentration of dissolved oxygen in isopropanol solution.

The Effect of the Oxygen Concentration.— When the oxygen concentration is of the same order as that of acridine, the rate of the reaction at first is practically the same as that of the air-saturated solution, but after a certain time there appears a sharp break, after which the rate becomes approximately the same as that of the degassed solution. The length before the break is approximately proportional to the concentration of oxygen. This phenomenon is common to both methanol and isopropanol and is quite similar to that already reported in ethanol.[1] There is no doubt that an interpretation similar to that given for ethanol in the previous paper can be applied to methanol and isopropanol. Thus, in such circumstances, the oxygen-consuming reaction (accompanied by the recovery of acridine from some transient intermediate) and the acridan-producing reaction go parallel and that, when the oxygen is exhausted only the latter reaction proceeds by the mechanism prevailing in oxygen-free solution.

The plot of the consumed acridine up to the breaking point against the initial oxygen concentration is given in Figs. 5 and 6. Although the average deviation from the drawn line is rather large especially in the latter case, the ratio between the quantities of acridine and of oxygen consumed before the break is, respectively, about 3 and 5.3 for methanol and isopropanol. The fact that the plot in Fig. 5

cuts the abscissa instead of passing through the origin, might be due to the participation of some other reaction like the following in such a low concentration of oxygen;

$$A^* + RH_2 \rightarrow AH\cdot + RH\cdot$$

$$RH\cdot + O_2 \rightarrow RH\cdots O_2$$

$$AH\cdot + RH\cdots O_2 \rightarrow A + R + H_2O_2$$

A similar tendency, although much less conspicuous, is observed in the case of ethanol described in the preceding paper (see Fig. 5 in Ref. 1). Table II gives a summary of γ and

TABLE II. γ AND k_d/k_a

Solvent	γ	k_d/k_a
Methanol	ca. 3	4
Ethanol	ca. 2	3
Isopropanol	ca. 5.3	2.8

k_d/k_a values. In the case of ethanol, the reaction rate under the air-saturation could be restored when a small quantity of air was dissolved after the break in Fig. 4. Similar experiments were undertaken for isopropanol, but the results proved to be as shown in Fig. 7.

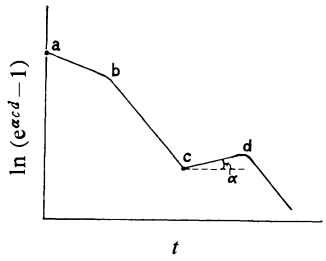

Fig. 7. A typical decay curve for supplementary experiments. At time dissolved oxygen would be exhausted. At c, the cell was shaken and oxygen was introduced into the liquid phase. At d, the oxygen would be exhausted again. The longer the interval bc is, the larger the value of α becomes.

Thus, when 10^{-4} M oxygen is added again after the exhaustion of oxygen (period ab) at c, the optical density does not fall, but rises. It was found that the longer the bc interval (the reaction in the absence of oxygen), the larger the value of α and, so, the larger the increase in the optical density. When bc is extremely short, then the slopes of ab and cd become practically the same. A similar phenomenon was also observed in the case of ethanol, and methanol although to a lesser extent. This is the reason why the phenomenon was overlooked in the preceding paper. At d, oxygen is consumed and the reaction goes on at the rate of the degassed solution.

The rise in the optical density during the cd period seems to be due to the oxidation of acridan to acridine by some unknown process, the extent of this reaction exceeding the usual reduction of acridine to acridan. This view is supported by the following facts. First, as is shown in Fig. 7, the spectra of acridine increase during the cd period while the spectra of the product (280~285 mμ) decrease, and second, this change goes on with an isosbestic point at 325 mμ. The dependence of α on the length of bc strongly suggests that some reaction products during the bc (degassed condition) period play an essential role in the reaction during cd period. To confirm this, the effect of the addition of acridan to various systems was examined. The addition of acridan (0.5×10^{-4} M) to an ethanol solution of acridine (0.5×10^{-4} M) containing 0.7×10^{-4} M of oxygen ($P_{air}=27.5$ mmHg at 18°C) did not have any effect. No effect was observed either when the same amount of acridan was added to an isopropanol solution of acridine (0.5×10^{-4} M) or when 1×10^{-4} M of acridan was added to an ethanol solution of acridine (1×10^{-5} M), both saturated with air.

Thus there is no simple sensitized oxidation of acridan by the excited acridine molecule. This is rather natural in view of the finding that $\ln(e^{\alpha cd}-1)\sim t$ gives a very satisfactory linear plot until more than a half of the acridine is consumed.

Next, the effect of any other conceivable by-product during bc was examined. Of these, acetaldehyde would be most probable in the case of ethanol. The addition of ~1 M acetaldehyde to an air-saturated ethanol solution of acridine (1×10^{-4} M) does not affect the rate, the rate being practically the same as that of an air-saturated solution of acridine. However, the ultraviolet spectra of the product as shown in Fig. 8 resembles that of diacridan. Using the ethanol solution of acridine (0.1×10^{-4} M) and acridan (0.9×10^{-4} M) to which 1.2 M acetal-

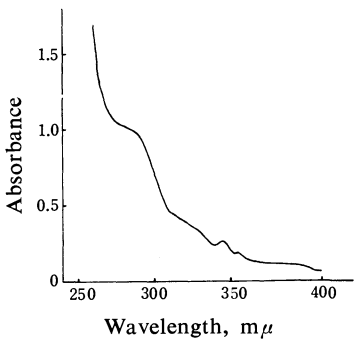

Fig. 8. The Absorption spectrum of photoproduct in air-saturated ethanol solution containing, 0.9×10^{-4} M acridan, 0.1×10^{-4} acridine and ~1 M acetaldehyde.

dehyde had been added, three cases were examined, i.e.; (1) an air-saturated solution; (2) 0.8×10^{-4} M oxygen ($P_{air}=29.0$ mmHg at 17.5°C), and (3) a completely degassed solution. The results was that for 1 the reduction proceeds at a much slower rate, k being approximately 3×10^{-3}, while for 3 the reaction goes on at just the same rate as when no acridan and acetaldehyde are added, (i.e., $k=0.13$); in case of 2, however, the rise in the optical density occurs first and, at a point where oxygen may be expected to be exhausted, a break appears and the optical density then decreases, but at a slower rate than that for the degassed solution of acridine. When oxygen is introduced again, the back reaction becomes apparent. A similar phenomenon, though to a lesser extent, was observed when acetone (1.0 M) and oxygen (1×10^{-4} M) ($P_{air}=36.2$ mmHg at 23.0°C) were added to an isopropanol solution containing acridan (0.9×10^{-4} M) and acridine (0.1×10^{-4} M).

Thus one can conclude that a certain quantity of aldehyde or ketone is necessary in order for acridan to be oxidized by the sensitization of acridine. However, there is rather a great possibility that some other oxidative by-products take part in the cd reaction shown in Fig. 7.

Discussion

The scheme presented in the preceding paper for the reaction under the degassed condition is as follows:

$$\left.\begin{aligned} &A + h\nu \rightarrow A^* \\ &A^* + RH_2 \rightarrow AH + RH \end{aligned}\right\} \quad (0)$$

$$AH\cdot + RH\cdot \rightarrow AH_2 + R \quad (1)$$

$$AH\cdot + RH\cdot \rightarrow A + RH_2 \quad (2)$$

$$AH\cdot + AH\cdot \rightarrow AH_2 + A \quad (3)$$

$$RH\cdot + RH\cdot \rightarrow RH_2 + R \text{ or } HR\text{–}RH \quad (4)$$

where A, RH_2 and R are acridine, ethanol and acetaldehyde respectively. A* is an excited singlet or triplet, but the latter is more plausible since the transient spectra for the degassed solution of acridine observed in our laboratory, perfectly coincides with that reported by Porter[4] and has interpreted to be due to the acridine triplet.

From the above scheme, one can easily derive the following rate formula by means of the steady state method:

$$-\frac{d[A]}{dt}=\frac{d[AH_2]}{dt}=\frac{\phi I_{abs}(k_1+\sqrt{k_3k_4})}{k_1+k_2+2\sqrt{k_3k_4}}$$

$$=\phi\beta I_{abs}$$

$$\beta=\frac{k_1+\sqrt{k_3k_4}}{k_1+k_2+2\sqrt{k_3k_4}}$$

where ϕ is the quantum yield of the formation of AH· and RH·, and k_1, k_2, k_3 and k_4 are the respective rate constants of processes 1, 2, 3 and 4. From the results in Table I, one can discuss the mechanism to some extent. First, the values of k for the degassed solution of methanol, ethanol and isopropanol are not consistent with the well-known fact that the order of ease of α-hydrogen abstraction in an alcohol molecule is isopropanol > ethanol > methanol. This relation was observed to hold[5] in, for instance, the case of the photoreduction of eosine in a degassed alcohol solution, for which the overall quantum yield is very small, of the order of 10^{-4}. Wells[6] also observed the same order for the photoreduction of sodium-anthraquinone-2-sulfonate. Perhaps the tendency of excited acridine to deprive α-hydrogen atom from alcohol is so large that the general ralation does not hold in this case. The small value of isopropanol may perhaps be due to its small number of α-hydrogen atoms (1, while it is 3 or 2 for methanol and ethanol) or to a certain steric factor. The independence of k of the temperature favors the view that the process following (0) goes along a single path, (1) or (3), and not along (1) and (3) both. As to whether (1) or (3) prevails, one cannot give a definite answer at this stage. The separate determination of ϕ and of the quantum yield of the triplet formation is desirable. It is worth mentioning that the triplet is observed in the flash experiment. If the triplet state is very easily reduced by alcohol, as has been mentioned above, then its life-time might be expected to be very small. Perhaps the relative orientation of the alcohol molecule and acridine must be suitable in order for the hydrogen atom transfer to occur, and this will be a chief reason why the life-time of the triplet is not very short.

Next let us consider the reaction in which oxygen takes part. In the preceding paper we tentatively proposed for the case of ethanol that oxygen very efficiently attacks the half-hydrogenated state of acridine on the grounds that the reaction goes on even in the presence of oxygen and that the rate is almost constant as long as the concentration of oxygen is larger than a certain small value ($\sim10^{-4}$ M). Since similar results were obtained for methanol and isopropanol, it can be said that the pro-

4) G. Jackson and G. Porter, *Proc. Roy. Soc.*, **A260**, 13 (1961).

5) M. Imamura and M. Koizumi. This Bulletin, **29**, 899 (1956).

6) C. F. Wells, *Trans. Faraday Soc.*, **57**, 1703 (1961).

posed scheme was largely substantiated. Therefore, we will discuss it on the basis of the analogous mechanism. However, it is to be noted here that the overall reaction will be somewhat different in methanol and isopropanol. In the former case, the final product will be acid, as in the case of ethanol, but for isopropanol, acetone instead of acid is the most plausible product. For methanol the scheme is exactly the same as for ethanol, which runs as follows:

$$AH\cdot + O_2 \rightarrow AH\cdots O_2 \quad (5)$$

$$RH\cdot + O_2 \rightarrow RH\cdots O_2 \quad (5')$$

$$2AH\cdots O_2 \rightarrow AH_2 + A + 2O_2 \quad (6)$$

$$2AH\cdots O_2 \rightarrow 2A + H_2O_2 + O_2 \quad (7)$$

$$2RH\cdots O_2 \rightarrow 2Acid + H_2O_2 \quad (8)$$

$$AH\cdots O_2 + RH\cdots O_2 \rightarrow AH_2 + R + 2O_2 \quad (9)$$

$$AH\cdots O_2 + RH\cdots O_2 \rightarrow A + R + H_2O_2 + O_2 \quad (10)$$

$$AH\cdots O_2 + R\cdots HO_2 \rightarrow A + RH_2 + 2O_2 \quad (11)$$

In the case of isopropanol, the above scheme will be partly altered in the following way; i.e., instead of 6,

$$2AH\cdots O_2 \rightarrow AH\text{–}AH + 2O_2 \quad (6')$$

and instead of 8,

$$2RH\cdots O_2 \rightarrow 2R + H_2O_2 + O_2 \quad (8')$$

6' of course corresponds to the formation of diacridan.

In the above scheme we consider that, in the presence of oxygen, reaction 5 proceeds so fast that 1, 2, and 3 do not occur at all. Of course, the above scheme is too simple and the real situation might involve the participation of $HO_2\cdot$; moreover, some chain reaction might also occur. For example, if the following chain reaction occurs:

$$RH\cdots O_2 \rightarrow R + HO_2\cdot$$

$$HO_2\cdot + RH_2 \rightarrow RH\cdot + H_2O_2$$

$$RH\cdot + O_2 \rightarrow RH\cdots O_2$$

then the oxygen consumption would be much increased. It is to be noted that such a possibility is disregarded in the following discussion because this possibility is very small in view of the consistency of the analysis.

Putting k_d/k_a (the ratio of the rate in the deaerated solution to that in the aerated solution) as n, let us now consider which process, 6, 7 and 8 (case I) or 9, 10 and 11 (case II), is more plausible.

As in the previous paper only two extreme cases will be considered.

Case I.—In this case 6 (or 6' for isopropanol) and 7 occur, and, naturally, 8 (or 8' for isopropanol) accompanies them. The steady state method gives

$$-\frac{d[A]}{dt} = \begin{cases} \dfrac{k_6\phi I_{abs}}{2(k_6+k_7)} & \text{for methanol} \\ \dfrac{k_6\phi I_{abs}}{k_6+k_7} & \text{for isopropanol} \end{cases}$$

$$-\frac{d[O_2]}{dt} = \begin{cases} \dfrac{\phi I_{abs}(2k_6+3k_7)}{2(k_6+k_7)} & \text{for methanol} \\ \dfrac{\phi I_{abs}(k_6+2k_7)}{2(k_6+k_7)} & \text{for isopropanol} \end{cases}$$

Hence,

$$\begin{cases} \dfrac{k_6}{2(k_6+k_7)} = \dfrac{\beta}{n} & \text{for methanol} \\ \dfrac{k_6}{k_6+k_7} = \dfrac{\beta}{n} & \text{for isopropanol} \end{cases}$$

and

$$\gamma = \frac{d[O_2]/dt}{d[A]/dt} = \begin{cases} 2+3\dfrac{k_7}{k_6} & \text{for methanol} \\ \dfrac{1}{2}+\dfrac{k_7}{k_6} & \text{for isopropanol} \end{cases}$$

From these two equations,

$$\gamma = \begin{cases} \dfrac{3n}{2\beta}-1 & \text{for methanol} \\ \dfrac{n}{\beta}-\dfrac{1}{2} & \text{for isopropanol} \end{cases}$$

In the case of methanol, $n=4$ and $\gamma=3$; therefore,

$$\gamma = \frac{6}{\beta}-1$$

For γ to be 3, β must be 1.5. This is nonsense, however, because β should be $\leqq 1$. For ethanol, $n=3$, $\gamma=2$ and, from these values, $\beta=1.5$. In the case of isopropanol, $n=2.8$ and $\gamma=5.3$; therefore, $\beta=0.48$.

Case II. — In this case both methanol and isopropanol can be treated in the same way provided that acridan is a main product in the latter case. When 9, 10 and 11 are the main reactions, the steady state method leads to the following equation:

$$-\frac{d[A]}{dt} = \phi I_{abs} k_9/(k_9+k_{10}+k_{11})$$

$$-\frac{d[O_2]}{dt} = \phi I_{abs} k_{10}/(k_9+k_{10}+k_{11})$$

Hence,

$$k_9/(k_9+k_{10}+k_{11}) = \frac{\beta}{n}$$

and

$$\gamma = \frac{k_{10}}{k_9}$$

From these two equations,

$$\frac{k_{11}}{k_9}=\frac{n}{\beta}-(\gamma+1)$$

In the case of methanol, $n=4$ and $\gamma=3$, and for some values of β, k_{11}/k_9 are calculated as follows:

β	1	0.8	0.6	0.5
k_{11}/k_9	0	1	2.6	4

For ethanol, $n=3$, $\gamma=2$, and, as has been reported already:[1]

β	1	0.8	0.6	0.5	0.4
k_{11}/k_9	0	0.75	2	3	4.5

In the case of isopropanol, $n=2.8$ and $\gamma=5.3$; therefore,

β	1	0.5	0.45
k_{11}/k_9	−3.5	−0.7	0

From the above analysis it can be said that, with ethanol and methanol, only case II fits the experimental results if alcohol is oxidized to acid. If, on the other hand, the oxidation stops at the stage of aldehyde, case I is also conceivable; the calculation requires that $\beta=1$ for both methanol and ethanol.

As for the case of isopropanol, one can not decide from the above analysis whether case I or case II is suitable. However, in this case the product contains a considerable quantity of diacridan, and so case I seems to be more plausible. This would perhaps be because $RH\cdots O_2$ has a great tendency to decompose in the following way:

$$\begin{matrix}CH_3\\CH_3\end{matrix}\!\!>\!\!\begin{matrix}COH\\\vdots\\O_2\end{matrix}\rightarrow CH_3\overset{\displaystyle O}{\overset{\|}{C}}CH_3+HO_2\cdot$$

At any rate, in the case of isopropanol the above analysis requires that $\beta\fallingdotseq 0.5$, whether case I or case II holds. This implies that, in the case of the degassed solution of isopropanol, (3) and (4) prevail instead of (1). On the other hand, in the cases of ethanol and methanol, case I requires that $\beta=1$ (on the condition that the product is aldehyde and not acid); $\beta=1$ holds also in case II if it is assumed that reaction 11 does not occur. Thus, in either case reaction 1 is more favorable.

The above discussion is of itself rather speculative, and we have aimed only at the plausible scheme. For example, the deduction would not hold if the chain reaction participates. However, as to the participation of the chain process, this can be safely denied on the basis of the rather small consumption of oxygen and also from the consistency of the above analysis. Moreover, very recently, it has definitely been established from the pulse radiolysis of ethanol that recombination and disproportionation are the only processes possible for ethanol radicals and that these occur as diffusion rate-determining processes.[7]

This makes our deduction very reasonable. It seems certain that, in the cases of ethanol and methanol, $AH\cdot + RH\cdot \rightarrow AH_2 + R$ occurs, while in the case of isopropanol, $AH\cdot + AH\cdot \rightarrow AH_2 + A$ and $RH\cdot + RH\cdot \rightarrow$ proceed. If such is the case, the existence of different values of k for methanol and ethanol on the one hand and for isopropanol on the other, is at least partly due to the different processes following (0). Wilkinson[8] proposed, for the photoreduction of isopropanol by quinone, the following process:

$$(CH_3)_2\dot{C}OH + Q \rightarrow QH\cdot + (CH_3)_2CO$$

However, such a process is not applicable in our case probably because of a rather small tendency of reduction for acidine. At any rate, the complete analysis of the products is desirable in order to obtain a definite answer. Lastly, it should be added that the experimental evidence for the formation of $AH\cdots O_2$ is lacking, but that the present deduction is not altered if $AH\cdots RH$ is formed and reacts with oxygen in any of three different ways, as has been mentioned in the preceding paper.[1]

As to the sensitized oxidation of acridan into acridine in the presence of aldehyde or acetone and a small quantity of oxygen, the discussion of this will be postponed until much more data have been accumulated.

Summary

The photoreduction of acridine in methanol and isopropanol has been studied and the following results obtained:

1) The quantum yield for the photoreduction in the dagassed solution is, for methanol, 0.13 and, for isopropanol, 0.09. The photoreduction can take place even in an air-saturated solution with quantum yields of 0.032 for methanol) and of 0.032 (for isopropanol).

2) In case of a degassed solution, the product is acridan for both isopropanol and methanol, while in an aerated solution the product is acridan in the case of methanol and mainly diacridan in the case of isopropanol.

3) When the concentration of oxygen is of the order of that of acridine, the reaction proceeds at first at a rate equal to that of an air-saturated solution and then, from the point at which the oxygen is exhausted, the rate

7) I. A. Taube and L. M. Dorfman, *J. Am. Chem. Soc.*, **84**, 4053 (1962).
8) F. Wilkinson, *J. Phys. Chem.*, **66**, 2569 (1962).

increases up to the value of a degassed solution.

4) The ratio of the quantities of oxygen and of acridine consumed before the break is, for methanol, about 3 and, for isopropanol, 5.3.

5) By the sensitizing action of acridine, acridan is oxidized to acridine in the presence of aldehyde (or acetone) and a small quantity of oxygen.

6) On the basis of the scheme proposed in the preceding paper and from the reaction product, some tentative discussion of the scheme has been undertaken. It seems plausible that, in the case of ethanol and methanol, $AH\cdot + RH\cdot \rightarrow AH_2 + R$ occurs, while in the case of isopropanol, $AH\cdot + AH\cdot \rightarrow AH_2 + A$ and $RH\cdot + RH\cdot \rightarrow$ take place (for a degassed solution).

Department of Chemistry
Faculty of Science
Tohoku University
Katahira-cho, Sendai

The Preparation of Strictly Halide Complexes of Copper(II) and Their EPR Spectra

By Masayasu MORI and Shizuo FUJIWARA

(Received July 17, 1963)

Copper(II) complexes are probably some of the most thoroughly studied of all the metal complexes, and many new findings in the field of EPR study have recently been obtained with these complexes. However, most of the copper complexes so far studied have been those in which ligands are coordinated through oxygen or nitrogen atoms; structurally they form elongated octahedra, with two atoms in the trans positions somewhat far from the central copper ion.

On the other hand, very little information has been obtained with copper complexes in which all the ligands are coordinated through halogen atoms. Bailar and Busch term such a compound "a strictly halide complex";[1] it is indeed in these compounds that various anomalies, both in structure and in spectra, are observed. Thus, in Cs_2CuCl_4 and Cs_2CuBr_4, tetrahalogenocuprate(II) anions form distorted tetrahedra,[2] while in $[Cr(NH_3)_6][CuCl_5]$, pentachlorocuprate(II) anion forms a trigonal bipyramid.[3] Brown compounds, $CsCuCl_3$[4] and $KCuCl_3$[5] of a polymer structure with Cl–Cu–Cl–Cu chains or the like, and a series of mixed valence compounds, $[Cr(NH_3)_6]CuCl_{5-x}$ or $[Cr(NH_3)_6]_4Cu_5Cl_{17+x}$,[6] also belong to this category. Research into these anomalous chlorocuprates seems to be necessary for a more complete understanding of the coordinate linkage in copper complexes.

As a means of studying this subject, the present authors chose to examine electron paramagnetic resonance, since it usually affords useful information, especially in connection with the state of the d electrons, electron delocalization, exchange interaction, and other problems. In particular, the accumulation of such fundamental EPR data as the *g*-values for pure copper halogen linkages can be made possible only by the use of these strictly halide complexes as specimens.

Experimental

Samples.—The chlorocuprates studied in the present research are: (1) hexamminecobalt(III) pentachlorocuprate(II), (2) hexamminecobalt(III) chlorocuprates(I, II), (3) chlorocuprates(II) of chain organic polyamines, (4) chlorocuprate(I, II) and chlorocuprate(I) of a chain organic polyamine, and (5) chlorocuprates(II) of *s*-triazine derivatives. The preparation of 1 and 2 has been described in

1) J. C. Bailer, Jr., and D. H. Busch, "Chemistry of the Coordination Compounds," Reinhold Publishing Corp., New York (1956), p. 5.
2) L. Helmholz and R. F. Kruh, *J. Am. Chem. Soc.*, **74**, 1176 (1952).
3) M. Mori, Y. Saito and T. Watanabe, This Bulletin, **34**, 295 (1961).
4) A. F. Wells, *J. Chem. Soc.*, **1947**, 1662.
5) R. D. Willett, C. Dwiggins, Jr., R. F. Kruh and R. E. Rundle, *J. Chem. Phys.*, **38**, 2429 (1963).
6) M. Mori, This Bulletin, 33, 985 (1960). The series of chlorocuprates(I, II) reported on in this literature may be expressible by either of the above formulae. The former expresses compounnds with a ratio of copper(I) and copper(II) smaller than 1 : 1 and in which x is, therefore, smaller than 0.5. The latter expresses compounds with a low copper(II) content and in which x is, therefore, small. Compounds of the intermediate domain have not yet been thoroughly analyzed to afford an appropriate formula by which they can be expressed.

a previous paper.[6] Most of the compounds of group 3 are those reported by Jonassen et al.[7] In this section the procedure for preparing compounds of groups 4 and 5 will be described.

Diethylenetriammonium Chlorocuprate(I, II).—A cooled mixture of 2.5 g. of diethylenetriamine and 3 ml. of water is slowly acidified with 10 ml. of 12 N hydrochloric acid. To the mixture are added 0.5 g. of copper(I) chloride and 1 g. of copper(II) chloride dihydrate, dissolved together in a mixture of 2.5 ml. of water and 10 ml. of 12 N hydrochloric acid. When the mixture is slowly shaken 2~3 times and allowed to stand for 1 min., small, very dark green, glistening crystals will be deposited. These are separated from the mother liquor by suction, washed with 12 N hydrochloric acid and ethanol, and dried under evacuation. Yield, 1.5 g.

Rubbing the sides of the glassware during the crystallization or allowing the mixture to stand for too long a period should be avoided, as this will cause a crystallization of a colorless copper(I) compound which is very difficult to remove from the substance to be prepared. Once colorless crystals are deposited, preparation should be repeated anew.

Found: Cu, 18.20; Cu(II), 17.85; Cl, 50.77; N, 12.16. Calcd. for $(H_3N\cdot C_2H_4\cdot NH_2\cdot C_2H_4\cdot NH_3)$-$CuCl_{5-x}$, ($x$=0, i. e., for a divalent compound for simplicity's sake): Cu, 18.31; Cl ,51.09; N, 12.11%.

When the analytical value is considered, the copper(I) content is seen to be quite low. Nevertheless, the color (very dark green) is quite different from the yellow color of a pure copper(II) compound; moreover, the copper(II) content and the color are changed when the ratio of mixing in the preparation is changed. Thus, for example, if 0.2 g. of copper(I) chloride is used instead of 0.5 g. in the above procedure, the color of the product is more yellowish but still far deeper than the color of the pure copper(II) compound, while the composition is now almost identical with that of the copper(II) compound. An increase in the quantity of copper(I) chloride used also seems to bring about a color change, but in this case preparation becomes more difficult owing to the readiness with which a colorless copper(I) compound separates out.

Diethylenetriammonium Pentachlorodicuprate(I). The procedure is similar to that for chlorocuprate-(I, II), but 2 g. of copper(I) chloride should be used instead of a mixture of copper(1) chloride and copper(II) chloride. It forms colorless, scaly crystals.

Found: Cu, 30.76; Cl, 43.52; N, 10.64. Calcd. for $(H_3N\cdot C_2H_4\cdot NH_2\cdot C_2H_4\cdot NH_3)Cu_2Cl_5$: Cu, 30.95; Cl, 43.18; N, 10.23%.

Ethylenediammonium Tetrachlorocuprate(II), Diethylenetriammonium Pentachlorocuprate(II) and Triethylenetetrammonium Hexachlorocuprate(II).—These compounds were first reported by Jonassen et al.[7] The present research has revealed, however, that they can be much more easily prepared. For example, diethylenetriammonium pentachlorocuprate(II) can be prepared by a procedure similar to that used in preparing the chlorocuprate-(I, II) described above, except that copper(II) dihydrate is used instead of a mixture of copper(I) chloride and copper(II) chloride. The other cases are analogous.

Chlorocuprates(II) of *s*-Triazine Derivatives.—(*a*) *Dimelammonium Hexachlorocuprate(II)*.—One and three-tenths grams of melamine is dissolved as quickly as possible in 20 ml. of boiling 6 N hydrochloric acid. To this solution is added, without delay, 1.7 g. of copper(II) chloride dihydrate dissolved in 10 ml. of 6 N hydrochloric acid; the mixture is then allowed to cool for several minutes. The yellow crystals that form are collected on a glass filter and washed with 6 N hydrochloric acid and with acetone; after being dried by strong suction, they are immediately sealed in a dry glass tube.

Found: Cu, 11.72; Cl, 39.85; N, 31.62. Calcd. for $\{C_3N_3(NH_2)_3H_2\}_2CuCl_6$: Cu, 11.93; Cl, 39.95; N, 31.56%.

(*b*) *Melammonium Hexachlorodicuprate(II)*.—One gram of melamine is dissolved in 10 ml. of boiling 6 N hydrochloric acid as quickly as possible, and the solution is mixed with 3 g. of copper(II) chloride dihydrate which has previously been dissolved in 20 ml. of 12 N hydrochloric acid. The brown needles thus formed are filtered, washed with 12 N hydrochloric acid and acetone, and kept in a desiccator.

Found: Cu, 26.44; Cl, 44.84; N, 18.21. Calcd. for $\{C_3N_3(NH_2)_3H_2\}Cu_2Cl_6$: Cu, 27.15; Cl, 45.47; N, 17.96%.

(*c*) *Benzoguanammonium Trichlorocuprate(II)*.—Two grams of benzoguanamine are dissolved in 30 ml. of hot glacial acetic acid. Two grams of copper(II) chloride dihydrate dissolved in 5 ml. of 6 N hydrochloric acid are then added, and the yellowish brown needles which precipitate out are washed on a glass filter with a mixture of glacial acetic acid and ether, and dried at about 100°C. Yield, 3.0 g.

Found: Cu, 18.57; Cl, 28.57. Calcd. for $\{C_6H_5\cdot C_3N_3(NH_2)_2H\}CuCl_3$: Cu, 17.74; Cl, 29.70.

The somewhat poorer agreement in the analytical value is probably due to a contamination of the free benzoguanamine or copper(II) chloride; the contaminating to materials are difficult to remove because of their low solubility in a mixture of glacial acetic acid and ether. Washing with such other liquids as hydrochloric acid brings about a decomposition of the preparation.

The Apparatus of EPR Measurement.—The apparatus used in EPR measurements has the same features as a spectroscope working at any other wavelength. The essential components are a source of radiation, an absorption cell, and a detector. In the microwave region the source of radiation is provided by a klystron tube which can be highly stabilized to give a very monochromatic radiation. The absorption cell is a resonant cavity tuned to the klystron frequency, and the specimen can be placed in a region of high r, f. magnetic field strength. The output from the cavity absorption cell is fed to a silicon-tungsten crystal, which detects the microwave radiation and feeds its modulated

7) H. B. Jonassen, T. B. Crumpler and T. D. O'Brien, *J. Am. Chem. Soc.*, 67, 1709 (1945).

envelope on to amplifiers. The resonance condition is

$$h\nu = g\beta H$$

where ν is the microwave frequency; β, the Bohr magneton, and H, the applied magnetic field, and where g is termed the spectroscopic splitting factor and has a value depending on the electronic state of the atom. In the present study, EPR spetra of chlorocomplexes of copper were taken at 9375 Mc., requiring magnetic fields in the 2700~3500 of range. The apparatus used in this experiment is one of Japan Electron Optics Company, of the JES-118, type, using an X-band generated by a Varian X-13 klystron tube. The magnetic field is modulated at 80 c. p. s. The field strength was calibrated by taking the spectra of the DPPH powder of an aqueous solution of manganese(II) sulfate.

The EPR spectra of powdered samples of chlorocuprates are shown in Fig. 1 (a)—(j). In Figs. (a) to (h), the upper curves are the derivatives of the absorption lines observed, and the lower curves, the integrated absorption lines. With the records of (i) and (j), integration could not be performed because of the extreme broadness of the absorption lines.

Results and Discussion

The Composition and the Color of the Chlorocuprates.—All strictly chloride complexes of copper(II) with an atomic ratio of chlorine to copper greater than 4 : 1 are yellow. This is probably due to the fact that the LF bands which impart blue or green colors to aquo or ammine complexes lie in the infrared region in chlorocuprates, while charge transfer bands come into the visible region in chloro complexes and give these compounds their yellowish color.

There is a group of chlorocuprates with the chlorine to copper ratio of 3 : 1. They are crystallized from solutions of high copper(II) concentration or from media of relatively concentrated acetic acid, and they are usually brown in color. Well-known examples are potassium copper(II) trichloride and cesium copper(II) trichloride, both of which have been found to be kinds of coordination polymers.[4,5] Additional examples found in the present research are melammonium hexachlorodicuprate(II) and benzoguanammonium trichlorocuprate(II), although their crystal structures are not yet known. All these compounds show characteristic EPR spectra, as will be discussed later.

The dark green color of diethylenetriammonium chlorocuprate(I, II) is probably due to the interaction of univalent and divalent copper ions.

EPR Absorption Spectra.—Most of the EPR data presented here are those of powdered samples. Kneubühl[8] developed a method to get EPR data from the spectra of powdered samples and applied it to the interpretation of the spectra of anisotropic copper ions. The method seems particularly convenient for the comparison of the EPR spectra of more or less analogous componuds.

Among the chlorocuprates studied in the present research, dimelammonium hexachlorocuprate(II) was the only compound that showed the fine structure of an anisotropic g-tensor. (Fig. 1(h)). By means of the method described by Kneubühl, the components of the g-tensor were evaluated as $g_{//}=2.32$ and $g_{\perp}=2.08$ for this compound.

All the other chlorocuprates studied showed single lines with half-widths ranging from 110 to 220 oe. Generally speaking, a single line can be observed either when three components of a g-tensor coincide with each other or when the superexchange interaction is great enough to smear out the effect of crystal anisotropy. The former can hardly be the case for Cu^{2+} ions in solid samples, as has in many cases been confirmed experimentally and theoretically.[9] The appearance of single lines in some copper compounds is, therefore, to be explained in terms of the latter effect.[10] In order to smear out the fine structure with the components of the g-tensor ranging from 2.08 to 2.32, the interaction energy corresponding to the exchange should be about $10^9\,sec^{-1}$. The fact that only dimelammonium hexachlorocuprate showed the superfine structure of an anisotropic g-tensor may be due to the screening effect of large planar organic molecules present in the crystal lattices of this compound.

There are two ways in which the superexchange of paramagnetic ions influence the line width of the EPR spectra: one is to broaden the width, and the other is to reduce it. The former effect, termed exchange broadening, is observed in a critical case when the exchange frequency is nearly equal to the energy separation between the resonance points divided by Planck's constant. The EPR spectra of the chlorocuprates of chain organic polyamines seem to exemplify such a case; the half width is about 200 oe, and the shape of the curve is of a bell type, with an assymmetric contour (Figs. 1 (d)—(f)).

The latter case (exchange narrowing) is the one in which the exchange frequency is greater than that in the critical case above mentioned; it is characterized by a line shape of the Lorenzian type. The EPR spectra of hexamminecobalt(III), pentachlorocuprate(II) and related

8) F. K. Kneubühl, *J. Chem. Phys.*, **33**, 1074 (1960).
9) L. E. Orgel and J. D. Dunitz, *Nature*, **179**, 462 (1957).
10) D. M. S. Bagguley and J. H. E. Griffiths, *Proc. Roy. Soc.*, **A201**, 366 (1950).

TABLE I. THE EPR DATA OF CHLOROCUPRATES

Compound	g.	ΔH_{msl}	$\Delta H_{1/2}$	$\Delta H_{1/2}/\Delta H_{msl}$	$\sqrt{\Delta H^2}$	$Cu^{II}/Cu \times 100$
$[Co(NH_3)_6]CuCl_5$	2.17	86	140	1.63		100
$[Co(NH_3)_6]CuCl_{5-x}$	2.16	64	105	1.64	80	78
$[Co(NH_3)_6]_4Cu_5Cl_{17+x}$	2.17	68	116	1.70	90	10
$[Co(NH_3)_6]_4Cu_5Cl_{17+x}$	2.17	88	183	2.10		
$dienH_3CuCl_{5-x}$	2.14	162	218	1.35		98
enH_2CuCl_4	2.14	148	222	1.50		100
$dienH_3CuCl_5$	2.14	139	185	1.33	108	100
$trienH_4CuCl_6$	2.14	139	218	1.57		100
$(melamine)_2H_4CuCl_6$	2.31 2.08					100

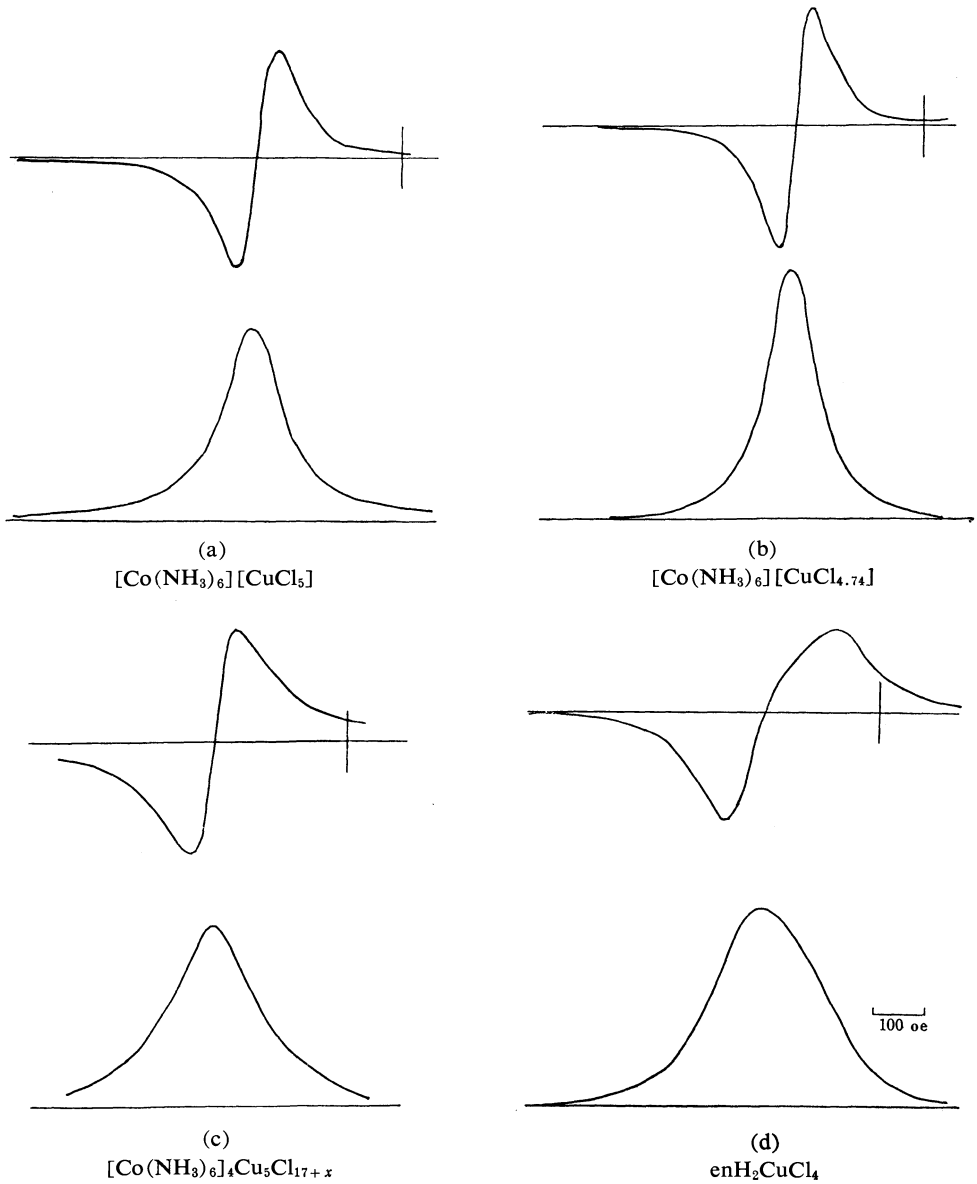

(a) $[Co(NH_3)_6][CuCl_5]$

(b) $[Co(NH_3)_6][CuCl_{4.74}]$

(c) $[Co(NH_3)_6]_4Cu_5Cl_{17+x}$

(d) enH_2CuCl_4

Fig. 1. EPR spectra of chlorocuprates.
The short vertical line on the right hand side of each derivative curve is the marker of the maximum point of a DPPH absorption line.

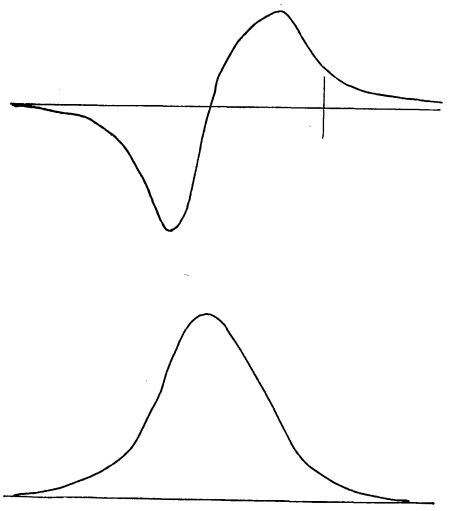

(e)
dien H_3CuCl_5

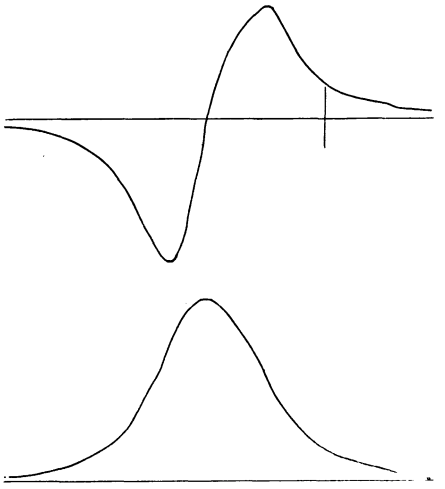

(f)
trien H_4CuCl_6

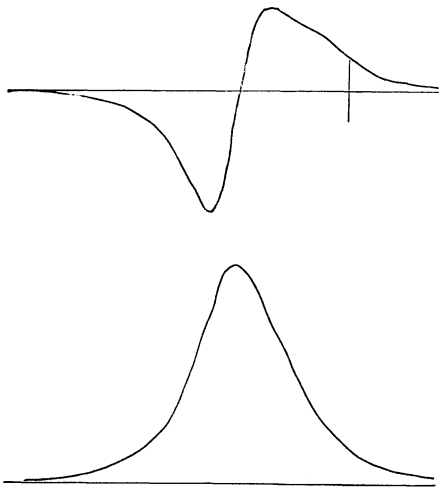

(g)
dien $H_3CuCl_{4.95}$

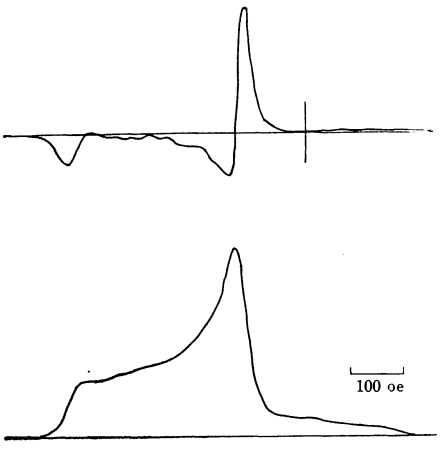

(h)
$(melamine)_2H_4CuCl_6$

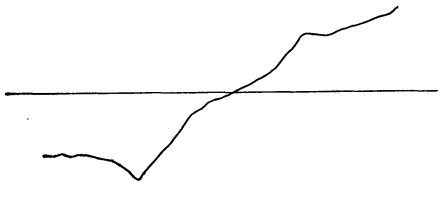

(i)
melamine $H_2Cu_2Cl_6$

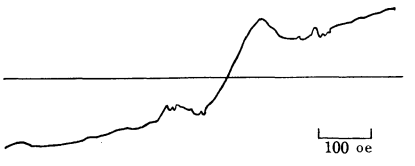

(j)
Benzoguanamine $HCuCl_3$

Fig. 1. continued.

mixed valence chlorocuprates(I, II) seem to fall in this category, since the lines are comparatively narrow (80 oe) and the ratio of the line width at the half-maximum point, $\Delta H_{1/2}$, to that at the points of maximum slopes, ΔH_{msl}, is about 1.7. The symmetric line shape of the EPR absorption spectra may be taken as partly due to the special character of the $CuCl_5^{3-}$ ion, with all the Cu–Cl distance almost identical to one another.[3] Even the line shape of the spectra of a single crystal showed scarcely any angular dependence on the field directions.

The width of the curve is narrower in the chlorocuprates(I, II) than in chlorocuprate(II) in this series when the content of copper(I) is not high. It seems, however, difficult to decide whether this is due to the effect of the dilution of copper(II) or to enhanced exchange interaction caused by the presence of copper(I). When the content of copper(I) becomes overwhelmingly higher than that of copper(II), the width again increases; this is probably due to the increased field anisotropy. The main EPR data of chlorocuprates of various compositions are presented in Table I.

As has been pointed out at the beginning of this discussion, chlorocuprates with a chlorine to copper ratio of 3:1 have a brown color and are considered to have polynuclear structures. The EPR spectra of such compounds have invariably a very broad line width to cover thousands of oersteds, and the *g*-values of these lines can be evaluated only with difficulty (Figs. 1 (i) and (j)). This broadening can perhaps be attributed to the strong exchange and dipolar action and to the great anisotropy of the crystal field, both arising from the linear structure in the crystal lattices.

Summary

Some copper complexes which have only chloride ions in the coordination spheres have been prepared and their EPR spectra examined at the microwave frequency of the X-band. Most of these compounds gave single EPR lines with half-widths ranging from 110 to 220 oe; this seems to indicate the existence of superexchange interaction. Only the yellow plates of dimelammonium hexachlorocuprate-(II) showed the fine structure of an anisotropic *g*-tensor, from which fact the *g*-components were evaluated as $g_{\parallel}=2.32$ and $g_{\perp}=2.08$ for this compound. The dark green color of diethylenetriammonium chlorocuprate(I, II) is probably due to the interaction of Cu^{+} and Cu^{2+} in the crystal lattices. Brown chlorocuprates with a chlorine to copper ratio of 3:1 are probably coordination polymers; the EPR lines of these compounds are so broad as to cover thousands of oersteds.

The authors are very grateful to Dr. Toschitake Iwamoto and Mr. Yasuhito Eguchi for their kind coorperation in the EPR measurements.

Faculty of Science
Osaka City University
Sumiyoshi-ku, Osaka (*M. M.*)

Faculty of Science
The University of Tokyo
Hongo, Tokyo (*S. F.*)

On the Jacobsen Reaction. IV.[1] *Character and Reaction Mechanism*

By Hitomi SUZUKI*

(Received July 22, 1963)

In the electrophilic substitution of highly-substituted aromatic compounds, the migration or replacement of substituents by the attacking groups has often been observed.[2-6] Although these phenomena have long been recognized, however, there have been few systematic studies on the scope of such anomalous substitution. The position at which substitution occurs is determined by the group already present in the aromatic ring and can usually be predicted from the rules governing aromatic substitution. As the compounds become more complex, however, it is difficult to predict the position precisely from the so-called "rules for orientation." This may be because the course of the reaction and the ease with which it takes place become much more influenced by such factors as the number, structure, and type of groups attached to the ring, as well as by the electronic and steric effects of these groups. Thus, the tendency towards an orthodox reaction, in which the replacement of hydrogen by an attacking group is in accordance with the rules of directive influence, is decreased while, at the same time, the reaction leading to the production of anomalous products becomes prominent.

The most typical of these anomalous reactions is the Jacobsen reaction.[7-10] This name has been given to the migration of an alkyl group or halogen atom of polysubstituted benzene derivatives containing only halogen atoms, only alkyl groups or a combination of the two, a migration which occurs when these substances are sulfonated or when their sulfonic acids are allowed to stand in contact with sulfuric acid. One of the most interesting features of this reaction is the migration of an alkyl group or halogen atom to the vicinal position. At first sight, this is in direct contrast to the orienting effects in the Friedel-Crafts reaction and has long been the object of much study.

Jacobsen reaction

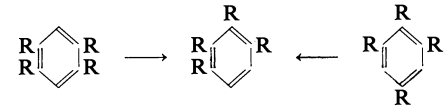

Friedel-Crafts reaction[11]

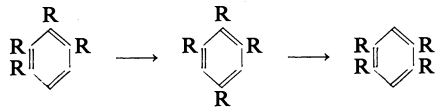

Although several mechanisms have been proposed for this reaction,[10,12-14] none of these proposals seem to be satisfactory. Some of them will, however, be cited here.

Arnold and Barnes[15] have proposed the following mechanism for the formation of the vicinal compound;

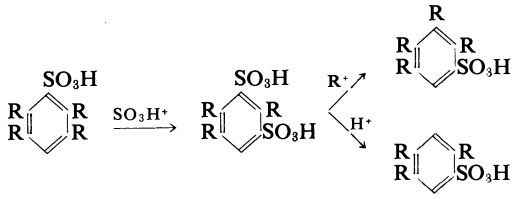

According to this theory, the migrating alkyl group is detached from the sulfonic acid molecule as a cation by the entrance of a second sulfonic acid group; this cation then replaces the more hindered sulfonic acid group

* Present address: Institute for Chemical Research, Kyoto University, Takatsuki, Osaka.

1) Previous papers in this series: a) R. Goto and H. Suzuki, *J. Chem. Soc. Japan, Pure Chem. Sec.* (*Nippon Kagaku Zasshi*), **84**, 167 (1963); b) H. Suzuki and R. Goto, ibid., **84**, 284 (1963); c) R. Goto and H. Suzuki, ibid., **84**, 435 (1963).

2) G. F. Hennion and SF. de C. McLeese, *J. Am. Chem. Soc.*, **64**, 2421 (1942).

3) P. W. Robertson and H. V. A. Briscoe, *J. Chem. Soc.*, **101**, 1964 (1912).

4) D. V. Nightingale, *Chem. Revs.*, **40**, 117 (1947).

5) D. V. Nightingale and H. B. Hucker, *J. Org. Chem.*, **18**, 1529 (1953).

6) H. Hopf and A. K. Wick, *Helv. Chim. Acta*, **43**, 1473 (1960); ibid., **44**, 19 (1961).

7) L. I. Smith, "Organic Reactions I," John Wiley & Sons, Inc., New York (1942), p. 370.

8) C. M. Suter, "The Organic Chemistry of Sulfur," John Wiley & Sons, Inc., New York (1944), p. 212.

9) C. M. Suter and A. W. Weston, "Organic Reactions 3," John Wiley & Sons, Inc., New York (1946).

10) C. L. Moyle and L. I. Smith, *J. Org. Chem.*, **2**, 112 (1937).

11) C. A. Thomas, "Anhydrous Aluminum Chloride in Organic Chemistry," Reinhold, New York (1941).

12) J. Herzig, *Monatsh.*, **2**, 192 (1881).

13) O. Jacobsen, *Ber.*, **19**, 1215 (1886).

14) G. Schroeter and S. Götzky, ibid., **60**, 2035 (1927).

15) R. T. Arnold and R. A. Barnes, *J. Am. Chem. Soc.*, **66**, 960 (1944).

of the di-sulfonic acid. This mechanism is, however, not tenable in view of: (a) the failure to isolate the postulated intermediary di-sulfonic acid; (b) the fact that the migration of an alkyl group occurs, even under the mild conditions under which the formation of di-sulfonic acid is improbable; (c) the failure to explain many reactions involving the migration of halogen atoms, and (d) the fact that the conversion of the sulfonic acid group into amide or ester exerts an inhibitory effect on the reaction.

Dewar[16] has assumed the intramolecular migration of the sulfonic acid group; applied to durene, the reaction can be written as follows:

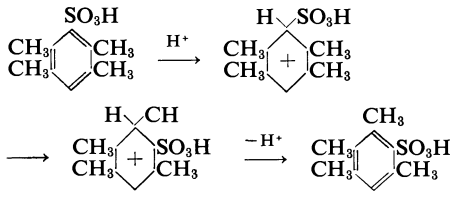

While a plausible explanation for some reactions of simple compounds, this mechanism fails when attempts are made to apply it to a variety of compounds which undergo the reaction. For example, since the sulfonic acid group always takes the less blocked position, the sulfonation of 5-substituted pseudocumene occurs preferrentially at the 3-position. Thus, one would, according to his theory, expect, 4-substituted hemimellitene to be the sole product from 5-substituted pseudocumene. This is not the case, however, as 5-ethylpseudocumene affords chiefly 3-ethylpseudocumene, whereas 5-isopropylpseudocumene gives no vicinal compound. Moreover, this mechanism is inconsistent with the fact that durene itself undergoes the Jacobsen reaction more readily than isodurene. His mechanism also cannot be applied to the halogen migration.

Fieser and Fieser[17] have explained the reaction on the basis of an allylic-type rearrangement of the substituent groups:

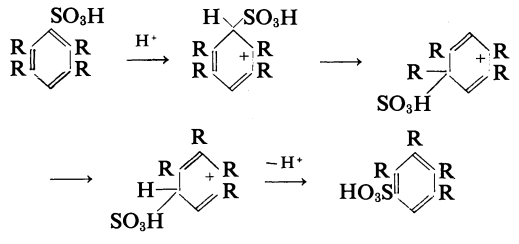

16) M. J. S. Dewar, "The Electronic Theory of Organic Chemistry," Oxford Press, London (1956).
17) L. F. Fieser and M. Fieser, "Advanced Organic Chemistry," D. C. Heath and Company, Boston (1961), p. 665.

In above mechanism the sulfonic acid is first protonated to form the aronium ion, which undergoes the allylic migration of a sulfonic acid group and the reverse migration of a methyl group, followed by the expulsion of a proton, to form prehnitene sulfonic acid. This mechanism is untenable since it cannot be used satisfactorily to explain the formation of vicinal compounds from either *unsym*-tetraalkyl or pentaalkylbenzenes as well as most of the reaction involving the migration of a halogen atom.

Thus no mechanism has yet been found which will satisfactorily explain all the available data. This is probably because several mechanisms are responsible for the Jacobsen reaction. Many of the studies of the mechanism of the reaction so far have been concerned with the reactions involved in the formation of vicinal compounds. In addition to these somewhat peculiar reactions, however, there exist a number of reactions which should be classed as Jacobsen reactions in the sense that they involve the migration of an alkyl group or halogen atom in the course of sulfonation. Therefore, it is apparent that a single mechanism capable of accounting for all the variations of the Jacobsen reaction cannot be postulated on the basis of such simple assumptions as have been mentioned above.

In this paper, the author would like first to summarize all the results of his studies, together with those of some previous workers, of the Jacobsen reactions, and then, classifying them according to their reaction types into three groups, to propose a more reasonable mechanism consistent with all the data.

Experimental Procedure

The details of the experimental procedure and findings have been given in the previous papers of the series, I-III,[1] they will not be repeated here.

The Jacobsen Reaction.—*Polyalkylbenzenes.*—The general procedure was as follows: a mixture of hydrocarbon and sulfuric acid was magnetically stirred and gradually heated on a water bath. The color changed from yellow to red; it then deepened to reddish brown, and finally to black. The complete solution of the hydrocarbon was usually effected at 60~80°C. The mixture was kept at this temperature range for 4~6 hr. and then allowed to stand for a day or two at room temperature. The mixture was diluted somewhat with water, and all solids were removed by filtration. The filtrate was distilled with superheated steam, the distillate was extracted with ether, and the extract was washed with aqueous sodium hydroxide and dried over calcium chloride. Then the solvent was evaporated and the residual oily material was fractionated.

Polyalkylhalogenobenzenes and Polyhalogenobenzenes.—The standard procedure for conducting the experiments with these compounds was divided into two parts, depending upon the solubilities of the reaction products. In procedure I, the whole reaction mixture was poured onto ice and all solids were removed by filtration. The solid was washed, dried and subjected to chromatographic separation on an alumina column. To the acidic filtrate a saturated sodium chloride solution was added to precipitate the sodium sulfonate. The salt was filtered and converted to sulfonamide, which was then fractionally crystallized. Procedure II was the same as I except for the method of handling the filtrate. The sulfonic acid solution was hydrolyzed by passing superheated steam through the filtrate, and the distillate was subjected to fractional distillation.

The Identification of the Reaction Products.—*Polyalkylbenzenes.*—All the specimens obtained from the Jacobsen reactions were inspected by gas-chromatography and infrared spectroscopy and then identified by conversion to known polybromo or polynitro compounds. The structure proof that all the groups attached to the ring were located vicinally, was effected either by the oxidation with diluted nitric acid of a portion of the specimen to benzene polycarboxylic acid, or by the transformation of the specimen into a phenanthrophenazine derivative through the dinitro and diamino compounds, which proved that the two vacant positions were ortho to each other, that is, all four alkyl substituents were in vicinal positions.

Polyalkylhalogenobenzenes and Polyhalogenobenzenes.—The oils obtained from the hydrolysis of sulfonic acids were carefully fractionated, and each fraction was subjected to gas-chromatographic and infrared spectroscopic inspection. The vicinal location of all substituent groups was established by the conversion of a specimen to a phenanthrophenazine derivative by the same method as that used in I. Solid crystalline materials were, after chromatographic separation on an alumina column, recrystallized from ethanol or benzene; they were identified by mixed melting determination with an authentic specimen prepared by other methods.

Results and Discussion

All the Jacobsen reactions may be divided into two general types, intramolecular and intermolecular; in both cases there are transfers of an alkyl group and/or halogen atom.

Polyalkylbenzenes.—The compounds which yield "abnormal products" are limited almost exclusively to tetra or pentaalkylbenzenes containing tetramethylene rings and/or alkyl groups with a short, straight chain, such as methyl, ethyl and *n*-propyl, while those with alkyl groups of a branched structure, such as isopropyl and *t*-butyl, the elimination of these or other alkyl groups are the only reactions taking place. Mono, di and trialkylbenzenes merely yield sulfonic acids, which are quite stable towards sulfuric acid.[18]

The Jacobsen reaction embodies an electrophilic attack upon the ring of polysubstituted benzenes and is dependent upon increased electron density at the position of sulfonation. It is readily apparent that an electron-attracting group, such as the nitro or carboxyl group, would inhibit the reaction. The conversion of sulfonic acid group to sulfonamide or ester exerts an inhibitory influence on the migration of an alkyl group. Reagents also exert a definite effect over the course of the reaction; fuming sulfuric acid usually favors sulfonation, whereas common sulfuric acid often brings about the migration of alkyl groups. These, and other known facts, suggest that the reversibility of sulfonation is the factor of greatest importance in determining whether a Jacobsen reaction will take place or not.

The process of the Jacobsen reaction of polyalkylbenzenes may be divided into two stages; both stages must be gone through before any Jacobsen reaction can be expected to occur in the sulfonation of polyalkylbenzenes.

(a) The elimination of an alkyl group, which occurs during the sulfonation of polyalkylbenzene relatively resistant to sulfonation owing to its highly crowded structure. In most cases the combined effects of steric hindrance and the entrance of a powerful electron-attracting group are necessary to bring about the expulsion of the migrating group.

(b) The alkyl cation thus ejected migrates, according to its stability, intramolecularly (vicinal orientation) or intermolecularly (disproportionation). The formation of the vicinal compound occurs when the migrating alkyl group can readily take the vacant position meta to the entering acid group.

Thus, with polyalkylbenzenes containing isopropyl or a *t*-butyl group, the first stage *a* readily takes place to give a bulky cation, which is, however, incapable of participating in the next stage *b* of the reaction.[19] On the other hand, mono, di and trialkylbenzenes are simply sulfonated to give stable sulfonic acids, from which no alkyl group can be removed at all. Therefore, with these compounds no Jacobsen reaction proceeds. *sym*-Hydrindacene has a structure formally similar to those present in octahydroanthracene and durene, but it does not undergo the reaction when left standing with sulfuric acid. This may possibly be

18) With some di- and trialkylbenzenes containing bulky groups, such as isopropyl or *t*-butyl, the elimination of one of these is observed.

19) Recently, an interesting reaction involving the intramolecular migration of *t*-butyl group has been reported by M. Menard, D. Awang and F. L. Chubb, *Can. J. Chem.*, **40**, 1738 (1962).

explained by the small hindering effects of five-membered rings.

In the Jacobsen reaction of tetraalkylbenzene, small amounts of trialkylbenzenes and hexaalkylbenzene were always formed. Trialkylbenzene fractions obtained from mixed tetraalkylbenzene were mixtures of several compounds. These facts indicate that there is a possibility of the formation of two or more vicinal isomers, depending on which alkyl group may shift towards the vacant position meta to the sulfonic acid group. For example, 5-ethylpseudocumene afforded two vicinal isomers, together with considerable amounts of prehnitene.[20]

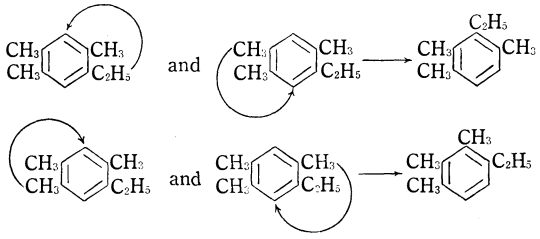

An experiment conducted upon a mixture of durene and *sym*-tetraethylbenzene led to a complex mixture of polyalkylbenzenes, in which the main products were also prehnitene and *vic*-tetraethylbenzene. This fact indicates that the migration of an alkyl group to the vicinal position proceeds intramolecularly. There is apparently an inverse correlation between the ease with which a compound undergoes the Jacobsen reaction and the ease with which the compound can be sulfonated. Thus, when durene and isodurene were subjected to the action of sulfuric acid under the same conditions, it was noted that the time required for the complete migration of the methyl group was much less with durene than with isodurene.

The conversion of 6, 7-dialkyltetralins to vicinal compounds can theoretically proceed by two different routes: the alkyl group may migrate from the 6 (or 7) position to the 8 (or 5), and the tetramethylene ring may open and then close in the ortho position to the alkyl group.

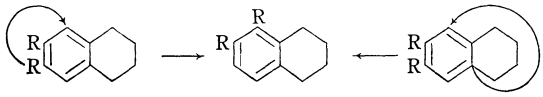

20) The isolation of neither of these isomers was successful. Although all possible isomeric products were undoutedly formed in the reaction of mixed polyalkylbenzene, their presence had been demonstrated or inferred only by a combination of gas-chromatography and infrared spectroscopy because of the experimental difficulties involved in separation.

The evidence that the main reaction takes place through the latter course may be briefly summarized as follows: (a) the reaction products contained only small amounts of monoalkyltetralins; (b) octahydroanthracene, in comparison to *sym*-tetraalkylbenzene, was much more readily converted to the vicinal compound under the same conditions; (c) when 5, 7- and 6, 7-dimethyltetralin were subjected to the same conditions of the Jacobsen reaction, the former gave only a small amount of an oily product which could not be identified, whereas the latter readily converted into the vicinal compound.

Although the opening of a ring, followed by the migration of an intermediate with a cationic terminal carbon atom, would involve the simultaneous isomerization of the group to the more stable secondary carbonium ion, no hydrindene derivative was detected in the reaction products from dialkyltetralins. This may be explained both by the well-known preference for the formation of a six-membered rather than a five-membered ring in cyclization, and by the tendency for a bulky cation to avoid a highly blocked position. Dialkyltetralins containing a isopropyl group were always converted into the compounds in which the isopropyl group was eliminated.

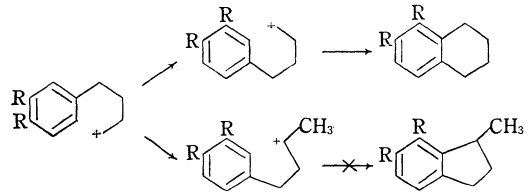

The relatively high yields of *vic*-dialkyltetralins compared to those of *vic*-tetraalkylbenzenes are attributed to the fact that one end of the long chain cation is attached to the ring and so cannot leave the molecule freely. Therefore, although *sym*-tetra-*n*-butylbenzene, with which an analogous process might be expected to occur, has not yet been studied, the formation of a vicinal compound can hardly be expected.

Reaction products from mixed polyalkylbenzenes are usually complex mixtures and require extensive purification. Furthermore, the yields are low, and the probable structure inferred from analogy should be investigated by independent methods. Thus, the Jacobsen reaction cannot be considered as a general synthetic method for *vic*-tetraalkylbenzenes.

Polyalkylhalogenobenzenes and Polyhalogenobenzenes.—An extensive study of the reaction of polyalkylhalogenobenzenes has shown, as can be predicted on theoretical grounds, that increasing the number of alkyl groups attached to the benzene ring favors both the migration

of the halogen atom and the decomposition of the compound to tarry materials. Thus, there exists a certain limited scope within which the reaction can proceed smoothly. For example, monochloroxylenes are merely sulfonated, while monoiodoxylenes afford polyiodoxylenes in high yields; with monochlorotetramethylbenzenes the migration of the methyl group is observed, whereas with monoiodotetramethylbenzenes, the reaction proceeds too readily, yielding intractable resinous materials.

The iodine atom is most readily, and the chlorine atom is least easily, replaced by the sulfonic acid group; therefore, the disproportionation is most prevalent with iodine compounds, whereas the formation of vicinal compounds is found with chlorine compounds. Bromine compounds occupies an intermediate place with respect to ease of replacement; hence, they show both disproportionation and intramolecular migration simultaneously. The three reactions which follow illustrate this statement well:

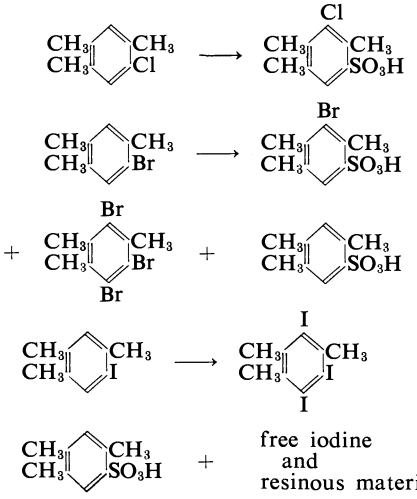

The iodine cation is unable to re-enter the molecule because of its bulkiness and so is set free as elementary iodine.

The behavior of a number of *sym*-polyhalogenobenzenes and *sym*-polyalkylhalogenobenzenes towards sulfuric acid is summarized in the following table:

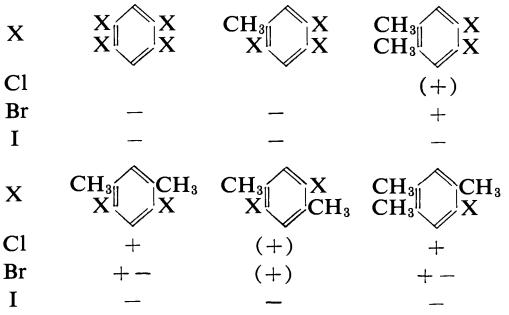

where sign + denotes the formation of the vicinal compound and sign −, disproportionation. The parentheses mean that the reaction occurs only under drastic conditions.

With polyhalogenobenzenes, the Jacobsen reaction is confined almost entirely to polybromo and polyiodobenzenes. A few special cases involving chlorine migration have been found, but for the most part the chlorine atom does not undergo the migration. It appears that the halogen atom always migrates intermolecularly if any reaction occurs at all, and all the available evidence indicates that the ease of migration in these compounds is in the order of I>Br>Cl. As the ring-bonded fluorine atom is unable to form a cation, it, of course, cannot take part in the migration.

In order to determine the effect of various substituents upon the ease, course and limits of the reaction, the action of sulfuric acid upon a number of halogenobenzene derivatives was studied. Electron-attracting groups, such as the nitro, carboxyl and carbonyl, hindered the reaction so greatly that it usually failed to take place when any of these were attached to the ring. On the other hand, an accumulation of electron-releasing groups, such as hydroxy and alkoxy, facilitated the reaction so much that it was often difficult to prevent the compounds from decomposing to tarry materials. The presence of bulky groups, such as isopropyl and *t*-butyl, on the aromatic ring also interfered with the reaction. The importance of the steric factor was revealed by an examination of the products from monoiodoalkylbenzenes; with the methyl and ethyl groups, the migration products were obtained in high yields, whereas with the isopropyl and *t*-butyl groups, the reaction was that leading to the formation of resinous materials, with no definite product.

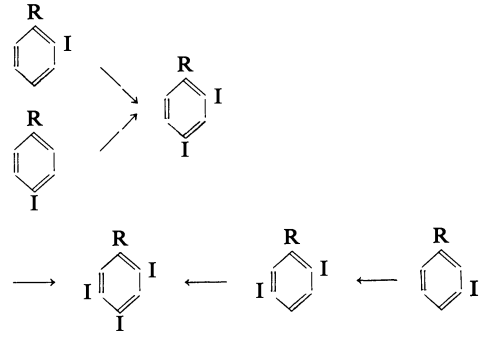

R=Methyl or ethyl

No attack of halogen atom upon the alkyl group was observed.

In some cases, slight changes in the structure of the compound may cause great differences in the ease of the migration of the halogen

atom. For example, *o*- and *p*-iodoanisol readily gives polyiodo compounds, but *m*-isomer is simply sulfonated to give a stable 6-sulfonic acid.

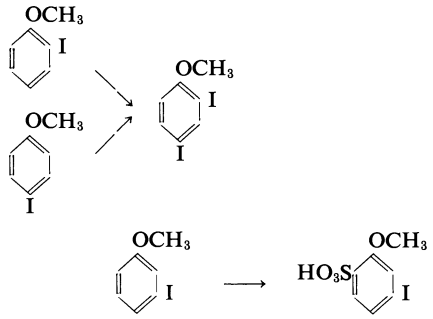

The reaction usually proceeds as the progressive halogenation of the parent compound, and a certain isomer is always formed in preference to others. For example,

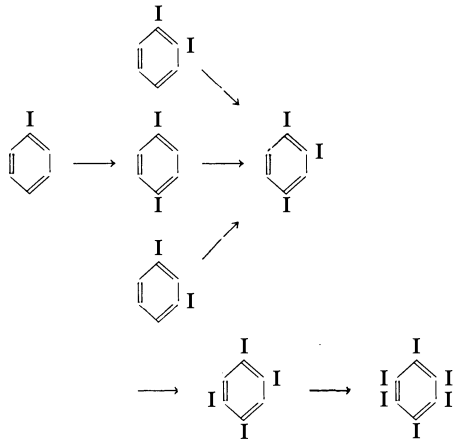

When there exist more than one halogen atom capable of migration, the preferential replacement occurs with those present at the positions that have a higher electron density or a greater steric hindrance.

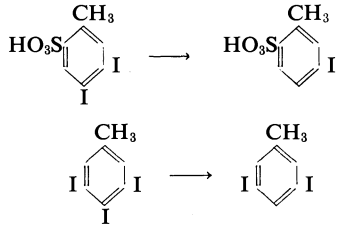

The reaction is considered of much value for the direct synthesis of some polyiodo compounds.[21]

Mechanism.—All the Jacobsen reactions so far observed can be divided into three groups according to their reaction types: *the first*, shown by a compound relatively resistant to sulfonation because of its highly crowded structure, involves an anomalous sulfonation leading to the elimination of an alkyl group or a halogen atom, followed by its migration; *the second*, in which the normal sulfonation of a compound constitutes the initial phase of the reaction, is most often encountered with these compounds which are readily sulfonated to form a stable sulfonic acid (the migration of substituent groups on the ring gradually occurs intra- or intermolecularly, depending on their structures and experimental conditions); *the third* is shown by some polyiodo compounds, in which no sulfonation can be expected at all because of their highly crowded structures and reduced reactivities (the protonation of the compound, followed by the expulsion of the iodine cation, must constitute the initial phase of this reaction).

In the following discussion, for each individual group of reactions the author has attempted to formulate a mechanism with which to explain satisfactorily the experimental findings so far obtained on the Jacobsen reaction.

(I) The first group involves compounds relatively difficult to sulfonate and may be represented by the following generalized scheme:

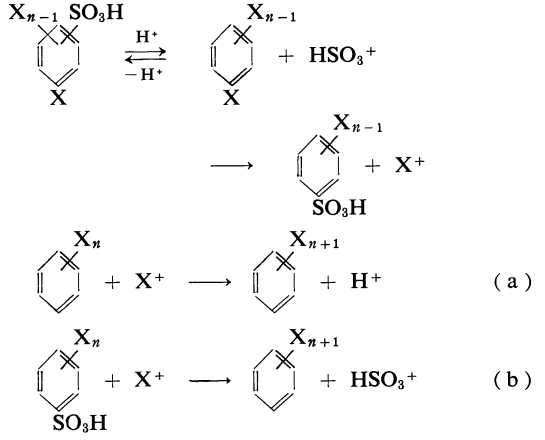

This is a two-stage reaction initiated by the electrophilic attack of a sulfonic acid group, which will, of course, seek a position with high electron density and small steric hindrance. The alkyl group or halogen cation which is eliminated during sulfonation will react with the parent compound according to Eq. a, or with the sulfonic acid according to Eq. b. The most typical reactions of this group are those observed in the sulfonation of *sym*-tetraalkylbenzenes, in which vicinal compounds are formed. Applied to durene, this may be outlined as follows:

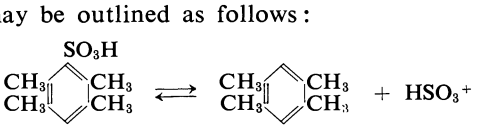

21) H. Suzuki and R. Goto, This Bulletin, **36**, 389 (1963).

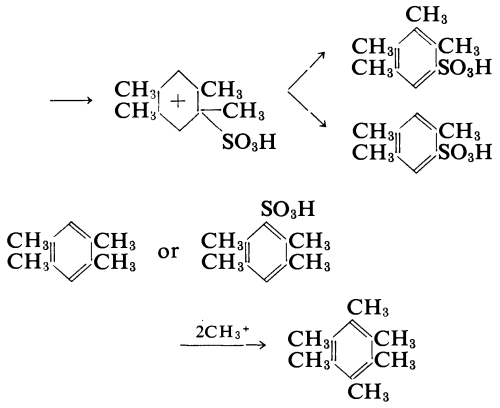

The formation of the vicinal compound may be interpreted as follows: a partially positive methyl group may be ejected from durene by the attack of a sulfonic acid group, but, never becoming completely free, it may form a π-complex with the ring and then pass to the vacant position meta to the sulfonic acid group. The remarkable color changes involved in the initial phase of the reaction support the theory that the reaction proceeds through the intermediary complex described above. The ability of several migrating groups to take this vacant position, giving vicinal compounds, is influenced to a large extent by steric requirements. This can readily be visualized by a series of 5-substituted pseudocumenes: the combined inductive and mesomeric effects of methyl groups give rise to a high electron density at the 5-position of pseudocumene derivatives and hence facilitate the electrophilic attack at this position by a sulfonic acid group, which expels a substituent group there as a cation. When the cationic group ejected is reactive and is sterically small enough, there a vicinal orientation is always observed. This is the case with 5-methyl, 5-ethyl, 5-chloro and 5-bromopseudocumene. If larger groups are involved in the reaction, the elimination of these groups is the only reaction that proceeds. These are found, for example, with 5-isopropyl and 5-iodopseudocumene.

The reactions of dialkyltetralin and pentaalkylbenzene may also be incorporated into this group. For example, with pentamethylbenzene:

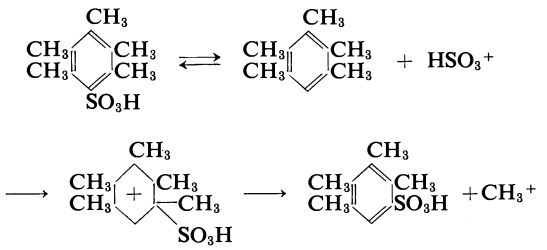

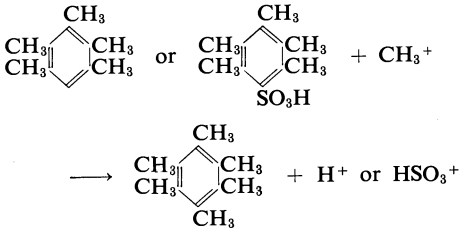

Next, let us consider compounds with only a few substituent groups. It has long been known that the sulfonation of *p*-diiodobenzene is always accompanied by disproportionation, thus giving *p*-iodobenzene sulfonic acid and mixtures of polyiodobenzenes. This process is also represented by an analogous two-stage mechanism, in which the following processes take place:

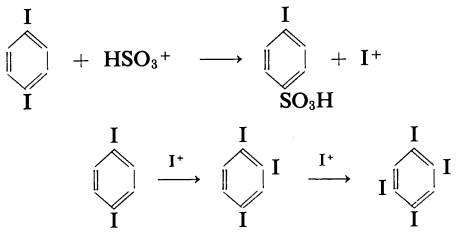

When some polyalkylbenzenes containing *t*-butyl groups are allowed to stand in contact with sulfuric acid, the elimination of the *t*-butyl group is observed to some extent. In these cases, however, the extreme aversion of the *t*-butyl group to the entry in a position ortho to the alkyl groups in the ring inhibits the further alkylation of the parent hydrocarbons; thus, no reaction analogous to the Jacobsen proceeds.

(II) The second group includes the reactions which are most often encountered with compounds readily subject to the action of sulfuric acid. As has been mentioned above, the ease of sulfonation is inversely related to that of migration; hence, the compounds of this group need more time for the completion of the reaction. It is best represented by the following generalized scheme:

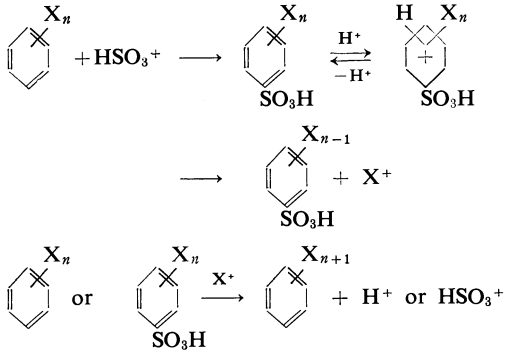

The reaction scheme above is interpreted at follows: sulfonic acid is first protonated to form an intermediate complex, from which the group present at the position of higher electron density and larger steric hindrance is ejected. The alkyl group or halogen atom thus expelled may migrate, according to its stability, intramolecularly to form vicinal compounds or intermolecularly to yield disproportionation products.

The formation of polybromobenzenes from monobromobenzene is one example:

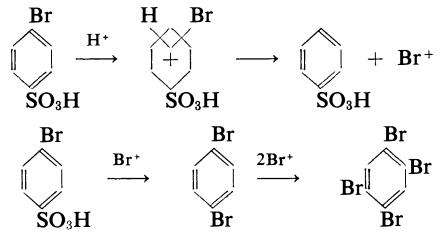

There are two possible routes by which a vicinal compound can be formed from a non-vicinal compound: one is that just described in group I, the other belongs to group II. For example, *unsym*-tetraalkylbenzenes are necessarily sulfonated ortho to both alkyl groups unless one of them is displaced by the entering sulfonic acid group. Thus, there arises a great steric hindrance which forces the migration of one of the alkyl groups so as to reduce the blocking action on the sulfonic acid group. Applied to ethylmesitylene, this may be outlined as follows:

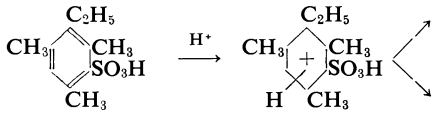

The vicinal orientation found with *unsym*-tetraalkylbenzene sulfonic acid is attributed to the buttressing effect of the alkyl group meta to the sulfonic acid group, because *sym*-trialkylbenzenes in which no buttressing effect of meta alkyl group is present can never show the Jacobsen reaction.

Another interesting example was found in the reaction of 2-iodo-*m*-xylene and 2, 3-diiodotoluene (cf. a future communication), where was formed not the expected 2, 4-diiodo-*m*-xylene nor 2, 3, 6-triiodotoluene, but the symmetrically-substituted 4, 6-diiodo-*m*-xylene and 2, 4, 5-triiodotoluene. These must have been formed as a result of initial sulfonation at the 6-position, followed by the intramolecular shift of the iodine atom from the hindered position 2 to the 4.[22]

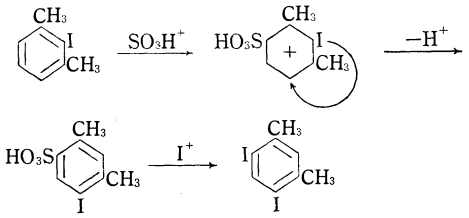

These resuits further support the concept that the entry of a bulky group at the meta position has a great influence on the stability of the substituent group sterically hindered by two ortho substituents.

The sulfonation of iodomesitylene might be another example where no reaction proceeds without accompanying the disproportionation of the iodine atom;[23]

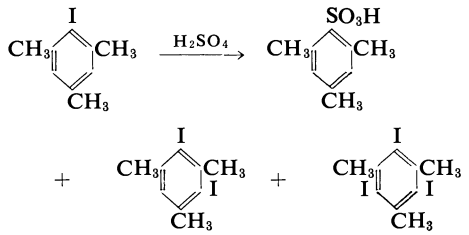

These two types of reaction routes, I and II, however, must be regarded as extremes; a number of the reactions may possibly take place through a course which could be regarded as a combination of the two. Which type

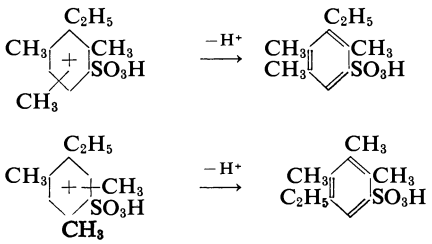

of reaction predominates depends on the steric requirements of the compound subjected to the Jacobsen reaction. With highly crowded compounds, the reaction scheme I, involving direct displacement, seems important, whereas with less crowded compounds the reaction scheme II predominates.

(III) The third group is quite different from the two mentioned above; here sulfuric acid appears to act only as a protic solvent. Some polyiodo compounds with highly crowded structures, with which no sulfonation can be

22) As *m*-xylene sulfonic acid and iodine afford no iodinated compound under the same conditions, the intermolecular migration of iodine atom is less probable.

23) A. Tohl and R. Eckel, *Ber.*, **26**, 1099 (1893).

expected to occur, undergo this type of reaction under drastic conditions. For example:

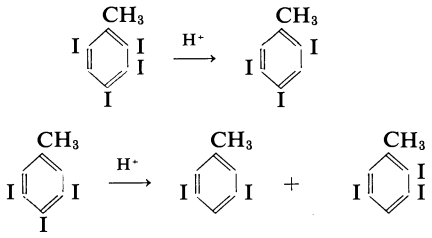

These can not be classed as true Jacobsen reactions, however, because no sulfonation is involved in the above reactions. There are, however, many interesting observations in the literature on the migration of an alkyl group or halogen atom, analogous to the Jacobsen reaction, where neither sulfonation nor a sulfonic acid group is concerned. The following are some examples:

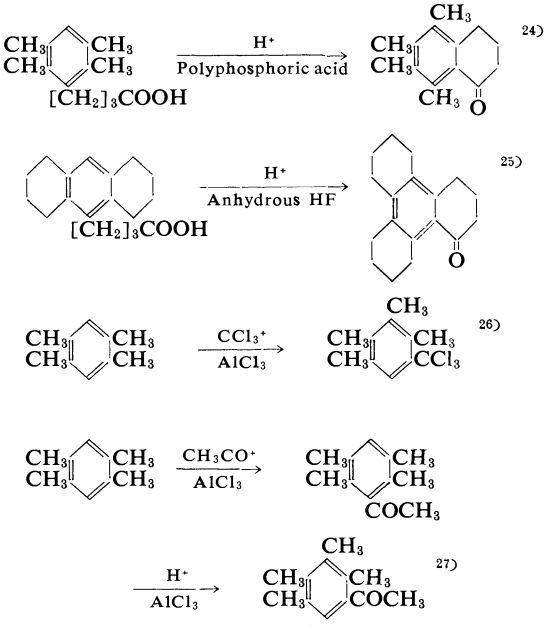

24) W. L. Mosby, *J. Am. Chem. Soc.*, **74**, 2564 (1952); *J. Org. Chem.*, **18**, 483 (1953).
25) G. M. Badger, W. Carruthers and J. W. Cook, *J. Chem. Soc.*, **1949**, 2044.
26) H. Hart and R. W. Fish, *J. Am. Chem. Soc.*, **83**, 4460 (1961).
27) G. Baddeley and A. G. Pendlum, *J. Chem. Soc.*, **1952**, 807.

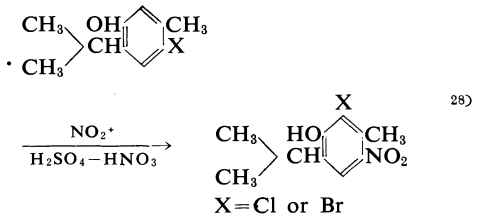

28) P. W. Robinson and H. V. A. Brisooe, ibid., **101**, 1964 (1912).

All cases contain intra- and/or intermolecular migration in the presence of an acidic medium, of an alkyl group or of a halogen atom, involving the vicinal orientation of these groups. If we consider that the nitro, carbonyl or acetyl group plays the same role as that of the sulfonic acid group in the Jacobsen reaction, then we may suppose that the above reactions are Jacobsen types and may indeed take place by analogous processes.

For the purpose of classifying these anomalous reactions, it seems convenient to give the term "Jacobsen Reaction" a much wider meaning, that is, to extend the definition to the general cases of anomalous electrophilic substitution, in which there is observed an intra- or intermolecular migration of substituent groups expelled by the entry of electrophilic attacking groups under the very influence of acidic solvents. Therefore, the term "Jacobsen Reaction" will no longer mean only abnormal sulfonation in a narrow sense, but a variety of anomalous electrophilic substitutions of a similar nature which are at present not systematized and are included in other categories.

The author wishes to express his gratitude to Professor Ryozo Goto of Kyoto University for his continuous encouragement and helpful discussions throughout this work.

Department of Chemistry
Faculty of Science
Kyoto University
Sakyo-ku, Kyoto

Photoconductive Polymer: Its Preparation and Photoconductive Behavior

By Kazuhisa MORIMOTO, Yoshiki HAYASHI and Akira INAMI

(Received July 30, 1963)

The photoconductive properties of 1, 3, 4,-triphenyl-2-pyrazoline, its derivatives and homologues have already been established,[1] and the present authors have reported in another paper[2] on their photoconductive and electrophotographic characteristics. A poly-[1, 3-diphenyl-5-(4-vinylphenyl)-2-pyrazoline] is considered to be perhaps the simplest polymer with a triphenyl-2-pyrazoline group to synthesize. Recently several polymers containing heterocyclic group have been reported,[3-5] but because vinyl monomers containing a heterocyclic group are chemically unstable, in most cases only solvent-insoluble high polymers can be obtained. The most successful synthetic route, therefore, is first to prepare polyvinylbenzalacetophenone from polystyrene, and then to let the product react with phenylhydrazine. This sequence produces poly[1, 2-diphenyl-5-(4-vinylphenyl)-2-pyrazoline] of a considerable purity. Under carefully controlled preparative conditions, a high degree of substitution is obtained without the substance's being insoluble in an organic solvent. The photoconductive behavior of this material is then measured.

Experimental

Synthesis of the Polymer. — The polymer was synthesized in three steps as follows:

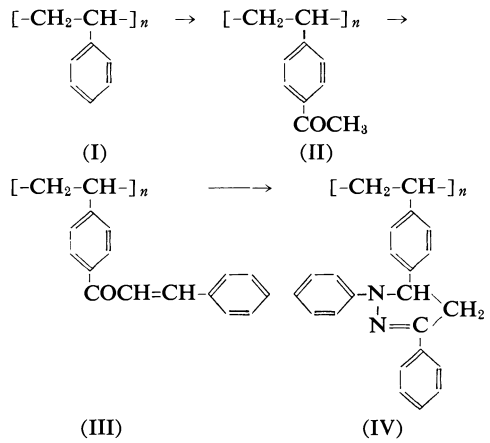

Polyvinylacetophenone (II) from Acetyl Chloride and Polystyrene (I).[6] — In a stirred flask with a dropping funnel and reflux condenser, 500 ml. of carbon disulfide, 134 g. (1 mol.) of aluminum chloride, and 59 g. (0.5 mol.) of polystyrene ($[\eta]=0.68$, at 25°C in benzene) dissolved in 500 ml. of carbon disulfide were placed in that order. The mixture was refluxed gently for about one hour, and the mass was heated in water to remove the carbon disulfide. The product was broken up and washed in water, then dried to yield about 63 g. of a nearly white powder. The product was soluble in acetophenone, acetone, acetic acid and dioxane.

Found: C, 81.53; H, 6.95. Calcd. for $C_{10}H_{10}O$: C, 82.15; H, 6.90%.

$[\eta]=0.33$, at 25°C in acetone.

Polyvinylbenzalacetophenone (III) from Polyvinylacetophenone with Benzaldehyde.[7]—To a solution of 10.0 g. of polyvinylacetophenone dissolved in 100 ml. of benzaldehyde, 2 g. of concentrated sulfuric acid dissolved in 30 ml. of benzaldehyde were added. After this mixture had stood in the dark for 96 hr., 10 g. of anhydrous sodium acetate was added to decompose the sulfuric catalyst. The solid substance was removed by centrifuging, and the remaining liquid was then poured into methanol. The pale yellow precipitate was twice reprecipitated from a monochlorobenzene solution by pouring it into methanol, and then it was dried in the dark at room temperature. The product was soluble in benzene, monochlorobenzene, ethyl methyl ketone and dioxane.

Found: C, 87.47; H, 6.69. Calcd. for $C_{17}H_{14}O$: C, 87.15; H, 6.02%.

$[\eta]=0.73$, at 25°C in dioxane.

Poly[1, 3-diphenyl-5-(4-vinylphenyl)-2-pyrazoline] (IV). — To a solution of 5 g. (0.02 mol.) of polyvinylbenzalacetophenone dissolved in a mixture of 50 ml. of dioxane and 6.5 g. of glacial acetic acid, 2.5 g. of phenylhydrazine were added. After the mixture had been stirred for 90 min. at 90°C, the solution was poured into methanol. The yellow precipitate was twice reprecipitated from dioxane solution by pouring it into methanol; it was then dried to yield about 4.8 g. of yellow powder. The product was soluble in benzene, toluene, monochlorobenzene, dioxane and methylene chloride.

Found: C, 81.67; H, 6.06; N, 8.72. Calcd. for $C_{23}H_{20}N_2$: C, 85.18; H, 6.17; N, 8.64%.

1) Japanese Pat. 261667 (1960)
2) K. Morimoto, Y. Murakami and A. Inami, *Electrophotography (Japan)*, **4**, No. 2, 13 (1963).
3) R. Kern, *J. Polymer Sci.*, **43**, 549 (1960).
4) A. Coscia, R. Kugel and J. Pellon, ibid., **55**, 303 (1961).
5) Brit. Pat. 915621 (1963).
6) W. Kenyon and G. Waugh, *J. Polymer Sci.*, **32**, 83 (1958).
7) C. Unruh, *J. Appl. Polymer Sci.*, **2**, 358 (1959).

$[\eta]=0.68$, at 25°C in benzene.

The Infrared Spectra of the Polymers. — The polymers synthesized were identified by comparing the infrared absorption bands of those compounds which do not have a vinyl group, such as acetophenone, benzalacetophenone and 1,3,4-triphenyl-2-pyrazoline. The infrared absorption spectra were measured with a Hitachi double-beam spectrometer. The polymers used were in the form of a thin film.

The Photoconductivity of Polymer, IV. — The conductivity cell used for the polymer was the so-called "sandwich-type photoconductivity cell," a schematic diagram of which is shown in Fig. 1.

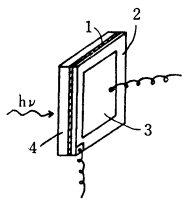

Fig. 1. The sandwich-type cell.
1, NESA coated layer; 2, polymer specimen film; 3, aluminum evaporated layer; 4, glass substratum

The preparation of the cell was carried out by the following technique: a 10% polymer solution of monochlorobenzene was placed uniformly flat onto a NESA conductive glass plate used as a transparent electrode with the aid of a Baker-type film applicator; then the solvent was throughly evaporated in the drying oven. After the solvent had been evaporated, the specimen film was 20 μ thick. The second electrode was formed thereafter by the evaporation of aluminum onto the surface of the specimen film.

The sandwich-type cell thus obtained was then placed in a closed glass chamber (as shown in Fig. 2), which was kept in a vacuo of $<10^{-3}$ mmHg. The

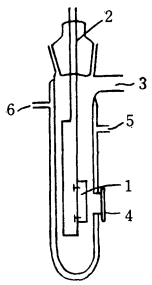

Fig. 2. The schematic diagram of the sandwich type cell placed in glass chamber.
1, Tefron casing of the cell; 2, metal-to-glass seal; 3, evacuation pipe; 4, quartz window; 5, 6, input and output of water from thermostat bath

temperature of the specimen was always kept at 25°C. The applied field to the specimen was 1500 V.-cm^{-1} (taken from a 3 V. dry battery source), and the current measurement was carried out with the aid of a vibration-reed electronic micro-micro ammeter (Takeda Riken, type TR-85) and an electronic X-T recorder (Toa-dempa, type EPR-2).

As the resistance of the polymer in both dark and light showed a considerably high value, the glass chamber was completey shielded to avoid all noises. The light source used for measuring the photocurrent of the cell was a 100 W tungsten lamp. When necessary, an interference filter was placed in the path of the light beam to obtain monochromatic light.

The sandwich-type celles tested were stored in a dark desiccator immediately after they had been coated. The cell that had been exposed to light was tested after it had been in the dark at least 24 hr. A diagram of the entire photoconductivity apparatus is shown in Fig. 3.

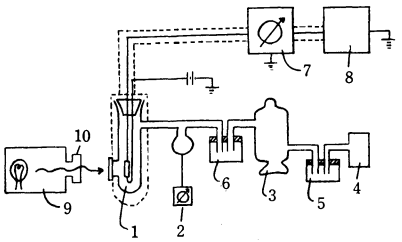

Fig. 3. Set up experimental apparatus.
1, Glass chamber containing the cell; 2, cold cathode ion gauge; 3, Hg diffusion pump; 4, rotary pump; 5, 6, cold traps; 7, vibration-reed micro-micro ammeter; 8, X-T recorder; 9, light source casing; 10, shutter

Results and Discussion

Identification of the Polymers. — *Polyvinylacetophenone.*—The infrared spectrum of polyvinylacetophenone indicates the absorptions of the acetyl group.

Wave number, cm^{-1}	Absorbing structure
1680	Carbonyl
1268	Aromatic ketone
1360	Methyl

Polyvinylbenzalacetophenone. — The absorption bands at 1304 and 975 cm^{-1} may be assigned to disubstituted ethylene, those at 765 and 696 cm^{-1}, to monosubstituted benzene, that at 1576 cm^{-1}, to benzal; that at 1663 cm^{-1}, to carbonyl, and that at 1216 cm^{-1}, to aromatic ketone. As the absorption band at 1360 cm^{-1} resulting from the methyl group is not present, it is considered that the reaction is complete.

Poly[1,3-diphenyl-5-(4-vinylphenyl)-2-pyrazoline].—As is shown in Fig. 4, the absorption bands at 1663 and 1216 cm^{-1}, resulting from the carbonyl group, completely disappear, and the bands at 1304 and 975 cm^{-1} resulting from the disubstituted ethylene group are barely present.

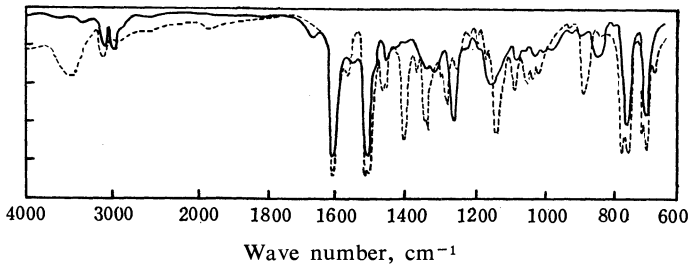

Fig. 4. IR spectra of poly[1,3-diphenyl-5-(4-vinylphenyl)-2-pyrazoline] (solid line) and of 1,3,4-triphenyl-2-pyrazoline (dotted line).

Photoconductivity Behavior. — *V-I Characteristic in the Dark.*—From Fig. 5 it may be seen that the V-I plot in the dark passes through the point of origin, showing that the dark

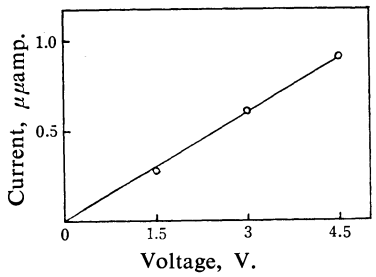

Fig. 5. Relation between voltage applied and photocurrent.

current of the specimen obeys Ohm's law. It may, therefore, be assumed that the contacts between the specimen film and the aluminum layer or NESA conductive surface are perfect.

The Photocurrent in an Incandescent Lamp.— When the cell is illuminated with an intense luminous flux, the photocurrent rises instantly and reaches a maximum value in less than 2 sec. Also, when the light source is switched off, the current decreases to the initial dark value in the same period. When illuminated with a weak light beam or monochromatic light, however, it takes several seconds to attain the peak current. Also, a longer time is required for it to come to equilibrium when the light is switched off to neutralize the space charge to zero.

A large photocurrent value is observed for this type of cell when the illuminated electrode is negative. This behavior suggests that the charge carriers in this polymer are mainly electrons rather than positive holes. The same relation was observed by Northrop and Simpson,[8-10] who used this type of cell for lower molecular weight polyaromatics. The

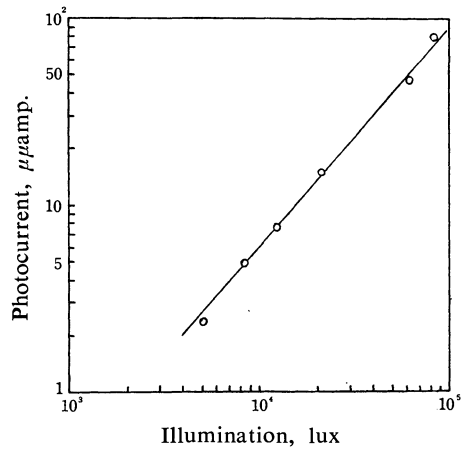

Fig. 6. Photoconductivity curve.

value of I_p(photocurrent)/I_d(dark current) is 34 or 147 depending on whether the illuminated electrode is positive or negative respectively.

When a powerfull incandescence (10^3 to 10^5 luxes) is applied o the cell, as is shown in Fig. 6, the empirical formula

$$I_p = KL^{1.2}$$

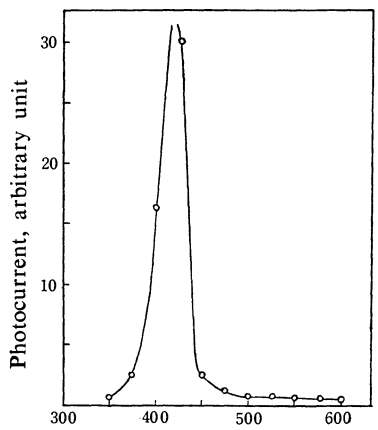

Fig. 7. Photocurrent sensitivity.

8) D. Northrop and O. Simpson, *Proc. Roy. Soc.*, **A234**, 124, 136 (1956).
9) D. Northrop and O Simpson, ibid., **A244**, 377 (1958).
10) H. Inokuchi and H. Akamatu, *Solid State Phys.*, **12**, 93 (1961).

can be applied, where K is a constant and L, the illumination.

Monochromatic Photoresponses. — The monochromatic responses of the polymer specimen are shown in Fig. 7. As may be seen from these results, remarkable responses occur in the wavelength of 400 and 425 mμ.

Summary

A photoconductive polymer, poly[1, 3-diphenyl-5-(4-vinylphenyl)-2-pyrazoline], has been synthesized from polystyrene via polyvinylacetophenone and polyvinylbenzalacetophenone. Under carefully controlled preparative conditions, a high degree of substitution has been obtained without its being insoluble. The photoconductive behavior of the polymer has been measured using a sandwich-type cell. The current obeyed Ohm's law, and the value of I_p/I_d was 34 or 147 depending on whether the illuminated electrode was positive or negative respectively.

Research Laboratory
Wireless Division
Matsushita Electric Industrial Co., Ltd.
Kadoma, Osaka

Studies on Fluorene Derivatives. XXI. The Radical Bromination of Dibiphenyleneethane and Its Derivatives by N-Bromosuccinimide*

By Kazuo SUZUKI and Minoru FUJIMOTO

(Received July 30, 1963)

N-Bromosuccinimide (NBS) has been used as a brominating agent[1] for a wide variety of organic compounds and as an oxidizing agent for some alcohols.

The present investigation is concerned with the reaction of NBS with dibiphenyleneethane and its bromoderivatives in order to introduce, selectively, a bromine atom on a methine group adjacent to an aromatic ring. These compounds were used further to prepare tribiphenylene-propane and its bromo derivatives by a halogen-metal interconversion reaction between 9-fluorenyl lithium and substituted 9-bromodibiphenyleneethane.[2]

The bromination reaction was carried out readily by refluxing the hydrocarbons with equimolar quantites of NBS in absolute benzene for 4 hr. Fluorene,[3] 2-bromofluorene (70%)[4] and 2,7-dibromofluorene (89%) react with NBS in benzene to give fairly good yields of the corresponding 9-bromosubstituted fluorenes. With dibiphenyleneethane it was possible, by selective bromination, to prepare mono or dibromosubstituted ethanes with high yields.

Two isomers were expected in the reaction of NBS with 2-bromodibiphenyleneethane. The structure of one, 2,9'-dibromodibiphenyleneethane (see Table I, Run 6), was confirmed by synthesis from hydrogen bromide and 2-bromo-9'-hydroxydibiphenyleneethane. The reaction of 2,7-dibromodibiphenyleneethane[5] with NBS also yielded two isomers, the structures of which were proved by independent syntheses.

The reaction of the symmetrical compounds, 2,2'-,[6] 3,3'-[7] and 4,4'-dibromodibiphenyleneethanes,[8] with equimolar quantities of NBS gave the corresponding 2,2',9-, 3,3',9- and 4,4',9-tribromodibiphenyleneethanes.

These results are summarized in Table I, which gives data on several preparations made under almost identical conditions.

It is very difficult to introduce a bromine atom on the 9-position of 1,1'-dibromodibiphenyleneethane[9] with NBS. Both of the starting materials were recovered even after having been refluxed for 10 hr. periods, per-

* XX of this series: S. Kajigaeshi, *J. Chem. Soc. Japan, Pure Chem. Sec.* (*Nippon Kagaku Zasshi*), **84**, 185 (1963).

1) C. Djerassi, *Chem. Revs.*, **43**, 271 (1948).

2) K. Suzuki et al., unpublished.

3) S. D. Ross, M. Finkelstein and R. C. Peterson *J. Am. Chem. Soc.*, **80**, 4327 (1958).

4) E. D. Bergmann et al., *Chem. Abstr.*, **47**, 3835 (1953).

5) A. Sieglitz, *Ber.*, **53**, 2249 (1920); K. Suzuki, *J. Chem. Soc. Japan, Pure Chem. Sec.* (*Nippon Kagaku Zassi*), **72**, 825 (1951).

6) J. Schmidt and H. Wagner, *Ann.*, **387**, 153 (1912).

7) K. Suzuki, S. Kajigaeshi and M. Sano, *J. Soc. Org. Synth. Chem. Japan* (*Yûki Gôsei Kagaku Kyôkaishi*), **16**, 82 (1958).

8) K. Suzuki, S. Kajigaeshi and S. Katô, ibid., **16**, 304 (1958).

9) K. Suzuki and S. Kajigaeshi, This Bulletin, **35**, 408 (1962).

TABLE I

Run	Compd. g.		Brominating agent g.		Solvent ml.		Reaction condition time or temp.	Reaction product	Recryst. solvent	M. p. °C	Yield g.	Analyses and mixed m. p. Mol. Formula	Bromine, % Found	Calcd.
1	D	1.0	NBS	0.54	Benzene	20	4 hr.	9-Bromo-D[10]	Benzene	168～170(d)	1.03	By mixed melting points and IR absorption spectrum		
2	D	1.0	NBS	0.7	Benzene	20	4 hr.	9, 9'-Dibromo-D[11]	Benzene	243(d)	1.12	By mixed melting points and IR absorption spectrum		
3	D	1.0	Br_2	0.5	$CHCl_3$	10	8 hr. 25°C	2-Bromo-D[12]	Alcohol	227～229	0.39			
								9-Bromo-D	Benzene	166～168(d)	0.05	By mixed melting points and IR absorption spectrum		
								9, 9'-Dibromo-D	Benzene	240～242(d)	0.1			
								Oily product			0.3			
4	D	1.0	Br_2	0.5	CCl_4	100	9 hr. 25°C	Fluorenone[13]	Alcohol	83～ 84	0.3			
								9, 9'-Dibromo-D	Benzene	240～241(d)	0.65	By mixed melting points and IR absorption spectrum		
								10, 10-Diphenylene-9-phenanthrone	Benzene	256～259(d)	0.02			
5	D	1.0	Br_2	0.5	CS_2	50	8 hr. 25°C	9-Bromo-D	Benzene	166～167(d)	0.74			
								Dibiphenylene-ethylene[15]	Acetic ester	187	0.01	By mixed melting points and IR absorption spectrum		
								9, 9'-Dibromo-D	Benzene	241(d)	0.09			
6	2-Bromo-D	1.0	NBS	0.43	Benzene	20	4 hr.	2, 9-Dibromo-D[12]	Benzene	197～199(d)	0.33	By mixed melting points and IR absorption spectrum		
								2, 9'-Dibromo-D	Cyclohexane	146～148(d)	0.05	$C_{26}H_{16}Br_2$	32.51	32.74
7	2-Bromo-D	1.0	NBS	0.86	Benzene	20	4 hr.	2, 9, 9'-Tribromo-D	Benzene	198～200(d)	0.5	$C_{26}H_{15}Br_3$	42.05	42.27
8	2, 2'-Dibromo-D	1.0	NBS	0.35	Benzene	20	4 hr.	2, 2', 9-Tribromo-D	Acetic ester Benzene	195～196(d)	0.41	$C_{26}H_{15}Br_3$	42.45	42.27
9	2, 2'-Dibromo-D	1.0	NBS	0.7	Benzene	20	5 hr.	2, 2', 9, 9'-Tetrabromo-D	Acetic ester Benzene	214～215(d)	0.3	$C_{26}H_{14}Br_4$	49.08	49.48
10	2, 7-Dibromo-D	1.0	NBS	0.35	Benzene	20	4 hr.	2, 7, 9-Tribromo-D	Acetic ester	216～217(d)	0.01	$C_{26}H_{15}Br_3$	42.10	42.27
								2, 7, 9'-Tribromo-D	Benzene	206～207(d)	0.43	$C_{26}H_{15}Br_3$	42.47	42.27
11	3, 3'-Dibromo-D	1.0	NBS	0.35	Benzene	20	4 hr.	3, 3', 9-Tribromo-D	Cyclohexane Benzene	208～210(d)	0.25	$C_{26}H_{15}Br_3$	41.70	42.27
12	4, 4'-Dibromo-D	1.0	NBS	0.35	Benzene	20	4 hr.	4, 4', 9-Tribromo-D	Cyclohexane Benzene	201～203(d)	0.28	$C_{26}H_{15}Br_3$	41.80	42.27

D: Dibiphenyleneethane

(d): Decomposition: These compounds were red colored because of the formation of dibiphenyleneethylenes at their melting points.

Run 5: Three products were separated by chromatography in benzene on alumina.

haps, because of the greater steric hindrance of the bromine atoms at the 1-positions.

These reactions proceed through a thermal, homolytic dissociation of the N–Br bond in NBS, followed by the abstraction of hydrogen from the methine groups by the free radical, and they involve chain termination accompanied by the formation of succinimide. The general mechanism acceptable for the bromination of dibiphenyleneethane derivatives may be visualized as follows:

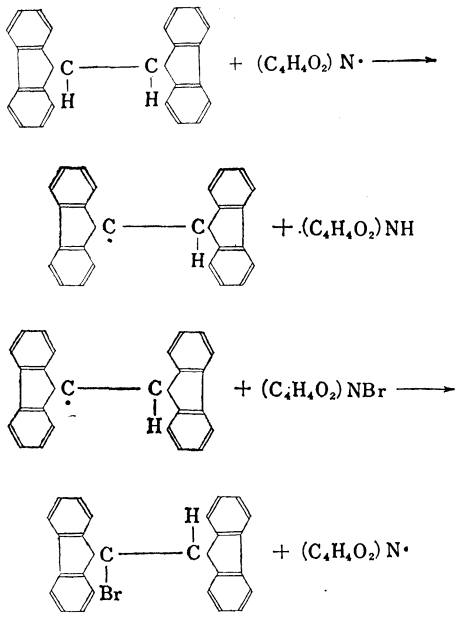

However, it should be mentioned in connection with these results that, from the direct action of equimolar quantities of bromine on dibiphenyleneethane, small amounts of fluorenone and 10, 10-diphenylen-9-phenanthrone were isolated in carbon tetrachloride. In carbon disulfide, dibiphenylene-ethylene was formed. These compounds result from the formation of 9-bromo-substituted products followed by the evolution of hydrogen bromide. In addition, a small amount of nuclear-substituted 2-bromodibiphenyleneethane was obtained in the reaction carried out in chloroform. From these results, it seems likely, that the reactions with bromine proceed by an ionic mechanism.

10) S. Kajigaeshi, *J. Chem. Soc. Japan, Pure Chem. Sec.* (*Nippon Kagaku Zasshi*), **82**, 1712 (1962).
11) A. Hantzch and W. H. Golver, *Ber.*, **39**, 4153 (1906); C. Graebe and B. Mantz, *Ann.*, **290**, 238 (1896).
12) S. Kajigaeshi, *J. Chem. Soc. Japan, Pure Chem. Sec.* (*Nippon Kagaku Zasshi*), **82**, 102 (1962).
13) E. H. Huntress, Y. Hershberg and I. S. Cliff, *J. Am. Chem. Soc.*, **53**, 2721 (1931).
14) H. Klinger and C. Lonnes, *Ber.*, **29**, 2152 (1896).
15) J. Schmidt and H. Wagner, ibid., **43**, 1799 (1910).

Experimental*

The General Reaction Procedure of Dibiphenyleneethanes with *N*-Bromosuccinimide.—To dibiphenyleneethane (1 g., 0.003 mol.) in dry benzene (20 ml.) *N*-bromosuccinimide (0.54 g., 0.003 mol.) was added, and the mixture was refluxed for 4 hr. The orange solution turned red. After this solution had cooled, the succinimide (0.3 g., m. p. 123°C) formed was filtered, and the benzene was removed in vacuo. The crystal mass was digested with water, then recrystallized from cyclohexane after it had been dried. When it had been cooled, a first crop of 0.91 g. of 9-bromodibiphenyleneethane was obtained. The concentration of the mother liquor gave a second crop of 0.12 g. of almost colorless hexagonal crystals. The yield was 84.4%; m. p. 168~170°C. The structure was proved by a mixed melting point determination with an authentic sample of 9-bromodibiphenyleneethane, with had been prepared by the reaction of 9-hydroxydibiphenyleneethane and hydrogen bromide in acetic acid.

The Reaction of 2-Bromofluorene or 2, 7-Dibromofluorene with *N*-Bromosuccinimide.—A mixture of *N*-bromosuccinimide (3.6 g., 0.02 mol. or 5.5 g., 0.03 mol.) and 2-bromofluorene (5.0 g., 0.02 mol.) or 2, 7-dibromofluorene (10.0 g., 0.03 mol.) respectively in dry benzene (20 ml. or 50 ml.) was refluxed for 4 or 5 hr. After the mixture had been cooled, the succinimide was filtered off. Evaporation of the solvent, and recrystallization of the residue from dry cyclohexane or dry benzene, resulted in 4.5 g. (70.3%) of 2, 9-dibromofluorene (m. p. 118~120°C) and 11.0 g. (88.6%) of 2, 7, 9-tribromofluorene (m. p. 190~192°C). These products were identified by a comparison of mixed melting points and infrared absorption spectrum with authentic samples.

The General Reaction Procedure for the Bromination of Dibiphenyleneethane. — To a stirred solution of 1.0 g. (0.003 mol.) of dibiphenyleneethane in 20 ml. of chloroform, there was added very slowly, over an 8 hr. period, 0.5 g. (0.003 mol.) of bromine in 10 ml. of a chloroform solution at 25°C, followed by an additional hour of stirring. Shortly after the addition had begun, hydrogen bromide was evolved. The orange-red reaction mixture was washed with water and dried over anhydrous calcium chloride, and the chloroform was evaporated to a small volume at reduced pressure; when this had been cooled, the deposited material was filtered and recrystallized from benzene to give 9, 9'-dibromodibiphenyleneethane (m. p. 238~242°C (decomp.)) (0.1 g.).

The first chloroform mother liquor was evaporated to one-half its original volume, and the precipitate was digested with hot cyclohexane. 2-Bromodibiphenyleneethane was obtained in the form of colorless needles, which recrystallized from alcohol to give 0.39 g. (m. p. 227~229°C).

The second chloroform mother liquor was evaporated to dryness, and the oily solid was recrystal-

* All the melting points are uncorrected.

lized from benzene, giving 0.05 g. of 9-bromodibiphenyleneethane (m. p. 166~168°C (decomp.)). These three compounds were identified by a comparison of melting points, mixed melting points and infrared absorption spectrum with authentic samples.

Syntheses of 2-Bromo-9'-hydroxydibiphenyleneethane and 2, 9'-Dibromodibiphenyleneethane.—Over a period of 2 hr., in an atmosphere of dry and oxygen-free nitrogen, 40 ml. of an ether solution containing 8.6 g. (0.062 mol.) of *n*-butyl bromide was added to a rapidly stirred mixture of 40 ml. of sodium-dried ether and 0.86 g. (0.12 g. atom) of freshly-cut lithium metal pieces. To this dark, *n*-butyl lithium solution, there was added, drop by drop, over a 45-min. period, a solution of 15.0 g. (0.061 mol.) of 2-bromofluorene in 100 ml. of an anhydrous xylene solution (exothermic reaction). The dark yellow-green color turned orange-red upon being heated. The ether was distilled off until a temperature of 120°C was reached, the solution turned dark-red, and a greenish-yellow solid deposited. Heating was continued for 30 min. at this temperature.

Into this resultant solution there was stirred, drop by drop, a solution of anhydrous xylene containing 11.0 g. (0.061 mol.) of fluorenone. The reaction mixture, which changed brown, was then heated to 100°C over a 90-min. period. The brown precipitate was filtered, hydrolyzed with a dilute ammonium chloride solution, and then recrystallized from cyclohexane to give 11.9 g. (m. p. 123~125°C) of 2-bromo-9'-hydroxydibiphenyleneethane.

Found: Br, 18.26. Calcd. for $C_{26}H_{17}OBr$: Br, 18.79%.

IR: 3270 (ν_{O-H}), 1155 (ν_{C-O}) cm^{-1} (KBr-disk).

The xylene mother liquor was also hydrolyzed with the same solution and dried over anhydrous sodium sulfate. Evaporation in vacuo gave a residual product which was chromatographed in benzene on alumina. 2-Bromo-9'-hydroxydibiphenyleneethane (m. p. 123~125°C) (2.6 g., total 58%) and 2-bromofluorene (0.5 g.) were obtained from the column.

2, 9'-Dibromodibiphenyleneethane.—A solution of 1.0 g. of 2-bromo-9'-hydroxydibiphenyleneethane in 10 ml. of acetic acid was saturated with dry hydrogen bromide. The product was filtered off and recrystallized from cyclohexane to give 2,9'-dibromodibiphenyleneethane (m. p. 146~148°C (decomp.)) (0.6 g.), identical in melting point, mixed melting point and infrared absorption spectrum with the compound obtained by the reaction of 2-bromodibiphenyleneethane and *N*-bromosuccinimide.

Found: Br, 32.51. Calcd. for $C_{26}H_{16}Br_2$: Br, 32.74%.

Syntheses of 2, 7-Dibromo-9'-hydroxydibiphenyleneethane and 2,7,9'-Tribromodibiphenyleneethane.—The former compound was prepared by the same procedure as was 2-bromo-9'-hydroxydibiphenyleneethane. Yield, 20.4% (m. p. 198~200°C).

Found: Br, 31.54. Calcd. for $C_{26}H_{16}OBr_2$: Br, 31.70%.

IR: 3260 (ν_{O-H}), 1154 (ν_{C-O}) cm^{-1} (KBr-disk).

2, 7, 9'-Tribromodibiphenyleneethane.—A solution of 1.0 g. of 2, 7-dibromo-9'-hydroxydibiphenyleneethane in 40 ml. of acetic acid was saturated with dry hydrogen bromide. The solid which was thus formed was recrystallized from benzene to give 2, 7, 9'-tribromodibiphenyleneethane; m. p. 206~207°C (decomp.); 0.8 g. (70%).

Found: Br, 42.10. Calcd. for $C_{26}H_{15}Br_3$: Br, 42.27%.

This product was identical in mixed melting point and infrared absorption spectrum with that obtained by the reaction of 2, 7-dibromodibiphenyleneethane and *N*-bromosuccinimide.

The Syntheses of 2, 7-Dibromo-9-hydroxydibiphenyleneethane and 2, 7, 9-Tribromodibiphenyleneethane.—The former compound was prepared by a method similar to that used for 2, 7-dibromo-9'-hydroxydibiphenyleneethane. Yield, 73%, m. p. 225~226°C.

Found: Br, 31.58. Calcd. for $C_{26}H_{16}OBr_2$: Br, 31.70%.

IR: 3230 (ν_{O-H}), 1155 (ν_{C-O}) cm^{-1} (KBr-disk).

2, 7, 9-Tribromodibiphenyleneethane.—2, 7-Dibromo-9-hydroxydibiphenyleneethane (1.5 g.) was dissolved in 60 ml. of acetic acid, which was then saturated with dry hydrogen bromide. The product deposited was recrystallized from benzene; (1.4 g., 83.3%) m. p. 216~217°C (decomp.). This product was identical in mixed melting point and infrared absorption spectrum with the product obtained by the reaction of 2, 7-dibromodibiphenyleneethane and *N*-bromosuccinimide.

Found: Br, 42.44. Calcd. for $C_{26}H_{15}Br_3$: Br, 42.27%.

The authors wish to express their gratitudes to Drs. John and Elizabeth Weisburger of the National Institutes of Health, U. S. A., for valuable information, and also to Dr. Shôji Kajigaeshi of Kyushû University, for the mixing test of the 2-bromodibiphenyleneethane.

Department of Chemistry
Faculty of Technology
Yamaguchi University
Tokiwadai, Ube

Studies on the Complex Formation between Uranium and Thiomalic Acid

By V. K. MATHUR, H. L. NIGAM and S. C. SRIVASTAVA

(Received July 31, 1963)

Attempts to study the complex formation between thiomalic acid and UO_2(II) has been made using spectrophotometric, potentiometric and magnetic susceptibility measurements. Thiomalic acid gives coloured complexes and has chiefly been used as an analytical reagent.[1-3] Some recent investigations[4-11] on thiomalic acid show it to be a powerful coordinating agent as is expected from the ideal position occupied by the sulphydryl group and two carboxylic groups in the molecule. Thiomalic acid is found to behave as a bidentate ligand with UO_2(II). The complex formed, however, exhibits anamolous magnateic behaviour.

The orangish-yellow coloured complex formed between UO_2(II) and thiomalic acid between pH 3.0~7.0 was studied at a pH 4.5±0.2.

Experimental

Material and Apparatus.—Standard solution of uranyl acetate was prepared from the 'Baker Analysed' $UO_2(C_2H_3O_2)_2 \cdot 2H_2O$ by direct weighing.

Fresh solutions of thiomalic acid were prepared by direct weighing whenever needed. pH of the solutions were fixed by sodium hydroxide and hydrochloric acid.

All the spectrophotometric measurements were carried out by means of a 'Unicam' SP 500 spectrophotometer, connected to a 220 V./50 cycles A. C. mains. Absorbance measurements were observed against distilled water blanks. Two lamps, one tungsten filament and the other hydrogen were used for visible and ultraviolet region respectively.

pH titrations were done with a Leeds and Northrup pH meter supplied with all purpose glass electrode operated at 220 V. mains.

Magnetic susceptibility measurements were done by Gouy's method. The assembly consisted of a semi-micro sartorius balance with a Leybold electromagnet. The field obtained was about 5500 gauss with a 2 cm. pole gap.

Experimental Results

Absorbance Studies.—The absorbance of TMA was zero at the wavelength of maximum absorbance of UO_2-TMA complex. The absorbance of UO_2^{2+} was very little at the wavelength of maximum absorbance of the complex, but this could not be neglected. Hence a few blank sets of observations for uranyl acetate solution were taken at different concentrations. These observations were utilized to introduce necessary corrections in the absorbance values for the complex.

TABLE I

Fig. No.	Curve	c $\times 10^3$ M	p	λ_{max}	Vol. of uranyl acetate at the peak	Composition of the chelate UO_2(II) : TMA
1	A	4.00	1	390	24.0	1 : 1
	B	2.50	1	390	25.0	1 : 1
	C	2.00	1	390	25.0	1 : 1
2	A	4.00	1	410	25.0	1 : 1
	B	2.50	1	410	25.0	1 : 1
	C	2.00	1	410	24.5	1 : 1
3	A	3.33	1.50	390	20.0	1 : 1
	B	3.33	1.50	410	20.0	1 : 1
4	A	2.22	0.66	390	29.5	1 : 1
	B	2.22	0.66	410	29.5	1 : 1

1) M. E. Roselli, *Anales direc. nacl quim.*, **7**, 35, (1954).
2) S. Sharma, *Sci & Culture (Ind.)*, **23**, 434 (1958).
3) O. König and W. R. Crowell, *Mikrochemic ver Mickrochim acta*, **33**, 300 (1948).
4) H. L. Nigam, Uma Kâpoor and V. K. Mathur, 7, ICCC, Stockholm (1962), 7B6, p. 332.
5) I. M. Klotz, G. H. Czexlinski and H. A. Fiess, *J. Am. Chem. Soc.*, **80**, 2920 (1958).
6) Uma Kapoor, D. Phil., Thesis, Allahabad Varsity, India (1961).
7) G. E. Cheney et al., *J. Phys. Chem.*, **63**, 2055 (1959).
8) J. H. Yoe and V. L. Wagner, *Talanta*, **2**, 239 (1959).
9) V. K. Mathur, D. Phil., Thesis, Varsity of India (1963).
10) R. C. Kapoor and O. P. Agrawal, 7, ICCC, Stockholm Allahabad, 7B7, p. 333.
11) M. Cefola, R. C. Taylor, P. S. Gentile and A. V. Celiano, *J. Phys. Chem.*, **66**, 790 (1962).

The method of Vosburgh and Cooper[12] was employed to determine the nature of the complex formed in solution. Mixtures containing 1:0.5, 1:1, 1:1.5, 1:2, 1:3, 1:4 ratios of uranium(VI) oxide to TMA were prepared, the total volume was kept 50 ml. in each case. Absorbance readings were recorded between a range of 320 mμ to 600 mμ at suitable intervals. The observations when plotted graphically show that the region of maximum absorbance of the solution lies at 390 mμ. Hence only one stable complex is formed under the conditions of study.

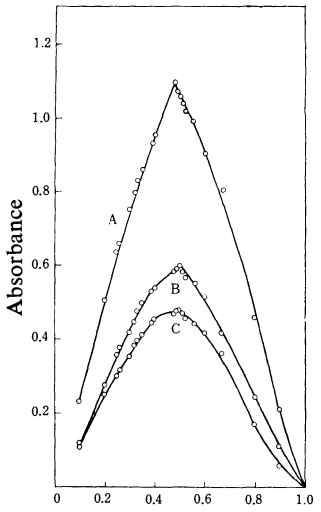

Fig. 1. Absorbance studies of equimolar mixtures of uranyl acetate and thiomalic acid at 390 mμ.
Curve A: Concn. of uranyl acetate, M/250
Curve B: Concn. of uranyl acetate, M/400
Curve C: Concn. of uranyl acetate, M/500

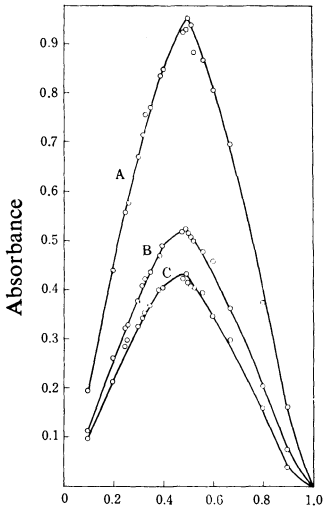

Fig. 2. Absorbance studies of equimolar mixtures of uranyl acetate and thiomalic acid at 410 mμ.
Concentrations is the same as in Fig. 1.

12) W. C. Vosburgh and G. R. Cooper, *J. Am. Chem. Soc.*, **63**, 437 (1941).

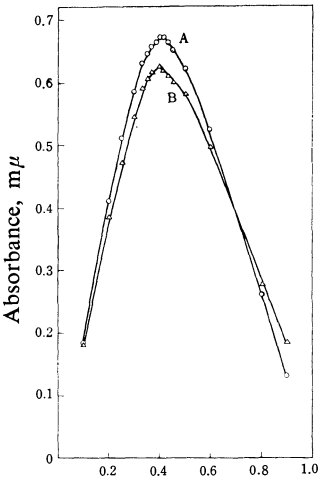

Fig. 3. Absorbance studies of non-equimolar mixtures of uranyl acetate and thiomalic acid.
$p=1.5$
Concn. of uranyl acetate, M/300
Curve A: 390 mμ
Curve B: 410 mμ

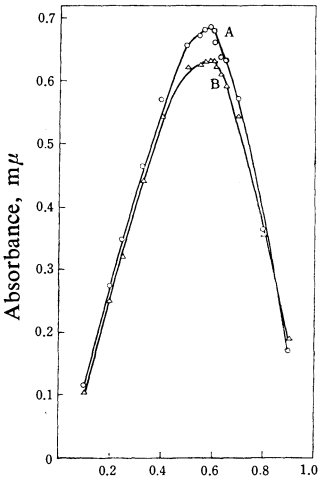

Fig. 4. Absorbance studies of non-equimolar mixtures of uranyl acetate and thiomalic acid.
$p=0.66$
Concn. of uranyl acetate, M/450
Curve A: Wavelength 390 mμ
Curve B: Wavelength 410 mμ

Effect of pH on the Complex.—The absorbances of mixtures containing uranyl acetate and thiomalic acid in the ratio 1:3 (each 1×10^{-2}M) at different pH values were observed. It is seen that λ_{max} (390 mμ) of the yellow coloured complex UO_2(II)-TMA remains the same between pH 3.0~7.0; hence the complex is stable in this range of pH.

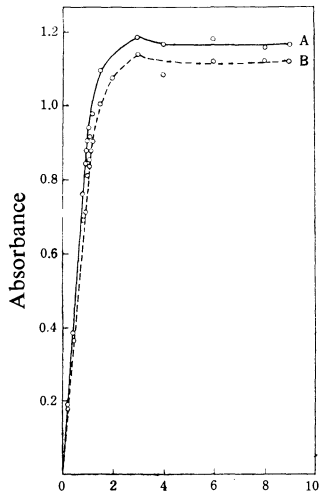

Fig. 5. Absorbance studies of mixtures of uranyl acetate and thiomalic acid by mole ratio method.
Concn. of uranyl acetate, M/300
Curve A: 390 mμ, Curve B: 410 mμ

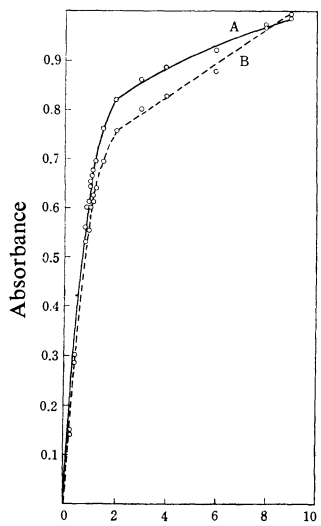

Fig. 6. Absorbance studies of mixtures of uranyl acetate and thiomalic acid by mole ratio method.
Concn. of thiomalic acid, M/400
Curve A: 390 mμ, Curve B: 410 mμ

Stiochiometry of the Components.—The stoichiometric ratio of uranyl to thiomalic acid was determined by the methods of continuous

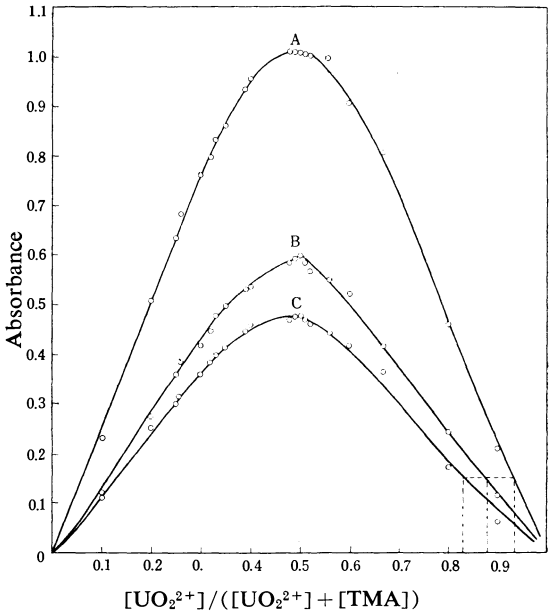

Fig. 7. Evaluation of the stability constant from absorbance measurements.
Concentrations is the same as in Fig. 1.
390 mμ, $p=1$

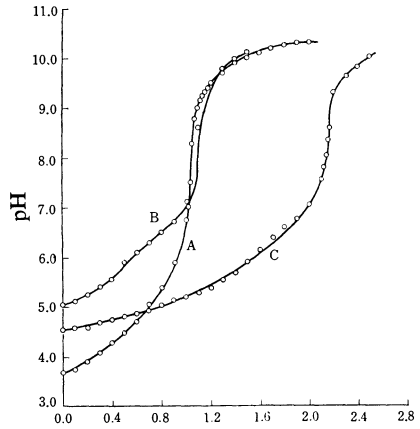

Fig. 8. Potentiometric titration curves with a standard alkali.
Concn. of uranyl acetate, M/100
Concn. of TMA, M/100
Concn. of NaOH, M/10
Curve A: 5 ml. TMA+5 ml. KNO_3+100 ml. water
Curve B: 5 ml. uranyl acetate+5 ml. KNO_3 +100 ml. water
Curve C: 5 ml. uranyl acetate+5 ml. TMA +5 ml. KNO_3+100 ml. water

variation[13] and mole ratio[14]. A large number of observations were taken, some of the typical results are plotted in Figs. 1—6.

Table I records the resuls obtained from the method of continuous variation (Figs. 1—4) where 'c' denotes the concentration of the metal ion and 'c'' the concentration of the ligand. 'p' is equal to c'/c.

The 1 : 1 composition of the chelate has been confirmed by the mole ratio method (Figs. 5 and 6).

Stability of the Complex. — The formation constant $\log k$ (at fixed pH and ionic strength) has been calculated from the curves of continuous variation (Fig. 7) using the formula $K=x/\{(a-x)(b-x)\}$, where the symbols have their usual meaning.[14] An average value of $\log k=3.0\pm0.1$ has been obtained. The corresponding free energy of formation ΔF° has been calculated as -4.2 ± 0.2 at 25°C.

Potentiometric Study.—Different solutions of ligand, metal ion and the complex were titrated respectively with a standard solution of sodium hydroxide. The plot between pH values and the volume of sodium hydroxide are shown in Fig. 8.

Magnetic Susceptibility Measurements.—Very dilute solutions can not be utilised for magnetic susceptiblity measurements since additivity law does not hold good at low concentrations. As the solubility of uranyl acetate was not very high, uranyl nitrate BDH Analar grade was used for the preparation of the solution.

λ_{max} of the complex being same in both the cases uranyl nitrate and TMA (0.1 M each) were mixed in the ratio 1 : 1. The susceptibility of this mixture was measured. The results are tabulated in Table II.

TABLE II

No.	β	Temp., °C	V, ml.	W, g.
1	0.523	32.5	2.589	2.62864
2	0.523	32.5	2.589	2.62984
3	0.523	32.5	2.589	2.62773

No.	ΔW, mg.	$\chi_{sop}\cdot10^6$	$\chi_{Mcorr}:10_6$	μ_{eff}, B.M.
1	−3.40	−0.625	739.11	1.34
2	−3.40	−0.624	792.16	1.35
3	−3.31	−0.630	681.71	1.30

Mean : 1.33

Discussion

Uranyl usually has a coordination number of four, out of which two appear to be satisfied by thiomalic acid in the complex under investigation. The third hydrogen of TMA is not liberated during complexation, is shown by potentiometric studies in which no shift at the inflexion point is observed, i.e., the amount of sodium hydroxide required at the inflexion point for metal and ligand together is equal to the amount required for the complex. From the spectrophotometric curves of continuous variation and mole ratio, it is clear that the complex formed is 1 : 1. The two remaining coordination positions may assumed to be occupied by water molecules. The magnetic moment of hexavalent uranium should have been zero, however, a moment which is slightly less than that expected for one unpaired electron, is observed. There is a lot of uncertainties about the magnetism exhibited by transuranic elements. There are a many complicating factors, e. g., for many uranium(VI) compounds magnetic moment is sufficiently close to the spin only value for two unpaired electrons to suggest $6d^2$ rather than $5f^2$ arrangement. Moreover, it might be showing a temperature independent paramagnetism which can be confirmed if the observations are taken in a wide range of temperature. Thus the formula of the compound on the basis of the above facts may be written as

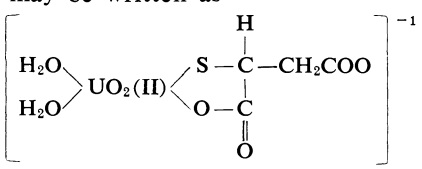

Summary

Uranyl ion has been found to form an orange-yellow coloured complex with thiomalic acid. Spectrophotometric measurements reveal a composition of 1 : 1 as UO_2(II) : TMA in the complex, where TMA stands for thiomalic acid. Thiomalic acid is found to behave as a bidentate ligand with UO_2(II) in this complex. This has been concluded by potentiometric method. Magnetic susceptibility measurements, however, show an anomolous magnetic behaviour. The formation constant $\log K$, at fixed pH and ionic strength as calculated from the spectrophotometric curves, comes out to be 3.0 ± 0.1 and the corresponding free energy of formation has been calculated as -4.2 ± 0.2 at 25°C.

The authors are thankful to the Council of Scientific and Industrial Research, New Delhi for the award of a fellowship to one of them (V. K. Mathur). Thanks are also due to Dr. A. K. Dey for providing the facilities to work.

Chemical Laboratories
University of Allahabad
Allahabad, India

13) P. Job, *Ann. Chim.*, **9**, 113 (1928).
14) J. H. Yoe and A. L. Jones, *Ind. Eng. Chem. Anal. Ed.*, **16**, 111 (1944).

The Nature of the Metal-Ligand Bonds in Hexahalostannates(IV) and Ammonium Hexachloroplumbate(IV) Studied by the Pure Quadrupole Resonance of Halogens

By Daiyu NAKAMURA

(Received July 31, 1963)

We have previously observed the pure quadrupole resonance of halogens in various metal halide complexes and discussed the nature of the metal-ligand bonds in these complexes.[1-6] From the investigations of hexahalo complexes, it has been brought to light that the covalent character of the metal-ligand bonds is linearly dependent only on the electronegativity difference between metal and ligand atoms in the case of central metal ions having the same outer electronic configuration. Both tin and lead have the same outer electronic configuration, different from those of selenium, tellurium, palladium and platinum, the hexahalo complexes of which have already been studied. The present investigation of hexahalostannates(IV) and ammonium hexachloroplumbate(IV) has been undertaken in order to confirm the above conclusion and to establish a linear relation between the ionic character of tin-halogen (or lead-halogen) bonds and the electronegativity difference between metal and halogen atoms.

Experimental

Materials. — Potassium hexachlorostannate(IV), ammonium hexachlorostannate(IV) and rubidium hexachlorostannate(IV) were prepared[7] by adding potassium chloride, ammonium chloride and rubidium chloride respectively to a solution of tin(IV) tetrachloride in hydrochloric acid containing a small amount of chlorine. All these compounds were separated as white crystals. Ammonium hexachloroplumbate(IV) was synthesized[8] by adding ammonium chloride to a solution of lead(IV) tetraacetate in concentrated hydrochloric acid. Yellow crystals were obtained. Rubidium hexabromostannate(IV) was prepared[9] from rubidium bromide and tin(IV) tetrabromide. Pale yellow crystals were separated and washed with concentrated hydrobromic acid containing a small quantity of bromine. Rubidium hexaiodostannate(IV) was obtained[10] by adding rubidium iodide to an alcoholic solution of hydrogen iodide. It formed black crytals. For identifying all these compounds, except for ammonium hexachloroplumbate(IV), quantitative analysis was made for halogens. All the samples were treated with an alkaline solution. Subsequently, the volumetric determination of the halogens was carried out by Volhard-Drechel's method. Ammonium hexachloroplumbate(IV) was identified by its X-ray powder patterns[11] as taken with a Norelco X-ray diffractometer.

Calcd. for K_2SnCl_6: Cl, 51.9. Found: Cl, 51.8. Calcd. for $(NH_4)_2SnCl_6$: Cl, 57.9. Found: Cl, 57.8. Calcd. for Rb_2SnCl_6: Cl, 42.3. Found: Cl, 42.0. Calcd. for Rb_2SnBr_6: Br, 62.3. Found: Br, 62.3. Calcd. for Rb_2SnI_6: I, 72.4. Found: I, 72.0.

Apparatus. — Self-quenching super-regenerative spectrometers which have already been described[1] were employed for the determination of the frequencies of the pure quadrupole resonance of halogens. A hexane thermometer was used in the range from −80 to 0°C.

Results and Discussion

Measurements were made at liquid nitrogen, dry ice and room temperatures. Additional measurements were carried out on potassium hexachlorostannate(IV) at 5~10°C intervals between dry ice and room temperatures for the determination of the transition points. The results are shown in Table I, from which data of less abundant isotopes ^{37}Cl and ^{81}Br are omitted because they give correct isotope frequency ratios.

Potassium hexachlorostannate(IV) yielded a single resonance line at room temperature, in

1) D. Nakamura, Y. Kurita, K. Ito and M. Kubo, *J. Am. Chem. Soc.*, **82**, 5783 (1960).
2) K. Ito, D. Nakamura, Y. Kurita, K. Ito and M. Kubo, ibid., **83**, 4526 (1961).
3) D. Nakamura, K. Ito and M. Kubo, ibid., **84**, 163 (1962).
4) K. Ito, K. Ito, D. Nakamura and M. Kubo, This Bulletin, **35**, 518 (1962).
5) D. Nakamura, K. Ito and M. Kubo, *Inorg. Chem.*, **1**, 592 (1962).
6) D. Nakamura, K. Ito and M. Kubo, ibid., **2**, 61 (1963).
7) W. E. Henderson and W. C. Fernelius, "Inorganic Preparation," McGraw-Hill Book Co., Inc., New York (1935), p. 118.
8) H. S. Booth, "Inorganic Syntheses," Vol. I, McGraw-Hill Book Co., Inc., New York (1939), p. 49.
9) J. W. Mellor, "A Comprehensive Treatise on Inorganic and Theoretical Chemistry," Vol. 7, Longmans, Green and Co., London (1940), p. 456.
10) J. C. Bailar, Jr., "Inorganic Syntheses," Vol. IV, McGraw-Hill Book Co., Inc., New York (1953), p. 121.
11) ASTM Cards. 1-0163, American Society for Testing Materials.

TABLE I. PURE QUADRUPOLE RESONANCE FREQUENCIES OF HALOGENS IN HEXAHALOSTANNATES(IV) AND AMMONIUM HEXACHLOROPLUMBATE(IV)

Compound	Temp., °C	Frequency Mc./sec.
K_2SnCl_6	25.5	15.065±0.002
	−76	15.379±0.003 15.507±0.003 15.548±0.003
	Liquid N_2	15.73 ±0.05
$(NH_4)_2SnCl_6$	23.0	15.474±0.002
	−76	15.539±0.003
	Liquid N_2	15.61 ±0.03 15.65 ±0.03
Rb_2SnCl_6	23.0	15.60 ±0.02
	−77	15.61 ±0.02
	Liquid N_2	15.63 ±0.03
$(NH_4)_2PbCl_6$	20.6	17.061±0.002
	−76	17.142±0.003
	Liquid N_2	17.26 ±0.05
Rb_2SnBr_6	23.5	128.34 ±0.03
	−77	128.62 ±0.05
	Liquid N_2	128.91 ±0.05
Rb_2SnI_6	20.1	130.48 ±0.10
	Liquid N_2	132.57 ±0.10

agreement with its cubic structure of the potassium hexachloroplatinate(IV) type as established by X-ray analysis.[12,13] As the temperature was lowered, the single resonance line was observed to disappear at about −9.5°C. The resonance frequency measured at −6.6°C was 15.068 Mc./sec. The temperature coefficient of the resonance line was about zero in the range from 5 to −8°C. As the temperature was raised, the resonance line appeared abruptly at about −8.5°C. These observations prove the existance of a transition point in the vicinity of −8.5°C. Below this transition point, at least two resonance lines were barely observed. Accordingly, the crystal structure of this compound is less symmetric below the transition point. At the dry ice temperature, three resonance lines were clearly observed. Therefore, another transition point might be expected to exist between the first transition point and the dry ice temperature, as has already been observed in the case of potassium hexabromoselenate(IV). However, above −70°C the intensity of the resonance lines was too weak to permit the determination of another transition point definitely. At the liquid nitrogen temperature, two weak resonance lines were observed, revealing the presence of at least one transition point between dry ice and liquid nitrogen temperatures. In their study of heat capacity,[17] Morfee et al. have reported no transition except for a λ-point, which is in agreement with the first transition point mentioned above.

Ammonim hexachlorostannate(IV) showed a single absorption line at room and dry ice temperatures. This indicates that all the chlorine atoms in the crystal are crystallographically equivalent, a fiinding which is in agreement with the results of X-ray structural analysis.[12] At the liquid nitrogen temperature, two very weak resonance lines were observed. Although Morfee et al. have obtained a normal heat capacity curve[14] between dry ice and liquid nitrogen temperatures, at least one transition point is likely to exist in this temperature range, because doublet absorption lines were observed at the liquid nitrogen temperature.

Rubidium hexachlorostannate(IV), ammonium hexachloroplumbate(IV) and rubidium hexabromostannate(IV) yielded a single absorption line at all the temperatures studied, as was expected from the potassium hexachloroplatinate(IV)-type structure established by X-ray analysis.[15]

Rubidium hexaiodostannate(IV) showed a very weak single resonance line, ν_1, at room and liquid nitrogen temperatures, in agreement with the results of X-ray crystal analysis.[16] At the dry ice temperature, no resonance line could be observed. As the nuclear spin of ^{127}I is 5/2, two resonance lines, ν_1 and ν_2, are expected to be observed. Our attempt to find the ν_2 resonance frequency was, however, unsuccessful, probably because the sensitivity of our spectrometer was low in this frequency range.

Since the crystals of hexahalostannates(IV) and hexachloroplumbates(IV) are known to consist of cations and complex anions with the O_h symmetry,[17] the asymmetry parameter of the electric field gradient about the halogen nucleus vanishes. Therefore, the quadrupole coupling constant, eQq (in Mc./sec.), is equal to twice the resonance frequency for the case of a 3/2 nuclear spin and to 20/3 times the ν_1 resonance frequency for a 5/2 nuclear spin.[18]

12) G. Engel, *Z. Krist.*, **90**, 341 (1935).
13) H. E. Swanson, N. T. Gilfrich and M. I. Cook, "Standard X-ray Diffraction Powder Patterns," NBS Circular 539, Vol. 6 (1956), p. 38.
14) R. G. S. Morfee, L. A. K. Staveley, S. T. Walters and D. L. Wigley, *J. Phys. Chem. Solids*, **13**, 132 (1960).
15) See Ref. 12 for Rb_2SnCl_6 and $(NH_4)_2PbCl_6$. For Rb_2SnBr_6: J. A. A. Ketelaar, A. A. Rietdijk and C. H. Staveren, *Rec. trav. chim.*, **56**, 907 (1937).
16) W. Werker, ibid., **58**, 257 (1939).
17) R. W. G. Wyckoff, "Crystal Structures," Interscience Publishers, Inc., New York (1948).
18) See for instance, T. P. Das and E. L. Hahn, "Solid State Physics," Supplement 1. Academic Press, Inc., New York (1958).

From the calculated quadrupole coupling constants (data at liquid nitrogen temperature were used, and the frequencies of the doublet components were averaged), the ionic character, i, of the metal-halogen bonds was evaluated by Townes and Dailey's procedure.[19,20] Fifteen per cent s-hybridization of the halogen σ bond orbitals was assumed in accordance with the data of Dailey and Townes.[20] From the evaluated ionic character, i, of the metal-halogen bonds, the net charge, ρ, on a central metal atom was calculated by

$$\rho = 4 - 6(1 - i)$$

The results are given in Table II, in which the corresponding data for hexahalotellurates(IV)[4] and hexabromostannates(IV)[5] are included for purposes of comparison.

TABLE II, THE QUADRUPOLE COUPLING CONSTANT OF ^{35}Cl, ^{79}Br AND ^{127}I AT LIQUID NITROGEN TEMPERATURE, THE IONIC CHARACTER, i, OF METAL-LIGAND BONDS, AND THE NET CHARGE, ρ, ON A CENTRAL METAL ATOM IN HEXAHALO COMPLEXES

Compound	eQq Mc./sec.	i	ρ
K_2SnCl_6	31.46	0.66	1.96
$(NH_4)_2SnCl_6$	31.26	0.66	1.96
Rb_2SnCl_6	31.26	0.66	1.96
$(NH_4)_2PbCl_6$	34.52	0.63	1.78
K_2SnBr_6[a]	261.1	0.60	1.60
$(NH_4)_2SnBr_6$[a]	253.7	0.61	1.66
Rb_2SnBr_6	257.8	0.61	1.66
Rb_2SnI_6	883.8	0.55	1.30
$(NH_4)_2TeCl_6$[b]	30.27	0.68	2.08
R_2TeBr_6[b,c]	273.5	0.58	1.48
R_2TeI_6[b,d]	1017.6	0.48	0.88

a) See Ref. 5.
b) See Ref. 4.
c) Average over R=K, NH_4, Cs and NMe_4.
d) Average over R=K, NH_4, Rb and Cs. Data of Rb_2TeI_6 to be published.

The ionic character of the tin-halogen bonds in hexahalostannates(IV) decreases with the decreasing electronegativity difference between tin(IV) and halogens, as has already been observed for various complexes.[1-6] Judging from the same electronegativity values of the central metal atoms, it is reasonable to assume that the extent of the ionic character of hexachlorostannates(IV) is very close to that of ammonium hexachloroplumbate(IV). The electronegativity values selected by Gordy were used in this paper.[21]

Although tin(IV) and lead(IV) are more electropositive than tellurium (as much as 0.3 in electronegativity units), the extent of the ionic character for hexachlorostannates(IV) and ammonium hexachloroplumbate(IV) is almost equal to that of ammonium hexachlorotellurate(IV). This fact must be attributed to the difference in the electronic structure of the central metal atoms. We have already pointed out, from the results for hexabromostannates(IV),[5] that a tin(IV) atom has one 5s orbital, as well as three 5p orbitals, available for forming bonds with halogen atoms in a $[SnX_6]^{2-}$ ion. On the other hand, tellurium(IV) can use only three 5p orbitals for bond formation.[4] Therefore, tin(IV)-halogen bonds are more covalent in character than tellurium(IV)-halogen bonds, if the electronegativity differences between metal and ligand atoms are the same. This interpretation is also valid for ammonium hexachloroplumbate(IV), because the outer electronic configuration of a lead(IV) atom is equivalent to that of a tin(IV) atom provided that all the principal quantum numbers are increased by one.

In a preceding paper[6] we reported, on the basis of a study of various hexahalo complexes, that the covalent character of the bonds between a central metal atom, M, and ligands, X, is in linear relation to the electronegativity difference $\Delta\chi = \chi_X - \chi_M$. The present investigation adds another series of linear relations, as is illustrated in Fig. 1. The three straight lines in Fig. 1 indicate that the only factor

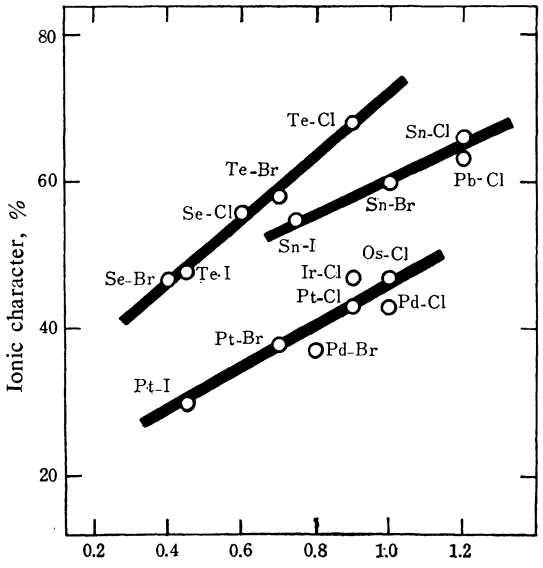

Fig. 1. Dependence of the ionic character of metal-ligand bonds in hexahalo complexes on the difference between the electronegativities of ligands and the central atom.

19) C. H. Townes and B. P. Dailey, *J. Chem. Phys.*, **17**, 782 (1949).
20) B. P. Dailey and C. H. Townes, ibid., **23**, 118 (1955).
21) W. Gordy and W. J. O. Thomas, ibid., **24**, 439 (1956).

determining the ionic character of the metal-ligand bonds in a hexahalo complex is the electronegativity difference between ligands and the central metal atom if the central metal atoms belong to the same family of the periodic table. This linear relation offers useful information, because with it one can estimate the extent of ionic character of metal-ligand bonds whenever necessary data are avaialable for hexahalo complexes.

The author wishes to acknowledge his indebtedness to Professor Masaji Kubo, under whose supervision this research was carried out.

Department of Chemistry
Faculty of Science
Nagoya University
Chikusa-ku Nagoya

The Electron Spin Resonance and Electronic Spectra of the Anion Radicals of 4-Nitropyridine and 4-Nitropyridine 1-Oxide

By Michiya ITOH, Toshihiko OKAMOTO and Saburo NAGAKURA

(Received August 1, 1963)

Recently, both experimental and theoretical studies of aromatic anion radicals have made remarkable progress. Ward and others[1-3] have made electron spin resonance (ESR) studies of various hetero aromatic anion radicals and have determined the coupling constants from proton and nitrogen hyperfine splittings. Furthermore, theoretical studies of odd electron distribution have been carried out with some anion radicals by the aid of a simple molecular orbital method;[4] the results are considerably consistent with the spin densities estimated from the ESR coupling constants.

Hoijtink et al. observed the electronic spectra of the anion radicals of some aromatic hydrocarbons such as benzene and naphthalene, and discussed their electronic structures by comparing the observed results with the theoretical results.[5]

In these circumstances, the present authors have attempted to study the electronic structures of the anion radicals of 4-nitropyridine and its 1-oxide by combining the experimental results of the electronic spectra and electron spin resonance spectra with the theoretical studies based on the semi-empirical molecular orbital method, including "configuration interaction."

Nitrogen hetero aromatic *N*-oxide compounds such as pyridine 1-oxide are known to have some interesting properties.[6,7] The non-bonding electrons of the oxygen atom are strongly conjugated with the π-electron system of the nitrogen hetero aromatic ring. This conjugation usually exerts a predominant effects upon various substitution reactions in the nitrogen hetero aromatic ring, and also upon various physical properties, such as the ultraviolet[8,9] and infrared spectra[10,11] and the nuclear magnetic resonance absorption.[12,13] One of the principal purposes of the present study is to get some knowledge about the conjugation effect in the anion radical of 4-nitropyridine 1-oxide.

In order to analyze exactly the ESR spectra of 4-nitropyridine and its 1-oxide, the measurements were also carried out with the respective compounds containing ^{15}N instead of ^{14}N in the nitro group. Furthermore, for the purpose of getting experimental data necessary for the present semi-empirical calculations, the electronic spectrum of the 3, 5-lutidine[2] anion radical was measured.

1) R. L. Ward, *J. Am. Chem. Soc.*, **84**, 3623 (1962); ibid., **84**, 332 (1962).
2) N. M. Atherton, F. Gerson and J. N. Murrell, *Mol. Phys.*, **5**, 500 (1962).
3) A. Carrington, and J. dos Santos-Veiga, ibid., **5**, 21 (1962).
4) A. Carrington, *Quart. Revs.*, **17**, 67 (1963); P. H. Rieger and C. K. Fraenkel, *J. Chem. Phys.*, **37**, 2735 (1962); ibid., **37**, 2811 (1962).
5) G. J. Hoijtink, *Mol. Phys.*, **2**, 85 (1959).
6) E. Ochiai, *J. Org. Chem.*, **18**, 534 (1953).
7) D. V. Ioffe and I. S. Efrons, *Uspekhi. Khimii.*, **30**, 1325 (1961).
8) T. Kubota and H. Hirayama, *J. Pharm. Soc. Japan (Yakugaku Zasshi)*, **72**, 1025 (1952); T. Kubota, *J. Chem. Soc. Japan, Pure Chem. Sec. (Nippon Kagaku Zasshi)*, **79**, 930 (1958); ibid., **80**, 578 (1959).
9) M. Ito and S. Mizushima, *J. Chem. Phys.*, **23**, 485 (1956); N. Hatta, This Bulletin, **29**, 82 (1956); M. Ito and N. Hatta, ibid., **28**, 260 (1955).
10) H. Shindo, *Chem. Pharm. Bull. (Japan)*, **4**, 460 (1956); ibid., **6**, 117 (1958).
11) G. Costa and P. Blasina, *Z. physik. Chem. N. F.*, **4**, 24 (1955); R. H. Wiley and S. C. Slaymaker, *J. Am. Chem. Soc.*, **97**, 2233 (1957).
12) L. M. Jackman and J. A. Elvidge, *J. Chem. Soc.*, **1961**, 859.
13) A. R. Katritzky and J. M. Lagowski, ibid., **1961**, 43.
14) E. Ochiai, M. Ishikawa and K. Arima, *J. Pharm. Soc. Japan (Yakugaku Zasshi)*, **63**, 79 (1943).

Experimental

Materials. — 4-Nitropyridine and 4-nitropyridine 1-oxide were prepared by the methods given in literatures[14,15] and were purified by repeating recrystallization before use. The melting points of these nitro compounds were in good agreement with those reported in the literatures.[14,15] 4-Nitropyridine 1-oxide with a heavy nitrogen atom (^{15}N) in the nitro group was prepared by the nitration of pyridine 1-oxide with potassium nitrate ($K^{15}NO_3$) containing the heavy nitrogen atom in sulfuric acid.[14] 4-Nitropyridine with the heavy nitrogen atom in the nitro group was obtained by the deoxygenation of 4-nitropyridine 1-oxide (containing $^{15}NO_2$) with phosphorus tribromide.[15] Commercial 3,5-lutidine was purified by repeating distillation:

The Preparation of Anion Radicals and Measurements.—The 4-nitropyridine, 4-nitropyridine 1-oxide and 3,5-lutidine anion radicals were prepared at room temperature by the reduction of the respective parent compounds with potassium metal in 1,2-dimethoxy ethane (abbreviated hereafter to DME). In order to remove reactive impurities, the solvent was kept in contact with sodium metal and the parent compound in vacuo before use. The potassium metal was purified by repeating sublimation in vacuo.

The preparation of the anion radicals and the measurements of electronic absorption spectra and ESR spectra were performed in vacuo by using a vacuum line system similar to that shown in a previous paper.[16] The ESR and electronic spectra were measured by a Hitachi x-band ESR spectrometer Model MPU-2B and a Cary recording spectrophotometer Model-14 M, respectively.

Experimental Results

The 4-Nitropyridine Anion Radical. — The DME solution of the 4-nitropyridine anion radical was colored yellow. The ESR spectrum observed with this solution is shown in Fig. 1a. The ESR spectrum of the 4-nitropyridine anion radical with the heavy nitrogen atom in the nitro group was also measured with the result shown in Fig. 1b. The heavy nitrogen atom leads to a splitting into doublets since ^{15}N has the nuclear spin of 1/2 (the nuclear magnetic moment, $\mu_N=0.404$), while ^{14}N causes a splitting into triplets.

From these spectra, the coupling constants associated with the nitrogen (^{14}N and ^{15}N) and hydrogen atoms were determined to be as shown in Table I. Reconstructions based on these coupling constants are also shown in Figs. 1a and 1b. The reconstructions match well with the observed spectra. Furthermore, the ratio of the nitrogen coupling constants associated with ^{14}N and ^{15}N of the nitro group is in good agreement with that of the nuclear moments of these two nitrogen isotopes. These facts show the high reliability of the coupling constants determined in the presents study.

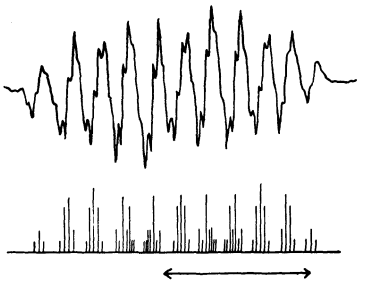

Fig. 1a. The ESR spectrum (first derivative) of 4-nitropyridine anion and the reconstruction based on the coupling constants.

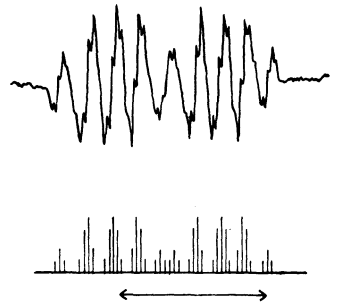

Fig. 1b. The ESR spectrum of the same compound containing ^{15}N in the nitro group and the reconstruction based on the coupling constants.

TABLE I. THE COUPLING CONSTANTS OF THE OBSERVED NITROGEN AND HYDROGEN HYPERFINE SPLITTINGS

Position	4-Nitropyridine anion gauss	4-Nitropyridine 1-oxide anion gauss
$^{14}NO_2$	8.72	7.49
$^{15}NO_2$	12.3	10.32
3-H	0.53*	1.58*
2-H	3.00*	3.58*
Ring N	2.55	4.58

* These assignments were made taking into account spin densities obtained by the molecular orbital calculation.

The electronic absorption spectrum of the DME solution of the 4-nitropyridine anion was measured parallel with the ESR spectrum. The result is shown in Fig. 2. The spectrum consists of three bands at 313, 440 and 640 mμ. It was found that these absorption bands disappeared or decreased remarkably their intensities when the solution was exposed to

15) M. Hamana, ibid., **75**, 135 (1955).
16) A. Ishitani, K. Kuwata, H. Tsubomura and S. Nagakura, This Bulletin, **36**, 1357 (1963).

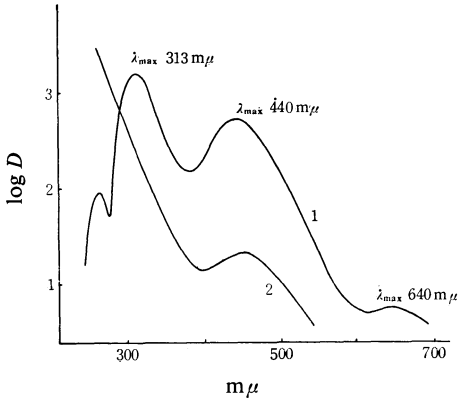

Fig. 2. The electronic absorption spectrum of 4-nitropyridine anion. (The scale factor of vertical axis is arbitrary.)
1) The spectrum of the DME solution of the anion.
2) The spectrum of the solution exposed to air.

air. From this fact, it is inferred that all three bands can be ascribed to the 4-nitropyridine anion. This opinion was also supported by the theoretical consideration based upon molecular orbital calculations which will be described later.

The 4-Nitropyridine 1-Oxide Anion Radical.— When the DME solution of 4-nitropyridine 1-oxide was kept in contact with pure potassium metal in vacuo, the DME solution became yellow after about 2 or 3 days. The ESR spectrum of this colored solution was measured, with the result given in Fig. 3a. The ESR spectrum of the 4-nitropyridine 1-oxide anion containing the heavy nitrogen atom in the nitro group was also measured in order to obtain useful information for the analysis of the hyperfine structure of the ESR spectrum. The result is shown in Fig. 3b. The ESR coupling constants of the 4-nitropyridine 1-oxide anion radical were finally determined to be as shown in Table I. Reconstructions from

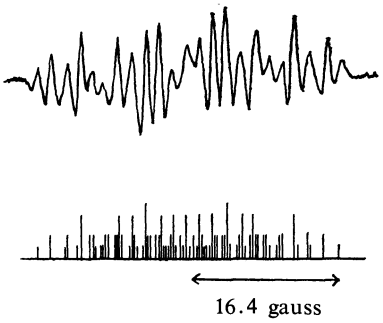

Fig. 3a. The ESR spectrum of 4-nitropyridine 1-oxide anion and the reconstruction based on the coupling constants.

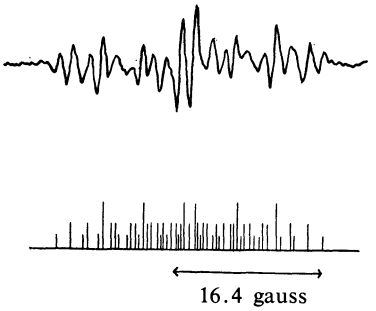

Fig. 3b. The ESR spectrum of the same compound containing ^{15}N in the nitro group and the reconstruction based on the coupling constants.

the coupling constants are also shown in Figs. 3a and 3b for the 4-nitropyridine 1-oxide anion radicals containing ^{14}N and ^{15}N respectively. The reconstructions are well coincident with the observed spectra.

We could not succeed in measuring the electronic absorption spectrum of the DME solution of the 4-nitropyridine 1-oxide anion. This may be because the concentration of the radical is not high enough for the electronic spectrum to be observed.

The Electronic Spectrum of the 3, 5-Lutidine Anion Radical. — The ESR spectrum of the 3, 5-lutidine anion radical was measured by Atherton et al.,[2] but the electronic spectrum has never been observed. Therefore, we measured the electronic spectrum of this anion radical. The DME solution of the 3, 5-lutidine anion shows the electronic absorption band at 355 mμ. This band disappeared parallel with the ESR spectrum by introducing air into the reaction tube.

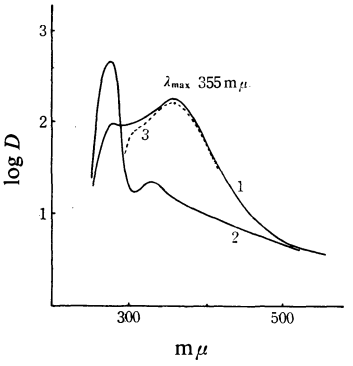

Fig. 4. The electronic absorption spectrum of 3,5-lutidine anion. (The scale factor of vertical axis is arbitrary.)
1) The spectrum of DME solution of the anion.
2) The spectrum of the solution exposed to air.
3) 1)−2).

Theoretical

Molecular orbital calculations were carried out with the π-electron system of the 4-nitropyridine anion in order to ascertain the assignment of the observed electronic spectrum and to obtain some knowledge about the electronic structure of this anion.

In the present calculations, the 4-nitropyridine anion was separated into the two components; the pyridine anion and the nitro group. The interaction between the components was taken into consideration by the aid of the configurational interaction among several π-electron configurations. For accomplishing this theoretical treatment, we need empirical knowledge about the π-electron structure of the pyridine anion radical. Therefore, calculations were first made with the π-electron structure of this anion.

The calculation of the pyridine anion was carried out by taking into account the configurational interaction among the ground and ten excited π-electron configurations which are obtained by putting seven π-electrons into the SCF-molecular orbitals of neutral pyridine.[17] The wave functions and energy values of the electron configurations taken up in the present calculations are shown in Table II. The off-diagonal matrix elements of the total electronic Hamiltonian, H_{ij}'s, are given in Table III. A detailed explanation of the calculation procedure may be omitted since similar calculations have been made for the benzene anion by Hoijtink[5] and by Ishitani et al.[16] In the actual calculation, the approximation of zero-differential overlap was adopted and the one-center Coulomb repulsion integrals of the type of (ii/ii) were calculated from the ionization potentials and electron affinities of the appropriate valence states.[18] The two-center Coulomb repulsion integrals of the type of (ii/jj) were calculated by the aid of quadratic equations* obtained by Pariser and Parr's method.[18]

The finally obtained energy levels and wave functions of the pyridine anion are summarized in Table IV. The transition energy for the transition between the ground and lowest excited states was evaluated to be 3.75 eV. Unfortunately, the electronic absorption of the pyridine anion has never been observed, since it easily converts into the 4, 4'-dipyridyl anion.[1] However, we succeeded in measuring the absorption spectrum of the 3, 5-lutidine anion. Therefore, we compared the calculated transition energy of the pyridine anion with that observed with the 3, 5-lutidine anion.** The calculated transition energy of the former (3.75 eV.) is in good agreement with that of the latter (3.54 eV.).

Table II. The π-electron configurations of the pyridine anion

Wave function	Energy, eV.
$\psi_1=\lvert\varphi_1\bar{\varphi}_1\varphi_2\bar{\varphi}_2\varphi_3\bar{\varphi}_3\varphi_4\rvert$	0
$\psi_2=\lvert\varphi_1\bar{\varphi}_1\varphi_2\bar{\varphi}_2\varphi_3\bar{\varphi}_3\varphi_5\rvert$	0.416
$\psi_3=\lvert\varphi_1\bar{\varphi}_1\varphi_2\bar{\varphi}_2\varphi_3\bar{\varphi}_5\varphi_5\rvert$	10.222
$\psi_4=\lvert\varphi_1\bar{\varphi}_1\varphi_2\varphi_3\bar{\varphi}_3\varphi_5\bar{\varphi}_5\rvert$	10.938
$\psi_5=\lvert\varphi_1\bar{\varphi}_1\varphi_2\bar{\varphi}_2\varphi_3\varphi_4\bar{\varphi}_4\rvert$	9.790
$\psi_6=\lvert\varphi_1\bar{\varphi}_1\varphi_2\varphi_3\bar{\varphi}_3\varphi_4\bar{\varphi}_4\rvert$	10.812
$\psi_{7a}=\frac{1}{\sqrt{2}}(\psi_7^1-\psi_7^2)$	10.936
$\psi_{7b}=\frac{1}{\sqrt{6}}(\psi_7^1+\psi_7^2-2\psi_7^3)$	9.895
$\psi_{8a}=\frac{1}{\sqrt{2}}(\psi_8^1-\psi_8^2)$	11.026
$\psi_{8b}=\frac{1}{\sqrt{6}}(\psi_8^1+\psi_8^2-2\psi_8^3)$	9.717
$\psi_9=\lvert\varphi_1\bar{\varphi}_1\varphi_2\bar{\varphi}_2\varphi_3\bar{\varphi}_3\varphi_6\rvert$	4.292

In this table, φ_i is the i-th molecular orbital of pyridine obtained by Mataga and Nishimoto,[17] and ψ_7^1, ψ_7^2,..... are as follows:

$$\psi_7^1=\lvert\varphi_1\bar{\varphi}_1\varphi_2\bar{\varphi}_2\varphi_3\varphi_4\bar{\varphi}_5\rvert$$
$$\psi_7^2=\lvert\varphi_1\bar{\varphi}_1\varphi_2\bar{\varphi}_2\varphi_3\varphi_4\varphi_5\rvert$$
$$\psi_7^3=\lvert\varphi_1\bar{\varphi}_1\varphi_2\bar{\varphi}_2\varphi_3\bar{\varphi}_4\varphi_5\rvert$$
$$\psi_8^1=\lvert\varphi_1\bar{\varphi}_1\varphi_2\varphi_3\bar{\varphi}_3\bar{\varphi}_4\varphi_5\rvert$$
$$\psi_8^2=\lvert\varphi_1\bar{\varphi}_1\bar{\varphi}_2\varphi_3\bar{\varphi}_3\varphi_4\varphi_5\rvert$$
$$\psi_8^3=\lvert\varphi_1\bar{\varphi}_1\varphi_2\varphi_3\bar{\varphi}_3\varphi_4\bar{\varphi}_5\rvert$$

Table III. The off-diagonal matrix elements (in the units of eV.) used in the calculation of the pyridine anion

$H_{14}=0$	$H_{7a9}=0.629$
$H_{16}=0$	$H_{7b9}=1.245$
$H_{17a}=0$	$H_{23}=0$
$H_{17b}=0.138$	$H_{25}=0$
$H_{19}=0$	$H_{28a}=0$
$H_{46}=0.292$	$H_{28b}=0.247$
$H_{47a}=0.545$	$H_{35}=0.292$
$H_{47b}=-0.651$	$H_{38a}=-0.545$
$H_{49}=-0.900$	$H_{38b}=0.651$
$H_{67a}=0.505$	$H_{58a}=0.228$
$H_{67b}=0.147$	$H_{58b}=-0.276$
$H_{69}=0.957$	$H_{8a8b}=-0.276$
$H_{7a7b}=-0.394$	

17) N. Mataga and K. Nishimoto, *Z. physik. Chem., N. F.*, **13**, 140 (1957).

18) R. Pariser and R. G. Rarr, *J. Chem. Phys.*, **21**, 466, 767 (1953); R. G. Parr, ibid., **20**, 1499 (1952).

* The Actual forms of the quadratic equations are as follows: $(11/22)_{CC}=11.08-2.978r+0.270r^2$ $(11/22)_{CN}=10.72-2.710r+0.228r^2$ $(11/22)_{NN}=12.27-3.634r+0.34r^2$ where r is an appropriate interatomic distance.

** Since the effect of the methyl group on the peak wavelength may conceivably be small, it is not unreasonable to compare the transition energy observed with the 3, 5-lutidine anion with that calculated with the pyridine anion.

TABLE IV. ENERGY LEVELS AND WAVE FUNCTIONS OF PYRIDINE ANION

Wave function	Energy, eV.
$\Phi_1 = 0.9998\phi_1 - 0.0005\phi_4 - 0.0001\phi_6 - 0.0007\phi_{7a} - 0.0145\phi_{7b} - 0.0042\phi_9$	−0.002
$\Phi_2 = 0.9996\phi_2 + 0.0017\phi_3 - 0.0008\phi_5 - 0.0006\phi_{8a} - 0.0267\phi_{8b}$	0.406
$\Phi_3 = -0.0068\phi_1 + 0.1161\phi_4 - 0.1248\phi_6 - 0.0946\phi_{7a} - 0.1860\phi_{7b} + 0.9629\phi_9$	3.757
$\Phi_4 = 0.0052\phi_1 - 0.4419\phi_4 + 0.6891\phi_6 + 0.2859\phi_{7a} + 0.4286\phi_{7b} + 0.2535\phi_9$	11.278
$\Phi_5 = 0.0198\phi_2 - 0.5429\phi_3 + 0.4927\phi_5 - 0.1132\phi_{8a} + 0.6703\phi_{8b}$	9.040
$\Phi_6 = -0.0035\phi_1 + 0.6381\phi_4 + 0.3595\phi_6 + 0.6069\phi_{7a} - 0.3071\phi_{7b} - 0.0300\phi_9$	11.977
$\Phi_7 = 0.0079\phi_2 + 0.6796\phi_3 + 0.4332\phi_5 + 0.5003\phi_{8a} + 0.3163\phi_{8b}$	10.309
$\Phi_8 = 0.0119\phi_1 + 0.4469\phi_4 - 0.3109\phi_6 + 0.1353\phi_{7a} + 0.8240\phi_{7b} + 0.0784\phi_9$	9.542
$\Phi_9 = 0.0153\phi_2 - 0.0136\phi_3 - 0.7509\phi_5 + 0.2953\phi_{8a} + 0.5903\phi_{8b}$	9.923
$\Phi_{10} = -0.0012\phi_1 - 0.4293\phi_4 - 0.5325\phi_6 + 0.7229\phi_{7a} - 0.0902\phi_{7b} + 0.0364\phi_9$	10.321
$\Phi_{11} = -0.0071\phi_2 - 0.4931\phi_3 + 0.0754\phi_5 + 0.8060\phi_{8a} - 0.3185\phi_{8b}$	11.489

Using the above-mentioned results obtained with the pyridine and 3, 5-lutidine anions, the energy levels and wave functions of the 4-nitropyridine anion were calculated by a method similar to that used for the theoretical consideration of the π-electron structures of the nitromethyl anion,[19] the nitrobenzene anion[16] and other neutral nitro compounds.[20] That is to say, the effect of the nitro group on the energy levels of the pyridine anion was considered by means of the configuration interaction between the ground, locally-excited and charge-transfer configurations. In the actual calculations, the geometrical arrangements of the pyridine ring and the nitro group were assumed to be equal to those of neutral pyridine[21] and the nitro group in nitrobenzene[22] respectively.

The energy of the ground configuration was evaluated by taking electrostatic interaction between the benzene anion and the nitro group into account, since there is a large heterogenity in the π-electron distribution of the nitro group with a large positive charge on the nitrogen atom and a negative charge on the oxygen atoms.

We considered the fourteen locally excited configurations whose wave functions and energy values are shown in Table V, together with those of the other electron configurations. Ten of them are brought about by one-electron excitation within the pyridine ring. Except for the lowest locally excited configuration, the energies of the other nine configurations were calculated by adding the electrostatic interaction energies to the calculated excitation energies of the pyridine anion. The energy of the lowest locally excited configuration was estimated by combining the experimental value which had been determined from the peak wavelength of the 3, 5-lutidine anion with the electrostatic interaction energy. The energy of the locally excited configuration within the nitro group was determined from the experimental value of the $\pi \rightarrow \pi^*$ transition energy of the nitromethane[19] and the electrostatic energy.

In addition to these configurations, a charge-transfer configuration which is caused by one electron transfer from the highest-occupied orbital of the pyridine anion toward the lowest vacant orbital of the nitro group was taken into account. The energy of this configuration, E_{CT}, was evaluated by the following equation:

$$\begin{aligned} E_{CT} &= A_P A_N + \Delta E \\ &= -0.4 - 0.4 + \Delta E \\ &= -0.8 + \Delta E \end{aligned}$$

where A_P and A_N are the electron affinities of pyridine and the nitro group respectively, and ΔE is the electrostatic interaction energy between the neutral pyridine ring and the negatively charged nitro group. ΔE was calculated to be −0.1 eV. A_N was determined to be 0.4 eV. for a series of nitro compounds.[16,20] The electron affinity of pyridine has not been determined. Therefore, assuming that it may be almost equal to or a little larger than the value of benzene (−0.54∼−1.62 eV.[23,24]), the authors adopted the two values, −0.4 and 0.1 eV., as the electron affinity of pyridine. The two calculations gave similar results for the transition energies (see Table VIII).

The off-diagonal matrix elements H_{ij}'s of the total electronic Hamiltonian were evaluated by the aid of the method presented by Pople[25] and by Murrell and Longuet-Higgins.[26] The Coulomb repulsion integrals necessary for the evaluation of the interaction energies between

19) S. Nagakura, *Mol. Phys.*, 3, 152 (1960).
20) S. Nagakura, M. Kojima and Y. Maruyama, to be published in *J. Mol. Spectroscopy*.
21) B. Bak, L. Hannsen and J. Rastrup-Andersen, *J. Chem. Phys.*, 22, 2013 (1954).
22) J. Trotter, *Acta. Cryst.*, 12, 884 (1959).
23) N. S. Hush, and J. A. Pople, *Trans. Faraday Soc.*, 51, 600 (1955).
24) R. M. Hedges and F. A. Matsen, *J. Chem. Phys.*, 28, 950 (1958).
25) J. A. Pople, *Trans. Faraday Soc.*, 49, 1375 (1953).
26) H. C. Longuet-Higgins and J. M. Murrell, *Proc. Phys. Soc.*, A68, 601 (1955).

Table V. The π-electron configurations of the 4-nitropyridine anion

Wave function	Energy, eV.
Ground configration :	
$\Psi_1=\Phi_1\lvert\varphi_a\bar{\varphi}_a\varphi_b\bar{\varphi}_b\rvert$ [a]	−0.888
Locally-excited configurations within the pyridin ring :	
$\Psi_2=\Phi_2\lvert\varphi_a\bar{\varphi}_a\varphi_b\bar{\varphi}_b\rvert$	−0.216
$\Psi_3=\Phi_3\lvert\varphi_a\bar{\varphi}_a\varphi_b\bar{\varphi}_b\rvert$	2.815 [c]
$\Psi_4=\Phi_4\lvert\varphi_a\bar{\varphi}_a\varphi_b\bar{\varphi}_b\rvert$	10.594
$\Psi_5=\Phi_5\lvert\varphi_a\bar{\varphi}_a\varphi_b\bar{\varphi}_b\rvert$	8.335
$\Psi_6=\Phi_6\lvert\varphi_a\bar{\varphi}_a\varphi_b\bar{\varphi}_b\rvert$	11.363
$\Psi_7=\Phi_7\lvert\varphi_a\bar{\varphi}_a\varphi_b\bar{\varphi}_b\rvert$	9.519
$\Psi_8=\Phi_8\lvert\varphi_a\bar{\varphi}_a\varphi_b\bar{\varphi}_b\rvert$	8.819
$\Psi_9=\Phi_9\lvert\varphi_a\bar{\varphi}_a\varphi_b\bar{\varphi}_b\rvert$	9.346
$\Psi_{10}=\Phi_{10}\lvert\varphi_a\bar{\varphi}_a\varphi_b\bar{\varphi}_b\rvert$	9.607
$\Psi_{11}=\Phi_{11}\lvert\varphi_a\bar{\varphi}_a\varphi_b\bar{\varphi}_b\rvert$	10.835
Locally-excited configurations within the nitro group : [b]	
$\Psi_{12a}=\frac{1}{\sqrt{2}}(\Psi^1_{12}-\Psi^2_{12})$	9.331
$\Psi_{12b}=\frac{1}{\sqrt{6}}(\Psi^1_{12}+\Psi^2_{12}-2\Psi^3_{12})$	6.331
$\Psi_{13a}=\frac{1}{\sqrt{2}}(\Psi^1_{13}-\Psi^2_{13})$	5.811
$\Psi_{13b}=\frac{1}{\sqrt{6}}(\Psi^1_{13}+\Psi^2_{13}-2\Psi^3_{13})$	5.811
Charge-transfer configuration :	
$\Psi_{14}=\lvert\varphi_1\bar{\varphi}_1\varphi_2\bar{\varphi}_2\varphi_3\bar{\varphi}_3\varphi_a\bar{\varphi}_a\varphi_b\bar{\varphi}_b\varphi_c\rvert$	$A_P-A_N+\Delta E$

a) The φ_a, φ_b and φ_c are the molecular orbitals of the nitro group obtained by Tanaka. (*J. Chem. Soc. Japan, Pure Chem. Sec. (Nippon Kagaku Zassi)*, **78**, 1643 (1957)).

b) The Ψ^1_{12}, Ψ^2_{12},..... are as follows :

$\Psi^1_{12}=\lvert\varphi_1\bar{\varphi}_1\varphi_2\bar{\varphi}_2\varphi_3\bar{\varphi}_3\varphi_5\varphi_a\bar{\varphi}_a\varphi_b\bar{\varphi}_c\rvert$
$\Psi^2_{12}=\lvert\varphi_1\bar{\varphi}_1\varphi_2\bar{\varphi}_2\varphi_3\bar{\varphi}_3\varphi_5\varphi_a\bar{\varphi}_a\bar{\varphi}_b\varphi_c\rvert$
$\Psi^3_{12}=\lvert\varphi_1\bar{\varphi}_1\varphi_2\bar{\varphi}_2\varphi_3\bar{\varphi}_3\bar{\varphi}_5\varphi_a\bar{\varphi}_a\varphi_b\varphi_c\rvert$
$\Psi^1_{13}=\lvert\varphi_1\bar{\varphi}_1\varphi_2\bar{\varphi}_2\varphi_3\bar{\varphi}_3\varphi_4\varphi_a\bar{\varphi}_a\varphi_b\bar{\varphi}_c\rvert$
$\Psi^2_{13}=\lvert\varphi_1\bar{\varphi}_1\varphi_2\bar{\varphi}_2\varphi_3\bar{\varphi}_3\varphi_4\varphi_a\bar{\varphi}_a\bar{\varphi}_b\varphi_c\rvert$
$\Psi^3_{13}=\lvert\varphi_1\bar{\varphi}_1\varphi_2\bar{\varphi}_2\varphi_3\bar{\varphi}_3\bar{\varphi}_4\varphi_a\bar{\varphi}_a\varphi_b\varphi_c\rvert$

c) The energy of this configuration was estimated by combining the experimental value which was determined from the peak wavelength of the 3,5-lutidine anion with the electrostatic interaction energy.

locally excited configurations were obtained by the same method as described for the calculation of the pyridine anion. The interaction energies between the charge transfer configuration and the others are calculated through the core resonance integral (β_{CN}) between the carbon atom at the 4-position and the neighboring nitrogen atom of the nitro group. The β_{CN} value was estimated to be −3.0 eV., the same value as that used for the calculation of the nitrobenzene anion.[16] The matrix elements thus evaluated are given in Table VI.

Table VI. The off-diagonal matrix elements (in units of eV.) used in the calculation of the 4-nitropyridine anion

$H_{1.3}=0$	$H_{8.14}=0.018\beta_{CN}$
$H_{1.4}=0$	$H_{10.12a}=-0.007$
$H_{1.6}=0$	$H_{10.12b}=0$
$H_{1.8}=0$	$H_{10.14}=0.011\beta_{CN}$
$H_{1.10}=0$	$H_{12a.12b}=0$
$H_{1.12a}=0$	$H_{12a.14}=0$
$H_{1.12b}=0$	$H_{12b.14}=0$
$H_{1.14}=-0.413\beta_{CN}$	$H_{2.5}=0$
$H_{3.4}=0$	$H_{2.7}=0$
$H_{3.6}=0$	$H_{2.9}=0$
$H_{3.8}=0$	$H_{2.11}=0$
$H_{3.10}=0$	$H_{2.13a}=-0.109$
$H_{3.12a}=0.177$	$H_{2.13b}=0$
$H_{3.12b}=0$	$H_{5.7}=0$
$H_{3.14}=0.281\beta_{CN}$	$H_{5.9}=0$
$H_{4.6}=0$	$H_{5.11}=0$
$H_{4.8}=0$	$H_{5.13a}=0.226$
$H_{4.10}=0$	$H_{5.13b}=0$
$H_{4.12a}=0.194$	$H_{7.9}=0$
$H_{4.12b}=0$	$H_{7.11}=0$
$H_{4.14}=0.071\beta_{CN}$	$H_{7.13a}=-0.115$
$H_{6.8}=0$	$H_{7.13b}=0$
$H_{6.10}=0$	$H_{9.11}=0$
$H_{6.12a}=-0.266$	$H_{9.13a}=-0.098$
$H_{6.12b}=0$	$H_{9.13b}=0$
$H_{6.14}=-0.007\beta_{CN}$	$H_{11.13a}=0.263$
$H_{8.10}=0$	$H_{11.13b}=0$
$H_{8.12a}=0.076$	$H_{13a.13b}=0$
$H_{8.12b}=0$	

The secular equation composed of the matrix elements given in Table VI was solved by the aid of an electronic computer IBM 7090. The evaluated energy levels and wave functions of the 4-nitropyridine anion are given in Table VII. Oscillator strengths were calculated for the three longer wavelength transitions by the following usual equation : $f=1.085\times10^{-5}Q^2\nu$, where Q and ν are the transition moment (in units of Å) and the peak wave number (in units of cm^{-1}) respectively. The calculated transition energies and oscillator strengths for the transitions between the ground level and the lowest three excited levels are shown in Table VIII, together with the observed transition energies.

Discussion

Karplus and Fraenkel proposed that the hyperfine coupling constants for nuclei such as ^{14}N and ^{13}C in aromatic ring depend not only on the spin densities of the respective atoms, but also on the spin densities of the

TABLE VII. THE ENERGY LEVELS AND WAVE FUNCTIONS OF THE 4-NITROPYRIDINE ANION

Energy	Wave function
$W_1 = -2.185$	$\Psi_{W_1} = -0.6716\Psi_1+0.1232\Psi_3+0.0122\Psi_4-0.0012\Psi_6+0.0036\Psi_8+0.0020\Psi_{10}-0.0029\Psi_{12a}+0.7304\Psi_{14}$
$W_2 = -0.218$	$\Psi_{W_2} = 0.9998\Psi_2-0.0005\Psi_5+0.0002\Psi_7+0.0002\Psi_9-0.0004\Psi_{11}+0.0181\Psi_{13a}$
$W_3 = 0.241$	$\Psi_{W_3} = 0.7370\Psi_1+0.2107\Psi_3+0.0133\Psi_4-0.0014\Psi_6+0.0041\Psi_8+0.0023\Psi_{10}-0.0066\Psi_{12a}+0.6419\Psi_{14}$
$W_4 = 3.008$	$\Psi_{W_4} = -0.0748\Psi_1+0.9684\Psi_3-0.0052\Psi_4-0.0011\Psi_6-0.0015\Psi_8-0.0012\Psi_{10}-0.0513\Psi_{12a}-0.2323\Psi_{14}$
$W_5 = 5.773$	$\Psi_{W_5} = -0.0181\Psi_2-0.0877\Psi_5+0.0305\Psi_7+0.0273\Psi_9-0.0516\Psi_{11}+0.9940\Psi_{13a}$
$W_6 = 6.314$	$\Psi_{W_6} = -0.0007\Psi_1+0.0514\Psi_3-0.0454\Psi_4+0.0525\Psi_6-0.0303\Psi_8+0.0021\Psi_{10}+0.9958\Psi_{12a}-0.0044\Psi_{14}$
$W_7 = 8.355$	$\Psi_{W_7} = -0.0011\Psi_2+0.9961\Psi_5+0.0086\Psi_7+0.0086\Psi_9-0.0092\Psi_{11}+0.0869\Psi_{13a}$
$W_8 = 8.822$	$\Psi_{W_8} = 0.0007\Psi_1+0.0017\Psi_3-0.0039\Psi_4+0.0032\Psi_6+0.9995\Psi_8+0.0000\Psi_{10}+0.0300\Psi_{12a}-0.0057\Psi_{14}$
$W_9 = 9.348$	$\Psi_{W_9} = 0.0003\Psi_2-0.0060\Psi_5-0.0183\Psi_7+0.9994\Psi_9+0.0048\Psi_{11}-0.0271\Psi_{13a}$
$W_{10} = 9.522$	$\Psi_{W_{10}} = 0.0004\Psi_2-0.0060\Psi_5+0.9993\Psi_7+0.0174\Psi_9+0.0063\Psi_{11}-0.0313\Psi_{13a}$
$W_{11} = 9.607$	$\Psi_{W_{11}} = -0.0004\Psi_1+0.0003\Psi_3-0.0003\Psi_4-0.0003\Psi_6+0.0000\Psi_8+0.9999\Psi_{10}-0.0021\Psi_{12a}-0.0032\Psi_{14}$
$W_{12} = 10.606$	$\Psi_{W_{12}} = -0.0020\Psi_1+0.0030\Psi_3+0.9987\Psi_4+0.0162\Psi_6+0.0025\Psi_8+0.0003\Psi_{10}+0.0445\Psi_{12a}-0.0189\Psi_{14}$
$W_{13} = 10.849$	$\Psi_{W_{13}} = -0.0005\Psi_2+0.0047\Psi_5-0.0045\Psi_7-0.0034\Psi_9+0.9986\Psi_{11}+0.0523\Psi_{13a}$
$W_{14} = 11.377$	$\Psi_{W_{14}} = 0.0002\Psi_1-0.0013\Psi_3-0.0137\Psi_4+0.9984\Psi_6-0.0016\Psi_8+0.0002\Psi_{10}-0.0532\Psi_{12a}+0.0020\Psi_{14}$

TABLE VIII. THE CALCULATED AND OBSERVED RESULTS FOR THE LOWEST THREE ELECTRONIC TRANSITIONS OF THE 4-NITROPYRIDINE ANION

Transition	λ_{max}, eV. calcd.	obs.	Calcd. oscillator strength	Direction of transition moment
$W_1 \rightarrow W_2$	1.96 (1.73)*	1.90	1.44×10^{-3}	↔
$W_1 \rightarrow W_3$	2.42 (2.40)*	2.81	6.07×10^{-1}	↕
$W_1 \rightarrow W_4$	5.18 (4.97)*	4.00	8.63×10^{-1}	↕

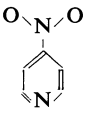

* The results calculated by assuming the electron affinity of pyridine to be 0.1 eV.

adjacent aromatic ring atoms via indirect polarization and that the coupling constant for the ring nitrogen atom, A_N, can be represented by the following equation:[27]

$$A_N = Q_N\rho_N + \sum_i Q_{C_i}\rho_{C_i} \quad (1)$$

where ρ_N and ρ_{C_i} are the spin densities of the concerned nitrogen and adjacent carbon atoms, respectively, and Q_N and Q_{C_i} are constants. Carrington and Santos-Veiga, however, suggested that the indirect coupling is apparently less important for ^{14}N in hetero aromatic anion radicals.[3] They proposed the following equation for the relationship between A_N and ρ_N:

$$A_N = Q_N\rho_N \quad (2)$$

and estimated the value of Q_N to be 25.3 gauss.

A similar relation is found also for the coupling constant due to the nitrogen nucleus of the nitro group, but the Q_N value is larger for this case than for the above case.[16] In the present study, the Q_N value was tentatively assumed to be 40 gauss for the nitrogen atom of the nitro group. Furthermore, it is well known that the proton coupling constants, A_H's, are related to the spin densities on carbon atoms, ρ_C's, by the following equation:[28]

$$A_H = Q_H\rho_C \quad (3)$$

where Q_H is a constant and is estimated to be 22.5 gauss.

By combining the observed coupling constants with the relations mentioned above, we have evaluated the spin densities on the nitrogen and carbon atoms of the 4-nitropyridine and 4-nitropyridine 1-oxide anions. The results are shown in Table IX, together with the theoretical values evaluated for the 4-nitropyridine anion by the aid of the wave function, Ψ_{W1}, in Table VII. The spin densities on the nitrogen and carbon atoms of the 4-nitropyridine anion estimated from the observed coupling constants are in good agreement with the calculated values except for the 2-carbon atom.

As is shown in Table IX, the spin densities on the ring nitrogen and carbon atoms are undoubtedly larger in the 4-nitropyridine 1-oxide anion than in the 4-nitropyridine anion, while the spin density on the nitrogen atom of the nitro group of the former decreases compared with that of the latter. This seems to be attributed to the resonance and inductive effects of the *N*-oxide group.***

Now let us turn our attention to the problem of the electronic absorption spectrum of

27) M. Karplus and G. K. Fraenkel, ibid., **35**, 1312 (1961).
28) H. M. McConell and D. B. Chesnut, *J. Chem. Phys.*, **28**, 107 (1958).

*** The details of this problem will be discussed in a future publication.

Table IX. The spin densities of nitrogen and carbon atoms of the 4-nitropyridine and 4-nitropyridine 1-oxide anions

Position	4-Nitropyridine anion		4-Nitropyridine 1-oxide anion
	Calcd. from molecular orbitals	Fstimated from the coupling const.	Estimated from the coupling const.
$^{14}NO_2$	0.261	0.218	0.187
3-C	0.033	0.024*	0.069*
2-C	0.052	0.133*	0.159*
Ring N	0.124	0.101	0.181

* These assignments were made taking into account spin densities obtained by the molecular orbital calculation.

the 4-nitropyridine anion. As is shown in Table VIII, the 313, 440 and 640 mμ bands can safely be ascribed to the $W_1 \rightarrow W_4$, $W_1 \rightarrow W_3$ and $W_1 \rightarrow W_2$ transitions respectively. From the wave functions Ψ_{W_1} and Ψ_{W_3} given in Table VII, it can be seen that the W_1 and W_3 states are in principle brought about by the resonance between the ground and charge-transfer configurations, and that the 440 mμ band corresponding to the $W_1 \rightarrow W_3$ transition may be regarded as the intramolecular charge-transfer band. Since, in the wave function of the W_4 state, the contribution of the locally excited configuration within the pyridine ring amounts to 94%, the 313 mμ band corresponding to the $W_1 \rightarrow W_4$ transition can be interpreted as the shifted band of the 355 mμ band of the 3, 5-lutidine (or pyridine) anion. It is noticeable that the 355 mμ band of the 3, 5-lutidine (or pyridine) anion shows a large blue shift upon the introduction of the nitro group. This is because the charge-transfer configuration is rather close to the ground configuration and therefore the ground configuration is largely stabilized by the resonance interaction with the charge-transfer configuration.

A similar blue shift phenomenon was observed with the nitrobenzene anion.[16] The weak 640 mμ band may conceivably correspond to the $W_1 \rightarrow W_2$ transition with a small transition moment.

Summary

The ESR and electronic spectra of the 4-nitropyridine and 4-nitropyridine 1-oxide anions have been measured. The nitrogen and hydrogen hyperfine splitting constants of these two compounds have been determined. In order to analyze the ESR spectra exactly, the measurements have also been carried out with respective compounds containing ^{15}N instead of ^{14}N in the nitro group. The spin densities on the nitrogen and carbon atoms of these two anions have been estimated from the splitting constants. It has thus been found that the spin densities on the ring nitrogen and carbon atoms are undoubtedly larger in the 4-nitropyridine 1-oxide anion than in the 4-nitropyridine anion.

The electronic spectrum of the 4-nitropyridine anion has been measured and three peaks found at 313, 440 and 640 mμ. According to the molecular orbital calculations carried out with the π-electron system of the 4-nitropyridine anion, it has been concluded that the 440 mμ band may be regarded as the intramolecular charge transfer band, and that the 313 mμ band can be interpreted as the blue shifted band of the pyridine anion.

The authors wish to express their sincere thanks to Mr. Koichi Itoh of the Institute for Solid State Physics for his kind help in measuring the ESR spectra.

The Institute for Solid State Physics
The University of Tokyo
Azabu, Tokyo (M. I. & S. N.)

The Faculty of Pharmaceutical Sciences
The University of Tokyo
Hongo, Tokyo (T. O.)

The Electronic Structure of the t-Butyl Cation

By Ichiro HANAZAKI, Haruo HOSOYA and Saburo NAGAKURA

(Received August 12, 1963)

There is considerable experimental evidence to show that methyl or other alkyl substituents increase the stability of hydrocarbon molecules.[1-10] The stabilization may be attributed in general to the steric hindrance, inductive effect and hyperconjugation. Although in the case of neutral molecules there is a little doubt about the stabilization effect of hyperconjugation, the effect seems to be vivid and extensive in the case of carbonium ions.[9,10]

In the present paper, we have studied the electronic structure of the *t*-butyl cation, paying special attention to the hyperconjugation effect. One of ourmain purposes is to estimate as accurately as possible the hyperconjugation effect on the electronic structure of the carbonium ion. The fact that the *t*-butyl cation shows a strong absorption band at 290~295 mμ[11,12] in spite of the complete absence of any unsaturated bond may be unexpected from the π-electron theory developed so far and seems to be closely related to the hyperconjugation effect. Another important aim of the present study is to clarify the nature of this band.

The Configuration of the *t*-Butyl Cation

There is a little doubt about the configuration of the *t*-butyl cation.[9,11,12] In the present calculation, however, the ion is reasonably assumed to take a planar configuration, the central carbon atom being in a sp^2 hybrid valence state and a $2p\pi$ AO perpendicular to the molecular plane being vacant. The configuration and the numbering of atoms are shown in Fig. 1.

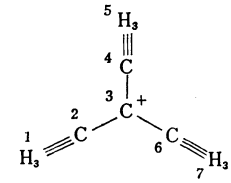

Fig. 1. The structure and numbering of *t*-butyl cation.
The distance between carbon atoms 2 and 3 is assumed to be 1.52Å (same as the distance between the carbon of methyl group and the ring carbon in toluene). The methyl group is assumed to have the same geometrical configuration as methane ($\angle HCH = 109°28'$ and $R_{C-H} = 1.091$Å).

Another possibility is a configuration of the π-complex type:

$$(H_3C)_2C \overset{H^+}{\uparrow\!\!\!\!\!\!\rightleftharpoons} CH_2$$

This possibility, however, may be disregarded because $B(CH_3)_3$, which is isoelectronic with the *t*-butyl cation, has a planar configuration.[12]

According to the usual treatment of hyperconjugation,[13] the following three pseudo AO's can be constructed from the 1s AO's of the hydrogen atoms:

$$\left.\begin{aligned} \chi_1 &= N_1 \cdot [\chi_a - 1/2(\chi_b + \chi_c)] \\ \lambda_2 &= N_2 \cdot (\chi_b - \chi_c) \\ \lambda_3 &= N_3 \cdot (\chi_a + \chi_b + \chi_c) \end{aligned}\right\} \quad (1)$$

where χ_1, λ_2 and λ_3 are three independent and orthonormal pseudo AO's, χ_a, χ_b and χ_c are the hydrogen 1s AO's, and N_i's are normalization constants. Of these, χ_1 can be regarded as a $p\pi$-type pseudo AO antisymmetric with regard to the molecular plane; it can construct a π-type MO together with the $2p\pi$ AO of the carbon atom in the methyl group.[14]

1a) V. A. Crawford, *Quart. Revs.*, **3**, 226 (1949).
1b) C. A. Coulson and V. A. Crawford, *J. Chem. Soc.*, **1953**, 2052.
1c) V. A. Crawford, ibid., **1953**, 2058, 2061.
2a) Y. I'Haya, *J. Chem. Phys.*, **23**, 1165 (1955).
2b) Y. I'Haya, *J. Chem. Soc. Japan, Pure Chem. Sec.* (*Nippon Kagaku Zassi*), **77**, 314 (1956).
3a) T. Morita, *J. Chem. Phys.*, **27**, 1442 (1957).
3b) T. Morita, This Bulletin, **31**, 322 (1958).
3c) T. Morita, ibid., **32**, 893 (1959).
4) M. M. Kreevoy, *Tetrahedron*, **5**, 233 (1959).
5) Wei-Chuwan Lin, *J. Chinese Chem. Soc.*, **4**, 14 (1957).
6) R. S. Mulliken, *Tetrahedron*, **5**, 253 (1959).
7) R. S. Mulliken, ibid., **6**, 68 (1959).
8) R. S. Mulliken, C. A. Rieke and W. G. Brown, *J. Am. Chem. Soc.*, **63**, 41 (1941).
9) N. Muller and R. S. Mulliken, ibid., **80**, 3489 (1958).
10) N. Muller, L. W. Pickett and R. S. Mulliken, ibid., **76**, 4770 (1954).
11) J. Rosenbaum and M. C. R. Symons, *Mol. Phys.*, **3**. 205 (1960).
12) J. Rosenbaum and M. C. R. Symons, *Proc. Chem. Soc.*, **1959**, 92.
13) C. A. Coulson, "Valence," Oxford Universtiy Press, Oxford (1961), p. 360.
14) The carbon atom is in a sp^3 hybrid valence state. However, taking a proper combination of the hybrid orbitals, we can tentatively obtain a pure $2p\pi$ AO whose node is in the molecular plane.

TABLE I. THE VALENCE STATE ENERGIES AND IONIZATION POTENTIAL OF H_3 GROUP[a,b]

	I_{χ_1}	I_{λ_2}	I_{λ_3}	J_{12}	J_{23}	J_{31}	K_{12}	K_{23}	K_{31}
^4E	1	1	1	1	1	1	−1	−1	−1
^2E	1	1	1	1	1	1	1	−1/2	−1/2
$^2E'$	1	1	1	1	1	1	−1	1/2	1/2
E	1	1	1	1	1	1	−1/2	−1/2	−1/2
$^3E^+$	0	1	1	0	1	0	0	−1	0
$^1E^+$	0	1	1	0	1	0	0	1	0
E^+	0	1	1	0	1	0	0	−1/2	0
$-I_p(\chi_1)$	1	0	0	1	0	1	−1/2	0	−1/2

a) The numbers in a given row give the coefficients of the integrals, I's, J's and K's, in the formula representing the energy listed in the first column.

b) $$I_\mu = \int \mu(1) H_h^c(1) \mu(1) \mathrm{d}v$$

where $\mu = \chi_1$, λ_2 or λ_3 and $H_h^c(1) = T(1) - \sum_{p=a,b,c} e^2/R_p(1)$

$T(1)$ and $R_p(1)$ being the kinetic energy operator and the distance between the electron (1) and the hydrogen core p respectively. Coulomb and exchange repulsion integrals are defined by

$$J_{\mu\mu'} = \int \mu(1) \mu(1) e^2/r_{12} \mu'(2) \mu'(2) \mathrm{d}v$$

and

$$K_{\mu\mu'} = \int \mu(1) \mu'(1) e^2/r_{12} \mu(2) \mu'(2) \mathrm{d}v$$

where μ and μ' are χ_1, λ_2 or λ_3.

The Ionization Potential of the H_3 Group

In the present calculation, the *t*-butyl cation was separated into four components; namely, the three methyl groups and the carbon ion with a positive charge. The interaction among them was accounted by the configurational interaction among several electron configurations constructed by putting the electrons into the orbitals of the components. In order to accomplish this kind of calculation, it is necessary to obtain accurate knowledge about the wave functions and energy values of the components. Therefore, we undertook first to evaluate the energy levels and wave functions of the H_3 group necessary for the calculation of the methyl group.

A neutral H_3 group in a methyl group has one electron in each of the pseudo AO's, χ_1, λ_2 and λ_3, so that following wave functions can be constructed as antisymmetrized wave functions:

$$\text{quartet}: \quad {}^4\psi = |\chi_1, \lambda_2, \lambda_3|^{15} \tag{2}$$

$$\text{doublet}: \quad {}^2\psi = (2)^{-1/2}\{|\chi_1, \overline{\lambda_2}, \lambda_3| + |\lambda_2, \overline{\chi_1}, \lambda_3|\} \tag{3}$$

$${}^2\psi' = (6)^{-1/2}\{|\chi_1, \overline{\lambda_2}, \lambda_3| - |\lambda_2, \overline{\chi_1}, \lambda_3| + 2|\chi_1, \overline{\lambda_3}, \lambda_2|\} \tag{4}$$

15) An abbreviated notation of the antisymmetrized wave function. For example,

$$|a, b, \bar{c}| = (3!)^{-1/2} \begin{vmatrix} a(1)\alpha(1), & b(1)\alpha(1), & c(1)\beta(1) \\ a(2)\alpha(2), & b(2)\alpha(2), & c(2)\beta(2) \\ a(3)\alpha(3), & b(3)\alpha(3), & c(3)\beta(3) \end{vmatrix}$$

The energies for the states, ^4E, ^2E and $^2E'$, can be written in terms of integrals over the pseudo AO's, as is summarized in Table I. A valence state energy, E, of the neutral H_3 group can be calculated as an average of them over spin natural abundance;

$$E = (4 \cdot {}^4E + 2 \cdot {}^2E + 2 \cdot {}^2E')/8 \tag{5}$$

Similarly, the H_3^+ ion, in which an electron in χ_1 is removed, has two electronic states, corresponding to the singlet and triplet states, whose energies are represented by $^1E^+$ and $^3E^+$ respectively. An average energy over spin natural abundance is:

$$E^+ = ({}^1E^+ + 3 \cdot {}^3E^+)/4 \tag{6}$$

Therefore, the valence state ionization energy of an electron in χ_1 is:

$$I_p(\chi_1) = E^+ - E \tag{7}$$

Now, taking Slater-type 1s AO's with the effective charge $Z=1$ for χ_a, χ_b and χ_c, the integrals in Table I can be reduced to integrals over AO's;

$$I_{\chi_1} = (\alpha_H - \beta_H)/(1 - S_H) \tag{8}$$

$$\alpha_H = \int \chi_a(1) H_h^c(1) \chi_a(1) \mathrm{d}v^{16} = W_H + 2\langle b \mid aa \rangle \tag{9}$$

$$\beta_H = \int \chi_a(1) H_h^c(1) \chi_b(1) \mathrm{d}v = S_H W_H + \langle b \mid ab \rangle + \langle c \mid ab \rangle \tag{10}$$

16) See the footnote of Table I for the definition of $H_h^c(1)$.

TABLE II. ELECTRONIC REPULSION INTEGRALS IN TERMS OF THE INTEGRALS OVER ATOMIC ORBITALS[a]

	eV.					eV.
	$(aa\|aa)$[b] 17.0025	$(aa\|bb)$[b] 7.8892	$(aa\|22)$[c] 12.2564	$(bb\|22)$[c] 11.3329	$(22\|22)$[b] 16.9304	
J_{12}	1/6	5/6	—	—	—	9.4081
J_{23}	1/3	2/3	—	—	—	10.9270
J_{31}	1/3	2/3	—	—	—	10.9270
K_{12}	1/6	−1/6	—	—	—	1.5189
K_{23}	x[d]	$-x$	—	—	—	3.5165
K_{31}	x	$-x$	—	—	—	3.5165
$(22\|\lambda_2\lambda_2)$	—	—	—	1	—	11.3329
$(22\|\lambda_3\lambda_3)$	—	—	1/3	2/3	—	11.6407
$(12\|\lambda_2\lambda_2)$	$S/12$[e]	$5S/12$	—	$S/2$	—	6.6911
$(12\|\lambda_2\lambda_3)$	$S/6$	$S/3$	$S/6$	$S/3$	—	7.2803
$(11\|11)$	1/2	1/2	—	—	—	12.4459
$(11\|22)$	—	—	2/3	1/3	—	11.9486
$(11\|12)$	$S/4$	$S/4$	$S/3$	$S/6$	—	7.8697
$(12\|12)$	$S^2/8$	$S^2/8$	$S^2/3$	$S^2/6$	$S^2/4$	5.5442
$(12\|22)$	—	—	$S/3$	$S/6$	$S/2$	9.3164

a) The first column contains integrals including the pseudo AO's. J_{ij}'s and K_{ij}'s are defined in Table I. For the last nine integrals in the first column, notations 1 or 2 means χ_1 or χ_2 respectively.
For example,

$$(12|\lambda_2\lambda_2) = \int \chi_1(1)\chi_2(1)e^2/r_{12}\lambda_2(2)\lambda_2(2)dv$$

They are reduced into the integrals over AO's by means of Mulliken's approximation. The latters are shown in the first row, for example,

$$(aa|22) = \int \chi_a(1)\chi_a(1)e^2/r_{12}\chi_2(2)\chi_2(2)dv$$

Calculated values for the integrals in the first column are shown in the last column (See also the footnote a of the Table I).

b) Values of $(aa|aa)$, $(aa|bb)$ and $(22|22)$ are taken from the table given by Roothaan.[17]

c) See Appendix for the evaluation of $(aa|22)$ and $(bb|22)$.

d) $x=(2+S_H)^2/12(1+2S_H)(1-S_H)$.

e) $S=\int \chi_1(1)\chi_2(1)dv$.

TABLE III. CORE ATTRACTION AND OTHER BASIC INTEGRALS[a]

	eV.					eV.
	$\langle 2\|aa\rangle$ −12.5410	$\langle a\|aa\rangle$ −27.2040	$\langle a\|bb\rangle$ −8.0385	$\langle a\|22\rangle$ −14.6474	$\langle b\|22\rangle$ −11.9043	
$\langle 2\|11\rangle$	1	—	—	—	—	−12.5410
$\langle a\|12\rangle$	—	$S/3$[b]	$S/6$	$S/2$	—	−11.4404
$\langle b\|12\rangle$	—	$S/12$	$5S/12$	—	$S/2$	−7.4641

	eV.		eV.
$\langle a\|bc\rangle$	−2.2548	$\langle a\|ab\rangle$	−4.1015
$-W_H$[c]	13.595	$-W_2$[c]	11.28
S_H[d]	0.2805	S_{12}[d]	0.6452

a) Values for basic core integrals are shown in the second row of the first part of this table. See Appendix for the evaluation of these integrals. See also Table I, note a.

b) $S=S_{12}=\int \chi_1(1)\chi_2(1)dv$.

c) W_H and W_2 are experimental ionization energies of hydrogen 1s and carbon 2p AO respectively.

d) Taken from the table given by Mulliken et al.[18]

17) C. C. J. Roothaan, "Special Issue of Technical Report of Laboratory of Molecular Structure and Spectroscopy," The University of Chicago (1955).

18) R. S. Mulliken, C. A. Rieke, D. Orloff and H. Orloff, *J. Chem. Phys.*, **17**, 1248 (1949).

where W_H is the orbital energy of hydrogen 1s AO, S_H is the overlap integral between two hydrogen 1s AO's, and the integrals of the $\langle r \mid pq\rangle$ type are defined by:

$$\langle r \mid pq\rangle = -\int \chi_p(1) e^2/R_r(1) \chi_q(1) \mathrm{d}v \qquad (11)$$

Here $R_r(1)$ is the distance between the electron (1) and the r-th hydrogen core. The electronic repulsion integrals, $J_{\mu\mu'}$ and $K_{\mu\mu'}$ can be reduced to two integrals over atomic orbitals by using Mulliken's approximation,[19] as shown in Table II. Using theoretically calculated values for the integrals over atomic orbitals (Table III), the ionization potential, $I_p(\chi_1)$, is evaluated at 9.2880 eV.

The Ionization Potential of the Methyl Group

The next step in the calculation is to consider the interaction between the pseudo π AO, χ_1, and the 2pπ AO of the carbon atom of the methyl group—in other words, to treat the methyl group as an unsaturated diatomic molecule. The actual calculation was carried out by the aid of the SCF MO method.[20,21]

Denoting carbon 2pπ AO in a methyl group by χ_2, the molecular orbital in question has the form:

$$\varphi = c_1\chi_1 + c_2\chi_2 \qquad (12)$$

The familiar SCF matrix elements in this case are:

$$L_{pq} = I_{pq} + G_{pq} \qquad (13)$$

$$I_{pq} = \int \chi_p(1) H_m^c(1) \chi_q(1) \mathrm{d}v \qquad (14)$$

$$G_{pq} = \int \varphi(1)\varphi(1) e^2/r_{12} \chi_p(2) \chi_q(2) \mathrm{d}v \qquad (15)$$

Here,

$$H_m^c(1) = T(1) + A(1) - e^2/R_2(1)$$

$T(1)$ and $A(1)$ being a kinetic energy operator and a Coulomb potential from the H_3 core (including attractions from three hydrogen cores and repulsions from two electrons in λ_2 and λ_3) respectively.

$$\left.\begin{aligned} I_{11} &= W_1 + \langle 2 \mid 11\rangle \\ I_{22} &= W_2 + (22 \mid \lambda_2\lambda_2) + (22 \mid \lambda_3\lambda_3) \\ &\quad + \langle a \mid 22\rangle + 2\langle b \mid 22\rangle \\ I_{12} &= SW_2 + (12 \mid \lambda_2\lambda_2) + (12 \mid \lambda_3\lambda_3) \\ &\quad + \langle a \mid 12\rangle + 2\langle b \mid 12\rangle \end{aligned}\right\} \qquad (16)$$

Also,

$$\left.\begin{aligned} G_{11} &= c_1^2(11 \mid 11) + 2c_1c_2(12 \mid 11) + c_2^2(22 \mid 11) \\ G_{22} &= c_1^2(11 \mid 22) + 2c_1c_2(12 \mid 22) + c_2^2(22 \mid 22) \\ G_{12} &= c_1^2(11 \mid 12) + 2c_1c_2(12 \mid 12) + c_2^2(22 \mid 12) \end{aligned}\right\} \qquad (17)$$

Here W_1 corresponds to $I_p(\chi_1)$ computed above. W_2 is the 2p atomic orbital energy of carbon and can be taken to be -11.28 eV.[19] (the ionization potential of carbon). The other integrals are given in Tables II and III.

After the usual SCF procedure had been performed, the following secular equation was finally obtained:

$$\begin{vmatrix} 9.6837+\varepsilon, & 10.8957+0.6452\varepsilon \\ 10.8957+0.6452\varepsilon, & 11.6492+\varepsilon \end{vmatrix} = 0 \qquad (18)$$

The resultant orbital energies and molecular orbitals are:

$$\varepsilon_1 = -13.245 \text{ eV.} \quad \varphi_1 = 0.4362\chi_1 + 0.6619\chi_2 \qquad (19)$$

and,

$$\varepsilon_2 = +0.708 \text{ eV.} \quad \varphi_2 = 1.2347\chi_1 - 1.1299\chi_2 \qquad (20)$$

The ionization potential to remove an electron from the orbital φ_1 is the minus of the lower energy:

$$I_p(\text{methyl}) = 13.245 \text{ eV.}$$

The Electronic Structure of the *t*-Butyl Cation

Now let us consider the interaction among the three methyl groups and the central carbon atom. The wave function for the ground configuration is

$$\Phi_G = |A, \overline{A}, B, \overline{B}, C, \overline{C}| \qquad (21)$$

where A, B and C are abbreviated notations of φ_A, φ_B and φ_C, the pseudo π molecular orbitals of the three methyl groups.[22] In the ground configuration, the +1 charge is localized on the central carbon atom.

In addition to the above ground configuration, we must take the three CT (charge-transfer) configurations into account:

$$\left.\begin{aligned} \Phi_1 &= (2)^{-1/2} \cdot \{|A, \overline{3}, B, \overline{B}, C, \overline{C}| \\ &\quad + |3, \overline{A}, B, \overline{B}, C, \overline{C}|\} \\ \Phi_2 &= (2)^{-1/2} \cdot \{|A, \overline{A}, B, \overline{3}, C, \overline{C}| \\ &\quad + |A, \overline{A}, 3, \overline{B}, C, \overline{C}|\} \\ \Phi_3 &= (2)^{-1/2} \cdot \{|A, \overline{A}, B, \overline{B}, C, \overline{3}| \\ &\quad + |A, \overline{A}, B, \overline{B}, 3, \overline{C}|\} \end{aligned}\right\} \qquad (22)$$

19) R. S. Mulliken, *J. chim. phys.*, **46**, 497 (1949).
20) C. C. J. Roothaan, *Rev. Mod. Phys.*, **23**, 69 (1951).
21) R. G. Parr and R. S. Mulliken, *J. Chem. Phys.*, **18**, 1338 (1950).

22) φ is defined by Eq. 19. In this case, however, it is renormalized according to the zero-overlap approximation;

$$\varphi = 0.5505\chi_1 + 0.8348\chi_2$$

Similarly, φ_B and φ_C can be constructed using the AO's (and pseudo AO's) χ_4 and χ_5, and χ_6 and χ_7, respectively.

where number 3 is an abbreviated notation of χ_3, the $2p\pi$ AO of the central carbon atom. Locally excited configurations may be omitted because the excitation energies are considerably high.[23]

The following three new wave functions can be constructed by taking linear combinations of Φ_1, Φ_2 and Φ_3:

$$\left.\begin{aligned}\Phi_{\mathrm{I}} &= (3)^{-1/2}\cdot\{\Phi_1+\Phi_2+\Phi_3\}\\ \Phi_{\mathrm{II}} &= (2)^{-1/2}\cdot\{\Phi_2-\Phi_3\}\\ \Phi_{\mathrm{III}} &= (6)^{-1\ 2}\cdot\{2\cdot\Phi_1-(\Phi_2+\Phi_3)\}\end{aligned}\right\} \quad (23)$$

Among these, only Φ_{I} interacts with Φ_{G}, so that the ground state energy is obtained as the lower root of the secular equation:

$$\begin{vmatrix} -E, & H_{\mathrm{GI}} \\ H_{\mathrm{GI}}, & (H_{\mathrm{II}}-H_{\mathrm{GG}})-E \end{vmatrix}=0 \quad (24)$$

H_{GG} and H_{II} are defined by

$$H_{\mathrm{GG}}=\int \Phi_{\mathrm{G}} H \Phi_{\mathrm{G}} \mathrm{d}v \quad (25)$$

and

$$H_{\mathrm{II}}=\int \Phi_{\mathrm{I}} H \Phi_{\mathrm{I}} \mathrm{d}v \quad (26)$$

where H is the total electronic Hamiltonian of the system. Each element in Eq. 24 can be represented as follows:

$$H_{\mathrm{II}}-H_{\mathrm{GG}}=-I_p(3)+I_p(\mathrm{methyl}) \quad (27)$$

$$H_{\mathrm{GI}}=2.044\cdot\beta \quad (28)$$

where $I_p(3)$ is the ionization potential of an electron in χ_3, $I_p(\mathrm{methyl})$ is the ionization potential of the methyl group computed above, and β is the resonance integral between the carbon $2p\pi$ AO of a methyl group and χ_3.[24]

Φ_{II} and Φ_{III} both correspond to the lower excited state (doubly degenerate) and their energies (taking H_{GG} as the standard of energy) are:

$$\begin{aligned}E_{\mathrm{L}} &= H_{\mathrm{II\ II}}-H_{\mathrm{GG}}\\ &= H_{\mathrm{III\ III}}-H_{\mathrm{GG}}\\ &= -I_p(3)+I_p(\mathrm{methyl})\end{aligned}$$ [25]

Now taking $I_p(3)=11.28$ eV.[19] and $I_p(\mathrm{methyl})=13.245$ eV.;

$$H_{\mathrm{II}}-H_{\mathrm{GG}}=E_{\mathrm{L}}=1.965 \text{ eV}. \quad (29)$$

If we assume $\beta=-1.52$ eV. which is reasonable as will be described later (in Discussion), the roots of Eq. 24 are calculated as follows:

$$E_{\mathrm{G}}=-2.28 \text{ eV}.$$

$$E_{\mathrm{U}}=4.24 \text{ eV}.$$

The first excitation energy is

$$E_{\mathrm{L}}-E_{\mathrm{G}}=4.25 \text{ eV}.$$

which is in good agreement with the empirical value (290~295 mμ=4.27~4.20 eV.) obtained by Symons et al.[11,12] (see Fig. 2).

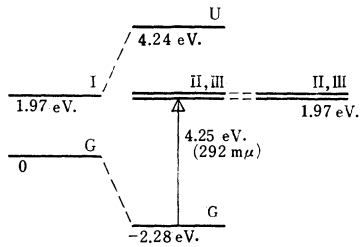

Fig. 2. The energy diagrams of the *t*-butyl cation.

The wave functions for the states are:

$$\left.\begin{aligned}\Psi_{\mathrm{G}} &= 0.8067\Phi_{\mathrm{G}}+0.5909\Phi_{\mathrm{I}}\\ \Psi_{\mathrm{L}_1} &= \Phi_{\mathrm{II}}\\ \Psi_{\mathrm{L}_2} &= \Phi_{\mathrm{III}}\\ \Psi_{\mathrm{U}} &= 0.5909\Phi_{\mathrm{I}}-0.8067\Phi_{\mathrm{G}}\end{aligned}\right\} \begin{matrix}\\ \\ \text{(doubly}\\ \text{degenerate)}\\ \\ \end{matrix} \quad (30)$$

The charge distributions for the ground and first excited states calculated from the above wave functions are shown in Fig. 3. The transition moments for the $\Psi_{\mathrm{G}}\rightarrow\Psi_{\mathrm{L}_1}$ and $\Psi_{\mathrm{G}}\rightarrow\Psi_{\mathrm{L}_2}$ transitions (μ_1 and μ_2 respectively) were evaluated as:

$$|\mu_1|=|\mu_2|=0.681 \text{ Å}$$

by the usual formula

$$\mu_{\mathrm{K}}=\int \Psi_{\mathrm{L_K}} \sum_i \boldsymbol{r}_i \Psi_{\mathrm{G}} \mathrm{d}v$$

The oscillator strength for the first excitation was determined to be 0.346 from the equation:

$$f=(1.085\times10^{-5})\nu G|\mu^2|$$

where ν is the wave number (in cm^{-1} units) for the transition and G is a degeneracy factor (in this case, $G=2$).[26]

23) The local excitation energy in the methyl group is given by

$$\varepsilon_2-\varepsilon_1-J_{\varphi_1\varphi_2}+2K_{\varphi_1\varphi_2}=5.228 \text{ eV}.$$

where ε_1 and ε_2 are the lower and upper roots of Eq. 18 and

$$J_{\varphi_1\varphi_2}=\int \varphi_1(1)\varphi_1(1)\mathrm{e}^2/r_{12}\varphi_2(2)\varphi_2(2)\mathrm{d}v$$

$$K_{\varphi_1\varphi_2}=\int \varphi_1(1)\varphi_2(1)\mathrm{e}^2/r_{12}\varphi_1(2)\varphi_2(2)\mathrm{d}v$$

The values of these integrals can be calculated using the basic integrals in Table II:

$J_{\varphi_1\varphi_2}=13.2592$ eV.

$K_{\varphi_1\varphi_2}=2.2670$ eV.

The effect of the locally excited configurations will be discussed below.

24) See Appendix for the reduction of $H_{\mathrm{II}}-H_{\mathrm{GG}}$ and H_{GI}.

25) Note $H_{\mathrm{II}}=H_{\mathrm{II\ II}}=H_{\mathrm{III\ III}}$ in this approximation.

26) In the evaluation of charge distributions and transition moments, the assumption of zero-differential overlap[27] is invoked. This is in accordance with the fact that overlap integrals are disregarded formally in the above calculation of the interactions between the configurations, G, L_1, L_2 and U.

27) R. Pariser and R. G. Parr, *J. Chem. Phys.*, **21**, 466 (1953).

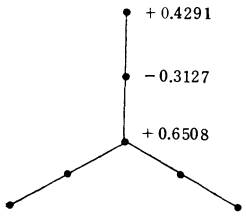

(a) The ground state.

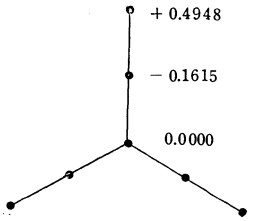

(b) The first excited state.

Fig. 3. The charge distributions of the *t*-butyl cation.

Finally, the hyperconjugation energy, $-E_G$, of the *t*-butyl cation can be obtained as follows:

$$-E_G = 2.28 \text{ eV.}$$
$$= 53.9 \text{ kcal./mol.}$$

Discussion

In the above calculation, the resonance integral, β, was determined to be -1.52 eV. If one plots the resonance integrals against the overlap integrals for this cation,[28] benzene, ethylene and butadiene,[29] all the points fit a straight line well. This seems to mean that the β value assumed for the *t*-butyl cation is reasonable.

From the absorption band of the *t*-butyl cation observed by Symons et al.,[11,12] the oscillator strength can be determined as follows:

$$f_{obs.} = 4.32 \times 10^{-9} \cdot \varepsilon_{max} \cdot \Delta H$$
$$= 0.13 \qquad (31)$$

where ε_{max} and ΔH are the peak molar extinction coefficient and the half-breadth in cm^{-1} units respectively. The theoretical *f* value (0.346) is about two or three times greater than the observed value. A discrepancy of this order of magnitude is usually found between observed and theoretical oscillator strength values. Moreover, the observed value is based on the assumption that the parent molecules (butyl alcohols, isobutene and *t*-butyl halides) can be completely converted into the cation in concentrated sulfuric acid. If they are not converted completely, or if the cation undergoes some futher reactions, the "apparent" extinction coefficient will be lower than the real one. In this connection, a further experimental check may be needed for a more quantitative comparison between the theoretical and observed oscillator strength values.

The calculated hyperconjugation energy (53.9 kcal./mol.) may be said to be unexpectedly large. However, this large stabilization energy due to hyperconjugation is thought to be reasonable from the experimental point of view. Franklin et al.[30] obtained the value 84 kcal./mol. for the stabilization energy of the *t*-butyl cation. Although there is a little question whether or not the observed stabilization energy corresponds to the *t*-butyl cation with the planar structure,[9] the calculated and observed results on the stabilization energy seem to show that the hyperconjugation effect is extraordinarily large in this cation.

As was mentioned in the introductory part of the present paper, the appearance of the absorption band in the 290 mμ region is difficult to be accounted for in molecules without any unsaturated bond. However, it has been established by the present calculations that the absorption can be understood in terms of the electron releasing ability (hyperconjugation effect) of the methyl groups. The excited state of the 290 mμ band is composed of the charge-transfer configurations caused by the electron transfer from the methyl groups towards the central carbon cation. Therefore, the transition corresponding to the 290 mμ band is accompanied by an electron transfer in the same direction. This may easily be seen from the electron distributions in the ground and first excited states shown in Fig. 3. In this interpretation, the band may be regarded as the intramolecular charge-transfer absorption,[31,32] the methyl groups and the carbon cation being the electron donor and the acceptor respectively.

Finally, let us check the effect of locally excited configurations within the methyl groups which were excluded in the above-mentioned calculations. The wave functions for these configurations are:

28) $S_{23} = 0.211$ for the overlap integral between a methyl group and the central carbon atom.
29) R. Pariser and R. G. Parr, *J. Chem. Phys.*, **21**, 767 (1953).
30) L. L. Franklin and H. E. Lumpkin, ibid., **20**, 745 (1952).
31) S. Nagakura and J. Tanaka, ibid., **22**, 236 (1954); S. Nagakura, ibid., **23**, 1441 (1954); *Mol. Phys.*, **3**, 105 (1960).
32) J. N. Murrell, *Quart. Revs.*, **15**, 191 (1960).

$$\left.\begin{aligned}\Phi_1^{\mathrm{L}} &= (2)^{-1/2}\{|A, \overline{A'}, B, \overline{B}, C, \overline{C}| \\ &\quad + |A', \overline{A}, B, \overline{B}, C, \overline{C}|\} \\ \Phi_2^{\mathrm{L}} &= (2)^{-1/2}\{|A, \overline{A}, B, \overline{B'}, C, \overline{C}| \\ &\quad + |A, \overline{A}, B', \overline{B}, C, \overline{C}|\} \\ \Phi_3^{\mathrm{L}} &= (2)^{-1/2}\{|A, \overline{A}, B, \overline{B}, C, \overline{C'}| \\ &\quad + |A, \overline{A}, B, \overline{B}, C', \overline{C}|\}\end{aligned}\right\} \quad (32)$$

where A', B' and C' denote $\varphi_{A'}$, $\varphi_{B'}$ and $\varphi_{C'}$ respectively, the upper MO's in each methyl group. If we take three linear combinations:

$$\left.\begin{aligned}\Phi_{\mathrm{I}}^{\mathrm{L}} &= (3)^{-1/2}(\Phi_1^{\mathrm{L}} + \Phi_2^{\mathrm{L}} + \Phi_3^{\mathrm{L}}) \\ \Phi_{\mathrm{II}}^{\mathrm{L}} &= (2)^{-1/2}(\Phi_2^{\mathrm{L}} - \Phi_3^{\mathrm{L}})\end{aligned}\right\} \quad (33)$$

and

$$\Phi_{\mathrm{III}}^{\mathrm{L}} = (3/2)^{-1/2}\{\Phi_1^{\mathrm{L}} - (1/2)(\Phi_2^{\mathrm{L}} + \Phi_3^{\mathrm{L}})\}$$

$\Phi_{\mathrm{I}}^{\mathrm{L}}$ interacts with Φ_{I} and Φ_{G}; $\Phi_{\mathrm{II}}^{\mathrm{L}}$, with Φ_{II}, and $\Phi_{\mathrm{III}}^{\mathrm{L}}$, with Φ_{III}.

The secular equations are:

$$\begin{vmatrix} -E & 2.04\beta & 1.83 \\ & 1.97-E & -0.551\beta \\ & & 6.23-E \end{vmatrix} = 0 \quad (34)$$

[33]

and

$$\begin{vmatrix} -E & -0.551\beta \\ & 3.72-E \end{vmatrix} \quad (35)$$

Assuming the same value of β (-1.52 eV.) as before, the results are:

Ground state: $E_{\mathrm{G}} = -2.71$ eV. (taking H_{GG} as the standard of energy)

$$\Psi_{\mathrm{G}} = 0.795\Phi_{\mathrm{G}} + 0.566\Phi_{\mathrm{I}} - 0.216\Phi_{\mathrm{I}}^{\mathrm{L}} \quad (36)$$

First excited state: $E_{\mathrm{L}} = 1.79$ eV.

$$\Psi_{\mathrm{L}_1} = 0.977\Phi_{\mathrm{II}} - 0.210\Phi_{\mathrm{II}}^{\mathrm{L}} \quad (37)$$

$$\Psi_{\mathrm{L}_2} = 0.977\Phi_{\mathrm{III}} - 0.210\Phi_{\mathrm{III}}^{\mathrm{L}} \quad (38)$$

The first excitation energy is, then, 4.50 eV., and the corresponding oscillator strength is calculated to be 0.365. From these results, we can see that the inclusion of the locally excited configurations does not bring about any significant change in the transition energy or in the oscillator strength.

The Institute for Solid State Physics
The University of Tokyo
Azabu, Tokyo

Appendix

Electronic Repulsion Integrals.—The integrals $(aa \mid 22)$ and $(bb \mid 22)$ are evaluated as follows: let us denote the direction of the axis of 2p AO, χ_2, as the z-axis, the carbon core C_2 as an origin, and the angle between the z-axis and the direction of hydrogen atom a as θ (see Fig. 1). Similarly, φ is the angle between $-$z and the direction of hydrogen atom b. 2p AO, χ_2, then, can be represented by:[18]

$$\begin{aligned}\chi_2 &= \cos\theta\cdot\chi_{\sigma a} + \sin\theta\cdot\chi_{\pi a} \\ &= -\cos\varphi\cdot\chi_{\sigma b} + \sin\varphi\cdot\chi_{\pi b}\end{aligned} \quad (1A)$$

where $\chi_{\sigma a}$ is the 2p AO of carbon atom 2 directed toward hydrogen atom a, and $\chi_{\pi a}$ is that perpendicular to it. $\chi_{\sigma a}$ and $\chi_{\pi b}$ are defined similarly for b. The integrals $(aa \mid 22)$ and $(bb \mid 22)$ are, then:[34]

$$\begin{aligned}(aa \mid 22) &= \cos^2\theta\cdot(aa \mid \sigma\sigma) + \sin^2\theta\cdot(aa \mid \pi\pi) \\ &= 0.8889(aa \mid \sigma\sigma) + 0.1112(aa \mid \pi\pi)\end{aligned} \quad (2A)$$

and

$$\begin{aligned}(bb \mid 22) &= \cos^2\varphi\cdot(bb \mid \sigma\sigma) + \sin^2\varphi\cdot(bb \mid \pi\pi) \\ &= 0.2221(bb \mid \sigma\sigma) + 0.7778(bb \mid \pi\pi)\end{aligned} \quad (3A)$$

$\cos\theta$, $\sin\theta$, $\cos\varphi$ and $\sin\varphi$ being determined from the assumed bond distance and bond angles. The integrals, $(aa \mid \sigma\sigma)$ etc., are taken from the table given by Roothaan,[17] for the Slater-type 2p AO of the carbon, with $Z=3.18$, and for the 1s AO of the hydrogen, with $Z=1.00$.

Core Attraction Integrals.—The core attraction integrals $\langle a \mid bb\rangle$ and $\langle a \mid ab\rangle$ were calculated non-empirically:

$$\begin{aligned}\langle a \mid bb\rangle &= -\int \chi_b(1)e^2/R_a(1)\chi_b(1)\mathrm{d}v \\ &= -(2/R)\cdot[1-(1+R)e^{-2R}]\end{aligned} \quad (4A)$$

and

$$\begin{aligned}\langle a \mid ab\rangle &= -\int \chi_a(1)e^2/R_a(1)\chi_b(1)\mathrm{d}v \\ &= -2(R+1)e^{-R}\end{aligned} \quad (5A)$$

where R is the distance (in atomic units) between hydrogen cores a and b ($R=3.367$) and χ_a and χ_b are AO's with $Z=1.00$. The three-center integral $\langle a \mid bc\rangle$ is reduced to the form:

$$\begin{aligned}\langle a \mid bc\rangle &= (S_{\mathrm{H}}/2)(\langle a \mid bb\rangle + \langle a \mid cc\rangle) \\ &= S_{\mathrm{H}}\langle a \mid bb\rangle\end{aligned} \quad (6A)$$

using Mulliken's approximation. $\langle 2 \mid aa\rangle$ is obtained from Eq. 4A, putting $R=2.062$, the distance

33) In the evaluation of the off-diagonal element (H_{GL}) between the ground and locally excited configurations, only the inductive effect by the central carbon ion was taken into account; i.e., the off-diagonal element belonging to the field of the methyl group, $H_{\mathrm{GL}}^{\mathrm{Me}}$, was disregarded. This is true when the MO's φ_A and $\varphi_{A'}$ are self-consistent with respect to the methyl group. As has been mentioned above (see footnote 22), however, φ_A and $\varphi_{A'}$ were renormalized in accordance with the zero-overlap approximation, so that we can not put the $H_{\mathrm{GL}}^{\mathrm{Me}}$ value at zero with the same values of α's and β as in the SCF calculation mentioned above (the overlap integral was not disregarded there). However, if we put $\beta=-2.35$ eV., the $H_{\mathrm{GL}}^{\mathrm{Me}}$ value vanishes. This value of β seems to be reasonable in the case of the zero-overlap approximation.

34) Note, $(aa \mid \sigma\pi) = (bb \mid \sigma\pi) = 0$.

between carbon core 2 and hydrogen core a.[35]

$\langle a \mid 22\rangle$ is reduced to the form:

$$\langle a \mid 22\rangle = \cos^2\theta\cdot\langle a \mid \sigma\sigma\rangle + \sin^2\theta\cdot\langle a \mid \pi\pi\rangle \quad (7A)$$

using Eq. 1A. $\langle a \mid \sigma\sigma\rangle$ is evaluated non-empirically, giving the formula:

$$\langle a \mid \sigma\sigma\rangle = -(Z/2)\rho^{-3}\cdot[2(\rho^2+12)-(\rho^5/4 + 3\cdot\rho^4/2+11\cdot\rho^3/2+14\cdot\rho^2+24\cdot\rho+24)e^{-\rho}] \quad (8A)$$

where $\rho=(Z/2)R$, with $Z=3.18$ and $R=2.062$ a. u. The integrals $\langle a \mid \pi\pi\rangle$ and $\langle b \mid 22\rangle$ are calculated by the aid of the "uniformly charged sphere" approximation,[27] in which $\chi_2(1)\chi_2(1)e$ is replaced by a pair of tangent uniformly-charged spheres of the diameter:

$$D=4.597/Z \text{ Å} \quad (9A)$$

where Z is the effective charge of the carbon 2p AO χ_2 ($Z=3.18$).[36]

The Evaluation of Matrix Elements.—The matrix elements necessary for the calculation of the configuration interaction between the ground and charge-transfer configurations of the *t*-butyl cation were evaluated under the approximation of zero-differential overlap:[27]

$$H_{GG}=\int |A, \overline{A}, B, \overline{B}, C, \overline{C}|H|A, \overline{A}, B, \overline{B}, C, \overline{C}|\,dv = 2(I_A+I_B+I_C)+J_{AA}+J_{BB}+J_{CC} + 4(J_{AB}+J_{BC}+J_{CA}) \quad (10A)$$

where

$$I_i=\int \varphi_i H^c \varphi_i dv \quad (11A)$$

$$J_{ij}=\int \varphi_i\varphi_i e^2/r_{12}\varphi_j\varphi_j dv \quad (12A)$$

and

$$H^c = T - \sum_{i=1}^{7}(e^2/R_i) \quad (13A)$$

T and R_i being the kinetic energy operator and the distance of an electron from the i-th core. Similarly,

$$H_{II}=I_A+I_3+2(I_B+I_C)+J_{BB}+J_{CC} + 2(J_{AB}+2J_{BC}+J_{CA})+J_{A3}+2(J_{B3}+J_{C3}) \quad (14A)$$

Accordingly,

$$H_{II}-H_{GG}=I_3-I_A-J_{AA}-2(J_{AB}+J_{CA}) + J_{A3}+2(J_{B3}+J_{C3}) \quad (15A)$$

On the other hand,

$$I_A=\int \varphi_A(T-e^2/R_1-e^2/R_2)\varphi_A dv+\sum_{i=3}^{7}\langle i \mid AA\rangle = I_A^A-2(J_{AB}+J_{CA})-J_{A3} \quad (16A)$$

where the approximate relations

$$\langle 3 \mid AA\rangle \fallingdotseq -J_{A3},\ \langle 4 \mid AA\rangle+\langle 5 \mid AA\rangle \fallingdotseq -2J_{AB} \text{ and } \langle 6 \mid AA\rangle+\langle 7 \mid AA\rangle \fallingdotseq -2J_{CA} \quad (17A)$$

are used. I_A^A is a core integral in the absence of an attraction from the other two methyl groups and from carbon core 3, so that we have a relation:

$$-I_p(\text{methyl}) = I_A^A + J_{AA} \quad (18A)$$

Similarly, we have:

$$I_3 = I_3^3 - 2(J_{A3}+J_{B3}+J_{C3}) \quad (19A)$$

and

$$-I_p(3) = I_3^3 \quad (20A)$$

Putting Eqs. 16A, 18A, 19A and 20A into Eq. 15A, we have

$$H_{II}-H_{GG}=I_p(\text{methyl})-I_p(3) \quad (21A)$$

The off-diagonal element H_{GI} is reduced as follows:

$$H_{GI}=(3)^{-1/2}(H_{G1}+H_{G2}+H_{G3})=(3)^{1/2}H_{G1} \quad (22A)$$

$$H_{G1}=(2)^{1/2}\int \varphi_A H^c \chi_3 dv = (2)^{1/2}\int (0.5525\chi_1+0.8348\chi_2)H^c\chi_3 dv \fallingdotseq (0.8348)(2)^{1/2}\int \chi_2 H^c \chi_3 dv \quad (23A)$$

Denoting $\int \chi_2 H^c \chi_3 dv = \beta$ and putting Eq. 23A into Eq. 22A,

$$H_{GI}=2.044\beta.$$

35) Under the assumption of disregarding a Coulomb penetration integral, the core attraction integral $\langle 2 \mid aa\rangle$, as is well known, can be approximated as equal to the two-center Coulomb integral $-(22 \mid aa)$. This value, -12.256 eV., is rather close to the value, -12.541 eV., obtained by the above-mentioned method.

36) If the "uniformly charged sphere" model is applied directly to $\langle a \mid 22\rangle$, hydrogen core a is "inside" of one of the spheres. Therefore, rigorous computation was carried out for $\langle a \mid \sigma\sigma\rangle$.

*The Electrical Conduction of the p-Phenylenediamine Iodine Complex**

By Shun-ichiro NISHIZAKI and Hideaki KUSAKAWA

(Received August 2, 1963)

Extensive work has by now been carried out on the electronic conduction in molecular complexes of aromatic hydrocarbon with iodine,[1-5] or antimony pentachloride,[6] and amines with quinones,[7-9] but on complexes of amines with iodine, except in solutions, there have been only a few papers.[10]

It seems that iodine is stronger as an electron acceptor[11] than are quinones, therefore, it is to be expected that the complexes constituted of amine and iodine have a lower electrical resistivity than that of amine and quinone.

This paper will report on the electrical conductivity of the complex of paraphenylenediamine with iodine. This complex appeared to have a nonstoichiometrical composition, and its electrical resistivity varied according to the iodine contents. Therefore, it was the objective of the present work to investigate the relation between the magnitude and temperature dependence of the electrical resistivities and the coordination numbers of the iodine.

Experimental

Materials.—The purification of *p*-phenylenediamine (*p*-PDA) and iodine (I_2) was carried out by distillation and sublimation, which were repeated twice.

p-PDA and iodine were dissolved in benzene. When both solutions were mixed, dark-colored complexes of *p*-PDA with iodine precipitated. In order to vary the iodine content in the complexes, the mole ratio of iodine/amine was arranged at 2/4, 3/4, 4/4, 5/4, 6/4 and 7/4. The complexes precipitated were left to stand for 24 hr. in the mixed solution, they were then filtered and dried.

All the complexes gave a rich yield above 90% for the mixed *p*-PDA and iodine, especially in cases of the mixed mole ratios of 2/4 and 3/4, when the yield was approximately 99%.

Electrical Conduction.—The electrical resistivities of the complexes were measured by means of the dc method, using crystalline powder which had been packed into a glass capillary (about 2 mm.) in a dry box and compressed with a pressure of 15 kg. between metal electrodes, the diameters of which were 2.0 mm. (about 500 kg./cm^2). This electrode cell was exposed to an atmosphere of dry air. By applying a dc field of about 50 V./cm. across the electrodes, the current through the specimen was measured with a micro or electronic micro-micro ammeter.

In order to isolate the ionic conduction, for over 15 hr. the d. c. field was applied through the specimen at room temperature (about 30°C). After this treatment, there was no change in the infrared absorption spectra of the specimens, the temperature of the specimen, which was controlled with an electric furnace placed around the cell, was raised to 85°C.

The relation between the electrical resistivities and the temperature for calculating the activation energy was measured during the first cooling.

Apparent Densities.—The apparent densities of the complexes were measured with tablets which had been compressed in a manner similar to that used potassium bromide tablet for the infrared-spectrum. The tablet of the potassium bromide compressed under the same conditions indicated 2.52 g./cm^3 at 30°C, but the density of potassium bromide is 2.7 g./cm^3 at 25°C.

Results and Discussion

The results of this investigation are shown in Fig. 1, as semilogarithmic plots of the resistivity vs. temperature for the complexes. In this case the coordination numbers of iodine (Table I) are noted on the figure. The activation energy for the electrical conduction process, E_c, can be calculated from the slope of the plots, $\rho=\rho_0 \exp(E/\boldsymbol{k}T)$, their values are listed in the last column in Table I.

It may be seen that the electrical conductivities of complexes are remarkably enhanced with a small increase in the iodine content in complexes and that a minimum value for both

* This paper has been presented in part at the 16th Annual Meeting of the Chemical Society of Japan, April, Tokyo.

1) H. Akamatu, H. Inokuchi and Y. Matsunaga, *Nature*, **173**, 168 (1954).
2) H. Akamatu, H. Inokuchi and Y. Matsunaga, This Bulletin, **29**, 213 (1956).
3) J. Kommandeur and F. R. Hall, *J. Chem. Phys.*, **34**, 129 (1961).
4) T. Uchida and H. Akamatu, This Bulletin, **34**, 1015 (1961).
5) T. Uchida and H. Akamatu, ibid., **35**, 981 (1962).
6) G. E. Blongrein and J. Kommandeur, *J. Chem. Phys.*, **35**, 1635 (1962).
7) M. M. Labes, R. Sehr and M. Bose, ibid., **32**, 1570 (1960).
8) D. L. Kronik and M. M. Labes, ibid.. **35**, 2016 (1961).
9) D. D. Eley, H. Inokuchi and M. P. Wilis, *Discussions Faraday Soc.*, **28**, 54 (1959).
10) J. A. Van Der Hoek, J. H. Lupinski and L. J. Oosterhoff, *Mol. Phys.*, **3**, 299 (1960).
11) D. C. Heosterey, *J. Chem. Phys.*, **36**, 557 (1962).

TABLE I. ELECTRICAL RESISTIVITY AT ROOM TEMPERATURE (30°C)
Activation energy and density of *p*-PDA-I_2 complexes

Sample No.	Coordination No. of I	30°C ohm-cm.	ρ_0 ohm-cm.	E_c eV.	Density g./cm³
1	0.45	5.9×10^{9}	3.3×10^{-4}	0.80	2.54
2	0.67	3.5×10^{7}	2.9×10^{-3}	0.61	2.62
3	0.82	1.7×10^{5}	2.4×10^{-2}	0.41	2.81
4	1.03	2.7×10^{5}	1.56×10^{-2}	0.44	3.78
5	1.36	1.04×10^{6}	1.07×10^{-2}	0.48	2.57
6	1.62	5.4×10^{6}	8.5×10^{-3}	0.59	1.88

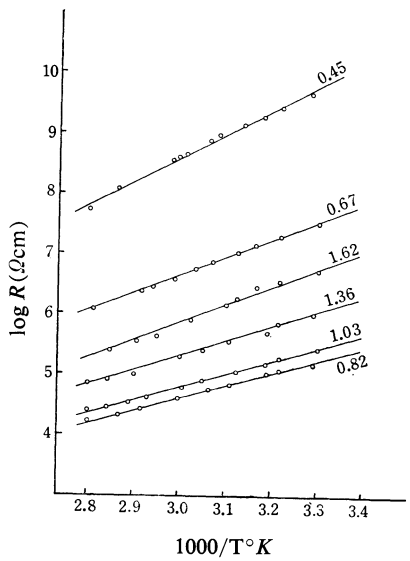

Fig. 1. Electrical resistivities vs. temperature for *p*-PDA-I_2 complexes.

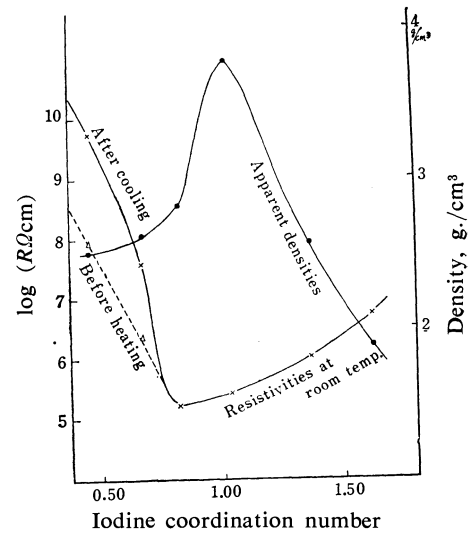

Fig. 2. The relationship between the I_2 coordination number and electrical resitivities, density.

the magnitude and the temperature dependence of the electrical resistivity appears in the complex the coordination number of the iodine of which is around 0.8. Over this range, the magnitude and temperature dependence of the resistivity gradually increase with the iodine content. However, on the other hand, the maximum value of density exists in the vicinity of the coordination number 1.0. These results are shown in Fig. 2.

In view of the fact that the resistivities increased with time when the current was run through the specimens the coordination numbers of which were 0.45 and 0.67, and so did not follow Ohm's law, it seems that ionic conduction formed most of the conduction in these complexes. The different values of resistivities between before heating and after cooling were especially conspicuous in these cases. However, even if these specimens were heated and cooled twice, there was no remarkable change in resistivity.

In the complexes the iodine coordination number of which was above the neighborhood of 0.8, ionic conduction was inferior to electronic conduction, because the current ran in an Ohmic pattern and the resistivity did not change between before heating and after cooling.

As Table II shows, the values for both the magnitude and the temperature dependence of

TABLE II. COMPARISON WITH *p*-PDA-I_2 AND *p*-PDA-CHLORANIL ON THE ELECTRICAL RESISTIVITY AND ACTIVATION ENERGY

	$\rho_{25°C}$ ohm-cm.	ρ_0 ohm-cm.	E_c eV.
p-PDA-I_2	2.1×10^{5}	2.4×10^{-2}	0.41
p-PDA-Chloranil	6×10^{6}	1.9×10^{-5}	0.67

the resistivity of an amine-iodine complex are smaller than those of an amine-chloranil complex[12] when the amine is *p*-PDA. On the other hand, the redox potential of iodine is 0.536 V. and that of chloranil is 0.742 V. From this point of view, chloranil seems to be a

12) R. Sehr, M. M. Labes, M. Bose and H. Ur. F. Wilhelm, "Symposium on Electrical Conductivity in Organic Solid," John Wiley & Sons Inc., New York (1961) p. 309.

stronger oxidative reagent than iodine, although, as an electron-acceptor, iodine is superior to chloranil for *p*-PDA. In the cases of bromine and iodine with benzidine,[10,13] one can see the same results. For this reason it is presumed that the polarization terms in the following equation play an important role[3,14].

$$2E_c \simeq \varepsilon = [I_G(D) - A_G(A)] - [P(D_+) + P(A_-)]$$

where ε is the energy of charge transfer band, $I_G(D)$ is the ionization potential of the donor, $A_G(A)$ is the electron affinity of the acceptor in the gas phase, and the contributions, $P(D_+)$ and $P(A_-)$, from the polarization energy around the positive and negative ion are represented.

The complexes of *p*-PDA with iodine were thermally stable up to the vicinity of 120°C, and their melting points were not lower than those of the two conpenents (*p*-PDA : 140°C iodine : 114°C). Iodine had been freed upon being heated before the complexes were melted therefore, the phase diagram for *p*-PDA-iodine could not be obtained in this atmosphere.

13) H. Kusakawa, unpublished.
14) H. Kuroda, *J. Japanese Chem.* (*Kagaku no Ryoiki*) **17**, 113 (1963).

Summary

In the case of a complex of *p*-phenylenediamine with iodine, a nonstoichiometrical composition has been established; the minimum values for both the magnitude and the temperature dependence of resistivity exist on the complex the coordination number of which is around 0.8. On the other hand, the maximum value of the apparent density appears in the vicinity of 1.0.

In comparison with the complex of *p*-phenylenediamine-iodine and that of *p*-phenylenediamine-chloranil, even though the redox potential of chloranil is larger than that of iodine, the resistivity and the activation energy of the *p*-phenylenediamine-iodine system are smaller than those of the chloranil complex.

Mitsubishi Electric Corporation
Research Laboratory
Amagasaki, Hyogo

The Pectic Acid from the Pulp of Jackfruit (Artocarpus Integrifolia). I. Methylation Studies

By U. K. Sen Gupta and C. V. N. Rao

(Received August 27, 1963)

The presence of pectic substances in the pulp of jackfruit has been reported earlier by different workers.[1,2] However, no detailed investigations seem to have been carried out on the structure of these pectic substances. The present paper reports some structural studies of the pectic acid isolated from the soft fleshy pulp of the ripe jackfruit.

The polysaccharide obtained from jackfruit pulp by extraction with hot water gave a blue color with iodine. The product obtained after treatment with diastase to remove starch, on hydrolysis gave L-rhamnose, D-xylose, L-arabinose, D-glucose, D-galactose and D-galacturonic acid.

Ammonium pectate was isolated from the water-extracted residue of the jackfruit pulp with a hot ammonium oxalate solution. The polysaccharide was purified by converting it to insoluble calcium salt, and then to ammonium pectate, and finally by treating the material with diastase to destroy any starch. The hydrolysis of the resulting polysaccharide yielded D-galacturonic acid, D-glucose, and traces of arabinose. The polysaccharide was subjected to further purification by different processes, viz., conversion into sodium salt followed by precipitation as calcium salt, complexing with cetyltrimethylammonium bromide[3,4] and repeated fractional precipitation with acetone from an aqueous solution. However, no pure polygalacturonic acid free from neutral sugar components could be isolated by any of these processes, though xylose, rhamnose and galactose containing moieties were removed after repeated purification. Different

1) C. R. Krishnamurti and K. V. Giri, *Proc. Ind. Acad. Sci.*, **29B**, 155 (1949).
2) H. W. Scharpenseel, *Landwirtsch Forsch*, **10**, 191 (1957).
3) A. S. Jones, *Biochim. et Biophys. Acta.*, **10**, 607 (1953).
4) B. C. Bera, A. B. Foster and M. Stacey, *J. Chem. Soc.*, **1955**, 3788.

methods of purification yielded polysaccharides with different specific rotation and uronic acid content values. The hydrolyzates of each material gave different amounts of galacturonic acid, together with glucose and traces of arabinose. It was also found that only galacturonic acid residues were released when ammonium pectate was hydrolyzed under mild conditions using 0.1 N sulphuric acid. As the uronic acid content was highest in sample A, this was used in further investigations.

The purified polysaccharide was dissolved in phosphate buffer and subjected to electrophoresis using a potential gradient of 7.0 V. per cm. Two distinct peaks were observed, one of them migrating towards the anode presumably because of the polyuronic acid constituents. A known mixture of quite divergent groups of polysaccharides has been reported[5] to have been separated by this method.

The results of the electrophoretic experiment, together with the earlier findings, viz., the variation of uronic anhydride content in polysaccharides obtained by different methods of purification and the failure to obtain an aldobiouronic acid by mild hydrolysis, indicate that the material under investigation is a mixture of at least two different polysaccharides, one being a polygalacturonan. Another interesting observation is that glucose was detected in the hydrolyzate of the purified polysaccharide even after the treatment with diastase, showing that glucose may be an artifect of a glucan which is different from starch.

Ammonium pectate was methylated first by treatment with methyl sulfate and sodium hydroxide and then by the addition of methyl iodide to the silver salt. The methylated polysaccharide was purified by adding cold ethanolic sodium hydroxide to remove the associated neutral methylated polysaccharide. The methylated sodium pectate so obtained was, as usual, reconverted into methylated methyl pectate, which showed no hydroxyl absorption band in the infrared spectrum.

The methylated product after methanolysis was saponified with aqueous barium hydroxide. The acid portion was separated from the neutral portion by absorbing the former on an anion-exchange resin. On hydrolysis the neutral portion yielded a mixture of methyl sugars which was separated and estimated[6] by paper chromatography to give 2, 3, 4, 6-tetra- (1 mol.), 2, 3, 6-tri- (10.2 mol.), 2, 4, 6-tri- (9.8 mol.) and 2, 3-di-*O*-methyl-D-glucose (1.1 mol.) ; each of these methyl sugars was identified through a suitable crystalline derivative. As no methyl arabinose was found in the hydrolyzate of the neutral polysaccharide, it is assumed that arabinose was eliminated during the methylation and the subsequent purification processes.

The acidic component was displaced from the resin and reduced with lithium aluminum hydride, and the resulting product on hydrolysis gave a mixture of neutral methyl sugars. The mixture was separated on a cellulose column to give 2, 3, 4-tri- and 2, 3-di-*O*-methyl-D-galactose, which were characterised through their crystalline anilides. The relative amounts of sugars were estimated by alkaline hypoiodite. The molar ratio of the tri- and di-methyl galactose was 1 : 91.

From the above results it is possible to assign structures to the pectic acid and to the glucan associated with it. It is clear from these results that the main component, 2, 3-di-*O*-methyl-D-galactose, has arisen from the residues of 2, 3-di-*O*-methyl-D-galacturonic acid, that the jackfruit pectic acid contains chains of 1 : 4 linked D-galacturonic acid residues, and that the 2, 3, 4-tri-*O*-methyl-D-galactose originates from the nonreducing D-galacturonic acid end groups. As no monomethyl galactose could be isolated, the molecule is considered to be unbranched. From the ratio of the amounts of trimethyl and dimethyl galactose, the average length of each molecules is calculated to be 92 hexouronic acid units. Hence, the structure of the pectic acid is as follows:

$$Ga_pU{=}_1{\longrightarrow}_4\ (Ga_pU)_{90}\ {}_1{\longrightarrow}_4\ Ga_pU$$

(Ga_pU represents the galactopyranosyl uronic acid residue).

From the methoxyl content of the original polysaccharide, it can be concluded that some of the carboxyl groups are involved in methyl ester linkages. Since the pectic acid and its methylated derivative have high positive rotations, the glycosidic linkages are considered to be of the α-type.

The demonstration of the presence of 2, 3, 4, 6-tetra-*O*-methyl-D-glucose in the tetra-methyl fraction of the neutral hydrolyzate indicates that the non-reducing ends of the glucan are occupied by the glucopyranose residues. The characterization of the two trimethyl sugars, 2, 3, 6-tri- and 2, 4, 6-tri-*O*-methyl-D-glucose, shows the existence of two kinds of linkages, 1→4 and 1→3, in the main a chain. The presence of a considerable amount of 2, 3-di-*O*-methyl-D-glucose suggests that the glucose residues at the branch points are joined through C_1, C_4 and C_6 and that the branches

5) J. R. Colvin, W. H. Cook and G. A. Adams, *Can. J. Chem.*, **30**, 603 (1952).
6) E. L. Hirst, L. Hough and J. K. N. Jones, *J. Chem. Soc.*, **1949**, 928.

originate from certain glucose units linked through the C_1 and C_4 positions and not those through the C_1 and C_3 positions in the chain. On the basis of the above results, one of the possible structures for the repeating unit of the glucan may be given as follow:

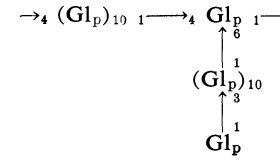

(Gl_p represents the glucopyranose unit)

However, it is not possible to stipulate exactly the distribution of 1→3 and 1→4 linked glucopyronose units in the polysaccharide in the light of present knowledge.

Further support for the proposed structure for the pectic acid was obtained from periodic acid oxidation studies of the pectic acid. It was found that one molar proportion of formic acid was liberated for every 30 mol. of anhydrouronic acid residues in 28 hr. and that 0.94 mol. of the oxidant were consumed per anhydrouronic acid residue in 30 hr., the theoretical figure for the consumption of periodate being 0.96 mol. The findings regarding periodate uptake are thus in good agreement with those theoretically expected.

The molecular weight of the methylated pectic acid, as determined by the light-scattering method, is 1.50×10^5.

The pectic acid obtained from the pulp of the jackfruit is similar to those obtained from apple,[7] strawberry,[8] citrus,[9,9a] and sisal.[10] The pectic acid obtained from these sources is generally associated with a neutral polysaccharide such as araban and galactan. In the case of jackfruit pectic acid, the neutral component is a glucan of a rather unusual structure, one which is similar to that isolated from mangifera indica.[11]

Experimental

All specific rotations are equilibrium values. Unless otherwise stated, all evaporations were carried out in vacuo at 30~40°C. Paper partition chromatography was carried out on Whatman No. 1 filter paper with the following solvent systems (v/v): (A) ethyl acetate: pyridine: water (8:2:1); (B) *n*-butanol: acetic acid: water (4:1:5) upper layer; (C) *n*-butanol: ethanol: water (40:11:19); (D) ethyl methyl ketone-water azeotrope; (E) *n*-butanol: ethanol: water (5:1:4) upper layer; (F) ethyl acetate: acetic acid: water (9:2:2). The spray reagents used were: (a) aniline hydrogen oxalate (a saturated aqueous solution), (d) *p*-anisidine hydrochloride (a 3% solution in butanol). Unless otherwise stated, the R_G values of methyl sugars refer to rates of movement relative to 2, 3, 4, 6-tetra-*O*-methyl-D-glucose in solvent E. Methyl sugars were demethylated with hydrobromic acid.[12]

The Isolation and Examination of Water-soluble Polysaccharides.—The pulp of jackfruit was freed from the seed and pericarp, and the soft fleshy material was macerated in a blender in the presence of ethanol. After the product had been kept overnight, the slurry was filtered through a cloth and the residue dried in air. The material (100 g.) so obtained was allowed to swell in water (2 l.); it was then heated, while being stirred, on a boiling-water bath for 4 hr. The slurry was diluted with water (2 l.) and filtered through a cloth. The filtrate was further clarified by passing it through a Cepa supercentrifuge, and the polysaccharide was precipitated as a white gelatinous material by adding thrice its volume of acidified ethanol. The precipitate was filtered, washed with ethanol, triturated and dried. The material isolated gave a blue color when iodine was added, indicating the presence of starch which was removed by the action of diastase. The polysaccharide recovered in the usual way was a white amorphous powder; yield, 18 g.; moisture, 8.8%; ash, 1.02%; OMe,[13] 1.1%; nitrogen, nil; equivalent weight, 388.9; anhydrouronic acid,[14] 46.76%; $[\alpha]_D^{29}+168.7°$ (*c* 1.1, in water). The water-extracted polysaccharide (0.8 g.) was heated with 1 N sulfuric acid (50 ml.) for 10 hr. on a boiling water-bath when the hydrolysis, followed iodometrically,[15] was complete. The cooled solution was neutralized, and the filtrate was concentrated to a sirup. On paper chromatography using solvents A, B and F, the sirup was found to contain rhamnose, xylose, arabinose, glucose, galactose and galacturonic acid. A portion of the sirup (460 mg.) was separated on a cellulose column (60×3.5 cm.), using *n*-butanol half-saturated with water as the eluent, to give five fractions and the sugars L-rhamnose, D-xylose, L-arabinose, D-glucose and D-galactose were identified through their specific rotations and the preparation of suitable crystalline derivatives. The sixth fraction, obtained as barium salt by elution with water, was deionised with Amberlite IR-120 (H) to give D-galacturonic acid, which was characterised through its specific rotation and the preparation of crystalline mucic acid.

The Isolation and Purification of Pectic Acid from Jackfruit Pulp.—The residue left (1.5 kg.) after the water-soluble polysaccharide had been removed from the jackfruit pulp was treated with

7) E. L. Hirst and J. K. N. Jones, ibid., **1939**, 454.
8) G. H. Beavan and J. K. N. Jones, ibid., **1947**, 1218.
9) G. H. Beavan, E. L. Hirst and J. K. N. Jones, ibid., **1939**, 1865.
9a) S. Luckett and F. Smith, ibid., **1940**, 1106.
10) G. O. Aspinall and A. Cañas-Rodríguez, ibid., **1958**, 4020.
11) A. Das and C. V. N. Rao, unpublished results.
12) L. Hough, J. K. N. Jones and W. H. Wadman, *J. Chem. Soc.*, **1950**, 1702.
13) E. P. Clark, "Semi-micro Quantitative Organic Analysis," Academic Press, Inc., New York (1943), p. 68.
14) C. Doree, "The Methods of Cellulose Chemistry," 2nd ed., Chapman & Hall Ltd., London (1947), p. 391.
15) F. L. Baker and H. F. E. Halton, *Biochem. J.*, **14**, 754 (1920).

a 0.5% ammonium oxalate solution (12 l.) and the polysaccharide was isolated as usual. A calcium chloride solution (5%) was added to a 2% aqueous solution of this material until no further precipitate was formed. The resulting calcium pectate was suspended in water (1 l.) and heated at 90°C for one hour with ammonium oxalate (6 g.). The calcium oxalate was then filtered off, and the polysaccharide was precipitated by adding ethanol. The above process was repeated once more, after which the solution was dialysed aganst distilled water and then treated with diastase. The purified polysaccharide was isolated in the usual way; yield, 85 g. The hydrolysis of the polysaccharide, followed by a chromatographic examination of the resulting sirup, revealed the presence of galacturonic acid and glucose, together with trace amounts of arabinose. D-Galacturonic acid and D-glucose were characterised through their crystalline derivatives. A portion of the ammonium pectate in the aqueous solution was passed through a column of Amberlite IR-120(H); the pectic acid so obtained had $[\alpha]_D^{29}$ +229° (*c* 0.45, in water) [equiv. 221 corresponds to 79.6% of anhydrouronic acid; found: anhydrouronic acid, 81.5%]; OMe, 1.3%.

The Attempted Fractionation of Ammonium Pectate.—(1) A suspension of crude ammonium pectate (40 g.) in ethanol (800 ml.) was treated with a sodium hydroxide solution (40%, 50 ml.) and the mixture kept at 2°C for 48 hr. while occasionally being shaken. After filtration the solid was washed with ethanol-water (1 : 1). An equal volume of ethanol was added to the aqueous solution to precipitate sodium pectate. The product, after extraction with hot ethanol-water (1 : 1), was dissolved in water, precipitated as calcium pectate, and finally converted into ammonium pectate. The above process was repeated once more to yield a polysaccharide (29 g., sample A); $[\alpha]_D^{29}$ +213.4° (*c* 0.6, in water), [equiv. 203 corresponds to 86.7% of anhydrouronic acid; found: anhydrouronic acid, 87.5%]. The hydrolysis of a portion of sample A yielded galacturonic acid, glucose, and a trace of arabinose; the amount of glucose was estimated[16] and found to be 9.5%.

(2) A solution of crude ammonium pectate (15 g.) in water (700 ml.) was treated with an aqueous solution of "Cetavlon" (cetyltrimethylammonium bromide) (10%, 200 ml.); the precipitate was then filtered. 5 N-Acetic acid was stirred into an aqueous suspension of the precipitate to decompose the complex. The polysaccharide was precipitated by ethanol, redispersed in water, shaken for 2 hr. with Amberlite IR-120(H) and filtered. The pectic acid was precipitated as usual and subjected to further purification as above to yield a polysaccharide (9.5 g., sample B); $[\alpha]_D^{29}$ +209.5° (*c* 0.5, in water) [equiv. 217 corresponds to 81.1% of anhydrouronic acid; found: anhydrouronic acid, 84.5%]. The hydrolysis of a portion of sample B gave galacturonic acid, glucose, and arabinose.

(3) An aqueous solution of crude ammonium pectate (2%, 500 ml.) was precipitated with acetone (600 ml.). The process was repeated several times, and the polysaccharide was extracted with hot ethanol-water (1 : 1) and reprecipitated from the aqueous solution by adding ethanol. The polysaccharide (5 g., sample C) had $[\alpha]_D^{29}$ +202° (*c* 0.7, in water) [equiv. 219 corresponds to 80.3% anhydrouronic acid; found: anhydrouronic acid, 81.7%]. The hydrolysis of a sample yielded galacturonic acid, glucose, and arabinose.

Repeated purification by each of these methods did not increase the uronic acid content.

The Electrophoresis of the Polysaccharide.—The purified polysaccharide (116 mg., sample A) was dissolved in a 0.1 M phosphate buffer (10 ml., pH 7.1). The solution was centrifuged on a high speed centrifuge at 20000 G for 15 min. in order to clarify it. The supernatant liquor was dialysed against the same buffer (500 ml.) for 18 hr. at 15°C. The conductivity of the resultant solution was determined, after which electrophoresis was carried out in a Perkin-Elmer electrophoresis apparatus (Model 38A) at 15°C using a potential gradient of 7.0 V./cm. Photographs of the migrating boundaries were taken at the beginning and at regular intervals. The photographs shown above were taken after one hour interval; the boundaries became diffused afterwards.

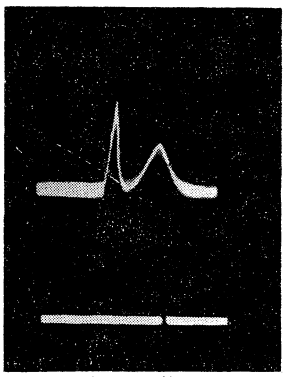

Descending

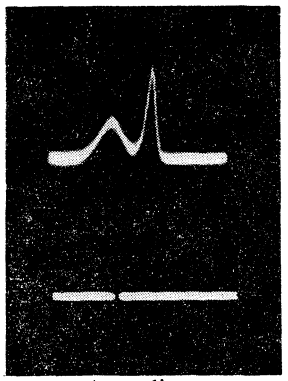

Ascending

Photo. 1

The Mild Hydrolysis of Ammonium Pectate.—Ammonium pectate (5 g., sample A) was heated with 0.1 N sulfuric acid (200 ml.) for 50 hr. at

16) E. L. Hirst and J. K. N. Jones, *J. Chem. Soc.*, **1949**, 1659.

85~90°C. The solution was then neutralized, filtered, and deionised by passing it through Amberlite IR-120(H). The acid was absorbed on a column of Dowex 1X-4 anion-exchange resin, and the column was freed from neutral sugars by washing it with water. The acid was displaced from the column by sulfuric acid, neutralized, and filtered, and the filtrate was deionized and concentrated to a sirup. The paper chromatographic examination of the sirup using solvent F gave a single spot corresponding to galacturonic acid; [6] $[\alpha]_D^{30}$ +80.5°, equiv. 188. The acid was characterised as D-galacturonic acid by converting it to crystalline D-galactose and to mucic acid.

The Methylation of Ammonium Pectate.—Ammonium pectate (22 g., sample A), was methylated by treatment with methylsulfate and sodium hydroxide[17] and then with methyl iodide and silver oxide,[18] according to the method adopted by Aspinall et al.,[10] to yield a methylated polysaccharide (15.3 g.), $[\alpha]_D^{29}$ +196° (*c* 0.8, in chloroform), OMe 39.8%. The methylated polysaccharide (15 g.) was purified by treating it with cold ethanolic sodium hydroxide according to the method of Aspinall et al.[10] The resulting methylated sodium pectate was converted into methylated methyl pectate (9.7 g.), which showed no hydroxyl absorption band in the infrared spectrum, $[\alpha]_D^{29}$ +208° (*c* 1.1, in chloroform) (Found: OMe, 40.5. Calcd. for $C_8H_{14}O_6$: OMe, 42.6%).

The Molecular Weight Determination of the Methylated Methyl Pectate.—All measurements of the intensities of scattered light for the molecular weight determination of the methyl pectate were carried out with a Brice-Phoenix light-scattering photometer (Model OM 1000A) using a semi-octagonal cell. The concentration used was over a range of $(0.4\sim3.0)\times10^{-3}$ g./ml. The molecular weight was found to be 1.503×10^5 as calculated by the dissymmetry method.[19] The value of *r*, corresponding to the root-mean-square end-to-end distances of the polymer, was calculated to be 1998 Å for the methylated polysaccharide at the wavelength of 5461 Å.

The Methanolysis of the Methylated Methyl Pectate and the Separation of Neutral and Acidic Methyl Sugars.—A solution of methylated methyl pectate (3.5 g.) in methanolic hydrogen chloride (4%, 125 ml.) was heated in a sealed tube at 100°C for 8 hr. Neutralization, filtration and evaporation yielded a sirup which was then heated with a barium hydroxide solution (2%, 50 ml.) at 80°C for 4 hr. The solution, after having been neutralized by passing carbon dioxide gas through it, was filtered and passed through a column of Amberlite IR-120(H) and Dowex 1 X-4 (bicarbonate form). The neutral solution was evaporated to a sirup, and the resulting mixture of methyl glycosides was hydrolysed with 1 N hydrochloric acid at 100°C for 8 hr. The hydrolyzate was neutralised (silver carbonate) and filtered, and the resulting solution after deionization was evaporated to a sirup (346 mg.). On paper partition chromatography using solvents D and E, the sirup gave four spots corresponding to 2, 3, 4, 6-tetra-, 2, 3, 6-tri-, 2, 4, 6-tri-, and 2, 3-di-*O*-methyl-D-glucose.

The mixture of neutral methyl sugars (ca. 335 mg.) was separated on Whatman No. 3MM papers using solvent D. The respective zones were eluted with water and evaporated to sirups.

The Identification of 2, 3, 4, 6-Tetra-O-methyl-D-glucose.—The sirup (15.5 mg.) had $[\alpha]_D^{29}$ +82° (*c* 0.4, in water) and R_G 1.0. Demethylation gave glucose. The sugar was characterised as 2, 3, 4, 6-tetra-*O*-methyl-D-glucose by conversion into the crystalline aniline derivative; m. p. and mixed m. p. 136~137°C; lit.[20] 136~138°C.

The Identification of 2, 3, 6-Tri-O-methyl-D-glucose.—The sirup (150.2 mg.) had $[\alpha]_D^{29}$ +67° (*c* 0.8, in water) and R_G 0.82 (Found: OMe, 41.6. Calcd. for trimethyl hexose: OMe, 41.8%). Demethylation gave glucose. The 2, 3, 6-tri-*O*-methyl-D-glucose was identified by preparing crystalline 2, 3, 6-tri-*O*-methyl-D-glucose-1, 4-di-*p*-nitrobenzoate; m. p. and mixed m. p. 190~191°C; lit.[21] 190~192°C.

The Identification of 2, 4, 6-Tri-O-methyl-D-glucose.—The sirup (148.1 mg.) with $[\alpha]_D^{29}$ +71° (*c* 1.0, in water), R_G 0.76 (Found: OMe, 41.1. Calcd. for trimethyl hexose: OMe, 41.8%.) gave glucose on demethylation. The sugar was identified as 2, 4, 6-tri-*O*-methyl-D-glucose by converting it to the crystalline anilide; m. p. and mixed m. p. 162~163°C; lit.[22] 162~166°C.

The Identification of 2, 3-Di-O-methyl-D-glucose.—The sirup (16 mg.) had $[\alpha]_D^{29}$ +65° (*c* 0.3, in water) and R_G 0.58. The sugar was characterised has 2, 3-di-*O*-methyl-D-glucose by conversion into 2, 3-di-*O*-methyl-D-gluconophenylhydrazide; m. p. and mixed m. p. 160~161°C; lit.[20] 160~162°C.

A portion of the mixture of methyl sugars was quantitatively separated by paper chromatography using solvent E, and each component was estimated by alkaline hypoiodite. The molar ratio of 2, 3, 4, 6-tetra-, to 2, 3, 6-tri- to 2, 4, 6-tri- to 2, 3-di-*O*-methyl-D-glucose was 1.0 : 10.2 : 9.8 : 1.1.

The Examination of the Acidic Component of the Methylated Methyl Pectate.—The Dowex 1 X-4 resin, after a thorough washing with water, was eluted with 1 N sulfuric acid (500 ml.). The eluted acid was neutralized ($BaCO_3$) and filtered, and the resulting solution was, after deionization, evaporated to a light yellowish sirup (2.95 g.).

The sirup (2.9 g.) was refluxed with methanolic hydrogen chloride (4%, 200 ml.) for 8 hr. The solution was neutralised, filtered and evaporated to a sirup. Lithium aluminium hydride (1.5 g.) in dry tetra hydrofuran (100 ml.) was added in portions with occassional shaking to the hot solution of the dry sirup in dry tetrahydrofuran (200 ml.). The mixture was heated for 1 hr., kept at room temperature for 2 hr., and then treated with water. The residue obtained after drying the mixture was extracted with acetone and ethanol;

17) W. N. Haworth, ibid., **107**, 8 (1915).
18) T. Purdie and J. C. Irvine, ibid., **83**, 1021 (1903).
19) P. Debye, *J. Phys. Chem.*, **51**, 18 (1947).
20) G. O. Aspinall, E. L. Hirst and W. McArthur, *J. Chem. Soc.*, **1955**, 3075.
21) P. A. Rebers and F. Smith, *J. Am. Chem. Soc.*, **76**, 6097 (1954).
22) H. Granichstädten and E. G. V. Percival, *J. Chem. Soc.*, **1943**, 54.

the combined extract was diluted with water, deionized, and evaporated. Hydrolysis of the resulting product, followed by the usual treatment, gave a sirupy mixture of sugars (2.36 g.).

The mixture of sugars (ca. 2.35 g.) was separated on a cellulose column (60×3.5 cm.) using solvent D, and the total eluate was separated into three fractions.

Fraction I.—The chromatographically-pure sirup (24.5 mg.) had $[\alpha]_D^{30}$ +112° (*c* 0.4, in water) and R_G 0.69 (Found: OMe, 41.6. Calcd. for trimethyl hexose: OMe, 41.8%). Demethylation gave galactose. The sugar was identified as 2, 3, 4-tri-*O*-methyl-D-galactose by conversion into a crystalline aniline derivative; m. p. and mixed m. p., 163~164°C; lit.[10] 163~165°C.

Fraction II.—The sirup (150.3 mg.) having $[\alpha]_D^{30}$ +82° (*c* 0.5, in water) gave galactose on demethylation. Paper partition chromatography using solvent D indicated that the mixture contained 2, 3, 4-tri-, and 2, 3-di-*O*-methyl-D-galactose.

Fraction III. — The sirup (2.05 g.) having $[\alpha]_D^{30}$ +79° (*c* 1.5, in water) and R_G 0.48 (Found: OMe, 29.6. Calcd. for dimethylhexose: OMe, 29.8%) was chromatographically homogenous and gave galactose on demethylation. The 2, 3-di-*O*-methyl-D-galactose was identified as its crystalline aniline derivative; m. p. and mixed m. p. 152~153°C; lit.[10] 152~154°C.

A small quantity of the mixture of methyl sugars was separated quantitatively by paper chromatrography, and the sugars were estimate by alkaline hypoiodite. The molar ratio of 2, 3, 4-tri- to 2, 3-di-*O*-methyl-D-galactose was 1 : 91.

The Periodate Oxidation of Ammonium Pectate.—The polysaccharide (sample A, 100.2 mg.) was dispersed in water (50 ml.) and oxidised by shaking it with 0.2 M periodic acid (50 ml.) in the dark at 15°C. The liberated formic acid and the amount of periodic acid consumed during the reaction were estimated in the usual way[23] at regular intervals. The liberation of formic acid became constant in 28 hr., corresponding to 30 mol. of anhydrouronic acid residues per mole of formic acid, while the periodate uptake became constant after 30 hr., corresponding to 0.94 mol. of the oxidant per anhydrouronic acid residue.

Summary

Water-soluble polysaccharide extracted from the pulp of jackfruit (*Artocarpus Integerifolia*) has been shown to be composed of L-rhamnose, D-xylose, L-arabinose, D-glucose, D-galactose and D-galacturonic acid. The jackfruit pectic acid has subsequently been extracted with ammonium oxalate and purified. The results of electrophoresis, mild hydrolysis and methylation studies indicate the presence of chains of 1 : 4 linked α-D-galacturonic acid residues in the pectic acid, which is physically associated with a neutral polysaccharide, a glucan. Periodate oxidation studies have also been reported.

The authors are grateful to Dr. P. Bagchi, Director of Research, East India Pharmaceutical Works, Ltd., Calcutta, for his valuable advice and his interest in this paper. They also wish to thank Dr. J. J. Ghosh and Dr. P. Sarkar of University College of Science and Technology, Calcutta, for conducting the electrophoresis experiment.

Department of Macromolecules
Indian Association
for the Cultivation of Science
Calcutta-32, India

23) P. Fleury and J. Lange, *J. Pharm. Chim.*, **17**(8), 107 (1933).

NOTES

A Spectrophotometric Study of the Metal Chelates of Resacetophenone Oxime. III. Nickel Chelate

By K. S. BHATKI,* A. T. RANE and M. B. KABADI**

(Received July, 16, 1963)

The first two parts of the study of resacetophenone oxime (RAPOX) chelates of copper and iron were published in the Proceedings of the Symposium on the Chemistry of Coordination Compounds, Agra, February, 1959. This paper is an extension of the study of RAPOX chelates of the nickel system.

Experimental

The Preparation and Standardisation of the Reagent Solutions.—*Nickel Solution.*—The solution of nickel sulphate was prepared using Merck's G. R. quality reagent. It was standardised using RAPOX.[1] The solution was found to be 7.675×10^{-2} M. Dilute solutions were prepared from the standard solution.

RAPOX.—RAPOX (resacetophenone oxime) was prepared and crystallised in a way which has been described previously.[2] The solutions of the required strength were prepared in freshly-distilled cyclohexanone using the recrystallised reagent.

Cyclohexanone.—Cyclohexanone of a B. D. H. technical quality was treated as described by Vogel[3] and distilled. A fraction distilling between 153°C and 156°C was collected and stored in amber-coloured glass-stoppered bottles.

The other reagents, such as glacial acetic acid, potassium dihydrogen phosphate, and sodium hydroxide, etc. were of either Merck's (G. R.) or B. D. H. (AnalaR) quality.

Besides cyclohexanone, the other organic solvents were used in the solubility study[4] of nickel RAPOXimate. They were chemically-pure reagents supplied by Eastman Organic Chemicals & Co.

Nickel RAPOXimate.—A measured volume of nickel solution was treated with a solution of sodium carbonate to neutralise the mineral acid present. The slight turbidity that developed was eliminated by adding dilute acetic acid. The pH of the resulting solution adjusted to a pH a little higher than 6.2, the required optimum pH for complete precipitation,[2] using sodium acetate. The nickel RAPOXimate was then precipiated by the dropwise addition of a two per cent alcoholic solution of RAPOX. After the precipitate had been digested for some time on a hot water bath, it was filtered using a sintered glass crucible with a porocity of 4 (2G4). It was then washed thoroughly free from impurities with hot distilled water. The precipitate was first dried in a vacuum desiccator to a constant weight. Thereafter the precipitate was dried in an air oven at 110°C. The weight of the precitate even after this treatment was the same, indicating the absence of water molecules in the complex in the solid state. It was preserved over fused calcium chloride in a desiccator.

A weighed quantity of the dried complex was treated in a silica crucible, first with nitric acid and then with perchloric acid. After the organic matter had been completely decomposed, the residue was treated in order to estimate the nickel volumetrically.[5] The nitrogen in the complex was also estimated by Kjeldahl's method.[6] The nickel and nitrogen contents were found to agree with the theory that the composition of the complex is $Ni(C_8H_8O_3N)_2$

The Spectral Study of Nickel RAPOXimate in Cyclohexanone.—A weighed quantity of nickel RAPOXimate was dissolved, and the solution made up to a known volume using freshly distilled cyclohexanone. The spectral examination of the resulting solution was first accomplished on a Beckman DU spectrophotometer, using cyclohexanone as a blank liquid. The detailed study was then carried out using a Lumetron photoelectric colorimeter, model 402-E. The data obtained from these experiments at different wavelengths are given in Fig. 1.

* Member, Chemistry Division, Atomic Energy Establishment Trombay, Government of India, Bombay.

** Present address: Maharshi Dayanand College, Bombay-12.

1) K. S. Bhatki and M. B. Kabadi, *J. Sci. Industr. Res.*, **11B**, 346 (1952); **12B**, 226 (1953).

2) K. S. Bhatki and M. B. Kabadi, *J. Univ. Bombay*, **24**(3), 51-57 (1955).

3) A. I. Vogel, "A Text Book of Practical Organic Chemistry," 3rd Ed., Longmans, Greeen & Co., London (1957), pp. 342-343.

4) K. S. Bhatki, A. T. Rane and M. B. Kabadi, *Proc. Indian Acad, Sci.*, **58A**(4), 202-208 (1963).

5) A. I. Vogel, "Quantitative Inorganic Analysis," 2nd Ed., Longmans, Green & Co., London (1953), p. 264.

6) J. J. Sudborough and T. C. James, "Practical Organic Chemistry," Blackie & Son Ltd., London (1937), p. 61.

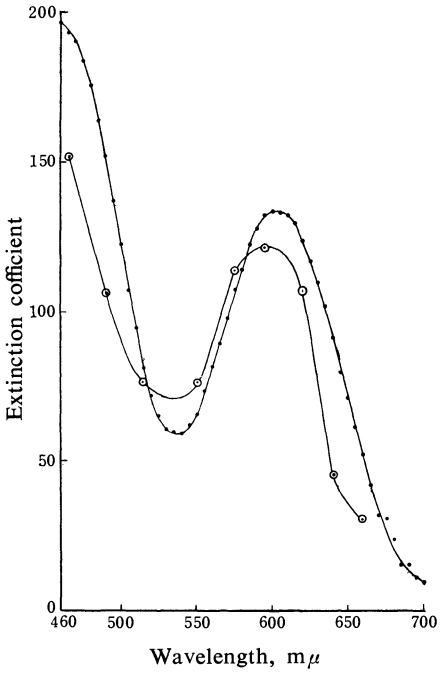

Fig. 1. Spectrum of nickel RAPOXimate in cyclohexanone in the visible region.
- Beckman spectrophotometer DU
- ⊙ Lumetron colorimeter-402E

A Standard Curve for Nickel.—Since the point of maximum absorption using the Lumetron was observed at 595 M (monochromatric filter), the obedience of Beer's law by the system was checked using the same filter. Several solutions of the complex in cyclohexanone, possessing different concentrations, were subjected to the Lumetron study. The results are recorded in Fig. 2. It is observed under these conditions that the smallest amount of nickel that can be determined is six parts per million. The molar extinction coefficient was found to be $\varepsilon_{595}=132.5$.

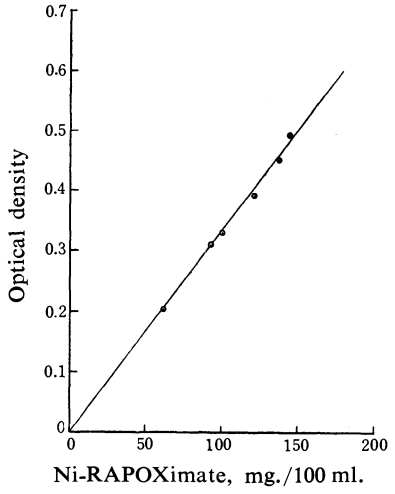

Fig. 2. Standard curve for nickel RAPOXimate in cyclohexanone using 595 M filter.

The Choice of the Solvent for the Extraction Study.—In order to extract nickel from an aqueous solution, it was necessary to choose a suitable water-immiscible solvent. A precise solubility study[4] of nickel RAPOXimate in a few typical water-immiscible solvents was, therefore, undertaken. The different solvents were benzene, nitrobenzene, chloroform, carbon tetrachloride, diisopropyl ether, *n*-butyl ether, amyl acetate, ethyl methyl ketone, methyl isobutyl ketone, diisobutyl ketone and cyclohexanone. In these experiments, the important observation was made that the same amount of nickel RAPOXimate present gave the same optical density, irrespective of the solvent employed, the monochromatic filter being also the same (595 M). Consequently, the standard curve for cyclohexanone can be used as a standard curve for the other solvents also. This observation establishes that the behaviour of nickel RAPOXimate in all the solvents is similar and shows neither association, dissociation nor any complex formation with the solvent itself if no such phenomenon existed in cyclohexanone. It can also be inferred from these findings that in all these solvents the molecular condition of the complex is the same.

Experiments were carried out at a temperature of 30±1°C. From these,[4] it was evident that the solubility of the complex in cyclohexanone was the maximum, 1.710 g. of nickel RAPOXimate per 100 ml. of the solution.

The Partition Study of Nickel RAPOXimate at Various pH Values.—A known and constant volume of the standard nickel solution was pipetted out into several glass-stoppered pyrex centrifuge

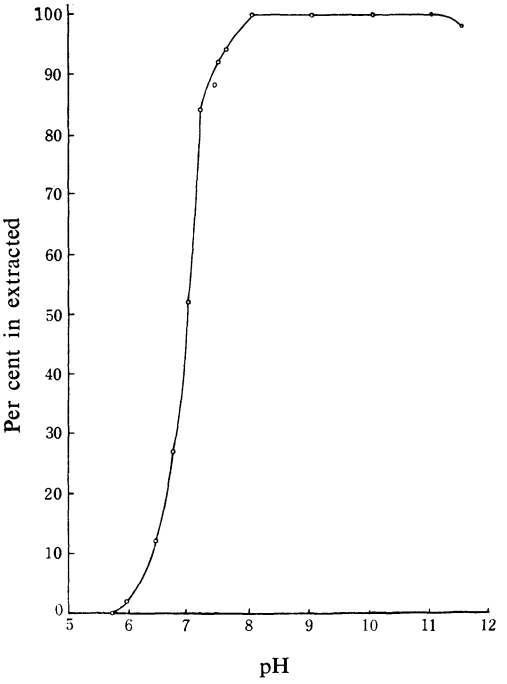

Fig. 3. Extraction of nickel at various pH using RAPOX in cyclohexanone.

tubes. To each of this was added a requisite amount of the buffer solution to fix the pH and then an equal volume of cyclohexanone containing RAPOX. For the sake of maintaining uniformity in the experiment, it was decided to take five times the amount of RAPOX required for the formation of 1 : 2 complex. The tubes were then shaken vigorously on a shaking machine for about eight hours. The phases were separated by centrifuging, and the optical density of the upper organic layer was noted using Lumetron 402-E and 595 M filter. The readings are shown in Fig. 3.

Composition of Nickel RAPOXimate.—The composition of the nickel complex of RAPOX was determined with the help of (i) Job's method[7] of continuous variation as extended to a two-phase system by Irving and Pierce[8] and (ii) the slope ratio method[9,10] modified similarly. These methods, which are generally applicable in case of complexes soluble in an aqueous medium or in an organic medium miscible with water, were employed because they could be so utilised in the present case with the same degree of accuracy. Moreover, the authors experienced no difficulty in extending the slope ratio method to a two-phase system.[11]

(*i*) *Job's Method.*—In this method x ml. of nickel sulphate solution (7.675×10^{-3} M) were mixed with a fixed volume of the buffer solution and diluted to 25 ml. $(10-x)$ ml. of the RAPOX solution of the same molarity in cyclohexanone diluted to 25 ml. was added to the former aqueous solution, and the mixture was shaken vigorously for a few minutes. The upper layer was then separated carefully after centrifuging and examined by Lumetron using a 595 M filter. The results are surveyed in Fig. 4.

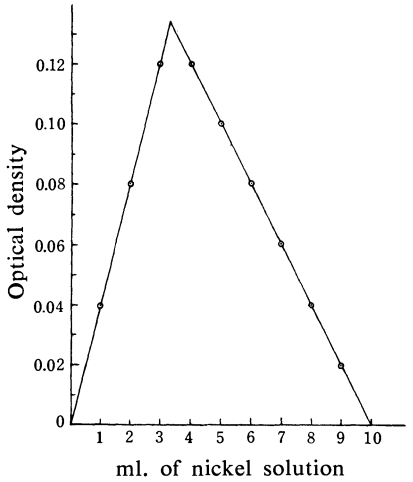

Fig. 4. Job's method in a two phase system.

(*ii*) *The Slope Ratio Method.*—For this purpose two sets of experiments had to be performed. In one, the volume of the nickel solution was kept constant, while that of the reagent was varied. In the other set the volume of the reagent in cyclohexanone was kept constant, whereas that of metal solution was varied. The molarity of the nickel solution and RAPOX in cyclohexanone was the same, namely, 9.225×10^{-3} M.

In the actual experiment different volumes of the standard nickel solution were diluted, each to a fixed volume of 25 ml., after the requisite buffer had been added to bring the pH to 9.0. This mixture was shaken for a few hours with an excess of RAPOX in cyclohexanone, the volume of which was also 25 ml.

In the second set the process was reversed. The volume of the standard RAPOX solution in cyclohexanone was varied and the volume of nickel solution, kept constant. The final volumes of both the aqueous and the organic phase were the same, namely, 25 ml.

The data so collected is surveyed in Fig. 5.

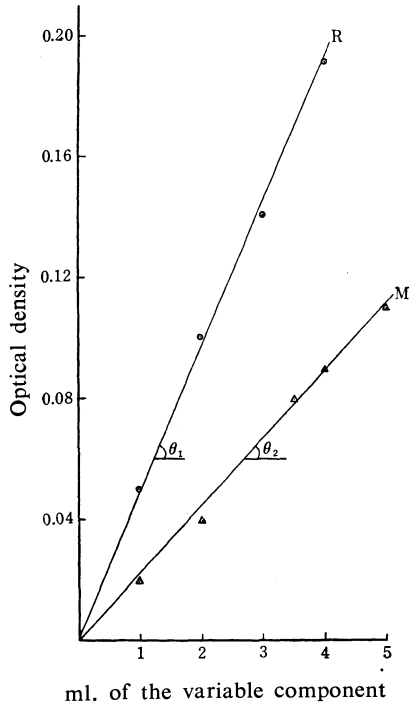

Fig. 5. Slope ratio method in a two phase system.
$\theta_1=67.2°$, $\theta_2=48°$
$\therefore \quad \dfrac{\tan\theta_1}{\tan\theta_2}=\dfrac{2.3789}{1.1106}=2.14$
⊙ RAPOX in constant excess
△ Ni in constant excess

Back Extraction.—Whenever the extraction of a metal chelate is achieved by an organic solvent, it becomes necessary to recover the metal in a pure form from the organic phase. For this purpose a back extraction study was undertaken.

7) P. Job, *Ann. Chim.*, **9(10)**, 113 (1928),
8) H. Irving and T. B. Pierce, *J. Chem. Soc.*, **1959**, 2565.
9) J. H. Yoe and A. L. Jones, *Ind. Eng. Chem., Anal. Ed.*, **16**, 111 (1944).
10) A. E. Harvey and D. L. Manning, *J. Am. Chem. Soc.*, **72**, 4488 (1950),
11) K. S. Bhatki, Ph.D. thesis, Univ. of Bombay, 1962, pp. 87, 102.

TABLE I. BACK EXTRACTION OF NICKEL FROM ORGANIC PHASE

10 ml. of cyclohexanone containing nickel-RAPOXimate (O. D.=0.59) is shaken for about 4 hr. with equal volume of aqueous solution at various pH.

Filter, 595 M Temp., 30±1°C Cuvette, 0.5 cm.

Nature of the aqueous solution	O. D. of the org. phase after shaking	Per cent of Ni back extrd.	Remarks
Dilute HCl about 1 N	0.00	100	Even hand shaking for a few minutes was sufficient.
Dilute acetic acid about 2N	0.00	100	RAPOX remained in the org. phase whereas nickel got back extrd. quantitatively as seen by dimethylglyoxime test on aq. phase.
Sodium acetate-HCl buffer pH=1.09	0.00	100	
Sodium acetate-HCl buffer pH=2.0	0.00	100	
M/20 K-biphthalate pH=4.05	0.00	100	
Borate Buffer pH=8.0	0.59	0.00	Neither the metal nor the reagent got transferred to the aq. phase.
Borax 0.01 M pH=9.14	0.59	0.00	
Dilute NaOH about 1 N	0.00	100	Reagent too was transferred to the aq. phase with the metal.

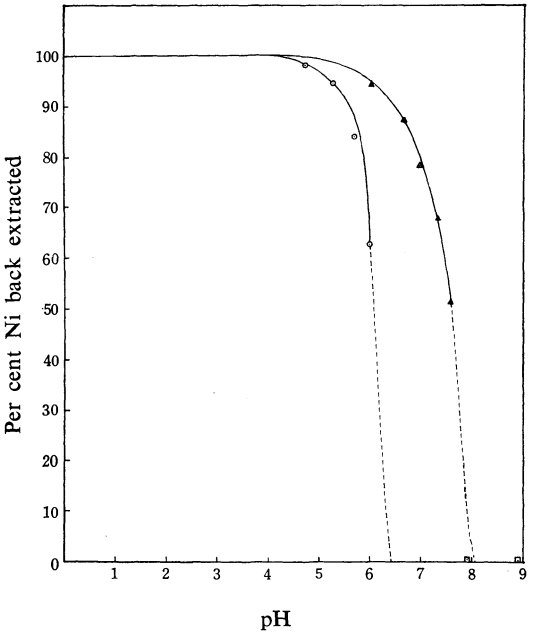

Fig. 6. Back extraction of nickel.
⊙ Phthalate buffer
△ Phosphate buffer
▣ Borate buffer

A cyclohexanone solution of the nickel complex of a known volume and possessing a known optical density was shaken for about four hours with the same volume of an acidic or alkaline solution. The organic layer was centrifuged and its optical density observed. It diminished with an increase in the acidity and also in the alkalinity. The results are given in Table I.

In another experiment a solution of nickel complex was prepared in cyclohexanone saturated with water. A known volume of this was shaken for about eight hours with an equal volume of a buffer solution previously saturated with cyclohexanone. The results are given in Fig. 6.

Discussion

The foregoing study shows a definite complex formation between nickel and RAPOX in the molecular ratio of 1 : 2. An important observation demanding careful consideration is that the extraction of this complex does not appear feasible below pH 6.0 and above 12.00. Under the former condition the formation of the complex is not quantitative, whereas in the latter circumstance the complex seems to decompose, resulting in the transfer of the reagent, along with the nickel ions, to the aqueous phase.

The plot in Fig. 4 is observed to consist of two intersecting straight lines. The point of intersection shows the presence of the complex in solution and corresponds to the concentrations of nickel and RAPOX given by the ratio 3.3 : 6.7 (i. e., 1 : 2). The inference follows that the composition of the complex must be $Ni(C_8H_8O_3N)_2$, in agreement with that composition determined for the complex in the solid state.

The plot in Fig. 4 is observed to be made up of perfectly straight lines, which suggests that a highly stable single complex is formed.

In the case of the slope ratio method, the ratio of slopes of the straight lines in Fig. 5 is found to be 2.14, confirming the formation of the complex containing nickel and RAPOX in the ratio 1 : 2, an inference drawn from Job's method.

Summary

RAPOX (resacetophenone oxime) in certain water-immiscible organic solvents is found to extract nickel from an aqueous medium as a nickel RAPOXimate complex. Cyclohexanone was found to be the best solvent for this

purpose. The brilliant green-coloured solution of the complex in cyclohexanone gave a maximum absorption at 600 mμ on a Beckman spectrophotometer DU. The coloured solution obeyed Beer's law in the lowest range—six parts per million. The extraction of this complex was quantitative in the pH range from 8 to 11.

The composition of the complex as determined by Job's method and the slope ratio method in a two-phase system was 1 : 2 (nickel to RAPOX). The back extraction study for the metal from the complex in the organic solvent was carried out and quantitative results obtained using an aqueous solution with a pH value below four.

The grateful thanks of the authors are due to Professor B. V. Thosar of the Tata Institute of Fundamental Research for making available the good working facilities of the Institute.

Tata Institute of Fundamental Research
Bombay-5, India (K. S. B. & A. T. R.)

Institute of Science
Bombay, India (M. B. K.)

*Some Observations on the Synthesis of 3-Bromofluorenone**

By Kazuo SUZUKI and Masaaki MOMOI

(Received July 30, 1963)

A synthetic pathway leading to 3-bromofluorenone by the following sequence has been investigated and found to result in a better yield than the method starting with 2-(4'-bromobenzoyl)-benzoic acid:[1] 2-Nitrofluorene→ 2-nitrofluorenone → 2-aminofluorenone (I) → 2-amino-3-bromofluorenone (II) → 3-bromofluorenone.

The deamination reaction of II is the crucial step in this route. Fletcher and Pan[2] attemted this reaction, but have not yet reported on the yield.

In the present work the deamination of II was carried out in an 82% yield by diazotization and decomposition in concentrated sulfuric acid. 2-Nitrofluorene, 2-nitrofluorenone[3] and I[4] were obtained in good yields. The bromination of I by the action of 48% aqueous hydrogen bromide in dimethyl sulfoxide[2] resulted in an 80% yield. However, in the present experiments we re-examined[5] the bromination of the same base by the action of an equimolar quantity of bromine in acetic acid; the main product was II (60%), accompanied by a small amount of a new bromoketone, III (6%, m.p. 254°C).

The following experiments proved that the bromine atoms were indeed in the 1, 3-positions of III. The analytical results agreed with a dibromo compound. Reduction and acetylation gave 1, 3-dibromo-2-aminofluorene and its acetyl derivative;[2] deamination gave 1, 3-dibromofluorenone.

The electron-releasing substituent at carbon 2 of I makes carbons 1, 3, 5 and 7 susceptible to an electrophilic attack. This was illustrated by the attack of the second bromine atom at the 1-position of the same ring. The same compound (92%) was obtained by the bromination of II.

Experimental[6]

Bromination of 2-Aminofluorenone (I). — Into a solution of 128 g. of I in 2140 ml. of acetic acid, 32.8 ml. of bromine in 50 ml. of acetic acid were stirred drop by drop over a 1.5 hr. period at about 20°C. The precipitate was filtered and digested with a hot dilute alkali solution; then it was filtered and washed with water. The crude product was extracted several times with hot benzene. The first fraction was a mixture of I, II and III. On being heated with alcohol, it was separated into a soluble (I and II) and an insoluble part (III).

The insoluble part was recrystallized from benzene to give III; 12.3 g. (6%), m. p. 254°C.

* Studies on Fluorene Derivatives. XXII. Part XXI: K. Suzuki and M. Fujimoto, **36**, 1654 (1963).

1) F. Ullmann and M. Sone, *Ann.*, **380**, 337 (1911); H. F. Miller and G. B. Bachman, *J. Am. Chem. Soc.*, **57**, 2444 (1935); K. Suzuki, S. Kajigaeshi and M. Sano, *J. Soc. Org. Synth. Chem. Japan* (*Yūki Gōsei Kagaku Kyōkaishi*), **16**, 82 (1958).

2) T. L. Fletcher and H.-L. Pan, *J. Am. Chem. Soc.*, **78**, 4812 (1956). The yield was not good according to a private communication from Dr. M. J. Namkung of the same laboratory.

3) O. Diels, *Ber.*, **34**, 1758 (1901).

4) C. L. Arcus and M. M. Coombs, *J. Chem. Soc.*, **1954**, 3978.

5) T. L. Fletcher, M. J. Namkung and H.-L. Pan, *Chem. & Ind.*, **25**, 660 (1957).

6) All melting points are uncorrected.

Found: C, 44.39; H, 2.20; N, 3.88; Br, 45.55%. Calcd. for $C_{13}H_7ONBr_2$: C, 44.23; H, 2.00; N, 3.97; Br, 45.27%.

IR: 3380, 3280 (ν N-H), 1710 (ν C=O), 1600 cm^{-1} (δ N-H).

III was acetylated, and the product was recrystallized from benzene, melting at 248~249°C.

Found: N, 3.37; Br, 40.46%; Calcd. for $C_{15}H_9O_2NBr_2$: N, 3.55; Br, 40.45%.

IR: 3175 (ν N-H), 1710 cm^{-1} (ν C=O).

The soluble part was evaporated to dryness, and the residue was extracted with hot dilute hydrochloric acid. Crude I (12.4 g.) was recovered by the addition of alkali. II (41 g.) was obtained from the acid-insoluble part.

A small amount of III was isolated from the benzene mother liquor by means of chromatography in benzene on alumina. On the other hand, the second and later benzene extractions contained II almost entirely; this was recrystallized from benzene to give 55.6 g. (total 96.6 g., 60%) (m. p. 215°C).

3-Bromofluorenone. — Finely-powdered sodium nitrite (13 g.) was stirred into a solution of 42.8 g. of II in 234 ml. of concentrated sulfuric acid over a period of 1 hr. at 10~15°C. Stirring was continued for an additional 30 min., and then the brown, diazotized solution was poured into 750 g. of ice, and 310 ml. of 50% hypophosphorous acid was added to the reaction mixture. Upon gradual heating, the vigorous evolution of nitrogen occurred at 60°C; after this stirring was continued at 80°C for 20 min.

The yellow precipitate was filtered and chromatographed in benzene on alumina. The crude product was recrystalized from benzene; weight, 33 g. (82%); m.p. 164~165°C, IR: 1703 cm^{-1} (ν C=O); this compound was identified by melting point and mixed melting point determination and by comparing its infrared absorption spectrum with an authentic sample of 3-bromofluorenone.

Deamination of III, the New Bromoketone (M.p. 254°C).—This deamination was carried out under the same conditions as in the case of II. 1,3-Dibromofluorenone was obtained from the mixture of 3 g. of III, 16.4 ml. of sulfuric acid, 0.87 g. of sodium nitrite and 21.9 ml. of hypophosphorous acid. The crude product was recrystallized from benzene to yield 2.3 g. (80%); m.p. 216~218°C (reported[7] m.p. 225°C), (Found: Br, 46.84%; Calcd. for $C_{13}H_6OBr_2$: Br, 47.28%; IR: 1710 cm^{-1} (ν C=O)).

Reduction of III.—a) A mixture of 0.5 g. of III in 6 ml. diethylene glycol, and 1 ml. of 50% hydrazine hydrate was heated under reflux at 160°C for 1 hr. and at 200°C for 2 hr. The reaction mixture was poured into water, and the product was filtered and recrystallized from cyclohexane to give 1,3-dibromo-2-aminofluoren (0.36 g. (74%), m. p. 183~185°C). (Found: Br, 47.58%; Calcd. for $C_{13}H_9NBr_2$: Br, 47.14%). IR: 3240 cm^{-1} (ν N-H), 1610 cm^{-1} (δ N-H). This was identified with an authentic sample by mixed melting point determination and infrared spectrum comparison.

b) A mixture of 0.5 g. of the same sample, 31 ml. of acetic acid, 3 ml. of hydrogen iodide and 0.1 g. of red phosphorus was refluxed for 7 hr. When poured into cold water, 2-aminofluorene (m.p. 125.5~127.5°C; 0.12 g., 46%) was obtained.

Bromination of II.—A solution of 1.6 g. of bromine in 5 ml. of acetic acid was vigorously stirred into 274 g. of II in 200 ml. of acetic acid over a period of 20 min. at 20°C. The product deposited was filtered, washed with water, and then recrystallized from benzene to give III (m.p. 254°C, 1.6 g.). From the mother liquor, 1.4 g. of II was recovered (balance yield, 92%).

The authors wish to express their gratitude to Drs. John and Elizabeth Weisburger of the National Institutes of Health, U.S.A., for valuable information, and also to Dr. Moses J. Namkung and Dr. Nobuo Ishikawa of the University of Washington, Seattle, for furnishing helpful information on the diazotization of 2-amino-3-bromofluorenone.

Department of Chemistry
Faculty of Technology
Yamaguchi University
Tokiwadai, Ube

Semiconductivity and Color of Pyranthrene

By Mizuka SANO and Hideo AKAMATU

(Received August 22, 1963)

The color of pyranthrene is a reddish brown. However, in the process of purification by a sublimation method, a yellow-colored pyranthrene is often obtained. When pyranthrene is sublimed slowly in the relatively high vacuum of 10^{-4} mmHg, a brown powder is obtained, whereas rapid sublimation in a low vacuum ($10^{-1}\sim10^{-2}$ mmHg) produces a soft yellow powder. The latter is also obtained when a molten sample is vaporized onto a cold glass plate. These two forms of pyranthrene with different colors can be changed to each other by the sublimation procedure; thus, we can obtain the yellow powder from the brown one, and vise versa.

The semiconductivities of these two forms of pyranthrene are of interest in relation to their crystal structures and absorption spectra; this paper will concern itself with these questions.

Pyranthrene was obtained from pyranthrone by zinc-dust fusion.[1] It was purified by a combination of repeated sublimations in vacuo and prolonged boiling in benzene. The two forms of powder were prepared by the procedure described above. A film specimen for each form was also made on a glass plate by a sublimation procedure in the way mentioned above. A single crystal, approximately $5\times0.1\times0.03$ mm^3, was grown in a sealed glass tube by a slow sublimation method. This crystal is brown in color.

The electrical resistivity (ρ) was measured by means of a dc method as a function of the temperature, which ranged from 40 to 200°C for the single crystal, both compressed powders (with the pressure of 116 kg./cm^2) and film specimens in vacuo. The results are summarized in Table I, where the ε-value, the energy gap or twice the activation energy for conduction, can be observed to be definitely lower for the yellow form than for the brown form.

TABLE I. SEMICONDUCTIVE DATA FOR PYRANTHRENE

		ε, eV.	ρ_{15}°, Ω·cm.
Single crystal		1.8	1.4×10^{15}
Powder	Brown	1.6	1.7×10^{16}
	Yellow	1.2	1.3×10^{14}
Film	Brown	1.7	7.3×10^{14}
	Yellow	1.1	3.0×10^{16}

1) E. Clar, *Ber. deut. Chem. Ges.*, **72**, 1648 (1939).

The absorption spectra of pyranthrene in a solid state and in a solution are shown in Fig. 1. Both forms of pyranthrene gave the same absorption spectrum when they were dissolved in benzene. However, film specimens of two forms gave different spectral curves. The brown form exhibited its absorption maxima at 516, 468, 429 and 358 mμ, while the yellow form showed its maxima at 491, 417 and 358 mμ. The absorption at 358 mμ corresponds to the β-band of the molecular spectrum, while the others correspond to the para-band. However, when a KBr-disk technique was employed for the powder specimens, both forms gave the same spectral curve, with absorption maxima at 498, 449 and 425 mμ. Furthermore, both forms exhibited the same fluorescence spectrum.

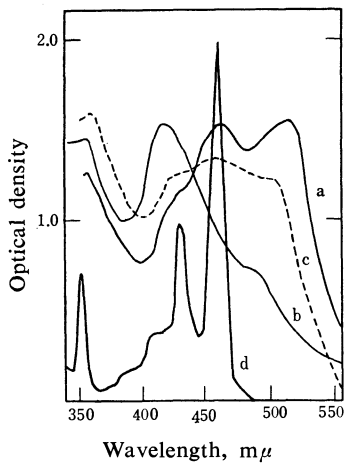

Fig. 1. Absorption spectra of pyranthrene.
(a) Brown film
(b) Yellow film
(c) KBr-disk of powder
(d) Solution in benzene

X-ray diffraction patterns for the powder specimens were obtained with the aid of a diffractometer. The patterns are shown in Fig. 2, which shows that the reflection peaks of the brown form are sharp and distinct, while those of the yellow form are very broad and diffuse. However, the crystal structure may be assumed to be the same for both forms.

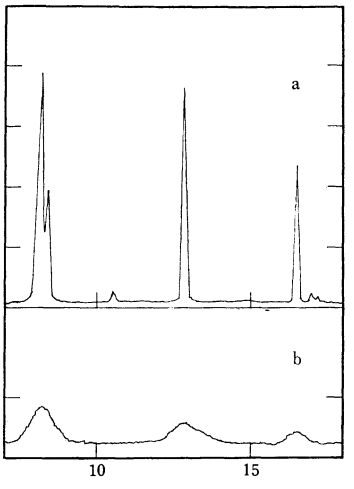

Fig. 2. X-ray diffraction patterns of (a) brown form and (b) yellow form (CuK_α).

An electron microscope revealed that both forms of powder and film specimens consist of flake-like minute crystals. The electron diffraction gave the same powder pattern for both forms of specimen; however, intensive spots could be observed in the reflection rings for the brown form but not for the yellow form.

All of these observations lead to the conclusion that the principal structure is the same for these two forms of pyranthrene, but that they result from different degrees of crystallinity. The yellow form consists of crystallites less perfect than those of the brown form.

The variation in apparent color may be explained mainly by the effect of the light scattering, which varies with the mode of aggregation of crystallites and hence depends on their crystallinity.

It is of interest to see that different semiconductive data were obtained for two forms of pyranthrene. If it can be assumed that the observed value of ε for the brown form corresponds to the intrinsic energy gap for pyranthrene, the lower value of activation energy observed for the yellow form can be related to an extrinsic conduction process which is associated with imperfections in the crystal.

Northrop and Simpson[2] and Parkyns and Ubbelohde[3] have observed the effect of impurities on the semiconductivity of organic crystals. Inokuchi and Ohki[4] have shown that the semiconductive data for pyrene varied according to the purification procedures. Eley and Parfitt[5] and Wihksne and Newkirk[6] have found that the semiconductivity of phthalocyanine changes with the transformation of the crystal structure. The present investigation has found an example of the semiconductivity of an organic crystal which is structure-sensitive and which varies with its crystallinity.

Department of Chemistry
Faculty of Science
The University of Tokyo
Hongo, Tokyo

2) D. C. Northrop and O. Simpson, *Proc. Roy. Soc.*, **A234**, 124 (1956).
3) N. Parkyns and A. R. Ubbelohde, *J. Chem. Soc.*, **1960**, 4188.
4) H. Inokuchi and K. Ohki, This Bulletin, **36**, 105 (1963).
5) D. D. Eley and G. D. Parfitt, *Trans. Faraday Soc.*, **51**, 1529 (1955).
6) K. Wihksne and A. E. Newkirk, *J. Chem. Phys.*, **34**, 2184 (1961).

The Polymerization of Trioxane Catalyzed by Rhenium Pentachloride and Molybdenum Pentachloride

By Hajime MIYAMA and Mikiharu KAMACHI

(Received August 24, 1963)

It is well known that the polymerization of trioxane is catalyzed by such Lewis acids as boron fluoride, tin(IV) chloride and antimony-(V) chloride.[1] Also, it has been recently found[2] that rhenium pentachloride and molybdenum pentachloride act as Lewis acids and are effective catalyst for alkylation and carbonylation. Therefore, the present authors have tried to polymerize trioxane by using these catalysts. Three types of polymerization, that is, solid state polymerization by the simultaneous sublimation of monomer and catalyst,[3]

1) S. Okamura, T. Higashimura and M. Fugawa, *J. Chem. Soc. Japan, Ind. Chem. Sec.* (*Kogyo Kagaku Zasshi*), **66**, 712 (1962); S. Okamura, T. Higashimura and K. Takeda, *Makromol. Chem.*, **51**, 217 (1962).

2) J. Tsuji and M. Morikawa, Private Communication.

3) H. Miyama and M. Kamachi, *J. Polymer Sci.*, **B 1**, 465 (1963).

solution polymerization, and bulk polymerization, were performed.

In the solid state polymerization by simultaneous sublimation, commercial trioxane (American Celanese Co.) was purified by repeated sublimation at a high vacuum and then introduced, at the pressure $10^{-4}\sim10^{-5}$ mmHg, into an ampoule cooled by liquid nitrogen. At the same time, the desired quantity of rhenium pentachloride or molybdenum pentachloride, which had also been purified by repeated vacuum sublimation, was introduced into the ampoule. After it had been sealed off, the ampoule was placed in a thermostat of a definite temperature for a definite time and then opened. In this reaction, as soon as the polymerization occurred, the color of the reaction system changed from yellow to blue-violet in the case of rhenium pentachloride, and from light yellow to dark yellow in the case of molybdenum pentachloride. The polymer obtained was washed completely with benzene, methyl alcohol, and water to remove any unreacted monomers and catalyst. The inherent viscosity of the polymer was measured in a *p*-chlorophenol solution (0.1 g./100 ml.) containing 2% of α-pinene by using a Ostwald viscometer at 60°C. The results obtained are shown in Table I.

Table I

Catalyst	Concn. of catalst wt. %	Polymn. time min.	Polymn. temp. °C	Yield %	η_{inh}
$ReCl_5$	0.6	60	62	90.5	2.60
			65	84.5	2.81
			43	81.4	2.77
			−10	25.0	3.11
$MoCl_5$	0.6	30	62	93.3	1.36
			50	82.7	0.71
			30	63.1	1.43
			21	64.3	1.47
			0	23.9	2.14
			−10	20.7	1.77
			−20	20.1	1.82

In the solution polymerization, 0.1 g. of the catalyst was dissolved or suspended in 50 cc. of benzene or another solvent. This solution was then mixed with a solution consisting of 20 cc. of benzene and 10 g. of trioxane. The mixture was made to react in the stream of nitrogen. The color of the system changed as soon as the polymerization occurred. For example, when rhenium pentachloride was used in a benzen-ethyl chloroacetate solution, the color changed from green to gray-green. The results are shown in Table II where "solvent" means the reagent used for dissolving of dispersing the catalyst.

In the bulk polymerization, 2 g. of trioxane and 0.01 g. of the catalyst were dispersed into 10 cc. of petroleum ether. After moisture and air had been removed by evacuation at the temperature of liquid nitrogen, the petroleum ether was evaporated; the reaction vessel was then sealed off and kept at 80°C for one hour. Results are shown in Table III.

In the solid state polymerization of trioxane by the simultaneous sublimation of monomer

Table II

Catalyst	Solvent	Polymn. time hr.	Polymn. temp. °C	Yield %	η_{inh}
$ReCl_5$	Benzene	4	60	88	0.63
	Benzene	2	40	34	0.63
	Benzene	4	40	46	0.80
	Ethylene dichloride	2/3	40	91	0.37
	Cyclohexane	1	40	48	0.85
	Acetone	1	40	62	0.64
	Methyl ethyl ketone	1	40	54	0.81
	Tetrahydrofrane	1	40	18	0.59
	Ethyl chloroacetate	2/3	40	93	0.65
	Ethyl chloroacetate	1	25	90	0.76
$MoCl_5$	Benzene	4	60	54	0.65
	Benzene	4	55	52	0.71
	Benzene	3	40	47	0.64
	Cyclohexane	3	55	69	0.88
	Cyclohexane	5.5	40	66	0.78
	Acetone	3	40	74	0.66
	Acetone	3	25	52	0.73
	Ethyl chloroacetate	3	40	91	0.75
	Ethyl chloroacetate	3	25	87	0.68

TABLE III

Catalyst	Yield, %	η_{inh}
$ReCl_5$	90	1.6
$MoCl_5$	70	1.4

and iodine,[3] it was once suggested by the present authors that the initiation of radical polymerization takes place in association with the crystal dislocations caused by the simultaneous sublimation and that polymerization occurs in the temperature range between 0°C and 15°C. However, the situation is very different for the present case because the polymerization occurs even at the temperature of −20°C and also in solution and in bulk.

Moreover the color of the polymerization system changes as soon as the polymerization occurs, and the coexistence of a polar solvent increases the polymer yield markedly. On the basis of these findings, it is considered that rhenium pentachloride and molydenum pentachloride catalyze the ionic polymerization of trioxane by forming a complex with trioxane.

The authors wish to express their thanks to Dr. Jiro Tsuji and Mr. Masanobu Morikawa for their advice.

Basic Research Laboratories
Toyo Rayon Company, Ltd.
Kamakura

SHORT COMMUNICATIONS

The Synthesis of Glycidylferrocences

By Kazuo HATA, Izumi MOTOYAMA and Hamao WATANABE

(Received October 15, 1963)

Since the discovery of ferrocene, a great number of its derivatives have been synthesized in studies of their chemical properties. However, only a few ferrocence derivatives have been reported which are available as monomers for polymerization to homopolymers in the presence of an adequate initiator.[1] Ketazine derivatives prepared by the present authors from diacetylferrocene and hydrazine have been shown to be novel polymers, the electric resistivities of which are near to those of organic semi-conductors.[2] Now we wish to report the synthesis of a new type of ferrocene derivatives, with one or two glycidyl substituents to provide promising monomers for the formation of a homopolymer. The sequence of the synthesis and the products of the reactions are as follows:

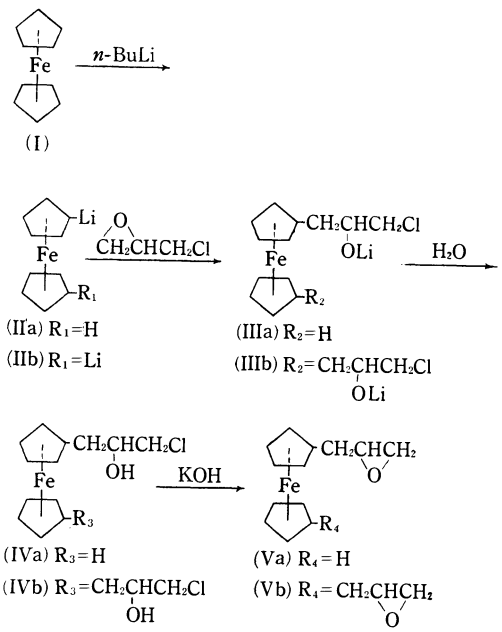

Ferrocene (I) was converted into the lithium derivative (IIa) by treatment with butyllithium

1) F. S. Arimoto and A. C. Haven, Jr., *J. Am. Chem. Soc.*, **77**, 6295 (1955); V. V. Korshak, S. L. Sosin and M. V. Chistyakova, *Vysokomolekularnye Soedineniya*, **1**, 937 (1959); *Chem. Abstr.*, **54**, 19451 (1960); V. V. Korshak, S. L. Sosin and B. P. Alekseeva, *Doklady Akad. Nauk S. S. S. R.*, **132**, 360 (1960); *Chem. Abstr.*, **54**, 20982 (1960).

2) K. Hata, I. Motoyama and K. Azuma, unpublished, read before the 16th Annual Meeting of The Chemical Society of Japan, Tokyo, April, 1963.

in anhydrous ether under an atmosphere of nitrogen.[3] The suspension was cooled to ca. −50°C. in a dry ice—acetone bath, and the ethereal solution of epichlorohydrin was added slowly.[4] After the reaction was over, the reaction mixture was poured into ice water to hydrolyze the lithium compound IIIa. The ethereal layer was separated and evaporated to remove the ether. On concentration, a large quantity of unreacted ferrocene separated as orange crystals, which were then removed by filtration. The filtrate was further evaporated under reduced pressure to obtain crude chlorohydrin (IVa), which was submitted to vacuum distillation to obtain the pure substance, a very viscous liquid, dark red in color; b.p. 156~158°C/0.8~0.9 mmHg.

Found: C, 56.09; H, 5.33. Calcd. for $C_{13}H_{15}FeClO$: C, 56.05; H, 5.43%.

Glycidylferrocene (Va) was obtained by the epoxidation of the chlorohydrin (IVa) with alkali.[5] An ethanolic solution of the crude chlorohydrin was cooled in an ice water bath, and an aqueous solution of potassium hydroxide was added with vigorous stirring. After the reaction was over, a large quantity of water and ether was added, and the crude epoxide was obtained from the ethereal layer. The crude product was purified by vacuum distillation to a slightly viscous, dark red liquid; b.p. 111~115°C/0.1~0.2 mmHg, n_D^{20} 1.6093. The overall yield of Va was ca. 13% based on ferrocene.

Found: C, 64.41; H, 5.57. Calcd. for $C_{13}H_{14}FeO$: C, 64.50; H, 5.83%. Epoxy equivalent, 0.99 (HCl-dioxane method).

From the residue of the vacuum distillation of Va, a small quantity of diglycidylferrocene (Vb) was obtained. The purification of Vb was unsuccessful by simple vacuum distillation. The distillation residue was treated with a hydrochloric acid dioxane mixture to open the epoxide ring. The products were dissolved in benzene and chromatographed on alumina, followed by elution with the same solvent. The bischlorohydrin (IVb) thus obtained was reconverted into the epoxide (Vb) with potassium hydroxide in the manner described above. The crude epoxide was dissolved in benzene and purified by chromatography on alumina, using a mixture of benzene and ether (1 : 1 by volume) for elution. Pure diglycidylferrocene was obtained as a dark red liquid with a low viscosity. The yield of Vb was ca. 0.3% based on ferrocene.

Found: C, 64.40; H, 6.18. Calcd. for $C_{16}H_{18}FeO_2$: C, 64.45; H, 6.09%.

The chlorohydrins (IVa and IVb) and the epoxides (Va and Vb) were characterized by their infrared absorption spectra (liquid film). The characteristic absorption peaks for the epoxide group in Va and Vb were found at 3050 and 2970 cm^{-1} (ν_{C-H}) and at 1256, 960~900, and 845 cm^{-1} (the epoxy ring). The figures of the two chlorohydrins and of the two epoxides are essentially identical in each pair except for the lack of peaks at 1100 and 1000 cm^{-1} in the disubstituted compounds IVb and Vb, as has been pointed out by Rosenblum in disubstituted ferrocene derivatives.[6]

Thanks are due to the Ministry of Education for the financial support granted for this research.

Department of Chemistry
Faculty of Science
Tokyo Metropolitan University
Setagaya-ku, Tokyo

3) R. A. Benkeser, D. Goggin and G. Schroll, *J. Am. Chem. Soc.*, **76**, 4025 (1954); M. Rausch, M. Vogel and H. Rosenberg, *J. Org. Chem.*, **22**, 900 (1957).
4) H. Gilmann, B. Hofferth and J. B. Honeycutt, *J. Am. Chem. Soc.*, **74**, 1594 (1952).
5) S. Winstein, T. L. Jacobs, G. B. Linden, D. Seymour, E. F. Levy, B. F. Day, J. H. Robson, R. B. Henderson and W. H. Florsheim, *J. Am. Chem. Soc.*, **68**, 1831 (1946).
6) M. Rosenblum and R. B. Woodward, *J. Am. Chem. Soc.*, **80**, 5443 (1958).

A. C. Polarography and Reversibility: Behaviour of Methyl Orange

By H. H. BAUER, T. BIEGLER and D. C. S. FOO

(Received November 4, 1963)

The appearance or non-appearance of an a.c. polarographic wave provides information on the mechanism and rate of an electrochemical process. If no wave is observed, the process may be a relatively complex one (reactions preceding or following the electron-transfer step); or a simple one (diffusion and electron transfer only) in which the rate of the electron-transfer is relatively small. If one or other of these factors is involved, it may be that a small a.c. wave is still observed; consequently, preliminary studies by a.c. polarography are usually carried out with comparatively large (~mM) concentrations of depolarizer in order to facilitate the detection of even a small wave. Such a procedure may, however, produce misleading information in the case of processes that are "reversible" at low concentrations but "irreversible" at higher concentrations; the reduction of methyl orange in alkaline solution represents, as far as we are aware, the first system in which such behaviour has actually been observed.

Methyl orange in 1M potassium nitrate and 0.05M sodium hydroxide produces a detectable a.c. polarographic wave at concentrations less than 10^{-6} M; the wave has a maximum height at concentrations of ca. 2×10^{-5} M, and at concentrations above ca. 2×10^{-4} M no a.c. wave is observed (cf. Fig. 1). The d.c. polarographic calibration curve is quite normal in this range of concentrations; but the d.c. step exhibits a maximum at concentrations above ca. 10^{-4} M, and the logarithmic plot changes with concentration (slope = 31 mV. at 10^{-5} M, 38 mV. at 2×10^{-5} M, 44 mV. at 5×10^{-5} M).

Solutions of methyl orange show deviations from Beer's law at concentrations above ca. 10^{-5} M, both in acid and in alkaline media; however, the a.c. polarographic calibration curve is anomalous (in the sense indicated above) only in alkaline solution (cf. Fig. 1) and not in acid (cf. Fig. 2).

Elucidation of the mechanism of the reduction requires additional data; our present purpose, however, is merely to report this new type of effect and to point to the implication that, in the testing of reversibility by a.c. polarography, it is essential to bear in mind the possible effect of concentration of the depolarizer.

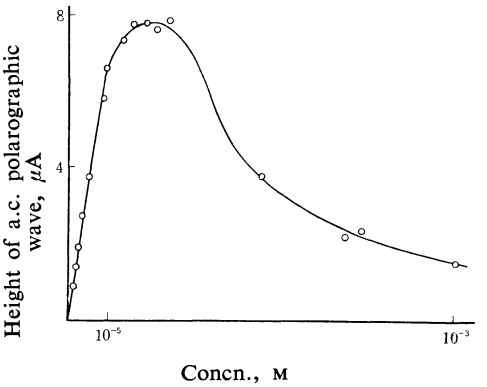

Fig. 1. Calibration curve for solutions of methyl orange in 1M KNO_3 and 0.05M NaOH; 15mV. r.m.s., 50 c.p.s.

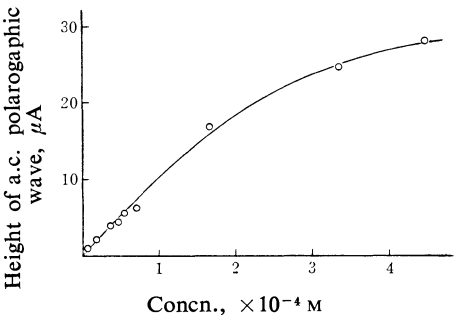

Fig. 2. Calibration curve for solutions of methyl orange in 1M KNO_3 and 0.005M H_2SO_4; 15 mV. r.m.s., 50 c.p.s.

Faculty of Agriculture
The University of Sydney
Sydney, Australia (H. B. & D. F.)

Department of Chemistry
University of Illinois
Urbana, Ill., U.S.A. (T. B.)